Superconductivity

Yury Holubeu *

October 31, 2025

The note is not intended for distribution. Superconductivity and its applications is discussed in detail. The note has solved problems and summary of special topics. Readers who have opened this note for the first time are highly recommended to read the preface.

Contents

Preface and main motivation **18**

I —— Superconductivity in a Nutshell —— **20**

1 Main Models and Properties of Superconductors **20**
1.1 Main Theories for Superconductors . . . 20
1.1.1 Main properties of SC and overview of theoretical methods . . . 20
1.1.2 GL theory . . . 25
1.1.3 BCS theory . . . 29
1.1.4 Electrodynamics of superconductors . . . 33
1.1.5 BdG equations, BTK formalism, Andreev states . . . 33
1.1.6 Currents, Thermodynamics, Susceptibilities . . . 36
1.1.7 General important features of superconductors and theories . . . 38
1.2 Typical SC Effects . . . 38
1.2.1 Josephson equations, SNS, SQUID, RCSJ . . . 38
1.2.2 NS, NIS, SIS, other typical junctions . . . 48
1.2.3 Skin effect, inductance, impedance . . . 50
1.2.4 Thin films, plates . . . 52
1.2.5 Vortices: basic models . . . 54
1.3 Basic concepts of condensed matter for SC . . . 56
1.4 Mathematics . . . 56
1.5 Materials, experimental facts . . . 57

2 Most Useful Special Methods **58**
2.1 Very useful special methods for special applications . . . 58
2.1.1 Functional integral for SC . . . 58
2.1.2 Scattering Matrix, Beenkker method for SC Junctions . . . 59

II Fundamentals of Superconductivity **60**

3 Framework for understanding superconductivity **60**
3.1 General ideas about fundamental nature of superconductivity . . . 60
3.1.1 How to predict existence of SC from literally nothing? . . . 60
3.1.2 How to predict existence of SC from high-T properties? . . . 60
3.1.3 Taking into account shape of the Fermi surface (????) . . . 60
3.1.4 Intuitive understanding of GL theory . . . 60
3.1.5 How to guess about GL theory? . . . 60
3.1.6 Intuitive understanding of BCS theory . . . 60
3.1.7 How to guess about BCS theory? . . . 60
3.2 Basic Experimental Facts about Typical SC . . . 61
3.2.1 Overview of Basic Experimental Facts about Typical SC . . . 61
3.2.2 The Isotope Effect . . . 64
3.2.3 The Anisotropy Effect. . . . 67

*https://yuriholubeu.github.io/, yuri.holubev@gmail.com

3.2.4 Meissner effect . . . 67
3.2.5 Advanced Experimental Facts about Typical SC . . . 67
3.3 Other Ideas for Introduction to Superconductivity . . . 72
3.3.1 General Introduction to Superconductivity . . . 72
3.3.2 I-I A new condensed state by de Gennes . . . 76
3.4 Professional Choice of Model for SC . . . 77
3.5 Linear Electrodynamics of Superconductors: Basics . . . 77
3.5.1 The London Equations: Basics . . . 77
3.5.2 The London Equations: Another Theories . . . 79
3.5.3 2.2 Magnetic Field Penetration Depth . . . 85
3.5.4 2.3 Nonlocal Electrodynamics of Superconductors . . . 86
3.5.5 Propagation of a electric field inside the SC . . . 87
3.5.6 2.4 Quantum Generalization of the London Equations. . . . 87
3.5.7 Magnetic Flux Quantization . . . 88
3.6 Ginzburg Landau Theory: Basics . . . 90
3.6.1 General GL philosophy of phase transitions . . . 90
3.6.2 3.2 Equations of the Ginzburg-Landau Theory . . . 93
3.6.3 Characteristic Lengths, Proximity Effect, Thermodynamic Critical Field . . . 101
3.6.4 Characteristic Lengths of the Ginzburg-Landau Theory . . . 106
3.6.5 Energy of a Normal Metal-Superconductor Interface . . . 111
3.6.6 Limits of Applicability of GL Theory . . . 115
3.6.7 1-4 Two kinds of superconductors by de Gennes . . . 115
3.6.8 The Wall Energy, derivation of $\varkappa_c = 1/2$ . . . 117
3.7 Ginzburg Landau theory: advanced general features and details . . . 123
3.7.1 Anderson-Higgs mechanics and Goldstone Theorem in SC . . . 123
3.7.2 Typical Subtle Features of GL theory . . . 125
3.7.3 Fluctuation effects near SC phase transitions: basic concepts . . . 126
3.7.4 Intuitive understanding of GL theory . . . 133
3.7.5 Short Examples of Applications of GL theory . . . 133
3.8 Background for Real Understanding of BCS Theory . . . 134
3.8.1 Speedrun of Condensed Matter for Superconductivity . . . 134
3.8.2 Superfluid Fermi Gas: Energy Spectrum . . . 134
3.8.3 Superfluid Fermi Gas: Thermodynamic Properties . . . 134
3.8.4 Green's Functions of Superfluid Fermi Gas . . . 134
3.8.5 Temperature Green's Functions of Superfluid Fermi Gas . . . 134
3.8.6 QFT formalism for bound states of two particles . . . 135
3.9 BCS Theory: Basic General Properties . . . 135
3.9.1 Cooper Pairs: General Idea and Physical Picture . . . 135
3.9.2 Cooper Pairs: Basic Calculations . . . 144
3.9.3 Cooper Pairs: QFT framework . . . 147
3.9.4 BCS Hamiltonian: Derivation and Features . . . 153
3.9.5 Mean-field Approximation of BCS Hamiltonian, Diagonalization . . . 165
3.9.6 Meaning of the gap Δ, gap equation . . . 175
3.9.7 Tight-binding 1D BCS model . . . 184
3.9.8 Ground State Energy and Wavefunction in BCS . . . 188
3.9.9 What exactly happens at a ground state of a SC (at $T = 0$)? . . . 192
3.9.10 System of QFT GF Equations for a Superconductor . . . 197
3.9.11 The Superconductivity QFT Equations: Derivation . . . 205
3.9.12 Δ_0 and T_c, The Universal BCS Relation . . . 208
3.9.13 Gap Δ as a function of T . . . 212
3.9.14 The gap Δ: 1001 questions and statements about details . . . 216
3.9.15 The gap Δ: Measurement and Effects from It . . . 218
3.9.16 Chemical Potential of a Superconductor . . . 221

3.9.17 The Coupling Constant of BCS Model . . . 221
3.10 BCS: Advanced Features and Details of a Typical Setups . . . 222
3.10.1 Overview of general important features of BCS . . . 222
3.10.2 How Good and Useful Is BCS Theory? . . . 224
3.10.3 Cooper Pairs: Deeper Understanding . . . 224
3.10.4 Cooper Pairs: Spatial Structure, Life Time, Speed . . . 227
3.10.5 BCS theory in 1D, 2D: General Features . . . 232
3.10.6 Original 1957 BCS Paper 1: Conclusion, Introduction, General Questions . . . 232
3.10.7 Original 1957 BCS Paper 1: Ground State . . . 239
3.10.8 Original 1957 BCS Paper: Excited States . . . 247
3.10.9 Original 1957 BCS Paper: Calculation of Matrix Elements . . . 257
3.10.10 Original 1957 BCS Paper: Electrodynamic Properties . . . 264
3.10.11 Original 1957 BCS Paper: Appendices . . . 274
3.10.12 Phase and Particle Number Operators in SC . . . 284
3.10.13 BCS model with net motion of electrons . . . 285
3.11 BCS: Formalisms for Special Setups . . . 286
3.11.1 BCS in a Framework of Path Integral . . . 286
3.11.2 Nambu Notation, Hole Interpretation . . . 286
3.11.3 Gap in Unconventional Superconductors: Basics . . . 287
3.11.4 Anderson's Random-Phase Approximation in SC . . . 290
3.11.5 Impurities in BCS: General Idea How to Take Them into Account . . . 290
3.11.6 Impact of Lattice Configuration in BCS . . . 290
3.11.7 BCS theory in the Density Matrix Framework . . . 291
3.11.8 Time-Dependent BCS . . . 294
3.12 General Formalisms for Typical Effects . . . 294
3.12.1 Currents and Tunneling Effects: Basic Concepts 1 . . . 294
3.12.2 Currents and Tunneling Effects: Basic Concepts 2 . . . 304
3.12.3 6.5 Persistent Current and the Meissner-Ochsenfeld Effect . . . 311
3.12.4 Formalism for Thermodynamic Effects of the Meissner State . . . 314
3.12.5 Introduction to Thermodynamics of Superconductors . . . 322
3.12.6 Which Equilibrium Properties will Be Not Present in Nonequilibrium? . . . 325
3.13 General Ideas of Other Effects . . . 325
3.13.1 Dissipative and open BCS: General Concepts . . . 325
3.13.2 Magnetic Field, Created by Cooper Pairs (???) . . . 326

4 Basic Effects of Superconductors 326
4.1 General Effects . . . 326
4.1.1 Critical supercurrent: basics . . . 326
4.1.2 Critical supercurrent: advanced features 1 . . . 331
4.1.3 Critical supercurrent: advanced features 2 . . . 339
4.1.4 Description of Isotope effect . . . 356
4.1.5 Description of Meissner effect . . . 356
4.1.6 Flux quantization . . . 357
4.1.7 Flux quantization: Experimental confirmation . . . 358
4.1.8 Levitation over Superconductor: Basic understanding . . . 358
4.1.9 1-2 Diamagnetism by de Gennes . . . 359
4.1.10 1-3 Absence of low energy excitations by de Gennes . . . 362
4.2 Thermodynamic Effects . . . 364
4.2.1 Specific heat, Free Energy, Entropy 1 . . . 364
4.2.2 Specific heat, Free Energy, Entropy 2 . . . 369
4.2.3 Specific Heat: Experimental confirmation . . . 372
4.2.4 Thermal Conductivity . . . 374
4.2.5 Vortices: General Properties . . . 376
4.2.6 Critical field of superconductors 1 . . . 378

4.2.7 Critical field of superconductors 2 . . . 381
4.2.8 Critical Magnetic Field of Thin Films in a Field Parallel to the Surface . . . 386
4.2.9 The Intermediate State . . . 387
4.2.10 Critical Magnetic Fields for Type-II SC . . . 390
4.2.11 38. Superconductors Close to the T_c in an Arbitrary Magnetic Field . . . 412

5 Details of Fundamental Effects and Other Basic Properties 416
5.1 Basics of Determination of Physical Parameters . . . 416
5.1.1 Determination of the value of T_c . . . 416
5.2 Important general features of theories of superconductivity . . . 416
5.2.1 Connection of the Ginzburg-landau and BCS theory . . . 416
5.2.2 What is Different in Equilibrium and Non-Equilibrium Superconductors? . . . 424
5.2.3 Derivation of phenomena of GL theory in the framework of BCS theory . . . 424
5.2.4 Derivation of phenomena of BCS theory in the framework of GL theory . . . 424
5.2.5 Existence of 1D superconductors . . . 425
5.2.6 General idea of dissipation in superconductors . . . 425
5.2.7 Other General Fundamental Concepts . . . 425
5.2.8 How can we theoretically prove that other low-energy effects do not destroy SC? 426
5.3 Other Typical Properties . . . 426
5.3.1 Velocity of superconductive electrons . . . 426
5.3.2 Parity Effect in SC by Shmidt 48* . . . 426
5.3.3 Unconventional superconductivity: Relation to the Basic Theory . . . 429

III Bulk Properties of Superconductors 434

6 Methods from De Gennes 434
6.0.1 3-3 Nonequilibrium Properties . . . 434
6.1 Description of the Condensed State . . . 441
6.1.1 4-1 Instability of the Normal State in the Presence of an Attractive Interaction 441
6.1.2 4-2 Origin of the Attractive Interaction . . . 444
6.1.3 4-3 Ground State and Elementary Excitations . . . 450
6.1.4 4-4 Calculations at Finite Temperature . . . 462
6.2 The Self-Consistent Field Method . . . 473
6.2.1 5-1 The Bogoliubov Equations . . . 473
6.2.2 5-2 Theorems on the Pair Potential and the Excitation Spectrum . . . 480
6.2.3 5-3 The Meissner Effect in Metals and Alloys . . . 491
6.3 Phenomenological Landau-Ginsburg Equations . . . 499
6.3.1 6-1 Introduction . . . 499
6.3.2 6-2 Construction of the Free Energy . . . 499
6.3.3 6-3 Equilibrium Equations . . . 502
6.3.4 6-4 The Two Characteristic Lengths . . . 503
6.3.5 6-5 Situations Where $|\psi|$ Is Constant . . . 507
6.3.6 6-6 Situations Where $|\psi|$ Varies Spatially . . . 517
6.3.7 6-7 Structure of the Vortex Phase in Strong Fields ($H \sim H_{C2}$) . . . 521
6.4 Microscopic Analysis of the Landau-Ginsburg Equations . . . 527
6.4.1 7-1 Linearized Self-Consistency Equation . . . 527
6.4.2 7-2 Landau-Ginsburg Equations . . . 534
6.4.3 7-3 Surface Problems in the Landau-Ginsburg Region . . . 540
6.5 Effects of Strong Magnetic Fields and of Magnetic Impurities . . . 555
6.5.1 8-1 Relation Between Transition Temperature and Time-Reversal Properties . . . 556
6.5.2 8-2 Ergodic Versus Nonergodic Behavior - Gapless Superconductivity . . . 561
6.5.3 8-3 Dirty Superconductors in High Magnectic Fields . . . 570

7 Well-known phenomena of superconductors **574**
7.1 Magnetic properties of first kind superconductors by de Gennes . . . 574
7.1.1 2-1 Critical field of a long cylinder . . . 574
7.1.2 2-2 Penetration depths . . . 577
7.1.3 2-3 Magnetic properties of a sample of arbitrary shape: intermediate state . . . 582
7.2 Magnetic properties of second kind superconductors by de Gennes . . . 596
7.2.1 3-1 Magnetization curves of a long cylinder . . . 596
7.2.2 3-2 Vortex state: microscopic description . . . 600
7.3 Thin films . . . 620
7.3.1 3.5 Critical Field of a Thin Film . . . 620
7.3.2 3.6 Critical Current of a Thin Film . . . 623
7.4 2. Some Effects in Scope of Linear Electrodynamics of Superconductors . . . 627
7.4.1 2.5 Magnetic Field and Current Distributions in Simple Configurations . . . 627
7.4.2 2.6 Kinetic Inductance . . . 633
7.4.3 2.7 Complex Conductivity of a Superconductor . . . 635
7.4.4 2.8 Skin Effect and Surface Impedance . . . 636
7.5 Other Bulk Effects in Electromagnetic Field . . . 638
7.5.1 Superconductors in a Weak Electromagnetic Field by AGD . . . 638
7.6 5. Type-II Superconductors . . . 649
7.6.1 5.1 Introduction . . . 649
7.6.2 5.2 Field of an Isolated Vortex . . . 651
7.6.3 5.3 The Lower Critical Field . . . 653
7.6.4 5.4 Interaction Between Vortices . . . 655
7.6.5 5.5 The Upper Critical Field . . . 657
7.6.6 5.6 Reversible Magnetization of a Type-II Superconductor . . . 657
7.6.7 5.7 Surface Superconductivity. The Third Critical Field . . . 659
7.6.8 5.8 Surface Barrier. Superheating of the Meissner State . . . 662
7.6.9 5.9 Some Remarks About High-Temperature Superconductors . . . 666
7.6.10 5.10 Critical Current of a Type-II Superconductor. Critical State . . . 668
7.6.11 5.11 Interaction of Vortices with Pinning Centers . . . 670
7.6.12 5.12 Resistive State . . . 675
7.7 Type II Superconductors: Advanced Properties . . . 679
7.7.1 35*. Anisotropic Type-II Superconductors . . . 679
7.7.2 36*. Разрушение сверхпроводимости в тонкой пленке тепловыми вихрями . . . 681
7.7.3 37*. Melting of the Vortex Lattice . . . 687
7.7.4 38. Critical current in type-II SC . . . 689
7.7.5 41*. Collective Pinning of Vortices by Weak Defects . . . 691
7.7.6 42*. Magnetic Flux Creep and Nonlinear Conductivity in HTSC . . . 696

8 Superconductivity by Abrikosov **701**
8.1 15 Macroscopic theory of superconductivity . . . 701
8.1.1 15.1. General properties of superconductors . . . 701
8.1.2 15.2. Thermodynamics of the superconducting transition . . . 704
8.1.3 15.2. Thermodynamics of the superconducting transition . . . 705
8.1.4 15.3. The intermediate state . . . 706
8.1.5 15.4. Destruction of superconductivity by a current . . . 711
8.1.6 15.4. Destruction of superconductivity by a current . . . 712
8.1.7 15.4. Destruction of superconductivity by a current . . . 713
8.1.8 15.5. The London equations . . . 717
8.2 16 Basic ideas of the microscopic theory . . . 721
8.2.1 16.1. The superfluidity condition . . . 721
8.2.2 16.2. Phonon attraction . . . 722
8.2.3 16.3. Cooper pairs . . . 724
8.2.4 16.3. Cooper pairs . . . 725

8.2.5 16.4. The energy spectrum . . . 727
8.2.6 16.5. Temperature dependence of the energy gap . . . 734
8.2.7 16.6. Thermodynamics of superconductors . . . 736
8.2.8 16.7. London and Pippard superconductors (qualitative theory) . . . 742
8.2.9 16.8. The Meissner effect at $T = 0$ . . . 743
8.2.10 16.9. The relationship between current and field at finite temperatures. The London limit . . . 749
8.2.11 16.10. The superconducting correlation and surface energy. Two types of superconductors. The role of impurities . . . 751
8.2.12 16.11. High-temperature superconductivity . . . 755
8.3 17 The Ginzburg-Landau theory . . . 765
8.3.1 17.1. Derivation of the Ginzburg-Landau equations . . . 765
8.3.2 17.2. Surface energy at the interface between the normal and superconducting phases . . . 775
8.3.3 17.2. Surface energy at the interface between the normal and superconducting phases . . . 776
8.3.4 17.3. The critical field and magnetization of a thin film. Supercooling and superheating . . . 777
8.3.5 17.4. The critical current of a thin wire with $x \ll 1$ . . . 782
8.3.6 17.4. The critical current of a thin wire with $x \ll 1$ . . . 783
8.3.7 17.5. Quantization of the magnetic flux . . . 787
8.4 18 Type II superconductivity . . . 791
8.4.1 18.1. Magnetic properties of type II superconductors. The qualitative picture . 791
8.4.2 18.2. Magnetic properties of type II superconductors. Quantitative theory for the vicinity of H_{c2} . . . 795
8.4.3 18.3. Magnetic properties of type II superconductors. Metals with $x > 1$ . . . 803
8.4.4 18.3. Magnetic properties of type II superconductors. Metals with $x \gg 1$ . . . 804
8.4.5 18.4. Surface superconductivity . . . 814
8.4.6 18.5. Type II superconductors at low temperatures . . . 820
8.4.7 18.6. A thin film of a type II superconductor in a magnetic field . . . 827
8.4.8 18.7 Anisotropic type II superconductor in a magnetic field . . . 833
8.4.9 18.8. Superconducting magnets. Pinning . . . 838
8.5 19 Kinetics of superconductors . . . 843
8.5.1 19.1. Electronic thermal conductivity . . . 843
8.5.2 19.2. Thermoelectric phenomena . . . 846
8.5.3 19.3. The behavior of superconductors in a weak high-frequency field . . . 851
8.5.4 19.3. The behavior of superconductors in a weak high-frequency field . . . 852
8.5.5 19.4. Absorption of ultrasound . . . 854
8.5.6 19.5. Stimulation of superconductivity by high-frequency, high-intensity field and sound . . . 856
8.5.7 19.5. Stimulation of superconductivity by high-frequency, high-intensity field and sound . . . 857
8.5.8 19.6. Paraconductivity . . . 860
8.6 20 The interface between a superconductor and a normal metal . . . 866
8.6.1 20.1. The proximity effect . . . 866
8.6.2 20.2. Superconductivity of twinning planes . . . 873
8.6.3 20.3. Andreev reflection . . . 892
8.6.4 20.4. Low-temperature heat capacity of the intermediate state . . . 894
8.7 21 Superconductivity and magnetism . . . 896
8.7.1 21.1. Superconductors containing magnetic impurities. Gapless superconductivity 896
8.7.2 21.2. The inhomogeneous superconducting state . . . 902
8.7.3 21.3. Ferromagnetic superconductors . . . 908
8.7.4 21.4. The Knight shift . . . 916

8.8 22 Tunnel junctions. The Josephson effect . . . 920
8.8.1 22.1. Single-particle tunnel current . . . 920
8.8.2 22.2. The Josephson effect . . . 928
8.8.3 22.3. Microscopic derivation of the Josephson current . . . 935
8.8.4 22.3. Microscopic derivation of the Josephson current . . . 936
8.8.5 22.3. Microscopic derivation of the Josephson current . . . 936
8.8.6 22.4. The Josephson effect in a magnetic field . . . 942
8.8.7 22.5. The ac Josephson effect . . . 947
8.8.8 22.5. The ac Josephson effect . . . 947
8.8.9 22.6. Waves in the Josephson junction . . . 951
8.8.10 22.7. Josephson junctions with a normal metal or a semiconductor layer . . . 955
8.8.11 22.7. Josephson junctions with a normal metal or a semiconductor layer . . . 956
8.8.12 22.8. Practical applications of the Josephson effect . . . 959
8.8.13 22.9. The dynamical resistive state of a thin superconductor at supercritical currents . . . 962

IV Junctions, tunneling 972

9 Typical Methods for Junctions with Examples 972
9.1 Reminder of Tunneling in Mesoscopic Physics and in Semiconductors . . . 972
9.2 Josephson Junction: Basic Models and Effects . . . 972
9.2.1 4.1 Phase Coherence and Types of Weak Links . . . 972
9.2.2 4.2 The DC Josephson Effect . . . 974
9.2.3 4.3 The AC Josephson Effect . . . 979
9.2.4 1001 Questions about what exactly happens in JJ? . . . 981
9.2.5 Experimental Confirmation of CPR in JJ . . . 981
9.2.6 Shapiro Steps . . . 981
9.2.7 Josephson Junction in an External Magnetic Field . . . 981
9.2.8 SQUIDs (Superconducting Quantum Interferometers): Basic Concepts . . . 988
9.2.9 SQUIDs: Typical Modifications . . . 995
9.2.10 46. Tunneling Effects by Shmidt . . . 996
9.2.11 7.4 Andreev Reflection . . . 1003
9.2.12 Andreev Reflection: Experimental Consequences . . . 1004
9.3 Overview and Comparison of Methods for different JJ . . . 1004
9.4 Special properties and Deeper Understanding of SC Contacts . . . 1005
9.4.1 22. Nonstationary Josephson Effect, Resistive Characteristics . . . 1005
9.4.2 23*. Fluctuations of Critical Current, Macroscopic Tunneling . . . 1012
9.4.3 Ambegoakar-Baratoff formula . . . 1018
9.4.4 Superconducting weak links by Likharev: Main Statements . . . 1018
9.4.5 Current-phase relation in JJ by Golubov et al.: Main Statements . . . 1018
9.4.6 Other basic features of Josephson junctions . . . 1018
9.4.7 Inelastic tunneling: Main Concepts . . . 1019
9.4.8 Josephson radiation . . . 1019
9.4.9 Junctions by de Gennes book . . . 1019
9.5 Bogliubov-de Gennes Equations for Superconductors in the Continuum Model . . . 1019
9.5.1 1.2 Hopping in a Quantum Many-Body Hamiltonian . . . 1019
9.5.2 1.3 Second Quantization of Hopping Hamiltonians . . . 1023
9.5.3 1.5 Derivation of the BdG Equations in the Continuum Model . . . 1026
9.5.4 1.7 Solution to the BdG Equations in Homogeneous Systems . . . 1032
9.5.5 1.8 Relation of BdG Method to the Abrikosov-Gor'kov Equations . . . 1037
9.6 Transport Across Normal-Metal/Superconductor Junctions . . . 1040
9.6.1 6.1 Blonder-Tinkham-Klapwijk Scattering Formalism . . . 1040
9.6.2 6.2 Tunneling Conductance Through a NS Junction . . . 1045

9.6.3 6.3 Suppression of Andreev Reflection in a FS Junction . . . 1052
9.6.4 Transport Properties Through a TI-S Junction . . . 1054
9.7 BdG Equations in Tight-Binding Model . . . 1060
9.7.1 2.1 Derivation of BdG Equations in a Tight-Bind Model . . . 1060
9.7.2 Local Density of States and Bond Current in the Lattice Model . . . 1066
9.7.3 Nambu Notation for SC Junctions . . . 1067
9.7.4 Optical Conductivity and Superfluid Density in the Lattice Model . . . 1067
9.7.5 2.2 Solution to the Lattice BdG Equations for a Uniform Superconductor . . . 1076
9.7.6 2.3 Lattice Abrikosov-Gorkov Equations . . . 1078
9.8 Junctions in Microscopic Framework: Basics . . . 1082
9.9 Junctions in Microscopic Framework: Other Features . . . 1082
9.10 GF method for JJ . . . 1082
9.10.1 Caroli's GF Method . . . 1082
9.10.2 GF method for JJ: Examples . . . 1082
9.11 Beeankker's Determinant Framework: Basics . . . 1083
9.12 Beeankker's Determinant Framework: Other Features . . . 1083
9.13 Green's function for SC Junctions: Other Working Methods . . . 1083
9.14 "Classic" theoretical results of Josephson Junctions: An Overview . . . 1083

10 Well-Known Models of Junctions 1083
10.1 Very Famous Models . . . 1083
10.1.1 Blonder Tinkham Klapwijk Original Model 1: Basics . . . 1083
10.1.2 Blonder Tinkham Klapwijk Original Model 1: Advanced Sratements . . . 1093
10.1.3 Josephson Junction with impurity by Bagwell . . . 1106
10.1.4 Josephson Junction with impurity by Bagwell: Calculations . . . 1118
10.1.5 Ballistic JC through an asymmetric SNS by Chang, Bagwell . . . 1127
10.1.6 Josephson and Andreev transport through quantum dots . . . 1127
10.1.7 JJ through a Semiconductor Nanowire . . . 1127

11 Specific Junctions, Applications 1128
11.1 SFS Junction (Junction Through a Ferromagnet) . . . 1128
11.1.1 47*. SFS junction by Shmidt . . . 1128
11.2 Multiterminal junctions . . . 1133
11.3 Very exotic models and properties of junctions . . . 1133
11.3.1 Casimir froce in Josephson Junctions . . . 1133
11.4 Application of Junctions: Main Ideas . . . 1133
11.4.1 4.6 Applications of Weak Superconductivity . . . 1133

V Very Useful Methods 1136

12 Methods for BCS SC 1136
12.1 Transformations . . . 1136
12.1.1 Selected GF methods for superconductivity . . . 1136
12.1.2 Matrix transformations for BCS . . . 1137
12.2 Numerical methods . . . 1137
12.2.1 Typical examples of numerical methods . . . 1137

13 Bogliubov-de Gennes Equations: Methods and Applications by Jian-Xin Zhu 1139
13.1 3 Local Electronic Structure Around a Single Impurity in Superconductors . . . 1139
13.1.1 3.1 Introduction . . . 1139
13.1.2 3.2 Yu-Shiba-Rusinov Impurity States in an s-Wave Superconductor . . . 1140
13.1.3 3.3 Majorana Fermion in an s-Wave SC with a Chain of Localized Spins . . . 1145
13.1.4 3.4 Impurity Resonance State in a d-Wave Superconductor . . . 1149

13.2 4 Disorder Effects on Electronic and Transport Properties in Superconductors 1153
13.2.1 4.1 Anderson Theorem for Disordered *s*-Wave Superconductor 1153
13.2.2 4.2 Suppression of Superconductivity in a Disordered *d*-Wave Superconductor . 1157
13.2.3 4.3 Quasiparticle Localization in a Disordered *d*-Wave Superconductor 1162
13.3 5 Local Electronic Structure in Superconductors Under a Magnetic Field 1169
13.3.1 5.1 Effect of the Magnetic Field 1169
13.3.2 5.2 Vortex Core State in an *s*-Wave Superconductor 1171
13.3.3 5.2.1 Single Isolated Vortex 1171
13.3.4 5.2.2 High Field Limit 1178
13.3.5 5.3 Vortex Core States in a *d*-Wave Superconductor 1179
13.3.6 5.3.1 Single Isolated Vortex 1179
13.3.7 5.3.2 Quasiparticle States in a Mixed-State of d-Wave Superconductors 1181
13.3.8 5.4 Fulde-Ferrell-Larkin-Ovchinikov State due to a Zeeman Magnetic Field . . . 1187
13.4 7 Topological and Quantum Size Effects in SC at Reduced Length Scale 1190
13.4.1 7.1 Persistent Current in a Mesoscopic *s*-Wave SC Ring 1190
13.4.2 7.2 Current in Multiply Connected Mesoscopic *d*-Wave SC Geometries 1196
13.4.3 7.2.1 Cylindrical Geometry 1196
13.4.4 7.2.2 Square Loop Geometry 1198
13.4.5 7.3 Quantum Size Effects in Nanoscale Superconductors 1199

VI Problems and Questions 1203

14 Typical problems 1203
14.1 Simplified problems about SC phenomena 1203
14.1.1 Problems about superconductors in magnetic field 1203
14.1.2 Qualitative, basic problems about SC 1 1203
14.1.3 Qualitative, basic problems about SC 2 1212
14.2 Problems about Typical Methods, Effects 1216
14.2.1 Framework of BCS: Problems about Basic Transformations 1216
14.2.2 Framework of BCS: Basic, General Properties 1225
14.2.3 Problems about the Gap Equation 1229
14.2.4 Problems about Exotic Transformations in BCS Model 1237
14.2.5 Problems about Numerical Computations in BCS Model 1239
14.2.6 Questions about Applicability of Formulas 1242
14.2.7 Problems about phenomena in the theoretical BCS 1 1242
14.2.8 Dirty Superconductors: Basic Problems 1 1252
14.2.9 Dirty Superconductors: Basic Problems 2 1257
14.2.10 Problems about tunneling, junctions 1: Basic Models 1264
14.2.11 Problems about tunneling, junctions 2: Basic Models 1271
14.2.12 Problems about tunneling, junctions 3: Basic Models 1273
14.2.13 Ginzburg-Landau Formalism: Problems about phenomena [SEE COND MATT] 1278
14.2.14 Type II superconductors: Basic Problems 1 1282
14.2.15 Other Problems by Shmidt's book 1283
14.3 Questions about Checking Basic Knowledge 1283
14.3.1 Questions about Understanding Basics 1 1283
14.3.2 Questions about Understanding Basics 2 1286
14.3.3 Questions about Understanding Basics 3 1288
14.3.4 Questions about Understanding Typical Phenomena 1 1289
14.3.5 Questions about Understanding Typical Phenomena 2 1290
14.3.6 Questions about Understanding Special Models 1290
14.3.7 Problems about Understanding Special Effects 1290
14.3.8 Hypothetical questions about сверхпроводниках 1290
14.4 Other Questions about Superconductivity 1290

14.4.1 Questions about what is exactly going on in BCS? . . . 1290

15 Problems about specific phenomena and properties 1291
15.1 Problems about Special Useful Methods . . . 1291
15.1.1 Problems about GF Special Methods for SC 1 . . . 1291
15.1.2 Problems about GF Special Methods for SC 1 . . . 1294
15.2 Problems about Special Effects . . . 1296
15.2.1 Problems about Nambu Notation for Applications . . . 1296
15.2.2 Problems Transformations of SC Green's functions . . . 1301
15.2.3 Problems about флуктуационные эффекты в слабых контактах . . . 1302
15.2.4 Problems about GF Special Methods for SC . . . 1303
15.2.5 Problems about Majorana states in SC-s . . . 1306
15.2.6 Problems about vortices . . . 1306
15.2.7 Problems about fluctuation effects . . . 1307
15.2.8 Problems about properties of unconventional superconductors . . . 1308
15.2.9 Problems about models with unconventional superconductors . . . 1309
15.3 Creation of Special Models . . . 1309
15.3.1 Problems about Creation of a Model for Special Superconductors 1 . . . 1309
15.3.2 Problems about Creation of a Model for Special Superconductors 2 . . . 1310
15.4 Problems about Special Methods . . . 1311
15.4.1 Problems about numerical evaluation . . . 1311
15.5 Problems about Special Devices, Junctions . . . 1311
15.5.1 Problems about Creation of a Model for SC Devices 1 . . . 1311
15.5.2 Problems about Creation of a Model for SC Devices 2 . . . 1312
15.5.3 Problems about special junctions with SC . . . 1312
15.5.4 Problems about Creation of a Model of Special MTJJ . . . 1313
15.5.5 Problems about Special Junctions 1 . . . 1313
15.5.6 Problems about Special Junctions 2 . . . 1314
15.5.7 Problems about Special Junctions 3 . . . 1315
15.5.8 Problems about MTJJ . . . 1315

VII —— Specific Superconductivity in a Nutshell —— 1316

16 Special also useful theories and properties 1316
16.1 Details of general properties of superconductors . . . 1316
16.2 Details of basic theories . . . 1318
16.2.1 Details of GL theory . . . 1318
16.2.2 Details of BCS theory . . . 1320
16.2.3 BCS: examples of diagrammatic methods . . . 1322
16.2.4 Gorkov formalism . . . 1331
16.2.5 General details of theories of SC . . . 1336
16.3 Details of well-known SC models . . . 1336
16.3.1 Josephson junctions: other methods and properties . . . 1336
16.3.2 RCSJ, SQUID: other methods and properties . . . 1337
16.3.3 Superconductors of II kind: other well-known properties . . . 1340
16.4 Other well-known methods for SC junctions . . . 1341
16.4.1 Tight-binding SC models . . . 1341
16.4.2 Overview of other tunneling properties . . . 1341
16.4.3 BTK Method . . . 1342
16.4.4 Beenakker's Determinant Method . . . 1346
16.4.5 Majorana wires and junctions . . . 1347
16.4.6 Fluctuation effects in weak contacts . . . 1349
16.5 Other well-known theories and formalisms for typical SC . . . 1349

16.5.1 Superconductors with dissipation . . . 1349
16.5.2 Theory of Superconducting Alloys by Abrikosov–Gorkov . . . 1350
16.5.3 Other experimental hints for a true SC theory . . . 1350
16.5.4 Effects of Temperature and Magnetic Field . . . 1350
16.5.5 Eliashberg Theory of Electron–Phonon Interaction (???) . . . 1350
16.6 Unconventional Superconductivity in a Nutshell . . . 1350
16.6.1 Overview of UC SC . . . 1351
16.6.2 Fundamentals of UC SC . . . 1351
16.6.3 Advanced properties of basic UC SC . . . 1354
16.6.4 9 Paramagnetic Susceptibility and Knight Shift . . . 1356
16.6.5 11 Superconducting States with Multicomponent Order Parameters . . . 1356
16.6.6 12 Ginzburg-Landau Equations and Upper Critical Field . . . 1356
16.6.7 13 Boundary Conditions and Surface Superconductivity . . . 1356
16.6.8 14 Meissner and Mixed States in Unconventional Superconductors . . . 1356
16.6.9 15 Magnetic Superconductors . . . 1356
16.6.10 18 Ginzburg-Landau Functional for UC SC . . . 1356
16.6.11 19 Upper Critical Field in a p-wave Superconductor . . . 1356
16.6.12 20 Boundary Conditions for the Order Parameter . . . 1356
16.6.13 21 Effect of Impurities on Unconventional Superconductivity . . . 1356
16.6.14 22 Electronic Thermal Conductivity of Unconventional Superconductors . . . 1356
16.7 Special effects . . . 1356
16.7.1 Thermoelectric effects . . . 1356
16.7.2 Heat Capacity from Fluctuation, Diamagnetism of SC II kind . . . 1356
16.7.3 Functional integral for Gor'kov and GL theories . . . 1359

17 Very special theories and models 1360
17.1 Very special SC junctions . . . 1360
17.1.1 Tight-biding models of SC junctions . . . 1360
17.1.2 Special Voltage States of JJ . . . 1360
17.1.3 Fluctuation Effects in Weak Junctions . . . 1361
17.1.4 SFS junctions . . . 1361
17.1.5 MTJJ methods and models . . . 1361
17.1.6 Overview of other not so used methods for SC contacts . . . 1363
17.2 Disorder in Superconductors in a Nutshell . . . 1364
17.2.1 Disorder of superconductors: Basic Models . . . 1364
17.2.2 Superconductor-insulator Phase Transition . . . 1370
17.2.3 2D Superconductors . . . 1370
17.2.4 Materials with Localization and SC . . . 1370
17.2.5 Superconductivity of a Graph . . . 1370
17.3 Less currently applicable, but potentially useful theories . . . 1371
17.3.1 Kitaev's 1D chain . . . 1371
17.3.2 Majorana Fermions in a Superconductors . . . 1371
17.3.3 London's theory . . . 1371
17.3.4 London equations, consequences . . . 1373
17.3.5 On 1D superconductors . . . 1373
17.3.6 BCS-BEC Crossover . . . 1373
17.4 High-T SC . . . 1373

18 Overview of special phenomena and applications 1375
18.1 Other Phenomena In a Nutshell . . . 1375
18.1.1 Thermoelectric Effects in Superconductors . . . 1375
18.1.2 Vortex Lattice Melting and Pinning in a Nutshell . . . 1375
18.1.3 Fluctuation Effects by Varlamov, Larkin in a Nutshell (????) . . . 1375
18.1.4 Other Magnetic Phenomena . . . 1375

18.1.5 On induced superconductivity of 2D materials (???) . . . 1376
18.2 Superconductivity for quantum computation (???) . . . 1376
18.3 Applications of superconductivity . . . 1376
18.3.1 On superconductivity for qubits and quantum computers . . . 1376
18.3.2 Overview of typical applications of superconductivity . . . 1379
18.3.3 Digital Electronics . . . 1379
18.3.4 Superconducting Photon and Particle Detectors . . . 1379
18.3.5 Microwave Applications . . . 1379
18.3.6 Applications of SC junctions and SQUIDS . . . 1380

VIII Other Properties, Theories and Effects 1381

19 Other Known Phenomena and Models 1381
19.1 Unconventional Superconductivity by Mineev, V.P. Samokhin, K., part 1 . . . 1381
19.1.1 1. Cooper Pairing in General . . . 1381
19.1.2 2. Spin Structure of Paired States . . . 1384
19.1.3 3. Phases of Superfluid Helium-3 . . . 1386
19.1.4 4. Superconducting States in Crystals . . . 1389
19.1.5 5. Energy of Elementary Excitations of a Superconductor . . . 1398
19.1.6 6. Gap in the Excitation Spectrum and Critical Temperature . . . 1405
19.1.7 7. Temperature Behavior of Thermodynamic Quantities as $T \to 0$ . . . 1408
19.1.8 8. Parity Effects of the Number of Electrons in Superconductors . . . 1410
19.1.9 9. Paramagnetic Susceptibility and Knight Shift . . . 1417
19.1.10 10. Landau Expansion of the Free Energy of Superconductors . . . 1421
19.1.11 11. Superconducting States with Multicomponent Order Parameters . . . 1424
19.1.12 12. Ginzburg–Landau Equations and the Upper Critical Field . . . 1428
19.1.13 13. Boundary Conditions and Surface Superconductivity . . . 1436
19.1.14 14. Meissner and Mixed States in Unconventional Superconductors . . . 1444
19.1.15 15. Magnetic Superconductors . . . 1452
19.1.16 16. Эффект Джозефсона . . . 1457
19.2 Unconventional Superconductivity by Mineev, V.P. Samokhin, K., part 2 . . . 1461
19.2.1 17. Gor'kov Equations . . . 1461
19.2.2 18. Ginzburg–Landau Functional . . . 1468
19.2.3 19. Upper Critical Field in p-wave Superconductors . . . 1474
19.2.4 20. Boundary Conditions for the Order Parameter . . . 1481
19.2.5 21. Influence of Impurities on Unconventional Superconductivity . . . 1489
19.2.6 22. Electronic Thermal Conductivity of Unconventional Superconductors . . . 1498
19.3 Eliashberg Theory: a short review by F. Marsiglio . . . 1508
19.3.1 Introduction . . . 1508
19.3.2 The Eliashberg Equations . . . 1510
19.3.3 Results on the imaginary axis: T_c . . . 1514
19.3.4 Validity of the Theory . . . 1516
19.3.5 Results on the imaginary axis: in the superconducting state . . . 1519
19.3.6 Results on the real axis . . . 1519
19.3.7 Summary and Outlook . . . 1525
19.4 Open superconductive systems . . . 1530
19.4.1 Choice of the Dissipator and the Model . . . 1530
19.4.2 Models of Open Superconductors . . . 1530
19.4.3 Experimental Results of Open Superconductors . . . 1530
19.5 Some phenomena by Abrikosov, Gor'kov, Dzyaloshinsky . . . 1530
19.5.1 Superconductor in an Arbitrary Magnetic Field Near the T_c . . . 1530
19.5.2 Theory Of Superconducting Alloys by AGD [see cond matter about it] . . . 1535

20 Fluctuation Phenomena in Superconductors by Larkin, Varlamov **1535**
20.1 Introduction . . . 1535
20.2 Ginzburg-Landau formalism. Thermodynamics . . . 1539
20.2.1 Fluctuation contribution to heat capacity . . . 1539
20.2.2 Ginzburg-Levanyuk criterion . . . 1544
20.2.3 Scaling and renormalization group . . . 1545
20.2.4 Fluctuation diamagnetism . . . 1550
20.3 Ginzburg-Landau formalism. Transport . . . 1559
20.3.1 Time dependent GL equation . . . 1559
20.3.2 Paraconductivity . . . 1561
20.3.3 General expression for paraconductivity . . . 1563
20.3.4 Fluctuation conductivity of layered superconductor . . . 1565
20.3.5 Magnetic field angular dependence of paraconductivity . . . 1568
20.4 Fluctuations near S-I transition . . . 1570
20.4.1 Quantum phase transition . . . 1570
20.4.2 3D superconductors . . . 1571
20.4.3 2D superconductors . . . 1575
20.5 Microscopic derivation of the TDGL equation . . . 1577
20.5.1 Preliminaries . . . 1577
20.5.2 The Cooper channel of electron-electron interaction . . . 1578
20.5.3 Superconductor with impurities . . . 1581
20.5.4 Microscopic theory of fluctuation conductivity of layered superconductor . . . 1585
20.6 Manifestation of fluctuations in various properties . . . 1599
20.6.1 The effects of fluctuations on magnetoconductivity [97, 127, 154, 155] . . . 1600
20.6.2 Fluctuations far from T_c or in strong magnetic fields . . . 1604
20.6.3 The effect of fluctuations on the Hall conductivity[174] . . . 1607
20.6.4 Fluctuations in the ultra-clean case [175] . . . 1609
20.6.5 The effect of fluctuations on the one-electron density of states and on tunneling measurements . . . 1611
20.6.6 Nonlinear fluctuation effects [14] . . . 1616
20.6.7 The effect of fluctuation on the optical conductivity [199] . . . 1618
20.6.8 Thermoelectric power above the superconducting transition [203, 201] . . . 1620
20.6.9 The effect of fluctuations on NMR characteristics [176] . . . 1622
20.7 Conclusions . . . 1626

21 Nonequilibrium SC **1627**
21.1 General Properties of Nonequilibrium Superconductors . . . 1627
21.1.1 General Understanding of Physics in Nonequilibrium SC . . . 1627
21.1.2 Choosing a Framework for Nonequilibrium SC . . . 1628
21.2 Typical Experiments with Nonequilibrium Superconductors . . . 1630
21.3 7. Some Nonequilibrium Effects in Superconductors by Shmidt . . . 1630
21.3.1 7.1 Quasiparticles: Electrons and Holes . . . 1631
21.3.2 7.2 Charge of a Quasiparticle in the Superconductor . . . 1632
21.3.3 7.3 Relaxation Time for the Quasiparticle Charge . . . 1634
21.3.4 7.5 Branch Imbalance of the Elementary Excitation Spectrum and Electric Field in the Superconductor . . . 1635
21.3.5 7.6 Experimental Study of a Nonequilibrium State at a Normal Metal-Superconductor Interface . . . 1639
21.3.6 7.7 Phase-Slip Centers . . . 1642
21.3.7 7.8 Nonequilibrium Enhancement of Superconductivity . . . 1643
21.3.8 7.9 Thermoelectric Effect in Superconductors . . . 1644
21.3.9 7.10 Superconducting 'Thermocouple' and the Magnetic Flux Induced by a Heat Flow . . . 1645
21.3.10 7.11 Thermoelectric Effects in Josephson Junctions . . . 1647

21.3.11 Solutions . . . 1651
21.4 Nonequlibrim Superconductors: Other Models, Features, Approaches . . . 1657

22 Disorder SC **1657**
22.1 Usadel theory . . . 1657

23 Other theoretical models **1657**
23.0.1 Strange, useless statements about typical theories of SC . . . 1657
23.1 Possibility of superconductivity type phenomena in a one-dimensional system . . . 1657
23.2 Very exotic models and properties of superconductors . . . 1658
23.3 Interesting Ideas, which are proven to be unphysical . . . 1658
23.3.1 On proposal by W. Heisenberg: Z. Naturforsch. 2a, 185 (1947) . . . 1658
23.3.2 On proposal by H. Welker: Z. Phys. 114, 525 (1939) . . . 1658
23.3.3 On proposal by M. Born, K. C. Cheng: Nature (London) . . . 1658

24 BCS-BEC Crossover by Chen et al. **1658**
24.1 Conclusions . . . 1658
24.2 Introduction to Qualitative Crossover Picture . . . 1659
24.2.1 Fermionic Pseudogaps and Meta-stable Pairs: Two Sides of the Same Coin . . . 1660
24.2.2 Introduction to high T_c Superconductivity: Pseudogap Effects . . . 1664
24.2.3 Introduction to High T_c SC: Mott Physics and Possible Ordered States . . . 1670
24.2.4 Overview of the BCS-BEC Picture of High T_c SC in the Underdoped Regime . . . 1672
24.2.5 Many Body Hamiltonian and Two Body Scattering Theory: Mostly Cold Atoms 1674
24.2.6 Cold Atom Experiments: Crossover in the Presence of Feshbach Resonances . . . 1679
24.2.7 T-Matrix-Based Approaches to BCS-BEC Crossover in the Absence of Feshbach Effects . . . 1681
24.2.8 Superconducting Fluctuations: a type of Pre-formed Pairs . . . 1685
24.3 Quantitative Details of Crossover . . . 1688
24.3.1 $T = 0$, BEC Limit without Feshbach Bosons . . . 1688
24.3.2 Extending conventional Crossover Ground State to $T \neq 0$ 1 . . . 1689
24.3.3 Extending conventional Crossover Ground State to $T \neq 0$ 2 . . . 1690
24.3.4 Nature of the Pair Dispersion: Size and Lifetime of noncondensed Pairs Below T_c 1694
24.3.5 T_c Calculations: Analytics and Numerics . . . 1695
24.4 Self Consistency Tests . . . 1696
24.4.1 Important check: behavior of ρ_s . . . 1697
24.4.2 Collective Modes and Gauge Invariance . . . 1698
24.4.3 Investigating the Applicability of a Nambu Matrix Green's Function Formulation 1701
24.5 Other Theoretical Approaches to the Crossover Problem . . . 1701
24.5.1 $T \neq 0$ Theories . . . 1701
24.5.2 Boson-Fermion Models for High T_c Superconductors . . . 1703
24.6 Physical Implications: Ultracold Atom Superfluidity . . . 1704
24.6.1 Homogeneous case . . . 1704
24.6.2 Superfluidity in Traps . . . 1712
24.6.3 Comparison Between Theory and Experiment: Cold Atoms . . . 1714
24.7 Physical Implications: High T_c Superconductivity . . . 1716
24.7.1 Phase Diagram and Superconductor-Insulator Transition: Boson Localization Effects . . . 1716
24.7.2 Superconducting Coherence Effects . . . 1717
24.7.3 Electrodynamics and Thermal Conductivity . . . 1719
24.7.4 Thermodynamics and Pair-breaking Effects . . . 1721
24.7.5 Anomalous Normal State Transport: Nernst and Other Precursor Transport Contributions . . . 1722
24.8 Derivation of the $T = 0$ variational conditions . . . 1725
24.9 Proof of Ward Identity Below T_c . . . 1726

24.10 Quantitative Relation between BCS-BEC crossover and Hartree-TDGL . . . 1727
24.11 Convention and Notation . . . 1729
24.11.1 Notation . . . 1729
24.11.2 Convention for units . . . 1730
24.11.3 Abbreviations . . . 1730

IX High Temperature Superconductivity 1731

25 High-T Superconductivity in the Cuprates by Banerjee et al. 1731
25.1 Introduction . . . 1731
25.2 Materials, structure and minimal electronic model . . . 1732
25.3 Phase diagram and phenomena . . . 1733
25.3.1 Superconducting state . . . 1733
25.3.2 Strange metal . . . 1736
25.3.3 Pseudogap phase . . . 1737
25.3.4 Spectroscopic characteristics of superconducting, strange metal and pseudogap phases . . . 1741
25.4 Phenomenological theory of superconducting and pseudogap states . . . 1744
25.4.1 Phenomenological GL-like functional . . . 1746
25.4.2 Thermodynamic quantities obtained from the phenomenological theory . . . 1750
25.5 Extensions of the phenomenological theory to describe thermoelectric transport and low-energy electronic spectra . . . 1750
25.5.1 Relaxation dynamics using the phenomenological theory . . . 1750
25.5.2 Pairing fluctuations and low-energy electronic spectra in cuprates . . . 1751
25.6 Results from the phenomenological theory and comparison with experiments . . . 1755
25.7 Conclusion and future directions . . . 1759
25.8 Parameters of the phenomenological theory . . . 1761

X Experiments and Other Applications 1762

26 Devices with Superconductivity 1762
26.0.1 Levitation over superconductors . . . 1762

27 Experiments with Superconductors 1762
27.1 Measurement methods . . . 1762
27.1.1 Measurement of a resistance by microwave photons (???) . . . 1762
27.2 "Classical" Experiments with Superconductors . . . 1762
27.2.1 Meissner's Experiment . . . 1762
27.3 Some Modern Well-Known Experiments . . . 1762

28 Other Phenomena and Applications 1762
28.0.1 Levitation over a superconductor . . . 1762
28.0.2 Superconducting Train: Main Ideas . . . 1762

29 Atomic physics and quantum optics using SC circuits by You, Nori 1762

30 Spin-polarized supercurrents for spintronics 1778
30.1 Introduction: historical background . . . 1778
30.1.1 Superconductivity interacting with magnetism . . . 1778
30.1.2 Pair breaking by paramagnetic impurities and external fields . . . 1779
30.1.3 Ferromagnetic superconductors . . . 1780
30.1.4 Cooper pairs with finite center of mass momentum . . . 1781
30.1.5 Proximity effect . . . 1783

30.1.6 Andreev reflection . . . 1784
30.1.7 Josephson effect . . . 1788
30.2 Symmetry classification of Cooper pairs in superconductors . . . 1789
30.2.1 Consequences of Pauli principle and Fermi statistics . . . 1789
30.2.2 Odd-frequency pairing amplitudes . . . 1791
30.3 Magnetically active interfaces . . . 1793
30.3.1 Scattering phase delays . . . 1793
30.3.2 Spin-mixing angle and spin-dependent scattering phase shifts . . . 1793
30.3.3 Scattering matrix and induced triplet correlations . . . 1796
30.4 Theoretical tools . . . 1800
30.4.1 Bogoliubov-de Gennes equations . . . 1801
30.4.2 Quasiclassical theory of superconductivity . . . 1804
30.4.3 Eilenberger equations . . . 1805
30.4.4 Normalization condition and transport equation in spin-space . . . 1807
30.4.5 Usadel equations . . . 1809
30.4.6 General features of the S/F proximity effect . . . 1811
30.4.7 Strongly spin-polarized ferromagnets . . . 1812
30.5 Pair amplitude oscillations and π-Josephson junctions . . . 1813
30.5.1 $0-\pi$ transitions in Josephson junctions . . . 1813
30.5.2 Phase sensitive measurements . . . 1816
30.5.3 φ-Josephson junctions . . . 1818
30.6 Long-range triplet supercurrents . . . 1819
30.6.1 Length scales for superconducting correlations in ferromagnets . . . 1819
30.6.2 Experimental "pre-history" . . . 1820
30.6.3 Theory of long-range proximity amplitudes . . . 1820
30.6.4 Recent experimental observations . . . 1828
30.7 Modern developments . . . 1832
30.7.1 Spin-valve devices and spin-filter junctions . . . 1832
30.7.2 Flux Qubits and semifluxons . . . 1832
30.7.3 Non-equilibrium quasiparticle distribution . . . 1833
30.7.4 Dynamical effects . . . 1834
30.7.5 Spin-orbit coupling and topological materials . . . 1835

XI Appendix 1839

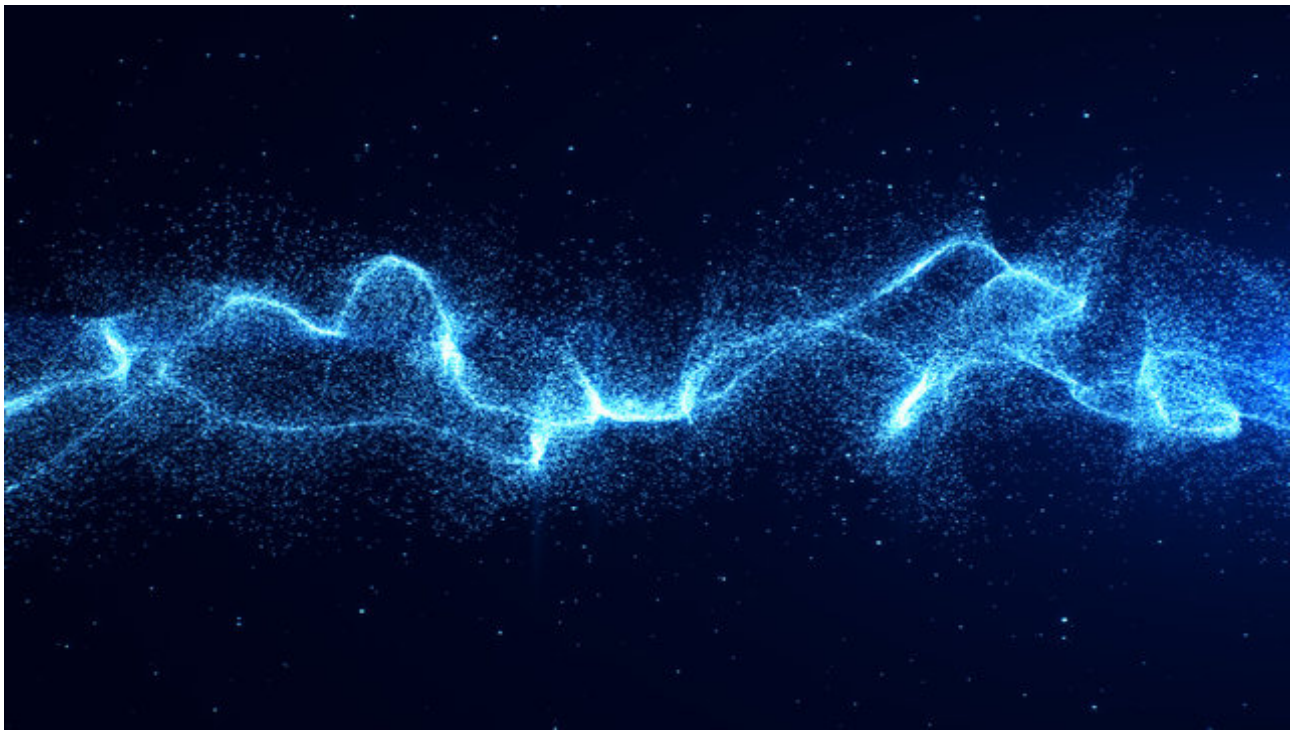
A Introduction to Superconductivity 1839
A.1 Other Motivation . . . 1839
A.1.1 Other General Motivation . . . 1839
A.1.2 Amazing Facts . . . 1839
A.1.3 Motivation for Specific Topics in SC . . . 1839
A.2 Thinking as a Professional in Superconductivity . . . 1839
A.2.1 Essence of Superconductivity . . . 1839
A.2.2 Ways to Earn Money Using Superconductivity . . . 1839
A.2.3 Everyday-Life Uses of Superconductivity . . . 1839
A.2.4 Overview of Most Relevant Applications . . . 1839
A.2.5 Ways to Guess All Main Ideas . . . 1839
A.2.6 Thinking for Effective Learning . . . 1840
A.3 Acknowledgements . . . 1840
A.4 Literature . . . 1840
A.4.1 Main Literature . . . 1840
A.4.2 Additional Literature and Articles on Various Phenomena and Methods . . . 1841
A.5 General overview of superconductivity . . . 1844
A.5.1 Popular Introduction to Superconductivity . . . 1845

A.5.2 Overview of Rare Phenomena in Superconductivity . . . 1846
A.5.3 Overview of Theoretical Approaches . . . 1846
A.5.4 Overview of Further Developments . . . 1846
A.5.5 Connections with Other Sciences . . . 1846
A.6 Description of the Note . . . 1847
A.7 History of Superconductivity in a Nutshell . . . 1847
A.8 Puzzles for Different Situations in Life . . . 1849
A.8.1 Typical Puzzles . . . 1850
A.8.2 Everyday Puzzles . . . 1850
A.8.3 Fundamental Puzzles . . . 1850
A.8.4 Puzzles about Details . . . 1850
A.8.5 Puzzles for Mastering Typical Concepts . . . 1850

B Mathematics and Physics for Reference **1850**
B.0.1 Quantum Mechanics for Superconductivity (??) . . . 1850
B.0.2 Some Mathematics for Superconductivity (??) . . . 1850

C References **1852**
C.1 References from Very Useful Books . . . 1854
C.2 References from Theoretical Articles and Books about Specific Models . . . 1870

Preface and main motivation



The key sections are:

Fundamentals of superconductivity

Basics of Ginzburg-Landau theory

Basics of BCS theory

Junctions with superconductors.

This note also includes theory of superconductive fluctuations by Varlamov, Larkin, Mineev's and Samokhin's unconventional superconductivity. I used the following literature.

Let's discuss some minimum knowledge and motivation that would be good to understand for studying the subject.

Сверхпроводимость - раздел, позволяющий соприкоснуться с результатами чело- веческого гения

(все-таки это одно из наиболее сильно мотивирующих! потом раскрою эту мысль.)

Best fundamental questions

(потом добавлю из ЛШ пару задач тут, пока в другом месте тренируюсь.)

I-motiv-1. Nature of Superconductivity

(вопрос про то, почему вообще есть сверхпро- водимость? по сути для этого во многом мы и изучаем сверхпроводники.)

I-motiv-2. Dielectric properties of superconductor (???)

Why do we have a Meissner effect?
(потом напишу подробнее вопрос и ответ, почему такое вообще??? совсем не тривиально, что такое происходит.)

I-motiv.3 Levitation of superconductor

(??? почему такое явление есть????)

Best technical questions

(потом добавлю из ЛШ пару задач тут, пока в другом месте тренируюсь.)

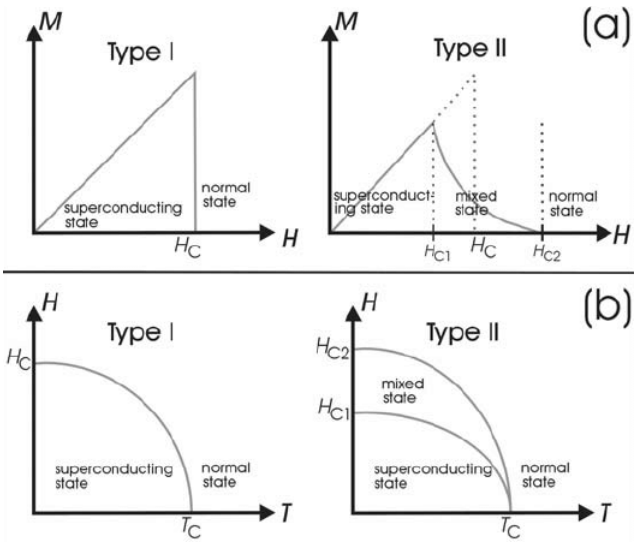
Part I
Superconductivity in a Nutshell

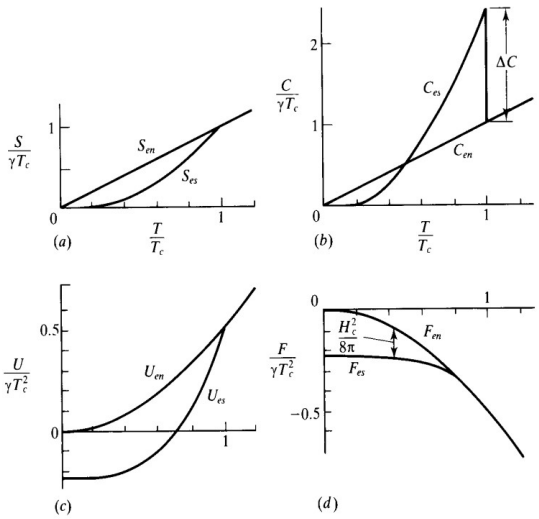
1 Main Models and Properties of Superconductors

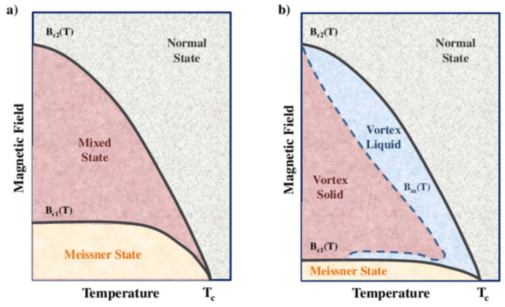
1.1 Main Theories for Superconductors

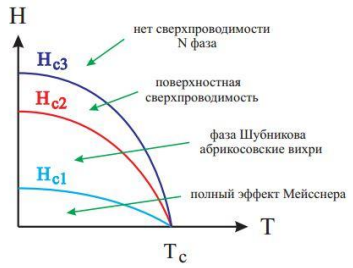
1.1.1 Main properties of SC and overview of theoretical methods

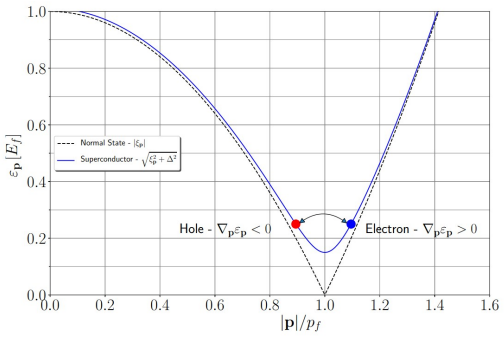
Main physical properties of superconductors

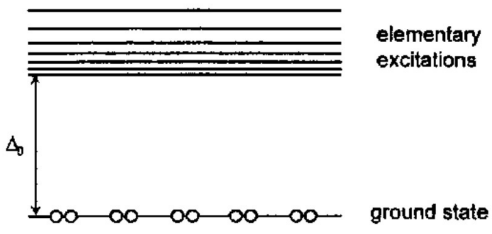




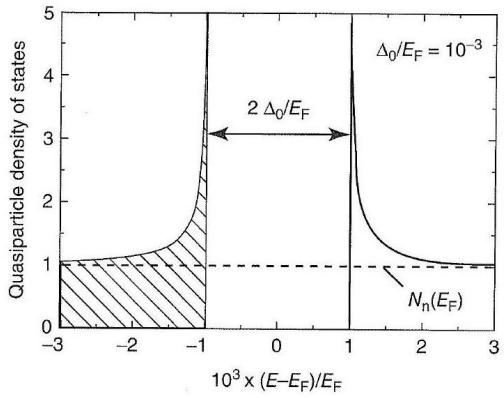


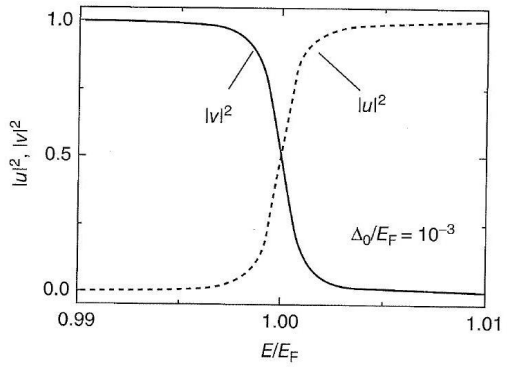


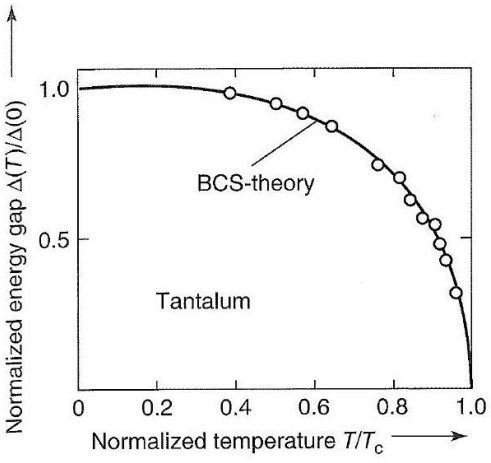


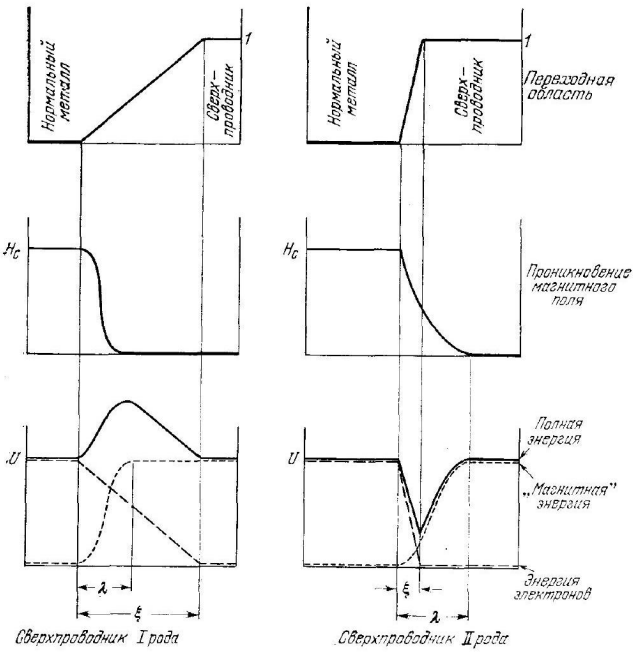


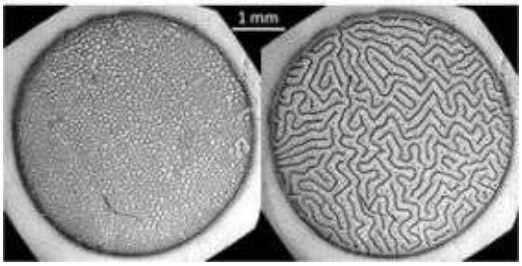
This is a spectrum of an unpaired electrons, that are excited above the superconductive paired ones. The superconductive ones are located below the Fermi surface.


Quasiparticle density of states
$\Delta_0/E_F = 10^{-3}$
$2\,\Delta_0/E_F$
$N_n(E_F)$
$10^3 \times (E-E_F)/E_F$


$|u|^2, |v|^2$
$|v|^2$
$|u|^2$
$\Delta_0/E_F = 10^{-3}$
E/E_F


Normalized energy gap $\Delta(T)/\Delta(0)$
BCS-theory
Tantalum
Normalized temperature T/T_c


Нормальный металл
Сверх-проводник
Переходная область
H_c
Проникновение магнитного поля
U
Полная энергия
„Магнитная" энергия
Энергия электронов
λ
ξ
Сверхпроводник I рода
Сверхпроводник II рода



Fundamental relations and concepts of superconductors

$$\Psi(r) \sim |\Delta| \sim \sqrt{n_s}.$$

$$\Psi(\mathbf{r}) = \sqrt{\frac{n_s}{2}} e^{i\phi}.$$

$$T_c \propto \omega_D \propto \frac{1}{\sqrt{M}} \qquad \text{Isotope effect}$$

$$T_c = 1,13 \frac{\hbar \omega_D}{k_B} \exp\left(-\frac{1}{N_n\left(E_F\right) V}\right)$$

$$\varepsilon(p) = \sqrt{\Delta^2 + v_F^2 (p - p_F)^2}$$

Основные экспериментальные факты

1. Идеальные проводники ниже критической температуры T_c. Температура перехода $T_c \sim 10$ K (Камерлинг-Оннес, 1911).

2. Разрушение сверхпроводимости магнитным полем $H_c \sim 300$ Э или транспортным током $j_c \sim 10^6$ A $\cdot$ cm^{-2} (Камерлинг-Оннес, 1914).
(??? в итоге, почему это, словами????)

3. Эффект Мейсснера (Мейсснер, Оксенфельд, 1933). Сверхпроводник - идеальный диамагнетик. Ниже критической температуры магнитное поле полностью выталкивается из сверхпроводника. Это важное обстоятельство. Поскольку $B = 0$ при $T < T_c$ независимо от предыстории возникновения сверхпроводимости, сверхпроводимость - это новая термодинамическая фаза металла.
(??? в итоге, почему это, словами????)

4. Экспоненциальная зависимость теплоемкости от температуры

$$C_e \sim \exp(-\Delta/T)$$

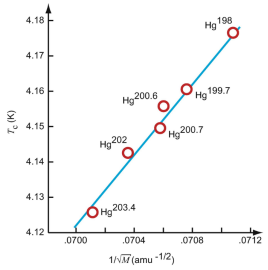
(W. S. Corak, et. al., 1954). Это означает, что возбуждённые состояния сверхпроводника отделены от основного «энергетической щелью» Δ как в полупроводнике. Поскольку при $T = T_c$ происходит фазовый переход II рода со скачком теплоемкости, то $\Delta(T) = 0$ в точке перехода. Далее электронная теплоемкость имеет нормальное поведение $C_e \sim T$.
(???)

5. Изотопический эффект (Максвелл, Рейнольдс, 1950):

$$T_c \propto (\text{Atomic mass of the metal})^{-1/2}.$$

Это значит, что ключевую роль при возникновении сверхпроводимости играет решётка металла. Электроны могут взаимодействовать между собой посредством обмена фононов, типичная энергия которых $\hbar\omega_D \approx 300$ K. Это могут быть виртуальные фононы, которые возбуждает в решётке движущийся в кристалле электрон. Испущенный одним электроном фонон может поглотиться другим электроном, и между ними возникает эффективное притяжение. Энергия связи такой пары $\Delta \sim T_c$. Поэтому

$$T_c \propto \hbar\omega_D.$$



(????)

Lengths of superconductors

$$\kappa = \lambda_L/\xi_{GL}$$

$\kappa = \frac{\lambda_L}{\xi_{GL}} < 1/\sqrt{2}$ Type-I superconductors, positive wall energy.
$\kappa = \frac{\lambda_L}{\xi_{GL}} > 1/\sqrt{2}$ Type-II superconductors, negative wall energy.
Characteristic lengths:

$$\lambda_L := \sqrt{m/\left(\mu_0 q^2 n_s\right)} \quad \xi_{GL} := \sqrt{-\hbar^2/2m\alpha} \quad \xi_0 := 0,18\frac{\pi\hbar v_F}{2k_B T_c}$$

$$\xi^2 = \frac{\hbar^2}{4ma\left(T_c - T\right)},$$
$$\lambda^2 = \frac{mc^2 b}{8\pi e^2 a\left(T_c - T\right)}.$$

London penetration depth $\lambda_{\mathrm{L}}(T)$ - typical distance it takes to screen the magnetic field inside a superconductor

Coherence length ξ_0 (BCS, Pippard) characterizes the length scale over which the correlation between the electrons in a Cooper pair is active. It is the typical size of a Cooper pair.

GL-coherence length $\xi_{\mathrm{GL}}(T)$ Gives the typical distance over which the superconducting order parameter can vary.

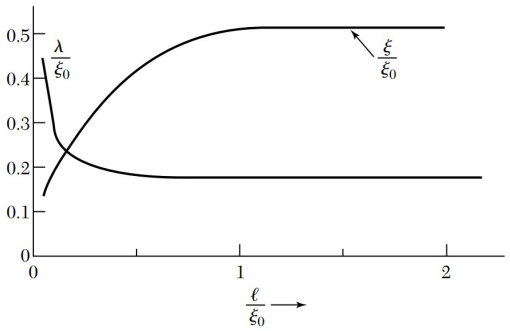
Dependence of$\lambda_{\mathrm{L}}, \xi_{\mathrm{GL}}$ and ξ_0 on impurities:

$$\lambda_L(T) = 0,71\frac{\lambda_L(0)}{\sqrt{1 - T/T_c}} \quad \xi_{GL}(T) = 0,74\frac{\xi_0}{\sqrt{1 - T/T_c}} \qquad \text{(clean limit)}$$

$$\lambda_L(T) = 0,64\lambda_L(0)\sqrt{\frac{\xi_0}{l^*\left(1 - T/T_c\right)}} \quad \xi_{GL}(T) = 0,855\sqrt{\frac{\xi_0 l^*}{1 - T/T_c}} \quad \xi_0 \approx l^* \qquad \text{(dirty limit)}$$

(?????!!!)

$$\xi_0 = 0,18\frac{\pi\hbar v_F}{2k_B T_c} \quad \xi_0 \approx l^*$$



(???)
$\lambda_L(T) \sim \frac{1}{\sqrt{1-T/T_c}}, \qquad \xi_{GL}(T) \sim \frac{1}{\sqrt{1-T/T_c}}$
$\xi = \frac{1}{\sqrt{2m\Delta}}$ (???)

$$\nu = mp_F/2\pi^2\hbar^3$$

- плотность состояний электрона на уровне Ферми в нормальном состоянии (без учета спина)

$$\hbar\boldsymbol{\nabla}\varphi = m_\mathrm{s}\boldsymbol{v}_\mathrm{s} + q_\mathrm{s}\boldsymbol{A}$$

(????? откуда такая формула??)

$$\boldsymbol{j}_\mathrm{s} = q_\mathrm{s}n_\mathrm{s}\boldsymbol{v}_\mathrm{s} = \frac{q_\mathrm{s}n_\mathrm{s}}{m_\mathrm{s}}\left(\hbar\boldsymbol{\nabla}\varphi - q_\mathrm{s}\boldsymbol{A}\right)$$

$$\boldsymbol{\nabla}\varphi = \frac{2\pi}{\Phi_0}\left(\mu_0\lambda_\mathrm{L}^2\boldsymbol{j}_\mathrm{s} + \boldsymbol{A}\right)$$

$$a \approx T_c/\varepsilon_F \qquad b \approx T_c^2/n\varepsilon_F$$

Wall energy per unit area:
(type-I) $\alpha_w \approx (\xi_{GL} - \lambda_\mathrm{pen})\frac{B_{ch}^2}{2\mu_0}$
(type-II) $\alpha_w \approx \xi_{GL}\frac{B_{ch}^2}{2\mu_0} - \lambda_L\frac{B^2}{2\mu_0}$

Magnetic fields

Effective field $B_\mathrm{eff} = \frac{1}{1-N_M}B_a$

$$B_{c1} = \frac{1}{\sqrt{2}\kappa}(\ln\kappa + 0.08)B_{clh} = \frac{\Phi_0}{4\pi\lambda_L^2}(\ln\kappa + 0.08)$$
$$B_{c2} = \sqrt{2}\kappa B_{cth} = \frac{\Phi_0}{2\pi\xi_{GL}^2}$$

$$g_n - g_s = \frac{B_{cth}^2}{2\mu_0}$$

Overview of methods for taking into account different effects

Taking into account Coulomb repulsion of electrons is done in Abricosov-Gorkov formalism. I don't know, how to do it in other way.

(?? add some formulas)

For fluctuation effects the functional integral approach works, but it is a special part of superconductivity.

(?? add some formulas)

(??? how to take into account structure of a lattice??)

1.1.2 GL theory

Idea and main properties of GL theory

There is an order parameter that is non-zero in ordered state and zero in the disordered state. (??)

$$\text{(order parameter)} \qquad \Psi(r) \sim |\Delta| \sim \sqrt{n_s}.$$

$$\Psi(\mathbf{r}) = \sqrt{\frac{n_s}{2}} e^{i\phi}.$$

$$\Omega_s[\Psi(\mathbf{r}), \mathcal{A}(\mathbf{r})] \overset{\text{(series)}}{\approx} \Omega_n + \int \left[\alpha |\Psi|^2 + \frac{b}{2}|\Psi|^4 + \frac{1}{2 \cdot 2m^*} \left| -i\hbar\nabla\Psi - \frac{2e}{c}\mathcal{A}\Psi \right|^2 + \frac{(\nabla \times \mathcal{A})^2}{8\pi} \right] dV.$$

$$\alpha = a\,(T - T_c)\,, \qquad a \geq 0 \qquad b \geq 0 \qquad e := -|e|$$

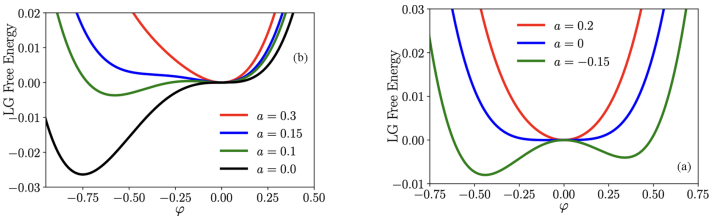
(??? слова про отсутствие нечетных членов!)

$$a \approx T_c/\varepsilon_F; \qquad b \approx T_c^2/n\varepsilon_F; \qquad c = \frac{\hbar^2}{4m}.$$

$$a^2/b = 4\Delta_0^2 n/\varepsilon_F T_c^2 \approx n/\varepsilon_F.$$

(add proof!)

$$a^2/b = 4\Delta_0^2 n/\varepsilon_F T_c^2 \approx n/\varepsilon_F \qquad (T = 0)$$



$$\alpha\Psi + b\Psi|\Psi|^2 + \frac{1}{4m}\left(i\hbar\nabla + \frac{2e}{c}\mathcal{A}\right)^2 \Psi = 0, \qquad \text{(1 GL eq.)}$$

$$\left(i\hbar\nabla\Psi + \frac{2e}{c}\mathcal{A}\Psi\right)_S \bar{n} = 0.$$

$$\nabla \times \nabla \times \mathcal{A} = \frac{4\pi}{c}\mathbf{j}_\mathrm{s}, \qquad \mathbf{j}_\mathrm{s} = -\frac{ie\hbar}{2m^*}\left(\Psi^*\nabla\Psi - \Psi\nabla\Psi^*\right) - \frac{2e^2}{m^*c}|\Psi|^2\mathcal{A}. \qquad \text{(2 GL eq.)}$$

$\psi = \dfrac{\Psi}{\Psi_0} \equiv |\psi|e^{i\phi}$

$$\xi^2\left(i\nabla + \frac{2\pi}{\Phi_0}\mathcal{A}\right)^2\psi - \psi + \psi|\psi|^2 = 0, \qquad \xi^2 := \frac{\hbar^2}{4ma\left(T_c - T\right)},$$
$$\lambda^2\nabla\times\nabla\times\mathcal{A} + |\psi|^2\mathcal{A} = \frac{-\Phi_0}{2\pi}|\psi|^2\nabla\phi, \qquad \lambda^2 := \frac{mc^2b}{8\pi e^2 a\left(T_c - T\right)}.$$

$\Phi_0 := \frac{\pi\hbar c}{e} = 2\cdot 10^{-7}\frac{\mathrm{Gs}}{\mathrm{cm}^2}$

$$\Psi(r) = \mathrm{const},\ B = 0 \ \Rightarrow\ (\min) \ \Rightarrow\ \frac{n_s}{2} \equiv |\Psi_0|^2 = \begin{cases} -\frac{a(T-T_c)}{b}, & T < T_c, \\ 0, & T > T_c. \end{cases}$$
$$n_s(T)|_{T=0} = 2aT_c/b.$$

Без внешнего поля $\Omega_n - \Omega_s(\mathcal{H}=0) \equiv V\alpha^2/2b$ может быть скомпенсирован проигрышем в энергии из-за магнитного поля $\Omega_s(\mathcal{H}) - \Omega_s(\mathcal{H}=0) = V\mathcal{H}^2/8\pi$ (ибо $\mathcal{M} = -\mathcal{H}/4\pi$ и $-V\int\limits_0^{\mathcal{H}}\mathcal{M}d\mathcal{H} = \mathcal{H}^2/8\pi$). Отсюда

$$\mathcal{H}_c^2 = \frac{4\pi a^2\left(T - T_c\right)^2}{b}.$$

$$\lambda_L = \sqrt{m/\left(\mu_0 q^2 n_s\right)} \qquad \lambda_L(T) = \frac{1}{\sqrt{1 - T/T_c}}$$
$$\xi_{GL} = \sqrt{\hbar^2/(2m|\alpha|)} \qquad \xi_{GL}(T) \sim \frac{1}{\sqrt{1 - T/T_c}}$$

(discuss what it means?)

$$\kappa = \lambda/\xi = \frac{mc}{\hbar e}\left(\frac{\beta}{2\pi}\right)^{1/2}$$

Критерий применимости теории Гинзбурга–Ландау

GL theory is applicable everywhere, except the little region near the critical temperature. (def?)
(here are Pukhov arguments)

$$\mathrm{Gi} = T_c b^2/ac^3 \approx \left(\frac{T_c}{\varepsilon_F}\right)^4 \ll 1.$$

so GL theory is applied well. Fluctuation effects are also big, if Gi number is little (???)

Proof 2:

$$\mathrm{Gi} = \Delta_\mathrm{fl}C_\phi/\Delta_\mathrm{gap}C = \left(\frac{T_c}{\varepsilon_F}\right)^4 \ll 1$$

since $\qquad \Delta_\mathrm{fl}C_\phi = \dfrac{T_c^2 V a^{3/2}}{16c^{3/2}\pi\sqrt{T - T_c}} \qquad \Delta_\mathrm{gap}C \sim C\left(T_c\right) \approx g_F T_c/\varepsilon_F,$

$c := \hbar^2/4m$, $a = T_c m\pi^2/p_F^2$ (?).

Second option to view it is by:
(???)

$$\left\| 1 - \frac{T}{T_c} \right\| \geq \left(\frac{kT_c}{H^2_{\mathrm{cm}(0)}\xi_0^3} \right) \equiv \mathrm{Gi}$$

(add some formulas for disorder and D=2, D=1)
(а в нетипичном - см ниже от Варламова Ларкина особые темы, потом добавлю что-то сюда тоже)

Типичные эффекты в рамках уравнений Гинзбурга-Ландау (???)

(чисто с точки зрения УМФ допишу уравнения и указания про решения потом)

Энергия границы раздела между сверхпроводящей и нормальной фазами и два рода сверхпроводников по ГЛ (!!!!!!!)

(!!!????)

$$\mathcal{H}_c = \frac{\Phi_0}{2\sqrt{2}\pi\lambda\xi} \qquad \text{(therm crit f)}$$

(add here words about proofing that $\varkappa = \sqrt{2}$!)
Wall energy per unit area
(type-I) $\alpha_w \approx (\xi_{GL} - \lambda_{\mathrm{pen}}) \frac{B^2_{ch}}{2\mu_0}$
(type-II) $\alpha_w \approx \xi_{GL} \frac{B^2_{ch}}{2\mu_0} - \lambda_L \frac{B^2}{2\mu_0}$

$$B_{c1} = \frac{1}{\sqrt{2}\kappa}(\ln\kappa + 0.08) B_{clh} = \frac{\Phi_0}{4\pi\lambda_L^2}(\ln\kappa + 0.08)$$
$$B_{c2} = \sqrt{2}\kappa B_{cth} = \frac{\Phi_0}{2\pi\xi_{GL}^2}$$
$$g_n - g_s = \frac{B^2_{cth}}{2\mu_0}$$

Верхнее и нижнее критические магнитные поля

(сперва подумаю про рассуждения, потом уже напишу их!)

Эффект Мейсснера по ГЛ

$\lambda^2 \nabla \times \nabla \times \mathcal{A} + |\psi|^2 \mathcal{A} = \frac{-\Phi_0}{2\pi} |\psi|^2 \nabla\phi$ rot $\nabla \times \mathcal{A} = \mathcal{B}$, $\nabla \cdot \mathcal{B} = 0$, $|\psi|^2 \overset{\text{d ins}}{=} 1$,

$$\lambda^2 \cdot \nabla^2 \mathcal{B} - \mathcal{B} = 0. \qquad \text{(London's eq)}$$

$$\mathcal{B} = \mathcal{B}_0 \exp(-z/\lambda)$$

(?? ниже - додумаю теорпол - пойму это??) Возникновение эффекта Мейсснера связано со спонтанным нарушением симметрии при $T < T_c$ и калибровочной инвариантности Ω-потенциала сверхпроводника. Он совершенно аналогичен эффекту Хиггса возникновения массы m у частицы при спонтанном нарушении симметрии

теории. Подобно тому, как кулоновский потенциал безмассовых частиц заменяется юкавским потенциалом массивных частиц с конечным радиусом действия $\lambda \sim m^{-1}$, в сверхпроводнике ниже точки перехода магнитное поле экспоненциально «зарезается» мейсснеровскими токами на масштабе лондоновской глубины проникновения λ.

Квантование потока по ГЛ

$$\Phi = n\Phi_0 \qquad \Phi_0 = \pi\hbar c/e = 2 \cdot 10^{-7}\text{Гс} \cdot \text{см}^{-2}$$

Proof. $j_S = \frac{-c|\psi|^2}{4\pi\lambda^2}\left(\frac{\Phi_0}{2\pi}\nabla\phi + \mathcal{A}\right)$, в топологически неодносвязном образце (СП торе), в котором «заморожен» некоторый магнитный поток, этот поток создаётся текущими по внутренней поверхности полости сверхпроводящими токами. Проинтегрируем ток по контуру, охватывающий дырку и проходящий глубоко ($\ll \lambda$) в сверхпроводник, $|\psi|^2 = 1$ и $\mathbf{j}_\text{s} = 0$:

$$\frac{\Phi_0}{2\pi}\oint \nabla\phi \cdot d\mathbf{l} = \oint \mathcal{A} \cdot d\mathbf{l}$$

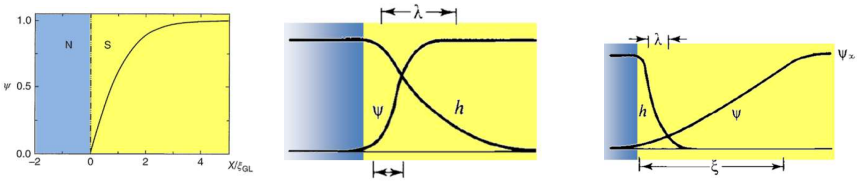
Тут интеграл от фазы не ноль, потому что у нас топологически не связный образец, а $\oint \nabla\phi \cdot d\mathbf{l} = 2\pi n$.

(?? так вот ловко обошли теорему Гаусса)

□

(?!?!?!? пара слов про флюксоид, что это за понятие. не супер важное. и что же там в итоге квантуется то? и в теорию про это допишу)

Глубина проникновения поля в сверхпроводник 1го и 2го родов по ГЛ

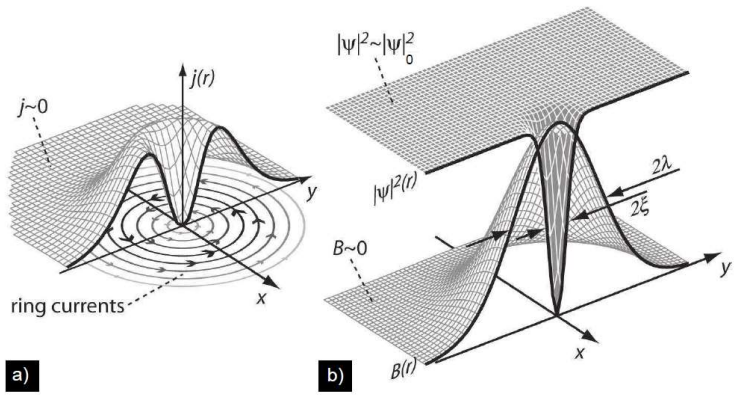


Уравнение Лондонов справедливо если $\lambda_L \gg \xi_0$, потому что при его выводе неявно предполагалось, что волновой пакет сверхпроводящих частиц целиком повержен магнитному полю, мы получили, что магнитное поле изменяется на масштабе λ_L. Если $\xi_0 \gg \lambda_L$, то лишь малая часть волнового пакета подвержена влиянию магнитного поля (СП 2го рода). Для оценки глубины проникновения считаем, что концентрация будет теперь $n = n_s\lambda/\xi_0$, в остальном вывод такой же, получаем:

$$\lambda = \left(\frac{mc^2\xi_0}{4\pi n_s e^2 \lambda}\right)^{1/2} \qquad \Rightarrow \qquad \lambda = \lambda_L\left(\frac{\xi_0}{\lambda_L}\right)^{1/3} \gg \lambda_L.$$

Solution ур ГЛ для абрикосовского вихря

$$\mathcal{B}(0) = \frac{\Phi_0}{2\pi\lambda^2}\ln\frac{\lambda}{\xi}.$$



(тут коротко про вывод!)

Другие типичные свойства и методы для ГЛ

Overview of methods for effective usage of GL theory

(??? мб это численно решается, пока не знаю, и не важно это)

Derivation of GL equations from GL functional

(I'll write key formulas of that boring variations)

Functional integral methods for GL theory

(if it is very useful, I'll add it to the top)

Broken symmetry and Goldstone mode in GL theory

(??? still don't understand what is meant by this?)

1.1.3 BCS theory

Idea and main properties of BCS theory

$$\hat{H}-\mu\hat{N}=\sum_{\mathbf{p}\sigma}\xi_{\mathbf{p}}\hat{a}^{\dagger}_{\mathbf{p}\sigma}\hat{a}_{\mathbf{p}\sigma}-\lambda\sum_{\mathbf{p}\mathbf{p}'}{}'\hat{a}^{\dagger}_{\mathbf{p}'+}\hat{a}^{\dagger}_{-\mathbf{p}'-}\hat{a}_{\mathbf{p}+}\hat{a}_{-\mathbf{p}-},$$

prime - region n. F. surf.

$\left\{\hat{a}_{\mathbf{p}\sigma},\hat{a}^{+}_{\mathbf{p}'\sigma'}\right\}=\delta_{\mathbf{p}\mathbf{p}}\delta_{\sigma\sigma'}$

$\hat{a}^{\dagger}_{\mathbf{p}'+}\hat{a}^{\dagger}_{-\mathbf{p}'-}$ – cr mode of Coop p

$$\Delta^{*}=\lambda\cdot\sum_{\mathbf{p}'}{}'\langle\hat{a}^{\dagger}_{\mathbf{p}',+}\hat{a}^{\dagger}_{-\mathbf{p}',-}\rangle,\qquad \Delta=\lambda\cdot\sum_{\mathbf{p}'}{}'\langle\hat{a}_{-\mathbf{p}',-}\hat{a}_{\mathbf{p}',+}\rangle\,.$$

$$\Delta_0=2\hbar\omega_D e^{-\frac{2}{\lambda g_F}}.\qquad g_F:=p_F m/\pi^2\hbar^3,$$

$$E_{\text{condens-n}}=-N\left(E_F\right)\Delta_0^2/2$$

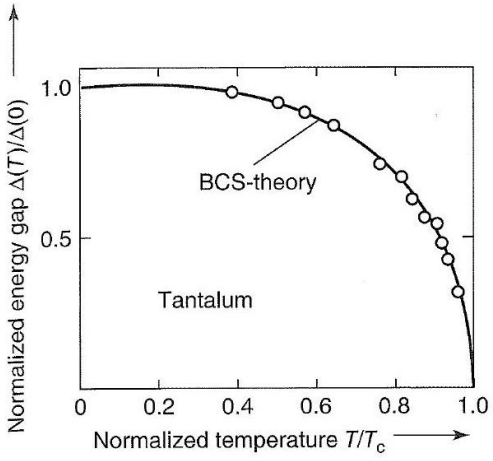
$$E_{\text{paired el.}}=2E_F-2\hbar\omega_D e^{-2/N(E_F)V}$$

$$T_c = 1,13\frac{\hbar\omega_D}{k_B}\exp\left(-\frac{1}{N_n\left(E_F\right)V}\right) \qquad T \sim \omega_D \sim M_{\text{isotope}}^{-1/2}$$

(write what are the parameters)

$$\frac{\Delta_0}{k_B T_c} \approx 1.76$$

It is proven by comparison two solutions of the Gap equation (at $T = T_c$ and $T = 0$).



Typical derivations in scope of BCS theory

Approximation and diagonalization of BCS Hamiltonian

$$\hat{H} - \mu\hat{N} = \sum_{\mathbf{p}\sigma}\xi_{\mathbf{p}}\hat{a}^{\dagger}_{\mathbf{p}\sigma}\hat{a}_{\mathbf{p}\sigma} - \lambda\sum_{\mathbf{p}\mathbf{p}'}{}'\underbrace{\hat{a}^{\dagger}_{\mathbf{p}'+}\hat{a}^{\dagger}_{-\mathbf{p}'-}}_{\text{crate C. pair}}\hat{a}_{\mathbf{p}+}\hat{a}_{-\mathbf{p}-}, \qquad \begin{matrix}\text{prime - region n. F. surf.}\\ \left\{\hat{a}_{\mathbf{p}\sigma}, \hat{a}^{+}_{\mathbf{p}'\sigma'}\right\} = \delta_{\mathbf{p}\mathbf{p}}\delta_{\sigma\sigma'}\end{matrix}$$

$$\Delta^* = \lambda\cdot\sum_{\mathbf{p}'}{}'\langle\hat{a}^{\dagger}_{\mathbf{p}',+}\hat{a}^{\dagger}_{-\mathbf{p}',-}\rangle, \qquad \Delta = \lambda\cdot\sum_{\mathbf{p}'}{}'\left\langle\hat{a}_{-\mathbf{p}',-}\hat{a}_{\mathbf{p}',+}\right\rangle.$$

(??????)

$$\hat{H} - \mu\hat{N} = \sum_{\mathbf{p}\sigma}\xi_{\mathbf{p}}\hat{a}^{\dagger}_{\mathbf{p}\sigma}\hat{a}_{\mathbf{p}\sigma} + \frac{1}{\lambda}|\Delta|^2 + \sum_{\mathbf{p}}\left[\Delta^*\hat{a}_{\mathbf{p}+}\hat{a}_{-\mathbf{p}-} + \Delta\hat{a}^{\dagger}_{-\mathbf{p}-}\hat{a}^{\dagger}_{\mathbf{p}+}\right]$$

$$\widehat{b}_{\mathbf{p}-} = u_p\widehat{a}_{\mathbf{p}-} + v_p\widehat{a}^{+}_{-\mathbf{p},+} \qquad \widehat{a}_{\mathbf{p}-} = u_p\widehat{b}_{\mathbf{p}-} - v_p\widehat{b}^{+}_{-\mathbf{p},+}$$
$$\widehat{b}_{\mathbf{p}+} = u_p\widehat{a}_{\mathbf{p}+} - v_p\widehat{a}^{+}_{-\mathbf{p},-} \qquad \widehat{a}_{\mathbf{p}+} = u_p\widehat{b}_{\mathbf{p}+} + v_p\widehat{b}^{+}_{-\mathbf{p},-}$$

$$\left\{\hat{b}_{\mathbf{p}\sigma}, \hat{b}^{\dagger}_{\mathbf{p}'\sigma'}\right\} = \delta_{\mathbf{p}\mathbf{p}}\delta_{\sigma\sigma'}$$

$$\hat{H} - \mu\hat{N} = \Omega_0 + \sum_{\mathbf{p}}{}'\varepsilon(p)\left(\hat{b}^{\dagger}_{\mathbf{p}+}\hat{b}_{\mathbf{p}+} + \hat{b}^{\dagger}_{\mathbf{p}-}\hat{b}_{\mathbf{p}-}\right)$$

$$\varepsilon(p) := \sqrt{\xi^2_{\mathbf{p}} + \Delta^2} \qquad \Omega_0 := 2\sum_{\mathbf{p}}{}'\left[\xi_{\mathbf{p}}v^2_{\mathbf{p}} - \Delta u_{\mathbf{p}}v_{\mathbf{p}}\right] + \frac{1}{\lambda}\Delta^2,$$

$$u^2_{\mathbf{k}} = \frac{1}{2}\left(1 + \frac{\xi_{\mathbf{k}}}{\sqrt{\xi^2_{\mathbf{k}} + \Delta^2}}\right), \qquad v^2_{\mathbf{k}} = \frac{1}{2}\left(1 - \frac{\xi_{\mathbf{k}}}{\sqrt{\xi^2_{\mathbf{k}} + \Delta^2}}\right)$$

Ground state and excitations

Ground state energy: $E_0 := \Omega_0(\Delta_0) - \Omega_0(0)$

$$E_0 = \frac{1}{2} g_F (\hbar\omega_D)^2 - \frac{1}{2} g_F \hbar\omega_D \Delta_0 \sqrt{1 + \left(\frac{\hbar\omega_D}{\Delta_0}\right)^2} \overset{\Delta_0 \ll \hbar\omega_D}{\approx} -g_F \Delta_0^2/4 \quad \text{(negative)}$$

$$E_{\text{Coop p}} = 2\sqrt{\Delta_0^2 + \xi_{\text{p}}^2}$$

(????)

$$|\text{BCS}\rangle = \prod_{\mathbf{k}} \left(u_{\mathbf{k}} + v_{\mathbf{k}} \hat{c}^\dagger_{\mathbf{k},\uparrow} \hat{c}^\dagger_{-\mathbf{k},\downarrow}\right) |\text{vac}\rangle.$$

Gap equation: obtaining $\Delta(T=0)$ and T_c

$$\Delta_0 = 2\hbar\omega_D e^{-\frac{2}{\lambda g_F}}; \qquad T_c = \frac{\gamma}{\pi}\Delta_0 \approx 0,57\Delta_0, \qquad \gamma = 1,78; \quad g_F := p_F m/\pi^2\hbar^3$$

Proof:

$$\Delta := \lambda \sum_{\mathbf{p}'}{}' \langle \hat{a}^\dagger_{\mathbf{p}',+} \hat{a}^\dagger_{-\mathbf{p}',-} \rangle \qquad \Rightarrow \qquad \begin{aligned} \widehat{a}_{\mathbf{p}+} &= u_p \widehat{b}_{\mathbf{p}+} + v_p \widehat{b}^+_{-\mathbf{p},-} \\ \widehat{a}_{\mathbf{p}-} &= u_p \widehat{b}_{\mathbf{p}-} - v_p \widehat{b}^+_{-\mathbf{p},+} \end{aligned}$$

$\left\langle \hat{b}^\dagger_{\text{p}+} \hat{b}_{\text{p}+} \right\rangle = \bar{n}_{\text{p}} = \left\langle \hat{b}^\dagger_{\text{p}-} \hat{b}_{\text{p}-} \right\rangle = [\exp(\varepsilon(p)/T) + 1]^{-1},$

$$\frac{1}{\lambda} = \frac{1}{2} \sum_{\mathbf{p}}{}' \frac{1 - 2\bar{n}_{\mathbf{p}}}{\sqrt{\xi^2_{\mathbf{p}} + \Delta^2}}. \qquad \text{(gap eq.)}$$

For Δ_0, we set $\bar{n}_{\text{p}}(T=0) \equiv 0$,
(???)

$$1 = \frac{\lambda}{2} \frac{4\pi}{(2\pi\hbar)^3} \frac{p_F^2}{v_F} \int_{-\hbar\omega_D}^{+\hbar\omega_D} \frac{d\xi_{\text{p}}}{\sqrt{\xi_{\text{p}}^2 + \Delta_0^2}} = \frac{\lambda}{2} \frac{4\pi}{(2\pi\hbar)^3} \frac{p_F^2}{v_F} 2 \int_0^{\hbar\omega_D/\Delta_0} \frac{dx}{\sqrt{1+x^2}},$$

$\int dx/\sqrt{1+x^2} = \ln\left|x + \sqrt{1+x^2}\right| \qquad \Rightarrow \qquad \Delta_0 \approx 2\hbar\omega_D e^{-\frac{2}{\lambda g_F}}.$

For T_c, we set $\Delta(T = T_c) = 0$:

$$1 = \frac{\lambda}{2} \int{}' \frac{d^3\mathbf{p}}{(2\pi\hbar)^3} \frac{1 - 2\bar{n}_{\mathbf{p}}}{|\xi_{\mathbf{p}}|} = \frac{\lambda g_F}{2} \int_{-\hbar\omega_D}^{+\hbar\omega_D} \frac{d\xi_{\mathbf{p}}}{2\xi_{\mathbf{p}}} \text{ th } \frac{|\xi_{\mathbf{p}}|}{2T_c} = \frac{\lambda g_F}{2} \int_0^{\hbar\omega_D/2T_c} \frac{\text{th}x}{x} dx.$$

$$\varepsilon(p) = |\xi_{\text{p}}|, \qquad 1 - 2\bar{n}_{\text{p}} = \text{th}\left(|\xi_{\text{p}}|/2T_c\right).$$

$\int_0^x (\text{th}x/x)dx \overset{x \gg 1}{\approx} \int_1^x dx/x = \ln|x|.$

$$2T_c \approx \hbar\omega_D \exp\left(-2/\lambda g_F\right) = 0,5\Delta_0.$$

Finding gap as a function of T

(??? it is done only numerically, I'll summarize it here later)
It was obtained numerically and from it we see that $\sqrt{1-T/T_c}$ is a nice approximation.

Green's function derivation, transformation for BCS

(??? I'll write it later)

Other Typical BCS ideas

Nambu spinors for BCS superconductors

(I'll write about it from my master's thesis later)
Often the hole interpretation is used, then we associate one real excitation with one non-real excitation with the negative energy:

$$h_k = c^\dagger_{-k,\bar{s}}$$

So, creating an electron is the same as destroying a hole.

Tight-binding BCS model

(I'll write about it from my master's thesis)

BCS for the case, when net momenta of pair not equal to zero

(see AGD about it later! maybe it is written there)

Density of BCS ground state

(it is typically computed)

Cooper pair from more Shorodinger equation

Fermi-liquid проявляет неустойчивость относительно образования связанных пар квазичастиц при сколь угодно слабом притяжении вблизи поверхности Ферми.

$$\hat{H}_0(\mathbf{r}_1)\,\psi_{\mathbf{p}}(\mathbf{r}_1) = |\xi_{\mathbf{p}}|\,\psi_{\mathbf{p}}(\mathbf{r}_1), \qquad \text{(free part-l near Fermi surf-s)}$$

$$\psi_{\mathbf{p}}(\mathbf{r}) = V^{-\frac{1}{2}} e^{\frac{i\mathbf{p}\mathbf{r}}{\hbar}}, \qquad \xi_{\mathbf{p}} = v_F(p - p_F).$$

$$\psi_{\text{pair}}(\mathbf{r}_1, \mathbf{r}_2) := \sum_{\mathbf{p}} c_{\mathbf{p}} \psi_{\mathbf{p},+}(\mathbf{r}_1)\,\psi_{-\mathbf{p},-}(\mathbf{r}_2),$$

$$\left[\hat{H}_0(\mathbf{r}_1) + \hat{H}_0(\mathbf{r}_2) + \hat{V}(\mathbf{r}_1, \mathbf{r}_2)\right]\psi(\mathbf{r}_1, \mathbf{r}_2) = E\psi(\mathbf{r}_1, \mathbf{r}_2). \qquad \hat{V}(\mathbf{r}_1, \mathbf{r}_2) \neq V(\mathbf{r}_1 - \mathbf{r}_2)$$

$$2|\xi_{\mathbf{p}}|\,c_{\mathbf{p}} + \sum_{\mathbf{p}'} V_{\mathbf{p}\mathbf{p}'} c_{\mathbf{p}'} = E c_{\mathbf{p}} \qquad V_{\mathbf{p}\mathbf{p}'} := \left\langle \mathbf{p}, +, -\mathbf{p}, - | \hat{V} | \mathbf{p}', +, -\mathbf{p}', - \right\rangle$$

$$2\hbar\omega_D \ll \varepsilon_F; \qquad V_{\mathbf{pp}'} \overset{\text{model}}{=} \begin{cases} -\lambda, & p_F - \frac{\hbar\omega_D}{v_F} < |\mathbf{p}|, |\mathbf{p}'| < p_F + \frac{\hbar\omega_D}{v_F} \\ 0, & \text{otherwise.} \end{cases}$$

$$c_{\mathbf{p}} = \frac{\lambda I}{2\,|\xi_{\mathrm{p}}| - E} \qquad I := \sum_{\mathbf{p}'}{}' c_{\mathbf{p}'} = \text{const}$$

$$-\frac{1}{\lambda} = \sum_{\mathbf{p}'}{}' \frac{1}{E - 2\,|\xi_{\mathbf{p}'}|}$$

(finish writing??)

(??? how does this model connects with Γ as two-point green's function??)

Typical Generalization of BCS Model

(max 1 page most useful general formulas about UC SC)

$$H = E_0 + \sum_{\mathbf{k}} E_{\mathbf{k}} b^+_{\mathbf{k}\alpha} b_{\mathbf{k}\alpha}$$

$$E_0 = \frac{1}{2}\sum_{\mathbf{k}} \Delta_{\mathbf{k},\alpha\beta} H^+_{\mathbf{k},\beta\alpha} + \frac{1}{2}\sum_{\mathbf{k}\alpha} (\xi_k - E_{\mathbf{k}}) \qquad \text{energ of gr state}$$

$$E_{\mathbf{k}} = \sqrt{\xi_k^2 + \Delta^2 |g(\mathbf{k})|^2}$$

$$E_{0\ \mathrm{s}} = E_{0\mathrm{n}} - \frac{1}{2} N_0 \Delta^2 \qquad \text{(сингл спар)}$$

$$E_{0\ \mathrm{s}} = E_{0\mathrm{n}} - \frac{1}{4} N_0 \mathrm{tr} \int \frac{d\Omega}{4\pi} \Delta^+_{\mathbf{k}} \Delta_{\mathbf{k}} \qquad \text{(произв спар)}$$

1.1.4 Electrodynamics of superconductors

Equations of electrodynamics of SC

(write Londons eq)

Examples

(write some comments which results can they give??)

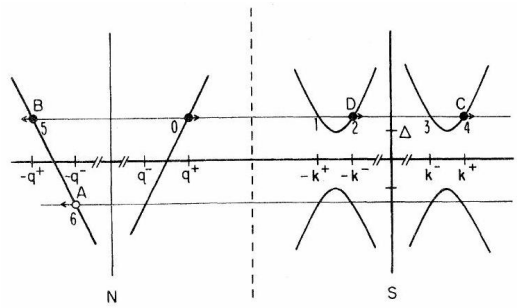
1.1.5 BdG equations, BTK formalism, Andreev states

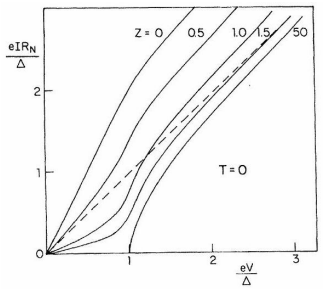
BdG equations

(see note on cond matter for now)

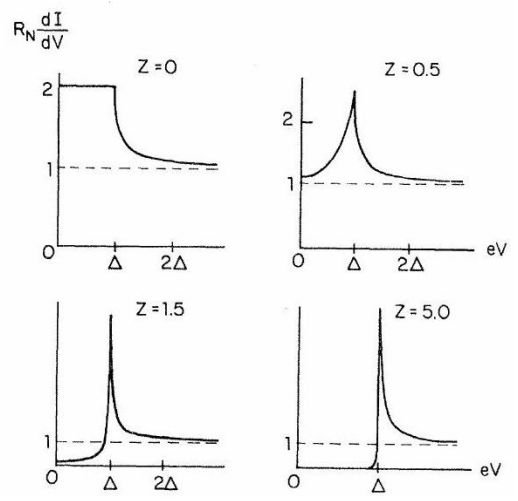
BTK method

(here are main formulas!!!)





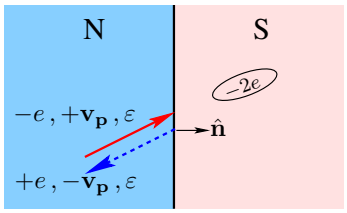
These curves attain their asympototic limits only for very high voltages. For example, the tunnel junction ($Z = 50$) curve will be within 1% of the normal-state curve (dotted line) only when $eV \geq 7\Delta$.

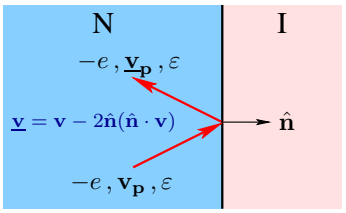


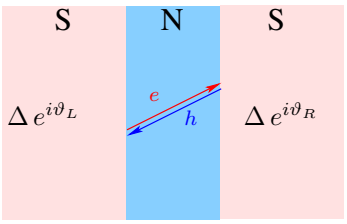
Differential conductance vs voltage for various barrier strengths Z at $T = 0$. This quantity is proportional to the transmission coefficient for electric current for particles at $E = eV$.

	A	B	C	D
Normal state	0	$\frac{Z^2}{1+Z^2}$	$\frac{1}{1+Z^2}$	0
General form				
$E<\Delta$	$\frac{\Delta^2}{E^2+(\Delta^2-E^2)(1+2Z^2)^2}$	$1-A$	0	0
$E>\Delta$	$\frac{u_0^2v_0^2}{\gamma^2}$	$\frac{(u_0^2-v_0^2)^2Z^2(1+Z^2)}{\gamma^2}$	$\frac{u_0^2(u_0^2-v_0^2)(1+Z^2)}{\gamma^2}$	$\frac{v_0^2(u_0^2-v_0^2)Z^2}{\gamma^2}$
No barrier ($Z=0$)				
$E<\Delta$	1	0	0	0
$E>\Delta$	v_0^2/u_0^2	0	$1-A$	0
Strong barrier $[Z^2(u^2-v^2)>>1]$				
$E<\Delta$	$\frac{\Delta^2}{4Z^2(\Delta^2-E^2)}$	$1-A$	0	0
$E>\Delta$	$\frac{u_0^2v_0^2}{Z^4(u_0^2-v_0^2)^2}$	$1-\frac{1}{Z^2(u_0^2-v_0^2)}$	$\frac{u_0^2}{Z^2(u_0^2-v_0^2)}$	$\frac{v_0^2}{Z^2(u_0^2-v_0^2)}$

The Andreev Reflection and States





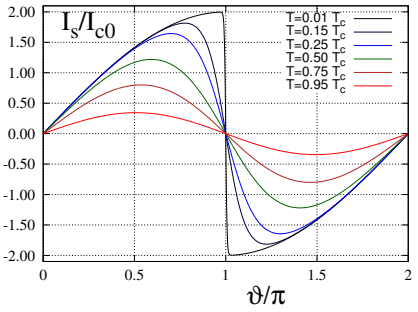


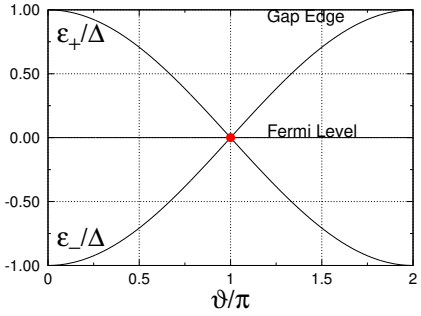
$$|r_{\mathrm{A}}|^2 = \begin{cases} 1 & \varepsilon \le |\Delta|, \\ \dfrac{|\Delta|^2}{(\varepsilon + \sqrt{\varepsilon^2 - |\Delta|^2})^2} & \varepsilon > |\Delta|\ . \end{cases} \tag{1.1}$$

$$\varphi - 2\arccos\left[\frac{E(\varphi)}{\Delta}\right] - 2\frac{E(\varphi)}{\Delta}\frac{L_N}{\xi} = 2\pi n, \qquad n \in \mathbb{Z}, \tag{1.2}$$

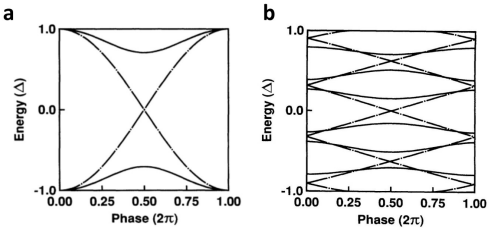
(for general length of a junction L_N)

$$E_i(\varphi) = \pm\Delta\sqrt{1 - T_N^i \sin^2\frac{\varphi}{2}}. \tag{1.3}$$

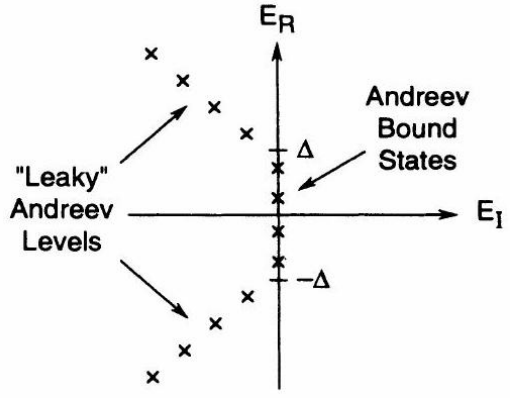




$$I_{c0} = \frac{\pi\Delta(0)}{2e\,R_{\mathrm{N}}}.$$



Spectrum of Andreev bound state. a) Short ballistic junction with (solid) and without (dotted) the presence of impurity b) Long ballistic junction. The discrete Andreev levels are shown with (solid) and without (dashed) the presence of an impurity. In both (a) and (b), an energy gap is opened in this quasi-particle spectrum.



Тепловая длина когерентности, введение в метод квазиклассических функций Грина.

Контакт сверхпроводников через ферромагнетик (S-F-S) и инверсия фазы (π–контакт).

1.1.6 Currents, Thermodynamics, Susceptibilities

Critical currents in SC from GL

$\Delta(T) \sim (T_c - T)^{1/2}$ from numerical solution of gap eq.

$$\Delta := \lambda \cdot \sum_{\mathbf{p}'} \langle \hat{a}_{-\mathbf{p}',-} \hat{a}_{\mathbf{p}',+} \rangle \qquad \Rightarrow \qquad \Delta^2 \sim n_s.$$

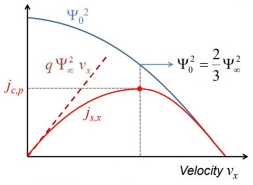
$$v_c = \min \frac{\varepsilon(p)}{p} = \min \frac{\sqrt{\xi_{\mathrm{p}}^2 + \Delta^2}}{p} \approx \frac{\Delta}{p_F}. \qquad \text{(superfluid crit)}$$

$$j_c = e n_s v_c \sim \Delta^3 \sim (T_c - T)^{3/2}$$

$n_s \approx 10^{22}\ \mathrm{cm}^{-3}, \Delta \approx 5\ \mathrm{K}, \varepsilon_F \approx 5\mathrm{eV} \qquad \Rightarrow \qquad j_s \approx 10^7\ \mathrm{A/cm}^2.$

Critical currents from current maximum by GL theory:

$$j_{s,x} = q\Psi_0^2(v_x)\, v_x \qquad \Psi_0^2(v_x) = \Psi_\infty^2 \left(1 - \frac{m v_x^2}{2|\alpha|}\right)$$



$$v_{\max,p} = \sqrt{\frac{2|\alpha|}{3m}}; \qquad j_{c,p} = q\frac{2}{3}\sqrt{\frac{2|\alpha|}{3m}}\Psi_\infty^2 = \frac{2}{3}\sqrt{\frac{2}{3}} B_{\mathrm{cth}} \frac{1}{\mu_0 \lambda_L}$$

(???)

(There is also another derivation from looking at Cooper pair (see par. 50 in Shmidt), I'll add it later)

Энергия и теплоемкость сверхпроводника

$$C_s \sim \exp(-\Delta/T) \qquad \text{(gapped)}$$

Proof 1: $\varepsilon(p) := \sqrt{\Delta^2 + v_F^2 \left(p - p_F\right)^2}, \quad g_s := 2s + 1 = 2$

$$E(T) = \int\limits_0^\infty \frac{g_s V 4\pi p^2 dp \varepsilon(p)}{(2\pi\hbar)^3 \left(e^{\frac{\varepsilon(p)}{T}} + 1\right)} \approx \frac{8V\pi p_F^2}{(2\pi\hbar)^3} e^{-\frac{\Delta}{T}} \int\limits_0^\infty \left(\Delta + \frac{v_F^2 \left(p - p_F\right)^2}{2\Delta}\right) e^{-\frac{v_F^2 (p-p_F)^2}{2T\Delta}} dp \approx$$
$$\approx \frac{8V\pi p_F^2}{(2\pi\hbar)^3} \frac{\sqrt{\pi T\Delta}}{v_F} e^{-\frac{\Delta}{T}} \sim e^{-\frac{\Delta}{T}}$$

Proof 2:

$$S = -\sum_k \left\{(1 - f_k)\ln(1 - f_k) + f_k \ln f_k\right\}$$

$$C_\mathrm{s} = \sum_{\mathrm{k}\alpha} E_\mathrm{k} \frac{\partial f_\mathrm{k}}{\partial T}$$

$$C_\mathrm{s} = 2N_0 \int\limits_{-\infty}^{+\infty} d\xi \sqrt{\xi^2 + \Delta^2} \frac{\partial}{\partial T} \left(\frac{1}{\exp\left(\sqrt{\xi^2 + \Delta^2}/T^1\right) + 1}\right) \overset{T\to 0}{\approx}$$
$$\approx \frac{2N_0\Delta^2}{T^2} e^{-\Delta/T} \int\limits_{-\infty}^{+\infty} d\xi e^{-\xi^2/(2\Delta T)} \approx N_0 \left(\frac{\Delta_0}{T}\right)^2 \sqrt{2\pi T\Delta_0} e^{-\Delta_c/T}.$$

Also, the total number of electrons:

$$N(T) = \int\limits_0^\infty \frac{g_s V 4\pi p^2 dp}{(2\pi\hbar)^3 \left(e^{\frac{\varepsilon(p)}{T}} + 1\right)} \approx \frac{8V\pi p_F^2}{(2\pi\hbar)^3} e^{-\frac{\Delta}{T}} \int\limits_{-\infty}^{+\infty} dp' e^{\frac{-v_F^2 p'^2}{2T\Delta}} = \frac{8V\pi p_F^2 \sqrt{2\Delta}}{(2\pi\hbar)^3 v_F} T^{1/2} e^{-\frac{\Delta}{T}} \propto e^{-\frac{\Delta}{T}} \ll 1.$$

Jump of heat capacity

$$\left(C_s - C_n\right)/C_s = 1.43. \qquad \text{BCS}$$

$$C = T\frac{\partial S}{\partial T} \qquad S_s - S_n = \frac{H_{cm}}{4\pi}\left(\frac{\partial H_{cm}}{\partial T}\right)_R$$
$$C_s - C_n = \frac{T}{4\pi}\left[\left(\frac{\partial H_{cm}}{\partial T}\right)^2 + H_{cm}\frac{\partial^2 H_{cm}}{\partial T^2}\right] = \frac{T_c}{4\pi}\left(\frac{\partial H_{cm}}{\partial T}\right)^2_{T_c} \qquad \text{(Rutgers),}$$

ибо при $T = T_c$ критическое поле $H_{cm} = 0$.

(??maybe the derivation is done in Levitos Shitov, I'll check later)

Entropy of a superconductor

(see Shmidt for now, sec. 3)

Diamagnetic susceptibility of a SC

(add ideas from Shmidt)

(maybe here I'll show some plots from calculations or from experiments)

(here there will be formulas from LS)

(maybe I'll write some important formulas from Varlamov Larkin)

1.1.7 General important features of superconductors and theories

General questions about measurements

Как измеряют нулевое сопротивление?

Как измеряют ток при нулевом сопротивлении?

Как измеряют такие малые температуры?

General questions about all theories

Connection of BCS and GL theory

(a short basic answer to this question is here)

Why SC doesn't work at low dimensions and what is meant by this?

(I'll write formulas, how fluctuations destroy it and why?)

1.2 Typical SC Effects

1.2.1 Josephson equations, SNS, SQUID, RCSJ

Finally, what is going on with tunneling?

Consider just NS border. Помимо термоактивационного вклада в ток, описываемого $I_{N-S}(V,T) = \frac{\sqrt{2\pi\Delta T}}{eR} e^{-\Delta/T} \operatorname{sh} \frac{eV}{T}$, под порогом $eV = \Delta$ существует еще один весьма интересный вклад, не исчезающий при $T \to 0$. Он связан с когерентным туннелированием пары электронов с противоположными импульсами и спинами.

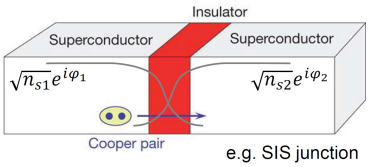
(??? add before that we don't consider two paericle tunnelings. why???)

Оказавшись в сверхпроводнике, такие два электрона могут образовать куперовскую пару. Туннелирование пары, в отличие от одночастичного туннелирования, не требует затраты энергии Δ на каждую частицу, и поэтому такой вклад не «вымерзает» при низких температурах. Когерентное туннелирование пар электронов часто называют андреевским отражением, поскольку описанный процесс перехода двух электронов из нормального металла в сверхпроводник можно рассматривать как превращение электрона в дырку при отражении от поверхности сверхпроводника. Вероятность двухчастичного туннелирования пропорциональна $|T_0|^4$, а не $|T_0|^2$, как для одночастичного туннелирования. Поэтому при $|T_0| \ll 1$ и не слишком низкой температуре двухчастичные процессы очень редки по сравнению с одночастичными. Вследствие этого андреевское отражение вносит существенный вклад в туннельный ток лишь при достаточно низких температурах.

Finally, what ideas are used in the most useful methods for tunneling?

(for now, see theoretical section with discussion of it)

Josephson effect and equations



$$I_s = I_c \sin(\varphi_2 - \varphi_1) \qquad (1^{\text{st}} \text{ Joseph. eq./current-phase})$$

$$\frac{\partial(\varphi_2 - \varphi_1)}{\partial t} = \frac{2e}{\hbar}U \equiv \frac{2\pi}{\Phi_o}U \qquad (2^{\text{nd}} \text{ Joseph. eq./voltage-phase})$$

$I_c := \frac{4eK\sqrt{N_1 N_2}}{\hbar}$, K - model const.

Particular cases are as follows:

DC Josephson effect: At zero applied voltage we have a finite supercurrent, upto a maximum 'critical' current.

AC Josephson effect: A DC voltage causes variation over time of the gauge invariant phase difference and thus produces an AC current. The frequency of the current is proportional to the voltage.

In formulas: from $\frac{\partial\gamma}{\partial t} = \frac{2\pi}{\Phi_0}U = \frac{2e}{\hbar}U$ we get $\gamma(t) = \gamma(0) + \frac{2\pi}{\Phi_0}Ut$, thus $I(t) = I_c \sin\left(\frac{2\pi}{\Phi_0}Ut + \gamma(0)\right)$, here

$$f_J := \frac{1}{\Phi_0}U \equiv \frac{2e}{h}U$$

Josephson constant

$$K_J := 2e/h = 483,5979\text{GHz/mV} \qquad (\text{material independent})$$

The inverse AC Josephson effect: Microwave radiation of a single frequency can induce quantized DC voltages across the Josephson junction, in which case the Josephson phase takes the form $\varphi(t) = \varphi_0 + n\omega t + a\sin(\omega t)$,

$$V(t) = \frac{\hbar}{2e}\omega(n + a\cos(\omega t)), \qquad I(t) = I_c \sum_{m=-\infty}^{\infty} J_m(a)\sin(\varphi_0 + (n+m)\omega t)$$

$$V_{\text{DC}} = n\frac{\hbar}{2e}\omega, \qquad I_{\text{DC}} = I_c J_{-n}(a)\sin\varphi_0.$$

A Josephson junction can act like a perfect frequency-to-voltage converter, which is the theoretical basis for the Josephson voltage standard (???? see wiki).

$$I_{\text{max, JJ}} = \frac{\pi\Delta}{2eR}\,\text{th}\,\frac{\Delta}{2T} \qquad (\text{Ambegaokar–Baratoff})$$

(add idea of the proof. It is done in Levitov Sitov, for example, and it is a long ones.)

Proof of Josephson relations

Proof from Schrödinger eq.:

$$\psi_A = \sqrt{n_A}e^{i\phi_A} \qquad \psi_B = \sqrt{n_B}e^{i\phi_B}$$

$$\frac{\partial}{\partial t}\begin{pmatrix}\sqrt{n_{s1}}e^{i\varphi_1}\\ \sqrt{n_{s2}}e^{i\varphi_2}\end{pmatrix} = \frac{-i}{\hbar}\begin{pmatrix}E_1 & K\\ K & E_2\end{pmatrix}\begin{pmatrix}\sqrt{n_{s1}}e^{i\varphi_1}\\ \sqrt{n_{s2}}e^{i\varphi_2}\end{pmatrix} \qquad \text{(Schrödinger)}$$

$$E_1 - E_2 = 2eV \qquad \sqrt{n_A} + i\sqrt{n_A}\dot{\phi}_A = \frac{1}{i\hbar}\left(eV\sqrt{n_A} + K\sqrt{n_B}e^{i\varphi}\right)$$

$$\varphi := \phi_B - \phi_A. \qquad \sqrt{n_B} + i\sqrt{n_B}\dot{\phi}_B = \frac{1}{i\hbar}\left(-eV\sqrt{n_B} + K\sqrt{n_A}e^{i\varphi}\right)$$

$$\dot{n}_A = \frac{2K\sqrt{n_A n_B}}{\hbar}\sin\varphi \qquad \dot{\phi}_A = -\frac{1}{\hbar}\left(eV + K\sqrt{\frac{n_B}{n_A}}\cos\varphi\right).$$

$$\dot{n}_B = -\frac{2K\sqrt{n_A n_B}}{\hbar}\sin\varphi, \qquad \dot{\phi}_B = \frac{1}{\hbar}\left(eV - K\sqrt{\frac{n_A}{n_B}}\cos\varphi\right).$$

Adding, using $I_s := 2eV\frac{\partial n_s}{\partial t}$ we get 1-st; subtracting, we get 2-nd Josephson equation.

Josephson inductance, energy, (etc...)

$$\text{J inductance} \qquad L(\varphi) = \frac{\Phi_0}{2\pi I_c\cos\varphi} = \frac{L_J}{\cos\varphi} \qquad L_J := L(0) = \frac{\Phi_0}{2\pi I_c}$$

Which is from $\frac{\partial I}{\partial t} = \frac{\partial I}{\partial\varphi}\frac{\partial\varphi}{\partial t} = I_c\cos\varphi\cdot\frac{2\pi}{\Phi_0}V$, so $V = \frac{\Phi_0}{2\pi I_c\cos\varphi}\frac{\partial I}{\partial t} \equiv L(\varphi)\frac{\partial I}{\partial t}$. Note that although the kinetic behavior of the Josephson junction is similar to that of an inductor, there is no associated magnetic field. This behavior is derived from the kinetic energy of the charge carriers, instead of the energy in a magnetic field.

Energy storage in JJ → Nonlinear reactance

$$\frac{dI_s}{dt} = I_c\cos\varphi\frac{d\varphi}{dt} \quad \Rightarrow \frac{dI_s}{dt} = I_c\cos\varphi\frac{2\pi}{\Phi_0}V$$

$$I_s(t) = I_c\sin\varphi(t)$$

$$\frac{d\varphi}{dt} = \frac{2\pi}{\Phi_0}V$$

For small variations near $I_s = I_c\sin\varphi \rightarrow$ JJ equivalent to inductance

$$L_s = \frac{\Phi_0}{2\pi I_c\cos\varphi} = L_c\frac{1}{\cos\varphi}$$

with $L_c = \frac{\hbar}{2el_c}$ Josephson inductance

Properties of the Josephson inductance: Negative for $\pi/2+2\pi n < \varphi < 3\pi/2+2\pi n$ (V > 0 → Oscillating Josephson current)

$\cos\varphi = \pm\sqrt{1-\left(\frac{I_s}{I_c}\right)^2}$

Josephson energy:

$$U_J(\delta) = E_J(1-\cos\delta)$$

Because the superconducting phase evolution equation is analogous to Faraday's law: $V = \mathrm{d}\Phi/\mathrm{d}t$. Assume that at time t_1, the Josephson phase is φ_1; At a later time t_2, the Josephson phase evolved to φ_2.

$$\Delta E = \int_1^2 IV\ \mathrm{d}t = \int_1^2 I\ \mathrm{d}\Phi = \int_{\varphi_1}^{\varphi_2} I_c\sin\varphi\mathrm{d}\left(\Phi_0\frac{\varphi}{2\pi}\right) = -\frac{\Phi_0 I_c}{2\pi}\Delta\cos\varphi.$$

This shows that the change of energy in the Josephson junction depends only on the initial and final state of the junction and not the path. Therefore, the energy stored in a Josephson junction is a state function, which can be defined as:

$$E(\varphi) = -\frac{\Phi_0 I_c}{2\pi}\cos\varphi = -E_J\cos\varphi$$

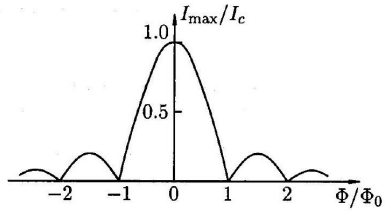
Here $E_J = |E(0)| = \frac{\Phi_0 I_c}{2\pi}$ is a characteristic parameter of the Josephson junction, named the Josephson Energy. It is related to the Josephson Inductance by $E_J = L_J I_c^2$.

$$E_s = \int_0^t I_s V dt \qquad \Rightarrow \qquad I_s V = \frac{\partial E_s}{\partial t} = \frac{\partial E_s}{\partial \varphi}\frac{\partial \varphi}{\partial t} = \frac{2eV}{\hbar}\frac{\partial E_s}{\partial \varphi} \qquad \Rightarrow$$

$$I_s = \frac{2e}{\hbar}\frac{\partial E_s}{\partial \varphi}$$

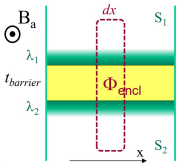
Magnetic field in single JJ

Fraughofer pattern:



$$I_c(\Phi_J) = I_c(0)\left|\frac{\sin[\pi\Phi_J/\Phi_0]}{\pi\Phi_J/\Phi_0}\right|$$

$\Phi_J = B_a t_{\text{eff}} a$ - flux through the junction, $t_{\text{eff}} = t_{\text{barrier}} + \lambda_{L,1} + \lambda_{L,2}$, $I_c(0) = j_c ab$ - critical current at zero magnetic field.



We consider a little contour, in which $\gamma_2 - \gamma_1 = \frac{2\pi}{\Phi_0}\Phi$. Then, we move along side of a junction $\gamma(x+dx) - \gamma(x) = \frac{2\pi}{\Phi_0}\Phi_{\text{encl}} = \frac{2\pi}{\Phi_0}B_a t_{\text{eff}} dx$, from here:

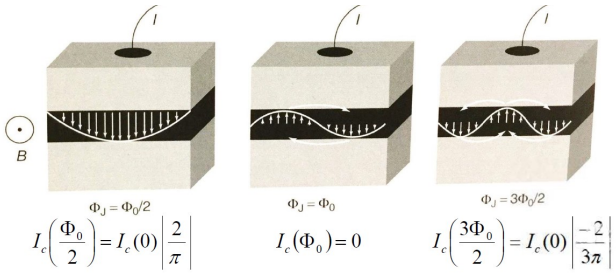
$$\frac{d\gamma}{dx} = \frac{2\pi}{\Phi_0}B_a t_{\text{eff}}$$

$$\gamma(x) = \gamma(0) + \frac{2\pi}{\Phi_0}B_a t_{\text{eff}} x$$

$$j_s(x) = j_c \sin\left[\gamma(0) + \frac{2\pi}{\Phi_0}B_a t_{\text{eff}} x\right]$$

$$I_c(\Phi_J) = I_c(0)\left|\frac{\sin[\pi\Phi_J/\Phi_0]}{\pi\Phi_J/\Phi_0}\right|$$

If we fix total flux, spatial distribution of current can be:

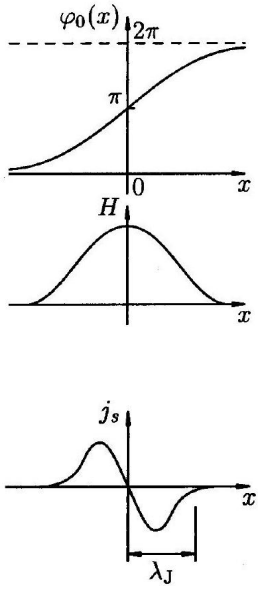


another theory, by Shmiedt:

$$\hbar\nabla\theta = 2m\mathbf{v}_s + \frac{2e}{c}\mathbf{A} \qquad \theta - \text{phase}$$

$j_{s,y} = \frac{c}{4\pi}\frac{dH}{dx}$

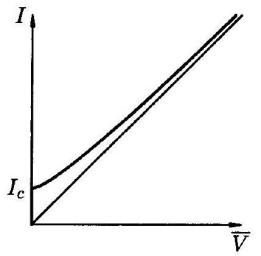
$$\frac{d^2\varphi}{dx^2} = \frac{1}{\lambda_J^2}\sin\varphi \qquad \lambda_J := \left(\frac{c\Phi_0}{8\pi^2 j_c d}\right)^{1/2}$$



On RCSJ, RSJL Josephson Junctions

RSJ

If we have just a JJ with resistance:



$$I = \frac{V}{R} + I_c\sin(\phi) = \frac{\hbar}{2eR}\frac{\partial\phi}{\partial t} + I_c\sin(\phi)$$

(???)

$$I_c > I \qquad \phi = \arcsin\left(I/I_c\right)$$

$$I_c < I \qquad \frac{\hbar}{2eR}\frac{d\phi}{I - I_c\sin(\phi)} = dt \quad \Rightarrow \quad \int_0^{t_0}, \int_0^{2\pi} \quad \Rightarrow$$

$$t_0 = \frac{\hbar}{2eR}\frac{2\pi}{\sqrt{I^2 - I_c^2}}$$

$$\langle V\rangle = \frac{1}{t_0}\int_0^{t_0} V dt = \frac{\hbar}{2e}\frac{1}{t_0}\int_0^{t_0}\frac{d\phi}{dt}dt = \frac{2\pi\hbar}{2e}\frac{1}{t_0}$$

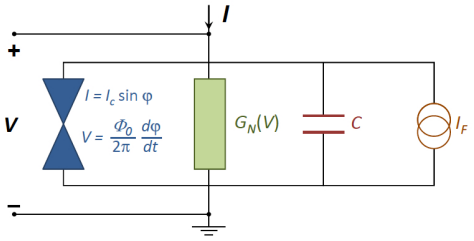
If we average $V(t) = R\frac{I^2 - I_c^2}{I + I_c\cos\omega t}$, where $\omega = \frac{2e}{\hbar}R\sqrt{I^2 - I_c^2}$, we get

$$2e\bar{V} = \hbar\omega.$$

Если среднее расстояние по энергиям между уровнями куперовских пар в двух половинках перехода равно $2e\bar{V}$, то при переходе одной пары через область слабой связи такая энергия выделяется в виде кванта электромагнитного излучения. (????)

Resistively and Capacitively Shunted Junction (RCSJ)

Junction $\Leftrightarrow$



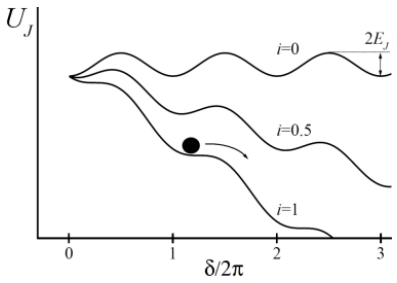
$$\frac{\hbar}{2e}C\frac{d^2\gamma}{dt^2} + \frac{1}{R}\frac{\hbar}{2e}\frac{d\gamma}{dt} + [I_c\sin\gamma - I] = 0$$

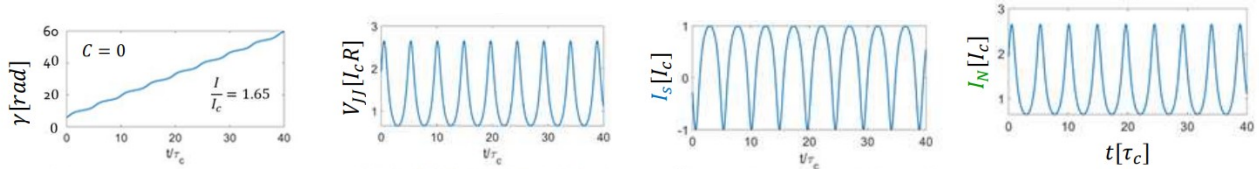
$$\beta_C\frac{d^2\gamma}{d\tau^2} + \frac{d\gamma}{d\tau} + \sin\gamma - i = 0$$

$$\left(\frac{\hbar}{2e}\right)^2 C\frac{d^2\gamma}{dt^2} + \frac{1}{R}\left(\frac{\hbar}{2e}\right)^2\frac{d\gamma}{dt} + \frac{d}{d\gamma}\{E_0[1 - cos\gamma - i\gamma]\} = 0$$

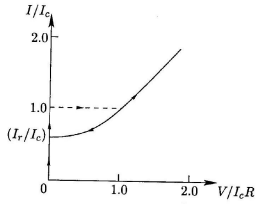
$$\left(\frac{\hbar}{2e}\right)^2 C\frac{d^2\gamma}{dt^2} + \frac{1}{R}\left(\frac{\hbar}{2e}\right)^2\frac{d\gamma}{dt} + \frac{d}{d\gamma}\{E_{J0}[1 - \cos\gamma - i\gamma]\} = 0 \qquad M\frac{d^2x}{dt^2} + \eta\frac{dx}{dt} + \nabla U = 0$$

$$x(t) \leftrightarrow \gamma(t) \qquad M \leftrightarrow \left(\frac{\hbar}{2e}\right)^2 C \qquad \eta \leftrightarrow \frac{1}{R}\left(\frac{\hbar}{2e}\right)^2 \qquad U \leftrightarrow E_{J0}[1 - \cos\gamma - i\gamma]$$





For $\beta_c = 4$

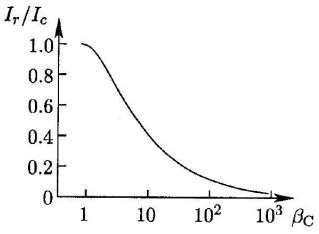


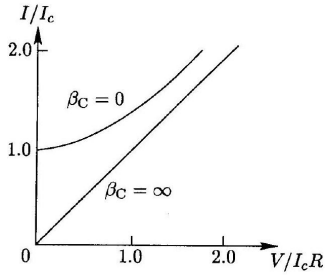
With inductance:

$$\beta_C := (2e/\hbar) I_c C R^2.$$

$$\omega_c := (2e/\hbar) I_c R$$

$$I/I_c = \beta_C \omega_c^{-2} \ddot{\varphi} + \omega_c^{-1} \dot{\varphi} + \sin\varphi.$$





Shapiro spikes (AC voltage circuits)

$$I_s(t) = I_c \sum_{-\infty}^{+\infty} (-1)^n \mathcal{J}_n\left(\frac{2\pi V_1}{\Phi_0 \omega_1}\right) \sin[(\boldsymbol{\omega_{DC}} - n\omega_1)t + \gamma_0]$$

$\mathcal{J}_n$ is the nth order Bessel function of the first kind

$$\boldsymbol{\omega_{DC}} \equiv \frac{2\pi}{\Phi_0} \boldsymbol{V_{DC}}$$

The Josephson frequency associated with the V_{DC} bias

$$V = V_0 + V_1 \cos(\omega t)$$

$$\phi = \int \frac{2eV}{\hbar} dt = \frac{2e}{\hbar} \int \left[V_0 + V_1 \cos(\omega t)\right] dt = \phi_0 + \frac{2e}{\hbar} V_0 t + \frac{2e}{\hbar\omega} V_1 \sin(\omega t)$$

$$I_s = I_c \sin(\phi) = I_c \,\mathrm{Im}\left[\exp\left(i\left(\phi_0 + \frac{2e}{\hbar} V_0 t + \frac{2eV_1}{\hbar\omega}\sin(\omega t)\right)\right)\right]$$

Inverse AC Josephson effect:

$$I = I_s + \frac{V_0}{R} = I_c \sum_{k=-\infty}^{\infty} (-1)^k J_k\left(\frac{2eV_1}{\hbar\omega}\right) \sin\left(\phi_0 + \frac{2e}{\hbar} V_0 t - k\omega t\right) + \frac{V_0}{R}$$

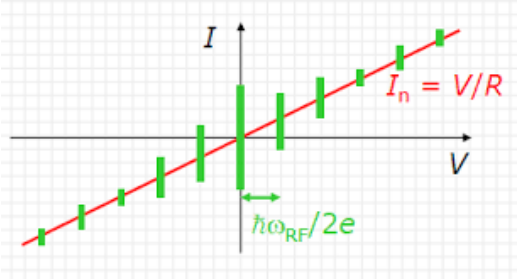
The DC part of the current is V_0/R unless

$$V_0 = \frac{k\hbar\omega}{2e}, \quad k = 0, \pm 1, \pm 2, \ldots$$

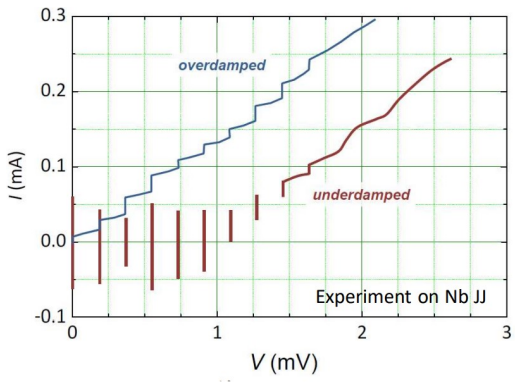
Then the supercurrent has the DC component

$$I_s = I_c (-1)^k J_k\left(\frac{2eV_1}{\hbar\omega}\right) \sin\left(\phi_0\right)$$

If the potential is not precisely given by Eq. (46) the supercurrent will oscillate slowly with an amplitude given by Eq. (47) with $\phi_0 = \pi/2$, i.e. given by the Bessel function value.

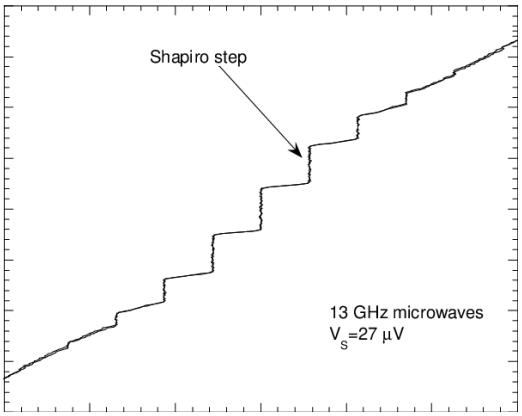


(???)



Shapiro steps (AC current circuits)

We don't know how to solve analytically equations, but we know numerical results:



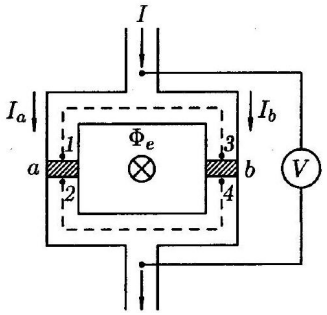
We have some hysteresis effect here (???)

The currents jump at the Shapiro step by an amount given by the Bessel function expression above.

The plateau appears and a Shapiro step occurs when the voltage match an integer value of $\hbar\omega/(2e)$

Typical SQUID in a nutshell

Typical SQUID



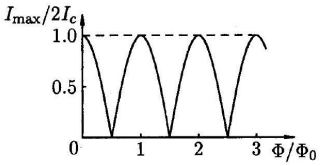
$$I_{s,\max} = 2I_c \left|\cos \pi \frac{\Phi_a}{\Phi_0}\right| \qquad \begin{matrix} I_{c,1} = I_{c,2} = I_c, \\ \beta_L \equiv \dfrac{2LI_c}{\Phi_0} \ll 1 \end{matrix}$$

$$I = I_1 + I_2, \qquad \begin{matrix} I_1 = \dfrac{I}{2} + J = I_c \sin \gamma_1, \\ I_2 = \dfrac{I}{2} - J = I_c \sin \gamma_2 \end{matrix} \qquad I_{c,1} = I_{c,2}$$

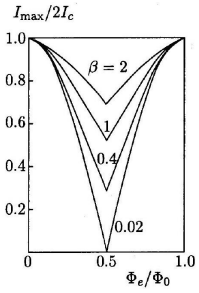
$$\gamma_2 - \gamma_1 = \frac{2\pi}{\Phi_0} \underbrace{(\Phi_a + LJ)}_{\text{tot flux}} \overset{\beta_L := \frac{2LI_c}{\Phi_0} \ll 1}{\approx} \frac{2\pi\Phi_a}{\Phi_0}$$

(????)

$$I_{s,\max} = 2I_c \left\|\cos \pi \frac{\Phi_a}{\Phi_0}\right\|$$



(???)



Другие типичные свойства и типичные джозефсоновы контакты

Overview other theoretical general properties of JJ

Free energy of a JJ at temperature T:

$$\Omega = -gT \int_0^\infty d\varepsilon \rho(\varepsilon) \ln[2\cosh(\varepsilon/2T)].$$

The spectrum of H_{BdG} consists of bound states (Andreev levels) for $\varepsilon < \Delta_0$ and a continuous spectrum for $\varepsilon > \Delta_0$.

$$\rho(\varepsilon) = -\frac{1}{\pi}\mathrm{Im}\frac{d}{d\varepsilon}\ln\det\left[1 - R_{\mathrm{A}}\left(\varepsilon + i0^+\right) S_{\mathrm{N}}\left(\varepsilon + i0^+\right)\right],$$

where R_{A} is an Andreev reflection matrix and S_{N} is the scattering matrix of the junction in the normal state.

Энергия связи в S-I-S контакте и критический ток.

(see Feigelman's lectures about it later, I am not sure what is meant here)

Температурная зависимость тока, формула Амбегаокара-Баратова для симметричного S-I-S.

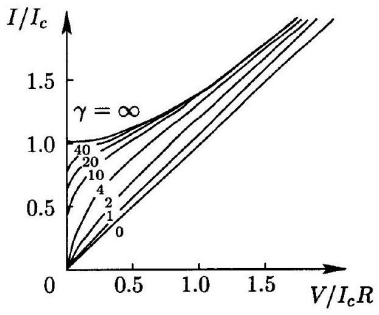
(maybe I'll write from LS main ideas)

Влияние тепловых флуктуаций на эффект Джохефсона (????7)

Shmidt cites some literature and states:

$$U_0(I) = \frac{4\sqrt{2}}{3} E_{\mathrm{J}} \left(1 - I/I_c\right)^{3/2}.$$

$$\omega(I) = \omega_p \left[1 - (I/I_c)^2\right]^{1/4},$$

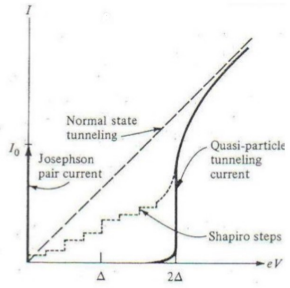


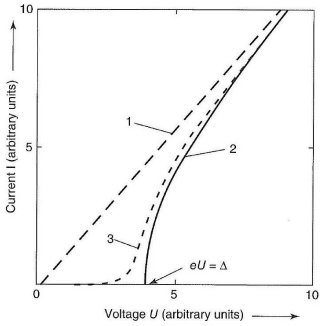
(I'll add later some conclusions from Varlamov, Larkin)

1.2.2 NS, NIS, SIS, other typical junctions

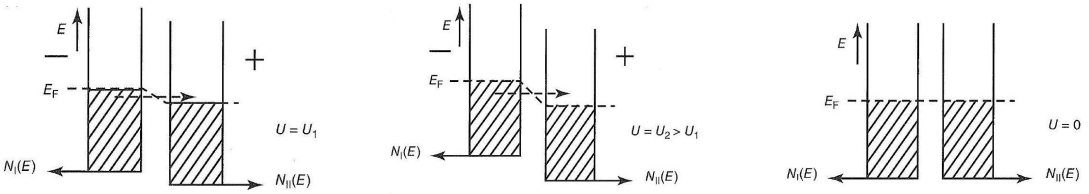
Свойства типичных сверхпроводящих контактов

Основные свойства NS контактов

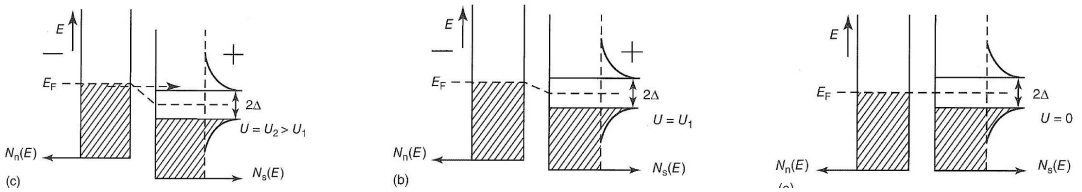




$N - N$ junction



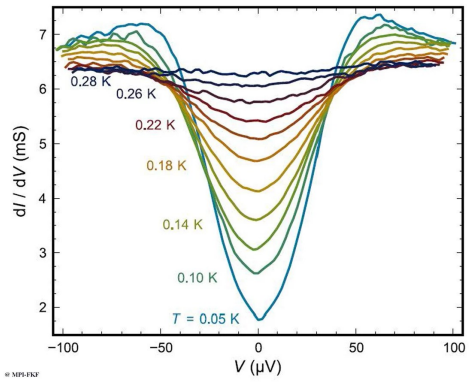
$N - S$ junction



At low temperatures the tunneling provides direct information on the superconducting state. Figure 2 shows d//dV(V) tunneling characteristics at temperatures below the superconducting transition. The characteristics reveal a clear superconducting gap and allow the gap of the 2DEL to be measured for the first time: it equals $\Delta(50\text{mK}) \approx 40\mu\text{V}$. This value is derived

from fitting the data with a quasiparticle lifetimebroadened BCS s-wave quasiparticle density of states. The gap vanishes at 280mK and the temperature dependence is well described by that expected from the BCS theory. (????)

(?????? how to get a gap from it????)



Типичное явление - эффект близости: проникновение ψ в нормальный металл. Это же и для двух разных сверхпроводников.

Из ГЛ:

$$-\xi^2(d\psi/dx)^2 - \psi^2 + \frac{1}{2}\psi^4 = C,$$

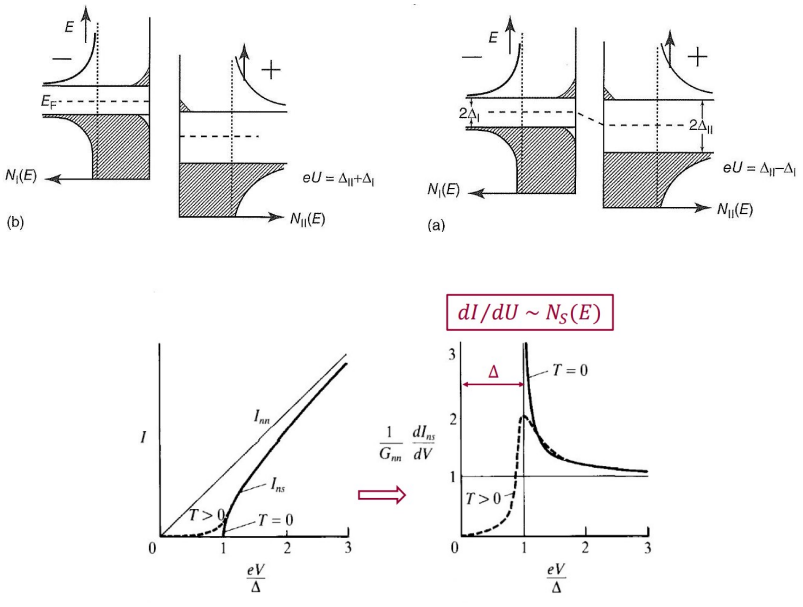
$(d\psi/dx) \overset{x\to\infty}{\to} 0, \psi \to 1 \;\Rightarrow\; C = -1/2,$

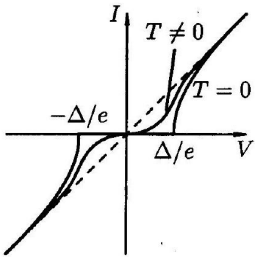
$$\psi = \text{th}\left[(x - x_0)/\sqrt{2}\xi\right]. \qquad x_0 = \text{const}$$

$$\frac{1}{\psi}\frac{d\psi}{dx} = \frac{1}{b}$$

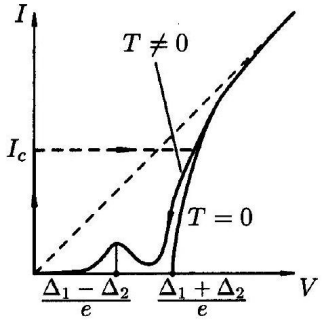
(снова тут картинка!)

$S - N - S$ **junction**





Superconductor-Insulator-Superconductor (SIS) контакт



Normal–Insulator-Superconductor (NIS) junctions

(??????)

(есть также Эффект близости в SIN-контакте, см. Шелкочева, за минут 20 додумаю, если будет нужно)

SINIS junction

(см Щелкочева, просто, интересно, но пока не до этого)

1.2.3 Skin effect, inductance, impedance

(просто саммари 1й части Шмидта, хорошие темы там)

Принцип замыкания по Шмидту

(есть такой принцип, Шмидт говорит, что он хороший, я пока не читал, не нужно это было.)

Кинетическая индуктивность

(!!?? нужно додумать еще смысл этого!)

$$\mathcal{F}^{\mathrm{M}} = \frac{1}{8\pi}\int H^2 dV = \frac{1}{2c^2} L^{\mathrm{M}} I^2;$$

$$L^K := c^2 \Lambda \int j_s^2 dV / I^2$$

Примеры кинетической индуктивности

(см Шмидт пар 10.)

Комплексная проводимость сверхпроводника

$$\mathbf{E} = \Lambda d\mathbf{j}_s/dt.$$

$$e\mathbf{E} - \frac{m}{n_n e}\frac{\mathrm{j}_n}{\tau} = \frac{m}{n_n e}\frac{d\mathrm{j}_n}{dt}. \qquad \Rightarrow \qquad \mathbf{E} = \frac{n_s}{n_n}\Lambda\frac{d\mathrm{j}_n}{dt} + \frac{n_s}{n_n}\Lambda\frac{\mathrm{j}_n}{\tau}.$$

$$\mathbf{j}_n \propto e^{i\omega t},$$

$$\mathbf{j} = \mathrm{j}_s + \mathrm{j}_n, \qquad \mathbf{j}_s = -i\frac{1}{\Lambda\omega}\mathbf{E}, \qquad \mathrm{j}_n = \frac{n_n}{n_s}\frac{\tau}{\Lambda}\frac{1-i\omega\tau}{1+(\omega\tau)^2}\mathbf{E}$$

$$\mathbf{j} = \sigma\mathbf{E}, \qquad \sigma = \sigma_1 - i\sigma_2, \qquad \sigma_1 := \frac{n_n}{n_s}\frac{\tau}{\Lambda}\frac{1}{1+(\omega\tau)^2} \qquad \sigma_2 := \frac{1}{\Lambda\omega}\left[1 + \frac{n_n}{n_s}\frac{(\omega\tau)^2}{1+(\omega\tau)^2}\right].$$

Скин эффект

Нормальный скин-эффект

$$\mathrm{rot}\mathbf{H} = \frac{4\pi}{c}\sigma\mathbf{E}, \qquad \mathrm{rot}\mathbf{E} = -\frac{1}{c}\frac{\partial\mathbf{H}}{\partial t}.$$

$$-\nabla^2\mathbf{H} = -\frac{4\pi}{c}\sigma\frac{\partial\mathbf{H}}{\partial t}.$$

$$k^2 = -i\frac{4\pi}{c^2}\sigma\omega,$$

$$k = (1-i)/\delta$$

$$\delta = \left(\frac{c^2}{2\pi\sigma\omega}\right)^{1/2}.$$

$$\sigma = \frac{n_n}{n_s}\frac{\tau}{\Lambda} - i\frac{1}{\Lambda\omega}.$$

$$\delta = \frac{\sqrt{2}\lambda}{\left(\frac{n_n}{n_s}\omega\tau - i\right)^{1/2}}.$$

Поверхностный импеданс

$$Z := \frac{4\pi}{c}\frac{E}{H}$$

$$ikH = \frac{4\pi}{c}\sigma E.$$

$$Z = \frac{ik}{\sigma} = \frac{1+i}{\sigma\delta}.$$

$$Z = R_\square + iX_{L\square},$$
$$R_\square = \frac{2\pi\omega^2\lambda}{c^2}\frac{n_n}{n_s}\tau$$
$$X_{L_\square} = 4\pi\lambda\omega/c^2 = \omega L_\square/c^2$$

$\lambda \propto (1-t^4)^{-1/2}$, $t = T/T_c$. Поскольку $\lambda \propto n_s^{-1/2}$, то $n_s \propto (1-t^4)$, или $n_s = n\,(1-t^4)$, n-плотность свободных электронов металла. Тогда $n_n = nt^4$, таким образом,

$$R_\square \propto t^4/\left(1-t^4\right)^{3/2}, \quad X_{L_\square} \propto \left(1-t^4\right)^{-1/2}.$$

$$Z = \frac{2\pi}{c^2}\left(2\omega\tau\frac{n_s}{n_n}\right)^{1/2}\frac{\lambda}{\tau}(1+i) = \frac{1+i}{\sigma_n\delta_n}$$

(картинку добавлю)

1.2.4 Thin films, plates

(выпишу Шмидта и ЛЛ9, добавлю задачи в каталог. не так акутально просто, но тут много нетривиального)

Critical field of a thin film ($d \ll \xi, \lambda$)

$$-\left(1-(2\pi\xi A/\Phi_0)^2\right)\psi + \psi^3 = 0$$
$$d^2A/dx^2 = \left(\psi^2/\lambda^2\right)A$$
$$H(\pm d/2) = H_0$$

(words)

$$H = A_1(\psi/\lambda)\,\mathrm{sh}(\psi x/\lambda) + A_2(\psi/\lambda)\,\mathrm{ch}(\psi x/\lambda)$$

(words)

$$\psi^2 = 1 - \frac{1}{24}\frac{H_0^2 d^2}{H_{cm}^2\lambda^2}$$

Finally,

$$H_\mathrm{K} = 2\sqrt{6}H_{cm}\frac{\lambda}{d}$$

Если толщина пленки на порядок меньше ее глубины проникновения, $\lambda/d \sim 10$, а $H_{cm} \sim 10^3$, то $H_\mathrm{K} \sim 40000$. Физически это вполне понятно. Поскольку магнитное поле проникает в пленку, она имеет существенно меньший диамагнитный момент на единицу объема, чем массивный образец. Но малый диамагнитный момент во внешнем поле - это маленькая магнитная стрелка, ориентированная навстречу полю. Такая ситуация энергетически более выгодна, чем в случае большого диамагнитного момента. Поэтому пленка оказывается во внешнем поле гораздо более устойчивой, чем массивный образец, и может сохранить сверхпроводимость в существенно больших полях.

Критический ток тонкой пленки

(words, somehting very similar to the previous par)

$$2\lambda^2 H_I^2 / \left(d^2 H_{cm}^2\right) = \psi^4 - \psi^6$$

$$\frac{d}{d\psi}\left(2\lambda^2 H_I^2 / d^2 H_{cm}^2\right) = 4\psi_c^3 - 6\psi_c^5 = 0,$$

отсюда $\psi_c^2 = 2/3$

$$H_{I_c} = \frac{\sqrt{2}}{3\sqrt{3}} H_{cm} \frac{d}{\lambda}.$$

$2H_{I_c} = (4\pi/c) I_c$

$$j_c = \frac{\sqrt{2}}{6\pi\sqrt{3}} \frac{cH_{cm}}{\lambda}.$$

1. Поле, созданное критическим током на поверхности пленки, оказывается пропорциональным ее толщине: $H_{I_c} \propto d$, т.е. падает с уменьшением толщины пленки, в то время как критическое поле пленки $H_к \propto 1/d$, т.е. растет с уменьшением толщины. Так, если $d/\lambda \sim 0.1$, а $H_{cm} = 1000$ Э, то $H_\kappa \sim 4 \cdot 10^4$, а $H_{I_c} \sim 30$. Это значит, что для тонкой пленки разрушение сверхпроводимости током никак нельзя сводить к разрушению сверхпроводимости магнитным полем этого тока.

2. Критическая плотность тока j_c, согласно (18.5), не зависит от толщины пленки. Из этой формулы следует, что j_c просто является характеристикой токонесущей способности данного материала.

3. Отметим, наконец, еще один очень важный момент. Разрушение сверхпроводимости током не сопровождается каким-либо фазовым переходом. При этом мы, конечно, имеем в виду, что пленка с током хорошо омывается жидким гелием и все выделяющееся в ней тепло сразу отводится, т. е. ее температура остается равной температуре гелиевой ванны. В этом случае даже при токе I_c свободная энергия сверхпроводящего состояния все еще остается меньше свободной энергии нормального состояния.

(by the way, it is similar to considerations about critical current. (??? how??))

Проникновение потока

(тут основное указание про то, как по итогу это вообще получается!!!)

Глубина проникновения по Ландау 9 (????)

(??? там много соображений, потом подумаю про них еще раз)

Пластина толщиной d в однородном параллельном магнитном поле B_0

$$\vec{h} + \lambda^2 \text{ rot rot } \vec{h} = 0$$

$$h - \lambda^2 \frac{d^2 h}{dx^2} = 0$$

$$h(x) = h_1 \text{ch}(x/\lambda) + h_2 \text{sh}(x/\lambda)$$

$$h(\pm d/2) = B_0$$
$$h(x) = B_0 \frac{\mathrm{ch}(x/\lambda)}{\mathrm{ch}(d/(2\lambda))}$$
$$j_s(x) = -\frac{c}{4\pi}\frac{dh}{dx} = -\frac{cB_0}{4\pi\lambda}\frac{\mathrm{sh}(x/\lambda)}{\mathrm{ch}(d/(2\lambda))}$$

(?? там ур Максвелла в конце??)

Пластна с током

В единичной полосе вдоль оси z течет ток I. На поверхностях пластины ($x = \pm d/2$) он создает магнитное поле $H(\pm d/2) = \mp H_I$. Подставляя эти граничные условия в общее решение (9.2), найдем поле в пластине:

$$H(x) = -H_I \frac{\mathrm{sh}(x/\lambda)}{\mathrm{sh}(d/2\lambda)}, \qquad H_I := 2\pi I/c$$

$$j_s(x) = \frac{cH_I}{4\pi\lambda}\frac{\mathrm{ch}(x/\lambda)}{\mathrm{sh}(d/2\lambda)}$$

$$H = -H_I \cdot 2x/d, \quad j_s = \frac{cH_I}{2\pi d} = \frac{I}{d}.$$

(картинку из Шмидта добавлю)

Пленка над экраном.

(изучу у Шмидта, пока не нужно это)
(тоже картинки у него есть)

Квантование потока

Little–Parks oscillations

Суть эффекта заключается в незначительном подавлении сверхпроводимости незатухающим током.

Результаты схематически показаны на рис. где наблюдаются периодические осцилляции критической температуры (Tc) на параболическом фоне.

(поизучаю мб потом, не самый важный эффект, если усвою основы, по идее быстро и решу его сам)

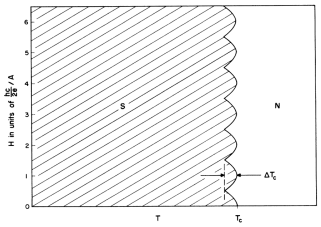


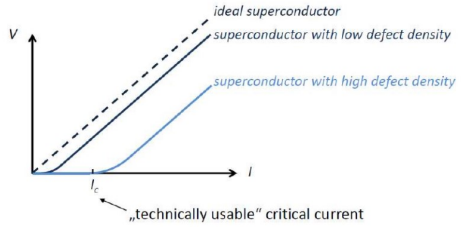
FIG. 1. Phase diagram for a thin cylindrical superconductor in an axial magnetic field. The scalloped edge of the superconducting phase results from the periodicity in the free energy of the bound pairs, in the magnetic flux through the cylinder.

1.2.5 Vortices: basic models

Основные свойства вихрей

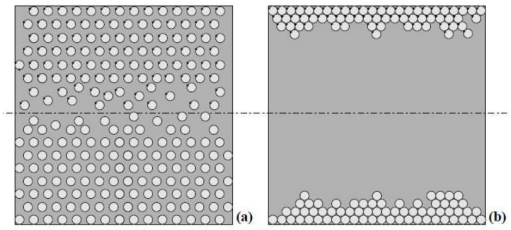
Мы рассматриваем сверхпроводники 2го рода при магнитном поле между 1м и 2м критическом, потому что это наиболее типичный случай.

"Lorentz"-like force $\boldsymbol{F}_L$ between current and magnetic flux lines.
→ force ⊥ current and ⊥ magnetic field
→ Flux lines move ⊥ current and ⊥ magnetic field
→ Moving flux lines create dissipation (electrical resistance!):
→ $j_c << j_{c,p}$ 'Ideal' superconductors have zero critical current density



Silsbee's hypothesis for the critical current:
"The threshold value of the current is that at which the magnetic field due to the current itself is equal to the critical magnetic field."
For type-II superconductors: $I_c = B_{c1} 2\pi R/\mu_0$
(????? как оценить размер вихря???? они супер мелкие, но я пока не умею их оценивать)

Вихри проникают именно через границу, потому что так им выгоднее (? когда-то мб пойму, почему?). Внутри они так вот просто не возникают. Если пининг сильный, то они особо и не двигаются, если же малый, то особо и не двигаются.



Решение Абрикосова для решетки вихрей и верхнее критическое поле.

Взаимодействие вихрей (в лондоновском приближении).

Вихрь в тонкой пленке.

Описание пиннинга вихрей в двух словах (???)

(?? там тоже часть лекции про это)

Критический ток при зацеплении вихрей на линейных дефектах.

Взаимодействие вихрей с точечными дефектами.

Типичные следствия вихрей

28 Поле одиночного вихря 159

29 Первое критическое поле 161

30 Взаимодействие вихрей 163

31 Второе критическое поле 165

32 Обратимый магнитный момент сверхпроводника 2го рода

33 Поверхностная сверхпроводимость. Третье критическое поле

34 Поверхностный барьер. Перегрев мейсснеровского состояния

Флуктуации вблизи температуры перехода (оценка ширины флуктуационной области, диамагнетизм, парапроводимость).

1.3 Basic concepts of condensed matter for SC

(I'll write useful background here)

Green's functions basics for SC

(for now it is written in cond. matter and applications are summarized in 2nd 1st section.)

Matsubara summation method for SC

(for now it is written in cond. matter and applications are summarized in 2nd 1st section.)

1.4 Mathematics

Типичный интеграл БКШ

(?? строчка - откуда он???)

$$I(u)=\int\limits_0^\infty \frac{dx}{\sqrt{x^2+u^2}\left(e^{\sqrt{x^2+u^2}}+1\right)}=\begin{cases}\left(\frac{\pi}{2u}\right)^{1/2}e^{-u} & \text{при } u\gg 1,\\ \ln\frac{\pi}{\gamma u}+\frac{7\zeta(3)}{8\pi^2}u^2 & \text{при } u\ll 1.\end{cases}$$

Полезные интегралы

$$\int\limits_0^{2\pi}\cos^2\theta\frac{d\theta}{2\pi}=\frac{1}{2} \qquad \int\limits_0^{2\pi}\cos^2\theta\sin^2\theta\frac{d\theta}{2\pi}=\frac{1}{8} \qquad \int\limits_0^{2\pi}\cos^4\theta\frac{d\theta}{2\pi}=\frac{3}{8}$$

$$\int\limits_{-\infty}^{\infty}\frac{x^2}{\left(1+x^2\right)^2}dx=\frac{\pi}{2} \qquad \int\limits_{-\infty}^{\infty}\frac{x^4}{\left(1+x^2\right)^2}dx=\frac{\pi}{2}dx=\frac{\pi}{16} \qquad \int\limits_{-\infty}^{\infty}\frac{x^2}{\left(1+x^2\right)^4}dx=\frac{\pi}{16}$$

$$\int\limits_{-\infty}^{\infty}\frac{1}{\left(1+x^2\right)^4}dx=\frac{5\pi}{16} \qquad \int\limits_{-\infty}^{\infty}\frac{1}{(2n+1)^5}=\frac{1}{32}\zeta(5) \qquad \int\limits_0^{\infty}\frac{1+4x^2}{\left(1+x^2\right)^{\frac{7}{2}}}dx=0$$

$$\sum_0^\infty \frac{1}{(2n+1)^3} = \frac{7}{8}\zeta(3) \qquad \sum_0^\infty \frac{1}{(2n+1)^5} = \frac{31}{32}\zeta(5)$$

$$\int_0^\pi dx \frac{\sin^2 x}{p + q\cos x} = \frac{\pi p}{q^2}\left(1 - \sqrt{1 - \frac{q^2}{p^2}}\right), |p| > |q|$$

(соберу потом, решая задачи)

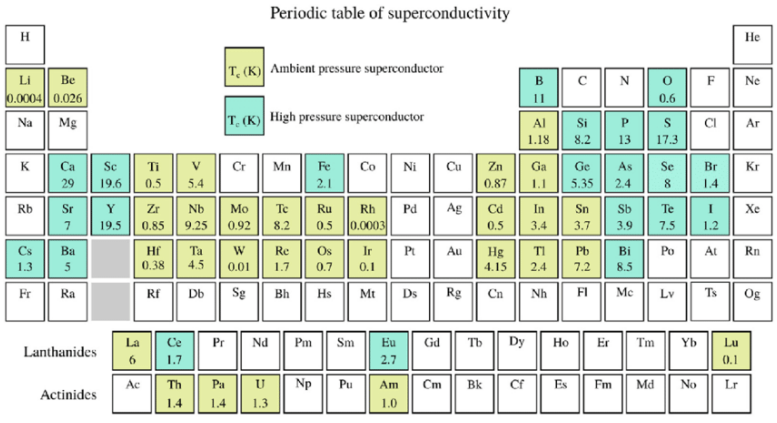
1.5 Materials, experimental facts

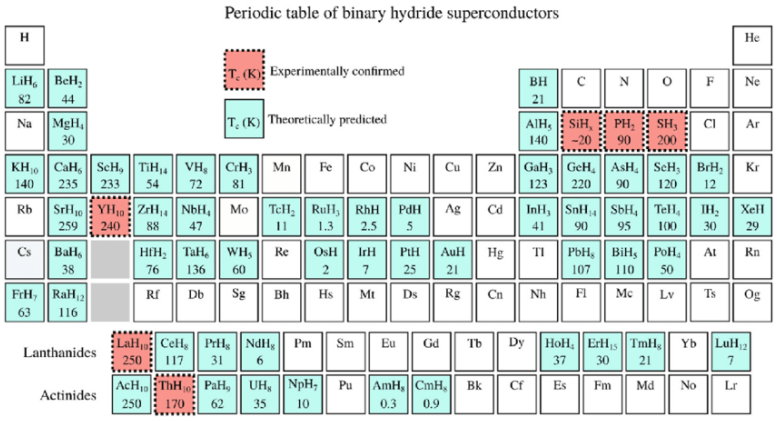
Typical SC materials

Examples of type one SC: Hg, Pb, Zn,etc
Examples of type two SC: NbTi, Nb3Sn

Metal	Θ_D(K)	T_c(K)	$N(0)V$
Zn	235	0.9	0.18
Cd	164	0.56	0.18
Hg	70	4.16	0.35
Al	365	1.2	0.18
In	109	3.4	0.29
Tl	100	2.4	0.27
Sn	195	3.75	0.25
Pb	96	7.22	0.39

P.G. de Gennes Superconductivity of Metals and Alloys, Westview (1999), table 4.





Название материала	Критическая температура T_c, К	Критическое поле B_c, Тл	Год опубликования обнаружения сверхпроводимости
Сверхпроводники I рода			
Pb (свинец)	7,26[3]	0,08[4]	1913[3]
Sn (олово)	3,69[3]	0,031[4]	1913[3]
Ta (тантал)	4,38[3]	0,083[4]	1928[3]
Al (алюминий)	1,18[3]	0,01[4]	1933[3]
Zn (цинк)	0,88[4]	0,0053[4]	
W (вольфрам)	0,01[4]	0,0001[4]	

Сверхпроводники II рода			
Nb (ниобий)	9,20[3]	0,4[4]	1930[3]
V_3Ga	14,5[4]	>35[4]	
Nb_3Sn	18,0[4]	>25[4]	
$(Nb_3Al)_4Ge$	20,0[4]		
Nb_3Ge	23[4]		
GeTe	0,17[4]	0,013[4]	
$SrTiO_3$	0,2—0,4[4]	>60[4]	
MgB_2 (диборид магния)	39	?	2001
H_2S (сероводород)	203[6]	72[6]	2015[6]

Calculated intrinsic coherence length and London penetration depth, at T=0 Meservey and B. B. Schwartz (from Kittel):

Metal	Intrinsic Pippard coherence length ξ_0, in 10^{-6} cm	London penetration depth λ_L, in 10^{-6} cm	λ_L/ξ_0
Sn	23.	3.4	0.16
Al	160.	1.6	0.010
Pb	8.3	3.7	0.45
Cd	76.	11.0	0.14
Nb	3.8	3.9	1.02

(???? why Nb is a SC? are they confirmed experimentally???? can I prove it theoretically????)

Link between properties of material and its superconducting properties (!!!)

(this is highly important for creating high T SC)

2 Most Useful Special Methods

2.1 Very useful special methods for special applications

2.1.1 Functional integral for SC

(I'll write soon)

Main formulas for Path integral for BCS

$$Z = \int \mathcal{D}[\bar{c}, c] e^{-S}, \qquad S = \int_0^\beta \sum_{\mathbf{k}\sigma} \bar{c}_{\mathbf{k}\sigma} \left(\partial_\tau + \epsilon_{\mathbf{k}}\right) c_{\mathbf{k}\sigma} - \frac{g_0}{V} \bar{A} A$$

$$-g\bar{A}A \to \bar{\Delta}A + A\bar{\Delta} + \frac{V}{g_0}\bar{\Delta}\Delta$$

$$Z = \int \mathcal{D}[\bar{\Delta}, \Delta, \bar{c}, c] e^{-S}$$
$$S = \int_0^\beta d\tau \left\{ \sum_{\mathbf{k}\sigma} \bar{c}_{\mathbf{k}\sigma} \left(\partial_\tau + \epsilon_{\mathbf{k}}\right) c_{\mathbf{k}\sigma} + \bar{\Delta} A + A\bar{\Delta} + \frac{V}{g_0}\bar{\Delta}\Delta \right\}$$

$$Z = \int \mathcal{D}[\bar{\Delta}, \Delta, \bar{\psi}, \psi] e^{-S}$$
$$S = \int_0^\beta d\tau \left\{ \sum_{\mathbf{k}} \bar{\psi}_{\mathbf{k}} \left(\partial_\tau + \underline{h}_{\mathbf{k}}\right) \psi_{\mathbf{k}} + \frac{V}{g_0}\bar{\Delta}\Delta \right\},$$

$$Z = \int \mathcal{D}[\bar{\Delta}, \Delta] e^{-S_E[\bar{\Delta},\Delta]}$$
$$e^{-S_E[\bar{\Delta},\Delta]} = \prod_{\mathbf{k}} \det\left[\partial_\tau + \underline{h}_{\mathbf{k}}(\tau)\right] e^{-V\int_0^\beta d\tau \frac{\bar{\Delta}\Delta}{g_0}}$$

$$S_E[\bar{\Delta}, \Delta] = V\int_0^\beta d\tau \frac{\bar{\Delta}\Delta}{g_0} + \sum_{\mathbf{k}} \mathrm{Tr}\ln\left(\partial_\tau + \underline{h}_{\mathbf{k}}\right)$$

Mean-field theory as a saddle point of the path integral:

$$Z_{BCS} = \int \prod_{\mathbf{k}n} d\bar{\psi}_{\mathbf{k}n} d\psi_{\mathbf{k}n} e^{-S_{MFT}\left[\bar{\psi}_{\mathbf{k}n}, \psi_{\mathbf{k}n}\right]} \qquad S_{MFT}\left[\bar{\psi}_{\mathbf{k}n}, \psi_{\mathbf{k}n}\right] = \sum_{\mathbf{k}n} \bar{\psi}_{\mathbf{k}n}\left(-i\omega_n + h_{\mathbf{k}}\right)\psi_{\mathbf{k}n} + \beta V \frac{\bar{\Delta}\Delta}{g_0}.$$

Proof.

$$Z = \int \mathcal{D}[\bar{\Delta}, \Delta] e^{-S_E[\bar{\Delta},\Delta]}.$$

$S_E = VS_0$,
$\delta S_E/\delta\Delta = 0$,

□

free energy: BCS pair condensate

$$\mathcal{F}[\Delta, T] = \frac{S_E}{\beta} = -T\sum_{\mathbf{k}n} \ln\left[\omega_n^2 + \epsilon_{\mathbf{k}}^2 + |\Delta|^2\right] + V\frac{|\Delta|^2}{g_0}$$

Proof.

$$\det\left[\partial_\tau + \underline{h}_{\mathbf{k}}\right] = \prod_n \det\left[-i\omega_n + \underline{h}_{\mathbf{k}}\right] = \prod_n \left[\omega_n^2 + \epsilon_{\mathbf{k}}^2 + |\Delta|^2\right]$$

$$Z_{BCS} = \prod_n \left[\omega_n^2 + \epsilon_{\mathbf{k}}^2 + |\Delta|^2\right] \times e^{-\frac{\beta V|\Delta|^2}{g_0}} = e^{-S_E}$$

□

(see Coleman)

2.1.2 Scattering Matrix, Beenkker method for SC Junctions

(I'll write later)

Part II
Fundamentals of Superconductivity

3 Framework for understanding superconductivity

3.1 General ideas about fundamental nature of superconductivity

3.1.1 How to predict existence of SC without knowing anything about low-temperature physics?

(good question, I'll think later about it when I'll have nothing important to do)

3.1.2 How to predict properties of SC if one knows everything about a material at normal state?

(good question, I'll think later about it when I'll have nothing important to do)

3.1.3 Taking into account shape of the Fermi surface (????)

(good question, I'll think later about it when I'll have nothing important to do. we always have $N(E_F)$, so there is a way to calculate it somehow for a different metals??? what is the dependence on the metal of it??? are there are articles about such examples, that for some concrete Fermi surface there are some concrete features of SC?)

3.1.4 Intuitive understanding of GL theory

Analogies of GL theory in life

(??? I had some ideas, but they are not strong now and it is not important)

3.1.5 How to guess about GL theory?

(how to get this idea? I don't know a good answer now)

But anyway, GL theory is not the only one way how one can see superconductivity. Sometimes it is useless to see it this way. There is a BCS and other theories (?? which??) and frameworks that are also useful.

3.1.6 Intuitive understanding of BCS theory

Analogies of BCS theory in life

(??? I had some ideas, but they are not strong now and it is not important)

3.1.7 How to guess about BCS theory?

(how to get this idea? I don't know a good answer now)

But anyway, BCS theory is not the only one way how one can see superconductivity. Sometimes it is useless to see it this way. There is a GL and other theories (?? which??) and frameworks that are also useful.

3.2 Basic Experimental Facts about Typical SC

3.2.1 Overview of Basic Experimental Facts about Typical SC

1.1.1 The Discovery of Superconductivity

Superconductivity was discovered in 1911 at the Leiden Laboratory. While studying the temperature dependence of the electrical resistivity of mercury, H. Kamerlingh-Onnes discovered that at a temperature T^* in the vicinity of 4 K the resistance of the sample dropped suddenly to zero and remained unmeasurable at all attainable temperatures below T^* [6]. Importantly, as the temperature decreased, the resistance disappeared instantly rather than gradually. It was obvious that the sample had undergone a transformation into a novel, as yet unknown, state characterized by zero electrical resistance. This phenomenon was named 'superconductivity'.

All attempts to find at least traces of resistance in bulk superconductors were to no avail. On the basis of the sensitivity of modern equipment, we can argue that the resistivity of superconductors is zero, at least at the level of $10^{-24}\Omega$ cm. For comparison, we note that the resistivity of high-purity copper is of the order $10^{-9}\Omega$ cm at 4.2 K.

Soon after the discovery of superconductivity in mercury, the same property was found in several other metals: tin, lead, indium, aluminum, niobium, and others. Many alloys and intermetallic compounds also turned out to be superconductors.

The temperature of the transition from the normal to the superconducting state is called the critical temperature T_c. Shortly after the discovery, it was found that superconductivity can be destroyed not only by heating the sample, but also by placing it in a relatively weak magnetic field. This field is called the critical field of bulk material, $H_{\rm cm}$. In most of the English-language literature, $H_{\rm cm1}$ is called the thermodynamic critical field, $H_{\rm ct/h}$.

Table 1.1 gives values of $T_{\rm c}$ and $H_{\rm crn}$ for a number of superconducting elements. Here $H_{\rm cm}(0)$ is the critical field extrapolated to absolute zero. The temperature dependence of $H_{\rm cm}$ is well described by the empirical formula

$$H_{\rm cm}(T) = H_{\rm cm}(0)\left[1 - (T/T_{\rm c})^2\right]. \tag{1.1}$$

Table 1.1. Critical temperatures and critical magnetic fields of superconducting elements [7]

Element	T_c/K	$H_{\rm cm}$ (0)/Oe	Element	$T_{\rm c}$/K	$H_{\rm cm}(0)$/Oe
Al	1.175 ± 0.002	104.9 ± 0.03	Pa	1.4	
Be	0.026		Pb	7.196 ± 0.006	803 ± 1
Cd	0.517 ± 0.002	28 ± 1	Re	1.697 ± 0.006	200 ± 5
Ga	1.083 ± 0.001	59.2 ± 0.3	Ru	0.49 ± 0.015	69 ± 2
Hf	0.128		Sn	3.722 ± 0.001	305 ± 2
Hg(α)	4.154 ± 0.001	411 ± 2	Ta	4.47 ± 0.04	829 ± 6
Hg (β)	3.949	339	Tc	7.8 ± 0.01	1410
In	3.408 ± 0.001	281.5 ± 2	Th	1.38 ± 0.02	160 ± 3
Ir	0.1125 ± 0.001	16 ± 0.05	Ti	0.40 ± 0.04	56
La (α)	4.88 ± 0.02	800 ± 10	Tl	2.38 ± 0.04	178 ± 5
La (β)	6.0 ± 0.1	1096, 1600	V	5.40 ± 0.05	1408
Lu	0.1	< 400	W	0.0154 ± 0.0005	1.15 ± 0.03
Mo	0.915 ± 0.005	96 ± 3	Zn	0.850 ± 0.01	54 ± 0.3
Nb	9.25 ± 0.02	2060 ± 50	Zr	0.61 ± 0.15	47
Os	0.66 ± 0.03	70			

This dependence is shown in Fig. 1.1 which essentially represents the $H-T$ phase diagram of the superconducting state. Within the dashed area, any point in the $H-T$ plane corresponds to the superconducting state.

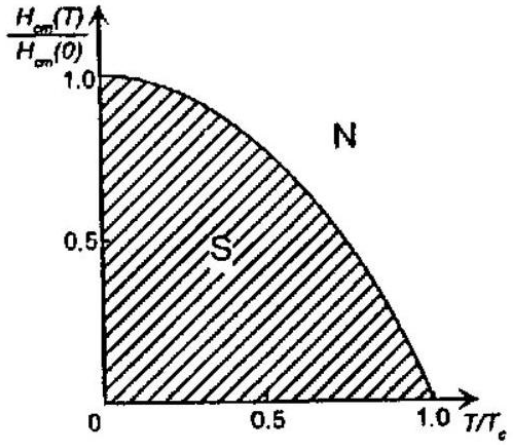


Fig. 1.1. Temperature dependence of the critical field $H_{\rm cm}$

Isotope Effect: Basics

(I'll add here about it from Shmidt's book, it is written below)

Isotope Effect: Experiments

(write articles about it shortly)

Magnetic Flux Quantization: Basics

An electric current in a superconducting ring can persist for an infinitely long time. Naturally, this does not require a power supply, since the resistance of the ring is zero. Such a persistent current can be produced as follows. Let us place the ring at $T > T_c$ in an external magnetic field so that the magnetic
external magnetic field is switched off. At the first moment after switch off the field, the magnetic flux through the ring decreases and, accordi to Faraday's law of electromagnetic induction, induces a current in the ri which will be persistent from this moment on. This current prevents a furtl decrease of the magnetic flux through the ring, i.e., now that the extern field is zero, the current itself supports the flux through the ring at the init level. Indeed, if the ring had a finite resistance R, the flux through the ri would decay during the time of the order of L/R, where L is the inductance the ring. In a superconducting ring, since $R = 0$, it takes the flux infinite ti to decay. This means that the magnetic flux becomes 'frozen' while the ri carries a persistent current usually referred to as a superconducting curr or a supercurrent.

At first sight it may seem that the 'frozen' magnetic flux can take on arbitrary value. However, a number of experiments [8, 9] intended to clar this situation established a very important experimental fact: The magne flux through a hollow superconducting cylinder may only assume values th are integral multiples of $\Phi_0 = 2.07 \times 10^{-7}\mathrm{Gcm}^2$. The latter is called t magnetic flux quantum and can be written as a combination of fundamen constants: $\Phi_0 = \pi\hbar c/e$, where $\hbar$ is Planck's constant, c is the speed of lig and e is the electron charge. In MKSA units $\Phi_0 = h/2e$.

It is surprising that these studies (1961) were not attempted earlier, sir by the mid-1930s superconductivity had already been generally perceived a quantum phenomenon.

Magnetic Flux Quantization: Experiments

(write articles about it shortly)

1.1.3 Josephson Effects

Another manifestation of the quantum nature of superconductivity was pl vided by the so-called weak superconductivity, or Josephson, effects [1 They were predicted in 1962 and soon verified experimentally. The ter 'weak superconductivity' refers to a situation in which two superconduct are coupled together by a weak link. The weak link can be provided by a tu nel junction or a short constriction in the cross-section of a thin film. Mc generally, this can simply be a weak contact between two superconductc over a small area or other arrangements where the superconducting conta between two superconductors is somehow 'weakened'.

There are two Josephson effects to distinguish: stationary (the dc Josep son effect) and nonstationary (the ac Josephson effect).

Consider first the dc effect. Let us apply a current through a weak lis (or, in other words, through a Josephson junction). Then, if the current sufficiently small, it passes through the weak link without resistance, ev if the material of the weak link itself is not superconducting (for examp) if it is an insulator in a tunnel junction). Here we directly come across tl most important property of a superconductor: the coherent behavior of s
in a different way. Having penetrated via the weak link into the second superconductor, the wavefunction of electrons from the first superconductor interferes with the 'local' electron wavefunction. As a result, all superconducting electrons on both sides of the weak link are described by the same wavefunction. The presence of the weak link should not change significantly the wavefunctions on the two sides, compared to what they had been before the link was established.

The ac Josephson effect is even more remarkable. Let us increase the dc current through the weak link until a finite voltage appears across the junction. Then, in addition to a dc component V, the voltage will also have an ac component of angular frequency ω, so that

$$\hbar\omega = 2\mathrm{eV}. \tag{1.2}$$

A fundamental experiment intended to record this so-called Josephson radiation (i.e., the electromagnetic radiation emitted by a Josephson junction) was successfully carried out by I.K. Yanson, V.M. Svistunov, and I.M. Dmitrenko [11].

1.1.4 The Meissner-Ochsenfeld Effect

For as long as 22 years after the discovery of superconductivity, scientists believed that a superconductor was simply an ideal conductor, that is, a piece of metal with zero resistance.

Let us work out how such an ideal conductor should behave in an external magnetic field that is weak enough so as not to destroy the specimen's ideal conductivity.

Suppose that initially the ideal conductor is cooled down below the critical temperature in zero external magnetic field. After that an external field is applied. From general considerations, it is easy to show that the field does not penetrate the interior of our sample, as shown schematically in Fig. 1.2. Indeed, immediately after the field penetrates the surface layer of the ideal conductor, an induced current is set up which, according to Lenz's law, generates a magnetic field in the direction opposite to that of the external field. Therefore, the total field in the interior of the specimen is zero.

Let us prove this with the help of Maxwell's equations. As the induction B changes, an electric field E must be induced in the specimen with

$$\operatorname{curl} \boldsymbol{E} = -\frac{1}{c}\frac{\partial \boldsymbol{B}}{\partial t},$$

where c is the speed of light in vacuum. In the ideal conductor $E = 0$, since $E = j\rho$, where ρ is the resistivity (which in our case is zero) and j is the density of the induced current. It follows that $\boldsymbol{B} = \text{const}$ and, taking into account that $\boldsymbol{B} = 0$ before applying the external field, we arrive at $\boldsymbol{B} = 0$ also after the field is applied. This phenomenon can also be interpreted in a

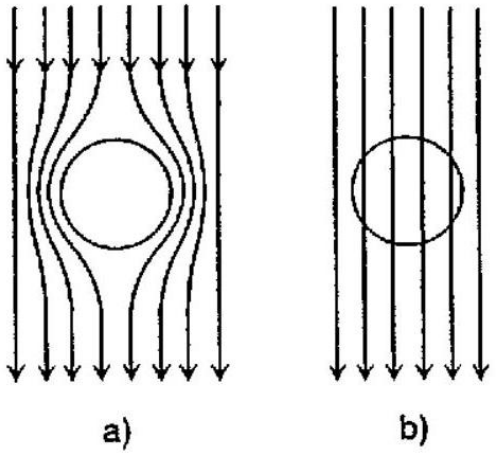


Fig. 1.2. For an ideal conductor, its magnetic state at $T < T_c, H > 0$ depends on its history: (a) magnetic field applied to an ideal conductor at $T < T_c$; (b) field applied at $T > T_c$

Thus, we have established that $\boldsymbol{B} = 0$ at any point of an ideal conductor placed in an external magnetic field. However, the same situation (an ideal conductor at $T < T_c$ in an external magnetic field) can be reached through a different sequence of events, that is, by first applying the external field to a 'warm' specimen and then cooling it down to $T < T_c$.

In that case, for the ideal conductor, electrodynamics predicts an entirely different result. At $T > T_c$, the resistivity of the specimen is finite and, therefore, the magnetic field penetrates into it. After cooling the specimen down through the superconducting transition, the field remains in it, as illustrated in Fig. 1.2 (b).

Note that in the above reasoning we always referred to the specimen characterized by $\rho = 0$ as an ideal conductor and not a superconductor.

It was generally believed before 1933 that the superconductor was indeed simply an ideal conductor. But the experiment by W. Meissner and R. Ochsenfeld [12] revealed that this was not true! They found that at $T < T_c$ the field inside a superconducting specimen was always zero ($B = 0$) in the presence of an external field, independent of which procedure had been chosen to cool the superconductor through T_c.

This discovery was immensely important. Indeed, if $B = 0$ independent of the specimen's history, the zero induction can be treated as an intrinsic property of the superconducting state at $H < H_{cm}$. Furthermore, it implies that we can treat a transition to the superconducting state as a phase transition and, consequently, apply all the might of the thermodynamic approach to examine the superconducting phase.

Thus, the superconducting state obeys the equations

$$\rho = 0, \tag{1.3}$$

$$\boldsymbol{B} = 0. \tag{1.4}$$

3.2.2 The Isotope Effect

The Isotope Effect

Already in 1922, Kamerlingh-Onnes [10] studied the question of whether the nuclear mass of the lattice atoms has an influence on superconductivity, that is, if superconductivity depends on

the lattice of the atomic ions, or whether it is restricted only to the system of the electrons. At the time, only the kinds of lead naturally occurring at different locations ($M = 206$ "uranium lead" and $M = 207.2$ "natural lead") were at his disposal. Within his experimental accuracy, he could not detect any difference in the transition temperature. Also subsequent experiments with lead samples by Justi in 1941 [11] did not show an influence of atomic mass on T_c .

With the advent of modern nuclear physics, it was possible to produce isotopes with a larger mass difference in sufficient concentration within nuclear reactors. In 1950 in mercury a dependence of the transition temperature on nuclear mass was observed [12, 13]. Some results are listed in Table 3.1.

We have already mentioned that these results were highly important for the development of superconductivity, since they appeared just in time to confirm perfectly the idea of the electron-phonon interaction. Already the initial rather qualitative discussions of Fröhlich or Bardeen suggested that the transition temperature T_c should be inversely proportional to the square root of the atomic mass M

$$T_c \propto M^{-1/2}$$

This dependence also remained valid in the BCS theory appearing only 7 years later, as we have discussed in Section 3.1.2.

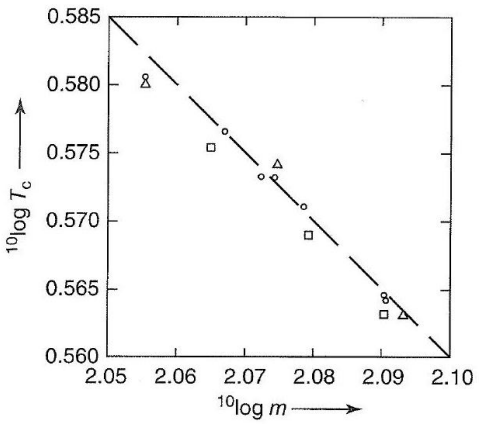


Figure 3.8 Isotope effect in tin: O Maxwell; □ Lock, Pippard, and Shoenberg; and Δ Serin, Reynolds, and Lohman. (From [14]])

Table 3.2 Isotope effect.

Element	Hg	Sn	Pb	Cd	TI	Mo	Os	Ru
Isotope exponent $\rho^{a)}$	0.50	0.47	0.48	0.5	0.5	0.33	0.2	0.0

a) The exponent β is obtained from experiment by fitting to the relation $T_c \propto M^{-\beta}$. The values shown are taken from Ref. [15].

The relation (3.8) is well satisfied for a series of superconductors. In Figure 3.8 we show the results for tin. Tin is a favorable substance, since its possible variations of the nuclear mass are relatively large, namely from $M = 113$ up to $M = 123$ In Figure 3.8 the results from different laboratories are shown [14]. The dashed line corresponds to the exponent $-1/2$ in relation (3.8). The agreement between experiment and the theoretical expectation is excellent.

From our current point of view this agreement is surprising, since the theory leading to relation (3.8) is strongly simplified. However, the agreement shows that apparently these simplifications are justified for a large number of superconductors. On the other hand, we see from Table 3.2, which lists measurements of the isotope effect in different superconductors, that this is not always the case.

The nontransition metals display well the exponent $\beta = 1/2$, the transition metal show strong deviations from this value. In spite of the great difficulties of these experiments, [8] the deviations are well reproduced. Measurements for uranium even indicate a value of $\beta = -2.2$, that is, an isotope effect with opposite sign [16].

For small changes of T_c sufficient accuracy of the experiments cannot be achieved easily. The measurements of T_c must be performed for different samples. Hence, all oher pdedesty The mea-

Because of the great success of the BCS theory, one is tempted to find an explanation of the isotope exponent deviating from 1/2 within the framework of this theory. This is quite possible, if we closely analyze the parameter V in Eq. (3.6) characterizing the interaction. Essentially, this interaction parameter results from the difference between the attractive electron - phonon interaction and the repulsive Coulomb interaction between the electrons. If both interactions are explicitly introduced into the theory, which became possible during further development of the theory, one obtains an improved and also more complicated formula for T_c[17]:

$$T_\mathrm{c} \propto \omega_\mathrm{D} \exp\left(\frac{\lambda^* + 1}{\lambda^* - \mu^* \left(1 + \lambda^* \langle\omega\rangle / \omega_\mathrm{D}\right)}\right)$$

Here, the electron-phonon interaction is characterized by λ^*, the Coulomb interaction by μ'', and $\langle\omega\rangle$ denotes a certain average value taken over all frequencies of the crystal lattice."

We do not want to discuss this formula in more detail. As the essential point, we note that in such a more detailed analysis the lattice frequencies also appear explicitly in the exponent, as expected. Hence, depending on the magnitude of λ^* and μ^*, the influence of the factor ω_D upon T_c (see Eq. (3.9)) is changed to a greater or lesser degree. Therefore, deviations of the quantity β in the relation $T_\mathrm{c} \propto M^{-\beta}$ from the value 1/2 cannot be taken as evidence against the importance of the electron-phonon interaction in these superconductors. The same applies even to the complete absence of any dependence of T_c upon M.

An important advance was achieved by tunneling experiments with superconductors, which we will discuss in the following section. The electron-phonon interaction shows up in the voltage - current characteristic of tunnel junctions, if the interaction is sufficiently strong. A careful analysis of such curves allows one to determine the quantities λ'' and μ''.

The isotope effect demonstrates most directly the influence of lattice vibrations. Because of its quantitative agreement with the theory, at least for many superconductors, it confirms the crucial role of the electron-phonon interaction. Here, the progress of nuclear physics, allowing the production of new isotopes in nuclear reactors, has strongly affected the development of superconductivity. This is one of the many examples in the field of superconductivity where different areas of physics have influenced each other during the progress that has been accomplished.

Also newly discovered superconductors have been investigated regarding the isotope effect, if possible. The results for the high-temperature superconductor will be discussed in Section 3.2.2. Here, as further examples, we mention the fullerides K_3C_{60} and Rb_3C_{60} [18] as well as magnesium diboride MgB_2 [19].

The order of magnitude of these parameters can be indicated as follows: λ° varies between 0 and 0.1 and 0.2 ; and $< \omega > |\omega_D$ is about 0.6. In the fullerides, the carbon isotope ^{12}C was partly or completely replaced by the isotope ^{13}C. Since carbon is a relatively light element, in this case a relatively large shift of T_c in the percent range could be observed. An isotope exponent of about 0.3 was found with a large scattering of the data. This value agrees well with the electron-phonon coupling, if we assume that the intramolecular vibrations of the C_{60} molecules provide the dominant contribution to the Cooper pairing. For MgB_2 the isotope effect was studied regarding both Mg and B. For the variation of the boron isotopes (^{10} B $\leftrightarrow$ ^{11} B) an exponent of about 0.3 was found, and the variation of the magnesium isotopes (^{26}Mg $\leftrightarrow$ ^{27}Mg)

only yielded an exponent of 0.02. This indicates that the vibrations of the boron ions apparently play an important role for the Cooper pairing in MgB_2.

3.2.3 The Anisotropy Effect.

(??? I forgot, where did I take it)

The correlation of the electrons, leading to the formation of Cooper pairs, is due to the elastic vibrations of the lattice, that is, the phonons. This interaction may depend on the direction within the crystal. In the presence of such anisotropy, in a simplified way we can say that certain crystal directions are more favorable for superconductivity than others.

For example, the energy gap Δ_0 can have different values along different directions. The strength of this anisotropy is quantified in terms of the averaged square of a parameter α[16] A value $\langle\alpha^2\rangle = 0.02$, as observed, say, for tin, means that in the different crystal directions the energy gap deviates from the average value by about $14\% \approx 0.02^{1/2}$. Such differences in the energy gap have been detected, for example, by means of tunneling experiments or by measurements of the absorption of ultrasound (see Section 3.1.3.2).

The transition temperature T_c is essentially determined by the more favorable spatial directions, since the transition into the superconducting state takes place when the first Cooper pairs are formed under equilibrium. [17] If lattice defects exist in the crystal, the electrons will be scattered at these imperfections. However, this means that the momentum of an electron quickly covers all spatial directions because of the scattering. Therefore, the interaction leading to superconductivity will be averaged. The most favorable directions will not become fully active anymore, since electrons with momentum along these directions are scattered quickly into other less favorable directions. This leads to an overall reduction of the transition temperature with an increasing concentration of the scattering centers.

The microscopic theory of superconductivity allows one to calculate this influence of the lattice defects on T_c. In Figure 3.22 we show some results for tin [42]. The scattering centers are formed by impurity atoms. Since the impurity atoms have different scattering properties, for convenience we take the residual resistance ratio $\rho'' = R_n/(R_{273} - R_n)$ as a measure of the electron mean free path. Here, R_n is the resistance extrapolated to low temperatures, and R_{273} is the resistance at 273 K. In Figure 3.22 the transition temperature is plotted versus ρ ". The anisotropy effect is dominated by the universal, linear decrease in T_c at small impurity concentrations (see Figure 3.22b), in good agreement with the theory. For large impurity concentrations, that is, for small values of the electron mean free path, complete averaging over all spatial directions is accomplished. For the anisotropy effect alone, T_c should then approach a limiting value a small percentage below the value of the defect-free superconductor.

Figure 3.22 indicates that this behavior is not observed anymore for large defect concentrations. Apparently, in this case, specific properties of the impurities become important, leading to various dependences of the transition temperature on the different impurity atoms. Presently we are still unable to understand

The averaging must be performed over all the electrons on the Fermi surface. the direction.

3.2.4 Meissner effect

(???? TODO: read about Experimental confirmation)

3.2.5 Advanced Experimental Facts about Typical SC

According to their magnetic properties, superconductors are divided into type-I superconductors and type-II superconductors. Type-I superconductors include all superconducting elements except niobium. Niobium, superconducting alloys and chemical compounds make up

the second group, type-II superconductors. The so-called high- T_c superconductors also belong to this group.

The chief difference between the two groups lies in their different response to an external magnetic field. The Meissner-Ochsenfeld effect (Sect. 1.1.4) is observed in type-I superconductors only.

1.2.1 Magnetic Properties of Type-I Superconductors

Let us consider the magnetization curve of a superconductor. Suppose that the specimen is a long cylinder in a longitudinal external magnetic field $\boldsymbol{H}_0$. As the field $\boldsymbol{H}_0$ increases, the induction inside the specimen does not change at first; it remains $B = 0$. As soon as H_0 reaches the value of H_{cm}, the superconductivity is destroyed, the field penetrates into the superconductor, and $\boldsymbol{B} = \boldsymbol{H}_0$. Therefore, the magnetization curve $B = B(H_0)$ appears as shown in Fig. 1.3 (a). The magnetic induction $\boldsymbol{B}$ and the magnetic field $\boldsymbol{H}_0$ are related to each other by the well-known expression

$$B = H_0 + 4\pi M \tag{1.5}$$

where M is the magnetic moment per unit volume. The magnetization curve is often plotted as $-4\pi M$ versus H_0, as illustrated in Fig. 1.3 (b). We shall now derive the basic magnetic properties of type-I superconductors proceeding from equations (1.3) and (1.4) [13].

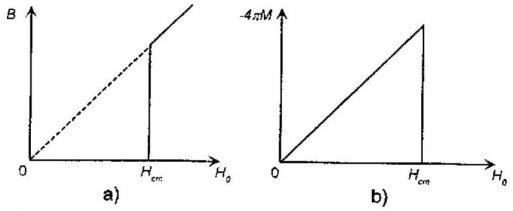


Fig. 1.3. (a) Magnetization curve of a superconductor: (b) magnetic moment per unit volume, M, versus H_0

(1) Magnetic field lines outside a superconductor are always tangential to its surface. Indeed, we know from electrodynamics that magnetic field lines,
be written as the equation

$$\operatorname{div} B = 0$$

from which it follows that the components of B normal to the surface must be equal on both sides of the surface, that is, inside and outside a piece of material. However, the field in the interior of a superconductor is $\boldsymbol{B}^{(i)} = 0$ and, consequently, $\boldsymbol{B}_{\mathrm{n}}^{(\mathrm{i})} = 0$. It follows that the normal component $\boldsymbol{B}_{\mathrm{n}}^{(\mathrm{e})}$ at the outside of the superconductor's surface is zero, too: $\boldsymbol{B}_{11}^{(\mathrm{e})} = 0$. And the meaning of the last equation is exactly that the magnetic field lines are tangential to the surface of the superconductor.

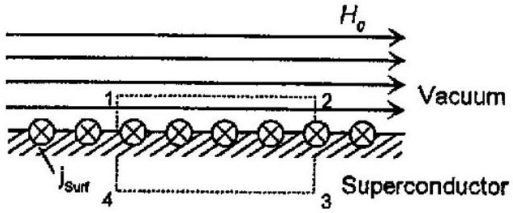


Fig. 1.4. A superconductor placed in an external magnetic field carries a surface current j_{surf}

(2) One of the consequences of the previous property is that a superconductor in an external magnetic field always carries an electric current near its surface. This statement is illustrated in Fig. 1.4. Let $\boldsymbol{H}_0$ be the field at a certain point of the surface of a superconductor. Then

it follows from Maxwell's equation curl $B = (4\pi/c)j$ and the requirement $B = 0$ that the volume current in the interior of the superconductor is zero ($j = 0$) and only a surface current is possible. To elucidate this statement, let us consider the contour $1-2-3-4-1$ in Fig. 1.4. First we find the circulation of B about this contour: $\oint \boldsymbol{B}\mathrm{d}l$. Along the section $1-2$, which is parallel to the surface, we have $\int_1^2 B\ \mathrm{d}l = H_0 l_{12}$, where l_{12} is the length of the section $1-2$. The contributions from the sections $2-3$ and $1-4$ are both zero because, from symmetry arguments, the vector $\boldsymbol{B}$ in these two sections is orthogonal to the integration path. The contribution from the section $3-4$ is zero, too, because $\boldsymbol{B} = 0$ in the interior of the superconduction. The result is $\oint \boldsymbol{B}\mathrm{d}l = H_0 l_{12}$. On the other hand, we find from Maxwell's equation

$$\oint B\ \mathrm{d}l = \frac{4\pi}{c} I$$

where I is the total current through the surface bounded by the contour 1-2-3-4-1. It follows that there must be a surface current at the surface of the superconductor, flowing 'into the page' (as shown in Fig. 1.4) and of linear density j_{surf} defined by

$$H_0 l_{12} = \frac{4\pi}{c} j_{\mathrm{s1rff}} l_{12}$$

The relation between the surface current and th

$$j_{\mathrm{surf}} = \frac{c}{4\pi}\,[n \times H_0] \tag{1.6}$$

where n is the unit vector along the normal to the surface.
Thus, the surface current $\boldsymbol{j}_{\mathrm{surf}}$ is completely defined by the magnetic field H_0 at the surface of a superconductor. In other words, the surface current automatically assumes a value such that the magnetic field generated by it inside a superconductor is exactly equal in value and opposite in direction to the external field. This assures zero total field in the interior: $\boldsymbol{B} = 0$.
(3) Let us point out one more, almost obvious, property: In a simply connected superconductor [1] surface currents can exist only when the superconductor is placed in an external magnetic field. Indeed, if the surface current remained after switching off the external field, it would create its own field in the superconductor which is impossible.

1.2.2 The Intermediate State

We already know that for a type-I superconductor in the shape of a long cylinder placed in a uniform magnetic field parallel to its surface, the superconductivity is destroyed when the field reaches the critical value H_{cm} . It is much harder, however, to destroy the superconductivity of the same cylinder if it is placed in a transverse magnetic field. The same is true for an ellipsoid, a sphere, or other bodies of more complicated geometries.

Consider, for example, the behavior of a superconducting sphere placed in an external magnetic field (Fig. 1.5). Since the magnetic field lines are always tangential to the surface of a superconductor, for our sphere it is obvious that the field lines have a higher density at the 'equator' thereby producing a local increase of the magnetic field. At the same time, the field at the 'poles' is zero. Far away from the sphere, where any perturbations caused by it average out, the uniform external field H_0 is lower than that at the 'equator'.

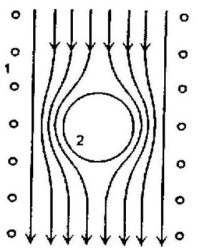


Fig. 1.5. Superconducting sphere in the homogeneous field of a solenoid; 1 - the winding of the solenoid, 2 - the superconducting sphere

A natural question now arises: what happens when the equatorial field reaches the critical value, $H_{\rm cm}$? Clearly, H_0 at that moment is below $H_{\rm cm}$ i A simply
and, therefore, it is not permitted for the whole sphere to revert to the normal state. On the other hand, it is not permitted for the whole sphere to be superconducting either, because the field at the 'equator' has already reached the critical value.

This contradiction is reconciled by a coexistence of alternating superconducting and normal regions within the sphere which is called the intermediate state. The interfaces between these regions are always parallel to the external field, while in the cross-section perpendicular to the field they may assume various intricate configurations.

Assume that before a superconducting body goes into the intermediate state, the maximum field at its surface (in the case of a sphere, at the 'equator') is $H_{\rm m}$ and the external field far away from the body is H_0. It is clear then that, on the one hand, $H_{\rm m} > H_0$ and, on the other hand, $H_{\rm m}$ is proportional to H_0, with the proportionality coefficient dependent on the exact shape of the body. This can be written in the form

$$H_{\rm m} = \frac{H_0}{1-n} \tag{1.7}$$

The values of n for various geometries [2] are given in Table 1.2.

Table 1.2. The demagnetizing factor n for various geometries

Sample geometry	n
Cylinder in parallel field	0
Cylinder in transverse field	1/2
Sphere	1/3
Thin plate in perpendicular field	1

With the help of Table 1.2 we can readily calculate the field H_0 corresponding to the transition into the intermediate state for a body of a certain shape. The transition occurs when the field $H_{\rm m}$ reaches the value of $H_{\rm cm}$. Therefore, for a sphere it takes place when, from (1.7), the external field H_0 reaches the value of

$$H_0 = H_{\rm cm}(1 - 1/3) = 2/3 H_{\rm cm}$$

A thin slab in a perpendicular magnetic field shows the intermediate state starting from an infinitesimal magnetic field H_0. This follows both from (1.7) ($n = 1$) and from general physical arguments, as we shall now demonstrate. Consider a thin disk in a perpendicular magnetic field. Since the magnetic field lines must go around the disk, their density increases substantially at the disk edges. The larger the radius of the disk, the larger the increase of
the field line density, i.e., of the field H_m, will be. For a disk of infinite radius, the transition to the intermediate state occurs in an infinitesimal field H_0.

A thin slab in the intermediate state is shown in Fig. 1.6,

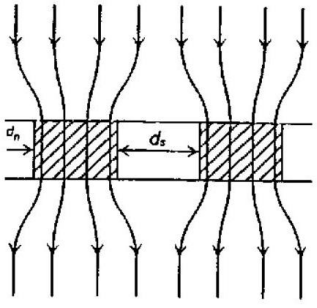


Fig. 1.6. Intermediate state of a thin superconducting plate in a perpendicular field; d_β is the width of a superconducting region, d_n is the width of a normal region

Let us now consider the conditions for thermodynamic equilibrium in the intermediate state.

We shall show that the field in the normal regions always equals the critical field $H_{\rm cm}$, and these regions automatically adjust their size $d_{\rm n}$ so as to provide the correct value of the field (see Fig. 1.6). Assume that the field in one of the normal regions exceeds $H_{\rm cm}$. Then it must destroy the superconductivity of the adjacent superconducting regions. Conversely, if the field in a normal region is less than $H_{\rm cm}$, this region must be superconducting. Therefore, a stable coexistence of the normal and superconducting regions is only possible if the field in the normal regions equals $H_{\rm rm}$.

In the cross-section perpendicular to the magnetic field, the domain patterms of the intermediate state can be very irregular. Classic experiments intended to clarify their configurations were performed by A.I. Shalnikov and A.G. Meshkovskii [14, 15]. They used a thin bismuth wire to study the magnetic field distribution in the equatorial cross-section of a tin sphere. In order to do this, they cut the sphere along the equatorial plane and then placed the two half-spheres slightly apart, with a very narrow gap between them, so that the external field was perpendicular to the surfaces of the cut. Then a bismuth wire was inserted into the gap. At low temperatures, the resistivity of the wire depends strongly on the external magnetic field and can be used as a probe of the field. By moving this probe inside the gap it was possible to examine the magnetic flux pattern. The result is shown in Fig. 1.7. The intermediate state was also studied by other methods, for example, by sputtering tiny ferromagnetic particles onto the superconducting surface and thereby producing a replica of the magnetic flux pattern (Fig.1.8).

The intermediate state assumes an interesting and unusual pattern in a cylindrical wire carrying an electric current. As soon as the current reaches a
distribution of normal (blank) and superconducting (shaded) regions in such a wire is shown in Fig. 1.9, for a current exceeding the critical value.

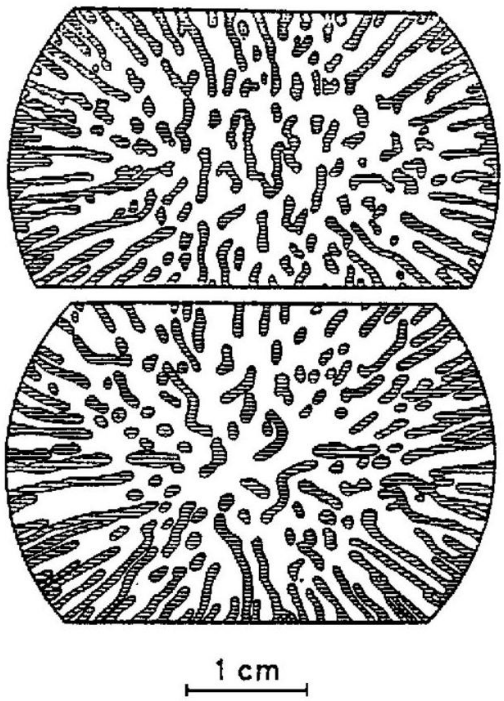


Fig. 1.7. Superconducting and normal regions in a tin sphere [15]. Shaded regions are superconducting

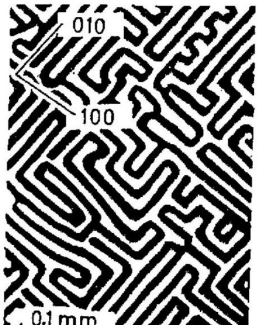


Fig. 1.8. Intermediate state of a single-

As one can see, a normal layer of thickness $(R-a)$ forms at the surface of the wire, and its thickness grows in proportion to the excess current, above the critical value.

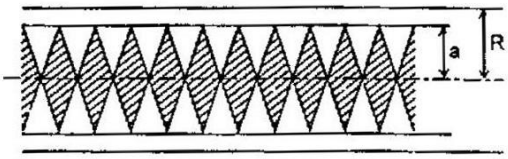


Fig. 1.9. Intermediate state of a wire carrying a supercritical electric current

1.2.3 Magnetic Properties of Type-II Superconductors

In contrast to type-I superconductors, type-II superconductors do not show the Meissner-Ochsenfeld effect. A magnetic field penetrates into these materials in a quite extraordinary way.

Let us take a type-II superconductor in the form of a long cylinder and place it in a longitudinal magnetic field. The field is increased from zero. At first the cylinder pushes all the field out, i.e., the magnetic induction in the interior of the cylinder is zero. This means that we initially observe the Meissner-Ochsenfeld effect. However, beginning from a certain value of the field we shall start to register a finite induction in the cylinder. This field is called the lower critical field and denoted by H_{c1}. With further increase of the external field H_0, the induction will build up until the average field in the cylinder becomes equal to the external field H_0 and the cylinder goes to the normal state. This will happen at the so-called upper critical field H_{c2}. However, in a thin surface layer the superconductivity will remain even at $H_0 > H_{c2}$, until $H_0 = 1.69H_{c2}$. This field is strong enough to destroy the superconductivity in the surface layer as well. It is called the third critical field and denoted by H_{c3}.

The physics of type-II superconductors will be discussed in more detail in Chap. 5.

3.3 Other Ideas for Introduction to Superconductivity

3.3.1 General Introduction to Superconductivity

Basic estimations

Сделаем предварительные оценки. Энергия конденсации куперовских пар на 1см^3, равна $H_c^2/8\pi \sim 10^5{}_{9\text{pr}}/\text{cm}^3$, если принять $H_c \sim 10^3$. Число электронов в 1 cm^3 по порядку величины равно 10^{22}. Таким образом, за сверхпроводимость отвечает энергия примерно равная $10^5/10^{22} = 10^{-17}$ эрг / электрон $= 10^{-5}$ эВ электрон. Заметим, что современная квантовая теория металлов прекрасно описывает многие их свойства даже в пренебрежении кулоновской энергией, имеющей порядок 1эВ электрон. Таким образом, предстояло объяснить природу явления, которой соответствует энергия на много порядков меньше энергии других взаимодействий, которыми обычно пренебрегают.

Abstract introduction for people who se superconductivity first time in their life

In daily life, one is frequently encountered with the states of classical matter, and transformation among these states or so called phases. For example, water can exist in the forms of ice, liquid, and vapor. The transition between these forms can be realized by varying temperature and pressure. These classical phenomena are the outcomes of the collective motion of atoms and molecules, the understanding of which constitutes the main subject of classical statistical physics.

In solid-state electronic materials, electrons are the major players. Since each of them possesses charge $-e(e > 0)$ and spin (an intrinsic degree of freedom), the electronic states exhibit insulating, metallic, and even superconducting and magnetic behaviors. The Mott-Hubbard-type insulating state occurs when the Coulomb repulsion among valence electrons are too large as compared with their kinetic energy (i.e., narrow electron energy band) in a pristine crystal [1, 2]. Therefore, these electrons have no nearby empty sites for them to hop to and they are trapped around ions. In an Anderson insulator, the electrons are localized due to the random distributed impurities in an impure metal, in which one can think of these electrons as waves and these waves cannot propagate beyond the localization length due to the wave-like interference effect [3-5]. Ideally, no conductivity exists in both types of insulators. In the metallic state, they can sneak by all ions in the presence of an electric field and conduct electricity. The difference between metallic and insulating states is striking in real materials. For example, the resistivity in copper is about $1.7 \times 10^{-8}\Omega$ m while the resistivity in undoped Sm_2CuO_{4+y} is as large as $\sim 1\Omega$ m at low temperatures [6]. In the magnetic state, electronic spins can be aligned into parallel, antiparallel, or other patterns.

More interestingly, in the superconducting state, electrons move throughout the whole system with zero resistance. These unique properties have formed the basis for operating electronic devices. Some of them have already been used in nowadays power plants, computers, and wind turbines, to list a few. Therefore, a microscopic understanding of the origin of these electronic states as well as how to control them has significant implications to technological applications. For superconductivity, it is now well accepted that the superconducting current arises from the formation of Cooper pairs [7] mediated by some kind of bosons such as phonons, which is originally proposed by Bardeen, Cooper, and Schrieffer (BCS) [8]. The singleparticle excitations in the superconducting state can not only provide insight into the fundamental properties of superconductivity itself such as pairing nature but also serve as new entities of significant technology implications as a response to defects or magnetic field etc. The Bogoliubov-de Gennes (BdG) [9] approach, which is the main focus of this text, is now a very powerful method to describe these singleparticle approximations in inhomogeneous superconductors. Before we proceed to bring out the BdG mathematical formalism, it should be helpful for the readers to be exposed with a quantum many-body framework in a more broad area of strongly correlated electronic systems.

1. Superconductivity

The problem of superconductivity is one of the most important and difficult presented to quantum statistics. It is well known that many metals undergo a phase change to a new "superconducting" state at sufficiently low temperatures. In this state the metal has thermodynamic and electromagnetic properties that are quite different from those in the normal state. Perhaps the most striking way in which the transition manifests itself experimentally is that the metal, on cooling to a critical temperature, suddenly ceases to present a resistance to electric current. In other words, there is no dissipation of energy when a current flows in a superconductor.

Experimental investigations have shown that the properties of a superconductor in a magnetic field are very different from the relatively simple properties of the normal metal. The

magnetic field does not penetrate into the body of the superconductor (the Meissner-Ochsenfeld effect). The effective depth, measured from the surface of a superconductor located in a constant magnetic field, at which the field is still different from zero (the so-called penetration depth) is extremely small, of the order of 10^{-5} to 10^{-6} cm. The thermodynamic transition from the normal to the superconducting state is a phase transition of the second kind and is characterized by a discontinuity in the specific heat at the transition temperature.

A substantial advance in the understanding of this phenomenon has been achieved in recent years. It has been found that the development of a theory of superconductivity requires a wide use of the methods of quantum field theory. These methods will be treated in subsequent sections; in the present section, we shall dwell mainly on the physical side of the subject.

It has been clear for a long time that superconductivity is somewhat akin to superfluidity. This is evident, first of all, from the fact that the maintainance of an electric current in a superconductor does not require an external potential difference, i.e. does not require work from external
sources. The current carriers in a metal are electrons; we are therefore concerned with none other than superfluidity of the electron liquid.

In Chap. I, in reference to the superfluidity of helium, we dwelt in detail on the properties of the energy spectrum of the excitations required for producing superfluidity. It must be remarked right away, however, that, at small momenta, the spectrum for a superconductor cannot be of the same type as that which we have to associate with liquid helium. For helium has a phonon acoustic branch as the initial part of its spectrum. As is well known, the propagation of sound is connected with long-wavelength density oscillations. But, for an electron liquid in a metal, a change in density involves a fairly substantial amount of energy, since it is hindered by the Coulomb forces acting between the electrons and the lattice, and between the electrons themselves. A change in the density of the electron liquid destroys the condition of electric neutrality, so that the corresponding spectrum of the long-wavelength oscillations starts at some finite frequency, just as in the case of a plasma. This frequency is in fact extremely high in a metal ($\sim$ 1eV $\simeq 10^{4}$°K). Our remarks naturally do not apply to the short-wavelength excitations, with a wave vector of the order of the reciprocal of an inter-atomic distance. We know that it is precisely these electron excitations that play the main role in a normal metal. In accordance with the results of Chap. I, a sufficient condition for the existence of superfluidity is that such excitations be separated by a gap from the ground state, i.e. that the spec-

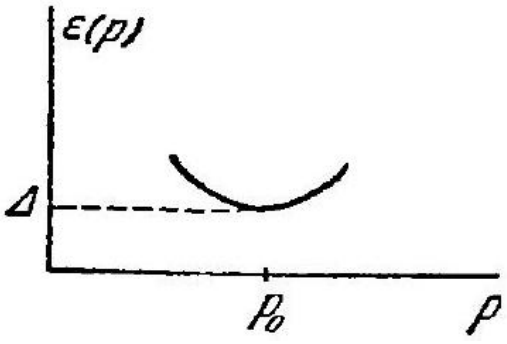


Fig. 88 trum has the shape illustrated in Fig. 88. It may be remarked that, apart from the arguments adduced above, the presence of a spectrum of this type in superconductors has been indicated by experimental data on the electronic specific heat at low temperatures; these data lead to a temperature dependence of the spccific heat of the form $e^{-\Delta/T}$.
We shall not dwell here on a treatment of various phenomenological theories; though they often give an adequate description of experimental data. they cannot provide an explanation of the microscopic mechanism involved.

The isotopic effect discovered in 1950 [5] provided a key to an understanding of the relative roles of the different interactions in a metal when it becomes superconducting. The critical tem-

perature T_c (the temperature at which the transition from the normal to the superconducting state occurs) was found to be a function of the mass of an isotope, of the form $T_c \sim (MI)^{-1/2}$. Frhlich [56] proposed independently that the main interaction corresponding to superconductivity must be of electrons with phonons. This interaction involves a strong dependence on the mass of the ions.

Short introduction with review of materials

Superconductivity was discovered by H. Kamerlingh Onnes in 1911 on mercury. Thereafter, it has also been discovered in other elemental solids like lead and niobium, and other simple compounds. The highest temperature superconductor has been Nb_3Sn until the year of 1986, when the high temperature superconductivity was discovered in copper-based oxides. In the copper-family of superconductors, the highest temperature superconductor is the ceramic $HgBa_2Cu_2Cu_3O_{8+8}$ with a transition temperature $T_c \sim 130$ degrees of Kelvin. In 2008, the iron-based superconductors was discovered with a highest transition temperature of 55 K obtained in SmO_{1-x} F_xFeAs. A chronicle for the discovery of superconductors is shown in Fig. 1.3.

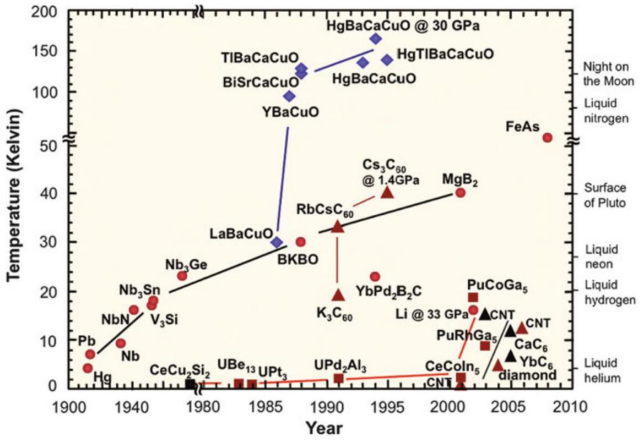


Fig. 1.3 Timeline of the superconductor discovery. Image courtesy of U.S. DOE Office of Basic Energy Sciences

The hallmarks of the superconductors are the zero resistivity and perfect diamagnetism as they are cooled below a critical temperature T_c. For all the superconductors discovered so far, the flux quantization experiments have provided strong evidence that the superconductivity arises from the formation of Cooper pairs [7] by electrons. However, the mechanism for glueing the electrons can be very different from materials to materials. The Cooper pairs are mediated by phonons, that is, lattice vibrational modes, in conventional superconductors while they are via a more exotic process (e.g., the fluctuations of the electron spins) in unconventional superconductors. Accordingly, the pairing symmetry that describes the relative orbital motion of the paired electrons can be different. An s-wave pairing symmetry is commonly observed in conventional superconductors, while other unconventional pairing symmetry like $p-, d-, f$ - and $s_{\pm}$-wave can occur in unconventional superconductors. The latter includes Sr_2RuO_4, ^{3}He, high-temperature cuprates, heavy fermion inter-metallic compounds, and recently discovered ironbased superconductors. On the one hand, the unconventional superconductors are accompanied with multiple electronic phases, a typical feature of strongly correlated electronic materials. On the other hand, although the BCS [8] theory, invoking the electron-phonon coupling as a pairing mechanism, is originally developed for the conventional superconductors, it seems that the quasiparticle properties in the superconducting state can be described by the BCS theory for the unconventional superconductors. This is the underlying basic assumption for the BdG [9] approach.

3.3.2 I-I A new condensed state by de Gennes

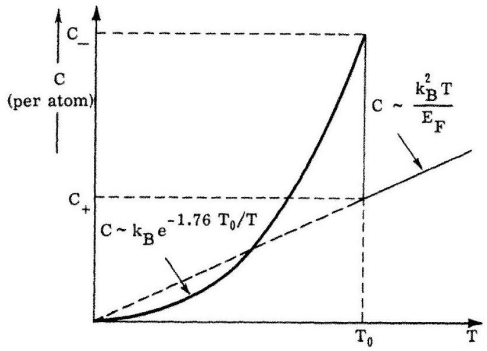
We take a piece of tin and cool it down; at a temperature $T_0 = 3.7°K$ we find a specific heat anomaly (Fig. 1-1a). Below T_0 the tin is in a new thermodynamical state. What has happened?

It is not a change in the crystallographic structure, as far as x rays can tell. It is not a ferromagnetic, or antiferromagnetic, transition. (It can be seen by magnetic scattering of neutrons, that tin carries no magnetic moment on an atomic scale.) The striking new property is that the tin has zero electrical resistance. (For instance, a current induced in a tin ring has been observed to persist over times > 1 year.) We say that tin, in this particular phase, is a superconductor, and we call the permanent current a supercurrent.

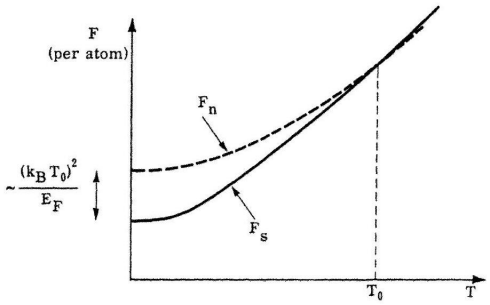
A large number of metals and alloys are superconductors, with critical temperatures T_0 ranging from less than 1°K to 18°K. Even some heavily doped semiconductors have been found to be superconductors.

Historically, the first superconductor (mercury) was discovered by Kammerling Onnes in 1911.

The free energy F_S in the superconducting phase can be derived from the specific heat data and is represented on Fig. 1-1b (solid line). The dotted line gives the corresponding curve F_n for the normal metal. The difference $(F_S - F_n)_{T=0}$ is called the condensation energy. It is not of order $k_B T_0$ per electron; it is, in fact, much smaller, of order $(k_B T_0)^2 / E_F$ (where E_F is the Fermi energy of the conduction electrons in the normal metal). Typically $E_F \sim 1$eV and $k_B T_0 \sim 10^{-3}$eV. Only a fraction $k_B T_0 / E_F$ $(\sim 10^{-3})$ of the metallic electrons have their energy significantly modified by the condensation process.



(a)



(b)

Figure 1-1

(a) The electronic specific heat C of a superconductor (in zero magnetic field) as a function of temperature (qualitative plot). Above T_0 (in the normal phase) $C_{(\text{per atom})} \sim k_B^2 \, T/E_F$ where E_F is the Fermi energy. At the transition point T_0, C has a discontinuity. At $T \ll T_0, C$ is roughly exponential $C \sim \exp(-1.76 \, T_0/T)$.

(b) Free energy of the superconducting phase (F_S) and of the normal phase (F_n) versus temperature. The two curves meet (with the same slope) at the transition point $T = T_0$. At $T = 0$ the difference $F_n - F_S$ is of order $(k_B T_0)^2 / E_F$ per atom.

3.4 Professional Choice of Model for SC

(an answer about which model to take???)

How accurate the predictions of the gap in scope of an operator approach compared to Gor'kov's approach are? Is it good idea to use it?

(????????????/)

(if all results are obtained by Gor'kov's formalism, then should we use at all in research such methods?)

Why to choose operator BCS model?

Why to choose Dorkov's QFT BCS model?

Why to choose GL model?

3.5 Linear Electrodynamics of Superconductors: Basics

3.5.1 The London Equations: Basics

In order to understand the behavior of a superconductor in an external electromagnetic field, let us use the so-called two-fluid model. We assume that all free electrons of the superconductor are divided into two groups: superconducting electrons of density n_8 and normal electrons of density n_n. The total density of free electrons is $n = n_\mathrm{s} + n_\mathrm{n}$. As the temperature increases from 0 to T_c, the density n_s decreases from n to 0.

Let us start our systematic study of the superconductor in an electromagnetic field with the simplest case. Assume that both the electric and magnetic fields are so weak that they do not have any appreciable influence on the superconducting electron density. Assume, in addition, that the density n_8 is the same everywhere, i.e., spatial variations of n_s are disregarded. The relation between the current, electric field, and magnetic field in this case is linear and described by the London equations [17].

2.1.1 The First London Equation

The equation of motion for superconducting electrons in an electric field is

$$n_\mathrm{s} m \frac{\mathrm{d}\boldsymbol{v}_\mathrm{s}}{\mathrm{d}t} = n_\mathrm{s} e E \tag{2.1}$$

where m is the electron mass, e is the electron charge, v_s is the superfluid velocity, and n_s is the number density of the superfluid. Taking into account that the supercurrent density is $j_\mathrm{s} = n_\mathrm{s} e v_\mathrm{s}$, we have

$$\boldsymbol{E} = \frac{\mathrm{d}}{\mathrm{d}t} (\Delta \boldsymbol{j}_\mathrm{s}) \tag{2.2}$$

with

$$A = m / n_\mathrm{s} e^2 \tag{2.3}$$

Equation (2.2) is simply Newton's second law for the superconducting electrons. It follows from this equation that in the stationary state, that is, when
superconducting electrons. Such variations become important, for example, when one considers the interface between a superconducting and a normal region, with a non-zero current passing through the interface. More details about this situation can be found in Chap. 7.

2.1.2 The Second London Equation

Let us now work out the relation between the supercurrent and the magnetic field in a superconductor. We denote the true microscopic magnetic field at a given point of a superconductor by $\boldsymbol{H}(\boldsymbol{r})$. Here an additional explanation is needed. We remember from Chap. 1 that magnetic field does not penetrate the interior of a type-I superconductor. Now we shall find that this is true only to a certain extent. Magnetic field does in fact penetrate to a shallow depth (of the order of $500 - 1000$Å) at the surface of a body. Our task at the moment is to work out how this field, $\boldsymbol{H}(\boldsymbol{r})$, varies in space.

Assume that the free energy of a superconductor in zero magnetic field is $\mathcal{F}_{50}$. The kinetic energy density of the supercurrent is

$$W_{\rm kin} = \frac{n_{\rm s} m v_{\rm s}^2}{2} = \frac{m j_{\rm s}^2}{2 n_{\rm s} e^2} \tag{2.4}$$

Taking into account Maxwell's equation

$$\operatorname{curl} H = \frac{4\pi}{c} j_{\rm s} \tag{2.5}$$

expression (2.4) for $W_{\rm kin}$ becomes

$$W_{\rm kin} = \frac{\lambda^2}{8\pi} (\operatorname{curl} \boldsymbol{H})^2 \tag{2.6}$$

where we have defined

$$\lambda^2 = \frac{mc^2}{4\pi n_{\rm s} e^2} \tag{2.7}$$

As we already know, the magnetic energy density at some point of the superconductor is $H^2/8\pi$. Therefore, the free energy of the superconductor as a whole, including both the kinetic energy of the supercurrent and the magnetic field energy, is

$$\mathcal{F}_{{\rm s}H} = \mathcal{F}_{\rm s0} + \frac{1}{8\pi} \int \left[\boldsymbol{H}^2 + \lambda^2 (\operatorname{curl} \boldsymbol{H})^2 \right] {\rm d}V \tag{2.8}$$

The integration is carried out over the entire volume of the superconductor.
Let us now solve a variational problem, namely, let us find the identity of the function $\boldsymbol{H}(\boldsymbol{r})$ corresponding to the minimum value of $\mathcal{F}_{{\rm s}H}$. We note that a more accurate approach would be to minimize the Gibbs free energy. We shall indeed do that when deriving the Ginzburg-Landau equations (see Sect. 3.2). However, the result is independent of which particular function is examined for a minimum, $\mathcal{F}_{{\rm B}H}$ or $\mathcal{G}_{{\rm B}H}$. Therefore, we examine $\mathcal{F}_{{\rm B}H}$ as it is easier to do.

Let us ascribe a small variation $\delta\boldsymbol{H}(\boldsymbol{r})$ to the function $\boldsymbol{H}(\boldsymbol{r})$. The resulting change in $\mathcal{F}_{{\rm B}H}$ will be $\delta\mathcal{F}_{{\rm s}H}$:

$$\delta\mathcal{F}_{{\rm s}H} = \frac{1}{8\pi} \int \left(2\boldsymbol{H} \cdot \delta\boldsymbol{H} + 2\lambda^2 \operatorname{curl} \boldsymbol{H} \cdot \operatorname{curl} \delta\boldsymbol{H} \right) {\rm d}V \tag{2.9}$$

The function $\boldsymbol{H}(\boldsymbol{r})$ to be found is the function that makes $\mathcal{F}_{{\rm B}H}$ a minimum, that is,

$$\delta \mathcal{F}_{BH} = 0. \tag{2.10}$$

Using the identity

$$\boldsymbol{a} \cdot \operatorname{curl} \boldsymbol{b} = \boldsymbol{b} \cdot \operatorname{curl} \boldsymbol{a} - \operatorname{div}[\boldsymbol{a} \times \boldsymbol{b}] \tag{2.11}$$

and combining (2.9) and (2.10), we obtain

$$\int \left[\boldsymbol{H} + \lambda^2 (\operatorname{curl} \operatorname{curl} \boldsymbol{H})\right] \cdot \delta \boldsymbol{H} \mathrm{d}V - \int \operatorname{div}[\operatorname{curl} \boldsymbol{H} \times \delta \boldsymbol{H}] \mathrm{d}V = 0 \tag{2.12}$$

The second integral in (2.12) is zero, as one can see from the following. By Gauss's theorem, the second term in (2.12) can be written in the form $\oint [\operatorname{curl} \boldsymbol{H} \times \delta \boldsymbol{H}] \cdot \mathrm{d}\boldsymbol{S}$, where the integration is carried out over the surface of the superconductor. But the field at the surface is fixed, it is the external field; therefore $\delta \boldsymbol{H}(\boldsymbol{r}) = 0$ there.

We have arrived at the equation $\int (\boldsymbol{H} + \lambda^2 \operatorname{curl} \operatorname{curl} \boldsymbol{H}) \cdot \delta \boldsymbol{H} \mathrm{d}V = 0$. For an arbitrary variation $\delta \boldsymbol{H}(r)$, this equation can be satisfied only if the sum in parentheses is zero. Thus we have obtained the equation for the magnetic field in a superconductor:

$$\boldsymbol{H} + \lambda^2 \operatorname{curl} \operatorname{curl} \boldsymbol{H} = 0 \tag{2.13}$$

This is the second Iondon equation. It can also be written in a different form. Using Maxwell's equation (2.5) and the equality $\boldsymbol{H} = \operatorname{curl} \boldsymbol{A}$, we obtain from (2.13)

$$j_{\mathrm{s}} = -\frac{c}{4\pi\lambda^2} \boldsymbol{A} \tag{2.14}$$

One can go from (2.13) to (2.14) only on the condition that the so-called London gauge is chosen for the vector potential:

$$\operatorname{div} \boldsymbol{A} = 0, \tag{2.15}$$

$$\boldsymbol{A} \cdot \boldsymbol{n} = 0, \tag{2.16}$$

where n is the unit vector normal to the superconductor's surface.
Equation (2.15), together with (2.14), specifies the conditions of continuity of the current and absence of a supercurrent source, while (2.16) assures that

It is assumed, of course, that there are no external circuits or contacts to current leads.

Using (2.3) and (2.7), we can write (2.14) in the form

$$j_{\mathrm{s}} = -\frac{1}{cA} \boldsymbol{A} \tag{2.17}$$

$$A = 4\pi\lambda^2/c^2 \tag{2.18}$$

In the rest of the book, we shall often use the second London equation in the form (2.17).

3.5.2 The London Equations: Another Theories

вывод уравнения Лондонов из минимума свободной энергии

просто посчитаем свободную энергию и найдем ее минимум.

Запишем полную свободную энергию сверхпроводника в виде

$$\mathcal{F} = \int F_s dV + E_{kin} + E_{mag}$$

здесь F_s - плотность свободной энергии сверхпроводящих электронов в отсутствие тока, E_{kin} - кинетическая энергия электронов, ответственных за сверхпроводящий ток:

$$E_{kin} = \frac{1}{2}\int n_s m v^2 dV$$

В рамках макроскопической электродинамики имеем

$$\operatorname{rot}\mathbf{B} = \frac{4\pi}{c}\mathbf{j}_s$$
$$\operatorname{divB} = 0$$

Запишем $\mathbf{j}_s$ по определению и через магнитное поле:

$$\mathbf{j}_s(\mathbf{r}) = n_s e\mathbf{v}(\mathbf{r}) = \frac{c}{4\pi}\operatorname{rot}\mathbf{B}$$

Тогда

$$E_{kin} = \frac{1}{2}\int n_s m\left(\frac{c}{4\pi n_s e}\operatorname{rot}\mathbf{B}\right)^2 dV$$

Магнитная энергия

$$E_{mag} = \int \frac{\mathbf{B}^2}{8\pi} dV$$

связана с энергией магнитного поля, индуцированного сверхпроводящими токами.

Здесь m, e - соответственно масса и заряд электрона, n_s - концентрация сверхпроводящих электронов.

Из (17),(18),(19) следует, что

$$\mathcal{F} = \int dV\left[\mathcal{F}_s + \frac{1}{8\pi}\left(\mathbf{B}^2 + \lambda_L^2(\operatorname{rot}\mathbf{B})^2\right)\right]$$

где

$$\lambda_L = \left(\frac{mc^2}{4\pi n_s e^2}\right)^{1/2}$$

Проварьируем свободную энергию по магнитному поло h:

$$\delta\mathcal{F} = \frac{1}{4\pi}\int\left(\mathrm{B}\delta\mathrm{B} + \lambda_L^2\mathrm{rotB}\cdot\mathrm{rot}\delta\mathrm{B}\right)dr$$

Попробуем вытащить δB.

Второе слагаемое преобразуется:

$$\operatorname{rot}\mathbf{B}\cdot\operatorname{rot}\delta\mathbf{B} = \delta\mathbf{B}\operatorname{rot}\mathbf{B}\cdot\operatorname{rot}\operatorname{rot}\mathbf{B} - \operatorname{div}[\operatorname{rot}\mathbf{B}\times\delta\mathbf{B}]$$

потому что

$$\operatorname{arot}\mathbf{b} = \operatorname{brot}\mathbf{a} - \operatorname{div}[\mathbf{a}\times\mathbf{b}] \qquad \mathbf{a} = \operatorname{rot}\mathbf{B},\ \mathbf{b} = \delta\mathbf{B}$$

Учтем, что член с дивергенцией преобразуется в поверхностный интеграл, равный нулю (так как на поверхности равна нулю вариация δB). (????)

Тогда оставшийся объемный интеграл должен равняться нулю при произвольном δB внутри тела.

Поэтому

$$\mathbf{B} + \lambda_L^2\operatorname{rot}\operatorname{rot}\mathbf{B} = 0$$

Это уравнение называется уравнением Лондонов и является следствием существования незатухающих токов.

границы применимости уравнения Лодонов

При выводе уравнения Лондонов мы неявно использовали тот факт, что размер сверхпроводящих электронов много меньше глубины проникновения λ.

Если это не так, и размер электрона $\xi > \lambda$, то в зоне действия магнитного поля находится только "часть электрона" и поэтому уравнение Лондонов несправедливо.

Приведем простейшие физические соображения, как можно прийти к рассмотрению задачи на этом уровне.

Очевидно, что при температуре T_c за сверхпроводимость должны отвечать электроны с энергией порядка T_c.

В соответствии с основными положениями теории ферми-жидкости характерный импульс сверхпроводящих электронов таков, что (????)

$$E_F - T_c < \frac{p^2}{2m} < E_F + T_c$$
$$T_c \ll E_F$$

где E_F - энергия Ферми.

Элементарные возбуждения в такой системе представляют собой волновые пакеты шириной $\delta p \sim T_c/v_F$, где $v_F = p_F/m$. Тогда характерная протяженность волнового пакета равна

$$\xi_0 \sim \frac{\hbar v_F}{T_c}$$

При вы воде уравнения Лондонов неявно предполагалось, что этот волновой пакет целиком повержен влиянию внешнего магнитного поля.

При этом мы получили, что магнитное поле изменяется на масштабе лондоновской глубины проникновения λ_L.

Если $\xi_0 \gg \lambda_L$, то лишь малая часть волнового пакета подвержена влиянию магнитного поля. Таким образом, уравнение Лондонов справедливо если $\lambda_L \gg \xi_0$. Такие сверхпроводники называются сверхпроводниками второго рода.

Парадоксально, но после открытия эффекта Мейсснера, главным образом, исследовались сверхпроводники первого рода, когда $\lambda_L \ll \xi_0$, для которых уравнение Лондонов не работает.

Оценим глубину проникновения магнитного поля λ в другом предельном случае, когда $\lambda \ll \xi_0$.

В этом случае, только λ/ξ_0 часть волнового пакета подвержена влиянию магнитного поля, то есть участвует в формировании незатухающего тока. Для оценки можно считать, что это эквивалентно уменьшению концентрации n. Тогда вычислениеλ можно провести тем же способом, каким получалась лонлоновская глубина проникновения, но с концентрацией $n_s\lambda/\xi_0$. В результате получаем самосогласованное уравнение

$$\lambda = \left(\frac{mc^2\xi_0}{4\pi n_s e^2 \lambda}\right)^{1/2}$$

Отсюда слелует, что

$$\lambda = \lambda_L \left(\frac{\xi_0}{\lambda_L}\right)^{1/3} \gg \lambda_L$$

Мы видим, что квантовомеханические соображения позволяют чисто феноменологически ввести парметр ξ_0.

Пойдем немного дальше.

Пусть сверхпроводяшщие электроны описы ватотся некоторой эффективной волновой функцией Ψ. Квалрат модуля этой функции определяет плотность сверхпроводяшщих

электронов. Это плотность обранцается в нуль в нормальном металле и увеличиваясь на NS гра- нице достигает своего максимального значения в толше сверхпроводника. Таким образом на границе $|\nabla\Psi|^2 \neq 0$.

Из квантовой механики известно, что эта величина пропорционалына плотности кинетической энергии.

Кинетическая энергия - положительна и дает положительный вклад в поверхностную энергию.

Таким образом, можно ожидать, что последовательный учет неоднородности позволит изменить знак результирующего поверхностного натяжения на $\sigma > 0$ и расслоение станет невыгодным.

эффект Мейсснера из уравнения Лондонов

Покажем, как из уравнения Лондонов следует эффект Мейсснера.

простейший случай уравнения лондонов - это когда два ротора становятся тупо второй производной. (Как???)

ну и в таком случае понятно, что решение - это затухающая экспонента, то есть простейшее явление проникновения поля в тело можно описать.

поэтому оно и сойдет для эффекта Мейсснера.

Ограничившись рассмотрением цилиндра большого радиуса, его границу можно считать полоской. Пусть продольное внешнее магнитное поле B_0 направлено по оси z, а нормаль к поверхности сверхпроводника направлена по осиx.

Тогда уравнение Лондонов (???) перепишется в виде:

$$B_z - \lambda_L^2 \frac{\partial^2}{\partial x^2} B_z = 0$$

Магнитная инлукция, конечная внутри сверхроводиика, имеет вид

$$B_x = B(0) e^{-\frac{x}{\lambda_L}} = B_0 e^{-\frac{x}{\lambda_L}}$$

что описывает эффект Мейсснера.

Во избежание недоразумений напомним, что в макроскопической электродинамике непрерывными являются тангенциальная составляющая напряженности магнитного поля и нормальная составляющая магнитной индукции.

При этом тангенциальная составляющая магнитной индукции может, вообще говоря иметь скачок, связанный с существованием поверхностных токов.

Если интересоваться масштабами, много большими глубины проникновения, масштаб λ следует считать бесконечно малым.

Это приводит к тому, что плотность сверхпроводящих токов обращается в бесконечность и их следует рассматривать как поверхностные.

Наличие поверхностных токов приводит к скачку тангенциальной составляющей магнитной индукции.

Заметим попутно, что при таком рассмотрении не определена напряженность магнитного поля внутри сверхпроводника.

В самом деле, магнитное поле определяется как вариация энергии по магнитной индукции. В сверхпроводнике $B \equiv 0$. (??)

Поэтому вариационная производная не определена.

Из уравнений (24),(21) и (15) имеем

$$\operatorname{rot} \mathbf{j}_s = -\frac{ne^2}{mc}\mathbf{B}$$

Введем потенциал A

$$\mathbf{B} = \mathrm{rot}\,\mathbf{A}$$

Этот потенциал определен неоднозначно, с точностью до градиента некоторой функции $\nabla\phi$. Тогда

$$\mathbf{j}_s = -\frac{ne^2}{mc}\left(\mathbf{A}' - \nabla\phi\right)$$

A′ - один из возможных потенциалов.

Если потребовать, чтобы $\mathrm{div j}_s = 0$, то $\mathrm{div}\left(\mathbf{A}' - \nabla\phi\right) = 0$.

Поэтому можно вектор-потенциал выбрать так, чтобы

$$\mathrm{div}\,\mathbf{A} = 0$$

Такой выбор потенциала A называется лондоновской калибровкой.

В этой калибровке получаем

$$\mathrm{j}_s = -\frac{ne^2}{mc}\,\mathrm{A}$$

Из уравнения Максвелла следует, что

$$\mathrm{j} = \frac{c}{4\pi}\mathrm{rotrotA}$$

Подставляя это выражение в уравнение Лондонов получим еще одну форму уравнения Лондонов

$$\mathrm{rotrot}\,\mathbf{A} = -\frac{1}{\lambda_L^2}\mathbf{A}, \quad \lambda_L = \frac{4\pi}{c}\frac{ne^2}{mc}$$

Итак, характерный масштаб затухания магнитного поля и токов в глубь сверхпроводника определяется параметром λ_L, называемым лондоновской глубиной проникновения.

(по факту тупое преобразование уравнения и все, и что тут такого? перепишу наверное с позиции, что это очевидно)

недостатки теории Лондонов

Обсудим теперь основные недостатки теории Лондонов.

В первую очередь, обратим внимание, что оно не является калибровочно инвариантным.

Это основной, так сказать, "фунламентальный" недостаток теории Лондонов.

Но из теории Лондонов следует, что во внешнем магнитном поле сверхпроводнику всегда термодинамически выгодно расслоиться на максимально мелкую сеть чередующихся нормальных и сверхпроводящих областей, так называемое промежуточное состояние.

Это означает, что на границе поверхностное натяжение $\sigma_{ns} < 0$.

Докажем это, используя уравнение Лондонов.

Пусть образец находится во внешнем магнитном поле.

Для простоты рассмотрим плоскую NS -границу между нормальной и сверхпроводящей частями образца.

Граница расположена перпендикулярно оси x. В левом полупространстве $x < 0$ имеем сверхпроводник, справа при$x > 0$ - нормальный металл.

Металл считаем немагнитным.

Поэтому в нем магнитная индукция равна магнитному полю.

Из условия сосуществования нормальной и сверхпроводящей фаз следует, что в нормальной фазе автоматически устанавливается магнитное поле $H = H_c$.

Поэтому можно считать, что мы имеем дело с образцом находящимся в заданном внешнем поле напряженностью H_c.

Тогда минимум должен иметь термо динамический потенциал G:

$$G = F - \frac{\mathrm{BH}_c}{4\pi}$$

Вдали от границы (где B = 0!) в сверхпроводящей части имеем

$$G_s = F_s(\mathbf{B}) - \left.\frac{\mathbf{BH}_c}{4\pi}\right|_{\mathbf{B}=0} = F_{s0}$$

Вдали от границы в нормальной фазе $H = B = H_c$.

Поэтому

$$G_n = F_n + \frac{\mathrm{B}^2}{8\pi} - \frac{\mathrm{BH}_c}{4\pi} = F_n - \frac{\mathrm{H}_c^2}{8\pi}$$

Учитывая (6), получаем, что, как и следовало ожидать в равновесии

$$G_s = G_n$$

Магнитное поле проникает в сверхпроводник на глубину λ и изменяет свободную энергию сверхпроводящей области.

Для анализа рассмотрим плоскую границу между нормальной и сверхпроводящей фазами.

Напомним, что если нормальная и сверхпроводящая фазы сосуществуют только если магнитное поле в нормальной фазе равно H_c.

Термодинамический потенциал Гиббса сверхпроводящего полупространства ($x > 0$) имеет вид

$$\mathcal{G} = \int\limits_{x>0} dV \left[F_{s0} + \frac{B^2}{8\pi} - \frac{H_c B}{4\pi} + \frac{\lambda^2}{8\pi}\left(\frac{dB}{dx}\right)^2 \right]$$

Здесь первый член - плотность свободной энергии Гиббса$G_s = F_{s0}$ в отсутствие магнитного поля, второй - энергия магнитного поля в сверпроводнике, третий - аналог члена HB в (14), последний - кинетическая энергия сверхпроводящих токов.

Если бы магнитное поле не проникало в сверхпроводник, то последние три члена обращались бы в нуль.

Из решения уравнения Лондонов следует, что $B = H_c \exp(-x/\lambda)$(cm.(25)).

Подставляя это выражение в потенциал Гиббса, вычислим поправку к свободной энергии за счет частичного проникновения магнитного поля в сверхпроводник:

$$\Delta\mathcal{G} = \gamma S$$

где S - площадь поверхности, σ - поверхностное натяжение

$$\sigma = \int\limits_{x>0} dx \left[\frac{B^2}{8\pi} - \frac{H_c B}{4\pi} + \frac{\lambda^2}{8\pi}\left(\frac{dB}{dx}\right)^2 \right] = -\frac{H_c^2}{8\pi}\lambda$$

Отсюда следует, что образование поверхности энергетически выгодно и упомянутое расслоение должно происходить всегда!

(????)

Такое расслоение действительно наблюдается, но далеко не для всех сверхпроводников и скорее является исключением, чем правилом.

Если с отсутствием калибровочной инвариантности в теории Лондонов экспериментаторы еще могли смириться, то с необходимостью расслоения - нет.

Пришлось теоретикам искать причину, по которой в большинстве сверхпроводников образование поверхности между сверхпроводящим и нормальным состоянием невыгодно.

Во введении мы определили сверхпроводники первого рода как вещества, в которых имеет место полный эффект Мейсснера - магнитное поле в них не проникает.

Как будет показано ниже для них $\sigma > 0$ и уравнение Лондонов несправедливо.

В противоположном случае $\sigma < 0$ мы имеем дело со сверхпроводниками второго рода, для которых имеет место смешанное (вихревое) состояние.

3.5.3 2.2 Magnetic Field Penetration Depth

Let us apply the London equations to examine how a magnetic field penetrates a superconductor. Consider a superconducting semispace $x > 0$. The surface of the superconductor coincides with the plane $x = 0$. An external magnetic field H_0 is oriented along the z axis. To solve this problem, we shall use (2.13). Taking into account the symmetry of the problem and that curl curl $\boldsymbol{H} = -\nabla^2 \boldsymbol{H}$, we can rewrite (2.13) in the form

$$\mathrm{d}^2 H/\mathrm{d}x^2 - \lambda^{-2} H = 0 \tag{2.19}$$

The boundary conditions are: $H(0) = H_0, H(\infty) = 0$. The second boundary condition takes account of the Meissner-Ochsenfeld effect. The solution of (2.19) is

$$H = H_0 \mathrm{e}^{-x/\lambda} \tag{2.20}$$

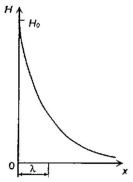


Fig. 2.1. Magnetic field penetration into a bulk superconductor. The field at the surface is H_0

It means that the magnetic field falls off with increasing distance from the surface of the superconductor. The characteristic deca len th is λ (see

Fig. 2.1). This length clarifies the physical significance of the quantity λ formally defined by (2.7) and is called the London magnetic field penetration depth:

$$\lambda = \left(\frac{mc^2}{4\pi n_8 e^2} \right)^{1/2} \tag{2.21}$$

It follows that the screening (Meissner) supercurrent at the surface falls off over the same length. Indeed, the supercurrent is $\boldsymbol{j}_\mathrm{s} = (c/4\pi)$ curl $\boldsymbol{H}$, which in our simple geometry reduces to $j_\mathrm{s} = (c/4\pi)\mathrm{d}H/\mathrm{d}x$. Substituting (2.20) in the last expression, we get

$$j_\mathrm{s} = \frac{cH_0}{4\pi\lambda} \mathrm{e}^{-x/\lambda} \tag{2.22}$$

One can see from (2.21) that λ is temperature-dependent because it depends on n_s. A good approximation for the temperature dependence of λ is given by the empirical formula

$$\lambda(T) = -\frac{\lambda(0)}{\left[1 - (T/T_\mathrm{c})^4\right]^{1/2}} \tag{2.23}$$

Let us now evaluate $\lambda(0)$. At $T = 0$ all electrons are superconducting, that is, $n_s = n \approx 10^{22}$ cm^{-3} (??? this is not true, right??? not all). Substituting this in (2.21), together with $m \sim 10^{-27}$ g, $c \sim 3 \times 10^{-10}$ cm s^{-1}, $e = 4.8 \times 10^{-10}$ esu, we obtain $\lambda(0) \sim 600$Å.

The values of $\lambda(0)$ for some superconductors are given in Table 2.1.

Table 2.1. London penetration depths for some superconductors [2]

Element	Al	Cd	Hg	In	Nb	Pb	Sn	Tl	$YBa_2Cu_3O_7$
$\lambda(0)$/A	500	1300	380 − 450 (anisotropy)	640	470	390	510	920	1700

3.5.4 2.3 Nonlocal Electrodynamics of Superconductors

Equations of Nonlocal Electrodynamics of Superconductors

Everything said so far about the electrodynamics of superconductors falls into the category of the so-called local electrodynamics. For instance, London's equation (2.17) relates the supercurrent density j_s (that is, the velocity of the supercurrent carriers, $\boldsymbol{v}_s$) to the vector potential $\boldsymbol{A}$ at the same point. Therefore, strictly speaking, (2.17) is applicable only if the size of the current carriers is much smaller than the characteristic length over which the vector potential changes, that is, smaller than the penetration deoth λ. We know
the size of a pair by ξ_0. For pure metals, ξ_0 is of the order $\xi_0 \sim 10^{-4}$ cm, as we shall find out later on, in Chap. 6. On the other hand, the penetration depth is $\lambda \sim 10^{-5} - 10^{-6}$ cm. Therefore, the local London electrodynamics is not applicable to pure superconductors, because the magnetic field changes appreciably over the length ξ_0.

Hence, the local equation (2.17) must be replaced by a nonlocal one relating the velocity of a particle to the magnetic field which is allowed to change substantially over the size of the particle, ξ_0. Such a nonlocal relation was proposed by A.B. Pippard [18] several years before the microscopic theory of superconductivity appeared.

In its general form, the nonlocal relation between $\boldsymbol{j}_5$ and $\boldsymbol{A}$ can be written as

$$j_\varepsilon(r) = \int \hat{Q}\,(r - r')\,A\,(r') \cdot \mathrm{d}r' \tag{2.24}$$

where $\hat{Q}$ is an operator which, operating on the vector $\boldsymbol{A}$, converts it into the vector $\hat{Q}A$. The operation range of the operator $\hat{Q}\,(\boldsymbol{r} - \boldsymbol{r}')$ is taken to be ξ_0, that is, $\hat{Q}\,(\boldsymbol{r} - \boldsymbol{r}')$ is nonzero only for $|\boldsymbol{r} - \boldsymbol{r}'| \leq \xi_0$. This is how the effect of the vector $\boldsymbol{A}$ on a large particle (a supercurrent carrier) is averaged out. If we now let the operation range go asymptotically to zero, $\hat{Q}$ turns into the δ-function, and we come back to local electrodynamics.

Pippard's proposal was to choose $\hat{Q}A$ in the form

$$\hat{Q}\,(\boldsymbol{r} - \boldsymbol{r}')\,\boldsymbol{A}\,(\boldsymbol{r}') = -\frac{3n_e e^2}{4\pi mc\xi_0}\frac{(\boldsymbol{r} - \boldsymbol{r}')}{(\boldsymbol{r} - \boldsymbol{r}')^{\frac{4}{4}}}\left[\boldsymbol{A}\,(\boldsymbol{r}') \cdot (\boldsymbol{r} - \boldsymbol{r}')\right] \mathrm{e}^{-|\boldsymbol{r} - \boldsymbol{r}'|/\xi_0} \tag{2.25}$$

The exact form of the magnetic field penetration into a superconductor in the nonlocal case differs from the exponential dependence. However, in this case one can also speak of a magnetic field penetration depth defined as

$$\lambda = \frac{1}{\bar{H}_0}\int_0^\infty H\ \mathrm{d}x \tag{2.26}$$

Here H_0 is the field at the surface of a semi-infinite superconductor. If the field near the surface falls off exponentially, all three definitions of λ[(2.26), (2.19), and (2.20)] coincide.

We shall not attempt here to solve the nonlocal problem explicitly. Rather, we shall show how to find an estimate of the correct answer [4]. Assume that the true dependence $H(x)$

is approximated by an exponential dependence with a new penetration depth denoted by λ_P (Pippard's penetration depth). Then, the vector potential $\boldsymbol{A}$ acts on a particle of size ξ_0 only within the depth $\lambda_P \ll \xi_0$ near the surface of the particle. The result is that, although the particle still participates in creating the current density j_5, the effect of A on it is reduced, because only the part of it λ_P/ξ_0 'feels' the presence of the vector potential. Accordingly, the current density is reduced by a factor

$$j_\mathrm{s} = -\frac{c}{4\pi\lambda^2}\frac{\lambda_\mathrm{P}}{\xi_0}\boldsymbol{A} \tag{2.27}$$

Rewriting (2.27) in the form

$$j_s = -\frac{c}{4\pi\lambda_P^2}A \tag{2.28}$$

we obtain, just as we wished, the exponential penetration of the magnetic field to the depth λ_P. Comparing (2.27) and (2.28), we get $\lambda_\mathrm{P}^2 = \lambda^2\xi_0/\lambda_\mathrm{P}$, which leads to the following estimate for λ_P:

$$\lambda_\mathbf{P} \approx \left(\lambda^2\xi_0\right)^{1/3} \tag{2.29}$$

The quantity λ in (2.29) is defined by (2.7). Then it follows from (2.29) that, in the case $\lambda \ll \xi_0$, we have $\lambda_\mathrm{P} \gg \lambda$, i.e., the nonlocal electrodynamics predicts deeper penetration of the magnetic field than would be expected from the London equations. This statement assumes, of course, that λ_p also satisfies the inequality $\lambda_\mathrm{P} \ll \xi_0$, which is not always the case even for pure metals.

A typical representative of superconductors which are well-described by the nonlocal relations (the so-called Pippard superconductors) is Al. In contrast, Pb, even of high purity, is a London superconductor. When the temperature T approaches T_c, all superconductors become local (London superconductors) because λ diverges at $T \to T_\mathrm{c}$ while ξ_0 is independent of temperature.

Everything said so far applies to pure metals, that is, those characterized by a mean free path $l \gg \xi_0$. If a metal contains a large number of impurities, $l \ll \xi_0$ can occur. We shall refer to such metals as dirty superconductors. Alloys also fall into this category. In very dirty metals, the role of the coherence length is played by the mean free path l. With the help of the microscopic theory, one can show that the magnetic field penetration depth for dirty superconductors is $\lambda_\mathrm{d} \approx \lambda\left(\xi_0/l\right)^{1/2}$ at $l \ll \xi_0$. Thus, superconducting alloys are described well by the local London equations. In the rest of the book we shall use local equations only.

Examples of Nonlocal Electrodynamics of Superconductors

(??? I'll write later)

3.5.5 Propagation of a electric field inside the SC

(this may be done in scope of linear electrodynamics of SC, I'll later write, how it works. See note on ED also about it)

3.5.6 2.4 Quantum Generalization of the London Equations.

2.4.1 Generalized London Equation

It was already mentioned in Chap. I that the elementary carrier of the supercurrent is a pair of electrons called the Cooper pair. All pairs occupy the same energy level, or the same

quantum state, i.e., they form a condensate. The wavefunction of a particle in the condensate can be written in the form
$\Psi(r) = (n_8/2)^{1/2}\, \mathrm{e}^{\mathrm{j}\theta(r)}$, where θ is the phase of the wavefunction. The normalization of $\Psi(r)$ has taken into account that the density of electron pairs is $n_5/2$, where n_5 is the density of the superconducting electrons.

Consider a particle of mass $2m$ and charge $2e$ moving in a magnetic field. Let us show that its momentum can be written as

$$\hbar\nabla\theta = 2mv_\mathrm{s} + \frac{2e}{c}A \tag{2.30}$$

where $\hbar$ is Planck's constant. In the absence of magnetic field, the particle flow density $n_5 v_5/2$ can be written in the form $(\mathrm{i}\,\hbar/4m)\,(\Psi\nabla\Psi^* - \Psi^*\nabla\Psi)$. Substituting here the expression $\Psi(\boldsymbol{r}) = (n_s/2)^{1/2}\,\mathrm{e}^{\mathrm{i}\theta}$, we get $\hbar\nabla\theta = 2mv_s$. Thus the total momentum of a particle moving in a magnetic field, $\hbar\nabla\theta$, is a sum of the momentum $2mv$ and the momentum $(2e/c)A$ due to the magnetic field.

Taking the expression for the supercurrent density in the form

$$j_\mathrm{s} = n_\mathrm{s} e v_\mathrm{s} \tag{2.31}$$

and using (2.7) and (2.18); it is easy to obtain from (2.30) the generalized second London equation:

$$j_\mathrm{s} = \frac{1}{cA}\left(\frac{\Phi_0}{2\pi}\nabla\theta - A\right) \tag{2.32}$$

Here we use the notation $\Phi_0 = \pi\hbar c/e$. The quantity Φ_0 has the dimensions of magnetic flux. Its physical significance will become clear in the following section.

3.5.7 Magnetic Flux Quantization

2.4.2 Magnetic Flux Quantization

We now proceed to a remarkably interesting phenomenon: magnetic flux quantization in superconductors.

Consider a hole through a bulk superconductor, such as shown in Fig. 2.2. At first, the temperature is $T > T_\mathrm{c}$ and the superconductor is in the normal state. Then we apply an external field H_0 parallel to the axis of the cylinder, and lower the temperature so that the specimen goes into the superconducting state. The field is now pushed out of the interior of the superconductor; while in the hole some frozen magnetic flux remains. This flux is produced by the supercurrent generated at the internal surface of the hole. Let us find this frozen magnetic flux.

Consider the contour C inside the superconductor, as in Fig. 2.2, enclosing the hole so that the distance between the contour and the internal surface of the hole is everywhere well in excess of λ. Then at any point of the contour, the supercurrent is $\boldsymbol{j}_\mathrm{s} = 0$ and the path integral of (2.32) along the contour reduces to

$$\frac{\Phi_0}{2\pi}\oint \nabla\theta \cdot \mathrm{d}\boldsymbol{l} = \oint \boldsymbol{A}\cdot\mathrm{d}\boldsymbol{l} \tag{2.33}$$

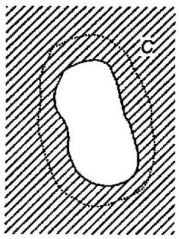


Fig. 2.2. Solid superconductor (dashed area) contains a hole. The contour C goes around the hole through the interior of the superconductor

Taking into account that

$$\oint_C \boldsymbol{A} \cdot \mathrm{d}\boldsymbol{l} = \Phi \tag{2.34}$$

we have

$$\Phi = \frac{\Phi_0}{2\pi} \oint_C \nabla\theta \cdot \mathrm{d}l \tag{2.35}$$

Here Φ is the total magnetic flux through the contour C. From (2.35), one can see immediately that θ is a multiple-valued function; it changes by a certain value after every full circle around the hole. But the wavefunction Ψ must be single-valued. Therefore, we have to stipulate that the change in θ after a full circle around the hole containing the magnetic flux must be an integral multiple of $2\pi n$, where $n = 0, 1, 2 \ldots$. Indeed, the addition of $2\pi n$ to $\theta(\boldsymbol{r})$ does not change the function $\Psi(\boldsymbol{r}) = (n_\mathrm{s}/2)^{1/2}\,\mathrm{e}^{\mathrm{i}\theta}$, because $\mathrm{e}^{\mathrm{i}2\pi n} = 1$. Therefore, $\oint_C \nabla\theta \cdot \mathrm{d}l = 2\pi n$ and (2.35) can finally be written as

$$\Phi = n\Phi_0 \tag{2.36}$$

where

$$\Phi_0 = \frac{\pi\hbar c}{e} = \frac{hc}{2e} \tag{2.37}$$

It follows from (2.36) that the magnetic flux enclosed in the hole (or, more accurately, the magnetic flux through the contour C) can only assume values that are integral multiples of the minimum possible value of magnetic flux, the magnetic flux quanturn Φ_0. The value of Φ_0 is defined by (2.37):

$$\Phi_0 = 2.07 \times 10^{-7}\mathrm{Gcm}^2$$

Physically, the origin of the magnetic flux quantization is the same as the quantization of electron orbits in atom. The wavefunction of electrons moving along a closed orbit must contain an integral number of wavelengths over the

Experimentally, magnetic flux quantization was discovered in 1961 almost simultaneously in the USA (B. Deaver and W. Fairbank) [8] and in Germany (R. Doll and M. Nbauer) [9]. It is interesting to note that F. London, who predicted the flux quantization, believed that the flux quantum should be hc/e, that is, he predicted a value twice as large as Φ_0. But that is not surprising because he believed that the charge of an elementary supercurrent carrier was equal to the electron charge e. Experiment confirmed the validity of (2.37). Thus the experiments that detected the quantization of magnetic flux also provided direct evidence that the supercurrent is carried by pairs of electrons.

3.6 Ginzburg Landau Theory: Basics

3.6.1 General GL philosophy of phase transitions

(discuss why in general we can view phase transitions this way? and how it is exactly?)

3.1 Introduction to GL by Shmidt

The London theory (Chap. 2) did not take into account quantum effects. The first quantum (phenomenological) theory of superconductivity was the Ginzburg-Landau (GL) theory [23].

A quantum theory should take into account, firstly, that the superconducting state is more ordered than the normal one and, secondly, that the transition from one state to the other (without magnetic field) is a secondorder phase transition. This implies the existence of an order parameter for a superconductor, which is nonzero at $T < T_c$ and vanishes at $T \geq T_c$. At the same time, in order to develop a quantum theory, it is necessary to introduce an effective wavefunction of the superconducting electrons, $\Psi(r)$.

Ginzburg and Landau decided to combine the two prerequisites: they decided to consider $\Psi(r)$ as an order parameter. This step required great scientific courage and deep physical intuition.

The GL theory is based on the theory of second-order phase transitions developed by Landau [24]. According to this theory, a phase transition of second order occurs when the state of a body changes gradually while its symmetry changes discontinuously at the transition temperature. Furthermore, the low-temperature phase is the one of reduced symmetry, i.e., it is more ordered. Such phenomena as the ferromagnetic transition at the Curie point, the transition of helium to the superfluid state, a number of orderdisorder transitions in alloys, and the superconducting transition all fall into the category of second-order phase transitions.

Let us explain how a gradual change of the state of a body can be accompanied by a discontinuous change of its symmetry. It becomes apparent from the following example of a structural transition leading to a more ordered state. Consider a linear chain of atoms of two different types: A and B. Assume that at a sufficiently high temperature the probabilities that the atoms of type A and type B occupy one of the sites in the chain are equal (this state corresponds to complete disorder, as in Fig. 3.1 (a)). At lower temperatures, $T < T_c$, the probability that the atoms of type A occupy the various sites in the chain is sketched in Fig. 3.1 (b). Now the arrangement of the atoms is
η appeared and gradually started to increase, while the period of the structure, which was a above T_c, underwent a discontinuous change at $T = T_c$ and became $2a$.

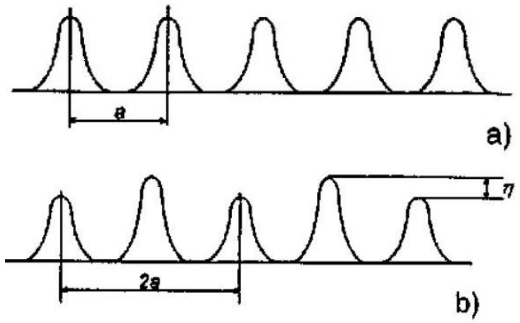


Fig. 3.1. Illustration of the discontinuous symmetry change in a structural phase transition of second order; (a) probability of finding an atom of type A at a given point of the crystal at $T > T_c$; (b) the same at $T < T_c$

Let us now go back to superconductivity. The Landau theory of second order phase transitions is based on an expansion of the free energy in powers of the order parameter, which is

small near the transition temperature. Such a starting point for the theory implies that it is valid only at temperatures close to the critical temperature, $T_c - T \ll T_c$. The range of validity of the GL theory will be discussed in more detail in Sect.6.6.

Let us assume that the wavefunction of superconducting electrons $\Psi(r)$ is the order parameter. In addition, let us choose normalization of this wavefunction such that $|\Psi(r)|^2$ gives the density of Cooper pairs:

$$|\Psi(r)|^2 = n_3/2 \tag{3.1}$$

Consider first the simplest case: a homogeneous superconductor without external magnetic field. In this case Ψ does not depend on r and the expansion of the free energy in powers of $|\Psi|^2$ near T_c becomes

$$F_{50} = F_n + \alpha|\Psi|^2 + \frac{\beta}{2}|\Psi|^4. \tag{3.2}$$

Here F_{s0} is the free energy density of the superconductor in the absence of magnetic field, F_n is its free energy density in the normal state and α and β are some phenomenological expansion coefficients which are characteristics of the material.

Let us find the value of $|\Psi|^2$ for which the free energy of a homogeneous superconductor, F_{s0}, is a minimum. This value, $|\Psi_0|^2$, is the solution of the equation

$$\frac{dF_{50}}{d|\Psi|^2} = 0$$

Substituting here (3.2) and carrying out elementary calculations we obtain

$$|\Psi_0|^2 = -\alpha/\beta. \tag{3.3}$$

$$F_n - F_{B0} = \alpha^2/2\beta \tag{3.4}$$

Recalling that, from (1.12), this difference equals $H_{cm}^2/8\pi$, we have

$$H_{cm}^2 = 4\pi\alpha^2/\beta \tag{3.5}$$

Let us discuss the temperature dependence of the coefficients α and β. Since the order parameter must be zero at $T = T_c$ and finite at $T < T_c$, it follows from (3.3) that $\alpha = 0$ at $T = T_c$ and $\alpha < 0$ at $T < T_c$. Therefore we can write, to first order in $(T_c - T)$,

$$\alpha \propto (T - T_c)\,. \tag{3.6}$$

This temperature dependence of α correlates (3.5) with the empirical formula (1.1) near T_c.

The coefficient β is positive and independent of temperature. Indeed, as follows from (3.3), at $T < T_c$ and $\alpha < 0, |\Psi_0|^2$ can be positive only if $\beta > 0$. On the other hand, if $T > T_c$ (and consequently, from (3.6), $\alpha > 0$) and $\beta > 0$, the energy F_{50} reaches its minimum at $|\Psi_0|^2 = 0$. This means that there is no superconducting state at $T > T_c$ as indeed ought to be the case. Thus we have $\beta > 0$ both at $T < T_c$ and at $T > T_c$. Therefore, to a first approximation in $(T_c - T)$, we may assume $\beta = \text{const}$.

Discussion of possible terms in the GL functional

(discuss why there are also exotic models with φ^3 and so on)

Seeing the Phase Transitions in the GL functional

Применим теорию среднего поля к сверхпроводящему переходу в присутствии магнитного поля. Вблизи температуры перехода Ψ и $\nabla\Psi$ малы, и Ω - потенциал, как обычно, может быть разложен в ряд. Нужно только учесть два обстоятельства. Во-первых, следует добавить кинетическую энергию сверхпроводящих электронов; плотность кинетической энергии в квантовой механике может быть представлена как $|(-i\hbar\nabla - e\mathcal{A}/c)\Psi|^2/2m$. Во-вторых, следует добавить энергию магнитного поля; ее плотность равна $\mathcal{B}^2/8\pi$. В общем случае $\Psi(\mathbf{r})$ и $\mathcal{A}(\mathbf{r})$ распределения по образцу неоднородны, и Ω-потенциал становится функционалом $\Omega_s = \Omega_s[\Psi(\mathbf{r}), \mathcal{A}(\mathbf{r})]$. Итак,

$$\Omega_s[\Psi(\mathbf{r}), \mathcal{A}(\mathbf{r})] = \Omega_n + \int \left[\alpha|\Psi|^2 + \frac{b}{2}|\Psi|^4 + \frac{1}{4m}\left| -i\hbar\nabla\Psi - \frac{2e}{c}\mathcal{A}\Psi \right|^2 + \frac{(\nabla\times\mathcal{A})^2}{8\pi} \right] dV.$$

Здесь, как обычно, $\alpha = a\,(T - T_c)\,, a$ и b положительны и мы заранее учли, что носителями заряда являются куперовские пары с $m \to 2m, e \to 2e$. Здесь и далее мы полагаем $e = -|e|$.

В однородном случае $\Psi(\mathbf{r}) = \text{const}$ в отсутствии поля внутри образца ($\mathcal{B} = 0$) функционал (12.2) превращается в обычную функцию. Минимизация этой функции, Ω-потенциала, как и ранее (см. лекцию 10), даёт

$$|\Psi_0|^2 = \begin{cases} -\frac{a(T-T_c)}{b}, & T < T_c \\ 0, & T > T_c \end{cases}$$

Это позволяет найти концентрацию сверхпроводящих электронов $|\Psi_0|^2 = n_s/2$. Например, при нулевой температуре $n_s = n$ получаем оценку

$$n_s = 2aT_c/b$$

Далее, «выигрыш» в энергии сверхпроводящей фазы в отсутствии внешнего поля $\Omega_n - \Omega_s(\mathcal{H} = 0) = V\alpha^2/2b$ может быть скомпенсирован «проигрышем» энергии из-за помещения образца во внешнее магнитное поле $\Omega_s(\mathcal{H}) - \Omega_s(\mathcal{H} = 0) = V\mathcal{H}^2/8\pi$. Действительно, поскольку в силу эффекта Мейсснера $\mathcal{B} = 0$ сверхпроводник - идеальный диамагнетик $\mathcal{M} = -\mathcal{H}/4\pi$, то плотность его дополнительной энергияи из-за поля равна $-V\int_0^{\mathcal{H}} \mathcal{M}d\mathcal{H} = \mathcal{H}^2/8\pi$. Это дает величину термодинамического критического поля:

$$\mathcal{H}_c^2 = \frac{4\pi a^2\,(T - T_c)^2}{b}.$$

И, наконец, выигрыш энергии сверхпроводящей фазы (например, в отсутствии поля) мы можем рассматривать как энергию конденсации куперовских пар. Поскольку энергия пары 2Δ, а образуются они из электронов, расположенных в слое толщиной $\Delta \ll \varepsilon_F$ вблизи энергии Ферми ε_F, то $\alpha^2/2b = 2\Delta^2 n/\varepsilon_F$. Здесь явно предполагается, что при $T = 0$ все электроны сверхпроводящие $n_s = n$ (см. лекцию 12). Это позволяет при нулевой температуре получить еще одно соотношение между коэффициентами функционала (13.2) a и b:

$$a^2/b = 4\Delta_0^2 n/\varepsilon_F T_c^2 \approx n/\varepsilon_F$$

Таким образом, из (13.4) и (13.6) получаем выражения для коэффициентов разложения (13.2) $a \approx T_c/\varepsilon_F$ и $b \approx T_c^2/n\varepsilon_F$ через микроскопические параметры сверхпроводника.

How to chose an order parameter of a superconductor?

(??? here, discuss how it is related to wave function of a condensate)

(write that this idea is also telling us that there exist a some gap, which will be introduced later. this is a non-trivial statement that it exist.)

3.6.2 3.2 Equations of the Ginzburg-Landau Theory

3.2.1 Free Energy Density

Let us now go over to the general case of an inhomogeneous superconductor in a uniform external magnetic field.

Near T_c, the Gibbs free energy can be expanded in powers of Ψ as

$$G_{sH} = G_n + \alpha|\Psi|^2 + \frac{\beta}{2}|\Psi|^4 + \frac{1}{2m^*}\left|-i\hbar\nabla\Psi - \frac{2e}{c}A\Psi\right|^2 + \frac{H^2}{8\pi} - \frac{\boldsymbol{H}\cdot\boldsymbol{H}_0}{4\pi} \tag{3.7}$$

where G_n is the free energy density of a superconductor in the normal state and $\boldsymbol{H}_0$ is the external magnetic field. The last but one term in (3.7) simply represents the magnetic energy density, where H is the exact microscopic field at a given point of the superconductor. The term before that is the kinetic energy density of the superconducting electrons. Let us analyze the latter in more detail.

In quantum mechanics, the kinetic energy density of a particle of mass m is

$$\frac{1}{2m}|-i\hbar\nabla\Psi|^2$$

operator $-i\hbar\nabla$ in the expression for the kinetic energy density has to be modified:

$$-i\hbar\nabla \to -i\hbar\nabla - \tfrac{e}{c}\boldsymbol{A} = mv$$

Therefore, the velocity operator is

$$v = -(i\hbar/m)\nabla - (e/cm)\boldsymbol{A}$$

Since it is the velocity v that enters the expression for the kinetic energy density, we can now understand why the corresponding term in (3.7) looks as it does. It should only be added that a substitution $e \to 2e$ has been made in (3.7) which takes into account that the elementary charge carrier of the supercurrent is $2e$. Accordingly, m^* in (3.7) is twice the electron mass.

Parameters of GL functional

(?? maybe I'll add several other derivations)

Let's discuss the coefficients in

$$\Omega_s[\Psi(\mathbf{r}), \mathcal{A}(\mathbf{r})] = \Omega_n + \int\left[\alpha|\Psi|^2 + \frac{b}{2}|\Psi|^4 + \frac{1}{4m}\left|-i\hbar\nabla\Psi - \frac{2e}{c}\mathcal{A}\Psi\right|^2 + \frac{(\nabla\times\mathcal{A})^2}{8\pi}\right]dV.$$

Derivation 1

И, наконец, выигрыш энергии сверхпроводящей фазы (например, в отсутствии поля) мы можем рассматривать как энергию конденсации куперовских пар. Поскольку энергия пары 2Δ, а образуются они из электронов, расположенных в слое толщиной $\Delta \ll \varepsilon_F$ вблизи энергии Ферми ε_F, то $\alpha^2/2b = 2\Delta^2 n/\varepsilon_F$. Здесь явно предполагается, что при $T = 0$ все электроны сверхпроводящие $n_s = n$ (см. лекцию 12). Это позволяет при нулевой температуре получить еще одно соотношение между коэффициентами функционала (13.2) a и b:

$$a^2/b = 4\Delta_0^2 n/\varepsilon_F T_c^2 \approx n/\varepsilon_F$$

Таким образом, из (13.4) и (13.6) получаем выражения для коэффициентов разложения (13.2) $a \approx T_c/\varepsilon_F$ и $b \approx T_c^2/n\varepsilon_F$ через микроскопические параметры сверхпроводника.

Derivation 2

Коэффициенты a и b уже оценивались в параграфе 3. Проделаем это еще раз, другим способом. Соотношения $a \approx T_c/\varepsilon_F$ и $b \approx T_c^2/n\varepsilon_F$ получаются, если воспользоваться формулами (13.4) и (13.15) при $T = 0$. В последнюю нужно подставить размер куперовской пары ξ_0, полученный из соотношения неопределенностей $\xi_0 \cdot \delta p \sim \hbar$, связывающего его с неопределенностью импульса $v_F \cdot \delta p \sim \Delta_0$. При этом следует учесть, что $\Delta_0 \approx T_c$ и $\varepsilon_F \sim m v_F^2 \sim \hbar^2 n_s^{2/3}/m$. Соотношение $c = \hbar^2/4m$ следует из сравнения функционалов (10.31) и (13.2).

3.2.2 Derivation of Ginzburg-Landau (GL) Equations from free energy

Derivation of the first equation

By (3.7), the Gibbs free energy of a superconductor as a whole is

$$\mathcal{G}_{sH} = \mathcal{G}_n + \int \left[\alpha|\Psi|^2 + \frac{\beta}{2}|\Psi|^4 + \frac{1}{4m}\left| -i\hbar\nabla\Psi - \frac{2e}{c}\boldsymbol{A}\Psi \right|^2 + \frac{(\operatorname{curl}\boldsymbol{A})^2}{8\pi} - \frac{(\operatorname{curl}\boldsymbol{A})\cdot\boldsymbol{H}_0}{4\pi} \right] \mathrm{d}V \tag{3.8}$$

where the integration is carried out over the entire volume of the superconductor. Our task now is to find equations for the functions $\Psi(r)$ and $A(r)$ such that their solutions, when substituted in (3.8), give the minimum value of $\mathcal{G}_{sH}$.

In order to do that we shall first assume that $\Psi(\boldsymbol{r})$ and $\boldsymbol{A}(\boldsymbol{r})$ are invariant and then solve the variational problem with respect to $\Psi^*(r)$:

$$\delta_{\Psi^*}\mathcal{G}_{\delta H} = 0 \tag{3.9}$$

$$\delta_{\Psi^*}\mathcal{G}_{sH} = \int \mathrm{d}V \left[\alpha\Psi\delta\Psi^* + \beta\Psi|\Psi|^2\delta\Psi^* + \frac{1}{4m}\left(i\hbar\nabla\delta\Psi^* - \frac{2e}{c}\boldsymbol{A}\delta\Psi^* \right)\cdot\left(-i\hbar\nabla\Psi - \frac{2e}{c}\boldsymbol{A}\Psi \right) \right] \tag{3.10}$$

The term $\delta\Psi^*$ could be taken out of the square brackets but for the term $i\hbar\nabla\delta\Psi^*$. Let us make some modifications. We write

$$\varphi = \left(-\mathrm{i}\hbar\nabla\Psi - \frac{2e}{c}A\Psi\right)$$

Using the identity

$$\nabla\left(\delta\Psi^*\varphi\right) = \varphi\nabla\delta\Psi^* + \delta\Psi^*\nabla\varphi$$

$$\int \mathrm{d}V\nabla\delta\Psi^*\varphi = -\int \delta\Psi^*\nabla\varphi\ \mathrm{d}V + \int \nabla\left(\delta\Psi^*\varphi\right)\mathrm{d}V \tag{3.11}$$

By Gauss's theorem, the last integral in (3.11) can be converted into a surface integral:

$$\int \nabla\left(\delta\Psi^*\varphi\right)\mathrm{d}V = \oint_S \delta\Psi^*\varphi\ \mathrm{d}S$$

Substituting (3.11) into (3.10) and (3.10) into (3.9), we obtain

$$\delta_{\Psi^*}\mathcal{G}_{\mathrm{s}H} = \int \mathrm{d}V\left[\alpha\Psi + \beta\Psi|\Psi|^2 + \frac{1}{4m}\left(-\mathrm{i}\hbar\nabla - \frac{2e}{c}\boldsymbol{A}\right)^2\Psi\right]\delta\Psi^* + \oint_S\left[-\mathrm{i}\hbar\nabla\Psi - \frac{2e}{c}A\Psi\right]\delta\Psi^*\ \mathrm{d}S = 0$$

For an arbitrary function $\delta\Psi^*$, this expression can be zero only if both expressions in square brackets are zero. From this requirement we obtain the first equation of the GL theory and its boundary condition:

$$\alpha\Psi + \beta\Psi|\Psi|^2 + \frac{1}{4m}\left(\mathrm{i}\hbar\nabla + \frac{2e}{c}\boldsymbol{A}\right)^2\Psi = 0 \tag{3.12}$$

$$\left(\mathrm{i}\hbar\nabla\Psi + \frac{2e}{c}A\Psi\right)\cdot n = 0$$

where n is the unit vector normal to the surface of the superconductor. One can easily verify that minimization of $\mathcal{G}_{\mathrm{B}H}$ with respect to Ψ leads to the complex-conjugate of (3.12). Thus, we have obtained the equation for the order parameter Ψ.

Derivation of the second equation

One variable still remains: $\boldsymbol{A}$. In order to obtain the equation for A, we shall minimize the expression for $\mathcal{G}_{sH}$ (3.8) with respect to A:

$$\begin{aligned}\delta_A\mathcal{G}_{sH} = \int \mathrm{d}V\Bigg\{\frac{1}{4m}\delta_{\boldsymbol{A}}\left[\left(\mathrm{i}\hbar\nabla\Psi^* - \frac{2e}{c}\boldsymbol{A}\Psi^*\right)\cdot\left(-\mathrm{i}\hbar\nabla\Psi - {}^{2e}_{c}\boldsymbol{A}\Psi\right)\right] + \\ + \frac{1}{4\pi}\operatorname{curl}\boldsymbol{A}\cdot\operatorname{curl}\delta\boldsymbol{A} - \frac{\boldsymbol{H}_0}{4\pi}\cdot\operatorname{curl}\delta\boldsymbol{A}\Bigg\} = \\ = \int\Bigg\{\frac{1}{4m}\left(-\frac{2e}{c}\Psi^*\delta\boldsymbol{A}\right)\cdot\left(-\mathrm{i}\hbar\nabla\Psi - \frac{2e}{c}\boldsymbol{A}\Psi\right) + \\ + \frac{1}{4m}\left(\mathrm{i}\hbar\nabla\Psi^* - \frac{2e}{c}\boldsymbol{A}\Psi^*\right)\cdot\left(-\frac{2e}{c}\Psi\delta\boldsymbol{A}\right) + \frac{1}{4\pi}\left(\operatorname{curl}\boldsymbol{A} - \boldsymbol{H}_0\right)\cdot\operatorname{curl}\delta\boldsymbol{A}\Bigg\}\mathrm{d}V\end{aligned} \tag{3.13}$$

One notices that δA in (3.13) could be taken out of the brackets but for the term $(1/4\pi)\left(\operatorname{curl}\boldsymbol{A} - \boldsymbol{H}_0\right)\cdot\operatorname{curl}\delta\boldsymbol{A}$. Using the identity

(??? restore it from rus version)
we can carry out the integration in the last term of (3.13):

$$\frac{1}{4\pi}\int \mathrm{d}V\,(\operatorname{curl}\boldsymbol{A}-\boldsymbol{H}_0)\cdot\operatorname{curl}\delta\boldsymbol{A}=\frac{1}{4\pi}\int \mathrm{d}V\delta\boldsymbol{A}\cdot\operatorname{curl}\operatorname{curl}\boldsymbol{A}-\frac{1}{4\pi}\oint \mathrm{d}\boldsymbol{S}\cdot[\delta\boldsymbol{A}\times(\operatorname{curl}\boldsymbol{A}-\boldsymbol{H}_0)] \tag{3.15}$$

When doing so we have used Gauss's theorem to convert the volume integral into a surface integral:

$$\int \mathrm{d}V\,\operatorname{div}[\delta\boldsymbol{A}\times(\operatorname{curl}\boldsymbol{A}-\boldsymbol{H}_0)]=\oint \mathrm{d}\boldsymbol{S}\cdot[\delta\boldsymbol{A}\times(\operatorname{curl}\boldsymbol{A}-\boldsymbol{H}_0)]\,.$$

The surface integral is zero because the magnetic field at the surface of the superconductor is fixed; hence $\delta\boldsymbol{A}|_S=0$.

Substituting now (3.15), without the last term, into (3.13) and equating the free energy variation to zero, we get, after elementary modifications,

$$\delta_A\mathcal{G}_{\mathrm{s}H}=\int\left[\frac{i\hbar e}{2mc}\left(\Psi^*\nabla\Psi-\Psi\nabla\Psi^*\right)+\frac{2e^2}{mc^2}\boldsymbol{A}|\Psi|^2+\frac{1}{4\pi}\operatorname{curlcurl}\boldsymbol{A}\right]\cdot\delta\boldsymbol{A}\mathrm{d}V=0 \tag{3.16}$$

For arbitrary δA, the integral in (3.16) can be zero only if the expression in square brackets is zero. This condition determines the second equation of the GL theory, for the vector potential $\boldsymbol{A}$:

$$j_{\mathrm{s}}=-\frac{i\hbar e}{2m}\left(\Psi^*\nabla\Psi-\Psi\nabla\Psi^*\right)-\frac{2e^2}{mc}|\Psi|^2A \tag{3.17}$$

where, by Maxwell's equation, the current density $\boldsymbol{j}_{\mathrm{s}}$ in the superconductor is

$$j_{\mathrm{s}}=\frac{c}{4\pi}\operatorname{curlcurl}A,\quad H=\operatorname{curl}A \tag{3.18}$$

Let us go over to a dimensionless wavefunction $\psi(r)$ by setting

$$\psi(\boldsymbol{r})=\Psi(\boldsymbol{r})/\Psi_0 \tag{3.19}$$

where ${\Psi_0}^2=n_{\mathrm{s}}/2=|\alpha|/\beta$. In addition, we introduce two more definitions:

$$\xi^2=\frac{\hbar^2}{4m|\alpha|} \tag{3.20}$$

$$\lambda^2=\frac{mc^2}{4\pi n_s e^2}=\frac{mc^2\beta}{8\pi e^2|\alpha|} \tag{3.21}$$

Now the GL equations can be written in a more concise and convenient form:

$$\xi^2\left(\mathrm{i}\nabla+\frac{2\pi}{\Phi_0}\boldsymbol{A}\right)^2\psi-\psi+\psi|\psi|^2=0 \tag{3.22}$$

$$\operatorname{curl}\operatorname{curl}\boldsymbol{A}=-\mathrm{i}\frac{\Phi_0}{4\pi\lambda^2}\left(\psi^*\nabla\psi-\psi\nabla\psi^*\right)-\frac{|\psi|^2}{\lambda^2}\boldsymbol{A} \tag{3.23}$$

Furthermore, if ψ is written as $\psi=|\psi|\mathrm{e}^{i\theta}$, the second GL equation becomes

$$\operatorname{curl}\operatorname{curl}\boldsymbol{A} = \frac{|\psi|^2}{\lambda^2}\left(\frac{\Phi_0}{2\pi}\nabla\theta - \boldsymbol{A}\right) \tag{3.24}$$

From (3.12) we obtain a boundary condition for ψ. If the superconductor has an interface with vacuum or an insulator, the condition will be

$$\left(\mathrm{i}\nabla + \frac{2\pi}{\Phi_0}\boldsymbol{A}\right)\cdot n\psi = 0 \tag{3.25}$$

where n in the unit vector normal to the surface of the superconductor. It is easy with the help of (3.17) to verify that (3.25) satisfies a very natural physical requirement, that is, it assures that no supercurrent passes through the superconductor-dielectric interface. However, the same requirement (that the normal component of the supercurrent through the interface is zero) will also be satisfied if a more general condition is imposed:

$$\left(\mathrm{i}\nabla + \frac{2\pi}{\Phi_0}A\right)\cdot n\psi = \mathrm{i}a\psi \tag{3.26}$$

where a is an arbitrary real number. With the help of the microscopic theory of superconductivity one can show that (3.26) is appropriate for the interface between a superconductor and a normal metal.

3.2.3 Gauge Invariance of the GL Theory

The GL equations contain the vector potential $\boldsymbol{A}$. But it is well-known that the choice of $\boldsymbol{A}$ is not unique. Indeed, the transformation

$$A = A' + \nabla\varphi, \tag{3.27}$$

where $\varphi(\boldsymbol{r})$ is a single-valued scalar function, does not change the magnetic field:

$$\boldsymbol{H} = \operatorname{curl}\boldsymbol{A} = \operatorname{curl}\boldsymbol{A'}$$

because

$$\operatorname{curl}\nabla\varphi = 0$$

To ensure that the theoretical results are independent of the choice of the vector potential, or, in other words, that they are gauge invariant, one has to impose the condition that the GL equations themselves are gauge invariant.

It is easy to verify that this condition is satisfied if we use the following transformations to go from the variables $\boldsymbol{A}$ and ψ to variables $\boldsymbol{A'}$ and ψ':

$$A = A' + \nabla\varphi \tag{3.28}$$

$$\psi = \psi' \exp\left[\mathrm{i}\frac{2\pi}{\Phi_0}\varphi(r)\right] \tag{3.29}$$

Let us verify this for (3.24). We proceed from $\boldsymbol{A}$ and ψ to $\boldsymbol{A'}$ and ψ' following (3.28) and (3.29). Then we see immediately that the second GL equation remains unaffected:

$$\operatorname{curl}\operatorname{curl}\boldsymbol{A'} = \frac{|\psi'|^2}{\lambda^2}\left(\frac{\Phi_0}{2\pi}\nabla\theta' - \boldsymbol{A'}\right)$$

Similarly, one can verify the gauge invariance of the first GL equation (3.22).
The gauge invariance of the GL equations implies a conclusion which is very important for our future discussions: For a simply connected superconductor, it is always possible to choose a gauge for the vector potential $\boldsymbol{A}$ such that the function $\psi(\boldsymbol{r})$ is real. (Recall that a simply connected body is a body in the interior of which an arbitrary closed contour can be reduced to a point without having to cross the boundaries of the body. In other words, there are no unbroken holes in a simply connected body. A toroid is an example of a doubly connected body.)

The requirement that a superconductor be simply connected is essential because, in a multiply connected superconductor, the phase of the order parameter, θ, is no longer a single-valued function. On going around a cavity in a multiply connected superconductor, the phase can vary by an integral multiple of 2π. Therefore, $\theta(r)$ becomes unsuitable as the corresponding gauge for $\boldsymbol{A}$.

Ginzburg-Landau Theory

So far in our thermodynamic discussions we have treated the Gibbs function of the system in an integrated way, such that spatial variations of the superconducting state did not appear explicitly. Furthermore, we have not yet utilized the fact that the superconducting state can be described in terms of a macroscopic wave function with a well-defined phase.

Both aspects were incorporated by Ginzburg and Landau into their theory published in 1950. This theory represents an important extension of the London theory [20], in which a spatially constant density of the superconducting charge carriers was assumed. Surprisingly, for a long time, the Ginzburg-Landau theory did not receive the proper attention. It was only after the development of a microscopic theory that the importance of this extended phenomenological theory was generally recognized. Only gradually it has become clear that the theory accounts for important physical properties of the superconducting state. It was shown by Gor'kov that for temperatures near T_c the theory can be derived from the BCS theory [21]. One of the great successes of the theory was the prediction of the vortex state by Abrikosov [22]. Often the theory is now referred to as GLAG theory after the four scientists Ginzburg, Landau, Abrikosov, and Gor'kov. In 2003, A. A. Abrikosov and V. L. Ginzburg together with A. J. Leggett received the Nobel Prize in physics for the development of the theory of superconductivity and superfluidity.

The GLAG theory starts from the argument that in the normal superconducting transition in the absence of a magnetic field, we are dealing with a secondorder phase transition (see Section 4.1). Landau had developed a theory exactly for such phase transitions. In the theory a parameter, the so-called order parameter, was defined, which in the new phase (here the superconducting phase) should increase continuously from zero at T_c up to the value 1 at $T = 0$. To describe the superconducting state, Ginzburg and Landau introduced a function $\Psi(\mathbf{r})$ as the order parameter. The quantity $|\Psi(\mathbf{r})|^2$ can be interpreted as the density of the superconducting charge carriers. Since in the superconducting state $|\Psi(\mathbf{r})|^2$ must approach zero continuously for $T \to T_\mathrm{c}$, near T_c we can expand the Gibbs function g_s of the superconducting phase in a Taylor series of the density $|\Psi(\mathbf{r})|^2$. Then we obtain

$$g_\mathrm{s} = g_\mathrm{n} + \alpha|\Psi|^2 + \frac{1}{2}\beta|\Psi|^4 + \cdots$$

Here, the Gibbs function g_n of the normal conducting phase appears, since for $\Psi = 0$ the Gibbs function g_s must be equal to g_n. Since for $T < T_\mathrm{c}$ we also have $g_\mathrm{s} < g_\mathrm{n}$ (stability criterion), we find $\alpha < 0$.

Sufficiently close to T_c an approximation that includes only the first two terms of the series is satisfactory, that is, one that cuts off the series after the $|\Psi|^4$ term. For temperatures close to the transition temperature, very general statements about the sign of the coefficients α and β are possible:

The coefficient β must be positive, otherwise a very large value of $|\Psi|$ would always lead to a value of g_s that is smaller than g_n. The "minimum" of g_s would only be reached for $|\Psi| \to \infty$.

For $T < T_c$, the coefficient α must be negative, otherwise g_s would always be larger than g_n, since β is positive.

For $T > T_c, \alpha$ must be positive. In this regime the normal state should have the smaller value of the Gibbs function, leading to $|\Psi| = 0$ as the most favorable solution.

Therefore, for temperatures close to T_c, the coefficients α and β can also be expanded in Taylor series of the temperature. Here, we include only the first nonvanishing coefficient. For α, we can write

$$\alpha(T) = \alpha(0)\left(\frac{T}{T_c} - 1\right)$$

However, the coefficient β can be taken as constant:

$$\beta(T) = \beta = \text{ const.}$$

The rather abstract expansion coefficients α and β can now be connected in a simple way with the so-called "thermodynamic critical field" B_{cth} and with the equilibrium density n_s in zero field. In the following, we will deal with B_{cth} many times. If we denote the equilibrium value of Ψ sufficiently far away from any interface by Ψ_∞, then we have the relation $n_s = |\Psi_\infty|^2$. We introduce the magnetic field B_{cth} based on the difference $g_n - g_s$:

$$g_n - g_s = -\alpha |\Psi_\infty|^2 - \frac{1}{2}\beta |\Psi_\infty|^4 = \frac{1}{2\mu_0} B_{cth}^2$$

In Section 4.6.1 we will see that for a type-I superconductor under certain conditions B_{cth} exactly corresponds to the critical field B_c.

We denote the Gibbs function by the letter g to indicate that it is an energy density. Since the equiminimum, one should use the terminology of energy functional. However, for simplicity in the following we continue to denote g as Gibbs function.

One obtains an additional equation for α and β from the fact that at equilibrium $g_s\left(|\Psi_\infty|^2\right)$ reaches a minimum. For the equilibrium value $|\Psi_\infty|^2$, we must have also $dg_s/\mathrm{d}|\Psi|^2 = 0$. Tis yields

$$\alpha + \beta |\Psi_\infty|^2 = 0$$

From this we obtain

$$n_s = |\Psi_\infty|^2 = -\frac{\alpha}{\beta}$$

and from Eq. (4.21) we find

$$B_{cth}^2 = \mu_0 \frac{\alpha^2}{\beta}$$

From the temperature dependences of Eqs. (4.20a) and (4.20b) for α and β, we see immediately that, near T_c, n_s and B_{cth} are proportional to $(1 - T/T_c)$, that is, for $T \to T_c$ they linearly approach zero. So we have [144]

$$n_\mathrm{s}(T) = n_\mathrm{s}(0)\,(1 - T/T_\mathrm{c}) \qquad \text{and} \qquad B_\mathrm{cth}(T) = B_\mathrm{cth}(0)\,(1 - T/T_\mathrm{c})$$

By solving for α and β, we find

$$\alpha = -\frac{1}{\mu_0}\frac{\beta_\mathrm{cth}^2}{n_\mathrm{s}}$$
$$\beta = -\frac{1}{\mu_0}\frac{\beta_\mathrm{cth}^2}{n_\mathrm{s}^2}$$

Now we can see directly that a second-order phase transition is described by Eq. (4.19) or (4.21):

For $T = T_\mathrm{c}$ we have $g_\mathrm{s} = g_\mathrm{n}$, since $|\Psi| = 0$.

The derivative $\partial g_\mathrm{s}/\partial T$ is

$$\frac{\partial g_\mathrm{s}}{\partial T} = \frac{\partial g_\mathrm{n}}{\partial T} - \frac{B_\mathrm{cth}}{\mu_0}\frac{\partial B_\mathrm{cth}}{\partial T} = \frac{\partial g_\mathrm{n}}{\partial T} + \frac{B_\mathrm{cth}^2(0)}{\mu_0}\left(1 - \frac{T}{T_\mathrm{c}}\right)\frac{1}{T_\mathrm{c}}$$

At T_c the second-term vanishes, that is, $\partial g/\partial T$ passes through T_c continuously - For the second derivative $\partial^2 g_\mathrm{s}/\partial T^2$, one finds

$$\frac{\partial^2 g_\mathrm{s}}{\partial T^2} = \frac{\partial^2 g_\mathrm{n}}{\partial T^2} - \frac{B_\mathrm{cth}^2(0)}{\mu_0}\frac{1}{T_\mathrm{c}^2}$$

We see that $\partial^2 g/\partial T^2$ jumps by the amount $B_\mathrm{cth}^2(0)/\left(\mu_0 T_\mathrm{c}^2\right)$, as it must for a second-order phase transition.

We note that we can also describe a first-order phase transition in a similar way. In this case we must supplement the series expansion in Eq. (4.19) by a term $|\Psi|^6$, and a negative sign of β must be allowed.

Note that these expressions are valid only near T_c. The crucial extension of the phenomenological description is achieved by the ansatz of the Gibbs function of the superconductor in a magnetic field under the assumption of a possible spatial variation of Ψ. Hence, one uses the ansatz

$$g_s(B) = g_\mathrm{n} + \alpha|\Psi|^2 + \frac{1}{2}\beta|\Psi|^4 + \frac{1}{2\mu_0}\left|\mathbf{B}_\mathrm{a} - \mathbf{B}_\mathrm{i}\right|^2 + \frac{1}{2m}\left|\left(\frac{\hbar}{i}\nabla - q\mathbf{A}\right)\Psi\right|^2$$

where m and q are the mass and charge, respectively, of the particles described by Ψ, that is, $m = 2m_\mathrm{e}$ and $|q| = 2e$ for Cooper pairs, and ∇ is a differential operator namely the gradient

$$\nabla\Psi = \mathrm{grad}\,\Psi = \frac{\partial\Psi}{\partial x}\mathbf{e}_x + \frac{\partial\Psi}{\partial y}\mathbf{e}_y + \frac{\partial\Psi}{\partial z}\mathbf{e}_z$$

operating on the function Ψ

We see that two additional terms appear. The first term refers to the energy needed to change the magnetic field from $\mathbf{B_a}$, the external field in the absence of the superconductor, to the value $\mathbf{B}_\mathrm{i}$. For the Meissner phase with $\mathbf{B}_i = 0$, this term yields the total energy to be supplied for the magnetic field expulsion. The second term takes into account a possible spatial variation of $\mathbf{B}_\mathrm{i}$ and Ψ within the superconductor. It includes the supercurrents leading to a variation of the magnetic field. Furthermore, it contains the energy needed to establish a spatial variation of the Cooper pair density. This contribution introduces a "stiffness" of the wave function, which gains importance at the phase boundary between the superconducting and normal conducting phases. We note that this second term is constructed quite analogously to the expression in the Schrödinger equation of the kinetic energy of a particle with mass m and charge q.

One obtains the Gibbs function for the total superconducting sample from an integration of Eq. (4.26) over the volume V of the sample:

$$\int_V \left\{ g_\mathrm{n} + \alpha|\Psi|^2 + \frac{1}{2}\beta|\Psi|^4 + \frac{1}{2\mu_0}\left|\mathbf{B}_\mathrm{a} - \mathbf{B}_\mathrm{i}\right|^2 + \frac{1}{2m}\left|\left(\frac{\hbar}{i}\nabla - q\mathbf{A}\right)\Psi\right|^2 \right\} \cdot \mathrm{d}V \quad (4.27)$$

This function G_s must be minimized by the variation of Ψ and A. The variation then yields the two equations of the Ginzburg-Landau theory:

$$\frac{1}{2m}\left(\frac{\hbar}{i}\nabla - q\mathbf{A}\right)^2 \Psi + \alpha\Psi + \beta|\Psi|^2\Psi = 0$$

$$\mathbf{j}_\mathrm{s} = \frac{q\hbar}{2mi}\left(\Psi^*\nabla\Psi - \Psi\nabla\Psi^*\right) - \frac{q^2}{m}|\Psi|^2\mathbf{A}$$

Here, Ψ " is the complex conjugate function to Ψ.

This system of differential equations must still be supplemented by a proper boundary condition. Frequently, in this case, one applies the obvious condition that the supercurrent cannot flow out of the superconductor, that is, that the current (Eq. (4.29)) perpendicular to the surface of the superconductor must vanish.

Next we will look in detail at the Ginzburg-Landau equations (4.28) and (4.29) or at the Gibbs function (4.27) in various limiting cases and compare the theoretical predictions with the experimental results.

3.6.3 Characteristic Lengths, Proximity Effect, Thermodynamic Critical Field

3.3.1 The Coherence Length and the Penetration Depth

In the preceding section, we formally introduced a quantity ξ in (3.20). Now we shall find its physical significance.

Let us consider a simple example. A thin film of a normal metal is deposited onto a clean flat surface of a superconductor. This will cause a local reduction in the superconducting electron density near the surface of the superconductor. In other words, the order parameter $|\psi|$ at the surface will be somewhat different from its equilibrium value deep inside the superconductor, where $|\psi| = 1$. What then is the characteristic length over which the order parameter returns to unity?

Let us take the x axis perpendicular to the surface of the superconductor ($x = 0$ at the surface). Then it is obvious that ψ can vary only along the x axis, i.e., $\psi = \psi(x)$. In addition, ψ can be presumed real because we are dealing with a simply connected superconductor (see Sect.3.2). Then the first GL equation (3.22) reduces to a simple form:

$$-\xi^2 \frac{\mathrm{d}^2}{-\frac{1}{r} - \frac{\psi}{2}} - \psi + \psi^3 = 0 \quad (3.30)$$

Suppose that the normal layer at the surface is so thin that the magnitude of ψ at the surface is not very different from 1, that is,

$$\psi = 1 - \varepsilon(x), \quad \varepsilon(x) \ll 1$$

Substituting this into (3.30) and keeping only linear terms in $\varepsilon(x)$, we obtain

$$\xi^2 \frac{\mathrm{d}^2\varepsilon(x)}{\mathrm{d}x^2} - 2\varepsilon(x) = 0 \quad (3.31)$$

Allowing for the fact that as $x \to \infty$ the order parameter $\psi \to 1$, we have $\varepsilon(\infty) = 0$. Then the obvious solution of (3.31) is

$$\varepsilon = \varepsilon(0)\mathrm{e}^{-\sqrt{2}x/\xi}$$

It follows that ξ is indeed the characteristic scale over which variations of the order parameter ψ occur. This length is called the coherence length.

Another quantity, λ, introduced in (3.21), is already known to us (Sect.2.2). This is the penetration depth for a weak magnetic field. Both ξ and λ are temperature dependent:

$$\lambda^2 = \frac{mc^2\beta}{8\pi|\alpha|e^2} \tag{3.32}$$

$$\xi^2 = \frac{\hbar^2}{4m|\alpha|} \tag{3.33}$$

In the vicinity of T_c, we have $|\alpha| \propto (T_\mathrm{c} - T)$. Therefore, in the temperature interval close to T_c

$$\lambda \propto (T_\mathrm{c} - T)^{-1/2}\,, \quad \xi \propto (T_\mathrm{c} - T)^{-1/2}\,. \tag{3.34}$$

In the entire temperature interval, a good approximation for $\lambda(T)$ is given by the empirical formula

$$\lambda(T) = \lambda(0)\,(1 - T/T_\mathrm{c})^{-1/4} \tag{3.35}$$

The values of $\lambda(0)$ for a number of superconducting materials are given in Table 2.1. Using (3.3) and (3.1), one can verify that the penetration depth (3.32) is the same as that introduced earlier in (2.7).

Now we can introduce another important quantity, the GL parameter κ:

$$\kappa = \lambda/\xi \tag{3.36}$$

Another expression for κ can be obtained from (3.32), (3.33) and (3.36):

$$\kappa = 2\sqrt{2}\frac{e}{\hbar c}\lambda^2 H_\mathrm{cm} \tag{3.37}$$

An additional, very useful, formula follows from (3.37) and the expression for the flux quantum $\Phi_0 = \pi\hbar c/e$:

$$\sqrt{2}H_\mathrm{cm} = \frac{\Phi_0}{2\pi\lambda\xi} \tag{3.38}$$

Before concluding this section, let us discuss the effect of magnetic field on the order parameter and the penetration depth.

Suppose that a superconducting specimen characterised by $\kappa \ll 1$ (or $\lambda \ll \xi$) occupies the semispace $x > 0$, with an external magnetic field along the z axis. Since by assumption $\lambda \ll \xi$, the magnetic field penetrates the specimen only to a small depth, $d \ll \xi$. This implies that the order parameter Ψ is affected by the magnetic field only over a small depth λ, while it can be expected to vary in a substantial way over a much larger length, ξ. Therefore, over the major part of the coherence length, the order parameter is 'not aware' of the existence of the magnetic field and is close to $\Psi_0 = (|\alpha|/\beta)^{1/2}$. Hence we can conclude that, for $\kappa \ll 1$, the effect of the magnetic field on the order parameter is insignificant.

It follows immediately that the magnetic field penetration depth, which depends on $|\Psi|^2$, is also only slightly affected by the magnetic field. Rigorous calculations show that, in the

presence of an external magnetic field H_0, the amplitude of the order parameter ψ is reduced near the surface of the superconductor by [23]

$$\frac{1}{4\sqrt{2}}\kappa\frac{H_0^2}{H_{\rm cm}^2}$$

For $\lambda \gg \xi$, the effect of an external magnetic field on the order parameter is much greater and brings about a number of qualitatively new and interesting effects. We shall discuss these in detail in the following sections.

Thermodynamic Critical Field

«Выигрыш» в энергии сверхпроводящей фазы в отсутствии внешнего поля $\Omega_n - \Omega_s(\mathcal{H} = 0) = V\alpha^2/2b$ может быть скомпенсирован «проигрышем» энергии из-за помещения образца во внешнее магнитное поле $\Omega_s(\mathcal{H}) - \Omega_s(\mathcal{H} = 0) = V\mathcal{H}^2/8\pi$. Действительно, поскольку в силу эффекта Мейсснера $\mathcal{B} = 0$ сверхпроводник - идеальный диамагнетик $\mathcal{M} = -\mathcal{H}/4\pi$, то плотность его дополнительной энергияи из-за поля равна $-V\int_0^{\mathcal{H}} \mathcal{M}d\mathcal{H} = \mathcal{H}^2/8\pi$. Это дает величину термодинамического критического поля:

$$\mathcal{H}_c^2 = \frac{4\pi a^2 \left(T - T_c\right)^2}{b}$$

This is it!

3.3.2 The Proximity Effect

The role of the coherence length becomes particularly evident when we consider a normal metal N and a superconductor S in good contact with each other. The Cooper pairs can penetrate from S into N and 'live' there for some time. As a result, a thin layer near the NS interface becomes superconducting. On the other hand, the penetration of the Cooper pairs from S into N results in their density being reduced in S. That is, in the vicinity of the interface, the order parameter ψ in the superconductor becomes less than 1, even without magnetic field.

This is the so-called proximity effect.

Consider the simplest case. Suppose that two superconductors, with slightly different critical temperatures ($T_{\rm cn}$ and $T_{\rm cs}$), are in good contact: $T_{\rm cs} > T_{\rm cn}, T_{\rm cs} - T_{\rm cn} \ll T_{\rm cn}$. The temperature of the specimen T is chosen to satisfy the inequality $T_{\rm cn} < T < T_{\rm cs}$, hence the material with the critical temperature $T_{\rm cn}$ is in the normal state. The interface between the two materials is flat and coincides with the plane $x = 0$. The superconductor occupies the semispace $x > 0$, and the normal metal $x < 0$.

The behavior of the order parameter in the S region ($x > 0$) can be determined by solving the first GL equation (3.12) of the form (3.30). The

$$-\xi^2\left(\frac{{\rm d}\psi}{{\rm d}x}\right)^2 - \psi^2 + \frac{1}{2}\psi^4 = C \tag{3.39}$$

where C is the integration constant. Since at $x \to \infty$ we have $({\rm d}\psi/{\rm d}x) \to 0$ and $\psi \to 1$, the integration constant is $C = -1/2$. Substituting this into (3.39) and carrying out the integration, we obtain

$$\psi = \tanh\left[\left(x - x_0\right)/\sqrt{2}\xi\right] \tag{3.40}$$

Here x_0 is the integration constant to be determined from the boundary condition at $x = 0$. In our case this condition is

$$\frac{1}{\psi}\frac{\mathrm{d}\psi}{\mathrm{d}x} = \frac{1}{b} \tag{3.41}$$

The value of b, in general, should be calculated using the microscopic theory. Its geometrical significance becomes evident from Fig.3.2.

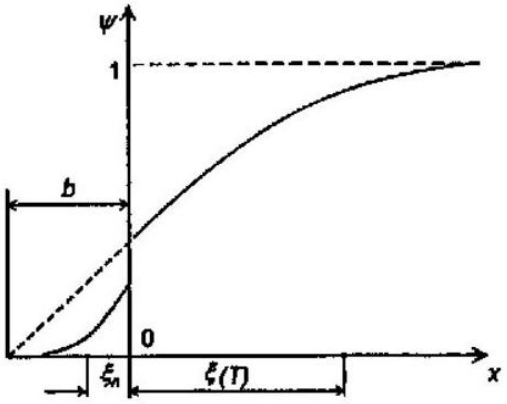


Fig. 3.2. Order parameter $\psi(x)$ near the interface between a superconductor ($x > 0$) and a normal metal ($x < 0$)

On substitution of (3.40) into (3.41), we find how the integration constant x_0 relates to b:

$$-\sinh\left(\sqrt{2}\frac{x_0}{\xi}\right) = \sqrt{2}\frac{b}{\xi}$$

Consider now the behavior of the order parameter ψ in the normal region ($x < 0$). The first GL equation is also applicable in this case (see, for example, [25]). Indeed, by (3.6), we have $\alpha_\mathrm{n} \propto (T - T_\mathrm{cn})$ so that $\alpha_\mathrm{n} < 0$ at $T < T_\mathrm{cn}$ and $\alpha_\mathrm{n} > 0$ at $T > T_\mathrm{cn}$. Hence, for the N region, the first GL equation (3.12) subject to the condition $T - T_\mathrm{cn} \ll T_\mathrm{cr}$ becomes

$$-\xi_\mathrm{n}^2\frac{\mathrm{d}^2\psi}{\mathrm{d}x^2} + \psi + \psi^3 = 0$$

where ${\xi_\mathrm{n}}^2 = \hbar^2/4m\alpha_\mathrm{n}$.

The order parameter in the normal region is small ($\psi \ll 1$), therefore the cubic term can be neglected. Then

$$-{\xi_\mathrm{n}}^2\frac{\mathrm{d}^2\psi}{1\ldots} + \psi = 0$$

Subject to the condition $\psi \to 0$ at $x \to \infty$, the solution is

$$\psi = \psi_0 \exp\left(-|x|/\xi_\mathbf{n}\right) \tag{3.42}$$

From (3.42) we see that the order parameter penetrates the N region to the depth ξ_n while decaying exponentially over this distance. Since T_cn and T_cs are close to each other, ψ and $\mathrm{d}\psi/\mathrm{d}x$ can be assumed continuous at the NS interface. Then, from (3.42), we have $b = \xi_\mathrm{n}$.

In the general case of a superconductor in contact with a true normal metal ($T_\mathrm{cn} = 0$), the GL equations are not applicable to the normal region, Nevertheless, qualitatively, the phenomenon remains, that is, the order parameter penetrates the normal region to a certain depth ξ_n. Rigorous calculations based on the microscopic theory give the following results [26].

In a pure N metal, that is, when the electron mean free path is $l_\mathrm{n} \gg \xi_\mathrm{n}$, the coherence length is

$$\xi_\mathrm{n} = \frac{\hbar v_\mathrm{Fn}}{2\pi k_\mathrm{B} T} \tag{3.43}$$

where v_{Fn} is the Fermi velocity and k_{B} is the Boltzmann constant. One should bear in mind, however, that at $T \to 0$ the decay of the order parameter in the N region is much slower than exponential.

In a 'dirty' N metal ($l_{\mathrm{n}} \ll \xi_{\mathrm{n}}$) the coherence length is

$$\xi_{\mathrm{n}} = \left(\frac{\hbar v_{\mathrm{Fn}} l_{\mathrm{n}}}{6\pi k_{\mathrm{B}} T} \right)^{1/2} \tag{3.44}$$

Evaluations by (3.43, 44) give values for ξ_{n} in the range $10^{-5} - 10^{-4}$ cm.
The behavior of the order parameter in the general case is sketched in Fig. 3.2. According to [27], the value of b in the 'dirty' case is

$$b = \frac{\sigma_{\mathrm{s}}}{\alpha \sigma_{\mathrm{n}}} \xi_{\mathrm{n}}, \tag{3.45}$$

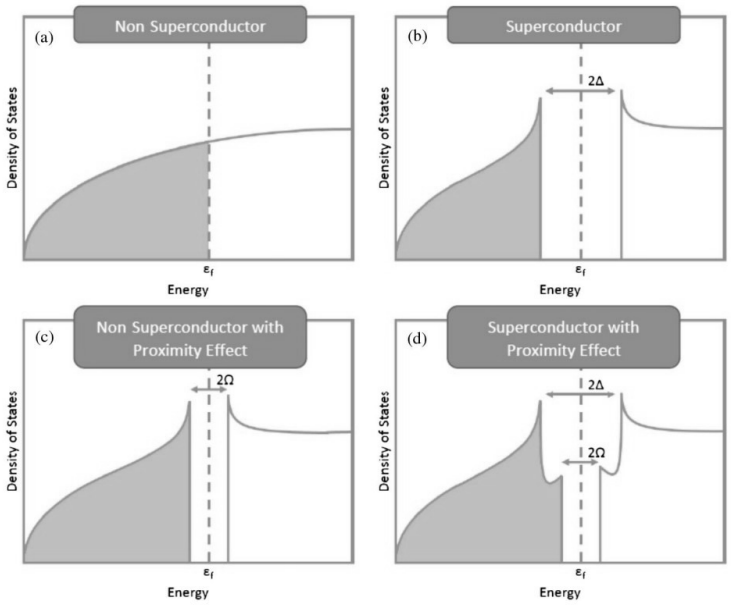
where σ_{s} and σ_{n} are the conductivities in the S and N regions, respectively, ξ_{n} is defined by (3.44), and the coefficient α is of the order 1. The exact values of α for a number of situations can be found in [27].

The existence of the proximity effect has been reliably established by experiment. If a superconducting film is deposited onto the surface of a normal metal, the critical temperature of the film decreases. Such a system was studied, for instance, in [28], namely a Pb film deposited on top of an Al film of thickness 4400Å and $T_{\mathrm{c}} = 1.2$ K. When the thickness of the Pb film was $d($ Pb$) = 900$Å, the critical temperature of the whole system, T_{c}, was close to the critical temperature of bulk lead (7.2 K). However, as the Pb film was made thinner, $d($ Pb$) = 600$Å$, T_{\mathrm{c}}$ fell to approximately 5.6 K, and at $d($ Pb$) = 200$Å it became $T_c = 1.6$ K, that is, close to the critical temperature of Al.

The proximity effect is utilized in SNS Josephson junctions where the phase coherence between the superconducting electrodes is established via a

Иллюстрация эффекта близости (????)

(????)



Other about coherence lengths

What else coherence length is?

The coherence length is a size, on which the order parameter is changed. By an "order parameter" I mean some complex variable Δ, that characterizes a condensate. This order parameter somehow is related to the concentration of superconducting electrons (??? how exactly??), which are determined by a Cooper pairs. Thus, GL coherence length is the size of a Cooper pair in the BCS model.

(????? this is a strange statement, I'll write theoretical sections, then return to it again.)

Are there several coherence lengths?

(??? I am not sure, maybe no, there is only one, the GL one. I'll think later. if there are many, I'll list them here)

3.6.4 Characteristic Lengths of the Ginzburg-Landau Theory

In the following, we will show that the Ginzburg-Landau equations contain two characteristic lengths, namely the London penetration depth λ_L and the Ginzburg-Landau coherence length ξ_GL. At this stage we cannot avoid a number of derivations and formulas. However, they are not very difficult.

We start by looking at Eq. (4.29). We want to rewrite this equation by normalizing Ψ to the value Ψ_∞. With the notation $\psi = \Psi/\Psi_\infty$, we find

$$\mathbf{j}_\mathrm{s} = \frac{q\hbar\left|\Psi_\infty\right|^2}{2mi}\left(\psi^*\nabla\psi - \psi\nabla\psi^*\right) - \frac{q^2\left|\Psi_\infty\right|^2}{m}|\psi|^2\mathbf{A}$$

With the definition (1.10) of the London penetration depth, $\lambda_\mathrm{L} = \sqrt{m/\left(\mu_0 q^2 n_\mathrm{s}\right)}$, and the relation $n_\mathrm{s} = \left|\Psi_\infty\right|^2$, we find

$$\mathbf{j}_\mathrm{s} = \frac{\hbar}{2iq}\frac{1}{\mu_0\lambda_\mathrm{L}^2}\left(\psi^*\nabla\psi - \psi\nabla\psi^*\right) - \frac{1}{\mu_0\lambda_\mathrm{L}^2}|\psi|^2\mathbf{A}$$

Using $\psi = \psi_0 \mathrm{e}^{i\varphi}$ for calculating the gradient in the brackets ($\nabla\psi = \mathrm{e}^{i\varphi}\nabla\psi_0 + \psi_0\mathrm{e}^{i\varphi}i\nabla\varphi$), we obtain

$$\mathbf{j}_\mathrm{s} = \psi_0^2\frac{\hbar}{q}\frac{1}{\mu_0\lambda_\mathrm{L}^2}\nabla\varphi - \frac{1}{\mu_0\lambda_\mathrm{L}^2}\psi_0^2\mathbf{A}$$

If the function Ψ is spatially constant, $\nabla\varphi$ vanishes, and $|\psi| = 1.0$. Then we have

$$\mathbf{j}_\mathrm{s} = -\frac{1}{\mu_0\lambda_\mathrm{L}^2}\mathbf{A}$$

Taking the curl on both sides and using curl $\mathbf{A} = \mathbf{B}$, we obtain the second London equation (1.14):

$$\mathbf{B} = -\mu_0\lambda_\mathrm{L}^2\,\mathrm{curl}\,\mathbf{j}_\mathrm{s}$$

We see that we recover the London theory in the case of a spatially constant Cooper pair density $n_{\mathrm{s}'}$. However, going beyond this case, the second Ginzburg-Landau equation apparently can take into account the supercurrents for a spatially varying wave function.

Let us turn to the first Ginzburg-Landau equation (4.28). Again we normalize Ψ to the value Ψ_∞. After a short calculation we find

$$\frac{1}{2m}\left(\frac{\hbar}{i}\nabla - q\mathbf{A}\right)^2\psi + \alpha\psi - \alpha|\psi|^2\psi = 0$$

Here, we must use the relation (4.23) to change the term $\beta\,|\Psi_\infty|^2$, appearing on the left-hand side, into $-\alpha$. We divide both sides by α and obtain

$$\frac{\hbar^2}{2m\alpha}\left(\frac{1}{i}\nabla - \frac{q}{\hbar}\mathbf{A}\right)^2\psi + \psi - |\psi|^2\psi = 0$$

Here, we have taken Planck's constant $\hbar$ in front of the bracket on the left-hand side. The quantity $-\hbar^2/(2m\alpha)$ has the dimension of [length] ^{2}. Obviously, it yields a second characteristic length of the Ginzburg-Landau theory, the Ginzburg-Landau coherence length ξ_{GL}, given by

$$\xi_{\mathrm{GL}} = \sqrt{\frac{-\hbar^2}{2m\alpha}}$$

Then the second Ginzburg-Landau equation can be written as

$$-\xi_{\mathrm{GL}}^2\left(\frac{\nabla}{i} - \frac{q}{\hbar}\mathbf{A}\right)^2\psi + \psi - |\psi|^2\psi = 0$$

With the temperature dependence of α (Eq. (4.20a)), we find immediately also the temperature dependences of λ_{L} and ξ_{GL}:

$$\lambda_{\mathrm{L}}(T) = \frac{\lambda_{\mathrm{L}}(0)}{\sqrt{1 - T/T_{\mathrm{c}}}}$$
$$\xi_{\mathrm{GL}}(T) = \frac{\xi_{\mathrm{L}}(0)}{\sqrt{1 - T/T_{\mathrm{c}}}}$$

For $T \to T_{\mathrm{c}}$ both quantities approach infinity. We note that Eqs. (4.35) and (4.36) are valid only close to T_{c}, although $\lambda_{\mathrm{L}}(0)$ and $\xi_{\mathrm{GL}}(0)$ appear in the equations. The Ginzburg-Landau theory is valid only in this limit.

Now we can introduce the ratio

$$\kappa = \frac{\lambda_{\mathrm{L}}}{\xi_{\mathrm{GL}}}$$

referred to as the Ginzburg-Landau parameter. Within the Ginzburg-Landau equations presented earlier, it is independent of the temperature and of the magnetic field.

In Eqs. (4.30b) and (4.34) we could also have normalized the other quantities having a dimension. Then we would find that the dimensionless Ginzburg-Landau equations would depend only on the Ginzburg-Landau parameter κ. Hence, this parameter is crucial for the behavior of these equations. Which length is indicated by ξ_{GL}? This is illustrated by a simple situation, in which the superconductor extends in the x-direction from $x = 0$ up to $x \to \infty$. In the y and z directions, the superconductor is assumed to be extended infinitely. For $x = 0$ we assume $|\psi| = 0$. Furthermore, we assume $\mathbf{A} = 0$. Then we can find a real solution for ψ from the equation

$$\xi_{\mathrm{GL}}^2\frac{\mathrm{d}^2\psi}{\mathrm{d}x^2} + \psi - \psi^3 = 0$$

which depends only on x. For $x \geq 0$, this equation has the solution

$$\psi(x) = \tanh\left(x/\sqrt{2}\xi_{\mathrm{GL}}\right)$$

shown in Figure 4.6. According to Eq. (4.39), $\psi(x)$ first increases linearly from 0 and then it approaches the limiting value 1 in the interior of the superconductor. We see that, at least in the situation we have discussed, ξ_{GL} can be interpreted as the characteristic length within which the order parameter ψ can change.

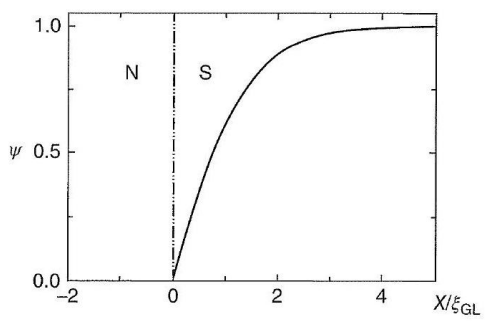


Figure 4.6 Variation of the function $\psi(x)$ according to Eq. (4.39) at the edge of a superconducting half-space.

Now we know the two length scales of the Ginzburg-Landau theory. The fact that the Ginzburg-Landau theory is valid only close to T_{c} should not diminish the importance of λ_{L} and ξ_{GL} as the characteristic length scales within which the supercurrents (or the magnetic field) and the Cooper pair density (or Ψ) can change. Both lengths are fundamental to the superconducting state. They can be analyzed further within the microscopic theory.

At very low temperatures, in the case of conventional superconductors, one finds that λ_{L} is approximately constant. The deviation from this constant value $\lambda_{\mathrm{L}}(0)$ decreases exponentially with decreasing temperature. On the other hand, in the case of unconventional superconductors, for which the energy gap has locations with value zero along certain crystal directions, the difference $\Delta\lambda = \lambda_L\ (T) - \lambda_L(0)$ increases from zero following a power law. In the case of the $d_{x^2-y^2}$ symmetry, $\Delta\lambda$ is proportional to T, if the samples are sufficiently pure. For impure samples, one observes a T^2 law. In Chapter 2 we listed the values of $\lambda_{\mathrm{L}}(0)$ for many conventional and unconventional superconductors.

Figure 4.7 shows experimental results for the temperature dependence of the penetration depth in mercury. Here, λ_{L} was determined from the magnetization of mercury colloid, that is, from small Hg balls [23]. For this material, as well as for many other conventional superconductors, the observed temperature dependence can be approximated over a wide temperature range by the empirical expression

$$\frac{\lambda_{\mathrm{L}}(T)}{\lambda_{\mathrm{L}}(0)} \propto \left[1 - \left(\frac{T}{T_{\mathrm{c}}}\right)^4\right]^{-1/2}$$

For $T \to T_{\mathrm{c}}$ this relation yields Eq. (4.35), in agreement with the Ginzburg-Landau theory. [15)] The plot in Figure 4.7 allows the comparison with Eq. (4.40). The solid straight line corresponds to this equation. The agreement between the analytic expression and the experimental data is excellent.

To see this we write $\left[1 - (T/T_c)^4\right] = \left[1 - (T/T_{\mathrm{c}})^2\right]\left[1 + (T/T_{\mathrm{c}})^2\right]$ and for $T \to T_{\mathrm{c}}$ replace the second factor by the factor 2. We apply the same procedure to $\left[1 - (T/T_{\mathrm{c}})^2\right]$ and finally obtain Eq. (4.35). 4.5 Characteristic Lengths of the Ginzburg-Landau Theory |219

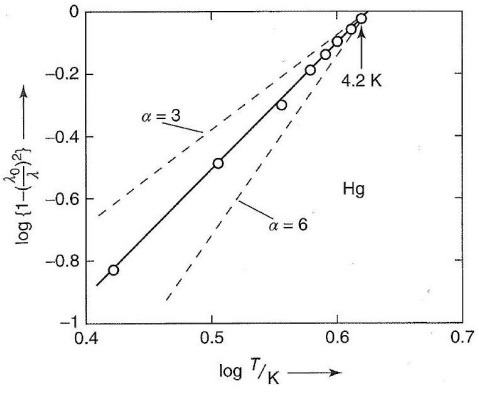


Figure 4.7 Temperature dependence of the penetration depth of Hg [23]. The solid line corresponds to the exponent $a = 4$ in the bracket of Eq. (4.40). For comparison, the cases $a = 3$ and $a = 6$ are also shown by the dashed curves.

For comparison we show in Figure 4.8 the experimental results obtained for a highly pure $YBa_2Cu_3O_7$ single crystal. The penetration depth was determined from the surface impedance of the crystal (see also Section 7.5.1). The latter was found from the frequency shift of a resonating cavity into which the crystal had been inserted. The data referring to the left vertical axis show the ratio $\lambda_L(0)^2/\lambda_L(T)^2$, which is proportional to the density of Cooper pairs according

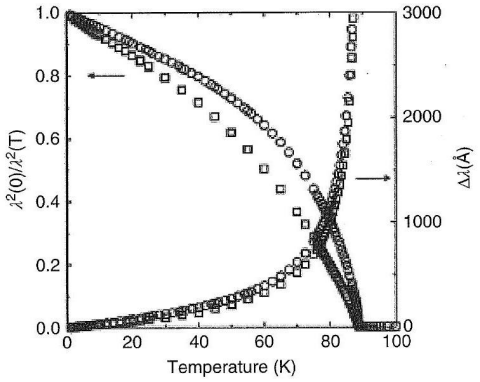


Figure 4.8 Temperature dependence of the crystal, and the squares indicate the penemagnetic penetration depth in highly pure tration depth along the b-direction. At low values $\lambda_g(0) = 160$ nm and $\lambda_b(0) = 80$ nm[24].

to Eq. (1.10). The data referring to the right vertical axis show the difference $\Delta\lambda = \lambda_L(T) - \lambda_L(0)$. For each axis there are two curves, which correspond to the penetration depth along the a and b directions of the crystal, respectively. We clearly see the linear increase in $\Delta\lambda$ over a wide temperature range.

The Ginzburg-Landau coherence length ξ_{GL} is much more difficult to determine experimentally than the penetration depth λ_L. (Numerical values of ξ_{GL} are listed in Chapter 2 for a number of superconductors.) Usually one employs indirect methods. The value of ξ_{GL} is closely connected with the upper critical field of type-II superconductors, from which it can be determined (see Section 4.7.1). Another indirect method uses the analysis of the electrical conductivity above the transition temperature. Because of thermal fluctuations, superconducting small regions always appear temporarily closely above T_c, contributing to an enhanced electrical conductivity. We will return to this subject in Section 4.8.

Within the Ginzburg-Landau theory, λ_L and ξ_G represent material properties, which depend on the Cooper pair density and on the thermodynamic critical field B_{ot} because of the parameters α and β. The microscopic theory provides us with another important relation: the

dependence of λ_L and ξ_{GL} on the electron mean free path l^*.[16] For conventional superconductors in the limit $T \to 0$, one finds

$$\lambda_L(T=0,l^*) = \lambda_L(T=0,l^* \to \infty)\left\{1 + \frac{\xi_{GL}(T=0,l^* \to \infty}{l^*}\right\}^{1/2}$$

and for $l^* \ll \xi_{GL}(T=0,l^* \to \infty)$ one has

$$\xi_{GL}(T=0,l^*) = \{\xi_{GL}(T=0,l^* \to \infty)\, l^*\}^{1/2}$$

This dependence is not yet taken into account by the expressions (4.35), (4.36), and (4.40), which are valid only in the limit of very large mean free paths, $l^* \to \infty$. From Eqs. (4.41) and (4.42) we see that, with decreasing l^*, the length λ_L increases and the length ξ_{GL} decreases. Hence, the Ginzburg-Landau parameter κ strongly depends on l^*. It increases with decreasing l^*.

The length l^* depends on the purity of the samples and can be controlled by the admixture of impurities. In Section 4.7 we will see that by varying the degree of purity, one can change a type-I superconductor into a type-II superconductor.

Together with the BCS coherence length presented in Section 3.1.1, we have introduced three different characteristic lengths of a superconductor:

penetration depth λ_L measuring the decay of the magnetic field in the interior of the superconductor

average extension ξ_0 of a Cooper pair as a measure of the distance within which the correlation forming Cooper pairs is active;

coherence length ξ_{GL} as the smallest length within which the Cooper pair density can vary - it is always larger than ξ_0, since the number density of Cooper pairs cannot vary within a distance smaller than the average extension of a Cooper pair.

The electron mean free path l indicates the average distance that a conduction electron can propagate between two collisions.

The coherence length ξ_0 is nearly temperature-independent, and in the limit $l^* \to 0$ it is about equal to l^*. In different limiting cases, we can also find simple relations for this length. For example, in the BCS theory:

$$\xi_0(T=0,l^* \to \infty) = 0.18\frac{\pi\hbar v_F}{2k_B T_c}$$

$$\xi_{GL} \approx \xi_0 \frac{\lambda_L(T,l^*)}{\lambda_L(T=0,l^* \to \infty)}$$

where v_F is the Fermi velocity and k_B is Boltzmann's constant. Such relations represent good approximations mostly only within specific regimes of T and l^*. In general, their mathematical derivation from the microscopic theory requires appreciable effort.

It is interesting to note that in 1951 Pippard postulated a coherence length for the interpretation of high-frequency measurements [25]. Based on this coherence length, which is closely related to ξ_0, Pippard could extend the London theory y claiming that the supercurrent density $j_s(x,y,z)$ should depend not only on the magnetic field $B(x,y,z)$ at the location (x,y,z) but also on the average field in a region with an extension of about the coherence length.

In the following, we return again to the thermodynamic properties of the superconducting state, and we start with type-I superconductors.

3.6.5 Energy of a Normal Metal-Superconductor Interface

Theory by Shmidt

Type-I and type-II superconductors, as we already know, can show entirely different responses to an external magnetic field. The reason is that the surface energy of the interface between a normal and a superconducting region, $\sigma_{\rm ns}$, is positive for type-I superconductors and negative for those of type-II. We are now in a position to understand the origin of this difference. It turned out that for type-I superconductors $\lambda < \xi$, and for those of type-II $\lambda > \xi$. The dividing line between the superconductors of type-I and type-II will be determined more precisely later. Let us start with a type-I superconductor.

Consider a flat NS interface within a superconductor in the intermediate state. Assume that far away to the left of the interface, the material is superconducting, and far away to the right of the interface, it is normal. The interface is perpendicular to the x axis and the magnetic field is parallel to the z axis. Since we consider a superconducting semispace, i.e., a simply connected superconductor, we can always choose an appropriate gauge so that the wavefunction of the GL theory is real. In addition, due to the simple geometry of the problem, all variables depend only on x, and the vector potential A may be assumed parallel to the y axis. The origin $x = 0$ is chosen at the interface.

Thus the initial data are:
(1) $\boldsymbol{H} = (0, 0, H(x))$,
(2) $\psi = \psi(x)$ is a real function,
(3) $\boldsymbol{A} = (0, A(x), 0)$.

Then the GL equations (3.22) and (3.24) can be rewritten in the form

$$-\xi^2 \frac{\mathrm{d}^2\psi}{\mathrm{d}x^2} + \left(\frac{2\pi\xi}{\Phi_0}\right)^2 A^2\psi - \psi + \psi^3 = 0$$
$$\frac{\mathrm{d}^2 A}{\mathrm{d}x^2} = \left(\frac{\psi^2}{\lambda^2}\right) A \tag{3.46}$$

One can easily verify that the first integral of these equations is

$$\left[1 - \left(\frac{2\pi\xi A}{-\Phi_0}\right)^2\right]\psi^2 - \frac{1}{2}\psi^4 + \left(\frac{2\pi\lambda\xi}{\Phi_0}\right)^2 \left(\frac{\mathrm{d}A}{\mathrm{d}x}\right)^2 + \xi^2 \left(\frac{\mathrm{d}\psi}{\mathrm{d}x}\right)^2 = C, \tag{3.47}$$

where C is the integration constant which can be found from the boundary conditions: at $x \to -\infty, \psi \to 1,\ \mathrm{d}\psi/\mathrm{d}x \to 0$, and $A \to 0$.

Indeed, at the far left, that is, as $x \to -\infty$, there is no magnetic field and the wavefunction of the GL theory tends to 1. On substitution of these boundary conditions into (3.47), we obtain $C = 1/2$ and, using (3.38), we finally have

$$\left[\left(\frac{2\pi\xi A}{\pi}\right)^2 - 1\right]\psi^2 + \frac{1}{n}\psi^4 = \xi^2 \left(\frac{\mathrm{d}\psi}{1\ldots}\right)^2 + \frac{H^2}{\pi\pi^7\bar{n}} - \frac{1}{n}. \tag{3.48}$$

Now, after these preliminary preparations, let us turn to calculation of the surface energy per unit area of the interface between a normal and a superconducting region. But first a little bit of physics. When inspecting a superconducting domain, we shall need to know the exact value of the external magnetic field surrounding it. As this domain is a part of the specimen in the intermediate state, there must be a normal domain next to it, which is penetrated by a magnetic field of strength $H_{\rm cm}$. (Recall that this is the field strength established automatically in the normal regions of a superconductor in the intermediate state.)

Thus, with respect to the superconducting domain, the external field is always $H_{\rm cm}$. Let us now write down the density of the Gibbs free energy deep in the interior of the superconducting domain, that is, far away to the left of the interface. From (1.22) we have

$$G_{\rm s} = F_{\rm s0} - HH_{\rm cm}/4\pi$$

Since at the far left $H = 0$, we get $G_{\rm s} = F_{\rm s0}$, where $F_{\rm s0}$ is the free energy density of the superconductor without magnetic field. Far to the right of the NS interface, i.e., in the normal metal where the magnetic field is $H_{\rm cm}$, the free energy density is

$$F = F_{\rm n} + H_{\rm cm}^2/8\pi$$

where the second term is simply the energy density of the magnetic field.

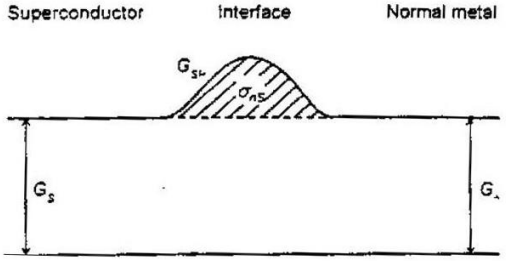


Fig. 3.3. Density of the Gibbs free energy G_{sH} in the vicinity of a normal metal-superconductor interface

In the normal domain, the Gibbs free energy density is

$$\begin{aligned} G_{\rm n} &= F - HH_{\rm cm}/4\pi = F_{\rm n} + H_{\rm cm}^2/8\pi - H_{\rm cm}^2/4\pi \\ &= F_{\rm n} - H_{\rm cm}^2/8\pi = F_{\rm s0} \end{aligned} \tag{3.49}$$

Here we have used the well-known relation between $F_{\rm n}$ and $F_{\rm s0}$ (1.12):

$$F_{\rm n} - F_{\rm s0} = H_{\rm cm}^2/8\pi$$

and the condition that in the normal domain $H = H_{\rm cm}$.

Thus we have arrived at a result which is precisely what one should have expected: In equilibrium, the density of the Gibbs free energy far to the left of the interface equals the energy density far to the right.

But what should be happening at the interface? The answer is given by

At the interface, the Gibbs free energy density may differ from G_n. Then it is natural to define the surface energy of the interface, $\sigma_{\rm ns}$, as

$$\sigma_{\rm ns} = \int_{-\infty}^{\infty} (G_{{\rm s}H} - G_{\rm n})\,{\rm d}x \tag{3.50}$$

where

$$G_{{\rm s}H} = F_{{\rm s}H} - HH_{\rm cm}/4\pi \tag{3.51}$$

$$F_{{\rm s}H} = F_{\rm n} + \frac{H^2}{8\pi} + \frac{H_{\rm cm}^2}{4\pi}\left[-|\psi|^2 + \frac{1}{2}|\psi|^4 + \xi^2\left|{\rm i}\nabla\psi + \frac{2\pi}{\Phi_0}A\psi\right|^2\right] \tag{3.52}$$

$$G_{\rm n} = F_{\rm n} - H_{\rm cm}^2/8\pi \tag{3.53}$$

Formula (3.51) follows from the general expression for the Gibbs free energy (where H is the magnetic field in the superconductor), formula (3.52), which forms the basis of the GL theory, can be easily derived from (3.7), and (3.53) was obtained earlier (see (3.49)).

On substitution of (3.51-53) into (3.50), we have

$$\sigma_{\rm ns} = \int_{-\infty}^{\infty} \left\{ \frac{H_{\rm cm}^2}{4\pi} \left[-|\psi|^2 + \frac{1}{2}|\psi|^4 + \xi^2 \left| {\rm i}\nabla\psi + \frac{2\pi}{\Phi_0}\boldsymbol{A}\psi \right|^2 \right] + \frac{H^2}{8\pi} - \frac{H H_{\rm cm}}{4\pi} + \frac{H_{\rm cm}^2}{8\pi} \right\} {\rm d}x$$

After recalling that $\boldsymbol{A} = (0, A, 0)$ and ψ is real, this becomes

$$\sigma_{\rm ns} = \int_{-\infty}^{\infty} \left\{ \frac{H_{\rm cm}^2}{4\pi} \left[-\psi^2 + \frac{1}{2}\psi^4 + \xi^2 \left(\frac{{\rm d}\psi}{{\rm d}x} \right)^2 + \left(\frac{2\pi\xi A}{\Phi_0} \right)^2 \psi^2 \right] + \frac{H^2}{8\pi} - \frac{H H_{\rm cm}}{4\pi} + \frac{H_{\rm cm}^2}{8\pi} \right\} {\rm d}x$$

Finally, using (3.48), we obtain

$$\sigma_{\rm ns} = \frac{H_{\rm cm}^2}{2\pi} \int_{-\infty}^{\infty} \left[\xi^2 \left(\frac{{\rm d}\psi}{{\rm d}x} \right)^2 + \frac{H\left(H - H_{\rm cm}\right)}{2H_{\rm cm}^2} \right] {\rm d}x \tag{3.54}$$

Let us analyze the result. First of all, the field penetrating the superconducting region is always less than the field at the interface, that is, less than $H_{\rm cm}$. Therefore, the second term in square brackets is always negative.

Now we understand why $\sigma_{\rm ns} < 0$ in the London theory: because quantum effects are not taken into account and, consequently, there is no term $\xi^2(\,{\rm d}\psi/{\rm d}x)^2$. One can see from (3.54) that this inadequacy of the London theory is removed by the GL theory. By taking into account quantum effects, a positive term $\xi^2(\,{\rm d}\psi/{\rm d}x)^2$ has appeared that leads to the energy $\sigma_{\rm ns}$ being positive.

Let us now make some evaluations. On going from N to S, the order parameter changes from 0 to 1 in the vicinity of the interface. This change takes place over a distance of the order of the coherence length ξ. Therefore, ${\rm d}\psi/{\rm d}x \sim 1/\xi$ and $\xi^2(\,{\rm d}\psi/{\rm d}x)^2 \sim 1$. This term is nonzero over a distance $x \sim \xi$ near the interface. Therefore,

$$\int_{-\infty}^{\infty} \xi^2(\,{\rm d}\psi/{\rm d}x)^2\,{\rm d}x \sim \xi \tag{3.55}$$

The term $H\left(H - H_{\rm cm}\right)/2H_{\rm cm}^2$ reaches approximately -1 at the interface and becomes zero deep in the interior of both S and N domains. The area where it is nonzero extends over a distance of the order of the penetration depth λ. Hence the contribution of this term to the integral in (3.54) is roughly $-\lambda$.

Consider two limiting cases.

(1) $\kappa \ll 1$, i.e., $\lambda \ll \xi$. Then, by (3.55), the dominant contribution to the integral in (3.54) comes from the gradient term and

$$\sigma_{ns} \sim H_{\rm cm}^2 \xi > 0.$$

Exact integration of (3.54) using the GL theory yields

$$\sigma_{\rm ns} = 1.89 \frac{H_{\rm cm}^2}{8\pi} \xi \tag{3.56}$$

(2) $\kappa \gg 1$, i.e., $\lambda \gg \xi$. In this case, the dominant contribution to the integral in (3.54) comes from the term $H\left(H - H_{\rm cm}\right)/2H_{\rm cm}^2$ and the surface energy of the interface is

$$\sigma_{\rm ns} \sim -H_{\rm cm}^2 \lambda$$

Exact calculations yield

$$\sigma_{\rm ns} = -\frac{H_{\rm cm}^2}{8\pi}\lambda. \tag{3.57}$$

Let us now interpret the results physically.
(1) The case $\kappa \ll 1, \lambda \ll \xi$. Figure 3.4 shows how the order parameter ψ and the magnetic field H vary in the vicinity of the interface. The former falls off over a distance ξ and the latter over a distance λ. As a result, there is a region of thickness $\sim \xi$ where the order parameter is already sufficiently small and the magnetic field is kept out. This region enjoys 'the privilege' of the superconductor: it is free of magnetic field; but the order parameter is still very small there compared to the superconducting regions. This ought to area at the far left. In other words, the energy of this region exceeds that of the superconducting region by the additional energy required to break the electron (Cooper) pairs within the region and thus to reduce the order parameter ψ. The density of the additional energy is $H_{\rm cm}^2/8\pi$, hence the energy of the region is $\sim H_{\rm cm}^2\xi/8\pi$, in accord with (3.56).

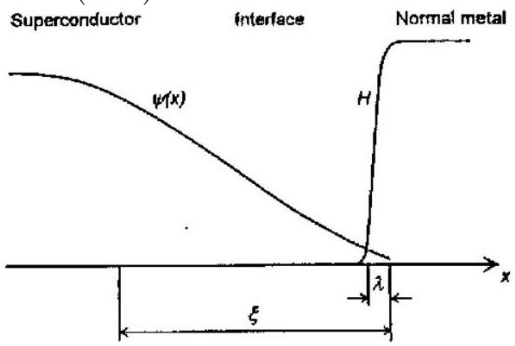


Fig. 3.4. Spatial variations of the order parameter ψ and the magnetic field H in the vicinity of the NS interface for $\kappa \ll 1$

This situation can be looked at from a different perspective. To keep the magnetic field out of the region with a reduced value of ψ (i.e., with the energy close to the energy of the normal metal), work must be done on the magnetic field to expel it from this region. This means that one must overcome a 'pressure' from the magnetic field $H_{\rm cm}^2/8\pi$ and shift its boundary by the distance ξ to the right. For this, the work $(H_{\rm cm}^2/8\pi)\,\xi$ must be done.

Fig. 3.5. Spatial variations of the order parameter ψ and the magnetic field H in the vicinity of the NS interface for $\kappa \gg 1$

(2) The case $\kappa \gg 1, \lambda \gg \xi$. The variations of $\psi(x)$ and $H(x)$ in this case are sketched in Fig. 3.5. This time, ψ varies much more rapidly than the magnetic field so that there is a region of thickness $\sim \lambda$ where the order parameter is $\psi \sim 1$ but a relatively strong magnetic field still remains. The presence of the magnetic field compels us to compare this region with the normal metal. Unlike the latter, the electrons in the region are coupled in Cooper pairs ($\psi \sim 1$). Hence its energy is less than the energy of the normal region to the right by the value of the condensation energy. As the thickness of the region is $\sim \lambda$ and the condensation energy density is $H_{\rm cm}^2/8\pi$, it is mordnotthnt - - tri2 to-il

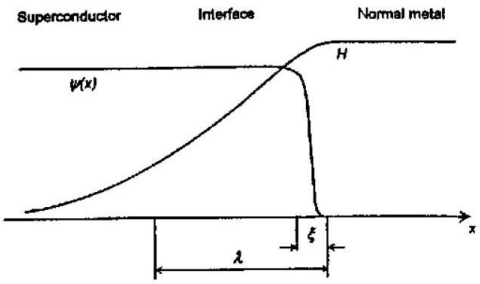


Fig. 3.5. Spatial variations of the order parameter ψ and the magnetic field H in the vicinity of the NS interface for $\kappa \gg 1$ field H in the vicinity of the NS in-(??)

From a different perspective, one can say that, in the case $\kappa \gg 1$, there is a region of thickness $\sim \lambda$ with $\psi \sim 1$ near the interface which is penetrated by the magnetic field. It implies that the energy of the system as a whole has decreased by the value of the work done to shift the field $H_{\rm cm}$ by the distance λ. We come to the following conclusions.

If $\kappa \ll 1$, then $\sigma_{\rm ns} > 0$. Such materials are called type-I superconductors.
If $\kappa \gg 1$, then $\sigma_{\rm ns} < 0$. Such materials are called type-II superconductors.
Evidently, at some value $\kappa \sim 1$, the energy $\sigma_{\rm ns}$ must be zero. Exact calculations show that this occurs at $\kappa = 1/\sqrt{2}$. Our conclusions are summarized in Table 3.1:

Table 3.1.

Type I	Type II
$\kappa < 1/\sqrt{2}$	$\kappa > 1/\sqrt{2}$
$\sigma_{\rm ne} > 0$	$\sigma_{\rm ns} < 0$

3.6.6 Limits of Applicability of GL Theory

Short Estimation

(write the background here!)

Теория Гинзбурга-Ландау является типичной теорией среднего поля. Учет флуктуаций ограничивает пределы применимости таких теорий. Критерием применимости является малость числа Гинзбурга-Леванюка $\mathrm{Gi} = T_c b^2/ac^3$.

(?? comment, why it is so??)

Подставляя полученные выше a, b и c, для числа Гинзбурга-Леванюка получаем оценку $\mathrm{Gi} \approx (T_c/\varepsilon_F)^4$. Таким образом, область применимости теории среднего поля в сверхпроводниках определяется критерием

$$\mathrm{Gi} = \left(\frac{T_c}{\varepsilon_F}\right)^4 \ll 1$$

Для реальных сверхпроводников число, стоящее в (13.33), как минимум на десять порядков меньше единицы. Это значит, что флуктуационная область на много порядков меньше тех вариаций температуры, которые можно контролировать в эксперименте. Таким образом, теория Гинзбурга-Ландау для сверхпроводников применима с огромной точностью.

3.6.7 1-4 Two kinds of superconductors by de Gennes

Our derivation of the London equation (1-9) assumes a slow variation in space of $v(r)$ or of the supercurrent $f_s(r)$. What do we mean by the word "slow"? In the condensed state, the

velocities of two electrons (1) and (2) are correlated if the distance between them R_{12} is smaller than a certain range. For pure metals, the correlation length is called ξ_0. Our derivation applies when $v(r)$ has a negligible variation over distances $\sim \xi_0$. To estimate ξ_0 we notice that the important domain in momentum space is defined by

$$\mathrm{E_F} - \Delta < \frac{\mathrm{p}^2}{2\ \mathrm{m}} < \mathrm{E_F} + \Delta \tag{1-18}$$

where $\mathrm{E_F}$ is the Fermi level. The thickness of the shell in p space defined by Eq. $(1-18)$ is $\delta \mathrm{p} \cong (2\Delta/\mathrm{v_F})$ (where $\mathrm{v_F} = \mathrm{p_F}/\mathrm{m}$ is the velocity at the Fermi level; we have made use of the fact that $\Delta \ll \mathrm{E_F}$ in all cases). A wave packet formed of plane waves whose momentum has an uncertainty $\delta \mathrm{p}$ has a minimum spatial extent $\delta \mathrm{x} \sim (\hbar/\delta \mathrm{p})$. This leads us to take

$$\xi_0 = \frac{\hbar v_F}{\pi \Delta} \tag{1-19}$$

(The factor $1/\pi$ is arbitrary but will become convenient later.) The length ξ_0 defined by Eq. $(1-19)$ is called the coherence length of the superconductor.

Equations (1-15) and (1-13) show that h, j_s, or v vary on a scale λ_L. Thus our derivation of the London equation holds only if $\lambda_L \gg \xi_0$.

(1) In simple (nontransition) metals as we have seen, λ_L is small (~ 300Å). The Fermi velocity v_F is large ($v_F > 10^8$ cm/sec) and according to Eq. (1-19) ξ_0 is also large ($\xi_0 \cong 10^4$ A for aluminum). Thus for these metals the London equation does not apply. In fact, they do exhibit the Meissner effect, but in order to calculate the penetration depth it is necessary to replace Eq. (1-9) by a somewhat more complicated relation, the form of which has been suggested by Pippard. We call these first kind (Type I) or Pippard superconductors and discuss them in Chapter 2.

(2) For transition metals and intermetallic compounds of the type $\mathrm{Nb_3Sn}, \mathrm{V_3Ga}$, the effective mass is very large, λ_L is large (~ 2000Å) and the Fermi velocity is small ($\sim 10^6$ cm/sec). Also, in these
compounds the transition temperature T_0 above which superconductivity disappears is found to be high (18°K in $\mathrm{Nb_3Sn}$). As we will see later, Δ is roughly proportional to T_0 and is therefore larger. For all these reasons ξ_0 is very small (~ 50Å). Therefore for this class of materials Eq. $(1-9)$ is well applicable in weak fields. We call these second kind (Type II) or London superconductors.

In order to complete this discussion, it is necessary to mention the case of superconducting alloys, for which the coherence length and penetration depth are modified by mean free path effects, which we will discuss later. Qualitatively, if the mean free path due to disorder in the structure is short, the coherence length becomes smaller than $\hbar v_F/\pi\Delta$ and λ_L is increased with respect to Eq. (1-7). Therefore it frequently occurs that the addition of impurities into a Pippard superconductor transforms it into a London superconductor.

The distinction here between the two classes is crucial for all experiments made in the presence of external fields. Historically, during a period of 20 years after the discovery of the Meissner effect, experiments were mainly carried out in first kind superconductors. The detailed study of second kind superconductors is much more recent. Paradoxically, the theory has followed the inverse order. Equation (1-9) was introduced by the London brothers in 1935, but the necessary modifications for first type superconductors was only proposed by Pippard in 1953. We now study in detail the magnetic properties of the two types.

3.6.8 The Wall Energy, derivation of $\varkappa_c = 1/2$

$$\kappa = \lambda/\xi = \frac{mc}{\hbar e}\left(\frac{\beta}{2\pi}\right)^{1/2}$$

Next we want to look more closely at the wall energy associated with an interface between a normal conducting domain and a superconducting domain. This positive [23] wall energy has been crucial for our understanding of the intermediate state. We will find that under certain conditions the generation of an interface does not require an expense of energy. This has to do with the type-II superconductors, the properties of which will be described in Section 4.7.

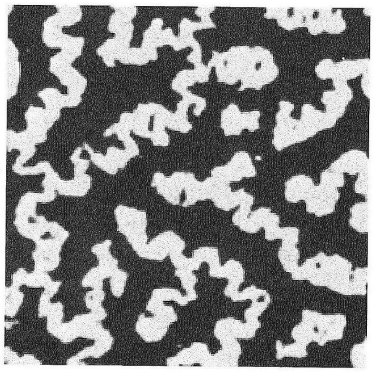


Figure 4.16 Intermediate state structure of an indium plate. The dark regions represent the superconducting domains. In purity: 99.999 at%; thickness: 11.7 mm; diameter: 38 mm; $B_\mathrm{a}/B_\mathrm{cth} = 0.1; T = 1.98$ K; T_c of indium: 3.24 K.

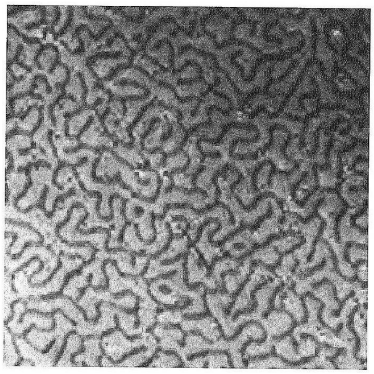


Figure 4.17 Intermediate state structure imaged by means of the Faraday effect. Pb layer with $7\mu m$ thickness; thickness of about 100 nm; magnetic fieds and EuF B_2:

In Chapter 1 we discussed other techniques in conjunction with the imaging of vortices perpendicular to the layer. The dark regions represent the superconducting domains. The imaged area is about 0.5 mm $\times$ 0.5 mm [34]. (By courtesy of Dr Kirchner, Siemens, the superconductor much larger than λ_L, and a constant assumptions, at an interface the magnetic fied must be ju equa to the cicica field B_cth . In the normal conductor we have $B > B_c$, vanishes within a layer thickness of about λ_L

The difference between a normal conducting domain and a superconducting domain within the same material comes from the fact that in the normal state doma cooper pair density n is zero, whereas in the superconductor it has a definite value $n_\mathrm{s}(T)$ depending on the material and the temperature. We recall that it is the condensation into Cooper pairs that effects the lowering of the free enthalpy and that below T_c results in the thermodynamic stability of the superconductor instead of the normal conductor

For our further discussion, it is crucial that at the interface the number density $n_s(T)$ cannot drop discontinuously from $n_{\rm s}(T)$ to zero. Because of the strong correlation between the Cooper pairs, a spatial variation of $n_{\rm s}(T)$ is stossible only within a distance larger than the Ginzburg-Landau coherence length $\xi_{\rm GL}$.

Figure 4.18 schematically indicates the situation at such an interface. In the normal domain on the left ($x < 0$), the magnetic field is just $B_{\rm cth}$ or larger. Therefore, within this domain the normal conducting state is stabilized, since the expulsion of the magnetic field would require more free enthalpy than can be supplied by he tanstion into the superconducting state [24)] In the superconducting domain

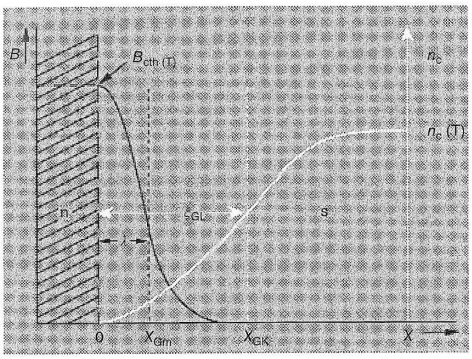


Figure 4.18 Spatial variation of B and n_s at an interface between a normal conducting (Here, x_{Gm} = "magnetic boundary" and x_{GK} = "condensate boundary.")

The boundy is only table if d diphcement to the left or to the right would lead to an increase or a decrease in the magnetic field, respectively.

($x > 0$), the Cooper pair density increases up to the equilibrium value $n_{\rm s}(T)$ within about the coherence length. Here, we have assumed that for the superconductor we have

$$\xi_{\rm GL} > \lambda_{\rm L}$$

At the boundary layer we must compare two contributions to the energy, namely the energy $E_{\rm B}$ associated with the expulsion of the magnetic field, and the energy $E_{\rm C}$ gained because of the condensation into Cooper pairs. In the normal conductor we have $E_{\rm B} = E_{\rm C} = 0$. The magnetic field is not expelled, and no Cooper pairs exist. Deep within the interior of the superconducting domain, for the application of the critical field $B_{\rm cth}$, we have at the boundary $E_{\rm B} = E_{\rm C} = (1/2\mu_0)\, B_{\rm cth}^2\, V$ (see Eq. (4.50)). The magnitude of the full condensation energy is just equal to the expulsion energy.

Within the boundary layer, the two energies do not have their full value. The magnetic field is not completely screened. Instead, it penetrates up to a depth $\lambda_{\rm L}$. The expulsion energy is reduced by the amount

$$\Delta E_{\rm B} = F\lambda_{\rm L}\frac{1}{2\mu_0}B_{\rm cth}^2$$

(where F is the area of the discussed boundary layer) compared to the case of complete expulsion up to the boundary line $x = 0$ in Figure 4.18. However, within the boundary layer the condensation energy is also reduced, since the number density of Cooper pairs is smaller than the equilibrium value $n_s(T)$. This reduction of the condensation energy is given by

$$\Delta E_{\rm C} = -F\xi_{\rm GL}\frac{1}{2\mu_0}B_{\rm cth}^2$$

where F is the area of the discussed boundary layer and ξ_{GLI} is the Ginzburg-Landau coherence length

For simplicity, we have defined λ_{L} and ξ_{GL} in such a way that the energy values ΔE_{B} and ΔE_{C} are equivalent to the case in which the magnetic field penetrates ΔE_{B} and ΔE_{C} are equivalent to the case in which the magnetic field penetrates completely up to the depth λ_{L} and then abruptly drops to zero and, on the other hand, the Cooper pair density abruptly jumps up to its full value $n_s(T)$ at ξ_{GL}. In this way, we have defined a "magnetic boundary" and a "condensate boundary." For the present case $\xi_{\mathrm{GL}} > \lambda_{\mathrm{L}}$, we find

$$\Delta E_{\mathrm{C}} - \Delta E_{\mathrm{B}} = (\xi_{\mathrm{GL}} - \lambda_{\mathrm{L}})\, F \frac{1}{2\mu_0} B^2_{\mathrm{cth}} > 0$$

Because of relation (4.67), the loss in condensation energy is larger than the gain in expulsion energy. In order to generate such a boundary, we must deliver the following wall energy α_{w} per unit area to the system:

$$\alpha_{\mathrm{w}} = (\xi_{\mathrm{GL}} - \lambda_{\mathrm{L}})\, F \frac{1}{2\mu_0} B^2_{\mathrm{cth}}$$

In Figure 4.19 we show the spatial variation of the energy densities ε_{B} and ε_{C} and their difference, which passes through a maximum.

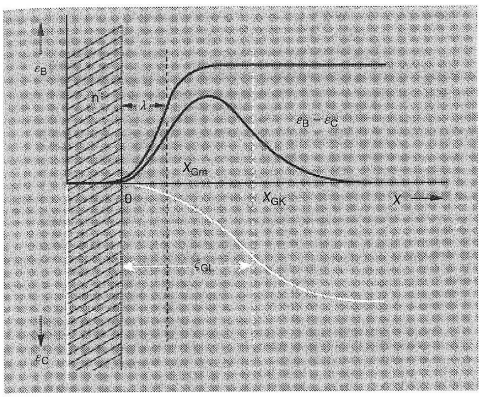


Figure 4.19 Spatial variation of the expulsion energy ε_B and of the condensation energy ε_C per unit volume at the boundary. We have $\int_0^{x \to x_{\mathrm{GK}}} (\varepsilon_{\mathrm{B}} - \varepsilon_{\mathrm{C}})\, F \mathrm{d}x = (\xi_{\mathrm{GL}} - \lambda_{\mathrm{L}})\, F \frac{1}{2\mu_0} B^2_{\mathrm{cth}}$.

Here we see very clearly that the generation of a boundary layer between a normal conducting domain and a superconducting domain in a homogeneous material requires energy if ξ_{GL} is larger than λ_{L}[2525] In the case where $\xi_{\mathrm{GL}} = \lambda_{\mathrm{L}}$, that is, if the magnetic boundary and the condensate boundary coincide, we have $\alpha_{\mathrm{w}} = 0$. In the case where $\xi_{\mathrm{GL}} < \lambda_{\mathrm{L}}$ formally we would obtain a negative wall energy. Now a new state, the so-called mixed state, is established. However, we must emphasize that these arguments based on the Ginzburg-Landau theory are valid only close to T_{c}

We will return to our discussion of the boundary between a normal conducting domain and a superconducting domain in conjunction with type-II superconductors. Next we want to discuss the pressure dependence of the superconducting state. Again we can apply the rules of thermodynamics. This section will conclude our treatment of type-I superconductors.

Influence of Pressure on the Superconducting State

In Sections 4.6.1 and 4.6.2 we discussed the difference between the free enthalpies of the normal and the superconducting states at constant pressure as a function of

We must note that the magnetic penetration depth at the boundary area in a metal can be slightly Cooper pair density. Here, we have ignored this difference.

the temperature. In order to simplify the formulas, for the quantitative discussion we have made three assumptions:

In the superconducting state, an external magnetic field should be completely expelled from the superconducting material, that is, there should be an ideal Meissner-Ochsenfeld effect. This assumption is well satisfied for macroscopic type-I superconductors over the whole stability range. It yielded the connection between the external field and the magnetization.

In order to find the magnetic moment m from the magnetization M, we must know the sample volume. In this context, we have used an approximation by ignoring the dependence of the volume upon the magnetic field B. Experience indicates that this dependence is very small.

Finally, we have taken the temperature dependence of the critical field B_c from experiment, and we have used the parabolic dependence $B_\mathrm{c}(T) = B_\mathrm{c}(0)\left[1 - (T/T_\mathrm{c})^2\right]$ as an analytic, satisfactory approximation.

All our discussions have been restricted to constant pressure. In this section, we take up the influence of pressure on superconductivity,

Already by 1925, Sizoo and Kamerlingh-Onnes had observed such an influence on the transition temperature T_c [35]. In Figure 4.20 we show the change of the transition temperature with increasing pressure for tin in the absence of an external magnetic field [36]. The transition temperature decreases with increasing pressure. The effect is not very large. In order to change T_c in tin by 0.1 K, we must apply pressures of about 2000bar[26)]

The behavior shown in Figure 4.20 is typical for many superconductors. However, there are also some materials (e.g., Ti, Zr, V, La, U) whose transition temperature increases with increasing pressure [37, 38].

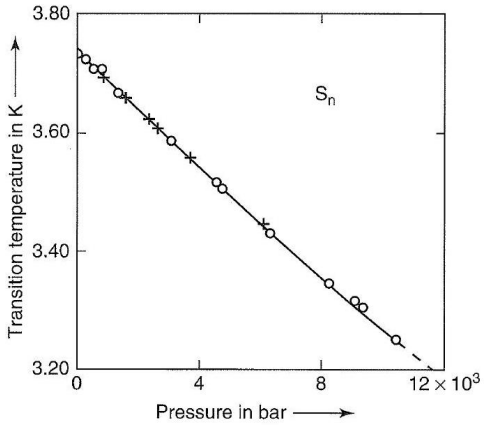


Figure 4.20 Pressure dependence of the transition temperature of tin [36]. 26) Pressure conversions: $1\mathrm{bar} = 10^5\ \mathrm{Pa} = 10^5\ \mathrm{N/m^2} = 1\mathrm{kp/cm^2}$.

The change of T_c under pressure in zero magnetic field must be connected with The of the critical field B_c with pressure. This influence of pressure on B a change of the chosen the results for cadis shown in Fgure 4.21 for cadmium [39]. We have cho sene resis cad mium, since they repres lemperatures combined with the application of high techniques. The very low temperatures combined

The pressure was generated in a so-called "ice bomb" [40]. A steel vessel is completely filled with water. During cooling below the freezing point a pressure of about 1800 bar develops, since the volume is kept constant. At constant pressure, the freezing of water is accompanied by a volume expansion of about 10%. If the liquid-solid phase transition takes place at constant volume, the resulting ice must develop under a pressure that is sufficiently high to effect a 10% volume reduction of the ice. This ice bomb method has served for performing many experiments on the behavior under pressure.

For the studies of Cd, the ice bomb was cooled down to about 6×10^{-2} K by means of so-called adiabatic demagnetization (a magnetic cooling technique), and the critical field B_c was measured down to these temperatures. In the case of C, the critical field B_c decreases with increasing pressure, as expected from the pressure dependence of T at zero magnetic field.

The reduction of the critical field under pressure means that the difference $G_n - G_0$ decreases with increasing pressure at constant B and T. If we know the $G_n - G_s$ decreases with increasing pressure at constant B and T. If we know the volumes of the normal conductor V_n and of the superconductor V_s as a function of our independent variables T, p, and B, we can calculate the p dependence of $G_1 - G$. However, the volume changes $\Delta V/V$ are very small, namely only a few 10^{-8}. Therefore, it represents an experimental challenge to demonstrate these

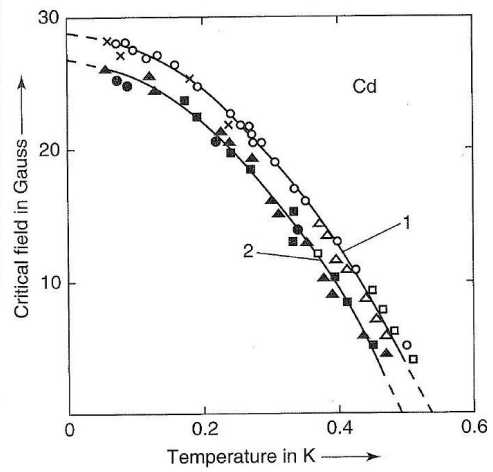


Figure 4.21 Temperature dependence of the critical field ($1\text{G} = 10^{-4}$ T) of cadmium at atmospheric pressure (curve 1) and at 1550 bar (curve 2). (From [39].) The original curves have many more data points than this reproduction.

changes convincingly. The measurements of B_c under pressure are somewhat simpler, and Figure 4.21 gives an example. From these measurements, we can determine the volume change during the phase transition by means of the Gibbs function G.

In general, we have the expression given in Eq. (4.11):

$$(\mathrm{d}G/\mathrm{d}p)_{T,B} = V$$

At the phase transition, we obtain [27]

$$(V_n - V_s)_{B=B_c} = V_s(B_c)\,\frac{\partial}{\partial p}\left(\frac{B_c^2}{2\mu_0}\right) = V_s(B_c)\,\frac{B_c}{\mu_0}\frac{\partial B_c}{\partial p}$$

This is analogous to the expression we have indicated in Section 4.2 for the entropy difference. From this expression we see that $V_n - V_s$ vanishes at T_c, because B_c is zero. Furthermore, we see that for $T < T_c$ we have $V_s > V_d$ if B_c decreases with p, that is, if $\partial B_c/\partial p < 0$, which is generally the case. The additional derivative with respect to p or T yields the difference of the compressibilities κ_s and κ_n or the difference of the thermal expansion coefficients α_s and α_n in the superconducting state and the normal state, respectively.

During the transition from the superconducting to the normal state, the volume changes have been measured directly using highly sensitive methods. Primarily, the length change of a sample in the form of a rod or a strip was determined. In Figure 4.22 we show the results for tin [41]. We see that $l_s > l_n$ for all temperatures $T > T_c$, as expected, where T_c denotes the transition temperature in zero magnetic field.

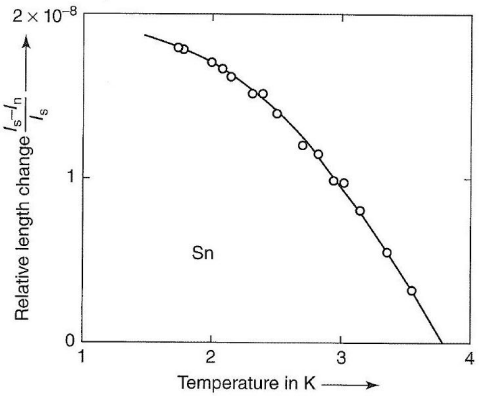


Figure 4.22 Relative length change $(I_s - I_n)\, I_s$ of a tin rod at the transition into the superconducting state. (From [41].)

At the transition from the superconducting to the normal conducting state, the volume change possible dependenced V_s/dp has been ignored

At the transition into the superconducting state, the sample expands. This is At tistent with the indications of our Gibbs function, for which we had assumed consise whe a perfect expusint of this length change near T_c requires a sensitivity of the length measurement of about 10^{-8} cm

Since the development of a microscopic theory, the BCS theory, studies of the pressure dependence of the transition temperature have gained much in importance. The application of hydrostatic pressure allows the continuous variation o the lattice constant of a substance. However, the lattice constant represents an important parameter for the quantum states of the electrons as well as of the lattice vibrations, the phonons. Since both quantities are highly important for superconductivity, new information for quantitative improvements of the microscopic conductivity, new information for quantits ive deressure. In Section 1.2 we have theory can be extracted from experiments under pressure. In Section 1.2 we have seen that our knowledge about the quantitative connections between the parameters of metals and superconductivity is still highly incomplete. For the transition the relation [28] (see Section 3.1.2, Eq. (3.6)):

$$T_c \propto \Theta_D \exp\left(-\frac{1}{N_n\left(E_F\right) V^*}\right)$$

We take the derivative with respect to p and obtain

$$\frac{\partial T_c}{\partial p} \propto \frac{\partial \Theta_D}{\partial p} \exp\left(-\frac{1}{N\left(E_F\right) V^*}\right) + \Theta_D \exp\left(-\frac{1}{N\left(E_F\right) V^*}\right)\left(\frac{1}{N\left(E_F\right) V^*}\right)^2 \frac{\partial\left(N\left(E_F\right) V^*\right)}{\partial p}$$

For determining the relative change of T_c, we divide by T_c

$$\frac{1}{T_c}\frac{\partial T_c}{\partial p} = \frac{1}{\Theta_D}\frac{\partial \Theta_D}{\partial p} + \left(\frac{1}{N\left(E_F\right) V^*}\right)^2 \frac{\partial\left(N\left(E_F\right) V^*\right)}{\partial p}$$

From the determination of the pressure dependence of T_c and from the Deby temperature Θ_D, we obtain information on the pressure dependence of the quantity $N\left(E_F\right) V^*$[38]

The change of the transition temperature under hydrostatic pressure can also serve for the construction of a superconducting manometer. Lead is particularly suitable, since it does not have any phase transition up to about 160kbar, and it is insensitive to lattice defects. Therefore, one can place a small lead wire into the pressure cell and determine the pressure within the cell at low temperatures from the transition temperature T_c of the wire. A calibration of this Pb manometer up to about 160 kbar has been carried out by Eichler and Wittig [42]. The insensitivity

Here, we denote the interaction potential between the electrons by V°, in order to distinguish it from the volume of the superconductor.

of T_c to lattice defects is important, since at the high pressures there is always a certain amount of plastic deformation, leading to the generation of lattice defects. This is even more pronounced at low temperatures.

So far we have discussed the influence of pressure within a single-crystalline phase. For many substances, under pressure one can obtain new crystalline phases, new modifications. Then we expect that during such a phase transition the superconducting properties are also changed. The high-pressure modification simply represents a new material.

Substances that do not show superconductivity at room pressure, but have superconducting phases at high pressure, are very interesting. In recent years, a number of such superconducting high-pressure phases have been found in semiconductors and in the transition range between metals and semiconductors (see also Table 2.1 and Figure 2.1).

Frequently, newly discovered superconductors are also studied early under high pressure. So in the case of the lanthanum-barium cuprate, one found a surprisingly large increase in T_c under hydrostatic pressure [43]. Since hydrostatic pressure reduces the lattice constant, also a "chemical" reduction of the lattice constant by inserting particularly small ions into the lattice could lead to T_c enhancement. C. W. Chu and coworkers utilized this argument and replaced the lanthanum by the smaller yttrium ion. In this way, they discovered the system $Y - Ba - Cu - O$ and prepared samples with values of T_c above 80 K[44][29]

Careful studies of the thermal expansion and of the effect of pressure were performed with single crystals without twin boundaries. The thermal expansion of $YBa_2Cu_3O_{7-x}$ was measured with a resolution of 10^{-9} cm. It shows a strong anisotropy also within the $Cu - O$ layers [45]. For a uniaxial pressure along the a-axis (Section 2.8.1), the experiments indicated a reduction of T_c, but along the b-axis an increase in T_c was found [46]. Similar results were obtained for other cuprates [47]. These observations were interpreted in terms of a change of concentration of the charge carriers in the Cu-O layers.

In the case of MgB_2, with increasing pressure a linear decrease in T_c was observed, in good agreement with the behavior expected from the BCS theory [48]. In the case of the iron pnictides, depending on the doping, one finds an increase or decrease in T_c[49].

3.7 Ginzburg Landau theory: advanced general features and details

3.7.1 Anderson-Higgs mechanics and Goldstone Theorem in SC

This Section is related to the Chapter on symmetry breaking. The idea is to put the Meissner effect into a wider perspective. Therefore, we will also use somewhat simpler notation in this Section and we will assume a relativistically invariant model, so that the expressions are more familiar. Apart from this, the Lagrangian that we write below is very much related to the functional $\mathcal{F}$ above.

Matter field

Asssume a matter field $\psi : \mathbb{R}^4 \to \mathbb{C}$ with Lagrangian

$$\mathcal{L}_M = \partial^\mu \psi^* \partial_\mu \psi - r_0 \psi^* \psi - \frac{u_0}{2} (\psi^* \psi)^2$$

where we use the signature $(1, -1, -1, -1)$ for the metric, so that the first term corresponds to $|\partial_t \psi|^2 - |\nabla \psi|^2$.

This is of course (apart from the temporal dependence) exactly the Gross-Pitaevskii functional. The extremal points of this Lagrangian (with uniform ψ) are

$$\begin{aligned} r_0 > 0 \Rightarrow &\text{ symmetric phase } \psi = 0 \\ r_0 < 0 \Rightarrow &\text{ symmetry broken phase } |\psi|^2 = -r_0/u_0 \end{aligned}$$

In the symmetry broken phase, it is instructive to choose new coordinates

$$\begin{aligned} \psi &= \mathrm{e}^{\mathrm{i}\phi}\left(\psi_0 + \eta\right) \\ \psi^* &= \mathrm{e}^{-\mathrm{i}\phi}\left(\psi_0 + \eta\right) \end{aligned}$$

Expanding the Lagrangian to second order gives

$$\mathcal{L} = -\frac{r_0}{u_0}\partial^\mu\phi\partial_\mu\phi + \partial^\mu\eta\partial_\mu\eta + 2r_0\eta^2$$

and ones sees that ϕ is massless whereas η has mass $-2r_0$. Again, this calculation was already done in the section on superfluids. We recall that the appearance of a massless field ϕ is a consequence of the Goldstone theorem.

EM field

Consider now also the EM Lagrangian, with gauge field $A : \mathbb{R}^d \to \mathbb{R}^4$

$$\mathcal{L}_{EM} = \mathcal{L}(A) = -\frac{1}{4}F^{\mu,\nu}F_{\mu,\nu}, \quad F^{\mu,\nu} = \partial^\mu A^\nu - \partial^\nu A^\mu$$

As one knows very well, this theory is free (quadratic) and has two massless modes (two physical polarizations)

Let us know couple the two fields

$$\mathcal{L} = \mathcal{L}_{EM} + \left(D^\mu\psi\right)^* D_\mu\psi - \left(u_0/2\right)\left(\psi^*\psi\right)^2, \quad D_\mu = \partial_\mu - \mathrm{i}qA_\mu$$

note the gauge invariance

$$\begin{aligned} \psi &\to \psi\mathrm{e}^{\mathrm{i}\chi(\boldsymbol{r})} \\ \psi^* &\to \psi^*\mathrm{e}^{-\mathrm{i}\chi(\boldsymbol{r})} \\ A^\mu &\to A^\mu + \frac{1}{q}\partial^\mu\chi \end{aligned}$$

(we chose units here such that $\hbar, c$ do not appear)

Symmetry broken phase

We start by again expanding around the solution $\psi = \psi_0$. We assume that the phase ϕ is small and in particular a univalued function (winding number 0). For the moment we do not yet expand the A field (anticipating the fact that instead of expanding around $A = 0$, we might as well expand around a pure gauge $A = \nabla\chi$). By performing the expansion in η, we get

$$\mathcal{L} = \left(D^\mu\eta\right)^* D_\mu\eta + \left|\psi_0\right|^2\left(D^\mu\mathrm{e}^{\mathrm{i}\phi}\right)^*\left(D_\mu\mathrm{e}^{\mathrm{i}\phi}\right) + 2r_0\eta^2 + \mathcal{L}_{EM}$$

Now we do the crucial step by choosing a gauge: Perform the gauge transformation with $\chi := \phi$ (gauge away the field ϕ, which is possible because of the assumption that it has vanishing winding number), then

$$\left|\psi_0\right|^2\left(D^\mu\mathrm{e}^{\mathrm{i}\phi}\right)^*\left(D_\mu\mathrm{e}^{\mathrm{i}\phi}\right) \to \left|\psi_0\right|^2 A^\mu A_\mu$$

Moreover, we will now also drop terms higher than of second order in the fields, including the field A (which can still be assumed small because χ was small as well.) This allows to simplify

$$(D^\mu \eta)^* D_\mu \eta \to \partial^\mu \eta \partial_\mu \eta$$

Finally, we use that $\mathcal{L}_{EM}$ is gauge invariant, so that $\mathcal{L}_{EM}(A - (\mathrm{i}/q)\phi) = \mathcal{L}_{EM}(A)$. Then we end up with the Lagrangian

$$\mathcal{L} = \partial^\mu \eta \partial_\mu \eta + |\psi_0|^2 A^\mu A_\mu + 2r_0 \eta^2 + \mathcal{L}_{EM}(A)$$

The big deal about this Lagrangian is that there is now a mass term for the A-field, whereas the Goldstone mode ϕ has dissappeared. As one says, the gauge particle (photon) has eaten the Goldstone boson (ϕ) and it has become massive. The symmetry breaking of ϕ has been traded for a breaking of gauge invariance. Indeed, if you interpret the resulting Lagrangian, with variables η, A as given, it does not have gauge-invariance. This should of course not be taken seriously, the gauge invariance is not really a symmetry but a redundancy in the description, so it cannot be broken. It is just that in the gauge where $\phi = 0$, the result is most transparent.

How did the 'Goldstone Theorem' get violated?

The Goldstone theorem, as stated in Section 3.2, relied on the intuition that, if one has continuous symmetry breaking, than one can form spin waves as excitations. The energy of such a spin wave then vanishes when the momentum goes to 0. However, this intuition relies crucially on the fact that the interaction is local, i.e. merely a function of the difference between nearby spins. If we allow long-range interactions, than the calculation of the energy of a smooth domain wall (and hence of a spin wave) would break down. In fact, this was explicitly demonstrated for the case of a discrete domain wall in Section??.

Hence, the Goldstone theorem should not be expected to hold for long-range interactions. This is why the Higgs-Anderson mechanism is possible, because electromagnetism is a long-range interaction.

3.7.2 Typical Subtle Features of GL theory

В уравнениях ГЛ m - это масса электрона или эффективная масса электрона? (???)

This is an effective mass.
(?? proof from comparison to some experiment???)

What is the order parameter?

(maybe I'll write it in the beginning of GL theory)

Why GL theory is written not in terms of Hamiltonian?

(I'll answer later, maybe we can do it by Hamiltonian as well??)

How to take into account field from moving electrons and what is exactly B in the functional?

(I'll think later about it)

When do we need F, or G, or Ω functionals for GL theory?

(I'll think later about it)

3.7.3 Fluctuation effects near SC phase transitions: basic concepts

19.1. Оценка ширины флуктуационной области.

Теория Гинзбурга - Ландау оперирует с распределением параметра порядка $\Psi(\mathbf{r})$, предполагая, что оно реализует минимум свободной энергии $G(\Psi)$ (при заданных температуре и магнитном поле), т.е. при его определении уже проведено усреднение по всем термодинамическим флуктуациям. Как представить себе такие флуктуации? Самый наглядный пример - критическая точка жидкость-пар: вблизи критической точки плотность пара флуктуирует во времени и пространстве, $n(\mathbf{r},t) = \bar{n} + \delta n(\mathbf{r},t)$. Явления вблизи критической точки тоже можно, до известной степени, представлять себе как аналогичные фазовому переходу II рода; здесь роль параметра порядка играет отклонение Δn средней плотности $\bar{n}$ от ее значения в критической точке n_0. Таким образом, флуктуации плотности $\delta n(\mathbf{r},t)$ приводят к появлению "флуктуационных зародышей" жидкости в паре (когда $\Delta n + \delta n(\mathbf{r},t) > 0$) и наоборот. Чем ближе система к критической точке, тем больше оказывается амплитуда характерных флуктуаций плотности и характерное время t_c существования таких зародышей. Аналогичным образом, выше точки сверхпроводящего перехода возникают и исчезают зародыши сверхпроводящего состояния, т.е. на большое (в микроскопическом масштабе - по сравнению с $\hbar/k_{\mathrm{B}}T_c$) время возникают локально сверхпроводящие области. Параметр порядка, описываемый теорией Гинзбурга - Ландау, возникает после усреднения по всем таким флуктуациям. При этом считается, что можно усреднять по различным флуктуациям независимо, т.е. пренебрегая корреляциями между ними. Такое предположение в любом случае оправдано, пока пространственный размер L рассматриваемых флуктуаций мал по сравнению с корреляционной длиной параметра порядка $\xi(T)$, однако при $L \sim \xi(T)$ оно справедливо лишь при условии $|\delta\Psi(\mathbf{r},t)| \equiv |\Psi(\mathbf{r},t) - \Psi| \ll |\Psi|$. Более точно это же условие записывается как

$$\langle \delta\Psi^*(\mathbf{r})\delta\Psi(0)\rangle|_{r\sim\xi(T)} \ll \left|\Psi^2(T)\right| \tag{19.1}$$

В теории Гинзбурга-Ландау предполагается, что условие (19.1) выполнено. Из общей теории фазовых переходов II рода [28], [34] известно, что это предположение становится неверным достаточно близко к точке фазового перехода. Окрестность температуры перехода $(\Delta T)_{\text{флукт}} = T - T_c$, где флуктуации оказываются сильными, называется флуктуационной областью. Поскольку теория Гинзбурга - Ландау строилась для окрестности точки перехода, $|\Delta T| \ll T_c$, область ее применимости существует лишь при условии $(\Delta T)_{\text{флукт}} \ll T_c$, или, иначе говоря, при условии малости так называемого параметра Гинзбурга $\mathrm{Gi} \equiv (\Delta T)_{\text{флукт}}/T_c$. Величина параметра Гинзбурга определяется микроскопической природой взаимодействия, приводящего к фазовому переходу II рода.

В некоторых случаях, как, например, при фазовом переходе ^{4}He в сверхтекучее состояние (который с точки зрения феноменологической теории фазовых переходов очень похож на сверхпроводящий фазовый переход), $\mathrm{Gi} \sim 1$, и область применимости теории Гинзбурга - Ландау вообще отсутствует. В большинстве сверхпроводников, напротив, флуктуационные эффекты очень слабы в объемных образцах. Исключение составляют ВТСП и некоторые другие сильно анизотропные сверхпроводники, например, $NbSe_2$ [35]. Кроме того, даже в «обычных» сверхпроводниках величина флуктуаций сильно возрастает при переходе от объемных образцов к тонким пленкам или проволокам. Ниже мы найдем связь между относительной шириной

флуктуационной области Gi и микроскопическими параметрами сверхпроводника для различных размерностей $d = 1, 2, 3$ образца.

Начнем с простой качественной оценки: изменение свободной энергии $F_{sn} = F_{s0} - F_n$ вследствие перехода в сверхпроводящее состояние в области размером с длину корреляции $\xi(T)$ имеет порядок $F_{sn}(T) \sim H_{cm}^2(T)\xi^3(T) \sim H_{cm}^2(0)\xi_0^3 \cdot (1 - T/T_c)^{1/2} = F_{sn}(0)(1 - -T/T_c)^{1/2}$. Это изменение свободной энергии положительно при $T > T_c$, т.е. сверхпроводящие области возникают лишь флуктуационно; напротив, при $T < T_c$ устойчиво сверхпроводящее состояние, а флуктуации приводят к его временному разрушению, т.е. появлению зародышей нормальной фазы. Вероятность флуктуационного образования зародышей с пространственным масштабом $L \sim \xi(T)$ определяется соотношением $F_{sn}(T)$ и тепловой энергии $k_{\mathrm{B}}T$: если $k_{\mathrm{B}}T \ll F_{sn}(T)$, то зародыши размера порядка $\xi(T)$ образуются экспоненциально редко, и условие (19.1) выполнено. Таким образом, получаем условие

$$\left|1 - \frac{T}{T_c}\right| \geqslant \left(\frac{k_{\mathrm{B}}T_c}{H_{cm}^2(0)\xi_0^3}\right)^2 \equiv \mathrm{Gi} \tag{19.2}$$

Убедимся, что величина Gi, определяемая правой частью (19.2), действительно очень мала. Для этого воспользуемся формулой (15.8) для H_{cm} и оценкой $\xi_0 \simeq \hbar v_{\mathrm{F}}/2\pi k_{\mathrm{B}}T_c$, которая будет обсуждаться ниже. Используя также выражение (6.3) для глубины проникновения $\lambda(0)$ и считая, что плотность сверхпроводящих
электронов n_s порядка полной их плотности $n \sim k_{\mathrm{F}}^3$, окончательно получим

$$\mathrm{Gi} \sim (k_{\mathrm{F}}\xi_0)^{-4} \ll 1. \tag{19.3}$$

Во всех известных сверхпроводниках длина когерентности ξ_0 велика по сравнению с межэлектронным расстоянием k_{F}^{-1}, что связано со слабостью куперовского притяжения; напротив, межатомное взаимодействие в жидком ^{4}He очень сильное, и аналогичная длина когерентности $\xi_{\mathrm{ст}}(0)$ для сверхтекучего состояния близка к межатомному расстоянию. Для сверхпроводников наименьшее известное значение параметра $k_{\mathrm{F}}\xi_0 \simeq 10$ относится к ВТСП и некоторым органическим сверхпроводникам [36]. Здесь надо заметить, что формулы (19.2), (19.3) неприменимы непосредственно к упомянутым сильно анизотропным материалам, т.к. были получены для изотропных трехмерных сверхпроводников. [1)] В большинстве «классических» сверхпроводников $k_F\xi_0 \geqslant \geqslant 100$, так что ширина флуктуационной области Gi пренебрежимо мала. Надо, однако, заметить, что сделанное при выводе оценки (19.3) предположение, что $n_s \sim k_{\mathrm{F}}^3$, применимо (по порядку величины) лишь для чистых сверхпроводников с длиной свободного пробега на примесях $l \gg \xi_0$. В «грязном» пределе $l \ll \ll \xi_0$ (что иначе может быть выражено как условие $k_{\mathrm{B}}T_c\tau/\hbar \ll 1$, где $\tau = l/v_{\mathrm{F}}$ - время свободного пробега) длина когерентности существенно уменьшается: $\xi_{0d} \simeq \sqrt{\xi_0 l} \simeq \sqrt{\hbar D/2\pi k_{\mathrm{B}}T_c}$, где $D = \frac{1}{3}v_{\mathrm{F}}l$-коэффициент диффузии в металле с примесями. В то же время термодинамическое критическое поле H_{cm} и температура перехода T_c не зависят (в главном приближении) от концентрации примесей (доказательство этого утверждения, называемого иногда "теоремой Андерсона», мы обсудим в 45). Приведенные выше оценки для ξ_0 и ξ_{0d} можно понять следующим образом: масштаб времени, соответствующий по соотношению неопределенности энергии связи пары $\Delta \sim k_{\mathrm{B}}T_c$ (см. §§44, 45), есть $\tau_p \sim \hbar/\Delta \sim \hbar/k_{\mathrm{B}}T_c$ и по порядку величины определяет время прохождения электроном области размером в

• Формулу (19.2) можно обобщить с учетом анизотропии, если заменить ξ_0^3 на произведение длин когерентности $(\xi_{0x}\xi_{0y}\xi_{0z})$ по всем трем направлениям.

длину когерентности. Учитывая независимость Δ от беспорядка, получаем в чистом случае $\xi_0 \sim v_{\rm F}\tau_p \sim \hbar v_{\rm F}/k_{\rm B}T_c$, а в грязном $-\xi_{0d} \sim \sim (D\tau_p)^{1/2} \sim (\hbar D/k_{\rm B}T_c)^{1/2}$, т. е. $\xi_{0d}^2 \sim \xi_0 l$.

Влияние примесей на ширину флуктуационной области ${\rm Gi}_d$ в грязном пределе проще всего усмотреть тогда из уравнения (19.2):

$$ {\rm Gi}_d \simeq {\rm Gi}\left(\frac{\hbar}{k_{\rm B}T_c\tau}\right)^3 \sim \frac{1}{\left(k_{\rm F}^2\xi_{0d}l\right)^2} \tag{19.4} $$

Перейдем теперь к оценке параметра Gi для низкоразмерных сверхпроводников - тонких пленок толщиной d и проволок поперечным сечением S. Теперь в качестве объема характерного «зародыша» следует брать либо $\xi^2(T)d$, либо $\xi(T)S$; будем также считать, что T_c и ξ_0 не меняются при уменьшении d или S. В результате для чистого сверхпроводника вместо (19.2) получим

$$ {\rm Gi}^{(2D)} = \frac{k_{\rm B}T_c}{H_{cm}^2(0)\xi_0^2 d} \sim \frac{1}{k_{\rm F}^2\xi_0 d} \tag{19.5} $$

$$ {\rm Gi}^{(1D)} = \left(\frac{k_{\rm B}T_c}{H_{cm}^2(0)\xi_0 S}\right)^{2/3} \sim \left(k_{\rm F}^2 S\right)^{-2/3}. \tag{19.6} $$

Разумеется, формулы (19.5) и (19.6) имеют смысл постольку, поскольку получающиеся из них значения ${\rm Gi}^{(2D)}, {\rm Gi}^{(1D)} \gg {\rm Gi}$. При выводе этих оценок мы предполагали, что толщина пленки d или поперечный размер проволоки $S^{1/2}$ малы по сравнению с длиной корреляции $\xi(T)$ в интересующей нас окрестности вблизи точки перехода - чем и вызвано эффективное уменьшение размерности образца. При этом низкотемпературная длина когерентности ξ_0 может быть и меньше $d, S^{1/2}$, и тогда при низких температурах сверхпроводник эффективно трехмерен. Как правило, низкоразмерные сверхпроводники имеют (по технологии их приготовления) довольно малую длину пробега $l \ll \xi_0$, т. е. реализуется грязный предел. Для оценки ширины флуктуационной области можно
в этом случае использовать первые из равенств (19.5), (19.6), заменяя ξ_0 на ξ_{0d} и учитывая независимость H_{cm} от беспорядка. В результате получим

$$ {\rm Gi}_d^{(2D)} \sim \left(k_{\rm F}^2 l d\right)^{-1} \sim g^{-1} \tag{19.7} $$

$$ {\rm Gi}_d^{(1D)} \sim \left(\frac{\xi_{0d}}{k_{\rm F}^2 S l}\right)^{2/3} \tag{19.8} $$

где $g = \frac{\hbar}{e^2}\sigma_{2d}$-безразмерная проводимость пленки на квадрат, а σ_{2d} - проводимость пленки на квадрат в нормальном состоянии. Интересно, что оценки (19.6) и (19.7) для Gi в одномерном чистом и двумерном грязном случаях оказались не зависящими от ξ или других собственно сверхпроводящих параметров, они определяются чисто металлическими свойствами - числом каналов проводимости $N_{\rm кан} \sim S/\lambda_{\rm F}^2 \sim k_{\rm F}^2 S$ в проволоке, либо безразмерной проводимостью g пленки, соответственно. Для совсем тонких пленок и проволок оценки (19.7), (19.8) должны быть уточнены, т. к. рассеяние электронов на поверхности образца может в этом случае оказаться наиболее сильным источником беспорядка, уменьшающим длину когерентности ξ_0 и тем самым увеличивающим Gi. Наконец, необходимо заметить, что формулы (19.3), (19.5) - (19.8) были получены лишь как порядковые оценки, указывающие на зависимость Gi от параметров, но не содержащие правильных численных коэффициентов; более аккуратное вычисление показывает, например, что ${\rm Gi}_d^{(2D)} \simeq 0.1g^{-1}$ (см. (19.17)).

19.2. Флуктуационные эффекты в окрестности T_c. Обсудим теперь, к каким наблюдаемым физическим эффектам приводят флуктуации параметра порядка, причем начнем со

[2)] Дело в том, что при решении задач по электропереносу вдоль тонких пленок удобно пользоваться величинами сопротивления на квадрат R^{2D} и проводимости на квадрат σ^{2D}, т.е. величинами для пленки с толщиной d и одинаковыми планарными размерами $L \times L$. Легко видеть, что эти величины от размера квадрата L не зависят и связаны с удельными сопротивлением и проводимостью соотношениями $R^{2D} = \rho/d, \sigma^{2D} = \sigma d$.

случая трехмерного сверхпроводника. Самый универсальный из таких эффектов, присутствующий при всех фазовых переходах II рода - изменение поведения теплоемкости $C(T)$ при $T \simeq T_c$ по сравнению с предсказанием теории Ландау. Например, при сверхтекучем фазовом переходе в ^{4}He (где Gi $\sim$ 1) теплоемкость логарифмически расходится в точке перехода, $C(T) \propto -\ln|1 - -T/T_c|$, вместо того чтобы испытывать конечный скачок при $T = T_c$. Общая теория фазовых переходов II рода [34] предсказывает, что в непосредственной окрестности T_c поведение системы описывается лишь симметрией параметра порядка и пространственной размерностью. Сверхтекучий фазовый переход в ^{4}He, как и обычный сверхпроводящий, описывается комплексным однокомпонентным параметром порядка, поэтому такая же логарифмическая аномалия теплоемкости должна наблюдаться и в сверхпроводниках в узкой окрестности точки перехода $|1 - T/T_c| \leqslant$ Gi Однако, из-за крайней малости Gi в объемных сверхпроводниках это явление почти никогда не наблюдается. Исключение представляют высокотемпературные сверхпроводники; в частности, на рис. 19.1 приведен график теплоемкости, измеренной вблизи сверхпроводящего перехода в YBaCuO в работе [37]. Вне флуктуационной области (т. е. при $|1 - T/T_c| \geqslant$ Gi) поправки к теплоемкости, обусловленные флуктуациями, малы:

$$\frac{\delta C(T)}{C_0} \sim \begin{cases} \left(\frac{\text{Gi}}{|1-T/T_c|}\right)^{1/2} & \text{при } d = 3, \\ \frac{\text{Gi}^{(2D)}}{|1-T/T_c|} & \text{при } d = 2, \end{cases} \tag{19.9}$$

где $C_0 \equiv C_s - C_n = T_c\widetilde{\alpha}^2/\beta$ - скачок теплоемкости при сверхпроводящем переходе (см. (3.12), (13.5) и (13.6)). Как видно из (19.9), в случае $d = 2$ поправки к теплоемкости растут заметно быстрее с приближением к T_c, однако измерять теплоемкость тонких пленок очень сложно из-за их малого объема. Интересный компромисс обнаруживается, если рассмотреть квазидвумерный (слоистый) объемный сверхпроводник с очень слабой связью между слоями (например, ВТСП семейства BiSrCaCuO): с понижением температуры в довольно широкой окрестности T_c взаимодей ствие между слоями несущественно и применима вторая из формул (19.9), описывающая "двумерные" флуктуации параметра порядка.

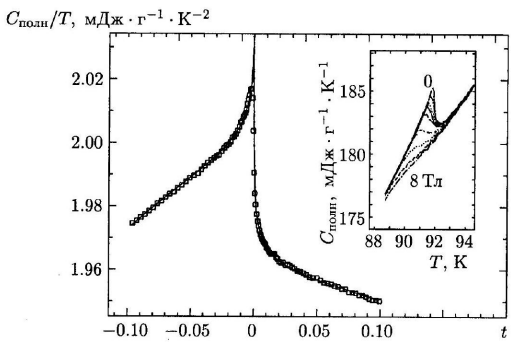


Рис. 19.1. Критическая аномалия теплоемкости монокристалла YBaCuO[37], близкая по форме к «-особенности» при сверхтекучем переходе в ^{4}He.

Взаимодействие критических флуктуаций меняет в области $\left(\frac{T}{T_c}-1\right) \leqslant \mathrm{Gi}$ вид температурных зависимостей и других величин, помимо теплоемкости. Так, длина корреляции $\xi(T) \propto (T - -T_c)^{-\nu}$, а глубина проникновения $\lambda \propto (T-T_c)^{-\nu/2}$, где критический показатель ν близок к 2/3 для трехмерной системы с комплексным параметром порядка [34].

Другая интересная для наблюдения флуктуационных поправок величина - диамагнитная восприимчивость $\chi(T)$. Действительно, в нормальном металле χ очень мала (обычно $\chi \leqslant 10^{-5}$); в то же время в сверхпроводнике имеется полный диамагнетизм, $\chi = -(4\pi)^{-1}$, т.е. в узкой окрестности перехода происходит скачок диамагнитной восприимчивости на несколько порядков. Поэтому следует ожидать, что сверхпроводящие флук туации будут давать относительно заметный вклад в χ и при $(1-T/T_c) \gg \mathrm{Gi}$. Магнитный момент сверхпроводника $M = -\partial G/\partial H_0$, где G - свободная энергия во внешнем поле H_0, определяемая согласно общим правилам статистической физики как

$$\exp\left(-G/k_{\mathrm{B}}T\right) = \int \mathcal{D}\Psi(\mathbf{r}) \exp\left(-G[\Psi(\mathbf{r})]/k_{\mathrm{B}}T\right) \tag{19.10}$$

где значок $\mathcal{D}$ обозначает интегрирование по всем возможным конфигурациям параметра порядка $\Psi(\mathbf{r})$ с весом, определяемым свободной энергией Гинзбурга-Ландау $G[\Psi(\mathbf{r})]$ (см. уравнение (14.1)). При $\left(\frac{T}{T_c}-1\right) > \mathrm{Gi}$ членом $|\Psi|^4$ в (14.1) можно пренебречь, и функциональный интеграл (19.10) сводится к произведению независимых интегралов

$$\exp\left(-G/k_{\mathrm{B}}T\right) = \prod_{\mu} da_\mu d\bar{a}_\mu \exp\left(-E_\mu \left|a_\mu\right|^2\right) \tag{19.11}$$

где использовано разложение $\Psi(\mathbf{r}) = \sum\limits_{\mu} a_\mu \psi_\mu(\mathbf{r})$ поля параметра порядка по собственным функциям оператора

$$\mathcal{H}_2 = \frac{1}{4m}\left(-i\hbar\nabla - \frac{2e}{c}\mathbf{A}\right)^2 + \alpha$$

соответствующего квадратичной части функционала Гинзбурга-Ландау (здесь $\alpha = \widetilde{\alpha}\,(T-T_c)$, где $\widetilde{\alpha} = \mathrm{const}$); величины E_μ - соответствующие собственные значения. Интеграл по каждой паре переменных $a_\mu, \bar{a}_\mu$ дает множитель $\pi k_{\mathrm{B}}T/E_\mu$. В результате диамагнитный момент равен

$$M = -\frac{\partial G}{\partial H_0} = -k_{\mathrm{B}}T \sum_{\mu} \frac{\partial \ln E_\mu}{\partial H_0} \tag{19.12}$$

Вычислим флуктуационную диамагнитную восприимчивость для самого простого случая [38] - шарика радиуса $R \ll \xi(T)$, когда в сумме (19.12) достаточно оставить лишь член с наименьшим собственным значением E_0, соответствующим постоянной по объему шарика собственной функции $\psi_0 = (4\pi R^3/3)^{-1/2}$ с нормировкой $\int d^3r \psi_0^2(\mathbf{r}) = 1$. Величину E_0 найдем просто как среднее значение оператора $\mathcal{H}_2$:

$$E_0 = \alpha + \psi_0^2 \int\limits_{r<R} d^3r \frac{e^2}{mc^2} A^2(\mathbf{r}) = \alpha + \frac{e^2 H_0^2 R^2}{10mc^2} \tag{19.13}$$

При вычислении интеграла в (19.13) мы выбрали векторный потенциал в виде $\mathbf{A} = \frac{1}{2}\left[\mathbf{H}_0\mathbf{r}\right]$; при этом $\mathbf{A}$ везде перпендикулярен нормали к поверхности шара, что необходимо

для удовлетворения граничного условия $\left(-i\nabla\psi - \frac{2e}{\hbar c}\mathbf{A}\right)_{r=R} = 0$ при $\psi_0 = \text{const}$ внутри шара. Комбинируя уравнения (19.12) и (19.13), получаем

$$M(H_0) = -\frac{e^2 T_c R^2 H_0}{5m^2c^2\left(\widetilde{\alpha}(T - T_c) + \frac{e^2 H_0^2 R^2}{10mc^2}\right)} \tag{19.14}$$

Таким образом, линейная часть флуктуационной диамагнитной восприимчивости шарика на единицу его объема равна

$$\chi_{\text{флукт}}(T) = \frac{3e^2 T_c}{20\pi mc^2 R\widetilde{\alpha}(T - T_c)} \tag{19.15}$$

Магнитная восприимчивость металла имеет порядок $\chi_0 \sim \frac{e^2 k_\text{F}}{mc^2}$; выражая по порядку величины $\tilde{\alpha}$ через ξ_0 и T_c с помощью (14.14), находим отношение флуктуационного вклада в восприимчивость к нормальному:

$$\frac{\chi_{\text{флукт}}(T)}{\chi_0} \sim \frac{\min(\xi_0, l)}{R}\frac{T_c}{T - T_c} \tag{19.16}$$

Как видно из (19.16), флуктуационный вклад в восприимчивость не выражается через число Gi, более того, он падает при уменьшении длины когерентности ξ_0 либо (в грязном пределе) примесной длины пробега l, несмотря на то, что число Gi при этом растет. В случае объемного сверхпроводника отношение $\chi_{\text{флукт}}/\chi_0 \sim \left(\frac{T_c}{T - T_c}\right)^{1/2}$ (вычисление см. в [39]) вообще не зависит от параметров материала. Такое отличие флуктуационных поправок к магнитной восприимчивости (по сравнению с поправками к теплоемкости и проводимости - см. ниже) происходит из-за того, что диамагнитный отклик сверхпроводника нелокален в пространстве; иначе говоря, он определяется экранирующими токами, текущими по его поверхности. Именно поэтому, в частности, в выражение (19.16) входит радиус шарика R.

Флуктуации сверхпроводящего параметра порядка приводят также к росту проводимости металла с понижением температуры к T_c. Этот эффект был предсказан Асламазовым и Ларкиным [40] и надежно подтвержден экспериментально. Мы качественно обсудим происхождение эффекта Асламазова - Ларкина в следующем разделе, а здесь приведем лишь результаты вычислений отношения флуктуационных поправок к нормальной проводимости грязных сверхпроводников различных размерностей d вблизи T_c:

$$\begin{gathered}
\left(\frac{\Delta\sigma_{AL}}{\sigma}\right)^{(1D)} = \frac{3\sqrt{\pi}}{4\sqrt{2}}\frac{1}{k_\text{F}^2 l}\sqrt{\frac{T_c}{D}}\left(\frac{T_c}{T - T_c}\right)^{1/2} = \\
= \left(\frac{\text{Gi}_d}{T/T_c - 1}\right)^{1/2}, \\
\left(\frac{\Delta\sigma_{AL}}{\sigma}\right)^{(2D)} = \frac{1}{16g}\frac{T_c}{T - T_c} = \frac{\text{Gi}_d^{(2D)}}{T/T_c - 1}, \\
\left(\frac{\Delta\sigma_{AL}}{\sigma}\right) = \left(\frac{\Delta\sigma_{AL}}{\sigma}\right)^{(3D)} = \frac{5.4}{(T_c\tau)^{1/2}}\frac{1}{k_\text{F}^2 S}\left(\frac{T_c}{T - T_c}\right)^{3/2} = \\
= \left(\frac{\text{Gi}_d^{(1D)}}{T/T_c - 1}\right)^{3/2}.
\end{gathered} \tag{19.17}$$

Iараметры $\mathrm{Gi}_d, \mathrm{Gi}_d^{(2D)}$ и $\mathrm{Gi}_d^{(1D)}$, введенные в формулах (19.17), сошпадают по порядку величины с оценками (19.4), (19.7) и (19.8);
мы выбрали флуктуационные поправки именно к проводимости, чтобы дать точное определение параметров Gi, поскольку проводимость удобнее всего измерять экспериментально. Микроскопическое вычисление поправок к теплоемкости [40] показывает, что численные коэффициенты в формулах (19.9) порядка единицы, т.е. ширина флуктуационной области, определенная по критическому поведению теплоемкости, такая же, как и при ее определении по проводимости.

19.3. Парапроводимость (эффект Асламазова-Ларкина). Флуктуационный вклад в проводимость металла вблизи сверхпроводящего перехода называют также парапроводимостью. Мы приведем сейчас качественное объяснение этого эффекта (см. также [41]), предсказанного Асламазовым и Ларкиным при помощи микроскопической теории [40]. Начнем с известной формулы Друде для остаточной (низкотемпературной) проводимости металла с примесями:

$$\sigma = \frac{e^2 n_e \tau_{tr}}{m} \tag{19.18}$$

В этой формуле n_e - плотность электронов проводимости, τ_{tr} транспортное время свободного пробега электронов на примесях (т. е. время за которое электрон заметно меняет направление своего импульса), m - масса электрона. В окрестности сверхпроводящего перехода в металле имеются флуктуационно возникшие куперовские пары. Их дополнительный вклад в проводимость мы и оценим с помощью формулы типа (19.18). Для этого необходимо понять, чем следует заменить параметры n_e и τ_{tr} в случае переноса заряда флуктуационными парами.

Мы уже знаем, что при $T < T_c$ величина $\langle\Psi\rangle^2$ играет роль плотности куперовских пар. Выше точки перехода эта величина равна нулю, в соответствии с тем, что настоящих пар с бесконечным временем жизни здесь нет. Однако можно рассмотреть величину $n(p) = \langle\psi_{\mathbf{p}}\psi_{-\mathbf{p}}\rangle$, которая представляет собой плотность флуктуационных пар, имеющих импульс $\mathbf{p}$. Величине $n_e\tau_{tr}$ в формуле (19.18) будет соответствовать теперь $\int d\mathbf{p} n(\mathbf{p})\tau(\mathbf{p})$.

Здесь $\tau(\mathbf{p})$ - время жизни флуктуационной пары с импульсом p, которое, как мы покажем ниже, сильно зависит от величины импульса $|\mathbf{p}|$. Начнем с оценки зависимости $n(\mathbf{p})$. Для этого надо лишь представить квадратичную часть функционала Гинзбурга-Ландау в виде (19.11), где теперь собственными функциями $\psi_\mu(\mathbf{r})$ являются просто плоские волны $e^{i\mathrm{p}r}$, а собственные значения $E_p = \hbar^2 p^2/4m + \alpha$. Соответственно, для $n(\mathbf{p}) = \langle\psi_{\mathbf{p}}\psi_{-\mathbf{p}}\rangle$ получаем

$$n(\mathbf{p}) = \frac{k_\mathrm{B}T}{\alpha + \hbar^2 p^2/4m} \tag{19.19}$$

Займемся теперь оценкой времени $\tau(\mathbf{p})$. В отличие от времени жизни τ_{tr} электрона с заданным импульсом, время жизни флуктуационной пары определяется не рассеянием на примесях, а распадом на отдельные электроны. Это время можно оценить без использования микроскопической теории, если произвести простейшее обобщение уравнений ГинзбургаЛандау для слабонеравновесной ситуации, когда параметр порядка $\Psi(\mathbf{r})$ не совпадает со своим равновесным значением Ψ_0. В этом случае вариация функционала ГЛ не равна нулю и (пределяет скорость возвращения величины параметра порядка к равновесному значению (в данном случае к нулю, т.к. $T >> T_c$:

$$\gamma\frac{\partial\Psi(\mathbf{r})}{\partial t} = -\frac{\delta F[\Psi]}{\delta\Psi(\mathbf{r})} \equiv \frac{\hbar^2}{4m}\nabla^2\Psi(\mathbf{r}) - \alpha\Psi(\mathbf{r}) - \beta|\Psi(\mathbf{r})|^2\Psi(\mathbf{r}) \tag{19.20}$$

'де γ имеет смысл кинетического коэффициента; порядок вели'ины этого параметра мы определим чуть ниже. Считая флукгуации малыми, пренебрегаем последним членом

в (19.20), после 'іго это уравнение становится линейным. Теперь можно перейти к переменным $\psi(\mathbf{p}) = \int d\mathbf{r}\Psi(\mathbf{r})e^{i\mathbf{p}r}$, в которых уравнение (19.20) чринимает простой вид:

$$\gamma\partial\psi(\mathbf{p})/\partial t = -\left(\alpha + \hbar^2 p^2/4m\right)\psi(\mathbf{p}) \tag{19.21}$$

Из уравнения (19.21) видно, что время релаксации флуктуаций параметра порядка с импульсом p равно

$$\tau(\mathbf{p}) = \frac{\gamma}{\alpha + \hbar^2 p^2/4m} \tag{19.22}$$

В результате, собирая вместе (19.19) и (19.22), получим

$$\sigma_{\mathrm{AL}} \sim \frac{e^2}{m}\sum_{\mathbf{p}} \frac{k_{\mathrm{B}}T\gamma}{\left(\alpha + \hbar^2 p^2/4m\right)^2} \tag{19.23}$$

Рассмотрим случай тонкой сверхпроводящей пленки (толщина $d \ll \xi$), когда выражение для парапроводимости имеет особенно простой и универсальный вид. Заменяя $\sum_{\mathbf{p}}$ на интеграл $(1/d)\int d^2p/(2\pi)^2$, получаем для проводимости на квадрат пленки

$$\sigma_{\mathrm{AL}}^{2D} = \sigma_{\mathrm{AL}} \cdot d \sim \frac{e^2 k_{\mathrm{B}} T_c \gamma}{\alpha\hbar^2} \sim \frac{e^2}{\hbar}\frac{T_c}{T - T_c} \tag{19.24}$$

Чтобы получить последнее выражение в правой части (19.24), мы учли, что при $(T - T_c) \sim T_c$ время релаксации сверхпроводящего параметра порядка $\tau_0 \sim \gamma/\widetilde{\alpha}T_c$ должно быть порядка $\hbar/k_{\mathrm{B}}T_c$, поэтому $\gamma \sim \hbar\widetilde{\alpha}$. Таким образом, в двумерном случае вклад в проводимость от флуктуационньг пар определяется только относительной близостью к точке перехода, и вообще не зависит от параметров сверхпроводника. Микроскопическое вычисление [40] подтверждает качественную оценку (19.24) и определяет численный коэффициент в правой части, равный 1/16.

Для тонких проволок и массивных сверхпроводников (размерность $d = 1, 3$) оценка, аналогичная (19.24), дает вклад в проводимость

$$\sigma_{\mathrm{AL}}^{(d)} \sim \left(\frac{T_c}{T - T_c}\right)^{(4-d)/2} \tag{19.25}$$

Коэффициент перед этой зависимостью уже не является универсальным; используя выражения из 51 для параметра $\alpha(T)$
и оценку для γ, можно получить (по порядку величины) формулы (19.17). В заключение заметим, что в отличие от обычного стационарного уравнения Гинзбурга-Ландау, неравновесное его обобщение применимо, строго говоря, только при $T > T_c$. Дело в том, что наличие конечной щели Δ в спектре нормальных возбуждений сверхпроводника при $T < T_c$ (см. 45) делает неверным предположение о простой релаксационной динамике параметра порядка, использованное в (19.20). Мы обсудим неравновесные процессы в сверхпроводящем состоянии в главе VII.

3.7.4 Intuitive understanding of GL theory

Analogies of GL theory in life

(???)

3.7.5 Short Examples of Applications of GL theory

(just model-solution, to finish basics)

3.8 Background for Real Understanding of BCS Theory

3.8.1 Speedrun of Condensed Matter for Superconductivity

(See Landau)

Brillouin zone

(???? write what is it and how is it related to superconductivity)

Fermi surface

(???? write what is it and how is it related to superconductivity)
(??? which it can be? not a ball, but why???)

Density of states near Fermi surface

(write that typical derivations from cond matter)

(??? when the DOS is not constant in the Debye's window? when it is constant?? we assume that it is so and that is all)

(??? what about TB models? is the DOS constant in them? maybe no, I'll derive it here)

Debye model

(???? write the idea that we have phonons, they are quantized and somehow we approximate it)

(???? how important the Debye approximation for SC? maybe it does not matter that there are more complicated dispersion relation of phonons? or ir is very inexact approximation? I think that there would be no consequences of the fact that the Debye model is only an approximation. It is true???)

3.8.2 Superfluid Fermi Gas: Energy Spectrum

(See Landau)

3.8.3 Superfluid Fermi Gas: Thermodynamic Properties

(See Landau)

3.8.4 Green's Functions of Superfluid Fermi Gas

(See Landau)

3.8.5 Temperature Green's Functions of Superfluid Fermi Gas

(See Landau)

3.8.6 QFT formalism for bound states of two particles

(I'll write from QFT and maybe from QM, how in general we are describing such situations? It is an important question to understand BCS!)

3.9 BCS Theory: Basic General Properties

3.9.1 Cooper Pairs: General Idea and Physical Picture

6.1 Introduction. Electron-Phonon Interaction by Shmidt

The physical mechanism of superconductivity became clear only 46 years after the phenomenon had been discovered, when Bardeen, Cooper and Schrieffer published their theory (the BCS theory).

The following estimates will help us to understand how serious were the difficulties facing theoreticians at the time. The difference in free energy between the normal metal and the superconductor is, as we already know, $H_{\rm cm}^2/8\pi \sim 10^5$ erg cm^{-3}, for $H_{\rm cm} \sim 10^3$ Oe.

(??? why it is so???)

The number of conduction electrons in 1 cm^3 is approximately 10^{22}. Then the energy responsible for superconductivity (??? what is meant by it???) is approximately $10^5/10^{22} = 10^{-17}$ erg/electron $\sim 10^{-5}$eV/ electron.

This energy should be compared with the Coulomb interaction energy $\sim$ 1eV which is sufficiently small to be neglected in many applications of the modern quantum theory of metals, without affecting the results.

The comparison implies that it was necessary to explain the coherent behavior of electrons coupled by an interaction of energy many orders of magnitude smaller than that of other interactions, which are often neglected exactly because of their small energies.

The first hint at the origin of superconductivity came with the discovery of the isotope effect. It was found that different isotopes of the same superconducting metal have different critical temperatures, $T_{\rm c}$, for the superconducting transition and that they obey the relation

$$T_{\rm c} M^a = \text{const}$$

where M is the mass of the isotope. For the majority of superconducting elements, a is close to 0.5.

Thus it became clear that the lattice of ions in a metal is an active participant in creating the superconducting state. Further theoretical analysis has demonstrated that the interaction between electrons and quantized excitations of the crystal lattice, phonons, can bring about an additional interaction between the electrons. Under certain circumstances, this interaction takes the form of electron-electron attraction. Furthermore, if the attraction proves to be stronger than the Coulomb repulsion, the electrons become effectively coupled which gives rise to the superconducting state.

Let us first try to understand how electrons can interact with each other via phonons (the latter are characterized by the energy $\hbar\omega_q$ and the wave vector q).

Consider a metal at $T = 0$. Evidently, at absolute zero, there are no phonons. How is it possible then that the electrons interact via them?

There is exactly zero phonons at $T = 0$ (???? why????) The default answer is as follows. In a perfect crystal treated harmonically, the $T = 0$ state is the phonon vacuum: every mode has occupation $n_{{\rm q},s} = 0$. The lattice still has zero-point energy $E_0 = \frac{1}{2}\sum_{{\rm q},s} \hbar\omega_{{\rm q},s}$ but that

doesn't correspond to real phonons being present. (Phonon number isn't conserved and, with anharmonicity/e-ph coupling, it's not even a sharply defined observable, but the ground state still has no thermally excited phonons.)

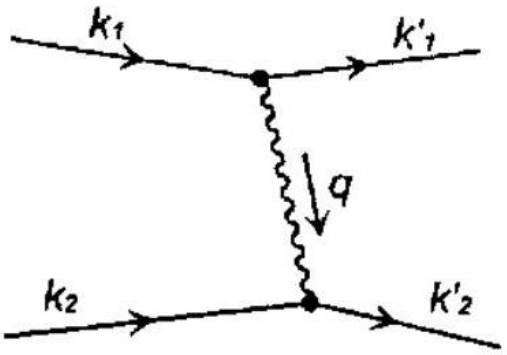


Fig. 6.1. Diagram illustrating electron-electron interaction via emission and subsequent absorption of a phonon of momentum $\hbar \boldsymbol{q}$

Consider a free electron of wave vector k_1 moving in a crystal. At some moment of time it excites a lattice vibration. In other words, the electron creates a phonon (which did not exist before) and goes to a new state k_1'.

(??? so the speed of phonon is much bigger than speed of moving out of each other electrons???)

Let the wavevector of the created phonon be $\boldsymbol{q}$. Then, by the law of momentum conservation,

$$k_1 = k_1' + q$$

The phonon q is almost immediately absorbed by another electron $\boldsymbol{k}_2$ which goes to the state k_2' as a result. Now, what has happened? Two electrons which at first occupied the states k_1 and k_2, ended up in the states k_1' and k_2'. This means that they were scattered by one another so that

$$k_1 + k_2 = k_1' + k_2'$$

But two particles can be mutually scattered only if they interact with each other. Therefore, we conclude that the above process, which is illustrated in Fig. 6.1, describes an effective electron-electron interaction. Let us consider the sign of this interaction. At the moment when one of the electrons goes from the state k_1 to the state k_1', it causes local oscillations of electron density at the frequency $\omega = \left(\bar{\varepsilon}_{k1} - \bar{\varepsilon}_{k1'}\right)/\hbar$, where $\bar{\varepsilon}_{k1}$ and $\bar{\varepsilon}_{k1'}$ are the electron energies in the states $\boldsymbol{k}_1$ and $\boldsymbol{k}_1'$, respectively. Suppose, more specifically, that at a given moment a local electron density (negative charge) has increased. The surrounding ions will then be attracted to this location and will start moving towards it, gradually compensating the electron density increase. However, due to their large mass, the ions will continue their motion even after the density increase has been compensated and will thereby create an excess positive charge. As a result, the second electron with momentum k_2 will be immediately attracted to it, that is, the particles k_1 and k_2 will be effectively attracted to each other. Such an attraction arises only if the lattice vibrations are in phase with the external force (its role in our case is played by the electron density oscillations of frequency $\omega = \left(\bar{\varepsilon}_{k1} - \bar{\varepsilon}_{k1'}\right)/\hbar$). Furthermore this ran only happen if the frequency of the external force, ω.

This will be only in case when the driving frequency ω is less than the characteristic frequency of the ion system, that is, the Debye frequency (which is also the maximum possible frequency [1]). Therefore, the condition for the attraction can be formulated as $\omega < \omega_{\mathrm{D}}$.

To elucidate the above statement, let us consider a simple oscillator of mass m and eigenfrequency ω_0 subjected to an external force $fe^{\mathrm{i}\omega t}$. The equation of motion for such a system reads

$$\ddot{x} + \omega_0^2 x = \frac{f}{m} e^{\mathrm{i}\omega t} \tag{6.1}$$

We seek the solution of the form $x = x_0 \mathrm{e}^{\mathrm{i}\omega t}$. Substituting it into (6.1), we have

$$x_0 = \frac{f}{\omega_0^2 - \omega^2}$$

that is, as long as $\omega^2 < \omega_0^2$, the oscillations $x = x_0 \mathrm{e}^{\mathrm{i}\omega t}$ are in phase with the external force f. At $\omega^2 > \omega_0^2$, the oscillations are out of phase with f.

Let us go back to our clectrons. To enable an electron to go from the state k_1 to the state k_1', the latter must be free (due to the Pauli exclusion principle) which is possible only in the vicinity of the Fermi surface. (Recall that the latter is represented by a sphere of radius k_F in momentum space.)

Now we are ready to formulate the law of phonon-mediated interaction between electrons which forms the foundation of the BCS theory: Electrons with energies that differ from the Fermi energy by no more than $\hbar\omega_\mathrm{D}$ are attracted to each other. We shall denote the energy of their interaction by $-V$. The rest of the electrons do not interact.

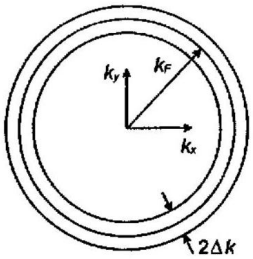


Fig. 6.2. In the BCS picture, only the electrons within the $2\Delta k$ layer near the Fermi surface interact via phonons

Let us write the matrix element of the electron interaction in the form

$$V_{kk'} = \begin{cases} -V, |\bar{\varepsilon}_k - \varepsilon_F| \le \hbar\omega_D, & |\bar{\varepsilon}_{k'} - \varepsilon_F| \le \hbar\omega_D \\ 0, |\bar{\varepsilon}_k - \varepsilon_F| > \hbar\omega_D, & |\bar{\varepsilon}_{k'} - \varepsilon_F| > \hbar\omega_D \end{cases} \tag{6.2}$$

Thus, in the BCS model, only those electrons that occupy the states within a narrow spherical layer near the Fermi surface experience mutual attraction. The thickness of the layer, $2\Delta k$, is determined by the Debye energy (see Fig. 6.2):

$$\frac{\Delta k}{k_\mathrm{F}} \sim \frac{\hbar\omega_\mathrm{D}}{\varepsilon_\mathrm{F}}, \quad \varepsilon_\mathrm{F} = \frac{\hbar^2 k_\mathrm{F}^2}{2m}.$$

Cooper Pairing by Means of Electron-Phonon Interaction by a book for experimenters

Following our discussion in Chapter 1, it appears relatively easy to arrive at a theory of superconductivity based on the microscopic interaction between the electrons themselves and between electrons and the surrounding crystal lattice. (?????)

[1] The existence of a maximum possible frequency for atom vibrations in crystals is easy to understand: a sound wave in a crystal is meaningless if its wavelength is less than the crystal lattice period. The existence of a minimum possible wavelength, which implies the existence of a maximum possible frequency, is then evident.

However, historically such a theory was confronted with extreme difficulties Because of the striking change of the electrical conductivity and the magnetic effects during the onset of superconductivity, one could presume that essentially one is dealing with an ordering process within the system of conduction electrons As we saw in Section 1.1, because of the Pauli principle the conduction electrons have fairly large energies up to a few electronvolts (1eV corresponds to thermal energy $k_{\mathrm{B}}T$ at a temperature of about 11000 K). However, the transition into the superconducting state occurs at only a few kelvins. Hence, one had to find an interaction that could lead to ordering within the electron system in spite of the high electron energies.

There exists a multitude of possible interactions between the conduction electrons in a metal. It had been imagined [W. Heisenberg: Z. Naturforsch. 2a, 185 (1947)] that Coulomb repulsion between the electrons could lead to a spatial ordering of the electrons in the form of a lattice. (??? what is there????)

Also [H. Welker: Z. Phys. 114, 525 (1939)] a magnetic interaction seemed possible. (I'll read later) The electrons propagating through the metal lattice with impressive velocities (electrons having energies near the Fermi energy can reach velocities near 1% of the velocity of light) generate a magnetic field because of the associated currents and can then interact with each other due to this magnetic field.

Other interactions can result from the structure of the electron states (allowed energy bands, see Section 1.1) [M. Born, K. C. Cheng: Nature (London) 161, 968 and 1017 (1948).]

All these attempts did not lead to a satisfactory microscopic theory of superconductivity. Only in 1950/1951 was an interaction between the electrons mediated by the vibrations of the lattice discussed simultaneously and independently by Fröhlich [H. Fröhlich: Phys. Rev. 79, 845 (1950)] and Bardeen [J. Bardeen: Phys. Rev. 80, 567 (1950)]. As it turned out later, these ideas would lead to a fundamental understanding of superconductivity in terms of established concepts about the behavior of metals. Starting from this interaction, in 1957 Bardeen (Bardeen-Cooper-Schrieffer) theory, which was able to explain quantitatively many known experimental facts, and which turned out to be extremely stimulating. Motivated by this theory, after 1957 a large number of completely new experiments were performed, which strongly expanded our ideas about superconductivity and which basically changed our underlying concepts.

Still the road from the suggestion of a new interaction (1950) to the formulation of a satisfactory theory (1957) was a very difficult one. It was thus highly favorable when, nearly simultaneously with the theoretical discussion of this new interaction and of its possible importance for superconductivity, a surprisingly clear experimental confirmation of the basic correctness of the theory reached the scene. During the study of the different isotopes of the same superconductor, it had been found that the transition temperature T_{c} of superconductivity depends on the mass of the lattice atoms. Furthermore, the experimentally observed dependence exactly corresponded to that expected from the theoretical concepts of Fröhlich. This has shown that apparently the theory had hit the correct point, independent of all formal difficulties. This confirmation of the basic concepts had an important influence on the subsequent development.

How can we understand the interaction between the electrons that is mediated through the lattice vibrations? In the following, we will discuss some model ideas regarding this interaction. However, we must keep in mind that these model ideas are of little value if we try to extract further conclusions.

We start with a static model. The lattice of the atomic ions, in which the conduction electrons propagate as a Fermi gas, has elastic properties. The atomic ions are not stiffly

bound to their lattice sites at rest. Instead, they can be deflected from their sites. At finite temperatures, they oscillate in an irregular way around these sites, as we have discussed. If we consider just two negative charges within this lattice of atomic ions, and in an oversimplified way ignore all other electrons, the negative charge of both electrons will slightly distort the lattice by attracting the surrounding positive charges. In other words, the lattice is polarized because of the negative charge. This situation is shown schematically in Figure 3.1.

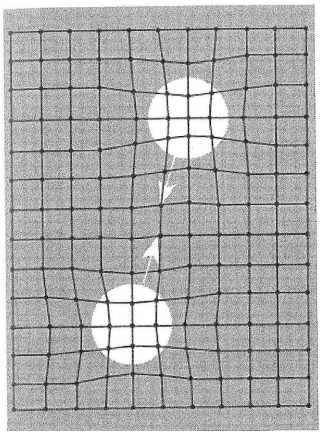


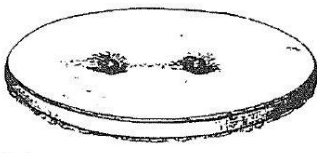
Figure 3.1 Polarization of the lattice of atomic ions due to the electrons. Within a static model, this polarization cannot overcompensate the repulsion between the electrons because of their equal charge. It can only strongly reduce the repulsion.

Compared to the uniform distribution of the positive charges, the polarization leads to an accumulation of positive charge near the polarizing negative charge. The second electron with its polarization then feels the polarization of the first electron It experiences an attraction to the location of the polarization and, hence, to the first electron. In this way, we have described an attractive interaction between two electrons due to the polarization of the lattice.

(??? does the analogy below makes sense at all??? maybe it is just a nonsense)

We can present a mechanical analogy for this static, attractive interaction. We represent the elastically deformed lattice of atomic ions by an elastic membrane, say, by a thin, stretched rubber sheet or by the surface of a liquid. Due to the surface tension it costs energy to deform the equilibrium configuration of the surface of a liquid. Next, we place two small balls onto this membrane. In the case of the liquid, the balls must remain non-wetted. If the distance between the balls is sufficiently large because of its weight, each ball will locally deform the membrane independent of the other (Figure 3.2a).

This corresponds to the deformation of the lattice. We recognize intuitively that the energy of the total system (membrane with the two balls) can be lowered if the the energy of the total system (membrane with the two balls) can be lowered if the two small balls lie in the same hollow. They will sink in more deeply (Figure 3.2b), which corresponds to a decrease of the potential energy in the gravitational field. Hence, also the total energy of the system decreases, and the difference between the mechanical energy at the beginning and at the end is changed into heat due to frictional effects. We see that we obtain an interaction between the small balls because of the elastic membrane, resulting in a bound state, that is, in a state where the two small balls are spatially located very close to each other.



(a)

Figure 3.2 Attraction between two small balls on an elastic membrane. The configuration (a) is unstable and changes into configuration (b).

The model illustrates that an attractive interaction can be realized by means of elastic deformations, no more than that. In a metal, the electrons have impressive velocities. They do not polarize the lattice statically. One could presume that rather, during this motion through the lattice, the polarization takes place along the way, which sensitively depends on how quickly the lattice can follow the polarizing action of the electron. The time during which the lattice of atomic ions can respond to any displacements should be crucial.

(??? I don't know what is below, I propose to delete it)

However, for an elastic system, this means that the characteristic internal frequencies are important (????). Because of this overall incorporation of a dynamical aspect, we have achieved an essential advance. Now we understand at least qualitatively that the strength of the polarization (????????), and hence of the interaction for the same other conditions, can depend on the characteristic frequency of the lattice and, therefore, also on the mass of the atomic ions. Heavy isotopes oscillate somewhat slower, that is, they have smaller frequencies of the lattice. They can follow the polarizing action only more slowly compared to lighter isotopes. Hence, the polarization remains smaller. From this, we expect that the interaction becomes weaker and that the superconducting transition temperature is smaller. With increasing isotope mass the transition temperature decreases, in agreement with the experimental results. However, we must keep in mind that these last discussions are meaningful only in a heuristic sense and do not allow any quantitative conclusions. (??? so that is why I'll later just delete these nonsense)

Only a quantum mechanical treatment can yield the frequencies of the lattice, which are essential for this interaction.

At this stage, we have introduced dynamic aspects into the interaction throug the polarization of the lattice. However, we have kept the concepts of a static discussion, which yielded the energy gain of an electron due to the polarization achieved by another electron (????). In order to extend our dynamic model a little further, we can imagine that the second electron propagates within the polarization trail of the first electron and thereby lowers its energy, since it experiences the lattice already in a polarized state.

(??? I don't know, how polarization is connected to the SC.... I mean, in terms of formulas. virtual phonon - one thing, polarization - another thing)

There are two possibilities. The first is that both electrons can propagate with the same momentum $\mathbf{p} = hbar\mathbf{k}$. Then we can justifiably treat this object a particle, namely an electron pair. However, the total momentum of this particle would be twice the momentum of a single electron. The other possibility would be that the electrons have opposite momentum. Again, one electron can propagate within the polarization trail of the other. However, in this case, the idea of a new particle, an electron pair, is more difficult. By a little abstraction, we note that in the first case the individual electrons are correlated due to the requirement that they have the same momentum, that is, $\mathbf{p}_1 = \mathbf{p}_2$ or $\mathbf{k}_1 = \mathbf{k}_2$.

(????????? so what is wrong physically with this model, when they are moving to the same direction???)

An equally definite correlation is obtained by the requirement that $\mathbf{p}_1 = -\mathbf{p}_2$ or $\mathbf{k}_1 = -\mathbf{k}_2$. We are justified to treat these strongly correlated electrons also as a pair. The latter electron pair has total momentum zero. Such pairs are referred to as Cooper pairs, since Cooper was the first to show that such a correlation leads to a decrease in the total energy [7]. If we take into account also the intrinsic angular momentum (spin) of the electrons, which is important for the statistical behavior of the new particles, a Cooper pair consists of two electrons with

opposite momentum of equal magnitude and with opposite spins:

Cooper pair: $\{\mathbf{k}\uparrow, -\mathbf{k}\downarrow\}$

The center of mass of the following Cooper pair is at rest, with a total momentum $\mathbf{P} = \hbar\mathbf{K} = 0$. However if we want to describe a state in which a supercurrent flows, the Cooper pairing must be performed for $\mathbf{K} \neq 0$, that is, for a state $\{\mathbf{k}+\mathbf{K}\uparrow, -\mathbf{k}+\mathbf{K}\downarrow\}\}$.

(???? why when I consider current, I haven't consider such pairs and just stationary pairs????)

The correlation leading to Cooper pairs is energetically favored because of the lattice of positive atomic ions.

Exchange interaction

Since the possibility of a pair correlation represents the crucial key of the microscopic theory of superconductivity and, hence, for an understanding of the superconducting state, we also want to present another more general consideration We can also understand the formation of electron pairs in a lattice from the very general formalism of the so-called exchange interaction.

Systems that exchange some physical quantities among themselves must experience an interaction for trivial reasons. This statement is very general. The exchange interaction of quantum mechanics deals with the fact that the exchange can lead to an attraction between two physical systems. For instance, two particles can experience an attraction because of the exchange of a third particle, leading to a state in which both particles are bound to each other.

A repulsion because of cally. Two people, throwing a ball back and forth between themselves, experience ach a repulsion. This seems obvious and can be checked easily by placing the people on two mobile platforms, which can move along the line connecting the two people. Because the ball is thrown back and forth, the two cars move away from each other. Here, it is only the exchange of the ball and the corresponding exchange of momentum that causes the repulsive interaction. action. Instead, we want to discuss an example of modern physics.

It is well known that two hydrogen atoms form a hydrogen molecule, and that the chemical bond in this molecule is very strong. In order to break this bond, one needs an energy of 26×10^4 W s/mol(62.5kcal/mol), that is, for dissociating 2 g of H_2. How can we understand such a strong bond between neutral H atoms in an H_2 molecule? To explain the principle, we look at a slightly simpler system, namely H_2^+, that is, a positively charged H_2 molecule. This ion consists of two hydrogen nuclei (two protons) and one electron. The two possible states of this system are shown in Figure 3.3a,b for a large distance between the two protons.

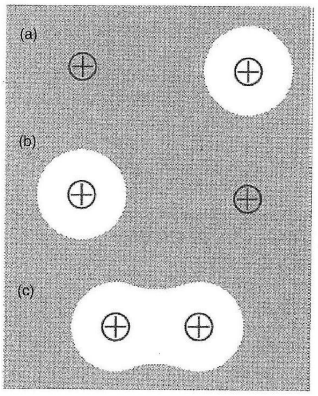


Figure 3.3 Binding of the H_2^+molecule. The scales are arbitrary. (a), (b): Two possible electron distributions for a large distance between the protons. (c) electron distribution for a small distance between the protons.

The electron resides near one of the two protons. If we bring the protons closer together, the electron will hop from one proton to the other, with a certain probability, as we know from

quantum mechanics. In our terminology, the electrons are exchanged. The probability for the exchange increases with decreasing distance. Then the electron belongs equally to both protons, as indicated in Figure 3.3c. As an important result of quantum mechanics, for this problem one finds that the total energy of the system can be lowered because of the exchange. However, this means that smaller distances R are energetically more favorable. A bond between the two protons appears because of the common electron. The equilibrium distance results from the condition that the attractive force of the electron exchange is exactly balanced by the repulsive force between the two protons.

We can understand the energy gain due to the exchange of electrons in a particularly simple way, if we apply a highly fundamental principle of modern physics, namely the uncertainty principle. This principle says that both the spatial location and the momentum of a particle cannot simultaneously be determined exactly. The accuracy of the observation of both quantities is limited by the famous relation

$\Delta p_x \Delta x = \hbar$

For our system this means that the smearing of the momentum Δp_x can be reduced if the electron is allowed to exist near both protons, since the smearing of its location Δx is enhanced in this case. As a result the energy smearing is reduced, and the energy of the electron is lowered [8].

If this energy gain is larger than the energy increase due to the Coulomb repulsion between the two protons, a net attraction is obtained. We see that the chemical bond of the H_2 molecule represents a typical quantum mechanical effect. These arguments briefly outlined provide the key for the understanding of the chemical bond.

Using similar arguments, we can also understand the attractive interaction between the conduction electrons in a metal. In the metal, a new kind of particle can be exchanged, namely the phonons. The phonons are the quantized elementary vibrations of the crystal lattice. Any complex vibrational state of the lattice can be separated into normal modes, that is, into harmonic waves. This corresponds to the description in terms of a Fourier series. For a macroscopic body, the normal modes have well-defined energies. They also have definite wavelengths and, because of the relation $p = h/\lambda$, definite momenta. Hence, they represent particles and are referred to as phonons or as quanta of sound.

So an electron in a lattice can interact with another electron by the exchange of phonons. One speaks of the electron-electron interaction via phonons. The exchanged phonons only exist virtually during their transfer from one electron to another, since they cannot escape from the electrons into the lattice as real phonons.3) Here, we note an important difference compared to the interaction within the H_2 molecule. In the latter case, the exchanged electrons are real particles. This interaction via phonons is shown schematically in Figure 3.4. In certain cases, namely in superconductors, it can be so strong that it becomes larger than the repulsion between the electrons due to the electrostatic forces.) [4] Then we obtain the pair correlation we have discussed.

For pure superconductors, the average distance within which this pair correlation is active ranges between 100 and 1000 nm.[5]) This length is referred to as the *BCS* coherence length ξ_0 of the Cooper pair. This length must not be mixed up with the Ginzburg-Landau coherence length ξ_{GL}, which indicates the length scale within which the total system of Cooper pairs can change.

The BCS coherence length ξ_0 can also be interpreted as the average size of a Cooper pair. In a highly simplified way we can say that in a pure superconductor a Cooper pair has an average size between 10^2 and 10^3 nm. This size is large compared to the average distance between two conduction electrons, which amounts

3) If real phonons are generated by an electron, we are dealing with a process causing

electrical resistance, since energy is transferred from the electrons to the lattice in this case.

4) We note that the electrostatic repulsion is highly screened by the positive charges of the atomic ions.

5) The interaction via the exchange of phonons is so weak that it cannot localize the electrons of a Cooper pair more sharply than within about ξ_0. Because of the uncertainty principle, a sharper localization would result in a kinetic energy of the electrons larger than the binding energy of the pair. However, these intuitive arguments quickly run into difficulties. For instance one can ask if the whole pair correlation is not destroyed by the high Fermi velocity. The answer is "no", but we do not attempt to justify this. Here, we would overextend the simple particle picture.

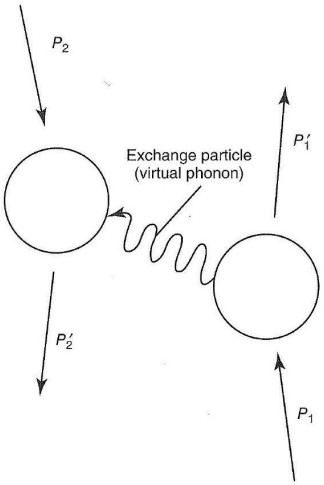


Figure 3.4 Electron-electron interaction via phonons.

to a few times 10^{-1} nm. The Cooper pairs strongly overlap. Within the space of a single pair there exist $10^6 - 10^7$ other electrons, each being correlated in pairs. Intuitively we expect that a system of such strongly overlapping particles must have unusual properties. This will be discussed in the next section.

Two pictures of BCS excitations

(write what Kabanov told me, this is very useful for understanding)

Despite Fermions are repulsive by Pauli's principle, they still can form a bound states

This is the main statement of Cooper pairs. This is because two electrons on top of a Fermi sea are effectively in 2D.

(?? I'll write more about it)

What is the virtual phonon?

It is not a real phonon.

In a perfect crystal treated harmonically, the $T = 0$ state is the phonon vacuum: every mode has occupation $n_{\mathrm{q},s} = 0$. The lattice still has zero-point energy $E_0 = \frac{1}{2}\sum_{\mathrm{q},s} \hbar\omega_{\mathrm{q},s}$ but that doesn't correspond to real phonons being present. (Phonon number isn't conserved and, with anharmonicity/e-ph coupling, it's not even a sharply defined observable, but the ground state still has no thermally excited phonons.)

(??? I'll answer here, what is it???)

Density of states near the Fermi surface

In many formulas below we will use the fact that

$$g_F := p_F m/\pi^2\hbar^3.$$

This is an important formula to keep in mind, because many quantities are deduced from it.

(write formulas for gap at 0, Tc, and maybe something else, I'll check later)

So let us derive it here.

(I'll do this trivial derivation later)

Other questions about BCS pairing

What happens with other excitations, higher than the cutoff of the BCS interaction?

Like, the electrons in the Debye's window are coupled, but what about those who are even higher in energies? Why they can't exchange a phonon? Yes, there are a very little number of them.

So, why phonons can make electrons attract each other?

(I'll write again an answer, but with formulas and precise!!! I don't have a good answer now, since all this story about lattice deformation is not enough to write the well-known formulas)

3.9.2 Cooper Pairs: Basic Calculations

Introduction about calculations of Cooper instability

(I'll add comments about this feature of theory)

This is not needed for anything (at least, now I haven't found any application of it).

And there are slightly different approaches to this derivation, though it is the same idea and same equations.

Cooper instability by Coleman

(write his derivation here)

The Cooper problem by Chalker

This is an attractive interaction for pairs of electrons with $|\epsilon(\mathbf{k}) - \epsilon(\mathbf{k}-\mathbf{q})| < \hbar\omega$: that is, for pairs within the Debye energy $\hbar\omega_{\mathrm{D}}$ of the Fermi surface. It is, however, typically very weak. This leads us to a puzzle: for two particles moving in free space in three dimensions, an attractive interaction must exceed a critical strength to produce a bound state. So how can a weak attraction generate superconductivity? The Cooper problem takes us one step towards answering this question: we consider a pair of particles moving not in free space, but above a filled Fermi sea, and will find that Pauli exclusion facilitates binding.

Consider the wavefunction for this pair of particles. We want to write a low-energy state, and so we set the centre-of-mass momentum to zero. To take advantage of a local attractive interaction, we choose the pair to be in a spin-singlet state so that the spatial wavefunction is symmetric. And to respect Pauli exclusion from a filled Fermi sea, we require the wavefunction to be built from orbitals outside the Fermi surface. The general form is then

$$\psi\left(\mathbf{r}_1\sigma_1, \mathbf{r}_2\sigma_2\right) = \left(\uparrow_1\downarrow_2 - \downarrow_1\uparrow_2\right) \cdot \sum_{|\mathbf{k}|>k_\mathrm{F}} g_\mathbf{k} \mathrm{e}^{\mathrm{i}\mathbf{k}\cdot\left(\mathbf{r}_1-\mathbf{r}_2\right)}$$

with $g_\mathbf{k}$ determined by requiring this to be a solution to the two-particle Schrödinger equation. Writing the pair energy as E and the pair potential as $U\left(\mathbf{r}_1 - \mathbf{r}_2\right)$, we have

$$\sum_{|\mathbf{k}|>k_\mathrm{F}} g_\mathbf{k} \mathrm{e}^{\mathrm{i}\mathbf{k}\cdot\left(\mathbf{r}_1-\mathbf{r}_2\right)} U\left(\mathbf{r}_1 - \mathbf{r}_2\right) = \sum_{|\mathbf{k}|>k_\mathrm{F}} \left(E - 2\epsilon(\mathbf{k})\right) g_\mathbf{k} \mathrm{e}^{\mathrm{i}\mathbf{k}\cdot\left(\mathbf{r}_1-\mathbf{r}_2\right)}.$$

To solve this Schrödinger equation, we operate on both sides with

$$\frac{1}{V}\int \mathrm{d}^d\left(\mathbf{r}_1 - \mathbf{r}_2\right) \ldots \mathrm{e}^{-\mathrm{i}\mathbf{q}\cdot\left(\mathbf{r}_1-\mathbf{r}_2\right)}$$

(where V is the system volume) and introduce the notation $\int \mathrm{d}^d\mathbf{r} U(\mathbf{r}) \mathrm{e}^{\mathrm{i}(\mathbf{k}-\mathbf{q})\cdot\mathbf{r}} = U_{\mathbf{kq}}$. Then Eq. (43) becomes

$$\frac{1}{V}\sum_{|\mathbf{k}|>k_\mathrm{F}} g_\mathbf{k} U_{\mathbf{kq}} = \left(E - 2\epsilon(\mathbf{q})\right) g_\mathbf{q}$$

We can understand the essentials in a simple way by taking

$$U_{\mathbf{kq}} = \begin{cases} -U & \text{if } \epsilon(\mathbf{k}) \text{ and } \epsilon(\mathbf{q}) \text{ are within } \hbar\omega_\mathrm{D} \text{ of } E_\mathrm{F} \\ 0 & \text{otherwise} \end{cases}$$

Then

$$\frac{U}{V}\sum_{\mathbf{k}}{}' g_\mathbf{k} = \left(2\epsilon(\mathbf{q}) - E\right) g_\mathbf{q}$$

where $\sum\limits_{\mathbf{k}}{}'$ is a sum over states within $\hbar\omega_\mathrm{D}$ of E_F.

$$\frac{1}{V}\sum_{\epsilon=E_\mathrm{F}}^{\epsilon=E_\mathrm{F}+\hbar\omega_\mathrm{D}} \frac{1}{2\epsilon - E} = \frac{1}{U}.$$

With a constant density of states ρ per unit volume, this yields

$$\int_{E_\mathrm{F}}^{E_\mathrm{F}+\hbar\omega_\mathrm{D}} \mathrm{d}\epsilon \frac{\rho}{2\epsilon - E} = \frac{\rho}{2} \ln\left[\frac{2\left(E_\mathrm{F} + \hbar\omega_\mathrm{D}\right) - E}{2E_\mathrm{F} - E}\right] = \frac{1}{U}.$$

There is a bound state for any positive U, and at weak coupling the binding energy is

$$2E_\mathrm{F} - E = 2\hbar\omega_\mathrm{D} \mathrm{e}^{-2/\rho U}.$$

Strikingly, this form is non-perturbative in ρU.

феномен Купера by Micheenkov

Прежде, чем заниматься многочастичной проблемой,

рассмотрим поведение двух выделенных электронов с локальным взаимодействием, которые двигаются на фоне остальных электронов, заполняющих сферу Ферми.

Это движение описывается стационарным уравнение Шредингера:

$$\left[\left(\frac{\hat{p}_1^2}{2m} - \mu\right) + \left(\frac{\hat{p}_2^2}{2m} - \mu\right) + U_0\delta\left(\mathbf{r}_1 - \mathbf{r}_2\right)\right]\psi\left(r_1, r_2\right) = E\psi\left(r_1, r_2\right)$$

Роль заполненной ферми-сферы сводится к тому, что из фазового пространства, доступного этим электронам, в силу принципа Паули исключены состояния, находяпциеся внутри этой сферы. Тогда волновая функция основного состояния есть функция покоюшейся пары электронов. Эта функция зависит только от расстояния межлу электронами $\mathbf{r} = (\mathbf{r}_1 - \mathbf{r}_2)$ и может быть представлена в форме

$$\psi(\mathbf{r}_1, \mathbf{r}_2) = \sum_{k>k_F} \psi_k e^{i\mathbf{kr}}$$

При суммировании по импульсам учтено, что все состояния внутри поверхности Ферми заняты. Для краткости здесь и далее мы полагаем$\hbar = 1$. Подставляя в(12), получим

$$\sum_{k'>k_F} \left[2\left(\frac{k'^2}{2m} - \mu\right) - E\right] \psi_{k'} e^{i\mathbf{k'r}} + U_0 \sum_{k'>k_F} \psi_{k'} \delta(\mathbf{r}) = 0$$

Умножая это уравнение на $e^{-i\mathrm{kr}}$ и интегрируя по объему V, находим

$$V\left[2\left(\frac{k^2}{2m} - \mu\right) - E\right] \psi_k + U_0 \sum_{k'>k_F} \psi_{k'} = 0$$

отсюда

$$\psi_k = -\frac{U_0/V}{2\left(\frac{k^2}{2m} - \mu\right)) - E} \sum_{k'>k_F} \psi_{k'}$$

Суммируя по импульсам и сокращая на $\sum\limits_{k'>k_F} \psi_{k'}$, получаем интегральное уравнение

$$1 = -\sum_{k>k_F} \frac{U_0/V}{2\left(\frac{k^2}{2m} - \mu\right) - E}$$

которое сводится к интегралу по $\xi = \frac{k^2}{2m} - \mu$.

Напомним, что

$$\sum_{k>k_F} = \frac{1}{2} V \int_0^{\omega_D} d\xi \nu(\xi), \nu(\xi) - \text{плотность состояний.}$$

Tor/a

$$-\frac{1}{2} g \int_0^{\omega_D} d\xi \frac{\nu(\xi)}{2\xi - E} = 1$$

Верхний предел интегрирования мы формально обозначили через ω_D, имея в виду, что впоследствии будет установлено $(***)$, что в металле притягиваготся электроны вблизи энергии Ферми в корочке толшиной порядка энергии Дебая ω_D При $g < 0$ сушествует решение этого уравнения с отрицательным собственное значением $E = -|E|$. Пренебрегая зависимостыо плотности $\nu(\xi)$ электронных состояний от энергии возбужления, получаем

$$\frac{1}{2} |U_0| \nu(0) \ln \frac{2\omega_D}{|E|} = 1$$

Откуда следует, что

$$|E| = \omega_D \exp\left[-\frac{2}{|U_0| \nu(0)}\right]$$

Cooper instability by Pukhov

(write his derivation here)

3.9.3 Cooper Pairs: QFT framework

Instability Of The Ground State Of A System Of Non-interacting Fermions With Respect To Arbitrarily Weak Attractions Between The Particles

1. Equation for the vertex part

We consider the properties of the system with the interaction (32.3). For this, we return to a study of the vertex part $\Gamma_{\alpha\beta,\gamma\delta}(p_1,p_2;p_3,p_4)$ at absolute zero. Let us write down the perturbation theory series for this quantity. The vertex part is, to a first approximation:

$$\lambda\left(\delta_{\alpha\gamma}\delta_{\beta\delta}-\delta_{\alpha\delta}\delta_{\gamma\beta}\right) \tag{33.1}$$

The diagrams corresponding to the first terms of the perturbation theory scries are illustrated in Fig. 90.

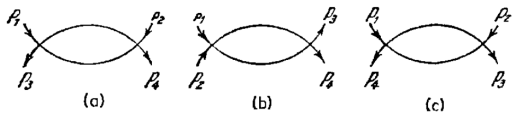


Fig. 90

As we know, singularities in the vertex part of "zero sound" type are connected with diagrams (a) and (c), i.e. these singularities are important for small momentum transfer. The diagrams of type (b) are connected with singularities in $\Gamma_{\alpha\beta,\gamma\delta}(p_1,p_2;p_3,p_4)$ at small values of the total 4 -momentum $q=p_1+p_2$. Let us investigate the last case in more detail. By using the concrete properties of the model in question, we can obtain more detailed information on the vertex part in the region of small q in comparison with the general results of (20.8).

The matrix element for the diagram of Fig. 90*b* is equal to

$$\lambda^2\frac{i}{(2\pi)^4}\left(\delta_{\alpha\gamma}\delta_{\beta\delta}-\delta_{\alpha\delta}\delta_{\gamma\beta}\right)\int \mathrm{d}^4k G(k)G(q-k)$$

where $q=\{\omega_0,q\}=\{\omega_1+\omega_2,p_1+p_2\}$. On substituting in this the expressions for the Green functions and integrating over the frequencies, we gct

$$\begin{gathered}\frac{\lambda^2}{(2\pi)^3}\left(\delta_{\alpha\gamma}\delta_{\beta\delta}-\delta_{\alpha\delta}\delta_{\beta\gamma}\right)\int\frac{\mathrm{d}^3k}{\omega_0-\varepsilon_0(k)-\varepsilon_0(q-k)+2\mu+i\delta}\\ (\varepsilon_0(k)>\mu,\varepsilon_0(q-k)>\mu)\\ -\frac{\lambda^2}{(2\pi)^3}\left(\delta_{\alpha\gamma}\delta_{\beta\delta}-\delta_{\alpha\delta}\delta_{\beta\gamma}\right)\int\frac{\mathrm{d}^3k}{\omega_0-\varepsilon_0(k)-\varepsilon_0(q-k)+2\mu-i\dot{\delta}}\\ (\varepsilon_0(k)<\mu,\varepsilon_0(q-k)<\mu)\end{gathered} \tag{33.2}$$

In the model which we are discussing, the only electrons that interact are those in a narrow region of energies close to the Fermi cnergy $\varepsilon_F\simeq\mu$. The integration over k in integrals (33.2) is therefore limited by the conditions $|\varepsilon_0(k)-\mu|,|\varepsilon_0(q-k)-\mu|<\omega_D$. On putting $\omega_0,|q|v\ll\omega_D$, we change in the ordinary way to an integration over $\xi=v(|k|-p_0)$. If we also neglect in the integrals a change in the upper limit of the order ω_0, or $|q|v$, we can transform (33.2) as follows:

$$-\frac{\lambda^2 m p_0}{2\pi^2}\left(\delta_{\alpha\gamma}\delta_{\beta\delta}-\delta_{\alpha\delta}\delta_{\beta\gamma}\right)\int_0^{\omega_D}\mathrm{d}\xi\int_0^1\left[\frac{1}{\omega_0+2\xi+2v|q|x-i\delta}+\frac{1}{2\xi+v|q|x-\omega_0-i\delta}\right]\mathrm{d}x$$

(where $x=\cos\theta,\theta$ is the angle between the directions of the vectors q and k). The remaining integrations are performed by elementary methods. Having chosen the branches of the logarithms from the condition that the integral of the first term in the square brackets be positive for $\omega_0>0$, and of the second, for $\omega_0<0$, we get the following expression for the diagram:

$$-\frac{\lambda^2 m p_0}{2\pi^2}\left(\delta_{\alpha\gamma}\delta_{\beta\delta}-\delta_{\alpha\delta}\delta_{\beta\gamma}\right)\left[1+\frac{1}{2}\ln\frac{2\omega_D-i\delta}{\omega_0+v|q|-i\delta}\right.$$
$$\left.+\frac{1}{2}\ln\frac{2\omega_D-i\delta}{-\omega_0+v|q|-i\delta}+\frac{\omega_0}{2v|q|}\left(\ln\frac{\omega_0-i\delta}{\omega_0+v|q|-i\delta}+\ln\frac{v|q|-\omega_0-i\delta}{-\omega_0-i\delta}\right)\right]. \qquad (33.3)$$

The principal term in this expression becomes, for small ω_0 and $v|q|$:

$$-\lambda^2\frac{mp_0}{2\pi^2}\left(\delta_{\alpha\gamma}\delta_{\beta\delta}-\delta_{\alpha\delta}\delta_{\beta\gamma}\right)\ln\frac{\omega_D}{\max\{\omega_0,v|q|\}}$$

Thus, when $\omega_D\gg\omega_0,v|q|$, the smallness of the interaction constant λ can be compensated by the large value of the logarithm, as a result of which this term becomes of the same order as the first term of the perturbation theory (33.1). In order to find the vertex part in the neighborhood of small ω_0 and $v|\boldsymbol{q}|$, when $\lambda\ln\omega_D/\max\{\omega_0,v|\boldsymbol{q}|\}\sim 1$, we must therefore sum the set of principal terms of the perturbation theory series, as in Chap. IV.

For this purpose, we write the equation for the vertex part in a form in which the terms leading to singularities of $\Gamma_{\alpha\beta,\gamma\delta}(p_1,p_2;p_3,p_4)$ for small $q=p_1+p_2$ are distinguished:

$$\Gamma_{\alpha\beta,\gamma\delta}(p_1,p_2;p_3,p_4)=\widetilde{\Gamma}_{\alpha\beta,\gamma\delta}(p_1,p_2;p_3,p_4) \qquad (33.4)$$
$$+\frac{i}{2(2\pi)^4}\int\tilde{\Gamma}_{\alpha\beta,\xi\eta}(p_1,p_2;k,q-k)\,G(k)G(q-k)\Gamma_{\xi\eta,\gamma\delta}(k,q-k;p_3,p_4)\,\mathrm{d}^4k$$

In this equation $\tilde{\Gamma}_{\alpha\beta,\gamma\delta}(p_1,p_2;p_3,p_4)$ is the sum of all the matrix elements whose diagrams are irreducible in the sense that interests us, i.e. cannot be split into two parts, one containing only incoming and the other only outgoing exterior ends and connected by two electron lines. The kernel of integral equation (33.4) contains a large logarithmic term from the integration of the two Green functions. In view of the smallness of the interaction constant, it is sufficient for us to take for $\tilde{\Gamma}$ its expression in terms of the first terms of the perturbation theory, since the corresponding expressions for $\tilde{\Gamma}$ do not contain large quantities. We have made it our aim, however, to calculate the kernel of equation (33.4) without confining ourselves to terms of order $\lambda\ln\omega_D/\omega_0\sim 1$; we try to find an expression for it up to and including terms of order λ. It would therefore seem at first sight that we need to know $\tilde{\Gamma}$ up to terms of order λ^2 in the perturbation theory, since the logarithmic integration in (33.4) can compensate one of the orders of λ. Let us consider terms of the second order of perturbation theory for $\tilde{\Gamma}$. The relevant diagrams are illustrated in Fig. 91.

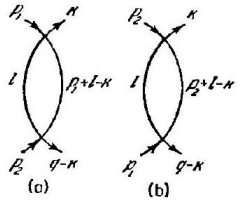


Fig. 91

Let us find the order of the matrix element corresponding to, say, diagram (a). Omitting numerical coefficients, we get

$$\lambda^2 \int G(l) G\left(l-k+p_1\right) \mathrm{d}^4 l.$$

On substituting the expressions for the Green functions, we can integrate over the frequency: (???? how to get these equations???)

$$\begin{aligned} &\lambda^2 \int \frac{\mathrm{d}^3 l}{\omega_k - \omega_\lambda + \varepsilon_0\left(l-k+p_1\right) - \varepsilon_0(l)} \left(\varepsilon_0(l) > \mu; \varepsilon_0\left(l-k+p_1\right) < \mu\right), \\ &-\lambda^2 \int \frac{\mathrm{d}^3 l}{\omega_k - \omega_1 + \varepsilon_0\left(l-k+p_1\right) - \varepsilon_0(l)} \left(\varepsilon_0(l) < \mu; \varepsilon_0\left(l-k+p_1\right) > \mu\right). \end{aligned} \tag{33.5}$$

The domain of integration over l is in fact much narrower than if it were determined only by the last conditions. This is connected with the properties of the model, in which only electrons with momenta in the neighbourhood of the Fermi momentum $|v\left(|\boldsymbol{p}| - p_0\right)| < \omega_D$ can interact. The actual domain of integration is shaded in Fig. 92 for the first condition in (33.5) and shown in black for the second In both cases the expression $\varepsilon\left(\boldsymbol{l}-\boldsymbol{k}+\boldsymbol{p}_1\right) - \varepsilon(\boldsymbol{l})$ in the denominator of the integrand is equal to ω_D in order of magnitude in the domain in question, whereas the volume of the domain over which the integration is carried out is $\sim m^2\omega_D^2/p_0$.

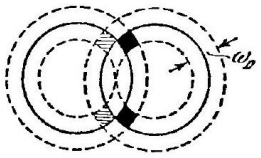


Fig. 92

The matrix element for the diagrams of Fig. 91 is therefore of order $\lambda^2 m^2 \omega_D/p_0$, i.e. their relative order compared with the simple vertex is $(\lambda m p_0)\, \omega_D/\varepsilon_T$. (As is clear from (33.3), the quantity $\lambda m p_0 \ll 1$ is a small dimensionless parameter in our model.) Since, by its physical meaning, $\omega_D \ll \varepsilon_F$, this extra order of smallness cannot be compensated in the domain considered by the large value of the logarithm. In view of this, we can confine ourselves in equation (33.4) for $\tilde{\Gamma}$ to the simple first order vertex of perturbation theory (33.1).

The equation obtained for the vertex part can now be solved easily. We notice that, as is clear from (33.3), $\Gamma_{\alpha\beta,\gamma\delta}\left(p_1, p_2; p_3, p_4\right)$ depends only on the sum of the variables $q = p_1 + p_2$. Hence the integral on the righthand side of (33.4) reduces to the integral already calculated by us for the matrix element of the second order of perturbation theory (33.3). We obtain as a result ($\omega_0 > v|\boldsymbol{q}|$):

$$\Gamma_{\alpha\beta,\gamma\delta}\left(p_1, p_2; p_3, p_4\right) \equiv \Gamma(q)\left(\delta_{\alpha\gamma}\delta_{\beta\delta} - \delta_{\alpha\delta}\delta_{\beta\gamma}\right)$$

$$\Gamma(q) = \lambda\left\{1 + \left(\frac{\lambda m p_0}{2\pi^2}\right)\left[1 + \ln\left|\frac{2\omega_D}{\omega_0}\right| + \frac{\pi i}{2} + \frac{1}{2}\ln\left|\frac{\omega_0^2}{\omega_0^2 - v^2|q|^2}\right| + \frac{\omega_0}{2v|q|}\ln\left|\frac{\omega_0 - v|q|}{\omega_0 + v|q|}\right|\right]\right\}^{-1} \tag{33.6}$$

2. Properties of the vertex part

Let us first consider for simplicity (33.6) with $q = 0$. We have for real and positive ω_0:

$$\Gamma\left(\omega_0\right) = \frac{\lambda}{1 + \left(\frac{\lambda m p_0}{2\pi^2}\right)\left[\ln\left|\frac{2\omega_D}{\omega_0}\right| + \frac{\pi i}{2}\right]} \tag{33.7}$$

We shall now regard $\Gamma(\omega_0)$ as a function of the complex variable ω_0, defining it as the analytic continuation of (33.7) in the upper half-plane $\operatorname{Im}\omega_0 > 0$. We now get

$$\Gamma(\omega_0) = \frac{\lambda}{1 + \left(\frac{\lambda m p_0}{2\pi^2}\right)\left[\ln\left|\frac{2\omega_D}{\omega_0}\right| + \frac{\pi i}{2} - i\varphi\right]}$$

Hence, if the interaction is an attraction $(\lambda < 0), \Gamma(\omega_0)$ has a pole at the point $\omega_0 = i\Omega$, where

$$\Omega = 2\omega_D \exp\left[-2\pi^2/|\lambda| m p_0\right] \tag{33.8}$$

In the neighbourhood of the pole $\Gamma(\omega_0)$ has the form

$$\Gamma(\omega_0) = -\frac{2\pi^2}{m p_0}\frac{i\Omega}{\omega_0 - i\Omega}$$

This result has to be connected with the above-mentioned idea of Cooper about the formation of bound-electron pairs. The vertex part $\Gamma_{\alpha\beta,\gamma\delta}(p_1, p_2; p_3, p_4)$ is defined in terms of the Fourier components of the two-particle Green function by the relation (10.17). Thus the fact that Γ has a pole means that the two-particle Green function has the same pole. The formation of bound pairs implies the instability of the ground state of the gas of interacting fermions from which we started out. The imposition of arbitrarily weak forces of attraction between the particles implies a readjustment of the entire system. The existence of an instability finds its reflexion in the appearance of poles in the vertex function with respect to the variable $\omega_0 = \omega_1 + \omega_2$ in the upper halfplane. This pole, being pure imaginary, determines the relaxation time of the unstable ground state. By the principle of indeterminacy, this time corresponds to the binding energy of the actual pair. In the new ground state the pairs behave as Bose formations and, as is the case for bosons, are capable of any degree of accumulation at the level of least energy. In the superconducting state these pairs are at the zero momentum level of the motion of the pair as a whole, in complete analogy with what occurs on the "Bose condensation" of ordinary bosons.

When $v|\boldsymbol{q}|$ is non-zero, (33.6) can be written as $(\omega_0 > v|\boldsymbol{q}|)$:

$$\Gamma(q, \omega_0) = \lambda\left\{1 + \frac{\lambda m p_0}{2\pi^2}\left[1 + \ln\left|\frac{2\omega_D}{\omega_0}\right| + \frac{i\pi}{2} - \frac{1}{2}\ln\left(1 - \frac{v^2|q|^2}{\omega_0^2}\right) + \frac{\omega_0}{2v|q|}\ln\left(\frac{\omega_0 - v|q|}{\omega_0 + v|q|}\right)\right]\right\}^{-1}.$$

After continuation into the half-plane $\operatorname{Im}\omega_0 > 0$ and use of definition (33.8) for Ω, we get

$$\Gamma(q, \omega_0) = -\frac{2\pi^2}{m p_0}\left\{\ln\frac{\omega_0}{i\Omega} - 1 + \frac{1}{2}\ln\left(1 - \frac{v^2|q|^2}{\omega_0^2}\right) - \frac{\omega_0}{2v|q|}\ln\left(\frac{\omega_0 - v|q|}{\omega_0 + v|q|}\right)\right\}^{-1}. \tag{33.9}$$

With small $v|\boldsymbol{q}| \ll \Omega$,

$$\Gamma(q, \omega_0) = -\frac{2\pi^2}{m p_0}\frac{i\Omega}{\omega_0 - i\Omega + i\left(v^2|q|^2/6\Omega\right)}$$

Equating to zero the denominator of (33.9) determines the pole of $\Gamma(\boldsymbol{q}, \omega_0)$ as a functions of $|\boldsymbol{q}|$. At small $|\boldsymbol{q}|$,

$$\omega_0 = i\Omega\left(1 - \frac{v^2|\boldsymbol{q}|^2}{6\Omega^2}\right)$$

i.e. the absolute value of ω_0 has decreased. At some value, $v|\boldsymbol{q}|_{\max}$, the pole ω_0 becomes zero, after which for greater $v|q|$ there is no pole of Γ. We can easily find the value of $v|q|_{\max}$ for which $\omega_0 = 0$:

$$v|q|_{\max} = e\Omega. \tag{33.10}$$

Since q is the momentum of the system of two particles as a whole, this result means that only those electrons which are moving almost towards one another reveal a tendency to the formation of bound pairs.

3. Determination of the transition temperature

Let us remark once more that the arguments adduced throw light on the instability of the ordinary ground state of a system of "attracting" particles at low temperatures. This instability amounts to an ability of two particles whose centre of mass is almost at rest to form bound pairs, i.e. a type of bosons, which "condense" in the lowest level.

The temperature at which such an instability first appears will be the transition temperature of the metal from the normal to the superconducting state.

To determine this, we can make use of the above-mentioned analogy with a boson gas. In the approximation in which we neglect the scattering of particles by one another (the weak interaction model), the bound pairs form an ideal gas. We know that the temperature-dependent Green function of an ideal boson gas is

$$\mathfrak{G}(\boldsymbol{q}, i\omega_n) = \left[i\omega_n - \frac{\boldsymbol{q}^2}{2m} + \mu\right]^{-1}$$

and represents the values at the points $\omega = i\omega_n = i2n\pi T$ of a function $G^R(q, \infty)$, analytic in the upper half-plane of ω. This function is equal to $[\mu - (q^2/2m)]^{-1}$ at $\omega_n = 0$. The latter first becomes infinite at the point $q = 0$ at some temperature $T = T_0$, called the temperature of the "Bose condensation". The temperature T_0 is determined by the condition $\mu = 0$.

The analogue of the boson Green function is, for a bound pair, the twoparticle fermion Green function (16.5). At the transition point, this latter must have analogous properties in the sense of its dependence on the variables $\omega_{0n} = (\omega_1 + \omega_2)_n$ and $\boldsymbol{q} = \boldsymbol{p}_1 + \boldsymbol{p}_2$, corresponding to the centre of mass of the pair. The fermion Green functions in (16.5) have no singularities with respect to these variables. We therefore consider the vertex part $\Gamma_R(q, \omega_0)$ (we shall omit the spin indices everywhere; the meaning of q and ω_0 is indicated above) and define it as an analytic function in the upper half-plane of ω_0, coinciding at the points $\omega_0 = i(\omega_1 + \omega_2)_n$ with the vertex part in the thermodynamic method. In other words, the function $\Gamma_R(\boldsymbol{q}, \omega_0)$ is the analytic continuation of the thermodynamic vertex part $\mathscr{T}_{\alpha\beta,\gamma\delta}(p_1\omega_1, p_2\omega_2; p_3\omega_3, p_4\omega_4) \equiv \mathcal{T}(q, \omega_0)(\delta_{\alpha\gamma}\delta_{\beta\delta} - \delta_{\alpha\delta}\delta_{\beta\gamma})$ (we shall show below that, in the approximation of interest to us, this function, like (33.9), actually depends only on the variables $\boldsymbol{q}$ and ω_0). We assume at the basis of the above that, at temperatures below the transition temperature, $\Gamma_R(\boldsymbol{q}, \omega_0)$ has poles $\operatorname{Im}\omega_0 > 0$. At the transition temperature, a pole $\omega_0 = 0$ first makes its appearance in the function $\Gamma_R(q, \omega_0)$.

The necessary equation for the thermodynamic vertex part has the same structure as (33.4):

$$\begin{aligned}\mathscr{T}_{\alpha\beta,\gamma\delta}(\boldsymbol{p}_1\omega_1, \boldsymbol{p}_2\omega_2; \boldsymbol{p}_3\omega_3, \boldsymbol{p}_4\omega_4) &= \tilde{\mathscr{T}}_{\alpha\beta,\gamma\delta}(\boldsymbol{p}_1\omega_1, \boldsymbol{p}_2\omega_2; \boldsymbol{p}_3\omega_3, \boldsymbol{p}_4\omega_4) \\ &- \frac{T}{2(2\pi)^3}\sum_{\omega'}\int \tilde{\mathscr{T}}_{\alpha\beta,\xi\eta}(\boldsymbol{p}_1\omega_1, \boldsymbol{p}_2\omega_2; \boldsymbol{k}\omega'; \boldsymbol{q} - \boldsymbol{k}, \omega_0 - \omega')\,\mathfrak{G}(k)\mathfrak{G}(q - k)\cdot \\ &\cdot \mathscr{T}_{\xi\eta,\gamma\delta}(\boldsymbol{k}\omega', \boldsymbol{q} - \boldsymbol{k}, \omega_0 - \omega'; \boldsymbol{p}_3\omega_3, \boldsymbol{p}_4\omega_4)\,\mathrm{d}^3\boldsymbol{k}, \end{aligned} \tag{33.11}$$

where $\tilde{\mathscr{T}}$ again is the sum of the matrix elements for all the diagrams which cannot be split by a vertical line into two parts, joined by two lines in the same direction. For the same reasons as above, we can confine ourselves to the first approximation of perturbation theory for $\tilde{\mathscr{T}}_{\alpha\beta,\gamma\delta}(\boldsymbol{p}_1\omega_1, \boldsymbol{p}_2\omega_2; \boldsymbol{p}_3\omega_3, \boldsymbol{p}_4\omega_4)$. The problem of finding the vertex part now reduces to finding the sum and the integral in the matrix element:

$$-\frac{\lambda^2}{(2\pi)^3} T \sum_{\omega'} \int \mathfrak{G}(k)\mathfrak{G}(q-k)\mathrm{d}^3k \tag{33.12}$$

On substituting (14.6) for the Green functions in this, we can easily perform the elementary summation over the frequencies.

We shall not evaluate (33.12) for arbitrary values of ω_0 and $|\boldsymbol{q}|$. It is clear from uniformity considerations that, as in a Bose gas, a pole first makes an appearance in $\Gamma_R(\boldsymbol{q}, \omega_0)$ for values $\omega_0 = |\boldsymbol{q}| = 0$. It is therefore sufficient to find the solution of equation (33.11) for $|\boldsymbol{q}| = \omega_0 = 0$. The instant at which this quantity becomes infinite determines the transition temperature from the normal to the superconducting state. When $|q| = \omega_0 = 0$, integral (33.12) can be transformed to

$$-\frac{\lambda}{2\pi}^2 mp_0 \int_0^{\omega_D} \tanh\left(\frac{\xi}{2T}\right)\frac{\mathrm{d}\xi}{\xi} = -\lambda^2 \frac{mp_0}{2\pi^2}\left(\ln\frac{\omega_D}{2T} - \int_0^\infty \frac{\ln x\ \mathrm{d}x}{\cosh^2 x}\right) \tag{33.13}$$

(after integration by parts, since the remaining integral is convergent, the limit $x = \omega_D/2T$ can be replaced by infinity. The integral is equal to $-\ln(2\gamma/\pi)$, where $\ln\gamma = C = 0.577$). Hence

$$\Gamma_R(0,0) = \mathscr{T}(0,0) = \frac{\lambda}{1 + \frac{\lambda mp_0}{2\pi^2}\ln\left(\frac{2\omega_D\gamma}{\pi T}\right)}$$

Close to the transition temperature, this expression can be written as

$$\mathscr{T}(0,0) = -\frac{2\pi^2}{mp_0}\frac{T_c}{T - T_c} \tag{33.14}$$

where the transition temperature T_c is equal to

$$T_c = \frac{\gamma}{\pi} 2\omega_D \exp\left[-\left(2\pi^2/|\lambda| mp_0\right)\right]. \tag{33.15}$$

The value of the frequency Ω, introduced above and characterising the instability of the system at absolute zero, is equal to

$$\Omega = \frac{\pi}{\gamma} T_{c*} \tag{33.16}$$

Cooper Pairs in QFT framework: The most important general questions

Why in general a two particle Green's function for BCS model is useful?

(????? can some one tell me??? where does it come from in the course of QFT? why in general when one looks at the BCS Hamiltonian, one says "Aha, I need to use the two-particle Green's function")

How to guess that such an approach exists?

(this is the deeper version of the previous question. Suppose we don't know that it exist. How to guess that this framework exists? I have no idea now....)

3.9.4 BCS Hamiltonian: Derivation and Features

BCS Hamiltonian

(here we will discuss why do we write it this way???)
(write that well-known expression)
(discuss here what it the momenta that corresponds to Debye frequency??)

Different way of writing original BCS Hamiltonians

Here, I'll summarize the different way of writing original BCS Hamiltonians without mean-field approximation.
(??? which are general version of which??)
from LS:

$$\widehat{\mathcal{H}}_{\text{ВКШ}} = \sum_p \xi_p a_p^+ a_p - \frac{1}{2} \sum_{p+p'=q+q'} V_{pp'qq'} a_{p\alpha}^+ a_{p'\beta}^+ a_{q\beta} a_{q'\alpha}$$

Как и раньше, будем считать, что взаимодействие отлично от нуля только вблизи ферми-поверхности:

$$V_{pp'qq'} = \begin{cases} \lambda & \text{при } \xi_{\max} < \omega_D, \\ 0 & \text{при } \xi_{\max} > \omega_D, \end{cases}$$

где $\xi_{\max} = \max\{|\xi_p|, |\xi_{p'}|, |\xi_q|, |\xi_{q'}|\}$. Выражение (10.10) называется гамильтонианом теории Бардина-Купера-Шриффера (БКШ).

$$\hat{H} - \mu\hat{N} = \sum_{\mathbf{p}\sigma} \xi_{\mathbf{p}} \hat{a}_{\mathbf{p}\sigma}^\dagger \hat{a}_{\mathbf{p}\sigma} - \lambda \sum_{\mathbf{pp}'}{}' \hat{a}_{\mathbf{p}'+}^\dagger \hat{a}_{-\mathbf{p}'-}^\dagger \hat{a}_{\mathbf{p}+} \hat{a}_{-\mathbf{p}-},$$

(??? here we have just all q-s, so which is more right?)

(discuss some notations with some minuses in some places)

(discuss here the order of operators. we have first two dagger, then two non-dagger in the coupling term. why is it so? answer! currently, I am not sure, but there is a derivation before, so the answer is already before)

Choice of model for AGD method

The interaction Hamiltonian has can be written as

$$H_{int}(x) = g\psi^+(x)\psi(x)\varphi(x) \tag{32.1}$$

Let us find the matrix clement of the scattering of two electrons by one another, in the process of which the electrons exchange one phonon. This process is illustrated schematically in Fig. 89. The dotted line represents the exchange of a phonon, which corresponds in the matrix element to the phonon D-function,

$$g^2 D(\varepsilon_3 - \varepsilon_1; p_3 - p_1) = g^2 \frac{u^2 (p_3 - p_1)^2}{(\varepsilon_3 - \varepsilon_1)^2 - u^2 (p_3 - p_1)^2}$$

where $\varepsilon_3 - \varepsilon_1, p_3 - p_1$ are respectively the changes in the cnergy and momentum of one of the electrons on collision. Close to the Fermi surface the momentum change on collision is in general of the order p_0 (i.e. $u\,|p_3 - p_1|$ is of the order of the Dcbye frequency ω_D, since $p_0 \sim a^{-1}$), so that the change in the cnergy of the electrons may be fairly small. In this region, i.e. when $|\varepsilon_3 - \varepsilon_1| \ll \omega_D$, the effective interaction, which is determined by the foregoing expression, simply reduces to

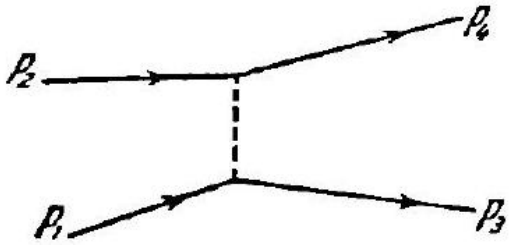


Fig. 89 the constant $-g^2$, i.e. there is an attraction.

L. Cooper [57] discovered in 1957 that the effective attraction between electrons close to the Fermi surface, resulting from an arbitrarily weak electron-phonon interaction, necessarily leads to the formation of bound electron pairs. Since binding involves an increase in energy, a readjustment of the ground state of the system must result when interaction takes place. Excitation of such a system requires the expenditure of a finite energy, cqual to the binding cnergy of the pair, which will in fact play the role of a gap in the excitation spectrum. It proved possible, on the basis of this idea, to construct a complete theory of superconductivity, explaining the vast mass of facts accumulated in several decades of intensive study of the phenomenon.

The basis chosen for our statement of the theory is not the same as in the original statements (Bardeen, Cooper and Schrieffer [58], Bogolyubov [59](†)), since it secms to us that the methods of quantum field theory offer substantial advantages. Apart from its simplicity and harmony, the approach described below enables a number of important new results to be obtained.

Before procecding further, let us remark that the electron-phonon interaction is not the only one for electrons in a metal. Repulsive Coulomb forces also operate between the electrons. The effective interaction between them will therefore be either an attraction or a repulsion, depending on

(†) See also [60].

the ratio of the magnitudes of the electron-phonon attraction and the Coulomb repulsion of the electrons. In general, the problem of taking into account both interactions for actual metals is extremely difficult. In addition to this, actual superconductors are anisotropic. A proviso must therefore be made regarding the present-day theory of superconductivity, that in essence it considers a simple model with a quadratic dispersion law for the clectrons, in which it is postulated in advance that the interaction of the electrons has the nature of an attraction in a narrow band of their energies close to the Fermi surface. This energy region is obviously of the order of the maximum energy of the emitted phonons, i.e. $\sim \omega_D$, where ω_D is the Debye frequency. In addition, we shall assume below, for simplicity, that the interaction is constant in this region and is fairly small.

To date, no theory of superconductivity has been developed on the basis of the Fermi liquid concept and which also takes the anisotropic properties into account. Nevertheless, it is interesting to note that, in spite of the crudity of the model, the theory not only explains the phenomena qualitatively, but also lcads to good quantitative agreement with the available experimental data.

We write down the effective interaction Hamiltonian of the electrons with one another in the second quantization representation as follows:

where $\lambda < 0$, and θ_p are the cut-off factors:

$$\theta_p = \begin{cases} 1, |\varepsilon(p) - \varepsilon_F| < \omega_D, \\ 0, |\varepsilon(p) - \varepsilon_F| > \omega_D. \end{cases}$$

The presence of these factors denotes that the only electrons taking part in the interaction are those with energies in a narrow band of width $2\omega_D$ close to the Fermi surface ($\omega_D \ll \varepsilon_F$). This Hamiltonian will often be written below in terms of the operators $\psi_\alpha(r)$ and $\psi_\beta^+(r)$ in the coordinate representation

$$H_{inl} = \frac{\lambda}{2} \int \psi_\alpha^+(r)\psi_\beta^+(r)\psi_\beta(r)\psi_\alpha(r)\mathrm{d}^3r. \tag{32.3}$$

It should be understood, of course, that the values of the four arguments of the ψ-operators in (32.3) are in fact somewhat different. This last is connected with the presence of the factors θ_p in expression (32.2) for the Hamiltonian. It would be more exact to write, instead of (32.3):

$$\begin{aligned} H_{\text{int}} = \frac{\lambda}{2} \iiint \iint \theta\left(r-\xi_1\right)\theta\left(r-\xi_2\right)\theta\left(r-\xi_3\right)\theta\left(r-\xi_4\right) \\ \times \psi_\alpha^+\left(\xi_1\right)\psi_\beta^+\left(\xi_2\right)\psi_\beta\left(\xi_3\right)\psi_\alpha\left(\xi_4\right)\mathrm{d}^3r\ \mathrm{d}^3\xi_1 \cdots\ \mathrm{d}^3\xi_4 \end{aligned} \tag{32.4}$$

where $\theta(x)$ is the Fourier transform of θ_p:

$$\theta(x) = \frac{1}{(2\pi)^3} \int e^{i(p\cdot x)}\theta_p\ \mathrm{d}^3p \tag{32.5}$$

It is easily verified by Fourier transforming that the functions $\theta(x)$ have δ-function characteristics:

$$\int \theta(x-y)f(y)\mathrm{d}^3y = f(x)$$

if the function $f(x)$ has noll-zero Fourier components f_p only for momenta p close to the Fermi surface. It is precisely with these functions that we shall be concerned in the theory described below. Expression (32.3) is to be understood in this sense.

Derivation of BCS Hamiltonian from electron-phonon interactions by Chalker

Experiments on the isotope effect showed that phonons are central to superconductivity. In the ideal case, for different isotopes of the same superconductor the energy scales represented by the critical temperature T_c and the critical field H_c vary with isotope mass like phonon frequencies, as (ionic mass) $^{-1/2}$. For a pair of electrons that are close in energy, phonon exchange generates an attractive interaction that beats the obvious screened Coulomb repulsion.

To derive this effective interaction we start from the Hamiltonian $\mathcal{H} = \mathcal{H}_0 + \mathcal{H}_1$ written in terms of electron operators $c_\mathbf{k}^\dagger$ and $c_\mathbf{k}$, and phonon operators $a_\mathbf{q}^\dagger$ and $a_\mathbf{q}$ as

$$\mathcal{H}_0 = \sum_\mathbf{k} \epsilon(\mathbf{k}) c_\mathbf{k}^\dagger c_\mathbf{k} + \hbar\omega \sum_\mathbf{q} a_\mathbf{q}^\dagger a_\mathbf{q} \quad \text{and} \quad \mathcal{H}_1 = \sum_\mathbf{kq} \left(M c_{\mathbf{k}+\mathbf{q}}^\dagger c_\mathbf{k} a_\mathbf{q} + \text{ h.c. } \right).$$

Here $\epsilon(\mathbf{k})$ is the electron dispersion relation and the phonons are represented as Einstein oscillators, all with frequency ω; the electron-phonon coupling is represented by the matrix element M; and we have omitted spin labels, though they will be crucial later.

We wish to focus on the electron system. To this end we eliminate the electron-phonon coupling by means of a canonical transformation, which we determine perturbatively. We write

$$\tilde{\mathcal{H}} = \mathrm{e}^{-S}\mathcal{H}\mathrm{e}^S = \mathcal{H} + [\mathcal{H}, S] + \frac{1}{2}[[\mathcal{H}, S], S] + \ldots$$

and at leading order we fix S simply by setting

$$\mathcal{H}_1 + [\mathcal{H}_0, S] = 0,$$

yielding

$$\tilde{\mathcal{H}} = \mathcal{H}_0 + \frac{1}{2}[\mathcal{H}_1, S] \equiv \mathcal{H}_0 + \mathcal{H}_{\text{int}}$$

To find S explicitly, we take matrix elements of Eq. (41) in eigenstates of $\mathcal{H}_0$, which satisfy $\mathcal{H}_0|n\rangle = E_n|n\rangle$. In this way we obtain

$$\langle n|S|m\rangle = \frac{\langle n\,|\mathcal{H}_1|\,m\rangle}{E_m - E_n} \quad \text{and} \quad \langle f\,|\mathcal{H}_{\text{int}}\,|\,i\rangle = \frac{1}{2}\sum_v \langle f\,|\mathcal{H}_1|\,v\rangle\,\langle v\,|\mathcal{H}_1|\,i\rangle \left(\frac{1}{E_i - E_v} + \frac{1}{E_f - E_v}\right).$$

From its matrix elements we can read off $\mathcal{H}_{\text{int}}$ in operator form, as

$$\mathcal{H}_{\text{int}} = \frac{1}{2}\sum_{\mathbf{pkq}} c^\dagger_{\mathbf{p}+\mathbf{q}} c_{\mathbf{p}} c^\dagger_{\mathbf{k}-\mathbf{q}} c_{\mathbf{k}} |M|^2 \left(\frac{1}{\epsilon(\mathbf{k}) - \epsilon(\mathbf{k}-\mathbf{q}) - \hbar\omega} + \frac{1}{\epsilon(\mathbf{p}+\mathbf{q}) - \epsilon(\mathbf{p}) - \hbar\omega}\right).$$

Derivation from электрон-фононное взаимодействие 2

Покажем, каким образом электрон-фононное взаимодействие может привести к эффективному притяжению электронов.

В отсутствие взаимодействия между электронами и решеткой гамильтониан системы имеет вид

$$H_0 = \sum_q \hbar\omega_q c_q^+ c_q + \sum_k \varepsilon_k a_k^+ a_k$$

Когда атомы решетки колеблотся возникает локальная леформация решетки и возникает локальная поляризация, описываемая дипольным моментом $\mathbf{P}(\mathrm{r})$.

Возникаюшее при этом изменение плотности связанного заряда выражается чepes диполыны й момент соотношением $\rho(\mathrm{r}) = -\operatorname{div}\mathrm{P}(\mathrm{r})$. Взаимолействие электрона, находящегося в точке $\mathbf{r}$, с этой поляризалией лается выражением

$$e\int Q\left(\mathbf{r} - \mathbf{r}'\right) \operatorname{div}\mathbf{P}$$

Если бы не было дебаевской экранировки (см. наши Лекиии по физической ки- экранировки, кулоновское взаимодействие обрезается на межатомном расстоянии $a \sim \hbar/p_F$. Поэтому можно считать, что

$$Q\left(\mathbf{r} - \mathbf{r}'\right) = a^2\delta\left(\mathbf{r} - \mathbf{r}'\right)$$

Дипольный момент $P \sim$ neu, где n - концентрания этомов, по поря дку величины равная концентрании электронов, u - смепение узла решетки из положения равновесия. Рассмотрим вклад в divP от некоторой фурье-компоненты флуктуацией $\operatorname{div}\mathbf{P}_k \sim V^{-1/2} iku_k$. Поэтому

$$V_k \sim V^{-1/2} ie^2a^2n(\omega/s)u_k$$

Оператор смещения есть линейная комбинация операторов рождения и уничтожения фононов c^+ и это разложение операторы рождения и уничтожения входят в комбинации

$i\sqrt{\frac{\hbar}{2nM\omega_k}}\left(c_k + c_k^+\right)$. Поэтому процесс, при котором происходит поглощение или испускание фонона описывается оператором

$$V_k \sim V^{-1/2} i e^2 a^2 n \left(\omega_k/s\right)^{1/2} \sqrt{\frac{\hbar}{2nM\omega_k}} \left(c_k + c_k^+\right) \sim$$

$$iV^{-1/2}\frac{ne^2a^2}{s}\sqrt{\frac{\omega_k\hbar}{2nM}} = iV^{-1/2}\left(na^3\right)\frac{e^2}{as}\sqrt{\frac{\omega_k\hbar}{2nM}}\left(c_k + c_k^+\right)$$

Типичный масштаб энергий в металле есть $e^2/$ a. Приравнивая эту величину кинетической части энергии колебаний $Ms^2/2$, получим для скорость звука оценку $s \sim a\omega_D \sim \sqrt{e^2/aM} \sim \sqrt{p_F^2/mM}$. Кроме того $na^3 \sim 1$. Подставляя эти оценки в (94), получим

$$V_k \sim iV^{-1/2} p_F \sqrt{\frac{\hbar\omega_k}{2nm}} \left(c_k + c_k^+\right)$$

Поглошение или испускание фонона, происходит при рассеянии электрона. Полный гамильтониан системы электронов и фононов с учетом взаимолействия между ними может, таким образом, быть представлен в виде

$$H = H_0 + V$$
$$H_0 = \sum_q \hbar\omega_q c_q^+ c_q + \sum_k \varepsilon_k a_k^+ a_k; V = D\sum_{kq}\sqrt{\hbar\omega_q}a_{k+q}^+ a_k\left(c_q + c_{-q}^+\right)$$

Здесьc_q^+, c_q - операторы рождения и уничтожения фононов с импульсом и энергией q и ω_q соответственно; a_k^+, a_k - операторы рожления и уничтожения электронов с импульсомk и энергией ε_k, соответственно. Последний член в (95) описывает рассеяние электронов на колебаниях решетки с испусканием (поглошением)

фонона, причем D - матричный элемент перехода. Гамильтониан V описы вает рассеяние электрона с испусканием или поглошением электрона. Гамильтониан рассеяния (БКII) возникает как процесс второго порядка теории возмущений. Вместо станлартной теории возмущений удобно применить каноническое преобразовние, предложенное Фрелихом,

$$\tilde{H} \equiv e^{-S} H e^S = H + [H, S] + \frac{1}{2}[[H, S], S]\ldots$$

Переход от H к $\tilde{H}$ с помонцьо унитарного канонического преобразования означает просто переход к другому базису, в котором гамильтониан может выглядеть проше.

Будем считать V малым возмупением по параметру D. Тогда S также мало по этому параметру. Выберем S из условия обращения в нуль в $\tilde{H}$ линейных по D членов:

$$V + [H_0, S] = 0$$

Во втором порялке теории возмунцений

$$\tilde{H} \equiv e^{-S} H e^S = H_0 + [V, S] + \frac{1}{2}\left[\left[H_0, S\right], S\right] + O\left(D^3\right) =$$
$$= H_0 + \frac{1}{2}[V, S] + O\left(D^3\right)$$

Перепишем (97) в базисе собственных функцций гамильтонтана H_0 с собственными значениями E_m. Тогда

$$S_{mn} = \frac{V_{mn}}{E_n - E_m}$$

и эффективный гамильтониан рассеяния электронов через обмен виртуальным фононом равен

$$H_2 = \frac{1}{2}[V, S]$$

Для простоты ограничимся случаем нулевых температур (когда фононы возникают лишь виртуальным образом). Для вычисления энергии $\tilde{H}$ нас интересует матричный элемент$\langle 0|\tilde{H}|0\rangle$ (являющийся оператором по отношению к электронному гильбертову пространству). Здесь $|0\rangle$ - фононная компонента полной волновой функции электрон-фононной системы при отсутствии фононов. При вычислении энергии во втором порядке теории возмущений нас интересуют матричные элементы

$$\langle 1_q|S|0\rangle = D\sum_k \frac{\sqrt{\hbar\omega_q}a^+_{k-q}a_k}{\varepsilon_k - \varepsilon_{k-q} - \hbar\omega_q}$$

$$\langle 0|S|1_q\rangle = D\sum_k \frac{\sqrt{\hbar\omega_q}a^+_{k+q}a_k}{\varepsilon_k + \hbar\omega_q - \varepsilon_{k+q}}$$

здесь $|1\rangle$ - фононная компонента волновой функции электрон-фононной системы с одним фононом в состоянии q. Очевидно, что

$$\langle 0|V|1_q\rangle = D\sqrt{\hbar\omega_q}\sum_k a^+_{k+q}a_k$$

$$\langle 1_q|V|0\rangle = D\sqrt{\hbar\omega_q}\sum_k a^+_{k-q}a_k$$

Используя (100) – (102), получим

$$\frac{1}{2}[V, S] = \frac{1}{2}D^2\sum_{kqk'} a^+_{k'+q}a_{k'}\frac{\hbar\omega_q a^+_{k-q}a_k}{\varepsilon_k - \varepsilon_{k-q} - \hbar\omega_q} - \frac{\hbar\omega_q a^+_{k+q}a_k}{\varepsilon_k + \hbar\omega_q - \varepsilon_{k+q}}a^+_{k'-q}a_{k'}$$

Учитывая, что$\omega_q = \omega_{-q}$, во втором слагаемом делаем замену $q \to -q$ и переставим пары операторов $a^+_{k+q}a_k$ и $a^+_{k'-q}a_{k'}$. (Коммутатор этих операторов есть квацратичная форма по операторам и может быть включен в перенормировку ε_k.)

$$\frac{1}{2}D^2\sum_{kqk'}\hbar\omega_q a^+_{k'+q}a_{k'}a^+_{k-q}a_k\left(\frac{1}{\varepsilon_k - \varepsilon_{k-q} - \hbar\omega_q} - \frac{1}{\varepsilon_k + \hbar\omega_q - \varepsilon_{k-q}}\right) =$$

$$= D^2\sum_{kqk'} a^+_{k'+q}a_{k'}a^+_{k-q}a_k\frac{(\hbar\omega_q)^2}{(\varepsilon_k - \varepsilon_{k-q})^2 - (\hbar\omega_q)^2} =$$

$$= D^2\sum_{kqk'} a^+_{k-q}a^+_{k'+q}a_{k'}a_k\frac{(\hbar\omega_q)^2}{(\varepsilon_k - \varepsilon_{k-q})^2 - (\hbar\omega_q)^2}$$

Отсюда следует, что если

$$|\varepsilon_k - \varepsilon_{k-q}| < \hbar\omega_q$$

то амплитуда рассеяния двух электронов имеет отрицательный знак. Итак, после канонического преобразовния гамильтоноан электрон-фононной системы имеет вид

$$H = H_0 + D^2\sum_{kqk'}\frac{(\hbar\omega_q)^2}{(\varepsilon_k - \varepsilon_{k-q})^2 - (\hbar\omega_q)^2}a^+_{k-q}a^+_{k'+q}a_{k'}a_k$$

Наиболыпий фазовый объем $\sim q^2$ отвечает процессам, в которых импульс q достигает своего максимального значения $q \sim \hbar/a$. Этому имульсу отвечает дебаевская энергия $\hbar\omega_D$. Поэтому в (106) можно заменить $\hbar\omega_q$ на $\hbar\omega_D$. Рассмотрим теперь только состояния, дуя которых $|\varepsilon_k - \varepsilon_{k-q}| \ll \hbar\omega_D$. Тогда

$$H = H_0 - D^2 \sum_{kqk'} a^+_{k-q} a^+_{k'+q} a_{k'} a_k$$

Если перейти в этом выражении в координатное представление то мы получим для взаимодействия выражение типа (11). Это означает, обмен фононами во втором порядке теории возмунений, эквивалнетен точечному притяжению. В силу принципа Паули это может иметь место, только если взаимодействуют элекроны с противоположными спинами.

Очевидно, что если рассеиваются электроны с противоположными импульсами $\mathrm{k} = -\mathrm{k}'$, то в результате рассеяния должны получиться два электрона также с противоположными импульсами, причем это может быть любой импульс из этой корочки корочки. Если же рассеивалтся электроны с одинаковыми импульсами (близкими к импульсу Ферми) то фазовый объем, доступный рассеянным электронам исчезагоше мал. Поэтому основной вклал в рассеяние датт процессы в которых электроны имегот практически противоположные импульсы.

мы рассматриваем модель, в которой только такое рассеяние и учитывается. Соображения, описанные выше обосновывают модель БКШ, описываемую гамильтонианом

$$H = H_0 - g \sum_{kq} a^+_{k+q,\sigma} a^+_{-k+q,-\sigma} a_{-k,-\sigma} a_{k,\sigma}, \quad g > 0$$

Why in the BCS Hamiltonian is what is there?

Why there is a plus sign in front of the part with Δ?

(I'll write that some initial Hamiltonians have different order of operators, in that nonation in a mean field approximation, there is a minus sign)

(??? I believe that it does not matter, but later maybe I'll explicetely write why it does not matter. It is not obvious)

What if one writes operators in a different position in the interaction term?

(??? I'll write later)

What exactly the meaning of $\mu\hat{N}$ in the BCS Hamiltonian?

The basic answer is that we have a chemical potential, which is the Fermi energy, so this term is just a subtraction of all the states below the Fermi energy.

(????? right???)

(???? see my thesis for deeper discussion.)

BCS model is nonlocal $\hat{V}(\mathbf{r}_1, \mathbf{r}_2) \neq V(\mathbf{r}_1 - \mathbf{r}_2)$

(??? I'll explain in details, why it is so???)

(???? why local theory would not work??)

Overview of other derivations of BCS coupling

Idea of derivation from functional integral

(??? maybe integration out phonon field will also give it. I'll derive it in the section on BCS in functional integral and explain this idea here. It is a very nontrivial idea!)

BCS Hamiltonian in the real space

This is an old scary notation, which is still a good thing to learn to understand it in a different way.

(translate it!)

Полный гамильтониан подсистемы электронов в представлении вторичного квантования для большого канонического ансамбля запишем в форме суммы кинетической энергии электронов и эффективного парного взаимодействия

$$\hat{H} = \int d^3 r \hat{\Psi}_\sigma^+(t,\mathbf{r}) \left(\frac{\left(\hat{\mathbf{p}} - \frac{e}{c}\mathbf{A}\right)^2}{2m} + e\varphi - \mu \right) \hat{\Psi}_\sigma(t,\mathbf{r}) + \\ + \frac{1}{2} \int d^3 r_1 d^3 r_2 \hat{\Psi}_\sigma^+(t,\mathbf{r}_1)\, \hat{\Psi}_{\sigma'}^+(t,\mathbf{r}_2)\, U(\mathbf{r}_1 - \mathbf{r}_2)\, \hat{\Psi}_{\sigma'}(t,\mathbf{r}_2)\, \hat{\Psi}_\sigma(t,\mathbf{r}_1)$$

где $\hat{\Psi}_\sigma(t,\mathbf{r})$ - оператор уничтожения электрона в (r,t)-представлении, $\hat{\mathbf{p}}$ - operagor импульса электрона, A, φ - потенциалы электромагнитного поля. В (2) мы пренебрегаем кристаллической структурой тела, $\sigma = \pm 1$ есть удвоенная проекция спина на одну из осей, постоянная μ есть химический потенциал электронов. Вы пишем также оператор полного числа частиI

$$\hat{N} = \int d^3 r \hat{\Psi}_\sigma^+(t,\mathbf{r}) \hat{\Psi}_\sigma(t,\mathbf{r})$$

Квантовое поле ферми-частиц удовлетворяет коммутащионным соотношениям:

$$\left\{ \hat{\Psi}_\sigma(t,\mathbf{r}_1), \hat{\Psi}_{\sigma'}^+(t,\mathbf{r}_2) \right\} = \delta_{\sigma\sigma'} \delta(\mathbf{r}_1 - \mathbf{r}_2) \\ \left\{ \hat{\Psi}_\sigma(t,\mathbf{r}_1), \hat{\Psi}_{\sigma'}(t,\mathbf{r}_2) \right\} = 0$$

где $\{\ldots\}$ - антикоммутатор. Обратим внимание, что в (2) операторы ферми-поля стоят в иормалъиом порядке - слева операторы рожления фермионов, справа операторы поглопения.

Потенциал $U(\mathrm{r}_1 - \mathrm{r}_2)$ равен сумме кулоновского отталкивания электронов и притяжения, которое возникает как результат взаимодействия летяшцх навстречу друг другу электронов благодаря обмену фононом или магноном. Обмен фононами - процесс второго порялка, и, согласно теории возмунений, приводит к понижению энергии, т. е. к притяжению (см. раздел$* * **$). В металлах кулоновское взаимодействие заэкранировано и сильно ослаблено. Если притяжение превалирует, то металл при достаточно низких температурах переходит в сверхпроводянее состояние. В таких металлах какCu преоблалает отталкивание, и перехола в сверхпроводящее состояния нет. Интересно, что в соединениях, которые называлотся купратами, причиной сверхпроводимости является сильное взаимодействие электронов проводимости с подсистемой спинов ионов меди во внутрикристаллических плоскостях CuO_2.

Короткодействующий парны й потенциал эффективного притяжения электронов можно заменить на локальны й

$$U(\mathbf{r}_1 - \mathbf{r}_2) = U_0 \delta(\mathbf{r}_1 - \mathbf{r}_2)$$

Параметр U_0 имеет размерность энергия хобъем и записы вается в виле

$$U_0 = \frac{4\pi\hbar^2 a}{m}$$

Величина a назы вается длиной рассеяния. В случае притяжения величины U_0 и a отрицательны. Итак, гамильтониан (2) принимает вид

$$\hat{H} = \int d^3r \left[\hat{\Psi}^+_\sigma(t,\mathbf{r}) \left(\frac{\left(\hat{p} - \frac{e}{c}\mathbf{A}\right)^2}{2m} + e\varphi - \mu \right) \hat{\Psi}_\sigma(t,\mathbf{r}) + \frac{1}{2} U_0 \hat{\Psi}^+_\sigma(t,\mathbf{r}) \hat{\Psi}^+_{-\sigma}(t,\mathbf{r}) \hat{\Psi}_{-\sigma}(t,\mathbf{r}) \hat{\Psi}_\sigma(t,\mathbf{r}) \right]$$

Потенциал (6) подразумевает, что взаимодействуют электроны находяпиеся в одном месте. В силу принципа Паули, для этого они должны иметь разные проекции спина, что и отражено в (8). Производная по времени от гайзенберговских операторов равна

$$i\hbar \frac{\partial}{\partial t} \hat{\Psi}_\sigma(t,\mathbf{r}) = \left[\hat{\Psi}_\sigma(t,\mathbf{r}), \hat{H} \right]$$

Вычисляя коммутатор с помощью (4), (5), приходим к "нелинейному уравнению Шредингера":

$$i\hbar \frac{\partial}{\partial t} \hat{\Psi}_\sigma(t,\mathbf{r}) = \left(\frac{\left(\hat{p} - \frac{e}{c}\mathbf{A}\right)^2}{2m} + e\varphi - \mu \right) \hat{\Psi}_\sigma(t,\mathbf{r}) + U_0 \hat{\Psi}^+_{-\sigma}(t,\mathbf{r}) \hat{\Psi}_{-\sigma}(t,\mathbf{r}) \hat{\Psi}_\sigma(t,\mathbf{r})$$

В отсутствие внешнего электромагнитного поле имеем

$$i\hbar \frac{\partial}{\partial t} \hat{\Psi}_\sigma(t,\mathbf{r}) = \left(\frac{\hat{p}^2}{2m} - \mu \right) \hat{\Psi}_\sigma(t,\mathbf{r}) + U_0 \hat{\Psi}^+_{-\sigma}(t,\mathbf{r}) \hat{\Psi}_{-\sigma}(t,\mathbf{r}) \hat{\Psi}_\sigma(t,\mathbf{r})$$

Современная наука не может решить это уравнение точно. Но в случае слабого взаимодействия ($nU_0 \ll \mu$), чтобы найти элементарные возбуждения достаточно нелинейный член учесть приближенно. Рассмотрение его в рамках теории возмущений дает только перенормировку массы электрона и слабое затухание возбужлений. Чтобы увидеть в (10) сверхпроводимость, неоходимо в решение задачи ввести илего, которая бы отражала физическую причину качественной перестройки электронной подсистемы, аналогичную той, которая привела к микроскопическому объяснению сверхтекучести бозе-газа. В бозе-газе - это конленсация Бозе-Эйнштейна. Явления конденсации в ферми-газе не может супествовать из-за принципа Паули. Но на уровне коллективных бозе-возбуждений конденсация становится возможной. Такими коллективными возбуждениями в ферми-газе являются куперовские пары.

Diagonalization of BCS Hamiltonian in the Real space

Двухчастичная задача Купера поучительна в том смысле, что она демонстрирует, что при $U_0 < 0$ электроны вблизи поверхности Ферми связываются в покоящиеся пары - бозе-частицы с нулевым суммарным импульсом.

Этот результат подсказывает, в каком направлении нужно двигаться.

Если таких пар много, то, по аналогии с бозе-газом, можно говорить о конденсате покоящихся пар.

Основной недостаток задачи Купера заключается в том, что она не учитывает тождественности электронов внутри сферы Ферми и двух выделенных электронов.

Из теории атома водорода и теории позитрония (связанного состояния электрон-позитрон) мы знаем, что волновая функция связанного состояния двух частиц есть произведение волновых функций этих частиц.

Поэтому произведение $\hat{\Psi}_\sigma(t,\mathbf{r})\hat{\Psi}_{-\sigma}(t,\mathbf{r})$ в (11) можно интерпретировать как оператор уничволновой функции куперовской пары.

Поскольку число куперовских пар есть макроскопическое число, то это произведение можно заменить на с-число.

$$\hat{\Psi}_{-\sigma}(t,\mathbf{r})\hat{\Psi}_\sigma(t,\mathbf{r}) \to \left\langle \hat{\Psi}_{-\sigma}(t,\mathbf{r})\hat{\Psi}_\sigma(t,\mathbf{r}) \right\rangle = \lim_{N\to\infty} \left(\mathrm{Sp}\,\rho_N \left\langle N \left| \hat{\Psi}_{-\sigma}(t,\mathbf{r})\hat{\Psi}_\sigma(t,\mathbf{r}) \right| N+2 \right\rangle \right)$$

В отличие от сверхтекучести, здесь мы хотим рассмотреть свойства сверхпроводника при всех температурах вплоть до критической температуры перехода в нормальное состояние.

Поэтому в (16) справа символ усреднения $\langle \ldots \rangle$ означает двойное усреднение по когерентному состоянию конденсата куперовских пар и по распределению Гиббса сN -частичной матрицей плотности ρ_N.

В однородном случае среднее (16) не зависит ни от времени, ни от координаты, но,как следует из (5), меняет знак при изменении знака σ. В приближении (16) уравнение (11) формально становится линейным

$$i\hbar\frac{\partial}{\partial t}\hat{\Psi}_\sigma(t,\mathbf{r}) = \left(\frac{\hat{p}^2}{2m} - \mu\right)\hat{\Psi}_\sigma(t,\mathbf{r}) + U_0\hat{\Psi}^+_{-\sigma}(t,\mathbf{r})\left\langle \hat{\Psi}_{-\sigma}(t,\mathbf{r})\hat{\Psi}_\sigma(t,\mathbf{r}) \right\rangle$$

Введем обозначения

$$\xi_k = \frac{k^2}{2m} - \mu, \sigma\Delta = U_0\left\langle \hat{\Psi}_{-\sigma}(t,\mathbf{r})\hat{\Psi}_\sigma(t,\mathbf{r}) \right\rangle$$

Аномалыное среднее Δ, вообне говоря, есть комплексная величина. Разложим поле $\hat{\Psi}_\sigma(t,\mathbf{r})$ по плоским волнам $|\mathbf{k}\sigma\rangle = |\mathbf{k}\rangle|\sigma\rangle$ $\left(|\mathbf{k}\rangle = \frac{1}{\sqrt{V}}e^{ikr}, |\sigma\rangle -\right.$ спиновая волновая функция):

$$\hat{\Psi}_\sigma(t,\mathbf{r}) = \sum_{k\sigma'}\langle \mathbf{k}\sigma'|r\sigma\rangle\,\hat{a}_{k\sigma'} = \sum_{k\sigma'}\langle\sigma'|\sigma\rangle\,\langle k|r\rangle\hat{a}_{k\sigma'} = \sum_k \frac{1}{\sqrt{V}}e^{ikr}\hat{a}_{k\sigma}$$

Тогда из (17) имеем уравнение для $\hat{a}_{k\sigma}$:

$$i\hbar\frac{\partial}{\partial t}\hat{a}_{k\sigma} = \xi_k\hat{a}_{k\sigma} + \sigma\Delta\hat{a}^+_{-k-\sigma}$$

Диагонализуем это уравнение с помоп,ью преобразования Боголобова

$$\hat{a}_{k\sigma} = u_k\hat{b}_{k\sigma} - \sigma v^*_k\hat{b}^+_{-k-\sigma}$$

Операторы поглошщения и рожления квазичастиI$\hat{b}_{k\sigma}, \hat{b}^+_{-k-\sigma}$ должны быть собственными функциями оператора энергии $i\hbar\frac{\partial}{\partial t}$:

$$i\hbar\frac{\partial}{\partial t}\hat{b}_{k\sigma} = \varepsilon_k\hat{b}_{k\sigma}, i\hbar\frac{\partial}{\partial t}\hat{b}^+_{-k-\sigma} = -\varepsilon_k\hat{b}^+_{-k-\sigma}$$

Кроме того,.операторы частиц и квазичастиц должны удовлетворять одинаковым правилам антикоммутации

$$\left\{\hat{a}_{k\sigma}, \hat{a}^+_{k'\sigma'}\right\} = u_k^2\left\{\hat{b}_{k\sigma}, \hat{b}^+_{k'\sigma'}\right\} + v_k^2\left\{\hat{b}^+_{-k-\sigma}, \hat{b}_{-k'-\sigma'}\right\} = \delta_{kk'}\delta_{\sigma\sigma'}$$

и, следовательно:

$$u_k^2 + v_k^2 = 1$$

Подстановка (21) в (20) дает

$$(\varepsilon_k - \xi_k)\, u_k \hat{b}_{k\sigma} + (\varepsilon_k + \xi_k)\, \sigma v_k^* \hat{b}^+_{-k-\sigma} = \sigma\Delta \left(u_k^* \hat{b}^+_{-k-\sigma} + \sigma v_k \hat{b}_{k\sigma} \right)$$

Orciola

$$\begin{gathered}(\varepsilon_k - \xi_k)\, u_k = \Delta v_k \\ (\varepsilon_k + \xi_k)\, v_k = \Delta^* u_k\end{gathered}$$

Репая эту систему уравнений находим энергию квазичастиц

$$\varepsilon_k = \sqrt{\xi_k^2 + |\Delta|^2}$$

и коэффициенты преобразования [9]

$$u_k = \sqrt{\frac{1}{2}\left(1 + \frac{\xi_k}{\varepsilon_k}\right)}, v_k = \frac{\Delta^*}{|\Delta|}\sqrt{\frac{1}{2}\left(1 - \frac{\xi_k}{\varepsilon_k}\right)}, 2u_k v_k^* = \frac{\Delta}{\varepsilon_k}, |u_k|^2 - |v_k|^2 = \frac{\xi_k}{\varepsilon_k}$$

Преобразование от операторов поглошения и рожления электронов к операторам квазичастиц диагонализует гамильтониан (8), и он равен сумме энергии основного состояния и энергии квазичастиц

$$H_s = E_0 + \sum \varepsilon_k \hat{b}^+_{k\sigma} \hat{b}_{k\sigma}$$

Filling factor, chemical potential, N-operator

(how does it exactly work??? why we define N as we define it??)

The constant in BCS Hamiltonians

(here will be a detailed discussion about what is its value???)

Connection of BCS model and weakly interacting Bose gas

The BCS model is basically

$$\hat{H} - \mu\hat{N} = \frac{1}{\lambda}|\Delta|^2 + \sum_{\mathbf{p}\sigma} \xi_{\mathbf{p}} \hat{a}^\dagger_{\mathbf{p}\sigma} \hat{a}_{\mathbf{p}\sigma} + \sum_{\mathbf{p}}{}' \left[\Delta^* \hat{a}_{\mathbf{p}+} \hat{a}_{-\mathbf{p}-} + \Delta \hat{a}^\dagger_{-\mathbf{p}-} \hat{a}^\dagger_{\mathbf{p}+} \right]$$

(write meaning of indices and that we have fermions here)

and Bose gas is described by

$$\hat{H} - \mu\hat{N} = \sum_{\mathbf{p}} \left(\frac{\mathbf{p}^2}{2m} - \mu \right) \hat{a}^+_{\mathbf{p}} \hat{a}_{\mathbf{p}} + \frac{U_0}{2V} \sum_{\mathbf{p}_1 + \mathbf{p}_2 = \mathbf{p}_1' + \mathbf{p}_2'} \hat{a}^+_{\mathbf{p}_1'} \hat{a}^+_{\mathbf{p}_2'} \hat{a}_{\mathbf{p}_1} \hat{a}_{\mathbf{p}_2}.$$

(??? explain this formula)

(write that even in the model, the model is basically the same, just a different constant and different type of operators.)

(write also that summation in bose gas is over much more momenta than just p, -p like in BCS, this is why constant is different(???))

(point out that Δ has its meaning)

then the $\hat{a}_0^+ = \hat{a}_0 = \sqrt{N_0}$ was introduced.

(??? write that finally we see that Δ is the same as a_0. Pukhov wrote that it is so. I'll study Bose gas, than I'll return to this statement.)

In Bose liquid, only excitations are temperature dependent (higher temperature - higher levels are excited). Here, also the spectrum is temperature dependent (not only higher levels are are excited, but also all excitation levels will change)

(??? maybe I'll write more explicit how is it? but maybe it is already very clear)

How from BCS Hamiltonian one can get some superconductivity?

(write question that one has the Hamiltonian, so what, we can approximate it, then diagonalize it, so where is the SC?)

(currently, the answer is that there are no excitations, so it will be still in the ground state thus no resistance. But I'll write the better answer!!!!)

(another argument is that superfluidity criterion is satisfied, so there is a superfluid....)

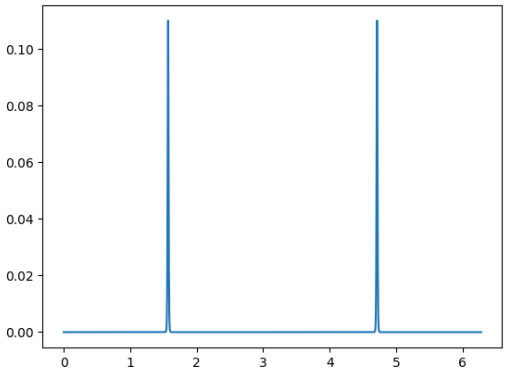
Still, there is a question, where is the current in the Hamiltonian? I don't see it.

What is exactly the excited state of a superconductor?

Plot of excitations

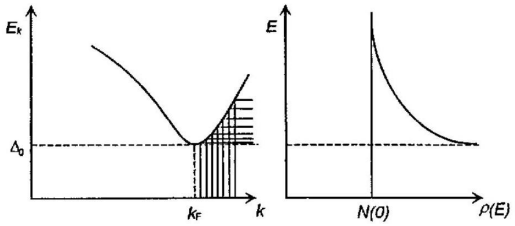
Here we will show, how typical excitations in a superconductor look like?

They look as follows:



(make this plot better, add axes, titles)

In this plot we just show how many excitations there are over the gap. Another plot which shows their energy values is:



(explain why they are about the same, it is rather obvious)

This is the case for BCS TB model and can be obtained by the code:

```
import numpy as np
import matplotlib.pyplot as plt
from scipy.optimize import brentq

EXP_MAX = 700.0
TINY    = 1e-12

init_tempr_fraction = 0.7
```

```
L      = 2000

p_vals = np.linspace(0, 2*np.pi, L, endpoint=False)


t_hop  = 1.0

mu     = 0.0
xi_vec = - 2*t_hop * np.cos(p_vals) - mu

cutoff = 0.4
mask   = (np.abs(xi_vec) <= cutoff)

lambd = 1.7


def gap_eq_thermal(Delta, T):
    E = np.sqrt(xi_vec**2 + Delta**2)
    f = np.exp(-E/T) / (1.0 + np.exp(-E/T))
    val = np.sum((1.0 - 2.0 * f[mask]) / E[mask])
    return 0.5 * val / L - 1.0 / lambd

Tc     = brentq(lambda T: gap_eq_thermal(1e-8, T), 1e-4, 1.0, maxiter=200)
Delta0 = brentq(lambda D: gap_eq_thermal(D, 1e-4), 1e-6, 2.0, maxiter=200)

Delta_init = brentq(lambda D: gap_eq_thermal(D, T_init), 1e-8, 2.0, maxiter=200)
T_init = init_tempr_fraction * Tc

E_init = np.sqrt(xi_vec**2 + Delta_init**2)
n_init = np.exp(-(E_init/T_init)) / (1.0 + np.exp(-E_init/T_init))


plt.plot(p_vals, n_init,   label='Initial')
plt.show()
```

What is the positive and what is the negative excitation?

(does an excited electron give the positive energy? if it has a negative charge, is still his energy positive? I think, yes, I'll explain why here.)

(now, there are excitation below Fermi surface. what are these holes exactly? are they an absence of electron with the positive energy? so totally what happens, do we have twice energy of the only excitations near Fermi surface?)
(how does it relate to having two branches n_+ and n_-? both of them have holes?)

(why there is no gap in the excitation spectrum (we don't see any gap on the plot)? well, because there are just excitations with the new spectrum (that square root), that it all)

(how can we see that energy is indeed bigger that the Fermi energy? well, we just plug the ξ_p into $E = \sqrt{\xi^2 + \Delta^2}$. in the plot, we assume that these are excitations, so we everything else is already assumed)

3.9.5 Mean-field Approximation of BCS Hamiltonian, Diagonalization

Mean-field approximation of BCS Hamiltonian by introduction of condensate by a common sense

We know that there is a sense of the model with

$$\hat{H} - \mu\hat{N} = \sum_{\mathbf{p}\sigma} \xi_{\mathbf{p}} \hat{a}^\dagger_{\mathbf{p}\sigma} \hat{a}_{\mathbf{p}\sigma} - \lambda \sum_{\mathbf{p}\mathbf{p}'} \hat{a}^\dagger_{\mathbf{p}'+} \hat{a}^\dagger_{-\mathbf{p}'-} \hat{a}_{\mathbf{p}+} \hat{a}_{-\mathbf{p}-},$$

(??? somehow) We know that there is a condensate, so we need to introduce it. We have seen that if there is an attraction between two electrons on the Fermi surface, then they form a bound state. Thus we understand that condensate will be formed by these paired electrons. There are a lot of them, so we need to average over all those who are near the Fermi surface.

(??? is it a good reasoning???)

Thus, we introduce an operator of creation of a Cooper pair $\hat{a}^\dagger_{\mathbf{p},+}\hat{a}^\dagger_{-\mathbf{p},-}$ and its annihilation $\hat{a}_{-\mathbf{p}-}\hat{a}_{\mathbf{p}+}$.

Why does operators in exactly this order and not vice versa? (????????? this I don't know, but one can see that exactly this order is in the interaction term in the BCS Hamiltonian, so it makes more sense then to do it than to do it vice versa)

Thus we can just write

$$\Delta^* = \lambda \cdot \sum_{\mathbf{p}'} \left\langle \hat{a}^\dagger_{\mathbf{p}',+}\hat{a}^\dagger_{-\mathbf{p}',-} \right\rangle,$$

$$\Delta = \lambda \cdot \sum_{\mathbf{p}'} \left\langle \hat{a}_{-\mathbf{p}',-}\hat{a}_{\mathbf{p}',+} \right\rangle.$$

Note that operators in Δ^* are exactly ordered as first two operators in the interaction term in the BCS Hamiltonian. This is not the case for Δ, its operators are changed compared to the two latter operators in the interaction term in the BCS Hamiltonian. This is important to understand, because otherwise some minus signs will appear (because we work with fermions).

This is how we get

$$\hat{H} - \mu\hat{N} = \frac{1}{\lambda}|\Delta|^2 + \sum_{\mathbf{p}\sigma} \xi_{\mathbf{p}}\hat{a}^\dagger_{\mathbf{p}\sigma}\hat{a}_{\mathbf{p}\sigma} + \sum_{\mathbf{p}}{}' \left[\Delta^*\hat{a}_{\mathbf{p}+}\hat{a}_{-\mathbf{p}-} + \Delta\hat{a}^\dagger_{-\mathbf{p}-}\hat{a}^\dagger_{\mathbf{p}+}\right]$$

Proof. (add a little derivation here. I forgot it....)

□

And here we have all terms with positive sign. Initially the interaction term was with negative sign.

(??? I can't explain it right now...)

Mean-field approximation of BCS Hamiltonian by path integral

(write several ways how to get there and what it the meaning of the new Hamiltonian?)

Mean-field approximation of BCS Hamiltonian by (another way)

(write several ways how to get there and what it the meaning of the new Hamiltonian?)

How exact is the mean-field approximation of BCS Hamiltonian?

(discussion of it. Yusbashyan said that it is very exact. I'll write it later)

Features of mean-field approximation of BCS Hamiltonian

Position of operators in the coupling term

The coupling term looks like this:

$$\sum_{kk'} V_{kk'} c^\dagger_{k\uparrow} c^\dagger_{-k\downarrow} c_{-k'\downarrow} c_{k'\uparrow}.$$

But how exactly it should be? What should be the proper position of the operators? Or it does not matter?

(answer here, currently I am not sure)

Which averages are zero, and which are nonzero?

(write what I understood after discussion with Zala that there are actually nonzero avearages because the Hamiltonian in general are not diagonal. or how???)

Does mean-field approximation of BCS Hamiltonian work in nonequilibrium?

I think that yes, it works. However, it is a complicated topic, so I don't have some good arguments.

(one can say that it does not work, because everything is more complicated there, but it is also not an argument that it does not works. Even I can't estimate, how much does it not work? So, answer on this question requires a month of studying nonequilibrium superconductivity)

In the mean-field Hamiltonian we neglect collisions, so all nonequilibrium effects are neglected

This is important to understand if one wants to look at some dynamical

Different forms of the mean-field BCS Hamiltonian

The H_{BCS} can be written in the matrix form as:

$$\sum_k \left(\xi_{\mathbf{k}} \sum_\sigma c^\dagger_{\mathbf{k}\sigma} c_{\mathbf{k}\sigma} + \left[\bar{\Delta} c_{-\mathbf{k}\downarrow} c_{\mathbf{k}\uparrow} + c^\dagger_{\mathbf{k}\uparrow} c^\dagger_{-\mathbf{k}\downarrow} \Delta \right] \right) = \sum_k \left(c^\dagger_{\mathbf{k}\uparrow}, c_{-\mathbf{k}\downarrow} \right) \begin{bmatrix} \xi_{\mathbf{k}} & \Delta \\ \bar{\Delta} & -\xi_{\mathbf{k}} \end{bmatrix} \begin{pmatrix} c_{\mathbf{k}\uparrow} \\ c^\dagger_{-\mathbf{k}\downarrow} \end{pmatrix} + \sum_k \xi_{\mathbf{k}}.$$

Note that in the raw and the column, †-s are at different positions. The constant term $\xi_{\mathbf{k}}$ originates from the term $-\xi_{\mathbf{k}} c_{-\mathbf{k}\downarrow} c^\dagger_{-\mathbf{k}\downarrow}$ and it is not a matrix. Note that the conjugation of gap $\bar{\Delta}$ is exactly at the upper right position (not lower left).

There is a one very similar form:

$$\sum_k \left(\xi_{\mathbf{k}} \sum_\sigma c^\dagger_{\mathbf{k}\sigma} c_{\mathbf{k}\sigma} + \left[\bar{\Delta} c_{-\mathbf{k}\downarrow} c_{\mathbf{k}\uparrow} + c^\dagger_{\mathbf{k}\uparrow} c^\dagger_{-\mathbf{k}\downarrow} \Delta \right] \right) = \sum_k \left(c^\dagger_{\mathbf{k}\uparrow}, c_{-\mathbf{k}\downarrow} \right) \begin{bmatrix} \xi_{\mathbf{k}} & \Delta \\ \bar{\Delta} & -\xi_{\mathbf{k}} \end{bmatrix} \begin{pmatrix} c_{\mathbf{k}\uparrow} \\ c^\dagger_{-\mathbf{k}\downarrow} \end{pmatrix}.$$

Now, there is no term $\xi_{\mathbf{k}}$ if one compares it to the previous version. This is because this sum is symmetric (runs from $-k$ to k), so it is zero.

(???? is there indeed no mistakes if one leaves this constant or neglects it??? Currently, I think that it is so.)

(write this in the Nambu notation)
The Nambu notation will be discussed below.

The Hamiltonian can be written in a diagonal basis:

$$\sum_k \left(\xi_{\mathbf{k}} \sum_\sigma c^\dagger_{\mathbf{k}\sigma} c_{\mathbf{k}\sigma} + \left[\bar{\Delta} c_{-\mathbf{k}\downarrow} c_{\mathbf{k}\uparrow} + c^\dagger_{\mathbf{k}\uparrow} c^\dagger_{-\mathbf{k}\downarrow} \Delta \right] \right) = \\ = 2 \sum_{\mathbf{p}} \left[\xi_{\mathbf{p}} v_p^2 - u_p v_p \Delta \right] + \sum_{\mathbf{p}} \sqrt{\Delta^2 + \varepsilon^2} \left[\hat{b}^\dagger_{\mathbf{p}-} \hat{b}_{\mathbf{p},-} + \hat{b}^\dagger_{\mathbf{p}+} \hat{b}_{\mathbf{p},+} \right].$$

This is the Bogoliubov transformation, which is discussed below. This "constant term" in front can be transformed since $u_p^2 = \frac{1}{2}\left(1 + \frac{\xi_p}{\varepsilon_p}\right),\ v_p^2 = \frac{1}{2}\left(1 - \frac{\xi_p}{\varepsilon_p}\right)$ as

$$2(\xi_p v_p^2 - u_p v_p \Delta) = \xi_p \left(1 - \frac{\xi_p}{\varepsilon_p}\right) - \sqrt{\left(1 - \frac{\xi_p^2}{\varepsilon_p^2}\right)}\Delta = \xi_p - \frac{\xi_p^2}{\varepsilon_p} - \frac{\sqrt{\xi_p^2 + \Delta^2 - \xi_p^2}}{\varepsilon_p}\Delta =$$
$$= \xi_p - \frac{\xi_p^2 + \Delta^2}{\varepsilon_p} = \xi_p - \varepsilon_p$$

so, this means that we can also write:

$$\sum_k \left(\xi_{\mathbf{k}} \sum_\sigma c^\dagger_{\mathbf{k}\sigma} c_{\mathbf{k}\sigma} + \left[\bar{\Delta} c_{-\mathbf{k}\downarrow} c_{\mathbf{k}\uparrow} + c^\dagger_{\mathbf{k}\uparrow} c^\dagger_{-\mathbf{k}\downarrow} \Delta\right]\right) =$$
$$= \sum_{\mathbf{p}} \left[\xi_p - \varepsilon_p\right] + \sum_{\mathbf{p}} \sqrt{\Delta^2 + \varepsilon^2} \left[\hat{b}^\dagger_{\mathbf{p}-} \hat{b}_{\mathbf{p},-} + \hat{b}^\dagger_{\mathbf{p}+} \hat{b}_{\mathbf{p},+}\right] =$$
$$= \sum_{\mathbf{p}} (-\varepsilon_p) + \sum_{\mathbf{p}} \varepsilon_p \left[\hat{b}^\dagger_{\mathbf{p}-} \hat{b}_{\mathbf{p},-} + \hat{b}^\dagger_{\mathbf{p}+} \hat{b}_{\mathbf{p},+}\right] =$$
$$= \sum_{\mathbf{p}} (-\varepsilon_p) + \sum_{\mathbf{p}} \varepsilon_p + \sum_{\mathbf{p}} \begin{pmatrix} \hat{b}^\dagger_{\mathbf{p}+} & \hat{b}_{\mathbf{p},-} \end{pmatrix} \begin{pmatrix} \varepsilon_p & 0 \\ 0 & -\varepsilon_p \end{pmatrix} \begin{pmatrix} \hat{b}_{\mathbf{p},+} \\ \hat{b}^\dagger_{\mathbf{p}-} \end{pmatrix} =$$
$$= \sum_{\mathbf{p}} \begin{pmatrix} \hat{b}^\dagger_{\mathbf{p}+} & \hat{b}_{\mathbf{p},-} \end{pmatrix} \begin{pmatrix} \varepsilon_p & 0 \\ 0 & -\varepsilon_p \end{pmatrix} \begin{pmatrix} \hat{b}_{\mathbf{p},+} \\ \hat{b}^\dagger_{\mathbf{p}-} \end{pmatrix}.$$

I don't have $\hat{b}^\dagger_{-\mathbf{p}-}$ instead of $\hat{b}^\dagger_{\mathbf{p}-}$ (like in the Nambu notation), because anyway the sum over p is symmetric, so both options will give the same result.

Different forms of the mean-field BCS Hamiltonian: Features

What role the constant term plays in the diagonalized BCS Hamiltonian?

(point out, when the constant term is important, when it is non-zero and when is it zero?)

Are there effects beyond mean-field approximation to the BCS Hamiltonian?

(I don't know, but some papers maybe consider it. I'll think later)

Diagonalization by Bogoliubov transformations: Matrix notation

The matrix notation is the most convenient approach for the derivation of a diagonal form.

(here, it will be written for an abstract fermionic Hamiltonian for now, later I'll change it to exacctly BCS notation)

We start with

$$\mathcal{H} = \epsilon \left(c_1^\dagger c_1 + c_2^\dagger c_2\right) + \lambda \left(c_1^\dagger c_2^\dagger + c_2 c_1\right),$$

and we rewrite it in the matrix form

$$\mathcal{H} = \frac{1}{2} \begin{pmatrix} c_1^\dagger & c_2 & c_2^\dagger & c_1 \end{pmatrix} \begin{pmatrix} \epsilon & \lambda & 0 & 0 \\ \lambda & -\epsilon & 0 & 0 \\ 0 & 0 & \epsilon & -\lambda \\ 0 & 0 & -\lambda & -\epsilon \end{pmatrix} \begin{pmatrix} c_1 \\ c_2^\dagger \\ c_2 \\ c_1^\dagger \end{pmatrix} + \epsilon$$

For conciseness, consider just the upper block

$$\begin{pmatrix} c_1^\dagger & c_2 \end{pmatrix} \begin{pmatrix} \epsilon & \lambda \\ \lambda & -\epsilon \end{pmatrix} \begin{pmatrix} c_1 \\ c_2^\dagger \end{pmatrix}$$

and write the Bogoliubov transformation also in matrix form as

$$\begin{pmatrix} c_1 \\ c_2^\dagger \end{pmatrix} \begin{pmatrix} \cos\theta & \sin\theta \\ -\sin\theta & \cos\theta \end{pmatrix} \begin{pmatrix} d_1 \\ d_2^\dagger \end{pmatrix}.$$

We pick θ so that

$$\begin{pmatrix} \cos\theta & -\sin\theta \\ \sin\theta & \cos\theta \end{pmatrix} \begin{pmatrix} \epsilon & \lambda \\ \lambda & -\epsilon \end{pmatrix} \begin{pmatrix} \cos\theta & \sin\theta \\ -\sin\theta & \cos\theta \end{pmatrix} = \begin{pmatrix} \tilde{\epsilon} & 0 \\ 0 & -\tilde{\epsilon} \end{pmatrix},$$

where $\tilde{\epsilon} = \sqrt{\epsilon^2 + \lambda^2}$. Including the other 2×2 block of $\mathcal{H}$, we conclude that

$$\mathcal{H} = \tilde{\epsilon}\left(d_1^\dagger d_1 + d_2^\dagger d_2\right) + \epsilon - \tilde{\epsilon}$$

Diagonalization by Bogoliubov transformations: Explicit substitution

The BCS Hamiltonian

$$\hat{H} = \sum_{\mathbf{p}\sigma} \varepsilon_{\mathbf{p}} \hat{a}^\dagger_{\mathbf{p}\sigma} \hat{a}_{\mathbf{p}\sigma} + \sum_{\mathbf{p}} \left[\Delta^* \hat{a}_{\mathbf{p}+} \hat{a}_{-\mathbf{p}-} + \Delta \hat{a}^\dagger_{-\mathbf{p}-} \hat{a}^\dagger_{\mathbf{p}+}\right]$$

is diagonalized by introduction of new operators b

$$\begin{aligned} \hat{b}_{\mathbf{p}-} &= u_p \hat{a}_{\mathbf{p}-} + v_p \hat{a}^\dagger_{-\mathbf{p},+}, \\ \hat{b}_{\mathbf{p}+} &= u_p \hat{a}_{\mathbf{p}+} - v_p \hat{a}^\dagger_{-\mathbf{p},-}; \end{aligned} \qquad u^2 + v^2 = 1.$$

This is rather a direct calculation.

It is not hard to remember them: first operators are the same as at the l.h.s., the second is purely opposite: opposite spin, momenta, it is daggered.

Note that we have a minus here in one of the terms.

(???? will it work if I change a minus to another similar place??? I'll discuss it below, here I'll just write the statement)

Now, here is the main part of this paragraph, that if we plug them, we will get

$$\hat{H} - \mu\hat{N} = \Omega_0 + \sum_{\mathbf{p}}{}' \varepsilon(p) \left(\hat{b}^\dagger_{\mathbf{p}+} \hat{b}_{\mathbf{p}+} + \hat{b}^\dagger_{\mathbf{p}-} \hat{b}_{\mathbf{p}-}\right)$$

$$\Omega_0 = 2\sum_{\mathbf{p}} \cdot \left[\xi_{\mathbf{p}} v_{\mathbf{p}}^2 - \Delta u_{\mathbf{p}} v_{\mathbf{p}}\right] + \frac{1}{\lambda}\Delta^2$$

$$\varepsilon(p) = \sqrt{\xi_{\mathbf{p}}^2 + \Delta^2}$$

Diagonalization by Bogoliubov transformations: Matrix eigenvalues

There is an easy way of obtaining spectrum of BCS Hamiltonian without knowing much about Bogoliubov transformation: One can just write the Hamiltonian in a matrix form, and then just find its eigenvalues.

(write that matrix!!!s)

To do this, we define the Bogoliubov transformation:

$$\begin{pmatrix} \gamma_{\mathbf{k}\uparrow} \\ \gamma^\dagger_{-\mathbf{k}\downarrow} \end{pmatrix} = \begin{pmatrix} u_{\mathbf{k}} & -v_{\mathbf{k}} \\ v^*_{\mathbf{k}} & u^*_{\mathbf{k}} \end{pmatrix} \begin{pmatrix} c_{\mathbf{k}\uparrow} \\ c^\dagger_{-\mathbf{k}\downarrow} \end{pmatrix}.$$

For this transformation to diagonalize $H_{\mathbf{k}}$, the eigenvalues of $H_{\mathbf{k}}$ must satisfy:

$$\det \begin{pmatrix} \xi_{\mathbf{k}} - E_{\mathrm{k}} & -\Delta \\ -\Delta^* & -\xi_{\mathrm{k}} - E_{\mathrm{k}} \end{pmatrix} = 0$$

And by solving for $E_{\mathbf{k}}$

$$E^2_{\mathrm{k}} = \xi^2_{\mathrm{k}} + |\Delta|^2,$$

we get the spectrum:

$$E_{\mathrm{k}} = \pm\sqrt{\xi^2_{\mathrm{k}} + |\Delta|^2}$$

(??? comment, do we need to know Bogoliubov transformations at all if this approach works?)

Diagonalization by Bogoliubov transformations: Using angle of rotation

We know that Bogoliubov transformations are mixing electrons and holes

$$c^\dagger_{\mathbf{k}\uparrow} = u_{\mathbf{k}}\gamma^\dagger_{\mathbf{k}0} + v^*_{\mathbf{k}}\gamma_{\mathbf{k}1} \quad \text{and} \quad c^\dagger_{-\mathbf{k}\downarrow} = u_{\mathbf{k}}\gamma^\dagger_{\mathbf{k}1} - v^*_{\mathbf{k}}\gamma_{\mathbf{k}0},$$

where we require $|u_{\mathbf{k}}|^2 + |v_{\mathbf{k}}|^2 = 1$ to preserve anticommutation relations, and $2\xi_{\mathbf{k}}u_{\mathbf{k}}v_{\mathbf{k}} + \Delta v^2_{\mathbf{k}} - \Delta^* u^2_{\mathbf{k}} = 0$ to eliminate number-changing terms from the transformed Hamiltonian. Writing $\Delta = \mathrm{e}^{\mathrm{i}\phi}|\Delta|$ these conditions are met by

$$u_{\mathbf{k}} = \mathrm{e}^{\mathrm{i}\phi/2}\cos\theta_{\mathbf{k}}, \quad v_{\mathbf{k}} = \mathrm{e}^{-\mathrm{i}\phi/2}\sin\theta_{\mathbf{k}} \quad \text{and} \quad \cot 2\theta_{\mathbf{k}} = \frac{\xi_{\mathbf{k}}}{|\Delta|}.$$

(??? I'll just write this formalism)

Diagonalization by exact diagonalization

(???????????)

I just think that in statistical physics there are methods of diagonalization that can be used here without any problem.

(??? I'll write it in stat phys and then try to apply them here. I can't do it now)

The spectrum of BCS model when particles are moving

(??? that statement from de Gennes book. (????))

Bogoliubov transformations: Features

Formula for averaging of electron and hole operators in superconductor

Using the Bogoliubov transform and $\langle b^\dagger b\rangle = n$, one gets

$$\begin{aligned}\langle c^\dagger c\rangle &= v^2 + \frac{\xi}{\varepsilon}n,\\ \langle cc^\dagger\rangle &= u^2 - \frac{\xi}{\varepsilon}n, \quad u^2 = \frac{1}{2}\left(1+\frac{\xi}{\varepsilon}\right), v^2 = \frac{1}{2}\left(1-\frac{\xi}{\varepsilon}\right), uv = \frac{\Delta}{2\varepsilon}.\\ \langle c^\dagger c^\dagger\rangle &= \langle cc\rangle = uv(1-2n),\end{aligned}$$

(add some other later.)

This formulas might be very helpful for doing similar Bogoliubov transformations in some special cases.

How to understand physically Bogoliubov transformations?

What is physically a superposition of electron and a hole?
(it was discussed some time ago, I'll study it later)

Physical meaning of coefficients of Bogoliubov transformations?

(it is already written in Schmidt... I'll write it later)

In general u was near annihilation operator, so u^2 is the probability that this state is free. Also, v was in front of a creation operator, so v^2 is the probability that this state is occupied.

(????? why???? and why we have square???? I don't understand it now)

Diagonalization of BCS by matrix notation from Coleman book

Here, I'll write the same Bogoliubov's transformations, but in different notation.

(??? I don't understand it, it uses that (u, v) vector diagonalizes the h, but I didn't find the proof of it)

$$\begin{aligned}a^\dagger_{\mathbf{k}\uparrow} &= \psi^\dagger_{\mathbf{k}}\cdot\begin{pmatrix}u_{\mathbf{k}}\\ v_{\mathbf{k}}\end{pmatrix} = c^\dagger_{\mathbf{k}\uparrow}u_{\mathbf{k}} + c_{-\mathbf{k}\downarrow}v_{\mathbf{k}}\\ a_{-\mathbf{k}\downarrow} &= \psi^\dagger_{\mathbf{k}}\cdot\begin{pmatrix}-\mathrm{v}^*_{\mathbf{k}}\\ u^*_{\mathbf{k}}\end{pmatrix} = c_{-\mathbf{k}\downarrow}u^*_{\mathbf{k}} - c^\dagger_{\mathbf{k}\uparrow}\mathrm{v}^*_{\mathbf{k}}.\end{aligned}$$

Bogoliubov transformation

This transformation, mixing particles and holes, is named after its inventor, Nikolai Bogoliubov. If one takes the complex conjugate of the quasihole operator and reverses the momentum, one obtains $a^\dagger_{\mathbf{k}\downarrow} = c^\dagger_{\mathbf{k}\downarrow}u_{\mathbf{k}} - c_{-\mathbf{k}\uparrow}v_{\mathbf{k}}$, which defines the spin-down quasiparticle. The general expression for the spin-up and spin-down quasiparticles can be written

$$a^\dagger_{\mathbf{k}\sigma} = c^\dagger_{\mathbf{k}\sigma}u_{\mathbf{k}} + \mathrm{sgn}(\sigma)c_{-\mathbf{k}-\sigma}\mathbf{v}_{\mathbf{k}}.$$

Let us combine the two expressions (14.96) into a single Nambu spinor $a^\dagger_{\mathbf{k}}$:

$$a_{\mathbf{k}}^\dagger = \left(a_{\mathbf{k}\uparrow}^\dagger, a_{-\mathbf{k}\downarrow}\right) = \psi_{\mathbf{k}}^\dagger \overbrace{\begin{pmatrix} u_{\mathbf{k}} & -\mathrm{v}_{\mathbf{k}}^* \\ \mathrm{v}_{\mathbf{k}} & u_{\mathbf{k}}^* \end{pmatrix}}^{U_{\mathbf{k}}} = \psi_{\mathbf{k}}^\dagger U_{\mathbf{k}}.$$

Taking the Hermitian conjugate $a_{\mathbf{k}} = U_{\mathbf{k}}^\dagger \psi_{\mathbf{k}}$, then $\psi_{\mathbf{k}} = U_{\mathbf{k}} a_{\mathbf{k}}$, since $UU^\dagger = 1$. Using (14.94),

$$\psi_{\mathbf{k}}^\dagger h_{\mathbf{k}} \psi_{\mathbf{k}} = a_{\mathbf{k}}^\dagger U_{\mathbf{k}}^\dagger \overbrace{U_{\mathbf{k}}^\dagger h_{\mathbf{k}} U_{\mathbf{k}}}^{U_{\mathbf{k}} E_{\mathbf{k}} \tau_{\mathbf{k}}} a_{\mathbf{k}} = a_{\mathbf{k}}^\dagger E_{\mathbf{k}} \tau_3 a_{\mathbf{k}},$$

so that, as expected,

$$H = \sum_{\mathbf{k}} a_{\mathbf{k}}^\dagger E_{\mathbf{k}} \tau_3 a_{\mathbf{k}} + V \frac{\bar{\Delta}\Delta}{g_0}$$

Bogoliubov Transformations as a change of basis

Indeed, c operators were one basis, b operators are the basis where the Hamiltonian is diagonal.

(????????????? here, I'll write what exactly is meant by this????? how is it related to the basis of the vector space in linear algebra?)

Why Bogoliubov transformations are called "canonical transformations"?

(??? connect them to the can. tr-s from mechanics??? write this from Levitov Shitov)

Position of a minus in fermionic Bogoliubov transformations

(??? here, I'll discuss, does it matter or not, in front of what)

Bogoliubov transformations for abstract fermionic model Hamiltonian

One can use the Bogoliubov Transformations to diagonalize more abstract Hamiltonians:

(this is exactly the SC Hamiltonian, but with different indices, so it is kind of very stupid statement, but okay)

Bogoliubov coefficients interpolate between electrons and holes

We know that Bogoliubov transformations are mixing electrons and holes

$$c_{\mathbf{k}\uparrow}^\dagger = u_{\mathbf{k}} \gamma_{\mathbf{k}0}^\dagger + v_{\mathbf{k}}^* \gamma_{\mathbf{k}1} \quad \text{and} \quad c_{-\mathbf{k}\downarrow}^\dagger = u_{\mathbf{k}} \gamma_{\mathbf{k}1}^\dagger - v_{\mathbf{k}}^* \gamma_{\mathbf{k}0},$$

Main statement: Note that for $\xi_{\mathbf{k}} \gg |\Delta|, \theta_{\mathbf{k}} \to 0$ and so $c_{\mathbf{k}\uparrow}^\dagger \sim \gamma_{\mathbf{k}0}^\dagger$ and $c_{-\mathbf{k}\downarrow}^\dagger \sim \gamma_{\mathbf{k}1}^\dagger$. Conversely, for $\xi_{\mathbf{k}} \ll -|\Delta|, \theta_{\mathbf{k}} \to \pi/2$ and so $c_{\mathbf{k}\uparrow}^\dagger \sim \gamma_{\mathbf{k}1}$ and $c_{-\mathbf{k}\downarrow}^\dagger \sim \gamma_{\mathbf{k}0}$. The Bogoliubov coefficients thus interpolate between electrons and holes, and at the Fermi energy, where $\xi_{\mathbf{k}} = 0$ and $\theta_{\mathbf{k}} = \pi/4$, have equal electron and hole content.

Spectrum of the BCS Hamiltonian in the presence of current

(I'll point out, why in general, the spectrum should change if there is a passing current?)

Connection of mean field approximation and conservation of particle number (???)

https://physics.stackexchange.com/questions/306515/mean-field-equations-in-the-bcs-theory-of-superconductivity?noredirect=1&lq=1

In BCS theory, one takes the model Hamiltonian

$$\sum_{k\sigma}(E_k-\mu)c^\dagger_{k\sigma}c_{k\sigma}+\sum_{kk'}V_{kk'}c^\dagger_{k\uparrow}c^\dagger_{-k\downarrow}c_{-k'\downarrow}c_{k'\uparrow}$$

This Hamiltonian clearly conserves particle number. Thus, we expect the ground state to have a definite particle number. It's possible the ground state is degenerate, but that could be lifted by perturbing μ.

Then, one makes a mean field approximation. One replaces

$$c^\dagger_{k\uparrow}c^\dagger_{-k\downarrow}c_{-k'\downarrow}c_{k'\uparrow}$$

with

$$\langle c^\dagger_{k\uparrow}c^\dagger_{-k\downarrow}\rangle c_{-k'\downarrow}c_{k'\uparrow}+c^\dagger_{k\uparrow}c^\dagger_{-k\downarrow}\langle c_{-k'\downarrow}c_{k'\uparrow}\rangle-\langle c^\dagger_{k\uparrow}c^\dagger_{-k\downarrow}\rangle\langle c_{-k'\downarrow}c_{k'\uparrow}\rangle$$

This doesn't make any sense to me. This seems to be saying that we know the terms $c^\dagger_{k\uparrow}c^\dagger_{-k\downarrow}$ and $c_{-k'\downarrow}c_{k'\uparrow}$ don't fluctuate much around their mean values. But we also know that in the actual ground state, the mean values are given by $\langle c_{-k'\downarrow}c_{k'\uparrow}\rangle=\langle c^\dagger_{k\uparrow}c^\dagger_{-k\downarrow}\rangle=0$ since the ground state will have definite particle number. Thus the fluctuations about the mean value aren't small compared to the mean value.

How can this mean field treatment be justified?

Answer

> First, why do we choose those terms to put the brakets around? Do we > somehow know that these are the terms that won't fluctuate much?

The heuristic motivation is that the superconductivity phenomenon can be understood as the non-relativistic analog of the Higgs mechanism for the EM $U_{\rm EM}(1)$ (this idea explains the main properties of the superconductor, such as absence of resistivity, magnetic field expulsion and other). For the Higgs mechanism one need a condensate of some particles. In the solid body, the only candidates are electrons. The simplest choice of the condensate is the scalar condensate (very-very heuristically, we require the Galilei invariance into the superconductor). Therefore the only allowed simplest scalar bounded state $|\psi\rangle$ is constructed from the electron pair with zero total spin, which can be imagine as two fermions moving in opposite directions:

$$|\psi\rangle=c^\dagger_{\mathbf{k},\uparrow}c^\dagger_{-\mathbf{k},\downarrow}|0\rangle$$

This is indeed realized when we calculate the four-fermion vertex in the microscopic theory of electron-phonon interactions. Indeed, we start from the interaction Hamiltonian

$$H_{\rm int}=g\psi^\dagger\psi\varphi,$$

where ψ is electron field, while φ is phonon field, and assume the second order in g diagrams of electron-electron scattering; let's denote their momenta as $\mathbf{p}_i$. After tedious calculations of the corresponding diagram one finds that the vertex $\Gamma^{(4)}(\mathbf{p}_1,\mathbf{p}_2,\mathbf{p}_3,\mathbf{p}_4)$ (with $\mathbf{q}=\mathbf{p}_1+\mathbf{p}_2$) has the pole at zero momentum $\mathbf{q}$ and zero total spin of fermions $1,2$ and $3,4$ or ($1,4$ and $2,3$). The pole quickly disappears once one enlarges $|\mathbf{q}|$.

Finally, since 4-fermion vertex is expressed through two-particles Green $G^{(2)}$ function, then the presence of the pole in $\Gamma^{(4)}$ means the presence of the pole in $G^{(2)}$. This means that bounded states of electrons appear.

> Second, why can't we just immediately say $\langle c_{-k'\downarrow}c_{k'\uparrow}\rangle = \langle c^\dagger_{k\uparrow}c^\dagger_{-k\downarrow}\rangle = 0$ since we know the ground state will > have definite particle number, and $c_{-k'\downarrow}c_{k'\uparrow}$ > and $c^\dagger_{k\uparrow}c^\dagger_{-k\downarrow}$ don't conserve > particle number?

(Added) Let's again use the idea of Higgs mechanism. It is clearly that the number of particles isn't strictly conserved in superconducting state. Really, because of the SSB of $U_{\text{EM}}(1)$ group the system loses the definition of the conserved particle number (being associated to the global phase invariance current) in the ground state.

Microscopically the formation of the condensate is argued in a following way: the presence of the two-fermions bounded states leads to instability of the electron gas inside the superconductor, and fermions are converted in Cooper pairs. Really, for bosons the lowest energy state can be filled by infinitely many number of particles, while for fermions this is not true due to Pauli principle. This (under some assumptions, see below) leads to formation of new vacuum state on which the operator $\hat{c}^\dagger_{\mathbf{k},\uparrow}\hat{c}^\dagger_{-\mathbf{k},\downarrow}$ has non-zero VEV:

$$\langle \text{vac}|\hat{c}^\dagger_{\mathbf{p},\uparrow}\hat{c}^\dagger_{-\mathbf{p},\downarrow}|\text{vac}\rangle = \Psi \neq 0$$

It's not hard to construct this state:

$$|\text{vac}\rangle = \prod_{\mathbf{k}=\mathbf{k}_1\ldots k_{\frac{N}{2}}} (u_{\mathbf{k}} + v_{\mathbf{k}}\hat{c}^\dagger_{\mathbf{k},\uparrow}\hat{c}^\dagger_{-\mathbf{k},\downarrow})|0\rangle, \quad |v_{\mathbf{k}}|^2 + |u_{\mathbf{k}}|^2 = 1$$

This state called **the coherent state** really doesn't have definite number of particles.

For the particles number operator $\hat{N} = \sum_{\mathbf{k}} \hat{c}^\dagger_{\mathbf{k},\uparrow}\hat{c}^\dagger_{-\mathbf{k},\downarrow}$ the VEV $\langle \text{vac}|\hat{N}|\text{vac}\rangle$ is

$$1N = \langle \text{vac}|\hat{N}|\text{vac}\rangle \sim \sum_{\mathbf{k}} |v_{\mathbf{k}}|^2,$$

Why the number of particles is not so indefinite

However, the root $\sqrt{\Delta N^2}$ of quadratic deviation from while the quadratic deviation $\langle \text{vac}|(\hat{N} - N)^2|\text{vac}\rangle$ is

$$2\Delta N^2 = \langle \text{vac}|(\hat{N} - N)^2|\text{vac}\rangle = \sum_{\mathbf{k}} |u_{\mathbf{k}}|^2|v_{\mathbf{k}}|^2$$

is negligible in the limit of large particle number (and volume). Really, both of (1) and (2) are proportional to the volume V (note only one summation over wave-numbers $\mathbf{k}$ in (2)), and hence $\sqrt{\Delta N^2} \sim \sqrt{V}$ which is negligible in the large volume limit. This argument is seemed to be first published in the BCS article.

(Added) This means that the state of superconductor with good accuracy can be projected on the state with definite particle number N. Precisely, define the phase dependent ground state

$$|\text{vac}(\theta)\rangle = |\text{vac}[c^\dagger_{\mathbf{k},\uparrow/\downarrow} \to c^\dagger_{\mathbf{k},\uparrow/\downarrow}e^{-i\theta}]\rangle$$

The state with definite particle number N is defined as

$$|N\rangle = \int_0^{2\pi} d\theta e^{i\hat{N}\theta}|\text{vac}(\theta)\rangle$$

Why there can be excitations below Fermi energy?

(write that because we have holes)

3.9.6 Meaning of the gap Δ, gap equation

The Meaning of Energy Gap and Addition of an Electron

Let us focus on an arbitrary pair of states $(\boldsymbol{q}, -\boldsymbol{q})$ in a superconductor, in momentum space. First we find the contribution of this pair, w_q, to the total energy of the superconductor. One can see from $E_s = \sum_k 2\varepsilon_k v_k^2 + \sum_{k.k'} V_{kk'} v_{k'} u_k v_k u_{k'}$ that

$$w_q = 2\varepsilon_q v_q^2 - 2V v_q u_q \sum_k{}' v_k u_k \tag{6.21}$$

(???? why???)

Here the first term is the kinetic energy of the pair $(\boldsymbol{q}, -\boldsymbol{q})$ and the second term is the pair's contribution to the negative part of the ground-state energy. The latter arises from various interactions in which our pair participates. As a result of these interactions, the pair can go to any other state $(k, -k)$ or, conversely, any other pair $(\boldsymbol{k}, -\boldsymbol{k})$ can go to the state $(\boldsymbol{q}, -\boldsymbol{q})$ which we have earmarked for our analysis.

The coefficient 2 in the second term takes into account that the pair $(\boldsymbol{q}, -\boldsymbol{q})$ is encountered twice as the summation in $E_s = \sum_k 2\varepsilon_k v_k^2 + \sum_{k.k'} V_{kk'} v_{k'} u_k v_k u_{k'}$ is carried out: first time when the sum runs over k, and the second time when it runs over $\boldsymbol{k'}$. Using the expression $\Delta_0 = V \sum_k{}' v_k u_k$, as well as $E_k = \sqrt{\varepsilon_k^2 + \Delta_0^2}$ and $v_k^2 = \frac{1}{2}\left(1 - \frac{\varepsilon_k}{E_k}\right)$, we obtain

$$w_q = 2\varepsilon_q \frac{1}{2}\left(1 - \frac{\varepsilon_q}{E_q}\right) - 2\left[\frac{1}{4}\left(1 - \frac{\varepsilon_q^2}{E_q^2}\right)\right]^{1/2} \Delta_0 = \varepsilon_q - \frac{\varepsilon_q^2}{E_q} - \frac{\Delta_0^2}{E_q} = \varepsilon_q - E_q \tag{6.22}$$

Let us now make use of (6.22). Suppose that the pair state $(\boldsymbol{q}, -\boldsymbol{q})$ in the ground state of a superconductor is empty. How will the energy of the system change if we add one more electron to it from outside and place it in the state $\boldsymbol{q}$? Since we then have a single electron in the state $\boldsymbol{q}$, the pair state $(\boldsymbol{q}, -\boldsymbol{q})$ is not allowed to take part in the scattering events, that is, it cannot contribute to the ground-state energy of the superconductor. Its potential contribution is known to us, it equals w_q. Hence the energy of the superconductor with one 'extra' electron in the state q will be

$$W_q = W - w_q + \varepsilon_q \tag{6.23}$$

We shall refer to this 'extra' uncoupled electron as an elementary excitation of our system, or quasiparticle. The quantity W in (6.23) is the ground-state energy of the superconductor and the third term accounts for the kinetic anarer of nur 'extra' plectron. Substituting (6.22) into (6.23) vields

$$W_q = W + E_q \tag{6.24}$$

This relation is very important. Since, according to $E_k = \sqrt{\varepsilon_k^2 + \Delta_0^2}$,

$$E_q = \sqrt{\varepsilon_q^2 + \Delta_0^2},$$

it is evident that, by adding one extra electron to a superconductor in the ground state, we increase the energy of the system by at least the value of Δ_0 (the minimum increase corresponds to $\varepsilon_q = 0$, that is, to the state q being on the Fermi surface). This means that the spectrum of elementary excitations of the superconductor is separated from the ground-state energy level by an energy gap.

To elucidate this statement, let us go back to the superconductor in the ground state. Suppose that, as a result of an external effect, one of the electrons from the pair $(q, -q)$ is moved to a neighboring state in momentum space. Recall that initially all states were either occupied in pairs or empty in pairs. Then the transfer of one electron from the pair $(\boldsymbol{q}, -\boldsymbol{q})$ to the neighboring state implies that two uncoupled (excited) electrons have appeared. One of them stays in one of the states $(q, -q)$ while the other turns up in the neighboring k state and, naturally, does not have a partner in the $-k$ state. But we have just found out that, in order to break a pair, one needs at least the energy $2\Delta_0$, as illustrated by the diagram in Fig. 6.6.

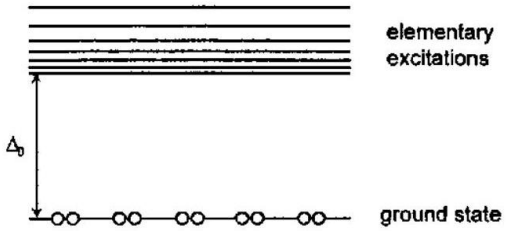


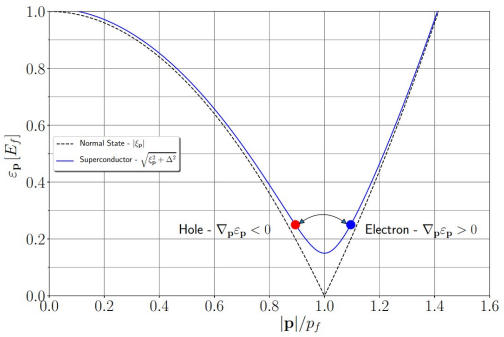
Fig. 6.6. The energy gap Δ_0 separates the energy levels of elementary excitations from the groundstate level (the energy level of electron pairs in the condensate)

(??? what is meant by this picture? that literally all electrons, even the one which are far below Fermi surface are in the ground state? then why?)

All pair states belong to the condensate occupying the ground-state energy level. A single extra electron is not allowed to be at this level and must therefore occupy the first empty level available in the elementary excitation spectrum. If a pair is broken, both electrons must go up to the elementary excitation levels which requires an energy larger than $2\Delta_0$.

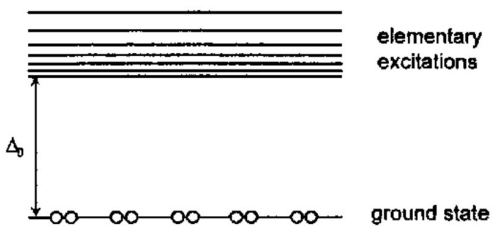
The existence of this energy gap is a very important property of the superconductor and explains many aspects of its behavior.

Picture of the dispersion of electrons and holes in a superconductor



(write here how to understand this plot! and also how one should not understand it!!! it is not obvious what is meat here!)

Simple picture of the dispersion of a superconductor and a ground state



(write here how to understand this plot! and also how one should not understand it!!! it is not obvious what is meat here!)

What happens physically with the Fermi sphere, when the gap opens?

(we had a ball, now what? I imagine that there are particles still up to Fermi level, but a lot of them are shifted down. and very few are excited.)
(??? what if Fermi surface goes out of the Brillouin zone???)

At $T = 0$, there are no particles above the filled Fermi surface.

Basically, we have renormalization of the Fermi surface at $T = 0$, it becomes suddenly lower than we would expect.

In BCS model, we assumed that the Fermi surface is nearly filled, but now there is a gap near Fermi surface, so is our assumption is still valid?

(?????????? maybe yes, but I have never seen answer to this question)

What physically happens with the system, when the gap decreases?

(!!!! this is a very important question, since we don't measure the gap. maybe we measure the current. So, what happens physically with the system?????)

What physically means by the excitation above the gap?

(these are electron-hole pares, so electron and the absence of electron)
(I'll discuss more how exactly is it?)

Density of States of Elementary Excitations in the Superconductor and the Coherence Length

The lower part of the elementary excitation spectrum is illustrated in Fig. 6.6. An expression for the density of states in this spectrum can be easily derived from $E_k = \sqrt{\varepsilon_k^2 + \Delta_0^2}$. Indeed. E_k is the energy of an elementary excitation (see (6.24)), it tells us how much the energy of the system increases when an extra electron with momentum k is added to the superconductor:

$$E_k = \sqrt{\varepsilon_k^2 + \Delta_0^2} = \sqrt{\left(\frac{\hbar^2 k^2}{2m} - \frac{\hbar^2 k_F^2}{2m}\right)^2 + \Delta_0^2}.$$

The dependence of E_k on k given by this expression is shown in Fig. 6.7.

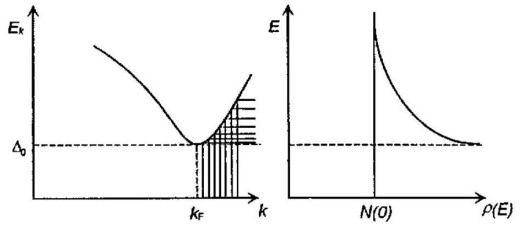


Fig. 6.7. Spectrum of elementary excitations, E_k, of the superconductor and the density of states $\rho(E)$

It is easy to see from the plot that the energy levels of elementary excitations become denser at $E_k \to \Delta_0$. The density of states or, in other words, the number of the energy levels per unit energy interval and unit volume (1 cm^3) of the material, is

$$\rho(E) = \mathrm{d}\nu/\mathrm{d}E,$$

where $\mathrm{d}\nu$ is the number of energy levels in the energy interval $\mathrm{d}E$, in the vicinity of the level E. We recall that $\mathrm{d}\nu/\mathrm{d}\varepsilon$ gives the density of states near the Fermi level (??? why near it?? is it an approximation???) for the normal metal, i.e.,

$$\mathrm{d}\nu/\mathrm{d}\varepsilon = N(0)$$

Therefore

$$\rho(E) = \frac{\mathrm{d}\nu}{\mathrm{d}\varepsilon}\frac{\mathrm{d}\varepsilon}{\mathrm{d}E} = N(0)\frac{E}{\sqrt{E^2-\Delta_0^2}}. \tag{6.25}$$

It follows from (6.25) that, at $E \to \Delta_0$, the density of states of elementary excitations in the superconductor is indeed $\rho(E) \to \infty$, as illustrated in Fig. 6.7.

Overview of different forms of the gap equation

Different forms of a trivial gap equation

$$\Delta_0 = V \sum_k{}' v_k u_k$$

$$\Delta = \lambda \sum_p{}' \langle c_{-p,-} c_{p,+} \rangle .$$

$$\Delta = V \sum_k{}' v_k u_k \left(1 - 2f_k\right)$$

$$\Delta = V \sum_k{}' \frac{\Delta}{2E_k}\left(1 - \frac{2}{\exp\left(E_k/k_\mathrm{B}T\right)+1}\right)$$

$$\frac{1}{N(0)V} = \int_0^{\hbar\omega_\mathrm{D}} \frac{\mathrm{d}\varepsilon}{\sqrt{\varepsilon^2+\Delta^2(T)}} \tanh\frac{\sqrt{\varepsilon^2+\Delta^2(T)}}{2k_\mathrm{B}T}.$$

The most typical form of the gap equation is:

$$\frac{1}{\lambda} = \frac{1}{2}\sum_{\mathbf{p}} \frac{1+2\bar{n}_{\mathbf{p}}}{\sqrt{\xi_{\mathbf{p}}^2+\Delta^2}}$$

where $\bar{n}_{\mathbf{p}} = \left\langle \hat{b}^\dagger_{\mathbf{p}+}\hat{b}_{\mathbf{p}+}\right\rangle = \left\langle \hat{b}^\dagger_{\mathbf{p}-}\hat{b}_{\mathbf{p}-}\right\rangle = [\exp(\varepsilon(p)/T)+1]^{-1}$

$$\Delta = V \sum_k{}' v_k u_k \left(1 - 2f_k\right)$$

After plugging $v_q^2 = \frac{1}{2}\left(1 - \frac{\varepsilon_q}{E_q}\right)$ where $E_q = \sqrt{\varepsilon_q^2+\Delta^2(T)}$, it becomes equivalent to

$$\Delta = V \sum_k{}' \frac{\Delta}{2E_k}\left(1 - \frac{2}{\exp\left(E_k/k_\mathrm{B}T\right)+1}\right)$$

Replacing summation with integration yields, after simple algebra,

$$\frac{1}{N(0)V} = \int_0^{\hbar\omega_\mathrm{D}} \frac{\mathrm{d}\varepsilon}{\sqrt{\varepsilon^2+\Delta^2(T)}} \tanh\frac{\sqrt{\varepsilon^2+\Delta^2(T)}}{2k_\mathrm{B}T}. \tag{6.35}$$

Here, again, we approximated the integral by extracting $N(0)$ out.

Basically the same equation, but with

$$1 = \frac{|\lambda| m p_0}{2\pi^2} \int_0^{\omega_D} \mathrm{d}\xi \frac{\tanh \frac{\sqrt{\xi^2+\Delta^2(T)}}{2T}}{\sqrt{\xi^2+\Delta^2(T)}}. \tag{34.37}$$

One can write the gap equation as integral with parameter in the integration range and inside of the integral:

$$\Delta = \lambda\Delta \int_{|\Delta|}^{\omega_\mathrm{D}} \mathrm{d}\epsilon \frac{\tanh \epsilon/2T}{\sqrt{\epsilon^2-|\Delta|^2}}$$

To bring it to well-known form, one changes variables as $\xi = \sqrt{\epsilon^2-|\Delta|^2}$ to write $\epsilon = \sqrt{|\Delta|^2+\xi^2}$, and finds $1 = \lambda \int_0^{\omega_\mathrm{D}} \left(\mathrm{d}\xi/\sqrt{|\Delta|^2+\xi^2}\right) \tanh \sqrt{|\Delta|^2+\xi^2}/2T$.

(??? do it! I haven't checked it, I believe Kamenev)

(this a general summary of what will be written above)
(add a very brief discussions of all the forms)

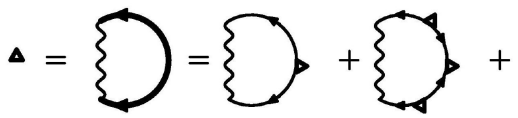
In the GF formalism, it is:

$$\Delta_{\alpha\beta} = \lambda \int F_{\alpha\beta}(\varepsilon, \mathbf{p}) \frac{d\varepsilon d^3p}{(2\pi)^4},$$

$$\Delta = \lambda T \sum_{\omega_n} \int F\left(i\omega_n, \mathbf{p}\right) \frac{d^3p}{(2\pi)^3} = \lambda T \sum_{\omega_n} \int \frac{\Delta}{\omega_n^2 + \xi_\mathbf{p}^2 + \Delta^2} \frac{d^3p}{(2\pi)^3},$$

(write def of F)

In diagrammatic representation it is



(describe what is here)

(??? explain the below formula)

$$\tilde{\Delta}(i\varepsilon) = T \sum_{\varepsilon'} \Gamma^0\left(i\varepsilon, i\varepsilon'\right) F\left(i\varepsilon', \mathbf{r}=\mathbf{r}'\right),$$

$$F\left(i\varepsilon, \mathbf{r}=\mathbf{r}'\right) := \int \frac{\tilde{\Delta}(i\varepsilon)}{\varepsilon^2 + \xi_p^2 + \tilde{\Delta}^2(i\varepsilon)} \frac{d^3p}{(2\pi)^3}. \qquad \Gamma^0\left(i\varepsilon, i\varepsilon'\right) = \lambda v(i\varepsilon) v\left(i\varepsilon'\right), \qquad \tilde{\Delta}(i\varepsilon) \equiv \Delta(T) v(i\varepsilon),$$

$$\Delta(T) = \lambda T \sum_{\varepsilon} \int \frac{v^2(i\varepsilon)\Delta(T)}{\varepsilon^2 + \xi_\mathbf{p}^2 + v^2(i\varepsilon)\Delta^2(T)} \frac{d^3p}{(2\pi)^3}.$$

Вычисляя интеграл по ξ (?????)

$$\frac{1}{\lambda\nu_0} = \pi T \sum_{\varepsilon} \frac{v^2(i\varepsilon)}{\sqrt{\varepsilon^2 + \Delta^2(T) v^2(i\varepsilon)}}.$$

$v(i\varepsilon) = \frac{\omega_D}{\sqrt{\varepsilon^2+\omega_D^2}}$

Some trivial transformation:

$$\frac{\Delta}{\lambda}=\frac{\Delta}{2}\sum_{\mathbf{p}}{}'\frac{1-2\bar{n}_{\mathbf{p}}}{\sqrt{\xi_{\mathbf{p}}^2+\Delta^2}}=\frac{\Delta}{2}\sum_{\mathbf{p}}{}'\frac{1-2\frac{1}{e^{\beta\varepsilon_p}+1}}{\sqrt{\xi_{\mathbf{p}}^2+\Delta^2}}=\frac{\Delta}{2}\sum_{\mathbf{p}}{}'\frac{1}{\sqrt{\xi_{\mathbf{p}}^2+\Delta^2}}\frac{(e^{\beta\varepsilon_p}-1)}{(e^{\beta\varepsilon_p}+1)}=\frac{\Delta}{2}\sum_{\mathbf{p}}{}'\operatorname{th}\frac{\varepsilon_p}{2T}$$

with $\varepsilon_p=\sqrt{\xi_p^2+\Delta^2}$

$$\frac{1}{\lambda\nu_0}=\pi T\sum_{\varepsilon}\frac{v^2(i\varepsilon)}{\sqrt{\varepsilon^2+\Delta^2(T)v^2(i\varepsilon)}};\qquad v(i\varepsilon)=\omega_D/\left(\omega_D^2+\varepsilon^2\right)^{1/2}$$

(write comments that here we have a different cutoffs! explain that it it the same equation, it is not obvious!)

$$2\sum_{n=0}^{\infty}\frac{\omega_D^2}{\left(\omega_D^2+\pi^2T_c^2(2n+1)^2\right)(2n+1)}=\frac{1}{\lambda\nu_0}$$

$$\frac{1}{\lambda\nu_0}=\sum_{k}\frac{\tanh\frac{\sqrt{\varepsilon^2+|\Delta|^2}}{2T}}{2\sqrt{\varepsilon^2+|\Delta|^2}}$$

Different forms of a gap equation for specific superconductors

Now, I'll collect some gap equations for some non-trivial models.
For a dirty superconductors:

$$\Delta=\lambda T\sum_{\omega_n}\int_{-\infty}^{\infty}\frac{\nu_0 d\xi\tilde{\Delta}}{\tilde{\omega}_n^2+\tilde{\Delta}^2+\xi^2}\qquad\begin{aligned}\tilde{\omega}_n&:=\omega_n\left(1+\frac{1}{2\tau\sqrt{\omega_n^2+\Delta^2}}\right),\\ \tilde{\Delta}&:=\Delta\left(1+\frac{1}{2\tau\sqrt{\omega_n^2+\Delta^2}}\right)\end{aligned}$$

$$\Delta=\pi\lambda\nu_0T\sum_{\omega_n}\frac{\tilde{\Delta}}{\sqrt{\tilde{\omega}_n^2+\tilde{\Delta}^2}}=\pi\lambda\nu_0T\sum_{\omega_n}\frac{\Delta}{\sqrt{\omega_n^2+\Delta^2}}$$

(I'll collect others later!)

Overview of working approaches for derivation of the gap equation

Обычные богол трансф

U v подстановка как в Шмидте, по сути тот же Боголюбов, только в другом формализме

(something similar is in original BCS article about it, it is very interesting, how did they do it, without any Bogoliubov transformations?)

Метод Дениса через матричное преобр

Метод Лункина через эксп и перестановку так, чтобы потом получить щель и ещё что-то

Derivation of the gap equation from plugging Bogoliubov operators in the definition

We know that $\Delta = \lambda \cdot \sum'_{\mathbf{p}'} \langle \hat{a}_{-\mathbf{p}',-} \hat{a}_{\mathbf{p}',+} \rangle$ and that $\begin{matrix} \hat{b}_{\mathbf{p}^-} = u_{\mathbf{p}} \hat{a}_{\mathbf{p}_-} + v_{\mathbf{p}_-} \hat{a}^\dagger_{-\mathbf{p}_+}, \\ \hat{b}_{\mathbf{p}^+} = u_{\mathbf{p}_-} \hat{a}_{\mathbf{p}_+} - v_{\mathbf{p}_-} \hat{a}^\dagger_{-\mathbf{p}_-}. \end{matrix}$, if one plugs them, one will get

$$\frac{1}{\lambda} = \frac{1}{2} \sum_{\mathbf{p}} \frac{1 + 2\bar{n}_{\mathbf{p}}}{\sqrt{\xi^2_{\mathbf{p}} + \Delta^2}}$$

where $\bar{n}_{\mathbf{p}} = \left\langle \hat{b}^\dagger_{\mathbf{p}+} \hat{b}_{\mathbf{p}+} \right\rangle = \left\langle \hat{b}^\dagger_{\mathbf{p}-} \hat{b}_{\mathbf{p}-} \right\rangle = [\exp(\varepsilon(p)/T) + 1]^{-1}$

(write more explanation)

Derivation of the gap equation using equations of motion for Nambu operators and interchanging them

(write Lunkin's method!)

Derivation of the gap equation from free energy

(??? not sure about this method)

As the temperature increases, the energy gap Δ decreases (the notation Δ_0 will be kept for $T = 0$). This is easy to understand. As we already know, in order to break a Cooper pair and create two elementary excitations, the energy 2Δ is needed. If the temperature T is such that

$$k_{\mathrm{B}} T \approx 2\Delta,$$

it is evident that many Cooper pairs will be broken through thermal processes. Accordingly, a large number of states in momentum space will be filled by elementary excitations (single electrons). But this implies that these states can no longer participate in the pair transitions and, therefore, cannot contribute to the net reduction of the superconductor's energy. (the energy of the superconductor has to increase). These states will likewise be unable to participate in forming the energy gap ($\Delta_0 = V \sum'_k v_k u_k$).

(??? by the way, why finally we have $4k_{\mathrm{B}}T \approx 2\Delta$, approximately, 4 times bigger??)

Since the elementary excitations obey the Fermi-Dirac statistics, the probability that the state k is occupied by a single electron is

$$f_k = \frac{1}{\exp\left(\frac{E_{\mathrm{k}}}{k_{\mathrm{B}}T}\right) + 1} \tag{6.29}$$

where E_k is the energy of an elementary excitation. One can see that $f_k \ll 1$ at $k_{\mathrm{B}}T \ll E_k$, and $f_k \simeq 0.5$ at $k_{\mathrm{B}}T \gg E_k$. This is how Fermi distribution function works for the case of zero chemical potential.

If at least one of the states, (k) or $(-k)$, is occupied, the pair state $(k, -k)$ cannot take part in creating the superconducting state. The probability of this is $2f_k$. Hence, the probability that the pair state $(k, -k)$ can participate in the scattering processes, i.e., can take part in creating the superconducting state, is $1 - 2f_k$.

The expression for the total energy of the superconductor at $T \neq 0$ can then be written in the form (see Sect.6.2) (??? why it is so????)

$$W = \sum_k 2\left|\varepsilon_k\right| f_k + 2\sum_k \varepsilon_k \left(1 - 2f_k\right) v_k^2 - V \sum_{kk'}{}' v_k u_k v'_k u'_k \left(1 - 2f_k\right)\left(1 - 2f_{k'}\right). \tag{6.30}$$

Here the first term is the kinetic energy of the elementary excitations, the second term is the kinetic energy of the superconducting electrons and the last term is the energy of the phonon-mediated electron interaction which is the prime cause of the superconducting state. The two last factors account for the probability of this interaction.

The free energy density of the superconductor is

$$F = W - TS \tag{6.31}$$

where S is the entropy of the material. The functions v_k^2, describing the distribution of the supeconducting electrons in momentum space at thermodynamic equilibrium, can be found from the condition that the free energy density F is a minimum:

$$\frac{\partial F}{\partial \left(v_q^2\right)} = 0 \tag{6.32}$$

Substituting F in terms of W and W in terms of u, v in this equation yields (??? what to do with entropy???? or derivative of it is zero?? I'll check later)

$$\frac{v_q u_q}{1 - 2v_q^2} = \frac{\Delta}{2\varepsilon_q} \tag{6.33}$$

where

$$\Delta = V \sum_k{}' v_k u_k \left(1 - 2f_k\right) \tag{6.34}$$

This last expression gives the temperature dependence of the energy gap. As $T \to 0$, the gap is $\Delta \to \Delta(0)$, where $\Delta(0) = \Delta_0$ is the gap at $T = 0$ defined earlier. The only thing that is left, is to simplify it. First, we write $v_q^2 = \frac{1}{2}\left(1 - \frac{\varepsilon_q}{E_q}\right)$ where $E_q = \sqrt{\varepsilon_q^2 + \Delta^2(T)}$.

Then $\Delta = V \sum_k{}' v_k u_k \left(1 - 2f_k\right)$ reduces to (??? I'll check later)

$$\Delta = V \sum_k{}' \frac{\Delta}{2E_k}\left(1 - \frac{2}{\exp\left(E_k/k_{\mathrm{B}}T\right) + 1}\right)$$

Replacing summation with integration yields, after simple algebra,

$$\frac{1}{N(0)V} = \int_0^{\hbar\omega_{\mathrm{D}}} \frac{\mathrm{d}\varepsilon}{\sqrt{\varepsilon^2 + \Delta^2(T)}} \tanh \frac{\sqrt{\varepsilon^2 + \Delta^2(T)}}{2k_{\mathrm{B}}T}. \tag{6.35}$$

Here, again, we approximated the integral by extracting $N(0)$ out.

Thus we have obtained an implicit temperature dependence of the energy gap.

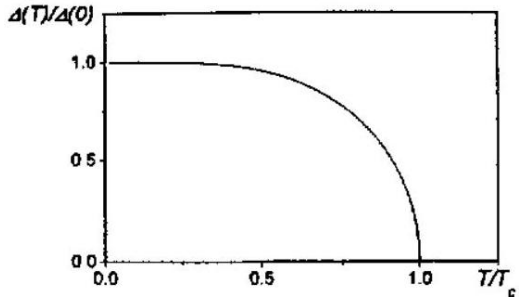


Fig. 6.8. Temperature dependence of the energy gap in the BCS theory

This dependence is sketched in Fig. 6.8: Near T_c, the variation of the gap with temperature obeys $\Delta \propto (T_c - T)^{1/2}$. The discussion of numerical obtaining this results are below.

How one should not derive of the gap equation

To get the gap equation, we need to calculate basically

$$\langle c_{-k,-} c_{k,+} \rangle = \mathrm{Tr}\left(\frac{\exp\Big[-\beta H \Big]}{\mathrm{Tr}[e^{-\beta H}]} c_{k,+} c_{-k,-} \right); \qquad H_{\mathrm{BCS}} = \sum_{p,\sigma} \Big(\xi_p c^\dagger_{p\sigma} c_{p\sigma} + \Delta \big(c_{p\uparrow} c_{-p\downarrow} + c^\dagger_{-k\downarrow} c^\dagger_{k\uparrow} \big) \Big), \quad \xi_p = v_F(p - p_F).$$

To do it, we need to plug the eigenstates under trace. They are obtain from the diagonalized Hamiltonian. These states are the excitations, not the Cooper pairs that are inside the condensate! Thus, one can't just plug states to the trace, because one needs to understand, what are these states? To understand, what are they, one needs to diagonalize the Hamiltonian. So, approaches by some clever transformation of just c operators inside the trace (without diagonalization of Hamiltonian) is, maybe, just impossible, since then anyway we need to plug states, which are known only when we know how to diagonalize the Hamiltonian. Nor matrix exponent of the Hamiltonian, nor expansion the exponent in series will not work, since evaluation of the trace by plugging states with some number of electrons or holes there is just a wrong approach. A real eigenstate under the trace is a superposition of electron and a hole.

Another, also maybe impossible approach is that suppose we have diagonalized the Hamiltonian and we know that the excitation is the Bogoliubov particles, then one might again try to massage the electron and hole operators, such that they will combine to some expression which will be evaluatable. I don't think that is also possible. Writing all in c operators is still a terrible idea, the only solution is to rotate the basis to b operators.

(??? okay, maybe there is a way how to do it using only c operators and evaluating trace explicitly, but I don't know this. Maybe one needs to plug two states there, with $b^\dagger b = 1$ and $b^\dagger b = 0$ in terms of c operators in the trace and see what is left? Sounds still complicated, because we have an exponent there. So, my conclusion is as was before: don't use this method unless you read some good article which tells you how to do it)

Mathematical properties of the gap equation

(??? about this sum)

Properties of the gap equation for numerical evaluation

(write that methods of finding a middle point)

If numerical function in Python says that it sees no root, increase the number of lattice sites!

```
L      = 300
p_vals = np.linspace(0, 2*np.pi, L, endpoint=False)
```

this is the good lattice cites, for a L=30 it was giving an error.

Other properties of the gap equation

(they will be discussed in detail below, in the special sections about special methods, here I'll just write main ideas and formulas)

What is more fundamental, the form of summation or the integral form of the gap equation?

This question can be important because the integral form can be approximated differently and there could be different cutoffs. Thus, to understand, what is the most exact solution, we need to understand, what is the most exact equation?

Idea of derivation of the gap equation using the density matrix

(??? I'll just write why it can be done so?? and key things about it)
(it is written in detail in the section of BCS in density matrix framework)

3.9.7 Tight-binding 1D BCS model

The 1D BCS tight-binding is a basic model of a simplest superconductor. It is very useful for research, so it is a basic model.

Reminder: The idea of tight-binding models

Derivation of the tight-binding BCS model

(write here the search of the spectrum $-2tcos\phi$)

Limit of applicability of 1D TB BCS models

(???? write it after learning that fluctuations)

Features of TB BCS models

Division by number of lattice sites N when sums are computed

(write that these sums should be understood as they were with division by N)
(??? explain, why??? I don't know, why?)

Remember that the division by N is also assumed sometimes if there is no sum, but it was originally there.
(write example of the dissipator that we used)

Parameters of tight-binding BCS model

At this stage we understand that there is a TB BCS model that explains superconductivity in 1D, but it is not clear which parameters to put into it? Here, we will answer this question.

Comparison of BCS relation at different parameters

We have a criterion that we need such parameters of the tight-binding model that the universal BCS relation is fulfilled.
(??? why??? the conclusion is that analytic derivation is very important)

```
import numpy as np
import matplotlib.pyplot as plt

J = 1.0
mu = 0.0

Nk = 2000
```

```
g_min, g_max = 1.0, 2.5
g_num = 30
g_list = np.linspace(g_min, g_max, g_num)

omega_D_list = np.linspace(0.1, 0.5, 5)

k  = np.linspace(-np.pi, np.pi, Nk, endpoint=False)
xi = -2.0 * J * np.cos(k) - mu

def kernel_linearized_Tc(x, T):
    y = x / (2.0 * T)
    out   = np.empty_like(x, dtype=float)
    small = np.abs(y) < 1e-8
    out[~small] = np.tanh(y[~small]) / (2.0 * x[~small])
    out[small]  = 1.0 / (4.0 * T)
    return out

def bisection(f, a, b, tol=1e-12, maxit=100):
    fa, fb = f(a), f(b)
    if not (np.isfinite(fa) and np.isfinite(fb)):
        raise ValueError("Non-finite f at bracket endpoints.")
    if fa * fb > 0:
        raise ValueError("Bisection bracket does not change sign.")
    left, right, fleft, fright = a, b, fa, fb
    for _ in range(maxit):
        mid  = 0.5 * (left + right)
        fmid = f(mid)
        if abs(fmid) < tol or (right - left) < tol:
            return mid
        if fleft * fmid < 0:
            right, fright = mid, fmid
        else:
            left,  fleft  = mid, fmid
    return 0.5 * (left + right)

def Tc_from_g(g_abs, xi_w, omega_D):
    def F(T):
        return g_abs * kernel_linearized_Tc(xi_w, T).sum()/Nk - 1.0
    T_low  = 1e-8
    F_low  = F(T_low)
    T_high = max(2.0 * omega_D, 2.0 * J)
    F_high = F(T_high)
    tries = 0
    while F_low * F_high > 0 and tries < 30:
        T_high *= 1.5
        F_high  = F(T_high)
        tries  += 1
    if F_low * F_high > 0:
        return np.nan
    return bisection(F, T_low, T_high)

def Delta0_from_g(g_abs, xi_w, omega_D):
    def F(Delta):
        E = np.sqrt(xi_w**2 + Delta**2)
        return g_abs * (0.5 / E).sum()/Nk - 1.0
    D_low, D_high = 1e-12, max(2.0 * omega_D, 2.0 * J)
    F_low, F_high = F(D_low), F(D_high)
    if F_low < 0:   # слишком слабая связь
        return np.nan
    tries = 0
    while F_high > 0 and tries < 40:
        D_high *= 1.5
        F_high  = F(D_high)
        tries  += 1
        if D_high > 100 * max(omega_D, J):
            break
    if F_low * F_high > 0:
        return np.nan
    return bisection(F, D_low, D_high)


plt.figure()
for omega_D in omega_D_list:
    window = np.abs(xi) <= omega_D
    xi_w   = xi[window].astype(float)
```

```
    #if xi_w.size < 50:
    #     # слишком мало состояний в окне - пропустим эту кривую
    #     continue

    Tc_list = []
    D0_list = []
    for g_abs in g_list:
        Tc  = Tc_from_g(g_abs, xi_w, omega_D)
        D0  = Delta0_from_g(g_abs, xi_w, omega_D)
        Tc_list.append(Tc)
        D0_list.append(D0)

    Tc_arr = np.array(Tc_list, dtype=float)
    D0_arr = np.array(D0_list, dtype=float)
    with np.errstate(invalid='ignore', divide='ignore'):
        ratio = D0_arr / Tc_arr

    # рисуем кривую для данного cutoff
    plt.plot(g_list, ratio, marker='o', linestyle='-', label=fr'$\omega_D$={omega_D:.2f}')

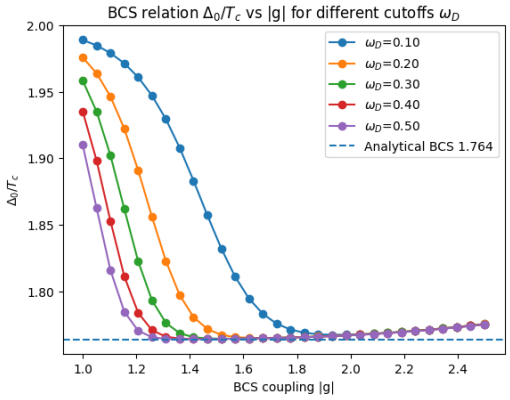

om_d_custom=2.3
Tc_list_2 = []
D0_list_2 = []

for g_abs in g_list:
    Tc_2  = Tc_from_g(g_abs, xi_w, om_d_custom)
    D0_2  = Delta0_from_g(g_abs, xi_w, om_d_custom)
    Tc_list_2.append(Tc_2)
    D0_list_2.append(D0_2)

Tc_arr_2 = np.array(Tc_list_2, dtype=float)
D0_arr_2 = np.array(D0_list_2, dtype=float)
ratio_2 = D0_arr_2 / Tc_arr_2

plt.axhline(y=1.76388, linestyle='--', label="Analytical BCS 1.764")
plt.xlabel("BCS coupling |g|")
plt.ylabel(f"$\\Delta_0/T_c$")
plt.title(f'BCS relation $\\Delta_0/T_c$ vs |g|, $N$={Nk}')
plt.legend()
plt.show()
```

And now we can compare parameters graphically:



Which values should have a hopping parameter?

(??? discuss of it!!)

Значения t зависят от конкретного материала и выбора единиц:

1. В модельных расчётах t обычно просто выбирают равным 1 . Тогда все энергии (включая щель Δ, температуру T, дебаевский срез ω_D) выражаются в единицах t.

Это упрощает численные вычисления, так как остаётся лишь безразмерный набор параметров: $|g|, \omega_D/t, \mu/t$, и т.д.

2. В реальных материалах t лежит в диапазоне порядка десятков - сотен мэВ:
- В органических проводниках и оптических решётках холодных атомов t может быть $\sim 0.01 - 0.1$eV.
- В медь-оксидных высокотемпературных сверхпроводниках $t \approx 0.3 - 0.5$eV.
- В простых металлах или модельных tight-binding системах часто берут $t \sim 1$ eV .
3. Отношение t и щели: у обычных сверхпроводников щель Δ и дебаевская частота ω_D существенно меньше t. Обычно

$$\Delta, k_B T_c, \omega_D \ll t,$$

чтобы зона была «широкой» и условие приближения БКШ выполнялось.
Причина в том, что в tight-binding BCS модели t играет роль масштабного параметра энергии, а сама модель безразмерна.

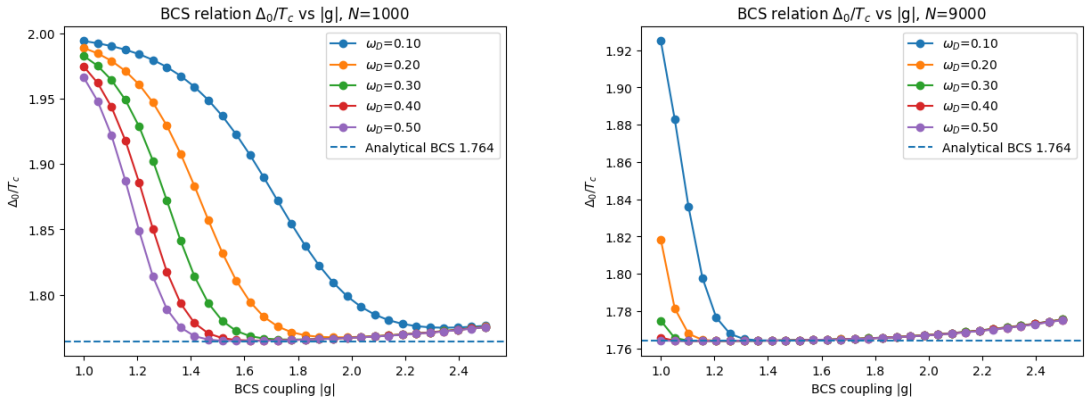
(how Tc and the gap Delta depend on the hopping parameter???? I can check numerically, but I don't understand it analytically)

Which values should have a Debye cutoff?

(??? discuss of it!!)

Which values should have a grid of the Brillouin zone (N)?

If we increase N, we'll get closer and closer to the real BCS relation.



(write that we have an increase of the BCS relation with increase of the coupling constant because it becomes not little compared to the kinetic energy. but why??? I'll answer here)

Which values should have a BCS coupling constant?

(??? discuss of it!!)
It can be lower and bigger than the hopping parameter t, but not too little and not too big. (????)

Which values should have a chemical potential?

We take it always to zero.
(why??? discuss of it!!)

Overview of different notations of tight-binding BCS model

(detalis of it will be later, here is just an intro to it)

Other general questions about TB BCS models

Relation of TB BCS model to the Ising and other spin models from statistical physics?

(??? there was an article about it by Zurek, so I'll point it out here)

How to take into account another orthogonal dimensions in 1D TB BCS models?

(???? good general question, I don't know. there is a discussion of degeneration of quantization, but I don't unerstand it)

How the basic TB BCS model can be generalized?

(??? there may be next nearest neighbor hopping and maybe something else? why? Ask Rock Zitko maybe about it later)

3.9.8 Ground State Energy and Wavefunction in BCS

Short calculation of BCS ground state energy

(?? add from Pukhov)

Long calculation of BCS ground state energy by Mexeenkov

Энергия основного состояния есть значение E при нулевой температуре. (??? почему??? у нас же разное число электронов будет в граунд стейте???)

Температуре $T = 0$ отвечают числа заполнения $n_p = 0$. Поэтому в основном состоянии для перестроенного спектра энергия равна:

(????? remind the formulas here?!!!)

$$E_g(\Delta) = \sum_p \xi_p \left(1 - \frac{\xi_p}{\sqrt{\xi_p^2 + \Delta^2}}\right) - \Delta^2 \sum_p \frac{1}{2\sqrt{\xi_p^2 + \Delta^2}} =$$
$$= \sum_p \left[\left(\xi_p - \sqrt{\xi_p^2 + \Delta^2}\right) + \frac{\Delta^2}{2\sqrt{\xi_p^2 + \Delta^2}}\right]$$

Если бы взаимодействия не было, то энергия основного нормального состояния равнялась бы энергии ферми-сферы

$$E_g = 2 \sum_{p<p_F} \xi_p$$

Запишем изменение энергии основного состояния:

$$E_g(\Delta) - E_g = \sum_{p>p_f}\left[\left(\xi_p - \sqrt{\xi_p^2+\Delta^2}\right) + \frac{\Delta^2}{2\sqrt{\xi_p^2+\Delta^2}}\right] + \sum_{p<p_f}\left[\left(-\xi_p - \sqrt{\xi_p^2+\Delta^2}\right) + \frac{\Delta^2}{2\sqrt{\xi_p^2+\Delta^2}}\right] =$$
$$= \sum_{p}\left[\left(|\xi_p| - \sqrt{\xi_p^2+\Delta^2}\right) + \frac{\Delta^2}{2\sqrt{\xi_p^2+\Delta^2}}\right] =$$
$$= 2\sum_{p>p_f}\left[\left(\xi_p - \sqrt{\xi_p^2+\Delta^2}\right) + \frac{1}{2}\frac{\Delta^2}{\sqrt{\xi_p^2+\Delta^2}}\right]$$

Докажем, что для перестроенного состояния $E_g(\Delta) < E_g$. We have:

$$I_1 = 2\sum_{p>p_f}\xi_p = 2\frac{\nu_F}{2}\int\limits_0^{\hbar\omega_D}\xi_p d\xi_p = \frac{\nu_F}{2}\left(\hbar\omega_D\right)^2$$

$$I_2 = 2\sum_{p>p_F}\sqrt{\xi_p+\Delta^2} = 2\frac{\nu_F}{2}\int\limits_0^{\hbar\omega_D}\sqrt{\xi^2+\Delta^2}d\xi = \Delta^2\nu_F\int\limits_0^{\hbar\omega_D/\Delta}\sqrt{x^2+1}dx$$

After $x = \sinh y$, we have

$$\int\sqrt{x^2+1}dx = \int dy\cosh^2 y = \frac{1}{4}\sinh(2y) + \frac{y}{2} = \frac{1}{2}\left(x\sqrt{x^2+1} + \operatorname{Arsh} x\right)$$

thus

$$I_2 = \Delta^2\frac{\nu_F}{2}\left(\hbar\omega_D/\Delta\right)\left[1+\left(\hbar\omega_D/\Delta\right)^2\right]^{1/2} + \Delta^2\frac{\nu_F}{2}\operatorname{Arsh}\left(\hbar\omega_D/\Delta\right)$$

From (??) следует, что

$$\sum_{p>p_f}\frac{\Delta^2}{\sqrt{\xi_p^2+\Delta^2}} = \frac{\Delta^2}{g}$$

Итак,

$$E_g(\Delta) - E_g = \frac{\nu_F}{2}\left(\hbar\omega_D\right)^2 - \Delta^2\frac{\nu_F}{2}\left(\hbar\omega_D/\Delta\right)\left[1+\left(\hbar\omega_D/\Delta\right)^2\right]^{1/2} - \Delta^2\frac{\nu_F}{2}\operatorname{Arsh}\left(\hbar\omega_D/\Delta\right) + \frac{\Delta^2}{g}$$

В силу (??) последняя строка в (58) обращается в нуль. Из выражения (58) немелленно слелует, что $E_g(\Delta) - E_g < 0$. При $\hbar\omega_D/\Delta \gg 1$

$$E_g(\Delta) - E_g = \frac{\nu_F}{2}\left(\hbar\omega_D\right)^2 - \Delta^2\frac{\nu_F}{2}\left(\hbar\omega_D/\Delta\right)\left[1+\left(\hbar\omega_D/\Delta\right)^2\right]^{1/2} \approx -\frac{\nu_F\Delta^2}{4}$$

Таким образом, энергия основного состояния сверхпроводящего состояния ($\Delta \neq 0$) ниже энергии нормального состояния.

Calculation of the ground state energy

Reminder: (write shortly what we have and where did we take it?) we know that $\Delta_0 = ...$
(statement about Δ_0, from which it follows? I moved it lower, the derivation was here)

The general expression for E_s is given by $E_s = \sum_k 2\varepsilon_k v_k^2 + \sum_{k.k'} V_{kk'}v_{k'}u_k v_k u_{k'}$. In the normal state, when the interaction between the electrons is switched off and all states below the Fermi level are full, the ground-state energy is given by

$$E_{\mathrm{n}} = \sum_{k<k_{\mathrm{F}}} 2\varepsilon_k \tag{6.17}$$

Here the coefficient 2 appears because the sum is taken over pairs of states $(k, -k)$.

The ground-state energy of the superconductor is measured from the ground-state energy of the normal metal, i.e., we seek the quantity

$$W = E_{\mathrm{s}} - E_{\mathrm{n}}$$

Using $E_s = \sum_k 2\varepsilon_k v_k^2 + \sum_{k.k'} V_{kk'} v_{k'} u_k v_k u_{k'}$ and (6.17), we obtain

$$W = \sum_{k<k_{\mathrm{F}}} 2\varepsilon_k \left(v_k^2 - 1\right) + \sum_{k>k_{\mathrm{F}}} 2\varepsilon_k v_k^2 - V \sum_{kk'}{}' v_k u_k v_{k'} u_{k'} \tag{6.18}$$

The prime on the last summation sign indicates that the sum is taken over the layer $\pm\hbar\omega_D$ near the Fermi surface. Substituting here $v_k^2 = \frac{1}{2}\left(1 - \frac{\varepsilon_k}{E_k}\right)$ yields, after elementary transformations,

$$W = \sum_{k<k_F} |\varepsilon_k| \left(1 - \frac{|\varepsilon_k|}{E_k}\right) + \sum_{k>k_F} \varepsilon_k \left(1 - \frac{\varepsilon_k}{E_k}\right) - V \sum_{kk'}{}' v_k u_k v_{k'} u_{k'} =$$

$$= 2 \sum_{k>k_F} \varepsilon_k \left(1 - \frac{\varepsilon_k}{E_k}\right) - V \sum_{kk'}{}' v_k u_k v_{k'} u_{k'}.$$

Taking into account the definition of $\Delta_0 = V \sum_k' v_k u_k$, we find

$$\sum_{kk'}{}' v_k u_k v_{k'} u_{k'} = \frac{\Delta_0^2}{V^2}$$

Then

$$W = 2 \sum_{k>k_{\mathrm{F}}} \varepsilon_k \left(1 - \frac{\varepsilon_k}{E_k}\right) - \frac{\Delta_0^2}{V}.$$

Going over from summation to integration, we have

$$W = 2N(0) \int_0^{\hbar\omega_{\mathrm{D}}} \varepsilon \left(1 - \frac{\varepsilon}{\sqrt{\varepsilon^2 + \Delta_0^2}}\right) \mathrm{d}\varepsilon - \frac{\Delta_0^2}{V}$$

Integrating yields

$$W = N(0)\Delta_0^2 \left\{ \left(\frac{\hbar\omega_{\mathrm{D}}}{\Delta_0}\right)^2 - \frac{\hbar\omega_{\mathrm{D}}}{\Delta_0} \left[1 + \left(\frac{\hbar\omega_{\mathrm{D}}}{\Delta_0}\right)^2\right]^{1/2} + \operatorname{arcsinh} \frac{\hbar\omega_{\mathrm{D}}}{\Delta_0} \right\} - \frac{\Delta_0^2}{V}.$$

Using (6.15), we obtain for $\hbar\omega_{\mathrm{D}} \gg \Delta_0$ the final result:

$$W = -\frac{1}{2} N(0) \Delta_0^2 \tag{6.19}$$

Thus, at $T = 0$, the difference in energy between the superconducting and the normal state is negative, that is, the superconducting state is more favorable energetically. And, of course, it is the state of lower energy that will be preferred by Nature.

The BCS wavefunction by Chalker

Given a wavefunction for a pair of electrons of the form we have been considering

$$\phi\left(\mathbf{r}_1, \mathbf{r}_2\right) = \left(\uparrow_1\downarrow_2 - \downarrow_1\uparrow_2\right) g\left(\mathbf{r}_1 - \mathbf{r}_2\right)$$

we can attempt to write a wavefunction for $2N$ electrons in which pairs are Bose condensed, of the form

$$\psi\left(\mathbf{r}_1 \ldots \mathbf{r}_{2N}\right) = \mathcal{A} \prod_{n=1}^{n=N} \phi\left(\mathbf{r}_{2n}, \mathbf{r}_{2n+1}\right)$$

where $\mathcal{A}$ denotes antisymmetrisation. It is initially unclear whether Pauli exclusion allows this - whether a nonzero wavefunction survives after the operation of $\mathcal{A}$ when N is large. That it does is clearer when we write both these states in k-space and using operator notation, as

$$|\phi\rangle = \sum_{\mathbf{k}} g_{\mathbf{k}} c^\dagger_{\mathbf{k}\uparrow} c^\dagger_{-\mathbf{k}\downarrow} |0\rangle$$

and

$$|\psi\rangle = \prod_{n=1}^{N} \left(\sum_{\mathbf{k}_n} g_{\mathbf{k}_n} c^\dagger_{\mathbf{k}_n\uparrow} c^\dagger_{-\mathbf{k}_n\downarrow} \right) |0\rangle$$

since when we expand the product, terms with all $\mathbf{k}_n$'s different will survive. The form of the wavefunction in Eq. (45) is not very convenient, because the occupation of different orbitals is correlated through the constraint that exactly $2N$ electrons are present. The BCS wavefunction relaxes this condition (passing to it is analogous to going from the cannonical to the grand canonical distributions in statistical mechanics). It has the form

$$|\mathrm{BCS}\rangle = \prod_{\mathbf{k}} \left(u_{\mathbf{k}} + v_{\mathbf{k}} c^\dagger_{\mathbf{k}\uparrow} c^\dagger_{-\mathbf{k}\downarrow} \right) |0\rangle.$$

Here $u_{\mathbf{k}}$ is the amplitude for a pair of orbitals to be empty, and $v_{\mathbf{k}}$ is the amplitude for them to contain a Cooper pair, so we require $|u_{\mathbf{k}}|^2 + |v_{\mathbf{k}}|^2 = 1$ for normalisation, and $\sum_{\mathbf{k}} |v_{\mathbf{k}}|^2 = N$ in a system containing $2N$ electrons on average.

In fact, a wavefunction of the form of Eq. (46) can represent a variety of states, depending on the choice of coefficients $v_{\mathbf{k}}$. A filled Fermi sea simply has $v_{\mathbf{k}} = 1$ for $\mathbf{k}$ inside the Fermi surface and $v_{\mathbf{k}} = 0$ outside. By contrast, in a state containing many Cooper pairs, we expect $v_{\mathbf{k}}$ to vary smoothly between 1 and 0 across a window of width $\hbar\omega_{\mathrm{D}}$ around the Fermi energy. One approach to finding $v_{\mathbf{k}}$ is variational, and the subject of Question 2 on Problem Sheet 2. An alternative is a mean field treatment of the Hamiltonian, as described next.

BCS ground state by Coleman

(??)

After Cooper's discovery, it took a further six months of intense exploration of candidate wavefunctions before Bardeen, Cooper and Schrieffer succeeded in formulating the theory of superconductivity in terms of a pair condensate [15]. It was the graduate student in the team, J. Robert Schrieffer, who took the next leap. Schrieffer's insight was to identify the superconducting ground state as a coherent state of the Cooper pair operator:

$$|\psi_{BCS}\rangle = \exp\left[\Lambda^\dagger\right] |0\rangle$$

where $|0\rangle$ is the electron vacuum and $\Lambda^\dagger = \sum_{\mathbf{k}} \phi_{\mathbf{k}} c^\dagger_{\mathbf{k}\uparrow} c^\dagger_{-\mathbf{k}\downarrow}$ is the Cooper pair creation operator (14.13). If we expand the exponential as a product in momentum space,

$$|\psi_{BCS}\rangle = \prod_{\mathbf{k}} \exp\left[\phi_{\mathbf{k}} c^\dagger_{\mathbf{k}\uparrow} c^\dagger_{-\mathbf{k}\downarrow}\right] |0\rangle = \prod_{\mathbf{k}} \left(1 + \phi_{\mathbf{k}} c^\dagger_{\mathbf{k}\uparrow} c^\dagger_{-\mathbf{k}\downarrow}\right) |0\rangle$$

BCS wavefunction

3.9.9 What exactly happens at a ground state of a SC (at $T = 0$)?

6.2.1 Electron Distribution in the Ground State

In this section, our objective is to investigate the state of a superconductor at $T = 0$, i.e., when its energy is a minimum.

First it is appropriate to recall the basic postulates of quantum mechanics which we shall need for what comes later. Suppose that $\psi_n(\boldsymbol{r}_1, \boldsymbol{r}_2, \ldots, \boldsymbol{r}_N)$ is a complete system of functions, where n runs over a set of values which we use to assign numbers to these functions. Then an arbitrary wavefunction $\Psi(r_1, r_2, \ldots, r_N)$ can be expanded in a series

$$\Psi = \sum_n a_n \psi_n \tag{6.3}$$

where a_n stands for the amplitude of the state ψ_n and $|a_n|^2$ defines the probability of finding the system in the state ψ_n.

Suppose that the Hamilton operator $\hat{H}$ is

$$\dot{H} = \hat{H}_{\text{kin}} + \hat{V} \tag{6.4}$$

where $\hat{H}_{\text{kin}}$ is the kinetic energy operator and $\hat{V}$ is the interaction energy operator. Then the mean value of energy $\bar{E}$ in the state Ψ can be written as

$$\vec{E} = \int \Psi^* \hat{H} \Psi \, \mathrm{d}\tau \tag{6.5}$$

the integration is carried out over all N variables. Substituting (6.3) and (6.4) into (6.5) yields

$$\bar{E} = \bar{E}_{\text{kin}} + \bar{V},$$

where

$$\bar{V} = \int \Psi^* \hat{V} \Psi \, \mathrm{d}\tau = \int \sum_n a_n^* \psi_n^* \hat{V} \sum_m a_m \psi_m \, \mathrm{d}\tau = \sum_{n,m} a_n^* a_m V_{nm} \tag{6.6}$$

Here V_{nm} is the matrix element for the transition from the state ψ_m to the state ψ_n:

$$V_{nm} = \int \psi_n^* \hat{V} \psi_m \, \mathrm{d}\tau \tag{6.7}$$

Let us go back to the ground state of the superconductor. The ground state of the normal metal in well known. At $T = 0$, the lowest energy belongs to the state, in momentum space (k space), in which all electron states inside the Fermi surface are occupied while all those outside it are empty. The kinetic energy of such a state is obviously a minimum while the potential energy is simply absent, i.e., it is zero.

Let us now switch on the interaction energy between electrons near the Fermi level, as discussed in the foregoing section. Since this energy is associated with the effective attraction between the electrons, its contribution will be negative and the total energy of the system will be reduced. But this can happen only if the electrons are allowed to scatter from the state $(\boldsymbol{k_1}, \boldsymbol{k_2})$ to the state (k_1', k_2'), that is, if, just before the event of scattering, the state (k_1, k_2) is full while the state (k_1', k_2') is empty.

Therefore, the Fermi sphere with all states below the Fermi level occupied and all states above it empty no longer corresponds to the state of minimum energy at $T = 0$.

What happens is that Nature risks a certain loss in kinetic energy in the hope of winning it back in potential energy. The total energy is now a minimum when the Fermi surface is 'smeared out', i.e., when some of the states in k space above the Fermi level are occupied while some of those below the Fermi level are empty. Moreover, when the states are being filled up, it happens in pairs: if the state $\boldsymbol{k} \uparrow$ becomes occupied, the state $-\boldsymbol{k} \downarrow$ must also be occupied (the arrows indicate the directions of electron spins). This process is illustrated in Fig. 6.3. The same applies to the empty states.

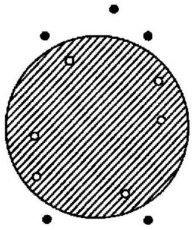


Fig. 6.3. Schematic diagram of an electron state, the energy of which can be lower than the energy of the main state (characterized by all k states below the Fermi level occupied and those above it empty)

Let us now explain why the most favorable way of coupling the electrons is such that the pairs - which are called Cooper pairs - are made of electrons with opposite momenta. A transition of an electron pair from the state (k_1, k_2) to the state (k_1', k_2') must obey the law of momentum conservation: $k_1 + k_2 = k_1' + k_2'$. The sum in (6.6) includes all possible transitions of this kind. The larger the number of allowed transitions, the larger the отрицательный вклад $\bar{V}$ в среднюю энергию $\bar{E}$ сверхпроводника.

If coupled electrons have a total momentum q, the interaction involves only the electrons occupying k states within the dashed areas

Consider, for example, $\boldsymbol{k}_1 + \boldsymbol{k}_2 = \boldsymbol{q}$ as illustrated in Fig. 6.4.

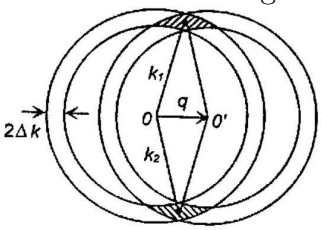


Fig. 6.4.

Here only the electrons occupying the k states in the dashed areas of momentum space are allowed to participate in the transitions. If we now reduce $\boldsymbol{q}$, the dashed areas will grow larger. Finally, at $q = 0$, all states within a band of width $\sim 2\hbar\omega_{\mathrm{D}}$ near the Fermi surface will contribute to the reduction of the average energy.

Let us identify all possible states similar to those shown in Fig. 6.3. Let us assign an index n to them. Then they form a complete system of functions which can be used as a basis for a series expansion of the ground state wavefunction Ψ. The mutual scattering of two coupled electrons $(k, -k)$ to the new state $(\boldsymbol{k}', -\boldsymbol{k}')$ can then be described as a transition from the state ψ_n to another state ψ_m. The state ψ_n corresponds to all states $(\boldsymbol{k}, -\boldsymbol{k})$ full and all states

$(\boldsymbol{k}', -\boldsymbol{k}')$ empty, while the state ψ_m is analogous to the state ψ_n with a single exception: here all states $(k, -k)$ are empty and all states $(\boldsymbol{k}', -\boldsymbol{k}')$ are full (the spin indices have been omitted).

Let us introduce a new function of k, v_k^2. Suppose that it gives the probability that the pair state $(k, -k)$ is occupied. Then the amplitude of the state corresponding to all states $(\boldsymbol{k}, -\boldsymbol{k})$ occupied and all states $(\boldsymbol{k}', -\boldsymbol{k}')$ empty reads

$$a_n = \left[v_k^2 \left(1 - v_{k'}^2\right)\right]^{1/2} = v_k u_{k'}, \quad \text{where} \quad u_k^2 = 1 - v_k^2.$$

By analogy, the amplitude of the state ψ_m corresponding to all states $(k, -k)$ empty and all states $(\boldsymbol{k}', -\boldsymbol{k}')$ occupied is

$$a_m = v_{k'} u_k$$

Using (6.6) we can write the total energy of a superconductor in the state described by the distribution v_k^2 as

$$E_s = \sum_k 2\varepsilon_k v_k^2 + \sum_{k,k'} V_{kk'} v_{k'} u_k v_k u_{k'} \tag{6.8}$$

The first term here gives the total kinetic energy of the system, where ε_k is the energy of an electron in the state k measured from the Fermi level, that is,

$$\varepsilon_k = \frac{\hbar^2 k^2}{2m} - \frac{\hbar^2 k_F^2}{2m} = \bar{\varepsilon}_k - \varepsilon_F.$$

The second term is, according to (6.6), the mean potential energy of electron interaction, where the matrix element $V_{kk'}$ is defined by (6.2).

Now we should find the identity of the function v_k^2 such that the total energy E_s is a minimum. This requires that v_k^2 satisfies the equation

$$\frac{\partial E_{\mathrm{B}}}{\partial v_k^2} = 0.$$

Substituting here $E_s = \sum_k 2\varepsilon_k v_k^2 + \sum_{k.k'} V_{kk'} v_{k'} u_k v_k u_{k'}$ and (6.2), we obtain

$$2\varepsilon_k - V \frac{1 - 2v_k^2}{v_k u_k} \sum_{k'}{}' v_{k'} u_{k'} = 0$$

It follows that

$$\frac{v_k u_k}{1 - 2v_k^2} = \frac{\Delta_0}{2\varepsilon_k} \tag{6.9}$$

where

$$\Delta_0 = V \sum_k{}' v_k u_k \tag{6.10}$$

The prime on the summation sign indicates that the summation is carried out only over the states k within the spherical layer near the Fermi surface, where the matrix element $V_{kk'}$ is nonzero (see (6.2)).

Expressing v_k^2 from (6.9) yields a quadratic equation for v_k^2:

$$v_k^4 - v_k^2 + \frac{\Delta_0^2}{4\bar{E}_k^2} = 0,$$

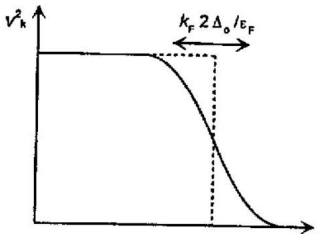
where

$$E_k = \sqrt{\varepsilon_k^2 + \Delta_0^2} \tag{6.11}$$

Then

$$v_k^2 = \frac{1}{2}\left(1 - \frac{\varepsilon_k}{E_k}\right). \tag{6.12}$$

The minus sign in (6.12) stems from a general argument that, as $k \to 0$, we ought to have $v_k^2 \to 1$ while $\varepsilon_k \to -\varepsilon_{\mathrm{F}}$.



The dependence of v_k^2 on k is plotted in Fig. 6.5. As one can see, the total energy of the system reaches its minimum when the electron distribution in the vicinity of the Fermi level is 'smeared out' over the energy interval $\sim 2\Delta_0$. Let us emphasize once more that this occurs at absolute zero! This is the identity of the ground state of the superconductor.

At $T = 0$ not all electrons are superconducting

This is because BCS model assumes the filled Fermi surface, which is field by typical electrons, not paired. Pairing comes into the game only near the Fermi surface, which is already created by some other electrons.

(??? need to discuss this with someone)

At $T = 0$ not all electrons are superconducting: Answers to some questions

(??????? don't know yet, how does it work????)

Proof that all they are in SC state

Газ электронов в сверхпроводнике характеризуется разделением его плотности n на нормальную n_n и сверхтекучую n_s части. Величину нормальной плотности, переносящей импульс, мы уже вычислили в прошлой лекции. Заменяя в (11.23) бозевскую функцию распределения квазичастиц на фермиевскую и умножая на 2 с учетом спина электронов, получаем

$$\rho_n = -\frac{8\pi}{3(2\pi\hbar)^3}\int_0^\infty \frac{dn_F}{dp} p^4 dp$$

Поскольку интеграл (12.29) «набирается» в окрестности импульса Ферми $p \approx p_F$, его можно представить приближенно в виде

$$\rho_n = -\frac{p_F^4}{3\pi^2\hbar^3 v_F}\int_{-\infty}^{+\infty} \frac{dn_F}{d\varepsilon} d\xi$$

Полная же плотность электронного газа $\rho = \rho_n + \rho_s$ равна $\rho = mN/V = = p_F^3 m/3\pi^2\hbar^3$. Таким образом, плотность нормальной компоненты равна

$$\frac{\rho_n}{\rho} = -2\int_0^{+\infty} \frac{dn_F}{d\varepsilon} d\xi$$

Интеграл в правой части (12.31) определяется температурной зависимостью щели $\Delta(T)$. Дифференцируя (12.23) по T и подставляя в (12.31), получаем

$$\frac{\rho}{\rho_n} = 1 - \frac{d\ln T}{d\ln \Delta}$$

Из (12.32) следует важный вывод. При $T \to 0$ плотность нормальной компоненты обращается в ноль $\rho_n \to 0$.

Это значит, что с точки зрения переноса массы и заряда при нулевой температуре все электроны становятся сверхпроводящими. Действительно, поскольку $\rho_{n,s} = mn_{n,s}$ и $n = n_s + n_n$, то $n_s(0) = n$. Тот же вывод можно получить из (12.32), представленный в форме

$$\frac{\rho_s}{\rho} = -\frac{d\ln T}{d\ln(\Delta/T)}$$

(???? so, what to say about it??? is it wrong???)

Other conceptually important statements about the ground state

At $T = 0$ real electrons are distributed according to "tilted Fermi distribution", not the Fermi distribution

(here I'll write that one expects for all fermions at ground state to have step distribution because of from of Fermi distribution)

(but for SC (and for interacting fermions) this is not the case)

(discuss it, add plot)

Critical field from the ground state energy

At the beginning of this book we established that (??? why it is so??) the difference in free energy between the normal and the superconducting state equals $H_{\rm cm}^2/8\pi$, where $H_{\rm cm}$ is the thermodynamic critical field. It then follows that at $T = 0$

$$\frac{H_{\rm cm}^2(0)}{8\pi} = \frac{1}{2}N(0)\Delta_0^2$$

or

$$H_{\rm cm}(0) = \Delta_0\sqrt{4\pi N(0)} \tag{6.20}$$

Thus we have expressed the thermodynamic critical field in terms of characteristic parameters of the superconductor, i.e., parameters describing its electron spectrum and electron-phonon interaction.

Let us check whether (6.20) gives reasonable orders of magnitude for relevant physical quantities. 1 cm^3 of metal contains $\sim 10^{22}$ electrons and the width of the conduction band is $\sim 10\text{eV} = 10 \times 1.6 \times 10^{-12}$erg. Then the density of states is $N(0) \sim 10^{22}/\left(10 \times 1.6 \times 10^{-12}\right) \sim 10^{33}\text{erg}^{-1}\ \text{cm}^{-3}$. According to our previous estimates, $\Delta_0 \sim 10$ K $\sim 10^{-15}$erg. This leads to $H_{\rm cm} \sim 10^{-15} \times \sqrt{10^{34}} = 100$Oe, which is a reasonable value for the thermodynamic critical field.

Argument that distribution of electrons $n_{\mathbf{FD}}(T=0)$ is a step regardless spectra doesn't work.

(!!! I'll write, why it is so. because the Hamiltonian is non-diagoanal in terms of operators of real electron. I'll elaborate, why)

3.9.10 System of QFT GF Equations for a Superconductor

Why do we need any QFT superconductivity equations

(?????? write, why???)

Why can we work with GF for superconductors?

(I need a really good answer to it!!! I'll think later)

1. Superconductor at absolute zero

We now proceed to the derivation of a system of equations for the Green functions describing the properties of a metal in the superconducting state (Gor'kov [61]). We shall confine ourselves for a start to the case of absolute zero. In our model, the complete Hamiltonian of the system of electrons in the second quantisation representation has the form

$$\hat{H} = \int \left\{ -\left(\psi^{+} \frac{\nabla^2}{2m} \psi \right) + \frac{\lambda}{2} \left(\psi^{+} \left(\psi^{+} \psi \right) \psi \right) \right\} \mathrm{d}^3 r$$

where $(\psi^{+}\psi) \equiv \psi_{\alpha}^{+}\psi_{\alpha}$ and the operators $\psi(\boldsymbol{r}), \psi^{+}(\boldsymbol{r})$ in the Schrdinger representation satisfy the usual commutation relations

$$\begin{aligned} \left\{ \psi_{\alpha}(\boldsymbol{r}), \psi_{\beta}^{+}\left(\boldsymbol{r}'\right) \right\} &= \delta_{\alpha\beta} \delta\left(\boldsymbol{r} - \boldsymbol{r}'\right) \\ \left\{ \psi_{\alpha}(\boldsymbol{r}), \psi_{\beta}\left(\boldsymbol{r}'\right) \right\} &= \left\{ \psi_{\alpha}^{+}(\boldsymbol{r}), \psi_{\beta}^{+}\left(\boldsymbol{r}'\right) \right\} = 0 \end{aligned} \tag{34.1}$$

We change to the Heisenberg representation, in which the operators $\tilde{\psi}, \tilde{\psi}^{+}$depend on the time and obey the following operator equations:

$$\begin{aligned} \left\{ i\frac{\partial}{\partial t} + \frac{\nabla^2}{2m} \right\} \tilde{\psi}_{\alpha}(x) - \lambda \left(\tilde{\psi}^{+}(x) \tilde{\psi}(x) \right) \tilde{\psi}_{\alpha}(x) = 0 \\ \left\{ i\frac{\partial}{\partial t} - \frac{\nabla^2}{2m} \right\} \tilde{\psi}_{\alpha}^{+}(x) + \lambda \tilde{\psi}_{\alpha}^{+}(x) \left(\tilde{\psi}^{+}(x) \tilde{\psi}(x) \right) = 0 \end{aligned} \tag{34.2}$$

The equation for the Green function of the system

$$G_{\alpha\beta}\left(x, x'\right) = -i \left\langle T \left(\tilde{\psi}_{\alpha}(x) \tilde{\psi}_{\beta}^{+}\left(x'\right) \right) \right\rangle$$

can be obtained in an obvious way from equations (34.2):

$$\left\{ i\frac{\partial}{\partial t} + \frac{\nabla^2}{2m} \right\} G_{\alpha\beta}\left(x, x'\right) + i\lambda \left\langle T \left(\left[\tilde{\psi}^{+}(x) \tilde{\psi}(x) \right] \tilde{\psi}_{\alpha}(x), \tilde{\psi}_{\beta}^{+}\left(x'\right) \right) \right\rangle = \delta\left(x - x'\right).$$

(???? I am not sure, how????)

This equation contains the mean of the product of four $\tilde{\psi}$-operators for a system of non-interacting electrons, which can be expanded by Wick's theorem into averages of pairs of operators $\tilde{\psi}, \tilde{\psi}^{+}$. The product of four $\tilde{\psi}$-operators for interacting particles is already expressible

in terms of the vertex part, i.e. includes the contribution of the different scattering processes. In our weak interaction model, the scattering of different particles by one another can be neglected. At the same time we have to take into account that the ground state of the system differs from the ordinary state with a filled Fermi sphere by the presence of bound electron pairs. As already mentioned in the previous section, such pairs are Bose formations and therefore possess the ability to accumulate in any amount at the level with the lowest energy. In the absence of an external field, and neglecting scattering processes, the pairs obviously "condense" in the state in which they are at rest as a whole.

Let us consider the product of operators $\tilde{\psi}\tilde{\psi}$ or $\tilde{\psi}^+\tilde{\psi}^+$. The first annihilates, whilst the second creates, two electrons. In particular, these two electrons may find themselves in a bound state, in other words, the operators $\tilde{\psi}\tilde{\psi}$ and $\tilde{\psi}^+\tilde{\psi}^+$contain terms corresponding to the annihilation and creation of bound pairs, including pairs at the lowest level. Since there are many such pairs (the number of them is proportional to the total number of particles), the corresponding contribution to the operators $\tilde{\psi}\tilde{\psi}$ and $\tilde{\psi}^+\tilde{\psi}^+$can be regarded as a c-number, just as in the case of a system of bosons.

Notice that there are special reasons, in a metal, why we do not consider pairs which are not at the lowest level: a bound pair of electrons, when the motion as a whole has finite momentum, is a Bose excitation with zero spin.

(??????)

As we have already remarked, the condition for electric neutrality in a metal actually implies that a substantial energy ($\sim$ 1eV) is required for the excitation of such a "Bose condensate" pair, this being much greater than the characteristic energies which we encounter when developing the theory of superconductivity.

Returning to equation (34.3) for the Green function, in the light of what has been said, the average of the product of four ψ-operators can be written as follows, e.g.

$$\begin{aligned}\left\langle \mathrm{T}\left(\tilde{\psi}_\alpha(x_1)\,\tilde{\psi}_\beta(x_2)\,\tilde{\psi}^+_\gamma(x_3)\,\tilde{\psi}^+_\delta(x_4)\right)\right\rangle = \\ = -\left\langle T\left(\tilde{\psi}_\alpha(x_1)\,\tilde{\psi}^+_\gamma(x_3)\right)\right\rangle\left\langle T\left(\tilde{\psi}_\beta(x_2)\,\tilde{\psi}^+_\delta(x_4)\right)\right\rangle + \\ + \left\langle T\left(\tilde{\psi}_\alpha(x_1)\,\tilde{\psi}^+_\delta(x_4)\right)\right\rangle\left\langle T\left(\tilde{\psi}_\beta(x_2)\,\tilde{\psi}^+_\gamma(x_3)\right)\right\rangle + \\ + \langle N|T\left(\tilde{\psi}_\alpha(x_1)\,\tilde{\psi}_\beta(x_2)\right)|N+2\rangle\langle N+2|T\left(\tilde{\psi}^+_\gamma(x_3)\,\tilde{\psi}^+_\delta(x_4)\right)|N\rangle \quad (34.4)\end{aligned}$$

where $|N\rangle$ and $|N+2\rangle$ are the ground states of the systems with N and $N+2$ particles.

(????? why there is the last term here???)

This way of writing the average implies that we have neglected all the effects of scattering of particles by one another. The existence of interactions is only taken into account in so far as it leads to the formation of bound pairs. The third term on the right-hand side of (34.4) is written in complete analogy with the case of a Bose gas, in accordance with the fact that a large number of bound pairs has "condensed" into the lowest level. The quantity

$$\langle N|T(\tilde{\psi}\tilde{\psi})|N+2\rangle\langle N+2|T\left(\tilde{\psi}^+\tilde{\psi}^+\right)|N\rangle$$

is obviously of the order of the density of the number of pairs.

It is easily verified that the functions thus introduced can be written as

$$\begin{aligned}\langle N|T\left(\tilde{\psi}_\alpha(x)\tilde{\psi}_\beta(x')\right)|N+2\rangle = e^{-2i\mu t}F_{\alpha\beta}(x-x') \\ \langle N+2|T\left(\tilde{\psi}^+_\alpha(x)\tilde{\psi}^+_\beta(x')\right)|N\rangle = e^{2i\mu t}F^+_{\alpha\beta}(x-x') \quad (34.5)\end{aligned}$$

(??????????????????????)

For the uniform problem (in the absence of an external field), the Green function $G(x-x')$ depends only on the coordinate difference $x-x'$. The source of the extra dependence on t in expressions (34.5) is clear from the general formulae of quantum mechanics for the time derivative of an arbitrary operator $\tilde{A}(t)$:

$$\frac{\partial}{\partial t}\langle N|\tilde{A}(t)|N+2\rangle = i\left(E_N - E_{N+2}\right)\langle N|\tilde{A}(t)|N+2\rangle.$$

By definition, the chemical potential $\mu = \partial E/\partial N$, so that the energy difference $E_{N+2} - E_N$ is equal to 2μ.

When substituting expression (34.4) into equation (34.3) for the Green function, we shall always omit the first two terms on the right-hand side of (34.4), since they may easily be shown to lcad, in the equations for functions G, F, F^+, to an additive correction to the chemical potential, and are of no interest. As a result, we get the following equation connecting G and F^+:

$$\left\{i\frac{\partial}{\partial t} + \frac{\nabla^2}{2m}\right\}\hat{G}(x-x') - i\lambda\hat{F}(0+)\hat{F}^+(x-x') = \delta(x-x') \tag{34.6}$$

(Here, $\hat{G}, \hat{F}, \hat{F}^+$denote the matrix forms of the functions $G_{\alpha\beta}, F_{\alpha\beta}, F^+_{\alpha\beta}$ in the spin indices, their products being the matrix products.)

The function $\hat{F}(0+)$ is defined as follows:

$$F_{\alpha\beta}(0+) := e^{2i\mu t}\langle N|\tilde{\psi}_\alpha(x)\tilde{\psi}_\beta(x)|N+2\rangle \equiv \lim_{r\to r', t\to t'+0} F_{\alpha\beta}(x-x'). \tag{34.7}$$

The equation for $\hat{F}^+(x-x')$ can be obtained in the same way by using the second of equations (34.2):

$$\left\{i\frac{\partial}{\partial t} - \frac{\nabla^2}{2m} - 2\mu\right\}\hat{F}^+(x-x') + i\lambda\hat{F}^+(0+)\hat{G}(x-x') = 0. \tag{34.8}$$

In accordance with (34.7),

$$F^+_{\alpha\beta}(0+) = e^{-2i\mu t}\langle N+2|\tilde{\psi}^+_\alpha(x)\tilde{\psi}^+_\beta(x)|N\rangle. \tag{34.9}$$

In the absence of spin-dependent interactions, the Green function $\hat{G}(x-x')$ is proportional to the unit matrix $\delta_{\alpha\beta}$ in the spin variables:

$$\hat{G}_{\alpha\beta}(x-x') = \delta_{\alpha\beta}G(x-x')$$

The functions $\hat{F}, \hat{F}^+$are proportional to the matrix $\hat{I}$, anti-symmetric with respect to its indices. Since the operators $\tilde{\psi}_\alpha(x)$ and $\tilde{\psi}_\beta(x')$ anticommute at the same instant, $F_{\alpha\beta}(r-r', 0) = -F_{\beta\alpha}(r'-r, 0)$. It follows from this that

$$\left\{F^+_{\alpha\beta}(\boldsymbol{r}-\boldsymbol{r}', 0)\right\}^* = -\boldsymbol{F}_{\alpha\beta}(\boldsymbol{r}-\boldsymbol{r}', 0) \tag{34.10}$$

In particular,

$$\left\{F^+_{\alpha\beta}(0+)\right\}^* = -F(0+) \tag{34.11}$$

It is convenient to write $\hat{F}, \hat{F}^+$as

$$\hat{F}^{+}(x-x') = \hat{I}F^{+}(x-x') \qquad (34.12)$$
$$\hat{F}(x-x') = -\hat{I}F'(x-x')$$

where $\left(\hat{I}^2\right)_{\alpha\beta} = -\delta_{\alpha\beta}$.

It is clear from (34.10) that $F^{+}(x-x')$ and $F(x-x')$ satisfy the relationship

$$\left\{F^{+}(r-r',0)\right\}^{*} = F(r-r',0)$$

The anti-symmetry of $\hat{F}, \hat{F}^{+}$with respect to the spin indices corresponds to the fact that the bound pairs are at a displaced level. The function $F_{\alpha\beta}(r-r',0)$ can obviously, apart from a factor, be regarded as the wave function of a pair of particles in a bound state (the centre of mass of the pair is at rest).

Let us write down the system of equations for these functions, omitting everywhere the dependence on the spin variables:

$$\left\{i\frac{\partial}{\partial t} + \frac{\nabla}{2m}\right\} G(x-x') - i\lambda F'(0+)F^{+}(x-x') = \delta(x-x') \qquad (34.13)$$
$$\left\{i\frac{\partial}{\partial t} - \frac{\nabla^2}{2m} - 2\mu\right\} F^{+}(x-x') + i\lambda F^{+}(0+)G(x-x') = 0$$

where $(F(0+))^{*} = F^{+}(0+)$.

Fourier transforming everywhere (†) we obtain:

$$\left(\omega - \frac{p^2}{2m}\right) G(p) - i\lambda F(0+)F^{+}(p) = 1 \qquad (34.14)$$
$$\left(\omega + \frac{p^2}{2m} - 2\mu\right) F^{+}(p) + i\lambda F^{+}(0+)G(p) = 0$$

(†) This system of equations has a great similarity to the system for the functions G' and $\hat{G}$ in the Bose system. It must be borue in mind, however, that the analogues of the functions F and $F^{+}$are in this case the operators $\xi_0, \xi_0^{+}$of the condensate particles. We therefore use the notations G and F^{+}as distinct from Q' and $\hat{G}$ for bosons.

The foregoing discussion has been carried through in the thermodynamic variables, where the number of particles is given. It is much more convenient to use the chemical potential μ as the independent variable. As usual, the transformation to this variable can be accomplished formally by substituting $\omega = \omega' + \mu$.

(???? why????)

Omitting the primes from the frequency, (34.14) can be rewritten as

$$(\omega - \xi)G(p) - i\lambda F(0+)F^{+}(p) = 1$$
$$(\omega + \xi)F^{+}(p) + i\lambda F^{+}(0+)G(p) = 0 \qquad (34.15)$$

where $\xi = v(|\boldsymbol{p}| - p_0), p_0 \simeq \sqrt{2m\mu}$ is the Fermi limiting momentum, and $v = p_0/m$.

The solution is

$$G(p) = \frac{\omega + \xi}{\omega^2 + \xi^2 - \Delta^2}, \qquad F^+(p) = -i\lambda \frac{F^+(0+)}{\omega^2 - \xi^2 - \Delta^2}$$

where

$$\Delta^2 = \lambda^2 \left| F^+(0+) \right|^2 \tag{34.16}$$

The determinant of the left-hand side of system (34.15) vanishes at the points $\omega = \pm\varepsilon(p)$, where $\varepsilon(p) = \sqrt{\xi^2 + A^2}$. The solution of (34.15) is therefore obtained up to arbitrary terms of the form

$$A_1(p)\delta(\omega - \varepsilon(p)) + A_2(p)\delta(\omega + \varepsilon(p)).$$

The boundary condition, determining the choice of the arbitrary A_1 and A_2 in the functions G and F^+, is supplied by Landau's theorem (Chap. II), in accordance with which the sign of the imaginary part of the Green function G is opposite to the sign of ω, whilst the function

$$G_R(\omega, p) = \operatorname{Re} G(\omega, p) + i \operatorname{sign}(\omega) \operatorname{Im} G(\omega, p)$$

must be analytic and cannot have singularities in the upper half-plane. It may easily be verified that the solution satisfying these requirements is (†)

$$G(p) = \frac{u_p^2}{\omega - \varepsilon(p) + i\delta} + \frac{v_p^2}{\omega + \varepsilon(p) - i\delta}, \tag{34.17}$$

$$F^+(p) = -i\lambda \frac{F^+(0+)}{(\omega - \varepsilon(p) + i\delta)(\omega + \varepsilon(p) - i\delta)}, \tag{34.18}$$

where the functions u_p^2 and v_p^2 are equal to

$$u_p^2 = \frac{1}{2}\left(1 + \frac{\xi}{\varepsilon(p)}\right); \quad v_p^2 = \frac{1}{2}\left(1 - \frac{\xi}{\varepsilon(p)}\right) \tag{34.19}$$

(†) We have chosen $F^+(0+)$ to be real. This is always possible in the absence of an external field, since equations (34.13) admit of the transformations $\{F(x - x'), F(0+)\} \to \{F(x - x')\, e^{2i\varphi}, F(0+)e^{2i\varphi}\}$ and $\{F^+(x - x'), F + (0+)\} \to \{F^+(x - x')\, e^{-2i\varphi}, F^+(0+)e^{-2i\varphi}\}$ with constant phase. For more details about this, see subsection 2 below.

The positive pole $\omega = \varepsilon(p)$ in Green function (34.17) determines the excitation spectrum $\varepsilon(p) = \sqrt{\xi^2 + \Delta^2}$. This spectrum has a gap Δ, which we find by starting from the relation

$$F^+(0) = (2\pi)^{-4} \int F^+(p) \mathrm{d}\omega \ \mathrm{d}^3 p \tag{34.20}$$

On substituting (34.18) in this, we get the equation
(??? I'll think later about this derivation and writ it here!!!!)

$$1 = -\frac{\lambda}{2(2\pi)^3} \int \frac{\mathrm{d}^3 p}{\sqrt{\xi^2 + \Delta^2}} \tag{34.21}$$

The divergence is cut out of this integral due to the condition that, in our model, the only electrons taking part in the interaction are those with energies in a layer of width $2\omega_D$ about the Fermi surface. We find on performing the integration that

$$1 = -\frac{\lambda}{2\pi^2} m p_0 \ln \frac{2\omega_D}{\Delta}.$$

We get as a result:

$$\Delta = 2\omega_D e^{-1/\eta}, \tag{34.22}$$

where $\eta = |\lambda| m p_0 / 2\pi^2$. On comparing this expression with the result of the previous subsection, we find that the size of the gap in the energy spectrum at absolute zero has the following relation with the transition temperature:

$$\Delta = \frac{\pi}{\gamma} T_c \tag{34.23}$$

2. The equations in the presence of an external electromagnetic field. Gauge-invariance

If a superconductor is located in an external field, say in an electromagnetic field, system (34.13) becomes rather more complicated. Notice, first of all, that in an external field the functions are no longer functions of the coordinate difference only. The electromagnetic field can be brought into (34.13) in the usual way by the following substitution:

$$\nabla \to \nabla - ieA \text{ or } \nabla \to \nabla + ieA, \tag{34.24}$$

depending on whether the differentiation refers to the operator $\tilde{\psi}$ or $\tilde{\psi}^+$. (It is generally convenient to use the gauge in which the scalar potential φ is zero.) The equations for G and F^+in the case of a field are

$$\begin{aligned} &\left\{ i\frac{\partial}{\partial t} + \frac{1}{2m}\left(\frac{\partial}{\partial r} - ieA(r)\right)^2 + \mu \right\} G(x,x') - i\lambda F(x,x) F^+(x,x') = \delta(x-x'), \\ &\left\{ i\frac{\partial}{\partial t} - \frac{1}{2m}\left(\frac{\partial}{\partial r} + ieA(r)\right)^2 - \mu \right\} F^+(x,x') + i\lambda F^+(x,x) G(x,x') = 0. \end{aligned} \tag{34.25}$$

Notice the obvious gauge-invariance of these equations. A gauge transformation of the vector potential,

$$A \to A + \frac{\partial \varphi}{\partial r} \tag{34.26}$$

leads to different transformations of the functions G, F' and F^+:

$$\begin{aligned} G(x,x') &\to G(x,x')\, e^{ie[\varphi(r)-\varphi(r')]} \\ F(x,x') &\to F(x,x')\, e^{ie[\varphi(r)+\varphi(r')]} \\ F^+(x,x') &\to F^+(x,x')\, e^{-ie[\varphi(r)+\varphi(r')]} \end{aligned} \tag{34.27}$$

whilst the "gap" $|\lambda| F(x,x)$ or $|\lambda| F^+(x,x)$, which, in an external field, is generally speaking a function of x, transforms in accordance with

$$F(x,x) \to F(x,x) e^{2ie\varphi(r)}, \quad F^+(x,x) \to F^+(x,x) e^{-2ie\varphi(r)}. \tag{34.28}$$

The gauge-invariance of the equations enables us to study now the properties of a superconductor in a magnetic field. It must be emphasized, as regards the gauge-invariance of (34.25), that it is connected with the use of the form (32.3) for writing the interaction Hamiltonian. Strictly speaking, Hamiltonian (32.2) is not gauge-invariant, this being, of course, a property

of the model. It may easily be shown that, in this model, equation (34.13) contains, instead of $F(0+)$ and $F^+(0+)$ - the values of the functions F and F^+at coincident points - the functions

$$\overline{F'(x,x)} = \int \theta(r-y)\theta(r-z)F(y,z)\mathrm{d}^3z\ \mathrm{d}^3y$$

and $\overline{F^+(x,x)}$ respectively. As the wave function of a pair, $F(y,z;t=t')$ has a correlation radius of the order of the pair dimensions $\xi_0 \sim hv/T_c$, and falls off rapidly when $|y-z| \gg \xi_0$. The functions θ are of the δ function type, as mentioned in par. 32, with a half-width of the order v/ω_D. Hence replacing of $\overline{F(x,x)}$ by $F(x,x)$ involves an error of the order T_c/ω_D, which is always small in real superconductors.

(??? write, where these equations are used???)

3. GF Equations for Superconductor at finite temperatures

We shall end the present section by considering the question of extending the above approach to the case of non-zero temperatures. This extension is obviously possible on the basis of the method described in Chap. III for $T \neq 0$. A system is characterised in the superconducting state by the non-zero averages

$$\mathfrak{F}(x,x') = \frac{\langle T_\tau(\psi(x)\psi(x')\mathfrak{S})\rangle}{\langle\mathfrak{S}\rangle}, \quad \mathfrak{F}^+(x,x') = \frac{\left\langle T_\tau\left(\psi(x)\bar{\psi}(x')\mathfrak{S}\right)\right\rangle}{\langle\mathfrak{S}\rangle}$$

(the meaning of the averaging and the definition of operators $\psi(x)$, $\bar{\psi}(x)$ being the same as in Chap. III. Remember that the chemical potential is chosen as the independent thermodynamic variable). If we regard the ensemble averages in the definitions of $\mathfrak{F}(x,x')$ and $\mathfrak{F}^+(x,x')$ as quantum mechanical averages over the state with energy equal to the mean energy $\bar{E}$, and with a number of particles equal to the average number of particles, this means that the creation or annihilation of a pair of electrons leaves the state virtually unchanged. It is necessary for this that the pair of electrons in question belong to those bound pairs that find themselves in the "Bose condensate" state. Since the number of these pairs is very large (proportional to the total number of particles in the total volume of the system), the addition or annihilation of one such pair makes no difference to the total state of the system.

(????)

In other words, as in the case of absolute zero, in the system the superconducting state possesses terms in the operator products $\psi\psi$ and $\psi^+\psi^+$that can be regarded as c-numbers. We assume that the (thermodynamic) average of the product of four ψ-operators can be written in terms of the Green function $\mathfrak{G}(x,x') = -\left\langle T_\tau\left(\psi(x)\bar{\psi}(x')\mathfrak{S}\right)\right\rangle/\langle\mathfrak{S}\rangle$ and the functions $\mathfrak{F}(x,x')$, $\mathfrak{F}^+(x,x')$, just as was done in expression (34.4) at absolute zero. As above, this implies neglecting the effects of scattering of particles by one another. We have:

$$\frac{\left\langle T_\tau\left(\psi_\alpha(x_1)\psi_\beta(x_2)\bar{\psi}_\gamma(x_3)\bar{\psi}_\delta(x_4)\mathfrak{S}\right)\right\rangle}{\langle\mathfrak{S}\rangle} = -\mathfrak{G}_{\alpha\gamma}(x_1,x_3)\mathfrak{G}_{\beta\delta}(x_2,x_4) + \\ + \mathfrak{G}_{\alpha\delta}(x_1,x_4)\mathfrak{G}_{\beta\gamma}(x_2,x_3) + \mathfrak{F}_{\alpha\beta}(x_1,x_2)\mathfrak{F}^+_{\gamma\delta}(x_3,x_4). \quad (34.29)$$

We shall not repeat here the derivation of the equations for the functions () and $\mathfrak{F}^+$. It is very similar to the derivation of (34.13); we shall just quote the final form of these equations:

$$\left\{-\frac{\partial}{\partial\tau}+\frac{\nabla^2}{2m}+\mu\right\}\mathfrak{G}\left(x-x'\right)+\Delta\mathfrak{F}^{+}\left(x-x'\right)=\delta\left(x-x'\right),$$
$$\left\{\frac{\partial}{\partial\tau}+\frac{\nabla^2}{2m}+\mu\right\}\mathfrak{F}^{+}\left(x-x'\right)-\Delta^{*}\mathfrak{G}\left(x-x'\right)=0 \tag{34.30}$$

where

$$\Delta=|\lambda|\mathfrak{F}\left(0^{+}\right),\quad \Delta^{*}=|\lambda|\mathfrak{F}^{+}\left(0^{+}\right). \tag{34.31}$$

It sometimes proves necessary to determine the function $\mathfrak{F}\left(x-x'\right)$. The corresponding equation is easily obtained:

$$\left\{-\frac{\partial}{\partial\tau}+\frac{\nabla^2}{2m}+\mu\right\}\mathfrak{F}\left(x-x'\right)-\Delta\mathfrak{G}\left(x'-x\right)=0.$$

This contains the function $\mathfrak{G}$ with arguments interchanged.

It is easy to show that the set of four equations for $\mathfrak{G}\left(x-x'\right),\mathfrak{F}^{+}\left(x-x'\right)$, $\mathfrak{F}\left(x-x'\right)$ and $\mathfrak{G}\left(x'-x\right)$ can be written symbolically in the matrix form

$$\begin{pmatrix}\left\{-\frac{\partial}{\partial\tau}+\frac{\nabla^2}{2m}+\mu\right\} & \Delta\\ -\Delta^{*} & \left\{\frac{\partial}{\partial\tau}+\frac{\nabla^2}{2m}+\mu\right\}\end{pmatrix}\times\begin{pmatrix}\mathfrak{G}\left(x-x'\right) & \mathfrak{F}\left(x-x'\right)\\ \mathfrak{F}^{+}\left(x-x'\right) & -\mathfrak{G}\left(x'-x\right)\end{pmatrix}=\hat{\mathbf{1}}. \tag{34.32}$$

In other words, the four functions form one Green function matrix for the operator on the left-hand side of (34.30).

In the temperature-dependent method, as we know, all the functions are expanded into Fourier series, rather than into a Fourier integral over the frequency. It is clear from these equations that. if we Fourier transform the functions $\mathfrak{F}$ and $\mathfrak{F}^{+}$, in the same way as we Fourier transformed the Green function in Chap. III:

$$\mathfrak{F}^{+}\left(x-x'\right)=(2\pi)^{-3}T\sum_{n}e^{-i\omega_n\tau}\int\mathrm{d}^3pe^{i(p\cdot r)}\mathfrak{F}_{\omega}^{+}(p)$$
$$\mathfrak{F}\left(x-x'\right)=(2\pi)^{-3}T\sum_{n}e^{-i\omega_n\tau}\int\mathrm{d}^3pe^{i(p\cdot r)}\mathfrak{F}_{\omega}(p) \tag{34.33}$$

where $\omega=(2n+1)\pi T$, equations (34.15) now correspond to the set

$$(i\omega-\xi)\mathfrak{G}_{\omega}(p)+\Delta\mathfrak{F}_{\omega}^{+}(p)=1$$
$$(i\omega+\xi)\mathfrak{F}_{\omega}^{+}(p)+\Delta^{*}\mathfrak{G}_{\omega}(p)=0 \tag{34.34}$$

which is satisfied by

$$\mathfrak{G}_{\omega}(\boldsymbol{p})=-\frac{i\omega+\xi}{\omega^2+\xi^2+\Delta^2},\qquad \mathfrak{F}_{\omega}^{+}(\boldsymbol{p})=\frac{\Delta^{*}}{\omega^2+\xi^2+\Delta^2}. \tag{34.35}$$

Notice also that, in the absence of a field, $\mathfrak{F}$ and $\mathfrak{F}^{+}$are equal to one another, and Δ is real. This solution is single-valued, as distinct from the situation holding for the system (34.15).

This is connected with the fact that the analytic properties of the thermodynamic functions are uniquely defined. The size of the gap is determined from the condition

$$1 = \frac{|\lambda| T}{(2\pi)^3} \sum_n \int \frac{\mathrm{d}^3 p}{\omega + \xi^2 + \Delta^2} \tag{34.36}$$

The series over the frequencies is easily summed. Instead of condition (34.21) at $T = 0$, a new relation is obtained, from which we can find the size of the gap at finite temperatures:

$$1 = \frac{|\lambda| m p_0}{2\pi^2} \int_0^{\omega_D} \mathrm{d}\xi \frac{\tanh \frac{\sqrt{\xi^2+\Delta^2(T)}}{2T}}{\sqrt{\xi^2+\Delta^2(T)}}. \tag{34.37}$$

At the point of the phase transition, i.e. at the temperature $T = T_c$, the gap $\Delta(T)$ vanishes and, as must be the case, condition $1 = \frac{|\lambda| m p_0}{2\pi^2} \int_0^{\omega_D} \mathrm{d}\xi \frac{\tanh \frac{\sqrt{\xi^2+\Delta^2(T)}}{2T}}{\sqrt{\xi^2+\Delta^2(T)}}$ turns into (33.15), from which the transition temperature T_c can be determined.

3.9.11 The Superconductivity QFT Equations: Derivation

Theory

Let us dwell on the derivation of the superconductivity equations in the model in which the electrons interact with one another through the electron-phonon interaction. Of course, such a model suffers from the same defect as the approach described above, inasmuch as no account is taken in it of the Coulomb forces acting in the metal. Nevertheless it evidently has a more direct physical significance than the model with a four-fermion interaction, even though the latter is more useful when it comes to obtaining practical results. The basic advantage of the phonon model lies, first of all, in the electron-phonon interaction Hamiltonian (32.1) being gauge-invariant right from the start, as distinct from the method with the four-fermion interaction Hamiltonian (32.2), which is only approximately gauge-invariant, by virtue of the relation $T_c \ll \omega_D$. As regards this relation, it is in general fulfilled only in the weak binding approximation(†). We shall show below that the restriction to weak binding is not essential in the theory of superconductors and that only the ratio $\omega_D/\varepsilon_F \ll 1$ is actually a small parameter of the theory ($\omega_D/\varepsilon_F \sim u/v \sim 10^{-2} - 10^{-3}$, where u is the sound velocity in the body, and v is the electron velocity on the Fermi surface ($\overset{(+)}{*}$)). We shall confine ourselves to deriving the equations at absolute zero.

Suppose, then, that the interaction Hamiltonian of the system of electrons and phonons is

$$H_{int}(x) = g\left(\tilde{\psi}^+(x)\tilde{\psi}(x)\right)\tilde{\varphi}(x)$$

If the system is in the superconducting state, its properties are characterised by two functions F, F^+, in addition to the Green function G. Hence, instead of the usual Dyson equation (21), it is generally necessary to investigate three equations, connecting the three functions

$$\begin{aligned}
\hat{G}_{\alpha\beta}(x,x') &= -i\left\langle T\left(\tilde{\psi}_\alpha(x), \tilde{\psi}^+_\beta(x')\right)\right\rangle \equiv \delta_{\alpha\beta} G(x-x'), \\
\hat{F}^+_{\alpha\beta}(x,x') &= \left\langle T\left(\tilde{\psi}^+_\alpha(x), \tilde{\psi}^+_\beta(x')\right)\right\rangle = I_{\alpha\beta} F^+(x-x'), \\
\hat{F}_{\alpha\beta}(x,x') &= \left\langle T\left(\tilde{\psi}_\alpha(x), \tilde{\psi}_\beta(x')\right)\right\rangle = -I_{\alpha\beta} F(x-x').
\end{aligned} \tag{35.1}$$

As regards the equation for the phonon Green function

$$D(x_1 - x_2) = -i \langle T(\varphi(x_1), \varphi(x_2)) \rangle ,$$

it remains almost unchanged, as we shall see.

The equation for the Green function can be obtained from the diagram technique of perturbation theory. Just as in the case of a boson system below the "Bose condensation" point, the set of possible diagrams of perturbation theory is widened due to the appearance in them of lines corresponding to the functions F and F^+. Let us agree to represent on the diagram the functions $G, F^+$and F by heavy lines with two arrows, the directions of which at the points x, x' are chosen in accordance with (35.1) in such a way that the operator $\tilde{\psi}$ at the point in question corresponds to an arrow directed away from the point, whereas $\tilde{\psi}^+$corresponds to an arrow directed towards the point. All three lines are illustrated in Fig. 93.

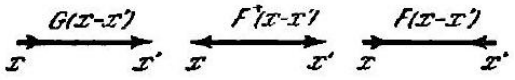


Fig. 93

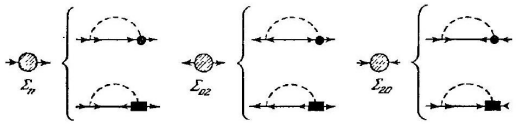


Fig. 94

(†) We always have, however, $T_c \ll \omega_D$ for actual superconductors.

(‡) Electron-phonon interactions in the theory of superconductors were investigated in [59], [60].

It may easily be seen now that, in complete analogy with a boson gas, there are three types of irreducible self-energy parts, which we denote by $\Sigma_{11}(x, x')$, $\Sigma_{20}(x, x')$ and $\Sigma_{02}(x, x')$. In Fig. 94, illustrating the $\sum_{ik}$ diagrams, the dotted line corresponds to the phonon D-functions, the point to a simple vertex, or factor g, and the heavy point or rectangle denotes the modification to the simple vertex as a result of the different elec-tron-phonon interactions.

Let us Fourier transform all the functions and consider one of the selfenergy diagrams, say $\Sigma_{11}(p)$. It will easily be seen that, up to terms of order ω_D/ε_F, we can neglect all the phonon corrections to the electron-phonon vertex part in the simplest diagram for $\Sigma_{11}(p)$ of Fig. 95.



Fig. 95

In fact, as we proved in 21, the values of the D-function (and phonon vertex) of importance in the relevant integrand are those for phonons with momenta of the order of the Fermi momentum of the electrons. For this reason, the estimate obtained in 21 for the corrections to the phonon vertex resulting from the electron-phonon interaction still remains valid in the present case. since the size of these corrections is determined by the values of the Green functions in the energy and momentum region remote from the Fermi surface. It is quite rlear that the Fourier components of the electron Green function for a metal in the superconducting state differ from their values in the normal metal only in a narrow region close to the Fermi surface, with excitation energies not greater than the order of the maximum phonon energies, i.c. of order ω_D. To the same degree, the functions $F^+(p), F(p)$, which are characteristic of the superconducting state, also differ from zcro only in the region mentioned. Fig. 94 illustrates the two possible types of self-energy diagram, for each of the parts Σ_{11}, Σ_{20} and Σ_{02}, depending on the choice of the modification to the phonon vertex. On the basis of what has just been said, we can immediately onit the diagrams of the sccond type. where the phonon vertex is marked by a

heavy rectangle, since the diagrams of this kind can be formed only by using the superconductor Green functions F and F^+.

We can therefore confine ourselves to the zero order approximation of perturbation theory for the phonon vertex in the irreducible parts of Σ_{11}, Σ_{20} and Σ_{02}.

For the same reasons, the phonon Green function $D(x_1 - x_2)$ will remain unchanged, and we can use (21.14) directly for its Fourier component. The structure of the equations for G and $F^+$is illustrated in Fig. 96 and is clear without further explanation.

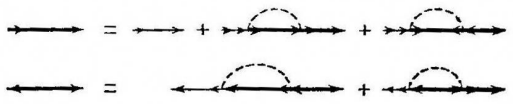


Fig. 96

Let us write these equations in analytic form. In the coordinate representation.

$$\begin{aligned}
\left\{i\frac{\partial}{\partial t}+\frac{\nabla^2}{2m}+\mu\right\}G(x-x') &= \delta(x-x') + g^2 i\int G(x-z)D(x-z)G(z-x')\,\mathrm{d}^4z \\
&\quad + g^2 i\int F(x-z)D(x-z)F^+(z-x')\,\mathrm{d}^4z \\
\left\{-i\frac{\partial}{\partial t}+\frac{\nabla^2}{2m}+\mu\right\}F^+(x-x') &= g^2 i\int G(z-x)D(z-x)F^+(z-x')\,\mathrm{d}^4z \\
&\quad + g^2 i\int F^+(x-z)D(x-z)G(z-x')\,\mathrm{d}^4z
\end{aligned} \tag{35.2}$$

(!!!! write here, what it the meaning of this equations????)

An electromagnetic field can be included in these equations in the usual way, precisely as was done above in 34. Let us emphasise that the resulting system is completely gauge-invariant, as distinct from system (34.13), in which the gauge-invariance was only approximate, up to terms T_c/ω_D. Unfortunately, as is clear from (35.2), this system has a much more complicated form, with a non-linear integral term, which makes it less suitable for solution in the coordinate representation, as is required in a number of problems in which a non-uniform magnetic field exists. On the other hand, the practical results obtained are as a rule equivalent for the two models.

In the absence of a magnetic field, on transforming to the momentum representation in equations (35.2), we easily get equations for the Fourier components of all the functions:

$$\begin{aligned}
\left(\omega-\xi-g^2 i\bar{G}_\omega\right)G(p) - g^2 i\bar{F}_\omega F^+(p) &= 1, \\
\left(-\omega-\xi-g^2 i\bar{G}_{-\omega}\right)F^+(p) - g^2 i\bar{F}^+_\omega G(p) &= 0.
\end{aligned} \tag{35.3}$$

Here, we have written

$$\begin{aligned}
\bar{G}_\omega &= \frac{1}{(2\pi)^4}\int G(p-k)D(k)\mathrm{d}^4k, \qquad \bar{F}_\omega = \frac{1}{(2\pi)^4}\int F(p-k)D(k)\mathrm{d}^4k, \\
\overline{F^+_\omega} &= \frac{1}{(2\pi)^4}\int F^+(p-k)D(k)\mathrm{d}^4k, \qquad G_{-\omega} = \bar{G}_\omega(-p).
\end{aligned} \tag{35.4}$$

This system is completely analogous to the system (34.15) obtained above. The only difference is this: whereas, in equations (34.15), $\bar{G}_\omega, \bar{F}_\omega$ and $\bar{F}^\top_\omega$ are constant in the region $|v(|p|-p_0)| < \omega_D$ about the Fermi surface and vanish outside this region, the functions (35.4) are in general functions of ω and p, smoothly decreasing to zero when ω, $|v(|p|-p_0)| \gg \omega_D$.

Let us express G and F^+in terms of $\bar{G}_\omega, \bar{F}_\omega$ and $\overline{F^+_\omega}$:

$$G(p) = \frac{\omega - g^2 i\bar{G}_\omega + \xi}{\left[\omega - \xi - g^2 iG_\omega\right]\left[\omega + \xi + g^2 i\bar{G}_{-\omega}\right] - g^4\left|\bar{F}^+_\omega\right|^2}$$
$$F^+(p) = \frac{-ig^2\bar{F}^+_\omega}{\left[\left(\omega - \xi - g^2 i\bar{G}_\omega\right)\left[\omega + \xi + g^2 i\bar{G}_{-\omega}\right] - g^4\left|\overline{F^+_\omega}\right|^2}$$

After substituting these expressions into the definitions (35.4) of $\bar{Q}_\omega$ and $\overline{F^+_\omega}$, we get two integral equations for these functions instead of the one equation (21.16) of 21. The solution of these equations was obtained by Eliashberg [62]. We shall give the final result, without dwelling on the details. It turns out that, at small energies, the excitation spectrum has the form

$$\varepsilon(p) = \sqrt{\xi^2 + \Delta^2},$$

where, however, $\xi = v_1\,(p - p_0)$ contains, in accordance with §21, the renormalised velocity on the Fermi surface v_1. The gap at absolute zero is connected with $\overline{F^+_\omega} = 0$ by the relation

$$\Delta = g^2\frac{v_1}{v_0}\left|\overline{F^+_{\omega=0}}\right|.$$

In the weak interaction limit, $g^2 \ll 1$, these formulae are the same as the results of the previous section.

3.9.12 Δ_0 and T_c, The Universal BCS Relation

Overview of approaches for establishing the gap at $T = 0$, Δ_0

(write later, not that important)

Calculations of the Δ_0

Calculation of Δ_0 from substitution of u, v into the gap equation and integration

(write what do we have to start doing it??)

We know that $\Delta_0 = V\sum'_k v_k u_k$, and that $v_k^2 = \frac{1}{2}\left(1 - \frac{\varepsilon_k}{E_k}\right)$ and $v_k^2 = \frac{1}{2}\left(1 + \frac{\varepsilon_k}{E_k}\right)$. So, we just transform the gap:

$$\Delta_0 = V\sum_k{}' \left[\frac{1}{2}\left(1 - \frac{\varepsilon_k}{E_k}\right)\frac{1}{2}\left(1 + \frac{\varepsilon_k}{E_k}\right)\right]^{1/2} = \frac{V}{2}\sum_k{}' \left(\frac{E_k^2 - \varepsilon_k^2}{E_k^2}\right)^{1/2} = \frac{V\Delta_0}{2}\sum_k{}' \left(\varepsilon_k^2 + \Delta_0^2\right)^{-1/2}$$

Here we have used the definition $E_k := \sqrt{\varepsilon_k^2 + \Delta_0^2}$.

Thus the equation for Δ_0 has the form:

$$1 = \frac{V}{2}\sum_k{}' \left(\varepsilon_k^2 + \Delta_0^2\right)^{-1/2} \tag{6.13}$$

Let us use the formula

$$\sum_k{}' \cdots = \int_{-\hbar\omega_D}^{\hbar\omega_D} \ldots N(\varepsilon)\mathrm{d}\varepsilon$$

to go from the summation over k to an integration over ε, where $N(\varepsilon)$ is the density of states at the energy ε. Then (6.13) reduces to

$$1 \approx \frac{N(0)V}{2} \int_{-\hbar\omega_{\rm D}}^{\hbar\omega_{\rm D}} \left(\varepsilon^2 + \Delta_0^2\right)^{-1/2} \, {\rm d}\varepsilon \tag{6.14}$$

Here $N(0)$ is the density of states at the Fermi level (recall that the energy ε is measured from the Fermi level) and we have taken into account that the integration is carried out over the energy interval $(2\hbar\omega_D)$ which is small compared to the Fermi energy ε_F. Therefore, any variations of the density of states $N(\varepsilon)$ over this are neglected. Since the function under the integral sign in (6.14) is even and the integration limits are symmetric, it can be written as

$$1 = N(0)V \int_{0}^{\hbar\omega_D} \left(\varepsilon^2 + \Delta_0^2\right)^{-1/2} \, {\rm d}\varepsilon$$

Since $\frac{d}{dx}\operatorname{arsinh} x = \frac{1}{\sqrt{x^2+1}}$, we get $\frac{1}{N(0)V} = \operatorname{arcsinh}\left(\frac{\hbar\omega_{\rm D}}{\Delta_0}\right)$, or

$$\frac{\hbar\omega_{\rm D}}{\Delta_0} = \sinh\left(\frac{1}{N(0)V}\right) \tag{6.15}$$

Recalling that for the majority of superconductors $N(0)V \leq 0.3$, we obtain Δ_0 in the form

$$\Delta_0 \simeq 2\hbar\omega_{\rm D} \exp\left(-\frac{1}{N(0)V}\right) \tag{6.16}$$

Let us estimate Δ_0: Taking the Debye temperature $\hbar\omega_{\rm D} \sim 100$ K and $N(0)V \sim 0.3$, we obtain $\Delta_0 \sim 4$ K.

Calculation of Δ_0 from the gap equation

One can use the gap equation in the form $\frac{1}{\lambda} = \frac{1}{2}\sum_{\mathbf{p}} \frac{1+2\bar{n}_{\mathbf{p}}}{\sqrt{\xi_{\mathbf{p}}^2+\Delta^2}}$.

При $T = 0$ квазичастиц нет $\bar{n}_{\rm p} = 0$. Заменяя в (12.23) сумму на интеграл с плотностью состояний $v_F g_F/2$ (??? this is the change to ξ, write about it!), we get

$$1 = \frac{\lambda}{2}\frac{4\pi}{(2\pi\hbar)^3}\frac{p_F^2}{v_F}\int_{-\hbar\omega_D}^{+\hbar\omega_D} \frac{d\xi_{\rm p}}{\sqrt{\xi_{\rm p}^2+\Delta_0^2}} = \frac{\lambda}{2}\frac{4\pi}{(2\pi\hbar)^3}\frac{p_F^2}{v_F} 2\int_{0}^{\hbar\omega_D/\Delta_0} \frac{dx}{\sqrt{1+x^2}}$$

Безразмерный интеграл в (12.24), как известно, равен «длинному логарифму» $\int dx/\sqrt{1+x^2} = \ln\left|x+\sqrt{1+x^2}\right|$. Если Вам это неизвестно, то его недолго и оценить асимптотически. Действительно, поскольку верхний предел интегрирования в (12.24) велик $\hbar\omega_D/\Delta_0 \gg 1$, то $\int_0^x dx/\sqrt{1+x^2} \propto \propto \int_1^x dx/x \propto \ln|x|$. Точность этой оценки обусловлена соотношениями $\Delta_0 \sim T_c \ll \hbar\omega_D \ll \varepsilon_F$. Отсюда получаем

$$\Delta_0 = 2\hbar\omega_D e^{-\frac{2}{\lambda g_F}}$$

Stability of numerical calculations of the gap equation

(discuss, for which parameters it is stable and fro which it will break. I have no idea, this question is in scope of computational mathematics)

Overview of approaches for establishing the T_c

Calculations of the T_c

Calculation of the T_c by known integral gap equation

(add comments, where does this formula come from?)

From $\frac{1}{N(0)V} = \int_0^{\hbar\omega_{\rm D}} \frac{{\rm d}\varepsilon}{\sqrt{\varepsilon^2+\Delta^2(T)}} \tanh \frac{\sqrt{\varepsilon^2+\Delta^2(T)}}{2k_{\rm B}T}$, an explicit expression for the critical temperature $T_{\rm c}$ can be derived as follows. At $T = T_{\rm c}$, the gap is $\Delta = 0$. Hence, replacing T in this equation with $T_{\rm c}$ and setting $\Delta = 0$ yields an equation for $T_{\rm c}$:

$$\frac{1}{N(0)V} = \int_0^{\hbar\omega_{\rm D}} \frac{{\rm d}\varepsilon}{\varepsilon} \tanh \frac{\varepsilon}{2k_{\rm B}T_{\rm c}} \tag{6.36}$$

Carrying out the integration (???? do it!!!), we get

$$k_{\rm B}T_{\rm c} = 1.14\hbar\omega_{\rm D} \exp\left(-\frac{1}{N(0)V}\right) \tag{6.37}$$

(??? what is exactly constant there???)

On the other hand, we already know from setting $T = 0$ in the gap equation that $\Delta_0 = 2\hbar\omega_{\rm n} \exp\left(-\frac{1}{N(0)V}\right)$. Then

$$2\Delta_0 = 3.52k_{\rm B}T_{\rm c} \tag{6.38}$$

Calculation of the T_c by transforming the gap equation to integral form and approximating

This derivation is basically the same as before, but in a different notation.

При конечных температурах величина щели уменьшается и в точке перехода $T = T_c$ обращается в ноль $\Delta = 0$:

$$1 = \frac{\lambda}{2} \int \frac{d^3\mathbf{p}}{(2\pi\hbar)^3} \frac{1-2\bar{n}_{\mathbf{p}}}{|\xi_{\mathbf{p}}|} = \frac{\lambda g_F}{2} \int_{-h\omega_D}^{+h\omega_D} \frac{d\xi_{\mathbf{p}}}{2\xi_{\mathbf{p}}} \ {\rm th} \ \frac{|\xi_{\mathbf{p}}|}{2T_c}$$

Здесь мы учли, что при $T = T_c$ и $\Delta = 0$ спектр квазичастиц имеет вид $\varepsilon(p) = |\xi_{\rm p}|$, а также $1 - 2\bar{n}_{\rm p} = {\rm th}\left(|\xi_{\rm p}|/2T_c\right)$. Таким образом,

$$1 = \frac{\lambda g_F}{2} \int_0^{\hbar\omega_D/2T_c} \frac{{\rm th}\, x}{x} dx$$

Безразмерный интеграл в (12.27) легко оценить, его главная асимптотика при больших $x \gg 1$ есть $\int_0^x ({\rm th}\, x/x)dx \approx \int_1^x dx/x = \ln|x|$. Отсюда получаем для критической температуры $2T_c \approx \hbar\omega_D \exp(-2/\lambda g_F) = 0,5\Delta_0$. Это лишь численным множителем отличается от точного расчета, который дает

$$T_c = \frac{e^\gamma}{\pi}\Delta_0 \approx 0,57\Delta_0$$

где $e^\gamma = 1,78$ - постоянная Эйлера.

The physical picture is as follows. Due to thermal processes, some of the Cooper pairs become broken and turn into uncoupled single electrons which can also be classified as normal electrons (aka elementary excitations). The single electrons occupy certain k states in momentum space thereby excluding these states (and their partner states) from the sum in $\Delta_0 = V \sum_k' v_k u_k$ which defines the gap Δ. As a result, the gap shrinks. When it finally becomes zero, the superconductor goes to the normal state, so all excitations above Fermi surface will be possible.

Calculation of the T_c by numerical summation

We could just sum the terms in the gap equation and get T_c numerically, and not think about any integrals at all.

General preparation:

```
import numpy as np
import matplotlib.pyplot as plt
from scipy.optimize import bisect

# Parameters
tttt = 0.3        # hopping parameter
lambd = 1.0       # coupling strength
cutoff = 0.3      # energy window near Fermi surface
N = 500          # number of momentum points
p_vals = np.linspace(-np.pi, np.pi, N)

def disp(p):
    return -2 * tttt * np.cos(p)

def fermi(E, beta):
    x = beta * E
    x = np.clip(x, -700, 700)  # safe range to avoid overflow
    return 1 / (np.exp(x) + 1)
```

And the function is:

```
def linearized_gap_eq(T):
    beta = 1 / T
    sum_val = 0.0
    for p in p_vals:
        xi = disp(p)
        if abs(xi) > cutoff:
            continue
        Ep = abs(xi)
        f = fermi(Ep, beta)
        sum_val += (1 - 2 * f) / Ep
    return 0.5 * sum_val / N - 1 / lambd

from scipy.optimize import brentq
Tc = brentq(linearized_gap_eq, 0.001, 0.1)
```

(??? finish writing it!)

The universal BCS relation $T_c = \frac{e^\gamma}{\pi}\Delta_0$

Derivation of $T_c = \frac{e^\gamma}{\pi}\Delta_0$ by comparison of Δ_0 and T_c

(write exactly about it)

And we see that this relation does not depend on the material (on the Debye's frequency and Fermi energy).

How accurate the universal BCS relation for continuous (not tight binding) model? (???)

(??? I don't know, I tested it only for TB model now)

Is it okay that in some model the universal BCS relation is not fulfilled by 10% or by 40%?

One can say "it is also just approximation", so it is fine. But is it really fine?

Other basic questions about T_c and Δ_0

Are there some divergences in the gap equation?

(???? I don't know them. My answer is that no, there are no them. But I'll think more about it. Is it because we have a cut-off of the integral?)

3.9.13 Gap Δ as a function of T

Overview of approaches for solving the gap equation (for general temperature)

(numerical approach)

Numerical Calculation of $\Delta(T)$ by `fsolve` in Python

(??? write the background better!!!!)
We know that

$$\Delta_0 \approx 1.76 k_B T_c; \qquad \frac{\hbar\omega_D}{\Delta_0} = \sinh\eta;$$

(?? explain!!)
We start from the gap equation and some introduced variables:

$$\eta := \frac{1}{N(0)V}; \quad \eta = \int_0^{\hbar\omega_D} \tanh\frac{\sqrt{\Delta^2+\xi^2}}{2k_BT}\frac{d\xi}{\sqrt{\Delta^2+\xi^2}};$$

We introduce

$$\delta := \Delta(T)/\Delta_0, \qquad \tau := T/T_c$$

and transform it as follows:

$$\begin{aligned}\eta &= \int_0^{\hbar\omega_D} \tanh\left(\frac{\Delta_0}{2k_BT_c}\frac{1}{T/T_c}\frac{\Delta}{\Delta_0}\sqrt{1+\xi^2/\Delta^2}\right)\frac{d\xi/\Delta}{\sqrt{1+\xi^2/\Delta^2}} \\ &\approx \int_0^{\delta^{-1}\sinh\eta} \tanh\left(0.882\frac{\delta}{\tau}\sqrt{1+z^2}\right)\frac{dz}{\sqrt{1+z^2}}\end{aligned}$$

here $\hbar\omega_D/\Delta = \Delta_0\hbar\omega_D/(\Delta_0\Delta) = \sinh\eta/\delta$. The number 0.882 is more precise than 1.76/2 for the computer.

The numerical strategy is as follows. We fix δ and find τ, change δ and solve for $\tau, \ldots$ up to obtain $\delta(\tau)$.

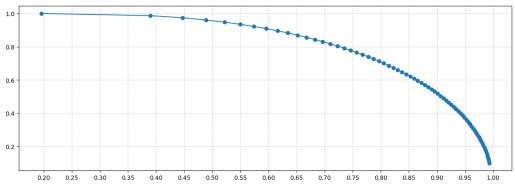
(discuss just these lines blow more!!!)

```
def bcs_gap_equation(d, t):
    integral, _ = quad(lambda z: np.tanh(0.882 * d * np.sqrt(1 + z**2) / t) / np.sqrt(1 +
    z**2), 0, np.sinh(eta) / d)
    return eta - integral

d_vals = np.linspace(0.1, 0.9999, 70)  # don't set zero here, since we are deviding by d.

t0 = 0.1
t_vals = [fsolve(lambda t: bcs_gap_equation(d, t), t0)[0] for d in d_vals]
```

We get what we expected:



The disadvantage of this approach is that there are no homogeneous points on temperature axes, only on gap axes. But still, it is fine.

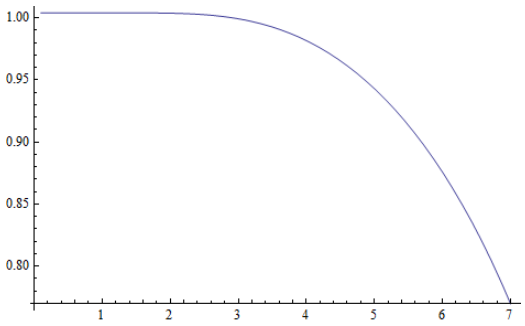
(????) This is simpler than first fixing τ to solve for δ, because of the $1/\delta$ in the boundary, but maybe Im wrong on this point. (??? I'll maybe try later it and write here code for this way)

Numerical Calculation of $\Delta(T)$ by `FindRoot` in Wolfram

(discuss just these lines blow more!!!)

```
Delta[T_]:=
  Block[{a = Log[1.13*hbar*omegad/kb/Tc], b = hbar *omegad/2/kb},
   Return[     FindRoot[     NIntegrate[
         Tanh[b/T*Sqrt[\[Epsilon]^2 + x^2]]/
          Sqrt[\[Epsilon]^2 + x^2], {\[Epsilon], 0, 1},  AccuracyGoal -> 2] - a, {x, 0.01,
    0.1}][[1, 2]]*hbar* omegad]];
Plot[Delta[x]/Delta0, {x, 0.1, 7}]
```

We get what we expected:



(??? there are warnings and the T axes is not normalized. so maybe it is a bad code, but still, it can teach us about using wolfram for superconductivity, so I'll keep it for now.)

Gap at $T \approx 0$

Analytical approximation of the gap at $T \sim 0$ by Bessel functions

Let us investigate in greater detail the temperature-dependence of the gap. We first take the case of low temperatures $T \ll T_0$ and carry out a suitable expansion of condition $1 = \frac{|\lambda| m p_0}{2\pi^2} \int_0^{\omega_D} \mathrm{d}\xi \frac{\tanh \frac{\sqrt{\xi^2+\Delta^2(T)}}{2T}}{\sqrt{\xi^2+\Delta^2(T)}}$. We have identically:

$$\frac{1}{\eta} = \int_0^{\omega_D} \frac{\mathrm{d}\xi}{\sqrt{\xi^2+\Delta^2}} - 2\int_0^{\infty} \frac{\mathrm{d}\xi}{\sqrt{\xi^2+\Delta^2}} \frac{1}{\exp\left(\sqrt{\xi^2+\Delta^2}/T\right)+1}, \tag{36.1}$$

where

$$\eta := |\lambda| m p_0 / 2\pi^2$$

(the second integral is convergent, so that its upper limit can be put equal to infinity). This is the gap equation.

By expanding with respect to the exponent in the second integrand, changing to an integration over ε, and using the definitions of the corresponding Bessel functions, we can write the gap equation as a series in zero order Bessel functions:

(!!!! do the derivations here!!!)

$$\ln \frac{\Delta_0}{\Delta} = 2 \sum_{n=1}^{\infty} (-1)^{n+1} K_0 \left(\frac{n\Delta}{T} \right) \tag{36.2}$$

(here $\Delta_0 \equiv \Delta(T=0)$).

At low temperatures $\Delta \gg T$, we obtain on using the asymptotic expansions of the Bessel functions:

(!!!! do the derivations here!!!)

$$\Delta = \Delta_0 - \sqrt{2\pi T \Delta_0} \left(1 - \frac{T}{8\Delta_0} \right) e^{-\Delta_0/T}. \tag{36.3}$$

The behavior of the gap at temperatures close to the transition temperature T_c is most conveniently determined by starting from $1 = \frac{|\lambda| T}{(2\pi)^3} \sum_n \int \frac{\mathrm{d}^3 p}{\omega + \xi^2 + \Delta^2}$.

Gap at $T \approx T_c$

Analytical approximation of the gap at $T \sim T_c$ by decomposing into series

The gap is small close to T_c, so that we can expand in powers of A^2/T^2 in it:
(!!!! do the derivations here!!!)

$$\frac{1}{\eta} = T \sum_n \int_{-\omega_D}^{\omega_D} \mathrm{d}\xi \left\{ \frac{1}{\omega^2 + \xi^2} - \frac{\Delta^2}{\left(\omega^2 + \bar{\xi}^2\right)^2} + \frac{\Delta^4}{\left(\omega^2 + \xi^2\right)^3} + \cdots \right\}.$$

On interchanging the order of summation over the frequency and integration over ξ in the convergent terms on the right-hand side we get

$$\frac{1}{\eta} = \int_0^{\omega_D} \frac{\mathrm{d}\xi}{\xi} \tanh \frac{\xi}{2T} - \frac{\Delta^2}{(\pi T)^2} \sum_0^{\infty} \frac{1}{(2n+1)^3} + \frac{3}{4} \frac{\Delta^4}{(\pi T)^4} \sum_0^{\infty} \frac{1}{(2n+1)^5} + \cdots \tag{36.4}$$

The series that appear here can be expressed in terms of the Riemann ζ-functions:

$$\sum_0^{\infty} \frac{1}{(2n+1)^z} = \frac{2^z - 1}{2^z} \zeta(z). \tag{36.5}$$

We find on substituting this into the previous expression:

$$\ln \frac{T}{T_c} = -\frac{7\zeta(3)}{8} \frac{\Delta^2}{(\pi T)^2} + \frac{93\zeta(5)}{128} \frac{\Delta^4}{(\pi T)^4} + \cdots$$

We obtain to a first approximation for the size of the gap close to T_c:

$$\Delta = \pi T_c \sqrt{\frac{8}{7\zeta(3)}} \sqrt{1 - \frac{T}{T_c}} \simeq 3.06 T_c \sqrt{1 - \frac{T}{T_c}}. \tag{36.6}$$

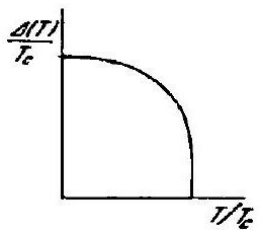


Fig. 97

Fig. 97 illustrates the graph of the temperature-dependence of the gap throughout the temperature interval.

Analytical approximation of the gap at $T \sim T_c$ by strange change the limit of integration

(???? need to think about it again, forgot the method)

Установим закон, по которому вблизи T_c шель обрашается в нуль. Из (51) и (??) имеем

$$1 = \frac{g\nu_F}{2} \int\limits_0^{\hbar\omega_D} d\xi \frac{\tanh \frac{\sqrt{\xi^2+\Delta^2}}{2T}}{\sqrt{\xi^2+\Delta^2}}$$

Из подынтегрального выражения (68) вылелим его значение с нулевой шелью

$$1 = \frac{g\nu_F}{2} \int\limits_0^{\hbar\omega_D} d\xi \frac{\tanh \frac{\xi}{2T}}{\xi} + \frac{g\nu_F}{2} \int\limits_0^{\hbar\omega_D} d\xi \left[\frac{\tanh \frac{\sqrt{\xi^2+\Delta^2}}{2T}}{\sqrt{\xi^2+\Delta^2}} - \frac{\tanh\left(\frac{\xi}{2T}\right)}{\xi} \right]$$

Первый член справа определяется (65), а второй член на верхнем прелеле сходится, и этот прелел можно заменить на бесконечность:

$$J = \int\limits_0^{\infty} d\xi \left[\frac{\tanh \frac{\sqrt{\xi^2+\Delta^2}}{2T}}{\sqrt{\xi^2+\Delta^2}} - \frac{\tanh\left(\frac{\xi}{2T}\right)}{\xi} \right] = \int\limits_0^{\infty} dx \left[\frac{\tanh \frac{\sqrt{x^2+(\Delta/T)^2}}{2}}{\sqrt{x^2+(\Delta/T)^2}} - \frac{\tanh \frac{x}{2}}{x} \right] \simeq -A(\Delta/T)^2$$

где $A \simeq 0.1$. Уравнение (69) принимает вид

$$1 \equiv \frac{g\nu_F}{2} \ln \frac{2\hbar\omega_D\gamma}{\pi T_c} = \frac{g\nu_F}{2} \ln \frac{2\hbar\omega_D\gamma}{\pi T} - A(\Delta/T)^2$$

Тогда

$$0 = \left(\ln \frac{T_c}{T} - A(\Delta/T)^2 \right)$$

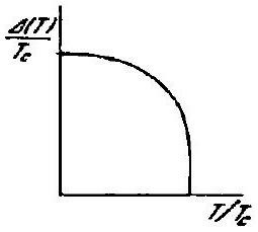
Поэтому вблизи T_c

$$\Delta = \sqrt{T_c \frac{T_c - T}{A}}$$

Analytical properties of the gap equation: Other questions

Do we need to know, how the gap looks in its asymptotics analytically?

No. One can just solve numerically the gap eq. and stop on it. But still, this purely mathematical question can be asked, and there are beautiful answers to it. And also, one can see the main features of the plot



just by analytical methods, which is also a powerful physical statement. However, still, in experiment we have just a plot, so to make a prediction of the behavior of the gap, it is very irrelevant to think about its analytical asymptotics, if one can just obtain it numerically.

(????? this is maybe a bad answer, since maybe I saw in one place that someone used the form of the gap as function of T at T≈0. I don't remember, but I am not sure that we don't need it 100%)

What do we need to know, to do these derivations analytically?

(I'll just select some not obvious mathematical statements that were used and write it here. also a good, but useless question.)

3.9.14 The gap Δ: 1001 questions and statements about details

The cutoff for the gap equation

The dependence of physical quantities on a cutoff in the interaction potential

(write how it is dependent!)

What if we sum over all little and not near a little region near Fermi surface?

Seems that if we have sum over

(write an argument, why is it so??? someone might say that it will be fine to sum over all the lattice, how to explain him that he is wrong?)

Range of summation near Fermi surface matters for the value of the gap

(I'll just explicitly write that)

(we know that there are expressions for Δ and T_c, and they depend on Debye's frequency, which determines exactly the range of integration.)

Thus, if we have an input $T_c = 1$ (we'll calculate temperature in units of critical temperature), then there will be only a fixed range of summation. If we increase the range of summation, there will be extra terms that will be added to the T_c and it will never be 1 again.

We can never sum over all the range of moments.

(?? what LS wrote about it, why did they sum over all the momenta?)

(??? how much is the rest contribution??? Is it little (change by 10% the results), or it will makes the results x20 times different?)

The cutoff of the AGD method versus cutoff of the typical method

(???? how are they related??)

The meaning of energy gap and the gap equation: Extra statements

The Gap is the wave-function of the superconductor (?????)

(??? or it is not???)
(add formulas about it)
(??? why there are such statements??? there is also a BCS wavefunction, which is not the gap!)
(??? what with a wave function of a two-particles which make a Cooper pair, this is not the w.f. of SC??? Currently, I think so.)

Δ sets the energy scale on which the occupation numbers change

This is obvious from the formula

$$\langle n_{k,\sigma} \rangle = \left\langle c^{\dagger}_{k,\sigma} c_{k,\sigma} \right\rangle = \sin^2 \theta_{\boldsymbol{k}} = \frac{1}{2}\left(1 - \frac{\xi_{\boldsymbol{k}}}{\xi^2_{\boldsymbol{k}} + \Delta^2}\right)$$

(!!! check it, there is most likely a typo. De Roeck's notation)
For $\Delta \to 0$, this converges to the function $\theta(-\xi_k)$, as it should, and that Δ sets the energy scale on which the occupation numbers change.

What is meant by self-consistency of the gap equation?

The default answer is that Hamiltonian depends on the gap and gap depends on the Hamiltonian.
How can we see that it is indeed self-consistent?
(????? I don't understand it that deep. why for example a gap which is x2 bigger is not self-consistent???)

(I'll add a comment that some people might say that by self-consistency something different is meant. Can it be?)

(comment about self-consistency for the case of current. Why at that situation, there is a change of a spectrum???)

How can there be a pseudogap?

(??? some strange gap??? I'll think some time later)

How can there be a two gaped superconductors?

(??? some strange gap??? I'll think some time later)

The isotope effect from the gap equation

Remarkably, $k_{\mathrm{B}}T_{\mathrm{c}} = 1.14\hbar\omega_{\mathrm{D}} \exp\left(-\frac{1}{N(0)V}\right)$ also provides an explanation for the isotope effect: For different isotopes of the same superconducting element, the critical temperatures are different and follow the rule

$$T_{\mathrm{c}} M^{1/2} = \text{ const}$$

where M is the mass of the isotope. Recalling that the Debye frequency varies as

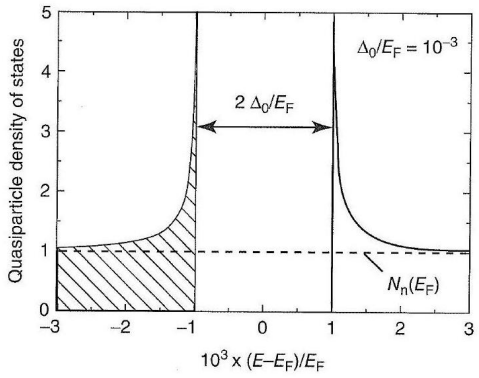
$$\omega_{\mathrm{D}} \propto M^{-1/2}$$

we immediately obtain the isotope effect from (6.37).

(??? why do we change the sum to integral? what is going on with dimensions???)

3.9.15 The gap Δ: Measurement and Effects from It

In figure below:



we have shown the normalized density of states of unpaired electrons in the superconducting state for $T = 0$. The existence of a forbidden energy range ("energy gap") has given us a simple means to understand the fact that, below a critical kinetic excitation energy, Cooper pairs cannot interact with the crystal lattice. We can use different methods for the measurement of this energy gap, which we will discuss in the following.

How in general a gap can be measured?

(I'll have below big discussions of each method, here I'll just write shortly later an answer. It is a hard question, if one was reading just a textbook on statistical physics)

Getting gap by Absorption of Electromagnetic Radiation

The energy gap can be determined by measuring the absorption of electromagnetic radiation. The first experiment proving the existence of a gap in the energy spectrum of the unpaired electrons for $T < T_c$ was reported in 1957 by Glover and Tinkham [20]. They observed the infrared transmission of thin superconducting films. (??? what was there?)

Already by the early 1930 s, it had been pointed out that electromagnetic waves of suitable frequency should serve well to break up the ordered state of a superconductor below its transition temperature. This should show up as an anomaly in the absorption. In the 1930s, such experiments could not be carried out, since the required range of electromagnetic wavelengths was not yet experimentally available. Assuming a binding energy E_{B} of about 10^{-3}eV, for this energy we need radiation quanta with a frequency $f = E_{\mathrm{B}}/h = 2.4 \times 10^{11}$ Hz(240GHz). These are waves with about 1 mm wavelength, for which no generation or detection methods were available in the 1930s. Only 20 years later, however, this method was applied successfully for measuring the energy gap, [20]. Today, for the range of wavelengths between about 500μm and 3 cm, we have sufficient, well-functioning experimental techniques for performing such measurements for quantitative determination of the energy gap.

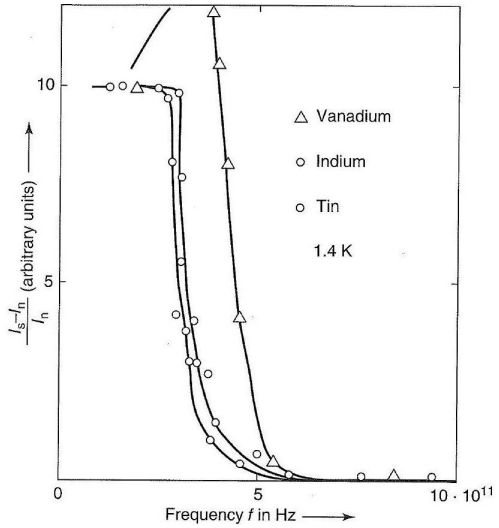


Figure 3.9 Absorption of electromagnetic waves with frequency f in superconductors. Transition temperatures Measurement temperature is 1.4 K. In vanadium for $f < 2\Delta_0/h$, a frequency dependence is observed, the possible origin of which can- not be discussed here. (From [22].) are V, 5.3 K; In, 3.42 K; and Sn, 3.72 K

The quantitative data analysis for this method is somewhat complicated, and we do not want to discuss it in more detail. In Figure 3.9 we just show an example of such a measurement [22]. Here, the radiation was guided into a small cavity, made from the material to be studied. Within the cavity the radiation is reflected many times before it is detected. The stronger the absorption of the radiation in the cavity wall, the smaller is the detected power. For the measurement, at a fixed temperature (here about 1.4 K), the power in the superconducting and in the norma states, I_s and I_n, respectively, is determined for each wavelength. In this experiment, the superconductivity can be eliminated by a sufficiently high magnetic field. The difference between the two power values yields the difference between the reflection for both states.

In Figure 3.9 this difference, normalized by the power in the normal conducting state, is plotted versus the frequency. At small frequencies, we see a distinct difference between the reflection in the superconducting and in the normal conducting states. In the superconducting state the reflection is larger. At a certain frequency the difference drops abruptly, and at higher frequencies it reaches zero. Apparently, the abrupt drop sets in as soon as the quantum energy of the radiation is large enough to break up the Cooper pairs. This results in an additional absorption. For energies $hf > 2\Delta_0$ the energy gap practically does not influence the absorption, since the electrons can be excited far beyond the energy gap by the radiation quanta. In Table 3.3 we list the values of the energy gap at $T = 0$ obtained from such measurements for different superconductors. Table 3.4 presents values of the energy gap for some selected superconducting compounds and alloys.

Table 3.3 Energy gap $2\Delta_0$ in units of $k_B T_C$ for some superconducting elements.

Element		Method		
	T_c(K)	Tunnel junctions	Ultrasound	Light absorption
Sn	3.72	$3.5 \pm 0.1(1.15)$	-	3.5
In	3.4	$3.5 \pm 0.1(1.05)$	3.5 ± 0.2	3.9 ± 0.3
Tl	2.39	$3.6 \pm 0.1(0.75)$	-	-
Ta	4.29	$3.5 \pm 0.1(1.30)$	3.5 ± 0.1	3.0
Nb	9.2	3.6 (2.90)	4.0 ± 0.1	2.8 ± 0.3
Hg	4.15	$4.6 \pm 0.1(1.65)$	-	4.6 ± 0.2
Pb	7.2	$4.3 \pm 0.05(2.70)$		4.4 ± 0.1

The numbers in brackets indicate the energy gap in megaelectronvolts. The values are taken from Ref. [23]. For special details see Superconductivity Data, no. 19-1 (1982), Fachinformationszentrum Karlsruhe GmbH.

Material	T_c(K)	$2\Delta_0$(meV)	$2\Delta_0/k_BT_c$	References	cf. Section
Nb_3Sn	18	6.55	4.2	[24]	2.3.1
NbN	13	4.6	4.1	[25]	2.3.1
MgB_2	40	3.6-15	1.1-4.5	[19]	2.3.2
Rb_3C_{60}	29.5	10-13	4.0-5.1	[18]	2.4
$ErRh_4$ B_4	8.5	2.7-3	3.8-4.2	[26]	2.5
$PbMo_6$ S_3	12	4-5	4-5	[27]	2.5
YNi_2 B_2C	15.5	4.7	3.5	[28]	2.5
$NbSe_2$	7	2.2	3.7	[29]	2.7
$BaPb_{0.75}Bi_{0.25}O_3$	11.5	3.5	3.5	[30]	2.8.2
$Ba_{0.6}$ $K_{0.4}BiO_3$	25-30	8	3.5	[31]	2.8.2

Table 3.4 Energy gap $2\Delta_0$ for selected superconducting compounds (s-wave Cooper pairing).

Experimental methods tunneling effect, optical methods, nuclear spin resonance, specific heat, and so on. Much data can also be found in the monograph [M14].

Getting gap by Ultrasound Absorption

(??? what is it????)

Sound waves also interact with the system of conduction electrons in a metal. We can look at a sound wave as a current of coherent phonons. Until recently, only sound waves with frequencies up to about 30GHz were available. Most measurements were carried out using frequencies from a few megahertzs up to 10MHz. The energies of these frequencies are much smaller than the width of the energy gap. Only very close to T_c, where the energy gap $2\Delta_0(T)$ approaches zero, it is possible that the sound energy of these frequencies becomes comparable to $2\Delta_0(T)$. Hence, in addition to other mechanisms, absorption essentially depends on the number of unpaired electrons. Below T_c this number decreases rapidly with decreasing temperature. Correspondingly, the damping of sound also decreases rapidly below T_c. In Figure 3.10 we present an example of such a measurement [32]. Since for a given temperature the number

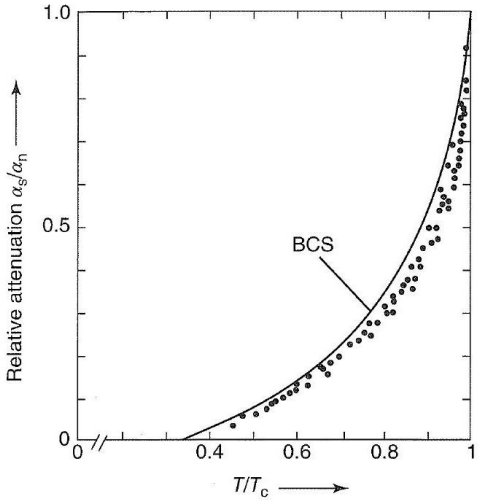


Figure 3.10 Ultrasound absorption in superconducting tin and indium. The solid line indicates the behavior expected from the BCS theory for the energy gap $2\Delta_0 = 3.5k_BT_C$. (From [32].)

of unpaired electrons depends on the width of the energy gap, the latter can be determined from such absorption measurements by means of a comparison with the theoretically expected behavior. In Figure 3.10 the curve expected from the BCS theory for $2\Delta_0(T = 0) = 3.5k_BT_c$ (Eq. (3.7)) is shown.

Here, we cannot discuss in detail the analysis of such measurements, which is not quite simple. We just want to point out that, compared to electromagnetic waves, sound waves have the great advantage of penetrating more deeply into the metal, whereas high-frequency electromagnetic waves only reach a thin layer at the surface, namely within the skin depth.

3.9.16 Chemical Potential of a Superconductor

(just all what I think about it, that it is zero because of quasiparticles.... or not zero, because it is a Fermi energy. I don't understand it fully yet, that is why there is a section about it here)

3.9.17 The Coupling Constant of BCS Model

Typical values of the coupling constant

This is also important for any numerical calculation.

Can the coupling constant be determined experimentally?

(????? I am not sure, since the measured quantities have many parameters, so currently, i don't know, is it possible at all to do it????)

Theoretical derivation of the coupling constant

(????? maybe no one knows how to do it, so it is an unsolved question)

Determining the Coupling BCS Constant for a Given Material

(???? TODO: write clear, how to do it?)

Determining using McMillan's formula (???)

McMillan's formula can help $T_c = \frac{\Theta_D}{1.45} \exp\left(-\frac{1.04(1+\lambda)}{\lambda-\mu^*(1+0.62\lambda)}\right)$, assuming $\mu^* \approx 0.1$.

From Tunneling Experiments or Spectroscopy

(??? maybe it is also possible)

Can the coupling constant change?

(??? there are articles about quenches, so maybe in some effective superconductors it can. I don't know yet, how)

3.10 BCS: Advanced Features and Details of a Typical Setups

3.10.1 Overview of general important features of BCS

Coherence length from BCS

Рассмотрим теперь, как микроскопическая теория сверхпроводимости позволяет оценить длину когерентности сверхпроводника. Волновая функция основного состояния сверхпроводника нами уже рассматривалась в п.44.1. Основное состояние может быть изображено распределением спаренных электронов в $\mathbf{k}$-пространстве, что дается функцией $v_{\mathbf{k}}^2$. График зависимости $v_{\mathbf{k}}^2$ от k представлен на рис. 44.3. Видно, что область k-пространства, где функция $v_{\mathbf{k}}^2$ испытывает сильные изменения, имеет размер порядка

$$\Delta k \sim 2\Delta_0 \frac{k_{\mathrm{F}}}{\varepsilon_{\mathrm{F}}}$$

Отсюда следует, что область Δx в x-пространстве, где волновая функция основного состояния сверхпроводника будет существенно изменяться, должна определяться соотношением

$$\Delta x \Delta k \sim 1$$

Отсюда следует, что

$$\Delta x \sim \frac{\varepsilon_F}{2\Delta_0 k_F} = \frac{1}{2\Delta_0 k_F}\frac{\hbar^2 k_F^2}{2m} = \frac{\hbar p_F}{4\Delta_0 m} = \frac{\hbar v_F}{4\Delta_0}. \tag{45.6}$$

Здесь p_{F} - импульс электрона на поверхности Ферми, v_{F} - фермиевская скорость электрона. Но по самому смыслу Δx-это как раз та величина, которую при изучении теории Гинзбурга-Ландау мы называли длиной когерентности ξ. Поэтому мы теперь можем говорить, что из (45.6) следует оценка для длины когерентности ξ_0 при $T = 0$:

$$\xi_0 \sim \hbar v_{\mathrm{F}}/4\Delta_0 \tag{45.7}$$

Скоро будет показано, что $\Delta_0 \sim k_{\mathrm{B}} T_c$, где k_{B} - постоянная Больцмана, T_c-критическая температура. Точный расчет дает

$$\xi_0 = 0.18\hbar v_{\mathrm{F}}/k_{\mathrm{B}} T_c \tag{45.8}$$

Эту величину ξ_0 можно также рассматривать как размер электронной пары, для оценки которого можно принять, что $v_F \sim \sim 10^8$ cm/c, $T_c \sim 1$ K, тогда

$$\xi_0 \simeq 0.18 \frac{10^{-27} \cdot 10^8}{1.38 \cdot 10^{-16} \cdot 1} \sim 10^{-4} \text{ cm}$$

Это очень большое, вполне макроскопическое расстояние.

Averaging of operators in BCS model

(remind the formalism, that ψ is the initial operator, in which the Hamiltonian is non-diagonal)

$$F_{\alpha\beta}(x, x') := -i \langle \mathrm{T}\psi_\alpha(x)\psi_\beta(x') \rangle .$$

It is nonzero for superconductor.

Proof. (???? I'll open the bra-kets and write explicitly...)

(but the idea is that the interacting term in Hamiltonian has also non-diag terms in ψ, that is why it is not zero)

□

(remind the formalism, that b below are those, in which the Hamiltonian is non-diagonal)

Statement:

$$-i \langle \mathrm{T}b_\alpha(x)b_\beta(x') \rangle = 0$$

Proof. (???? I'll open the bra-kets and write explicitly... and since the Hamiltonian is diagonal, we have zero)

□

Can perturbation theory be applicable to the BCS Hamiltonian?

When we see the BCS Hamiltonian, we can think: "Oh, another correction to a free Hamiltonian, let's use the perturbation theory for it!" Here we will discuss what would be if we do so?

(I'll try and report here what happens???)

(??? Pukhov said that no, PT is not applicable, but why?)

(?????)

How to work with BCS without Bogoliubov transformations?

(This is what Gor'kov's formalism is doing, so I'll write exactly, how it works?)

BCS model without Bogoliubov transformations

(here I'll show, what we can do with BCS model if we don't use Bogoliubov transformations at all. a good question.)

Proof that indeed in BCS theory the resistance of the current is zero

(here I'll show just that it is so. not so obvious)

(maybe we use the Landau criteria for superfluids, but I want to write here more explicitly that it is so? maybe I'll repeat the proof of Landau's criterion in the context of superconductors)

3.10.2 How Good and Useful Is BCS Theory?

Is it fine that one can't reproduce any effects in scope of electrodynamics of SC?

(I have no idea how to reproduce it. maybe it means the BCS theory is not that useful and rather specific? I don't know, I'll discuss here)

The problem with a Debye model

Debye model is an approximate model. So from the beginning we start from a simplified abstraction.

In which cases of metals at low temperatures the BCS model is not applicable?

(experimental intro to generalization of bcs)

3.10.3 Cooper Pairs: Deeper Understanding

Physical picture of Cooper pairs

(?? all about interpretation)

Механизм притяжения электронов в решётке по Вайскопфу (1981 г.).

Пусть электрон движется через ионную решётку металла. Интерес представляют только электроны, импульс которых лежит вблизи поверхности Ферми. Действительно, электроны вдали от этой поверхности ($\varepsilon < \varepsilon_F$) не могут менять своё состояние, поскольку отсутствуют близлежащие свободные состояния, в которые они могли бы переходить в результате взаимодействия с фононами. Тогда

$$\varepsilon \approx \varepsilon_F, v \approx v_F$$

«Пролетая» мимо иона, электрон взаимодействует с ним с силой $f \sim e^2/a^2$, где a - постоянная решётки. Длительность взаимодействия $\tau \sim a/v_F$. Полагая для оценки $a \sim 10^{-8}$ cm, $v_F \sim 10^8$ cm/c, получаем $\tau \sim 10^{-16}$ c. Это время много меньше характерного периода колебаний атома в решётке $\omega_D^{-1} \sim (10^{-12} - 10^{-13})$ c. Однако за это время ион приобретает импульс $p_\perp \sim f\tau \sim \frac{e^2}{a^2} \cdot \frac{a}{v_F} = \frac{e^2}{av_F}$. Поскольку $e^2/a \sim \varepsilon_\text{B} \sim \varepsilon_F$, то $p_\perp \sim \varepsilon_F/v_F \sim p_F$. Таким образом, ион приобретает импульс $p_\perp$ порядка фермиевского импульса электрона, направленный к траектории электрона. Максимальное смещение иона массой M можно оценить из соотношения

$$\frac{p_\perp^2}{2M} \sim \frac{\kappa x^2}{2} \Rightarrow x \sim \frac{p_F}{\sqrt{M\kappa}}$$

Эффективная жёсткость связи к иона в решётке оценивается из тех соображений, что смещение иона на величину порядка межатомного расстояния существенно меняет энергию электронной конфигурации, т.е.

$$\frac{\kappa a^2}{2} \sim \varepsilon_B \sim \varepsilon_F \Rightarrow \kappa \sim \frac{\varepsilon_F}{a^2}$$

С учётом этого получаем оценку результирующего смещения иона:

$$x \sim \frac{p_\perp}{\sqrt{M\kappa}} \sim \frac{p_F}{\sqrt{M\varepsilon_F/a^2}} \sim a\sqrt{\frac{m}{M}}$$

где $\varepsilon_F = p_F^2/2m, m$ - масса электрона. Следовательно, смещение иона мало: $x \sim 10^{-2}a \ll a$. В процессе своего движения электрон вызывает смещение ионов, мимо которых он пролетает, возникает «хвост». Длина этого «хвоста» L определяется тем, что смещение ионов существует в течение конечного промежутка времени $\sim T/2 = \pi/\omega_D$. Учитывая, что $\omega_D \sim \sqrt{\kappa/M} \sim \sqrt{\varepsilon_F/Ma^2}$, находим длину «хвоста»:

$$L \sim \frac{v_F}{\omega_D} \sim v_F\sqrt{\frac{Ma^2}{\varepsilon_F}} \sim a\sqrt{\frac{Mv_F^2}{\varepsilon_F}} \sim a\sqrt{\frac{M}{m}} \sim 10^2 a \gg a.$$

Заметим, что оценке величины L можно придать иной вид:

$$L \sim \frac{v_F T}{2} = \frac{\pi v_F}{\omega_D} = \frac{\pi v_F}{(\pi s/a)} \approx \frac{\pi v_F}{s\,(p_F/\hbar)} = \frac{\pi\hbar}{ms}$$

Полагая $m = m_e, s \sim 3 \cdot 10^5$ cm/c, получим $L \sim 10^3$Å. Смещение ионов приводит к повышению плотности положительных зарядов вдоль траектории электрона на нейтральном фоне, присутствующем «в среднем» в металле. Оценим полный заряд «хвоста». На участке длиной a прирост заряда, обусловленный смещением одного иона, составляет

$$\Delta q \sim |e|\frac{x}{a} \sim |e|\sqrt{\frac{m}{M}}$$

а на участке длиной L полный заряд составляет

$$q \sim \Delta q\frac{L}{a} \sim |e|\sqrt{\frac{m}{M}}\sqrt{\frac{M}{m}} = |e|$$

Таким образом, этот заряд приблизительно равен заряду электрона, но имеет положительный знак. К сформировавшемуся «хвосту» уже может притягиваться второй электрон. При этом электроны сильно разнесены в пространстве, и вследствие дебаевского экранирования их прямое кулоновское отталкивание уже практически отсутствует.

Interpretation, why superconductivity is destroyed when some parameters are increased?

Беспорядок не разрушает куперовские пары, хоть импульс и становится плохим квантовым числом. Качественно это можно пояснить так. В присутствии примесей электроны двигаются по ломаным, от одной примеси к другой. За каждым электроном вдоль линии его движения остается деформация решетки, представляющая собой шлейф из виртуальных фононов, рассасывающийся за время порядка ω_D^{-1}. Этот «ароматический след» притягивает другие электроны, причем эффект притяжения максимален для электрона, движущегося в точности по той же траектории, но в обратном направлении.

Такие состояния есть при любой степени беспорядка, поскольку увеличение концентрации примесей лишь делает траектории более изломанными, но не выделяет определенного направления движения на каждой из них (в отличие, скажем, от траекторий в магнитном поле). Из этого рассуждения видно, что чисто потенциальное рассеяние на примесях, оставляющее систему инвариантной по отношению к обращению времени, не подавляет сверхпроводимость. А магнитное поле, например, подавляет.

Two-particle density matrix

(????)

Why do we need two-particle density matrix?

(answer to this question, I don't know)

Construction of two-particle density matrix

As in the case of BEC, it is instructive to consider the (in this case) two-particle density matrix $\rho^{(2)}$, whose kernel in momentum space is

$$\hat{\rho}^{(2)}\left(\boldsymbol{k}_1', \sigma_1', \boldsymbol{k}_2', \sigma_2'; \boldsymbol{k}_1, \sigma_1, \boldsymbol{k}_2, \sigma_2\right) := \left\langle c^\dagger_{\boldsymbol{k}_2'} c^\dagger_{\boldsymbol{k}_1'} c_{\boldsymbol{k}_1} c_{\boldsymbol{k}_2} \right\rangle$$

Note that $\hat{\rho}^{(2)}$ is a self-adjoint operator on $P_a(\mathcal{H} \otimes \mathcal{H})$, where $\mathcal{H} = L^2(\Lambda) \otimes \mathbb{C}^2$ is the one-particle Hilbert space and P_a projects to antisymmetric functions. Just as in BEC, BCS is marked by the appearance of a macroscopic eigenvalue of this operator. We are interested only in the case $\boldsymbol{k}_1 = -\boldsymbol{k}_2, \sigma_1 = -\sigma_2$ and analogously for the primes, so in the kernel

$$\hat{\rho}^{(\text{pair})}\left(\boldsymbol{k}', \sigma', \boldsymbol{k}, \sigma\right) = \hat{\rho}^{(2)}\left(\boldsymbol{k}', \sigma', -\boldsymbol{k}', -\sigma'; \boldsymbol{k}, \sigma, -\boldsymbol{k}, -\sigma\right) = \left\langle c^\dagger_{\boldsymbol{k}', \sigma'} c^\dagger_{-\boldsymbol{k}', -\sigma'} c_{\boldsymbol{k}, \sigma} c_{-\boldsymbol{k}, -\sigma} \right\rangle$$

The reason that it is legitimate to make the reduction form $\hat{\rho}^{(2)}$ to $\hat{\rho}^{(\text{pair})}$ is that the system is assumed to be translation and rotation invariant and does not contain spin-orbit coupling. Therefore, the operator $\rho^{(2)}$ commutes with the total momentum (of two particles) and with the total spin, therefore, the space spanned by the base states $|\boldsymbol{k}, \sigma, -\boldsymbol{k}, -\sigma\rangle$ is mapped into itself. It follows that any eigenvalue of the restriction of $\rho^{(\text{pair})}$ to this space is also an eigenvalue of $\rho^{(2)}$.

(Reminder: in this notation $\hat{F}_k := \langle c_{k,\downarrow} c_{-k,\uparrow} \rangle$)

If we neglect fluctuations (in the spirit of BCS), then $\hat{\rho}^{(\text{pair})}$ equals $\hat{F}^*_{\boldsymbol{k}'} \hat{F}_{\boldsymbol{k}}$, up to signs that are irrelevent since all different choices for σ, σ' are related by antisymmetry and the symmetry under $\boldsymbol{k} \to -\boldsymbol{k}$. Fourier-transforming $\boldsymbol{k} \leftrightarrow \boldsymbol{r}, \boldsymbol{k}' \leftrightarrow \boldsymbol{r}'$, we get

$$\rho^{(\text{pair})}\left(\boldsymbol{r}', \uparrow, \boldsymbol{r}, \uparrow\right) \approx F^*\left(\boldsymbol{r}'\right) F(\boldsymbol{r})$$

Hence $F(\boldsymbol{r})$ is an eigenfunction with eigenvalue $N_0 = \int \mathrm{d}\boldsymbol{r} |F(\boldsymbol{r})|^2$. However, note that $\boldsymbol{r}$ is a relative coordinate! The condensate is uniform in space, corresponding to the fact that we assumed pairing with center of mass momentum 0.

Two-particle density matrix: Other Statements

(????)

Applications

(??? what can one do with it???)

Cooper pair creation operator

(???)
Cooper pair creation operator by Coleman:

$$\Lambda^\dagger = \sum_{\mathbf{k}} \phi_{\mathbf{k}} c^\dagger_{\mathbf{k}\downarrow} c^\dagger_{-\mathbf{k}\uparrow},$$

where

$$\phi_{\mathbf{k}} = \int d^3x e^{-i\mathbf{k}\cdot\mathbf{x}} \phi(\mathbf{x})$$

(??? so why do we sum over spins?)

Influence of Lattice Defects on Conventional Cooper Pairing

We use the term defects to denote all deviations from perfect periodicity of the crystal lattice, independent of whether they are due to the presence of foreign atoms or due to only structural perturbations, that is, displacements of the atoms from their regular sites. Primarily, such lattice defects act as scattering centers for the system of conduction electrons, reducing the electron mean free path.

However, in general, the lattice defects influence all the properties of a superconductor. In this section, we will discuss some of these effects.

3.10.4 Cooper Pairs: Spatial Structure, Life Time, Speed

(есть целая статья про это, но не уверен, что она полезная. Так или иначе, ответ на этот вопрос тоже должен быть)

Size of cooper pair and unsetainty relation for it (???)

(a special section about the question: why can we use unsetainty relation to find size of a cooper pair? Can we show some similar examples of usage of this method? Now I just belive that we just can do so.)

Introduction and overview: The Superconducting State, Quasiparticles, and BCS Theory

At least qualitatively we have seen that two electrons attract each other momentarily because of the electron-phonon interaction, and in this way they form a Cooper pair $\{\mathbf{k}\uparrow, -\mathbf{k}\downarrow\}$. Next we deal with the question of how these pairs collectively can occupy the same quantum state. Here, BCS found an ingenious answer, which we want to outline for the case of zero temperature.

Let us recall first the situation of the unpaired electrons. At $T = 0$ they occupy the lowest possible energy states. If we treat the electrons as free particles, their energy is given by

$$\varepsilon_k = \frac{1}{2m}\left(p_x^2 + p_y^2 + p_z^2\right)$$

or, with $\mathbf{p} = \hbar\mathbf{k}$,

$\varepsilon_k = \frac{\hbar^2}{2m}\left(k_x^2 + k_y^2 + k_z^2\right)$

The possible values of $\mathbf{k}$ are discrete (see Section 1.2), and in the simplest case in k-space the electrons occupy the Fermi sphere (see Figure 1.18). All states within the Fermi sphere must be occupied by an electron, and all states outside the Fermi sphere must remain unoccupied.

The electrons near the Fermi energy will interact attractively with each other. The attractive interaction energy is taken as a negative constant $-V$ for the electrons, with its energy range distributed over the interval $\pm\hbar\omega_c$ near the Fermi energy.6) Everywhere else the interaction is assumed to be zero. It is not necessary that the interaction energy V results from the electron-phonon interaction. However, if this is the case, it is likely that the energy $\hbar\omega_\mathrm{c}$ is associated with a characteristic phonon energy, or the frequency ω_c with a characteristic phonon frequency, namely the Debye frequency.

Around the surface of the Fermi sphere, the Cooper pairs constitute a highly peculiar state, in which, within a certain interval around the Fermi energy E_F, the pair states $\{\mathbf{k}\uparrow, -\mathbf{k}\downarrow\}$ are simultaneously unoccupied with probability $|u_k|^2$ and occupied with probability $|v_k|^2$. In general, the probability amplitudes u_k and v_k are complex numbers, which depend on the wave vector k. The condition $|u_k|^2 + |v_k|^2 = 1$ must be valid, since the two probabilities must add up to 1. Classically, such a state cannot be imagined. However, in quantum mechanics such superpositions are quite possible.

Next we must determine the parameters u and v. This can be done by inserting the ansatz of the wave function of the Cooper pairs given above into the Schrödinger equation of the system. Then one calculates the energy of the system as a function of u and v, and finally one chooses u and v such that the energy reaches a minimum [M3, M4]. Then we have found the energetically optimum state consistent with the assumed wave function.

Using this procedure, for $|v_k|^2$ one finds the expression

$$|v_k|^2 = \frac{1}{2}\left[1 - \frac{\varepsilon_k - E_\mathrm{F}}{\sqrt{|\Delta|^2 + (\varepsilon_k - E_\mathrm{F})^2}}\right]$$

Here, the energy of the individual electrons in the absence of the interaction V is denoted by ε_k as in Eqs. (3.2a) and (3.2b), and E_F is the Fermi energy. The quantity Δ will become highly important in the following. It is given by the sum $\Delta = -V\sum u_k v_k$. Hence, it is different from zero only for values of ε_k within the interval $\pm\hbar\omega_c$, similar to the interaction V. In general, Δ is a complex number, which we write in the following as $\Delta = \Delta_0 \mathrm{e}^{i\varphi}$ with real amplitude Δ_0. Then we have $|\Delta|^2 = \Delta_0^2$. For $|u_k|^2 = 1 - |v_k|^2$, one finds

$$|u_k|^2 = \frac{1}{2}\left[1 + \frac{\varepsilon_k - E_\mathrm{F}}{\sqrt{|\Delta|^2 + (\varepsilon_k - E_\mathrm{F})^2}}\right] = \frac{1}{2}\left[1 + \frac{\varepsilon_k - E_\mathrm{F}}{\sqrt{\Delta_0^2 + (\varepsilon_k - E_\mathrm{F})^2}}\right] \quad (3.3b)$$

In a more general way, we can also allow the interaction between the electrons to depend on the momentum or the wave vector of the electrons.

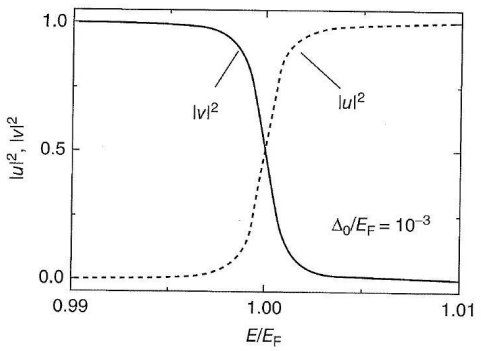


Figure 3.5 The functions $|u_k|^2$ and $|v_k|^2$, indicating the probability that a pair state $\{\mathbf{k}\uparrow, -k\downarrow\}$ is occupied $\left(|v_k||^2\right)$ or unoccupied $\left(|u_k|^2\right)$. For the figure, the values $E_F = 1\text{eV}$ and

The two functions $|u_k|^2$ and $|v_k|^2$ are shown in Figure 3.5. Here, we have assumed for E_F a value of 1eV and for Δ_0 a value of 1meV, which are typical for metallic superconductors. Deep within the Fermi sphere (i.e., for $\varepsilon_k \ll E_\mathrm{F}$), the probability $|v_k|^2$ of finding an electron pair in the state $\mathbf{k}$ (or $|\mathbf{k}|$) is practically equal to one, as would also be in the case for noninteracting electrons. Analogously, for energies $e_k \gg E_\mathrm{F}$, the probability $|u_k|^2$ that this state is unoccupied is nearly equal to one. However, within an interval of about $\pm\Delta_0$ around the Fermi energy, both functions $|u_k|^2$ and $|v_k|^2$ strongly deviate from the value one. For independent, unpaired electrons, exactly this would not be the case. We see that the Cooper pair system shows nontrivial behavior in this energy interval. In Figure 3.5, the ratio $\Delta_0/E_\mathrm{F} = 10^{-3}$. Hence, we can say that only about 0.1% of all electrons, namely hose near the Fermi energy, participate in the superconductivity.

The quantity Δ depends on all states k because of the product $u_k v_k$ This shows that all Cooper pairs are collectively connected with each other. Contrary to this, for independent electrons, Δ would always be zero, since either u_k or v_k always vanishes.

In the state described by the BCS theory, all pairs show the same values of all physical quantities. In particular, the motion of the center of mass is the same for all pairs. So we have arrived at the macroscopic matter wave, the properties of which we have described in detail in Chapter 1. What further information is provided by the microscopic theory?

First one can calculate the energy gain because of the Cooper pairing, that is, the condensation energy. One finds that this is given by $-N\left(E_\mathrm{F}\right)\Delta_0^2/2$, where $N\left(E_\mathrm{F}\right)$ is the density of states at the Fermi energy (see Section 1.1). In addition to $N\left(E_\mathrm{F}\right)$, the condensation energy also depends on the pair interaction V because of Δ_0^2. Apparently, it is favorable for superconductivity if both quantities become very large.

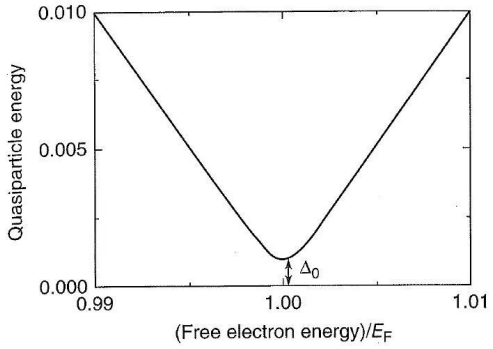


Figure 3.6 Energy of an unpaired electron (quasiparticle) in a superconductor, plotted versus the energy the electron would have without the pair interaction.

The next important question concerns the possible excitations of the supercon ducting ground state. As a very simple excitation we can imagine that a Cooper pair is broken, yielding two independent electrons. Here, we can look at a single unpaired electron as an "elementary process," and we can ask how its (excitation) energy compares with the energy ε_k of the same electron in the normal state. The resulting electron is referred to as quasiparticle. Due to the pair interaction in the superconductor, this quasiparticle does not satisfy any longer the energy-momentum relation (3.2 b).

Instead, one finds that the energy of this unpaired electron is given by [M3, M4]

$$E_k = \sqrt{\left(\varepsilon_k - E_\mathrm{F}\right)^2 + \Delta_0^2}$$

This function is shown in Figure 3.6. If Δ_0 were zero, we would have $E_k = \pm\left(\varepsilon_k - E_\mathrm{F}\right)$, and we would recover the energy of the noninteracting electrons. However, for $\Delta_0 \neq 0, E_k$ attains a

minimum value Δ_0. This also means that at least twice this amount must be supplied, in order to break a Cooper pair and to generate two quasiparticles.

At this stage, we can already see the influence of the Cooper pair interaction on the density of states of unpaired electrons. Even without this interaction, the density of states is in general a very complicated function depending on the crystal structure. We denote this function by $N_n(E)$. However, here we are concerned only with a small interval $\pm\Delta_0$ near the Fermi energy. In this interval, we can treat the density of states of the noninteracting electrons as constant: $N_{\mathrm{n}}(E) \approx N_{\mathrm{n}}(E_{\mathrm{F}})$. In this case there are states already very close to the Fermi energy, into which the electrons can be excited. However, this is by no means possible for the quasiparticles. According to Eq. (3.4), for this the minimum energy Δ_0 is needed.

For the density of states of the quasiparticles, this means that a gap appears in an interval $\pm\Delta_0$ at the Fermi energy. Within this gap, no states exist anymore. The exact expression for the density of states of the quasiparticles, which we want to denote by $N_s(E)$, is given from the BCS theory by

$$N_{\mathrm{s}}(E) = N_{\mathrm{n}}(E_{\mathrm{F}}) \frac{|E - E_{\mathrm{F}}|}{\sqrt{(E - E_{\mathrm{F}})^2 - \Delta_0^2}}$$

for energies $|E - E_{\mathrm{F}}| \geq \Delta_0$. For $|E - E_{\mathrm{F}}| < \Delta_0$, the function $N_{\mathrm{s}}(E)$ is zero. This density of states is shown in Figure 3.7.

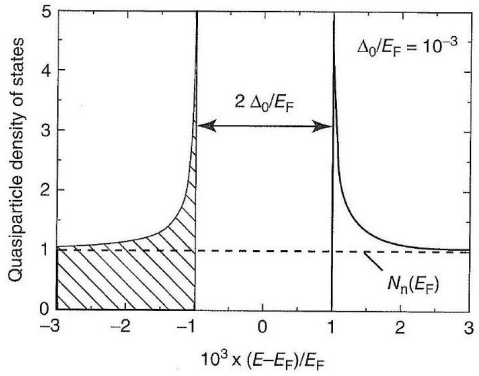


Figure 3.7 Normalized density of states $N_{\mathrm{s}}(E)/N_n(E_{\mathrm{F}})$ of the quasiparticles in a superconductor according to the BCS theory. The ratio Δ_0/E_F was taken as 10^{-3}. At the temperature $T = 0$, all states below the Fermi energy are occupied (hatched region).

At energies $E = E_{\mathrm{F}} \pm \Delta_0$ it reaches infinity, and for large values of $|E|$ it rapidly approaches the density of states $N_{\mathrm{n}}(E_{\mathrm{F}})$. Within the energy interval $E_{\mathrm{F}} \pm \Delta_0$, there are no states." Therefore, $2\Delta_0$ is also referred to as the energy gap of the superconductor.

At this point we note that the energy states of the unpaired electrons are energetically redistributed because of the Cooper pair interaction, but they are not annihilated. If we integrate $N_{\mathrm{s}}(E)$ over all energies, we obtain the same number of states as in the normal state. Most of the states between E_{F} and $E_{\mathrm{F}} + \Delta_0$ in the normal conductor appear at energies slightly above $E_{\mathrm{F}} + \Delta_0$ in a superconductor. As we will see in Section 3.1.3, the energy gap in a superconductor can be observed very nicely in infrared absorption experiments and also by means of superconducting tunnel junctions. These experiments perfectly confirm our ideas about the superconducting state.

Next we turn to the properties of superconductors at finite temperatures. At $T > 0$ some Cooper pairs are broken because of thermal fluctuations, and thermally excited quasiparticles are generated. These quasiparticles are fermions, exactly like the electrons in a normal conductor. Hence, the probability of finding a quasiparticle in a given energy state is indicated by the Fermi distribution function (1.3).

In Section 3.2 we will see that this property changes if the.Cooper pairs do not form an $L = 0$ state (see Section 21) In this case, quasiparticles exist for all energies.

We note that a quasiparticle in the quantum state $\mathbf{k}$ is blocking this state for the condensation of Cooper pairs, thereby affecting a reduction of the total number of Cooper pairs and also a reduction of their binding energy. One obtains a decrease in Δ_0 with increasing temperature. For $T \to T_c, \Delta_0$ approaches zero.

How does the density n_s of Cooper pairs depend on Δ_0? One finds that n is proportional to Δ_0^2. We see that, on the one hand, the quantity Δ_0 appears as (half) the "energy gap" of the superconductor. On the other hand, it also determines the number of Cooper pairs. In Chapter 1, we described the Cooper pair density in terms of the absolute square of the macroscopic wave function $\Psi = \Psi_0 e^{i\varphi}$. One can show that $\Delta \propto \Psi$[9]. Hence, pair amplitude Ψ_0 and Δ_0 are often used synonymously.

Finally, from the BCS theory one can derive a very simple connection between T_c and the quantities $N_n(E_F), \hbar\omega_c$, and the Cooper pair interaction V: it is [M3, M4]

$$T_c = 1.13 \frac{\hbar\omega_c}{k_B} \exp\left(-\frac{1}{N_n(E_F)V}\right)$$

If we identify ω_c with the Debye frequency ω_D, we also obtain immediately a connection between the transition temperature and the mass M of the elements building the lattice, since the frequency of the lattice vibrations is inversely proportional to the square root of M. If we substitute an isotope on a lattice site by another one, the interaction between these elements building the lattice remain unchanged. This results in the isotope effect, which we expect for Cooper pairing because of the electron-phonon interaction

Furthermore, from the BCS theory, we can derive the following important relation between Δ_0 at zero temperature and T_c:

$$2\Delta_0(T = 0) = 3.5 k_B T_c$$

In the following section, we turn to the experimental results dealing with the microscopic concepts of the superconducting state.

3.1.3

Experimental Confirmation of Fundamental Concepts about the Superconducting Stat

In the previous section we have outlined a picture of the superconducting state based on the BCS theory, which represents a most successful microscopic theory of superconductivity. In principle, it is the total sum of all experimental observations explained quantitatively or at least qualitatively by the theory, which completely justifies the essential concepts. There are a few experimental results that particularly strongly illuminate certain characteristic properties of the superconducting state.

In Chapter 1 we discussed results showing directly that superconductivity manifests itself in terms of a macroscopic quantum state with a well-defined phase. In the following section, we will present additional results that should strengthen our confidence in the somewhat complicated ideas about the

Table 3.1 Isotope effect in mercury [13].

Average atomic mass	199.7	200.7	202.0	203.4
Tran				

superconducting state, and which should deepen our understanding by means of concrete experiments. Except for the isotope effect, these characteristic properties are independent of the special interaction leading to the pair correlation.

Some of the experimental facts, such as, say, the behavior of the specific heat or the isotope effect, were already known before the development of the BCS theory. Other experiments, such as, say, measurements of the tunneling effect and of the Josephson effects (discussed already in

Chapter 1), were stimulated only by the microscopic theory. However, the flux quantization, also discussed in Chapter 1, is a special case, since it was already predicted by F. London long before the BCS theory arrived. On the other hand, it was experimentally observed only after the development of this theory and represents an impressive quantitative confirmation of the concept of Cooper pairing.

Time of Cooper Pair coherence

(???? how long are they correlated??? there are articles about it)

3.10.5 BCS theory in 1D, 2D: General Features

(what with BCS in d=1 or d=2?)

Main ideas

3.10.6 Original 1957 BCS Paper 1: Conclusion, Introduction, General Questions

Abstract

A theory of superconductivity is presented, based on the fact that the interaction between electrons resulting from virtual exchange of phonons is attractive when the energy difference between the electrons states involved is less than the phonon energy, $\hbar\omega$. It is favorable to form a superconducting phase when this attractive interaction dominates the repulsive screened Coulomb interaction. The normal phase is described by the Bloch individual-particle model. The ground state of a superconductor, formed from a linear combination of normal state configurations in which electrons are virtually excited in pairs of opposite spin and momentum, is lower in energy than the normal state by amount proportional to an average $(\hbar\omega)^2$, consistent with the isotope effect. A mutually orthogonal set of excited states in one-to-one correspondence with those of the normal phase is obtained by specifying occupation of certain Bloch states and by using the rest to form a linear combination of virtual pair configurations. The theory yields a second-order phase transition and a Meissner effect in the form suggested by Pippard. Calculated values of specific heats and penetration depths and their temperature variation are in good agreement with experiment. There is an energy gap for individual-particle excitations which decreases from about $3.5kT_c$ at $T = 0°\mathrm{K}$ to zero at T_c. Tables of matrix elements of single-particle operators between the excited-state superconducting wave functions, useful for perturbation expansions and calculations of transition probabilities, are given.

VI. CONCLUSION

Although our calculations are based on a rather idealized model, they give a reasonably good account of the equilibrium properties of superconductors. When the parameters of the theory are determined empirically, we find that we get agreement with observed specific heats and penetration depths to within the order of 10%. Only the critical temperature involves the superconducting phase; the other two parameters required (density of states and average velocity at the Fermi surface) are determined from the normal phase. This quantitative agreement, as well as the fact that we can account for the main features of superconductivity is convincing evidence that our model is essentially correct.

The basis for the theory is a net attractive interaction between electrons for transitions in which the energy difference between the electron states involved is less than the phonon energy, $\hbar\omega$. For simplicity we have assumed a constant matrix element, $-V$, for transitions within an

average energy $\hbar\omega$ of the Fermi surface and have neglected the repulsive interaction outside this region. In more accurate calculations one should take an interaction region dependent on the initial states of the electron and the transition involved, and also take into account any anisotropy in the Fermi surface and in the matrix elements. The fact that there is a law of corresponding states is empirical evidence that such effects are not of great importance. Neglect of the repulsive part of the interaction is in the spirit of the Bloch approximation for normal metals, and appears to be well justified in first approximation. Our theory may be regarded as an extension of the Bloch theory to superconductors in which we introduce only those interactions responsible for the transition.

An improvement in the general formulation of the theory is desirable. We have used that of Bardeen and Pines in which screening of the Coulomb field is taken into account by the Bohm-Pines collective model, and the phonon interaction between electrons is determined only to second order. Diagonal or self-energy terms in the net interaction have been omitted with the assumption that they are included in the Bloch energies of the normal state. When the phonon interaction is so large as to give superconductivity, higher order terms than the second may well be important. One should really have used a renormalized interaction in which such higher order terms are taken into account as well as possible. Very likely the assumption of two-particle interactions is a reasonably good one, so that the only effect would be a redefinition of the interaction constant V in terms of microscopic quantities.

The discussion of the matrix elements in Sec. IV should be a good starting point for calculation of transport properties in the superconducting phase. Our excited state many-particle wave functions are not
much more difficult to use in such calculations than the determinantal wave functions of the Bloch theory.

For calculation of boundary energies and related problems, one would like to introduce an order parameter which can decrease continuously from an equilibrium value for the superconducting phase to zero in the normal phase as the boundary is crossed. The Ginsburg-Landau theory and its extensions [7] appear to give a good phenomenological description of such effects. Perhaps the energy gap, $2\epsilon_0$, or, what is equivalent, the coherence distance, ξ_0, could be used for such a parameter.

Another problem, not yet solved, is the calculation of the paramagnetic susceptibility of the electrons in a superconductor, such as is required to account for Reif's data [38] on the Knight shift in the nuclear paramagnetic resonance of colloidal mercury. Our ground state is for total spin $S = 0$. It is possible that there is no energy gap between this state and those for $S \neq 0$. While a finite energy is required to turn over an individual spin, it might be possible to construct states analogous to those used in spin-wave theory in which each virtual pair has a small net spin, and for which the energy varies continuously with S. The explanation of the observed electronic paramagnetism (about twothirds that of the normal metal) would then be similar to that suggested by Reif himself.

In view of its success with equilibrium properties, it may be hoped that our theory will be able to account for these and for other so far unsolved problems.

The authors are indebted to many of their associates for discussions which have helped to clarify the problems involved. We should like to mention particularly discussions with C. P. Slichter and L. C. Hebel on calculation of matrix elements, with D. Pines on the criterion for superconductivity, and with K . A. Brueckner on the exactness of the solution for the ground state.

I. INTRODUCTION

The main facts which a theory of superconductivity must explain are (1) a second-order phase transition at the critical temperature, T_c, (2) an electronic specific heat varying as

$\exp(-T_0/T)$ near $T = 0°\mathrm{K}$ and other evidence for an energy gap for individual particle-like excitations, (3) the MeissnerOchsenfeld effect ($\mathbf{B} = 0$), (4) effects associated with infinite conductivity ($\mathbf{E} = 0$), and (5) the dependence of T_c on isotopic mass, $T_c\sqrt{M} = \text{const}$. We present here a theory which accounts for all of these, and in addition gives good quantitative agreement for specific heats and penetration depths and their variation with temperature when evaluated from experimentally determined parameters of the theory.

When superconductivity was discovered by Onnes [1] (1911), and for many years afterwards, it was thought to consist simply of a vanishing of all electrical resistance below the transition temperature. A major advance was the discovery of the Meissner effect [2] (1933), which showed that a superconductor is a perfect diamagnet; magnetic flux is excluded from all but a thin penetration region near the surface. Not very long afterwards (1935), London and London [3] proposed a phenomenological theory of the electromagnetic properties in which the diamagnetic aspects were assumed

basic. F. London [4] suggested a quantum-theoretic approach to a theory in which it was assumed that there is somehow a coherence or rigidity in the superconducting state such that the wave functions are not modified very much when a magnetic field is applied. The concept of coherence has been emphasized by Pippard, [5] who, on the basis of experiments on penetration phenomena, proposed a nonlocal modification of the London equations in which a coherence distance, ξ_0, is introduced. One of the authors [6,7] pointed out that an energy-gap model would most likely lead to the Pippard version, and we have found this to be true of the present theory. Our theory of the diamagnetic aspects thus follows along the general lines suggested by London and by Pippard. [7]

The Sommerfeld-Bloch individual-particle model (1928) gives a fairly good description of normal metals, but fails to account for superconductivity. In this theory, it is assumed that in first approximation one may neglect correlations between the positions of the electrons and assume that each electron moves independently in some sort of self-consistent field determined by the other conduction electrons and the ions. Wave functions of the metal as a whole are designated by occupation of Bloch individual-particle states of energy $\epsilon(\mathbf{k})$ defined by wave vector $\mathbf{k}$ and spin σ; in the ground state all levels with energies below the Fermi energy, $\mathcal{E}_F$, are occupied; those above are unoccupied. Left out of the Bloch model are correlations between electrons brought about by Coulomb forces and interactions between electrons and lattice vibrations (or phonons).

Most of the relatively large energy associated with correlation effects occurs in both normal and superconducting phases and cancels out in the difference. One of the problems in constructing a satisfactory microscopic theory of superconductivity has been to isolate that part of the interaction which is responsible for the transition. Heisenberg [8] and Koppe [9] proposed a theory based on long-wavelength components of the Coulomb interaction, which were presumed to give fluctuations in electron density described roughly by wave packets localizing a small fraction of the electrons on lattices moving in different directions. A great break-through occurred with the discovery of the isotope effect, [10] which strongly indicated, as had been suggested independently by Fröhlich, [11] that electronphonon interactions are primarily responsible for superconductivity.

[1] H. K. Onnes, Comm. Phys. Lab. Univ. Leiden, Nos. 119, 120, 122 (1911).
[2] W. Meissner and R. Ochsenfeld, Naturwiss. 21, 787 (1933).
[3] H. London and F. London, Proc. Roy. Soc. (London) A149, 71 (1935) ; Physica 2, 341 (1935).
[4] F. London, Proc. Roy. Soc. (London) A152, 24 (1935); Phys. Rev. 74, 562 (1948).
[5] A. B. Pippard, Proc. Roy. Soc. (London) A216, 547 (1953).
[6] J. Bardeen, Phys. Rev. 97, 1724 (1955).
[7] For a recent review of the theory of superconductivity, which includes a discussion of the diamagnetic properties, see J. Bardeen, Encyclopedia of Physics (Springer-Verlag, Berlin, 1956), Vol. 15, p. 274.

Early theories based on electron-phonon interactions have not been successful. Fröhlich's theory, which makes use of a perturbation-theoretic approach, does give the correct isotopic mass dependence for H_0, the critical field at $T = 0°\mathrm{K}$, but does not yield a phase with superconducting properties and further, the energy difference between what is supposed to correspond to normal and superconducting phases is far too large. A variational approach by one of the authors [12] ran into similar difficulties. Both theories are based primarily on the self-energy of the electrons in the phonon field rather than on the true interaction between electrons, although it was recognized that the latter might be important. [13]

The electron-phonon interaction gives a scattering from a Bloch state defined by the wave vector $\mathbf{k}$ to $\mathbf{k}' = \mathbf{k} \pm \boldsymbol{k}$ by absorption or emission of a phonon of wave vector $\boldsymbol{k}$. It is this interaction which is responsible for thermal scattering. Its contribution to the energy can be estimated by making a canonical transformation which eliminates the linear electron-phonon interaction terms from the Hamiltonian. In second order, there is one term which gives a renormalization of the phonon frequencies, and another, H_2, which gives a true interaction between electrons, independent of the vibrational amplitudes. A transformation of this sort was given first by Fröhlich [14] in a formulation in which Coulomb interactions between electrons were disregarded. In a later treatment, Nakajima [15] showed how such interactions could be included. Particularly for the longwavelength part of the interaction, it is important to take into account the screening of the Coulomb field of any one electron by other conduction electrons. Such effects are included in a more complete analysis by Bardeen and Pines, [16] based on the Bohm-Pines collective model, in which plasma modes are introduced for long wavelengths.

We shall call the interaction, H_2, between electrons resulting from the electron-phonon interaction the "phonon interaction." This interaction is attractive when the energy difference, $\Delta\epsilon$, between the electron states involved is less than $\hbar\omega$. Diagonal or self-energy terms of H_2 give an energy of order of $-N(\mathcal{E}_F)(\hbar\omega)^2$, where $N(\mathcal{E}_F)$ is the density of states per unit energy at the Fermi surface. The theories of Fröhlich and Bardeen mentioned above were based largely on this part of the energy. The observed energy differences between superconducting and normal states at $T = 0°\mathrm{K}$ are much smaller, of the order of $-N(\mathcal{E}_F)(kT_c)^2$ or about 10^{-8} ev/ atom. The present theory, based on the off-diagonal elements of H_2 and the screened Coulomb interaction, gives energies of the correct order of magnitude. While the self-energy terms do depend to some extent on the distribution of electrons in $\mathbf{k}$ space, it is now believed that this part of the energy is substantially the same in the normal and superconducting phases. The self-energy terms are also nearly the same for all of the various excited normal state configurations which make up the superconducting wave functions.

In a preliminary communication, [17] we gave as a criterion for the occurrence of a superconducting phase that for transitions such that $\Delta\epsilon < \hbar\omega$, the attractive H_2 dominate the repulsive short-range screened Coulomb interaction between electrons, so as to give a net attraction. We showed how an attractive interaction of this sort can give rise to a cooperative many-particle state which is lower in energy than the normal state by an amount proportional to $(\hbar\omega)^2$, consistent with the isotope effect. We have since extended the theory to higher temperatures, have shown that it gives both a second-order transition and a Meissner effect, and have calculated

[8] W. Heisenberg, Two Lectures (Cambridge University Press, Cambridge, 1948).
[9] H. Koppe, Ergeb. exakt. Naturw. 23, 283 (1950) ; Z. Physik 148, 135 (1957).
[10] E. Maxwell, Phys. Rev. 78, 477 (1950); Reynolds, Serin, Wright, and Nesbitt, Phys. Rev. 78, 487 (1950).
[11] H. Fröhlich, Phys. Rev. 79, 845 (1950).
[12] J. Bardeen, Phys. Rev. 79, 167 (1950) ; 80, 567 (1950) ; 81, 829 (1951).
[13] For a review of the early work, see J. Bardeen, Revs. Modern Phys. 23, 261 (1951).
[14] H. Fröhlich, Proc. Roy. Soc. (London) A215, 291 (1952).
[15] S. Nakajima, Proceedings of the International Conference on Theoretical Physics, Kyoto and Tokyo, September, 1953 (Science Council of Japan, Tokyo, 1954).

specific heats and penetration depths.

In the theory, the normal state is described by the Bloch individual-particle model. The ground-state wave function of a superconductor is formed by taking a linear combination of many low-lying normal state configurations in which the Bloch states are virtually occupied in pairs of opposite spin and momentum. If the state $\mathbf{k}\uparrow$ is occupied in any configuration, $-\mathbf{k}\downarrow$ is also occupied. The average excitation energy of the virtual pairs above the Fermi sea is of the order of kT_c. Excited states of the superconductor are formed by specifying occupation of certain Bloch states and by using all of the rest to form a linear combination of virtual pair configurations. There is thus a one-to-one correspondence between excited states of the normal and superconducting phases. The theory yields an energy gap for excitation of individual electrons from the superconducting ground state of about the observed order of magnitude.

The most important concribution to the interaction energy is given by short- rather than long-wavelength phonons. Our wave functions for the suerconducting phase give a coherence of short-wavelength components of the density matrix which extend over large distances in real space, so as to take maximum advantage of the attractive part of the interaction. The coherence distance, of the order of Pippard's ξ_0, can be estimated from uncertainty principle arguments. [5,7] If intervals of the order of $\Delta k \sim (kT_c/\mathcal{E}_F)\, k_F \sim 10^4$ cm^{-1} are important in $\mathbf{k}$ space, wave functions in real space must extend over distances of at least $\Delta x \sim 1/\Delta k \sim 10^{-4}$ cm. The fraction of the total number of electrons which have energies within kT_c of the Fermi surface, so that they can interact effectively, is approximately $kT_c/\mathcal{E}_F \sim 10^{-4}$. The number of these in an interaction region of volume $(\Delta x)^3$ is of the order of $10^{22} \times (10^{-4})^3 \times 10^{-4} = 10^6$. Thus our wave functions must describe coherence of large numbers of electrons. [18]

In the absence of a satisfactory microscopic theory, there has been considerable development of phenomenological theories for both thermal and electromagnetic properties. Of the various two-fluid models used to describe the thermal properties, the first and best known is that of Gorter and Casimir, [19] which yields a parabolic critical field curve and an electronic specific heat varying as T^3. In this, as well as in subsequent theories of thermal properties, it is assumed that all of the entropy of the electrons comes from excitations of individual particles from the ground state. In recent years, there has been considerable experimental evidence [20] for an energy gap for such excitations, decreasing from $\sim 3kT_c$ at $T = 0°$K to zero at $T = T_c$. Two-fluid models which yield an energy gap and an exponential specific heat curve at low temperatures have been discussed by Ginsburg [21] and by Bernardes. [22] Koppe's

theory may also be interpreted in terms of an energygap model. [7] Our theory yields an energy gap and specific heat curve consistent with the experimental observations.

The best known of the phenomenological theories for the electromagnetic properties is that of F . and H . London. [23] With an appropriate choice of gauge for the vector potential, A, the

[16] J. Bardeen and D. Pines, Phys. Rev. 99, 1140 (1955).

17 Bardeen, Cooper, and Schrieffer, Phys. Rev. 106, 162 (1957).

[18] Our picture differs from that of Schafroth, Butler, and Blatt, Helv. Phys. Acta 30, 93 (1957), who suggest that pseudomolecules of pairs of electrons of opposite spin are formed. They show if the size of the pseudomolecules is less than the average distance between them, and if other conditions are fulfilled, the system has properties similar to that of a charged Bose-Einstein gas, including a Meissner effect and a critical temperature of condensation. Our pairs are not localized in this sense, and our transition is not analogous to a Bose-Einstein condensation.

[19] C. J. Gorter and H. B. G. Casimir, Physik. Z. 35, 963 (1934); Z. techn. Physik 15, 539 (1934).

[20] For discussions of evidence for an energy gap, see Blevins, Gordy, and Fairbank, Phys. Rev. 100, 1215 (1955); Corak, Goodman, Satterthwaite, and Wexler, Phys. Rev. 102, 656 (1956);
W. S. Corak and C. B. Satterthwaite, Phys. Rev. 102, 662 (1956);
R. E. Glover and M. Tinkham, Phys. Rev. 104, 844 (1956), and to be published.

[21] W. L. Ginsburg, Fortschr. Physik 1, 101 (1953); also see reference 7.

[22] N. Bernardes, Phys. Rev. 107, 354 (1957).

London equation for the superconducting current density, $\mathbf{j}$, may be written

$$-c\Lambda\mathbf{j} = \mathbf{A} \tag{1.1}$$

The London penetration depth is given by:

$$\lambda_L^2 = \Lambda c^2/4\pi \tag{1.2}$$

F. London has pointed out that (1.1) would follow from quantum theory if the superconducting wave functions are so rigid that they are not modified at all by the application of a magnetic field. For an electron density n/cm^3, this approach gives $\Lambda = m/ne^2$.

On the basis of empirical evidence, Pippard [5] has proposed a modification of the London equation in which the current density at a point is given by an integral of the vector potential over a region surrounding the point:

$$\mathbf{j}(\mathbf{r}) = -\frac{3}{4\pi c\Lambda\xi_0}\int \frac{\mathbf{R}\left[\mathbf{R}\cdot\mathbf{A}\left(\mathbf{r}'\right)\right]e^{-R/\xi_0}}{R^4}d\tau' \tag{1.3}$$

where $\mathbf{R} = \mathbf{r} - \mathbf{r}'$. The "coherence distance," ξ_0, is of the order of 10^{-4} cm in a pure metal. For a very slowly varying $\mathbf{A}$, the Pippard expression reduces to the London form (1.1).

The present theory indicates that the Meissner effect is intimately related to the existence of an energy gap, and we are led to a theory similar to, although not quite the same as, that proposed by Pippard. Our theoretical values for ξ_0 are close to those derived empirically by Pippard. We find that while the integrand is relatively independent of temperature, the coefficient in front of the integral (in effect Λ) varies with T in such a way as to account for the temperature variation of penetration depth.

Our theory also accounts in a qualitative way for those aspects of superconductivity associated with infinite conductivity and a persistent current flowing in a ring. When there is a net current flow, the paired states $(\mathbf{k}_1\uparrow, \mathbf{k}_2\downarrow)$ have a net momentum $\mathbf{k}_1 + \mathbf{k}_2 = \mathbf{q}$, where $\mathbf{q}$ is the same for all virtual pairs. For each value of $\mathbf{q}$, there is a metastable state with a minimum in free energy and a unique current density. Scattering of individual electrons will not change the value of $\mathbf{q}$ common to virtual pair states, and so can only produce fluctuations about the current determined by $\mathbf{q}$. Nearly all fluctuations will increase the free energy; only those which involve a majority of the electrons so as to change

the common $\mathbf{q}$ can decrease the free energy. These latter are presumably extremely rare, so that the metastable current carrying state can persist indefinitely. [24]

It has long been recognized that there is a law of corresponding states for superconductors. The various properties can be expressed approximatly in terms of a small number of parameters. If the ratio of the electronic specific heat at T to that of the normal state at $T_c, C_s(T)/C_n\left(T_c\right)$, is plotted on a reduced temperature scale, $t = T/T_c$, most superconductors fall on nearly the same curve. There are two parameters involved: (1) the density of states in energy at the Fermi surface, $N\left(\mathcal{E}_F\right)$, determined from $C_n(T) = \gamma T$ and (2) one which depends on the phonon interaction, which can be estimated from T_c. A consequence of the similarity law is that $\gamma {T_c}^2/V_m {H_0}^2$ (where V_m is the molar volume and H_0 the critical field at $T = 0°\mathrm{K}$) is approximately the same for most superconductors.

A third parameter, the average velocity, v_0, of electrons at the Fermi surface,

$$v_0 = \hbar^{-1}|\partial\mathcal{E}/\partial\mathbf{k}|_F \tag{1.4}$$

is required for penetration phenomena. As pointed out by Faber and Pippard, [25] this parameter is most conveniently determined from measurements of the anomalous skin effect in

[23] An excellent account may be found in F. London, Superfluids (John Wiley and Sons, Inc., New York, 1954), Vol. 1.

normal metals in the high-frequency limit. The expression, as given by Chambers [26] for the current density when the electric field varies over a mean free path, l, may be written in the form:

$$\mathbf{j}_n(r) = \frac{e^2 N(\mathcal{E}_F) v_0}{2\pi} \int \frac{\mathbf{R}[\mathbf{R}\cdot\mathbf{A}(\mathbf{r}')] e^{-R/l}}{R^4} d\tau'. \tag{1.5}$$

The coefficient $N(\mathcal{E}_F) v_0$ has been determined empirically for tin and aluminum.

Pippard based his Eq. (1.3) on Chambers' expression. London's coefficient, Λ, for $T = 0°\mathrm{K}$ may be expressed in the form:

$$\Lambda^{-1} = \frac{2}{3} e^2 N(\mathcal{E}_F) v_0^2. \tag{1.6}$$

Faber and Pippard suggest that if ξ_0 is written:

$$\xi_0 = a\hbar v_0/kT_c, \tag{1.7}$$

the dimensionless constant a has approximately the
same value for all superconductors and they find it equal to about 0.15 for Sn and Al.[27]

Our theory is based on a rather idealized model in which anisotropic effects are neglected. It contains three parameters, two corresponding to $N(\mathcal{E}_F)$ and v_0, and one dependent on the electron-phonon interaction which determines T_c. The model appears to fit the law of corresponding states about as well as real metals do ($\sim 10\%$ for most properties). We find a relation corresponding to (1.7) with $a = 0.18$. It thus appears that superconducting properties are not dependent on the details of the band structure but only upon the gross features.

Section II is concerned with the nature of the ground state and the energy of excited states near $T = 0°\mathrm{K}$, Sec. III with excited states and thermal properties, Sec. IV with calculation of matrix elements for application to perturbation theory expansions and transition probabilities and Sec. V with electrodynamic and penetration phenomenon. Some of the computational details are given in Appendices.

We give a fairly complete account of the equilibrium properties of our model, but nothing on transport or boundary effects. Starting from matrix elements of single-particle scattering operators as given in Sec. IV, it should not be difficult to determine transport properties in the superconducting state from the corresponding properties of the normal state.

How did they derive the gap as function of temperature without Bogoliubov transformations?

(??? this was always in my mind... I'll read later)

[24] Blatt, Butler, and Schafroth, Phys. Rev. 100, 481 (1955) have introduced the concept of a "correlation length," roughly the distance over which the momenta of a pair of particles are correlated. M. R. Schafroth, Phys. Rev. 100, 502 (1955), has argued that there is a true Meissner effect only if the correlation length is effectively infinite. In our theory, the correlation length (not to be confused with Pippard's coherence distance, ξ_0) is most reasonably interpreted as the distance over which the momentum of virtual pairs is the same. We believe that in this sense, the correlation length is effectively infinite. The value of $\mathbf{q}$ is exactly zero everywhere in a simply connected body in an external field. When there is current flow, as in a torus, there is a unique distribution of $\mathbf{q}$ values for minimum free energy.

[25] T. E. Faber and A. B. Pippard, Proc. Roy. Soc. (London) A231, 53 (1955).

[26] See A. P. Pippard, Advances in Electronics (Academic Press, Inc., New York, 1954), Vol. 6, p. 1.

3.10.7 Original 1957 BCS Paper 1: Ground State

II. THE GROUND STATE

The interaction which produces the energy difference between the normal and superconducting phases in our theory arises from the virtual exchange of phonons and the screened Coulomb repulsion between electrons. Other interactions, such as those giving rise to the single-particle self-energies, are thought to be essentially the same in both states, their effects thus cancelling in the energy difference. The problem is therefore one of calculating the ground state and excited states of a dense system of fermions interacting via two-body potentials.

The Hamiltonian for the fermion system is most conveniently expressed in terms of creation and annihilation operators, based on the renormalized Bloch states specified by wave vector $\mathbf{k}$ and spin σ, which satisfy the usual Fermi commutation relations:

$$\left[c_{\mathrm{k}\sigma}, c_{\mathrm{k}'\sigma'}\right]_+\Big]_+ = \delta_{\mathrm{k}\mathrm{k}'}\delta_{\sigma\sigma'}, \tag{2.1}$$

$$\left[c_{\mathrm{k}\sigma}, c_{\mathrm{k}'\sigma'}\right]_+ = 0. \tag{2.2}$$

The single-particle number operator $n_{\mathrm{k}\sigma}$ is defined as

$$n_{\mathrm{k}\sigma} = {c_{\mathrm{k}\sigma}}^* c_{\mathrm{k}\sigma} \tag{2.3}$$

The Hamiltonian for the electrons may be expressed in the form

$$H = \sum_{k>k_F} \epsilon_{\mathrm{k}} n_{\mathrm{k}\sigma} + \sum_{k<k_F} |\epsilon_{\mathrm{k}}| \left(1 - n_{\mathrm{k}\sigma}\right) + H_{\mathrm{Coul}} + \\ + \frac{1}{2} \sum_{\mathbf{k},\mathbf{k}',\sigma,\sigma',\mathbf{k}} \frac{2\hbar\omega_k \left|M_{\mathbf{k}}\right|^2 c^*\left(\mathbf{k}'-\mathbf{k},\sigma'\right) c\left(\mathbf{k}',\sigma'\right) c^*(\mathbf{k}+\mathbf{k},\sigma) c(\mathbf{k},\sigma)}{\left(\epsilon_{\mathrm{k}} - \epsilon_{\mathrm{k}+\alpha}\right)^2 - \left(\hbar\omega_k\right)^2} \\ = H_0 + H_I, \tag{2.4}$$

where ϵ_{k} is the Bloch energy measured relative to the Fermi energy, $\mathcal{E}_F$. We denote by $k > k_F$ states above the Fermi surface, by $k < k_F$ those below. The fourth term on the right of (2.4) is H_2, the phonon interaction, which comes from virtual exchange of phonons between the electrons. The matrix element for phonon-electron interaction, M_κ, calculated for the zero-point amplitude of the lattice vibrations, is related to the v_κ introduced by Bardeen and Pines [16] by

$$\left|M_\kappa\right|^2 = \left|v_\kappa\right|^2 \left\langle q_\kappa^2 \right\rangle_{\mathrm{Av}} = \left|v_\kappa\right|^2 \left(\hbar/2\omega_\kappa\right). \tag{2.5}$$

Since $\left|M_\kappa\right|^2$ varies with isotopic mass in the same way that ω_κ does, the ratio $\left|M_\kappa\right|^2/\hbar\omega_\kappa$ is independent of isotopic mass. We consider only the off-diagonal interaction terms of H_2, assuming that the diagonal terms are taken into account by appropriate renormalization of the Bloch energies, ϵ_{k}. The third term is the screened Coulomb interaction.

Following Bardeen and Pines, [16] the phonons are assumed to be decoupled from the electrons by a renormalization procedure and their frequencies are taken to be unaltered by the transition to the superconducting state. While this assumption is not strictly valid, the shift in self-energy can be taken into account after we have solved for the electronic part of the wave function. This

[27] From analysis of data on transmission of microwave and far infrared radiation through superconducting films of tin and lead, Glover and Tinkham (reference 20) find $a = 0.27$.

separation is possible because the phonons depend only upon the average electron distribution in momentum space and the wave function for electrons at any temperature is formed from configurations with essentially the same distribution of particles. The Bloch energies are also assumed to be constant; however, their shift with temperature could be treated as in the phonon case.

The form of the phonon interaction shows that it is attractive (negative) for excitation energies $|\epsilon_{\mathrm{k}} - \epsilon_{\mathrm{k+k}}| < \hbar\omega_\kappa$. Opposed to this is the repulsive Coulomb interaction, which may be expressed in a form similar to H_2. For free electrons in a system of unit volume the interaction in momentum space is $4\pi e^2/\kappa^2$. In the BohmPines theory, the long-wavelength components are expressed in the form of plasma oscillations, so that κ can be no smaller than minimum value κ_c, usually slightly less than the radius of the Fermi surface, k_F. One could also take screening into account by a FermiThomas method, in which case κ^2 would be replaced by $\kappa^2 + {\kappa_s}^2$, where κ_s depends on the electron density. Our criterion for superconductivity is that the attractive phonon interaction dominate the Coulomb interaction
for those matrix elements which are of importance in the superconducting wave function:

$$-V \equiv \left\langle -\frac{2\left|M_\kappa\right|^2}{\hbar\omega_\kappa} + \frac{4\pi e^2}{\kappa^2} \right\rangle_{\mathrm{Av}} < 0 \tag{2.6}$$

The most important transitions are those for which $|\epsilon_{\mathrm{k}} - \epsilon_{\mathrm{k+k}}| \sim kT_c \ll \hbar\omega_{\mathrm{k}}$. A detailed discussion of the criterion (2.6) has been given by Pines, [28] who shows that it accounts in a reasonable way for the empirical rules of Matthias [29] for the occurrence of superconductivity. Numerically, the criterion is not much different from one given earlier by Fröhlich, [11] based on a different principle.

To obtain the ground state function, we observe that the interaction Hamiltonian connects a large number of nearly degenerate occupation number configurations with each other via nonzero matrix elements. If the matrix elements were all negative in sign, one could obtain a state with low energy by forming a linear combination of the basis functions with expansion coefficients of the same sign. The magnitude of the interaction energy obtained in this manner would be approximately given by the number of configurations which connect to a given typical configuration times an average matrix element. This was demonstrated by one of the authors [30] by solving a problem in which two electrons with zero total momentum interact via constant negative matrix elements in a small shell above the Fermi surface. It was shown that the ground state of this system is separated from the continuum by a volume independent energy. This type of coherent mixing of Bloch states produces a state with qualitatively different properties from the original states.

In the actual problem, the interaction which takes a pair from ($\mathbf{k}_1\sigma_1, \mathbf{k}_2\sigma_2$) to ($\mathbf{k}_1'\sigma_1, \mathbf{k}_2'\sigma_2$) contains the operators,

$$c^*\left(\mathbf{k}_2', \sigma_2\right) c\left(\mathbf{k}_2, \sigma_2\right) c^*\left(\mathbf{k}_1', \sigma_1\right) c\left(\mathbf{k}_1, \sigma_1\right). \tag{2.7}$$

Conservation of momentum requires that

$$\mathbf{k}_1 + \mathbf{k}_2 = \mathbf{k}_1' + \mathbf{k}_2' \tag{2.8}$$

Because of Fermi-Dirac statistics, matrix elements of (2.7) between arbitrary many electron configurations alternate in sign so that if the configurations occur in the ground state with roughly equal weight, the net interaction energy would be small. We can, however, produce a coherent low state by choosing a subset of configurations between which the matrix elements are negative. Such a subset can be formed by those configurations in which the Bloch states are occupied in pairs, ($\mathbf{k}_1\sigma_1, \mathbf{k}_2\sigma_2$); that is, if one member of the pair is occupied in any configuration in the subset, the other is also. Since the interaction conserves momentum, a

maximum number of matrix elements will be obtained if all pairs have the same net momentum, $\mathbf{k}_1 + \mathbf{k}_2 = \mathbf{q}$. It is further desirable to take pairs of opposite spin, because exchange terms reduce the interaction for parallel spins. The best choice for q for the ground state pairing is $q = 0$, ($k \uparrow, -k \downarrow$).

We start then by considering a reduced problem in which we include only configurations in which the states are occupied in pairs such that if $\mathbf{k} \uparrow$ is occupied so is $-\mathbf{k} \downarrow$. A pair is designated by the wave vector $\mathbf{k}$, independent of spin. Creation and annihilation operators for pairs may be defined in terms of the singleparticle operators as follows:

$$b_{\mathrm{k}} = c_{-\mathrm{k}\downarrow} c_{\mathrm{k}} \uparrow \tag{2.9}$$

$$b_{\mathrm{k}}{}^{*} = c_{\mathrm{k}} \uparrow^{*} \, c_{-\mathrm{k}\downarrow}{}^{*} \tag{2.10}$$

These operators satisfy the commutation relations

$$[b_{\mathrm{k}}, b_{\mathrm{k}'} *]_{-} = (1 - n_{\mathrm{k}} \uparrow - n_{-\mathrm{k}\downarrow}) \, \delta_{\mathrm{k}\mathrm{k}'} \tag{2.11}$$

$$[b_{\mathrm{k}}, b_{\mathrm{k}'}]_{-} = 0 \tag{2.12}$$

$$[b_{\mathrm{k}}, b_{\mathrm{k}'}]_{+} = 2 b_{\mathrm{k}} b_{\mathrm{k}'} \, (1 - \delta_{\mathrm{k}\mathrm{k}'}) \tag{2.13}$$

where $n_{\mathrm{k}\sigma}$ is given by (2.3). While the commutation relation (2.12) is the same as for bosons, the commutators (2.11) and (2.13) are distinctly different from those for Bose particles. The factors ($1 - n_{\mathrm{k}} \uparrow - n_{-\mathrm{k}\downarrow}$) and ($1 - \delta_{\mathrm{k}\mathrm{k}'}$) arise from the effect of the exclusion principle on the single particles.

That part of the Hamiltonian which connects pairs with zero net momentum may be derived from the Hamiltonian (2.4) and expressed in terms of the b 's. Measuring the energy relative to the Fermi sea, we obtain:

$$H_{\mathrm{red}} = 2 \sum_{k > k_F} \epsilon_{\mathrm{k}} b_{\mathrm{k}} * b_{\mathrm{k}} + 2 \sum_{k < k_F} |\epsilon_{\mathrm{k}}| b_{\mathrm{k}} b_{\mathrm{k}}^{*} - \sum_{\mathrm{k}\mathrm{k}'} V_{\mathrm{k}\mathrm{k}'} b_{\mathrm{k}'}^{*} b_{\mathrm{k}} \tag{2.14}$$

We have defined the interaction terms with a negative sign so that $V_{kk'}$ will be predominantly positive for a superconductor. There are many other terms in the complete interaction which connect pairs with total momentum $\boldsymbol{q} \neq 0$. These have little effect on the energy, and can be treated as a perturbation. Although the interaction terms kept in H_{red} may appear to have a negligible weight, it is this part which contributes overwhelmingly to the interaction energy.

We have used a Hartree-like method to determine the expansion coefficients, which appears to give an excellent approximation, and may, indeed, even be correct in the limit of a large number of particles. [31] (See Appendix A.)

Excited states are treated in much the same way as the ground state. One must distinguish between singly excited particles, in which one and only one of a pair ($\mathbf{k} \uparrow, -\mathbf{k} \downarrow$) is occupied, and excited or "real" pair states. We treat singly excited particles in the Bloch scheme, as in the normal metal. They contribute a negligible amount to the interaction energy directly, but reduce the amount of phase space available for real and virtual pairs. Thus the interaction

28 D. Pines (to be published).

[29] B. Matthias, Progress in Low Temperature Physics (NorthHolland Publishing Company, Amsterdam, 1957), Vol. 2.

[30] L. N. Cooper, Phys. Rev. 104, 1189 (1956).

[31] Since (2.14) is quadratic in the b 's, one might hope to get an exact solution for the ground state by an appropriate redefinition of the single-particle states, as can be done for either Fermi-Dirac or Einstein-Bose statistics. Our pairs obey neither of these, and no such simple solution appears possible.

portion of H_{red} is modified by deleting from the sums over $\mathbf{k}$ and $\mathbf{k}'$ all singly occupied states, and the remainder is used to determine the interaction energy associated with the pairs.

One might expect to get some interaction energy from singly occupied states by associating them in various pairs with $\boldsymbol{q} \neq 0$. However, an appreciable energy is obtained only if a finite fraction of the pairs have the same $\mathbf{q}$, and this will not be true for randomly excited particles. States with a net current flow can be obtained by taking a pairing ($\mathbf{k}_1 \uparrow, \mathbf{k}_2 \downarrow$), with $\mathbf{k}_1 + \mathbf{k}_2 = \mathbf{q}$, and $\boldsymbol{q}$ the same for all virtual pairs.

The most general wave function satisfying the pairing condition ($\mathbf{k} \uparrow, -\mathbf{k} \downarrow$) is of the form

$$\sum_{\mathbf{k}_1 \cdots \mathbf{k}_n} \left[h\left(\mathbf{k}_1 \cdots \mathbf{k}_n\right)\right]^{\frac{1}{2}} f\left(\cdots 1\left(k_1\right) \cdots 1\left(k_n\right) \cdots\right) \tag{2.15}$$

where the sum extends over all distinct pair configurations. To construct our ground state function we make a Hartree-like approximation in which the probability that a specific configuration of pairs occurs in the wave function is given by a product of occupancy probabilities for the individual pair states. If for the moment we relax the requirement that the wave function describes a system with a fixed number of particles, then a function having this Hartree-like property is

$$\Psi = \prod_{\mathrm{k}} \left[(1 - h_{\mathrm{k}})^{\frac{1}{2}} + h_{\mathrm{k}}^{\frac{1}{2}} b_{\mathrm{k}}^*\right] \Phi_0 \tag{2.16}$$

where Φ_0 is the vacuum. It follows from (2.16) that the probability of the n states $\mathbf{k}_1 \cdots \mathbf{k}_n$ being occupied is $h\left(\mathbf{k}_1\right) \cdots h\left(\mathbf{k}_n\right)$, and since n is unrestricted we see that Ψ is closely related to the intermediate coupling approximation.

For any specified wave vector $\mathbf{k}'$, it is convenient to decompose Ψ into two components, in one of which, φ_1, the pair state designated by $\mathbf{k}'$ is certainly occupied and the other, φ_0, for which it is empty:

$$\Psi = h_{\mathbf{k}'}^{\frac{1}{2}} \varphi_1 + (1 - h_{\mathbf{k}'})^{\frac{1}{2}} \varphi_0 \tag{2.17}$$

The coefficient $h_{\mathrm{k}'}$ is the probability that state $\mathbf{k}'$ is occupied and the φ 's are the normalized functions:

$$\varphi_1 = b_{\mathrm{k}'} * \varphi_0 = b_{\mathrm{k}'} * \prod_{\mathrm{k}(\neq \mathrm{k}')} \left[(1 - h_{\mathrm{k}})^{\frac{1}{2}} + h_{\mathrm{k}^2}^{\frac{1}{2}} b_{\mathrm{k}} *\right] \Phi_0 \tag{2.18}$$

In the limit of a large system, the weights of states with different total numbers of pairs in Ψ will be sharply peaked about the average number, N, which will be dependent on the choice of the h 's. We take for our
ground state function, Ψ_N, the projection of Ψ onto the space of exactly N pairs. [32] This function may also be decomposed as in (2.17), but since φ_{N1} and φ_{N0} now have the same number of pairs, φ_{N1} is not equal to ${b_{\mathrm{k}'}}^* \varphi_{N0}$. To decompose Ψ_N, we suppose that $\mathbf{k}$ space is divided into elements, $\Delta\mathbf{k}$, with $\mathfrak{U}_{\mathbf{k}}$ available states of which in a typical configuration m_{k} are occupied by pairs. The m_{k} 's are restricted so that the total number of pairs is specified:

$$\sum_{\text{all } \Delta\mathrm{k}} m_{\mathrm{k}} = N = \sum_{\text{all } \Delta\mathrm{k}} \left\langle m_{\mathrm{k}} \right\rangle_{\mathrm{Av}} \tag{2.19}$$

The total weight of a given distribution of m_{k} 's in Ψ is

$$W\left(m_{\mathrm{k}}\right) = \prod_{\text{all } \Delta\mathrm{k}} \frac{\mathfrak{N}_k!}{m_{\mathrm{k}}!\left(\mathfrak{V}_{\mathrm{k}} - m_k\right)!} h_{\mathrm{k}}^{m_k} \left(1 - h_{\mathrm{k}}\right)^{\mathfrak{N}_{\mathrm{k}} - m_{\mathrm{k}}} \tag{2.20}$$

and the total weight of functions with specified N is

$$W_N = \sum_{(\Sigma m_{\mathrm{k}}=N)} W\left(m_{\mathrm{k}}\right) \tag{2.21}$$

where the sum is over-all distributions of the m_{k} 's subject to the conditions (2.19).

The decomposition of Ψ_N into a part in which a specified pair state $\mathbf{k}'$ is occupied and one where it is not can be carried out by calculating from Ψ_N the total weight, $W_{N,\mathrm{k}'}$, corresponding to $\mathbf{k}'$ occupied with the restriction $\sum m_{\mathrm{k}} = N$. When $\mathbf{k}'$ is occupied, there are $\mathscr{C}_{k'} - 1$ other states in the cell over which the remaining $m_{\mathrm{k}'} - 1$ particles can be distributed and this cell will contribute a factor

$$\frac{(\mathfrak{C}_{\mathfrak{k}'} - 1)! h_{\mathfrak{k}'}, m_{\mathfrak{k}'} \left(1 - h_{\mathfrak{k}'}\right)^{\mathfrak{C}_{\mathfrak{k}'} - m_{\mathfrak{k}'}}}{\left(m_{\mathfrak{k}'} - 1\right)! \left(\mathfrak{l}_{\mathfrak{k}'} - m_{\mathfrak{k}'}\right)!} \tag{2.22}$$

to the weight for a given distribution of m_{k} 's. It follows that

$$W_{N,\mathrm{k}'} = \sum_{(\Sigma m_{\mathrm{k}}=N)} \frac{m_{\mathrm{k}'}}{\mathfrak{T}_{\mathrm{k}'}} W\left(m_{\mathrm{k}}\right) = h_{\mathrm{k}'} W_N. \tag{2.23}$$

The last equality holds except for terms which vanish in the limit of a large system because the state vector Ψ gives a probability $\left\langle m_{\mathrm{k}'} / \mathscr{T}_{\mathrm{k}'} \right\rangle_{\mathrm{Av}} = h_{\mathrm{k}'}$ that a given state in $\Delta\mathbf{k}'$ is occupied. Now the weights for different numbers of pairs in Ψ are strongly peaked about the most probable number N and therefore the average over distributions with exactly N pairs is essentially equal to the average over all distributions. Since all terms in the wave function come in with a positive sign, it follows that the normalized Ψ_N may be decomposed in the form

$$\Psi_N = {h_{\mathrm{k}'}}^{\frac{1}{2}} \varphi_{N1} + \left(1 - h_{\mathrm{k}'}\right)^{\frac{1}{2}} \varphi_{N0} \tag{2.24}$$

where φ_{N1} and φ_{N0} are normalized functions.
For purposes of calculating matrix elements and

interaction energies, a further decomposition into states in which occupancy of two pair states, $\mathbf{k}$ and $\mathbf{k}'$, is specified is often convenient. Thus we may write:

$$\begin{aligned} \Psi_N = (hh')^{\frac{1}{2}} \varphi_{N11} + \left[h\left(1 - h'\right)\right]^{\frac{1}{2}} \varphi_{N10} + \left[(1 - h)h'\right]^{\frac{1}{2}} \varphi_{N01} \\ + \left[(1 - h)\left(1 - h'\right)\right]^{\frac{1}{2}} \varphi_{N00} \end{aligned} \tag{2.25}$$

where the first index gives the occupancy of $\mathbf{k}$ and the second of $\mathbf{k}'$. It follows from the definition of the functions that

$$b_{\mathrm{k}'}, {}^*b_{\mathrm{k}} \varphi_{N10} = \varphi_{N01} \tag{2.26}$$

Thus the diagonal matrix element of $b_{\mathrm{k}'} * b_{\mathrm{k}}$ is

$$\left(\Psi_N \left| {b_{\mathrm{k}'}}^* b_{\mathrm{k}} \right| \Psi_N\right) = \left[h_{\mathrm{k}}\left(1 - h_{\mathrm{k}}\right) h_{\mathrm{k}'}\left(1 - h_{\mathrm{k}'}\right)\right]^{\frac{1}{2}} \tag{2.27}$$

Ground-State Energy

If the wave function (2.24) is used as a variational approximation to the true ground-state function, the ground-state energy relative to the energy of the Fermi sea is given by

$$W_0 = \left(\Psi_0, H_{\mathrm{red}} \Psi_0\right) \tag{2.28}$$

[32] It is easily seen that Ψ_N has zero total spin, corresponding to a singlet state.

where Ψ_0 is the N-pair function Ψ_N, for the ground state. The Bloch energies, ϵ_{k}, are measured with respect to the Fermi energy and

$$-V_{\mathbf{k}\mathbf{k}'} = (-\mathbf{k}'\downarrow, \mathbf{k}'\uparrow|\ H_I\ |-\mathbf{k}\downarrow, \mathbf{k}\uparrow) + (\mathbf{k}'\uparrow, -\mathbf{k}'\downarrow|H_I|\,\mathbf{k}\uparrow, -\mathbf{k}\downarrow)\,. \tag{2.29}$$

The decomposition (2.23) leads to the Bloch energy contribution to W_0 of the form

$$W_{\mathrm{KE}} = 2\sum_{k>k_F} \epsilon_{\mathrm{k}} h_{\mathrm{k}} + 2\sum_{k<k_F} |\epsilon_{\mathrm{k}}|\,(1-h_{\mathrm{k}}) \tag{2.30}$$

where "KE" stands for kinetic energy. The matrix elements of the interaction term in H_{red} are given by (2.27) and the interaction energy is

$$W_I = -\sum_{\mathbf{k},\mathbf{k}'} V_{\mathbf{k}\mathbf{k}'} \left[h_{\mathbf{k}}\,(1-h_{\mathbf{k}})\,h_{\mathrm{k}'}\,(1-h_{\mathrm{k}'})\right]^{\frac{1}{2}} \tag{2.31}$$

and therefore

$$W_0 = W_{\mathrm{KE}} + W_I = 2\sum_{k>k_F} \epsilon_{\mathrm{k}} h_{\mathrm{k}} + 2\sum_{k<k_F} |\epsilon_{\mathrm{k}}|\,(1-h_{\mathrm{k}}) - \sum_{\mathbf{k},\mathbf{k}'} V_{\mathrm{k}\mathbf{k}'} \left[h_{\mathrm{k}}\,(1-h_{\mathrm{k}})\,h_{\mathrm{k}'}\,(1-h_{\mathrm{k}'})\right]^{\frac{1}{2}}. \tag{2.32}$$

By minimizing W_0 with respect to h_{k}, we are led to an integral equation determining the distribution function:

$$\frac{\left[h_{\mathrm{k}}\,(1-h_{\mathrm{k}})\right]^{\frac{1}{2}}}{1-2h_{\mathrm{k}}} = \frac{\sum_{\mathrm{k}'} V_{\mathrm{k}\mathrm{k}'} \left[h_{\mathrm{k}'}\,(1-h_{\mathrm{k}'})\right]^{\frac{1}{2}}}{2\epsilon_{\mathrm{k}}}. \tag{2.33}$$

We shall neglect anisotropic effects and assume for simplicity that the matrix element $V_{\mathbf{k}\mathbf{k}}$, can be replaced by a constant average matrix element,

$$V = \langle V_{\mathrm{k}\mathrm{k}\mathbf{k}'}\rangle_{\mathrm{Av}}\,, \tag{2.34}$$

for pairs making transitions in the region $-\hbar\omega < \epsilon < \hbar\omega$
and by zero outside this region, where ω is the average phonon frequency. This cutoff corresponds to forming our wave function from states in the region where the interaction is expected to be attractive and not mixing in states outside this region. The average is primarily one over directions of $\mathbf{k}$ and $\mathbf{k}'$ since the interaction is insensitive to the excitation energy for those transitions of importance in describing the superconducing phase. The average may also be viewed as choosing h to be a function of energy alone, thus neglecting the details of band structure. The laws of similarity indicate this to be a reasonable assumption and the good agreement of our theory with a wide class of superconductors supports this view.

Introduction of the average matrix element into (2.33) leads to

$$h_{\mathrm{k}} = \frac{1}{2}\left[1 - \frac{\epsilon_{\mathrm{k}}}{(\epsilon_{\mathrm{k}}^2 + \epsilon_0^2)^{\frac{1}{2}}}\right], \tag{2.35}$$

and

$$\left[h_{\mathrm{k}}\,(1-h_{\mathrm{k}})\right]^{\frac{1}{2}} = \frac{\epsilon_0}{2\,(\epsilon_{\mathrm{k}}^2 + \epsilon_0^2)^{\frac{1}{2}}}, \tag{2.36}$$

where

$$\epsilon_0 = V \sum_{\mathrm{k}'} \left[h_{\mathrm{k}'} \left(1 - h_{\mathrm{k}'}\right)\right]^{\frac{1}{2}}, \tag{2.37}$$

the sum extending over states within the range $|\epsilon_{\mathrm{k}}| < \hbar\omega$. If (2.36) and (2.37) are combined, one obtains a condition on ϵ_0 :

$$\frac{1}{V} = \sum_{\mathbf{k}} \frac{1}{2\left(\epsilon_{\mathbf{k}}^2 + \epsilon_0^2\right)^{\frac{1}{2}}} \tag{2.38}$$

Replacing the sum by an integral and recalling that $V = 0$ for $|\epsilon_{\mathrm{k}}| > \hbar\omega$, we may replace this condition by

$$\frac{1}{N(0)V} = \int_0^{\hbar\omega} \frac{d\epsilon}{\left(\epsilon^2 + \epsilon_0^2\right)^{\frac{1}{2}}} \tag{2.39}$$

Solving for ϵ_0, we obtain

$$\epsilon_0 = \hbar\omega / \sinh\left[\frac{1}{N(0)V}\right] \tag{2.40}$$

where $N(0)$ is the density of Bloch states of one spin per unit energy at the Fermi surface.

The ground state energy is obtained by combining the expressions for h_{k} and ϵ_0, (2.35), (2.36), and (2.37), with (2.32). We find

$$\begin{aligned} W_0 &= 4N(0) \int_0^{\hbar\omega} \epsilon h(\epsilon) d\epsilon - \frac{\epsilon_0^2}{V} \\ &= 2N(0) \int_0^{\hbar\omega} \left[\epsilon - \frac{\epsilon^2}{\left(\epsilon^2 + \epsilon_0^2\right)^{\frac{1}{2}}}\right] d\epsilon - \frac{\epsilon_0^2}{V} \end{aligned} \tag{2.41}$$

where we have used the fact that $[1 - h(-\epsilon)] = h(\epsilon)$, that is, the distribution function is symmetric in electrons and holes with respect to the Fermi surface.

Using the relations (2.40), we find that the difference in energy between the superconducting and normal states at the absolute zero becomes
$W_0 = N(0)(\hbar\omega)^2 \left\{1 - \left[1 + \left(\frac{\epsilon_0}{\hbar\omega}\right)^2\right]^{\frac{1}{2}}\right\} = \frac{-2N(0)(\hbar\omega)^2}{e^{[2/N(0)V]} - 1}$.

If there is a net negative interaction on the average, no matter how weak, there exists a coherent state which is lower in energy than the normal state. Thus our criterion for superconductivity is that $V > 0$, as given in (2.6).

For excitations which are small compared to $\hbar\omega$, the phonon interaction is essentially independent of isotopic mass and therefore the total mass dependence of W_0 comes from $(\hbar\omega)^2$, in agreement with the isotope effect. Empirically, W_0 is of the order of $N(0)\left(kT_c\right)^2$ and in general kT_c is much less than $\hbar\omega$. According to (2.42), this will occur if $N(0)V < 1$, that is, the weak coupling limit.

It should be noted that the ground state energy cannot be obtained in any finite-order perturbation theory. In the strong-coupling limit, (2.42) gives the correct result, $-N(0)(\hbar\omega)^2 V$, for the average interaction approximation and it is possible that our solution is accurate in the statistical limit over the entire range of coupling. (See Appendix A.)

In the weak-coupling limit, the energy becomes

$$W_0 = -2N(0)(\hbar\omega)^2 \exp\left[-\frac{2}{N(0)V}\right] \tag{2.43}$$

which may be expressed in terms of the number of electrons, n_c, in pairs virtually excited above the Fermi surface as

$$W_0 = -\frac{1}{2} n_c^2 / N(0), \tag{2.44}$$

where

$$n_c = 2N(0)\hbar\omega \exp\left[-\frac{1}{N(0)V}\right] \tag{2.45}$$

In this form, the cooperative nature of the ground state is evident. Using the empirical order of magnitude relation between W_0 and kT_c, we might estimate

$$kT_c \sim \hbar\omega \exp\left[-\frac{1}{N(0)V}\right]. \tag{2.46}$$

In the next chapter we shall see that the explicit calculation of kT_c from the free energy as a function of temperature leads to nearly this result.

Energy gap at $T = 0°\mathrm{K}$

An important feature of the reduced Hamiltonian is that there are no excitations from the ground state, analogous to single-particle excitations of the Bloch theory, with vanishing excitation energy. This is easily
seen by considering a function

$$\Psi_{\mathrm{exc}} = \left\{ \prod_{\mathrm{k} \neq \mathrm{k}', \mathrm{k}''} \left[(1 - h_{\mathrm{k}})^{\frac{1}{2}} + h_{\mathrm{k}^2}^{\frac{1}{2}} b_{\mathrm{k}} * \right] \right\} c_{-\mathrm{k}'\downarrow} * c_{\mathrm{k}'\prime\uparrow} * \Phi_0 \tag{2.47}$$

which is orthogonal to the ground state function and corresponds to breaking up a pair in $\mathbf{k}'$, the spin-up member going to $\mathbf{k}'' \uparrow$. The projection of Ψ_{exc} onto the space with N pairs is also orthogonal to Ψ_0. The decomposition of $\Psi_{N\,\mathrm{exc}}$ is the same as that of Ψ_0, except that $-\mathbf{k}' \downarrow$ and $\mathbf{k}'' \uparrow$ are definitely known to be occupied and $\mathbf{k}' \uparrow$ and $-\mathbf{k}'' \downarrow$ are unoccupied. This leads to the excitation energy

$$\begin{aligned} W_{\mathbf{k}',\mathbf{k}''} - W_0 = {} & \epsilon_{\mathrm{k}'} (1 - 2h_{\mathrm{k}'}) + \epsilon_{\mathrm{k}''} (1 - 2h_{\mathrm{k}''}) \\ & + 2V \sum_{\mathbf{k}} \left[h_{\mathrm{k}} (1 - h_{\mathrm{k}}) \right]^{\frac{1}{2}} \left\{ \left[h_{\mathrm{k}'} (1 - h_{\mathrm{k}'}) \right]^{\frac{1}{2}} \right. \\ & \left. + \left[h_{\mathrm{k}''} (1 - h_{\mathrm{k}''}) \right]^{\frac{1}{2}} \right\} \end{aligned} \tag{2.48}$$

the decrease in interaction energy arising from the fact that pairs cannot make transitions into or out of pair states $\mathbf{k}'$ and $\mathbf{k}''$ in the excited function because these states are occupied by single particles. Combining (2.35), (2.36), and (2.37) with (2.48), we find

$$\begin{aligned} W_{\mathrm{k}',\mathrm{k}''} - W_0 = {} & \frac{{\epsilon_{\mathrm{k}'}}^2}{E_{\mathrm{k}'}} + \frac{{\epsilon_{\mathrm{k}''}}^2}{E_{\mathrm{k}''}} + \epsilon_0^2 \left(\frac{1}{E_{\mathrm{k}'}} + \frac{1}{E_{\mathrm{k}''}} \right) \\ & = E_{\mathrm{k}'} + E_{\mathrm{k}''} \end{aligned} \tag{2.49}$$

where

$$E_{\mathrm{k}} = \left(\epsilon_{\mathrm{k}}^2 + \epsilon_0^2 \right)^{\frac{1}{2}} \tag{2.50}$$

When $\epsilon_k \to 0$, then $E_k \to \epsilon_0$ and (2.49) shows that the minimum excitation energy is $2\epsilon_0$. These single-particlelike excitations have the new dispersion law (2.50) which goes over to the normal law when $\epsilon_k \gg \epsilon_0$.

To obtain a complete set of excitations, we must include excited state pair functions generated by

$$\left[(1-h_k)^{\frac{1}{2}} b_k^* - h_k^{\frac{1}{2}}\right], \tag{2.51}$$

which by construction are orthogonal to the ground state pair functions generated by

$$\left[(1-h_k)^{\frac{1}{2}} + h_k^{\frac{1}{2}} b_k^*\right]. \tag{2.52}$$

The decomposition of an excited state with an excited pair in $\mathbf{k}'$ and a ground pair in $\mathbf{k}$ would be

$$\begin{aligned}\Psi_{k'} = {} & [h_k (1-h_{k'})]^{\frac{1}{2}} \varphi_{11} - [h_k h_{k'}]^{\frac{1}{2}} \varphi_{10} \\ & + [(1-h_k)(1-h_{k'})]^{\frac{1}{2}} \varphi_{01} - [(1-h_k) h_{k'}]^{\frac{1}{2}} \varphi_{00}\end{aligned} \tag{2.53}$$

where the functions φ are normalized and the second script denotes the occupancy of $\mathbf{k}'$. Taking the expectation value of H_{red} with respect to (2.53), we find the energy to form an excited pair in state $\mathbf{k}'$ is:

$$\begin{aligned}W_{k'} - W_0 = {} & 2\epsilon_{k'}(1-2h_{k'}) \\ & + 4V \sum_k [h_k (1-h_k) h_{k'} (1-h_{k'})]^{\frac{1}{2}} = 2E_{k'}\end{aligned} \tag{2.54}$$

Again the minimum energy required to form an excitation is $2\epsilon_0$ and an energy gap of width $2\epsilon_0$ appears in
the excitation spectrum in a natural way. It follows that in general the energy difference between two states, 1 and 2, is given by the difference in the sums of the excited-particle energies,

$$W_1 - W_2 = \sum_1 E_k - \sum_2 E_k \tag{2.55}$$

and it is unnecessary to distinguish between single particles and two members of an excited pair in calculating the sums.

Collective excitations corresponding to long-range density fluctuations are suppressed by the subsidiary condition on the wave function resulting from the collective description of the electron-ion interaction. [16] The effect of the terms neglected in the Hamiltonian, $H - H_{\text{red}} = H'$, can be estimated by a perturbation expansion of H' in eigenfunctions of H_{red}. This expansion is carried out to second order in Appendix A and it is concluded that H' will contribute little to the condensation energy. The shift in the zero-point energy of the lattice associated with the transition at the absolute zero is estimated in Appendix B and it is shown that this effect contributes a small correction to W_0. The electron self-energy shift has not been calculated at the present time; however, it is also believed that the correction is small.

3.10.8 Original 1957 BCS Paper: Excited States

III. EXCITED STATES

An excited state of the system will be formed by specifying the set of states, $\mathcal{S}$, which are occupied by single particles and the set of states, $\mathcal{P}$, occupied by excited pairs. The rest

of the states, $\mathcal{G}$, will be available for occupation by ground pairs. The term "singleparticle" occupation means that either $\mathbf{k}\uparrow$ or $-\mathbf{k}\downarrow$ is occupied by an electron, but not both. "Excited pair" and "ground pair" occupation refers to pairs which are in functions generated by operators of the form (2.51) and (2.52) respectively. Wave functions with different distributions of single particles and excited pairs are orthogonal to each other and the totality of such functions constitutes a complete set of excited states which are in one-to-one correspondence with the Bloch-type excitations in the normal metal.

The energy of the excited states will be evaluated by using the reduced Hamiltonian plus the Bloch energy for single particles:

$$H_e = \sum_{k>k_F,\sigma} \epsilon_{\mathrm{k}} n_{\mathrm{k}\sigma} + \sum_{k<k_F,\sigma} |\epsilon_{\mathrm{k}}| \left(1 - n_{\mathrm{k}\sigma}\right) - \sum_{\mathbf{k},\mathbf{k}'} V_{\mathbf{k}\mathbf{k}'} b_{\mathbf{k}'} * b_{\mathbf{k}} \tag{3.1}$$

where the second term gives the Bloch energy of the holes and the energies ϵ_{k} are measured relative to the Fermi energy. Since H_I contains only terms for transitions by ground pairs and excited pairs, the single particles contribute only to the Bloch energy and hence they are treated as in the Bloch scheme.

The equilibrium condition of the system at a specified temperature will be determined by minimizing the free
energy with respect to the distribution function for excited particles, f, and ground pairs, h.

It turns out that h_{k} is a function of temperature and therefore excited and ground pairs are not necessarily orthogonal to each other at different temperatures, although the excited states form a complete orthonormal set at each temperature. The most probable distribution of single particles also varies with temperature and thus the great majority of states contributing to the free energy at different temperatures will be orthogonal in any event. The situation is similar to taking the lattice constant temperature dependent as a result of thermal expansion. This freedom in choosing h_{k} allows us to work in that representation which minimizes the free energy at the specified temperature.

A typical excited state wave function can be written as the projection of

$$\Psi_{\mathrm{exc}} = \prod_{\mathbf{k}(\mathcal{G})} \left[(1-h_{\mathrm{k}})^{\frac{1}{2}} + h_{\mathrm{k}^2}^{\frac{1}{2}} b_{\mathrm{k}^2}^*\right] \prod_{\mathbf{k}'(\mathcal{P})} \left[(1-h_{\mathrm{k}'})^{\frac{1}{2}} b_{\mathrm{k}'}{}^* - h_{\mathrm{k}'}^{\frac{3}{2}}\right] \prod_{\mathbf{k}''(\mathcal{S})} c_{(\mathrm{k}'')^*\Phi_0} \tag{3.2}$$

onto the space with N pairs, where $\mathcal{G}, \mathcal{P}$, and $\mathcal{S}$ specify the states occupied by ground pairs, excited pairs, and single particles respectively and $c_{(\mathrm{k}'')}{}^*$ denotes either $\mathbf{k}''\uparrow$ or $-\mathbf{k}''\downarrow$ is included in the product. For any specified $\mathbf{k}$, this function can be decomposed into a portion with $\mathbf{k}$ occupied and a portion with $\mathbf{k}$ unoccupied. The decompositions for the three cases in which $\mathbf{k}$ is in the sets $\mathcal{G}, \mathcal{P}$, and $\mathcal{S}$ are
Ground:

$$\Psi = h_{\mathrm{k}}^{\frac{1}{2}} \varphi_1 \left(\cdots 1_{\mathrm{k}} \cdots\right) + (1-h_{\mathrm{k}})^{\frac{1}{2}} \varphi_0 \left(\cdots 0_{\mathrm{k}} \cdots\right), \tag{3.3}$$

Excited:

$$\Psi = (1-h_{\mathrm{k}})^{\frac{1}{2}} \varphi_1 \left(\cdots 1_{\mathrm{k}} \cdots\right) - h_{\mathrm{k}^2}^{\frac{1}{2}} \varphi_0 \left(\cdots 0_{\mathrm{k}} \cdots\right), \tag{3.4}$$

Single in $\mathbf{k}\uparrow$:

$$\Psi = c_{\mathrm{k}}\uparrow^{*}\varphi_0\left(\cdots 0_{\mathrm{k}}\cdots\right), \tag{3.5}$$

where the φ 's are normalized functions with 1_{k} representing pair state k being occupied and 0_{k} unoccupied.

To determine the distribution functions, we need the free energy

$$F = W - TS \tag{3.6}$$

where W is the energy calculated by an ensemble average over the wave functions of the form (3.2) and S is the entropy.

To enumerate the systems in the ensemble we divide k-space into cells $\Delta\mathbf{k}$ containing $\mathfrak{I}_k$ pair states as before. Let there be S_{k} single particles and P_{k} excited pairs in $\Delta\mathbf{k}$, with the rest of the $\mathfrak{N}_{\mathbf{k}}$ states being occupied by ground pairs. The probability that either $\mathbf{k}\uparrow$ or $-\mathbf{k}\downarrow$ is occupied by a single particle is $s_{\mathrm{k}} = S_{\mathrm{k}}/\mathfrak{V}_{\mathrm{k}}$, while the probability for an excited pair in state $\mathbf{k}$ is $p_{\mathrm{k}} = P_{\mathrm{k}}/\mathscr{C}_{\mathrm{k}}$ and therefore the probability for a ground pair is $(1 - s_k - p_k)$. Above the Fermi surface, $h < \frac{1}{2}$ and s
and p refer to excited electrons; below the Fermi surface, $h > \frac{1}{2}$ and s and p refer to holes.

The diagonal element of $n_{\mathrm{k}\sigma}$ follows immediately from (3.3), (3.4), and (3.5). Including the factor giving fractional number of configurations for which each decomposition applies, we have

$$\begin{aligned}
(\psi\,|n_{\mathrm{k}\sigma}|\,\psi) &= (1/2)s_{\mathrm{k}} + p_{\mathrm{k}}\,(1-h_{\mathrm{k}}) \\
&\quad + (1 - s_{\mathrm{k}} - p_{\mathrm{k}})\,h_{\mathrm{k}}, \quad \epsilon > 0; \\
(\psi\,|1-n_{\mathrm{k}\sigma}|\,\psi) &= (1/2)s_{\mathrm{k}} + p_{\mathrm{k}}h_{\mathrm{k}} \\
&\quad + (1 - s_{\mathrm{k}} - p_{\mathrm{k}})\,(1-h_{\mathrm{k}}), \quad \epsilon < 0.
\end{aligned} \tag{3.7}$$

Upon using (3.7) and the fact that $1 - h_{\mathrm{k}}(-\epsilon) = h_{\mathrm{k}}(\epsilon)$, the Bloch energy contribution to W,

$$\left(\psi\left|\sum_{\mathrm{k}>k_F\sigma}\epsilon_{\mathrm{k}}n_{\mathrm{k}\sigma} + \sum_{\mathrm{k}<k_F\sigma}\right|\epsilon_{\mathrm{k}}\,|(1-n_{\mathrm{k}\sigma})|\,\psi\right), \tag{3.8}$$

becomes
$W_{\mathrm{KE}} = \sum_{\mathrm{k}}|\epsilon_{\mathrm{k}}|\,[s_{\mathrm{k}} + 2p_{\mathrm{k}} + 2\,(1 - s_{\mathrm{k}} - 2p_{\mathrm{k}})\,h_{\mathrm{k}}\,(|\epsilon_{\mathrm{k}}|)]$,
where we have carried out the spin sum.

To calculate the matrix elements of the pair interaction operator $\sum V_{\mathrm{kk}'}b_{\mathrm{k}'}{}^{*}b_{\mathrm{k}}$, we assume that $V_{\mathrm{kk}'}$ varies continuously with $\mathbf{k}$ and $\mathbf{k}'$ so that $V_{\mathbf{kk}'}$ may be considered to be the same for all transitions from states in $\Delta\mathbf{k}$ to states in $\Delta\mathbf{k}'$. Let $\mathbf{k}$ and $\mathbf{k}'$ represent two specified wave vectors in $\Delta\mathbf{k}$ and $\Delta\mathbf{k}'$. To obtain nonvanishing matrix elements for $b_{\mathrm{k}'}{}^{*}b_{\mathrm{k}}$, these states must be occupied by either excited (-) or ground (+) pairs, giving the four possibilities,,,+−+−+− for $\mathbf{k}$ and $\mathbf{k}'$, respectively. For any one of these cases, a typical wave function may be decomposed into components in which the pair occupancy of $\mathbf{k}$ and $\mathbf{k}'$ is specified:

$$\begin{aligned}
\Psi_{\mathrm{k},\mathrm{k}'} = \alpha_{11}\varphi_{11}(&\cdots 1_{\mathrm{k}}\cdots 1_{\mathrm{k}'}\cdots) \\
&+ \alpha_{10}\varphi_{10}\,(\cdots 1_{\mathrm{k}}\cdots 0_{\mathrm{k}'}\cdots) \\
&+ \alpha_{01}\varphi_{01}\,(\cdots 0_{\mathrm{k}}\cdots 1_{\mathrm{k}'}\cdots) \\
&+ \alpha_{00}\varphi_{00}\,(\cdots 0_{\mathrm{k}}\cdots 0_{\mathrm{k}'}\cdots)
\end{aligned} \tag{3.10}$$

where the φ 's are normalized functions. Table I gives the values of the α 's for the different cases along with the fractional number of configurations for which they apply.

The diagonal elements of $b_{\mathrm{k}'}, {}^{*}b_{\mathrm{k}}$ are given by $\alpha_{10}\alpha_{01}$ in each case. If we sum these, weighted according to the probability they occur in the ensemble, we obtain

$$\begin{aligned}
&[h(1-h)h'(1-h')]^{\frac{1}{2}}\{(1-s-p)(1-s'-p') \\
&+pp'-(1-s-p)p'-p(1-s'-p')\} \\
&\quad=[h(1-h)h'(1-h')]^{\frac{1}{2}} \\
&\quad\times\{(1-s-2p)(1-s'-2p')\} \qquad (3.11)
\end{aligned}$$

Introducing these matrix elements into the ensemble average of the interaction Hamiltonian, we find

$$\begin{aligned}
W_I=-\sum_{\mathrm{k},\mathrm{k}'}V_{\mathrm{k}\mathrm{k}'}&[h_{\mathrm{k}}(1-h_{\mathrm{k}})h_{\mathrm{k}'}(1-h_{\mathrm{k}'})]^{\frac{1}{2}} \\
&\times\{(1-s_{\mathrm{k}}-2p_{\mathrm{k}})(1-s_{\mathrm{k}'}-2p_{\mathrm{k}'})\}. \qquad (3.12)
\end{aligned}$$

Table I. Coefficients for the decomposition of Ψ according to Eq. (3.10).

Wave function						
k	$\mathbf{k'}$	Fractional No. of cases	α_{11}	$\boldsymbol{\alpha_{10}}$	α_{01}	α_{00}
+	+	$(1-s-p)(1-s'-p')$	$[hh']^{\frac{1}{2}}$	$[h(1-h')]^{\frac{1}{2}}$	$[(1-h)h']^{\frac{1}{2}}$	$[(1-h)($
-	-	pp'	$[(1-h)(1-h')]^{\frac{1}{2}}$	$-[(1-h)h']^{\frac{1}{2}}$	$-[h(1-h')]^{\frac{1}{2}}$	$[hh']^{\frac{1}{2}}$
+	-	$(1-s-p)p'$	$[h(1-h')]^{\frac{1}{2}}$	$-[hh']^{\frac{1}{2}}$	$[(1-h)(1-h')]^{\frac{1}{2}}$	$-[(1-h$
-	+	$p(1-s'-p')$	$[(1-h)h']^{\frac{1}{2}}$	$[(1-h)(1-h')]^{\frac{1}{2}}$	$-[hh']^{\frac{1}{2}}$	$-[h(1-$

It should be noted that the Bloch energy (3.9) and the interaction energy (3.12) depend on ($s+2p$) or the total occupancy probability. The energy does not depend upon the relative probability for single-particle and excited-pair occupation. Thus one may use a distribution function f which gives the over-all probability of occupancy, where

$$s_{\mathrm{k}}=2f_{\mathrm{k}}(1-f_{\mathrm{k}}), \qquad (3.13)$$

and

$$p_{\mathrm{k}}=f_{\mathrm{k}}^2, \qquad (3.14)$$

which follows from the fact that s_{k} is the probability that either $\mathbf{k}\uparrow$ is occupied and $-\mathbf{k}\downarrow$ is empty or the reverse and $p_{\mathbf{k}}$ is the probability that both $\mathbf{k}\uparrow$ and $-\mathbf{k}\downarrow$ are occupied. The free energy can be minimized directly with respect to $h_{\mathrm{k}}, p_{\mathrm{k}}$, and s_{k} without introducing f_{k} and one indeed finds that (3.13) and (3.14) hold.

Since the excited particles are specified independently for each system in the ensemble, the usual expression for the entropy in terms of f may be used:
$-TS=2kT\sum_{\mathrm{k}'}\{f_{\mathrm{k}'}\ln f_{\mathrm{k}'}+(1-f_{\mathrm{k}'})\ln(1-f_{\mathrm{k}'})\}$.

Minimization of the Free Energy

If the expressions (3.13) and (3.14) are introduced into (3.9) and (3.12), the free energy becomes

$$F = 2\sum_{\mathbf{k}} |\epsilon_{\mathbf{k}}| \left[f_{\mathbf{k}} + (1-2f_{\mathbf{k}})\, h_{\mathbf{k}}\left(|\epsilon_{\mathbf{k}}|\right)\right]$$
$$- \sum_{\mathbf{k},\mathbf{k}'} V_{\mathbf{k}\mathbf{k}'} \left[h_{\mathbf{k}}\left(1-h_{\mathbf{k}}\right) h_{\mathbf{k}'}\left(1-h_{\mathbf{k}'}\right)\right]^{\frac{1}{3}}$$
$$\times \left\{\left(1-2f_{\mathbf{k}}\right)\left(1-2f_{\mathbf{k}'}\right)\right\} - TS \tag{3.16}$$

When we minimize F with respect to h_{k}, we find that

$$2\epsilon_{\mathrm{k}} - \sum_{\mathrm{k}'} V_{\mathrm{k}\mathrm{k}'} \left[h_{\mathrm{k}'}\left(1-h_{\mathrm{k}'}\right)\right]^{\frac{1}{2}} \left(1-2f_{\mathrm{k}'}\right)$$
$$\times \frac{\left(1-2h_{\mathrm{k}}\right)}{\left[h_{\mathrm{k}}\left(1-h_{\mathrm{k}}\right)\right]^{\frac{1}{2}}} = 0, \tag{3.17}$$

or

$$\frac{\left[h_{\mathrm{k}}\left(1-h_{\mathrm{k}}\right)\right]^{\frac{1}{2}}}{1-2h_{\mathrm{k}}} = \sum_{\mathrm{k}'} \frac{V_{\mathrm{k}\mathrm{k}'}\left[h_{\mathrm{k}'}\left(1-h_{\mathrm{k}'}\right)\right]^{\frac{1}{2}}\left(1-2f_{\mathrm{k}'}\right)}{2\epsilon_{\mathrm{k}}}, \tag{3.18}$$

where the energy ϵ_{k} is measured relative to the Fermi energy and $\epsilon_{\mathrm{k}} < 0$ for $k = k_F$. Assuming as before that the interaction can be replaced by a constant average matrix element $-V$, defined by (2.34) for $|\epsilon_{\mathrm{k}}| < \hbar\omega$ and by zero outside this region, it follows that h_{k} is again of the form

$$h_{\mathrm{k}} = \frac{1}{2}\left[1 - \left(\epsilon_{\mathrm{k}}/E_{\mathrm{k}}\right)\right], \tag{3.19}$$

and

$$\left[h_{\mathrm{k}}\left(1-h_{\mathrm{k}}\right)\right]^{\frac{1}{2}} = \frac{1}{2}\epsilon_0/E_{\mathrm{k}}. \tag{3.20}$$

The energy E_{k}, a positive definite quantity, is defined as

$$E_{\mathrm{k}} = +\left(\epsilon_{\mathrm{k}}^2 + \epsilon_0^2\right)^{\frac{1}{2}}, \tag{3.21}$$

where

$$\epsilon_0 = V\sum_{\mathrm{k}'} \left[h_{\mathrm{k}'}\left(1-h_{\mathrm{k}'}\right)\right]^{\frac{1}{2}}\left(1-2f_{\mathrm{k}'}\right) \tag{3.22}$$

It will turn out that $2\epsilon_0$ is the magnitude of the energy gap in the single-particle density of states and therefore the distribution of ground pairs is determined by the magnitude of the gap at that temperature.

When we minimize F with respect to f_{k}, we find that

$$2\epsilon_{\mathrm{k}}\left(1-2h_{\mathrm{k}}\right) + 4\sum_{\mathrm{k}'} V_{\mathrm{k}\mathrm{k}'}\left[h_{\mathrm{k}'}\left(1-h_{\mathrm{k}'}\right) h_{\mathrm{k}}\left(1-h_{\mathrm{k}}\right)\right]^{\frac{1}{2}}$$
$$\times\left(1-2f_{\mathrm{k}'}\right) + 2kT\ln\left(f_{\mathrm{k}}/\left(1-f_{\mathrm{k}}\right)\right) = 0 \tag{3.23}$$

and using (3.19) through (3.22), we find that

$$-\ln\left(f_{\mathrm{k}}/\left(1-f_{\mathrm{k}}\right)\right)=\beta\left[\frac{\epsilon_{\mathrm{k}}^{2}}{E_{\mathrm{k}}}+\frac{\epsilon_{0}^{2}}{E_{\mathrm{k}}}\right]=\beta E_{\mathrm{k}} \tag{3.24}$$

where $\beta = 1/kT$ and E_{k} is a positive quantity. The solution for f_k is

$$f_{\mathrm{k}}=\frac{1}{e^{\beta E_{\mathrm{k}}}+1}=f\left(E_{\mathrm{k}}\right). \tag{3.25}$$

Thus the single particles and excited pairs describe a set of independent fermions with the modified dispersion law (3.21). For $k > k_F$, f_{k} specifies electron occupation while for $k < k_F$, f_{k} specifies hole occupation. These electrons and holes are identified with the normal component of the two-fluid model.

When $\epsilon_{\mathrm{k}} \to 0^{+}$, then $E_{\mathrm{k}} \to \epsilon_0$ for the electron and when $\epsilon_{\mathrm{k}} \to 0^{-}$, then $E_{\mathrm{k}} \to \epsilon_0$ for the hole or the corresponding electron energy $\to -\epsilon_0$. Thus the new density of states has an energy gap of magnitude $2\epsilon_0$ centered about the Fermi energy. The modified density of states is given by

$$\frac{dN(E)}{dE}=\frac{dN(\epsilon)}{d\epsilon}\frac{d\epsilon}{dE}=N(0)\frac{E}{\left(E^{2}-\epsilon_{0}^{2}\right)^{\frac{1}{2}}}, \tag{3.26}$$

which is singular at the edges of the gap, $E = \epsilon_0$. The total number of states is of course unaltered by the interaction.

If the distribution functions (3.19) and (3.25) are introduced, the condition determining the energy gap

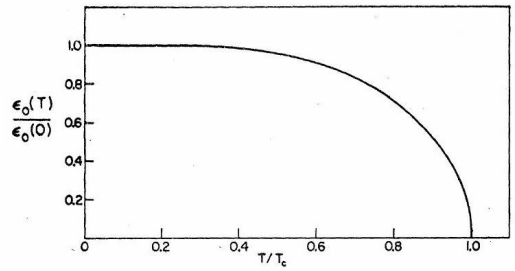


Fig. 1. Ratio of the energy gap for single-particle-like excitations to the gap at $T = 0°\mathrm{K}$ vs temperature.

(3.22) becomes (dividing by ϵ_0)

$$\frac{1}{N(0)V}=\int_{0}^{\hbar\omega}\frac{d\epsilon}{\left(\epsilon^{2}+\epsilon_{0}^{2}\right)^{\frac{1}{2}}}\tanh\left[\frac{1}{2}\beta\left(\epsilon^{2}+\epsilon_{0}^{2}\right)^{\frac{1}{2}}\right] \tag{3.27}$$

where we have replaced the sum by an integral and used the fact that the distribution functions are symmetric in holes and electrons with respect to the Fermi energy. The transition temperature, T_c, is defined as the boundary of the region beyond which there is no real, positive ϵ_0 which satisfies (3.27). Above T_c therefore, $\epsilon_0 = 0$ and $f\left(E_{\mathrm{k}}\right)$ becomes $f\left(\epsilon_{\mathrm{k}}\right)$, so that the metal returns to the normal state. Below T_c the solution of (3.27), $\epsilon_0 \neq 0$, minimizes the free energy and we have the superconducting phase. Thus (3.26) can be used to determine the critical temperature and we find

$$\frac{1}{N(0)V}=\int_{0}^{\hbar\omega}\frac{d\epsilon}{\epsilon}\tanh\left(\frac{1}{2}\beta_{c}\epsilon\right) \tag{3.28}$$

or

$$kT_{c}=1.14\hbar\omega\exp\left[-\frac{1}{N(0)V}\right] \tag{3.29}$$

as long as $kT_c \ll \hbar\omega$, which corresponds to the weakcoupling case discussed in Sec. II. The transition temperature is proportional to $\hbar\omega$, which is consistent with the isotope effect. The small magnitude of T_c compared to the Debye temperature is presumably due to the cancellation of the phonon interaction and the screened Coulomb interaction for transitions of importance in describing the superconducting state, and the resulting effect of the exponential.

The transition temperature is a strong function of the electron concentration since the density of states enters exponentially. It should be possible to make estimates of the change in transition temperature with pressure, alloying, etc., from (3.29).

A plot of the energy gap as a function of temperature is given in Fig. 1. The ratio of the energy gap at $T = 0°\mathrm{K}$ to kT_c is given by combining (2.36) and (3.28):

$$2\epsilon_0/kT_c = 3.50 \tag{3.30}$$

From the law of corresponding states, this ratio is predicted to be the same for all superconductors. Near
T_c, the gap may be expressed as

$$\epsilon_0 = 3.2kT_c\,[1 - (T/T_c)]^{\frac{1}{2}} \tag{3.31}$$

which has the form suggested by Buckingham. [33]
It can be seen from the distribution functions that our theory goes over into the Bloch scheme above the transition temperature. As $T \to T_c, E_\mathrm{k} \to |\epsilon_\mathrm{k}|$, and h_k vanishes for $k > k_F$ and is unity for $k < k_F$. According to (3.4) the excited-pair function specifies complete electron occupancy for $k > k_F$ and complete hole occupancy for $k < k_F$ in this case. Thus, in the normal state, the ground pairs vanish above the Fermi surface and form the Fermi sea below, while the single particles and excited pairs combine to describe excited electrons for $k > k_F$ and excited holes for $k < k_F$.

Critical Field and Specific Heat

The critical field for a bulk specimen of unit volume is given by

$$H_c^2/8\pi = F_n - F_s \tag{3.32}$$

where F_n is the free energy of the normal state:

$$\begin{aligned} F_n &= -4N(0)kT\int_0^\infty d\epsilon \log(1 + e^{-\beta\epsilon}) \\ &= -\frac{1}{3}\pi^2 N(0)(kT)^2 \end{aligned} \tag{3.33}$$

With the aid of (3.25) the entropy in the superconducting state, (3.15) may be expressed as

$$TS = 4kT\sum_{k>k_F}\left[\ln\left(1 + e^{-\beta E_\mathrm{k}}\right) + \beta E_\mathrm{k} f_\mathrm{k}\right] \tag{3.34}$$

Replacing the sum by an integral and performing a partial integration, we find

$$TS = 4N(0)\int_0^\infty d\epsilon \left[\frac{\epsilon^2}{E} + E\right] f(\beta E) \tag{3.35}$$

where the upper limit has been extended to infinity because $f(\beta E)$ decreases rapidly for $\beta\epsilon > 1$. If (3.34) and (3.16) are combined with the distribution functions (3.19) and (3.25), the free energy becomes

$$F_s = -4N(0)\int_0^\infty d\epsilon E f(\beta E) + 2N(0)\int_0^{\hbar\omega} d\epsilon \left[\epsilon - \frac{\epsilon^2}{E}\right] - \frac{\epsilon_0^2}{V} \tag{3.36}$$

which with the aid of (3.27) may be expressed as

$$F_s = -2N(0)\int_0^\infty d\epsilon \left[\frac{2\epsilon^2+\epsilon_0^2}{E}\right] f(\beta E) - N(0)(\hbar\omega)^2 \left\{\left[1+\left(\frac{\epsilon_0}{\hbar\omega}\right)^2\right]^{\frac{1}{2}} - 1\right\} \tag{3.37}$$

The critical field is given by combining (3.31), (3.32), and (3.37):

$$\frac{H_c^2}{8\pi} = N(0)(\hbar\omega)^2 \left\{\left[1+\left(\frac{\epsilon_0}{\hbar\omega}\right)^2\right]^{\frac{1}{2}} - 1\right\} - \frac{\pi^2}{3}N(0)(kT)^2 \times \left\{1 - \beta^2\int_0^\infty d\epsilon \left[\frac{2\epsilon^2+\epsilon_0^2}{E}\right] f(\beta E)\right\} \tag{3.38}$$

A plot of the critical field as a function of $(T/T_c)^2$ is given in Fig. 2. The curve agrees fairly well with the $1-(T/T_c)^2$ law of the Gorter-Casimir two-fluid model, [19] the maximum deviation being about four percent. There is good experimental support for a similar deviation in vanadium, thallium, indium, and tin; however, our deviation appears to be somewhat too large to fit the experimental results.

The critical field at $T = 0$ is

$$H_0 = [4\pi N(0)]^{\frac{1}{2}}\epsilon_0(0) = 1.75[4\pi N(0)]^{\frac{1}{2}}kT_c \tag{3.39}$$

where $2\epsilon_0(0)$ is the energy gap at $T = 0$ and the density of Bloch states $N(0)$ is taken for a system of unit volume.

A law of corresponding states follows from (3.39) and may be expressed as

$$\gamma T_c^2/H_0^2 = \frac{1}{6}\pi\left[kT_c/\epsilon_0(0)\right]^2 = 0.170 \tag{3.40}$$

where the electronic specific heat in the normal state is given by

$$C_{en} = \gamma T\left(\text{ergs}/^\circ\text{C cm}^3\right), \tag{3.41}$$

and

$$\gamma = \frac{2}{3}\pi^2 N(0)k^2. \tag{3.42}$$

The Gorter-Casimir model gives the value of 0.159 for the ratio (3.40). The scatter of experimental data is too great to choose one value over the other at the present time.

[33] M. J. Buckingham, Phys. Rev. 101, 1431 (1956).

Near $T = 0$, the gap is practically independent of temperature and large compared to kT, and hence for

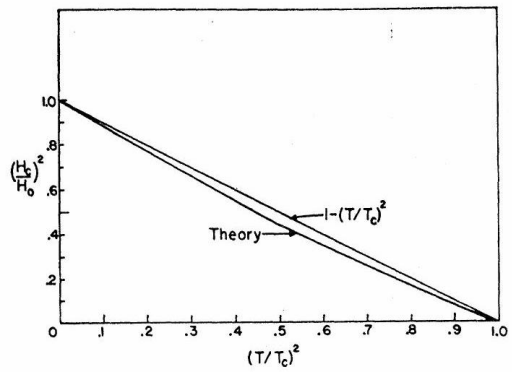


Fig. 2. Ratio of the critical field to its value at $T = 0°$K vs $(T/T_c)^2$. The upper curve is the $1 - (T/T_c)^2$ law of the GorterCasimir theory and the lower curve is the law predicted by the theory in the weak-coupling limit. Experimental values generally lie between the two curves.
$T/T_c \ll 1$ we have the relation
or

$$H_c^2 = H_0^2 \left[1 - \frac{2}{3}\pi^2 \left(kT/\epsilon_0\right)^2\right], \tag{3.43}$$

$$H_c \cong H_0 \left[1 - 1.07 \left(T/T_c\right)^2\right]. \tag{3.44}$$

This approximation corresponds to neglecting the freeenergy change of the superconducting state, the total effect coming from F_n.

The electronic specific heat is most readily obtained from the entropy, (3.34):

$$C_{es} = T\frac{dS}{dT} = -\beta\frac{dS}{d\beta} = -4k\beta \sum_{k>kF} \beta E_{\mathrm{k}} \frac{df_{\mathrm{k}}}{d\beta}, \tag{3.45}$$

or

$$C_{es} = 4k\beta^2 \sum_{k>k_F} f_{\mathrm{k}} \left(1 - f_{\mathrm{k}}\right) \left[E_{\mathrm{k}}^2 + \frac{\beta}{2}\frac{d\epsilon_0^2}{d\beta}\right] \tag{3.46}$$

The expression for C_{es} is simply interpreted as the specific heat due to electrons and holes with the modified spectrum (3.21) plus the change in condensation energy with temperature.

At the transition temperature, the energy gap vanishes and the jump in specific heat associated with the second order transition is given by

$$\begin{aligned}\left(C_{es} - C_{en}\right) \mid T_c &= 2k\beta^3 \sum_{k>kF} f_{\mathrm{k}n} \left(1 - f_{\mathrm{k}n}\right) \left[\frac{d\epsilon_0^2}{d\beta}\right]_{T_c} \\ &= kN(0)\beta_c^2 \left[\frac{d\epsilon_0^2}{d\beta}\right]_{T_c}\end{aligned} \tag{3.47}$$

where

$$f_{\mathrm{k}n} = 1/\left(e^{\beta\epsilon_{\mathrm{k}}} + 1\right) \tag{3.48}$$

The derivative $d{\epsilon_0}^2/d\beta$ can be obtained from the relation between ϵ_0 and T, (3.27). After some calculation we find

$$\left.\frac{d\epsilon_0^2}{d\beta}\right|_{T_c} = \frac{10.2}{\beta_c^3} \tag{3.49}$$

and the jump in specific heat becomes

$$\left.\frac{C_{es} - \gamma T_c}{\gamma T_c}\right|_{T_c} = 1.52 \tag{3.50}$$

The Gorter-Casimir model gives 2.00 and the Koppe theory [9] gives 1.71 for this ratio. The experimental data in general range between our value and 2.00 .

The initial slope of the critical-field curve at the transition temperature is given by the thermodynamic relation

$$\left.\frac{T_c}{4\pi}\left(\frac{dH_c}{dT}\right)^2\right|_{T_c} = (C_s - C_n)|_{T_c} \tag{3.51}$$

With use of (3.47) this becomes

$$\left.\frac{1}{\gamma}\left(\frac{dH_c}{dT}\right)^2\right|_{T_c} = 19.4 \tag{3.52}$$

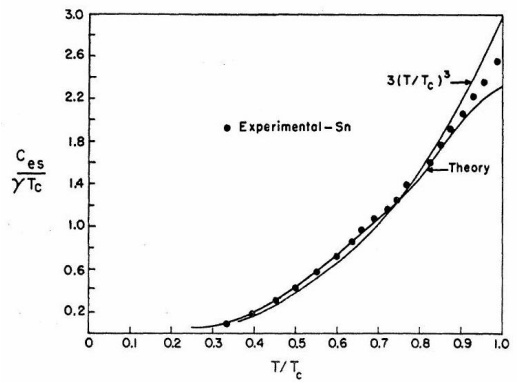


Fig. 3. Ratio of the electronic specific heat to its value in the normal state at T_c vs T/T_c for the Gorter-Casimir theory and for the present theory. Experimental values for tin are shown for comparison. Note added in proof.-The plotted theoretical curve is incorrect very near T_c; the intercept at T_c should be 2.52 .

or with (3.39),

$$\left.\frac{dH_c}{dT}\right|_{T_c} = -\frac{1.82 H_0}{T_c}. \tag{3.53}$$

When $\beta\epsilon_0 \gg 1$, the specific heat can be expressed in the form

$$\begin{aligned}\frac{C_{es}}{\gamma T_c} = \frac{3}{2\pi^2}\left(\frac{\epsilon_0}{kT_c}\right)^3\left(\frac{T_c}{T}\right)^2\left[3K_1(\beta\epsilon_0) + K_3(\beta\epsilon_0)\right] \\ \cong 8.5 e^{-1.44 T_c/T}\end{aligned} \tag{3.54}$$

where K_n is the modified Bessel function of the second kind.

The ratio $C_{es}/(\gamma T_c)$ is plotted in Fig. 3 from (3.46) and compared with the T^3 law and the experimental values for tin. The agreement is rather good except near T_c where our specific heat is somewhat too small. The logarithm of the same ratio is plotted in Fig. 4 to bring out the experimental deviation from the T^3 law. The recent work of Goodman et al. [20] shows that the data for tin and vanadium fit the law:

$$C_{es}/\left(\gamma T_c\right) = ae^{-bT_c/T} \tag{3.55}$$

with high accuracy for $T_c/T > 1.4$, where $a = 9.10$ and $b = 1.50$. These values are in good agreement with our results in this region, (3.54).

Thus we see that our theory predicts the thermodynamic properties of a superconductor quite accurately and in particular gives an exponential specific heat for $T/T_c \ll 1$ and explicitly exhibits a second-order phase transition in the absence of a magnetic field.

3.10.9 Original 1957 BCS Paper: Calculation of Matrix Elements

IV. CALCULATION OF MATRIX ELEMENTS

There are many problems for which one would like to determine matrix elements of a single-particle scattering operator of the form $U = \sum_j H_j$, where H_j involves only the coordinates of particle j. In terms of creation and destruction operators,

$$U = \sum_j H_j = \sum_{\mathbf{k},\mathbf{k}',\sigma,\sigma'} B_{\mathbf{k}\sigma\mathbf{k}'\sigma'} C_{\mathbf{k}'\sigma'} * C_{\mathbf{k}\sigma} \tag{4.1}$$

where

$$B_{\mathrm{k}\sigma\mathrm{k}'\sigma'} = \int \psi_{\mathrm{k}'\sigma'} * H_j \psi_{\mathrm{k}\sigma} d\tau_j \tag{4.2}$$

is the matrix element for scattering of a single electron from $\mathbf{k}\sigma$ to $\mathbf{k}'\sigma'$. In this section we shall determine matrix elements of U between two of our many-particle excited-state wave functions for a superconductor and give tables which should be useful for application to perturbation theory and transport problems. We first give a brief review of the corresponding problems for the normal state.

The matrix element of ${c_{\mathrm{k}'\sigma'}}^* c_{\mathrm{k}\sigma}$ between two normal state configurations is zero unless the occupation numbers differ only in transfer of an electron from $\mathbf{k}\sigma$ in the initial to $\mathbf{k}'\sigma'$ in the final configuration, in which case it is unity. If one wishes to calculate the probability that at temperature T an electron be scattered from a state of spin σ in an element $\Delta\mathbf{k}$ to one of spin σ' in $\Delta\mathbf{k}'$, one must multiply the usual single-particle expression by $f\left(1-f'\right)$, the probability that $\mathbf{k}\sigma$ be occupied and $\mathbf{k}'\sigma'$ unoccupied in a typical initial configuration. A similar factor occurs in the second-order perturbation theory expansion of U :

$$\sum_{\mathrm{k},\sigma,\mathrm{k}',\sigma'} \frac{\left|B_{\mathrm{k}\sigma\mathrm{k}'\sigma'}\right|^2 f\left(1-f'\right)}{\epsilon-\epsilon'}. \tag{4.3}$$

If H_j is independent of spin, $\sigma' = \sigma$ and the sum reduces to

$$2\sum_{\mathbf{k},\mathbf{k}'} \frac{\left|B_{\mathrm{k}\mathrm{k}'}\right|^2 f\left(1-f'\right)}{\epsilon-\epsilon'} = -\sum_{\mathbf{k},\mathbf{k}'} \left|B_{\mathbf{k}\mathbf{k}'}\right|^2 \left(\frac{f'-f}{\epsilon-\epsilon'}\right) \tag{4.4}$$

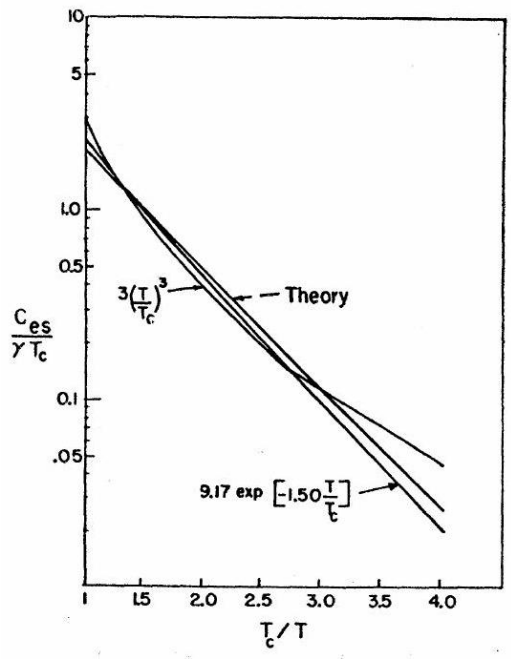


Fig. 4. A logarithmic plot of the ratio of the electronic specific heat to its value in the normal state at T_c vs T_c/T. The simple exponential fits the experimental data for tin and vanadium well for $T_c/T > 1.4$.

Table II. Matrix elements of single-particle scattering operator.

Wave functions [a]							
Initial, Ψ_i		Final, Ψ_f		Ground (+)		Energy	
(k ↑, ($\mathbf{k}'$ ↑, −k ↓), $-k'$ ↓)		(k ↑, $-k$ ↓),			k $\mathbf{k}'$	difference $W_i - W_f$	Probability of initi
				+	+	$E - E'$	$\frac{1}{2}s\,(1 - s' - p')$
X0	00	00	X0	-	-	$E' - E$	$\frac{1}{2}sp'$
X0	XX	XX	X0	+	-	$E + E$	$\frac{1}{2}sp'$
				-	+	$-\,(E + E')$	$\frac{1}{2}s\,(1 - s' - p')$
	(b)			+	+	$E' - E$	$\frac{1}{2}s'(1 - s - p)$
XX 00		$0X$	XX	-	-	$E - E'$	$\frac{1}{2}s'p$
	$0X$	$0X$	00	+	-	$-\,(E + E')$	$\frac{1}{2}s'(1 - s - p)$
				-	+	$E + E'$	$\frac{1}{2}s'p$
	(c)			+	+	$E + E'$	$\frac{1}{4}ss'$
X0		00	XX	-	-	$-\,(E + E')$	$\frac{1}{4}ss'$
		XX	00	+	-	$E - E'$	$\frac{1}{4}ss'$
				-	+	$E' - E$	$\frac{1}{4}ss'$
	(d)			+	+	$-\,(E + E')$	$(1 - s - p)\,(1 - s'$
XX 00	00	$0X$	X0	-	-	$E + E'$	pp'
	XX			+	-	$E' - E$	$(1 - s - p)p'$
				-	+	$E - E'$	$p\,(1 - s' - p')$

[a] For transitions which change spin, reverse designations of ($\mathbf{k}' \uparrow, -\mathbf{k}' \downarrow$) in the initial and in the final states.

The factor of two comes from the sum over spins in the initial configuration and the second form from the fact that $|B_{\mathbf{k}\mathbf{k}'}|^2$ is symmetric in $\mathbf{k}$ and $\mathbf{k}'$.

The calculation of the corresponding factors for the superconducting case is complicated by the fact that any given state $\mathbf{k}\sigma$ may be occupied singly or by either ground or excited pairs, and these possibilities must be weighted by the probability that they occur in a typical initial wave function. First consider matrix elements of an operator which does not give a spin change:

$$\left(\Psi_f \left| \sum_{\mathrm{k},\mathrm{k}',\sigma} B_{\mathrm{k}\mathrm{k}'} {c_{\mathrm{k}'\sigma}}^* c_{\mathrm{k}\sigma} \right| \Psi_i \right) \tag{4.5}$$

Nonvanishing matrix elements of ${c_{\mathrm{k}'\uparrow}}^* c_{\mathrm{k}\uparrow}$ are obtained only when the single and excited-pair occupancy of Ψ_i and Ψ_f is the same except for those designated by wave vectors $\mathbf{k}$ and $\mathbf{k}'$. Further, Ψ_i must contain a configuration in which $\mathbf{k}\uparrow$ is occupied and $\mathbf{k}'\uparrow$ unoccupied and Ψ_f one in which $\mathbf{k}'\uparrow$ is occupied and $\mathbf{k}\uparrow$ unoccupied. The various possible transitions along with the matrix elements are listed in Table II. While the individual matrix elements are complicated, fairly simple results are obtained when a sum is made over all transitions in which $\mathbf{k}$ is in a volume element $\Delta\mathbf{k}$ and $\mathbf{k}'$ in $\Delta\mathbf{k}'$, it being assumed that $B_{\mathbf{k}\mathbf{k}'}$ is a continuous function of $\mathbf{k}$ and $\mathbf{k}'$.

The first type of transition, (a), listed in Table II corresponds to single occupancy of $\mathbf{k}\uparrow$ in the initial and of $\mathbf{k}'\uparrow$ in the final state. Pair occupancy of $\mathbf{k}'$ (i.e., the pair $\mathbf{k}'\uparrow, -\mathbf{k}'\downarrow$) in Ψ_i and of $\mathbf{k}$ in Ψ_f may be either excited or ground, giving the four possible combinations listed in the second column. These have components in
which the pair states $\mathbf{k}'$ in Ψ_i and $\mathbf{k}$ in Ψ_f are unoccupied, designated by $X000$ for Ψ_i and $00X0$ for Ψ_f. There is a nonvanishing matrix element of ${c_{\mathrm{k}'\uparrow}}^* c_{\mathrm{k}\uparrow}$ between these components. Other components of the same wave functions have the pair states $\mathbf{k}'$ in Ψ_i and $\mathbf{k}$ in Ψ_f occupied, as is indicated by the designations $X0XX$ and $XXX0$, respectively. While the matrix element of ${c_{k'}}^* c_k \uparrow$ between these latter vanishes, that of ${c_{-k\downarrow}}^* c_{-k'\downarrow}$ does not. Since both ${c_{\mathrm{k}'}}^* c_{\mathrm{k}} \uparrow$ and ${c_{-\mathrm{k}\downarrow}}^* c_{-\mathrm{k}'\downarrow}$ are included in the sum in (4.5), they will give coherent contributions and must be considered together. Matrix elements between these states of all other terms in the sum are zero.

Matrix elements of type (b) are for single-particle occupancy of $-\mathbf{k}'\downarrow$ in Ψ_i and of $-\mathbf{k}\downarrow$ in Ψ_f, while $\mathbf{k}$ in Ψ_i and $\mathbf{k}'$ in Ψ_f may be occupied by either excited or ground pairs. With interchange of spin and of $\mathbf{k}$ and $\mathbf{k}'$, they are similar to type (a). Type (c) represents single occupancy of $\mathbf{k}\uparrow$ and $-\mathbf{k}'\downarrow$ in Ψ_i and either excited or ground pair occupancy of both $\mathbf{k}$ and $\mathbf{k}'$ in Ψ_f. Transitions of ${c_{\mathrm{k}'\uparrow}}^* c_{\mathrm{k}} \uparrow$ are allowed for the component $00XX$ of Ψ_f and of ${c_{-\mathrm{k}\downarrow}}^* c_{-\mathrm{k}'\downarrow}$ for the component $XX00$. Again, these are coherent. Finally, type (d) represents excited or ground pair occupancy of Ψ_i and single particle occupancy of $-\mathbf{k}\downarrow, \mathbf{k}'\uparrow$ in Ψ_f.

The energy differences $W_i - W_f$ listed in the third column are obtained by taking an energy $2E$ for an excited pair, E for single occupancy, and zero for a ground pair. We have used the notation $E = E(\mathbf{k})$; $E' = E(\mathbf{k}')$, etc.

In column 4 are given the probabilities of the initial state designations, based on taking $\frac{1}{2}s$ for a specified
single occupancy, p for an excited pair, and ($1-s-p$) for a ground pair. For example, Ψ_i in the top row corresponds to $\mathbf{k}\uparrow$ occupied and a ground pair in $\mathbf{k}'$, and the fraction of the states $\mathbf{k}$ in the volume element $\Delta\mathbf{k}$ and $\mathbf{k}'$ in $\Delta\mathbf{k}'$ which have this designation is $\frac{1}{2}s(\mathbf{k})\left[1 - s(\mathbf{k}') - p(\mathbf{k}')\right]$.

To calculate the matrix elements, it is convenient to decompose the wave functions into components corresponding to definite occupancy of excited and ground pairs as in (3.10). Thus, for the top row in which $\mathbf{k}'$ in Ψ_i and $\mathbf{k}$ in Ψ_f are both ground pairs,

$$\Psi_i = c_{\mathrm{k}} \uparrow^* \left[h'^{\frac{1}{2}} \varphi_{01}(0_{\mathrm{k}}, 1_{\mathrm{k}'}) + (1-h')^{\frac{1}{2}} \varphi_{00}(0_{\mathrm{k}}, 0_{\mathrm{k}'})\right] \tag{4.6a}$$

$$\Psi_f = c_{\mathrm{k}'} \uparrow^* \left[h^{\frac{1}{2}} \varphi_{10}(1_{\mathrm{k}}, 0_{\mathrm{k}'}) + (1-h)^{\frac{1}{2}} \varphi_{00}(0_{\mathrm{k}}, 0_{\mathrm{k}'})\right] \tag{4.6b}$$

where

$$\varphi_{10} = b_{\mathrm{k}}^{*} b_{\mathrm{k}'} \varphi_{01}$$

The matrix element of $c_{\mathrm{k}'}{}^{*} c_{\mathrm{k}} \uparrow$ is

$$\begin{aligned}(\Psi_f \left| c_{\mathrm{k}'\uparrow} * c_{\mathrm{k}} \uparrow \right| \Psi_i) &= \left[(1-h)\left(1-h'\right)\right]^{\frac{1}{2}} \left(c_{\mathrm{k}'\uparrow} * \varphi_{00} \mid c_{\mathrm{k}'\uparrow}{}^{*} \varphi_{00}\right) \\ &= \left[(1-h)\left(1-h'\right)\right]^{\frac{1}{2}} \end{aligned} \tag{4.7}$$

The matrix element of $c_{-\mathrm{k}\downarrow}{}^{*} c_{-\mathrm{k}'\downarrow}$ is given by

$$\begin{aligned}&(\Psi_f \left| c_{-\mathrm{k}\downarrow} * c_{-\mathrm{k}'\downarrow} \right| \Psi_i) \\ &\quad = \left(hh'\right)^{\frac{1}{2}} \left(c_{\mathrm{k}'\uparrow} * b_{\mathrm{k}} * b_{\mathrm{k}'} \varphi_{01} \mid c_{-\mathrm{k}\downarrow} * c_{-\mathrm{k}'\downarrow} c_{\mathrm{k}} \uparrow * \varphi_{01}\right)\end{aligned} \tag{4.8}$$

Since

$$c_{\mathrm{k}'\uparrow}{}^{*} b_{\mathrm{k}} * b_{\mathrm{k}'} \varphi_{01} = -c_{-\mathrm{k}'\downarrow} b_{\mathrm{k}}{}^{*} \varphi_{01} \tag{4.9}$$

$$c_{-\mathrm{k}\downarrow}{}^{*} c_{-\mathrm{k}'\downarrow} c_{\mathrm{k}} \uparrow^{*} \varphi_{01} = c_{-\mathrm{k}'\downarrow} b_{\mathrm{k}}{}^{*} \varphi_{01} \tag{4.10}$$

the matrix element is $-\left(hh'\right)^{\frac{1}{2}}$. The other matrix elements of types (a) and (b) may be calculated in a similar manner.

For types (c) and (d) we make use of the decomposition (3.10). For example, for type (d),

$$\begin{aligned}\Psi_i = \alpha_{11}\varphi_{11}\left(1_{\mathrm{k}}, 1_{\mathrm{k}'}\right) + \alpha_{10}\varphi_{10}\left(1_{\mathrm{k}}, 0_{\mathrm{k}'}\right) \\ + \alpha_{01}\varphi_{01}\left(0_{\mathrm{k}}, 1_{\mathrm{k}'}\right) + \alpha_{00}\varphi_{00}\left(0_{\mathrm{k}}, 0_{\mathrm{k}'}\right)\end{aligned} \tag{4.11}$$

where the α 's are as listed in Table I. The final wave function is

$$\Psi_f = c_{\mathrm{k}'\uparrow} * c_{\mathrm{k}\uparrow} \uparrow \varphi_{10} \tag{4.12}$$

Thus the matrix element of $c_{\mathrm{k}'}|^{*} c_{\mathrm{k}} \uparrow$ is just α_{10}. The matrix element of $c_{-\mathrm{k}\downarrow}{}^{*} c_{-\mathrm{k}'\downarrow}$ is found from

$$\begin{aligned}c_{-\mathrm{k}\downarrow} * c_{-\mathrm{k}'\downarrow} \varphi_{01} &= c_{-\mathrm{k}\downarrow} * c_{-\mathrm{k}'\downarrow} b_{\mathrm{k}'} * b_{\mathrm{k}} \varphi_{10} \\ &= c_{\mathrm{k}'\uparrow} * c_{\mathrm{k}} \uparrow \varphi_{10},\end{aligned} \tag{4.13}$$

so that we find

$$(\Psi_f \left| c_{-\mathrm{k}\downarrow}{}^{*} c_{-\mathrm{k}'\downarrow} \right| \Psi_i) = \alpha_{01} \tag{4.14}$$

Those for type (c) can be obtained by interchanging initial and final states and spin up and spin down.

We have so far assumed a spin-independent interaction. One involving a spin flip may be treated by exactly similar methods. Initial and final states differ from the parallel spin case by interchange of spin designation of $\mathbf{k}'$ in the initial and in the final state. There is a coherence between the matrix elements for $c_{-k'} \downarrow^{*} c_{k} \uparrow$ and
$c_{-\mathrm{k}}{}^{*} c_{\mathrm{k}'} \uparrow$. They are the same as the corresponding matrix elements for parallel spin, except for

a reversal of sign of the reverse spin transitions. For example, for the type (a) transition of the top row, the final state is now

$$\Psi_f = c_{-\mathrm{k}'\downarrow^*}\left[h^{\frac{1}{2}}\varphi_{10}\left(1_\mathrm{k}, 0_{\mathrm{k}'}\right) + (1-h)^{\frac{1}{2}}\varphi_{00}\left(0_\mathrm{k}, 0_{\mathrm{k}'}\right)\right] \tag{4.15}$$

The matrix element of $c_{-\mathrm{k}'\downarrow}{}^* c_\mathrm{k} \uparrow$ is $\left[(1-h)(1-h')\right]^{\frac{1}{2}}$ as before. To obtain matrix element of $c_{-k} \downarrow^* c_{k'} \uparrow$, we now have, corresponding to (4.9) and (4.10),

$$c^*_{-\mathrm{k}'\downarrow^*} b_{\mathrm{k}'} b^*_\mathrm{k} \varphi_{01} = c_{\mathrm{k}'\uparrow} \uparrow b^*_\mathrm{k}\varphi_{01}$$
$$c_{-\mathrm{k}\downarrow}{}^* c_{\mathrm{k}'} \uparrow c_\mathrm{k} \uparrow^* \varphi_{01} = c_{\mathrm{k}'\uparrow} b^*_\mathrm{k}\varphi_{01}$$

giving $+(hh')^{\frac{1}{2}}$. We have indicated the change in sign in the table by listing $-c_{-\mathrm{k}\downarrow}{}^* c_{\mathrm{k}'} \uparrow$ at the top of column 6.
In a second-order perturbation theory calculation, one is interested in determining

$$\sum_f \frac{\left|\left(\Psi_f \left| \sum_{\mathbf{k},\mathbf{k}',\sigma} B_{\mathrm{k}\mathrm{k}'} c_{\mathrm{k}'\sigma}{}^* c_{\mathrm{k}\sigma} \right| \Psi_i\right)\right|^2}{W_i - W_f} \tag{4.16}$$

where the sum is over all intermediate states, f. The initial state should be a typical one for a given temperature T. In general, one might have either

$$B_{\mathrm{k}\mathrm{k}'} = +B_{-\mathrm{k}',-\mathrm{k}}, \quad (\text{ case I}) \tag{4.17}$$

or

$$B_{\mathrm{k}\mathrm{k}'} = -B_{-\mathrm{k}',-\mathrm{k}}. \quad (\text{ case II }) \tag{4.18}$$

The latter applies to the magnetic interaction. To take the coherence into account, one may take the spinindependent sum over $\mathbf{k}$ and $\mathbf{k}'$, which designate initial and intermediate states: $+\sum_{\mathrm{k},\mathrm{k}'} \frac{|B_{\mathrm{k}\mathrm{k}'}|^2 \langle |\left(\Psi_f \left| c_{\mathrm{k}'\uparrow}{}^* c_{\mathrm{k}\uparrow} \pm c_{-\mathrm{k}\downarrow}{}^* c_{-\mathrm{k}'\downarrow} \right| \Psi_i\right)|^2 \rangle_{\mathrm{Av}}}{W_i - W_f}$,
where the average is taken over volume elements $\Delta\mathbf{k}$ and $\Delta\mathbf{k}'$ for the initial state.

For terms with an energy denominator $W_i - W_f = E - E'$, we have

$$\begin{aligned}\left\{\left[(1-h)(1-h')\right]^{\frac{1}{2}} \mp (hh')^{\frac{1}{2}}\right\}^2 &\left[\frac{1}{2}s(1-s'-p')\right. \\ &\left. + \frac{1}{2}ps' + \frac{1}{4}ss' + p(1-s'-p')\right] \\ &= \frac{1}{2}\left\{1 + \frac{\epsilon\epsilon' \mp \epsilon_0^2}{EE'}\right\} f(1-f')\end{aligned} \tag{4.20}$$

Table III lists the average matrix elements for the various values of $W_i - W_f$.
The second-order perturbation theory sum may be written

$$-\sum_{\mathbf{k},\mathbf{k}'} |B_{\mathbf{k}\mathbf{k}'}|^2 L(\epsilon, \epsilon') \tag{4.21}$$

Table III. Mean square matrix elements for possible values of $W_i - W_f$.

$W_i - W_f$	$\left\langle \left\vert \left(\Psi_f \left\vert {c_{\mathrm{k}'\uparrow}}^* c_{\mathrm{k}\uparrow} \pm {c_{-\mathrm{k}\downarrow}}^* c_{-\mathrm{k}'\downarrow}\right\vert \Psi_i\right)\right\vert^2 \right\rangle_{\mathrm{Av}}$
$E - E'$	$\frac{1}{2}\left(1 + \frac{\epsilon\epsilon' \mp {\epsilon_0}^2}{EE'}\right) f\left(1 - f'\right)$
$E' - E$	$\frac{1}{2}\left(1 + \frac{\epsilon\epsilon' \mp {\epsilon_0}^2}{EE'}\right) f'(1 - f)$
$-\left(E + E'\right)$	$\frac{1}{2}\left(1 - \frac{\epsilon\epsilon' \mp {\epsilon_0}^2}{EE'}\right) (1 - f)\left(1 - f'\right)$
$E + E'$	$\frac{1}{2}\left(1 - \frac{\epsilon\epsilon' \mp {\epsilon_0}^2}{EE'}\right) f f'$

where

$$\begin{aligned} L\left(\epsilon, \epsilon'\right) =& \frac{1}{2}\left(1 + \frac{\epsilon\epsilon' \mp \epsilon_0^2}{EE'}\right)\left(\frac{f' - f}{E - E'}\right) \\ &+ \frac{1}{2}\left(1 - \frac{\epsilon\epsilon' \mp \epsilon_0^2}{EE'}\right)\left(\frac{1 - f - f'}{E + E'}\right) \\ =& \frac{1}{2}\left(\frac{(1 - 2f)E - \left(1 - 2f'\right)E'}{\epsilon^2 - \epsilon'^2}\right) \\ &+ \frac{1}{2}\left(\frac{\epsilon\epsilon' \mp \epsilon_0^2}{EE'}\right)\left(\frac{(1 - 2f)E' - \left(1 - 2f'\right)E}{\epsilon^2 - \epsilon'^2}\right) \end{aligned} \tag{4.22}$$

The upper signs correspond to case I, the lower to case II.

To determine the probability of a transition in which an energy quantum $h\nu$ is absorbed, we have a sum of the form

$$\begin{aligned} \tfrac{2\pi}{\hbar} \textstyle\sum_{\mathbf{k},\mathbf{k}'} \left|B_{\mathrm{kk}'}\right|^2 \left\langle \left\vert \left(\Psi_f \left\vert {c_{\mathrm{k}'\uparrow}}^* c_{\mathrm{k}} \uparrow \pm c_{-\mathrm{k}\downarrow} c_{-\mathrm{k}'\downarrow}\right\vert \Psi_i\right)\right\vert^2 \right\rangle_{\mathrm{Av}} \\ \times \delta\left(W_f - W_i - h\nu\right) \end{aligned} \tag{4.23}$$

For the matrix elements for which $W_f - W_i = E - E'$, we may interchange $\mathbf{k}$ and $\mathbf{k}'$ in the sum and combine them with those for which $W_f - W_i = E' - E$. This just gives either one multiplied by a factor of two:

$$\begin{aligned} \frac{2\pi}{\hbar} \sum_{\mathbf{k},\mathbf{k}'} 2\left|B_{\mathbf{kk}'}\right|^2 \frac{1}{2}(1 + \frac{\epsilon\epsilon' \mp \epsilon_0^2}{EE'}\Big) \\ \times f\left(1 - f'\right)\delta\left(W_f - W_i - h\nu\right) \end{aligned} \tag{4.24}$$

One may interpret the factor of two as accounting for the sum over the two spin possibilities of the initial state. If $\left|B_{\mathrm{kk}'}\right|^2$ is symmetric with respect to the Fermi surface, so that we may sum over + and - values of ϵ and ϵ', terms odd in ϵ and ϵ' drop out, and we find

$$\begin{aligned} \frac{2\pi}{\hbar} \sum_{k,k' > kF} 4\left|B_{\mathrm{kk}'}\right|^2 (1 \mp \frac{\epsilon_0^2}{EE'}\Big) \\ \times f\left(1 - f'\right)\delta\left(E' - E - h\nu\right) \end{aligned} \tag{4.25}$$

The corresponding expressions for $W_f - W_i = E + E'$ and $-\left(E + E'\right)$ are:

$$\begin{aligned} \frac{2\pi}{\hbar} \sum_{k,k' > k_F} 2\left|B_{\mathrm{kk}'}\right|^2 \left(1 \pm \frac{\epsilon_0^2}{EE'}\right) \\ \times (1 - f)\left(1 - f'\right)\delta\left(E + E' - h\nu\right) \end{aligned} \tag{4.26}$$

$$\frac{2\pi}{\hbar} \sum_{k,k' > k_F} 2\left|B_{\mathrm{kk}'}\right|^2 \left(1 \pm \frac{\epsilon_0^2}{EE'}\right) f f'\delta\left(E + E' + h\nu\right) \tag{4.27}$$

respectively, where again we have dropped terms odd in ϵ and ϵ'.

Hebel and Slichter [34] have used (4.25) to estimate the temperature dependence of the relaxation time for nuclear spin resonance in the superconducting state from the corresponding value in the normal state. They are able to account for an observed initial decrease in relaxation time in Al as the temperature is lowered below T_c. The increased density of states in energy in the superconducting phase more than makes up for the decrease in number of excited electrons at temperatures not too far below T_c. For this problem, the lower sign (+) is appropriate.

These expressions may also be used to determine transport properties, such as electrical conductivity in the microwave region and thermal conductivity.

Note added in proof.-The marked effect of coherence on the matrix elements is verified experimentally by comparing absorption of ultrasonic waves, which follows case I, with nuclear spin relaxation or electromagnetic absorption, both of which follow case II. For frequencies such that $h\nu \ll kT_c$, one expects for case II an initial increase in absorption just below T_c, followed by a decrease to values below that of the normal state as the temperature is lowered, as is observed experimentally. On the other hand, for case I one expects the absorption to drop with an infinite slope at T_c, such as is found for ultrasonic waves.

The expressions for the transition probabilities are simplified if we change our convention for the moment to give E the same sign as ϵ, so that $E = -\left(\epsilon^2 + \epsilon_0^2\right)^{\frac{1}{2}}$ below the Fermi surface. One may then write (4.26) and (4.27) in the same form as (4.25), with E and E' now taking on both positive and negative values. Considering both direct absorption and induced emission, the net rate of absorption of energy in the superconducting state is proportional to

$$\alpha_s \propto \int \left(1 \mp \frac{\epsilon_0^2}{EE'}\right) \left[f\left(1 - f'\right) - f'(1 - f)\right] \rho(E)\rho\left(E'\right) dE \tag{4.28}$$

where $E' = E + h\nu$ and $\rho(E) = N(0)E/\left(E^2 - \epsilon_0^2\right)^{\frac{1}{2}}$ is the density of states in energy.

With the upper sign (case I) and with $h\nu \ll kT$, the density of states terms are cancelled by the first factor, and the expression reduces to

$$\alpha_s \propto 2[N(0)]^2 \int_{\epsilon_0}^{\infty} \left(f - f'\right) dE \cong 2[N(0)]^2 h\nu f\left(\epsilon_0\right)$$

The factor 2 comes from adding contributions above and below the Fermi surface. The corresponding expression for the normal

state is similar, except that $\epsilon_0 = 0$. We thus find

$$\alpha_s/\alpha_n = 2f\left(\epsilon_0\right) \tag{4.29}$$

R. W. Morse and H. V. Bohm (to be published) have used (4.29) for analysis of data on ultrasonic attenuation in an indium specimen for which the electronic mean free path is large compared with the wavelength of the ultrasonic wave, so that one might expect the theory to apply. Values of $\epsilon_0(T)$ estimated from the data by use of (4.29) are in excellent agreement with our theoretical values (Fig. 1).

For case II, the integral may be expressed in the form:

$$\frac{\alpha_s}{\alpha_n} = \frac{1}{h\nu} \int \frac{\left(EE' + \epsilon_0^2\right)\left(f - f'\right) dE}{\left\{\left(E^2 - \epsilon_0^2\right)\left[(E + h\nu)^2 - \epsilon_0^2\right]\right\}^{\frac{1}{2}}} \tag{4.30}$$

The integral diverges at $E = \epsilon_0$ if $h\nu$ is set equal to zero in the denominator. Numerical evaluation of the integral indicates that for $h\nu \sim \frac{1}{2}kT_c$ or less, (4.30) gives an increase in

[34] L. C. Hebel and C. P. Slichter, Phys. Rev. 107, 901 (1957). We are indebted to these authors for considerable help in working out the details of the calculation of matrix elements, particularly in regard to taking into account the coherence of matrix elements of opposite spin.

absorption just below T_c as observed by Hebel and Slichter in nuclear magnetic resonance and by Tinkham and co-workers (private communication) for microwave absorption in thin superconducting films.

In order to have absorption at $T = 0, h\nu$ must be greater than the energy gap, $2\epsilon_0$. We take E negative and E' positive, and find for this case:

$$\frac{\alpha_s}{\alpha_n} = \frac{1}{h\nu} \int_{\epsilon_0 - h\nu}^{-\epsilon_0} \frac{[E(E + h\nu) + \epsilon_0^2]\, dE}{\{(E^2 - \epsilon_0^2)\,[(E + h\nu)^2 - \epsilon_0^2]\}^{\frac{1}{2}}} \tag{4.31}$$

The integral may be evaluated in terms of the complete elliptic integrals, $E(\gamma)$ and $K(\gamma)$ as follows:

$$\frac{\alpha_s}{\alpha_n} = \left(1 + \frac{2\epsilon_0}{h\nu}\right) E(\gamma) - 2\left(\frac{2\epsilon_0}{h\nu}\right) K(\gamma) \tag{4.32}$$

where

$$\gamma = (h\nu - 2\epsilon_0) \,/\, (h\nu + 2\epsilon_0)\,. \tag{4.33}$$

This expression is in excellent agreement with data of Glover and Tinkham (reference 20, Fig. 6) on infrared absorption in thin films.

3.10.10 Original 1957 BCS Paper: Electrodynamic Properties

V. ELECTRODYNAMIC PROPERTIES

The electrodynamic properties of our model are determined using a perturbation treatment in which the first order change in the wave function is used to calculate the current as a functional of the field. For such properties as the Meissner effect this approach is quite rigorous since we are interested in the limit as $\mathbf{A}(\mathbf{r})$ approaches zero. It is assumed that the medium is infinite and that the sources of the field may be introduced by inserting current sheets in the interior. This method has been applied previously to the calculation of the diamagnetic properties of an electron gas. [35]

We first derive an expression, valid for arbitrary temperatures, relating the current density to the total field (the field due to the sources and to the induced currents). The fact that the system displays a Meissner effect is established by investigating the Fourier transform of the current density in the limit that $q \to 0$. In this limit we obtain the equation,

$$\lim_{\mathbf{q}\to 0} \mathbf{j}(\mathbf{q}) = -\frac{1}{c\Lambda_T} \mathfrak{a}(\mathbf{q}) \tag{5.1}$$

where Λ_T is a function of temperature, increasing, in the free-electron approximation, from the London value $\Lambda = m/ne^2$ at $T = 0$ to infinity at the transition temperature.

The limiting expression (5.1) is valid only for values of q smaller than those important for most penetration phenomena. In general we find the current density is a functional of the vector potential A which, with $\operatorname{div} \mathbf{A} = 0$, may be expressed in a form similar to that proposed by Pippard (1.3):

$$\mathbf{j}(\mathbf{r}) = -\frac{3}{4\pi c\Lambda_T \xi_0} \int \frac{\mathbf{R}\,[\mathbf{R} \cdot \mathbf{A}\,(\mathbf{r}')]\, J(R,T) d\mathbf{r}'}{R^4} \tag{5.2}$$

[35] This method was first applied to the calculation of the diamagnetic properties of an electron gas by O. Klein, Arkiv Mat. Astron Fysik, A31, No. 12 (1944). Our treatment follows that of one of the authors as given in reference 7, pp. 303-321, where further references to the literature may be found.

The kernel, $J(R,T)$, is a relatively slowly varying function of temperature, and at $T = 0°\mathrm{K}$ is not far different from Pippard's $\exp(-R/\xi_0)$.

To calculate penetration depths, it is more convenient to use the Fourier transform of (5.2), which may be expressed in the form

$$\mathbf{j}(\mathbf{q}) = -(c/4\pi)K(q)\mathfrak{a}(\mathbf{q}), \tag{5.3}$$

where $K(q)$ is a scalar which approaches the constant value $4\pi/(\Lambda_T c^2)$ in the limit $q \to 0$. One may determine $K(q)$ directly from the perturbation expansion of the wave function, or one may first calculate $J(R,T)$ and then find the transform of (5.2). The latter procedure is followed in Appendix C, where an explicit expression for $K(q)$ valid for q not too small is derived. In this section we shall give a direct derivation of the transform which can be used to investigate the limit $q \to 0$, and then give the derivation of (5.2). A comparison of calculated and observed values of penetration depths is given at the end of the section.

In the absence of the electromagnetic field, the system at a given temperature is characterized by the complete orthonormal set of wave functions which we denote by

$$\Psi_0(T), \Psi_1(T), \cdots \Psi_n(T), \cdots$$

with corresponding energies

$$W_0(T), W_1(T) \cdots W_n(T) \cdots \tag{5.4}$$

We choose for $\Psi_0(T)$ a typical wave function of the type described in the previous sections, where the occupation of "single particles" and "excited pairs" is given by the s and p distributions, respectively, appropriate to the temperature T; the rest of the phase space is available for "ground pairs" whose distribution is specified by h which is also a function of T. The set of orthogonal states is obtained by varying s and p (in analogy with the normal metal) and not changing h. We thus are choosing a representative configuration of the most probable distribution and taking system averages with respect to this representative configuration.

The electromagnetic interaction term for an electron of charge $q = -e, e > 0$, is, in second quantized form,

$$H_I = \int d\mathbf{r}\psi^*(\mathbf{r}) \left[\frac{-ie\hbar}{2mc}(\mathbf{A}\cdot\nabla + \nabla\cdot\mathbf{A}) + \frac{e^2}{2mc^2}\mathbf{A}^2(\mathbf{r}) \right] \psi(\mathbf{r}) \tag{5.5}$$

We choose a gauge in which $\boldsymbol{\nabla}\cdot\mathbf{A} = 0$ and in which $\mathbf{A} = 0$ if the magnetic field is zero.

We expand ψ and ψ^* in creation and annihilation operators [36] :

$$\psi(\mathbf{r}) = \frac{1}{\Omega^{\frac{1}{2}}} \sum_{\mathbf{k},\sigma} c_{\mathrm{k},\sigma} u_\sigma e^{i\mathbf{k}\cdot\mathbf{r}}$$
$$\psi^*(\mathbf{r}) = \frac{1}{\Omega^{\frac{1}{2}}} \sum_{\mathbf{k}',\sigma'} c_{\mathbf{k}',\sigma'}{}^* u_{\sigma'}{}^* e^{-i\mathbf{k}'\cdot\mathbf{r}} \tag{5.6}$$

where the c 's satisfy the usual fermion anticommutation relations, (2.1) and (2.2), u_σ is a two-component spinor, and Ω is the volume of the container. The interaction Hamiltonian becomes, when one neglects the term of higher order in A,

$$H_I = \frac{e\hbar}{mc}\frac{(2\pi)^{\frac{3}{2}}}{\Omega}\sum_{\mathbf{k},\mathbf{q},\sigma} {c_{\mathbf{k}+\mathbf{q},\sigma}}^* c_{\mathbf{k},\sigma}\mathfrak{a}(\mathbf{q})\cdot\mathbf{k} \tag{5.7}$$

where

$$\mathfrak{a}(\mathbf{q}) = \left(\frac{1}{2\pi}\right)^{\frac{3}{2}}\int d\mathbf{r}\mathbf{A}(\mathbf{r})e^{-i\mathbf{q}\cdot\mathbf{r}}$$

The current operator $\mathfrak{I}(\mathbf{r})$ is

$$\begin{aligned}\mathfrak{J}(\mathbf{r}) = \frac{ie\hbar}{2m}(\psi^*\nabla\psi - \text{ Herm. conj. }) - \frac{e^2}{mc}\psi^*\mathbf{A}\psi \\ = \mathfrak{J}_P(\mathbf{r}) + \mathfrak{J}_D(\mathbf{r})\end{aligned} \tag{5.8}$$

Expanding ψ and ψ^* as in (5.6), we get

$$\begin{aligned}\mathfrak{J}_P(\mathbf{r}) &= \frac{e\hbar}{2m\Omega}\sum_{\mathbf{k},\mathbf{q},\sigma} {c_{\mathbf{k}+\mathbf{q},\sigma}}^* c_{\mathbf{k},\sigma}e^{-i\mathbf{q}\cdot\mathbf{r}}(2\mathbf{k}+\mathbf{q}), \\ \mathfrak{J}_D(\mathbf{r}) &= -\frac{e^2}{mc}\frac{1}{\Omega}\sum_{\mathbf{k},\mathbf{q},\sigma} {c_{\mathbf{k}+\mathbf{q},\sigma}}^* c_{\mathbf{k},\sigma}e^{-i\mathbf{q}\cdot\mathbf{r}}\mathbf{A}(\mathbf{r}).\end{aligned} \tag{5.9}$$

In the presence of the electromagnetic field the wave function for the system may be written

$$\Phi(\mathbf{A}) = \Phi_0 + \Phi_1 + \left(\text{ terms of order } \mathbf{A}^2\cdots\right), \tag{5.10}$$

where the usual perturbation expression for Φ_1 is

$$\Phi_1 = \sum_{i\neq 0}\frac{(\Psi_i\,|H_I|\,\Psi_0)}{W_0 - W_i}\Bigg|\ \Psi_i\Bigg) \tag{5.11}$$

To the lowest order in $\mathbf{A}(\mathbf{r})$, the expectation value of the current operator is then

$$\begin{aligned}\mathbf{j}(\mathbf{r}) = (\Phi|\text{Im}\,(\mathbf{r})|\Phi) = (\Phi_1\,|\text{Im}_{\,P}(\mathbf{r})|\,\Phi_0) \\ + (\Phi_0\,|\text{Im}_{\,P}(\mathbf{r})|\,\Phi_1) + (\Phi_0\,|\text{Im}_{\,D}(\mathbf{r})|\,\Phi_0)\end{aligned} \tag{5.12}$$

where the last equality follows if the current in the field free state, $\mathbf{j}_0(\mathbf{r}) = (\Phi_0|\mathfrak{J}(\mathbf{r})|\Phi_0)$, vanishes. [36a]

If (5.7), (5.9), and (5.11) are combined with (5.12) and the condition $\mathbf{q}\cdot\mathfrak{a}(\mathbf{q}) = 0$ is used, we obtain for the paramagnetic part of the current density,

$$\begin{aligned}\mathbf{j}_P(\mathbf{r}) = -\frac{e^2\hbar^2(2\pi)^{\frac{3}{2}}}{2m^2c\Omega^2}\sum_{i\neq 0}\sum_{\mathbf{k},\mathbf{q},\sigma}\sum_{\mathbf{k}',\mathbf{q}',\sigma'}(2\mathbf{k}+\mathbf{q})\mathbf{k}' \\ \cdot\left[\mathfrak{a}(\mathbf{q}')\,e^{-i\mathbf{q}'\cdot\mathbf{r}}\,(\Psi_0(T)\,|c_{\mathbf{k}'+\mathbf{q}',\sigma'}c_{\mathbf{k}'\sigma'}|\,\Psi_i(T))\right. \\ \times(\Psi_i(T)\,|c_{\mathbf{k}+\mathbf{q},\sigma^*}c_{\mathbf{k},\sigma}|\,\Psi_0(T))\,\frac{1}{W_0 - W_i} \\ \left.+\text{ complex conjugate }\right]\end{aligned} \tag{5.13}$$

[36] At this point we insert plane waves for the Bloch functions. It would be possible to carry through an analogous procedure formally with Bloch functions. The average matrix elements which enter cannot be evaluated explicitly, but can be expressed in terms of empirically determined parameters. The appropriate modifications of the free-electron expressions are as indicated in the introduction.

while for the diamagnetic part we have

$$\mathbf{j}_D(\mathbf{r}) = -\left(ne^2/mc\right)\mathbf{A}(\mathbf{r}) \tag{5.14}$$

where n is the number of conduction electrons, of both spin directions, per unit volume.

The spin sums and the calculation of the average matrix elements can be carried out as indicated in Sec. IV, (4.16) to (4.22). We then obtain

$$\mathbf{j}_P(\mathbf{r}) = \frac{e^2\hbar^2}{2m^2c}\frac{(2\pi)^{\frac{3}{2}}}{\Omega^2}\sum_{\mathbf{k},\mathbf{q}}(2\mathbf{k}+\mathbf{q})\mathbf{k} \cdot\mathfrak{a}(-\mathbf{q})e^{-i\mathbf{q}\cdot\mathbf{r}}L\left(\epsilon_{\mathbf{k}},\epsilon_{\mathbf{k}+\mathbf{q}}\right) \tag{5.15}$$

where $L\left(\epsilon_{\mathrm{k}},\epsilon_{\mathrm{k+q}}\right)$ is given by (4.22) with the lower signs, corresponding to case II. Setting $\epsilon_{\mathrm{k}} = \epsilon$ and $\epsilon_{\mathrm{k+q}} = \epsilon'$, the explicit expression for L is

$$\begin{aligned} L\left(\epsilon,\epsilon'\right) = \frac{1}{2}\left(\frac{1-f-f'}{E+E'}\right)\left(1-\frac{\epsilon\epsilon'+\epsilon_0^2}{EE'}\right) \\ +\frac{1}{2}\left(\frac{f'-f}{E-E'}\right)\left(1+\frac{\epsilon\epsilon'+\epsilon_0^2}{EE'}\right) \end{aligned} \tag{5.16}$$

To show how (5.16) reduces to the usual expression for a free-electron gas in the limit $\epsilon_0 \to 0$, we note that E is defined so that it is intrinsically positive, while the Bloch energy ϵ may be either positive or negative. As $\epsilon_0 \to 0, E \to |\epsilon|$. If ϵ is negative,

$$f(\epsilon) = f(-|\epsilon|) = 1 - f(|\epsilon|) = 1 - f(E), \tag{5.17}$$

To get a nonvanishing contribution from the first line, ϵ and ϵ' must have opposite signs, while for the second line they must have the same signs. We thus find that $L\left(\epsilon,\epsilon'\right) \to \left(f'-f\right)/\left(\epsilon-\epsilon'\right)$, as it should [see (4.4)].

The Meissner Effect

To establish the existence of the Meissner effect, we investigate the Fourier transform of $\mathbf{j}(\mathbf{r})$ in the limit $\mathbf{q} \to 0$. If $\mathbf{j}(\mathbf{q})$ does not go to zero in this limit, and is opposite in sign to $\mathfrak{a}(\mathbf{q})$, then the system will expel the field from its interior and behave like a perfect diamagnet.

The Fourier transform of the paramagnetic part of the current density, $\mathbf{j}_P(\mathbf{r})$, is given by

$$\mathbf{j}_P(\mathbf{q}) = \left(\frac{1}{2\pi}\right)^{\frac{3}{2}}\int d\mathbf{r}\mathbf{j}_P(\mathbf{r})e^{-i\mathbf{q}\cdot\mathbf{r}} \tag{5.18}$$

Referring to (5.15), this can be written as
$\mathbf{j}_P(\mathbf{q}) = \frac{e^2\hbar^2}{m^2c}\left(\frac{1}{2\pi}\right)^3\int d\mathbf{k}(2\mathbf{k}+\mathbf{q})\mathbf{k}\cdot\mathfrak{a}(\mathbf{q})L\left(\epsilon_{\mathbf{k}},\epsilon_{\mathbf{k}+\mathbf{q}}\right)$,
where in the limit that $\mathbf{q} \to 0, \epsilon_{\mathrm{k}} = \epsilon_{\mathrm{k+q}}$ and $L\left(\epsilon_{\mathrm{k}},\epsilon_{\mathrm{k+q}}\right)$ becomes

36a Note added in proof.-We neglect the effects of the momentum dependent cutoff on the expression for the current density; as shown explicitly by P. W. Anderson (private communication) errors introduced are negligible in the weak coupling limit. In a general gauge, $\mathrm{A} = \mathrm{A}_0 + \mathrm{grad}\,\varphi$, with $\mathrm{div}\ \mathrm{A}_0 = 0$, it would be necessary to include in the perturbation expansion collective excitations of the electrons, the simplest of which corresponds to a uniform displacement of all of the electrons in momentum space. Energies and matrix elements of collective excitations are nearly the same in normal and superconducting phases. We assume the collective excitations make a negligible contribution to the current form $\mathbf{A}_0$ (see J. Bardeen, Nuovo Cimento 5, 1766 (1957)).

$$\lim_{\mathrm{q}\to 0} L\left(\epsilon_{\mathrm{k}}, \epsilon_{\mathrm{k+q}}\right) = \frac{\beta e^{\beta E}}{\left(1+e^{\beta E}\right)^2}. \tag{5.20}$$

Thus we want to evaluate

$$\lim_{\mathbf{q}\to 0} \mathbf{j}_P(\mathbf{q}) = \frac{e^2\hbar^2}{m^2 c}\left(\frac{1}{2\pi}\right)^3 2\beta \int d\mathbf{kkk}\cdot\mathfrak{a}(\mathbf{q})\frac{e^{\beta E}}{\left(1+e^{\beta E}\right)^2}. \tag{5.21}$$

Choosing $\mathfrak{a}(\mathbf{q})$ as the polar axis, the angular integration can be done; then, using the relations $n = {k_F}^3/3\pi^2$ and $\mathcal{E}_F = \hbar^2 {k_F}^2/2m$, we get

$$\lim_{\mathbf{q}\to 0} \mathbf{j}_P(\mathbf{q}) = \frac{ne^2}{mc}\left(1-\frac{\Lambda}{\Lambda_T}\right)\mathfrak{a}(\mathbf{q}), \tag{5.22}$$

where

$$1-\frac{\Lambda}{\Lambda_T} \equiv \frac{2\beta\mathcal{E}_F}{{k_F}^5}\int_0^\infty k^4 dk e^{\beta E}\left(1+e^{\beta E}\right)^{-2} \tag{5.23}$$

Letting $y = \epsilon/kT$, and using the sharp maximum of the integrand at $\epsilon = 0$, we find

$$1-\frac{\Lambda}{\Lambda_T} = 2\int_0^\infty dy \frac{\exp\left(y^2+\beta^2\epsilon_0^2\right)^{\frac{1}{2}}}{\left[1+\exp\left(y^2+\beta^2\epsilon_0^2\right)^{\frac{1}{2}}\right]^2}. \tag{5.24}$$

The London constant Λ_T can also be expressed in terms of derivatives of ϵ_0, as is done in Appendix C where the following result is derived

$$\Lambda_T = \Lambda\left(1+\frac{\beta}{\epsilon_0}\frac{d\epsilon_0}{d\beta}\right). \tag{5.25}$$

The total induced current thus becomes:

$$\lim_{\mathbf{q}\to 0}\mathbf{j}(\mathbf{q}) = \mathbf{j}_P + \mathbf{j}_D = -\frac{\Lambda}{\Lambda_T}\frac{ne^2}{mc}, \quad \mathfrak{a}(\mathbf{q}) = -\frac{1}{\Lambda_T c}\mathfrak{a}(\mathbf{q}). \tag{5.26}$$

In the two limiting situations $T\to 0$ and $T\to T_c, \Lambda/\Lambda_T$ can very easily be evaluated. As $T\to 0, \beta$ becomes infinite, so that Λ_T becomes equal to Λ, the London value

$$\lim_{T\to 0}\left(\Lambda/\Lambda_T\right) = 1-2\int_0^\infty dy \exp\left[-\left(y^2+\beta^2\epsilon_0^2\right)^{\frac{1}{2}}\right] = 1 \tag{5.27a}$$

This could have been seen immediately from (5.19) since in the $T\to 0$ limit $L\left(\epsilon_{\mathrm{k}}, \epsilon_{\mathrm{k+q}}\right) = 0$ and the paramagnetic part of the current density is zero. This limit just gives the equation obtained by London assuming complete rigidity of the unperturbed system wave function in the presence of an electromagnetic field. When $T\to T_c, \epsilon_0\beta$ goes to zero and Λ/Λ_T also goes to zero, since

$$\lim_{T\to T_c}\left(\frac{\Lambda}{\Lambda_T}\right) = 1-2\int_0^\infty \frac{e^y dy}{\left(1+e^y\right)^2} = 0 \tag{5.27b}$$

The small Landau diamagnetism would appear only in a higher order. We thus find that when the system is in the superconducting phase, the current density in the London limit has the form (5.1), with Λ_T varying from Λ to ∞ as T goes from 0 to T_c.

It is interesting to note that the Meissner effect occurs for any value of $\epsilon_0 \neq 0$. If $\epsilon_0 = 0$ (for example if we let $V = 0$), then, for $T > 0, \beta\epsilon_0 = 0$ and from (5.27b) we see that $\Lambda/\Lambda_T = 0$. The paramagnetic part of the current density is then

$$\lim_{\mathbf{q}\to 0}\mathbf{j}_P(\mathbf{q}) = \frac{ne^2}{mc}\mathfrak{a}(\mathbf{q}), \tag{5.28}$$

and the total current in the $\mathbf{q}\to 0$ limit becomes

$$\lim_{\mathbf{q}\to \mathbf{0}}\mathbf{j}(\mathbf{q}) = 0. \tag{5.29}$$

This is also true when $T = 0$, though in this case one must be careful of the order in which the various limits are taken.

Current Density

We now evaluate the spacial distribution of the current density and exhibit it in a form similar to that proposed by Pippard. The method we use follows that of one of the authors [7] who carried out a similar calculation for an energy-gap model.

Beginning with (5.15), setting $\mathbf{q} = \mathbf{k}' - \mathbf{k}$, and using the fact that $\mathbf{q}\cdot\mathfrak{a}(\mathbf{q}) = 0$ and that we can write terms like $\mathbf{k}e^{i\mathbf{k}\cdot\mathbf{r}}$ as

$$\mathbf{k}e^{i\mathbf{k}\cdot\mathbf{r}} = -i\nabla e^{i\mathbf{k}\cdot\mathbf{r}}, \tag{5.30}$$

we can reduce all of the angular integrations to integrals of the form

$$\int_0^\pi \sin\theta d\theta e^{\pm ik\cdot(r-r')} = \frac{2}{kR}\sin kR \tag{5.31}$$

where $R = |\mathbf{r}-\mathbf{r}'|$. Then, using the relation

$$\nabla\left(\frac{\sin kR}{kR}\right) = \frac{kR\cos kR - \sin kR}{kR^2}\nabla R, \tag{5.32}$$

we finally obtain

$$\mathbf{j}_P(\mathbf{r}) = \frac{e^2\hbar^2}{2m^2c\pi^4}\int d\mathbf{r}'\frac{(\mathbf{A}(\mathbf{r}')\cdot\nabla' R)\,\nabla R G_s(R)}{R^4} \tag{5.33}$$

where

$$G_s(R) = \int_0^\infty dk\int_0^\infty dk' kk' f(k,R) f(k',R)\, L(\epsilon,\epsilon') \tag{5.34}$$

and

$$f(k,R) = kR\cos kR - \sin kR. \tag{5.35}$$

These equations correspond to (21.4)-(21.6) of reference 7. The entire current density $\mathbf{j}(\mathbf{r})$ can now be written

$$\mathbf{j}(\mathbf{r}) = \mathbf{j}_P(\mathbf{r}) - \frac{ne^2}{mc}\mathbf{A}(\mathbf{r}). \tag{5.36}$$

It is convenient to subtract and add $G_n(R)$ inside the integral (5.33), where $G_n(R)$ is $G_s(R)$ evaluated at $\epsilon_0 = 0$. The integral evaluated with $G_n(R)$ gives the paramagnetic current contribution of a free electron gas and just cancels the term $-(ne^2/mc)\,\mathbf{A}(\mathbf{r})$, leaving the small Landau diamagnetic term in which we are not interested. We have left the interesting part of the current density:
$\mathbf{j}(\mathbf{r}) = \frac{e^2\hbar^2}{2m^2c\pi^4}\int d\mathbf{r}'\frac{[G_s(R)-G_n(R)]\mathbf{R}[\mathbf{A}(\mathbf{r}')\cdot\mathbf{R}]}{R^6}$.
An inspection of $G_s(R)$, (5.34), reveals that the major contribution to the integral comes

from the region $k, k' \simeq k_F$ (i.e., very close to the Fermi surface). Since we are interested in values of $R \gtrsim$ penetration depth which is $\simeq 10^{-5}$ cm, in the region of the major contribution, $kR \simeq k'R \gg 1$. With this in mind, the product $f(k,R)f(k'R)$ becomes

$$\begin{aligned} f(k,R)f(k',R) &\simeq kk'R^2 \cos kR \cos k'R \\ &= \frac{1}{2}kk'R^2 \left[\cos(k+k')R + \cos(k-k')R\right] \\ &\simeq \frac{1}{2}kk'R^2 \cos(k-k')R \end{aligned} \tag{5.38}$$

as $\cos(k+k')R$ is very rapidly oscillating in the region of interest.

Now, making the change of variable $dk = (dk/d\mathcal{E})d\epsilon$, approximating the slowly varying terms $k + k' \simeq 2k_F$ and $dk/d\mathscr{E} \simeq 1/\hbar v_0$, where v_0 is the velocity of an electron at the Fermi surface, and using the rapid convergence of the integral to extend large finite limits to infinite ones, we obtain

$$\begin{aligned} &G_s(R) - G_n(R) \\ &\quad = -\frac{1}{2}k_{F^4}R^2 \left(\frac{dk}{d\mathcal{E}}\right)_F^2 \pi^2 \epsilon_0(0) \frac{\Lambda}{\Lambda_T} J(R,T) \end{aligned} \tag{5.39}$$

where

$$J(R,T) = I(R,0) - I(R,\epsilon_0) \tag{5.40}$$

and

$$\begin{aligned} I(R,\epsilon_0) = \frac{\Lambda_T}{\Lambda\pi^2\epsilon_0(0)} \iint_{-\infty}^{+\infty} d\epsilon d\epsilon' L(\epsilon,\epsilon') \\ \times \cos\left[(\epsilon-\epsilon')\frac{R}{\hbar v_0}\right]. \end{aligned} \tag{5.41}$$

The current density then becomes

$$\mathbf{j}(\mathbf{r}) = \frac{-3}{4\pi c\Lambda_T} \frac{\pi\epsilon_0(0)}{\hbar v_0} \int d\mathbf{r}' \frac{J(R,T)\mathbf{R}\left[\mathbf{A}(\mathbf{r}')\cdot\mathbf{R}\right]}{R^4} \tag{5.42}$$

where Λ_T has been given by (5.25).

The current density has now been written in a form in which it is easily comparable to Eq. (1.3), proposed by Pippard for a pure superconductor, where we identify $1/\xi_0$ with the microscopic quantities:

$$\frac{1}{\xi_0} = \frac{\pi\epsilon_0(0)}{\hbar v_0} \tag{5.43}$$

and where $J(R,T)$ is to be compared with the exponential function, $\exp[-R/\xi_0]$. We have defined $J(R,T)$ so that it has the same integral as $\exp[-R/\xi_0]$:

$$\int_0^\infty J(R,T)dR = \xi_0 \tag{5.44}$$

As evaluated in Appendix C, $J(R,T)$ is given by

$$J(R,T) = \frac{\Lambda_T}{\Lambda}\frac{\epsilon_0(T)}{\epsilon_0(0)}\left[\tanh\frac{\epsilon_0(T)}{2kT} - \frac{2\epsilon_0(T)}{\pi}\int_0^\infty d\epsilon' \sin\left(\frac{2R}{\hbar v_0}\epsilon'\right)\frac{1-2f(E')}{\epsilon' E'}\right] \tag{5.45}$$

from which (5.44) can be established. In the London limit, where $\mathbf{A}(\mathbf{r})$ varies so slowly compared to the coherence distance ξ_0 that it may be taken out of the integral sign, we obtain

$$\mathbf{j}(\mathbf{r}) = -\frac{1}{c\Lambda_T}\mathbf{A}(\mathbf{r}), \tag{5.46}$$

as has been shown previously.

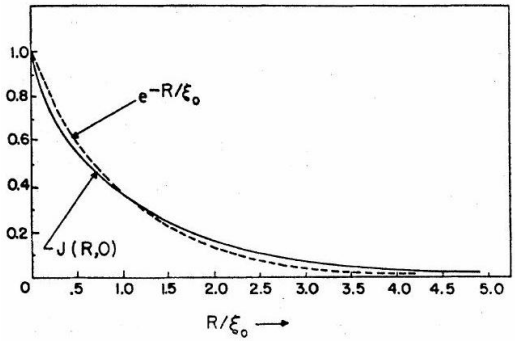


Fig. 5. The kernel $J(R,0)$ for the current density at $T = 0°\mathrm{K}$ vs R/ξ_0, compared with the Pippard kernel, $\exp(-R/\xi_0)$.

With this normalization of $J(R,T)$ it turns out that most of the temperature variation of the current density is contained in Λ_T, and that the integral does not produce effects that vary very much with the temperature. This will be made clear later in the calculation of the penetration depth as a function of the temperature.

At $T = 0, J(R,0)$ has the simple form

$$J(R,0) = \frac{2}{\pi}\int_{2\epsilon_0(0)R/\hbar v_0}^\infty K_0(y)dy \tag{5.47}$$

and when $R = 0$

$$J(0,0) = 1 \tag{5.48}$$

Thus $J(R,0)$ not only has the same integral as the exponential but also the same value at $R = 0$. A comparison of the two given in Fig. 5 shows that they are quite similar.

We may express ξ_0 in a form similar to that suggested by Faber and Pippard [25] :

$$\xi_0 = a\,(\hbar v_0/kT_c) \tag{5.49}$$

where a was adjusted empirically from observed penetration depths. From (5.43), we find

$$\xi_0 = \frac{\hbar v_0}{\pi\epsilon_0(0)} = \frac{1}{\pi\epsilon_0(0)}\frac{kT_c}{kT_c} = 0.18\frac{\hbar v_0}{kT_c} \tag{5.50}$$

Our theoretical value of 0.18 is between the empirical estimates of 0.15 by Faber and Pippard [25] and of 0.27 by Glover and Tinkham. [27] Thus at the absolute zero our theory gives a current density very much like that proposed by Pippard. Since $J(R,T)$ varies slowly with T, most of the temperature variation is contained in the constant Λ_T.

Penetration Depths

A most important application of the equations we have derived for the current density is to the calculation of field penetration at a plane surface. The results depend to some extent on the boundary conditions for scattering of electrons at the surface. Pippard [26] has given general solutions for the limiting cases for specular
reflection and for random scattering, based on corresponding expressions derived by Reuter and Sondheimer [37] for the anomalous skin effect. The penetration depth, defined by

$$\lambda = \frac{1}{H(0)} \int_0^\infty H(x)dx \tag{5.51}$$

is given by

$$\lambda = \frac{2}{\pi} \int_0^\infty \frac{dq}{q^2 + K(q)} \tag{5.52}$$

for specular reflection and by

$$\lambda = \frac{\pi}{\int_0^\infty \ln\left[1 + q^{-2}K(q)\right]} \tag{5.53}$$

for random scattering, where $K(q)$ is defined by (5.3).
Limiting expressions have been given for ξ_0/λ large or small compared with unity. The London limit corresponds to $\xi_0 \ll \lambda$, in which case $K(q)$ is a constant $= 4\pi/\Lambda_T c^2$ over the important range of integration. The penetration depth is then

$$\lambda_L(T) = \left(4\pi/\Lambda_T c^2\right)^{\frac{1}{2}}. \tag{5.54}$$

For a free-electron gas, this reduces to the London value ($mc^2/4\pi ne^2$) at $T = 0°\mathrm{K}$. Since, for most metals, $\xi_0 \simeq 10^{-4}$ cm and $\lambda \simeq 5 \times 10^{-6}$ cm, it is the opposite limit, $\xi_0 \gg \lambda$, which is more applicable (except possibly near T_c). In this limit $J(R,T)$ does not vary much over the penetration depth, so that it is only the value at $R = 0, J(0,T)$, which enters. Pippard [25] has given expressions for λ in this limit, called λ_∞. For random scattering,

$$\lambda_\infty = \frac{3^{1/6}}{(2\pi)^{\frac{1}{3}}} \left(\frac{\xi_0 \lambda_L^2}{J(0,T)}\right)^{\frac{1}{3}}, \tag{5.55}$$

while the value for specular reflection is smaller by a factor 8/9.

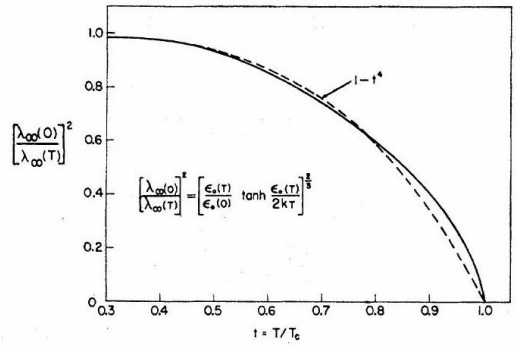


Fig. 6. The temperature variation of the penetration depth, λ_∞, in the infinite coherence distance limit, $(\xi_0/\lambda) \to \infty$, compared with the empirical law, $[\lambda(0)/\lambda(T)]^2 = 1 - t^4$.

Table IV. Penetration depth, λ, at $T = 0°\mathrm{K}$.[a]

[37] G. E. H. Reuter and E. H. Sondheimer, Proc. Roy. Soc. (London) A195, 336 (1948).

	(1)	(2)	(3)	(4)	(5)	(6)	(7)	(8)
					Specular reflection		Random scattering	
Metal	$10^6\lambda_L$ cm	$10^4\hbar v_0/kT_c$ cm	$10^4\xi_0$ cm	ξ_0/λ_L	$\lambda/\lambda L$	$10^6\lambda$	λ/λ_L	$10^6\lambda$
Tin	3.5	1.4	0.25	7.3	1.4	4.8	1.6	5.7
Aluminum	1.6	8.2	1.5	93.			3.2	5.2

[a] Values of λ_L and v_0 are those estimated by Faber and Pippard [25] from high-frequency skin resistance and normal electronic specific heat. The value of ξ_0 is $0.18hv_0/kT_c$, as in (5.43). Ratios in columns 5 and 7 are taken from Fig. 6. Observed values are from reference 25.

The temperature dependence of λ_∞ can be obtained directly from (5.45). The second term vanishes when $R = 0$, so that we have

$$\frac{\lambda_\infty^2(0)}{\lambda_\infty^2(T)} = \left[\frac{\epsilon_0(T)\tanh\left[\frac{1}{2}\beta\epsilon_0(T)\right]}{\epsilon_0(0)}\right]^{\frac{2}{3}} \tag{5.56}$$

A plot of this quantity on a reduced temperature scale is given in Fig. 6. It is plotted in this way so that a comparison can be made with the empirical law:

$$\lambda^2(0)/\lambda^2(t) = 1 - t^4 \tag{5.57}$$

based on the Gorter-Casimir two-fluid model. It is seen that our theory is very close to the empirical law except for temperatures very close to T_c. It is in this region that the approximation $\xi_0 \gg \lambda$ becomes invalid as a result of λ increasing with T. The corrections are such as to reduce the theoretical values so as to bring them closer to the experimental values.

To determine $\lambda(T)$ for intermediate cases, we plot in Fig. 7 the quantity $\lambda(T)/\lambda_L(T)$ as a function of $\xi_0/\ \lambda_L(T)$. The calculations are based on use of the asymtotic forms for $K(q)$ near $T = 0°$ and $T = T_c$ given in Appendix C, and numerical integrations of (5.52) and (5.53). The curves for the two limiting temperatures are quite close together, indicating that the effect of the variation of $J(R, T)$ with temperature is rather small. This procedure is analogous to that of Pippard [5] who gave a plot by means of which one can determine λ from known values of ξ_0 and λ_L for the case $J(R, 0) = \exp(-R/\xi_0)$.

Using our theoretical expression (5.50) for ξ_0 and empirically estimated values of v_0 and $\lambda_L(0)$ for tin and aluminum, [25] we have obtained $\xi_0/\lambda_L(0)$, and, using Fig. 7, have determined $\lambda(0)/\lambda_L(0)$ for these two metals (Table IV). The agreement between theory and experiment is reasonably good, the experimental values falling between the theoretical values calculated for random scattering and specular reflection.

The theory we have presented applies to a pure metal. Pippard [5] has shown experimentally that the existence of a finite mean free path, l, due to impurity scattering, has the effect of increasing the penetration depth, and has suggested that it may be taken into account by introducing an extra factor, $\exp(-R/l)$, into the kernel for the current density. One of the authors [7] has shown why such a factor may be expected from a theory of the diamagnetic properties based on
an energy-gap model. Similar considerations apply to the theory developed in this section; however, effects of coherence on the scattering matrix elements introduce complications and the proper correction factor has not yet been worked out.

To complete the electrodynamics we should give a relation corresponding to the second London equation, the one which gives the time-rate of change of current when an electric field is present. Such a theory would require a calculation, not yet completed, of transport properties with our excited-state wave functions. We expect to find something similar to a two-fluid model, in which thermally excited electrons correspond to the normal component of

the fluid. For frequencies such that $h\nu \ll \epsilon_0$, one may determine $\partial \mathbf{j}/\partial t$ for the superconducting component by taking the time derivative of the integral relation (5.2) and then setting $\partial \mathbf{A}/\partial t = -c\mathbf{E}$ in the result (see reference 7).

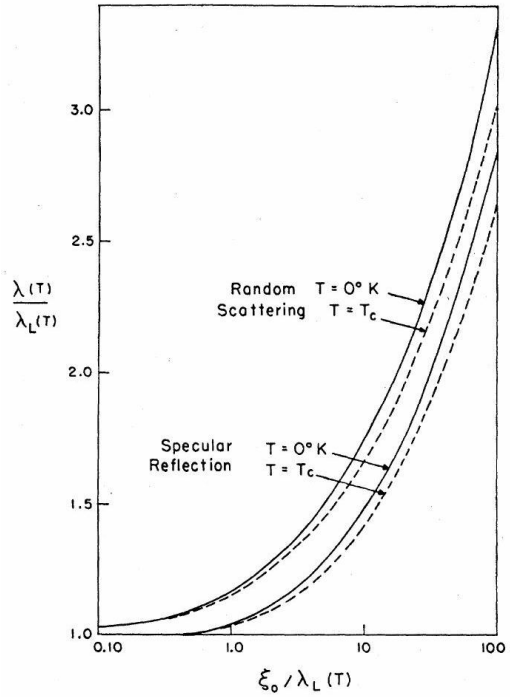


Fig. 7. The ratio $\lambda(T)/\lambda_L(T)$ vs $\xi_0/\lambda_L(T)$ for the boundary conditions of random scattering and specular reflection and for temperatures near $T = 0°\mathrm{K}$ and near $T = T_c$. The temperature variation of $\lambda_L(T)$ is given by $\lambda_L(T) = (\Lambda_T c^2/4\pi)^{\frac{1}{2}}$.

3.10.11 Original 1957 BCS Paper: Appendices

APPENDIX A. CORRECTIONS TO GROUND STATE ENERGY

We may estimate the accuracy of our superconducting ground state energy, W_0, measured relative to that of the normal state, by making a perturbation theory expansion, using the complete set of excited state superconducting wave functions as the basis functions of the expansion. We first consider the reduced, H_{red} , which includes only pair transitions for pair momentum $q = 0$, and then the effect of the neglected portion of the Hamiltonian, $H' = H - H_{\mathrm{red}}$.

To the second order, the ground state energy of H_{red} is:

$$\begin{aligned} \mathscr{W}_0 &= (\Psi_0 \left|H_{\mathrm{red}}\right| \Psi_0) + \sum_{i\neq 0} \frac{\left|(\Psi_i \left|H_{\mathrm{red}}\right| \Psi_0)\right|^2}{W_0 - W_i} + \cdots \\ &= W_0 + W_0^{(2)} + \cdots \end{aligned} \tag{A1}$$

[38] F. Reif, Phys. Rev. 106, 208 (1957).

Since the smallest excitation energy is $2\epsilon_0$, the second order energy is overestimated by setting $|W_0 - W_i| = 2\epsilon_0$ and performing a closure sum. We obtain the inequality

$$\begin{aligned} W_0^{(2)} &\leq \left[\left(\Psi_0 \left|H_{\mathrm{red}}^2\right| \Psi_0\right) - (\Psi_0 \left|H_{\mathrm{red}}\right| \Psi_0)^2\right] / (-2\varepsilon_0) \\ &= \frac{w_a + w_b + w_c}{-2\epsilon_0}, \end{aligned} \tag{A2}$$

where

$$w_a = \left(\Psi_0 \left| H_0^2 \right| \Psi_0\right) - \left(\Psi_0 \left| H_0 \right| \Psi_0\right)^2 \tag{A3}$$

$$w_b = \left(\Psi_0 \left| H_0 H_v + H_v H_0 \right| \Psi_0\right) - 2\left(\Psi_0 \left| H_0 \right| \Psi_0\right)\left(\Psi_0 \left| H_v \right| \Psi_0\right) \tag{A4}$$

$$w_c = \left(\Psi_0 \left| H_v^2 \right| \Psi_0\right) - \left(\Psi_0 \left| H_v \right| \Psi_0\right)^2 \tag{A5}$$

and

$$H_0 = \sum_{k>k_F} \epsilon_{\mathrm{k}} b_{\mathrm{k}}^* b_{\mathrm{k}} + \sum_{k<k_F} \left|\epsilon_{\mathrm{k}}\right| b_{\mathrm{k}} b_{\mathrm{k}}^* \tag{A6}$$

$$H_v = -V \sum_{\mathrm{k},\mathrm{k}'} b_{\mathrm{k}'}^* b_{\mathrm{k}} \tag{A7}$$

the sum in (A7) being carried out over the region $|\epsilon_k|$ and $|\epsilon_{k'}| < \hbar\omega$. If terms in ${W_0}^{(2)}$ linear in the volume of the system are evaluated, the following expressions may be derived with the aid of the decomposition (2.25) :

$$w_a = 8N(0)\int_0^{\hbar\omega} d\epsilon h(\epsilon)[1-h(\epsilon)]\epsilon^2 \tag{A8}$$

$$\begin{aligned} w_b = &-16N(0)V\int_0^{\hbar\omega} d\epsilon_1 \int_0^{\hbar\omega} d\epsilon_2 \left\{h\left(\epsilon_1\right)\left[1-h\left(\epsilon_1\right)\right]\right. \\ &\left.\times h\left(\epsilon_2\right)\left[1-h\left(\epsilon_2\right)\right]\right\}^{\frac{1}{2}}\left[1-2h\left(\epsilon_1\right)\right]\epsilon_1 \\ w_c = &\, 8[N(0)V]^2\left[\int_0^{\hbar\omega} d\epsilon_1 h\left(\epsilon_1\right)\left[1-h\left(\epsilon_1\right)\right]\right]^2 \\ &\times \int_0^{\hbar\omega} d\epsilon_2\left[1-2h\left(\epsilon_2\right)\right]^2 \end{aligned} \tag{A9}$$

With the use of the relations (2.35), (2.36), and (2.37), terms linear in the volume in (A2) become

$$\begin{aligned} -2\varepsilon_0 W_0^{(2)} \leq 8N(0)\int_0^{\hbar\omega} d\epsilon\epsilon^2\{h(\epsilon)[1-h(\epsilon)] \\ -\frac{\epsilon_0^2}{2E^2}+\frac{\epsilon_0^2}{4E^2}\Bigg\} = 0 \end{aligned} \tag{A11}$$

and therefore ${W_0}^{(2)}/W_0$ vanishes in the limit of a large system.

It is likely that $\left(\Psi_0 \left| {H_{\mathrm{red}}}^n \right| \Psi_0\right) - \left(\Psi_0 \left| H_{\mathrm{red}} \right| \Psi_0\right)^n$ also vanishes in this limit for n small compared with the total number of valance electrons in the system. For Ψ_0 to be an exact eigenfunction of H_{red} , in the statistical limit, it is required that the above condition hold for all n. Since this requirement can be shown to hold in
the strong coupling limit, it is possible that Ψ_0 is exact in the statistical limit for all values of the coupling constant, although no proof has been found at this time.

We may estimate the effect of the neglected portion of the Hamiltonian, $H' = H - H_{\mathrm{red}}$ by a similar perturbation calculation. To second order in H' the correction to the superconducting ground state energy W_0 (measured relative to the normal ground state) is

$$W' = \sum_i \frac{|(i\,|H'|\,0)|^2}{W_0 - W_i}, \tag{A12}$$

where

$$\begin{aligned}(i\,|H'|\,0) = -V \Big\{ &[h(\mathbf{k}_0)\,(1-h(\mathbf{k}_0{}'))\,h(\mathbf{k})\,(1-h(\mathbf{k}'))]^{\frac{1}{2}} \\ &- [h(\mathbf{k}_0{}')\,(1-h(\mathbf{k}_0))\,h(\mathbf{k}')\,(1-h(\mathbf{k}))]^{\frac{1}{2}} \Big\}\end{aligned} \tag{A13}$$

The first term in ($i\,|H'|\,0$) may be identified with breaking up a pair in $\mathbf{k}_0$, the spin-down member going to $-\mathbf{k}_0{}' \downarrow$ and breaking up a pair in $\mathbf{k}$, the spin-up member going into $\mathbf{k}' \uparrow$. The second term arises from $\mathbf{k}_0{}'$ and $\mathbf{k}'$ being occupied in the ground state and arriving at the same intermediate state by $\mathbf{k}_0{}' \uparrow \rightarrow \mathbf{k}_0 \uparrow$ and $-\mathbf{k}' \downarrow \rightarrow -\mathbf{k} \downarrow$. The transitions involving particles with parallel spin have been neglected since their contribution is reduced by exchange.

Since the distribution of particle changes differs only over an energy region several ϵ_0 wide, it is to be expected that most of W' will cancel between the normal and superconducting phases. To estimate the energy difference, we shall carry out the sums over a region $6\epsilon_0$ wide. Inserting typical values in (A12), we find

$$W' \sim -\frac{V^2\,[3N(0)\epsilon_0]^3}{2\epsilon_0}\left(\frac{3\epsilon_0}{E_F}\right) \sim 10^{-3} W_0 \tag{A14}$$

where the factor ($3\epsilon_0/E_F$) comes from the average reduction in phase space as a result of conservation of momentum of the pairs making transitions.

These estimates indicate that although the total energy associated with H' may be significant, the effect of H' on the condensation energy is very small. It should be possible to obtain any required quantitative corrections to W_0 by use of perturbation theory.

APPENDIX B. CHANGE IN ZERO-POINT ENERGY OF LATTICE VIBRATIONS

The contribution to the condensation energy from the change in zero-point energy of the lattice can be estimated on the basis of the Bardeen and Pines collective ion-electron treatment. [16] Their theory gives

$$\begin{aligned}&W_{ZP}{}^{(s)} - W_{ZP}{}^{(n)} \\ &\quad = \sum_{\mathbf{k},\boldsymbol{k}} \frac{|M_{\mathbf{k}}|^2 \left\{ \left(n_{\mathbf{k}}^{(s)} - n_{\mathbf{k}}^{(n)}\right) - \left(n_{\mathrm{k}+\kappa}^{(s)} - n_{\mathrm{k}+\kappa}^{(n)}\right) \right\}}{\epsilon_{\mathrm{k}} - \epsilon_{\mathrm{k}+\kappa} - \hbar\omega}\end{aligned} \tag{B1}$$

where $n_{\mathrm{k}}{}^{(s)}$ is the average occupation number in the superconducting state and $n_{\mathrm{k}}{}^{(n)}$ that for the normal
state. The sum over $\boldsymbol{\kappa}$ ranges over the first zone and $\mathbf{k} + \boldsymbol{k}$ is to be interpreted as the corresponding reduced wave vector so that Umklapp processes may be taken into account. If $\mathbf{k} + \boldsymbol{\kappa}$ is replaced by $\mathbf{k}$ and $\boldsymbol{\kappa}$ by $-\boldsymbol{\kappa}$ in the terms containing $n_{\mathrm{k}+\kappa}$, (B1) reduces to

$$\begin{aligned}&W_{ZP^{(s)} - W_{ZP^{(n)}}} \\ &\quad = \sum_{\mathrm{k,k}} \frac{2\,|M_{\mathrm{k}}|^2\,(\epsilon_{\mathrm{k}} - \epsilon_{\mathrm{k+k}})\left(n_{\mathrm{k}}^{(s)} - n_{\mathrm{k}}^{(n)}\right)}{(\epsilon_{\mathrm{k}} - \epsilon_{\mathrm{k}+\kappa})^2 - (\hbar\omega_\kappa)^2}\end{aligned} \tag{B2}$$

If the sum over $\boldsymbol{\kappa}$ is carried out, it is seen that the quantity multiplying the difference in occupation numbers is almost independent of $\mathbf{k}$. Since ${n_{\mathrm{k}}}^{(s)} - {n_{\mathrm{k}}}^{(n)}$ is antisymmetric with respect to the Fermi surface and differs from zero only in a range of the order of several ϵ_0, it follows that the change in zero-point energy will be small compared to W_0.

A rough estimate of the sum gives

$$\begin{aligned} W_{ZP^{(s)}-W_{ZP^{(n)}}=-2\langle|M_\kappa|^2\rangle\int_0^{\hbar\omega}N(0)h(\epsilon)d\epsilon} & \\ \times\int_{\mathcal{E}_F}^{\mathcal{E}_Z}N(\epsilon')\left\{\frac{\epsilon-\epsilon'}{(\epsilon-\epsilon')^2-(\hbar\omega)^2}+\frac{\epsilon+\epsilon'}{(\epsilon+\epsilon')^2-(\hbar\omega)^2}\right\}d\epsilon' & \\ \simeq -2\langle|M_\kappa|^2\rangle\int_0^{\hbar\omega}N(0)h(\epsilon)d\epsilon\cdot 2\epsilon\left[N(\mathcal{E}_Z)/\mathcal{E}_Z\right] & \\ \simeq -2\frac{\langle|M_\kappa|^2\rangle}{\mathcal{E}_Z}[N(0)]^2\epsilon_0^2\simeq(\hbar\omega/\mathcal{E}_Z)W_0\simeq 10^{-3}W_0, \quad \text{(B} & \end{aligned} \tag{B3}$$

where $\mathcal{E}_Z$ is the energy at the zone boundary and typical values have been inserted for the parameters. Thus, it appears that the lattice zero-point energy should have little effect on the condensation energy.

APPENDIX C. EVALUATION OF THE KERNEL IN THE PIPPARD INTEGRAL

According to (5.41), the kernel of the Pippard integral expression for the current density at any temperature T may be written

$$\begin{aligned} J(R,T) &= I(R,0)-I(R,\epsilon_0) \\ &= \frac{\Lambda_T}{\pi^2\epsilon_0(0)\Lambda}\iint_{-\infty}^{+\infty}\left\{\frac{f(\epsilon')-f(\epsilon)}{\epsilon-\epsilon'}-L(\epsilon,\epsilon')\right\}\cos\alpha(\epsilon-\epsilon')\,d\epsilon d\epsilon' \end{aligned} \tag{C1}$$

where $\alpha = R/\hbar v_0$. The limits should really be $\pm\hbar\omega$, but the convergence is sufficiently rapid in the weak coupling limit so that we may replace $\hbar\omega$ by ∞ without appreciable error. One integration can be performed if use is made of the symmetry of the integrand in ϵ and ϵ'. We shall use the second form given for $L(\epsilon,\epsilon')$ in (4.22), with the lower (+) signs. From the symmetry
for positive and negative values of ϵ and ϵ', the integral may be written as the sum of two integrals with limits 0 and ∞ :

$$J(R,T) = \left[\Lambda_T/\pi^2\epsilon_0(0)\Lambda\right](I_1+I_2) \tag{C2}$$

where

$$I_1 = 2\int_0^\infty\int_0^\infty\frac{[F(\epsilon)-F(\epsilon')]\cos\alpha\epsilon\cos\alpha\epsilon'}{\epsilon^2-\epsilon'^2}d\epsilon d\epsilon' \tag{C3}$$

$$I_2 = 2\int_0^\infty\int_0^\infty\frac{[G(\epsilon)-G(\epsilon')]\,\epsilon\epsilon'\sin\alpha\epsilon\sin\alpha\epsilon' d\epsilon d\epsilon'}{\epsilon^2-\epsilon'^2} \tag{C4}$$

and

$$F(\epsilon) = [1-2f(\epsilon)]\epsilon-[1-2f(E)]\left(E+\epsilon_0^2E^{-1}\right) \tag{C5}$$

$$G(\epsilon) = [1-2f(\epsilon)]\epsilon^{-1}-[1-2f(E)]E^{-1} \tag{C6}$$

Unless the argument is given explicitly, $\epsilon_0 \equiv \epsilon_0(T)$.
If integration over the region about $\epsilon' = \epsilon$ is made by principal parts, each of the two terms in I_1 (and each of the two terms in I_2) will give equal contributions. Care must be taken to take the same limits for ϵ and ϵ'. Thus we may write

$$I_1 = 4 \odot' \lim_{a\to 0, b\to\infty} \int_a^b \int_a^b \frac{F(\epsilon)\cos\alpha\epsilon\cos\alpha\epsilon' d\epsilon d\epsilon'}{\epsilon^2 - \epsilon'^2} \tag{C7}$$

Here $\mathscr{P}'$ indicates the principal part of the integral of ϵ' past $\epsilon' = \epsilon$ is to be taken. Since $F(\epsilon) \to 0$ as $\epsilon \to \infty$, the value of the integral does not depend on how the upper limits of the integrals over ϵ and ϵ' are approached. Thus we may set $b = \infty$ for both, and integrate over ϵ' first. This would not have been true if we had not included $I(R, 0)$, the normal state contribution, which is equivalent to the term proportional to $\mathbf{A}$ in the expression for the current density. The lower limit is more critical; we must take a the same for both ϵ and ϵ' and approach the limit $a = 0$ only in the final result. The integral over ϵ' may be obtained from

$$\int_a^\infty \frac{\cos\alpha\epsilon' d\epsilon'}{\epsilon^2 - \epsilon'^2} = \int_0^\infty \frac{\cos\alpha\epsilon' d\epsilon'}{\epsilon^2 - \epsilon'^2} - \int_0^a \frac{d\epsilon'}{\epsilon^2 - \epsilon'^2} \tag{C8}$$

In the second integral on the right we have assumed that a is sufficiently small so that $\cos\alpha\epsilon'$ may be replaced by unity. The first integral on the right may be evaluated by contour integration and the second directly to give

$$\mathscr{O}' \int_a^\infty \frac{\cos\alpha\epsilon' d\epsilon'}{\epsilon^2 - \epsilon'^2} = \frac{1}{2}\pi\frac{\sin\alpha\epsilon}{\epsilon} - \frac{1}{2\epsilon}\ln\left(\frac{\epsilon + a}{\epsilon - a}\right) \tag{C9}$$

Similarly, to evaluate I_2, we have

$$\mathscr{P}' \int_0^\infty \frac{\epsilon' \sin\alpha\epsilon' d\epsilon'}{\epsilon^2 - \epsilon'^2} = -\frac{1}{2}\pi\cos\alpha\epsilon \tag{C10}$$

In this integral we may take $a = 0$, since the integrand is not singular at the origin. Combining I_1 and I_2, we find

$$\begin{aligned} I_1 + I_2 = -2\int_a^\infty F(\epsilon)\ln\left(\frac{\epsilon + a}{\epsilon - a}\right)\frac{d\epsilon}{\epsilon} \\ + \pi\int_0^\infty \left[F(\epsilon) - \epsilon^2 G(\epsilon)\right]\frac{\sin 2\alpha\epsilon}{\epsilon} d\epsilon \end{aligned} \tag{C11}$$

In the limit $a \to 0$, the first integral gives a contribution only near $\epsilon = 0$. We may therefore replace $F(\epsilon)$ by $F(0)$. The logarithmic integral may then be evaluated, and we find

$$\begin{aligned} I_1 + I_2 = \pi^2\epsilon_0\left[1 - 2f\left(\epsilon_0\right)\right] \\ - 2\pi\epsilon_0^2\int_0^\infty \frac{1 - 2f(E)}{E}\sin 2\alpha\epsilon d\epsilon \end{aligned} \tag{C12}$$

Note that this expression vanishes in the two limits $\epsilon_0 \to 0$ and α (or R) $\to \infty$, as it should. The second term vanishes as $R \to 0$.

From (C2) and (C12), we may write

$$\begin{aligned} J(R,T) = \frac{2\Lambda_T\epsilon_0^2}{\pi\epsilon_0(0)\Lambda}\int_0^\infty \left\{\frac{1 - 2f\left(\epsilon_0\right)}{\epsilon_0}\right. \\ \left. - \frac{1 - 2f(E)}{E}\right\}\frac{\sin 2\alpha\epsilon}{\epsilon} d\epsilon \end{aligned} \tag{C13}$$

which is equivalent to (5.45) of the text.
Since $f = 0$ when $T = 0$, we can write

$$J(R,O) = \frac{2\epsilon_0(0)}{\pi}\left(\frac{\pi}{2\epsilon_0(0)} - \int_0^\infty \frac{\sin 2\alpha\epsilon}{\epsilon E}d\epsilon\right) \tag{C14}$$

This can be put into a form convenient for evaluation by using

$$\begin{aligned}\frac{\partial}{\partial\alpha}\int_0^\infty \frac{\sin 2\alpha\epsilon}{\epsilon E}d\epsilon &= 2\int_0^\infty \frac{\cos 2\alpha\epsilon}{E}d\epsilon \\ &= 2K_0\left(2\alpha\epsilon_0\right)\end{aligned} \tag{C15}$$

where K_0 is a modified Bessel function [39] which falls off exponentially for large values of its argument. If we now observe that $\int_0^\infty K_0(y)dy = \pi/2$, we obtain

$$J(R,O) = \frac{2}{\pi}\int_{2R/\pi\xi_0}^\infty K_0(y)dy \tag{C16}$$

We next consider the integral of $J(R,T)$ with respect to R. If we introduce a convergence factor, we may
integrate under the sign in (C13):

$$\lim_{\gamma\to 0}\int_0^\infty e^{-\gamma R}\sin\left(2\epsilon R/\hbar v_0\right)dR = \frac{1}{2}\hbar v_0/\epsilon \tag{C17}$$

Thus, remembering that $\xi_0 = hv_0/\left[\pi\epsilon_0(0)\right]$, we find

$$\begin{aligned}&\frac{1}{\xi_0}\int_0^\infty J(R,T)dR \\ &\quad = \frac{\epsilon_0^2\Lambda_T}{\Lambda}\int_0^\infty\left\{\frac{1-2f\left(\epsilon_0\right)}{\epsilon_0} - \frac{1-2f(E)}{E}\right\}\frac{d\epsilon}{\epsilon^2}\end{aligned} \tag{C18}$$

According to (5.44) of the text, Λ_T is defined so that the expression on the left is equal to unity. If we integrate the right hand side by parts, we find that

$$\frac{\Lambda}{\Lambda_T} = -\epsilon_0^2\int_0^\infty \frac{d}{dE}\left(\frac{1-2f(E)}{E}\right)\frac{d\epsilon}{E} \tag{C19}$$

This integral may be expressed in terms of ϵ_0 and its temperature derivative by differentiating the defining integral for ϵ_0 with respect to $\beta = 1/kT$. By a change of variable, $\beta\epsilon = x, \beta\epsilon_0 = y$, we may write

$$\begin{aligned}\frac{1}{N(0)V} &= \int_0^{\hbar\omega}\frac{1-2f(E)}{E}d\epsilon \\ &= \int_0^{\beta\hbar\omega}\frac{1-2f\left(\left(x^2+y^2\right)^{\frac{1}{2}}\right)}{\left(x^2+y^2\right)^{\frac{1}{2}}}dx\end{aligned} \tag{C20}$$

We now differentiate with respect to β, remembering that y depends on β. In the weak-coupling limit $[\epsilon_0 \ll \hbar\omega, f(\beta\hbar\omega) \simeq 0]$, we find:

[39] See Erdelyi, Magnus, Oberhettinger, and Tricomi, Higher Transcendental Functions (McGraw Hill Book Company, Inc., New York, 1953), Vol. 2, pp. 5 and 19.

$$0 = \frac{1}{\beta} + \frac{d(\beta\epsilon_0)}{d\beta} \cdot \frac{\epsilon_0}{\beta} \int_0^{\hbar\omega} \frac{d}{dE}\left(\frac{1-2f(E)}{E}\right) \frac{d\epsilon}{E} \tag{C21}$$

The integral converges sufficiently rapidly so that we may replace the upper limit by ∞. Comparing (C19) and (C21), we find that

$$\frac{\Lambda_T}{\Lambda} = \frac{1}{\epsilon_0} \frac{d(\beta\epsilon_0)}{d\beta} \tag{C22}$$

as stated in (5.25).

Finally, we shall derive an approximate expression for the transform $K(q)$ valid when $qhv_0 > \epsilon_0(0)$. First we express $K(q)$ as an integral of $J(R,T)$. The transform of $\mathbf{j}(\mathbf{r})$ may be written

$$\begin{aligned} \mathbf{j}(\mathbf{q}) &= -\frac{c}{4\pi} K(q) \mathfrak{a}(\mathbf{q}) \\ &= -\frac{3}{4\pi c \Lambda_T \xi_0} \int \frac{\mathbf{R}[\mathbf{R}\cdot\mathfrak{a}(\mathbf{q})] e^{i\mathbf{q}\cdot\mathbf{R}}}{R^4} J(R,T) d\tau \end{aligned} \tag{C23}$$

To carry out the integration over angles, we take the polar axis in the direction of $\mathbf{q}$ and set $u = \cos\theta$. This gives

$$K(q) = \frac{3\pi}{c^2 \Lambda_T \xi_0} \int_0^\infty \int_{-1}^{+1} \left(1-u^2\right) e^{iRqu} J(R,T) du dR.$$

When (C13) is substituted for $J(R,T)$, we require the following integral:

$$g(b) = \int_0^\infty \int_{-1}^{+1} e^{iRqu} \left(1-u^2\right) \sin\left(\epsilon Rq/\epsilon_1\right) du dR = \left(1-b^2\right) \ln\left(\frac{1+b}{1-b}\right) + 2b \tag{C25}$$

where $\epsilon_1 = \frac{1}{2} q\hbar v_0$ and $b = \epsilon/\epsilon_1$. We thus find

$$K(q) = \frac{6\pi\epsilon_0^2}{qc^2\Lambda\hbar v_0} \int_0^\infty \left\{ \frac{1-2f(\epsilon_0)}{\epsilon_0} - \frac{1-2f(E)}{E} \right\} g(b) \frac{d\epsilon}{\epsilon}.$$

Expansions of $g(b)$ for b small and b large are

$$b < 1 : g(b) = 4\left(b - \frac{1}{3}b^3 - \frac{1}{15}b^5 \cdots\right) \tag{C27}$$

$$b > 1 : g(b) = 4\left(\frac{1}{3b} + \frac{1}{15b^3} + \cdots\right) \tag{C28}$$

Further,

$$\int_0^\infty g(b) \frac{db}{b} = \frac{1}{2}\pi^2 \tag{C29}$$

We may change the variable of integration in (C26) from ϵ to b, and then use different expansions for $b < 1$ and $b > 1$. One of the integrals required is

$$\begin{aligned} &4\int_0^1 \frac{1-2f(E)}{E} \left\{ b - \frac{1}{3}b^3 - \frac{1}{15}b^5 - \cdots \right\} \frac{db}{b} \\ &+ 4\int_1^\infty \frac{1-2f(E)}{E} \left\{ \frac{1}{3b} + \frac{1}{15b^3} + \cdots \right\}_{\frac{db}{b}} \end{aligned} \tag{C30}$$

In terms of b,

$$E = \epsilon_1 \left(b^2 + b_0^2\right)^{\frac{1}{2}} \tag{C31}$$

where

$$b_0 = \epsilon_0/\epsilon_1. \tag{C32}$$

An approximate expression valid in the limit $b_0 \ll 1$ may be obtained by neglecting b_0 in the integral for $b > 1$, and also in terms in b^3 and higher in the integral for $b < 1$. The only integral in which ${b_0}^2$ is not neglected in comparison with b^2 is the first term,

$$4\int_0^1 \frac{1-2f(E)}{E} db = \frac{4}{\epsilon_1}\int_0^{\epsilon_1} \frac{1-2f(E)}{E} d\epsilon \tag{C33}$$

which can be determined from (C20), the defining integral for ϵ_0. For $\epsilon > \epsilon_1$ we may take $f(E) = 0$. Thus we find

$$\frac{4}{\epsilon_1}\int_0^{\epsilon_1} \frac{1-2f(E)}{E} d\epsilon \simeq \frac{4}{\epsilon_1}\left(\frac{1}{N(0)V} - \ln\frac{\hbar\omega}{\epsilon_1}\right) = \frac{4}{\epsilon_1}\ln\frac{q\hbar v_0}{\epsilon_0(0)} \tag{C34}$$

The latter form follows from the expression for $\epsilon_0(0)$ in the weak-coupling limit. The remaining terms cancel when ${b_0}^2$ is neglected:

$$\int_0^1 \left\{\frac{b^3}{3} - \frac{b^5}{15} - \cdots\right\}\frac{db}{b^2} + \int_1^\infty \left\{\frac{1}{3b} + \frac{1}{15b^3} + \cdots\right\}\frac{db}{b^2} = 0 \tag{C35}$$

Thus we find that for $q\hbar v_0/\epsilon_0(0) = \pi q\xi_0 \gg 1$,

$$K(q) = \frac{3\pi^2\epsilon_0}{qc^2\Lambda\hbar v_0}\left\{1 - 2f\left(\epsilon_0\right) - \frac{16\epsilon_0}{\pi^2 q\hbar v_0}\ln\left(\pi q\xi_0\right)\right\}. \tag{C36}$$

For q very small, $K(q)$ approaches the constant value,

$$K(q) = \lambda_L^{-2}(T) = 4\pi/\left(\Lambda_T c^2\right), \quad (q \to 0) \tag{C37}$$

where Λ_T is the temperature-dependent London constant defined by (C22). For intermediate values of q, one may interpolate between this constant value for $\pi q\xi_0 < 1$ and the asymptotic form (C36) for large q.

The two limiting cases are $T = 0°\mathrm{K}$ and T close to T_c. At $T = 0°\mathrm{K}, \epsilon_0 \to \epsilon_0(0)$ and $f\left(\epsilon_0\right) \to 0$, and we find

$$K(q) = 4\pi/\left(\Lambda c^2\right) = 1/{\lambda_L}^2(0), \quad (q \to 0); \tag{C38}$$

$K(q) = \frac{3\pi}{4q{\lambda_L}^2(0)\xi_0}\left\{1 - \frac{16}{\pi^3 q\xi_0}\ln\left(\pi q\xi_0\right)\right\}$, (large q).

Near T_c, one may determine Λ_T from (C22) and (3.49):

$$\Lambda/\Lambda_T = 0.23\beta_c^2\epsilon_0^2(T) = 2(1-t) \tag{C40}$$

where $\beta_c = 1/kT_c$ and $t = T/T_c$. When $\epsilon_0(T)$ is small,

$$1 - 2f\left(\epsilon_0\right) = \tanh\left(\frac{1}{2}\beta\epsilon_0\right) \to \frac{1}{2}\beta_c\epsilon_0(T) \tag{C41}$$

Thus the limiting expressions for $K(q)$ as $T \to T_c$ are

$$K(q) = \frac{1}{{\lambda_L}^2(T)} = \frac{2(1-t)}{{\lambda_L}^2(0)}, \quad (q \to 0); \tag{C42}$$

$K(q) = \frac{3.75\pi}{4q{\lambda_L}^2(T)\xi_0}\left\{1 - \frac{18.3}{\pi^3 q\xi_0}\ln(\pi q\xi_0)\right\}, \quad (\text{ large } q).$

The close similarity of the expressions for the two limiting cases is evident. The reason for the similarity is that $J(R,T)$ varies slowly with T.

At temperatures very close to T_c, λ becomes larger than ξ_0, so that $\lambda(T)$ approaches $\lambda_L(T)$. A comparison of penetration depths measured near T_c to those measured at low temperatures would then be expected to give

$$\frac{\lambda(0)}{\lambda(T)} = \frac{\lambda(0)}{\lambda_L(0)}\frac{\lambda_L(0)}{\lambda(T)} = \frac{\lambda(0)}{\lambda_L(0)}\sqrt{2}(1-t)^{\frac{1}{2}} \tag{C44}$$

This is to be compared with the ratio $2(1-t)^{\frac{1}{2}}$ which the empirical law, $(1-t^4)^{\frac{1}{2}}$, gives as $t \to 1$.

APPENDIX D. CORRELATION OF ELECTRONS OF OPPOSITE SPIN

Insight into the coherent structure of our ground state wave function may be obtained by an investigation of the correlation function for electrons of opposite spin. For the normal metal (in the Bloch approximation), electrons of antiparallel spin are entirely uncorrelated while for electrons of parallel spin there is the exchange correlation.

The correlation function $\rho_{\sigma'\sigma''}(\mathbf{r}', \mathbf{r}'')$ for an n-electron system is defined as

$$\begin{aligned}\rho_{\sigma'\sigma''}(\mathbf{r}', \mathbf{r}'') = \sum_{i,j=1}^{2n} \int \cdots \int d\tau_1 \cdots d\tau_n \Psi^*(\mathbf{r}_1 \cdots r_n) \\ \times \Psi(\mathbf{r}_1 \cdots r_n)\, \delta_{\sigma'}(\mathbf{r}_i - \mathbf{r}')\, \delta_{\sigma''}(\mathbf{r}_j - \mathbf{r}'')\end{aligned} \tag{D1}$$

This can be written in second quantized form, following the notation of Sec. V, as

$$\begin{aligned}\rho_{\sigma'\sigma''}(\mathbf{r}', \mathbf{r}'') = (\Psi_0 \left|\psi_{\sigma''} * (\mathbf{r}'')\, \psi_{\sigma'} * (\mathbf{r}')\, \psi_{\sigma'}(\mathbf{r}')\, \psi_{\sigma''}(\mathbf{r}'')\right| \Psi_0) \\ = \sum_{\mathbf{k}_1,\mathbf{k}_2,\mathbf{k}_3,\mathbf{k}_4} (\Psi_0 \left|c^*(\mathbf{k}_1, \sigma'')\, c^*(\mathbf{k}_2, \sigma')\, c(\mathbf{k}_3, \sigma')\, c(\mathbf{k}_4, \sigma'')\right| \Psi_0) \\ \times e^{i(\mathbf{k}_4 - \mathbf{k}_1)\cdot\mathbf{r}'' + i(\mathbf{k}_3 - \mathbf{k}_2)\cdot\mathbf{r}'},\end{aligned} \tag{D2}$$

where Ψ_0 is our ground-state wave function.

Of particular interest is the correlation function for electrons of opposite spin. If we define

$$\rho_A = \rho_{\uparrow\downarrow} + \rho_{\downarrow\uparrow} \tag{D3}$$

use the matrix elements obtained in Sec. IV, and set $\mathbf{r} = \mathbf{r}' - \mathbf{r}''$, we get at the absolute zero of temperature

$$\rho_A(r) = n\left[\frac{1}{2}n + P_A(r)\right]$$

where

$$P_A(r) = \frac{1}{2n}\left(\frac{1}{2\pi}\right)^6 \iint_{\mathcal{R}} d\mathbf{k} d\mathbf{k}' \left\{e^{i(\mathbf{k}' - \mathbf{k})\cdot\mathbf{r}} \frac{\epsilon_0^2(0)}{EE'}\right\} \tag{D4}$$

The integration is over $\mathcal{R}$, the region of interaction ($|\epsilon| < \hbar\omega$), and n is the number of electrons of both spin directions per unit volume. The terms in the bracket give the number of

electrons of opposite spin per unit volume one would find a distance r away from an electron of given spin direction. The first term is just the average density, while the second gives the effects of correlation.

The integral of $P_A(r)$ gives the number of electrons of opposite spin correlated with a given electron. This is

$$\begin{aligned}\int P_A(r)d\tau &= \frac{\epsilon_0^2(0)}{2n}\left(\frac{1}{2\pi}\right)^3\int_{\mathscr{R}} dk\frac{1}{\epsilon^2+\epsilon_0^2(0)} \\ &\simeq \frac{\epsilon_0^2(0)}{2n}\frac{1}{\pi^2}\frac{dk}{d\mathscr{E}}\Big]_F k_{F^2}\int_0^{\hbar\omega}\frac{d\epsilon}{\epsilon^2+\epsilon_0^2(0)} \\ &\simeq \frac{3}{4}\frac{1}{k_F\xi_0} = \frac{\pi n_c}{2}\end{aligned} \tag{D5}$$

where we have given slowly varying functions their value at the Fermi surface, and have used (5.43) and $n_c = N(0)\epsilon_0(0)$. Thus the number of electrons of given spin correlated to one of opposite spin is of the order of the ratio of the number of electrons in coherent pairs to the total number of electrons in the system.

The range of the spacial correlation may be determined by investigating $P_A(r)$. We must then evaluate

$$I = \left(\frac{1}{2\pi}\right)^3\int_{\mathcal{R}} d\mathbf{k}\frac{e^{i\mathbf{k}\cdot\mathbf{r}}}{E} = \frac{1}{2\pi^2 r}\int_{k_F-\delta}^{k_F+\delta}\frac{k\sin krdk}{\left[\epsilon^2+\epsilon_0^2(0)\right]^{\frac{1}{2}}} \tag{D6}$$

To evaluate this, we make use of the sharp maximum of the integral near $\epsilon = 0$ and the fact that the sine function is rapidly oscillating in this region for values of r of interest, $k_F r \gg 1$. We set (as in Sec. V)

$$k \simeq k_F + \frac{dk}{d\mathscr{E}}\Big]_F \epsilon = k_F + \epsilon/\left(hv_0\right) \tag{D7}$$

and

$$\sin\left(k_F+\frac{\epsilon}{hv_0}\right)r \simeq \sin k_F r\cos\left(\frac{\epsilon}{hv_0}r\right) \tag{D8}$$

give slowly varying functions their value at the Fermi surface, and drop terms antisymmetric in ϵ. Then, setting $x = \epsilon/\epsilon_0$, we get

$$I = \frac{k_F}{\pi^2 r}\frac{1}{hv_0}\sin k_F r\int_0^a\frac{\cos\left(rx/\pi\xi_0\right)dx}{\left(x^2+1\right)^{\frac{1}{2}}} \tag{D9}$$

where $a = \hbar\omega/\epsilon_0 \gg 1$. The integral may be expressed as

$$\int_0^a\frac{\cos\left(r/\pi\xi_0\right)x}{\left(x^2+1\right)^{\frac{1}{2}}}dx = K_0\left(\frac{r}{\pi\xi_0}\right) - \int_a^\infty\frac{\cos\left(rx/\pi\xi_0\right)}{\left(x^2+1\right)^{\frac{1}{2}}}dx \tag{D10}$$

where K_0 is a modified Bessel function. [39] Since $a \gg 1$ except for very small values of $r, \left(x^2+1\right)^{\frac{1}{2}} \simeq x$ in the last integral. Then, setting $t = rx/\left(\pi\xi_0\right)$, we have

$$I = \frac{k_F}{\pi^2 r}\frac{1}{hv_0}\sin k_F r\left[K_0\left(\frac{r}{\pi\xi_0}\right) - \int_{ar/\pi\xi_0}^\infty\frac{\cos t}{t}dt\right].$$

Asymptotically

$$-\int_x^\infty \frac{\cos t}{t} dt \sim \frac{\sin x}{x}, \quad x \gg 1$$

while $K_0(x)$ falls off exponentially. Thus the asymptotic behavior of $P_A(r)$ is given by

$$P_A(r) \sim \frac{9n\epsilon_0^2(0)}{2(\hbar\omega)^2} \frac{\sin^2 k_F r \sin^2\left(\frac{\epsilon_0}{\hbar\omega}\frac{r}{\pi\xi_0}\right)}{(k_F r)^4}.$$

Since $a = h\omega/\epsilon_0 \gg 1$, the range of correlation is determined by the K_0 function which drops off rapidly when $r/(\pi\xi_0) \gtrsim 1$. Thus correlation distance is the order of $\pi\xi_0 \simeq 10^{-4}$ cm.

3.10.12 Phase and Particle Number Operators in SC

Calculation of the Number of Particles

One gets the number of particles from $F_{\boldsymbol{k}}$, which has the meaning of a 'condensate wave-function' (apart from normalization)

$$\frac{N_0}{|\Lambda|} := \frac{1}{|\Lambda|}\sum_{\text{band}} |F_{\boldsymbol{k}}|^2 = \frac{1}{|\Lambda|}\sum_{\text{band}} \Delta^2/(2E_{\boldsymbol{k}})^2 = \frac{N(0)}{4}\int_{\text{band}} \mathrm{d}\xi \frac{\Delta^2}{\xi^2+\Delta^2}$$

For obvious reasons, N_0 is identified with the number of particles in the condensate. In the limit $\Delta \ll \omega_c$, the integral can be extended to the full line and this yields

$$\frac{N_0}{|\Lambda|} = \frac{\pi}{4}\Delta N(0)$$

In the free-electron approximation, we have

$$N(0) \sim (3\epsilon_F)^{-1} N/\Lambda$$

where N/Λ is the total density, then

$$N_0/N = \pi\Delta/(12\epsilon_F)$$

what is in particular clear from this relation, is that the condensate density vanishes with Δ. This is logical because only the electrons near the FS participate in the condensate.

Particle number is not conserved in superconductors

(here I'll explain, why it is so?)

Particle number and phases have uncertainty

It's common knowledge (and has been discussed in other questions on this site) that the standard BCS ground state $|\Psi_{BCS}\rangle = \prod_k \left(u_k + v_k c^\dagger_{k\uparrow} c^\dagger_{-k\downarrow}\right)|0\rangle$ does not have a well-defined particle number and that this doesn't matter in bulk superconductors because the standard deviation is $\Delta N \propto \sqrt{N}$ and hence irrelevant for $N \to \infty$.

But I also read that you can arrive at a BCS state with well-defined particle number by first defining

$$|\Psi_{BCS}(\phi)\rangle = \left(|u_k| + e^{i\phi}|v_k|c^\dagger_{k\uparrow}c^\dagger_{-k\downarrow}\right)|0\rangle$$

and then "integrating out" the phase according to

$$|\Psi_{BCS}(N)\rangle = \int_0^{2\pi} \mathrm{d}\phi\, e^{-iN\phi/2}\,|\Psi_{BCS}(\phi)\rangle \ ,$$

which gives you a BCS state with precisely N particles **at the cost of having a completely ill-defined phase**.

If that is true, then surely this is the actual "physical" state of a superconductor and the original BCS state is merely used for convenience.

But that, in turn, *would make the well-defined phase of the superconducting state a mere mathematical artifact*, when every other textbook highlights it as something very fundamental (and if I remember correctly, it's very important for things like the Josephson effect as well).

So, can anyone point to the error in the logic above?

The important point is that $[N, \phi] = i$, with N the number of electron et ϕ the phase. So you can apply the Heisenberg uncertainty principle, of which you gave the two extremum situations of 1) either perfectly defined N and completely unknown ϕ or 2) perfectly defined ϕ and completely unknown N. In general varying a bit the phase ϕ let a bit of electron N flowing, which is the basic situation in mesoscopic systems (e.g. Josephson junctions).

Conceptually, isolate a part of a superconductor (or any macroscopic system behaving as quantum mechanics), if you can count the number of electrons precisely, there is no current and so no phase difference, so ϕ is not a good quantum number. If you can define a current (and so fix a phase *difference*) you can not count the electrons in your control volume of superconductor.

Note that it is not that obvious to demonstrate the commutation relation $[N, \phi] = i$ in the general case, and discussions using this relation are usually subtle.

from https://physics.stackexchange.com/questions/284314/bcs-state-with-well-defined-particle-number-interpretation/284355#284355

3.10.13 BCS model with net motion of electrons

(??? write it later here! it is already written before in Shmid's theory and in Gor'kov's theory)

Net motion of Cooper pairs in BCS

(оставил этот вопрос, внятного ответа не читал, самому думать про это нет времени)

Электроны в паре Купера все-таки куда-то в общей массе двигаются, пусть и имеют противоположные импульсы, потому что их импульсы противоположны только в их СО, а не в нашей. (???? никак это не соотношу с формулой?????????????77)

BCS model with net motion of Cooper pairs

(write solution to it here)

How can each electron move in the Cooper pair to the different directions?

(подробно отвечу на этот вопрос, потому что давно он весит. не знаю пока удовлетворяющего меня ответа! потом пропишу. ну да, говорим, что это в СО электронов, а эта СО и движется. но где конкретно это в формулах?)

3.11 BCS: Formalisms for Special Setups

3.11.1 BCS in a Framework of Path Integral

(write this later here! also, before there will be paragraphs with it)

Why path integral is applicable for the BCS model?

(because this is a general framework of the cond matter. but I'll write a really good answer here)

What do we mean by path integral for the BCS model?

(now, there is no that interpretation of paths, so what do we mean by these formulas?)

Formulation of BCS using Path Integral

(see Coleman and others, add it here)

Advantages of path integral approach?

(discuss advantages)

Should we really use path integral approach?

(??? currently, I think that no, without it all works fine. but maybe later I'll see that it is better to formulate all in it...)

3.11.2 Nambu Notation, Hole Interpretation

(I'll write about it from my master's thesis)

Formulation of the Nambu formalism

(??? write a good theory)
There are several ways of introduction of the Nambu notation.

The typical Nambu spinor is defined as

$$\psi_{\mathbf{k}} = \begin{pmatrix} c_{\mathbf{k}\uparrow} \\ c^{\dagger}_{-\mathbf{k}\downarrow} \end{pmatrix} \quad \text{electron}$$

with the corresponding Hermitian conjugate

$$\psi^{\dagger}_{\mathbf{k}} = \left(c^{\dagger}_{\mathbf{k}\uparrow}, c_{-\mathbf{k}\downarrow} \right)$$

Nambu spinors behave like conventional electron fields, with an algebra

$$\left\{ \psi_{\mathbf{k}\alpha}, \psi^{\dagger}_{\mathbf{k}'\beta} \right\} = \delta_{\alpha\beta}\delta_{\mathbf{k},\mathbf{k}'}$$

but instead of up and down electrons, they describe electrons and holes. These spinors enable us to unify the kinetic and pairing energy terms into a single vector field, analogous to a magnetic field, that acts in isospin space.

The kinetic energy can be written as

$$\sum_{\mathbf{k}} \epsilon_{\mathbf{k}} \left(c^{\dagger}_{\mathbf{k}\uparrow} c_{\mathbf{k}\uparrow} - c_{-\mathbf{k}\downarrow} c^{\dagger}_{-\mathbf{k}\downarrow} + 1 \right) = \left(c^{\dagger}_{\mathbf{k}\uparrow}, c_{-\mathbf{k}\downarrow} \right) \begin{bmatrix} \epsilon_{\mathbf{k}} & 0 \\ 0 & -\epsilon_{\mathbf{k}} \end{bmatrix} \begin{pmatrix} c_{\mathbf{k}\uparrow} \\ \bar{c}^{\dagger}_{-\mathbf{k}\downarrow} \end{pmatrix} + \sum_{\mathbf{k}} \epsilon_{\mathbf{k}},$$

where the sign reversal in the lower component derives from anticommuting the downspin electron operators. The energy $-\epsilon_{\mathbf{k}}$ is the energy to create a hole. We will drop the constant remainder term $\sum_{\mathbf{k}} \epsilon_{\mathbf{k}}$. We can now combine the kinetic and pairing terms into a single matrix:

$$\epsilon_{\mathbf{k}} \sum_{\sigma} c^{\dagger}_{\mathbf{k}\sigma} c_{\mathbf{k}\sigma} + \left[\bar{\Delta} c_{-\mathbf{k}\downarrow} c_{\mathbf{k}\uparrow} + c^{\dagger}_{\mathbf{k}\uparrow} c^{\dagger}_{-\mathbf{k}\downarrow} \Delta \right] = \left(c^{\dagger}_{\mathbf{k}\uparrow}, c_{-\mathbf{k}\downarrow} \right) \begin{bmatrix} \epsilon_{\mathbf{k}} & \Delta \\ \bar{\Delta} & -\epsilon_{\mathbf{k}} \end{bmatrix} \begin{pmatrix} c_{\mathbf{k}\uparrow} \\ c^{\dagger}_{-\mathbf{k}\downarrow} \end{pmatrix}$$

And in this notation one can work with BCS Hamiltonian further.

Another way of introducing another Nambu notation, more in matrix from is as follows:

$$\begin{aligned} \mathcal{H} &= \epsilon \left(c^{\dagger}_1 c_1 + c^{\dagger}_2 c_2 \right) + \lambda \left(c^{\dagger}_1 c^{\dagger}_2 + c_2 c_1 \right) = \\ &= \frac{1}{2} \begin{pmatrix} c^{\dagger}_1 & c_2 & c^{\dagger}_2 & c_1 \end{pmatrix} \begin{pmatrix} \epsilon & \lambda & 0 & 0 \\ \lambda & -\epsilon & 0 & 0 \\ 0 & 0 & \epsilon & -\lambda \\ 0 & 0 & -\lambda & -\epsilon \end{pmatrix} \begin{pmatrix} c_1 \\ c^{\dagger}_2 \\ c_2 \\ c^{\dagger}_1 \end{pmatrix} + \epsilon \end{aligned}$$

(??? by the way, how to derive it???)
Maybe it is not exactly a Nambu notation, just it also works. And we can find spectrum by just computing eigenvalues of the obtained squared matrix.

(here, about extended Nambu notation, see my thesis or articles)
(discuss that actually there are two ways of introducing it)
(and that there is an important minus in the last component)

(and there are other notations from articles, which I'll list here)

Hole interpretation of excitation of SC

(it is an easy idea, I'll write later)

Nambu Notation: Other features

Nambu Notation for MTJJ

(a good example, I'll write from my thesis that we have such SC Hamiltonian, so let's write it in Nambu notation. A good illustration)

What was Nambu originally doing when he introduced his notation?

(I don't know, since his article is a very complicated one, but the question is very interesting)

3.11.3 Gap in Unconventional Superconductors: Basics

(this is not needed, just to connect it with NC SC section)

Theory

The spin wavefunction of a singlet state is antisymmetric upon an interchange of the particles (spin indices). It enables us to write the order parameter as

$$\hat{\Delta}(\mathbf{k}) = d_0(\mathbf{k}) \begin{pmatrix} 0 & 1 \\ -1 & 0 \end{pmatrix} = d_0(\mathbf{k}) i\hat{\sigma}_2 = d_0(\mathbf{k})\hat{\chi}_0 \tag{1.81}$$

In terms of the spin up ($\uparrow$) and spin down ($\downarrow$) wavefunctions of individual electrons, the quantity

$$\hat{\chi}_0 = i\hat{\sigma}_2 = \begin{pmatrix} 0 & 1 \\ -1 & 0 \end{pmatrix}, \tag{1.82}$$

corresponds to the singlet wave function $\frac{1}{\sqrt{2}}[|\uparrow\rangle|\downarrow\rangle - |\downarrow\rangle|\uparrow\rangle]$. The factor $\hat{\chi}_0$ is antisymmetric upon interchanging spin variables of the order parameter while $d_0(\mathbf{k})$ is symmetric upon interchanging orbital variables of the order parameter, that is, $d_0(-\mathbf{k}) = d_0(\mathbf{k})$. The singlet pairing symmetry has been discovered in most of the conventional superconductors [28], high-temperature cuprates [29], ironbased superconductors [30], and $\mathrm{Ce}-115$ [31] and $\mathrm{Pu}-115$ [32, 33] heavy fermion superconductors.

For the triplet pairing state, the total spin is $S = 1$ for the two paired electrons and accordingly there are three spin wavefunctions. Therefore, the pairing amplitude for each of these spin states can be different and $\mathbf{k}$-dependent. The order parameter may then be written in the form:

$$\hat{\Delta}(\mathbf{k}) = \mathbf{d}(\mathbf{k}) \cdot \hat{\boldsymbol{\sigma}} i\hat{\sigma}_2 = \mathbf{d}(\mathbf{k}) \cdot \hat{\chi}, \tag{1.83}$$

where the vector $\mathbf{d}$ measures the amplitude of the order parameter and the matrices

$$\hat{\chi}_1 = i\hat{\sigma}_1\hat{\sigma}_2 = \begin{pmatrix} -1 & 0 \\ 0 & 1 \end{pmatrix}, \tag{1.84}$$

$$\hat{\chi}_2 = i\hat{\sigma}_2\hat{\sigma}_2 = \begin{pmatrix} i & 0 \\ 0 & i \end{pmatrix}, \tag{1.85}$$

and

$$\hat{\chi}_3 = i\hat{\sigma}_3\hat{\sigma}_2 = \begin{pmatrix} 0 & 1 \\ 1 & 0 \end{pmatrix}. \tag{1.86}$$

They correspond to the spin wavefunctions

$$\hat{\chi}_1 \to \frac{-1}{\sqrt{2}}[|\uparrow\rangle|\uparrow\rangle - |\downarrow\rangle|\downarrow\rangle] \tag{1.87}$$

$$\hat{\chi}_2 \to \frac{i}{\sqrt{2}}[|\uparrow\rangle|\uparrow\rangle + |\downarrow\rangle|\downarrow\rangle] \tag{1.88}$$

and

$$\hat{\chi}_3 \to \frac{1}{\sqrt{2}}[|\uparrow\rangle|\downarrow\rangle + |\downarrow\rangle|\uparrow\rangle]. \tag{1.89}$$

Now all three of these wavefunctions are symmetric upon interchanging the spin indices. In an expanded form, the triplet order parameter is written as:

$$\hat{\Delta}(\mathbf{k}) = \begin{pmatrix} -d_x(\mathbf{k}) + id_y(\mathbf{k}) & d_z(\mathbf{k}) \\ d_z(\mathbf{k}) & d_x(\mathbf{k}) + id_y(\mathbf{k}) \end{pmatrix}. \tag{1.90}$$

Recall that $\hat{\Delta}$ must satisfy the Pauli antisymmetric property $\hat{\Delta}_{\beta\alpha}(-\mathbf{k}) = -\hat{\Delta}_{\alpha\beta}(\mathbf{k})$, so we have $\mathbf{d}(-\mathbf{k}) = -\mathbf{d}(\mathbf{k})$. Also notice that the parity of spherical harmonics is $(-1)^{-l}$, the above behavior is in accord with our intuition for p-wave ($l = 1$) (or more generally, odd angular momentum) pairing.

If the vector $\mathbf{d}(\mathbf{k})$ has the form $\mathbf{d}(\mathbf{k}) = a(\mathbf{k})\hat{\mathbf{n}}(\mathbf{k})$, where $a(\mathbf{k})$ is a complex number and $\hat{\mathbf{n}}(\mathbf{k})$ is a real unit vector, we then have the property

$$\mathbf{d}(\mathbf{k}) \times \mathbf{d}^*(\mathbf{k}) = 0 \tag{1.91}$$

This property leads to the constraint

$$\hat{\Delta}^\dagger(\mathbf{k})\hat{\Delta}(\mathbf{k}) = |\mathbf{d}|^2\hat{\mathbf{1}} + i\hat{\boldsymbol{\sigma}} \cdot [\mathbf{d}(\mathbf{k}) \times \mathbf{d}^*(\mathbf{k})] \;=\; |\mathbf{d}|^2\hat{\mathbf{1}} \tag{1.92}$$

We refer to a state where $\mathbf{d}$ has the property as given by Eq.(1.91) as the unitary state because $\hat{\Delta}^\dagger\hat{\Delta}$ is then proportional to the unit matrix. A rigorous classification of the symmetry properties of triplet superconductors was given by Blount [34], and Ueda and Rice [35] based on the group theory.

For the p-wave pairing state, the most general gap structure would involve a sum over all possible spin-orbital wavefunction products, each with its own complex amplitude, which we may write as

$$\hat{\Delta} = \sum_{i,\alpha} D_{\alpha i}\hat{\chi}_\alpha \hat{k}_i \tag{1.93}$$

Here the indices α and i denotes the three component in spin and orbitals spaces with $\hat{k}_x = \sin\theta\cos\phi, \hat{k}_y = \sin\theta\sin\phi$, and $\hat{k}_z = \cos\theta$ while χ_α already given above. The matrix $D_{\alpha i}$ allows nine complex (equivalently, 18 real) coefficients and suggests the possibility of 18 types of pairing states.

So far, the spin triplet pairing states has been discovered in ^{3}He superfluid [36] and possibly in Sr_2RuO_4 [37] and heavy-fermion UPt_3 and UBe_{13} [38-40] superconductors. In superfluid ^{3}He, two phases are stabilized at zero magnetic field and very low temperatures, depending on pressure [41]. They can be represented by the $D_{\alpha i}$ matrices:

$$\text{(B phase): } \hat{D} = \Delta_0 \begin{pmatrix} 1 & 0 & 0 \\ 0 & 1 & 0 \\ 0 & 0 & 1 \end{pmatrix}, \tag{1.94}$$

$$\text{(A phase): } \hat{D} = \Delta_0 \begin{pmatrix} 0 & 0 & 0 \\ 0 & 0 & 0 \\ 1 & i & 0 \end{pmatrix}. \tag{1.95}$$

The corresponding gap matrices are:

$$\begin{aligned} \text{(B phase): } \hat{\Delta} &= \Delta_0 \begin{pmatrix} -\hat{k}_x + i\hat{k}_y & \hat{k}_z \\ \hat{k}_z & \hat{k}_x + i\hat{k}_y \end{pmatrix}, \\ (\text{ A phase for } \mathbf{d}\|\hat{\mathbf{z}}): \quad \hat{\Delta} &= \Delta_0 \begin{pmatrix} 0 & \hat{k}_x + i\hat{k}_y \\ \hat{k}_x + i\hat{k}_y & 0 \end{pmatrix}. \end{aligned} \tag{1.97}$$

The B-phase is also called the BW phase proposed by Balian and Werthamer [42]. In this phase, the single particle spectrum and the energy gap are isotropic; the total spin and orbital angular momenta are each equal to 1 ; the spin susceptibility is finite at zero temperature. The A-phase is also called the ABM-phase proposed by Anderson, Brinkman, and Morel [43]. In this phase, the S_z channel is completely suppressed and the spin susceptibility is very similar to that in the normal state.

3.11.4 Anderson's Random-Phase Approximation in SC

(add it later here)

Main ideas

3.11.5 Impurities in BCS: General Idea How to Take Them into Account

Остановимся теперь кратко на вопросе о влиянии примесей на спаривание электронов. В присутствии примесей направление импульса электрона не сохраняется, поэтому строить пары из электронов с противоположными импульсами $\hbar\mathbf{k}$ и $-\hbar\mathbf{k}$, как мы это делали выше, затруднительно. Однако ничто не мешает использовать вместо электронных плоских волн $e^{i\mathbf{kr}}$ точные волновые функции $\chi_n(\mathbf{r})$ электронов с учетом потенциала примесей $U(\mathbf{r})$, описывающие диффузионное распространение электронных волн. Точный вид этих функций нам неизвестен, но он и не войдет в окончательные уравнения типа (44.11) и (45.15) на величину щели Δ. Единственное, но важное условие состоит в том, чтобы для всякого электронного состояния n с волновой функцией $\chi_n(\mathbf{r})$ имелось «парное» состояние $\bar{n}$ с волновой функцией $\chi_{\bar{n}}(\mathbf{r}) = \chi_n^*(\mathbf{r})$, отвечающее движению электрона "вспять" но диффузионной траектории, соответствующей состоянию n. Комплексное сопряжение волновых функций в квантовой механике эквивалентно операции обращения времени, поэтому в одном и том же случайном потенциале $U(\mathbf{r})$ существуют одновременно точные состояния $\chi_n(\mathbf{r})$ и $\chi_n^*(\mathbf{r})$, если $U(\mathbf{r})$ не меняется при:амене $t \to -t$. Это условие выполнено для обычных примесей, которые поэтому очень слабо влияют на Δ_0 и другие термодинамические свойства сверхпроводника даже в "грязном" пределе, когда длина свободного пробега $l \ll \xi_0$ (т. наз. "теорема Андерсона», подробнее см. [7]).

Совсем иначе обстоит дело, если в сверхпроводнике имеются магнитные примеси, непосредственно взаимодействующие со спинами электронов (или если к грязному сверхпроводнику приложено магнитное поле). В этом случае 'имметрия электронных состояний по отношению к обращению «ремени нарушается, и температура сверхпроводящего перехода резко падает с концентрацией таких примесей.

3.11.6 Impact of Lattice Configuration in BCS

(here we will discuss in details, how to take into account lattice structure. (????))
(??? I don't know it at all now)

General Idea How to Take Lattice Configuration into Account

(???? still, have no idea, I need to read papers about it)

3.11.7 BCS theory in the Density Matrix Framework

Do we need the density matrix for superconductivity?

(I don't know, actually, distribution of particles are fine. but maybe I'll write later, when it is useful?zx)

Formulation of BCS theory in the density matrix framework

(no, currently I don't understand how to write it)

(write here how the density matrix of a SC look like!!!)

Conceptual details of formulation of BCS theory in the density matrix framework

What is a density matrix for BCS in general?

(write, how to understand it????)

Evolution of BCS theory in the density matrix framework

(write how we deal with BCS in it????)
(no, currently I don't understand how to write it)
(??? how to answer it???? Read Brower Petrucione, this is the only way I know)

Gap in the density matrix framework

(???? I don't know, how is it related to the density matrix, but okay, I'll learn it later)
Here, we will present the evaluation of a gap in a notation of diagonalization of Hamiltonian. First, we write the Hamiltonian in the Nambu notation:

$$\epsilon_{\mathbf{k}} \sum_{\sigma} c^{\dagger}_{\mathbf{k}\sigma} c_{\mathbf{k}\sigma} + \left[\bar{\Delta} c_{-\mathbf{k}\downarrow} c_{\mathbf{k}\uparrow} + c^{\dagger}_{\mathbf{k}\uparrow} c^{\dagger}_{-\mathbf{k}\downarrow} \Delta \right] = \left(c^{\dagger}_{\mathbf{k}\uparrow}, c_{-\mathbf{k}\downarrow} \right) \begin{bmatrix} \epsilon_{\mathbf{k}} & \Delta \\ \bar{\Delta} & -\epsilon_{\mathbf{k}} \end{bmatrix} \begin{pmatrix} c_{\mathbf{k}\uparrow} \\ c^{\dagger}_{-\mathbf{k}\downarrow} \end{pmatrix}$$

we will introduce a matrix and an index notation

$$H = \psi^{\dagger} h \psi = \sum_{jl} h_{jl} \psi^{\dagger}_{j} \psi_{l}$$

Our goal is to obtain the gap, which is the average of two hole operators. For this, we need to go to a basis where the Hamiltonian is diagonal.

The Hamiltonian matrix is diagonalized by a unitary matrix U:

$$h = U^{\dagger} D U$$

or in index notation,

$$h_{jl} = \sum_{kk'} \left(U_{kj} \right)^{\dagger} D_{kk'} U_{k'l} = \sum_{k} U^{*}_{jk} D_{kk} U_{kl},$$

where we used that $D_{kk'}$ is diagonal and that $\left(U_{kj} \right)^{\dagger} = U^{*}_{jk^{*}}$. By the algorithm of diagonalization, the U_{kl} and U_{kj} are constructed by the right eigenvector matrices, i.e., matrices where the columns are the right eigenvectors of h.

The full Hamiltonian is rewritten in terms of the diagonal basis

$$H = \sum_{jl,k} U^*_{jk} D_{kk} U_{kl} c^\dagger_j \psi_l = \sum_{jl,k} D_{kk} (U^*_{jk} \psi^\dagger_j)(U_{kl}\psi_l) = \sum_k D_{kk} \eta^\dagger_k \eta_k,$$

where we introduced a new basis

$$\eta_k = \sum_l U_{kl}\psi_l \qquad \eta^\dagger_k = \sum_j (U_{kj})^\dagger \psi^\dagger_j = \sum_j U^*_{jk}\psi^\dagger_j$$

and the back transformation is

$$\psi_l = \sum_k U^*_{lk}\eta_k, \qquad \psi^\dagger_j = \sum_k \left(U^*_{jk}\right)^\dagger \eta^\dagger_k = \sum_k U_{kj}\eta^\dagger_k$$

This is obvious from looking at the previous transformations as a multiplication of a matrix to a column.

Now, we can notice that all the combination of daggered and non-daggered operators in general can be expressed as

$$\begin{aligned}
A_{jl} &= \left\langle \psi^\dagger_j \psi_l \right\rangle \\
&= \frac{1}{Z} \operatorname{Tr}\left[e^{-\beta H} \psi^\dagger_j \psi_l \right] \\
&= \frac{1}{Z} \operatorname{Tr}\left[e^{-\beta \sum_k D_{kk}\eta^\dagger_k \eta_k} \sum_{k'} U_{k'j}\eta^\dagger_{k'} \sum_{k''} U^*_{lk''}\eta_{k''} \right] \\
&= \sum_{k'k''} U_{k'j} U^*_{lk''} \underbrace{\frac{1}{Z} \operatorname{Tr}\left[e^{-\beta \sum_k D_{kk}\eta^\dagger_k\eta_k} \eta^\dagger_{k'}\eta_{k''} \right]}_{F_{kk'} = \delta_{k,k'} \operatorname{diag}(f(D_{kk},\beta))} \\
&= \sum_k U^*_{lk} F_{kk} U_{kj}
\end{aligned}$$

Here, the f is the Fermi function. This is because we now can easily compute the trace, because we have just two states with $\eta^\dagger_k\eta_k = 0$ and $\eta^\dagger_k\eta_k = 1$.

(??? don't understand the density matrix!!! what about other states??? or it is just a matrix from our common sense, but not a density matrix of thermal superconductor???)

In matrix notation, this corresponds to

$$A = U^\dagger F U$$

Thus, we can just take the 10-component to get the conjugated gap (this component corresponds to $\psi^\dagger_1\psi_0 = c_{-k\downarrow}c_{k\uparrow}$). This is the exactly its definition. Note that the 01-component will give us also exactly the definition of the conjugated gap (this component corresponds to $\psi^\dagger_0\psi_1 = c^\dagger_{k\uparrow}c^\dagger_{-k\downarrow}$). There are no problems with minus sign which could arise from the order of Fermi operators under the averaging.

Other (00 and 11) components have no meaning. This is not a Fermi function, since $c\,\dagger\,c$ is not an excitation (the excitations are Bogoliubov operators). (????? yes?)

Now, we need to find the U matrix. For this, we find normalized eigenvalues and just plug them into the columns.

(??? write it analytically)

This is realized in Wolfram as follows:

```
ham = {{\[Xi],
    Conjugate[\[CapitalDelta]]}, {\[CapitalDelta], -\[Xi]}};

Eigenvectors[ham]

norm1 = Sqrt[(\[Xi] +
       Sqrt[\[Xi]^2 + \[CapitalDelta] ^2])^2/\[CapitalDelta]^2 + 1];
norm2 = Sqrt[(\[Xi] -
       Sqrt[\[Xi]^2 + \[CapitalDelta] ^2])^2/\[CapitalDelta]^2 + 1];

Uinv = {{-((-\[Xi] -
       Sqrt[\[CapitalDelta]^2 + \[Xi]^2])/\[CapitalDelta]) 1/
     norm1, -((-\[Xi] +
       Sqrt[\[CapitalDelta]^2 + \[Xi]^2])/\[CapitalDelta]) 1/
     norm2}, {1/norm1, 1/norm2}} // MatrixForm
```

we get

$$U = \begin{pmatrix} -\frac{-\xi-\sqrt{\Delta^2+\xi^2}}{\Delta\sqrt{\frac{\left(\xi+\sqrt{\Delta^2+\xi^2}\right)^2}{\Delta^2}+1}} & -\frac{\sqrt{\Delta^2+\xi^2}-\xi}{\Delta\sqrt{\frac{\left(\xi-\sqrt{\Delta^2+\xi^2}\right)^2}{\Delta^2}+1}} \\ \frac{1}{\sqrt{\frac{\left(\xi+\sqrt{\Delta^2+\xi^2}\right)^2}{\Delta^2}+1}} & \frac{1}{\sqrt{\frac{\left(\xi-\sqrt{\Delta^2+\xi^2}\right)^2}{\Delta^2}+1}} \end{pmatrix}$$

And then we get the stated expression:

```
FullSimplify[ConjugateTranspose[Uinv].ham.Uinv,
 Assumptions -> {\[CapitalDelta] > 0, \[Xi] > 0}]

fermi[\[Epsilon]_, \[Beta]_] := 1/(1 + Exp[\[Beta] \[Epsilon]]);

rhodiag =
  DiagonalMatrix[{fermi[Sqrt[\[Xi]^2 + \[CapitalDelta]^2], \[Beta]],
    fermi[- Sqrt[\[Xi]^2 + \[CapitalDelta]^2], \[Beta]]}];

FullSimplify[ConjugateTranspose[Uinv].rhodiag.Uinv,
  Assumptions -> {\[CapitalDelta] > 0, \[Xi] > 0}] // MatrixForm
```

after taking the 01- component we get the gap equation:
(copy it from wolrfam!)
This is how by knowing the density matrix, we can obtain the gap.

Gap in the density function framework: Features

Derivation of the gap equation by plugging the diagonal basis

(this is a slightly different approach as the one above, which gives the same result. I'll write it later)

Is it possible to evaluate the gap by matrix exponent?

(write this statement that we have these series, so we know the answer and it is interesting to obtain it. but it is very complicated)
(see section of problems for my attempt of evaluating it)

How does the approach of rotating with eigenvectors related to the typical Bogoliubov transformations?

(???? there is a question about it. I am not sure now)

Overview about what is done about BCS theory in the density matrix framework

There are some articles that connect DFT and SC, but currently I consider them as bad and non-practical.
(??? maybe later I'll write something about them or I'll a=find a good article)

Other features and questions of the BCS in the density function framework

Advantages of BCS in the density function framework

(discuss, why it is useful to do it??)

Generalization of BCS theory in the density matrix framework for the case of open superconducting systems

(see also a subsubsection about it below)

Don't solve Loiuville equation using exponents

(write that we don't use exponents. this is an unsolvable approach. I'll summarize what we tried to do in Ljubljana and why it did not work)

3.11.8 Time-Dependent BCS

(there are articles, I'll read them later)
(???)

Time-dependent BCS in the density function framework

(that theory that Zala told me)

Time-dependent BCS: Other features and questions

(??)

3.12 General Formalisms for Typical Effects

3.12.1 Currents and Tunneling Effects: Basic Concepts 1

Experimental Introduction to Tunneling

In 1961, Giaever pointed out the possibility of determining the energy gap by means of tunneling experiments [33, 34]. We will treat this method in some detail, since it yielded much new information far beyond just the measurement of the energy gap. The method is based on the observation of the tunneling current across a thin insulating layer between a reference sample and the superconductor to be studied. In contrast to the Josephson current we treated in Chapter 1, now we are concerned with the tunneling of the unpaired electrons.

The arrangement is shown schematically in Figure 3.11a. Two metallic conductors, for instance, two aluminum layers, are separated from each other by mean of a thin insulating layer, for instance, Al_2O_3. The Al_2O_3 is an excellent electrical insulator, which can be fabricated nearly perfectly also with a thickness of only a few nanometers.

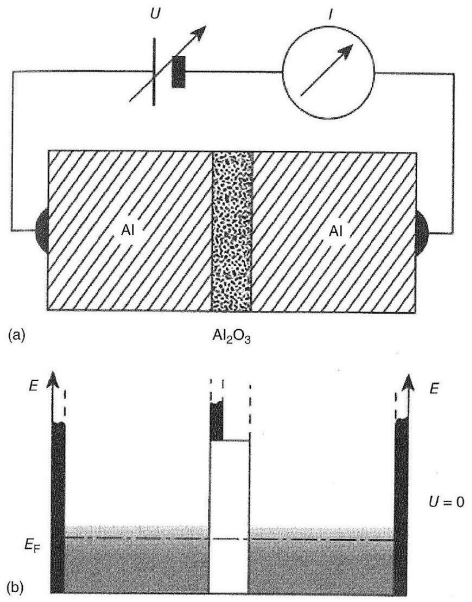


Figure 3.11 (a) The arrangement for measuring a tunneling current. (b) The allowed energy values (black areas) and their occupation (gray shaded areas).

Because of the great importance of this tunneling effect, for instance, also in semiconductor physics, we want to look at it in more detail. Therefore, in Figure 3.11b we have indicated schematically the allowed and forbidden energy ranges near the Fermi energy for the three parts of the tunneling arrangement. The black vertical areas indicate the allowed energy bands. The gray shaded areas show the occupation of the bands. The thermal smearing of the occupation is also indicated. In the electrical insulator the nearest allowed and unoccupied energy values are much higher.

We can also understand the tunneling effect without a detailed calculation, if we recall the wave character of our particles. If a wave encounters the surface of a medium into which it cannot enter, the wave must be totally reflected. Here, we recognize intuitively that the wave must penetrate a small distance into the forbidden portion. In some sense, the wave tests the possibility of whether it can exist in this medium. At the same time, its amplitude decreases exponentially, this decrease being faster, the larger the difference between the energy of the wave and

an allowed energy value, that is, the higher the barrier. From this highly qualitative argument, we see immediately that for a sufficiently thin barrier there is a finite probability that the wave can extend beyond the barrier. This is always the case if the thickness of the barrier is comparable with the decay length of the wave amplitude in the forbidden regime. In this case, a finite amplitude arrives at the back side where it can exit again into the allowed regime. However, there the amplitude is very small, that is, the probability for the passage of a particle decreases rapidly with increasing barrier thickness along with the wave amplitude. We see that the tunneling probability depends on the energetic height and on the thickness of the barrier. Here, the energetic height of the barrier must be taken from the particle energy, that is, in our case of Figure 3.11b practically from E_F.

In our present discussion we are dealing with electrons, that is, with Fermi particles. They must satisfy the Pauli principle (see Section 1.1). In order to traverse the barrier, the electron must find an unoccupied state on the other side. If all states are already occupied on the other side, the passage of the electron is impossible, even for a sufficiently thin barrier. Therefore, the number of particles passing across the barrier depends on the following three quantities:

number of electrons reaching the barrier;

tunneling probability across the barrier;

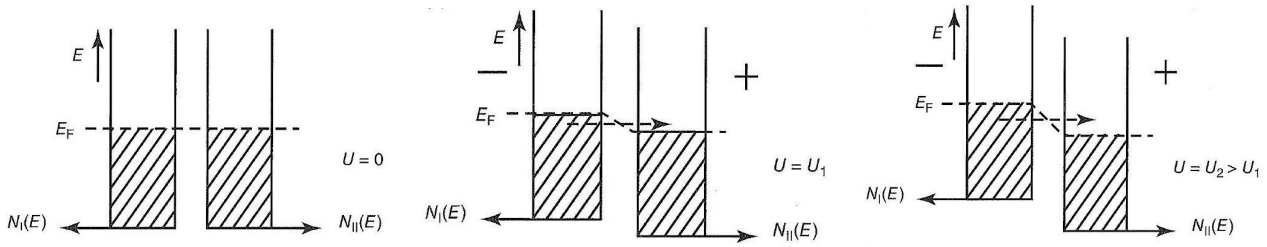
number of unoccupied energy levels on the other side.

In a quantitative treatment of the tunneling current of electrons, all three quantities must be taken into account

In Figure 3.11b we have shown the tunneling arrangement without an external voltage. If electrons can be exchanged between two systems, the equilibrium state is fixed by the fact that the Fermi energy is located at the same height, that is, the Fermi energy is displayed by a horizontal line in our schematic diagram. For this state the net exchange of particles is exactly zero. The same number of electrons tunnel to the right as to the left.

Next we apply a voltage $U \neq 0$ to the arrangement. Practically, the voltage drop is completely restricted to the barrier layer. This means that the Fermi energies on the right and on the left of the barrier differ by the amount eU. Now the tunneling currents in both directions no longer compensate each other, and a net current I flows.

To illustrate the magnitude of the current and its dependence on the voltage U, in Figure 3.12 we present a schematic diagram that also includes the density of states. Close to the Fermi energy, within the model of free electrons, the density of states can be taken approximately as constant. In Figure 3.12 the tunneling arrangement is shown for the voltages $U = 0, U_1$, and $U_2 > U_1$. The occupation of the states is indicated by the hatched areas. For simplicity we have taken the case $T = 0$. On the positive side of the voltage, the energy of the electrons with their negative charge is lowered compared to the negative side. In this case, more electrons can tunnel from left to right than in the opposite direction, that is, an electron current is flowing, as shown by the horizontal arrow in Figure 3.12b,c. Since we have assumed a constant density of states, the number of electrons that can



a) b) c)

Figure 3.12 Tunneling current between normal metals for three values of applied voltage, (a) $U = 0$, (b) $U = U_1$ and (c) $U = U_2 > U_1$. For simplicity, the distribution for $T = 0$ is shown. Near the energy E_F there are no states in the insulating barrier.

tunnel from left to right increases proportional to the voltage U. Therefore, the net tunneling current I is also proportional to the applied voltage U (see Figure 3.14, dashed curve. Here, we neglect the influence of the applied voltage on the energetic height of the barrier. At this point we emphasize again that we are only considering tunneling processes at constant energy, that is, transitions indicated horizontally in our scheme. During the tunneling process, for instance, within the barrier, an electron can absorb or emit a phonon. Such processes are referred to as "phonon-assisted tunneling". They are relatively rare and will be neglected initially.

The current-voltage characteristic of such a tunneling arrangement changes if one or both sides are in the superconducting state. This is immediately obvious, if we recall that in the superconducting state an energy gap appears in the energy spectrum of the unpaired electrons, which strongly changes the density of states near the Fermi energy.

In Figure 3.13 we show the first case, a normal conductor against a superconductor, following the scheme of Figure 3.12. Again, for simplicity we take the case $T = 0$. The corresponding current-voltage characteristic is shown in Figure 3.14 as curve 2. No tunneling current can flow

up to the voltage $U = \Delta_0/e$, since the electrons from the normal conductor do not find any states in the superconductor. At $U = \Delta_0/e$ the tunneling current sets in with a vertical slope. This steep rise is caused by the high density of unoccupied states in the superconductor. At higher voltages, the curve approaches the tunneling characteristic between two normal conductors (curve 1). At finite temperatures, in the normal conductor the distribution is thermally smeared, and also a few unpaired electrons exist in the superconductor above the energy gap. Furthermore, the energy gap is slightly reduced, as we have discussed in Section 3.1.2. The resulting characteristic is shown schematically in Figure 3.14 as curve 3.

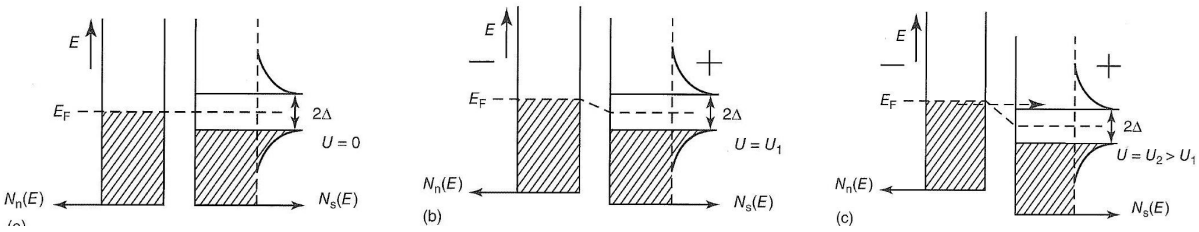
From such characteristics the energy gap can be determined easily. From the function $I(U)$, for a given density of states of the normal conductor, we can also extract quantitative information on the energy-dependent density of states of the unpaired electrons in the superconductor. For $T = 0$ and $N_{\mathrm{n}}(E) =$ constant, the derivative $\mathrm{d}//\mathrm{d}U$ directly yields the density of states of the unpaired electrons $N_{\mathrm{S}}(E)$.

We note that the tunneling characteristic is independent of the direction of the voltage. During reversal of the voltage, only the role of the unoccupied and occupied states is changed. If the superconductor is connected to the negative side, at $U = \Delta_0/e$ the unpaired electrons can tunnel into the free states of the normal conductor. We must recall that because of the Pauli principle during the tunneling process of single electrons, in addition to the electrons of the state at the starting point (for instance, on the left side in Figure 3.13), the free energy sites at the terminal point (on the right side in Figure 3.13) must also exist.

Before we turn to case 2, namely the tunnel junction between two superconductors, we want to look at the quantitative relation between the important quantities. As we have seen, the tunneling probability depends on the height and width of the barrier. Within the small energy range near the Fermi energy with which we are concerned, we can treat this probability as a constant (independent of the energy). We denote it by D. The number of electrons tunneling per unit time at energy E from left to right is proportional to the number of occupied states $^{13}N_{\mathrm{I}}(E)f(E)$ on the left side and to the number of unoccupied states on the right side. The probability of finding an unoccupied state at energy E is 1 minus the probability that this state is occupied, that is, $1 - f(E)$. In the case of a voltage drop U across the barrier, the electrons tunnel from a state with energy E on the left side into a state with energy $E + eU$ on the right side. Hence, at the voltage U, their number is

$N_{\mathrm{II}}(E + eU)[1 - f(E + eU)]$

We denote the density of states in the electrodes by the indices I or II.



a) b) c)

Figure 3.13 Tunneling current between a normal conductor and a superconductor for $T = 0$ and three values of applied voltage, (a) $U = 0$, (b) $U = U_1$ and (c) $U = U_2 > U_1$.

Basic Intuitive Formulas for Tunneling

In the following we measure the electron energy from the Fermi energy: $\varepsilon = E - E_\mathrm{F}$. So in a small energy interval $\mathrm{d}\varepsilon$ at the energy ε, we have the following small contribution to the tunneling current from left to right:

$$\mathrm{d}I_{\mathrm{I}\to\mathrm{II}} \propto DN_\mathrm{I}(\varepsilon)f(\varepsilon)N_\mathrm{II}(\varepsilon + eU)[1 - f(\varepsilon + eU)]\mathrm{d}\varepsilon$$

The total tunneling current $I_{\mathrm{I}\to\mathrm{II}}$ is obtained by integration over all energies. One finds

$$I_{\mathrm{I}\to\mathrm{II}} \propto D \int_{-\infty}^{\infty} N_\mathrm{I}(\varepsilon)f(\varepsilon)N_\mathrm{II}(\varepsilon + eU)[1 - f(\varepsilon + eU)]\mathrm{d}\varepsilon$$

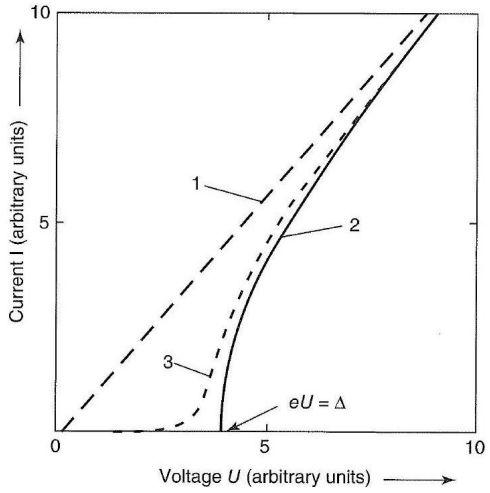


Figure 3.14 Current-voltage characteristic of tunnel junctions: curve 1, normal conductor/normal conductor (Figure 3.12); curve 2, normal conductor/superconductor, $T = 0$ K (Figure 3.13); and curve 3, normal conductor/superconductor, $0 < T < T_c$.

Since we measure the energy from E_F, we must integrate from $-\infty$ to $+\infty$. Similarly we obtain the tunneling current $I_{\mathrm{II}\to 1}$ from right to left:

$$I_{\mathrm{II}\to\mathrm{I}} \propto D \int_{-\infty}^{\infty} N_\mathrm{II}(\varepsilon + eU)f(\varepsilon + eU)N_\mathrm{I}(\varepsilon)[1 - f(\varepsilon)]\mathrm{d}\varepsilon$$

The difference between the two yields the net tunneling current:

$$I = I_{\mathrm{I}\to\mathrm{II}} - I_{\mathrm{II}\to\mathrm{I}} \propto D \int_{-\infty}^{\infty} N_\mathrm{I}(\varepsilon)N_\mathrm{II}(\varepsilon + eU)[f(\varepsilon) - f(\varepsilon + eU)]\mathrm{d}\varepsilon$$

Here, according to Eq. (1.3), we have

$$f(\varepsilon) = \frac{1}{\mathrm{e}^{\varepsilon/k_\mathrm{B}T} + 1} \quad \text{with } \varepsilon = E - E_\mathrm{F}$$

We have indicated this brief derivation, since it yields in a simple way the quantitative connection in the form of a balance equation. For the situation in Figure 3.13, for example, we can assume $N_\mathrm{n}(\varepsilon) = \text{constant}$, and for $N_\mathrm{s}(\varepsilon)$ we can use relation (3.5) from Section 3.1.2 after changing it from E to ε:

$$N_\mathrm{s}(\varepsilon) = N_\mathrm{n}(0)\frac{|\varepsilon|}{\sqrt{\varepsilon^2 - \Delta_0^2}} \text{ for } |\varepsilon| \geq \Delta_0$$

Now we can calculate the tunneling characteristic. The case of a tunnel junction between two normal conductors shown in Figure 3.12 represents a very simple example for further exercise. [14])

Next we turn to the case of a tunnel junction between two superconductors. Such a junction is shown in Figure 3.15a,b in the usual way. However, the case $U = 0$ is omitted. In Figure 3.15c the current-voltage characteristic is presented schematically.

In this case the characteristic for finite temperatures differs strongly from that for $T = 0$. Therefore, we have assumed a distribution for $T \neq 0$. The dashed line in Figure 3.15c would be obtained for $T = 0$. At $eU = \Delta_{\mathrm{II}} - \Delta_{\mathrm{I}}$ a maximum of the tunneling current is reached, since now all single electrons of superconductor I can tunnel to the right, where they encounter a particularly high density of unoccupied states. Then the current decreases with a further increase in the voltage, since the density of the unoccupied states in II decreases. Finally, at $eU = \Delta_{\mathrm{I}} + \Delta_{\mathrm{II}}$ one observes a particularly steep increase in the current because of the high density of the occupied as well as the unoccupied states. It is this extremely steep slope that provides the important advantage of measurement using two superconductors.

Tunneling experiments have provided much important information about the energy gap. In most cases, two thin evaporated layers with an oxide layer as the barrier are used. However, also compact bulk samples can be used for studying substances that are difficult to evaporate. In the latter case, the barrier can consist also of a natural oxide layer, or it can be fabricated by the evaporation of an insulator. The study of compact bulk samples is necessary if the energy gap is to be determined in a specific crystallographic direction by using single crystals.

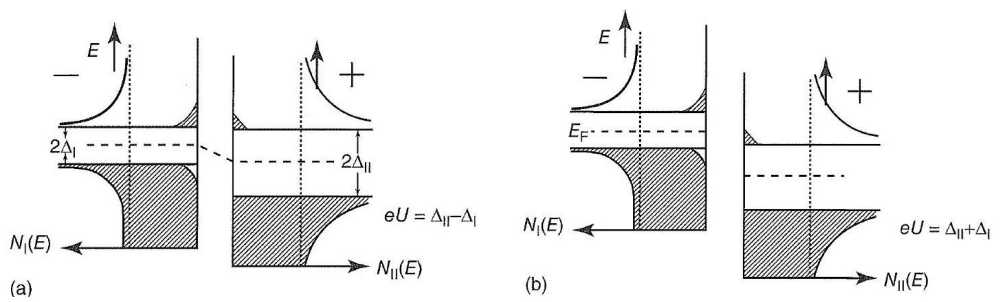
In Figure 3.16 we present an arrangement of evaporated layers. It is advantageous to keep the tunneling area small, in order to avoid large tunneling currents and to reduce the chances for the appearance of holes in the oxide layer.

Figure 3.17 shows the results obtained for an $\mathrm{Al} - \mathrm{Al_2O_3} - \mathrm{Pb}$ tunnel junction at four different temperatures [35]. For the curves $1 - 3$, the Al is normal conducting. Only for curve 4 do we deal with a junction of two superconductors. However, although in the latter case the measuring temperature of 1.05 K is only slightly below the transition temperature of Al(1.2 K), the different shape of the characteristic is clearly visible

Figure 3.18 shows the characteristic of a typical junction between two superconductors, namely Nb-niobium oxide- Sn at 3.4 K [36]. At this temperature Nb ($T_{\mathrm{c}} = 9.3$ K) and Sn ($T_{\mathrm{c}} = 3.7$ K) are both superconducting. The solid line is

In the case of Figure 3.12, for all $\varepsilon > 0$, the term in brackets $[f(\varepsilon) - f(\varepsilon - eU)]$ is equa to zero, since both Fermi functions are zero. Independent of the sign of the electron charge, we have assumed $ell > 0$. For $\varepsilon < -ell$ the term in brackets is zero again, since both Fermi functions have the value 1. Only in the (??? text is missing) antain the value 1. The density of states, of the integral. 'Then we obtain (see curve 1 in Figure 3.14):

$$I \propto DN_{\mathrm{I}}N_{\mathrm{n}} \int_{-eU}^{0} 1 \, \mathrm{d}\varepsilon \propto U$$



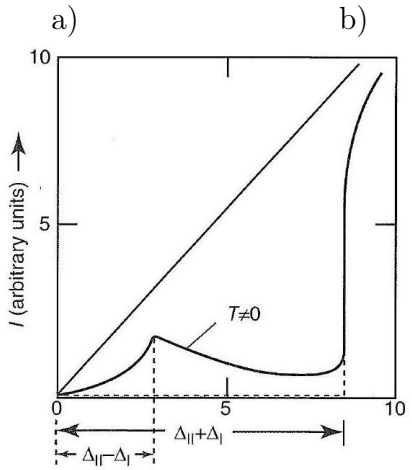


Figure 3.15 Tunneling current between two superconductors; $0 < T < T_c$. (a) and (b) show the density of states and (c) displays the current voltage characteristic.

the experimentally recorded result. The dots are calculated from Eq. (3.13) using proper values of the energy gaps ($2\Delta_{\mathrm{Sn}} = 0.74\mathrm{meV}; 2\Delta_{\mathrm{Nb}} = 2.98\mathrm{meV}$).

How one should see BCS to deal with tunneling problems

(write the question that we have a Hamiltonian and so what? okay, there is a gap. but how to approach a current?)

Continuing Experimental Discussions

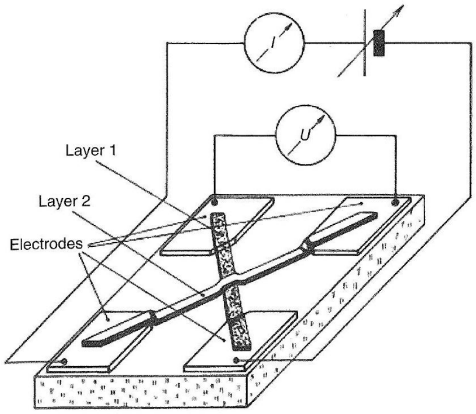


Figure 3.16 Tunnel junction between two layers. Layer 1 was oxidized before the depobelow 1μm. Usually, the oxide barriers are about 3 nm thick.

We see from Tables 3.3 and 3.4, which only contain a small part of the many possible results, that in a series of metals the ratio $2\Delta_0/k_{\mathrm{B}}T_{\mathrm{c}}$ for $T = 0$ is close to the value 3.5 predicted by the BCS theory (Eq. (3.7)). Deviations from this value in metals such as Nb can be caused easily by impurities near the surface. For such tors Pb and Hg show strong deviations from the values of the BCS theory. These deviations can be understood in terms of a particularly strong electron-phonon interaction in these metals.

From tunneling experiments, we can find out if the interaction leading to Cooper pairing is indeed the exchange of phonons. If the coupling between the lattice vibrations and the electron system is sufficiently strong, the density of states of the quasiparticles will be changed due to this coupling. These changes manifest themselves in the tunneling characteristic and can be measured using equipment with sufficiently high sensitivity. With some numerical work it is then possible to determine the coupling constant λ^* of the attractive electron-phonon

interaction and the constant μ' of the repulsive Coulomb interaction (see Eq. (3.9)). In this way, one obtains the so-called Eliashberg function $\alpha^2 F(\omega)$, which is closely connected with λ°. Here, $F(\omega)$ is the density of states of the phonons. In order to avoid any confusion with the density of states of the electrons, here we denote the energy by ω.

The tunneling measurements only deal with the phonons coupling to the electron system. On the other hand, neutron diffraction experiments can measure the

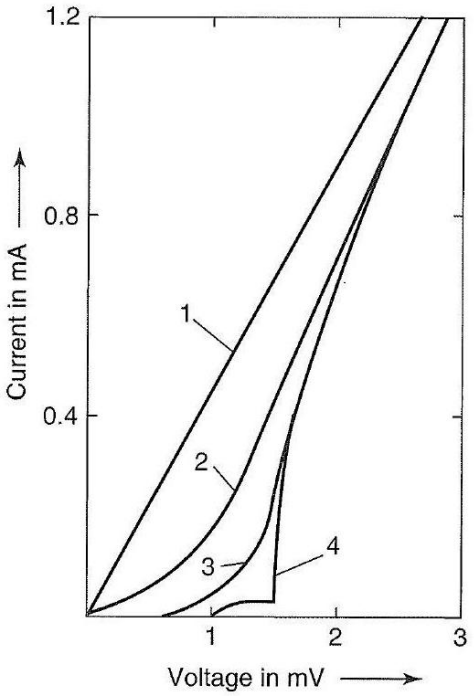


Figure 3.17 Voltage-current characterMeasuring temperature: curvel junction. curve $2, T = 4.2$ K; curve $3, T = 1,64$ K; curve 4 $T = 1.05$ K. At 1.05 K the Al is also superconclearly be seen. Transition temperatures are

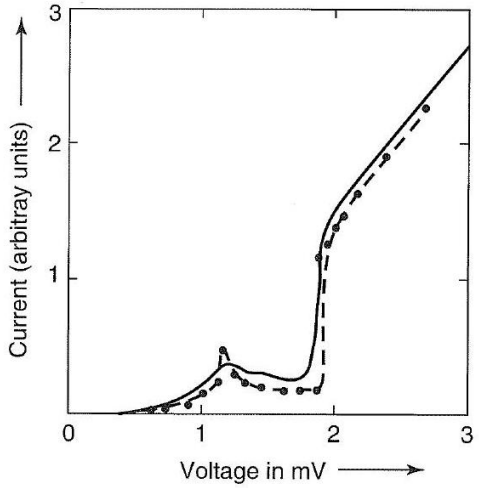


Figure 3.18 Current-voltage characteristic of a Nb-insulator-Sn tunnel junction at $T = 3.38$ K. The solid line is the experimentally recorded curve. The dots are calculated from Eq. (3.13) using the values $2\Delta_{\mathrm{sn}} = 0.74$meV and $2\Delta_{\mathrm{Nb}} = 2.98$meV. (From [36].)

density of states of the phonons independent of whether or not the latter couple to the electrons. Hence, from the comparison of both measurements, one obtains information about the coupling. Figure 3.20 shows such a comparison for Pd-D samples, the properties of which we

discussed in Section 2.3.3 [38, 39]. In spite of the strongly different deuterium concentration, we clearly see that prominent structures appear in both measurements. In particular, the phonons with high energies, resulting from the implanted deuterium, are also visible in the tunneling measurements, indicating that these vibrations couple well to the

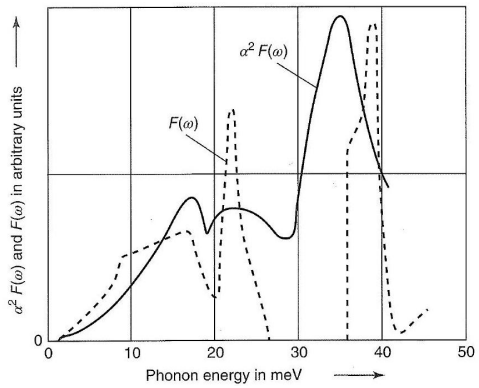


Figure 3.20 Plot showing $\alpha^2 F(\omega)$ obtained from tunneling measurements and $F(\omega)$ from neutron diffraction experiments as functions of the phonon energy ω for Pd − D samples (see Section 2.3.3). (From [38, 39].

electrons. These results explain the relatively high transition temperatures of the palladium-hydrogen system.

The determination of the function $\alpha^2 F(\omega)$ from the detailed structure of the tunneling conductivity and the comparison with the phonon spectrum $F(\omega)$ obtained, say, from neutron diffraction, represented the key experiment demonstrating that in conventional superconductors Cooper pairing is due to the electron-phonon interaction.

In a similar way, for each newly discovered superconductor one can try tò measure accurately the quasiparticle density of states by means of tunneling spectroscopy, if a tunnel junction with high quality can be fabricated. In the following (Section 3.2), we will see that, for high-temperature superconductors, not only tunneling spectroscopy but also other methods yield highly peculiar results, which are not yet completely understood. However, they clearly indicate that in this case the Cooper pairing is unconventional.

At this stage, we want to mention three additional aspects in context with the energy gap, which will be discussed in more detail in Section 3.1.4.

The energy gap can have different magnitudes along different crystallographic directions. Such superconductors are referred to as anisotropic. This anisotropy can lead to different results in various experiments. Depending on the evaporation conditions, special crystal directions can also be distinguished in experiments performed with thin layers. Measurements with single crystals along different directions yield information about the magnitude of the anisotropy.

It appears that in some compounds at least two energy gaps exist. As an example we mention $SrTiO_3$ doped with niobium, which becomes superconducting below 0.7 K [40]. Another example is MgB_2 [41]. In these materials, two or more different Fermi surfaces or energy bands contribute to the superconductivity, each forming its own energy gap, respectively ("two-band superconductivity". So in the case of MgB_2 one finds one energy gap around 2meV and another one around 7meV).

In principle, the energy gap can be changed even by very small concentrations of impurities, having an atomic angular momentum and, hence, a magnetic moment (paramagnetic impurities). In this way, superconductors can be generated without an energy gap ("gapless superconductor"). However, they are still superconducting, since they display pair correlation.

So far in our discussion of the tunneling experiments with superconductors, we have only been concerned with the unpaired electrons. For the interpretation of the experimental observations, we have taken into account only the density of states of the unpaired electrons in the

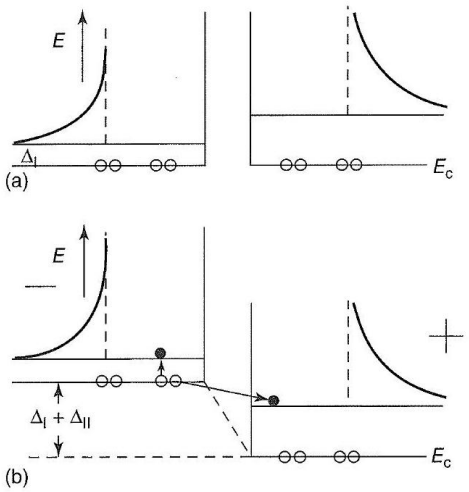
superconducting state. The Cooper pairs and their binding energy have never been mentioned. This also could not be expected, since within our picture of the individual electrons the total interaction was expressed in terms of the change of the density of states of the unpaired electrons.

On the other hand, since the superconducting state is based entirely on the concept of Cooper pairs, we are also interested in a picture where the Cooper pairs become distinctly visible. In the following, we will briefly discuss such a picture. However, there is a certain difficulty within this picture, since states of pairs, that is, collective states, and states of single electrons are shown in a single scheme. For our discussion we take the case of a tunnel junction between two different superconductors (Figure 3.15), and for simplicity we assume $T = 0$. Now superconductors are characterized by showing the Cooper pairs in one state and indicating the states that are occupied by the single electrons after breaking a pair (Figure 3.21). In equilibrium without an external voltage, the Cooper pair states are shown at the same energy level. This configuration is established if we allow the exchange of particles. At an applied voltage, in the case $T = 0$, according to Figure 3.15 we do not expect a tunneling current I in the range $\mathrm{e}U < \Delta_\mathrm{I} + \Delta_\mathrm{II}$. At $eU = \Delta_\mathrm{I} + \Delta_\mathrm{II}$, we expect a steep rise of I. In Figure 3.21 b, c, we show the situation for the two possible polarities of the voltage $U = (\Delta_\mathrm{I} + \Delta_\mathrm{II})/e$. In our present picture, we must explain the appearance of a tunneling current at this voltage in terms of the breaking of Cooper pairs. The applied voltage must be at least large enough that a pair can decay into an electron in superconductor I and an electron in superconductor II. This is exactly the process we want to describe, namely the transfer of a particle across the insulating layer. With increasing voltage U, the possibility for such a process first appears at $U = (\Delta_\mathrm{I} + \Delta_\mathrm{II})/e$. If the energy of superconductor II is lowered compared to that of superconductor I by means of the voltage, at $U = (\Delta_\mathrm{I} + \Delta_\mathrm{II})/e$, a pair in I can be broken up. As a result, a single electron appears in the lowest state of I, whereas the other single electron tunnels into the lowest state of II. During this process the energy remains conserved. The excitation energy of the one electron can be supplied by the transfer of the other electron in the electric field of the external voltage. The final states occupied by the two electrons are crucial for the necessary value of the voltage. At voltages $U < (\Delta_\mathrm{I} + \Delta_\mathrm{II})/e$, the electrons of a pair cannot be transferred into two single-electron states in I and II, respectively, at constant energy. If the superconductor II is connected to the negative side, again at $|U| = (\Delta_\mathrm{I} + \Delta_\mathrm{II})/e$ a pair can break up, however, this time in superconductor II, and the single electrons occupy states in I and II, respectively. [15] Because of the extremely large density of states for single electrons at $E = \Delta_\mathrm{I}$, the tunneling current sets in very steeply at $|U| = (\Delta_\mathrm{I} + \Delta_\mathrm{II})/e$. The argument is now similar as in the other picture. The number of processes is proportional to the number of possible final states.

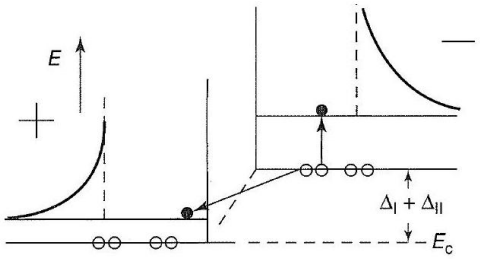
If we want to keep this picture also for finite temperatures and to derive from it at least the qualitative form of the current-voltage characteristic, for single electrons existing in thermal equilibrium we must use the first picture discussed earlier.

In Section 4.2 we will discuss another possibility for determining the energy gap in conjunction with the specific heat in the superconducting state. Furthermore, we will see in Chapter 4 that, for example, the temperature dependence of the London penetration depth, being a property of the Cooper pairs, depends on the energy gap. In principle, each physical property depending on the density of states of the single electrons can be used for determining Δ_0. We have discussed three of these possibilities, namely the absorption of light, the damping of ultrasound, and the tunneling of single electrons. These techniques yielded many results, and the underlying physics is particularly clear.

The condition $I(U) = -I(-U)$, which must always be valid for tunnel junctions, is satisfied.



(b)



(c) $N_1(E) \longleftarrow \quad \longrightarrow N_N(E)$

Figure 3.21 Tunneling effect between superconductors in the picture of Cooper pairs and to (c) are for different values of applied voltage.

3.12.2 Currents and Tunneling Effects: Basic Concepts 2

Another theory, by Shmidt

The most direct way of examining the energy gap is by tunneling experiments. This technique was developed by Giaever in 1960 [63]. Its principle is very simple (see Fig. 6.9). A narrow film of the first metal is deposited onto a glass substrate with contact pads made in advance. Then the film is oxidized, so that it is covered with an insulating oxide layer of several nanometers thickness (the barrier layer). After that, a narrow film of the second metal is deposited in the transverse direction. The intersection of the two films (of area ~ 1 mm^2) forms a tunnel junction. The experiment consists in examining the current-voltage characteristic of this junction. Physically, the experiment employs the special quantum-mechanical ability of electrons to pass through thin potential barriers (in our case, through the insulating layer) by means of tunneling.

Let us discuss the current-voltage characteristics expected for different types of tunnel junctions.

The simplest case is when both the first and the second metal are normal. As soon as the two metals are in contact, their Fermi levels become equal.

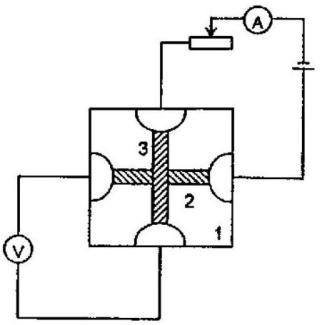


Fig. 6.9. Scheme of an electron tunneling experiment: 1 - glass substrate; 2 - thin film of the first metal; 3-thin film of the second metal

V is then applied to the junction (see Fig. 6.10 (b)), the Fermi levels will shift apart by the amount of eV and a tunneling current will begin to flow. If the density of states in the energy interval of interest is assumed to be constant, the current will be directly proportional to eV, as is evident from Fig. 6.10 (b). In other words, the current will obey Ohm's law.

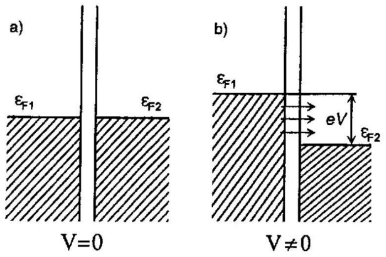


Fig. 6.10. Energy-level diagram for two normal metals brought into contact: (a) $V = 0$; (b) $V \neq 0$, a tunneling current proportional to eV passes through the junction

Let us now consider the case when one of the metals is normal and the other superconducting. The elementary excitation spectrum of the superconductor is already known to us (see Figs. 6.6 and 6.7). The energy of elementary excitations is measured from the ground-state level of the superconductor. In the normal metal, the energy of elementary excitations is measured from the Fermi level. Hence, when a tunnel junction is established between a normal metal and a superconductor, the energy levels to be equalized (due to the voltage drop) are the Fermi level of the normal metal and the ground-state level of the superconductor, as illustrated in Fig. 6.11 (a).

Let us apply a voltage V to the junction. Suppose that, as a result, the Fermi level of the normal metal has moved up by the value of eV above the ground-state level of the superconductor. A current from N to S can flow

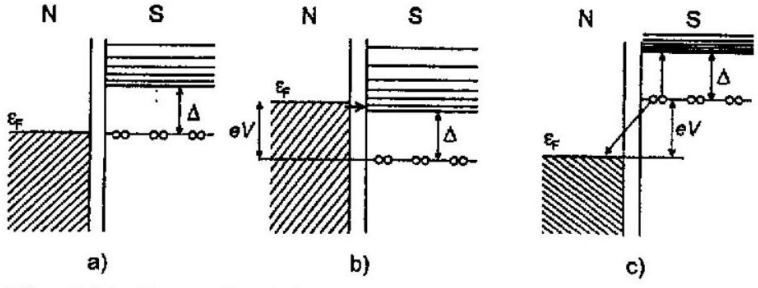


Fig. 6.11. Energy-level diagram for an NS tunnel junction: (a) $V = 0, \epsilon_{\mathrm{F}}$ coincides with the ground-state level of the superconductor; (b) $V \neq 0, |eV| > \Delta$, a finite tunneling current passes from N to S ; (c) $V \neq 0, |eV| > \Delta$, a finite tunneling current passes from S to N

gap of the superconductor. The result will be the same if the polarity of the applied voltage is reversed. In that case, electrons will tunnel from S to N and a current will start to flow when the break-up of Cooper pairs in S becomes possible. That is, the energy released as a result of the tunneling of one electron from the pair has to be sufficient for the second electron to be excited into the energy band allowed for single electrons, i.e., above the energy gap (see Fig.

6.11 (c)).

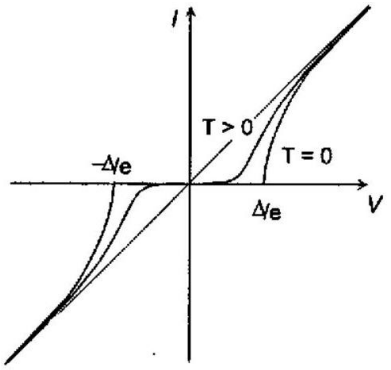
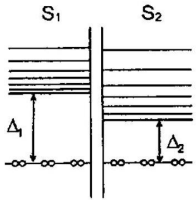


Fig. 6.12. Current-voltage characteristic of an NS tunnel junction

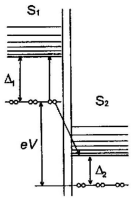
Thus the current-voltage characteristic of such a junction must be an odd function of V, as illustrated in Fig. 6.12. In the case $T \neq 0$, the currentvoltage characteristic will be somewhat smeared out, as one would expect.

Let us turn to the tunneling effects which occur when both metals (S_1 and S_2) are superconducting. Then the cases $T = 0$ and $T \neq 0$ are essentially different.

Consider the case $T = 0$ first. It follows from Fig. 6.13 that a tunneling current can start to flow only when the voltage across the junction is $V > (\Delta_1 + \Delta_2)/e$. Indeed, it is only on this condition that the tunneling process shown in Fig. 6.13 becomes possible? Cooper pair in S? break up and one of the electrons of the pair tunnels to S_2 thereby releasing an energy equal to, or greater than, Δ_1. The released energy is absorbed by the second electron of the broken pair, which is subsequently excited to the quasiparticle energy band of S_1.



$V = 0, I = 0$



$eV > \Delta_1 + \Delta_2, I \neq 0$

Fig. 6.13. Energy-level diagrams for an S_1 S_2 tunnel junction at $T = 0$

In a real experiment, when $T \neq 0$, the pattern is somewhat more complicated. At finite temperatures, there is always a certain number of excited single (unpaired) electrons in both superconductors; their equilibrium number is determined by the temperature.

The energy-level diagrams for this case are shown in Fig. 6.14. The number of dots at a given energy level roughly corresponds to the number of excited states at this energy. One can see that, at $V = 0$ (Fig. 6.14 (a)), the number of excited states at the levels of the same energy in S_1 and S_2 are equal despite the fact that the energy gaps in S_1 and S_2 are different. Therefore, the number of particles tunneling from S_1 to S_2 is exactly the same as the number of particles tunneling in the opposite direction, from S_2 to S_1. That is, at equilibrium, the net tunneling current is $I = 0$, as one would expect.

If we now apply a voltage V, the equilibrium will be immediately lifted and a flow of

quasiparticles will start from one superconductor to the other, even if the voltage is very small. One should bear in mind, however, that the quasiparticle density of states in the superconductor has a singularity at $E = \Delta$ (see (6.25) and Fig. 6.7). Hence, if the applied voltage is precisely $eV = \Delta_1 - \Delta_2$ (see Fig. 6.14 (b)), the equalized energy levels in S_1 and S_2 will be those having a density of states $\rho = \infty$. This will result in a sharp rise of the tunneling current. As the voltage V is increased further, the energy levels with $\rho = \infty$ will move apart again and the tunneling current will decrease. This implies that the current-voltage characteristic exhibits a maximum at

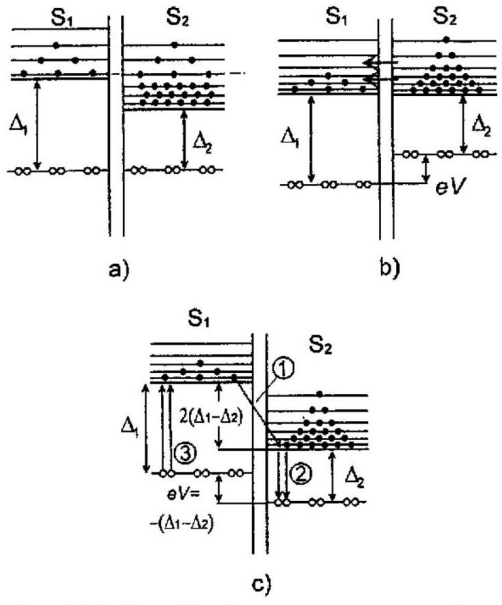


Fig. 6.14. Tunneling between two superconductors at $T \neq 0$: (a) $V = 0$, the numbers of excitations of the same energy are identical in S_1 and S_2 and the current is zero; (b) $eV = \Delta_1 - \Delta_2$, the finite current is due to the transfer of excited particles from S_1 to S_2; (c) $eV = -(\Delta_1 - \Delta_2)$, an excited particle passes from S_2 to S_1 (process 1); in S_2, it couples with one of the electrons there and relaxes back to the ground level (process 2); the energy $2\ \Delta_1$ released during process 2 is sufficient to break a Cooper pair in S_1 (process 3)

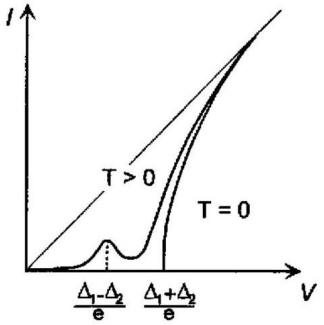


Fig. 6.15. Current-voltage characteristic of an S_1 S_2 tunnel junction

the corresponding energy-level diagram will be that shown in Fig. 6.14 (c). A sharp rise of current will be observed at $|V| = (\Delta_1 - \Delta_2)/e$ in this case, too. Hence the current-voltage characteristic of the tunnel junction formed by two superconductors is an odd function of the voltage V.

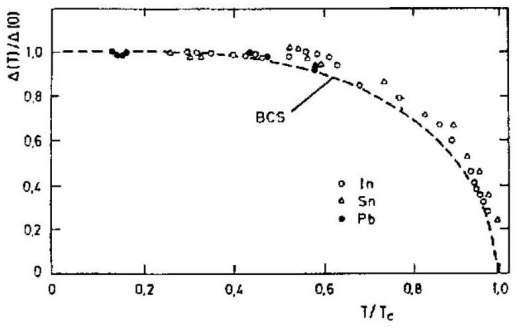


Fig. 6.16. Experimental temperature dependences of the energy gap in indium (open circles), tin (triangles), and lead (solid circles). The dashed line is $\Delta(T)$ given by the BCS theory

To conclude this section, we show the results of the tunneling experiment by Giaever and Megerle [64] who studied the details of the energy gap and its temperature dependence for different superconductors (see Fig. 6.16). The dashed line shows the variation of the gap given by the BCS theory.

Теория (?)

Уравнение Шредингера для одного электрона в ЭМ поле имеет вид

$$i\hbar\frac{\partial\psi}{\partial t} = \left(\frac{1}{2m}\left(-i\hbar\nabla - \frac{e}{c}\mathbf{A}\right)^2 + e\varphi\right)\psi$$

Введем фазовое преобразование $\chi = \chi(r,t)$

$$\psi = \psi_0 e^{i\chi}$$

Тогда

$$i\hbar\frac{\partial\psi}{\partial t} = e^{i\chi}\left(i\hbar\frac{\partial\psi_0}{\partial t} - \hbar\frac{\partial\chi}{\partial t}\psi_0\right)$$

$$\left(-i\hbar\nabla - \frac{e}{c}\mathbf{A}\right)\psi = e^{i\chi}\left(-i\hbar\nabla - \frac{e}{c}A + (\hbar\nabla\chi)\right)\psi_0$$

$$\left(-i\hbar\nabla - \frac{e}{c}A\right)^2\psi = e^{i\chi}\left(-i\hbar\nabla - \frac{e}{c}A + (\hbar\nabla\chi)\right)^2\psi_0$$

Одновременно рассмотрим градиентное преобразование

$$-\frac{e}{c}A_0 = -\frac{e}{c}A + (\hbar\nabla\chi), e\varphi_0 = e\varphi + \hbar\frac{\partial\chi}{\partial t}$$

Выбираем фазу преобразования, так, чтобы в представлении с индексом нуль отсутствовал электрический потенциал

$$\frac{\partial\chi}{\partial t} = -\frac{e}{\hbar}\varphi$$

Уравнение (73) преобразуется к виду

$$i\hbar\frac{\partial\psi_0}{\partial t} = \left[\frac{1}{2m}\left(-i\hbar\nabla - \frac{e}{c}\mathbf{A}_0\right)^2\right]\psi_0$$

Переход от (73) к (76) называется калибровочным преобразованием. При этом преобразовании меняются и потенциалы поля, и фаза волновой функции. Это формальное преобразование, и оба уравнения описывают одно и то же движение электрона.

В такой калибровке во вторичном квантовании гамильтониан системы электронов (8) имеет вид:

$$\hat{H} = \int d^3r \left[\hat{\Psi}^+_{0\sigma}(t,\mathbf{r}) \left(\frac{\left(\hat{\mathbf{p}} - \frac{e}{c}\mathbf{A}_0\right)^2}{2m} - \mu \right) \hat{\Psi}_{0\sigma}(t,\mathbf{r}) + \frac{1}{2} g \hat{\Psi}^+_{0\sigma}(t,\mathbf{r}) \hat{\Psi}^+_{0-\sigma}(t,\mathbf{r}) \hat{\Psi}_{0-\sigma}(t,\mathbf{r}) \hat{\Psi}_{0\sigma}(t,\mathbf{r}) \right]$$

Введем обозначение $-\frac{e}{c}\mathbf{A}_0 = \mathbf{v}_s m$, и ограничимся линейным приближением по магнитному поло (квалратичный член содержит скорость света c в знаменателе). Тогда

$$\hat{H} = \hat{H}_1 + \hat{H}_2$$

$$\hat{H}_1 = \int d^3r \left[\hat{\Psi}^+_{0\sigma}(t,\mathbf{r}) \left(\frac{\hat{\mathbf{p}}^2}{2m} - \mu \right) \hat{\Psi}_{0\sigma}(t,\mathbf{r}) + \frac{1}{2} g \hat{\Psi}^+_{0\sigma}(t,\mathbf{r}) \hat{\Psi}^+_{0-\sigma}(t,\mathbf{r}) \hat{\Psi}_{0-\sigma}(t,\mathbf{r}) \hat{\Psi}_{0\sigma}(t,\mathbf{r}) \right]$$

$$\hat{H}_2 = \int d^3r \hat{\Psi}^+_{0\sigma}(t,\mathbf{r}) \left(\hat{\mathbf{p}}\mathbf{v}_s\right) \hat{\Psi}_{0\sigma}(t,\mathbf{r})$$

(Здесь мы воспользовались тем, что, если дополнительно потребовать, чтобы $\operatorname{div} \mathbf{A} = 0$, то операторы $\hat{\mathbf{p}}$ и $\mathbf{A}$ коммутируют) Первый член H_1 - гамильтониан сверхпроводника без поля, который в импульсном представлении имеет вид (39), а второй член равен

$$\hat{H}_2 = \int d^3r \hat{\Psi}^+_{0\sigma}(t,\mathbf{r}) \left(\hat{\mathbf{p}}\mathbf{v}_s\right) \hat{\Psi}_{0\sigma}(t,\mathbf{r}) = \int d^3r \sum_{\mathbf{k}\sigma} \frac{1}{\sqrt{V}} e^{-i\mathbf{k}\mathbf{r}} \hat{a}^+_{\mathbf{k}} \left(\hat{\mathbf{p}}\mathbf{v}_s\right) \sum_{\mathbf{k}'\sigma} \frac{1}{\sqrt{V}} e^{i\mathbf{k}'\mathbf{r}} \hat{a}_{\mathbf{k}'} = \mathbf{v}_s \sum_{\mathbf{k}\sigma} \mathbf{k} \hat{a}^+_{\mathbf{k}} \hat{a}$$

В основном состоянии без поля система электронов находится в состоянии покоя. Поэтому импульс системы в поле равен импульсу квазичастиц. Это легко доказать с помоїью преобразования Боголюбова, оставив только диагональные члены

$$\mathbf{P} = \sum_{\mathbf{k}\sigma} \mathbf{k} \hat{a}^+_{\mathbf{k}} \hat{a}_{\mathbf{k}} = \sum_{\mathbf{k}\sigma} \mathbf{k} \hat{b}^+_{\mathbf{k}\sigma} \hat{b}_{\mathbf{k}\sigma}$$

В результате гамильтониан сверхпроводника в поле принимает вид

$$H = E_0 + \sum \varepsilon_{\mathbf{k}} \hat{b}^+_{\mathbf{k}\sigma} \hat{b}_{\mathbf{k}\sigma} + \mathbf{v}_s \sum \mathbf{k} \hat{b}^+_{\mathbf{k}\sigma} \hat{b}_{\mathbf{k}\sigma} = E_0 + \sum \tilde{\varepsilon}_{\mathbf{k}} \hat{b}^+_{\mathbf{k}\sigma} \hat{b}_{\mathbf{k}\sigma}$$

Мы видим, что энергия квазичастицы в поле деформируется

$$H = E_0 + \sum \tilde{\varepsilon}_{\mathbf{k}} \hat{b}^+_{\mathbf{k}\sigma} \hat{b}_{\mathbf{k}\sigma}, \tilde{\varepsilon}_{\mathbf{k}} = \varepsilon_{\mathbf{k}} + \mathbf{v}_s \mathbf{k}, \mathbf{v}_s = -\frac{e}{mc}\mathbf{A}_0$$

Поскольку для спаренных электронов характерное значение импульса есть p_F то минимальная энергия возбуждения

$$\min \tilde{\varepsilon}_{\mathbf{k}} = |\Delta| - v_s p_F$$

В соответствии с критерием Ландау (27) сверхпроводянее состояние разрупается если $\min \tilde{\varepsilon}_{\mathbf{k}} \leq 0$. Значит, сильное магнитное поле разрушает сверхпроводник, если

$$v_s = \frac{e}{mc}\mathbf{A}_0 > v_c = \frac{|\Delta|}{p_F}$$

Свяжем величину v_s с электрическим током, который в сверхпроводнике генерируется не электрическим, а магнитным полем. Согласно квантовой механике, плотность электрического тока, создаваемого электронами в присутствии магнитного потенциала,

равна (вспомним, что скорость заряженной частицы есть отношение кинематического импульса $\left(\mathrm{p}-\frac{e}{c}\,\mathrm{A}_0\right)$ к массе)

$$\mathbf{j}=e\mathbf{v}n=e\left\langle \mathrm{Re}\,\hat{\Psi}_0^+\frac{\left(\hat{\mathbf{p}}-\frac{e}{c}\mathbf{A}_0\right)}{m}\hat{\Psi}_0\right\rangle=e\sum\left(\frac{\mathrm{k}}{m}+\mathbf{v}_s\right)\left\langle \hat{a}_k^+\hat{a}_k\right\rangle$$

Внесем знак суммы под знак статистического усреднения

$$\mathbf{j}=e\mathbf{v}_s\left\langle\sum\hat{a}_k^+\hat{a}_k\right\rangle+\frac{e}{m}\left\langle\sum\mathbf{k}\hat{a}_k^+\hat{a}_k\right\rangle$$

Тогда в первом члене получаем полное число электронов N_e, а во втором - с учетом (79) - ток квазичастиц

$$\mathbf{j}=e\mathbf{v}_sN_e+\frac{e}{m}\left\langle\sum\mathbf{k}\hat{b}_{\mathbf{k}\sigma}^+\hat{b}_{\mathbf{k}\sigma}\right\rangle$$

(Заметим, что в силу (83) ток обрандается в нуль, когда $P=\left\langle\sum\mathrm{k}\hat{b}_{\mathrm{k}\sigma}^+\hat{b}_{\mathrm{k}\sigma}\right\rangle=-m\mathbf{v}_sN_e$ т.е. когда импульс квазичастиц полностью компенсирует суммарный импульс электронов, двигагопихся как целое со скоростью v_s)

При нулевой температуре квазичастиц нет, и в системе сунествует незатухающий ток

$$\mathbf{j}=e\mathbf{v}_sN_e$$

Из этой формулы следует, что в образовании сверхтекучего электрического тока приниматот участие все электроны. Это удивительно, поскольку при переходе в сверхпроводяпее состояние по Боголобову перестраиватотся только электроны в узкой корочке около поверхности Ферми.

(????????????????????????????????????)

При $T\neq 0$ в термодинамическом равновесии число квазичастиц в заданном состоянии равно

$$n_{bk}=\left\langle\hat{b}_{k\sigma}^+\hat{b}_{k\sigma}\right\rangle=\frac{1}{e^{\beta\tilde{\varepsilon}_k}+1}$$

Энергия квазичастиц зависит от направления. Если скорость мала, то $\tilde{\varepsilon}_k\approx\varepsilon_k+\mathrm{v}_s\mathrm{k}$ и

$$n_{bk}\left(\tilde{\varepsilon}_k\right)\approx n_{bk}\left(\varepsilon_k\right)+\left(\mathbf{v}_s\mathbf{k}\right)\frac{\partial n_{bk}}{\partial\varepsilon_k}$$

Только поправка в (85) дает вклал квазичастиц в электрический ток при подстановке (85) в (84):

$$\tilde{\mathbf{j}}=\frac{e}{m}\sum\mathbf{k}\left(\mathbf{v}_s\mathbf{k}\right)\frac{\partial n_{bk}}{\partial\varepsilon_k}=-\frac{e}{3m}\mathbf{v}_s\sum k^2\left|\frac{\partial n_{bk}}{\partial\varepsilon_k}\right|$$

Здесь мы воспользовались тем, что, если перейти от суммирования к интегрированиго по k, то

$$\sum_{\mathbf{k}}\mathbf{k}\left(\mathbf{v}_s\mathbf{k}\right)\frac{\partial n_{bk}}{\partial\varepsilon_k}=\frac{V}{(2\pi)^3}\int dk\frac{\partial n_{bk}}{\partial\varepsilon_k}\int\mathbf{k}\left(\mathbf{v}_s\mathbf{k}\right)d\Omega_k=$$

$$\frac{V}{(2\pi)^3}\int dk\frac{\partial n_{bk}}{\partial\varepsilon_k}(4\pi/3)\mathbf{v}_sk^2=\mathbf{v}_s/3\frac{V}{(2\pi)^3}\int dk\frac{\partial n_{bk}}{\partial\varepsilon_k}(4\pi/3)k^2=\mathbf{v}_s/3\sum_{\mathbf{k}}k^2\frac{\partial n_{bk}}{\partial\varepsilon_k}$$

Возникающий(87) здесь интеграл по углам считается так:

$$\int d\Omega\mathbf{k}\left(\mathbf{v}_s\mathbf{k}\right)=a\mathbf{v}_s$$

Домножив обе части скалярно на $\mathbf{v}_s$, получим

$$av_s^2 = \int d\Omega \left(\mathbf{v}_s\mathbf{k}\right)^2 = 2\pi v_s^2 \int\limits_0^\pi d(-\cos\theta)\cos^2(\theta) = v_s^2 4\pi/3$$

То есть $a = 4\pi/3$. Обратим внимание, что квазичастицы создагот электрический ток (86), противоположный скорости $\mathbf{v}_s$, в направлении которой течет элекрический ток электронов в основном состоянии. Таким образом, при фиксировантом значении v_s с увеличением температуры сверхтекучий ток падает

$$\mathbf{j} = e\mathbf{v}_s N_s(T)$$

где плотность сверхтекучих электронов равна

$$N_s(T) = N_e + \frac{1}{3}\sum_{\mathbf{k}} k^2 \frac{\partial n_{bk}}{\partial \varepsilon_k}$$

Когда

$$N_s(T) = 0$$

сверхтекучесть пропалает. Это происходит при $T = T_c$

$$\frac{1}{3}\sum_{\mathbf{k}} k^2 \left(\frac{\partial n_{bk}}{\partial \varepsilon_k}\right)_{T_c} = \frac{1}{3}\sum_{\mathbf{k}} k^2 \left(\frac{\partial n_{bk}}{\partial \left|\xi_k\right|}\right)_{\Delta=0} = -N_e$$

Используя (82), напишем максимальный (критический) ток

$$\mathbf{j} = e\frac{\Delta}{p_F} N_s$$

С помошыо формул (74) вернемся в исходное представление

$$\mathbf{j} = \frac{e}{m} N_s \left(-\frac{e}{c}\mathbf{A} + (\hbar\nabla\chi)\right)$$

Это есть калибровочно-инвариантная формула для плотности тока сверхпроводящик электронов в электромагнитном поле. При калибровочном преобразовании меняется векторный потенциал и фаза волновой функции, но вил выражения в скобках остается неизменным. Этот ток супествует в состоянии термодинамического равновесия, в отличие от тока электронов в нормальном состоянии, который есть проявление необратимого процесса с вылелением тепла.

Features of tunneling density of states

Smoothness of the dI/dV over E plot

(??? does it often smoothed? I think so. But Kiselev told me that it is only if there is a pseudogap. so how does it work???)

3.12.3 6.5 Persistent Current and the Meissner-Ochsenfeld Effect

Earlier in this chapter, we discussed the basic ideas of the superconducting state. We gave a description of the ground state of the superconductor, examined the elementary excitation spectrum, and proved the existence of the energy gap. However, the reader may have wanted

to ask whether there is any proof that everything said so far has anything to do with superconductivity. After all, at this moment, all we know about superconductivity from the microscopic theory is only the following.

The existence of electron-phonon interaction in some metals can result in an effective attraction between the electrons. This, in turn, reduces the energy of the ground state which is then represented by an electron distribution smeared out in momentum space about the Fermi surface. The elementary excitation spectrum of such a metal has an energy gap, that is, the lowest energy level allowed for elementary excitations is separated from the ground state by the energy gap. However, we have not found any indication so far that a material having all these properties is a superconductor.

In this section, we shall demonstrate that the possibility of a persistent current - a fundamental property of the superconductor - follows directly examine the normal metal. In particular, we are interested in the electron distribution in momentum space in the presence of a constant current passing through a normal metal. At $T = 0$ and zero current, all electrons of the metal occupy the states within the Fermi surface while all states outside it are empty. If we then apply an electric field to the metal (for example, in the direction of the x axis), the electrons will start accelerating in this direction. But accelerated motion of electrons in real space is equivalent to their steady motion in momentum space, with constant velocity. This means that the Fermi sphere as a whole will start to move at a steady rate in the direction of the k_x axis in momentum space. This steady motion can be considered uninterrupted as long as electron collisions with crystal defects or impurity atoms can be neglected. When this is no longer possible, there arises a dynamic equilibrium: As a resultof scattering, the electrons having the maximum value of momentum component k_x are carried to the empty states in momentum space until an equilibrium is attained. This implies that, despite the electric field and the steady motion of electrons in momentum space in the direction of k_x, their scattering results in an electron distribution in momentum space which is on average stationary. The Fermi surface shifts somewhat with respect to the origin and the electron scattering results in a transfer of energy to the crystal lattice, that is, in heating up the conductor.

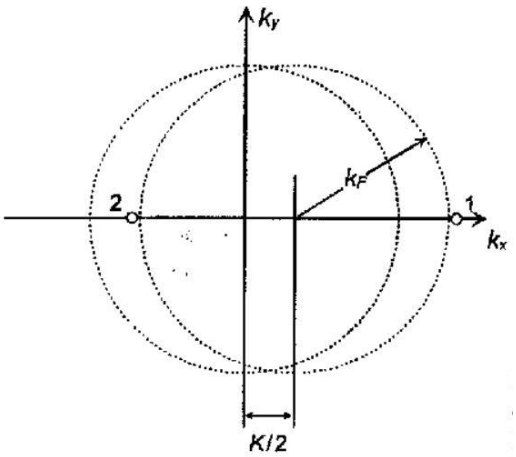


Fig. 6.17. Electron states in a superconductor carrying a current. The 'smeared' Fermi sphere shifts as a whole by $K/2$

Consider now the superconductor. In this case, a current can start to flow (in the absence of an electric field!) if all Cooper pairs have the same momentum K. Suppose that the direction of the current coincides with the x axis, that is, $K = (K, 0, 0)$. This is equivalent to a shift of the 'smeared' Fermi sphere in momentum space by the value of $K/2$ in the direction of the k_x axis, as illustrated in Fig. 6.17. Let us follow the transformations of a Cooper pair (1,2) of momentum $(k_\mathrm{F} + K/2, 0, 0)$ indicated in the figure. Electron 1 having the maximum kinetic energy $(\hbar^2/2m)\,(k_F + K/2)^2$ would have benefited from a transition to an empty state

somewhere near electron 2. Such a process would have been accompanied by an energy decrease by the value of

$$\frac{\hbar^2}{2m}\left(k_F+\frac{K}{2}\right)^2-\frac{\hbar^2}{2m}\left(k_F-\frac{K}{2}\right)^2=\frac{\hbar^2}{m}k_FK$$

where m is the electron mass and k_F is the radius of the Fermi sphere. But then the pair (1, 2) must be broken, which would cause an increase of the total energy of the system by 2Δ, where Δ is the energy gap.

It is now evident that, at sufficiently small currents (or sufficiently small K), the energy gain $\hbar^2k_\mathrm{F}K/m$ cannot compensate for the energy loss 2Δ and the pair will not break up. Of course, on the whole, such a state is less favored energetically than the state without a current ($K=0$), but it can happen to be metastable and exist for an infinitely long time. An example of such a state is provided by a closed superconducting ring carrying a current: A break-down of the current state begins when it becomes energetically favorable to break Cooper pairs, that is, when

$$\frac{\hbar^2k_FK_c}{m}\approx 2\Delta$$

where $\hbar K_\mathrm{c}=P_\mathrm{c}$ is the critical momentum of a pair. Hence

$$P_\mathrm{c}=\hbar K_\mathrm{c}\approx\frac{2m\Delta}{p_\mathrm{F}}=\frac{2\Delta}{v_\mathrm{F}} \tag{6.39}$$

where v_F is the electron velocity on the Fermi surface.
Let us evaluate the current density corresponding to the critical momentum. Since the critical velocity of a pair is

$$v_\mathrm{c}=\frac{P_\mathrm{c}}{2m} \tag{6.40}$$

the critical current density will be, according to (6.39) and (6.40),

$$j_\mathrm{c}=n_\mathrm{s}ev_\mathrm{c}=n_\mathrm{s}e\frac{\Delta}{mv_\mathrm{F}} \tag{6.41}$$

where n_s is the density of the superconducting electrons, which, at $T=0$, is equivalent to the total density of electrons in the metal. Expressing n_s in terms of the London magnetic penetration depth λ, according to (2.7), and Δ_0 in terms of the coherence length ξ, according to (6.27), we obtain the critical current density at $T=0$ in the form

$$j_\mathrm{c}=\frac{\hbar c^2}{16\pi e}\frac{1}{\bar{\lambda}^2\dot{\xi}_0} \tag{6.42}$$

To estimate the order of magnitude of j_c, we assume $\lambda\sim10^{-5}$ cm and $\xi_0\sim10^{-4}$ cm. Then

$$j_\mathrm{c}\sim\frac{10^{-27}\left(3\times10^{10}\right)^2}{16\pi\times4.8\times10^{-10}}\frac{1}{\left(10^{-5}\right)^2\,10^{-4}}\sim4\times10^{15}\ \text{CGS units}$$

$$j_\mathrm{c}=\frac{4\times10^{15}}{3\times10^9}\approx1.3\times10^6\ \text{A cm}^{-2}$$

The critical current density j_c in (6.41) can be expressed in terms of $H_\mathrm{cm}(0)$ and λ. Using the expressions for the density of states near the Fermi surface, $N(0)=k_\mathrm{F}m/\left(\pi^2\hbar^2\right)$, and the electron density $n_\mathrm{s}=k_\mathrm{F}^3/3\pi^2$, together with (6.20) and (6.27), we obtain

$$j_c = \frac{1}{\sqrt{3}4\pi}\frac{cH_{cm}(0)}{\lambda} \tag{6.43}$$

It is interesting to compare the result (6.43) with the critical current density (3.67) given by the Ginzburg-Landau theory. One can easily verify that the two results are equivalent except for a numerical factor (if, of course, (6.43) is extrapolated to temperatures close to T_c). The discrepancy in the numerical factor is not surprising because (6.43) is only intended as an estimate.

Thus we can draw a very important conclusion: the critical current (3.67) given by the Ginzburg-Landau theory has the physical significance of a pairbreaking current, that is, of a current that causes electron pairs in the condensate to become unstable.

Let us now turn to a discussion of how the existence of the energy gap in the elementary excitation spectrum of the superconductor explains the Meissner-Ochsenfeld effect, i.e., the exclusion of weak magnetic fields from the interior of the superconductor. Rigorous calculations which prove that the existence of the energy gap is a sufficient condition for the Meissner effect are beyond the scope of this book. Nevertheless, we shall attempt an interpretation of the Meissner effect using the language of microscopic theory.

Following London [65], one can introduce the so-called 'rigidity' of the electron wavefunction of the superconductor. This means that, owing to the energy gap and the coherent behavior of the whole body of electrons, a weak magnetic field is unable to change the wavefunction in any significant way. From this the Meissner effect follows immediately.

Indeed, assume that $\Psi(\boldsymbol{r}_1, \boldsymbol{r}_2, \ldots, \boldsymbol{r}_N)$ is the wavefunction of N electrons in the superconductor. Note that here Ψ is not an effective wavefunction of the superconducting electrons, as in the Ginzburg-Landau theory (which depends on only one coordinate r), but a true wavefunction. Then the following expression for a current in the presence of a magnetic field can be derived using general relations of quantum mechanics:

$$j(r) = \sum_{n=1}^{N} \int \ldots \int \left\{ \frac{e\hbar}{2im} \left[\Psi^* \nabla_n \Psi - \Psi \nabla_n \Psi^*\right] - \frac{e^2}{mc} \boldsymbol{A}(r_n) |\Psi|^2 \right\} \delta(\boldsymbol{r} - \boldsymbol{r}_n) \, \mathrm{d}^3\boldsymbol{r}_1 \ldots \, \mathrm{d}^3\boldsymbol{r}_N \tag{6.44}$$

Here $\boldsymbol{A}$ is the vector potential of the magnetic field. If the magnetic field is zero ($A = 0$), the current and the integral of the first term are zero, too:

$$\sum_{n=1}^{N} \int \ldots \int \left[\Psi^* \nabla_n \Psi - \Psi \nabla_n \Psi^*\right] \delta(r - r_n) \, \mathrm{d}^3 r_1 \ldots \, \mathrm{d}^3 r_N = 0 \tag{6.45}$$

But we have assumed that the wavefunction is 'rigid', that is, it is not affected by the magnetic field. Hence, formula (6.45) must hold in a nonzero magnetic field. Then, omitting the first term of (6.44), we obtain, after elementary integration

$$\boldsymbol{j}(r) = -\text{ const } \times \boldsymbol{A}(r) \tag{6.46}$$

This last formula is equivalent to the well-known London equation (2.17) and, therefore, is indeed a mathematical expression of the Meissner effect.

3.12.4 Formalism for Thermodynamic Effects of the Meissner State

Formalism 1

In the following, we discuss the consequences for other properties of a superconductor resulting from the temperature dependence of the critical field according to Eq. (4.51). Here, we

will use the strong advantage of the thermodynamic treatment, namely that all the important quantities can be obtained from the Gibbs function by means of simple differential operations.

We recall that the entropy S is found from G according to Eq. (4.10): $S = -\left(\frac{\partial G}{\partial T}\right)_{B,p}$

In the absence of a magnetic field, we have

$$S_{\mathrm{n}} - S_{\mathrm{s}} = -V \frac{B_{\mathrm{cth}}}{\mu_0} \frac{\partial B_{\mathrm{cth}}}{\partial T}$$

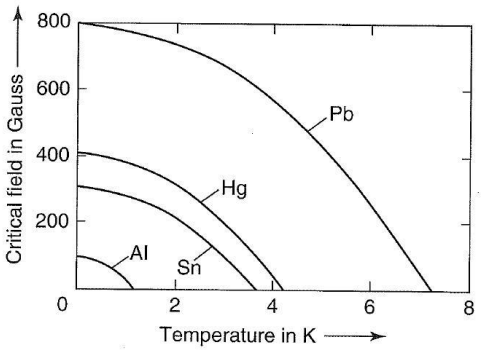


Figure 4.12 Critical magnetic field plotted versus the temperature for different typesuperconductors (1G = 10^{-4} T).

Again we have neglected the T dependence of V, since it is very small. In Section 4.6.6 we will return to this change of V, making the justification of our approximation more clear.

By looking at the temperature dependence of the critical field B_{cth} , as seen in Figure 4.12 and as approximated by Eq. (4.51), we can immediately find the general behavior of $S_{\mathrm{n}} - S_{\mathrm{s}}$. For $T \to T_{\mathrm{c}}$ we have $B_{\mathrm{cth}} \to 0$. Hence, we conclude that $S_{\mathrm{n}} - S_{\mathrm{s}} \to 0$ for $T \to T_{\mathrm{c}}$. At T_{c} (in the absence of a magnetic field) the entropies of the normal conducting and of the superconducting phases are equal, and no heat of transition appears at T_{c} . Hence, we are dealing with a second-order or higherorder phase transition. In our discussion of the specific heat (see Section 4.2), we have derived this result already in a different way.

At temperatures $T < T_{\mathrm{c}}$ the entropy difference $S_{\mathrm{n}} - S_{\mathrm{s}}$ takes a positive value, since in the total range $0 < T < T_{\mathrm{c}}$ we have $\mathrm{d}B_{\mathrm{cth}}/\mathrm{d}T < 0$. According to the third law of thermodynamics, for $T \to 0$ also $S_{\mathrm{n}} - S_{\mathrm{s}}$ must approach zero (the approximation (Eq. (4.51)) satisfies this condition). However, this means that $S_{\mathrm{n}} - S_{\mathrm{s}}$ passes through a maximum. This fact has important consequences for the specific heat. Further we note that at all temperatures $0 < T < T_{\mathrm{c}}$, there exists a finite entropy difference $S_{\mathrm{n}} - S_{\mathrm{s}}$, that is, in this temperature range we have a first-order phase transition with a finite heat of transition.

Figure 4.13 shows the temperature dependences of $G_{\mathrm{n}}, G_{\mathrm{s}}$, and $S_{\mathrm{n}} - S_{\mathrm{s}}$ plotted in arbitrary units on the vertical axis. At $T = T_{\mathrm{c}}$ the two curves $G_{\mathrm{n}}(T)$ and $G_{\mathrm{s}}(T)$ must not only take the same value but also have the same slope, as we have seen. This is the signature of a first-order phase transition. The transition to superconductivity is a second-order phase transition (as we will see explicitly in a moment), since at T_{c} the second derivatives of the Gibbs functions G_{n} and G_{s} are different.

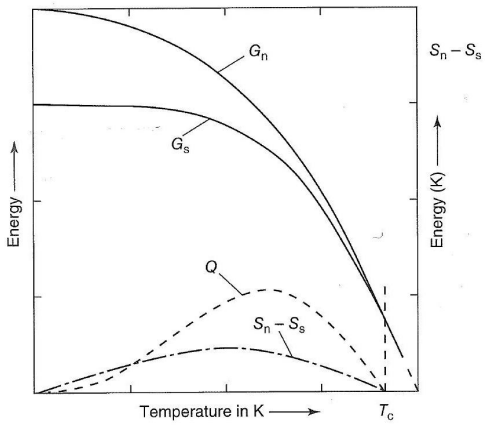


Figure 4.13 Gibbs functions G_n and $G_{s'}$ entropy difference $S_\mathrm{n} - S_{s'}$ and heat of transition Q plotted versus the temperature. Numerical example for 1 molSn : $T_C = 3.72$ K $(G_\mathrm{n} - G_\mathrm{s})_{T=0} = 5 \times 10^{-3}$ Ws; $(S_\mathrm{n} - S_\mathrm{s})_\mathrm{max} = 2.28 \times 10^{-3}$ W s/K; and $Q_\mathrm{max} = 5 \times 10^{-3}$Ws.

These results that we have derived from thermodynamics fit very well into our microscopic picture, as they should. From $S_\mathrm{n} - S_\mathrm{s} > 0$, we conclude that the superconducting phase has a smaller entropy than the normal conducting phase. Without going into details, we recall that the entropy is a measure of the disorder of a physical system. Hence, from $S_\mathrm{n} > S_\mathrm{s}$, we conclude that the degree of order in the superconducting phase is larger than in the normal conducting phase. This higher degree of order can immediately be associated with the correlation between single electrons forming Cooper pairs and between the Cooper pairs themselves. This correlation amounts to an additional order in our system.

For $T \to T_\mathrm{c}$, the Cooper pair density and the energy gap continuously approach zero. Hence, at T_c we cannot expect a heat of transition. Instead, our microscopic picture indicates that we deal with a transition of higher than first order. However, below T_c there exists a finite density of Cooper pairs. In an applied magnetic field permanent currents are generated. However, in type-I superconductors the Cooper pair density practically remains constant until the critical field is reached. At the critical field, the superconductivity breaks down, and all the Cooper pairs are broken up. This requires a finite heat of transition. At the transition from the superconducting to the normal conducting state, heat energy is consumed, namely $(S_\mathrm{n} - S_\mathrm{s})\,T$. In an isothermal process this energy must be delivered to the system. However, if the transition from normal conducting to superconducting state is performed adiabatically, that is, thermally insulated with $\mathrm{d}Q = 0$, the sample becomes colder, since the heat energy is extracted from the other degrees of freedom. Superconductors represent a substance that can be cooled by means of adiabatic demagnetization [26]. However, since much more effective cooling techniques have been developed, this particular method has not become an important application.

Formulas

The second derivative of the Gibbs function with respect to the temperature yields the specific heat, here at constant pressure and constant B (see Eq. (4.13)). From Eq. (4.50),

$$G_\mathrm{n} - G_\mathrm{s} = V \frac{B_\mathrm{cth}^2}{2\mu_0}$$

for the difference $c_\mathrm{n} - c_\mathrm{s}$ of the specific heat in the normal state and in the superconducting state, we obtain

$$c_\mathrm{n} - c_\mathrm{s} = -\frac{VT}{\mu_0} \left\{ \left(\frac{\partial B_\mathrm{cth}}{\partial T} \right)^2 + B_\mathrm{cth} \frac{\partial^2 B_\mathrm{cth}}{\partial T^2} \right\}$$

$$c_\mathrm{s} - c_\mathrm{n} = \frac{VT}{\mu_0}\left\{\left(\frac{\partial B_\mathrm{cth}}{\partial T}\right)^2 + B_\mathrm{cth}\frac{\partial^2 B_\mathrm{cth}}{\partial T^2}\right\}$$

Again we have taken the volume V as constant. Further we note that we insert here the specific volume, that is, the volume per unit mass. In this way we obtain specific quantities, here the specific heat, which refers to the amount of 1 g of the substance. The result of Eq. (4.54) was derived by Keesom [2] in 1924, but without a solid justification of the existence of a superconducting phase in the thermodynamic sense.

From Eq. (4.54) we see that at $T = T_\mathrm{c}$, we have $c_\mathrm{s} > c_\mathrm{n}$. At T_c the critical field vanishes, $B_\mathrm{cth} = 0$, and, hence, $c_\mathrm{s} - c_\mathrm{n} > 0$. At T_c the specific heat displays a jump, which is given by

$$(c_\mathrm{s} - c_\mathrm{n})_{T=T_\mathrm{c}} = \frac{VT_\mathrm{c}}{\mu_0}\left(\frac{\partial B_\mathrm{cth}}{\partial T}\right)^2_{T=T_c}$$

In the literature this important relation is referred to as the Rutgers formula [27]. It connects a thermal quantity, namely the jump of the specific heat, with the critical magnetic field. For a number of superconductors this relation is well satisfied. In Table 4.1 we list some values of $(c_\mathrm{s} - c_\mathrm{n})_{T=T\mathrm{c}}$, as obtained from thermal data and from measurements of the critical field.

Since we found $\mathrm{d}^2 B_\mathrm{cth}/\mathrm{d}T^2 < 0$ and since $\mathrm{d}B_\mathrm{cth}/\mathrm{d}T$ becomes smaller and smaller with decreasing temperature, we find a temperature $0 < T < T_\mathrm{c}$ at which $c_\mathrm{s} = c_\mathrm{n}$. Below this temperature we have $c_\mathrm{s} < c_\mathrm{n}$. The intersection of $c_\mathrm{s}(T)$ and $c_\mathrm{n}(T)$ must appear at the temperature at which $S_\mathrm{n} - S_\mathrm{s}$ reaches a maximum (see Figure 4.13). Since the density of states represents an important quantity for superconductivity, we discuss the possibility for its determination from $B_{cth}(T)$. We start from Eq. (4.54). In many cases, the contribution of the lattice to the specific heat practically does not change at the onset of superconductivity. Hence, we can attribute the difference $c_\mathrm{s} - c_\mathrm{n}$ completely to the electron system. So we obtain

$$c_\mathrm{sE} - c_\mathrm{nE} = \frac{VT}{\mu_0}\left\{\left(\frac{\partial B_\mathrm{cth}}{\partial T}\right)^2 + B_\mathrm{cth}\frac{\partial^2 B_\mathrm{cth}}{\partial T^2}\right\}$$

According to Figures 4.2 and 4.3 and due to the higher degree of order of the superconducting state, we can assume that in the superconducting state the specific heat of the electrons for $T \to 0$ approaches zero faster than in the normal conducting state. We can express this as follows: $c_\mathrm{sE} \propto T^{1+a}$ with $a > 0$. This means that c_sE/T

Table 4.1 Values of $(c_s - c_n)_{T=T_c}$ obtained from thermal and magnetic data.

Element	T_c (K)	$(c_s - c_n)$ thermal data (10^{-3} W s/(mol K))	$(c_s - c_n)$ magnetic data (10^{-3} W s/(mol K))
Sn[a)]	3.72	10.6	10.6
In[a)]	3.40	9.75	9.62
Tl[b)]	2.39	6.2	6.15
Ta[a)]	4.39	41.5	41.6
Pb[b)]	7.2	52.6	41.8

Test of the "Rutgers formula."
a) Ref. [28].
b) Ref. [29].

approaches zero for $T \to 0$. Then for sufficiently small temperatures, if c_sE/T is

$$-\frac{c_\mathrm{nE}}{T} = \frac{V}{\mu_0}\left\{\left(\frac{\partial B_\mathrm{cth}}{\partial T}\right)^2 + B_\mathrm{cth}\frac{\partial^2 B_\mathrm{cth}}{\partial T^2}\right\}$$

According to Eq. (4.14), the quantity c_nE/T is equal to the Sommerfeld coefficient γ, which is proportional to $N(E_\mathrm{F})$ due to Eq. (4.16). If we also assume that

$$\left(\frac{\partial B_{\mathrm{cth}}}{\partial T}\right)^2 \ll B_{\mathrm{cth}}\frac{\partial^2 B_{\mathrm{cth}}}{\partial T^2}$$

which is always valid for sufficiently small temperatures, we find

$$\gamma = -\frac{V}{\mu_0}B_{\mathrm{cth}}\frac{\partial^2 B_{\mathrm{cth}}}{\partial T^2}$$

and finally with Eq. (4.51) we get

$$\gamma = -\frac{V}{\mu_0}2B_{\mathrm{cth}}\frac{B^2_{\mathrm{cth}}(0)}{T_{\mathrm{c}}^2}$$

We see that at sufficiently low temperatures, the observation of B_{cth} is independent of the special temperature dependence of the critical field and can serve for determining γ and thereby yield information about $N(E_{\mathrm{F}})$.

Связь между B и H в промежуточном состоянии

Рассмотрим сверхпроводник первого рода.

Казалось бы, поскольку в нем, $\sigma > 0$, то он должен находится в одиородиом состоянии. Несложный анализ показывает, что в этом случае форма образца существенно опрелеляет распрелеление магнитного поля внутри сверхпроводника.

В сверхпроводниках первого рода глубина проникновения $\lambda = 0$, если он находится во внешнем магнитном поле $H < H_c$. Рассмотрим сверхпроводянций шар, помешенный в изначально однородное магнитное поле.

Применим уравнение Максвелла divB = 0 к области, вблизи одного из полюсов. В силу симметрии залачи, в этом месте магнитное поле может быть направлено только по нормали к поверхности. Но поскольку в сверхпроводнике B = 0 то и снаружи вблизи полюса магнитное поле H = 0.

Рассмотрим теперь область вблизи экватора. В силу симметрии залачи магнитная индукция как внутри, так и вне шара по-прежнему может быть направлена параллельно оси, соединяюшей полюса. Внутри пара B = 0. А вне шара может сунествоать ненулевая тангенциальная сосавляюшдая магнитного поля. В этом случае условие divB = 0 не наклалывает на внешнее тангенциальное поле никаких ограничений. Поэтому экваториальный участок находится в ненулевом магнитном поле. Итак, при движении вдоль меридиана, магнитное поле вблизи поверхности шара. изменяется от нуля до некоторого максимального, пропорционального исходному внепнему полю.

Будем постепенно увеличивать внешнее поле. Тогда в тот момент, когда на экваторе поле достигло значение H_c в оствльных точках поверхности шара поле меньше H_c. Это означает, что экваториальная часть шара должна перейти в нормальное состояние (магнитное поле разрушило сверхпроводимость), в то время как часть шара ближе к полюсам может сохраняет сверхпроводимость. То есть мы имеем сосуществование двух фаз - нормальной и сверхпроводяней. Из теории фазовых переходов следует, что это в этом случае имеет место фазовый переход первого рода.

Можно поставить залачу, какая часть образца находится в сверхпроводяней фазе в магнитном поле. Рассмотрим, для простоты плоскую пластинку в нормальном внешнем поле. В этом случае, сколь угодно слабое магнитное поле переводит пластину в промежуточное состояние. В самом деле, если пластина находится в однородном сверхпроводяпем состоянии, то в ней $B = 0$.

Очевидно, что, поскольку вне пластины $B \neq 0$, то это несовместимо с условием divB = 0.

В то же время пластина не может находиться полностью в нормальном состоянии, так как проникшее в нее поле слабо, чтобы разрушить сверхпроводимость.

Таким образом пластина находится в промежуточном состоянии.

Очевидно, что в нормальной фазе в равновесии напряженность магнитного поля есть H_c и совпадает в ней с магнитной индукцией.

В сверхпроводящей фазе магнитная индукция равна нуло.

Пусть вне образца магнитное поле, равное магнитной индукции, есть H.

Тогда, в силу сохранения магнитного потока через поверхность ($\operatorname{div} \mathrm{B} = 0$!) имеем

$$H = H_c(1 - \rho)$$

гдеρ - доля пластинки, находяпейся в сверхпроводящем состоянии. Переход из промежуточного в нормальное состояние имеет место, если $\rho = 0$, что происходит при $H = H_c$ Несложно показать, что д,линный цилиндр из сверхпроводника первого рода в продольном магнитном поле в промежуточное состояние не переходит никогда. То есть магнитное поле в него не проникает.

(????)

Критическое поле для сверхпроводника первого рода

Рассмотрим металлический цилиндр в однородном продольном магнитном поле. Свободная энергия системы есть свободная энергия иилиндра в отсутствие магнитного поля + энергия поля (в отсутствие цилиндра) +энергия взаимодействия цилиндра с полем. Свободную энергию системы будем отсчитывать от состояния в котором имеется только поле. Тогда плотность энергии нормального цилиндра есть F_n. Будем охлаждать систему до тех пор, пока цилиндр не перейдет в сверхпроводяпее состояние. Тогда его магнитный момент станет равным $\mathrm{M} = -\mathrm{H}/4\pi$.

Для энергии этого цилиндра в магнитном поле

$$dE_m = -\mathrm{M}d\mathrm{H} = \frac{HdH}{4\pi}$$

поэтому

$$E_m = H^2/8\pi = \frac{MH}{2}$$

Пусть F_{s0} - своболная энергия сверхпроводника в нулевом магнитном поле. Тогда $F_{sH} = F_{s0} + H^2/8\pi$ - свободная энергия сверхпроводника в магнитном поле. Очевилно, что в равновесии

$$F_n = F_{sH}$$

Это имеет место при критическом поле H_c :

$$F_n - F_{s0} = H_c^2/8\pi$$

Итак, в иулевом внешнем магнитном поле внутренняя энергия сверхпроводника меньше энергии нормального состояния (при той же температуре и объеме) на величину $H_c^2/8\pi$. При включении внешего магнитного поля, появление магнитного момента у сверхпроводящего металла приводит к увеличению его энергии на величину (5). Ло тех пор, пока $H_0 < H_c$, сверхпроводнику выгодно оставаться в сверхпроводяпем состоянии. Поле H_c назы вагот критическим термодинамическим магитным полем. Обратим внимание, что конечно же, это поле есть свойство только материала.

13.3.2 Энтропия и теплоемкость сверхпроводника

Из термодинамики известно, что энтропия

$$S = -(\partial F/\partial T)_V$$

Из (6) и (7) следует, что

$$S_s - S_n = \frac{H_c}{4\pi}\left(\frac{\partial H_c}{\partial T}\right)_V$$

состояние является чем-то более упорядоченным, чем нормальное. Это наталкивает на мысль описы вать переход в сверхпроводящее состояние как фазовый переход в духе теории Ландау. (см. соответствующую главу).

При $T = T_c$ магнитное поле $H_c = 0$. Тогда $S_s - S_n = 0$. Следовательно, переход в сверхпроводящее состояние в этом случае является фазовым переходом второго рода. При $T < T_c$, имеет место скачок энтропии, то есть при переходе в сверхпроводящее состояние из нормального скрытая теплота выделяется, и наоборот, при переходе из сверхпроводящего в нормальное - поглощается. Это переход первого рода. Удельная теплоемкость $C = T(\partial S/\partial T)$. Из выражения (8) следует, что

$$C_s - C_n = \frac{T}{4\pi}\left[\left(\frac{\partial H_c}{\partial T}\right)^2 + H_c\frac{\partial^2 H_c}{\partial T^2}\right]$$

$$S_s - S_n = \frac{H_c}{4\pi}\left(\frac{\partial H_c}{\partial T}\right)_V$$

состояние является чем-то более упорядоченным, чем нормальное. Это наталкивает на мысль описы вать переход в сверхпроводящее состояние как фазовый переход в духе теории Ландау. (см. соответствующую главу).

Термодинамические потенциалы

Макроскопическая электродинамика описывает электромагнитные поля в веществе, усредненные по временам, много большим времени изменения молекулярных полей τ_a и по расстояниям, много большим межатомных расстояний a. то есть макроскопическая электродинамика описывает низкочастотные и длинноволновые поля, удовлетворяющие условиям

$$\omega \ll \frac{1}{\tau_a}, a \ll \lambda$$

Магнитной индукцией в веществе называется усредненная по достаточно большим временам и размерам полная напряженность магнитного поля - сумма внешнего магнитного поля и молекулярного поля. При изменении внешнего магнитного поля происходит изменение магнитной индукции внутри тела δB. При этом изменение энергии системы "магнитное поле + тело":

$$\delta R = \frac{1}{4\pi}\int dV \mathbf{H}\delta\mathbf{B}$$

Входящий в это выражение параметр **H** назвается напряженностью магнитного поля в веществе. Он не обязательно совпадает с внешним магнитным полем.

Совпадение, например, имеет место в случае длинного цилиндра в продолыном внешнем магнитном поле. В соответствии с теоремой о малых добавках, в равновесии для свободной энергии $\mathcal{F}$ имеем внешнем магнитном поле. В соответствии с теоремой о малых добавках, в равновесии для своболной энергии $\mathcal{F}$ имеем

$$\delta\mathcal{F} = -S\delta T - pdV + \frac{1}{4\pi}\int dV \mathrm{H}\delta\mathrm{B}$$

мъи поле+тело. Определенный таким образом термодинамический потенциал $\mathcal{F}$ $(T, V, \mathbf{B})$ в равновесии имеет минимум. Предположим, что мы хотим измерять теплоемкость при заданных значениях T, V, B. На эксперименте контролировать значение магнитной инлукции B внутри тела неудобно, а в случае тел с нецилиндрической геометрией попросту невозможно. Фактически эксперимент проводится в заланном виеинем магнитном поле.

Для исследования термодинамики сверхпроводника в таких условиях введем термодинамический потенциал

$$\mathcal{G} = \mathcal{F} - \int dV \frac{\mathrm{HB}}{4\pi}$$

Этот прием в теоретической механике назывался преобразованием. Лежандра.

Тогда

$$\delta\mathcal{G} = -S\delta T - \frac{1}{4\pi}\int dV\ \mathrm{B}\delta\mathrm{H}$$

В соответствии с обнцми принципами термодинамики именно этот потенциал имеет минимум при заданных температуре T, объеме и магнитном поле H. Напомним лишний раз, что в формуле (13) H - магнитное поле виутри образиа. В случае цилиндрической геометрии в продолыном магнитном поле напряженность магнитного поля в веществе совпалает с напряженностыо внешнего магнитного поля. Полезно также ввести плотность потенциала $\mathcal{G}$:

$$G = F - \frac{\mathrm{HB}}{4\pi}$$

В случае других геометрий для описания термодинамики вешества во внешнем магнитном поле вводят другие термодинамические потенциалы. Например

$$\tilde{\mathcal{G}} = \mathcal{F} - \frac{\mathrm{H_0M}}{2}$$

где $\mathrm{H_0}$ - внешнее магнитное поле, а M - полный магнитный момент образца. Для простоты считаем тело однородным. Рассмотрим некоторый термодинамический потенциал, например свободную энергию F. Она является функцией объема, энтропии, и магнитной индукции внутри телаB. Если поле B постоянно, то свободная энергия F имеет минимум.

В равновесии, при малом изменении B для изменения свободной энергии имеем

$$dF = SdT - pdV + HdB/4\pi$$

Если равновесия нет, то

$$\delta F \leq S\delta T - p\delta V + H\delta B/4\pi$$

Пусть процессы в теле происходят таким образом, что постоянны H, T и V. Из последнего соотношения следует, что

$$d(F - HB/4\pi) \leq .0$$

Поэтому в теле могут происходить только такие процессы, что потенциал $F - HB$ может только уменьшаться и в состоянии равновесия он имеет минимум

Как правило теоретики выводят (либо постулируют) вид свободной энергии F, как функции магнитной индукции B. В тоже время, экспериментаторы работают с системами, помешенными во внешнем поле, которым они и управляют. Если образец - длинный цилиндр, то магнитное поле внутри образца численно равно внешнему магнитному полю. Тогда в условиях эксперимента минимум имеет потенциал $\mathcal{G}$.

3.12.5 Introduction to Thermodynamics of Superconductors

Just Intro

In the last chapter we saw that a well-established theory exists for conventional superconductors. The theory explains how a coherent matter wave is constructed by means of the formation of Cooper pairs. However, we also saw that, in particular for unconventional superconductors, the microscopic details often remain unclear. On the other hand, based on only a few basic symmetry arguments, we were able to account for many properties of the pair wave function.

Next we want to treat superconductivity on a macroscopic scale. We will se that by means of a rigorous application of the general laws of thermodynamics we can reach a deep understanding of the properties of the superconducting state. This will lead us to the Ginzburg-Landau theory [1], which was developed in the early 1950s, and which turned out to be highly powerful for the solution of many practical problems. It serves for the description of conventional as well as unconventional superconductors

Already in 1924 Keesom [2] had tried to apply thermodynamics to superconductivity. At the time there was the difficulty that the superconducting state could not be interpreted in terms of a single new thermodynamic phase. Then in 1933 the discovery of the Meissner-Ochsenfeld effect brought crucial progress. At the onset of superconductivity, a magnetic field is expelled from the interior of a type-I superconductor, independent of the experimental details. This represented a clear experimental confirmation of the existence of a single superconducting phase. The thermodynamic equilibrium state is unequivocally determined by the specification of T and B also in the case of a type-II superconductor, where the magnetic field penetrates into the superconductor

Before we turn to the details, we make some general remarks on the thermodynamic treatment of physical systems.

Reminder: General Aspects of Thermodynamics

A crucial quality of the thermodynamic treatment of a macroscopic physical system arises from the fact that the immense number of independent coordinates of the individual particles is reduced to only a few macroscopic variables of the system. For instance, for the thermodynamic treatment of an ideal gas, one does not start from the $3N$ spatial coordinates and the $3N$ momentum coordinates of the N gas atoms. Instead, one describes the behavior by such variables as the temperature T, the volume V, the particle number N, and so on

One is interested in the macroscopic behavior of the system, say, in the stability of the different phases, such as the solid, liquid, and gaseous phases, during the variation of one variable while the other variables are kept constant. The thermodynamic equilibrium states of a system under specified conditions play an important role. Here, we deal with the following question. A system, say, a liquid-vapor mixture, is specified by fixing the temperature T, the volume V, and the total particle number N. We want to know the number N of atoms in the vapor in thermodynamic equilibrium, that is, in the state that is established if all other quantities can be freely adjusted under the given conditions. The system then exists in a definite state, where the particles can be freely exchanged between the vapor and the liquid, and where a definite heat exchange with a thermal bath must be possible.

At this point we mention that frequently the thermodynamic equilibrium state is not established at all or only very slowly, because the free exchange of some quantity is not possible in the particular experiment. The thermodynamic prediction on the equilibrium state is completely independent of the question of the chances for it to become realized.

All such questions are dealt with by specifying suitable thermodynamic functions, the Gibbs

functions, or thermodynamic potentials. These Gibbs functions are constructed from the variables in such a way that a certain Gibbs function is associated with a definite set of independent variables. The system is completely accounted for by means of this Gibbs function.

To find the correct Gibbs function of a system is not easy. First, we must find a set of independent variables, which is sometimes difficult. Standard sets of variables are temperature T, volume V, and particle number N; or temperature T, pressure p, and particle number N. Other variables must be added if a system is also affected, for example, by electric or magnetic fields. The behavior in a magnetic field will be highly important for superconductors

If we have found the Gibbs function associated with a set of variables, the equilibrium states are determined by the extrema of the Gibbs function.") Two phases of a system are in equilibrium if their Gibbs functions have the same value. In principle, from this we can already answer the question of the stability of a phase. If the equilibrium state is determined by the minimum of the Gibbs function, then 1) A well-known case is the condition for the extremum of the entropy S as the Gibbs observed macroscopic state of the wyst the realized. Systems having the entropy as the Gibbs function move in the direction of

increasing entropy. The equilibrium state corresponds to a state wh maximum entropy, of course, always under the given cibbs functions, the rium states with other extremum can always be related to the second law of thermodynamics. function which, in the end, is a measure of

phase I will be unstable relative to phase II if the Gibbs function of phase I is larger than that of phase II..2)

The Gibbs functions are distinguished by the fact that, for a differential variation, just the differentials of the independent variables appear. For illustration, we present a few known examples.

For the internal energy U, we have

$$\mathrm{d}U = T\ \mathrm{d}S + \delta A$$

If we include only the compressional work $\delta A^V = -p\ \mathrm{d}V$, we obtain

$$\mathrm{d}U = T\ \mathrm{d}S - p\ \mathrm{d}V$$

U is the Gibbs function for the variables S and V. We note that these two variable change with the size of the system ("extensive state variables"), whereas this is not so in the case of the variables T and p (intensive state variables"). In the Gibbs functions there always appear products of extensive and intensive quantities. The negative sign of the term $p\ \mathrm{d}V$ is needed, since we define that all energies added to a system are counted as positive. For a reduction of the volume, that is, $\mathrm{d}V < 0$ work is added to the system.3. Of course, other variables, for example, the particle number N, may also appear. In the following, we always keep the particle number constant. Hence, we can ignore this variable.

The free energy F is given as

$$F = U - TS$$

leading to

$$\mathrm{d}F = \mathrm{d}U - T\ \mathrm{d}S - S\ \mathrm{d}T = -S\ \mathrm{d}T - p\ \mathrm{d}V$$

We see that F is the Gibbs function for the variables T and V.

Frequently, the arbitrary variation of the pressure p is much easier than that of V and, hence, p is introduced as the independent variable. The Gibbs function for the variables T and p is the enthalpy G with

$$G = U - TS + pV$$

and

$$\mathrm{d}G = -S\ \mathrm{d}T + V\ \mathrm{d}p$$

In our above-mentioned discussion, we have considered only the variables pressure and temperature. For the thermodynamic treatment of the superconducting phase,") we must include an additional variable, which accounts for the behavior in a magnetic field. As the additional independent variable, we choose the magnetic

At this stage we should mention that phase transitions also exist at $T = 0$. They originate from quantum mechanics. The transition point is referred to as quantum-critical point. of this kind are discussed in connection with he cuprate superconductors, and also in the case of materials such as the heary fermions Superconductivity can appear near a and many other substances [3]

In technical thermodynamics mostly one proceeds differently. There the work that is done by the 4) system is counted as positive (representing the interesticin palt for tecchnologs)

field $\mathbf{B}$. The Gibbs function associated with the variables T, p, and $\mathbf{B}$ for constant particle number is

$$G = U - TS + pV - \mathbf{m} \cdot \mathbf{b}$$

are always parallel or antiparallel, and since we indicate this in the sign of m, we can ignore the vector property in this discussion. For the variation of the internal energy, we obtain [6]

$\mathrm{d}U = T\ \mathrm{d}S - p\ \mathrm{d}V + B\ \mathrm{d}m$

as is shown in standard textbooks on the theory of heat. Hence, one finds?

$\mathrm{d}G = -S\ \mathrm{d}T + V\ \mathrm{d}p - m\ \mathrm{d}B$

For our choice of the Gibbs function $G(T, p, B)$, the independent variables T, p, and B appear in the differentials, as expected.

If we know the Gibbs function of a system, we can calculate from it very easily many thermodynamic quantities by means of suitable derivatives with respect to the variables. In this way, we find the entropy S from G:

$$S = -\left(\frac{\partial G}{\partial T}\right)_{p,B}$$

Here, the symbol $\partial/\partial T$ indicates the partial derivative with respect to temperture. At the same time, the pressure p and the magnetic field B must be kept constant. This is indicated by the subscript index p, B. In this way the dependence of the entropy on the temperature, on the magnetic field, and on the pressure is obtained: $S = S(T, B, p)$. If G depends on additional variables, these must also be kept constant. In this case these variables also appear in the subscript index after the bracket

Analogously, we can also derive other thermodynamic quantities from G. From the partial derivative with respect to the pressure at constant temperature, we find the sample volume V (as a function of T, B, and p):

$$V = \left(\frac{\partial G}{\partial p}\right)_{T,B}$$

The specific heat c is another important quantity that we will need in the following It is defined by the relation

$$\Delta Q = cm'\Delta T$$

where ΔQ is the amount of heat we must introduce into a substance of mass m' in order to raise its temperature by ΔT. We distinguish between different kinds

magnetic moment m always appears together with B, confusion with the mass is unlikely.

The differential work $\delta A^m = B\ \mathrm{d}m$ exactly corresponds to the compressional work $\delta A^V = -p\ \mathrm{d}V$ where B and the magnetic moment m appear in place of the pressure p and the negative vol ume $-V$, respectively. We take paramagnetic materials as an example. Then **m** is paralifel to B. During an increase in m, that is, dm>0, work is added to the system, which appears as heat of 7) See, for example, [4] f secific heat, depending on the conditions under which the addition of heat fres example, if the pressure is kept constant, we speak of the energy taks place. For exant pressure.

From the function G the specific heat is obtained directly by means of the expression

$$-T\left(\partial^2 G/\partial T^2\right)_{p,B} = T(\partial S/\partial T)_{p,B} = c_{\mathrm{p}}$$

Relations such as Eq. (4.13) are highly important for calculating the entropy from he measured temperature dependence of the specific heat. There exist specific characteristic relations between the different thermodynamic quantities. In this chapter, we will deal with several examples.

As the last general aspect we will discuss the order of the transition between two thermodynamic phases. We have mentioned already that at a phase transition the relevant Gibbs functions have the same value. If the first derivative of the Gibbs function with respect to the temperature is discontinuous at the phase transibs one speaks of a first-order phase transition. In this case, the entropy iumps by a finite value. Analogously, if the entropy is continuous at the phase transition, but if the second derivative of the Gibbs function, which is proportional to the specific heat, shows a jump, one speaks of a second-order phase transition For such higher-order phase transitions, L. D. Landau has developed a powerful theory [5].

Also the superconducting phase transition in the absence of a magnetic field of second order. The application of the concepts of the Landau theory to the superconducting phase transition will lead us to the Ginzburg-Landau theory. However, before we turn to this theory, we want to show by means of specific-heat measurements that the superconducting phase transition is, indeed, of second order. Also we want to discuss the thermal conductivity of superconductors.

3.12.6 Which Equilibrium Properties will Be Not Present in Nonequilibrium?

(an intro to nonequilibrim SC. theory of it will be present in detail in some latter part)

3.13 General Ideas of Other Effects

3.13.1 Dissipative and open BCS: General Concepts

(here there will be a discussion about how to work with it? just an intro, details are presented later)

Physical Examples of Dissipative SC

(??? overview of effects)

Some models of Dissipative SC

(??? overview of models)

Physical Examples of open SC

(??? overview of effects)

Some models of open SC

(??? overview of models)

3.13.2 Magnetic Field, Created by Cooper Pairs (???)

(???? what is know about it??? maybe it is just negligible???)

4 Basic Effects of Superconductors

4.1 General Effects

(отсюда многое, возможно, в главы дальше перенесу)

4.1.1 Critical supercurrent: basics

Gap from spectrum leads to supercurrent by Shmidt

Наличие электрон-фононного взаимодействия в некоторых металлах может привести к эффективному притяжению электронов металла друг к другу. Это приводит к понижению энергии основного состояния, которое теперь представляет собой размазанное около поверхности Ферми распределение электронов в k-пространстве. Спектр элементарных возбуждении такого материала имеет энергетическую щель, т.е. первые разрешенные уровни спектра элементарных возбуждений отделены от уровня основного состояния энергетической щелью. Но мы до сих пор никак не показали, что материал, обладающий этими свойствами, - сверхпроводник.

Сейчас мы покажем, как из существования энергетической щели следует возможность незатухающего тока - основного свойства сверхпроводника. Для того чтобы это лучше понять, обратимся сперва к нормальному металлу. Нас будет интересовать распределение электронов нормального металла в **k**-пространстве, когда по металлу идет постоянный ток. Если тока нет, то при $T = 0$ все электроны заполняют состояния внутри сферы Ферми, и все состояния вне этой сферы пусты. Создадим в металле электрическое поле (пусть в направлении оси x), тогда электроны начнут ускоряться в этом направлении, а ускоренному движению электронов в x-пространстве будет отвечать равномерное движение с постоянной скоростью электронов в k-пространстве. В результате вся сфера Ферми начнет с постоянной скоростью перемещаться в **k**-пространстве в направлении оси k_x. Так будет происходить до тех пор, пока мы можем пренебрегать процессами соударений электронов с примесями и дефектами кристаллической решетки. Если эти процессы учесть, то окажется, что в результате рассеяния электроны, имеющие максимальное значение компоненты импульса k_x, будут переки дываться в свободные ячейки k-пространства и, в конце концов, возникнет динамическое равновесие. Это значит, что, несмотря на электрическое поле и равномерное движение электронов в **k**-пространстве в направлении оси k_x, рассеяние на дефектах приводит к тому, что в целом распределение электронов в **k**-пространстве становится стационарным. Сфера Ферми оказывается несколько сдвинутой относительно начала координат, что естественно для токового состояния. Рассеяние электронов приводит к передаче энергии решетке, к разогреву проводника.

Теперь рассмотрим сверхпроводник. Ток в сверхпроводнике (в отсутствие электрического поля!) может возникнуть, если все электронные пары будут иметь один и тот же импульс $\hbar$ K. Пусть ток течет вдоль оси x сверхпроводника, т.е. $\mathbf{K} = (K, 0, 0)$. Это значит, что "размазаннал» сфера Ферми будет сдвинута в k-пространстве на

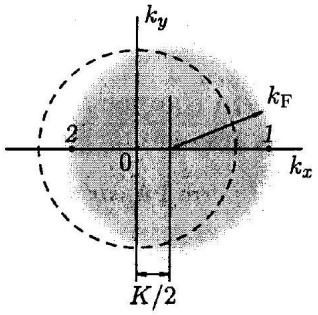
величину $K/2$ в направлении оси k_x. Это схематически изображено на рис. 50.1. Проследим за поведением показанной там электронной пары $(1,2)$, имеющей состояние $(\pm k_{\mathrm{F}} + K/2, 0, 0)$. Электрону 1, имеющему наибольшую кинетическую энергию $(\hbar^2/2m)\,(k_{\mathrm{F}} + K/2)^2$, конечно, было бы выгодно перейти в свободную ячейку где-нибудь около электрона 2. При этом энергия системы понизится на величину

$$\frac{\hbar^2}{2m}\left(k_{\mathrm{F}} + \frac{K}{2}\right)^2 - \frac{\hbar^2}{2m}\left(k_{\mathrm{F}} - \frac{K}{2}\right)^2 = \frac{\hbar^2}{m} k_{\mathrm{F}} K$$

Но тогда пара $(1,2)$ будет разрушена и, как мы уже знаем, энергия системы повысится на 2Δ, где Δ-энергетическая щель, m-масса электрона, k_{F} - радиус сферы Ферми.

Отсюда ясно, что при достаточно маленъких токах (достаточно малых K) выигрыш в энергии $\hbar^2 k_F K/m$ не может скомпенсировать проигрыш 2Δ, и пара разрываться не будет. Конечно, в целом такое состояние энергетически менее выгодно, чем состояние без тока ($K = 0$), но оно может оказаться метастабильным и существовать бесконечно долго. Примером тому служит замкнутое сверхпроводящее кольцо с током. Разрушение такого состояния начнется тогда, когда разрыв пар станет энергетически оправданным. Правильную оценку мы получим, если

Рис. 50.1. Токовое состояние в сверхпроводнике. Вся "размазаннал» сфера Ферми сдвинута на $K/2$.



напишем

$$\hbar^2 k_{\mathrm{F}} K_c/m \simeq 2\Delta,$$

где $\hbar K_c$ - критический импульс пары. Следовательно, критический импульс пары равен

$$P_c = \hbar K_c \simeq 2m\Delta/p_{\mathrm{F}} = 2\Delta/v_{\mathrm{F}} \tag{50.1}$$

здесь v_F - скорость электрона на поверхности Ферми.

Оценим, какой плотности тока соответствует такой критический импульс. Поскольку критическая скорость пары

$$v_c = P_c/2m \tag{50.2}$$

то критическая плотность тока, согласно (50.1) и (50.2), будет

$$j_c = n_s e v_c = n_s e \frac{\Delta}{m v_{\mathrm{F}}} \tag{50.3}$$

где n_s-плотность сверхпроводящих электронов, которая при $T = 0$ просто равна электронной плотности металла. Выражая n_s через лондоновскую глубину проникновения магнитного поля λ, согласно (5.7), и Δ_0 через длину когерентности ξ_0, согласно (45.7), получим окончательно плотность критического тока при $T = 0$ в виде

$$j_c = \frac{\hbar c^2}{16\pi e}\frac{1}{\lambda^2 \xi_0} \tag{50.4}$$

Оценим порядок получившейся величины. Пусть $\lambda \sim 10^{-5}$см, $\xi_0 \sim 10^{-4}$см, тогда

$$j_c \sim \frac{10^{-27}\left(3\cdot 10^{10}\right)^2}{16\pi \cdot 4.8 \cdot 10^{-10}}\frac{1}{\left(10^{-5}\right)^2 10^{-4}} \text{ абс. ед. } \sim 4\cdot 10^{15} \text{ абс. ед.}$$

Учитывая, что 1 А содержит $3\cdot 10^9$ абс. ед. силы тока, имеем

$$j_c = \frac{4\cdot 10^{15}}{3\cdot 10^9} \text{ A/cm}^2 \simeq 1.3\cdot 10^6 \text{ A/cm}^2.$$

Выразим критическую плотность тока j_c в формуле (50.3) через $H_{cm}(0)$ и λ. Воспользовавшись выражением для плотности состояний у поверхности Ферми $N(0) = k_F m/\left(\pi^2\hbar^2\right)$, формулой (44.18), выражением для электронной плотности $n_s = k_{\mathrm{F}}^3/3\pi^2$ и формулой (45.7), получим

$$j_c = \frac{1}{\sqrt{3}4\pi}\frac{cH_{cm}(0)}{\lambda}. \tag{50.5}$$

Интересно сравнить результат (50.5) с плотностью критического тока, полученной в теории Гинзбурга-Ландау (18.5). С точностью до численного коэффициента эти результаты совпадают (если, конечно, формулу (50.5) проэкстраполировать в область температур, близких к T_c). Расхождение в численном коэффициенте вполне естественно, так как формула (50.5) носит оценочный характер.

Следовательно, мы можем сформулировать теперь важный физический вывод: критический ток (18.5), даваемый теорией Гинзбурга-Ландау, имеет смысл критического тока распаривания, т. е. такого тока, при котором теряется устойчивость электронных пар, образующих сверхпроводящий конденсат.

Intro: Currents in Type-I and Type-ll Superconductors

We have already seen several times that a superconductor can carry only a limited electric current. As the first example, in Section 1.5.1 we discussed the critical current in a Josephson junction. However, also in the case of homogeneous superconductors the strong correlation of the Cooper pairs leads to the existence of a critical velocity and, hence, of a critical current density j_c. If this critical value is exceeded, Cooper pairs will be broken up.

Next we want to discuss some relations resulting from the existence of a critical current density, for the maximum possible current in a superconductor. We will restrict ourselves to simple geometric situations.

Our discussions of the critical current are highly important for the technical applications of superconductivity. In type-II superconductors we have materials that can still remain superconducting also for technically interesting magnetic fields. However, for applications it is also important that these superconductors can still transport high electric currents sufficiently without resistance in high magnetic fields. As we will see, here we are confronted with another problem, which has been solved only with the so-called hard superconductors.

Before we turn in detail to the special features in type-I and type-II superconductors, we want to investigate the magnitude of the critical supercurrent density in the ideal case of a thin and homogeneous superconducting wire.

Limit of the Supercurrent from Superfluidity Criterion

Более точное разложение $E_0 = \frac{1}{2} g_F (\hbar\omega_D)^2 - \frac{1}{2} g_F \hbar\omega_D \Delta_0 \sqrt{1 + \left(\frac{\hbar\omega_D}{\Delta_0}\right)^2}$ вблизи точки перехода $T = T_c$ позволяет получить зависимость $\Delta(T) \sim (T_c - T)^{1/2}$. Из $\Delta = \lambda \cdot \sum'_{\mathbf{p}'} \langle \hat{a}_{-\mathbf{p}',-} \hat{a}_{\mathbf{p}',+} \rangle$. видно, что щель Δ пропорциональна оператору уничтожения куперовских пар, что означает $\Delta^2 \sim n_s$. Это позволяет оценить температурную зависимость критического j_c тока от температуры T. В соответствии с критерием сверхтекучести для куперовских пар со спектром $\varepsilon(p) = \sqrt{\xi_{\mathrm{p}}^2 + \Delta^2}$, их критическая скорость $v_c = \Delta / p_F$. Это значит, что при скоростях, больших v_c, пары утрачивают свойство сверхтекучести и разваливаются. Поэтому плотность критического тока $j_c = e n_s v_c \sim \Delta^3 \sim (T_c - T)^{3/2}$ еще называют током распаривания.

(!!! elaborate!!!)

Limit of the Supercurrent Due to Pair Breaking in scope of GL formalism

In order to determine the maximum supercurrent density that can be reached under the most favorable conditions, we consider a homogeneous superconducting wire extending along the x-direction. The diameter of the wire is assumed to be smaller than the London penetration depth λ_{L} and the Ginzburg-Landau coherence length ξ_{GI}. In this case, the Cooper pair density can be taken as constant over the cross-section of the wire, and the Ginzburg-Landau equations (4.28) and (4.29) can be solved for this problem.

In order to keep our calculation no more complicated than necessary and to uncover the underlying physics, resulting in the maximum supercurrent of our wire, we use a few simplifications. For the wave function Ψ of the superconductor, we use the ansatz

$$\Psi = \Psi_0 \mathrm{e}^{ikx}$$

Here, the amplitude Ψ_0 is independent of location. This means that the Cooper pair density $n_s = |\Psi|^2$ is spatially homogeneous. The exponential function is taken such that the wave with wavenumber k is running along the wire.

In order to see how Ψ is connected with the supercurrent or the supercurrent density along the wire, we insert Eq. (5.1) into the second Ginzburg-Landau equation (4.29):

$$j_{\mathrm{s}} = \frac{q\hbar}{2mi} (\Psi^* \nabla\Psi - \Psi \nabla\Psi^*) - \frac{q^2}{m} |\Psi|^2 \mathbf{A}$$

Then we obtain for the x component of the current density

$$j_{\mathrm{s},x} = \frac{q\hbar k}{m} \Psi_0^2 - \frac{q^2}{m} \Psi_0^2 A_x = q\Psi_0^2 \frac{\hbar k - q A_x}{m}$$

According to Eqs. (1.5) and (1.6), the ratio on the right-hand side is just the Cooper pair velocity. Hence, we have

$$j_{\mathrm{s},x} = q\Psi_0^2 v_x$$

This corresponds exactly to the relation $j = qnv$ for the current density of electrically charged particles.

Next, we turn to the first Ginzburg - Landau equation (4.28):

$$\frac{1}{2m} \left(\frac{\hbar}{i} \nabla - q\mathbf{A} \right)^2 \Psi + \alpha\Psi + \beta |\Psi|^2 \Psi = 0$$

By inserting Eq. (5.1) and by assuming the vector potential to be also independent of x,[1)] we obtain

$$\frac{(\hbar k - qA_x)^2}{2m}\Psi + \alpha\Psi + \beta\Psi_0^2\Psi = 0$$

or by introducing the velocity v_x and after dividing by Ψ

$$\frac{1}{2}mv_x^2 + \alpha + \beta\Psi_0^2 = 0$$

With $\alpha < 0$, this yields

$$\Psi_0^2 = -\frac{\alpha}{\beta}\left(1 - \frac{mv_x^2}{2|\alpha|}\right) = \Psi_\infty^2\left(1 - \frac{mv_x^2}{2|\alpha|}\right)$$

Here, we have used the relation $-\alpha/\beta = \Psi_\infty^2$ (Eq. (4.23)), and we have introduced the wave function Ψ_∞ of the homogeneous system in the absence of a supercurrent. We see that the Cooper pair density Ψ_0^2 decreases with increasing kinetic energy $^1/2mv_x^2$. It vanishes if this energy is equal to $|\alpha|$.

The calculation can also be performed using a spatially varying A_{x_x}, resulting in a more complicated calculatio This dependence of the Cooper pair density on the velocity must also be taken into account in the expression (5.2b) for the supercurrent density. If the Cooper pair density were constant, $j_{s,x}$ would simply increase linearly with the velocity of the charge carriers. This is exactly what happens at small velocities. However the larger v_x, the more pronounced is the decrease of the Cooper pair density. A the larger v_x, the more pronounced is the decrease of the Cooper pair density. As soon as Ψ_0^2 reaches zero, j_x vanishes. Between $v_x = 0$ and this limiting value, j_x has a maximum as a function of v_x, which we want to determine next.

For this, we must calculate the derivative $\mathrm{d}j_s/\mathrm{d}v_w$, set it equal to zero, and find v_x. For the velocity yielding the maximum supercurrent density, we obtain

$$v_{x,p} = \sqrt{\frac{2|\alpha|}{3m}}$$

According to Eq. (5.5), at this velocity the Cooper pair density attains the value $2/3\Psi_\infty^2$, and Eq. (5.2b) yields

$$j_{\mathrm{c,p}} = q\frac{2}{3}\sqrt{\frac{2|\alpha|}{3m}}\Psi_\infty^2$$

This current density is also referred to as the critical pair-breaking current density. Using expression (4.25a), connecting α with B_{cth}, and with expression (1.10) for the London penetration depth, we can write it also in the form [2)]

$$j_{\mathrm{c,p}} = \frac{2}{3}\sqrt{\frac{2}{3}}B_{\mathrm{cth}}\frac{1}{\mu_0\lambda_{\mathrm{L}}}$$

This critical current density can become very large. If for B_{cth} we take a value of 1 T and for λ_{L} a value of 100 nm, we obtain for $j_{c,p}$ a value of about 4.3×10^8 A/cm^2. In the following sections, we will see to what extent this high critical current density can be achieved in real superconductors.

4.1.2 Critical supercurrent: advanced features 1

Experimental Overview of Type-I Superconductors (??)

As the simplest geometric example, we consider a wire with circular cross-section carrying a current I. The wire is assumed to be much thicker than the London penetration depth

At sufficiently small currents, the superconducting wire resides in the Meissner phase. In this phase, the interior of the superconductor must remain free of magnetic flux. However, this also means that the interior cannot carry an electric current, since otherwise the magnetic field due to the current would exist. From this we also conclude that the current passing through a superconductor is restricted to the thin surface layer, into which the magnetic field can penetrate in the Meissner phase. The external currents applied to a superconductor are

Since Eq. (5.7b) has been obtained from an analysis of the Ginzburg-Landau equations, this expression is valid only near T_c. From the microscopic bCS theory, one finds that $j_{c,p}$ is proportional to obtain again $j_{c,p} = B_{cth}/\mu_0\lambda_L$ 286 Fritical Currents in Type-l and Type-ll Superconductors

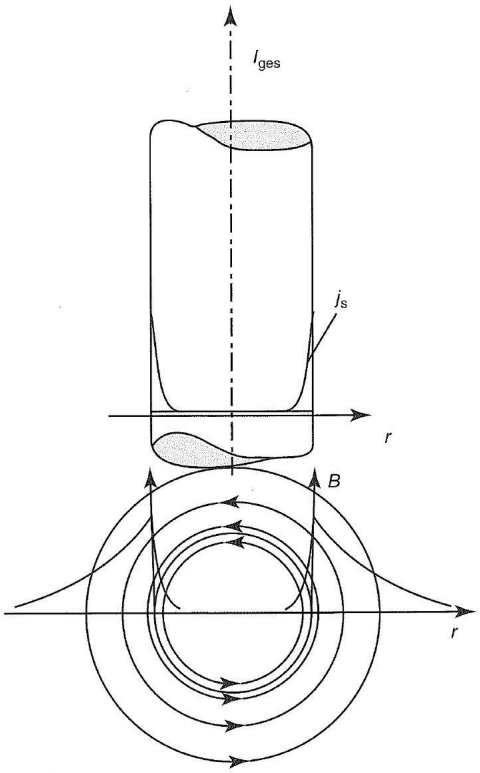


Figure 5.1 Distribution of the current density and of the magnetic field in a currentcarrying superconducling wire. The surface layer has the thickness of only the penetration depth λ_L.

referred to as transport currents, in contrast to the shielding currents appearing in the superconductor as circulating currents.

In Figure 5.1 we show schematically the spatial distribution of a transport current in a wire with circular cross-section in a plot of the current density versus the wire radius. The total current is given by the integral of the current density over the cross-sectional area

$$I = \int_F j_s df$$

The magnetic field of this current is also shown in Figure 5.1

Silsbee hypothesis

Already by 1916, Silsbee [1] had proposed the hypothesis that in the case of "thick" superconductors, that is, for superconductors with a fully developed shielding layer, the critical current is reached exactly when the magnetic field of the current at the surface attains the value B_{cth} . This hypothesis has been confirmed perfectly. In other words, it means that the magnetic field and the current density at a surface with a well-developed shielding layer are strongly correlated (Eq. (4.60)). The critical value of the current density is associated with a certain critical field, namely B_{cth}, where it is completely irrelevant whether the current density is due to shielding currents or a transport current.

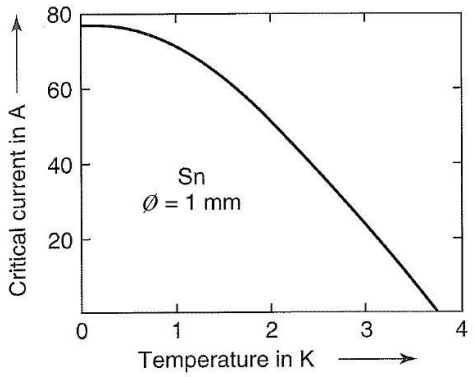


Figure 5.2 Critical current of a tin wire with 1 mm diameter plotted versus the temperature.

Because of the validity of the Silsbee hypothesis, it is very simple to calculate the critical currents of wires with circular cross-section from the critical fields, for example, from those of Figure 4.12. The magnetic field at the surface of such a wire carrying the current I is given by

$$B_0 = \mu_0 \frac{1}{2\pi R}$$

where B_0 is the field at the surface, I is the transport current, R is the wire radius, and $\mu_0 = 4\pi \times 10^{-7}$ V s/Am. The only requirement is cylindrical symmetry of the current distribution. The radial dependence of the current density is arbitrary.

It follows from Eq. (5.9) that the critical current shows the same temperature dependence as the critical magnetic field (at I_{c} the field B_{c} is reached). As an example, in Figure 5.2 we show the temperature dependence of the critical current for a tin wire with 1 mm diameter. According to Eq. (5.9), the critical field of about 300G at 0 K corresponds to a critical current $I_{\mathrm{c0}} = 75$ A. This critical current increases proportional to the wire radius, since the total current only flows within the thin shielding layer

We can also find an average critical current density at the surface. In this case we replace the exponentially decaying current density (Figure 5.1) by a distribution in which the full current density at the surface remains constant to a depth λ_{L}, the penetration depth, and then abruptly drops to zero.3) Based on this argument, for the tin wire, for example, at 0 K we obtain a critical current density

Since the penetration depth is only a few times 10^{-6} cm, for macroscopic wires we always have plane

$$j_{\mathrm{c0}} = \frac{I_{\mathrm{c0}}}{2\pi R \lambda_{\mathrm{L}}(0)} = 7.9 \times 10^7 \ \mathrm{A/cm^2}$$

with $R = 0.5$ mm, $\lambda_{\mathrm{L}}(0) = 3 \times 10^{-6}$ cm, and $I_{00} = 75$ A. This critical current density is similar to the critical pair-breaking current density of a thin wire treated in Section 5.1. It would allow very high transport currents if the shielding effect, leading to the restriction of the current to

a thin surface layer, could be avoided. Such substances have been developed in the form of the hard superconductors.

Using Silsbee's hypothesis, we can also calculate the critical currents of a superconductor in an external magnetic field. For this purpose, we only have to add the vectors of the external field and of the field of the transport current at the surface. The critical current density is reached when this resulting field attains the critical value. We consider a wire of radius R and a magnetic field B_a applied perpendicula to the wire axis. At first, no transport current is passing through the wire. Due to the Meißner effect, the field B_a is expelled from the wire, as shown in Figure 5.3a.

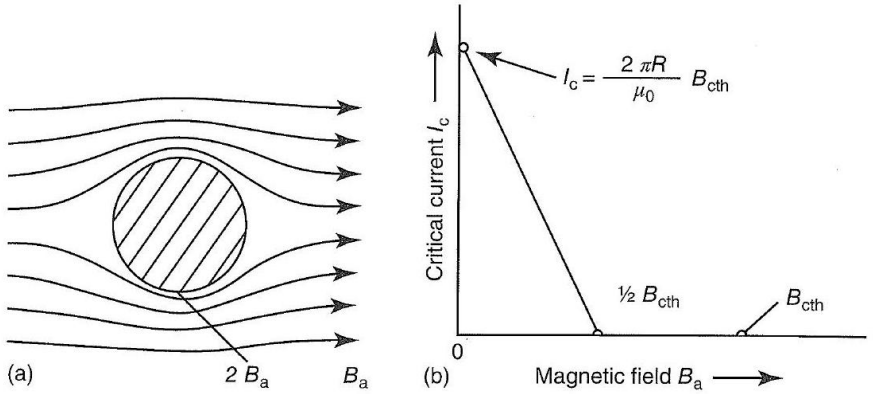


Figure 5.3 (a) Field distribution around a superconducting wire in the Meissner phase without a transport current. (b) Critical current of a wire with circular cross-section in external field B_a oriented perpendicular to the wire axis.

In the case of a wire in a perpendicular magnetic field, the demagnetization factor is 1/2. Therefore, at the top and the bottom side of the wire, the effective field is $B_\mathrm{eff} = 2B_\mathrm{a}$. A transport current I passing through the wire generates a magnetic field as indicated in Figure 5.1. At the top side of the wire, this field is directed opposite to the applied field. At the bottom side of the wire both fields add to each other. Hence, here one observes the highest total field, $B_\mathrm{ges} = 2B_2 + \mu_0 I/2\pi R$. The critical current is reached in the case $B_\mathrm{ges} = B_\mathrm{cth}$, that is,

$$I_\mathrm{c} = \frac{2\pi R}{\mu_\mathrm{o}} (B_\mathrm{cth} - 2B_\mathrm{a})$$

This dependence is plotted in Figure 5.3b

Next we turn to the question of how the superconductor enters the normal state upon reaching the critical current. For this, we again consider a wire with cir cular cross-section. If the critical current is exceeded, the Meissner phase with its complete flux expulsion must become unstable. One would expect that the superconductor becomes completely normal conducting. However, in this case

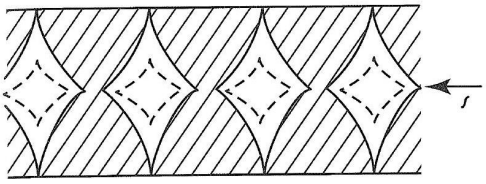


Figure 5.4 Intermediate-state structure of symmetry around the cylinder axis. For a (????) ical current. Hatched domains are normal conducting. The structure shows rotationa

the transport current would be distributed over the total cross-section. The magnetic field at the surface would remain unaffected by this redistribution. However then everywhere in the superconductor the current density would be smaller than its critical value. Since the critical

current density represents the crucial quantity for the stability of the superconducting state, we expect that the transition cannot take place in such a way that the current density is everywhere smaller than the critical value.

'This assumption is confirmed by experiment. If the critical current is exceeded, the superconductor enters the intermediate state, that is, there appear normal conducting domains. Several models have been proposed to describe this intermediate state. In this case, configurations of the normal conducting or superconducting domains are sought that yield the critical field B_{cth} at all interfaces as much as possible. For the macroscopic structure of the intermediate state, this critical field value also yields the critical current density because of the fully developed shielding. A model of this kind is shown in Figure 5.4 [2]. Since the magnetic field of the transport current consists of circular field lines, the phase boundaries must also run perpendicularly to the wire axis. Because of the requirement that for each radius the field must be equal to B_{cth}, the current density must increase toward the wire axis. This is accomplished also by an increase in the thickness of the superconducting domains toward the wire axis.

The geometrical details can only be found from a calculation. In this case certain additional assumptions are necessary. The various models of this current-induced intermediate state are different because of these additional assumptions.

The domain structure of this intermediate state has been demonstrated beautifully by means of the powder decoration method (see Section 4.6.4). An example of this structure is shown in Figure 5.5 [3]. Upon exceeding the critical current density, the superconducting wire jumps into a state where the superconducting domains still extend to the sample surface. Upon a further increase in the current, a normal conducting ring-shaped domain appears, which surrounds a core region resing in the intermediate state, the thickness of which increases with increasing current.

In Figure 5.6 we show the electrical resistance of the wire plotted versus the transport current [2]. At I_{c} the resistance jumps; however, the full normal resistance is not yet established. The latter is obtained only upon a further 290 5 Critical Currents in Type-l and Type-ll Superconductors



Figure 5.5 Intermediate-state structure of current 30 A, external field B_{a} perpendicua current-carrying In cylinder. The bright lar to the cylinder axis 0.01 T, temperature stripes indicate normal conducting domains. $T = 2.1$ K (T_c of IIn : 3.42 K), normal conduct- Length 38 mm, diameter 6 mm, transport ing $\rightarrow$ superconducting transition. (From [3].)

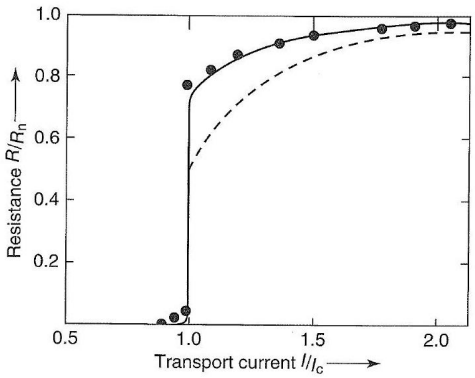


Figure 5.6 Electrical resistance plotted against the transport current. Solid line: model calculation from [2]; dashed line: model of London [4]; data points; from [5] (see also [6].

increase in I. Such measurements are quite difficult, since in the current-induced intermediate state at finite resistance the dissipated joule heat can easily lead to an increase in temperature and, hence, to instabilities."

Regarding the stability of the intermediate state, a "thick" wire carrying a transport current corresponds to a sample with a demagnetization coefficient different from zero in the external field (see Section 4.6.4). In both cases, by means of the transition into the intermediate state, the superconductor can respond to the constraint of the external variables (current or magnetic field) by splitting up into normal conducting and superconducting domains. In this way, the critical value can be kept constant over a range of external variables.

So far we have treated static models of the intermediate state. For a given state, the superconducting or normal conducting domains remain fixed within the sample, except for thermal fluctuations. Gorter [7] has proposed a dynamic model, according to which domain motion appears in the presence of a transport current, leading to a resistance. In this case, within this model, the interfaces are oriented

For sufficiently small resistance in the external circuit, the voltage-current characteristic can be traversed completely. However, the dissipated joule heat results in an increase in the average temperature. 5.3 Type-ll Superconductors 291

parallel to the direction of the transport current. In the static model discussed earlier (Figure 5.4), they were oriented perpendicular to the current direction. Decoration experiments using Nb powder have shown that for sufficiently large transport current the domains, indeed, move across the superconductor perpendicular to the current [8].

Very complicated intermediate state structures are obtained in wires that carry large transport currents in the presence of a longitudinal magnetic field. In this case, the longitudinal external field and the circular field of the current are superimposed such that the phase boundaries, which must always be oriented parallel to the field, display a screw pattern. Therefore, the transport current is also wound in a screw pattern. In this case, unexpected effects occur. For example, field enhancement is observed in the interior of the sample, which can be understood from the structure of the intermediate state, and which demonstrates impressively the general rule (see Section 4.6.4) that the phase boundaries must always be oriented parallel to the magnetic field [9].

5.3 Type-II Superconductors

Next we turn to type-II superconductors, which differ in an important fundamental way from type-I superconductors. For small magnetic fields and, hence, also for small transport currents, type-II superconductors reside in the Meissner phase. In this phase they behave like type-I superconductors, that is, they expel the magnetic field and the current into a thin surface layer.

A difference from type-I superconductors first appears when the magnetic field at the surface exceeds the value B_{c1}. Then a type-II superconductor must enter the Shubnikov phase, that is, flux lines must penetrate into the superconductor One finds that in the Shubnikov phase the ideal [5] type-II superconductor has a finite electrical resistance even at very small transport currents [10]. In the next section, we will treat this in detail. On the other hand, in type-II superconductors containing a large amount of defects, we can observe very large supercurrents. These "hard superconductors" will be discussed in Section 5.3.2.

5.3.1

Ideal Type-II Superconductor

We consider a rectangular plate carrying a current parallel to the plane of the plate and kept in the Shubnikov phase due to a magnetic field $B_{\mathrm{a}} > B_{\mathrm{c1}}$ oriented perpendicular to the plate (Figure 5.7).

In Section 4.7.1, an ideal type-II superconductor was defined by the fact that reversibly for increasing and decreasing evernal magnetic field In this case the corresponding equilibrium flux-line

configuration must be established arbitrarily easily, that is, arbitrarily easy flux-line motion must be possible. Hence, an ideal homogeneous with respect to the locations of the flux lines. 2925 Critical Currents in Type-l and Type-ll Superconductors

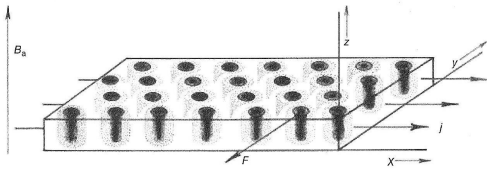


Figure 5.7 Shubnikov phase in the presence of a transport current density j. The flux line experience a force F driving them along the y-direction. The magnetic field distribution around the flux lines is indicated by the shading.

As the first important result of such an experiment, one finds that under these conditions the transport current I is distributed over the total cross-section of the plate, that is, it is no longer completely restricted to a thin surface layer. After the penetration of the magnetic flux into the superconducting sample, the transport current can also flow within the interior of the superconductor

In this case there exists an important interaction between the transport current and the vortices. The transport current, say, along the x-direction, also passes through the vortices, that is, through regions where a magnetic field exists.) Between an electric current and a magnetic field, there exists the Lorentz force. In the case of a current I along a wire of length L in a perpendicular magnetic field B_2, the absolute magnitude of this force is

$F = ILB$

This force is oriented perpendicular to B and to the current (here given by the wire axis). It is also this Lorentz force that drives our electric motors.

the Shubnikov phase carrying a transport current, the Lorentz force acts between the vortices and the current. Since the transport current is spatially fixed by the boundaries of the plate, under the influence of the Lorentz force the vortices must move perpendicular to the current direction and to the magnetic field, that is, perpendicular to their own axis [11]. For ideal type-II superconductors, in which free motion of the vortices is possible, this vortex motion should appear already at arbitrarily small forces and, hence, at arbitrarily small transport currents.

However, the vortex motion across the superconductor causes dissipation, that is, electrical energy is changed into heat. This energy can only be taken from the

In the illustration of the Shubnikov phase, for simplicity cylindrical vortices are presented (see, e.g., Figures 1.8 and 5.7). This picture could lead to the wrong conclusion that the by flowing around them, and thereby also avoids the magnetic field regions. However in this case, because of the vortex motion, we are dealing with a complicated nonequilibrium phenomenon, and a more detailed discussion can be found in monograph [M17].

transport current by means of an electrical voltage appearing along the sample. Hence, the sample shows electrical resistance.

The dissipation of electrical energy into heat during vortex motion may be due to two fundamentally different processes. The first loss mechanism is associated with the appearance of local electric fields generated by the moving vortices. This electric field also accelerates the unpaired electrons. They can deliver their energy taken up from the electric field to the lattice and thereby generate heat.

In addition to this process for energy dissipation, associated with the spatial variation of the magnetic field in a vortex, there exists another process caused by the spatial variation of

the Cooper pair density in a vortex. If a vortex moves across the location P a temporal change of the Cooper pair density n_s also appears at this location, since n_s increases from its value zero in the vortex center toward the outside. In this case we must take into account that, following a deviation from equilibrium, this equilibrium value of n_n is re-established only after a finite time τ (the relaxation time, see Section 4.9). If n_s changes very slowly, that is, within times much larger than τ, the system only passes through equilibrium states. In his case the energy consumed at the front side of the vortex during breaking up of Cooper pairs will be delivered back at the back side during pair formation. Therefore, practically no net heat is generated in this process. However, if the vortex moves sufficiently fast, such that the Cooper pair density cannot pass only through equilibrium states anymore, energy will be dissipated during the temporal change of n_s, and heat will be generated.

We can understand this in the following way. The high magnetic field within the vortex core moves sufficiently fast that the equilibrium concentration of Cooper vortex core moves sufficiently fast that the equilibrium concentration of Cooper pairs corresponding to each field value cannot be established anymore. In this case, at the front side of the vortex, the Cooper pairs are broken up in a magnetic field that is too high. On the other hand, at the back side the Cooper pairs recombine in a field that is already too small for the corresponding concentration. Since the heat of reaction of the breaking of a Cooper pair decreases with increasing magnetic field," during the break-up process less heat energy is consumed than is delivered back during the recombination. Therefore, heat will be generated, if the temporal variation of n_s is made fast enough such that deviations from equilibrium appear between all parameters.

What we just have described for the example of the Cooper pair density is exactly the mechanism of all relaxation processes for changes of external parameters during times comparable to the relaxation time. Other well-known examples are the polarization losses of a dielectric substance in an alternating electric field or the magnetization losses of a ferromagnetic material in an alternating magnetic field.

So we summarize: As soon as the vortices in the Shubnikov phase start to move due to a transport current, we have losses and, hence, electrical resistance.

In the Shubnikoy phase, with increasing magnetic field, the Cooper pair density and, hence, the binding energy decrease. 2945 Critical Currents in Type-I and Type-ll Superconductors

Since in an ideal type-II superconductor arbitrarily small transport currents already lead to vortex motion, the critical current of such a superconductor in the Shubnikov phase is zero [10]. Therefore, such superconductors are useless for technical applications, say, for building magnets, in spite of their high critical field B_{c2}. Finite critical currents in the Shubnikov phase can only be obtained if the vortices in some way are bound to their locations. Such pinning of the vortices can, indeed, be achieved. Type-II superconductors containing such pinning centers are referred to as hard superconductors. Their properties will be discussed in the next section.

So far in our discussions of the critical current in type-II superconductors, we have stabilized the Shubnikov phase by means of an external magnetic field. Now we return to the question of the critical current in the absence of an external magnetic field, with which we had started. Again, we assume a wire with circular cross-section carrying the transport current I. Upon exceeding the value $I_c = B_{c1} 2\pi R/\mu_0$, which generates just the field B_{c1} at the surface, the superconductor enters the Shubnikov phase. Since the magnetic field of the transport current circulates around the wire axis, in this geometry circular closed vortices are also generated. Under the influence of the Lorentz force they move toward the wire axis by shrinking and vanish at the axis. So for an ideal type-II superconductor with this geometry, we expect a critical current I_c determined from B_{c1} in the same way as for a type-I superconductor from B_{cth} (see Section 5.2). Since B_{c1} is smaller than B_{cth}, in ideal type-II superconductors this critical current will always be smaller than in the corresponding type-I superconductors.

For a long time, there has been an animated discussion on the role of vortex motion in the

generation of electrical voltage. Within this context many experiments were contemplated and carried out. Here, we want to treat only one example.

In 1996 Giaever [12] performed an experiment, the idea of which is illustrated with the configuration shown in Figure 5.8. A thin film of a superconductor (A) is driven into the Shubnikov phase by means of an external magnetic field, and a transport current is applied. In this case, motion of the flux lines should occur. In order to detect this flux motion, on top of film A Giaever deposited a second superconducting film B, which was electrically insulated from film A by means of a thin insulating layer. In this configuration the magnetic flux lines in both films are coupled to each other.9) If the vortices move across the superconductor A under the influence of the transport current, the vortices in B are dragged along because of the coupling. If, as felt by Giaever, an electrical voltage appears between the ends of the superconductor because of the vortex motion, this voltage must also be observed along the film B, which is completely separated from the primary circuit. Therefore, the arrangement represents some kind of "flux transformer,"

Here, "corresponding" means that the superconductors have the same geometry and the same $B_{\text{cht.}}$.

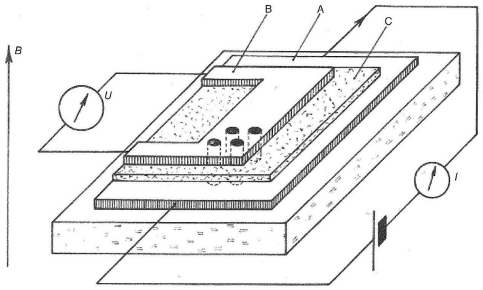


Figure 5.8 Generation of an electrical voltage U during vortex motion. A and B are superconductors, C is an insulating layer. All layer thicknesses are strongly exaggerated. (From [12].)

Giaever performed the experiment in the absence of an external magnetic field. Also in this case, the magnetic field of the transport current applied to film A penetrates into both films in the form of flux lines. These flux lines have opposite sign at the left and the right sides of the film, respectively, and they move from both sides of the film A to the center, where they annihilate each other. This vortex motion resulted in the expected voltage also along the electrically completely separated film B. If both films were normal conducting, no electrical voltage was observed along film B for the same conditions otherwise. This experiment clearly demonstrated the importance of vortex motion for the appearance of an electrical voltage in the Shubnikov phase.

Recently, the geometry of the flux transformer has been taken up again in order to investigate if in high-temperature superconductors the vortices can move independently of each other in the form of pancakes (see Section 4.7.2) [13]. For this purpose, at one side, for example, of a $Bi_2Sr_2CaCu_2O_8$ single crystal a transport current is injected parallel to the layer structure, and the voltage drop is measured resulting from the vortex motion. If the vortices represent compact, continuous flux lines across the crystal, at the opposite crystal surface a voltage of equal magnitude will be induced. However, if the pancakes move independently of each other, this secondary voltage will be smaller than the primary voltage. In this way, the existence of pancake vortices in $Bi_2Sr_2CaCu_2O_8$ could be beautifully demonstrated. On the other hand, it turned out that the vortices in $YBa_2Cu_3O_7$ behave more like compact, continuous flux lines. 296 F critical Currents in Type-I and Type-ll Superconductors

5.3.2

Hard Superconductors

In Section 4.7.1 we have discussed the magnetization curves of type-II superconductors (Figure 4.23). We started with ideal, homogeneous substances, that is, substances in which the vortices of the Shubnikov phase are freely mobile, having no energetically favorable locations. This discussion only represents a limiting case, which is approximated only more or less poorly by real samples.

In this section we will discuss the case in which the vortices of the Shubnikov phase are energetically strongly bound to favorable locations. These superconductors are referred to as hard superconductors and represent technically useful materials.

4.1.3 Critical supercurrent: advanced features 2

Pinning of Flux Lines

First we want to discuss how vortices in type-II superconductors can be pinned. We will deal with a series of different types of pinning centers.

In the simplest way we can understand the effect of pinning centers by means of an energy consideration. The formation of a vortex requires a certain amount of energy. This energy is contained, say, in the circulating currents flowing around the vortex core. We see that for the given conditions a vortex is associated with a the vortex core. We see that for the given conditions a vortex is associated with a certain amount of energy per unit length, that is, the longer the flux line, the larger the energy needed for its generation.

We denote this energy by ε^*. It can be estimated from the lower critical field B_{c1} above which magnetic flux starts to penetrate into a type-II superconductor. The resulting gain in expulsion energy suffices to generate vortices in the interior. For simplicity, we consider again a long cylinder in a magnetic field parallel to its axis, that is, a geometry with zero demagnetization coefficient. At B_{c1} the penetration of the magnetic flux results in n flux lines per unit area. Each flux line carries just one flux quantum Φ_0. This requires the energy

$$\Delta E_F = n\varepsilon^* LF$$

where n = number of flux lines per unit area, ε^* = energy per unit length of vortex, L = sample length, and F = sample cross-section. The gain in magnetic expulsion energy is

$$\Delta E_M = B_{c1}\Delta MV$$

where $\triangle M$ = change of the magnetization of the sample and $V = LF$ = sample volume. ΔM can be expressed in terms of the penetrated flux quanta. We have

$$\Delta M = n\Phi_0/\mu_0$$

This yields for the gain in expulsion energy

$$\Delta E_M = \frac{1}{\mu_0} B_{c1} n\Phi_0 LF$$

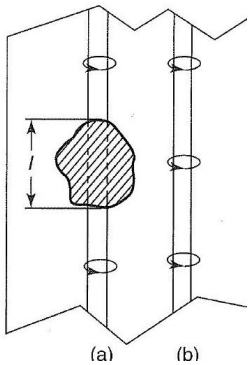


Figure 5.9 Pinning effect of normal conducting precipshorter compared to that in location " b," since there are no circulating currents in the normal conducting region.

If the two energy changes are being set equal ($\Delta E_{\mathrm{F}} = \Delta E_{\mathrm{M}}$), from the definition of B_{c1} we obtain

$n\varepsilon^* LF = \frac{1}{\mu_0} B_{\mathrm{c1}} n \Phi_0 LF$

and hence [10)]

$$\varepsilon^* = \frac{1}{\mu_0} B_{c1} \Phi_0$$

In the case of the estimate given above, we have considered only the fieldexpulsion energy. However, the loss of condensation energy on the scale of the coherence length also affects the value of ε^*. From our knowledge of the vortex energy ε^*, we can easily understand the pinning effect of normal precipitates. If a vortex can pass through a normal conducting inclusion, its length within the superconducting phase and thereby its energy are reduced. This is schematically indicated in Figure 5.9. The hatched region indicates the normal inclusion. A vortex in location "a" has an energy smaller by the amount $\varepsilon^* l$ compared to one in location "b." This means that we must supply the energy $\varepsilon^* l$ to the vortex in order to move it from "a" to "b." Hence, a force is needed to effect this change in location.

If there are many pinning centers, the vortices will attempt to occupy the energetically most favorable locations. As shown in Figure 5.10, they will also bend in order to reach the minimum value of the total energy. The length increment caused by the bending must be overcompensated by the effective shortening within the

The energy per unit length, $\varepsilon^{\|\prime}$, can also be currents (see, e.g, [M8], Chapter 3, p. 57). One obtains the expression

$\varepsilon^* = \frac{1}{\mu_0} \left(\Phi/\lambda_{\mathrm{L}}\right)^2 \ln\left(\lambda_{\mathrm{L}}/\xi_{\mathrm{GL}}\right)$

We see that the energy $\varepsilon^\star$ increases proportional to the square of the magnetic flux Φ in a vortex. Therefore, vortices containing more than one flux quantum Φ_0 are energetically unfavorable In a type-II superconductor or in hard superconductors, such vortices can only exist if they are strongly promoted by other conditions such as inhomogeneities in the material.
298 5 Critical Currents in Type-l and Type-ll superconductors

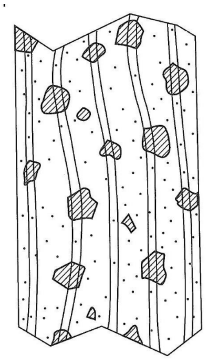


Figure 5.10 Vortex configuration in a hard superconductor. The hatched regions represent pinning centers. The dots indicate atomic defects.

normal conducting regions. In a vortex lattice as it is generated in the Shubnikov phase, we must take into account in the total energy balance also the repulsive forces acting between the flux lines.

(We must note, however, that often the details are difficult, and that a complete account of the effects of all pinning centers is impossible)

In principle, other pinning centers, say, lattice defects, can also be understood in the same way..1) Every inhomogeneity of the material that is less favorable for superconductivity acts as a pinning center, with the completely normal state representing the limiting case. For example, superconducting precipitates, however, with a lower transition temperature, in general act as pinning centers.

If for a certain material the superconductivity is associated with an expansion of If for a certain material the superconductivity is associated with an expansion of less favorable for superconductivity and, hence, will act as pinning centers. This may be the case within grain boundaries and dislocation configurations, as they are generated during plastic deformation.

Atomic defects within the crystal lattice represent a particular issue with respect Atomic defects within the crystal lattice represent a particular issue with respect to the coherence length ξ_{GL}, which amounts to many lattice constants in many superconductors. Hence, one could expect that atomic defects are not effective pinning centers. However, it could be shown that the scattering of electrons at atomic defects leads to an appreciable pinning effect [14]. On the other hand, since each flux line usually covers many atomic defects, in the case of a homogeneous distribution of the atomic defects the effective pinning force vanishes, since no particular location within the material is distinguished. Such distinction only appears if the density of the atomic defects varies spatially.

In the case of superconductors with an extremely small value of the coherence length as, for example, the cuprates, the situation is completely different. Here, spatially very small defects can act as pinning centers in different ways.22)

In the extreme case, even the crystal structure itself can have an effect. In Section 4.7.2 we have already discussed that, in the case of the cuprates, in magnetic fields oriented parallel to the superconducting CuO_2 planes, there develop Josephson vortices with their axis being located in the nonsuperconducting or only weakly superconducting intermediate layers. These intermediate layers represent highly effective pinning centers against vortex motion perpendicular to the planes. One speaks of “intrinsic pinning” [15] On the other hand, the vortices can still move easily parallel to the layer structure.

In a similar way grain boundaries or twin boundaries between single-crystalline regions act as defects, preventing vortex motion perpendicular to these defects. [13] Line defects and point defects are also important. Dislocation lines represent a example. Line defects and point defects were also artificially generated by irradiating high-temperature superconductors with high-energy heavy ions or also with protons [16]. During irradiation with heavy ions, along the path of the beam particles there appears a straight, highly perturbed region across the crystal, which is referred to as a columnar defect. On the other hand, irradiation with protons results in accumulations of point defects.

For the generation of well-controlled pinning centers, the continuously improved techniques of nanotechnology are applied. A summary can be found in [17]. During the deposition of thin films one can incorporate nanoparticles into the superconducting matrix. Equally distributed "round" nanoparticles consisting, for example, of Y_2O_3, result in a nearly isotropic pinning of flux lines. On the other hand, in the case of rod-like structures, a preferential direction is obtained. As an example we mention $BaZrO_3$ nanorods, which grow on the film during its deposition by means of pulsed laser ablation [18]. In the case of pulsed laser deposition by means of pulsed $YBa_2Cu_3O_7$ thin film, in an oxygen atmosphere of about 0.3mbar, highly intensive laser pulses are directed onto a "target" made of massive $YBa_2Cu_3O_7$. The ablated

material condenses on a single-crystalline $SrTiO_3$ substrate such that the CuO_2 planes of the cuprate are oriented parallel to the surface of the substrate. In order to incorporate $BaZrO_3$ nanorods in addition, one uses a target containing some $BaZrO_3$ in addition to

Furthermore, the vortices can form not only more or less crystalline lattices, but also liquid and even gaseous phases (see Section 4.7.2). In the later phases the

13) However, we do not want to suggest that centers. In high-temperature superconductors, for not too small tilting angles between two grains, the grain pinning forces, and, hence, the critical current I_c are small, Frequently, above I_c the electric resistance increases grad boundaries act as Josephson junctions, even in the absence of an external magnetic field. In a magnetic field this supercurrent is strongly reduced further. 300 5 Critical Currents in Type-l and Type-ll Superconductors

$YBa_2Cu_3O_7$. If this mixture is deposited, in addition to the $YBa_2Cu_3O_7$ matrix, also $BaZrO_3$ rods of about 10 nm diameter grow on the substrate, which penetrate the total thickness of the film and act as rod-shaped pinning centers.

In thin films of metallic superconductors and also in the cuprates, one can fabricate "defects" in a well-controlled way in the form of microholes within the material. In this case one often speaks of "antidots" [19]. Also the opposite of the antidots, magnetic particles placed on the film surface ("magnetic dots"), have been studied [20]

Another "defect" we want to mention is the surface of the superconductor itself. If the external magnetic field is increased (decreased), vortices enter (exit) the sample at the edge. This process is already prevented by the flow of the shielding currents, and the vortices must traverse a surface barrier. This is also referred to as the Bean-Livingston barrier [21]

The effect of the pinning centers can also be described in terms of an energy landscape. Now the pinning center represents a potential well of depth E_p. The vortex is located at its most favorable position, similar to a ball at the lowest point of a bowl. If the ball is to be displaced from this location, one needs a force in order to supply the increase of the potential energy. To remove the ball from its most favorable location, we must supply the energy needed to lift the ball out of the bowl. Usually, in a material there are many pinning centers, which are irregularly distributed and have different energy depths E_p. If the superconductor is cooled below T_c in a magnetic field, the vortices will quickly occupy the potential wells, instead of generating a regular triangular lattice. At best, we have a distorted lattice, or in the extreme case even a glassy state [22].

The deviation of an individual vortex from its ideal location within the triangular vortex lattice depends on the depth of the potential wells, and also on the configuration of all other vortices, because of the repulsive interaction between them. An energetically highly unfavorable arrangement of the vortices will be changed quickly because of the thermal fluctuations. These fluctuations can provide the energy difference ΔE needed to leave the potential well, with a probability $w = \exp(-\Delta E/k_B T)$. In this case, the thermodynamic fluctuations can reduce the depth of the potential well, or they can supply the missing energy to the vortex. At low temperatures and for large values of ΔE, this probability can become very small, such that the state with the lowest energy cannot be occupied any more. Furthermore, because of the interaction between the vortices, ΔE can approach infinity. In this case we are dealing with the state of a vortex glass, which experiences no changes anymore within finite times.

A special effect occurs if two pinning centers are located very close to each other. In this case a vortex can jump very easily back and forth between the two potential wells because of thermal fluctuations. This effect is highly important in the context of superconducting quantum interferometers (SQUIDs) made from high-temperature superconductors. The magnetic field of a flux quantum located within the superconducting material of the SQUID is recorded as a measuring signal by the SQUID. If this flux quantum moves, then this (unwanted) signal changes

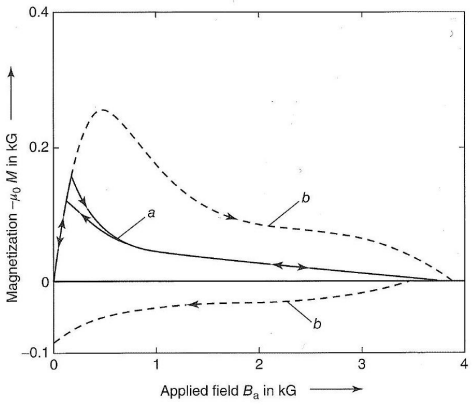


Figure 5.11 Magnetization curves of a Nb_{55} T_{45} alloy: curve a, well annealed; curve b, with many lattice defects (1kG = 0.1 T),from [23])

and causes a reduction of the SQUID sensitivity for real measuring signals..[14)] Therefore, the investigation of such pinning centers and the development of most effective and strong pinning centers are highly important.

What is the effect of the pinning centers if in the superconducting state the magnetic field is changed or a transport current is applied to the superconductor? These questions will be discussed in the next two sections. We start with the magnetization curves of hard superconductors.

Magnetization Curve of Hard Superconductors

If in the Shubnikov phase the vortices are attached to certain locations within the material, then in an external field the magnetization corresponding to thermodynamic equilibrium cannot establish itself. The prerequisite for this is the free mobility of the vortices. Hence, we have to expect quite different magnetization curves. Furthermore, it represents an important difference, whether the superconductor is cooled in a field B_a, or this field is applied only after the superconducting state is established. First, we treat the properties of massive metallic superconductors, and then we turn to the high-temperature superconductors and to special thin-film structures, in which pinning centers were artificially generated.

In Figure 5.11 as an example we show the behavior of a Nb-Ta alloy [23]. Niobium and tantalum can be mixed in any ratio. After careful annealing one obtains 14) This effect is to be compared with Figure 1.10e. In this case, the displacement of flux quanta by means of an electron beam was specifically utilized for the imaging of vortices. 302 5 Critical Currents in Type-I and Type-II Superconductors

highly homogeneous mixed crystals. They yield a nearly reversible magnetization curve (curve a). After deformation of such a mixed crystal, say, by pulling for the fabrication of wires, many lattice defects exist within the crystal, acting as pinning centers for vortices. In this case the magnetization curve is completely different (curve b). First we note that a much higher magnetization is reached. This also means that in external fields much higher than B the deformed sample can still display nearly perfect diamagnetic shielding. Furthermore, any trace of reversibility has disappeared. For decreasing field, magnetic flux remains trapped in the sample also at $B_2 = 0$. In this case the trapped flux is oriented parallel to the previously applied external field.

Only the upper critical field B_{c_2} remains unchanged. This can be understood from the fact that a mixed crystal of the alloy $Nb_{55}Ta_{45}$ already has a very small mean free path l^*. Hence, the additional defects can hardly change κ and also B_{c2} (see Section 4.7.1) any more. If we assume that the vortices are more or less strongly pinned within the deformed material, we can easily understand this magnetization curve qualitatively. We look at the curve starting at field

zero. Up to the external field B_{c1} there is no difference. The sample resides in the Meissner phase, which is hardly influenced by perturbations..[15)]

If B_{c1} is exceeded, vortices enter the sample at the surface. At first, these vortices are attached to their locations immediately below the surface, and they cannot distribute themselves equally over the volume as in a homogeneous material. However, within the surface layer, where the pinned vortices are, shielding current can also flow. As a result, the total shielding current, determining the diamagnetic behavior, extends further into the superconductor than in the Meissner phase where it is restricted only to a layer with the thickness of the penetration depth. As a result, the shielding current and, hence, the diamagnetic signal in the vortex state can exceed those in the Meissner phase.

At B_{c2} the Cooper pair density is zero, and the superconductivity disappears. [10] The magnetic field homogeneously penetrates the superconductor. If the externa field is decreased below B_{c2}, the sample again enters the Shubnikov phase. Again the magnetic flux is divided into multiples of the flux quantum Φ_0, and the vortices are more or less strongly pinned to the perturbations in the crystal lattice. Hence, with decreasing external field they can leave the material only with difficulty. The field within the sample then becomes larger than the external field, and the magnetization of the sample becomes positive. Even at $B_a = 0$ there remains a finite magnetic flux along the field direction trapped within the sample. 15) Here, we ignore the small influence of the perturbation on the penetration depth λ_1. 16) Here, we do not include the surface superconductivity in a thin layer near the surface, which can exist in parallel fields up to $B_a = 1.7B_{c2}$

We note that this irreversible behavior was observed already in very early experimen isistercefic alloys [24]. At the nerise Therefore, a frest attempt at explaining tie hysteretic magnetization curves was based on the assumption of a sponge-like

As a second example, in Figure 5.12 we show the magnetization curve of a lead-bismuth alloy containing 53at%Bi [26]. At low fields-we see abrupt changes of the magnetization, which are due to so-called flux jumps. In this case large flux-line bundles or regions of the vortex lattice tear off the pinning sites and thereby result in a jump of the magnetization toward thermodynamic equilibrium. In superconducting magnets such flux jumps are very dangerous, since, because of the generated heat energy, the superconductor can become normal conducting over its whole cross-section (see Section 7.1.2) and the magnetic field can break down

Flux jumps can look spectacular and can develop into avalanches. In Figure 5.13 we show an example in the case of an MgB_2 thin film [27]. The image was obtained by magneto-optics (see Figure 1.10b). The branching bright regions represent the locations where magnetic flux has penetrated into the sample. This is also referred to as dendritic flux avalanches.

In high-temperature superconductors the situation is still more complicated, since a number of different vortex phases can exist even in the absence of pinning centers, as we have discussed in Section 4.7.2 (see Figures 4.33-4.38). The pinning centers act differently in the different phases. Different glassy states can develop, like the amorphous vortex glass [28] or the "Bragg glass" [29]. In the latter case, at small distances the vortices are somewhat disordered. However, at large distances the vortices again approach a vortex lattice because of the interactions between them. Another example is the "Bose glass" appearing in the presence of columna defects along a certain direction [30]. This is illustrated in Figure 5.14 based on a phase diagram calculated for cuprates in magnetic fields oriented perpendicular to the layer structure [31]. Here the vortices were treated as continuous lines, that is, additional degrees of freedom due to the pancake vortices were ignored

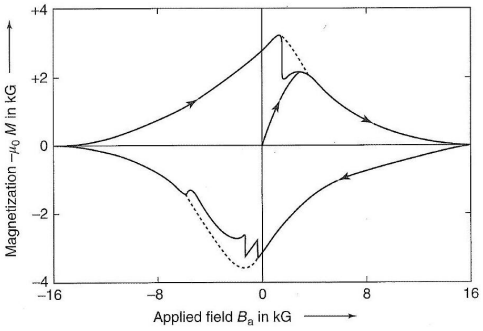


Figure 5.12 Complete magnetization cycle of a Pb-Bi alloy (53at% Bi). The dashed curve is expected if there are no flux jumps (1kG = 0.1 T).(from [26]

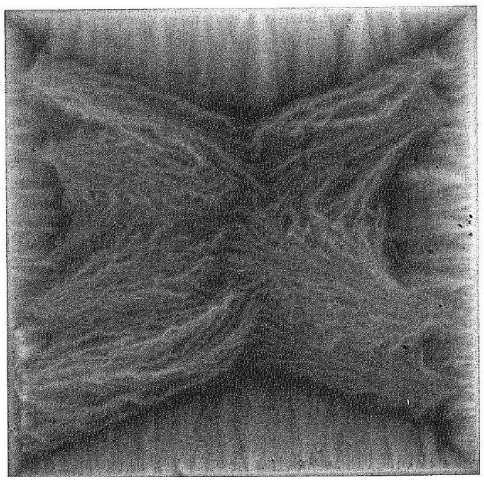


Figure 5.13 Dendritic flux avalanches, which have penetrated into an MgB_2 thin film. Sample area: 5×5 mm^2, film thickness: 200 nm. The magnetic field (8mT) was applied perpendicular to the thin film. Temperature: 10 K. (Courtesy by J. Albrecht, College Aalen,

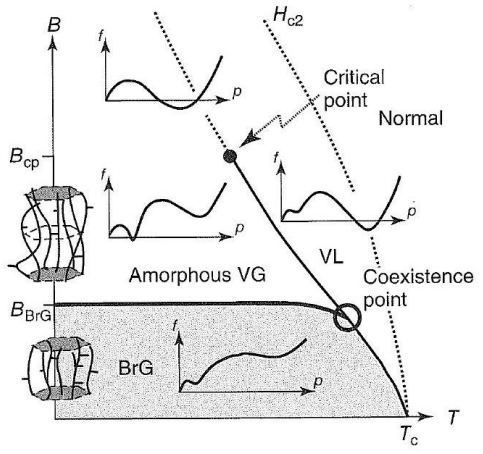


Figure 5.14 Glass-like vortex phases in the how the Gibbs energy in the corresponding cuprates in the presence of pinning centers [31]. BrG, Bragg glass; VG, vortex glass; tion density in the vortex lattice.

VL, vortex liquid, The small insets indicate

In the magnetization curve, the transition between two vortex phases sometimes shows up as a maximum, which is also referred to as a second peak or as a fishtail. This is shown in Figure 5.15 based on a measurement for a $YBa_2Cu_3O_{7-\delta}$ 5.3 Type-ll Superconductors | 305

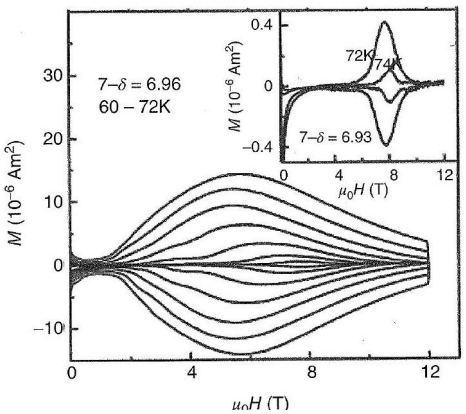
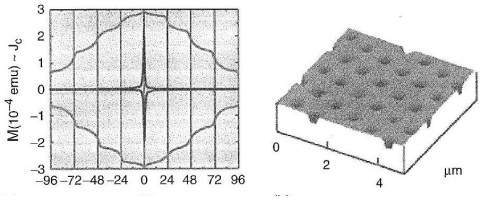


Figure 5.15 Magnetization curve of a $YBa_2Cu_3O_{7-\delta}$ single crystal at temperatures between 60 and 72 K. At fields above 4 T, we note a second peak [32].

single crystal [32]. This effect can also be well observed in $Bi_2Sr_2CaCu_2O_8$ [33]. During the transition between the Bragg glass and the vortex glass observed here, the elastic constants of the vortex ensemble decrease, so that the vortices can adjust themselves better to the pinning centers in the material.

As a last example of the interaction between vortices and pinning centers, in Figure 5.16 we show the magnetization curve of a PbGe film, in which microholes (antidots) with a separation of 1μm were fabricated [34]. If a magnetic field is applied to this film, there are certain field values at which the number of vortices



(a)

H(G)

Figure 5.16 Magnetization curve of a PbGe of microholes. For comparison, the magnefilm (a) in which a regular lattice of micro- tization curve of a PbGe film without antiholes was fabricated (b). The magnetization dots is also shown. In the latter case, the (being proportional to the critical current magnetization strongly decreases already density in the film) shows a very large hys- at small fields. Measuring temperature: netic field values at which the number of Elsevier.)

vortices is an integer multiple of the number 306 5 critical Currents in Type-I and Type-ll Superconductors

in the film is an integer multiple of the number of antidots. At these matching fields the vortices are distributed regularly onto the antidots. It is also possible that more than one vortex can be trapped within one antidot. In Figure 5.15 in the diagram on the left the matching-field values are indicated by vertical lines. At the matching fields the vortex lattice is particularly strongly pinned. [18] For comparison, Figure 5.15 also shows the magnetization curve of a PbGe film without antidots. In this case the magnetization curve strongly decreases already at small fields

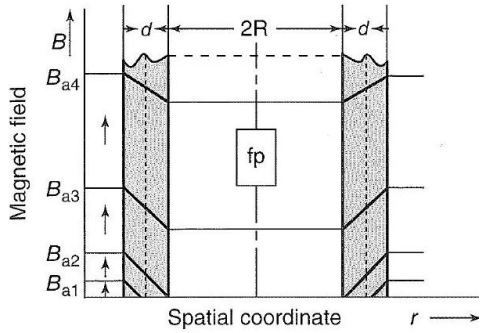
The possibility of fabricating pinning centers in thin films allows the investigation of specific models of the interaction between vortices and pinning centers. This is interesting for both the fundamental physics and technical applications. For example, in SQUID magnetometers, antidots can be placed strategically in such a way that the perturbing signals due to the vortex motion are minimized [35].

Next we want to discuss the origin of the hysteresis in the magnetization curve more quantitatively and look at the connection between the magnetization and the maximum possible supercurrent in the sample. Frequently, the direct measurement of the maximum supercurrent is difficult, since currents of 100 A or higher must be measured. Hence, it is advantageous to have a procedure for measuring the critical current without electrical contacts. This method turns out to be particularly important for the study of sintered materials, which mostly are not available in the form of wires or sheets and, hence, cannot be investigated with the standard methods.

In this context Bean [36] has proposed a model, which we want to discuss in the following in a slightly simplified version. We consider a simple geometry, namely a long, hollow cylinder (length L, diameter $2R$, wall thickness $d \ll 2R$). If a circulating current I flows within this cylinder, it generates a magnetic field $B_\mathrm{i} = \mu_0 I/L$, which can also be written in terms of the average current density $j = I/(Ld)$ as $B_\mathrm{i} = \mu_j j$ j

The cylinder is assumed to be cooled in zero applied magnetic field. Upon the application of the field B_a parallel to the cylinder axis, at the outside of the superconducting cylinder a circulating current is generated shielding the interior of the cylinder (Figure 5.17). As long as the hard superconductor resides in the Meissne phase, the shielding current only flows within the penetration depth near the surface of the cylinder. If B_2 exceeds the value B_{c1}, which we can assume to be ver small, magnetic flux can penetrate into the superconductor in the form of vortices. Initially, the vortices are trapped by the pinning centers below the surface. In this case, the Bean model simply assumes that the critical transport current within the region of the superconductor penetrated by the vortices just has the homogeneous critical current density j_c. For simplicity, this current density is taken as constant, that is, it is assumed to be independent of the magnetic field in the superconductor. This state carrying the critical current density is referred to as the critical state.

A similar but weaker effect also appears for rational values of the ratio: (number of antidots)/(number of vortices). 5.3 Type-ll Superconductors | 307



(a)

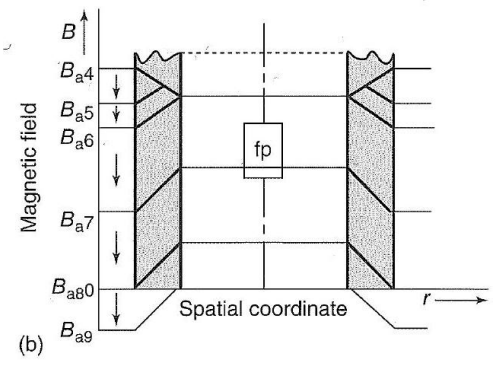


Figure 5.17 Magnetic field distribution in a hollow cylinder of a hard superconductor for increasing B is indicated by a less steep field slope [36]. f = field probe.

If the field B_a is increased further beyond the value B_{c1}, a thicker and thicker layer below the cylinder surface is filled with vortices. The total shielding current increases proportional to the thickness of this layer which, according to our assumption, carries the constant current density j_i[19] The critical state grows into the superconductor. Because of the shielding current, the magnetic field within the superconductor decreases toward the cylinder axis. If the radius R is large compared to the thickness d of the cylinder wall, we can well approximate the latter in terms of a planar layer. In this case, the magnetic field decreases linearly toward the axis. [20)] In Figure 5.17a this field variation is indicated for different values of the external field. At B_{21} only part of the cylinder wall is filled with vortices (dashed lines, part a). At B_{22} the shielding current has reached its maximum value, since now the current density j_c flows homogeneously in the whole cylinder wall. However, in the interior of the cylinder, the field B_i still remains zero. Only during a further increase in B_a does a magnetic field also appear in the interior. In our simple model this field is equal to $B_a - B_{22}$ (with $B_a > B_{22}$)

Of course, for large fields our assumption j_C = constant cannot be valid anymore, since j_c must approach zero for $B_a \to B_{c2}$. So we must improve our model by requiring that j_c decreases with increasing B_2. In this case with increasing field B_a, the difference $B_2 - B_i$ gradually approaches zero.

In Figure 5.18 the field B_i in the interior of the cylinder is plotted versus the external field B_a for a $V_3(Ga_{0.54}Al_{0.46})$ sample (high-field superconductor). Up to the value B_{22} the field B_i remains zero. In this case, with j_c = constant, we would always have $B_i = B_a - B_{a2}$ (dashed line). However, since j_c decreases with increasing field, the curve $B_i(B_2)$ more and more approaches the straight line $B_i = B_a$. From the behavior of $B_i(B_a)$, or from the magnetization curve 19) If the thickness of the cylinder wall is very small compared to the radius R, we can ignore the vari20) Wion of r within the wall thickness. Within the superconductor, because

netic field In our discussion of the model, the field in the, we have a spatial varia tion

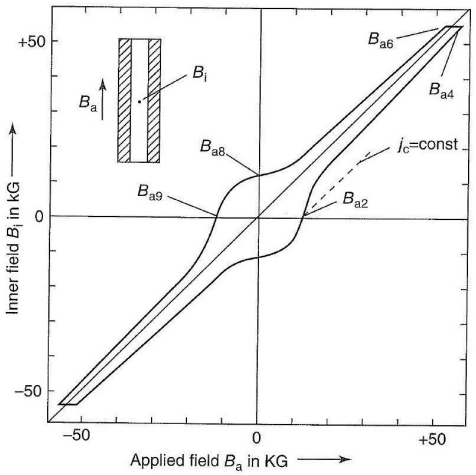


Figure 5.18 Magnetic shielding of a hollow cylinder made from $V_3(Ga_{0.54}Al_{0.46})$. Inner field B_i plotted versus the external field B_a(1kG = 0.1 T). Measuring temperature: 4.2 K; transition temperature: 12.2 K. (By courtesy of DrH. Voigt, Siemens.)

$M(B_2) = (B_i - B_a)/\mu_0$, within our model (which assumes the existence of a critical state) we can determine the critical current density of the material investigated Frequently, this elegant method is applied in the study of novel superconductors. In the case of a long hollow cylinder, one obtains

$$|M(B_a)| = j_c(B_a)\, d$$

where d is the wall thickness of the hollow cylinder. Analogously, for a solid cylinder with diameter $2R$ one finds the magnetization $|M| = j_c R/3$ (from, e.g., [M4]).

We want to also discuss the case where the external field is lowered starting say, from B_{24}. Now, because of the negative field change ($\Delta B < 0$), an induction process takes place, which slows down the shielding current flowing at the outer part of the cylinder and generates a critical current in the opposite direction. In igure 5.17 b the magnetic field variation is indicated for a few sequential values B_{a5} up to B_{a7}. Again a critical state exists in the whole cylinder. However, now the ortex density increases toward the interior. In this case the vortices appear to exit om the outer cylinder wall. Up to the value B_{26} the field B_1 remains constant. Then B_i decreases. At $B_a = 0$ a certain magnetic flux and, hence, a field B_i is trapped. The corresponding points are indicated in Figure 5.18.

If in the next step we increase the external field in the opposite direction, then at $-B_{29} = B_{a2}$ we just obtain the field $B_i = 0$. This can clearly be seen from Figure 5.17b. In Figure 5.18 we show the corresponding variation of B_i together with the complete hysteresis loop traversed in such an experiment. In many hard superconductors, this dependence is well described by the expression [37]

$$j_c = \frac{\alpha_c}{B + B_0}$$

Here, the constants α_c and B_0 are characteristic for the particular material. In samples with a more complicated shape, for example, in thin films or irreguarly shaped crystals, and also in materials with an inhomogeneous structure, the enetration of magnetic flux can occur in a highly complicated way. However, in this case techniques such as magneto-optics provide the possibility to measure the spatially resolved magnetization and to derive from this the supercurrent density in the material. Here, we do not want to discuss the details and, instead, refer to the review articles [38, 39].

If, like during the measurement of the magnetization curve, the magnetic field B_2 is changed, within a hard superconductor an inhomogeneous distribution of vortices develops, which by no means corresponds to thermodynamic equilibrium. Now we want to investigate what happens if the magnetic field is raised to a certain value and then is kept constant at this value. In this case we will deal with the phenomenon of flux creep.

In the critical state all locations at which magnetic flux has penetrated into the sample carry the critical current density j_c, which in turn acts with the Lorentz force on the vortices. If the applied field is kept at the value B, the Lorentz force is exactly compensated by the force originating from the pinning centers. Therefore, without thermal fluctuations, the vortex distribution would remain unchanged. However, because of thermal fluctuations, the energy needed to leave a pinning site can be supplied to a vortex. In this case, under the influence of the Lorentz force, the vortex will move a short distance until it is trapped again at another pinning center. Eventually, all vortices will move in this way, such that the magnetization gradually decreases and a state with lower energy is established. During this process the supercurrent density quickly falls below its critical value. This thermally activated vortex motion is referred to as flux creep.

If the supercurrent density is not too close to the critical current density, the velocity of the vortex motion will be proportional to $\exp(-\Delta E/k_B T)$. In general, one can show that the temporal change is then given by $\mathrm{d}j/\mathrm{d}t = -j_c \exp(-\Delta E/k_B T)/t_0$. Here, t_0 denotes a characteristic time constant that depends on the material parameters. However, the height ΔE of the energy barrier in turn depends on the supercurrent density. It must vanish when the critical current is reached, since in this case the vortices are torn off from the pinning centers. Near the critical state this behavior can be expressed by the relation

$$\Delta E\,(j \to j_c) \approx E_c\,(1 - j/j_c)^{\alpha}$$

with a certain exponent α. In the case $\alpha = 1$, this just leads to a reduction of the supercurrent density or of the magnetization, which is logarithmic initially:

$$|M(t)| \propto j(t) \approx j_c \left[1 - \frac{k_B T}{E_c} \ln(1 + t/t_0)\right]$$

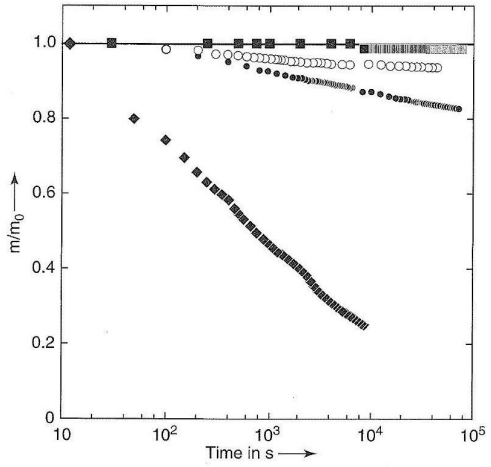


Figure 5.19 Temporal decay of the mag- were turned on [40]. □NbTi at 4.2 K; O, netization of different superconductors. The $YBa_2Cu_3O_7$ with oriented grains at 77 K; magnetization is normalized to its value

In Figure 5.19 we show the temporal decay of the magnetization of some superconductors [40]. This decay occurs by means of flux creep. In NbTi, a classical superconductor, at about 4.2 K, that is, at about $T_c/2$, within more than 10^5 s (slightly more than 1 day) hardly any change is observed. On the other hand, in $YBa_2Cu_3O_7$ the supercurrents clearly decrease, particularly in the single-crystalline sample. The data shown here are from the year 1990, that is, from the early period of high-temperature superconductivity. In the meantime, also $YBa_2Cu_3O_7$ samples have been prepared in such a way that well above 15 T they can trap magnetic fields for a long time. We will discuss this subject in more detail in Section 7.2.

In the high-temperature superconductors, we must note that the different vortex phases can behave much differently. In particular, in the region of the vortex liquid one observes no or at most only a weak pinning force. In this case the magnetization curves are reversible. Therefore, the phase boundary line at the transition between the vortex liquid and the crystalline or glass-like vortex phases is referred to as the irreversibility line.

Critical Currents and Current-Voltage Characteristics

Next we want to discuss the effect of the pinning centers during current transport in superconducting wires or thin films. In Section 5.3.1 we saw that an ideal type-II superconductor in the Shubnikov phase cannot carry a current perpendicular to

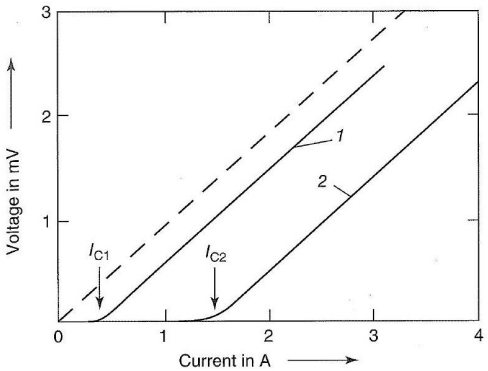


Figure 5.20 Current-voltage characteristics of an $Nb_{55}Ta_{50}$ alloy in the Shubnikov phase. $T = 3.0$ K; external field $B_a = 0.2$ T; T_c in zero field: 6.25 K. (From [41].)

the direction of the magnetic field without dissipation, since due to the influence of the Lorentz force the vortices start moving, resulting in dissipative processes. However, in a real superconductor, the vortices are never completely freely mobile. There is always a perhaps very small force necessary in order to tear the vortices off the pinning centers that are practically always present. The strength of the pinning forces acting on the individual vortices will have a certain distribution about an average value F_H. Also the whole vortex lattice will affect the pinning forces due to collective effects. However, for simplicity we will only speak of a single pinning force F_H.

As long as the Lorentz force F_L is smaller than the pinning force F_H, the vortices cannot move. Therefore, also in every real type-II superconductor in the Shubnikov phase, we will be able to observe current flow without dissipation. If the transport current exceeds its critical value at which $F_L = F_H$, the vortex motion sets in, and electrical resistance appears. [21)] We see that the critical current is a measure of the force F_H with which the vortices are pinned at energetically favored locations.

In Figure 5.20 we show the current-voltage characteristics of two samples of an $Nb_{50}Ta_{50}$ alloy with a different amount of internal disorder [41]. Both samples were cooled in the magnetic field and were measured in the Shubnikov phase. For the more strongly disordered sample 2, no electrical voltage is observed up to a transport current I_{c2} of about 1.2 A.22 On the other hand, the less perturbed

If the pinning forces acting on the individual vortices are different, initially the most weakly pinned vortices will start moving, resulting in only a relatively small resistance. With increasing current 22) Of of course, the terminology "no voltage" represents a strong simplification. Since for currents $I < I_c$ usually a finite and also very weak dissipation is possible, we will also observe small voltages in this case. The curves in Figure 5.19 indicate this by gradually approaching the linear part.

sample 1 shows a voltage and, hence, resistance already at about 0.2 A. The currents I_{c1} and I_{c2}, respectively, are referred to as the critical currents of both samples. An ideal sample of the same material, that is, a completely homogeneous sample, for the same conditions would display a current-voltage characteristic indicated by the dashed line.

In hard superconductors, the pinning forces must be made particularly high in order to allow the highest possible transport currents to flow without resistance. Before we discuss a few examples of hard superconductors, we want to look at the linear part of the characteristics in Figure 5.20. Also in this part of the characteristic, the voltage along the superconductor is generated by vortex motion. The resulting differential resistance $\mathrm{d}U/\mathrm{d}I = R_f$, the flux-flow resistance, clearly has the same value in both samples, that is, it is independent of the pinning centers acting on the vortices.

This observation can be understood in the following way: If the vortices are removed from the pinning centers, they move through the material under the influence of the force difference $F^* = \mathrm{F_L} - \mathrm{F_H}$. Because of the dissipative processes during the motion, resulting in a kind of "friction" for the vortex in the superconductor, a flux-flow velocity v develops, which is proportional to F^*. We have

$$v \propto F^* \propto (I - I_c)$$

On the other hand, the electrical voltage U is proportional to v, that is, one finds

$$U \propto v \propto I - I_c$$

and hence

$\mathrm{d}U/\mathrm{d}I = \text{const.}$

The equal values of $\mathrm{d}U/\mathrm{d}I$ for samples with different amounts of imperfections (Figure 5.20) indicate clearly that the pinning centers do not affect the relation between F^* and v. Independent of the nature of the pinning centers, the same value of F^* yields the same velocity v and, hence, the same voltage U. The characteristics are only shifted parallel to each other along the current axis.

According to these arguments, we have two components of the energy dissipation UI, namely UI_c and $U\,(I - I_c)$. We start with the component UI_c. The vortices move through the material under the influence of the Lorentz force due to a transport current. This means that they must pass through a number of potential wells. To raise a vortex out of a well costs energy. One could imagine that this energy is recovered when the vortex falls into the next (equally deep) well. In this case, there would be no net energy dissipation during vortex motion across the potential wells. However, there is the crucial fact that during their motion across the pinning centers the vortices are always elastically deformed [42, M17]. These deformations lead to the energy losses described by the component UI_{c}.

Next we turn to the component $U\,(I - I_{\mathrm{c}})$ of the dissipated power determining the vortex velocity according to Eq. (5.23). The most important energy losses during the vortex motion are caused by the appearance of local electric fields acting on the unpaired electrons. This means that the flux-flow resistance depends on

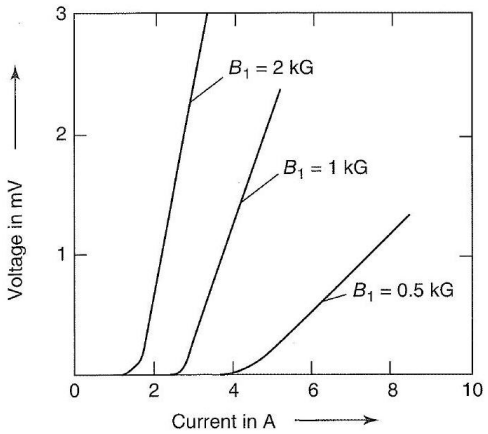


Figure 5.21 Current-voltage characteristics of a Pb-In alloy in the Shubnikov phase. Material: Pb + 17at%In; T = 2.0 K; transition temperature in zero field: about 7.1 K. (From [41].)

the normal resistance of the material. One finds that R_{f} is proportional to R_{n}[23)] Furthermore, the same dissipative effects appear at each vortex. Therefore, the dynamic (flux-flow) resistance is proportional to the vortex density. This density increases with increasing external field B_{a}. With increasing magnetic field, the $U - I$ characteristics become steeper. This dependence of the flux-flow resistance on the external field is shown in Figure 5.21 for a lead-indium alloy (Pb + 17 at% In) [41].

With increasing magnetic field, the critical current I_{c} decreases. This decrease can be caused in different ways. For increasing vortex density, not all vortices can experience the same pinning force. Hence, the average pinning force becomes smaller. On the other hand, for one and the same pinning center, with increasing external field, the pinning force decreases and approaches zero for $B_{\mathrm{a}} \to B_{\mathrm{c2}}$. The behavior of the critical current for increasing external field will be seen particularly clearly in a plot of the field dependence of I_c (see Figures 5.22 and 5.23). [24]

In our discussion of Figure 5.20 we have already seen that the critical current I_{c} depends on the degree of disorder within the sample. This internal disorder

Under otherwise the same conditions, with increasing R_{n} the vortex velocity v due to the given force $F^2 = \mathrm{F}_L - \mathrm{F}_{\mathrm{H}}$ (i.e., for a given current $I = I_c + F_1$) increases. $_{\mathrm{H}}$ (ilis can be seen

from a simple but instructive discussion of velocity v through the material dwe to the force F^v, the force F^s generates the power $P^*_= = F^*\nu$. This power must be turned into

heat because of the local electric fields E_1 thus $P^*_F = P_{el}$. For the resistivity ρ_n of the aterial in the normal state, the electrical power P_{el} is proportional to $L^2\rho_n$. n the ther hand, w, he serise $E^2/\rho, \propto F^* v\alpha\gamma^2/\rho^2$ and hence, $F^{*\prime}\alpha\nu$ For a given F^* the velocity v increases with

$P^*_F = F^*\nu$. This power must be turned into increasing ρ_n.

24) We mention that the shape of the current–voltage characteristic in an external magnetic field als

depends on the sample geometry. For example, for the same material, different characteristics are observed in a tape than in a circular disk with the current running fiom the center to the outer edge (“Corbino disk")

(!!!!!!!!!!)

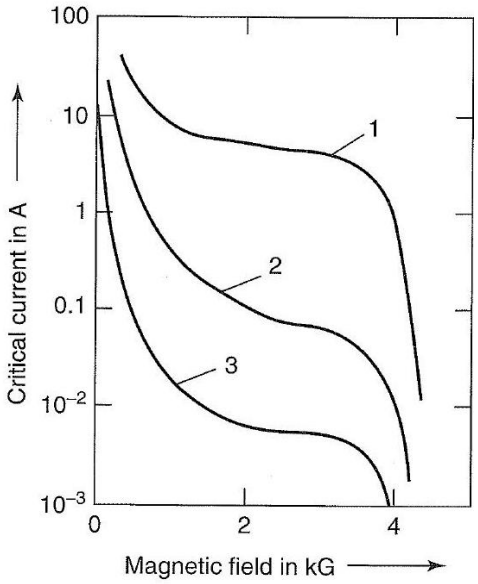


Figure 5.22 Critical current of an Nb_{55} T_{45} alloy in an external magnetic field (1kG = 0.1 W) oriented perpendicular to the current. Wire diameter: 0.38 mm; measuring temperature: 4.2K. Curve 1, immediately 1800 K; curve 3, after 48 h at 1800 K. (From [23].)

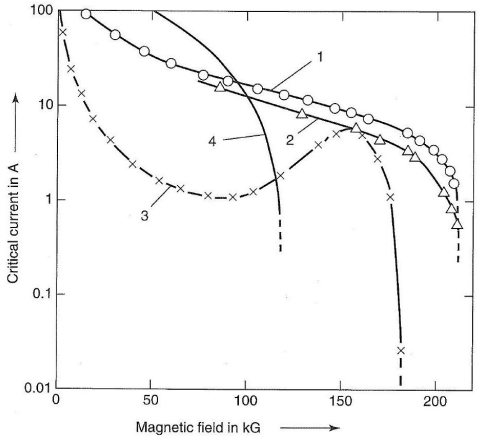


Figure 5.23 Critical currents of thin wires In each case the compound exists only of metallic high-field superconductors within a surface layer obtained by diffu(1kG = 0.17). Measuring temperature: 4.2 K. sion of the second component into the base Wire diameter of all three samples: 0.5 mm. eter 0.15 mm. (From [43, 44].) can be caused, for example, by plastic deformation. If a metal wire (such as Cu) is pulled through a die at room temperature to

reduce the cross-section, many imperfections, that is, regions in which the periodic structure of the metallic lattice is strongly perturbed, are generated within the wire. Grain boundaries (i.e., transition regions between individual grains), for example, are such regions. If subsequently the metal is heated, these disordered regions gradually can be annealed out and can be transformed more and more into well-ordered regions.

If the disordered regions act as pinning sites for the vortices, a plastically deformed superconductor is expected to display a particularly high value of the critical current immediately after deformation. During heating, along with the gradual removal of the disordered regions, the critical current should also decrease

In Figure 5.22 we clearly see this effect [23]. For an $Nb_{55}Ta_{45}$ alloy the critical current is plotted versus the external magnetic field oriented perpendicular to the current for different degrees of disorder. Immediately after the mechanical pulling process, that is, in a state with a high degree of disorder, the critical current in the Shubnikov phase is large.. [25]) During the removal of the perturbations by means of annealing, the pinning centers disappear more and more. The critical current strongly decreases as expected. In Figure 5.11 the corresponding magnetization curves are shown for the same alloy. In this case, the pinning centers lead to strong irreversibilities of the magnetization curve.

In Figure 5.23 we show the values of the critical current of wires of a few metallic high-field superconductors. Since the critical current is strongly influenced by the previous treatment of the sample because of its dependence on the degree of disorder, as we have discussed, the data of Figure 5.23 can serve only as a rough indication. The curves are chosen arbitrarily from a large number of examples. However, they show that suitably prepared hard superconductors, with a wire diameter of only 0.5 mm and for external fields above 10 T, can carry supercurrents of more than 10 up to 100 A without dissipation. Wires containing many thin filaments, so-called multifilamentary wires, can even carry still much higher currents. Of course, such superconductors are highly important for the construction of superconducting magnets (see Section 7.1).

In Figure 5.23 we show a curve (V_3Ga) having a maximum of the critical current near B_2 (the so-called peak effect, see also Figure 5.15). Apparently, with increasing external field, conditions can develop leading to a more effective pinning of the vortices. In this case the elastic properties of the vortex lattice are essential [M17]. The lattice becomes more elastic, and the vortices can adjust themselves better to the configuration of the pinning sites. Furthermore, near B_{c2} also normal conducting regions can appear, which act as additional pinning centers and cause an increase in the critical current.

By means of a systematic study of hard superconductors, it has been possible empirically to develop quite useful materials. However, the detailed dependence

The steep drop of the critical current at very small magnetic fields occurs in the Meissner phase of the superconductor at fields $B_2 < B_{cc}$ (see Figure 5.3b).

of the critical current on the defect structures is still by no means completely clarified.

This is even more valid for the high-temperature superconductors [45]. In thi case the initial measurements of the critical currents in polycrystalline, sintered samples yielded disappointingly small values of the critical current density. At 77 K, the boiling point of liquid nitrogen, even in zero applied magnetic field, frequently the critical current density was found to be less than 10^3 A/cm^2. However it soon became clear that to a large extent the critical current was limited by grain boundaries. In this case, the critical current of a grain boundary strongly decreases with increasing relative tilt angle between the crystal axes in the two grains. This could be demonstrated by transport measurements in thin films of $YBa_2Cu_3O_7$ deposited onto $SrTiO_3$ bicrystal substrates [26][47].

In 2010 the details of current limitation by means of grain boundaries could be explained theoretically [48]. Apparently, the dominating mechanism of the critical-current reduction is

due to the fact that near the dislocation lines the grain boundary is electrically charged. Many additional properties of curren transport across grain boundaries are summarized in the review articles [49, 50] An additional limitation of the critical current results from the layered structure of the cuprates. Along the CuO_2 planes a high value of the critical current is observed, whereas perpendicular to the planes the value is very small, and in some cases it is limited by the Josephson effect (see Figure 1.22f). Also in the case of current flow parallel to the CuO_2 planes it is important, how the external magnetic field is oriented relative to the crystal structure. This effect is shown in Figure 5.24 for the example of a $YBa_2Cu_3O_7$ thin film [51]. The film was prepared by mean of laser ablation. In the figure the critical current density in the case of current flow along the CuO_2 planes is plotted versus the applied magnetic field for different temperatures. The field was oriented either perpendicular to the CuO_2 planes (i.e., along the crystallographic c-direction) or perpendicular to the c-axis. We see hat at 4.2 K critical current densities of several 10^7 A/cm^2 are reached, and at 77 K still values of several 10^6 A/cm^2. As long as the magnetic field is applied parallel to the planes, these values remain also in high fields (in fact, in fields up to far above 20 T) at least at 4.2 K [52]. However, the critical current density decrease rapidly, if the magnetic field is oriented perpendicular to the lavered structure. O the other hand, in the meantime (the measurements in Figure 5.24 are from 1990) appreciable improvements could be achieved. Now, for example, $YBa_2Cu_3O_7$ thin films in a field of 5 T perpendicular to the layers can carry supercurrents of several 0^5 A/cm^2 also at 77 K[17]

If $YBa_2Cu_3O_7$ is condensed on a single-crystalline $SrTiO_3$ substrate under low oxygen pressure (about 0.1mbar), the thin se show the crystal orientation mostly fabrica. In this case the substrates are CuO_2 pabicas in such a way that the to the surface of the substrate. This technique served in the early days for preparing $YBa_2Cu_3O_7$ thin fins with redaively high

quality [46]. In a bicrystal substrate, two single-crystalline parts are rotated relative to each other. In this case the grain boundary Im on top and, transmitted into the thin can be studied systematically. Such grrain boundaries have been discussed already in Section 1.5 in the context of Josephson junctions (see Figure 1.22e),

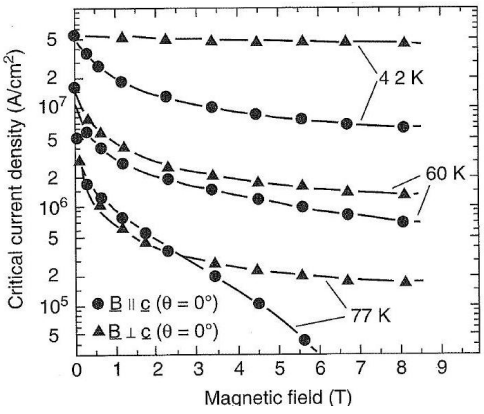


Figure 5.24 Critical current density of $YBa_2Cu_3O_7$ thin film for three temperatures plotted versus the applied magnetic field. The field was oriented either perpendicular to the layered structure (i.e., parallel to the crystallographic c-axis) or parallel to it. (From [51].)

In general, to achieve a high supercurrent density, in the case of the cuprates it is necessary to avoid grain boundaries, and the transport currents must flow parallel to the layered structure as much as possible. By means of thin-film technology, the corresponding epitaxial film growth can be achieved relatively easily, long as the substrate size is not too large [53]. However, if one is interested in high-current-carrying wires or tapes fabricated from the cuprates, obviously the material must have a high critical-current value over long lengths. Furthermore, the fabrication technique should be relatively simple and not too expensive. In recent years a number of procedures have been developed, which we will discuss in Section 7.1.2. Enormous progress

has also been achieved in the field of massive materials, which are needed, for example, for magnetic levitation or for magnetic energy storage (see Section 7.2). These developments are by no means finished. In addition, MgB_2 and the iron pnictides can become important for the conductor development. On the one hand, the upper critical field can reach very high values. On the other hand, at least in the case of MgB_2 grain boundaries practically do not suppress the supercurrent density [54]

We want to conclude our discussion of the critical currents in superconductors with a few general remarks. We have seen that the mechanism of pair breaking results in an intrinsic maximum supercurrent density. However, in cases that are technically relevant, the critical current of a superconductor is determined by extrinsic properties. On the one hand, the latter properties in the form of pinning centers in the Shubnikov phase only allow a finite supercurrent, and on the other hand, for example, in the form of grain boundaries in high-temperature superconductors, they represent weak regions in the material, strongly reducing the maximum supercurrent. Whether a new material, say, MgB_2, finds interesting technical applications depends on the concrete problems, and often can be answered only after a long development period. In Chapter 7, we will discuss some examples in more detail.

Change of the state if current approaches the Critical supercurrent

(??? see De Gennes??)

4.1.4 Description of Isotope effect

(main section about it, what is known about it, where it works, where does not??)

4.1.5 Description of Meissner effect

Gap from spectrum leads to Meissner effect by Shmidt

Обсудим теперь, как существование щели в спектре элементарных возбуждений сверхпроводника объясняет выталкивание слабого магнитного поля, т. е. эффект Мейсснера - Оксенфельда. Существуют строгие расчеты, выходящие за рамки настоящего курса, из которых следует, что существование энергетической щели является достаточным условием для эффекта Мейсснера.

Тем не менее, мы попытаемся все же проинтерпретировать эффект Мейсснера на языке микротеории. Следуя Лондону [154], можно предположить так называемую "жесткость" волновой функции электронов сверхпроводника. Это значит, что наличие энергетической щели, когерентное поведение всего коллектива электронов приводят к тому, что слабое магнитное поле не может сколь-нибудь существенно иэменить эту волновую функцию. Но отсюда эффект Мейсснера следует мгновенно.

Действительно, пусть $\Psi(\mathbf{r}_1, \ldots, \mathbf{r}_N)$ - волновая функция N электронов сверхпроводника. Заметим, что здесь Ψ-это не эффективная волновая функция сверхпроводящих электронов теории Гинзбурга - Ландау (которая, кстати, зависит только от одной переменной $\mathbf{r}$), а истинная волновая функция. Тогда из общих соотношений квантовой механики следует такое выражение для тока при наличии магнитного поля:

$$\mathbf{j}(r) = \sum_{n=1}^{N} \int \dots \int \left\{ \frac{e\hbar}{2im} \left[\Psi^* \nabla_n \Psi - \Psi \nabla_n \Psi^* \right] - \right.$$
$$\left. - \frac{e^2}{mc} \mathbf{A}\left(r_n\right) \left|\Psi\right|^2 \right\} \delta\left(\mathbf{r} - \mathbf{r}_n\right) d^3\mathbf{r}_1 \dots d^3\mathbf{r}_N \tag{50.6}$$

здесь $\mathbf{A}$ - векторный потенциал магнитного поля. Если магнитного поля нет ($\mathbf{A} = 0$), то, конечно, и тока в сверхпроводнике нет, и тогда интеграл от первого слагаемого должен равняться нулю:

$$\sum_{n=1}^{N} \int \dots \int \left[\Psi^* \nabla_n \Psi - \Psi \nabla_n \Psi^* \right] \delta\left(\mathbf{r} - \mathbf{r}_n\right) d^3\mathbf{r}_1 \dots d^3\mathbf{r}_N = 0 \tag{50.7}$$

Но мы предполагаем "жесткосты" волновой функции, т. е. ее неизменность под действием магнитного поля. Это значит, что и при наличии магнитного поля равенство (50.7) сохраняется. Опуская поэтому первое слагаемое в (50.6), получим после элементарного интегрирования

$$\mathbf{j}(r) = -\text{const} \cdot \mathbf{A}(r) \tag{50.8}$$

А это равенство есть математическое выражение эффекта Мейсснера, поскольку оно является известным уравнением Лондонов (5.17).

4.1.6 Flux quantization

Description of flux quantization

(theory is here)

Во многих квантово-механических задачах (квантование потока в полости сверхпроводника, эффект Ааронова-Бома, монополь Дирака) возникает необходимость вычислить изменение фазы ϕ волновой функции $\exp(i\phi)$ вдоль некоторого контура. По определению для контура, связывающего начальную 1 и конечную 2 точки имеем

$$\int_1^2 \nabla\phi(\mathbf{r}) \cdot |d\mathbf{r} = \phi_2 - \phi_1$$

Для замкнутого контура $\mathbf{r}_1 = \mathbf{r}_2$ из (25.1) казалось бы получаем ноль.

Этот же вывод дает применение теоремы Стокса:

$$\oint \nabla\phi(\mathbf{r}) \cdot d\mathbf{r} = \int \nabla \times \nabla\phi \cdot d\mathbf{S} = 0$$

Однако это верно не для всех функций $\phi(\mathbf{r})$.

Если речь идет о фазе волновой функции $\exp(i\phi(\mathbf{r}))$, то величина (25.1) определяется топологией области, охватываемой замкнутым контуром.

Это связано с требованиями однозначности и гладкости волновой функции $\exp(i\phi(\mathbf{r}))$, которые вытекают из экспериментов по интерференции волновой функции.

Если область односвязна, то контур можно стянуть в точку.

В процессе такого стягивания волновая функция на контуре должна оставаться однозначной и гладкой.

Это можно обеспечить только при обращении интеграла (25.1) в ноль.

Если же контур охватывает неодносвязную область, например, в образце имеется полость (дырка), то при обходе такой дырки изменение фазы может быть ненулевым:

$$\oint \nabla\phi(\mathbf{r}) \cdot d\mathbf{r} = 2\pi n$$

где n целое число, возможно, и ноль. Конкретное значение n определяется физическими условиями в полости.

Например, в сверхпроводнике ве личина n определяется числом квантов магнитного потока, введенного в полость внешним источником.

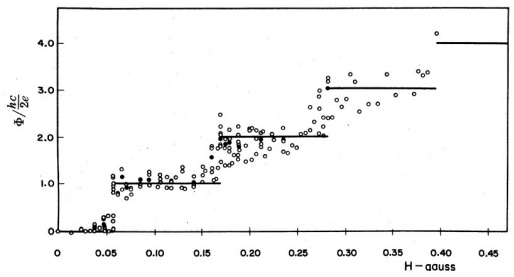
4.1.7 Flux quantization: Experimental confirmation

(????? read articles about it)

Experiments that prove flux quantization

Deaver and Fairbank

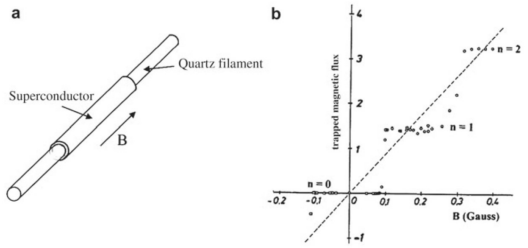
Deaver and Fairbank prooved in 1961 that: (?????? how???)



Расплывание потока они свели к погрешностям, а было ли это перемерено еще раз (??????)

Doll and Näbauer

in 1961 showed (?????? how???) that field in rod is quantized if (????)



They did this: 1. The sample was heated above the transition temperature; then a defined field to be frozen in, Hy, was applied. 2. After recooling below the transition temperature, Hy was switched off. 3. The resonance amplitude was measured, and it is proportional to the product (measuring field H) times (magnetic moment of the sample). The latter in turn is proportional to the frozen-in flux. (???? need to discuss it with someone who knows it)

4.1.8 Levitation over Superconductor: Basic understanding

(??? Later I'll create some formulas for it. Currently, nothing is prepared to describe this)

4.1.9 1-2 Diamagnetism by de Gennes

The London Equation

We now extend our energy considerations to situations where there are supercurrents $j_S(r)$ and associated magnetic fields $h(r)$ in the sample. [1] We see that in the limit where all fields, currents, and so on, are weak and have a slow variation in space the condition of minimum free energy leads to a simple relation between fields and currents (F. and H. London, 1935).

We consider a pure metal with a parabolic conduction band; the electrons have an effective mass m. The free energy now has the following form:

$$F = \int F_S dr + E_{\text{kin}} + E_{\text{mag}} \tag{1-1}$$

where F_S is the energy of the electrons in the condensed state at rest and E_{kin} is the kinetic energy associated with the permanent currents. Let us call $v(r)$ the drift velocity of the electrons at point r. It is related to the current density j_S by

$$\mathrm{n_S ev(r) = j_S(r)} \tag{1-2}$$

(where e is the electron charge, and $\mathrm{n_S}$ the number of superconducting electrons per cm^3). Then we have simply

$$\mathrm{E_{kin}} = \int \mathrm{dr} \frac{1}{2} \mathrm{mv^2 n_s} \tag{1-3}$$

the integral being extended over the sample volume. Equation (1-3) would be exact for situations of uniform flow (v = const). It remains approximately correct for our present problem, provided that $\mathrm{v}(\mathbf{r})$ is a slowly varying function of $\mathbf{r}$. (We return to this limitation later.)

Finally, $\mathrm{E_{mag}}$ is the energy associated with the magnetic field $\mathbf{h}(\mathbf{r})$

$$\mathrm{E_{mag}} = \int \frac{\mathrm{h}^2}{8\pi} \mathrm{dr} \tag{1-4}$$

The field is related to j_S by Maxwell's equation

$$\operatorname{curl} h = \frac{4\pi}{c} j_s \tag{1-5}$$

Using (1-3), (1-4), and (1-5) we rewrite the energy E as

$$E = E_0 + \frac{1}{8\pi} \int \left[h^2 + \lambda_L^2 |\operatorname{curl} \ h|^2 \right] dr$$

$$E_0 = \int F_S dr \tag{1-6}$$

where the length λ_L is defined by

$$\lambda_{\mathrm{L}} = \left[\frac{\mathrm{mc}^2}{4\pi \mathrm{n_S e}^2} \right]^{1/2} \tag{1-7}$$

At $\mathrm{T} = 0, \mathrm{n_s}$ is equal to n, the total number of conduction electrons per cubic centimeter. We can then compute λ_L explicitly. In simple metals such as Al, Sn, and so on, where m is

[1] We use **h** to denote a local field value. H will be reserved for the thermodynamic field.

close to the free electron mass, we find $\lambda_L \sim 500$Å. For transition metals and compounds with narrow d bands, m is larger and λ_L is also larger (up to 2000Å).

We wish to minimize the free energy (1-6) with respect to the field distribution $h(r)$. If $h(r)$ changes by $\delta h(r), E$ changes by δE:

$$\begin{aligned}\delta E &= \frac{1}{4\pi}\int \left[h\cdot\delta h + \lambda_L^2 \operatorname{curl} h\cdot\operatorname{curl}\delta h\right] dr \\ &= \frac{1}{4\pi}\int \left[h + \lambda_L^2 \operatorname{curl}\operatorname{curl} h\right]\cdot\delta h dr \end{aligned} \tag{1-8}$$

where we have integrated the second term by parts. The field configuration, in the interior of the specimen, which minimizes the free energy, must therefore satisfy the condition

$$h + \lambda_L^2 \operatorname{curl}\operatorname{curl} h = 0 \tag{1-9}$$

Equation (1-9) was first proposed (with a slightly different notation) by $F.$ and $H.$ London. When combined with the Maxwell equation (1-5), it allows us to calculate the distribution of fields and currents.

Meissner Effect

We now apply the London equation and discuss the penetration of a magnetic field h into a superconductor. We choose the simplest geometry. The surface of the specimen is the xy plane, the region $z < 0$ being empty (Fig. 1-2). The field h and the current j_S depend only

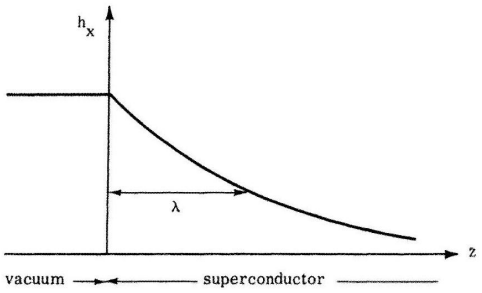


Figure 1-2

Field penetration in a superconductor. The field becomes negligibly small at distances larger than a few penetration depths λ. When the simple London equation (1-9) holds, the penetration is exponential $\mathrm{h} = h_0 \exp(-z/\lambda_L)$.

on z. In addition to the relation (1-9), h and j_s are always related by the Maxwell equations

$$\operatorname{curl}\mathrm{h} = \frac{4\pi \mathrm{J_S}}{\mathrm{c}} \tag{1-10}$$

$$\operatorname{div}\mathrm{h} = 0 \tag{1-11}$$

Two cases are possible:

(1) h is parallel to z. Then $(1-11)$ reduces to $\partial h/\partial z = 0$ and h is spatially constant. Therefore curl $h = 0$ and $j_S = 0$ from Eq. (1-10). Inserting this into Eq. (1-11) we find $h = 0$. Therefore it is not possible to have a field normal to the surface of the specimen.

(2) h is tangential (and directed along the x axis). Then Eq. (1-9) is automatically satisfied. From Eq. $(1-10) j_S$ is directed along the y axis:

$$\frac{dh}{dz} = \frac{4\pi j_S}{c} \tag{1-12}$$

Finally, from Eq. (1-9),

$$\frac{\mathrm{dj}s}{\mathrm{dz}} = \frac{n\mathrm{e}^2}{\mathrm{mc}}\mathrm{h} \tag{1-13}$$

$$\frac{\mathrm{d}^2\ \mathrm{h}}{\mathrm{dz}^2} = \frac{\mathrm{h}}{\lambda_\mathrm{L}^2} \quad \lambda_\mathrm{L}^2 = \frac{\mathrm{mc}^2}{4\pi n\mathrm{e}^2} \tag{1-14}$$

The solution that remains finite in the superconductor is exponentially decreasing,

$$h(z) = h(0)\exp\left(-z/\lambda_L\right) \tag{1-15}$$

The field h penetrates only to a depth λ_L inside the sample. This result, established here for a semiinfinite slab, is easily generalized to a macroscopic specimen of arbitrary shape. As we have seen, the "penetration depth" λ_L is small. Therefore, in all cases, a weak magnetic field practically does not penetrate at all into a macroscopic specimen. [2] The lines of force are excluded as shown on Fig. 1-3.

The superconductor finds an equilibrium state where the sum of *ki* netic and magnetic energies is minimum, and this state, for macroscopic samples, corresponds to the expulsion of magnetic flux.

Experimentally, the expulsion of lines of force was shown by Meissner and Ochsenfeld in 1933. The Meissner result was particularly important in proving that a true equilibrium state was achieved.

Three remarks concerning the above derivation:

(1) Assuming the existence of permanent currents plus thermodynamic equilibrium, we are led to the diamagnetic properties. It is more usual to go the other way round: Taking the Meissner effect as a starting point, conclude that there exist permanent currents. I chose the first way because I wanted to show you the different contributions to the energy in a superconductor (Eq. 1-6). This list of energies will be useful later (Chapter 3).

(2) We obtained Eq. (1-9) from a minimum condition on the free energy $\mathfrak{F}$. This is the correct thermodynamic potential when the external field sources are permanent magnets. When the source is a coil, with a fixed current I, the correct potential is not $\mathcal{F}$ but a different function S (the "Gibbs potential"). Fortunately, both potentials can be shown to lead to the same local equilibrium condition in the sample. (See Chapter 2 for a discussion of $\mathcal{F}$ and $\mathcal{S}$.)

(3) Note that the above calculation is valid only for weak applied fields. In higher fields it may become energetically more favorable

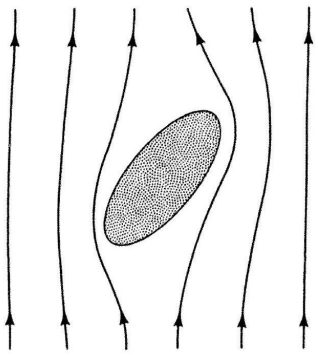


Figure 1-3

Distortion of the magnetic lines of force around a macroscopic superconductor ("macroscopic" means dimensions much larger than the penetration depth). If the fields are not too strong, the superconductor expels the lines completely (Meissner effect).

[2] In higher field different catastrophes may occur.

to destroy superconductivity in some parts of the sample and to allow the flux lines to penetrate. This will be considered in detail in Chapters 2 and 3.

4.1.10 1-3 Absence of low energy excitations by de Gennes

Let us begin by considering a free electron gas without interactions. The ground state is obtained by placing an electron into each individual momentum state p, of energy $p^2/2m$, until the Fermi energy $\mathbf{E}_F = \mathrm{p_F^2}/2$ m is reached. Above the Fermi energy $\mathrm{E_F}$, all the levels are empty. (The condition $p = p_F$ defines the Fermi sphere, in momentum space.) In order to construct an excited state of the gas, it suffices to take an electron of momentum p from an initially occupied state ($p \leq p_F$) and to place it into a state p' initially empty ($p' \geq p_F$) (Fig. 1-4). The excitation energy of this electron-hole pair is

$$E_{pp'} = \frac{p'^2 - p^2}{2m} \geq 0 \tag{1-16}$$

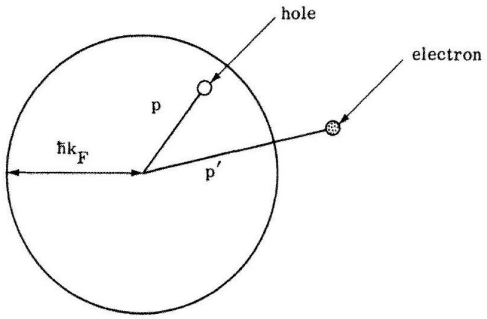


Figure 1-4

An excited state of the electrongas in a normal metal. One electron has been taken from a state of momenturn p inside the Fermi sphere, to a state of momentum p' outside the Fermi sphere. The excitation energy $\left(p'^2 - p^2\right)/2m$ is very low if p and p' are close to the Fermi momentum $\mathrm{p_F} = \hbar \mathrm{k_F}$.

If both p and p' are close to the Fermi momentum, $E_{pp'}$ is very small; in a free electron gas there are numerous low energy excitations. In a normal metal, this free electron picture is not qualitatively modified. The low energy excitations are displayed by the following experiments:

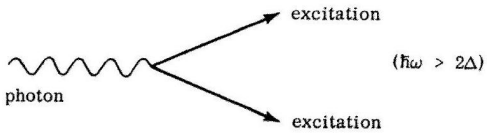
(a) The specific heat is relatively large and proportional to T (of order $\mathrm{k}_B \cdot (\mathrm{k_B T/E_F})$ per electron).

(b) Strong dissipative effects appear when the electrons are submitted to low frequency external perturbations (electromagnetic waves, ultrasonic waves, nuclear spin precession, and so on).

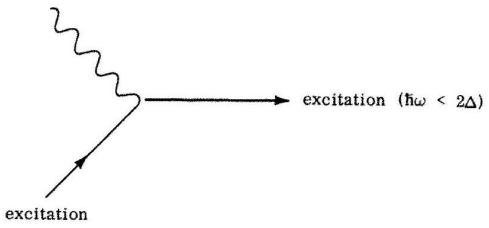
In most superconductors, the situation is completely different. The energy $E_{pp'}$ necessary to create a pair of excitations is no longer given by Eq. (1-16). It is necessary to at least furnish a certain "pairing energy" 2Δ:

$$E_{pp'} \geq 2\Delta \tag{1-17}$$

Roughly speaking, this "gap" 2Δ is related to the transition temperature by $2\Delta = 3.5\mathrm{k_B T_0}$. Thus typically 2Δ is of order 10°K (Table 1-1).



(a)



(b)

Figure 1-5

Typical dissipative processes in a superconductor. Fig. 1-5a shows the creation of a pair of excitations by one photon. This process can occur only if $\hbar\omega > 2\Delta$. Fig. $1-5$ b shows the absorption of the photon by a preexisting excitation. This process can occur even if $\hbar\omega < 2\Delta$, but it is weak at low temperatures, where there are very few thermal excitations. Similar processes are obtained by replacing "photon" by "phonon" in 1-5a and $1-5b$.

Note that 2Δ is the energy needed to create two excitations. The energy per excitation is Δ.

Various experiments measure Δ. Here are some of them:

(a) The low temperature specific heat is now exponential and proportional to $\exp(-\Delta/k_BT)$.

(b) Absorption of electromagnetic energy. For $\hbar\omega \geq 2\Delta$ a photon of frequency ω can create an electron-hole pair. [This corresponds to photons in the far infrared; typical wavelengths are in the 1 mm range (Fig. 1-5a).]

(c) Ultrasonic attenuation. Here the phonon is of low frequency and cannot decay by creation of a pair of excitations. But it can be absorbed by collision with a preexisting excitation (Fig. 1-5b). This

Table 1-1

Values of the energy gap 2Δ (at 0°K) in °K[a]

	P	A	T
Zn		3.17	
Cd	1.8		
Hg	18.4		18.0
Al	6.01	4.4	4.2
In	13.6	11.9	11.9
Ga		4.03	
Sn	13.0		12.9
Pb	28.7		30.9
V	18.0	18.5	18.0
Nb	27.4	37.4	35.0
Ta		15.7	16.1
La			

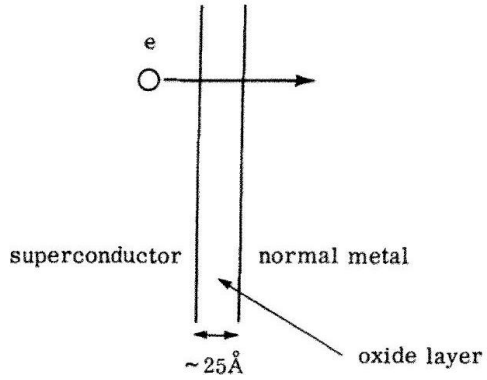
process is proportional to the number of preexisting excitations, thus to $\exp(-\Delta/k_BT)$.

(d) Tunnel effect. A superconductor S and a normal metal N are separated by a thin insulating barrier (typical thickness 25Å) (Fig. 1-6a). The quantum mechanical tunnel effect allows

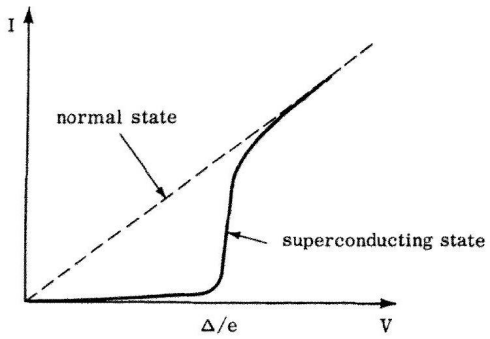
a For a bibliography on energy gap measurements see D. H. Douglas, Jr., and L. M. Falicov, Low Temperalure Physics, Vol. IV, edited by C. G. Gorter (Amsterdam: North Holland Publishing Co., 1964). The experiments are classified as follows: P photon absorption (microwave or far infrared photons); A ultrasonic attenuation; T tunneling. The ultrasonic experiments are often performed in single crystals, in which case, 2Δ depends slightly on the direction of the sound wave, [Fond]

individual electrons to pass through the barrier. The electron must have been excited from the condensed phase, and this requires an energy Δ. There is no current at low temperatures unless we apply a voltage V across the junction such that the energy gain eV is larger than Δ. The current voltage characteristic has the form shown in Fig. 1-6b.

Question: Is the existence of an energy gap a necessary condition for the existence of permanent current (superfluidity)? The answer is no. A number of situations have been found where superfluidity occurs with no gap in the one particle excitation spectrum. The simplest example is "surface super-



(a)



(b)

Figure 1-6

A tunneling junction between a normal metal and a superconductor. (a) Shows the geometry. (b) Shows the current-voltage characteristic when s is superconducting ($T \ll T_0$) and also when s is normal ($T > T_0$). Typically for a junction 1 mm$\times$ 1 mm the resistance V/I when both metals are normal may range from 10^{-2} to 10^4ohms. When $T \ll T_0$, to extract one electron from the superconducting condensate requires a minimum energy Δ. Essentially no current flows until $eV = \Delta$.

conductivity" - certain metals or alloys, in a suitable range of field, are superconducting only in a thin sheath (typically 1000Å) near the sample surface. Excitations from the inner (normal) regions can leak up to the surface-there is no gap in the energy spectrum. (This has been checked recently by tunneling experiments.) However the sheath is superconducting! There are other examples, some of which we shall discuss later.

4.2 Thermodynamic Effects

4.2.1 Specific heat, Free Energy, Entropy 1

2. Specific heat by AGD

(!! write the background here!!)

To find the different thermodynamic functions, we use the relation derived above for the derivative of the thermodynamic potential with respect to the interaction constant:

$$\frac{\delta\Omega}{\delta\lambda} = \frac{1}{\lambda}\langle H_{\text{int}} \rangle .$$

In our case H_{int} is given by (32.3). If we retain in this average terms which differ from zero only in the superconducting phase, we obtain, since $\lambda < 0$,

$$\frac{\delta\Omega}{\delta|\lambda|} = -\frac{1}{\lambda^2}|\Delta|^2$$

The connection between $1/|\lambda|$ and Δ at a given temperature is determined by the relation (36.1). Hence the difference between the potentials Ω for the metal in the superconducting and normal phases is

$$\Omega_s - \Omega_n = \int_0^{\Delta} \left(\frac{\mathrm{d}\frac{1}{|\lambda|}}{\mathrm{d}\Delta} \right) \Delta^2 \, \mathrm{d}\Delta$$

By a general rule of statistical physics, this added correction, when expressed in suitable variables, is the same for all the thermodynamie potentials. Using (36.2), according to which

$$\frac{1}{|\lambda|} = \frac{mp_0}{2\pi^2} \left\{ \ln \frac{2\omega_D}{\Delta} - 2\sum_{n=1}^{\infty} (-1)^{n+1} K_0 \left(\frac{n\Delta}{T} \right) \right\}$$

and using the familiar formula of Bessel function theory: $K_0'(x) = -K_1(x)$ we get

$$F_s - F_n = -\left(\frac{mp_0}{2\pi^2} \right) \left\{ \frac{A^2}{2} - 2\sum_{n=1}^{\infty} (-1)^{n+1} \frac{T^2}{n^2} \int_0^{n\Delta/T} K_1(x) x^2 \, \mathrm{d}x \right\}$$

At low temperatures $\Delta/T \gg 1$. In this case $\int_0^{n\Delta/T} K_1(x)x^2 \, \mathrm{d}x = 2 - \int_{n\Delta lT}^{\infty} K_1(x)x^2 \, \mathrm{d}x$. The latter integral only needs to be found for $n = 1$. the asymptotic expansion of $K_1(x)$ being used for this purpose.

The remaining series over n is easily summed. We get as a result:

$$F_s - F_n = \frac{mp_0 T^2}{6} - \frac{mp_0}{2\pi^2} \left[\frac{\Delta^2}{2} + \sqrt{2\pi\Delta_0^3 T} \left(1 + \frac{15}{8}\frac{T}{\Delta_0} \right) e^{-\Delta_v/T} \right] \tag{36.7}$$

The first term on the right-hand side is equal to the main term (with reversed sign) in the expansion of the free energy of the normal metal in powers of T. We know that this latter term leads to a linear law for
the electron part of the specific heat in the normal phase:

$$C_n = \frac{mp_0 T}{3}$$

On substituting (36.3), we find that the entropy in the superconducting phase at low temperatures is equal to

$$S_s = \frac{mp_0}{\pi^2} \sqrt{\frac{2\pi\Delta_0^3}{T}} e^{-\Delta_0/T}$$

whilst the specifie heat is

$$C_s = \frac{mp_0}{\pi^2} \left| \frac{\sqrt{2\pi\Delta_0^5}}{\pi^3} e^{-\Delta_d/T} \right.$$

This gives us, with the aid of (34.23), for the ratio of the specific heats of the superconducting phase in the region $T \ll T_c$ and of the normal phase at $T = T_0$:

$$\frac{C_s(T)}{C_n\,(T_c)} = \frac{3}{\gamma}\sqrt{\frac{2}{\pi}}\left(\frac{\Delta_0}{T}\right)^{3/2} \exp\left(-\frac{\Delta_0}{T}\right). \tag{36.8}$$

In order to obtain asymptotic formulae in the temperature region close to T_c, we start from expansion (36.4):

$$\delta\frac{1}{|\lambda|} = -\left(\frac{mp_0}{2\pi^2}\right)\frac{7\zeta(3)}{(2\pi T)^2}\Delta\delta\Delta$$

We find with the aid of (36.6) for the difference between the free energies:

$$F_s - F_n = -\left(\frac{mp_0}{2\pi^2}\right)\frac{7\zeta(3)}{16(\pi T)^2}\Delta^4 = -\frac{2mp_0T_c^2}{7\zeta(3)}\left(1-\frac{T}{T_c}\right)^2 \tag{36.9}$$

Hence the entropy in the superconducting phase is

$$S_s = -\frac{4mp_0T_c}{7\zeta(3)}\left(1-\frac{T}{T_c}\right) + S_n$$

On differentiating a second time and retaining the main terms, we get the following expression for the specific heat of the superconductor at the transition point:

$$C_s\,(T_c) = C_n\,(T_c) + \frac{4mp_0}{7\zeta(3)}T_c$$

Thus the specific heat of a metal has a jump of $4mp_0T_c/7\zeta(3)$ at the point of the phase transition to the superconducting state. If we take into account higher order terms in $T_c - T$ in expansion (36.9), we can find the ratio of the specific heat $C_s(T)$ to the specific heat $C_n\,(T_c)$ in the normal phase close to T_c:

$$\frac{C_s(T)}{C_n\,(T_c)} = 2\cdot 43 + 3\cdot 77\left(\begin{array}{cc} T & \\ T_c & -1\end{array}\right)$$

This behaviour of the electron part of the specific heat of a metal close to T_c is illustrated in Fig. 98 on p. 304.

1.3.1 Critical Field of Bulk Material. Thermodynamic Critical Field

Consider a long cylinder of a type-I superconductor in a uniform longitudinal magnetic field H_0. We shall now work out the value of the field which destroys its superconductivity, that is, we shall find the value of $H_{\rm cm}$.

At $H_0 < H_{\rm cm}, B$ is zero due to the Meissner-Ochsenfeld effect. The

$$M = -H_0/4\pi \tag{1.8}$$

When a value $\mathrm{d}\boldsymbol{H}_0$ is added to the magnetic field $\boldsymbol{H}_0$, an external source of magnetic field does a work on the superconductor, per unit volume, of

$$-\boldsymbol{M}\mathrm{d}\boldsymbol{H}_0 = \boldsymbol{H}_0\ \mathrm{d}\boldsymbol{H}_0/4\pi \tag{1.9}$$

Consequently, when the field changes from 0 to H_0, the work done by the field source is

$$-\int_0^{H_0}\boldsymbol{M}\ \mathrm{d}\boldsymbol{H}_0 = H_0^2/8\pi \tag{1.10}$$

This work is stored in the free energy of the superconductor placed in the field H_0. Thus, if the free energy density of a superconductor in zero magnetic field is $F_{\rm so}$, that of the superconductor in a finite magnetic field is

$$F_{sH} = F_{\rm s0} + H_0^2/8\pi \tag{1.11}$$

A transition to the normal state occurs when the free energy F_{sH} reaches the level of the free energy of the normal metal, i.e., $F_{sH} = F_{\rm n}$ at $H_0 = H_{\rm cm}$. This means that

$$F_{\rm n} - F_{\rm s0} = H_{\rm cm}^2/8\pi \tag{1.12}$$

It follows from (1.12) that the critical field of a bulk superconductor is a measure of the extent to which the superconducting state is preferable to the normal one from the standpoint of free energy. In other words, it measures the difference in free energy between the normal and superconducting states. The field $H_{\rm cm}$ is often called the thermodynamic critical field.

1.3.2 Entropy of a Superconductor

By the first law of thermodynamics we have

$$\delta Q = \delta R + \delta U \tag{1.13}$$

where δQ is the element of the thermal energy density for the body under consideration, δR is the work done by the body on external bodies, per unit volume, and δU is the element of its internal energy. By definition, the free energy density F is

$$F = U - TS \tag{1.14}$$

where T is the temperature of the body and S is the entropy per unit volume. Then

$$\delta F = \delta U - T\delta S - S\delta T$$

Since for a reversible process $\delta Q = T\delta S$, we have

$$\delta F = -\delta R - S\delta T. \tag{1.16}$$

It follows from (1.16) that

$$S = -(\partial F/\partial T)_R \tag{1.17}$$

Let us use (1.17) to calculate the difference in entropy between the normal and superconducting states. Substituting (1.12) into (1.17) we get

$$S_{\rm s} - S_{\rm n} = \frac{H_{\rm cm}}{4\pi}\left(\frac{\partial H_{\rm cm}}{\partial T}\right)_R \tag{1.18}$$

From (1.18), important physical results can be derived.
(1) According to Nernst's theorem, the entropy of a body at $T = 0$ is zero. Therefore $(\partial H_{\rm cm}/\partial T)_{T=0} = 0$, i.e., at $T = 0$ the curve $H_{\rm cm}(T)$ has zero derivative.
(2) It is known from experiment that, as the temperature T increases, the dependence $H_{\rm cm}(T)$ has the form of a monotonically descending curve (see Fig. 1.1). That is, for the entire temperature interval from 0 to $T_{\rm c}$, we have $\partial H_{\rm cn}/\partial T < 0$ and $S_{\rm s} < S_{\rm n}$,
(3) Since $H_{\rm cm} = 0$ at $T = T_{\rm c}$, we get $S_{\rm s} = S_{\rm n}$ at $T = T_{\rm c}$. A sketch of the $S_8 - S_{\rm n}$ dependence

on temperature is shown in Fig. 1.10.

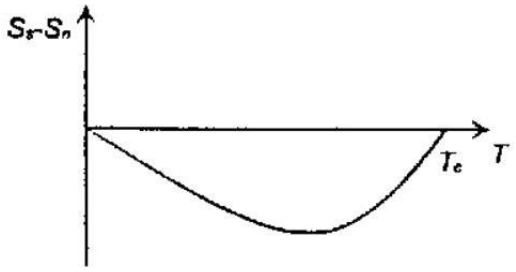


Fig. 1.10. Temperature dependence of the entropy difference $S_k - S_n$

We now arrive at some very important conclusions.

(1) The superconducting state is a more ordered state than the normal one because it is characterised by lower entropy.

(2) Since $S_\mathrm{s} = S_\mathrm{n}$ at $T = T_\mathrm{c}$, the transition at $T = T_\mathrm{c}$ does not involve latent heat. Therefore, the transition at $T = T_\mathrm{c}$ is a second-order phase transition.

(3) At $T < T_\mathrm{c}$, a transition from the superconducting to the normal state occurs when a sufficiently strong magnetic field is applied. Since, as we know, $S_\mathrm{s} < S_\mathrm{n}$, such a transition is accompanied by absorption of latent heat. For the transition from the superconducting to the normal state, it is the other way round, i.e., the latent heat is given up. Therefore, in the presence of a magnetic field, all the transitions at $T < T_\mathrm{c}$ are first-order phase transitions.

It is amazing how a couple of formulas from thermodynamics and a single experimental fact - the dependence of H_cm on T (Fig. 1.1) - have led to such fundamental conclusions! Fundamental indeed, because from our new knowledge that the superconducting state is more ordered (i.e., possesses a lower entropy) than the normal one, we come straight to the understanding that superconductivity is based on the coherent behavior of electrons.

1.3.3 Heat Capacity

The specific heat of matter can be defined as $C = T(\partial S/\partial T)$. Therefore, we can write the difference in specific heat between the superconducting and normal states as

$$C_\mathrm{s} - C_\mathrm{n} = \frac{T}{4\pi}\left[\left(\frac{\partial H_\mathrm{cm}}{\partial T}\right)^2 + H_\mathrm{cm}\frac{\partial^2 H_\mathrm{cm}}{\partial T^2}\right] \tag{1.19}$$

In order to obtain (1.19), we have taken the derivative of (1.18). Now, since $H_\mathrm{cm} = 0$ at $T = T_\mathrm{c}$, we have

$$C_\mathrm{s} - C_\mathrm{n} = \frac{T_\mathrm{c}}{4\pi}\left(\frac{\partial H_\mathrm{cmn}}{\partial T}\right)^2_{T_\mathrm{c}} \tag{1.20}$$

Expression (1.20), known as the Rutgers formula, implies that there must be a discontinuous jump at $T = T_\mathrm{c}$ in the specific heat as a function of temperature. The Rutgers formula defines the height of the jump. The temperature dependence of the specific heat is plotted in Fig.1.11. At $T > T_\mathrm{c}$, the specific heat decreases linearly with decreasing temperature, as is usually the case for normal metals (electronic specific heat).

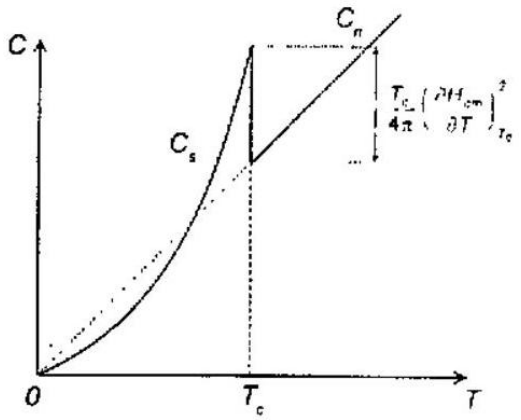


Fig. 1.11. Temperature dependence of the specific heat of a superconductor

For the moment we shall consider the form of the $C(T)$ dependence in Fig. 1.11 simply as an experimental fact, i.e., not supported by theoretical analysis. However, the fact that there exists a point at $T < T_c$ where the two curves - $C_{\rm s}(T)$ and the extrapolation of $C_{\rm n}(T)$ - intersect, fol-

1.3.4 Free Energy

Let us consider in more detail the basic properties of those thermodynamic potentials that we shall often deal with when studying superconductivity. These potentials are equally suitable for analysis of any sori of matter, superconductors in particular. Definitions and detailed arguments can be found in [13].

Consider a body in an external magnetic field H_0 such that its temperature and the magnetic induction in its interior are constant. The body attains thermodynamic equilibrium when the free energy $\mathcal{F} = \int F \, \mathrm{d}V$ is a minimum, where the free energy density F is defined by (1.14). The quantity $\mathcal{F}$ is sometimes referred to as the Helmholtz free energy.

For many calculations, making use of this potential is awkward because normally the quantities presumed to be constant for a body in an external magnetic field are the temperature and the external magnetic field H_0. In the latter case, thermodynamic equilibrium is attained when another thermodynamic potential is a minimum, that is, the Gibbs free energy $\mathcal{G}$ defined as

$$\mathcal{G} = \int G \, \mathrm{d}V, \tag{1.21}$$

$$G = F - \boldsymbol{B} \cdot \boldsymbol{H}_0/4\pi, \tag{1,22}$$

4.2.2 Specific heat, Free Energy, Entropy 2

Typical Derivation of Heat Capacity

To get the Heat Capacity, one needs just to calculate energy and then take a derivative. But first, let us calculate the number of particles, since it is easy and the method is the same.

При низких температурах число возбуждений в сверхпроводнике невелико. Термодинамика любой системы вблизи основного состояния определяется считалочкой: каков спектр возбуждений, такова и теплоёмкость. Для спектра с щелью Δ при $T \ll T_c$ получается экспоненциальная зависимость теплоемкости $C_s \sim \exp(-\Delta/T)$. Такая зависимость является типичной при наличии щели в спектре возбуждений. Покажем это на примере числа квазичастиц в сверхпроводнике. Полное равновесное число квазичастиц равно

$$N(T) = \int_0^\infty \frac{g_s V 4\pi p^2 dp}{(2\pi\hbar)^3 \left(e^{\frac{\varepsilon(p)}{T}} + 1\right)}$$

где $\varepsilon(p) = \sqrt{\Delta^2 + v_F^2 \left(p - p_F\right)^2}, g_s = 2s + 1 = 2$ - кратность вырождения по спину. Поскольку $T \ll \Delta$, экспонента велика по сравнению с единицей; а поскольку $\sqrt{T\Delta} \ll v_F p_F$, интеграл (12.34) «набирается» в узкой $|p - p_F| \approx \sqrt{T\Delta}/v_F \ll p_F$ области около p_F. С экспоненциальной точностью $\exp(-\Delta/T) \ll 1$ получаем

$$N(T) \approx \frac{8V\pi p_F^2}{(2\pi h)^3} e^{-\frac{\Delta}{T}} \int_{-\infty}^{+\infty} dp' e^{\frac{-v_F^2 p^2}{2T\Delta}} = \frac{8V\pi p_F^2 \sqrt{2\Delta}}{(2\pi h)^3 v_F} T^{1/2} e^{-\frac{\Delta}{T}} \propto e^{-\frac{\Delta}{T}}.$$

Число квазичастиц экспоненциально мало, поэтому предэкспоненциальный множитель можно не выписывать.

(??? check these formulas!!!)

Теперь вычислим энергию квазичастиц:

$$E(T) = \int_0^\infty \frac{g_s V 4\pi p^2 dp \varepsilon(p)}{(2\pi\hbar)^3 \left(e^{\frac{\varepsilon(p)}{T}} + 1\right)}$$

Учитывая отмеченные выше приближения, получаем

$$E(T) \approx \frac{8V\pi p_F^2}{(2\pi\hbar)^3} e^{-\frac{\Delta}{T}} \int_0^\infty \left(\Delta + \frac{v_F^2 \left(p - p_F\right)^2}{2\Delta}\right) e^{-\frac{v_F^2 (p-p_F)^2}{2T\Delta}}$$

Поскольку интеграл «набирается» в узкой окрестности $|p - p_F| \ll \sqrt{T\Delta}/v_F \ll p_F$, вторым слагаемым в (12.37) можно пренебречь:

$$E(T) \approx \frac{8V\pi p_F^2 \sqrt{2\pi}\Delta^{3/2}}{(2\pi\hbar)^3 v_F} T^{1/2} e^{-\frac{\Delta}{T}}$$

Учитывая крайнюю малость экспоненты, предэкспоненциальный множитель можно не удерживать. Для теплоемкости это дает

$$C_s(T) \propto e^{-\frac{\Delta}{T}}$$

типичную экспоненциальную зависимость теплоемкости для спектра возбуждений со щелью.

Jump of Heat Capacity

При температуре перехода теплоемкость испытывает скачок. Модель Бардина-Купера-Шриффера предсказывает для него значение $\left(C_s - C_n\right)/C_s = 1.43$.

Let us proof it.

Тепловые свойства сверхпроводника определяются его возбуженими - квазичастицами, которые можно рассматривать как ферми-газ с нулевым химическим потенциалом. Энтропия этого газа равна

$$S = -\sum [n \ln n + (1-n)\ln(1-n)]$$

здесь $n = \left(e^{\beta\varepsilon}+1\right)^{-1}$, $\varepsilon = \sqrt{\xi^2+\Delta^2}$

Теплоемкость дается формулой из термодинамики:

$$C = T\frac{\partial S}{\partial T} = \sum T\frac{\partial S}{\partial n}\frac{\partial n}{\partial T} = -\sum T[\ln n - \ln(1-n)]\frac{\partial n}{\partial T}$$

$$\ln n - \ln(1-n) = \ln\frac{n}{1-n} = -\ln\left(\frac{1}{n}-1\right) = -\beta\varepsilon$$

Таким образом

$$C = \sum \varepsilon\frac{\partial n}{\partial T}$$

При низких температурах теплоемкость экспоненциально мала.

Вблизи критической температуры самое сложное - найти производную от распределения квазичастиц

$$\frac{\partial n}{\partial T} = \frac{\partial n}{\partial \beta\varepsilon}\frac{\partial \beta\varepsilon}{\partial T} = T\frac{\partial n}{\partial \varepsilon}\left(-\frac{\varepsilon}{T^2}+\frac{1}{T}\frac{1}{2\varepsilon}\frac{\partial\Delta^2}{\partial T}\right)$$

Квадрат пели линейно зависит от температуры

$$\frac{\partial\Delta^2}{\partial T} = \frac{\partial}{\partial T}T_c\frac{T_c-T}{A} = -\frac{T_c}{A}$$

Тогда теплоемкость

$$C_s = \sum\left|\frac{\partial n}{\partial\varepsilon}\right|\left(\frac{\varepsilon^2}{T}+\frac{T_c}{2A}\right) = C_n + \frac{T_c}{2A}\sum\left|\frac{\partial n}{\partial\varepsilon}\right| = C_n + \frac{T_c}{2A}\nu(0)$$

Так как $C_n = \frac{\pi^2}{3}\nu(0)T$, то скачек теплоемкости в точке фазового перехода равен

$$\frac{C_s - C_n}{C_n} = \frac{T_c\nu(0)}{2A\frac{\pi^2}{3}\nu(0)T} = \frac{3}{2A\pi^2} = 1,43$$

Флуктуационная теплоемкость сверхпроводника

(write the background!!!!)

Используя уравнения Гинзбурга-Ландау, можно определить флуктуационную поправку к Ω-потенциалу, энтропии и теплоемкости. Это позволяет еще раз независимым образом установить область применимости уравнений Гинзбурга-Ландау.

Решение этой задачи основывается на ранее (см. лекцию 10) полученной формуле для флуктуационной поправки к теплоемкости:

$$\Delta C_\phi = \frac{T_c^2 V a^{3/2}}{16c^{3/2}\pi\sqrt{T-T_c}}$$

Следует только правильно выразить величины a и c через микроскопические параметры сверхпроводника. Выше мы видели, что в функционале (13.2) $c = \hbar^2/4m$ и $a = T_c m\pi^2/p_F^2$. Сравнивая флуктуационую теплоемкость (13.38) со скачком теплоемкости $\Delta C \sim C\left(T_c\right) \approx g_F T_c/\varepsilon_F$, снова получаем критерий (13.37).

4.2.3 Specific Heat: Experimental confirmation

(????? read articles about it)

In Figure 4.1 as an example we show the specific heat of tin as a function of temperature [6]. Tin is a type-I superconductor. The solid curve is observed in the absence of a magnetic field. We clearly see the jump of the specific heat at T_c, indicating a second-order phase transition. In the case of a first-order phase transition, at the transition temperature c_p would have become infinitely large.

In magnetic fields above the critical field B_c, the specific heat c_n of the normal conducting state can also be determined for $T < T_c$ (solid dots in Figure 4.1). In this case no discontinuity is observed, since there is no phase transition.

The specific heat of the normal conductor can be separated into two components, the contribution of the conduction electrons c_{nE} and the contribution of the lattice vibrations c_{nL}, thus $c_n = c_{nE} + c_{nL}$

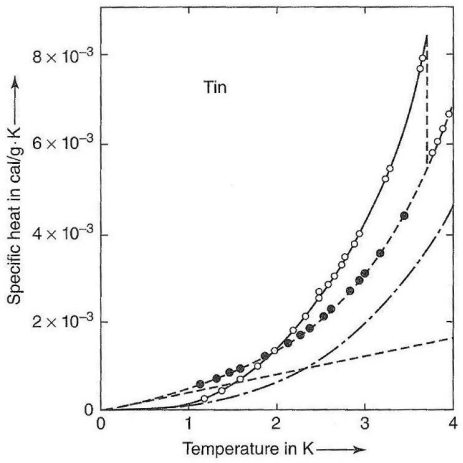


Figure 4.1 Specific heat of tin plotted versus the temperature. Open circles: without a trons for $B > B_c$ dashed-i: with a magnetic field $B > B_c$; dashed line: contribution of the elec(6) $> B_c$; dash

In good approximation we have

$$c_{nE} = \gamma T$$
$$c_{nL} = \alpha \left(T/\Theta_D\right)^3$$

γ and α are constants, and Θ_D is the Debye temperature. The Sommerfeld coefficient γ is proportional to the density of states of the electrons at the Fermi energy (see Section 1.1). It is given by

$$\gamma = \frac{2}{3}\pi^2 k_B^2 N\left(E_F\right)$$

where $k_B = 1.38 \times 10^{-23}$ W s/K is Boltzmann's constant and $N\left(E_F\right)$ is the density of states at the Fermi energy in (W s mol) $^{-1}$.

In the superconducting state for medium temperatures, the temperature dependence of the specific heat is well approximated by a power law of third order According to Eqs. (4.14) and (4.15), this means that the lattice component domi-

Also we want to discuss briefly which temperature dependence of the specific heat in the superconducting state results from the microscopic theory. First we look at conventional superconductors.

For temperatures near T_c, the Cooper pair density and the energy gap chang strongly with temperature. In this temperature range we cannot expect simple theoretical relations. However,

at very low temperatures the energy gap is nearly independent of T. The introduction of energy into the electron system then essentially

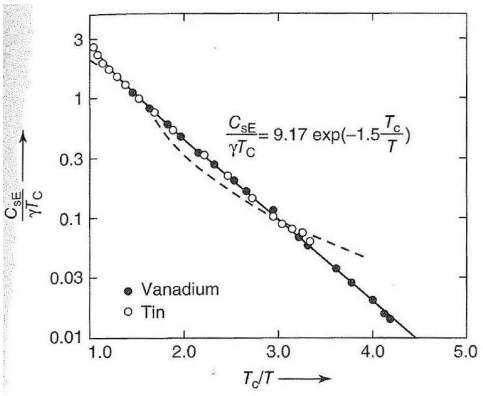


Figure 4.2 Electronic component of the specific heat of tin and vanadium. The straight line represents the relation predicted by the BCS theory. The dashed curve indicates a T^3 law according to Eq. (4.15). (From [7].)

results in the breaking up of Cooper pairs." [8] For this, excitations beyond the energy gap are needed. Since the probability of such excitations should decrease following an exponential function of the kind $\exp(-A/k_{\mathrm{B}}T)$, at very low temperatures we expect essentially an exponential decrease in the electronic component c_{sE} of the specific heat. Here, A is a constant, essentially the excitation energy.

For $T \to 0$, the Bardeen-Cooper-Schrieffer (BCS) theory yields for the specific heat of conventional superconductors

$$c_{\mathrm{sE}} = 9.17\gamma T_{\mathrm{c}} \exp\left(-\frac{1.5T_{\mathrm{c}}}{T}\right)$$

In Figure 4.2 we show an example of this exponential dependence [7]. Corresponding to Eq. (4.17), $c_{\mathrm{S}}/\gamma T_{\mathrm{c}}$ is plotted versus T_{c}/T. The straight line represents sponding to Eq. (4.17), $c_{\mathrm{sE}}/\gamma T_{\mathrm{c}}$ is plotted versus T_{c}/T. The straight line represents the relation (4.17). Also, before the advent of the BCS theory, highly accurate specific-heat measurements had already indicated exponential dependences at very low temperatures. This result confirmed at the time the prediction by Daunt and Mendelssohn [8] of an energy gap in the excitation spectrum of a superconductor For the relative jump of the electronic component of the specific heat, $(c_{\mathrm{sE}} - c_{\mathrm{nE}})/c_{\mathrm{nE}}$, near T_{c}, the BCS theory yields the value 1.43, in excellent agreement with the experimental observations.

On the other hand, in unconventional superconductors, the excitation spectrum does not have an energy gap. Instead, the gap function $\Delta_0(\mathbf{k})$ vanishes along certain directions in $\mathbf{k}$-space. Hence, even at very low temperatures there exist an appreciable number of unpaired electrons, which contribute to the specific heat

The density of the free, unpaired electrons has become so small that its energy absorption can be neglected.

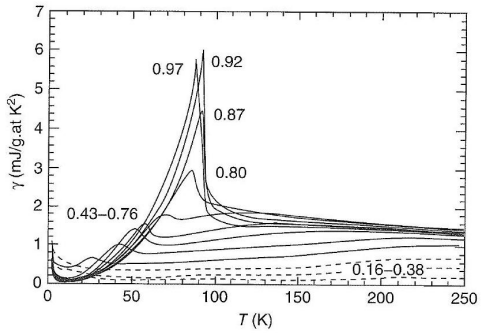


Figure 4.3 Sommerfeld coefficient $\gamma = c_{el}/T$ plotted versus temperature T for $YBa_2Cu_3O_{6+x}$ crystals with different

of the electron system. As we have seen in Section 3.2, the function $\Delta_0(\mathbf{k})$ can vanish at individual points or along extended lines in $\mathbf{k}$-space. Therefore, $c_{sE}(T)$ ncreases with temperature following a power law: $c_{sE}(T) \propto T^a$. Depending on the dimension of the locations with zero gap (points or lines) and on the exponent with which $\Delta_0(\mathbf{k})$ vanishes with $|\mathbf{k}|$ near these locations, one finds $a = 2$ or $a = 3$. Also the relative magnitude of the jump $(c_{sE} - c_{nE})/c_{nE}$ of the electronic specific heat at T_c depends on the exact behavior of $\Delta_0(\mathbf{k})$ near the locations with zero gap. Hence, it yields information about these locations.

For the cuprates it is very difficult to determine the electronic component of the specific heat over a large temperature range, since (except for very low temperatures) the contribution of the phonons to the specific heat is relatively large [9-11]. Furthermore, it is impossible to suppress the superconductivity simply by the application of a magnetic field, because of the large values of the upper critical fields. Therefore, the difference between the specific heat in the normal and in the superconducting states cannot be extracted in the simple way shown in Figure 4.1. Instead, one can use undoped samples for comparison, say, comparing $YBa_2Cu_3O_6$ with $YBa_2Cu_3O_7$. In Figure 4.3 we show the temperature dependence of the quantity $\gamma = c_{el}/T$ for different levels of oxygen doping x in $YBa_2Cu_3O_{6+x}$ The jumps at the different transition temperatures can clearly be seen.

The specific heat c_{sE} has also been analyzed exactly in the limit of low temperatures, and a surprisingly large linear term has been found, that is, $a = 1$ [13] However, for a superconductor with $d_{x^2-y^2}$ symmetry of the pair wave function in the absence of a magnetic field, in the simplest case one would have expected quadratic temperature dependence of c_{sE}.) Subsequent experiments have confirmed the T^2 term [14] and, on the other hand, have identified paramagnetic mpurities as the origin of the linear term [15]. 9) For d-wave superconductors in the vortex state, one expects a linear term increasing proportional to $B^{1/2}$. Such a term was also confirmed experimentally. 4.3 Thermal conductivity 209

For the three examples of superconductors, tin, vanadium, and $YBa_2Cu_3O_7$, we have seen that the transition into the superconducting state represents a secondorder phase transition. [10]

4.2.4 Thermal Conductivity

If we establish a temperature difference ΔT along a rod of length l (taking a simple geometry), heat energy is transported from the hot end to the cold end. The thermal conductivity λ_T is a material parameter and is defined by the equation

$$\frac{\Delta Q}{\Delta t} = \lambda_T \frac{F}{l} \Delta T$$

where $\Delta Q/\Delta t$ is the heat energy per unit time, F and l are the cross-section and length of the rod, respectively, and ΔT is the temperature difference. Here, we assume a linear change of T along the length of the rod.

In a metal, heat transport is due to the conduction electrons as well as lattice vibrations. In general, the contribution of the electrons is much larger than that of the lattice. In this case, from our basic understanding of the superconducting state, we can easily predict how the thermal conductivity should behave for temperatures below T_c . Below T_c, with decreasing temperature more and more conduction electrons are correlated, forming Cooper pairs, and hence are decoupled from the energy exchange. Therefore, below T_c the contribution of the electrons to the thermal conduction becomes smaller and smaller. So we expect that in the superconducting state the thermal conductivity is smaller than in the normal conducting state, as long as it is dominated by the electrons.

This behavior is shown in Figure 4.4 for tin and mercury [17]. Here, we do not want to discuss the temperature dependence of the thermal conductivity in the normal conducting state. We only emphasize the fact that in the superconducting state the thermal conductivity is smaller than in the normal conducting state, as expected. At sufficiently low temperatures, at which practically no free electrons exist anymore in the superconducting state, because of the nearly complete correlation in the form of Cooper pairs, the behavior in a superconductor corresponds exactly to that in an electrically insulating crystal. The electron system is simply decoupled from the thermal behavior. If the superconductivity is suppressed by means of an overcritical magnetic field, then the metal recovers the much larger thermal conductivity of the electron system. Therefore, a superconductor can serve as a thermal switch. In the overcritical fields we have high thermal conductivity; analogous to electric circuits, the switch is closed. At zero field the thermal conductivity is much smaller, and the switch is open. Often such thermal switches represent an important feature of experiments at temperatures below 1mK.

This only applies in the absence of a magnetic field. Otherwise, the phase transition can be of first transition into the normal state, the magnetization changes discontinuously [16].

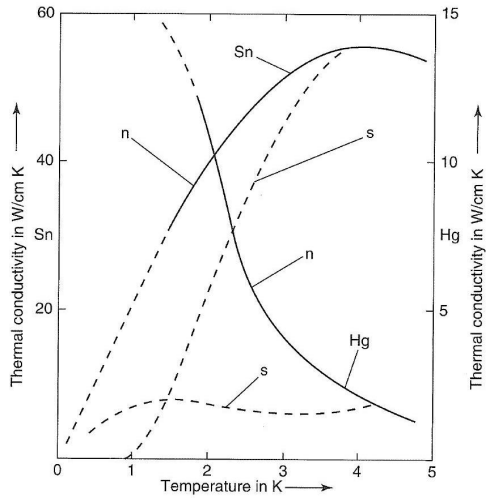


Figure 4.4 Thermal conductivity of pure tin and mercury. (From [16].) The left scale is for

The behavior discussed earlier is characteristic of many metals. However, in alloys or highly impure metals, the situation is much more complex. If chemical impurities are introduced into a metal lattice, the electron mean free path becomes shorter due to collisions between the electrons and the impurities. At low temperatures the corresponding additional electrical resistance is observed in the form of a residual resistance. The reduction of the electron mobility also leads to an increase in the thermal resistance.

In contrast to the electrons, the lattice vibrations, the phonons, are much less hindered in their propagation by atomic lattice defects. [11)] Therefore, the contribution of the phonons to the thermal conductivity is much less affected by such impurities. As a result, the thermal conductivity of the electrons can become smaller than that of the phonons. Then the thermal conductivities in the superconducting and in the normal conducting states differ only little from each other. As an example, we show in Figure 4.5 the thermal conduction of lead-bismuth alloys containing 0.1%Bi[18].

The scattering of a wave at an obstacle becomes strong if the wavelength and the the Fermi energy the matter wave of the electrons has a wavelength of a few

angstroms. Therefore, the electrons are srongly scattered at atomic obstacles. On much longer wavelengths, experience much weaker interaction with the obstacle. If the electronic component of the thermal conductivity becomes much smaller the component due to the phonons, in the superconducting state the thermal than the tivity can become even larger than in the

normal conducting state. This can conductivity in some alloy systems. As an example of this behavior, in Figure 4.5 we show the thermal conductivity of a lead-bismuth alloy containing 0.5%Bi. This behavior can be understood by noting that the electron and phonon systems can also interact with each other, that is, there are collisions between the electrons and the phonons. Such collisions of the electrons with the phonons dominate the total temperature dependence of the electrical resistance. With increasing temperature the lattice vibrations, that is, the number of phonons, increase. As a result, the collisions of the electrons and, hence, the electrical resistance increase with increasing temperature.

In substances in which the phonons provide the dominant contribution to the hermal conduction, we must look at the electron-phonon collisions from the viewpoint of the phonons. These collisions reduce the propagation and, hence, the thermal conduction of the phonons. If the electrons are decoupled in the superconducting state, these collisions are eliminated. The thermal conductivity of the phonon system increases. In this way, we can understand why thermal conduction in the superconducting state can become larger than in the normal conducting state. This is the explanation of the results shown for the Pb − Bi alloys in Figure 4.5. Here we do not want to go any further in our discussion of thermal conductivy. We just mention that, in unconventional superconductors, with decreasing temperature the electronic contribution vanishes much more slowly than in conventional superconductors. This results from the relatively large number of quasiparticles existing in the former also at low temperatures [19]. A similar argument applies if superconducting and normal conducting regions exist next to each other in a sample. This happens in the vortex state of type-II superconductors and also in the so-called intermediate state of type-I superconductors. The latter will be discussed in Section 4.6.4 in more detail.

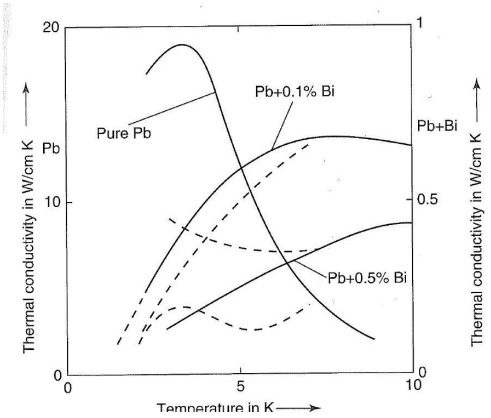


Figure 4.5 Thermal conductivity of lead and lead-bismuth alloys. Solid lines: normal state; dashed lines: superconducting state. (From [18]].)

4.2.5 Vortices: General Properties

Выше мы установили, что для них энергия границы между нормальной и сверхпроводящей фазами $\sigma_{ns} < 0$.

Это означает, что становится энергетически выгодным расслоение образца на области нормальной и сверхпроводящей фаз.

Вначале этой части пособия мы описали, каким образом магнитное поле проникает в сверхпроводник второго рода.

Так, внутри цилиндрического образца образуются вихри.

Каждый вихрь представляет собой цилиндр с нормальной сердцевиной, радиус которого порядка длины когерентности ξ.

В сердцевине параметр порядка $\psi = 0$.

Вокруг этой нормальной сердцевины течет незатухающий сверхток.

Создаваемое им магнитное поле направлено вдоль сердцевины.

Вихревой ток захватывает область радиуса порядка λ - глубины проникновения. Эта область может быть достаточно большой, поскольку для сверхпроводников второго рода $\lambda \gg \xi$.

Один вихрь несет один квант магнитного потока.

Образование вихрей становится энергетически выгодным при внешнем поле $H_0 > H_{c1}$.

Вихри, образовавшись в сверхпроводнике, располагаются на расстоянии порядка λ и образуют в поперечном сечении правильную треугольную решетку.

Возникающее состояние называется смешанным. Это состояние существует при повышении величины внешнего поля до значения H_{c2}, называемого вторым критическим полем.

В этом случае период решетки становится порядка ξ.

Это означает, что вихри соприкасаются своими нормальны ми сердцевинами и параметр порядка ψ обращается в нуль во всем объеме образца.

Вблизи верхнего поля есть область, где решетка плавится.

Кривая намагниченности лля сверхпроводника второго рода ведет себя как показано на рисунке..

(хз как, нет рисунка)

одиночный вихрь

Рассмотрим сверхпроводник второго рода, то есть случай $\lambda \gg \xi$.

Мы хотим показать, что существует область магнитных полей, при которых выгодно образование в толпе сверхпроводника нормальных тонких цилиндрических областей радиуса ξ - вихрей.

Параметр порядка внутри этой области изменяется от 0 до 1.

Вне сердцевины $|\psi|^2 = 1$. Поэтому для больших расстояний $\rho \gg \xi$.

уравнение ГЛ (58) перепишется

$$\operatorname{rotrot} \mathbf{A} = \frac{1}{\lambda^2}\left(\frac{\Phi_0}{2\pi}\nabla\theta - \mathbf{A}\right), \qquad \rho \gg \xi$$

Проинтегрируем его по замкнутому контуру охватывающему нормальную сердцевину вихря.

$$\oint dl \left(\lambda^2 \operatorname{rotrot} \mathbf{A} + \mathbf{A}\right) = \frac{\Phi_0}{2\pi} \oint dl \nabla\theta$$

Если бы не магнитная сердцевина, то фаза волновой функции была бы однозначной аналитической функцией и интеграл в правой части равнялся бы нулю.

Наличие нормальной сердцевины делает сверхпроводянций образец миогосвязным.

В то же время остется требование однозначности волновой функциии.

Это означает, что при обходе по замкнутому контуру фаза может измениться на $2\pi n$ - значение интеграла в правой части (68).

Преобразуем левую часть (68) к поверхностному интегралу, учитывая, что $\operatorname{rot}\mathbf{A} = \mathrm{B}$:

$$\int d\mathbf{S} \left(\lambda^2 \operatorname{rotrot} \mathbf{B} + \mathbf{B}\right) = n\Phi_0$$

Поскольку интеграл в левой части не зависит от контура (главное, что он охватывает сердцевину!), то формально можно считать, что подынтегральная функция есть δ -функция. Поэтому

$$\lambda^2 \operatorname{rot}\, \operatorname{rot}\mathbf{B} + \mathbf{B} = n\Phi_0\delta(\rho)$$

Всюлу вне сердцевины при$\rho \gg \xi$ имеем

$$\text{rotrot}\,\mathbf{B} = -\frac{1}{\lambda^2}\mathbf{B}$$

Раскры вая левую часть этого выражения по известной формуле, получим

$$\Delta \mathrm{B} = \frac{1}{\lambda^2}\ \mathrm{B}$$

В цилинлрических координатах имеется только одна z -компонента h_z. Поэтому для нее имеем

$$\frac{1}{\rho}\frac{\partial}{\partial\rho}\rho\frac{\partial}{\partial\rho}h_z = \frac{\rho}{\lambda^2}$$

$\Pi_{\text{vCTb}} h_z = f(x), x = \rho/\lambda$. Тогда

$$xf'' + f' - xf = 0$$

Это - уравнение Бесселя. Нас инересует его решение в окрестности вихря, то есть при $\rho < \lambda$. При малых значениях аргумента $f = \ln x$.(Это легко проверить непосредственной подстановкой). Поэтому магнитное поле в окрестности оси вихря имеет вид

$$h \sim \ln\left(\frac{\lambda}{\rho}\right), \xi < \rho < \lambda$$

Точное решение уравнения (69) при условии$h(\infty) = 0$ имеет вил

$$h = \frac{\Phi_0}{2\pi\lambda^2}K_0(\rho/\lambda)$$

K_0 - функция Макдональда, ассимптотика которой $K_0(z) \propto \ln(1/z)$ при $z \ll 1$ приводит к (72). Это позволяет оценить поле в центре вихря с логарифмической точностью

$$h(0) \simeq h(\xi) \simeq \frac{\Phi_0}{2\pi\lambda^2}\ln(\xi/\lambda)$$

(???????)

4.2.6 Critical field of superconductors 1

Using the methods of thermodynamics, we look at the stability of the Meissner phase of type-I superconductors as a function of the temperature and of the applied magnetic field. We will see that in the simplest case the critical field of these superconductors, at which the transition from the Meissner phase into the hormal conducting phase sets in, is identical with the thermodynamic critical field discussed in Section 4.4. However, we will also see that one observes a much more complex behavior if the magnetic field at the sample edge differs from the applied field because of the shape of the sample.

We will also use thermodynamics to understand the behavior of superconductors under pressure.

Первое критическое поле

Исходим из функционала Гинзбурга-Ландау для свободной энергии

$$\mathcal{F}_{sH} = \mathcal{F}_n + \int dV\left[\alpha|\Psi|^2 + \tfrac{\beta}{2}|\Psi|^4 + \tfrac{1}{4m}\left|-i\hbar\nabla\Psi - \tfrac{2e}{c}\mathbf{A}\Psi\right|^2 + \tfrac{(\text{rot}\,\mathbf{A})^2}{8\pi}\right]$$

Напомним выражения для длины когерентности и глубины проникновения магнитного поля

$$\xi^2 = \frac{\hbar^2}{4m|\alpha|}$$
$$\lambda^2 = \frac{mc^2}{4\pi n_s e^2} = \frac{mc^2\beta}{8\pi e^2|\alpha|}$$

Если вихря нет, то поскольку внутри сверхпроводника микроскопическое поле B = 0, то вклал в свободнут энергиго (74) дает только верхняя строка.

Энергией вихря будем называть свободную энергиго, определяемую нижней строкой в, то есть будем ее отсчиты вать от свобоной энергии состояния без вихрей. Нас интересует случай $\lambda \gg \xi$.

Поэтому можно пренебречь свободной энергией, сосредоточенной в объеме нормальной сердцевины.

Кроме того, поскольку мы интересуемся расстояниями $\rho > \xi$, где параметр порядка практически не изменяется, можно считать $|\Psi|^2 = |\Psi_0|^2 = \frac{|\alpha|}{\beta}$. По этой причине в (39) можно пренебречь квантовым членом$-i\hbar\nabla\Psi$. Поэтому из (39) для вычисления энергии вихря остается только выражение

$$\varepsilon = \int dV \left(\frac{e^2}{mc^2}\mathbf{A}^2\frac{|\alpha|}{\beta} + \frac{h^2}{8\pi} \right)$$

Во втором уравнении ГЛ (58)

$$\operatorname{rotrot}\mathbf{A} = \frac{|\psi|^2}{\lambda^2}\left(\frac{\Phi_0}{2\pi}\nabla\theta - \mathbf{A}\right)$$

опустим квантовый градиентный член. Тогда

$$\mathbf{A} = \left(\frac{\lambda}{|\psi|}\right)^2 \operatorname{rotrot} A = \left(\frac{\lambda}{|\psi|}\right)^2 \operatorname{rot}\mathbf{B}$$

Подставляя (77) в (78), получим

$$\varepsilon = \frac{1}{8\pi}\int dV \left(\lambda^2(\operatorname{rot}\mathbf{B})^2 + \mathbf{B}^2\right)$$

Заметим, что, как и следовало ожидать при$\lambda \gg \xi$, это есть Лондоновское вы ражение, (20),

$$\operatorname{rotrot}\mathbf{A} = \frac{|\psi|^2}{\lambda^2}\left(\frac{\Phi_0}{2\pi}\nabla\theta - \mathbf{A}\right)$$

опустим квантовый градиентный член. Тогда

$$\mathbf{A} = \left(\frac{\lambda}{|\psi|}\right)^2 \operatorname{rotrot} A = \left(\frac{\lambda}{|\psi|}\right)^2 \operatorname{rot}\mathbf{B}$$

Подставляя (77) в (78), получим

$$\varepsilon = \frac{1}{8\pi}\int dV \left(\lambda^2(\operatorname{rot}\mathbf{B})^2 + \mathbf{B}^2\right)$$

Заметим, что, как и следовало ожидать при$\lambda \gg \xi$, это есть Лондоновское вы ражение, (20),

Применим к выражению $(\mathrm{rot}\,\mathbf{B})^2 = \mathrm{rot}\,\mathbf{B}\cdot\mathrm{rot}\,\mathbf{B}$ формулу

$$\mathrm{arot}\,\mathbf{b} = \mathrm{b\ rota} - \mathrm{div}[\mathbf{a},\mathbf{b}]$$

Tor/a

$$(\mathrm{rot}\,\mathbf{B})^2 = \mathbf{B}\,\mathrm{rotrot}\,\mathbf{B} - \mathrm{div}[\mathrm{rot}\,\mathbf{B},\mathbf{B}]$$

По теореме Гаусса

$$\int \mathrm{div}[\mathrm{rot}\,\mathbf{B}\times\mathbf{B}] = \oint d\mathbf{S}[\mathrm{rot}\,\mathbf{B}\times\mathbf{B}]$$

Напомним, что нас интересует цилиндрическая геометрия, когда вектор B направлен по осиz. Вычислим энергию вихря единичной длины, ограниченного плоскостями$z = 0, z = 1$. Интеграл по торцевым окружностям равен нули, так как вектор [rotB$\times$ B] лежит в плоскости этих торцов. Поскольку поле вихря B $\to$ 0, при $\rho \to \infty$, то интеграл и по бесконечно удаленной цилиндрической поверхности в (81) обрашается в нуль. Итак,

$$\varepsilon = \frac{1}{8\pi}\int dV\left[\mathbf{B}\left(\lambda^2\,\mathrm{rotrot}\,\mathbf{B} + \mathbf{B}\right)\right]$$

В силу уравнения (69), выражение в круглых скобках есть δ -функция. Поэтому, используя (73), получим

$$\varepsilon = \frac{\Phi_0\mathbf{B}(0)}{8\pi} = \left(\frac{\Phi_0}{4\pi\lambda}\right)^2\ln(\xi/\lambda)$$

Во внешнем поле минимум должна иметь энергия Гиббса

$$\varepsilon_1 = \varepsilon - \int\frac{\mathrm{BH_0}}{4\pi}dV$$

$\mathrm{H_0}$ можно вынести за знак интеграла. Если считать, что вихрь несет один квант

$$\int\frac{\mathrm{B}}{4\pi}dV = \int\limits_0^1 dz\int\frac{\mathrm{B}}{4\pi}d\ \mathrm{S} = \frac{\Phi_0}{4\pi}$$

Итак

$$\varepsilon_1 = \left(\frac{\Phi_0}{4\pi\lambda}\right)^2\ln(\xi/\lambda) - \frac{\Phi_0\mathrm{H_0}}{4\pi}$$

Отсюда следует, что в слабом магнитном поле$\varepsilon_1 > 0$ и образование вихря невыгодно. Из (86) следует, что минимальное поле при котором $\varepsilon_1 < 0$ есть

$$H_{c1} = \frac{\Phi_0}{4\pi\lambda^2}\ln(\xi/\lambda) = \frac{\Phi_0}{4\pi\lambda^2}\ln(x)$$

Это поле называется первъи критическим полем, при котором внешнее магнитное поле начинает проникать в сверхпроводник. Вспоминая оценку (66), получим

$$H_{c1}\,(T\to T_c) \sim H_{c1}(0)\,(T_c - T)$$

второе критическое поле

Найдем теперь второе критическое поле, при котором почти весь образец находится в нормальном состоянии, то есть параметр порядка Ψ - мал. Из первого уравнения Гинзбурга-Ландау имеем

$$\xi^2\left(i\nabla + \frac{2\pi}{\Phi_0}\mathbf{A}\right)^2\psi = a\psi, a = 1 - |\psi|^2$$

В сильном поле сверхпроводящая фаза слаба, и в уравнении (89) нелинейность проявляется только в том смысле, что собственное значение линейного уравнения

$$a < 1$$

Подставим в уравнение (89) потенциал $\mathbf{A} = (0, Bx, 0)$:

$$-\xi^2 \frac{\partial^2 \psi}{\partial x^2} + \xi^2/\hbar^2 \left(i\hbar\nabla + \frac{2e}{c} Bx \right)^2 \psi - \xi^2 \frac{\partial^2 \psi}{\partial z^2} = a\psi$$

Похожее уравнение решалось в разделе о магнетизме электронного газа. Если установить соответствие

$$m' = \frac{\hbar^2}{2\xi^2}, e' = 2e$$

то получим уравнение движения электрона в магнитном поле

$$-\frac{\hbar^2}{2m'} \frac{\partial^2 \psi}{\partial x^2} + \frac{1}{2m'} \left(-i\hbar\nabla - \frac{e'}{c} Bx \right)^2 \psi - \frac{\hbar^2}{2m'} \frac{\partial^2 \psi}{\partial z^2} = a\psi$$

Минимальное собственное значение уравнения (91) есть$a = \frac{\hbar e' B}{2m'c} = \frac{2eB\xi^2}{\hbar c}$. Нас интересует решение этого уравнения, когда$a < 1$. Итак, решение уравнения (90) cymecrisyer($npua <$ 1), если

$$\frac{2eB\xi^2}{\hbar c} < 1$$

Тогда верхнее критическое поле опрелелится критерием

$$H_{c2} = \frac{\hbar c}{2e\xi^2}$$

Это условие имеет простой физический смысл. Во внешнем поле $H \sim H_{c2}$ поле почти полностью проникает в образец. Это означает, что расстояние между вихрями становится поря,ха толщины сердцевины вихря.и поле внутри сверхпроводника $h \sim .H_{c2}$. Слеловательно о дин вихрь несет магнитны й поток по порядку величины равный$\xi^2 H_{c2}$. С другой стороны, этот поток равенΦ_0, что и отражает критерий (92)

Заметим, что при приближении H_0 к H_{c2} параметр порядка $|\Psi|^2 = 1 - H_0/H_c$ Строгий анализ, основанный на уравнениях Гинзбурга-ландау, показывает, что в сверхпроводниках второго рода, для которых $x > 1/\sqrt{2}$, в интервале $H_{c1} < H_0 < H_{c2}$ образуются вихри. Эти вихри отталкивалтся друг от друга и образуют двумерную решетку, составленную из равносторонних треугольников. При наличии гралиента внешнего магнитного поля вихри могут двигаться, но примеси их останавливают (пиннинг). Это явление аналогично движению и пиннингу дислокаций в реальных кристаллах.

4.2.7 Critical field of superconductors 2

Critical Field and Magnetization of Rod-Shaped Samples

Figure 4.9 shows again the Meissner-Ochsenfeld effect for a rod-shaped superconductor. If the length l of the rod is much larger than the diameter, the magnetic field is slightly distorted only at the ends. Along the rod practically we have the same field B_2 as in a large distance from the rod. For simple shapes of the sample (ellipsoids with principal axis parallel to the field), we can

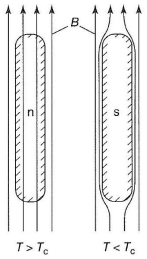


Figure 4.9 Magnetic field expulsion for a rod-shaped sample. The sample is cooled down in the field *B*.

express the influence of the sample geometry by a number, the demagnetization coefficient N_{M}. For a long rod in a magnetic field parallel to its axis, the demagnetization coefficient is $N_{\mathrm{M}} = 0$. In this case, the magnetic field at the surface must not be corrected, since it is identical with the external field B_{a} at a large distance from the sample. This illustrates the particular simplicity of this sample geometry.

Because of its significance, we want to also present the field expulsion in the Meissner phase in a different way. Because of the shielding currents, which completely compensate the external field in the interior of the rod-shaped sample, the rod carries a magnetic moment m. Formally, we can speak of a magnetization M by writing $M = m/V$, where V is the sample volume. This magnetization corresponds to that of an ideal diamagnet with the susceptibility [17)] $\chi = -1$.

In Figure 4.10 we show this magnetization M as a function of the external field B_{a} for a long rod with its axis oriented parallel to the field. Following the standard custom, the negative magnetization is plotted versus the external magnetic field. The magnetization increases proportional to the external field. The superconductivity breaks down only if the critical field is exceeded.

In Figure 4.11 the magnetic field B_i observed in the interior of the sample, say, within a narrow channel parallel to the axis, is plotted versus the external field B Because of the shielding current, the inner field B_{i} remains exactly zero until the critical field B_{c} is reached. [18)] For all external fields $B_{\mathrm{a}} > B_{\mathrm{c}}$ we have $B_{\mathrm{i}} = B_{\mathrm{a}}$, since the sample is normal conducting in this case.

The thin surface layer, into which the magnetic field penetrates, can be neglected for this integral look at the sample.

Here, we explicitly utilize the fact that the external field is compensated by the macroscopic currents flowing at the surface. To describe the magnetic fields in the interior of a substance, we must know the mechanism causing the magnetic behavior. How the magnetization is accomplished remains for the external magnetic field

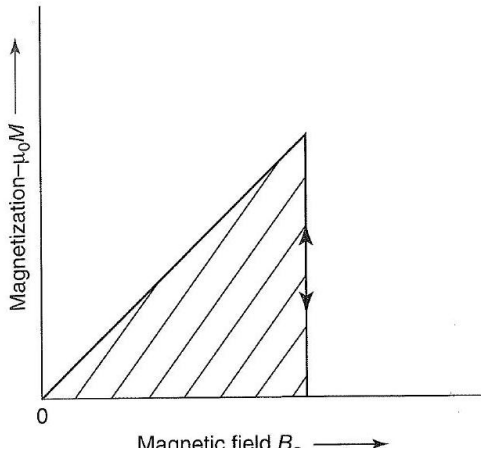
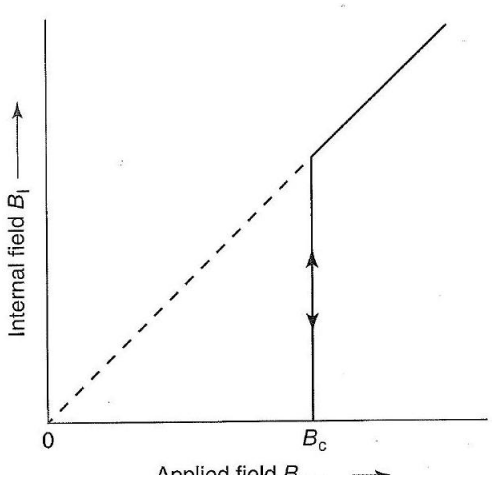


Figure 4.10 Magnetization of a rod-shaped sample ($N_M = 0$) in a magnetic field parallel to the axis, During a reversible transition, the same curve is followed for increasing and decreasing field B.



Applied field B_a $\longrightarrow$ Figure 4.11 Magnetic field in the interior of a rod-shaped sample ($N_M = 0$) in a mag- netic field parallel to the axis. During a reversible transition, the same curve is followed for increasing and decreasing field B.

Figures 4.10 and 4.11 present the same information. Both plots are used frequently, and they are adjusted to different experiments: measurement of M by means of the induction or of B_i, say, by using a Hall probe. [19] The difference between type-I and type-II superconductors is clearly seen from the variation of M or of B_i as a function of B_a (see Section 4.7.1).

Modern Hall probes allow measurements of the magnetic field with high sensitivity. One observes the electrical voltage generated perpendicular to the electric current and to the magnetic fied because of the Lorentz force. The Hall voltage is proportional to the applied magnetic field.

We note that the measurement of the magnetization represents a very simple method for determining the transition temperature T_c. One places the sample within an induction coil and measures the self-inductance as a function of the temperature using a small a.c. magnetic field. The self-inductance drops abruptly if superconductivity sets in. Compared to a measurement of the electrical resistance by means of a current-voltage curve (see Section 1.1), this magnetic measurement of the transition temperature has the advantage that the shielding currents must flow along the total sample surface in order to provide the shielding. Frequently, inhomogeneous samples, where the current-voltage measurement can indicate superconductivity because of a single continuous current path, do not show perfect shielding, in this way signaling the inhomogeneity. [20]

Now we apply the rules of thermodynamics to the Meissner state. We start from the Eq. (4.9):

$$\mathrm{d}G = -S\ \mathrm{d}T + V\ \mathrm{d}p - m\ \mathrm{d}B$$

First, we consider the superconducting phase in the absence of a magnetic field. Then the term mB vanishes. Furthermore, we keep the superconductor at con stant pressure and only vary the temperature. For $T < T$ the Gibbs function G_s of the superconductor must be smaller than G_n, the Gibbs function of the normal conductor. At $T = T_c$, we have $G_s = G_n$

We can determine the difference $G_n - G_s$, which is a measure of the stability of the superconducting state, as a function of the temperature. We use the fact that the superconducting phase becomes unstable in the presence of a sufficiently strong external magnetic field. The reason for this is an increase in G_s with increasing field B, resulting in the fact that above a critical field G_s will be larger than G_n and, hence, will become unstable. Practically, the Gibbs function G_n of the normal conducting phase is independent of the magnetic field, since at least in most cases in the normal conductor the generated magnetic moments are very small.

For obtaining $G_\mathrm{n} - G_\mathrm{s}$ as a function of T, we must determine the critical field B_c at different temperatures. Then the term $\int_0^{B_c} m \, \mathrm{d}B$ yields $G_\mathrm{n} - G_\mathrm{s}$ at the corresponding temperature. We have

$$G_\mathrm{s}(B) - G_\mathrm{s}(0) = -\int_0^B m \, \mathrm{d}B$$
$$G_\mathrm{n}(B) - G_\mathrm{n}(0) = 0$$
$$G_\mathrm{n}\left(B_\mathrm{c}\right) - G_\mathrm{s}\left(B_\mathrm{c}\right) = 0$$

The first equation is found by integrating Eq. (4.9) at constant temperature and constant pressure. At B_c the Gibbs functions G_s and G_n must be just equal. From these three equations, one finds

$$G_\mathrm{n}(T) - G_\mathrm{s}(T) = -\int_0^{B_\mathrm{c}(T)} m \, \mathrm{d}B$$

Since in equilibrium the magnetic moment of the superconductor must always be oriented antiparallel to B, we have $G_\mathrm{n}(T) > G_\mathrm{s}(T)$ for all $T < T_\mathrm{c}$.

For a more quantitative statement about the difference between the Gibbs funcions of the superconducting and normal conducting phases, we must know the agnetic moment m as a function of B. Now we restrict ourselves to the rodhaped sample geometry, and we assume a spatially constant external magnetic field. In this case, the local magnetic moment m and the magnetization M are simply connected with each other:

$$m = MV$$

Here, V is the sample volume, taken to be independent of the magnetic field, the pressure, and the temperature. With these conditions, we have

$$G_\mathrm{n} - G_\mathrm{s} = -V \int_0^{B_\mathrm{c}} M \, \mathrm{d}B$$

For additional information, we must know the magnetization M as a function of B. For a "thick" rod of a type-I superconductor, [21)] we have $\chi = -1$. Then the magnetization is in good approximation

$$M = \chi \frac{B}{\mu_0} = -\frac{B}{\mu_0}$$

where $\mu_0 = 4\pi \times 10^{-7}$ V s/A m. This yields the following simple expression for $G_\mathrm{n} - G_\mathrm{s}$

$$G_\mathrm{n} - G_\mathrm{s} = \frac{V}{\mu_0} \int_0^{B_\mathrm{c}} B \, \mathrm{d}B = V \frac{B_\mathrm{c}^2}{2\mu_0} = V \frac{B_\mathrm{cth}^2}{2\mu_0}$$

Now we can calculate quantitatively the difference $G_n - G$ if we have determined the critical field B_c as a function of T for our simple geometry.

For a "thick" superconductor with fully developed shielding, the critical field B is identical to the thermodynamic field B_cth . We can see this from Eq. (4.21), if we integrate the latter over the sample volume. However, for a "thin" superconductor, with dimensions comparable to the London penetration depth, B_c is larger than B_cth (see Section 4.6.3).

The area under the magnetization curve of the "thick," rod-shaped type-I superconductor, multiplied by the sample volume V, yields the difference of the thermodynamic potentials, $G_{\mathrm{n}} - G_{\mathrm{s}}$, in the field $B = 0$. However, we also emphasize that in

In principle, we can also use Eq. (4.48) for a type-II superconductor. Then we must integrate up to the upper critical field B_{c2}, and the particular dependence $M(b)$ of these superconductors n us be

the case of a more complicated dependence of the magnetization on the external field, as we will see for type-II superconductors, the area under the magnetization curve $M(B)$ always yields the difference of the Gibbs functions, $G_{\mathrm{n}} - G_{\mathrm{s}}$. The only assumption is that the magnetization is reversible, that is, it is established only by means of equilibrium states. Reversibility exists if the same magnetization curve is obtained for increasing and for decreasing external fields. In the case of the "hard superconductors," which we will discuss in Section 5.3.2, this reversibility is absent.

In Figure 4.12 the critical field B_{c} is plotted versus the temperature for different type-I superconductors. For all temperatures $T < T_{\mathrm{c}}$, the experimental data are well approximated by the empirical expression:

$$B_{\mathrm{c}}(T) = B_{\mathrm{c}}(0)\left[1 - (T/T_{\mathrm{c}})^2\right]$$

Near T_{c}, this dependence approaches the linear dependence on temperature, as described by the Ginzburg-Landau theory.

3. Critical field by AGD

The so-called critical magnetic field H_0 is an important thermodynamic quantity in the theory of superconductivity. At a given temperature

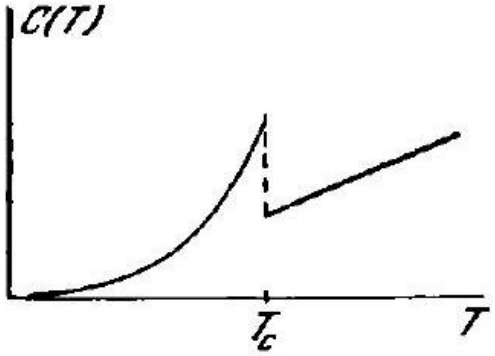


Fig. 98 $T < T_c$, a metal in a magnetic field may find itsclf both in the superconducting and in the normal state.

If a superconductor is situated in a magnetic field, the surface currents screening the field produce a magnetic moment, which interacts with the external field. The additional energy arising from this interaction is - (H.M)/2 (per unit volume). Let us consider a superconducting cylinder located in a field parallel to the cylinder axis. Having found the surface current from the condition that the magnetic field be equal to zero in the body of the superconductor, and having determined the magnetic moment produced by these currents, we discover that the extra magnetic energy is $H^2/8\pi$, i.e. the free energy of the superconductor in the magnetic field is $\boldsymbol{F_{8H}} = \boldsymbol{F_B} + (\boldsymbol{H}^2/8\pi)$. Thus a transition from the superconducting to the normal phase occurs when the magnetic field is increased at a given temperature; this transition is a first order transition. The critical ficld is

$$\frac{H_c^2}{8\pi} = F_n - F_s.$$

We shall again confine ourselves to limiting cases. At low temperatures ($T \ll T_c$), we obtain from (36.3) and (36.7), neglecting exponentially small terms:

$$H_c(0) = \sqrt{\frac{2mp_0}{\pi}}\Delta_0 = T_c\frac{\pi}{\gamma}\left|\frac{\sqrt{2mp_0}}{\pi}\right. \tag{36.10}$$

and

$$H_c(T) = H_c(0)\left(1 - \frac{\gamma^2}{3}\frac{T^2}{T_c^2}\right) \tag{36.11}$$

On using (36.9) and expressing $H_c(T)$ close to the transition point in terms of $H_c(0)$ with the aid of (36.10), the temperature dependence $H_c(T)$ in the region close to T_c is found to be

$$H_c(T) = H_c(0)\gamma/\left.\frac{\overline{8}\bar{\zeta}(3)}{7\bar{\zeta}\left(1-\frac{T}{T_c}\right)}\right) \simeq 1\cdot 73H_c(0)\left(1-\frac{T}{T_c}\right). \tag{36.12}$$

Notice that the experimental data usually correspond to the function

$$H_c(T) = H_c(0)\left(1 - \frac{T^2}{T_c^2}\right) \tag{36.13}$$

The theoretical formulac (36.11) and (36.12) are in fairly close agreement with the experimental relationship (36.13) in both the limiting cases (see [58], [63]).

4.2.8 Critical Magnetic Field of Thin Films in a Field Parallel to the Surface

The behavior of thin films depends sensitively on the penetration depth, if the film thickness d becomes comparable to λ_{L}. We discussed this already in Section 1.4 (Figures 1.14 and 1.15). As a result, we found that the magnetic field varies within the plate as given by Eq. (1.22):

$$B_z(x) = B_{\mathrm{a}}\frac{\cosh\left(x/\lambda_{\mathrm{L}}\right)}{\cosh\left(d/2\lambda_{\mathrm{L}}\right)}$$

The critical field in a thin film represents a highly important subject. As the critical field, we understand the field that must be applied to completely destroy the superconductivity, that is, to make G_{s} equal to G_{n}. With decreasing film thickness, this critical field B_{c} becomes larger and larger. For a thickness $d \ll \lambda_{\mathrm{L}}$ it can be larger by more than a factor 10 than the thermodynamic field B_{cth} we observe, when the shielding layer is fully developed.

This surprising result can be understood in a simple way. In Section 4.1 we saw that the free enthalpy of the superconducting state increases with the external field B_{a}. Because of Eq. (4.45) we have $G_{\mathrm{s}}(B) - G_{\mathrm{s}}(0) = -\int_0^B m\,\mathrm{d}B$, where m denotes the magnetic moment of the sample, which is generated by the shielding toward the interior of the superconductor is fixed current density j_{s} and its decay dently of the macroscopic sample dimensions. For samples that are smaller than or comparable to the penetration depth in at least one dimension, the connection between the external field and the shielding current becomes dependent on the sample geometry. With decreasing thickness, say, of our film, for constant B_{a}, the shielding currents become smaller and smaller. This means that for the thin superconductor, the free enthalpy increases more slowly with increasing B_{a} than for the "thick" superconductor. Therefore, higher fields B_{a} are needed to make G_{s} equal to G_n.

Qualitatively, we can see this very clearly from Figure 1.16. The decrease in the magnetic field in the interior of the layer is a measure of the diamagnetic sample behavior. With decreasing layer thickness, the decrease in the field in the interior and, hence, the diamagnetism become smaller and smaller. In order to make G_s equal to G_n by means of an external magnetic field, with decreasing layer thickness we must apply larger and larger external magnetic fields.

We want to estimate this in the limit $d \ll \lambda_L$. From the general relation $B(x) = B_2 + \mu_0 M(x)$ and Eq. (1.22) or (4.60), within the adopted approximation, we find $M(x) \approx B_a (4x^2 - d^2) / (8\mu_o \lambda_L^2)$. Following a simple calculation, for the magnetization averaged over the plate one finds

$$M \approx -B_a d^2 / \left(12\mu_0 \lambda_L^2\right)$$

which differs from expression (4.49) for the "thick" superconductor by a factor $d^2/(12\lambda_L^2)$. By inserting this magnetization into Eq. (4.48), we obtain a critical magnetic field that is larger than the critical field B_{cth} of the "thick" superconductor by a factor $12^{1/2}\lambda_r/d$.

We summarize the important result of this section: For superconductors that are comparable with the penetration depth in at least one dimension, the external field B_a needed for canceling the superconductivity is larger than the thermodynamic critical field. This result will be highly important in the following.

4.2.9 The Intermediate State

Following the results of the last section, the following question comes up: Why is it possible that the superconducting state becomes unstable because of an overcritical magnetic field? From the results of Section 4.6.3 we could expect that, upon reaching the critical field, the superconductor splits up into very fine domains parallel to the magnetic field and alternately consisting of superconducting and normal conducting phase. Then the superconducting domains could be thin compared to the penetration depth and could sustain a larger magnetic field without becoming unstable.

From experience we know that this is not the case. Instead, the superconducting state of a rod-shaped sample ($N_M = 0$) becomes unstable when the critical field is reached. From this, we must conclude that a separation into many fine domains is energetically unfavorable. This can be understood from a simple idea. Each interface between a normal conducting domain and a superconducting domain carries an additional energy, the wall energy. This energy does not allow the splitting of a type-I superconductor into many fine domains. The energy needed for this would make this state energetically less favorable than the normal conducting state.

This wall energy is taken into account by the gradient term in the Ginzburg-Landau theory (see Eq. (4.26)). It controls the magnetic flux structure of the so-called intermediate state. The intermediate state refers to situation in which a homogeneous type-I superconductor is neither completely superconducting nor completely normal conducting. Such configurations can be realized very simply by means of the geometric shape of the sample.

We consider a superconducting sphere in a homogeneous external field B_a (Figure 4.14). The shielding currents flowing within a thin surface layer keep the interior of the sphere free of magnetic field. As we can see from Figure 4.14, at the surface of the sphere near the equator, this expulsion of the magnetic field results in an enhancement of the field. The actual behavior of the field is given by the superposition of the homogeneous external field B_a and the field generated by the shielding currents.

Apparently the field enhancement results from the sample geometry. For simple geometric shapes it can be taken care of by the demagnetization coefficient (see Section 4.6.1). One can show that homogeneous samples with the shape of an ellipsoid display a homogeneous magnetization in a homogeneous external magnetic field. If one principal axis of the ellipsoid is

oriented parallel to the external field, then the magnetization is also parallel to this field. This magnetization changes the magnetic field experienced by the sample. The maximum value of this field is referred to as the effective magnetic field B_{eff} .

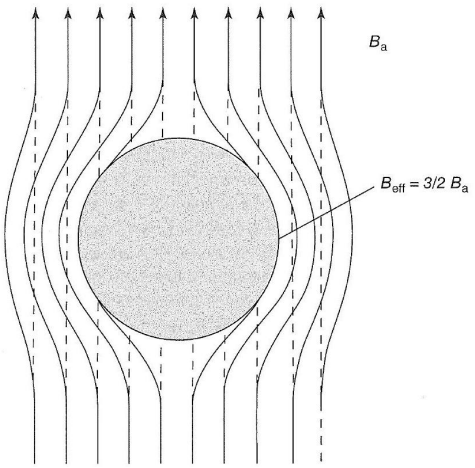


Figure 4.14 Expulsion of magnetic field (solid field lines) from a superconducting sphere. In the absence of the sphere, the field is homogeneous (dashed field lines).

It is given by

$$B_{\text{eff}} = B_{\text{a}} - N_{\text{M}}\mu_0 M$$

For a superconductor with a complete Meissner effect, the magnetization M is related to the effective field B_{eff}

$$M = -\frac{B_{\text{eff}}}{\mu_0}$$

Hence, we have

$$B_{\text{eff}} = B_{\text{a}} + N_{\text{M}} B_{\text{eff}}$$

$$B_{\text{eff}} = \frac{1}{1 - N_{\text{M}}} B_{\text{a}}$$

The effective magnetic field is just the field at the equator at the surface. If the demagnetization coefficient N_{M} is known, the field at the equator can be calculated. For example, for a sphere we have $N_{\text{M}} = 1/3$. Hence, for the ideal diamag netic sphere, we obtain

$$B_{\text{eff}} = \frac{3}{2} B_{\text{a}}$$

Because of the field expulsion, for a demagnetization coefficient $N_{\text{M}} > 0$ it is possible to choose a value of the external field B_{a} at which the superconductor is neither completely superconducting nor completely normal conducting. We look at the sphere somewhat closer. If we increase the external field B_{a}, at the value $B_{\text{a}} = 2/3\ B_{\text{eff}}$ the critical field B_{c} is reached at the equator. If B_{a} is increased further, at the equator the superconductivity must be destroyed. However, the sphere cannot become completely normal conducting, since in this case the field in the interio would be equal to the external field and, hence, would be smaller than B_c. The superconductor enters the intermediate state, that is, it splits up into superconducting and normal conducting domains.

Before we discuss this domain structure in more detail, we want to describe the behavior in the intermediate state phenomenologically. At $B_{\text{a}} = B_{\text{c}}$ the sample must be completely

superconducting. It turns out that, in the total regime $2/3B_c < B_a < B_c$, at the equator exactly B_c is observed. With increasing B_a, the normal conducting fraction in the interior of the sphere increases exactly in such a way that the remaining field expulsion yields the value B_c at the equator.

We could say also that in the intermediate state the demagnetization coefficien N_M becomes dependent on B_a. If we measure the magnetic flux by means of an induction coil wound around the equator, then this flux Φ increases monotonically with increasing B_2. This behavior is shown in Figure 4.15.

The magnetic flux structure of a sphere in the intermediate state has been investigated in detail [29, 30]. There exist normal conducting and superconducting domains next to each other. Hence, there are interfaces separating the normal conducting from the superconducting phase. These interfaces are stabilized because

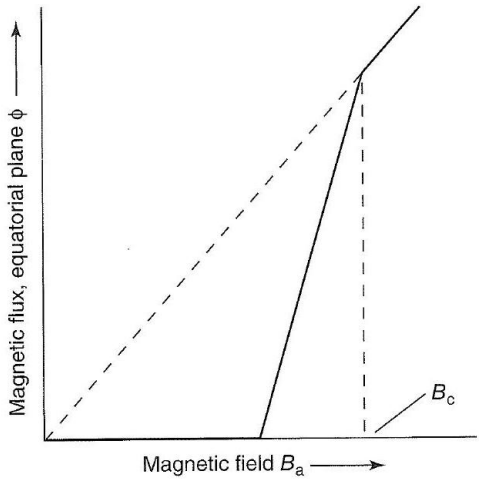


Figure 4.15 Magnetic flux Φ passing through the equatorial plane of a sphere plotted versus the external field B

of the appearance of the critical field parallel to the external magnetic field. For each intermediate state structure, the phase boundaries must be oriented parallel to the magnetic field. This statement is always valid. In the case of more complicated intermediate state structures, as can appear in superconductors in an external magnetic field and for a simultaneous flow of an electric transport current (see Section 5.2), this can lead to surprising effects.

Since the development of the phase boundaries requires an amount of wall energy, the splitting into domains cannot take place on an arbitrarily fine scale. The sample must adopt a state in which larger superconducting and normal conducting domains exist next to each other. This configuration is determined by the fact that the free enthalpy of the system reaches a minimum. This requirement allows us to determine the wall energy from measurements of the intermediate state structure.

We cannot discuss such calculations in detail. We want to mention only a few particularly simple results. In the case of a sphere, the transition into the intermediate state should happen at the field $B_a = 2/3B_c$. However, this transition is accompanied by the generation of interfaces. Because of the positive wall energy, a finite amount of energy is needed for this. This energy must be supplied by the magnetic field. Therefore, the transition into the intermediate state does not occur exactly at $B_2 = 2/3B_c$, but at a slightly higher field instead. The field is expelled beyond the critical field until the stored field energy suffices for generating the necessary interfaces. This excess field was observed for wires in a perpendicular magnetic field and was interpreted in the way we have discussed [29].

The magnetic flux structures in the intermediate state have been investigated in detail by means of different experimental methods. Small bismuth wires were used to probe the

superconducting and normal conducting domains of a sphere fabricated from tin [30]. For this purpose the sphere was cut into two halves along a plane through the equator, and subsequently the two halves were fixed togethe in such a way that a small opening of only a few tenths of a millimeter remained. The bismuth wires acting as magnetic field probes could be inserted into this opening. Then their electrical resistance, which for bismuth depends sensitively on the magnetic field, was measured. The normal conducting domains are detected by means of the magnetic field that they carry. On the other hand, the superconducting domains remain free of field. The small opening between the two hemispheres distorts these domains only very little, since the domain boundaries are oriented parallel to the magnetic field. With this technique the configuration of the intermediate state could be imaged [31]

Much more direct methods have since been utilized, which provide immediately a complete image of the flux structure. Among others, these are the following:22)

the decoration of superconducting domains using a diamagnetic powder; 2) the imaging of normal conducting domains by means of the Faraday effect.

In the first method, a fine powder of a superconducting material is sprinkled onto the sample residing in the intermediate state. Mostly one uses niobium pow der [32], which remains fully superconducting for the magnetic fields needed to establish the intermediate state, in the case of many superconductors with a value superconducting niobium grains are ideal diamagnets. They are expelled from the regions with a high magnetic field, and they accumulate on the locations at the surface where the superconducting domains are. Figure 4.16 shows such an image of the intermediate state of an indium plate [32]. Another example is presented in Figure 5.5 for the case of the intermediate state in a wire carrying an electric transport current [33].

The second method has been described already in Section 12 Compared to the powder decoration, it has the advantage that it can also record movements, that is, temporal changes, of the intermediate state structure. Highly impressive motion pictures of the intermediate state in motion have been produced. In Figure 4.17 we present an image of the intermediate state obtained in this way.

4.2.10 Critical Magnetic Fields for Type-II SC

Fast Estimations of H_{c1}

У сверхпроводников II рода разрушение сверхпроводимости магнитным полем происходит в два этапа. По сложившейся традиции будем считать, что образец представляет собой длинный, вытянутый вдоль поля цилиндр. Тогда из равенства тангенциальных составляющих внешней $\mathcal{H}_0$ и внутренней $\mathcal{H}$ напряженностей следует, что внешнее поле задает внутри сверхпроводника величину именно напряженности магнитного поля $\mathcal{H}$.

Если внешнее магнитное поле меньше нижнего критического поля $\mathcal{H}_{c1}$, то сверхпроводник ведёт себя так же, как и сверхпроводник I рода, обнаруживая идеальный диамагнетизм (полный эффект Мейсснера, $\mathcal{M} = -\mathcal{H}/4\pi$). Выше $\mathcal{H}_{c1}$ становится выгодным проникновение с поверхности вглубь образца вихрей Абрикосова, которые образуют в материале устойчивую треугольную решётку и уменьшают намагниченность. При увеличении внешнего поля вихревая решётка становится всё плотней, и при верхнем критическом поле $\mathcal{H}_{c2}$ «коры» вихрей сливаются. Образец полностью переходит в нормальное состояние. Оценим верхнее и нижнее критические поля.

Первое (нижнее) критическое поле $\mathcal{H}_{c1}$ означает, что величины внешнего поля достаточно, чтобы обеспечить поле в центре вихря (13.27), Или, что то же самое, магнитный поток через сечение вихря $\sim \lambda^2$ достигает кванта потока Φ_0. Это дает нам оценку $\mathcal{H}_{c1} \approx \Phi_0 \ln(\lambda/\xi)/2\pi\lambda^2$. Проверим её точным расчётом. Вычислим свободную энергию единицы длины вихря.

Вихрь возникает в образце с достаточно большой ($\gg \xi, \lambda$) длинной вдоль поля. Как отмечалось выше, будем считать, что образец представляет собой длинный, вытянутый вдоль поля цилиндр. Из граничных условий следует, что при этом в образце тангенциальное поле $\mathcal{H}$ совпадает с внешним $\mathcal{H}_0$. Поскольку задано внешнее поле $\mathcal{H}_0 = \mathcal{H}$, то здесь нам нужно перейти от Ω-потенциала, заданного, как отмечалось выше, в переменных T, V, μ, B к соответствующему потенциалу Гиббса G в переменных $T, V, \mu, \mathcal{H}$. Переход к потенциалу Гиббса осуществляется преобразованием Лежандра, совершенно аналогично тому, как переходят по паре P, V от $F(T, V)$ к $\Phi(T, P)$. Приращение плотности энергии системы поле + вещество равно $d\Omega = \mathcal{H}d\mathcal{B}/4\pi + \ldots$ (см. приложение 26), следовательно, для потенциала Гиббса G получаем:

$$G = \Omega - \frac{\mathcal{H}\mathcal{B}}{4\pi}.$$

Сверхпроводники II рода $\lambda \gg \xi$ представляют собой типично лондоновский случай, когда поправками в (13.2) за счёт $\nabla\psi \sim \xi/\lambda$ можно пренебречь. Энергия единицы длины вихря складывается из энергии поля и кинетической энергии сверхпроводящих электронов:

$$G_1 = \int \left[\frac{\mathcal{B}^2}{8\pi} + \frac{\lambda^2}{8\pi}(\nabla \times \mathcal{B})^2 - \frac{\mathcal{H}\mathcal{B}}{4\pi}\right] dV.$$

Воспользовавшись формулой

$$(\nabla \times \mathcal{B})^2 = \mathcal{B} \cdot \nabla \times \nabla \times \mathcal{B} + \nabla(\mathcal{B} \times \nabla \times \mathcal{B}),$$

получаем

$$G_1 = \int \left[\frac{\mathcal{B}\left(\mathcal{B} + \lambda^2 \nabla \times \nabla \times \mathcal{B}\right)}{8\pi} - \frac{\mathcal{H}\mathcal{B}}{4\pi}\right] dV - \frac{\lambda^2}{8\pi} \int \mathcal{B}\nabla \times \mathcal{B} d\mathbf{S}$$

Поверхностный интеграл берётся по ∞ удалённому цилиндру и горизонтальным плоскостям $z = 0$ и $z = 1$. Поскольку $\mathcal{B} \perp$ этим плоскостям, а $\nabla \times \mathcal{B}$ лежит на них, поверхностный интеграл в (13.31) обращается в ноль. Далее всё просто: используя (13.25), получаем

$$G_1 = \frac{\Phi_0 \mathcal{B}(0)}{8\pi} - \frac{\Phi_0 \mathcal{H}}{4\pi}$$

где $\mathcal{B}(0)$ поле в центре вихря (13.27). Таким образом, возникновение абрикосовского вихря в сверхпроводнике становится энергетически выгодным, когда внешнее поле достигает половины поля в центре вихря:

$$\mathcal{H}_{c1} = \frac{\Phi_0}{4\pi\lambda^2} \ln \frac{\lambda}{\xi}$$

Fast Estimations of H_{c2}

Второе (верхнее) критическое поле $\mathcal{H}_{c2}$ соответствует ситуации, когда вихрей так много, что их коры соприкасаются и весь образец становится нормальным. Это значит,

что поток одного вихря Φ_0 пронизывает площадь $\sim \xi^2$, что соответствует внешнему полю $\mathcal{H}_{c2} \approx \Phi_0/\xi^2$. Подтвердим эту оценку точным расчётом. Вблизи поля $\mathcal{H}_{c2}$ могут существовать только малые зародыши сверхпроводящей фазы. Это значит, что параметр порядка мал $|\psi| \ll 1$ и в уравнении Гинзбурга-Ландау (13.9) можно выбросить нелинейный член:

$$\frac{1}{4m}\left(i\hbar\nabla + \frac{2e}{c}\mathcal{A}\right)^2 \Psi = -\alpha\Psi.$$

При этом в силу $\xi \ll \lambda$ поле $\boldsymbol{\mathcal{A}}(\mathbf{r})$ в зародыше можно считать однородным. Видно, что уравнение (13.34) полностью идентично уравнению

Шредингера для частицы с массой $2m$, зарядом $2e$ и энергией $-\alpha$ в однородном магнитном поле $\mathcal{H} = \nabla \times \mathcal{A}$. Как известно, его собственными значениями являются уровни Ландау, так что спектр ненулевых решений (13.34) начинается с $-\alpha = \hbar\omega/2$, где циклотронная частота $\omega = 2e\mathcal{H}/2m$. С учетом (13.15) это соответствует верхнему критическому полю:

$$\mathcal{H}_{c2} = \frac{\Phi_0}{2\pi\xi^2}$$

Relation of critical field

(add formulas and comment where they come from)

Сравнивая (13.21), (13.33) и (13.35) мы видим, что с логарифмической точностью термодинамическое критическое поле является средним геометрическим верхнего и нижнего критических полей:

$$\mathcal{H}_c = \sqrt{\mathcal{H}_{c1}\mathcal{H}_{c2}}.$$

Theory

As we have already discussed, below the lower critical magnetic field B_{c1} type-II superconductors exist in the Meissner phase, if geometric effects are ignored. However, above B_{c1} the magnetic field penetrates into the sample in the form of 29) Chinese scientists independently also found the system $\mathrm{Y-Ba-Cu-O}$. Upon being questioned by "Since replacing Ba by Sr resulted in an enhancement of T, it appeared obvious to us also to replace La by Y."

quantized flux lines or vortices. Above the upper critical magnetic field B_{c2}, the superconductivity vanishes. In the following, we will look in more detail at these properties from a thermodynamic point of view. [30]

The discussion of the boundary layer between a normal conducting domain and a superconducting domain in Section 4.6.5 has shown that in the case $\lambda_{\mathrm{L}} > \xi_{\mathrm{GL}}$ the formation of the boundary layer is accompanied by an energy gain. In this case the following condition must be (approximately) satisfied:

$$\xi_{\mathrm{GL}} F \frac{1}{2\mu_0} B_{\mathrm{cth}}^2 - \lambda_{\mathrm{L}} F \frac{1}{2\mu_0} B^2 < 0$$

Hence,

$$\xi_{\mathrm{GL}} B_{\mathrm{cth}}^2 < \lambda_{\mathrm{L}} B^2$$

$$\frac{B_{\mathrm{cth}}^2}{B^2} < \frac{\lambda_{\mathrm{L}}}{\xi_{\mathrm{GL}}}$$

Therefore, we expect that, for superconductors with $\lambda_{\mathrm{L}} > \xi_{\mathrm{GL}}$, the magnetic field can penetrate into the superconductor already at fields B that are smaller than B_{cth} . In this case, spatial variations of B and of the Cooper pair density n_{s} are expected, similar to the situation at a boundary layer. From the relations 4.41 and 4.42 in Section 4.5, we see that the condition $\xi_{\mathrm{GL}} < \lambda_{\mathrm{L}}$ can always be achieved by making the electron mean free path l^* sufficiently small. According to Eq. (4.41), λ_{L} increases weakly with decreasing l^*. On the other hand, according to Eq. (4.42), ξ_{GL} decreases with $(l^*)^{1/2}$. The mean free path can be reduced easily by alloying the superconductor with a small amount of impurities. The electrons are scattered at the impurities and, hence, their mean free path is reduced. Indeed, as we will see, alloys are in general type-II superconductors

Already in the 1930s, this particular behavior of superconducting alloys was observed experimentally. De Haas and Voogd reported [50] that in magnetic fields up to about 2 T lead-bismuth alloys still remain superconducting. These are magnetic fields that are larger by more than the factor 20 than the critical field of pure lead. There were attempts to understand such high critical fields in terms of the so-called sponge model proposed by Mendelssohn [51]. According to this model, the high critical fields should be caused by a network of fine precipitates, say, at grain boundaries. If these precipitates were assumed to be small compared to the penetration depth at least in one dimension, then the high critical fields could be understood qualitatively simply because of this geometry (see Section 4.6.3). Today we know that this sponge model may apply to many alloys, but that there exist also homogeneous superconductors, namely the type-II superconductors, which remain superconducting up to very high magnetic fields.

Qualitatively, we can understand in a simple way why a superconductor can tolerate higher magnetic fields, if at least a partial penetration of the field is possible.

A more detailed discussion of the properties of vortices can be found in the monograph [M17].

During the penetration of the field, the expulsion energy, which increases the free enthalpy of the superconducting state in the magnetic field, is reduced. Therefore, higher external fields are needed, in order to make the free enthalpy of the superconducting state equal to that of the normal state. Using similar arguments, we have understood the increase in the effective critical field of thin superconductors, into which the field can also penetrate.

According to Section 4.6.5 we expect that, together with the penetration of the field, also the condensation energy is reduced. However, for $\lambda_{\mathrm{L}} \gg \xi_{\mathrm{GL}}$, the gain due to the reduction of the expulsion energy can be much larger than the loss of condensation energy. Qualitatively, this situation is well accounted for by the Ginzburg-Landau theory. The prediction of the vortex state by Abrikosov [22] was one of the great successes of this theory.

Magnetization Curve and Critical Fields

The difference between type-I and type-II superconductors is clearly seen in the form of the magnetization curve. In Figure 4.23 we schematically show the magnetization curve of a type-II superconductor. Again we consider a rod-shaped sample, the demagnetization coefficient N_M of which is practically zero. At the lower critical field B_{c1}, the gain of expulsion energy due to the field penetration becomes larger than the loss of condensation energy caused by the local variation of the Cooper pair density n_5. As a result, the magnetic field penetrates into the superconductor in the form of quantized flux lines.

As a result of the magnetic field penetration, with increasing field the magnetization of the superconductor decreases monotonically. At a value B_{c2}, the upper

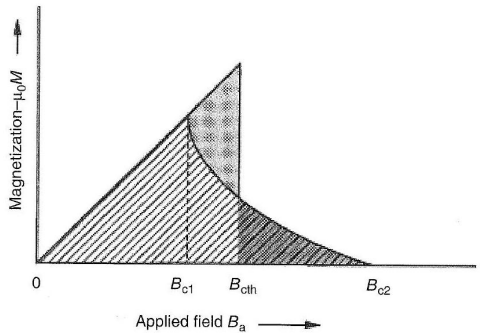


Figure 4.23 Magnetization curve of a type-ll superconductor. Rod-shaped sample with $N_{\mathrm{M}} = 0$. Because of the definition of B_{cth}, the shaded areas must be equal.

critical field, the magnetization reaches zero - the external field has canceled the superconductivity. [31)]

From the general thermodynamic arguments (see Sections 4.1 and 4.6.1), at constant temperature T and constant pressure p, the difference of the free enthalpies is given by

$$G_{\mathrm{n}} - G_{\mathrm{s}} = -\int_0^{B_{\mathrm{c2}}} MV \, \mathrm{d}B$$

If we ignore (as in Section 4.6.1) the very small changes of the volume V as a function of the magnetic field, we can extract V as a constant in front of the integral. The integral is proportional to the area under the magnetization curve

$$\int_0^{B_{\mathrm{c2}}} M \, \mathrm{d}B \propto \mu_0 F_{\mathrm{M}}$$

Here, F_{M} is the area under the magnetization curve. [32)]

If we take a type-I superconductor for comparison, with the same difference of the free enthalpies, its magnetization curve would be given by the vertical line at B_{cth} in Figure 4.23. The areas under both magnetization curves must be equal. Now we see clearly the difference between a type-I superconductor and a typeII superconductor. A type-I superconductor completely expels the field up to the thermodynamic critical field B_{cth} , that is, it stays in the Meissner phase up to this field. On the other hand, at the lower critical field B_{cI} a type-II superconductor enters a state with a penetrated field, the so-called Shubnikov phase. In the Shubnikov phase, with increasing field the magnetization decreases monotonically and completely vanishes only at the upper critical field B_{c2}. The latter field can be much larger than the thermodynamic critical field of the corresponding type-I superconductor

In Figure 4.24 we present this important fact again. Here, the average magnetic field in the interior of the rod-shaped sample is plotted versus the external field. Figure 4.24 exactly corresponds to Figure 4.11 in Section 4.6.1. At B_{c1} the field starts to penetrate into the superconductor However, only at B_{c} is the average starts to penetrate into the superconductor Again the behavior of the corresponding type-I superconductor is indicated by the dashed line. The "corresponding" type-I superconductor denotes again one that has the same difference of the free enthalpies $G_{\mathrm{n}} - G_{\mathrm{s}}$ as the type-II superconductor.

We have already mentioned that a type-I superconductor can turn into a type-II superconductor if the electron mean free path is reduced sufficiently. This result of the Ginzburg-Landau theory has been well confirmed experimentally. By alloying

Under certain conditions, superconductivity can survive within a thin surface layer for fields in the range $B_{\mathrm{c2}} < B_{\mathrm{a}} \leq X, \hat{y}' B_{\mathrm{c3}}$. The value of B_{c3} is about $1.7 B_{\mathrm{c2}}$. Here, we ignore this surface superconductivity.

In Figure 4.23 (as in Figure 4.10) we have plotted the quantity $-\mu_0 M$ instead of the magnetization M. For ideal fiedd expulsion we ha the ordinate, we obtain a straight line with a 45° angle.

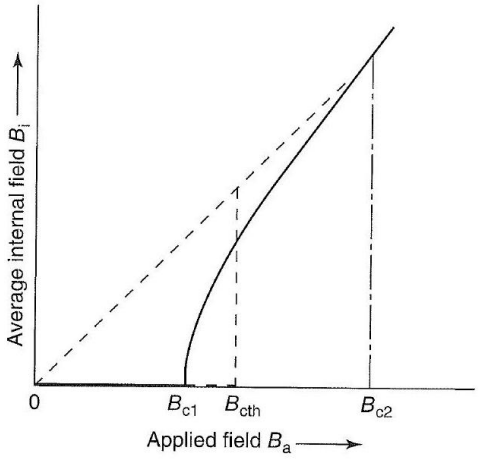


Figure 4.24 Average magnetic field in the interior of a type-ll superconductor plotted versus the external field.

with impurity atoms, which reduce the electron mean free path, all type-I superconductors can be changed into type-II superconductors. One of many examples is shown in Figure 4.25. Here, the ideal magnetization curve of pure lead and the measured curve of a lead-indium alloy with 13.9at% indium are shown [52] Pure lead is a type-I superconductor. The alloy shows typical type-II behavior. The superconductivity of the alloy is completely canceled only at an upper critical field of about 0.24 T(2400G). On the other hand, for the temperature of 4.2 K of this experiment, the thermodynamic field of lead is only about 0.055 T(550G).

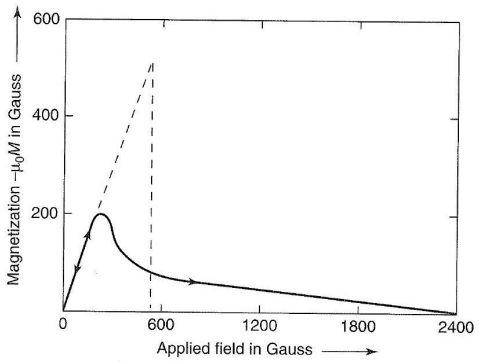


Figure 4.25 Magnetization curve of lead with 13.9 at% of indium (solid line). Rod-shaped sample with a small demagnetization coefficient. The dashed line shows the ideal curve of pure lead ($1\text{G} = 10^{-4}$ T). (From [52],)

Following these qualitative considerations, now we must turn to a few quantitative relations between the fields B_{c1}, B_{c2}, and B_{cth}. All these relations are obtained from the Ginzburg-Landau theory. Here, we must keep in mind that this theory is valid only close to T_c. The crucial parameter is the Ginzburg-Landau parameter κ, that is, the ratio of the penetration depth λ_L and the coherence length ξ_g

Using the Ginzburg - Landau parameter, all the quantitative relations can be formulated in a simple way. For the upper critical field B_{c2}, one obtains

$$B_{c2} = \sqrt{2}\kappa B_{cth}$$

Here, for each type-II superconductor B_{cth} is defined from the difference of the free enthalpies given by Eq. (4.50):

$$G_{\mathrm{n}} - G_{\mathrm{s}} = \frac{1}{2\mu_0} V B_{\mathrm{cth}}^2$$

From the solution of the Ginzburg-Landau equations one also finds [33)] a simple relation between the Ginzburg-Landau coherence length ξ_{GL} and B_{c2}

$$B_{\mathrm{c2}} = \frac{\Phi_0}{2\pi\xi_{\mathrm{GL}}^2}$$

Frequently, this relation is used for determining ξ_{GL} from the measurement of the upper critical field. However, frequently B_{c2} is too large to be measured directly in the limit of low temperatures. In this case, one extrapolates the experimental data from temperatures near T_{c} down to $T \to 0$. For conventional superconductors, the microscopic theory yields the important relation [53]:

$$B_{\mathrm{c2}}(0) \approx 0.7 T_{\mathrm{c}} \left.\frac{\mathrm{d}B_{\mathrm{c2}}}{\mathrm{d}T}\right|_{T_{\mathrm{c}}}$$

Furthermore, we note that Eqs. (4.82) and (4.83) are valid only for isotropic superconductors. If the superconducting properties depend strongly on the crystallographic direction, as in the high-temperature superconductors, Eq. (4.82), for example, must be replaced by $B_{\mathrm{c2}}^a = \Phi_0 / (2\pi\xi_b\xi_c)$. Here, the magnetic field is applied parallel to the crystallographic a direction, and ξ_b and ξ_c are the Ginzburg-Landau coherence lengths in the directions perpendicular to the field, respectively. Analogous expressions are obtained for the field orientation along the other crystal axes. In addition, we note that the results of this section apply to single-band superconductors

Also the lower critical field can be calculated from the Ginzburg-Landau equations. According to Abrikosov [22], in the limit $\kappa \gg 1/\sqrt{2}$ one obtains

$$B_{\mathrm{c1}} = \frac{1}{2\kappa}(\ln\kappa + 0.08) B_{\mathrm{cth}}$$

The value 0.08 in the bracket originates from the interaction between the vortices in the triangular lattice. We see that, with increasing κ, B_{c1} decreases

The details are too complicated to be presented here.

and B_{c2} increases. The lower critical field can also be related to the London penetration depth:

$$B_{\mathrm{c1}} = \frac{\Phi_0}{4\pi\lambda_{\mathrm{L}}^2}(\ln\kappa + 0.08)$$

Equations (4.84) and (4.85) are valid for isotropic superconductors and can be modified for anisotropic superconductors analogously to Eq. (4.82). Equation 4.85 provides a simple possibility for estimating λ_{L} from the measurement of the lower critical field.

Since in alloys the mean free path l^* decreases monotonically with increasing concentration of the impurities, for each system we can indicate a specific "critical" concentration at which the host metal turns into a type-II superconductor This transition is determined by the condition $B_{\mathrm{c2}} \geq B_{\mathrm{cth}}$. According to Eq. (4.81) this condition is equivalent to $\kappa \geq 1/\sqrt{2}$. We see that type-I and type-II superconductors are simply distinguished by the value of κ:

$$\text{type-I superconductors: } \kappa < 1/\sqrt{2}$$

$$\text{type-II superconductors:} \kappa \geq 1/\sqrt{2}$$

This discrimination is strictly valid only near T_c. For $T < T_c$, for κ values only slightly larger than $1/\sqrt{2}$ there exists a transition into a state in which both the Meissner phase and the Shubnikov phase appear next to each other. We will return to this point in Section 4.7.2.

In Table 4.2 some values of κ for In-Bi alloys are indicated. In this system the transition into type-II superconductivity occurs at about 1.5 at% Bi. Similar concentrations were found also for other systems. From this we see that it is very easy to obtain a type-II superconductor. The κ_1 values in the table are obtained from measurements of the upper critical field B_c. However, the κ_2 values are calculated using a formula given by Gor'kov and Goodman. In this formula, the relation between κ and the electron mean free path is summarized as [55]

$$\kappa_2 \approx \kappa_0 + 7.5 \times 10^{-4} \rho \gamma^{1/2}$$

Here, κ_0 is the Ginzburg-Landau parameter of the pure superconductor, that is, for the limiting case $l^* \to, \infty, \gamma$ is the Sommerfeld coefficient of the specific heat of the electron system (in the unit J/cm^3 K^2), and ρ is the resistivity in the normal conducting state (in Ωcm). In this formula, the electron mean free path is expressed in terms of ρ and γ.

Table 4.2 The κ valuesa) of $\ln - Bi$ alloys.

A − %Bi	1.55	1.70	1.80	2.0	2.5	4.0
κ_1 at T_c	0.76	0.88	0.91	1.10	1.25	1.46
κ_2 at T_c	0.74	0.85	0.88	1.15	1.29	1.53

a) $\kappa_1 = \frac{B_c}{\sqrt{2}}$; $\kappa_2 = \kappa_0 + 7.5 \times 10^{-4} \rho \gamma^{1/2}$.
From [54].
Frin

A comparison of lines 2 and 3 in Table 4.2 indicates that the quite differently determined values of κ agree very well. For the application of Eq. (4.87), we must now the values of κ_0. These κ_0 values can be obtained by extrapolating the κ values of alloys to zero concentration of the impurity atoms (Table 4.3)

One might ask if the constant κ_0 for type-I superconductors has a physical meaning. Such a meaning, indeed, results from the GLAG theory. In this case, (4.81) defines a field B which is smaller than B_{cth} . This field yields a definite Eq. (4.81) it for the so-called supercooling experiments.

In a magnetic field the transition from the normal conducting into the superIn a magnetic field the transition from the normal conducting into the supertransitions, supercooling or superheating effects can occur. For example, water can be cooled down carefully to a few degrees below its freezing point withou the formation of ice. For superconductivity this means, for example, that the magric field can be lowered below its critical value without the immediate appearance of the superconducting state. The magnitude of this effect depends on the detailed features of the experiment. For $B < B_{\text{cth}}$ the normal conducting state is thermodynamically unstable. However, the new phase cannot yet form itself. First, nucleation seed for this phase must appear, which subsequently can grow further. During such experiments, the magnetic field cannot fall below the value B_{c2} $(\sqrt{2})\kappa_0 B_{\text{cth}}$ without the appearance of the superconducting state. So if we have a uperconductor with a κ_0 value very close to $1/\sqrt{2}$, no supercooling effects can se observed. However, in superconductors like pure Al or pure In, the magnetic be observed. However, in superconductors cold be well confirmed experimentally.

Finally, we mention another possibility for determining κ. Also the slope of the magnetization curve near B_{c2} is determined by κ, and we have

$$\mu_0(\,\mathrm{d}M/\mathrm{d}B)_{B=B_{c2}} = -\frac{1}{1.16\,(2\kappa^2-1)}$$

So far we have indicated four possibilities for determining κ: Eqs. (4.81), (4.84), (4.87), and (4.88). Near T_c all four methods yield closely similar κ values. However, for temperatures $T \ll T$ the values differ from each other. This is due to the fact hat the Ginzburg-Landau theory is strictly valid only close to T_c. Furthermore, beyond this range of validity, K is temperature-dependent.

Because of their relation to B_{cth}, the two critical fields B_{c1} and B_{c2} are also dependent on the temperature. Neglecting all details, in Figure 4.26 we show schematically the three critical fields of a type-II superconductor. We can clearly see the stability regimes of the different phases. Below B_{c1}, the Meissner phase, that is the phase with complete field expulsion, is stable. Between B_{c1} and B_{c2} we have

Table 4.3 The κ_0 values [a)] of superconducting elements.

Element	Al	In	Pb	Sn	Ta	Tl	Nb	V
κ_0 at T_c	0.03	0.06	0.4	0.1	0.35	0.3	0.8	0.85

a) See also [56]

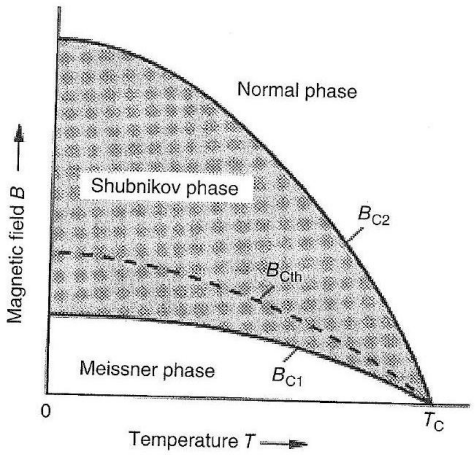


Figure 4.26 Schematics of the phase diagram of a type-Il superconductor.

the mixed state, the Shubnikov phase, as the stable phase; and above B_{c2} there is normal conduction. In Figure 4.27 we show this diagram for an indium-bismuth alloy (In +4 at% Bi) [54].

For some substances, the upper critical field can reach rather large values (see also Chapter 2). In this case one often speaks of "high-field superconductors." For example, the Chevrel phases [57] (ternary molybdenum sulfides, see Section 2.5)

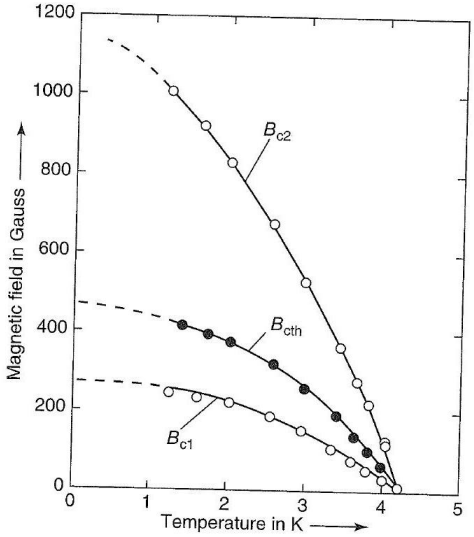


Figure 4.27 The critical fields ($1\text{G} = 10^{-4}$ T) of an indium bismuth alloy, In +4 at% Bi. (From [54].)

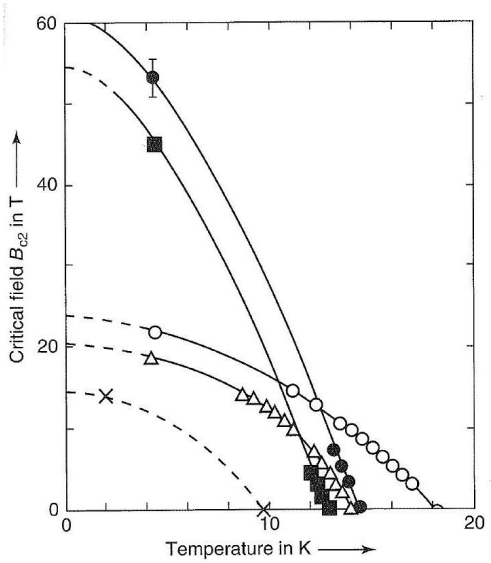
represent materials that can tolerate extreme magnetic fields up to about 60 T without losing their superconductivity [57, 58]. In Figure 4.28 we show B_{c2} plotted versus the temperature for some high-field superconductors. The critical fields of these materials can be a few hundred times larger than those of the type-I superconductors (Figure 4.12).

In the high-temperature superconductors, still larger values of B_{c2} are reached. In this case the layered structure of the materials plays an important role. In order to understand this, we consider a stack of thin superconducting plates of thickness d placed in a magnetic field. The plates should represent the layers of the structure, that is, the CuO_2 planes in the case of the high-temperature superconductors. If the magnetic field is oriented perpendicular to these layers, the supercurrents completely flow within the plates. We do not expect a particular influence of the layered structure. For the upper critical field, one finds the value

$$B_{c2\perp} = \frac{\Phi_0}{2\pi\xi_{\parallel}^2}$$

which essentially is identical to the expression (4.82) for isotropic superconductors. We have only denoted the Ginzburg - Landau coherence length by $\xi_{\parallel}$to indicate that in this case the change of Ψ parallel to the planes is relevant.

On the other hand, if the magnetic field is oriented parallel to the layers, the supercurrents are restricted to a region with the thickness d of the plates, if



Upper critical field of some high-field superconductors: ONb_3Sn, wire ow between neighboring sample [59]; $\times Nb_{5n}Ti_{5n}$ [60]; ■$PbMo_{635}$ S_8 [61]; $PbGd_{03}Mo_6$ S_8 [61]. (See also Ref. [62])

no supercurrents can flow between neighboring plates. If the plate thickness is smaller than the coherence length $\xi_\perp$ perpendicular to the plates, we can expect that in the expression of the upper critical field the plate thickness appears instead of $\xi_\perp$. This is exactly the result one obtains. One finds [63].

$$B_{\mathrm{c2}\|}^{TP} = \sqrt{6}\frac{\Phi_0}{\pi\xi_{||}d}$$

The notation " TP " indicates that we are dealing with the upper critical field of a hin plate. For $d \ll \xi_{\|},, B_{\mathrm{c2}}^{TP}$ is much larger than B_{c2}

For a single thin plate, the upper critical field can be found also in the case of an arbitrary field orientation. If we denote the angle between the magnetic field and the plane of the plate by ϑ, the upper critical field of the plate is obtained from the quadratic equation [61]

$$B_{\mathrm{c2}}^{TP}(\vartheta)\left|\frac{\sin\vartheta}{B_{\mathrm{c2},\perp}}\right| + \left[B_{\mathrm{c2}}^{TP}(\vartheta)\frac{\cos\vartheta}{B_{\mathrm{c2},\|1}^{DP}}\right]^2 = 1$$

The quantity $B_{c2}^{TP}(\vartheta)$ has a sharp peak at $\vartheta = 0°$, and then decreases monotonically with increasing angle. The minimum B_{02} is reached for $\vartheta = 90°$. In Figure 4.29 this curve is shown in comparison with experimental data of the upper critical field for the two high-temperature superconductors $YBa_2Cu_3O_7$ and $Bi_2Sr_2CaCu_2O_8$. Although the measurements were performed only a few

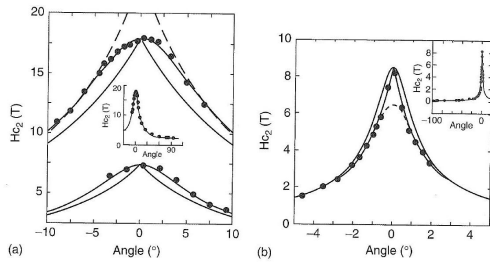


Figure 4.29 Upper critical field $B_{C2} = \mu_0 H_{c2}$ of the two high-temperature superconductors $Ba_2Ca_3O_7$ ($T_c \approx 91$ K, a) and $Bi_2Sr_2CaCu_2O_8$ ($T_c \approx 85$ K, b) obtained from resistance measurements ploted the angle between the cuo planes and the applied field. The main plots show the angles near the parallel orientation. The insets refer to the full range of angles. Measuring temperatures: for $YBa_2Cu_3O_7$, 89 K (upper curve) and 84.5 K (lower curve); for

$Bi_2Sr_2CaCu_2O_8$ 80.4K. The sharply peaked carves correspond to Eq. (4.91) for the angle dependence of the upper critical field of a thin plate. The rounded curves refer to spatially homogneous, superconduct (From [64].) kelvins below the transition temperature, the upper critical field parallel to the kelvins below the transilin the layers already reaches values of 10 T and higherin th the figue wee the experimental data for $Bi_2Sr_2CaCu_2O_8$ closely follow the angle dependence expected for a thin plate (or a stack of such plates). Weak Josephson currents are flowing between the CuO_2 layers of this compound (see Sections 1.5.1 and 6.1.1). However, they are so small that we can speak of a stack of independent plates in good approximation.

For field orientations nearly parallel to the layers, in contrast to $Bi_2Sr_2CaCu_2O_8$ he experimental data for $YBa_2Cu_3O_7$ follow a rounded curve. In the latter matethe coupling between the CuO_2 planes is relatively strong. Hence, this compound is better described in terms of a spatially nearly homogeneous superconductor. However, the superconducting properties depend on direction. In particular, much larger supercurrents can flow within the CuO_2 planes than perpendicular to the planes. This dependence on direction can be well reproduced by the Ginzburg-Landau theory if in the gradient term of the Gibbs function yy (4.26) one introducs difient vales of the effective Foss for the gradients of the upper critical field, in this "anisotropic Ginzburg-Landau theory" one obtains the expressio

$$B_{c2}(\vartheta) = \frac{1}{\sqrt{(\sin\vartheta/B_{c2,\perp})^2 + \left(\cos\vartheta/B_{c2,\parallel}\right)^2}}$$

Here, $B_{c2,\perp}$ is given by Eq. (4.89). For $B_{c2,\|]}$ one obtains

$$B_{c2,\parallel} = \frac{\Phi_0}{2\pi\xi_\parallel\xi_\perp}$$

At low temperatures, for both materials one obtains extremely high values of At special laboratories. For field orientations perpendicular to the layers, for $T \to 0$ in the case of $Bi_2Sr_2CaCu_2O_8$ for the lower limit of $B_{c,2\perp}$ one obtains a value of at least 60 T, and for $YBa_2Cu_3O_7$ even values above 100 T. This correspond to Ginzburg-Landau coherence lengths $\xi_\parallel$(also referred to as ξ_{ab}) of about $1.5 - 3$ nm. For $YBa_2Cu_3O_7$ and for field orientations parallel to the layers, measurements were carried out using explosive flux-compression technique [66]. From this it appears that this material remains superconducting up to at least 240 T. Such fields correspond to coherence lengths $\xi_\perp$ (also referred to as ξ_c) of about 0.3 nm. For $Bi_2Sr_2CaCu_2O_8$ from such measurements near T_c, one even extrapolates critical fields in the range of 1000 T. The latter value corresponds to "plate thickness" d of about 0.4 nm, or to a coherence length $\xi_c \approx 0.1$ nm, if we use Eq. (4.93). These atomically small values, together with the angle dependence of the upper critical field, clearly show that in $Bi_2Sr_2CaCu_2O_8$ the superconductivity is practically exclusively concentrated on the CuO_2 planes.

Actually, the measurements were limited by the fact that the vortices within the material became mobile (see Section 47.2). The true values of B are much higher; for example, see [65].

So far we have discussed a number of superconductors with a very high uppe critical field. From Eq. (4.90) for $B_{c2,||}$ we even conclude that the upper critical fiel can become arbitrarily large if the plate thickness d becomes sufficiently small hysically, this is unreasonable. Therefore, we must look for other mechanisms that limit the superconductivity in high magnetic fields.

In the case of spin-singlet Cooper pairing a limitation is reached by the Zeeman splitting, which the two electrons of the pair experience in the magnetic field We have discussed this in Section 3.2.4. At a sufficiently high magnetic field, this energy splitting becomes so large that it is more favorable to abandon superconductivity and to orient the spins of both electrons parallel to the field. Based on these arguments, one can derive a critical field B_p that is connected with the energy gap Δ_o via the relation [67, 68]

$B_{\mathrm{p}} = \frac{\Delta_0}{\sqrt{2}\mu_{\mathrm{B}}} \approx 1.84[T/K]T_{\mathrm{c}}$

Here, μ_{B} denotes Bohr's magneton. This limitation of the superconducting state is also referred to as the Clogston-Chandrasekhar-limit or the paramagnetic limit. In the case of a strong coupling between the electron spin and the orbital ngular momentum, this value can still be strongly increased, as well as by the Fulde-Ferrell-Larkin-Ovchinnikov (FFLO)-states discussed in Section 3.2.4. For a superconductor with a transition temperature of 10 K, from Eq. (4.94) we obtain a value of 18.4 T, and for a superconductor with $T_{\mathrm{c}} = 100$ K a value of 184 T. For most superconductors, B_{p} is much larger than B_{c2} according to Eq. (4.82). At the end of our discussion of the magnetization curve and the critical fields of type-II superconductors, we emphasize that all the results presented in this section are restricted to magnetization curves that can be followed reversibly. For an increasing external magnetic field, the same curve must appear as in a decreasing field. This is only the case if the thermodynamic equilibrium state is established for each external field B_{a}. In Chapter 5 we will see that generally this is not the case, and that, instead, all kinds of inhomogeneities hinder the spatial equilibrium distribution of the field. In this case, the form of the magnetization curve depends on the previous history of the superconductor. Only the value of B_{c}, at which the superconductivity completely vanishes, remains unequivocally fixed.

4.7.5

The Shubnikov Phase

In the Shubnikov phase, which is stable in a type-II superconductor at external fields B_{a} in the range between B_{c1} and B_{c2}, magnetic flux penetrates into the superconductor in the form of quantized flux lines (vortices). In the case of conventional superconductors, the lowest enthalpy value is obtained for a configuration of the vortices at the corners of equilateral triangles (see Section 1.2).

In Figure 4.30 the Cooper pair density, the spatial field distribution, and the supercurrent density associated with a vortex are shown schematically. In the center of the vortex the density of Cooper pairs is zero, and it reaches its

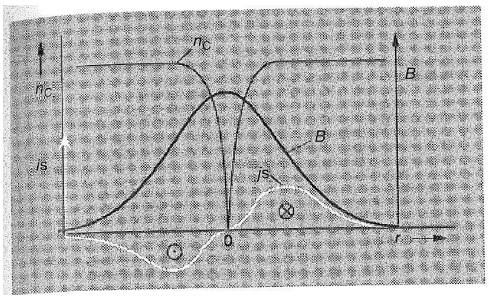


Figure 4.30 Spatial variations of Cooper pair density, magnetic field, and supercurrent density for a planar cut across a vortex, shown schematically.

equilibrium value $n_{\mathrm{s}}(T)$ at a distance of about ξ_{GL}. In the center the magnetic field has its maximum with a value of about $2B_{\mathrm{C1}}$, and it decreases toward the outside This decrease in B is controlled by the penetration depth. Superconducting circulating currents flow around the vortex core, resulting in the spatial variation of the magnetic field.

Only after a lengthy calculation can one show that the lowest enthalpy and thereby the stable state is attained for a state with a triangular vortex lattice with one flux quantum at each lattice site. It is easy to see that only a vortex structure can appear, where each vortex contains exactly an integer multiple of the elementary flux quantum. In Section 1.2 we have derived the flux quantization, or more accurately the fluxoid quantization, from the condition that, during one turn around the superconducting ring, the wave function of the Cooper pairs must just reproduce itself. This condition is also valid for the vortices of the Shubnikov phase. From this we conclude that each vortex can contain only an integer multiple of the flux quantum

Φ_0. If the configuration of a normal conducting core along the axis of a vortex is energetically favorable, we expect that each vortex contains exactly one Φ_0 such that as many vortices can be generated as possible. However, the fact that such a vortex lattice indeed represents the state with the smallest enthalpy can only be shown by detailed calculations. In Figure 4.31 we present the spatial variation of the Cooper pair density and of the magnetic field ang one direction. With increasing external field B, the distance between the vortices becomes smaller. However, at the same time also the average Cooper the vortices becomes smaller. pair density n_s decreases. For external fields only slightly below B_{c2}, the because of approach each other down to a distance of about $2\xi_{GL}$. In this case, because of the strong overlap of the circulating current systems, distinguishing between the individual vortices is no longer meaningful. For $B \to B_{c2}$, the Cooper pair density continuously approaches zero. Because of these features, the phase transition into the normal state at B_{c2} represents a second-order phase transition. On the other hand, in type-I superconductors, the phase transition in a magnetic field is of first order (see Section 4.6.2)

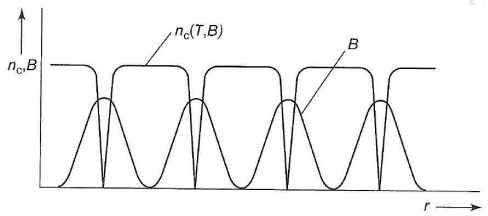


Figure 4.31 Spatial variations of Cooper to the given values of T and B. Since pair density and magnetic field in the $\lambda_L > \xi_L$, with increasing field the magnetic field between the vortices is not completely Between the vortices the Cooper pair density expelled any more. attains the equilibrium value corresponding

Today we can investigate the Cooper pair density near a vortex with high spatial resolution using scanning tunneling microscopy [69] (see Section 1.2, Figure 1.10f). With this method, for example, ξ_{GL} can be determined directly, and the density of states of the unpaired electrons within the vortex can be studied in detail. Such experiments were particularly interesting for the high-temperature superconductors. In this case, ξ_{GL} (more precisely, ξ_{ab}) is so small that the unpaired electrons can occupy only a few discrete energy states, in contrast to many other superconductors, where these electrons can form a continuous energy spectrum.

So far, our discussion of the vortex lattice has been restricted to samples with zero demagnetization coefficient. The magnetic flux penetration was not determined by the geometry as in the case of the intermediate state experiments (see Section 4.6.4). Now the question comes up, whether some kind of intermediate state also exists in a type-II superconductor, and which phases coexist in this intermediate state. As long as the type-II superconductor resides in the Meissner phase, it expels the field in the same way as a type-I superconductor. However, if the field B_{cl} is reached at the surface of the sample, flux must penetrate into the type-II superconductor. In this case, a state is established in which macroscopic domains of the Meissner phase and of the Shubnikov phase exist next to each other. An example of this new state is shown in Figure 4.32. Instead of the normal phase of a type-I superconductor, for the type-II superconductor we have the Shubnikov phase.

Structures of this type are referred to as intermediate-mixed state. They are observed only for values of κ close to $1/\sqrt{2}$. Neumann and Tewordt [70] have extended the Ginzburg-Landau theory to temperatures below T_c. From this extension, one finds that there is a narrow range of κ values near $1/\sqrt{2}$ where the interaction between vortices becomes attractive. Due to this attraction, domains without flux lines coexist with domains containing vortices. Further details can be found in the monograph [M17].

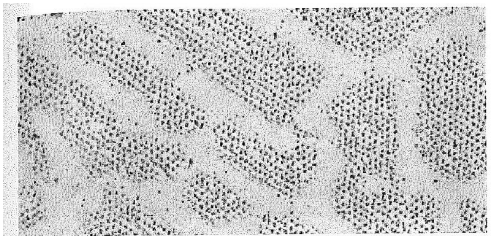


Figure 4.32 Coexistence of the Meissner phase and of the Shubnikov phase in a type-ll superconductor with κ close to $1/\sqrt{2}$. Material: Pb + 1.89at% T

diameter and 1 mm thickness; external field B_a = 36.5mT; magnification 4800x. This state can be established in samples with a finte value of the demagnetization coefficient. (By $\kappa = 0.73, T = 1.2K$; sample: disk with 2 mm courtesy of Dr U. Essmann.)

Turning now to the Shubnikov phase in the high-temperature superconductors, we note that several of their properties have a strong impact on this phase:

the atomically small Ginzburg-Landau coherence length;

the high transition temperature T_c;

the layered structure of the superconducting state in combination with the Josephson coupling between the superconducting CuO_2 layers in many cuprates.

As an additional property, we could mention the $d_{x^2-y^2}$ symmetry of the pair wave function. However, this affects the vortex properties that we want to discuss in the following only very little.

We can treat the "coherence volume" $V_c = {\xi_{ab}}^2 \xi_c$ as the volume element [355] in which the Cooper pair density changes only very little, whereas large variations can appear on larger scales. In the cuprates, this volume is smaller by $2-4$ orders of magnitude compared to that in conventional superconductors. We can write the condensation energy per unit volume of the superconducting state as $E_c = B_{cth}^2/2\mu_0$. In the cuprates, the value of B_{cth} can be about 1 T.

The condensation energy stored within V can be compared to the thermal energy $k_B T$. Here, we use the transition temperature T_c for an upper limit of $k_B T$. Obviously, the ratio $k_B T_c / (E_c V_c)$ represents a characteristic measure indicating the sensitivity of a superconductor against thermal fluctuations. The ratio $(k_B T_c / E_c V_c)^2 / 2$ is also referred to as the Ginzburg number G_i. In materials such as $YBa_2Cu_3O_7$ or $Bi_2Sr_2CaCu_2O_8$ it has a value of about 10^{-2}. However, in conventional superconductors, one obtains values that are smaller by 5 or more orders of magnitude. [36)] This indicates that in the cuprates thermal fluctuations play a much more important role than in conventional superconductors.

In the case of compounds such as $Bi_2Sr_2CaCu_2O_8$, instead of ξ_c, we can use the thickness d of the superconducting layers.

W G_{cice} can can reach values of a few 10^{-3}

In conventional superconductors, the vortices generate a triangular lattice. Due to thermal fluctuations, the vortices can move around their equilibrium lattice site without leaving it altogether. In some sense the vortices form a crystal, which exists up to the upper critical field. However, if the fluctuations around the equilibrium site become comparable to the distance between the vortices, then the vortices will leave their lattice site, and we are dealing with a vortex liquid.

This "melting" of the vortex lattice was proposed in 1985 by Nelson and coworkers [71], and was subsequently studied in many theoretical and experimental papers, in particular for $YBa_2Cu_3O_7$. A summary can be found in the Refs [72-74] and in the monograph [M17]. In $YBa_2Cu_3O_7$ the supercurrents between the CuO_2 planes are relatively strong. So in this case we can speak of a highly anisotropic, but spatially nearly homogeneous, superconductor. [37]

In Figure 4.33 we show schematically the vortex structure in the solid and liquid phases, and also a possible phase diagram. In the liquid phase there can still exist a certain amount of

short-range order of the vortices ("hexatic vortex liquid"). In magnetic fields only slightly above B_{c1}, initially one expects a vortex liquid, which turns into a vortex lattice only with decreasing inter-vortex distance. At very high fields or very small distance between the vortices, the lattice melts again, and one

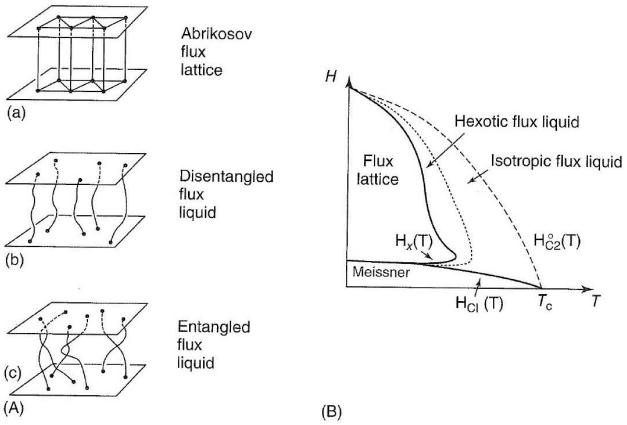


Figure 4.33 Possible phases of the socalled vortex matter in a spatially homogethermal fluctuations play an important role [75]. (A) We see schematically different vortex configurations: (a) vortex lattice, (b) a liquid phase where the vortices still remain

(B)

separated, and (c) a liquid phase with entanis shown 7761 in the liquid phase a diagram amount of short-range order is possible ("hexatic vortex liquid"). One must note also that the liquid phase is inserted between the Meissner phase and the vortex lattice. obains the vortex liquid. It is interesting that this melting represents a first-order obtains transition, in contrast to the second-order phase transition observed in conphastional type-II superconductors at B_{c2}.

In the early experiments, often the dissipation due to the vortex motion was In the early experiments, often the dissipation due to the vortex motion was were discussed highly controversially for a long time. One reason is that the studied materials contain a large concentration of defects. Then, instead of the regular vortex lattice, one obtains a vortex glass. Furthermore, in the liquid phase, the vortices are not freely mobile. However, with improving quality of the crystals, the melting of the vortex lattice could be demonstrated nicely in measurements of the magnetization [78] and even of the specific heat [79]. In Figure 4.34 we show a recent experimental phase diagram obtained from such measurements with $YBa_2Cu_3O_7$[80]. We note that the deviations from the theoretical phase diagram of Figure 4.33 are still very large. In particular, there appears a glass phase caused by the defects in the vortex lattice.

Liquid vortex phases could also be detected in other anisotropic superconductors such as NbSe (indexes?) and also in the iron pnictide $BaCo_xFe_{2-x}As_2$. In the case of these compounds, the Ginzburg number is about 10^{-4}.

Now we turn to the superconducting, lavered compounds, in which the layers are only weakly coupled with each other by means of the Josephson effect. ers are only weakly coupled with each other by means of the Josephson effect. First we consider the case $T = 0$, and we assume that the magnetic field is oriented

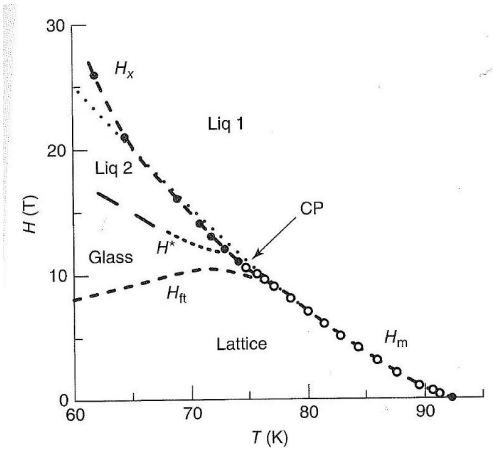


Figure 4.34 Experimental phase diagram state caused by defects in the vortex crystal. of the vortex state in $YBa_2Cu_3O_7$ in mag (???) Above the line H^* the magnetization curves A the planes.

The plot shows the melting line H_m hysteresis. The dashed line corresponds to a $H_{\rm ft}$ separates the vortex lattice from a glassy lattice. (From [80], Θ2001 Nature.)

perpendicular to the layered structure. Also in this case above the field $B_{\rm c1,\perp}$ there appear vortices each carrying one flux quantum Φ_0. The field $B_{\rm c1,\perp}$ is given by

$$B_{\rm c1,\perp} = \frac{\Phi_0}{4\pi\lambda_{ab}^2}\left(\ln\frac{\lambda_{ab}}{\xi_{ab}} + 0.08\right)$$

corresponding exactly to expression 4.85. Here, we have denoted the London penetration depth by λ_{ab}, since the shielding currents flow within the ab plane of the superconducting layers.

In the present case, the supercurrents flow around the vortex axis exclusively in the superconducting layers separated from each other, that is, within the planes marked by the crystallographic a and b axes. Hence, we can speak of stacks of nearly two-dimensional vortices. In each layer the vortex can be imagined as an independent, individual object. J. R. Clem introduced the term pancakes for these vortices [83].

The case of a single thin superconducting layer of thickness d was studied by J. Pearl in 1966 [84]. It was found that within the layer the circulating current around the vortex decay with a characteristic length $\lambda_{\rm eff} = \lambda_{\rm L}^2/d$ from the axis toward the outside. Obviously, for $d \ll \lambda_{\rm I}$ the length $\lambda_{\rm eff}$ can become much larger than $\lambda_{\rm L}$. However, also in this two-dimensional case, the vortices generate a triangular lattice within the layer.

If we have a stack of many superconducting layers, the pancakes within the different planes will interact with each other. This interaction results, on the one hand, from the magnetic field generated by each vortex, and, on the other, from the osephson supercurrents between the planes. Two vortices in neighboring planes attract each other if they have the same sign. Hence, in a perpendicular magnetic field the pancakes order themselves on top of each other along common axes. So one again obtains essentially a triangular lattice of flux lines penetrating the whole sample.

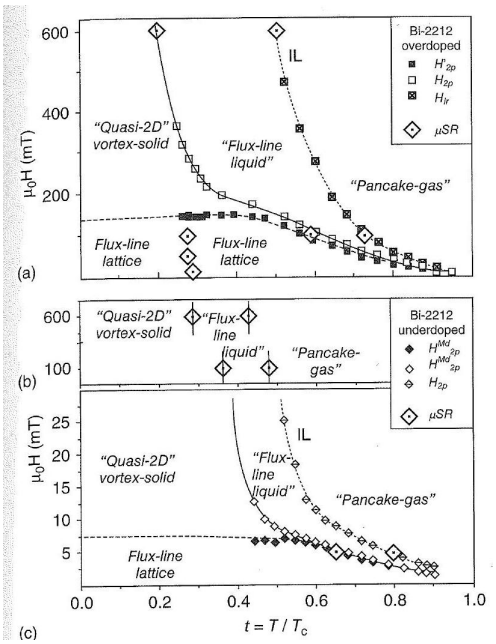
However, now it costs only little energy to shift the individual pancakes away from their common axis. Therefore, at finite temperatures, a number of different vortex phases are possible [85]

the "crystalline" state, in which the pancakes form a triangular flux-line lattice; - a flux-line liquid, in which the pancakes still form flux lines, which are freely mobile;

a quasi-2D vortex solid, in which the pancakes form a triangular lattice within a plane, but where the lattices in different planes are freely shifted relative to each other;

a pancake gas, in which the pancakes are freely mobile within a plane and also are not ordered any more perpendicular to it.

In Figure 4.35 we show a vortex phase diagram of two $Bi_2Sr_2CaCu_2O_{8+x}$ single crystals with different oxygen concentrations, determined from measurements of the muon-spin resonance and magnetization [86]. We can see the phases discussed above. However, we also note that the details strongly depend on the



(c)

Figure 4.35 Vortex phase diagrams of (μSR) and of the magnetization. (a) Overdoped crystal, $T_c = 77$ K[86].

doping level of the samples. Furthermore, disorder plays an important role, similarly as in $YBa_2Cu_3O_7$, such that the "crystalline" phases rather represent glassy states. Similar phase diagrams were also determined using other experimental methods, say, using the vortex penetration into the crystal [87] or using the magnetic permeability [88]. Frequently, these measurements differ in a number of details, but they clearly indicate that in $Bi_2Sr_2CaCu_2O_8$ there exist a number of different vortex states.

Further we note that mostly a Gibbs function serves as the starting point of the theoretical calculations, which is constructed similar to Eq. (4.27) of the Ginzburg-Landau theory. This "Lawrence-Doniach model" [89] was developed in 1970. In this model one considers a stack of two-dimensional superconducting layers, which are coupled to each other by means of Josephson currents. However, the calculation of the different vortex phases is extremely difficult and can be done only using various approximations.

Let us look at the superconducting layered structure at $T = 0$ in a magnetic field oriented parallel to the layers. If the applied field is very weak, the Meissner phase appears again. The shielding currents flow across the superconductin layers. However, the maximum value of this current is much smaller than in the case where the field is applied perpendicular to the layers. As a result the penetration depth λ_c of the magnetic field parallel to the layers is much larger than perpendicular to them. The value of λ_c can reach up to 100μm or more.

Vortices can also be generated in a parallel orientation of the field, if the magnetic field exceeds a lower critical field $B_{c1,\parallel}$. In the Lawrence-Doniach model for $B_{c1,\parallel}$, one finds the expression [90]

$$B_{c1,\parallel} = \frac{\Phi_0}{4\pi\lambda_{ab}\lambda_c}\left(\ln\frac{\lambda_{ab}}{s} + 1.12\right)$$

Here, s is the distance between the superconducting layers. Because of the larg value of $\lambda_c, B_{c1,\parallel}$ is smaller by a factor λ_{ab}/λ_c than the field $B_{c1,\perp}$ for perpendicular field orientation

given by Eq. (4.95). The factor λ_{ab}/λ_c can attain values of 10^{-3} or smaller. Further, we note that in Eq. (4.96) compared to Eq. (4.95) the coherence ength ξ_{ab} is replaced by the layer distance

Within the planes the vortices have a diameter of about $2\lambda_c$ and perpendicular to the planes a diameter of about $2\lambda_{ab}$. Hence, they are very flat objects, extending also over many superconducting planes, since λ_{ab} in general is much larger than the layer distance. Figure 4.36 schematically shows the current distribution of one of these so-called "Iosephson vortices." The magnetic field distribution of such vortices can be imaged experimentally by means of scanning superconducting quantum interference device (SQUID) microscopy (see Section 1.2) [92].

Near the vortex axis the Josephson vortices differ strongly from the Abrikosov vortices in homogeneous type-II superconductors or from the pancake vortices in superconducting layered structures. In the Abrikosov vortices or pancake vortices the Cooper pair density decreases toward the vortex axis down to zero on a length scale ξ_{GL} (see Figure 4.30). On the other hand, in the Josephson vortices the axis is located within a non-superconducting layer, such that the Cooper pair density does not have to be suppressed anymore.

In Figure 4.36 b we show the current density between the two superconducting layers where the vortex axis is located. The supercurrent density increases from the vortex axis toward the outside on a length scale λ_1, the Josephson penetration depth (see Eq. (1.69)). It passes through a maximum value and then decreases gradually. A Josephson vortex also has a core, which is given perpendicular to the ayers by the thickness of the insulating barrier and parallel to the layers by λ_T.

A Josephson vortex can move easily only parallel to the layers. [38)] During a displacement in the z direction the vortex axis must cross a superconducting layer, which is only possible by suppressing the Cooper pair density within this layer at the vortex axis down to zero. However, this costs a large amount of condensation energy, and as a result the superconducting layers develop an energy barrier against the displacement of the Josephson vortex in the z-direction.

In Chapter 6 we will discuss in detail the highly interesting dynamic properties of moving Josephson vortices. (!?!?!?)

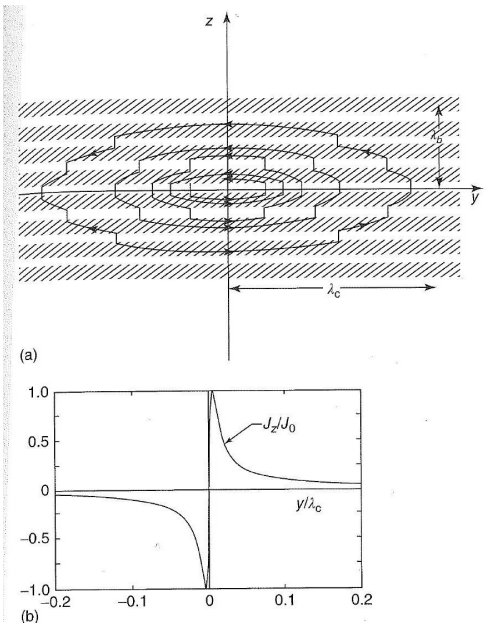


Figure 4.36 (a) Schematic of the circulat- vortex axis runs along the x-direction, that is ing currents around a "Josephson vortex" perpendicular to the paper. (b) The superconducting layers are the hatched two layers, between which the vortex axis is located. (From [91].)

In parallel magnetic fields also the Josephson vortices generate a triangular vortex lattice [93]. If the applied magnetic field is slightly tilted away from the parallel orientation, initially the Josephson vortices cannot cross the superconducting lay ers [94]. We have the situation that

is highly unusual for superconductors in which the magnetization generated by the circulating currents and the applied magnetic field are not parallel to each other. This matching effect, which can be demonstrated, for example, by the measurement of the torque trying to reorient the sample parallel to the field, is frequently used to find out if the superconductor has an internal layered structure.

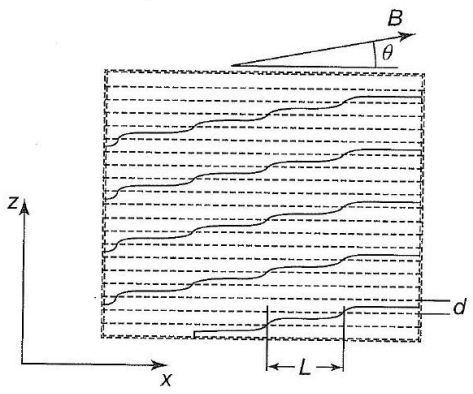


Figure 4.37 Staircase pattern of flux lines in a magnetic field applied at an angle θ to the superconducting layers [95]. The flux lines pass across the planes in the form of pancake vortices joined together by short segments (of length $\llcorner$) of Josephson vortices.

Only when the magnetic field component perpendicular to the layers reaches a value corresponding to about the lower critical field $B_{\mathrm{cl},1}$ can the magnetic field also pass through the superconducting planes. Depending on the magnitude of the maximum supercurrents that can flow between the layers, different types of vortex structures are possible. For example, independent sublattices of Josephson vortices and of pancake vortices can be formed. In the case of strong coupling between the layers, one obtains vortices that are arranged like a staircase around the direction of the applied field. This latter situation is shown schematically in Figure 4.37. The flux lines cut across the superconducting planes in the form of pancake vortices. In between there appear short segments of Josephson vortices.

We expect that at finite temperatures, the situation becomes even more versatile. As an example, in Figure 4.38 we show the vortex phases observed for a $Bi_2Sr_2CaCu_2O_8$ single crystal in the temperature range $77-88$ K by means of Hall magnetometry [96]. The diagram indicates the different vortex phases in the $\left(\mathrm{H}_{\|}, H_{\perp}\right)$ plane. One finds a vortex liquid (VII), slightly tilted lattices from pancake vortices (II), weakly interacting crossing lattices (III), composite lattices (IV), or configurations in which the pancakes are arranged in the form of chain structures above the Josephson vortices (V, 1D chains; or VI, sublimed 1D chain state).

We do not want to discuss the various possibilities any further. However, we emphasize that the special properties of high-temperature superconductors have resulted in a number of novel phenomena, which had not been observed previously in superconductors.

At the end of this section we briefly want to discuss what happens if we deal only with a single, very thin superconducting plane instead of a superconducting layered structure. We have already treated the case of thin plates several times in the context of the Ginzburg-Landau theory or of the critical magnetic fields, but we have ignored the influence of thermal fluctuations.

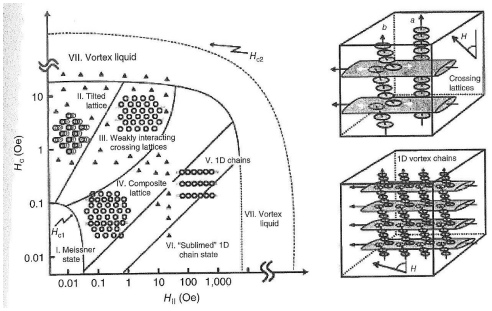


Figure 4.38 Phase diagram of means of Hall probe microscopy. Measuring $Bi_2Sr_2CaCu_2O_8$ single crystal as a function temperature: $77 - 88$ K. The two figures on and H_1 The vortex phases were observed by vortex phases (From [96], @2001 Nature.)

It turns out that for two-dimensional or one-dimensional systems, these fluctuations can become sufficiently large that the macroscopic wave function characterizing the superconducting state is destroyed. This result was derived by Hohenberg [97] and by Mermin and Wagner [98] in the 1960s. We can understand this easily by looking again at the coherence volume $V_c = \xi_{ab}^2 \xi_c$. If the superconducting byer is very thin, we must replace ξ_c by the layer thickness d. However, for $d \to 0$ we have $V_c \to 0$, and the condensation energy stored in V_c vanishes. Then it costs less and less energy to generate a vortex by means of thermal fluctuations. [39] In the absence of an external magnetic field, positive and negative vortices will be generated spontaneously in equal numbers such that the average magnetization of the sample vanishes. If these vortices can move independently of each other they result in dissipation and, hence, in a finite resistance. The superconducting state is destroyed.

Berezinskii [99] as well as Kosterlitz and Thouless [100] have shown that at a somewhat lower temperature, namely at the now so-called Berezinskii-Kosterlitz-Thouless transition temperature T_{BKT}, vortex-antivortex

A more accurate calculation, which takes into account also the energy contribution of the shielding the decay length of the circulating currents in a nearly two-dimensional layer

pairs are generated. These pairs again stabilize a superconducting state, in which the Cooper pairs are not correlated with each other anymore over arbitrarily large distances.

If below T_{BKT} a magnetic field is applied perpendicular to the layer, free vortices appear with their orientation given by the applied field. At low temperatures, these vortices again form a triangular lattice. However, this lattice is also highly sensitive to thermal fluctuations. Again one can obtain a vortex liquid, perhaps having a certain hexatic short-range order [101]. Hence, also for the two-dimensional system there exists a phase diagram containing a Meissner phase, a triangular vortex lattice, and liquid vortex phases.

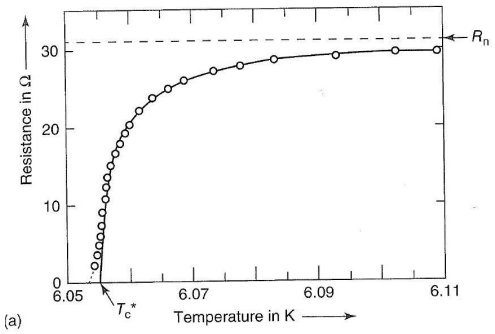
In the last section, but also briefly in Section 1.4, we considered the influence of thermal fluctuations on the vortex state below the transition temperature T_c Obviously, these fluctuations of the equilibrium state also exist above T_c. In the normal conducting state, the deviation from equilibrium can lead to the transient appearance of the superconducting state within certain regions, that is, to the formation of "puddles" of Cooper pairs. These deviations from equilibrium are not stable, and they will disappear more or less quickly. The statistical appearance of Cooper pairs will become more and more rare the higher the temperature, since with increasing temperature the normal conducting state becomes more and more stable compared to the superconducting state. Therefore, with increasing temperature, larger and larger deviations from equilibrium are needed to generate the superconducting state.

If we note further that the puddles of Cooper pairs represent perfectly conducting regions, we understand immediately that already above T_c due to the fluctuations in the normal conducting state the statistically appearing puddles of Cooper pairs result in an additional electrical conductivity, which must strongly increase on approaching $T_.$

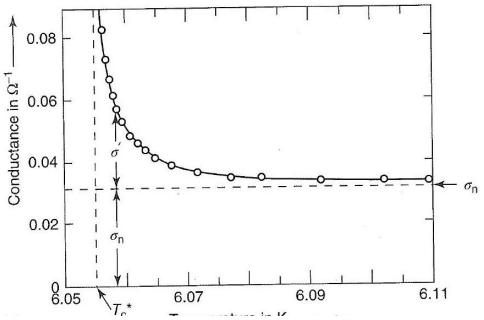
This influence of the thermal fluctuations can be clearly detected for a number of super-

conductors. In Figure 4.39a we show the transition curve of a bismuth film near the critical temperature T_c [102]. We see clearly that the full normal resistance is reached only at temperatures considerably above T_c . In Figure 4.39 b the electrical conductance is plotted instead of the resistance. In this plot the additional conductance σ' of the Cooper pair puddles, statistically appearing and vanishing again, is particularly clearly visible. [40)] We note that here and in the following we are not dealing with the specific conductance σ^*, but with the conductance $\sigma' = \sigma^* d\,(d = \text{ thickness})$ in the unit $\mathrm{A/V} = \Omega^{-1}$.

In Figures 4.39 and 4.40, the resistance or the conductance is normalized to the film geometry of square (length l = width b).



(a)



(b)

Figure 439 Transition curve of an amorphous bismuth film of 47 nm thickness: (a) resis-

The additional conductance due to the Cooper pairs can be calculated from the existing theories of superconductivity in combination with the theory of fluctuations. For a film that is thinner than ξ_{GL}, one obtains [103]

$$\sigma'(T) = \frac{e^2}{16\hbar} \frac{T_c^*}{T - T_c^*} \frac{b}{l}$$

where e is the elementary charge, $\hbar$ is Planck's constant $h/2\pi$, T_c^* is the transition temperature obtained by fitting Eq. (4.97) to the experimental data, b is the width and l is the length of the film

We see that the additional conductance σ' must be proportional to $1/\left(T - T^*\right)$. This theoretical result is well confirmed by experiment. The curves shown in Figure 4.39 exactly reproduce this temperature dependence. Furthermore, according to Eq. (4.97), the additional conductance σ' should be independent of

4.2.11 38. Superconductors Close to the T_c in an Arbitrary Magnetic Field

Theory by AGD

The properties of superconductors close to the critical temperature provide a special case. Here the size of the gap is fairly small, as a result of which all the equations are greatly simplified. It is easily scen from the results of 36 (expression (36.4)) that it is now possible to expand the equations in the quantity $1 - T/T_c \gg 1$. In addition, as we have already remarked in the previous section, close to T_c the depth of penetration of a weak magnetic field $\delta \ll \xi_0$, i.e. all the functions in the field, including the field itself, vary at distances which are much greater than the parameters $\xi_0 \sim v/T_c$ of the theory. This fact enables us to develop a theory in this temperature range (Gor'kov [68]), which describes the behaviour of superconductors in arbitrary magnetic fields (of the order of the critical field).

With this aim, we again rewrite cquations (37.6):

$$\left\{ i\omega + \frac{1}{2m}\left(\frac{\partial}{\partial r} - ieA(r)\right)^2 + \mu \right\} \mathfrak{G}_\omega(r, r') + \Delta(r)\mathfrak{F}^+_\omega(r, r') = \delta(r - r')$$
$$\left\{ -i\omega + \frac{1}{2m}\left(\frac{\partial}{\partial r} + ieA(r)\right)^2 + \mu \right\} \mathfrak{F}^+_\omega(r, r') - \Delta^*(r)\mathfrak{G}_\omega(r, r') = 0$$

together with the equation that determines the gap size:

$$\Delta^*(\boldsymbol{r}) = |\lambda| T \sum_{\omega}^{\searrow} \mathfrak{F}^+_\omega(\boldsymbol{r}, \boldsymbol{r}). \tag{38.1}$$

Since $|\Delta|$ is small, we expand $\mathfrak{F}^+_\omega(r, r')$ in powers of $|\Delta|$ and, on substituting this expansion in (38.1), find an equation for $\Delta^*(r)$. It is useful here to introduce the Fourier components of the Green function $\tilde{\mathscr{F}}^{(0)}_\omega(r, r')$ for the electrons in the normal metal (in the given field $A(r)$). The equation which $\tilde{\mathfrak{G}}^{(0)}_\omega(r, r')$ satisfies can be written in two ways:

$$\left\{ i\omega + \frac{1}{2m}\left(\frac{\partial}{\partial r} - ieA(r)\right)^2 + \mu \right\} \tilde{\mathfrak{G}}^{(0)}_\omega(r, r') = \delta(r - r') \tag{38.2}$$

or

$$\left\{ i\omega + \frac{1}{2m}\left(\frac{\partial}{\partial r'} + ieA(r')\right)^2 + \mu \right\} \tilde{\mathfrak{H}}^{(0)}_\omega(r, r') = \delta(r - r'). \tag{38.2'}$$

Taking the second form of the Green function, we can use it to roduce the system of equations for $\mathfrak{B}_\omega$ and $\mathfrak{F}^+_\omega$to the integral form:

$$\mathfrak{G}_\omega(r, r') = \tilde{\mathfrak{G}}^{(0)}_\omega(r, r') - \int \tilde{\mathfrak{G}}^{(0)}_\omega(r, l)\Delta(l)\mathfrak{F}^+_\omega(l, r')\,\mathrm{d}^3 l,$$
$$\mathfrak{F}^+_\omega(r, r') = \int \tilde{\mathfrak{G}}^{(0)}_{-\omega}(l, r)\Delta^*(l)\mathfrak{G}_\omega(l, r')\,\mathrm{d}^3 l. \tag{38.3}$$

Before proceeding further, we find the value of $\mathfrak{S}^{(0)}_\omega(r, r')$. In the absence of a magnetie ficld, $\tilde{\mathscr{F}}^{(0)}_\omega(r - r')$ is equal to ($R = |r - r'|$):

$$\mathfrak{G}^{(0)}_\omega(R) = \begin{cases} -\frac{m}{2\pi R} e^{ip_0 R - |\omega| R/v} \text{ for } \omega > 0, \\ -\frac{m}{2\pi R} e^{-ip_0 R - |\omega| R/v} \text{ for } \omega < 0. \end{cases} \tag{38.4}$$

This can be verified either by direct substitution of (38.4) in (38.2) in the absence of field, or by using the now familiar expression for the Fourier component $\mathrm{G}_\omega^{(0)}(p) = [i\omega - \xi]^{-1}$:

$$\begin{aligned}\mathfrak{G}_\omega^{(0)}(R) &= \frac{1}{(2\pi)^3}\int \mathfrak{G}_\omega^{(0)}(p)\mathrm{d}^3 p e^{i(p\cdot R)} \\ &= -\frac{m}{(2\pi)^2} iR \int \frac{e^{ip_0 R + i\xi R/v} - e^{-ip_0 R - i\xi R/v}}{i\omega - \xi}\mathrm{d}\xi\end{aligned}$$

(we are of course interested in the form of $\mathscr{G}_\omega^{(0)}(R)$ at distances which are larged compared with the atomie distances: $Rp_0 \gg 1$). On integrating over ξ, we obtain (38.4) immediately.

The function $\mathscr{G}_\infty^{(0)}(R)$ oscillates rapidly. Since $p_0 R \gg 1$, this fact enables us to find $\tilde{\mathfrak{G}}_\omega^{(0)}(r, r')$ in a magnetic field by making use of the quasi-classical approximation. In fact, we look for $\widetilde{\mathfrak{S}}_\omega^{(0)}(r, r')$ in the form

$$\tilde{\mathfrak{G}}_\omega^{(0)}(r, r') = e^{iq(r,r')}\mathfrak{G}_\omega^{(0)}(r - r'), \tag{38.5}$$

where $\varphi(r, r) = 0$. On substituting (38.5) into (38.2) and differentiating only the principal terms, we obtain an equation for the extra term $\varphi(r, r')$ in the action:

$$(n \cdot \nabla_r \varphi(r, r')) = e(n, A(r)); \quad \left(n = \frac{R}{|R|}\right). \tag{38.6}$$

We have thrown away the terms quadratic in A in this equation, since the radius of curvature of the electrons ep_0/H in the fields of interest is extremely large by comparison with the depth of penetration: $p_0 \gg Ae \sim eH\delta$ (δ is the order of the depth of penetration).

We now return to equations (38.3) and carry out expansions in them in powers of $|\Delta(r)|$. As is clear from (38.4) and (38.6), it is sufficient to carry out this expansion in $\mathfrak{F}_\omega^+(r, r')$ up to the third power in $|\Delta|$. As regards the Green function $\mathfrak{G}_\omega(r, r')$, we only need to know it up to second order terms in $|\Delta|$:

$$\mathfrak{G}_\omega(r, r') = \tilde{\mathfrak{G}}_\omega^{(0)}(r, r') - \int \tilde{\mathfrak{G}}_\omega^{(0)}(r, l)\Delta(l)\tilde{\mathfrak{G}}_\omega^{(0)}(m, r')\,\Delta^*(m)\tilde{\mathfrak{G}}_{-\omega}^{(0)}(m, l)\mathrm{d}^3 m\ \mathrm{d}^3 l. \tag{38.7}$$

On substituting this expression in the second of equations (38.3), we obtain the expansion of $\mathfrak{F}_\omega^+(r, r')$, with the aid of which the following equation in $\Delta^*(r)$ is obtained from (38.1):

$$\begin{aligned}\Delta^*(r) =& |\lambda| T \sum_\omega \int \widetilde{G}_\omega^{(0)}(l, r)\Delta^*(l)\widetilde{G}_{-\omega}^{(0)}(l, r)\mathrm{d}^3 l \\ &- |\lambda| T \sum_\omega \iiint \widetilde{G}_\omega^{(0)}(l, m)\Delta(m)\widetilde{G}_\omega^{(0)}(s, r)\Delta^*(s)\widetilde{G}_{-\omega}^{(0)}(s, m) \\ &\times \Delta^*(l)\widetilde{G}_{-\omega}^{(0)}(l, r)\mathrm{d}^3 l\ \mathrm{d}^3 m\ \mathrm{d}^3 s\end{aligned} \tag{38.8}$$

The important distances in the integrals in this equation are of order ξ_0, since, as is clear from (38.4) and (38.5), the function $\tilde{\mathcal{G}}_\omega^{(0)}(r, r')$ de-
creases exponentially for $|r - r'| > \xi_0$. The change in the gap $\Delta(r)$ and field $A(r)$ occur at distances of the order of the penetration depth, which is much greater than ξ_0 close to the critical temperature. For the same reasons, the phase $\varphi(r, r')$ in (38.5) can be written as

$$\varphi(r, r') \simeq e\,(A(r) \cdot r - r').$$

Close to T_c, $A(r) \sim H\delta \sim \sqrt{1 - (T/T_c)}$, so that the phase $\varphi(r, r')$ is small and the exponent can be expanded in powers of φ.

We start by considering the first term on the right-hand side. Let

$$K(l,r) = T\sum_{\omega} \mathscr{G}_{\omega}^{(0)}(l,r)\tilde{\mathfrak{G}}_{-\omega}^{(0)}(l,r) = K_0(l-r)\exp[2ie(A(r)\cdot l - r)]$$

Using the representation (38.4) for the Green function in coordinate space and performing a summation over the frequencies, we get the following expression for $K_0(R)$:

$$K_0(R) = \frac{m^2 T}{(2\pi R)^2}\frac{1}{\sinh\frac{2\pi TR}{v}} \tag{38.9}$$

As we have already remarked, all the functions change little over distances of the order of ξ_0, so that we can expand all the functions in the integral

$$\int K_0(l-r)\exp[2ie(A(r)\cdot l - r)]\Delta^*(l)\mathrm{d}^3 l$$

into series in powers of $(l-r)$ about the point r. On confining ourselves to second order terms in $(l-r)$, we get

$$\Delta^*(r)\int K_0(R)\mathrm{d}^3 R + \frac{1}{6}\left(\frac{\partial}{\partial r} + 2ieA(r)\right)^2 \Delta^*(r)\int K_0(R)R^2\ \mathrm{d}^3 R$$

By (38.9), the function $K_0(R)$ tends to infinity as $1/R^3$ at $R=0$. The first of these two integrals is therefore formally divergent. It is more convenient to perform the cut-off of the divergent expression in momentum space. We obtain as a result the familiar expression:

$$\int K_0(R)\mathrm{d}^3 R = \frac{mp_0}{2\pi^2}\int_0^{\omega_D}\tanh\left(\frac{\xi}{2T}\right)\frac{\mathrm{d}\xi}{\xi}$$

The second term contains no singularities on integrating close to $\boldsymbol{R}=0$. On evaluating this integral directly in the coordinate representation, we get:

$$\int R^2 K_0(R)\mathrm{d}^3 R = \frac{7\zeta(3)v^2}{8(\pi T)^2}\cdot\frac{mp_0}{2\pi^2}$$

In the term of third order in $|\Delta|$ in equation (38.8), we can neglect the dependence of $\Delta(r)$ on the coordinates. This term is therefore equal to $\left(\frac{mp_0}{2\pi^2}\right)\Delta^*(r)|\Delta(r)|^2 T\sum\limits_{\omega}\int \mathrm{d}\xi\frac{1}{(\omega^2+\xi^2)^2} = \left(\frac{mp_0}{2\pi^2}\right)\frac{7\zeta(3)}{8(\pi T)^2}\Delta^*(r)|\Delta(r)|^2$.

On collecting the results obtained, we find that $\Delta^*(r)$ satisfies the following equation close to the critical temperature:

$$\left\{\frac{1}{4m}\left(\frac{\partial}{\partial r} + 2ieA(r)\right)^2 + \frac{1}{\varrho}\left[\frac{T_c - T}{T_c} - \frac{7\zeta(3)}{8\left(\pi T_c\right)^2}|\Delta(r)|^2\right]\right\}\Delta^*(r) = 0,$$

where

$$\varrho = \frac{7\zeta(3)}{6\left(\pi T_c\right)^2}\varepsilon_F \tag{38.10}$$

In the absence of a field Δ is constant in space and equation (38.10) is the same as the first terms of expansion (36.4).

We now turn to evaluating the current density $\boldsymbol{j}(\boldsymbol{r})$. Obviously (37.5) of the previous section still holds in this case. If, however, we use the fact that Δ is small by comparison with T_c, we can also carry out here an expansion in A and Δ up to the first non-vanishing terms. Notice that the term in the current density (37.5)

$$-\frac{2e^2A(r)}{m}\mathscr{G}_{l'=t+0}(r,r) \equiv -\frac{e^2}{m}A(r)N.$$

Here N is the density of the total number of electrons, which is equal to its value for a normal metal. Variation of N would contradict the condition for neutrality. (The solution of (38.7) satisfies this requirement, i.e. if

$$\mathfrak{G}_\omega(r,r') = \tilde{\mathfrak{G}}_\omega^{(0)}(r,r') + \delta\mathfrak{G}_\omega(r,r'), \text{ then } T\sum_\omega \delta\mathfrak{G}_\omega(r,r) \equiv 0.\Big)$$

On substituting (38.7) in (37.5), we find that

$$T\sum_\omega \frac{ie}{m}\left(\nabla_{r'} - \nabla_r\right)\underset{r'\to r}{\tilde{\mathfrak{G}}_\omega^{(0)}}(r,r') - \frac{e^2}{m}NA(r) \equiv 0$$

since the current in a normal metal is zero in a constant magnetic field. Therefore

$$j(r) = \frac{ie}{m}\left(\nabla_{r'} - \nabla_r\right)_{r'\to r} T\sum_\omega \delta\mathfrak{G}_\omega(r,r')$$

where

$$\delta\mathfrak{G}_\omega(r,r') = -\int \mathfrak{G}_\omega^{(0)}(r,l)\Delta(l)\tilde{\mathfrak{G}}_\omega^{(0)}(m,r')\,\Delta^*(m)\tilde{\mathfrak{G}}_{-\omega}^{(0)}(m,l)\mathrm{d}^3m\ \mathrm{d}^3l$$

On substituting (38.5) in this, expanding all the functions about the point r up to first order terms and omitting terms which yield zero an integration over the angle, we get:

$$j(r) = \left[\frac{ie}{m}\left(\Delta\frac{\partial\Delta^*}{\partial r} - \Delta * \frac{\partial\Delta}{\partial r}\right) - \frac{4e^2|\Delta|_-^2}{m}A(r)\right]C \tag{38.11}$$

where

$$C = \frac{1}{3}T\sum_\omega \iint \left\{\left[\left(\nabla_r\mathfrak{G}_\omega^{(0)}(r-l)\right)\mathfrak{G}_\omega^{(0)}(m-r) - \mathfrak{G}_\omega^{(0)}(r-l)\right.\right.$$
$$\left.\left.\times\left(\nabla_r\mathfrak{G}_\omega^{0}(m-r)\right)\right]\cdot m\right\}\mathfrak{G}_{-\omega}^{(0)}(m-l)\mathrm{d}^3m\ \mathrm{d}^3l$$

The evaluation of C is best performed in Fourier components, after making the usual substitution $r \to i(\ \mathrm{d}/\mathrm{d}\boldsymbol{p})$. We shall omit the details of this fairly simple calculation and give the final result:

$$C = \frac{7\zeta(3)N}{16\left(\pi T_c\right)^2}$$

The system of equations (38.10) and (38.11) describes the properties of a superconductor in a constant magnetic field close to $\boldsymbol{T_c}$. We introduce the wave function $\psi(r)$, proportional to $\Delta(r)$:

$$\psi(r) = \sqrt{\frac{7\zeta(3)N}{8\left(\pi T_c\right)^2}}\Delta(r). \tag{38.12}$$

On taking the complex conjugate of equation (38.10) and substituting (38.12) throughout, we can derive these equations as follows:

$$\left\{\frac{1}{4m}\left(\frac{\partial}{\partial r}-2ieA(r)\right)^2+\frac{1}{\varrho}\left[\frac{T_c-T}{T_c}-\frac{1}{N}|\psi|^2\right]\right\}\psi(r)=0$$

$$j(r)=-\frac{2ie}{4m}\left(\psi^*\nabla\psi-\psi\nabla\psi^*\right)-\frac{(2e)^2}{2m}A(r)|\psi|^2 \tag{38.13}$$

The point in introducing the wave function $\psi(r)$ now becomes clear: the resulting equations are in a form similar to the quantum mechanical equations for particles with mass $2m$ and charge $2e$. This result is quite obvious physically, since $\Delta(r)$ has the significance of a function which is proportional to the wave function of a bound pair, or, more precisely, the wave function in the centre of mass coordinates. It is of interest that equations of a similar form where proposed in the phenomenological Ginzburg-Landau theory [69], where, however, a single elementary charge occurred. Apart from this essential difference, the new theory of superconductivity, which supports the correctness of the Ginzburg-Landau theory close to T_c, enables us to compute the constants featured in the latter theory.

Let us again mention in conclusion the fact that our derivation employed the smallness of the variation of all the functions over distances of the order ξ_0. Since, as may clearly be seen from (38.13) and (37.19), all the functions are in the general case variable at distances of the order of the London penetration depth close to T_c, whilst this depth becomes greater than ξ_0 only in the immediate neighbourhood of T_c in the case of Pippard metals, the domain of applicability of these equations for metals of the Pippard type is an extremly limited neighbourhood of temperatures close to the critical transition temperature. For metals of the London type, or intermediate metals, the equations are valid in a fairly wide temperature range close to T_c. This is a range of the greatest interest from the experimental point of view, and it must be remarked that equation (38.13) leads to a very good agreement between the theory and experimental results in this range.

5 Details of Fundamental Effects and Other Basic Properties

5.1 Basics of Determination of Physical Parameters

5.1.1 Determination of the value of T_c

(maybe I'll create later a subsection about it. still, it is not clear, how to do it from basic BCS. and how to take into account properties of materials? I'll try to discuss it here, but see special my note about this very big question. It is a big and unsolved problem for science now)

5.2 Important general features of theories of superconductivity

5.2.1 Connection of the Ginzburg-landau and BCS theory

Statements of connection of GL and BCS theories by Shmidt

The Ginzburg-Landau (GL) theory is, as we already know, phenomenological, that is, it does not allow its coefficients to be interpreted on the microscopic level. A detailed interpretation of the quantities involved in the GL theory became possible only after the rigorous microscopic theory of superconductivity had been developed by Bardeen, Cooper, and Schrieffer. This task was accomplished by Gorkov [66]. Here we shall only outline the final results, which

differ for 'clean' and 'dirty' superconductors. In what follows, all quantities corresponding to 'clean' superconductors will be labeled with an index ' p ' and those corresponding to 'dirty' superconductors with an index ' d '. A superconductor is considered clean if $l \gg \xi_0$, where l is the electron mean free path. A dirty superconductor is characterized by $l \ll \xi_0$.

As one should expect, the energy gap $\Delta(T)$ represents the order parameter in the superconductor and, therefore, at $T \to T_c$, must be proportional to the order parameter Ψ of the GL theory. Indeed, the exact result is:

$$\Psi_p = \left[\frac{7\zeta(3)}{2}\frac{mv_F^2 N(0)}{k_B^2 T_c^2}\right]^{1/2}\Delta(r), \quad \zeta(3) \approx 1.202$$
$$\Psi_d = \left[\frac{\pi m v_F}{12}\frac{N(0)l}{k_B T_c}\right]^{1/2}\Delta(r)$$

where $\zeta(x)$ is the Riman function.

At $T \to T_c$ we have

$$\Delta(T) = \left(\frac{8\pi^2}{7\zeta(3)}\right)^{1/2} k_B T_c \left(1 - \frac{T}{T_c}\right)^{1/2}$$

or

$$\Delta(T) \approx 3.1 k_B T_c \left(1 - \frac{T}{T_r}\right)^{1/2}.$$

The coherence length and the magnetic penetration depth are, accordingly,

$$\xi_p = 0.74\xi_0 \left(1 - \frac{T}{T_c}\right)^{-1/2}$$
$$\xi_d = 0.85\left(\xi_0 l\right)^{1/2}\left(1 - \frac{T}{T_c}\right)^{-1/2}$$
$$\lambda_p = \frac{\lambda(0)}{\sqrt{2}}\left(1 - \frac{T}{T_c}\right)^{-1/2}$$
$$\lambda_d = 0.615\lambda(0)\left(\frac{\xi_0}{l}\right)^{1/2}\left(1 - \frac{T}{T_c}\right)^{-1/2}$$
$$\lambda^2(0) = \frac{3c^2}{8\pi e^2 v_F^2 N(0)}$$

The GL coefficients α and β in the expansion of the free energy in powers of the order parameter Ψ are:

$$\alpha_p = 1.83\frac{\hbar^2}{2m}\frac{1}{\xi_0^2}\left(\frac{T}{T_c} - 1\right)$$
$$\alpha_d = 1.36\frac{\hbar^2}{2m}\frac{1}{\xi_0 l}\left(\frac{T}{T_c} - 1\right)$$
$$\beta_p = 0.35\frac{1}{N(0)}\left(\frac{\hbar^2}{2m\xi_0^2}\right)^2\frac{1}{(k_B T_c)^2}$$
$$\beta_d = 0.2\frac{1}{N(0)}\left(\frac{\hbar^2}{2m\xi_0 l}\right)^2\frac{1}{(k_B T_c)^2}$$

The GL parameter takes the values

$$\kappa_{\mathrm{p}} = 0.96\frac{\lambda(0)}{\xi_0}, \quad \kappa_{\mathrm{d}} = 0.725\frac{\lambda(0)}{l}$$

Let us now establish the range of validity for the GL theory. In the series expansion (3.7) of the Gibbs free energy density G_{BH} in powers of $|\mathrm{i}\hbar\nabla\Psi - (2e/c)A\Psi|^2$, only the first term has been kept. This means that only slow changes of Ψ and $\boldsymbol{A}$ are assumed over distances comparable with the characteristic size of an inhomogeneity in the superconductor, that is, over the size of the Cooper pair.

In the case of a clean superconductor, when the electron mean free path satisfies the inequality $l \gg \xi_0$, the GL theory is valid if $\xi(T), \lambda(T) \gg \xi_0$. Since $\xi(T) \sim \xi_0 (1 - T/T_{\mathrm{c}})^{-1/2}$, the quantity $\xi(T)$ always exceeds ξ_0 at $T \sim T_{\mathrm{c}}$ and the first condition of validity is satisfied automatically.

The second condition, $\lambda(T) \gg \xi_0$, represents the requirement that local electrodynamics is applicable, or, in other words, that the superconductor is of the London type. Since $\lambda(T) \sim \lambda(0) (1 - T/T_c)^{-1/2}$ and $\kappa \sim \lambda(0)/\xi_0$, the

$$\kappa^2 \gg 1 - \frac{T}{T_{\mathrm{c}}} \tag{6.47}$$

This is a rather strict condition because κ in type-I superconductors can assume a small value. For example, $\kappa(\mathrm{Al}) = 0.01, \kappa(\mathrm{\ Pb}) = 0.23$. In 'dirty' superconductors ($l \ll \xi_0$), the validity interval for the GL theory is much wider. In this case, the characteristic scale of inhomogeneity is the mean free path l and the GL theory can be applied if $\xi(T), \lambda(T) \gg l$. Since $\xi(T) \sim (\xi_0 l)^{1/2} (1 - T/T_{\mathrm{c}})^{-1/2}$, the condition $\xi(T) \gg l$ reduces to $\xi_0/l \gg 1 - T/T_c$. Furthermore, since $\xi_0 \gg l$, this condition is much less strict than the general condition of validity for the Landau theory of the second-order phase transitions, $T_{\mathrm{c}} - T \ll T_{\mathrm{c}}$.

Consider the second condition: $\lambda(T) \gg l$. Recalling that, for dirty superconductors, $\lambda(T) \sim \lambda(0) (\xi_0/l)^{1/2} (1 - T/T_{\mathrm{c}})^{-1/2}$ and $\kappa \sim \lambda(0)/l$, it can be rewritten as $\kappa^2 (\xi_0/l) \gg 1 - T/T_c$. If $\kappa \sim 1$, we find once again that it is less strict than the general condition $T_{\mathrm{c}} - T \ll T_{\mathrm{c}}$.

Thus, in the case of dirty superconductors (alloys), the GL theory is valid within a rather wide temperature interval - at least, qualitatively - and, provided the condition $T_{\mathrm{c}} - T \ll T_{\mathrm{c}}$ is satisfied, also quantitatively.

Superconducting coherence length from the microscopic theory

The wavefunction of the ground state of the superconductor is already known to us from Sect.6.2.1. The ground state can be represented by the distribution of electron pairs in momentum space given by the function v_k^2. The dependence of v_k^2 on k is plotted in Fig. 6.5.

(add it here)

One can see that large variations of v_k^2 can occur only within the

$$\Delta k \sim 2\Delta_0 \frac{k_{\mathrm{F}}}{\varepsilon_{\mathrm{F}}}$$

Then, in real space, large variations of the ground state wavefunction can be expected within the interval Δx defined by the relation

$$\triangle x \triangle k \sim 1$$

It follows that

$$\Delta x \sim \frac{\varepsilon_{\mathrm{F}}}{2\Delta_0 k_{\mathrm{F}}} = \frac{1}{2\Delta_0 k_{\mathrm{F}}} \frac{\hbar^2 k_{\mathrm{F}}^2}{2m} = \frac{\hbar p_{\mathrm{F}}}{4\Delta_0 m} = \frac{\hbar v_{\mathrm{F}}}{4\Delta_0} \tag{6.26}$$

Here p_{F} is the electron momentum and v_{F} the velocity of electrons on the Fermi surface. But, in terms of its physical significance, the quantity Δx is exactly the same as the quantity that we called the coherence length ξ, when studying the Ginzburg-Landau theory: Hence, we conclude that (6.26) provides an estimate of the coherence length ξ_0 at $T = 0$:

$$\xi_0 \sim \frac{\hbar v_{\mathrm{F}}}{4\Delta_0}. \tag{6.27}$$

It will be demonstrated below that $\Delta_0 \sim k_{\mathrm{B}} T_{\mathrm{c}}$, where k_{B} is the Boltzmann constant and T_{c} is the critical temperature. A rigorous calculation yields

$$\xi_0 = 0.18 \frac{\hbar v_{\mathrm{F}}}{k_{\mathrm{B}}} \frac{T_{\mathrm{c}}}{T_{\mathrm{c}}} \tag{6.28}$$

The quantity ξ_0 can also be treated as the size of a Cooper pair which can be evaluated as

$$\xi_0 \simeq 0.18 \frac{10^{-27} \times 10^8}{1.38 \times 10^{-16} \times 1} \sim 10^{-4} \text{ cm}$$

where $v_{\mathrm{F}} \sim 10^8$ cm s^{-1} and $T_{\mathrm{c}} \sim 1$ K. This is a large, macroscopic distance.

Microscopic Derivation Of The Ginzburg-landau Equations In The Theory Of Superconductivity by Gor'kov

It is shown that the phenomenological Ginzburg-Landau equations follow from the theory of superconductivity in the London temperature region in the neighborhood of $\mathrm{T_c}$. In these equations there occurs, however, twice the electronic charge; this is related to the physical meaning of $\Psi(x)$ as the wave function for Cooper pairs. The constant κ turns out to be small. The problem of the surface energy for the boundary between the normal and superconducting phases in the neighborhood of $\mathrm{T_c}$ is discussed.

Gor'kov's derivations

(???? think about them more later!!!!)

It is well known that the behavior of superconductors in a magnetic field in the neighborhood of the critical temperature is qualitatively well described by Ginzburg and Landau's phenomenological theory. We shall show in the present paper that equations of the same type as those in Ginzburg and Landau's theory follow indeed from the theory of superconductivity.

We shall start from the equations for the thermodynamic Green functions [3,4] which we obtained earlier. [2] These equations are in a magnetic field of the form

$$\left\{ -\frac{\partial}{\partial \tau} + \frac{1}{2m} \left(\frac{\partial}{\partial \mathrm{r}} - ie\mathbf{A}(\mathrm{r}) \right)^2 + \mu \right\} G(x, x') + \Delta(\mathrm{r}) F^+(x, x') = \delta(x - x')$$

$$\left\{ \frac{\partial}{\partial \tau} + \frac{1}{2m} \left(\frac{\partial}{\partial \mathrm{r}} + ie\mathbf{A}(\mathrm{r}) \right)^2 + \mu \right\} F^+(x, x') - \Delta^*(\mathrm{r}) G(x, x') = 0; \tag{1}$$

where

$$\Delta^*(\mathbf{r}) = g F^+(\tau, \mathbf{r}; \tau, \mathbf{r}).$$

The last relation expresses $\Delta(\mathbf{r})$ in terms of the coupling constant and the value of the function $F^+(x, x')$ for equal arguments. If there is no field, $\Delta = \text{const}$. The quantity 2Δ is in that case the energy gap in the spectrum. $\mathrm{F^+(x, x')}$ tends, in fact, logarithmically to infinity as

$x = x'$; this corresponds to the well known logarithmic divergence in the equation determining the gap when one integrates in momentum space. In the papers by Bardeen, Cooper, and Schrieffer [5] and Bogolyubov [6] this divergence was removed by cutting-off the energy of the interacting electrons at distances of the order of the Debye frequency $\widetilde{\omega}$ from the Fermi surface; we
shall do the same in the following. One verifies easily that such a cut-off corresponds in the coordinate representation to a "spread out" in Eq. (1') over a distance of the order $\hbar v/\bar{\omega}$.

Let us go over to the Fourier components of the Green functions $G(x, x')$ and $F^+(x, x')$ with respect to the difference of the variables $u = \tau - \tau'$, for instance,

$$G(\mathbf{r}, \mathbf{r}'; u) = T \sum_n e^{-i\omega_n u} \mathfrak{G}_\omega(\mathbf{r}, \mathbf{r}'),$$
$$\mathfrak{G}_\omega(\mathbf{r}, \mathbf{r}') = \frac{1}{2} \int_{-1/T}^{+1/T} e^{i\omega_n u} G(\mathbf{r}, \mathbf{r}'; u)\, du$$

where $\omega_n = \pi(2n+1)T (n = \ldots -1, 0, 1, \ldots)$. Equations (1) go over into the following equations for the Fourier components $\mathscr{G}_\omega(\mathbf{r}, \mathbf{r}')$ and $\mathfrak{F}^+_\omega(\mathbf{r}, \mathbf{r}')$:

$$\left\{ i\omega_n + \frac{1}{2m}\left(\frac{\partial}{\partial \mathbf{r}} - ie\ \mathrm{A}(\mathbf{r})\right)^2 \div \mu \right\} \mathfrak{G}_\omega(\mathbf{r}, \mathbf{r}') + \Delta(\mathbf{r}) \mathfrak{F}^+_\omega(\mathbf{r}, \mathbf{r}') = \delta(\mathbf{r} - \mathbf{r}'),$$
$$\left\{ -i\omega_n + \frac{1}{2m}\left(\frac{\partial}{\partial r} + ie\ \mathrm{A}(\mathbf{r})\right)^2 + \mu \right\} \mathfrak{F}^+_\omega(\mathbf{r}, \mathbf{r}') - \Delta^*(\mathbf{r}) \mathfrak{G}_\omega(\mathbf{r}, \mathbf{r}') = 0, \tag{2}$$

and condition (1') can be written in the form

$$\Delta^*(\mathbf{r}) = T \sum_n \mathfrak{F}^+_\omega(\mathbf{r}, \mathbf{r}).$$

We introduce, finally, $\tilde{\mathfrak{G}}_\omega(\mathbf{r}, \mathbf{r}')$, the Fourier component of the Green function for an electron in the normal metal in a magnetic field. The equation satisfied by $\mathfrak{G}_\omega(\mathbf{r}, \mathbf{r}')$ can be written in two ways:

$$\left\{ i\omega_n + \frac{1}{2m}\left(\frac{\partial}{\partial \mathbf{r}} - ie\mathbf{A}(\mathbf{r})\right)^2 + \mu \right\} \tilde{\mathfrak{G}}_\omega(\mathbf{r}, \mathbf{r}') = \delta(\mathbf{r} - \mathbf{r}') \tag{3}$$
$$\left\{ i\omega_n + \frac{1}{2m}\left(\frac{\partial}{\partial \mathbf{r}'} + ie\mathbf{A}(\mathbf{r}')\right)^2 + \mu \right\} \tilde{\mathfrak{G}}_\omega(\mathbf{r}, \mathrm{r}') = \delta(\mathbf{r} - \mathbf{r}').$$

It is convenient to use the function $\tilde{\mathfrak{G}}_\omega(\mathbf{r}, \mathbf{r}')$ to write Eqs. (2) in integral form, using the second of Eqs. (3):

$$\mathfrak{G}_\omega(\mathbf{r}, \mathbf{r}') = \tilde{\mathfrak{G}}_\omega(\mathbf{r}, \mathbf{r}') - \int \tilde{\mathfrak{G}}_\omega(\mathbf{r}, \mathbf{s}) \Delta(\mathbf{s}) \mathfrak{F}^+_\omega(\mathbf{s}, \mathbf{r}) d^3\mathbf{s},$$
$$\mathfrak{F}^+_\omega(\mathbf{r}, \mathbf{r}') = \int \mathfrak{G}(\mathbf{s}, \mathbf{r}')\, \Delta^*(\mathbf{s}) \tilde{\mathfrak{G}}_{-\omega}(\mathbf{s}, \mathbf{r}) d^3\mathbf{s} \tag{4}$$

Before we proceed, we find out what the function $\tilde{\mathfrak{G}}_\omega(\mathbf{r}, \mathbf{r}')$ is equal to. If there is no magnetic field, one sees from (3) that

$$\mathfrak{G}^0_\omega(\mathbf{r} - \mathbf{r}') = -\frac{m}{2\pi R} \exp\left\{ \left[i \operatorname{sign} \omega p_0 - \frac{|\omega_n|}{v} \right] R \right\}. \tag{5}$$

Here

$$\operatorname{sign}\omega = \omega/|\omega|, \quad R = |\mathbf{r}-\mathbf{r}'|, \quad \mu = p_0^2/2m \gg |\omega|.$$

$\tilde{\mathfrak{G}}_\omega(\mathbf{r},\mathbf{r}')$ in a magnetic field differs from (5) by a phase factor. Indeed, because p_0 is a large quantity we can use the quasi-classical approximation to determine $\tilde{\mathfrak{G}}_\omega(\mathbf{r},\mathbf{r}')$, i.e., write it in the following form:

$$\tilde{\mathfrak{G}}_\omega(\mathbf{r},\mathbf{r}') = e^{i\varphi(r,r')}\tilde{\mathfrak{G}}^0_\omega(\mathbf{r}-\mathbf{r}'), \qquad \varphi(\mathbf{r},\mathbf{r}')\,|_{\mathbf{r}=\mathbf{r}'} = 0. \tag{6}$$

Substituting (6) into (3) we find for the addition to the action of $\varphi(\mathbf{r},\mathbf{r}')$

$$(\mathbf{n}, \nabla_r\varphi(\mathbf{r},\mathbf{r}')) = \frac{e}{c}(\mathbf{n},\mathbf{A}(\mathbf{r})), \qquad \mathbf{n} = (\mathbf{r}-\mathbf{r}')/|\mathbf{r}-\mathbf{r}'|.$$

Near the transition temperature $\Delta(\mathbf{r})$ (and at the same time $\hat{y}^+_\omega(\mathbf{r},\mathbf{r}')$) is small. We shall therefore expand Eq. (4) in powers of Δ and Δ^* and express $\mathfrak{F}^+_\omega(\mathbf{r},\mathbf{r}')$ up to terms of the fourth order, and $\mathfrak{G}_\omega\omega(\mathbf{r},\mathbf{r}')$ up to terms of second order in Δ, inclusive. The substitution of the expression obtained for $\mathfrak{F}^+_\omega(\mathbf{r},\mathbf{r}')$ into (2′) gives one equation connecting $\Delta(\mathbf{r})$ and A(**r**):

$$\Delta^*(\mathbf{r}) = gT\sum_n \int \tilde{\mathfrak{G}}_\omega(\mathbf{r},\mathbf{r}')\,\tilde{\mathfrak{G}}_{-\omega}(\mathbf{r},\mathbf{r}')\,\Delta^*(\mathbf{r}')\,d^3\mathbf{r}'$$
$$- gT\sum_n \iiint \tilde{\mathfrak{G}}_\omega(\mathbf{s},\mathbf{r})\tilde{\mathfrak{G}}_{-\omega}(\mathbf{s},\mathbf{l})\tilde{\mathfrak{G}}_\omega(\mathbf{m},\mathbf{l})\tilde{\mathfrak{G}}_{-\omega}(\mathbf{m},\mathbf{r})\Delta(\mathbf{s})\Delta^*(\mathbf{l})\Delta^*(\mathbf{m})d^3\mathbf{s}d^3|d^3\mathbf{m} \tag{8}$$

The important distances in Eq. (8) are of the order $\xi = \hbar v/T_c$, since it can be seen from (5) and (6) that the Green function $\tilde{\mathfrak{G}}_\omega(\mathbf{r},\mathbf{r}')$ decreases exponentially for $R > \xi_0$. At the same time, the changes in the gap $\Delta(\mathbf{r})$ and the field $\mathbf{A}(\mathbf{r})$ take place at distances of the order of the penetration depth which is much larger than ξ_0 near the critical temperature. For the same reason the phase $\varphi(\mathbf{r},\mathrm{r}')$ in (6) is small near $\mathrm{T_c}$ and equal to

$$\varphi(\mathbf{r},\mathbf{r}') \approx \frac{e}{c}(\mathbf{A}(\mathbf{r}'),\mathbf{r}-\mathbf{r}') \tag{9}$$

Using these facts we can perform the integration in Eq. (8).

The first term on the right hand side is of the form

$$g\int K(\mathbf{r},\mathbf{r}')\,\Delta^*(\mathbf{r}')\,d^3\mathbf{r}'$$

where the kernel

$$K(\mathbf{r},\mathbf{r}') = K_0(\mathbf{r}-\mathbf{r}')\exp\left\{\frac{2ie}{c}(\mathbf{A}(\mathbf{r}'),\mathbf{r}-\mathbf{r}')\right\}$$

has a singularity for $R = |\mathbf{r}-\mathbf{r}'| = 0$:

$$K_0(R) = m^2T/(2\pi R)^2\sinh(2\pi TR/v)$$

This singularity is connected, as was pointed out already in the foregoing, with the cut-off of the interaction at the Debye frequencies $\tilde{\omega}$.

Introducing this cut-off we get

$$\int K_0(R)d^3R = \frac{m\rho_0}{2\pi^2}\int_0^{\tilde{\omega}}\frac{\tanh(\xi/2T)}{\xi}d\xi = \frac{m\rho_0}{2\pi^2}\ln\left(\frac{2\gamma}{\pi}\frac{\tilde{\omega}}{T}\right) = \frac{m\rho_0}{2\pi^2}\left(\frac{1}{g}+\ln\frac{T_c}{T}\right) \tag{10}$$

*This was pointed out by L. D. Landau.

where the transition temperature $\mathrm{T_c}$ is connected to the gap in the energy spectrum at absolute zero in the well-known way [5]:

$$\frac{\Delta_0 \mathcal{Y}}{\pi} = T_c \quad \left(\frac{1}{g} = \frac{m\rho_0}{2\pi^2} \ln \frac{2\tilde{\omega}}{\Delta_0}\right).$$

Expanding the exponents in the Green functions in terms of $\varphi(\mathbf{r}, \mathbf{r}')$ using the fact that $\Delta(\mathbf{r})$ and $\mathrm{A}(\mathbf{r})$ vary slowly near T_c, and eliminating $\tilde{\omega}$ and g by using (10) we get the following equation

$$\left\{\frac{1}{2m}\left(\frac{\partial}{\partial \mathbf{r}} + 2ie\mathbf{A}(\mathbf{r})\right)^2 + \frac{1}{\lambda}\left[\frac{T_c - T}{T_c} - \frac{7\zeta(3)}{8\left(\pi T_c\right)^2}|\Delta(\mathbf{r})|^2\right]\right\}\Delta^*(\mathbf{r}) = 0 \tag{11}$$

where $\lambda = 7\zeta(3)\epsilon_{\mathrm{F}}/12\left(\pi\ \mathrm{T_c}\right)^2$ (ζ(x) is here Riemann's zeta function).

To get a second equation connecting Δ and A we shall now calculate what the current density f(r) is equal to. To do this we use the relation expressing $j(r)$ in terms of a Green function:

$$\mathrm{j}(\mathbf{r}) = \left\{\frac{ie}{m}\left(\nabla_{\mathbf{r}'} - \nabla_{\mathrm{r}}\right)G\left(x, x'\right) - \frac{2e^2}{mc}\mathbf{A}(\mathbf{r})G\left(x, x'\right)\right\}_{t'=t+0; r=r'}$$

(the additional factor of 2 is due to a summation over spin). We note that if we substitute everywhere the Green function for the normal metal in the form (6) and then sum over frequencies we get no contribution to the expression for the current, as should be the case. The total current is thus equal to

$$\mathrm{j(r)} = \frac{ie}{m}\left(\nabla_{\mathrm{r}'} - \nabla_{\mathrm{r}}\right)\delta G\left(x, x'\right)\Big|_{x=x'}, \tag{12}$$

where

$$\delta G\left(x, x'\right)|_{x=x'} = -T\sum_n \iint \tilde{\mathfrak{G}}_\omega(\mathbf{r}, \mathbf{s})\tilde{\mathfrak{G}}_\omega(\mathbf{l}, \mathbf{r})\tilde{\mathfrak{G}}_{-\omega}(1, \mathbf{s})\Delta^*(\mathbf{l})\Delta(\mathbf{s})d^3\mathbf{s}d^3\mathbf{l}$$

Restricting ourselves in the expression for the current to terms linear in A and assuming $A(r)$ to vary slowly with $\mathbf{r}$ in the London temperature range near $\mathrm{T_c}$ we get

$$\mathrm{j(r)} = \left\{\frac{ie}{m}\left(\Delta\frac{\partial\Delta^*}{\partial \mathrm{r}} - \Delta^*\frac{\partial\Delta}{\partial \mathrm{r}}\right) - \frac{4c^2|\Delta|^2}{mc}\mathbf{A}\right\}\frac{7\zeta(3)N}{16(\pi T)^2} \tag{14}$$

We shall introduce a "wave function" $\Psi(\mathbf{r})$, proportional to $\Delta(\boldsymbol{r})$:

$$\Psi(r) = \Delta(r)\sqrt{7\zeta(3)N}/4\pi T_c \tag{15}$$

The set of Eqs. (11) and (14) takes then a form completely analogous to the equations of the phenomenlogical Ginzburg-Landau theory:

$$\left\{\frac{1}{2m}\left(\frac{\partial}{\partial \mathrm{r}} - ie^*A(\mathrm{r})\right)^2 + \frac{1}{\lambda}\left[\frac{T_c - T}{T_c} - \frac{2}{N}|\Psi(\mathrm{r})|^2\right]\right\}\Psi(\mathrm{r}) = 0 \tag{16}$$

$$\mathrm{j(r)} = -\frac{ie^*}{2m}\left(\Psi^*\frac{\partial\Psi}{\partial \mathrm{r}} - \Psi\frac{\partial\Psi^*}{\partial \mathrm{r}}\right) - \frac{e^{*2}}{mc}\mathbf{A}\left|\Psi^*\right|^2,$$

where $e^* = 2e$, N is the number density of the electrons in the normal metal and λ was defined after Eq. (11). There is a difference, however, in that (16) contains the electronic charge e twice, clearly owing to the physical meaning of $\Psi(r)$ as the wave function of a Cooper pair.

These equations arise thus in a natural way in the theory of superconductivity in the London region* near T_c. The phenomenological constant defined in the same way as in the old theory, but with $e^* = 2e$, can now be evaluated and turns out to be equal to

$$x = 3T_c(\pi/v)^{1/2}\,(c/ep_0)\,\sqrt{2/7\zeta(3)} \tag{17}$$

The region of applicability of Eqs. (16) is small for sharply expressed Pippard metals and occurs very near T_c; at large distances from T_c the local relation (14) ceases to be valid.

For metals of the London type the region of applicability of (16) is determined solely by the smallness of the ratio $(\mathrm{T} - \mathrm{T_c})/\ \mathrm{T_c}$.

The possibility to apply (16) to describe the properties of thin films in a magnetic field with the microscopic value (17) of the constant κ is limited by the fact that usually films are polycrystalline specimens with grain sizes of the order of the film thickness. The presence of boundaries between different crystals will act like the presence of foreign impurities. One must therefore possibly describe real films in the microscopic theory from the same point of view as superconducting alloys.

We note now that to evaluate the difference in the free energy of the metal in the normal state and in the superconducting state in a magnetic field we can use the following formula:

$$F_{sH} - F_n = -(1/\lambda N)\int |\Psi(r)|^4 d^3\mathbf{r} \tag{18}$$

Indeed, we shall use the thermodynamic relation

$$\delta\Omega/\delta g(\mathbf{r}) = -\langle H_{\mathrm{int}}(\mathbf{r})\rangle/g(\mathbf{r})$$

where according to (5)

$$H_{\mathrm{int}}(r) = \frac{1}{2}g(r)\left(\hat{\Psi}^+(r)\left(\hat{\Psi}^+(r)\hat{\Psi}^+(r)\right)\hat{\Psi}^{(r)}(r)\right.$$

Ω is the thermodynamic potential [we introduce here for the sake of convenience a variable "interaction constant" $g(r)$]. Taking averages we get

$$\Omega_s - \Omega_n = -\int d^3r \int_0^g \frac{\delta g(r)}{g^2(r)}|\Delta(r)|^2 \tag{19}$$

Equation (8) determines $1/g(\mathbf{r})$ as a functional of $\Delta(r)$ [for the sake of simplicity we shall consider the real solution for $\Delta(r)$ as is usually done in one-dimensional problems]. Using (8) to integrate (19), and using the fact that small additions to all thermodynamic potentials in the corresponding variables are equal, we get Eq. (18).

The constant κ of (17) is connected with the magnitude of the critical field $\mathrm{H_{cm}}$ of a bulk specimen and the penetration depth δ_0 by the relation (which contains the charge e^*):

$$x = \frac{\sqrt{2}e^*}{\hbar c}H_{cm}\delta_0^2 \tag{20}$$

For metals of the London type or such intermediate metals as tin the region of applicability of Eqs. (16) is fairly large and in that case we should consistently use the experimental data* for $\mathrm{H_{cm}}$ and δ_0^2 to compare the theory with experiments. For Pippard metals δ_0 is the penetration depth only in a very narrow range of temperatures near T_c. It is thus convenient in this case to turn to the theoretical formulae for a definition of κ. It can easily be verified that (17) can be written in the form

$$x \approx 0.96\delta_L/\xi_0 \tag{21}$$

where $\delta_{\mathrm{L}}^{-1} = \left(4\pi \mathrm{Ne}^2/mc^2\right)^{1/2}$ is the London penetration depth and $\xi_0 = 0.18\hbar \mathrm{v}/\mathrm{kT_c}$ is the non-localization parameter introduced in Bardeen, Cooper, and Schrieffer's paper. Using the data given in reference 5 we get from (21) for tin $\kappa \approx 0.14$, and for aluminum $\kappa \approx 0.01$.

We note an interesting consequence of (21). The condition that a superconductor be a London one requires $\kappa \approx \delta_L/\xi_0 \gg 1$. At the same time if $\kappa \gg 1/\sqrt{2}$ a metal displays in a strong field the same behavior as for alloys. A metal which in weak fields at $T = 0$ must be assigned to the London class will thus behave in strong fields near $\mathrm{T_c}$ as an "alloy." At the same time the case of small κ corresponds to a Pippard metal.

Let us now stop a moment at the problem of the surface energy at the boundary between the normal and the superconducting phase. For strongly expressed Pippard superconductors we can, because κ is small, use the limiting solution [1]

$$\sigma_{ns}\left(8\pi/H_{cm}^2\right) = 1.89\delta_0/x \tag{22}$$

where

$$\delta_0 = \delta_L(T=0)/\sqrt{2\,(1-T/T_c)}.$$

We note that for these metals the applicability of Eq. (22) in an appreciable temperature interval near $\mathrm{T_c}$ is just connected with the fact that κ is small, since, as was shown in reference 1, in that case the quantity σ_{ns} does not depend on the distribution of the field in the transition region.

For tin the accuracy of this equation is insufficient and one must use the results of numerical calculations. Estimating σ_{ns} from Ginzburg's calculations [8] we get for $\kappa \approx 0.14$

$$\sigma_{ns}\left(8\pi/H_n^2\right) \approx (2 \div 3)\cdot 10^{-5}/\sqrt{1-T/T_c}$$

According to Sharvin's data [9]

$$\sigma_{ns}\left(8\pi/H_c^2\right) = 2.5\cdot 10^{-5}/\sqrt{1-T/T_c}$$

and according to Faber's data [10]

$$\sigma_{ns}\left(8\pi/H_c^2\right) = 1.88\cdot 10^{-5}/\sqrt{1-T/T_c}$$

These results do, apparently, not contradict the theory (See reference 7).

5.2.2 What is Different in Equilibrium and Non-Equilibrium Superconductors?

(discuss what will chenge? for non-eq sc - see some sections at the end of the note)

5.2.3 Derivation of phenomena of GL theory in the framework of BCS theory

(??? a very hard section, I have no idea how to do it now)

5.2.4 Derivation of phenomena of BCS theory in the framework of GL theory

(??? a very hard section, I have no idea how to do it now)

5.2.5 Existence of 1D superconductors

(here will be a detailed discussion about it, since there are always questions about it!)
(still, often we use such formulas)

5.2.6 General idea of dissipation in superconductors

(!!! I'll crate here theory about basics, more details - in another note or at some latter part of this note)

Formalism for dissipation for BCS model

We can just add a Lindblad operator, because it is often done in open systems.
(????)

Connection of Lindblad operator and physical processes

(??? how can we make if from some coupling???)

Choice of Lindblad operators and dissipator

(????)
(here is about the dissipator that was used in the work with Zala)
(write that it acts on all the momenta, not in the Debye's window because we have electron and hole excitations, all with positive energy)

Lindblad operators for BCS theory: Other questions

Why some Lindblad operators are broken if there are some reasonable parameters in the BCS TB model?

(this is the question which I tried to answer in September 2025)
(remind the form of the lindbladian)
(write that with this code we get these plots, which are broken)
(??? and then answer the question. I don't know yet the answer)

Other about basics of dissipation in superconductivity

5.2.7 Other General Fundamental Concepts

How Exactly Temperature of Superconductor is Established?

Suppose we are in an empty space (where there are only vacuum fluctuations) and we have a material. What will fix its temperature? How would electrons know, if they should be in superconductive state or in normal?

Answer

They "feel" energy of an atom, then collect statistics and compare it with the fundamental constant $\hbar$.
(??? but how exactly??)
(????? this is a question on statistical physics, so I'll write answer there and then these ideas will be applied to the superconductivity)

How Exactly Electrons will know, where spin of each points?

(??? should there be a selected axes? maybe yes, because withought it spin will be in different directions and there will be on +,- spins.)

5.2.8 How can we theoretically prove that other low-energy effects do not destroy SC?

(it is maybe impossible, and also very hard and also not needed at all. but later I'll maybe think about it)

5.3 Other Typical Properties

5.3.1 Velocity of superconductive electrons

(here we will discuss in details the question about what is the velocity of electrons in SC?)

5.3.2 Parity Effect in SC by Shmidt 48*

При температурах $T \ll T_c$ большая часть электронов в сверхпроводнике образует куперовские пары и лишь экспоненциально малая их доля (порядка $e^{-\Delta/k_{\rm B}T}$) находится в возбужденных состояниях с энергией $E > \Delta$ (это следует из выражения (45.9) для функции распределения $f_{\mathbf{k}}$). Это означает, что для изолированного островка сверхпроводящего металла имеет смысл вопрос о четности полного числа электронов на нем. Действительно, если число электронов четно, то при $T = 0$ все они образуют пары; в противном случае какой-то электрон остается неспаренным, т. е. энергия всего островка будет выше на величину минимальной энергии возбуждения Δ_0. Напомним (см. (44.17)), что плотность энергии сверхпроводящего спаривания равна $|W_0| = \frac{1}{2}N(0)\Delta_0^2$, т.е. полное изменение энергии островка объема V из-за сверхпроводящего спаривания состояния имеет порядок $\mathcal{N}_{\text{полн}}\,\Delta_0^2/\varepsilon_{\rm F}$, где $\mathcal{N}_{\text{полн}} \sim N(0)V\varepsilon_{\rm F}$ - полное число электронов. Таким образом, изменение числа куперовских пар на единицу приводит к изменению энергии лишь на величину Δ_0^2/ε_F, много меньшую, чем Δ_0. Пренебрегая этой малой поправкой, получаем, что при добавлении к "нечетному" островку еще одного электрона его полная энергия понизится на Δ_0, т. к. квазичастица (возбуждение) исчезнет и образуется дополнительная куперовская пара (с энергией на уровне Ферми).

Можно ли экспериментально обнаружить периодическое изменение свойств сверхпроводящего островка с периодом $2e$? В работе [147] было впервые продемонстрировано, что это возможно, несмотря на то, что полное число $\mathcal{N}_{\text{полн}}$ электронов на островке было порядка 10^9. Прежде чем описать этот эксперимент, мы выясним, как обобщить приведенное выше простое рассуждение, справедливое при $T = 0$, на случай отличных от нуля температур.

Самое простое соображение таково: полное число квазичастиц на островке есть

$$N_{qp} = \sum_{\mathbf{k}} f_{\mathbf{k}} = N(0)V \int\limits_0^\infty \frac{d\varepsilon}{\exp\left(\sqrt{\varepsilon^2+\Delta^2}/k_{\rm B}T\right)+1} \sim$$
$$\sim \mathcal{N}_{\text{эфф}}\, e^{-\Delta/k_{\rm B}T} \tag{48.1}$$

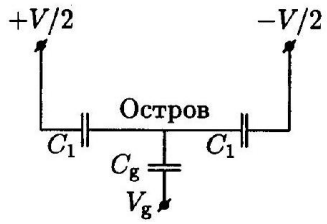
где $\mathcal{N}_{\text{эфф}} \approx N(0)V\sqrt{T\Delta}$ близко по порядку величины к числу электронов на островке, имеющих энергии в полосе порядка Δ_0 вблизи ферми-поверхности (действительно,

электроны с энергиями, много большими Δ_0, в любом случае "ничего не знают" о сверхпроводящем спаривании). Если величина N_{qp} окажется много меньше единицы, то вероятность найти на островке хотя бы одно возбуждение мала и картина такая же, как при $T = 0$; отсюда получается условие $k_{\mathrm{B}}T \ll \Delta_0/\ln \mathcal{N}_{\text{эфф}}$. Более аккуратное рассмотрение необходимо, чтобы понять, что происходит при $k_{\mathrm{B}}T \sim \Delta_0/\ln \mathcal{N}_{\text{эфф}}$. Оно проводится следующим образом: при $T > 0$ вместо энергии неспаренного электрона следует использовать его свободную энергию $F_1(T) = \Delta - TS_1$, где соответствующая энтропия $S_1 = k_{\mathrm{B}} \ln \mathcal{N}_{\text{эфф}}$. В таком случае эффект четности имеет место, если появление неспаренного электрона увеличивает свободную энергию островка, т.е. при $F_1(T) > 0$, что имеет место при температурах

$$T < T^* = \frac{\Delta_0}{k_{\mathrm{B}} \ln \mathcal{N}_{\text{эфф}}} \tag{48.2}$$

Таким образом, можно ожидать (при $\ln \mathcal{N}_{\text{эфф}} \gg 1$), что эффект четности возникает при определенной температуре, как это бывает при фазовом переходе. В условиях экспериментов по эффекту четности [147] число $\mathcal{N}_{\text{эфф}} \sim 10^4$, так что ожидаемое $k_{\mathrm{B}}T^* \simeq 0.1\Delta_0$, что и было подтверждено экспериментально. Точное вычисление (приведенное, например, в книге [2]) показывает, что полученное выше из качественных соображений выражение для $F_1(T)$ является правильным с точностью до численного коэффициента в выражении для $\mathcal{N}_{\text{эфф}}$. Поскольку в ответ входит лишь логарифм $\mathcal{N}_{\text{эфф}}$, это отличие малосущественно.

Рис. 48.1. Электрическая схема электрометра с кулоновской блокадой.

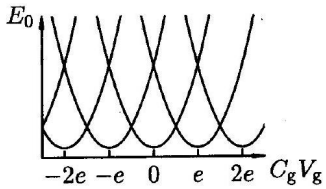


Перейдем теперь к описанию проведенных в [147, 148] экспериментов, где был использован прибор, называемый сверхпроводящим одноэлектронным транзистором (СОЭТ). Его электрическая схема изображена на рис. 48.1: алюминиевый островок в виде тонкой пленки (раэмерами $0.2 \times 0.6 \times 2$ мкм ^{3} в условиях эксперимента [147]) соединялся со включенными в цепь алюминиевыми берегами высокоомными ($R_{1,2} \gg h/e^2 \simeq 26$ кОм, смысл этого условия будет прояснен ниже) туннельными контактами с емкостями C_1, C_2. Кроме того, около островка располагался электрический затвор, позволявший создавать на островке заданный потенциал V_g, от которого зависит электростатическая энергия $U_{el}(n, V_g)$ островка с добавленными на него n электронами:

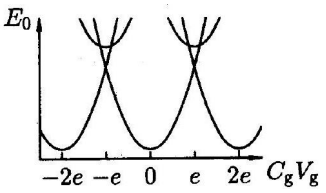
$$U_{el}(n, V_g) = \frac{(en)^2}{2C} - \frac{ne}{C} C_g V_g, \quad C = C_g + C_1 + C_2 + C_0 \tag{48.3}$$

(здесь C_0-собственная емкость островка). Пусть $k_{\mathrm{B}}T \ll E_C = e^2/2C$, а островок находится в нормальном состоянии (что достигается, например, приложением магнитного поля $H > H_c$, разрушающего сверхпроводимость). Число электронов на островке определяется из условия минимума энергии $U_{el}(n)$ по n и меняется на единицу при полуцелых значениях $C_g V_g/e = m + 1/2$, когда энергии состояний с $n = m, m+1$ совпадают. Графически это удобно представлять как точки пересечения парабол $\widetilde{U}_{el}(n, V_g) = \frac{(\,\mathrm{en} - C_g V_g)^2}{2C}$, изображенных на рис. 48.2, a (добавление не зависящего от n члена $(C_g V_g)^2/2C$ к $U_{el}(n, V_g)$ не меняет результат минимизации энергии по n).

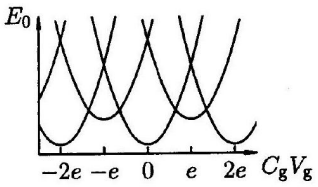
Рассмотрим теперь ту же систему в сверхпроводящем состоянии, причем $T < T^*$, так что свободная энергия одного возбуждения велика: $F_1(T) > E_C \gg k_{\mathrm{B}}T$. Теперь все кривые $\widetilde{U}_{el}(V_g)$ с нечетными n поднимутся вверх на величину $F_1(T) > e^2/2C$, см. рис. 48.2, 6, так что минимум электростатической энергии всегда достигается на кривых с четным числом электронов $n = 2k$ и изменение этого числа происходит при $C_gV_g/e = 2m + 1$. Скачок заряда на островке при этих значениях потенциала означает, что эффективная дифференциальная емкость островка по отношению к затвору $C_{\text{эфф}} = d(en)/dV_g$ имеет резкие пики с периодом $\Delta V_g = 2e/C_g$ (вместо e/C_g в нормальном состоянии). Таким образом, измерение дифференциальной емкости позволяет пронаблюдать возникновение эффекта четности как переход от - к $2e$-периодичности в зависимости $C_{\text{эфф}}(V_g)$. Этот метод был использован в работе [148].



а)



б)



в)

Рис. 48.2. Качественное поведение энергии островка в зависимости от заряда C_gV_g на затворе: a) островок в нормальном состоянии; б) $F_1(T) > E_C \gg k_{\mathrm{B}}T; \theta)\, E_C > F_1(T) \gg k_{\mathrm{B}}T$.

В работе [147] использовался другой метод - измерялась зависимость критического джозефсоновского тока I_c через островок от V_g. Рассмотрим происхождение этой зависимости для слу'ая $F_1(T) > E_C$, когда реализуются только "четные" состояпия на островке. В отличие от обычного джозефсоновского контакта (с прямым туннелированием пар с одного берега на другой), здесь туннелирование куперовской пары с первого берега на второй происходит через промежуточное виртуальное (в квантовомеханическом смысле) состояние островка. Энергия этого промежуточного состояния $U_2(V_g) = U_{el}(n_{\min} + 2) - U_{el}(n_{\min}) = 4E_C \min_k \left|2k + 1 - \frac{C_gV_g}{e}\right|$ зависит от C_gV_g периодически с пе риодом $2e$. В эксперименте с СОЭТ E_C много больше матричного элемента K туннелирования пары в каждом контакте; предполагая также, что $K \ll U_2(V_g)$, получаем с помощью квантовомеханической теории возмущений энергию джозефсоновской связи между берегами $K^{\text{эфф}} = K^2/U_2(V_g)$ (более подробный вывод, аналогичный фейнмановскому выводу выражения (21.9) для джозефсоновского тока, приведен в книге [2]). Поэтому максимальный джозефсоновский ток через СОЭТ равен

$$I_c\left(V_g\right)=\frac{2e}{\hbar}\frac{K^2}{U_2\left(V_g\right)} \tag{48.4}$$

Электростатическая энергия $U_2\left(V_g\right)$ зависит от C_gV_g с периодом $2e$, что и приводит к такой же периодичности в $I_c\left(V_g\right)$ с резкими максимумами при $V_g=\frac{e}{C_g}(2m+1)$, где $U_2\left(V_g\right)$ обращается

в нуль (вблизи этих максимумов $U_2\left(V_g\right)$ становится меньше K, так что формула (48.4) там неприменима; критический ток в максимумах имеет порядок $I_c^{\max}\sim(2e/\hbar)K$, см. [149]).

При выводе (48.4) мы подразумевали, что $F_1(T)>E_C\gg k_{\mathrm{B}}T$, так что "нечетные» состояния островка не реализуются ни при каких V_g. С повышением температуры величина $F_1(T)$ становится меньше E_C, и тогда вырожденными по полной энергии $U_{el}\left(V_g\right)+F_1(T)\frac{1-(-1)^n}{2}$ оказываются состояния различной четности (отличающиеся по заряду на e), см. рис. 48.2, в. Это означает, что состояния островка, переходящие друг в друга при туннелировании одной куперовской пары, т.е. отличающиеся на $2e$ по заряду, имеют разность кулоновских энергий порядка E_C при всех V_g. В результате "кулоновский знаменатель" в (48.4) всегда остается величиной порядка E_C, так что максимальное значение критического тока резко падает; при $F_1(T)\ll E_C$ эффектами четности можно полностью пренебречь, и зависимость $I_c\left(V_g\right)$ имеет период e с максимумами при $V_g=\frac{e}{2C_g}(2m+1)$. Последовательный микроскопический вывод зависимостей $I_c\left(V_g\right)$ во всех упомянутых случаях приведен в работах [149].

Остановимся в конце на вопросе о том, почему для наблюдения эффекта четности с помощью СОЭТ необходимо иметь высокоомные контакты островка с берегами, $R\gg h/e^2$. Рассмотрим сначала случай островка в нормальном состоянии, когда время релаксации неравновесного заряда на островке имеет порядок $\tau=RC$. Согласно соотношению неопределенностей, величина $\Delta E\sim h/\tau$ характеризует ширину возбужденного уровня энергии островка (т.е. уровня с неоптимальным значением n). Требование малости этой ширины по сравнению с характерной энергией возбуждения $E_C=e^2/2C$ и приводит к условию $R\gg\gg R_K=h/e^2$. Для сверхпроводящего состоянии островка то же самое условие следует из требования малости туннельного матричного элемента: $\Delta>E_C\gg K\simeq\frac{\hbar}{Re^2}\Delta$, где для оценки K использовано соотношение (46.14).

5.3.3 Unconventional superconductivity: Relation to the Basic Theory

(just about connection of these two topics)

by par 49 by Schmidt

При обсуждении куперовского спаривания в §§44, 45 мы неявно предполагали, что матричный элемент межэлектронного взаимодействия $V_{\mathrm{k},\mathbf{k}'}$, ответственный за спаривание, не зависит от направлений векторов $\mathbf{k}$ и $\mathbf{k}'$ на поверхности Ферми. В таком слу'ае амплитуда спаривания $v_{\mathbf{k}}$ электронов с импульсами $\hbar\mathbf{k}$ и $-\hbar\mathbf{k}$ и противоположными спинами также не зависит от направления вектора $\mathbf{k}$. Иначе говоря, два электрона, составляющие пару, находятся в состоянии взаимного движения с орбитальным угловым моментом $L=0$, называемом также s-состоянием (по аналогии с классификацией электронных оболочек в атомах). Поскольку полная волновая функция двух электронов должна быть по принципу Паули антисимметрична при их перестановке, а орбитальное s-состояние симметрично, антисимметрия должна быть беспечена за счет спиновой части волновой функции; поэтому лектроны в паре

находятся в синглетном по спину состоянии (полный спин куперовской пары $S = 0$) - это более точная формулировка уже упомянутого в §44 обстоятельства - электроны ппариваются с противоположными спинами.

В действительности, синглетное s-спаривание - самый распространенный, но не единственный возможный тип куперов ских пар. Прежде всего здесь надо напомнить о сверхтекучих фазах ^{3}He, изотопа гелия с фермиевской статистикой атомов (изза полуделого спина ядра ^{3}He). Объединение двух атомов ^{3}He в пару наподобие куперовской происходит аналогично обычному спариванию электронов, описанному в 44. Однако взаимодействие в ^{3}He устроено так, что в s-состоянии атомы отталкиваются, а притяжение возникает только в p-состоянии (взаимный орбитальный момент пары равен $L = 1$). Волновая функция этого орбитального состояния антисимметрична при перестановке, соответственно, и полный спин пары здесь равен $S = 1$ («спиновый триплет»). Такой вид куперовского состояния называется триплетным p-спариванием. Спаривание такого типа, по-видимому, реализуется и в недавно открытом сверхпроводнике Sr_2RuO_4 (см., например, [150]). Мы не будем здесь обсуждать весьма интересные свойства состояний с p-спариванием (об этом можно прочитать в книге [2]), а остановимся на другом примере, связанном с высокотемпературными сверхпроводниками семейств $YBa_2Cu_3O_{7-x}, La_{2-x}Sr_xCuO_4$ и $Bi_2Sr_2CaCu_2O_8$.

Прежде всего заметим; что при синглетном ($S = 0$) спаривании допустимо не только s-состояние, но и все высшие состояния с четными орбитальными моментами пары, $L = 2k$, поскольку такие волновые функции не меняют знака при повороте на угол 180°, т.е. симметричны при перестановке частиц в паре. Считается экспериментально установленным (мы обсудим соответствующие эксперименты позднее), что спаривание в этих ВТСПсоединения имеет такую же качественно структуру, какая получается в обобщении простой БКШ-модели на случай синглетного d-спаривания (орбитальный момент $L = 2$). Микроскопический механизм, приводящий к появлению сильного притяжения в ВТСП-соединениях, до сих пор не вполне ясен, и, скорее всего, он сильно отличается от обычного электрон-фононного механизма притяжения. Однако наиболее важные черты спаривания в ВТСП можно понять на примере «минимального обобщения» теории БКШ, которое состоит в постулировании сильно анизотропного потенциала притяжения $V_{\mathbf{k},\mathbf{k}'}$ подходящего вида (он должен соответствовать тетрагональной симметрии кристаллов ВТСП
и приводить к спариванию с моментом $L = 2$). Основные качественные свойства d-спаривания и вытекающие из них методы экспериментального обнаружения таких состояний мы и обсудим далее в этом параграфе.

В d-состоянии амплитуда (волновая функция) пары $v_{\mathbf{k}}$ меняет знак в зависимости от направления вектора k на поверхности Ферми. Поскольку ВТСП-кристаллы имеют слоистую структуру, в простейшем приближении можно считать поверхность Ферми почти цилиндрической и ограничиться рассмотрением "фермилинии" - сечения ферми-поверхности плоскостью сильной связи (x, y). Тогда соответствующая d-состоянию угловая зависимость волновой функции [1)] пары имеет вид

$$v_{\mathbf{k}} \propto \left(k_x^2 - k_y^2\right) \propto \cos 2\theta_k \tag{49.1}$$

где угол θ_k отсчитывается от направления кристаллографической оси x. Тем самым, в четырех точках на ферми-линии, задаваемых равенствами $k_x = \pm k_y$, волновая функция пары, а вместе с ней и вероятность $v_{\mathbf{k}}^2$ заполнения ячейки $(\mathbf{k}, -\mathbf{k})$ с такими $\mathbf{k}$ обращается в нуль. Это очень важное свойство d-спаривания сейчас мы покажем, что и спектр возбуждений в таком состоянии оказывается анизотропным, причем возбуждения с $k_x = \pm k_y$ могут иметь сколь угодно низкую энергию; о такой ситуации говорят как о нулях щели в спектре на линиях (линии появляются, если вспомнить о наличии импульса $\hbar k_z$).

Амплитуду спаривания вида (49.1) можно получить, выбрав потенциал притяжения электронов, например, в виде $V_{\mathbf{k},\mathbf{k}'} = -2V_d \cos 2\theta_{\mathbf{k}} \cos 2\theta_{\mathbf{k}'}$. Такой выбор означает, что наиболее сильно притягиваются электроны с импульсами, близкими к осям x и y, в то время как вблизи диагоналей $k_x = \pm k_y$ притяжение отсутствует. Проводя с таким потенциалом вывод, совершенно аналогичный сделанному в §44, получим вместо (44.8) - (44.9) следующие уравнения (выражение (44.10) для v_{k}^2 при этом сохраняет свой вид) на спектр при температуре $T = 0$:

$$\Delta_{\mathbf{k}} = 2V_d \cos 2\theta_{\mathbf{k}} \sum_{\mathbf{k}'} v_{\mathbf{k}'} u_{\mathbf{k}'} \cos 2\theta_{\mathbf{k}'} \tag{49.2}$$

$$E_{\mathbf{k}} = \sqrt{\varepsilon_{\mathbf{k}}^2 + \Delta_{\mathbf{k}}^2} \tag{49.3}$$

Обозначив $\Delta_{\mathbf{k}} = \Delta_0 \cos 2\theta_{\mathbf{k}}$, получим уравнение на Δ_0 почти такого же вида, как (44.12),

$$1 = N(0)V_d \int_0^{2\pi} \frac{d\theta}{2\pi} \int_0^{\hbar\omega_{\mathrm{D}}} \frac{d\varepsilon}{\sqrt{\varepsilon^2 + \Delta_0 \cos^2 2\theta}} \tag{49.4}$$

решение которого отличается от (44.14) лишь численным коэффициентом перед экспонентой. Зависимость парной амплитуды $\Delta_{\mathbf{k}}$ от направления вектора $\mathbf{k}$ относительно осей кристалла наглядно изображена на рис. 49.1 в виде "розетки", аналогичной обычной электронной d-орбитали в атоме.

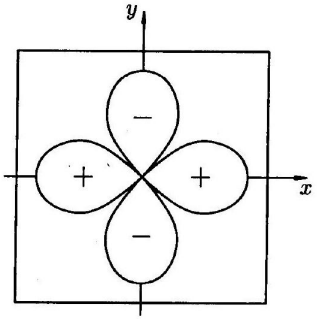


Рис. 49.1. Схематическая зависимость d-волнового параметра порядка $\Delta_{\mathbf{k}}$ от направления импульса пары $\hbar\mathbf{k}$ на фермиповерхности.

Уравнения (49.2), (49.3) имеет важное следствие, проявляющееся при малых энергиях - плотность квазичастичных состояний $\rho(E)$ нигде не обращается в нуль, а лишь плавно убывает при $E \to 0$. Действительно, рассмотрим квазичастичное состояние с $\mathbf{k} = (k_{\mathrm{F}} + q_\perp) \cdot \left(\frac{1}{\sqrt{2}}, \frac{1}{\sqrt{2}}\right) + q_\parallel \cdot \left(\frac{1}{\sqrt{2}}, -\frac{1}{\sqrt{2}}\right)$, где обе компоненты вектора q малы по сравнению с k_{F}. Согласно (49.3), его энергия равна

$$E_{\mathbf{q}} = \hbar \sqrt{v_{\mathrm{F}}^2 q_\perp^2 + \left(\frac{2\Delta_0}{\hbar k_{\mathrm{F}}}\right)^2 q_\parallel^2} \tag{49.5}$$

Как видно из выражения (49.5), энергия возбуждения стремится к нулю при $q \to 0$, т.е. при импульсе $\hbar\mathbf{k}$ вблизи точки $\left(\frac{1}{\sqrt{2}}, \frac{1}{\sqrt{2}}\right)$. Всего таких выделенных точек на ферми-линии четыре: $\left(\pm\frac{1}{\sqrt{2}}, \pm\frac{1}{\sqrt{2}}\right)$.

[1] В действительности, влияние поля кристаллической решетки в ВТСП столь велико, что фермиповерхность оказывается сильно анизотропной в плоскости (x, y), так что классификация состояний пар по угловому моменту вообще отсутствует, и правильнее говорить просто о смене знака волновой функции пары при дискретных поворотах на угол 90°.

Найдем теперь плотность состояний $\rho(E)$ при $E \ll \Delta_0$. Вводя вектор $\tilde{\mathbf{q}} = \left(q_\perp, q_\parallel \frac{2\Delta_0}{v_\mathrm{F} k_\mathrm{F}}\right)$, запишем энергию возбуждения (49.5) в приведенном к изотропному виде: $E_{\tilde{q}} = \hbar v_\mathrm{F} \tilde{q}$. Переписывая элемент фазового объема $d^3\mathrm{k}/(2\pi)^3$ в виде

$$\frac{dk_z}{2\pi}\frac{dk_x dk_y}{(2\pi)^2} = \frac{dk_z}{2\pi}\frac{dq_\perp dq_\parallel}{(2\pi)^2} = \frac{v_F k_F}{2\Delta_0}\frac{dk_z}{2\pi}\frac{d^2\widetilde{\mathbf{q}}}{(2\pi)^2} = \frac{k_F}{2v_\mathrm{F}\Delta_0}\frac{dk_z}{2\pi}\frac{EdE}{2\pi}$$

Сравнивая с выражением для плотности состояний $N(\varepsilon)$ в нормальном металле и умножая на четыре, получаем низкоэнергетическую плотность состояний в сверхпроводнике с d-спариванием:

$$\rho(E) = N(0)\frac{2E}{\Delta_0} \tag{49.6}$$

Иначе говоря, плотность состояний в d-сверхпроводнике лишь на множитель порядка $E/k_\mathrm{B}T_c$ меньше, чем в нормальном металле. :)то означает, что число элементарных возбуждений $\nu_{qp}(T)$ при низких температурах не является, в отличие от обычного сверхцроводника (см. (48.1)), экспоненциально малым:

$$\nu_{qp}(T) = \sum_{\mathbf{k}} f_{\mathbf{k}} = V\int\limits_0^\infty dE\rho(E)f(E) \sim N(0)V\frac{T^2}{\Delta_0} \tag{49.7}$$

Поэтому условие $\nu_{qp}(T) \ll 1$, необходимое для наблюдения эффекта четности (см. 48), очень трудно выполнить для d-сверхпроводника - оно требует температур $T < T_d^* \simeq (\Delta_0 \delta E)^{1/2}$, где $\delta E = (N(0)V)^{-1}$ - расстояние между электронными уровнями в образце в нормальном состоянии, имеющее порядок 10^{-4} К в экспериментах по эффекту четности [147]. Более того, при низких температурах $T \ll T_d^*$ связанная с присутствием неспаренного электрона дополнительная свободная энергия $F_1(T)$ очень мала, $F_1(0) \sim \delta E$. Дело в том, что квазичастица может занять ячейку k-пространства, сколь угодно близкую к одной из четырех точек вырождения. Можно показать (см. [2]), что максимальная величина $F_1^{\max}(T)$ для d-сверхпроводников имеет порядок $k_\mathrm{B}T_d^*$ и достигается при $T \simeq T_d^*$. Таким образом, отсутствие (или аномальная слабость) эффекта четности может служить одним из доказательств аномальной природы спаривания.

Другое важное свойство d-сверхпроводника - относительно большая величина низкотемпературной электронной теплоемкости $C_s(T)$. Используя комбинаторное выражение (см. [28]) для энтропии ферми-газа

$$S\left(f_{\mathbf{k}}\right) = -\sum_{\mathbf{k}}\left[\left(1-f_{\mathbf{k}}\right)\ln\left(1-f_{\mathbf{k}}\right) + f_{\mathbf{k}}\ln f_{\mathbf{k}}\right]$$

и выражения (45.5) и (49.6) для $\rho(E)$, получим теплоемкость сверхпроводника в следующем виде (окончательные выражения написаны для $T \ll T_c$):

$$\begin{aligned} C_s(T) =& T\frac{\partial S}{\partial T} = \sum_{\mathbf{k}} E_{\mathbf{k}}\frac{\partial f_{\mathbf{k}}}{\partial T} = N(0)\int\limits_0^\infty dE\rho(E)\frac{(E/T)^2}{\left(e^{E/T}+1\right)^2} = \\ &= \begin{cases} N(0)\frac{\pi^2 T}{6}\sqrt{\frac{2\pi\Delta_0^5}{T^5}}e^{-\Delta_0/T} & \text{для } s\text{-спаривания,} \\ 0.55N(0)\frac{T^2}{\Delta_0} & \text{для } d\text{-спаривания.} \end{cases} \end{aligned} \tag{49.8}$$

Отсутствие щели в спектре при d-спаривании приводит к возбуждению большего количества квазичастиц и к существенно более быстрому, чем при s-спаривании,

убыванию параметра спаривания $\Delta_0(T)$ с температурой. Обобщение уравнения (49.4) на ненулевые температуры производится так же, как при выводе (45.15), и имеет вид

$$1 = N(0)V_d \int_0^{2\pi} \frac{d\theta}{2\pi} \int_0^{\hbar\omega_{\rm D}} \frac{d\varepsilon}{\sqrt{\varepsilon^2 + \Delta_0(T)\cos^2 2\theta}} \,\mathrm{th}\, \frac{\sqrt{\varepsilon^2 + \Delta_0(T)\cos^2 2\theta}}{2T}. \tag{49.9}$$

Основной вклад в зависимость $\Delta(T)$ при низких температурах дают низколежащие возбуждения с $\varepsilon \sim k_{\rm B}T$ и $\cos 2\theta \sim k_{\rm B}T\Delta_0 \ll \ll 1$. Вычисляя приближенно разность интегралов (49.4) и (49.9), получаем

$$\Delta_0 - \Delta_0(T) \simeq \frac{2\ln 2}{\pi} \frac{T}{\Delta_0} \tag{49.10}$$

в отличие от экспоненциально малых поправок порядка $e^{-\Delta/T}$ при s-спаривании. В эксперименте бывает удобнее измерять температурную зависимость лондоновской глубины проникновения, которая тоже оказывается линейной [151] : $(\lambda(T)/\lambda(0) - 1) \sim T/\Delta_0$. Соответствующие расчеты проведены в работах [152].

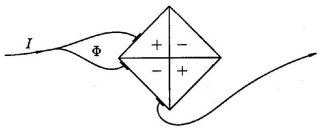


Рис. 49.2. Двухконтактный сквид, подсоединенный к соседним граням тетрагонального кристалла с противоположными знаками параметра порядка.

До сих пор мы обсуждали особые свойства d-сверхпроводника, связанные с наличием в нем бесщелевых возбуждений.

Другая важная черта d-спаривания - зависимость знака парной амплитуды $\Delta_{\mathbf{k}}$ от направления вектора k относительно кристаллических осей.2) Это свойство и было использовано [153] для доказательства существования d-спаривания в $YBa_2Cu_3O_{7-x}$. В работе [153] измерялся критический ток двухконтактного сквид-интерферометра с контактами между обычным сверхпроводником (свинец) и двумя соседними гранями монокристалла $YBa_2Cu_3O_{7-x}$, см. рис. 49.2. Если спаривание в $YBa_2Cu_3O_{7-x}$ имеет вид d-волны, типа изображенной на рис.49.1, то знаки волновых функций куперовских пар, проходящих через контакты a и b, будут противоположны. Рассмотрим (аналогично 25) зависимость критического тока сквида $I_{\max}(\Phi)$ от проходящего через его кольцо магнитного потока Φ. Различие знаков $\Delta_{\mathbf{k}}$ на гранях a и b приведет к замене уравнения (25.2) на $\varphi_a - \varphi_b = 2\pi\Phi/\Phi_0 + \pi$, что эквивалентно сдвигу Φ на величину $\Phi_0/2$. Таким образом, d-спаривание в $YBa_2Cu_3O_{7-x}$ должно приводить к зависимости $I_{\max}(\Phi)$ вида

$$I_{\max}(\Phi) = 2I_c \left| \sin \frac{\pi\Phi}{\Phi_0} \right| \tag{49.11}$$

с максимумами при полуцелых значениях магнитного потока. Именно такая зависимость и была обнаружена в эксперименте [153].

[2)] По этой причине для сверхпроводников с d-спариванием (как и с другими типами нетривиального спаривания) неверна "теорема Андерсона" об отсутствии влияния потенциальных примесей на сверхпроводимость-рассеяние перепутывает состояния с разными направлениями импульса, имеющие теперь разные знаки парных волновых функций, так что спаривание подавляется [2].

Part III
Bulk Properties of Superconductors

6 Methods from De Gennes

6.0.1 3-3 Nonequilibrium Properties

Up to now, we have restricted our attention to the reversible behavior of second type superconductors. We have seen that when the coherence length ξ is small, they can remain superconducting up to very high fields, of order $H_{c_2} \sim \phi_0/\xi^2$.

From a technical point of view, however, what is most interesting is to obtain superconducting wires that can carry high currents. But this condition cannot be realized at thermal equilibrium, as shown by the following argument: Consider a cylindrical wire of radius a carrying a total current I. (When I is weak, this current is, in fact, entirely carried by a surface sheet, of thickness λ, around the cylinder.) The field at the surface of the wire is

$$H = \frac{2I}{ca} \tag{3-69}$$

The situation is stable when $H < H_{c_1}$. When $H > H_{c_1}$, vortex lines begin to appear. They are bent in circles (following the lines of force). Once created at the surface, with radius a, they tend to shrink (to decrease their line energy) and finally annihilate near the axis of the wire. This process dissipates energy. Thus in an ideal specimen we have 0 resistance only if $H < H_{c_1}$ or $I < (ca/2)H_{c_1}$. If we want to carry higher currents with our wire, we need to pin the vortex lines, that is, to quench their motion by suitably chosen lattice defects, and achieve a nonequilibrium situation. While the field H_{c_2} is an intrinsic property of the metal (or alloy), the critical current measured on a wire is extremely sensitive to the metallurgical state of the sample. This distinction between the factors ruling H_{C_2} and I was stressed first by Gorter.

In practice, a favorable defect structure is obtained by the following procedures:
(1) imperfect sintering (e.g., Nb_3Sn)
(2) cold work (e.g., MoRe alloys)
(3) precipitation processes (e.g., lead alloys)

The resulting materials, with high critical currents, are called hard superconductors.

The coupling mechanisms between the lines and the defects are only vaguely known at the present time. A rather simple case is met when we have large cavities, due to imperfect sintering, in the superconducting material. A vortex tends to remain pinned to the cavity, since this corresponds to a smaller length of line in the superconducting material, and thus to a smaller line energy. The mechanical stresses realized by cold work impose slight modifications to the condensation
energy and to the local density of superconducting electrons n_s. This results in local modifications of λ, ξ, and thus of the line energies $\mathfrak{J}$ and interactions U. These interactions are rather complex, and in the following we only present a phenomenological description of their effects.

Critical State at Zero Temperature

Consider a hard superconductor in an applied magnetic field H (along Oz). In equilibrium the line density would have the value $B(H)/\phi_0$ and be the same at all points. We now consider a metastable situation where the induction B is not equal to $B(H)$ but varies from point to point - say in the x direction. Thus (1) the line density is not constant, (2) there is a macroscopic current $J = (c/4\pi)(\partial B/\partial x)$ flowing in the y direction. The forces acting on the line system can

be decomposed in the following way: First, because of the repulsive interactions between lines, the regions of high line density (high B) tend to expand towards the regions of low density. This may be described in terms of the pressure p in our two-dimensional line system. [6] The force (per cm^3) is $-\partial \mathrm{p}/\partial \mathrm{x}$. This has to be balanced by a pinning force due to the structural defects. This pinning force, however, cannot become arbitrarily large. It must stay below a certain threshold value α_m

$$\left|\frac{\partial \mathrm{p}}{\partial \mathrm{x}}\right| < \alpha_m \tag{3-70}$$

If at some point $|\partial \mathbf{p}/\partial \mathbf{x}|$ is larger than α, then the lines start moving and dissipation occurs until condition (3-70) is again satisfied. In practice the line density $(1/\phi_0)\,\mathrm{B(x)}$ will thus adjust itself so that the threshold condition is just realized at all points [equality in (3-70)]. The state thus realized is called the critical state, and was first described by Bean. We can get some physical feeling for this critical state by thinking of a sand hill. If the slope of the sand hill exceeds some critical value, the sand starts flowing downwards (avalanche). The analogy is, in fact, rather good, since it has been shown (by careful experiment with pickup coils) that, when the system becomes overcritical, the lines do not move by single units, but rather in the form of avalanches including typically 50 lines or more.

We now proceed to compute explicitly the pressure p of the line system, to be inserted in (3-70). We consider a group of N lines intersecting a surface S in the xy plane. Their energy (per cm along Oz) is

$$\mathcal{G} = SG$$

where G is the thermodynamic potential introduced by Eq. (3-64). The pressure is obtained from S by differentiating with respect to S (that is, to the volume) at constant N .

$$p = \left(-\frac{\partial G}{\partial S}\right)_N = -G - S\frac{\partial G}{\partial S}$$

For fixed N we have $\mathrm{dS/S} = -\mathrm{dB/B}$

$$p = -G + B\frac{\partial G}{\partial B} \tag{3-71}$$

Thus when we know the form of the thermodynamic potential G, we know $p(B)$, that is, the pressure-density relation. It is, in fact, possible to write the pressure gradient $\partial p/\partial x$ in a very simple way. Set

$$G(B) = F(B) - \frac{BH}{4\pi}$$

where $F(B)$ describes the line self-energies and interaction. The equilibrium relation $B(H)$ or $H(B)$ is obtained by imposing $\partial G/\partial B = 0$. Thus $\mathrm{H(B)} = 4\pi(\partial\ \mathrm{F}/\partial \mathrm{B})$. Now

$$\begin{aligned} \frac{\partial p}{\partial x} &= B\frac{\partial^2 G}{\partial B^2}\frac{\partial B}{\partial x} = \frac{B}{4\pi}\frac{\partial H(B)}{\partial B}\frac{\partial B}{\partial x} \\ \frac{\partial p}{\partial x} &= \frac{B}{4\pi}\frac{\partial H(B)}{\partial x} \end{aligned} \tag{3-72}$$

Thus, if we know H(B), we can immediately compute the pressure gradient as a function of B and $\partial \mathrm{B}/\partial \mathrm{x}$.

[6] We make an isotropic approximation and neglect the tensor properties of p.

In fact, in materials where $H_{c_1} \ll H_{c_2}$, if $H \gg H_{c_1}, H(B)$ is nearly equal to B as is clear from the magnetization curve of Fig. 3-2. In this region we have simply

$$-\frac{\partial p}{\partial x} = -\frac{B}{4\pi}\frac{\partial B}{\partial x} = \frac{BJ_y}{c} \quad (H \gg H_{c_1}) \tag{1'}$$

The critical state is then defined by

$$\left|\frac{B}{4\pi}\frac{\partial B}{\partial x}\right| = \left|\frac{BJy}{c}\right| = \alpha_m \quad (H(B) \gg H_{c_1}) \tag{3-73}$$

(a)

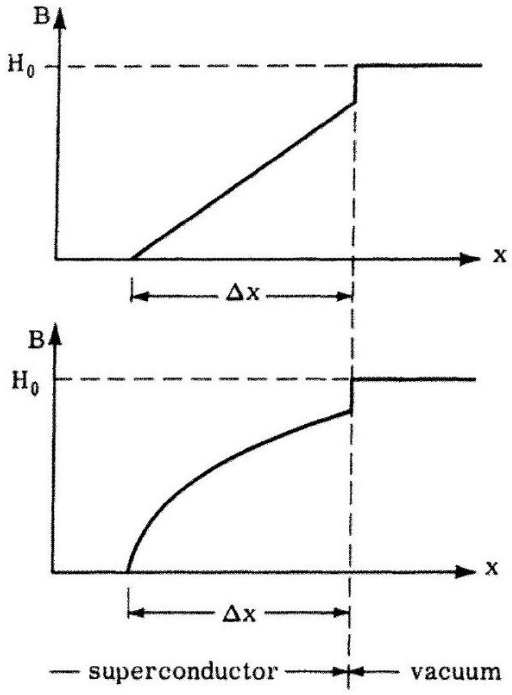


Figure 3-13
Irreversible penetration of flux in a hard superconductor: (a) Bean model; (b) AndersonKim model (parabolic profile).

To compute B(x) in the critical state we now need to know what is the dependence of the maximum pinning force α_m on B (that is,on the line density). It was originally assumed by Bean that α_m was linear in B; that is, J_y was a constant in the critical state. (J_y would typically be of order 10^5 A/cm^2.) A series of experiments by Kim and co-workers on NbZr alloys and on Nb_3Sn indicates that for these systems (in the particular metallurgical condition realized, and for fields in the 10^4Oe range), a good approximation amounts to taking α_m independent of B. This very simple result is not fully explained theoretically at the present time. In particular, we would expect the pinning centers to be most efficient when their size is comparable to the interline distance, and the latter depends on B (like $B^{-1/2}$).

The shape of the profile $B(x)$ in the critical state is represented for the Bean model and for the Kim model (Fig. 3-13). For typical hard superconductors and applied fields of order 10^4Oe, the total thickness Δx of the zone where flux lines have penetrated is of order 1 mm . To determine $B(x)$ experimentally [or equivalently to determine $\alpha_m(B)$], the simplest method amounts to measuring the flux ϕ in cylindrical samples of radius R (Fig. 3-14) for increasing values of the applied field H.

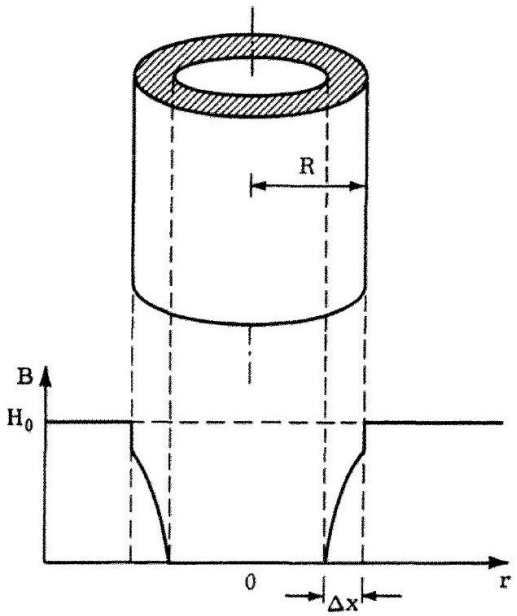


Figure 3-14
Magnetization measurements on a cylinder (external field increasing). The flux lines penetrate only in the hatched area.
(1) If R is much smaller than Δx, the induction is nearly uniform in the sample, B = B(H), $\phi = \pi \mathrm{R}^2$ B(H).[7]
(2) If $R \gg \Delta x$ we have essentially a one-dimensional situation. If x denotes the radial distance, we may write

$$\phi = 2\pi R \int_{R-\Delta x}^{R} dx B(x) \tag{3-74}$$

At the edge of the flux ($x = R - \Delta x$), we have $B = 0, H(B) = H_{C_1}$. At the surface of the cylinder ($x = R$), again assuming no surface barriers, we have the equilibrium value of B corresponding to the external field H. B = B(H). Transforming dx by (3-72) and (3-70), we get

$$\phi = 2\pi R \int_{H_{C_1}}^{H} dH \frac{B^2(H)}{4\pi \alpha_{mH}}$$

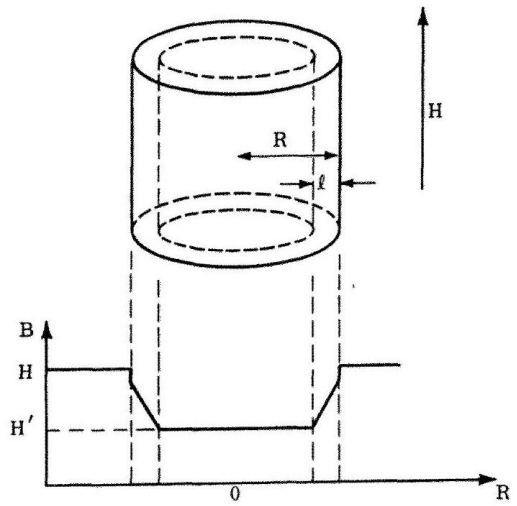


Figure 3-15
Principle of the Kim experiments on hollow cylinders of hard superconductors. An external

[7] We assume that there is no surface barrier impeding the entrance of vortex lines in the cylinder. Surface barriers do occur sometimes, but their effects can easily be separated.

field H is applied. The field H′ inside the cylinder is measured.
where α_{mH} stands for α_m[B(H)]. Of particular interest is the derivative of ϕ

$$\frac{\mathrm{d}\phi}{\mathrm{dH}} = \frac{\mathrm{R}}{2}\frac{\mathrm{B}^2(\mathrm{H})}{\alpha_{\mathrm{mH}}} \tag{3-75}$$

Thus from magnetization measurements in increasing fields, we may derive α_{mH} and α_m (B). Another method, devised by Kim and coworkers, makes use of hollow cylinders as shown in Fig. 3-15. A field H is applied on the outside of the cylinder and the field H′ in the cylinder is measured. When H is increased from $0, \mathrm{H}'$ first stays strictly equal to 0 . Then, when the flux front reaches the inner surface of the cylinder, H′ starts to increase (ideally H′ would first jump abruptly to H_{c_1}, and then grow steadily). The interest of the method is to give a direct determination of Δx, for that particular value of H where H′ starts to increase.

More complicated situations are met if the field H is alternatively increased and decreased, as shown in Fig. 3-16. Then we meet regions

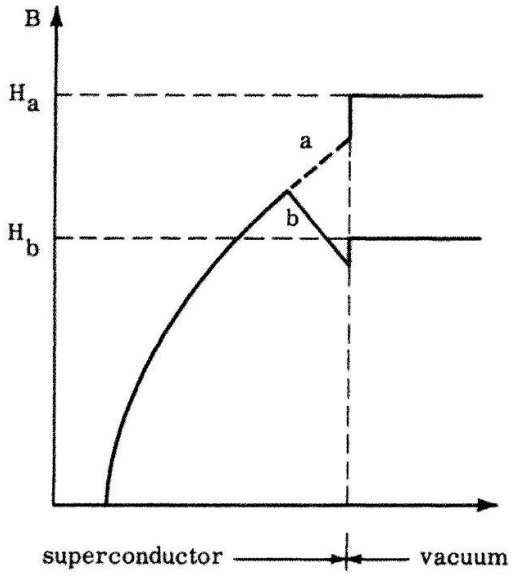
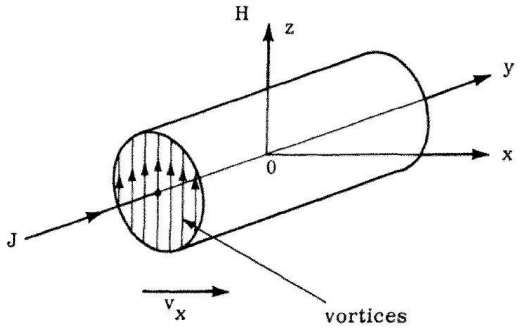


Figure 3-16
Flux distribution in a hard superconductor when the applied field is first raised to $\mathrm{H_a}$ (broken curve) and decreases to $\mathrm{H_b}$ (full curve).
with $\mathrm{dB/dx} > 0$ and regions with $\mathrm{dB/dx} < 0$, but the absolute value $|\partial \mathrm{p}/\partial \mathrm{x}|$ stays equal to α_m. This permits a detailed calculation of all hysteresis cycles when $\alpha_m{}^{(\mathrm{B})}$ is known.

Flux Creep at Finite Temperatures

At finite temperatures, if $\partial \mathrm{p}/\partial \mathrm{x} \neq 0$, the vortex lines will tend to move (from the regions of high B towards the regions of low B) by activated jumps across the pinning barriers. We call the average flow velocity of the lines (in the x direction) v_x. Various methods can be used to detect this flow, or "creep":
(1) Magnetic measurements, with thick cylinders or hollow cylinders. In the latter case, for instance, if H has been raised from 0 to some value and then kept constant, we observe that H′ increases slowly in time.
(2) Electrical measurements. If the lines of force are moving, they create electromotive forces that can be measured directly. The most simple situation is represented in Fig. 3-17. A wire (in the y direction) carries a current of density J, and is submitted to an external



vortex drift velocity
Figure 3-17
Electrical measurements on a hard superconductor wire. There is a current $J = -(c/4\pi)(\partial B/\partial x)$ in the y direction, thus $\partial B/\partial x < 0$. The lines are more closely packed on the left side of the wire: they drift with a velocity v_X towards the positive x axis.
field H in the z direction. Thus we have a nonzero $\partial B/\partial x = 4\pi$ J/c and the lines (pointing along Oz) tend to drift in the x direction. The resulting electric field E_y is along the wire axis (Oy) and in the limit $H \gg H_{c_1}$, it is given by

$$E_y = \frac{Bv_x}{c} \tag{3-76}$$

To prove (3-76) we compute the power dissipation per unit volume; this is the work done by the presence of gradient on the lines, that is. $(\partial p/\partial x)v_x$.
By setting this equal to $E_y J$ and making use of (3-72'), we get (3-76). Thus we need an electric field E_y to maintain the current J. As pointed out by Anderson and Kim, this dissipative effect in the superconducting state explains many features of the resistive behavior of hard superconductors.

The main difference between (1) the magnetic measurements and (2) the electric ones lies in the order of magnitude of the velocities involved. In case (1) the creep typically is measured over intervals of hours or days, and the velocities are of order 1 mm/ day or 10^{-6} cm/sec. In case (2) taking $B = 10^4 E_y = 1\mu$ V/cm, we get $v_x \sim 10^{-2}$ cm/sec. The main difficulty of (2) is related to possible inhomogeneities in the wire; experimentally it is found that different portions of the same wire have different E_y 's.

The results show unambiguously that
(a) the creep velocity has an activation energy behavior

$$v_x = v_0 \exp\left(-E/k_B T\right) \tag{3-77}$$

v_0 is not very accurately known, but may be in the range of 10^3 cm/sec in typical cases. The energy E may be as high as 100°K.
(b) the energy E depends on the pressure gradient $\partial p/\partial x$

$$E = E_0 - \left|\frac{\partial p}{\partial x}\right| \rho^4 \tag{3-78}$$

where ρ has the dimensions of a length, and is typically of order 500Å. We can relate E_0 and ρ to the critical pressure gradient α_m, if we notice that for $T \to 0$ the velocity v_X will depart from 0 only when $E = 0$

$$\alpha_m = \frac{E_o}{\rho^4} \tag{3-79}$$

These results (mainly obtained by Anderson, Kim, and co-workers) have various important consequences. First, since v_x varies rapidly with E according to (3-77), it is possible to extend

the crictical state concept to finite temperatures. Define a limiting velocity $v_{\min}$ below which the line motion cannot be detected. Then, if

$$\frac{E}{k_B^T} > \log \frac{v_0}{v_{\min}}$$

the line structure is frozen. Thus the critical state at temperature T corresponds to

$$\begin{aligned} E_0 - \rho^4 \left|\frac{dp}{dx}\right| &= k_B T \log \frac{v_0}{v_{\min}} \\ \left|\frac{dp}{dx}\right| &= \alpha_m \left(1 - \frac{k_B T}{E_0} \log \frac{v_0}{v_{\min}}\right) \end{aligned} \tag{3-80}$$

In general α_m will depend on T (since α_m involves λ, ξ, and the condensation energy, which are all temperature dependent). But if T is much smaller than the transition point T_0 this dependence may be neglected and all the temperature variation in (3-80) comes from the factor $k_B T$. A linear dependence of |dp/dx| on T has indeed been observed experimentally by Kim on various alloys and compounds the critical currents of hard superconductors are strongly temperature dependent even when $T \ll T_0$.

Another important consequence of (3-77), pointed out by Anderson, is the possibility of severe thermal instabilities. If in a small region of the sample the pinning energy E_0 is slightly smaller than elsewhere, the vortex lines in this region will dissipate a large power, $[(\partial p/\partial x) v_X]$ per cm^3, and this will tend to raise the local temperature, if the thermal conductivity of the material is low. This temperature rise will, in turn, increase the line velocity v_x according to (3-77) and may finally result in an instability. These thermal processes have to be taken into account in the design of superconducting coils.

CONCLUDING REMARKS

Our description of pinning and creep has been strictly phenomenological. Of course, we would like to interpret E_0, ρ, and v_0 in terms of microscopic processes. There are two difficulties: (1) What is the coupling between defects and lines? As pointed out earlier an important term is related to local modifications of the penetration depth λ by strain or by impurity gradients. Another, more obvious, contribution stems from local modifications of the superconducting condensation energy. There may be other contributions.
(2) How can we describe the metastable equilibrium and the irreversible motions of strongly coupled vortex lines in the presence of random perturbations? Coming back to the sand-hill analogy, we need a theory for the equilibrium slope of the sand hill and a theory for the avalanches -both are complicated. For the vortex line system there is an interesting suggestion, due to Frank-creep may take place by a motion of dislocations in the two-dimensional line lattice.

REFERENCES

Vortex line structure:
A. Abrikosov, Zh. Eksperim. i Teor. Fix., 32, 1442 (1957), translated by Soviet Phys. -JETP, 5, 1174 (1957).
B. B. Goodman, Rev. Mod. Phys., 36, 12 (1964).

Reversible magnetization curves:
J. D. Livingston, Phys. Rev., 129, 1943 (1963).
T. Kinsel, E. A. Lynton, and B. Serin, Phys. Letters, 3, 30 (1962).

Neutron diffraction by lines:
D. Cribier, B. Jacrot, L. M. Rao, and B. Farnoux, Phys. Letters, 9, 106 (1964).
Pinning of vortex lines and creep effects:
C. P. Bean, Phys. Rev. Letters, 8 (1962), Rev. Mod. Phys., 36, 31 (1964).
P. W. Anderson, Phys. Rev. Letters, 9, 309 (1962).
Y. B. Kim, C. F. Hempstead, and A. R. Strnad, Phys. Rev., 129, 528 (1963).
J. Friedel, P. G. de Gennes, and J. Matricon, Appl. Phys. Letters, 2, 199 (1963).
Viscous motion of vortices:
Y. B. Kim, C. F. Hempstead, A. R. Strnad, Phys. Rev., 139, A1163 (1965).

6.1 Description of the Condensed State

6.1.1 4-1 Instability of the Normal State in the Presence of an Attractive Interaction

The ground state of a free electron gas corresponds to complete filling of the one-electron energy levels of wavevector $\mathbf{k}$ and energy $\hbar^2\mathrm{k}^2/2m$ up to a certain energy $E_F = \hbar^2\mathrm{k}_F^2/2m$ (the Fermi energy). However, in the presence of an attractive interaction, no matter how weak, this state becomes unstable (Cooper, 1957). The instability can be understood by considering two particular electrons of coordinates r_1 and r_2, the other electrons still being treated as a free electron gas. The only effect of this electron gas is to forbid the two electrons to occupy all states $\mathrm{k} < \mathrm{k_F}$ by the exclusion principle. Let $\psi(\mathrm{r}_1, \mathrm{r}_2)$ be the wavefunction of the two electrons. Consider only states where the center of gravity of the pair (r_1, r_2) is at rest; ψ is then only a function of $\mathbf{r}_1 - \mathbf{r}_2$. Expand ψ in plane waves

$$\psi(r_1 - r_2) = \sum_k g(k) e^{ik\cdot(r_1 - r_2)} \tag{4-1}$$

$g(k)$ is the probability amplitude for finding one electron in the planewave state of momentum $\hbar\mathrm{k}$ and the other electron in the state $(-\hbar\mathrm{k})$. Since the states $\mathrm{k} < \mathrm{k_F}$ are already occupied, the Pauli principle imposes

$$g(\mathbf{k}) = 0 \text{ for } \mathbf{k} < \mathbf{k_F} \tag{4-2}$$

The Schrdinger equation for our two electrons is

$$-\frac{\hbar^2}{2m}\left(\nabla_1^2 + \nabla_2^2\right)\psi(r_1, r_2) + V(r_1, r_2)\,\psi = \left(E + \frac{\hbar^2 k_F^2}{m}\right)\psi \tag{4-3}$$

(E is the energy of the pair relative to the state where the two electrons are at the Fermi level.) On inserting (4-1) into (4-3), we find an equation for $g(k)$,

$$\frac{\hbar^2}{m}k^2 g(k) + \sum_{k'} g(k')\, V_{kk'} = (E + 2E_F)\, g(k) \tag{4-4}$$

$$V_{kk'} = \frac{1}{L^3}\int V(r) e^{-i(k-k')\cdot r} dr$$

is the matrix element of the interaction between the electronic states $\mathbf{k}$ and $\mathbf{k}'$. L^3 is the volume of the system. Equation (4-4) together with the Pauli condition (4-2) is sometimes called the Bethe-Goldstone equation for the two-electron problem. For $\mathrm{E} > 0$ it has a continuous spectrum describing the collisions of the two electrons from the initial state $(\mathbf{k}, -\mathbf{k})$ towards

final states $(\mathbf{k}', -\mathbf{k}')$ of the same energy. But if the interaction V is attractive there may also be bound state solutions, with $\mathrm{E} < 2\mathrm{E_F}$. To see this, consider the simplified interaction

$$\begin{aligned} V_{kk'} &= -\tfrac{V}{L^3} \text{ for } \quad \tfrac{\hbar^2 k^2}{2m} < E_F + \hbar\omega_D \\ &= 0 \qquad\qquad\qquad\qquad \tfrac{\hbar^2 k^{*2}}{2m} < E_F + \hbar\omega_D \\ &= 0 \qquad\qquad\qquad\qquad \text{otherwise} \end{aligned} \tag{4-5}$$

(This interaction is attractive and constant in an energy band $\hbar\omega_D$ above the Fermi level.) Then (4-4) becomes

$$\left(-\frac{\hbar^2 k^2}{m} + E + 2E_F\right) g(k) = C \tag{4-6}$$

where C is independent of k

$$\mathrm{C} = -\frac{\mathrm{V}}{\mathrm{L}^3} \sum_{\mathrm{k}'} \mathrm{g}\left(\mathbf{k}'\right) \tag{4-7}$$

$$\mathrm{E_F} < \frac{\hbar^2 \mathrm{k}'^2}{2m} < \mathrm{E_F} + \hbar\omega_\mathrm{D}$$

Comparing (4-6) and (4-7), we find the self-consistency condition

$$1 = \frac{V}{L^3} \sum_{k'} \frac{1}{-E + \frac{\hbar^2 k'^2}{m} - 2E_F} \tag{4-8}$$

$$E_F < \frac{\hbar^2 k'^2}{2m} < E_F + \hbar\omega_D$$

If we set

$$\xi' = \frac{\hbar^2 \mathrm{k}'^2}{2m} - \mathrm{E_F} \tag{4-9}$$

and introduce the density of states per unit energy interval

$$\mathrm{N}\left(\xi'\right) = (2\pi)^{-3} 4\pi \mathrm{k}'^2 \frac{\mathrm{dk}'}{\mathrm{d}\xi'}$$

the condition becomes

$$1 = V \int_0^{\hbar\omega} DN\left(\xi'\right) \frac{1}{2\xi' - E} d\xi' \tag{4-10}$$

If we assume $\hbar\omega_\mathrm{D} \ll \mathrm{E_F}, \mathrm{N}\left(\xi'\right)$ can be considered as constant and replaced by its value $N(0)$ at the Fermi level; we can perform the integration

$$1 = \frac{1}{2} N(0) V \ln \frac{E - 2\hbar\omega_D}{E} \tag{4-11}$$

and in the limit of weak interactions $N(0)V \ll 1$

$$E = -2\hbar\omega_D e^{-2/N(0)V} \tag{4-12}$$

Therefore there exists a two-electron bound state of energy $\mathrm{E} < 0$. If we start from a free electron gas, and turn on the interaction V, we predict that the electrons will group themselves in pairs giving up energy to the external world. The normal state is thus unstable.

A few important remarks.

(1) The instability persists even if V is very weak provided that it is attractive. This is a very remarkable difference from the usual two-body problem. If we had only two particles coupled by an attractive interaction of finite range, they would not form bound states unless the attractive interaction exceeded a certain threshold.

For the two-body problem ($k_F = 0$), the density of states N(ξ) varies as $\xi^{1/2}$ as $\xi \to 0$ and the expression

$$f(E) = V \int N(\xi) \frac{d\xi}{-E + 2\xi} \tag{4-13}$$

converges even for E = 0. Therefore, if V is small, f(0) < 1 and f(E) < f(0) < 1 for $E < 0$. The condition $f(E) = 1$ cannot be satisfied in the domain of bound states. On the contrary, for our problem, $N(\xi)$ is nearly constant, $f(0) = \infty$, and there is always a value of E < 0 such that f(E) = 1.

(2) The binding energy is proportional to $e^{-2/NV}$. It cannot be expanded in powers of V for $V \to 0$. This algebraic difficulty considerably hindered the development of the theory of superconductivity.

(3) In the preceding calculation, we have taken account of the exclusion principle between the electron (1) and the electrons in the Fermi sphere and between (2) and the Fermi sphere. It is also necessary to insure that the wavefunction be antisymmetric in $(\mathbf{r}_1, \mathbf{r}_2)$. With the simplified interaction V, of $(4-5), g(k)$ depends only on ξ, that is, the magnitude of k. Therefore the spatial part of the wave function $\psi(r_1, r_2)$ is symmetric from (4-1), and the spin part of the wave function must be antisymmetric, of the form $(1/\sqrt{2})(\alpha_1\beta_2 - \beta_1\alpha_2)$ in Schiff's notation. [1]

This function describes a state where the total spin of the pair is zero, that is, antiparallel coupling. If the interaction V_{kk}', instead of having the simple form (4-5), depended strongly on the angle between k and k', one could find:

(a) several bound states;

(b) spatially anisotropic solutions and therefore more complicated spin dependences. In practice, in the superconducting metals, it appears that the angular dependence of V_{kk} ' is not strong enough to bring in very spectacular effects.

Problem.

Calculate the mean square radius ρ of a Cooper pair.

Solution.

By definition

$$\rho^2 = \frac{\int |\psi(r_1 - r_2)|^2 R^2 dR}{\int |\psi|^2 dR}, \quad R = r_1 - r_2$$

$$\rho^2 = \frac{\Sigma |\nabla_k g(k)|^2}{k\Sigma_k |g(k)|^2}$$

$$\cong \frac{N(0)\left(\frac{\partial \xi}{\partial k}\right)^2_{\xi=0} \int_0^\infty d\xi \left(\frac{\partial g}{\partial \xi}\right)^2}{N(0)\int_0^\infty g^2 d\xi}$$

In the approximation of (4-5), $g = C/(E - 2\xi)$. Also, $(\partial k/\partial \xi)_{\xi=0} = 1/\hbar v_F$ where v_F is the Fermi velocity. Performing the integration, one finds

$$\rho = \frac{2}{\sqrt{3}} \frac{\hbar v_F}{E}$$

6.1.2 4-2 Origin of the Attractive Interaction

In a simple electron gas, the only interactions are Coulomb repulsions, and thus not favorable for the Cooper phenomenon. To obtain an attractive matrix element $V_{kk'}$, the electrons must be coupled to

another system of particles, or excitations, in the solid. There are many varieties of such excitations we might try for that purpose-phonons, electrons from other bands, spin waves in magnetic media, and so on. Only one of these couplings is really known to be important (at the present time). This is the electron-phonon interaction, first proposed in that connection by Frlich (1950), which we now discuss.

The Quantum Mechanical Picture

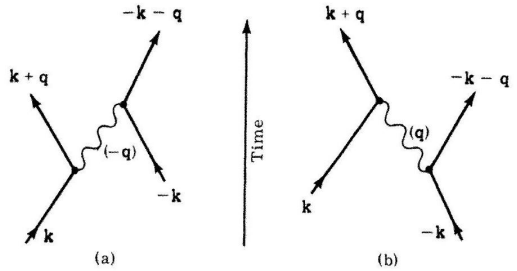
We wish to know the matrix element $V_{kk'}$ of the electron-electron interaction between an initial state (I) where two electrons are in the plane wave states $\mathbf{k}$ and $-\mathbf{k}$, and a final state (II) where the electrons are in $(\mathbf{k}', -\mathbf{k}')$. $V_{kk'}$ will, in general, contain two terms:
(a) There is a direct Coulomb repulsion $U_C(\mathbf{r}_1 - \mathbf{r}_2)$ between the two electrons. The corresponding matrix element is

$$\langle I|\mathscr{H}_c|II\rangle = \int dr_1 dr_2 e^{-i\mathbf{k}\cdot(r_1-r_2)} U_c(r_1 - r_2)\, e^{i\mathbf{k}'\cdot(r_1-r_2)} \tag{4-14}$$

(the wave functions being normalized in a unit volume)

$$\langle I|\mathscr{H}_c|II\rangle = \int U_c(\rho) d\rho e^{iq\cdot\rho} = U_q \quad q = \mathbf{k}' - \mathbf{k} \tag{4-15}$$

(b) One electron may emit a phonon later reabsorbed by the other electron. This process is displayed in Fig. 4-1. The initial state (I) has energy



Electron-electron interaction via phonons. In process (a) the electron k emits a phonon of wave-vector $-q$. The phonon is absorbed later by the second electron. In process (b) the second electron in state $(-\mathbf{k})$ emits a phonon $\mathbf{q}$, subsequently absorbed by the first electron.

$$E_I = 2\xi_k$$

where ξ_K is defined by Eq. (4-9) (for convenience we always measure the one-electron energies from the Fermi level). The final state (II) has energy

$$E_{II} = 2\xi_{k'}$$

[1] L. I. Schiff, Quantum Mechanics(New York: McGraw-Hill, 1955), Chapter 9.

There are two intermediate states allowed by momentum conservation:
(i1): Electron 1 in state $\mathbf{k}' = \mathbf{k} + \mathbf{q}$, electron 2 in $-\mathbf{k}$, one phonon created with wave vector -q, energy $\hbar\omega_{\mathrm{q}}$

$$E_{i1} = \xi_{k'} + \xi_k + \hbar\omega_q$$

(notice that ξ_{k} and ω_{k} are even functions of k)
(i2): electron 1 in state k

$$2 \text{ in state } -\mathbf{k}' = -(\mathbf{k} + \mathbf{q})$$

one phonon created with wave vector q, energy $\hbar\omega_q$

$$E_{i2} = \xi_{k'} + \xi_k + \hbar\omega_q = E_{i1}$$

The second-order matrix element coupling states (I) and (II) is

$$\langle I|\mathscr{H}_{\text{indirect}}\,|II\rangle = \sum_i \langle I|\mathscr{H}_{ep}|i\rangle \frac{1}{2}\left(\frac{1}{E_{II} - E_i} + \frac{1}{E_I - E_i}\right)(i\,|\mathscr{H}_{ep}|\,II) \tag{4-16}$$

Here the sum Σ_{i} is over the allowed intermediate states. $\mathscr{C}_{\mathrm{ep}}$ is the electron phonon coupling, the matrix element of which we shall call $\mathrm{W_q}$ (for emission or absorption of a phonon of wave vector q)

$$\langle I|\mathscr{H}_{\text{indirect}}\,|II\rangle = \frac{|W_q|^2}{\hbar}\left(\frac{1}{\omega - \omega_q} - \frac{1}{\omega + \omega_q}\right) \tag{4-17}$$

where we have defined a frequency ω by

$$\hbar\omega = \xi_{\mathrm{k}'} - \xi_{\mathrm{k}} \tag{4-18}$$

Thus $\hbar\omega$ and $\hbar$q are, respectively, the energy and momentum change of electron 1 in the transition I $\rightarrow$ II. The total matrix element is

$$\langle \mathrm{I}|\mathscr{H}|\mathrm{II}\rangle = \mathrm{U_q} + \frac{2\,|\,\mathrm{W_q}|^2}{\hbar}\frac{\omega_{\mathrm{q}}}{\omega^2 - \omega_{\mathrm{q}}^2} \tag{4-19}$$

When $\omega < \omega_{\mathrm{q}}$ the indirect term is negative (attractive); we have found an attractive interaction, provided that $\mathrm{U_q}$ is not too large.

Description in Terms of a Dielectric Constant

It is also possible to present the effective electron-electron interaction in the following way. The bare Coulomb interaction between the two electrons is e^2/r, leading to a repulsive matrix element $4\pi e^2/q^2$. But this interaction is screened-by the other electrons and also by the positive ions in the lattice. If we work near the resonance frequency (ω_{q}) of the ion motion, the ions give a very large response: They can "overscreen" the negative charge of electron 1 ; the resultant, positive cloud will be attracted by electron 2 .

In practice, we describe this screening effect by a dielectric constant $\epsilon(q\omega)$ (which is a function of wave vector and frequency). The effective interaction is the bare interaction divided by ϵ

$$\langle I|\mathscr{H}|II\rangle = \frac{4\pi e^2}{q^2\epsilon(q,\omega)} \tag{4-20}$$

It only remains to calculate ϵ. We do this for a very simple model, and show that Eqs. (4-19) and (4-20) agree.

JELLIUM

Consider a system formed of n electrons per cm^3 (of mass m and charge -e) and of ions, of mass M and charge + Ze. (The entire system being electrically neutral, the number of ions per cm^3 is n/Z.) We take into account only the electrostatic interactions between particles. Also we treat the ions as fluid, not as an ordered solid. This simple model of a metal has been called "jellium." [2] It neglects mainly
(1) the short-range repulsive interactions between ions due to repulsion of their deep electronic levels;
(2) the fact that the electronic wave functions must be orthogonal to the wave function of the deep-lying levels of each ion. (This gives rise to an effective repulsive electron-ion interaction.)
(3) the possibility of transverse oscillations (transverse phonons) of the ion system, which exist in a real solid, but not in our fluid model.

All these simplifications are rather arbitrary, but the simple model that results is useful for a qualitative understanding of the interactions. The dielectric constant $\epsilon(q\omega)$ is defined in the following way: Assume that small external charges, of density

$$\delta\rho(r) = \delta\rho\cos(q\cdot r)e^{i\omega t} + \text{ C.C.} \tag{4-21}$$

are added to the system. The latter will build up screening charges, of distribution

$$\rho(r) = \rho\cos(q\cdot r)e^{i\omega t} + \text{ C.C.} \tag{4-22}$$

The dielectric constant is the ratio of the external charge to the total charge

$$\epsilon(q\omega) = \frac{\delta\rho}{\rho+\delta\rho} \tag{4-23}$$

We must calculate the charge response ρ. In our case

$$\rho = \rho_{\mathrm{e}} + \rho_{\mathrm{i}}$$

is a sum of an electronic component and an ionic component. Our starting equations are
(a) Poisson's equation relating the electrostatic potential V to the charge densities $\delta\rho, \rho_{\mathrm{i}}, \rho_{\mathrm{e}}$:

$$\nabla^2 V = -4\pi\left(\delta\rho + \rho_i + \rho_e\right) \tag{4-24}$$

(b) the equation of motion of the ions in the presence of the electric field $\mathbf{E} = -\nabla\mathbf{V}$:

$$M\frac{dj_i}{dt} = nZe^2E \tag{4-25}$$

where j_i is the current carried by the ions, related to ρ_i by the continuity equation

$$\frac{\partial\rho_i}{\partial t} + \operatorname{div} j_i = 0 \tag{4-26}$$

In the small motion approximation, the total derivative $\mathrm{dj_j/dt}$ in Eq. (4-25) can be replaced by the partial derivative $\partial j_i/\partial t$. Eliminating j_i between (4-25) and (4-26), we obtain

$$\frac{\partial^2\rho_i}{\partial t^2} = \frac{nZe^2}{M}\nabla^2 V \tag{4-27}$$

Writing $\partial/\partial\mathrm{t} = \mathrm{i}\omega$ and making use of (4-24), we arrive at

[2] The jellium model was first applied to superconductivity by Pines [Phys. Reu., 109, 280 (1958)]; the phonon-induced part of that interaction had been earlier derived by Bardeen and Pines [Phys. Reu., 99, 1140 (1955)]; a description of the electron-ion system in terms of the overall dielectric constant was first worked out by Nozires (unpublished) and generalized slightly by Pines in his 1958 Les Houches lectures.

$$\omega^2\rho_{\mathrm{i}}(\mathrm{q},\omega) = \omega_{\mathrm{i}}^2\left[\rho_{\mathrm{i}}(\mathrm{q},\omega) + \rho_{\mathrm{e}}(\mathrm{q},\omega) + \delta\rho(\mathrm{q},\omega)\right] \tag{4-28}$$

with

$$\omega_{\mathrm{i}} = \sqrt{\frac{4\pi \mathrm{nZe}^2}{\mathrm{M}}} \tag{4-29}$$

As we shall see later, ω_i gives essentially the width of the phonon spectrum for our simple model. Typically $\omega_{\mathrm{i}} \sim 10^{13}\mathrm{sec}^{-1}$.
(c) We need an equation describing the response of the electron gas (that is, ρ_{e}) as a function of the electrostatic potential V. There is one simplifying feature in this calculation-the two characteristic frequencies of the electron gas are $\mathrm{E_F}/\hbar$ and the plasma frequency

$$\omega_p = \left(\frac{4\pi ne^2}{m}\right)^{1/2} \sim \omega_i\left(\frac{M}{m}\right)^{1/2}$$

Both these frequencies are very high. On the other hand ω is low ($\omega \sim \omega_{\mathrm{i}}$). Thus, in this part of the calculation, we may neglect ω completely and compute ρ_{e} simply for a static perturbation V .

We make a further approximation and derive ρ_e by the method of Thomas and Fermi (this is strictly correct only at long wavelengths $q \ll k_F$). In this approximation the electronic density at r is proportional to $[E_F + eV(r)]^{3/2}$. Its relative variation for small V is therefore given by

$$\frac{\rho_{\mathrm{e}}}{-\mathrm{ne}} = \frac{3}{2}\frac{\mathrm{eV}}{\mathrm{E_F}} \tag{4-30}$$

For a Fourier component of wave vector q this may be rewritten, according to Eq. (4-24), in the form

$$\rho_{\mathrm{e}} = \frac{-\mathrm{k_S^2}}{\mathrm{q}^2}(\rho + \delta\rho) \tag{4-31}$$

where

$$\mathrm{k_S^2} = \frac{6\pi n\mathrm{e}^2}{\mathrm{E_F}}$$

Collecting (4-28) and (4-31), we have

$$\rho = \rho_{\mathrm{i}} + \rho_{\mathrm{e}} = \left(\frac{\omega_{\mathrm{i}}^2}{\omega^2} - \frac{\mathrm{k_s^2}}{\mathrm{q}^2}\right)(\rho + \delta\rho)$$

and

$$\epsilon(q\omega) = \frac{\omega^2\left(k_S^2 + q^2\right) - \omega_i^2 q^2}{\omega^2 q^2} \tag{4-32}$$

Let us first determine from this expression the phonon frequency ω_{q}
for wave vector **q**. The spontaneous modes of vibration of our system correspond to 0 external charge $\delta\rho = 0$ or $\epsilon(q\omega) = 0$. For each q this defines one frequency ω_q given by

$$\omega_q^2 = \omega_i^2\frac{q^2}{k_S^2 + q^2} \tag{4-33}$$

For long wavelengths, $\omega_{\mathrm{q}} \sim (\omega_{\mathrm{i}}/\mathrm{k_S})\,\mathrm{q}$ is a linear function of q and the sound velocity ω_i/k_S. This formula gives, in fact, a rather realistic value for the velocity of sound for all the nontransition metals if we choose Z as the valence of the metal. In terms of ω_{q} we may rewrite Eq. (4-32) in the form

$$\frac{1}{\epsilon(q\omega)} = \frac{q^2}{k_s^2 + q^2}\left[1 + \frac{\omega_q^2}{\omega_i^2 - \omega_q^2}\right] \tag{4-34}$$

and the interaction matrix element is

$$\langle II|\mathscr{H}|I\rangle = \frac{4\pi e^2}{q^2\epsilon(q\omega)} = \frac{4\pi e^2}{k_S^2 + q^2} + \frac{4\pi e^2}{k_S^2 + q^2} \times \frac{\omega_q^2}{\omega^2 - \omega_q^2} \tag{4-35}$$

This has exactly the form predicted by Eq. (4-19), but with precise numerical coefficients. The first term is a (screened) Coulomb repulsion. The second term is the phonon-mediated interaction and i^+ is attractive for $\omega < \omega_{\mathrm{q}}$.

For an average phonon: $\omega_{\mathrm{q}} \sim \omega_{\mathrm{D}}$, the Debye frequency of the material. Thus the energy interval in which we find an attraction is of order $\hbar\omega_D = k_B\theta_D$ where k_B is Boltzmann's constant, and Θ_D (the Debye temperature) is typically of order $300°\mathrm{K}$ ($\mathrm{k_B}\ominus_{\mathrm{D}} \sim 0.03\mathrm{eV}$). Note that ω_{q} (or ω_{D}) depends on the mass M of the ions. Equations (4-29) and (4-33) show that $\omega_{\mathrm{q}} \sim \mathrm{M}^{-1/2}$. Thus two isotopes of the same superconductor have different attractive bandwidths, and their transition temperatures differ slightly - such isotope effects were first predicted by Frlich and observed soon after (Maxwell, Reynolds, et al., 1950). They prove that the vibrational motions of the lattice give an important contribution to the electron-electron interactions.

Numerical Values of the Interaction Constants

At the present time we cannot compute the matrix elements $\mathrm{V_{kk'}}$ in a very reliable way - we know too little about the relevant band structures, electron-phonon couplings, and so on. The calculation is particularly difficult for the following reason: At low frequencies ω, there is a rather strong compensation between the Coulomb repulsion and the indirect interaction. For "jellium," in particular, we notice that $\epsilon(\mathrm{q}\omega) \to \infty$ when $\omega \to 0$. In this model a static perturbation $\delta\rho$ is completely screened. Nothing prevents the positive ions from piling up with an arbitrary density in order to neutralize the charges $\delta\rho$.[3] If the short range repulsion between ions is taken into account, this effect disappears, the screening is not complete, and $\epsilon(q, 0)$ is then finite. This remark shows that the width of the attractive band and the attractive force are rather sensitive to the details of the physical model. It is important to make exactly the same approximations in the calculations of the direct and indirect interactions to avoid gross errors in the sum.

Problem.

Estimate $N(0)V_p$ for simple metals, using the "jellium" approximation.

Solution.

We define V_p as being the attractive part of interaction for $\omega = 0$. Then

$$V_p = \frac{4\pi e^2}{k_s^2 + q^2}$$

For q we take the root mean square average $q^2 = \frac{3}{5}q_D^2$ where q_D (the Debye cutoff) is defined by

$$v_0(2\pi)^{-3}\frac{4\pi}{3} \quad q_D^3 = 1$$

v_0 being the atomic volume. Finally

$$N(0) = \frac{mk_F}{2\pi^2\hbar^2} \tag{4-36}$$

$$N(0)V_p = \frac{2}{\pi}\frac{me^2}{\hbar^2}\frac{k_F}{q^2 + k_s^2} \tag{4-37}$$

$\mathrm{k_S^2}$ is defined below Eq. (4-31) as a function of the number n of electrons per cm^3

$$\mathrm{n} = \frac{\mathrm{k_F^3}}{3\pi^2} = \frac{\mathrm{Z}}{\mathrm{v_0}} \tag{4-38}$$

Finally, we recall that $\hbar^2/\mathrm{me}^2 = \mathrm{a_0} = 0.529\text{Å}$ is the Bohr radius. Collecting all these remarks, we find [4]

$$N(0)v_p = \frac{1}{2 + 4.7a_0\,|v_0 Z|^{-1/3}} \tag{4-39}$$

Problem.

Study the sign of the interaction between electrons at low frequencies in a magnetic medium.

Solution.

Suppose that the interaction between an electron situated at the point r, of spin S_i, and the local magnetization $M(r')$ of the medium is of the scalar form

$$\mathrm{H_1} = -\mathrm{TS_i} \cdot \mathrm{M(r)}$$

Since we are only interested in the zero frequency limit, we shall calculate the static response of the magnetic medium to the perturbation $\mathrm{H_1}$. To first order in Γ, this is of the form

$$\delta\mathrm{M}_\alpha(\mathbf{r}') = \sum_\beta \chi_{\alpha\beta}(\mathbf{r} - \mathbf{r}')\,\Gamma\mathrm{S_{i\beta}}$$

where χ is a generalized susceptibility tensor and $\alpha, \beta = \mathrm{x, y, z}$. Consider now the interaction V of δM with a second electron at r', of spin S_j,

$$V(r - r') = -\Gamma S_j \cdot \delta M(r') = -\Gamma^2 \sum_{\alpha\beta} S_{j\alpha}\chi_{\alpha\beta}(r - r')\,S_{i\beta}$$

Here again it is useful to consider the Fourier transform

$$V(q) = -\Gamma^2 \sum_{\alpha\beta} S_{i\alpha}\chi_{\alpha\beta}(q)S_{j\beta}$$

The static susceptibility tensor $\chi_{\alpha\beta}(q)$ is symmetric and can be diagonalized by a convenient choice of axes. The three principal susceptibilities ${\chi_{\alpha\alpha}}^{(q)}$ are necessarily positive. (Otherwise the magnetic material would be unstable with respect to a sinusoidal distortion of the magnetization of wavevector q.) If the spins S_i and S_j are antiparallel (singlet state), the static interaction

[4] This result differs from that of Anderson and Morel (Phys. Rev., 125, 1263 (1962) I. Their equation (14) uses $\omega_q = (\omega_i q)/k_s$ instead of the consistent form

[3] One physical case where this extraordinary screening effect can play an important role seems to be that of protons dissolved in palladium. These protons are very mobile. If a metallic impurity is added to the hydrogenated palladium, the screening charge around the impurity may be made largely of protons and not of electrons.

$$\omega_{\mathrm{q}} = \omega_{\mathrm{i}} \frac{\mathrm{q}}{(\mathrm{k_s^2} + \mathrm{q^2})_{1/2}}$$

A recent discussion of the effective interaction, with the allowance for periodicity, more accurate screening, and so on, may be found in Pines, Elemenlary Excilations in Solids (New York: Benjamin, 1963), Chapter 5.
will be positive (repulsive). By continuity, this will remain true at finite frequencies small compared to the exchange frequencies of the magnetic medium. (In an ordered system, the change of sign occurs for $\omega = \omega_{\mathrm{q}}$, the lowest spin wave frequency for the wave vector q.) Therefore, in the presence of a magnetic medium, there exists an interaction whose low frequency part is repulsive for Cooper pairs of antiparallel spin. On the contrary, for parallel pairs (triplet states), one can, in principle, find an attractive interaction at low frequencies.

6.1.3 4-3 Ground State and Elementary Excitations

Choice of a Trial Wave Function

The Cooper argument (Section 4-1) suggests that in the presence of attractive interactions the normal ground state of a free electron gas becomes unstable. The argument is of course only suggestive. In particular, it does not allow for the scattering of electrons above the Fermi sea against the electrons inside. We now calculate in more detail the structure of the condensed state, treating all electrons on the same footing.

In Section 4-1 we considered a pair of electrons described by a wave function $\psi(r_1 - r_2)$. In order to treat N electrons on the same footing, a natural generalization leads us to look for a wave function of the form

$$\phi_N(r_1, r_2, \ldots, r_N) = \phi(r_1 - r_2)\,\phi(r_3 - r_4) \cdots \phi(r_{N-1} - r_N) \tag{4-40}$$

In the state described by ϕ_N, the electrons are grouped in pairs, each pair having the same wave function ϕ. We can determine the function by minimizing the energy of the state ϕ_{N}.

Three technical remarks.
(a) The function ϕ_N can only be constructed for an even number N of electrons. For odd N, it would be necessary to place the last electron in a separate state. For an electron gas ($\mathrm{N} \sim 10^{23}$), the presence of this electron only gives rise to effects of the order of 1/N on the energy per particle and the other properties of the condensed stat; therefore it will not be important. On the other hand, for superfluids of fermions with small N (atomic nuclei), the even or odd character of N plays an important role especially on the form of the excitation spectrum.
(b) We have not yet included spin indices in ϕ_N. Guided by analogy with the situation in Section 4-1, we select the spin states $\uparrow\downarrow$, opposite for the two electrons of a pair. The function ϕ thus chosen will be the most favorable if the interaction V_{kk} ' is weakly dependent on the angle between k and k'.
(c) The function ϕ_{N} must be antisymmetrized, which we represent by an operator A:

$$\phi_N = A\phi(r_1 - r_2) \cdots \phi(r_{N-1} - r_N)\,(1t)(2t) \cdots (N-1t)(Nt) \tag{4-41}$$

Algebraic Transformations

The form (4-41) of ϕ_N has the merit of being explicit, but on the other hand it would be rather complicated to calculate directly from it. Introduce the Fourier transform of the pair function

$$\phi(r) = \sum_k g_k e^{ik\cdot r} \tag{4-42}$$

$$\phi_N = \sum_{k_1} \cdots \sum_{k_N/2} g_{k_1} \cdots g_{k_N/2} \cdots A e^{ik_1(r_1 - r_2)} \cdots$$
$$e^{ik_N/2\cdot(r_N - 1 - r_N)} (1\uparrow)(2\downarrow)\cdots(Nt) \tag{4-43}$$

The function $A \exp\left[ik_1\left(r_1 - r_2\right)\right] \cdots \exp\left[ik_{N/2}\cdot\left(r_{N-1} - r_N\right)\right] \times (14) \times (2t) \cdots (Nt)$ has a simple interpretation. It describes a state where one electron occupies the state $k_1 t$, another the state $(-k_1 t)$, a third $(\mathbf{k}_2\mathbf{1})$, and so on. Because of A, it is conveniently antisymmetrized. This is what is usually called a Slater determinant formed with the states

$$(k_1 t)\,(-k_1 t)\,(k_2 t)\,(-k_2 t)\cdots\left(k_{N/2}t\right)\left(-k_{N/2}t\right)$$

In order to represent such a Slater determinant, we use the more convenient Wigner-Jordan notation

$$a^{+}_{k_1 t^+} \cdots a^{a^+_{-k_N/2}\,\phi_0}_{k^+_{N/2}} \tag{4-44}$$

The operator $\mathrm{a}^+_{\mathrm{k}\alpha}$creates an electron in the state $(\mathrm{k}\alpha)$ when operating on the vacuum state designated by ϕ_0. We also use the destruction operator $\mathrm{a}_{\mathrm{k}\alpha}$, which is the adjoint of $\mathrm{a}^+_{\mathrm{k}\alpha}$and is such that $\mathrm{a}_{\mathrm{k}\alpha}\phi_0 = 0$. Wigner and Jordan have shown that all properties of the Slater determinant are correctly reproduced by the form (4-44) if anticommutation [5] relations are imposed on the operators a and a^+:

$$\begin{aligned} a^+_{k\alpha}a^+_{\ell\beta} + a^+_{\ell\beta}a^+_{k\alpha} &= 0 \\ a^+_{k\alpha}a_{\ell\beta} + a_{\ell\beta}a^+_{k\alpha} &= \delta_{k\ell}\delta_{\alpha\beta} \\ a_{k\alpha}a_{\ell\beta} + a_{\ell\beta}a_{k\alpha} &= 0 \end{aligned} \tag{4-45}$$

Our function ϕ_N takes the form

$$\phi_N = \sum_{k_1} \cdots \sum_{k_{N/2}} g_{k_1} \cdots g_{k_{N/2}} a^+_{k_1\uparrow} a^+_{-k_1\downarrow} \cdots a^+_{k_{N/2t}} a^+_{-k_{N/2t}} \phi_o \tag{4-46}$$

It is still not very easy to manage. Consider instead the generating function

$$\tilde{\phi} = C \prod_k \left(1 + g_k a^+_{k\uparrow} a^+_{-k\downarrow}\right) \phi_0 \tag{4-47}$$

where the product Π_k extends over all plane wave states [5a] and C is a normalization constant. By comparing (4-46) and (4-47), it is easy to see that to within the factor C, ϕ_N is the part of $\widetilde{\phi}$ that has N creation operators acting upon ϕ_0, that is, the component of $\tilde{\phi}$ that describes an N particle state. We make a slight transformation on $\tilde{\phi}$ by incorporating the factor C into the product Π_k

$$\tilde{\phi} = \prod_k \left(u_k + v_k a^\dagger_{kt} a^\dagger_{-kt}\right) \phi_o \tag{4-48}$$

[5] See Landau and Lifshitz, Nonvelativistic Quantum Mechanics (New York: Pergamon, 1959), Chap. 9.

with

$$\frac{v_k}{u_k} = g_k \quad u_k^2 + v_k^2 = 1 \tag{4-49}$$

The latter condition assures the normalization of $\tilde{\phi}$. We have assumed g_k, u_k, and v_k to be real. (We see later that this restriction is unimportant.) The function $\tilde{\phi}$ was introduced by Bardeen, Cooper, and Schrieffer in their fundamental paper of 1957. $\tilde{\phi}$ is much simpler than ϕ_N. For large N, all calculations can be performed from $\tilde{\phi}$ rather than ϕ_{N}. In order to understand this, write the expansion

$$\tilde{\phi} = \sum_N \lambda_N \phi_N \tag{4-50}$$

with $\Sigma_N \left|\lambda_N\right|^2 = 1$ to assure normalization. (Note that, with the above choice of phase for u_k and v_k, the coefficients λ_N are, in fact, real.)

For large N and whatever is the detailed form of the $\mathrm{g_k}$ ' s, the form of $\left|\lambda_N\right|^2$ as a function of N is that represented in Fig. 4-2. $\left|\lambda_N\right|^2$ has a sharp maximum. We can obtain the position of this maximum by calculating the average number of particles in the state

$$N^* = \langle N \rangle = \sum_k 2v_k^2 = \frac{\Omega}{(2\pi)^3} \int dk 2v_k^2 \tag{4-51}$$

where Ω is the volume of the sample. In the same way we can calculate the mean square of the distribution $\left|\lambda_N\right|^2$. From (4-44), we find

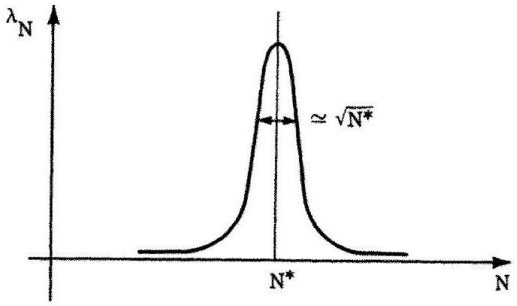


Figure 4-2 The probability amplitude λ_{N} to find a configuration with N particles in the BCS wave function (4-44). λ_N is strongly peaked around $\mathrm{N} = \mathrm{N}^*$.

$$\left\langle N^2 \right\rangle - \langle N \rangle^2 = \sum_k 4v_k^2 u_k^2 = \frac{\Omega}{(2\pi)^3} \int d\mathbf{k} \cdot 4v_k^2 u_k^2 \tag{4-52}$$

$\langle N^2 \rangle - \langle N \rangle^2$ is proportional to Ω, therefore to N^*-the halfwidth of the curve is a quantity of the order of $\sqrt{\mathrm{N}^*}$. Under these conditions, the relative fluctuations of N are of the order $1/\sqrt{\mathrm{N}^*}$-very small. On the contrary, $\sqrt{N^*}$ is still large with respect to 1 and the variations of λ_N are negligible when N varies by one or two

$$\lambda_{\mathrm{N+p}} \sim \lambda_{\mathrm{N}} \quad \text{for } \mathrm{p} \ll \sqrt{\mathrm{N}^*} \tag{4-53}$$

We now investigate the correspondence between the matrix elements of an arbitrary operator F taken between the ϕ_N or $\tilde{\phi}$.

$$\langle \tilde{\phi} | F | \tilde{\phi} \rangle = \sum_{N'} \lambda_{N^*} \lambda_{N'} \left\langle \phi_{N'} \right| F \left| \phi_{N'} \right\rangle \tag{4-54}$$

[52] Note that all factors in the product Π_k commute, as can be seen from (4-45).

Suppose first that F conserves the number of particles, then

$$\langle\tilde{\phi}|F|\tilde{\phi}\rangle = \sum_N |\lambda_N|^2 \langle\phi_N| F |\phi_N\rangle \tag{4-55}$$

The matrix element $\langle\phi_N| F |\phi_N\rangle$ is a slowly varying function of N and we can replace it by its value at the peak. As $\Sigma_N |\lambda_N|^2 = 1$, we obtain

$$\langle\tilde{\phi}|F|\tilde{\phi}\rangle = \langle\phi_{N^*}| F |\phi_{N^*}\rangle \tag{4-56}$$

In the same way, if F acting on ϕ_{N} gives a state of N + p particles,

$$\begin{aligned}\langle\tilde{\phi}|F|\tilde{\phi}\rangle &= \sum_N \lambda_{N^*+p'}\lambda_N \langle\phi_{N+p}| F |\phi_{N'}\rangle \\ &\cong \sum_N |\lambda_{N'}|^2 \langle\phi_{N+p}| F |\phi_N\rangle \\ &= \langle\phi_{N^*+p}| F |\phi_{N^*}\rangle\end{aligned} \tag{4-57}$$

Therefore in practice $\widetilde{\phi}$ gives the same information as ϕ_{N}.

Calculation of the Energy

Let $\mathscr{H}$ be the Hamiltonian of the interacting electron system. With the wave function ϕ_{N} we could apply the variational principle directly and look for the minimum of $\langle\phi_N| \mathscr{H} |\phi_N\rangle$. With the wave function $\widetilde{\phi}$ there is one slight difference-the number of particles is not fixed, and what we must minimize is

$$(\tilde{\phi}|\mathscr{H}|\tilde{\phi}) - E_F(\tilde{\phi}|N|\tilde{\phi}) \tag{4-58}$$

where N is the number of particles and $\mathrm{E_F}$ is a Lagrange multiplier we call the Fermi level. Now list the contributions to $\mathscr{H} - E_F N$. The kinetic energy term is

$$\begin{aligned}\mathscr{H}_0 &= \sum_{\mathrm{k}\alpha} \xi_{\mathrm{k}} \mathrm{a}^+_{\mathrm{k}\alpha} \mathrm{a}_{\mathrm{k}\alpha} \\ \xi_{\mathrm{k}} &= \frac{\hbar^2 \mathrm{k}^2}{2m} - \mathrm{E_F}\end{aligned} \tag{4-59}$$

The potential energy term $\mathcal{H}_{\mathrm{int}}$ has matrix elements describing the scattering of 2 electrons,

$$\begin{aligned}&(\mathbf{k}\alpha)\,(\mathbf{k}'\beta) - (\mathbf{k}+\mathbf{q},\alpha)\,(\mathbf{k}'-\mathbf{q},\beta) \\ \mathscr{H}_{\mathrm{int}} =& \frac{1}{2}\sum_{\mathbf{k},\mathbf{k}',\mathbf{q}} \mathrm{V}\,(\mathbf{k}+\mathbf{q},\mathbf{k}'-\mathbf{q}|\mathbf{k},\mathbf{k}') \\ &\alpha\beta \\ &\times a^+_{\mathbf{k}+\mathbf{q},\alpha} a^+_{\mathbf{k}'} - \mathbf{q},\beta a_{\mathbf{k}'\beta} a_{\mathbf{k}\alpha}\end{aligned} \tag{4-60}$$

The form (4-60) takes into account conservation of momentum and of total spin.

In the state $\widetilde{\phi}$, the probability of finding a state $\mathbf{k}$ occupied is $v^2_{\mathbf{k}}$. Therefore the kinetic energy becomes

$$\langle\tilde{\phi}|\mathscr{H}_0|\tilde{\phi}\rangle = \sum_{\mathrm{k}\alpha} \mathrm{v}^2_{\mathrm{k}} \xi_{\mathrm{k}} \tag{4-61}$$

The only terms contributing in $\mathscr{H}_{\text{int}}$ are
(1) the diagonal terms $\mathbf{V}(\mathbf{kk'kk'})$;
(2) the exchange terms $V(\mathbf{kk'k'k})$;
(3) the terms describing the transition of a pair from the state $(\mathbf{k}\uparrow, -\mathbf{k}\downarrow)$ to the state $(\ell\downarrow, -\ell\downarrow)$, $\mathbf{V}(\ell, -\ell|\mathbf{k}, -\mathbf{k}) = V_{k\ell}$.

The contributions of (1) and (2) are already present in a normal metal. We see later that they can be simply incorporated into ξ_k. We neglect them for the moment. The interesting contribution comes from (3). It is derived in the following way. We can first analyze the wave function $\widetilde{\phi}$ in two parts ϕ_{k1} and ϕ_{k0} in which the pair state $(\mathbf{kt} - \mathbf{kt})$ is, respectively, occupied and unoccupied. From (4-48) we have

$$\tilde{\phi} = v_k\phi_{k1} + u_k\phi_{k0} \tag{4-62}$$

Similarly we can analyze $\widetilde{\phi}$ into four components describing the occupancy of two different pair states $(\mathbf{kt} - \mathbf{kt})$ and $(\boldsymbol{\ell t} - \boldsymbol{\ell t})$

$$\tilde{\phi} = \mathrm{v_k v_\ell}\phi_{\mathrm{k1\ell 1}} + \mathrm{v_k u_\ell}\phi_{\mathrm{k1\ell 0}} + \mathrm{u_k v_\ell}\phi_{\mathrm{k0\ell 1}} + \mathrm{u_k u_\ell}\phi_{\mathrm{k0\ell 0}} \tag{4-63}$$

When computing the contribution of $V_{k\ell}$ to the interaction energy $\langle\widetilde{\phi}|\mathscr{H}_{\text{int}}|\widetilde{\phi}\rangle$, we must use the components

$$\mathrm{v_k u_\ell}\,\langle\phi_{\mathrm{k1\ell 0}}|\,\mathcal{H}_{\text{int}}\,\,|\phi_{\mathrm{k0\ell 1}}\rangle\,\mathrm{u_k v_\ell}$$

and the remaining matrix element is simply $V_{k\ell}$. Thus we find

$$\langle\tilde{\phi}|\mathscr{H} - E_F N|\tilde{\phi}\rangle = 2\sum_k \xi_k v_k^2 + \sum_{k\ell} v_{k\ell}u_k v_k u_\ell v_\ell \tag{4-64}$$

In order to minimize $\langle\tilde{\phi}|\mathscr{H}|\tilde{\phi}\rangle$ taking account of the relation $u_{\mathrm{k}}^2 + v_{\mathrm{k}}^2 = 1$, it is useful to put

$$u_k = \sin\theta_k \quad v_k = \cos\theta_k \tag{4-65}$$

$$\langle\tilde{\phi}|\mathrm{Im}\,C|\tilde{\phi}\rangle = 2\sum_k \xi_k \cos^2\theta_k + \frac{1}{4}\sum_{k\ell}\sin 2\theta_k \sin 2\theta_\ell v_{k\ell} \tag{4-66}$$

The minimization equations are

$$0 = \frac{\partial}{\partial\theta_{\mathrm{K}}}\langle\tilde{\phi}|\mathscr{H}|\tilde{\phi}\rangle = -2\xi_{\mathrm{k}}\sin 2\theta_{\mathrm{k}} + \sum_\ell \cos 2\theta_{\mathrm{k}}\sin 2\theta_\ell \mathrm{V_{k\ell}}$$

or

$$\xi_{\mathrm{k}}\tan 2\theta_{\mathrm{k}} = \frac{1}{2}\sum_\ell \mathrm{V_{k\ell}}\sin 2\theta\ell \tag{4-67}$$

We define

$$\Delta_k = -\sum_\ell v_{k\ell}u_\ell v_\ell \tag{4-68}$$

$$\epsilon_k = \sqrt{\xi_k^2 + \Delta_k^2} \tag{4-69}$$

and we find

$$\tan 2\theta_{\mathrm{k}} = -\frac{\Delta_{\mathrm{k}}}{\xi_{\mathrm{k}}} \tag{4-70}$$

$$2\mathrm{u_k v_k} = \sin 2\theta_{\mathrm{k}} = \frac{\Delta_{\mathrm{k}}}{\xi_{\mathrm{k}}} \tag{4-71}$$

$$-\mathrm{u_k^2} + \mathrm{v_k^2} = \cos 2\theta_{\mathrm{k}} = -\frac{\xi_{\mathrm{k}}}{\epsilon_{\mathrm{k}}} \tag{4-72}$$

(The choice of the sign in the last equation is such that for very large positive $\xi_{\mathrm{K}}, \mathrm{u_k} = 1, \mathrm{v_k} = 0$, and the total number of electrons $\Sigma_{\mathrm{k}} \mathrm{v_k^2}$ converges.)

With the insertion of the value of $u_\ell v_\ell$ into (4-68), we finally obtain an equation for Δ,

$$\Delta_{\mathrm{k}} = -\sum_{\ell} \mathrm{V_{k\ell}} \frac{\Delta_\ell}{2\left(\xi_\ell^2 + \Delta_\ell^2\right)^{1/2}} \tag{4-73}$$

We first notice that this equation always has the trivial solution $\Delta_{\mathrm{k}} = 0$, corresponding to

$$v_k = \begin{cases} 1 & \xi_k < 0 \\ 0 & \xi_k > 0 \end{cases} \tag{4-74}$$

The associated function $\widetilde{\phi}$ is simply

$$\tilde{\phi}_{\mathrm{n}} = \prod_{\mathrm{k}<\mathrm{k_F}} \mathrm{a_k^+ a_{-k}^+} \phi_0 \tag{4-75}$$

This represents a Slater determinant formed of all states of energy less than $E_F = \hbar^2 k_F^2/2m$; and is the wave function of a noninteracting electron gas. To show explicitly that there can be other solutions we choose the simplified interaction

$$V_{k\ell} = \begin{cases} -V & \text{if } |\xi_k|, |\xi_\ell| \leq \hbar\omega_D \\ 0 & \text{otherwise} \end{cases} \tag{4-76}$$

We call this simple form the BCS interaction. V is a positive constant. Then

$$\begin{array}{ll} \Delta_{\mathrm{K}} = 0 & \text{for } |\xi_{\mathrm{K}}| > \hbar\omega_{\mathrm{D}} \\ \Delta_{\mathrm{K}} = \Delta & \text{(independent of k) for } |\xi_{\mathrm{K}}| < \hbar\omega_{\mathrm{D}} \end{array} \tag{4-77}$$

We can then rewrite (4-73) by first summing over all orientations of ℓ for a fixed ξ_ℓ. This gives a factor $\mathrm{N}(\xi_\ell)$, the density of states per unit energy in the normal state for a given spin direction. Since we are interested in an energy interval of width $\hbar\omega_D \ll E_F$, we can replace $\mathrm{N}(\xi_\ell)$ by its value at the Fermi level N(0),

$$\Delta = N(0)V \int_{-\hbar\omega_D}^{\hbar\omega_D} \Delta \frac{d\xi}{2\sqrt{\Delta^2 + \xi^2}} \tag{4-78}$$

$$\frac{1}{N(0)V} = \int_0^{\hbar\omega_D} \frac{d\xi}{\sqrt{\Delta^2 + \xi^2}} = \sinh^{-1}\left(\frac{\hbar\omega_D}{\Delta}\right) \tag{4-79}$$

This equation only has a solution for positive V, that is, an attractive interaction. Then

$$\Delta = \frac{\hbar\omega_D}{\sinh \frac{1}{N(0)V}} \tag{4-80}$$

In everything that follows we are only interested in the weak coupling limit $\mathrm{N(0)V} \ll 1$, for which

$$\Delta = 2\hbar\omega_D e^{-1/N(0)V} \tag{4-81}$$

How is this limit justified? We shall see later that in this simple model the transition temperature is given by $\Delta = 1.75\mathrm{k_B T_0}$. Therefore $e^{-1/N(0)V} = 0.88T_0/\Theta_D$ where Θ_D is the Debye temperature defined by $\hbar\omega_D = \mathrm{k}_B\Theta_D$. For most superconducting metals $\Theta_D \sim 300°\mathrm{K}, \mathrm{T_0} \sim 10°\mathrm{K}$. Therefore we empirically conclude that $\mathrm{N(0)V} < 0.3$. (Lead and mercury are two notable exceptions with very low θ_D 's, giving, respectively, $\mathrm{N(0)V} = 0.39$ and 0.35 .)

Once Δ is known, we can explicitly calculate the kinetic and potential energies. In the weak coupling limit, one finds from (4-64)

$$\langle\tilde{\phi}|\mathscr{H}_0|\tilde{\phi}\rangle = 2\sum_{\mathrm{k}<\mathrm{k_F}} \xi_{\mathrm{k}} + \frac{\Delta^2}{\mathrm{V}} - \frac{\mathrm{N(0)}\Delta^2}{2} \tag{4-82}$$

The first term is the kinetic energy of the normal state ($\Delta = 0$). In the same way, we find

$$\langle\tilde{\phi}|\mathscr{H}_{\mathrm{int}}\,|\tilde{\phi}\rangle = -\frac{\Delta^2}{V} \tag{4-83}$$

The energy difference between the state $\widetilde{\phi}$ and the normal state is

$$\langle\tilde{\phi}|\mathscr{H}|\tilde{\phi}\rangle - \langle\phi_{\mathrm{n}}|\,\mathscr{H}\,|\phi_{\mathrm{n}}\rangle_{(\Delta=0)} = -\frac{\mathrm{N(0)}\Delta^2}{2} \tag{4-84}$$

The condensed state energy is lower than that of the normal state. Thus energy gain is, however, very small, of the order Δ^2/E_F per particle. For $\Delta = 10°\mathrm{K}$ and $\mathrm{E_F} = 10^{4\circ}$ K, this gives $\Delta^2/\mathrm{E_F} = 10^{-2\circ}$ K. We cannot calculate the energy of the normal state with this accuracy. Fortunately the unknown terms are very nearly the same in the normal state and in the condensed state. Each term in (4-82) is incorrect, but the difference is very nearly correct, and it is this difference that is measured experimentally.

Certain simple properties can be determined from the function $\tilde{\phi}$:
(a) Let us study the probability of finding an electron condensed into the state $(\mathbf{k}\alpha)$. It is given by

$$\langle\tilde{\phi}|\mathrm{a}^+_{\mathrm{k}\alpha}\mathrm{a}_{\mathrm{k}\alpha}|\tilde{\phi}\rangle = \mathrm{v}^2_{\mathrm{k}} = \frac{1}{2}\left(1 - \frac{\xi_{\mathrm{k}}}{\sqrt{\xi^2_{\mathrm{k}} + \Delta^2_{\mathrm{k}}}}\right) \tag{4-85}$$

from (4-70) and (4-55). It is shown as a function of k in Fig. 4-3. v_k^2 gives the momentum distribution in the ground state. Ideally v^2_{k} can be measured by the Compton effect, positron annihilation, and so on. In fact, high accuracy would be required to measure v^2_{k} directly in the domain of interest. For $\mathrm{k} \ll \mathrm{k_F}, \mathrm{v_k} = 1$. For $\mathrm{k} \gg \mathrm{k_F}, \mathrm{v_k} = 0$. The distribution function v^2_{K} is continuous in contrast to the normal state where it has a discontinuity at $\mathrm{k_F}$. The transition region, where $\mathrm{v_k}$ goes from 1 to 0, has an energy width Δ and a momentum width $\delta\mathrm{k}$.

$$\begin{aligned} &\frac{\hbar^2}{2m}\left[(k_F + \delta k)^2 - k_F^2\right] \cong \Delta \\ &\delta k = \frac{m\Delta}{\hbar^2 k_F} = \frac{\Delta}{\hbar v_F} \end{aligned} \tag{4-86}$$

(b) Let us add two electrons to the states $\mathbf{k} \notin$ and $-\mathbf{k} \neq$ in the condensed state $\tilde{\phi}_{\mathrm{N}}$. What is the probability amplitude for obtaining the state $\phi_{\mathrm{N}+2}$? This is the quantity

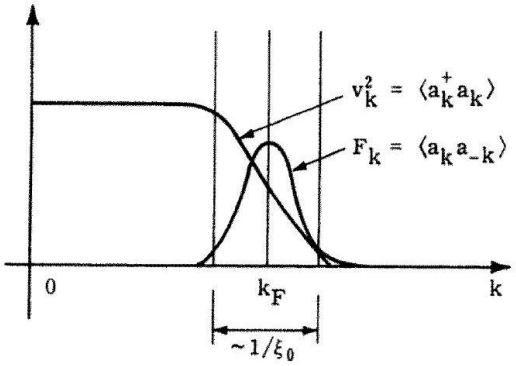


Figure 4-3
The momentum distribution ($|v_k|^2$) of electrons in the BCS ground state. In a normal metal, the distribution drops discontinuously at $k = k_F$. In the superconductor, this drop is smeared out on an interval $\delta \mathrm{k} \sim 1/\xi_0 \sim \Delta/\hbar \mathrm{v_F}$. Also shown is the condensation amplitude $\mathrm{F_k}$.

$$\mathrm{F_k} = \langle \phi_{\mathrm{N}+2} |\, \mathrm{a}^+_{\mathrm{k}\uparrow} \mathrm{a}^+_{-\mathrm{k}\downarrow} \,| \phi_{\mathrm{N}} \rangle = \langle \widetilde{\phi} | \mathrm{a}^+_{\mathrm{k}\downarrow} \mathrm{a}^+_{-\mathrm{k}\downarrow} | \widetilde{\phi} \rangle \tag{4-87}$$

We call $\mathrm{F_k}$ the condensation amplitude in the state $\mathbf{k}$. On using the definition of $\widetilde{\phi}$, we find

$$F_k = u_k v_k \tag{4-88}$$

$\mathrm{F_k}$ is only nonvanishing in the transition zone and is maximum for $\mathrm{k} = \mathrm{k_F}$.

First Excited States

We have constructed a ground state function ϕ_{N} where N particles are coupled in pairs. We now try to add one particle in the plane wave state $(m\alpha)$. We obtain a state

$$\begin{aligned} \phi_{\mathrm{N}+1,\mathrm{m}\,\alpha}\,(\mathrm{r}_1 \cdots \mathrm{r}_{\mathrm{N}+1}) &= \mathrm{A}\phi\,(\mathrm{r}_1 - \mathrm{r}_2) \cdots \phi\,(\mathrm{r}_{\mathrm{N}-1} - \mathrm{r}_{\mathrm{N}}) \\ &\times \exp\,(\mathrm{im} \cdot \mathrm{r}_{\mathrm{N}+1})\,(1\uparrow) \cdots (\mathrm{N}\downarrow)(\mathrm{N}+1, \alpha) \end{aligned} \tag{4-89}$$

We introduce the corresponding generating function

$$\widetilde{\phi}_{m\alpha} = \sum_{\mathrm{N}} \lambda_{\mathrm{N}} \phi_{\mathrm{N}+1}, m\alpha \tag{4-90}$$

By repeating for $\phi_{m\alpha}$ our earlier arguments on ϕ we find

$$\widetilde{\phi}_{m\alpha} = \prod_{k \neq m} \left(u_k + v_k a^+_{k\uparrow} a^+_{-k\downarrow} \right) a^+_{m\alpha} \phi_0 \tag{4-91}$$

$\widetilde{\phi}_{m\alpha}$ is orthogonal to $\widetilde{\phi}$. What is the energy of the state $\phi_{m\alpha}$? For the kinetic energy we find

$$\left\langle \widetilde{\phi}_{m\alpha} \right| \mathscr{H}_0 \left| \tilde{\phi}_{m\alpha} \right\rangle = \langle \widetilde{\phi} | \mathscr{H}_0 | \widetilde{\phi} \rangle + \left(1 - 2\mathrm{v}^2_m\right) \xi_m \tag{4-92}$$

since $\tilde{\phi}_{m\alpha}$ has an electron in the orbital state $m\alpha$, while in the state $\tilde{\phi}$ there is a probability $2v_m^2$ of finding an electron (mt) or (mt). For the potential energy, we notice that only the terms corresponding to the transitions $(\mathbf{k}, \alpha)(-\mathbf{k}, -\alpha) \rightarrow (\mathbf{k}'\alpha)\,(-\mathbf{k}' - \alpha)$ with $\mathbf{k} \neq \mathbf{m}$ and $\mathbf{k}' \neq \mathrm{m}$ contribute since no pair can use the state $m\alpha$. Therefore

$$\left\langle \tilde{\phi}_{m\alpha} \right| \mathscr{H}_{\text{int}} \left| \tilde{\phi}_{m\alpha} \right\rangle = \langle \tilde{\phi} | \mathscr{H}_{\text{int}} | \tilde{\phi} \rangle - 2 \sum_{\ell} \mathrm{v}_{m\ell} \mathrm{u}_m \mathrm{v}_\ell \mathrm{u}_\ell \mathrm{v}_m \tag{4-93}$$

The total energy becomes

$$\begin{aligned} \left\langle \tilde{\phi}_{m\alpha} \right| \varkappa \left| \tilde{\phi}_{m\alpha} \right\rangle &= E_0 + \left(1 - 2v_m^2\right) \xi_m + 2u_m v_m \Delta_m \\ &= E_0 + \frac{\xi_m^2}{\epsilon_m} + \frac{\Delta_m^2}{\epsilon_m} \\ &= E_0 + \epsilon_m \end{aligned} \tag{4-94}$$

Since E_0 is the energy in the ground state $\tilde{\psi}, \epsilon_m = \sqrt{\Delta_m^2 + \xi_m^2}$ is the energy necessary to place a new particle into the state m. Notice that even when $\xi_m = 0, \epsilon_m$ is finite and equal to $\Delta_{\mathrm{k_F}} = \Delta$.

We can try to construct states with $2, 3 \ldots . n$ excitations in the same way. For the states with two excitations. for example, we are tempted to take the function

$$\Xi_{m\alpha, n\beta} = \prod_{k \neq m,n} \left(u_k + v_k a_{kt}^+ a_{-kt}^+\right) a_{m\alpha}^+ a_{n\beta}^+ \phi_0 \tag{4-95}$$

Unfortunately such functions are not necessarily orthogonal to $\widetilde{\phi}$. For example,

$$\left\langle \tilde{\phi} | \Xi_{mt} - m \right\rangle^{\rangle} = \mathrm{v}_m \neq 0 \tag{4-96}$$

Two methods to avoid this difficulty are
(a) Add to Ξ a component $\lambda\widetilde{\phi}$ where λ is chosen in such a way as to make the total function orthogonal to $\widetilde{\phi}$. This is the original BCS method, which is numerically rather tedious.
(b) Reconsider the wave functions of single excitation $\widetilde{\phi}_{m\alpha}$. Let us try to place these functions into the form

$$\tilde{\phi}_{m\alpha} = \gamma_{m\alpha}^* \tilde{\phi} \tag{4-97}$$

where $\gamma_{m\alpha}^+$will appear as a creation operator for one elementary excitation. If the operators $\gamma^+$and their adjoints γ can be found such that
(1) the γ and γ^+obey the fermion commutation rules (analogous to (4-45),
(2) $\gamma_{m\alpha}\widetilde{\phi} = 0$, that is, $\widetilde{\phi}$ is the state of no excitation,
then it is easy to see by manipulating the commutation relations that all the states obtained by applying an arbitrary number of operators $\gamma^+$to $\tilde{\phi}$ are orthogonal to each other, normalized, and orthogonal to the ground state $\widetilde{\phi}$. From the kinematic point of view, these wave functions can therefore conveniently describe states of multiple excitations.

We must now find the γ^+. As a first attempt, we notice that

$$\tilde{\phi}_{m\alpha} = \frac{1}{u_m} a_{m\alpha}^+ \tilde{\phi} \tag{4-98}$$

as is easy to verify from (4-91) by noting that $a_{m\alpha}^+ a_{m\alpha}^+ = 0$ and so on. However $(1/u_m)\, a_{m\alpha}^*$ does not obey the above anticommutation rules. As a second attempt, we notice that

$$\tilde{\phi}_{m\downarrow} = \frac{1}{v_m} a_m \, \phi \tag{4-99}$$

However, we again encounter the same difficulty with the commutation rules. We then try to define γ^+as a linear combination of the preceding forms. If we take

$$\gamma^+_{m\uparrow} = u_m a^+_{m\uparrow} - v_m a_{-m}\dagger$$
$$\gamma^+_{m\neq} = u_m a^+_{m+} + v_m a_{-m\uparrow} \tag{4-100}$$

we find that (4-97) and conditions (1) and (2) are verified. For example, condition (2) becomes

$$\begin{aligned}\gamma_{mt}\tilde{\phi} &= \prod_{k\neq m}\left(u_k + v_k a^+_{kt} a^+_{-kt}\right)\left(u_m a_{mt} - v_m a^+_{-mt}\right)\\ &\times \left(u_m + v_m a^+_{mt} a^+_{-mt}\right)\phi_0\\ &= \prod_{k\neq m}\left(u_k + v_k a^+_{kt} a^+_{-kt}\right) u_m v_m \left(a^+_{-mt} - a^+_{-mt}\right)\phi_0\\ &= 0\end{aligned} \tag{4-101}$$

where we have used the relations $a_{-m\alpha}\phi_0 = 0$, $a_{m\alpha}a^+_{m\alpha}\phi_0 = \phi_0$, and the anticommutation relations. We thus obtain the operators γ^+, which create excited states that are mutually orthogonal and also orthogonal to the ground state. The use of the γ and γ^+enormously simplifies all calculations in which the excited states play a role (Bogolubov, Valatin, 1958). We designate the excitations created by the γ^+'s as quasiparticles.

Physical remarks.

(a) The fact that $\gamma^+_{m\alpha}$is a linear combination of $\mathrm{a}^+_{m\alpha}$and $\mathrm{a}_{m-\alpha}$ expresses the fact that it is possible to create the state $\phi_{\mathrm{N}+1,\mathrm{k}\alpha}$ either by adding an electron $(\mathrm{k}\alpha)$ to the condensed state ϕ_{N} or by removing an electron $(-\mathrm{k}-\alpha)$ from the state $\phi_{\mathrm{N}+2}$.
(b) Suppose we start from the ground state ϕ_N. We have seen that if we add a particle in a state k, it must at least have an energy equal to $E_F + \Delta$. Such an "injection" experiment is not a purely theoretical invention. It can be accomplished by bringing electrons into a superconductor across a thin oxide layer. This is the previously mentioned tunnel effect (Giaever, 1959), which permits us to determine the gap Δ.
(c) However, except from the tunneling experiments, the excited states are usually studied without changing **N** (for example, infrared radiation). If **N** is even, the first excited states of this type correspond to breaking a pair. They correspond to wave functions of the form $\gamma^+_{\mathrm{k}\alpha}\gamma^+_{\ell\beta}(\mathrm{k}\alpha \neq \ell\beta)$. The excitation energy is easily calculated and becomes $\epsilon_k + \epsilon_\ell$. The minimum of this energy (corresponding to the infrared absorption energy gap) is 2Δ. If N is odd (N = 2 K + 1), the state consists of K pairs plus one unpaired electron. There are then 2 kinds of excitations: either a pair is decoupled as previously (gap 2 Δ) or the state of the unpaired electron is changed (gap 0). However the absorption intensity of the first process is $\sim N$ times greater than that of the second process. In practice, since $\mathrm{N} \sim 10^{23}$, one always measures an absorption threshold at 2Δ.
(d) The excitation energy is at least 2Δ, but the energy per excited particle is Δ. At low temperatures the probability of finding a particle excited into a given state k (k near k_F) varies as $\exp(-\Delta/k_B T)$.

Case of Two Coupled Superconductors

Consider two superconductors S and S' separated by an insulating layer. If the layer is thick, the electrons cannot cross it, and S and S' become completely independent. If the layer is thin (thickness < 30Å), the electrons can traverse it by the tunneling effect. This gives rise

to a coupling between the regions S and S', which we consider now. Algebraically, the transfer of the electrons can be described by adding to the Hamiltonian operator $\mathscr{H}_{\mathrm{SS'}}$ of the electrons for S and S', a small term $\mathscr{H}_T$, which causes an electron to tunnel from S to S' and vice versa.

$$\begin{aligned}\mathscr{H} &= \mathscr{H}_{\mathrm{SS'}} + \mathscr{H}_{\mathrm{T}} \\ \mathscr{H}_{\mathrm{T}} &= \sum_{\mathrm{k}\ell} \left(\mathrm{a}^{+}_{\mathrm{ks}}\mathrm{a}_{\ell\mathrm{s'}}\mathrm{T}_{\mathrm{k}\ell} + \mathrm{a}^{+}_{\ell\mathrm{s'}}\mathrm{a}_{\mathrm{ks}}\ \mathrm{T}^{+}_{\mathrm{k}\ell}\right)\end{aligned} \tag{4-102}$$

where a^*_{ks} created an electron in the state k on the side S and $a_{\ell s'}$ destroys an electron in the state ℓ on the side S'. The matrix element $\mathrm{T}_{\mathrm{k}\ell}$ can be calculated explicitly from a solution of the one-electron Schroedinger equation in the barrier. (Notice that $'\mathcal{H}_{\mathrm{SS'}}$ is the complete Hamiltonian of S and S$'$. It contains the electron interactions V.) An eigenstate for $\mathscr{H}_{\mathrm{SS}}$, will be a product of two functions of the type (4-43), one relative to S and one relative to S'. Let

$$\psi_\nu = \phi^{(\mathrm{s'})}_{2(\mathrm{N}-\nu)}\phi^{(\mathrm{s})}_{2\nu} \quad \mathcal{F}_{\mathrm{SS'}}\psi_\nu = \mathrm{E}_\nu\psi_\nu \tag{4-103}$$

ψ_ν describes 2ν electrons coupled in pairs on the side S and $2(\mathrm{N}-\nu)$ electrons coupled in S'. The total number of electrons $2N$ is fixed. On the contrary, ν is not known in advance. How does the energy E_ν vary with respect to ν ? If ν is augmented by 1,2 electrons are created on the side S at the expense of S'. Thermodynamics gives us

$$E_{\nu+1} - E_\nu = 2\left(E^{(s)}_F - E^{(s')}_F\right) \tag{4-104}$$

where $E^{(s)}_F$ is the chemical potential (Fermi level) on the side S. For the moment, let us suppose that there is no voltage applied between S and S'. Then $E^{(S)}_F = E^{(S')}_F$ and the functions ψ_ν are degenerate ($E_\nu =$

E independent of ν). The perturbation $\mathscr{H}_{\mathrm{T}}$ removes this degeneracy. To second order in $\mathscr{H}_{\mathrm{T}}$ there is a matrix element coupling the functions ψ_ν and $\psi_{\nu+1}$

$$\begin{aligned}\mathrm{J}_0 = &\sum_{\substack{\mathrm{k},\ell \\ \mathrm{k'},\ell'}} \langle\nu+1|\mathrm{T}_{\mathrm{k}\ell}\mathrm{a}^{+\,\mathrm{a}}_{\mathrm{ks}}\ell\ \mathrm{s'}|\mathrm{I}\rangle \frac{1}{\mathrm{E}-\mathrm{E}_\mathrm{I}} \\ &\times \langle\mathrm{I}|\mathrm{T}_{\mathrm{k'}\ell'}\mathrm{a}^{+\,\mathrm{a}}_{\mathrm{k's}}\ell'\mathrm{s'}|\nu\rangle\end{aligned} \tag{4-105}$$

where |I) is an intermediate state with $2\nu+1$ electrons on the S side and $2(\mathrm{N}-\nu)-1$ electrons on the S$'$ side. The tunneling Hamiltonian $\mathscr{H}_{\mathrm{T}}$ acting on the state with ν pairs on side S creates a state |I⟩ with one "bachelor electron" of wave vector $\mathbf{k}$ ' on side S . Then $\mathscr{H}_{\mathrm{T}}$ acting on | 1) creates another electron of wave vector k on side S. The final state onto which this is projected is composed of $(\nu+1)$ pairs on side S; thus we must save $k = -k'$. Similarly $\ell = -\ell'$. Then, using the symmetry relation $\mathrm{T}_{-\mathrm{k}-\ell} = \mathrm{T}^{+}_{\mathrm{k}\ell}$and our results on excited states, we find

$$J_0 = -4\sum_{k\ell} |T_{k\ell}|^2 \frac{u_k v_k u_\ell v_\ell}{\epsilon_k + \epsilon_\ell} \tag{4-106}$$

To second order in $\mathscr{H}_{\mathrm{T}}$, one can write

$$\mathscr{H}\psi_\nu = \mathrm{E}\psi_\nu + \mathrm{J}_0\left(\psi_{\nu+1} + \psi_{\nu-1}\right) \tag{4-107}$$

The correct wave function will be a linear combination of the ψ_ν. This problem is formally identical to that of the motion of an electron in a linear atomic chain. ψ_ν is then the analog

of an atomic orbital localized around the ν th atom. In the tight binding approximation, one attempts to form the wave function as a linear combination of the ψ_ν 's. The form of this combination ψ_k is imposed in Bloch's theorem

$$\psi_\mathrm{k} = \sum_\nu \psi_\nu \mathrm{e}^{\mathrm{ik}\nu} \tag{4-108}$$

where k is analogous to a wave vector. The corresponding energy $E(k)$ is

$$E(k) = E + 2J_0 \cos k \tag{4-109}$$

Suppose that we now construct a wave packet of the ψ_k 's corresponding to wave vectors in the interval between k and $k + \Delta k$. In our "linear chain" analogy, the wave packet has a spatial extent $\Delta\nu \sim 1/\Delta\mathrm{k}$. As ν is enormous ($\nu \sim 10^{22}$), we can take $\Delta\nu$ to be very large (for example, $\Delta\nu \sim \sqrt{\nu} \sim 10^{11}$), therefore having a verv small Δk and at
the same time $\Delta\nu/\nu$ very small ($\sim 10^{-11}$). Therefore it is possible to specify k and ν simultaneously with good accuracy. Such a wave packet moves with group velocity

$$\frac{\hbar d\langle\nu\rangle}{dt} = \frac{\partial E(k)}{\partial k} = -2J_0 \sin k \tag{4-110}$$

For the state described by our wave packet, there is a time variation of ν and therefore a current passing from S to S'

$$I = 2e\frac{d\langle\nu\rangle}{dt} = -4e\frac{J_0}{\hbar}\sin k \tag{4-111}$$

In other words, if S and S' are attached to a generator, a current ($< 4\mathrm{eJ}_0/\hbar$) can flow from S to S′ under zero voltage. Equation (4-111) shows us in a simple example why the condensed state has superfluid properties. Note that for a normal system ($u_k v_k \equiv 0$) J_0 vanishes (Eq. 4-106). This effect was predicted by Josephson (1961) and observed first by Anderson and Rowell. The present derivation is due to Ferrel (1963). (Typical current values are of order 10^{-2} A/cm^2.)

How are these results modified when a voltage is applied between S and S' ? We then have $E_{\nu+1} - E_\nu = 2eV$. This is the analog of a uniform electric field applied on the "chain." The wave packet moves according to the force equation

$$\frac{d}{dt}\langle\hbar k\rangle = 2eV \tag{4-112}$$

Equations (4-111) and (4-112) completely determine the behavior of the junction. For example, if the voltage V is held constant, k varies linearly with time and I is an alternating current of frequency $2eV/\hbar$.

Problem.

A Josephson junction SS′ is placed in series with a resistance R′ and connected to a generator of voltage U. Calculate the currents.

Solution.

The voltage across the junction is

$$V = U - RI = U + \frac{4eJ_0R}{\hbar}\sin k$$

From (4-112)

$$\frac{\mathrm{dk}}{\mathrm{dt}} = \frac{2\mathrm{e}}{\hbar}\left(\mathrm{U} + \frac{4\mathrm{eJ_0R}}{\hbar}\sin\mathrm{k}\right) = \omega_0(1 - \lambda\sin\mathrm{k})$$

with

$$\omega_0 = \frac{2\mathrm{eU}}{\hbar} \quad \lambda = -\frac{4\mathrm{eJ_0R}}{\hbar\mathrm{U}} = \frac{\mathrm{RJ}_m}{\mathrm{U}}$$

(J_m = maximum supercurrent allowable through the junction).
The force equation can be integrated in the form

$$\omega_0\,(t - t_0) = \int \frac{\mathrm{dk}}{1 - \lambda\sin k}$$

We consider two cases:
(a) If $\lambda > 1$, the denominator has pole for $k = k_0$, where $\sin k_0 = 1/\lambda$. t tends towards ∞ for $k \to k_0$. The current tends toward the limiting value U/R. When this value is reached, the voltage across the junction $SS', U - RI$, will fall to zero. There is therefore a regime in which there is a permanent continuous current.
(b) If $\lambda < 1$, the denominator never vanishes. The relation between k and t can be integrated explicitly by setting

$$m = \tan\frac{\mathrm{k}}{2} \quad \mathrm{I} = \frac{2\ \mathrm{J}mm}{1 + m^2}$$

One obtains

$$m = \lambda + \sqrt{1 - \lambda^2}\tan\left[\frac{1}{2}\sqrt{1 - \lambda^2}\omega_0\,(t - t_0)\right]$$

m, and consequently k, is a periodic function of time with period $2\pi/\omega_0\sqrt{1 - \lambda^2}$. Notice that the current is not sinusoidal except for $\lambda = 0$.

6.1.4 4-4 Calculations at Finite Temperature

Construction of the Free Energy

For $\mathrm{T} \neq 0$, the states $\gamma_\mathrm{k}^+\tilde{\phi}, \gamma_\mathrm{k}^+\gamma_\ell^+\tilde{\phi}$, and so on, are thermally excited. When $\mathrm{k_B T} \ll \Delta$, there are only a few of these excitations and they are independent. However, when $\mathrm{k_B T} \sim \Delta$, the number of excitations are large. We now study the average effect of the interaction between them, and show that it can be simply described by allowing the energy gap Δ to vary with temperature.

We still define the fermion operators $\gamma_\mathrm{k}^+$by the transformation (4-100) where the u_k and v_k are not yet determined. We treat the excitations of the system as a gas of independent quasiparticles. At temperature T, there is a probability

$$f_{k\alpha} = \left\langle \gamma_{k\alpha}^+\gamma_{k\alpha} \right\rangle = 1 - \left\langle \gamma_{k\alpha}\gamma_{k\alpha}^+ \right\rangle \tag{4-113}$$

of finding a quasiparticle of wave vector $\mathbf{k}$ and spin α.[6] The symbol
denotes a thermal average. We shall calculate the free energy F (where the f_k are arbitrary), then minimize F with respect to u_k and v_k and with respect to f_k.
(1) Calculation of the average kinetic energy from (4-92):

[6] In most usual cases $f_{k\alpha}$ will be independent of the index α and written simply f_k.

$$\langle \mathscr{H}_0 \rangle = \sum_{\mathrm{k}\alpha} \xi_{\mathrm{k}} \left[u_{\mathrm{k}}^2 \left\langle \gamma_{\mathrm{k}\alpha}^+ \gamma_{\mathrm{k}\alpha} \right\rangle + v_{\mathrm{k}}^2 \left\langle \gamma_{\mathrm{k}\alpha} \gamma_{\mathrm{k}\alpha}^+ \right\rangle \right]$$
$$= \sum_{\mathrm{k}} 2\xi_{\mathrm{k}} \left[u_{\mathrm{k}}^2 f_{\mathrm{k}} + v_{\mathrm{k}}^2 \left(1 - f_{\mathrm{k}}\right) \right] \tag{4-114}$$

(2) Potential energy: With our approximations, the only terms that come into play are still those that describe the collisions $(\mathrm{k}\uparrow -\mathrm{k}\downarrow)$ $(lt - lt)$.

$$\langle \mathscr{H}_{\mathrm{int}} \rangle = \sum_{\mathrm{k}\ell} \left\langle \mathrm{a}_{\mathrm{k}t}^+ \mathrm{a}_{-\mathrm{k}t-\ell t}^+ {}^{\mathrm{a}}{}_{\ell t} \right\rangle \mathrm{V}_{\mathrm{k}\ell} \tag{4-115}$$

In Eq. (4-115) the operators a^+, a, are linear combinations of the operators γ^+, γ, and the $\gamma\gamma^+$describe a set of independent fermions. Then we have the simple property

$$\langle 0_1 0_2 0_3 0_4 \rangle = \langle 0_1 0_2 \rangle \langle 0_3 0_4 \rangle + \langle 0_1 0_4 \rangle \langle 0_2 0_3 \rangle - \langle 0_1 0_3 \rangle \langle 0_2 0_4 \rangle \tag{4-116}$$

where each of the 0 is an a or an a^+operator. This property (a particular application of a theorem by Wick) can be checked by writing explicitly the transformation from the a's to the γ 's and then taking the averages. It simplifies the algebra considerably. In the present case, we find 3 terms for the interaction. Two of them involve only averages $\left\langle \mathrm{a}_{\mathrm{k}}^+ \mathrm{a}_{\mathrm{k}} \right\rangle$ and lead to a Hartree and an exchange contributionboth are essentially temperature independent and we drop them as before. The remaining term $\langle a^+ a^+ \rangle \langle a \rangle$ leads to

$$\langle \mathscr{H}_{\mathrm{int}} \rangle = \sum_{\mathrm{k}\ell} v_{\mathrm{k}\ell} u_{\mathrm{k}} v_{\mathrm{k}} u_\ell v_\ell \left(1 - 2f_{\mathrm{k}}\right) \left(1 - 2f_\ell\right) \tag{4-117}$$

(3) Entropy S. The entropy for a system of independent fermions is given by

$$S = -k_B \sum_{k\alpha} \left[f_k \ln f_k + \left(1 - f_k\right) \ln \left(1 - f_k\right) \right] \tag{4-118}$$

(4) The total energy F becomes

$$\mathrm{F} = \langle \mathscr{H}_0 + \mathscr{H}_{\mathrm{int}} \rangle - \mathrm{TS} \tag{4-119}$$

We first require that F be stationary with respect to u_k and v_k. Again setting $u_k = \sin\theta_k, v_k = \cos\theta_k$, we obtain

$$+2\xi_{\mathrm{k}} \left(1 - 2\mathrm{f}_{\mathrm{k}}\right) \sin 2\theta_{\mathrm{k}} = \sum_{\ell} \mathrm{V}_{\mathrm{k}\ell} \cos 2\theta_{\mathrm{k}} \sin 2\theta_\ell \left(1 - 2\mathrm{f}_{\mathrm{k}}\right) \left(1 - 2\mathrm{f}_\ell\right) \tag{4-120}$$

If we define

$$\Delta_{\mathrm{k}} = -\frac{1}{2} \sum_{\ell} \mathrm{v}_{\mathrm{k}\ell} \sin 2\theta_\ell \left(1 - 2\mathrm{f}_\ell\right) \tag{4-121}$$

we recover the solution (4-69)-(4-72). The only modification arises from the fact that Δ_k(4−121) differs from (4-68) by the excitation occupation number f_ℓ. If we now minimize F with respect to f_k, we obtain

$$2\xi_k \left(u_k^2 - v_k^2\right) - 4 \sum_{\ell} v_{k\ell} u_k v_k u_\ell v_\ell \left(1 - 2f_\ell\right)$$
$$+ 2k_B T \ln \left(\frac{f_k}{1 - f_k} \right) = 0 \tag{4-122}$$

Then, using (4-69)-(4-72), we find

$$f_k = \frac{1}{1 + \exp\left(\epsilon_k / k_B T\right)} \tag{4-123}$$

This is the usual form for the distribution function for fermions of energy ϵ_k. However, the variation of f_k with temperature is not simple because ϵ_{K} and Δ_{K} depend on the temperature.

Variation of the Gap with Temperature and Transition Point

The self-consistency equation [analogous to (4-73)] becomes

$$\Delta_{\mathrm{k}} = -\sum_{\ell} \mathrm{v}_{\mathrm{k}\ell} \frac{\Delta_\ell}{2\epsilon_\ell} \left[1 - 2\mathrm{f}\left(\epsilon_\ell\right)\right] \tag{4-124}$$

Let us first take for $V_{k\ell}$ the simple BCS interaction (4-76). The condition becomes

$$1 = \mathrm{N}(0)\mathrm{V} \int_0^{\hbar\omega_{\mathrm{D}}} \frac{\mathrm{d}\xi}{\sqrt{\xi^2 + \Delta^2}} \left[1 - 2\mathrm{f}\left(\sqrt{\xi^2 + \Delta^2}\right)\right] \tag{4-125}$$

This is an implicit relation between T and Δ. For $T = 0$, the Fermi function $f(E)$ is zero (E being positive), and one recovers the condition (4-79). The form of $\Delta(T)$ is given in Fig. 4-4. Δ decreases as T increases, and finally vanishes at a certain temperature T_0. Above T_0.

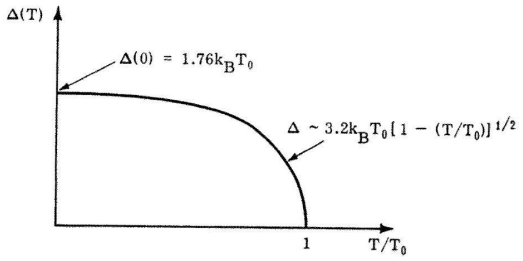


Figure 4-4
Variation of the order parameter Δ with temperature in the BCS approximation.
the normal state ($\Delta_{\mathrm{k}} \equiv 0$) is the only solution of (4-124). T_n is therefore the transition temperature between the (S) and (N) states (in zero magnetic field). Numerically T_0 is defined by setting $\Delta = 0$ in (4-125)

$$1 = \mathrm{N}(0)\mathrm{V} \int_0^{\hbar\omega} \mathrm{D} \frac{\mathrm{d}\xi}{\xi} \tanh \frac{\xi}{2\mathrm{k_B}\ \mathrm{T}_0} \tag{4-126}$$

For $\hbar\omega_D \gg k_B T_0$, it is clear that the integral has the asymptotic form $\ln\left(\hbar\omega_D / k_B T_0\right) + C$ since the hyperbolic tangent is equal to unity in the major part of the domain of integration. A detailed calculation gives $\mathrm{C} = \ln 1.14$. Therefore

$$1 = \mathrm{N}(0)\mathrm{V} \ln \frac{1.14\hbar\omega_{\mathrm{D}}}{\mathrm{kB_B}\ \mathrm{T}_0}$$

or

$$k_B T_0 = 1.14\hbar\omega_D e^{-1/N(0)V} \tag{4-127}$$

Taking $\hbar\omega_D = k_B\theta_D$, where Θ_D is the Debye temperature deduced from specific heat measurements, one can determine the coupling constant $\mathrm{N}(0)\mathrm{V}$ from T_0. The values for the non-transition metals are given in Table 4-1. In most cases, the coupling constant is rather small and $\mathrm{T}_0 \ll \Theta_{\mathrm{D}}$, the only important exceptions being Hg and Pb . (In these two metals, the self-consistent field method is probably inaccurate.) From the exponential form of (4-127). it can be seen that if $N(0)V$ falls below ~ 0.1, with $\Theta_D \sim 200°\mathrm{K}$. then T_0 falls into the region

10^{-30} K. For such small values of T_0. superconductivity might be masked by parasitic effects (such as the magnetic field of the earth. nuclear spins, and so on). It is therefore possible that certain metals

Table 4-1

Metal	θ_{D} (°K)	T_0 (°K)	$[\mathrm{N}(0)\mathrm{V}]_{\mathrm{exp}}$
Zn	235	0.9	0.18
Cd	164	0.56	0.18
Hg	70	4.16	0.35
Al	375	1.2	0.18
In	109	3.4	0.29
Tl	100	2.4	0.27
Sn	195	3.75	0.25
Pb	96	7.22	0.39

not known to be superconducting have, nevertheless, weakly attractive interactions. Finally the qualitative predictions of the "jellium" theory are verified in the sense that $N(0)V$ is large when the valence Z and the atomic volume V_0 are large. [7]

THE ISOTOPE EFFECT

With the BCS interaction (4-76), T_0 is proportional to the cutoff frequency ω_{D}. As already mentioned, for two isotopes, with the same electronic properties but different ionic masses, ω_D will be different and vary as $\mathrm{M}^{-1/2}$. (This is a general result; it comes from the fact that the equation of motion of an ion is of the form $Md^2x/dt^2 = F$ where F is a restoring force independent of M.) Equation (4-127) therefore predicts an isotope effect on the transition temperature ($T_0 \propto \mathrm{M}^{-1/2}$). This dependence on $\mathrm{M}^{-1/2}$ has indeed been observed in a number of nontransition metals (Hg, Pb, Mo, Sn, Tl). However, in many other superconductors (transition metals and compounds), the isotope effect is much smaller, or even nearly absent (Ru, Os). There are various possible explanations for this, notably
(1) The interaction is still mediated by phonons, but the BCS form for $V_{k\ell}$ is oversimplified.
(2) The interaction is mediated by some other low-frequency mode of the solid, involving no lattice motion.
Explanation (2) may well apply in some cases, but it is very hard to prove (or disprove) it experimentally. We discuss only explanation (1).

INCLUSION OF COULOMB REPULSION

In fact, when we discussed the electron-electron interactions earlier in this chapter, we obtained two terms: a repulsive Coulomb term,

essentially frequency independent, and a phonon term (attractive at frequencies $\omega < \omega_D$, and negligible for $\omega \gg \omega_D$).

As before, we neglect completely the dependence of the matrix $V_{k\ell}$ on the angle between $\mathbf{k}$ and $\boldsymbol{\ell}$. We write

$$V_{k\ell} = V(\omega) = V_c - V_p(\omega)$$
$$\omega = \frac{\xi_\ell - \xi_k}{\hbar} \tag{4-128}$$

[7] Numerically, however, the jellium model gives theoretical values for N(0)V which are too large, even when one includes the Coulomb repulsion.

Equation (4-124) for the transition temperature is now replaced by

$$\Delta(\xi) = -\mathrm{N}(0) \int \mathrm{d}\xi' \mathrm{V} \left(\frac{\xi - \xi'}{\hbar} \right) \Delta(\xi') \frac{1 - 2\mathrm{f}(\xi')}{2\xi'} \tag{4-129}$$

Unfortunately, even with the simple interaction (4-128), this integral equation is hard to solve, and we shall discuss it in a sloppy way. We separate the Coulomb term and call its contribution A

$$A = -N(0) \int d\xi' V_C \Delta(\xi') \frac{1 - 2f(\xi')}{2\xi'} \tag{4-130}$$

A is independent of ξ. The equation for Δ is

$$\Delta(\xi) = \mathrm{N}(0) \int \mathrm{d}\xi' \mathrm{V_p} \left(\frac{\xi - \xi'}{\hbar} \right) \Delta(\xi') \frac{1 - 2\mathrm{f}(\xi')}{2\xi'} + \mathrm{A} \tag{4-131}$$

When $|\xi| \gtrsim \hbar\omega_D$ the integral is not large, because the factors $V_p\left(\frac{(\xi-\xi')}{\hbar}\right)$ and $1/\xi'$ cannot be simultaneously large. Thus in this region we may roughly set $\Delta(\xi) = \mathrm{A}$. On the other hand, the integral is important when $|\xi|$ is small. Call B the average value of Δ in the region $\hbar\omega_D > |\xi|$.
Then we have

$$\begin{aligned} B &\cong N(0) V_p \int_{-\hbar\omega_D}^{\hbar\omega_D} d\xi' B \frac{1 - 2f(\xi')}{2\xi'} + A \\ &\cong N(0) V_p \log \frac{\hbar\omega_D}{k_B T_0} + A \end{aligned} \tag{4-132}$$

where V_p is some average of $V_p(\omega)$ over the interval $-\omega_D < \omega < \omega_D$. Finally, Eq. (4-130) defining A may be rewritten as

$$\begin{aligned} A \cong & - N(0) V_c \left[B \int_{-\hbar\omega_D}^{\hbar\omega_D} + A \int_{-\hbar\omega_D}^{\hbar\omega_D} + A \int_{-\hbar\omega_D}^{\hbar\omega_c} + A \int_{-\hbar\omega_c}^{\hbar\omega_D} \right] \\ & \times d\xi' \frac{1 - 2f(\xi')}{2\xi'} \\ \cong & - N(0) V_c \left[B \log \frac{\hbar\omega_D}{k_B T_0} + A \log \frac{\omega_c}{\omega_D} \right] \end{aligned} \tag{4-133}$$

ω_c is a high-frequency cutoff for the Coulomb interaction (in practice, of the order of $\mathrm{E_F}/\hbar$). Writing that (4-133) and (4-130) are compatible, we arrive at the condition

$$\begin{aligned} 1 &= \log \frac{\hbar\omega_D}{K_B T_0} \left(K_p - \frac{K_C}{1 + K_C \log \frac{\omega_C}{\omega_D}} \right) \\ K_p &= N(0) V_p \quad K_C = N(0) V_C \end{aligned} \tag{4-134}$$

An equation of the form (4-134) for the transition temperature was first derived by Bogolubov (1958). It has some remarkable implications:
(1) The Coulomb repulsion described by K_C is not very efficient in counteracting superconductivity, because of the factor

$$\frac{1}{1 + K_C \log \frac{\omega_C}{\omega_D}}$$

In particular, we might have $K_p < K_c$, that is, an over-all interaction constantly repulsive, and still find superconductivity lprovided that $K_p\,(1 + K_c \log\,(\omega_c/\omega_D) > K_c]$.
(2) The isotope effect is modified: If the ionic mass has a relative variation $\delta M/M$, the Debye frequency is changed according to $\delta\omega_D/\omega_D = -\frac{1}{2}\delta M/M$ and the transition temperature shifts according to the law

$$\frac{\delta \mathrm{T}_0}{\mathrm{T}_0} = \frac{\delta \omega_\mathrm{D}}{\omega_\mathrm{D}} \left[1 - \frac{\mathrm{K}_\mathrm{C}^2}{1 + \mathrm{K}_\mathrm{C} \log \frac{\omega_\mathrm{C}}{\omega_\mathrm{D}}}\right]$$

The amplitude of the isotope effect is reduced. This reduction should be particularly strong in metals with narrow bands (ω_c small). This may explain why the isotope effect is strongly reduced in transition metals and in related compounds (Garland, 1963).

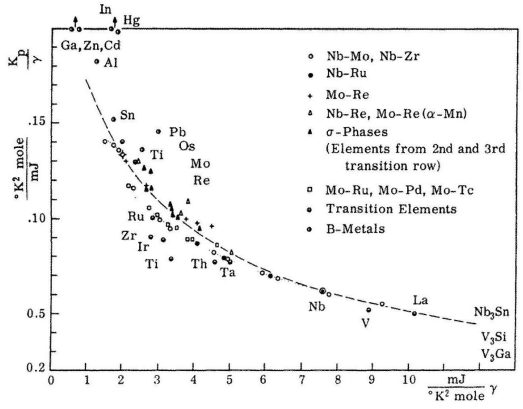


Figure 4-5
An empirical relation between the coupling constant K_p describing the elec-tron-electron interaction via phonons, and the electronic specific heat parameter γ (courtesy J. Muller).

Conversely, from the experimental values of T_0 and of the isotope effect, one can deduce K_p and K_c, assuming that the model is valid. The results for K_p in various metals show a strong correlation between K_p and the electronic specific heat coefficient γ in the normal phase [8] (Muller, 1963) (Fig. 4-5).

Calculation of the Thermodynamic Functions

Combining the expressions for the kinetic and potential energies (4-114) and (4-115) together with the expressions derived for u_k and v_k in the previous section, we obtain for the total energy

$$E = \sum_k \frac{1}{2\epsilon_k} \left[(\epsilon_k + \xi_k)^2 f\,(\epsilon_k) - (\epsilon_k - \xi_k)^2\,(1 - f\,(\epsilon_k))\right] \tag{4-135}$$

In particular, at absolute zero ($f = 0$), we recover the energy calculated in Section 4-3. Writing the entropy (4-118) we find

$$TS = 2\sum_k \left[\epsilon_k f\,(\epsilon_k) + k_B T \ln\,(1 + \exp\,(\epsilon_k/k_B T))\right] \tag{4-136}$$

The specific heat, for example, is determined by

[8] γ is proportional to the density of states at the Fermi level. There is, however, one difference between γ and N(0) : γ is defined per atom, while N(0) is defined per unit volume.

$$C = T\frac{dS}{dT} \tag{4-137}$$

Recalling that ϵ_k depends on T in (4-136), we find

$$\mathrm{C} = 2\beta^2 \mathrm{k_B} \sum_{\mathrm{k}} \mathrm{f}\left(\epsilon_{\mathrm{k}}\right)\left(1 - \mathrm{f}\left(\epsilon_{\mathrm{k}}\right)\right)\left[\epsilon_{\mathrm{k}}^2 + \beta\epsilon_{\mathrm{k}}\frac{\mathrm{d}\epsilon_{\mathrm{k}}}{\mathrm{d}\beta}\right] \tag{4-138}$$

In the BCS approximation, $\epsilon_{\mathrm{k}}\mathrm{d}\epsilon_{\mathrm{k}}/\mathrm{dT} = \Delta\mathrm{d}\Delta/\mathrm{dT}$ is independent of k. Then,

$$\begin{aligned}\mathrm{C} &= 2\beta^2 \mathrm{k_B}\ \mathrm{N}(0)\int_0^\infty \mathrm{d}\xi \mathrm{f}(\epsilon)(1-\mathrm{f}(\epsilon))\left[\epsilon^2 - \mathrm{T}\Delta\frac{\mathrm{d}\Delta}{\mathrm{dT}}\right] \\ \epsilon &= \sqrt{\xi^2 + \Delta^2}\end{aligned} \tag{4-139}$$

The form of this specific heat is represented in Fig. 1-1. At very low temperatures ($\beta\Delta \gg 1$), the term $\Delta\mathrm{d}\Delta/\mathrm{dT}$ is negligible and

$$\begin{aligned}\mathrm{C} &\sim 2\beta^2 \mathrm{k_B}\ \mathrm{N}(0)\Delta^2 \int_0^\infty \mathrm{d}\xi \mathrm{e}^{-\beta\sqrt{\Delta_0^2+\xi^2}} \\ &\sim 2\beta^2 \mathrm{k_B}\ \mathrm{N}(0)\Delta^2 \mathrm{e}^{-\beta\Delta_0}\int_0^\infty \mathrm{d}\xi \mathrm{e}^{-\beta\xi^2/2\Delta_0}\end{aligned} \tag{4-140}$$

where $\Delta_0 = \Delta_{\mathrm{T}} = 0$. The integral is

$$\sqrt{\frac{\pi}{2}}\left(\mathrm{k_B}\ \mathrm{T}\Delta_0\right)^{1/2}$$

The dominant factor in C is the term $e^{-\beta\Delta_0}$, which we have already predicted. A measurement of the low-temperature specific heat allows us to determine Δ_0. Also, Eq. (4-139) predicts a discontinuity in the specific heat at the transition temperature because of the $\Delta d\Delta/dT$ term

$$\begin{aligned}\mathrm{C_S} - \mathrm{C_n} &= \mathrm{k_B}\ \mathrm{N}(0)\beta_0^2\left(\frac{\mathrm{d}\left(\Delta^2\right)}{\mathrm{d}\beta}\right)\mathrm{T_n} \\ \beta_0 &= 1/\mathrm{k_B}\ \mathrm{T}_0\end{aligned} \tag{4-141}$$

Numerically from (4-125), one obtains $\left(\mathrm{d}\Delta^2/\mathrm{d}\beta\right)\ \mathrm{T}_0 = 10.2/\beta_0^3$ and

$$C_s - C_n = 10.2 k_B^2 T_c N(0) \tag{1-142}$$

Finally the Gibbs function is obtained by adding (4-135) and (4-136).

$$\begin{aligned}G &= \sum_k \frac{1}{2\epsilon_k}\left[\left(\epsilon_k + \xi_k\right)^2 f + \left(\epsilon_k - \xi_k\right)(f-1) - 4f\left(\epsilon_k^2 + \xi_k^2\right)\right] \\ &= \sum_k \left[\left(-\epsilon_k + \frac{\Delta^2}{2\epsilon_k}\right)(2f+1) + \xi_k\right]\end{aligned} \tag{4-143}$$

This expression can be transformed by noting that

$$\sum_k \frac{(2f+1)}{2\epsilon_k}\Delta^2 = \sum_k \frac{(2f-1)\Delta^2}{2\epsilon_k} + \sum_k \frac{\Delta^2}{\epsilon_k}$$

The first term on the right is determined from the self-consistency condition (4-124) and is $-\Delta^2/V$. Then

$$G = -2\sum_k \left(\epsilon_k f\left(\epsilon_k\right) - \frac{\Delta^2}{V} + \xi_k - \frac{\xi_k^2}{\epsilon_k}\right) \tag{4-144}$$

Knowing G, we can calculate the critical thermodynamic field defined in Chapter 2, from the equation

$$G_n - G_s = \frac{H_c^2}{8\pi} \tag{4-145}$$

In particular, for $T = 0$, we have $H_c = H_{C_0}$,

$$\mathrm{H}_{\mathrm{C}_0}^2 = 4\pi\ \mathrm{N}(0)|\Delta(0)|^2$$

For finite T, from (4-144), we find a curve $H_c(T)$ rather close to the empirical approximation

$$\frac{\mathrm{H_c}}{\mathrm{H_{C0}}} = 1 - \left(\frac{\mathrm{T}}{\mathrm{T_c}}\right)^2 \tag{4-146}$$

If we look at finer details, we find that, for superconductors where N(0)V is not too large (weakly coupled superconductors), the detailed theoretical curve of $\mathrm{H_c}$ versus T derived from the BCS theory gives even a better fit to the experimental data than does the simplified law (4-146).

Calculation of Transition Probabilities

Suppose that a time-dependent exterior perturbation is applied to a gas of superconducting electrons.

Examples:

(1) Ultrasonics: A longitudinal acoustic wave modifies the potential energy of each electron by a term $\mathrm{U}\theta(\mathrm{rt})$, where θ is the local dilatation of the lattice and U is a constant (the "deformation potential") of the order of several electron volts. The matrix element of this perturbation between the electron plane wave states $\mathbf{k}$ and $\mathbf{k}'$ is $U\theta_{\mathbf{k}-\mathbf{k}'}$ [where θ_{q} is the Fourier transform of $\theta(r)$]. The perturbation acting on the electron system is then

$$\mathscr{H}_1 = \sum_{\mathbf{k},\mathbf{k}',\alpha} \mathrm{U}\theta_{\mathbf{k}-\mathbf{k}'} \mathrm{a}_{\mathbf{k}\alpha}^{+} \mathrm{a}_{\mathbf{k}'\alpha} \tag{4-147}$$

(2) Microwaves: The effect of an electromagnetic perturbation described by a vector potential $A(r,t)$ is given by replacing $p^2/2m$ by $(1/2m)[p-(e/c)A]^2$ in the electronic energy. To first order in A the perturbation is $(-\mathrm{e}/2\mathrm{mc})\ (\mathrm{pA} + \mathrm{Ap})$ and as a function of a and a^{+}it becomes

$$\mathscr{H}_1 = \sum_{\mathrm{k},\mathrm{k}',\alpha} -\frac{\mathrm{e}\hbar}{2\mathrm{mc}}\ \mathrm{A_k} - \mathrm{k}' \cdot (\mathrm{k} + \mathrm{k}')\, \mathrm{a}_{\mathrm{k}\alpha}^{+} \mathrm{a}_{\mathrm{k}'\alpha} \tag{4-148}$$

More generally, the perturbations have the form

$$\mathscr{H}_1 = \sum_{\mathrm{k}\alpha,\mathrm{k}'\alpha'} \mathrm{B}\left(\mathrm{k}\alpha|\mathrm{k}'\alpha'\right) \mathrm{a}_{\mathrm{k}\alpha'}^{+} \mathrm{a}_{\mathrm{k}'\alpha'} \tag{4-149}$$

We find two effects in the presence of $\mathscr{H}_1$:

(1) $\mathfrak{K}_1$ induces transitions between the different excited states described by the γ^{+}. To classify these transitions, we write $\mathfrak{K}_1$ as a function of the γ, γ^{+}operators. Inverting (4-100)

$$\mathrm{a}^{+}_{m\alpha} = \mathrm{u}_m \gamma^{+}_{m\alpha} + \sum_{\beta} \rho_{\alpha\beta} \mathrm{v}_m \gamma_{-m\beta} \tag{4-150}$$

$$\rho = \begin{pmatrix} 0 & -1 \\ 1 & 0 \end{pmatrix}$$

This gives

$$\begin{aligned} \mathscr{H}_1 = \sum_{\mathrm{k}\alpha} \mathrm{B}\left(\mathrm{k}\alpha|\mathrm{k}'\alpha'\right) \Big\{ & \mathrm{u}_\mathrm{k}\mathrm{u}_{\mathrm{k}'}\gamma^{+}_{\mathrm{k}\alpha}\gamma_{\mathrm{k}'\alpha'} \\ & + \mathrm{v}_\mathrm{k}\mathrm{v}_{\mathrm{k}'} \sum_{\beta,\beta'} \rho_{\alpha\beta}\rho_{\alpha'\beta'}\gamma_{\mathrm{k}\beta}\gamma^{+}_{\mathrm{k}'\beta'} \\ & + \mathrm{u}_\mathrm{k}\mathrm{v}_{\mathrm{k}'} \sum_{\beta} \rho_{\alpha'\beta'}\gamma^{+}_{\mathrm{k}\alpha}\gamma^{+}_{-\mathrm{k}'\beta'} + \mathrm{u}_{\mathrm{k}'}\mathrm{v}_\mathrm{k} \sum_{\beta} \rho_{\alpha\beta}\gamma_{-\mathrm{k}\beta}\gamma_{\mathrm{k}'\alpha'} \Big\} \end{aligned} \tag{4-151}$$

The terms in $\gamma^{+}_i\gamma_j$ and $\gamma_i\gamma^{+}_j$describe transitions where a quasiparticle in the state i is scattered into the state j (and vice versa). The $\gamma^{+}_1\gamma^{+}_2$create two quasiparticles and the terms $\gamma_1\gamma_j$ destroy two of them.

(2) $\mathscr{H}_1$ can also modulate the parameters, such as Δ, which describe the structure of the condensed state, and this modulation also leads to an absorption. In many cases this effect is negligible; consider for instance the ultrasonic attenuation problem. The direct perturbation is $\mathrm{U}\theta(\mathrm{r})$. If the pair potential is also modulated, it will shift by an a mount $\delta\Delta = C\Delta\theta(r)$, where C is a constant of order unity. This gives a modification in the generalized self-consistent field. But U is of order $1 - 10\mathrm{eV}$ and $C\Delta$ is of order $10^{-3}\mathrm{eV}$. Thus the modulation of Δ is unimportant here. In the present paragraph, we neglect it (but we return to it later when we consider the Meissner effect).

We now return to the form (4-151) for $\mathfrak{K}_1$ and consider transitions where a quasiparticle passes from the state $(\mathbf{k}'\alpha')$ into the state $(\mathbf{k}\alpha)$. The matrix element $\mathrm{M}\left(\mathrm{k}\alpha|\mathrm{k}'\alpha'\right)$ is the coefficient of $\gamma^{\dagger}_{\mathrm{k}\alpha}\gamma_{\mathrm{k}'\alpha'}$. The first two terms of (4-151) contribute since $\gamma_1\gamma^{+}_2 = -\gamma^{+}_2\gamma_1$ for $1 \neq 2$. Then

$$\begin{aligned} \mathrm{M}\left(\mathrm{k}\alpha|\mathrm{k}'\alpha'\right) = & \mathrm{B}\left(\mathrm{k}\alpha|\mathrm{k}'\alpha'\right) \mathrm{u}_\mathrm{k}\mathrm{u}_{\mathrm{k}'} \\ & - \mathrm{v}_\mathrm{k}\mathrm{v}_{\mathrm{k}'} \sum_{\sigma,\sigma'} \rho_{\sigma'\alpha'}\rho_{\sigma\alpha}\mathrm{B}\left(-\mathrm{k}'\sigma' \mid -\mathrm{k}\sigma\right) \end{aligned} \tag{4-152}$$

The term $\Sigma_{\sigma\sigma'}\mathrm{B}\left(-\mathrm{k}'\sigma' \mid -\mathrm{k}\sigma\right)\rho_{\sigma'\alpha'}\rho_{\sigma\alpha}$ is essentially the matrix element B where the spins and momenta of the electrons are reversed.

For the interactions $\mathscr{H}_1$, which we consider, it differs at most from $\mathrm{B}\left(\mathrm{k}\alpha|\mathrm{k}'\alpha'\right)$ by a sign

$$\sum_{\sigma\sigma'} \mathrm{B}\left(-\mathrm{k}'\sigma' \mid -\mathrm{k}\sigma\right)\rho_{\sigma\alpha}\rho_{\sigma'\alpha'} = \eta\mathrm{B}\left(\mathrm{k}\alpha|\mathrm{k}'\alpha'\right) \tag{4-153}$$

$$\text{with } \eta = \begin{cases} +1 & \text{case I} \\ -1 & \text{case II} \end{cases}$$

Then

$$\mathrm{M}\left(\mathrm{k}\alpha|\mathrm{k}'\alpha'\right) = \mathrm{B}\left(\mathrm{k}\alpha|\mathrm{k}'\alpha'\right)\left[\mathrm{u}_\mathrm{k}\mathrm{u}_{\mathrm{k}'} - \eta\mathrm{v}_\mathrm{k}\mathrm{v}_{\mathrm{k}'}\right] \tag{4-154}$$

The factor $[u_k u_{k'} - \eta v_k v_{k'}]$ is called the coherence factor of the transition. The number of transitions $(\mathrm{k}'\alpha' \to \mathrm{k}\alpha)$ per unit time less the number of inverse transitions is

$$\begin{aligned}\dot{\nu} =& \frac{2\pi}{\hbar} \left|M\left(k\alpha|k'\alpha'\right)\right|^2 \left\{f\left(\epsilon_{k'}\right)\left[1 - f\left(\epsilon_k\right)\right] - f\left(\epsilon_k\right)\left[1 - f\left(\epsilon_{k'}\right)\right]\right\} \\ & \times \delta\left(\epsilon_k - \epsilon_{k'} - \hbar\omega\right)\end{aligned} \tag{4-155}$$

where we have assumed that $\mathscr{H}_1$ is a sinusoidal perturbation of frequency ω. The power absorbed is

$$\mathrm{W}_1 = \sum_{\mathrm{k},\mathrm{k}'} \nu\hbar\omega \tag{4-156}$$

In order to calculate W_1, we first average over the angles of $\mathbf{k}$ and $\mathbf{k}'$ and the spin indices of the matrix element B,

$$\mathrm{B}^2 = \sqrt{\mathrm{B}\left(\mathrm{k}\alpha|\mathrm{k}'\alpha'\right)\Big|^2}$$

Since $|\xi_\mathrm{k}|$ and $|\xi_{\mathrm{k}'}|$ are small with respect to $\mathrm{E_F}$ [this is ensured by the factors f in (4-155)], B can be treated as a constant, and

$$\begin{aligned}\mathrm{W}_1 = & 2\pi\omega\ \mathrm{B}^2 \int_\Delta^\infty \mathrm{N_S}(\epsilon)\mathrm{N_S}\left(\epsilon'\right) \mathrm{d}\epsilon d\epsilon' \left(uu' - \eta vv'\right)^2 \\ & \times \left[\mathrm{f}\left(\epsilon'\right) - \mathrm{f}(\epsilon)\right] \delta\left(\epsilon - \epsilon' - \hbar\omega\right)\end{aligned} \tag{4-157}$$

In this formula, $N_S(\epsilon) = N(0)|d\xi/d\epsilon|$ is the density of states for the Bogolubov excitations

$$N_S(\epsilon) = N(0)\frac{\epsilon}{\sqrt{\epsilon^2 - \Delta^2}} \quad \epsilon > \Delta \tag{4-158}$$

By using the definitions (4-71) and (4-72) of u and v, we can write

$$\left[\mathrm{uu}' - \eta\mathrm{vv}'\right]^2 = \frac{1}{2}\left[1 + \frac{\xi\xi'}{\epsilon\epsilon'} - \eta\frac{\Delta^2}{\epsilon\epsilon'}\right] \tag{4-159}$$

Each value of ϵ is obtained for two opposite values of ξ. The term $\xi\xi'/\epsilon\epsilon'$ disappears when summed over these two values. Finally

$$\begin{aligned}\mathrm{W}_1 =& 4\pi\omega\ \mathrm{B}^2\ \mathrm{N}(0)^2 \int_\Delta^\infty d\epsilon \int_\Delta^\infty d\epsilon' \frac{\epsilon\epsilon' - \eta\Delta^2}{\left(\epsilon^2 - \Delta^2\right)^{1/2}\left(\epsilon'^2 - \Delta^2\right)^{1/2}} \\ & \times \left[\mathrm{f}\left(\epsilon'\right) - \mathrm{f}(\epsilon)\right] \delta\left(\epsilon - \epsilon' - \hbar\omega\right)\end{aligned} \tag{4-160}$$

An analogous calculation can be made for the power W_2 absorbed by creation and annihilation of two quasiparticles. W_2 is nonzero if $\hbar\omega > 2\Delta$. The final formula for $W = W_1 + W_2$ differs from (4-160) only by the domain of integration,

$$\begin{aligned}W =& 2\pi\omega B^2 N(0)^2 \int_{-\infty}^\infty \int_{-\infty}^\infty d\epsilon d\epsilon' \frac{\epsilon\epsilon' - \eta\Delta^2}{\left(\epsilon^2 - \Delta^2\right)^{1/2}\left(\epsilon'^2 - \Delta^2\right)^{1/2}} \\ & \times \left[f\left(\epsilon'\right) - f(\epsilon)\right] \delta\left(\epsilon - \epsilon' - \hbar\omega\right)\end{aligned} \tag{4-161}$$

Here ϵ and ϵ' are of arbitrary sign, but $|\epsilon| > \Delta$ and $|\epsilon'| > \Delta$. In practice one always compares W to the absorption W_N, which would be obtained in the normal state [W_N is simply obtained from (4-161) by setting $\Delta = 0$],

$$\frac{W}{W_N} = \frac{1}{\hbar\omega} \int d\epsilon d\epsilon' \frac{\epsilon\epsilon' - \eta\Delta^2}{\left(\epsilon^2 - \Delta^2\right)^{1/2} \left(\epsilon'^2 - \Delta^2\right)^{1/2}} \times \left[f\left(\epsilon'\right) - f(\epsilon)\right] \delta\left(\epsilon - \epsilon' - \hbar\omega\right) \tag{4-162}$$

APPLICATIONS

(1) Absorption of sound: In this case $\eta = 1$ and the coherence factor is small when ϵ and ϵ' are simultaneously close to Δ or $-\Delta$. If we study the case where $\hbar\omega$ is small compared to Δ or $k_B T$, then (4-162) reduces to

$$\frac{W}{W_N} = -\int_{|\epsilon|>\Delta} d\epsilon \frac{\epsilon^2 - \Delta^2}{\epsilon^2 - \Delta^2} \frac{\partial f}{\partial \epsilon} = \frac{2}{1 + e^{\beta\Delta}} \tag{4-163}$$

The attenuation is very small at low temperatures and increases rapidly as $T \to T_0$. This therefore gives a way to measure $\Delta(T)$, which has been widely applied, notably by Morse and his co-workers (see Fig. 4-6).

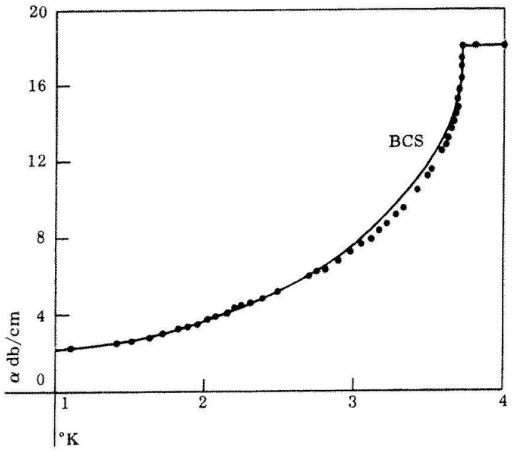


Figure 4-6
Ultrasonic measurements in tin compared with the BCS prediction [after R. W. Morse, IBM J., 6, 58 (1963)].

(2) Nuclear Relaxation: The interaction $\mathscr{H}_1$ between the nuclear spins and the conduction electrons is complicated, but at any rate Case II applies: $\eta = -1$. One can measure the time T_1 for the nuclear spins to equalize their temperature with the electrons in zero field. The ratio T_{1n}/T_1 of the relaxation rates in the superconducting and normalstates is still given by (4-162). The frequency ω, which comes into play here, is the precession frequency of the nuclear spins in the local field of the other nuclei. This is small ($\omega \sim 10^4$). Therefore we can let $\omega \to 0$ and obtain

$$\frac{T_{1n}}{T_1} = -\int_{|\epsilon|>\Delta} d\epsilon \frac{df}{d\epsilon} \frac{\epsilon^2 + \Delta^2}{\epsilon^2 - \Delta^2} \tag{4-164}$$

Here the coherence factor doesn't vanish at the same time as the denominator (for $|\epsilon| = \Delta$): the integral diverges logarithmically. But in a real metal, Δ_k is anisotropic. The singularity in density of states $N_S(\epsilon)$ is then smeared out somewhat and the integral converges. The results depend in detail on the anistropy of Δ_k. In practice, Δ is rather weakly anisotropic; then the

variation of T_{1n}/T_1 with temperature is as shown on Fig. 4-7. The relaxation rate for T slightly less than T_c is greater than in the normal state. This remarkable result arises

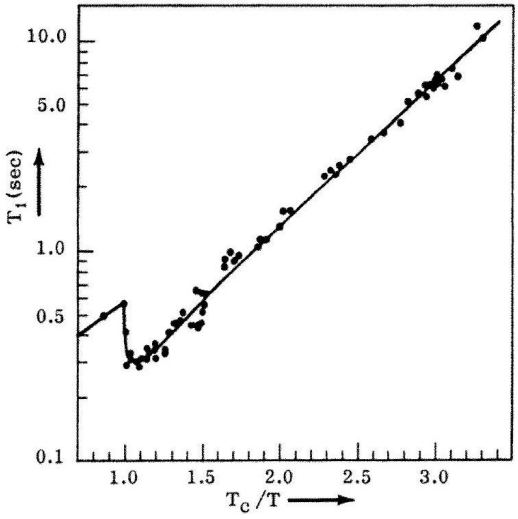


Figure 4-7
Nuclear relaxation rates in aluminum [after A. G. Redfield, Phys. Rev., 125, 159 (1962)]. Notice the dip of T_1 at temperatures below the transition point. The theoretical curve is calculated on the assumption that the peak in the BCS density of states is smeared out on an energy interval $\Delta/5$.

from the increase in the density of states $N_S(\epsilon)$. At low temperatures $T \ll T_c$, on the contrary, the relaxation becomes very slow because of the population factor $df/d\epsilon$. This type of variation of $1/T_1$ with T was first observed in 1957 by Hebel and Slichter. The prediction of the different coherence factors and of the resulting very different behaviors of the ultrasonic attenuation and nuclear relaxation has been one of the great successes of the BCS theory.

REFERENCES

M. Tinkham, "Superconductivity," in Low Temperature Physics, Les Houches lecture notes (New York: Gordon & Breach, 1962).
E. A. Lynton, Superconductivity (London: Methuen, 1964, 2nd edition), Chap. 8, 9, 10, 11.

6.2 The Self-Consistent Field Method

6.2.1 5-1 The Bogoliubov Equations

In the preceding chapter, we studied a homogeneous electron gas with attractive interactions. We now consider the more general case where the electrons also experience an arbitrary external potential $U_0(r)$ (this will be important to describe the effects of impurities and of the specimen surface) and a magnetic field $\mathbf{H} = \text{curl } \mathbf{A}$.

The most natural method, at first sight, to treat $U_0(r)$ would be the following:

(1) Find the wave function w_n of the one-electron Hamiltonians, which are solutions of

$$\xi_n w_n = \left(-\frac{\hbar^2}{2m}\nabla^2 + U_0(r) - E_F \right) w_n \tag{5-1}$$

(2) Notice that there exist at least two solutions for each energy ξ_n:

$$w_n = w_n(r)|t\rangle \quad \text{and} \quad w_{\bar{n}} = w_n^*(r)|t\rangle \tag{5-2}$$

where $|\alpha\rangle$ denotes the spin states.

(3) Construct a trial function of the BCS type describing a pairing of electrons in the degenerate energy states w_n and $w_{\bar{n}}$,

$$\tilde{\phi} = \prod_n \left(u_n + v_n a_n^+ a_{\bar{n}}^+\right) \phi_0 \tag{5-3}$$

where $a_{\bar{n}}^+$is the creation operator for an electron in the state $w_{\bar{n}}$. The analysis follows that of Section 3.

In fact, this method has several defects: (a) it is not applicable in the presence of a magnetic field; (b) above all, it does not allow enough freedom in the trial function. In fact, the energy can often be lowered if we pair the electrons in states that are better choices than w_n.

We now describe a more powerful method (Bogolubov, 1959), which is essentially a generalization of the Hartree-Fock equations to the case of superconductivity. We begin by rewriting the Hamiltonian $\mathscr{H}$ of the electron system, not with the operators $\mathrm{a_{k\alpha}}$ (which are only ($\alpha =\uparrow$ or $\downarrow$ is again a spin index.) The operators Ψ satisfy the anticommutation rules

$$\begin{aligned} \Psi(r\alpha) &= \sum_k e^{ik\cdot r} a_{k\alpha} \\ \Psi^+(r\alpha) &= \sum_k e^{-ik\cdot r} a_{k\alpha}^+ \end{aligned} \tag{5-4}$$

($\alpha =\uparrow$ or $\downarrow$ is again a spin index.) The operators Ψ satisfy the anticommutation rules

$$\begin{aligned} \Psi(\mathbf{r}\alpha)\Psi\left(\mathbf{r}'\beta\right) + \Psi\left(\mathbf{r}'\beta\right)\Psi(\mathbf{r}\alpha) &= 0 \\ \Psi^+(\mathbf{r}\alpha)\Psi^+\left(\mathbf{r}'\beta\right) + \Psi^+\left(\mathbf{r}'\beta\right)\Psi^+(\mathbf{r}\alpha) &= 0 \\ \Psi^+(\mathbf{r}\alpha)\Psi\left(\mathbf{r}'\beta\right) + \Psi\left(\mathbf{r}'\beta\right)\Psi^+(\mathbf{r}\alpha) &= \delta_{\alpha\beta}\delta\left(\mathbf{r}-\mathbf{r}'\right) \end{aligned} \tag{5-5}$$

The operator associated with the number of particles is

$$N = \sum_{k\alpha} a_{k\alpha}^+ a_{k\alpha} = \sum_\alpha \int dr \Psi^+(r\alpha)\Psi(r\alpha) \tag{5-6}$$

The Hamiltonian $\mathscr{H}$ is also very simply written in terms of Ψ and Ψ^+.[1]

$$\mathscr{H} = \mathscr{H}_0 + \mathscr{H}_1 \tag{5-7}$$

$$\mathscr{H}_0 = \int \mathrm{dr} \sum_\alpha \Psi^+(\mathrm{r}\alpha) \left[\frac{\left(\mathrm{p} - \frac{\mathrm{e}}{\mathrm{c}}\,\mathrm{A}\right)^2}{2m} + \mathrm{U}_0(\mathrm{r})\right] \Psi(\mathrm{r}) \tag{5-8}$$

$$\mathscr{H}_1 = -\frac{1}{2}\,\mathrm{V} \int \mathrm{dr} \sum_{\alpha\beta} \Psi^+(\mathrm{r}\alpha)\Psi^+(\mathrm{r}\beta)\Psi(\mathrm{r}\beta)\Psi(\mathrm{r}\alpha) \tag{5-9}$$

We have taken $U_0(r)$ to be independent of spin (it will eventually be necessary to add a spin-dependent term to describe the exchange potential existing in magnetic media). Also, for the electron-electron coupling $\mathfrak{K}_1$, we have assumed the simplest form describing an interaction, which is

(a) independent of spin (this is correct for a nonmagnetic material),

(b) pointlike and thus characterized by only one coefficient V (BCS approximation).

Also notice that we have neglected the effect of the magnetic field on the conduction electron spins in $\mathscr{H}_0$. (This is correct for $\mathrm{e}\hbar\mathrm{H/mc} < \Delta$.) It will be useful to define

[1] See Landau and Lifschitz, Nonrelativistic Quantum Mechanics (New York: Pergamon, 1959), Chap. 9.

$$H_0 - E_F N = \sum_\alpha \int \Psi^+(r\alpha)\mathscr{H}_e\Psi(r\alpha)dr \tag{5-10}$$

with

$$\mathscr{H}_e(r) = \frac{1}{2m}\left(-i\hbar\nabla - \frac{eA}{c}\right)^2 + U_0(r) - E_F \tag{5-11}$$

Definition of the Effective Potentials

We now replace the interaction $V\Psi^+\Psi^+\Psi\Psi$ by an average potential acting on only one particle at a time (therefore only containing two operators Ψ or Ψ^+). We try an effective hamiltonian of the form

$$\begin{aligned}\mathscr{H}_{\text{eff}} = \int dr \Big\{ &\sum_\alpha \Psi^+(r\alpha)\mathscr{H}_e(r)\Psi(r\alpha) + U(r)\Psi^+(r\alpha)\Psi(r\alpha) \\ &+\Delta(r)\Psi^+(r\uparrow)\Psi^+(r\downarrow) + \Delta^*(r)\Psi(r\downarrow)\Psi(r\uparrow)\Big\}\end{aligned} \tag{5-12}$$

The term U destroys and creates one electron and therefore conserves the number of particles. On the other hand, the terms in Δ increase or decrease the number of particles by two. This should not disturb us, since $\mathscr{H}_{\text{eff}}$ will operate on wave functions such as $\tilde{\phi}$, which are not eigenfunctions of the number operator. In the simple case of the preceding section, an average such as $\langle\widetilde{\phi}|\mathrm{a_k^+ a_{-k}^+}|\widetilde{\phi}\rangle$ is nonzero. Here, in the same way, the mean of the product $\Psi^+\Psi^+$will be nonvanishing and this term will play an important role. We call Δ the pair potential. [Note that terms such as $\Psi(r\uparrow)\Psi(r\uparrow)$ vanish identically because of the commutation rules (5-5).]

Energy Levels of the Effective Hamiltonian $\mathscr{H}_{\text{eff}}$

Let us assume, for the moment, that $\mathscr{H}_{\text{eff}}$ is known; we try to determine its eigenstates and corresponding energies. $\mathscr{H}$ eff is a quadratic
form in Ψ and Ψ^+. We can diagonalize it by performing a unitary transformation which is the exact analog of Eq. (4-100)

$$\begin{aligned}\Psi(r\uparrow) &= \sum_n \left(\gamma_{n\uparrow}u_n(r) - \gamma^+_{n\downarrow}v^*_n(r)\right) \\ \Psi(r\downarrow) &= \sum_n \left(\gamma_{n\downarrow}u_n(r) + \gamma^+_{n\uparrow}v^*_n(r)\right)\end{aligned} \tag{5-13}$$

where the γ and $\gamma^+$are new operators still satisfying the fermion commutation relations

$$\begin{aligned}\gamma^+_{\mathrm{n}\alpha}\gamma_{m\beta} + \gamma_{m\beta}\gamma^+_{\mathrm{n}\alpha} &= \delta_{\mathrm{mn}}\delta_{\alpha\beta} \\ \gamma_{\mathrm{n}\alpha}\gamma_{m\beta} + \gamma_{m\beta}\gamma_{\mathrm{n}\alpha} &= 0\end{aligned} \tag{5-14}$$

The transformation (5-13) must diagonalize $\mathscr{H}_{\text{eff}}$, that is,

$$\mathscr{H}_{\text{eff}} = \mathrm{E_g} + \sum_{\mathrm{n},\alpha} \epsilon_{\mathrm{n}}\gamma^+_{\mathrm{n}\alpha}\gamma_{\mathrm{n}\alpha} \tag{5-15}$$

where E_g is the ground state energy of $\mathscr{H}_{\text{eff}}$ and ϵ_n is the energy of the excitation n . We can also write this condition by taking the commutator of $\mathscr{H}_{\text{eff}}$ with $\gamma_{\mathrm{n}\alpha}$ and $\gamma^+_{\mathrm{n}\alpha}$

$$\begin{aligned}[\mathscr{H}_{\text{eff}}, \gamma_{\text{n}\alpha}] &= -\epsilon_{\text{n}}\gamma_{\text{n}\alpha} \\ \left[\mathscr{H}_{\text{eff}}, \gamma^{+}_{\text{n}\alpha}\right] &= \epsilon_{\text{n}}\gamma^{+}_{\text{n}\alpha}\end{aligned} \tag{5-16}$$

These conditions fix the functions u_n and v_n in (5-13). To derive the equations for u and v, we calculate the commutator $[\mathscr{H}_{\text{eff}}\,, \Psi]$, using the definition (5-12) of $\mathscr{H}_{\text{eff}}$ and the anticommutation properties of the Ψ, obtaining

$$\begin{aligned}[\Psi(r\uparrow), \mathscr{H}_{\text{eff}}\,] &= [\mathscr{H}_{\text{e}} + \text{U}(r)]\,\Psi(r\uparrow) + \Delta(r)\Psi^{+}(r\downarrow) \\ [\Psi(r\downarrow), \mathscr{H}_{\text{eff}}] &= [\mathscr{H}_{\text{e}} + \text{U}(r)]\,\Psi(r\downarrow) - \Delta^{*}(r)\Psi^{*}(r\uparrow)\end{aligned} \tag{5-17}$$

In this equality, we replace the Ψ 's by the γ 's by means of (5-13). Then we apply the commutation relations (5-16). Comparing the coefficients of γ_{n} (and γ^{+}_{n}) on the two sides of the equation, we obtain the Bogolubov equations:

$$\begin{aligned}\epsilon u(r) &= [\mathscr{H}_{e} + U(r)]\,u(r) + \Delta(r)v(r) \\ \epsilon v(r) &= -\,[\mathscr{H}^{*}_{e} + U(r)]\,v(r) + \Delta * (r)u(r)\end{aligned} \tag{5-18}$$

The $\binom{u_n}{v_n}$ are eigenfunctions of a linear system with corresponding eigenvalues ϵ_{n}:

$$\epsilon\begin{pmatrix}u\\v\end{pmatrix} = \hat{\Omega}\begin{pmatrix}u\\v\end{pmatrix} \tag{5-19}$$

Remarks.

(1) The operator $\mathcal{H}^{*}_{\text{e}}$ differs from $\mathcal{H}_{\text{e}}$ when a magnetic field is present:

$$\begin{aligned}\mathscr{H}_{\text{e}} &= \frac{1}{2m}\left(-\text{i}\hbar\nabla - \frac{\text{eA}}{\text{c}}\right)^{2} + \text{U}_0(\text{r}) - \text{E}_{\text{F}} \\ \mathscr{H}^{*}_{\text{e}} &= \frac{1}{2m}\left(\text{i}\hbar\nabla - \frac{\text{eA}}{\text{c}}\right)^{2} + \text{U}_0(\text{r}) - \text{E}_{\text{F}} \neq \mathscr{H}_{\text{e}}\end{aligned}$$

Both $\mathscr{H}_{\text{e}}$ and $\mathscr{H}^{*}_{\text{e}}$ are Hermitian.
(2) The operator $\hat{\Omega}$ is Hermitian; consequently different eigenfunctions $\binom{u}{v}$ are orthogonal.
(3) If $\binom{u}{v}$ is the solution for the eigenvalue ϵ, $\binom{-v^{*}}{u^{*}}$ is the solution for the eigenvalue $-\epsilon$.[2] In agreement with (5-15) we only keep the solutions with positive ϵ.

Choice of the Potentials U and Δ

We now determine $\mathscr{H}_{\text{eff}}$ by requiring that the free energy F calculated from the states which diagonalize $\mathscr{H}_{\text{eff}}$ be stationary. By definition

$$\text{F} = \langle\mathscr{H}\rangle - \text{TS} \tag{5-20}$$

where $\mathscr{H}$ is the initial Hamiltonian $\mathscr{H} = \mathscr{H}_0 + \mathscr{H}_1 (5-7-9)$ and the average $\langle\mathscr{H}\rangle$ is given by

$$\langle\mathscr{H}\rangle = \frac{\Sigma_\phi \langle\phi|\mathscr{H}|\phi\rangle \exp\left(-\beta E_\phi\right)}{\Sigma_\phi \exp\left(-\beta E_\phi\right)} \tag{5-21}$$

The matrix elements are taken with respect to the eigenfunctions $|\phi\rangle$ of $\mathscr{H}_{\text{eff}}$:

$$\mathscr{H}_{\text{eff}}\,|\phi\rangle = E_\phi|\phi\rangle \tag{5-22}$$

A general method to calculate $\langle\mathscr{H}\rangle$ is to replace the Ψ 's (5-7) by the γ 's according to (5-13), then to use the mean value rules

$$\begin{aligned}\left\langle\gamma^+_{\text{n}\alpha}\gamma_{m\beta}\right\rangle &= \delta_{\text{nm}}\delta_{\alpha\beta}\text{f}_\text{n}\\ \langle\gamma_{\text{n}\alpha}\gamma_{m\beta}\rangle &= 0\\ \text{f}_\text{n} &= \frac{1}{\exp(\beta\epsilon_\text{n})+1}\end{aligned} \tag{5-23}$$

However it will not be necessary to perform this entire calculation. We write $\langle\mathscr{H}\rangle$ in the form

$$\begin{aligned}\langle\mathscr{H}\rangle =& \sum_\alpha\int \text{dr}\left\langle\Psi^+(\text{r}\alpha)\mathscr{H}_\text{e}\Psi(\text{r}\alpha)\right\rangle\\ &-\sum_{\alpha\beta}\frac{\text{V}}{2}\int\text{dr}\left\langle\Psi^+(\text{r}\alpha)\Psi^+(\text{r}\beta)\Psi(\text{r}\beta)\Psi(\text{r}\alpha)\right\rangle\end{aligned} \tag{5-24}$$

The product $\langle\Psi^*\Psi^*\Psi\Psi\rangle$ can be simplified thanks to a theorem by Wick, which makes use only of the fact that the $\Psi^+$and Ψ are linear functions of the γ^+,γ. The theorem gives

$$\begin{aligned}\left\langle\Psi^+(1)\Psi^+(2)\Psi(3)\Psi(4)\right\rangle =& \left\langle\Psi^+(1)\Psi(4)\right\rangle\left\langle\Psi^+(2)\Psi(3)\right\rangle\\ &-\left\langle\Psi^+(1)\Psi(3)\right\rangle\left\langle\Psi^+(2)\Psi(4)\right\rangle\\ &+\left\langle\Psi^+(1)\Psi^+(2)\right\rangle\langle\Psi(3)\Psi(4)\rangle\end{aligned} \tag{5-25}$$

We now vary amplitudes $\binom{u}{v}$ to $\binom{\delta u}{\delta v}$ and the occupation numbers f_n to δf_n. The free energy (5-20) then varies by δF:

$$\begin{aligned}\delta\text{F} = \int\text{dr}\Bigg\{&\sum_\alpha\delta\left[\left\langle\Psi^+(\text{r}\alpha)\mathscr{H}_\text{e}\Psi(\text{r}\alpha)\right\rangle\right]\\ &-\text{V}\sum_{\alpha\beta}\left\langle\Psi^+(\text{r}\alpha)\Psi(\text{r}\alpha)\right\rangle\delta\left[\left\langle\Psi^+(\text{r}\beta)\Psi(\text{r}\beta)\right\rangle\right]\\ &+\text{V}\sum_\alpha\left\langle\Psi^+(\text{r}\alpha)\Psi(\text{r}\alpha)\right\rangle\delta\left|\left\langle\Psi^+(\text{r}\alpha)\Psi(\text{r}\alpha)\right\rangle\right|\\ &-\text{V}\left[\langle\Psi^+(\text{r}\uparrow)\Psi^+(\text{r}\downarrow)\rangle\delta(\langle\Psi(\text{r}\downarrow)\Psi(\text{r}\uparrow)\rangle+\text{ C.C. })\right]\Bigg\}-\text{T}\delta\text{ S}(5-26)\end{aligned}$$

where we have assumed $\langle\Psi^+(\mathbf{rt})\Psi(\mathbf{rt})\rangle = 0$ as is correct for our "nonmagnetic" situations. Now notice that the quantity

$$\text{F}_1 = \langle\mathscr{H}_{\text{eff}}\,\rangle - \text{TS} \tag{5-27}$$

is stationary with respect to $\delta\text{u}_\text{n}, \delta\text{v}_\text{n}$, and δf_n since our excitations diagonalise $\mathscr{H}_{\text{eff}}$ exactly. Using (5-12), this condition becomes explicitly:

[2] These two properties allow us to verify that the transformation (5-13) is indeed unitary.

$$
\begin{aligned}
0 =& \delta \left\langle \mathscr{H}_{\text{eff}} \right\rangle - \mathrm{T}\delta\ \mathrm{S} \\
=& \int \mathrm{d}\mathbf{r} \left\{ \sum_{\alpha} \delta \left\langle \Psi^{+}(\mathbf{r}\alpha) \left(\mathscr{H}_{\mathrm{e}} + \mathrm{U}(\mathbf{r})^{n} \right) \Psi(\mathbf{r}\alpha) \right\rangle \right. \\
& \left. + \left\lfloor \Delta(\mathbf{r}) \delta \left(\left\langle \Psi^{+} \left(\mathbf{r}^{\sharp} \right) \Psi^{+}(\mathbf{r}\mathbf{t}) \right\rangle \right) + \text{ C.C. } \right\rceil \right\} - \mathrm{T}\delta\ \mathrm{S}
\end{aligned}
\tag{5-28}
$$

Comparing (5-26) and (5-28), we see that F will be stationary if we take as effective potentials

$$
U(r) = -V \left\langle \Psi^{+}(rt)\Psi(rt) \right\rangle = -V \left\langle \Psi^{+}(rt)\Psi(rt) \right\rangle \tag{5-29}
$$

(the standard Hartree-Fock result for a point interaction), and

$$
\Delta(r) = -V \langle \Psi(r\downarrow)\Psi(r\uparrow) \rangle = V \langle \Psi(r\uparrow)\Psi(r\downarrow) \rangle \tag{5-30}
$$

If we replace the Ψ 's by the γ 's by means of (5-13) and if we use the mean value rules (5-23), we can put these conditions into the explicit form

$$
U(r) = -V \sum_{n} \left[|u_n(r)|^2 f_n + |v_n(r)|^2 (1 - f_n) \right] \tag{5-31}
$$

$$
\Delta(r) = +V \sum_{n} v_n^*(r) u_n(r) (1 - 2f_n) \tag{5-32}
$$

These conditions assure that the potentials U and Δ are self-consistent.

In practice there is an important distinction between $U(r)$ and $\Delta(r)$. The Hartree-Fock potential $U(r)$ comes from an integral Σ_n involving all states below the Fermi level. Consequently, $U(r)$ is nearly independent of temperature, and U can be approximated by the HartreeFock potential calculated in the normal state. This represents a considerable simplification. On the contrary, the pair potential $\Delta(r)$ is a sum of terms of the form $u_n v_n^*$. Such terms, as we already have seen for the homogeneous gas, are nonzero only in the neighborhood of the Fermi surface. For this reason $\Delta(r)$ is a strong function of temperature.

For the case of the homogeneous gas considered in the previous chapter, $\Delta(r)$ is spatially constant and the self-consistency equation (5-31) reduces to a determination of the constant Δ. When $\Delta(r)$ varies spatially, it is much more difficult to ensure the self-consistency of Δ. We shall return several times to this problem.

Problem. Spectrum for a state with a current flow

Discuss the quasiparticle spectrum for a state of uniform current flow, in a pure superconductor. A state of uniform flow is described by a pair potential of the form $\Delta = |\Delta| e^{2iq\cdot r}$ where q is a vector in the direction of flow (the average momentum per electron in this state is $\hbar q$).

Solution.

The solution of (5-18) is then of the form

$$
\begin{aligned}
u(r) &= U_k e^{i(k+q)\cdot r} \\
v(r) &= V_k e^{i(k-q)\cdot r}
\end{aligned}
$$

and the eigenvalue equation reads

$$(\epsilon_{\mathrm{k}} - \xi_{\mathrm{k+q}})\,\mathrm{U_k} - |\Delta|\mathrm{V_k} = 0$$
$$-|\Delta|\mathrm{U_k} + (\xi_{\mathrm{k}} + \xi_{\mathrm{k-q}})\,\mathrm{V_k} = 0$$

The positive eigenvalue ϵ_{k} is given by

$$\epsilon_{\mathrm{k}} = \frac{\xi_{\mathrm{k+q}} - \xi_{\mathrm{k-q}}}{2} + \left[\left(\frac{\xi_{\mathrm{k+q}} + \xi_{\mathrm{k-q}}}{2}\right)^2 + |\Delta|^2\right]^{1/2}$$

As we shall see, the region of major interest is $q \sim \Delta/\hbar v_F$, thus $q \ll k_F$. Retaining only terms of first order in q, we can write

$$\frac{\xi_{k+q} - \xi_{k-q}}{2} = \frac{\hbar^2 k}{m} \cdot q$$
$$\frac{\xi_{k+q} + \xi_{k-q}}{2} \cong \xi_k$$
$$\epsilon_k = \epsilon_k^0 + \frac{\hbar^2 k}{m} \cdot q$$

where ϵ_{k}^0 is the excitation energy for $\mathrm{q} = 0, \epsilon_{\mathrm{k}}^0 = \sqrt{|\Delta|^2 + \xi_{\mathrm{k}}^2}$, and $\hbar\mathrm{q}/m$ is usually called the superfluid velocity $\mathrm{v_s}$. Notice that the gap in the energy spectrum goes to 0 when $v_S = |\Delta|/\hbar k_F = |\Delta|/p_F$. (In application of these
formulas it must be recalled that, in general, the self-consistent value of $|\Delta|$ depends on $\mathrm{v_S}$.)

Theory

In principle, this spectrum could be studied in thin films of pure metals; in practice it cannot for the following reasons: The film thickness d must be smaller than the penetration depth λ (to have a uniform current), but d must be large compared with ξ_0 (if not, the diffuse scattering on the film boundaries can bring some important changes in the spectrum). Thus we would have to work with a pure Type II material, with $\lambda \gg \xi_0$. But then comes another difficulty: for $v_s \sim |\Delta|/p_F$, the current density $n_s e v_s$ is high. The field at the surface of the film is of order

$$\frac{1}{c}\,(\mathrm{n_S e v_S})\,\mathrm{d} \sim \frac{\phi_0\ \mathrm{d}}{\lambda^2 \xi_0} \quad \text{for } \mathrm{T} = 0$$

It is larger than the first penetration field $\mathrm{H_{Cl}}$ by a factor $\sim \mathrm{d}/\xi_0 > 1$. Thus vortex lines come in the film and the situation is not the one desired.

On the other hand, the above calculation can be of use for a discussion of quasiparticles in the Schubnikov phase of bulk, pure, Type II superconductors (M. Cyrot, 1964). Assume that
(a) the Landau-Ginsburg parameter $\kappa = \lambda/\xi$ is much larger than unity,
(b) the field H is much smaller than the upper critical field $\mathrm{H_{C_2}}$.

Then the distance d between lines is much larger than ξ, and most of the excitations (with energies $\epsilon \sim \Delta_\infty$, where Δ_∞ is the amplitude of the pair potential far from the line) can be obtained as follows: At point r compute the superfluid velocity $v_s(r)$ and write that locally the excitations have a shifted BCS spectrum

$$\epsilon(\mathrm{k, r}) = \left\{\Delta_\infty^2 + \xi_{\mathrm{k}}^2\right\}^{1/2} + \hbar \mathrm{v_S} \cdot \mathrm{k} \quad \text{where } \xi_{\mathrm{k}} = \frac{\hbar^2\,(\mathrm{k}^2 - \mathrm{k_F^2})}{2m}$$

Since the minimum spatial extension of wave packets made with these excitations is of order ξ, while the fields and the velocities v_s are modulated on a scale $\mathrm{d} > \xi$, in general, this procedure is correct.

It fails however for the low-lying excited states ($\epsilon \ll \Delta_\infty$) localized very near one line where v_S and the order parameter Δ vary rapidly. These particular excitations are discussed in the next problem, page 153.

6.2.2 5-2 Theorems on the Pair Potential and the Excitation Spectrum

Gauge Invariance

The one-electron Hamiltonian

$$\mathscr{H}_e(A) = \frac{1}{2m}\left(p - \frac{eA}{c}\right)^2 + U - E_F$$

and its complex conjugate

$$\mathscr{H}_e^*(\mathrm{A}) = \frac{1}{2m}\left(\mathrm{p} + \frac{\mathrm{eA}}{\mathrm{c}}\right)^2 + \mathrm{U} - \mathrm{E_F}$$

depend on the choice of the vector potential $\mathbf{A}$. This choice of $\mathbf{A}$ is not unique. If $\mathbf{A}$ is replaced by $\mathbf{A}'$ such as

$$\mathbf{A}' = \mathbf{A} + \nabla \times (\mathbf{r}) \tag{5-33}$$

where X is an arbitrary function, then

$$\operatorname{curl} \mathbf{A}' = \operatorname{curl} \mathbf{A} = \mathrm{h}$$

A and A' are equally acceptable to describe the field configuration $\mathbf{h}(\mathbf{r})$. All physically measurable quantities will have the same values when calculated with A or A'. We shall prove this property for the quasiparticle excitation energies, that is, for the eigenvalues of Eq. (5-18).

Suppose that the eigenfunctions $\binom{u_n}{v_n}$ of (5-18) with vector potential A are known. Now consider Eq. (5-18) with vector potential $\mathbf{A}'$. Two things are modified:
(a) the eigenfunctions $\binom{u'_n}{v'_n}$ differ from $\binom{u_n}{v_n}$.

$$\left.\begin{aligned} u'_n(r) &= u_n(r)\exp\left[\tfrac{\mathrm{ie}}{\hbar \mathrm{c}}\chi(r)\right] \\ v'_n(r) &= v_n(r)\exp\left[-\tfrac{\mathrm{ie}}{\hbar \mathrm{c}}\chi(r)\right] \end{aligned}\right\} \tag{5-34}$$

(b) the pair potential is modified: if $\Delta(r)$ was associated with A, the pair potential $\Delta'(r)$ is given by

$$\Delta'(r) = \Delta(r)\exp\left[\frac{2\mathrm{ie}}{\hbar \mathrm{c}}\chi(r)\right] \tag{5-35}$$

Proof of (5-34): The function u'_n defined by (5-34) satisfies the equation

$$\begin{aligned} \left(p - \frac{eA'}{c}\right) u'_n(r) &= \left(-i\hbar\nabla - \frac{e}{c}A'\right)\exp\left[\frac{ie}{\hbar c}\chi(r)\right] u_n(r) \\ &= \exp\left[\frac{ie}{\hbar c}\chi\right]\left(-i\hbar\nabla - \frac{eA'}{c} + \frac{e}{c}\nabla\chi\right) u_n(r) \\ &= \exp\left[\frac{ie}{\hbar c}\chi\right]\left(p - \frac{e}{c}A\right) u_n \end{aligned} \tag{5-36}$$

where we have made use of (5-33). Iterate this property:

$$\left(p-\frac{eA'}{c}\right)^2 u'_n = \exp\left[\frac{ie}{\hbar c}x\right]\left(p-\frac{eA}{c}\right)^2 u_n \tag{5-37a}$$

$$\mathscr{H}_e\left(A'\right)u'_n = \exp\left[\frac{ie}{\hbar c}x\right]\mathscr{H}_e(A)u_n$$

Similarly

$$\mathscr{H}^*_{\mathrm{e}}\left(\mathrm{A}'\right)\mathrm{v}'_{\mathrm{n}} = \exp\left[\frac{-\mathrm{ie}}{\hbar\mathrm{c}}\chi\right]\mathscr{H}^*_{\mathrm{e}}(\mathrm{A})\mathrm{v}_{\mathrm{n}} \tag{5-37b}$$

Since $\binom{u_n}{v_n}$ is an eigenfunction of (5-18) we have

$$\mathscr{H}_e(\mathrm{A})\mathrm{u}_{\mathrm{n}} + \Delta\mathrm{v}_{\mathrm{n}} = \epsilon_{\mathrm{n}}\mathrm{u}_{\mathrm{n}}$$

Multiply by exp lie χ/hcl and make use of (5-37a). The equation becomes

$$\mathscr{H}_{\mathrm{e}}\left(\mathrm{A}'\right)\mathrm{u}'_{\mathrm{n}} + \Delta'\mathrm{v}'_{\mathrm{n}} = \epsilon_{\mathrm{n}}\mathrm{u}'_{\mathrm{n}} \tag{5-38a}$$

and similarly

$$-\mathscr{H}^*_{\mathrm{e}}\left(\mathbf{A}'\right)v'_{\mathrm{n}} + \Delta'u'_{\mathrm{n}} = \epsilon_{\mathrm{n}}v'_{\mathrm{n}} \tag{5-38b}$$

The $\binom{\mathrm{u}'_{\mathrm{n}}}{\mathrm{v}'_{\mathrm{n}}}$ is the set of eigenfunctions of the vector potential A′ and the pair potential Δ'. Furthermore if Δ satisfied the self-consistency relation (5-32) with the set $\binom{u}{v}$, Δ' also satisfies (5-32) with the set $\binom{u'}{v'}$.

Conclusion: The wave functions, and even the pair potential, have changed by the "gauge transformation" $A \rightarrow A$ '. We say that Δ, for instance, is "gauge covariant." But the eigenvalues ϵ_{n} are unchanged: We say that they are "gauge invariant." We can prove in the same way that all physically measurable quantities (such as the current density at one point...) are gauge invariant.

Remarks.

Restrictions on the possible gauge functions χ. The self-consistent field $\Delta(r)$ must be a single-valued function of r, whatever gauge we choose. Take for instance a sample in the form of a hollow cylinder, $0z$ being the cylinder axis and φ the rotation angle around 0 z . Try a gauge function of the form

$$\chi = \frac{\hbar c}{2e}m\varphi \tag{5-39}$$

where m is an arbitrary constant. Then

$$\Delta'(r) = \Delta(r)e^{im\varphi} \tag{5-40}$$

Both Δ and Δ' must be single values: This imposes that m be an integer. More generally, for an arbitrary ring shaped specimen, the increment of χ when performing one term around the ring must be $2\pi(\mathrm{ch}/2\mathrm{e}) = \mathrm{ch}/2\mathrm{e}$ times an integer.

SPECIAL CHOICES OF GAUGE

Starting from a given A, the transformation function X can be chosen to impose some convenient properties to A'.

Example 1. For a singly connected specimen, we impose

$$\begin{aligned} \operatorname{div} A' &= 0 \text{ in the sample} \\ A' \cdot n &= 0 \text{ at the surface} \end{aligned} \tag{5-41}$$

(where **n** is a unit vector normal to the surface). The transformation function χ is derived from the equations

$$\begin{aligned} \nabla^2 \chi &= -\operatorname{div} \mathbf{A} \text{ in the sample} \\ \mathbf{n} \cdot \nabla \chi &= -\mathbf{n} \cdot \mathbf{A} \text{ at the surface} \end{aligned} \tag{5-42}$$

According to general theorems in electrostatics, the solution χ of (5-42) is unique for a singly connected specimen. Thus A' is well defined. We say that A' is the vector potential in the London gauge.

Example 2. With A as vector potential, we have a certain pair potential $\Delta(r)$. Separate the amplitude and phase of Δ:

$$\Delta(r) = |\Delta(r)| e^{i\varphi(r)} \tag{5-43}$$

Then transform to A' using as gauge function

$$\chi = -\frac{\hbar c}{2e} \varphi \tag{5-44}$$

Since Δ was single valued, this choice χ is always acceptable. [3] The new pair potential is simply

$$\Delta'(r) = |\Delta(r)|$$

Thus it is always possible to choose a gauge where the pair potential is real. For a singly connected superconductor with no external current leads, this gauge coincides in fact with the London gauge, but it is defined for more general situations.

Flux Quantization

Consider the superconducting ring of Fig. 5-1 (diameter and thickness much larger than the penetration depth).

[3] This property was pointed out to the writer by Dr. P. Marcus.

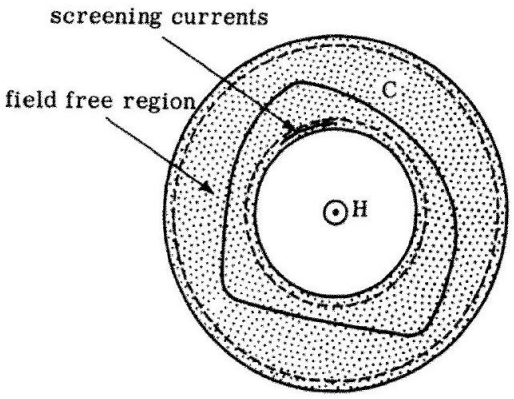


Figure 5-1
Flux trapped in a large superconducting ring. The thickness of the ring is assumed to be very large compared with the penetration depth; then it is possible to find a contour C in the superconductor along which the current and the field are 0 .

Experiments by Doll and Nabauer, and by Deaver and Fairbanks (1961), have shown that the flux ϕ, which passes through the ring, can only take on certain discrete values:

$$\begin{aligned} \phi &= \mathrm{n}\phi_0 \\ \phi_0 &= \frac{\mathrm{ch}}{2\mathrm{e}} \simeq 2.10^{-7}\mathrm{G}\times\mathrm{cm}^2 \\ \mathrm{n} &= \text{ any integer} \end{aligned} \tag{5-45}$$

(Such measurements of small fluxes are done on metallic films deposited on the surface of a capillary $\sim 10\mu$ in diameter. The flux unit ϕ_0 then corresponds to a sizeable field ~ 0.1G.)

This "flux quantization" is a consequence of the condition that $\Delta(r)$ be a single-valued function.

Proof. Introduce a vector

$$u = \hbar\nabla\phi - \frac{2e}{c}A \tag{5-46}$$

where ϕ is the phase of Δ defined as above. Note first that u is gauge invariant, as can be seen from the transformation laws (5-34), (5-35). Physically, for situations where $|\Delta|$ is constant in space, u is proportional to the local supercurrent density (take for instance the situation of uniform flow and $A = 0$ described in the last problem). Now consider an inner point P of the ring (Fig. 5-1). At P, no field penetrates; there is no current and $u = 0$. Integrate this relation around the countour C, which comes nowhere close to the surface ($\mathbf{u} = 0$ along $\mathbf{C}$)

$$\int_{\mathrm{c}} \mathrm{d}\ell \cdot \left(\hbar\nabla\phi - \frac{2\mathrm{e}}{\mathrm{c}}\,\mathrm{A}\right) = 0 \tag{5-47}$$

$\int \mathrm{c}A\cdot d\ell = \phi$ is the flux in the ring. $\int \nabla\phi\cdot d\ell = [\phi]$ is the change of phase of $\Delta(r)$ after one turn around C. Since Δ must be single valued: $[\phi] = 2n\pi$ (n integer). Inserting these results in (5-47) we obtain (5-45).

Flux quantization was first considered by London. He predicted a flux quantization ch/e = twice the experimental value. We now repeat his argument (for a pure metal, at $T = 0$) and then try and correct it. Let $\phi_0\,(r_1\cdots r_N)$ be the ground state wavefunction of the superconducting electrons i (a state of no current). A state of uniform current flow is obtained if we replace ϕ_0 by

$$\phi_0 \exp \mathrm{iq} \cdot \lfloor \mathbf{r}_1 + \mathbf{r}_2 + \ldots + \mathbf{r_N} \rfloor \tag{5-48}$$

leading to a current density $ne\hbar q/m$. A more general state of macroscopic motion would be

$$\phi_0 \exp \mathrm{i} [\, \mathrm{S}(\mathrm{r}_1) + \ldots + \mathrm{S}(\mathrm{r_N})] \tag{5-49}$$

where S(r) is a slowly varying function in space. If there is also a vector potential A, the resulting current has the form

$$j = \frac{ne}{m} \left(\hbar \nabla S - \frac{eA}{c} \right) \tag{5-50}$$

If we assume that the only states that can be realized in the superconductor are of the form (5-49) we immediately find the Meissner effect: Taking the curl of (5-50) leads to the London equation. Furthermore, we find flux quantization: Consider again our superconducting ring. In the interior, far from the surface, $\mathbf{j} = 0$, and the vector potential is given by

$$A = \frac{c\hbar}{e} \nabla S \tag{5-51}$$

If some flux ϕ passes through the annulus, S cannot be single valued. Consider a contour C as shown in Fig. 5-1. If C is nowhere close to the surface, (5-51) is valid along C and the flux enclosed by C is given by

$$\int \mathrm{Hd}_\sigma = \oint \mathrm{A} \cdot \ \mathrm{d}l = \frac{\mathrm{ch}}{\mathrm{e}} \oint \nabla \ \mathrm{S} \cdot \ \mathrm{d}l = \frac{\mathrm{ch}}{\mathrm{e}} \not{\mathrm{S}} \tag{5-52}$$

where the integrals $\oint dl$ are taken along C, and $\varnothing$ is the increase in S when one makes one complete path around the contour. $\not{S}$ cannot take on arbitrary values. The wave function must be a single-valued function of $r_1 \ldots r_N$. If we allow one of the coordinates r_1 to vary along C, after a complete cycle we must find the same function. Since ϕ_0 is single valued, this imposes the condition that $\not{S} = 2n\pi$, where n is an integer. From (5-52) this gives ch/e as the flux quantum.

This argument has one weak point, however (Brenig, 1961). In reality the states $\phi_0 \exp \{i [S(r_1) + \ldots + S(r_N)]\}$ are not the only states of macroscopic motion we can construct in a superconductor. To see this, we have to look into the detailed shape of ϕ. Let us do it on a simple problem: a superconducting electron gas with periodic boundary conditions

$$\phi(x_i \ldots x_i \ldots x_N) \equiv \phi(x_i \ldots x_i + L \ldots x_N) \qquad \text{for all } i \tag{5-53}$$

We construct states of translational motion with momentum hq per electron. Pairing electrons $(\mathbf{k} + \mathbf{q}, \uparrow)$ and $(-\mathbf{k} + \mathbf{q}, \downarrow)$, we can build BCS wave functions:

(1) If $qL = \phi = 2n\pi$ (n integer), we use one-electron states k satisfying the usual periodic boundary conditions

$$k_X L = 2n_X \pi \quad (n_X \text{ integer }) \tag{5-54}$$

Then Eq. (5-53) is obeyed.

(2) If qL = \$ = $(2\mathrm{n} + 1)\pi$ (n integer), we use one-electron states k satisfying the opposite boundary condition

$$k_X L = (2n_X + 1)\, \pi \tag{5-55}$$

Again (5-53) is obeyed.

The functions of class (1) are of the London type: they differ from the BCS function at rest only by the factor $\exp[iq(x_1 + \ldots + x_N)]$. The functions of class (2) are not ot the London type. Both classes are acceptable. In all cases the energy is given by

$$E = E_0 + \frac{\hbar^2 q^2}{2m} N \tag{5-56}$$

Equation (5-56) applies to both classes, provided that

$$\mathrm{k_F\ L} \gg 1 \quad \text{and} \quad \frac{\mathrm{L}}{\xi_0} \gg 1 \tag{5-57}$$

When (5-57) is satisfied, all sums Σ_k on the allowed k values can be replaced by integrals which are independent of the choice of conditions (5-54) or (5-55).

Finally, it is easy to transpose these results to the case of an annulus. Again we find $\$ = n\pi$ and the resulting flux quantum is $ch/2e$.

How do the Bogolubov amplitudes $\binom{u}{v}$ change after one turn around the ring?

Answer.

This of course depends on the gauge chosen. Choose the gauge where Δ is real. Then, after one turn around the ring, the amplitudes are multiplied by $(-1)^n$, where n is the number of flux quanta in the ring.

Solution.

Return again to the simple case of uniform translation with the boundary condition (5-53). In the gauge where $\Delta = |\Delta| e^{21qx}$, we have

$$\binom{u}{v} = \begin{pmatrix} U_k & e^{i(k+q)\cdot r} \\ V_k & e^{i(k-q)\cdot r} \end{pmatrix} \tag{5-58}$$

as discussed in the last problem. For $\not{S} = n\pi$, we have just seen that the one-electron states e^{ikr} must be chosen such that

$$\exp(ik_x L) = (-1)^n$$

Also

$$e^{iqL} = (-1)^n$$

Thus $\binom{u}{v}$ is periodic in this gauge. If we now transform to the gauge where Δ is real, we get the amplitudes

$$\binom{u'}{v'} = \binom{U_k e^{ik\cdot r}}{V_k e^{ik\cdot r}} \tag{5-59}$$

and $\binom{u'}{v'}$ is multiplied by $(-1)^n$ if we change x into $x + L$.

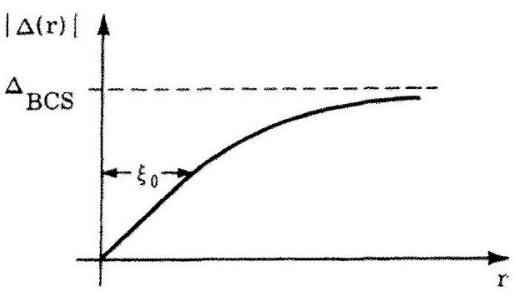


Figure 5-2
The amplitude of the order parameter Δ around a single vortex line in a pure Type II superconductor. Δ vanishes at $z = 0$ and has a finite slope for $r \to 0$. The region in which Δ is lowered from the BCS value has a radius $\sim \xi_0$.

Discuss the low energy excitations in the core of a vortex line

(C. Caroli, P. G. de Gennes, and J. Matricon, 1964).

Solution.

We restrict our attention to pure superconductors of Type II. The starting point is Eq. (5-18). We use cylindrical coordinates $(r\theta z)$, the line being along the z axis, and a gauge where the pair potential $\Delta(r) = |\Delta(r)|e^{-i\theta}$: We call A the vector potential in this particular gauge. $|\Delta(r)|$ vanishes for $r = 0$, then increases (linearly at small r) and finally reaches the BCS value Δ_∞ at distances $r > \xi$. We rewrite (5-18) in a condensed spinor notation $\hat{\phi} = \binom{u}{v}$ and eliminate the phase of Δ by setting

$$\hat{\phi} = \exp\left(-\frac{1}{2}\sigma_z\theta\right)\hat{\psi}$$

where $\sigma_x\sigma_y\sigma_z$ are Pauli matrices. Equation (5-18) becomes

$$\sigma_z\left\{\frac{1}{2m}\left(p - \sigma_z\frac{eA}{c} - \sigma_z\frac{\hbar}{2}\nabla\theta\right)^2 - E_F\right\}\hat{\psi} + \sigma_x\Delta\hat{\psi} = \epsilon\hat{\psi}$$

Note that $\mathrm{A} \sim \mathrm{Hr}$ and

$$\frac{\frac{\mathrm{eA}}{\mathrm{c}}}{\hbar\nabla\theta} \sim \left(\frac{\mathrm{H}}{\phi_0}\right)\mathrm{r}^2$$

(where $\phi_0 = \mathrm{ch}/2\mathrm{e}$ is the flux quantum). For the excitations on interest, $\mathrm{r} \lesssim \xi$ and

$$\frac{\mathrm{eA}}{\mathrm{ch}\,\nabla\theta} \sim \frac{\mathrm{H}_\xi^2}{\phi_0} \sim \frac{\mathrm{H}}{\mathrm{H_{c2}}} \ll 1$$

Thus we can neglect all magnetic field effects.

We then look for solutions of the form $\hat{\psi} = \exp\left(\mathrm{ik_F z}\cos\alpha\right)\exp(\mathrm{i}\mu\theta)\hat{\mathrm{f}}(\mathrm{r})$ where k_F is the Fermi wave vector, α an arbitrary angle, and 2μ an odd integer. The latter condition ensures that ϕ is multiplied by (-1) after one complete turn, as required for one flux quantum in the gauge where Δ is real.

Dropping the Δ term in the equation for $\hat{\psi}$, we get

$$\sigma_z\frac{\hbar^2}{2m}\left\{-\frac{d^2\hat{f}}{dr^2} - \frac{1}{r}\frac{d\hat{f}}{dr} + \left(\mu - \frac{\sigma_z}{2}\right)^2\frac{\hat{f}}{r^2} - k_F^2\sin^2\alpha\hat{f}\right\} + \sigma_x\Delta(r)\hat{f} = \epsilon\hat{f}$$

It is possible to solve this equation completely in the region $0 < \mu \ll \mathrm{k_F}\xi$, which turns out to be the important one. Consider a radius r_c such that

$$(\mu + 1/2)k_F^{-1} \ll r_c \ll \xi$$

For $r < r_c$, the Δ term can be neglected and $\hat{f} = \binom{f^+}{f_-}$is given by

$$f_\pm(r) = A_{\pm\mu\mp1/2}J_{\mu\mp1}\left\{\left(k_F\sin\alpha \pm q\right)r\right\}$$

where J is a Bessel function, A_+, $A_-$are arbitrary coefficients, and $\mathrm{q} = \epsilon/\hbar \mathrm{v_F} \sin\alpha$.

For $r > r_c$, we put

$$\hat{f} = \hat{g}(r) H_m\left(k_F r \sin\alpha\right) + \text{ C.C.} \qquad \left(m = \sqrt{\mu^2 + \frac{1}{4}}\right)$$

where H is a Hankel function and g a slowly-varying envelope. The equation for 8 may be reduced to

$$-i\sigma_z \hbar v_F \sin\alpha \frac{d\hat{g}}{dr} + \Delta\sigma_x \hat{g} = \left(\epsilon + \frac{\mu\hbar^2}{2mr^2}\right)\hat{g} \quad v_F = \frac{\hbar k_F}{m}$$

For $\epsilon \ll \Delta_\infty$ and $k_F r \gg \mu$, the right-hand side is a small perturbation. Treating it to first order, we get

$$\begin{aligned}
\hat{g} &= \text{const } \times \begin{pmatrix} e^{i\psi/2} \\ -ie^{-i\psi/2} \end{pmatrix} e^{-K} \\
K(r) &= \left(\hbar v_F \sin\alpha\right)^{-1} \int_0^r \Delta(r) dr \\
\psi(r) &= -\int_r^\infty \exp\left\{2K(r) - 2K\left(r'\right)\right\} \left(2q + \frac{\mu}{k_F r'^2 \sin\alpha}\right) dr \\
\psi\left(r_c\right) &\cong -\mu\left(k_F r_c \sin\alpha\right)^{-1} + 2qr_c - 2\int_0^\infty dr' e^{-2K(r')} \left(q - \frac{\mu\Delta\left(r'\right)}{\hbar k_F v_F \sin^2\alpha}\right)
\end{aligned}$$

Finally we match the solutions at $r = r_c$, making use of the asymptotic forms

$$J_m(z) = \text{ const } z^{-1/2} \sin\left\{z + \frac{m^2}{2z} - \frac{\pi}{2}\left(m - \frac{1}{2}\right)\right\}$$

etc., and obtain the condition (for $\mu \neq 0$)

$$\psi\left(r_c\right) = 2qr_c - \mu\left(k_F r_c \sin\alpha\right)^{-1}$$

Comparing with our earlier result for $\psi\left(r_c\right)$, we see that all the r_c dependent terms cancel out, and find the eigenvalue

$$\begin{aligned}
\epsilon_{\mu\alpha} = hqv_F \sin\alpha &= \mu\left(k_F \sin\alpha\right)^{-1} \frac{\int_0^\infty \frac{\Delta(r)}{r} e^{-2K(r)} dr}{\int_0^\infty e^{-2K(r)} dr} \\
&= \mu\left(k_F \sin\alpha\right)^{-1} \left(\frac{d\Delta}{dr}\right)_{r=0} g(\alpha) \quad (\mu \neq 0, \mu \ll k_F \xi)
\end{aligned}$$

The dimensionless function $g(\alpha)$ thus defined depends on the exact shape assumed for $\Delta(r)$ but is always close to 1 . In particular $g(0) = g(\pi) = 1$. Thus the eigenvalues are of order $\mu\Delta_\infty/\mathrm{k_F}\xi \sim \mu\Delta^2/\mathrm{E_F}$, the lowest one corresponding to $\mu = \frac{1}{2}$. The density of states N_ℓ associated with the levels is (for one spin direction and for a unit length of line)

$$\mathrm{N}_\ell(\epsilon) = \frac{1}{2\pi}\left\{\left(\frac{\mathrm{d}\Delta}{\mathrm{dr}}\right)_{r=0}\right\}^{-1} \mathrm{k_F^2} \int_0^\pi \mathrm{d}\alpha \frac{\sin^2\alpha}{\mathrm{g}(\alpha)} \quad \left(\frac{\Delta_\infty^2}{\mathrm{E_F}} < \epsilon \ll \Delta_\infty\right)$$

Note that $\mathrm{N}_\ell(\epsilon) \sim \mathrm{N}(0)\xi^2$, that is, each line is equivalent to a normal region of radius $\sim \xi$. The low-lying states occupy only a fraction $\sim (\xi^2/\mathrm{d}^2) \sim (\mathrm{B}/\mathrm{H_{c2}})$ of the volume. They will be of importance mainly at low temperatures T (roughly when $(\xi/\mathrm{d})^2 \exp(\Delta\infty/\mathrm{T}) > 1$). Then the specific heat will be linear in T, the thermal conductivity will be anisotropic (maximum along

the lines) and the nuclear relaxation may, in some cases, become limited by the spin diffusion rate.

Excitation Threshold in Inhomogeneous Systems

Consider a pure metal in the absence of field or currents. Usually the pair potential Δ is constant throughout the sample. The functions u and v are then plane waves and it is easily verified that the energy gap is Δ. However, it is possible for sufficiently thin samples to impose a spatial variation in $\Delta(r)$ (for example, by depositing metals of different characteristics on the superconductor). We now study the particularly simple case described in Fig. 5-3.

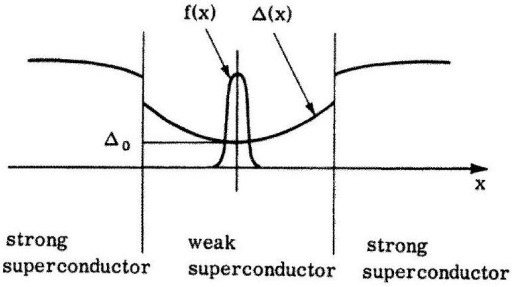


Figure 5-3
The pair potential $\Delta(x)$ for a system of three metallic layers, the central layer being the weakest superconductor. Δ has a minimum Δ_0. It is possible to construct a quasiparticle with an amplitude $f(x)$ very localized around Δ_0; such a quasiparticle has an excitation energy essentially equal to Δ_0

The pair potential varies only in the x direction and it has a minimum Δ_n at $x = 0$. For $x \neq 0$, Δ increases; the spatial scale of the variation in Δ is rather large (at least $\sim \xi_0$). We show that the threshold energy ϵ_0 for the quasiparticles, that is, the smallest positive eigenvalue of (5-18), is nearly equal to Δ_0. Writing (5-18) in a more condensed form, we have

$$\epsilon\hat{\psi} = (\mathscr{H}_{\mathrm{e}}\sigma_{\mathrm{z}} + \Delta\sigma_{\mathrm{x}})\,\hat{\psi} = \hat{\Omega}\hat{\psi} \tag{5-60}$$

where $\hat{\psi} = \binom{u}{v}, \sigma_z = \begin{pmatrix} 1 & 0 \\ 0 & -1 \end{pmatrix}$, and $\sigma_x = \binom{01}{10}$ are the Pauli matrices. We wish to use a variational principle to show that ϵ_0 is close to Δ_0. However $\hat{\Omega}$ is not a positive definite operator [ϵ and $(-\epsilon)$ are simultaneously eigenvalues]. It is therefore necessary to study

$$\hat{\Omega}^2 = \mathscr{H}_{\mathrm{e}}^2 + \Delta^2 + \mathrm{i}\,[\mathscr{H}_{\mathrm{e}}, \Delta]\,\sigma_{\mathrm{y}} \tag{5-61}$$

[In order to obtain (5-61), we have used $\sigma_x\sigma_z + \sigma_z\sigma_x = 0$ and $\sigma_x\sigma_z$ - $\sigma_z\sigma_x = -2i\sigma_y$.] Take as a trial function

$$\hat{\psi}(r) = \exp(\mathrm{ik}_F z)\,\mathrm{f(x)}\hat{\phi}_{\mathrm{y}} \tag{5-62}$$

where z designates an arbitrary direction normal to the x axis and $\hat{\phi}_y$ is a constant spinor such that $\sigma_y\hat{\phi}_y = \pm\hat{\phi}_y$. Since $\mathscr{H}_e$ is the energy measured from the Fermi level, we have simply

$$\mathscr{H}_e\hat{\psi} = \exp(\mathrm{ik}_F z)\left(-\frac{\hbar^2}{2m}\right)\frac{d^2 f(x)}{dx^2}\hat{\phi}_y \tag{5-63}$$

(This choice of wave vector leads us to a nodeless function f in the ground state, which is favorable for having a low kinetic energy.) Calculating the average value of $\hat{\Omega}^2$, we obtain

$$\epsilon^2 = \langle\hat{\psi}|\hat{\Omega}^2|\hat{\psi}\rangle = \int dx f^*(x)\left[\frac{\hbar^4}{4m^2}\frac{d^4 f}{dx^4} + |\Delta(x)|^2\right] f(x) \pm i\int dx f^*(x)\left[-\frac{\hbar^2}{2m}\frac{d^2}{dx^2}, \Delta(x)\right] f(x) \tag{5-64}$$

If f is taken as real, the last integral vanishes. If f is chosen as a regular function of spatial extent L, then the kinetic energy term gives a contribution $\alpha\left(\hbar^2/2mL^2\right)^2$ where α is a numerical coefficient of the order unity. For the pair potential term, we assume that Δ varies parabolically around Δ_0,

$$\Delta(\mathrm{x}) = \Delta_0\left(1 + \frac{\mathrm{x}^2}{\delta^2}\right) \tag{5-65}$$

with $\delta \gg L$. Then the potential term becomes $\Delta_0^2\left[1 + \beta\left(L^2/\delta^2\right)\right]$ where β is another numerical coefficient, and finally

$$\epsilon^2 = \Delta_0^2 + \alpha\left(\frac{\hbar^2}{2mL^2}\right)^2 + \beta\Delta_0^2\frac{L^2}{\delta^2} \tag{5-66}$$

Minimizing this expression with respect to L, we obtain

$$\epsilon_0^2 \cong \Delta_0^2\left(1 + \mu^{2/3}\right) \tag{5-67}$$

where $\mu \sim \hbar^2/2m\delta^2\Delta_0$. For $\delta \sim \xi \sim \hbar v_\mathrm{F}/\Delta_0$, we have $\mu \sim 1/\mathrm{k_F}\xi_0 \sim 10^{-2}$ to 10^{-3}. Therefore, in practice, ϵ_0 is very close to Δ_0.

Nonmagnetic Alloys: Anderson's Theorem

We now study the excitation spectrum in a superconducting alloy, in zero field. We must solve the system of equations (5-18):

$$\begin{aligned}\epsilon u &= \left(-\frac{\hbar^2}{2m}\nabla^2 + U(r) - E_F\right)u + \Delta v \\ \epsilon v &= \left(\frac{\hbar^2}{2m}\nabla^2 - U(r) + E_F\right)v + \Delta^* u\end{aligned} \tag{5-68}$$

U(r) is now the complete Hartree potential for one electron in the normal state. In (5-68), we have assumed, as always, that the electronelectron coupling is nearly a point interaction $[-V\delta(r_1 - r_2)]$ and that the potential $U(r)$ does not depend on the spin indices (nonmagnetic alloy). Still $U(r)$ contains the impurity potentials, and (5-68) includes the multiple scattering effects from all of the impurities; it is therefore a very complicated system. The situation is much improved if we assume that $\Delta(r)$ is independent of r even in the presence of impurities. This is not rigorously correct, but has been shown to be acceptable if the impurities are not too different chemically from the matrix (C. Caroli, 1962). Then a large simplification occurs if we introduce the one-electron wave functions in the normal state $w_n(r)$ defined by:

$$\xi_n w_n(r) = \left[-\frac{\hbar^2}{2m}\nabla^2 + U(r) - E_F\right]w_n(r) \tag{5-69}$$

For pure metal, the $w_n(r)$ are Bloch functions. In an alloy, the $w_n(r)$ are complicated functions describing the successive scattering of an electron by all of the impurities. Fortunately, we shall not need to know these wave functions in detail for the following calculation. When

the pair potential $\Delta(r)$ reduces to a constant Δ, the solutions of (5-68) have the same spatial dependence as the $w_n(r)$. If we set

$$\begin{aligned} u_n(r) &= w_n(r) u_n \\ v_n(r) &= w_n(r) v_n \end{aligned} \tag{5-70}$$

it is easy to see that (5-68) is satisfied when

$$\begin{aligned} \left(\epsilon_n - \xi_n\right) u_n - \Delta v_n &= 0 \\ \Delta^* u_n - \left(\epsilon_n + \xi_n\right) v_n &= 0 \end{aligned} \tag{5-71}$$

which implies as usual

$$\epsilon_{\mathrm{n}}^2 = \xi_{\mathrm{n}}^2 + |\Delta|^2 \tag{5-72}$$

The coefficients u_n and v_n depend only on ξ_n. From the normalization condition, they must satisfy

$$|u_n|^2 + |v_n|^2 = 1 \tag{5-73}$$

Using (5-71), one can write explicitly

$$\begin{aligned} |u_n|^2 &= \frac{1}{2}\left(1 + \frac{\xi_n}{\epsilon_n}\right) \\ |v_n|^2 &= \frac{1}{2}\left(1 - \frac{\xi_n}{\epsilon_n}\right) \end{aligned} \tag{5-74}$$

It is convenient to choose u_n, v_n and $w_n(r)$ to be real. This is possible because the $w_n(r)$ are eigenfunctions of a real operator. This choice of standing waves rather than traveling waves will be useful for the discussion of alloys. The self-consistency equation (5-32) becomes

$$\Delta(\mathbf{r}) = V \sum_n |w_n(\mathbf{r})|^2 \frac{\Delta}{2\sqrt{\Delta^2 + \xi_n^2}} \left[1 - 2f\left(\sqrt{\xi_n^2 + \Delta^2}\right)\right] \tag{5-75}$$

It is useful to introduce the density of states $\mathrm{N}(r)$ at the point r in the normal metal, at the Fermi energy

$$N(r) = \sum_n |w_n(r)|^2 \, \delta\left(\xi_n\right) \tag{5-76}$$

The condition (5-75) becomes

$$\Delta(r) = V N(r) \int_{-\hbar\omega_D}^{\hbar\omega_D} d\xi \frac{\Delta(1-2f)}{2\sqrt{\xi^2 + \Delta^2}} \tag{5-77}$$

Thus the self-consistency cannot be exact since Δ was assumed to be constant, but here $\Delta(r)$ is proportional to $N(r)$ and is therefore modified by the impurities. However, if the impurities are chemically similar to the matrix, $N(r)$ is not very different from its average $\bar{N}$ and the self-consistency requirement becomes

$$1 = \bar{N} V \int_{-\hbar\omega_D}^{\hbar\omega_D} d\xi \frac{1 - 2\mathrm{f}}{2\sqrt{\xi^2 + |\Delta|^2}} \tag{5-78}$$

This is of the same form as for a pure metal. To a first approximation, the excitation spectrum and all of the thermodynamic properties are the same for the alloy as for the pure metal. This property was first pointed out by Anderson (1959). Experimentally, it has been verified that nonmagnetic impurities do not have spectacular effects on the transition temperature in superconducting metals. [4]

6.2.3 5-3 The Meissner Effect in Metals and Alloys

The Magnetic Field Treated as a Perturbation

We shall now study the currents j induced by a weak magnetic field $h = \text{curl } A$ in a gas of superconducting electrons. The mathematical machinery necessary for this calculation is contained in the preceding section. We start from the reduced form of the self-consistent field equations with a one-electron energy

$$\mathscr{H}_{\mathrm{e}} = \frac{\left(p - \frac{\mathrm{e}}{\mathrm{c}}\,\mathrm{A}\right)^2}{2m} + \mathrm{U(r)} - \mathrm{E_F} \tag{5-79}$$

We do not demand that $U(r)$ be spatially constant, or even periodic. Thus we are able to discuss simultaneously pure metals and alloys. To first order in h (or A), we set

$$\begin{aligned} u_n(r) &= u_n^{(0)}(r) + u_n^{(1)}(r) \\ v_n(r) &= v_n^{(0)}(r) + v_n^{(1)}(r) \end{aligned} \tag{5-80}$$

where $v_n^{(0)}$ and $u_n^{(0)}$ are the eigenfunctions of the Bogolubov system (5-18) for the case $\mathrm{A} = 0$, and are written more explicitly in Eq. (5-70). Also,

$$\Delta(r) = \Delta_0 + \Delta_1(r)$$

In general Δ_1 is nonzero, that is, the self-consistent field Δ is modified when a magnetic field is applied. This remark, due to Bogolubov, is necessary to preserve the gauge invariance.

A typical case where Δ_1 is nonzero can be found in the following way: Suppose that $A = \nabla\chi(r)$ where χ is an arbitrary function (then $H = \text{curl}\, A = 0$). One can verify that the system of equations (5-18) and the self-consistency equation (5-32) have a solution

$$\begin{aligned} u_n &= e^{(ie/\hbar c)\chi(r)} u_n^0 \\ v_n &= e^{(-ie/\hbar c)\chi(r)} v_n^0 \\ \Delta(r) &= \Delta_0 e^{(2ie/\hbar c)\chi(r)} \end{aligned} \tag{5-81}$$

and that, as expected, $j = 0$. Expanding to first order in χ (or A) we obtain

$$\begin{aligned} u_n^{(1)} &= \frac{ie}{\hbar c} u_n^0 \chi \\ v_n^{(1)} &= \frac{-ie}{\hbar c} v_n^0 \chi \\ \Delta_1 &= \frac{2ie}{\hbar c} \Delta_0 \chi \end{aligned} \tag{5-82}$$

[4] There exist certain effects (??? which???) that cannot be described by our crude interaction - V $\delta\,(r_1 - r_2)$. However the smallness of these effects shows that this interaction is at least a good starting point.

and thus Δ_1 is nonzero for that particular case. More generally, when Δ_1 is first order in A, the most general form it can have is

$$\Delta_1(r) = \sum_\alpha \int p_\alpha (r, r') A_\alpha (r') \, dr' \tag{5-83}$$

where the integral is extended over the entire volume of the sample and $\alpha = \mathrm{x}, \mathrm{y}, \mathrm{z}$. If we are considering an isotropic, homogeneous metal, $P(r, r')$ must only be a function of $R = |r - r'|$ and must be a vector in the direction of $R.P(R)$ can be completely determined by returning to our special case for which

$$\frac{2\mathrm{ie}}{\hbar \mathrm{c}} \Delta_0 \chi(r) = \int \mathrm{P}(r' - r) \cdot \nabla \chi(r') \, \mathrm{d}r' \tag{5-84}$$

Let us now restrict our attention to a particular class of functions $\chi(r')$ such that $\chi(r')$ vanishes at large distances from $r, (|r - r'| \to \infty)$. Then the integration can be performed by parts to give $-\int \chi(r')$ div $\mathbf{P}\times$ $(\mathbf{r}' - \mathbf{r}) \, \mathrm{d}\mathbf{r}'$. Therefore we must have div $\mathbf{P}(\mathbf{r}' - \mathbf{r}) = -(2\mathrm{ie}/\hbar \mathrm{c}) \Delta_0 \delta(R)$. Since $\mathbf{P}$ is a radial vector, the unique solution is

$$P(R) = -\frac{ie\Delta_0}{2\pi\hbar c} \frac{R}{R^3} = \frac{ie\Delta_0}{2\pi\hbar c} \nabla \left(\frac{1}{R} \right) \tag{5-85}$$

This form of $\mathbf{P}(\mathbf{R})$ is also applicable in an alloy if we calculate the average of Δ_1 over all impurity configurations (because on averaging the system becomes homogeneous and isotropic).

Knowing $\mathbf{P}(\mathbf{R})$, the following theorem can be proved: If $\mathbf{A}$ is chosen in the gauge div $A = 0$ and if A has no component normal to the surface of the sample (London gauge), then Δ_1 is zero. In fact,

$$\begin{aligned} \Delta_1(r) &= \frac{ie\Delta_0}{2\pi\hbar c} \int \nabla \left(\frac{1}{R} \right) \cdot A(r') \, dr' \\ &= -\frac{ie\Delta_0}{2\pi\hbar c} \left[\int \frac{1}{R} \operatorname{div} A dr' - \int \frac{1}{R} A \cdot n d\sigma \right] = 0 \end{aligned} \tag{5-86}$$

($\mathbf{n}$ is a unit vector normal to the sample surface). It is important to realize that this theorem is valid only when the following conditions occur: (1) isotropic metal, (2) point interaction between electrons. In fact, if the interaction has a finite range, the pair potential $\Delta(r, r')$ must depend on two arguments. Then the change in Δ takes the form

$$\Delta_1(r, r') = \int dr'' K_\alpha (r, r', r'') A_\alpha (r'') \tag{5-87}$$

We no longer have a symmetry argument to allow us to introduce the gradient of a function. Detailed numerical calculations show that the corrections resulting from such a spread-out interaction are small and have little influence on the diamagnetism: See G. Rickayzen, Phys. Rev., 115, 795 (1959).

We now explicitly calculate the corrections $u^{(1)}$ and $v^{(1)}$ in the London gauge, where $\Delta_1 = 0$; this choice of gauge greatly simplifies the calculations. We first write the system of equations (5-18) with (5-19) only keeping terms to first order in A,

$$\begin{aligned} \left[\epsilon + \frac{\hbar^2}{2m} \nabla^2 - U(r) \right] u_n^{(1)}(r) - \Delta v_n^{(1)}(r) &= \frac{ie\hbar}{2mc} (A \cdot \nabla + \nabla \cdot A) u_n^{(0)}(r) \\ \left[\epsilon - \frac{\hbar^2}{2m} \nabla^2 + U(r) \right] v_n^{(1)}(r) - \Delta^* u_n^{(1)}(r) &= \frac{ie\hbar}{2mc} (A \cdot \nabla + \nabla \cdot A) v_n^{(0)}(r) \end{aligned} \tag{5-88}$$

We now expand $u_n^{(1)}$ and $v_n^{(1)}$ in terms of the orthonormal set $w_n(r)$ (remember incidentally that we choose the w_n 's as real)

$$u_n^{(1)}(r) = \sum_m a_{nm} w_m(r)$$
$$v_n^{(1)}(r) = \sum_m b_{nm} w_m(r) \tag{5-89}$$

replace $u_n^{(0)}$ and $v_n^{(0)}$ by their values (5-70), multiply each of (5-88) by w_m and integrate over r. We then obtain

$$\begin{aligned} a_{nm}(\epsilon_n - \xi_m) - \Delta b_{nm} &= iF_{nm}u_n \\ -\Delta a_{nm} + b_{nm}(\epsilon_n + \xi_m) &= iF_{nm}v_n \end{aligned} \tag{5-90}$$

where

$$F_{nm} = \frac{e\hbar}{2mc}\int w_m(A\cdot\nabla + \nabla\cdot A)w_n dr = -F_{mn} \tag{5-91}$$

The solution of (5-90) is

$$\begin{aligned} \mathrm{a_{nm}} &= \frac{\mathrm{i\ F_{nm}}}{\xi_\mathrm{n}^2 - \xi_m^2}\left[(\epsilon_\mathrm{n} + \xi_m)\,\mathrm{u_n} + \Delta \mathrm{v_n}\right] \\ \mathrm{b_{nm}} &= \frac{\mathrm{i\ F_{nm}}}{\xi_\mathrm{n}^2 - \xi_m^2}\left[(\epsilon_\mathrm{n} - \xi_m)\,\mathrm{v_n} + \Delta \mathrm{u_n}\right] \end{aligned} \tag{5-92}$$

Once $u_n^{(1)}$ and $v_n^{(1)}$ are calculated from these formulas, you can return to the self-consistency equation (5-32) and verify directly that in the London gauge Δ_1 is zero, as predicted.

Relation between the Diamagnetic Response and the Conductivity in the Normal State

Knowing the wave functions to first order in A, we calculate the current

$$j(r) = \mathrm{Re}\left\{\langle\Psi^+(r)\left(p - \frac{eA}{c}\right)\Psi(r)\rangle\right\}$$

We limit our discussion to the case where $T = 0$. To zeroth order in A, $j = 0$. To first order, expressing the Ψ 's in terms of the γ 's, taking the average and expanding $u = u^0 + u'$, and so on, we find

$$\begin{aligned} j(r) &= -\frac{e\hbar i}{2m}\sum_n \left[v_n^{*(0)}\nabla v_n^{(1)} + v_n^{*(1)}\nabla v_n^{(0)} - C.C.\right] \\ &= -\frac{e\hbar i}{2m}\sum_{n,m} v_n\left[w_n\nabla w_n b_{nm} + w_m\nabla w_n b_{nm}^* - C.C.\right] \qquad (5\text{-}93) \\ &= -\frac{e\hbar i}{2m}\sum_{n,m} v_n\left(b_{nm} - b_{nm}^*\right)\left(w_n\nabla w_m - w_m\nabla w_n\right) \qquad (5\text{-}94) \end{aligned}$$

From (5-92), we determine the following properties

$$b_{nm}^{*} = -b_{nm}$$
$$v_n b_{nm} = iF_{nm}R_{nm}$$

where

$$\mathrm{R_{nm}} = \frac{1}{2\epsilon_{\mathrm{n}}\left(\xi_{\mathrm{n}}^2 - \xi_m^2\right)}\left[\left(\epsilon_{\mathrm{n}} - \xi_{\mathrm{n}}\right)\left(\epsilon_{\mathrm{n}} - \xi_m\right) + \Delta^2\right]$$

The symmetric part of $\mathrm{R_{nm}}$ is

$$\frac{1}{2}\,\mathrm{L}\left(\xi_{\mathrm{n}}, \xi_m\right) = \frac{\mathrm{R_{nm}} + \mathrm{R_{mn}}}{2} = \frac{\Delta^2 + \xi_{\mathrm{n}}\xi_m - \epsilon_{\mathrm{n}}\epsilon_m}{\epsilon_{\mathrm{n}}\epsilon_m\left(\epsilon_{\mathrm{n}} + \epsilon_m\right)}$$

The relation between the current and vector potential takes the form (???? why???)

$$j_\mu(r) = \sum_\nu \int dr' A_\nu\left(r'\right) S_{\mu\nu}\left(r, r'\right) \tag{5-95}$$

where $\mu, \nu = \mathrm{x}, \mathrm{y}, \mathrm{z}$ and

$$S_{\mu\nu}\left(r, r'\right) = \left(\frac{e\hbar}{2m}\right)^2 \frac{1}{c}\sum_{n,m} L\left(\xi_n, \xi_m\right) p_{\mu nm}(r) p_{\nu nm}\left(r'\right) - \frac{ne^2}{mc}\delta\left(r - r'\right)\delta_{\mu\nu} \tag{5-96}$$

and we have defined

$$p_{\mu nm}(r) = \left[w_n(r)\frac{\partial}{\partial r_\mu} w_m(r) - w_m(r)\frac{\partial}{\partial r_\mu} w_n(r)\right]$$

For a pure infinite metal, the w_n are plane waves and the p_{nm} can be calculated immediately. However, in practice, we must take account of the presence of impurities and the surface of the sample. It is then impossible to construct the $\mathrm{w_n}$ explicitly.

However, $\mathrm{S}_{\mu\nu}$ can be obtained without much work by noticing that the electrical conductivity $\sigma_{\mu\nu}$ in the normal state involves the same matrix elements. This observation also explains the success of Pippard's phenomenological model, which led to a (j, A) relation for a superconductor analogous to the (j, E) relation in a normal metal.

More precisely, the conductivity $\sigma_{\mu\nu}\left(r, r', \Omega\right)$ at a frequency Ω is defined in the following way: At each point of the sample r', an electric field $\mathbf{E}\left(\mathbf{r}'\right)\mathrm{e}^{-\mathrm{i}\Omega\mathrm{t}}+$ C.C. is applied. The current induced at the point $r, f(r)e^{-i\Omega t}+$ C.C., is measured. The current is a linear function of the fields

$$\mathrm{j}_\mu(r) = \int d_3 r' \sigma_{\mu\nu}\left(rr', \Omega\right)\mathrm{E}_\nu\left(r'\right)$$

In practice we know the explicit form of $\sigma_{\mu\nu}$. The field current relation is given by the Chambers equation

$$j_\mu(r) = \frac{e^2 v_F}{2\pi} N(0)\sum_\nu \int dr' E_\nu\left(r'\right)\frac{R_\mu R_\nu}{R^4}\exp\left[\left(i\Omega/v_F - 1/\ell\right)R\right] \quad R = \left|r' - r\right| \tag{5-97}$$

where $\mathbf{R} = \mathbf{r}' - \mathbf{r}$. In (5-97), ℓ represents the transport mean free path. The integral extends only over the volume of the sample. Three assumptions are necessary to establish (5-97):

(1) The reflection of the electrons from the surface must be diffuse, which is realized in most cases.

(2) The fields **E** and the currents **j** are transverse (div **E** = 0, div j = 0). E and j have no components normal to the surface. This restriction doesn't disturb us since in the superconducting state our perturbation (the vector potential A) will also be transverse (London gauge).

(3) The frequency Ω is less than $k_B T/\hbar$. From (5-97) we see that σ has the form

$$\sigma_{\mu\nu}(rr') = \begin{array}{ll} \dfrac{e^2 v_f}{2\pi} N(0) \dfrac{R_\mu R_\nu}{R^4} \exp(i\Omega R/v_F)\, e^{-R/\ell} & (r, r' \text{ inside the sample}) \\ 0 & (\text{ if } r \text{ or } r' \text{ is outside the sample}) \end{array} \tag{5-98}$$

In fact, we only need the real part of $\sigma_{\mu\nu}$, which gives the power dissipated W

$$\mathrm{W} = \sum_{\mu\nu} \int \mathrm{dr}\ \mathrm{d}\mathbf{r}' \left[\mathrm{E}^*_\mu(\mathbf{r})\mathrm{E}_\nu(\mathbf{r}') + \text{ C.C. }\right] \mathrm{Re}\left\{\sigma_{\mu\nu}(\mathbf{r}, \mathbf{r}', \Omega)\right\} \tag{5-99}$$

We now calculate $\sigma_{\mu\nu}$ from the one-electron wave functions in the normal metal $w_n(r)$ and show that $\mathrm{Re}\,\sigma_{\mu\nu}$ can be expressed by a formula analogous to (5-96) for $S_{\mu\nu}$. In the normal metal the one-electron energy has the form

$$\mathscr{H}_e = \frac{1}{2m}\left(p - \frac{e}{c}A\right)^2 + U_0(r) \tag{5-100}$$

where $U_0(r)$ is the lattice potential energy including impurities and surfaces. On the other hand, the alternating electric field is not in U_0, but derived from the vector potential by

$$E = -\frac{1}{c}\frac{\partial A}{\partial t} = \frac{i\Omega}{c}A \tag{5-101}$$

Because the field **E** is a weak perturbation,

$$\begin{aligned} \mathscr{H}_e &= \mathscr{H}_0 + \mathscr{H}_1 \\ \mathscr{H}_0 &= \frac{\mathrm{p}^2}{2m} + U_0 \\ \mathscr{H}_1 &= -\frac{\mathrm{e}}{2\mathrm{mc}}(\mathrm{p}\cdot\ \mathrm{A} + \mathrm{A}\cdot\mathrm{p}) \end{aligned} \tag{5-102}$$

The eigenfunctions of $\mathscr{H}_0$ are the $w_n(r)$. The oscillating perturbation $\mathscr{H}_1$ induces transitions, $\mathrm{n} \to m$, such that $\xi_m - \xi_\mathrm{n} = \pm\hbar\Omega$. The transition probability per unit time is given by

$$g_{nm} = \frac{2\pi}{\hbar} f(\xi_n)\left[1 - f(\xi_m)\right] |\langle n|\mathscr{H}_1|m\rangle|^2\ \left[\delta(\xi_n - \xi_m + \hbar\Omega) + \delta(\xi_n - \xi_m - \hbar\Omega)\right] \tag{5-103}$$

where

$$\begin{aligned} \langle n|\mathscr{H}_1|m\rangle &= \frac{ei\hbar}{2mc}\int w_n(\nabla\cdot A + A\cdot\nabla)w_m dr \\ &= \frac{ei\hbar}{2mc}\sum_\nu \int A_\nu(r) p_{\nu nm}(r) dr \end{aligned} \tag{5-104}$$

The power dissipated is

$$\mathrm{w} = \sum_{\mathrm{n},m} \mathrm{g_{nm}}\left(\xi_m - \xi_\mathrm{n}\right) \tag{5-105}$$

Comparing this equation with (5-99), we find

$$\mathrm{Re}\left\{\sigma_{\mu\nu}\left(\mathrm{r},\mathrm{r}',\Omega\right)\right\} = \frac{2\pi}{\hbar}\left(\frac{\mathrm{e}\hbar}{m}\right)^2 \sum_{\mathrm{n},m} \frac{\mathrm{f}\left(\xi_\mathrm{n}\right) - \mathrm{f}\left(\xi_m\right)}{\hbar\Omega} \mathrm{p}_{\mu\mathrm{nm}}(\mathrm{r})\mathrm{p}_{\nu\mathrm{nm}}(\mathrm{r}')\delta\left(\xi_\mathrm{n} - \xi_m - \hbar\Omega\right) \tag{5-106}$$

In order to compare this with Chamber's formula we must consider the region $\hbar\Omega \ll \mathrm{k_B T}$. In this region,

$$\frac{f\left(\xi_n\right) - f\left(\xi_m\right)}{\hbar\Omega} = \frac{f\left(\xi_n\right) - f\left(\xi_m\right)}{\xi_n - \xi_n} \cong \frac{\delta f}{\delta\xi}$$

which is nearly $-\delta(\xi)$. Then (5-106) reduces to

$$\mathrm{Re}\left\{\sigma_{\mu\nu}\right\} = \frac{2\pi}{\hbar}\left(\frac{e\hbar}{m}\right)^2 \mathrm{N}(0) \sum_m \overline{\mathrm{p}_{\mu\mathrm{nm}}(\mathrm{r})\mathrm{p}_{\nu\mathrm{nm}}\left(\mathrm{r}'\right)}\delta\left(\xi_\mathrm{n} - \xi_m - \hbar\Omega\right) \tag{5-107}$$

where the symbol () denotes an average over one-electron states at the Fermi surface, in the normal state. [6]

Calculation of the Diamagnetic Currents

Equations (5-107) and (5-96) show that the conductivity $\sigma_{\mu\nu}$ in the normal state involves the same matrix elements as the diamagnetic response $S_{\mu\nu}$ in the superconducting state. Replacing Σ_n by $\mathrm{N}(0)\int \mathrm{d}\xi_\mathrm{n}$ in (5-96), we write the fundamental relation

$$\mathrm{S}_{\mu\nu}\left(\mathbf{r},\mathbf{r}'\right) = \frac{\hbar}{2\pi\mathrm{c}} \int \mathrm{d}\xi\ \mathrm{d}\xi' \mathrm{L}\left(\xi,\xi'\right) \mathrm{Re}\left\{\sigma_{\mu\nu}\left(\mathbf{r},\mathbf{r}',\frac{\xi-\xi'}{\hbar}\right)\right\} - \frac{\mathrm{ne}^2}{\mathrm{mc}}\delta(\mathbf{r})\delta_{\mu\nu} \tag{5-108}$$

We now insert Chambers' formula for $\sigma_{\mu\nu}$ to obtain

$$\mathrm{S}_{\mu\nu}\left(\mathrm{r},\mathrm{r}'\right) = \frac{3\mathrm{ne}^2}{4\pi\mathrm{mc}\xi_0}\frac{\mathrm{R}_\mu\mathrm{R}_\nu}{\mathrm{R}^4}\mathrm{e}^{-\mathrm{R}/\ell}\mathrm{J}(\mathrm{R}) - \frac{\mathrm{ne}^2}{\mathrm{mc}}\delta(\mathrm{R})\delta_{\mu\nu} \tag{5-109}$$

where we have set $\xi_0 = \hbar v_F/\pi\Delta(0), R = r' - r$, and

$$J(R) = \frac{1}{\pi^2\Delta(0)}\int_{-\infty}^{\infty} d\xi d\xi' L\left(\xi,\xi'\right)\cos\left[\frac{\left(\xi-\xi'\right)R}{\hbar v_F}\right] \tag{5-110}$$

From the form of $L\left(\xi,\xi'\right)$ we predict that the important contribution to the integral occurs when $\xi - \xi' \sim \Delta$. This leads to a range for I(R) of the order of ${}^{hv}{}_F/\Delta(0) \sim \xi_0$ (the choice of the numerical coefficient in the definition of ξ_0 will be useful later). For an explicit calculation of I(R), we change variables to: $\xi = \Delta\sinh\theta, \xi' = \Delta\sinh\theta'$, then set $\alpha = \left(\theta - \theta'\right)/2, \beta = \left(\theta + \theta'\right)/2$ to obtain

[6] Note that the average depends strongly on $\hbar\Omega$ but only slightly on ξ_m when $|\xi_n| \ll E_F$.

$$J(R) = \frac{1}{\pi^2}\int d\alpha d\beta \frac{\sinh^2\alpha}{\cosh\alpha\cosh\beta}\cos\left[\frac{2\Delta(0)R}{hv_F}\sinh\alpha\cosh\beta\right]$$
$$= \frac{1}{\pi^2}\int_{-\infty}^{\infty}\frac{d\beta}{\cosh\beta}\int_{-\infty}^{\infty}du\left(1-\frac{1}{1+u^2}\right)\cos\left(\frac{2\Delta(0)R}{\cosh\beta}\right)$$
$$(u=\sinh\alpha) \tag{5-111}$$

and

$$J(R) = \frac{1}{\pi}\frac{hv_F}{\Delta(0)}\delta(R) - \frac{1}{\pi}\int_{-\infty}^{\infty}\frac{d\beta}{\cosh\beta}\exp\left(-2\Delta(0)R\cosh\beta/hv_F\right) \tag{5-112}$$

The first term represents a contribution localized at the origin. On performing the $\mathbf{r}'$ integration in (5-95), we find that this term exactly cancels $(-ne^2/mc)\ \delta(\mathrm{R})\delta_{\mu\nu}$. Then, finally, we have

$$\mathrm{S}_{\mu\nu}\left(\mathrm{r},\mathrm{r}'\right) = \frac{-3\mathrm{ne}^2}{4\pi\mathrm{mc}\xi_0}\frac{\mathrm{R}_\mu\mathrm{R}_\nu}{\mathrm{R}^4}\mathrm{e}^{-\mathrm{R}/\ell}\mathrm{I}(\mathrm{R}) \tag{5-113}$$

where

$$\mathrm{I}(\mathrm{R}) = \frac{2}{\pi}\int_{-\infty}^{\infty}\frac{\mathrm{d}\beta}{\cosh\beta}\exp\left[-(2/\pi)\left(\mathrm{R}/\xi_0\right)\cosh\beta\right] \tag{5-114}$$

Formulas (5-95), (5-113), and (5-114) give a complete solution to the problem of the currents induced by a static, weak, magnetic field in a superconductor.

Conclusions.

(1) For A $\neq 0$ (in the London gauge), permanent currents exist in a superconductor. Unfortunately this crucial result has been obtained only after a long calculation and the physical content is obscure; it will become clearer in Chapter 6.

(2) In a pure metal ($\ell = \infty$), the range of the kernel $S_{\mu\nu}\left(r,r'\right)$ is governed by I(R) and is of the order of ξ_0. Pippard's formula assumes $I(R) = \exp\left(-R/\xi_n\right)$. The exact result (5-114) is not an exponential but only differs from it slightly. Note in particular that

$$I(0) = 1$$
$$\int_0^{\infty} I(R)dR = \xi_0 \quad \text{for } T = 0$$

which are common to the exact result and Pippard's formula.

(3) For a pure infinite metal, if $\mathbf{A}\left(\mathbf{r}'\right)$ varies slowly relative to ξ_0, we can take it outside of the integral (5-95), and integrate to obtain the London relation

$$j(r) = \frac{-ne^2}{mc}A(r) \tag{5-115}$$
$$\operatorname{curl} j = \frac{-ne^2}{cm}H$$

(4) In the presence of impurities, the kernel $S\left(r,r'\right)$ is reduced by the factor $e^{-R/\ell}$, where ℓ is the transport mean free path of the electrons in the normal state. This result was also predicted by Pippard before the development of the microscopic theory.

(5) In an impure metal, if A varies slowly with respect to $\left(\xi_0^{-1}+\ \ell^{-1}\right)^{-1}$, A can still be taken out from under the integral sign and we then obtain a new London relation, which is usually written in the form

$$\begin{aligned} -c\Lambda_0 j(r) &= A(r) \\ -c\Lambda_0 \operatorname{curl} j(r) &= H \end{aligned} \tag{5-116}$$

where

$$\Lambda_0^{-1} = \frac{ne^2}{m}\int_0^\infty \frac{dR}{\xi_0} I(R) e^{-R/\ell} < \frac{ne^2}{m} \quad (T=0) \tag{5-117}$$

In particular for $\ell \ll \xi_0$, I(R) can be taken to be unity and we find

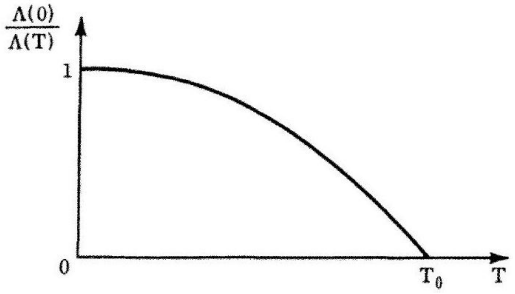


Figure 5-4
Strength of the diamagnetic response of the superconductor as a function of temperature.

$$\Lambda_0^{-1} = \frac{ne^2}{m}\left(\frac{\ell}{\xi_0}\right) \quad (\ell \ll \xi_0) \tag{5-118}$$

(6) We have limited this calculation to $T = 0$. It can be performed in the same way for $\mathrm{T} \neq 0$. The equation (5-95) still applies, but the definitions of $L\left(\xi, \xi'\right)$ must be generalized for $T \neq 0$. The integration must be performed numerically with the following results: The spatial form of the kernel $\mathrm{S}_{\mu\nu}\left(\mathbf{r}, \mathbf{r}'\right)$ is nearly independent of temperature. Its range of pure metal remains ξ_n even for $\mathrm{T} \to \mathrm{T}_0$. On the other hand, its normalization changes: The supercurrents become weaker as T increases, and finally vanish at $\mathrm{T} = \mathrm{T}_0$. This normalization is usually defined in terms of the coefficient Λ_T given by

$$\int S_{\mu\nu}\left(r, r', T\right) dr' = \frac{1}{c\Lambda_\mathrm{T}} \tag{5-119}$$

where Λ_T depends only on temperature. The temperature dependence of $\Lambda_0/\Lambda_\mathrm{T}$ is given in Fig. 5-4. We shall come back later to a discussion of parameters related to Λ_T near $\mathrm{T} = \mathrm{T}_0$ in terms of the Landau-Ginsburg equations.

REFERENCES

The self-consistent field method and the Anderson theorem:
P. W. Anderson, Proceedings of the 8th Conference on Low Temperature Physics (Toronto: University of Toronto Press, 1961).

Flux quantization and long range order in superconductors:
C. N. Yang, Rev. Mod. Phys., 34, 694 (1962).

Meissner effect: a simple approach relating the Meissner effect to the energy gap in BCS superconductors:

M. Tinkham, "Superconductivity" in Low Temperature Physics, Les Houches Lecture Notes 1961. (New York: Gordon and Breach, 1965.)

6.3 Phenomenological Landau-Ginsburg Equations

6.3.1 6-1 Introduction

Let us first recapitulate our knowledge of the microscopic behavior of a superconductor in the presence of a static magnetic field **H**. Our first method of determining the currents j induced by the field was to use the London equation

$$\operatorname{curl} j = \frac{-c}{4\pi\lambda^2(T)} H \tag{6-1}$$

However, Eq. (6-1) is applicable only when the following conditions are satisfied:
(1) $\lambda(T)$ must be much larger than $(1/\xi_0 + 1/\ell)^{-1}$, where $\xi_0 = 0.18^{\hbar} v_F/\mathrm{k}_B T_c$ and ℓ is the mean free path;
(2) H is small and can be treated as a perturbation;
(3) the superconducting electron density $n_S(r)$ is nearly constant in space.

Finally we were able to relax the first condition by replacing (6-1) by the nonlocal Pippard equation. However conditions (2) and (3) remain and we are not able to attack such problems as that of a wall separating a normal region ($H = H_C, n_S = 0$) from a superconducting region ($\mathrm{H} = 0, \mathrm{n_S}$ finite) in a Type I superconductor.

In principle, we can return to the general method:
(a) Write the equations of motion for the excitations

$$\epsilon u(r) = \frac{1}{2m}\left[\left(p - \frac{e}{c}A\right)^2 - E_F\right] u(r) + \Delta(r) v(r)$$
$$\epsilon v(r) = -\frac{1}{2m}\left[\left(p + \frac{e}{c}A\right)^2 - E_F\right] v(r) + \Delta * (r) u(r)$$

(b) Assume a spatial form of the pair potential $\Delta(r)$. (c) Calculate u and v, which give us current densities and other physical properties. (d) Verify that the form chosen for $\Delta(r)$ is correct by means of the self-consistency equation

$$\Delta(r) = \sum_n u_n v_n^* \left[1 - 2f\left(\epsilon_n\right)\right]$$

This program is, however, extremely tedious and difficult in practice.
There is considerable simplification if we restrict our attention to the neighborhood of the transition temperature T_0. For $T \to T_0$:
(1) the penetration depth $\lambda(T)$ becomes large [in the London limit $\lambda(\mathrm{T})$ is proportional to $\mathrm{n_S}^{-1/2}$ and $\mathrm{n_S}$ tends to zero as $\mathrm{T} \to \mathrm{T_0 l}$; (2) the thickness of the walls separating N and S regions also becomes large. Empirically, in a first-kind material, this depth varies roughly as $\xi_0 \lfloor \mathrm{T_0}/\left(\mathrm{T_0} - \mathrm{T}\right)]^{1/2}$ (for a pure metal).

More generally, in many physical situations the current $j(r)$ and the pair potential $\Delta(r)$ have only slow spatial variations if one is sufficiently close to the transition temperature. Under these conditions, the physical properties can be determined from more simple equations, which we now describe.

6.3.2 6-2 Construction of the Free Energy

We consider a homogeneous superconducting metal or alloy. We first form the free energy for a configuration where the pair potential $\Delta(r)$ and the vector potential $A(r)$ have arbitrary, but slowly varying, spatial forms. Then, by minimizing the energy, we obtain explicit equations for $\Delta(r)$ and for the current $j(r)$.

(a) First return to the trivial case when (1) Δ is the same at each point, and (2) there is no magnetic field. If we fix an arbitrary value for Δ, we can determine u and v and calculate, by the methods of Chapter 4, the free energy F (per cm^3) as a function of Δ. In particular, for small Δ, which is the case in the region near T_0, we find

$$\mathrm{F} = \mathrm{F_n} + \mathrm{A(T)}|\Delta|^2 + \frac{\mathrm{B(T)}}{2}|\Delta|^4 + \cdots \tag{6-2}$$

for Δ constant and zero field. Only the even terms in Δ appear in the expansion. F_n is the free energy in the normal phase; A and B are coefficients which in the BCS approximation are given by

$$\begin{aligned} A(T) &= N(0)\frac{T - T_0}{T_0} \\ B(T) &= 0.1066\frac{N(0)}{(k_B T_0)^2} \quad T \to T_0 \end{aligned} \tag{6-3}$$

More generally, we assume that the exact free energy can be represented by an expansion of the type (4-2) with the coefficients A and B having the following properties: A is negative for $T < T_0$ and vanishes at $T = T_0$, the slope $(dA/dT)T_0$ being finite. B is positive and finite at $T = T_0$ and can, in practice, be replaced by its value at T_0.

For $\mathrm{T} < \mathrm{T_0}$, the minimum of F corresponds to a nonvanishing value of Δ,

$$\begin{aligned} \Delta &= \Delta_0(\mathrm{T}) \\ \Delta_0^2 &= -\frac{\mathrm{A}}{\mathrm{B}} = 9.38\mathrm{k_B^2}\ \mathrm{T_0}\,(\mathrm{T_0} - \mathrm{T}) \end{aligned} \tag{6-4}$$

This is the value that will occur in equilibrium in the absence of a magnetic field. The corresponding free energy is

$$F = F_S = F_n - \frac{A^2}{2B} \tag{6-5}$$

Because of our assumptions about A and B, the difference $F_n - F_S = \mathrm{H_C^2}/8\pi$ is proportional to $(\mathrm{T_0} - \mathrm{T})^2$. This is characteristic of all sec-ond-order transitions.

(b) We now allow Δ to have a slow variation from point to point, however, still keeping $\mathbf{H} = \mathbf{A} = 0$. How will the free energy (6-2) be modified? Since in the absence of a magnetic field equilibrium corresponds to $\Delta = \text{const}$, the first significant terms will be of the form $(\partial\Delta/\partial x)^2$ or $(\partial\Delta/\partial x)(\partial\Delta/\partial y)$, and so on. For simplification, from now on we only consider cubic crystals. Then,

$$\mathrm{F} = \mathrm{F_n} + \mathrm{A}|\Delta|^2 + \frac{\mathrm{B}}{2}|\Delta|^4 + \mathrm{C}\left[\left|\frac{\partial\Delta}{\partial \mathrm{x}}\right|^2 + \left|\frac{\partial\Delta}{\partial \mathrm{y}}\right|^2 + \left|\frac{\partial\Delta}{\partial \mathrm{z}}\right|^2\right] \tag{(6-6)}$$

We take C to be nonzero and positive for $\mathrm{T} = \mathrm{T_0}$. In fact, a microscopic calculation will show later that for a pure metal $\mathrm{C} \sim \mathrm{N}(0)\xi_0^2$, that is, the "torsion energy" represented by the last term in (6-6) is of the order $N(0)\Delta^2\xi_0^2[(1/\Delta)(\partial\Delta/\partial x)]^2$.

The relation (6-6) between the free energy F and the order parameter Δ in the neighborhood of the transition temperature has been assumed as a starting point by Landau for a general theory of second-order phase transitions. (In a ferromagnet, for instance, the order parameter is the magnetization. [1])

Problem.

Calculate the fluctuation in the pair potential Δ in the normal phase ($T > T_0$), in zero field.

Solution.

The probability of finding a configuration where the pair potential has a determined spatial form $\Delta(r)$ is proportional to $\exp(-\mathfrak{J}/\mathrm{k_B T})$, where $\mathfrak{J}$ is the free energy of the sample calculated from (6-6). For $T > T_0$, it suffices to keep only the terms of order of Δ^2 in (6-6). In the gauge where $A = 0$ and Δ is real, we have

$$\mathcal{F} = \int \mathrm{dr}\left[A|\Delta(r)|^2 + C|\nabla\Delta(r)|^2\right] = L^3 \sum_k |\Delta_k|^2 \left(A + Ck^2\right)$$

where

$$\Delta_\mathrm{k} = \mathrm{L}^{-3} \int \mathrm{dre}^{\mathrm{ikr}}\Delta(\mathrm{r})$$

and L^3 is the volume of the sample. (As we shall see later, this equation is valid, in a pure superconductor, when $\xi_0 k \ll 1$.) One then finds the thermal averages

$$\langle\Delta_k\rangle = 0$$
$$\left\langle|\Delta_k|^2\right\rangle = \frac{\int \exp\left(-\mathfrak{F}/k_B T\right)|\Delta_k|^2\, d\Delta_k}{\int \exp\left(-\mathfrak{F}/k_B T\right) d\Delta_k} = \frac{1}{2L^3}\frac{k_B T}{A + Ck^2}$$

(??? check the calculations!!!)

On the other hand $\left\langle|\Delta_\mathrm{K}|^2\right\rangle$ is related to the spatial correlation function of Δ:

$$\left\langle|\Delta_\mathrm{k}|^2\right\rangle = \mathrm{L}^{-6}\int \mathrm{d}\mathbf{r}\ \mathrm{d}\mathbf{r}'\left\langle\Delta(\mathbf{r}\rangle\Delta\left(\mathbf{r}'\right)\right\rangle \mathrm{e}^{\mathrm{ik}\cdot(\mathbf{r}-\mathbf{r}')}$$
$$= \mathrm{L}^{-3}\int \mathrm{dR}\langle\Delta(0)\Delta(\mathrm{R})\rangle \mathrm{e}^{\mathrm{ik}\cdot\mathrm{R}}$$

[$\langle\Delta(\mathbf{r})\Delta\left(\mathbf{r}'\right)\rangle$ only depends on $\mathbf{r} - \mathbf{r}'$.] On taking the inverse of this expression we find the correlation function

$$\langle\Delta(0)\Delta(R)\rangle = \frac{1}{(2\pi)^3}\int dk \frac{k_B T}{2\left(A + Ck^2\right)} e^{-ik\cdot R} = \frac{k_B T}{8\pi C R} e^{-qR}$$

where $q^2 = A/C, q > 0$. For a pure metal, ($C \sim N(0)\xi_0^2$):

$$\frac{\langle\Delta(0)\Delta(R)\rangle}{\left(k_B T_0\right)^2} \sim \frac{k_B T}{E_F}\frac{1}{k_F R} e^{-qR}$$

which is very small. Thus short-range order effects are indeed negligible in most superconductors.

(c) Eq. (6-6) must be completed by adding a vector potential $\mathbf{A}$, which gives rise to the field $h = \mathrm{curl}\ A$. The free energy must be independent of the gauge chosen for A. (If we set $A' = A + \nabla\chi$, the magnetic field derived from A' is the same as that derived from A. If H is

[1] For magnetic materials, recent experiments and theoretical calculations indicate that the Landau hypothesis on the analytic form of F is, in fact, too restrictive; the real situation is more complicated. However, in superconductors, (6-6) is excellent. The complications encountered in the magnetic case stem from short-range order effects. These effects are large in magnetic materials, but are very small in superconductors (see problem above).

unchanged, the free energy F must also be unchanged.) As we have seen in Chapter 5, the pair potential does change according to the law

$$\Delta'(r) = \Delta(r)e^{2ie\chi(r)/hc}$$

Thus in order to insure the invariance of F, we must replace (6-6) by

$$\mathrm{F} = \mathrm{F_n} + \mathrm{A}|\Delta|^2 + \frac{\mathrm{B}}{2}|\Delta|^4 + \mathrm{C}\left|\left(-\mathrm{i}\nabla - \frac{2\mathrm{eA}}{\hbar c}\right)\Delta\right|^2 + \frac{\mathrm{h}^2}{8\pi} \tag{6-7}$$

(The last term $h^2/8\pi$ represents the magnetic field energy in the vacuum.) There is a formal analogy between the terms of order $|\Delta|^2$ in (6-7) and the equation giving the energy density of a particle of charge 2 e described by a wave function $\psi(\mathbf{r})$. More precisely, if we set

$$\begin{aligned} &\psi(r) = \frac{(2mC)^{1/2}}{\hbar}\Delta(r), \quad \alpha = \frac{\hbar^2}{2m}\frac{A}{C}, \quad \beta = \left(\frac{\hbar^2}{2m}\right)^2\frac{B}{C^2} \\ &\frac{\alpha^2}{2\beta} = \frac{H_C^2}{8\pi} \end{aligned} \tag{6-8}$$

Then

$$\mathrm{F} = \mathrm{F_n} + \alpha|\psi|^2 + \frac{\beta}{2}|\psi|^4 + \frac{1}{2m}\left|\left(-\mathrm{ih}\nabla - \frac{2\mathrm{eA}}{\mathrm{c}}\right)\psi\right|^2 + \frac{\mathrm{h}^2}{8\pi} \tag{6-9}$$

This is the free energy form proposed by Landau and Ginsburg in 1951 well before the development of the microscopic theory. At that time the physical significance of $\psi(\mathbf{r})$ was far from being clear; furthermore, the value e^* of the charge that appears in $-i\hbar\nabla - e^*A/c$ was not known (initially Landau and Ginsburg took $e^* = e$). This construction of (6-9) independent of any detailed theory of the superconducting state represented a tour de force of physical intuition.

Notice that the choice of the free electron mass m as a factor in (6-8) and (6-9) is entirely arbitrary. We could just as well have chosen the mass of the sun. [2]. So there is no way for theoretical physicist to construct this constant from microscopic theory (??? right???).

On the contrary, the presence of the charge 2 e in the factor 2eA/c is not a convention, but expresses a fundamental property of the pair potential: $\Delta = V\langle\psi t(r)\psi t(r)\rangle$ is the average of the product of two annihilation operators.

6.3.3 6-3 Equilibrium Equations

We must now minimize the free energy with respect to: (1) the order parameter $\Delta(r)$; and (2) the magnetic field distribution, therefore $A(r)$. We set $\mathfrak{F} = \int \mathrm{F}d\mathrm{r}$ where the integral is extended over the volume of the specimen. If we vary $\psi(\mathbf{r})$ by $\delta\psi(\mathbf{r})$ and $\mathbf{A}(\mathbf{r})$ by $\delta\mathbf{A}(\mathbf{r})$, we obtain the variation in the free energy which after an integration by parts becomes

$$\begin{aligned} \delta\mathcal{F} = &\int d\mathbf{r}\left\{\delta\psi^*\left[\alpha\psi + \beta|\psi|^2\psi + \frac{1}{2m}\left(-\mathrm{i}\hbar\nabla - \frac{2\mathrm{eA}}{\mathrm{c}}\right)^2\psi\right] + \text{ C.C. }\right\} \\ &+ \int \mathrm{d}\mathrm{r}\delta\ \mathrm{A}\cdot\left\{\frac{1}{4\pi}\,\mathrm{curl}\ \mathrm{h} - \frac{\mathrm{e}}{\mathrm{mc}}\left[\psi^*\left(-\mathrm{i}\hbar\nabla - \frac{2\mathrm{e}}{\mathrm{c}}\ \mathrm{A}\right)\psi + \text{ C.C. }\right]\right\} \end{aligned} \tag{6-10}$$

In the second term, notice that $(1/4\pi)$ curl h is the current density j/c from Maxwell's equations. By setting $\delta\mathfrak{F} = 0$, we obtain the conditions

$$\alpha\psi + \beta|\psi|^2\psi + \frac{1}{2m}\left(-i\hbar\nabla - \frac{2eA}{c}\right)^2\psi = 0 \tag{6-11}$$

$$j = \frac{e\hbar}{im}\left(\psi^*\nabla\psi - \psi\nabla\psi^*\right) - \frac{4e^2}{mc}\psi^*\psi\mathbf{A} \tag{6-12}$$

Equations (6-11) and (6-12) are the fundamental Landau-Ginsburg equations. The first gives the order parameter and the second gives the currents, that is, the diamagnetic response of a superconductor.

Remarks.

(1) The relation (6-12) giving the current is identical to that which would occur for particles of charge $2e$, mass m, and wavefunction $\psi(r)$.

(2) Boundary condition: In deriving (6-10) we neglected the surface integral

$$\int \delta\psi^*\left(-i\hbar\nabla - \frac{2eA}{c}\right)\psi\frac{i\hbar}{2m}\cdot d\sigma + C.C.$$

If we keep this term and require that it vanishes, we obtain the boundary condition

$$\left(-i\hbar\nabla - \frac{2eA}{c}\right)_n\psi = 0 \tag{6-13}$$

where the subscript n designates the component normal to the surface. This procedure was followed by Landau and Ginsburg in their original paper. It implicitly assumes that the form (6-9) for the free energy remains valid even in the neighborhood of a surface. We shall see, in fact, from the microscope theory that for a superconductor-insulator interface (6-13) is correct, but that for a superconductor-normal metal junction the boundary condition is severely modified.

On substituting (6-13) into the equation (6-12) for the current, we see that $j_n = 0$; that is, there is no current entering or leaving the superconductor. If we do the inverse, and impose $j_n = 0$, we do not obtain (6-13), but only

$$\left(-i\hbar\nabla - \frac{2eA}{c}\right)_n\psi = i\lambda\psi$$

where λ is an arbitrary real constant. In practice, this is the type of boundary condition encountered for a superconductor-normal metal junction.

6.3.4 6-4 The Two Characteristic Lengths

The Landau-Ginsburg equations (6-11) and (6-12) introduce two characteristic lengths, which we now discuss.

[2] Some authors do in fact use 2 m instead of m . Our normalization follows the original paper of Landau and Ginsburg.

First characteristic length

(a) First consider a situation where there are neither currents nor magnetic fields. Choose the gauge in which ψ is real. Then in one dimension, for example, (6-11) becomes simply

$$\frac{-\hbar^2}{2m}\frac{d^2\psi}{dx^2} + \alpha\psi + \beta\psi^3 = 0 \tag{6-14}$$

There are two obvious solutions: (1) $\psi = 0$ which describes the normal state, (2) $\psi = \psi_0$ with

$$\psi_0^2 = -\frac{\alpha}{\beta} > 0 \tag{6-15}$$

which describes the usual superconducting state. This second solution exists and is lower in energy when $\alpha < 0$, that is, $\mathrm{T} < \mathrm{T}_0$. However we would like to consider more general solutions. For example, if,
by means of exterior constraints, we impose that $\psi(x)$ have a different value than ψ_0 at one point, how does the order parameter deform about this point?

In order to fix the length scale, it is useful to write (6-14) in terms of reduced variables

$$\psi = \psi_0 \mathrm{f} \tag{6-16}$$

$$\frac{\hbar^2}{2m|\alpha|} = \xi^2(\mathrm{T}) \tag{6-17}$$

where $\xi(T)$ has the dimensions of a length. Equation (6-14) becomes

$$-\xi^2(\mathrm{T})\frac{\mathrm{d}^2\mathrm{f}}{\mathrm{dx}^2} - \mathrm{f} + \mathrm{f}^3 = 0 \tag{6-18}$$

The natural unit of length for the variation of f is $\xi(\mathrm{T})$, which we call the coherence length at the temperature T. What is its order of magnitude? First notice that $\hbar^2/2m|\alpha| = -\mathrm{C}/\mathrm{A}$ from (6-8). For a pure material we have already mentioned that $\mathrm{A} \simeq \lfloor(\mathrm{T} - \mathrm{T}_0)/\mathrm{T}_0\rfloor\,\mathrm{N}(0)$ and $\mathrm{C} \sim \mathrm{N}(0)\xi_0^2$; thus

$$\xi(\mathrm{T}) = 0.74\xi_0\left(\frac{\mathrm{T}_0}{\mathrm{T}_0 - \mathrm{T}}\right)^{1/2} \tag{6-19}$$

(where we have inserted the exact numerical coefficient).
Conclusion: The variations in ψ, which take place within the length $\xi(\mathrm{T})$, are slow with respect to ξ_0 if T is close to T_0.

Problem.

From (6-18) calculate the energy of a NS wall in a Type I superconductor where the penetration depth is negligible. The field distribution and $|\psi|$ are represented in Fig. 6-1.

Solution.

By hypothesis, the field does not penetrate into the region where ψ is nonzero. We can therefore use (6-18) with the boundary conditions

$$\begin{aligned} f &= 0, \quad x = 0 \\ f &\to 1, \quad x \to \infty \end{aligned}$$

By multiplying (6-18) by df/dx and integrating, we obtain the first integral

$$-\xi^2(T)\left(\frac{df}{dx}\right)^2 - f^2 + \frac{1}{2}f^4 = \text{ const}$$

In order to satisfy the boundary condition as $x \to \infty$, we must take the constant to be equal to $-\frac{1}{2}$. This gives

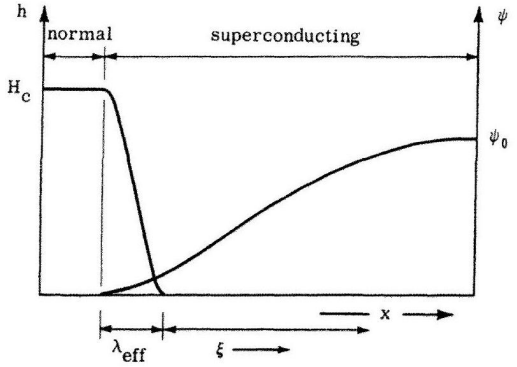


Figure 6-1
Spatial variation of the field and order parameter near a N-S wall for $\xi(T) \gg \lambda(T)$. The effective penetration depth λ_{eff} is of order $\sqrt{\lambda\xi}$ (see problem, page 178).

$$\xi^2(\mathrm{T})\left(\frac{\mathrm{df}}{\mathrm{dx}}\right)^2 = \frac{1}{2}\left(1-\mathrm{f}^2\right)^2$$

The solution satisfying our boundary conditions is

$$f = \tanh\left[\frac{x}{\sqrt{2}\xi(T)}\right]$$

Energy per unit area of the wall:

$$F_p = \int_0^\infty dx \frac{\hbar^2}{2m}|\nabla\psi|^2 + \alpha|\psi|^2 + \frac{\beta}{2}|\psi|^4$$

The surface energy $(\mathrm{H_c^2}/8\pi)\,\delta$ is the difference between $\mathrm{F_p}$ and the condensation energy, which we would find if the medium were uniformly superconducting from the point $x = 0$:

$$\frac{\mathrm{H_c^2}}{8\pi}\delta = \mathrm{F_p} - \int_0^\infty \left(-\frac{\mathrm{H_c^2}}{8\pi}\right)\mathrm{dx}$$

Inserting the reduced parameter f and the relations (6-8), we obtain

$$\delta = \int_0^\infty \mathrm{dx}\left[2\xi^2(\mathrm{T})\left(\frac{\mathrm{df}}{\mathrm{dx}}\right)^2 + \left(1-\mathrm{f}^2\right)^2\right]$$

By making use of the first integral for $\mathrm{df/dx}, \delta$ can be transformed into

$$\delta = 2\int_0^\infty dx\left(1-f^2\right)^2 = 2\int_0^1 \left(1-f^2\right)^2 \frac{dx}{df}df = 2\sqrt{2}\xi(T)\int_0^1 df\left(1-f^2\right) = \frac{4}{3}\sqrt{2}\xi(T) = 1.89\xi(T)$$

Second characteristic length

(b) A second characteristic length comes into play if we introduce electromagnetic effects - for example, the penetration depth in weak fields. In order to define this length, we consider a superconductor occupying the half-space $z > 0$. The region $z < 0$ is either empty or filled with an insulator where the boundary condition (6-13) applies.

In weak fields, and to first order in h. $|\psi|^2$ in the region z > 0 can be replaced by its equilibrium value in the absence of a field $|\psi_0|^2$ defined by (6-15). Because ψ_n is independent of position, when we take the curl of both sides of (6-12), we obtain a London-type equation:

$$\operatorname{curl} j = -\frac{4e^2}{mc}\psi_0^2 h \tag{6-20}$$

On adding Maxwell's equations, we find, as in Chapter 2, nonvanishing solutions only if h is in the xy plane; for example, taking h along the x axis.

$$h_x = h_x(0)e^{-z/\lambda(T)} \tag{6-21}$$

$$\lambda(T)^{-2} = \frac{16\pi e^2\psi_0^2}{mc^2} = \frac{32\pi e^2}{\hbar^2 c^2} C\Delta_0^2 \tag{6-22}$$

where Δ_0 is the equilibrium value of the pair potential. Equation $\frac{32\pi e^2}{\hbar^2 c^2} C\Delta_0^2$ allows C to be related to directly measurable quantities. [3] Note that $\lambda(T)$ is proportional to ψ_0^{-1} and therefore to $[T_0/(T_0 - T)]^{1/2}$. For a pure metal in the free electron approximation, the microscopic calculation in the BCS approximation gives

$$\lambda(T) = \frac{1}{\sqrt{2}}\lambda_L(0)\left(\frac{T_0}{T_0 - T}\right)^{1/2} \quad T - T_0 \tag{6-23}$$

where $\lambda_L(0)$ is the London penetration depth at absolute 0, given in terms of the number of electrons per cm^3n by the equation $\lambda_L{}^2(0) = 4\pi ne^2/mc^2$. Except for the numerical coefficient, (6-23) can be predicted from (6-22) if we guess (as stated earlier) that $C \sim N(0)\xi_n^2$ and that

$$\Delta_0^2 \sim k_B^2\, T_0\,(T_0 - T)$$

Conclusions.

The Landau-Ginsburg hypothesis, in particular the form of the free energy (6-7) in the presence of a field, has led us to a local relation (6-12) between the current and vector potential. We know from the microscopic analysis of Chapter 5 that in the special case where $|\Delta|$ is constant and h small, the exact relation is nonlocal; that is, the current density $j(r)$ depends on $A(r')$ for $|r - r'| \leq \xi_0$ in a pure metal. In order for the local approximation to be valid, it is necessary that A or the current have a slow variation on the scale of ξ_0, therefore, $\lambda(T) \gg \xi_0$,

$$\lambda_L{}^{(0)}\left(\frac{T_0}{T_0 - T}\right)^{1/2} \gg \xi_0 \tag{6-24}$$

For a pure metal, this condition will be satisfied if T is sufficiently close to T_0. [However, for certain nontransition metals, notably aluminum, $\lambda_L(0)$ is so much smaller than ξ_0 that the temperature interval allowed by (6-24) is very small.]

(c) We have defined two characteristic lengths $\xi(T)$ and $\lambda(T)$, which determine the behavior of a superconductor near the transition point. They both diverge as $(T_0 - T)^{-1/2}$ as $T \to T_0$. It is therefore particularly interesting to form their ratio

[3] Note that for a noncubic crystal it is necessary to take into account the tensorial nature of C.

$$\kappa = \frac{\lambda(\mathrm{T})}{\xi(\mathrm{T})} \tag{6-25}$$

By using the definitions (6-17) and $\lambda(T)^{-2} = \frac{16\pi e^2\psi_0^2}{mc^2}$ of $\xi(\mathrm{T})$ and $\lambda(\mathrm{T})$, one obtains

$$\kappa = \frac{\mathrm{mc}}{2\mathrm{e}\hbar}\left(\frac{\beta}{2\pi}\right)^{1/2} = \frac{\hbar\mathrm{c}}{4\mathrm{Ce}}\left(\frac{\mathrm{B}}{2\pi}\right)^{1/2} \tag{6-26}$$

κ is called the Landau-Ginsburg parameter of the substance. When $\kappa \lesssim 1 (\lambda < \xi)$, the material is of the first kind, when $\kappa > 1 (\lambda > \xi)$, material is of the second kind. We see later that the exact separation between the two types of behavior occurs for $\kappa = 1/\sqrt{2}$. For a pure substance we show later that

$$\kappa = 0.96\frac{\lambda_{\mathrm{L}}(0)}{\xi_0} \tag{6-27}$$

It is interesting to notice that κ can be defined directly from experimentally obtained numbers on the penetration depth and thermodynamic field $\mathrm{H_c}$ measured in the region of validity of the Landau-Ginsburg equations. By making use of $\lambda(T)^{-2} = \frac{16\pi e^2\psi_0^2}{mc^2}$, (6-15), (6-9), and (6-8), one can put (6-26) in the form

$$\kappa = 2\sqrt{2}\frac{\mathrm{e}}{\hbar\mathrm{c}}\mathrm{H_C}(\mathrm{T})\lambda^2(\mathrm{T}) \tag{6-28}$$

Another way of writing (6-28), often useful for numerical calculations, is the following

$$\mathrm{H_c}(\mathrm{T}) = \frac{\phi_0}{2\pi\sqrt{2}\xi(\mathrm{T})\lambda(\mathrm{T})} \tag{6-29}$$

where $\phi_0 = \mathrm{ch}/2\mathrm{e}$ is the flux quantum.
In this chapter we also study other methods that allow the determination of κ.

6.3.5 6-5 Situations Where $|\psi|$ Is Constant

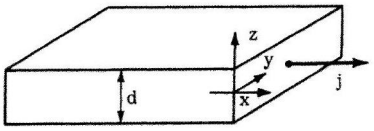
We now apply the Landau-Ginsburg equations to some concrete examples. First, consider the particularly simple cases where the amplitude $|\psi|$ of the order parameter is the same at all points. Such a situation has already been encountered (the penetration depth of a weak magnetic field in a bulk sample). The examples we now consider are rather different. They concern thin samples (films, wires, and so on) where ψ cannot vary through the depth without catastrophically increasing the term $|\nabla\psi|^2$ in the free energy. But allow the field h (or currents j) to be strong and $|\ \psi\ |$, though constant, will not necessarily be equal to its unperturbed value ψ_0.

Critical Current in a Thin Film

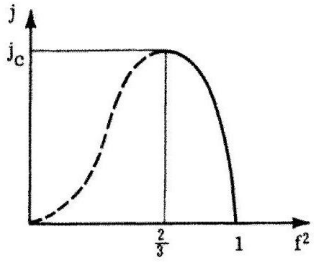
The situation envisaged is that represented in Fig. 6-2a. The film of thickness d carries a current density f along the x axis. We assume that

$$\begin{aligned} \mathrm{d} &\ll \xi(\mathrm{T}) \quad \text{in order to have } |\psi| \text{ constant } [4] \\ \mathrm{d} &\ll \lambda(\mathrm{T}) \quad \text{in order to have } j \text{ constant} \end{aligned}$$

Then our equations become particularly simple. If we set $\psi = |\psi|e^{i\phi(r)}$ where $|\psi|$ is independent of r, the current becomes



(a)



(b)

Figure 6-2
(a) Geometry to measure the critical current of a thin film (thickness d). The current flows along the x axis. (b) Current density (normalized to the critical current density) as a function of the order parameter f (normalized to the order parameter in zero current). For $j > j_c$, there is no solution to (6-35) and f falls abruptly to zero.

$$\mathrm{j} = \frac{2\mathrm{e}}{m}|\psi|^2\left(\hbar\frac{\partial\phi}{\partial \mathrm{x}} - \frac{2\mathrm{e}}{\mathrm{c}}\,\mathrm{A_x}\right) = 2\mathrm{e}|\psi|^2\mathrm{v} \tag{6-30}$$

$$\mathrm{v} = \frac{1}{m}\left(\hbar\frac{\partial\phi}{\partial \mathrm{x}} - \frac{2\mathrm{e}}{\mathrm{c}}\,\mathrm{A_x}\right) \tag{6-31}$$

where v is the velocity of the "particles" described by the wave function ψ. The free energy (6-9) is simply

$$\mathrm{F} = \mathrm{F_n} + |\psi|^2\left[\alpha + \frac{\beta}{2}|\psi|^2 + \frac{1}{2}\mathrm{mv}^2\right] + \frac{\mathrm{h}^2}{8\pi} \tag{6-32}$$

and contains a term with the form of a kinetic energy. The minimum of F with respect to $|\psi|$ is obtained for

$$\alpha + \beta|\psi|^2 + \frac{1}{2}mv^2 = 0 \tag{6-33}$$

If we set, as usual, $|\psi| = \psi_0 \mathrm{f}$ with $\psi_0^2 = -\alpha/\beta$ and eliminate v between (6-30) and (6-33), we find

$$j = 2e\psi_0^2\left(\frac{2|\alpha|}{m}\right)^{1/2} f^2\left(1-f^2\right)^{1/2} \tag{6-34}$$

$$= 2e\psi_0^2\left(\frac{\hbar}{m\xi(T)}\right) f^2\left(1-f^2\right)^{1/2} \tag{6-35}$$

The relation between f and j is represented in Fig. 6-2b. For $j = 0$, $f = 1$. As j increases, f decreases. Finally when j becomes larger than $\mathrm{j_c}$ given by

$$\mathrm{j_c} = \frac{4\mathrm{e}\psi_0^2}{3\sqrt{3}}\frac{\hbar}{m\xi(\mathrm{T})} \tag{6-36}$$

[4] It is easy to verify that $|\psi|$ = constant is compatible with the boundary condition (6-13).

there do not exist any solutions with $f \neq 0$. Thus for $j > j_c$ the film becomes normal and f changes abruptly from 0.8 to 0 . The current $\mathrm{j_c}$ is the critical current of the film. It is given in (6-36) as a function of ψ_0^2 and $\xi(\mathrm{T})$, that is, as a function of the Landau-Ginsburg parameters α and β. In order to determine its order of magnitude, it is interesting to rewrite j_c in terms of the velocity v_c. When $j = j_c$, the velocity is $\mathrm{v_c} \sim \mathrm{h}/m\xi(\mathrm{T})$. For a pure metal

$$\xi(T) \sim \xi_0 \left(\frac{T_0}{T_0 - T}\right)^{1/2} \sim \frac{\hbar v_F}{k_B T_0} \left(\frac{T_0}{T_0 - T}\right)^{1/2} \sim \frac{\hbar v_F}{\Delta_0(T)} \tag{6-37}$$

and consequently

$$\mathrm{v_c} \sim \frac{\Delta_0(\mathrm{T})}{\mathrm{m v_F}} \tag{6-38}$$

It is also interesting to compare (6-38) to the maximum velocities associated with the currents giving rise to the Meissner effect in bulk superconductors. If H is an applied field, then the current near the surface is $\sim \mathrm{cH}/\lambda$, where λ is the penetration depth. If one is sufficiently close to T_0, λ is correctly given by $\lambda(T)^{-2} = \frac{16\pi e^2 \psi_0^2}{mc^2}$; the velocity v near the surface becomes

$$\mathrm{v} \sim \frac{\mathrm{j}}{2\mathrm{e}\psi_0^2} \sim \frac{\mathrm{cH}}{2\lambda \mathrm{e} \psi_0^2} \tag{6-39}$$

In a first kind superconductor, the maximum field is $\mathrm{H_c} = (4\pi/\beta)^{1/2}|\alpha|$ which, by using the definition (6-25, 6-26) of κ, becomes

$$\mathrm{v} \sim \frac{\kappa\hbar}{m\lambda} \sim \frac{\hbar}{m\xi(\mathrm{T})}$$

Thus the order of magnitude is the same as (6-38). In a type 2 superconductor, the maximum field for which there is a complete Meissner effect is $H_{C_1} \sim H_C/\kappa$ and $v \sim \hbar/m\lambda(T) \ll \hbar/m\xi(T)$. The supercurrents are less stable because of the possible formation of vortex lines.

The critical velocity is proportional to $(T_0 - T)^{1/2}$ and the critical current varies as $\mathrm{v_C}\psi_0^2$ and thus as $(\mathrm{T_0} - \mathrm{T})^{3/2}$.

Experimentally, the measurement of $\mathrm{j_c}$ is very delicate. (a) It is necessary to control the magnetic field distribution by shielding the film with other superconducting foils. (b) In practice, the transition appears at a "hot point" and then the remainder of the film becomes normal by a purely thermal effect. The situation is improved by using supports that are good thermal conductors and operating in a pulsed regime. (c) The transition as determined by a current-voltage diagram is not abrupt, but continuous.

At any rate, certain careful experiments (Newhouse and Bremer) on thin tin films [$\xi_0 \sim 2300$Å, d ~ 3000Å, $\mathrm{T_0} - \mathrm{T} \sim 3 \times 10^{-2}$ K, $\lambda_\mathrm{L}(\mathrm{T}) \sim$ d, $\xi(\mathrm{T}) \gg$ d] seem to be in agreement with theory. Typically $\mathrm{j_c} \sim 10^4$ A/cm^2 in this temperature region. The variation of $|\psi|$ or $|\Delta|$ with current could, in principle, be followed by a tunneling measurement of the gap. (Detailed calculations show that, for the present geometry, the gap in the excitation spectrum is nearly equal to $|\Delta|$.)

There are two precautions that must be taken in the discussion of critical current experiments:

(1) When $\lambda(T) \sim d$, it is necessary to take account of the variation of the current density through the thickness of the film. This calculation is feasible because in the region of validity of the Landau-Ginsburg equations when $|\psi|$ is constant in space, the current j obeys a simple London equation.

(2) When d $< \xi$(T = 0) in addition to d $< \xi$(T), the bulk Landau-Ginsburg equations no longer apply (see problem, page 225).

The Experiment of Little and Parks

Consider now a superconducting film deposited on a cylindrical insulating support of radius R as is shown in Fig. 6-3. The film has a thickness $d \ll R(d \sim 300 - 1000\text{Å})$. A uniform magnetic field H (typically several tens of gauss) is applied along the axis of the cylinder. How does the transition temperature vary with H?

We shall calculate it by a method due to Tinkham (1962) based on the Landau-Ginsburg equations. We still assume that $d \ll \xi(T)$ and $d \ll \lambda(T)$ and we take $|\psi|$ to be constant in the film. As usual we set $\psi = |\psi|e^{i\theta(r)}$ and the free energy is still given by (6-32).

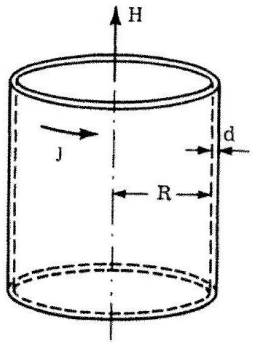


Figure 6-3
Experimental geometry for the Little-Parks experiment. One measures the critical temperature of a thin film (thickness d) deposited on a cylinder (radius $R \gg$ d) in an axial field H .

If the cylinder does not carry a current along its axis, v will be a tangential vector of constant length. How is **v** determined? In the preceding case, the current at the boundaries of the film was fixed and v was determined from the current density by $\mathbf{v} = \text{j}/2\text{e}|\psi|^2$. Here we fix the exterior magnetic field H. In order to relate it to v we study the velocity circulation $\oint \mathbf{v} \cdot \text{d}\boldsymbol{\ell}$ around the cylinder. The contour of integration will be a circle of radius R and the circulation becomes

$$\oint v \cdot d\ell = 2\pi Rv = \frac{\hbar}{m}[\theta] - \frac{2e}{mc}\oint A \cdot d\ell \tag{6-40}$$

[θ] represents the change in phase after a complete revolution about the cylinder. $\psi(r)$, proportional to the self-consistent field $\Delta(r)$, must be a single-valued function as explained in Chapter 5. Therefore $[\theta] = 2\pi\text{n}$, where n is an arbitrary integer. The second term in (6-40) is proportional to

$$\oint \text{A} \cdot \text{ d}\boldsymbol{l} = \int \text{H} \cdot \text{ d}\sigma = \phi = \pi\text{R}^2\text{H} \tag{6-41}$$

which represents the flux contained in the interior of the cylinder. Finally,

$$\text{v} = \frac{\hbar}{\text{mR}}\left[\text{n} - \frac{\phi}{\phi_0}\right] \tag{6-42}$$

where $\phi_0 = \text{hc}/2\text{e}$ is the quantum of flux.
For H fixed, ϕ is fixed, but v can take on an infinity of discrete values from (6-42). However, we see from (6-32) that the free energy will be minimized by choosing the integer n in (6-42) such that $|v|$ is minimum.

$$v = \min\left\{\frac{\hbar}{mR}\left|n - \frac{\phi}{\phi_0}\right|\right\} \tag{6-43}$$

Thus v is a periodic function of H with period $\phi_0/\pi R^2$. For $R = 7 \times 10^3 \text{Å}$, $\phi_0/\pi R^2 \cong 14\text{G}$. Since v is known, we can minimize the free energy with respect to $|\psi|$ and find

$$|\psi|^2 = \left(-\alpha - \frac{mv^2}{2}\right)\beta^{-1} \tag{6-44}$$

This solution exists when $-\alpha > \frac{1}{2}mv^2$. The transition point T_H therefore corresponds to $-\alpha\,(\mathrm{T_H}) = \frac{1}{2}\mathrm{mv}^2$ and $\mathrm{T_H}$ is also a periodic function of H . Since $\alpha(\mathrm{T}) \sim (\mathrm{T} - \mathrm{T_0})$, we see finally that the theoretical curve $\mathrm{T_H}$ is a series of arcs of parabolas. The maximum displacement of the transition point corresponds to

$$\begin{aligned} v &= \frac{\hbar}{2mR} \\ -\alpha\,(T_H) &= \frac{\hbar^2}{2m\xi^2\,(T_H)} = \frac{1}{2}m\left(\frac{\hbar}{2mR}\right)^2 \\ \xi\,(T_H) &= 2R \end{aligned} \tag{6-45}$$

For a pure substance film (for $\mathrm{d} > \xi_0$), we already have the relation $\xi(T) = 0.74\xi_0\,[T_0/\,(T_0 - T)]^{1/2}$, which gives

$$(\mathrm{T_0} - \mathrm{T_H})_{\max} = 0.55\ \mathrm{T_0}\left(\frac{\xi_0}{2\mathrm{R}}\right)^2 \tag{6-46}$$

Remarks

(1) Equation(6-45) shows that the conditions $\mathrm{d} \ll \xi(\mathrm{T})$ and $\mathrm{d} \ll \lambda(\mathrm{T})$ will be satisfied in practice if

$$\mathrm{d} \ll 2\mathrm{R} \qquad \mathrm{d} \ll 2\mathrm{R}\kappa$$

(2) One often uses films for which $\mathrm{d} < \xi_0$. In this case, (6-46) is modified to $(T_0 - T_H) \sim T_0\,[\xi_0 d/(2R)^2]$. We see the justification for this formula later (problem, page 225). The effects we are describing were discovered by Little and Parks (1961) on tin films. In order to have a measurable displacement $T_0 - T_H$, it is evidently necessary to have a small R. As we have already mentioned, R is typically of the order of 0.7μ (the support is a thin plastic fiber) and $\mathrm{d} \sim 350\text{Å}$. The resistance is measured along the axis of the cylinder with as small a current as possible.

(3) In zero field, the relation $\mathrm{R(H} = 0,\ \mathrm{T})$ between resistance and temperature has the form represented in Fig. 6-4a. The transition is spread over $0.05°\mathrm{K}$.

(4) A temperature T^* is chosen in the transition region and the resistance $R\,(H, T^*)$ is measured as a function of field. The result is the curve in Fig. $6-4$ b, which displays the oscillation with a period of 14 G for $\mathrm{R} = 0.7\mu$. The experiment therefore gives a direct determination of the quantum of flux ϕ_0. On the contrary, the amplitude of the oscillations in $R(H)$ is not well understood. The dissipation mechanisms that take place in the transition zone are not fully elucidated. (In particular, in the presence of a field H, the curve R(T) is not only shifted along the temperature axis, but also deformed.]

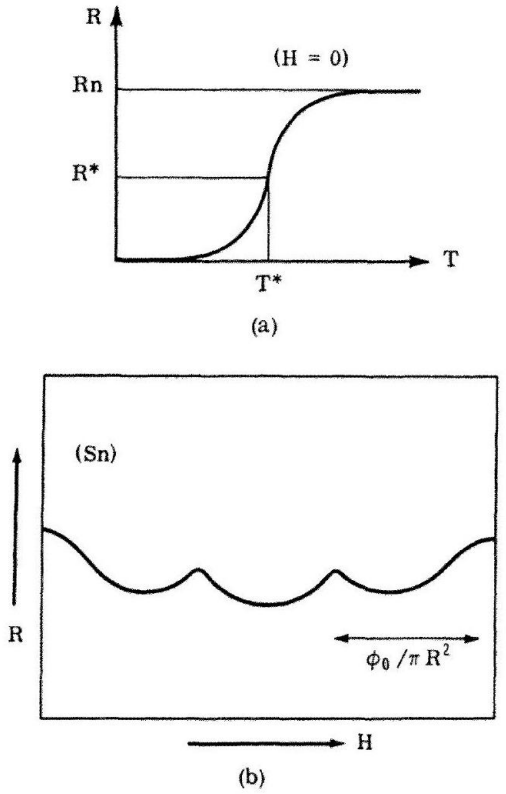


Figure 6-4
(a) Resistance of the film in Fig. 6-3 in zero field as a function of temperature. A temperature is chosen in the transition region (T*). (b) The "quantum scallop." At a fixed temperature T^* (close to T_0), the resistance $R(H)$ oscillates as a function of field. One period corresponds to one quantum of flux in the cylinder $\Delta H = \phi_0/\pi R^2$. [After Little and Parks, Phys. Rev., 133A, 97 (1964).] The parabolic "background" is probably due to a slight misorientation of the field with respect to the axis of the cylinder.

In Fig. 6-4b, there is a continuous increase proportional to H^2 superimposed on the oscillations, which is related to the diamagnetism of the sample. In the preceding calculation we have assumed that H is parallel to the axis of the cylinder and $d \ll \lambda(T)$. Under these conditions, h does not vary through the thickness of the film, and the lines of the force are nearly undisplaced when the sample undergoes the superconducting transition-the diamagnetism is negligible. This is not the case if H is not perfectly aligned along the axis of the cylinder. Then, in the superconducting state, the lines of force are more severely distorted and the energy is increased by a term proportional to H^2. This term is responsible for the continuous increase. (It is experimentally verified that the H^2 contribution is very sensitive to the orientation of the cylinder.)

Plane Film in a Parallel Field

We consider a film of thickness $d[< \xi(T)]$ in an external field H applied parallel to the plane of the film and having the same value at both faces. In this case, the film does not carry a macroscopic current. This is the difference with the previously discussed experiments. In order to understand this, we consider the Maxwell equation curl $h = (4\pi/c)j$ and take h along the y axis, j along the x axis, the film being defined by the planes $z = \pm d/2$. Then

$$\frac{\partial h(z)}{\partial z} = -\frac{4\pi}{c} j$$

$$0 = h\left(\frac{d}{2}\right) - h\left(-\frac{d}{2}\right) = -\frac{4\pi}{c}\int_{-d/2}^{d/2} j dz \tag{6-47}$$

There are currents that cancel on the average and we wish to examine their distribution in detail. We begin with the London equation which, as we have seen previously, is a consequence of the Landau-Ginsburg equation in the case where $|\psi|$ is spatially constant. It is written as

$$\frac{\partial j}{\partial z} = -\frac{4e^2}{mc}|\psi|^2 h \tag{6-48}$$

Therefore

$$\frac{\partial^2 h}{\partial z^2} = \frac{f^2 h}{\lambda^2(T)} \tag{6-49}$$

(as usual we set $\mathbf{f} = |\psi|/\psi_0$). Application of the boundary condition $h(\pm d/2) = H$ gives

$$h = H\frac{\cosh(zf/\lambda(T))}{\cosh(\epsilon f/2)} \tag{6-50}$$

where $\epsilon = \mathrm{d}/\lambda(\mathrm{T})$. From h, we can calculate j from (6-47) or (6-48). As usual, we introduce the drift velocity

$$v = \frac{j}{2e|\psi|^2} = -\frac{2eH\lambda(T)}{mcf}\frac{\sinh(zf/\lambda(T))}{\cosh(\epsilon f/2)} \tag{6-51}$$

A knowledge of v allows us to calculate the free energy from (6-32). We must determine the average value of the kinetic energy through the thickness of the film

$$\overline{v^2} = \frac{1}{d}\int_{-d/2}^{d/2} v^2 dz = \frac{1}{2}\left[\frac{2eH\lambda(T)}{mcf\cosh(\epsilon f/2)}\right]^2\left(\frac{\sinh\epsilon f}{\epsilon f} - 1\right) \tag{6-52}$$

On minimizing (6-32) with respect to f, we obtain

$$\mathrm{f}^2 = 1 + \frac{m\overline{\mathrm{v}^2}}{2\alpha} \tag{6-53}$$

Using our basic equations (6-8), (6-15), and (6-22), we can place this result in the form

$$\left(\frac{\mathrm{H}}{\mathrm{H_c}}\right)^2 = 4\mathrm{f}^2\left(1-\mathrm{f}^2\right)\frac{\cosh^2\frac{\epsilon\mathrm{f}}{2}}{\frac{\sinh\epsilon\mathrm{f}}{\epsilon\mathrm{f}} - 1} \tag{6-54}$$

Equation (6-54) gives the decrease in f as H increases. The behavior for $\epsilon\mathfrak{f} \ll 1$ is

$$\left(\frac{\mathrm{H}}{\mathrm{H_C}}\right)^2 = \frac{24}{\epsilon^2}\left(1-\mathrm{f}^2\right), \quad \mathrm{d} < \frac{\lambda(\mathrm{T})}{\mathrm{f}} \tag{6-55}$$

On the other hand, for $\epsilon f \gg 1$, we later see that f is close to 1 in the important region and then (6-54) reduces to

$$\left(\frac{\mathrm{H}}{\mathrm{H_c}}\right)^2 = 2\epsilon\left(1-\mathrm{f}^2\right), \quad \mathrm{d} > \lambda(\mathrm{T}) \tag{6-56}$$

What is the critical field of the film, that is, the maximum value allowed for H? If the transition to the normal state is first order, we must calculate and compare the Gibbs potential G (at fixed H and T) in the superconducting phase [with f given by (6-54)] and in the normal phase.

We first calculate the free energy F_S (per cm^3) in the superconducting state from (6-32) and (6-52). Upon using the equilibrium condition (6-53) and the equations (6-8), (6-15), we can put it in the form

$$F_s = F_n - \frac{H_c^2}{8\pi} f^4 + \frac{\overline{h^2}}{8\pi} \tag{6-57}$$

where

$$\overline{h^2} = \frac{1}{d}\int_{-d/2}^{d/2} h^2 dz = H^2 \frac{\epsilon f + \sinh \epsilon f}{\epsilon f(1+\cosh \epsilon f)} \tag{6-58}$$

We also need the induction B (which is the average of h)

$$B = H \frac{2}{\epsilon f} \tanh \frac{\epsilon f}{2} \tag{6-59a}$$

The reader can verify that $\mathrm{dF/dB = H/4\pi}$ and therefore that H is the thermodynamic field as could be predicted from the analysis of Chapter 2 . We finally form the Gibbs potential

$$G_S = F_S - \frac{BH}{4\pi} = F_n + \frac{H^2}{8\pi}\left[\frac{\sinh \epsilon f + \epsilon f}{\epsilon f(1+\cosh \epsilon f)} - \frac{4}{\epsilon f}\tanh\left(\frac{\epsilon f}{2}\right)\right] - \frac{H_c^2}{8\pi} f^4 \tag{6-59b}$$

On the other hand, $G_n = F_n - H^2/8\pi$ and the critical field H is obtained by setting $G_n = G_s$ or

$$\left(\frac{\mathrm{H}_\ell}{\mathrm{H_c}}\right)^2 \left[1 + \frac{\epsilon \mathrm{f}_\ell + \sinh \epsilon \mathrm{f}_\ell}{\epsilon \mathrm{f}_\ell\,(1+\cosh \epsilon \mathrm{f}_\ell)} - \frac{4}{\epsilon \mathrm{f}_\ell}\tanh\left(\frac{\epsilon \mathrm{f}_\ell}{2}\right)\right] = \mathrm{f}_\ell^4 \tag{6-60}$$

Equations (6-54) and (6-60) define H_ℓ and the corresponding order parameter $\psi_\ell = \psi_0 \mathrm{f}_\ell$. One can eliminate H_ℓ to obtain

$$1 + \frac{1}{6}\frac{\mathrm{f}_\ell^2}{1-\mathrm{f}_\ell^2} = \frac{1}{3}\frac{\epsilon \mathrm{f}_\ell\,[\cosh \epsilon \mathrm{f}_\ell - 1]}{\sinh(\epsilon \mathrm{f}_\ell) - \epsilon \mathrm{f}_\ell} \tag{6-61}$$

In Fig. 6-5a we plot both sides of (6-61) as a function of f_ℓ on the interval $(0 \to 1)$. For $f \to 0$, the left side behaves as $1 + \frac{1}{6} f_\ell^2$ and the right-hand side as $1 + (\epsilon \mathrm{f}_\ell)^2/30$. If $\epsilon > \sqrt{5}$, the right-hand side increases faster than the left. Since the left-hand side diverges for $\mathrm{f} = 1$, there must be an intersection between $\mathrm{f}_\ell = 0$ and $\mathrm{f}_\ell = 1$. On the contrary, there will be no intersection for $\epsilon < \sqrt{5}$ (see Fig. 6-5b).

Therefore, if $d > \sqrt{5}\lambda(T)$, we have a first-order transition with a critical field H_ℓ deduced from (6-61) and (6-60). If $\mathrm{d} < \sqrt{5}\lambda(\mathrm{T}), \mathrm{G_S}$ always remains less than G_n when the solution exists; ψ decreases as H increases, according to (6-54) and finally vanishes for

$$\mathrm{H} = \mathrm{H}'_\ell = \frac{\sqrt{24}}{\epsilon}\mathrm{H_c} \tag{6-62}$$

The transition that occurs at H'_ℓ is of the second order. These two types of behavior, depending on the ratio $\mathrm{d}/\lambda(\mathrm{T})$, were predicted by Ginsburg in 1952. They have been qualitatively verified in a series of tunneling experiments by Douglass (1961) (metal used: aluminum, $\xi_0 = 16{,}000\text{Å}\Big)$. He showed that

(1) The energy gap ϵ_0 in the excitation spectrum was a decreasing function of the field.
(2) For T $\cong$ 0.75 T_0 in films with thicknesses d > 3.500Å, the gap dropped abruptly from a finite value to 0 when the critical field was reached.
(3) At the same temperature, in films with $d < 3.500\text{Å}, \epsilon_0$ dropped smoothly to 0 when the field was increased up to the critical value.

These results are represented on Fig. 6-5c. The distinction between first- and second-order transitions is very apparent. Unfortunately it is not possible to go beyond this qualitative statement for the following reasons:

Both $\lambda(T)$ and d are much smaller than ξ_0 in all the films. The currents j_S have a rapid variation on the scale ξ_0 (note that j_S reverses its sign when one goes from one side of the film to the other). In such a situation the Landau-Ginsburg equations cannot be applied, even if one allows for a change of κ with thickness. [5] Note: the energy

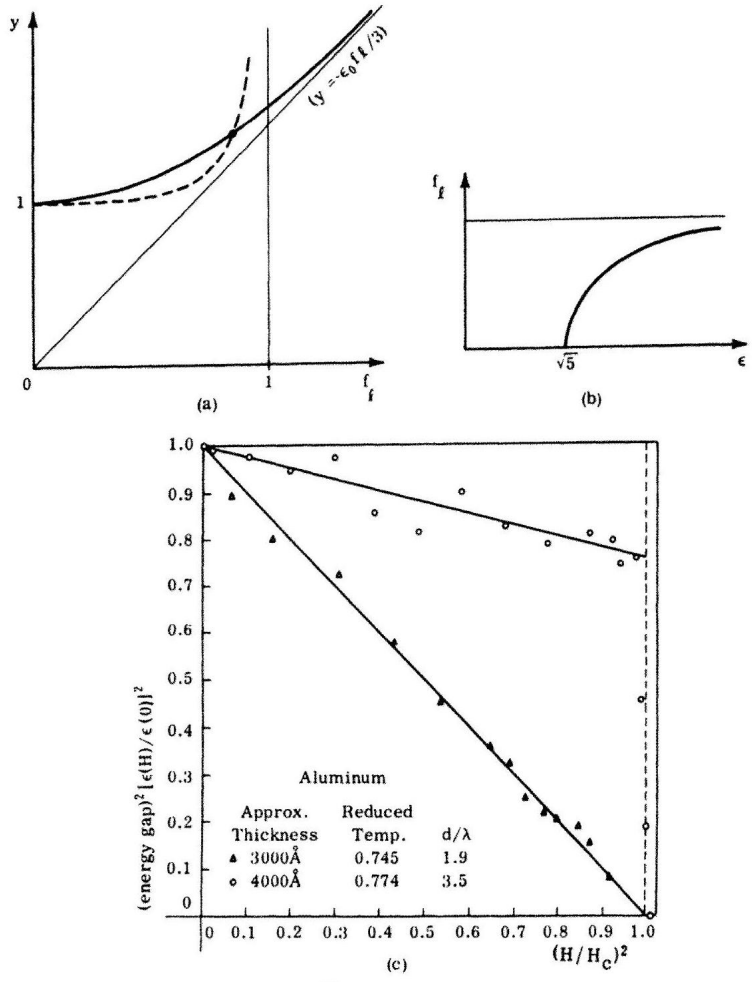


Figure 6-5
(a) A plot of the left-and right-hand sides of Eq. (6-61) as a function of the normalized order parameter f_ℓ. Left side: broken curve. Right side: continuous curve. The two curves have an intersection if $d > \sqrt{5}\lambda$ (T). (b) The dependence of the order parameter at the first-order transition as a function of $\epsilon = \text{d}/\lambda(\text{T})$. Note that for $\epsilon < \sqrt{5}$ there is a second-order transition and the critical value f_ℓ is zero. (c) Tunneling measurement of the energy gap versus magnetic field in two aluminum samples of different thicknesses. For the film with $\varepsilon > \sqrt{5}$, note the first-

[5] The space variations of j_s depend on two parameters d and $\lambda(T)$. Thus, in general, an "effective κ " for the present geometry would depend on $\lambda(T)$ and lose its intrinsic significance. Furthermore, even in the limit $\lambda(T) \gg d$, this effective κ would be numerically different from the one required by a critical current measurement on the same film.

order transition; for the thinner film we see a much less abrupt behavior. [After D. Douglas, Jr., IBM J. Res. Develop., 6, 47 (1962).]
gap ϵ_0 is different from $|\Delta|$ in thin films under strong magnetic fields. In particular there is a finite region of the (H, T) plane where $\epsilon_0 = 0$ while $\Delta \neq 0$ (gapless superconductivity). This complicates somewhat the analysis of the tunneling results.

Problem.

Consider a superconducting cylindrical film (radius R) of thickness 2d ($d \ll R$). A small axial external field h_0 is applied to the cylinder; determine the field in the core when
(a) the fluxoid Φ_f is held fixed,
(b) the fluxoid Φ_f can adjust and reach its most favorable value.

Solution.

By definition, the fluxoid Φ_f is proportional to the change in phase $[\phi]$ of the order parameter after one revolution around the cylinder

$$\Phi_{\mathrm{f}} = \frac{\mathrm{ch}}{2\mathrm{e}}[\phi]$$

In practice the adjustment of $|\phi|$ allowed in (b) can take place only by the penetration of vortices or macroscopic flux bundles.
(a) The current density on the film is given by (6-12)

$$\mathrm{j} = 2\frac{\mathrm{e}}{m}|\psi|^2\left(\mathrm{h}\nabla\phi - \frac{2\mathrm{e}}{\mathrm{c}}\ \mathrm{A}\right)$$

For small $h_0, |\psi|$ is equal to its value ψ_0 in zero field.
Integrating the current density around a circle running along the inner surface of the cylinder, we find

$$\oint \mathrm{j}\cdot\ \mathrm{d}l = \frac{\mathrm{c}}{4\pi\lambda^2}\left(\Phi_{\mathrm{f}} - \Phi_{\mathrm{i}}\right)$$

where λ is the penetration depth defined in $\lambda(T)^{-2} = \frac{16\pi e^2\psi_0^2}{mc^2}$ and Φ_1 is the flux contained within the core of the cylinder. The field distribution is still given by

$$\frac{d^2h}{dx^2} = \frac{h}{\lambda^2}$$

within the film, and thus

$$h = \frac{(h_0 - h_i)}{2}\frac{\sinh(x/\lambda)}{\sinh(d/\lambda)} + \frac{(h_0 + h_i)}{2}\frac{\cosh(x/\lambda)}{\cosh(d/\lambda)}$$

where h_0 is the applied field and h_i is the field within the core (to be determined). Comparing $\Phi \mathrm{j}\cdot \mathrm{d}l$ derived from this field distribution with the previous equation involving the fluxoid, we find

$$\begin{aligned} h_i &= \frac{\frac{\Phi_f}{\pi\lambda R} + \frac{2h_0}{\sinh(2d/\lambda)}}{2\coth(2d/\lambda) + R/\lambda} \\ &\simeq \frac{\Phi_f}{\pi R^2} + \frac{2h_0\lambda}{R\sinh(2d/\lambda)} \quad \left(R \gg \frac{\lambda^2}{d}\right) \end{aligned}$$

If the fluxoid is held fixed, for example, $\Phi_f = 0$, we find

$$h_i \simeq \frac{2h_0\lambda}{R\sinh(2d/\lambda)}$$

h_i is, in general, quite small compared to the applied field h_0, except of course for extremely thin films ($d \leq \lambda^2/R$).
(b) Let us now assume that the fluxoid is allowed to vary. For a fixed applied field h_0, we must minimize the Gibbs potential S with respect to the fluxoid. S may conveniently be written as

$$S = \frac{\lambda^2}{8\hbar}\int\left(\frac{dh}{dx}\right)^2 dr + \frac{1}{8\pi}\int (h-h_0)^2\, dr + \text{ const}$$

Using the explicit form derived above for the field, one finds that the minimum corresponds to $h_i = h_0$.

Thus in thermodynamic equilibrium the field within the core is equal to the applied field. However it often occurs in A.C. experiments that the fluxoid cannot adjust itself to its equilibrium value during the time of observation and we then find a situation where the core field is small.

6.3.6 6-6 Situations Where $|\psi|$ Varies Spatially

Nucleation in the Bulk

We consider a superconducting metal in a high magnetic field. For sufficiently high fields, superconductivity is destroyed and the field is uniform in the sample. If we continuously decrease the field, at a certain field $H = H_{C_2}$, superconducting regions begin to nucleate spontaneously. We see that H_{C_2} does not coincide with the thermodynamic field H_c; depending on the case it can be either larger or smaller.

In the regions where the nucleation occurs, superconductivity is just beginning to appear and therefore $|\psi|$ is small. The Landau-Ginsburg equation can be linearized to give

$$\frac{1}{2m}\left(-i\hbar\nabla - \frac{2eA}{c}\right)^2 \psi = -\alpha\psi \tag{6-63}$$

Also, in (6-63) we can set curl $A = H$ where H is only the applied field. This is valid because the supercurrents are of order $|\psi|^2$ and the resulting corrections to the field are therefore negligible in the linear approximation. Equation (6-63) is then formally identical to the Schrdinger equation for a particle of charge $2e$ and mass m in a uniform magnetic field.

First consider the case of an infinite medium. The particle has a
constant velocity v_z along the field and moves in a circle in the xy plane with the frequency

$$\omega_c = 2eH/mc \tag{\prime}$$

The energies corresponding to the bound states of (6-63) have the form $\frac{1}{2}mv_Z^L + \left(n+\frac{1}{2}\right)\hbar\omega_c$ where n is a positive integer. In particular, the lowest level corresponds to $v_Z = 0, n = 0$, and gives $-\alpha = e\hbar H/mc$.

The field H thus obtained is the field H_{c_2}. (The other levels with n or v_Z nonzero will give, for the same α, lower values of H .) By using the relation $\alpha^2/2\beta = H_C^2/8\pi$ and the definition (6-26) of the Lan-dau-Ginsburg parameter, one finally obtains

$$\begin{aligned} H_{C2} &= \kappa\sqrt{2}H_c \\ &= \frac{\phi_0}{2\pi\xi(T)^2} \end{aligned} \tag{6-64}$$

Discussion of this formula.

(1) When $\kappa > 1/\sqrt{2}, (\mathrm{H_c} < \mathrm{H_{c_2}})$, a condensed phase ($\psi \neq 0$) will appear in the bulk of the sample for fields $\mathrm{H} < \mathrm{H_{C_2}}$. This phase cannot correspond to a complete exclusion of the magnetic flux, since a complete Meissner effect is energetically unfavorable at fields $\mathrm{H} > \mathrm{H_c}$ and we can choose $\mathrm{H_c} < \mathrm{H} < \mathrm{H_{c_2}}$. In fact, what we obtain here below $\mathrm{H_{c_2}}$ is the Schubnikov phase discussed in Chapter 3. As predicted there, we see that the upper critical field is of order $\phi_0/\xi(\mathrm{T})^2$. It corresponds to a close packing of vortex lines, each of them carrying the flux unit ϕ_0 and having a core radius $\xi(\mathrm{T})$.
(2) When $\kappa < 1/\sqrt{2}\,(\mathrm{H_{c_2}} < \mathrm{H_c})$, if we decrease the field we first meet the value H_c, at which a complete Meissner effect takes place-we are dealing here with a first type superconductor.

$$\begin{array}{ll} \kappa < \frac{1}{\sqrt{2}} & \text{first type} \\ \kappa > \frac{1}{\sqrt{2}} & \text{second type} \end{array} \tag{6-65}$$

Nucleation on the Sample Surface

The calculation that led to (6-64) is only valid in an infinite medium. It neglects boundary effects. In fact, for an ideal substance, nucleation always takes place first on the surface (D. Saint-James and P. G. de Gennes, 1963). We now analyze in greater detail the effects of the sample surface in a simple case. The surface is assumed to be a plane [radius of curvature much larger than $\xi(T)$] and the boundary separates the superconductor from either an insulator or a vacuum such
that the boundary conditions (6-13) apply. We consider two cases:
(1) The field (along z) is normal to the surface (xy plane). Then the function ψ corresponding to the lowest level of (6-63) is also an eigenfunction of $\Pi_2 = -i\hbar\partial/\partial z - 2eA_2/c$ with eigenvalue 0 . Therefore (6-13) is automatically satisfied and the surface does not modify the nucleation field.
(2) The field is in the surface of the sample; **H** is directed along the z axis, the surface is in the yz plane and the superconductor occupies the region $x > 0$. We select the gauge $A_Z = A_X = 0, A_Y = Hx$ and look for solutions of the form

$$\psi = e^{iky} f(x) \tag{6-66}$$

Equation (6-63) becomes

$$-\frac{\hbar^2}{2m}\frac{d^2 f}{dx^2} + \frac{1}{2m}\left(\hbar k - \frac{2eHx}{c}\right)^2 f = -\alpha f \tag{6-67}$$

and the boundary condition is

$$\left(\frac{df}{dx}\right)_{x=0} = 0 \tag{6-68}$$

Equation (6-67) is analogous to the Schrdinger equation of a harmonic oscillator of frequency ω given by (6-63), the equilibrium position being the point

$$\mathrm{x_0} = \frac{\hbar \mathrm{kc}}{2\mathrm{eH}} \tag{6-69}$$

However (6-68) introduces a complication. If $\mathrm{x_0} \gg \xi(\mathrm{T})$, the wavefunction will be localized around x_0 and nearly zero at the surface; therefore (6-68) will automatically be satisfied. In this case, we have

$$f \cong \exp\left[-\frac{1}{2}\left(\frac{x-x_0}{\xi(T)}\right)^2\right] \tag{6-70}$$

the eigenvalue still being given by (6-63). If x_0 is zero, on the other hand, the function (6-70) still satisfies the boundary condition (6-68), and (6-63) is still obtained. We now show that between the two extreme cases, namely for $x_0 \sim \xi(T)$, the lowest eigenvalue is lower than (6-63). In order to see this, we can replace (6-67), valid for $x > 0$, by an equation valid over the interval $-\infty < x < \infty$

$$-\frac{\hbar^2}{2m}\frac{d^2f}{dx^2} + V(x)f = -\alpha f \tag{6-71}$$

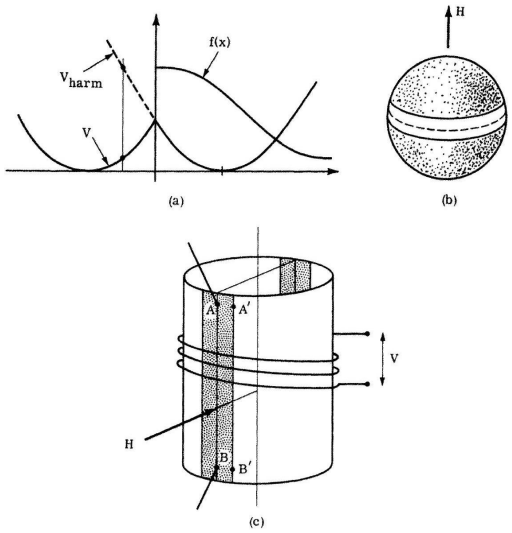


Figure 6-6
(a) The harmonic potential $V_{\text{harm}} = \text{const}\ (x-x_0)^2$ and the symmetrical potential V. Since $V < V_{\text{harm}}$, the first level in V is lower than the first level in V_{harm} . Also shown is the shape of the eigenfunction $f(x)$. (b) Surface superconductivity in a sphere. The band around the equator represents the superconducting sheath when H is just below H_{C3}. As H decreases, this band broadens and reaches the poles at H_{C_2}. (c) Principle of the determination of H_{C2} and H_{C3} on hollow cylinders lafter J. P. Burger, G. Deutscher, E. Guyon, and A. Martinet, Solid State Commun., 2, 101 (1964)]. A field H > H $_{c2}$ is applied normal to the cylinder axis. Two normal strip appears on the cylinder (shaded areas). Their onset is detected with a coil wound around the cylinder: the self-inductance of the coil increases abruptly when the strips appear. The width of the strips is measured with the resistive probes AB. The current flows from A to A', then in the superconducting regions from A' to B', and finally from B' to B. The resistance is proportional to the length AA'.

The potential V(x) coincides with that of (6-67) for x > 0. For x < 0, we continue it symmetrically (Fig. 6-6a):

$$V(x) = \begin{cases} \frac{2e^2H^2}{mc^2}(x-x_0)^2 & x > 0 \\ V(-x) & x < 0 \end{cases} \tag{6-72}$$

The eigenfunction corresponding to the lowest eigenvalue of (6-71) has no nodes, is an even function of x, and automatically satisfies (6-68). For $x < 0$, we see from the figure that the potential $V(x)$ is always less than $(2e^2H^2/mc^2)(x-x_0)^2$ and therefore the lowest eigenvalue of V(x) is lower than (6-63). Hence, nucleation is favored by the presence of a surface.

A detailed calculation shows that the optimum value of x_0 is $0.59\xi(T)$ and that the corresponding eigenvalue becomes

$$-\alpha = 0.59\frac{e\hbar H}{mc} \tag{6-73}$$

The eigenfunction is a rather complicated Weber function. But, as first noticed by C. Kittel, a good approximation to the exact eigenvalue (6-73) can be obtained more simply from the variational principle applied to the Schrdinger equation (6-67). Taking as a trial function a gaussian of adjustable width

$$f(x) = e^{-rx^2}$$

and minimizing $|\alpha|$ with respect to r and x_0, one finds

$$|\alpha| = \sqrt{1 - \frac{2}{\pi}}\frac{e\hbar H}{mc} = 0.60\frac{e\hbar H}{mc}$$

The nucleation field, which we call H_{C3}, is given by (6-73). By making use of (6-64), it can be written as

$$H_{c3} = 2.4\kappa H_c = 1.7H_{c_2} \tag{6-74}$$

Discussion of Eq. (6-74).
(1) Materials of the second type. The above calculation shows us that above H_{c2}, in the interval $H_{c2} < H < H_{c3}$, superconductivity is not entirely destroyed. The bulk of the material is normal, but a superconducting sheath subsists in certain surface regions. For a long cylinder placed in an axial field, this sheath occupies the entire lateral surface of the cylinder. For a sphere, the situation is quite different. When H is slightly less than H_{C_3}, the sheath is limited to a narrow band around the equatorial circle (Fig. 6-6b). As H decreases, this band broadens and finally reaches the poles at $H = H_{C_2}$.

A number of methods have been used to detect the surface sheath: resistance measurements (at low currents, the sheath acts as a short circuit); inductive measurements at low frequencies-a typical geometry is shown in Fig. 6−6c. When the sheath is present on the cylinder surface, flux lines cannot pass it and the self-inductance of the coil is low. When H reaches H_{C3}, the sheath disappears and the full self-inductance is restored (Fig. 6-7a). Similar but more complicated experiments can also be carried out in the microwave region.

In films [much thicker than ξ(T)], various sensitive techniques can be applied: (a) tunneling experiments display a density of states that deviates significantly from the normal state value; (b) the sheath acts as a small diamagnetic region that can be detected by torque measurements.

All these experiments have shown that for clean sample surfaces [radius of curvature $\gg \xi(T)$] there is, indeed, a sheath in an interval $H_{c_2} < H < H_{c_3}(\theta)$, where θ is the angle between the field and the surface. For $\theta = 0$ the experimental value $H_{c_3}(0)$ is close to the theoretical value (6-74). For $\theta \neq 0, H_{C3}(\theta)$ varies as shown on Fig. 6-7b. For $\theta = \frac{1}{2}\pi, H_{C3}(\theta) \to H_{C2}$.
(2) Type 1 superconductors with $0.42 < \kappa < 1/\sqrt{2}$. Here $H_{C2} < H_C$, but $H_{C3} > H_C$. Thus in the field range $H_C < H < H_{C_3}$ there still exists a superconducting

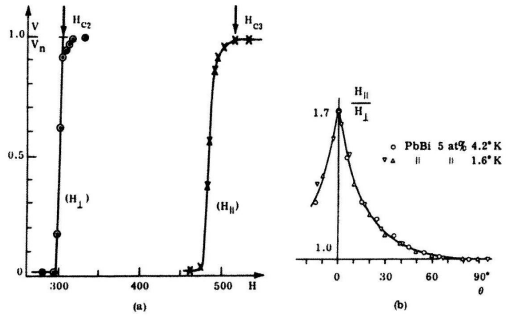


Figure 6-7 (a) Results of induction measurements (with the coil of Fig.6-6c) on hollow cylinders of a Snin alloy. When the field H is normal to the cylinder axis ($H_\perp$), the voltage V (proportional to the self-inductance of the coil) increases for $H = H_{c_2}$. When H is parallel to the axis $\left(H_\parallel\right)$, the increase occurs only when H = H_{c3} (after Burger et al.). (b) Angular dependence of the critical field in PbBi alloys at various temperatures. (After P. Burger, G. Deutscher, E. Guyon, and A. Martinet, Phys. Rev., 137A, 853 (1965).]

sheath (in the regions where H is parallel or nearly parallel to the sample surface). This sheath in a Type I superconductor has been observed in a few cases such as lead and dilute lead alloys. (3) Type I superconductors with $\kappa < 0.42$. Here $H_{c_3} < H_c$ and it is not possible to observe the sheath in a state of thermodynamic equilibrium. It is still possible, however, to measure H_{C_3} in the following way: In very good samples it is possible to lower the field below H_c while still retaining the sample in the normal (metastable) state, In aluminum, for instance, the field can be lowered to $< H_c/10$ with no transition occurring. However, the metastable normal phase never extends down to 0 applied field; the reason is that, when we reach the field H_{c_3}, it becomes possible to create weakly superconducting regions near the sample surface, with no energy expense. The normal phase becomes strictly unstable when $H \leq H_{C3}$. The corresponding nucleation process has, in fact, been studied very carefully by Faber on various Type I superconductors. He showed experimentally that nucleation took place near the sample surface (however, without realizing at the time that this was a fundamental property) and he measured the nucleation field we now identify with H_{C3}. From his results one could, in principle, derive the corresponding κ values by Eq. (6-74). If we do this blindly, we find

$\kappa = 0.015$Al
0.07 In
0.10 Sn

This procedure is probably not quite correct for these pure metals where the Landau-Ginsburg equations are valid only for temperatures T very close to T_0, while the supercooling fields are usually measured at lower temperatures. For the sake of completeness, we quote the "theoretical" values of κ derived from the definition (6-27) where $\lambda_I, (0)$ and ξ_0 are determined from Fermi surface measurements in the normal state (plus the experimental value of T_0). They are

$$\begin{aligned} \kappa &= 0.010\text{Al} \\ &0.05\text{In} \\ &0.15\text{Sn} \end{aligned}$$

6.3.7 6-7 Structure of the Vortex Phase in Strong Fields (H ~ H_{C2})

Consider a cylindrical sample of a second type material ($\kappa > 1/\sqrt{2}$) placed in an exterior field H parallel to the axis of the cylinder. Let H decrease. When H becomes equal to H_{C_2}, nucleation of the superconducting state begins in the volume of the sample. The order parameter $|\psi|$ is small and the form of ψ on nucleation is obtained from the linearized Landau-Ginsburg equations (6-63). If H still decreases,

the nucleation region develops, $|\psi|$ becomes larger and in order to determine the nature of the order it is necessary to solve the complete nonlinearized Landau-Ginsburg equations. This represents a formidable numerical problem.

Things become simpler if H is taken to be only slightly less than H_{C_2} (A. Abrikosov, 1956). By continuity, the solution ψ of the complete Landau-Ginsburg equations must have a strong resemblance to a certain solution ψ_L of the linearized equation. This does not mean that the problem is immediately solved. We only know that the ψ_L satisfies

$$\frac{1}{2m}\left(-i\hbar\nabla - \frac{2eA_0}{c}\right)^2 \psi_L = -\alpha\psi_L \tag{6-75a}$$

with

$$\operatorname{curl} A_0 = (0, 0, H_{C_2}) \tag{6-75b}$$

However, the eigenvalues of (6-75a) are strongly degenerate, that is, there exist many independent solutions describing nucleation in one or another part of the sample. For example, in the gauge ($A_X = A_Z = 0,\ A_y = H_{C_2}x$) we have seen that the solutions are of the form

$$\begin{aligned} \psi_{\mathrm{k}} &= \mathrm{e}^{\mathrm{iky}}\mathrm{e}^{-\left(\frac{1}{2}\right)(\mathrm{x}-\mathrm{x}_0)^2/\xi^2(\mathrm{T})} \\ \mathrm{x}_0 &= \frac{\hbar\mathrm{ck}}{2\mathrm{eH}_{\mathrm{C}_2}} \end{aligned} \tag{6-76}$$

where k is an arbitrary parameter. The nucleation region for such a situation is a band of width $\xi(T)$ perpendicular to the x axis. Its average abscissa x_n depends on the value chosen for k. We know that ψ_L must be a linear combination of the ψ_k. In fact, from our simplified discussion in Chapter 3, we expect to find $|\psi|$ to have a periodic structure in x and y. If $2\pi/q$ is the spatial period in the y direction, such a function ψ_L will be the combination

$$\begin{aligned} \psi_L &= \sum_n C_n e^{inqy} \exp\left[-\frac{1}{2}(x - x_n)^2/\xi^2(T)\right] \\ x_n &= \frac{n\hbar cq}{2eH_{c2}} \end{aligned} \tag{6-77}$$

In order that $|\psi_L|$ also be periodic in x, it is necessary to impose a periodicity on the $C_n's$. The form of condition chosen by Abrikosov was $C_{n+\nu} = C_n$, where ν is a fixed integer. Then

$$\psi_L\left(x + \frac{\nu\hbar cq}{2\mathrm{eH}_{\mathrm{C}_2}}, y\right) = e^{i\nu qy}\psi_L(x, y)$$

However, independent of the detailed structure of ψ_{L} postulated in (6-77), it is possible to establish certain general theorems:
(1) Normalization of ψ_{L}: As the starting equations (6-11) and (6-12) are nonlinear in ψ, the normalization adopted for ψ_L plays a nontrivial role. Let us assume that the free energy (6-9) is stationary if the trial function ψ_L is changed to $(1 + \epsilon)\psi_L$ where ϵ is small and independent of r. To first order in ϵ the variation in the free energy is

$$\delta\mathcal{F} = 2\epsilon \int \mathrm{dr}\left[\alpha\left|\psi_{\mathrm{L}}\right|^2 + \beta\left|\psi_{\mathrm{L}}\right|^4 + \frac{1}{2m}\left|\left(-\mathrm{i}\hbar\nabla - \frac{2\mathrm{eA}}{\mathrm{c}}\right)\psi_{\mathrm{L}}\right|^2\right] \tag{6-78}$$

In order to simplify the notation, we shall write an integral such as $\int \left|\psi_{\mathrm{L}}\right|^2 \mathrm{dr}$ extended over a macroscopic volume V in the form $\mathrm{V}\left|\psi_{\mathrm{L}}\right|^2$. From (6-78). the condition $\delta\mathcal{F} = 0$ can be written

$$\overline{\alpha \left|\psi_L\right|^2} + \overline{\beta \left|\psi_L\right|^4} + \frac{1}{2m}\overline{\left|\left(-i\hbar\nabla - \frac{2eA}{c}\right)\psi_L\right|^2} = 0 \tag{6-79}$$

This equation can be simplified by using (6-75a), which is satisfied by ψ_{L}. Set $\mathrm{A} = \mathrm{A}_0 + \mathrm{A}_1$ where A_0 (defined by 6-75b) is the vector potential which would exist in the presence of the field H_{C_2} and where A_1 represents the modifications due to the facts that (a) the applied field is slightly smaller than H_{C_2}: and (b) there exist supercurrents, which also contribute to the fields. Expanding (6-79) to first order in A_1 and using (6-75a), we obtain

$$\beta \left|\psi_{\mathrm{L}}\right|^4 - \frac{1}{\mathrm{c}}\overline{\mathbf{A}_1 \cdot \mathrm{j_L}} = 0 \tag{6-80}$$

where

$$j_L = \frac{e}{m}\left[\psi_L^*\left(-i\hbar\nabla - \frac{2eA_0}{c}\right)\psi_L + C.C.\right] \tag{6-81}$$

j_L represents the current associated with the unperturbed solution. If we integrate the second term in (6-80) by parts and set curl $A_1 = h_1$ and curl $h_s = (4\pi/c)j_L$, we obtain

$$\beta\overline{\psi_{\mathrm{L}}|^4} - \frac{1}{4\pi}\overline{\mathrm{h_t} \cdot \ \mathrm{h_S}} = 0 \tag{6-82}$$

(2) Relation between field and order parameter: In order to make
the condition (6-82) explicit, we must calculate the fields h_1 and h_s. (From the results of Chapter 3, we predict that h_1 and h_S are everywhere parallel to the z axis.) We can write

$$h_1(r) = H - H_{C_2} + h_S(r) \tag{6-83}$$

The term $\mathrm{H}-\mathrm{H}_{\mathrm{C}_2}$ represents the contribution (α) and $\mathrm{h_S}$ gives the effect of the supercurrents.
6

When ψ_{L} is a solution of (6-75a) corresponding to the lowest eigenvalue $-\alpha = \frac{1}{2}\hbar\omega_{\mathrm{C}}$, the lines of current associated with j_{L} coincide with the lines $|\psi_{\mathrm{L}}| = \text{const}$. This property allows us to calculate $\mathrm{h_S}$ simply.

Proof.

$$\text{Set } \Pi = (2m\hbar\omega_c)^{-1/2}\left(-i\hbar\nabla - \frac{2eA_0}{c}\right)$$

and $\Pi^{\pm} = \Pi_{x^{\pm}} = i\Pi_y$. The commutator $[\Pi^+, \Pi^-]$is one and (6-75a) can be written in the form

$$\Pi^+\Pi^-\psi_L = 0$$

whose bound state solutions correspond to

$$\Pi^-\psi_L = 0 \tag{6-84}$$

We still set

$$\psi_{\mathrm{L}} = |\psi_{\mathrm{L}}|\,\mathrm{e}^{\mathrm{i}\vartheta} \tag{6-85}$$
$$\mathrm{j_L} = \frac{2\mathrm{e}}{m}|\psi_{\mathrm{L}}|^2\left(\hbar\nabla\psi - \frac{2\mathrm{e}}{\mathrm{c}}\ \mathrm{A}_\theta\right)$$

On equating the real and the imaginary parts of $\Pi^+\psi_L$ to zero and using (6-85), we find

$$\mathfrak{j}_{Lx} = -\frac{e\hbar}{m}\frac{\partial}{\partial y}|\psi_L|^2 \tag{6-86}$$
$$\mathfrak{j}_{Ly} = \frac{e\hbar}{m}\frac{\partial}{\partial x}|\psi_L|^2$$

[6] $\int_L = (c/4\pi)$ curl h_s is not exactly the supercurrent since it is A_n and not A_1 which enters in (6.81). However we shall see that $H_{c2} - H$ and $|\psi|^2$ are of the same order and small, and therefore $\overline{(A_0 - A)|\psi|^2}$ is of order $|\psi|^4$ and negligible at this stage

We see that the current lines are the lines of constant $|\psi_L|$.
By comparing (6-86) to the definition curl $h_S = (4\pi/c)j_L$, we find explicitly that the field h_s due to the supercurrents is given by

$$h_s = -4\pi\frac{e\hbar}{mc}|\psi_L|^2 \tag{6-87}$$

The constant of integration is such that, for $\overline{|\psi_L|^2} = 0, h_s$ disappears. By regrouping (6-82), (6-83), and (6-87), we obtain the explicit condition

$$\beta\overline{|\psi_L|^4} + \frac{e\hbar}{mc}\overline{|\psi_L|^2\left(H - H_{C_2} - \frac{4\pi e\hbar}{mc}|\psi_L|^2\right)} = 0 \tag{6-88a}$$

It is again useful to set $|\psi_L| = \psi_0 f$, to use the definition (6-26) of κ, and (6-64) for H_{C_2}, to find

$$\overline{\mathrm{f}^4}\left(1 - \frac{1}{2\kappa^2}\right) - \overline{\mathrm{f}^2}\left(1 - \frac{\mathrm{H}}{\mathrm{H}_{c_2}}\right) = 0 \tag{6-88b}$$

The relation (6-88b) is important because it is independent of the detailed form of the hypothesis for ψ_L, that is, independent of the nature of the lattice formed by the flux lines. If we now select a given lattice, that is, fix q and the periodicity of the coefficients C_n, we can explicitly calculate the ratio

$$\frac{\overline{f^4}}{\left(\overline{f^2}\right)^2} = \beta_A \tag{6-89}$$

which corresponds to this lattice. If β_A is known, (6-88b) and (6-89) can be solved for $\overline{f^4}$ and $\overline{f^2}$. This is all that is necessary to calculate the induction and free energy.
(1) Induction B: This is the average value of the field $\mathrm{H} + \mathrm{h_S}$ and is found from (6-87) to be

$$B = H + \overline{h_S} = H - \frac{4\pi e\hbar}{mc}\sqrt{\psi_L T^2}$$
$$= H - \frac{H_c}{\kappa\sqrt{2}}\overline{f^2} \tag{6-90}$$

(2) The free energy per unit volume F is calculated using (6-11) to simplify (6-9)

$$F = -\frac{\beta}{2}|\psi_L|^4 + \frac{\overline{h^2}}{8\pi} = -\frac{H_C^2}{8\pi}\overline{f^4} + \frac{\overline{h^2}}{8\pi} \tag{6-91}$$

By returning to (6-87) we can express h^2 as a function of H, f^2, and f^4. We then eliminate $\mathrm{H}, \mathrm{f}^2, \mathrm{f}^4$ by means of (6-88b), (6-89), and (6-90) to obtain the free energy only as a function of B:

$$F = \frac{B^2}{8\pi} - \frac{(H_{C_2} - B)^2}{1 + (2\kappa^2 - 1)\beta_A}\frac{1}{8\pi} \tag{6-92}$$

Conclusions.

(1) For fixed B, F is an increasing function of β_A (since $\kappa > 1/\sqrt{2}$). The most favorable "lattice" will correspond to the smallest β_A. (Note that from (6-89) $\beta_A \geq 1$.]

The choice of lattice corresponds algebraically to a certain choice of the periodicity conditions satisfied by the C_n 's in Eq. (6-77). Two lattices have been studied in practice: a square lattice of vortex lines is obtained when all C_n 's are taken as being equal; a triangular lattice is obtained with the conditions

$$C_{n+2} = C_n$$
$$C_1 = iC_0$$

(after minimization of β_A with respect to q). It is found that $\beta_A = 1.18$ for the square lattice, and $\beta_A = 1.16$ for the triangular lattice. The latter is thus slightly more stable. The contour diagram of $|\psi|^2$ for the triangular solution is shown on Fig. 3-5, p. 67.
(2) Once β_A is known, the usual thermodynamic calculations can be performed with the free energy (6-92). We can first verify that

$$4\pi \frac{dF}{dB} = H$$

as expected. Then the magnetization $M = (B - H)/4\pi$ can be calculated. M is of order $|\psi|^2$ as expected, and given explicitly by

$$M = \frac{B - H}{4\pi} = \frac{H - H_{c2}}{4\pi\beta_A (2\kappa^2 - 1)}, \quad \frac{H_{c2} - H}{H_{c2}} \ll 1 \tag{6-93}$$

The magnetization vanishes at $H = H_{c_2}$-the transition at $H = H_{c_2}$ is of second order. (However, if κ is only slightly greater than $1/\sim \ddot{2}$, the slope $|dM/dH|$ becomes very large.) A detailed test of Eq. (6-93) has been carried out by Kinsel, Lynton, and Serin on an alloy In Bi with 2.5%Bi, an example of a Type II superconductor with a nearly reversible magnetization curve. The phase diagram deduced from their magnetic measurements on this alloy is shown in Fig. 6-8. From the experimental values of H_{c2} near T_0, one finds

$$\kappa = \frac{1}{\sqrt{2}} \frac{H_{C2}}{H_C} = 1.80$$

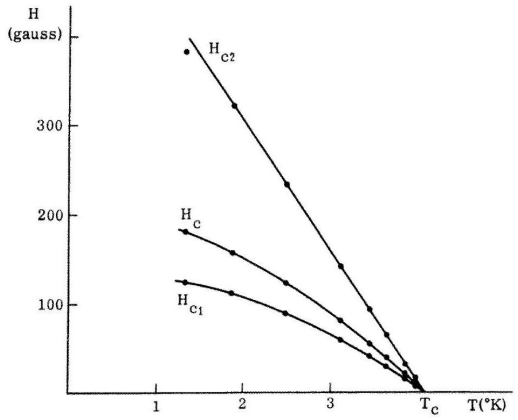


Figure 6-8
The phase diagram of a Type II superconductor (InBi alloy). (After T. Kinsel, E. A. Lynton, and B. Serin, Phys. Letters, 3, 30 (1962).]

From (6-93), taking $\beta_A = 1.16$, one finds from the magnetization curves

$$\kappa = 1.81$$

This very good agreement [7] is further confirmed by a theoretical calculation of κ described later.

Problem.

Show that the wall energy in a Type I superconductor vanishes for $\kappa = 1/\sqrt{2}$.

Solution.

We follow a method due to G. Sarma. By taking the fields h to be along the z direction, we first reduce the Landau-Ginsburg equation to a twodimensional form

$$\frac{1}{2m}\left(n_x^2 + n_y^2\right)\psi + \alpha\psi + \beta|\psi|^2\psi = 0$$

where $\Pi = p - 2eA/c$. By putting $\Pi^{\pm} = \Pi_x \pm i\Pi_y$, we have

$$n_x^2 + n_y^2 = n^- n^+ + \frac{2e\hbar}{c}h$$

We now look for solutions ψ such that

$$\Pi^+\psi = 0$$

For these particular "Sarma solutions" the field h at any point is a known function of the order parameter ψ at the same point, given by

$$\frac{e\hbar}{mc}h + \alpha + \beta|\psi|^2 = 0$$

We must furthermore ensure that the fields and currents associated with the Sarma solution are self-consistent:

$$\begin{aligned}
\operatorname{curl}\mathbf{h} = \frac{4\pi}{\mathrm{c}}\mathbf{j} &= \frac{4}{\mathrm{mc}}\mathbf{e}\left[\psi^*\Pi\psi + \psi\Pi\psi^*\right] \\
\frac{\partial \mathrm{h}}{\partial \mathrm{y}} - \mathrm{i}\frac{\partial\ \mathrm{h}}{\partial \mathrm{x}} &= \frac{4\pi\mathrm{e}}{\mathrm{mc}}\left(\psi^*\Pi^+\psi + \psi\Pi^+\psi^*\right) \\
&= \frac{4\pi\mathrm{e}}{\mathrm{mc}}\psi\Pi^+\psi^*
\end{aligned}$$

This relation must agree with the $h(\psi)$ relation obtained earlier. Differentiation of the $h(\psi)$ relation gives

$$\frac{e\hbar}{mc}\left(\frac{\partial h}{\partial y} - i\frac{\partial h}{\partial x}\right) + \beta\psi^*\left(\frac{\partial\psi}{\partial y} - i\frac{\partial\psi}{\partial x}\right) + \beta\psi\left(\frac{\partial\psi^*}{\partial y} - i\frac{\partial\psi^*}{\partial x}\right) = 0$$

This may be transformed in the following way: The condition $\Pi^+\psi = 0$ may be written as

$$\hbar\left(\frac{\partial\psi}{\partial y} - i\frac{\partial\psi}{\partial x}\right) = \frac{2e}{c}\left(A_x + iA_y\right)\psi$$

from which we obtain

[7] The agreement is even surprising since the experimental magnetization curves are not perfectly reversible, which implies a certain uncertainty in $(\mathrm{dM/dH})^{\mathrm{H_{c_2}}*}$

$$\frac{\partial h}{\partial y} - i\frac{\partial h}{\partial x} = \frac{\beta mc}{e^{\hbar}}\psi\Pi^{+}\psi^{*}$$

This does agree with the equation for the current provided that

$$\frac{4\pi e}{mc} = \frac{\beta mc}{e\hbar^2} \quad \text{or} \quad \kappa = \frac{1}{\sqrt{2}}$$

Consider now more specifically a wall in the yz plane. For $x \to -\infty$ (normal side), $h = H_c$ and $\psi = 0$. For $x \to +\infty$ (superconducting side), $h = 0$ and
$|\psi|^2 = -\alpha/\beta$. These two conditions are in agreement with the $h(\psi)$ relation for the Sarma solution-thus the Sarma solution does apply to the present problem. The thermodynamic potential (per unit area in the yz plane) S is given by

$$S = \int \mathrm{dx}\left[\alpha|\psi|^2 + \frac{1}{2}\beta|\psi|^4 + \frac{1}{2m}|\Pi\psi|^2 + \frac{\mathrm{h}^2}{8\pi} - \frac{\mathrm{hH_c}}{4\pi}\right]$$

The last term is the microscopic analog of the - BH/4π term, the thermodynamic field H being here equal to H_C. Since ψ satisfies the Landau-Ginsburg equation, ρ can be integrated by parts to give

$$\mathrm{s} = \int \mathrm{dx}\left[-\frac{1}{2}\beta|\psi|^4 + \frac{\mathrm{h}^2 - 2\mathrm{H_c\ h}}{8\pi}\right]$$

To obtain the wall energy S_{wall} , we subtract from S the term $\int (H_c^2/8\pi)\, dx$, which corresponds to the potential in the normal (or in the superconducting) phase:

$$\mathrm{S_{wall}} = \int \mathrm{dx}\left[-\frac{1}{2}\beta|\psi|^4 + \frac{(\mathrm{h} - \mathrm{H_c})^2}{8\pi}\right]$$

The $h(\psi)$ relation can be rewritten as

$$\mathrm{h} = \mathrm{H_c} - \frac{\mathrm{mc}}{\mathrm{e}\hbar}\beta|\psi|^2$$

and

$$\frac{(\mathrm{h} - \mathrm{H_c})^2}{8\pi} = \frac{1}{8\pi}\beta^2\left(\frac{\mathrm{mc}}{\mathrm{eh}}\right)^2|\psi|^4 = \frac{1}{2}\beta|\psi|^4 \quad \text{when } \kappa = \frac{1}{\sqrt{2}}$$

Thus $S_{\text{wall}} = 0$ for $\kappa = 1/\sqrt{2}$.
A similar calculation in terms of Sarma solutions can be done for the energy of an isolated vortex line, when $\kappa = 1/\sqrt{2}$. The conclusion there is that the first penetration field $\mathrm{H_{c_1}}$ is equal to $\mathrm{H_c}$. For that particular value of κ, $\mathrm{H_{C_1}}, \mathrm{H_{C2}}$, and $\mathrm{H_C}$ coincide.

REFERENCES

A much more detailed study of the various applications of the Landau-Ginsburg equation is to be published by Saint-James, Sarma, Thomas (Pergamon).

6.4 Microscopic Analysis of the Landau-Ginsburg Equations

6.4.1 7-1 Linearized Self-Consistency Equation

In the preceding chapter we constructed the Landau-Ginsburg equations from a postulated form of the free energy F, which introduces an unknown coefficient [for example, the coefficient

C of (6-7)] giving the energy associated with spatial variations in the order parameter. Gorkov (1959) has shown that it is possible to establish the Landau-Ginsburg equations from the microscopic theory and to calculate in particular the coefficient C. Here we give a simplified version of this calculation.

Δ Treated as a Perturbation

Our starting point will be the self-consistency equation

$$\Delta(r) = V \sum_n v_n^*(r) u_n(r) \left[1 - 2f\left(\epsilon_n\right)\right] \tag{7-1}$$

where u_n and v_n are solutions corresponding to positive eigenvalues of the Bogolubov system

$$\begin{aligned} \epsilon_n u_n &= \left[\frac{1}{2m}\left(p - \frac{e}{c}A\right)^2 + U - E_F\right] u_n + \Delta v_n \\ \epsilon_n v_n &= -\left[\frac{1}{2m}\left(p + \frac{e}{c}A\right)^2 + U - E_F\right] v_n + \Delta^* u_n \end{aligned} \tag{7-2}$$

As usual, the effects of impurities, and so on, are included in U. We expand the right-hand side of (7-1) as a power series in Δ and set

$$\begin{aligned} u_n &= u_n^0 + u_n^1 + \cdots \\ v_n &= v_n^0 + v_n^1 + \cdots \end{aligned} \tag{7-3}$$

From (7-2), we see that u_n^0 and v_n^0 are proportional to the eigenfunctions ϕ_n of one electron in a normal metal, defined by

$$\xi_\mathrm{n}\phi_\mathrm{n} = \left[\frac{1}{2m}\left(\mathrm{p} - \frac{\mathrm{eA}}{\mathrm{c}}\right)^2 + \mathrm{U} - \mathrm{E_F}\right]\phi_\mathrm{n} \tag{7-4}$$

To zeroth order, we have

$$\begin{aligned} u_n^0 &= \phi_n, \quad v_n^0 = 0 \quad (\xi_n > 0) \\ u_n^0 &= 0, \quad\ v_n^0 = \phi_n^* \quad (\xi_n < 0) \end{aligned} \tag{7-5}$$

and $\epsilon_n^0 = |\xi_n|$. Since $u_n^0 v_n^0 = 0$, there is no term of lowest order on the right-hand side of (7-1). In order to determine the first-order corrections u_n^1 and v_n^1, we set

$$\begin{aligned} \mathrm{u_n^1} &= \sum_m \mathrm{e_{nm}}\phi_m \\ \mathrm{v_n^1} &= \sum_m \mathrm{d_{nm}}\phi_m^* \end{aligned} \tag{7-6}$$

If we insert these values into (7-2), multiply the first equation by ϕ_m^*, the second by ϕ_m, and integrate, we find

$$\begin{aligned} \left(|\xi_n| - \xi_m\right) e_{nm} &= \int \Delta(r)\phi_m^*(r) v_n^0(r) dr \\ \left(|\xi_n| + \xi_m\right) d_{nm} &= \int \Delta*(r)\phi_m(r) u_n^0(r) dr \end{aligned} \tag{7-7}$$

As usual, the diagonal terms such as e_{nn} are taken to be zero to preserve the normalization of $\binom{u}{v}$.

We can now insert u_n^1 and v_n^1 defined by (7-6) and (7-7) into the self-consistency equations (7-1). We obtain to first order:

$$\Delta(\mathbf{s}) = \int K(\mathbf{s},\mathbf{r})\Delta(\mathbf{r})d\mathbf{r} \tag{7-8}$$

where

$$\begin{aligned} K(s,r) =& V\sum_{n,m}\left[1-2f\left(|\xi_n|\right)\right] \\ &\times\left[\frac{u_n^{0*}(r)u_n^0(s)}{|\xi_n|+\xi_m}+\frac{v_n^{0*}(s)v_n^0(r)}{|\xi_n|-\xi_m}\right]\phi_m(s)\phi_m^*(r) \end{aligned}$$

u_n^0 is nonzero only for $\xi_n > 0$, while v_n^0 is nonzero for $\xi_n < 0$. Also the function $1-2\mathrm{f}\left(\xi_\mathrm{n}\right) = \tanh\left(\beta\xi_\mathrm{n}/2\right)$ is odd in ξ_n. These remarks enable us to collect the uu and vv terms into one single component. Finally, we can symmetrize the expression with respect to the indices n and m (since it is to be summed over n and m) and obtain

$$\begin{aligned} K(s,r) =& \frac{V}{2}\sum_{nm}\frac{\tanh\left(\frac{\beta\xi_n}{2}\right)+\tanh\left(\frac{\beta\xi_m}{2}\right)}{\xi_n+\xi_m} \\ &\times\phi_n^*(r)\phi_m^*(r)\phi_n(s)\phi_m(s) \end{aligned} \tag{7-9}$$

It is sometimes useful to transform this result in the following manner: Let us write

$$\tanh\frac{\beta\xi}{2} = 2\mathrm{k_B}\ \mathrm{T}\sum_\omega\frac{1}{\xi-\mathrm{i}\hbar\omega} \tag{7-10}$$

where $\hbar\omega = 2\pi k_B T\left(\nu+\frac{1}{2}\right)$ and Σ represents a sum over all positive or negative integers ν. Equation (7-10) can be verified by comparing the poles and residues of both sides of (7-10) in the complex ξ plane. (Also note that we can use either $\pm$i in the denominator of (7-10) since both ω and $-\omega$ contribute.)

Then

$$\begin{aligned} \frac{\tanh\left(\frac{\beta\xi}{2}\right)+\tanh\left(\frac{\beta\xi'}{2}\right)}{\xi+\xi'} &= 2\mathrm{k_B}\ \mathrm{T}\sum_\omega\frac{1}{\xi+\xi'} \\ &\times\left(\frac{1}{\xi-\mathrm{i}\hbar\omega}+\frac{1}{\xi'+\mathrm{i}\hbar\omega}\right) \\ &= 2\mathrm{k_B}\ \mathrm{T}\sum_\omega\frac{1}{\left(\xi-\mathrm{i}\hbar\omega\right)\left(\xi'+\mathrm{i}\hbar\omega\right)} \end{aligned}$$

and

$$K(s,r) = Vk_BT\sum_\omega\sum_{n,m}\frac{\phi_n^*(r)\phi_m^*(r)\phi_n(s)\phi_m(s)}{\left(\xi_n-i\hbar\omega\right)\left(\xi_m+i\hbar\omega\right)} \tag{7-11}$$

Equation (7-8) with the explicit form (7-11) for the kernel constitutes the linearized form of the self-consistency condition (7-7). The enormous advantage over (7-1) is that the functions u and v are eliminated, and $\Delta(r)$ is then the only unknown in (7-8). However we must remember that the linearized form only applies for very small Δ, that is, in the immediate neighborhood of a second-order transition.

Separation of Magnetic Effects

We now assume that the spatial variations in the vector potential are small. Then the eigenfunctions ϕ_n in the normal metal in the presence of A differ from the eigenfunctions w_n in the absence of A by only a phase factor.

$$\phi_n^*(r)\phi_n(s) \to w_n(r)w_n(s)e^{ieA\cdot(s-r)/\hbar c} \tag{7-12}$$

where the w_n are taken to be real. It is easy to verify that (7-12) is compatible with (7-4) and the definition of the w_n if the spatial variations in A are systematically neglected. What is the range of validity of this approximation?
(1) We see later that the range of the kernel K(s, r) in a pure metal is of the order of $\xi_0 = 0.18\hbar v_F/k_B T_0$. The spatial variations in the vector potential must therefore be small on this scale. A condition is thus obtained by requiring the field h to vary slowly, which implies that the penetration depth be large with respect to ξ_0

$$\lambda_{\mathrm{L}}(\mathrm{T}) \gg \xi_0 \tag{7-13}$$

(2) A slow variation of $h = \operatorname{curl} A$ does not guarantee that A varies slowly. Over the distance $|s - r| \sim \xi_0$, A can vary by $\sim \xi_0 h$. This results in an uncertainty in the phase

$$\frac{\mathrm{e}}{\hbar \mathrm{c}}\xi_0\ \mathrm{h}\xi_0 \sim \frac{\hbar\omega_{\mathrm{c}}\mathrm{E_F}}{(\mathrm{k_B}\ \mathrm{T}_0)^2}$$

This must be small compared to one, and we are then led to

$$\frac{(k_B T_0)^2}{E_F} \gg \hbar\omega_c \tag{7-14}$$

where $\omega_c = eh/mc$ is the cyclotron frequency of electrons in the normal metal in the field h. For a bulk, first-kind superconductor, h is at most equal to the thermodynamic field $\mathrm{H_c(T)}$. From Eqs. (6-25) and (6-19) we have, for a pure metal,

$$\mathrm{H_c} \sim \frac{\phi_0}{\kappa\xi_0^2}\frac{\mathrm{T}_0 - \mathrm{T}}{\mathrm{T}_0} \quad (\mathrm{T} - \mathrm{T}_0)$$

where κ is the Landau-Ginsburg parameter and $\phi_n = \mathrm{hc/2e}$ is the quantum of flux. The condition (7-14) then becomes $(T_0 - T)/T_0 < \kappa$. This is less restrictive than condition (7-13) which can be written as $\kappa > [(\mathrm{T}_0 - \mathrm{T})/\mathrm{T}_0]^{1/2}$. For a second-kind superconductor, h is at most of the order of $\mathrm{H_{C_2}} \sim (\phi_0/\xi_0^2)[(\mathrm{T}_0 - \mathrm{T})/\mathrm{T}_0]$ and (7-14) becomes $(\mathrm{T}_0 - \mathrm{T})/\mathrm{T}_0 \ll 1$.
(3) For (7-12) to be correct, it is evident that the radius $R = mcv_F/eh$ of the electronic orbits in the field h must be large with respect to the range of the kernel $K(s, r)$. This requirement assures that all effects related to Landau diamagnetism are negligible. The condition $\mathrm{R} \gg \xi_0$ can also be written

$$\hbar\omega_{\mathrm{c}} \ll \mathrm{k_B}\ \mathrm{T_n} \tag{7-15}$$

again less restrictive than (7-14). We conclude that for pure metals the substitution (7-12) is valid provided that T is close enough to T_n. This, as we shall see, leads directly to the Landau-Ginsburg equations. For "dirty" alloys, we show later that the situation is even more favorable, and that the linear integral equation (7-8) can be replaced at all temperatures by a second-order differential equation of the Landau-Ginsburg form. Finally we are led to

$$\Delta(s) = \int dr K_0(s, r) \exp\left[-\frac{2ie}{\hbar c}A\cdot(s - r)\right]\Delta(r) \tag{7-16}$$

$$K_o(s,r) = Vk_BT \sum_{\omega} \sum_{n,m} \frac{w_n(r)w_m(r)w_n(s)w_m(s)}{(\xi_n - i\hbar\omega)(\xi_m + i\hbar\omega)} \tag{7-17}$$

Infinite Homogeneous Medium

We usually consider the kernel K_n in an infinite homogeneous medium. Then, if this is a pure metal, it is clear that $K_0(s,r)$ depends only on $s-r$. On the contrary, for an alloy, this translational invariance is lost. In this case, the translational invariance is restored by making an additional approximation. In (7-16), the average is taken over all impurity configurations. On the right-hand side of (7-16) appears the average $\overline{K_0(s,r)\Delta(r)}$. We approximate this in the following way:

$$\overline{\mathrm{K_0}(s,r)\Delta(r)} \to \overline{\mathrm{K_0}(s,r)}\,\overline{\Delta(r)} \tag{7-18}$$

Equation (7-18) is not rigorous because it neglects certain distortions of the pair potential in the immediate neighborhood of each impurity. However, detailed calculations (C. Caroli, 1962) have shown that this approximation is reasonable when the impurity potentials can be treated as weak perturbations. We therefore limit our discussion to alloys whose constituents are not too different chemically. Then (7-18) is applicable and the integral equation for $\overline{\Delta(r)}$ can be written completely in terms of the average kernel $\overline{K_0(s,r)}$, which only depends on $\mathbf{s}-\mathbf{r}$.

Relation between K_0 and a Correlation Function

A priori, the product of the four functions $\mathrm{w_n}$ that occurs in (7-17) is rather discouraging. However, it can be shown that this product is related to rather simple physical concepts. Taking, for simplicity, an infinite homogeneous medium, we study the Fourier transform

$$\begin{aligned} K_0(q) &= L^{-3} \int dr ds K_0(s-r) e^{iq\cdot(s-r)} \\ &= VL^{-3}k_BT \sum_{\omega,n,m} \frac{\langle n|e^{iqx}|m\rangle\langle m|e^{-iqx}|n\rangle}{(\xi_n - i\hbar\omega)(\xi_m + i\hbar\omega)} \end{aligned} \tag{7-19}$$

where L^3 is the volume of the sample. We have taken q along the x direction and set

$$\langle n|e^{iqx}|m\rangle = \int w_n(r) e^{iq\cdot r} w_m(r) dr$$

It is useful to first discuss the real function

$$g(q,\Omega) = \sum_m \overline{\langle n|e^{iqx}|m\rangle\langle m|e^{-iqx}|n\rangle}\,\delta(\xi_m - \xi_n - \hbar\Omega) \tag{7-20}$$

sometimes called the spectral density of the one-electron operator e^{iqx}. The symbol represents an average over all states of fixed energy ξ_n (for example, $\xi_\mathrm{n}=0$ corresponds to the Fermi level). In practice, $g(q,\Omega)$ depends strongly on Ω but only slightly on ξ_n and the average will be taken at the Fermi level. If g is known, then $K_n(q)$ is immediately given by

$$K_0(q) = N(0)Vk_BT \sum_{\omega} \int \frac{d\xi d\xi' g\left(q, \frac{\xi-\xi'}{\hbar}\right)}{(\xi - i\hbar\omega)(\xi' + i\hbar\omega)} \tag{7-21}$$

Now $g(q,\Omega)$ has a simple physical significance. Introduce the Heisenberg operator

$$e^{iqx(t)} = \exp\left(i\mathscr{H}_e t/\hbar\right) e^{iqx} \exp\left(-i\mathscr{H}_e t/\hbar\right) \tag{7-22}$$

which describes the evolution of e^{iqx} in time for an electron in the pure normal metal described by the Hamiltonian $\mathscr{H}_e = (p^2/2m) + U(r)$. In terms of the operator $e^{iqx(t)}$, the spectral density takes a very simple form:

$$g(q,\Omega) = \frac{1}{2\pi\hbar}\int dt e^{i\Omega t}\overline{\langle n|e^{-iqx(0)}e^{iqx(t)}|n\rangle} \tag{7-23}$$

Equation (7-23) can be verified by writing explicitly the matrix elements of $e^{iqx(t)}$ between states $|n\rangle$ and $|m\rangle$.

In order to determine g, it is only necessary to determine the correlation function of e^{iqx},

$$\left\langle e^{-iqx(0)}e^{iqx(t)}\right\rangle_{E_F} = \overline{\langle n|e^{-iqx(0)}e^{iqx(t)}|n\rangle} \tag{7-24}$$

for an electron at the Fermi energy in a normal metal.

(1) First for a pure metal, we can assume that at $t = 0$ the electron has abscissa $\mathrm{x_0}$ and velocity $\mathrm{v_F}\cos\theta$ along the x axis (θ is the angle between q and the electron velocity vector).

$$\begin{aligned} e^{-iqx(0)} &= e^{-iqx_0} \\ e^{iqx(t)} &= \exp\left[iq\left(x_0 + v_F t\cos\theta\right)\right] \end{aligned}$$

Thus

$$\left\langle e^{-iqx(0)}e^{iqx(t)}\right\rangle_{E_F} = \frac{1}{2}\int_0^\pi \sin\theta d\theta \exp\left(iqv_F\cos\theta t\right) \tag{7-25}$$

and

$$\begin{aligned} \mathrm{g(q,\Omega)} &= \frac{1}{2\hbar}\int_0^\pi \sin\theta \mathrm{d}\theta\delta\left(\Omega - \mathrm{qv_F}\cos\theta\right) \\ &= \begin{cases} \left(2\mathrm{qv_F}\hbar\right)^{-1} & |\Omega| < \mathrm{qv_F} \\ 0 & |\Omega| > \mathrm{qv_F} \end{cases} \end{aligned} \tag{7-26}$$

(2) For an impure metal where the mean free path ℓ is small compared to the wavelength studied $q^{-1}, e^{iqx(t)}$ is controlled by a diffusion (random walk) process. If $D = v_F\ell/3$ is the diffusion coefficient, we have

$$\begin{aligned} &\left\langle e^{-iqx(0)}e^{iqx(t)}\right\rangle_{E_F} = e^{-Dq^2|t|} \quad q\ell \ll 1 \\ &g(q,\Omega) = \frac{1}{\pi\hbar}\frac{Dq^2}{\Omega^2 + D^2q^4} \end{aligned} \tag{7-27}$$

Explicit Calculation of the Kernel $\mathrm{K_0}$

Using the forms (7-26) and (7-27) for $\mathrm{g(q,\Omega)}$, one can explicitly calculate the kernel $\mathrm{K_0(q)}$ from (7-21). The variables of integration are taken to be ξ and $\hbar\Omega = \xi' - \xi$ and the first integration is performed by the theory of residues over ξ. For the pure metal, one finds

$$\begin{aligned} \mathrm{K_0(q)} &= \frac{\mathrm{N(0)Vk_B\ T}\pi}{\mathrm{qv_F}^{\mathrm{h}}} \sum_{\omega} \int_{-\mathrm{qv_F}}^{\mathrm{qv_F}} \frac{\mathrm{d}\Omega}{2\omega - \mathrm{i}\Omega} \\ &= \frac{2\pi\ \mathrm{N(0)Vk_B\ T}}{\hbar_{\mathrm{qv}}} \sum_{\omega} \tan^{-1}\left(\frac{\mathrm{qv_F}}{2|\omega|}\right) \end{aligned} \tag{7-28a}$$

and for the impure metal

$$\begin{aligned} \mathrm{K_0(q)} &= \mathrm{N(0)Vk_B\ T}\frac{2\mathrm{i}}{\hbar} \sum_{\omega} \int \mathrm{d}\Omega \frac{\mathrm{Dq}^2}{\left(\mathrm{Dq}^2 + \mathrm{i}\Omega\right)(2\mathrm{i}\omega + \Omega)} \\ &= \frac{\mathrm{N(0)Vk_B\ T}}{\hbar} \sum_{\omega} \frac{1}{\mathrm{Dq}^2 + 2|\omega|} \quad (\mathrm{q}\ell \ll 1) \end{aligned} \tag{7-28b}$$

Discussion of these results

(1) Precautions related to the frequency cut-off in the interaction V. Until now we have neglected the fact that the interaction V in the BCS approximation only couples those states of energy $|\xi| < \hbar\omega_D$. This causes the sums in (7-28) to diverge. However, this is easily remedied by writing

$$K_0(q) = K_0(0) + [K_0(q) - K_0(0)] \tag{7-29}$$

The only divergent term is $K_0(0)$, which can be calculated directly from (7-9).

$$\begin{aligned} K_0(0) &= V \sum_n \frac{\tanh(\beta\xi/2)\,|w_n(r)|^2}{2\xi_n} \\ &= N(0)V \int_{-\hbar\omega_D}^{\hbar\omega_D} \frac{d\xi}{2\xi} \tanh\left(\frac{\beta\xi}{2}\right) \\ &= N(0)V \ln\frac{1.14\hbar\omega_D}{k_B T} \end{aligned} \tag{7-30}$$

where the s integration was performed by using the orthogonality of the function $w_n(s)$.[1]
(2) Spatial form of the kernel K_0. On taking the inverse Fourier transform of (7-28), we find

$$K_0(8,r) = K_0(R) = \begin{cases} \frac{N(0)Vk_BT}{2\hbar D} \sum_\omega \frac{1}{R} \exp\left\{-(2|\omega|/D)^{1/2}R\right\} & (R \gg \ell) \\ \frac{N(0)Vk_BT}{2\hbar v_F} \sum_\omega \frac{1}{R^2} \exp\left\{(-2|\omega|R)/v_F\right\} & (R \ll l) \end{cases} \tag{7-31b}$$

$$R = s - r$$

For R $\neq 0$, the sums converge. It is particularly interesting to study the asymptotic form of $K_0(R)$ at large distances. The only important terms are then $\hbar\omega = \pm\pi k_B T\ (\simeq \pm\pi k_B T_0)$. Then we find for $T = T_0$

[1] We had already obtained the result (7-30) in the simpler case of an infinite homogeneous medium without fields or currents where we predicted that $\Delta(r)$ is constant in space. Then the linearized self-consistency equation is simply written $\Delta = K_0(0)\Delta$. This has a nonzero solution only if $K_0(0) = 1$. This condition gives the temperature T_0 at which a nonzero order parameter can appear, that is, the transition temperature.

$$\frac{K_0(R)}{N(0)V} = \frac{k_B T_0}{2\hbar v_F}\frac{1}{R^2}\exp\left[-\frac{2\pi k_B T_0 R}{\hbar v_F}\right] = \frac{k_B T_0}{2\hbar v_F}\frac{1}{R^2}\exp\left(-1.13R/\xi_0\right)$$
$$= \frac{k_B T_0}{\hbar D}\frac{1}{R}\exp\left[-\left(\frac{6\pi k_B T_0}{v_F \ell}\right)^{1/2} R\right] \tag{7-32a}$$
$$= \frac{k_B T_0}{\hbar D R}\exp\left(-1.8R/\sqrt{\xi_0 \ell}\right)$$

Conclusion. For a pure metal and $T \sim T_0$, the range of $K_0(R)$ is of the order of $\xi_0 = 0.18\hbar v_{\mathrm{F}}/\mathrm{kT}_0$ as we previously stated. On the contrary when ℓ is small, (7-32b) gives a range $\sqrt{\xi_n \ell}$. The range of validity of (7-32b) is limited by $\mathrm{R} \gg \ell$, which implies $(\xi_0 \ell)^{1/2} \gg \ell$ or

$$\xi_0 \gg \ell \quad \text{(dirty metal)} \tag{7-33}$$

[When (7-33) is satisfied, the alloy is said to be dirty following the terminology introduced by Anderson.) If the matrix is a nontransition metal, ξ_0 is generally high (for example, $\xi_0 = 16 \times 10^3$Å for Al), and a small fraction of impurities (10^{-3}) is sufficient to make the metal dirty.

It is interesting to compare K_0 with the kernel $S_{\mu\nu}$, studied in Chapter 5, which gives the current responds of a superconductor in the presence of a vector potential A . We have seen that in a dirty alloy the range of $S_{\mu\nu}$ is ℓ, but the range of K_0 is $\sqrt{\xi_0 \ell}$. What is the reason for this difference?

Answer. The kernels $\mathrm{S}_{\mu\nu}$ and K_0 can both be expressed as average one-electron correlation functions in a normal metal in the absence of fields:

$$S_{\mu\nu} = \frac{1}{4}\int d\xi d\xi' \int \frac{dt}{2\pi} L\left(\xi, \xi'\right) e^{i(\xi-\xi')t/\hbar} \left\langle j_\mu\left(r_1, 0\right) j_\nu\left(r_2, t\right)\right\rangle_{E_F}$$
$$K_0 = \frac{1}{2} N(0) V \int d\xi d\xi' \left[\frac{\tanh(\beta\xi/2) + \tanh\left(\beta\xi'/2\right)}{\xi + \xi'}\right] \tag{7-34}$$
$$\times \int \frac{dt}{2\pi} e^{i(\xi-\xi')t/\hbar} \left\langle \delta\left(r(0) - r_1\right) \delta\left(r(t) - r_2\right)\right\rangle_F \tag{7-35}$$

where $\langle j_\mu j_\nu \rangle$ is a transverse current correlation function and $\langle \delta\delta \rangle$ is a density correlation function. Equations (7-34) and (7-35) can easily be verified by explicitly calculating the matrix elements that appear in products such as $\mathrm{j}_\mu \mathrm{j}_\nu$.

For $\mathrm{T} \sim \mathrm{T}_0$, the integrations over ξ and ξ' in (7-34) and (7-35) limit the useful interval to $t \sim h/k_B T_0$. If there are no collisions, the distance traveled by an electron in the time t is $v_F t \sim \xi_0$. Then both $S_{\mu\nu}$ and K_0 have the range ξ_0. If the alloy is dirty, the velocity correlation function falls to zero after the electron travels a distance ℓ: the range of $S_{\mu\nu}$ is ℓ. However the density correlation function is not destroyed by a collision. It obeys a diffusion equation. The average distance traveled in time t is $v\overline{Dt}$, where D is the diffusion coefficient $\mathrm{D} = \frac{1}{3}\mathrm{v}_{\mathrm{F}}\ell$. Thus the range of the kernel K_0 becomes $\sqrt{\mathrm{Dt}} \sim \sqrt{\xi_0 \ell}$.

6.4.2 7-2 Landau-Ginsburg Equations

Addition of Nonlinear Terms to the Self-Consistency Equations

The linearized self-consistency equation (7-8) for the pair potential applies when Δ is infinitesimal, that is, at the transition point (provided that the transition of interest is of second order, that is, Δ goes to 0 continuously when the temperature is raised). Call T^* the highest temperature for which (7-8) has a nonzero solution $\Delta(r)$.T^* is the ordering temperature in the

conditions of the experiment: For instance, in a bulk Type II material, if we impose an external field H, T^* is such that $H_{c_2}(T^*) = H$. Later in this section we make extended use of this property. For the present time, our aim is slightly different. We want to extend our analysis to temperatures (slightly) below T*. Then, it is not sufficient to consider only a first-order approximation in Δ in the right-hand side of (7-1). To extend the calculation, u and v must be calculated to higher order in Δ. The result is of the form

$$\begin{aligned}\Delta(s) = &\int K_0(s,r)e^{-[2ieA\cdot(s-r)]/\hbar c}\Delta(r)dr \\ &+ \int R(s,r,\ell,m)\Delta^*(r)\Delta(\ell)\Delta(m)drd\ell dm \end{aligned} \tag{7-36}$$

Notice in particular that there are no terms of order Δ^2. The kernel $R(s,r,\ell,m)$ can be calculated but its only important property to remember is that in a pure metal its range is of the order of ξ_0. The only contributions to the integral $drd\ell dm$ come from regions where the three points r, ℓ, m are simultaneously near s. In an alloy, the ranges are further reduced. These remarks allow us to avoid a complete calculation of the kernel R.

Hypothesis of Slow Variation

We now assume that quantities such as $\Delta(r)e^{[2ieA\cdot(r-s)]/\hbar c}$ vary slowly with respect to the range of K_0 or of R. This restriction defines the Landau-Ginsburg domain. We can then expand $\Delta(r)$ in a Taylor series about the point s:

$$\begin{aligned}\Delta(r)e^{-2i\phi(r)} =&\Delta(s)e^{-2i\phi(s)} + (r-s)\cdot\nabla\left(\Delta e^{-2i\phi}\right) \\ &+ \frac{1}{2}\sum_{\alpha\beta}(r-s)_\alpha(r-s)_\beta\frac{\partial^2}{\partial r_\alpha \partial r_\beta}\left(\Delta e^{-2i\phi}\right)\end{aligned}$$

where we have introduced the phase parameter

$$\phi_S(r) = e[A(s)\cdot r]/\hbar c$$

By performing the differentiations, we get

$$\begin{aligned}\Delta(r)e^{-2i\phi(r)} =&e^{-2i\phi(s)}\left\{\Delta(s) + \sum_\alpha (r-s)_\alpha\delta_\alpha\Delta\right. \\ &\left. + \frac{1}{2}\sum_{\alpha\beta}(r-s)_\alpha(r-s)_\beta\delta_\alpha\delta_\beta\Delta\right\} \\ \delta_\alpha =&\frac{\partial}{\partial s_\alpha} - \frac{2ieA_\alpha(s)}{\hbar c}\end{aligned} \tag{7-37}$$

We insert the expansion (7-37) into the linear part of (7-36). For the correction term of order Δ^3 in Eq. (7-36), it will be sufficiently accurate to neglect completely the spatial variations of Δ, and to set $\Delta(r) = \Delta(\ell) = \Delta(m) = \Delta(s)$. Finally, in an infinite, homogeneous metal, terms such as $\int K_0(r,s)(r-s)dr$ vanish by symmetry. This finally gives

$$\Delta(s) = Q\Delta(s) + \frac{1}{2}\sum_{\alpha,\beta} L_{\alpha\beta}\delta_\alpha\delta_\beta\Delta(s) + R|\Delta(s)|^2\Delta(s) \tag{7-38}$$

$$\begin{aligned} Q &= \int K_0(s,r)dr \\ L_{\alpha\beta} &= \int K_0(s,r)\,(s_\alpha - r_\alpha)\,(s_\beta - r_\beta)\,dr \\ R &= \int R(s,r,\ell,m)drd\ell dm \end{aligned} \tag{7-39}$$

For a cubic crystal ($L_{\alpha\beta} = L\delta_{\alpha\beta}$), Eq. (7-38) has exactly the form predicted by Landau and Ginsburg (6-11). The coefficients Q, L, R introduced here are related to the coefficients A, B, C in (6-7) by

$$\frac{-Q+1}{A} = \frac{R}{B} = \frac{1}{2}\frac{L}{C} \tag{7-40}$$

Discussion of the Coefficients

We have already determined A and B for the case $A = 0, \Delta = \text{const}$ (6-3). Numerical values for Q and R can also be found by the same method. We know that for $\mathrm{A} = 0, \Delta = \text{const}$, and the complete self-consistency equation (7-1) reduces to

$$\begin{aligned} \Delta &= \mathrm{N(0)V}\int_0^{\mathrm{h}\omega} \mathrm{D}\Delta\frac{\tanh(\beta\epsilon/2)}{\epsilon}\mathrm{d}\xi \\ \epsilon &= \left(\xi^2 + \Delta^2\right)^{1/2} \end{aligned} \tag{7-41}$$

Anderson's theorem (Chapter 5) shows that (7-41) is valid for an alloy as well as for a pure metal. Expanding the right-hand side as a power series in Δ and performing the integration, we find

$$\begin{aligned} \mathrm{Q} &= \mathrm{N(0)V}\left[\ln\frac{1.14\hbar\omega_\mathrm{D}}{\mathrm{k_B\ T}}\right] \sim 1 + \mathrm{N(0)V}\frac{\mathrm{T_0 - T}}{\mathrm{T_0}} \\ \mathrm{R} &= -0.1066\frac{\mathrm{N(0)V}}{(\mathrm{k_B\ T_0})^2} \end{aligned} \tag{7-42}$$

The most interesting coefficient is L. which describes the effects of spatial variations of Δ. From the explicit form of the kernel $K_0(7-31)$, we find for a pure metal

$$\begin{aligned} L &= \frac{\pi}{6}N(0)Vv_F^2k_BT_0\sum_\omega\frac{1}{|\omega|^3} \\ &= 0.033N(0)V\left(\frac{\hbar v_F}{k_BT_0}\right)^2 \end{aligned} \tag{7-43a}$$

and for a dirty metal ($\ell \ll \xi_0$)

$$\begin{aligned} L &= \pi N(0)VD\frac{k_BT_0}{\hbar}\sum_\omega\frac{1}{|\omega|^2} \\ &= \frac{\pi}{12}N(0)V\frac{\hbar v_F\ell}{k_BT_0} \end{aligned} \tag{7-43b}$$

(The sum $\Sigma_\omega 1/|\omega|^3$ must be evaluated numerically while $\Sigma_\omega 1/|\omega|^2$ determined by differentiating (7-10) with respect to ξ and then setting ξ equal to zero.) These results can be expressed in various ways:
(1) The coefficient C of the free energy (6-7) becomes

$$C = \frac{L}{2}\frac{A}{1-Q} = \frac{1}{2}\frac{L}{V} \tag{7-44}$$

(2) The characteristic length $\xi(T)$ that appears in the Landau-Ginsburg equation in the absence of a field is obtained by comparing (6-17) to (6-8)

$$\xi(\mathrm{T}) = \left[\frac{\mathrm{L}}{2(\mathrm{Q}-1)}\right]^{1/2} \tag{7-45}$$

It diverges as $[T_0/(T_0 - T)]^{1/2}$ as predicted in (6-19).
(3) The Landau-Ginsburg parameter κ is given by Eq. (6-26)

$$\kappa = \frac{1}{4}\left(\frac{\mathrm{B}}{2\pi}\right)^{1/2}\frac{\hbar \mathrm{c}}{\mathrm{eC}} \tag{7-46}$$

For a pure metal, this formula leads to the previous result $\kappa = 0.96\lambda_{\mathrm{L}}(0)/\xi_0$. For a dirty metal, we have

$$\kappa = 0.75\frac{\lambda_L(0)}{\ell} \tag{7-47}$$

where $\lambda_L(0) = (mc^2/4\pi ne^2)^{1/2}$ is the London penetration depth in the pure metal at absolute 0 .

This result can be expressed in another way that involves directly measurable quantities in the normal state instead of ℓ and λ_L. The mean free path ℓ is related to the resistivity ρ by the equation [2]

$$\rho^{-1} = 2e^2N(0)D = \frac{2}{3}N(0)e^2v_F\ell \tag{7-48}$$

The Lodon penetration depth is given by [3]

$$\lambda_L(0) = \left(\frac{3c^2}{8\pi N(0)v_F^2e^2}\right)^{1/2} \tag{7-49}$$

Finally, N(0) can be expressed as a function of the electronic specific heat at low temperatures C_e (per cm^3):

$$\mathrm{C_e} = \gamma \mathrm{T}$$
$$\gamma = \frac{2\pi^3}{3}\,\mathrm{N(0)k_B^2}$$

Finally this gives

$$\frac{\lambda_{\mathrm{L}}(0)}{\ell} = \frac{1}{2\pi\sqrt{\pi}}\frac{\mathrm{ce}}{\mathrm{k_B}}\rho\gamma^{1/2} \tag{7-50}$$

If ρ is expressed in ohm.cm instead of cgs units, we find

[2] Proof of (7-48): In the normal state, the current j is given by $j = -eD\nabla n + E/\rho$ where n is the number of electrons per cm^3. At equilibrium, $n = n_0$ 2 N(0)eV where V is the potential such that $\mathrm{E} = \nabla \mathrm{V}$. On setting $\mathrm{j} = 0$ we obtain (7-48).

$$\kappa = 7.5 \times 10^3 \rho\gamma^{1/2} \quad (\xi_0 \gg \ell) \tag{7-51}$$

Remarks about Dirty Alloys.

(1) From (7-47), κ only depends on ℓ, that is, the transport properties of the alloy in the normal state.
(2) If the pure metal is a superconductor of the first kind ($\kappa_{\text{pure}} \ll 1$), then the alloy is of the second type ($\kappa > 1/\sqrt{2}$) when ℓ is less than a critical value $\ell_c = 1.06\lambda_L(0)$. This law has been verified by Seraphim for various impurities in indium. The critical concentrations vary a great deal according to the impurity used (0.8% for Bi, 7% for Tl). However, the value of ℓ_c is nearly independent of the nature of the impurity $\ell_C = 440 \pm 100$Å for Bi, Pb, Su, Cd, Tl, Hg). (The London penetration depth $\lambda_L(0)$ of indium is estimated to be 400Å.
(3) For the alloy InBi (2.5%Bi), studied by Kinsel, Lynton, and Serin, the magnetic measurements give $\kappa = 1.79$. The theoretical value deduced from $(7-51)$ is of the order of 1.7.

Table 7-1
Characteristic Lengths

	Pure Metal
Range of the kernel $S_{\mu\gamma}$ (relation between current and vector potential)	$\xi_0 = 0.18\frac{\hbar v_F}{k_B T_0}$
Range of the kernel K_0 Iself-consistency equation for $\Delta(r)$]	$\sim 5_0$
Scale of the spatial variations of $\lvert\Delta\rvert$ in the Landau-Ginsburg domain	$\xi(T) = 0.74\xi_0 \left(\frac{T_0}{T_0 - T}\right)^{L/2}$
Penetration depth in the Landau-Ginsburg domain	$\lambda(T) = \frac{1}{\sqrt{2}}\lambda_L(0) \left(\frac{T_0}{T_0 - T}\right)^{1/2}$

Final Remarks.

Our discussion has only dealt with the first Landau-Ginsburg equation (6-11), that is, the self-consistency equation for $\Delta(r)$ lor $\psi(r)$]. In order to complete the microscopic analysis, it is also necessary to calculate the current $f(r)$ at each point and show that it is given by a formula of the type (6-12). This calculation is performed just as the preceding one, by expressing $j(r)$ as a function of the Bogolubov u's and v's, and then calculating j to second order in Δ. We do not do this here since it is very analogous to the preceding calculation and gives no new information. The three coefficients A, B, C of the free energy (6-7) have already been determined. We could also have directly treated the free energy itself. All these approaches are equivalent. We chose to discuss the self-consistency equation for Δ, in view of other applications to be discussed later.

Problem.

Construct a Landau-Ginsburg equation for a thin film ($d \ll \xi_0$) with diffuse reflection at the boundaries of the film.

Solution.

In general, there is no solution. No Landau-Ginsburg equation applies to all cases. For instance the effective κ would depend on the angle between the magnetic field and the film

[3] Proof of (7-49): In the presence of a static vector potential A, the entire Fermi surface is displaced by a momentum $\delta p = eA/c$. The corresponding current is $\mathbf{j} = e\Sigma l\,(\partial f/\partial_p)\cdot\delta p|v_p$ where f is the distribution function. This gives $j = -A\left(2e^2/3c\right)N(0)v_F^2$ and thus $(7-49)$.

plane. Even more seriously, it may depend on the ratio d/λ(T) which is strongly temperature dependent.

However, in one case we can construct a well-defined (two-dimensional) Landau-Ginsburg equation. We need two conditions: (1) The amplitude of Δ must be constant in the film thickness. This will be true when d $< \xi_0$, and implies

$$\left(\frac{\partial}{\partial z} - \frac{2ie}{\hbar c}A_z\right)\Delta \to 0$$

(z is the direction normal to the film). (2) The variations of A in the film thickness are negligible. This requires that the field be normal to the film plane, and also that the film be thinner than some effective penetration depth (we come back to that condition later).

On the other hand, Δ and A shall be allowed to vary slowly in the plane of the film (xy plane). The free energy is then of the form

$$\mathrm{F} = \mathrm{A}|\Delta|^2 + \frac{\mathrm{B}}{2}|\Delta|^4 + \mathrm{C}\left\{\left|\left(\frac{\partial}{\partial \mathrm{x}} - \frac{2\mathrm{ie}}{\hbar \mathrm{c}}\ \mathrm{A_x}\right)\Delta\right|^2 + \left(\frac{\partial}{\partial \mathrm{y}} - \frac{2\mathrm{ie}}{\hbar \mathrm{c}}\ \mathrm{A_y}\right)\Delta\right|^2\right\}$$

In order to determine C, we start from the linearized self-consistency equation (7-16) and study the Fourier transform $K_0(q)$ of the kernel, where q is a vector in the xy plane. When d is small ($d \ll \xi_0$), most of the electrons experience several collisions with the walls during the time interval $\hbar/k_B T_0$ and the function $g(q, \Omega)$ is governed by a diffusion equation just as for a dirty superconductor. [4] The calculations are quite analogous to those giving rise to (7-43) and (7-44) and give

$$\mathrm{C} = \frac{\pi}{8}\ \mathrm{N}(0)\frac{\mathrm{hD}}{\mathrm{k_B}\ \mathrm{T_0}}$$

The diffusion coefficient D is no longer equal to $\frac{1}{3}v_F\ell$ but rather of the order of $v_F d$. The coefficient D can be related to the experimental conductivity $\bar{\sigma}$ of the film in the normal state by means of (7-48)

$$\bar{\sigma} = 2e^2 N(0) D$$
$$C = \frac{\pi}{16}\frac{\hbar\bar{\sigma}}{2k_B T_0}$$

Detailed calculations of $\bar{\sigma}$ can be found for instance in the book by Olsen, Electron Transport in Metals (New York: Interscience, 1962), p. 80. In practice of course it is better to extract $\bar{\sigma}$ from a measurement in the normal state on the same film.

Discussion.

(1) The order of magnitude of $\bar{\sigma}$ is $ne^2 d/mv_F$. Thus $C \sim N(0)\xi_0 d$ and $\kappa \sim \lambda_L(0)/d$.
(2) Once C is determined, we can write the equation for the current - in the x direction

$$\mathrm{j_X} = \frac{2\mathrm{eC}}{\mathrm{i}\hbar}\left(\Delta^*\frac{\partial\Delta}{\partial \mathrm{x}} - \Delta\frac{\partial\Delta^*}{\partial \mathrm{x}}\right) - \frac{8\mathrm{e}^2\mathrm{C}}{\hbar \mathrm{c}}\ \mathrm{A_X}$$

[4] There are a few electrons whose velocity is just in the plane of the film and which thus suffer no collisions. One can take account of them exactly. For simplification we here assume that there also exist volume impurities and therefore a bulk mean free path $\ell \lesssim \xi_0$ (but $\ell >$ d). Under this condition there is no significant contribution from these "anomalous electrons."

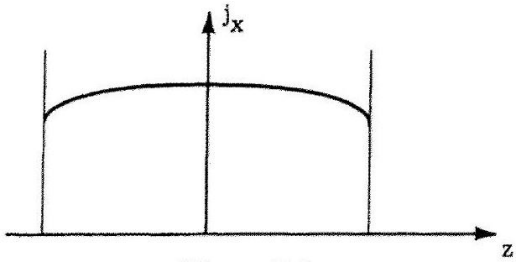


Figure 7-1
Current distribution across a thin film ($d < \xi_0$) with diffuse reflection at the surface.

However it is important to realize that, even if d is small, the current distribution $j_X(z)$ throughout the thickness of the film is not uniform (Fig. 7-1). The current j_X given by the preceding formula is just the average of j_X over the thickness.
(3) Although j is not independent of z, A is to a good approximation independent of z: using the relation $\partial^2 A_X/\partial z^2 = (4\pi/c)j_X$, it is easy to show that, when A_X is an even function of z, the relative variations of A_X through the thickness are of the order $d^3/\xi_0\lambda^2 \ll 1$.

6.4.3 7-3 Surface Problems in the Landau-Ginsburg Region

Boundary Conditions at an Interface

In the preceding section we have reconstructed the Landau-Ginsburg equations from the microscopic theory, for an infinite homogeneous medium. We shall now consider a superconducting specimen occupying the half-space $x > 0$. The region $x < 0$ is either an insulator or normal metal. In all cases, we shall assume that there is no current flowing through the boundary. [5]

Over a width ξ_0 at the surface, [6] $K_0(r, r')$ and $S_{\mu\nu}(r, r')$ are modified. On the microscopic scale it is necessary to calculate these modifications and then to determine the spatial distribution of the currents j and of the pair potential Δ in the perturbed layer. The result of such calculations is represented in (Fig. 7-2a) for Δ. On the other hand, on the Landau-Ginsburg scale [lengths of the order of $\xi(T), \lambda(T) \gg \xi_0$] the effect of the surface can be simply described by means of a boundary condition for $x = 0$ (Fig. 7-2b). What will be the form of this

[5] When normal currents and supercurrents coexist, the implied dissipative effects must be calculated by a dynamic equation more general than the Lan-dau-Ginsburg equations.
[6] We quote here the orders of magnitude that apply for a pure metal. In a dirty alloy, of course, the "transition width" would decrease to $\sqrt{\xi_0 l}$.

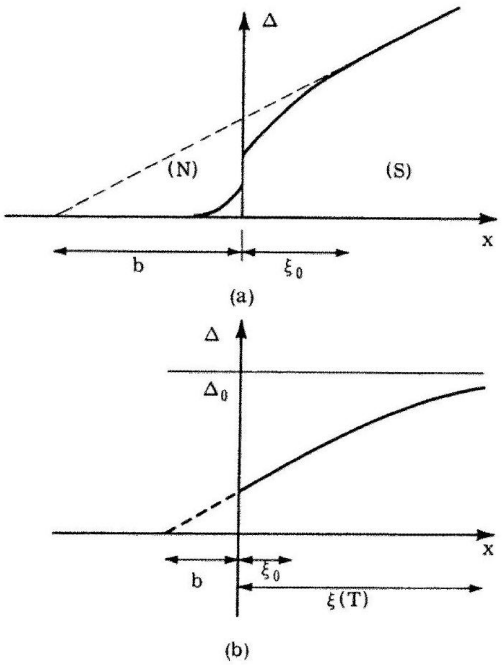


Figure 7-2
(a) The microscopic variation of the order parameter near a superconducting-normal metal boundary. (b) "Macroscopic" description of the same situation, at temperatures where $\xi(T) \gg b$.

condition? Let us first consider the case A = 0, Δ = real. The exact boundary condition will be of the form

$$\left(\frac{d\Delta}{dx}\right)_{x=0} = \frac{1}{b}\Delta_{x=0} + \frac{1}{c}\frac{\Delta^3_{x=0}}{(k_B T_0)^2} + \cdots \tag{7-52}$$

Justification of (7-52):
(1) From the general form of the self-consistency equation, only the odd powers of Δ occur in the expansion. Also the lengths b, c, and so on, are real.
(2) Higher derivatives do not occur in (7-52) because they can be expressed in terms of the first and zeroth derivatives by the Landau-Ginsburg equations.
(3) We expect nonlinear effects to become important when $\Delta \sim k_B T_0$. Thus the quantities $1/b, 1/c$, and so on, are of the same order

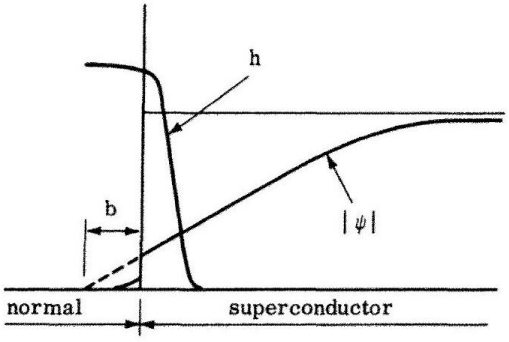


Figure 7-3
The magnetic field distribution at a normal-superconducting boundary.

of magnitude ($\sim 1/\xi_0$). The Δ^3 term in (7-52), smaller than the Δ term by $\sim (\Delta/k_B T_0)^2 \ll 1$, can be neglected. In the Landau-Ginsburg region, the boundary condition is linear, and the coefficient b can be obtained by solving the linearized self-consistency equation (7-8) in the neighborhood of the surface (for $T = T_0, A = 0$). In the presence of a magnetic field, we write, instead of (7-52),

$$\left(\frac{\mathrm{d}\Delta}{\mathrm{dx}} - \frac{2\mathrm{ie}}{\hbar\mathrm{c}}\,\mathrm{A_x}\Delta\right)_{\mathrm{x=0}} = \frac{(\Delta)_{\mathrm{x=0}}}{\mathrm{b}} \tag{7-53}$$

The form of (7-53) assures the gauge invariance dictated by the general formulas of Chapter 5. In (7-53), Δ may be replaced by ψ to which it is proportional. Using (7-53), it is easy to verify that for real b, the current (6-12) crossing the boundary is zero, as desired.

Contact between Superconductor and Insulator (or Vacuum)

We shall now show that $1/b$ is very small when the boundary separates the superconductor from an insulator. The equation to be solved (for A = 0 and T = $\mathrm{T_0}$) is

$$\Delta(s) = \int K_0(s,r)\Delta(r)dr \tag{7-54}$$

$K_0(s,r)$ is defined by (7-17) and therefore $\Delta(s)$ contains in particular a product of two functions $w_n(s)$ and $w_m(s)$, which decrease expotentially in the insulating region. Therefore $\Delta(s)$ vanishes rapidly for $\mathrm{s_x} < 0$.

On the other hand, for $s_x > \xi_0, \Delta(s)$ will have a linear form, [7]

$$\Delta(s) = \Delta_0\left(1 + \frac{s_X}{b}\right) \quad (s_X > \xi_0) \tag{7-55}$$

Proof of (7-55):
For $s_x, r_x > \xi_0$, the kernel $K_0(s,r)$ becomes identical to the kernel $K_p(s-r)$ in the bulk metal. For $T = T_0$, any linear function of the type (7-55) is a solution of $\Delta(s) = \int K_p(s-r)\Delta(r)dr$ because $\int K_p dr = 1$ and $\int K_p(s-r)[\Delta(r) - \Delta(s)]dr$ vanishes by symmetry.

In order to determine the length b in which we are interested, (7-54) is rewritten in the form

$$\begin{aligned}\Delta(s) - \int K_p(r-s)\Delta(r)dr &= \int \left[K_0(s,r) - K_p(r-s)\right]\Delta(r)dr \\ &= -H(s)\end{aligned} \tag{7-56}$$

The function H(s) vanishes for $\mathrm{s_x} > \xi_0$ (because $\mathrm{K_0} \to \mathrm{K_p}$) and also vanishes for $s_x < -\xi_0$ because $\Delta(r)$ is zero for $r_x < 0$ and the range of K_p is ξ_0. The advantage of (7-56) is that a localized perturbation appears on the right. For the moment we assume H(s) as known and solve for Δ by a Laplace transformation

$$\begin{aligned}\Delta(p) &= \int \Delta\left(s_X\right)\exp\left(-ps_X\right)ds \\ H(p) &= \int H\left(s_X\right)\exp\left(-ps_X\right)ds \\ K_p(p) &= \int K_p(r)\exp\left(-pr_X\right)dr \\ &= 1 + \frac{p^2}{2}L\cdots\end{aligned} \tag{7-57}$$

where $L = \int K_p(r)r_X^2 dr$ is given explicitly by (7-39). The transform of (7-56) is

[7] The linear dependence (7-55) might seem physically absurd since it leads to very large Δ 's at large distances from the boundary. In fact, when T is slightly below $\mathrm{T_0}$, the correct Δ(x) has a negative curvature and reaches the BCS values deep in the superconductor $[x > \xi(T)]$. But here we are interested in $x \sim \xi_0 \ll \xi(T)$ and the curvature is negligible.

$$\Delta(p)\left[1-K_p(p)\right]=-H(p) \tag{7-58}$$

Taking the limit $p \to 0$, from (7-57)

$$-\frac{L}{2}p^2\Delta(p) \to -H(0) = -\int H\left(s_X\right) ds$$

As $p \to 0$, the dominant term in (7-55) is the linear part,

$$\Delta(p) - \frac{\Delta_0}{b}\int_0^\infty s_X \exp\left(-ps_X\right) ds = \frac{\Delta_0 \Sigma}{bp^2} \tag{7-59}$$

where Σ is the surface area of the boundary. Combining (7-58) and (7-59), we find

$$\frac{1}{b} = \frac{2}{L\Sigma\Delta_0}\int H\left(s_X\right) ds = \frac{2}{L\Sigma\Delta_0}\int \left[K_p(s-r) - K_0(s,r)\right] \times \Delta(r) dr ds \tag{7-60}$$

In order to simplify (7-60), we shall assume that the interaction V is constant. Then $\int K_0(r,s)$ ds can be integrated by using the orthogonality of the functions $w_n(s)$ and we find

$$\int K_0(r,s) ds = N(r) V \ln \frac{1.14\hbar\omega_D}{k_B T_0} = \frac{N(r)}{N(0)} \tag{7-61}$$

where $N(r) = \Sigma_n \left|w_n(r)\right|^2 \delta\left(\xi_n\right)$ is the local density of states at the Fermi surface and $N(0)$ is its usual value for the bulk metal. Finally

$$\frac{1}{b} = \frac{2}{L}\int_{-\infty}^{\infty} dx \frac{\Delta(x)}{\Delta_0}\left[1 - \frac{N(x)}{N(0)}\right] \tag{7-62}$$

where $\Delta(x)/\Delta_0$ approaches zero in the insulating region and is of the order of 1 in the metallic region. $N(x)/N(0)$ passes from $0 \to 1$ in a few interatomic distances and the integrand is nonvanishing only in a width of order of the interatomic distance a. The effective distance b is given by

$$b \sim \frac{L}{a} \tag{7-63}$$

This is generally enormous: for a pure metal L $\sim \xi_0^2$ with $\xi_0 = 10^{-4}$ cm, which gives b ~ 1 cm. Therefore for a boundary separating
a superconductor from an insulator we can set $1/b = 0$. This leads to the boundary condition (6-13). More precisely, the criterion for the validity of (6-13) is that b $\gg \xi$(T), which is equivalent to $a/\xi_0 \ll \left[\left(T_0 - T\right)/T_0\right]^{1/2}$ [8]

Contact between Superconductor and Normal Metal

We now briefly discuss the case of the boundary between a superconductor and normal metal. If there is a good electrical contact between the N and S regions, the Cooper pairs can diffuse into the normal region. Algebraically this means that $\Delta(s)$ extends up to a rather long distance ξ_N into the N regions $(x < 0)$ $(\xi_N \sim \hbar v_{FN}/k_B T$ if N is a pure metal).

Equation (7-60) remains valid. It is, however, necessary to determine the exact form of $\Delta(x)/\Delta_0$ and therefore solve the integral equation (7-54) completely. Qualitatively the results can be represented in the form

$$\Delta \sim \Delta_0 \frac{^{\mathrm{N}}\mathrm{N}}{\mathrm{N}}\, \mathrm{T_j} \exp\left(\mathrm{x}/\xi_{\mathrm{N}}\right) \quad (\mathrm{x} < 0) \tag{7-64}$$

where $\mathrm{N_N/N}$ is the density of states factor occuring in (7-61) and $\mathrm{T_j}$ is the transmission coefficient at the boundary for an electron at the Fermi surface. By substituting (7-64) into (7-62), we find

$$b \sim \frac{N}{N_N} \frac{1}{T_j} \frac{L}{\xi_N} \tag{7-65}$$

If $(\mathrm{N_N/N})\,\mathrm{T_j} \sim 1$, we can have $\mathrm{b} \sim \xi_{\mathrm{N}}$, b is then short when compared to $\xi(\mathrm{T})$ and the boundary conditions are drastically modified from the insulator case.

Problem.

How is the penetration depth modified in a superconductor S when it is covered by a normal metal layer N? (P.G. de Gennes and J. Matricon, 1965).

Solution.

Consider the Landau-Ginsburg domain (see Fig. 7-3). Assume (as is often the case) that the N metal does not contribute to the screening of magnetic

fields. Then the field at the NS boundary is the applied field. For the order parameter, the presence of N imposes a boundary condition on the type (7-53) at the surface ($x = 0$) of the superconductor.

(1) In zero field, $\psi(x)$ is given by

$$f(x) = \frac{\psi(x)}{\psi_0} = \tanh \frac{x - x_0}{\sqrt{2}\xi(T)}$$

where x_0 is a parameter to be determined by the condition (7-53),

$$\left(\frac{1}{\psi}\frac{d\psi}{dx}\right)_{x=0} = \frac{1}{b}$$

If the electrical contact between N and S is good, if the density of states of N is comparable to S, and if N is thick compared to $\xi_0 \simeq \hbar v_{\mathrm{F}}/\mathrm{k_B T_0}$, b is of the order of ξ_0. Therefore we can make $\mathrm{b} \ll \xi(\mathrm{T})$ and decrease strongly the order parameter at the surface $f(0) \sim b/[\sqrt{2}\xi(T)] \ll 1$.

(2) If we now apply a weak magnetic field $h_z(x) = \partial A_y(x)/\partial x$ along the z axis, its distribution is determined by

$$\frac{\partial^2 A_y}{\partial x^2} = \frac{16\pi e^2}{mc^2} |\psi_0|^2 f^2 A_y = \frac{f^2}{\lambda^2(T)} A_y$$

In a weak field, we can use the unperturbed form f given above. It happens that the equation for A_y is then soluble exactly in terms of hypergeometric functions (for a similar problem, see Landau and Lifshitz, Quantum Mechanics, London: Pergamon Press, 1959, p. 69). We only quote here the result for the limiting case $b/\xi(T) \to 0\,[x_0 \to 0, f(0) \to 0]$. Then

$$\frac{\lambda}{\lambda(\mathrm{T})} = \frac{1}{\kappa\sqrt{2}} \frac{\Gamma\left(-\frac{\mathrm{S}}{2} + \frac{1}{\kappa\sqrt{2}}\right)\Gamma\left(\frac{1}{2} + \frac{\mathrm{S}}{2} + \frac{1}{\kappa\sqrt{2}}\right)}{\Gamma\left(\frac{1}{2} - \frac{\mathrm{S}}{2} + \frac{1}{\kappa\sqrt{2}}\right)\Gamma\left(1 + \frac{\mathrm{S}}{2} + \frac{1}{\kappa\sqrt{2}}\right)}$$

[8] Remark: Notice the difference in this behavior with that of liquid He [4], which is also a superfluid satisfying, at least approximately, a Landau-Ginsburg equation in the neighborhood of $\mathrm{T_C}$. In He^4, ξ_0 is of the order of a and $\mathrm{b} \sim \mathrm{a} \gg \xi(T)$. The correct boundary condition is then completely different and closer to $\psi_{\mathrm{X}=0} = 0$.

For small $\kappa, \lambda/\lambda(T) - 1.75\kappa^{-1/2}$. This could have been guessed by the following argument: If the penetration depth is small, we can replace the exact expression for f (with $x_0 = 0$) by the approximate form $f = x/[\sqrt{2}\xi(T)]$. This approximation will be correct in the region where the field penetrates. Then the equation for A_y reduces to

$$\frac{\partial^2 \mathrm{A}y}{\partial \mathrm{x}^2} = \frac{\mathrm{x}^2}{2\lambda^2\xi^2}\ \mathrm{A_y}$$

and the penetration depth is of the order of $(\lambda\xi)^{1/2}$.
The opposite limit $\kappa \to \infty$ leads to $[\lambda/\lambda(T)] \to 1$. This was also expected since, when $\xi(T) \ll \lambda(T)$, the distortion of $\psi(x)$ near the surface, due to the presence of the N layer, is present only in a small fraction of $\lambda(T)$.
(3) In strong fields, the penetration depth increases spectacularly if $\kappa \sim 1/\sqrt{2}$ and $b \ll \xi(T)$. This can be shown from the complete nonlinear Landau-Ginsburg equations, but has not yet been verified experimentally.

S-N-S' Junction

Consider now the system of three layers $\mathrm{S} - \mathrm{N} - \mathrm{S}'$ represented in Fig. (7-4); two superconductors S and S' separated bv either an insulating film N of thickness $d(\sim 20 - 50\text{Å})$, or a normal metal with d $\sim 10^3$ A. When d is not too large, the Cooper pairs can tunnel from S to S' and vice versa. We shall analyze this effect under the following assumptions:
(1) The conditions for the validity of the Landau-Ginsburg equations are satisfied in S and S'.
(2) The thickness d is small with respect to $\lambda(T)$ and $\xi(T)$.

The effect of the film N is simply to impose boundary conditions relating the values of Δ and $\mathrm{d}\Delta/\mathrm{dx}$ at one surface of N to the values at the other surface. As previously, the boundary conditions can be reduced to be linear. Consider first the case when the vector potential $A = 0$. Then

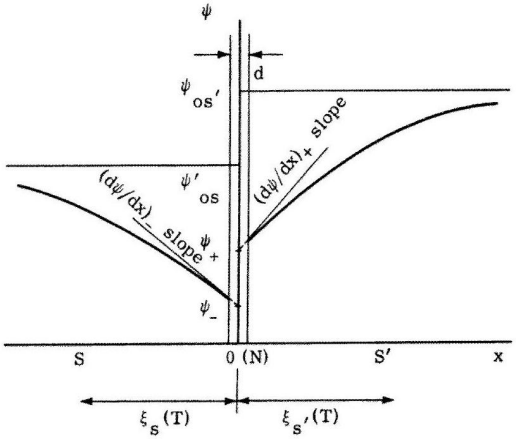


Figure 7-4
An S-N-S' junction where the normal layer may either be an insulator (d $\sim$ 50Å) or a metal (d $\sim 10^3$Å).

$$\begin{aligned} \Delta_+ &= L_{11}\Delta_- + L_{12}\left(\frac{d\Delta}{dx}\right)_- \\ \left(\frac{\partial\Delta}{\partial x}\right)_+ &= L_{21}\Delta_- + L_{22}\left(\frac{\partial\Delta}{\partial x}\right)_- \end{aligned} \tag{7-66}$$

(A=0)

Here the x axis is normal to the film; Δ_+represents the value of $\Delta(x, y, z)$ extrapolated to the point $(0, y, z)$ from the solution of the Lan-dau-Ginsburg equations in the S region as is

shown in Fig. (7-4), and so on. The coefficients L_{ij} are obtained by completely solving the linearized self-consistency equation (7-8) (for A = 0, T = T_0) in and around the N region. For $A = 0$, the kernel $K_0(s, r)$ of their equation is real, therefore, the L_{ij} are real. Sometimes it is more useful to deal with ψ instead of Δ, and then (7-66) can be rewritten

$$\psi_+ = M_{11}\psi_- + M_{12}\left(\frac{\partial\psi}{\partial x}\right)_-$$
$$\left(\frac{\partial\psi}{\partial x}\right)_+ = M_{21}\psi_- + M_{22}\left(\frac{\partial\psi}{\partial x}\right)_- \qquad (\prime)$$

(A=0)

[If the metals S and S' are different, the ratio ψ/Δ defined by (6-8) is not the same in S as in S'. Thus the coefficients M_{ij} are not identical to the L_{ij}. | The M_{ij} are real. They are not all independent, but are related to each other by one relation expressing current conservation through the boundary. The supercurrent I_x crossing a unit area of the wall is given by

$$I_x = \frac{-ie\hbar}{m}\left(\psi^*\frac{\partial\psi}{\partial x} - C.C.\right)_+ = \frac{-ie\hbar}{m}\left(\psi^*\frac{\partial\psi}{\partial x} - C.C.\right)_- \qquad (A = 0) \qquad (7\text{-}67)$$

By comparing (7-67) and (7-66'), we find

$$M_{11}M_{22} - M_{12}M_{21} = 1 \qquad (7\text{-}68)$$

and the current I_x can be written in the form

$$I_X = \frac{-ie\hbar}{m}\left\{\psi_-^*\left(\frac{1}{M_{12}}\psi_+ - \frac{M_{11}}{M_{12}}\psi_-\right) - \text{C.C. }\right\}$$
$$= \frac{-ie\hbar}{M_{12}m}\left(\psi_-^*\psi_+ - \text{C.C. }\right) \qquad (7\text{-}69)$$

Therefore a supercurrent must flow through the junction (B. D. Josephson, 1962). The junction cannot be too thick because then the coefficient M_{12} would become too large. Such currents have first been clearly observed by Anderson and Rowell (1963).

These results are easily generalized to the case $A \neq 0$. We always assume that, on the Landau-Ginsburg scale, the vector potential A is continuous at the boundary. [9] Then, putting $A_x = A_x(0, yz)$, we replace Eq. (7-66') by

$$\psi_+ = M_{11}\psi_- + M_{12}\left(\frac{\partial}{\partial x} - \frac{2ie}{\hbar c}A_x\right)\psi_- \qquad (7\text{-}70)$$
$$\left(\frac{\partial}{\partial x} - \frac{2ieA_x}{\hbar c}\right)\psi_+ = M_{21}\psi_- + M_{22}\left(\frac{\partial}{\partial x} - \frac{2ie}{\hbar c}A_x\right)\psi_-$$

The equation (7-69) for the current is not changed. [10]

In practice, the use of the current formula (7-69) is particularly simple when the region N is only slightly transparent to pairs, that is, when I_X is small relative to the critical currents in S or S' in their bulk states. With this assumption, the absolute values $|\psi_+|$and $|\psi_-|$are only slightly modified by the presence of the current and they can be replaced by their values $\psi_{S'}$ and ψ_S in the state without current:

$$\begin{matrix}\psi_+ \to \psi_{S'}\exp\left(i\phi_{S'}\right) \\ \psi_- \to \psi_S\exp\left(i\phi_S\right)\end{matrix} \qquad (\psi_S, \psi_{S'} \text{ are real })$$

The phases ϕ_{S} and $\phi_{\mathrm{S}'}$, on the other hand, will, in general, be very sensitive to the presence of currents and magnetic fields and nothing can be said about them a priori. With the substitution of these values into (7-69), the current takes the form

$$\mathrm{I_X} = \frac{2\mathrm{e}\hbar}{\mathrm{mM_{12}}}\psi_{\mathrm{S}}\psi_{\mathrm{s}'}\sin\left(\phi_{\mathrm{S}} - \phi_{\mathrm{S}'}\right) \tag{7-71}$$

Its maximum value is

$$\mathrm{I}_m = \frac{2\mathrm{e}\hbar}{\mathrm{mM_{12}}}\psi_{\mathrm{s}'}\psi_{\mathrm{s}'} \tag{7-72}$$

To determine ψ_S and $\psi_{S'}$, it is only necessary to solve the Landau-Ginsburg equation in S and S' in the simple case $A = 0$ and ψ real. We have already encountered the form of these solutions in one dimension

$$\psi(x) = \begin{cases} \psi_{0s'}\tanh\left(\frac{x+x_{s'}}{\sqrt{2}\xi_{s'}(T)}\right) & x > 0 \\ \psi_{0s}\tanh\left(\frac{-x+x_{s'}}{\sqrt{2}\xi_{s}(T)}\right) & x < 0 \end{cases} \tag{7-73}$$

where ψ_{os} and $\xi_{\mathrm{S}}(\mathrm{T})$ are, respectively, the order parameter in the bulk S metal and the coherence length at the temperature T in S . The lengths $\mathrm{x_S}$ and $\mathrm{x_{S'}}$ are related to ψ_{S} and $\psi_{\mathrm{S}'}$ by

$$\psi_S = \psi_{oS}\tanh\left(\frac{x_S}{\sqrt{2}\xi_S(T)}\right) \quad \psi_{S'} = \psi_{oS'}\tanh\left(\frac{x_{S'}}{\sqrt{2}\xi_{S'}(T)}\right) \tag{7-74}$$

They can be determined explicitly by demanding that (7-73) satisfy the boundary (7-66'), which gives

$$\begin{aligned} \psi_{\mathrm{s}'} &= \mathrm{M_{11}}\psi_{\mathrm{S}} - \mathrm{M_{12}}\frac{\psi_{\mathrm{oS}}}{\sqrt{2}\xi_{\mathrm{S}}(\mathrm{T})}\left(1 - \frac{\psi_{\mathrm{S}}^2}{\psi_{\mathrm{oS}}^2}\right) \\ \frac{\psi_{\mathrm{oS}'}}{\sqrt{2}\xi_{\mathrm{S}'}(\mathrm{T})}\left(1 - \frac{\psi_{\mathrm{S}'}^2}{\psi_{\mathrm{os}}^2}\right) &= \mathrm{M_{21}}\psi_{\mathrm{S}} - \mathrm{M_{22}}\frac{\psi_{\mathrm{oS}}}{\sqrt{2}\xi_{\mathrm{S}}}\left(1 - \frac{\psi_{\mathrm{S}}^2}{\psi_{\mathrm{oS}}^2}\right) \end{aligned} \tag{7-75}$$

The system of equations (7-75) can be solved numerically to obtain ψ_{S} and ψ_{S}. Certain limiting cases are simple:
(1) If N is an insulator, ψ(x) is only slightly modified by the presence of N ($\psi_S \sim \psi_{0S}$). Then M_{12} and M_{21} are small, and M_{11} is nearly 1. (See the microscopic calculation that follows later.)
(2) If N is metallic [sufficiently thick for $\mathrm{L_x}$ to be small, but thin compared to $\lambda(T)$ and $\xi(T)$], we predict that

$$\frac{\psi_{\mathrm{s}}}{\psi_{\mathrm{os}}} \sim \frac{\psi_{\mathrm{s}'}}{\psi_{\mathrm{os\ s}'}} \sim \frac{\mathrm{b}}{\xi(\mathrm{T})} \ll 1$$

by analogy with the NS boundary studied previously. In this case, (7-75) can be linearized.

[9] A could be discontinuous if a different choice of gauge was made on the two sides.
[10] A particularly simple case occurs when the junction is symmetric. Then $M_{11} = M_{22}$ and, by taking account of (7-68), we see that the M_{ij} depend on only two independent parameters.

Conclusions.

(1) If N is an insulating layer, the maximum current becomes

$$\mathrm{I}_m = \frac{2\mathrm{e}\hbar}{\mathrm{mM}_{12}}\psi_{0\ \mathrm{s}}\psi_{0\ \mathrm{s}'}$$

M_{12} is finite as $T \to T_0$; ψ_{0S} varies as $(T_0 - T)^{1/2}$ from (6-15) and consequently the maximum current varies as $T_0 - T$.

(2) If N is metallic, $\mathrm{I}_m \sim (\mathrm{e}\hbar/\mathrm{mM})[\mathrm{b}/\xi(\mathrm{T})]^2\psi_{\mathrm{o}S}\psi_{\mathrm{o}S}$, which varies as $(T_0 - T)^2$. (This latter result has not yet been experimentally verified.)

MICROSCOPIC CALCULATION OF $\mathrm{M_{ij}}$

FOR AN INSULATING JUNCTION

We consider a symmetric situation for $\mathrm{d} \ll \xi_0$. We start from the linearized self-consistency equation (7-8) for $A = 0$ and $T = T_0$.

From (7-35), the kernel $K_0(r, r')$ is essentially related to the function $\langle\delta[\mathbf{r} - \mathbf{r}(0)]\delta[\mathbf{r}' - \mathbf{r}(\mathrm{t})]_{\mathrm{E_F}}$, which represents the probability of finding an electron at $\mathbf{r}'$ at the time t (in the normal state) if it has been injected at r at time 0, with the Fermi energy. This allows us to write $K_0(r, r')$ directly in terms of $K_{\text{pure}}(r - r')$ which we have already studied for the infinite metal S. Equation (7-8) becomes

$$\begin{aligned}\Delta(r) = &\int_{\mathrm{I}} \mathrm{K_{pure}}\ (r - r')\,\Delta(r')\,dr' + \int_{\mathrm{II}} \mathrm{K_{pure}}\ (r - r') \\ &\times \left[\mathrm{T_j}\Delta(r') + \mathrm{R_j}\Delta\overline{(r')}dr'\right]\end{aligned} \tag{7-76}$$

where the first integral (I) corresponds to a direct propagation from r to r' and the region of integration is limited by the condition that r and r' be on the same side of the junction. The integral (II) gives the effects of transmission and reflection arising from the presence of the junction. The coefficient $T_j = 1 - R_j$ is the transmission coefficient of the function for an electron of energy E_F in the normal metal. The point $\overline{r'} = (-x', y', z')$ is the image point of r' with respect to the junction. For simplification we assume that the reflection is specular and that the reflection coefficient is independent of the angle of incidence.

Equation (7-76) has an even solution $\Delta(x) = \Delta(-x) =$ constant by virtue of the property $\int K_{\text{pure}}(r - s)dr = 1$ at $T = T_0$. In order to determine M_{12}, it is necessary to construct a second independent solution, for example, the odd solution $\Delta(x) = -\Delta(-x)$.

If we set $\Delta^+(x) = \Delta(s)S(x)$ where

$$S(x) = \begin{cases} 1 & x > 0 \\ 0 & x < 0 \end{cases}$$

Eq. (7-76) can be put into the form

$$\Delta^+(x) = S(x)\int \Delta^+(x')\left[K_0(r, r') + (1 - 2T_j)\,K_0(r, r')\right]dr'$$

or further

$$\begin{aligned}\Delta^+(r) - \int K_0(r, r')\,\Delta^+(r')\,dr' = &\int dr\Delta^+(r')\left[-S(-x)K_0(r, r')\right. \\ &\left.+S(x)\,(1 - 2T_j)\,K_0(r, r')\right] \\ = &-H(x)\end{aligned} \tag{7-77}$$

The function H(x) represents a source localized in the region $|x| < \xi_0$. The equation is very similar to (7-56) and can be solved in the same way,

$$\left(\frac{L}{2}\right)\left(\frac{d\Delta}{dx}\right)_{x\gg\xi_0} = \int H(x)dx = 2T_j \int_\infty^0 dx \int_\infty^0 dx' \times \int dy'dz'\Delta^+(x')\,K_0(r,r') \tag{7-78}$$

As the junction is insulating, $\Delta^*(x')$ does not vary much over the region of integration ($x' \sim \xi_0$), $\Delta^+(x) \to \Delta^+$. The integral that remains can be calculated by recalling the definition of K_{pure} ,

$$\int_{-\infty}^0 dx \int_0^\infty dx' \int dy'dz'K_{\text{pure}}\,(r-r') = \xi_0 \tag{7-79}$$

Finally, we find

$$\frac{\mathrm{L}}{2}\left(\frac{\mathrm{d}\Delta}{\mathrm{dx}}\right)_+ = \mathrm{T_j}\xi_0\Delta_+$$

and comparing this with (7-66),

$$L_{12} = M_{12} = \frac{L}{T_j\xi_0} \tag{7-80}$$

The coefficient $\mathrm{M_{12}}$ is of the order of $\xi_0/\mathrm{T_j}$ since $\mathrm{L} \sim \xi_0^2$. In practice the transmission coefficient T_j across an insulating wall is very small when d is larger than a few angstrms. This implies that the maximum supercurrent flowing across the junction is small

$$\mathrm{I}_m \sim \frac{\mathrm{eh}}{m\xi_0}\,|\psi_0|^2\;\mathrm{T_j} \tag{7-81}$$

DISTRIBUTION OF FIELDS AND CURRENTS NEAR A JUNCTION

A typical situation is shown on Fig. 7-5. The field H is applied in the plane of the junction. Surface currents appear on S and S' to screen out the field. How will the currents manage to go through the junction? Because the maximum current density I_m through the junction is small, the currents must go deep in between S and S'. Typically, for an insulating junction, they will penetrate on a length $\delta \sim 1$ mm. At higher fields, things will become even more dramatic, and vortex lines will pile up in the junction (Fig. 7-6).

The behavior of the junction in this type of situation is governed by a simple equation due to Ferrell and Prange. In order to obtain this equation, we consider a junction occupying the entire xy plane; the magnetic fields are directed along the z axis and it is convenient to describe them by a vector potential directed along the y axis:

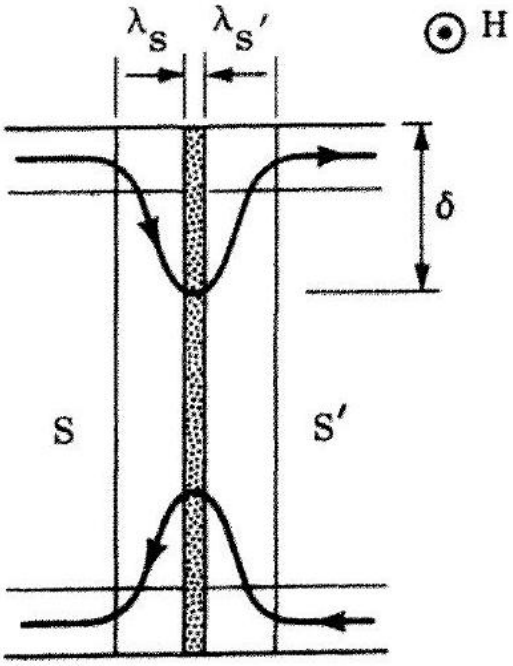
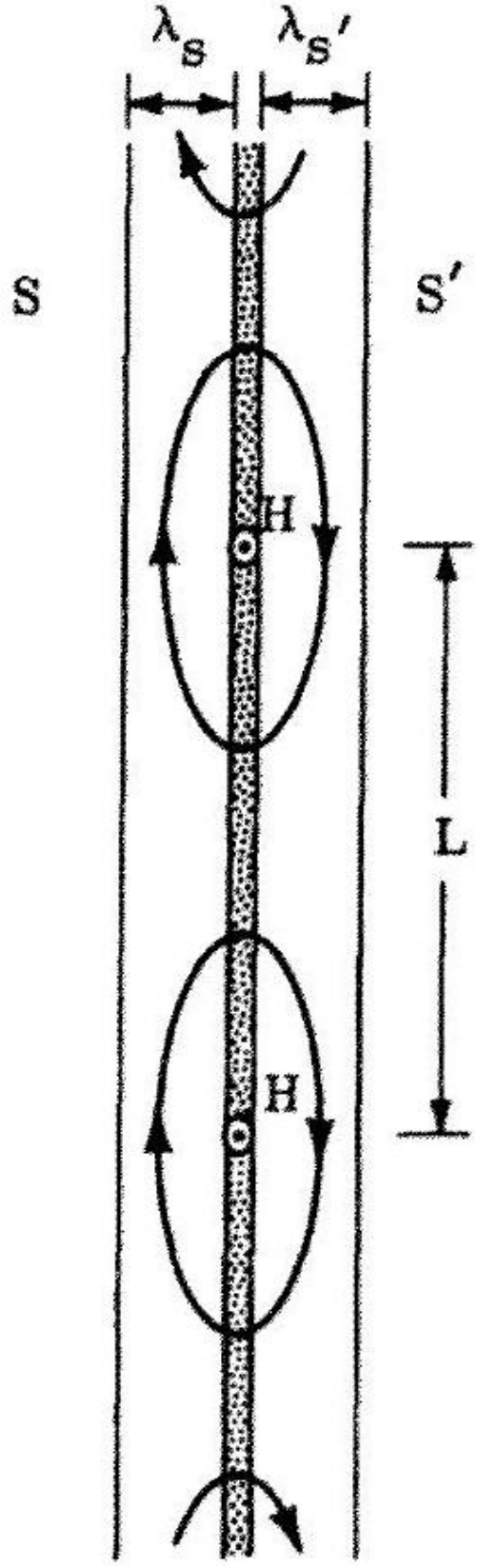


Figure 7-5
Current streamlines around an S-N-S' junction under a very weak applied field. Because of the weak current capacity of the junction, the field penetrates up to a large distance δ.

Figure 7-6 Current distribution in a junction at higher fields: Vortex lines are stacked along the junction.



$$h(x,y) = \frac{\partial}{\partial x} A_y(x,y)$$

We assume a solution of the Landau-Ginsburg equations of the form

$$\psi(x,y) = \begin{cases} \psi(x) \exp\left[i\phi_{S'}(y)\right] & x > 0 \\ \psi(x) \exp\left[i\phi_{S}(y)\right] & x < 0 \end{cases} \tag{7-82}$$

As we shall see, the variations of $\phi_{\mathbf{S}}$ (or $\phi_{\mathbf{S}'}$) take place over distances (δ) much larger than ξ(T). Then ψ(x) is essentially the solution (7-73).

Let us first consider the region $x > 0$ far from the junction ($x \gg \lambda_{s'}$). Here the Meissner effect is complete, no current flows and we find from Eq. (6-12)

$$\frac{2e}{\hbar c} A_y = \frac{\partial \phi_{s'}(y)}{\partial y} \quad (x \gg \lambda_{s'}) \tag{7-83a}$$

and similarly

$$\frac{2eA_y}{\hbar c} = \frac{\partial \phi_s(y)}{\partial y} \quad (x \ll -\lambda_s) \tag{7-83b}$$

Therefore $A_y(x, y)$ has well-defined limiting values, on either side far from the junction. Call these values $A_S(y), A_{S'}(y)$. At the junction itself (x = 0), we can, for convenience, take $\mathrm{A_y(x = 0, y) = 0}$. The magnetic field $\mathrm{H(x = 0, y) = h_0(y)}$ at the junction is simply deduced from the following considerations.

If we let λ_{S} and $\lambda_{\mathrm{S}'}$ be the penetration depths in S and S′ in the neighborhood of the junction, [11] then by definition

$$\begin{aligned} A_{s'} &= \int_0^{\infty} h dx = \lambda_{s'} h_0 \\ A_s &= \int_0^{-\infty} h dx = \lambda_s h_0 \end{aligned} \tag{7-84}$$

and by comparison with (7-83)

$$\mathrm{h_0 = \frac{\hbar c}{2e} \frac{1}{\lambda_{s'}} \frac{\partial \phi_{s'}}{\partial y} = \frac{\hbar c}{2e} \frac{1}{\lambda_s} \frac{\partial \phi_s}{\partial y}} \tag{7-85}$$

We now write the relation between field and current at the junction $\mathrm{curl}\, h = (4\pi/c)j$,

$$\mathrm{\frac{\partial h_0}{\partial y} = \frac{4\pi}{c} I_x = \frac{4\pi}{c} I_m \sin(\phi_s - \phi_{s'})} \tag{7-86}$$

where we have used (7-71). By combining (7-85) and (7-86), we obtain the Ferrell-Prange equation

$$\mathrm{\frac{\partial^2 \phi}{\partial y^2} = \frac{1}{\delta^2} \sin \phi} \tag{7-87}$$

where $\phi = \phi_S - \phi_{S'}$

$$\mathrm{\delta^2 = \frac{\hbar c^2}{8\pi e I_m (\lambda_s + \lambda_{s'})}} \tag{7-88}$$

We now estimate the characteristic length δ for an insulating junction. The order of magnitude of I_m is given by (7-81) and

$$\begin{aligned} \mathrm{\delta^2} &\sim \mathrm{\frac{mc^2}{16\pi e^2 |\psi_0|^2} \frac{\xi_0}{\lambda(T)} \frac{1}{T_j}} \\ &\sim \mathrm{\frac{\lambda(T) \xi_0}{T_j}} \end{aligned} \tag{7-89}$$

[11] When the N region is metallic, ψ(x) becomes small near the junction and the penetration depths must be calculated taking this into account, as we have previously seen for an NS boundary.

For an insulator of thickness $d \sim 20\text{Å}$, the transmission coefficient is typically of the order of 10^{-8}. If $\lambda(\mathrm{T}) \sim \xi_0 \sim 10^3$ A, then $\delta \sim 1$ mm.

Equation (7-87) can be completely discussed by noticing that it is formally identical to the equation of motion of a pendulum.

Two limiting cases are particularly interesting.

(1) Very weak fields. Then (7-87) can be linearized to give solutions of the form

$$\phi = \phi_0 e^{-y/\delta}, \quad h_0 = H_0 e^{-y/\delta} \tag{7-90}$$

where $y = 0$ corresponds to the intersection of the junction and the sample surface, and H_0 is the field just outside of the sample. Thus the penetration depth of the junction in weak fields is δ. This regime holds when $\Phi \ll 1$ or $\mathrm{H} \ll \phi_0/\left(\lambda_\mathrm{S} + \lambda_{\mathrm{S}'}\right)\delta$, that is, the flux that penetrates into the junction must be much less than the flux quantum ϕ_0.

(2) Domain of complete penetration. If $\mathrm{H} \gg \phi_0/\left(\lambda_\mathrm{s} + \lambda_{\mathrm{s}'}\right)\delta$, the field becomes nearly uniform along the junction and $h_0(y) \to H.\phi$ can be determined from (7-85),

$$\phi \approx \frac{2\pi \mathrm{y}}{\mathrm{L}} + \text{ const} \qquad \mathrm{L} = \frac{\phi_0}{\left(\lambda_\mathrm{s} + \lambda_{\mathrm{s}'}\right)\mathrm{H}} \tag{7-91}$$

The structure of the currents is then periodic with period L

$$I_x = I_m \sin\phi \cong I_m \sin\left(\frac{2\pi\left(y - y_0\right)}{L}\right) \tag{7-92}$$

By placing (7-91) into the right-hand side of (7-87), it is easy to verify that $\partial^2\phi/\partial y^2$ and $\partial h_0/\partial y$ are essentially negligible for $L \ll \delta$.

The current structure is shown on Fig. (7-6). Each period carries one quantum of flux. It resembles a series of vortex lines stacked in the plane of the junction. Because the penetration depth δ is very large ($\delta \gg \xi$), the situation is similar to a Type II superconductor where $\lambda \gg \xi$. In the limit $\mathrm{L} \ll \delta$, it can be shown, by a complete calculation of the thermodynamic potential, that the field h_0 is very nearly equal to the applied field.

It is also interesting to calculate the total current that flows from S to S' when the junction has a finite length $0 < y < D$. Per cm of length along the z axis, we have

$$\begin{aligned} I_{\text{total}} &= \int^D I_m \sin\phi dy \\ &\cong \frac{I_m L}{2\pi}\int d\phi \sin\phi \quad (L \ll \delta) \\ &= \frac{I_m L}{2\pi}\left[\cos\phi(0) - \cos\left(\phi(0) + \frac{2\pi D}{L}\right)\right] \end{aligned}$$

The maximum value of I_{total} is obtained when $\phi(0) = \pi/2 - \pi D/L$,

$$\mathrm{I}_{\text{total max}} = \frac{\mathrm{I}_m\ \mathrm{L}}{2\pi}\left|\sin\frac{\pi\mathrm{D}}{\mathrm{L}}\right| \quad (\mathrm{L} \ll \delta) \tag{7-93}$$

The factor D/L is the number of flux quanta in the junction. The total current vanishes when D/L is an integer, and is maximum when D/L is half-integral. Rather detailed verifications of (7-93) have recently been obtained by Fiske and by Rowell.

Problem.

Discuss the maximum superfluid current 1 of a system of two SNS junctions in parallel, as a function of the magnetic field H ("quantum interferometer"). The (schematic) arrangement

and the notation are shown on Fig. 7-7. A flux Φ is enclosed in the ring between the two junctions. For simplicity assume that (a) the junctions A and B are small, the flux trapped in each of the junctions is negligible ($2\ \mathrm{d}\lambda\mathrm{H} \ll \phi_0$); (b) the superconducting pieces (1) and (2) are much thicker than the penetration depth λ.

Solution.

The overall supercurrent flowing from (1) to (2) is

$$I = I_m d\left[\sin\left(\phi_{2A} - \phi_{1A}\right) + \sin\left(\phi_{2B} - \phi_{1B}\right)\right]$$

The different phases ϕ_{1A}, and so on, are coupled by a relation involving the flux ϕ, which we now derive. At any point in superconductor 1, for instance, the current density j_s is proportional to $\hbar\nabla\phi - 2eA/c$ (where ϕ is the local phase of the pair potential). Consider a path C_1 in the superconductor distant enough from the surface, so that $j_s \equiv 0$ on it. Then, on $C_1, \hbar\nabla\phi = 2eA/c$. Integrating this relation we obtain

$$\phi_{1\ \mathrm{B}} - \phi_{1\ \mathrm{A}} = \frac{2\mathrm{e}}{\hbar\mathrm{c}} \int_{\mathrm{C}_1} \mathrm{A} \cdot\ \mathrm{d}\boldsymbol{\ell}$$

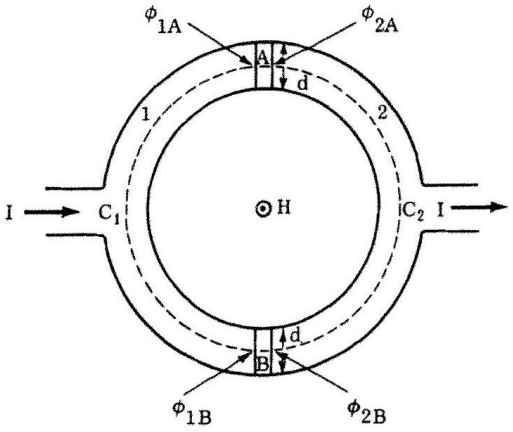


Figure 7-7
Principle of a "quantum interferometer." A and B are two Josephson junctions. The maximum superfluid current 1 is measured as a function of the field H in the loop.

and similarly

$$\phi_{2A} - \phi_{2B} = \frac{2e}{\hbar c} \int_{C_2} A \cdot d\ell$$

Adding these equations we arrive at

$$\phi_{1\ \mathrm{B}} - \phi_{2\ \mathrm{B}} + \phi_{2\ \mathrm{A}} - \phi_{1\ \mathrm{A}} = \frac{2\mathrm{e}}{\mathrm{hc}} \oint \mathrm{A} \cdot\ \mathrm{d}\boldsymbol{\ell} = 2\pi \frac{\Phi}{\Phi_0}$$

where Φ is the total flux in the loop.

Apart from this relation, the phases, ϕ_{1A}, and so on, are arbitrary. The current I is maximum when we choose

$$\phi_{2\ \mathrm{A}} - \phi_{1\ \mathrm{A}} = -\left(\phi_{2\ \mathrm{B}} - \phi_{1\ \mathrm{B}}\right) = \pi \frac{\Phi}{\Phi_0}$$

$$I = 2\mathrm{I}_m\ \mathrm{d} \left|\sin\left(\pi \frac{\Phi}{\Phi_0}\right)\right|$$

The maximum superfluid current is a periodic function of Φ or H . To observe the periodicity in field the surface S of the loop must be small. The experiment has been achieved by Jaklevic, Lambe, Silver, and Mercereau. A and B can be two Josephson junctions, or, even more simply, two mechanical contacts between superconducting wires.

REFERENCES

Microscopic derivation of the Landau-Ginsburg equations:

L. P. Gor'kov, Zh. Eksperim. i Teor. Fiz., 36, 1918; 37, 833 (1959); Translation Soviet Phys. JETP, 9, 1364; 10, 593 (1960).

Experimental data for κ in "dirty" alloys and comparison with Gor'kov's formula:

B. B. Goodman, I. B. M. Journal, 6, 62 (1962).
T. Kinsel, E. A. Lynton, B. Serin, Phvs. Lett.. 3, 30 (1962).

Boundary conditions and junctions:

B. D. Josephson, Rev. Mod. Phys., 36, 216 (1964).
P. G. de Gennes, Rev. Mod. Phys., 36, 225 (1964).

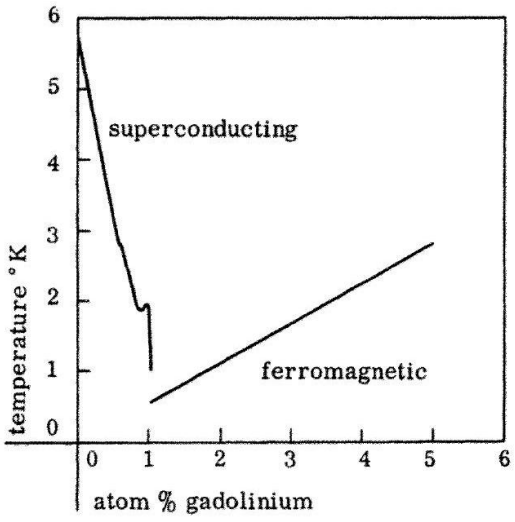
6.5 Effects of Strong Magnetic Fields and of Magnetic Impurities

We shall discuss two apparently very different physical situations:
(1) dirty superconductors and small superconducting samples in high magnetic fields;
(2) superconductors containing magnetic impurities.

There are in fact some crucial features shared by (1) and (2).
(a) In both cases the perturbation acts with opposite signs on the two members of a Cooper pair. In case (1) there is a term $(1/2m)$ $(\mathbf{p}\cdot\mathbf{A}+\mathbf{A}\cdot\mathbf{p})$ if the one-electron Hamiltonian, and this changes sign when going from p to -p. In case (2) we may often describe the effect of the magnetic impurity (i) of spin S_i on a conduction electron (of coordinate r_e and spin S_e) by an interaction of the form

$$\Gamma\,(r_e - r_i)\,S_e \cdot S_i$$

(Γ is called an exchange coupling constant, but in fact its origin is complex.) Γ has an arbitrary sign, and is typically of order 0.1eV $= 10^3$°K.[1] Since the two electrons of a Cooper pair have opposite spins, this Γ coupling acts with opposite signs on each.
(b) Experimentally, such "antisymmetric" perturbations lead to a



[1] Note that Γ has nothing to do with the dipolar field created by the magnetic impurity. The dipolar coupling energy is of order $\mu_B^2/a^3 \sim 1°K$ (μ_B = Bohr magneton, a = atomic distance) and much smaller than Γ (C . Herring, 1958).

Figure 8-1
Superconducting and ferromagnetic transition temperatures of La Gd alloys lafter B. T. Matthias, IBM J., 6, 250 (1962)]. Note the sharp drop of the superconducting transition point when the (magnetic) gadolinium atoms are added to lanthanum.

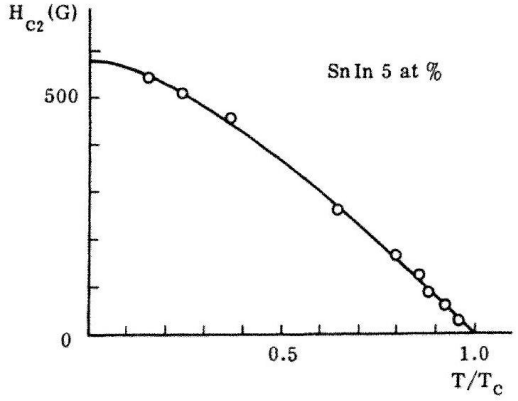


Figure 8-2
Relation between temperature and field at the upper transition point of a "dirty" Type II superconductor. Experimental points by E. Guyon and A. Martinet. The theoretical curve is derived from Eq. (8-40).

strong decrease of the transition temperature. This is shown on examples in Figs. 8-1 and 8-2. Note that the "antisymmetry" is crucial. Recall that nonmagnetic impurities (which give rise only to "symmetric" perturbations) have very little effect on the transition point (Anderson's theorem).

(c) Another important property is shared by classes (1) and (2). Electrons are randomly scattered by impurities or on the sample surface. Thus the "antisymmetric" perturbation seen by one given Cooper pair is modulated in time. This, as we shall see, can lead to a number of strange properties, and in particular to gapless superconductivity (A. Abrikosov and L. P. Gorkov, 1961).

6.5.1 8-1 Relation Between Transition Temperature and Time-Reversal Properties

Our problem is to translate the qualitative asymmetry property of the perturbation into more numerical terms. Consider for instance the calculation of a transition point, in a given field (case 1) or for a given concentration of magnetic impurities (case 2). Experimentally for both cases the transition is found to be of second order. $\Delta(r)$ is small near the transition and a linearized self-consistency equation like (7-8) can be used.

Let us first restrict our attention to case (1), where spin indices play no role, and where (7-8) thus applies directly. We rewrite the kernel $\mathrm{K}(\mathbf{r}_1\mathbf{r}_2)$ of (7-8) under a form equivalent to (7-11).

$$\mathrm{K}(\mathbf{r}_1\mathbf{r}_2) = \mathrm{k_B}\ \mathrm{T}\sum_{\omega} v\ \mathrm{N}(0)\mathrm{V}\int \frac{\mathrm{d}\xi\ \mathrm{d}\xi'}{(\xi - \mathrm{i}\omega\ \mathrm{h})(\xi' + \mathrm{i}\omega\ \mathrm{h})} \times \mathrm{f}\left(\mathbf{r}_1\mathbf{r}_2, \frac{\xi - \xi'}{\hbar}\right) \tag{8-1}$$

$$\mathrm{f}(\mathbf{r}_1\mathbf{r}_2\Omega) = \sum_{m} \langle \phi_{\mathrm{n}}^*(\mathbf{r}_1)\,\phi_m^*(\mathbf{r}_1)\,\phi_m(\mathbf{r}_2)\,\phi_{\mathrm{n}}(\mathbf{r}_2) \times \delta(\xi_m - \xi_{\mathrm{n}} - \hbar\Omega)\rangle \tag{8-2}$$

[U is the sample volume and $N(0)$ the density of states per unit volume in the normal state so that $\mathcal{U}\mathcal{N}(0)$ is the total density of states of the sample when it is normal. We have made the substitution $\Sigma_{\mathrm{n}} \rightarrow \int \cup N(0)\mathrm{d}\xi_{\mathrm{n}}\cdot\big]$ As usual, the sum Σ_ω runs over the values $\pi\left(\mathrm{k_B}T/\hbar\right)\times(2\nu+1)$. The average in Eq. (8-2) is taken over all states n at a fixed energy ξ_{n} (in practice, at the Fermi energy $\xi_{\mathrm{n}}=0$). We would like to express the product of two ϕ' s and two ϕ^* 's in terms of matrix
elements between one-electron states n and m. Obviously, the * symbols are not located as desired. We circumvent this by introducing an ad hoc operator K, which by definition changes a function into its complex conjugate

$$\mathrm{K}\phi_m = \phi_m^* \quad \text{(case 1)} \tag{8-3}$$

We call K the time-reversal operator. In terms of K we may write

$$\begin{aligned}
\phi_{\mathrm{n}}^*\left(\mathrm{r}_1\right)\phi_m^*\left(\mathrm{r}_1\right) &= \left(\mathrm{n}\left|\delta\left(\mathrm{r}-\mathrm{r}_1\right)\mathrm{K}\right|m\right)\\
\phi_{\mathrm{n}}\left(\mathrm{r}_2\right)\phi_m\left(\mathrm{r}_2\right) &= \left(m\left|\ \mathrm{K}^+\delta\left(\mathrm{r}-\mathrm{r}_2\right)\right|\mathrm{n}\right)\\
\mathrm{f}\left(\mathrm{r}_1\mathrm{r}_2\Omega\right) &= \sum_m \Big\langle\left(\mathrm{n}\left|\delta\left(\mathrm{r}-\mathrm{r}_1\right)\mathrm{K}\right|m\right)\left(m\left|\ \mathrm{K}^+\delta\left(\mathrm{r}-\mathrm{r}_2\right)\right|\mathrm{n}\right)\\
&\quad\times\delta\left(\xi_{\mathrm{n}}-\xi_m-\hbar\Omega\right)\Big\rangle
\end{aligned} \tag{8-4}$$

At this stage, as usual, we find it convenient to use the Fourier transform of f

$$\begin{aligned}
f\left(r_1r_2t\right) &= \int d\Omega e^{-i\Omega t} f\left(r_1r_2\Omega\right)\\
&= \left\langle\delta\left[r(t)-r_1\right]K(t)K^+(0)\delta\left[r(0)-r_2\right]\right\rangle
\end{aligned} \tag{8-5}$$

where $K(t)$ and $r(t)$ are Heisenberg operators describing the time evolution of K or r for one electron submitted to the forces described by the Hamiltonian

$$\begin{aligned}
\mathscr{H}_e &= \frac{1}{2m}\left(p-\frac{eA}{c}\right)^2 + U(r) - E_F \quad \text{(case 1)}\\
K(t) &= \exp\left(i\frac{\mathscr{H}_e t}{\hbar}\right)K\exp\left(+i\frac{\mathscr{H}_e t}{\hbar}\right)
\end{aligned} \tag{8-6}$$

(Note the unusual sign in the last exponent, due to the fact that Ki = -iK.) The rate of change of K is given by

$$\frac{dK}{dt} = \frac{i}{\hbar}\left[\mathscr{H}_e, K\right] = \frac{-ie}{m\hbar c}(p\cdot A + A\cdot p)K \quad \text{(case 1}\Big) \tag{8-7}$$

The motion of K is due only to the "antisymmetric" part of the magnetic perturbation in $\mathscr{H}_e$. (Rather than "antisymmetric," we now say: the part that changes sign under time reversal.)

Finally, our result is the following: The kernel $K\left(r_1r_2\right)$ of the integral equation giving the transition temperature is known in terms of a correlation function $f\left(r_1r_2t\right)$ defined in (8-5). This correlation
function is useful because, as in many cases discussed before, it is closely related to the transport properties in the normal state. All the complications due to "antisymmetric" perturbations are described in terms of the time-reversal operator $K(t)$.

These conclusions can be extended directly to cases where there are magnetic impurities, that is, where spin indices must be taken into account. We now briefly describe this extension. The complete Hamiltonian is

$$\begin{aligned}\mathscr{H} = \sum_{\sigma} \int \mathrm{d}\mathbf{r} \Bigg\{ & \psi^{+}(\mathbf{r},\sigma) \left[\frac{\left(\mathbf{p} - \frac{\mathrm{e}}{\mathrm{c}}\mathbf{A}\right)^2}{2m} - \mathrm{E_F} \right] \psi(\mathbf{r},\sigma) \\ & + \sum_{\sigma\nu} \psi^{+}(\mathbf{r},\sigma) \mathrm{U}_{\sigma\nu}(\mathbf{r}) \psi(\mathbf{r},\nu) \\ & - \mathrm{V} \sum_{\sigma\nu} \psi^{+}(\mathbf{r},\sigma)\psi^{+}(\mathbf{r},\nu)\psi(\mathbf{r},\nu)\psi(\mathbf{r},\sigma) \Bigg\} \end{aligned} \tag{8-8}$$

where $\psi^{+}(\mathbf{r},\sigma)$ creates an electron of spin σ at the point $\mathbf{r}$.$\mathrm{U}_{\sigma\nu}$ is the potential acting upon the electrons, which for magnetic alloys is spin dependent. (In order to simplify the notation, we assume that U be a local operator coupling $\psi^{+}$and ψ at the same point.) The main assumption made about the potential U is that it is static. We do not take into account possible motions of the impurity spins. (This, as we later see, is correct only for very dilute alloys. In more concentrated systems, the impurities are coupled among themselves and precess in the exchange field of their neighbors.) The pair potential $\Delta(r)$ is still defined by

$$\Delta(\mathbf{r}) = \mathrm{V}\langle\psi(\mathbf{r}\uparrow)\psi(\mathbf{r}\downarrow)\rangle = -\mathrm{V}\langle\psi(\mathbf{r}\downarrow)\psi(\mathbf{r}\uparrow)\rangle$$

which can be rewritten in the condensed form

$$\Delta = \frac{V}{2} \sum_{\sigma\mu} \rho_{\sigma\mu} \langle\psi(r,\sigma)\psi(r,\mu)\rangle \tag{8-9}$$

where

$$\rho = \begin{pmatrix} 0 & 1 \\ -1 & 0 \end{pmatrix}$$

As in Chapter 5, we write the equations of motion of ψ and $\psi^{+}$and linearize them, allowing for a nonzero Δ. The linearized equation of motion for ψ is

$$\begin{aligned} \frac{\partial\psi}{\partial \mathrm{t}}(\mathbf{r},\sigma) = & [\mathscr{H}, \psi(\mathbf{r},\sigma)] \\ \mathrm{it} \qquad = & \left(\frac{\mathbf{p}^2}{2m} - \mathbf{E_F} \right) \psi(\mathbf{r},\sigma) \\ & + \sum_{\mu} \mathrm{V}_{\sigma\mu}\psi(\mathbf{r},\mu) + \sum_{\mu} \rho_{\sigma\mu}\Delta(\mathbf{r})\psi^{+}(\mathbf{r},\mu) \end{aligned} \tag{8-10}$$

(As usual, we have subtracted the chemical potential $\mathrm{E_F}$.) The elementary excitations are found by performing the transformation

$$\psi(\mathbf{r},\sigma) = \sum_{\mathrm{n}} \left[\mathrm{u_n}(\mathbf{r},\sigma)\gamma_{\mathrm{n}} + \mathrm{v}^{*}_{\mathrm{n}}(\mathbf{r},\sigma)\gamma^{+}_{\mathrm{n}} \right]$$

and imposing the condition $[\mathscr{H}, \gamma_n] = -E_n\gamma_n$. The $\binom{u}{v}$ are eigenfunctions of the system

$$\begin{aligned}
\epsilon u(r,\sigma) &= \left(\frac{\left(p-\frac{eA}{c}\right)^2}{2m} - E_F\right) u(r,\sigma) \\
&\quad + \sum_\mu \left[V_{\sigma\mu}(r)u(r,\mu) + \Delta(r)\rho_{\sigma\mu}v(r,\mu)\right] \\
-\epsilon v(r,\sigma) &= \left[\left(p+\frac{eA}{c}\right)^2 \frac{1}{2m} - E_F\right] v(r,\sigma) \\
&\quad + \sum_\mu \left[V^*_{\sigma\mu}(r)v(r,\mu) + \Delta^*(r)\rho_{\sigma\mu}u(r,\mu)\right]
\end{aligned}$$

We are interested in the limit $\Delta \to 0$. To zeroth order in Δ, $\binom{u}{v}$ are related to the electronic eigenfunctions ϕ_n in the normal metal, defined by

$$\begin{aligned}
\xi\phi(\mathbf{r},\sigma) &= \left[\frac{1}{2m}\left(\mathbf{p} - \frac{\mathrm{eA}}{\mathrm{c}}\right)^2 - \mathrm{E_F}\right]\phi(\mathbf{r},\sigma) + \sum_\mu \mathrm{U}_{\sigma\mu}(\mathbf{r})\phi(\mathbf{r},\mu) \\
&\equiv \mathscr{H}_\mathrm{e}\phi(\mathbf{r},\sigma) \\
\mathrm{u}^0_\mathrm{n} &= \begin{cases} \phi_\mathrm{n} & \xi_\mathrm{n} > 0 \\ 0 & \xi_\mathrm{n} < 0 \end{cases} \\
\mathrm{v}^0_\mathrm{n} &= \begin{cases} 0 & \xi_\mathrm{n} > 0 \\ \phi^*_\mathrm{n} & \xi_\mathrm{n} < 0 \end{cases} \qquad \epsilon^0_\mathrm{n} = |\xi_\mathrm{n}|
\end{aligned}$$

To first order in Δ we write

$$\begin{aligned}
u_n &= u^0_n + \sum_{m\neq n} a_{nm}\phi_m \\
v_n &= v^0_n + \sum_{m\neq n} b_{nm}\phi^*_m
\end{aligned}$$

The coefficients a_{nm} and b_{nm} are obtained by the usual perturbation method:

$$\mathrm{a_{nm}} = \begin{cases} 0 & (\xi_\mathrm{n} > 0) \\ \frac{-1}{\xi_\mathrm{n}+\xi_m}\sum_{\sigma\mu}\int \mathrm{d}\mathbf{r}_2\phi^*_m(\mathbf{r}_2\sigma)\,\rho_{\sigma\mu}\phi^*_\mathrm{n}(\mathbf{r}_2\mu)\,\Delta(\mathbf{r}_2) & (\xi_\mathrm{n} < 0) \end{cases}$$

$$b_\mathrm{nm} = \begin{cases} \frac{-1}{\xi_\mathrm{n}+\xi_m}\sum_{\sigma\mu}\int \mathrm{d}r_2\phi_\mathrm{n}(r_2\sigma)\,\rho_{\mu\sigma}\phi_\mathrm{n}(r_2\mu)\,\Delta(r_2) & (\xi_\mathrm{n} > 0) \\ 0 & (\xi_\mathrm{n} < 0) \end{cases}$$

We now insert these corrected values for u and v into the self-consistency equation for Δ. The latter, when spin indices are taken into account, takes the form

$$\Delta(r_1) = \frac{1}{2}V\sum_{\sigma\mu}\sum_n \rho_{\sigma\mu}v^*_n(r,\sigma)u_n(r,\mu)\left[1-2f(\xi_n)\right]$$

To first order in Δ this again has the form

$$\Delta(r_1) = \int K(r_1r_2)\,\Delta(r_2)\,dr_2 \tag{8-11}$$

and the kernel can still be expressed in terms of a correlation function by Eq. (8-1) and (8-5). The only change is that the definition of the time-reversal operator in (8-5) now involves the spin indices. Explicitly we have

$$\begin{aligned} \mathrm{K}\phi(\mathrm{r}\uparrow) &= \phi^*(\mathrm{r}\downarrow) \\ \mathrm{K}\phi(\mathrm{r}\downarrow) &= -\phi^*(\mathrm{r}\uparrow) \end{aligned} \tag{$\prime$}$$

In terms of Pauli spin matrices, one often writes

$$K = i\sigma_y C$$

where $\mathrm{C}\phi = \phi^*$ and $i\sigma_y$ coincides with our earlier defined $\rho = \begin{pmatrix} 0 & 1 \\ -1 & 0 \end{pmatrix}$. Thus in all cases of interest we have reduced our problem to a study of the motion of the operator K for one electron in the normal metal.

At first sight, K is a rather unfamiliar object, but with some practice you can get a very physical understanding of it. Take for instance the case of orbital magnetic fields, where the equation of motion for K is (8-7). In Eq. (8-1) the order of magnitude of $|\xi - \xi'|$ is $\mathrm{k_B T}$. Thus in $f\,(r_1 r_2 t)$ the time scale of interest is $t \sim \hbar/k_B T$. The spatial distances traveled by an electron during such times are very large when compared to the Fermi wavelength. Then we can treat the motion of the operator K classically and write (8-7) in the form

$$\begin{aligned} \frac{dK(t)}{dt} &= -i\frac{d\phi}{dt}K \\ K(t) &= e^{-i\phi(t)}K(0) \\ \phi(t) &= \frac{2e}{\hbar cm}\oint_0^t A \cdot p dt \end{aligned} \tag{8-12}$$

In this last equation, the integral is to be taken along a classical one-electron trajectory in the normal metal. Replacing p by mv (the difference eA/c between p and mv being very small when compared to the Fermi momentum), we may rewrite the phase ϕ in the form

$$\phi = \frac{2e}{\hbar c}\int A \cdot v dt = \frac{2e}{\hbar c}\int A \cdot d\ell \tag{8-13}$$

In this case the correlation function $f\,(r_1 r_2 t)$ may be understood as follows: Consider all one-electron trajectories linking r_1 and r_2 in a time interval t. For a pure metal, there is only one such trajectory - essentially a straight line (the cyclotron radius being very large on our scale $v_F t$). For more "dirty" systems, there are many wiggly trajectories allowed. For each of these we compute $e^{i\phi}$. Finally we sum over the different allowed trajectories, each of them being weighted. according to its probability to occur in a succession of scattering processes: As announced, the calculation of f is reduced to a study of transport properties.

In case 2 (magnetic impurities), the equation of motion of K is derived in the following way: the one-electron Hamiltonian $\mathcal{K}_e$ is of the form

$$\mathscr{H}_e = A + B \cdot S_e \tag{8-14}$$

where A includes the kinetic energy and the spin-independent forces, while **B** stems from the Γ interaction with all impurities. Using the definition $(8-3')$ of K and the corresponding equations for the adjoint K^+, we can show that

$$\mathrm{K}^+ \mathscr{H}_\mathrm{e}\ \mathrm{K} = \mathrm{A}^* - \mathbf{B} \cdot \mathrm{S_e} \tag{8-15}$$

that is, $K^+ \mathscr{H}_e K$ is obtained from $\mathscr{H}_e$ by changing A into A^* (this amounts to changing p into $-p$ in the magnetic coupling term) and S_e into $-\mathrm{S_e}$. (This could be reached by changing the

direction of time for the conduction electrons and justifies the name "time-reversal operator.") We also notice that $K^+K = K^+ = 1$, and write

$$[\mathscr{H}_{\mathrm{e}},\ \mathrm{K}] = \mathscr{H}_{\mathrm{e}}\,\mathrm{K} - \mathrm{K}\mathscr{H}_{\mathrm{e}} = \mathrm{K}\,(\mathrm{K} + \mathscr{H}_{\mathrm{e}}\,\mathrm{K} - \mathscr{H}_{\mathrm{e}}) \tag{8-16}$$

Consider for instance pure case 2 (no orbital magnetic fields $A = A^*$). Then, by (8-15),

$$\frac{\mathrm{dK}}{\mathrm{dt}} = \frac{\mathrm{i}}{\hbar}\,[\mathscr{H}_{\mathrm{e}}, K] = -\frac{2\mathrm{i}}{\hbar}\,\mathrm{KB}\cdot\ \mathrm{S}_{\mathrm{e}} \tag{8-17}$$

Here we might also say that K acquires a time-dependent phase (due to the Γ coupling). However, we cannot treat the phase classically, because the potential B varies strongly in one atomic distance, or in one Fermi wavelength. We see later how the motion of K is analyzed in such situations. Before going into such details, we now discuss some general qualitative properties of $K(t)$ lin both cases (1) and (2) ⌋ related to the shape of the one-electron trajectories.

6.5.2 8-2 Ergodic Versus Nonergodic Behavior - Gapless Superconductivity

For the moment, let us restrict our attention to systems where the pair potential $\Delta(r)$ has an amplitude $|\Delta|$ constant in space. This greatly simplifies the discussion of the linear equations (8-8) or (8-11) and allows us to bring out directly the most important features. Also, it is not an academic case. It is found in the following situations:
(1) small superconducting colloids;
(2) thin superconducting films in fields parallel to the film surface;
(3) superconducting alloys, with magnetic impurities, in zero external field. In colloids, $|\Delta|$ cannot vary very much if all dimensions of the grains are small compared with $\xi(\mathrm{T})$. In thin films, we have to be more careful, since only one of the dimensions is small. In particular, if the field is normal to the film, it often penetrates by means
of vortices as in Type II superconductors (M. Tinkham, 1962), and then $|\Delta|$ is strongly varying in space. To avoid this, we only consider fields parallel to the surface. There is also another requirement on the colloids and films, related to the fact that we discuss second-order transition. In Type I materials, the transition is indeed observed to be of second order only if the sample thickness is smaller than one or two penetration depths.

Finally, for magnetic alloys (in zero field), it is also a reasonable starting point to take $|\Delta| =$ const. (This neglects only some rather weak local modulations of $\Delta(r)$ in the vicinity of each impurity.)

We now write down explicitly the equation for the transition temperature. For a singly connected specimen, we can choose a particular gauge for the vector potential $\mathbf{A}$, such that $\Delta(r)$ is real, and constant in space (since $|\Delta|$ is constant). This enables us to integrate the selfconsistency equation (8-11) on $\mathbf{r}_2$ and $\mathbf{r}_1$, obtaining

$$\Delta U = \int dr_1 dr_2 K\,(r_1 r_2)\,\Delta$$

By making use of (8-1), (8-5), and canceling out a factor Δv on both sides, we reach the condition

$$1 = \mathrm{N}(0)\mathrm{V}\int\ \mathrm{d}\xi\ \mathrm{d}\xi' \sum_{\omega} \frac{\mathrm{k_B\ T}}{(\xi - \mathrm{i}\omega\hbar)\,(\xi' + \mathrm{i}\omega\hbar)}\frac{1}{\hbar}\ \mathrm{g}\left[\frac{(\xi - \xi')}{\hbar}\right] \tag{8-18}$$

$$\mathrm{g}(\Omega) = \int \frac{\mathrm{dt}}{2\pi}\left\langle\ \mathrm{K}^+(0)\mathrm{K}(\mathrm{t})\right\rangle \mathrm{e}^{-\mathrm{i}\Omega\mathrm{t}}$$

$g(\Omega)$ is the power spectrum of the operator K. Instead of using the summation Σ_ω we may also, if we wish, write (8-18) in terms of Fermi functions $f(\xi)$

$$1 = N(0)V \int d\xi \, d\xi' \frac{1 - f(\xi) - f(\xi')}{\xi + \xi'} g\left[\frac{(\xi - \xi')}{\hbar}\right] \qquad (8\text{-}18')$$

[Some features are more striking on (8-18'), but (8-18) is more convenient for computational purposes.]

Discussion of this equation: First we notice that for all cases where the one-electron Hamiltonian $\mathcal{K}_e$ is invariant by time reversal ($[K, \mathscr{H}_e] = 0$), $K(t) = K(0)$:

$$\langle K^*(0)K(t)\rangle \equiv 1$$
$$g(\Omega) = \delta(\Omega)$$

The power spectrum of K has a single line at zero frequency. Then (8-18') reduces to

$$1 = N(0)V \int d\xi \frac{1 - 2f(\xi)}{2\xi}$$

This is the BCS condition for the transition temperature in conventional superconductors.

When $[K, \mathscr{H}_e] \neq 0$, we must study $g(t)$ in more detail. As pointed out, we are interested in $\Omega \sim k_B T/\hbar$ and $t \sim \hbar/k_B T$, that is, a very long time scale. Thus we consider first the limiting behavior of $\langle K^+(0)K(t)\rangle$ at very large times. There can be many types of limiting behavior. Two of them are particularly interesting:

(I) $\lim_{t\to\infty} \langle K^+(0)K(t)\rangle = \eta \neq 0$

(II) $\lim_{t\to\infty} \langle K^+(0)K(t)\rangle = \exp(-t/\tau_K)$

where η and τ_K are certain functions of the strength of the perturbation (the magnetic field, or the magnetic impurity concentration).

If our system is of class I, we say it is nonergodic.

If our system is of class II, we say it is ergodic and Markoffian.

Nonergodic Systems

We may write

$$\left\langle K^+(0)K(t)\right\rangle = \eta + R(t) \qquad (8\text{-}21)$$

where $R(t)$ is a rapidly decreasing function of time [for instance, in small samples of class I, the time constant of $R(t)$ is of order d/v_F where d is the sample dimension, and here $d \ll \xi_0$ or $d/v_F \ll \hbar/k_B T$].

Thus we may, in a first approximation, neglect completely $R(t)$ at the times of interest, and Eq. (8-18') takes again the BCS form

$$1 = N(0)V\eta \int_{-\hbar\omega_D}^{\hbar\omega_D} d\xi \frac{1 - 2f(\xi)}{2\xi} \qquad (8\text{-}22)$$

leading to a transition temperature

$$k_B\, T = 1.14\hbar\omega_D \exp\left(-\frac{1}{N(0)V\eta}\right) \qquad (8\text{-}23)$$

The behavior is close to that of a conventional superconductor in zero field, but the coupling constant $N(0) \vee \eta$ is now dependent on the strength of the perturbation (through η). The following problem discusses a physical system of class I.

Problem.

Discuss the behavior of $\langle K^+(0)K(t)\rangle$ at large times for a thin film (thickness d) with diffuse reflection on the boundaries but no volume defects, in a parallel field H (P. G. de Gennes and M. Tinkham, 1964).

Solution.

Consider an electron starting at point r_0 at time 0 (Fig. 8-3), then suffering collisions alternatively on both sides of the film at times $t_1, t_2, \ldots, t_n$ and finally arriving at r_t at time t. The phase ϕ defined by Eq. (8-13) is a sum of increments:

$$\phi = \Delta\phi_{01} + \Delta\phi_{12} + \cdots + \Delta\phi_{n-1n} + \Delta\phi_{nt}$$

The vector potential, in the gauge where Δ is real, has one nonzero component $A_y = Hx$. Then each of these increments (except $\Delta\phi_{01}$ and $\Delta\phi_{nt}$) is in fact equal to 0, as shown in Fig. 8-3.

$$\Delta\phi_{pp+1} = \frac{2eH}{\hbar c}\int_{x=-d/2}^{x=d/2} x\,dy = 0$$

The trajectory between two successive collisions is essentially a straight line; y is a linear function of x. Thus the above integral, taken between even limits, vanishes and $\phi = \Delta\phi_{01}+\Delta\phi_{\mathrm{nt}}$. Furthermore, when $\mathrm{t} \gg \mathrm{d}/\mathrm{v_F}$, the number of collisions n is large and the relevant time intervals $0 \to t_1$ and $t_n \to t$ are uncorrelated. We may thus write

$$\eta = \langle \exp(\mathrm{i}\Delta\phi_{01})\rangle \langle \exp(\mathrm{i}\Delta\phi_{\mathrm{nt}})\rangle \qquad \eta^{1/2} = \langle \exp(\mathrm{i}\Delta\phi_{01})\rangle$$

η is nonvanishing: in spite of the numerous collisions, the system is not ergodic in our sense. To compute η we consider an electron starting from an arbitrary point $\mathbf{r}$, with a randomly oriented velocity of length v_F, the projection of this velocity on the xy plane making an angle ψ with the x axis.

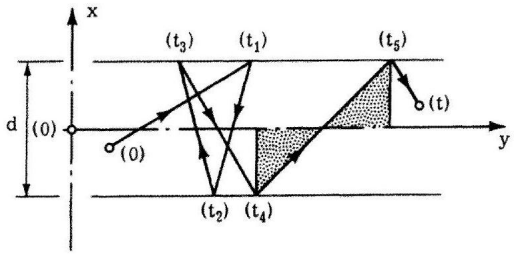


Figure 8-3
Successive collisions of one electron in a thin film with diffuse scattering on the boundaries.

$$\eta^{1/2} = \frac{1}{\pi d}\int_{-\pi/2}^{\pi/2} d\psi \int_{-d/2}^{d/2} dx \exp\left[i\pi\frac{H}{\phi_0}\left(\frac{d^2}{4} - x^2\right)\tan\psi\right]$$
$$= \frac{2}{d}\int_0^{d/2} dx \exp\left[\frac{\pi H}{\phi_0}\left(\frac{x^2 - d^2}{4}\right)\right]$$

where $\phi_0 = \mathrm{ch}/2\mathrm{e}$ is the flux quantum.

$$\eta = \begin{cases} 1 - \frac{\pi}{3}\frac{\mathrm{H}}{\phi_0}\,\mathrm{d}^2 & \mathrm{H} \ll \frac{\phi_0}{\mathrm{d}^2} \\ \left(\frac{2\phi_0}{\pi \mathrm{H d}^2}\right)^2 & \mathrm{H} \gg \frac{\phi_0}{\mathrm{d}^2} \end{cases}$$

Ergodic Markoffian Systems

If the exponential decay law (8-20) is obeyed at the times t of interest, we can write

$$\mathrm{g}(\Omega) = \frac{1}{\pi}\frac{{}^{\tau}\mathrm{K}}{1+\Omega^2\tau_{\mathrm{K}}^2} \tag{8-24}$$

and perform the integrations $\int \mathrm{d}\xi\mathrm{d}\xi'$ in Eq. (8-18). We arrive at the condition

$$1 = \mathrm{N}(0)\mathrm{V}\sum_{\omega} 2\pi\frac{\mathrm{k_B\ T}}{\hbar}\frac{1}{2|\omega| + \frac{1}{\tau_{\mathrm{K}}}} \tag{8-25}$$

The sum Σ_ω diverges. This is because we did not take into account the frequency cutoff ω_{D} of the interaction. A similar complication has been discussed after Eq. (7-28), p. 218. When the cutoff is taken into account, (8-25) becomes

$$1 = \mathrm{N}(0)\mathrm{V}\left[\ln\left(\frac{1.14\hbar\omega_{\mathrm{D}}}{\mathrm{k_B\ T}}\right) + \frac{2\pi\mathrm{k_B\ T}}{\hbar} \times\sum_{\omega}\left(\frac{1}{2|\omega| + \frac{1}{\tau_{\mathrm{K}}}} - \frac{1}{2|\omega|}\right)\right] \tag{I}$$

The sum is now convergent and can be expressed in terms of a tabulated function $\psi(z)$.

$$\psi(z) = \frac{\Gamma'(z)}{\Gamma(z)} = -0.577 - \frac{1}{z} + \sum_{\nu=1}^{\nu=\infty}\left(\frac{1}{\nu} - \frac{1}{\nu+z}\right)$$

$$\frac{2\pi k_B T}{\hbar}\sum_{\omega}\left(\frac{1}{2|\omega| + \frac{1}{{}^{\top}K}} - \frac{1}{2|\omega|}\right)$$

$$= \left(\frac{1}{2}\right) - \psi\left(\frac{1}{2} + \frac{\hbar}{4\pi{}^{\top}K^k k_B T}\right)$$

Finally the relation between $1/\tau_{\mathrm{K}}$ and T takes the implicit form

$$\ln\frac{\mathrm{T_0}}{\mathrm{T}} = -\psi\left(\frac{1}{2}\right) + \psi\left(\frac{1}{2} + \frac{\hbar}{4\pi\tau_{\mathrm{K}}\mathrm{k_B\ T}}\right) \tag{8-26}$$

Since a relation of this form occurs very often in the theory of superconductivity, we give a special name to it. We say that

$$\frac{\hbar}{\tau_K} = k_B T_0 \cup n\left(\frac{T}{T_0}\right) \tag{I}$$

The "universal function" Un(x) is shown in Fig. 8-4. For $\mathrm{x} \to 0$,

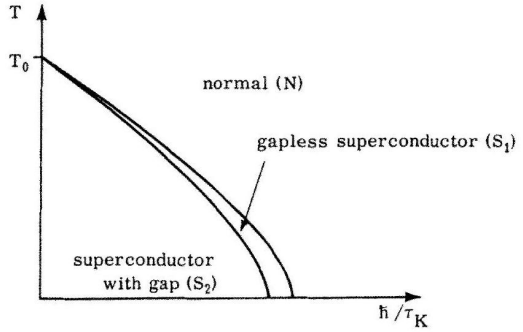


Figure 8-4

Phase diagram for a superconductor with "asymmetric" perturbations on the Cooper pairs + ergodicity. $\hbar/\tau_\kappa$ measures the strength of the perturbation.
Un(x) $\to$ 1.76 and $\hbar/\tau_{\mathrm{K}} \to 1.76\mathrm{k_B T_0} = \Delta_0$ [the BCS gap parameter in the unperturbed superconductor at $(T = 0)$]. For $x \to 1$

$$\mathrm{Un}(x) \to \frac{\pi}{8}(1-x) \tag{8-27}$$
$$\frac{\hbar}{\tau_K} \cong \frac{\pi}{8} k_B\,(T_0 - T) \quad (T \to T_0)$$

EXAMPLES OF "ERGODIC" SYSTEMS

(1) In a field H:
(a) small colloidal particles,
(b) thin films with both surface and volume scattering (for films of well controled thickness, surface scattering is not enough to bring in the ergodicity, as mentioned above) in parallel fields,
(c) thin films of irregular thickness.
(2) Alloys with magnetic impurities.

In the following problems, specific calculations of τ_{K} are described for Markoffian systems. In case (1) for instance, once $^{\top}$K is known as a function of magnetic field, we insert the result in Eq. (8-26) and obtain the critical field versus temperature curve.

Problem.

Compute τ_{K} for a small "dirty" sample of arbitrary shape under a field (K. Maki, 1963).

Solution.

We consider a sample of dimensions d much larger than the mean free path ℓ. It is important to realize, however, that there is an upper bound on d, related to our assumption $|\Delta| =$ const. At larger d's, we know in fact that the order parameter is not constant in space: The superconducting phase nucleates at a field $\mathrm{H_{C2}}$ or $\mathrm{H_{C3}}$, the nucleus having a size

$$\xi(\mathrm{T}) \sim \sqrt{\xi_0 \ell \frac{\mathrm{T_0}}{\mathrm{T_0 - T}}}$$

where $\xi_0 = 0.18\,(\hbar v_F/\mathrm{k}_B T_0)$. Thus, to be sure that $|\Delta|$ is constant, we must have

$$d < \sqrt{\xi_0 \ell \frac{\mathrm{T_0}}{\mathrm{T_0 - T}}}$$

and the inequalities

$$\ell < d < \sqrt{\xi_0 \ell \frac{\mathrm{T_0}}{\mathrm{T_0 - T}}}$$

allow only for a rather narrow range of d values. We discuss this region, however, since it is a simple example of ergodic behavior. From the point of view
of the one-electron trajectories, the condition $\sqrt{\xi_0 l} > d$ means that the diffusion length $\sqrt{Dt}$ (where $D = \frac{1}{3} v_F \ell$ and $t \sim \hbar/k_B T_0$) is larger than d, and consequently that at time t the electron has explored all regions of the sample. Then the phase $\phi(t)$ defined in Eq. (8-13) is a sum of many uncorrelated increments, and has a gaussian distribution. This implies that

$$\left\langle \mathrm{e}^{\mathrm{i}\phi(\mathrm{t})} \right\rangle = \mathrm{e}^{-1/2\left\langle \phi^2(\mathrm{t}) \right\rangle}$$

We write $\phi(\mathrm{t}) = \int_0^{\mathrm{t}} \mathrm{dt}'\omega\,(\mathrm{t}')$ with $\omega = 2\mathrm{ev}\cdot\mathrm{A}/\ \mathrm{hc}$. At times t much larger than the collision time $\tau = \ell/v_F$, we have

$$\left\langle \phi^2 \right\rangle - 2\mathrm{t}\int_0^\infty \langle \omega(0)\omega\,(\mathrm{t}')\rangle\,\mathrm{dt}' \quad (\mathrm{t} \gg \tau)$$

For trajectories originating from point r, we may write

$$\begin{aligned}\langle \omega(0)\omega\,(t')\rangle &= \left(\frac{2e}{\hbar c}\right)^2 \sum_{\alpha\beta} A_\alpha(r) A_\beta\,(r')\,\langle v_\alpha(0) v_\beta\,(t')\rangle \\ &= \left(\frac{2e}{\hbar c}\right)^2 A^2(r)\frac{v_F^2}{3} e^{-t'/\tau} \quad \alpha,\beta = x,y,z\end{aligned}$$

since at times of order τ the change of r along the trajectory is $\sim \ell$ and negligible on the scale of variation of $\mathbf{A}(\sim \mathrm{d})$. Then

$$\begin{aligned}\langle \exp[i\phi(t)]\rangle &= \exp\left(-t/\tau_K\right) \quad (t \gg \tau) \\ \frac{1}{\tau_K} &= \frac{1}{3}\tau\left(\frac{2\mathrm{ev}_F}{\hbar \mathrm{c}}\right)^2 \left\langle A^2(r)\right\rangle\end{aligned}$$

The average of A^2 is to be taken over the sample volume.
It is very important to realize that the choice of gauge for A is imposed by the condition: $\Delta =$ const.

For simple geometries, this gauge can be found by inspection:
(1) Thin film (of thickness d along $0x$) in uniform field (along 0z), carrying no over-all current.

$$\begin{aligned}A_x &= A_z = 0 \\ A_y &= Hx \quad \text{(where } x \text{ is measured from the midplane of the film)} \\ \left\langle A^2\right\rangle &= \frac{H^2 d^2}{12}\end{aligned}$$

(2) Spherical grain of radius R in uniform field

$$\begin{aligned}A &= \frac{1}{2} r \times H \\ \left\langle A^2\right\rangle &= \frac{H^2 R^2}{10}\end{aligned}$$

Problem.

Compute τ_{K} for a magnetic alloy (A. Abrikosov and L. P. Gorkov, 1961).

Solution.

The following is a "lowbrow" derivation. Start from the equation

$$\begin{aligned}g(\Omega) &= \frac{\sum}{m} |(n|K|m)|^2 \delta\left(\frac{\xi_m - \xi_n}{\hbar} - \Omega\right) \\ &= \frac{1}{\pi}\frac{\tau_k}{1+\Omega^2\tau_k^2}\end{aligned}$$

the average being taken over one-electron states at a fixed energy ξ_{n} (and in practice at the Fermi level). Choose a value $\Omega \gg 1/\tau_{\mathrm{k}}$ (although $\Omega \ll \mathrm{E_F}/\hbar$). Then $g(\Omega) \sim 1/\pi\Omega^2\tau_{\mathrm{K}}$ and we can write

$$\begin{aligned}\frac{1}{\tau_{\mathrm{K}}} &= \pi\hbar\sum_m \sqrt{\langle \mathrm{n}|\mathrm{K}|m\rangle|^2}\Omega^2\delta\left(\xi_{\mathrm{n}}-\xi_m-\hbar\Omega\right)\\ &= \frac{\pi}{\hbar}\sum_m \sqrt{\langle \mathrm{n}|\mathrm{K}|m\rangle|^2}\left(\xi_{\mathrm{n}}-\xi_m\right)^2\delta\left(\xi_{\mathrm{n}}-\xi_m-\hbar\Omega\right)\\ &= \frac{\pi}{\hbar}\sum_m \sqrt{\langle \mathrm{n}|\left[\mathcal{K}_{\mathrm{e}},\ \mathrm{K}\right]|m\rangle|^2}\delta\left(\xi_{\mathrm{n}}-\xi_m-\hbar\Omega\right)\end{aligned}$$

The commutator $[\mathscr{H}_e, K]$ has been derived in Eq. (8-17)

$$[\mathscr{H}_{\mathrm{e}}, K] = -2\ \mathrm{KB}\cdot\ \mathrm{S_e}$$

where $\mathrm{B} = \Sigma_{\mathrm{i}}\Gamma\left(r-r_{\mathrm{i}}\right)S_{\mathrm{i}}$.
To second order in the impurity potentials, we may now replace the exact one-electron states $|n\rangle, |m\rangle$ by plane waves $\phi_n \to L^{-3/2}e^{ik\cdot r}$

$$\frac{1}{\tau_{\mathrm{K}}} = \frac{\pi}{2\hbar}\sum_{\sigma,\mu}\sum_{\mathbf{k}'}\left(\sigma\mathbf{k}|2\mathbf{B}\cdot\mathbf{S}\rho|\mu\mathbf{k}'\right)\delta\left(\xi_{\mathbf{k}}-\xi_{\mathbf{k}'}-\hbar\Omega\right)$$

The summation on spin indices (σ, μ) is performed according to the rules

$$\begin{aligned}&\frac{1}{2}\sum_{\sigma\mu}\langle\sigma|\mathrm{S_e^X}|\mu\rangle\langle\mu|\mathrm{S_e^X}|\sigma\rangle = \frac{1}{2}\sum_{\sigma}\langle\sigma|\left(\mathrm{S_e^X}\right)^2|\sigma\rangle = \frac{1}{4}\\ &\frac{1}{2}\sum_{\sigma\mu}\langle\sigma|\mathrm{S_e^X}|\mu\rangle\langle\mu|\mathrm{S_e^Y}|\sigma\rangle = 0,\ \text{and so on}\end{aligned}$$

With the Γ interaction, the orbital part of the matrix element is given by

$$\langle k|\mathbf{B}\,|k'\rangle = L^{-3}\sum_{\mathbf{i}}\exp\left[i\left(k-\mathbf{k}'\right)\cdot\mathbf{r_i}\right]S_{\mathbf{i}}\Gamma\left(\mathbf{k}-\mathbf{k}'\right)$$

where

$$\Gamma(q) = \int_e^{iqr}\Gamma(r)dr$$

On squaring and only keeping terms of the form S_iS_i, not S_iS_j (no correlation between impurities), we obtain

$$\frac{1}{\tau_K} = \frac{\pi}{\hbar}\frac{n}{L^3}\frac{S_i\left(S_i+1\right)}{3}\sum_{k'}\left|\Gamma\left(k-k'\right)\right|^2\delta\left(\xi_k-\xi_{k'}-\hbar\Omega\right)$$

where n is the number of impurities per cm^3.
Finally we may simplify this by taking $\hbar\Omega \to 0$, because Σ_{k} ' is nearly independent of $\hbar\Omega$ (when $\hbar\Omega \ll E_F$) and $\xi_k \to 0$, that is, we calculate $1/\tau_K$ just at the Fermi surface. [2] Then

$$\frac{1}{\tau_K} = \frac{\pi}{\hbar}n\frac{S_i\left(S_i+1\right)}{3}N(0)\int\frac{d\Omega_{k'}}{4\pi}\left|\Gamma\left(k-k'\right)\right|^2$$

where $\int \mathrm{d}\Omega_{\mathrm{k}'}$ is an integration over the polar angles of $\mathbf{k}'$. The lengths are $k = k' = k_F$. If x is the impurity fraction and a^3 the atomic volume ($n = x/a^3$):

$$N(0) = \frac{1}{a^3E_F},\quad \Gamma(q) \sim \Gamma\cdot a^3$$

and thus

$$\frac{\hbar}{\tau_K} \sim x\frac{\Gamma^2}{E_F}$$

Comments on this formula:
(1) At small $x, 1/\tau_K$ is small and Eq. (8-27) may be used to derive the transition point T. Qualitatively, this gives

$$k_B\left(T_0 - T\right) \sim x\frac{\Gamma^2}{E_F}$$

T decreases very rapidly when magnetic impurities are added. Typically $\Gamma \sim 0.2\text{eV}, E_F \sim 2\text{eV}, \Gamma^2/E_F \sim 2.10^{3\circ}\text{K}$. For $x = 10^{-3}, T$ has dropped by 2°. Such rapid drops are indeed observed in practice. They are now, in fact,

one of the best methods to ascertain whether an impurity is, or is not, magnetic in a given matrix.
(2) The whole calculation is valid only when $x\left(\Gamma^2/E_F\right) \ll k_B T_0$. This comes from the following effect: In the presence of the Γ coupling, an indirect interaction appears between the impurities, of the form

$$H_{ij} = S_i \cdot S_j \frac{\Gamma^2}{E_F} f\left(k_F R_{ij}\right)$$

where $E_F = \hbar^2 k_F^2/2m$ is the Fermi energy of the conduction electrons and $f\left(k_F R_{ij}\right)$ is a dimensionless function which behaves at large distances as $\left(k_F R\right)^{-3}\cos 2k_F R$ (M. A. Ruderman and C. Kittel, 1954). Because of H_{ij}, the impurities order magnetically (ferro- or antiferromagnetically) at low temperatures. The magnetic transition point is roughly given by $k_B T_c = x\left(\Gamma^2/E_F\right)$. We need $T_c \ll T$ where T_c is the superconducting transition temperature of the alloy. Under these conditions:
(a) Each impurity is only weakly coupled to the others and its spin direction is nearly independent of time (static impurities).
(b) The spin correlation between two impurities is of the order of T_c/T and is thus negligible (independent impurities).
(3) Note that if a spin-orbit coupling term is added to $\mathscr{H}_e$, it does not contribute to $1/\tau_{\text{K}}$ since it is invariant under time inversion. This shows an important difference between τ_K and the electron spin relaxation time T_1 (the spin-orbit coupling contributes to T_1).
(4) The whole calculation is valid only to order Γ^2. In higher orders, the situation is complicated by the so-called "Kondo effect."

Gapless Superconductivity

At temperatures slightly below the transition point defined by (8-26), Δ is nonzero, but still small. We can treat it as a perturbation, and compute the excitation energies ϵ_{n} of the quasiparticles. As usual, knowledge of the wave functions u, v, to first order in Δ, permits the calculation of the eigenvalues ϵ to order Δ^2. Taking u and v from the calculations before Eq. (8-11), we arrive at

$$\epsilon_{\text{n}} = |\xi_{\text{n}}| + |\Delta|^2 \sum_m \text{p}\frac{|\langle \text{n}|\text{K}|m\rangle\,|^2}{\xi_{\text{n}} + \xi_m} \tag{8-28}$$

(P denotes a principal part, at $\xi_n = -\xi_m$).
If the one-electron Hamiltonian is invariant under time-reversal $[\mathcal{F}_{\text{e}}, K] = 0$ and $\langle \text{n}|\text{K}|m\rangle$ is

[2] We can pass to the limit $\Omega \to 0$ in the final expression even though in the initial expression we took $\Omega \gg 1/\tau_{\text{K}}$. This simplification is introduced when the true states $|\text{n}\rangle$ are replaced by the unperturbed states $|\text{k}\rangle$.

0 unless $\xi_m = \xi_\mathrm{n}$. Then the perturbation calculation is not good: If ξ_n is small, the energy denominator $2\xi_\mathrm{n}$ is small and the correction diverges. This is related to the existence of the BCS energy gap. The same properties appear in all nonergodic systems.

For an ergodic system, $\langle n|K|m\rangle$ is not singular at $\xi_m = \xi_n$ and has nonzero components in a finite band $|\xi_m - \xi_\mathrm{n}| \sim \hbar/\tau_\mathrm{K}$. Thus the energy denominator in (8-28) remains finite, even if ξ_n (or ξ_m) goes to 0 . The perturbation calculation works. The expansion parameter is now $\Delta/(\hbar/\tau_K) = \Delta\tau_K/\hbar$ instead of Δ/ξ_n. We can compute ϵ_n explicitly if we make use of (8-24) for the power spectrum of K; performing the integration, we get

$$\begin{aligned}\epsilon &= |\xi| + |\Delta|^2 \mathrm{P}\int \mathrm{d}\xi' \mathrm{g}\left(\frac{\xi-\xi'}{\hbar}\right)\frac{1}{\xi+\xi'} \\ &= |\xi| + \frac{2|\Delta|^2|\xi|}{(2\xi)^2 + (\hbar/\tau_\mathrm{K})^2} \quad \left(\frac{\Delta\tau_\mathrm{K}}{\hbar} \ll 1\right)\end{aligned} \tag{8-29}$$

The form of this dispersion law is shown on Fig. 8-4. For $\xi \gg \hbar/\tau_K$, $\epsilon \cong \xi + \Delta^2/2\xi \cong (\Delta^2+\xi^2)^{1/2}$. which is the BCS result for conventional superconductors. On the other hand, if $\xi \to 0, \epsilon \to \xi\left[1 + 2\left(\Delta\tau_\mathrm{K}/\hbar\right)^2\right]$ tends toward 0 linearly. There is no gap in the excitation spectrum. Equation (8-29) can also be expressed in terms of a density of states $N_S(\epsilon)$. To order Δ^2 we have

$$\mathrm{N_S}(\epsilon) = \mathrm{N}(0)\frac{\partial\xi}{\partial\epsilon} \cong \mathrm{N}(0)\left[1 + 2\left(\frac{\Delta\tau_\mathrm{K}}{\hbar}\right)^2 \frac{(2\epsilon)^2 - (\hbar/\tau_\mathrm{K})^2}{\left[(2\epsilon)^2 + (\hbar/\tau_\mathrm{K})^2\right]^2}\right] \tag{8-30}$$

$\mathrm{N_S}(\epsilon)$ is lower than the normal state value $\mathrm{N}(0)$ when $\epsilon < \hbar/2\tau_\mathrm{K}$, but still finite (Fig. 8-5).

The material has no gap, but it is still a superconductor. For instance, we can compute the screening currents induced by an applied magnetic field H, and we find that they do not vanish - they are of order Δ^2 as usual.

This remarkable "gapless superconductivity" takes place only in the region of small Δ 's ($\Delta\tau_K/\hbar < 1$) where our perturbation calculation converges. At larger Δ 's we find a gap again. This can be represented in a diagram where we plot along x the strength of the perturbation (measured by $\hbar/\tau_K$) and along y the temperature (Fig. 8-5). In such a plane, we find 3 regions:

$N =$ normal
$S_1 =$ gapless superconductor
$S_2 =$ superconductor with gap

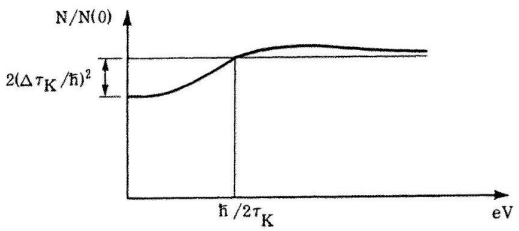


Figure 8-5
Gapless superconductivity: Density of states for Fermi-type excitations as a function of excitation energy. (The curve is valid when the pair potential Δ is small when compared with $\hbar/\tau_K$.) Note that the energy scale is given by $\hbar/\tau_K$ (not by Δ).

The boundary between N and $\mathrm{S_1}$ is given by the universal function of Eq. (8-26'). The boundary between S_1 and S_2 must be computed by more sophisticated techniques (in our language: summing the whole series in powers of Δ).

There is some evidence for the existence of region S_1 in magnetic alloys, from tunneling experiments on InFe (quenched) solid solutions (F. Reif and M. Woolf, 1962). Unfortunately, in the region of greatest interest $[x\,(\Gamma^2/E_F) \sim k_B T_0]$, the impurity spins precess rapidly in their mutual exchange fields and this complicates the interpretation of all data on magnetic alloys. Colloidal particles or films in a parallel field should also exhibit the region S_1, but, in the present state of the art, their dimensions are not accurately controlled (what an experimentalist calls a 500Å film is in most cases an irregular layer with bumps and holes maybe 100Å or more in amplitude). τ_{K} depends on the thickness. To display clearly the region S_1, ${}^{\top}K$ would have to be fixed to a few per cent, as is clear from Fig. 8-4. This is beyond present technical capability.

More convenient examples of gapless superconductivity will be mentioned in the next paragraph, where we allow $|\Delta|$ to vary in space.

6.5.3 8-3 Dirty Superconductors in High Magnectic Fields

From now on, we restrict our attention to "dirty," nonmagnetic alloys. More precisely we assume that the mean free path ℓ is much smaller than $\xi_0 = 0.18\,(\hbar v_{\mathrm{F}}/\mathrm{k_B T_0})$ and also much smaller than all
sample dimensions d. We also assume that the sample is surrounded only by insulators (no normal metal plated on the surface). Apart from these restrictions, the shape of the specimen is arbitrary, and we do not assume that $|\Delta|$ is constant in the whole volume.

We shall now show that, for such conditions, the linear self-consistency equation (7-8) can be replaced by a second-order differential equation generalizing the Landau-Ginsburg equation at all temperatures. Basically, this simplification occurs because the transport properties in the normal state are ruled by a diffusion equation-a second-order differential equation.

As we know, the kernel $\mathrm{K}\,(\mathbf{r}_1\mathbf{r}_2)$ of Eq. (7-8) can be expressed in terms of the correlation function $f\,(r_1 r_2 t)$ defined in Eq. (8-5). In the "dirty" limit, it is not hard to find out what is the differential equation satisfied by f. We consider two successive times $t(>0)$ and $t+\epsilon$ (ϵ being small) and write down that a particle reaching r_1 at time $t+\epsilon$ has come by diffusion from a point r' at time t. The average distance between r_1 and r' is small (of order $\sqrt{\epsilon}$) and thus the corresponding increment in phase $\Delta\phi$ of K is simply

$$\Delta\phi = \frac{2e}{c} A\,(r_1)\cdot(r_1 - r')$$

Thus

$$\mathrm{f}\,(\mathbf{r}_1\mathbf{r}_2, \mathrm{t}+\epsilon) = \int \mathrm{d}_3\mathbf{r}'\mathrm{f}\,(\mathbf{r}'\mathbf{r}_2, \mathrm{t})\,D\,(\mathbf{r}_1\mathbf{r}'|\epsilon)\,\mathrm{e}^{\mathrm{i}\Delta\phi} \tag{8-31}$$

Here $D\,(r_1 r'|\epsilon)$ is the function describing the spread of a point source at point $\mathbf{r}_1$ after a time ϵ has elapsed. It is a solution of the diffusion equation:

$$\frac{\partial}{\partial\epsilon}\mathfrak{D} = D\nabla'^2\mathfrak{D} \quad \nabla' = \left(\frac{\partial}{\partial \mathrm{x}'}, \frac{\partial}{\partial \mathrm{y}'}, \frac{\partial}{\partial \mathrm{z}'}\right)$$

together with the initial condition $\lim D = \delta\,(r_1 - r')$ and appropri-

$$\epsilon \to 0$$

ate boundary conditions on the sample surface $(\nabla' D)_{\mathrm{normal}} = 0$. For an infinite medium, for instance, we have

$$D\,(r_1 r'|\epsilon) = \frac{1}{(4\pi D\epsilon)^{3/2}} e^{-(r_1 - r')^2/4D\epsilon}$$

Expanding $f(r'r_2t)$ in a Taylor series around $r' = r_1$ in (8-31), retaining all terms up to first order in ϵ, and identifying coefficients on both sides, we obtain the required differential equation

$$\frac{\partial f}{\partial t} = D\left(\nabla_1 - \frac{2ieA}{c}\right)^2 f \quad (t > 0) \tag{8-32}$$

A similar calculation near the boundary of the specimen leads to the condition

$$\left(\nabla - \frac{2ieA}{c}\right)_n f = 0 \tag{8-33}$$

where n represents the direction of the normal to the surface. Finally, for $t \to 0$, the function f reduces to a δ function suitably normalized:

$$f(r_1r_2, 0) = V^{-1}\delta(r_2 - r_1) \quad V = \text{ sample volume} \tag{8-34}$$

Let us now assume that we have found the eigenfunctions $g_p(r)$ of the linear operator appearing in (8-32); the g's are defined by

$$-D\left(\nabla - \frac{2ieA}{c}\right)^2 g_p(r) = \frac{\epsilon_p}{\hbar} g_p(r) \tag{8-35}$$

with the boundary condition (8-33). We can then expand the delta function in (8-34) in terms of the g's, obtaining, for any $t > 0$,

$$f(r_1r_2t) = v^{-1}\sum_p g_p^*(r_2)\, g_p(r_1) \exp(-\epsilon_p t/\hbar) \tag{8-36}$$

We insert (8-36) in (8-1) and perform the integration over t, obtaining

$$\begin{aligned} K(r_1r_2) =& k_BT\sum_\omega 2\pi N(0)V \\ &\times \sum_p g_p^*(r_2)\, g_p(r_1)\, \frac{1}{2\hbar|\omega| + \epsilon_p} \end{aligned} \tag{8-37}$$

Finally, if we make use of (8-37), our starting equation (8-8) becomes

$$\begin{aligned} \Delta(r_1) =& N(0)V2\pi k_BT\sum_\omega\sum_p \frac{1}{2\hbar|\omega| + \epsilon_p} g_p(r_1) \\ &\times \int dr_2 \Delta(r_2)\, g_p^*(r_2) \end{aligned} \tag{8-38}$$

The eigenfunctions of this linear integral equation for Δ are simply the g's. For, if we choose $\Delta(r) = g_q(r)$, the orthogonality of the g's leaves only one term $p = q$ in the sum Σ_p and (8-38) is satisfied provided that

$$1 = N(0)V2\pi k_BT\sum_\omega \frac{1}{2\hbar|\omega| + \epsilon_q} \tag{8-39}$$

Equation (8-39) has a familiar form, and leads to

$$\epsilon_q = k_BT_0 \cup n\left(\frac{T}{T_0}\right)$$

where the universal function Un(x) has been discussed earlier. For a fixed field H and a given sample shape, the ϵ_{q} 's are fixed [and can be computed, more or less laboriously, by solving Eq. (8-35)]. What we want to know is the highest temperature T at which (8-38) has a nonzero solution $\Delta(r)$.
Un(x) is a decreasing function of x . Thus we must choose the lowest eigenvalue ϵ_0. Thus the recipe to compute a nucleation field for a "dirty" sample of arbitrary shape is the following: We find the lowest eigenvalue ϵ_0 of Eq. (8-35) plus the boundary condition corresponding to (8-33). This is then a known function of the field ϵ_0(H). To obtain the relation between nucleation field and temperature, we write

$$\frac{\epsilon_o(\mathrm{H})}{\mathrm{k_B\ T_0}} = \mathrm{Un}\left(\frac{\mathrm{T}}{\mathrm{T_0}}\right) \tag{8-40}$$

Problem.

Derive a formula for the critical field $\mathrm{H_{C2}}$ in a dirty superconductor, valid at all temperatures (K. Maki, P. G. de Gennes, and N. Werthamer, 1964).

Solution.

Equation (8-35) has the form of a Schrdinger equation for a particle of mass $\hbar/2D$ and charge $2e$. The cyclotron frequency for such a particle is

$$\omega_c = \frac{4eD}{c\hbar}H = 4\pi\frac{DH}{\phi_0}$$

where ϕ_0 is the flux quantum. The lowest eigenvalue is

$$\epsilon_0 = \frac{1}{2}\hbar\omega_{\mathrm{c}}$$

Writing that $\mathrm{H} = \mathrm{H_{C2}}$ and $\epsilon_0 = \mathrm{Un}\,(\mathrm{T}/\mathrm{T_0})$, we arrive at the implicit equation

$$\ln\left(\frac{\mathrm{T_0}}{\mathrm{T}}\right) = \psi\left(\frac{1}{2}\right) - \psi\left(\frac{1}{2} + \frac{\hbar\mathrm{DH_{C2}}}{2\phi_0\mathrm{k_B\ T}}\right)$$

Discussion of this equation: First, for T close to $T_0, \mathrm{H_{C2}}$ close to 0, we can make use of the aforementioned expansion of Un(T) and get

$$\mathrm{H_{C2}} = \frac{4}{\pi^2}\phi_0\frac{\mathrm{k_B}\,(\mathrm{T_0} - \mathrm{T})}{\hbar\mathrm{D}} \quad (\mathrm{T} - \mathrm{T_0})$$

It is easily verified that this agrees with the Landau-Ginsburg formula $\mathrm{H_{c2}} = \kappa\sqrt{2}\mathrm{H_c}$ when we take for κ the Gorkov expression in the dirty superconductor limit (Eq. 7-47), that is,

$$\kappa = 0.75\frac{\lambda_L(0)}{\ell}$$

For $T = 0$ on the other hand, we have

$$\frac{2\pi\hbar_{\mathrm{L2}}}{\phi_0} = k_{\mathrm{B}}\ \mathrm{T_0 Un}(0) = 1.76\mathrm{k_B\ T_0} = \Delta_{00}$$

while the bulk critical field is given by $H_{\mathrm{C}}^2/8\pi = \frac{1}{2}N(0)\Delta_{00}^2$, or

$$H_c = \sqrt{\frac{3}{2}}\frac{1}{\pi^2}\frac{\phi_0}{\xi_0\lambda_L{}^{(0)}}$$

This leads to

$$\frac{\mathrm{H_{C2}}}{\sqrt{2}\mathrm{H_c}} = \frac{\sqrt{3}}{2}\frac{\lambda_\mathrm{L}(0)}{\ell} = 0.87\frac{\lambda_\mathrm{L}(0)}{\ell}$$

Thus the ratio $\mathrm{H_{c2}}/\sqrt{2}\mathrm{H_c}$ increases only by 20 per cent when one goes from $T = T_0$ to $T = 0$. A similar calculation for a plane boundary shows that in a superconductor the ratio $\mathrm{H_{C3}}/\mathrm{H_{C2}}$ should remain equal to 1.69 at all temperatures. Also, when the field is applied at a finite angle θ from the surface, the angular dependence of $\mathrm{H_{C3}}(\theta)/\mathrm{H_{C2}}(0)$ has a form independent of temperature. Both these properties appear to be well confirmed by experiment. (In fact, it had been a surprise to notice that in dirty superconductors the Landau-Ginsburg linearized equation applied so well at low temperature.)

A THEOREM ON THE LOCAL DENSITY OF STATES

Just as in Section 8-2, we can, if we wish, study our system at temperatures slightly below the nucleation point T. In particular we can compute the density of states $\mathrm{N_S}(\mathbf{r}\epsilon)$ for excitation energy ϵ. It is now a function of the observation point $\mathbf{r}$ since the order parameter $\Delta(r)$ is not constant in space. This function can be measured by tunneling experiments. When N_S is computed to order $|\Delta|^2$, the results are remarkably simple (P. G. de Gennes, 1964).
(1) $\mathrm{N_S}(\mathrm{r}\epsilon)$ depends only on the value of $\Delta(\mathrm{r})$ at the observation point $\mathbf{r}$. This local relationship is at first sight very surprising. In the initial equation it is found in fact that $N_S(r\epsilon)$ depends on the values of $\Delta(r')$ within a radius $\sim \xi(T)$ from r. But just below the nucleation temperature, we know that the function $\Delta(r)$ has a simple shape. It is proportional to one of the eigenfunctions $\mathrm{g_0}(\boldsymbol{r})$ of Eq. (8-35). This remark permits one to carry out explicitly the required integrations in $N_S(r\epsilon)$ and the final result involves only $\Delta(r)$.
(2) $\mathrm{N_S}(\mathrm{r}\epsilon)$ is given by Eq. (8-30) where Δ is now the local value $\Delta(r)$, and where $\hbar/\tau_K = \epsilon_0$ is related to the temperature by Eq. (8-40). Thus, in the region of validity of the calculation $\left[\bar{\Delta}\tau_K/\hbar\tau 1\right.$, or (H nucleation -H) /H $\ll 1$ $\left.\right]$, our dirty systems are all gapless superconductors. These predictions have recently been confirmed by tunneling experiments on various alloys in both the $\mathrm{H_{C_3}}$ and $\mathrm{H_{C_2}}$ regions (E. Guyon and A. Martinet, 1964). In particular, these experiments show that the energy scale (given by $\hbar/\tau_\mathrm{K} = \epsilon_0$) on which the density of states deviates from N(0), is finite even when the order parameter $\Delta(r)$ becomes very small (that is, when H becomes close to the nucleation field). These measurements give in fact an accurate measurement of τ_K.

REFERENCES

Magnetic impurity effects and gapless superconductivity:
Theory:
A. Abrikosov and L. P. Gor'kov, Zh. Eksperim. i Teor. Fiz., 39, 1781 (1960), Translation Soviet Phys.-JETP, 10, 593 (1960).
Experiment:
M. A. Woolf and F. Reif, Phys. Rev., 137A, 557 (1965).
Magnetic field effects:
Theory:
K. Maki, Phys., 1, 21, 127 (1964).
P. G. de Gennes and M. Tinkham, Phys., 1, 107 (1964).
P. G. de Gennes, Phys. Condensed Matter, 3, 79 (1964).
Experiment:
E. Guyon, A. Martinet, J. Matricon, and P. Pincus, Phys. Rev., 138A, 746 (1965).

7 Well-known phenomena of superconductors

7.1 Magnetic properties of first kind superconductors by de Gennes

7.1.1 2-1 Critical field of a long cylinder

A long superconducting cylinder of radius r_0 is placed in a solenoid of radius $r_1 > r_0$ (Fig. 2-1).

A (weak) current I flows in the coil. The resulting field distribution $h(r)$ is shown in Fig. 2-2. Outside the sample, $h(r)$ takes a constant value H. In the sample the field falls rapidly (in a depth $\lambda \sim 500$Å) to 0. We restrict our attention to a macroscopic specimen ($r_0 \gg \lambda$). Then, on the scale r_0, the field does not penetrate into the sample.

This complete flux expulsion is observed for weak external fields H, but, when H reaches a critical value H_c, a radical modification occurs:

(1) The field becomes uniform across the entire section.

(2) The specimen is no longer superconducting (this we can see in principle by measuring the resistivity between the ends of the cylinder). With sufficiently perfect specimens, one can verify that this transition is reversible. If I is now decreased, the superconducting state reappears with total flux expulsion. Typical values of H_c are given in Table 2-1. The critical field decreases with increasing temperature, roughly according to the law

$$H_c(T) = H_c(0)\left[1 - \frac{T^2}{T_0^2}\right] \tag{2-1}$$

(For $T > T_0$ the material is normal even in zero field; T_0 is the

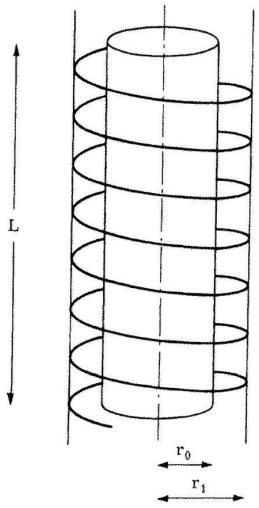


Figure 2-1

Experimental geometry to measure the critical field. The sample is a long cylinder (of length L and radius r_0). It is placed in a coil of radius r_1.

transition temperature in zero field.) From H_c, we can calculate the difference in free energy between the normal and superconducting states:

(a) When the cylinder is normal the field is uniform across the solenoid

$$h = \frac{4\pi NI}{cL} \tag{2-2}$$

(where N is the number of turns in the solenoid and L is its length, which is also the length of the specimen). The free energy of the system becomes

$$\mathcal{F}_{\mathrm{a}} = \pi \mathrm{r}_0^2 L F_{\mathrm{n}} + \pi \mathrm{r}_1^2 L \frac{\mathrm{h}^2}{8\pi} \tag{2-3}$$

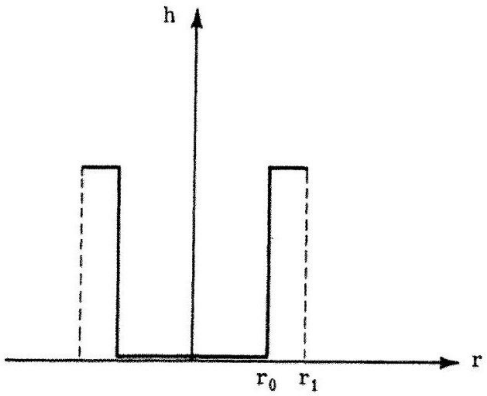


Figure 2-2 The field distribution of the coil and cylinder of Fig. 2-1 while the cylinder is superconducting. The field penetrates only up to one penetration depth in the sample. On the scale of the figure we may say that H drops abruptly to 0 inside the sample.

F_n is the free energy density of the normal sample and the second term is the magnetic energy stored in the coil.

(b) Suppose now that the cylinder becomes superconducting, the current being kept constant in the coil. The field is zero in the sample, but it maintains the value (2-2) in the region $r_0 < r < r_1$[1] The free energy becomes

$$\mathcal{F}_{\mathrm{b}} = \pi \mathrm{r}_0^2 L F_{\mathrm{s}} + \pi \left(\mathrm{r}_1^2 - \mathrm{r}_0^2\right) \mathrm{L} \frac{\mathrm{h}^2}{8\pi} \tag{2-4}$$

where F_S is the free energy density of the superconducting sample. Equation (2-4) neglects the penetration of the field in the thickness and

[1] In order to demonstrate this property, one writes curl $h = (4\pi/c)j$, from which

$$\oint \mathrm{h} \cdot \mathrm{dl} = \frac{4\pi}{\mathrm{c}} \int \mathrm{j} \cdot \mathrm{d}\boldsymbol{\sigma}$$

and one takes for a contour a line of force passing through the coil (in the region $r_0 < r < r_1$). The contributions to $\phi \mathrm{h} \cdot \mathrm{dl}$ from the parts of the line of force enclosing the magnetic current in the exterior of the coil are negligible if the solenoid is long, and one obtains $h = (4\pi \mathrm{NI/cL})$.

Table 2-1

Values of T_c and $\mathrm{H_c}(0)$ for some metals

	Zn	Cd	Hg(α)	Al	Ga	In	Tl	Sn	Pb
$\mathrm{H_c}(0)$(G)	53	30		99	51	283	162	306	803
$\mathrm{T_c}$(K)	0.88	0.56	4.15	1.19	1.09	3.41	1.37	3.72	7.18

also the kinetic energy of the surface currents - both these terms are surface effects, and are negligible for a macroscopic cylinder ($r_0 \gg \lambda$).

Note that $\mathcal{F}_{\mathrm{b}} < \mathcal{F}_{\mathrm{a}}$, because (1) $\mathrm{F_s} < \mathrm{F_n}$ and (2) the magnetic term is smaller in state b. What has become of the energy $\mathcal{F}_a - \mathcal{F}_b$ when the transition occurs? Answer: The flux ϕ passing through the coil diminishes when we go from (a) $\rightarrow$ (b). This induces a voltage V in the coil. The work done by this voltage V on the external circuit is

$$\int \mathrm{VI}dt = \int_{\mathrm{a}}^{\mathrm{b}} - \left(\frac{\mathrm{N}}{\mathrm{c}} \frac{\mathrm{d}\phi}{\mathrm{dt}}\right) \mathrm{I}dt \tag{2-5}$$

The current I is kept constant during the transition. Therefore,

$$\begin{aligned}\int \mathrm{VIdt} &= \frac{\mathrm{N}}{\mathrm{c}}\mathrm{I}\left(\phi_{\mathrm{a}} - \phi_{\mathrm{b}}\right) \\ &= \frac{\mathrm{NI}}{\mathrm{c}}\pi \mathrm{r}_0^2\ \mathrm{h} \\ &= \pi \mathrm{r}_0^2\ \mathrm{L}\frac{\mathrm{h}^2}{4\pi}\end{aligned} \tag{2-6}$$

At equilibrium between the two states ($\mathrm{h} = \mathrm{H_c}$), we must have $\mathcal{F}_{\mathrm{a}} - \mathcal{F}_{\mathrm{b}} = \mathrm{SVI\ dt}$. Using Eqs. (2-3) and (2-4), we obtain

$$F_n - F_S = \frac{H_c^2}{8\pi} \tag{2-7}$$

From these relations one can deduce a series of thermodynamical properties. Fix the current I and vary the temperature. The entropy (per cubic centimeter) of each phase is determined from the formulas

$$S_n = -\frac{dF_n}{dt} \quad S_s = -\frac{dF_s}{dT} \tag{2-8}$$

Therefore the difference in entropy between the two phases at equilibrium becomes

$$S_n - S_S = -\frac{1}{4\pi} H_c \frac{d_c}{dT} \tag{2-9}$$

The latent heat of the transition is

$$L = T\left(S_n - S_S\right) = -\frac{T}{4\pi} H_c \frac{dH_c}{dT} \tag{2-10}$$

This heat is positive; it is necessary to furnish this energy to pass from the superconducting state to the normal state. [2]

L vanishes when one considers the transition in zero field: for $\mathrm{T} = \mathrm{T_c}, \mathrm{H_c} = 0$, and experiment shows that for all superconductors studied until now $\mathrm{dH_c/dT}$ remains finite, therefore $[L]_{\mathrm{H}=0} = 0$.

Thus in zero field the superconducting transition is of the second order. There is a discontinuity in the specific heat

$$\begin{aligned}C_n - C_S &= T\frac{d}{dT}\left(S_n - S_S\right)_T = T_c \\ &= -\frac{T}{4\pi}\left(\frac{dH_c}{dT}\right)_T^2 = T_c\end{aligned} \tag{2-11}$$

Formulas $(2-10)$ and $(2-11)$ have been verified to better than 1% in several metals (notably $\mathrm{Sn}, \mathrm{In}, \mathrm{Ta}$); these experiments demand some care; it is especially necessary to assure that equilibrium has set in, that is, no flux is "frozen" in the superconductor, and so on. The practical interest of the relations $(2-10)$ and $(2-11)$ is to relate the thermodynamic quantities (latent heat and specific heat) to the critical field curve, which is often easier to measure.

[2] Consequence: If one passes from the superconducting state to the normal state in a thermally isolated specimen, the temperature of the sample decreases.

7.1.2 2-2 Penetration depths

Relation between Current and Field in a First Kind Superconductor

On the macroscopic scale, a weak field ($h < H_c$) does not penetrate into a first kind superconductor. However, on the microscopic scale, the field does not vary discontinuously at the surface. It penetrates a certain depth λ in the metal. We would like to compute λ.

In Chapter 1 we derived λ from the London equation

$$\operatorname{curl} j = -\frac{ne^2}{mc} h \tag{2-12}$$

But, in superconductors of the first kind ($\xi_0 > \lambda$), Eq. (2-12) is not valid. We need a more general relation between currents and fields, applicable even when f and h have rapid variations in space.

It turns out that the most convenient variable here is not the field h, but rather the vector potential A such that

$$\operatorname{curl} A = h \tag{2-13}$$

This equation does not define A completely. We often find it convenient to specify **A** exactly by adding the supplementary conditions

$$\begin{aligned} \operatorname{div} A &= 0 \\ A_n &= 0 \quad \text{on the sample surface} \end{aligned} \tag{2-14}$$

(A_n is the component of A normal to the surface). When Eqs. (2-14) are satisfied we say that A is chosen in the London gauge. In the London gauge (2-12) can be rewritten as

$$j = -\frac{ne^2}{mc} A \tag{2-15}$$

since insertion of (2-13) gives (2-12) and insertion of (2-14) gives

$$\begin{aligned} \operatorname{div} j &= 0 \text{ (continuity equation)} \\ j_n &= 0 \text{ on the surface} \end{aligned}$$

The latter surface condition is satisfactory if no external current is fed into the sample.

Equation (2-15) applies only when j and A vary slowly in space on the scale ξ_0. In general, we may guess that the current $j(\boldsymbol{r})$ at one point will depend on the vector potential $\mathbf{A}(\mathbf{r}')$ at all neighboring points $\mathbf{r}'$ such that $|\mathbf{r} - \mathbf{r}'| < \xi_0$. A phenomenological relation constructed to describe this effect, has been proposed by Pippard; in the London gauge it has the form

$$J(r) = C \int \frac{(A(r) \cdot R)R}{R^4} e^{-R/\xi_0} d\mathbf{r}' \quad \mathbf{R} = \mathbf{r} - \mathbf{r}' \tag{2-16}$$

The coefficient C is simply determined by noticing that when A varies slowly spatially (over distances $\sim \xi_n$), it can be taken out of the integral, and one must obtain the London value (2-15). This gives

$$\mathrm{C}\frac{4\pi}{3}\xi_0 = -\frac{\mathrm{ne}^2}{\mathrm{mc}} \quad \mathrm{C} = \frac{-3\mathrm{ne}^2}{\mathrm{mc}}$$

The choice of the simple form (2-16) for the relation between current and vector potential was a guess of Pippard. Later, after the development of the microscopic theory, it was verified that the exact relation between field and current is very close to $(2-16)$ if ones takes

$$\xi_0 = \frac{\hbar v_F}{\pi \Delta} \quad (\text{ for } T = 0) \tag{2-18}$$

The exact relation between j and A will be discussed in Chapter 4. It is much more complicated algebraically than (2-16) and the approximate Pippard form remains very useful. We now apply it to a study of penetration depths.

The Penetration Depth

Eq. $(2-16)$ is valid for a bulk superconductor. But we now want to study penetration phenomena near the sample surface: in general the relation between j and A is then modified. In practice, the following prescription applies: keep Eq. (2-16), but extend the integration $\int \mathrm{d}\mathbf{r}'$ only to points $\mathbf{r}'$ in the superconductor, and, more restrictively, to points $\mathbf{r}'$ from which an electron can travel in a straight line to point r. For instance, if there is a small empty cavity in the metal, one must exclude the "shadow" of the cavity, as shown in Fig. 2-3. (This prescription is the correct one for the (usual) case where reflection of individual electrons on the surface is diffuse. We shall derive it later from the microscopic theory.)

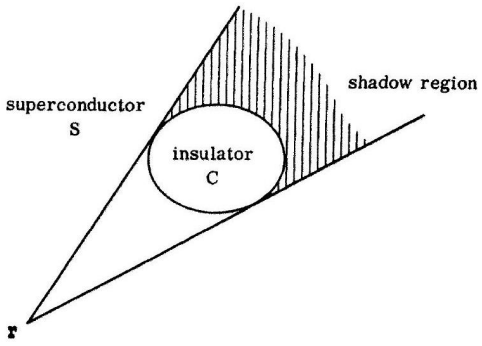


Figure 2-3

"Shadow effect" in the calculation of the current $j(r)$ induced by a magnetic perturbation $\mathbf{A}(\mathbf{r}')$. A cavity or an insulating precipitate occupies region C inside the superconductor S. Electrons are reflected diffusely at the SC boundary. The magnetic potentials $\mathbf{A}(\mathbf{r}')$. in C and in the shadow region do not contribute to $j(\mathbf{r})$.

Consider now a specimen with a plane surface x0y, the superconducting side being $z > 0$, A and j are directed along the x axis. The penetration depth λ can then be estimated by another intuitive argument of Pippard's: if $\mathbf{A}(\mathbf{z})$ was essentially constant on a thickness $\sim \xi_0$ near the surface, we would have, in this region, from Eq. (2-16): $j = -(\mathrm{ne}^2/\mathrm{mc})\,\mathbf{A}$ (the London result). But in fact $\mathbf{A}(\mathrm{z})$ is nonzero only in a smaller thickness λ. Thus the integral $(2-16)$ is reduced, roughly by the factor λ/ξ_0:

$$\mathrm{j} \simeq -\frac{\mathrm{ne}}{\mathrm{mc}} \cdot \frac{\lambda}{\xi_0}\,\mathrm{A} \quad (\lambda \ll \xi_0)$$

Using this relation in conjunction with curl $h = (4\pi/\mathrm{c})\mathrm{j}$, we obtain an (approximate) penetration law of the form $h(z) = h(0)e^{-z/\lambda}$, where λ is defined self-consistently by

$$\frac{1}{\lambda^2} = \frac{4\pi n e^2}{\mathrm{mc}^2}\frac{\lambda}{\xi_0}$$
$$\lambda^3 = \lambda_L^2 \xi_0 \quad (\lambda \ll \xi_0)$$

A (much more complicated) rigorous calculation gives $\lambda^3 = 0.62\lambda_{\mathrm{L}}^2\xi_0$.

The essential conclusions are that, in the Pippard limit, λ becomes larger than the London value $(\lambda/\lambda_L) \sim (\xi_0/\lambda_L)^{1/3} > 1$, but λ remains much smaller than the coherence length $(\lambda/\xi_0) \sim (\lambda_L/\xi_0)^{2/3} < 1$.

Methods to Measure the Penetration Depth

Historically, the first determinations of λ were made by measuring the magnetic susceptibility of very small specimens (colloids or films). Experimentally, one first verifies that the transition temperature of even very fine colloids ($\sim 100\text{Å}$) is not very different from that of bulk samples. One can therefore expect that the parameters $\lfloor n_S, \Delta(0) \rfloor$, which occur in ξ_0 and λ_L, are practically the same in small particles as in the bulk state, and this is encouraging. However, there are several difficulties:

(a) There is a rather large uncertainty in the grain dimensions of the colloid.

(b) In general, one has many lattice defects in such materials and therefore the electronic mean free path ℓ is rather short, and badly known. When ℓ is comparable to ξ_0, the Pippard formula (2-16) must be modified.

The other methods used to determine λ reduce to measuring the value of a self- or mutual inductance in the presence of the superconductor. The principle of the mutual inductance measurement is represented in Fig. 2-4.

The coil 1 creates a field h_e along the exterior of the film and a field $h_i = \rho h_e \ll h_e$ in the interior region. The field h_i is detected by the coil 2. From ρ one can determine λ by suitable theoretical analysis. In practice, one is able to measure coefficients $\rho \sim 10^{-9}$. This allows one to work with relatively thick films ($\sim 10\lambda$) for which the crystallographic state is well defined [and this minimizes objection (b)].

One can also measure the self-inductance of a coil surrounding a superconducting cylinder (method initially suggested by Casimir). If e is the distance between coil and specimen (see Fig. 2-5), the magnetic flux penetrates a surface $\sim \pi R(e + \lambda)$. As $\lambda \sim 10^3\text{Å}$ it is necessary to make e as small as possible (typically e $\sim$ 2 mm, R being 4 mm). In practice e is not known to sufficient precision and the method serves mainly to determine the temperature dependence of λ. Adifferent technique, but similar in principle, is to construct a microwave resonant cavity with the superconducting material.

(1) transmitting coil

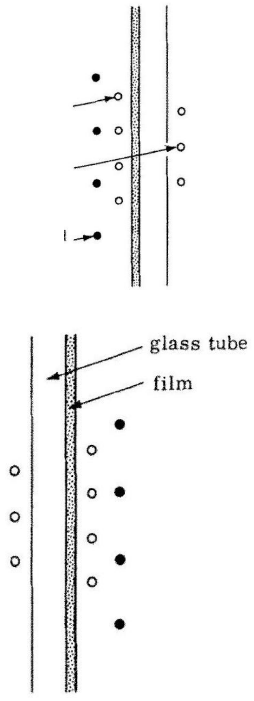


Figure 2-4 Inductive method to measure the penetration depths of thin cylindrical films lafter Sarachik, et al., Phy's. Rol. Lelters, 452(1960)]. The transmitting coil creates a field attenuated in the film. The receiving coil in the central region detects the field that has leaked

through the superconducting film. The solenoid is used to study the field dependence of the penetration depth.

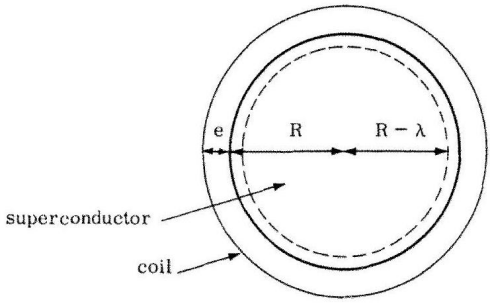


Figure 2-5

Self-induction method to measure penetration depths on a superconducting cylinder of radius R. The cylinder is surrounded by a coil of radius $R + e$. The flux is contained in a ring of thickness $e + \lambda$. In practice e is not known accurately and only the changes of λ with temperature can be measured.

Discussion

PENETRATION IN THE PURE METALS AT ABSOLUTE ZERO

Does the experimental determination of λ permit us to verify the phenomenological Pippard relation? For the pure metals at absolute zero we can calculate separately

$$\xi_0 = \frac{\hbar v_F}{\pi \Delta(0)} \quad \lambda_L = \left(\frac{mc^2}{4\pi n e^2}\right)^{1/2}$$

Taking v_F and n/m from measurements of specific heat, anomalous skin effect, and so on, in the normal state, and $\Delta(0)$ from measurements in the superconducting state, we can then predict a theoretical value for λ ($\lambda^3 = 0.62\lambda\lambda_L^2\xi_0$) for $\lambda_L \ll \xi_0$ (and more complex formulas when $\lambda_L \sim \xi_0$). Table 2-2 gives a comparison between such theoretical values and the experimental data (extrapolated to 0°K). There is satisfactory qualitative agreement, but it would be rather difficult to determine ξ_0 from λ if one had no other information. The detailed form of relation (2-16) cannot be considered established by this type of measurement.

We are now beginning to obtain finer verifications, mainly by measurement of magnetic field transmission through a thin film. In particular, the complete solution of Eq. $(2-16)$ for such a film predicts that when $\xi_0 \gg \lambda$, the field does not have a constant sign, but the ratio ρ can become negative; this has been observed experimentally (Drangeid and Sommerhalder, 1962).

Table 2-2

	λ_{L}	ξ_0	λ_{th}	λ_{exp}
Al	157	16,000	530	$490 - 515$
Sn	355	2,300	560	510
Pb	370	830	480	390

after Bardeen and Schrieffer, Low Temperature Physics, edited by C. J. Gorter (Amsterdam: North Holland, 1961), Vol. III, p. 170.

EXTENSION TO ALLOYS

When the electronic mean free path ℓ is limited by the presence of impurities, it is natural to expect that the relation between current (at the point $\mathbf{r}$) and vector potential (at the point $\mathbf{r}'$) contains an attenuation factor $e^{-|\mathbf{r}-\mathbf{r}'|/\ell}$. One is therefore led to assume, with Pippard,

$$j(\mathbf{r}) = C \int \frac{\lfloor \mathbf{A}(\mathbf{r}') \cdot \mathbf{R} \rfloor \mathbf{R}}{R^4} e^{-R(1/\xi_0 + 1/l)} dr \tag{2-19}$$

The normalization coefficient C is assumed to be independent of ℓ (therefore equal to its pure metal value $-3ne^2/4\pi mc\xi_0$); in other words, one assumes that the contributions to $j(r)$ coming from points $\mathbf{r}'$ in the neighborhood of $r, (|r' - r|\, z\ell)$ are not modified by the impurities. This hypothesis has permitted Pippard to explain a series of experiments on the dilute SnIn alloy system. One finds that λ increases with the concentration of impurities (Fig. 2-6) and the results are well interpreted by the formula (2-19). One limiting case is particulary remarkable. When $\lambda \gg \ell$ we can neglect the variations of $A(r')$ in Eq. (2-19) and perform the integration

$$j(\mathbf{r}) = CA(\mathbf{r}) \frac{4\pi}{3} \frac{1}{1/\xi_0 + 1/\ell} \tag{2-20}$$

This is a London type equation, but with a coefficient modified with respect to the pure metal. In particular, if $\ell \ll \xi_0$, we have

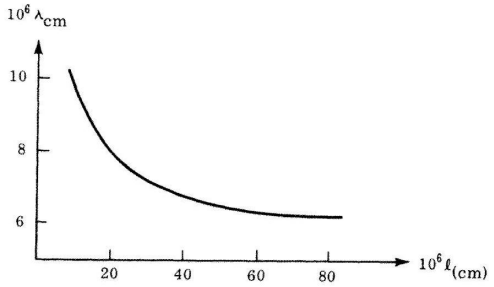


Figure 2-6

The variation of the penetration depth with mean free path in tin-indium alloys. (After A. B. Pippard, Proc. Roy. Soc. (London), A216, 547 (1953).) These results are in excellent agreement with Pippard's prediction (2-21).

$$j(\mathbf{r}) = -\frac{ne^2}{mc} \frac{\ell}{\xi_0} \mathbf{A}(\mathbf{r})$$

which leads to a penetration depth λ

$$\lambda = \lambda_L \left(\frac{\xi_0}{\ell} \right)^{1/2} \qquad (\lambda \gg \ell, \quad \xi_0 \gg \ell) \tag{2-21}$$

In this domain λ is proportional to $\ell^{-1/2}$ and therefore to the square root of the impurity concentration.

The agreement between theory and experiment in the SnIn system gives an excellent justification of the Pippard assumptions. In Chapter 4, we see that the microscopic theory confirms them to a large extent.

VARIATIONS OF λ WITH TEMPERATURE

Until now we have essentially limited our discussion to the case T = 0. For finite T, the situation can qualitatively be described in the following way: The Pippard equation $(2-16)$ remains valid with a value ξ_0 almost temperature independent. The normalization coefficient C is a function of temperature, and vanishes at the transition point T_c. Very near T_c, C is a linear function of $T_C - T$. A theoretical universal curve for C, derived from the microscopic theory, is given in Chapter 4 (Section 5). Once C is known, one computes λ by solving Eq. (2-20). In an attempt to short circuit this heavy machinery, the experimentalists often refer to the empirical law

$$\lambda^2(\mathrm{T}) = \lambda^2(0)\frac{\mathrm{T_c^4}}{\mathrm{T_c^4 - T^4}} \tag{2-22}$$

The form (2-22) gives a good fit to the experimental data on tin. It has also the correct feature that $\lambda \sim (\mathrm{T_c - T})^{-1/2}$ when $\mathrm{T} \to \mathrm{T_c}$. However, it must be emphasized that a universal law such as (2-22) cannot be applied to all superconductors, because two independent parameters (for instance, ξ_0 and the London penetration depth λ_L) are involved in the calculation of λ.

7.1.3 2-3 Magnetic properties of a sample of arbitrary shape: intermediate state

Origin of the Intermediate State

In order to define the critical field $\mathrm{H_c}$ we chose a cylindrical specimen placed in a field parallel to the axis of the cylinder. This geometry assures that the field h be the same over the entire surface of the specimen ignoring end effects. We now consider a less trivial case, for example, a superconducting sphere of radius a placed in a uniform external field $\mathrm{H_0}$. If $\mathrm{H_0}$ is small, the lines of force are expelled from the specimen and assume the form of Fig. 2-7.

The field configuration external to the sphere is determined by the equations

$$\mathrm{div\,h} = \mathrm{curl\,h} = 0 \qquad \mathrm{h} \to \mathrm{H_0 \text{ as } r} \to \infty \tag{2-23}$$

where r is the distance measured from the center of the sphere. Finally, the Meissner effect imposes the condition that no line of force can penetrate into the sphere. The normal component of h vanishes on the surface of the sphere

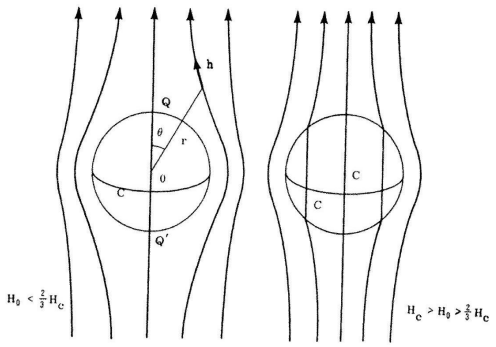


Figure 2-7 The magnetic field distribution about a superconducting sphere of radius a. For applied fields $\mathrm{H_0}$ less than $\frac{2}{3}\mathrm{H_c}$, there is a complete Meissner effect and the field at the equator (at any point on circle C) is $\frac{3}{2}\mathrm{H_0}$; the field at the poles (Q, Q') is zero. For $H_c = H_0 > \frac{2}{3}H_c$, the sphere is in the intermediate state.

$$(h_n)_{r=a} = 0 \tag{2-24}$$

The appropriate solution in the exterior region is

$$\mathrm{h} = \mathrm{H}_0 + \mathrm{H}_0 \frac{\mathrm{a}^3}{2} \nabla \left(\frac{\cos\theta}{\mathrm{r}^2} \right) \tag{2-25}$$

The component of h parallel to the surface of the specimen is

$$|\mathrm{h}_\theta|_{\mathrm{r=a}} = \frac{3}{2} \mathrm{H}_0 \sin\theta \tag{2-26}$$

At points Q and Q′, h is zero. On the equatorial circle ($\theta = \pi/2$) the tangential component is maximum and is $\frac{3}{2}\mathrm{H}_0$. The surface points experience fields between 0 and $\frac{3}{2}\mathrm{H}_0$. When H_0 attains the value $\frac{2}{3}\mathrm{H}_\mathrm{c}$, the field at the equatorial circle becomes equal to H_c. Therefore, for $\mathrm{H}_0 > \frac{2}{3}\mathrm{H}_\mathrm{c}$, certain regions of the sphere pass into the normal state. But there must still exist superconducting regions since $\mathrm{H}_0 < \mathrm{H}_\mathrm{c}$. (If the entire sphere were normal, the field would be equal to H_0 throughout and, because $\mathrm{H}_0 < \mathrm{H}_\mathrm{c}$, the system would be unstable and superconductivity would reappear.) Therefore in the domain

$$\frac{2\mathrm{H}_\mathrm{c}}{3} < \mathrm{H}_0 < \mathrm{H}_\mathrm{c} \tag{2-27}$$

there will be a coexistence of normal and superconducting regions. This situation is called the intermediate state.

Notice that the range of fields H_0 for which one will observe such an equilibrium between the two phases is given by $(2-27)$ only for a specimen in the form of a sphere. If instead of a sphere we had a prolate and/or oblate ellipsoid in the direction of H_0, then the equatorial field would be slightly and/or very different from H_0 and the domain of existence of the intermediate state would be small and/or large. In particular, if we consider a thin metallic slab, H_0 being perpendicular to the plane of the slab, we predict that the intermediate state will exist throughout the domain $0 < \mathrm{H}_0 < \mathrm{H}_\mathrm{c}$. (When H_0 is nonzero, if the slab were to remain entirely superconducting, the field at the edge of the slab would be very large, therefore $> \mathrm{H}_\mathrm{c}$ and it is thus necessary for normal regions to be established.)

Let us consider precisely such a slab of thickness e. The appearance of the normal (N) and superconducting (S) regions is represented in Fig. 2-8. The regions N and S form laminas perpendicular to the plane of the figure. The lines of force only penetrate in the region N. On the contact planes between the N and S regions, the field h must be equal to H_c in order to ensure equilibrium between the two planes.

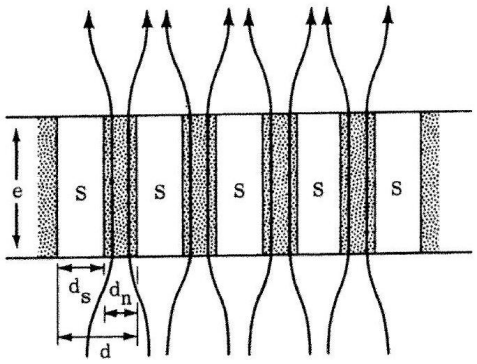


Figure 2-8

Field distribution in a slab in a perpendicular field. For all fields $\mathrm{H} < \mathrm{H}_\mathrm{c}$, the sample is in an intermediate state with a laminar structure of normal and superconducting domains (small distortions of the slabs near the surface are not taken into account).

In the N regions, h is parallel to the z axis, div h = 0 and curl h = 0. Thus h is constant and, therefore, equal to H_c through the N region. In the region S, h = 0. For this simple geometry, the fraction $\rho = d_S/(d_S + d_n)$ of S regions is fixed directly by the condition of conservation of flux-far from the film, the field is uniform, $h = H_0$, and the flux becomes SH_0 (where S is the surface area of the film). In the film, the flux is concentrated through a surface $S(1-\rho)$ and the field is H_c. Therefore

$$SH_0 = S(1-\rho)H_c \tag{2-28}$$
$$\rho = 1 - \frac{H_0}{H_c}$$

An important observation is that, for macroscopic samples (e $\gg \xi_0$) the thicknesses of the layers d_s, d_n are much smaller than the sample dimensions (smaller than e) (this has been verified by detailed experiments to be described later). Thus for many purposes we can ignore the microscopic structure of alternating layers, and we need to know only the relative amount of S regions given by ρ.

The derivation of ρ was very simple for the slab. For more complicated sample shapes, the determination of ρ and of the macroscopic
average field of any point requires a more general analysis (due to Peierls), discussed in the following sections and applied to several typical cases.

Preliminary Thermodynamics

We now define some macroscopic concepts (induction B, thermodynamic field **H**, and so on) useful for the description of situations where there is only a partial penetration of the lines of force. One such case is the intermediate state of macroscopic samples. Other applications will be found in Chapter 3 in connection with Type II superconductors.

DEFINITION OF THE FREE ENERGY

The system consists of a specimen + external objects (coils, generators). We define a free energy as follows: First, we take the energy of the electrons in the sample

$$U = \sum_i \left[\frac{1}{2m} \left(p_i - \frac{eA}{c} \right)^2 + V_i \right] + \sum_{i>j} V_{ij} \tag{2-29}$$

Here A is the vector potential, related to the field $h(r)$ by the relation curl $A = h$.V_{ij} represents the electron-electron interactions and V_i the one electron potentials. Second, we add an entropy term - TS. Then two contributions appear in practice as an integral over the sample volume.

$$U - TS = \int_{\text{sample}} F_S dr \tag{2-30}$$

Third, we include in the free energy the magnetic field energy $\int (h^2/8\pi)\, dr$. The sum of the three contributions we call the free energy

$$\mathcal{F} = \int_{\text{sample}} F_S dr + \int_{\text{all space}} \frac{h^2}{8\pi} dr \tag{2-31}$$

DEFINITION OF THE INDUCTION B

We often meet situations where the microscopic field $h(r)$ in the sample has strong variations in space on a scale Δx much smaller than the sample dimension (Example: the intermediate state pattern of Fig. 2-8). We then find it convenient to introduce a vector B($\mathbf{r}$) giving the average of h in a region around point r of dimensions small compared with the sample, but large compared with Δx.

$$B = \bar{h} \tag{2-32}$$

Outside of the sample, we take by definition $B = h$. On a microscopic scale, h satisfies to the equations

$$\begin{aligned} \operatorname{curl} h &= \frac{4\pi}{c} j \\ \operatorname{div} h &= 0 \end{aligned} \tag{2-33}$$

where f is the local current density. Thus the induction B satisfies to

$$\begin{aligned} \operatorname{curl} B &= \frac{4\pi}{c} j \\ \operatorname{div} B &= 0 \end{aligned} \tag{2-34}$$

j is the macroscopic current density.

DEFINITION OF THE THERMODYNAMIC FIELDH

Suppose that (by changing the currents in the coils) the field distribution $h(r)$ is changed slightly. At each point $\mathbf{r}, \mathbf{B}(\mathbf{r})$ changes by a small amount of $\delta\mathbf{B}(\mathbf{r})$. To first order in $\delta\mathbf{B}$ the change $\delta\mathcal{F}$ of the free energy is, in its most general form,

$$\delta\mathcal{F} = \int \frac{H(r)}{4\pi} \cdot \delta\mathbf{B}(\mathbf{r}) \mathrm{d}\mathbf{r} \tag{2-35}$$

where the factor $(1/4\pi)$ has been inserted for convenience, and $H(r)$ is some vector function of $\mathbf{r}$. We call $\mathbf{H}(\mathbf{r})$ the thermodynamic field at point $\mathbf{r}$[3] Outside of the sample we must have

$$\frac{\mathrm{h} \cdot \delta\mathrm{h}}{4\pi} = \frac{\mathrm{H} \cdot \delta\mathrm{B}}{4\pi} \tag{2-36}$$

and h = B. Thus h = H = B out of the sample. Equation (2-35) is a rather abstract definition of $\mathbf{H}$. To get a physical feeling for $\mathbf{H}$ consider only situations where no external currents are fed into the sample. Then we can write for the current

$$\bar{j} = \bar{j}_s + j_{\mathrm{ext}} \tag{2-37}$$

$\bar{j}_{\mathrm{s}}(\mathbf{r})$ is the average supercurrent at point r in the sample (by definition j_S is 0 out of the sample). j_{ext} is the current in the coils, generators, and so on. Since no current is fed directly into the sample, the distinction between $\mathrm{j_{ext}}$ and $\bar{\mathrm{j}}_{\mathrm{S}}$ is clear cut $\mathrm{j_{ext}} = 0$ in the sample). Then we have simply

$$\operatorname{curl} \mathrm{H} = \frac{4\pi}{\mathrm{c}} \mathrm{J_{ext}} \tag{2-38}$$

[3] Note that in the complete Meissner effect region, B ≡ 0 and H is undetermined.

Proof of Eq. (2-38): When $B(r)$ varies by $\delta B(r)$, in a time δt, an electric field E, given by

$$\operatorname{curl} \mathbf{E} = -\frac{1}{\mathrm{c}} \frac{\delta \mathbf{B}}{\delta \mathrm{t}}$$

is generated. The work done by E on the external currents is $\delta t \int j_{\text{ext}} \cdot \mathbf{E}\, \mathrm{dr}$ or conversely the work done by the external currents is

$$\delta W = -\delta t \int \boldsymbol{E} \cdot j_{\text{ext}}\, d\mathbf{r} \tag{2-39}$$

For a reversible transformation at constant temperature, we know from thermodynamics that $\delta \mathrm{W} = \delta \mp$. We want to compare this expression with (2-35). For that purpose we transform (2-35) as follows:

$$\begin{aligned} \delta \mathscr{F} &= \delta \mathrm{t} \frac{1}{4\pi} \int \mathbf{H} \cdot \frac{\delta \mathrm{B}}{\delta \mathrm{t}} \mathrm{d}\mathbf{r} \\ &= -\delta \mathrm{t} \frac{\mathrm{c}}{4\pi} \int \mathrm{H} \cdot \operatorname{curl} \mathbf{E} \mathrm{d}\mathbf{r} \\ &= -\delta \mathrm{t} \frac{\mathrm{c}}{4\pi} \int \mathbf{E} \cdot \operatorname{curl} \mathbf{H} \mathrm{dr} - \frac{\mathrm{c}\delta \mathrm{t}}{4\pi} \int (\mathbf{E} \times \mathbf{H}) \cdot \mathrm{d}\boldsymbol{\sigma} \end{aligned} \tag{2-40}$$

The last integral is to be taken over a distant surface surrounding the entire system. It represents the radiated energy and for a slow, reversible transformation it is negligible. Then comparing $(2-40)$ and $(2-39)$ we see that $(2-38)$ is satisfied.

Conclusion. All currents contribute to curl B (Eq. 2-34), but only j_{ext} contributes to curl H (Eq. 2-38). We might be tempted to say that H is the field that would exist in the absence of the specimen (the same j_{ext} being kept on the coils). This is correct for the cylindrical geometry of Fig. 2-1 but is wrong in general. Consider, for instance, the spherical sample of Fig. 2-7. Here the lines of force are distorted in the presence of the sphere and this implies a change of $\mathbf{H}(\mathbf{r})$ (though not of curl $\mathbf{H}$).

Remark on boundary conditions. The equation $\operatorname{div} \mathbf{B} = 0$ implies as usual that the normal component of B be continuous at the surface of the specimen. On the other hand, the tangential component of $\mathbf{B}$ is, in general, not continuous. Curl B contains the supercurrent. Often we find supercurrents localized on the surface (physically in a thickness λ near the surface). If we let S be the current per cm on the surface, then by integration of (2-34) we find

$$\mathbf{n} \times (B_{\text{ext}} - B_{\text{int}}) = \frac{4\pi}{c} S \tag{2-41}$$

(n is a unit vector normal to the surface and directed outward).

Thermodynamic Potential for Fixed T and j_{ext}

When both fields and temperatures are allowed to change, the free energy variation (2-35) becomes

$$\delta \mathcal{F} = \frac{1}{4\pi} \int \mathrm{H} \cdot \delta \mathrm{B} d\mathbf{r} - \mathrm{S}\delta \mathrm{T} \tag{2-42}$$

where S is the entropy. When the values of $B(r)$, at each point r, and the temperature T, are fixed, the equilibrium state corresponds to the minimum of $\mathfrak{F}$. Very often, however, this is not the situation of interest. The quantities fixed during the experiment are T and the currents j_{ext} in the coils. We now construct a thermodynamic potential S adapted to this situation. Define

$$\mathcal{S} = \mathcal{F} - \int \frac{\mathrm{B}\cdot\mathrm{H}}{4\pi}\mathrm{d}\mathbf{r} \tag{2-43}$$

Then

$$\delta S = -\int \frac{\mathrm{B}\cdot\delta\mathbf{H}}{4\pi}\mathrm{d}\mathbf{r} - \mathrm{S}\delta\mathrm{T} \tag{2-44}$$

Since $\operatorname{div}\mathbf{B} = 0$ we can set $\mathrm{B} = \operatorname{curl}\overline{\mathrm{A}}$ (where $\overline{\mathrm{A}}$ is the macroscopic vector potential) and integrate by parts

$$\begin{aligned}\mathrm{S}\delta\mathrm{T} + \delta S = -\frac{1}{4\pi}\int \operatorname{curl}\overline{\mathbf{A}}\cdot\delta\mathrm{H}d\mathbf{r} &= -\frac{1}{4\pi}\int \overline{\mathbf{A}}\cdot\operatorname{curl}\delta\mathrm{H}d\mathbf{r} \\ &= -\frac{1}{\mathrm{c}}\int \overline{\mathbf{A}}\cdot\delta j_{\mathrm{ext}}\mathrm{d}\mathrm{r}\end{aligned} \tag{2-45}$$

Thus $\delta\mathcal{G} = 0$ when T and j_{ext} are fixed. The equilibrium state for fixed T and $\mathrm{j_{ext}}$ corresponds to the minimum of G. In practice, we usually construct first $\mathfrak{F}$ and B on a microscopic model; then we form $\mathcal{S}$ and finally on minimizing $\mathcal{S}$ we have a condition defining the equilibrium state. This condition plays the same role as the relation $B = \mu\mathbf{H}$ in a paramagnetic or diamagnetic medium.

Relation between B and H in the Intermediate State

In order to obtain this relation, we calculate the Gibbs potential $\mathrm{G}d\mathbf{r}$ of a volume element dr of a specimen when it is in the intermediate state [a fraction ρ of the volume dr being superconducting (S) and a fraction $(1-\rho)$ being normal (N)]. In (N), the microscopic field takes on a certain value h_n; in (S) it is zero. We show that the condition of minimum S leads to $h_n = H_c$. In terms of ρ

$$\mathrm{B} = (1-\rho)\mathrm{h_n} + \rho\cdot 0 = (1-\rho)\mathrm{h_n} \tag{2-46}$$

The free energy per cubic centimeter becomes

$$F = F_n - \frac{\rho H_c^2}{8\pi} + (1-\rho)\frac{h_n^2}{8\pi} \tag{2-47}$$

The second term represents the condensation energy in the superconducting regions and the third term the magnetic energy. We neglect the (NS) surface energy and also the terms arising from the distortion of the lines of force in the neighborhood of the surface of the specimen; on the macroscopic scale these surface terms are negligible. Expressing F in terms of the variables ρ and $\mathbf{B}$, we obtain

$$\mathrm{F} = \mathrm{F_n} - \frac{\rho\mathrm{H_c^2}}{8\pi} + \frac{\mathrm{B}^2}{8\pi(1-\rho)} \tag{2-48}$$

Now forming the thermodynamic potential G, we find

$$\mathrm{G(B},\rho) = \mathrm{F} - \frac{\mathrm{BH}}{4\pi} = \mathrm{F_n} - \frac{\rho\mathrm{H_C^2}}{8\pi} + \frac{\mathrm{B}^2}{8\pi(1-\rho)} - \frac{\mathrm{BH}}{4\pi} \tag{2-49}$$

If we minimize G: (1) With respect to ρ, we obtain

$$|B| = H_c(1-\rho) \tag{2-50}$$

On comparing Eqs. $(2-50)$ and $(2-46)$, we see that the field in the normal regions h_n is equal to H_c (this property was previously cited for a simple example on page 26).

(2) With respect to B, we obtain

$$\frac{\partial G}{\partial B} = 0 \qquad B = H(1-\rho) \tag{2-51}$$

We conclude that (1) the field $\mathbf{H}$ is parallel to B, (2) the length of $\mathbf{H}$ must be constant and equal to $\mathrm{H_C}$ in the entire specimen. This is the condition equivalent to the relation $\mathrm{B} = \mu\mathrm{H}$ in a paramagnetic medium. But note that here the relation $B(H)$ is not linear. In order to calculate the field distribution in our sample, it it necessary to solve the equations

$$\operatorname{div}\mathbf{B} = 0 \quad (\text{and } \mathbf{B}_{\text{normal}} \text{ continuous at the surface}) \tag{2-52}$$

$$\operatorname{curl}\mathrm{H} = 0 \quad (\text{and } \mathbf{H}_{\text{tangential}} \text{ continuous}) \tag{2-53}$$

$$\mathbf{H} = \mathbf{B}\frac{\mathrm{H_c}}{|\mathrm{B}} \tag{2-54}$$

Equation 2-53 expresses our assumption that no current is fed into the sample (see Eq. 2-38).

Applications

We still limit ourselves to the (most usual) case where the specimen is not directly connected to the current generator. Then the lines of force, inside the sample, are straight lines. In order to show this, we write (proof due to London)

$$\mathrm{H}^2 = \mathrm{H_c^2} \qquad 0 = \nabla\left(\mathrm{H}^2\right) = 2(\mathrm{H}\cdot\nabla)\mathrm{H} + 2\mathrm{H}\times\operatorname{curl}\mathrm{H} \tag{2-55}$$

In the sample, curl $\mathbf{H} = 0$, then $(\mathbf{H}\cdot\nabla)\mathbf{H} = 0$. The vector $\mathbf{H}$ does not vary along a line of forces and therefore the line of force is straight.

Example. Let us return to a spherical sample placed on an exterior field $\mathrm{H_0}$ such that $\frac{2}{3}\mathrm{H_c} < \mathrm{H_0} < \mathrm{H_c}$. We can construct the solution of the system(2-52), $(2-53), (2-54)$ in the following manner.

In the interior of the sphere ($\mathrm{r} < \mathrm{a}$) we take H and B to be parallel to the z axis and constant. In magnitude, $\mathrm{H} = \mathrm{H_c}$ and B has a certain unknown value B_0. In the exterior, on the other hand,

$$\mathbf{H} = \mathbf{B} = \mathrm{H_0} - \mathrm{H_1}\frac{\mathrm{a}^3}{2}\nabla\frac{\cos\theta}{\mathrm{r}^2} \tag{2-56}$$

where $\mathrm{H_1}$ is a constant to be determined. The condition on the continuity of $\mathrm{H_{tang}}$ at the surface imposes

$$\left(\mathrm{H_0} + \frac{\mathrm{H_1}}{2}\right)\sin\theta = \mathrm{H_c}\sin\theta \tag{2-57}$$

The condition of the continuity of $\mathrm{B_{norm}}$ gives

$$(\mathrm{H_0} - \mathrm{H_1})\cos\theta = \mathrm{B_0}\cos\theta \tag{2-58}$$

Upon comparing these two equations we find

$$\begin{aligned} \mathrm{B}_0 &= 3\mathrm{H}_0 - 2\mathrm{H}_\mathrm{c} \\ \mathrm{H}_1 &= 2\,(\mathrm{H}_\mathrm{c} - \mathrm{H}_0) \end{aligned} \tag{2-59}$$

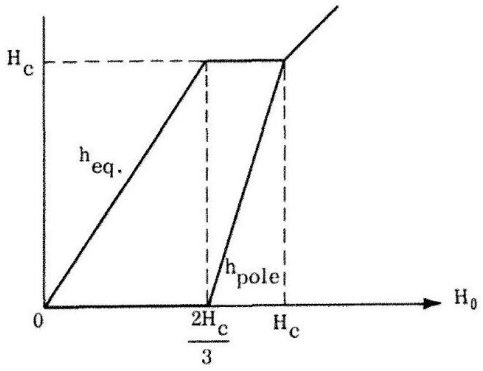


Figure 2-9
The field at the equator and the field at the poles of a superconducting sphere. For $\mathrm{H}_0 < \frac{2}{3}\mathrm{H}_\mathrm{c}$, there is a complete Meissner effect, and the polar field vanishes. For $\frac{2}{3}\mathrm{H}_\mathrm{c} < \mathrm{H}_0 < \mathrm{H}_\mathrm{c}$, the sphere is in the intermediate state; the equatorial field remains constant at H_c while the polar field increases from zero to H_c.

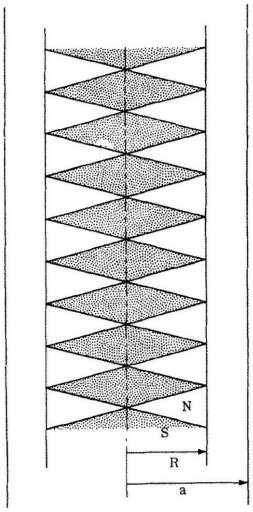


Figure 2-10 A schematic representation of the domain structure in a superconducting wire of radius a carrying a current $\mathrm{I} > I_C(2-60)$. There are a normal surface layer and an intermediate state core of radius R. The interface (R) is determined by $\mathrm{H(R)} = \mathrm{H}_\mathrm{c}$.

Conclusions.

(1) There exists a solution such that B is constant throughout the sphere. The fraction of superconducting regions $\rho = 1 - \mathrm{B}_0/\mathrm{H}_\mathrm{C}$ is therefore the same throughout the sphere.

(2) The induction B_0 is a linear function of the applied field H_0. In practice, one can measure B_0 by placing a magnetic probe in the neighborhood of the poles Q, Q' of the sphere. Since B_{norm} is continuous, the field immediately exterior to the sphere near Q or Q' is equal to B_0. The field H_c is measured by placing the probe on the equatorial circle (from the continuity of $\mathrm{H}_{\mathrm{tang}}$). Ex - perimentally one very nearly obtains diagrams of the theoretical form (Fig. 2-9) in clean samples.

CRITICAL CURRENT OF A SUPERCONDUCTING WIRE

The wire of radius a is connected to the poles of a generator that supplies a current I. The field at the surface of the wire is $H(a) = 2\mathrm{I}/\mathrm{ca}$. When $\mathrm{H(a)} < \mathrm{H_c}$, the wire can be completely superconducting. This defines a critical current

$$I_c = H_c \frac{ca}{2} \tag{2-60}$$

When I becomes larger than $\mathrm{I_c}, \mathrm{H(a)} > \mathrm{H_c}$, and the wire' must become normal near the surface. However it cannot become entirely normal, since, if it were, the current I would be spread uniformly through the section and the field h would be very small in the central region; therefore the wire must remain at least partially superconducting. Finally there is an exterior normal region $\mathrm{R} < \mathrm{r} < \mathrm{a}$ and a superconducting or intermediate interior region $0 < \mathrm{r} < \mathrm{R}$. In the exterior region $B = H$ and at the boundary $H(R) = H_c$. This allows us to predict the current I_1, which flows through the interior region

$$\mathrm{H(R)} = \mathrm{H_c} = \frac{2\mathrm{I_L}}{\mathrm{cR}} \tag{2-61}$$

$$\mathrm{I_1} = \frac{\mathrm{cRH_c}}{2} = \mathrm{I_c}\frac{\mathrm{R}}{\mathrm{a}} < \mathrm{I_c} \tag{2-62}$$

Therefore $\mathrm{I_1} < \mathrm{I_c} < \mathrm{I}$. The exterior region must carry a current $\mathrm{I} - I_1$. Since this is a normal region, there must be an electric field **E** directed along the axis of the wire; this field **E** must be the same throughout the wire since curl $E = 0$.

This shows that the interior region cannot be entirely superconducting since it would short circuit the field **E**. It must, in fact, be in the intermediate state with N and S laminas perpendicular to the axis of the cylinder (Fig. 2-10). This situation is discussed in detail in the book by London.

PRINCIPLE OF THE CRYOTRON

The cryotron is a control device invented by Buck in 1956; the principle is shown on Fig. 2-11. The "control" current I' creates a field $\mathrm{H}' = 4\pi\mathrm{NI}'/\mathrm{cL}$ in the solenoid (where N is the number of turns

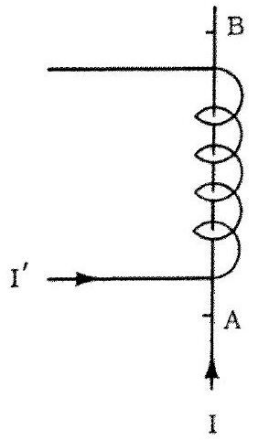


Figure 2-11

The principle of the cryotron. The current passing through the superconducting wire AB is controlled by the current I' flowing through the solenoid. When the field in the coil reaches H_C, the wire AB becomes normal.

and L is the length of the coil). A superconducting wire AB of diameter 2a and critical field H_c passes through the solenoid. For $H' < H_c$, the wire has zero resistance. For $H' > H_c$, the resistance is finite. It is therefore possible to control a current I passing through AB by the current I'. The minimum current value of I' required to make AB normal is

$$I'_m = \frac{cL}{4\pi N} H_c \tag{2-63}$$

On the other hand, the current I cannot be too large; otherwise the line AB passes into the intermediate state as we have previously seen

$$I \leq I_c = \frac{caH_c}{2} \tag{2-64}$$

The current gain of the cryotron is

$$G = \frac{I_c}{I'_m} = 2\pi N \frac{a}{L} \tag{2-65}$$

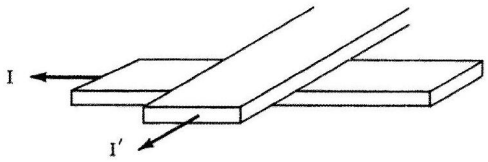


Figure 2-12

A more efficient (shorter time constants) cryotron can be constructed of two crossed metallic films separated by a thin insulated layer.

In Buck's first experiment, the control coil was made of a niobium wire (superconductor with a high critical field $\sim$ 2000G) of diameter $\sim$ 0.1 mm. The wire AB (of tantalum) had $H_c \sim 100$G at 4.2°K and a diameter 2a = 0.2 mm. For a coil of only one turn, this corresponds to Na/L $\sim$ 1, and G $\sim$ 6. In practice it is not useful to increase N for this increases the self-inductance of the coil and finally increases the time constant τ of the cryotron (for only one turn, the τ is not less than 10^{-5}sec). In practice, the time constants are reduced considerably by replacing the set up in Fig. 2-11 by two thin crossed metallic films (Fig. 2-12) separated by an insulating layer approximately 1000Å thick. Since the self-inductance is proportional to this thickness, it is quite small and the time constants fall into the domain $10^{-8} - 10^{-9}$sec.

Microscopic Structure of the Intermediate State

A slab (Fig. 2-13) of thickness e and lateral dimensions $L_x L_y$ (very large) is placed in a perpendicular field H_0 - normal and superconducting domains will occur. We assume that these domains are in the form of layers, as shown on the figure. (Experimentally, this arrangement is often found.) We wish to know the thickness d_n or d_s of the normal and of the superconducting regions, and the period $d = d_n + d_s$ of the domain structure.

To do this, we construct the free energy $\mathcal{F}$, and then minimize it (with respect to d_n, d_s, or equivalent parameters) for fixed H_0 (fixed H_o means fixed flux through the slab; thus the appropriate potential is $\mathcal{F}$, not $\mathcal{S}$).

In a zero-order approximation we consider the S and N domains as exactly plane layers and neglect all surface energies. Then the free energy is simply

$$\mathcal{F}_{\text{macroscopic}} = -\frac{H_c^2}{8\pi} L_x L_y e \frac{d_s}{d} + \frac{H_0^2}{8\pi} \frac{d}{d_n} \text{ e } L_x L_y \tag{2-66}$$

The first term is the condensation energy in the S regions. The second is the magnetic field energy $h^2/8\pi$, in the N regions, where $h = H_0 (d/d_n)$ by flux conservation.

Going now to a first-order approximation, one must add three corrections to $\mathfrak{F}$.

(1) To create a wall between an S region and an N region we need a certain surface energy γ per cm^2 of wall. Dimensionally it is convenient to write this γ in the form

$$\gamma = \frac{\mathrm{H_c^2}}{8\pi}\delta \tag{2-67}$$

where the length δ is of order $10^3 - 10^4$Å. The corresponding contribution to $\mathcal{F}$ is

$$\gamma e L_y \times \Bigg(\text{number of walls)} \ = \frac{H_c^2}{8\pi}\delta e L_y \frac{2L_x}{d} \tag{2-68}$$

(2) The lines of force "open up" near the sample surface and the superconducting domains become thinner near the ends. Thus we lose some condensation energy, in a volume of order $d_S^2 L_y$ for each S domain. This gives a contribution

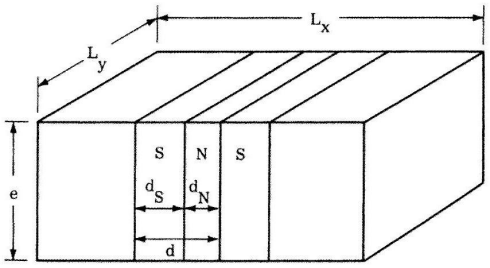


Figure 2-13

Microscopic structure of the normal and superconducting regions in the intermediate state of a slab. The domains form a laminar structure of period $d \sim \sqrt{e\delta}$(e = slab thickness, $\delta \cong$ thickness of a wall).

$$\frac{\mathrm{H_c^2}}{8\pi}\mathrm{d_S^2}\ \mathrm{L_y}\frac{\mathrm{L_x}}{\mathrm{d}}\mathrm{U_0}\left(\rho_\mathrm{s}\right) \tag{2-69}$$

where $\rho_\mathrm{S} = \mathrm{d_S/d}$ and $\mathrm{U_0}\left(\rho_\mathrm{S}\right)$ is a dimensionless function that can be computed when the exact shape of the "thinner" regions is known.

(3) The magnetic field energy $\int \left(\mathrm{h}^2/8\pi\right)\mathrm{dr}$ is also modified near the surface, and this gives a term of the form

$$\frac{\mathrm{H_0^2}}{8\pi}\mathrm{d_S^2}\ \mathrm{L_y}\frac{\mathrm{L_x}}{\mathrm{d}}\mathrm{V_0}\left(\rho_\mathrm{S}\right) \tag{2-70}$$

where $V_0\left(\rho_\mathrm{S}\right)$ is another dimensionless function. (The calculation of $\mathrm{U_0}$ and $\mathrm{V_0}$ is described in Landau and Lifshitz, Electrodynamics of Continuous Media.)

We can choose as independent variables ρ_S and d. If we first minimize the free energy with respect to ρ_S, we find that for a macroscopic sample ($e \gg \xi_0$)

$$1 - \rho_\mathrm{s} = \frac{\mathrm{H_0}}{\mathrm{H_c}} \tag{2-71}$$

This, as we know, expresses that the field in the normal regions is equal to $\mathrm{H_c}$. Then we minimize $\mathcal{F}$ with respect to d. The d-dependent terms are the three correction terms

$$\begin{aligned}\mathcal{F} =& \mathcal{F}_{\text{macroscopic}} + \frac{\mathrm{H_C^2}}{8\pi}\ \mathrm{e}\ L_\mathrm{x}\mathrm{L_y} \\ &\times \left[\frac{2\delta}{\mathrm{d}} + \left(\rho_\mathrm{S}^2\mathrm{U_0} + \rho_\mathrm{S}^2\left(1-\rho_\mathrm{S}\right)^2\ \mathrm{V_0}\right)\frac{\mathrm{d}}{\mathrm{e}}\right]\end{aligned} \tag{2-72}$$

The optimum d is given by

$$\mathrm{d}^2 = \frac{\delta \mathrm{e}}{\phi\left(\rho_{\mathrm{S}}\right)} \tag{2-73}$$

where $\phi = \frac{1}{2}\left[\rho_{\mathrm{S}}^2 \mathrm{U}_0 + \rho_{\mathrm{S}}^2\left(1-\rho_{\mathrm{S}}\right)^2\ \mathrm{V}_0\right]$. Typically, for $\mathrm{H_o/H_c} \sim 0.7$, $\phi \sim 10^{-2}$ and thus $\mathrm{d} \sim 10\sqrt{\delta \mathrm{e}}$. Taking $\mathrm{e} = 1\ \mathrm{cm}, \delta = 3000\mathring{\mathrm{A}}$, we arrive at $\mathrm{d} \sim 0.6$ mm. Near the ends ($\rho_{\mathrm{s}} \to 0$ or $\rho_{\mathrm{n}} \to 1$), ϕ tends toward 0 and d becomes still larger. How can we observe this domain structure? Various methods have been used:

(1) A fine bismuth wire (whose resistance is strongly dependent on field) is moved close to the surface of the sample. The resistance is large in the N regions and small in the S regions (Meshkovsky and Shalnikov, 1947).

(2) Niobium powder is placed on the sample. Niobium has a high critical field ($\sim$ 2000G). Thus the grains are always superconducting and diamagnetic, they tend to avoid the lines of force, and they gather on the S regions.

(3) The specimen is covered with a thin layer of cerium glass (typical thickness ~ 0.1 mm). This glass has a large Faraday rotation. Polarized light traveling along the magnetic field H_0 (normal to the sample surface) has its plane of polarization rotated by an angle θ when it traverses the glass; the total rotation after being reflected from the sample is then 2θ. Since, in general, θ is proportional to the field ($\theta \sim 0.02\%$ mm/G), if the specimen is observed between crossed analyzer and polarizer, the N regions, where $\mathrm{h} \neq 0$, appear bright. Ultimately, these measurements furnish a determination of the wall energy (characterized by the length δ).

Problem.

What are the corrections to the critical field of the plate due to the fact that the thickness e is finite?

Solution.

If we minimize the free energy with respect to d, keeping as other independent variables the reduced field $\mathrm{h_r} = \mathrm{H_0/H_c}$ and $\rho_{\mathrm{s}} = \mathrm{d_s/d}$ we find

$$\mathfrak{F} = \frac{\mathrm{H_c^2}}{8\pi}\mathrm{e_x L_y}\left[-\rho_{\mathrm{s}} + \frac{\mathrm{h_r^2}}{1-\rho_{\mathrm{s}}} + 4\left(\frac{\delta}{\mathrm{e}}\right)^{1/2}\phi^{1/2}\right]$$

$$\phi = \frac{1}{2}\rho_{\mathrm{S}}^2\left[\mathrm{U}_0\left(\rho_{\mathrm{s}}\right) + \mathrm{h_r^2}\ \mathrm{V}_0\left(\rho_{\mathrm{s}}\right)\right]$$

In the region of interest, $\mathrm{h_r}$ is close to 1, ρ_{s} is close to 0, and we may write for ϕ

$$\phi \cong \theta^2 \rho_{\mathrm{S}}^2$$

where $\theta^2 = \frac{1}{2}\left|\mathrm{U}_0(0) + \mathrm{V}_0(0)\right| = (1/\pi)\ln 2 = 0.22$ (this numerical value is obtained in the previously mentioned calculation of Landau and Lifshitz). Minimizing $\mathcal{F}$ with respect to ρ_{S}, we obtain the condition

$$-1 + \left(\frac{\mathrm{h_r}}{1-\rho_{\mathrm{s}}}\right)^2 + 4\theta\left(\frac{\delta}{\mathrm{e}}\right)^{1/2} = 0$$

The critical field of the plate is reached when $\mathcal{F}$ is equal to the normal state free energy $(\mathrm{H_0^2}/8\pi)\ \mathrm{e\ L_y L_x}$. This leads to the condition

$$\rho_{\mathrm{s}}\left(\frac{\mathrm{h_r^2}}{1-\rho_{\mathrm{s}}} - 1\right) + 4\theta\left(\frac{\delta}{\mathrm{e}}\right)^{1/2}\rho_{\mathrm{s}} = 0$$

Both conditions are satisfied when

$$\rho_s = 0$$
$$1 - h_r^2 = 4\theta \left(\frac{\delta}{e}\right)^{1/2}$$
$$H_0 \cong H_c \left(1 - 2\theta \left(\frac{\delta}{e}\right)^{1/2}\right)$$

By taking e = 1 mm and $\delta = 10^4$Å, we get a 3% decrease of the critical field. Similar deviations from the macroscopic theory occur in all geometries; very often they are important in the discussion of experimental results in type I superconductors.

A PARADOX

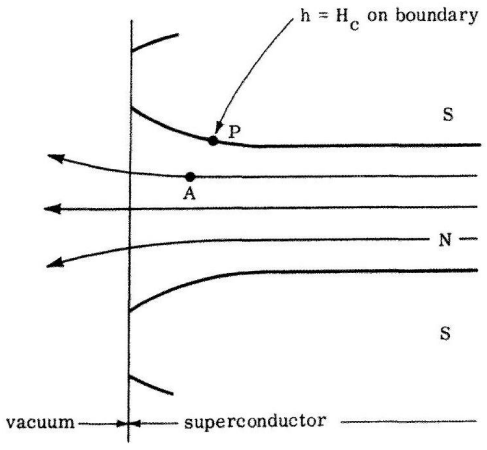
If we look carefully at the domain structure of Fig. 2-14a, we notice that at a point such as A, in the N regions, the lines of force have "opened up." Thus the field is significantly lower than at point P on the boundary, that is, lower than H_c. At first sight this is troublesome. We would expect a region near A to become superconducting again. This complication has been considered by Landau. He concluded that the normal regions should "branch" as shown on Fig. 2-14b, possibly up to such a fine scale that the domain structure would become unobservable. In fact, the simple domain structure is often observed. Branching does not take place in clean samples with dimensions of order 1 cm. The critical field at point A is reduced below H_c by an effect similar to that discussed in the problem above (but here the dimension of interest is d, not e, thus the effect is large). Thus A can remain normal in rather low fields.

If we had a superconductor of thickness $e = 1$ mile, d would be of order 1 cm, we could still apply macroscopic considerations in the neighborhood of P, and some branching would take place. The branching model is not wrong; it is simply not adequate for the usual scale of sample dimensions. (Another way to favor branching is not to increase e, but rather to reduce δ-this could be done in suitable alloy systems.)

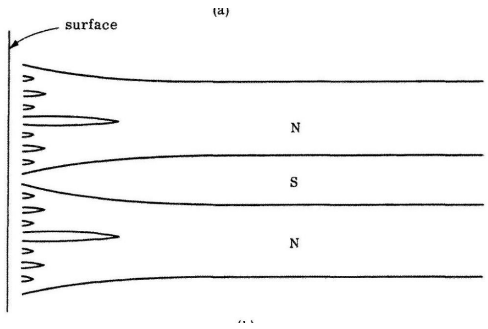
ORIGIN OF THE SURFACE ENERGY

We qualitatively discuss two extreme cases:

(1) $\xi_0 \gg \lambda$: In our previous macroscopic discussion, there was a sharp boundary between the normal region N and the superconducting region S (to fix ideas, we shall take this boundary as being the yz plane, the fields being along z and the N region corresponding to x < 0). On the N side, the thermodynamic potential was lowered by the magnetic



(a)



(b)

Figure 2-14

(a) The domain structure near the surface. Note that, at a point such as A, the field is smaller than at point P (as is indicated by the curvature of the lines of flux): $h(a) < h(P) = H_c$. There are some small normal regions near the ends where $h < H_c$! (b) Landau's branching model. Such a branching is required if one wants to keep $h > H_c$ everywhere in the normal regions. In fact branching does nol take place: The condition $h > H_c$ applies only to macroscopic normal regions. Here the small regions of interest near the surface have critical fields significantly lower than H_c; they can remain normal for $h < H_c$ and the simpler model of Fig. $2-14a$ is the correct one.

field terms $H_c^2/8\pi - H_c^2/4\pi$ (see Eq. 2-49). On the S side, S was lowered by the condensation energy $-H_c^2/8\pi$. Now, what does happen on a microscopic scale? If λ is small, it is still correct to assume that the field drops abruptly at the limiting plane $x = 0$. The new feature is that on the S side ($x > 0$), superconductivity is "damaged" in a region of thickness $\sim \xi_0$ near the boundary. Thus we lose the condensation energy $H_c^2/8\pi$ on an interval $\sim \xi_0$ and this gives a wall energy $\gamma \sim (H_c^2/8\pi)\,\xi_0$ (i.e., $\delta \sim \xi_0$).

(2) $\xi_0 \ll \lambda$: In this case the above contribution is negligible. We can calculate the field distribution by using London's equation (Fig. $2-15$). Let us put the wall in the yz plane, the fields being directed along the z axis. In the normal region $(x < 0), h = H_c$. In the S region $(x > 0), h = H_c e^{-x/\lambda}$. The thermodynamic potential becomes

$$S = \int_{x>0} dr \left(F_n - \frac{H_c^2}{8\pi} + \frac{h^2}{8\pi} - \frac{Hh}{4\pi} + \lambda^2 \frac{\left(\frac{dh}{dx}\right)^2}{8\pi} \right) \tag{2-74}$$

The first term is the free energy of the normal phase in zerofield; the second term is the condensation energy ($\rho = 0$ for $x < 0$ and $\rho = 1$ for $x > 0$); the third term is the magnetic field energy; the fourth is the microscopic equivalent of $-BH/4\pi$. Finally, the last term represents the kinetic energy of the currents.

We first verify that, far from the wall, the Gibbs function density is the same in the two phases (equilibrium condition) and $\mathcal{G}$ can be written in the form

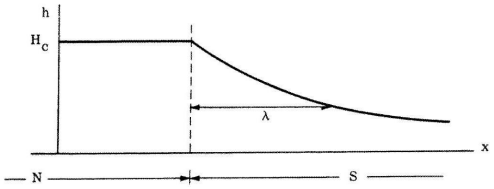


Figure 2-15

Microscopic field distribution at a wall separating normal and superconducting domains. In the normal domain, $h - H_c$; h falls to zero within a penetration depth on the superconducting side.

$$G = \int dr \left(F_n - \frac{H_c^2}{8\pi} \right) + \gamma S$$

where S is the surface area of the wall and γ is the surface tension given by

$$\gamma = \int_0^\infty dx \left[\frac{h^2 + \lambda^2 \left(\frac{dh}{dx}\right)^2}{8\pi} - \frac{hH_c}{4\pi} \right] = -\frac{H_c^2}{8\pi}\lambda \tag{2-75}$$

In this limit, the surface tension is negative and the system decreases its energy by creating new walls; the largest possible number of walls is created, and it is evident that the magnetic properties will be found to be considerably different from those cited previously. It is for this reason that materials having $\xi_0 < \lambda$ are called second kind superconductors. We study them in the next chapter.

7.2 Magnetic properties of second kind superconductors by de Gennes

7.2.1 3-1 Magnetization curves of a long cylinder

Type II superconductors are characterized by the following macroscopic properties:

(1) A cylinder placed in a longitudinal field H does not exhibit a "perfect" total flux expulsion (Meissner effect), except for weak field $H < H_{c_1}$.

If one calculates the critical field H_c defined by the difference in free energies between the normal and superconducting states in zero field:

$$F_n - F_s = \frac{H_c^2}{8\pi} \tag{3-1}$$

one finds that H_{c_1} is clearly smaller than H_c. For example, for the compound V_3Ga, caloric measurements in zero field (giving $F_n - F_S$) indicate $(H_c)_{T=0} \simeq 6000G$, and magnetic measurements give $(H_{C_1})_{T=0} \simeq 200G$.

(2) For $H > H_{C_1}$, lines of force penetrate the cylinder, but even

[1] The notation H_{Cl} for the first penetration field has been recommended by the participants of the Colgate Conference on Superconductivity (1963).

at thermal equilibrium this penetration is not complete. The flux ϕ passing through the cylinder remains less than its value when the sample is in the normal state. This implies the existence of permanent currents in the specimen, which is thus still superconducting. This situation exists for fields $H_{C_1} \leq H \leq H_{C_2}$.$H_{C_2}$ is larger than H_c and is sometimes very large-for V_3Ga $(H_{C_2})_T = 0 \sim 300,000G$.

(3) For $H > H_{C_2}$ a macroscopic sample does not show any expulsion of flux $B \equiv H$. However superconductivity is not completely destroyed. In an interval $H_{C_2} < H < H_{C_3}$ there remains on the surface of the cylinder a superconducting sheath (of typical thickness $10^3 \mathring{A}$). (In most cases $H_{c_3} \sim 1.69 H_{C_2}$.) The existence of this sheath can be shown, for instance, by measuring the resistance between two probes on the sample surface. It is found that for low measuring currents the resistance vanishes. Physically the sheath has the following origin: It is easier to nucleate a small superconducting region near the sample surface - just as it is easier to grow bubbles on the bottom of a glass of beer than to grow them from an arbitrary point in the beer. (A somewhat more sophisticated version of this argument will be discussed in Chapter 5.)

The variation with temperature of the fields $H_{C_1}, H_{c_2}, H_{c_3}$ is represented in Fig. 3-1. We now focus our attention on the region $H_{C_1} < H < H_{C_2}$ where partial flux penetration occurs. The existence of this region of the (H, T) plane was clearly shown for the first time in early

experiments on alloys by Schubnikov (1937). We call it the Schubnikov phase, or sometimes the vortex state. (The latter name comes from the microscopic picture to be derived in Section 3-2.)

The partial flux penetration in the Schubnikov phase can be described in terms of a diagram $B(H)$; the aspect of this diagram is shown in Fig. 3-2. Sometimes, instead of the induction B, the experimentalists prefer to plot the "magnetization" M defined by

$$M = \frac{B - H}{4\pi} \tag{3-2}$$

The $M(H)$ curve is shown in Fig. 3-3.

(In practice the observation of these curves is often complicated by difficulties in attaining equilibrium; for example, structural defects oppose the displacement of the lines of force.)

In Fig. 3-3 the dashed line represents the magnetization curve found for a first kind superconductor with the same H_c. These two curves are related by a remarkable property - the areas they subtend are equal.

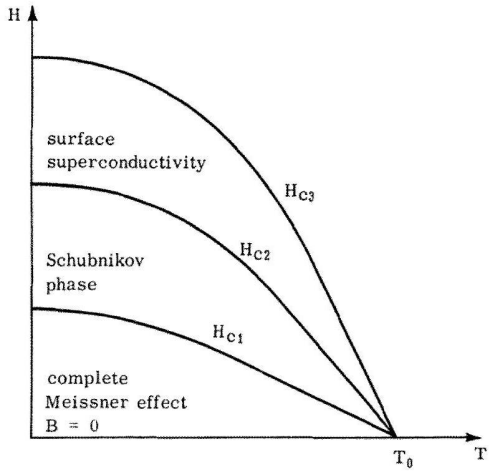


Figure 3-1 Phase diagram for a long cylinder of a Type II superconductor.

Proof: Let G_S be the Gibbs function per unit volume for the superconducting state

$$G_S = F_S(B) - \frac{BH}{4\pi} \tag{3-3}$$

G_S is a minimum for fixed H, that is, at equilibrium

$$\left(\frac{\partial G_S}{\partial B}\right)_H = 0 \tag{3-4}$$

Let G_n be the Gibbs function for the normal state

$$G_n = F_n + \frac{B^2}{8\pi} - \frac{BH}{4\pi} \tag{3-5}$$

At thermodynamic equilibrium in the normal phase $(\partial G_n/\partial B)_H = 0$; therefore, B = H and

$$G_n = F_n - \frac{H^2}{8\pi} \tag{3-6}$$

Let the field vary from H to H + δH. From (3-3) and (3-4)

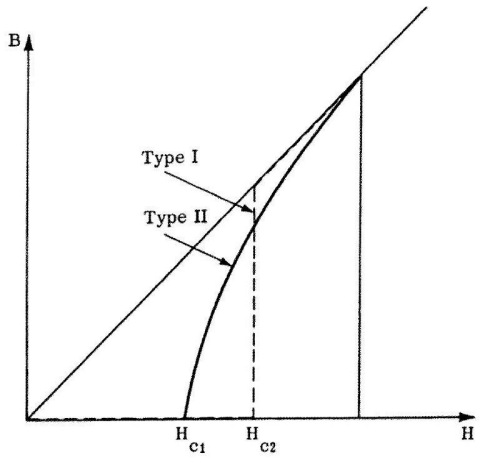


Figure 3-2 The induction (or flux /cm^2) in the cylinder as a function of the applied field H. The full curve applies for a Type II superconductor, the dotted curve for a Type I.

$$\frac{\partial \mathrm{G_S}}{\partial \mathrm{H}} = -\frac{\mathrm{B}}{4\pi} \tag{3-7}$$

and from (3-6)

$$\frac{\partial G_n}{\partial H} = -\frac{H}{4\pi} \tag{3-8}$$

$$\frac{\partial}{\partial H}\left(G_n - G_S\right) = \frac{B-H}{4\pi} = M \tag{3-9}$$

We now integrate this relation between H = 0 and H = $\mathrm{H_{C_2}}$. At H = $\mathrm{H_{C_2}}$, the two phases are in equilibrium and $G_n = G_S$. For $H = 0, B = 0$ we have $G_n = F_n$, $\mathrm{G_S} = \mathrm{F_S}$, and by definition

$$\left(F_n - F_s\right)_{B=0} = \frac{H_c^2}{8\pi}$$

The result is therefore

$$\int_0^{H_{c2}} \mathrm{MdH} = \frac{-\mathrm{H_C^2}}{8\pi} \tag{3-10}$$

and we conclude that the area subtended by the curve of Fig. 3-3 depends only on $\mathrm{H_c}$. From the equilibrium magnetization curves, one can therefore determine $\mathrm{H_c}$ and the condensation energy.

We now discuss the transition occurring when the applied field H becomes equal to one of the limiting values $\mathrm{H_{c_1}}$ or $\mathrm{H_{c_2}}$. Consider first the transition at $\mathrm{H_{C_2}}$. Experimentally this is a second-order transition in all cases studied up to now.

(1) Magnetization measurements show that the B(H) curve is continuous at H = $\mathrm{H_{C_2}}$.

(2) In the few cases ($\mathrm{V_3Ga}$) where thermal measurements have been performed, it appears that there is no latent heat for the transformation, but only a discontinuity in the specific heat.

It is possible to relate this discontinuity to the magnetization curves by a purely ther modynamic analysis (Goodman, 1962). Let i and j be the two phases of interest (for the case at hand i would represent the Schubnikov phase and j the phase with $B \equiv H$, where the bulk of the sample is normal)

$$G_i = F_i\left(T, B_i\right) - \frac{B_i H}{4\pi} \tag{3-11}$$

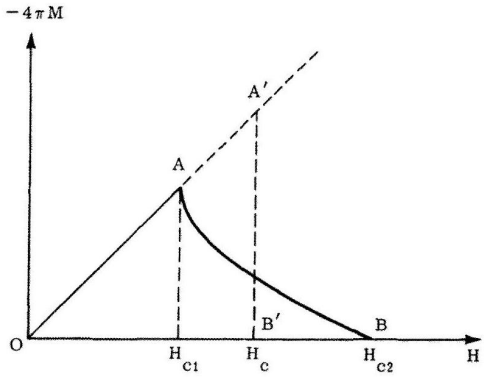


Figure 3-3

The reversible magnetization curve of a long cylinder of Type I (dotted line) or Type II (solid line) superconductor. If the two materials have the same thermodynamic field H_c, the areas OAB and OA′B′ are equal.

is the Gibbs function per cm^3 of the ith phase. The relation between the field H and the induction B in this phase is obtained by minimizing G for fixed H and T

$$\frac{\partial}{\partial B_i} F_i\,(T, B_i) = \frac{H}{4\pi} \tag{3-12}$$

the entropy S_i is deduced from the relations

$$S_i = -\left(\frac{\partial G_i}{\partial T}\right)_H = -\frac{\partial F_i}{\partial T} \tag{3-13}$$

When the field satisfies a certain condition $H = H^*(T)$, there is an equilibrium between the phases i and j (i.e., for the present case $H^* = H_{C2}$). On this curve, one has

$$G_i = G_j \tag{3-14}$$

Suppose that there is no latent heat associated with the transformation. Then, along the curve $H = H^*(T)$, the two phases have the same entropy

$$S_i = S_j \tag{3-15}$$

We first show that this excludes any discontinuity in B at the transition. To show this, we calculate the variation of F_i when one moves along the equilibrium curve $[dH = (dH^*/dT)\,dT]$

$$\frac{dF_i}{dT} = \frac{\partial F_i}{\partial T} + \frac{\partial F_i}{\partial B_i}\frac{dB_i}{dT} \tag{3-16}$$

From this equation and using (3-12) and (3-13), we obtain the variation of G along the equilibrium curve

$$\frac{dG_i}{dT} = -S_i - \frac{B_i}{4\pi}\frac{dH}{dT}d^* \tag{3-17}$$

Along the equilibrium curve we have constantly $G_i = G_j$, therefore $dG_i/dT = dG_j/dT$; if also $S_i = S_j$ we necessarily have $B_i = B_j$; B is continuous at the transition.

We now calculate the specific heat in constant field

$$C_i = T\left(\frac{\partial S_i}{\partial T}\right)_H \tag{3-18}$$

We can transform the second factor by calculating the total derivative of the entropy along the equilibrium curve

$$\frac{\mathrm{dS_i}}{\mathrm{dT}} = \left(\frac{\partial \mathrm{S_i}}{\partial \mathrm{T}}\right)_{\mathrm{H}} + \left(\frac{\partial \mathrm{S_i}}{\partial \mathrm{H}}\right)_{\mathrm{T}} \frac{\mathrm{dH^*}}{\mathrm{dT}} \tag{3-19}$$

From (3-15), $\mathrm{dS_i/dT} = \mathrm{dS_j/dT}$ along the equilibrium curve and

$$C_j - C_i = T\frac{dH^*}{dT}\left[\left(\frac{\partial S_i}{\partial H}\right)_T - \left(\frac{\partial S_j}{\partial H}\right)_T\right] \tag{3-20}$$

We transform $(\partial \mathrm{S_i}/\partial \mathrm{H})_{\mathrm{T}}$ by using (3-13) and (3-12)

$$\begin{aligned}\left(\frac{\partial S_i}{\partial H}\right)_T &= \left(\frac{\partial S_i}{\partial B_i}\right)_T \left(\frac{\partial B_i}{\partial H}\right)_T = -\frac{\partial^2 F_i}{\partial B_i \partial T}\left(\frac{\partial B_i}{\partial H}\right)_T \\ &= -\frac{1}{4\pi}\frac{\partial H\,(B_i T)}{\partial T}\left(\frac{\partial B_i}{\partial H}\right)_T\end{aligned} \tag{3-21}$$

Finally, we write the variation of H^* with respect to T in the form

$$\frac{dH^*}{dT} = \left(\frac{\partial H}{\partial T}\right)_{B_i} + \left(\frac{\partial H}{\partial B_i}\right)_T \frac{dB}{dT} \tag{3-22}$$

where $\mathrm{dB/dT} = \mathrm{dB_i/dT} = \mathrm{dB_j/dT}$ represents the variation of B along the equilibrium curve. On inserting $(\partial \mathrm{H}/\partial \mathrm{T})_B$ from (3-22) into (3-21) we find

$$\left(\frac{\partial S_i}{\partial H}\right)_T = -\frac{1}{4\pi}\frac{d^*}{dT}\left(\frac{\partial B_i}{\partial H}\right)_T + \frac{1}{4\pi}\frac{dB}{dT} \tag{3-23}$$

$$C_j - C_i = \frac{T}{4\pi}\left(\frac{dH^*}{dT}\right)^2\left[\left(\frac{\partial B_j}{\partial H}\right)_T - \left(\frac{\partial B_i}{\partial H}\right)_T\right] \tag{3-24}$$

Therefore, if one knows $H^*(T)$ and the permeabilities $(\partial B_i/\partial H)_T$ for each of the phases, one can predict the discontinuity in the specific heat. For the transition $(i \to j)$ we have a finite permeability (> 1) in the vortex state (i) from Fig. 3-2 and a permeability equal to 1 in the normal state (j). Therefore $C_i > C_j$. At this time all the necessary information is not available to compare (3-24) to experiment. However, for $\mathrm{V_3Ga}$, $\mathrm{C_i - C_j}$ and $\mathrm{dH_{C2}/dT}$ are known and if one makes a reasonable extrapolation for $\partial \mathrm{B}/\partial \mathrm{H}$ in order to predict its value at $\mathrm{H_{C_2}}$ one finds an agreement to within about 10% from magnetic and calorimetric measurements. A similar analysis can be carried out in principle for the transition at $\mathrm{H} = \mathrm{H_{C_1}}$. Here, however, the permeability $(\partial \mathrm{B}/\partial \mathrm{H})_{\mathrm{H}} = \mathrm{H_{C_1}}$ in the Schubnikov phase is probably infinite, as shown by the theoretical calculations of Section 3-2. From (3-24) this leads to an infinite peak in the specific heat at the transition. The singularity is, in fact, weak and easily masked by hysteresis effects. It has been observed recently (on Niobium) by the Rutgers group.

7.2.2 3-2 Vortex state: microscopic description

Negative Surface Energy

We have previously seen that in a London $(\xi < \lambda)$ superconductor the surface tension of a wall separating normal and superconducting regions becomes negative. Under these conditions, we guess that in the presence of a field a state is created where the N and S regions are finely divided and where the wall energy gives an important contribution to the thermodynamic potential. This situation is very different from that encountered for a Pippard superconductor

where the walls are less numerous and where their energy can be neglected in a macroscopic treatment.

Consider, for example, the limit where B is small (that is, few lines of force penetrate the specimen and only a small fraction of the sample is normal). There are essentially two possibilities to maximize the surface to volume ratio for the N regions:

We can form lamina of very small thickness ($\geq \xi$) or filaments of small diameter ($\sim \xi$). In the case of $\lambda \gg \xi$, theoretical calculations show that the second solution is lowest in energy. [2] We therefore find filaments. They are represented in Fig. 3-4a.

Each filament has a hard core of radius ξ where the superconducting electron density n_S falls as is shown in Fig. 3-4c. The lines of force are not confined to the hard core; the field is maximum at the center of the filament but extends a distance λ (Fig. 3-4b). Annular

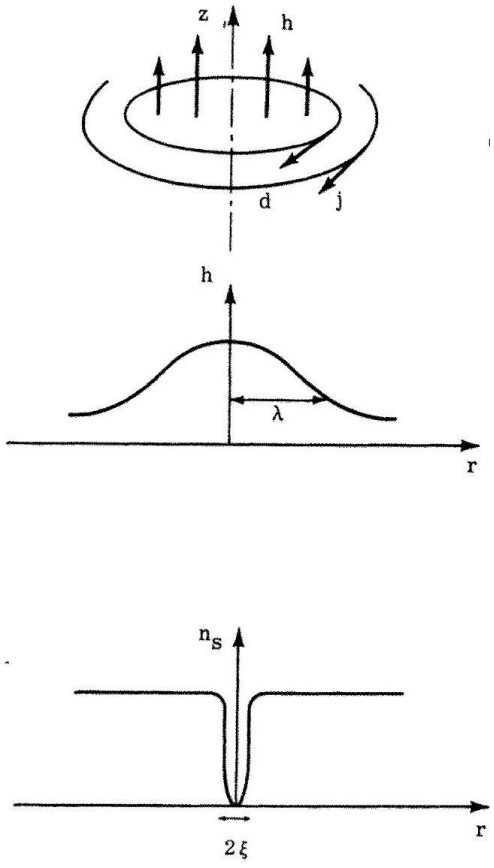


Figure 3-4

Structure of one vortex line in a Type II superconductor. The magnetic field is maximum near the center of the line. Going outwards, h decreases because of the screening in an "electromagnetic region" of radius $\sim \lambda$ (the penetration depth) (Fig. 3-4b). On the other hand, the number of superconducting electrons per $cm^3 n_S$ is reduced only in a small "core region" of radius ξ (Fig. $3-4c$).

currents j encircle the filament and screen out the field for $r > \lambda$. For $r > \xi$, that is, in most of the region of interest, the currents and fields can be simply calculated by London's equations. It will be shown that the radius and exact form of the hard core only appear in the argument of a logarithm; therefore it will not be necessary to know them accurately. In the limit $\xi \ll \lambda$ we shall, in fact, see that the properties of a filament are very easy to calculate.

What is the flux $\phi = \int$ hdo carried by a filament?

Experiment and theory show us that if a bulk superconducting annulus surrounds some lines of force the enclosed flux can only take on discrete values

[2] See problem, page 71.

$$\phi = \mathrm{k}\phi_0 \quad (\mathrm{k\ is\ an\ integer}) \tag{3-25}$$
$$\phi_0 = \frac{\mathrm{ch}}{2\mathrm{e}} = 2 \times 10^{-7}\mathrm{Gcm}^2$$

The explanation of this effect will be given at the end of Chapter 4. The same result applies here. In order to attain the state of maximum subdivision, each filament carries one quantum of flux ϕ_0. This condition fixes the field scale in Fig. $3-4$ b, and the structure of the filament is completely defined.

Such a quantized filament, formed of a very thin hard core surrounded by currents rotating about the axis, is very analagous to the vortex lines found in superfluid He^4 when the helium container is rotated. The only important difference is that the helium atoms are not charged, making $\mathrm{e} = 0$ in Eq. $(1-13)$. We see that the penetration depth λ in He^4 is infinite and the particle currents j, instead of decreasing exponentially for $r > \lambda$, decrease very slowly (as in $1/r$) far from the filament. Historically, vortex lines were first discussed for the He^4 problem by Onsager and Feynman; the generalization to superconductivity is due to Abrikosov (1956). When the superconducting metal contains a finite density of these lines, we say that it is in the vortex state.

Properties of One Isolated Vortex Line

We now study in detail the structure of one vortex line in the limit $\lambda \gg \xi$. The "hard core" of radius ξ is very small and we shall, for the moment, neglect completely its contribution to the energy.

Then the line energy is given by the formula

$$J = \int_{(\mathrm{r}>\xi)} \mathrm{dr} \frac{1}{8\pi} \left[h^2 + \lambda^2 (\mathrm{curl}\, h)^2\right] \tag{3-26}$$

Equation (3-26) has been derived in Chapter 1 (assuming $\lambda \gg \xi$). For a pure superconductor, the penetration depth λ has the London value

$$\lambda_{\mathrm{L}} = \left[\frac{\mathrm{mc}^2}{4\pi \mathrm{n_S e}^2}\right]^{1/2} \tag{3-27}$$

For a superconducting alloy, with $\lambda \gg \xi$, Eq. (3-26) still applies, but with a modified (larger) value of λ, as explained in Chapter 2 (see the discussion after Eq. 2-20). In Eq. (3-26) the integration is carried out in all space outside of the "hard core" ($r > \xi$). We also choose to compute the energy per unit length of line; the resulting energy per cm$J$ is called the line tension. Demanding that J be a minimum leads as usual to the London equation

$$\mathrm{h} + \lambda^2\ \mathrm{curl\ curl\ h} = 0 \quad |\mathrm{r}| > \xi \tag{3-28}$$

In the interior of the hard core Eq. (3-28) must be replaced by something more complicated. But, since the hard core has a very small radius, we can try to replace the corresponding singularity, simply by a two-dimensional delta function $\delta_2(r)$, and write

$$h + \lambda^2\ \mathrm{curl\ curl}\ h = \phi_0 \delta_2(r) \tag{3-29}$$

where ϕ_0 is a vector along the line direction. We now show that the strength ϕ_0 in (3-29) represents the total flux carried by the line.

Integrate (3-29) over the interior surface of a circle C of radius r encircling the axis of the cylinder and use the curl formula:

$$\int \mathrm{h}\cdot \mathrm{d}\sigma + \lambda^2 \oint \mathrm{curl}\,\mathrm{h}\cdot \mathrm{d}\ell = \phi_0 \tag{3-30}$$

if the circle has a radius $\mathrm{r} \gg \lambda$, the currents $j(\mathrm{r}) = \mathrm{c}/4\pi$ curl h are negligible and the line integral along the perimeter of the circle vanishes. Thus the total flux carried by the filament has the value ϕ_0.

We now pass on to the explicit solution of $(3-30)$ to which is added the Maxwell equation

$$\mathrm{div}\, h = 0 \tag{3-31}$$

The field h is directed along the z axis; the current lines are circles in the xy plane. It is easy to predict the value of curl h, that is, the current, in the region $\xi \ll \mathrm{r} \ll \lambda$. In fact, if we reconsider (3-30) with a circle C whose radius is in this domain, the term $\mathrm{Jh}\cdot \mathrm{d}\sigma$ is negligible (only a fraction r^2/λ^2 of the flux ϕ_0 passes through the circle C) and we have

$$\lambda^2 2\pi \mathrm{r}|\ \mathrm{curl}\ \mathrm{h}\ | = \phi_0 \tag{3-32}$$

and

$$|\,\mathrm{curl}\,\mathrm{h}| = \frac{\phi_0}{2\pi\lambda^2}\frac{1}{\mathrm{r}} \quad (\xi < \mathrm{r} \ll \lambda) \tag{3-33}$$

Since h is directed along the z axis, we have $|\,\mathrm{curl}\, h| = -dh/dr$ and upon integrating this relation

$$\mathrm{h} = \frac{\phi_0}{2\pi\lambda^2}\left[\ln\left(\frac{\lambda}{\mathrm{r}}\right) + \mathrm{const}\right] \quad (\xi < \mathrm{r} < \lambda) \tag{3-34}$$

In order to derive the constant of integration in (3-34), it is necessary to write the complete solution to $(3-30)$ and $(3-32)$, which is

$$\mathrm{h} = \frac{\phi_0}{2\pi\lambda^2}\ \mathrm{K}_0\left(\frac{\mathrm{r}}{\lambda}\right) \tag{3-35}$$

where K_0 is the zero-order Bessel function of an imaginary argument defined as in Morse and Feshbach. [3] The important properties of this solution are the asymptotic form (3-34) for $\mathrm{r} \ll \lambda$ (it is found that the constant vanishes) and the asymptotic form for large distances

$$\mathrm{h} = \frac{\phi_0}{2\pi\lambda^2}\sqrt{\frac{\pi\lambda}{2\mathrm{r}}}\mathrm{e}^{-\mathrm{r}/\lambda} \quad (\mathrm{r} \gg \lambda) \tag{3-36}$$

Once the fields are determined, it is easy to calculate the energy J. On integrating the second term in (3-28) by parts,

$$J = \frac{\lambda^2}{8\pi}\int \mathrm{d}\sigma \cdot h \times \mathrm{curl}\, h \tag{3-37}$$

where the integral $\int \mathrm{d}\sigma$ is to be taken over the surface of the hard core (cylinder of radius $\sim \xi$). It is convenient to calculate $\mathfrak{J}$ per cm of length along the filament. Then

$$J = \frac{\lambda^2}{8\pi} 2\pi\xi \mathrm{h}(\xi)|\,\mathrm{curlh}(\xi)| \tag{3-38}$$

which is, from (3-34) and (3-33),

$$J = \left(\frac{\phi_0}{4\pi\lambda}\right)^2 \ln\left(\frac{\lambda}{\xi}\right) \tag{3-39}$$

DISCUSSION OF THIS FORMULA

(1) J only depends upon ξ logarithmically.

(2) J is a quadratic function of the flux. Upon going to a situation where the flux is $2\phi_0$, it is preferable to have two filaments of flux ϕ_0 (total energy 2J) than a filament of double flux (energy 4J). This justifies the choice for ϕ_0 of the minimum flux value, that is, the quantum of flux.

(3) It is possible to rewrite J at $T = 0$ in a rather different form by using the relations

$$\phi_0 = \frac{\mathrm{ch}}{2\mathrm{e}}, \quad \xi = \xi_0 = \frac{\hbar \mathrm{v_F}}{\pi \Delta(0)} \tag{3-40}$$

and a relation (which will be proven by the microscopic theory) between the condensation energy and the energy gap $\Delta(0)$:

$$\frac{\mathrm{H_c^2}}{8\pi} = \frac{1}{2}\,\mathrm{N}(0)\Delta^2(0) \tag{3-41}$$

where $N(0) = m^2 v_F / 2\pi^2\hbar^3$ is the density of states (for one direction of spin) at the Fermi energy in the normal state per unit energy and per cm^3. Upon regrouping these formulas, we obtain

$$J = \frac{\pi^3}{3}\frac{\mathrm{H_c^2}}{8\pi}\xi^2 \ln\frac{\lambda}{\xi} \quad (\mathrm{T} = 0) \tag{3-42}$$

This formula is interesting for the following reason:

Until now we have neglected the contribution of the hard core to the line energy. In fact, superconductivity is more or less destroyed in the hard core section and this takes an extra energy $J_{\mathrm{int}} \sim (\mathrm{H_c^2}/8\pi)\,\xi^2$.

Dimensionally from (3-42) this energy is comparable to $\mathfrak{J}$. Numerically, however, it is much smaller. A more detailed calculation gives for the total energy

$$J = \left(\frac{\phi_0}{4\pi\lambda}\right)^2 \left(\ln\frac{\lambda}{\xi} + \epsilon\right) \quad (\lambda \gg \xi)$$

The numerical constant ϵ includes the effect of the hard core and is of the order of 0.1.

Problem.

Discuss the structure of vortices in a thin film, the applied magnetic field being normal to the film surface (J. Pearl, 1964).

Solution.

Again there is a "hard core" of radius ξ (which we assume to be small) surrounded by current rings. But since the currents are restricted to the thickness d of the film, their screening capacity is weak and the "electromagnetic region" is more spread out than in a long vortex line.

Inside the film, we apply Eq. (3-29)

$$\mathrm{h} + \frac{4\pi\lambda^2}{\mathrm{c}}\,\mathrm{curl\ j} = \phi_0\delta_2(r)\mathrm{n_z}$$

where f is the current density and n_z is a unit vector normal to the film. It is convenient to use the vector potential A rather than the field $h = \mathrm{curl}\,A$. In the London gauge, we find

[3] Methods of Theoretical Physics, (New York: McGraw-Hill, 1953), Chap. 10, p. 1321.

$$A + \frac{4\pi\lambda^2}{\mathrm{c}}\mathrm{J} = \Phi$$

where $\Phi_\mathrm{r} = \Phi_\mathrm{z} = 0$ and $\Phi_\theta = \phi_0/2\pi\mathrm{r}$.

Now average over the thickness d of the film. If $d \ll \lambda, A$ and J are nearly constant in the thickness. Call J the total current $J = jd$. Then

$$J = \frac{c}{4\pi}\frac{1}{\lambda_{\text{eff}}}(\Phi - A)$$
$$\lambda_{\text{eff}} = \frac{\lambda^2}{d}$$

Now replace the film by a infinitesimally small current carrying sheet in the plane z = 0, the current density being $J\delta(z)$. This will be valid when d is much smaller than the range of the electromagnetic region.

In terms of the current sheet the equation valid for all space is

$$\text{curl curl } A = \text{curl}\, h = \frac{4\pi}{c}j = \frac{1}{\lambda_{\text{eff}}}\delta(z)(\Phi - A)$$

or (since curl curl $A = -\nabla^2 A$ in the London gauge)

$$-\nabla^2 A + A\frac{1}{\lambda_{\text{eff}}}\delta(z) = \Phi\frac{1}{\lambda_{\text{eff}}}\delta(z)$$

This result was derived here from the London Eq.(3-29). In actual thin films, such a simple equation does not usually hold. But it is still correct to assume a linear current response of the form $J = (c/4\pi\lambda_{\text{eff}})(\Phi - A)$, where λ_{eff} is some unknown constant, which can be obtained from another experiment (λ_{eff} is, in fact, the effective penetration depth in parallel fields, which could be measured on a hollow cylinder made with the same film).

To solve the equation for A, introduce the three-dimensional Fourier transform

$$A_{qk} = \int A(xyz)\exp i\,(q_x x + q_y y + kz)\,dxdydz$$

and the two-dimensional transforms

$$A_q = \frac{1}{2\pi}\int dk A_{qk} = \int A\delta(z)\exp i\,(q_x x + q_y y)\,dxdydz$$
$$\Phi_q = \int \Phi(xy)\exp i\,(q_x x + q_y y)\,dxdy = i\frac{\phi_0}{q^2}n_z xq$$

Then

$$\left(q^2 + k^2\right)A_{qk} + \frac{1}{\lambda_{\text{eff}}}A_q = \frac{1}{\lambda_{\text{eff}}}\Phi_q$$

Solve for $\mathbf{A}_{\mathrm{qk}}$ and integrate over k:

$$A_q = -\frac{1}{2\pi}\int dk\frac{1}{q^2 + k^2}(A_q - \Phi_q)\frac{1}{\lambda_{\text{eff}}} = -\frac{1}{2q\lambda_{\text{eff}}}(A_q - \Phi_q)$$
$$A_q = \Phi_q\frac{1}{1 + 2q\lambda_{\text{eff}}}$$

From this, all required information can be extracted:

(a) The current has components

$$J_q = \frac{c}{4\pi\lambda_{\text{eff}}}\left(\Phi_q - A_q\right) = \frac{c}{4\pi\lambda_{\text{eff}}}\Phi_q \frac{2q\lambda_{\text{eff}}}{1+2q\lambda_{\text{eff}}}$$

When $q \gg \lambda_{\text{eff}}^{-1}$, J_q is proportional to Φ_q. Thus at small distances r from the center of the vortex

$$J(r) = \frac{c}{4\pi\lambda_{\text{eff}}}\mathbf{\Phi}(r)$$
$$J = \frac{c\phi_0}{8\pi^2\lambda_{\text{eff}}\, r} \quad (\xi \ll r \ll \lambda_{\text{eff}})$$

When $q \ll \lambda_{\text{eff}}^{-1}$

$$J_q \approx \frac{c}{4\pi\lambda_{\text{eff}}} 2q\lambda_{\text{eff}}\, \Phi_q = \frac{c\phi_0}{2\pi}\frac{i_z \times q}{q}$$
$$J = \frac{c\phi_0}{4\pi^2 r^2} \quad (r \gg \lambda_{\text{eff}})$$

The size of the screening region is λ_{eff}. But even beyond λ_{eff}, J decreases only slowly with distance.

(b) The normal field component $\mathrm{h_7}$ in the film is derived from

$$\mathrm{h_{zq}} = \left(-\mathrm{iq} \times \mathbf{A}_{\mathrm{q}}\right)_{\mathrm{z}} = \frac{\phi_{\mathrm{u}}}{1+2\mathrm{q}\lambda_{\text{eff}}}$$

When $q \gg \lambda_{\text{eff}}^{-1}$

$$\mathrm{h_{zq}} \sim \frac{\phi_0}{2\mathrm{q}\lambda_{\text{eff}}}$$
$$\mathrm{h_z(r)} \sim \frac{\phi_0}{4\pi\lambda_{\text{eff}}\,\mathrm{r}} \quad (\xi < \mathrm{r} \ll \lambda_{\text{eff}})$$

At large r we derive h_z most easily from the current J

$$\mathrm{h_2} = -\frac{4\pi\lambda_{\text{eff}}}{\mathrm{c}}\frac{1}{\mathrm{r}}\frac{\mathrm{d}}{\mathrm{dr}}(\mathrm{Jr})$$
$$\cong \frac{2}{\pi}\frac{\phi_0\lambda_{\text{eff}}}{\mathrm{r}^3}$$

(c) The self-energy of the vortex is derived from Eq. (3-26); the required components of h and curl h at the core surface ($\xi \ll \lambda_{\text{eff}}$) are quoted above. The result is

$$E = \left(\frac{\phi_0}{4\pi}\right)^2 \frac{1}{\lambda_{\text{eff}}} \log\frac{\lambda_{\text{eff}}}{\xi} = \frac{137}{16}\frac{\hbar c}{\lambda_{\text{eff}}} \log\frac{\lambda_{\text{eff}}}{\xi}$$

Typically $\lambda_{\text{eff}} \sim 1000\text{Å}$ and $E \sim 30\text{eV}$.

(d) The force between two vortices is

$$\mathbf{F}_{12} = \frac{\phi_0}{\mathrm{c}}\mathbf{n}_{\mathrm{z}} \times J\left(\mathrm{R}_{12}\right)$$

Note that at long distances $J \sim 1/R^2$ and the repulsion energy decreases only like $1/R$. This long range is due to the fact that most of the interaction takes place not through the superconductor, but through the empty space above and below.

Interactions between Vortex Lines

TWO VORTEX LINES

Consider two parallel lines directed along the z axis with positions $r_1 = (x_1, y_1), r_2 = (x_2 y_2)$. The magnetic field distribution is determined by the equations

$$h + \lambda^2 \text{ curl curl } h = \phi_0 \left[\delta\left(\mathbf{r} - \mathbf{r}_1\right) + \delta\left(\mathbf{r} - \mathbf{r}_2\right)\right]$$

which is the generalization of $(3-29)$. The solution h is the superposition of the fields h_1 and h_2 due to the filaments (1) and (2).

$$h(r) = h_1(r) + h_2(r)$$
$$h_1(r) = \frac{\phi_0}{2\pi\lambda^2} K_0\left(\frac{r - r_1}{\lambda}\right)$$

The energy of the system is still written

$$F = \int \frac{h^2 + \lambda^2(\text{curl h})^2}{8\pi} dr = \frac{\lambda^2}{8\pi} \int h \times \text{curl}\, h \cdot d\sigma$$

Here the integral $\int \mathrm{d}\sigma$ is to be taken over the surfaces of the two hard cores ($|r - r_i| = \xi$); writing explicitly the two contributions to h we obtain

$$F = \frac{\lambda^2}{8\pi} \int (d\sigma_1 + d\sigma_2) \cdot (h_1 + h_2) \times (\text{curl}\, h_1 + \text{curl}\, h_2)$$

There are 8 terms that we regroup as follows: First the individual energy of each filament

$$\frac{\lambda^2}{8\pi}\left[\int \mathrm{d}\sigma_1 \cdot h_1 \times \text{curl}\, h_1 + \int d\sigma_2 \cdot h_2 \times \text{curl}\, h_2\right] = 2J$$

then the terms

$$\int (h_1 + h_2) \cdot (\text{curl}\, h_1 \times d\sigma_2 + \text{curl}\, h_2 \times d\sigma_1)$$

which tend toward 0 in the limit where $\xi \ll \lambda$ because $h_1 + h_2$ and curl h_1 are finite in the domain of integration $\int d\sigma_2$. There remains an important contribution

$$U_{12} = \frac{\lambda^2}{8\pi} \int (h_1 \times \text{curl}\, h_2 \cdot d\sigma_2 + h_2 \times \text{curl}\, h_1 \cdot d\sigma_1)$$

In effect, curl h_2 is proportional to $1/|r - r_2|$ for $|r - r_2| \ll \lambda$ from (3-33) and after integration one obtains a finite result as $\xi \to 0$. If we set

$$h_{12} = h_1(r_2) = h_2(r_1) = \frac{\phi_0}{2\pi\lambda^2} K_0\left(\frac{r_1 - r_2}{\lambda}\right)$$

then using (3-33) we obtain

$$U_{12} = \frac{\phi_0 \, \mathrm{h}_{12}}{4\pi}$$

U_{12} represents the interaction energy (per cm) of two filaments. This is a repulsive energy which decreases as $\left(1/\sqrt{r_{12}}\right) \mathrm{e}^{-\mathrm{r}_{12}/\lambda}$ at large distances, and which diverges as $\ln\left(|\lambda/r_{12}|\right)$ at short distances.

A remark about forces. Let us compute the force f_2 experienced by line 2, as due to the interaction U_{12}

$$f_{2x} = -\frac{\partial U_{12}}{\partial x_2} = -\frac{\phi_0}{4\pi}\frac{\partial h_{12}}{\partial x_2}$$

Introduce now the current $f = n_s e v$, which would exist, in the presence of line 1 alone, at the point $x_2 y_2$. Then $j_y = -(c/4\pi)\,(\partial h_{12}/\partial x_2)$ by Maxwell's equation and we have

$$f_{2x} = \frac{\phi_0}{c} j_y = \frac{1}{2} h n v y$$

When more than one line is acting on line 2, Eq. (3-52) remains valid provided we interpret v as the total superfluid velocity at point $(x_2 y_2)$.

Conclusion. A line is in static equilibrium when the superfluid velocity at any point on the line is 0.

MAGNETIZATION CURVES

We now form the Gibbs function, minimize it, and deduce the density of vortices existing in the sample in thermal equilibrium.

$$G = n_L J + \sum_{ij} U_{ij} - \frac{BH}{4\pi}$$

The first term represents the individual energies of the lines, n_L is the number of lines per cm^2, related to the induction B by

$$B = n_L \phi_0$$

(This expresses the fact that each vortex carries a flux ϕ_0.) The second term in (3-53) describes the repulsive interactions between vor tices; the explicit form of U_{ij} is given by (3-49) and (3-50). Finally, the last term gives the effect of the field H and favors large values of B. It plays the role of a pressure that tends to increase the density of vortices.

In order to numerically evaluate the interaction term, it is useful to distinguish several regions:

(1) In the small induction region ($n_L \lambda^2 \ll 1$), only the interaction between nearest neighbor vortices is important and the sum ΣU_{ij} converges rapidly.

(2) When B is larger ($n_L \lambda^2 \gg 1$), the range λ of the interaction becomes large compared to the spacing of the filament lattice, and other methods are preferable to evaluate ΣU_{ij}.

(3) Finally, when n_L becomes comparable to $1/\xi^2$, the hard cores begin to overlap and the elementary methods used in this section are no longer valid. But, qualitatively, we may guess that when the hard cores do overlap, superconductivity is destroyed in the bulk. This corresponds to inductions $B \sim \phi_0/\xi^2$.

THE FIRST PENETRATION FIELD H_{C_1}

At very low line densities (low B), the interaction term in Eq. (3-53) is small and we shall first neglect it completely. Then, using Eq.(3-54) we get

$$G \cong B\left(\frac{5}{\phi_0} - \frac{H}{4\pi}\right)$$

When $H < 4\pi J/\phi_0$, G is an increasing function of B. The lowest G is obtained for $B = 0$ (complete Meissner effect).

When $H > 4\pi J/\phi_0$, we can lower G by choosing $B \neq 0$. There is some flux penetration.

We conclude that the first penetration field is given by

$$H_{c1} = \frac{4\pi J}{\phi_0} = \frac{\phi_0}{4\pi\lambda^2} \log \frac{\lambda}{\xi}$$

H_{c_1} is often much'smaller than the "thermodynamic" field H_c defined by $(3-1)$. For $T = 0$, for example, on using $(3-40)$ and $(3-41)$, we find

$$\frac{H_{c_1}}{H_c} = \frac{\pi}{\sqrt{24}} \frac{\xi}{\lambda} \ln\left(\frac{\lambda}{\xi}\right)$$

The result is therefore $H_{C_1}/H_c \sim \xi/\lambda$ and this may be much smaller than 1. A measurement of H_{c_1} and H_c, in principle, allows a determination of ξ and λ. For example, for V_3Ga, if at $T = 0, H_c \sim 6000G$ and $H_{c_1} \sim 200G$, one finds from (3-57) that $\lambda/\xi \sim 80$ and then, from (3-56), $\lambda \sim 2000$Å and $\xi \sim 25$Å. These orders of magnitude are still rather inaccurate because of current uncertainties in H_c and H_{C_1}, but it is hoped that the situation will improve in the near future.

FIELDS SLIGHTLY LARGER THAN H_{C_1}

For finite line densities (finite B's) we must take into account the interaction term in Eq. (3-53). To minimize this repulsive energy, the lines will take a regular arrangement. Detailed calculations based on (3-53) show that, at all B's, the most favorable arrangement is triangular, as shown on Fig. 3-5 (J. Matricon, 1964).

If H is only slightly larger than H_{c_1}, we can guess that the equilibrium density of lines n will be small, and thus the distance between neighboring lines d will be large. If $d > \lambda$, we may keep only the nearest neighbor contributions to the interaction term in (3-53) and write

$$G \cong \frac{B}{4\pi}\left[H_{c_1} - H + \frac{1}{2} z \frac{\phi_0}{2\pi\lambda^2} K_0\left(\frac{d}{\lambda}\right)\right]$$

where z is the number of nearest neighbors of one line ($z = 6$ for the triangular lattice), d is related to the induction B through the relation

$$B \equiv \phi_0 n_L = \frac{2}{\sqrt{3}} \frac{\phi_0}{d^2} \quad \text{(triangular lattice)}$$

Equation (3-59) can be easily verified on Fig. 3-5. The function $G(B)$ is represented in Fig. 3-6. Since $H > H_{C_1}$, the initial slope $(\partial G/\partial B)_{B=0}$

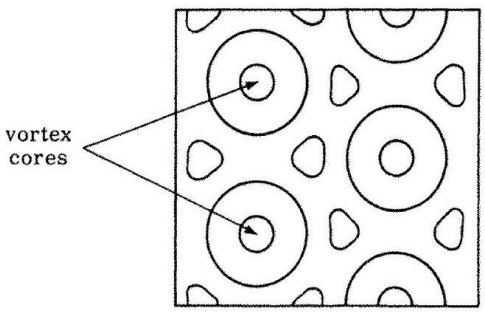


Figure 3-5

A triangular lattice of vortex line (after Kleiner, Roth, and Autler, Phy's. Ren., 133A, 1226 (1964). The plane of the figure is normal to the field direction. The contours give the lines of constant n_s. This figure describes the situation at high fields (nearly overlapping cores).

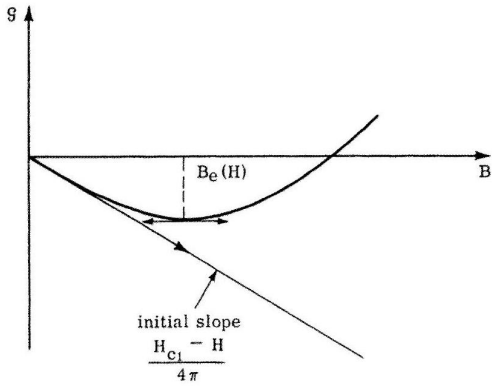


Figure 3-6 The thermodynamic potential S as a function of the induction B ($B = n_L\phi_0$ measures the number of vortices per $\mathrm{cm}^2 \mathrm{n}_L$). The equilibrium value of $B\,[B_e(H)]$ corresponds to the minimum of g.

is negative. As B increases, the interaction term begins to contribute but rather slowly, since it is proportional to $K_0(d/\lambda)$. When $d > \lambda$ we may write, according to (3-36)

$$\mathrm{K}_0\left(\frac{\mathrm{d}}{\lambda}\right) \sim \exp\left(-\frac{\mathrm{d}}{\lambda}\right) = \exp\left[-1.07\sqrt{\frac{\phi_0}{\mathrm{B}\lambda^2}}\right]$$

Thus the interaction term is exponentially small at small B's. At larger B 's however, it dominates the over-all behavior and $G(B)$ increases. There is a minimum of G for some value $B = B(H).B(H)$ is the induction found at equilibrium in the field H. The theoretical $B(H)$ or $M(H)$ has been computed along these lines by Goodman and is shown on Fig. 3-7, together with experimental results on a particularly good MoRe alloy.

The following points must be noticed:

The theoretical curve has an infinite slope $(\partial \mathrm{M}/\partial \mathrm{H})_{\mathrm{H}} = \mathrm{H}_{\mathrm{c}_1} = \infty$ at the first penetration field. Physically, this reflects the fact that the lines repel each other like $e^{-d/\lambda}$, that is, we may think of their interaction as having a finite range λ. At field slightly larger than H_{c_1} it is thus possible to form many lines in the sample without competing against the interaction energy. The experimental curve does not show

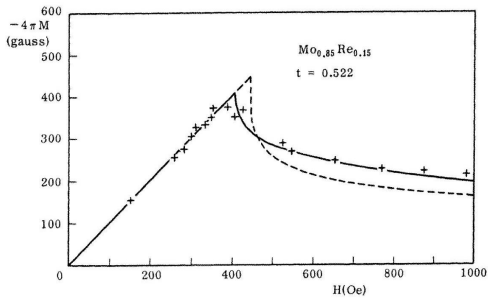


Figure $3-7$

Experimental magnetization of a molybdenum-rhenium alloy at $\mathrm{T} = 0.52\ \mathrm{T}_0$ (after Joiner and Blaugher, Rev. Mod. Phy',, 36, 67 (1964). Also shown are two theoretical magnetization curves (after B. B. Goodman). The broken curve is for a laminar model, the continuous one for vortex lines.

a very large slope $(\partial M/\partial H)_H = H_{c_1}$; this is not very surprising since in the region of interest the interactions between lines are very weak and the lines can easily be pinned by structural defects. However, as we depart from $\mathrm{H}_{\mathrm{c}_1}$ by more than 10%, we get good agreement between theory and experiment.

A similar theoretical curve can be drawn for another model where the flux-carrying units are not vortex lines, but laminas (see problem, p. 71). If the distance between laminas is d, we

again find a repulsion between units proportional to $e^{-d/\lambda}$. However, in this case, the induction B is proportional to d^{-1}, while in the line case it is proportional to d^{-2} as shown by Eq. (3-59). Thus the fall of M(H) for $\mathrm{H} > \mathrm{H}_{\mathrm{C}_1}$ is more rapid in the laminar model than in the vortex line model. The two theoretical curves are compared on Fig. 3-7; it is apparent that the vortex line gives a better fit, as emphasized by Goodman.

DOMAIN $\frac{1}{\lambda^2} \ll \mathrm{n_L} \ll \frac{1}{\xi^2}$

In this region the vortices form a rather dense lattice and the interactions extend to distant neighbors. The interaction energy can then be calculated by the following method: The field $h(r)$ directed along the z axis is the solution of

$$\mathrm{h} + \lambda^2 \ \mathrm{curl\ curl\ h} = \phi_0 \sum_{\mathrm{i}} \delta_2 \left(\mathbf{r} - \mathbf{r}_{\mathrm{i}}\right)$$

$$\mathrm{div\,h} = 0$$

where $r_i = (x_i, y_i)$ denotes the position of the ith vortex. The points $\mathbf{r}_{\mathrm{i}}$ form a two-dimensional periodic lattice. We define the Fourier transform h_J by

$$h_J = n_L \int_{\text{cell}} h\left(x_i, y_i\right) \exp\left[i\left(J_x x + J_y y\right)\right] dxdy$$

Since $h\left(x_i, y_i\right)$ is periodic, h_J is nonvanishing only when J is a reciprocal lattice vector. From (3-61),

$$\mathrm{h}_J = \frac{\mathrm{n_L}\varphi_0}{1 + \lambda^2\ \mathrm{J}^2}$$

Finally the free energy becomes

$$\begin{aligned}
\mathcal{F} &= \frac{1}{8\pi} \int \left(h^2 + \lambda^2 \operatorname{curl}^2 h\right) dr \\
&= \frac{1}{8\pi} \sum_J h_J^2 \left(1 + \lambda^2 J^2\right) = \frac{B^2}{8\pi} \sum_J \frac{1}{1 + \lambda^2 J^2} \\
&= \frac{B^2}{8\pi} + \frac{B^2}{8\pi} \sum_{J \neq 0} \frac{1}{1 + \lambda^2 J^2}
\end{aligned}$$

In the sum $\Sigma_{J\neq 0}$, the minimum magnitude of the vectors J is of the order $1/\mathrm{d} \sim \sqrt{\mathrm{n_L}}$ and $\lambda^2\ \mathrm{J}^2 \sim \mathrm{n_L}\lambda^2 \gg 1$ in the domain of interest. Therefore $1/\left(1 + \lambda^2\ \mathrm{J}^2\right)$ can be replaced by $1/\lambda^2\ \mathrm{J}^2$. Finally we must perform the sum $\Sigma_{J\neq 0} 1/J^2$, which depends on the particular lattice considered. Here, we will simplify the calculation by replacing the sum by an integral

$$\begin{aligned}
&\sum \frac{1}{J^2} \to \frac{1}{(2\pi)^2} \frac{1}{n_L} \int \frac{dJ_x dJ_y}{J^2} \to \frac{1}{2\pi n_L} \int_{J\,\min}^{J\,\max} \frac{JdJ}{J^2} \\
&= \frac{1}{2\pi n_L} \ln \left| \frac{\mathrm{J\,max}}{\mathrm{J\,min}} \right|
\end{aligned}$$

with $\mathrm{J\,min} \sim 1/\mathrm{d}$ and $\mathrm{J\,max} \sim 1/\xi$ (the Fourier components relative to the interior of the hard core must be excluded). We finally find

$$F = \frac{B^2}{8\pi} + \frac{B}{4\pi} H_{c_1} \frac{\ln \beta d/\xi}{\ln \lambda/\xi}$$

$$G = F - \frac{BH}{4\pi}$$

In (3-64) β is a numerical constant of the order unity (for the triangular lattice, Matricon has calculated $\beta = 0.381$). The B(H) relation is ob-tained as usual by imposing $\partial G/\partial B = 0$. This gives

$$H = B + H_{c_1} \frac{\ln\left(\beta' \frac{d}{\xi}\right)}{\ln \frac{\lambda}{\xi}}$$

where $\beta' = \beta e^{-1/2}$ and where d is always related to B by Eq. (3-59). The logarithmic dependences predicted by (3-65) are in rather good agreement with the experimental data on revrsible magnetization curves in materials with $\lambda \gg \xi$.

DOMAIN $n_L \sim \xi^{-2}$

Here, as already pointed out, our simple model breaks down, and we shall need a more elaborate approach based on the Landau-Ginsburg equations (Chapter 6). The upper critical field H_{C_2} is of order φ_0/ξ^2. This, physically, corresponds to the onset of overlap between the hard cores.

Problem.

Compare the Gibbs function in the filamentary structure described above with that of a possible laminar structure.

Solution.

As before, we shall limit our considerations to the case $\lambda \gg \xi$. The laminar structure will be formed of planes, for example, perpendicular to the x axis, and equidistant (spacing d)(Fig. 3-8). In the neighborhood of each of these planes, over a thickness $\sim 2\xi$, the superconductivity is strongly perturbed (N regions). In the remainder (S regions), the density of superconducting electrons has the value n_S. Such a model has been discussed in detail by Goodman (1961). The fields h(x) (parallel to the z axis) are determined by the London equation

$$h = \lambda^2 \frac{d^2 h}{dx^2}$$

except in the thin (N) regions. The solution is of the form

$$h = H_m \cosh(x/\lambda)/\cosh P$$

where $P = d/2\lambda$ and H_m is the field in the N regions. The free energy of the (S) regions becomes, from (3-26),

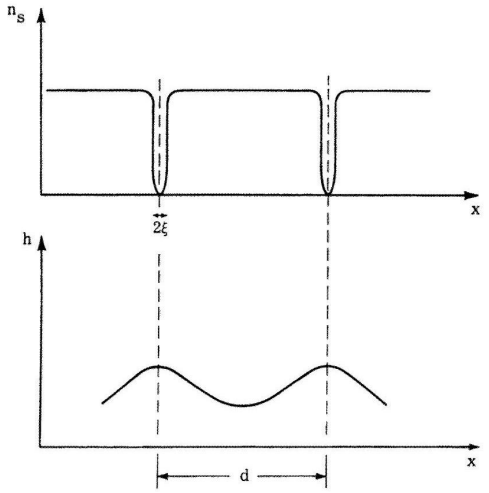


Figure 3-8
The laminar model for the Schubnikov phase. Thin normal sheets N of thickness $\sim 2\xi$ alternate with superconducting sheets S. The N sheets repel each other. The range of the repulsive forces is the penetration depth λ.

$$F_1 = \frac{2}{d}\int_0^{d/2} dx \frac{h^2 + \lambda^2\left(\frac{dh}{dx}\right)^2}{8\pi} = \frac{H_m^2}{8\pi}\frac{\tanh p}{p}$$

It is necessary to add the formation energy of the N regions

$$\mathrm{F_2} \cong \frac{\mathrm{H_c^2}}{8\pi}\frac{2\xi}{\mathrm{d}} = \frac{\mathrm{H_c^2}}{8\pi}\frac{1}{\mathrm{PK}}$$

where $\kappa = \lambda/\xi$. Finally, to obtain the Gibbs function, we must add a term

$$\begin{aligned} -\frac{BH}{4\pi} &= -H\frac{H_m}{4\pi}\frac{\tanh P}{P} \\ G_{\text{laminar}} &= \frac{1}{8\pi}\left[H_m^2\frac{\tanh P}{P} + \frac{H_c^2}{P.K} - 2HH_m\frac{\tanh P}{P}\right] \end{aligned}$$

On minimizing G with respect to H_m we obtain $\mathrm{H} = \mathrm{H}_m$.

$$\mathrm{G_{laminar}} = \frac{1}{8\pi\mathrm{P}}\left[-\mathrm{H^2}\tanh\mathrm{P} + \frac{\mathrm{H_c^2}}{\kappa}\right]$$

For $\mathrm{H} < \mathrm{H_C}/\sqrt{\kappa}$ the minimum G is obtained for infinite P, which corresponds to a complete Meissner effect. For $\mathrm{H} > \mathrm{H_c}/\sqrt{\kappa}$ the minimum occurs for finite P. The initial field for penetration is therefore $H_c/\sqrt{\kappa}$ for the laminar model. This is to be compared with the result for the vortex line model, Eq. (3-56).

$$\mathrm{H_{c1}} = \frac{\pi}{\sqrt{24}}\frac{\mathrm{H_c}}{\kappa}\ln\kappa(\kappa \gg 1)$$

for $\kappa \gg 1, \mathrm{H_{C_1}} < \mathrm{H_C}/\kappa$. For $\mathrm{H_{C1}} < \mathrm{H} < \mathrm{H_c}/\kappa^{1/2}$, we have

$$\begin{aligned} G_{\text{vortex}} &< G_{\text{Meissner}} \\ G_{\text{laminar}} &= G_{\text{Meissner}} \end{aligned}$$

therefore, $G_{\text{vortex}} < G_{\text{laminar}}$; that is, the vortex state is more favorable in the weak induction domain.

It is also possible to make the comparison in the region where H is larger ($\mathrm{H} \sim \mathrm{H_C}$, for example). We are then in the region $\mathrm{P} \ll 1$ for the laminar model By expanding $\tanh \mathrm{P} \cong \mathrm{P} - \mathrm{P}^3/3$ and minimizing G, we obtain

$$\mathrm{G_{laminar}} = -\frac{\mathrm{H^2}}{8\pi} + \left(\frac{3}{2\kappa}\right)^{2/3}\frac{\mathrm{H_c^{4/3}H^{2/3}}}{8\pi}$$

In the vortex line model, the potential is determined from (3-64) and (3-65)

$$\begin{aligned} \mathrm{G_{vortex}} &= -\frac{1}{8\pi}\left(\mathrm{H} - \mathrm{H}'\right)^2 \\ \mathrm{H}' &= \mathrm{H_{c1}}\frac{\ln \mathrm{d}/\xi}{\ln\kappa} = \nu\frac{\mathrm{H_c}}{\kappa} \end{aligned}$$

where ν is a constant of order unity. For $T = 0$

$$\nu = \frac{\pi}{\sqrt{24}} \ln \frac{d}{\xi}$$

In the region of interest $\mathrm{H}' \ll \mathrm{H}$ and

$$\mathrm{G_{vortex}} = -\frac{\mathrm{H}^2}{8\pi} + \nu \frac{H H_\mathrm{c}}{4\pi\kappa}$$

therefore

$$\frac{\mathrm{G_{laminar}} + \frac{\mathrm{H}^2}{8\pi}}{\mathrm{G_{vortex}} + \frac{\mathrm{H}^2}{8\pi}} = \text{ const } \left(\frac{\mathrm{KH}}{\mathrm{c}}\right)^{1/3}$$

when $\mathrm{H} < \kappa \mathrm{H_c}$ (which roughly corresponds to the upper critical field $\mathrm{H_{c2}}$), $\mathrm{G_{laminar}} > \mathrm{G_{vortex}}$. Thus the vortex state is still most stable in the intermediate and high field regions. [4]

Problem.

Discuss the equilibrium magnetization curves for a second kind superconductor in the form of an ellipsoid of revolution, the field being applied along the ellipsoidal axis.

Solution.

The equations $\operatorname{div} B = 0$, curl $H = 0$, and $B = (H/|H|)B_e(H)$, where $B_e(H)$ is the equilibrium induction in the presence of a field H measured for a long cylinder, allow a solution where B and H are constant in the ellipsoid with $\mathrm{H} = \mathrm{H_0} - \mathrm{NM} = \mathrm{H_0} - \mathrm{N(B - H)}/4\pi$ where N is the demagnetizing coefficient of the ellipsoid. The relation between B and the applied field is therefore given by the implicit formula

$$B = B_e \left(\frac{H_0 - \frac{NB}{4\pi}}{1 - \frac{N}{4\pi}} \right)$$

B is nonzero for $\mathrm{H_0} > \mathrm{H_{Cl}}(1 - \mathrm{N}/4\pi)$. The slope $(\mathrm{dB}/\mathrm{dH_0})_{B=0}$ is finite and equal to $4\pi/\mathrm{N}$. The upper critical field remains equal to $\mathrm{H_{C2}}$ since $\mathrm{B}\,(\mathrm{H_{C2}}) = \mathrm{H_{C2}}$ when the transition is second order.

Problem.

Discuss the scattering of slow neutrons by a regular lattice of vortex lines in a superconductor.

Solution.

The interaction between neutron and lines is $\mu_\mathrm{n} \mathrm{h}(\mathbf{r})$ where $\mu_\mathrm{n} = 1.91\mathrm{e}/2\mathrm{Mc}$ is the neutron moment and M the neutron mass. Consider a scattering event where the neutron momentum changes from $\hbar k_0$ to $\hbar\,(k_0 + q)$. The corresponding scattering amplitude is given by the Born approximation formula

$$a = \frac{M}{2\pi\hbar^2} \int \mu_n h(r) e^{iq \cdot r} dr$$

This is nonzero only if $q = J$, where J is a reciprocal lattice vector associated with the two-dimensional "line lattice." From (3-62) we find

These elementary calculations of G are not sufficient in the neighborhood of $\mathrm{H_{c2}}$. We return later to a study of the region using the Landau-Ginsburg equations.

$$\int h(r)e^{iJ\cdot r}dr = \frac{BV}{1+\lambda^2 J^2} = \frac{n_L \phi_0 V}{1+\lambda^2 J^2}$$

where V is the sample volume and n_L the number of lines per cm^2. Thus

$$\mathrm{a_J} = \frac{1}{2} 1.91 \frac{\mathrm{n_L V}}{1+\lambda^2\ \mathrm{J}^2}$$

For a triangular lattice of lines with nearest neighbor distance d, we have $\mathrm{n_L} = (2/\sqrt{3})\,(1/\mathrm{d}^2)$ and, for the first reflection, $\mathrm{J} = (4\pi/\sqrt{3})\mathrm{d}^{-1}$. Taking $\mathrm{B} = 2000\mathrm{G}\,(\mathrm{n_L} = 10^{10})$, we get $\mathrm{d} \sim 10^3 \mathring{\mathrm{A}}$ and $\mathrm{J} \sim 6.710^5\ \mathrm{cm}^{-1}$. For $\lambda = 1000\mathring{\mathrm{A}}$ this gives $(\lambda J)^2 \cong 45 \gg 1$. We compute the amplitude a per atom (since this is the quantity familiar to experimentalists). Inserting for V an atomic volume of $30\mathring{\mathrm{A}}^3$ we get $\mathrm{a} \cong 0.710^{-13}$ cm. The corresponding "coherent scattering cross section" is $4\pi \mathrm{a}^2 \sim 5 \times 10^{-28}\ \mathrm{cm}^2 = 0.5$ millibarns - a small, but measurable value.

The scattering angle θ for this first reflection is very small $\theta \cong (\mathrm{J/k_0}) = (2/\sqrt{3})\,(\lambda_n/d)$ where we have introduced the neutron wavelength $\lambda_n = 2\pi/k_0$. At best, with subthermal neutrons we can make λ_n as large as $\sim 5\mathring{\mathrm{A}}$. For the above example this leads to angles $\theta \sim 6.10^{-3}$rad (or $20'$ of arc). The experiment has been performed on Nb metal (Cribier, Jacrot, et al., 1964). Due to the $1/\left(1+\lambda^2 J^2\right)$ dependence of a, it has been possible only to observe the first reflection (with the smallest J). (See Fig 3-9.)

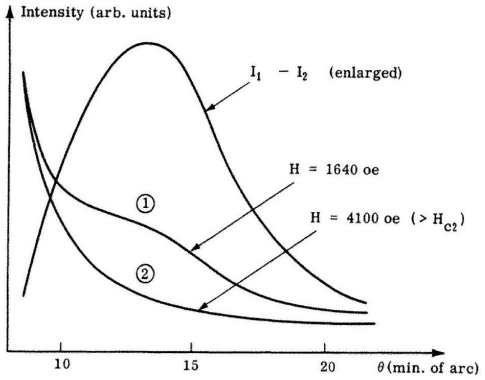


Figure 3-9
Neutron scattering by an array of vortex lines in niobium metal at T = 4.2°K. (Courtesy of D. Cribier.)

Problem.

Calculate the broadening of a nuclear magnetic resonance line arising from the field inhomogeneities associated with the vortex state (P. Pincus, 1964).

Solution.

In intermediate fields $\mathrm{H_{c_1}} \ll \mathrm{H} \ll \mathrm{H_{C2}}$ where the vortices form a dense lattice, the field distribution is given by the Fourier transform of Eq. (3-62). A knowledge of all the moments of the field distribution would completely determine the nuclear magnetic resonance line shape (if this were the only source of broadening). However if the line does not have anomalous wings, as is often the case (Jaccarino and Gossard, 1964), the second moment is a good measure of the line width (see A. Abragam, Principles of Nuclear Magnetism, Clarendon Press, 1961). Thus the line width is given by

$$\Delta H = \left[\left\langle h^2 \right\rangle - \langle h \rangle^2\right\}^{1/2}$$

where \langle\rangle denotes a spatial average. The term $\langle \mathrm{h} \rangle$ is just $\mathrm{n_L}\phi_0 = \mathrm{B}$. $\langle \mathrm{h}^2 \rangle$ can easily be calculated from Eq. (3-62):

$$\left\langle h^2 \right\rangle = S^{-1} \int h^2(r) d\sigma = \sum_J h_J h_{-J} = n_L^2 \phi_0^2 \sum_J \left[1 + (\lambda J)^2\right]^{-2}$$

where S is the surface area of the sample perpendicular to the field. On replacing the sum over reciprocal lattice vectors by an integral in a similar manner as is done in the text after Eq. (3-63), we obtain

$$\Delta H = \frac{B}{\sqrt{4\pi}} \frac{d}{\lambda} \left[1 + \left(\frac{2\pi\lambda}{d}\right)^2\right]^{-1/2}$$

where for simplicity we have assumed a square lattice. This result is valid in the domain $\mathrm{d} \gg \xi$. In the intermediate field region $\mathrm{d} \ll \lambda$, this leads to

$$\Delta H \cong \frac{1}{\sqrt{2}} \times \frac{\phi_0}{(2\pi)^{3/2}\lambda^2}$$

Notice that this width is of the order of $\mathrm{H_{C_1}}$ (for $\mathrm{V_3Ga}, \lambda \sim 2000\mathring{\mathrm{A}}, \Delta\mathrm{H} \approx 20\mathrm{Oe}$) and remains nearly field independent on to fields of the order of $\mathrm{H_{c_2}}$ where the inhomogeneous broadening vanishes. For fields near $\mathrm{H_{C_1}}(\mathrm{d} \approx \lambda)$, the broadening is more severe. More detailed calculations of the line shape using Eq. (3-62) have been performed by Matricon.

Problem.

Compute the energy of a vortex line near the surface of the specimen, the line being parallel to the surface.

Solution.

Let the line, and the fields, be parallel to the z axis, the limiting surface being the $y0z$ plane, the sample occupying the half-space $x > 0$. The field $h(r)$ is governed by the equation

$$\mathrm{h} + \lambda^2 \text{ curl curl } \mathrm{h} = \phi_0 \delta_2 (\mathbf{r} - \mathbf{r}_\mathrm{L})$$

where r_L represents the two-dimensional coordinate of the line lwe shall take $r_L = (x_L, 0)$] and ϕ_0 is a vector, of length ϕ_0, along z. The boundary conditions on the surface are

$$\mathrm{h} = \mathrm{H} \quad (\text{ curl h})_\mathrm{X} = 0 \quad (0 \text{ normal current})$$

where H is the applied field. The solution $h(r)$ will be written as

$$\mathbf{h} = \mathbf{h}_1 + \mathbf{h}_2$$

where $h_1 = H \exp(-x/\lambda_L)$ represents the field penetration in the absence of any line, while h_2 is due to the line, and can be obtained by a method of images. To the line $(x_L, 0)$ we add an image of opposite sign located at $(-x_L, 0)$ and take for h_2 the algebraic sum of the field due to the line and image. Thus h_2 automatically vanishes on the limiting surface $\mathrm{x} = 0$ and the boundary condition is satisfied.

Having constructed $h(r)$, we now compute the thermodynamic potential

$$S = \int dr \left\{ \frac{h^2 + \lambda^2 (\text{curl h})^2}{8\pi} - \frac{H \cdot h}{4\pi} \right\}$$

The integral is taken in the sample volume ($x > 0$) except for the core region of the line, which is excluded. The last term is the microscopic analog of the standard $\mathbf{B} \cdot \mathbf{H}/4\pi$ term for macroscopic systems. We transform S into a surface integral, using the London equation for h, and we obtain

$$S = \frac{\lambda^2}{4\pi} \int_{\text{(core and plane)}} \mathrm{d}\boldsymbol{\sigma} \cdot \left(\frac{1}{2}\,\mathrm{h} - \mathrm{H}\right) \times \operatorname{curl} h$$

The surface integral $\int \mathrm{d}\sigma$ includes the surface of the hard core (giving a contribution S′) and the surface of the specimen (giving a contribution S″). As usual the only important term in $\int_{\text{core}} d\sigma$ (in the limit $\xi \to 0$) comes from the singular term in curl h, and the result is

$$S' = \frac{\phi_0}{4\pi}\left(\frac{1}{2}h\left(r_L\right) - H\right)$$

The second term ς'' may be written as

$$\varrho'' = -\frac{\lambda^2}{8\pi} \int_{\text{plane}} d\sigma \cdot h_1 \times \ \text{curl}\ h$$

since on the sample surface $h = h_1 = H$. Writing curl $h = \operatorname{curl} h_1 + \operatorname{curl} h_2$ we can separate in G'' a term involving $h_1 \times \operatorname{curl} h_1$, which is the energy in the absence of the line, an additive constant we drop from now on. We are left with

$$\mathrm{S}'' = -\frac{\lambda^2}{8\pi} \int_{\text{plane}} \mathrm{d}\sigma \cdot h_1 \times \text{curl}\ \ h_2$$

We rewrite this integral as

$$\int_{\text{plane}} = \int_{\text{core + plane}} - \int_{\text{core}}$$

By making use of London's equation for $\mathbf{h}$, in the region outside the core, we have

$$\int_{\text{core + plane}} \mathrm{d}\sigma \cdot h_1 \times \operatorname{curl} h_2 = \int_{\text{core + plane}} d\sigma \cdot h_2 \times \operatorname{curl} h_1$$

h_1 is not singular near the line axis; thus the core contribution to the righthand side vanishes when $\xi \to 0$. The integral on the plane also vanishes since $(\mathbf{h}_2)_{\mathrm{X}=0} = 0$. Finally

$$S'' = \frac{\lambda^2}{8\pi} \int_{\text{core}} d\sigma \cdot h_1 \times \operatorname{curl} h_2 = \frac{\phi_0 h_1\left(r_L\right)}{8\pi}$$

$$S = \frac{\phi_0}{4\pi}\left[H \exp\left(-x_L/\lambda\right) + \frac{1}{2}h_2\left(r_L\right) - H\right]$$

[Note incidentally that $S = 0$ when $x_L = 0$, that is, when the line is just on the surface, since $h_2(x = 0) = 0$.] If we analyze $h_2\left(r_L\right)$ into a direct term and an image term, the direct term gives as a contribution to g the line self-energy $J = \phi_0 \mathrm{H}_{\mathrm{C}_1}/4\pi$. The image term describes an attraction between line and image, of value $-\left(\phi_0/8\pi\right) h\left(2x_L\right)$ where $h(r)$ is the function giving the field at distance r of a single line (Eq. 3-35). Finally

$$S = \frac{\phi_0}{4\pi}\left[H \exp\left(-x_L/\lambda\right) - \frac{1}{2}h\left(2x_L\right) + H_{C1} - H\right]$$

Discussion

(1) The term $(\phi_0 \mathrm{H}/4\pi)\exp(-\mathrm{x_L}/\lambda)$ describes the interaction of the line with the external field and the associated screening currents. It has the same form as Eq. (3-50). It is a repulsive term.

(2) The term $-\phi_0\ \mathrm{h}\,(2\mathrm{x_L})\,/8\pi$ represents the attraction between the line and its image. The magnitude of this energy differs from Eq. (3-50) by a factor $\frac{1}{2}$. But the force derived from it has the conventional magnitude ϕ_0j/c [when differentiating $h\,(2x_L)$ with respect to x_L, we get a factor 2).

(3) The aspect of $S\,(x_1)$ for various values of the applied field H is shown on Fig. 3-10. When $\mathrm{H} \sim \mathrm{H_{C_1}}$ there is a strong barrier opposing the entry of a line. We can understand this barrier as follows: When $H = H_{c_1}, S\,(x_L = 0) = S\,(x_L = \infty) = 0$. if we start from x_L large and bring the line closer to the surface,

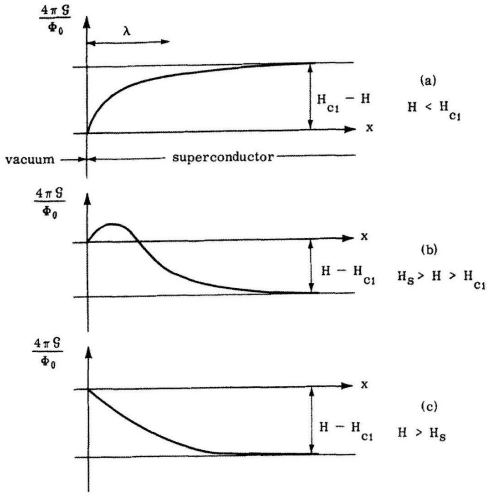


Figure 3-10

Surface barrier impeding the entry of the first flux line is a Type II superconductor. (a) When $\mathrm{H} < \mathrm{H_{C1}}$, the force on the line always points towards the surface: no lines can exist (in an ideal specimen). (b) When $\mathrm{H_S} > \mathrm{H} > \mathrm{H_{Cl}}$ the line gains an energy $(\phi_0/4\pi)\,(\mathrm{H} - \mathrm{H_{ci}})$ as it reaches the deep inside of the sample. But there is a barrier near the surface, and the line will not enter if the surface is clean. (c) When $\mathrm{H} > \mathrm{H}_S$, the barrier disappears.

the repulsive term $(\sim \exp(-x_L/\lambda)$ dominates the image term $(\sim \exp(-2x_L/\lambda)$. Thus S becomes positive and we have a barrier. The barrier disappears, however, in high fields as is clear in Fig. $3-10$ (c). When $\mathrm{H} > \mathrm{H_S} = \phi_0/4\pi\lambda\xi$, it can be seen from the equation for S that the slope $(\partial S/\partial x_L)\,x_L = \xi$ becomes negative. [5]

[5] We shall see later from the microscopic analysis that the field $\mathrm{H_S}$ thus defined is of the order of the thermodynamic critical field $\mathrm{H_c}$.

The conclusion is that, at field $\mathrm{H} < \mathrm{H}_S$, the lines cannot enter in an ideal specimen (although their entry is thermodynamically allowed as soon as $\mathrm{H} > \mathrm{H_{c1}}$). These surface barrier effects have been predicted independently by Bean and Livingston and by the Orsay group. They have been observed experimentally on lead thallium alloys (Tomash and Joseph) and on niobium metal (de Blois and de Sorbo). (The sample surface must have very few irregularities on the scale of λ.)

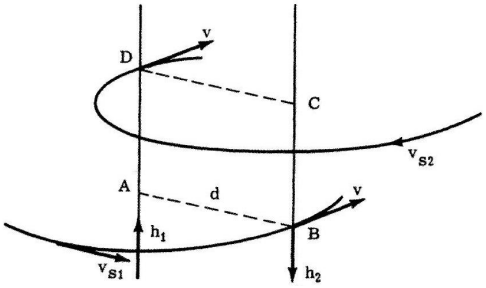
Vortex Line Motions

Consider the two antiparallel vortices of Fig. 3-11. According to Eq. $(3-50)$ they attract each other. Will they move under the action of this force, or will they stand still? This question is very much debated at the present time. My personal belief is that in a pure metal each line will drift in the other's velocity field. They will thus both move at right angle from their

common plane, with a velocity

$$v_{\text{drift}} = v_{12}$$

where v_{12} is the superfluid velocity at point 2 due to the presence of line 1.



(1) (2)
Figure 3-11

Two antiparallel vortex lines in a pure superconductor of Type II. $\mathbf{v_{S1}}$ ($\mathbf{v_{S2}}$) is the superfluid velocity induced by line 1 (2). Each line drifts with the local superfluid velocity v. For that particular geometry both lines go with the same velocity. Note that **v** is normal to the plane $ABCD$ of the lines.

Such drift motions should lead to amusing collective modes for an assembly of vortex lines in a very pure metal of Type II. (P. G. de Gennes, J. Matricon, 1962.)

In dirty superconductors, on the other hand, friction between the lines and the lattice will dominate the motion. The two antiparallel vortex lines AD and CB will then move toward one another, as shown on Fig. $3-12$, with a velocity

$$\mathrm{v_{drift}}\ (2) = -\mathrm{v_{drift}}\ \left(1; = \frac{\mathrm{f}}{\eta}\right.$$

where f is the attractive force between the lines, as given by Eq. (3-52) and η is a viscosity coefficient. We can estimate η with the following assumptions: suppose that the currents due to line 1 are not distorted near the core of line 2. This core then carries a current density $j = \mathrm{nev}_{12}$. But this core is essentially normal. Thus we expect a loss (per unit length of line 2)

$$w = \frac{j^2}{\sigma\pi\xi^2}$$

where $\sigma = \mathrm{ne}^2\tau/m$ is the normal state conductivity and ξ the core radius. This power dissipation must also be equal to $\mathrm{fv_{drift}}\ (2) = 1/\eta\mathrm{f}^2$. Recalling from Eq. $(3-52)$ that $f = \frac{1}{2}nhv_{12}$. we obtain

$$\eta = \frac{\mathrm{n}\tau\mathrm{h}^2}{4\pi m\xi^2}$$

Viscous motions which are reasonably well described by this type of damping have been observed in dirty materials by Kim and coworkers.

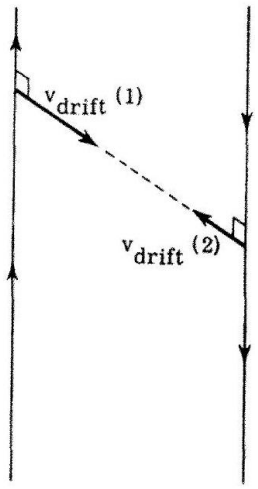


Figure 3-12
Two antiparallel vortex lines in a dirty superconductor of Type II: the lines move toward each other with a drift velocity controlled by friction with the lattice.

7.3 Thin films

7.3.1 3.5 Critical Field of a Thin Film

A thin superconducting film, of thickness less than the penetration depth, can remain superconducting in a parallel magnetic field even if the value of the field is well in excess of H_{cm}. We shall denote the magnetic field destroying the film's superconductivity by H_{c} .

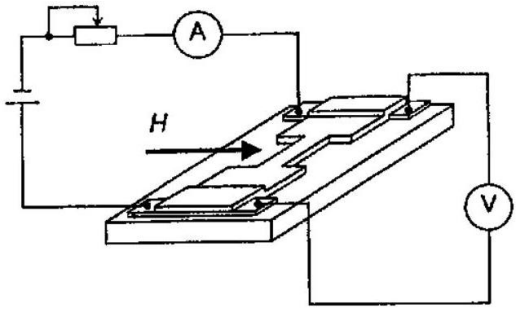


Fig. 3.6. Scheme of the critical magnetic field measurements on a thin film
Consider an experiment shown schematically in Fig. 3.6. A thin film of the material under study is deposited onto a clean glass substrate and connected to a measuring circuit by current and voltage leads. Then the specimen is mounted in a cryostat in such a way that an external magnetic field is parallel to its surface. The external field is increased and at a certain value of the

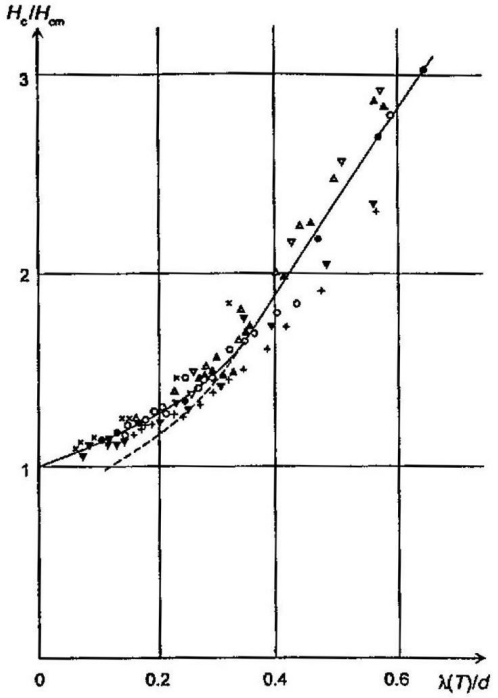


Fig. 3.7. Results of the critical magnetic field measurements on Sn films of various thicknesses [29]; d is the film thickness. The solid curve shows the result of the GinzburgLandau theory

field the film begins to show a finite resistance. This is the critical field of the film. A compilation of the results of such an experiment is shown in Fig. 3.7.

We remember from Sect. 1.3 that a bulk superconductor in an external field $H_{\rm cm}$ undergoes a first-order phase transition. Indeed, one notices in Fig. 3.7 that thick films show supercooling. This means that, when the film is in the normal state and the field decreases, the transition to the superconducting state may not occur at the appropriate value of the field, that is, at the field for which the free energies of the normal and superconducting states are equal. The transition may be delayed down to a lower field called the supercooling field. In Fig. 3.7 the supercooling fields are shown by the dashed curve. Thus we observe that, as the film thickness decreases, the effect of supercooling becomes weaker and weaker and finally, starting from a certain thickness, disappears completely. This leads to a natural conclusion: that the superconducting transition for films of this thickness or thinner is of second order.

Assume now that the thickness of our film is $d \ll \xi, \lambda$. Then we may neglect variations of ψ in the film and assume that the magnetic field penetrates the film completely. THe surfaces of the film are assumed to coincide with the planes $x = \pm d/2$. Since the film is a simply connected body, we can choose a gauge for the vector potential $\boldsymbol{A}$ such that the wavefunction ψ is real. Then the first GL equation can be written in the form

$$-\left[1-\left(\frac{2\pi\xi A}{\Phi_0}\right)^2\right]\psi+\psi^3=0 \tag{3.58}$$

$$\frac{\mathrm{d}^2A}{\mathrm{d}x^2}=\frac{\psi^2}{\lambda^2}A \tag{3.59}$$

Here the vector potential $\boldsymbol{A}$ is along the y axis and the magnetic field is subject to the boundary condition

$$H(\pm d/2)=H_0 \tag{3.60}$$

where H_0 is the external field parallel to the surface of the film. The solution of (3.59) is

$$A = A_1 \cosh(\psi x/\lambda) + A_2 \sinh(\psi x/\lambda)$$

where A_1 and A_2 are integration constants. The magnetic field H can be found simply by differentiating A:

$$H = A_1(\psi/\lambda)\sinh(\psi x/\lambda) + A_2(\psi/\lambda)\cosh(\psi x/\lambda).$$

The boundary conditions (3.60) are satisfied if

$$A_1 = 0, \quad A_2 = \frac{H_0\lambda}{\psi\cosh(\psi d/2\bar{\lambda})}$$

Then

$$H = H_0\frac{\cosh(\psi x/\lambda)}{\cosh(\psi d/2\lambda)}, \quad A = \frac{H_0\lambda}{\psi}\frac{\sinh(\psi x/\lambda)}{\cosh(\psi d/2\lambda)} \tag{3.61}$$

Let us now apply the results to a thin film ($d \ll \lambda$). In this case, $\psi x/\lambda \ll 1$ and $\psi d/2\lambda \ll 1$ and we can expand the hyperbolic functions in a Taylor's series. Keeping only linear terms, we have

$$\cosh(\psi d/2\lambda) = 1, \quad \sinh(\psi x/\lambda) = \psi x/\lambda$$

On substituting this into (3.61), we obtain: $A = H_0 x$ and then, from (3.58),

$$\psi^2 = 1 - \left(\frac{2\pi\xi}{\Phi_0}\right)^2 H_0^2 x^2$$

To find the average of the last expression over the thickness of the film, we integrate with respect to x from $-d/2$ to $+d/2$:

$$\psi^2 d = d - {H_0}^2\frac{1}{12}d^3\left(\frac{2\pi\xi}{\Phi_0}\right)^2$$

Taking into account (3.38), we finally obtain the dependence of the order parameter in the film on the applied magnetic field:

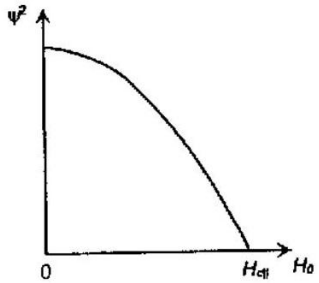


Fig. 3.8. Order parameter as a function of the parallel external magnetic field H_0 for a thin film ($d \ll \lambda$)

$$\psi^2 = 1 - \frac{1}{24}\frac{H_0^2 d^2}{H_{\rm cm}^2\lambda^2}$$

This dependence is sketched in Fig. 3.8. Thus, the order parameter ψ in a thin film is strongly dependent on the applied field H_0 and gradually goes to zero at the value of the field of $2\sqrt{6}H_{\rm cm}\lambda/d$. It is natural to select this field as the critical field of the film, $H_{\rm c\|}$.

Finally, the critical field of a thin film of thickness d in a parallel external field H_0 is

$$H_{c\parallel} = 2\sqrt{6} H_{cn1} \frac{\lambda}{d} \tag{3.62}$$

Thus, as the thickness of the film decreases, its critical field goes up. For example, if the thickness of a film is an order of magnitude less than the penetration depth, $\lambda/d \sim 10$, and $H_{cm} \sim 10^3$ Oe, we obtain, by (3.62), $H_{c\parallel} \sim 40000$ Oe. Physically, this is easy to understand. Since the magnetic field penetrates into the film, the film's diamagnetic moment per unit volume is substantially reduced compared to a bulk specimen. But a small diamagnetic moment in an external field is equivalent to a small magnetic needle oriented against the field. Such a situation is energetically more favorable than in the case of a large diamagnetic moment. Therefore, a film in an external field is much more stable than a bulk specimen and can remain superconducting up to much higher fields.

7.3.2 3.6 Critical Current of a Thin Film

Theory

Let us now consider a film carrying a current I, in the absence of external magnetic field. We assume, as before, that the surfaces of the film coincide with the planes $x = \pm d/2$ and that the current flows in the y direction. The current I is the total current through the film per unit length of the z axis.

The current generates a magnetic field H_I at the surfaces of the film. This imposes the boundary conditions

$$H(\pm d/2) = \mp H_I \tag{3.63}$$

As in the preceding section, we note that the film is a simply connected body and use this to choose a gauge for $\boldsymbol{A}$ so that ψ is real. In addition, we assume that the film is thin: $d \ll \lambda, \xi$. Then we may neglect variations of the order parameter over the thickness of the film and, as a result, we arrive at the GL equations of the form (3.58) and (3.59). We shall analyze these equations again but this time subject to the boundary conditions (3.63). The general solution of (3.59) is

$$A = A_1 \cosh(\psi x/\lambda) + A_2 \sinh(\psi x/\lambda).$$

Since for our problem $H = \mathrm{d}A/\mathrm{d}x$, we have

$$H = (A_1\psi/\lambda) \sinh(\psi x/\lambda) + (A_2\psi/\lambda) \cosh(\psi x/\lambda)$$

On substitution of the boundary conditions (3.63) into this expression we obtain two equations with two unknowns (A_1 and A_2). Their solution is

$$A_1 = \frac{\lambda H_I}{\psi \sinh(\psi d/2\lambda)}, \quad A_2 = 0$$

The final result is

$$H = H_I \frac{\sinh(\psi x/\lambda)}{\sinh(\psi d/2\lambda)}, \quad A = \frac{\lambda H_I \cosh(\psi x/\lambda)}{\psi \sinh(\psi d/2\lambda)} \tag{3.64}$$

Now we take into account that the thickness of the film is small, i.e., $\psi d \ll \lambda$. This implies that in the expression for A in (3.64) we can assume $\cosh(\psi x/\lambda) \approx 1$ and $\sinh(\psi d/2\lambda) \approx \psi d/2\lambda$. Then

$$A = 2\lambda^2 H_J/\psi^2 d$$

Substituting this into (3.58) and using (3.38), we obtain

$$\frac{2\lambda^2 H_I^2}{d^2 H_{\rm cm}^2} = \psi^4 - \psi^6. \tag{3.65}$$

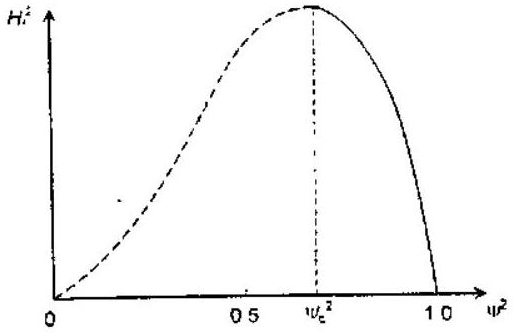


Fig. 3.9. Order parameter in a thin superconducting film as a function of the applied current. The heavy part of the curve corresponds to stable superconductivity

The dependence of $H_I{}^2$ on ψ^2 is plotted in Fig. 3.9. The heavy line emphasizes the part of the plot corresponding to stable states. When the film does not carry any current, equation (3.65) has two solutions: $\psi = 0$ and $\psi = 1$. From general arguments, it is clear that in this case the superconducting state ($\psi = 1$) is more favorable energetically and, therefore, it is this that will he roaligurl rather than the momal etato If wen now owiteh on o
very small current across the film, equation (3.65) will again have two solutions: one corresponding to $\psi \leq 1$, and the other corresponding to $\psi \ll 1$. It then follows from the requirement of continuity that it is the former that corresponds to the stable superconducting state.

But what is the maximum current that the film can sustain while remaining in the superconducting state?

The answer follows directly from the plot of Fig. 3.9: it is the current corresponding to the maximum in the plot. Let us work out its value. First, we find $\psi_{\rm c}$ corresponding to the maximum of $H_I{}^2$:

$$\frac{\rm d}{{\rm d}\psi}\left(2\lambda^2 H_I^2/d^2 H_{\rm cm}^2\right) = 4\psi_{\rm c}^3 - 6\psi_{\rm c}^5 = 0$$

which leads to $\psi_{\rm c}{}^2 = 2/3$.
Then

$$H_{I_{\rm c}} = \frac{\sqrt{2}}{3\sqrt{3}} H_{\rm cm} \frac{d}{\lambda}. \tag{3.66}$$

From (3.66) and the formula $H_{I_{\rm c}} = (4\pi/c) I_{\rm c}$, one can easily find the average critical current density $j_{\rm c}$ across the film:

$$j_{\rm c} = \frac{\sqrt{2}}{12\pi\sqrt{3}} \frac{c H_{\rm cm}}{\lambda}. \tag{3.67}$$

Let us summarize the major results of this section.
(1) The field generated by the critical current at the surface of a film is proportional to the thickness of the film: $H_{I_{\rm c}} \propto d$, namely, it becomes smaller when the thickness of the film decreases. At the same time, the critical field of the film varies as $H_{c\|} \propto 1/d$, that is, it increases when the film becomes thinner. For example, if $d/\lambda \sim 0.1$ and $H_{\rm cm} = 1000$Oe, then $H_{c\|} \sim 4 \times 10^4$ Oe and $H_{I_{\rm e}} \sim 30$Oe. Hence, for a thin film, the destruction of superconductivity by a current is not identical to its destruction by the magnetic field of this current.

(2) The critical current density j_c from (3.67) is independent of the thickness of the film. It follows that j_c is simply a characteristic of the currentcarrying capacity of a particular material. (3) Finally, let us emphasize one more important point. The destruction of superconductivity by a current is not accompanied by a phase transition. This is only true, of course, provided that the film is in good thermal contact with liquid helium such that all the heat given up by the film is immediately thermalized. Then the temperature of the film remains, at any moment, equal to the temperature of the helium bath. In this case, even if the current reaches the value of I_c, the free energy of the superconducting state remains below the free energy of the normal state.

What happens then when the current is $I = I_c$?

Why cannot a supercritical current pass through the film without dissipation? To answer these questions, we shall use the analysis proposed by Bardeen. Since the film is thin, we can neglect the energy of the magnetic field generated by the current and write the free energy density in the form

$$F_s = F_n - |\alpha| n_s + \frac{\beta}{2} n_s^2 + n_s \frac{m}{2} v_s^2$$

Here n_s is the superconducting electron density; α and β are the coefficients of the GL theory, which are already known to us. The last term describes the kinetic energy of the superconducting electrons and v_s is the velocity of their correlated motion, or 'superfluid' velocity.

The equilibrium value of $n_s(v_s)$ as a function of v_s can be found from the requirement that the free energy at equilibrium is a minimum:

$$\frac{\partial F_s}{\partial n_s} = -|\alpha| + \beta n_s + \frac{m v_s^2}{2} = 0$$

This yields

$$n_s = \frac{\left(|\alpha| - \frac{m v_s^2}{2}\right)}{\beta} \tag{3.68}$$

The current density j_s in this case is determined by the well-known expression

$$j_s = n_s e v_s \tag{3.69}$$

The dependences $n_s(v_s)$ and $j_s(v_s)$, corresponding to (3.68) and (3.69), respectively, are sketched in Fig. 3.10. Again, the part of the curve $j_s(v_s)$ corresponding to stable states is shown in bold. What does this plot tell us? As the superconducting current density increases, the electron velocity also increases. But this is accompanied by a decrease of the electron density $n_s(v_8)$. The electron pairs are being broken. Finally, a state is attained such that it is not possible to increase the superconducting current any further, because the superconducting electron density becomes so low. There are simply not enough carriers to maintain a higher current. This is the critical current given by (3.67). It is often called the pair-breaking current.

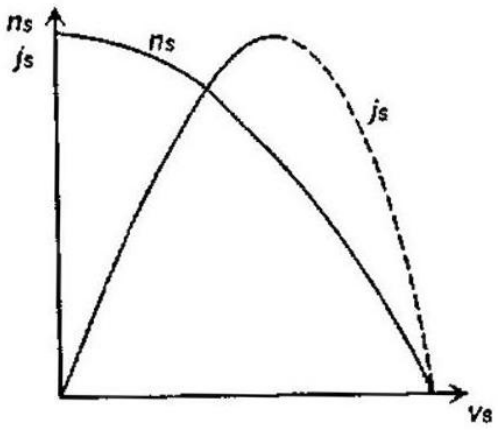


Fig. 3.10. Superconducting electron density n_s and supercurrent density j_s in a thin film as functions of the velocity of the superconducting component of the electron density

Problems

Problem 3.1. Consider a Pb cylinder at 4.2 K in a uniform magnetic field parallel to its axis. The field at the surface of the cylinder is $H_0 = 300$ Oe. Find the density w of the magnetic energy in the specimen at the distance $x = 300$Å from the surface. (The diameter of the cylinder is much larger than the magnetic field penetration depth.)

Problem 3.2. The critical temperature of Pb is 7.18 K . Find the ratio of the value of the penetration depth λ at $T = 7.10$ K to its value at $T = 4.2$ K. Estimate the density of the superconducting electrons at $T = 7.10$ K.

Problem 3.3. Consider a specimen of superconducting Sn. At $T = 0.9T_\mathrm{c}, \lambda = 8.7 \times 10^{-6}$ cm and $\xi = 4.35 \times 10^{-5}$ cm. Find the surface energy of the interface between a normal and a superconducting region, σ_ne.

Problem 3.4. Consider a Sn film of thickness $d = 1000$Å deposited onto a glass substrate. The film is placed in an external magnetic field $H_0 = 10$ Oe parallel to its surface. The temperature is $T = 0.9T_\mathrm{c}$. Find the field at the center of the film and the diamagnetic moment M_0 per unit area of the film's surface.

Problem 3.5. Consider a thick Sn film in a parallel magnetic field. The thickness of the film is 10^{-4} cm and the temperature is $T = 0.9T_c$. Find the critical field of the film, H_cll , on the assumption that the order parameter ψ is independent of the field and equals 1 (the first-order phase transition).

Problem 3.6. Consider a Pb film of thickness $d = 200$Å deposited onto a glass substrate. At $T = 0$, the magnetic field penetration depth is $\lambda(0) = 390$Å, and the thermodynamic critical field is $H_\mathrm{cm}(0) = 803$ Oe. Find the magnetic field generated by the critical current at the surface of the film. Compare it with the parallel critical field of the same film.

Problem 3.7. Find the critical current density for the film of the previous problem.

Problem 3.8. Consider a thin film ($d \ll \lambda$) of In in the superconducting state. The GL parameter of the film is $\kappa = 0.1$. The magnetic field penetration depth is $\lambda = 800$Å. Find the critical velocity of the superconducting electrons.

Problem 3.9. Consider a bulk type-I superconductor in an external magnetic field equal to the thermodynamic critical field H_cm. Compare the density of the Meissner current j_M at the surface of the superconductor with the critical current density j_c of a thin film made of the same material.

7.4 2. Some Effects in Scope of Linear Electrodynamics of Superconductors

7.4.1 2.5 Magnetic Field and Current Distributions in Simple Configurations

2.5.1 Thin Slab in a Parallel Magnetic Field

In this section we shall analyze magnetic field and current distributions in simple configurations of superconductors. We start with the case of an infinite slab of thickness d placed in a uniform magnetic field H_0 parallel to its surface. Assume that the plane $x = 0$ is in the center of the slab and that its surfaces coincide with the planes $x = \pm d/2$. The magnetic field is along the z axis.

In the interior of the slab, the magnetic field H must satisfy (2.13). Then, from symmetry arguments, H is along the z axis and depends only on the x coordinate. Therefore (2.13) can be rewritten as:

$$\mathrm{d}^2H/\mathrm{d}x^2 - \lambda^{-2}H = 0 \tag{2.38}$$

with the boundary conditions $H(\pm d/2) = H_0$. The general solution of (2.38) is

$$H = H_1 \cosh(x/\lambda) + H_2 \sinh(x/\lambda) \tag{2.39}$$

where H_1 and H_2 are integration constants. Substituting the boundary conditions into (2.39), we get two algebraic equations with two unknowns that can be solved easily. The final result is

$$H(x) = H_0 \frac{\cosh(x/\lambda)}{\cosh(d/2\lambda)} \tag{2.40}$$

The supercurrent density in the slab can be found by combining (2.40) and Maxwell's equation curl $\boldsymbol{H} = (4\pi/c)\boldsymbol{j}_\mathrm{s}$:

$$j_\mathrm{s} = -\frac{c}{4\pi}\frac{\mathrm{d}H}{\mathrm{d}x} \tag{2.41}$$

As a result, we get

$$cH_0 \quad \sinh(x/\lambda)$$

If the slab is thick ($d \gg \lambda$), it follows from (2.40) and (2.42) that both the magnetic field and the current penetrate into it only to a certain depth of the order λ. In the other limiting case, a thin film ($d \ll \lambda$), we get, in linear approximation and after expanding the hyperbolic functions in terms of the small parameters x/λ and $d/2\lambda$:

$$H = H_0, \quad j_\mathrm{s} = \frac{cH_0 x}{4\pi\lambda^2}$$

This means that the magnetic field penetrates the entire film, while the supercurrent density varies linearly with depth.

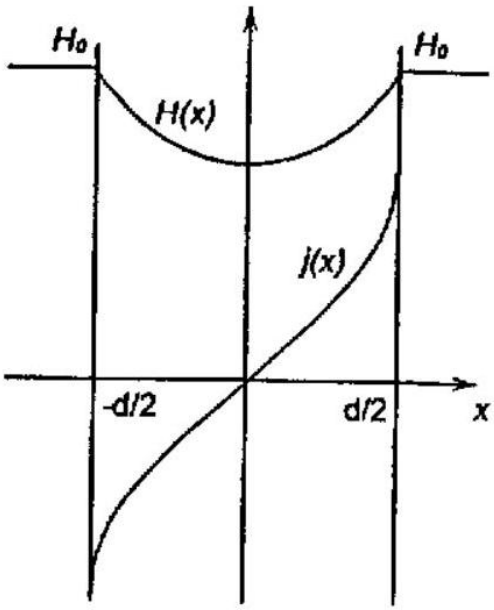


Fig. 2.3. Distribution of current and magnetic field across a thin film placed in a parallel uniform magnetic field

The current and field distributions obtained above are shown in Fig. 2.3. The current circulates at the edges of the slab so that the induced magnetic field cancels out the external field H_0 in its interior.

2,5.2 Thin Slab Carrying a Current

In this section we consider an infinite thin slab carrying a current in the absence of magnetic field. We assume that the slab is the same as in Sect. 2.5.1 and the current flows in the direction of the y axis. Further we assume that the current is uniform along the z axis, that is, edge effects are disregarded. Consider a part of the slab in the form of a strip of unit width parallel to the z axis. The current I flows along the z axis and generates a magnetic field $\pm H_I$ at the surfaces of the slab ($x = \pm d/2$). Substituting these boundary conditions into the general solution (2.39), we find the field distribution in the slab:

$$H(x) = -H_I \frac{\sinh(x/\lambda)}{\sinh(d/2\lambda)} \tag{2.43}$$

Using Maxwell's equation (2.41), we find the distribution of current:

$$j_{\mathrm{s}}(x) = \frac{cH_I}{4\pi\lambda} \frac{\cosh(x/\lambda)}{\sinh(d/2\lambda)} \tag{2.44}$$

It follows from (2.43) and (2.44) that, similarly to the previous case, for $d \gg \lambda$ both the magnetic field and the current are present only within a surface layer of thickness λ. If the film is thin ($d \ll \lambda$), the pattern is different; the current flows through its entire cross-section and the field is a linear function of the coordinate:

$$H = -H_I \frac{2x}{d}, \quad j_{\mathrm{s}} = \frac{cH_I}{2\pi d} = \frac{I}{d}$$

Recall that a uniform current in an infinite thin slab generates a uniform magnetic field outside the slab, independent of the coordinates. The field and current distributions are shown in Fig. 2.4.

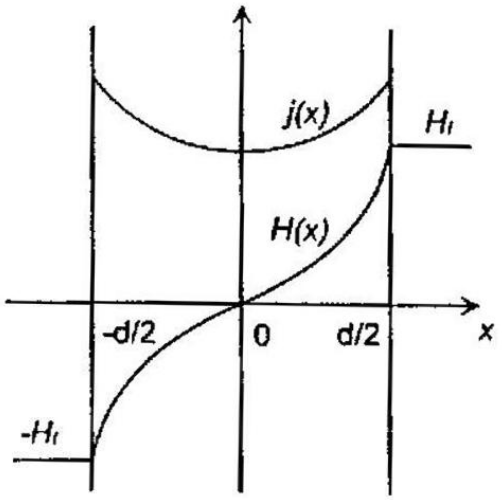


Fig. 2.4. Distribution of current and magnetic field across a thin film carrying a current

2.5.3 Thin Slab Carrying a Current in a Transverse Uniform Field

Consider a thin slab in a uniform external field H_0 parallel to the z axis. The slab carries a current along the y direction which is uniform along the z axis, as in Sect. 2.5.2. The total current through the cross-section of unit height is I. It generates a field $\pm H_I$ at the surfaces of the slab ($x = \pm d/2$). Thus, in this problem we have a superposition of the conditions from the two previous problems. Due to the linearity of the London equations, this should lead to a superposition of their solutions.

Consider a particular case $H_I = H_0$. The external field H_0 in this case cancels out the field generated by the current on one side of the slab and doubles it on the other side. As a result, the current I flows on one side of the

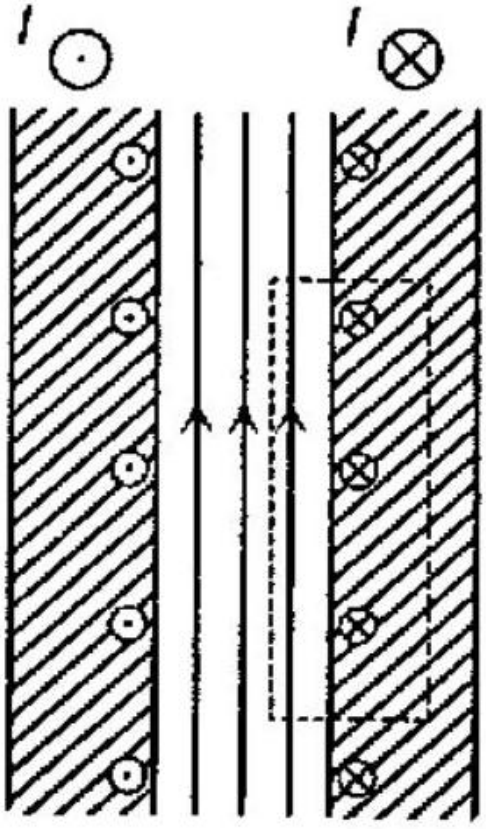


Fig. 2.5. If two parallel superconducting slabs carry currents which are equal in value and opposite in direction, the resulting magnetic field is 'locked' in the gap between the slabs

as in Fig. 2.5. The field in the gap between the slabs [1] is $H = (4\pi/c)I$. One can assume that this field is generated by both currents. Due to the current I flowing in the left-hand slab, there is a uniform field $H_I = 2\pi I/c$ directed upwards everywhere to the right of the slab and downwards everywhere to the left of it. Vice versa, the current from the right-hand slab generates a field H_I directed downwards everywhere to the right of the slab and upwards everywhere to the left of it. The result is that both to the right and to the left of the pair of slabs the fields cancel each other out while in the gap the field is doubled.

2.5.4 Thin Film Above a Superconducting Semispace

In this section we discuss a situation which is particularly important from a practical point of view: a thin film above a semi-infinite superconducting space (we shall refer to the latter as a superconducting screen). In order to find the distribution of the magnetic field when the film carries a certain current, we start with a very simple case.

Consider a rectilinear current-carrying conductor, which is placed above a superconducting screen and oriented along the y axis. Its distance from the screen is a. Let us find the magnetic field above the screen. If there were no screen, the magnetic field lines would form concentric circles centered on the conductor. But because the field lines cannot penetrate a superconductor (due to the Meissner-Ochsenfeld effect), it is obvious that, with the superconducting screen in place, the magnetic field around it will be distorted. Let us find this field.

In the semispace $z > 0$ and outside the conductor, there are no electric currents and curl $\boldsymbol{H} = 0$. Therefore, we can introduce a magnetic field potential satisfying the Laplace equation. On the other hand, we know that the magnetic field at the surface of a superconductor is always tangential to the

surface, that is, $H_z(z = 0) = 0$. This boundary condition assures that the solution of the Laplace equation is single-valued.

The correct field in the region $z > 0$ can be found very simply by means of the method of images. It is easy to see that it will be the field generated by two rectilinear currents, equal in value and opposite in direction, without the superconducting screen. For one of the currents, the distance from the plane $z = 0$ is a, i.e., the coordinates of its cross-section are $(0, a)$, while for the other (the image of the first) the coordinates are $(0, -a)$. Then in the semispace $z > 0$ and outside the conductor, the magnetic field still satisfies the equation curl $\boldsymbol{H} = 0$, and the boundary condition $H_z(z = 0) = 0$ is satisfied automatically due to symmetry of the problem.

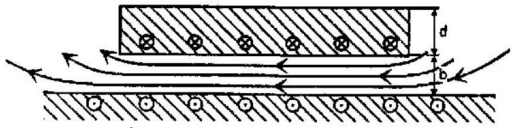


Fig. 2.6. Magnetic field generated by a currentcarrying film placed above a superconducting semispace

Thus we can apply the method of images to derive the field generated by a superconducting film placed above a semi-infinite superconducting screen. Let the thickness of the film be $d > \lambda$ and its width $w \gg \lambda$. The film is placed at a distance b from the screen and carries a current I. Let us find the current distributions in the film and in the screen and the magnetic field in the gap between the film and the screen.

Using the method of images, we replace the effect of the screen with that of an irnage film placed at a distance $2b$ from our film. The image also carries a current, but the direction of this current is opposite to that in the real film. Thus we have arrived at the problem of field and current distributions for two parallel films with opposite currents. This problem has just been solved in Sect. 2.5.3 (Fig. 2.5) and we already know the answer: in the gap between the

[1] Stokes' theorem states that $\oint \boldsymbol{H} \cdot \mathrm{d}\boldsymbol{l} = (4\pi/\mathrm{c})I$, where I is the total current through the surface bounded by the contour along which the path integral is

film and the screen, there is a uniform magnetic field $H_I = \frac{4\pi}{c}\frac{I}{w}$. The
current I in the film flows only near the surface adjacent current I in the film flows only near the surface adjacent to the screen, within a layer $\sim \lambda$. The current in the screen also flows within a layer $\sim \lambda$ near the surface and its surface density is I/w. The direction of this current is opposite to that of the current in the film. The relation between the field H_I and the current in the screen is given by the law of the total current. This situation is shown schematically in Fig. 2.6. The edge effects are disregarded in the above consideration. The magnetic field distribution incorporating the edge effects is shown in Fig. 2.7 [19].

The results that we have just obtained agree with reality if the real film playing the role of the screen can indeed be approximated by a semi-infinite screen. Below there is an example of a situation in which such an approximation is not valid

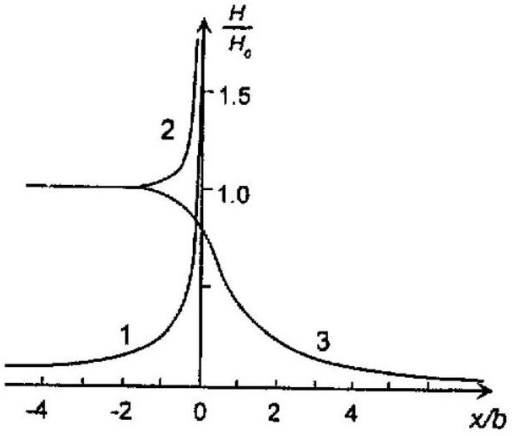


Fig. 2.7. Magnetic field distribution near the edge of a current-carrying superconducting film placed in the vicinity of a superconducting screen: 1 - field at the upper surface of the film; 2field at the lower surface of the screen; 3 - field at the surface of the screen

Consider a thick superconducting film (of thickness $d \geq \lambda$) of width w and length l deposited onto a glass substrate; $w \ll \lambda$. The film has been covered with a thin insulating layer of thickness b, such that $b \ll w$, and then another superconducting film has been deposited on top, also of thickness w and of length well in excess of l. Then a current from an external source is applied to the upper superconducting film. It is easy to realize that the

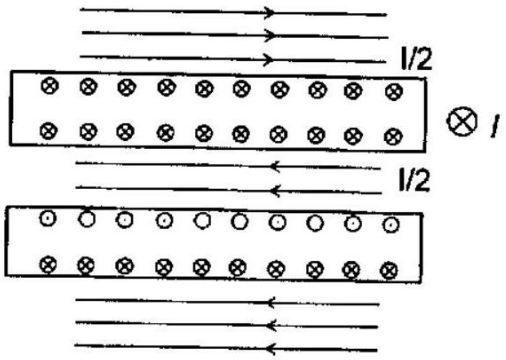


Fig. 2.8. Field and current distributions for two parallel closely spaced films. A current I is applied to the upper film. The lower film is not supplied with current
lower film cannot produce any screening effect in this situation. Indeed, if the upper film carries a certain current I, this current generates a magnetic field in the gap between the films. This means that the currents at the lower surface of the upper film and at the upper surface of the lower film must be equal in value. Furthermore, because the length of the lower film is finite, the current at its upper surface has to close at its lower surface, as in Fig. 2.8. As a result, the magnetic field at this surface is exactly the same as that in the gap between the films. Moreover, the current in the upper film is now split equally between its upper and lower surfaces, as illustrated in Fig. 2.8. Thus, the magnetic fields above and below the pair of films

and in the gap are exactly the same as those in the absence of the lower film. That is, the

2.5.5 Short-Circuit Principle

Quite often in modern superconducting electronics, when complex multilayer systems are being designed, it can be rather difficult to have an instant grasp of how the magnetic fields and electric currents will be distributed in such a system. Great help can be provided here by the so-called short-circuit principle [20]. It can be applied to thick films, of thicknesses larger than the penetration depth, provided their widths and lengths are well in excess of the distances between the films.

Consider two superconducting films separated by an insulating layer. If the films carry electric currents, the currents along the neighboring surfaces must be equal in value and opposite in direction. Indeed, the surface current is determined by the magnetic field at the surface of a superconductor, and the magnetic field in the gap between the two films is common to both of them. If the thickness of the insulating layer is small, the magnetic flux through this layer is also small and the magnetic field at the edges of the films, associated with this flux, is negligible. Hence we can ignore the magnetic field at the edges and argue that the other parts of the films 'are not aware' of the existence of this flux and 'will not notice' if it disappears. And it can disappear as a result of short-circuiting, that is, bringing into contact two neighboring superconducting surfaces carrying electric currents that are equal in value and opposite in direction.

We can now formulate the short-circuit principle [20]: In a complex system of superconducting films, if two neighboring film surfaces are short-circuited, it will not affect the current distribution in any other part of the system other than the two short-circuited surfaces.

Consider several examples illustrating this principle.

(1) Let us find the distribution of currents in two parallel and identical thick films separated by a thin gap. The first film carries a current I_1 and the second one carries a current I_2, in the same direction. The two films are short-circuited. As a result, we have one film carrying a total current $I_1 + I_2$ distributed uniformly over the outer surfaces of the short-circuited films. Thus, the current at each of those surfaces is $(I_1 + I_2)/2$. We now know the currents at the outer surfaces of our system of films. Let i denote the current at the inner surfaces of the films. Because the total current in the first film, I_1, is fixed, we have $(I_1 + I_2)/2 + i = I_1$, i.e., $i = (I_1 - I_2)/2$. All surface currents in our system are now defined.

Note that if $I_2 = 0$, we come straight to the result shown in Fig. 2.8, that is, to the absence of screening by a superconducting film.

(2) If an insulated current-carrying wire is covered with a superconducting sheath, the latter will not be capable of screening the magnetic field generated by the current in the wire. To elucidate this statement, let us short-circuit the inner surface of the sheath and the surface of the wire. Then the entire current from the wire flows at the outer surface of the sheath and generates

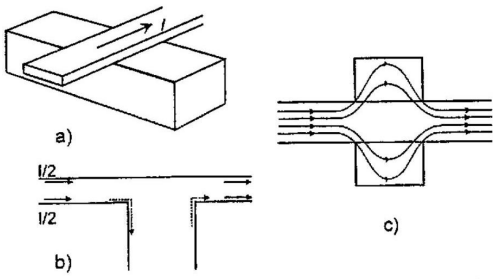


Fig. 2.9. Current-carrying film separated from the flat surface of a bulk superconductor by a thin gap: (a) general view; (b) side view after short-circuiting; (c) top view

(3) Let us find the distribution of currents in a system consisting of a thick superconducting

film carrying a current which is placed above a massive superconducting bar (see Fig. 2.9). If the lower surface of the film and the upper surface of the bar are short-circuited, the resulting distribution of currents is that sketched in Fig. 2.9 (b). Indeed, at first the current from the film spreads over the upper surface of the bar, but a small fraction of it goes around the bar, along its lower surface. As a result, the current density at the upper surface of the film decreases sharply. Taking this into account, one can argue that in the initial system, without the short-circuit, the current in the part of the film immediately above the bar flows predominantly at the lower surface of the film. A current of the same value and opposite in direction must then appear at the upper surface of the bar, in the part situated immediately below the film. Further, this current spreads over the upper surface of the bar and closes there, while a small fraction of it closes over a path around the bar.

One can conclude that the role of the bar in this system approaches the role of the semi-infinite screen (see Fig. 2.7).

7.4.2 2.6 Kinetic Inductance

The inductance of a section of an electric circuit is usually defined by the energy $\mathcal{F}^{\mathrm{M}}$ of the magnetic field generated by a current I through the circuit:

$$\mathcal{F}^{\mathrm{M}} = \frac{1}{8\pi}\int H^2 \,\mathrm{d}V = \frac{1}{2c^2}L^{\mathrm{M}}I^2 \tag{2.45}$$

The integral is taken over the entire space. We shall refer to this inductance as
the current I in the circuit requires a part of the energy to be converted into the kinetic energy $\mathcal{F}^{\mathrm{K}}$ of the current carriers (electrons). With this part of the energy can be associated the so-called kinetic inductance L^{K};

$$\mathcal{F}^{\mathrm{K}} = \int n\frac{mv^2}{2} \,\mathrm{d}V = \frac{1}{2c^2}L^{\mathrm{K}}I^2 \tag{2.46}$$

where n is the number density of the current carriers, m is the mass of one carrier and v is the velocity. The integration is carried out over the volume of the conductor.

If the section of the circuit is normal, the contribution of the kinetic inductance to the total resistivity is very small compared to its active resistivity and usually neglected. The contribution of the kinetic inductance in normal conductors can only be significant at very high frequencies (over 10^{13} Hz). In superconductors, however, the kinetic inductance sometimes plays an important role.

Recall that the supercurrent density is $j_{\mathrm{s}} = n_{\mathrm{s}}\boldsymbol{e}\boldsymbol{v}_{\mathrm{s}}$. Then, from (2.46), we obtain the following definition of the kinetic inductance of a superconductor:

$$L^{\mathrm{K}} = c^2\Lambda\int \frac{j_8^2}{I^2} \,\mathrm{d}V \tag{2.47}$$

where the integral is taken over the volume of the superconductor and I is the total current through the superconductor.

Let us illustrate the concept of kinetic inductance with specific examples.
(1) Consider a superconducting wire of length l and radius R. Assume that $R \gg \lambda$. If the wire carries a current I, this current must circulate near its surface. The current density j_{s} at a distance r from the center of the wire is $j_\varepsilon(x) = j_{30}\mathrm{e}^{-x/\lambda}$, where $x = R - r, j_{80} = j_8(0)$. The total current is $I = 2\pi R\lambda j_{50}$. Substituting these into (2.47) and carrying out the integration, we get $L^{\mathrm{K}} = l\lambda/R$.

Let us now introduce another quantity which is particularly useful in many applications: the inductance per square $L_\square$. For a flat superconductor, the greater its length, the larger

its inductance and resistivity. Furthermore, the greater its width, the smaller the inductance. Therefore, the inductance of a square is always the same for a given superconductor, whether one considers 1 km^2 or 1 mm^2 of it. For our wire, since the circumference of the cross-section is $2\pi R$, the kinetic inductance per square is

$$L_{\rm O}^{\rm K} = 2\pi\lambda. \tag{2.48}$$

If we use (2.45) and calculate the part of the magnetic inductance associated with the magnetic field penetrating the superconductor (more accurately, penetrating the layer of the order λ near the surface) we obtain the same result:

$$L_{\square}^{\rm M} = 2\pi\lambda. \tag{2.49}$$

The total inductance per square of the layer λ at the surface of a bulk superconductor is equal to the sum of (2.48) and (2.49):

$$L_{\square} = 4\pi\lambda \tag{2.50}$$

In the International System of Units (SI), equation (2.50) takes the form: $L_{\square} = \mu_0\lambda$, with $\mu_0 = 4\pi \times 10^{-7}{\rm H}/m$. As follows from (2.48-50), in CGS $L_{\square}$ is measured in cm, and in SI in H, where 1 cm corresponds to $10^{-9}{\rm H} = 1{\rm nH}$.

One can say that λ is a characteristic of the inertia of the current carriers since, for a semispace, $L_{\square}^{\rm K}$ depends only on the penetration depth. If $\lambda \approx 5 \times 10^{-6}$ cm, then $L_{\square} = 4\pi\lambda = 6.3 \times 10^{-5}$ cm $= 6.3 \times 10^{-14}$H.

(2) Consider the kinetic inductance of a thin superconducting film. Assume that the thickness of the film is $d \ll \lambda$ and, therefore, the current in the film is distributed uniformly over its thickness. We shall consider a small section of width w along the width of the film and assume that the current there is also uniform. Restricting the length of the section to the same value w, we obtain for the kinetic energy of the superconducting electrons within this section:

$$\mathcal{F}_{\square}^{\rm K} = \frac{\Lambda}{2} j_{\rm s}^2 w^2 d$$

Recalling that the current I through the cross-section is assumed to be uniform, we have $j_{\rm s} = I/wd$ and

$$\mathcal{F}_{\rm O}^{\rm K} = \frac{1}{2d} A I^2 = \frac{1}{2d}\frac{4\pi\lambda^2}{c^2} I^2 = \frac{1}{2c^2} L_{\rm O}^{\rm K} I^2.$$

From the last expression we immediately obtain $L_{\rm O}^{\rm K}$ for a thin film:

$$L_{\square}^{\rm K} = 4\pi\lambda^2/d \tag{2.51}$$

Now it is obvious that, for $d \ll \lambda$, the kinetic inductance can be significant. For example, for a thin film ($d \sim 10^{-6}$ cm) with the penetration depth $\lambda = 3 \times 10^{-5}$ cm, the kinetic inductance per square is, according to (2.51), $L_{\square}^{\rm K} \approx 10^{-2}$ cm $= 10^{-11}$H.

(3) Finally, consider a thick film above a massive superconducting screen. Assume that the distance between the film and the surface of the screen is b. If the film carries a current, there must be a magnetic field present in the gap between the film and the screen. After calculating the energy of this magnetic field, we find its contribution to the inductance of the film $L_{\square} = 4\pi b$. In addition, the magnetic field penetrates the film to the depth λ_1 and the screen to the depth λ_2. This penetrating field, from (2.50), makes an additional contribution to the inductance of the system as a whole so that its total inductance is

$$L_{\square} = 4\pi\left(b + \lambda_1 + \lambda_2\right). \tag{2.52}$$

One can see from (2.52) that, in order to reduce the inductance, the film should be placed as close to the screen as possible. However, making b sub-
and the kinetic inductance will remain within a layer of the order of the penetration depth, in the film as well as in the screen.

7.4.3 2.7 Complex Conductivity of a Superconductor

This section deals with the complex conductivity of a superconductor in an electromagnetic field. In what follows we assume that the electron mean free path l is small and, therefore, that the normal skin effect approximation is valid. In other words, l is small enough and the frequencies are low enough that l is less than the penetration depth of the electromagnetic field. The frequency of electron collisions is $\tau^{-1} = v_{\mathrm{F}}/l \gg \omega$, where ω is the frequency of the electromagnetic wave and v_F is the electron velocity on the Fermi surface.

In the following analysis we shall partly follow the monograph by Van Duzer and Turner [21].

In order to calculate the conductivity of a superconductor in a highfrequency field, we use the two-fluid model, that is, we assume that there are normal electrons of density n_{n} and superconducting electrons of density n_{s}, and the total density of conduction electrons is $n = n_{\mathrm{s}} + n_{\mathrm{n}}$. The motion of the superconducting electrons is governed by the first London equation (2.2):

$$E = \Lambda \mathrm{d}j_s/\mathrm{d}t \tag{2.53}$$

For the normal electrons we can write

$$eE - \frac{m}{n_{\mathrm{n}}e} j_{\mathrm{n}}^{\tau} = \frac{m}{n_{\mathrm{n}}e} \frac{\mathrm{d}j_{\mathrm{n}}}{\mathrm{d}t} \tag{2.54}$$

The left-hand side of (2.54) describes the forces on the normal electrons: the electric field and the average 'friction' due to electron collisions. The righthand side is the product of the electron mass and acceleration. For one normal electron, this Newton's second law can be written as

$$E = \frac{n_{\mathrm{s}}}{n_{\mathrm{n}}} \Lambda \frac{\mathrm{d}j_{\mathrm{n}}}{\mathrm{d}t} + \frac{n_{\mathrm{s}}}{n_{\mathrm{n}}} \Lambda \frac{j_{\mathrm{n}}}{\tau} \tag{2.55}$$

Assuming $j_s \propto \mathrm{e}^{\mathrm{i}\omega t}$, we can rewrite (2.53) and (2.55) as

$$j_s = -\mathrm{i} \frac{1}{A\omega} E \tag{2.56}$$

$$j_{\mathrm{n}} = \frac{n_{\mathrm{n}}}{n_{\mathrm{s}}} \frac{\tau}{A} \frac{1 - \mathrm{i}\omega\tau}{1 + (\omega\tau)^2} E \tag{2.57}$$

The total current density is $j = j_8 + j_{\mathrm{n}}$, and we finally have

$$j = \sigma E, \quad \sigma = \sigma_1 - \mathrm{i}\sigma_2 \tag{2.58}$$

$$\sigma_2 = \frac{1}{\lambda\omega} \left[1 + \frac{n_{\mathrm{n}}}{n_{\mathrm{B}}} \frac{(\omega\tau)^2}{1 + (\omega\tau)^2} \right] \tag{2.60}$$

Equations (2.58-60) describe the complex conductivity of a superconductor in a high-frequency electromagnetic field.

7.4.4 2.8 Skin Effect and Surface Impedance

2.8.1 Normal Skin Effect

It is well known that an electromagnetic field penetrates a normal metal to the so-called skin depth, or to the depth of a skin layer. In this section we shall consider how the field penetrates a superconductor. The surface of the superconductor coincides with the plane $x = 0$.

Let us write down Maxwell's equations

$$\operatorname{curl} \boldsymbol{H} = \frac{4\pi}{c}\sigma \boldsymbol{E}, \tag{2.61}$$

$$\operatorname{curl} \boldsymbol{E} = -\frac{1}{c}\frac{\partial \boldsymbol{H}}{\partial t}. \tag{2.62}$$

Assuming that the magnetic field in the superconductor is $\boldsymbol{H} \propto \mathrm{e}^{-\mathrm{i}(kx-\omega t)}$ and taking the curl of both sides of (2.61), we get

$$-\nabla^2 \boldsymbol{H} = -\frac{4\pi}{c}\sigma\frac{\partial \boldsymbol{H}}{\partial t}. \tag{2.63}$$

Here we have used the equations $\operatorname{div} \boldsymbol{H} = 0$ and $\operatorname{curl}\operatorname{curl} \boldsymbol{H} = -\nabla^2 \boldsymbol{H}$. Substituting $H \propto \mathrm{e}^{-\mathrm{i}(kx-\omega t)}$ in (2.63), we obtain

$$k^2 = -\mathrm{i}\frac{4\pi}{c^2}\sigma\omega \tag{2.64}$$

and

$$k = (1-\mathrm{i})/\delta \tag{2.65}$$

where

$$\delta = \left(\frac{c^2}{2\pi\sigma\omega}\right)^{1/2} \tag{2.66}$$

Our problem is now essentially solved. Indeed, the field penetration is defined by the quantity k which can be expressed through the conductivity σ using (2.65) and (2.66). Let us make some simplifications. Assume that the temperature is not too close to T_c so that $(n_\mathrm{n}/n_\mathrm{s})\,(\omega\tau)^2 \ll 1$. In addition, we assume, as always, that $\omega\tau \ll 1$. Then we obtain from (2.59) and (2.60)

Substituting (2.67) into (2.66), we get

$$\delta = \frac{\sqrt{2}\lambda}{\left(\frac{n_\mathrm{n}}{n_\mathrm{k}}\omega\tau - \mathrm{i}\right)^{1/2}} \tag{2.68}$$

At low frequencies, when $(n_\mathrm{n}/n_s)\,(\omega\tau) \ll 1$, we have $\delta = \sqrt{2}\mathrm{i}\lambda = \lambda(1+\mathrm{i})$. Substituting this into (2.65), we obtain $k = -\mathrm{i}/\lambda$, i.e., $H \propto \mathrm{e}^{-\mathrm{i}kx} = \mathrm{e}^{-x/\lambda}$. Thus, as one should have expected, a low-frequency magnetic field penetrates a superconductor in the same manner as a dc field, that is, it is exponentially damped over the magnetic field penetration depth. In the general case, the field penetration is described by (2.65) and (2.68).

2.8.2 Surface Impedance

By definition, the surface impedance is

$$Z = \frac{4\pi}{c}\frac{E}{H} \tag{2.69}$$

This expression has a clear physical meaning. Suppose that there are ac electric and magnetic fields at the surface of a metal, such that the vectors $\boldsymbol{E}$ and $\boldsymbol{H}$ are mutually orthogonal and tangential to the surface. Then $c\boldsymbol{H}/4\pi$ is the density of the surface current j_{surf} and, therefore, Z in (2.69) is E/j_{surf} , that is, it expresses the surface impedance per square.

Let us now work out the surface impedance of a superconductor. With the magnetic field written as $\boldsymbol{H} \propto \mathrm{e}^{-\mathrm{i}(kx-\omega t)}$, equation (2.61) becomes

$$\mathrm{i}kH = \frac{4\pi}{c}\sigma E \tag{2.70}$$

Then from (2.69) and (2.65) we have

$$Z\frac{\mathrm{i}k}{\sigma} = \frac{1+\mathrm{i}}{\sigma\delta} \tag{2.71}$$

Substituting (2.66) and (2.67) into (2.71), we get

$$Z = R_{\square} + \mathrm{i}X_{L\square} \tag{2.72}$$

$$R_{\square} = \frac{2\pi\omega^2\lambda}{c^2}\frac{n_{\text{n}}}{n_{\text{s}}}\tau \tag{2.73}$$

$$X_{L\square} = \frac{4\pi\lambda\omega}{c^2} = \frac{\omega L_{\square}}{c^2} \tag{2.74}$$

The real part of the impedance, $R_{\square}$, reflects the energy dissipation due to heating, while the imaginary part, $X_{L\square}$, is the inductive resistance.

Let us find the temperature dependences of $R_{\square}$ and $X_{L\square}$. Recalling the

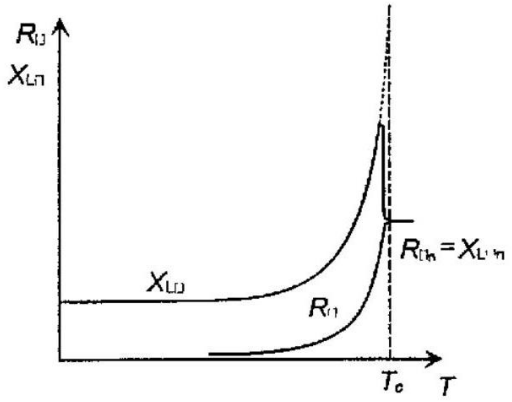


Fig. 2.10. Real and imaginary parts of the surface impedance as functions of temperature [22]

because $\lambda \propto {n_{\text{s}}}^{-1/2}$. Here $t = T/T_{\text{c}}$ and n is the density of free electrons in a metal. Then $n_{\text{n}} = nt^4$ and

$$R_{\square} \propto t^4/\left(1-t^4\right)^{3/2}, \quad X_{L\square} \propto \left(1-t^4\right)^{-1/2} \tag{2.75}$$

The above formulas reproduce the temperature dependences of both active and imaginary components of the impedance rather well (at least qualitatively), with an exception of temperatures close to T_{c}. In this temperature interval, (2.73) and (2.74) are no longer valid.

Recall that, while deriving these formulas, we used (2.67) obtained on the assumption that $(n_n/n_\varepsilon)(\omega\tau)^2 \ll 1$. But no matter how low the frequency is, the superconducting electron density at $T \to T_c$ is $n_s \to 0$ and the inequality is violated. Therefore, at $T \to T_c$ we have from (2.60): $\sigma = (n_n/n_s)\tau/\Lambda - i(n_n/n_s)(\omega\tau)^2/\Lambda\omega$. Neglecting the imaginary part and substituting this expression in (2.65) and (2.71) we obtain

$$Z = \frac{2\pi}{c^2}\left(2\omega\tau\frac{n_s}{n_n}\right)^{1/2}\frac{\lambda}{\tau}(1+i) = \frac{1+i}{\sigma_n\delta_n} \tag{2.76}$$

where σ_n and δ_n are the conductivity and the skin depth of the normal metal, respectively.

It follows from (2.76) that, at $T^\top \to T_c$, $R_\square$ and $X_{L\square}$ are equal in value and independent of temperature, since ${n_s}^{1/2}\lambda = \text{const}$.

The temperature dependences of $R_\square$ and $X_{L\square}$ obtained within the twofluid model are sketched in Fig. 2.10.

As far as high-temperature superconductors are concerned, many experiments indicate that they do not have a 'clean' gap. This means that even at zero temperature they have an intrinsic density of quasiparticle states in the gap down to zero energy. As a consequence, the temperature dependences of the two-fluid model are no longer valid for high- T_c materials.

Problems

Problem 2.1. Consider a bulk superconductor containing a cylindrical hole of 0.1 mm diameter. There are 7 magnetic flux quanta tra ped in the hole. Find the

Problem 2.2. Consider a bulk superconductor containing a cylindrical hole of 2 cm diameter. The magnetic field trapped in the hole is $H = 300$ Oe. Find the vector potential A at the distance $R = 2$ cm from the center of the hole. Find the phase gradient $\nabla\theta$ at the same distance.

Problem 2.3. Consider a thin superconducting film of thickness $d \ll \lambda$ deposited onto a dielectric fllament. The radius of the filament's cross-section is R. At room temperature, the filament is placed in a longitudinal magnetic field and then cooled down to a temperature below T_c. Then the external field is switched off. Find how the magnetic flux trapped by the filament is quantized.

Problem 2.4. Find the distribution of the magnetic field under the conditions of the previous problem.

7.5 Other Bulk Effects in Electromagnetic Field

7.5.1 Superconductors in a Weak Electromagnetic Field by AGD

(??????????????????)

1. Constant weak magnetic field

Let us return to the question of the electromagnetic properties of superconductors. We shall confine ourselves in this section to the behaviour of superconductors in fairly weak fields, which are small compared with the critical magnetic field. Suppose that a superconductor with a plane surface occupies the half-space $z < 0$ as illustrated in Fig. 99, and is located in a constant magnetic field, directed parallel to its surface. We introduce the vector potential A:

$$H = \text{curl}\, A.$$

In vacuo $\boldsymbol{H}$ = const and we can take the vector potential as, say,

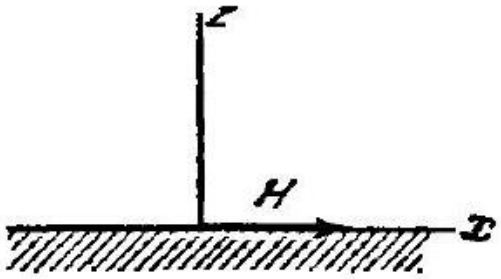


Fig. 99

$$A_y = -Hz, \quad A_x = A_z = 0 \tag{37.1}$$

Current is produced in the superconductor under the action of the magnetie field; the field distribution in the superconductor is subject to Maxwell's equation

$$\nabla^2 A = -4\pi j \tag{37.2}$$

Since the current density is in turn due to the presence of the field, it will be proportional to A in a linear approximation with respect to the field. It follows from uniformity considerations that, in an infinite superconductor, the connection of the current density with the ficld must in general be of the form

$$j(x) = -\int Q(x-y)A(y)\mathrm{d}^4 y \tag{37.3}$$

or in Fourier components:

$$j(k) = -Q(k)A(k) \tag{/}$$

We shall not dwcll in detail below on the solution of the actual electromagnetic problem as defined by (37.2), (37.3) for the half-space, but confine ourselves to deriving an expression for the kernel $Q(x-y)$, with a view to demonstrating the application of quantum field theory methods to this case.

As usual, the current density $\boldsymbol{j}$ at a given point is the thermodynamic average of the familiar quantum mechanical expression for the current operator $\boldsymbol{j}(x)$ in sccond quantisation:

$$j(x) = \frac{ie}{2m}\left(\nabla_{r'} - \nabla_r\right)_{r'\to r} \tilde{\psi}\,(x')\,\tilde{\psi}(x) - \frac{e^2 A(x)}{m}\tilde{\tilde{\psi}}(x)\tilde{\psi}(x) \tag{37.4}$$

The current density $\boldsymbol{j}(x)$ can thus be written directly in terms of the Green function of the system (we have put $c = 1$):

$$j(x) = 2\left\{\frac{ie}{2m}\left(\nabla_{r'} - \nabla_r\right)\circlearrowleft(x,x') - \frac{e^2 A(x)}{m}\circlearrowleft(x,x')\right\}_{r'\to r, z'=\tau+0} \tag{37.5}$$

We proceed to finding the Green function, or more precisely, the correction to the Green function of first order in the field. In a constant magnetic field all the Green functions $\mathfrak{G}, \mathfrak{F}$, and $\mathfrak{F}^+$depend only on the difference of the "time" coordinates $\tau = \tau_1 - \tau_2$. We change to the Fourier components $\mathfrak{K}_\omega$ and $\mathfrak{F}_\omega$. The system of equations for these latter reads as follows in a constant magnetic field:

$$\left\{ i\omega + \frac{1}{2m}\left(\frac{\partial}{\partial \boldsymbol{r}} - ieA(\boldsymbol{r})\right)^2 + \mu \right\} \mathfrak{G}_\omega(\boldsymbol{r}, \boldsymbol{r}') + \Delta(\boldsymbol{r})\mathfrak{F}^+_\omega(\boldsymbol{r}, \boldsymbol{r}') = \delta(\boldsymbol{r} - \boldsymbol{r}'),$$
$$\left\{ -i\omega + \frac{1}{2m}\left(\frac{\partial}{\partial \boldsymbol{r}} + ieA(\boldsymbol{r})\right)^2 + \mu \right\} \mathfrak{F}^+_\omega(\boldsymbol{r}, \boldsymbol{r}') - \Delta^*(\boldsymbol{r})\mathfrak{G}_\omega(\boldsymbol{r}, \boldsymbol{r}') = 0. \tag{37.6}$$

We write the Green functions $\mathfrak{G}$ and $\mathfrak{F}^+$as

$$\mathfrak{G} = \mathfrak{G}_0 + \mathfrak{G}^{(1)}; \quad \mathfrak{F} = \mathfrak{F}_0 + \mathfrak{F}^{(1)}; \quad \mathfrak{F}^+ = \mathfrak{F}^+_0 + \mathfrak{F}^{+(1)},$$

where $\mathfrak{G}_0, {}_0, \mathfrak{F}^+_0$are the Green functions in the absence of a field, and $\mathfrak{G}^{(1)}, \mathfrak{F}^{(1)}, \mathfrak{F}^{+(1)}$ are the added terms, linear in the field. We obtain on linearising equations (37.6):

$$\begin{aligned}
&\left\{ i\omega + \frac{\nabla^2}{2m} + \mu \right\} \mathfrak{G}^{(1)}_\omega(r, r') + \Delta_0 \mathfrak{F}^{+(1)}_\omega(r, r') \\
&\quad = -\Delta^{(1)}(r)\mathfrak{F}^+_{0\omega}(r - r') + \frac{ie}{2m}[(\nabla \cdot A) + (A \cdot \nabla)]\mathfrak{G}_{0\omega}(r - r') \\
&\left\{ -i\omega + \frac{\nabla^2}{2m} + \mu \right\} \mathfrak{F}^{+(1)}_\omega(r, r') - \Delta_0 \mathfrak{G}^{(1)}_\omega(r, r') \\
&\quad = \Delta^{*(1)}(r)\mathfrak{G}_{0\omega}(r - r') - \frac{ie}{2m}[(\nabla \cdot A) + (A \cdot \nabla)]\mathfrak{F}^+_{0\omega}(r - r')
\end{aligned} \tag{37.7}$$

Using these equations, we can very easily express $\mathfrak{W}^{(1)}_\omega(r, r')$ and $\mathfrak{F}^{+(1)}_\omega(r, r')$ in terms of the quantities on the right-hand sides of (37.7). This is best done by using expression (34.32) for the inverse operator to the left-hand sides of (37.7). Before writing down to result for $\mathfrak{G}^{(1)}_\omega(r, r')$, however, let us consider in more detail the structure of equations (37.7),

System (37.6) and hence (37.7) also are gauge-invariant, i.e. are invariant with respect to the transformations (34.26) and (34.27). Thus when finding the current $\boldsymbol{j}(\boldsymbol{r})$, which is equal in the linear approximation to

$$j(r) = \frac{ie}{m} T \sum_\omega (\nabla_{r'} - \nabla_r)_{r' \to r} \mathfrak{G}^{(1)}_\omega(r, r') - \frac{e^2 A(r) N}{m} \tag{37.8}$$

the final result can depend only on the transverse part of the vector potential A. In other words, the addition to A of the gradient of any scalar $\varphi : A \to A + \partial\varphi/\partial r$ cannot change the current $j(r)$.

As regards $\mathfrak{G}^{(1)}_\omega(r, r'), \mathfrak{F}^{+(1)}_\omega(r, r')$, by (34.27), they are by no means invariant with respect to a change of the vector potential. The same
applies to $\Delta^{(1)}(r), \Delta^{*(1)}(r)$, which appear on the right-hand sides of (37.7) and must themselves be determined from the integral equation

$$\Delta^{*(1)}(r) = |\lambda| T \sum_\omega \mathfrak{F}^{+(1)}_\omega(r, r')$$

Given any $A(r), \Delta(r)$ is in general an unknown function of the potential A. It can nevertheless be asserted that, in the linear approximation with respect to the field, by virtue of the uniformity of the problem, the function $\Delta^{*(1)}(r)$, being a scalar, depends only on div A. Owing to this fact, if we choose our gauge such that the vector potential $\boldsymbol{A(r)}$ satisfies the equation

$$\operatorname{div} A = 0$$

it proves possible to simplify the problem considerably, inasmuch as, with this choice of $A(r)$, the function $\Lambda^{*(1)}(r)$ vanishes identically. The result obtained below refers only to a purely "transverse" vector potential $\boldsymbol{A}(r)$.

The method described for making $\Delta^{*(1)}, \Delta^{(1)}$ vanish can be extended in such a way as to make it usable in problems that do not have spatial uniformity in the absence of a field (say superconductors of finite dimensions in a magnetic field). In these cases it is possible to form a scalar from the field $A(r)$ and the vector r or any other vector characterising the problem. In the general case of the non-uniform problem, therefore, the $\Delta^{(1)}(r), \Delta^{*(1)}(r)$ in equations (37.7) (where we now have to understand by $\mathfrak{G}_0$ and $\mathfrak{F}_0$ the Green functions of the body in question with the relevant boundary conditions) depend both on the longitudinal and on the transverse components of the vector $A(r)$. It is always possible, however, to choose the longitudinal part $A_{\text{long}} = \operatorname{grad}\varphi$ in such a way that $\Delta^{(1)}, \Delta^{*(1)}$ vanish. As regards the function φ, for which this condition is fulfilled, it can be found from the condition $\operatorname{div} \boldsymbol{j} = 0$, i.e. from the condition for charge conservation.

Let us now return to equations (37.7) for an infinite superconductor. Putting $\Delta^{(1)}(r) = 0$ and using (34.32), we obtain the following expression for the correction, linear in the field, to the Green function:

$$\mathfrak{G}_{\omega}^{(1)}(r, r') = \frac{ie}{m} \int \{\mathfrak{G}_{0\omega}(r-l)\,(A(l)\cdot\nabla_l)\,\mathfrak{G}_{0\omega}(l-r') + \mathfrak{F}_{0\omega}(l-r)\,(A(l)\cdot\nabla_l)\,\mathfrak{F}_{0\omega}^{+}(r'-l)\}\,\mathrm{d}^3 l \tag{37.9}$$

We have already made use of the condition $\operatorname{div} A = 0$ in this formula, so that it can be assumed that the differentiation in brackets $(A(l)\cdot\nabla)$ refers only to the functions $\mathfrak{G}_{0\omega}(\boldsymbol{l}-\boldsymbol{r'})$ and $\mathfrak{F}_{0\omega}^{+}(\boldsymbol{r'}-\boldsymbol{l})$. By (37.8), the current density $\boldsymbol{j}(\boldsymbol{r})$ is equal to

$$j(r) = \frac{e^2}{m^2} T \sum_{\omega} (\nabla_r - \nabla_{r'}) \int \{\mathfrak{G}_{0\omega}(r-l)\,(A(l)\cdot\nabla_l)\,\mathfrak{G}_{0\omega}(l-r') + \mathfrak{W}_{0\omega}(l-r)\,(A(l)\cdot\nabla_l)\,\mathfrak{F}_{0\omega}^{+}(r'-l)\}_{r'\to r}\,\mathrm{d}^3 l - \frac{Ne^2}{m} A(r) \tag{37.10}$$

It is convenient here to change to the Fourier transforms, introducing the Fourier components for the current density $j(r)$ and the potential $\boldsymbol{A}(\boldsymbol{r})$ in the usual way:

$$j(r) = \frac{1}{(2\pi)^3} \int j(k) e^{i(k-r)} \mathrm{d}^3 k; \quad A(r) = \frac{1}{(2\pi)^3} \int A(k) e^{i(k\cdot r)} \mathrm{d}^3 k$$

The equation for the connection between the components $\boldsymbol{j}(\boldsymbol{k})$ and $\boldsymbol{A}(\boldsymbol{k})$ is as follows:

$$j(k) = -\frac{2e^2 T}{(2\pi)^3} \overline{m^2} \frac{\Sigma}{\omega} \int p! p \cdot A(k) \Big) \{\mathfrak{G}_{\omega}(p_+)\,\mathfrak{G}_{\omega}(p_-) + \mathfrak{F}_{\omega}(p_+)\,\mathfrak{F}_{\omega}^{+}(p_-)\}\,\mathrm{d}^3 p - \frac{Ne^2}{m} A(k) \tag{37.11}$$

where $p_{\pm} = p \pm 1/2k$. Let us emphasise again that our result refers only to the purely transverse gauge. (It can be shown, however, that the formulae obtained remain in force for any gauge, i.e. the longitudinal part falls out from the final result.)

The field $A(r)$ and current $j(r)$ in a superconductor vary at distances of the order of the penetration depth δ, which is usually of the order $\sim 10^{-5}$ to 10^{-6} cm (i.e. at distances much greater than atomic distances). Hence only the components $\boldsymbol{j}(\boldsymbol{k})$ and $\boldsymbol{A}(\boldsymbol{k})$ in the range $k \sim$

$1/\delta \ll p_0$ are important in (37.11). We shall see below that the integration in the kernel (37.11) is performed essentially close to the Fermi surface over a narrow range of values of $|\boldsymbol{p}|$ of the order $||\boldsymbol{p}! - p_0| \sim| \boldsymbol{k} |$. Further, only the two vectors k and $A(k)$ figure in (37.11), and $(k \cdot A) = 0$. On choosing the vector k as the polar axis of coordinates for the variable of integration p and carrying out the averaging over the angle in the azimuthal plane, we find at once that the vector $\boldsymbol{j}(\boldsymbol{k})$ is directed along the vector $A(k)$. In view of what has bcen said above, on substituting expressions (34.35) for the functions (% and $\mathfrak{F}$, we get

$$j(k) = -\frac{Ne^2}{m} Q(k) A(k)$$

where

$$\bar{Q}(k) = 1 + \frac{3T}{4} \sum_{\omega} \int_0^{\pi} \sin^3 0 \, \mathrm{d}\theta \int_{-\infty}^{+\infty} \mathrm{d}\xi \frac{(i\omega + \xi_+)(i\omega + \xi_-) + \Delta^2}{[\omega^2 + \xi_+^2 + 1^2][\omega^2 + \xi_-^2 + \Delta^2]} \tag{37.12}$$

(we have used here the fact that $p_0^3/3\pi^2 = N$). For small $k, \xi_{\pm} = \xi \pm \frac{1}{2}(v \cdot k)$.
It must be borne in mind for future calculations that, for large ω and ξ, the integrand on the right-hand side of (37.12) behaves like ω^{-2} when $\omega \gg \xi$ and like ξ^{-2} when $\xi \gg \omega$. Strictly speaking, therefore, the integral over ξ and sum over the frequencies ω are divergent. To understand the esscuce of the matter, we consider the singularities of the expression for a normal metal (i.e. when $\Delta = 0$):

$$\frac{3}{4} T \sum_{\omega} \int \mathrm{d}\xi \int_0^{\pi} \sin^3 \theta \, \mathrm{d}\theta \frac{1}{(i\omega - \xi_+)(i\omega - \xi_-)}. \tag{37.13}$$

Notice, first of all, that an unusually important role is played in this integral by the order in which we carry out the summation over the frequencies and the integration over ξ. For, if we first integrate over ξ, the poles of the integrand, whatever the sign of ω, lic to one side of the real axis, so that the result is equal to zero. Suppose, now, that we first sum over the frequencics $\omega = (2n+1)\pi T$. It is easily shown that the following is obtained as a result of summation of this simple series:

$$\frac{3}{8} \int_0^{\pi} \sin^3 \theta \, \mathrm{d}\theta \int \frac{\mathrm{d}\xi}{(v \cdot k)} \left[\tanh \frac{\xi_-}{2T} - \tanh \frac{\xi_+}{2T} \right| = -1 \tag{37.14}$$

The reason why the final result changes on interchanging the order of the summation and integration is to be traced to the formal divergence of the entire expression. The essence of the matter is clearly, however, that the result when we first sum over the frequencies only differs from zero in a very narrow range of energies close to the Fermi surface (this region has a width $\sim (\boldsymbol{v} \cdot \boldsymbol{k})$, as follows from (37.14)). In this region the integral over the momentum proves to be rapidly convergent, and the expression for the excitation energy, measured from the Fermi surface, can be written approximately as $\xi = (\boldsymbol{p}^2 - p_0^2)/2m \simeq v(|\boldsymbol{p}| - p_0)$. It is for this reason that, in integrals of the type in question, we must first sum over the frequencies and then carry out the integration over ξ: otherwise, the integration over ξ embraces the domain $||p| - p_0| \sim p_0$, where our expansion of the functions about the Fermi surface becomes unsuitable.

However, it is possible to avoid the need for carrying out the fairly complicated summation over the frequencies in (37.12). We have to proceed as follows. We add to and subtract from the integrand of (37.12) the corresponding expression (37.13) for a normal metal. The integral and sum over the frequencies of the difference of the integrands is now rapidly convergent, as a result of which we can change the order of integration and summation. The relevant expression for the normal metal was evaluated in (37.14); it cancels the unity in (37.12). Integration over ξ gives us

$$Q(k) = \frac{3\pi T}{4} \sum_{\omega} \int_{-1}^{+1} \frac{(1-\beta^2)\,\mathrm{d}\beta}{\sqrt{\omega^2+\Delta^2}} \cdot \frac{1^2}{\omega^2+\Delta^2+\frac{1}{4}v^2|k|^2\beta^2}. \tag{37.15}$$

Further transformation of this kernel is difficult unless some assumptions are made about $|\boldsymbol{k}|$. It is clear from the structure of the integrand that
it is only the ratio of $v|k|$ to the transition temperature T_c that is important. For, when $T \ll T_c$, the gap Δ_0 is of the order T_c; close to T_c, i.e. when $|T-T_c| \ll T_c$, the gap is small, though now $\omega = (2n+1)\pi T \sim T_c$. The quantity $\xi_0 \sim v/T_c$, with the dimension of a length, plays the part of a characteristic parameter in present-day superconductor theory, and is in fact the radius of correlation of the bound electrons. The penetration depth δ can be either greater or less than ξ_0. In the former case the important region $|k| \sim 1/\delta$ satisfies the inequality $v|k| \ll T_c$ whereas in the latter case it is described by the reverse inequality $v|k| \gg T_c$.

Let us start with the first case. Let $v|\boldsymbol{k}| \ll T_0$. We retain in (37.15) only the first non-vanishing term of the expansion in $v|k|$:

$$\bar{Q}(k) = \frac{3\pi}{4}\Delta^2 T \sum_{\omega} \int_{-1}^{+1} \frac{(1-\beta^2)\,\mathrm{d}\beta}{(\omega^2+\Delta^2)^{3/2}} = \pi T \Delta^2 \sum_{\omega} \frac{1}{(\omega^2+\Delta^2)^{3/2}} \tag{37.16}$$

Thus, when $\delta \gg \xi_0$, the kernel $Q(k)$ is independent of k and the connection between the current and ficld is of a local kind, in the sense that the current at a given point r is determined by the field $A(r)$ at this point alone:

$$j(r) = -\frac{e^2 N_s}{m} A(r) \tag{37.17}$$

An equation of this type was first proposed by H. and F. London [64]. It will therefore be natural to describe a superconductor in which $\delta \gg \xi_0$ as a London type superconductor. The function $N_s(T)$ plays the role of the number of "superconducting" electrons. Formula (37.16) expresses the ratio $N_s(T)/N$ as a function of the temperature. Let us emphasise that the gap Δ figuring here is the equilibrium gap in the absence of field at a given temperature, determined by condition (34.37). When $T = 0$, the summation over the frequencies can be replaced by integration: $2\pi T \delta n = \mathrm{d}\omega$. On evaluating the integral, we find that, at $T = 0$, the number of superconducting electrons is equal to their total number N.

Close to T_c, $\Delta(T)$ is small compared with T_c and ω. Neglecting Δ^2 in the denominator, we get the series

$$\frac{N_s(T)}{N} = \frac{2\Delta^2}{\pi^2 T^2} \sum_{n>0} \frac{1}{(2n+1)^3}$$

which has already been evaluated in 36. Using expression (36.6) for the gap close to T_c, we find that in the present case

$$\frac{N_s(T)}{N} = 2\left(1 - \frac{T}{T_c}\right)$$

Let us now consider the second limiting case $v|k| \gg T_c$. The integrand has poles at the points $v|k|\beta/2 = \pm i\sqrt{\omega^2+\Delta^2}$. Since $v|k|$ is large, this means that the integrand has a sharp maximum in the region of
angles $\beta = \cos\theta \simeq T_c/v|k| \ll 1$. Hence the term containing β^2 in the numerator can be neglected by comparison with unity. The remaining expression is a rapidly convergent integral over β, since the integrand decreases as $1/\beta^2$ in the domain $T_d/v|k| \ll \beta \ll 1$. On making the substitution $v|k|\beta = x$ and putting the limits of integration equal to infinity, the integral can be found with the aid of theory of residues:

$$\bar{Q}(k) = \frac{3T\pi^2}{v|k|} \sum_{\omega>0} \frac{4^2}{\omega^2 + \Delta^2} = \frac{3\pi^2}{4v|k|} \Delta \tanh \frac{\Delta}{2T}. \tag{37.18}$$

We see that the kernel $Q(k)$ is in this case essentially dependent on k. Hence, if the field penetration depth $\delta \ll \xi_0$, relationship (37.3) is nonlocal, in other words, the current density $j(r)$ at a given point is determined by the values of the vector potential throughout a neighbourhood of the point with linear dimensions of order ξ_0. The non-local connection between the field and current for certain superconductors was first predicted by Pippard on the basis of an analysis of experimental data [65]. Throughout what follows we shall describe the case when $\delta \ll \xi_0$ as Pippard's case.

There is an important fact that must be mentioned at once. As we have already remarked, the only important factor for deciding which case actually holds is the ratio of the penetration depth δ to the parameter $\xi_0 \sim v/T_c$. If, therefore, the condition $\delta \ll \xi_0$ is fulfilled at low temperatures, the increase in δ as we approach T_c will mean that the reverse situation arises at temperatures sufficiently close to T_c, δ will become much greater than ξ_0. In other words, the London case will always hold in the immediate neighbourhood of T_c. A considerable number of the familiar superconductors belongs to the Pippard type almost throughout the whole temperature range and they only change over to the London type in an extremely narrow neighbourhood $T_c - T \ll T_c$. The remaining pure superconductors represent an intermediate case at low temperatures, i.e. they have a fairly wide London range of temperatures close to T_c We shall not touch here on the subject of alloys (see 39).

Having expression (37.15) for the kernel $\bar{Q}(k)$ at our disposal, we can use Maxwcll's equations to solve the problem of the field penetration into a superconductor with a plane surface. The solution is particularly simple in the London case: on substituting (37.17) into (37.2) and taking all the functions as functions of z only, we find that the vector potential distribution in the superconductor is described by

$$A_y(z) = -H_0 \delta e^{z/\delta}$$

where δ is the London penetration depth

$$\delta = \sqrt{\frac{m}{4\pi N_s e^2}} \left(\text{ in ordinary units } \delta = \int'_{4\pi N_s e^2} mc^2 \right) \tag{37.19}$$

The solution of the problem in the Pippard case is much more difficult and requires the use of special mathematical methods. We shall not dwell on this, but refer the reader who is interested in the theory of superconductors as such to the original literature (see [58], and also [63]).

2. Superconductor in variable fields

We have confined ourselves so far to a discussion of the properties of superconductors in constant magnetic fields. A problem of great physical interest is also the behaviour of a superconductor in an alternating electromagnetic field, or, in more concrete terms, the nature of the absorption and reflection of electromagnetic radiation incident on the surface of a superconductor. The thermodynamic, equilibrium approach on which the previous treatment has been based, is not immediately applicable in the case of an alternating field. We shall find extremely useful in these circumstances the analytic expressions obtained in Chap. III, connecting the various time-dependent functions with the corresponding functions determined by the thermodynamic method. Suppose that an alternating field A (as above, we shall assume that $\varphi = 0$) of frequency ω exists inside an infinite superconductor. The current in the superconductor resulting from the action of the field is obviously connected, as before, with the field

by a relationship of the type (37.3). The difference here is that, with an alternating field, we have to know the Fourier component $Q(k,\omega)$ at non-zero ω. (The kernel $\bar{Q}(k)$ defined above is evidently $\bar{Q}(k) \equiv Q(k,0)$.) We shall again start from the quantum mechanical expression for the current operator:

$$\begin{aligned}\tilde{\hat{j}}(x) &= \frac{ie}{2m}\left(\nabla_{r'} - \nabla_r\right)_{r'\to r} \tilde{\psi}^+(x')\,\tilde{\psi}(x) - \frac{e^2}{m}A(x)\tilde{\psi}^+(x)\tilde{\psi}(x) \\ &\equiv \tilde{\hat{j}}_1(x) - \frac{e^2}{m}A(x)\tilde{\psi}^+(x)\psi(x),\end{aligned}$$

where the operators are written in the Heisenberg representation and contain the field dependence. The connection with the corresponding operators in the interaction representations is, by (6.28), given by

$$\tilde{\hat{j}} = S^{-1}(t) j S(t)$$

where

$$S(t) = T\exp\left\{i\int_{-\infty}^{t}(j(x)A(x))\mathrm{d}^4x\right\}$$

In the approximation linear in the field:

$$\tilde{\hat{\boldsymbol{j}}}_\alpha(x) = \hat{\boldsymbol{j}}_{1\alpha}(x) - \frac{e^2}{m}\boldsymbol{A}_\alpha(x)\psi^+(x)\psi(x) + i\int_{-\infty}^{t}\left[\hat{\boldsymbol{j}}_{1\alpha}(x), \hat{\boldsymbol{j}}_{1\beta}(y)\right]\boldsymbol{A}_\beta(y)\mathrm{d}^4y.$$

The current in the superconductor at a given point and given instant is the average

$$j(x) = \langle\tilde{\hat{j}}(x)\rangle = {}_m\exp\left[\left(\Omega + \mu\nu_m - E_m\right)/T\right]\langle m|\tilde{\hat{j}}(x)|m\rangle$$

Since $\left\langle\hat{j}_1\right\rangle \equiv 0$,

$$j_\alpha(x) = -e_m^{e^2N}A_\alpha(x) + \int P^R_{\alpha\beta}(x-y)A_\beta(y)\mathrm{d}^4y \tag{37.20}$$

where we have introduced the notation

$$P^R_{\alpha\beta}(x-y) = \begin{cases} i\left\langle\left[\hat{j}_\alpha(x), \hat{j}_\beta(y)\right]\right\rangle & \text{for } t_x > t_y \\ 0 & \text{for } t_x < t_y \end{cases} \tag{37.21}$$

On Fourier transforming we get for the kernel of equation (37.3)

$$Q_{\alpha\beta}(k,\omega) = \frac{e^2N}{m}\delta_{\alpha\beta} - P^R_{\alpha\beta}(k,\omega)$$

We now consider the same problem in the technique at finite temperatures, $A(r,\tau)$ and $j(r,\tau)$ being formally regarded as functions of the "time" parameter τ. The following relation now occurs in place of (37.20):

$$\boldsymbol{j}_\alpha(\boldsymbol{r},\tau) = -\frac{e^2N}{m}\boldsymbol{A}_\alpha(\boldsymbol{r},\tau) + \int\mathrm{d}^3\boldsymbol{r}\int_0^\beta \mathscr{P}_{\alpha\beta}(x-y)\boldsymbol{A}_\beta(y)\mathrm{d}\tau_y$$

where

$$\mathscr{P}_{\alpha\beta}(r-r',\tau-\tau') = \left\langle T\left(\hat{j}_{\alpha1}(r,\tau), \hat{j}_{1\beta}(r',\tau')\right)\right\rangle. \tag{37.22}$$

On introducing the Fourier components of the thermodynamic functions, we find that the role of the kernel $Q_{\alpha\beta}(k,\omega_0)$ is played by

$$Q_{\alpha\beta}(k,\omega_0)=\frac{e^2N}{m}\delta_{\alpha\beta}-\mathscr{P}_{\alpha\beta}(k,\omega_0)$$

where the frequencies ω_0 run over the discrete values $\omega_0=2n\pi T$.
We shall shortly prove in a general form that the Fourier components $P^R_{\alpha\beta}(\boldsymbol{k},\omega)$ and $\mathscr{P}_{\alpha\beta}(\boldsymbol{k},\omega_0)$ are values of the same function of a complex variable ω, analytic in the upper half-plane, taken in the first case on the real axis, and in the second at the points $\omega=i\omega_0$. The method of proof is precisely the same as in previous chapters. We expand (37.21) and (37.22) into sums over intermediate states. We now find for the Fourier components, $P^R_{\alpha\beta}$, $\mathscr{P}_{\alpha\beta}$, suitably defined in this case:

$$\begin{aligned}P^R_{\alpha\beta}(\boldsymbol{k},\omega)&=-\sum_{m,p}\varrho_{pm}(\boldsymbol{k})\frac{1}{\omega-\omega_{pm}+i\delta}\\ \mathscr{P}_{\alpha\beta}(\boldsymbol{k},\omega_0)&=-\sum_{m,p}\varrho_{pm}(\boldsymbol{k})\frac{1}{i\omega_0-\omega_{pm}}\end{aligned}\tag{37.23}$$

where

$$\varrho_{pm}(k)=\mathrm{e}^{(\Omega+\mu N_m-E_m)/T}\left(1-\mathrm{e}^{-\omega_{pm}/T}\right)(j_{\alpha1})_{mp}(j_{\beta1})_{pm}(2\pi)^3\delta(k-k_{pm})$$

It is clear from (37.23) that $P^R_{\alpha\beta}(k,\omega)$ is obtained from $\mathscr{P}_{\alpha\beta}(k,\omega_0)$ by replacing ω_0 by $-i\omega$, whilst the values of $P^R_{\alpha\beta}(k,\omega)$ on the real axis must be chosen as the limits when ω tends to the axis from above.

Thus, if we find $\mathscr{P}_{\alpha\beta}(k,\omega_0)$ in the Matsubara technique and continue it analytically onto real frequencies $P^R_{\alpha\beta}(k,\omega)=\mathscr{P}_{\alpha\beta}(k,-i\omega)$ in such a way that the function obtained has no singularities in the upper halfplane of ω, we can in principle find the kernel $Q_{\alpha\beta}(k,\omega)$ which determines the connection between j and A in an alternating electromagnetic field.

Whilst keeping this purpose in mind, let us consider formally the equations for the thermodynamic functions $\mathfrak{G}$ and $\mathfrak{F}^+$in a field alternating in τ of the form $A(r,\tau)=A(k,\omega_0)\,e^{ikr-i\omega_0\tau}$. Instead of (37.11), we now get for the Fourier components of the current $j(k,\omega_0)$:

$$\begin{aligned}j(k,\omega_0)=-\frac{2e^2}{(2\pi)^3m^2}T\sum_{\omega}\int p\,(p\cdot A(k,\omega_0))[&\mathfrak{G}(p_+)\,\mathfrak{W}(p_-)\\ &+\mathfrak{F}(p_+)\,\mathfrak{F}^+(p_-)]\,\mathrm{d}^3p-\frac{Ne^2}{m}A(k,\omega_0)\end{aligned}$$

(here $p_\pm=\{p\pm1/2k;\omega'\pm1/2\omega_0\}$). On repeating the course of the arguments that led us, in the case of a constant field, to expression (37.15), we get after integration over ξ:

$$\begin{aligned}\bar{Q}(k,\omega_0)=&\frac{3\pi T}{4}\sum_{\omega'}\int_{-1}^{+1}(1-\beta^2)\,\mathrm{d}\beta\\ &\times\left\{\frac{i\left(\omega_++\sqrt{\omega_+^2+\Delta^2}\right)\left[i\left(\omega_-+\sqrt{\omega_+^2+\Delta^2}\right)-v|k|\beta\right]+\Delta^2}{\sqrt{\omega_+^2+\Delta^2}\left[\omega_-^2+\Delta^2+\left(v|k|\beta-i\sqrt{\omega_+^2+\Delta^2}\right)^2\right]}\right.\\ &\left.+\frac{i\left(\omega_-+\sqrt{\omega_-^2+\Delta^2}\right)\left[i\left(\omega_++\sqrt{\omega_-^2+\Delta^2}\right)+v|k|\beta\right]+\Delta^2}{\sqrt{\omega_-^2+\Delta^2}\left[\omega_+^2+\Delta^2+\left(v|k|\beta+i\sqrt{\omega_-^2+\Delta^2}\right)^2\right]}\right\}\end{aligned}\tag{37.24}$$

As above, certain assumptions must be made in regard to $v|\boldsymbol{k}|$ in order further to simplify this expression. We shall confine ourselves below to the case of most practical interest. when $v|k| \gg (T_c, \omega_0)$. In this case, as before, the main contribution to the expression for $\bar{Q}(k, \omega_0)$ comes from the range of angles where $\beta \sim T_c/v|k|, \omega'/v|k|$, so that we can neglect β^2 by comparison with unity in the numerator of the integrand. The remaining expression in curly brackets decreases when $\beta \gg T_c/v|k|$, $\omega'/v|k|$ rather more slowly than in the $T = 0$ case, namely, as $1/\beta$. It is therefore advisable to carry out a rearrangement of (37.24), separating out the more slowly decreasing terms:

$$\begin{aligned}
&\bar{Q}(k, \omega_0) \\
&= \frac{3\pi T}{4} \sum_{\omega'} \int_{-1}^{1} \mathrm{d}\beta \left\{ \frac{\Delta^2 - \left(\omega_+ + \sqrt{\omega_+^2 + \Delta^2}\right)\left(\omega_- + \sqrt{\omega_-^2 + \Delta^2}\right)}{\sqrt{\omega_+^{2+} + \Delta^2}\left[\omega_-^2 + \Delta^2 + \left(v|k|\beta - i\sqrt{\omega_+^2 + \Delta^2}\right)^2\right]} \right. \\
&+ \frac{\Delta^2 - \left(\omega_- + \sqrt{\omega_-^2 + \Delta^2}\right)\left(\omega_+ + \sqrt{\omega_+^2 + \Delta^2}\right)}{\sqrt{\omega_-^2 + \Delta^2}\left[\omega_+^2 + \Delta^2 + \left(v|k|\beta + i\sqrt{\omega_-^2 + \Delta^2}\right)^2\right]} \\
&- i \frac{\omega_+ + \sqrt{\omega_+^2 + \Delta^2}}{\sqrt{\omega_+^2 + \Delta^2}\left[v|k|\beta - i\left(\sqrt{\omega_+^2 + \Delta^2} + \sqrt{\omega_-^2 + \Delta^2}\right)\right]} \\
&\left. + i \frac{\omega_- + \sqrt{\omega_-^2 + \Delta^2}}{\sqrt{\omega_-^2 + \Delta^2}\left[v|k|\beta + i\left(\sqrt{\omega_+^2 + \Delta^2} + \sqrt{\omega_-^2 + \Delta^2}\right)^2\right]} \right\}
\end{aligned}$$

On carrying out the integration and passing to the limit as $v|k| \to \infty$, we get

$$\bar{Q}(k, \omega_0) = \frac{3\pi^2 T}{4v|k|} \sum_{\omega_1} \left[1 + \frac{\Delta^2 - \omega'(\omega' - \omega_0)}{\sqrt{\omega'^2 + \Delta^2}\sqrt{(\omega' - \omega_0)^2 + \Delta^2}} \right]. \tag{37.25}$$

When $\omega_0 = 0$ this result tranforms to (37.18).
Since ω runs over the values $(2n+1)\pi T$ in the summation of (37.25), $\bar{Q}(k, \omega_0)$ can be written as the contour integral:

$$\bar{Q}(k, \omega_0) = \frac{3\pi i}{16v|k|} \int_C \tan\frac{\omega'}{2T} \left\{ 1 + \frac{\Delta^2 - \omega'(\omega' - \omega_0)}{\sqrt{\omega^2 + \Delta^2}\sqrt{(\omega' - \omega_0)^2 + \Delta^2}} \right\} \mathrm{d}\omega \tag{37.26}$$

where the contour C consists of two pieces $C_+$and C_-, as illustrated in Fig. 100. The choice of the analytic branches of the functions $\sqrt{\omega^2 + \Delta^2}$ and $\sqrt{(\omega' - \omega_0)^2 + \Delta^2}$ is clear from the same figure: the values of these functions on the cuts are purely imaginary, the imaginary part being positive to the right of the upper cut and to the left of the lower cut. We pass from an integration over the contours C_+ and $C_-$to an integration over the four contours $C_+^{(1,2)}$ and $C_-^{(1,2)}$ (Fig. 101). It is easily seen that the integrals over $C_+^{(2)}$ and $C_-^{(2)}$, considered formally as functions of ω_0, have singularities at $\omega_0 = (2n+1)\pi T$, since the contour of integration passes in this case through the point $\omega' = (2n+1)\pi T$,

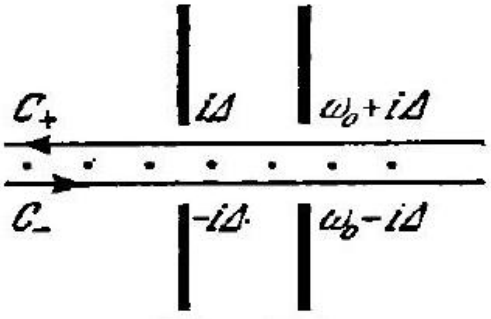


Fig. 100 where $\tan \omega'/2T$ becomes infinite. Hence, in order to find the branch of the function, analytic in the upper half-plane of the variable $\omega = i\omega_0$, we have to transform expression (37.26) at particular points $\omega = 2n\pi Ti$ in such a way that, on later extending this expression to arbitrary values of ω, the contour of integration does not pass through the singularities of the integrand. We observe for this, that if $\omega_0 = 2n\pi T$, by virtue of the periodicity of $\tan \omega'/2T$, the integral over the contour $C_-^{(2)}$ is equal to the integral over $C_+^{(1)}$ (and the same for contours $C_+^{(2)}$ and $C_-^{(1)}$). We can easily verify what has bcen said by replacing the variable of integration, say, in the integral over $C_-^{(2)}$ in accordance with $\omega' - \omega_0 = -\imath$. We can thus write (37.26) as

$$\bar{Q}(k, \omega_0)$$

$$= \frac{3\pi i}{8\vec{v}|\vec{k}|} \left(\int_{c_-^{(1)}} + \int_{c_+^{(1)}} \right) \left\{ \tan \frac{\omega'}{2T} \left[1 + \frac{\Delta^2 - \omega' (\omega' - \omega_0)}{\sqrt{\omega'^2 + \Delta^2} \sqrt{(\omega' - \omega_0)^2 + 1^2}} \right] \right\} d\omega.$$

The expression obtained, regarded formally as a function of $\omega = i\omega_0$, is analytic in the upper half-plane of ω, since the contour of integration, with $\operatorname{Im} \omega > 0$, never passes through a singularity of the integrand.

We can now write down directly the $Q(k, \omega)$ for

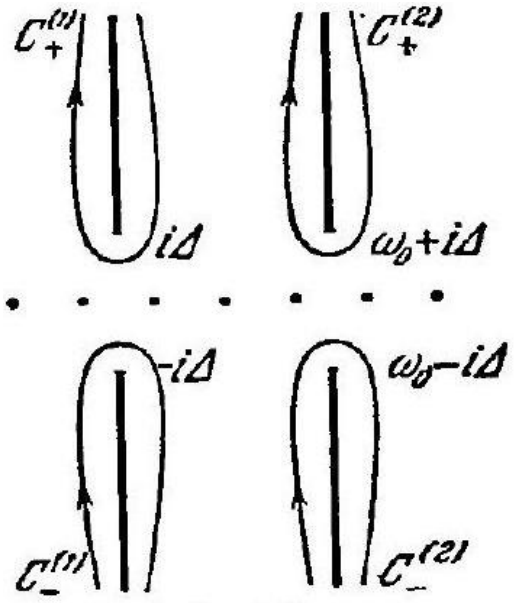


Fig. 101 $\omega > 0$ in which we are interested. Two cases arise: (a) $\omega < 2\Delta$ and (b) $\omega > 2\Delta$. The elementary calculation is performed in both cases in accordance with Fig. 102, where we have indicated in brackets the choice of sign of the imaginary part of the

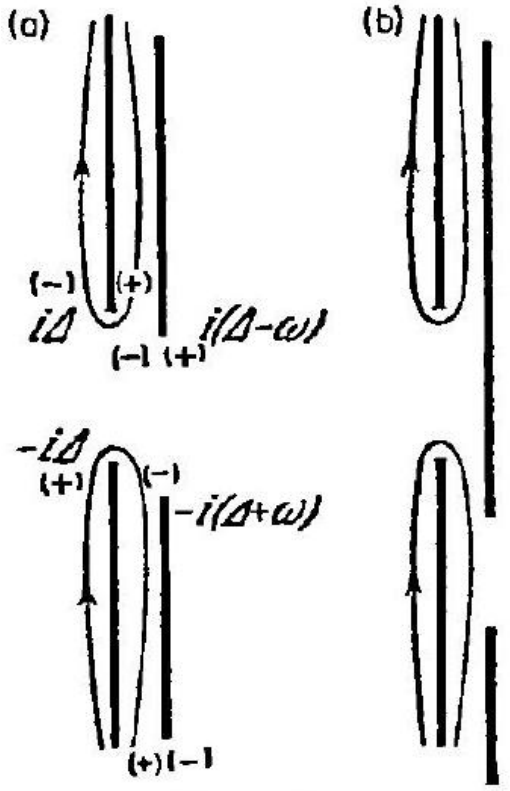


Fig. 102 functions on the different sides of the cuts. Let us quote the results obtained [66, 67]:

(a) $\omega < 2\Delta$:

$$\bar{Q}(k,\omega) = \frac{3\pi}{4v|k|}\left\{\int_{\Delta}^{\Delta+\omega} \tanh\frac{\omega'}{2}\bar{T}\frac{\omega'(\omega'-\omega)+\Delta^2}{\sqrt{\omega^2-\Delta^2}\sqrt{\Delta^2-(\omega'-\omega^2)^2}}\,\mathrm{d}\omega'\right.$$

$$\left.+i\int_{\Delta}^{\infty}\left[\tanh\frac{\omega'}{2T}-\tanh\frac{\omega'+\omega}{2T}\right]\frac{\omega'(\omega'+\omega)+\Delta^2}{\sqrt{\omega'^2-\Delta^2}}\frac{+\omega(\omega'+\omega)^2-\Delta^2}{\sqrt{(\omega'+\omega'}}\right\},$$

(b) $\omega > 24$:

$$\bar{Q}(k,\omega) = \frac{3\pi}{4}\frac{\pi}{i'k'}\left\{\int_{\omega-\Delta}^{\omega+\Delta}\tanh\frac{\omega'}{2T}\frac{\omega'(\omega'-\omega)+\Delta^2}{\sqrt{\omega'^2-\Delta^2}\sqrt{\nu'-(\omega'-\omega)^2}}\,\mathrm{d}\omega'\right.$$

$$+i\int_{\Delta}^{\omega-\Delta}\tanh\frac{\omega'}{2T}\frac{\omega'(\omega'-\omega)+\Lambda^2}{\sqrt{\omega'^2}-\Delta^2\sqrt{(\omega'-\omega^2-\Delta^2}}\mathrm{d}\omega'$$

$$\left.+i\int_{A}^{\infty}\left[\tanh\frac{\omega'}{2T}-\tanh\frac{\omega'+\omega}{2T}\right]\overline{\sqrt{\omega'^2}}(???)\omega'\left(\omega'+\Lambda^2\bar{V}\overline{\overline{(\omega'+\omega)^2-\Lambda^2}}\,\mathrm{d}\omega'\right\}.\right.$$

7.6 5. Type-II Superconductors

7.6.1 5.1 Introduction

The term 'type-II superconductors' was first introduced by Abrikosov in his classic paper [47] where he proposed a detailed phenomenological theory of these materials based on the GL theory and capable of explaining their magnetic properties. Later, with further development of the physics of superconductors, the theory received copious experimental verification.

Here we come across a rare case in which the development of an extensive branch of the

physics of superconductors was initiated by a single theoretical work. Originally, Abrikosov's theory was greeted with a certain skepticism: so much out of the ordinary were its predictions. It was generally accepted only several years later, when it proved to be capable of explaining the complex behavior of superconducting alloys and compounds in a consistent manner. In particular, it explained the very high critical fields of some materials.

We already know that, for type-II superconductors, the energy of an interface between a normal and a superconducting region is $\sigma_{11s} < 0$. This implies that, under certain circumstances, it is energetically favorable for these materials, when placed in an external magnetic field, to become subdivided into alternating normal and superconducting domains.

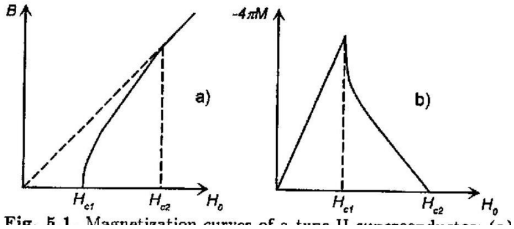


Fig. 5.1. Magnetization curves of a type-II superconductor: (a) magnetic induction B as a function of an external field H_0; (b) magnetic moment per unit volume, M, as a function of H_0

The magnetization curve of a type-II superconductor in the form of a long cylinder placed in a parallel magnetic field is shown schematically in Fig.5.1. As long as the external field is $H_0 < H_{\rm cl}$, the average field in the interior of the specimen is $B = 0$. However, at $H_{\rm c1} < H_0 < H_{\rm c2}$, a steadily increasing field B penetrates the superconductor. This field always remains below the external field H_0 and the specimen's superconductivity is not destroyed. At a certain field $H_0 = H_{\rm c2}$, the average field in the interior, B, becomes equal to H_0 and the bulk superconductivity disappears.

Thus, above $H_{\rm cl}$, a type-II superconductor does not show the MeissnerOchsenfeld effect. Magnetic field penetrates into these materials in a very special way: as quantized vortex filaments. Every filament (or vortex) has a normal core which can be approximated by a long thin cylinder with its axis parallel to the external magnetic field. Inside the cylinder, the order parameter ψ is zero. The radius of the cylinder is of the order ξ, the coherence length. The direction of the supercurrent circulating around the normal core is such that the direction of the magnetic field generated by it coincides with that of the external field and is parallel to the normal core. The vortex current circulates within an area of radius $\sim \lambda$, the penetration depth. The size of this area can be well in excess of ξ because $\lambda \gg \xi$ for type-II superconductors.

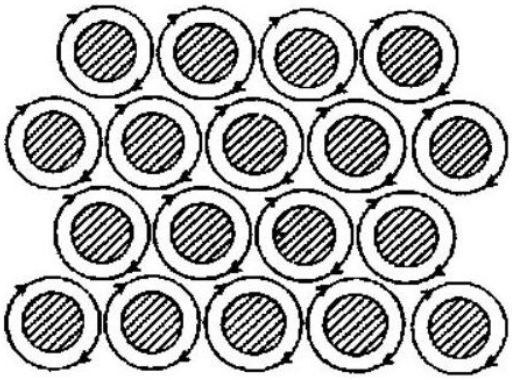


Fig. 5.2. Mixed state of a type-II superconductor. Superconducting vortices form a regular triangular lattice. Vortex cores (dashed areas) are normal

Each vortex carries one magnetic flux quantum. Penetration of vortices into the interior of a superconductor becomes thermodynamically favorable at $H_0 > H_{\rm c1}$. Once inside the superconductor, the vortices arrange themselves at distances $\sim \lambda$ from each other so that in the cross-section they form a regular triangular lattice, as sketched in Fig. 5.2.

This state of the superconductor is referred to as the mixed state because it is characterized

by a partial penetration of the magnetic field in the interior of the specimen. The mixed state is observed at fields from $H_{\rm cl}$ (the lower critical field) to $H_{\rm c2}$ (the upper critical field).

Once formed at $H_{\rm c1}$, the vortex lattice persists at much higher fields. As the external field increases, the lattice period steadily decreases and the density of the vortices rises. Finally, at a field $H_0 = H_{\rm c2}$, the vortex lattice grows so dense that the distance between the neighboring vortices, i.e., the lattice period, becomes of the order ξ. This means that the normal cores of becomes zero over the entire volume of the superconductor. In other words, a second-order phase transition occurs.

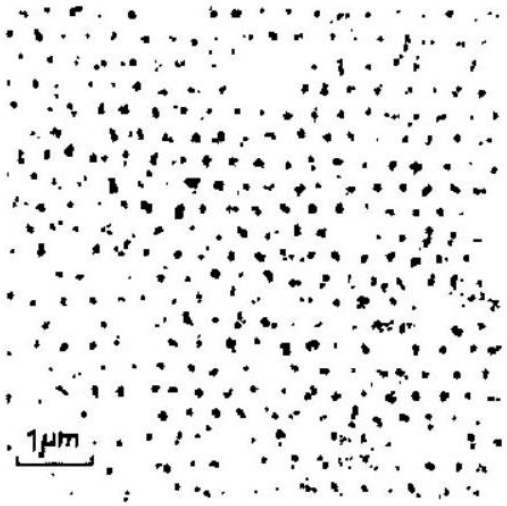


Fig. 5.3. Mixed state in niobium as observed in the electron microscope [48]

The existence of the mixed state in type-II superconductors has been reliably verified by experiment. In addition to numerous indirect proofs, a spectacular direct experimental demonstration of the vortex array is due to Truble and Essmann [48]. They covered the top of a type-II superconducting cylinder with a thin organic film and placed it in a magnetic field so that the specimen was driven to the mixed state. Then a thin layer of fine ferromagnetic particles was sputtered onto the surface covered with the film. As the ferromagnetic particles approached the surface, they were preferentially attracted to the sites where the magnetic field lines emerged from the superconductor, i.c., to the locations of the vortices. Then, having peeled the organic film off the specimen and placed it in the electron microscope, the authors were able to enjoy a direct view of the mixed state (see Fig. 5.3).

7.6.2 5.2 Field of an Isolated Vortex

Let us turn to a systematic study of the mixed state. We start with the simplest case: an isolated vortex. We already know that an isolated vortex in an infinite superconductor comprises a normal core of radius $\sim \xi$ and vortex currents circulating within an area $\sim \lambda$. Assume that the GL parameter is $\kappa \gg 1$. Then $\lambda \gg \xi$. At a distance $r \gg \xi$ we have $|\psi|^2 = 1$. Let us focus on this part of the vortex. The GL equation for the vector potential (3.24) can be written as

$$\text{curlcurl}\, \boldsymbol{A} = \frac{1}{\lambda^2}\left(\frac{\Phi_0}{2\pi}\nabla\theta - \boldsymbol{A}\right). \tag{5.1}$$

Noting that $\text{curl}\, \boldsymbol{A} = \boldsymbol{H}$, we obtain from (5.1)

$$\text{curl}\, \boldsymbol{H} = \frac{1}{\lambda^2}\left(\frac{\Phi_0}{2\pi}\nabla\theta - \boldsymbol{A}\right) \tag{5.2}$$

Evaluatng the curl of both parts of (5.2), we obtain

$$H + \lambda^2 \operatorname{curlcurl} H = \frac{\Phi_0}{2\pi} \operatorname{curl} \nabla\theta \tag{5.3}$$

At any point of the vortex, apart from its center, we have curl $\nabla\theta = 0$, since curl $\nabla_\varphi = 0$, where φ is an arbitrary function. But the center of the vortex represents a singularity, there we have $|\nabla\theta| \to \infty$. To understand how curl $\nabla\theta$ behaves at the center of the vortex, we shall take its integral over the surface of a small circle centered on the center of the vortex:

$$\int_{\odot} \operatorname{curl} \nabla\theta \cdot \mathrm{d}S.$$

By Stokes's theorem,

$$\int_{\odot} \operatorname{curl} \nabla\theta \cdot \mathrm{d}\boldsymbol{S} = \oint \nabla\theta \cdot \mathrm{d}l,$$

where the path integral is taken along the circumference of our circle. Since after every full circle around the center of the vortex, the phase changes by 2π (recall that each vortex carries one flux quantum), we have

$$\int_{\odot} \operatorname{curl} \nabla\theta \cdot \mathrm{d}\boldsymbol{S} = 2\pi \tag{5.4}$$

Thus the function curl $\nabla\theta$ is zero everywhere except for the center of the vortex. At the center, it is infinite but its integral, according to (5.4), equals 2π. This corresponds to the behavior of the δ-function and we therefore can write

$$\operatorname{curl} \nabla\theta = 2\pi\delta(r)e_{\mathrm{v}},$$

where e_v is the unit vector along the vortex.
As a result; (5.3) can be replaced by

$$\boldsymbol{H} + \lambda^2 \operatorname{curl} \operatorname{curl} \boldsymbol{H} = \Phi_0 \delta(\boldsymbol{r}) \boldsymbol{e}_{\mathrm{v}} \tag{5.5}$$

subject to the boundary condition $H(\infty) = 0$. The solution of (5.5) is

$$h = \frac{\Phi_0}{2\pi\lambda^2} K_0(r/\lambda), \tag{5.6}$$

where K_0 is the MacDonald function, or the Hankel function of imaginary argument.
The asymptotic behavior of this function is:

$$K_0(z) \sim \begin{cases} \ln(1/z) & \text{at } z \ll 1, \\ \mathrm{e}^{-z}/z^{1/2} & \text{at } z \gg 1. \end{cases} \tag{5.7}$$

Thus, K_0 diverges logarithmically at small arguments and goes exponentially to zero at large ones. As follows from (5.6) and (5.7), the magnetic field
because these expressions do not hold in the vicinity of the normal core (of radius $\sim \xi$). Therefore, the field at the center of the vortex can be obtained to logarithmic accuracy by setting a cut-off at $r = \xi$:

$$H(0) \approx \frac{\Phi_0}{2\pi\lambda^2} \ln \kappa \tag{5.8}$$

A more accurate value of $H(0)$ can be obtained by taking into account the actual variation of $\psi(r)$ in the vortex core and carrying out numerical integration of the GL equations [47]:

$$H(0) = \frac{\Phi_0}{2\pi\lambda^2}(\ln\kappa - 0.18). \tag{5.9}$$

The above correction is not essential since all the calculations are carried out on the assumption that $\kappa \gg 1$.

The spatial variation of the magnetic field of an isolated vortex is illustrated in Fig. 5.4.

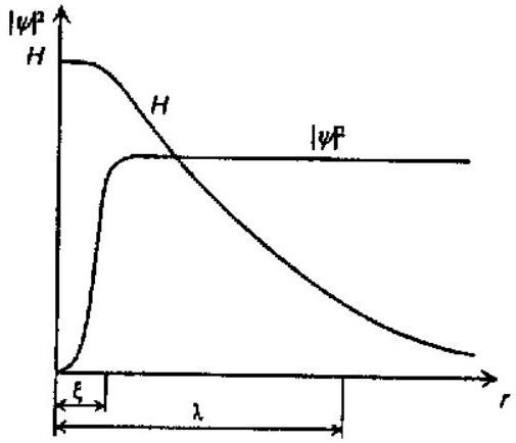


Fig. 5.4. Single vortex in an infinite superconductor. Shown are spatial distributions of the order parameter and the magnetic field of the vortex

7.6.3 5.3 The Lower Critical Field

Let us find the lower critical field $H_{\rm cl}$, that is, the lowest field at which formation of vortices in a type-II superconductor becomes thermodynamically favorable.

First we should find the free energy of a vortex, or, more accurately, the free energy of a superconductor containing one vortex, ε, measured relative to its free energy without the vortex. We shall consider the case $\kappa \gg 1$ or $\lambda \gg \xi$. Our specimen in this case is a typical London superconductor and the corrections due to $\nabla\psi$ are negligible. Therefore, we can use the London expression for the free energy (2.8):

$$\varepsilon = \frac{1}{8\pi}\int \left[\boldsymbol{H}^2 + \lambda^2(\operatorname{curl}\boldsymbol{H})^2\right] \mathrm{d}V, \tag{5.10}$$

where the integration is carried out over the space between two infinite parallel planes perpendicular to the vortex and separated by a unit length. Then (5.10) is simply the sum of the magnetic and kinetic energies of the superconducting electrons contained in the vortex, per unit length of the vortex. Making use of the formula

$$(\operatorname{curl}\boldsymbol{H})^2 = \boldsymbol{H}\cdot\ \operatorname{curl}\operatorname{curl}\ \boldsymbol{H} - \operatorname{div}[(\operatorname{curl}\boldsymbol{H})\times\boldsymbol{H}]$$

we have

$$\varepsilon = \frac{1}{8\pi}\int H\cdot\left(H + \lambda^2\operatorname{curlcurl} H\right)\mathrm{d}V - \lambda^2\int \operatorname{div}[(\operatorname{curl} H)\times H]\mathrm{d}V$$

By Gauss's theorem, we can convert the second integral into a surface integral:

$$\int \operatorname{div}[(\operatorname{curl}\boldsymbol{H})\times\boldsymbol{H}]\mathrm{d}V = \oint[(\operatorname{curl}\boldsymbol{H})\times\boldsymbol{H}]\cdot\mathrm{d}\boldsymbol{S}$$

where the surface integral is taken over an infinitely remote surface and the surfaces $z = 0$ and $z = 1$ (the vortex is assumed to be parallel to the z axis). Since H is perpendicular to the planes $z = 0$ and $z = 1$, the vector $(\operatorname{curl}\boldsymbol{H})\times\boldsymbol{H}$ is parallel to the planes $z = 0$ and $z = 1$ and

the vector $\mathrm{d}\boldsymbol{S}$ is perpendicular to them. Hence the expression under the integral sign is zero over these planes. On the other hand, at $r \to \infty$ we have $H \to 0$ and so the above expression is zero there, too. Then

$$\int \operatorname{div}[(\operatorname{curl} H) \times H]\mathrm{d}V = 0$$

and

$$\varepsilon = \frac{1}{8\pi} \int \boldsymbol{H} \cdot \left(\boldsymbol{H} + \lambda^2 \operatorname{curlcurl} \boldsymbol{H}\right) \mathrm{d}V$$

Noting that $\boldsymbol{H}$ must satisfy (5.5), we have

$$\varepsilon = \frac{\Phi_0}{8\pi} H(0) \tag{5.11}$$

Substituting (5.8) into this expression, we obtain

$$\varepsilon = \left(\frac{\Phi_0}{4\pi\lambda}\right)^2 \ln \kappa \tag{5.12}$$

In deriving (5.12), we neglected a small additional contribution to the vortex energy due to the fact that the core is normal. Indeed, the free energy density of the core exceeds that of the surrounding areas by $F_\mathrm{n} - F_{\mathrm{s}0} = H_\mathrm{cm}^2/8\pi$, that is, by the lost condensation energy. Then, if the core radius is taken to be ξ, the additional energy disregarded in (5.12) is $(H_\mathrm{cm}^2/8\pi)\,\pi\xi^2$. Using (3.38), it is easy to show that this energy is

$$\frac{1}{4}\left(\frac{\Phi_0}{4\pi\lambda}\right)^2 \ll \left(\frac{\Phi_0}{4\pi\lambda}\right)^2 \ln \kappa$$

More rigorous calculations of the condensation energy lost in the core lead to the following final expression for the energy of an isolated vortex line:

$$\varepsilon = \left(\frac{\Phi_0}{4\pi\lambda}\right)^2 (\ln \kappa + 0.08) \tag{5.13}$$

It follows from (5.13) that the energy of an isolated vortex is positive, that is, without an external field, the vortex cannot exist in the interior of a superconductor. Hence, if a bulk superconductor is placed in a weak external field, no vortices are formed: Their formation is not favored by the energy. Instead, the superconductor remains in the Meissner state, just as a type-I superconductor. Let us find the minimum value of the field at which vortex formation in a type-II superconductor becomes favorable.

We already know that, for a superconductor in an external magnetic field, the energy that is a minimum at equilibrium is the Gibbs free energy $\mathcal{G}$. Per unit length of the vortex, this energy is

$$\mathcal{G} = \varepsilon - \int \frac{\boldsymbol{B} \cdot \boldsymbol{H}_0}{4\pi}\, \mathrm{d}V \tag{5.14}$$

where H_0 is the external magnetic field and the free energy of a vortex of unit length is ε. Indeed, by (1.22), the Gibbs free energy density is

$$G = F - B \cdot H_0/4\pi$$

where F is the free energy density. Since H_0 is applied externally, it can be taken out of the integral sign in (5.14). Then, recalling that the vortex carries one magnetic flux quantum Φ_0, we have

$$\mathcal{G} = \varepsilon - \frac{\Phi_0 H_0}{4\pi} \tag{5.15}$$

Clearly, for a sufficiently weak external field $H_0, \mathcal{G} > 0$ and vortex formation is not favored. However, there exists such a field $H_{\rm cl}$, starting from which $\mathcal{G}$ becomes negative, i.e. formation of a vortex reduces the energy. It follows from (5.15) that

$$H_{\rm c1} = 4\pi\varepsilon/\Phi_0 \tag{5.16}$$

Making use of (5.13), we obtain the lower critical field for a type-II superconductor:

$$H_{\rm c1} = \frac{\Phi_0}{4\pi\lambda^2}(\ln\kappa + 0.08) \tag{5.17}$$

Comparing (5.17) and (5.8), one can see that the lower critical field is approximately half the field at the center of an isolated vortex.

Let us emphasize once again that all the above estimates are valid for superconductors with $\kappa \gg 1$ and are of logarithmic accuracy.

The field $H_{\rm cl}$ is a relatively weak field. For instance, if $\kappa \sim 100$ and $H_{r1,1} \sim 10^3$ Oe, we have $H_{r1} \sim 30$ Oe.

7.6.4 5.4 Interaction Between Vortices

In the preceding section we have analyzed the properties of an isolated vortex But the number of vortices in the mixed state is usually large and they interact strongly with each other. The objective of this section is to understand how they interact.

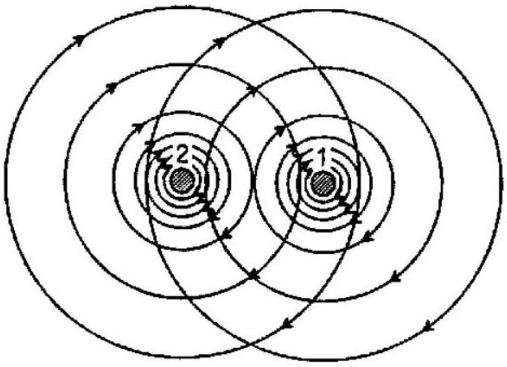


Fig. 5.5. Interaction of two parallel vortices of the same orientation

Consider two parallel vortices of the same orientation in an infinite superconductor. As before, we assume that $\kappa \gg 1$. As long as the distance between the vortices exceeds λ, they do not 'feel' each other. But when their distance becomes less than λ, the core of one vortex moves into the area where the supercurrents of the other vortex circulate, as illustrated in Fig. 5.5. It is evident from the figure that the superfluid components of the electron velocity to the right of vortex 1 and to the left of vortex 2 add up while those in between the vortices subtract from each other. This means that in the area adjoining the core of vortex 1 (to the right of it), the Bernoulli pressure is less than on its left. This results in a difference of Bernoulli pressures exerted on the core of vortex 1 in the direction from left to right. Applying similar arguments to vortex 2, one can conclude that two parallel vortices of the same sign repel each other and the repulsion force acts only on the vortex core.

Let us now work out the force between two parallel vortices. Assume that the coordinates of the vortex cores are r_1 and r_2, respectively. By (2.8), the energy of a superconductor containing two vortices measured from its energy without vortices is

$$\mathcal{F} = \frac{1}{8\pi} \int \left[\boldsymbol{H}^2 + \lambda^2 (\operatorname{curl} \boldsymbol{H})^2 \right] \mathrm{d}V \tag{5.18}$$

Here $\boldsymbol{H}$ is the total magnetic field generated by the two vortices. This field must satisfy an equation constructed by analogy with (5.5):

$$H + \lambda^2 \operatorname{curl} \operatorname{curl} H = \Phi_0 \left[\delta (r - r_1) + \delta (r - r_2) \right] e_{\mathrm{v}}$$

After a series of transformations analogous to those in the foregoing section,

$$\mathcal{F} = \frac{\Phi_0}{8\pi} \left[H (r_1) + H (r_2) \right] \tag{5.19}$$

Here $H (r_1)$ is the field at the center of vortex 1 . It incorporates the field generated by vortex 1 itself and the field $H_{12}(x)$ due to vortex 2 (the latter is separated from vortex 1 by the distance $x = |r_1 - r_2|$). The same applies to the field $H (r_2)$. Then it follows from (5.19) that

$$\mathcal{F} = 2\varepsilon + \frac{\Phi_0}{8\pi} 2 H_{12}(x) \tag{5.20}$$

where ε is the energy of an isolated vortex defined by (5.13).
The physical significance of (5.20) is evident: the first term is the energy of two noninteracting vortices and the second term is the energy of their interaction. Denote the latter by $U(x)$:

$$U(x) = \frac{\Phi_0 H_{12}(x)}{4\pi} \tag{5.21}$$

Then the interaction force per unit length of the vortex is

$$f = -\frac{\mathrm{d}U}{\mathrm{d}x} = -\frac{\Phi_0}{4\pi} \frac{\mathrm{d}H_{12}}{\mathrm{d}x}$$

Taking into account that for two parallel vortices, according to Maxwell's equations,

$$\frac{\mathrm{d}H_{12}}{\mathrm{d}x} = \frac{4\pi}{c} j_{12}(x)$$

where $j_{12}(x)$ is the current density induced by the first vortex at the center of the second vortex (or vice versa), we have

$$|f| = \frac{1}{c} j_{12} \Phi_0 \tag{5.22}$$

The above formula is also valid in a more general case: If there is an externally applied current j circulating around a vortex, it exerts a Lorentz force on the vortex core, per unit length,

$$f_{\mathrm{L}} = \frac{1}{c} \left[j \times \Phi_0 \right] \tag{5.23}$$

where j is the density of the external current at the location of the normal core and $\boldsymbol{\Phi}_0 = \boldsymbol{e}_{\mathrm{v}} \boldsymbol{\Phi}_0$.

7.6.5 5.5 The Upper Critical Field

The mixed state of a homogeneous type-II superconductor is characterized by a regular, usually triangular, vortex lattice. As the external field is increased, the lattice period decreases and when it becomes of the order of the coherence length ξ, a second-order phase transition occurs from the mixed to the normal
state. This happens when the external field reaches the value of the upper critical field H_{c2}.

We can estimate the order of magnitude of H_{c2} even without exact calculations, proceeding from the following arguments. For two neighboring vortices at a distance ξ from each other, the distance ξ can be interpreted as the thickness of a superconducting layer separating their normal cores. It can be roughly approximated by a thin film of thickness ξ. But we know from Sect. 3.5 that a thin film in a parallel magnetic field undergoes a second-order phase transition to the normal state at the field $H_{c||} \sim H_{cm}\,\lambda/d$, where d is the thickness of the film. If, as in our case, the film thickness is ξ, one should expect the transition to the normal state at an external field $\sim H_{cm}\lambda/\xi$. This provides us with a simple estimate of the upper critical field:

$$H_{c2} \sim \kappa H_{cm}. \tag{5.24}$$

Our estimate differs from the result of exact calculations only by a numerical factor $\sqrt{2}$ [47]:

$$H_{c2} = \sqrt{2}\kappa H_{cm} \tag{5.25}$$

The upper critical field can be rather large. For example, for $\kappa \sim 100$ and $H_{cm} \sim 10^3$ Oe we obtain $H_{c2} \sim 10^5$ Oe.

Using (5.25), the expression $\kappa = \lambda/\xi$, and (3.38), namely, $\sqrt{2}H_{cm} = \Phi_0/2\pi\lambda\xi$, we get

$$\Phi_0 = 2\pi\xi^2 H_{c2} \tag{5.26}$$

The last formula is very useful for determining the coherence length ξ because it relates ξ to a quantity which can be easily measured in experiment: the upper critical field.

7.6.6 5.6 Reversible Magnetization of a Type-II Superconductor

Let us work out an expression for the magnetic moment per unit volume of a type-II superconductor, when the latter is in the mixed state and when the external field is $H_0 \gg H_{c1}$. In other words, let us find the dependence $M(H_0)$.

This problem could be handled in the usual way by varying the energy of the system in order to find the equilibrium value of the magnetic moment. But we shall instead employ a somewhat artificial method which will allow us to shorten the computations.

Consider a bulk cylinder of a type-II superconductor, with its axis parallel to the z axis, in a longitudinal magnetic field H_0. Assume that the coherence length ξ depends only on the x coordinate and increases monotonically with x.
field H_{c2} will also depend on x, namely, it will decrease with increasing x. As a result, the magnetic flux density (induction) B will become a function of x, that means that a current j will start in the interior of the sample, in the direction of the y axis:

$$j = \frac{c}{4\pi}\frac{\mathrm{d}B}{\mathrm{d}x}$$

Recalling that $B = H_0 + 4\pi M$, we arrive at $M = M(x)$, that is,

$$j = c\frac{\mathrm{d}M}{\mathrm{d}x}.$$

Furthermore, the current exerts a Lorentz force on each vortex

$$f_{\mathrm{L}} = \frac{1}{c} j \Phi_0 = \Phi_0 \frac{\mathrm{d}M}{\mathrm{d}x}. \tag{5.27}$$

On the other hand, since the system of vortices is at equilibrium, the force f_{L} must be compensated by another force. The origin of this second force is evident: If $\xi = \xi(x)$, the self-energy of a vortex, ε, also becomes a function of x resulting in a force $-\nabla\varepsilon$ on the vortex, where (see (5.12))

$$\varepsilon = \left(\frac{\Phi_0}{4\pi\bar{\lambda}}\right)^2 \ln\kappa = \left(\frac{\Phi_0}{4\pi\bar{\lambda}}\right)^2 \ln\frac{\lambda}{\xi} \tag{5.28}$$

Differentiating (5.28) and equating it to the right-hand side of (5.27), we obtain a condition for equilibrium:

$$\Phi_0 \frac{\mathrm{d}M}{\mathrm{d}x} = \left(\frac{\Phi_0}{4\pi\dot{\lambda}^-}\right)^2 \frac{1}{\xi}\frac{\mathrm{d}\xi}{\mathrm{d}x}$$

Following integration, we obtain

$$M = \frac{\Phi_0}{16\pi^2\lambda^2} \ln\frac{\xi}{l} \tag{5.29}$$

where l is the integration constant with dimensions of length.
Now we seek the dependence $M(H_0)$. The only quantity in (5.29) depending on H_0 is l. We can find the relation between H_0 and l in the following way. Since an increase of x is followed by a monotonic increase of ξ and a monotonic decrease of H_{c2}, it is clear that, at some point x_0, the field H_{c2} becomes equal to the external field H_0. This means that at this particular point $M(x_0) = 0$, i.e., $l = \xi(x_0)$. On the other hand, the relation between ξ and H_{c2} is given by (5.26). Applying it to x_0, we have

$$2\pi l^2 H_0 = \Phi_0.$$

Hence the ratio ξ/l is

$$\frac{\xi}{l} = \left(\frac{H_0}{H_{\mathrm{c2}}}\right)^{1/2} \tag{5.30}$$

Substituting (5.30) in (5.29), we obtain
or

$$M = -\frac{\Phi_0}{16\pi^2\bar{\lambda}^2} \ln\left(\frac{H_{\mathrm{c2}}}{H_0}\right)^{1/2}$$

$$M = -\frac{\Phi_0}{32\pi^2\lambda^2} \ln\frac{H_{\mathrm{c2}}}{H_0} \tag{5.31}$$

From the last expression, one can derive the dependence $B(H_0)$:

$$B = H_0 - \frac{\Phi_0}{8\pi\lambda^2} \ln\frac{H_{\mathrm{c2}}}{H_0} \tag{5.32}$$

The above formulas are correct to logarithmic accuracy, provided $\kappa \gg 1$. Let us employ them to work out the details of the $M(H_0)$ dependence at fields H_0 close to H_{c2}. Writing H_{c2}/H_0 as

$$\frac{H_{\mathrm{c2}} - H_0}{H_0} + 1$$

we obtain, instead of (5.31),

$$M = -\frac{\Phi_0}{32\pi^2\lambda^2}\ln\left(1+\frac{H_{c2}-H_0}{H_0}\right) \approx -\frac{\Phi_0}{32\pi^2\lambda^2}\frac{H_{c2}-H_0}{H_0}.$$

Finally, using (5.26), we have

$$-4\pi M = \frac{H_{c2}-H_0}{4\kappa^2} \tag{5.33}$$

Thus we have found that $|M|$ decreases linearly as $H \to H_{c2}$. An exact calculation of $M(H_0)$ in this field range was carried out by Abrikosov [47] with the result

$$-4\pi M = \frac{H_{c2}-H_0}{1.16\,(2\kappa^2-1)} \tag{5.34}$$

It is easy to see that at $\kappa \gg 1$ we can omit the term -1 in parenthesis, Then the exact formula (5.34) will differ from the approximate one (5.33) only by a numerical coefficient ~ 1.

Let us clarify a question which might cause some confusion: What is $H_{\rm cm}$ for a type-II superconductor? In a type-I superconductor, it is the thermodynamic critical field at which the superconductor goes to the normal state. Now, what happens to a type-II superconductor at $H_{\rm cm}$? The answer is: nothing special. There are no special features on the magnetization curve at $H_{\rm cm}$. For a type-II superconductor, the quantity $H_{\rm cm}$ should be considered simply as a measure of the extent to which the superconducting state of a particular material is favored over its normal state in the absence of magnetic field:

$$F_{\rm n} - F_{\rm s0} = H_{\rm cm}^2/8\pi$$

Alternatively, one can say that, for a type-II superconductor, a transition to the normal state occurs when the work done to magnetize it is $F_n - F_{50}$:

$$-\int_0^{H_{c2}} M\ {\rm d}H_0 = H_{\rm cm}^2/8\pi$$

From the last expression we obtain the following definition of $H_{\rm cm}$ for a type-II superconductor:

$$H_{\rm cm}^2 = 2\int_0^{H_{c2}} [H_0 - B(H_0)]\,{\rm d}H_0 \tag{5.35}$$

7.6.7 5.7 Surface Superconductivity. The Third Critical Field

Consider a type-II superconductor in an external magnetic field H_0 decreasing from $H_0 > H_{c2}$. At the moment when H_0 falls just below H_{c2}, superconducting nuclei appear all over the volume of the superconductor and a tightly packed vortex lattice forms. The order parameter ψ at this field is small ($|\psi| \ll 1$). In other words, a phase transition of second order occurs as the material goes from the normal ($H_0 > H_{c2}$) to the mixed state ($H_0 \le H_{c2}$).

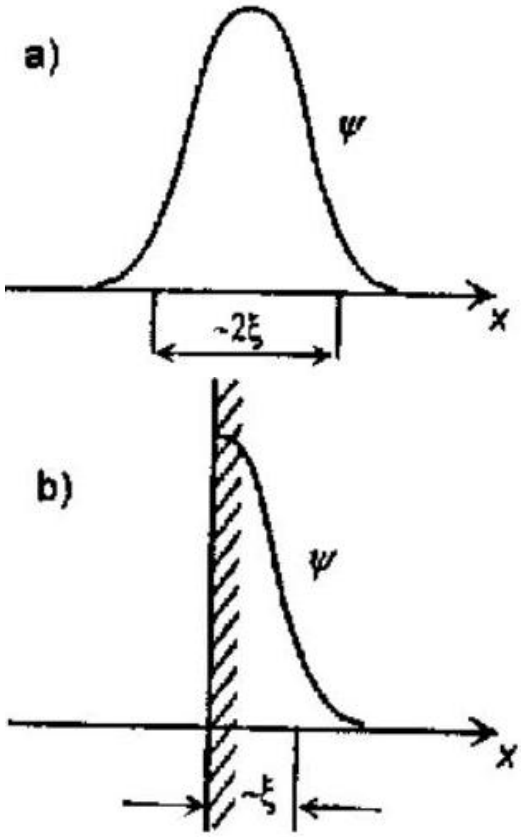


Fig. 5.6. (a) Wavefunction ψ of a nucleus of the superconducting state in an infinite superconductor, the size of the nucleus is $\sim 2\xi$; (b) the same for a superconducting semispace, the size of the nucleus is $\sim \xi$

The nucleus of superconductivity mentioned above is a region between the normal cores of two neighboring vortices. The thickness of this region is of the order $2\xi(T)$ because, if the vortex lattice is close-packed and the radius of the normal core is assumed to be ξ, the distance between the core centers is $\sim 2\xi$. The dependence of the order parameter on the coordinate along the line joining the vortex centers is sketched in Fig. 5.6 (a): The nucleus in this cross-section has the form of a dome-shaped curve.

This is how superconductivity arises in the bulk of a type-II superconductor at H_{c2}. It turns out, however, that at the surface of a superconductor, the superconducting state can exist in much higher fields, provided the surface is parallel to the external field.

Consider a semi-infinite superconducting space occupying the semispace $x > 0$, in an external magnetic field H_0 parallel to the z axis. Since the surface of the superconductor coincides with the plane $x = 0$, a nucleus of superconductivity, which forms at the surface, can be expected to have an
a surface nucleus is shown in Fig. 5.6 (b). Furthermore, the critical field for the formation of such a nucleus can be expected to be larger than the critical field for nucleation of bulk superconductivity. This follows from (3.62), the expression for the critical field of a thin film, which is the most relevant reference case when considering surface superconductivity. A decrease of the film thickness results in an increase of its critical field. Therefore, we should expect the critical field for nucleation of surface superconductivity to be approximately twice the critical field for bulk superconductivity. We shall refer to this new critical field as the third critical field and denote it by H_{c3}. Numerical calculations [49] have shown that

$$H_{c3} = 1.69 H_{c2} \tag{5.36}$$

Now we can draw some conclusions. It follows from the above argumentation that, as the

external magnetic field decreases and reaches the value H_{c3} from above, a thin superconducting layer appears at the surface of a superconductor. The thickness of the layer is of the order $\xi(T)$. The bulk of the superconductor remains normal and the magnetic field there is equal to the external field. In the surface superconducting layer, the magnetic field is somewhat weakened as is the case in thin superconducting films in a parallel magnetic field. The analogy with a thin film also implies the presence of screening currents circulating along both the inner and outer surfaces of the superconducting layer in opposite directions.

What happens to the surface superconducting layer as the external field decreases further, below H_{c3}? According to detailed calculations, both the amplitude of the order parameter, f_0, and the thickness of the superconducting layer, Δ, increase with decreasing field. Their field dependences for several values of the GL parameter κ are shown in Figs. 5.7 and 5.8.

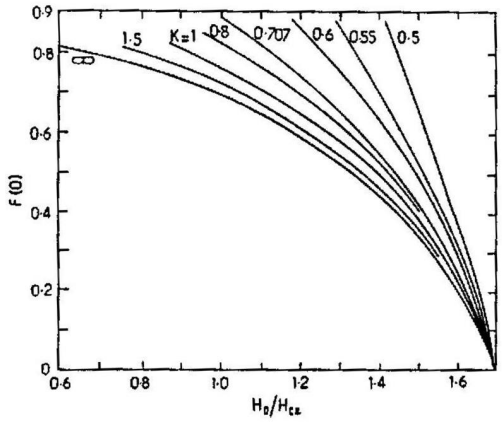


Fig. 5.7. Amplitude of the order parameter, $\mathrm{F}(0) = f_0$, at the surface of a superconductor versus external magnetic field, for several values of κ [50]

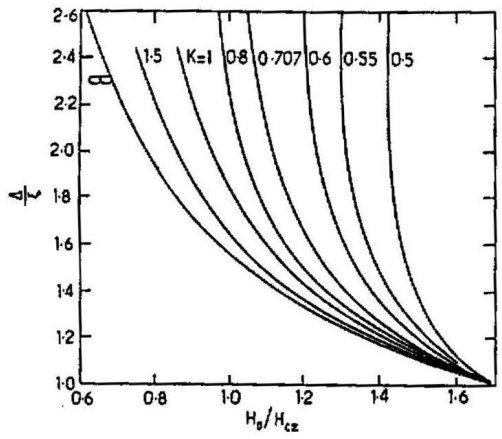


Fig. 5.8. Thickness Δ of a surface superconducting layer as a function of the external magnetic field, for several values of κ [50]

If the surface of a superconductor is covered with a layer of normal metal, it causes a reduction of H_{c3} to a value very close to H_{c2}.

It is interesting to note that the phenomenon of surface superconductivity can also be observed in some type-I superconductors. Indeed, nowhere in the above argumentation was it assumed that $\kappa > 1/\sqrt{2}$, and the result still was $H_{c3} = 1.69H_{c2} = 1.69\sqrt{2}\kappa H_{cm}$. Surface superconductivity arises if H_{c3} is larger than H_{cm}, i.e., provided

$$1.69\sqrt{2}\kappa H_{cm} > H_{crn} \tag{5.37}$$

Thus, the condition for the existence of surface superconductivity in a type-I superconductor is

$$\kappa > \frac{1}{1.69\sqrt{2}} = 0.42.$$

7.6.8 5.8 Surface Barrier. Superheating of the Meissner State

sAll situations considered so far corresponded to thermodynamic equilibrium. For example, we assumed that if penetration of vortices into a type-II superconductor becomes favorable at the lower critical field, the vortices indeed penetrate at that value of the field.

However, a more detailed analysis shows that, in order to penetrate into the interior of a superconductor, vortices must first overcome an energy barrier at the surface.

Consider an ideally smooth surface of a superconductor and an isolated vortex in the interior, parallel to the surface. For convenience, we assume

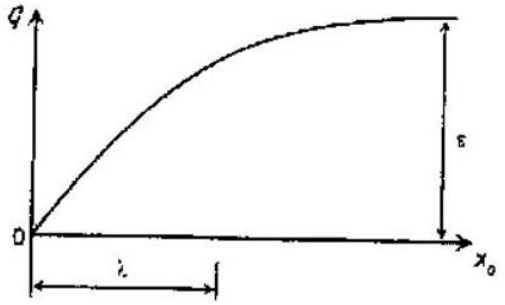


Fig. 5.9. Gibbs free energy of a superconductor containing an isolated vortex, as a function of the vortex distance from the surface, x_0

free energy $\mathcal{G}$ of such a superconductor with a vortex is a function of the distance x_0 between the vortex axis and the surface, as illustrated in Fig. 5.9. It is obvious from the figure that, without an external field, an isolated vortex in the interior of a superconductor is unstable, as expected, and that at sufficiently large distances from the surface, $\mathcal{G}$ is simply equal to the free energy of an isolated vortex, ε. Here, as well as in the following, the energy of a superconductor with a vortex is measured relative to its energy without the vortex.

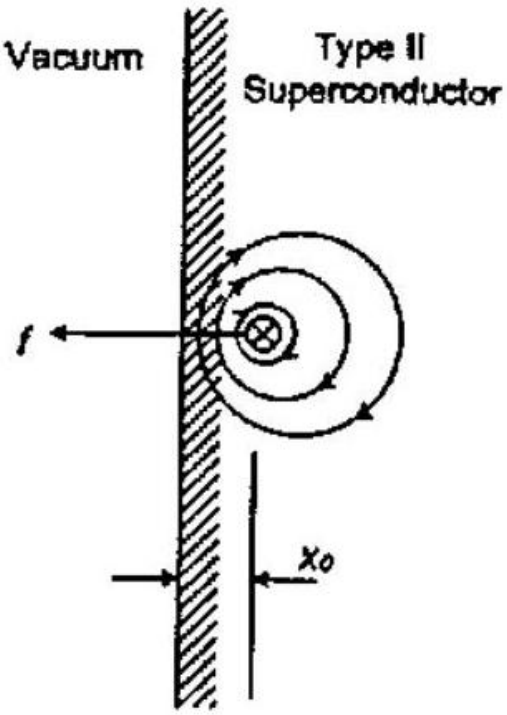


Fig. 5.10. Vortex currents near the surface of a superconductor

Let us explain the form of the function $\mathcal{G}(x_0)$. If $x_0 < \lambda$, the lines of current circulating

around the vortex core are as sketched in Fig. 5.10. It is then evident that, on the left-hand side of the core, the superfluid velocity is larger than on the right-hand side, and the vortex core is subjected to the difference of Bernoulli pressures. This brings about a force pushing the vortex towards the surface. It is easy to see that the same force $f(x_0)$ can be obtained by taking the derivative

$$f = -\mathrm{d}\mathcal{G}/\mathrm{d}x_0 \tag{5.38}$$

which explains the shape of $\mathcal{G}(x_0)$ in Fig.5.9.

To find the force pushing the vortex towards the surface, we shall use the method of images. Since we have assumed $\kappa \gg 1$, the field generated by the vortex satisfies the linear equation (5.5). At the same time, at the surface, the field due to the vortex is zero (this can be proved using arguments similar to those in the well-known problem of a long solenoid: Outside the solenoid, the
condition of zero field at the surface. When solving a linear problem, we may apply the superposition principle and can therefore replace our problem with another, equivalent, one.

Consider an infinite superconductor containing two vortices of opposite signs at $\pm x_0$. Due to the symmetry of the problem, the field at $x = 0$ is zero, while at $x > 0$ equation (5.5) must hold. Since this differential equation has a single-valued solution, the field generated by the two vortices in the semispace $x > 0$ is exactly equal to the field which would be generated by the vortex situated at x_0 if the real surface of a superconductor were present at $x = 0$.

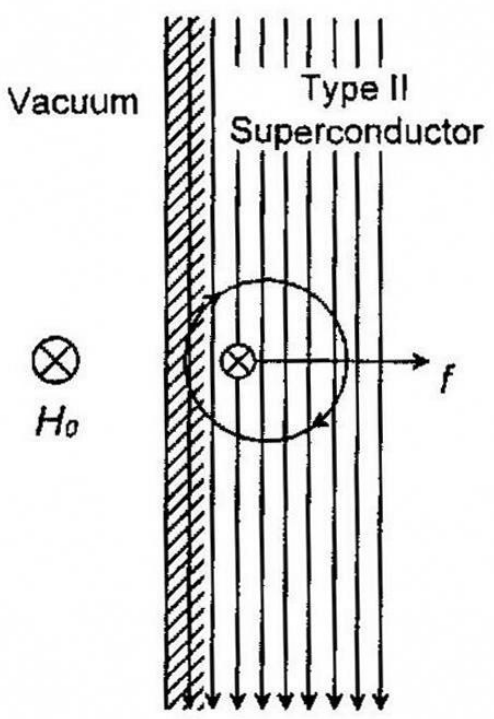


Fig. 5.11. The Meissner current, generated by an external field H_0, pushes the vortex away from the surface

Now it is easy to realize that the interaction of a vortex with the surface (attraction to the surface) can be interpreted as its interaction with its image (also attraction, because the real vortex and the image-vortex have opposite signs).

Let us now switch on an external field H_0 parallel to the surface of the superconductor, as illustrated in Fig. 5.11. This will immediately generate a Meissner current circulating near the surface which will start to push the vortex away from the surface. The result is that, on the one hand, the vortex is attracted to the surface by its own image and, on the other hand, it is repelled from it by the Meissner current. Corresponding variations of the Gibbs free energy with distance, for several values of the external field, are shown in Fig. 5.12. One can see

that at $H_0 < H_{c1}$, a metastable vortex state becomes possible, such that the presence of a vortex in the superconductor is not favored thermodynamically. However, in order to leave the superconductor, the vortex must first overcome an energy barrier. This is the so-called Bean-Livingston barrier.

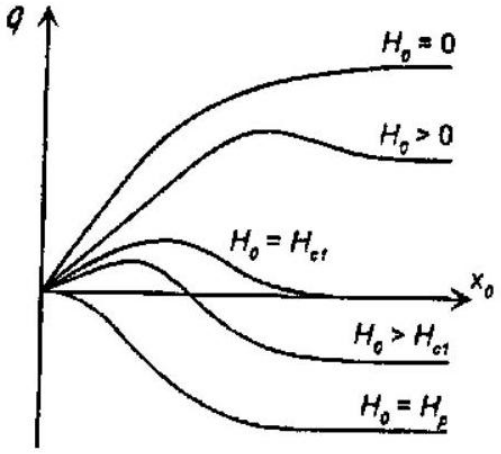


Fig. 5.12. Gibbs free energy of an isolated vortex as a function of its distance from the surface for different values of H_0

The field $H_0 = H_{c1}$ (see Fig. 5.12) is the lowest external field at which it becomes thermodynamically favorable for a vortex to enter the interior of the superconductor. However, the vortex penetration is now hampered by the Bean-Livingston barrier. As we continue to increase the field H_0, the barrier shrinks but does not disappear and the vortex is still unable to penetrate the superconductor. This means that the superconductor remains in the Meissner state which is now metastable and can be understood as a superheated Meissner state.

The barrier finally vanishes at a certain field $H_0 = H_{\mathrm{p}}$, which is sometimes referred to as the superheating field for the Meissner state, or the penetration field. Let us find this field.

Assume that the vortex center is at x_0. The force pushing the vortex towards the surface is the image force, that is, the force due to the interaction of the vortex with the currents generated by its image. From (5.23) we have

$$f_{\mathrm{image}} = \frac{1}{c}\frac{c}{4\pi}\frac{\mathrm{d}H_{\mathrm{v}}}{\mathrm{d}x}\mathbf{\Phi}_0 \tag{5.39}$$

where H_{v} is the field generated by the image vortex and $(c/4\pi)\,(\mathrm{d}H_{\mathrm{v}}/\mathrm{d}x)$ is the current that it generates at $x = x_0$. The interaction force between the vortex and the Meissner current is

$$f_{\mathrm{M}} = \frac{1}{c}\frac{c}{4\pi}\frac{H_0}{\lambda}\mathrm{e}^{-x/\lambda}\Phi_0 \tag{5.40}$$

where $(c/4\pi)\,(H_0/\lambda)\,\mathrm{e}^{-x/\lambda}$ is the current density in the Meissner state.
The Gibbs free energy is

$$\mathcal{G} = -\int f\ \mathrm{d}x \tag{5.41}$$

where $f = f_{\mathrm{M}} + f_{\mathrm{image}}$ is the total force exerted on the vortex. Substituting (5.39) and (5.40) into (5.41) and carrying out the integration, we obtain

$$\mathcal{G}\,(x_0) = -\frac{\Phi_0}{4\pi}H_{\mathrm{v}}\,(2x_0) + \frac{\Phi_0}{4\pi}H_0\mathrm{e}^{-x_0/\lambda} + \ \mathrm{const} \tag{5.42}$$

The field $H_{\mathrm{v}}\,(2x_0)$ in (5.42) is the field generated at x_0 by the image vortex
is still to be determined. At $x_0 \to \infty$, the first two terms in (5.42) are zero. On the other hand, the energy $\mathcal{G}$ at $x_0 \to \infty$ is the Gibbs free energy of a single vortex in an infinite superconductor,

which is defined by (5.15). Using (5.15) and (5.16), we obtain the integration constant in the form

$$\text{const} = \mathcal{G}(\infty) = \frac{\Phi_0}{4\pi}\left(H_{c1} - H_0\right)$$

so that

$$\mathcal{G} = \frac{\Phi_0}{4\pi}\left[H_0 e^{-x_0/\lambda} - H_v\left(2x_0\right) + H_{cl} - H_0\right]. \tag{5.43}$$

It can be easily verified that (5.43) gives a family of curves $\mathcal{G}\left(x_0\right)$ for different values of H_0 which is shown in Fig. 5.12.

The penetration field H_p can be found from a condition which is evident from Fig. 5.12:

$$d\mathcal{G}/dx_{0|x_0=0} = 0. \tag{5.44}$$

Substituting this into the expression for $\mathcal{G}$ (5.43) and using (5.6) and (5.7), we get

$$H_p \approx H_{crn} \tag{5.45}$$

While deriving (5.45) we had to take a derivative of $H_v\left(2x_0\right)$, which caused divergence at $x_0 = 0$. The reason is that at $x_0 = 0$ our approach is no longer appropriate because we have neglected spatial variations of the order parameter ψ. To bypass this difficulty, we assumed that the vortex emerges from the superconductor at $x_0 = \xi$, that is, when it touches the surface with its core, rather than at $x_0 = 0$. The exact calculation, due to de Gennes, leads to precisely the same result:

$$H_p = H_{cm} \tag{5.46}$$

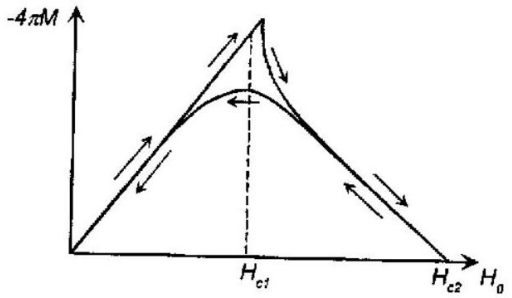


Fig. 5.13. Hysteresis in the magnetization due to the surface barrier

The existence of the Bean-Livingston barrier has been confirmed experimentally. It causes a small hysteresis in the magnetization curve of a homogeneous type-II superconductor near H_{cl}, as illustrated in Fig. 5.13. This hysteresis cannot be removed by improving bulk superconductivity. It is present even if the specimen is made ideally homogeneous.

There have also been direct measurements of H_p: de Blois and de Sorbo [52] studied Nb samples containing small amounts of oxygen, and Nb − Ta alloys. The following results were obtained for specimens with very smooth surfaces finished by electro-polishing: For oxygen-contaminated Nb, the fields were found to be $H_{c1} = 580\text{Oe}, H_{c2} = 7000\text{Oe}, H_{cm} = 1360\text{Oe}$, and $H_p = 1330\text{Oe}$; for Nb − Ta, the fields were $H_{c1} = 110\text{Oe}, H_{c2} = 1600\text{Oe}$, $H_{cm} = 310\text{Oe}$, and $H_p = 180 - 320\text{Oe}$. Comparison of the thermodynamic and penetration fields obtained in these experiments shows that (5.46) is fairly accurate.

In many cases, however, the Bean-Livingston barrier is strongly suppressed. For example, if the surface of a superconductor is rough, the vortices penetrate into it at $H_0 < H_p$.

Let us find the magnetic flux associated with a vortex parallel to the surface and positioned close to it. As follows from the general expression for the Gibbs free energy, for a superconductor with a vortex, one has

$$\mathcal{G} = \mathcal{F} - \Phi H_0/4\pi \tag{5.47}$$

where $\mathcal{F}$ is the free energy of the superconductor containing one vortex (which is independent of the external field H_0) and Φ is the magnetic flux associated with the vortex. On the other hand, the Gibbs free energy $\mathcal{G}$ is given by (5.43). Taking the H_0-dependent terms in (5.43) and comparing them with (5.47), we obtain the following expression for the magnetic flux associated with the vortex near the surface:

$$\Phi = \Phi_0 \left(1 - \mathrm{e}^{-x_0/\lambda}\right) \tag{5.48}$$

According to (5.48), as the vortex moves closer to the surface, its magnetic flux tends to zero. This result can be easily understood. The total magnetic flux of the vortex can be written as

$$\Phi = \int H \, \mathrm{d}S$$

where the integration is carried out over the semiplane $z = 0, x > 0$ and H is the true field due to the vortex. The latter can be considered as the result of a superposition of the fields of the vortex itself and of its image. Taking into account that the sign of the image is opposite to that of the real vortex, we finally have

$$\Phi < \Phi_0$$

7.6.9 5.9 Some Remarks About High-Temperature Superconductors

Despite the fact that there is still no definite theory to explain their high

Table 5.1. Critical temperatures and in-plane coherence lengths ξ_{ab} of some high- T_c superconductors

Material	T_c/K	ξ_{ab} /nm
$(La_{0.925}Sr_{0.075})\,CuO_4$	34	2.9
$YBa_2Cu_3O_7$	92.4	2.5
$Bi_2Sr_2CaCu_2O_8$	84	1.1
$Bi_2Sr_2Ca_2Cu_3O_{10}$	111	1.0
$Tl_2Sr_2Ca_2Cu_3O_{10}$	123	1.6
$HgBa_2Ca_2Cu_3O_8$	133	1.3

the classic sense. This means that the magnetic properties of these materials can be well described by the familiar BCS/Ginzburg-Landau theory. The main differences from the classic superconductors arise from intrinsic material properties such as the extremely short coherence length. Table 5.1 lists the critical temperatures and coherence lengths of some typical materials.

One of the consequences of the short coherence length was already discussed in Chap. 4. Even a grain boundary can be sufficient to suppress superconductivity, and can be used to fabricate weak-link-type Josephson devices from epitaxial films on bicrystalline substrates (see Fig. 4.1).

The second important property of high- T_c superconductors is their huge anisotropy caused by the layered crystal structure. As an example, let us consider the structure of $Bi_2Sr_2CaCu_2O_8$.

The crystal is a stacked sequence

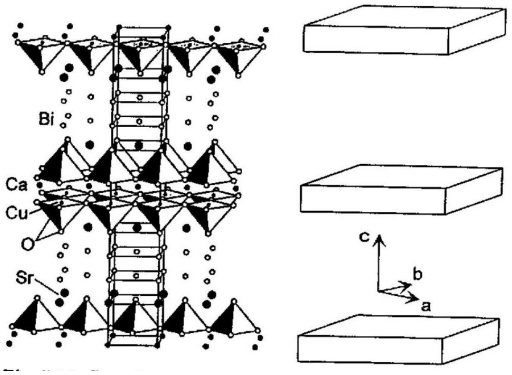


Fig. 5.14. Crystal structure of $Bi_2Sr_2CaCu_2O_8$ (left part). The Cu -O coordination polyhedra are marked for clarity. The right part shows corresponding superconduct-

of CuO_2 planes alternating with other oxide layers (Fig.5.14). The basic building block is the CuO_2 double layer (intercalated by Ca). These blocks are separated by two SrO and two $BiO_{1.5}$ oxide layers. In this structure, there are two principal axes, the in-plane direction and the direction perpendicular to the planes, or c axis. Consequently, we have two critical fields: $H_{c2\parallel}$ and $H_{c2\perp}$, corresponding to the field directions parallel and perpendicular to the planes. The London penetration depth and the coherence length are also anisotropic: $\lambda_{ab}, \lambda_c, \xi_{ab}, \xi_c$. The notation is as follows. Since, for instance, the upper critical field perpendicular to the planes, $H_{c2\perp}$, is determined by vortices whose screening currents flow parallel to the planes, we generalize the coherence length formula (5.26) to

$$H_{c2\perp} = \frac{\Phi_0}{2\pi\xi_{ab}^2} \tag{5.49}$$

Correspondingly, the indices of λ and ξ, 'ab' or 'c', always indicate the direction of the screening currents.

A number of experiments indicate that high- T_c superconductors are inhomogeneous superconductors, i.e., the layered crystal structure is linked to a modulation of the order parameter [53]. Then one can argue that the superconductivity is confined to the CuO_2 planes or double planes. They are separated from neighboring planes by weakly superconducting, normal, or even insulating regions of the crystal. Three-dimensional phase coherence is provided by Josephson currents between the planes.

In order to estimate the critical field parallel to the planes, we neglect the relatively weak coupling between different double planes and consider only a single bilayer. This situation is sketched in the right part of Fig. 5.14. Since the coherence length is about 1.5 nm and the thickness, d, of a CuO_2 double plane is 0.3 nm, we can use the thin film solution of Sect. 3.5. From (3.62) we have:

$$H_{c\parallel} = 2\sqrt{6} H_{cm} \frac{\lambda}{d}$$

The thermodynamic critical field can be calculated from (3.38):

$$H_{cm} = \frac{\Phi_0}{2\sqrt{2}\pi\lambda\xi}$$

which is valid for any pair of λ_i and ξ_i because H_{cm} is an isotropic quantity.
Since only a single bilayer is considered, we obtain:

$$H_{c\parallel} = \sqrt{3}\frac{\Phi_0}{\pi d \xi_{ab}} \tag{5.50}$$

Taking into account (5.49) and (5.50), we obtain for the anisotropy ratio

$$\frac{H_{\mathrm{cl}\parallel}}{H_{\mathrm{c2}\perp}} = 2\sqrt{3}\frac{\xi_{\mathrm{ab}}}{d}$$

This ratio is approximately 17 for $Bi_2Sr_2CaCu_2O_8$. Using the experimen-

10000 kOe, consistent with extrapolations from many experiments. However, in such high fields, pair-breaking effects due to spin-orbit coupling or Pauli paramagnetism are to be expected and these should decrease H_{cll} significantly. We note that, for a less anisotropic material, such as $YBa_2Cu_3O_7$, the assumption of independent superconducting layers might be inappropriate.

If, instead of the above argumentation, we assume a homogeneous order parameter and use the anisotropic Ginzburg-Landau description, $H_{\mathrm{c2}\parallel}$ becomes:

$$H_{\mathrm{c2}\parallel} = \frac{\Phi_0}{2\pi\xi_{\mathrm{ab}}\xi_{\mathrm{c}}}$$

Then the anisotropy ratio is

$$\frac{H_{\mathrm{c2}\parallel}}{H_{\mathrm{c2}\perp}} = \frac{\xi_{\mathrm{ab}}}{\xi_{\mathrm{c}}}$$

In the case of a highly anisotropic material, such as $Bi_2Sr_2CaCu_2O_8$, ξ_{c} would then be of the order of 0.1 nm, i.e., approaching atomic scales. In any case, this is inconsistent with the assumption of a homogeneous order parameter.

The extreme anisotropy is also responsible for many peculiar effects associated with the flux line lattice in high- T_{c} superconductors. A detailed analysis of these effects goes far beyond the scope of this book.

7.6.10 5.10 Critical Current of a Type-II Superconductor. Critical State

Consider a type-II superconductor in the mixed state to which a transport current (that is, a current from an external source) is applied in the direction perpendicular to the vortices. The current gives rise to a Lorentz force on the vortices. If the superconductor were absolutely homogeneous (free of defects), the vortices would start moving at an infinitely small Lorentz force.

Later (in Sect. 5.12) we shall find that vortex motion is accompanied by dissipation of energy. Therefore, the critical current of such an ideally homogeneous superconductor is zero.

In an inhomogeneous type-II superconductor containing various types of defects (grain boundaries, dislocation walls, dislocation tangles, voids, or second-phase precipitates), vortices can be pinned by the defects. A finite transport current is then required to set them moving, such that the Lorentz force produced by it is sufficient to tear the vortices off the defects. The latter are often referred to as pinning centers. The current density corresponding to the initiation of vortex break-off from the pinning centers is called the critical current density, j_{c}.

The critical current density is a structure-sensitive property and can vary by as much as several orders of magnitude as a result of thermal or mechanical
treatment of the material. At the same time, the critical temperature T_{c} and the critical field H_{c2} can remain virtually unaffected. In superconductors which are tailored for superconducting magnets or other superconducting devices, the critical current density can be as large as 10^6 A cm^{-2}.

Let us consider in more detail the flow of the critical current through a type-II superconductor containing a large number of pinning centers. In order for the transport current to

be distributed over the entire cross-section of the specimen, one has to stipulate that the distribution of vortices is inhomogeneous. Indeed, the total current density at a given location is

$$j_{\rm tr} = \frac{c}{4\pi} \operatorname{curl} B \tag{5.51}$$

Furthermore, $B = \Phi_0 n$ is the average field at this location, that is, the average magnetic induction in a region of dimensions much larger than the distance between the vortices; n is the average vortex density. Then it follows from (5.51) that $j_{\rm tr}$ is nonzero only if n is a function of the coordinates: $n = n(r)$.

How does such a state, with the critical current density established across the entire cross-section of the superconductor, set in?

Assume that an infinite plate of thickness d contains a large number of defects which can pin vortices, and $d \gg \lambda$. The surfaces of the plate coincide with the planes $x = \pm d/2$. To begin with, the external magnetic field H_0 is zero and a transport current is applied in the direction of the y axis. At first, the current will flow along the surfaces of the plate (Meissner-Ochsenfeld effect), just as in the case of a homogeneous superconductor. Furthermore, as soon as the field H_I generated by this surface current exceeds the critical value $H_{\rm cl}$, vortices will start to enter the plate from both surfaces, their signs being opposite when they penetrate from the opposite sides. While moving towards the center of the plate, the vortices will be pinned by the defects in the plate and, therefore, will not be able to penetrate far inside. This means that a gradient of the vortex density will appear. Evidently, it will be the maximum possible gradient, that is, the gradient corresponding to the critical value of the current. Thus, certain parts of the plate near the surfaces will carry the critical current while, in the rest of the plate, there will be no current at all. This situation is illustrated in Fig. 5.15 which shows the distribution of the magnetic field in the plate when it carries a current I_1 (per unit length along the z direction).

Let us now increase the current to a certain value I_2. The vortices, while keeping the gradient of their density at $(\nabla n)_c$, will move closer to the center so that only a small central part of the plate will remain free of transport current, while everywhere else the current density will have the critical value. If we continue to increase the current, at some moment it will reach such a value, I_c, that the current density at any point of the plate will be of the critical value, as illustrated in Fig. 5.15 (a). This is the critical state.

Let us now apply an external magnetic field H_0 parallel to the z axis, that is narallel to the surfaces of the nlate and pernendicular to the current.

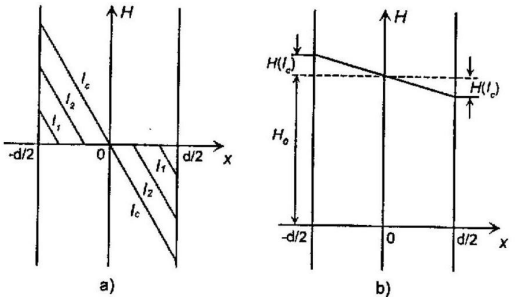


Fig. 5.15. Magnetic field distribution in a plate of thickness d containing pinning centers. The plate carries a current I: (a) the external field is zero and $I_1 < I_2 < I_{\rm c}$ are the currents circulating in the plate; (b) the external magnetic field is finite. Shown is the field distribution in the critical state

Assume that the field is $H_0 \gg H_I$. Neglecting a small difference between $H_0 + H_I$ and $H_0 - H_I$, we can assume that every point of the superconductor is in the field H_0. Then the distribution of current in the critical state will be as shown in Fig. 5.15 (b). The critical gradient of the vortex density in the presence of H_0 is less than that without the field because the critical current is reduced, as explained below.

Indeed, if the Lorentz force per unit length of a vortex is $f_{\mathrm{L}} = j_{\mathrm{tr}}\Phi_0/c$, the Lorentz force per unit volume is $F_{\mathrm{L}} = j_{\mathrm{tr}}B/c$ because the density of the vortices is $n = B/\Phi_0$. When the vortices are at rest, the Lorentz force is balanced by the pinning forces exerted on the vortices. If the average density of the pinning force per unit volume is denoted by F_p, the critical current must satisfy the following equation:

$$\frac{1}{c} j_{\mathrm{c}} B = F_{\mathrm{p}} \tag{5.52}$$

For F_{p} independent of the external field H_0, the critical current is $j_{\mathrm{c}} \propto B^{-1}$. This dependence has indeed been observed in many experiments.

If the distribution of pinning centers in a superconductor is random, they cannot pin an absolutely rigid vortex lattice. To elucidate this statement, let us shift the lattice by a small distance in the direction of the Lorentz force. This displacement obviously does not change the energy of the system because the random distribution of pinning centers relative to the rigid vortex lattice remains essentially the same as before. And since there is no variation of energy, there is no restoring force which would push the vortices to their old positions, that is, there is no pinning.

The situation is quite different if we assume that the vortex lattice is an elastic medium. Then every time when we shift the vortex lattice, it will
that the energy of the vortex system as a whole is a minimum. Therefore, if we try to shift the vortex lattice in this case, a certain effort is needed to overcome the restoring force and tear the vortices off the pinning centers. Clearly, the 'softer' the vortex lattice, i.e., the more pliable it is, the larger the pinning force.

At $H_0 \to H_{c2}$, the elastic moduli of the vortex lattice decrease, that is, the lattice becomes softer and pinning becomes stronger. This results in a maximum of the critical current at $H_0 \to H_{c2}$ (peak effect) which is often observed in experiment (see Fig. 5.16).

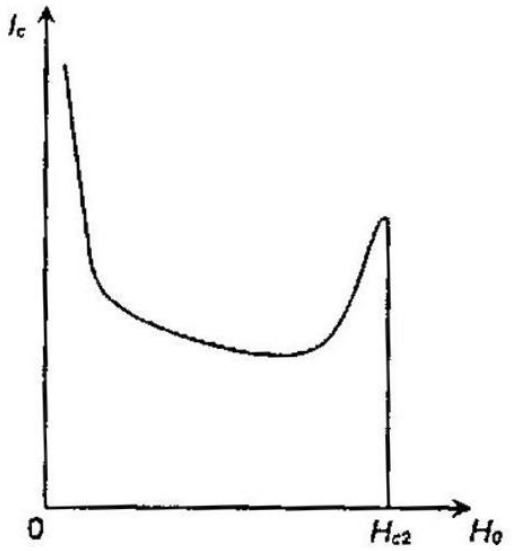


Fig. 5.16. Dependence of the critical current on perpendicular magnetic field. A pronounced peak effect is observed at $H_0 \approx H_{c2}$

7.6.11 5.11 Interaction of Vortices with Pinning Centers

Vortices interact with many different types of defects, which often leads to large values of the critical current. The objective of this section is to study in some detail several simple examples of defects and consider the physical mechanisms by which they interact with vortex lines. One should bear in mind that not every defect can interact with vortices effectively. In the classic

superconductors, for example, vacancies, individual second-phase atoms, or other similar tiny defects are not effective as pinning centers for an obvious reason: as a rule, the characteristic size of a vortex - the coherence length exceeds by far the atomic size, i.e., the characteristic size of such a defect. Therefore, a vortex simply 'does not notice' them. Conversely, structural defects with dimensions $\sim \xi$ and larger are very effective and can be the cause of very large critical current densities.

However, the situation is different for high- T_c superconductors. There, the coherence lengths are so small that point defects have sizes comparable to ξ. We shall discuss some aspects of this qualitatively new situation in Sect. 5.11.2.

5.11.1 Interaction of Vortices with the Surface of a Superconductor

Let us consider an ideally homogeneous type-II superconductor in the form of a plate of thickness $d \gg \lambda$. An external magnetic field H_0 is parallel to the surface of the plate; in addition, $H_{c1} \ll H_0 \ll H_{c2}$ and $\kappa \gg 1$. Then the vortices in the plate form a triangular lattice with period $a \ll d$. According to detailed calculations, the distance between the edge of the plate and the vortex row nearest to it is $\sim a$. To a good accuracy, a can be assumed constant over the plate.

As we switch on a small transport current through the plate, so that it is perpendicular to the magnetic field, the current generates a field H_I, and the total field at one side of the plate becomes $(H_0 + H_I)$ and at the other $(H_0 - H_7)$. We already know that a stable state with a gradient of the vortex density is not possible in a homogeneous superconductor. Therefore, in response to the applied current, the vortex structure must shift as a whole in the direction of the Lorentz force. Since the vortices had been at equilibrium before the current was applied, even a very small displacement from their equilibrium positions ought to bring about a restoring force. The result will be an elastic shift of the whole vortex structure by a certain distance determined by the balance between the Lorentz force and the restoring force. If the Lorentz force, acting against the restoring force, is sufficient to shift the vortices by a distance $\sim a$, a continuous flow of vortices will start. Indeed, as a vortex row comes to the edge of the plate on one side, it is annihilated by its image. At the same time, an identical row enters the plate from the opposite side and moves by a distance $\sim a$ thereby leaving enough room for a new vortex row to enter. Then a new row enters the plate, the whole structure shifts again by the distance $\sim a$, etc. This implies that the transport current shifting the vortex lattice by $\sim a$ is the critical current.

Assume that our superconductor is now in thermodynamic equilibrium. Then a magnetizing current I_M along its surface is determined by the difference between the external field H_0 at the surface and the average field B in the interior:

$$I_M = \frac{c}{4\pi} |B - H_0| = cM$$

The density of the magnetizing current can be written as

$$j_M = \frac{c|M|}{\lambda} \mathrm{e}^{-x/\lambda}, \tag{5.53}$$

where x is the distance of a given point from the edge of the plate. A vortex occupying the position x is then acted upon by the Lorentz force

$$f_M = \frac{1}{c} j_M \Phi_0 = \frac{|M|\Phi_0}{\lambda} \mathrm{e}^{-x/\lambda}$$

If the vortex shifts by a small distance δx, f_M changes by δf_M:

$$|\delta f_M| = \frac{M\Phi_0}{\lambda^2}\mathrm{e}^{-x/\lambda}\delta x$$

The force f_M is applied only to the vortices within a surface layer $\sim \lambda$. Therefore, the net change of the force on the vortex system, as it shifts by δx, is

$$\frac{|M|\Phi_0}{\lambda^2}\delta x\frac{\lambda}{a}$$

In order to obtain the final expression for the restoring force F_{restore} per unit area of the surface, we multiply the last expression by the number of vortices within the unit length along the direction of the current, i.e., by $1/a$, and further multiply it by 2 (in order to take into account the second edge of the plate):

$$F_{\text{restore}} = \frac{2|M|\Phi_0}{\lambda a^2}\delta x \tag{5.54}$$

Recalling that $a^2 \approx \Phi_0/B$, we have

$$F_{\text{restore}} = \frac{2|M|B}{\lambda}\delta x \tag{5.55}$$

As was already mentioned, the condition for equilibrium is that F_{restore} equals the Lorentz force per unit area of the surface,

$$\mathcal{F}_{\text{L}} = \frac{1}{c}I_{\text{tr}}B \tag{5.56}$$

where I_{tr} is the transport current per unit length of the plate. The current I_{tr} reaches its critical value when δx becomes equal to $a \approx (\Phi_0/B)^{1/2}$. Substituting this into (5.55) and equating it to (5.56) we get

$$I_c = \frac{2c|M|\sqrt{\Phi_0}}{\lambda\sqrt{\bar{B}}} \tag{5.57}$$

The average of the critical current density over the cross-section is

$$j_{\text{c}} = \frac{2c|M|\sqrt{\Phi_0}}{\lambda\sqrt{B}d} \tag{5.58}$$

The last formula agrees well with experiment.

Let us draw some conclusions. First, we shall outline our present understanding of the flow of transport current through a superconducting plate in the mixed state. If the current is below the critical value, the Lorentz force causes an elastic shift of the vortex structure as a whole by a certain distance $\delta x < a$. As soon as this happens, the Lorentz force is balanced by a restoring force brought about by the shift, and the vortex lattice comes to rest. The lattice period is the same everywhere; therefore, in the interior of the plate, the transport current is zero. In other words, the transport current flows within the layer $\sim \lambda$ near the surface.

Let us estimate the maximum transport current, i.e., the critical current.
$d \sim 10^{-4}$ cm. Then $|M|$ is $\sim$ 1G. Substituting these into (5.58) we obtain $j_{\text{c}} \sim 10^5$ A cm^{-2}. Thus, even a homogeneous superconducting plate in the mixed state is capable of carrying a rather large transport current. Now let us imagine a thick superconducting plate consisting of a set of thin superconducting plates, already familiar to us, which are separated from each other by thin layers of an insulator or a normal metal. In this construction, the transport current can flow along every surface of every thin plate (within the surface layer $\sim \lambda$, of course) so that the resulting transport current through our composite superconductor will be very large.

An experimental verification of (5.58) was obtained by Campbell, Evetts and Dew-Hughes [55] who studied the interaction of vortices with inclusions of a normal metal in a Pb – Bi alloy.

5.11.2 Interaction of a Vortex with a Cavity in a Superconductor

Consider an infinite superconductor containing a defect in the form of a cylindrical cavity. How will a single vortex parallel to the cavity interact with it?

Assume that the diameter of the cavity satisfies the inequality $d > \xi(T)$. Then the interaction energy can be very easily estimated. If the vortex is far away from the cavity, its normal core (of diameter $\sim 2\xi$) stores a positive energy (relative to the energy of the superconductor without the vortex) because the free energy of the normal state exceeds that of the superconducting state by $H_{\rm cm}^2/8\pi$ per unit volume. Then the energy of the normal core, per unit length, is

$$\frac{H_{\rm cm}^2}{8\pi}\pi\xi^2 \tag{5.59}$$

On the other hand, if the vortex is trapped by the cavity, i.e., passes through its interior, it does not have a normal core and, accordingly, the energy of the system is reduced by the amount of (5.59). This means that the vortex is attracted to the cavity. The interaction force per unit length, f_p, can be found easily if we recall that the energy changes by the value of (5.59) when the vortex changes its position near the edge of the cavity by $\sim \xi$:

$$f_{\rm p} \approx H_{\rm cm}^2\xi/8 \tag{5.60}$$

If, instead of a cylindrical cavity, the superconductor contains a spherical cavity of diameter d, the pinning force $f_{\rm pd}$ on the vortex can be obtained from (5.60):

$$f_{\rm pd} \approx H_{\rm cm}^2\xi d/8 \tag{5.61}$$

To get an idea of how large this force is, let us find the current that must be applied in the direction perpendicular to the vortex in order to produce

We know that the Lorentz force per unit length of a vortex is $j\Phi_0/c$. Then the force applied to the part of the vortex which actually interacts with the defect is $j\Phi_0 d/c$. Equating this to $f_{\rm pd}$(5.61), we get

$$j = \frac{cH_{\rm cm}^2}{8\Phi_0}\xi \tag{5.62}$$

Furthermore, since $H_{\rm cm} = \Phi_0/2\sqrt{2}\pi\lambda\xi$ (see (3.38)), we obtain from (5.62)

$$j = \frac{cH_{cm}}{16\sqrt{2\pi\lambda}}$$

One can easily verify that j in the last expression is of the same order of magnitude as the pair-breaking current considered earlier in Sect.3.6. Thus, in order to tear the vortex off a spherical void, one should apply the maximum possible current for a given superconductor.

The above reasoning is also valid in the case of a superconductor containing tiny dielectric inclusions. It will also remain valid (at least by the order of magnitude) if the inclusions are of a normal metal, provided the size of the inclusions is larger than ξ. The restriction is due to the proximity effect which is essential only at distances of the order ξ from the interface. We can then conclude that various types of normal inclusions represent effective pinning centers in superconductors. This property is widely used in technical applications when large critical currents and fields are involved.

Consider, for example, a Nb − Ti alloy used in many superconducting devices where large critical currents are of importance. A typical thermal treatment of such an alloy is as follows: a Nb-Ti wire is tempered from 800°C and then annealed for a short time ($\sim$ 30 minutes) at $\approx$ 400°C. This results in a partial transformation of the superconducting β-phase into a

nonsuperconducting α-phase, in the form of tiny precipitates of α-phase in the superconducting matrix. As a result of this treatment, the critical current increases by several orders of magnitude.

Among other effective pinning centers in superconductors are dislocations, dislocation walls, grain boundaries, and interfaces between superconductors with different parameters.

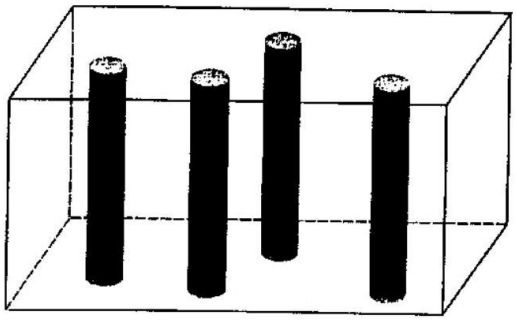


Fig. 5.17. Nuclear tracks of fast heavy ions form cylindrical amorphous regions in high- T_c superconductors

The above analysis of vortex-defect interactions forms the basis for interpreting the effects of the so-called columnar defects [56] produced in highT_c superconductors by heavy-ion irradiation. Nuclear tracks of high-energy heavy ions form cylindrical amorphous regions in the material (see Fig. 5.17). It is generally accepted that the material in the columnar defects is not superconducting.

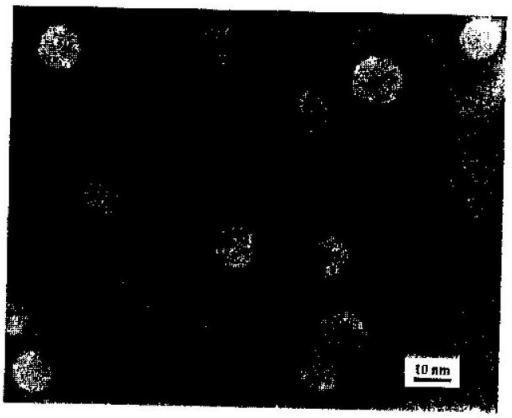


Fig. 5.18. Nuclear tracks in $Bi_2Sr_2CaCu_2O_8$ produced by irradiation with 865 MeV Pb ions. The fluence was 5×10^{10} cm^{-2}

The nuclear tracks have the useful property that their diameter is only $5 - 10$ nm, i.e., of the order of the coherence length. As we have just seen, cavities with such sizes make extremely effective pinning centers. This is one of the very few possibilities for producing artificial defects of sizes comparable with the coherence length of high- T_c superconductors. This length is so short that conventional metallurgical methods used to produce pinning centers such as precipitates or grain boundaries are either ineffective, due to the large sizes of the defects, or not applicable at all, due to the brittleness of the materials.

Fig. 5.18 shows a transmission electron micrograph of the nuclear tracks in $Bi_2Sr_2CaCu_2O_8$ [57]. The view is along the direction of the ion beam. Columnar defects show up as bright circular spots. Each defect is able to trap approximately one vortex. Hence the optimum pinning efficiency can be expected at fields for which the vortex lattice period is less than the average distance between the amorphous tracks. Decoration patterns (c.f. Sect.5.1) obtained on a virgin and an irradiated $Bi_2Sr_2CaCu_2O_8$ crystal (see Fig. 5.19) show the effect of columnar defects when the distance between the vortices just matches the average distance between the defects [58]. The originally regular vortex lattice is heavily deformed due to pinning by columnar defects. The defects were produced by 2.7GeV^{238}U ions.

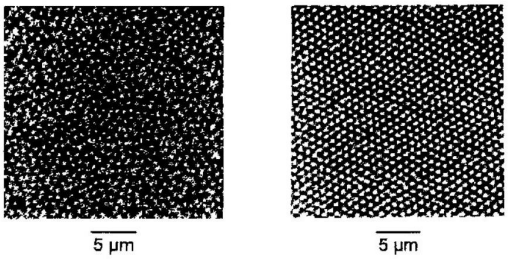


Fig. 5.19. Vortex lattice in $Bi_2Sr_2CaCu_2O_8$ with columnar defects observed by decoration (left part). The applied magnetic field of 40 Oe is such that the vortex spacing just matches the average distance between the defects. For comparison, the right part shows the decoration pattern for the unirradiated sample

7.6.12 5.12 Resistive State

Let us discuss what happens when the Lorentz force due to an applied current becomes larger than the pinning force and vortex flow in the direction perpendicular to the applied current sets in.

We shall show that such a vortex flow results in dissipation of energy and a finite electric resistance. This state of the vortex system is therefore referred to as the resistive state.

By Faraday's law of electromagnetic induction, a flow of magnetic flux generates an electric field E in the same direction as the applied current. [1] This means that an energy dissipation $Ej_{\rm tr}$ arises across the bulk of the superconductor. Assume that the velocity of the vortices in the direction of the Lorentz force, that is, in the direction perpendicular to both the current and the magnetic field, is $v_{\rm L}$. Then the work done by the external source to keep the vortices moving will be $F_{\rm L}v_{\rm L}$, per unit time, where $F_{\rm L}$ is the density of the Lorentz force. Obviously, this work is equal to the energy dissipated by the system per unit volume and unit time, that is,

$$F_{\rm L}v_{\rm L} = Ej_{\rm tr} \tag{5.63}$$

Recalling that $F_{\rm L} = j_{\rm tr}B/c$, we obtain

$$E = Bv_{\rm L}/c \tag{5.64}$$

The resistivity of a superconductor resulting from the flux flow is referred to as the flux-flow resistivity and denoted by $\rho_{\rm f}$:

$$\rho_{\rm f} = E/j_{\rm tr} \tag{5.65}$$

The fact that the vortex motion is accompanied by dissipation of energy allows us to assume that the vortices move in a viscous medium. We introduce
a viscosity coefficient η:

$$f_{\rm friction} = -\eta v_{\rm L}$$

where $f_{\rm friction}$ is the friction exerted on one vortex moving with the velocity $v_{\rm L}$. Neglecting the vortex mass, we obtain an equation of motion for the vortex in the form

$$f_{\rm friction} + f_{\rm L} = 0$$

After substituting the relevant expressions for the forces per unit volume, this equation becomes

$$\frac{B}{\Phi_0}\eta v_{\rm L} = \frac{1}{c}Bj_{\rm tr} \tag{5.66}$$

Using (5.64) and (5.65), we can rewrite (5.66) as

$$\rho_{\rm f} = \frac{\Phi_0 B}{c^2\eta} \tag{5.67}$$

If η is independent of magnetic field, the resistivity $\rho_{\rm f}$ is a linear function of B. The linear dependence is indeed observed in experiments at low temperatures. An empirical formula at $T \to 0$ reads:

$$\rho_{\rm n} = \frac{\Phi_0 H_{\rm c2}}{c^2\eta}$$

It can be used to determine the viscosity coefficient at low temperatures:

$$\eta = \frac{H_{\rm c2}(0)\Phi_0}{c^2\rho_{\rm n}} \tag{5.68}$$

Here $\rho_{\rm n}$ is the normal-state resistivity of the superconductor. It is of interest to evaluate the order of magnitude of the flux flow velocity in a real experiment. Assume that the electric field in the resistive state is $E \sim 10^{-6}$ V cm^{-1} and the magnetic induction is $B \sim 10^4$G. Then, by (5.64), we have

$$v_{\rm L} = \frac{cE}{B} = 3\times 10^{10}\frac{10^{-6}}{300}\frac{1}{10^4} = 10^{-2}\ \text{cm s}^{-1}$$

A typical current-voltage characteristic of a superconductor in the resistive state is shown in Fig. 5.20. A finite voltage appears at a certain value of current (the critical current) and, at small values of the voltage, the characteristic is nonlinear. The nonlinear part corresponds to a flow of vortices that is not yet stabilized, that is, to flux creep, where the vortices jump randomly from one pinning center to another. As the current is increased further, the current-voltage characteristic becomes linear. The linear part corresponds to the flow of the vortex structure as a whole.

There are two ways to define the critical current on an $I-V$ characteristic. The current $I_{\rm cs}$ - the minimum current giving rise to a finite voltage - is the static critical current. At I_{cs}, the process of vortex break-off from pinning

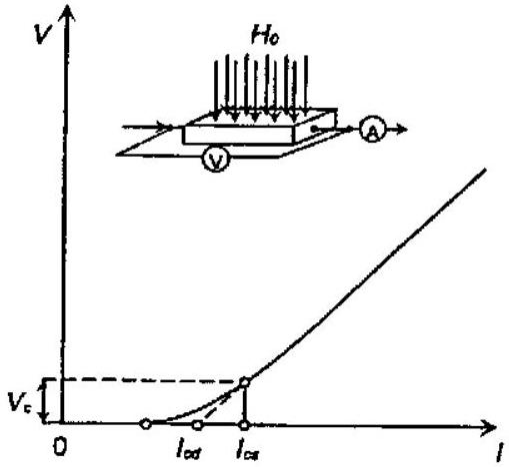


Fig. 5.20. Current-voltage characteristic of a superconductor containing crystal defects. Two ways of defining the critical current are illustrated: I_{cs} is the static and I_{cd} the dynamic critical current

depends on the actual value of the voltage that is assumed to correspond to the critical current.

[2] A series of experiments [59] was intended to clarify the extent to which the critical current I_{cs} depends on the voltage threshold (or, in other words, on the sensitivity of the voltage measurements). It was found that at $H_0 \ll H_{c2}$, an enhancement of the sensitivity by several orders of magnitude leads to negligibly small changes of the critical current.

The second definition of the critical current is I_{cd}, the dynamic critical current. This value is obtained by extrapolating the linear part of a currentvoltage characteristic until it intersects the I axis.

Finally, let us mention some features that are common to the resistive state of a type-11 superconductor and the ac Josephson effect (Josephson radiation) [60].

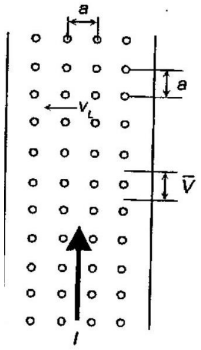


Fig. 5.21. Vortex structure in a type-II superconductor subjected to the Lorentz force moves with velocity v_L

Suppose that a bulk type-II superconductor is in the resistive state and the average magnetic induction in its interior is B. Assume, for the sake of simplicity, that the vortices form a square lattice as illustrated in Fig. 5.21. This assumption does not affect the generality of our discussion.

Under the Lorentz force from a current I applied to the superconductor, the vortex structure moves with velocity v_{L}, thereby generating an electric field

$$E = \frac{1}{c} B v_{\mathrm{L}}$$

The average voltage $\bar{V}$ over the vortex period a is then

$$\bar{V} = \frac{a}{c} B v_{\mathrm{L}} \tag{5.69}$$

(see Fig. 5.21). It is evident that the vortex lattice displacement has a translational symmetry with period a. One can therefore expect that the voltage V will have an ac component of frequency

$$\omega = 2\pi \frac{v_{\mathrm{L}}}{a}. \tag{5.70}$$

Substitution of this in (5.69) yields

$$\bar{V} = \frac{\omega B a^2}{2\pi c}$$

Note that Ba^2 is the magnetic flux associated with one vortex, i.e., the flux quantum Φ_0. Therefore

$$\bar{V} = \frac{\hbar \omega}{2e}$$

We have arrived at an expression identical to (4.21).

[2] A 10^{-6} V threshold is applied in the majority of technical applications, i.e., a

This radiation in type-II superconductors is very difficult to observe. Owing to the inevitable structural defects and inhmogeneities, the motion of the vortex lattice is random and turbulent, rather than coherent and laminar. However, if one takes special precautions to make the vortex motion well-ordered, it should be possible, in principle, to observe features in the resistive state of a type-II superconductor similar to those characteristic of the ac Josephson effect [61].

Problems

Problem 5.1. Two parallel superconducting vortices in an infinite superconductor are fixed at positions a and b. The distance between them is d (see Fig. 5.22). A third vortex of the same sign is allowed to move along the dashed line perpendicular to ab and passing through its middle. Find the force exerted on the third vortex as a function of the distance x from the line ab. All distances in the problem are much smaller than λ and $\kappa \gg 1$.

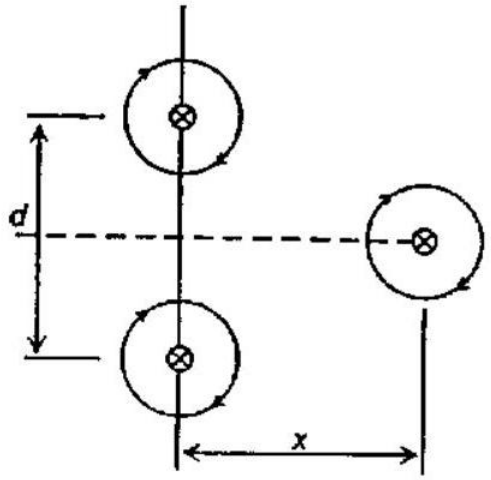


Fig. 5.22. See Problem 5.1. Two vortices are at a fixed distance d from each other. The third vortex is allowed to move along the dashed line

Problem 5.2. A superconducting alloy has an upper critical field of 30 kOe and a thermodynamic critical field of 1500 Oe. Find the magnetic field penetration depth.

Problem 5.3. Find the lower critical field of a superconducting specimen of Nb − Ta if $H_{c2} =$ 4000Oe and $\kappa = 3$.

Problem 5.4. Consider a superconductor with $\kappa \gg 1$. Find the density of vortex currents at the distance $r = \xi$ from the center of an isolated vortex.

Problem 5.5. A superconducting alloy has $H_{c2} =$ 150kOe and $\kappa = 96$. Find the energy of an isolated vortex in this alloy. Compare it with the condensation energy stored in the normal core of the vortex.

Problem 5.6. A superconducting alloy has $H_{c2} =$ 50kOe and $\kappa = 60$. Find the magnetic moment per unit volume, M, for an external field $H_0 =$ 10kOe.

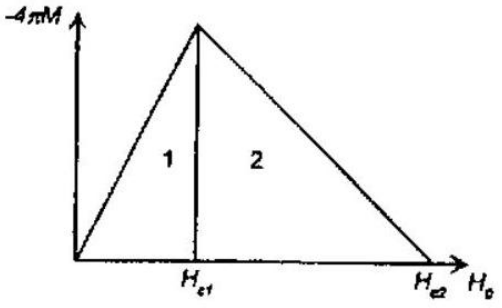


Fig. 5.23. Approximation of the magnetization curve by two triangles. Triangle (1) is defined by $-4\pi M = H_0$, triangle (2) by $-4\pi M = (H_{c2} - H_0) / [1.16\,(2\kappa^2 - 1)]$

Problem 5.7. A Nb -Ta superconducting alloy has an upper critical field $H_{c2} =$ 4000 Oe

and $\kappa = 3$. Approximate the magnetization curve of the alloy by two triangles, as illustrated in Fig. 5.23. Find the lower critical field H_{c1} and the thermodynamic critical field H_{cm}. Compare the value of H_{c1} with the answer to Problem 5.3 and that of H_{cm} with its true value (the latter can be found proceeding from the known value of H_{c2}).

Problem 5.8. Find the third critical field of a superconducting alloy that has $H_{cm} = 900$Oe and $\lambda = 2500$Å.

Problem 5.9. Find the third critical field of a superconductor with the coherence length $\xi = 90$Å.

Problem 5.10. Find the attractive force exerted on a vortex by the surface of a flat superconductor if the vortex is parallel to the surface at a distance $l = 500$Å,

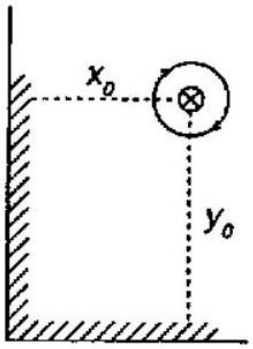


Fig. 5.24. See Problem 5.11

Problem 5.11. An isolated vortex is placed in the vicinity of the surface of a superconductor as shown in Fig. 5.24. Find the total force exerted on the vortex by the surfaces if $\lambda = 1500$Å, $x_0 = 400$Å, and $y_0 = 600$Å.

Problem 5.12. Find the force with which a vortex interacts with the Meissner current if the vortex is parallel to the flat surface of a superconductor and the distance between the surface and the vortex is $l = 400$Å. The external field is $H_0 = 50$Oe and $\lambda = 1000$Å.

Problem 5.13. Find the superheating field of the Meissner state if $\kappa = 24$ and $\lambda = 2000$Å.

Problem 5.14. A perfectly homogeneous superconducting plate of thickness $l = 5$ mm is placed in an external magnetic field $H_0 \approx B = 18$kG. The field is parallel to the surface of the plate and perpendicular to a transport current. Find the critical current of the plate if $H_{c2} = 75$kOe and $H_{c1} = 130$Oe.

Problem 5.15. Estimate the flux flow resistivity ρ_f if the external field is $H_0 = 5 \times 10^3$Oe, $T_c = 10$ K, and $H_{c2}(T = 4.2\text{ K}) = 40$kOe. The remnant normal-state resistivity of the specimen is $\rho_n = 3 \times 10^{-5}\Omega$ cm.

Problem 5.16. A superconducting wire of length $l = 8$ cm is placed in an external field $B = 5$ T and is in the resistive state. Find the velocity v_L of moving vortices if the voltage across the wire is $U = 1.5 \times 10^{-5}$ V.

7.7 Type II Superconductors: Advanced Properties

7.7.1 35*. Anisotropic Type-II Superconductors

Очень многие сверхпроводники II рода имеют сильно анизотропную (слоистую) кристаллическую структуру; таковы все представители семейства BTC, $NbSe_2$ и многие другие соединения. Вследствие этого и их электронные свойства оказываются анизотропными. Энергия электрона может быть выражена через эффективные электронные массы поперек $(m_\perp)$ и вдоль $(m_\parallel)$слоев:

$$E_p = \frac{p_z^2}{2m_\perp} + \frac{p_x^2 + p_y^2}{2m_\parallel}$$

причем $m_\perp \gg m_\parallel \sim m$, где m-обычная электронная масса. В результате оказываются

зависящими от направления и параметры, характеризующие сверхпроводящее состояние - длина когерентности, лондоновская глубина проникновения, первое и второе критические поля. Если интересующий нас анизотропный сверхпроводник имеет $\varkappa \gg 1$, можно применить простой прием, предложенный в работе [94], чтобы найти все эти угловые зависимости.

Начнем наше рассмотрение со свободной энергии ГинзбургаЛандау для анизотропного случая:

$$\mathcal{G}_{sH} = \mathcal{G}_n + \int \left[\alpha|\Psi|^2 + \frac{\beta}{2}|\Psi|^4 + \right.$$
$$+ \frac{1}{4m_\parallel}\left|-i\hbar\nabla_\parallel\Psi - \frac{2e}{c}\mathbf{A}_\parallel\Psi\right|^2 + \frac{1}{4m_\perp}\left|-i\hbar\nabla_z\Psi - \frac{2e}{c}\mathbf{A}_z\Psi\right|^2 +$$
$$\left. + \frac{(\nabla\times\mathbf{A})^2}{8\pi} - \frac{(\nabla\times\mathbf{A})\cdot\mathbf{H}_0}{4\pi}\right] dV \tag{35.1}$$

Далее удобно использовать параметр анизотропии ε, определенный как $m_\parallel/m_\perp = \varepsilon^2 \ll 1$. Сделаем в выражении (35.1) замену координат и компонент векторного потенциала:

$$x = \tilde{x}, \quad y = \tilde{y}, \quad z = \varepsilon\tilde{z}, \quad A_x = \tilde{A}_x, A_y = \widetilde{A}_y, \quad A_z = \frac{\tilde{A}_z}{\varepsilon}. \tag{35.2}$$

В новых переменных члены в (35.1), содержащие градиенты, станут изотропными, однако анизотропия появится в членах с магнитной энергией. Действительно, преобразования (35.2) для компонент вектора индукции $\mathbf{B} = \nabla\times\mathbf{A}$ имеют вид

$$B_x = \frac{\widetilde{B}_x}{\varepsilon}, \quad B_y = \frac{\widetilde{B}_y}{\varepsilon}, \quad B_z = \widetilde{B}_z \tag{35.3}$$

так что магнитная энергия запишется в виде

$$\mathcal{G}_M = \frac{1}{8\pi}\int\left[\frac{\widetilde{B}_\parallel^2}{\varepsilon^2} + \widetilde{B}_\perp^2 - 2\left(\frac{\widetilde{\mathbf{B}}_\parallel\mathbf{H}_\perp}{\varepsilon} + \widetilde{B}_\perp H_\perp\right)\right] dV. \tag{35.4}$$

Для сверхпроводников с очень большим параметром $\varkappa$ магнитную индукцию B можно часто считать постоянной по образцу, в то время как параметр порядка $\Psi(\mathbf{r})$ может быть сильно неоднороден (например, вблизи вихрей). Именно в таких случаях полезно преобразование (35.2): минимизируя G_M по компонентам вектора $\widetilde{\mathbf{B}}$, найдем

$$\widetilde{\mathbf{B}} = (\varepsilon H_x, \varepsilon H_y, H_z)\,, \tag{35.5}$$

что соответствует равенству B = $\mathbf{H}$ для изотропной системы; такое приближение пригодно при $B \gg H_{c1}$. Преобразование (35.2) не меняет длин в плоскости слоев, поэтому мы сохраним обозначения ξ и λ за длиной когерентности в плоскости слоев и глубиной проникновения токов, текущих вдоль них.

В качестве примера найдем с помощью преобразования (35.2) зависимость второго критического поля H_{c2} от угла ϑ между вектором магнитной индукции B и плоскостью слоев. Введем функцию $\varepsilon(\vartheta) \equiv \varepsilon_\vartheta$, определив ее равенством $\varepsilon_\vartheta^2 = \varepsilon^2\cos^2\vartheta + \sin^2\vartheta$. Тогда из соотношения (35.5) следует, что магнитное поле $\mathbf{H}$ действует на анизотропный сверхпроводник так же, как поле $\varepsilon_\vartheta H$ на сверхпроводник изотропный. Отсюда немедленно находим:

$$H_{c2}(\vartheta) = \frac{\Phi_0}{2\pi\varepsilon_\vartheta\xi^2} \tag{35.6}$$

В частном случае, когда поле направлено параллельно слоям, второе критическое поле максимально, $H_{c2}^{\parallel} = \varepsilon^{-1} H_{c2}^{\perp}$. Этот результат можно также выразить как $H_{c2}^{\parallel} = \Phi_0 / (2\pi\xi\xi_\perp)$, где $\xi_\perp = \varepsilon\xi$ длина когерентности в поперечном к слоям направлении; это соотношение между $\xi_\perp$ и ξ следует уже из вида свободной энергии (35.1).

Термодинамическое критическое поле H_{cm} не может зависеть от направления поля (поскольку оно просто определяет плотность энергии, выигранной при переходе в сверхпроводящее состояние, $\mathcal{G}_n - \mathcal{G}_s = H_{cm}^2/8\pi$). С другой стороны, обычно $H_{c1}H_{c2} = H_{cm}^2 \ln(\lambda/\xi)$, т. е. следует ожидать, что первое критическое поле будет зависеть от угла ϑ противоположным (по сравнению с (35.6)) образом. Для определения $H_{c1}(\vartheta)$ метод преобразования (35.2) непригоден, т.к. вблизи первого критического поля распределение $B(\mathbf{r})$ максимально неоднородно. Расчеты [95] в рамках лондоновского приближения дают

$$H_{c1}(\vartheta_H) = \frac{\Phi_0}{4\pi\lambda^2} \frac{\varepsilon}{\varepsilon_{\theta_H}} \ln\frac{\lambda}{\xi} \tag{35.7}$$

где $\theta_H = \pi/2 - \vartheta_H$, а ϑ_H - угол между направлением магнитного поля $\mathbf{H}$ и плоскостью слоев (в полях порядка первого критического направления магнитного поля H и индукции B, вообще говоря, отличаются). Первое критическое поле минимально в направлении слоев, что легко понять - плотность экранирующих токов, текущих в направлении поперек слоев, уменьшена по сравнению с токами вдоль слоев, так что длина экранирования возрастает, $\lambda_\perp = \varepsilon^{-1}\lambda$.

До сих пор мы подразумевали, начиная с выражения для свободной энергии (35.1), что сверхпроводник может быть описан как непрерывная трехмерная среда, хотя и анизотропная. Для того чтобы это было справедливо, поперечная длина когерентности $\xi_\perp(T)$ должна быть велика по сравнению с расстоянием d между сверхпроводящими слоями в слоистой структуре. Если и низкотемпературная длина когерентности $\xi_{0\perp} = \varepsilon\xi_0$ больше d, то сверхпроводник всегда можно считать непрерывным; в случве $\xi_{0\perp}/d < 1$ непрерывное описание пригодно достаточно близко к T_c, где длины когерентности $\xi(T)$ и $\xi_\perp(T)$ возрастают. В области $\xi_\perp(T)/d < 1$ материал естественно рассматривать как набор тонких сверхпроводящих слоев со слабыми (джозефсоновскими) связями между слоями. К этой категории относятся высокотемпературные сверхпроводники семейства $Bi - Sr - Ca - Cu - O$, у которых параметр анизотропии $\varepsilon^{-1} > 100$. В первом приближении при рассмотрении такого вещества джозефсоновской связью между слоями можно вовсе пренебречь и рассматривать его как набор двумерных сверхпроводящих слоев, связанных лишь магнитным взаимодействием. Мы не будем здесь останавливаться подробнее на свойствах слоистых квазидвумерных сверхпроводников; их обсуждение можно найти, например, в обзоре [96].

7.7.2 36*. Разрушение сверхпроводимости в тонкой пленке тепловыми вихрями

36.1. Фазовый переход Березинского-Костерлица Таулеса.

В тонких сверхпроводящих пленках (толщиной $d \ll \lambda$) вихри, аналогичные абрикосовским, могут не только рождаться внешним поперечным магнитным полем, но и возникать при $H_0 = 0$ (чисто флуктуационным образом). В этом случае плотности вихрей с положительной и отрицательной циркуляциями совпадают. Однако возникшие из-за тепловых флуктуаций вихри могут сильно влиять на сверхпроводящие свойства пленки; они приводят к ее переходу в нормальное состояние при температуре $T_{\text{ВКТ}}$,

более низкой, чем определенная по теории Гинзбурга-Ландау температура перехода T_{c0}. Подобный фазовый переход был впервые предсказан (для целого ряда двумерных систем - магнетиков, кристаллов, сверхтекучих пленок) В.Л. Березинским [97], а затем подробнее исследован в работах [98, 99] и (специально для случая сверхпроводников) в [100]; с тех пор его существование подтверждено многочисленными экспериментами. Мы рассмотрим здесь качественную картину фазового перехода Березинского - Костерлица - Таулеса (сокра щенно - БКТ-переход), а в следующем разделе - его наблюдаемые следствия для сверхпроводящих пленок.

В §30 было показано, что энергия взаимодействия (на единицу длины) двух абрикосовских вихрей на расстоянии $R \ll \lambda$, когда экранировкой можно пренебречь, равна $2q_1q_2\epsilon_0 \ln(R/\lambda)$, где $q_{1,2}$ принимают значения $+1$ для вихрей с положительной и -1 для вихрей с отрицательной циркуляцией соответственно, а $\epsilon_0 = (\Phi_0/4\pi\lambda)^2$. Главный вклад в ϵ_0 дает кинетическая энергия сверхтекучего движения вокруг каждого вихря $E_{\text{кин}} = \frac{1}{2}\int d\mathbf{r} m n_s v_s^2(r)$, где сверхтекучая скорость $v_s(r) = \frac{\hbar}{2m}\left(\nabla\theta - \frac{2e}{\hbar c}\mathbf{A}\right) \propto \frac{\hbar}{2mr}$ на малых расстояниях от центров вихрей (где можно пренебречь вкладом векторного потенциала). В случае пленки экранирующий сверхтекучий ток сосредоточен в тонком слое толщины $d \ll \lambda$, в то время как магнитное поле распределено во всем трехмерном пространстве. Поэтому экранировка магнитного поля вихря в пленке оказывается гораздо слабее, чем в объемном сверхпроводнике. Точный расчет, изложенный в книге [7], дает эффективную длину экранировки

$$\lambda_{2d} = \frac{2\lambda^2}{d} \tag{36.1}$$

Этот результат можно угадать и из сравнения формул (10.4) и (10.7) для кинетических индуктивностей поверхности массивного сверхпроводника и тонкой пленки - обе эти формулы можно записать в виде $L_{\square}^k = 2\pi\lambda_{\text{эфф}}$, где $\lambda_{\text{эфф}}$ равно либо λ, либо λ_{2d}.

При расстолниях между вихрями в пленке $R \ll \lambda_{2d}$ экранировкой можно пренебречь, и полная энергия взаимодействия $U_2(R) = 2q_1q_2d\epsilon_0 \ln(R/\lambda_{2d})$, а собственная энергия каждого из вихрей равна $U_1 = d\epsilon_0 \ln(\lambda_{2d}/\xi)$, так что полная энергия пары вихрей противоположных циркуляций равна

$$U_{\text{pair}}(R) = 2\epsilon_0 d \ln\frac{R}{\xi} = \frac{\Phi_0^2}{4\pi^2\lambda_{2d}} \ln\frac{R}{\xi} \tag{36.2}$$

В тонких пленках λ_{2d} может достигать макроскопических размеров. Так, при $\lambda = 3$ мкм (что легко достигается в близкой
окрестности T_{c0}) и толщине пленки $d = 50$Å получим $\lambda_{2d} \simeq \simeq 3.6$ мм. При этом энергия кора вихря, $U_{\text{core}} = d\epsilon_0$, мала: $U_{\text{core}}/k_{\text{B}} \simeq 10$ K, в то время как полная энергия гораздо больше, $U_1/k_{\text{B}} \simeq 100$ K (мы выбрали здесь для оценки $\xi \simeq 0.1$ мкм). Пусть, для примера, $T_{c0} = 5$ K. Тогда вероятность найти (на площади порядка размера кора ξ^2) отдельный вихрь, возникший вследствие тепловой флуктуации в бесконечной пленке, будет очень мала, порядка $e^{-U_1/T} \leqslant 10^{-8}$. Казалось бы, это значит, что такими вихрями всегда можно пренебречь. Однако в бесконечной пленке и число мест, где может находиться каждый вихрь, бесконечно. Для аккуратного анализа надо рассмотреть случай пленки конечного размера L, где есть порядка $(L/\xi)^2$ возможных "посадочных мест" для вихрей.

Поскольку λ_{2d} может быть очень велико, имеет смысл рассмотреть случай размеров L, малых по сравнению с λ_{2d} (мы обсудим влияние конечности длины λ_{2d} позже, в самом конце этого раздела). Тогда энергия вихря равна $U_1(L) = d\epsilon_0 \ln(L/\xi)$, а среднее число вихрей во всей пленке порядка

$$n(L) \simeq (L/\xi)^2 \exp(-U_1(L)/T) = (L/\xi)^{2-\alpha}$$

где $\alpha = \epsilon_0 d/k_\mathrm{B}T = \Phi_0^2/(8\pi^2\lambda_{2d}k_\mathrm{B}T)$. При достаточно низких температурах $\alpha > 2$ и среднее число вихрей во всей пленке убывает с ростом L; иначе говоря, в большой системе при $k_\mathrm{B}T < \epsilon_0 d/2$ отдельных флуктуационных вихрей нет. Напротив, при $\alpha < 2$ вероятность найти вихрь растет с L. Этот же результат можно выразить немного иначе, определив свободную энергию одиночного вихря по обычным правилам статистической механики как $F_1 = U_1 - TS_1$, где энтропия $S_1 = k_\mathrm{B}\ln(L^2/\xi^2)$ есть просто логарифм числа доступных для вихря мест на пленке. Тогда условие $\alpha < 2$ означает, что свободная энергия в расчете на один вихрь отрицательна, то есть вихрям выгодно рождаться (до тех пор, пока их взаимодействие, пока еще нами не учтенное, не остановит этот процесс). Температура $T_\mathrm{BKT} = \Phi_0^2/(16\pi^2 k_\mathrm{B}\lambda_{2d})$, при которой $\alpha = 2$, называется температурой перехода БерезинскогоКостерлица-Таулеса.

Но состояние пленки со свободными вихрями уже не является сверхпроводящим! Это можно понять с помощью двух различных рассуждений. Во-первых, фаза параметра порядка $\theta(\mathbf{r},t)$ в каждой точке сверхпроводника сильно зависит (в каждый данный момент времени) от положений всех вихрей, поскольку фаза меняется на 2π при обходе вокруг каждого вихря. Это означает, что вихри, передвигаясь подобно частицам жидкости, приводят к сильным флуктуациям фазы $\theta(\mathbf{r},t)$. Нетрудно показать, что в случае двумерной жидкости вихрей флуктуации эти столь велики, что среднее значение $\left\langle e^{i\theta(\mathrm{r},t)}\right\rangle$ обращается в нуль. Поэтому обращается в нуль и сверхпроводящий параметр порядка $\Psi \propto \left\langle e^{i\theta(\mathrm{r},t)}\right\rangle$, так что с позиций теории Гинзбурга-Ландау сверхпроводимость отсутствует. Второе рассуждение имеет более "практический" характер. В том случае, когда вихри индуцируются в сверхпроводнике внешним магнитным полем, они обычно образуют решетку, которая зацепляется за примеси и потому остается неподвижной при достаточно малых токах (подробнее это обсуждается в §§38, 39, 41). Транспортный ток с плотностью j, большей критического значения j_c, приводит (как будет объяснено в 40) к движению вихревой решетки, при котором происходит диссипация энергии. Вихри же, возникающие в тонкой пленке вследствие тепловых флуктуаций, взаимодействуют между собой с энергией порядка тепловой и решетки не образуют. Поэтому они не могут и зацепиться за примеси, т. е. движение тепловых вихрей (и потому диссипация) вызывается сколь угодно малым током. Мы пришли к важному выводу: разрушение сверхпроводящего состояния в тонкой пленке происходит в действительности при более низкой температуре, чем это предсказывается в теории Гинзбурга-Ландау, не учитывающей флуктуаций, причем с приближением к температуре T_BKT этого перехода снизу лондоновская глубина проникновения $\lambda(T)$ остается конечной:

$$\frac{1}{\lambda_{2d}(T_\mathrm{BKT})} = \frac{d}{2\lambda_-^2(T_\mathrm{BKT})} = \frac{16\pi^2 k_\mathrm{B}T_\mathrm{BKT}}{\Phi_0^2}. \tag{36.3}$$

Иначе говоря, макроскопическая (с учетом вихрей) сверхтекучая плотность пленки $n_s^{(2)} = n_s d$ испытывает при повышении температуры скачок от значения $n_s^{(2),\min}$, универсальным образом связанного с температурой перехода:

$$n_s^{(2),\min} = \frac{8mk_\mathrm{B}T_\mathrm{BKT}}{\pi\hbar^2} \tag{36.4}$$

до нуля. Найдем, используя теорию Гинзбурга-Ландау, насколько температура БКТ-перехода отличается от «затравочной» критической температуры T_{c0}. Вблизи T_{c0} сверхтекучая плотность $n_s(T) = \mathcal{A}n_s(0)(1 - T/T_{c0})$, где коэффициент $\mathcal{A}$ равен 2 в чистом пределе и примерно 2.6 - в грязном (см. 51), так что получаем

$$\frac{T_{c0} - T_\mathrm{BKT}}{T_{c0}} \simeq \frac{32\pi^2\lambda^2(0)k_\mathrm{B}T_{c0}}{\mathcal{A}\Phi_0^2 d} \tag{36.5}$$

где $\lambda(0)$ - глубина проникновения при $T \to 0$. Оценка (36.5) совпадает (с точностью до численного множителя) с приведенной ранее в 19 оценкой ширины флуктуационной области в двумерной системе Gi^{2D}. Хотя в 19 мы использовали совсем другие аргументы, не имеющие отношения к вихрям, результат получился такой же. Фактически T_{BKT} всегда близко к T_{c0} даже в тонких пленках грязных сверхпроводников: используя (36.5) и формулы из §51, для грязного предела получим

$$\frac{T_{c0} - T_{\mathrm{BKT}}}{T_{c0}} \simeq 3\mathrm{Gi}_d^{(2D)} = \frac{3}{16g} \tag{36.6}$$

где параметр $\mathrm{Gi}_d^{(2D)}$ определен в (19.17). Правая часть (19.17) может стать порядка 1 лишь при g, заметно меньшем единицы, что происходит лишь в окрестности перехода металл - диэлектрик. Во всех остальных случаях зависимость $n_s(T)$ должна иметь вид, изображенный схематически на рис.36.1. Этот вывод подтвержден экспериментально - путем измерения кинетической индуктивности тонких пленок [101].

Аргументы, которые мы использовали выше, чтобы найти условие $\alpha = 2$ фазового БКТ-перехода, были не вполне строги, однако последовательная теория приводит к точно такому

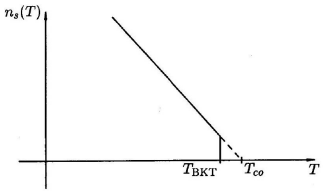


Рис. 36.1. Схематический вид характерной зависимости сверхтекучей плотности от температуры при БКТ-переходе в тонкой сверхпроводящей пленке.

же выводу. Тем не менее, мы сейчас опишем схематически этот более последовательный подход, т.к. эти идеи понадобятся нам ниже при обсуждении вида вольт-амперных характеристик вблизи точки БКТ-перехода.

При $T < T_{\mathrm{BKT}}$ в системе нет одиночных флуктуационных вихрей, однако существуют пары вихрей с противоположными циркуляциями ($q_1 q_2 = -1$), и вероятность найти такую пару с расстоянием R между вихрями есть $P(R) = \exp\left(-U_{\mathrm{pair}}(R)/k_{\mathrm{B}}T\right) \propto$ $\propto (R/\xi)^{-2\alpha}$. Мы можем формально рассматривать вихри как заряженные частицы, а их пары - как нейтральные «вихревые молекулы». Эта аналогия тем более разумна, что в двумерном пространстве обычный кулоновский потенциал точечного заряда (определяемый уравнением Гаусса $\varepsilon_v \nabla \mathbf{E} = -\varepsilon_v \nabla^2 \varphi = 2\pi\delta(\mathbf{r})$) логарифмически растет с расстоянием: $\varphi = \varepsilon_v^{-1} \ln(r)$. Здесь мы ввели обозначение ε_v для "диэлектрической постоянной» газа вихревых молекул. Тогда фазовый переход БКТ можно описать как переход между газом нейтральных вихревых молекул (где величина ε_v конечна) и "вихревой плазмой", состоящей из отдельных «заряженных» частиц, где $\varepsilon_v \to \infty$ и кэлектрическое» поле каждого отдельного «заряда» экранируется другими «зарядами" - вихрями. Начнем с низкотемпературной фазы, где
есть лишь малая плотность вихревых молекул. Они дают вклад в «диэлектрическую восприимчивость" среды $\kappa_v = (\varepsilon_v - 1)/2\pi$, пропорциональный среднему квадрату "дипольного момента" вихревой молекулы:

$$\kappa_v \propto \int_{\xi}^{L} R^2 P(R) 2\pi R dR \propto \int_{\xi}^{L} \frac{dR}{R^{2\alpha-3}}; \quad \alpha = \frac{\epsilon_0 d}{T\varepsilon_v} \tag{36.7}$$

Как видно из (36.7), при α, стремящемся к 2 сверху, интеграл, определяющий κ_v, начинает логарифмически расходиться как функция размера системы L. Второе

равенство в (36.7) учитывает (самосогласованным методом), что параметр α сам зависит от взаимодействия между вихрями (мы здесь подразумеваем, что величина λ, входящая в ϵ_0, определена в рамках теории Гинзбурга-Ландау и вихрей не учитывает). Самосогласованное уравнение типа (36.7) было выведено в работе Костерлица и Таулеса [98], а его аккуратное решение приведено в последующей работе Костерлица [99] (см. также [34]). Результат этого решения, как можно догадаться уже из (36.7), состоит в том, что $\alpha_{\min} = 2$ сохраняется как точное минимальное значение параметра α при учете всех поправок, что подтверждает универсальность скачка сверхтекучей плотности (36.4). Кроме того, это решение позволяет найти зависимость среднего расстояния между свободными вихрями $R_c(T)$ (т.е. масштаба длины, на котором разрушается сверхпроводимость) при $T > T_{\text{ВКТ}}$:

$$\ln \frac{R_c(T)}{\xi} = b \left(\frac{\text{Gi}^{(2D)} T}{T - T_{\text{ВКТ}}} \right)^{1/2} \tag{36.8}$$

где $\xi(T)$ - обычная сверхпроводящая длина корреляции, определяемая с помощью теории Гинзбурга - Ландау, а b - число порядка единицы. Появление множителя $\text{Gi}^{(2D)}$ в правой части (36.8) легко понять: при $\frac{T-T_{\text{ВКТ}}}{T} \geqslant \text{Gi}^{(2D)}$ температура уже столь близка к T_{c0}, что невозможно отличить флуктуационные вихри от обычных флуктуаций, поэтому $R_c(T) \sim \xi(T)$.

Весь предыдущий анализ был основан на логарифмической зависимости энергии пары вихрь-антивихрь от расстояния. На очень больших расстояниях $R \geqslant \lambda_{2D}$ энергия такой пары перестает расти с R; иначе говоря, энергия уединенного вихря остается конечной, а потому и отлична от нуля их концентрация при всякой отличной от нуля температуре. Формально говоря, это означает, что двумерный сверхпроводник всегда находится в резистивном состоянии. Однако фактически концентрация вихрей при $T < T_{\text{ВКТ}}$ имеет порядок $e^{-\alpha \ln(\lambda_{2D}/\xi)} < (\xi/\lambda_{2D})^2$, и ею можно пренебречь везде, кроме совсем узкой окрестности $T_{\text{ВКТ}}$, где корреляционный радиус, определяемый уравнением (36.8), мог бы оказаться больше λ_{2D}.

36.2. Вольт-амперные характеристики вблизи БКТперехода. В сверхпроводящем состоянии, реализующемся при $T < T_{\text{ВКТ}}$, по определению должно быть равно нулю линейное сопротивление, определяемое как $\rho_{\text{лин}} = (dV/dI)_{I=0}$. Это, однако, не означает, что напряжение должно быть равно нулю при малых токах. В тонкой пленке, как мы сейчас увидим, напряжение при низких температурах растет как высокая степень тока, $V \propto I^{\alpha+1}$. Действительно, рассмотрим «нейтральную" пару вихрей, повернутую перпендикулярно протекающему току с плотностью j, так что сила Лоренца стремится увеличить размер пары R. Полная энергия пары с учетом силы Лоренца равна

$$U_{\text{полн}}(R) = 2\epsilon_0 d \ln \frac{R}{\xi} - jd \frac{\Phi_0}{c} R \tag{36.9}$$

где j - плотность транспортного тока. При самых больших $R > R^* = (2c\epsilon_0/j\Phi_0)$ второй член в полной энергии всегда больше первого, т.е. внешний ток приводит к разрыву вихревых молекул на отдельные вихри. Иначе говоря, если по пленке протекает транспортный ток, в ней создается ненулевая плотность неспаренных вихрей $n_v(j)$ на единицу площади пленки. Но движение этих вихрей под действием тока приводит к диссипации энергии, т. е. к конечному сопротивлению $\rho(j) \sim n_v(j)\xi^2(T)\rho_n$ (эту оценку легко получить, сравнивая с проведенным в §40 выводом сопро тивления ρ_f в резистивном состоянии). Поэтому нам осталось найти стационарную плотность одиночных вихрей $n_v(j)$ (обоих знаков) при заданной плотности тока j.

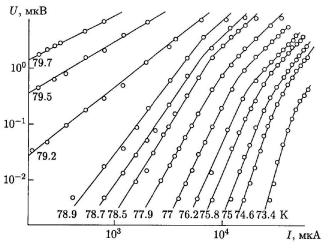


Рис. 36.2. Нелинейные вольт-амперные характеристики монокристалла $Bi_2Sr_2CaCu_2O_x$ при различных температурах $T \lesssim T_c$.

Стационарная величина $n_v(j)$ определяется равенством скорости рождения одиночных вихрей Γ_+из-за разрыва пар током и скорости аннигиляции Γ_-уже имеющихся вихрей противоположных знаков. Величину Γ_+оценим как вероятность термоактивационного процесса преодоления потенциального барьера $U_{\text{полн}}\ (R^*) = 2\epsilon_0 d \ln(2\epsilon_0 c/j\Phi_0\xi)$, определяемого максимумом по R выражения (36.9). Таким образом,

$$\Gamma_+ \sim \Gamma_0 \exp\left(-U_{\text{полн}}\ (R^*)/k_{\text{B}}T\right)$$

где Γ_0 - величина размерности частоты. Величина Γ_-определяется вероятностью (в единицу времени) того, что два вихря про тивоположных знаков приблизятся на расстояние порядка размера кора $\xi(T)$, после чего аннигилируют. При малой концентрации вихрей, $n_v(j)\xi^2(T) \ll 1$, вероятность такого «столкновения» вихрей пропорциональна квадрату их концентрации,

$$\Gamma_- \sim \Gamma_0 \left(n_v(j)\xi^2(T)\right)^2$$

Таким образом, приравнивая Γ_+к Γ_-, получаем равновесную концентрацию вихрей

$$n_v(j)\xi^2(T) \sim \exp\left(-U_{\text{полн}}\ (R^*)/2k_{\text{B}}T\right)$$

и для сопротивления получаем

$$\rho(j) \sim \rho_n j \left(\frac{j}{j_T}\right)^{\boldsymbol{\alpha}} \tag{36.10}$$

где

$$j_T = \frac{c\Phi_0}{16\pi^2\lambda^2(T)\xi(T)}$$

близко к плотности тока распаривания в теории Гинзбурга-Ландау.

Как мы уже знаем, минимальная величина параметра α в низкотемпературной фазе равна 2, так что показатель степени в вольт-амперной характеристике $V(I) \propto I^{1+\alpha}$ испытывает при понижении температуры скачок от 1 к 3. Пример измерения ВАХ, позволившего продемонстрировать существование БКТперехода в сильно анизотропном (слоистом) ВТСП монокристалле $Bi_2Sr_2CaCu_2O_8$ [103], показан на рис. 36.2

Зависимость линейного сопротивления от температуры при $T > T_{\text{ВКт}}$ можно определить аналогично выводу (36.10). Выше точки перехода плотность вихрей n_v остается ненулевой при $j \to \to 0$: по порядку величины $n_v \sim R_c^{-2}(T)$, где радиус корреляции $R_c(T)$ ведет себя согласно уравнению (36.8). Поэтому для сопротивления получаем

$$\rho(T) \sim n_v(T)\xi^2(T)\rho_n \sim \rho_n \exp\left(-2b\left(\frac{\text{Gi}_{2D}T}{T - T_{\text{ВКТ}}}\right)\right) \tag{36.11}$$

Зависимость сопротивления вида (36.11) была с хорошей точностью подтверждена на эксперименте [102].

7.7.3 37*. Melting of the Vortex Lattice

В теории Гинзбурга - Ландау - Абрикосова - Горькова фазовый переход в сверхпроводящее состояние в магнитном поле происходит при значении внешнего поля $H_0 = H_{c2}(T)$, когда одновременно появляется сверхпроводящий параметр порядка $\Psi(\mathbf{r}_\perp, z) \neq \neq 0$, периодически зависящий от координат $\mathbf{r}_\perp$, и возникает решетка вихрей (в центрах которых $\Psi(\mathbf{r}_\perp, z)$ обращается в нуль). С точки зрения изменения симметрии на линии $H_0 = H_{c2}(T)$ одновременно происходят два разных фазовых перехода: нарушается и градиентная инвариантность (параметр порядка Ψ неинвариантен при градиентном преобразовании, см. п. 14.3), и трансляционная инвариантность - поскольку возникает периодическая структура.

В отличие от большинства обычных сверхпроводников, в случае ВТСП тепловыми флуктуациями вблизи фазового перехода пренебрегать нельзя. Даже в отсутствие магнитного поля в $YBa_2Cu_3O_{7-x}$ с температурой перехода около 90 K ширина флуктуационной области имеет порядок 1 K, т.е. параметр Gi $\sim \sim 10^{-2}$, и она еще больше в сильно слоистых соединениях типа $Bi_2Sr_2CaCu_2O_8$. Фазовый переход в сверхпроводящее состояние в магнитном поле еще более чувствителен к флуктуационным эффектам: помимо обычных флуктуаций параметра порядка, имеющихся и при $B = 0$, здесь возможны также флуктуации положений вихревых линий в пространстве, которые очень сильно меняют фазу параметра порядка в окрестности каждой такой линии.

Последовательной теории фазового перехода сверхпроводник-металл в магнитном поле, которая учитывала бы флуктуационные эффекты, не создано до сих пор, однако качественную картину происходящего в ВТСП можно понять, рассмотрев решетку вихрей в лондоновском приближении, справедливом при $B \ll H_{c2}(T)$ (подразумевается сверхпроводник с $\varkappa \gg 1$, что характерно для ВТСП). В этом случае размер сердцевины вихря ξ мал по сравнению с расстоянием между вихрями $a_0 = \sqrt{\Phi_0/B}$, в большей части сверхпроводника абсолютная величина параметра порядка $|\Psi|$ близка к ее значению в отсутствие магнитного поля, и решетку вихрей можно рассматривать как аналог обычной кристаллической решетки. Отличие лишь в том, что вихревал решетка состоит из линий (в среднем параллельных направлению z внешнего магнитного поля $\mathbf{H}_0$). Известно, что всякий кристалл плавится при некоторой температуре, когда амплитуда $u_{\text{тепл}} = \sqrt{\langle u^2 \rangle_{\text{тепл}}}$ тепловых флуктуаций атомов (или электронов - если речь идет о вигнеровском кристалле из электронов на поверхности гелия) становится сравнимой с постоянной решетки a_0. Фактически отношение $u_{\text{тепл}}/a_0$ в точке плавления всегда остается численно малой величиной (называемой постоянной Линдеманна c_{L}, который и предложил использовать равенство $u_{\text{тепл}} = c_{\text{L}} a_0$ в качестве феноменологического критерия плавления обычных трехмерных кристаллов, где $c_{\text{L}} \simeq 0.1 \div 0.15$). Величину $u^2_{\text{тепл}}$ для вихревой решетки можно вычислить как сумму квадратов амплитуд флуктуаций с определенными волновыми векторами $\mathbf{q}$ - аналогичных обычным фононам. Мы не будем приводить здесь этот вывод (см., например, обзор [96]) и дадим вместо этого простую оценку величины поля плавления решетки $B_m(T)$, качественно справедливую в широком интервале полей, $H_{c1} \ll B \ll H_{c2}$. Чтобы ее получить, приравняем по порядку величины тепловую энергию $k_{\text{B}}T$ и энергию $E_{\text{упр}}$ сильной ($|\delta\mathbf{u}| \sim a_0$) деформации вихревой решетки в объеме порядка a_0^3. Для таких коротковолновых возмущений нет существенного различия между деформациями сжатия и сдвига, и потому $E_{\text{упр}}$ можно оценить просто через характерное значение

энергии взаимодействия вихрей на длине порядка постоянной решетки: $E_{\text{упр}} \sim \epsilon_0 a_0$, где $\epsilon_0 = (\Phi_0/4\pi\lambda)^2$. Приравнивая полученную таким образом величину $E_{\text{упр}}$ к тепловой энергии, получим для поля плавления решетки

$$B_m(T) \propto \frac{\Phi_0}{(k_{\text{B}}T)^2}\left(\frac{\Phi_0}{4\pi\lambda}\right)^4 \propto (1-T/T_c)^2 \quad \text{при} \quad T \to T_c. \tag{37.1}$$

Мы получили важный и несколько неожиданный результат: поле плавления решетки убывает с повышением температуры быстрее,
чем верхнее (и нижнее) критическое поле, которое ведет себя линейно вблизи температуры перехода, $H_{c2} \propto (1-T/T_c)$. Вспоминая определение ширины флуктуационной области Gi, данное в §19, оценку (37.1) для поля плавления решетки можно записать в виде

$$\frac{B_m(T)}{H_{c2}(T)} = \alpha_m \frac{1-T/T_c}{\text{Gi}} \tag{37.2}$$

где α_m - численный коэффициент. Более аккуратные аналитические [96] и численные [104] расчеты тоже приводят к результату (37.2), а также показывают, что α_m весьма мало, $\alpha_m \sim \sim 2 \cdot 10^{-2}$ (иначе этот результат может быть выражен в виде значения $k_{\text{B}}T_m(B)/\epsilon_0 a_0 \simeq 0.1$). Численные расчеты [104] позволяют определить и величину параметра Линдеманна для плавления вихревой решетки, $c_{\text{L}} \simeq 0.25$. Результат для линии плавления в форме (37.2) остается справедлив и для анизотропных сверхпроводников типа $YBa_2Cu_3O_{7-x}$, когда исходное выражение (37.1) должно быть модифицировано для учета анизотропии (поскольку характерный пространственный масштаб деформаций в направлении вихрей z теперь отличается от a_0 и имеет порядок ϵa_0, получаем $k_{\text{B}}T_m(B)/\epsilon_0 a_0 \simeq 0.1\epsilon$). Для сильно слоистых соединений типа $Bi_2Sr_2CaCu_2O_8$ оценка для линии $B_m(T)$ несколько отличается от (37.2), но качественно картина остается той же.

Конечно, оценка (37.2) имеет смысл лишь вне области сильных флуктуаций параметра порядка, т.е. при $(1-T/T_c) \geqslant \text{Gi}$. Кроме того, отношение B_m/H_{c2} должно быть мало, поскольку иначе энергия деформации оказывается [105] существенно меньше, чем использованная оценка $E_{\text{упр}} \sim \epsilon_0 a_0$. Эти два условия оказываются совместны в области температур $\text{Gi} \ll (1-T/T_c) \ll \ll \text{Gi} \cdot \alpha_m^{-1}$ в силу малости числа α_m. В результате мы приходим к важному выводу: в некотором интервале температур вблизи T_c смешанное состояние сверхпроводника II рода в форме решетки вихрей неустойчиво по отношению к тепловым флуктуациям - уже при полях B существенно меньших, чем H_{c2}. Обычно плавление кристаллической решетки - фазовый переход I рода (с ненулевым скачком энтропии и плотности). Плотность вихрей пропорциональна магнитной индукции B, поэтому если пла вление вихревой решетки - переход I рода, то на линии перехода должен наблюдаться скачок равновесной намагниченности образца. Именно такой результат был получен в очень красивых экспериментах [106, 107], где фазовые переходы плавления вихревой решетки в очень чистых монокристаллах $Bi_2Sr_2CaCu_2O_8$ и $YBa_2Cu_3O_{7-x}$ были зарегистрированы по слабым скачкам локального значения равновесной намагниченности $\Delta M_{\text{плавл}}$. В полях $B > B_m(T)$ в смешанном состоянии вихревые линии образуют жидкость. Количественной теории этого нового состояния пока не существует; также не вполне ясно, какой смысл следует придавать верхнему критическому полю H_{c2}, когда оно заметно превышает поле плавления $B_m(T)$. В любом случае, эти вопросы имеют практический смысл почти исключительно для высокотемпературных сверхпроводников - в большинстве остальных материалов величина Gi очень мала и эффекты плавления решетки почти ненаблюдаемы. В то же время для ВТСП наблюдаемые следствия плавления вихревой решетки весьма важны, они определяют собой аномальное поведение вольт-амперных характеристик в

смешанном состоянии при относительно высоких полях и температурах. Мы рассмотрим эти явления ниже в 42.

7.7.4 38. Critical current in type-II SC

Если сверхпроводник второго рода находится в смешанном состоянии и в направлении, перпендикулярном вихрям, идет транспортный ток (т.е. ток, созданный каким-то внешним источником), то на вихри действует сила Лоренца. Если бы сверхпроводник был совершенно однороден, бездефектен, то при любой, сколь угодно малой силе Лоренца, вихри бы начали свое движение под действием этой силы.

В 40 будет показано, что такое движение сопровождается диссипацией энергии. Это означает, что у такого абсолютно однородного образца критический ток равен нулю.

В неоднородном сверхпроводнике второго рода, когда существуют разные виды дефектов (границы зерен, включения дру гой фазы, дислокационные стенки, скопления дислокаций, поры и т.п.), вихри могут на них закрепиться. Тогда требуется уже конечный транспортный ток для начала движения вихрей. Этот ток создает такую силу Лоренца, действующую на вихри, которой достаточно для отрыва вихрей от дефектов. Эти дефекты часто называются центрами пиннинга, а закрепление на них вихрей - пиннингом. [1)] Плотность тока, при котором начинается отрыв вихрей от центров пиннинга, называется критической плотностью тока j_c.

Критическая плотность тока может очень сильно (на несколько порядков) меняться в результате термомеханической обработки материала, так как является чрезвычайно структурно чувствительным свойством. При этом критическая температура T_c и второе критическое поле H_{c2} могут практически не измениться. У некоторых сверхпроводников, предназначенных для использования в сверхпроводящих магнитах или других сверхпроводящих устройствах, величина критического тока может достигать значений порядка 10^6 A/cm^2. Такого же порядка величины, до $5 \cdot 10^6$ A/cm^2, достигают критические токи в не очень чистых кристаллах $YBa_2Cu_3O_{7-x}$ и других ВТСП при низких температурах.

Рассмотрим механизм протекания критического тока через сверхпроводник второго рода, в котором имеется много центров пиннинга. Для того чтобы транспортный ток шел по всему ссчению сверхпроводника, необходимо, чтобы существовало неоднородное распределение вихрей. Действительно, плотность полного тока, текущего в данном месте, равна

$$j_{\text{тр}} = \frac{c}{4\pi} \operatorname{rot} \mathbf{B} \tag{38.1}$$

но $B = \Phi_0 n$ - среднее поле в данном месте, т. е. напряженность магнитного поля, усредненная по области, размер которой намного больше расстояния между вихрями, n - средняя плотность вихрей в данном месте. Из (38.1) следует, что $\mathbf{j}_{\text{тр}}$ отличен от нуля в данном месте, если плотность вихрей $n = n(\mathbf{r})$.

Теперь нам надо понять, как возникает такое состояние, когда по всему сечению сверхпроводника устанавливается критическая плотность тока.

Пусть бесконечная пластина толщины d содержит очень много дефектов, на которых сверхпроводящие вихри могут хорошо закрепляться, при этом $d \gg \lambda$. Поверхности пластин совпадают с плоскостями $x = \pm d/2$. Внешнее магнитное поле H_0 пока отсутствует. Начнем пропускать транспортный ток через пластину (в направлении оси y). Сначала, как и у бездефектного сверхпроводника, ток пойдет по поверхности пластины (эффект Мейсснера Оксенфельда). Когда поле, созданное током на

[1)] От английского слова pin - булавка. Дословно pinning - это пришпиливание.

поверхностях, H_I, превысит поле H_{c1} материала пластины, внутрь пластины проникнут вихри. Они будут иметь разные направления на противоположных сторонах. Но далеко внутрь они не проникнут, так как закрепляются на неоднородностях пластины. При этом возникает градиент их плотности. Ясно, что это будет максимально возможный градиент, т.е. такой, который обеспечивает протекание критического тока. Итак, некоторая область вблизи поверхностей пластины будет нести критический ток, а остальная часть пластины вообще тока нести не будет. Это схематически изображено на рис. 38.1, a, где показано распределение магнитного поля внутри пластины при токе через пластину, равном I_1 (на единицу высоты пластины вдоль оси z).

Увеличим теперь ток до величины I_2. Вихри, сохранив критический градиент плотности $(\nabla n)_c$, продвинутся ближе к центру. Теперь только центральная часть пластины свободна от транспортного тока, а остальная часть пластины несет ток, плотность которого равна критической. Если продолжать увеличивать ток через пластину, мы придем к такому току I_c, когда в любой точке пластины плотность тока будет критической. Все это изображено на рис. 38.1, a.

Такое состояние, когда в любом месте поперечного сечения пластины течет критический ток, называется критическим состоянием.

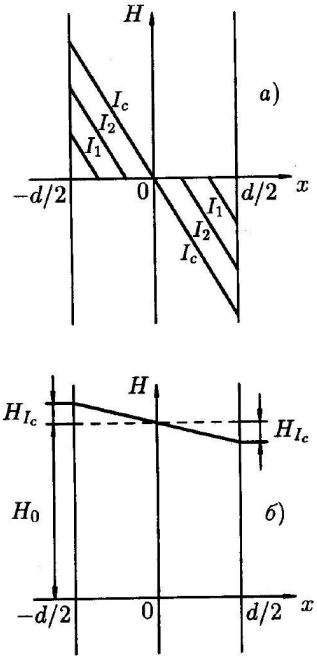


Рис. 38.1. Распределение поля в пластине (толщины d) с центрами пиннинга, когда по пластине течет ток I: а) внешнее поле отсутствует, $I_1 < I_2 < I_c$ - токи в пластине; б) случай пластины с током и во внешнем поле. Показано распределение в критическом состоянии.

Наложим теперь внешнее магнитное поле H_0, параллельное поверхности пластины и перпендикулярное току, т.е. поле H_0 параллельно оси z. Предположим, что $H_0 \gg H_I$. Тогда распределение тока в пластине в критическом состоянии будет таким, как показано на рис. 38.1, б. Пренебрегая небольшой разницей в полях $H_0 + H_I$ и $H_0 - H_I$, можно считать, что все точки проводника находятся в поле H_0. Плотность критического тока в поле H_0 меньше, чем в отсутствие поля, поэтому критический градиент плотности вихрей меньше.

Действительно, если сила Лоренца, действующая на единицу длины вихря, равна $f_{\mathrm{L}} = j_{\mathrm{тр}}\,\Phi_0/c$, то сила Лоренца, отнесенная к единице объема, равна $F_{\mathrm{L}} = j_{\mathrm{гр}}B/c$, поскольку суммарная длина всех вихрей в единице объема равна $n = B/\Phi_0$. Эта сила уравновешивается в стационарном состоянии силой закрепления вихрей на неоднородностях. Пусть удельная сила закрепления (пиннинга) вихрей в единице объема равна F_p. Тогда

критический ток должен удовлетворять уравнению

$$\frac{1}{c} j_c B = F_p \tag{38.2}$$

Если предположить, что F_p не зависит от внешнего поля H_0, то получим $j_c \propto B^{-1}$. Такая зависимость критического тока от внешнего поля наблюдалась во многих экспериментах.

Если дефекты структуры сверхпроводника, т. е. центры пиннинга, распределены хаотично, то абсолютно жесткая решетка вихрей на них не может закрепиться. Чтобы это стало понятно, сдвинем мысленно такую решетку на малое расстояние в направлении действия силы Лоренца. Очевидно, что энергия системы при этом не изменяется, так как новое хаотическое расположение центров пиннинга относительно жесткой вихревой решетки ничем не отличается в принципе от старого. А раз нет изменения энергии, то нет и возвращающей силы, нет и пиннинга.

Совсем другая картина возникает, если предположить, что решетка вихрей - это упругая среда. Тогда вихри каждый раз будут подстраиваться к данному хаотическому распределению центров пиннинга так, чтобы вся система вихрей имела минимум энергии. Поэтому теперь уже будет нужно некоторое усилие, ттобы, сдвинув вихри, превзойти предел возвращающей силы и оторвать их от центров пиннинга. Ясно поэтому, что чем "мягче» решетка вихрей, чем она податливее, тем больше сила пиннинга.

Расчеты [108] показали, что модули упругости вихревой решетки уменьшаются при $H_0 \to H_{c2}$. Решетка становится мягче, а пиннинг сильнее. Это приводит к довольно часто наблюдаемому пику критического тока при $H_0 \sim H_{c2}$ (рис. 38.2). Подробнее этот вопрос мы рассмотрим в конце 41.

7.7.5 41*. Collective Pinning of Vortices by Weak Defects

41.1. Одиночный вихрь в поле слабых примесей.

Как уже упоминалось выше в 39, дефекты кристаллической решетки с размером порядка атомного очень слабо взаимодействуют с вихрями, поскольку размер кора вихря ξ обычно весьма велик в атомном масштабе. Тем не менее, вихрь может быть эффективно зацеплен и такими дефектами, если их плотность достаточно велика. В таком случае говорят о коллективном пиннинге вихрей на многих дефектах одновременно. Такие слабые дефекты-это, например, кислородные вакансии в высокотемпературных сверхпроводниках (ВТСП) и атомные примеси Та (замещающие атомы Nb) в слоистом соединении $NbSe_2$. Теория коллективного пиннинга была развита в работах Ларкина и др. [114, 115, 96, 116]. В этом параграфе мы опишем качественный подход, позволяющий оценить величину критического тока при коллективном пиннинге.

Начнем с самого простого случая: одна вихревая линия в поле слабых дефектов. Как мы знаем (см. (29.3)), вихрь в изотропном чистом сверхпроводнике обладает определенной энергией на единицу длины, равной $\epsilon_1 = \left(\frac{\Phi_0}{4\pi\lambda}\right)^2 \ln\varkappa \equiv \epsilon_0 \ln\varkappa$. Это означает, что если вихревую линию изогнуть, то ее энергия увеличится, т. е. вихрь ведет себя как упругая струна. Добавка к энергии вихря из-за изгиба пропорциональна его удлинению и при плавных изгибах может быть записана как

$$E_{el} = \frac{\epsilon_1}{2} \int dz \left(\frac{d\mathbf{u}}{dz}\right)^2 \tag{41.1}$$

где $\mathbf{u}$-вектор смещения участка вихря, соответствующего координате z вдоль него. Предположим сначала, что коэффициент линейного натяжения ϵ_1 очень велик, так что

можно считать вихрь совершенно прямым, и рассмотрим его взаимодействие с мелкими дефектами. Каждый такой дефект изменяет энергию вихря (если находится вблизи его кора) на величину порядка e (???) прим и случайную по знаку (поскольку среднее изменение энергии вихря из-за дефектов не приводит к его зацеплению, мы можем считать, что среднее значение $\overline{\delta e_{\text{прим}}} = 0$). При концентрации примесей $n_{\text{прим}}$ на длине L вдоль вихря в коре находится примерно $\mathcal{N} \sim n_{\text{прим}}\,\xi^2 L$ дефектов, так что при перемещении вихря в другое положение (на расстояние порядка ξ) энергия взаимодействия с дефектами изменится на величину порядка $E_{\text{пинн}}(L) \simeq e_{\text{прим}}\sqrt{\mathcal{N}} \simeq e_{\text{прим}}\,\xi\,(n_{\text{прим}}\,L)^{1/2}$. Заметим здесь, что именно размер кора вихря ξ определяет характерный пространственный масштаб, на котором меняется энергия взаимодействия вихря с мелкими дефектами. Как видно, возможный выигрыш в энергии взаимодействия с дефектами (из-за того, что вихрь передвинулся в более "подходящее» место) растет с длиной сегмента вихря (если он абсолютно жесткий) как $\sqrt{L}$. Но сила Лоренца, действующая на тот же сегмент вихря со стороны транспортного тока, пропорциональна его длине: $F_{\text{L}}(L) = \frac{1}{c}\Phi_0 j L$, так что и выигрыш в энергии взаимодействия с этим током растет пропорционально L и при достаточно большой длине всегда превысит $E_{\text{пинн}}(L)$, каким бы слабым ни был ток j.

Казалось бы, мы получили "отрицательный» результат-отсутствие пиннинга, нулевой критический ток. Теперь, однако, надо вспомнить о сделанном в начале предположении, что вихрь можно считать совершенно жестким - оно и привело к такому странному результату. В действительности форма вихря определяется конкуренцией между его упругой энергией, возрастающей при изгибе, и выигрышем энергии при помещении его сегментов в наиболее подходящие "потенциальные ямы". Результат этой конкуренции и определяет характерную длину L_p вихревого сегмента, на которой он смещается в поперечном направлении на длину порядка ξ, т.е. «переползает" из одной потенциальной ямы в поле дефектов в другую. Чтобы найти L_p, приравняем по порядку величины упругую энергию $E_{el}(L_p)\,\epsilon_1\frac{\xi^2}{L_p}$ и энергию связи с примесями $E_{\text{пинн}}(L_p) = e_{\text{прим}}\,\xi\,(n_{\text{прим}}\,L_p)^{1/2} \equiv (\gamma\xi^2 L_p)^{1/2}$:

$$\epsilon_1\frac{\xi^2}{L_p} \simeq \left(\gamma\xi^2 L_p\right)^{1/2} \tag{41.2}$$

(мы здесь также ввели обозначение $\gamma = n_{\text{прим}}\,e^2_{\text{прим}}$, которое будет часто использоваться в дальнейшем). Уравнение (41.2) определяет "длину пиннинга" L_p, а с ее помощью и критический ток j_c, задаваемый соотношением $\frac{1}{c}\Phi_0 j_c \simeq E_{\text{пинн}}(L_p)/\xi$ (в правой части здесь стоит характерная сила, действующая на вихрь со стороны ансамбля примесей, расположенных на длине L_p):

$$E_{\text{пинн}}(L_p) \simeq \left(\gamma\epsilon_1\xi^4\right)^{1/3} \simeq H^2_{cm}\xi^3\frac{\xi}{L_p}, \quad L_p \simeq \left(\frac{\epsilon_1^2\xi^2}{\gamma}\right)^{1/3}, \tag{41.3}$$

$$j_c \simeq \frac{c}{\Phi_0}\left(\frac{\gamma}{L_p}\right)^{1/2} \simeq j_0\left(\frac{\xi}{L_p}\right)^2, \tag{41.4}$$

где j_0 - "ток распаривания", определенный выше в (18.5) как критический ток для тонкой пленки. Все величины, входящие в формулу (41.4), подразумеваются зависящими от температуры, эти зависимости вблизи T_c следуют, как правило, из теории Гинзбурга-Ландау. Оценки (41.4) применимы, по смыслу их вывода, для случая слабого пиннинга, $j_c \ll j_0$, что и соответствует относительно большой длине $L_p \gg \xi$. Более того, буквальный вид формул (41.4), в которые входит параметр нлинейного натяжения* вихря ϵ_1, справедлив лишь при более сильном условии $L_p \geqslant \lambda$; в:противном случае

множитель $\ln\kappa = \ln(\lambda/\xi)$ в выражении для ϵ_1 следует заменить на $\ln(L_p/\xi)$. Дело в том, что при коротковолновых ($q > \lambda$) деформациях вихря магнитное поле «не успевает» следовать за изгибом его кора и эффективная жесткость вихря уменьшается, $\epsilon(q) = \epsilon_0 \ln(1/q\xi)$.

Длина L_p (называемая далее длиной пиннинга) имеет важный физический смысл - вихрь можно считать упругой струной лишь на масштабах $L \ll L_p$, в то время как на много больших масштабах отдельные сегменты длины L_p зацепляются примесями почти независимо один от другого. В результате полная энергия пиннинга сегмента большой длины $L \gg L_p$ оказывается пропорциональной длине: $E_{\text{пинн}}(L) \propto L\left(E_{\text{пинн}}(L_p)/L_p\right)$. Таким образом, пиннинг на слабых дефектах возникает из-за того, что вихрь слегка изгибается в поле дефектов, выбирая конфигурации, реализующие локальные минимумы полной энергии. Соот ветственно, увеличение линейного натяжения ϵ_1 должно приводить и к увеличению L_p, и к уменьшению критического тока j_c, как и следует из формул (41.4).

41.2. Коллективный пиннинг вихревой решетки.

В описанной выше картине шла речь о единичном вихре, т. е. предполагалось, что его взаимодействие с другими вихрями много слабее, чем с дефектами. Легко понять, в каких случаях такое представление справедливо: надо сравнить энергию пиннинга на единицу длины $E_{\text{пинн}}/L_p$ и повышение энергии (тоже на единицу длины) упругого взаимодействия вихрей в вихревой решетке, возникающее при относительном сдвиге соседних вихрей на расстояние порядка пространственного масштаба случайного потенциала ξ, т.е. $\epsilon_0\left(\xi/a_0\right)^2$, где $a_0 = \sqrt{\Phi_0/B}$. Сравнивая эти две энергии, обнаруживаем, что упругостью вихревой решетки можно пренебречь, если решетка достаточно редкая, $a_0 \gg L_p$. В обратном случае взаимодействие между вихрями сильное и его надо учитывать с самого начала. Это можно сделать аналогично описанному выше случаю одиночного вихря, разница лишь в том, что вместо упругой линии надо теперь рассмотреть трехмерную упругую решетку. Мы будем сначала считать, что постоянная решетки $a_0 \gg \xi$, т.е. среднее магнитное поле $H \ll H_{c2}$, так что можно использовать лондоновское приближение (что имеет смысл для сверхпроводников "сильно II рода», т.е. имеющих параметр Гинзбурга-Ландау $\varkappa \gg 1$).

Теперь нам надо исходить из упругой энергии деформации трехмерной вихревой решетки, которую можно записать в виде

$$E_{el}^{3D} = \frac{1}{2}\int d^3r \left[\left(C_{11} - C_{66}\right)(\nabla\cdot\mathbf{u})^2 + \right. \\ \left. + C_{66}\left(\nabla_a u_b\right)^2 + C_{44}\left(\frac{d\mathbf{u}}{dz}\right)^2\right]. \tag{41.5}$$

Здесь $\mathbf{u}$ - двумерный вектор локального смещения вихревой решетки, имеющий компоненты в плоскости (x, y), перпендикулярной направлению внешнего поля H; постоянные C_{11}, C_{44}, и C_{66} упругие модули вихревой решетки, соответствующие деформациям сжатия, изгиба и сдвига, соответственно. Заметим, что в (41.5) написан общий вид упругой энергии для треугольной решетки линий с осью симметрии шестого порядка [117]. Далее нам понадобятся значения всех трех упругих модулей:

$$C_{11} - C_{66} = \frac{B^2}{4\pi}\frac{\partial H}{\partial B}, \quad C_{44} = \frac{BH}{4\pi}, \quad C_{66} = \frac{\Phi_0 B}{(8\pi\lambda)^2}. \tag{41.6}$$

Первые две формулы из (41.6) имеют общий характер и легко выводятся (см. ниже), результат же для модуля сдвига C_{66} приведен для наиболее интересного (при $\varkappa \gg 1$)

случая $H_{c1} \ll B \ll H_{c2}$, когда вихри все еще сильно взаимодействуют на длинах гораздо больших, чем a_0, а подавлением параметра порядка из-за близости к H_{c2} еще можно пренебречь. Формулы для C_{11} и C_{44} можно получить из простых макроскопических соображений. Действительно, $\nabla \mathbf{u} = \delta B/B$ есть относительное изменение плотности вихрей, поэтому первый член в интеграле (41.5) можно записать как $\frac{1}{2}(C_{11} - C_{66})(\delta B)^2/B^2$, т.е. $B^{-2}(C_{11} - C_{66}) = \partial^2 F/\partial B^2 = (1/4\pi)\partial H/\partial B$. Чтобы получить второе из равенств (41.6), рассмотрим однородную деформацию вихревой решетки, при которой все вихри наклоняются на малый угол $\theta = \partial u_x/\partial z$ по отношению к исходному направлению поля вдоль оси z. При этом возникает поперечная компонента магнитной индукции $B_\perp = B\theta$ и сохраняется проекция индукции на ось z, т. е. $B_\parallel = B$. В результате полная величина магнитной индукции $B_{\text{полн}} = \left(B_\parallel^2 + B_\perp^2\right)^{1/2}$ изменяется на $\delta|B| = \frac{B}{2}(\partial \mathrm{u}/\partial z)^2$, а свободная энергия - на величину $(\partial F/\partial B)\delta|B| = \frac{H}{4\pi} \cdot \frac{B}{2}(\partial \mathbf{u}/\partial z)^2$. Сравнивая это выражение с соответствующим членом в (41.5), получаем результат для C_{44} из (41.6). Модуль сдвига C_{66} нельзя определить из столь же общих соображений - его необходимо вычислять как некоторую бесконечную сумму по узлам вихревой решетки. Мы здесь не будем останавливаться на этом (в действительности не очень сложном) вычислении [105]; заметим лишь, что малость модуля сдвига C_{66} по сравнению с $C_{11} \simeq C_{44}$ (их отношение, как видно из (41.6), порядка $(n\lambda^2)^{-1} \ll 1$) легко понять: дальнодействующий характер отталкивания между вихрями приводит к очень малой сжимаемости решетки, но слабо влияет на энергию деформаций, не меняющих плотность вихрей; поэтому модуль сдвига можно оценить как энергию взаимодействия ближайших соседей (порядка ϵ_0), умноженную на плотность вихрей $n = B/\Phi_0$, что совпадает по порядку величины с (41.6).

Теперь мы готовы воспроизвести для решетки вихрей оценку силы коллективного пиннинга (по аналогии с (41.2)). Будем считать, что деформация вихревой решетки, вызванная ее подстройкой под случайный потенциал примесей, достаточно мала, так что относительное смещение вихрей $|\mathbf{u}(\mathbf{r}) - \mathbf{u}(\mathbf{r}')|$ достигает величины порядка ξ при $|z - z'| \geqslant L_p^{3D}$, либо $|\rho - \rho'| \geqslant R_p$ (здесь ρ и z - поперечные и продольная (к полю $\mathbf{B}$) компоненты вектора $\mathbf{r}$). Характерные длины пиннинга L_p^{3D} и R_p в продольном и поперечном направлениях существенно отличаются вследствие различия порядков величин упругих модулей C_{66} и C_{44}; кроме того, продольная длина L_p^{3D} отличается и от ранее введенной кодновихревой» длины пиннинга L_p. Для характерной величины энергии взаимодействия с дефектами получим теперь $E_{\text{пинн}}^{3D} \sim (\gamma \xi^2 n V_p)^{1/2}$, где $V_p = L_p^{3D} R_p^2$ - объем области упругого пиннинга. Далее, неравенство $C_{11} \gg C_{66}$ означает, что деформациями сжатия можно пренебречь по сравнению с деформациями сдвига, так что достаточно приравнять по порядку величины энергию взаимодействия с дефектами $E_{\text{пинн}}^{3D}$ и энергии сдвиговых и изгибных деформаций:

$$\frac{C_{44}\xi^2}{\left(L_p^{3D}\right)^2} V_p \simeq \frac{C_{66}\xi^2}{R_p^2} V_p \simeq \left(\gamma \xi^2 n V_p\right)^{1/2} \tag{41.7}$$

Кроме того, для определения критической плотности тока j_c следует, как и выпе, приравнять силу Лоренца $j_c \frac{1}{c} B V_p$ (теперь действующую на единицу объема вихревой решетки) к максимальной объемной силе пиннинга $\mathcal{F}_{\text{пинн}} \simeq E_{\text{пинн}}^{3D}/\xi$. В результате

получим

$$R_p \simeq \lambda \left(\frac{L_p}{a_0}\right)^3, \quad L_p^{3D} \simeq \frac{\lambda}{a_0} R_p \tag{41.8}$$

$$E_{\text{пинн}}^{3D} \simeq H_{cm}^2 \xi^3 \frac{\xi}{L_p} \left(\frac{\lambda}{a_0}\right)^2 \left(\frac{L_p}{a_0}\right)^4 \tag{41.9}$$

$$j_c^{3D} \simeq j_c \left(\frac{a_0}{\lambda}\right)^2 \left(\frac{a_0}{L_p}\right)^4 \propto B^{-3}. \tag{41.10}$$

Как видно из (41.9), (41.10), с увеличением магнитного поля (а потому и жесткости вихревой решетки) характерная энергия пиннинга в объеме V_p растет (вместе с самим объемом), в то время как критическая плотность тока падает. Это происходит потому, что энергия $E_{\text{пинн}}^{3D}$ растет с полем медленнее, чем объем, в то время как полная сила Лоренца при заданном токе пропорциональна объему.

Результаты (41.4) и (41.10) не переходят один в другой при $a_0 \sim L_p$, как этого можно было бы ожидать-формулы для коллективного пиннинга решетки (41.8) приводят к большим длинам пиннинга ($R_p \sim \lambda \gg a_0$) и меньшему критическому току $j_c^{3D} \ll\ll j_c$ по сравнению с формулой (41.4) для пиннинга одиночных вихрей. Дело в том, что при выводе оценок (41.8) - (41.10) мы предполагали, что вихревая решетка описывается обычной теорией упругости с постоянными упругими модулями (пока длина волны деформации много больше постоянной решетки). В действительности, это предположение справедливо для вихревой решетки лишь при длинах волн q^{-1}, больших чем лондоновская длина λ. При меньших длинах волн магнитное поле "не успевает" следовать за деформациями вихревых линий (оно не может меняться на длинах меньше λ) и макроскопический подход к выводу C_{11} и C_{44} отказывает. В области $q\lambda \geqslant 1$ вихревая решетка описывается нелокальной теорией упругости, в рамках которой упругие модули сжатия и изгиба следует рассматривать как функции волнового вектора деформации q (это похоже на ситуацию с нелокальным экранированием токов в пиппардовских сверхпроводниках, см. 7). В интервале волновых векторов $\lambda^{-1} \leqslant q \leqslant a_0^{-1}$ упругие модули $C_{11}(q)$ и $C_{44}(q)$ ведут себя при $B \gg H_{c1}$ одинаково [105, 115]:

$$C_{11}(q) = C_{44}(q) = \frac{B^2}{4\pi} \frac{1}{1 + (q\lambda)^2} \tag{41.11}$$

Аккуратный расчет [115, 116] с использованием (41.11) показывает, что имеется промежуточная область магнитных полей, в которой длина пиннинга и критический ток экспоненциально резко зависят от поля:

$$R_p \simeq a_0 e^{(B/B^*)^{3/2}-1}, \quad j_c^{3D} \simeq j_c \frac{B}{B^*} e^{-2(B/B^*)^{3/2}+2} \tag{41.12}$$

где $B^* \simeq (j_c/j_0)\, H_{c2} < B < B^\dagger$. Результаты же (41.8) - (41.8) справедливы при еще больших полях $B > B^\dagger$, когда длина R_p, определяемая из (41.12), становится больше λ. Как видно из сравнения формул (41.8) - (41.8) и (41.12), величины B^* и $B^\dagger$ всегда довольно близки.

Все полученные выше оценки показывают, что j_c монотонно убывает с ростом внешнего поля B; однако, как уже упоминалось в конце §38, в эксперименте часто наблюдается (например, [118, 35]) пик критического тока при $B \simeq H_{c2}$. Дело в том, что использованные нами здесь формулы (41.6) справедливы лишь в области слабых полей, когда коры соседних вихрей не перекрываются между собой (фактически это условие имеет вид $B \leqslant 0.2 H_{c2}$). Действительно, поскольку при $B > H_{c2}$ сверхпроводник непрерывно (фазовый переход II рода) переходит в нормальное состояние, где

квантованных вихрей вовсе нет, то и упругие модули (41.6), и параметр взаимодействия вихрей с примесями γ уменьшаются при $b = B/H_{c2} \to 1$. Расчеты [115, 105] показывают, что эффект от "смягчения" решетки сильнее, чем от ослабления связи вихрей с дефектами (так, максимальное значение $C_{66}(b)$ достигается при $b \simeq 0.6$, а затем модуль сдвига убывает пропорционально $(1-b)^2$), поэтому с ростом b критический ток $j_c(b)$ растет, а длина коллективного пиннинга R_p падает вплоть до величины порядка a_0 - т.е. происходит переход к одновихревому пиннингу. В области $a_0 < R_p < \lambda$ существенна пространственная дисперсия упругих модулей (41.11), поэтому рост критического тока происходит экспоненциально резко. При дальнейшем увеличении b взаимодействие между вихрями становится несущественным и $j_c(b)$ падает из-за ослабления взаимодействия каждого вихря с примесями ($\gamma_{\text{эфф}}(b) \propto (1-b)^2$). Таким образом, пик критического тока достигается (при слабом коллективном пиннинге) в полях B, близких к H_{c2}.

7.7.6 42*. Magnetic Flux Creep and Nonlinear Conductivity in HTSC

До открытия высокотемпературных сверхпроводников было естественно рассматривать критическое (38) и резистивное (40) состояния вихрей независимо друг от друга. Подразумевалось, что в критическом состоянии плотность тока j, возникшего из-за неоднородного распределения плотности вихрей при их проникновении в образец, равна критическому значению j_c, так что вихри неподвижны - в то время как в резистивном состоянии ток велик по сравнению с j_c, пиннингом вихрей можно вовсе пренебречь, и их движение характеризуется постоянным коэффициентом трения η. Однако ясно, что если потенциальные барьеры для движения вихрей обращаются в нуль при $j = j_c$ непрерывно, то при чуть меньших токах эти барьеры должны быть малы - и преодолимы для тепловых флуктуаций вихрей. Физическая причина, позволяющая провести упомянутое разделение явлений в обычных сверхпроводниках - очень большая при малых токах величина энергетических барьеров U_0 (по сравнению с тепловой энергией $k_{\text{B}}T$). Достаточно иметь плотность тока ниже j_c на малую величину порядка $k_{\text{B}}T/U_0$, чтобы пренебречь вероятностью тепловых перескоков вихрей через барьеры, созданные примесным потенциалом. В высокотемпературных сверхпроводниках характерные значения $k_{\text{B}}T/U_0$ на несколько порядков выше, и область термоактивированного движения (называемого обычно "крип" - от английского "creep", т. е. "переползание") вихрей оказывается широко представленной в эксперименте. Ниже мы рассмотрим с единой точки зрения как релаксацию критического состояния вследствие крипа ви хрей, так и нелинейные вольт-амперные характеристики $V(j)$ в ВТСП.

Вернемся к рассмотренной в 38 задаче о проникновении магнитного поля в пластину сверхпроводника толщиной d. Теперь мы не будем считать постоянным возникший в пластине (при проникновении в нее вихрей) ток и выведем макроскопическое уравнение, определяющее временную эволюцию плотности тока. удем считать магнитное поле направленным вдоль оси z, а ток плотности $\mathbf{j}$ и возникающее из-за движения вихрей электрическое поле $\mathbf{E} = (1/c)[\mathbf{Bv}]$ - вдоль оси y. Используя уравнения Максвелла $\partial B/\partial t = -c\partial E/\partial x$ и $\partial B/\partial x = -(4\pi/c)j$, получим для скорости релаксации тока

$$\frac{\partial j}{\partial t} = \frac{c}{4\pi}\frac{\partial^2(vB)}{\partial x^2} \tag{42.1}$$

В правой части этого уравнения содержится средняя скорость движения вихрей $v \simeq v_0 e^{-U(j)/k_{\text{B}}T}$, где $U(j)$-соответствующий плотности тока j потенциальный барьер. Для

простоты мы рас(:мотрим сейчас случай, когда величина B мало меняется по толщине пластины (см. рис. 38.1, б), а отношение $k_{\rm B}T/U(j)$ мало. Тогда распределение плотности тока по пластине оказывается по'ти однородным, $j(x,t) = j(t) + \delta j(x,t)$, где $\delta j/j \propto k_{\rm B}T/U(j) \ll \ll 1$, и для величины $j(t)$ можно вывести [96, 119] замкнутое уравгение

$$\frac{\partial j}{\partial t} = -\left(\frac{j_c}{\tau_0}\right) e^{-U(j)/k_{\rm B}T} \tag{42.2}$$

где $\tau_0 \sim d^2/c^2\rho_f$ имеет порядок времени диффузии магнитного поля в состоянии течения потока по толщине образца d. Соответствующий "коэффициент диффузии» для магнитного поля имеет вид $D_{\rm B} = c^2\rho_f/4\pi$, как это видно из уравнения $\dot{B} = (c^2\rho_f/4\pi)\,\nabla^2 B$, которое получается комбинированием уравнений Максвелла с законом Ома $E = \rho_f j$. При большой величине показателя экспоненты уравнение (42.2) можно решить приближенно, как говорят в таких случаях - с логарифмической точ ностью:

$$U(j) = k_{\rm B}T \ln\left(1 + \frac{t}{t_0}\right),$$
$$\text{где } t_0 = \tau_0 \frac{k_{\rm B}T}{j_c|\partial U/\partial j|} \sim \frac{k_{\rm B}T}{U_c}\frac{d^2}{c^2\rho_f}. \tag{42.3}$$

Физический смысл решения (42.3) очевиден-к моменту времени t после начала релаксации (крипа) величина плотности тока в образце устанавливается такой, что соответствующие этому току энергетические барьеры $U(j)$ как раз могут быть преодолены вихрями за время порядка t. Важное и заранее неочевидное обстоятельство состоит в том, что характерное "время попыток" t_0 для крипа оказывается зависящим от размера образца и вполне макроскопическим - в интервале $(10^{-6} \div 10^{-2})$ с.

Для того чтобы извлечь из соотношения (42.3) явную зависимость плотности экранирующих токов от времени, необходимо использовать какую-то оценку для функциональной зависимости $U(j)$. Рассмотрим сначала случай токов, близких к критическому. Тогда естественно предположить, что $U\,(j \to j_c) \simeq \simeq U_c\,(1 - j/j_c)^a$, где a - число порядка единицы. Используя это соотношение вместе с (42.3), находим, что

$$\frac{j(t)}{j_c} = 1 - \left[\frac{k_{\rm B}T}{U_c}\ln\left(1 + \frac{t}{t_0}\right)\right]^{1/a}. \tag{42.4}$$

Зависимость вида (42.4) с $a = 1$ была впервые получена в работе [120]. В эксперименте обычно измеряется зависимость магнитного момента сверхпроводника в течение длительного времени после включения (или изменения) внешнего магнитного поля, которое вызвало формирование критического состояния. Измеряемый магнитный момент $M(t)$ (пропорциональный протекающему в образце экранирующему току) в обычных сверхпроводниках ведет себя, как правило, логарифмически со временем, что соответствует показателю $a = 1$ и очень малому значению отношения $k_{\rm B}T/U_c \leqslant 10^{-3}$, так что полное изменение $M(t)$ при экспериментально достижимых временах остается много меньше
исходной величины $M(0)$. Иначе обстоит дело в ВТСП, где характерная величина $k_{\rm B}T/U_c$ часто бывает порядка 0.1 при $T \sim 0.5T_c$. Поскольку логарифмический множитель в (42.4) имеет порядок $10 \div 20$ при характерных временах релаксационных измерений $(10^2 \div 10^4)$ с, ток и намагниченность ВТСП должны релаксировать на величину порядка своих исходных значений, что и наблюдается экспериментально [121], рис. 42.1. Но в таком случае уже нельзя пользоваться формулой (42.4), выведенной в предположении малости изменения тока в процессе релаксации. Другой предельный

случай, в котором можно ожидать простой зависимости $U(j)$, - случай малых токов $j \ll j_c$. В случае коллективного пиннинга вихревой решетки слабыми примесями (или пиннинга отдельных вихревых линий) удается показать, что эта зависимость должна быть степенной, $U(j) \simeq U_c\,(j_c/j)^{\mu}$. Полуколичественная теория, приводящая к такому результату, была развита в работе [122] и называется теорией коллективного крипа (см. также [96]). Значение показателя μ в теории коллективного крипа зависит от соотношения длины пиннинга R_p, постоянной решетки a_0 и лондоновской длины λ, а также от отношения j/j_c и может меняться от значений порядка 0.1 до больших единицы. Простейшая интерполяционная формула, содержащая в себе и область $j \ll j_c$, и область $j_c - j \ll j_c$, может быть написана в виде

$$U(j) \simeq U_c \left[\left(\frac{j_c}{j} \right)^{\mu} - 1 \right] \tag{42.5}$$

Используя формулу (42.5) вместе с (42.3), получаем закон релаксации тока в виде

$$j(t) = j_c \left[1 + \frac{\mu k_{\mathrm{B}} T}{U_c} \ln \left(1 + \frac{t}{t_0} \right) \right]^{-1/\mu} \tag{42.6}$$

В тех случаях, когда $\mu \ll 1$, как, например, в случае слабо взаимодействующих между собой вихревых линий (т.е. при низких полях и температурах), выражение (42.6) можно приближенно эаписать в виде $j(t) \simeq j_c \exp\left[-\left(k_{\mathrm{B}}T/U_c\right) \ln\left(t/t_0\right)\right]$, т. е. измеряемый на
некотором масштабе времени t экранирующий ток оказьвается экспоненциальной функцией температуры и при этом степенной функцией времени t, что и наблюдалось экспериментально [123]. M, ед. СГСМ

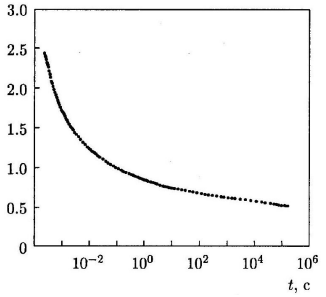


Рис. 42.1. Релаксация остаточной намагниченности в кристалле ВТСП на интервале времени в 9 порядков [121].

В общем случае величина, удобная для анализа экспериментальных данных по релаксации, - логарифмическая производная $S(t) = \partial \ln j(t)/\partial \ln t$. Используя (42.6), получаем предсказание для $S(t)$ в теории коллективного крипа:

$$S(t) = \frac{k_{\mathrm{B}} T}{U_c + \mu k_{\mathrm{B}} T \ln\left(1 + t/t_0\right)} \tag{42.7}$$

Важной чертой зависимости (42.7) является насыщение роста S как функции температуры при больших T и ее уменьшение как функции $\ln\left(t/t_0\right)$ в пределе больших времен. Оба эти предсказания, проистекающие из картины роста энергетических барьеров крипа по мере "старения" системы и релаксации в ней тока, нашли экспериментальное подтверждение; подробное обсуждение этих экспериментов можно найти в обзоре [124].

В теории коллективного крипа энергетические барьеры $U(j)$ растут при стремлении плотности тока j к нулю неограниченно. Следовательно, скорость движения вихрей

$v(j) \propto E(j)$, а дифференциальное сопротивление $dE/dj \propto \rho_f e^{-U(j)/k_B T}$ экспоненциально падает при уменьшении плотности тока. Это свойство очень важно - оно показывает, что равновесное состояние коллективного пиннинга вихревой решетки имеет нулевое линейное сопротивление, т.е. отличается от высокотемпературного состояния с конечной проводимостью качественным образом и потому должно быть отделено от него некоторым фазовым переходом.

Обычный способ нахождения линии перехода $H_{c2}(T)$ в сверхпроводящее состояние состоит в измерении линейного сопротивления $\rho(T, H)$ как функции температуры при различных значениях H: температура перехода $T_c(H)$ определяется по обращению $\rho(T, H)$ в нуль (функция же $H_{c2}(T)$ является обратной к $T_c(H)$). Фактически "нулевым» считается сопротивление ниже некоторой выбранной величины, например, 0.1 (или 0.01) от сопротивления в нормальном состоянии ρ_n, так что положение линии перехода определяется не вполне однозначно. У низкотемпературных сверхпроводников $\rho(T, H)$ очень резко падает с понижением температуры или поля ниже линии перехода, так что неоднозначность в определении $H_{c2}(T)$ очень мала. Совсем иначе дело обстоит в случае ВТСП; характерное семейство кривых $\rho(T, H)$ для $YBa_2Cu_3O_{7-x}$ показано на рис. 42.2. С увеличением H температурный интервал, в котором происходит падение сопротивления, очень заметно уширяется (причем верхние части кривых $\rho(T)$ зависят от величины H гораздо слабее, чем нижние), так что раэличные варианты выбора "нулевого" сопротивления (например, 0.1 или 0.01 от ρ_n) привели бы к существенно различным значениям температуры перехода $T_c(H)$. Поэтому в экспериментах с ВТСП фазовый переход приходится регистрировать по изменению (с температурой или полем) вида вольт-амперных характеристик $V(j)$: измерение ВАХ в широком (несколько порядков) интервале токов и напряжений позволяет надежно определить точку обращения линейного сопротивления в нуль.

На рис. 42.3 приведен в двойной логарифмической шкале на-

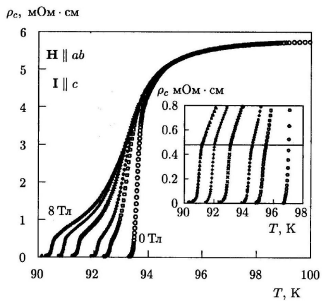


Рис. 42.2. Температурные зависимости сопротивления монокристалла YBaCuO при различных значениях H внешнего магнитного поля [125]. На вставке в более крупном масштабе показаны данные для области низких сопротивлений; участки кривых ниже сплошной линии практически совпадают для различных значений H.

бор вольт-амперных характеристик из эксперимента [126] на тонкой (толщина 0.4 мкм) пленке $YBa_2Cu_3O_{7-x}$, соответствующих различным значениям температуры, во внешнем поле $H_0 = 1$ Тл. Весь набор вольт-амперных характеристик делится на две части с качественно различным поведением. На графиках для температур $T < T_g \simeq 84.6$ К видна отрицательная кривизна в области малых токов, т.е. электрическое поле $E(j)$ убывает при $j \to 0$ по закону более быстрому, чем степенной, что качественно соответствует обсуждавшейся выше зависимости (42.5) энергии активации крипа. С другой стороны, кривые, соответствующие $T > T_g$, E, В/m

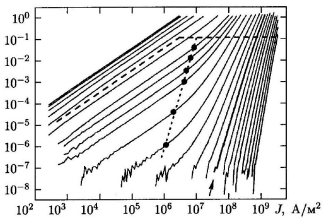


Рис. 42.3. Вольт-амперные характеристики тонкой пленки YBaCuO во внешнем магнитном поле 1 Тл [126] для различных температур в интервале между 80.5 и 91 K. Фазовый переход вихревая жидкость-вихревое стекло происходит при температуре $T_g = 84.6$ K, соответствующая вольт-амперная характеристика помечена стрелкой.

линейны в области малых токов, причем имеют единичный наклон, что означает линейную зависимость $E = \rho_{\text{эфф}}\, j$ при $j \to 0$. При этом значения эффективного сопротивления $\rho_{\text{эфф}}$ меняются на несколько порядков в довольно узком интервале температур чуть выше T_g. Наконец, в области не слишком малых токов $j > j_*(T)$ все кривые ведут себя примерно одинаково - линейно с наклоном больше единицы, что соответствует степенной зависимости $E(j) \propto j^{1+\alpha_j}$. С приближением T к T_g характерная величина тока $j_*(T)$ падает, так что сепаратрисе ($T = T_g$) семейства кривых соответствует степенное поведение ВАХ при всех значениях плотности тока. Оказывается возможным [126] представить совокупность всех этих данных единым образом при по мощи двух безразмерных функций $\mathcal{E}_\pm(x)$, соответствующих областям выше и ниже T_g:

$$\frac{E}{j\rho_f} \sim R\left(\frac{T-T_g}{T_g}\right)\mathcal{E}_\pm\left(\frac{j}{j_*}\right), \qquad \text{где} \qquad j_* \propto |T-T_g|^{\beta_j} \tag{42.8}$$

а безразмерные "скейлинговые" функции $\mathcal{E}_\pm(x)$ имеют асимптотики

$$\begin{aligned} &\mathcal{E}_\pm(x)|_{x\to\infty} \propto x^{\alpha_j}, \quad \mathcal{E}_+(x\to 0) = \text{const}, \\ &\mathcal{E}_-(x\to 0) \propto e^{-1/x^\mu} \end{aligned} \tag{42.9}$$

Функция $R(y)$ также ведет себя степенным образом, а показатель степени определяется тем, что ВАХ универсальны (т. е. слабо зависят от $T - T_g$) при относительно больших токах: из условия сокращения зависящих от T множителей в (42.8) при $j \gg j_*$ получаем, учитывая (42.9), что $R(y) \propto y^{\alpha_j\beta_j}$. Анализ ВАХ из эксперимента [126] приводит к значениям показателей $\alpha_j \simeq 4.0$ и $\beta_j \simeq 3.3$.

Масштабно-инвариантное поведение (scaling) описанного выше типа характерно для фазовых переходов II рода с сильно развитыми флуктуациями [28, 34]. Обычно свойства таких фазовых переходов можно описать теоретически как следствие изменения симметрии и появления параметра порядка, характеризующего степень нарушения симметрии в одной из фаз. В данном случае такое описание весьма затруднено, поскольку свойства уже самой низкотемпературной фазы определяются неоднородностями (примесями), приводящими к пиннингу вихревой решетки и, как следствие, к разрушению ее периодичности: корреляции положений вихревых линий пропадают на достаточно больших расстояниях (см. 41). Иначе говоря, низкотемпературная фаза, сформированная взаимодействием решетки вихрей с примесями, представляет собой «вихревое стекло", находящееся в одном из многих возможных метастабильных состояний, как это характерно вообще для стекол.

Что же представляет собой состояние, реализующееся при $T > T_g$? Как было объяснено в 37, идеальная (беспримесная)
вихревая решетка плавится при $B = B_m(T) < H_{c2}(T)$, вследствие чего образуется

жидкость из вихревых линий. Это фазовый переход I рода, но довольно близкий ко II роду (скачки энтропии и намагниченности малы). Пусть теперь в сверхпроводнике имеются примеси, создающие слабый случайный потенциал. В области на фазовой диаграмме сверхпроводника, достаточно удаленной (вверх) от линии плавления, выигрыш в свободной энергии за счет выгодного расположения вихрей в случайном потенциале меньше, чем разность свободных энергий твердого и жидкого состояний. Поэтому здесь беспорядок не меняет качественно состояния вихревой системы, однако он создает энергетические барьеры для течения вихревой жидкости [127]. Величины этих барьеров конечны при малых токах, $U(j,T,B) \underset{j\to 0}{\to} U_{\max}(T,B)$. В таком состоянии имеется ненулевое линейное сопротивление $(dE/dj)|_{j\to 0} = \rho_f e^{-U_{\max}/k_{\rm B}T}$. При совсем слабом беспорядке род фазового перехода не может измениться, так что переход из вихревой жидкости в стекло происходит скачком. Именно такая ситуация реализовалась в очень чистых монокристаллах, использованных в экспериментах [106, 128, 107, 129, 125]. При этом величина $U_{\max}$ может существенно превышать $k_{\rm B}T$, так 'то сопротивление в таком состоянии (называемом «термоактивированное течение потока», а в англоязычной литературе "thermally assisted flux flow", или сокращенно - TAFF) хотя и отлично от нуля, но может быть на несколько порядков меньше, чем сопротивление течения потока ρ_f. В особенно широкой области полей и температур термоактивированное течение потока наблюдается в слоистых ВТСП-материалах типа $Bi_2Sr_2CaCu_2O_8$, где зависимости $\rho_{\rm taff}\,(T,B)$ хорошо описываются как следствие поведения максимального энергетического барьера $U_{\max}(T,B) \propto \propto (T_c - T)\ln(H_{c2}/B)$ (см., например, работу [130]).

В образцах с большим количеством дефектов (особенно в тонких пленках, как в [126]) линия фазового перехода сдвигается по сравнению с линией плавления идеальной решетки, поэтому мы и обозначаем температуру этого перехода $T_g(B)$ новым подстрочным индексом g (от английского "glass»-стекло). Более того, скачки энтропии и намагниченности "размываются" беспорядком и фазовый переход становится непрерывным. В этом случае величина $U_{\max}$ неограниченно возрастает с приближением к линии перехода сверху, а линейное сопротивление обращается в нуль пропорционально $(T - T_g)^{\alpha_j\beta_j}$, как было объяснено в связи с рис. 42.3. В некоторых случаях при "промежуточном» количестве дефектов фазовый переход принадлежит к I роду при малых B и $(T_c - T)$ и становится непрерывным в более сильных полях, когда относительная роль случайного потенциала увеличивается; фазовая диаграмма такого типа приведена, в частности, в работе [131]. Теоретическое описание таких фазовых переходов еще недостаточно хорошо разработано.

8 Superconductivity by Abrikosov

8.1 15 Macroscopic theory of superconductivity

8.1.1 15.1. General properties of superconductors

In Part I we have been concerned with the various mechanisms of electrical resistance. Some of these mechanisms give a gradual decrease in resistance with temperature and other lead to a constant value or even to an increase in resistance at very low temperatures. However, in 1911 H. Kamerlingh Onnes, while studying the variation with temperature of the electrical resistance of mercury, observed that the resistance dropped sharply to zero at a temperature of 4.2 K . The same properties were later detected in some other metals. The new phenomenon was termed "superconductivity" and the corresponding metals were called "superconductors".

The temperature at which the resistance disappears is called the critical temperature, T_c; it

is different in different superconductors. The highest critical temperature among pure metals is shown by niobium: $T_c = 9.25$ K; the lowest has been found in tungsten: $T_c = 0.0154$ K. Although these are both low temperatures, in fact the temperature range is very wide, since the two extremes differ by about a factor of a thousand.

In what follows we shall also mention the practical applications of superconductors. Even at this moment they are rather numerous. However the recent discovery of so-called high-temperature superconducting ceramics arouses hopes for a further development of such applications. At the moment this book was written the highest critical temperature was registered for a composition $YBa_2Cu_3O_{7-8}$ and is equal to 93-95 K. But the discovery of even higher critical temperatures is not excluded. The importance of these discoveries is based on the fact that the superconductivity in such ceramics can be maintained in cryostats with liquid nitrogen (boiling point 77.4 K).

Subsequent investigations of the properties of superconductors have shown that superconductivity can be destroyed not only by increasing the temperature but also by applying a sufficiently strong magnetic field (Kamerlingh Onnes 1914). The critical field in which superconductivity is destroyed decreases with increasing temperature. It has been established empirically that the dependence $H_c(T)$ is described well by the formula

$$H_c(T) = H_c(0)\left[1 - \left(\frac{T}{T_c}\right)^2\right]. \tag{15.1}$$

Superconductivity is also destroyed by a strong electric current. If the superconductor is not too thin (see below), the critical current, at which resistance appears, satisfies Silsbee's rule (Silsbee 1916): the magnetic field produced by the critical current at the surface of a superconductor must be equal to H_c.

One of the basic properties of superconductors is the so-called Meissner effect (Meissner and Ochsenfeld 1933). If a metal is placed in a magnetic field smaller than H_c, then upon transition into the superconducting state the field is expelled from its interior, i.e., the true field $\boldsymbol{B} = \boldsymbol{0}$ in the superconductor (recall that the magnetic induction $\boldsymbol{B}$ is the average microscopic field)*. This is shown in fig. 93: (a) a superconductor; (b) a normal metal.

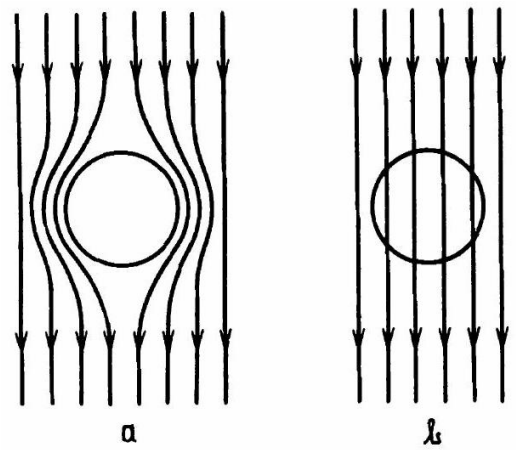


Fig. 93.

In more detailed investigations it has been found that the magnetic field is equal to zero only in the bulk of a massive sample. In a thin surface layer the field gradually decreases from a given value at the surface to zero. The thickness of this layer, which is called the penetration depth (δ), is usually of the order of $10^{-5} - 10^{-6}$ cm.

When a superconductor is placed in an external magnetic field, an undamped current appears in the surface layer, which produces a magnetic field of its own, and the latter compensates completely the external field inside the superconductor.

This can be traced out most simply on a cylinder in a longitudinal magnetic field. Suppose we have a solenoid with current i. Inside the solenoid a magnetic field is created, $H = (4\pi/c)i \cdot n$, where n is the number of turns in a coil per 1 cm of length. Instead of $i \cdot n$ we can write J, which is the current per 1 cm of the solenoid length. If the superconducting cylinder is placed in a field H, a current $J = cH/4\pi$ will

flow in the surface layer, which is directed so that the field produced by it will compensate the external field H.

The penetration depth δ depends on various factors, in particular on temperature. When the temperature approaches T_c, the penetration depth $\delta \to \infty$. The empirical formula that reflects in general aspects the temperature dependence of δ has the form

$$\delta(T) = \frac{\delta(0)}{\left[1 - (T/T_c)^4\right]^{1/2}} \tag{15.2}$$

As for the thermodynamic character of the transition of a metal from the superconducting to the normal state, it has been found that if the transition occurs at $H = 0$, i.e., at $T = T_c$, it is a second-order phase transition (see Appendix II). Upon this transition the latent heat of transition is not absorbed, but a jump in heat capacity takes place instead. But if the transition occurs at $H \neq 0$, i.e., at $T < T_c$, then it is a first-order transition at which the latent heat of transition is absorbed.

This change in the character of the transition may be associated with the behavior of the penetration depth. With $T \to T_c$ the penetration depth $\delta \to \infty$ and a superconductor does not differ at all at the transition point from a normal metal (with respect to the penetration of an infinitely weak field). Hence, the quantity δ that may serve as a characteristic of the extent of difference between a superconductor and a normal metal varies continuously and the transition should be second order. But if the transition occurs in a finite magnetic field, a discontinuous variation takes place in δ from a finite value in the superconducting phase to an infinite value in the normal phase (the field penetrates a normal metal completely, i.e., formally $\delta = \infty$).

The continuous variation of δ at T_c indicates that the state of the electron liquid in a metal varies continuously. This is also evidenced by measurements of thermal conductivity.

In Part I it has been pointed out that usually the major role in the thermal conductivity of a metal is played by electrons. But the vanishing of the resistance might indicate that the electrons cease to interact with the crystal lattice and, hence, are incapable of participating in thermal conductivity. In such a case, the overall coefficient of thermal conductivity at the transition point should decrease abruptly to a value determined by phonons alone. This does not occur. At $T = T_c$ the quantity x varies continuously.

The last of the fundamental properties that should be mentioned here is the behavior of heat capacity at low temperatures. In Part I we have described a construction (fig. 11), which enables one to separate the electronic part of the heat capacity from the lattice part. In this way we can find the coefficient in the Debye law $C = BT^3$ for the lattice (phonon) heat capacity. Assuming that the lattice heat capacity does not vary upon transition to the superconducting state, it is possible to determine the electronic heat capacity of a superconductor by subtracting BT^3 from the total value. As a result of such measurements it turned out that the electronic

- In superconducting alloys the behavior in a magnetic field is more complicated; in particular, the Meissner effect may be incomplete. We shall defer the discussion of this question until ch. 18.

heat capacity of a superconductor at temperatures substantially lower than T_c depends on temperature by an exponential law (Corak and Satterthwaite 1954,

Corak et al. 1954, 1956):

$$C_{\text{es}} = a \exp\left(\frac{-\Delta}{T}\right). \tag{15.3}$$

This means that the excited states of the electronic system are separated from the ground state by an "energy gap", just as in a semiconductor. On the other hand, a superconductor differs very strongly from a semiconductor in its electrical properties. Moreover, the phase transition at T_c is a second-order phase transition, which implies that the energy gap vanishes at T_{c}, i.e., the energy spectrum depends strongly on temperature. Such a dependence of the energy spectrum on temperature (in other words, on the state of the electron system) is contained in the Landau theory of the Fermi liquid (ch. 13). We shall use it in the derivation of the microscopic theory.

8.1.2 15.2. Thermodynamics of the superconducting transition

Let us consider a cylindrical sample in a longitudinal magnetic field. The condition for the superconducting transition is the equality of the free energies:

$$F_{\text{s}}(H,T) = F_{\text{n}}(H,T). \tag{15.4}$$

Here and henceforth the subscripts s and n designate the superconducting and the normal phase, respectively. Equilibrium may occur only at a field of $H = H_c(T)$.

The magnetic field enters a superconductor only to the penetration depth. In the presence of the field a superconducting current flows in the surface layer and screens the field in the bulk of the sample. This introduces a contribution to the energy of the order of $H_{\text{c}}^2/8\pi$ per unit volume of the surface layer. The total contribution to F_{s} from the currents and the field is of order $(H_{\text{c}}^2/8\pi)\,\delta S/V$, where S is the surface area of the sample (the free energy is referred to the unit volume).

The field penetrates a normal metal completely. Since we consider the equilibrium in a given field, we have to use the formula for F_{H} (Appendix III, formula AIII.10). Usually, superconducting metals are nonmagnetic, i.e., there $\mu \approx 1$. Hence, $F_{\text{n}}(H_{\text{c}},T) = F_{\text{n}}(T) - H_{\text{c}}^2/8\pi$. From this we see that the magnetic contribution to F_{n} is much larger than that to F_{s}, namely D/δ times as larger (D is the diameter of the sample). Therefore, for a massive cylinder the field contribution to F_{s} may be neglected; as a result, we obtain from eq. (15.4)

$$F_{\text{n}}(T) - F_{\text{s}}(T) = \frac{H_{\text{c}}^2}{8\pi} \tag{15.5}$$

Differentiating with respect to T, we find the entropy difference ($S = -\partial F/\partial T$):

$$S_{\text{n}} - S_{\text{s}} = \frac{-H_{\text{c}}}{4\pi}\frac{\mathrm{d}H_{\text{c}}}{\mathrm{d}T} \tag{15.6}$$

Corak et al. 1954, 1956):

$$C_{\text{es}} = a \exp\left(\frac{-\Delta}{T}\right). \tag{15.3}$$

This means that the excited states of the electronic system are separated from the ground state by an "energy gap", just as in a semiconductor. On the other hand, a superconductor differs very strongly from a semiconductor in its electrical properties. Moreover, the phase transition at T_c is a second-order phase transition, which implies that the energy gap vanishes at

T_c, i.e., the energy spectrum depends strongly on temperature. Such a dependence of the energy spectrum on temperature (in other words, on the state of the electron system) is contained in the Landau theory of the Fermi liquid (ch. 13). We shall use it in the derivation of the microscopic theory.

8.1.3 15.2. Thermodynamics of the superconducting transition

Let us consider a cylindrical sample in a longitudinal magnetic field. The condition for the superconducting transition is the equality of the free energies:

$$F_{\rm s}(H,T) = F_{\rm n}(H,T). \tag{15.4}$$

Here and henceforth the subscripts s and n designate the superconducting and the normal phase, respectively. Equilibrium may occur only at a field of $H = H_c(T)$.

The magnetic field enters a superconductor only to the penetration depth. In the presence of the field a superconducting current flows in the surface layer and screens the field in the bulk of the sample. This introduces a contribution to the energy of the order of $H_c^2/8\pi$ per unit volume of the surface layer. The total contribution to $F_{\rm s}$ from the currents and the field is of order $(H_c^2/8\pi)\,\delta S/V$, where S is the surface area of the sample (the free energy is referred to the unit volume).

The field penetrates a normal metal completely. Since we consider the equilibrium in a given field, we have to use the formula for $F_{\rm H}$ (Appendix III, formula AIII.10). Usually, superconducting metals are nonmagnetic, i.e., there $\mu \approx 1$. Hence, $F_{\rm n}\,(H_{\rm c},T) = F_{\rm n}(T) - H_c^2/8\pi$. From this we see that the magnetic contribution to $F_{\rm n}$ is much larger than that to $F_{\rm s}$, namely D/δ times as larger (D is the diameter of the sample). Therefore, for a massive cylinder the field contribution to $F_{\rm s}$ may be neglected; as a result, we obtain from eq. (15.4)

$$F_{\rm n}(T) - F_{\rm s}(T) = \frac{H_c^2}{8\pi}. \tag{15.5}$$

Differentiating with respect to T, we find the entropy difference ($S = -\partial F/\partial T$):

$$S_{\rm n} - S_{\rm s} = \frac{-H_{\rm c}}{4\pi}\frac{{\rm d}H_{\rm c}}{{\rm d}T}. \tag{15.6}$$

The quantity $q = T\,(S_{\rm n} - S_{\rm s})$ gives the latent heat of transition. Since ${\rm d}H_{\rm c}/{\rm d}T < 0$ (see eq. 15.1) it turns out that $q > 0$, i.e., the heat is absorbed upon transition from the superconducting to the normal phase.

A further differentiation with respect to temperature gives the difference in heat capacities ($C = T(\partial S/\partial T)_{\rm V}$

$$C_{\rm n} - C_{\rm s} = -\frac{T}{4\pi^i}\left[H_{\rm c}\frac{{\rm d}^2H_{\rm c}}{{\rm d}T^2} + \left(\frac{{\rm d}H_{\rm c}}{{\rm d}T}\right)^2\right]. \tag{15.7}$$

In particular, at $T = T_{\rm c}$ the field $H_{\rm c} = 0$ and we have

$$C_{\rm s}\,(T_{\rm c}) - C_{\rm n}\,(T_{\rm c}) = \frac{T_{\rm c}}{4\pi}\left(\frac{{\rm d}H_{\rm c}}{{\rm d}T}\right)^2 \tag{15.8}$$

It is interesting to note that this simple treatment, in which use is made of only a single experimental fact - the Meissner effect, enables one to derive rigorous formulae relating the critical magnetic field to the thermodynamic characteristics of the superconductor.

8.1.4 15.3. The intermediate state

So far we have considered a cylindrical geometry. Now suppose that the sample has an arbitrary shape or that, even if it is a cylinder, the field is not longitudinal. In this case the superconducting sample distorts the field, which becomes inhomogeneous in space. Let us see what happens if the specimen has the form of an ellipsoid. In such a case, the Maxwell field $\boldsymbol{H}_{\text{i}}$ inside it is homogeneous, although different from the external field at infinity $\boldsymbol{H_0}$. They are connected by the relation (Appendix III):

$$H_{\text{i}} = H_0 - 4\pi n M, \tag{15.9}$$

where M is the magnetization and n is the demagnetization factor.
Since the metal is in the superconducting state, inside $B = 0$, i.e.,

$$H_i + 4\pi M = H_0 + 4\pi(1-n)M = 0,$$

that is,

$$M = -\frac{H_0}{4\pi(1-n)}, \quad H_{\text{i}} = \frac{H_0}{1-n}. \tag{15.10}$$

According to the boundary conditions of the Maxwell theory, the normal component of $\boldsymbol{B}$ and the tangential component of $\boldsymbol{H}$ are continuous at the interface between the media. Outside the superconductor $\boldsymbol{B} = \boldsymbol{H}$. From the fact that $\boldsymbol{B} = 0$ in the superconductor one can conclude that $\boldsymbol{H}$ at the superconductor boundary has only a tangential component, i.e., the lines of force "by-pass" the superconductor (fig. 93a). From the continuity of the tangential component $\boldsymbol{H}$ at the interface one may conclude that at those points where the direction of $\boldsymbol{H}$ coincides with the
external field $\boldsymbol{H}_0$ the field at the boundary is at a maximum and equals $\boldsymbol{H}_0/(1-\boldsymbol{n})$, i.e., is larger than H_0. The superconductor moves apart the force lines of the field, which leads to their concentration outside the superconductor. We also see that along the superconductor surface the field varies and in some portions it may attain values of H_c, while $H_0 < H_c$.

Suppose that in a certain portion of the superconductor surface the field exceeds H_{c}. Then the superconductivity must vanish there. It will be most natural to presume that the picture will be as shown in fig. 94, where the shaded portion of the sample has passed to the normal state. However, this assumption leads to a contradiction. If the metal in the normal state is nonmagnetic, then for the magnetic field there is no difference between the normal metal and vacuum. Hence, departing from the superconducting region the field must decrease. If it is accepted that at the interface between the normal and the superconducting region $H = H_c$, then in the normal region the field $H < H_{\text{c}}$. But in this case the metal must be superconducting.

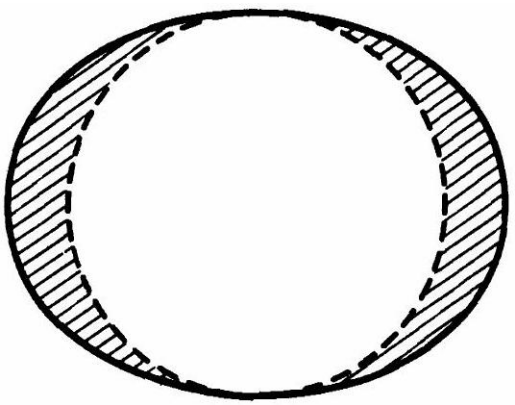


Fig. 94.

The way to remove this contradiction has been suggested by Peierls and London (Peierls 1936, London 1936) who advanced the idea of the "intermediate state". According to this idea, in the region of the external field

$$(1-n)H_c < H_0 < H_c \tag{15.11}$$

the superconductor passes to a special state characterized by the condition

$$H_i = H_c. \tag{15.12}$$

From eq. (15.9) we obtain

$$M = -\frac{H_c - H_0}{4\pi n}. \tag{15.13}$$

Substituting into the formula for the induction, we find

$$B = H_\mathrm{i} + 4\pi M = \frac{H_0}{n} - H_\mathrm{c}\frac{1-n}{n}. \tag{15.14}$$

From this we see that $B = 0$ at $H_0 = (1-n)H_2$ and $B = H_\mathrm{c}$ at $H_0 = H_\mathrm{c}$, and in the interval between these values the dependence of B on H_0 is linear. For the cylinder in the field perpendicular to its axis ($n = \frac{1}{2}$) the dependence $B\,(H_0)$ is shown in fig. 95.

In the Maxwell theory the field H_i does not always have a clear-cut microscopic meaning. Therefore, although the assumption $H_\mathrm{i} = H_\mathrm{c}$ and formula (15.14), which follows from it, agree well with experiment, they leave a feeling of dissatisfaction. Therefore, the intermediate state has been studied in more detail. It has been found that when a cylindrical specimen is placed in a perpendicular field and undergoes a transition to the intermediate state, its electrical resistance becomes anisotropic. Along the axis of the cylinder there is a finite resistance, and across the axis the resistance is equal to zero. This indicates that the cylinder splits up into thin layers of normal and superconducting phases perpendicular to its axis. When a current is passed along the axis, the layers are connected in series, but when it is passed across the axis they are connected in parallel, and the normal layers are shunted by the superconducting ones.

The picture in an infinite plate perpendicular to the magnetic field must be the simplest. In this case, $n = 1$, i.e., the intermediate state begins with $H_0 = 0$. If it is assumed that in the normal layers the field is $\boldsymbol{H}_\mathrm{c}$ and in the superconducting layers it is equal to zero, then the mean field, i.e., the induction in the plate, is $B = xH_c$, where x is the fraction of the normal phase. Outside the superconductor $B = H_0$. In this case, the field is directed normally to the interface. From the continuity condition for the normal component of $\boldsymbol{B}$ (i.e., in this particular case, $\boldsymbol{B}$ itself) we have

$$x = \frac{H_0}{H_c}. \tag{15.15}$$

No further conclusions can be made without studying the structure of the layers.
A detailed investigation of the structure of the intermediate state has been carried out by Landau (1937). We shall present here a simplified version of this theory. Let

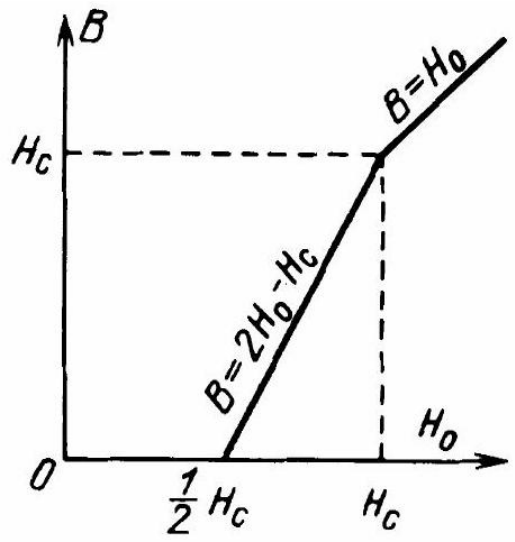


Fig. 95.

us consider a plate in a perpendicular field. If we assume that alternating plane layers of the normal and superconducting phases are formed in the plate, then the interfaces between the layers will coincide with the lines of force of the field. A kink in the lines of force would have led to a large additional energy. Therefore, we have to assume that the normal layers are slightly widened near the surface (fig. 96). If the thickness of the normal layers is a and that of the superconducting layer is b, then the characteristic size of the "corner" is of the order of

$$c \sim \frac{ab}{a+b}. \tag{15.16}$$

As $a \to 0$ or $b \to 0$ the "corners" disappear, as should be expected.
Let us calculate the energy of this structure. We use the formulas of Appendix III (AIII.12) and (AIII.13) for the free energy of a body of an arbitrary shape in a magnetic field. The magnetization M is defined with respect to the field H_0. But since outside the sample $B = H_0$ and B does not vary upon intersection of the boundary, the induction of the body $B = H_0$, i.e., $M = 0$. Hence, we may presume that the normal layers have an energy F_{n} and the superconducting layers an energy F_{s} per unit volume. We assume that the thickness of the plate (i.e., the length of the layers) is equal to L. The size in the direction perpendicular to the plane of the drawing is assumed to be equal to unity. If the free energy is counted off from F_{s}, the superconducting layers give a zero contribution and the total free energy will be equal to $H_c^2/8\pi$ multiplied by the volume of the normal phase. Considering that the number of layers per cm of length is $(a+b)^{-1}$, the energy per unit area of the plate will be

$$\frac{H_{\mathrm{c}}^2}{8\pi}\frac{1}{a+b}\left[La + \gamma\left(\frac{ab}{a+b}\right)^2\right], \tag{15.17}$$

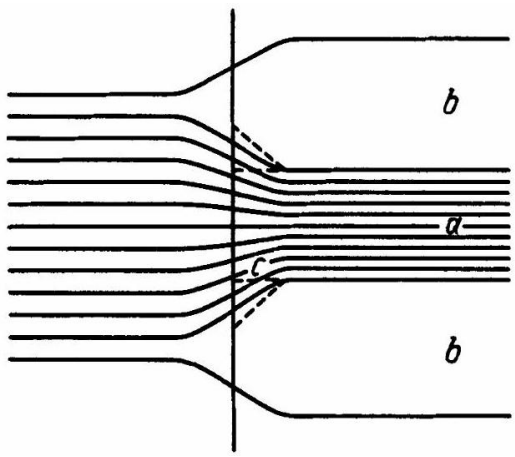


Fig. 96.

where $\gamma \sim 1$. The second term takes account of the "corners", i.e., the expansion of the normal layers near the surface.

However, if only this energy is taken into account, layers of finite size cannot be obtained. Therefore, Landau assumed the existence of an additional surface energy at the interface between the normal and the superconducting phase. The energy per unit area of the interface σ_{ns} has the dimension of erg/cm^2, while $H_{\mathrm{c}}^2/8\pi$ has the dimension of erg/cm^3. This makes it possible to introduce a new convenient parameter ξ having the dimension of length:

$$\sigma_{\mathrm{ns}} = \frac{H_{\mathrm{c}}^2}{8\pi}\xi. \tag{15.18}$$

At a later stage we shall see that the parameter ξ plays a fundamental role in the theory of superconductivity.

Considering that each normal layer has two boundaries of length $L + \beta c$, where $\beta \sim 1$ and c is the length of the corner (15.16), we obtain a contribution to the energy per unit area of the plate surface arising from the boundaries:

$$\frac{H_{\mathrm{c}}^2}{8\pi}\xi\frac{1}{a+b}2\left[L + \beta\frac{ab}{a+b}\right]. \tag{15.19}$$

Before finding the minimum of the total free energy, one has to take into account that the widths of the layers a and b are not independent but are determined by the external field H_0. According to eq. (15.19), we find the concentration of the normal phase:

$$x = \frac{a}{a+b} = \frac{H_0}{H_c}. \tag{15.20}$$

In the following all the lengths will be expressed in terms of a. Using eq: (15.20), we have

$$a + b = a\frac{H_{\mathrm{c}}}{H_0}, \quad b = a\frac{H_{\mathrm{c}} - H_0}{H_0}. \tag{15.21}$$

Substituting this into eqs. (15.17) and (15.19), we obtain the total free energy:

$$F = \frac{H_{\mathrm{c}}^2}{8\pi}\left\{L\frac{H_0}{H_{\mathrm{c}}} + \gamma a\frac{H_0}{H_{\mathrm{c}}}\frac{(H_{\mathrm{c}} - H_0)^2}{H_{\mathrm{c}}^2} + 2\xi\left[\frac{L}{a}\frac{H_0}{H_{\mathrm{c}}} + \beta\frac{H_0\,(H_{\mathrm{c}} - H_0)}{H_{\mathrm{c}}^2}\right]\right\}. \tag{15.22}$$

In this expression only two terms depend on a. Taking the minimum with respect to a, we find

$$a = \left(\frac{2\xi L}{\gamma}\right)^{1/2} \frac{H_c}{H_c - H_0}, \quad b = \left(\frac{2\xi L}{\gamma}\right)^{1/2} \frac{H_c}{H_0},$$
$$a + b = \left(\frac{2\xi L}{\gamma}\right)^{1/2} \frac{H_c^2}{H_0 (H_c - H_0)}. \tag{15.23}$$

In practice, $\xi \sim 10^{-5}$ cm. For a plate with a thickness of the order of 1 cm the period of the structure is of the order of 10^{-3} cm and it increases with thickness as $L^{1/2}$. Note the similarity between these results and the structure of diamagnetic domains (section 10.6). Chronologically, the theory of the intermediate state had been worked out earlier. According to eq. (15.23), the period of the structure $a + b$ increases at both boundaries of the intermediate state, i.e., with $H_0 \to 0$ and $H_0 \to H_c$. If $H_0 \to 0$, then $b \to \infty$ and $a \to$ const. and, conversely, with $H_0 \to H_c, a \to \infty$ and $b \to$ const.

The exact theory (Landau 1937) permits one to determine the shape of the layers from the condition that the interface between the normal and superconducting phase coincides with the line of force. The results of this theory are in qualitative agreement with those given above, the only difference being that at the boundaries of the intermediate state the thickness of the "foreign" layers does not remain constant and decreases slightly. For example, $a \sim [\xi L / \ln (H_c/H_0)]^{1/2}$ as $H_0 \to 0$.

In the experimental determination of the structure of the intermediate state, use is made of the inhomogeneity of the magnetic field which arises due to phase separation. The first experiments made use of a magnetic-field detector in the form of a bismuth wire of a very small size, whose resistance varied, depending on the magnetic field. The use of such a detector made it possible to trace out the emergence of the layers of the intermediate state to the sample surface (Meshkovskii and Shal'nikov 1947). In another method, ferromagnetic powders were used. If the sample is sprinkled with such a powder, the ferromagnetic particles are concentrated at the regions where the normal layers emerge (Sharvin and Balashova 1956, Sharvin 1957). Figure 97 shows a photograph of the normal layers obtained in this way in a superconducting plate. The field $\boldsymbol{H}_0$ is tilted relative to the normal n. The layers are parallel to the plane in which n and H_0 lie.

A further method of determining the structure of the intermediate state is covering the sample surface with a thin layer of a transparent substance having a large Faraday effect, i.e., capable of rotating the plane of polarization of light in a magnetic field. Illumination with polarized light and the observation of the reflected light with the aid of a polaroid gives a very contrasty picture of the layers of the normal and superconducting phases. It is also possible to follow their dynamics upon variation of the external field (Laeng and Rinderer 1972).

Owing to these experiments it has been possible to establish the existence of layers in the intermediate state and to determine the parameter ξ, i.e., the surface energy at the interface between the phases.

In conclusion, we return to the Maxwell field H_i. Although, as has been pointed out earlier (see Appendix III), the true physical significance is exhibited not by the Maxwell field H_i but by the induction B, which corresponds to the average of the microscopic field in the sample, the condition (15.12) $\boldsymbol{H}_i = \boldsymbol{H}_c$ must have a physical meaning. It turns out that in going from the microscopic description of the intermediate state to the "macroscopic" one, in which the averaging is made over distances larger than the thickness of the layers, it is necessary to introduce an additional

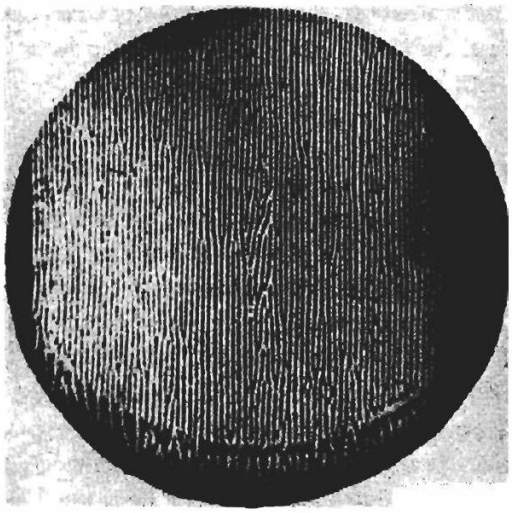


Fig. 97.

variable, namely, the average of the magnetic field taken only over the normal layers (Andreev 1966). It is exactly this average that corresponds to H_i; this clarifies the meaning of the condition (15.12).

8.1.5 15.4. Destruction of superconductivity by a current

Now we shall deal with another problem of the intermediate state. Suppose a current flows in a thick superconducting wire of radius r_0. In accordance with Silsbee's rule (Silsbee 1916), resistance can appear when the field generated by the current reaches the value H_c. Consider the Maxwell equation

$$\operatorname{rot} H = \left(\frac{4\pi}{c}\right) j.$$

Integrating over a circle of radius $r < r_0$ and using the rule of transformation of the curl, we obtain

$$\int \operatorname{rot} H \, \mathrm{d}S = \oint H \, \mathrm{d}l = H \cdot 2\pi r = \frac{4\pi}{c} \int j \, \mathrm{d}S = \left(\frac{4\pi}{c}\right) J(r).$$

Hence,

$$H(r) = 2\frac{J(r)}{cr}, \tag{15.24}$$

where $H(r)$ is the field at a distance r from the cylinder axis and $J(r)$ is the current flowing through a circle of radius r.

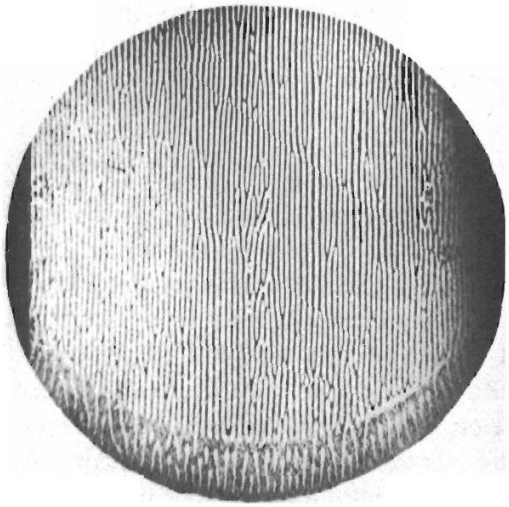


Fig. 97.

variable, namely, the average of the magnetic field taken only over the normal layers (Andreev 1966). It is exactly this average that corresponds to H_{i}; this clarifies the meaning of the condition (15.12).

8.1.6 15.4. Destruction of superconductivity by a current

Now we shall deal with another problem of the intermediate state. Suppose a current flows in a thick superconducting wire of radius r_0. In accordance with Silsbee's rule (Silsbee 1916), resistance can appear when the field generated by the current reaches the value H_{c}. Consider the Maxwell equation

$$\operatorname{rot} \boldsymbol{H} = \left(\frac{4\pi}{c}\right) \boldsymbol{j}$$

Integrating over a circle of radius $r < r_0$ and using the rule of transformation of the curl, we obtain

$$\int \operatorname{rot} \boldsymbol{H} \mathrm{d}\boldsymbol{S} = \oint \boldsymbol{H} \mathrm{d}\boldsymbol{l} = \boldsymbol{H} \cdot 2\pi r = \frac{4\pi}{c} \int \boldsymbol{j} \ \mathrm{d}\boldsymbol{S} = \left(\frac{4\pi}{c}\right) J(r).$$

Hence,

$$H(r) = 2\frac{J(r)}{cr}, \tag{15.24}$$

where $H(r)$ is the field at a distance r from the cylinder axis and $J(r)$ is the current flowing through a circle of radius r.

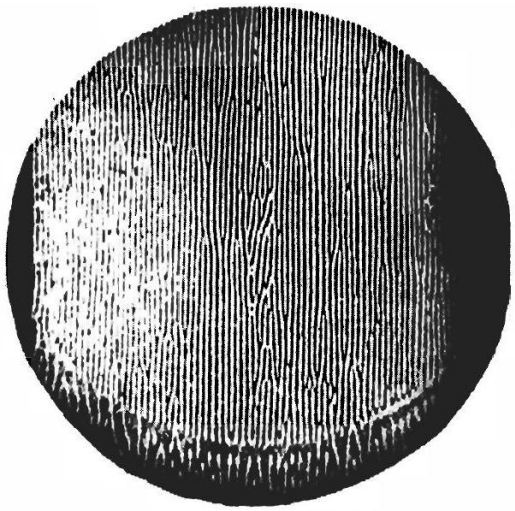


Fig. 97.

variable, namely, the average of the magnetic field taken only over the normal layers (Andreev 1966). It is exactly this average that corresponds to H_{i}; this clarifies the meaning of the condition (15.12).

8.1.7 15.4. Destruction of superconductivity by a current

Now we shall deal with another problem of the intermediate state. Suppose a current flows in a thick superconducting wire of radius r_0. In accordance with Silsbee's rule (Silsbee 1916), resistance can appear when the field generated by the current reaches the value H_{c}. Consider the Maxwell equation

$$\operatorname{rot} H = \left(\frac{4\pi}{c}\right) j.$$

Integrating over a circle of radius $r < r_0$ and using the rule of transformation of the curl, we obtain

$$\int \operatorname{rot} H \ \mathrm{d}S = \oint H \ \mathrm{d}l = H \cdot 2\pi r = \frac{4\pi}{c} \int j \ \mathrm{d}S = \left(\frac{4\pi}{c}\right) J(r).$$

Hence,

$$H(r) = 2\frac{J(r)}{cr}, \tag{15.24}$$

where $H(r)$ is the field at a distance r from the cylinder axis and $J(r)$ is the current flowing through a circle of radius r.

In the superconducting state the current flows only in a thin surface layer. Hence, $H = 0$ everywhere, except for this layer. The maximum field exists at the surface. It becomes equal to H_{c} with a current given by

$$J_{\text{c}} = \frac{1}{2} c r_0 H_{\text{c}}.$$

where r_0 is the radius of the conductor.

Let $J > J_c$. In this case, the superconductivity in the surface layer begins to be destroyed. It would appear as if a normal tube and a superconducting core were formed (fig. 98a). As a matter of fact, the entire current flows inside the superconducting cylinder. But it has a smaller

radius and from (15.24) it follows that with the same current the field H at the interface will be stronger. Hence, the process of destruction will go through the whole wire. But in this case the entire sample will become normal and the current will be distributed uniformly along the cross section. Then, $J(r) = j\pi r^2$, where j is the constant current density. According to eq. (15.24), the field in the vicinity of the cylinder axis will become lower than H_c; thus, the normal state is also unstable.

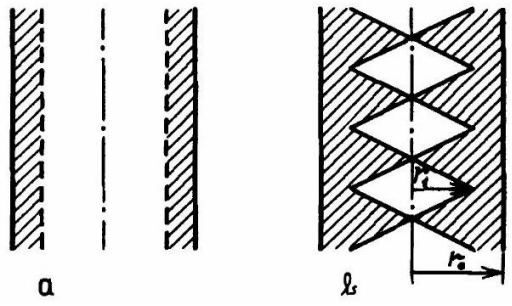


Fig. 98.

The solution lies in the assumption of the existence of the intermediate state (London 1937)*. We shall assume that the interior of the cylinder, with a radius r_1, is in the intermediate state and the external tube is in the normal state (fig. 98b). In the interior $\boldsymbol{H}(\boldsymbol{r}) = \boldsymbol{H}_c$. From eq. (15.24) we obtain

$$J(r) = \frac{1}{2} cr H_c. \tag{15.25}$$

The current density is given by

$$j_{r<r_1}(r) = \frac{\mathrm{d}J(r)}{\mathrm{d}S} = \frac{\mathrm{d}J(r)}{2\pi r\ \mathrm{d}r} = cH_c(4\pi r). \tag{15.26}$$

On the other hand, in the outer normal tube the current is distributed uniformly, i.e.,

$$j_{r>r_1}(r) = \frac{J - J\,(r_1)}{\pi\,(r_0^2 - r_1^2)} \tag{15.27}$$

In the superconducting state the current flows only in a thin surface layer. Hence, $H = 0$ everywhere, except for this layer. The maximum field exists at the surface. It becomes equal to $\boldsymbol{H}_c$ with a current given by

$$J_c = \frac{1}{2} cr_0 H_c.$$

where r_0 is the radius of the conductor.

Let $J > J_c$. In this case, the superconductivity in the surface layer begins to be destroyed. It would appear as if a normal tube and a superconducting core were formed (fig. 98a). As a matter of fact, the entire current flows inside the superconducting cylinder. But it has a smaller radius and from (15.24) it follows that with the same current the field H at the interface will be stronger. Hence, the process of destruction will go through the whole wire. But in this case the entire sample will become normal and the current will be distributed uniformly along the cross section. Then, $J(r) = j\pi r^2$, where j is the constant current density. According to eq. (15.24), the field in the vicinity of the cylinder axis will become lower than H_c; thus, the normal state is also unstable.

*The same idea was put forward at the same time by L.D. Landau (unpublished, see Shoenberg 1955).

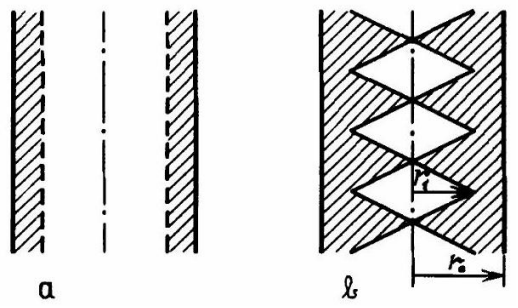


Fig. 98.

The solution lies in the assumption of the existence of the intermediate state (London 1937)*. We shall assume that the interior of the cylinder, with a radius r_1, is in the intermediate state and the external tube is in the normal state (fig. 98b). In the interior $H(r) = H_c$. From eq. (15.24) we obtain

$$J(r) = \frac{1}{2} cr H_c. \tag{15.25}$$

The current density is given by

$$j_{r<r_1}(r) = \frac{\mathrm{d}J(r)}{\mathrm{d}S} = \frac{\mathrm{d}J(r)}{2\pi r\ \mathrm{d}r} = cH_c(4\pi r). \tag{15.26}$$

On the other hand, in the outer normal tube the current is distributed uniformly, i.e.,

$$j_{r>r_1}(r) = \frac{J - J\,(r_1)}{\pi\,(r_0^2 - r_1^2)} \tag{15.27}$$

From the condition of the continuity of current density at $r = r_1$ we find that

$$\frac{cH_c}{4\pi r_1} = \frac{J - \frac{1}{2} cr_1 H_c}{\pi\,(r_0^2 - r_1^2)} \tag{15.28}$$

(here we have substituted $J\,(r_1)$ from eq. 15.25).
We now introduce new variables:

$$\frac{r_1}{r_0} = \rho, \quad \frac{J}{J_c} = \frac{2J}{cr_0 H_c} = \lambda. \tag{15.29}$$

Equation (15.28) will now be rewritten in the form

$$\rho^2 - 2\lambda\rho + 1 = 0.$$

The roots of this equation are

$$\rho = \lambda \pm \left(\lambda^2 - 1\right)^{1/2}.$$

Only one must be retained because the physical solution evidently corresponds to $\rho \to 0$ with $\lambda \to \infty$. Thus,

$$\rho = \lambda - \left(\lambda^2 - 1\right)^{1/2}. \tag{15.30}$$

• The same idea was put forward at the same time by L.D. Landau (unpublished, see Shoenberg 1955).

Let us draw two cross sections of the conductor at a certain distance from each other. Evidently, the potential must be constant along each cross section. The potential difference is the product of the current and the resistance. Let us denote the resistance of a normal metal by R_n. In such a case the resistance of the normal tube of $r_1 < r < r_0$ will be $R_n r_0^2/\left(r_0^2 - r_1^2\right)$. The potential difference is equal to the product of this resistance and the current flowing through the normal tube, on the one hand, and to the product of the total current and the total resistance R on the other:

$$JR = \left[J - J\left(r_1\right)\right] R_n \frac{r_0^2}{r_0^2 - r_1^2}. \tag{15.31}$$

Substituting $J\left(r_1\right)$ and passing over to the dimensionless variables ρ and λ, we obtain:

$$\frac{R}{R_\mathrm{n}} = \frac{1}{2}\left[1 + \left(1 - \lambda^{-2}\right)^{1/2}\right]. \tag{15.32}$$

This formula is applicable in the region of the intermediate state, i.e., for $\lambda > 1$. From this formula it follows that at $\lambda = 1$ a jump occurs in the resistance up to $\frac{1}{2}R_\mathrm{n}$, and then with increasing λ the resistance approaches asymptotically to R_n (the solid line in fig. 99). This prediction is in qualitative agreement with experiment, but the quantitative results are different. A jump $J = J_\mathrm{c}(\lambda = 1)$ occurs up to a value greater than $\frac{1}{2}R_\mathrm{n}$, and the subsequent asymptotic approach to R_n occurs more rapidly (the dashed line in fig. 99). This can be accounted for in the following manner. According to formula (15.26), the current density in the core is inversely proportional to r.

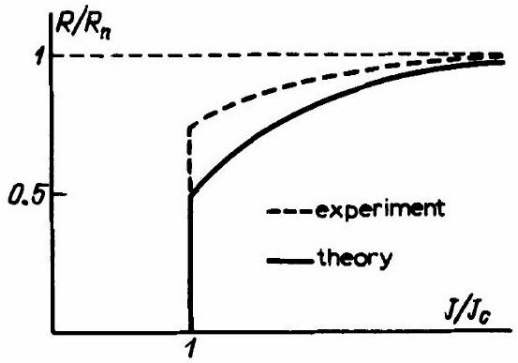


Fig. 99.

Hence, the structure of the intermediate state is such that the thickness of the normal layers increases proportionately to r, as shown in fig. 98b. If we recall the presence of the surface energy σ_ns, it will become clear that a boundary with a kink would have led to an infinite energy. Hence, the "discs" of the superconducting phase must have rounded edges, this being responsible for a certain delay in the transition and for the attainment of a larger total resistance. It is interesting to note that with an increase in the wire diameter the initial jump in the resistance decreases and tends towards $\frac{1}{2}R_\mathrm{n}$. This is in accord with the conceptions presented above, since the relative role of roundings-off decreases with increasing radius of the layers.

We do not describe here the complete microscopic theory (Andreev 1968). The result of this theory is as follows: the period of the structure at $J = J_c$ is of order $\left(\xi^2 r_0\right)^{1/3}$ and falls off with increasing current. The theory also predicts the value of the true critical current and the magnitude of the jump in the resistance at J_c, which are in good agreement with experiment. It is interesting to note that in accordance with the microscopic (BCS) theory the picture of the

intermediate state outlined above is observed only in the case of a not-too-pure metal. But if the metal is so pure that the Hall components of the resistivity tensor are comparable with the diagonal components, then the superconducting layers bend along the axis, forming a system of cones (a Christmas tree) instead of a system of planar discs, and move along the axis of the conductor.

In concluding this section, let us consider formula (15.32) from a somewhat different standpoint. Substituting λ into it according to eq. (15.29) and expressing $H_c(T)$ in accordance with formula (15.1), we obtain

$$\frac{R}{R_\mathrm{n}} = \frac{1}{2}\left\{1 + \left[1 - \left(\frac{cr_0 H_\mathrm{c}(0)}{2J}\right)^2 \left(1 - \frac{T^2}{T_\mathrm{c}^2}\right)^2\right]^{1/2}\right\}. \tag{15.33}$$

The formula can be applied as long as the expression in brackets is positive.
Let us specify the current J and consider $R(T)$. If $J \to 0$, then, according to this formula, the resistance appears near T_c and immediately becomes equal to R_n. But if we take a large current, the transition will be extended to a finite temperature range (fig. 100). From this it follows that we may speak of the jump in the resistance

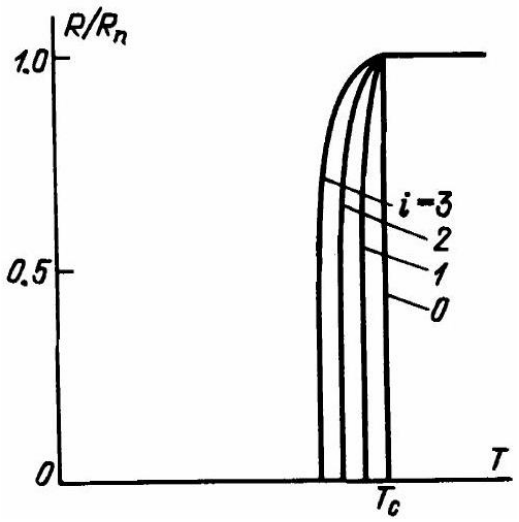


Fig. 100.

from zero to $\boldsymbol{R}_\mathrm{n}$ in the superconducting transition only if we mean a measurement in an infinitesimal current.

8.1.8 15.5. The London equations

The first attempt to develop the electrodynamics of superconductors was undertaken by the brothers F. London and H. London (1935). The purpose of this theory was to express in mathematical form the basic experimental facts: the absence of resistance and the Meissner effect, without consideration of the microscopic factors responsible for superconductivity.

If an electron does not undergo scattering, it is accelerated by an external field and, hence,

$$m\frac{\mathrm{d}v}{\mathrm{d}t} = eE. \tag{15.34}$$

This refers to all electrons. Hence, we can rewrite formula (15.34) for the current density. Introducing $j = n_e e v$, where n_e is the electron density and e is the charge, we get:

$$\frac{\mathrm{d}}{\mathrm{d}t}(\Lambda j) = E,$$

where $\Lambda = m/\left(n_e e^2\right)$.
In Part I we have already noted that the full derivative signifies the variation of the quantity in a given volume element moving together with the liquid. It is connected with the partial derivative, which describes the variation at a given point
of space by the relation

$$\frac{\mathrm{d}}{\mathrm{d}t} = \frac{\partial}{\partial t} + v\nabla.$$

Since the real current velocities v in a metal are small compared to the Fermi velocity, we can replace the total derivative by a partial derivative, in which case we have

$$\frac{\partial(\Lambda j)}{\partial t} = E. \tag{15.35}$$

According to the general equation of electrodynamics:

$$\operatorname{rot} E' = -c^{-1}\frac{\partial H}{\partial t}. \tag{15.36}$$

Taking the curl of eq. (15.35) and substituting (15.36), we get

$$\frac{\partial}{\partial t}\left(\operatorname{rot}\Lambda j + c^{-1}H\right) = 0.$$

This means that the quantity in parentheses does not change with time. But in the bulk of a massive superconductor $\boldsymbol{j} = 0$ and $\boldsymbol{H} = 0$. Hence, the quantity in parentheses is not simply conserved but is always equal to zero:

$$\operatorname{rot}\Lambda\boldsymbol{j} + c^{-1}\boldsymbol{H} = 0 \tag{15.37}$$

Equations (15.36) and (15.37) constitute the basis of London electrodynamics.
Let us consider the simplest problem: a bulk superconductor in an external magnetic field. According to the Maxwell equation,

$$\operatorname{rot} H = \frac{4\pi}{c} j \tag{15.38}$$

We take the curl of this equation:

$$\operatorname{rot}\operatorname{rot} H = \operatorname{grad}\operatorname{div} H - \Delta H = \frac{4\pi}{c}\operatorname{rot} j$$

Using the fact that $\operatorname{div}\boldsymbol{H} = \boldsymbol{0}$ and substituting $\operatorname{rot}\boldsymbol{j}$ from (15.37), we obtain

$$\Delta H - \delta^{-2}H = 0, \tag{15.39}$$

where

$$\delta = \left(\frac{\Lambda c^2}{4\pi}\right)^{1/2} = \left(\frac{mc^2}{4\pi n_{\mathrm{e}} e^2}\right)^{1/2} \tag{15.40}$$

of space by the relation

$$\frac{\mathrm{d}}{\mathrm{d}t} = \frac{\partial}{\partial t} + v\nabla.$$

Since the real current velocities v in a metal are small compared to the Fermi velocity, we can replace the total derivative by a partial derivative, in which case we have

$$\frac{\partial(\Lambda j)}{\partial t} = E. \tag{15.35}$$

According to the general equation of electrodynamics:

$$\operatorname{rot} E' = -c^{-1}\frac{\partial H}{\partial t}. \tag{15.36}$$

Taking the curl of eq. (15.35) and substituting (15.36), we get

$$\frac{\partial}{\partial t}\left(\operatorname{rot}\Lambda j + c^{-1}H\right) = 0.$$

This means that the quantity in parentheses does not change with time. But in the bulk of a massive superconductor $\boldsymbol{j} = 0$ and $\boldsymbol{H} = 0$. Hence, the quantity in parentheses is not simply conserved but is always equal to zero:

$$\operatorname{rot}\Lambda j + c^{-1}H = 0. \tag{15.37}$$

Equations (15.36) and (15.37) constitute the basis of London electrodynamics.
Let us consider the simplest problem: a bulk superconductor in an external magnetic field. According to the Maxwell equation,

$$\operatorname{rot} H = \frac{4\pi}{c}j \tag{15.38}$$

We take the curl of this equation:

$$\operatorname{rot}\operatorname{rot} H = \operatorname{grad}\operatorname{div} H - \Delta H = \frac{4\pi}{c}\operatorname{rot} j$$

Using the fact that $\operatorname{div}\boldsymbol{H} = \boldsymbol{0}$ and substituting $\operatorname{rot}\boldsymbol{j}$ from (15.37), we obtain

$$\Delta H - \delta^{-2}H = 0 \tag{15.39}$$

where

$$\delta = \left(\frac{\Lambda c^2}{4\pi}\right)^{1/2} = \left(\frac{mc^2}{4\pi n_{\mathrm{e}}e^2}\right)^{1/2} \tag{15.40}$$

of space by the relation

$$\frac{\mathrm{d}}{\mathrm{d}t} = \frac{\partial}{\partial t} + v\nabla.$$

Since the real current velocities v in a metal are small compared to the Fermi velocity, we can replace the total derivative by a partial derivative, in which case we have

$$\frac{\partial(\Lambda j)}{\partial t} = E. \tag{15.35}$$

According to the general equation of electrodynamics:

$$\operatorname{rot} E' = -c^{-1}\frac{\partial H}{\partial t}. \tag{15.36}$$

Taking the curl of eq. (15.35) and substituting (15.36), we get

$$\frac{\partial}{\partial t}\left(\operatorname{rot}\Lambda j + c^{-1}H\right) = 0$$

This means that the quantity in parentheses does not change with time. But in the bulk of a massive superconductor $\boldsymbol{j} = 0$ and $\boldsymbol{H} = 0$. Hence, the quantity in parentheses is not simply conserved but is always equal to zero:

$$\operatorname{rot}\Lambda j + c^{-1}H = 0 \tag{15.37}$$

Equations (15.36) and (15.37) constitute the basis of London electrodynamics.
Let us consider the simplest problem: a bulk superconductor in an external magnetic field. According to the Maxwell equation,

$$\operatorname{rot} H = \frac{4\pi}{c} j \tag{15.38}$$

We take the curl of this equation:

$$\operatorname{rot}\operatorname{rot} H = \operatorname{grad}\operatorname{div} H - \Delta H = \frac{4\pi}{c}\operatorname{rot} j$$

Using the fact that $\operatorname{div}\boldsymbol{H} = \boldsymbol{0}$ and substituting rot $\boldsymbol{j}$ from (15.37), we obtain

$$\Delta\boldsymbol{H} - \boldsymbol{\delta}^{-2}\boldsymbol{H} = \boldsymbol{0}, \tag{15.39}$$

where

$$\delta = \left(\frac{\Lambda c^2}{4\pi}\right)^{1/2} = \left(\frac{mc^2}{4\pi n_{\mathrm{e}} e^2}\right)^{1/2} \tag{15.40}$$

(we have used here the definition of Λ). Suppose the superconductor occupies the half-space $x > 0$ and the field is applied parallel to its surface in the direction z. From eq. (15.39) we find

$$H = H_0 \exp\left(\frac{-x}{\delta}\right) \tag{15.41}$$

where H_0 is the field at the surface. From eq. (15.37) we get

$$j_y = \frac{cH_0}{4\pi\delta}\exp\left(\frac{-x}{\delta}\right). \tag{15.42}$$

Thus, we conclude that London electrodynamics provides a correct qualitative description of the fact that the field and current are present only in a thin surface layer of the superconductor. Moreover, according to eq. (15.40), the quantity δ is of the order of $10^{-5} - 10^{-6}$ cm, consistent with experimental data.

Of course, in the derivation given above we proceeded from the assumption that all the electrons participate in the superconducting current. This contradicts the fact that δ depends on temperature and also that a second-order phase transition occurs at T_c, i.e., the state of electrons varies continuously. The theory may be "corrected" to a certain extent by introducing, instead of the total number of electrons, a certain number of "superconducting electrons" $n_{\mathrm{s}}(T)$, which decreases with temperature and turns to zero at T_c.

In conclusion, we note that eqs. (15.35) and (15.37) may be written in a different form, which will prove useful at a later stage. We introduce the vector potential A; $\boldsymbol{H}$ and $\boldsymbol{E}$ are expressed by the relations

$$H = \operatorname{rot} A, \quad E = -c^{-1}\frac{\partial A}{\partial t}.$$

Using A, we can write both London equations in the form of a single equation:

$$j = -\frac{1}{\Lambda c}A = -\frac{n_e e^2}{mc}A \tag{15.43}$$

At first glance this means that only one London equation is important and the second one is its corollary. But this is not the case: taking div of the Maxwell equation (15.38), we obtain the law of charge conservation:

$$\operatorname{div} j = 0. \tag{15.44}$$

But this is compatible with eq. (15.43) only if

$$\operatorname{div} A = 0. \tag{15.45}$$

This means that eq. (15.43) is valid not for any vector potential A but only for one that satisfies the condition (15.45). Thus, instead of the two London equations (15.35) and (15.37), we again have two equations, (15.43) and (15.45).

8.2 16 Basic ideas of the microscopic theory

8.2.1 16.1. The superfluidity condition

The microscopic theory of superconductivity was developed by J. Bardeen, L.N. Cooper and J.R. Schrieffer in 1957 and independently by N.N. Bogoliubov in 1957 (Bardeen et al. 1957, Bogoliubov 1958, Bogoliubov et al. 1958). It is quite natural to ask why superconductivity remained a puzzling phenomenon for nearly half a century after its discovery. Science was advancing; a great deal of experimental information was obtained and several useful phenomenological theories were developed (for example, the theory described in ch. 1).

The main cause is as follows. The phenomenon of superconductivity is very similar to the superfluidity of liquid helium discovered by P.L. Kapitza (Kapitza 1938). The theory of this phenomenon was developed by L.D. Landau in 1941 (Landau 1941a, b, 1944, 1947). One of the manifestations of superfluidity is the frictionless flow of helium in capillaries. It was natural to interpret superconductivity as the superfluidity of the electron liquid.

The Landau theory introduced a criterion for superfluidity. Imagine helium flowing in a capillary with a velocity v. If we pass to the coordinate system associated with helium, it will be at rest while the walls of the tube will move at a velocity - v. If viscosity arises, the moving tube will begin to entrain the resting helium. This means that the momentum $\boldsymbol{P}$ and the energy E of the helium will be changed. But, as we know from ch. 2, in a homogeneous quantum system the variation of energy and momentum occurs by way of the appearance of quasiparticles. Suppose a quasiparticle with momentum p and energy $\varepsilon(p)$ has appeared. Let us now pass to the laboratory coordinate system associated with the tube. In this system the energy and momentum are given by

$$\boldsymbol{P}' = \boldsymbol{P} + Mv, \quad E' = E + \boldsymbol{P}v + \frac{1}{2}\mathbf{M}v^2.$$

(M is the mass of the liquid). The variation of the energy resulting from the creation of a quasiparticle is $E + Pv = \varepsilon(p) + pv$. Hence, in order for the creation of a quasiparticle to be energetically favorable it is necessary that

$$\varepsilon(p) + pv < 0.$$

The lowest value of $\varepsilon + pv$ is attained with the opposite orientation of p and v; hence, in any case, $\varepsilon - pv < 0$ or

$$v > \frac{\varepsilon(p)}{p}.$$

This is the lowest velocity at which quasiparticles of momentum p and energy $\varepsilon(p)$ can appear. But we are interested in the velocity at which any quasiparticles can be created. Evidently, for this to occur it is necessary that

$$v > v_c = \min\left(\frac{\varepsilon(p)}{p}\right) \tag{16.1}$$

Thus, viscosity arises if the velocity exceeds v_c. In liquid helium the energy spectrum is such that v_c is a finite quantity. This means that at low flow velocities there is no viscosity.

We shall consider the Fermi liquid from this standpoint. The excitation of such a system consists of the creation of a particle-antiparticle pair. If such a pair is generated directly at the surface of the Fermi sphere, the energy may be as small as possible. At the same time, the total change in the momentum may reach $2p_0$ if the particle and the antiparticle are located on the opposite sides of the Fermi sphere. From this it follows that $v_c = 0$, i.e., in the Fermi system there is viscosity at any flow velocity.

Attempts have been made to find the solution on the assumption that electrons combine into pairs which are Bose particles and are analogous to helium atoms. However, no causes for such a combination could be found, since electrons have the same charge and according to the Coulomb law they repel each other. It is this circumstance that held back the development of the theory of superconductivity.

8.2.2 16.2. Phonon attraction

In 1950 a phenomenon was discovered which is known as the isotope effect (Maxwell 1950; Reynolds et al. 1950). In determining the T_c and H_c of superconductors of different isotopic composition it was found that T_c and H_c depend on the mass of ions forming the crystal lattice:

$$T_c \propto M^{-1/2}, \quad H_c \propto M^{-1/2} \tag{16.2}$$

The mass of the ions manifests itself only when lattice vibrations are taken into account. Hence, superconductivity is not a purely electronic phenomenon; phonons are also involved in it. On the basis of this fact Frölich (1950) and Bardeen (1950, 1951a, b) demonstrated independently that the electrons, while residing in the crystal lattice, are also capable of attracting one another*.

Let us consider the process shown schematically in fig. 101a. One electron with momentum p_1 emits a phonon of momentum $\hbar k$. The momentum of the electron

---

- We shall describe here the phonon mechanism of electron attraction which takes place in all superconductors known to date. The possibility is not excluded that the excitonic mechanism is operating in the newly found high-temperature ceramics (section 16.11). However, its principal scheme is very similar to phonon attraction.

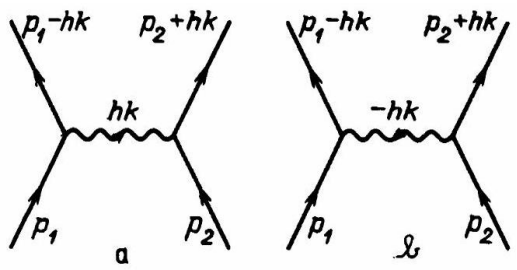


Fig. 101.

then becomes equal to $\boldsymbol{p}_1' = \boldsymbol{p}_1 - \hbar\boldsymbol{k}$. The phonon is absorbed by a second electron, which has had momentum p_2 before the absorption; after the phonon is absorbed the second electron acquires a momentum $\boldsymbol{p}_2' = \boldsymbol{p}_2 + \hbar\boldsymbol{k}$. The amplitude of this process, which is of second order according to perturbation theory, is given by

$$\frac{|V_k|^2}{\varepsilon(p_1) - \varepsilon(p_1 - \hbar k) - \hbar\omega(k),}$$

where $V_k = V_{p-ik,p}$ (section 4.3, formula 4.13).
On the other hand, the same finite momenta result if the electron of $\boldsymbol{p}_2$ emits a phonon with momentum - $\hbar k$, which is then absorbed by the electron of p_1 (fig. 101b). The amplitude of this process is

$$\frac{|V_k|^2}{\varepsilon(p_2) - \varepsilon(p_2 + \hbar k) - \hbar\omega(k)}.$$

Here it is taken into account that $\omega(k)$ and V_k are invariant under the replacement of $\boldsymbol{k}$ by $-\boldsymbol{k}$. The amplitudes obtained above must add up. Here one has to take account of the energy conservation law:

$$\varepsilon(p_1) + \varepsilon(p_2) = \varepsilon(p_1') + \varepsilon(p_2').$$

As a result, for the total amplitude we find

$$-\frac{2|V_k|^2 \hbar\omega(k)}{[\hbar\omega(k)]^2 - [\varepsilon(p_1) - \varepsilon(p_1 - \hbar k)]^2}.$$

Substituting expression (4.13) for V_k ($n_k = 0$ in this case), we obtain the order of magnitude of the total amplitude:

$$-\frac{\hbar^3}{p_0 m V}\frac{[\hbar\omega(k)]^2}{[\hbar\omega(k)]^2 - [\varepsilon(p_1) - \varepsilon(p_1 - \hbar k)]^2}. \tag{16.3}$$

Let us analyze this expression. At $\varepsilon(p_1) - \varepsilon(p_1') < \hbar\omega(k)$ we obtain a negative constant, which is independent of $\boldsymbol{k}$. If the electrons were involved in a direct point interaction with one another, i.e., $U = U_0\delta(r_1 - r_2)$, the matrix element corresponding to the first order perturbation theory for the scattering amplitude would be equal
to U_0. Hence, the interaction between the electrons transmitted by phonons is equivalent, with slight variations in the energy, to a point interaction, its sign corresponding to attraction.

Note also that since the interaction is independent of $\boldsymbol{k}$, i.e., of the rotation angle of the electron momenta, it follows that this is an interaction in the s-state, i.e., in a state with an orbital moment $l = 0$. Thus, the coordinate wave function of the interacting electrons is symmetric with respect to the interchange of particles. But since the electrons are Fermi

particles, their total wave function is antisymmetric under interchange. Hence, their spin wave function must be antisymmetric, i.e., the spins of the interacting electrons must be directed in opposite directions. The same may be put in a different way. The interaction found is equivalent to the attraction of particles if their coordinates coincide. The Pauli principle forbids two identical Fermi particles to be at a single point. Hence, they must differ in the spin direction.

If we take into account that the density of states of phonons is proportional to $k^2(\,\mathrm{d}k/\mathrm{d}\omega)$, i.e., falls off rapidly with decreasing k, and that the resultant amplitude is independent of k, then it becomes clear that the key role will be played by phonons with the largest k.values, i.e., with $k \sim k_\mathrm{D} \sim \pi/a$ and $\hbar\omega \sim \hbar\omega_\mathrm{D}$. At $\varepsilon(p) - \varepsilon(p') > \hbar\omega_\mathrm{D}$ the interaction rapidly decreases. Since the major role is played by electrons in the neighborhood of the Fermi boundary, it may be said that the phonon attraction occurs in a narrow layer near the Fermi boundary, whose thickness is of order $\hbar\omega_\mathrm{D}$ on the energy scale and of order $\Delta_p \sim \hbar\omega_\mathrm{D}/v$ on the momentum scale.

The fact that the interaction spreads over an energy interval $\Delta\varepsilon \sim \hbar\omega_\mathrm{D}$ implies, according to quantum mechanics, that it is "retarded" or, in other words, it operates during a finite time interval $\Delta t \sim \hbar/(\hbar\omega_\mathrm{D}) \sim \omega_\mathrm{D}^{-1}$. Its magnitude is of order $\left(p_0 m/\hbar^3\right)^{-1} \sim \nu^{-1}\mu\Big)$.

Simultaneously, Coulomb repulsion is operating. Taking account of the Debye screening (section 14.1), one can show that it operates at interatomic distances and may be written in the form $e^2a^2\delta(r_1 - r_2)$. for the same reason it is retarded with a characteristic time of order $\hbar/\varepsilon_\mathrm{F}$. The ratio of the interaction constants is of order

$$\frac{e^2a^2}{\hbar^3/p_0 m} \sim \frac{e^2\hbar^2}{p_0^2}\frac{p_0 m}{\hbar^3} \sim \frac{e^2}{\hbar v} \sim 1$$

that is, both interactions are of the same order of magnitude. Hence, in some metals phonon attraction may be dominant, while in others Coulomb repulsion predominates. This explains why some metals become superconductive and others remain normal at all temperatures.

To be more precise, it should be said that quantitative calculations always give some preference to the Coulomb repulsion. But its time of action is much shorter than that of the phonon attraction. This leads to an effective damping of the Coulomb repulsion: it is divided by the log of the time ratio, i.e., by $\ln(\varepsilon_\mathrm{F}/\hbar\omega_\mathrm{D}) = \ln(M/m)$.

In most cases, the two interactions differ quantitatively rather strongly to one or the other side, so that in studying superconductivity one may limit oneself to taking account of phonon attraction alone. Instead of the exact formula (16.3), we shall simulate its amplitude by a constant $-g\,(g \sim \hbar^3/p_0 m \sim (\nu/\mu)]^{-1}\Big)$ in the energy interval $\mu - \hbar\omega_\mathrm{D} < \varepsilon < \mu + \hbar\omega_\mathrm{D}$ and by zero at other energies.

8.2.3 16.3. Cooper pairs

It would appear that after the discovery of the attraction it became immediately possible to work out the theory of superconductivity. Nevertheless, several years were needed for this to be accomplished. The difficulty that had to be overcome was as follows. As has been explained earlier, the superfluidity of the electron liquid could have arisen upon binding of electrons into pairs. But from quantum mechanics it is known that if the interaction is not strong enough or has a small action radius, a bound state cannot be produced. Exceptions are the purely one- and twodimensional cases when the motion of particles is limited by a straight line or a plane; in these cases, any attraction leads to the formation of a bound state. But at first sight such models have nothing to do with the case under consideration.

A measure of the binding energy of a pair may be the critical temperature. If one considers that it is of the order of degrees, i.e., 10^4 times lower than the kinetic energy of electrons (the Fermi energy), the binding of electrons into pairs seems to be impossible.

The resolution of this paradox was found by Cooper (Cooper 1956), who noticed that pairs are formed not by free isolated electrons but by quasiparticles of the Fermi liquid. We shall present here a slightly modified version of Cooper's derivation which provides an answer correct in order of magnitude, in contrast to the original paper in which actually only quasiparticles of particle type were taken into account and this led to an incorrect result.

For the sake of simplicity we will consider the isotropic case. The energy spectrum of quasiparticles is shown in fig. 102 by a solid line (section 2.2). Here the right branch refers to quasiparticles of particle type and the left to quasiparticles of antiparticle type. On the whole, the energy spectrum may be written in the form $|\xi(p)|$, where $\xi = v\,(p - p_0)$. One should, however, keep in mind that antiparticles have a different sign of the charge. As will be seen below, we are interested in the

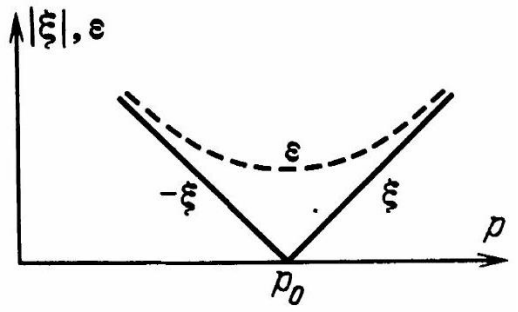


Fig. 102.

simulate its amplitude by a constant $-g\,(g \sim \hbar^3/p_0 m \sim (\nu/\mu)]^{-1}\Big)$ in the energy interval $\mu - \hbar\omega_{\mathrm{D}} < \varepsilon < \mu + \hbar\omega_{\mathrm{D}}$ and by zero at other energies.

8.2.4 16.3. Cooper pairs

It would appear that after the discovery of the attraction it became immediately possible to work out the theory of superconductivity. Nevertheless, several years were needed for this to be accomplished. The difficulty that had to be overcome was as follows. As has been explained earlier, the superfluidity of the electron liquid could have arisen upon binding of electrons into pairs. But from quantum mechanics it is known that if the interaction is not strong enough or has a small action radius, a bound state cannot be produced. Exceptions are the purely one- and twodimensional cases when the motion of particles is limited by a straight line or a plane; in these cases, any attraction leads to the formation of a bound state. But at first sight such models have nothing to do with the case under consideration.

A measure of the binding energy of a pair may be the critical temperature. If one considers that it is of the order of degrees, i.e., 10^4 times lower than the kinetic energy of electrons (the Fermi energy), the binding of electrons into pairs seems to be impossible.

The resolution of this paradox was found by Cooper (Cooper 1956), who noticed that pairs are formed not by free isolated electrons but by quasiparticles of the Fermi liquid. We shall present here a slightly modified version of Cooper's derivation which provides an answer correct in order of magnitude, in contrast to the original paper in which actually only quasiparticles of particle type were taken into account and this led to an incorrect result.

For the sake of simplicity we will consider the isotropic case. The energy spectrum of quasiparticles is shown in fig. 102 by a solid line (section 2.2). Here the right branch refers to quasiparticles of particle type and the left to quasiparticles of antiparticle type. On the whole, the energy spectrum may be written in the form $|\xi(p)|$, where $\xi = v\,(p - p_0)$. One should,

however, keep in mind that antiparticles have a different sign of the charge. As will be seen below, we are interested in the

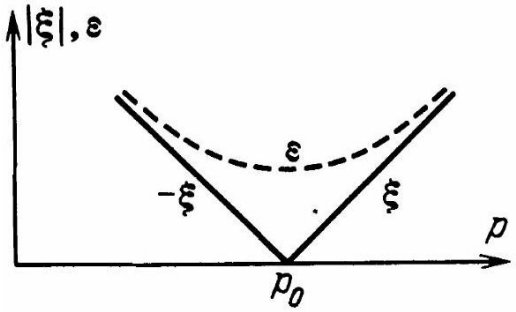


Fig. 102.

interaction of quasiparticles with the same $|p|$, i.e., the interaction of either two particles or two antiparticles. In either case, phonons produce attraction.

Let us write the Schrödinger equation for two quasiparticles:

$$\left[\mathscr{H}_0(r_1) + \mathscr{H}_0(r_2) + U(r_1, r_2)\right]\Psi(r_1, r_2) = E\Psi(r_1, r_2). \tag{16.4}$$

Here $\mathscr{H}_0(r_1)$ is the Hamiltonian of a free quasiparticle, i.e.,

$$\mathscr{H}_0(r_1)\,\psi_p(r_1) = |\xi(p)|\psi_p(r_1) \tag{16.5}$$

(in the free-quasiparticle model $\psi_p = V^{-1/2}\mathrm{e}^{\mathrm{i}pr/\hbar}$). In the ground state the total momentum and spin of a bound pair must be equal to zero. Hence, the wave function of the pair will be a superposition of the states of two free quasiparticles having opposite momenta and spins, i.e.,

$$\Psi(r_1, r_2) = \sum_p c_p \psi_{p,+}(r_1)\,\psi_{p,-}(r_2), \tag{16.6}$$

where the subscripts $\pm$ signify the projection of spin $\pm\frac{1}{2}$. Substituting this into eq. (16.4), we obtain

$$2|\xi(p)|c_p + \sum U_{pp'}c_{p'} = Ec_p. \tag{16.7}$$

We put

$$U_{pp'} = \begin{cases} -g, & p_0 - \frac{\hbar\omega}{v} < |p|, |p'| < p_0 + \frac{\hbar\omega_{\mathrm{D}}}{v}, \\ 0, & \text{outside this interval,} \end{cases} \tag{16.8}$$

and solve eq. (16.7) for c_p :

$$c_p = \frac{g\bar{I}}{2|\xi(p)| - E}, \tag{16.9}$$

where

$$I = \sum_{|p'|=p_0-\hbar\omega_{D'}/v}^{|p'|=p_0+\hbar\omega_{D'}/v} c_{p'} \tag{16.10}$$

Taking into account that we are looking for a bound state (a negative energy value), denoting $E = -2\Delta$ and substituting c_p from eq. (16.9) into eq. (16.10) we find

$$I = \frac{1}{2} \sum_{|p|=p_0-\hbar\omega_D/v}^{|p|=p_0+\hbar\omega_D/v} \frac{1}{|\xi(p)| + \Delta}.$$

Passing to integration over $\boldsymbol{\xi}$ and taking into account that the integral is taken over neighborhood of the Fermi surface, we get

$$1 = \frac{1}{2} g\nu(\mu) \ln\left(\frac{\hbar\omega_D}{\Delta}\right)$$

(the factor $\frac{1}{2}$ has appeared because the summation is carried out over states of one of the quasiparticles, for which the spin projection is specified, whereas the density of states defined earlier, $\nu = p_0 m/(\pi^2\hbar^3)$, included both projections of the spin).

Solving for Δ, we find

$$\Delta = \hbar\omega_D \exp\left(\frac{-2}{g\nu(\mu)}\right) \tag{16.11}$$

Thus, a pair of quasiparticles has a finite binding energy 2Δ. Such bound pairs are called Cooper pairs. At $T = 0$ they form a Bose condensate.

Below we shall obtain Δ from the exact theory. It will be twice as large as (16.11). The difference is associated with the fact that in the derivation given above we were concerned with the creation of a pair against the background of the unreconstructed ground state with a "normal" energy spectrum*.

In spite of a certain inaccuracy, the result (16.11) makes it possible to draw certain conclusions. First of all, note that since $g \sim \nu^{-1}(\mu)$, the expression in the exponent is formally of the order of unity. In fact, $g\nu$ is always somewhat smaller than unity. A certain numerical smallness in the exponent turns to a substantial smallness of the ratio $\Delta/\hbar\omega_D$, which, judging by the known values of T_c (it will be shown below that $\Delta \sim T_c$), is usually 10^{-2} or less**.

Further, from the result obtained it is seen that the binding energy of a Cooper pair 2Δ is finite at any g, which is not consistent with the above-given reasoning concerning the impossibility of the formation of a bound complex upon week interaction. In fact, we are speaking not of isolated particles but of quasiparticles with the Fermi sphere being occupied. This actually leads to the replacement of the three-dimensional problem by a two-dimensional one: the integrals over the momenta are transformed in accordance with the rule $\int d^3p/(2\pi\hbar)^3 \to \frac{1}{2}\nu \int d\xi$, and for the two-dimensional problem $\int d^2p/(2\pi\hbar)^2 \to 2\pi \int p\, dp/(2\pi\hbar)^2 \to 2\pi m \int d\varepsilon/(2\pi\hbar)^2$, since $\varepsilon = p^2/2m$. In a two-dimensional model, as has been said above, any attraction will be sufficient for the particles to be bound.

We thus see that the presence of a filled Fermi sphere plays a most important role in the formation of Cooper pairs.

It is clear that any change in temperature will have an effect on the binding energy. It is because of this that $\Delta(T)$ decreases with increasing temperature and vanishes at $T_c \sim \Delta(0)$. Such is the physical picture. We will now turn our attention to a more detailed description of the Bardeen-Cooper-Schrieffer (BCS) theory***.

8.2.5 16.4. The energy spectrum

While considering the quantization of lattice vibrations in section 4.3, we introduced operators u_k and u_k^+. Let us write these operators in the following

form:

$$u_k = \left(\frac{\hbar}{2nM\omega(k)}\right)^{1/2} b_k, \quad (b_k)_{n_k}^{n_k-1} = n_k^{1/2}$$

The operator b_k thus introduced is called the phonon annihilation operator and b_k^+, its Hermitian conjugate, is the phonon creation operator. The operator $b_k^+ b_k$ is diagonal with the matrix elements being equal to n_k. Thus,

$$b_k^+ b_k = n_k$$

is the operator of the number of particles in state $\boldsymbol{k}$. Analogously,

$$b_k b_k^+ = n_k + 1$$

Hence, the commutator of the operators $\boldsymbol{b_k}$ and $\boldsymbol{b_k^+}$is

$$b_k b_k^+ - b_k^+ b_k = \left[b_k b_k^+\right] = 1$$

Since operators with different $\boldsymbol{k}$ commute, we may write:

$$\left[b_k, b_k^+\right] = \delta_{kk'}$$

All this refers to phonons, which obey Bose statistics. Let us now consider electrons, which obey Fermi statistics. For them we can also introduce particle creation and annihilation operators. Consider a system of noninteracting Fermi particles. According to the Pauli principle, no more than one particle may exist in each state. We shall conventionally write the wave function of this system, noting in which states there are particles and in which there are no particles at all. For example,

$$\Phi\left(1_{p_1}, 0_{p_2}, 1_{p_3}, 1_{p_4}, 0_{p_5}\right)$$

denotes a system in which the states p_1, p_3 and p_4 are occupied and the states p_2 and p_5 are free.

Let the system be described by the wave function $\Phi\left(\ldots 0_p \ldots\right)$. Then the annihilation operator a_p acting on this system gives zero, because there are no particles in the state $\boldsymbol{p}$:

$$a_p \Phi\left(\ldots 0_p \ldots\right) = 0$$

But if there is a wave function $\Phi\left(\ldots 1_p \ldots\right)$, then under the action of the operator a_p it is transformed to $\Phi\left(\ldots 0_p \ldots\right)$, i.e.,

$$a_p \Phi\left(\ldots 1_p \ldots\right) = \Phi\left(\ldots 0_p \ldots\right).$$

Let us now act on these functions by means of the operator $a_p^+ a_p$. Since $a_p^+$is the creation operator, we obtain

$$\begin{aligned} a_p^+ a_p \Phi\left(\ldots 0_p \ldots\right) &= a_p^+ \cdot 0 = 0 = 0 \cdot \Phi\left(\ldots 0_p \ldots\right) \\ a_p^+ a_p \Phi\left(\ldots 1_p \ldots\right) &= a_p^+ \Phi\left(\ldots 0_p \ldots\right) = \Phi\left(\ldots 1_p \ldots\right) \\ &= 1 \cdot \Phi\left(\ldots 1_p \ldots\right) \end{aligned}$$

*The derivation performed in the original work (Cooper 1956) leads to a substantial error, giving an exponent twice as large in absolute magnitude.

** As for the high-temperature ceramics, if the idea of the excitonic mechanism of their superconductivity is confirmed, $\hbar\omega_D$ in formula (16.11) should be replaced by an essentially larger quantity (section 16.11).

*** As noted above, the same theory was developed practically at the same time by Bogoliubov. We shall refer to it as the BCS theory because this name has been generally adopted.

From these formulae if follows that the operator $a_p^+ a_p$ is diagonal and equal to the number of particles:

$$a_p^+ a_p = n_p.$$

Analogously, we find

$$a_p a_p^+ \Phi\left(\ldots 1_p \ldots\right) = 0, \quad a_p a_p^+ \Phi\left(\ldots 0_p \ldots\right) = \Phi\left(\ldots 0_p \ldots\right),$$

and, hence,

$$a_p a_p^+ = 1 - n_p, \quad \left\{a_p, a_p^+\right\} = a_p a_p^+ + a_p^+ a_p = 1.$$

This rule is known as the anticommutation rule of Fermi operators.
Consider now the action of operators $a_p^+ a_{p'}$ and $a_{p'} a_p^+$with different p and p'. In the first case we have

$$\begin{aligned} a_p^+ a_{p'} \Phi\left(\ldots 0_p \ldots 1_{p'} \ldots\right) &= a_p^+ \Phi\left(\ldots 0_p \ldots 0_{p'} \ldots\right) \\ &= \Phi\left(\ldots 1_p \ldots 0_{p'} \ldots\right) \end{aligned}$$

and in the second

$$\begin{aligned} a_{p'} a_p^+ \Phi\left(\ldots 0_p \ldots 1_{p'} \ldots\right) &= a_{p'} \Phi\left(\ldots 1_p \ldots 1_{p'} \ldots\right) \\ &= -a_{p'} \Phi\left(\ldots 1_{p'} \ldots 1_p \ldots\right) = -\Phi\left(\ldots 0_{p'} \ldots 1_p\right) \\ &= -\Phi\left(\ldots 1_p \ldots 0_{p'} \ldots\right) \end{aligned}$$

The change in sign is associated with the fact that when two particles are interchanged the wave function changes sign. This must be taken into account when there are several occupied states. From this it follows that the anticommutator $\left\{a_p^+ a_{p'}\right\}$ with different $\boldsymbol{p}$ and $\boldsymbol{p}'$ is equal to zero and, hence,

$$\left\{a_{p'}, a_p^+\right\} = a_{p'} a_p^+ + a_p^+ a_{p'} = \delta_{pp'}. \tag{16.12}$$

The use of the occupation numbers of the states as variables and the introduction of the operators $a_p, a_p^+$is called second quantization.

Using the operators of second quantization we can write the Hamiltonian of an interacting system of electrons. For a normal metal we have used two descriptions: quasiparticles with the energy spectrum $\varepsilon_{\mathbf{qp}} = |\xi|$ and the gas model. The difference between these two models consists, in particular, in that the former specifies the chemical potential while the latter specifies the total number of particles. As has been shown in section 2.4, the variation of the chemical potential in cases of physical interest is insignificant. Therefore, both descriptions are practically equivalent.

For superconductors it is more convenient to use the picture of quasiparticles, and this also corresponds to the specification of the chemical potential. With the chemical potential being specified the role of the Hamiltonian is played by $\mathscr{H} - \mu N$, where N is the operator of the total number of particles. As a matter of fact, this reduces to the replacement of the electron energy by $\xi = \varepsilon - \mu$, i.e., to a shift in the origin of the energy. Exactly such a Hamiltonian will be used here for the determination of the energy spectrum of quasiparticles.

Below we shall always consider the isotropic model of the metal because in this case it is easier to trace out the main properties of superconductors. For those cases where anisotropy is of fundamental importance a special analysis will be given.

After what has been said above we can write the Hamiltonian*:

$$\mathscr{H} - \mu N = \sum_{p,\sigma} \xi_p a^+_{p,\sigma} a_{p,\sigma} - g \sum_{p_1+p_2=p'_1+p'_2} a^+_{p'_1}, a^+_{p'_2}, , a_{p_2}, , a_{p_1}, , \cdot \tag{16.13}$$

The first term is simply $\sum_{p,\sigma} \xi_p n_{p,\sigma}$. The summation runs over momenta and spins ($\sigma = \pm$). The second term corresponds to the interaction of electrons. It describes how two electrons with initial momenta p_1 and p_2 acquire new momenta, p'_1 and p'_2, as a result of the interaction; in other words, electrons with initial momenta disappear and instead of them there are created electrons with new momenta. Here, the law of conservation of the total momentum is taken into account**. The sums over the momenta run over the intervals $p_0 \pm \hbar\omega_{\mathrm{D}}/v$; it is taken into account that at a single point only electrons with opposite spins are interacting. The coefficient in this term should have been written in the form g/V, but for simplicity we assume the normalizing volume $V = 1$ in this part of the book.

For a normal metal we may pass from electrons to quasiparticles. To do this, we have to assume that $a_{p,\sigma} = \alpha_{p,\sigma}$ at $p > p_0$ and that $a_{p,\sigma} = \alpha^+_{-p,-\sigma}$at $p < p_0$, where $\alpha_{p,\sigma}$ are the operators of second quantization for quasiparticles. As a matter of fact, the destruction of a particle with $p < p_0$ means the creation of a quasiparticle of antiparticle type. Thus, even in an ordinary Fermi system the ground state is such that the transition to quasiparticles requires the redefinition of the creation and annihilation operators.

In a superconductor an even more complicated change in the ground state takes place. For this change to be found and for the energy of quasiparticles to be calculated, we employ a variational method (Abrikosov and Khalatnikov 1958)***. We introduce the creation and annihilation operators for quasiparticles, $\alpha_{p,+}$ and $\alpha_{p,-}$ by using the Bogoliubov relations (Bogoliubov 1958):

$$a_{p,+} = u_p \alpha_{p+} + v_p \alpha^+_{-p,-}, \quad a_{p,-} = u_p \alpha_{p,-} - v_p \alpha^+_{-p,+}. \tag{16.14}$$

Note that with these transformations the momentum and spin are conserved.
Let us write the anticommutator $\left\{a_{p,+} a^+_{p,+}\right\}$and substitute into it formulae (16.14). As a result, we have

$$\begin{aligned}\left\{a_{p,+} a^+_{p,+}\right\} =& u_p^2 \left\{\alpha_{p,+} \alpha^+_{p,+}\right\} + v_p^2 \left\{\alpha^+_{-p,-} \alpha_{-p,-}\right\} \\ &+ u_p v_p \left\{\alpha_{p,+} \alpha_{-p,-}\right\} + u_p v_p \left\{\alpha^+_{-p,-} \alpha^+_{p,+}\right\} = 1\end{aligned}$$

Below we shall always consider the isotropic model of the metal because in this case it is easier to trace out the main properties of superconductors. For those cases where anisotropy is of fundamental importance a special analysis will be given.

After what has been said above we can write the Hamiltonian*:

$$\mathscr{H} - \mu N = \sum_{p,\sigma} \xi_p a^+_{p,\sigma} a_{p,\sigma} - g \sum_{p_1+p_2=p'_1+p'_2} a^+_{p'_1,+} a^+_{p'_2}, , a_{p_2}, , a_{p_1,+} \tag{16.13}$$

The first term is simply $\sum_{p,\sigma} \xi_p n_{p,\sigma}$. The summation runs over momenta and spins ($\sigma = \pm$). The second term corresponds to the interaction of electrons. It describes how two electrons

---

- Here and below $\xi_p \equiv \xi(p)$.
  ** In the second term of the Hamiltonian we omitted the term with $p_1 = p'_1$. This term is responsible for a slight variation in the chemical potential and can be compensated if we write $\xi - \Delta\mu$ in the first term. For simplicity we dispense with this procedure as being unimportant for the derivation.
  *** The method described here is simpler than the one used in the original work of Bardeen, Cooper and Schrieffer and is a generalization of the Bogoliubov method (Bogoliubov 1958; Bogoliubov et al. 1958) to finite temperatures.

with initial momenta p_1 and p_2 acquire new momenta, p_1' and p_2', as a result of the interaction; in other words, electrons with initial momenta disappear and instead of them there are created electrons with new momenta. Here, the law of conservation of the total momentum is taken into account**. The sums over the momenta run over the intervals $p_0 \pm \hbar\omega_{\mathrm{D}}/v$; it is taken into account that at a single point only electrons with opposite spins are interacting. The coefficient in this term should have been written in the form g/V, but for simplicity we assume the normalizing volume $V = 1$ in this part of the book.

For a normal metal we may pass from electrons to quasiparticles. To do this, we have to assume that $a_{p,\sigma} = \alpha_{p,\sigma}$ at $p > p_0$ and that $a_{p,\sigma} = \alpha^+_{-p,-\sigma}$at $p < p_0$, where $\alpha_{p,\sigma}$ are the operators of second quantization for quasiparticles. As a matter of fact, the destruction of a particle with $p < p_0$ means the creation of a quasiparticle of antiparticle type. Thus, even in an ordinary Fermi system the ground state is such that the transition to quasiparticles requires the redefinition of the creation and annihilation operators.

In a superconductor an even more complicated change in the ground state takes place. For this change to be found and for the energy of quasiparticles to be calculated, we employ a variational method (Abrikosov and Khalatnikov 1958)***. We introduce the creation and annihilation operators for quasiparticles, $\alpha_{p,+}$ and $\alpha_{p,-}$ by using the Bogoliubov relations (Bogoliubov 1958):

$$a_{p,+} = u_p\alpha_{p+} + v_p\alpha^+_{-p,-}, \quad a_{p,-} = u_p\alpha_{p,-} - v_p\alpha^+_{-p,+}. \tag{16.14}$$

Note that with these transformations the momentum and spin are conserved.
Let us write the anticommutator $\left\{a_{p,+}a^+_{p,+}\right\}$and substitute into it formulae (16.14). As a result, we have

$$\begin{aligned}\left\{a_{p,+}a^+_{p,+}\right\} =& u_p^2\left\{\alpha_{p,+}\alpha^+_{p,+}\right\} + v_p^2\left\{\alpha^+_{-p,-}\alpha_{-p,-}\right\} \\ &+ u_pv_p\left\{\alpha_{p,+}\alpha_{-p,-}\right\} + u_pv_p\left\{\alpha^+_{-p,-}\alpha^+_{p,+}\right\} = 1\end{aligned}$$

For the operators $\boldsymbol{\alpha_{p,\sigma}}$ to satisfy the ordinary anticommutation rules, it is necessary that

$$u_p^2 + v_p^2 = 1. \tag{16.15}$$

Thus, there is only one independent function, say v_p. We choose it so that the average energy be a minimum*. Here for the moment we leave the occupation numbers for quasiparticles undetermined. The average energy corresponds to the diagonal matrix element of the Hamiltonian (16.13). Substituting into it formulas (16.14) and retaining only

$$\left\langle\alpha^+_{p,-} - \alpha_{p,-}\right\rangle = n_{p,-}, \quad \left\langle\alpha^+_{p,+}\alpha_{p,+}\right\rangle = n_{p,+}$$

(here $\langle\cdots\rangle$ signifies the average over states with given occupation numbers), we obtain

---

- Here and below $\xi_p = \xi(p)$.
  ** In the second term of the Hamiltonian we omitted the term with $p_1 = p_1'$. This term is responsible for a slight variation in the chemical potential and can be compensated if we write $\xi - \Delta\mu$ in the first term. For simplicity we dispense with this procedure as being unimportant for the derivation.
  *** The method described here is simpler than the one used in the original work of Bardeen, Cooper and Schrieffer and is a generalization of the Bogoliubov method (Bogoliubov 1958; Bogoliubov et al. 1958) to finite temperatures.

$$
\begin{aligned}
E-\mu N &= \langle \mathscr{H} - \mu N \rangle \\
&= \sum_p \xi_p \left[u_p^2 \left(n_{p,+} + n_{p,-} \right) + v_p^2 \left(2 - n_{p,-} - n_{p,+} \right) \right] \\
&\quad - g \sum_p u_p v_p \left(1 - n_{p,+} - n_{p,-} \right) \sum_{p'} u_{p'} v_{p'} \left(1 - n_{p',+} - n_{p',-} \right). \qquad (16.16)
\end{aligned}
$$

Expressing u_p in accordance with (16.15) and varying with respect to v_p leads to the condition

$$
2\xi_p = \frac{\Delta \left(1 - 2v_p^2 \right)}{u_p v_p}, \qquad (16.17)
$$

where we have introduced the notation

$$
\Delta = g \sum_p u_p v_p \left(1 - n_{p,+} - n_{p,-} \right). \qquad (16.18)
$$

The solution of eq. (16.17) is

$$
u_p^2 = \frac{1}{2} \left(1 + \frac{\xi_p}{\varepsilon_p} \right), \quad v_p^2 = \frac{1}{2} \left(1 - \frac{\xi_p}{\varepsilon_p} \right), \qquad (16.19)
$$

where

$$
\varepsilon_p = \left(\xi_p^2 + \Delta^2 \right)^{1/2} \qquad (16.20)
$$

Substitution into eq. (16.18) leads to the condition

$$
\Delta = \frac{1}{2} g \sum_p \frac{\Delta}{\varepsilon_p} \left(1 - n_{p,+} - n_{p,-} \right). \qquad (16.21)
$$

For calculating the energy of quasiparticles we use the ideas of Landau's Fermi liquid theory (section 13.1). The energy of quasiparticles is defined as a variational
derivative of the total energy with respect to the distribution function

$$
\delta(E - \mu N) = \sum_p \varepsilon_{p,+} \delta n_{p,+} + \sum_p \varepsilon_{p,-} \delta n_{p,-} \qquad (16.22)
$$

With such a definition the equilibrium distribution function will be a Fermi function with $\varepsilon_{p,\sigma}$ as the energy*. Since $n_{p,+}$ and $n_{p,-}$ are included in the functional (16.16) in the same manner, the corresponding $\varepsilon_{p,\sigma}$ will also be the same. Varying (16.16) with respect to $\boldsymbol{n}_{\boldsymbol{p},+}$, for example**, we obtain

$$
\begin{aligned}
\varepsilon_{p,+} &= \frac{\delta(E - \mu N)}{\delta n_{p,+}} = \xi_p \left(u_p^2 - v_p^2 \right) + 2 u_p v_p \Delta \\
&= \left(\xi_p^2 + \Delta^2 \right)^{1/2} = \varepsilon_p.
\end{aligned}
$$

Thus, ε_p defined by formula (16.20) corresponds to the energy of quasiparticles (fig. 102, the dashed line). At $|\xi_p| > \Delta$, ε_p turns to $|\xi_p|$, which corresponds to quasiparticles of a normal metal.

- As has been said in section 14.1, the variational principle with the condition of the minimum average energy is equivalent to the Schrödinger equation.

This can also be seen from formulae (16.14) and (16.9). At $|\xi_p| \gg \Delta$ we have $u_p \to 1, v_p \to 0$ at $\xi_p > 0$ and $u_p \to 0$ and $v_p \to 1$ at $\xi_p < 0$. In such a case $\alpha_{p,+}$ and $\alpha_{p,-}$ play the role of the annihilation operators for quasiparticles of a normal metal.

From formula (16.20) it follows that there is an energy gap Δ in the quasiparticles spectrum. This not only agrees with experimental data but also accounts for the superconductivity. The critical velocity according to the Landau criterion (16.1) is finite: $v_c \sim \Delta/p_0$, i.e., at lower velocities the electron fluid exhibits superfluidity. Note also that the binding energy of a Cooper pair is equal to 2Δ. When it is broken up, two quasiparticles are formed, i.e., an energy Δ has to be consumed for each.

There arises, however, the following question: Are there excitations that are associated not with the breakdown of Cooper pairs but with their translational motion? The study of this question leads to the following results, which are rather understandable from a physical viewpoint. Cooper pairs form an interacting system. At low temperatures it may be regarded as a liquid and, hence, excitations with a low energy correspond to the propagation of sound waves (phonons). But sound is accompanied by density oscillations, and the liquid of Cooper pairs is charged. The density oscillations give rise to electric fields, which must be taken into account.

On the whole, we arrive at a situation resembling the problem of propagation of zero sound in the electron liquid (section 13.5). It has been found in section 13.5 that with the electric field taken into account the spectrum of vibrations is no longer linear, $\omega = ck$, and starts with a finite energy of order μ. This also occurs in

superconductors. It is clear that quasiparticles with such an energy cannot be of interest in a study of superconductivity.

Of course, just as in a normal metal, oscillations are possible, in principle, with a more complicated variation of the distribution function, which do not lead to a change in the electron density. However, because of a lack of clear-cut experimental evidence indicating their existence we shall not consider them.

A question may also be raised about pairing with a non-zero orbital moment, $l \neq 0$. The study of this question shows that if the amplitude of electron scattering is strongly dependent on the angle and there are negative coefficients in its expansion in spherical harmonics (each corresponding to a certain l), pairing may take place corresponding to the negative coefficient that is largest in absolute magnitude (see Abrikosov et al. 1962). An example of this kind in nature is a Fermi liquid - superfluid ^{3}He. In superfluid ^{3}He pairing actually occurs of quasiparticles with an orbital moment of $l = 1$ and parallel spins, which leads to superfluidity (see the review articles by Leggett 1975 and Wheatley 1975), but ^{3}He is a neutral Fermi liquid. Among metals a pairing with a nonzero orbital moment can possibly occur in so-called "systems with heavy fermions" (section 16.11), but this question has so far received no definite answer.

The difficulty lies in that scattering with a nonzero orbital moment implies a nonlocal interaction. However, as has been indicated in this book, phonon attraction and Coulomb repulsion are, in fact, local (i.e., they occur when electrons reside at a single point). Hence, we may speak only of some new, nonphonon mechanism of electron attraction, whose origin is not known at present (see the discussion of this question in section 16.11). In view of this, we shall not consider pairing with $l \neq 0$.

- In accordance with the generally adopted convention, here we denote the energy of quasiparticles by ε_p. It enters into the Fermi distribution without subtracting μ, i.e., $n_p = \left(e^{\varepsilon_p/T} + 1\right)^{-1}$. It should not be confused with the electron energy in the gas model, $\varepsilon(p)$, which has been used in Part I.
** Upon variation with respect to $n_{p,\sigma}$ the quantities u_p and v_p must be assumed to be constant, because these functions are themselves determined from the condition $\delta(E - N\mu)/\delta v_p = 0$.

8.2.6 16.5. Temperature dependence of the energy gap

We will begin the study of the thermodynamics of superconductors with the calculation of $\Delta(T)$. Substituting the Fermi function into formula (16.21) and passing to an integration over momenta, we arrive at the equation for determination of Δ :

$$\begin{aligned} 1 &= \frac{1}{2} g \int \frac{\mathrm{d}^3 p}{(2\pi\hbar)^3} \frac{1-2n_{\mathrm{F}}(\varepsilon)}{\varepsilon} \\ &= \frac{1}{2} g\nu(\mu) \int_0^{\hbar\omega_{\mathrm{D}}} \frac{\tanh\left[\left(\xi^2+\Delta^2\right)^{1/2}/2T\right]}{\left(\xi^2+\Delta^2\right)^{1/2}}\,\mathrm{d}\xi. \end{aligned} \tag{16.23}$$

Here we singled out the integration over ξ, took into account the symmetry with respect to $\xi \to -\xi$ and introduced the density of states $\nu(\mu) = p_0 m/\pi^2\hbar^3$) (remember that we are dealing with the isotropic model).

With $T \to 0, \tanh \to 1$. Taking the integral, we obtain:

$$1 = \frac{1}{2} g\nu(\mu) \ln\left(\frac{2\hbar\omega_{\mathrm{D}}}{\Delta(0)}\right)$$

(we assume that $g\nu(\mu) < 1$; therefore $\Delta < \hbar\omega_D$). From this it follows that

$$\Delta(0) = 2\hbar\omega_D \exp\left(\frac{-2}{g\nu}\right) \tag{16.24}$$

This formula differs from eq. (16.11) by a factor 2 , which results from taking account of the transformation of the energy spectrum.

As $T \to T_{\mathrm{c}}$, the energy gap tends to zero. In this case we have

$$1 = \frac{1}{2} g\nu(\mu) \int_0^{\hbar\omega_{\mathrm{D}}} \frac{\tanh(\xi)/2T_{\mathrm{c}}}{\xi}\,\mathrm{d}\xi = \frac{1}{2} g\nu(\mu) \ln\frac{2\hbar\omega_{\mathrm{D}}\gamma}{\pi T_{\mathrm{c}}}$$

where $\gamma = e^c = 1.78$. It follows that

$$T_c = \frac{2\hbar\omega_{\mathrm{D}}\gamma}{\pi} \exp\left(\frac{-2}{g\nu}\right). \tag{16.25}$$

Comparing this with eq. (16.23), we get

$$\Delta(0) = \frac{\pi}{\gamma} T_{\mathrm{c}} = 1.76 T_{\mathrm{c}}. \tag{16.26}$$

Let us consider the behavior of Δ near $T = 0$ and $T = T_{\mathrm{c}}$. Near $T = 0$ formula (16.23) is rewritten as follows: we divide it by $\frac{1}{2} g\nu(\mu)$ and then subtract and add $\left(\xi^2+\Delta^2\right)^{-1/2}$ under the integral. As a result we obtain

$$\ln\frac{\Delta(0)}{\Delta(T)} = \int_0^{\infty} \frac{1-\tanh\left[\left(\xi^2+\Delta^2\right)^{1/2}/2T\right]}{\left(\xi^2+\Delta^2\right)^{1/2}}\,\mathrm{d}\xi = 2f\left(\frac{\Delta}{T}\right) \tag{16.27}$$

where

$$f(x) = \int_1^{\infty} \frac{\mathrm{d}y\,\left(y^2-1\right)^{-1/2}}{1+\mathrm{e}^{yx}} \tag{16.28}$$

(the variable y corresponds to $\left(\xi^2+\Delta^2\right)^{1/2}/\Delta$). Since the integral in (16.27) converges at $\xi\sim\Delta$, we extended its upper limit to ∞. Since we are interested in large values of $x=\Delta/T$, we expand the integrand in (16.28) in e^{-yx} :

$$f(x)=\int_1^\infty\sum_{n=1}^\infty(-1)^{n+1}\mathrm{e}^{-nyx}\left(y^2-1\right)^{-1/2}\,\mathrm{d}y$$

Using the integral representation of the MacDonald functions (the Hankel function of imaginary argument)

$$K_\nu(z)=\frac{\Gamma\left(\frac{1}{2}\right)}{\Gamma\left(\nu+\frac{1}{2}\right)}\left(\frac{1}{2}z\right)^\nu\int_1^\infty\mathrm{e}^{-zy}\left(y^2-1\right)^{\nu-1/2}$$

($\Gamma(x)$ is the gamma function), we obtain

$$f(x)=\sum_{n=1}^\infty(-1)^{n+1}K_0(nx)\tag{16.29}$$

With large values of the argument the functions $\boldsymbol{K_0}$ fall off exponentially. Retaining only the first term and using the asymptotic

$$K_0(x)=\left(\frac{\pi}{2x}\right)^{1/2}\mathrm{e}^{-x}$$

we obtain, at $T<T_\mathrm{c}$,

$$\Delta\approx\Delta(0)-[2\pi\Delta(0)T]^{1/2}\mathrm{e}^{-\Delta(0)/T}.\tag{16.30}$$

This dependence is a consequence of the fact that the variation of Δ is associated with the appearance of quasiparticles and the number of quasiparticles is proportional to $\exp[-\Delta(0)/T]$.

If conversely $T\to T_\mathrm{c}$, then $\Delta\to0$. In this case, formula (16.23) can be conveniently expanded in Δ. We will proceed just as in the previous case. We divide (16.23) by $\frac{1}{2}\,\mathrm{g}\nu(\mu)$ and then subtract and add $\xi^{-1}\tanh(\xi/2T)$ in the integrand. As a result, we get

$$\ln\frac{T_c}{T}=\int_0^\infty\left(\frac{\tanh(\xi/2T)}{\xi}-\frac{\tanh\left[\left(\xi^2+\Delta^2\right)^{1/2}/2T\right]}{\left(\xi^2+\Delta^2\right)^{1/2}}\right)\mathrm{d}\xi\tag{16.31}$$

(because of the convergence of the integral at $\xi\sim T$, we again extended it up to ∞).
Let us use the following formula:

$$\tanh\frac{1}{2}\pi x=\frac{4x}{\pi}\sum_{k=0}^\infty\frac{1}{(2k+1)^2+x^2}$$

Substituting this into (16.31), expanding in Δ and integrating over ξ, we find that

$$\ln\frac{T_\mathrm{c}}{T}=2\sum_{n=1}^\infty(-1)^{n+1}\frac{(2n-1)!!}{2n!!}\left(\frac{\Delta}{\pi T}\right)^{2n}\sum_{k=0}^\infty\frac{1}{(2k+1)^{2n+1}},\tag{16.32}$$

where $n!!=n(n-2)(n-4)\ldots$. If we retain the first term, we will have

$$\Delta\approx\pi\left(\frac{8}{7\zeta(3)}\right)^{1/2}\left[T_\mathrm{c}\left(T_\mathrm{c}-T\right)\right]^{1/2}=3.06\left[T_\mathrm{c}\left(T_\mathrm{c}-T\right)\right]^{1/2}\tag{16.33}$$

($\zeta(x)$ is the Riemann zeta function: $\zeta(x)=\sum_{n=1}^\infty n^{-x}$).
This behavior is rather natural. In fact, Δ, while being finite at $T<T_\mathrm{c}$ and equal to zero at

$T > T_c$, may serve as the order parameter of the superconducting transition. The temperature dependence (16.33) is consistent with Landau's theory of secondorder phase transitions (see Appendix II). The question of the validity of this theory for superconductors will be discussed at a later time.

The graph of the function $\Delta(T)$ is shown in fig. 103.

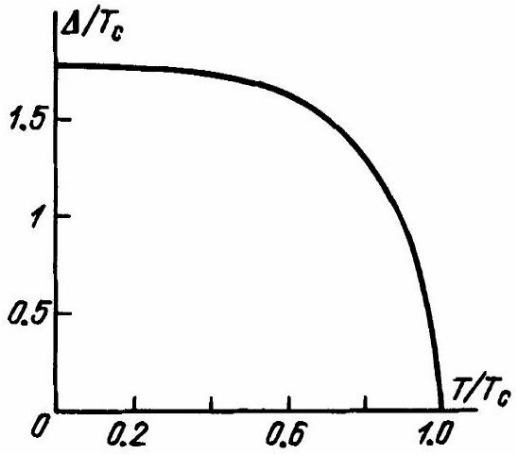


Fig. 103.

8.2.7 16.6. Thermodynamics of superconductors

Statistical physics gives the following expression for the thermodynamic potential*:

$$\Omega = -T \ln Z, \quad Z = \sum_{n,N} \exp\left(\frac{-E_{nN} + N\mu}{T}\right) \tag{16.34}$$

where $E_{n,N}$ are the energy levels, i.e., the eigenvalues of the Hamiltonian operator of a system of N particles. The expression for the statistical sum may be written in the form of a trace of the matrix $Z_{nm} = \int \Phi_n^* Z \Phi_m \, \mathrm{d}V$; $Z = \mathrm{e}^{-(\mathscr{H}-N\mu)/T}$ and Φ_n are wave functions of the system (the operation Sp is invariant with respect to the choice of the orthonormalized system of the functions $\boldsymbol{\Phi_n}$):

$$Z = \mathrm{Spe}^{-(\mathscr{H}-N\mu)/T}. \tag{16.35}$$

We substitute $\mathscr{H} - N\mu$ in the form of (16.13) and differentiate Ω (16.34) with respect to the interaction constant g. As a result, we have

$$\frac{\partial \Omega}{\partial g} = g^{-1} \frac{\mathrm{Sp}\left[\mathscr{H}_{\mathrm{int}} \, \mathrm{e}^{-(\mathscr{H}-N\mu)/T}\right]}{\mathrm{Spe}^{-(\mathscr{H}-N\mu)/T}} = g^{-1} \left\langle \mathscr{H}_{\mathrm{int}} \right\rangle, \tag{16.36}$$

where we have denoted the second term in the Hamiltonian (16.23) as $\mathscr{H}_{\mathrm{int}}$ (it describes the interaction of electrons). The angular brackets $\langle \cdots \rangle$ denote the average over the Gibbs distribution.

We express in (16.36) the operators $a_{p,\sigma}$ in terms of $\alpha_{p,\sigma}$ (16.15) and take the average. To within a factor we obtain the second term in formula (16.16). Using the definition of Δ (16.18), we can write:

$$\frac{\partial \Omega}{\partial g} = -\frac{\Delta^2}{g^2}. \tag{16.37}$$

Passing from the variable g to the variable Δ, we obtain

$$\Omega_{\rm s} - \Omega_{\rm n} = \int_0^{\Delta} \frac{{\rm d}g^{-1}\left(\Delta_1\right)}{{\rm d}\Delta_1} \Delta_1^2 \, {\rm d}\Delta_1. \tag{16.38}$$

Here we have used the fact that at $\Delta = 0$ the superconductor is converted to a normal metal. The expression for g^{-1} as a function of Δ is obtained from formulae (16.24) and (16.27):

$$g^{-1} = \frac{1}{2}\nu(\mu)\left[\ln\left(\frac{2\hbar\omega_{\rm D}}{\Delta}\right) - 2f\left(\frac{\Delta}{T}\right)\right]. \tag{16.39}$$

The function f is expressed by formula (16.28).
Let us find the asymptotic values of $\Omega_{\rm s} - \Omega_{\rm n}$ for $T \to 0$ and $T \to T_{\rm c}$. In the first case we use formula (16.29) for f. Substituting into eq. (16.38), we find

$$\Omega_{\rm s} - \Omega_{\rm n} = -\frac{1}{2}\nu(\mu)\left[\frac{1}{2}\Delta^2 - 2\sum_{n=1}^{\infty}(-1)^{n+1}\frac{T^2}{n^2}\int_0^{n\Delta/T} K_1(x)x^2 \, {\rm d}x\right]$$

where we have employed the relation $K_0'(x) = -K_1(x)$. The integral in brackets is taken in explicit form, $\int x^2 K_1(x) = -x^2 K_2(x)$. While inserting the lower limit we shall take into account that $\left[x^2 K_2(x)\right]_{x\to 0} = 2$. As a result, we obtain the sum

$$2T^2\nu(\mu)\sum_{n=1}^{\infty}(-1)^{n+1}n^2 = \frac{1}{6}\pi^2 T^2 \nu(\mu)$$

The free energy of a normal metal on the left-hand side is equal to $-\frac{1}{6}\pi^2 T^2\nu(\mu)$. This follows from formula (2.27) for the heat capacity and from the relation $C = -T\,(\,\partial^2\Omega/\partial T^2\,)$. Cancelling $-\Omega_{\rm n}$ on the left- and right-hand sides, we obtain

$$\Omega_{\rm s} = -\frac{1}{2}\nu(\mu)\left[\frac{1}{2}\Delta^2 + 2\sum_{n=1}^{\infty}(-1)^{n+1}K_2(n\Delta/T)\Delta^2\right]. \tag{16.40}$$

At $T = 0$ the second term vanishes and we obtain

$$\Omega_{\rm s}(0) = -\frac{1}{4}\nu(\mu)\Delta^2(0) \tag{16.41}$$

This formula is quite natural. It corresponds to the fact that the electrons in an energy band with a width of order Δ [their number is of order $\nu(\mu)\Delta$] are bound into pairs with a binding energy of order Δ.

At low temperatures we take into account the correction to $\Delta(0)$ and the term with $n = 1$ in the second term of (16.40). As a result, we find

$$\begin{aligned}\Omega_{\rm s}(T) - \Omega_{\rm s}(0) &= \nu(\mu)\Delta^2(0)\left[K_0\left(\frac{\Delta(0)}{T}\right) - K_2\left(\frac{\Delta(0)}{T}\right)\right] \\ &= -2\nu(\mu)\Delta(0)TK_1\left(\frac{\Delta(0)}{T}\right) \\ &\approx -\nu(\mu)\left[2\pi T^3\Delta(0)\right]^{1/2}{\rm e}^{-\Delta(0)/T}\end{aligned} \tag{16.42}$$

from which we obtain the entropy per unit volume,

- The potential Ω depends on the variables T, V and μ, while the free energy F is a function of T, V and N.

$$S_{\rm s} = -\frac{\partial \Omega_{\rm s}}{\partial T} \approx \nu(\mu) \left(\frac{2\pi \Delta^3(0)}{T} \right)^{1/2} {\rm e}^{-\Delta(0)/T} \tag{16.43}$$

and the heat capacity,

$$C_{\rm s} = T \frac{\partial S_{\rm s}}{\partial T} = \nu(\mu) \left(\frac{2\pi \Delta^5(0)}{T^3} \right)^{1/2} {\rm e}^{-\Delta(0)/T}. \tag{16.44}$$

Now we pass to the case $T \to T_{\rm c}$. We use formula (16.32). Expressing $T_{\rm c}$ via g with the aid of formula (16.25), we find g^{-1} as a function of Δ :

$$\begin{aligned} g^{-1} = & \frac{1}{2}\nu(\mu) \left[\ln \left(\frac{2\hbar\omega_{\rm D}\gamma}{\pi T} \right) \right. \\ & \left. -2 \sum_{n=1}^{\infty} (-1)^{n+1} \frac{(2n-1)!!}{(2n)!!} \left(\frac{\Delta}{\pi T} \right)^{2n} \sum_{k=0}^{\infty} (2k+1)^{-(2n+1)} \right]. \end{aligned}$$

Substitution into eq. (16.38) yields

$$\begin{aligned} \Omega_{\rm s} - \Omega_{\rm n} = & -\nu(\mu) \sum_{n=1}^{\infty} (-1)^{n+1} \frac{(2n-1)!!2n}{(2n+2)!!} \\ & \times \frac{\Delta^{2n+2}}{(\pi T)^{2n}} \sum_{k=0}^{\infty} (2k+1)^{-(2n+1)} \end{aligned} \tag{16.45}$$

Retaining only the first term, we find from eq. (16.45)

$$\Omega_{\rm s} - \Omega_{\rm n} \approx -\nu(\mu) \frac{7}{32} \zeta(3) \frac{\Delta^4}{(\pi T)^2} \tag{16.46}$$

Inserting the value of Δ for $T \to T_{\rm c}$ (16.33), we obtain

$$\Omega_{\rm s} - \Omega_{\rm n} \approx -\frac{2}{7\zeta(3)} \frac{p_0 m}{\hbar^3} \left(T_{\rm c} - T \right)^2 \tag{16.47}$$

from which we find the entropy:

$$S_{\rm s}(T) \approx S_{\rm n}(T) + \frac{4}{7\zeta(3)} \frac{p_0 m}{\hbar^3} \left(T - T_{\rm c} \right) \tag{16.48}$$

Differentiating once more, we obtain the heat capacity at the transition point:

$$C_{\rm s}\left(T_{\rm c}\right) = C_{\rm n}\left(T_{\rm c}\right) + \frac{4}{7\zeta(3)} \frac{p_0 m}{\hbar^3} T_{\rm c} \tag{16.49}$$

Recall (see eq. 2.29) that

$$C_{\rm n}(T) = S_{\rm n}(T) = \frac{p_0 m}{3\hbar^3} T \tag{16.50}$$

From (16.49) it follows that the heat capacity undergoes a jump at the transition point equal to $[4/7\zeta(3)]\,({\rm p_0\ m}/\hbar^3)\,{\rm T_c}$. In order to trace out the temperature course of the heat capacity in the vicinity of $T_{\rm c}$, it is necessary to take into account the following terms of the expansion in Δ in formulae (16.45) and (16.32). This being done, we substitute the numbers and obtain

$$\frac{C_{\rm s}(T)}{C_{\rm n}\left(T_{\rm c}\right)} = 2.42 + 4.76 \frac{T - T_{\rm c}}{T_{\rm c}}. \tag{16.51}$$

The dependence $C_{\rm s}(T)$ is shown in fig. 104.
A knowledge of the thermodynamic potentials makes it possible to determine the critical field H_c. For this purpose we use relation (15.5). We take into account that, according to thermodynamics, the corrections to all thermodynamic potentials are identical if they are expressed in terms of the corresponding variables. In particular,

$$(\delta F)_{N,T,V} = (\delta\Omega)_{\mu,T,V}$$

This enables one to determine H_c from the relation

$$\Omega_{\rm n} - \Omega_{\rm s} = \frac{H_{\rm c}^2}{8\pi} \tag{16.52}$$

First of all, at $T = 0$ we obtain from eq. (16.41) (recall that we assume $\Omega_{\rm n}(0) = 0$)

$$H_{\rm c}(0) = [2\pi\nu(\mu)]^{1/2}\Delta(0). \tag{16.53}$$

At low temperatures $\Omega_{\rm n}(T) = -\frac{1}{6}\pi^2T^2\nu(\mu)$, and the temperature conrection to $\Omega_{\rm s}(0)$ is exponentially small in accordance with (16.42). Hence,

$$\frac{H_{\rm c}^2(T)}{8\pi} = \Omega_{\rm n}(T) - \Omega_{\rm s}(T) \approx -\frac{1}{6}\pi^2T^2\nu(\mu) + \frac{1}{4}\nu(\mu)\Delta^2(0).$$

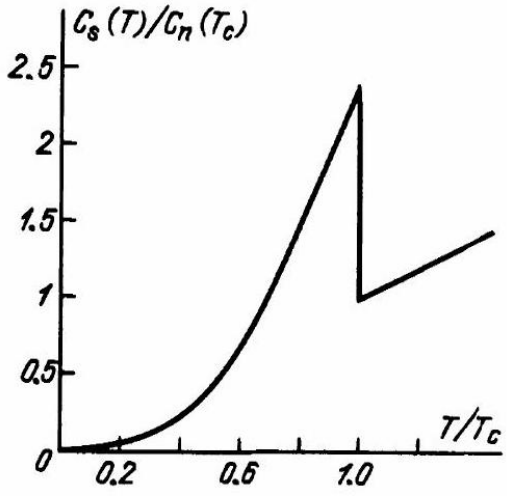


Fig. 104.

From (16.49) it follows that the heat capacity undergoes a jump at the transition point equal to $[4/7\zeta(3)]\,(\mathrm{p_0\ m}/\hbar^3)\,\mathrm{T_c}$. In order to trace out the temperature course of the heat capacity in the vicinity of T_c, it is necessary to take into account the following terms of the expansion in Δ in formulae (16.45) and (16.32). This being done, we substitute the numbers and obtain

$$\frac{C_{\rm s}(T)}{C_{\rm n}\,(T_{\rm c})} = 2.42 + 4.76\frac{T - T_{\rm c}}{T_{\rm c}}. \tag{16.51}$$

The dependence $C_{\rm s}(T)$ is shown in fig. 104.
A knowledge of the thermodynamic potentials makes it possible to determine the critical field $H_{\rm c}$. For this purpose we use relation (15.5). We take into account that, according to thermodynamics, the corrections to all thermodynamic potentials are identical if they are expressed in terms of the corresponding variables. In particular,

$$(\delta F)_{N,T,V} = (\delta\Omega)_{\mu,T,V}$$

This enables one to determine $\boldsymbol{H_c}$ from the relation

$$\Omega_{\rm n} - \Omega_{\rm s} = \frac{H_{\rm c}^2}{8\pi} \tag{16.52}$$

First of all, at $T = 0$ we obtain from eq. (16.41) (recall that we assume $\Omega_{\rm n}(0) = 0$)

$$H_c(0) = [2\pi\nu(\mu)]^{1/2}\Delta(0). \tag{16.53}$$

At low temperatures $\Omega_{\rm n}(T) = -\frac{1}{6}\pi^2T^2\nu(\mu)$, and the temperature conrection to $\Omega_{\rm s}(0)$ is exponentially small in accordance with (16.42). Hence,

$$\frac{H_c^2(T)}{8\pi} = \Omega_{\rm n}(T) - \Omega_{\rm s}(T) \approx -\frac{1}{6}\pi^2T^2\nu(\mu) + \frac{1}{4}\nu(\mu)\Delta^2(0).$$

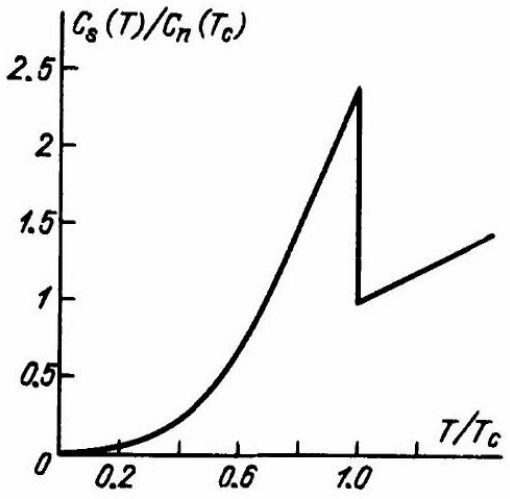


Fig. 104.

With the aid of eq. (16.53) we find from the last relation

$$\begin{aligned} H_c(T) &\approx H_c(0)\left(1 - \frac{1}{3}\pi^2\frac{T^2}{\Delta^2(0)}\right) \\ &= H_c(0)\left(1 - \frac{1}{3}\gamma^2\frac{T^2}{T_c^2}\right) = H_c(0)\left(1 - 1.05\frac{T^2}{T_c^2}\right) \end{aligned} \tag{16.54}$$

Here we have used the relationship between $\Delta(0)$ and $T_{\rm c}$(16.26).
Near $T_{\rm c}$ obtain in accordance with eq. (16.47):

$$\begin{aligned} H_c &\approx \left(16\pi\frac{p_0m}{7\zeta(3)\hbar^3}\right)^{1/2}(T_c - T) \\ &= H_c(0)\gamma\left(\frac{8}{7\zeta(3)}\right)^{1/2}\left(1 - \frac{T}{T_c}\right) \\ &= 1.735H_c(0)\left(1 - \frac{T}{T_c}\right) \end{aligned} \tag{16.55}$$

Formulae (16.55) and (16.49) are consistent with formula (15.8) for the jump in heat capacity, as was to be expected.

Let us consider certain consequences of the results obtained. According to formulas (16.26) and (16.53), the critical temperature T_c and the critical field $H_c(0)$ are proportional to $\Delta(0)$. In accordance with formula (16.24), $\Delta(0)$ is proportional to the Debye frequency ω_D, which depends on the mass of lattice ions by the law $\omega_D \propto M^{-1/2}$. This is in accord with the formulae for the isotope effect (16.2). Further, at low temperatures the heat capacity is described by the exponential law (16.44), this being in agreement with the experimental result (15.3). Finally, although the results for the critical field do not coincide completely with the empirical formula (15.1), the asymptotic formulas for $T < T_c$ and $T \to T_c$ (16.54) and (16.55) are rather close to it.

All the results given above refer to the isotropic model, whereas true metals are anisotropic. Therefore, it is surprising that these formulas agree well with experiment not only qualitatively but quantitatively as well. But there are certain differences, which call for consideration. First of all it should be noted that, according to the theory described here, any thermodynamic quantity expressed in dimensionless units, say $C_s(T)/C_n(T_c)$ or $H_c(T)/H_c(0)$, depends only on the ratio T/T_c, where T_c is connected with the gap in the energy spectrum at $T = 0$ by relation (16.26).

In an anisotropic metal the energy spectrum of quasiparticles looks somewhat different:

$$\varepsilon(\boldsymbol{p}) = \left[\Delta^2(\boldsymbol{n}) + \xi^2(\boldsymbol{n})\right]^{1/2} \tag{16.56}$$

where $\xi(n) = v(n)\,[p - p_0(n)]$, and n is the unit vector in the direction p. Thus, Δ depends on the direction $\boldsymbol{p}$. At low temperatures the role of the energy gap is played by the minimum value of $\Delta(n, 0)$, which we denote by Δ_{min}. It is exactly this value
that governs the temperature course of the heat capacity with $T \to 0 : C_s \propto \exp(-\Delta_{min}/T)$. On the other hand, $\Delta(n, T)$ depends on temperature: at $T \to T_c \Delta(n, T) \approx \Delta_0(n) f(T/T_c)$, where $f \to 0$ when $T \to T_c$ (Pokrovskii 1961).

For an anisotropic metal the statement that $C_s(T)/C_n(T_c)$ depends only on T/T_c over the entire temperature range from 0 to T_c does not conform to reality. As a matter of fact, if $\Delta(0)$ is determined from formula (16.26), we obtain a certain averaged value of $\Delta(0)$ and, hence, the low-temperature formula $C_s \propto \exp[-\Delta(0)/T]$ will differ from the true law, which includes Δ_{min}. Therefore, if we compare the experimental data for C_s with the theoretical curve for the isotropic model, then with $T \to 0$ the experimental points should be expected to lie above the theoretical curve, which is what occurs in reality. However, the anisotropy of Δ is not large in reality: $\left(\overline{\Delta(0)} - \Delta_{min}\right)/\overline{\Delta(0)} < 10\%$. This may be accounted for as follows: the phonon forces of attraction are mainly determined by short-wave length phonons with a frequency of order ω_D. Upon exchange of such phonons with $\hbar k \sim p_0$ the momenta of electrons vary significantly. This leads to a certain effective averaging along the entire Fermi surface.

Another assumption of the theory described above is that the interaction between the electrons is weak:

$$g\nu(\mu) < 1.$$

This assumption is not always justifiable. In fact, for lead, for example, $T_c = 7.2$ K and $\hbar\omega_D = 94.5$ K; hence, $g\nu(\mu) = 0.76$. It is not surprising that for such metals the above-described theory differs somewhat from experiment (this refers mainly to the dependence $H_c(T)$). However, after an appropriate correction of the theory the disagreement is markedly reduced.

8.2.8 16.7. London and Pippard superconductors (qualitative theory)

Before considering the microscopic derivation of the basic relations that characterize the behavior of superconductors in an electromagentic field, we shall give a simple qualitative analysis. In section 15.5 we have derived the equations of London electrodynamics. In particular, it has been noted that these equations may be written in the form (15.43), i.e.,

$$j = -QA, \quad (\operatorname{div} A = 0),$$

where

$$Q = \frac{n_e e^2}{mc}$$

In deriving the London equations it was assumed that the superconducting current is transported by electrons. At present, however, we know that the carriers of superconducting current are Cooper pairs. The main difference is that Cooper pairs
have a finite size. This size can be determined on the basis of the following considerations. The energy spectrum of quasiparticles $\varepsilon = \left[v^2 (p - p_0)^2 + \Delta^2\right]^{1/2}$ indicates that binding into pairs involves the momenta in the region of $\delta p \sim \Delta/v$ near the Fermi boundary. According to the uncertainty principle, $\delta p \delta r \sim \hbar$. From this we may infer that the size of the pair is $\hbar v/\Delta$. If we substitute here $v \sim 10^8$ cm/s, $\Delta \sim 10$ K $\sim 10^{-3}$eV $\sim 10^{-15}$erg, we obtain

$$\frac{\hbar v}{\Delta} \sim 10^{-4} \text{ cm}$$

that is, thousands of interatomic distances.
Hence, the pairs are very loose formations. A natural question arises: How could they be accommodated in a metal without interfering with one another? Of course, the Cooper pairs cannot, in fact, be visualized as a classical gas composed of particles, the distance between which is much larger than their size. The pairs penetrate each other and at the same time, just as gas particles, they are free and there is practically no interaction between them. This is, of course, possible only in quantum mechanics, in the same way as the flow of this gas through the lattice without scattering. In order to emphasize this nonclassical behavior, in the rigorous theory one speaks not of pairs having a certain size but of a pair correlation between electrons extending to a certain distance - a "correlation length", which is of order $\xi \sim \hbar v/\Delta^*$.

In view of the presence of a correlation the current is determined by the electromagnetic field not only directly at the point of observation but also in the entire region around this point, with a radius of order ξ. Therefore, the relationship between the current and the field becomes nonlocal and is expressed by the relation

$$j_i(r) = -\sum_k \int Q_{ik}(r - r') A_k(r') \, dV' \tag{16.57}$$

where the kernel Q_{ik} falls off at a distance of order ξ.
In the limiting case, when the field varies very slowly in space, in the integral of (16.57) $A_K(r')$ may be replaced by $A_k(r)$, which is taken outside the integral sign. Denoting $\int Q_{ik}(r - r') \, dV' = \delta_{ik} Q$, we obtain the London relationship between the current and the field. The characteristic length that determines the variation of the field in a superconductor is obviously the penetration depth δ. As a matter of fact, at this distance the field varies from a given value at the surface of the superconductor to zero. Hence, in a case where $\delta > \boldsymbol{\xi}$, we return to London electrodynamics. This limit is called the London limit.

In the opposite limiting case $\delta < \xi$ we may apply the inefficiency concept, just as in the anomalous skin effect (section 7.2). Indeed, the electrons (or, more exactly, pairs) that move at large angles to the surface of the superconductor emerge rapidly

from the penetration depth and practically do not interact with the field. Only those electrons which move at an angle not exceeding $\theta \sim \delta/\xi$ are effective. But the number of such electrons is $n_e\theta \sim n_e\delta/\xi$. Substituting this number into expression (16.40) for the penetration depth, we obtain

$$\delta \sim \left(\frac{mc^2}{4\pi e^2 n_e \delta \xi^{-1}}\right)^{1/2}.$$

This is an equation for δ. Solving it, we get

$$\delta_P \sim \left(\frac{mc^2}{4\pi n_e e^2}\xi\right)^{1/3} \sim \delta_L^{2/3}\xi^{1/3} \tag{16.58}$$

(the London penetration depth defined by eq. (15.40) was denoted as δ_L). The case $\delta < \xi$ was first considered by Pippard (1953). Therefore, such superconductors are called Pippard superconductors.

In experiment all pure superconductors are Pippard superconductors or intermediate superconductors, i.e., in them $\xi \geqslant \delta$. However, as we shall see below, the correlation length can be reduced and δ increased by introducing impurities or structural defects, from which the electrons are scattered. As a result, we can arrive at the London limit. Moreover, near T_c all superconductors become London superconductors.

In concluding this section we note that the expression for the London coefficient Q and the corresponding penetration depth does not depend on whether electrons or pairs are considered to be carriers. Indeed, making the replacement $e \to 2e, n_e \to \frac{1}{2}n_e$ and $m \to 2m$, we obtain the same formulas for Q and δ, (15.43) and (15.40), respectively.

8.2.9 16.8. The Meissner effect at $T = 0$

Now we shall deal with a quantitative microscopic derivation. Since the equations derived in the general case are cumbersome, we will consider here the simplest case: the behavior of superconductors at $T = 0$ in a weak magnetic field, which is independent of time.

The Hamiltonian is known from quantum mechanics to vary with the variations of the vector potential (Landau and Lifshitz 1974):

$$\delta\mathscr{H} = -\frac{1}{c}\int j\delta A \, \mathrm{d}V. \tag{16.59}$$

Here on the left under the integral is the current operator. Averaging this formula over a given state, say the equilibrium state, at temperature T, we obtain

$$\delta E = -\frac{1}{c}\int \langle j\rangle \delta A \, \mathrm{d}V, \tag{1'}$$

where $\langle \boldsymbol{j}\rangle$ is the average current. Thus, in order to find $\langle \boldsymbol{j}\rangle^*$, we are to find the average energy as a function of A, and to vary it with respect to A.

Since in the absence of the field $\boldsymbol{j} = 0$, it follows that at not too large fields the current is proportional to the field. From this we see that in order to find the current, we are to find the energy in the presence of the field to within terms that are second order in $\boldsymbol{A}$ and then to vary it with respect to $\boldsymbol{A}$.

*The symbol $\boldsymbol{\xi}$ is generally adopted for the correlation length. We use it because the correlation length and the electron energy $\xi = v\,(p - p_0)$ will not be encountered in the same formulas.

In the presence of a field the Hamiltonian (16.13) is transformed in such a manner that instead of the momentum operators $-\mathrm{i}\hbar\nabla$ the combination $-\mathrm{i}\hbar\nabla - (e/c)A$ is included. Hence, in the Hamiltonian we obtain

$$\frac{1}{2m}\left[-\hbar^2\nabla^2 + \mathrm{i}\hbar\frac{e}{c}(A\nabla + \nabla A) + \left(\frac{e}{c}\right)^2 A^2\right]. \tag{16.60}$$

While the first term retains the momentum of the particle, the other terms do not. If we expand $\boldsymbol{A}$ into a Fourier integral,

$$A(r) = \sum_q A_q \mathrm{e}^{\mathrm{i}qr} \tag{16.61}$$

we may interpret $\boldsymbol{A_q}$ as the operator of the absorption of an electromagnetic quantum with momentum $\hbar q$. In view of this, the operator A_q transfers a particle of momentum $\boldsymbol{p} - \boldsymbol{\hbar q}$ to a state of momentum $\boldsymbol{p}$. The terms of the Hamiltonian containing $\boldsymbol{A}$, which are of interest to us, may be written in the following form with the aid of the second-quantization operators:

$$\mathscr{H}_1 = -\frac{e}{2mc}\sum_{p,q,\sigma}\left[(p-\hbar q)a^+_{p,\sigma}a_{p-\hbar q,\sigma} + pa^+_{p,\sigma}a_{p-\hbar q,\sigma}\right]A_q, \tag{16.62}$$

$$\mathscr{H}_2 = \frac{e^2}{2mc^2}\sum_{p,q,q',\sigma} a^+_{p,\sigma}a_{p-\hbar q-\hbar q',\sigma}A_qA_{q'}. \tag{16.63}$$

Here it is taken into account, for example, that

$$-\mathrm{i}\hbar\nabla A_q\mathrm{e}^{\mathrm{i}qr} = A_q\mathrm{e}^{\mathrm{i}qr}(-\mathrm{i}\hbar\nabla + \hbar q).$$

Let us express the combinations $\sum_\sigma a^+_{p,\sigma}a_{p',\sigma}$ contained in $\mathscr{H}_1$ and $\mathscr{H}_2$ in terms of the operators $\alpha_+$and α_-. Substituting formulas (16.14) and collecting the terms, we find

$$\begin{aligned}\sum_\sigma a^+_{p,\sigma}a_{p',\sigma} =& u_pu_{p'}\left(\alpha^+_{p,+}\alpha_{p',+} + \alpha^+_{p,-}\alpha_{p',-}\right)\\ &+ v_pv_{p'}\left(\alpha_{-p,-}\alpha^+_{-p',-} + \alpha_{-p,+}\alpha^+_{-p',+}\right)\\ &+ u_pv_{p'}\left(\alpha^+_{p,+}\alpha^+_{-p',-} - \alpha^+_{p,-}\alpha^+_{-p',+}\right)\\ &+ v_pu_{p'}\left(\alpha_{-p,-}\alpha_{p',+} - \alpha_{-p,+}\alpha_{p',-}\right)\end{aligned} \tag{16.64}$$

Since the part of Hamiltonian $\mathscr{H}_2$(16.63) is second order in A, it is sufficient to take it into account only in the first order of perturbation theory, i.e., it will suffice to average it over the ground state. As a result, only the term with $v_pv_{p'}$ from expression (16.64) makes a contribution, and it appears that $p = p'$, i.e., $q = -q'$. Considering that $n_{p,+} = n_{p,-} = 0$ at $T = 0$, we obtain from this term

$$E_2 = \frac{e^2}{mc^2}\sum_{p,q} v_p^2A_qA_{-q} \tag{16.65}$$

The first order of perturbation theory in $\mathscr{H}_1$ turns to zero. Indeed, upon averaging over the ground state we obtain $\sum_p pv_p^2\delta_{q,0} = 0$, since v_p depends only on $|p|$. Therefore, we are to find the second order of perturbation theory:

*In the following we will omit the angular brackets for the average current.

$$E_1 = \sum_{m\neq 0} \frac{|(\mathscr{H}_1)_{m0}|^2}{E_{(0)} - E_{(m)}}$$

Since there are no quasiparticles in the ground state, the contribution to E_1 comes only from transitions involving the creation of two quasiparticles and their annihilation. Thus, we obtain

$$\begin{gathered}(\mathscr{H}_1)_{m0} = -\frac{e}{2mc}\left(u_p v_{p-\hbar q} - v_p u_{p-\hbar q}\right)(2p - \hbar q),\\ E_{(0)} - E_{(m)} = -\left(\varepsilon_p + \varepsilon_{p-\hbar q}\right),\\ E_1 = -\left(\frac{e}{2mc}\right)^2 \sum_p \frac{[(2p-\hbar q)A_q]\,[(2p-\hbar q)A_{-q}]}{\varepsilon_p + \varepsilon_{p-\hbar q}}\\ \times \left(u_p v_{p-\hbar q} - v_p u_{p-\hbar q}\right)^2. \qquad (16.66)\end{gathered}$$

Here we have used the reality of $\boldsymbol{A}(\boldsymbol{r})$. According to (16.61), it follows that $\boldsymbol{A}_{\boldsymbol{q}}^* = \boldsymbol{A}_{-\boldsymbol{q}}$. Moreover, it has been taken into account that the operators $\alpha_{p,-}$ and $\alpha_{p',+}$ anticommute, i.e., their permutation leads to a change in sign.

Before performing further calculations one remark should be made. As is known from electrodynamics, a correct theory must have the property of gauge invariance. In the static case this reduces to the invariance of the equations under the transformation $A \to A + \nabla\varphi$, where φ is any scalar function. This is because only the magnetic field $\boldsymbol{H} = \operatorname{rot}\boldsymbol{A}$ has a physical meaning. But if the Fourier component of the vector potential enters explicitly into the equations, then only the following combination is permissible:

$$A_{q\perp} = A_q - \frac{q\,(qA_q)}{q^2}$$

Indeed, the gauge transformation in the Fourier components has the form

$$A_q \to A_q + \mathrm{i}q\varphi_q.$$

With such a replacement $\boldsymbol{A}_{\mathbf{q}\perp}$ does not change.
The invariance under a gauge transformation is provided in quantum mechanics as a result of the vector potential entering into the Hamiltonian in combination with thc momentum operator $p - (e/c)A$. The addition of the gradient to A can be
compensated for by a change of the phase of the wave function. In view of this, there is no need to test the gauge invariance of the resultant equations and one can use the gauge of $\boldsymbol{A}$ that is most convenient. We will use a vector potential that satisfies the condition $\operatorname{div} A = 0$ or, in Fourier components, $qA_q = 0$ (section 15.5), because in such a case the derivation is simplified.

In order to obtain explicitly gauge-invariant equations that are valid for any gauge, we should have taken into account the change of the Bogoliubov transformation formulas (16.14) under the action of the field. Since u_p and v_p are scalars, they may have only corrections proportional to $\boldsymbol{qA_q}$, i.e., the ones which vanish in our gauging $\boldsymbol{qA_q} = 0$. But if this condition is not imposed, we obtain the same equations, but with $\boldsymbol{A_q}$ being replaced by $\boldsymbol{A}_{\boldsymbol{q}\perp}$. We shall not perform this complicated derivation here, since in choosing the correct initial Hamiltonian the result is known in advance.

We make the replacement $\boldsymbol{p} \to \boldsymbol{p} + \frac{1}{2}\hbar\boldsymbol{q}$ and introduce the notations

$$\xi_{p+\hbar q/2} \equiv \xi_+, \quad \xi_{p-\hbar q/2} \equiv \xi_-, \quad \xi = v\,(p - p_0)$$

and analogous ones for the other quantities. Substituting into eq. (16.66) the values of u_p and v_p in accordance with eq. (16.19), we have

$$E_1 = -\frac{1}{2}\left(\frac{e}{mc}\right)^2 \sum_p \frac{(pA_q)\,(pA_{-q})\,(\varepsilon_+\varepsilon_- - \xi_+\xi_- - \Delta^2)}{\varepsilon_+\varepsilon_-\,(\varepsilon_+ + \varepsilon_-)}. \tag{16.67}$$

Relation (16.59′) in Fourier components has the form

$$\delta E = -c^{-1}\sum_q j_q \delta A_q. \tag{16.68}$$

From eqs. (16.65) and (16.66) we obtain

$$\begin{aligned} j_q = &-\frac{2e^2}{mc}\sum_p v_p^2 A_q \\ &+ \frac{e}{m^2 c}\sum_p \frac{p\,(pA_q)\,(\varepsilon_+\varepsilon_- - \xi_+\xi_- - \Delta^2)}{\varepsilon_+\varepsilon_-\,(\varepsilon_+ + \varepsilon_-)}. \end{aligned} \tag{16.69}$$

In the first term $2\sum_p v_p^2 = n_\mathrm{e}$ is the electron density (recall that the normalization volume V has been assumed equal to unity). This equality can be obtained if in the expression for the operator of the number of particles (section 16.4)

$$n_\mathrm{e} = \sum_{p,\sigma} a_{p,\sigma} a_{p,\sigma} \tag{16.70}$$

we perform the Bogoliubov transformation and then average it over the ground state.
In the second term we assume that $|q| < p_0$. In such a case,

$$\xi_\pm = \frac{1}{2m}\left[\left(p + \frac{1}{2}\hbar q\right)^2 - p_0^2\right] \approx \xi \pm \frac{1}{2} v\hbar q\cos\theta,$$

where $v = p_0/m$; for the vector p we have introduced polar coordinates with the axis along q (the z axis). In accordance with our choice of $\boldsymbol{A}_q$, the current component along q is missing, and we shall find j_x (evidently, $j_x = j_y$). Passing from $\sum_p$ to
$(2\pi\hbar)^{-3}\int \mathrm{d}^3 p$, we have

$$j_{q_\perp} = -Q(q) A_{q_\perp} \tag{16.71}$$

where

$$\begin{aligned} Q(q) = &\frac{n_\mathrm{e} e^2}{mc} - \frac{1}{(2\pi\hbar)^3}\frac{e^2}{m^2 c} \\ &\times \frac{p_0^4}{v}\int_{-\infty}^{\infty} \mathrm{d}\xi\; \mathrm{d}\Omega \cos^2\varphi \sin^2\theta \frac{\varepsilon_+\varepsilon_- - \xi_+\xi_- - \Delta^2}{\varepsilon_+\varepsilon_-\,(\varepsilon_+ + \varepsilon_-)}. \end{aligned} \tag{16.72}$$

Since ξ of order Δ are important in the integral, we have put $p \approx p_0$ and passed from integration over p to integration over ξ, which may be extended to the interval $(-\infty, \infty)$. Without making further assumptions, we can take the integrals over φ and ξ. This leaves only the integral over $\mathrm{d}(\cos\theta)$. We introduce the notation $\cos\theta = t$. As a result, we have

$$Q(q) = \frac{n_e e^2}{mc}\left\{1 - \frac{3}{4}\int_{-1}^{1} \mathrm{d}t\,(1-t^2)\left[1 - \frac{4\Delta^2(0)}{\hbar q t v}\frac{\operatorname{arcsinh}[\hbar q t v/2\Delta(0)]}{[4\Delta^2(0) + (\hbar q t v)^2]^{1/2}}\right]\right\}$$
$$= \frac{3e^2 n_e \Delta(0)}{mc\hbar q v}\int_0^1 \frac{\mathrm{d}t}{t}\,(1-t^2)\,\frac{\operatorname{arcsinh}[\hbar q t v/2\Delta(0)]}{\{1 + [\hbar q t v/2\Delta(0)]^2\}^{1/2}} \tag{16.73}$$

The integral over t cannot be taken in explicit form in the general case. Therefore, we confine ourselves to the limiting formulas for large and small q.

The expression $Q(q)$ depends on the combination $q\hbar v/\Delta(0)$. The wave vector q characterizes the rapidity of the spatial variation of the current and field. The corresponding characteristic length is q^{-1}. In physical problems evidently $q^{-1} \sim \delta$ (the penetration depth). The quantity $\xi = \hbar v/\Delta(0)$ is the correlation length, as has been pointed out in the preceding section. Thus, the kernel Q depends on the ratio δ/ξ. A large value of this ratio corresponds to $q \to 0$. In this case we find from eq. (16.73)

$$Q = \frac{n_e e^2}{mc} \tag{16.74}$$

This formula corresponds to the London limit (see the preceding section and formula 15.43).

Conversely, large values of q corresponds to the Pippard limit $\delta/\xi < 1$. In the integral of (16.73) small values of t are important. Neglecting t^2 compared to unity and evaluating the integral, we obtain

$$Q(q) \approx \frac{3}{4}\pi^2 \frac{n_e e^2}{mc}\frac{\Delta(0)}{\hbar q} q^{-1} \tag{16.75}$$

This formula corresponds to the inefficiency concept. Indeed, assuming that $q^{-1} \sim \delta$, we see that formula (16.75) differs from (16.74) by the replacement of n_e by $n_e\delta/\xi$.

In coordinate space the relationship $\boldsymbol{j}(\boldsymbol{q}) = -\boldsymbol{Q}(\boldsymbol{q})\boldsymbol{A}(\boldsymbol{q})$ is expressed by formula (16.57). At $\xi > \delta$ the coupling is basically nonlocal because the field $A(r')$ varies rapidly at distances characteristic for the kernel $Q(r - r')$. Here, strictly speaking, the results we have obtained cannot be used because we have found Q for an infinite space, whereas in the problem of the penetration of the field the metal has a surface, i.e., let us say, it occupies a half-space $x > 0$. In such problems it is necessary to impose boundary conditions for electrons.

The condition of specular reflection from the boundary proves to be the simplest. In this case, just as for the anomalous skin effect, one may use the kernel Q for an infinite space, but then it is necessary to extend the vector potential in an even manner through the boundary (section 7.3). If the magnetic field is directed parallel to the surface of the metal along the z axis, then we may choose $A_y(x)$ along the y axis. On the strength of what has been said, $A_y(x) = A_y(-x)$.

According to the Maxwell equation

$$\operatorname{rot} H = \operatorname{rot}\operatorname{rot} A = \operatorname{grad}\operatorname{div} A - \nabla^2 A = \frac{4\pi}{c} j$$

The first term on the left-hand side is equal to zero, since $\operatorname{div}\boldsymbol{A} = 0$. The extension of the vector potential in an even manner through the boundary implies a kink in the $A_y(x)$ curve. Hence, if the field H_0 is given at the metal surface, i.e., $(\mathrm{d}A_y/\mathrm{d}x)_{x=+0} = H_0$, then $(\mathrm{d}A_y/\mathrm{d}x)_{x=-0} = -H_0$. But then the second derivative $\mathrm{d}^2A_y/\mathrm{d}x^2$ acquires a correction $2H_0\delta(x)$. Thus, we have

$$\frac{\mathrm{d}^2 A_y}{\mathrm{d}x^2} = 2H_0\delta(x) - \frac{4\pi}{c}j \tag{16.76}$$

Passing to Fourier components, substituting eq. (16.71) and solving the resultant equation, we find

$$A_q = -2H_0 \frac{1}{q^2 + \frac{4\pi}{c}Q(q)} \tag{16.77}$$

In the coordinate representation we have

$$A(x) = -\frac{2H_0}{\pi}\int_0^\infty \frac{\cos qx \ \mathrm{d}q}{q^2 + \frac{4\pi}{c}Q(q)} \tag{16.78}$$

(here it has been taken into account that Q depends on $|\boldsymbol{q}|$ alone). Differentiating with respect to H, we find the magnetic field*

$$H(x) = \frac{2H_0}{\pi}\int_0^\infty \frac{q\sin qx \ \mathrm{d}q}{q^2 + \frac{4\pi}{c}Q(q)} \tag{16.79}$$

We shall not analyze the behavior of the field in the general case; we only find the penetration depth, which we define as follows:

$$\delta = \frac{1}{H_0}\int_0^\infty H \ \mathrm{d}x = -\frac{A(0)}{H_0} = \frac{2}{\pi}\int_0^\infty \frac{\mathrm{d}q}{q^2 + \frac{4\pi}{c}Q(q)} \tag{16.80}$$

Let us assume that small q are important in the integral. In such a case, $Q(q)$ has the form (16.74) and we obtain from the integral the London penetration depth:

$$\delta_{\mathrm{L}} = \left(\frac{mc^2}{4\pi n_{\mathrm{e}} e^2}\right)^{1/2}. \tag{16.81a}$$

Note that in the integral $q \sim \delta^{-1}$ are important and, hence, our calculation is correct at $\delta > \hbar v/\Delta \sim \xi$.

In the opposite limiting case we substitute Q from eq. (16.75). Evaluating the integral, we find

$$\begin{aligned}\delta_{\mathrm{P}} &= 4\times 3^{-11/6}\pi^{-1}\left(\frac{mc^2}{n_{\mathrm{e}}e^2}\right)^{1/3}\left(\frac{\hbar v}{\Delta(0)}\right)^{1/3} \\ &= 2^{8/3}3^{-11/6}\pi^{-2/3}\delta_{\mathrm{L}}^{2/3}\left(\frac{\hbar v}{\Delta(0)}\right)^{1/3}\end{aligned} \tag{16.81b}$$

This formula corresponds to the estimate for the Pippard case (16.58) described in the previous section.

Upon passing to coordinate representation (16.57) in the general case it is essential that the kernel $Q(q)$ couples only the transverse components j and A (see eq. 16.71), i.e., strictly speaking, it is necessary to replace $Q(q)$ by $Q(q)\,(\delta_{ik} - q_i q_k/q^2)$. For the Pippard limit this leads to the following form for $Q_{ik}\,(r - r')$ in formula (16.57):

- In order to obtain H at the surface one cannot put $x = 0$ under the integral; instead, it is necessary to calculate it for small $x > 0$, after which x is made to tend towards zero.

$$Q_{ik}(r-r') = \frac{3}{4} n_e e^2 \frac{\Delta(0)}{hv} n_i n_k |r-r'|^{-2}, \tag{16.71'}$$

where

$$n = \frac{(r-r')}{|r-r'|}.$$

8.2.10 16.9. The relationship between current and field at finite temperatures. The London limit

We shall not examine the general case at finite temperatures because of its complexity. We only note the following points. When the temperature increases, the role of the correlation length in the kernel $Q(r-r')$ which couples the current to the field (16.57) gradually goes over from $\hbar v/\Delta(0)$ to $\hbar v/T$. Since $\Delta(0) \sim T_c$, at all
temperatures the correlation length is of order $\hbar v/T_c$. Use is commonly made of the standard correlation length equal to

$$\xi_0 = \frac{\hbar v}{\pi \Delta(0)} = \frac{\gamma}{\pi^2} \frac{\hbar v}{T_c} = 0.18 \frac{\hbar v}{T_c}. \tag{16.82}$$

In section 15.1 it has been pointed out that the penetration depth δ increases indefinitely as $T \to T_c$. This will also be obtained below. But it follows that even if $\delta(0) < \xi_0$ at $T = 0$, then $\delta(T)$ will sooner or later exceed ξ_0 with $T \to T_c$. Here the London situation occurs, i.e., the Fourier component of the kernel $Q(q)$ can be substituted by $Q(0)$. Hence the calculation of $Q(0)$ at a finite temperature enables one to establish the relationship between the current and the field at all temperatures for London superconductors, for which $\delta(0) > \xi_0$, and also at a temperature near T_c for Pippard superconductors, for which $\delta(0) < \xi_0$ (and, of course, for intermediate superconductors, for which $\delta(0) \sim \xi_0$).

We could have followed the previous path, i.e., we could have found $E\{A\}$ according to perturbation theory and calculated the current by varying with respect to $\boldsymbol{A}$. However, the result can be obtained more simply. At finite temperatures some of the Cooper pairs break down and quasiparticles appear. The latter interact with impurities and phonons and therefore make no contribution to the superconducting current. Hence, the effective number of electrons entering into formula (15.43) or formula (16.74), which coincides with (15.43), must begin to decrease, i.e., is replaced by a certain function $n_s(T)$, which had been known as the "number of superconducting electrons" before the appearance of the microscopic theory. The replacement of n_e by $n_s(T)$ in the London theory made it possible to account qualitatively for the temperature dependence of the penetration depth. We will define this quantity quantitatively.

Suppose that all the quasiparticles move with velocity $\boldsymbol{u}$. In this case, the argument of the distribution function will be $\varepsilon - pu$ rather than $\varepsilon(p)$. The motion of the quasiparticles will lead to the appearance of a momentum $\boldsymbol{P}$ given by

$$\begin{aligned} \boldsymbol{P} &= \int p\,(n_{p,+} + n_{p,-})\,\frac{\mathrm{d}^3 p}{(2\pi\hbar)^3} \\ &= 2\int p n_F(\varepsilon - pu)\frac{\mathrm{d}^3 p}{(2\pi\hbar)^3} \end{aligned}$$

(n_F is the Fermi function). Assuming u to be small and expanding in u, we obtain

$$P = -2\int p(pu)\frac{\partial n_F}{\partial \varepsilon}\frac{\mathrm{d}^3 p}{(2\pi\hbar)^3} \tag{16.83}$$

We transform the integral over $\mathrm{d}^3\boldsymbol{p}$ to an integral over $\mathrm{d}\xi$ and over the solid angle, as has been done in Part I. Here, however, one has to take into account that ε does not coincide with ξ, the energy of a normal metal. We have

$$2\int \frac{\mathrm{d}^3 p}{(2\pi\hbar)^3} \to \nu(\mu)\int \mathrm{d}\xi \frac{\mathrm{d}\Omega}{4\pi}.$$

Here we have taken account of the fact that the integral goes over the neighborhood of the Fermi surface. This also makes it possible to assume that $|p| = p_0$ in formula (16.83). Integrating over the solid angle, we obtain

$$\int p(pu)\frac{\mathrm{d}\Omega}{4\pi} \approx \frac{1}{3}p_0^2 u$$

Substituting $\varepsilon = (\xi^2 + \Delta^2)^{1/2}$ and introducing a new variable $\xi = \Delta \sinh\varphi$, we find (we have taken into account the rapid fall of the integral with increasing $|\xi|$ and replaced the limits of integration by $-\infty$ and ∞):

$$P = \frac{2}{3}p_0^2 u\nu(\mu)\frac{\Delta}{T}\int_0^\infty \frac{\cosh\varphi \mathrm{d}\varphi}{(\mathrm{e}^{\Delta\cosh\varphi/T}+1)\,(\mathrm{e}^{-\Delta\cosh\varphi/T}+1)}.$$

The proportionality factor between $\boldsymbol{P}$ and $\boldsymbol{mu}$ is called here the number of "normal electrons" n_n. Substituting $\nu(\mu) = p_0 m/\pi^2\hbar^3$ and taking into account that the total number of electrons is $n_\mathrm{e} = p_0^3/3\pi^2\hbar^3$, we obtain

$$\frac{n_\mathrm{n}}{n_\mathrm{e}} = 2\frac{\Delta}{T}\int_0^\infty \frac{\cosh\varphi \mathrm{d}\varphi}{(\mathrm{e}^{\Delta\cosh\varphi/T}+1)\,(\mathrm{e}^{-\Delta\cosh\varphi/T}+1)}. \tag{16.84}$$

If we make the same replacement of variables in formula (16.27), we get

$$\ln\frac{\Delta(0)}{\Delta(T)} = 2\int_0^\infty \frac{\mathrm{d}\varphi}{\mathrm{e}^{\Delta\cosh\varphi/T}+1}. \tag{16.85}$$

Differentiating with respect to temperature, we have

$$\Delta^{-1}\frac{\mathrm{d}\Delta}{\mathrm{d}T} = 2\int_0^\infty \frac{\cosh\varphi \mathrm{d}\varphi}{(\mathrm{e}^{\Delta\cosh\varphi/T}+1)\,(\mathrm{e}^{-\Delta\cosh\varphi/T}+1}\frac{\mathrm{d}}{\mathrm{d}T}\left(\frac{\Delta}{T}\right).$$

comparing with (16.84), we find

$$\frac{n_\mathrm{n}}{n_\mathrm{e}} = \frac{1}{T}\frac{\mathrm{d}\Delta}{\mathrm{d}T}\frac{1}{\frac{d}{\mathrm{d}T}\frac{\Delta}{T}}. \tag{16.86}$$

At $T = T_\mathrm{c}$ this quantity is equal to unity (which is seen from the fact that $\Delta \propto (T_\mathrm{c} - T)^{1/2}$), but with $T < T_\mathrm{c}$ it is less than unity. Hence, in contrast to a normal metal, the movement of quasiparticles alone does not correspond to the movement of the entire electron liquid. The remaining number of electrons is just the sought-for "number of superconducting electrons". Thus,

$$\frac{n_\mathrm{s}}{n_\mathrm{e}} = 1 - \frac{n_\mathrm{n}}{n_\mathrm{e}} = -\left[\frac{\mathrm{d}\ln(\Delta/T)}{\mathrm{d}\ln T}\right]^{-1}. \tag{16.87}$$

It is exactly this number that appears in the kernel $Q(T)$ instead of n_e.
Thus, in the London situation at $T \neq 0$ we have

$$Q = \frac{n_\mathrm{s}e^2}{mc}. \tag{16.88}$$

The same result is obtained by way of more lengthy calculations analogous to those in the preceding section. From eq. (16.88) it follows that the penetration depth is expressed, instead of (15.40), by the formula

$$\delta = \left(\frac{mc^2}{4\pi n_s e^2}\right)^{1/2} \tag{16.89}$$

Let us consider the limiting cases. At $T < T_c$ we obtain with the aid of formula (16.30)

$$\frac{n_s}{n_e} \approx 1 - \left(\frac{2\pi\Delta(0)}{T}\right)^{1/2} e^{-\Delta(0)/T}, \tag{16.90}$$

$$\delta_L(T) \approx \delta_L(0)\left[1 + \left(\frac{\pi\Delta(0)}{2T}\right)^{1/2} e^{-\Delta(0)/T}\right]. \tag{16.91}$$

At $T_c - T \ll T_c$ we find from eq. (16.33) that

$$\frac{n_s}{n_e} \approx \frac{T_c - T}{T_c} \tag{16.92}$$

$$\delta_L(T) \approx \delta_L(0)\left(\frac{T_c}{2(T_c - T)}\right)^{1/2}. \tag{16.93}$$

In concluding this section we note the following. In the limit $T \to T_c$ all superconductors become London superconductors and their penetration depth is described by the formulas derived above; but in a case where $\delta_L(0) < \xi_0$ at $T = 0$, the transition to the London limit occurs only in the immediate vicinity of T_c. For such superconductors, the Pippard situation exists practically over the entire temperature range; in particular, it also persists at $T_c - T < T_c$; for example, for aluminum the London Limit occurs only at $1 - T/T_c \sim 10^{-3}$. The complete derivation for the Pippard case, which is not given here, yields a result qualitatively similar to formula (16.81) for $T = 0$ with $\delta_L(0)$ replaced by $\delta_L(T)$. Hence, $\delta_P(T) \sim \delta_P(0)\,(1 - T/T_0)^{1/3}$ as $T \to T_c$. The complete formula has the form

$$\delta_P(T) = \delta_P(0)\left[\frac{\Delta}{\Delta(0)}\tanh\left(\frac{\Delta}{2T}\right)\right]^{-1/3}. \tag{16.94}$$

8.2.11 16.10. The superconducting correlation and surface energy. Two types of superconductors. The role of impurities

The concept of correlation length introduced in the preceding sections explains the surface energy at the interface between the normal and the superconducting phase, which was proposed by L.D. Landau in his theory of the intermediate state (section 15.3). Imagine a planar interface between the normal and superconducting phases,
which is formed in the intermediate state. Let us show how Δ and the magnetic field vary in the vicinity of the interface (fig. 105)*. The superconducting correlation does not allow Δ to vary discontinuously, because the states of electrons are correlated at a distance of order $\xi(T) = \hbar v/\Delta(T)$. It should be noted that the detailed theory yields somewhat different correlation lengths for different quantities. In section 16.8 it has already been said that in electrodynamics this is ξ_0(16.82), i.e., a temperature-independent quantity. The characteristic length over which Δ varies is $\xi(T) = \hbar v/\Delta(T)$. The difference manifests itself near T_c, where $\xi(T) \to \infty$.

Thus, in the region of contact between the normal and superconducting phases Δ varies as shown in fig. 105. On the other hand, the equilibrium between the normal and superconducting

phases can occur only if there is a magnetic field equal to H_c in the normal phase. The field is damped in the superconducting phase at a distance δ. Figure 105 shows the Pippard situation corresponding to $\xi \gg \delta$.

For the convenience of reasoning we replace the true picture by a rougher one with sharp boundaries along H (the line A) and along Δ (the line B) drawn so that the total free energy and the average field are the same as before. In such a case, there arises a region AB of order ξ, in which, on the one hand, $\Delta = 0$, corresponding to the normal phase, and, on the other hand, there is no magnetic field. Taking into account that $F_n - F_s = H_c^2/8\pi$, we obtain an excess energy equal to $H_c^2/8\pi$ per cm^3 of the region AB . But we are interested in the excess energy per cm^2 of the interface area. This is equal to $(H_c^2/8\pi) \cdot \mathrm{AB}$, i.e.,

$$\sigma_{ns} \sim \xi \frac{H_c^2}{8\pi}$$

(it is this parameter, ξ, that we introduced in section 15.3 instead of σ_{ns}).
As has been pointed out, the derivation described, just as fig. 105, refers to the Pippard case $\xi > \delta$. But if, conversely, $\delta \gg \xi$, then we find in the same way that at the interface there appears a negative surface energy of order $-\delta H_c^2/8\pi$. Naturally, this also occurs at $\xi = 0$, i.e., in the London theory. The impossibility of explaining the origin of the positive surface energy within the framework of the London theory has long been thought to be one of its main shortcomings.

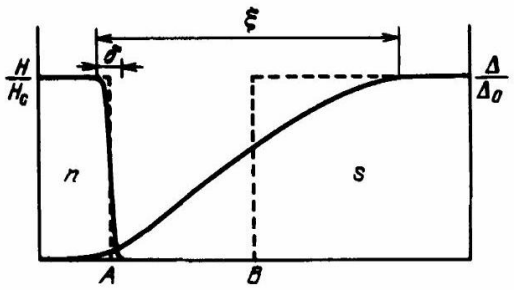


Fig. 105.

It has turned out that there really exist superconductors with a negative surface energy. Such superconductors exhibit an extremely unusual behavior in a magnetic field, which will be described in detail in ch. 18 . The existence of such superconductors was first predicted by Abrikosov and Zavaritsky (Abrikosov 1952; Zavaritsky 1952) on the basis of the analysis of experimental data on the critical fields of thin superconducting films prepared by different methods. They were called superconductors of the second group. At present they are known as type II superconductors. Accordingly, ordinary superconductors with $\sigma_{ns} > 0$ are called type I superconductors.

Since the sign of the surface energy depends on the ratio of the penetration depth δ and the correlation length ξ, it is natural to classify superconductors according to the value of the ratio δ/ξ. Especially attractive is the circumstance that with $T \to T_c$ this ratio tends to a constant, because both $\delta(T)$ and $\xi(T)$ depend on temperature by the law $(T_c - T)^{-1/2}$. The precise boundary between type I and type II superconductors is determined by the condition $x = \frac{1}{2}\sqrt{2}$, where, with $T \to T_c$, according to Gor'kov (1959) (see the derivation in ch. 17)

$$\varkappa(T_c) = \left(\frac{24}{7\zeta(3)}\right)^{1/2} \frac{\gamma}{\pi} \frac{\delta_L(0)}{\xi_0} = 0.96 \frac{\delta_L(0)}{\xi_0}. \qquad (16.95)$$

*The reasoning given below stems from Pippard (1955).

The quantity x was first introduced in the Ginzburg-Landau theory (ch. 17) and has come to be known as the Ginzburg-Landau parameter. Thus, in the vicinity of T_c we have

$$\begin{array}{ll} x < \frac{1}{\sqrt{2}}, & \sigma_{ns} > 0, \quad \text{type I}, \\ x > \frac{1}{\sqrt{2}}, & \sigma_{ns} < 0, \quad \text{type II}. \end{array} \tag{16.96}$$

This condition may also be extended to temperature far from T_c. To do this, the quantity x must be considered to be temperature-dependent, i.e.,

$$\varkappa(T) = \varkappa(T_c)\, A(T). \tag{16.97}$$

Calculations show that the function $A(T)$ varies little with temperature. This dependence is shown in fig. 106 (Gor'kov 1959).

Among pure metals presumably no type II superconductors are encountered. However, there is a method by means of which any type I superconductor can be converted to a type II superconductor. To this end, one has to introduce impurities.

The scattering from impurities first of all reduces the superconducting correlation*. Indeed, imagine an electron moving in the field of impurities. It performs a diffusive motion with a mean free path l and a velocity v; its mean displacement will be of order (section 3.5):

$$x \sim (Dt)^{1/2},$$

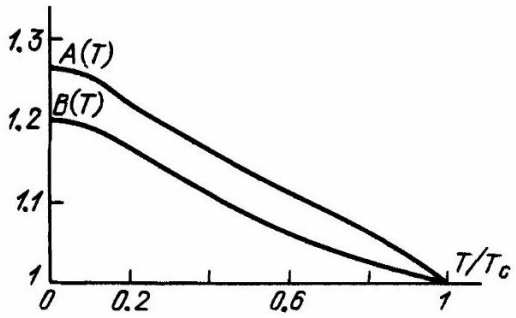


Fig. 106.

where D is the diffusion coefficient, which is of order $D \sim lv$. But its total path length is $t \cdot v$. If we take $tv \sim \xi$, then

$$x \sim \xi' \sim \left(lv \cdot \frac{\xi}{v}\right)^{1/2} \sim (\xi l)^{1/2}. \tag{16.98}$$

In other words, the effective correlation length decreases and becomes equal to ξ'. Of course, all these reasonings are valid as long as $\xi > l$. In case $l > \xi$, scattering on impurities practically has no effect on the superconducting correlation.

The incorporation of impurities alters the penetration depth too. In a case where $l < \xi$, one can estimate the modified quantity δ' rather simply. The presence of a finite mean free path leads to the appearance in the kernel $Q(r - r')$ of a damping at distance l, which can be taken into account by introducing a factor $f(r - r') = \exp(-|r - r'|/l)$. The Fourier

* The estimate given below refers to temperatures far from T_c.

component of the product of the functions $Q_0(r)f(r)$ is equal, as can be easily seen, to $\int Q_0(q-q_1)\,f(q_1)\,\mathrm{d}^3q_1(2\pi)^3$ (Q_0 refers to a pure metal). In our case, the characteristic length for $f(r)$ is l and, hence, for its Fourier component the characteristic values of $q_1 \sim l^{-1}$. The scale of the kernel $Q_0(q-q_1)$ is ξ^{-1}. If $l > \xi$, then $q_1\xi \sim \xi/l > 1$, i.e., the argument for Q_0 is large and one has to make use of the Pippard limit (16.75).

In subsequent calculations $q \sim \delta^{-1}$ are important. If $\delta/l < 1$, then $q > q_1$. In such a case

$$\int Q_0(q-q_1)\,f(q_1)\,\frac{\mathrm{d}^3q_1}{(2\pi)^3} = Q_0(q)\int f(q_1)\,\frac{\mathrm{d}^3q_1}{(2\pi)^3}$$

The last integral is $f(r)$ at $r=0$, i.e., unity. Thus, formula (16.75) is reproduced. But if $\delta/l > 1$, then $q < q_1$. In this case,

$$\int Q_0(q-q_1)\,f(q_1)\,\frac{\mathrm{d}^3q_1}{(2\pi)^3} \approx \int Q_0(q_1)\,f(q_1)\,\frac{\mathrm{d}^3q_1}{(2\pi)^3} \sim \frac{n_\mathrm{e}e^2}{mc}\,\frac{l}{\xi}$$

(here we have substituted expression (16.75) for Q_0). Since the resultant kernel is independent of q, we have the London situation. The penetration depth is $\delta = (4\pi Q/c)^{-1/2}$. Thus, we find

$$\delta' \sim \delta_\mathrm{L}\left(\frac{\xi}{l}\right)^{1/2} \tag{16.99}$$

Hence, in the presence of impurities

$$x \sim \frac{\delta'}{\xi'} \sim \frac{\delta_\mathrm{L}}{l}.$$

The values given by the exact theory at $l < \xi$ are* (Abrikosov and Gor'kov 1958, Gor'kov 1959, Helfand and Werthamer 1966):

$$\delta(T) = \left[\frac{mc^2\hbar}{4\pi n_\mathrm{e}e^2\tau_\mathrm{tr}\Delta\tanh(\Delta/2T)}\right]^{1/2}, \tag{16.100}$$

$$\tau_\mathrm{tr}^{-1} = \int W(\theta)(1-\cos\theta)\frac{\mathrm{d}\Omega}{4\pi},$$

$$x(T) = x(T_\mathrm{c})\,\mathrm{B}(T), \quad l = v\tau_\mathrm{tr},$$

$$x(T_\mathrm{c}) = [42\zeta(3)]^{1/2}\pi^{-2}\frac{\delta_\mathrm{L}(0)}{l} = 0.72\frac{\delta_\mathrm{L}(0)}{l}. \tag{16.101}$$

The plot of the function $B(T)$ is given in fig. 106. This value of $\varkappa$ must be substituted into the criterion (16.97). In the intermediate cases of $\xi \sim l$ one may use the interpolation

$$\varkappa(T) \approx \delta_\mathrm{L}(0)\left(0.96\frac{A(T)}{\xi_0} + 0.72\frac{B(T)}{l}\right). \tag{16.102}$$

At $\xi_0^{-1}l \gg 1$ this expression becomes equivalent to eqs. (16.97) and (16.95) and at $\xi_0^{-1}l \ll 1$ it transforms to eq. (16.101).

From what has been said above one may conclude that by reducing the mean free path, i.e., by increasing the impurity concentration (since $l \propto n_\mathrm{i}^{-1}$, section 4.1), one can increase x and convert any type I superconductor to a type II superconductor.

The following question may, however, arise: How do the impurities affect Δ, T_c and other thermodynamic characteristics of the superconductor? Investigations of this topic (Abrikosov and Gor'kov 1958, 1959, Anderson 1963) show that the variation of all these quantities is of order a/l, where a is the atomic dimension. Taking into account that $l \sim (n_i a^2)^{-1} \sim (c_i n a^2)^{-1} \sim a/c_i$, we find (section 4.1) that

the corrections to the thermodynamic quantities are of a relative order c_i, the atomic concentration of impurities. Hence, as long as $c_i < 1$ these corrections are small, in contrast to the correction to δ, which has a relative order of $\delta/l \sim 10^2 - 10^3 c_i$. The smallness of the corrections to thermodynamic quantities is a consequence of the fact that they are governed by the local properties of the superconductor, i.e., the properties at a given point, and are not associated with the motion of electrons from one point to another. Evidently, any damping of the type of $\exp(-|r - r'|/l)$ with $\boldsymbol{r} \to \boldsymbol{r}'$ becomes inefficient. As for the local properties, they are determined by the density of states, which will vary only by an amount of order c_i*.

Of course, if $c_i \sim 1$, all the quantities may vary strongly, but in this case we are dealing with a different substance.

The superconducting correlation helps us to understand one more result. In section 16.6 we have calculated the heat capacity, and it has been found to exhibit a discontinuity at T_c but with no singularities. This behavior of the heat capacity is associated with the neglect of fluctuations (Appendix II). However, in this particular case there is every ground to expect that the fluctuational region corresponds to an extrememly small neighborhood of T_c. In Appendix II it is shown that the size of this region is determined by the ratio of the mean separation between the particles and the correlation length far from T_c. In the case under discussion this ratio is of order

$$\frac{\hbar/p_0}{\hbar v/T_c} \sim \frac{T_c}{p_0 v} \sim \frac{T_c}{\mu} \sim 10^{-4},$$

that is, it is very small. The exact size of the fluctuational region will be found in section 17.1.

8.2.12 16.11. High-temperature superconductivity

As has been said in section 15.1, the highest critical temperature attained to date is 93−95 K for the compound $YBa_2Cu_30_{7-\delta}$. However, this composition is at present not satisfactory in its mechanical properties. Technological superconducting alloys are Nb_3Sn ($T_c = 17 - 18$ K) and $Nb - Zr - Ti$ ($T_c = 9 - 11$ K). In order to maintain such low temperatures, one has to employ special cryostats with liquid helium (boiling point at atmospheric pressure 4.2 K). Nevertheless, as will be seen in what follows, superconductivity has already found practical applications in spite of the difficulties

associated with cooling, since some properties that are important in practice are exhibited

---

• Here $W(\theta)$ is the probability of scattering of an electron from an impurity introduced in section 3.2 and τ_{tr} is the corresponding collision time (in section 3.2 it is denoted as τ; we use here the symbol adopted in the literature on superconductivity, τ_{tr}).

*The reasoning given is valid for the isotropic model. For an anisotropic superconductor the situation is different. In this case, the scattering of electrons from an impurity mixes the components of the wave function of a Cooper pair corresponding to different values of the momentum, i.e., different Δ. This leads to a decrease in the binding energy of the pair and to a change of all thermodynamic quantities. The exact theory (Hohenberg 1963) shows that the relative corrections are of order $\left[(\Delta(n) - \bar{\Delta})^2/\bar{\Delta}^2\right] \xi_0/l$. Since the anisotropy in real superconductors is small, $(\Delta(n) - \bar{\Delta})^2/\bar{\Delta}^2 \leqslant 10^{-2}$, these corrections, in fact, differ little from the corrections for an isotropic superconductor, which are of order c_i.

only by superconductors.

It is not difficult to visualize the technical revolution that could be brought about by substances exhibiting superconductivity at room temperatures. In the first place, this would include the possibility of producing lines transmitting electrical power over any distance without loss. It would be possible to solve the problem of energy storage in small volumes and, hence, to use electric motors for all transport facilities that run on petroleum products. Many other perspectives could also be visualized.

This is why at present many laboratories in several countries are concerned with the study of high-temperature ceramics. On the one hand, it is necessary to define the limiting critical temperature and to develop standard technology for preparing the substances required. On the other hand, a construction method for superconducting equipment must be designed, which could be of practical use. The possibility is not excluded that the latter will be a formidable task for ceramics and the search for high-temperature superconductors will be continued. Moreover, the mechanism of superconductivity in ceramics has not been definitely established. Therefore, we shall present here some ideas concerning high-temperature superconductivity [detailed information on this topic can be found in the book edited by Ginzburg and Kirzhnits (1977)].

We begin with a more detailed discussion of the familiar interaction between electrons: Coulomb repulsion and phonon attraction. Then we shall consider "quasiphonon" mechanisms for the interaction of electrons and, finally, turn to nonphonon or so-called "exciton" mechanisms for the interaction. At the end of the section we shall discuss the possibility of producing high critical magnetic fields.

The formula for the critical temperature was derived in the BCS theory (16.25). It took into account only electron-phonon interaction in its simplified form. A more detailed formula was found by McMillan (1968), who carried out a more accurate examination of the electron-phonon interaction and took account of Coulomb repulsion; the formula has the form

$$T_{\mathrm{c}} = \frac{\hbar\omega_{\mathrm{D}}}{1.45} \exp\left[-\frac{1.04(1+\lambda)}{\lambda - \mu^*(1+0.62\lambda)}\right], \tag{16.103}$$

where λ characterizes the electron-phonon interaction (λ corresponds to $\frac{1}{2}g\nu$ in the simplified theory) and μ^* characterizes the electron-electron repulsion. Since the Coulomb interaction is screened at interatomic distances, it may be treated as a point interaction and described by a constant μ. The quantity μ^* is connected with this constant by the relation*

$$\mu^* = \frac{\mu}{1 + \mu \ln(\varepsilon_{\mathrm{F}}/\hbar\omega_{\mathrm{D}})} \tag{16.104}$$

The large logarithm in the denominator results from the different action times of the Coulomb repulsion ($t_{\mathrm{c}} \sim \hbar/\varepsilon_{\mathrm{F}}$) and phonon attraction ($t_{\mathrm{ph}} \sim \omega_{\mathrm{D}}^{-1}$); $t_{\mathrm{c}}/t_{\mathrm{ph}} \sim \hbar\omega_{\mathrm{D}}/\varepsilon_{\mathrm{F}} < 1$. For $\lambda < 1$ and $\mu^* = 0$ formula (16.103) takes a form similar to eq. (16.25).

Since λ and μ^* appear in the exponent, it is clear that these constants are of prime interest. The Coulomb interaction constant μ is formally of the order of unity. However, μ^*, which enters into T_{c} according to (16.104), is weakened by the large logarithm. Estimates give $\mu^* \sim 0.1-0.2$. As for the constant λ, it is also formally of the order of unity. But it must be taken into account that electron-phonon interaction eventually occurs as a result of the interaction of electrons with ions, which is described by a small pseudopotential. Therefore, λ usually does not reach unity. On the whole, the difference $\lambda - \mu^*(1+0.62\lambda)$ appearing in (16.103) may have any sign, but

---

- We use the symbol μ for the dimensionless Coulomb interaction constant ($\mu \sim e^2/\hbar v$) since it is generally accepted in the literature. It should not be confused with the chemical potential, which is denoted here as ε_{F}.

substances for which this difference is close to zero are rare. At relatively small λ the substance is not a superconductor* and at relatively large λ the term with μ^* may be neglected.

It is therefore reasonable to concentrate our attention on the constant λ. This constant determines not only the critical temperature but also the magnitude of the electrical resistance that appears as a result of the scattering of electrons as phonons. Since at room temperature this mechanism dominates over others, a paradoxical consequence arises: poor conductors (at room temperature) are good superconductors (i.e., they have a high T_c). Examples illustrating this are Pb : $\rho\,(18^\circ\mathrm{C}) = 20.8\times10^{-6}\mathrm{ohm\cdot cm}, T_c = 7.2$ K, and Al: $\rho\,(18^\circ\mathrm{C}) = 3.2\times10^{-6}\mathrm{ohm\cdot cm}, T_c =$ 1.2 K. The superconducting ceramics that have lately been found are extremely bad conductors ($\rho \sim 10^{-3}\mathrm{ohm\cdot cm}$ at room temperature). If in formula (16.103) we assume that $\mu^* = 0$, then T_c will increase monotonically with increasing λ. Actually this formula does not apply when $\lambda > 1$. It has been shown (Allen and Mitrovic 1982) that

$$T_c \approx 0.18\hbar \left(\overline{\omega^2}\right)^{1/2} \lambda^{1/2},$$

i.e. grows monotonically with λ. However in reality the value of λ never exceeds unity by order of magnitude. The idea has been proposed that λ can increase strongly if the lattice is close to a structural transition. Such a transition is usually preceded by the formation of a "soft mode", i.e., by a pronounced decrease of $\omega(k)$ at a certain $\boldsymbol{k}$. Such a decrease could imply an increase in the action time of phonon attraction and this was the basis for speculations on the subject. However, it should be taken into account that a soft mode at a particular $\boldsymbol{k}$ has a very small statistical weight (the integral includes $k^2\,\mathrm{d}k$) and therefore it cannot play an essential role.

A special situation could take place for the "nesting" type of transitions in which, due to the change of the lattice period and the formation of a new Brillouin zone, some parts of the Fermi surface would be almost entirely superposed on each other. In the vicinity of such a transition an increase of the state density $\nu(\mu)$ would take place, i.e., an increase of λ in eq. (16.103) [more details can be found in the book edited by Ginzburg and Kirzhnits (1977)]. Such transitions are known to exist in nature, but their relation to superconductivity has not yet been established.

Apart from the increase of λ, one may think also of the increase of $\hbar\omega_D$. Considering that $\hbar\omega_D \sim sp_0 \sim \varepsilon_F(m/M)^{1/2}$, where M is the mass of the ion, an attempt must be made to reduce this mass. A unique possibility in this respect could be provided by solid hydrogen if it were a metal. Unfortunately, under ordinary conditions solid hydrogen is a dielectric crystal consisting of H_2 molecules. Theoretical calculations show that with increased pressure a phase transition must occur from molecular hydrogen to the atomic phase, which is analogous to alkali metals. The pressure of the transition is very high, of the order of 2.5 Mbar .

Of course, such a pressure is difficult to reach and to maintain and it is of no practical value. There exists, however, a possibility that, because of the large difference in specific volume between the molecular and the atomic phase, the latter can be preserved as a metastable phase even when the pressure is removed (an example is diamond, which is the metastable phase of carbon under ordinary conditions). Also, various methods have been proposed for producing

---

- Actually, the situation is in all probability more complicated. The interaction forces between electrons at large distances presumably always correspond to attraction. This may give rise to Cooper pairs with a nonzero orbital moment (if we deal with the isotropic model of course; in the anisotropic case there is no conserved orbital momentum, but there is another analogous classification of states, so that the qualitative conclusions do not change). The binding energy of such pairs is small, so that T_c will also be low. Nevertheless, this reasoning leads one to the conclusion that at sufficiently low temperatures any pure metal will become superconducting.

metallic hydrogen directly from the gas phase without applying high pressures (adsorption on carbon, condensation in a strong magnetic field, etc.). However, the question of the existence of a metastable metallic phase and the possibility of its prepration in the absence of pressure has not yet been clarified.

The difficulty in calculations for solid hydrogen lies in the fact that, in contrast to all other elements, its ions have no electron shells and are simply protons. Because of this, for hydrogen the pseudopotential coincides with the real coulomb potential and is not small (section 14.2). Usually, calculations for metallic hydrogen are based on the strongly compressed matter approximation (section 14.4). However, the resultant series do not converge rapidly enough, so that it is difficult to choose the energetically most favorable structure and to solve the problem of the possibility of the metastable state. At the same time the strong electron-ion interaction implies also a strong electron-phonon interaction, which may bring about a certain increase in λ in formula (16.103). Preliminary calculations show that $T_c \sim 100 - 200$ K (Schneider 1969).

It has also been suggested that the difficulties associated with the preparation of metallic hydrogen can be overcome by producing the hydrides, i.e., compounds of metals with hydrogen. In the phonon energy spectrum of such compounds branches may appear that correspond mainly to the vibrations of protons and exhibit high frequencies. However, the hydrides are dielectrics. Therefore, attempts have been made to take advantage of the good solubility of hydrogen in some metals, especially in platinum. Since the natural solubility is still insufficient, special methods have been applied to produce metastable solid solutions with an increased hydrogen concentration. Although these compounds were superconductors, however their T_{c} was below 10 K . It is possible that the interaction of electrons with the high-frequency vibrations of protons is weak for some reasons.

There is one more theoretical possibility, which in fact, makes use of the same advantages exhibited by metallic hydrogen (Abrikosov 1978). It concerns the production of a substance that might be called "metallic excitonium". Imagine an even metal containing equal numbers of electrons and holes. If the mass of the holes is much larger than the mass of electrons due to the specific nature of the energy spectrum*, their potential energy will then exceed their kinetic energy. As a result, the holes will become classical objects and will form a periodic superstructure, i.e., a "lattice in the lattice" (Herring 1968, see Halperin and Rice 1968). The periods of such a superstructure are determined by the density of electrons and holes and must not necessarily coincide with the periods of the main lattice. For the hole lattice to be stable, it is necessary that the amplitude of the zero-point vibrations of the holes be much less than (not more than $\frac{1}{5}$) the lattice period, which leads to the requirement $m_{\mathrm{h}}^*/m_{\mathrm{e}}^* > 50$. If, besides, m_{e} is less than the mass of a free electron m, then the ratio m_{h}^*/m must not be very large.

As a result, a "substance" is produced, which resembles metallic hydrogen, but with the protons being replaced by heavy holes [Abrikosov (1978) proposed the term "metallic excitonium" for this substance]. In such a substance "phonons" can propagate. Their velocity will be determined by the mass of holes, which may be of the order of $10 - 20$ m at best, i.e., 100 times less than the mass of the proton. With a not-too-small density of electrons and holes this may lead to $\hbar\omega_D$ in formula (16.103) being 10 times larger than in the case of hydrogen.

At present no such substances are known to exist and, of course, we still do not know whether they can be produced. They should most likely be sought for among compounds containing transition metals (and also metals similar to them, such as $\mathrm{Cu}, \mathrm{Ag}, \mathrm{Au}$) or rare-earth elements for the valence band to be formed from the weakly overlapping d - or f -shells of the atoms. In this case, the formation of heavy holes is possible. The search for such compounds is not a simple matter. However, on the other hand, there is no need for high pressures and the problem of the stability of the metastable metallic phase does not arise, as is the case with metallic hydrogen.

We have so far been concerned with the mechanism of electron attraction accomplished by

phonons (or by similar hole lattice vibrations in the hypothetical "metallic excitonium"). There naturally arises the question of the possibility of a different attraction mechanism. Since the direct interaction of electrons is a repulsion, we are to seek in metals a "transmitting system" different from the phonon system.

The general scheme of the interaction of electrons via the transmitting system A may be outlined as follows:

$$e_1 + A \to e_1' + A^*, \quad e_2 + A^* \to e_2' + A, \tag{16.105}$$

where e_i corresponds to an electron of momentum p_i; A is the ground state; A^* is the excited state of the transmitting system. As a result of this double "reaction" the system A reverts to the initial state and the momenta of electrons e_1 and e_2 undergo a change, i.e., they are scattered from each other. It can easily be shown that such an interaction is necessarily an attraction and if it is not too strong, we have

$$T_c \sim \Delta E \exp\left(-\frac{1}{\lambda}\right) \tag{16.106}$$

where ΔE is the energy difference between the states A and A^* and λ depends on the interaction of electrons with the system A. As a matter of fact, phonon attraction occurs according to an analogous scheme.

Let us examine some variants. The role of the transmitting system A could be played by a system of spins in a magnetic metal. The excitation of this system is described by a gas of quasiparticles called magnons or spin waves. Since ferromagnetism is antagonistic to superconductivity (see section 21.2 for more detail), we may speak here of antiferromagnetic metals. However, estimates of the quantities ΔE and λ, which determine T_c, provide no advantages in this case compared to phonons.

A mechanism of a rather similar type is an exchange of "virtual paramagnons". If the substance is close to the magneto-ordered state (ferro- or antiferromagnetic), there can exist strong fluctuations corresponding to the magnetic phase and they produce a strong interaction between quasiparticles. Such virtual paramagnons are involved in explaining the unusual properties of almost ferromagnetic metals (which have been mentioned in ch. 13) and the formation of Cooper pairs in superfluid He^3; they are also proposed as a possible explanation of the high-temperature superconductivity in ceramics (Anderson 1987, Fukuyama and Yoshida 1987) and of the unusual superconductivity in metals with "heavy fermions" (see pp. 378-379).

Another transmitting system could be electrons that are separated in some way from conduction electrons (i.e., their states are not mixed). The excitations of such electron systems are called "excitons" and therefore this fundamentally possible mechanism of superconductivity is called the "exciton" mechanism (Little 1964; Ginzburg 1964, 1968, 1970, 1976).

In particular, the electrons of the inner shells of atoms that are retained in the lattice ions of metals could be such an isolated system. The excitation energy ΔE is here of the order of 10 eV , i.e., 10^5 K. If this mechanism were efficient, all metals would be high-temperature superconductors. This is not the case in reality because of the weak interaction of the conduction electron with the inner-shell electrons and, accordingly, the smallness of λ in (16.105).

Let us consider the matrix element corresponding to the first of the processes (16.105). It is given by

$$M_{12} = \int \psi_{A^*}^* (r_1)\, \psi_A (r_1)\, V (|r_1 - r_2|)\, \mathrm{e}^{-\mathrm{i}(p'-p)r_2/\hbar} \times u_{p'}^* (r_2)\, u_p (r_2)\, \mathrm{d}V_1\, \mathrm{d}V_2$$

*This may occur if holes appear in a narrow band generated from the d- or f-levels of the atoms, whereas the electrons come from the s- or p-states of the atoms.

where $V(r)$ is the interaction; the functions ψ_A and ψ_A^* are the wave functions of one of the ionic electrons; the conduction electron is described here by the Bloch function $e^{ipr/\hbar}u_p(r)$. The essential values of r_2 in the integral over r_2 are $r_2 \sim a$, where a is the interatomic separation. The order of magnitude of the quantity r_1 is determined by the ionic radius r_i, which is appreciably smaller than a. Hence, we can expand $V(|r_1 - r_2|)$ in r_1/r_2, i.e.,

$$V(|r_1 - r_2|) \approx V(r_2) - \frac{r_1 r_2}{r_2} V'(r_2).$$

Since the functions ψ_A and ψ_A^* are orthogonal, the zeroth expansion term $V(r_2)$ gives no contribution and the matrix element M_{12} may be expected not to be larger than r_i/a in order of magnitude. Such smallness also results from the second process in (16.105). Hence, the effective electron interaction constant g will contain $(r_i/a)^2$, and this smallness will be included in λ (because $\lambda = \frac{1}{2}g\nu(\mu)$). It may be said that the ionic shells exhibit low polarizability.

Thus, an attempt must be made to find a transmitting system of electrons with high polarizability. Little was the first (Little 1964) to suggest the use of long polymeric organic molecules with so-called alternating bonds of carbon atoms, which behave as if they were one-dimensional metals. If the structure of the molecule includes strongly polarizable side atomic groups (fig. 107), these groups could serve as the transmitting system $\boldsymbol{A}$. In fact, apart from the technical infeasibility of manufacturing such conductors from unruptured polymeric molecules, a fundamental objection arises against this idea. The point is that a purely one-dimensional superconductor cannot exist because fluctuations of the order-parameter phase destroy the long-range order at any finite temperature (Rice 1965)*.

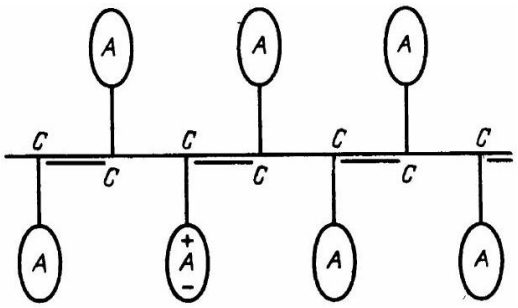


Fig. 107.

where $V(r)$ is the interaction; the functions ψ_A and ψ_A^* are the wave functions of one of the ionic electrons; the conduction electron is described here by the Bloch function $e^{ipr/\hbar}u_p(r)$. The essential values of r_2 in the integral over r_2 are $r_2 \sim a$, where a is the interatomic separation. The order of magnitude of the quantity r_1 is determined by the ionic radius r_i, which is appreciably

* What is really calculated is the correlation function $Z(x_1 - x_2) = \langle \Psi(x_1)\Psi(x_2)\rangle$, where Ψ is the Ginzburg-Landau order parameter which is proportional to Δ (ch. 17), and the average value is used with thermodynamic fluctuations taken into account. As a result, it is found that $Z \propto \exp\left(-|x_1 - x_2| mT/\Psi_0^2 h^2\right)$ with $|x_1 - x_2| \to \infty$. Here Ψ_0 is the equilibrium value of Ψ (in the one-dimensional problem Ψ_0^2 is normalized to the number of electrons per cm of length). Hence, $Z \to 0$ with $|x_1 - x_2| \to \infty$; this is an indication of the absence of long-range order at a finite temperature. In the presence of long-range order Ψ is coherent over the entire space and, hence, Z has a finite limit with $|x_1 - x_2| \to \infty$. The destruction of long-range order occurs because of the fluctuations in the phase of the complex function $\Psi = |\Psi|e^{i\varphi}$.

smaller than a. Hence, we can expand $V(|r_1 - r_2|)$ in r_1/r_2, i.e.,

$$V(|r_1 - r_2|) \approx V(r_2) - \frac{r_1 r_2}{r_2} V'(r_2).$$

Since the functions ψ_A and ψ_A^* are orthogonal, the zeroth expansion term $V(r_2)$ gives no contribution and the matrix element M_{12} may be expected not to be larger than r_i/a in order of magnitude. Such smallness also results from the second process in (16.105). Hence, the effective electron interaction constant g will contain $(r_\text{i}/a)^2$, and this smallness will be included in λ (because $\lambda = \frac{1}{2} g\nu(\mu)$). It may be said that the ionic shells exhibit low polarizability.

Thus, an attempt must be made to find a transmitting system of electrons with high polarizability. Little was the first (Little 1964) to suggest the use of long polymeric organic molecules with so-called alternating bonds of carbon atoms, which behave as if they were one-dimensional metals. If the structure of the molecule includes strongly polarizable side atomic groups (fig. 107), these groups could serve as the transmitting system A. In fact, apart from the technical infeasibility of manufacturing such conductors from unruptured polymeric molecules, a fundamental objection arises against this idea. The point is that a purely one-dimensional superconductor cannot exist because fluctuations of the order-parameter phase destroy the long-range order at any finite temperature (Rice 1965)*.

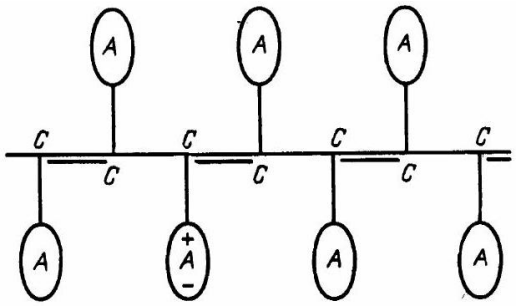


Fig. 107.

In order to overcome this difficulty, numerous "quasi-one-dimensional" compounds have been synthesized. These are mostly molecular crystals, which may be identified in the sense of conducting properties with bundles of weakly bound conducting filaments. The conductivity along the filaments is high, but the probability of an electron to be transferred from filament to filament is low, and therefore the conductivity anisotropy $\sigma_\parallel/\sigma_\perp$ may reach a few thousands. Apart from molecular crystals, polymers (for example, $(\text{SN})_x$ and $(\text{CH})_x$, where x stands for the multiple repetition of the group) have also been studied. Some of these compounds have been found to exhibit superconductivity, but with $T_c \leqslant 8$ K; the corresponding crystals were presumably more "three-dimensional" and the superconductivity mechanism was the ordinary phonon mechanism.

- What is really calculated is the correlation function $Z(x_1 - x_2) = \langle \Psi(x_1)\, \Psi(x_2) \rangle$, where Ψ is the Ginzburg-Landau order parameter which is proportional to Δ (ch. 17), and the average value is used with thermodynamic fluctuations taken into account. As a result, it is found that $Z \propto \exp\left(-|x_1 - x_2|\, mT/\Psi_0^2 h^2\right)$ with $|x_1 - x_2| \to \infty$. Here Ψ_0 is the equilibrium value of Ψ (in the one-dimensional problem Ψ_0^2 is normalized to the number of electrons per cm of length). Hence, $Z \to 0$ with $|x_1 - x_2| \to \infty$; this is an indication of the absence of long-range order at a finite temperature. In the presence of long-range order Ψ is coherent over the entire space and, hence, Z has a finite limit with $|x_1 - x_2| \to \infty$. The destruction of long-range order occurs because of the fluctuations in the phase of the complex function $\Psi = |\Psi| e^{i\varphi}$.

In this connection, it should be noted that the basic idea of Little was not one-dimensionality, which, as has already been pointed out, interferes with superconductivity, but rather the presence of strongly polarizable side groups that surround the main filament by a thick "coat". In currently available molecular quasi-onedimensional crystals the conductivity anisotropy occurs not because of the large distances between the filaments but because of the high anisotropy of the electronic wave functions, which overlap strongly along the filaments and weakly in the transverse direction. Hence, in compounds of this type there is no room for a strongly polarizable "coat".

The idea of Ginzburg (Ginzburg 1964) consists in producing heterogeneous structures, in which metal and insulator films would alternate [a semiconductor has also been proposed in place of an insulator (Allender et al. 1973)]. Due to the quantum tunnelling effect some of the electrons of the metal could get into the insulator and exchange the excitons of the insulator. A theoretical estimation of T_c is very difficult because it depends on the detailed assumptions of the properties of the interface. High T_c cannot probably be attained by this method because of the smallness of the layer in which the pairing occurs and because of the weakness of the effective interaction. No substantial increase in T_c has been achieved in experiments with this type of structure.

The following remark may be made concerning the possibility of superconductivity in thin boundary layers of a metal. We have already discussed superconducting correlation (sections 16.7 and 16.10). One of its manifestations is the so-called "proximity effect - the mutual influence of a superconductor and a normal metal which are in contact with each other (see section 20.1 for more detail). In particular, superconductivity in a film applied onto a normal metal will be destroyed if its thickness is smaller than ξ. Hence, even if superconductivity could have arisen in a thin layer near the point of contact between a metal and any polarizable dielectric medium, it would have been suppressed if the thickness of this layer is less than ξ. Superconductivity could be preserved provided the value of T_c attained is so high that $\xi_0 \sim \hbar v/T_c$ is of the order of the thickness of the superconducting layer; note that to room temperature there corresponds $\xi \sim 10^{-5} - 10^{-6}$, i.e., several hundreds of interatomic distances. The way out of this situation could be the use of thin
superconducting films between layers of an insulator, which is what has been done in experiments, though with no success yet.

The limiting case of heterogeneous structures are quasi-two-dimensional superconductors, in which the conducting layers have a thickness of one molecule and are separated by relatively thick nonconducting layers. Such compounds have readily been synthesized on the basic of lamellar chalcogenides, such as TaS_2 and $NbSe_2$. Due to the weakness of the interaction, large organic molecules (say pyridine, C_6H_5 N) can be incorporated into the spaces between the layers of a chalcogenide. Such crystals are called intercalation compounds. Here the separation between the layers may strongly increase (up to 50Å), which, in particular, affects the conductivity anisotropy (it may increase from 10 up to 10^5).

Although purely two-dimensional conductivity is impossible for the same reason as purely one-dimensional superconductivity [the fluctuational destruction of the long-range order (Rice 1965)], it turns out that even an insignificant interaction between the layers suppresses the fluctuations and restores the superconductivity (Dzyaloshinskii and Katz 1968). In experiments in some cases upon intercalation there has been observed an increase in T_c. For example, upon intercalation of TaS_2 by pyridine T_c increased from 0.3 K up to 3.5 K (Gamble et al. 1976). Although high critical temperatures have not yet been reached in such compounds, this path should nonetheless be regarded as promising*.

In connection with superconductivity of two-dimensional systems mention should be made of the increase in T_c at the twinning plane of crystals (Khaikin and Khlyustikov 1981, 1983). This phenomenon is considered in detail in section 20.2.

The effect of twinning planes may be of prime importance in the high-temperature ceramic $YBa_2Cu_3O_{7-\delta}$, in which, due to a phase transition at 750 K , twinning planes appear spontaneously upon lowering the temperature at a distance of $500 - 1500$Å. It appears that their critical temperature is 93 K , while the "bulk" T_c is $\sim$ 89 K; this could explain many peculiarities in the interval $89 - 93$ K. Traces of higher- T_c superconductivity sometimes observed in this ceramic could possibly be due to the occasional formation of dense arrays of twinning planes (Abrikosov and Buzdin 1988).

Recently one more variant has been proposed of the system transmitting the interaction between conduction electrons - the so-called two-level systems in metallic "glasses" with a strongly disordered crystalline structure. In such compounds, entire groups of atoms can be transferred from some positions to others, these transfers being associated with relatively small changes in energy. Such groups are called two-level systems. Usually, at each temperature T those systems are important, which have a level difference of order T.

Theoretical investigations (Harris et al. 1983) show that the interaction of electrons through two-level systems adds to the phonon attraction and brings about an increase

superconducting films between layers of an insulator, which is what has been done in experiments, though with no success yet.

The limiting case of heterogeneous structures are quasi-two-dimensional superconductors, in which the conducting layers have a thickness of one molecule and are separated by relatively thick nonconducting layers. Such compounds have readily been synthesized on the basic of lamellar chalcogenides, such as TaS_2 and $NbSe_2$. Due to the weakness of the interaction, large organic molecules (say pyridine, C_6H_5 N) can be incorporated into the spaces between the layers of a chalcogenide. Such crystals are called intercalation compounds. Here the separation between the layers may strongly increase (up to 50Å), which, in particular, affects the conductivity anisotropy (it may increase from 10 up to 10^5).

Although purely two-dimensional conductivity is impossible for the same reason as purely one-dimensional superconductivity [the fluctuational destruction of the long-range order (Rice 1965)], it turns out that even an insignificant interaction between the layers suppresses the fluctuations and restores the superconductivity (Dzyaloshinskii and Katz 1968). In experiments in some cases upon intercalation there has been observed an increase in T_c. For example, upon intercalation of TaS_2 by pyridine T_c increased from 0.3 K up to 3.5 K (Gamble et al. 1976). Although high critical temperatures have not yet been reached in such compounds, this path should nonetheless be regarded as promising*.

In connection with superconductivity of two-dimensional systems mention should be made of the increase in T_c at the twinning plane of crystals (Khaikin and Khlyustikov 1981, 1983). This phenomenon is considered in detail in section 20.2.

The effect of twinning planes may be of prime importance in the high-temperature ceramic $YBa_2Cu_3O_{7-8}$, in which, due to a phase transition at 750 K , twinning planes appear spontaneously upon lowering the temperature at a distance of $500 - 1500$Å. It appears that their critical temperature is 93 K , while the "bulk" T_c is $\sim$ 89 K; this could explain many peculiarities in the interval $89 - 93$ K. Traces of higher- T_c superconductivity sometimes observed in this ceramic could possibly be due to the occasional formation of dense arrays of twinning planes (Abrikosov and Buzdin 1988).

Recently one more variant has been proposed of the system transmitting the interaction between conduction electrons - the so-called two-level systems in metallic "glasses" with a

---

- Taking into account that high-temperature ceramics have a layered structure and that their conductivity is due to layers containing Cu and O , which are separated by relatively large distances, one may suppose that these ceramics are superconductors of the excitonic type.

strongly disordered crystalline structure. In such compounds, entire groups of atoms can be transferred from some positions to others, these transfers being associated with relatively small changes in energy. Such groups are called two-level systems. Usually, at each temperature T those systems are important, which have a level difference of order T.

Theoretical investigations (Harris et al. 1983) show that the interaction of electrons through two-level systems adds to the phonon attraction and brings about an increase

in T_c. An estimation of this effect in real metallic glasses shows that T_c may increase by $2-7\%$. This is in accord with experimental facts: the critical temperature of a disordered metal always decreases upon annealing (heating which leads to recrystallization); for example, it drops from 2.34 to 2 K in the alloy $Cu_{33}Zr_{67}$ and from 3.15 K to 3 K in $Zr_{76}Ni_{24}$. Although this effect is not strong, it is interesting from the standpoint of the demonstration of a nonphonon superconductivity mechanism.

Another idea has been proposed associated with the special centers in inhomogeneous metals (Schütter et al. 1987). Let us imagine that there exist centers for which it is energetically favorable to bind two electrons with opposite spins since attraction occurs between electrons of such centers. Although the existence of such centers can be justified, strictly speaking, only in semiconducting glasses, nevertheless their appearance in metals is not ruled out. In the latter case the hybridization of conduction electrons with these states, i.e., the possibility of virtual transitions from the band states to the centers, leads to an attraction and to the formation of Cooper pairs. The effectiveness of such a mechanism depends on the concentration of these special centers. In particular, such special centers may be regular structural units. This idea has also been proposed for the ceramics. For example, as an explanation of high-T_c superconductivity in ceramics it has been proposed that the holes of the conduction band (which transmit the current in those materials) can be localized at the double-negative oxygen ion (Zvezdin and Khomskii 1987).

Unusual superconductivity takes place in a number of compounds containing rare-earth metals and actinides, say YBe_{13} and $CeCu_2Bi_2$ (see Brandt and Moshchalkov 1984). Although the critical temperature of these compounds is not high ($T_c < 1$ K), their other properties are very interesting. First of all, they exhibit relatively strong critical fields. This may be interpreted as a consequence of an increase of the effective mass of carriers; estimates give values of m^* of the order of $200-400m$, where m is the mass of the free electron. It is for this reason that the term "heavy fermions" is used.

The study of the various characteristics in the normal state indicates that in such compounds the density of states has a narrow and large peak at the Fermi level (recall that the density of states $\nu = p_0 m^* / (\pi^2 \hbar^3)$. The origin of this peak is presumably associated with the electron screening of the spin of magnetic atoms of rare-earth elements and actinides. If the magnetic atoms are minor impurities, this leads to the Kondo effect in conductivity (section 4.6), but has no noticeable effect on the energy spectrum and thermodynamic properties. However, if the magnetic atoms become regular structural units and the exchange interaction constant J is so high that the Kondo temperature is higher than the freezing temperature of the spins, the Abrikosov-Suhl resonance in conductivity (see formula 4.49) may manifest itself as a peak in the density of states.

A further interesting property consists in that the low-temperature electronic heat capacity in UBe_{13} has been found to be proportional to T^3 or T^2. This is evidence
that at certain points or contours of the Fermi surface the energy gap Δ vanishes. In all proba-

- Taking into account that high-temperature ceramics have a layered structure and that their conductivity is due to layers containing Cu and O , which are separated by relatively large distances, one may suppose that these ceramics are superconductors of the excitonic type.

bility, the latter is associated with the nonphonon mechanism of electron attraction (probably the virtual paramagnons mentioned before).

Apart from increasing T_c, high critical fields are also important. In principle, in order to attain high critical fields two things are required: (a) the localization of electrons must be as large as possible; and (b) there must be attraction in the localized state. In this case, Cooper pairs could be "prepared in advance" from localized electrons and a certain probability of jumps could provide the supercurrent (Abrahams and Kulik 1977, Kulik and Pedan 1980, 1982, 1983, Bulaevskii et al. 1984, Alexandrov et al. 1986). In section 18.1 we shall see that the strongest critical fields can be attained in type II superconductors, and these are limited by two mechanisms: (1) Larmor twisting of pairs, and (2) the tendency of the magnetic field to flip the electron spins parallel to each other. These two mechanisms of pair collapse could be challenged successfully by superconductors of the "localized" type: the first mechanism could be challenged due to the large effective mass of carriers and the second due to the strong attraction of carriers with opposite spins in a single "well". However, it is still unknown whether such superconductors can be produced*. Metallic glasses in which a random potential could lead to localization of electrons could be of interest from this stand-point (section 11.6) (Kulik 1984).

8.3 17 The Ginzburg-Landau theory

8.3.1 17.1. Derivation of the Ginzburg-Landau equations

In ch. 16 we have been concerned with the application of the microscopic (BCS) theory for describing the thermodynamic properties of superconductors and their behavior in a weak magnetic field. A generalization of this theory (Gor'kov 1958) allows one to consider the behavior of superconductors in strong fields, including alternating fields. However, the corresponding equations are extremely complicated, which is why they are seldom used in practice for solution of physical problems. Instead, use is made of a simplified theory, which we shall describe in the present chapter.

In 1950, i.e., even before the microscopic (BCS) theory was developed, Ginzburg and Landau had proposed a theory currently known as the Ginzburg-Landau theory (Ginzburg and Landau 1950), which describes the properties of superconductors near T_c; this theory has successfully surmounted the difficulties of London electrodynamics. For example, it explained the origin of the positive surface energy σ_{ns}. The equations of this theory were derived on the basis of the ideas of Landau's theory of second-order phase transitions (Appendix II).

Later, Gor'kov (Gor'kov 1959a,b) demonstrated that the equations of the Ginzburg-Landau theory are the limit of the BCS equations provided that the following two conditions are satisfied: (a) $T_c - T < T_c$, and (b) $\delta > \xi_0$. For London superconductors the second condition is fulfilled at all temperatures and only the first condition (a) remains. For Pippard superconductors, conversely, the requirement (b) is more stringent. We shall deal here with the simple derivation given in the fundamental work of Ginzburg and Landau (1950).

We start with the definition of the order parameter. We take it as the wave function of Cooper pairs present in the Bose condensate. For an ideal Bose condensate under homogeneous conditions, the ground state is a state with $p = 0$. Below the point of Bose condensation in this state there is a finite number of particles with a wave function $\Psi = \text{const}$. (i.e., $e^{ipr/\hbar + i\alpha}$ at $p = 0$) identical for all particles; this is called coherence. It is believed that with a slight (long-wavelength) inhomogeneity due to the application of an external field, the coherence is preserved and the function $\Psi(r)$ characterizes all particles of the condensate.

*The possibility is not excluded that Chevrel phases and superconductors with "heavy fermions" could be such superconductors.

Near the critical temperature Ψ is small and the free energy Ω may be expanded into a series in Ψ. In the absence of an external field in a bulk superconductor Ψ
is independent of the coordinates. Since Ψ is a complex quantity and Ω is real, the expansion is carried out in powers of $|\Psi|^2$. Thus, we have (for unit volume)

$$\Omega_{\mathrm{s}} = \Omega_{\mathrm{n}} + a|\Psi|^2 + \frac{\mathrm{l}}{2}\,\mathrm{b}|\Psi|^4 + \cdots . \tag{17.1}$$

Since the theory is built up for the vicinity of T_{c}, the coefficients a and b can be expanded in $\tau = (T - T_{\mathrm{c}})/T_{\mathrm{c}}$ and only the first nonvanishing terms need be retained. Since the minimum of Ω_{s} corresponds to $\Psi = 0$ above T_{c} and $\Psi \neq 0$ below T_{c}, the coefficient a changes sign at the transition point; therefore, $a = \alpha\tau$, where $\alpha > 0$. From the condition that $\Psi = 0$ must correspond to the minimum of Ω_{s} at the transition point too, we have

$$b \approx b\,(T_c) > 0.$$

Differentiating with respect to Ψ^*, we obtain the condition of the minimum of Ω_{s} :

$$\Psi\left[\alpha\tau + |\Psi|^2\right] = 0$$

This yields the equilibrium values:

$$\begin{aligned} &\Psi = 0, \quad T > T_{\mathrm{c}}, \\ &|\Psi|^2 = -\frac{\alpha\tau}{b} \equiv \Psi_0^2, \quad T < T_{\mathrm{c}} \end{aligned} \tag{17.2}$$

Substituting the equilibrium value of $|\Psi|^2 = \Psi_0^2$ into (17.2) and comparing with (15.5), we have

$$\Omega_{\mathrm{n}} - \Omega_{\mathrm{s}} = \frac{(\alpha\tau)^2}{2b} = \frac{H_{\mathrm{cm}}^2}{8\pi} \tag{17.3}$$

In the present chapter we use the notation $\boldsymbol{H}_{\mathrm{cm}}$ for the thermodynamic critical field of a bulk superconductor in order to distinguish it from the critical field of a thin film and also from other critical fields that will be introduced later. Comparing eq. (17.3) with formula (16.55), we see that the Ginzburg-Landau theory gives a correct temperature dependence of H_{cm}. From this comparison we can also derive a microscopic formula for a certain combination of the coefficients α and b :

$$\frac{\alpha^2}{b} = \frac{4}{7\zeta(3)}T_{\mathrm{c}}^2\frac{mp_0}{\hbar^3} = \frac{4\pi^2}{7\zeta(3)}\nu(\mu)T_{\mathrm{c}}^2 \tag{17.4}$$

Suppose now that an external magnetic field is applied to the superconductor. In this case, both the field in the superconductor and Ψ depend on the coordinates. Here one has to examine the total free energy of the entire superconductor. The energy of the field per unit volume is $H^2/8\pi$. Moreover, one has to add the energy associated with the inhomogeneity of Ψ. We will assume that the variation of Ψ in space occurs slowly. This permits one to consider only the correction $|\nabla\Psi|^2$ to the free energy. However, the order parameter Ψ has the meaning of the wave function of Cooper pairs. In view of this, the momentum operator -i $\hbar\nabla$ must necessarily is independent of the coordinates. Since Ψ is a complex quantity and Ω is real, the expansion is carried out in powers of $|\Psi|^2$. Thus, we have (for unit volume)

$$\Omega_{\mathrm{s}} = \Omega_{\mathrm{n}} + a|\Psi|^2 + \frac{\mathrm{l}}{2}\,\mathrm{b}|\Psi|^4 + \cdots . \tag{17.1}$$

Since the theory is built up for the vicinity of T_c, the coefficients a and b can be expanded in $\tau = (T - T_c)/T_c$ and only the first nonvanishing terms need be retained. Since the minimum of Ω_s corresponds to $\Psi = 0$ above T_c and $\Psi \neq 0$ below T_c, the coefficient a changes sign at the transition point; therefore, $a = \alpha\tau$, where $\alpha > 0$. From the condition that $\Psi = 0$ must correspond to the minimum of Ω_s at the transition point too, we have

$$b \approx b(T_c) > 0.$$

Differentiating with respect to Ψ^*, we obtain the condition of the minimum of Ω_s :

$$\Psi\left[\alpha\tau + |\Psi|^2\right] = 0.$$

This yields the equilibrium values:

$$\begin{aligned} &\Psi = 0, \quad T > T_c, \\ &|\Psi|^2 = -\frac{\alpha\tau}{b} \equiv \Psi_0^2, \quad T < T_c. \end{aligned} \tag{17.2}$$

Substituting the equilibrium value of $|\Psi|^2 = \Psi_0^2$ into (17.2) and comparing with (15.5), we have

$$\Omega_n - \Omega_s = \frac{(\alpha\tau)^2}{2b} = \frac{H_{cm}^2}{8\pi} \tag{17.3}$$

In the present chapter we use the notation H_{cm} for the thermodynamic critical field of a bulk superconductor in order to distinguish it from the critical field of a thin film and also from other critical fields that will be introduced later. Comparing eq. (17.3) with formula (16.55), we see that the Ginzburg-Landau theory gives a correct temperature dependence of H_{cm}. From this comparison we can also derive a microscopic formula for a certain combination of the coefficients α and b :

$$\frac{\alpha^2}{b} = \frac{4}{7\zeta(3)} T_c^2 \frac{mp_0}{\hbar^3} = \frac{4\pi^2}{7\zeta(3)} \nu(\mu) T_c^2 \tag{17.4}$$

Suppose now that an external magnetic field is applied to the superconductor. In this case, both the field in the superconductor and Ψ depend on the coordinates. Here one has to examine the total free energy of the entire superconductor. The energy of the field per unit volume is $\boldsymbol{H^2/8\pi}$. Moreover, one has to add the energy associated with the inhomogeneity of Ψ. We will assume that the variation of Ψ in space occurs slowly. This permits one to consider only the correction $|\nabla\Psi|^2$ to the free energy. However, the order parameter Ψ has the meaning of the wave function of Cooper pairs. In view of this, the momentum operator $-i\hbar\nabla$ must necessarily is independent of the coordinates. Since Ψ is a complex quantity and Ω is real, the expansion is carried out in powers of $|\Psi|^2$. Thus, we have (for unit volume)

$$\Omega_s = \Omega_n + a|\Psi|^2 + \frac{1}{2}\, b|\Psi|^4 + \cdots . \tag{17.1}$$

Since the theory is built up for the vicinity of T_c, the coefficients a and b can be expanded in $\tau = (T - T_c)/T_c$ and only the first nonvanishing terms need be retained. Since the minimum of Ω_s corresponds to $\Psi = 0$ above T_c and $\Psi \neq 0$ below T_c, the coefficient a changes sign at the transition point; therefore, $a = \alpha\tau$, where $\alpha > 0$. From the condition that $\Psi = 0$ must correspond to the minimum of Ω_s at the transition point too, we have

$$b \approx b(T_c) > 0.$$

Differentiating with respect to Ψ^*, we obtain the condition of the minimum of Ω_s :

$$\Psi\left[\alpha\tau + |\Psi|^2\right] = 0.$$

This yields the equilibrium values:

$$\begin{aligned} &\Psi = 0, \quad T > T_c, \\ &|\Psi|^2 = -\frac{\alpha\tau}{b} \equiv \Psi_0^2, \quad T < T_c \end{aligned} \tag{17.2}$$

Substituting the equilibrium value of $|\Psi|^2 = \Psi_0^2$ into (17.2) and comparing with (15.5), we have

$$\Omega_\mathrm{n} - \Omega_\mathrm{s} = \frac{(\alpha\tau)^2}{2b} = \frac{H_\mathrm{cm}^2}{8\pi} \tag{17.3}$$

In the present chapter we use the notation H_cm for the thermodynamic critical field of a bulk superconductor in order to distinguish it from the critical field of a thin film and also from other critical fields that will be introduced later. Comparing eq. (17.3) with formula (16.55), we see that the Ginzburg-Landau theory gives a correct temperature dependence of $\boldsymbol{H}_\mathrm{cm}$. From this comparison we can also derive a microscopic formula for a certain combination of the coefficients α and b :

$$\frac{\alpha^2}{b} = \frac{4}{7\zeta(3)} T_\mathrm{c}^2 \frac{mp_0}{\hbar^3} = \frac{4\pi^2}{7\zeta(3)} \nu(\mu) T_\mathrm{c}^2. \tag{17.4}$$

Suppose now that an external magnetic field is applied to the superconductor. In this case, both the field in the superconductor and Ψ depend on the coordinates. Here one has to examine the total free energy of the entire superconductor. The energy of the field per unit volume is $H^2/8\pi$. Moreover, one has to add the energy associated with the inhomogeneity of Ψ. We will assume that the variation of Ψ in space occurs slowly. This permits one to consider only the correction $|\nabla\Psi|^2$ to the free energy. However, the order parameter Ψ has the meaning of the wave function of Cooper pairs. In view of this, the momentum operator $-\mathrm{i}\hbar\nabla$ must necessarily be included in the combination $-\mathrm{i}\hbar\nabla - (2e/c)A$, where A is the vector potential*; we took into account that the pair has a charge $2e$.

In order to impart the ordinary form to the new term in the free energy, we write it as the kinetic energy of a particle of mass $2m$ **:

$$\frac{1}{4m}|(-\mathrm{i}\hbar\nabla - (2e/c))A\Psi|^2.$$

Thus, we have

$$\begin{aligned} \int \Omega_\mathrm{s}\, \mathrm{d}V = &\int \Omega_\mathrm{n}^{(0)} \mathrm{d}V \\ &+ \int \left\{ \alpha\tau|\Psi|^2 + \frac{1}{2}b|\Psi|^4 + \frac{1}{4m}\left| \left(-\mathrm{i}\hbar\nabla - \frac{2e}{c}A\right)\Psi \right|^2 + \frac{H^2}{8\pi} \right\} \mathrm{d}V \end{aligned} \tag{17.5}$$

(here we have introduced the notation $\Omega_\mathrm{n}^{(0)}$ for the free energy of the normal phase without the field).

In order to obtain the minimum of the total free energy, we vary expression (17.5) with respect to Ψ^*. In such a case, we obtain

$$\int \left\{ \alpha\tau\Psi\delta\Psi + b|\Psi|^2\delta\Psi^* \right.$$
$$\left. + \frac{1}{4m}\left(-\mathrm{i}\hbar\nabla - \frac{2e}{c}A\right)\Psi\left(\mathrm{i}\hbar\nabla - \frac{2e}{c}A\right)\delta\Psi^* \right\} \mathrm{d}V = 0$$

In order to get rid of $\nabla\delta\Psi^*$, we integrate the corresponding term by parts and use Gauss' theorem. We find

$$\frac{\mathrm{i}\hbar}{4m}\int \delta\Psi^* n\left(-\mathrm{i}\hbar\nabla - \frac{2e}{c}A\right)\Psi \mathrm{d}S$$
$$+ \frac{1}{4m}\int \delta\Psi^*\left(-\mathrm{i}\hbar\nabla - \frac{2e}{c}A\right)^2\Psi \ \mathrm{d}V$$

where the integration in the first term runs over the surface of the superconductor (n is the unit vector of the normal).

The variation of $\delta\Psi^*$ is arbitrary. Assuming that $\delta\Psi^* = 0$ at the surface and equating to zero the factor at $\delta\Psi^*$ in the integral over the volume, we obtain the equation for Ψ :

$$\frac{1}{4m}\left(-\mathrm{i}\hbar\nabla - \frac{2e}{c}A\right)^2\Psi + \alpha\tau\Psi + b|\Psi|^2\Psi = 0. \tag{17.6}$$

be included in the combination - i $\hbar\nabla - (2e/c)A$, where A is the vector potential*; we took into account that the pair has a charge $2e$.

In order to impart the ordinary form to the new term in the free energy, we write it as the kinetic energy of a particle of mass $2m$ ** :

$$\frac{1}{4m}|(-\mathrm{i}\hbar\nabla - (2e/c))A\Psi|^2.$$

Thus, we have

$$\int \Omega_\mathrm{s}\ \mathrm{d}V = \int \Omega_\mathrm{n}^{(0)}\mathrm{d}V$$
$$+ \int \left\{ \alpha\tau|\Psi|^2 + \frac{1}{2}b|\Psi|^4 + \frac{1}{4m}\left|\left(-\mathrm{i}\hbar\nabla - \frac{2e}{c}A\right)\Psi\right|^2 + \frac{H^2}{8\pi} \right\} \mathrm{d}V \tag{17.5}$$

(here we have introduced the notation $\Omega_\mathrm{n}^{(0)}$ for the free energy of the normal phase without the field).

In order to obtain the minimum of the total free energy, we vary expression (17.5) with respect to Ψ^*. In such a case, we obtain

$$\int \left\{ \alpha\tau\Psi\delta\Psi + b|\Psi|^2\delta\Psi^* \right.$$
$$\left. + \frac{1}{4m}\left(-\mathrm{i}\hbar\nabla - \frac{2e}{c}A\right)\Psi\left(\mathrm{i}\hbar\nabla - \frac{2e}{c}A\right)\delta\Psi^* \right\} \mathrm{d}V = 0$$

- Recall that the theory must be invariant under a gauge transformation of the vector potential $A \to A + \nabla\varphi$. In the expression $[-\mathrm{i}\hbar\nabla - (2e/c)A]\Psi$ this is provided by the fact that $\nabla\varphi$ is compensated for by the change in the phase of the function Ψ.

**The mass m in this term is quite arbitrary, but it is convenient to take it to be equal to the mass of the electron (see below).

In order to get rid of $\nabla\delta\Psi^*$, we integrate the corresponding term by parts and use Gauss' theorem. We find

$$\frac{\mathrm{i}\hbar}{4m}\int \delta\Psi^* n\left(-\mathrm{i}\hbar\nabla-\frac{2e}{c}A\right)\Psi \mathrm{d}S + \frac{1}{4m}\int \delta\Psi^*\left(-\mathrm{i}\hbar\nabla-\frac{2e}{c}A\right)^2\Psi\ \mathrm{d}V$$

where the integration in the first term runs over the surface of the superconductor (n is the unit vector of the normal).

The variation of $\delta\Psi^*$ is arbitrary. Assuming that $\delta\Psi^*=0$ at the surface and equating to zero the factor at $\delta\Psi^*$ in the integral over the volume, we obtain the equation for Ψ :

$$\frac{1}{4m}\left(-\mathrm{i}\hbar\nabla-\frac{2e}{c}A\right)^2\Psi+\alpha\tau\Psi+b|\Psi|^2\Psi=0. \tag{17.6}$$

If now we assume $\delta\Psi^*$ to be arbitrary at the surface of the superconductor, the surface integral will give the following boundary condition:

$$n\left(-\mathrm{i}\hbar\nabla-\frac{2e}{c}A\right)\Psi\Big|_{\mathrm{b}}=0 \tag{17.7}$$

Variation of (17.5) with respect to $\delta\Psi$ gives an equation and a boundary condition which are complex-conjugate to (17.6) and (17.7).

Now we vary (17.5) with respect to the vector potential $\boldsymbol{A}$, assuming that $\boldsymbol{H}=\operatorname{rot}\boldsymbol{A}$. The variation of H^2 gives $2\operatorname{rot}A\operatorname{rot}\delta A$. We may use the formula $\operatorname{div}[ab]=b\operatorname{rot}a-a\operatorname{rot}b$. This yields $2\delta A\operatorname{rot}\operatorname{rot}A+2\operatorname{div}[\delta A\operatorname{rot}A]$. The volume integral of div is transformed to a surface integral and vanishes. Equating the variation to zero, we find

$$\operatorname{rot}\operatorname{rot}A=\operatorname{rot}H=\frac{4\pi}{c}j, \tag{17.8}$$

$$j=-\frac{ie\hbar}{2m}\left(\Psi^*\nabla\Psi-\Psi\nabla\Psi^*\right)-\frac{2e^2}{mc}|\Psi|^2A. \tag{17.9}$$

Equation (17.8) is a Maxwell equation. The boundary condition is the specification of the field at the superconductor surface. Expression (17.9) corresponds to the quantum-mechanical current in magnetic field if the wave function is equal to Ψ, the charge is $2e$ and the mass $2m$.

We now pass over to new units which will allow us to drop most of the constants in (17.6)-(17.9). We introduce the following notations:

$$\begin{array}{ll} \Psi'=\frac{\Psi}{\Psi_0}, & H'=\frac{H}{H_{\mathrm{cm}}\sqrt{2}},\\ r'=\frac{r}{\delta}, & \delta=\sqrt{\frac{2mc^2}{4\pi\Psi_0^2(2e)^2}},\\ A'=\frac{A}{H_{\mathrm{cm}}\sqrt{2}\delta}, & H_{\mathrm{cm}}=\frac{2\sqrt{\pi}\alpha\tau}{b^{1/2}},\\ \Psi_0^2=\alpha\frac{|\tau|}{b}. & . \end{array} \tag{17.10}$$

- Recall that the theory must be invariant under a gauge transformation of the vector potential $A\to A+\nabla\varphi$. In the expression $[-\mathrm{i}\hbar\nabla-(2e/c)A]\Psi$ this is provided by the fact that $\nabla\varphi$ is compensated for by the change in the phase of the function Ψ.
  ** The mass m in this term is quite arbitrary, but it is convenient to take it to be equal to the mass of the electron (see below).

As a result, the equations become (we omit the primes in the new quantities):

$$\left(-\frac{i\nabla}{x} - A\right)^2 \Psi - \Psi + |\Psi|^2\Psi = 0, \tag{17.6'}$$

$$n\left(-\frac{i\nabla}{x} - A\right)\Psi\Big|_{\mathrm{b}} = 0, \tag{17.7'}$$

$$\operatorname{rot}\operatorname{rot} A = -\frac{i}{2x}\left(\Psi^*\nabla\Psi - \Psi\nabla\Psi^*\right) - |\Psi|^2 A. \tag{17.8'}$$

Equations (17.6'), (17.7') and (17.8') contain only one constant, x, which is called the Ginzburg-Landau parameter; it is defined as

$$x = 2^{3/2} e H_{\mathrm{cm}} \frac{\delta^2}{\hbar c}. \tag{17.11}$$

This is the same constant introduced in section 16.9 (formula 16.95). This point will be discussed later.

Let us consider the simplest problem: the penetration of a weak magnetic field into the bulk of a superconductor with a planar boundary. Let the superconductor occupy the half-space $x = 0$. The field is applied to it along the z axis. The field penetrates the superconductor and decreases rapidly in the bulk, i.e., it depends on x. Therefore, we choose the vector potential A along the direction y. In this case,

$$H(x) = \frac{\mathrm{d}A_y}{\mathrm{d}x}.$$

It is natural to assume that Ψ is also dependent only on x. From eqs. (17.6) and (17.7) we obtain

$$-x^2\frac{d^2\Psi}{dx^2} - \Psi + A^2\Psi + |\Psi|^2\Psi = 0,$$

$$\frac{d\Psi}{dx}\Big|_b = 0.$$

We assume that $x < 1$. Then we obtain $\Psi = \text{const}$. From the condition in the bulk of the superconductor it follows that $|\Psi|^2 = 1$. The function Ψ may be chosen real. Equation (17.8') yields

$$\frac{\mathrm{d}^2 A}{\mathrm{d}x^2} - A = 0.$$

Differentiating with respect to x, we derive a similar equation for H. The solution that satisfies the boundary condition $H = H_0$ is $H = H_0\mathrm{e}^{-x}$ or, in conventional units,

$$H = H_0\mathrm{e}^{-x/\delta}, \tag{17.12}$$

where δ is defined in (17.10). But we know that this must give the London penetration depth near T_c. Choosing m in (17.10) to be equal to the mass of the electron, we find that $|\Psi_0|^2 = \frac{1}{2}n_s$, i.e., the number of Cooper pairs. Comparing (17.2) with the BCS formula (16.92), we find that

$$\frac{\alpha}{b} = n_{\mathrm{c}}. \tag{17.13}$$

Using formulae (17.13) and (17.14), we can define α and $b\,(n_{\mathrm{e}} = p_0^3/3\pi^2\hbar^3)$:

$$\alpha = \frac{12\pi^2}{7\zeta(3)}\frac{mT_c^2}{p_0^2}, \quad b = \frac{\alpha}{n_e}. \tag{17.14}$$

Substituting formulae (16.55) for $H_{cm}(T)$ and (16.93) for $\delta(T)$ into the expression for x (17.11), we obtain

$$x = 3\left(\frac{2}{7\zeta(3)}\right)^{1/2}\left(\frac{\pi\hbar}{v}\right)^{3/2}\frac{cT_c}{\hbar p_0}. \tag{17.15}$$

The constant x may be expressed through the ratio of $\delta_L(0) = (mc^2/4\pi n_e e^2)^{1/2}$ and $\xi_0 = (\gamma/\pi^2)\,\hbar v/T_c$ (see formula 16.82). As a result, we obtain formula (16.95).

Thus, all the constants that appear in the theory have a microscopic interpretation. Only the microscopic meaning of the order parameter Ψ remains unclear. However, this can be found by comparison with the microscopic theory. It is rather evident that Ψ is proportional to Δ. These two quantities are complex scalars in the general case, both are equal to zero at $T > T_c$ and proportional to $|\tau|^{1/2}$ at $T_c - T < T_c$. Therefore it is sufficient to compare the coefficients at $|\tau|^{1/2}$ for Ψ (17.2) and for Δ when $T \to T_c$ (16.33). From this we get

$$\Psi(r) = \frac{1}{\pi}\left(\frac{7}{8}\zeta(3)\right)^{1/2} n_e^{1/2}\frac{\Delta(r)}{T_c}. \tag{17.16}$$

The Ginzburg-Landau theory refers also to superconductors that contain impurities; such superconductors are usually called superconducting alloys or dirty superconductors in the literature. As has already been remarked in section 16.9, impurities in a small concentration exert but a slight effect on the thermodynamic properties, i.e., on T_c, Δ, and H_{cm}, but at $l < \xi$ they appreciably change the penetration depth. Inserting expressions (16.55) for H_{cm} and (16.100) for δ with $T \to T_c$ into the general formula (17.11) for x, we obtain formula (16.101), where $l = v\tau_{tr}$.

For convenience of comparison with experiment x may be expressed via the conductivity of a normal metal $\sigma = n_e e^2 l/p_0$ and the coefficient in the linear law of heat capacity $C_n = \gamma_c T, \gamma_c = p_0 m/3\hbar^3$ (Gor'kov 1959a,b):

$$x = \left(\frac{21\zeta(3)}{2\pi}\right)^{1/2}\frac{ce}{\pi^3}\frac{\gamma_c^{1/2}}{\sigma}. \tag{17.17}$$

In conventional units, when the temperature is measured in Kelvin and the heat capacity in erg/cm$^3\cdot$ K, our γ_c is measured in $\left(\text{erg}\cdot\text{cm}^{-3}\cdot\ \text{K}^{-2}\right)/k_B^2$, where k_B is Boltzmann's constant. Substituting the numerical values of c and e and expressing the resistivity $\sigma^{-1} = \rho$ in ohm ·cm, we obtain

$$\varkappa = 7.5\times 10^3\left[\gamma_c\left(\text{erg}\cdot\ \text{cm}^{-3}\cdot\ \text{K}^{-2}\right)\right]^{1/2}\rho(\text{ohm}\cdot\ \text{cm}). \tag{17.17'}$$

Using relation (17.4) derived from H_{cm}, which we assume to be constant, and expressions (16.100) and (17.10) for δ together with formula (16.33) for Δ (which
remains unchanged too), we find the coefficients α and b and the relationship between Δ and Ψ :

$$\alpha = \frac{6}{\pi}\frac{\hbar T_c}{\tau_{tr}}\frac{m}{p_0^2}, \quad \frac{\alpha}{b} = \frac{2\pi^3}{7\zeta(3)}\frac{T_c\tau_{tr}}{\hbar}n_e \tag{17.18}$$

$$\Psi(r) = \left(\frac{1}{4}\pi\right)^{1/2}\left(\frac{n_e\tau_{tr}}{hT_c}\right)^{1/2}\Delta(r)$$

Inserting these expressions into eq. (17.6), we obtain the form of this equation that is frequently used for alloys:

$$\frac{\pi D\hbar}{8T_{\rm c}}\left(\nabla-\frac{2{\rm i}e}{\hbar c}A\right)^2\Delta+\left(\frac{T_{\rm c}-T}{T_{\rm c}}\right)\Delta-\left(\frac{7\zeta(3)}{8\pi^2T_{\rm c}^2}\right)|\Delta|^2\Delta=0, \qquad (\prime\prime)$$

where $D=\frac{1}{3}v^2\tau_{\rm tr}$ is the diffusion coefficient (section 3.5). The corresponding expression for the current is

$$j=-{\rm i}\frac{\pi e\nu D}{4T_{\rm c}}\left(\frac{1}{2}\left(\Delta^*\nabla\Delta-\Delta\nabla\Delta^*\right)-\frac{2ie}{\hbar c}A|\Delta|^2\right) \qquad (\prime)$$

where $\nu=p_0m/\pi^2\hbar^3$ is the density of states.
For subsequent applications we transform the expression for the free energy (17.5). Passing to the reduced quantities and using formulas (17.10), we have

$$\int\Omega_{\rm s}\,{\rm d}V=\int\Omega_{\rm n}^{(0)}{\rm d}V + \frac{H_{\rm cm}^2}{4\pi}\int\left\{-|\Psi|^2+\frac{1}{2}|\Psi|^4+\left|\left(-{\rm i}\frac{\nabla}{\varkappa}-A\right)\Psi\right|^2+H^2\right\}{\rm d}V. \qquad (17.19)$$

As before, in the derivation of the equations, we integrate the term with $\nabla\Psi^*$ by parts. Here the surface integral vanishes due to the boundary condition (17.7) and in the volume integral left we use the fact that Ψ satisfies eq. (17.6'). As a result, we have

$$\int\Omega_{\rm s}\,{\rm d}V=\int\Omega_{\rm n}^{(0)}{\rm d}V+\frac{H_{\rm cm}^2}{4\pi}\int\left(H^2-\frac{1}{2}|\Psi|^4\right){\rm d}V \qquad (\prime)$$

In what follows we will be interested in the transition from the normal to the superconducting state under the influence of an external field. For a cylindrical geometry the free energy in a given external field is obtained by subtracting $\boldsymbol{H}_0\boldsymbol{B}/4\pi$, where $\boldsymbol{H}_0$ is the external field and $\boldsymbol{B}$ is the induction equal to the average field in the sample, $\boldsymbol{B}=\boldsymbol{V}^{-1}\int\boldsymbol{H}\,{\rm d}V$ (see Appendix III). For the normal phase $\Omega_{{\rm n}H}=\Omega_{\rm n}^{(0)}-H_0^2/8\pi$.

Thus, we obtain (in reduced units):

$$\int\left(\Omega_{{\rm s}H}-\Omega_{{\rm n}H}\right){\rm d}V=\frac{H_{\rm cm}^2}{4\pi}\int\left[\left(H-H_0\right)^2-\frac{1}{2}|\Psi|^4\right]{\rm d}V \qquad (17.20)$$

In concluding this section we evaluate the size of the region where the GinzburgLandau theory based on the Landau approximation for second-order phase transitions becomes inapplicable because of the fluctuational effects. According to Appendix II, the range of validity of the Landau approximation is determined by condition (AII.20):

$$1>|\tau|>\frac{b^2T_c^2}{\alpha c^3},$$

where $\tau=\left(T-T_{\rm c}\right)/T_{\rm c}$. In the Ginzburg-Landau theory the coefficients α and b have the same meaning as in the model considered in Appendix II, and the role of the parameter c (the coefficient in front of $\nabla\varphi$, where φ is the real scalar order parameter) is played by $\hbar^2/m$. Hence,

$$1>|\tau|>\frac{m^3b^2T_c^2}{\alpha\hbar^6}$$

Substituting α and b for a pure superconductor, we obtain in accordance with (17.14)

$$1 > |\tau| > \left(\frac{T_c}{\varepsilon_F}\right)^4, \tag{17.21}$$

where $\varepsilon_F \sim p_0^2/m$ is the Fermi energy. Usually, T_c/ε_F does not exceed 10^{-3}, i.e., the quantity that stands on the right is less than 10^{-12}, which is many orders of magnitude smaller than the fluctuations in temperature that can be controlled in experiments.

For superconductors containing impurities at $l < \xi$ in accordance with (17.18) we have

$$1 > |\tau| > \left(\frac{\hbar}{\tau_{tr}}\right)^3 \frac{T_c}{\varepsilon_F^4}. \tag{17.22}$$

This requirement is less stringent than (17.21), but it also practically rules out the fluctuational region.

From this it follows that the fluctuations are unimportant in the thermodynamics of bulk superconductors. The physical cause for this is the large correlation length, as has already been pointed out at the end of section 16.9*. Nevertheless, situations are possible where the role of fluctuations increases noticeably, and these are responsible for the observed effects. This occurs for the kinetic effects in small objects, say for the conductivity of thin films and filaments. This point will be discussed in section 19.6.

Thus, the Ginzburg-Landau theory can be applied practically up to the very critical temperature. What is the range of its validity on the low-temperature side? One of these conditions is known: this is $|\tau| < 1$. The other is $\delta < \xi_0$, i.e., the London

region. The latter can be seen, for example, from the fact that, according to section 16.7, the relation between the current and the field is nonlocal in the general case and changes to the local theory only in the London region. In the Ginzburg-Landau theory the relation between the current and the field is local.

As has been said above, the Ginzburg-Landau equations are the exact limit of the BCS theory at $|\tau| < 1$. We will not give the corresponding derivation here because it is cumbersome (see Gor'kov 1959a, b). We note only that the relation that generalizes formula (16.18) for Δ to the inhomogeneous case $\Delta(r)$ (here we are speaking of $T \to T_c$, i.e., small Δ) is a complex integral relation: the right-hand side contains terms of the type

$$\int K(r, r')\,\Delta(r')\,dV'$$

$$\int K(r, r', r'', r''')\,\Delta(r')\,\Delta(r'')\,\Delta(r''')\,dV'dV''dV'''$$

The distances that are important in the kernels of the integrals are of order ξ_0. On the other hand, the distances over which Δ varies are of order $\xi(T) \sim \hbar v/\Delta(T) > \xi_0$ (at $|\tau| < 1$). This makes it possible to consider the variations of $\Delta(r)$ to be slow and to pass from the integral to differential relations. An analogous situation occurs with the vector potential A if the condition $\delta(T) > \xi_0$ is satisfied.

Both requirements can be expressed in the form of a single relation. For this purpose we use the fact that $\xi_0 \sim \xi(0) \sim \delta_L(0)/x$ and also that $\delta(T) \sim \delta_L(0)|\tau|^{-1/2}$ at $|\tau| < 1$. The condition $\delta(T) > \xi_0$ may be written in the form $|\tau|^{1/2} < x$. Thus, the general condition for the validity of the Ginzburg-Landau theory reads

$$1 - \frac{T}{T_c} < \min\left(\chi^2, 1\right). \tag{17.23}$$

*There are indications that in high- T_c ceramics the fluctuation region is relatively large. Specific-heat data show that its width is ~ 2 K, i.e. $|\tau| \sim 0.02$. This could be due to the small correlation length (~ 30Å) or to the relatively large value of T_c/ε_F. Nevertheless this region is not so large as to make G-L theory inapplicable.

Although we have been speaking all the time of pure superconductors, formula (17.23) is also valid for dirty superconductors.

The Ginzburg-Landau theory is much simpler than the complete BCS theory for superconductors in an external field. Nevertheless, its content has proved to be very rich, since it has made it possible to account for all the basic equilibrium properties of superconductors. In spite of the limitation (17.23), it has turned out that GinzburgLandau theory provides a satisfactory quantitative agreement with experiment even at temperatures well below T_c if all the parameters are expressed in reduced units. This is associated with the slowness of the variation of x with temperature [the function $A(T)$ in eq. (16.97) and the function $B(T)$ in eq. (16.101)].

8.3.2 17.2. Surface energy at the interface between the normal and superconducting phases

Below we will demonstrate the solution of several problems using the GinzburgLandau theory. Consider a case where Ψ and A depend only on a single coordinate,
region. The latter can be seen, for example, from the fact that, according to section 16.7, the relation between the current and the field is nonlocal in the general case and changes to the local theory only in the London region. In the Ginzburg-Landau theory the relation between the current and the field is local.

As has been said above, the Ginzburg-Landau equations are the exact limit of the BCS theory at $|\tau| < 1$. We will not give the corresponding derivation here because it is cumbersome (see Gor'kov 1959a, b). We note only that the relation that generalizes formula (16.18) for Δ to the inhomogeneous case $\Delta(r)$ (here we are speaking of $T \to T_c$, i.e., small Δ) is a complex integral relation: the right-hand side contains terms of the type

$$\int K(\boldsymbol{r}, \boldsymbol{r}') \Delta(\boldsymbol{r}') \, \mathrm{d}V'$$

$$\int K(\boldsymbol{r}, \boldsymbol{r}', \boldsymbol{r}'', \boldsymbol{r}''') \Delta(\boldsymbol{r}') \Delta(\boldsymbol{r}'') \Delta(\boldsymbol{r}''') \, \mathrm{d}V' \mathrm{d}V'' \mathrm{d}V'''$$

The distances that are important in the kernels of the integrals are of order ξ_0. On the other hand, the distances over which Δ varies are of order $\xi(T) \sim \hbar v/\Delta(T) > \xi_0$ (at $|\tau| < 1$). This makes it possible to consider the variations of $\Delta(r)$ to be slow and to pass from the integral to differential relations. An analogous situation occurs with the vector potential A if the condition $\delta(T) > \xi_0$ is satisfied.

Both requirements can be expressed in the form of a single relation. For this purpose we use the fact that $\xi_0 \sim \xi(0) \sim \delta_L(0)/x$ and also that $\delta(T) \sim \delta_L(0)|\tau|^{-1/2}$ at $|\tau| < 1$. The condition $\delta(T) > \xi_0$ may be written in the form $|\tau|^{1/2} < x$. Thus, the general condition for the validity of the Ginzburg-Landau theory reads

$$1 - \frac{T}{T_c} < \min\left(x^2, 1\right). \tag{17.23}$$

Although we have been speaking all the time of pure superconductors, formula (17.23) is also valid for dirty superconductors.

The Ginzburg-Landau theory is much simpler than the complete BCS theory for superconductors in an external field. Nevertheless, its content has proved to be very rich, since it has made it possible to account for all the basic equilibrium properties of superconductors. In spite of the limitation (17.23), it has turned out that GinzburgLandau theory provides a satisfactory quantitative agreement with experiment even at temperatures well below T_c if all the parameters are expressed in reduced units. This is associated with the slowness of the variation of x with temperature [the function $A(T)$ in eq. (16.97) and the function $B(T)$ in eq. (16.101)].

8.3.3 17.2. Surface energy at the interface between the normal and superconducting phases

Below we will demonstrate the solution of several problems using the GinzburgLandau theory. Consider a case where Ψ and A depend only on a single coordinate,
say x, with A being directed perpendicular to x. Here the general equations (17.6'), (17.7') and (17.8') simplify and take the form

$$\frac{1}{x^2}\frac{\mathrm{d}^2\Psi}{\mathrm{d}x^2} + \Psi\left(1 - A^2\right) - \Psi^3 = 0, \tag{17.24}$$

$$\left.\frac{\mathrm{d}\Psi}{\mathrm{d}x}\right|_{\mathrm{b}} = 0, \tag{17.25}$$

$$\frac{\mathrm{d}^2 A}{\mathrm{d}x^2} - \Psi^2 A = 0 \tag{17.26}$$

(it is easy to see that Ψ may be taken to be real).
The integrals of eqs. (17.24) and (17.26) are easily evaluated. To this end, we multiply eq. (17.24) by $\mathrm{d}\Psi/\mathrm{d}x$ and eq. (17.26) by $\mathrm{d}A/\mathrm{d}x$, add up and integrate over x. With the boundary condition in the bulk of the superconductor being taken into account, we get

$$\frac{1}{x^2}\left(\frac{\mathrm{d}\Psi}{\mathrm{d}x}\right)^2 + \left(\frac{\mathrm{d}A}{\mathrm{d}x}\right)^2 + \Psi^2\left(1 - A^2\right) - \frac{1}{2}\Psi^4 = \text{ const. } = \frac{1}{2} \tag{17.27}$$

(the value of the constant is taken from the boundary conditions 17.28).
Let us find the surface energy between the normal and superconducting phases (Ginzburg and Landau 1950). Suppose that as $x \to \infty$ there is a superconducting phase and for $x \to -\infty$ there is a normal phase. We assume that $\boldsymbol{H} \| z, \boldsymbol{A} \| y$ and $H = \mathrm{d}A/\mathrm{d}x$. Then we have the following boundary conditions:

$$\begin{array}{lllll} x \to \infty: & \Psi = 1, & H = A = 0, & \frac{\mathrm{d}\Psi}{\mathrm{d}x} = 0, \\ x \to -\infty: & \Psi = 0, & H = H_0 = \frac{1}{\sqrt{2}}, & \frac{\mathrm{d}\Psi}{\mathrm{d}x} = 0 \end{array} \tag{17.28}$$

(in conventional units $\Psi = 1$ corresponds to Ψ_0 and $H_0 = 1/\sqrt{2}$ corresponds to H_{cm}). Since eqs. (17.24), (17.25) and (17.26) are not integrable in the general case, we will consider the limiting case $x < 1$.

This case corresponds to $\xi \gg \delta$ and is shown in fig. 105. Obviously, the major part of the surface energy arises from the region in which H and A are small. Assuming that $A = H = 0$ in eq. (17.27), we obtain

$$\frac{\mathrm{d}\Psi}{\mathrm{d}x} = \frac{x}{\sqrt{2}}\left(1 - \Psi^2\right). \tag{17.29}$$

The solution of this equation that satisfies the boundary condition $\Psi = 1$ for $x \to \infty$ and decreases towards diminishing x is

$$\Psi = \tanh\left(\frac{xx}{\sqrt{2}}\right). \tag{17.30}$$

Of course, we have to take into account that such a solution becomes incorrect in the region where the field penetrates, but this region makes a small contribution to surface energy. For convenience, we have chosen the origin at point $x = 0$, where $\Psi \approx 0$ (the boundary A in fig. 105).

Consider now the formula for the free energy difference (17.30). The integrand vanishes as $x \to \infty$ and also with $x \to -\infty$. A contribution comes only from the transition region. It is this region that corresponds to the excess energy associated with the boundary, i.e., σ_{ns} . Substituting into eq. (17.20) $H_0 = 1/\sqrt{2}, H = 0$ and Ψ according to (17.30), we obtain

$$\begin{aligned}
\sigma_{\text{ns}} &= \frac{H_{\text{cm}}^2}{8\pi} \int_0^\infty \left(1 - \Psi^4\right) \mathrm{d}x \\
&= \frac{H_{\text{cm}}^2}{8\pi} \int_0^\infty \left(1 - \tanh^4\left(\frac{xx}{\sqrt{2}}\right)\right) \mathrm{d}x \\
&= \frac{H_{\text{cm}}^2}{8\pi} \int_0^\infty \cosh^{-2}\left(\frac{xx}{\sqrt{2}}\right)\left(1 + \tanh^2\left(\frac{xx}{\sqrt{2}}\right)\right) \mathrm{d}x \\
&= \frac{H_{\text{cm}}^2}{8\pi} \frac{4\sqrt{2}}{3x}.
\end{aligned} \tag{17.31}$$

The lower limit of the integral over x is chosen where Ψ becomes small and the field begins to penetrate, i.e., $x = 0$. In conventional units we have

$$\delta_{\text{ns}} = \frac{H_{\text{cm}}^2}{8\pi} \frac{4\sqrt{2}\delta}{3x}. \tag{17.32}$$

For $x \geqslant 1$ the calculation of σ_{ns} is possible only by a numerical method. It turns out that σ_{ns} vanishes at $x = 1/\sqrt{2}$, and becomes negative at larger values of x. Since this contradicted the superconductivity picture known by the time the GinzburgLandau theory was developed (1950), this case was not considered. The experimental data on the size of the layers in the intermediate state (section 15.3) make it possible to determine x. For pure superconductors the values of x obtained are small: 0.16 for mercury, 0.15 for tin, and 0.026 for aluminum*.

Since the vanishing of σ_{ns} at $x = 1/\sqrt{2}$ is important, we shall give here a rigorous proof (Lifshitz and Pitaevskii 1978). Consider the complete free-energy expression (17.20) at $H_0 = H_{\text{cm}}$, or in reduced units $H_0 = 1/\sqrt{2}$. Evidently, the integrand and, hence, the whole integral turns to zero at

$$H = \frac{\mathrm{d}A}{\mathrm{d}x} = \frac{1 - \Psi^2}{\sqrt{2}}.$$

Substituting this expression into eq. (17.26), we find

$$\frac{\mathrm{d}\Psi}{\mathrm{d}x} = -\frac{A\Psi}{\sqrt{2}}.$$

It is easy to see that these formulae satisfy eq. (17.27) at $x = 1/\sqrt{2}$.

8.3.4 17.3. The critical field and magnetization of a thin film. Supercooling and superheating

Since $x < 1$ for many pure superconductors, it will be reasonable to solve the problems in this approximation, which considerably facilitates calculations. We shall consider the question

- It is easier to determine x experimentally from the supercooling field (section 18.4), though, strictly speaking, there is a risk of obtaining overestimated values of x.

of the properties of a thin superconducting film placed in a parallel magnetic field H_0 (Ginzburg and Landau 1950, Ginzburg 1952). Suppose $H \| z$ and the film occupies a volume $-\frac{1}{2}d < x < \frac{1}{2}d$. Equation (17.24) is rewritten in the form

$$\frac{\mathrm{d}^2\Psi}{\mathrm{d}x^2} = \varkappa^2\Psi\left(A^2 - 1 + \Psi^2\right). \tag{17.33}$$

At $x \ll 1$ in the zeroth approximation we neglect the right-hand side. As a result, we have (with eq. 17.25 taken into account):

$$\frac{\mathrm{d}^2\Psi}{\mathrm{d}x^2} = 0 \quad \text{and} \quad \left.\frac{\mathrm{d}\Psi}{\mathrm{d}x}\right|_{x=\pm\frac{1}{2}d} = 0.$$

This gives

$$\Psi = \text{ const.} \tag{17.34}$$

Substituting this, as yet unknown, constant into eq. (17.26) and using $H = \mathrm{d}A/\mathrm{d}x$ and the boundary condition $H\left(\pm\frac{1}{2}d\right) = H_0$, we get

$$H = H_0\frac{\cosh(\Psi x)}{\cosh\left(\frac{1}{2}\Psi d\right)} \tag{17.35}$$

$$A = \frac{H_0}{\Psi}\frac{\sinh(\Psi x)}{\cosh\left(\frac{1}{2}\Psi d\right)} \tag{17.36}$$

Let us consider eq. (17.33) in the next approximation. Substituting $\Psi + \Psi_1$ into it, we have

$$\frac{\mathrm{d}^2\Psi_1}{\mathrm{d}x^2} = \chi^2\Psi\left(A^2 - 1 + \Psi^2\right).$$

For this inhomogeneous equation to have a solution, it is necessary that the righthand side be orthogonal to the solution of a homogeneous equation with correct boundary conditions; such a solution is $\Psi_1 = \text{const}$. Hence,

$$\int_{-\frac{1}{2}d}^{\frac{1}{2}d}\left(A^2 - 1 + \Psi^2\right)\mathrm{d}x = 0 \tag{17.37}$$

whence we find the relation between Ψ and H_0 :

$$H_0^2 = \frac{2\Psi^2\left(1-\Psi^2\right)\cosh^2\left(\frac{1}{2}\Psi d\right)}{(\sinh(\Psi d)/\Psi d) - 1} \tag{17.38}$$

This relation is valid at any H_0 and gives an implicit expression for Ψ in terms of $\boldsymbol{H}_0$. From this we can find the magnetization of the film (in units of $\boldsymbol{H}_{\mathrm{cm}}\sqrt{2}$):

$$\begin{aligned} 4\pi M = B - H_0 &= \frac{1}{d}\int_{-\frac{1}{2}d}^{\frac{1}{2}d} H\ \mathrm{d}x - H_0 \\ &= -H_0\left[1 - \frac{\tanh\left(\frac{1}{2}(\Psi d)\right)}{\frac{1}{2}\Psi d}\right]. \end{aligned} \tag{17.39}$$

At $\Psi d > 1, 4\pi M = -H_0$, which corresponds to the Meissner effect - the nonpenetration of the field into the superconductor. If $\Psi d < 1$, then from (17.39) and (17.38) we find

$$4\pi M \approx -\frac{1}{12} H_0 \, \mathrm{d}^2\Psi^2, \quad H_0^2 \approx \frac{12\,(1-\Psi^2)}{d^2}, \tag{17.40}$$

from which we obtain

$$4\pi M \approx -\frac{1}{12} H_0 d^2 \left(1 - \frac{H_0^2 d^2}{12}\right). \tag{17.41}$$

For further applications we will find the free-energy difference for the superconducting and normal states in a given external field H_0 and a given $\Psi = \text{const}$. without using the equation for Ψ and relation (17.38) which follows from it. This means that we are dealing with a nonequilibrium state characterized by some constant Ψ. Adding $-\mathrm{H}_0\ \mathrm{B}/4\pi + \mathrm{H}_0^2/8\pi$ to (17.19) and passing to the reduced quantities, we obtain

$$\int_{-\frac{1}{2}d}^{\frac{1}{2}d} (\Omega_{\mathrm{sH}} - \Omega_{\mathrm{nH}})\, \mathrm{d}x = \frac{H_{\mathrm{cm}}^2}{4\pi} \int_{-\frac{1}{2}d}^{\frac{1}{2}d} \left[-\Psi^2 + \frac{1}{2}\Psi^4 + (H - H_0)^2 + A^2\Psi^2\right] \mathrm{d}x. \tag{17.42}$$

Note that the minimization of this expression with respect to Ψ^2 leads to the condition (17.38) and substitution of this condition into (17.42) gives the equilibrium formula (17.20).

Let us substitute the formulae for H and A, (17:35) and (17.36), into (17.42). This yields

$$\begin{aligned} &\int_{-\frac{1}{2}d}^{\frac{1}{2}d} (\Omega_{\mathrm{sH}} - \Omega_{\mathrm{nH}}) \frac{\mathrm{d}x}{(H_{\mathrm{cm}}^2/4\pi)\, d} \\ &\quad = H_0^2 \left(1 - \frac{\tanh\left(\frac{1}{2}\Psi d\right)}{\frac{1}{2}\Psi d}\right) - \Psi^2 + \frac{1}{2}\Psi^4. \end{aligned} \tag{17.43}$$

In a field equal to the critical field H_c this expression must be equal to zero. Hence,

$$H_{\mathrm{c}}^2 = \frac{\Psi^2\,(2-\Psi^2)}{2\left(1 - \frac{\tanh\frac{1}{2}\Psi d}{\frac{1}{2}\Psi d}\right)}. \tag{17.44}$$

Formulae (17.38) and (17.39) give the dependence of H_{c} on the film thickness.

Consider the limiting cases. If the film thickness is large, then at the transition point Ψ is close to unity. We put $\Psi = 1 - \varphi$, where $\varphi < 1$. Substituting this into (17.38) yields

$$\varphi \approx \frac{H_0^2}{2d}$$

that is, really $\varphi < 1$. Inserting $\Psi = 1 - \varphi$ into (17.44), we find that

$$H_{\mathrm{c}}^2 \approx \frac{(1-2\varphi)(1+2\varphi)}{2(1-2/d)} \approx \frac{1}{2}\left(1 + \frac{2}{d}\right)$$

Hence,

$$H_{\mathrm{c}} \approx \frac{1}{\sqrt{2}}\left(1 + \frac{1}{d}\right) \tag{17.45}$$

or, in conventional units,

$$H_{\mathrm{c}} \approx H_{\mathrm{cm}}\left(1 + \frac{\delta}{d}\right) \tag{17.46}$$

For a thin film we have already the expansion of formulae (17.38) in d - this is expression (17.40). From (17.44) at $d \ll 1$ we have

$$H_c^2 \approx \frac{6\,(2-\Psi^2)}{d^2} \tag{17.47}$$

Comparing with (17.40), we obtain at the transition point:

$$\Psi = 0, \quad H_c = \frac{2\sqrt{3}}{d} \tag{17.48}$$

or, in conventional units,

$$H_{\rm c} = 2\sqrt{6} H_{\rm cm} \frac{\delta}{d} \tag{17.48'}$$

Thus, while for $d \gg 1$ the transition to the normal state with $\Psi = 0$ occurs from the state with $\Psi \approx 1$ which means a first-order transition for $d < 1$ upon approach to the transition point $\Psi \to 0$, i.e., this is a second-order transition. Here H_c increases with decreasing thickness according to the law $H_c \propto d^{-1}$. The complete plot of $H_{\rm c}/H_{\rm cm}$ against δ/d is given in fig. 108.

Thus, at a certain film thickness the first-order phase transition changes to a second-order phase transition. In order to find out how this occurs, we return to the nonequilibrium formula (17.43). The graph of the function on the right-hand side (we denote it by Ω) versus Ψ^2 at various H_0 is shown in fig. 109, where (a) corresponds to $d/\delta = 4$ and (b) to $d/\delta = 1.6$. From these graphs it is seen that with small thickness Ω has one minimum, which corresponds to $\Psi \neq 0$ for low fields

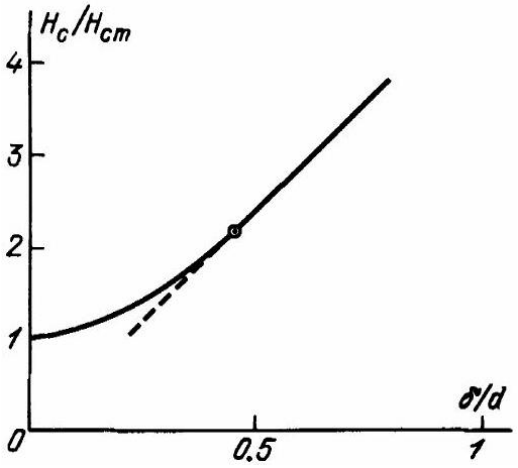


Fig. 108.

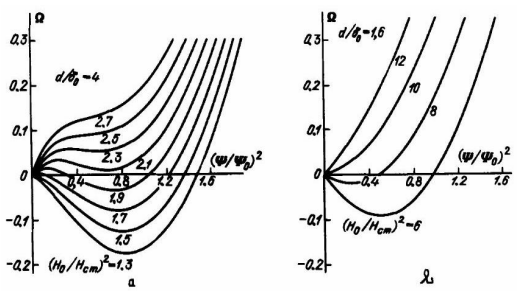


Fig. 109.

and to $\Psi = 0$ for high fields. This is the case of a second-order phase transition. For large film thicknesses in a general case we have two minima, one at $\Psi = 0$ and the other at finite Ψ. The field at which the depths of the minima become equal is just the transition field. This is obviously a first-order phase transition.

The boundary situation between (a) and (b) is the case where both minima merge at the point $\Psi = 0$. Evidently, at this point we have simultaneously $\Psi = 0$, $\mathrm{d}\Omega/\mathrm{d}(\Psi^2) = 0$ and $\mathrm{d}^2\Omega/(\mathrm{d}(\Psi^2))^2 = 0$. From these conditions we obtain

$$d_\mathrm{c} = \sqrt{5} \tag{17.49}$$

or, in conventional units,

$$d_\mathrm{c} = \sqrt{5}\delta \tag{17.49'}$$

(the circle in fig. 108).

In the case of a first-order phase transition, the lower of the two minima corresponds to the equilibrium state, and the higher-lying minimum corresponds to a metastable state. Indeed, a slight deviation of Ψ^2 from the value in the minimum
brings about an increase in free energy. When the magnetic field is changed, the metastable phase persists until the high minimum disappears. The result is that a hysteresis may be observed in an investigation of the transition in increasing and decreasing fields. The occurrence of hysteresis is the simplest way for identifying a first-order transition.

The limiting fields of the retardation of metastable phases are called the supercooling field (retardation of the normal phase) and the superheating field (retardation of the superconducting phase). The superheating field is difficult to observe because at the edges of the specimen there always occurs a concentration of the field lines of force, i.e., an increase in the field strength. Hence, the edges may serve as nucleation sites for the normal phase. It is much easier to observe the supercooling field. The disappearance of the minimum at $\Psi = 0$ occurs at $\mathrm{d}\Omega/\mathrm{d}(\Psi^2) = 0$. As has been pointed out, this condition gives formula (17.38). Substituting $\Psi = 0$ into it leads to

$$H_0 = H_{\mathrm{c}2} = \frac{2\sqrt{3}}{d}, \tag{17.50}$$

which coincides with (17.48). Hence, the critical field formula for a thickness $d < d_\mathrm{c}$ also determines the supercooling field for a thickness $d > d_\mathrm{c}$ (the dashed line in fig. 108).

In fact, this conclusion is valid only for not-too-large film thicknesses. The point is that it has been derived from the formula for the nonequilibrium free energy (17.43) obtained under the assumption $\Psi = \mathrm{const}$. At the same time it is clear that in a bulk specimen the minimal nucleus of the superconducting phase will be localized in a certain region of space, i.e., we shall have $\Psi(r) \neq \mathrm{const}$. (this will be shown in sections 18.2 and 18.4). The assumption of $\Psi = \mathrm{const}$. is evidently valid at $d < \xi$ or, in our units, $d < x^{-1}$, i.e., at $x < 1$ up to thicknesses much larger than d_c. At thicknesses $d \gg \xi$ the supercooling field coincides with the field $H_{\mathrm{c}3}$ (section 18.4.).

The experimental determination of magnetic properties of thin superconducting plates is carried out on films prepared by evaporation of drops of a molten metal on a dielectric substrate. Of course, in such a case it is rather difficult to control the film thickness. In view of this, use may be made of the fact that all the theoretical formulas contain the ratio d/δ, where δ is expressed by formula (18.93), i.e., it increases when the temperature approaches T_c. This makes it possible to use a single film instead of many films, and to carry out measurements at various temperatures. The reduced length that appears in the formulas will then be expressed, according to (16.93), by the following formula:

$$d_{\text{red}} = \frac{\mathrm{d}}{\delta_{\text{L}}(0)} \left[\frac{2\,(T_{\text{c}} - T)}{T_{\text{c}}}\right]^{1/2}.$$

The results of measurements on films deposited by sputtering onto the substrate at room temperature (Zavaritskii 1951) have confirmed the Ginzburg-Landau theory.

8.3.5 17.4. The critical current of a thin wire with $x \ll 1$

We will now consider another problem of the Ginzburg-Landau theory - the critical current of a thin cylindrical wire of radius R^*. According to the Maxwell equation, we have (see eq. 15.23):

$$H_J = \frac{2J}{cR}. \tag{17.51}$$

Hence, the specification of the total current is equivalent to specifying the field at the interface. We introduce cylindrical coordinates: ρ, φ, and z. Since the current flows along z, the field $\boldsymbol{H}$ has only the component $\boldsymbol{H}_\varphi$. We choose the vector potential A along the z axis. Then, from the general equations (17.6'), (17.7') and (17.8') we obtain

$$\frac{\mathrm{d}^2\Psi}{\mathrm{d}\rho^2} = \chi^2\left(A^2 - 1 + \Psi^2\right)\Psi, \tag{17.52}$$

$$\left.\frac{\mathrm{d}\Psi}{\mathrm{d}\rho}\right|_{\rho=R} = 0, \tag{17.53}$$

$$\frac{\mathrm{d}^2 A}{\mathrm{d}\rho^2} + \frac{1}{\rho}\frac{\mathrm{d}A}{\mathrm{d}\rho} - \Psi^2 A = 0, \tag{17.54}$$

$$H = -\frac{\mathrm{d}A}{\mathrm{d}\rho}. \tag{17.55}$$

From eqs. (17.52) and (17.53) it follows that in a first approximation with respect to $x < 1$ we have $\Psi = \text{const}$. Substituting this into eq. (17.54), we find that A is proportional to $I_0(\Psi\rho)$, where I_0 is the Bessel function of imaginary argument. According to (17.55), $H(\rho)$ is proportional to $I_1(\Psi\rho)$; due to the boundary condition we have

$$H = \frac{H_J I_1(\Psi\rho)}{I_1(\Psi R)} \tag{17.56}$$

$$A = -\frac{H_J}{\Psi}\frac{I_0(\Psi\rho)}{I_1(\Psi R)} \tag{17.57}$$

The solvability condition of the equation for the correction to Ψ is analogous to (17.37):

$$\int_0^R \left(A^2 - 1 + \Psi^2\right)\rho\mathrm{d}\rho = 0$$

- In their original work, Ginzburg and Landau (1950) considered a thin film and assumed that the current density varies only in the transverse direction and that along the film width the current is uniform. This does not correspond to reality because the current is redistributed over the film and becomes nonuniform in two directions. It is for this reason that we consider a cylinder with a current.

8.3.6 17.4. The critical current of a thin wire with $x \ll 1$

We will now consider another problem of the Ginzburg-Landau theory - the critical current of a thin cylindrical wire of radius R^*. According to the Maxwell equation, we have (see eq. 15.23):

$$H_J = \frac{2J}{cR}. \tag{17.51}$$

Hence, the specification of the total current is equivalent to specifying the field at the interface. We introduce cylindrical coordinates: ρ, φ, and z. Since the current flows along z, the field $\boldsymbol{H}$ has only the component $\boldsymbol{H}_\varphi$. We choose the vector potential A along the z axis. Then, from the general equations (17.6'), (17.7') and (17.8') we obtain

$$\frac{\mathrm{d}^2\Psi}{\mathrm{d}\rho^2} = \varkappa^2 \left(A^2 - 1 + \Psi^2\right)\Psi, \tag{17.52}$$

$$\left.\frac{\mathrm{d}\Psi}{\mathrm{d}\rho}\right|_{\rho=R} = 0, \tag{17.53}$$

$$\frac{\mathrm{d}^2 A}{\mathrm{d}\rho^2} + \frac{1}{\rho}\frac{\mathrm{d}A}{\mathrm{d}\rho} - \Psi^2 A = 0, \tag{17.54}$$

$$H = -\frac{\mathrm{d}A}{\mathrm{d}\rho}. \tag{17.55}$$

From eqs. (17.52) and (17.53) it follows that in a first approximation with respect to $x < 1$ we have $\Psi = \text{const}$. Substituting this into eq. (17.54), we find that A is proportional to $I_0(\Psi\rho)$, where I_0 is the Bessel function of imaginary argument. According to (17.55), $H(\rho)$ is proportional to $I_1(\Psi\rho)$; due to the boundary condition we have

$$H = \frac{H_J I_1(\Psi\rho)}{I_1(\Psi R)} \tag{17.56}$$

$$A = -\frac{H_J}{\Psi}\frac{I_0(\Psi\rho)}{I_1(\Psi R)} \tag{17.57}$$

The solvability condition of the equation for the correction to Ψ is analogous to (17.37):

$$\int_0^R \left(A^2 - 1 + \Psi^2\right)\rho \mathrm{d}\rho = 0$$

From this we get

$$H_J^2 = \frac{\Psi^2\left(1 - \Psi^2\right) I_1(\Psi R)}{I_0^2(\Psi R) - I_1^2(\Psi R)}. \tag{17.58}$$

We begin with the case $R < 1$. Assuming that $\Psi \leq 1$, we expand the right-hand side of (17.58) in R :

- In their original work, Ginzburg and Landau (1950) considered a thin film and assumed that the current density varies only in the transverse direction and that along the film width the current is uniform. This does not correspond to reality because the current is redistributed over the film and becomes nonuniform in two directions. It is for this reason that we consider a cylinder with a current.

$$H_J^2 \approx \frac{1}{4}\Psi^4\left(1-\Psi^2\right)R^2 \tag{17.59}$$

Evidently, the value of H_J is small at $R < 1$, i.e., superconductivity cannot be destroyed due to H_J becoming equal to $H_{\rm cm}$ (in conventional units), as in the case of a bulk specimen according to Silsbee's rule (section 15.4). The mechanism of destruction of superconductivity is different here. If we consider H_J^2 (17.59) as a function of Ψ^2, then we shall see that it vanishes at $\Psi = 0$ and $\Psi = 1$, and has a maximum in between. Hence, there is a certain maximum value of H_J which is compatible with superconductivity; at larger values of H_J superconductivity cannot exist. What happens at such large currents will be discussed in section 22.9. Here we will find the maximum of H_J.

Differentiating with respect to Ψ^2, we obtain for the maximum point:

$$\Psi^2 = \frac{2}{3}, \quad H_{J,\max} = \frac{R}{3^{3/2}}. \tag{17.60}$$

Passing to conventional units and using formula (17.51), we obtain the value of the critical current:

$$J_{\rm c} = \frac{{\rm c}R^2}{3\sqrt{6}}\frac{H_{\rm cm}}{\delta}. \tag{17.61}$$

Since $J_c \propto R^2$, it is reasonable to introduce the critical current density:

$$j_{\rm c} = \frac{J_{\rm c}}{\pi R^2} = \frac{1}{3\pi\sqrt{6}}\frac{cH_{\rm cm}}{\delta}. \tag{17.62}$$

The quantity $\boldsymbol{j_{\rm c}}$ is independent of size and is a characteristic of the superconducting metal.

The physical significance of this quantity can be understood if we substitute the BCS expressions for δ and $H_{\rm cm}$. Then we obtain

$$j_{\rm c} = \frac{1}{3\sqrt{2}}\frac{n_{\rm s}{\rm e}\Delta(T)}{p_0} \tag{17.63}$$

[here we have introduced $\Delta(T)$ in accordance with eq. (17.33) and $n_{\rm s}$ according to eq. (16.92)]. From this formula it follows that $j_{\rm c}$ corresponds to the motion of electrons with a velocity of the order of $\Delta(T)/p_0$. Thus, we conclude that Cooper pairing and, hence, superconductivity exists until the pairs begin to move at a velocity larger than Δ/p_0. This occurs not only near $T_{\rm c}$ but also at any temperature and is consistent with the Landau criterion (16.1).

It should be noted that the critical current density (17.62) is very large. If we substitute typical values for pure superconductors, $H_{\rm cm} \sim 10^2 - 10^3{\rm Oe}, \delta \sim 10^{-5} - 10^{-6}$ cm, we obtain:

$$j_c \sim 10^7 - 10^9 \ {\rm A/cm^2}. \tag{17.64}$$

For large thicknesses, $R > 1$, we obtain from formula (17.58):

$$H_J^2 \approx \Psi^3\left(1-\Psi^2\right)R.$$

At the maximum value of H_J^2 we have $\Psi^2 = \frac{3}{5}$ and

$$H_{J,\max} \approx 3^{3/4}2^{1/2}5^{-5/4}R^{1/2}.$$

Passing to conventional units and expressing J_c, we find

$$J_{\rm c} \approx 3^{3/4}5^{-5/4}cH_{\rm cm}R^{3/2}\delta^{-1/2}. \tag{17.65}$$

The complete curve of H_J^2 versus R in reduced units is shown in fig. 110 (curve 1).
The above-described mechanism of superconductivity destruction by the current occurs only as long as the radius of the cylinder is not too large. According to formula (17.59), the magnetic field of the current is of order $\boldsymbol{H}_{\rm cm}$ at $\boldsymbol{R} \sim \boldsymbol{\delta}$. Here the destruction of superconductivity by the magnetic field is possible according to Silsbee's rule. If the sample were massive, an intermediate state would arise (see section 15.4). However, in the intermediate state the sample must consist of layers of the normal and superconducting phases, i.e., the order parameter must vary in space. This is possible only at distances of order $\xi \sim \delta/x > \delta$. Thus, there exists a whole region of thicknesses from δ to ξ (or in reduced units from 1 to x^{-1}) at which neither the superconducting state nor the normal state (the field in the middle of the film is weaker than $\boldsymbol{H}_{\rm cm}$) nor the intermediate state can be realized at first sight.

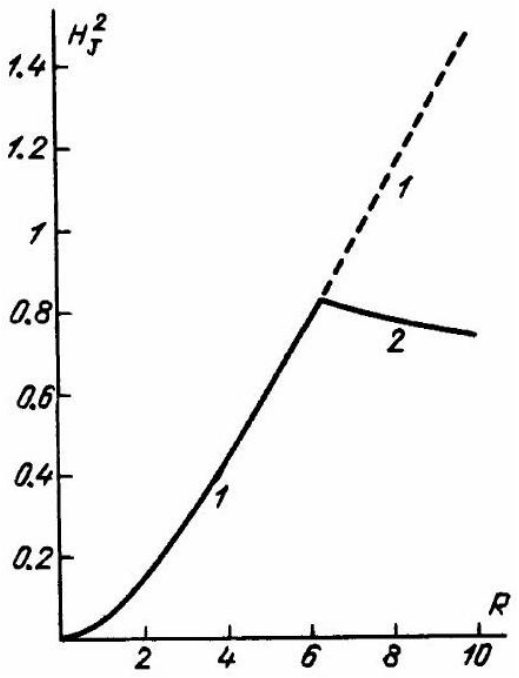


Fig. 110.

This means, in fact, that at a certain thickness a discontinuous transition occurs from the superconducting to the normal state. Strictly speaking, such a transition cannot be treated as a phase equilibrium because in the normal state energy is dissipated in the presence of a current, and the state is not an equilibrium state. However, because of the high conductivity of the metal the departure from equilibrium is very small. For the same reason the electric field is always small compared to the magnetic field. This enables one to consider the transition of the wire with a current as a first-order phase transition and to take into account the magnetic field alone.

In this particular case, the condition for the transition is the equality of the energies in a given field since the specification of the total current is equivalent to the specification of the field at the interface. Since the field is inhomogeneous in the normal phase too, we cannot use formula (17.20) and we have to find $\Omega_{{\rm s}H}$ and $\Omega_{{\rm n}H}$ with an appropriate distribution of H. From eq. (17.19) we have

$$\int \Omega_{\mathrm{sH}}\, \mathrm{d}V = \int \Omega_{\mathrm{n}}^{(0)} \mathrm{d}V + \frac{1}{2} H_{\mathrm{cm}}^2 \int_0^R \left(H^2 - \frac{1}{2}\Psi^4 - 2HH_J \right) \rho \mathrm{d}\rho, \tag{17.66}$$

$$\int \Omega_{\mathrm{nH}}\, \mathrm{d}V = \int \Omega_{\mathrm{n}}^{(0)} \mathrm{d}V + \frac{1}{2} H_{\mathrm{cm}}^2 \int_0^R \left(H^2 - 2HH_J \right) \rho \mathrm{d}\rho. \tag{17.67}$$

For a superconductor formula (17.56) must be substituted as $\boldsymbol{H}(\boldsymbol{\rho})$. For a normal metal we have $j = \text{const.} = J/\left(\pi R^2\right)$;

$$H = \frac{2J(\rho)}{c\rho} = \frac{2j\pi\rho^2}{c\rho} = \frac{2J\rho}{cR^2} = \frac{H_J \rho}{R} \tag{17.68}$$

(the last expression is also valid in reduced units).
Let us consider in more detail the case $R \gg 1$. Using the asymptotics of the functions I_ν at $z \gg 1$,

$$I_\nu(z) \approx \frac{1}{(2\pi z)^{1/2}} \mathrm{e}^z \left(1 - \frac{1}{2z} \left(\nu^2 - \frac{1}{4} \right) \right), \tag{17.69}$$

we find from eqs. (17.58) and (17.56)

$$\Psi \approx 1 - O\left(R^{-1}\right) \tag{17.70}$$

$$H \approx H_J \left(\frac{R}{\rho} \right)^{1/2} \mathrm{e}^{\rho - R}. \tag{17.71}$$

From this it follows that in the superconducting phase H is different from zero only in a layer of order δ, i.e., to within terms of order R^{-1} we may replace the integrand in (17.66) by $-\frac{1}{2}\Psi^4 \approx -\frac{1}{2}$. Calculating $\Omega_{\mathrm{n}H}$ with H (17.68) and using the condition $\Omega_{\mathrm{n}H} = \Omega_{\mathrm{s}H}$, we obtain $H_{J\mathrm{c}} = \sqrt{\frac{3}{5}}$ or, in conventional units,

$$H_{Jc} = \sqrt{\frac{6}{5}} \mathrm{H}_{\mathrm{cm}}. \tag{17.72}$$

As should be expected, $H_{J\mathrm{c}}$ is somewhat larger than H_{cm} since the field in the normal state varies from 0 to $H_{J\mathrm{c}}$ at the surface. However, this difference is only 10%. Since H_J is proportional to J, then from eq. (17.68) we obtain

$$J_c = J_{\text{Silsbee}} \sqrt{\frac{6}{5}}. \tag{17.73}$$

In the case $R \sim 1$, it is impossible to express $H_{J\mathrm{c}}$ in analytical form. The corresponding curve (2) is given in fig. 110. The intersection of curves 1 and 2 occurs at a rather large value of $R (R = 6.24)$. In this region J_{c} is well described by the asymptotics (17.65) on the left of the point of intersection. Note that continuation of curve 2 beyond the point of intersection to the left is meaningless since $\boldsymbol{H}_{\mathrm{J,max}}$ corresponds to the maximum field compatible with superconductivity.

Just as in any first-order phase transition, hysteresis is likely to occur. As the current increases the transition may be retarded up to the stability limit of the metastable superconducting state corresponding to the maximum of the field H_J (17.58) (curve 1 in fig. 110). When the current decreases, the transition may probably be retarded until $J = 0$.

Note that all the reasonings given in the present section are valid as long as $R \ll \xi$ ($R < x^{-1}$ in reduced units). At larger thicknesses an intermediate state is formed.

8.3.7 17.5. Quantization of the magnetic flux

Let us now consider a hollow cylinder or, to put it differently, a tube with wall thickness larger than δ. Suppose this cylinder is placed in an external longitudinal magnetic field weaker than the critical field ($H < H_{c1}$ in the case of a type II superconductor, ch. 18). Imagine that the external field varies with time. We have not considered the extension of the Ginzburg-Landau equations to nonstationary problems, but for our purposes it will suffice to use the London equation (17.36). We integrate this equation along a closed path, lying entirely within the superconductor and surrounding the cavity in the cylinder. Here we obtain

$$\frac{\partial}{\partial t}\oint \Lambda j \ \mathrm{d}l = \oint E \ \mathrm{d}l = \int \mathrm{d}S \,\mathrm{rot}\, E = -\frac{1}{c}\int \ \mathrm{d}S\frac{\partial H}{\partial t}$$

(we have used the Maxwell equation here). Hence,

$$\oint \Lambda j \ \mathrm{d}l + \frac{1}{\mathrm{c}}\int H \ \mathrm{d}S = \ \mathrm{const} \ .$$

Since the current can flow only in a surface layer, then along the closed path lying in the bulk of the superconductor $\boldsymbol{j} = 0$. Consequently,

$$\Phi = \int H \ \mathrm{d}S = \ \mathrm{const} \tag{17.74}$$

Thus, we have come to the conclusion that the magnetic flux through a loop lying within the superconductor cannot vary with time.

Note that this conclusion is valid not only for the problem of a hollow cylinder under consideration but also for an inhomogeneous superconductor, whose different portions have different critical parameters. In such a specimen multiply connected superconducting regions may form enclosing normal regions, as a result of which a phenomenon known as "trapped magnetic flux" arises with decreasing magnetic field.

Let us return, however, to the problem of the tube. We will now show that the magnitude of the magnetic flux trapped by the superconducting tube cannot be arbitrary. For this purpose we consider the expression for the superconducting current (17.9). We write the function Ψ in the form $\Psi = |\Psi|e^{ix}$, i.e., we introduce the modulus and the phase. The current is then written in the form

$$j = \frac{\hbar e}{m}|\Psi|^2\left(\nabla\chi - \frac{2e}{\hbar c}A\right) \tag{17.75}$$

We divide j by $|\Psi|^2$ and integrate along the same loop as before, i.e., along a closed path, which encloses the hole and passes in the bulk of the tube wall. Here we obtain

$$\oint \frac{j}{|\Psi|^2} \ \mathrm{d}l = \frac{\hbar e}{m}\left(\oint \nabla\chi \ \mathrm{d}l - \frac{2e}{\hbar c}\oint A \ \mathrm{d}l\right). \tag{/}$$

If the loop passes inside the wall, then $\boldsymbol{j} = 0$ on it. The second integral on the right-hand side is equal to

$$\oint A \ \mathrm{d}l = \int \mathrm{rot}\, A \ \mathrm{d}S = \int H \ \mathrm{d}S = \Phi.$$

As for the first integral, at first glance it must be equal to zero, just as any integral of the gradient of a function along a closed loop. However, in fact, this is not necessarily the case. For the function $\Psi = |\Psi|\mathrm{e}^{\mathrm{i}\chi}$ to be single-valued it is not required that the phase of χ return to the same value when we make a complete turn around the loop; it is sufficient only that it varies by $2\pi n$, where n is an integer. Thus, in a general case $\oint \nabla\chi \mathrm{d}l = 2\pi n$. We obtain

$$\Phi = n\Phi_0 \tag{17.76}$$

$$\Phi_0 = \pi\frac{\hbar c}{e} = 2.07 \times 10^{-7}\text{Oe}\cdot\ \text{cm}^2 \tag{17.77}$$

Thus, the magnetic field passing through the loop may take only a discrete series of values. This phenomenon is called magnetic flux quantization, and the quantity Φ_0 is known as the flux quantum.

The phenomenon of flux quantization in a superconductor was first predicted by F. London (1950). However, being unaware of Cooper pairing, London assumed the charge of the carriers to be equal to e instead of $2e$, and obtained a flux quantum equal to $2\Phi_0$. Recall that a flux quantum also appears in the theory for a normal
metal. In a metal placed in a magnetic field, the electrons move along spiral trajectories (in the case of a closed Fermi surface); these trajectories enclose a magnetic flux equal to $n \cdot 2\Phi_0$ (section 10.4). The magnetic flux quantum Φ_0 determines the period of interference oscillations of the resistance of a hollow normal cylinder (section 11.4).

In the case under consideration, the quantized magnetic flux Φ is the sum of the flux passing through the hole and the flux in the surface layer of the superconductor, of thickness δ, which adjoins the cavity. If the radius of the tube is much larger than δ, then the latter may be neglected.

For the experimental determination of the magnitude of the flux through the cavity it is not sufficient to simply vary the external field. According to the condition (17.74) the internal flux will not change in such a case. Therefore, one has to proceed as follows (Doll and Näbauer 1961, Deaver and Fairbank 1961). The superconductor is cooled in a given external field from a temperature above T_c to a certain temperature below T_c. Upon transition to the superconducting state a certain magnetic flux is frozen in it. The magnitude of this flux can be determined from the minimum condition for the free energy difference (17.20):

$$\int (\Omega_{\text{s}H} - \Omega_{\text{n}H})\,\mathrm{d}V$$
$$= \frac{H_\text{cm}^2}{4\pi}\left\{(H_\text{int} - H_0)^2\,\pi R_1^2 + \int_{R_1}^{R_2}\left[(H - H_0)^2 - \frac{1}{2}|\Psi|^4\right] 2\pi\rho\ \mathrm{d}\rho\right\} \tag{17.78}$$

where R_1 and R_2 are the inner and outer radii of the tube; H_int is the field inside the tube. The first term in brackets refers to the cavity, and the second to the superconducting tube. We are to find H_int satisfying the quantization condition (17.76) and corresponding to the minimum of expression (17.78). Since in the second term the dependence on $\boldsymbol{H}_\text{int}$ extends only to the layer of thickness $\boldsymbol{\delta}$, we may neglect it.

The minimization of the first term leads to the following result: a magnetic flux through the core equal to $\Phi_\text{int} = n\Phi_0$, is realized in that interval of the field H_0 in which $\Phi_\text{ext} = H_0\pi R_1^2$ lies within the interval $\left(n - \frac{1}{2}\right)\Phi_0 < \Phi_\text{ext} < \left(n + \frac{1}{2}\right)\Phi_0$. When the boundary of this interval is crossed, the transition to the next n occurs. This situation is shown in fig. 111.

According to the derivation given above, the quantization of magnetic flux is a consequence of the variation of the phase of the order parameter Ψ by $2\pi n$ upon making a complete turn around the closed loop. This behavior of the phase has been demonstrated in a very ingenious experiment (Little and Parks 1962, 1964). Let us take a thin cylindrical superconducting film whose thickness is much less than the penetration depth and apply the magnetic field along the axis of the cylinder. Such a thin film does not practically screen out the magnetic field (its magnetization in the field is equal to zero according to formula 17.40) and, hence, the field inside and outside the film is the same. The radius of the cylinder is assumed to be much

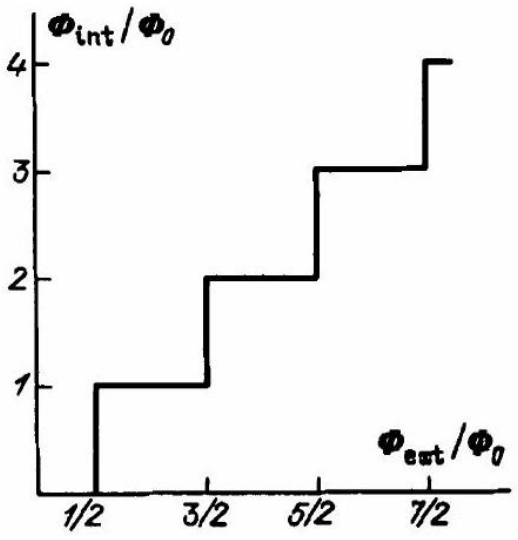


Fig. 111.

larger than the penetration depth. In this case all the quantities, including the vector potential A, do not practically vary along the film thickness.

Let us choose A such that it has only the component A_φ in cylindrical coordinates. We substitute $\Psi = |\Psi|e^{ix}$ into the free energy (17.5). The integrand has the form

$$\Omega_{\rm s} - \Omega_{\rm n}^{(0)} = \alpha\tau|\Psi|^2 + \frac{1}{2}b|\Psi|^4 + \frac{\hbar^2}{4m}\left(\nabla\chi - \frac{2e}{c\hbar}A\right)^2|\Psi|^2 + \frac{H^2}{8\pi} \tag{17.79}$$

(in accordance with the result of section 17.4 it may be assumed that $|\Psi| = \text{const.}$). The combination $\boldsymbol{A} - (c\hbar/2e)\nabla\chi$ is gauge invariant since any gradient added to $\boldsymbol{A}$ may be compensated by the variation of the phase.

Using the fact that $\nabla\chi$ and A are constant along the superconducting film, we write the combination that appears in parentheses in eq. (17.79) in the form of the average value:

$$\begin{aligned}\nabla\chi - \frac{2e}{c\hbar}A &= \frac{1}{2\pi R}\oint\left(\nabla\chi - \frac{2e}{c\hbar}A\right)\mathrm{d}l \\ &= \frac{1}{2\pi R}\left(2\pi n - \frac{2e}{c\hbar}\Phi\right) = \frac{1}{R}\left(n - \frac{\Phi}{\Phi_0}\right)\end{aligned}$$

where the integral is taken over the contour of the cylinder cross section perpendicular to the axis; $\Phi = H\pi R^2$ is the magnetic flux through the cylinder; Φ_0 is the flux quantum. Substituting into eq. (17.79) gives

$$\begin{aligned}\Omega_{\rm s} - \Omega_{\rm n}^{(0)} =& \alpha\tau|\Psi|^2 + \frac{\hbar^2}{2mR^2}\left(n - \frac{\Phi}{\Phi_0}\right)^2|\Psi|^2 \\ &+ \frac{1}{2}b|\Psi|^4 + \frac{H^2}{8\pi}.\end{aligned} \tag{17.80}$$

The number n has to be chosen so as to correspond to the minimum of the free energy, i.e., a given n is realized at

$$n - \frac{1}{2} < \frac{\Phi}{\Phi_0} < n + \frac{1}{2}. \tag{17.81}$$

In the formula (17.80) the second term can be added to the first term with τ being replaced by τ' :

$$\tau' = \tau + \frac{\hbar^2}{4mR^2\alpha}\left(n - \frac{\Phi}{\Phi_0}\right)^2.$$

From the condition $\tau' = 0$ we obtain the variation of the critical temperature:

$$\frac{\Delta T_c}{T_c} = -\frac{\hbar^2}{4mR^2\alpha}\left(\frac{\Phi}{\Phi_0} - n\right)^2. \tag{17.82}$$

Substituting the BCS expression for α from formulae (17.14) and (17.18), we find

$$-\frac{\Delta T_c}{T_c} = \begin{cases} C_1 \frac{\xi_0^2}{R^2}\left(\frac{\Phi}{\Phi_0} - n\right)^2, & \xi_0 < l, \\ C_2 \frac{\xi_0 l}{R^2}\left(\frac{\Phi}{\Phi_0} - n\right)^2, & \xi_0 > l, \end{cases} \tag{17.83}$$

where

$$C_1 = \frac{7\pi^2\zeta(3)}{48\gamma^2} = 0.55, \quad C_2 = \frac{\pi^3}{24\gamma} = 0.72, \quad l = v\tau_{\rm tr}$$

From (17.83) it follows that the dependence of $-\Delta T_c/T_c$ on Φ/Φ_0 consists of periodically recurring parabolic pieces, each of which corresponds to the interval (17.81) with the corresponding n (fig. 112). This prediction is consistent with experiment (Little and Parks 1962, 1964). Note that in the experiment carried out by Little and Parks the superconductor cannot trap the magnetic flux because of its small thickness, which is why no flux quantization occurs; however, the nonuniqueness of the phase is observed and it is the phase that is measured in the experiment.

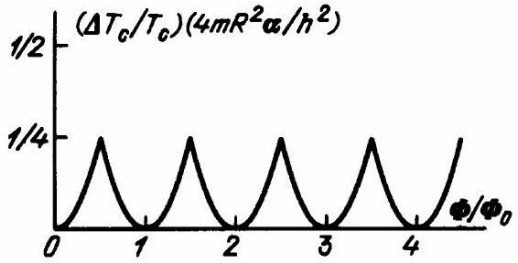


Fig. 112.

The number n has to be chosen so as to correspond to the minimum of the free energy, i.e., a given n is realized at

$$n - \frac{1}{2} < \frac{\Phi}{\Phi_0} < n + \frac{1}{2}. \tag{17.81}$$

In the formula (17.80) the second term can be added to the first term with τ being replaced by τ' :

$$\tau' = \tau + \frac{\hbar^2}{4mR^2\alpha}\left(n - \frac{\Phi}{\Phi_0}\right)^2.$$

From the condition $\tau' = 0$ we obtain the variation of the critical temperature:

$$\frac{\Delta T_c}{T_c} = -\frac{\hbar^2}{4mR^2\alpha}\left(\frac{\Phi}{\Phi_0} - n\right)^2. \tag{17.82}$$

Substituting the BCS expression for α from formulae (17.14) and (17.18), we find.

$$-\frac{\Delta T_c}{T_c} = \begin{cases} C_1 \frac{\xi_0^2}{R^2}\left(\frac{\Phi}{\Phi_0} - n\right)^2, & \xi_0 < l, \\ C_2 \frac{\xi_0 l}{R^2}\left(\frac{\Phi}{\Phi_0} - n\right)^2, & \xi_0 > l, \end{cases} \tag{17.83}$$

where

$$C_1 = \frac{7\pi^2\zeta(3)}{48\gamma^2} = 0.55, \quad C_2 = \frac{\pi^3}{24\gamma} = 0.72, \quad l = v\tau_{\text{tr}}$$

From (17.83) it follows that the dependence of $-\Delta T_c/T_c$ on Φ/Φ_0 consists of periodically recurring parabolic pieces, each of which corresponds to the interval (17.81) with the corresponding n (fig. 112). This prediction is consistent with experiment (Little and Parks 1962, 1964). Note that in the experiment carried out by Little and Parks the superconductor cannot trap the magnetic flux because of its small thickness, which is why no flux quantization occurs; however, the nonuniqueness of the phase is observed and it is the phase that is measured in the experiment.

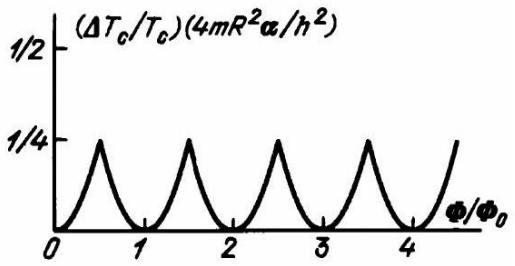


Fig. 112.

8.4 18 Type II superconductivity

8.4.1 18.1. Magnetic properties of type II superconductors. The qualitative picture

In this chapter we shall be concerned with the properties of type II superconductors, for which, according to eq. (16.96), $x > 1/\sqrt{2}$ and $\sigma_{\text{ns}} < 0$. First of all, we note that with $\sigma_{\text{ns}} < 0$ a first-order phase transition to the normal state is impossible, even if we are dealing with a superconducting cylinder in a longitudinal field. Indeed, suppose that the superconductor has been divided up into layers of the normal and superconducting phases parallel to the magnetic field. In section 17.4 we have defined the critical field of a thin layer, which was found to be proportional to $H_{\text{cm}}\delta/d$; this may considerably exceed H_{cm}. Hence, it is energetically favorable for such layers to retain superconductivity in fields stronger than $\boldsymbol{H_{\text{cm}}}$. In ordinary type I superconductors the splitting up into layers does not occur because of the surface energy σ_{ns} at the layer boundaries. But if $\sigma_{\text{ns}} < 0$, then nothing will hinder the splitting up of the superconductor into layers of the n - and s -phases.

Thus, the phase transition of a type II superconductor will proceed by way of a gradual expulsion of the superconducting phase, and the metal will become normal at a field in which even an infinitesimal superconducting region can no longer exist. Thus, it may be concluded

that the transition will extend over an interval of magnetic fields, and in this interval the external magnetic field will partially penetrate the superconductor, i.e., the Meissner effect will be incomplete. The superconductor will be in a special state, called the mixed state, which adjoins the superconducting phase at a certain field $H_{\rm cl}$ (the lower critical field) and the normal phase at another field $H_{\rm c2}$ (the upper critical field) (Abrikosov 1957).

The fields $H_{\rm c1}$ and $H_{\rm c2}$ can be determined in order of magnitude from qualitative considerations. We begin with $H_{\rm c2}$, the field at which the superconductivity disappears altogether. The breakup of Cooper pairs occurs as a result of curving of their trajectory in the magnetic field. Evidently, a pair can be preserved as long as the Larmor radius is larger than its size, i.e.,

$$r_{\rm L} \sim \frac{cp_\perp}{eH} > \xi.$$

In this formula $p_\perp$ is the perpendicular component of the momentum corresponding to the motion of the pair as a whole. Therefore, $p_\perp \leqslant p \sim mv_{\rm s}$, where $v_{\rm s}$ is the velocity of the pair. From the Landau criterion (see also formula 17.63) it follows that $v_{\rm s} < \Delta/p_0$, otherwise the pair will break up. The same condition may be written in the form $p_\perp < \hbar/\xi$. Thus, we have

$$\xi < \frac{cp_\perp}{eH} < \frac{ch}{\xi eH}$$

or

$$H < \frac{c\hbar}{e\xi^2} \sim H_{\rm c2} \tag{18.1}$$

The field $\boldsymbol{H}_{\rm c2}$ may be expressed in terms of $\boldsymbol{H}_{\rm cm}$:

$$\begin{aligned} H_{\rm c2} &\sim \frac{c\hbar}{e\xi}\frac{\Delta}{hv} \sim \frac{c}{e\xi v}\frac{H_{\rm cm}\hbar^{3/2}}{(mp_0)^{1/2}} \\ &\sim H_{\rm cm}\frac{\delta_{\rm L}}{\xi} \sim H_{\rm cm}x. \end{aligned} \tag{18.2}$$

We have so far considered a pure superconductor. But if it contains impurities and $l < \xi$, then in formula (18.1) ξ must be replaced by $\xi' \sim (\xi l)^{1/2}$. In this case we obtain

$$H_{c2} \sim \frac{c\hbar}{e\xi l} \sim \frac{c\hbar}{el}\frac{\Delta}{\hbar v} \sim H_{\rm cm}\frac{\delta_{\rm L}}{l} \sim H_{\rm cm}x. \tag{18.3}$$

Thus, in both cases the field $H_{\rm c2}$ is of order $H_{\rm cm}\varkappa$. However, the second case is more important. It follows from eq. (18.3) that by increasing the impurity concentration and, hence, by decreasing the mean free path (i.e. $l \propto n_i^{-1}$), one can strongly increase $\boldsymbol{H}_{\rm c2}$. Up to $\boldsymbol{H}_{\rm c2}$ the metal retains superconducting regions, i.e., a zeroresistance supercurrent can flow in it. The mean free path can, in principle, be decreased down to interatomic distances. Considering that the usual values of $H_{\rm cm} \sim 10^2 - 10^3$Oe and that $\delta_{\rm L} \sim 10^{-5} - 10^{-6}$ cm, we obtain a limiting estimate for the fields $\boldsymbol{H}_{\rm c2}$ (Gor'kov 1963):

$$H_{\rm c2} < 10^3\frac{10^{-5}}{10^{-8}}\text{Oe} \sim 10^6\text{Oe} \tag{18.4}$$

These fields are so high that a question arises: Would not the pairs be broken up earlier due to orientation of the spins of both electrons parallel to the magnetic field? (the Clogston paramagnetic limit; Clogston 1962). The order of magnitude of this limit is evidently determined by the condition

$$\beta H_{\rm cp} \approx 2\Delta, \tag{18.5}$$

where β is the Bohr magneton. Considering that the highest $T_{\rm c}$ value is of the order of 20 K , we obtain

$$H_{\rm cp} < 10^6 {\rm Oe} \tag{18.6}$$

hence, the upper limits for $H_{\rm cp}$ and $H_{\rm c2}$ coincide and the value 10^6Oe may be regarded as limiting.

What happens when the field is decreased below $H_{\rm c2}$? If the field penetrates the superconductor partially, then persistent eddy currents must exist in it. Near the limiting field $H_{\rm c1}$ the metal must be almost completely superconducting, i.e., regions with eddy currents must be rare. The field $H_{\rm c1}$ can be determined if it is taken into account that an elementary vortex is a quantum entity. This was first detected in the study of the superfluidity of liquid helium (Onsager 1949, Feynman 1955).

Suppose that Cooper pairs execute a vortex motion around a certain axis. Let us draw a circular loop around the axis. The velocity of the pairs along this loop is evidently constant. According to the Bohr quantization rule,

$$\oint p \, {\rm d}q = 2m \oint v_{\rm s} \, {\rm d}l = 2m v_{\rm s} \cdot 2\pi\rho = 2\pi n\hbar$$

Hence,

$$v_{\rm s} = n\hbar/(2m\rho),$$

that is, the velocity of the pairs falls off proportionately to the distance from the axis. This inference becomes invalid when $\rho \leqslant \xi$, the size of the pairs. On the other hand, we ignored the fact that the pairs are charged and their motion implies the generation of electric current and a magnetic field. The latter must vanish at a distance of the order of the penetration depth δ. Hence, the formula derived is valid only at $\rho < \delta$. Below we shall assume that $\delta > \xi$, i.e., $x > 1$.

As regards the number n, it may, in principle, be arbitrary. However, it is rather clear that we must take $n = 1$. First of all, it is evident that a small vortex is created more readily than a large one and therefore the lower critical field $H_{\rm cl}$ corresponds to the creation of the smallest vortex. With higher fields the problem is solved from the condition of the minimum free energy. From this condition one has to find the positions of the vortex axes. Suppose, for example, that $n = 2$. This corresponds to two fused vortices with $n = 1$. In order to find the position of the vortex axis we have to find the minimum free energy varying the coordinates of the axes, i.e., the points x and y of its intersection with the plane perpendicular to the magnetic field (the z-axis). But if the vortices did not stick together, we would be able to minimize Ω with respect to $x_1 y_1$ and $x_2 y_2$, i.e., a larger number of variables. In a general case this leads to a lower minimum of Ω. Thus, we will assume $n = 1$ and, hence*,

$$v_{\rm s} = \frac{\hbar}{2m\rho}, \quad \xi < \rho < \delta. \tag{18.7}$$

hence, the upper limits for $H_{\rm cp}$ and $H_{\rm c2}$ coincide and the value 10^6Oe may be regarded as limiting.

- Quantum vortices of supercurrent which are attenuated at a distance δ and which carry one magnetic flux quantum $\mathbf{\Phi_0}$ (see sections **18.2** and 18.3) are usually called fluxoids or Abrikosov vortices.

What happens when the field is decreased below H_{c2} ? If the field penetrates the superconductor partially, then persistent eddy currents must exist in it. Near the limiting field H_{cl} the metal must be almost completely superconducting, i.e., regions with eddy currents must be rare. The field H_{c1} can be determined if it is taken into account that an elementary vortex is a quantum entity. This was first detected in the study of the superfluidity of liquid helium (Onsager 1949, Feynman 1955).

Suppose that Cooper pairs execute a vortex motion around a certain axis. Let us draw a circular loop around the axis. The velocity of the pairs along this loop is evidently constant. According to the Bohr quantization rule,

$$\oint p \, \mathrm{d}q = 2m \oint v_\mathrm{s} \, \mathrm{d}l = 2mv_\mathrm{s} \cdot 2\pi\rho = 2\pi n\hbar.$$

Hence,

$$v_\mathrm{s} = n\hbar/(2m\rho),$$

that is, the velocity of the pairs falls off proportionately to the distance from the axis. This inference becomes invalid when $\rho \leqslant \xi$, the size of the pairs. On the other hand, we ignored the fact that the pairs are charged and their motion implies the generation of electric current and a magnetic field. The latter must vanish at a distance of the order of the penetration depth δ. Hence, the formula derived is valid only at $\rho < \delta$. Below we shall assume that $\delta > \xi$, i.e., $x > 1$.

As regards the number n, it may, in principle, be arbitrary. However, it is rather clear that we must take $n = 1$. First of all, it is evident that a small vortex is created more readily than a large one and therefore the lower critical field H_{cl} corresponds to the creation of the smallest vortex. With higher fields the problem is solved from the condition of the minimum free energy. From this condition one has to find the positions of the vortex axes. Suppose, for example, that $n = 2$. This corresponds to two fused vortices with $n = 1$. In order to find the position of the vortex axis we have to find the minimum free energy varying the coordinates of the axes, i.e., the points x and y of its intersection with the plane perpendicular to the magnetic field (the z-axis). But if the vortices did not stick together, we would be able to minimize Ω with respect to x_1y_1 and x_2y_2, i.e., a larger number of variables. In a general case this leads to a lower minimum of Ω. Thus, we will assume $n = 1$ and, hence*,

$$v_\mathrm{s} = \frac{\hbar}{2m\rho}, \quad \xi < \rho < \delta. \tag{18.7}$$

The energy of such a vortex is basically the kinetic energy of Cooper pairs. The energy per unit length of the vortex is given by (the density of the pairs is $\frac{1}{2}n_s$):

$$\begin{aligned}\xi_0 &= \frac{1}{2}n_\mathrm{s}\int_\xi^\delta \frac{2mv_\mathrm{s}^2}{2} 2\pi\rho \, \mathrm{d}\rho \\ &= \frac{\pi n_\mathrm{s}h^2}{4m}\int_\xi^\delta \frac{\mathrm{d}\rho}{\rho} = \frac{\pi n_\mathrm{s}\hbar^2}{4m}\ln\left(\frac{\delta}{\xi}\right) \\ &= \frac{\pi n_\mathrm{s}\hbar^2}{4m}\ln x\end{aligned}$$

* Quantum vortices of supercurrent which are attenuated at a distance δ and which carry one magnetic flux quantum $\boldsymbol{\Phi_0}$ (see sections 18.2 and 18.3) are usually called fluxoids or Abrikosov vortices.

(here we have substituted formula 18.7). The magnetic moment of the vortex per unit length is equal to

$$M = \frac{1}{2} n_s \frac{2e}{c} \int_\xi^\delta \rho v_s 2\pi\rho \, \mathrm{d}\rho = \pi \frac{e\hbar n_s}{mc} \int_\xi^\delta \rho \mathrm{d}\rho$$
$$\approx \frac{\pi e\hbar n_s}{2mc} \delta^2$$

(we have neglected ξ^2 as compared to δ^2).
In the presence of a magnetic field H the vortex acquires a magnetic energy -MH. The smallest field at which an elementary vortex can appear corresponds to $\varepsilon_0 - MH = 0$ or

$$H_{c1} = \frac{\varepsilon_0}{M} \sim \frac{c\hbar}{e\delta^2} \ln x.$$

Using the BCS formulae, we obtain

$$H_{c1} \sim \frac{H_{cm}}{x} \ln x. \tag{18.8}$$

Just as in the case of $\boldsymbol{H_{c2}}$, this formula also refers both to a pure superconductor and to the case $l < \xi_0$. From formula (18.8) it follows that the higher H_{c2} (i.e., the greater x) the lower ΔH_{cl}, i.e., the earlier the magnetic field begins to penetrate the superconductor.

In the following two sections we shall present the quantitative theory of the magnetic properties of type II superconductors based on the Ginzburg-Landau equations (Abrikosov 1957). Although this theory is valid, strictly speaking, only near T_c, yet, as has already been noted, all the basic conclusions are valid at any temperatures.

8.4.2 18.2. Magnetic properties of type II superconductors. Quantitative theory for the vicinity of H_{c2}

We begin with H_{c2}. Since this is the limiting field for the existence of superconductivity, it follows that an infinitesimal nucleus of the superconducting phase must
decrease with time at $H > H_{c2}$ and increase with time at $H < H_{c2}$. This means that at $H = H_{c2}$ there may exist a stationary infinitesimal superconducting nucleus.

Let us consider the homogeneous Ginzburg-Landau equations (17.24), (17.25) and (17.26)*. Assuming Ψ to be infinitesimal, we retain only terms of lower order in Ψ. In this case, we get

$$\frac{1}{x^2} \frac{\mathrm{d}^2\Psi}{\mathrm{d}x^2} + \Psi\left(1 - A^2\right) = 0, \tag{18.9}$$
$$\frac{\mathrm{d}^2 A}{\mathrm{d}x^2} = 0. \tag{18.10}$$

From eq. (18.10) we obtain $A = H_0 x$ (we assume that $H \| z, A \| y$); the origin $x = 0$ may be chosen at an arbitrary point. Substituting into (18.9), we have

$$-\frac{\mathrm{d}^2\Psi}{\mathrm{d}x^2} + \chi^2 H_0^2 x^2 \Psi = \chi^2 \Psi \tag{18.11}$$

We must find the solution that vanishes as $x \to \pm\infty$.
We have deliberately placed the terms of eq. (18.22) in such a manner that it becomes similar to the Schrödinger equation for a harmonic oscillator:

$$-\frac{\hbar^2}{2m} \frac{\mathrm{d}^2\Psi}{\mathrm{d}x^2} + \frac{1}{2} k x^2 \Psi = \varepsilon\Psi \tag{18.12}$$

As is well known from quantum mechanics, the last equation has solutions which vanish with $x \to \pm\infty$ at

$$\varepsilon = \hbar\omega\left(n + \frac{1}{2}\right)$$

where $\omega = (k/m)^{1/2}$. If we denote the coefficient in front of the first term of (18.12) as a and that the second term as b, then $\hbar\omega = 2\sqrt{ab}$. Comparing eq. (18.11) with eq. (18.12), we obtain $2\sqrt{ab} = 2\varkappa H_0$ and, hence, the required solutions exist at $\chi^2 = 2\chi H_0\left(n + \frac{1}{2}\right)$ or**

$$H_0 = \frac{x}{2n+1}.$$

We are interested in the strongest field at which the solution $\Psi \neq 0$ is possible. It corresponds to $n = 0$ and is equal to

$$H_{c2} = \varkappa \tag{18.13}$$

or, in conventional units,

$$H_{c2} = \varkappa\sqrt{2}H_{cm}. \tag{18.14}$$

This value is consistent with the qualitative estimate (18.2) and (18.3). Note that $H_{c2} > H_{cm}$ at $x > 1/\sqrt{2}$.

The solution corresponding to the lowest level of the oscillator has the form $\Psi \propto \exp\left[-\left(\sqrt{km}/2\hbar x^2\right]\right.$. Again, denoting the coefficients in (18.12) as a and b, we have $\Psi \propto \exp\left[-\frac{1}{2}(b/a)^{1/2}x^2\right]$. In our case we obtain $\Psi \propto \exp\left(-\frac{1}{2}xH_0x^2\right)$ or, in view of $H_0 = x$,

$$\Psi \propto \exp\left(-\frac{1}{2}\varkappa^2x^2\right). \tag{18.15}$$

As has been pointed out above, we may choose the coordinate origin $x = 0$ at any point, i.e., the nucleus of the superconducting phase may appear at any point in the superconductor. The change in the coordinate origin corresponds to the change in the gauge of the vector potential if we wish to use real Ψ. But if we wish to use a unified gauge, then we have to take a complex Ψ. Indeed, writing $\Psi = |\Psi|e^{i\chi}$ and substituting into (17.6'), we obtain

$$\left(-i\varkappa^{-1}\nabla + \varkappa^{-1}\nabla\chi - A\right)^2|\Psi| - |\Psi| + |\Psi|^3 = 0. \tag{18.16}$$

It is sufficient to take $\chi = ky$ and we obtain the same equation with the replacement $A_y \to A_y - k/x = H_0(x - k/xH_0)$. Hence, the small nucleus may not only have the form (18.15) but also

$$\Psi \propto \exp\left[iky - \frac{1}{2}\varkappa^2\left(x - \frac{k}{x^2}\right)^2\right]. \tag{18.17}$$

- At first sight, it may seem that the search for a nucleus which is dependent only on a single coordinate is a limitation on generality. In fact, for homogeneous magnetic field the vector potential depends linearly on the coordinates. Choosing $A_y = H_0x$, we see that the equation for Ψ contains explicitly only the coordinate x.

** The possibility of superconducting regions with small Ψ at $H_0 = x(2n+1)$ was pointed out by Ginzburg and Landau (1950). But they considered only type I superconductors with $x < 1/\sqrt{2}$, for which these values of H_0 were lower than H_{cm}, and the statement of the problem of small Ψ was meaningless (the supercooling field was not studied by Ginzburg and Landau).

Evidently, the solution may also be any linear combination of functions of the type (18.17). Since the conditions along the entire superconductor are uniform, it is most natural to suppose a linear combination of solutions centered through equal intervals, i.e.,

$$\Psi = \sum_{n=-\infty}^{\infty} C_n \exp\left[ikny - \frac{1}{2}\varkappa^2\left(x - \frac{kn}{\chi^2}\right)^2\right]. \tag{18.18}$$

Let us now consider the solution of eq. (17.6') at H_0 slightly smaller than $\varkappa$. We apply the method of successive approximations. First of all, we take into account
the term with Ψ in equation (17.8') for A. Substituting eq. (18.18), we obtain two equations:

$$\begin{aligned}
\frac{\partial^2 A}{\partial x \partial y} &= \frac{\partial H}{\partial y} \\
&= \frac{i}{2x}\sum_{n,m} C_n C_m^* \exp\left[ik(n-m)y - \frac{1}{2}x^2\left(x - \frac{kn}{x^2}\right)^2\right. \\
&\quad \left. -\frac{1}{2}x^2\left(x - \frac{km}{x^2}\right)\right]\cdot k(m-n), \\
-\frac{\partial^2 A}{\partial x^2} &= -\frac{\partial H}{\partial x} \\
&= \frac{1}{2x}\sum_{n,m} C_n C_m^* \exp\left[ik(n-m)y - \frac{1}{2}x^2\left(x - \frac{kn}{x^2}\right)^2\right. \\
&\quad \left. -\frac{1}{2}x^2\left(x - \frac{km}{x^2}\right)^2\right]\cdot\left[k(n+m) + 2x^2 x\right]
\end{aligned}$$

(we have taken $A = H_0 x$ on the right-hand side of eq. (17.8')). From this it is easy to see that

$$H = \frac{\partial A}{\partial x} = H_0 - \frac{|\Psi|^2}{2x}, \quad A = H_0 x - \frac{1}{2x}\int |\Psi|^2 \, \mathrm{d}x. \tag{18.19}$$

Consider now the next approximation to eq. (17.6'). We write

$$\Psi = \Psi^{(0)} + \sum_n \mathrm{e}^{\mathrm{i}kny}\psi_n^{(1)}(x),$$

where $\Psi^{(0)}$ is the function (18.18). We shall assume the second term to be a small correction and write eq. (17.6') to first order in this correction. Here we obtain a linear inhomogeneous equation, which may be split into equations for individual $\psi_n^{(1)}$. The vector potential is inserted in the form (18.19), the first term being written in the form $xx + (H_0 - x)\,x$ and the second term is assumed to be a first-order correction, just as the second term in (18.19). As a result, we find

$$\begin{aligned}
&\left(\frac{kn}{x} - xx\right)^2 \psi_n^{(1)} - \frac{1}{x^2}\frac{d^2\psi_n^{(1)}}{\mathrm{d}x^2} - \psi_n^{(1)} \\
&= 2\,(x - H_0)\,xx\left(x - \frac{kn}{x^2}\right) C_n \psi_n(x) \\
&\qquad + \sum_{m,p} C_p C_m^* C_{n-p+m}\left[\left(x - k\frac{n - \frac{1}{2}(p-m)}{x^2}\right)\psi_{n-p+m}(x)\int^x \psi_p\,(x')\,\psi_m\,(x')\,\mathrm{d}x'\right. \\
&\qquad\qquad \left. -\psi_p(x)\psi_m(x)\psi_{n-p+m}\right]
\end{aligned} \tag{18.20}$$

the term with Ψ in equation (17.8') for A. Substituting eq. (18.18), we obtain two equations:

$$\begin{aligned}
\frac{\partial^2 A}{\partial x \partial y} &= \frac{\partial H}{\partial y} \\
&= \frac{i}{2x} \sum_{n,m} C_n C_m^* \exp\left[\mathrm{i}k(n-m)y - \frac{1}{2}x^2 \left(x - \frac{kn}{x^2} \right)^2 \right. \\
&\quad \left. - \frac{1}{2}x^2 \left(x - \frac{km}{x^2} \right) \right] \cdot k(m-n), \\
-\frac{\partial^2 A}{\partial x^2} &= -\frac{\partial H}{\partial x} \\
&= \frac{1}{2x} \sum_{n,m} C_n C_m^* \exp\left[\mathrm{i}k(n-m)y - \frac{1}{2}x^2 \left(x - \frac{kn}{x^2} \right)^2 \right. \\
&\quad \left. - \frac{1}{2}x^2 \left(x - \frac{km}{x^2} \right)^2 \right] \cdot \left[k(n+m) + 2x^2 x \right]
\end{aligned}$$

(we have taken $A = H_0 x$ on the right-hand side of eq. (17.8')). From this it is easy to see that

$$H = \frac{\partial A}{\partial x} = H_0 - \frac{|\Psi|^2}{2x}, \quad A = H_0 x - \frac{1}{2x} \int |\Psi|^2 \, \mathrm{d}x \tag{18.19}$$

Consider now the next approximation to eq. (17.6'). We write

$$\Psi = \Psi^{(0)} + \sum_n \mathrm{e}^{\mathrm{i}kny} \psi_n^{(1)}(x),$$

where $\Psi^{(0)}$ is the function (18.18). We shall assume the second term to be a small correction and write eq. (17.6') to first order in this correction. Here we obtain a linear inhomogeneous equation, which may be split into equations for individual $\psi_n^{(1)}$. The vector potential is inserted in the form (18.19), the first term being written in the form $xx + (H_0 - x)\, x$ and the second term is assumed to be a first-order correction, just as the second term in (18.19). As a result, we find

$$\begin{aligned}
&\left(\frac{kn}{x} - xx \right)^2 \psi_n^{(1)} - \frac{1}{x^2} \frac{d^2 \psi_n^{(1)}}{\mathrm{d}x^2} - \psi_n^{(1)} \\
&\qquad = 2\,(x - H_0)\, xx \left(x - \frac{kn}{x^2} \right) C_n \psi_n(x) \\
&\qquad\quad + \sum_{m,p} C_p C_m^* C_{n-p+m} \left[\left(x - k \frac{n - \frac{1}{2}(p-m)}{x^2} \right) \psi_{n-p+m}(x) \int^x \psi_p(x')\, \psi_m(x')\, \mathrm{d}x' \right. \\
&\qquad\qquad \left. - \psi_p(x) \psi_m(x) \psi_{n-p+m} \right]
\end{aligned} \tag{18.20}$$

where

$$\psi_n(x) = \exp\left[-\frac{1}{2}x^2 \left(x - \frac{kn}{x^2} \right)^2 \right]. \tag{18.21}$$

In order for this inhomogeneous equation to have a solution, it is necessary that its right-hand side be orthogonal to the solution of a homogeneous equation with the same boundary conditions. Such is $\psi_n(x)$. From the orthogonality condition we obtain

$$2^{-1/2}\left(\frac{1}{2x^2}-1\right)\sum_{p,m}C_pC_m^*C_{n-p+m}\exp\left(-k^2\frac{(p-n)^2+(p-m)^2}{2x^2}\right)$$
$$+C_n\frac{x-H_0}{x}=0 \tag{18.22}$$

We multiply this equation by C_n^* and sum over n. The resultant relation may be written in the form (see eq. 18.18)

$$\left(\frac{x-H_0}{x}\right)\overline{|\Psi|^2}+\left(\frac{1}{2x^2}-1\right)\overline{|\Psi|^4}=0. \tag{18.23}$$

The induction, i.e., the average field, is obtained from formulae (18.19) and (18.23):

$$B=\bar{H}=H_0-\frac{\overline{|\Psi|^2}}{2\varkappa}=H_0-\frac{\overline{\left(|\Psi|^2\right)^2}}{\overline{|\Psi|^4}}\frac{\overline{|\Psi|^4}}{2\varkappa|\Psi|^2}$$
$$=H_0-\frac{1}{\beta_A}\frac{\varkappa-H_0}{2\varkappa^2-1} \tag{18.24}$$

where

$$\beta_A=\frac{\overline{|\Psi|^4}}{\overline{\left(|\Psi|^2\right)^2}} \tag{18.25}$$

is a quantity which does not depend on H_0.
Let us find the free energy using formula (17.19). Substituting eqs. (18.18) and (18.19) into it and expressing H_0 in terms of B, according to (18.24), we obtain (with all $\overline{|\Psi|^2}$ and $|\Psi|^4$ calculated using formulae 18.25 and 18.23):

$$\frac{\Omega_{\rm s}-\Omega_{\rm n}^{(0)}}{H_{\rm cm}^2/4\pi}=B^2-\frac{(\varkappa-B)^2}{1+(2\varkappa^2-1)\,\beta_A}. \tag{18.26}$$

This is the thermodynamic potential with respect to B. In order to obtain the external field from it, we have to calculate $\frac{1}{2}\partial\Omega_{\rm s}/\partial B$. So, we have

$$H_{\rm ext}=B+\frac{x-B}{1+(2x^2-1)\,\beta_A}. \tag{18.27}$$

Solving formula (18.24) for H_0, we obtain the same expression, i.e., $H_0=H_{\rm ext}$.
The minimum of free energy (18.26) is reached at the minimum value of β_A. This allows one to choose the coefficients C_n and k in formula (18.18) for Ψ. Note that,
according to eq. (18.25), $\beta_A>1$. Indeed, if $|\Psi|^2=\overline{|\Psi|^2}+q$, then $\bar{q}=0$. At the same time

$$\overline{|\Psi|^4}=\overline{\left(|\ \overline{\Psi|^2}+q\right)^2}=\overline{\left(|\Psi|^2\right)^2}+\overline{q^2}>\overline{\left(|\Psi|^2\right)^2}.$$

It is not difficult to see that eq. (18.22), which we derived from the solvability condition for the inhomogeneous equation (18.22), may be written in the following form:

$$\frac{\partial\beta_A}{\partial C_n^*}=0, \tag{18.28}$$

that is, it follows from the requirement of the minimum of $\boldsymbol{\beta}_A$.
A detailed analysis of the problem of choosing the correct solution is very time-consuming, so

we do not give it here (see Saint-James et al. 1969). If we consider the simplest variant, namely if all the coefficients C_n in (18.18) are assumed to be equal, it turns out that

$$\beta_A = \frac{k}{x\sqrt{2\pi}} \left[\sum_{n=-\infty}^{\infty} \exp\left(\frac{-k^2 n^2}{2x^2} \right) \right]^2 .$$

The minimum value is reached at $k = x(2\pi)^{1/2}$ and is equal to

$$\beta_A^{\square} = \left[\sum_{n=-\infty}^{\infty} \exp\left(-\pi n^2\right) \right]^2 = \vartheta_3^2(1;0) = 1.18, \tag{18.29}$$

where $\boldsymbol{\vartheta}_3$ is the theta function defined in the general case by

$$\vartheta_3(X;Y) = \sum_{n=-\infty}^{\infty} \exp\left(-\pi X n^2 + 2\pi \,\mathrm{i}\, n Y\right). \tag{18.30}$$

The function Ψ itself may be written in the form

$$\Psi^{\square} = C \exp\left(-\frac{1}{2} x^2 x^2 \right) \vartheta_3 \left(1; (2\pi)^{1/2} x \mathrm{i}(x + \mathrm{i}y)\right). \tag{18.31}$$

Using the properties of the ϑ_3-functions, one can show that upon rotation of the coordinate system by $\frac{1}{2}\pi$ the function Ψ is multiplied by a phase factor $\exp(\mathrm{i}x^2 xy)$, remaining unaltered in other respects. Thus, $|\Psi|^2$ has the symmetry of a square lattice. At points $x = (\sqrt{2\pi}/x)\left(m + \frac{1}{2}\right), y = (\sqrt{2\pi}/x)\left(n + \frac{1}{2}\right)$ (m and n are integers) the function Ψ vanishes. According to formula (18.19), the magnetic field at these points reaches the maximum value H_0.

As a result of a detailed analysis (Kleiner et al. 1964), it has been found that the lowest value of β_A is exhibited by a solution that has the symmetry of a triangular lattice; it may be written in the form

$$\Psi^{\Delta} = C \sum_{n=-\infty}^{\infty} \exp\left[\frac{1}{2}\pi \mathrm{i} n(n-1) - \frac{1}{2}\varkappa^2 \left(x - \frac{kn}{\varkappa^2} \right)^2 + \mathrm{i}kny \right], \tag{18.32}$$

where $k = x(\pi\sqrt{3})^{1/2}$. Other notations may also be used, but they differ only in the choice of the coordinate system. Comparison with formula (18.18) shows that in this case the coefficients C_n are chosen such that $C_{n+4} = C_n$ and $C_0 = C_1 = C$, $C_2 = C_3 = -C$. The solution (18.32) may be written in the following form:

$$\Psi^{\Delta} = \exp\left(-\frac{1}{2}\varkappa^2 x^2 \right) \vartheta_3 \left[\exp\left(-\frac{1}{6}\mathrm{i}\pi \right); \frac{1}{2}\varkappa \left(\frac{\sqrt{3}}{\pi} \right)^{1/2} (y - \mathrm{i}x) - \frac{1}{4} \right]. \tag{18.33}$$

The triangular lattice has a period $a = (2/x)(\pi/\sqrt{3})^{1/2}$ (the side of the triangle). The function Ψ^{Δ} vanishes at points $x = -\left(\frac{1}{2}a\sqrt{3}\right)\left(m + \frac{1}{2}\right), y = a\left(1 + \frac{1}{2}m + n\right)$, where m and n are integers. For this lattice

$$\beta_A^{\Delta} = 1.16. \tag{18.34}$$

We see that the two solutions considered are periodic and both have points at which $\Psi = 0$. In the neighborhood of each of these points Ψ is proportional to $x + \mathrm{i}y$, where x and y are counted off from the point where $\Psi = 0$. This may also be written in the form $\Psi \propto \rho \mathrm{e}^{\mathrm{i}\theta}$, where $\rho = (x^2 + y^2)^{1/2}, \theta = \arctan(y/x)$. The phase χ coincides with the angle of the cylindrical

coordinate system. We see that the phase varies by 2π upon each trip around such a point. Let us now examine formula (17.75) for the current written in conventional units and expressed in terms of the modulus and the phase Ψ. In cylindrical coordinates $\nabla\chi = \rho^{-1}\partial\chi/\partial\theta = \rho^{-1}$. At sufficiently small $\rho, \nabla\chi > (2e/\hbar c)A$. Hence,

$$j = \frac{\hbar e}{m}\frac{|\Psi|^2}{\rho}$$

If we write $j = en_s v_s$, we obtain ($|\Psi|^2 = \frac{1}{2}n_s$):

$$v_s = \frac{\hbar}{2m\rho},$$

which coincides exactly with formula (18.7) for a quantum vortex.

At the point $\rho = 0, v_s$ tends to infinity. For the physical quantity - electric current to be finite, it is necessary that $\Psi \to 0$ with $\rho \to 0$, and this does really occur. Another argument may be also be given: the vanishing of Ψ at $\rho = 0$ is necessary for the uniqueness of Ψ at this point. Such behavior of the wave function of the Bose condensate in the presence of a quantum vortex was first predicted by Feynman (1955) for superfluid liquid helium.

A natural question arises: we constructed the solutions of the Ginzburg-Landau equations without any preliminary assumptions and, in spite of this, in all the solutions there appear points where $\Psi = 0$ and the phase varies by 2π in each trip around this point. What is this associated with? The answer consists in the following. The equations contain the vector potential $\boldsymbol{A}$. If the magnetic field inside the superconductor is directed parallel to the external field, then $A_y = \int^x H\,\mathrm{d}x$ must increase with increasing x. But the physical quantity is not the vector potential but the magnetic field, which does not increase on the average in the specimen. Hence, the increase of the vector potential must be compensated. This is what really occurs. The point is that the equations always include the combination $\boldsymbol{x}^{-1}\boldsymbol{\nabla\chi} - \boldsymbol{A}$ (in reduced units).

Consider the solution $\Psi^{\square}$ (18.31) in the xy-plane (fig. 113). The solid circles designate the points where $\Psi = 0$. For the phase to be single-valued, we draw through these points branch cuts parallel to the y-axis. If one moves $\|y$ staying on the right

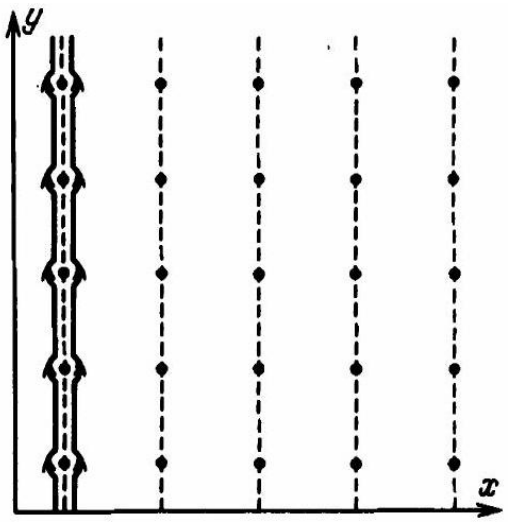


Fig. 113.

of such a branch cut, χ will vary according to the law

$$\chi(y) = \chi_{\mathrm{reg}}(y) + \pi\frac{y}{a}$$

where a is the period of the structure; $\chi_{\text{reg}}(y)$ is the regular part not associated with the vortices. But if one moves $\|y$ staying on the left of the branch cut, then

$$\chi(y) = \chi_{\text{reg}}(y) - \pi\frac{y}{a}$$

From this it follows that at each of the branch cuts the phase gradient undergoes a discontinuity:

$$\Delta\left(\frac{\partial\chi}{\partial y}\right) = \frac{2\pi}{a}$$

At the same time the vector potential increases by xa per period with increasing x ($A_y \approx H_0 x, H_0 \approx x$). In order to compensate this increase, it is necessary that

$$xa = \frac{1}{x}\Delta\left(\frac{\partial\chi}{\partial y}\right) = \frac{2\pi}{xa}.$$

It follows then that

$$a^{\square} = \frac{\sqrt{2\pi}}{x}.$$

This is what was exactly obtained for the square lattice.
As for the triangular lattice, the separation between the branch cuts is $\frac{1}{2}a\sqrt{3}$ and the compensation condition is

$$\frac{1}{2}xa\sqrt{3} = \frac{2\pi}{xa}$$

Hence,

$$a^{\Delta} = 2\left(\frac{\pi}{\sqrt{3}}\right)^{1/2}\frac{1}{x}$$

which corresponds to the solution of (18.33).
Let us find the current lines. Substituting eq (18.18) into the expression for the current (the right-hand side of eq. 18.8'), we obtain

$$\begin{aligned} j_x =& \sum_{n,m} C_n C_n^* \left(k\frac{n+m}{2x} - xx\right) \\ & \times \exp\left[\mathrm{i}(n-m)y - \frac{1}{2}x^2\left(x - \frac{kn}{x^2}\right)^2 - \frac{1}{2}x^2\left(x - \frac{km}{x^2}\right)^2\right] \\ =& -\frac{1}{2x}\frac{\partial|\Psi|^2}{\partial y} \\ j_y =& \frac{1}{2x}\frac{\partial|\Psi|^2}{\partial x} \end{aligned}$$

The equation for the current lines is

$$\frac{dx}{j_x} = \frac{dy}{j_y}.$$

Substituting j_x and j_y, we obtain

$$\frac{\partial|\Psi|^2}{\partial x}\,\mathrm{d}x + \frac{\partial|\Psi|^2}{\partial y}\,\mathrm{d}y = 0$$

or

$$|\Psi|^2 = \text{ const.}$$

According to eq. (18.19), these are simultaneously the lines of constant field. These lines are shown in fig. 114 for the quadratic solution (the numbers are the values of $|\Psi|^2/|\Psi|^2_{\max}$).

Consider the square contour in fig. 114 with vertices at the points marked by 1. It is not difficult to see that the integral $\oint j \, \mathrm{d}l$ taken along this contour is equal to zero. Hence, according to section 17.6, an integer number of magnetic flux quanta passes through this contour. We will show that this is one flux quantum. Indeed, we have

$$\Phi = BS^{\square} \approx x\frac{2\pi}{x^2} = \frac{2\pi}{x}. \tag{18.35}$$

Using conventional units and substituting the value of $\boldsymbol{\chi}$ (17.11), we get

$$\Phi = \frac{2\pi}{x} H_{\mathrm{cm}} \sqrt{2}\delta^2 = \frac{\pi\hbar c}{e} = \Phi_0. \tag{/}$$

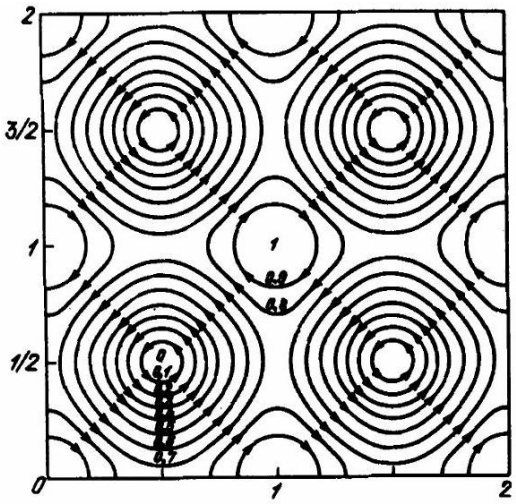


Fig. 114.

The situation is analogous for the triangular lattice (the contour is a hexagon which surrounds the point at which $\Psi = 0$).

In conclusion, we write formula (18.24) in a form more convenient for comparison with experiment:

$$-4\pi M = \frac{H_{c2} - H_0}{(2\varkappa^2 - 1)\,\beta_{\mathrm{A}}}, \tag{18.36}$$

that is, the dependence $M\,(H_0)$ near $H_0 = H_{c2}$ is linear.

8.4.3 18.3. Magnetic properties of type II superconductors. Metals with $x > 1$

In the present section we shall use an approximation that can be applied with fields smaller than H_{c2}. In order for this approximation to correspond to a real mixed state, it is necessary that $H_{c1} < H_{c2}$ or, according to the results of section 18.1, $x \gg 1$.

In the preceding section we have found the solution at fields close to H_{c2}. It is rather obvious that the main qualitative property of the function Ψ - the presence of points where $\Psi = 0$ and the fact that in going around these points the phase varies by 2π - must be preserved at lower fields too. This is associated with the necessity of the compensation of the increase of the vector potential by discontinuities in the phase gradient. But the lower the field the slower is the increase of A_y and, hence, the more seldom are the discontinuities. Indeed, the compensation condition (for the square lattice) with an arbitrary field has the form

$$\frac{2\pi}{xa} = A_y(a) - A_y(0) = \int_0^a H(x)\mathrm{d}x = \bar{H}a = Ba.$$

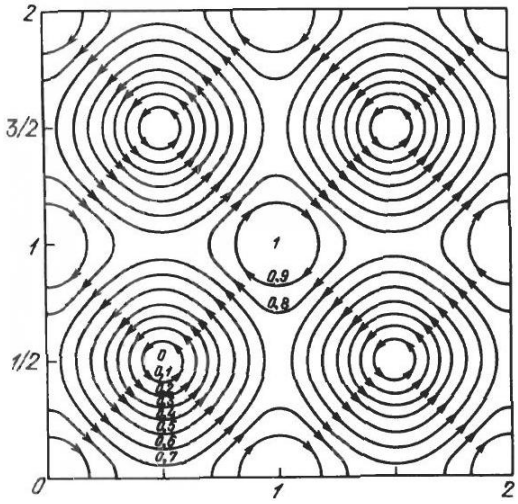


Fig. 114.

The situation is analogous for the triangular lattice (the contour is a hexagon which surrounds the point at which $\Psi = 0$).

In conclusion, we write formula (18.24) in a form more convenient for comparison with experiment:

$$-4\pi M = \frac{H_{c2} - H_0}{(2\varkappa^2 - 1)\,\beta_A}, \tag{18.36}$$

that is, the dependence $M\,(H_0)$ near $H_0 = H_{c2}$ is linear.

8.4.4 18.3. Magnetic properties of type II superconductors. Metals with $x \gg 1$

In the present section we shall use an approximation that can be applied with fields smaller than H_{c2}. In order for this approximation to correspond to a real mixed state, it is necessary that $H_{c1} \ll H_{c2}$ or, according to the results of section 18.1, $x \gg 1$.

In the preceding section we have found the solution at fields close to H_{c2}. It is rather obvious that the main qualitative property of the function Ψ - the presence of points where $\Psi = 0$ and the fact that in going around these points the phase varies by 2π-must be preserved at lower fields too. This is associated with the necessity of the compensation of the increase of the vector potential by discontinuities in the phase gradient. But the lower the field the slower is the increase of A_y and, hence, the more seldom are the discontinuities. Indeed, the compensation condition (for the square lattice) with an arbitrary field has the form

$$\frac{2\pi}{xa} = A_y(a) - A_y(0) = \int_0^a H(x)\mathrm{d}x = \bar{H}a = Ba.$$

From this it seen that $a = (2\pi/xB)^{1/2}$, i.e., the period of the structure increases with decreasing B.

At small fields the distance between the vortex lines becomes so large that they are almost independent and to a first approximation we may consider a single vortex line. We introduce the cylindrical system of coordinates (ρ, θ, z) and the z-axis is directed along the axis of the vortex line. The vector potential is chosen to be perpendicular to the radius-vector ρ, i.e., $A = A_\theta$.

If we write $\Psi = f\mathrm{e}^{\mathrm{i}x}(f = |\Psi|)$, then the current in Ginzburg-Landau units has the form $j = f^2(\nabla\chi/\chi - A)$. Since $f^2 = \frac{1}{2}n_\mathrm{s}$ is the density of pairs in the condensate (n_s is the density of "superconducting electrons"), then it follows that $\nabla\chi/x - A$ plays the role of their velocity. Therefore we introduce the following notation:

$$v_\mathrm{s} = \frac{\nabla\chi}{\chi} - A.$$

We emphasize that the vector $\boldsymbol{v}_\mathrm{s}$, which is convenient for the solution of equations, is not a true physical quantity, in contrast to the current $j = f^2 v_\mathrm{s}$, which can be measured. Equations (17.6) and (17.8) assume the following form in terms of the new notation:

$$-\frac{1}{\chi^2\rho}\frac{\mathrm{d}}{\mathrm{d}\rho}\left(\rho\frac{\mathrm{d}f}{\mathrm{d}\rho}\right) + v_\mathrm{s}^2 f = f - f^3, \tag{18.37}$$

$$-\frac{\mathrm{d}H}{\mathrm{d}\rho} = v_\mathrm{s} f^2, \tag{18.38}$$

$$H = (\mathrm{rot}\, A)_z = -\frac{1}{\rho}\frac{\mathrm{d}}{\mathrm{d}\rho}(\rho v_\mathrm{s}) + \frac{2\pi}{\chi}\delta(\rho). \tag{18.39}$$

In the last formula it is taken into account that in the vicinity of an individual filament $\chi = \theta$, i.e., it varies by 2π on encircling the line $\rho = 0$. Because of this, $\nabla\chi$ has an unusual property. If we take the integral of $\nabla\chi$ over an infinitesimal loop around the point $\rho = 0$, this will give, on the one hand

$$\oint \nabla\chi \mathrm{d}l = 2\pi$$

and on the other hand

$$\oint \nabla_\chi \mathrm{d}l = \int \mathrm{rot}\, \nabla_\chi \mathrm{d}S$$

Hence,

$$(\mathrm{rot}\, \nabla\chi)_z = 2\pi\delta(\rho) \tag{18.40}$$

The magnetic field $\boldsymbol{H} = \mathrm{rot}\, \boldsymbol{A} = -(\mathrm{rot}\, v_\mathrm{s} - \chi^{-1}\, \mathrm{rot}\, \nabla\chi)$, from which we obtain (18.39). The boundary conditions for eqs. (18.37), (18.38) and (18.39) are as follows. With $\rho \to \infty$ we have $f \to 1$ and $H \to 0$ (and, consequently, $v_s \to 0$). With $\rho \to 0$ we have $v_\mathrm{s} \to (x\rho)^{-1}$; this is associated with the fact that

$$\nabla_\theta\chi = \frac{1}{\rho}\frac{\partial\chi}{\partial\theta} \to \frac{1}{\rho}.$$

As for f, it must not increase indefinitely at any ρ.
The solution of the equations in a general case can be obtained only by numerical integration. However, at $x > 1$ the situation is substantially simplified. To demonstrate this, we note that the distances over which the function v_8 varies significantly is $\rho \sim 1$. As regards the function f, it varies appreciably at distances of $\rho \sim x^{-1} < 1$. In view of this, in eq. (18.38) the function f may be supposed to have reached the value $f = 1$ already. Substituting (18.39) for $\rho \neq 0$, we obtain the equation for v_s; its solution is

$$v_\mathrm{s} = \frac{K_1(\rho)}{\varkappa} \tag{18.41}$$

where K_1 is the MacDonald function, which has been introduced in section 16.5.
In the equation for f we may use the asymptotic form of v_s for small distances, i.e., $v_\mathrm{s} \approx (x\rho)^{-1}$. Inserting this into eq. (18.37) gives

$$\frac{1}{\chi^2}\left[\frac{1}{\rho}\frac{\mathrm{d}}{\mathrm{d}\rho}\left(\rho\frac{\mathrm{d}f}{d}\right) - \frac{f}{\rho^2}\right] = f^3 - f. \tag{18.42}$$

The solution of this equation at distances $\rho > x^{-1}$ (but, of course, $\rho < 1$) is

$$f^2 = 1 - \frac{1}{(x\rho)^2}. \tag{18.43}$$

At $\rho < x^{-1}$ we assume that $f < 1$ and find that

$$f = Cx\rho, \tag{18.44}$$

where C is a numerical constant, which can be found by numerical solution of eq. (18.42). The result $\Psi \propto \rho$ corresponds to what was observed in the vicinity of H_{c2}.

Let us determine the free energy per unit length of the vortex line. It must be measured from the energy of the superconductor in the absence of magnetic field. Using formula (17.19'), we obtain (in units of $\boldsymbol{H}_\mathrm{cm}^2\boldsymbol{\delta}^2/\boldsymbol{4\pi}$):

$$\varepsilon_0 = 2\pi\int\left[\Omega_\mathrm{s} - \Omega_\mathrm{s}^{(0)}\right]\rho\mathrm{d}\rho = 2\pi\int\left[H^2 + \frac{1}{2}\left(1 - f^4\right)\right]\rho\mathrm{d}\rho. \tag{18.45}$$

The principal part of this integral arises from the second term and is associated with distances much larger than x^{-1}. Substituting eq. (18.43) yields

$$\varepsilon_0 \approx \frac{2\pi}{x^2}\int\frac{1}{\rho}\,\mathrm{d}\rho \approx \frac{2\pi}{x^2}\ln x.$$

As a result of numerical integration, we find a more accurate result:

$$\varepsilon_0 = \frac{2\pi}{x^2}(\ln x + 0.081). \tag{18.46}$$

For the formation of vortex lines to be energetically favorable, we must have a field strength at which the free energy $\Omega_\mathrm{s} - \Omega_\mathrm{ns}^{(0)} - 2H_0B$ becomes negative. If the density of the vortex lines, i.e., the number of lines that intersect the unit area, is labeled as n, then

$$\Omega_\mathrm{s} - \Omega_\mathrm{s}^{(0)} = n\varepsilon_0, \quad B = \bar{H} = n\int H\,\mathrm{d}S = n\oint A\,\mathrm{d}l. \tag{18.47}$$

Because the contour passes at a distance $\rho = \infty$ and at such distances $v_\mathrm{s} = 0$ (see 18.41), we conclude that $A = \nabla\chi/x$ and is equal in magnitude to $(x\rho)^{-1}$. Hence,

$$B = \frac{2\pi n}{x}. \tag{18.48}$$

But since B is also the magnetic flux per unit area, it follows that the magnetic flux per vortex line is $2\pi/x$ or, according to eq. (18.35), one flux quantum Φ_0.

From the condition $\Omega_s - \Omega_s^{(0)} - 2H_0B = 0$ we obtain the value of the first critical field:

$$H_{cl} = \frac{\varepsilon_0 \chi}{4\pi}. \tag{18.49}$$

This formula applies for any x. In the case $x \gg 1$ we can substitute formula (18.46) for ε_0. In conventional units we have

$$H_{c1} = \frac{H_{cm}}{x\sqrt{2}}(\ln x + 0.08). \tag{18.50}$$

It is interesting to note that the field in the center of the vortex line is twice as large as H_{c1}. Indeed, according to eq. (18.38), $H(0) = \int_0^\infty v_s f^2 \, d\rho$. The principal part of the integral is taken over the region $x^{-1} < \rho < 1$. Inserting $f \approx 1$ and $v_s \approx (x\rho)^{-1}$, we find $H(0) \approx x^{-1} \ln x$. Numerical integration gives a more accurate formula:

$$H(0) = \frac{1}{x}(\ln x - 0.18). \tag{18.51}$$

The distribution of the field and $f(\rho)$ in the vortex is shown in fig. 115.
When $H_0 > H_{cl}$, there appear many vortices which begin to interact. In order to find the distribution of the fields and currents in this case and also the dependence

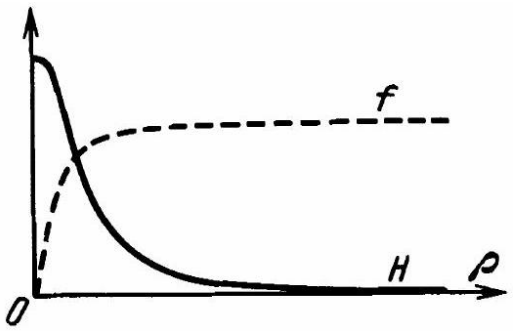


Fig. 115.

$B(H_0)$, we use the fact that the vortex axes come closer together to a distance of order x^{-1} only with $H_0 \to H_{c2}$, and at smaller fields the intervortex distance is substantially larger. In view of this, the vortex cores (of order x^{-1}) will simply play the role of singularities in the solution, and their detailed structure will be unimportant. We write the Maxwell equation in the form

$$\operatorname{rot} H = f^2 v_s$$

substitute $f = 1$, and take the curl. Taking into account that each vortex line gives a δ-function according to eq. (18.40), we obtain

$$\Delta H - H = -\frac{2\pi}{x} \sum_m \delta(\rho - \rho_m), \tag{18.52}$$

where ρ_m corresponds to the centers of the vortices ($\rho = (x, y)$). The solution of this equation is

$$H = \frac{1}{\chi} \sum_m K_0 \left(|\rho - \rho_m| \right), \tag{18.53}$$

where K_0 is the MacDonald function.
The free energy will be measured from the value for the superconducting phase in the absence of the field. We use formula (17.19), in which we assume that $\Psi = f e^{ix}$ and $\boldsymbol{f} = \mathbf{1}$. So, we have

$$\int \left(\Omega_s - \Omega_s^{(0)} \right) dV = \int \left(v_s^2 + H^2 \right) dV \tag{18.54}$$

Considering that in our approximation $\boldsymbol{v}_s = \operatorname{rot} \boldsymbol{H}$, integrating the first term by parts and substituting (18.52), we find that

$$\bar{\Omega}_s - \Omega_s^{(0)} = \overline{H(H - \Delta H)} = \frac{2\pi n}{x^2} \sum_m K_0 \left(|\rho_m| \right) \tag{18.55}$$

(n is the number of vortices intersecting 1 cm^2). The term that corresponds to $\rho_m = 0$ must be replaced by $n\varepsilon_0$.

Just as in the previous section, we are to choose the vortex lattice using the criterion of the minimal free energy. The triangle lattice turns out to be the most favorable. The period of the lattice is chosen in accordance with formula (18.48), i.e., on the basis of the fact that $B = n\Phi_0 = n(2\pi/x)$. So, we obtain $n^{-1} = a \cdot a\sqrt{3}/2$, from which it follows that

$$a = 2 \left(\frac{\pi}{\sqrt{3}} \right)^{1/2} \frac{1}{(Bx)^{1/2}} \tag{18.56}$$

(a is the side of the triangle).
The vector ρ_m is given by

$$\rho_m = a_1 q + a_2 l$$

where l and q are integers, and the basis vectors a_1 and a_2 have a length a and make an angle of 60°. In accordance with this,

$$|\rho_m| = a \left(q^2 + l^2 + ql \right)^{1/2}$$

Thus, we obtain

$$\Omega_s - \Omega_s^{(0)} = \frac{xB\varepsilon_0}{2\pi} + \left(\frac{B}{x} \right) \sum_{x_{q,l} \neq 0} K \left(x_{q,l} \right), \tag{18.57}$$

where

$$x_{q,l} = \left(4\pi \frac{q^2 + l^2 + ql}{\sqrt{3}Bx} \right)^{1/2} \tag{18.58}$$

The external field is expressed with the aid of the relation

$$H_0 = \frac{1}{2} \frac{\partial \left(\Omega_s - \Omega_s^{(0)} \right)}{\partial B}. \tag{18.59}$$

Substituting eq. (18.56) and using $K_0'(x) = -K_1(x)$, we obtain

$$x \left(H_0 - H_{c1} \right) = \frac{1}{4} \sum_{x_{q,l} \neq 0} \left[2K_0 \left(x_{q,l} \right) + x_{q,l} K_1 \left(x_{q,l} \right) \right] \tag{18.60}$$

We see that the dependence of xB on $x\,(H_0 - H_{c1})$ is a universal function. Let us examine the asymptotic forms of this dependence. With $H_0 - H_{c1} \to 0, B$ tends to zero, i.e., $x_{q,l} \to \infty$. Because of the exponential decrease of the MacDonald function it will be sufficient to retain only terms with the lowest x corresponding to $q^2 + l^2 + q^l = 1$. Since in the triangular lattice there are 6 neighbors at each point, a factor 6 appears in eq. (18.60). Using the asymptotics of the MacDonald functions $K_0(x) \approx K_1(x) \approx (\pi/2x)^{1/2} e^{-x}$, we get

$$x\,(H_0 - H_{c1}) \approx \frac{3}{2}\left(\frac{1}{2}\pi\right)^{1/2}\left(\frac{4\pi}{\sqrt{3}Bx}\right)^{1/4}\exp\left[-\left(\frac{4\pi}{\sqrt{3}Bx}\right)^{1/2}\right]. \tag{18.61}$$

It is not difficult to see that with $H_0 \to H_{cl}, B \to 0$ and $\mathrm{d}B/\mathrm{d}H_0 \to \infty$, i.e., the $B\,(H_0)$ curve has a vertical tangent at point H_{c1}.

Another limit that can be obtained is the relation between H_0 and B for fields at which the lattice period is much larger than ξ but less than δ, i.e., in reduced units $x^{-1} \ll a < 1$ or

$$x > B > \frac{1}{x}. \tag{18.62}$$

At $x \gg 1$ this occurs in most of the region of the mixed state, except the immediate neighborhood of H_{c1} and H_{c2}. We pass in formula (18.60) to the Fourier transforms of K_0 and K_1 :

$$x\,(H_0 - H_{cl}) = \pi \int \frac{2 + k^2}{(1 + k^2)^2} \sum_{\rho_{q,l} \neq 0} \mathrm{e}^{ik\rho_{q,l}} \frac{\mathrm{d}^2 k}{(2\pi)^2}. \tag{18.63}$$

If we add the term with $\rho_{q,l} = 0$ to the sum over $\rho_{q,l}$, we obtain

$$\sum_{\boldsymbol{\rho}_{q,l}} \mathrm{e}^{\mathrm{i}k\boldsymbol{\rho}_{q,l}} = (2\pi)^2 n \sum_{K} \delta(k - K) \tag{18.64}$$

where n is the number of vortices per cm^2; $\boldsymbol{K}$ are the reciprocal lattice vectors with respect to the planar lattice formed by the vectors $\rho_{q,l}$. These vectors are given by

$$\begin{aligned} &K = p_1 K_1 + p_2 K_2, \\ &K_1 = 2\pi\,[a_1 \times z_0]\,n, \quad K_2 = 2\pi\,[z_0 \times a_2]\,n, \end{aligned} \tag{18.65}$$

where n^{-1} is the area of the unit cell; a_1 and a_2 are basis vectors; z_0 is the unit vector with respect to z. Since $n = xB/2\pi$, it follows that K_1 and K_2 are equal, in magnitude, to $2(\pi/\sqrt{3})^{1/2}(xB)^{1/2}$ and the angle between them is equal to $\pi/3$, just as in the main lattice. Substituting (18.64) into (18.63), we get

$$x\,(H_0 - H_{c1}) = \pi\left(n \sum_{K} \frac{2 + K^2}{(1 + K^2)^2} - \int_0^\infty \frac{2 + k^2}{(1 + k^2)^2} \frac{\mathrm{d}^2 k}{(2\pi)^2}\right) \tag{18.66}$$

(the subtraction of the last integral corresponds to absence of the term with $\boldsymbol{\rho_{q,l}} = \mathbf{0}$ in (18.63).

Each of the expressions in brackets diverges logarithmically, but taken together they give a finite expression. We single out out from the first sum the term with $K = 0$. It is equal to $2\pi n = \varkappa B$. In the remaining terms and in the integral we shall first confine ourselves to the values $|K|, |k| < K_1 P = 2(\pi/\sqrt{3})^{1/2}(xB)^{1/2}P$; we shall then find the difference and pass to the limit $P \to \infty$. Since in the remaining sum over K the lowest K^2 is $K_1^2 \gg 1$ (according to eq 18.62), it may be replaced by

$$n\sum_K \frac{1}{K^2} = \frac{n}{K_1^2}\sum_{p_1\cdot p_2}\frac{1}{p_1^2+p_2^2+p_1p_2} = \frac{\sqrt{3}}{8\pi^2}\sum_{p_1,p_2}\frac{1}{p_1^2+p_2^2+p_1p_2}.$$

Evaluating the integral over k with the limit $K_1P \gg 1$, we get

$$\int_0^{K_1P}\frac{2+k^2}{(1+k^2)^2}\frac{d^2k}{(2\pi)^2} = \frac{1}{2\pi}\left(\ln K_1 + \ln P + \frac{1}{2}\right).$$

Collecting together all the terms, we find

$$\begin{aligned}\varkappa(H_0-H_{\rm cl}) \approx& \varkappa B - \frac{1}{4}\ln(\varkappa B) - \frac{1}{4}\ln\left(\frac{4\pi}{\sqrt{3}}\right) - \frac{1}{4} \\ &+ \lim_{P\to\infty}\left(\frac{\sqrt{3}}{8\pi}\sum_{0<\left(p_1^2+p_2^2+p_1p_2\right)<P^2}\frac{1}{p_1^2+p_2^2+p_1p_2} - \frac{1}{2}\ln P\right) \\ =& \varkappa B - \frac{1}{4}\ln(\varkappa B) - 0.49 \end{aligned} \tag{18.67}$$

If we substitute here formula (18.49) for $H_{\rm c1}$, we obtain

$$H_0 \approx B + \frac{1}{4\chi}\ln\left(\frac{\chi}{B}\right) - 0.45\frac{1}{\chi}. \tag{18.68}$$

From this formula we see that at $B \sim \varkappa, H_0 \approx B$ to within terms of order $\varkappa^{-1}$, as should be expected. On the basis of the limiting expressions (18.68) and (18.27) one can write an interpolation formula which reflects the logarithmic dependence of $H_0 - B$ on B in the region where the distance between the vortex cores is large and which changes to (18.27) with $B \to x \quad (x > 1)$:

$$H_0 \approx B + \frac{1}{2\beta_A x}\ln\left(\frac{x}{B}\right). \tag{18.69}$$

Of course, first this is only an interpolation and second it does not apply near $H_{\rm c1}$.
In concluding this section we will show that at $x = 1/\sqrt{2}$ the critical fields $H_{\rm cl}$, $H_{\rm c2}$ and $H_{\rm cm}$ coincide with each other. We put $x = 1/\sqrt{2}$ in eq. (18.37). It can be shown that

$$H = 2^{-1/2}\left(1-f^2\right) \tag{18.70}$$

Indeed, substituting into eq. (18.38), we get

$$fv_{\rm s} = 2^{1/2}\frac{\partial f}{\partial \rho} \tag{18.71}$$

We multiply eq. (18.37) (with $x = 2^{-1/2}$) by f and substitute eq. (18.71):

$$-\frac{1}{\rho}f\frac{\mathrm{d}}{\mathrm{d}\rho}\left(\rho\frac{\mathrm{d}f}{\mathrm{d}\rho}\right) + \left(\frac{\mathrm{d}f}{\mathrm{d}\rho}\right)^2 = \frac{1}{2}\left(1-f^2\right)f^2.$$

On the other hand, if we multiply eq. (18.39) by $\boldsymbol{f}^2$ and substitute eqs. (18.70) and (18.71), the same relation is obtained; this confirms the assumption (18.70). Now let us find ε_0 by using eq. (18.45). Substitution of eq. (18.70) yields

$$\varepsilon_0 = 2\pi \int \left(1 - f^2\right) \rho \mathrm{d}\rho = 2\pi\sqrt{2} \int H\rho \, \mathrm{d}\rho$$
$$= \sqrt{2}\Phi = \sqrt{2}\frac{2\pi}{x} \tag{18.72}$$

Here we have taken into account that there is one flux quantum per vortex, i.e., $2\pi/x$. Substituting this into (18.49), we obtain $H_{\mathrm{cl}} = 2^{-1/2}$ or, in conventional units, $H_{\mathrm{c1}} = H_{\mathrm{cm}}$. For H_{c2} this follows from (18.14). Thus, when x decreases to $1/\sqrt{2}$, the region of the mixed state is narrowed until it eventually disappears.

Thus, on the basis of qualitative arguments and quantitative calculations we have come to the conclusion that in type II superconductors in a magnetic field a mixed state arises with an incomplete Meissner effect, when the external field penetrates the superconductor in the form of filaments of the magnetic flux. Each filament is a tiny vortex current and carries one quantum of the magnetic flux. The order parameter is equal to zero on the vortex axis and is restored to the equilibrium value in the absence of the field at a distance $\xi = \delta/x$. This region is called the vortex core. The region of the mixed state disappears at $x \leqslant 1/\sqrt{2}$ and becomes large
at $x > 1$. Typical magnetization curves ($-4\pi M$ as a function of H_0) are shown in fig. 116.

Direct observation of the vortex structure was first made with the aid of neutron diffraction (Cribier et al. 1964). Since neutrons have a magnetic moment, they can be used for the analysis of magnetic structures in the same way as X-rays are used for the investigation of the electron density distribution. It is in this way that the existence of the vortex lattice was proved directly for the first time.

At a later time ferromagnetic powders were used for the observation of the vortex structure (Essmann and Träuble 1967), similar to what had been done for the intermediate state of type I superconductors. However, since the period of the structure is much smaller in this case, powders consisting of very small particles (diameter ~ 40Å) had to be used and the resultant picture was studied with the aid of an electron microscope using the replica technique (fig. 117). Usually, a triangular vortex lattice is obtained. However, when the magnetic field is directed along a fourth-order axis, a square lattice results. This is due to the small difference in energy between the two structures, which leads to the possibility of reconstitution under the influence of crystal anisotropy.

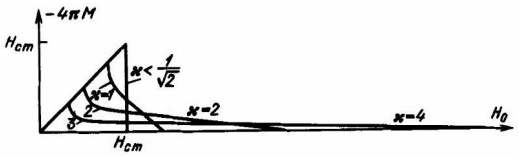


Fig. 116.

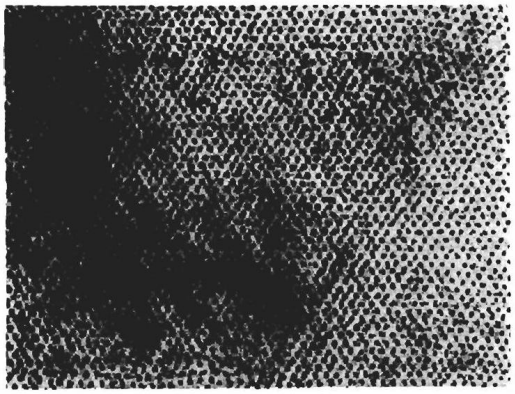


Fig. 117.

at $x \gg 1$. Typical magnetization curves ($-4\pi M$ as a function of H_0) are shown in fig. 116.

Direct observation of the vortex structure was first made with the aid of neutron diffraction (Cribier et al. 1964). Since neutrons have a magnetic moment, they can be used for the analysis of magnetic structures in the same way as X-rays are used for the investigation of the electron density distribution. It is in this way that the existence of the vortex lattice was proved directly for the first time.

At a later time ferromagnetic powders were used for the observation of the vortex structure (Essmann and Träuble 1967), similar to what had been done for the intermediate state of type I superconductors. However, since the period of the structure is much smaller in this case, powders consisting of very small particles (diameter ~ 40Å) had to be used and the resultant picture was studied with the aid of an electron microscope using the replica technique (fig. 117). Usually, a triangular vortex lattice is obtained. However, when the magnetic field is directed along a fourth-order axis, a square lattice results. This is due to the small difference in energy between the two structures, which leads to the possibility of reconstitution under the influence of crystal anisotropy.

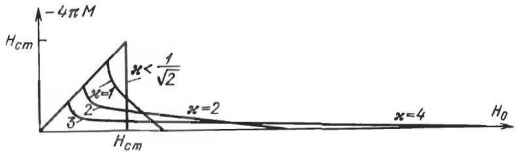


Fig. 116.

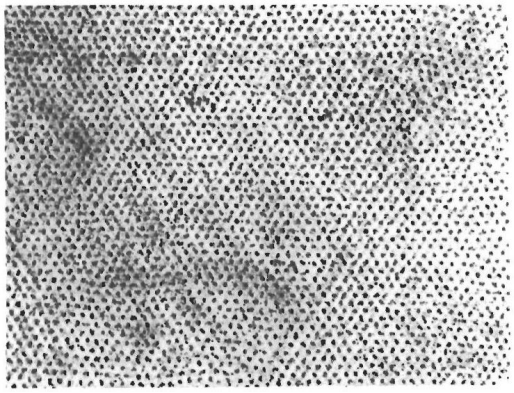


Fig. 117.

at $x \gg 1$. Typical magnetization curves ($-4\pi M$ as a function of H_0) are shown in fig. 116.

Direct observation of the vortex structure was first made with the aid of neutron diffraction (Cribier et al. 1964). Since neutrons have a magnetic moment, they can be used for the analysis of magnetic structures in the same way as X-rays are used for the investigation of the electron density distribution. It is in this way that the existence of the vortex lattice was proved directly for the first time.

At a later time ferromagnetic powders were used for the observation of the vortex structure (Essmann and Träuble 1967), similar to what had been done for the intermediate state of type I superconductors. However, since the period of the structure is much smaller in this case, powders consisting of very small particles (diameter ~ 40Å) had to be used and the resultant picture was studied with the aid of an electron microscope using the replica technique (fig. 117). Usually, a triangular vortex lattice is obtained. However, when the magnetic field is directed along a fourth-order axis, a square lattice results. This is due to the small difference in energy between the two structures, which leads to the possibility of reconstitution under the influence of crystal anisotropy.

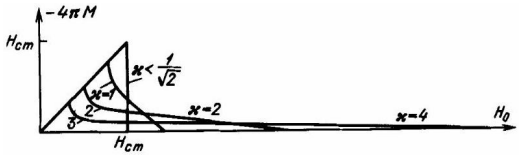


Fig. 116.

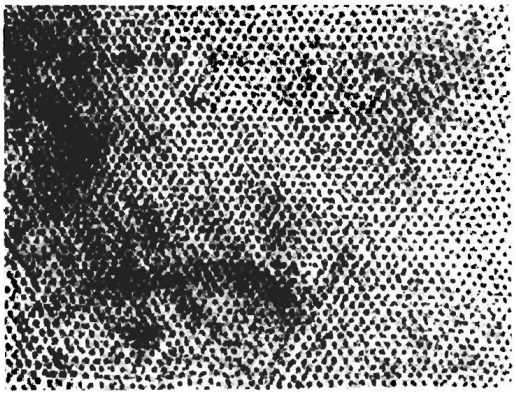


Fig. 117.

8.4.5 18.4. Surface superconductivity

Up until now we have dealt with an infinite superconducting space or, in other words, with phenomena that take place in the interior of a bulk superconductor. Investigations show that in the surface layer superconductivity may be retarded up to fields larger than H_{c2} (Saint-James and De Gennes 1963). The physical cause of this phenomenon consists in the following. While considering the nucleus of the superconducting phase in infinite space in section 18.2, we used the boundary condition $\Psi \to 0$ for $x \to \pm\infty$. In the presence of a surface the boundary condition is $\mathrm{d}\Psi/\,\mathrm{d}x|_{\mathrm{b}} = 0$.

Figure 118 shows the various possible cases: (a) a nucleus in the bulk; (b) a nucleus with its center at the surface; (c) a nucleus near the surface, but with a shifted center and, finally, (d) a nucleus in a thin film. In the last two cases the boundary condition on the surface requires an increase in Ψ near the surface as compared to the case of infinite space. This leads to an increase in the eigenvalue in the equation for Ψ(18.11) (the role of the energy is played by x^2), as a result, the value of the critical field increases. An example is the critical field of thin films (section 17.4), which is the same for type I and II superconductors with thicknesses of $d \ll \min(1, x^{-1})$ (section 18.6) and which increases with decreasing thickness.

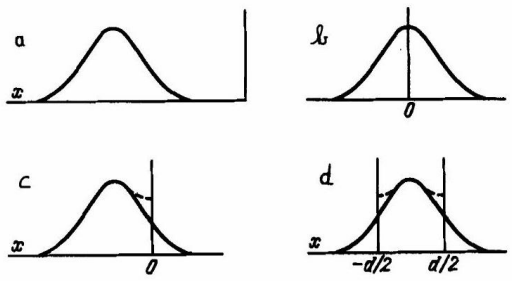


Fig. 118.

It is easy to see that the solutions with the center far from the surface and with the center directly at the surface differ only by the shift of the coordinate origin (in both cases $\mathrm{d}\Psi/\,\mathrm{d}x|_{\mathrm{b}} = 0$, see fig. 118) and, hence, they correspond to the same value of the field $H_0 = \varkappa$. The solution with the maximum slightly shifted relative to the surface corresponds to a larger value of the field. From this it follows that there exists a certain single solution, for which the field will have a maximum. Let us find this solution.

We begin with the case of the external field parallel to the surface. Here we may take the vector potential in the form $A = H_0(x - x_0)$ and use the boundary conditions $\Psi = 0$ for $x \to \infty$

and $\mathrm{d}\Psi/\mathrm{d}x = 0$ at $x = 0$. In this case, Ψ will depend only on x. Instead of this, we could have taken $A = H_0 x$, looking for Ψ in the form $\mathrm{e}^{\mathrm{i}ky}\Psi(x)$,
but, as has been shown in sections 18.2, these are equivalent statements of the problem. Thus, substituting $A = H_0\,(x - x_0)$ into eq. (18.9), we obtain

$$-\frac{\mathrm{d}^2\Psi}{\mathrm{d}x^2} + \chi^2 H_0^2\,(x - x_0)^2\,\Psi = \chi^2\Psi. \tag{18.73}$$

The solution of this equation in the general case is

$$\Psi = \exp\left(-\frac{1}{2}\zeta^2\right)\left\{C_1 F\left[\frac{1}{4}(1-\beta), \frac{1}{2}, (\zeta-\zeta_0)^2\right]\right.$$
$$\left. +\zeta C_2 F\left[\frac{1}{4}(3-\beta), \frac{3}{2}, (\zeta-\zeta_0)^2\right]\right\}, \tag{18.74}$$

where

$$\zeta = (xH_0)^{1/2}\,x, \quad \zeta_0 = (xH_0)^{1/2}\,x_0, \quad \beta = \frac{x}{H_0},$$

$F(\alpha, \gamma, z)$ is a degenerate hypergeometric function satisfying the equation

$$zF'' + (\gamma - z)F' - \alpha F = 0, \tag{18.75}$$

and C_1 and C_2 are arbitrary constants (see Landau and Lifshitz 1974).
The boundary conditions enable one to determine the ratio C_2/C_1 and β as a function of x_0. After this, minimizing β with respect to x_0, we obtain $\beta_{\min}$ or $H_{0,\,\max}$. This turns out to be equal to

$$H_{c3} = 1.695x = 1.695H_{c2}. \tag{18.76}$$

This is the critical field of surface superconductivity. It is larger than H_{c2}.
The procedure described allows one to obtain the exact value of H_{c3}, but requires cumbersome numerical calculations. We can, instead, use a simpler procedure, which will prove useful later on (Abrikosov 1964b). We write eq. (18.73) using the variables introduced earlier, ζ, ζ_0 and β :

$$-\frac{\mathrm{d}^2\Psi}{\mathrm{d}\zeta^2} + (\zeta - \zeta_0)^2\,\Psi = \beta\Psi \tag{18.77}$$

The problem of solving this equation may be presented as a variational problem of finding the minimum of a quantity:

$$\beta = \frac{\int_0^\infty \left[\left(\frac{\mathrm{d}\Psi}{\mathrm{d}\zeta}\right)^2 + (\zeta-\zeta_0)^2\,\Psi^2\right]\mathrm{d}\zeta}{\int_0^\infty \Psi^2\;\mathrm{d}\zeta}$$

Indeed, varying with respect to Ψ, we arrive at eq. (18.77).
We substitute into the functional (18.77) the trial function $\Psi = \exp\left(-\frac{1}{2}b\zeta^2\right)$, which satisfies the correct boundary conditions: $\Psi(\infty) = 0,\ \mathrm{d}\Psi/\mathrm{d}\zeta = 0$. The coefficient b
but, as has been shown in sections 18.2, these are equivalent statements of the problem. Thus, substituting $A = H_0\,(x - x_0)$ into eq. (18.9), we obtain

$$-\frac{\mathrm{d}^2\Psi}{\mathrm{d}x^2} + \chi^2 H_0^2\,(x - x_0)^2\,\Psi = \chi^2\Psi. \tag{18.73}$$

The solution of this equation in the general case is

$$\Psi = \exp\left(-\frac{1}{2}\zeta^2\right)\left\{C_1 F\left[\frac{1}{4}(1-\beta), \frac{1}{2}, (\zeta-\zeta_0)^2\right] + \zeta C_2 F\left[\frac{1}{4}(3-\beta), \frac{3}{2}, (\zeta-\zeta_0)^2\right]\right\} \tag{18.74}$$

where

$$\zeta = (xH_0)^{1/2}\, x, \quad \zeta_0 = (xH_0)^{1/2}\, x_0, \quad \beta = \frac{x}{H_0},$$

$F(\alpha, \gamma, z)$ is a degenerate hypergeometric function satisfying the equation

$$zF'' + (\gamma - z)F' - \alpha F = 0, \tag{18.75}$$

and C_1 and C_2 are arbitrary constants (see Landau and Lifshitz 1974).
The boundary conditions enable one to determine the ratio C_2/C_1 and β as a function of x_0. After this, minimizing β with respect to x_0, we obtain $\beta_{\min}$ or $H_{0,\,\max}$. This turns out to be equal to

$$H_{c3} = 1.695\chi = 1.695 H_{c2}. \tag{18.76}$$

This is the critical field of surface superconductivity. It is larger than $\boldsymbol{H_{c2}}$.
The procedure described allows one to obtain the exact value of H_{c3}, but requires cumbersome numerical calculations. We can, instead, use a simpler procedure, which will prove useful later on (Abrikosov 1964b). We write eq. (18.73) using the variables introduced earlier, ζ, ζ_0 and β :

$$-\frac{\mathrm{d}^2\Psi}{\mathrm{d}\zeta^2} + (\zeta - \zeta_0)^2\,\Psi = \beta\Psi \tag{18.77}$$

The problem of solving this equation may be presented as a variational problem of finding the minimum of a quantity:

$$\beta = \frac{\int_0^\infty \left[\left(\frac{\mathrm{d}\Psi}{\mathrm{d}\zeta}\right)^2 + (\zeta-\zeta_0)^2\,\Psi^2\right]\mathrm{d}\zeta}{\int_0^\infty \Psi^2\,\mathrm{d}\zeta}$$

Indeed, varying with respect to Ψ, we arrive at eq. (18.77).
We substitute into the functional (18.77) the trial function $\Psi = \exp\left(-\frac{1}{2}b\zeta^2\right)$, which satisfies the correct boundary conditions: $\Psi(\infty) = 0,\ \mathrm{d}\Psi/\mathrm{d}\zeta = 0$. The coefficient b
must be determined from the minimum condition for β. Evaluating the integrals, we get

$$\beta = \frac{1}{2}b + \frac{1}{2b} - \frac{2\zeta_0}{(\pi b)^{1/2}} + \zeta_0^2$$

Minimizing with respect to b, we obtain $\beta\,(\zeta_0)$. Then, we are to find the minimum with respect to ζ_0. Instead, we proceed in the reverse order, i.e., first we find the minimum with respect to ζ_0 and then with respect to b. By simple calculations we obtain

$$\beta_{\min} = b = \left(1 - \frac{2}{\pi}\right)^{1/2}, \quad \zeta_0 = \frac{1}{(\pi b)^{1/2}}. \tag{18.78}$$

This yields

$$H_0 = 1.66x,$$

which differs from the true value (18.76) by 2%.
Thus, we conclude that the superconductivity is retained in the surface layer up to fields larger than H_{c2} and, hence, in this layer persistent currents may be circulating. However, these currents cannot screen out the field inside the specimen. In fact, if the field inside the specimen were different from the external field, this would give rise to an additional bulk energy:

$$\int (H - H_0)^2 \ \mathrm{d}V$$

which could not be compensated by a decrease in energy in the surface sheath. Hence, the current density in the surface sheath is distributed so that $\int_0^\infty j_y \, \mathrm{d}x = 0$, i.e., j_y changes sign with depth. This is seen from the fact that j_y is equal to $-A\Psi^2 = -H_0 (x - x_0) \Psi^2$. If the result of the variational calculation is substituted, we obtain

$$\int_0^\infty (\zeta - \zeta_0) \exp(-b\zeta)^2 \, \mathrm{d}\zeta = \frac{1}{2} \left[\frac{1}{b} - \zeta_0 \left(\frac{\pi}{b} \right)^{1/2} \right]$$

According to eq. (18.79) this integral is equal to zero. This is also valid for the exact solution.

It is interesting to note that at $1/\sqrt{2} > x > (1.69\sqrt{2})^{-1}$ the superconductor will belong to type I, i.e., it passes to the normal state discontinuously at H_{cm}. However, the superconductivity in the surface sheath will persist up to $H_{c3} = 1.69\sqrt{2}\varkappa H_{\mathrm{cm}}$. From all this it follows that the determinations of the transition to the normal state in a magnetic field from the disappearance of the diamagnetic moment at the one hand and the appearance of resistance between contacts applied to the superconductor surface on the other may give different results.

The field H_{c3} plays another important role. In section 17.3 we have noted that the normal phase in type I superconductors may be retained when the field is decreased below the critical value. This retardation may occur up to the limiting supercooling field, when the free energy minimum corresponding to the normal phase vanishes. In the case of a bulk type I superconductor the supercooling field is determined from the condition of the possibility of existence of a small stationary nucleus of the superconducting phase in a normal conductor. As a matter of fact, at larger fields it must decrease with time and increase at lower fields. But this is exactly the condition from which the fields H_{c2} and H_{c3} were determined. Since $H_{c3} > H_{c2}$, the supercooling field is defined exactly as the field H_{c3}. Of course, this makes sense only for those type *I* superconductors for which $H_{c3} < H_{\mathrm{cm}}$, i.e., $x < (1.69\sqrt{2})^{-1}$. But if $1/\sqrt{2} > x > (1.69\sqrt{2})^{-1}$, the retardation of the normal phase does not occur because a superconducting nucleus appears at the surface even before the transition.

However, the surface can be "spoiled" deliberately, say by way of absorption of magnetic atoms (section 21.1) or by sputtering a film of a normal metal (section 20.1). In such a case, surface superconductivity is impossible, and the role of the supercooling field will be played by H_{c2}.

Let us now examine a case where the external field is directed at an angle to the sample surface. Let the superconductor occupy the half-space $x > 0$ and let the magnetic field have the following components:

$$H_z = H_0 \cos\theta, \quad H_x = H_0 \sin\theta. \tag{18.79}$$

The vector potential is chosen along the y axis:

$$A_y = H_0(x \cos\theta - z \sin\theta). \tag{18.80}$$

The equation for Ψ in the linear approximation is written as

$$-\frac{\partial^2\Psi}{\partial x^2}+\left[\mathrm{i}\frac{\partial}{\partial y}+\varkappa H_0(x\cos\theta-z\sin\theta)\right]^2\Psi-\frac{\partial^2\Psi}{\partial z^2}=x^2\Psi. \tag{18.81}$$

The boundary conditions are the same as before.
Along the boundary plane, in particular along the z direction, the conditions must be uniform. It is not difficult to see that the variation of z in eq. (18.81) can be compensated by the phase factor $\exp(\mathrm{i}ky)$ in the function Ψ, i.e., we are dealing here with a situation very similar to what occurs close to H_{c2} (section 18.2). But in order to obtain the critical field, it is sufficient to solve the linear equation, and the solution may be a superposition of the solutions localized near any z, and in particular, one solution of such a type. Therefore, it is sufficient to find Ψ which vanishes as $z\to\pm\infty$. Substituting $\Psi(x,y,z)=\exp(\mathrm{i}xH_0x_0y)\,\Psi(x,z)$ and introducing the variables

$$\zeta=(xH_0)^{1/2}\,x,\quad \zeta_0=(xH_0)^{1/2}\,x_0,\quad \eta=(xH_0)^{1/2}\,z,\quad \beta=x/H_0,$$

we obtain the generalization of eq. (18.77):

$$-\frac{\partial^2\Psi}{\partial\zeta^2}-\frac{\partial^2\Psi}{\partial\eta^2}+\left[(\zeta-\zeta_0)\cos\theta-\eta\sin\theta\right]^2\Psi=\beta\Psi$$

This equation is equivalent to the variational principle for determination of the minimum of β :

$$\beta=\frac{\int_0^\infty \mathrm{d}\zeta\int_{-\infty}^\infty \mathrm{d}\eta\left\{\left(\frac{\partial\Psi}{\partial\zeta}\right)^2+\left(\frac{\partial\Psi}{\partial\eta}\right)^2+\left[(\zeta-\zeta_0)\cos\theta-\eta\sin\theta\right]^2\Psi^2\right\}}{\int_0^\infty \mathrm{d}\zeta\int_{-\infty}^\infty \mathrm{d}\eta\Psi^2} \tag{18.82}$$

We shall assume the trial function $\Psi=\exp\left(-\frac{1}{2}a\eta^2-\frac{1}{2}b\zeta^2\right)$, which would satisfy the boundary conditions. We get

$$\beta=\frac{1}{2}\left(b+\frac{1}{b}\cos^2\theta\right)+\frac{1}{2}\left(a+\frac{1}{a}\sin^2\theta\right)+\cos^2\theta\left(\zeta_0^2-\frac{2\zeta_0}{(\pi b)^{1/2}}\right).$$

Minimizing this expression with respect to $\boldsymbol{a},\boldsymbol{b}$ and ζ_0, we find

$$\begin{aligned}&\beta=\cos\theta\left(1-\frac{2}{\pi}\right)^{1/2}+\sin\theta,\quad b=\cos\theta\left(1-\frac{2}{\pi}\right)^{1/2},\\&a=\sin\theta,\quad \zeta_0=\frac{1}{(\pi b)^{1/2}}.\end{aligned} \tag{18.83}$$

Substituting

$$\beta=\frac{\chi}{H_{c3}(\theta)},\quad H_{c3}(0)=\chi\left(1-\frac{2}{\pi}\right)^{-1/2},\quad H_{c2}=x,$$

we have

$$\frac{1}{H_{c3}(\theta)}=\frac{1}{H_{c3}(0)}\cos\theta+\frac{1}{H_{c2}}\sin\theta, \tag{18.84}$$

that is, a smooth variation of H_{c3} from $H_{c3}(0)$ at $\theta=0$ to H_{c2} at $\theta=\frac{1}{2}\pi$. This gives, in particular,

$$-\left(\frac{1}{H_{c3}}\frac{\mathrm{d}H_{c3}}{\mathrm{d}\theta}\right)_{\theta=0}=\frac{H_{c3}(0)}{H_{c2}}=1.66.$$

An exact calculation gives the value 1.35 (Saint-James 1965).
In order to determine the current distribution at fields somewhat lower than $\boldsymbol{H_{c3}(\theta)}$, we have to solve the nonlinear Ginzburg-Landau equation. The solution is
again taken in the form of a superposition of solutions of the type we found earlier, centered around various z :

$$\Psi = \exp\left(\mathrm{i}xH_0x_0y\right)\sum_{n=-\infty}^{\infty} C_n \mathrm{e}^{\mathrm{i}kny}\Psi_0\left(x, z - \frac{nk}{xH_0\sin\theta}\right). \tag{18.85}$$

A superposition of the same type, (18.18), was obtained close to $\boldsymbol{H_{c2}}$. The subsequent line of reasoning is quite analogous to section 18.2, and we shall not give it here. The result is a solution containing vortices, i.e., points which make the phase Ψ change by 2π when they are encircled (Kulik 1968a).

The periods of the vortex structure can be found using the idea that the rise of the vector potential is compensated by jumps of the phase gradient at branch cuts drawn through the vortex points parallel to the y axis. If the period along the y axis is a, then the jump in $\partial\varphi/\partial y$ at each line is $2\pi/a$. Compensation of the increase of the term $H_0z\sin\theta$ in (18.81) occurs with the condition

$$-\frac{2\pi}{a} + xH_0b\sin\theta = 0,$$

where b is the period in the z direction, or

$$ab = \frac{2\pi}{xH_0\sin\theta}. \tag{18.86}$$

In the case under consideration, as opposed to the neighborhood of $\boldsymbol{H_{c2}}$, anisotropy arises: the directions y and z are not equivalent because the field H lies in the xz plane. Nevertheless, if we assume a rectangular vortex lattice, the minimization of the free energy will lead to the result $a = b$, i.e., it will give a square lattice with a period given by

$$a = b = \left(\frac{2\pi}{xH_0\sin\theta}\right)^{1/2}. \tag{18.87}$$

Other variants have not been studied.
From formula (18.87) it follows that the period of the vortex structure increases with decreasing θ according to the law $a \sim \theta^{-1/2}$ (at small θ). Moreover, one of the basis vectors of the vortex lattice is directed along the component H in the plane of the surface (this is the z axis in the case under consideration).

The field H_{c3} has been detected in numerous experiments. There are also data in favor of the vortex structure of the surface currents with a tilted field. They refer to the critical current for surface superconductivity. A theoretical calculation of the critical current for the field parallel to the surface (Abrikosov 1964b), which is not given here, yields

$$J_c \sim j_c\xi,$$

where J_c is the critical current flowing through a cross-sectional area of length 1 cm (along the surface) and extending to infinity into the bulk of the metal; j_c is the
absolute critical value of the current density corresponding to the Landau criterion (see eq. 17.63). This result is obvious since the thickness of the superconducting sheath in the case of surface superconductivity is of order ξ. Formula (18.88) is an estimate of the value of the critical current within the interval $H_{c2} < H_0 < H_{c3}$. Actually the current depends on H_0 and vanishes at H_{c3}.

Much lower values of the critical current are always obtained in experiments. This may be accounted for by the fact that a field orientation exactly parallel to the surface cannot be realized in practice, and with a tilted field a vortex structure is formed. When current is flowing, the vortices are acted on by a force, which makes them move. As a result, electrical resistance arises (this point will be discussed in more detail in section 18.8). Strictly speaking, we must obtain zero critical current. However, in fact, the vortices cling to surface irregularities (pinning, see section 18.8) and therefore with a sufficiently small current they remain immobile. This effect can be enhanced by deliberately making the surface rougher. Indeed, in this case the critical current increases (Akhmedov et al. 1969).

8.4.6 18.5. Type II superconductors at low temperatures

In this section we shall draw certain conclusions concerning the behavior of type II superconductors at temperatures far from T_c, where the Ginzburg-Landau theory does not apply. We use conventional units.

It is rather obvious that at low temperatures the qualitative picture of the magnetic properties of superconductors is the same as in the vicinity of T_c. There is a surface energy σ_{ns}, which may be positive or negative. In type I superconductors it is positive; a first-order transition occurs at the field H_{cm}, and there is a supercooling field H_{c3} or H_{c2}. For type II superconductors σ_{ns} is negative, and the transition to the normal phase takes place by way of a second-order transition in the field $\boldsymbol{H}_{c2}$. Therefore, the ratio

$$\frac{H_{c2}(T)}{H_{cm}(T)\sqrt{2}} = \varkappa(T) \tag{18.89}$$

is a quantity that distinguishes the two types of superconductors (with $x < 1/\sqrt{2}$ and with $x > 1/\sqrt{2}$), and exactly this quantity was given in formulae (16.97) and (16.101).

In type II superconductors at all temperatures there arises a mixed state in a magnetic field. By order of magnitude the field H_{cl} has been defined in section 18.1. However, in case $x \gg 1$ (recall that, according to formulae 16.97 and 16.101x varies little with temperature) one can determine the value of H_{c1} rather precisely. To do this, we take into account that the major part of the vortex energy builds up in the region $\xi < \rho < \delta$, and in this region the detailed structure of its core, which has a radius of order ξ, is unimportant. The only important point is that the order parameter
and, hence, the current, begins to decrease at such distances and vanishes in the center.

Just as near T_c, each vortex carries one quantum of magnetic flux. This follows from the fact that at $\delta \gg \boldsymbol{\xi}$ far from the vortex axis the London equation (section 16.7) is valid. According to this equation, the current is connected with the vector potential by the relation $\mathbf{j} = -QA$, but in such a form the current is not gaugeinvariant, i.e., it depends on the choice of $\boldsymbol{A}$. To provide gauge invariance, it is necessary that $\boldsymbol{A}$ be included in the combination with the gradient of the phase of the complex order parameter $\Delta = |\Delta|e^{i\chi}$:

$$j = -Q\left(A - \frac{\hbar c}{2e}\nabla\chi\right). \tag{18.90}$$

But this expression is quite analogous to eq. (17.75).
Considering that far from the vortex axis $|\Delta|$ and, hence, Q are equal to their values in a superconductor in the absence of the field, i.e., are independent of the coordinates, it may be asserted that the flux is equal to an integer number of flux quanta inside the loop, for which $\oint j\, \mathrm{d}l = 0$. If we are dealing with a single vortex, then it is sufficient to choose the loop at $\rho \gg \delta$, where $j = 0$. In a case where there are many vortices and they form a lattice, one

can find such a loop around each vortex, on which $\oint j\ \mathrm{d}l = 0$ due to the lattice symmetry. Evidently, each vortex carries only one flux quantum.

As has been noted, at $\rho > \boldsymbol{\xi}$ we may consider Δ to be equal to its value in the absence of the field, which is why for H the London equation (15.39) is valid. Thus, we have

$$\Delta H - \delta^{-2} H = -\delta^{-2}\Phi_0 \delta(\rho). \tag{18.91}$$

The right-hand side takes account of the presence of a vortex with a magnetic flux Φ_0. Integrating over the cross-sectional area perpendicular to the vortex axis, we can see that the choice of the right-hand side is correct. The solution of eq. (18.91) is

$$H = \frac{1}{2\pi\delta^2}\Phi_0 K_0\left(\frac{\rho}{\delta}\right). \tag{18.92}$$

Now we must write the expression for the free energy corresponding to the London equation. It is made up of the field energy and the kinetic energy of the supercurrent. For unit volume we have

$$\Omega_\mathrm{s} - \Omega_\mathrm{s}^{(0)} = \frac{H^2}{8\pi} + \frac{1}{2} n_\mathrm{s} m v_\mathrm{s}^2 = \frac{H^2}{8\pi} + \frac{1}{2} n_\mathrm{s} m \left(\frac{j}{n_\mathrm{s} e}\right)^2 = \frac{H^2}{8\pi} + \frac{1}{2}\Lambda j^2, \tag{18.93}$$

where use is made of the expression $\Lambda = m/n_\mathrm{s}e^2$ (see eq. 15.35). Note that with this derivation it is immaterial whether we use the concept of superconducting electrons with density n_s, charge e and mass m or the concept of pairs with density $\frac{1}{2}n_\mathrm{s}$, charge $2e$ and mass $2m$.

The integral over the volume of the last term can be transformed using the Maxwell equation $\mathrm{rot}\,\boldsymbol{H} = (\boldsymbol{4}\pi/c)\boldsymbol{j}$:

$$\begin{aligned}
\frac{1}{2}\Lambda \int j^2\ \mathrm{d}V &= \frac{1}{2}\Lambda\left(\frac{c}{4\pi}\right)^2 \int (\mathrm{rot}\, H)^2\ \mathrm{d}V \\
&= \frac{\delta^2}{8\pi}\int \{\mathrm{div}[H\,\mathrm{rot}\,H] + H\,\mathrm{rot}\,\mathrm{rot}\,H\}\mathrm{d}V \\
&= \frac{\delta^2}{8\pi}\left\{\int_S [H\,\mathrm{rot}\,H]\mathrm{d}S - \int H\Delta H\ \mathrm{d}V\right\}
\end{aligned}$$

Here we have used the formula $\mathrm{div}[\boldsymbol{ab}] = \boldsymbol{b}\ \mathrm{rot}\ \boldsymbol{a} - \boldsymbol{a}\ \mathrm{rot}\ \boldsymbol{b}$, transformed the integral of div to an integral over the sample surface and took advantage of the fact that $\mathrm{rot}\,\mathrm{rot}\,\boldsymbol{H} = \mathrm{grad}\,\mathrm{div}\,\boldsymbol{H} - \Delta\boldsymbol{H}$ and $\mathrm{div}\,\boldsymbol{H} = 0$. Thus, we have

$$\begin{aligned}
\int \Omega_\mathrm{s}\ \mathrm{d}V = \int \Omega_\mathrm{s}^{(0)}\mathrm{d}V + \frac{\delta^2}{8\pi}\int_\mathrm{S} [H\,\mathrm{rot}\,H]\mathrm{d}S \\
+ \frac{1}{8\pi}\int H\left(H - \delta^2\Delta H\right)\mathrm{d}V
\end{aligned} \tag{18.94}$$

We give also another form of this expression. Since

$$[H\ \mathrm{rot}\ H] = \frac{1}{2}\nabla\left(H^2\right) - (H\nabla)H, \quad H\Delta H = \mathrm{div}\left[\frac{1}{2}\nabla(H)^2\right] - (\nabla H)^2,$$

we can obtain from eq. (18.94), for a case where $(\boldsymbol{H}\nabla)\boldsymbol{H} = 0$, i.e., $\boldsymbol{H}$ is directed along z and depends only on ρ :

$$\int \Omega_\mathrm{s}\ \mathrm{d}V = \int \Omega_s^{(0)} + \frac{1}{8\pi}\int \left[H^2 + \delta^2(\nabla H)^2\right]\mathrm{d}V \tag{18.94'}$$

In the case of a single vortex under consideration the surface integral in (18.94) is equal to zero. We must substitute formulae (18.91) and (18.92) into the second integral of (18.94). The logarithmic infinity $K_0(\rho)$ at $\rho = 0$ must be replaced by $\ln(\delta/\xi)$ because at a distance of order ξ from the axis eq. (18.91) is no longer valid and H ceases to depend on the coordinate (with a logarithmic accuracy). As a result, we obtain an extra energy per unit length of the vortex:

$$\varepsilon_0 \approx \frac{1}{(4\pi\delta)^2}\Phi_0^2 \ln\left(\frac{\delta}{\xi}\right) \tag{18.95}$$

We have limited ourselves to the calculation of the dominant term with $\ln(\delta/\xi)$ because higher accuracy requires a knowledge of the core structure.

The condition of the nucleation of a vortex is

$$\varepsilon_0 - \frac{1}{4\pi}H_0 \int H \ \mathrm{d}S = \varepsilon_0 - \frac{1}{4\pi}H_0\Phi_0 = 0$$

From this relation we obtain

$$H_{\mathrm{c1}} = 4\frac{\pi\varepsilon_0}{\Phi_0} \approx \frac{1}{4\pi}\frac{\Phi_0}{\delta^2}\ln\left(\frac{\delta}{\xi}\right) \tag{18.96}$$

This formula is consistent in order of magnitude with eqs. (18.8) and (18.50). Note that, in accordance with formula (18.91), the field in the vortex core is equal with logarithmic accuracy to

$$H(0) \approx \frac{1}{2\pi}\frac{\Phi_0}{\delta^2}\ln\left(\frac{\delta}{j}\right)$$

that is, just as near $T_{\mathrm{c}}, H(0)$ is about twice as large as H_{cl}.

The expression for the current is derived from the Maxwell equation $\boldsymbol{j} = (c/4\pi)\ \mathrm{rot}\ H$. In the case under consideration,

$$j_\varphi = \frac{c}{2\delta}\frac{1}{(2\pi\delta)^2}\Phi_0 K_1\left(\frac{\rho}{\delta}\right) \tag{18.97}$$

At $\rho < \delta, \quad K_1 \approx \delta/\rho$. Substituting $\Phi_0 = \pi\hbar c/e, \quad \delta = (mc^2/4\pi n_{\mathrm{s}}e^2)^{1/2}$ gives

$$j_\varphi \approx n_{\mathrm{s}}e\frac{\hbar}{2m\rho}$$

From this it follows that the velocity of Cooper pairs in the vortex at a distance of $\xi < \rho < \delta$ is equal to $\hbar/2m\rho$ and this is in agreement with formula (18.7) deduced from the Bohr quantization rule. At distances of $\rho \geqslant \delta$ it becomes important that the liquid consists of charged particles and its motion leads to generation of a magnetic field. As a result, at $\rho > \delta$ the current is damped according to the law $\exp(-\rho/\delta)$.

Taking into account the agreement between eq. (18.52) near T_{c} and eq. (18.91) and also between expressions (18.55) and (18.94) for the free energy, and considering that each vortex carries one flux quantum, we conclude that formulae (18.60) and (18.58) are also valid, provided that correct units are used, namely x has to be replaced by $2\pi\delta^2/\Phi_0$. This refers also to the limiting expressions (18.61) and (18.67) and also to formula (18.68) without the last term, which cannot be determined accurately because of the logarithmic accuracy in the calculation of H_{c1}. All these results characterize the dependence $B\,(H_0)$ at $H_{\mathrm{cl}} \leqslant H_0 < H_{\mathrm{c2}}$.

In what follows the estimates for critical fields expressed in terms of $\boldsymbol{\Phi_0}$ and characteristic lengths will be useful. Formula (18.96) gives an estimate for H_{c1}. With the field H_{c2} the vortices are moved together to distances of order ξ and since there is one flux quantum per vortex, it

follows that $\boldsymbol{H}_{c2} \sim \boldsymbol{\Phi}_0/\boldsymbol{\xi}^2$. Finally, because of $H_{c2} \sim H_{cm}x \sim H_{cm}\delta/\xi$, we have $H_{cm} \sim \Phi_0/\delta\xi$. Thus,

$$H_{c1} \sim \frac{\Phi_0}{\delta^2}, \quad H_{cm} \sim \frac{\Phi_0}{\delta\xi}, \quad H_{c2} \sim \frac{\Phi_0}{\xi^2}. \tag{18.98}$$

While comparing the theory with experiment, it is necessary to take into account a number of circumstances. First of all, large x values are attained only in superconductors with a large impurity concentration. We have already noted in section 16.9 that impurities present in a small concentration have a very slight effect on the thermodynamic properties of the superconductor, in particular on H_{cm}. However, at a large impurity concentration of the order of tens of percent, we are actually dealing with a new substance.

The boundaries of the mixed state are the fields H_{cl} and H_{c2}, which are sufficiently clearly seen in the $\boldsymbol{B}(\boldsymbol{H}_0)$ curve. It turns out that from this curve one can also easily determine $\boldsymbol{H}_{cm}$. Indeed, at $\boldsymbol{H}_{c2}$

$$\Omega_s(H_{c2}) = \Omega_n(H_{c2}).$$

From this it follows (see Appendix III) that

$$\Omega_s^{(0)} - \frac{1}{4\pi}\int_0^{H_{c2}} B(H_0)\,dH_0 = \Omega_n^{(0)} - \frac{H_{c2}^2}{8\pi}.$$

But since $\Omega_n^{(0)} - \Omega_s^{(0)} = H_{cm}^2/8\pi$, we find that

$$\frac{1}{2}H_{cm}^2 = \int_0^{H_{c2}} [H_0 - B(H_0)]\,dH_0 = \int_0^{H_{c2}} [-4\pi M(H_0)]\,dH_0. \tag{18.99}$$

In other words, H_{cm} is determined by the area under the curve of $-\boldsymbol{4\pi M}$ versus $\boldsymbol{H}_0$.
In experiments one often has to work with specimens of noncylindrical shape. If the specimen has the form of an ellipsoid, the role of the external field H_0 is played by the "internal" field H_i (Appendix III):

$$H_i = H_0 - 4\pi nM,$$

where M is the magnetization and n is the demagnetization factor. The magnetization M is connected with B by the relation

$$B = H_i + 4\pi M$$

Expressing M by this relation and substituting into the preceding formula, we obtain

$$(1-n)H_i + nB = H_0.$$

If the dependence $B(H_0)$ for cylindrical geometry obtained earlier is written in the form $H_0 = f(B)$, the same function will now relate H_i to B. As a result, we have

$$(1-n)f(B) + nB = H_0. \tag{18.100}$$

This is just the relation between B and H_0 for the ellipsoid. In particular, the onset of the mixed state corresponds to $B = 0, f(B) = H_{cl}$. Hence, for the ellipsoid it begins at

$$H_0 = (1-n)H_{c1}. \tag{18.101}$$

In particular, for an infinite plate in a perpendicular field ($n = 1$) it begins at $H_0 = 0$. The termination of the mixed state corresponds to $B = f(B) = H_0 = H_{c2}$.

While speaking of comparison with experiment, one more circumstance must be borne in mind. The variation of the induction with H_0 in the mixed state is the result of the variation of the vortex density. Hence, upon gradual variation of H_0 there is a displacement of the vortices. This displacement can be hindered by the microscopic irregularities of the specimen (pinning). We defer a more detailed discussion of this point until section 18.7; for the moment we only note that the dependence $B(H_0)$ for real specimens may prove to be rather far from the theoretical equilibrium curve, so that comparison of theory with experiment may be made only for specially prepared homogenized specimens. Homogenization can be achieved, in particular, by prolonged annealing at a temperature close to the melting point.

However, even in this case there is a certain inevitable potential barrier which impedes the free motion of the vortices. It is associated with the sample surface (Bean and Livingston 1964). Let us consider a vortex which is approaching the surface (fig. 119). We assume that $x > 1$, that the vortex axis is parallel to the sample surface (along the z axis), and that the distance x_1 from the axis to the surface by far exceeds the radius of the core. In the absence of the vortex the field is equal to $H_0 e^{-x/\delta}$. The vortex adds its own magnetic field, which is distorted by the surface so as, first, not to produce an extra field at the surface (because the field is specified and equals $\boldsymbol{H}_0$) and, second, to make the current normal to the surface vanish.

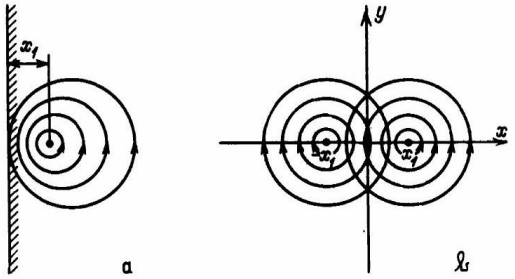


Fig. 119.

This can be realized if we add to the vortex its mirror image relative to the surface with the opposite direction of the field and current (fig. 119b). The vortex field will satisfy the London equation with two sources:

$$\Delta H - \frac{1}{\delta^2} H = -\frac{1}{\delta^2} \Phi_0 \left[\delta(\rho - \rho_1) - \delta(\rho - \rho_2)\right], \tag{18.102}$$

where $\rho_1 = (x, 0)$ and $\rho_2 = (-x_1, 0)$; the total magnetic field will be given by

$$H = H_0 e^{-x/\delta} + \frac{\Phi_0}{2\pi\delta^2} \left[K_0\left(\frac{|\rho - \rho_1|}{\delta}\right) - K_0\left(\frac{|\rho - \rho_2|}{\delta}\right)\right]. \tag{18.103}$$

Let us find the energy in a given field using these formulas:

$$\int \Omega_{sH} \, dV = \int \Omega_s \, dV - \frac{1}{4\pi} H_0 \int H \, dV.$$

We shall calculate the energy per unit length along z and integrate over the half-plane $x > 0$. In this case, as opposed to a single vortex in infinite space, the integral over the surface does not vanish, so we must be careful.

Let us, first, integrate eq. (18.102) over the half-plane $x > 0$. Then we obtain (the normal to the surface is directed along $-x$):

$$\int H \, dV = \Phi_0 + \delta^2 \int \Delta H \, dx \, dy = \Phi_0 - \delta^2 \int_{x=0} \frac{\partial H}{\partial x} \, dy.$$

Hence,

$$-\frac{H_0}{4\pi}\int H\ \mathrm{d}V = -\frac{H_0\Phi_0}{4\pi} + \frac{\delta^2 H_0}{4\pi}\int_{x=0}\frac{\partial H}{\partial x}\ \mathrm{d}y.$$

The surface integral in (18.94) is equal to

$$\frac{\delta^2}{8\pi}\int [H\,\mathrm{rot}\,H]\mathrm{d}S = -\frac{\delta^2}{8\pi}H_0\int_{x=0}\frac{\partial H}{\partial x}\ \mathrm{d}y.$$

The volume integral in eq. (18.94) is evaluated with the aid of formulae (18.102) and (18.103). Here we replace $K_0(0)$ by $\ln(\delta/\xi)$ because at distances smaller than ξ the theory presented here is no longer valid and we have to extrapolate H from $x \sim \xi$. We also make use of formula (18.96). Substituting formulas (18.103) for H into the integral $(\delta^2/8\pi)\,H_0\int_{x=0}(\partial H/\partial x)\mathrm{d}y$, we see that the first term gives $-(\delta H_0^2/8\pi)\int \mathrm{d}y$, which corresponds to the field energy in the layer δ without a vortex. This energy is neglected here.

As a result, the energy associated with the vortex is given by

$$U(x_1) = \frac{\Phi_0}{4\pi}\left\{H_0\exp\left(-\frac{x_1}{\delta}\right) - \frac{\Phi_0}{4\pi\delta^2}K_0\left(\frac{2x_1}{\delta}\right) - H_0 + H_{c1}\right\}. \tag{18.104}$$

At distances $x_1 \leqslant \xi$, $K_0(2x_1/\delta)$ must be replaced by $\ln(\delta/\xi)$. Comparing with (18.96), we see that over such distances $U(x_1)$ vanishes. With $x_1 \to \infty$ the first two terms of (18.104) vanish; $U(\infty) < 0$ at $H_0 > H_{c1}$ and $U(\infty) > 0$ at $H_0 < H_{c1}$, as should be expected. The graph of the function $U(x_1)$ is given in fig. 120 . We see that a potential barrier appears near the surface, which hinders both the entry of the vortex into the superconductor and its escape from it. An increase in the field leads to the disappearance of the barrier only at a certain field $H_0 = H'_{c1} > H_{c1}$.

This field can be estimated as follows. The condition $U'(x_1) = 0$ yields

$$\frac{\Phi_0}{4\pi\delta^2}\frac{2}{\delta}K_1\left(\frac{2x_1}{\delta}\right) - \frac{H_0}{\delta}\exp\left(-\frac{x_1}{\delta}\right) = 0.$$

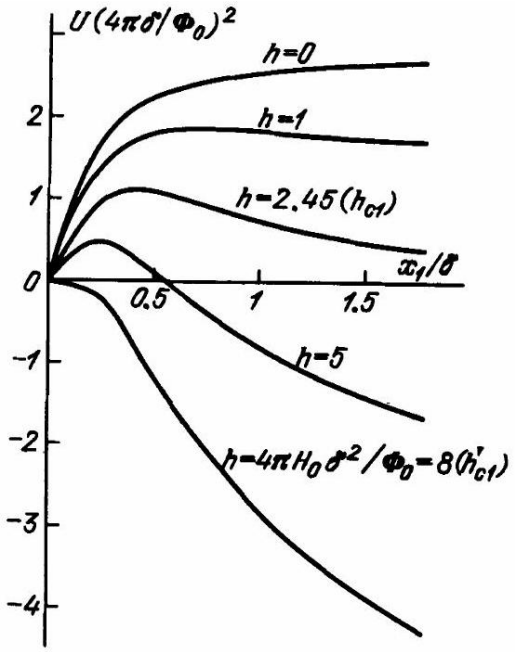


Fig. 120.

We are interested in the case where the top of the barrier reaches the surface, i.e., $x_1 = 0$. But as $x_1 \to 0, K_1(2x_1/\delta) \approx \delta/2x_1$. As has already been pointed out, at small x_1 we have to replace x_1 by ξ, i.e., $K_1(2x_1/\delta) \sim \delta/\xi$. As a result, we have (see eq. 18.97):

$$H'_{\rm cl} \sim \frac{\Phi_0}{\delta\xi} \sim H_{\rm cm}.$$

As the field decreases the barrier disappears only at $\boldsymbol{H_0} = \mathbf{0}$.
In real experiments, the field lines of force are always concentrated at the edges of the sample, and thus at these sites the external field may exceed $H'_{\rm c1}$. It is these edges that will be "weak places" through which the vortices will enter the sample. Therefore, the $B(H_0)$ curve taken in an increasing field may be regarded as an equilibrium curve*. However, when the field falls off, the sample surface has no portions where the field is zero and, hence, the barrier is preserved everywhere. Therefore, the magnetization curve taken in a decreasing field even in the most homogenized samples will be nonequilibrium. This is supported by experimental data (fig. 121).

We will now consider another property of the mixed state. As has been found earlier, at the vortex axis $\Delta = 0$. But the spectrum of quasiparticles in a superconductor begins with the energy Δ. In view of this, the possibility is not excluded that there exist special quasiparticles localized near the vortex axis, with zero excitation

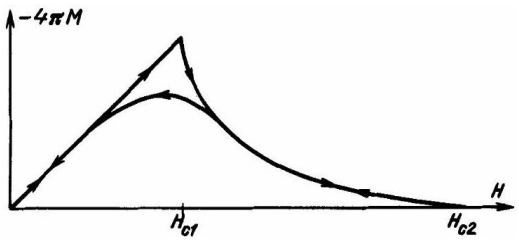


Fig. 121.

energy. This idea is confirmed by rigorous theoretical calculations (Caroli and Matricon 1965, Caroli et al. 1965). Indeed, in the mixed state the superconductor has quasiparticles which move along the vortex axis and which have finite density of states as $\varepsilon \to 0$, just as in cylinders of a normal metal with a radius of order ξ.

Since the cross-sectional area of the core of a single vortex is of the order of ξ^2 and the number of vortices that pass through 1 cm^2 is $n = B/\Phi_0$, the fraction of "normal metal" is $\xi^2 B/\Phi_0$ and, accordingly, the density of states is given by

$$\nu \sim \nu_n \xi^2 \frac{B}{\Phi_0},$$

where $\nu_{\rm n}$ is the density of states for a normal metal. At the field $H_{\rm c2}$ the vortices approach each other to a distance of the order of ξ; in this case $B \approx H_{\rm c2} \sim \Phi_0/\xi^2$ (see eq. 18.97). Hence, the density of states may be written as

$$\nu = \nu_{\rm n} \frac{B}{H_{\rm c2}} \tag{18.105}$$

- In specially prepared samples with a very smooth surface it is possible to succeed in retarding the transition in an increasing field. This provides good agreement with the result of the exact theory, $H'_{\rm c1} = H_{\rm cm}$.

(the equality sign is used because of the condition of matching with a normal metal at $B = H_{c2}$). But the finite density of states leads to a linear dependence of heat capacity on temperature. Thus, we arrive at the conclusion that at $T < T_c$ in type II superconductors in the mixed state the heat capacity is linear in temperature:

$$\Delta C(B) = \frac{1}{3}\pi^2 \nu_n \frac{TB}{H_{c2}} = C_n(T)\frac{B}{H_{c2}}. \tag{18.106}$$

In conclusion we note that, just as in the vicinity of $\boldsymbol{T}_c$, the generation of a superconducting nucleus near the surface is possible at fields larger than $\boldsymbol{H}_{c2}$. The ratio H_{c3}/H_{c2} depends on temperature and on electron scattering conditions at the sample surface. A calculation performed by means of a variational method similar to that employed in section 18.4 gives, at $T = 0, H_{c3}/H_{c2} \geqslant 1.99$ for specular reflection of electrons from the surface and $H_{c3}/H_{c2} \geqslant 2.09$ for diffuse reflection (Kulik 1968). We see that all the magnetic properties of type II superconductors are not only qualitatively similar to those observed in the vicinity of T_c but differ little quantitatively from them (in the corresponding units).

8.4.7 18.6. A thin film of a type II superconductor in a magnetic field

The critical field of thin films of type I superconductors with $x < 1$ has been calculated in section 17.3. The condition $x < 1$ enabled us to assume $\Psi \approx$ const. throughout the superconductor. In all subsequent computations x did not appear. Some of the results of section 17.3 may also be extended to type II superconductors. Indeed, with thicknesses of $d < \xi$ (in reduced units $d < x^{-1}$) Ψ must not vary throughout the film thickness. But for type II superconductors $\xi < \delta$ and, hence, one must employ the formulas for $d < \delta$ (in reduced units $d < 1$). In particular, the critical field of the transition to the normal state is expressed by formulae (17.48) or (17.48'). Note that for such films the ratio δ/d plays the role of the "effective" parameter $\varkappa$, therefore formula (17.48) is completely consistent with formulae (18.2) and (18.3) for the upper critical field of type II superconductors.

As far as real experimental objects are concerned, films of type II superconductors are prepared by vaporization of a small piece of metal and condensation of the vapor onto a non-metallic substrate kept at helium temperature. It turns out that the atoms of the metal upon contact with the substrate immediately stick to it and are not displaced. Therefore, the film formed is almost entirely amorphous, i.e., has a small mean free electron path and therefore belongs to type II, even if the parent pure metal was a type I superconductor and had $x < 1$. Thus, we see that a film of a type II superconductor is a rather common object. When such a film is annealed, i.e., its temperature is raised to several tens of degrees, recrystallization occurs, and it becomes a type I superconductor with H_{cm} and T_c close to the characteristics of the bulk material. The same occurs if the metal is vaporized onto a substrate kept at room temperature.

A question arises as to the possibility of realizing a mixed state in a film with $x > 1/\sqrt{2}$. The qualitative answer to this question is rather obvious: the mixed state is possible with thicknesses of $d \geqslant \xi$. From this it follows that with decreasing film thickness the field H_{cl} must increase more rapidly than the field H_{c2} and they must become equal at $d \sim \xi$.

Let us now consider the problem quantitatively. In order to find H_{cl}, we are to find the conditions for the creation of one vortex. From symmetry considerations it is clear that the lowest energy will be exhibited by a vortex in the center of the film. In the preceding section it has been shown that the boundary conditions on a planar boundary may be fulfilled by introduction of a specularly reflected vortex with an opposite direction of the field and current. In the case under consideration, there are two boundaries and, as a result, there arises an infinite

system of reflections which are alternating in field and current, with a distance d between the nearest vortices. Instead of eq. (18.102), we have

$$\Delta H - \frac{1}{\delta^2} H = \frac{1}{\delta^2} \Phi_0 \sum_{n=-\infty}^{\infty} (-1)^n \delta(\rho - \rho_n), \tag{18.107}$$

where $\rho_n = (nd, 0)$ and n assumes all integer values, positive and negative.

The total magnetic field, which satisfies the conditions $H = H_0$ at $x = \pm\frac{1}{2}d$ will be equal to (see eq. 18.102 and 18.103)

$$\begin{aligned} H =& H_0 \frac{\cosh(x/\delta)}{\cosh(d/2\delta)} \\ &+ \frac{\Phi_0}{2\pi\delta^2} \sum_{n=-\infty}^{\infty} (-1)^n K_0 \left(\frac{|\rho - \rho_n|}{\delta} \right). \end{aligned} \tag{18.108}$$

Let us now find the free energy. Using the same procedure as in the preceding section, we find the energy of one vortex in the field (per unit length):

$$\begin{aligned} \int \left(\Omega_{\mathrm{s}H} - \Omega_{\mathrm{s}H}^{(0)} \right) \mathrm{d}V = & \int \left(\Omega_{\mathrm{s}} - \Omega_s^{(0)} \right) \mathrm{d}V \\ & - \frac{1}{4\pi} H_0 \int \left[H(\rho) - H^{(0)}(\rho) \right] \mathrm{d}V, \end{aligned}$$

where $\Omega_{\mathrm{sH}}^{(0)}$ and $\Omega_{\mathrm{s}}^{(0)}$ correspond to the absence of a vortex and $H^{(0)}(\rho)$ is the first term in (18.108). Calculation gives

$$\begin{aligned} & \int_{-d/2}^{d/2} \mathrm{d}x \int_{-\infty}^{\infty} \mathrm{d}y \left(\Omega_{\mathrm{s}H} - \Omega_{\mathrm{sH}}^{(0)} \right) \\ & = \frac{1}{4\pi} \frac{\Phi_0 H_0}{\cosh(d/2\delta)} \\ & \quad + 2 \left(\frac{\Phi_0}{4\pi\delta} \right)^2 \sum_{n=1}^{\infty} (-1)^n K_0 \left(\frac{nd}{\delta} \right) + \frac{1}{4\pi} \left[H_{\mathrm{c}1}(\infty) - H_0 \right] \Phi, \end{aligned}$$

where $H_{\mathrm{c}1}(\infty)$ corresponds to an infinite sample. Equating this expression to zero, we obtain the first critical field for a sample of thickness d (Abrikosov 1964a):

$$H_{\mathrm{c}1}(d) = \frac{H_{\mathrm{c}1}(\infty) - \frac{\Phi_0}{2\pi\delta^2} \sum_{n=1}^{\infty} (-1)^{n+1} K_0 \left(\frac{nd}{\delta} \right)}{1 - \frac{1}{\cosh(d/2\delta)}} \tag{18.109}$$

The limiting formulas are as follows:

$$\begin{aligned} & H_{\mathrm{c}1}(d) \approx H_{\mathrm{c}1}(\infty) \left[1 + 2\exp\left(\tfrac{-d}{2\delta} \right) \right], && d > \delta \\ & H_{\mathrm{c}1}(d) \approx \tfrac{2\Phi_0}{\pi d^2} \ln\left(\tfrac{d}{\xi} \right), && d < \delta \end{aligned} \tag{18.110}$$

In the last formula we used the integral representation of the MacDonald function (preceding eq. 16.29) and expression (18.95) for $H_{\mathrm{c}1}$ at $x > 1$ (the expression is written with logarithmic accuracy). The asymptotic of (18.110) for $d < \delta$ is suitable
only at $d \gg$. From this asymptotic it follows that $H_{\mathrm{c}1}$ increases with decreasing thickness proportionately to d^{-2}, whereas $H_{\mathrm{c}2}$ increases proportionately to d^{-1} (see eq. 17.48). From the BCS theory it follows that $H_{\mathrm{cm}} \sim \Phi_0/(\delta\xi)$ (see eq. 18.98). Comparing $H_{\mathrm{c}2} \sim H_{\mathrm{cm}}\delta/d \sim \Phi_0/(\xi d)$ with $H_{\mathrm{c}1} \sim \Phi_0/d^2$, we see that the two fields become equal at $d \sim \xi$.

We shall now consider a thin plate in a perpendicular magnetic field. We assume the plate thickness to be much smaller than the penetration depth. Let us show that in this case vortices are also generated, and not only in a type II superconductor but in a type I superconductor as well (Pearl 1964).

Suppose that such a vortex has been formed and that the field and current are damped at a distance much larger than ξ. In this case, outside the core with a radius of order ξ we may use the London equation with the vortex (18.91), which is more conveniently written in the form

$$H + \frac{4\pi\delta^2}{c} \operatorname{rot} j = \Phi_0 z^0 \delta(\rho) \tag{18.111}$$

(we assume that the plate is perpendicular to the z axis and the vortex is at the point $\rho = 0$). We introduce a vector potential! $\boldsymbol{H} = \operatorname{rot} \boldsymbol{A}$. If use is made of a cylindrical system of coordinates, the current will apparently have only the component j_θ. In view of this, A is also chosen in the form $A = (0, A_\theta, 0)$.

Equation (18.111) may be integrated and the current density expressed through it:

$$j = \frac{c}{4\pi\delta^2}(S - A), \tag{18.112}$$

where $S = (0, S_\theta, 0)$,

$$S_\theta = \frac{\Phi_0}{2\pi\rho} \tag{18.113}$$

(in fact, rot $S = 0$ everywhere, except for $\rho = 0$, and $\int \operatorname{rot} S \, \mathrm{d}s = \oint S \, \mathrm{d}l = \Phi_0$ for any contour around $\rho = 0$).

If the plate thickness d is smaller than the penetration depth, the current and field vary slightly along the plate thickness. As will be shown later, the characteristic distance over which the field varies significantly is much larger than d and δ, and therefore we may assume the plate to be infinitesimally thin and use the following as the current density:

$$j(r) = J\delta(z) = j \, \mathrm{d}\delta(z) = \frac{cd}{4\pi\delta^2}(S - A)\delta(z). \tag{18.114}$$

This current produces a magnetic field throughout the entire surrounding space, which is determined from the Maxwell equation

$$\operatorname{rot} H = \frac{4\pi}{d} j = \frac{d}{\delta^2}(S - A)\delta(z).$$

only at $d > \boldsymbol{\xi}$. From this asymptotic it follows that $\boldsymbol{H}_{c1}$ increases with decreasing thickness proportionately to d^{-2}, whereas H_{c2} increases proportionately to d^{-1} (see eq. 17.48). From the BCS theory it follows that $H_{cm} \sim \Phi_0/(\delta\xi)$ (see eq. 18.98). Comparing $H_{c2} \sim H_{cm}\delta/d \sim \Phi_0/(\xi d)$ with $H_{c1} \sim \Phi_0/d^2$, we see that the two fields become equal at $d \sim \xi$.

We shall now consider a thin plate in a perpendicular magnetic field. We assume the plate thickness to be much smaller than the penetration depth. Let us show that in this case vortices are also generated, and not only in a type II superconductor but in a type I superconductor as well (Pearl 1964).

Suppose that such a vortex has been formed and that the field and current are damped at a distance much larger than ξ. In this case, outside the core with a radius of order ξ we may use the London equation with the vortex (18.91), which is more conveniently written in the form

$$H + \frac{4\pi\delta^2}{c} \operatorname{rot} j = \Phi_0 z^0 \delta(\rho) \tag{18.111}$$

(we assume that the plate is perpendicular to the z axis and the vortex is at the point $\rho = 0$). We introduce a vector potential: $H = \operatorname{rot} A$. If use is made of a cylindrical system of coordinates, the current will apparently have only the component j_θ. In view of this, $\boldsymbol{A}$ is also chosen in the form $\boldsymbol{A} = (0, \boldsymbol{A}_\theta, 0)$.

Equation (18.111) may be integrated and the current density expressed through it:

$$j = \frac{c}{4\pi\delta^2}(S - A), \tag{18.112}$$

where $S = (0, S_\theta, 0)$,

$$S_\theta = \frac{\Phi_0}{2\pi\rho} \tag{18.113}$$

(in fact, rot $S = 0$ everywhere, except for $\rho = 0$, and $\int \operatorname{rot} S \, \mathrm{d}s = \oint S \, \mathrm{d}l = \Phi_0$ for any contour around $\rho = 0$).

If the plate thickness d is smaller than the penetration depth, the current and field vary slightly along the plate thickness. As will be shown later, the characteristic distance over which the field varies significantly is much larger than d and δ, and therefore we may assume the plate to be infinitesimally thin and use the following as the current density:

$$j(r) = J\delta(z) = j \, \mathrm{d}\delta(z) = \frac{cd}{4\pi\delta^2}(S - A)\delta(z). \tag{18.114}$$

This current produces a magnetic field throughout the entire surrounding space, which is determined from the Maxwell equation

$$\operatorname{rot} H = \frac{4\pi}{d} j = \frac{d}{\delta^2}(S - A)\delta(z).$$

Substituting $\boldsymbol{H} = \operatorname{rot} \boldsymbol{A}$ and using the condition $\operatorname{div} \boldsymbol{A} = 0$, we obtain the equation for A :

$$-\Delta A + \delta_{\text{eff}}^{-1} A\delta(z) = \delta_{\text{eff}}^{-1} S\delta(z), \tag{18.115}$$

where the following definition is introduced:

$$\delta_{\text{eff}} = \frac{\delta^2}{d}. \tag{18.116}$$

This parameter, which has the dimension of length, will be the characteristic dimension of the problem. In order for our treatment to make sense, it is necessary that this characteristic dimension be much larger than ξ. For a type II superconductor, this follows from the fact that $\delta > \xi$ and $d < \delta$, and for a type I superconductor it is necessary that

$$d < \frac{\delta^2}{\xi} \sim \delta x \sim \xi x^2 \tag{18.117}$$

In order to solve eq. (18.115), we introduce the Fourier transformation

$$A(\rho, z) = \int A_{qk} \exp(\mathrm{i}q\rho + \mathrm{i}kz) \mathrm{d}^2 q \frac{\mathrm{d}k}{(2\pi)^3}$$

Here

$$A(\rho, z)\delta(z) = A(\rho, 0)\delta(z) = \int A_{qk} \exp(\mathrm{i}q\rho) \mathrm{d}^2 q \frac{\mathrm{d}k}{(2\pi)^3} \int_{-\infty}^{\infty} \exp(\mathrm{i}k_1 z) \frac{\mathrm{d}k_1}{2\pi}$$

From eq. (18.115) we get

$$\left(q^2+k^2\right)A_{qk}+\frac{1}{\delta_{\text{eff}}}A_q=\frac{1}{\delta_{\text{eff}}}S_q \tag{18.118}$$

where

$$\boldsymbol{A}_q=\int_{-\infty}^{\infty}\boldsymbol{A}_{qk}\frac{\mathrm{d}k}{2\pi} \tag{18.119}$$

and S_q is the Fourier component of $S(\rho)$.
Solving eq. (18.118), we find

$$A_{qk}=\frac{\left(S_q-A_q\right)\delta_{\text{eff}}^{-1}}{q^2+k^2} \tag{18.120}$$

Substitution of eq. (18.120) into eq. (18.119) gives

$$A_q=\frac{S_q}{1+2q\delta_{\text{eff}}} \tag{18.121}$$

The Fourier component $\boldsymbol{S_q}$ can easily be obtained from the condition

$$\operatorname{rot}S=\Phi_0 z^0\delta(\rho)$$

Inserting the Fourier expansion, we have

$$S_q=\mathrm{i}\Phi_0\frac{[qz^0]}{q^2} \tag{18.122}$$

According to formulae (18.112), (18.119) and (18.122), we obtain

$$\begin{aligned}J_q&=\frac{c}{4\pi\delta_{\text{eff}}}\left(S_q-A_q\right)=\frac{c}{2\pi}\frac{q}{1+2q\delta_{\text{eff}}}S_q\\&=\frac{c}{2\pi}\frac{\mathrm{i}\Phi_0\left[qz^0\right]}{q\left(1+2q\delta_{\text{eff}}\right)}.\end{aligned} \tag{18.123}$$

Considering that $\boldsymbol{H}=\operatorname{rot}\boldsymbol{A}$, we have for the field at $z=0$

$$H_q=\frac{\mathrm{i}\left[qS_q\right]}{1+2q\delta_{\text{eff}}}=\frac{z^0\Phi_0}{1+2q\delta_{\text{eff}}}. \tag{18.124}$$

From these formulas it is seen that there are two asymptotic regions: $q>\delta_{\text{eff}}^{-1}$, which corresponds to $\rho<\delta_{\text{eff}}$, and $q<\delta_{\text{eff}}^{-1}$, which corresponds to $\rho>\delta_{\text{eff}}$. In the first of these regions

$$J_q\approx\frac{c}{4\pi\delta_{\text{eff}}}S_q.$$

Hence, $\boldsymbol{J}(\boldsymbol{\rho})$ is simply proportional to $\boldsymbol{S}(\boldsymbol{\rho})$ and, according to eq. (18.113),

$$J(\rho)=\frac{\Phi_0 c}{8\pi^2\delta_{\text{eff}}\rho},\quad \rho<\delta_{\text{eff}} \tag{18.125}$$

At large distances, from (18.123) we obtain

$$\begin{aligned}J(\rho)&=\int J_q\mathrm{e}^{\mathrm{i}q\rho}\frac{\mathrm{d}^2q}{(2\pi)^2}=\operatorname{rot}\left[\frac{c\Phi_0 z^0}{2\pi}\int_0^{\infty}\mathrm{d}q\int_0^{2\pi}\mathrm{d}\theta\frac{\mathrm{e}^{\mathrm{i}q\rho\cos\theta}}{(2\pi)^2}\right]\\&=\operatorname{rot}\left[\frac{c\Phi_0 z^0}{4\pi^2}\int_0^{\infty}J_0(q\rho)\mathrm{d}q\right]=\frac{\Phi_0 c}{4\pi^2}\operatorname{rot}\left(\frac{z^0}{\rho}\right)\end{aligned}$$

($J_0(q\rho)$ is the Bessel function). From this we find that the current J has only a θ-component, equal to

$$J(\rho) \approx \frac{\Phi_0 c}{4\pi^2 \rho^2} \quad \rho > \delta_{\text{eff}} \tag{18.126}$$

The limiting expression for the magnetic field at $z = 0$ and $\rho < \delta_{\text{eff}}$ is derived with the aid of formula (18.124):

$$H(\rho, 0) \approx \frac{\Phi_0}{4\pi\delta_{\text{eff}}} \int_0^\infty \mathrm{d}q J_0(q\rho) = \frac{\Phi_0}{4\pi\delta_{\text{eff}}\rho}, \quad \rho < \delta_{\text{eff}} \tag{18.127}$$

For the case $\rho > \delta_{\text{eff}}$ it is better to use the London equation (18.111) and formula (18.126):

$$H(\rho, 0) = -\frac{4\pi\delta_{\text{eff}}}{c} \operatorname{rot}_z J = \frac{\Phi_0 \delta_{\text{eff}}}{\pi\rho^3}, \quad \rho > \delta_{\text{eff}}. \tag{18.128}$$

The distribution of the field outside the plate can be deduced using formula (18.120). Substituting eqs. (18.121) and (18.122), we obtain

$$A_{qk} = \frac{2qS_q}{(1 + 2q\delta_{\text{eff}})(q^2 + k^2)} = \frac{2\mathrm{i}\Phi_0 [qz^0]}{q(1 + 2q\delta_{\text{eff}})(q^2 + k^2)}.$$

Taking the curl, we find

$$\begin{aligned} H_{zqk} &= \mathrm{i}[qA_{qk}]_z = \frac{2\Phi_0 q}{(1 + 2q\delta_{\text{eff}})(q^2 + k^2)} \\ H_{\perp qk} &= -\frac{2\Phi_0 qk}{q(1 + 2q\delta_{\text{eff}})(q^2 + k^2)} \end{aligned} \tag{18.129}$$

In the coordinate representation we have

$$\begin{aligned} H &= -\nabla\varphi \operatorname{sign} z \\ \varphi &= \frac{\Phi_0}{2\pi} \int_0^\infty \frac{\mathrm{d}q}{1 + 2q\delta_{\text{eff}}} J_0(q\rho) \mathrm{e}^{-q|z|} \end{aligned} \tag{18.130}$$

At large distances we have $q < \delta_{\text{eff}}^{-1}$. Here

$$\varphi = \frac{\Phi_0}{2\pi r}, \quad H = \frac{\Phi_0}{2\pi} \frac{r}{r^3} \operatorname{sign} z. \tag{18.131}$$

It should be noted that, according to eq. (18.130), $\boldsymbol{H}_\perp \neq 0$ at $z = 0$. But if from the start we set $z = 0$, i.e., if we find $\int_{e-\infty}^{\infty} \boldsymbol{H}_{\perp qk}\, \mathrm{d}k/2\pi$, we shall obtain zero. This is associated with the replacement of the plate by an infinitesimally thin plane with a current. For such a film we have from the Maxwell equation rot $\boldsymbol{H} = (4\pi/c)\boldsymbol{j}$:

$$H_\perp(\rho, +0) - H_\perp(\rho, -0) = \frac{4\pi}{c} J(\rho).$$

This condition is satisfied by formulae (18.129) and (18.123). The changeover from $H_\perp(\rho, +0)$ to $H_\perp(\rho, -0)$ occurs at a distance $\Delta z \sim d$. Here, in the center of the plate $H_\perp = 0$.

We have considered one isolated vortex. In fact, of course, vortices arise when the plate is placed in a perpendicular magnetic field. This gives rise to a regular vortex structure. From the symmetry of the problem it is seen that, as before, around each vortex a contour can be drawn on which $\oint j\, \mathrm{d}l = 0$ and, hence, each vortex carries one flux quantum $\boldsymbol{\Phi}_0$. If the core

centers are located at the points $\boldsymbol{\rho}_m$, then in place of eq. (18.111) we obtain an equation with $\sum \delta(\rho - \rho_m)$ instead of $\delta(\rho)$.

All the subsequent expressions in which S_q is not specified are retained. A new $\boldsymbol{S_q}$ results from the condition

$$\operatorname{rot} S = \Phi_0 z^0 \sum_m \delta(\rho - \rho_m)$$

and is given by (compare with eq. 18.122)

$$S_q = \mathrm{i}\Phi_0 \left[q z^0\right] \sum_m \frac{\exp(-\mathrm{i}q\rho_m)}{q^2}. \tag{18.132}$$

Using formulae (18.121) and (18.120), we obtain $\boldsymbol{A_{qk}}$ and $\boldsymbol{H_{qk}}$. In particular, at $\boldsymbol{z} > 0$

$$H_z(\rho, z) = -\frac{\partial}{\partial z}\frac{\Phi_0}{2\pi}\int_0^\infty \frac{\sum_m J_0(q|\rho - \rho_m|)\, e^{-qz}}{1 + 2q\delta_{\text{eff}}}\, \mathrm{d}q.$$

At $z \gg \delta_{\text{eff}}$ we put $q\delta_{\text{eff}} < 1$. Taking the integral, we get

$$H_z(\rho, z) \approx \frac{\Phi_0}{2\pi} z \sum_m \left[z^2 + (\rho - \rho_m)^2\right]^{-3/2}. \tag{18.133}$$

At a distance z much larger than the period of the structure we can make the replacement

$$\sum_m \to n \int d^2\rho_m,$$

where n is the number of vortices per cm^2. Taking the integral, we obtain the obvious result

$$H_z(\rho, z) \approx n\Phi_0 = H_0 \tag{18.134}$$

(H_0 is the external field at infinity). The same result could have been obtained from the continuity condition for the normal component of the induction.

The formulae obtained are valid as long as the intervortex spacings are much larger than ξ, i.e., at

$$H_0 < \frac{\Phi_0}{\xi^2} \sim H_{c2}$$

(recall that for type I superconductors H_{c2} is the supercooling field).

8.4.8 18.7 Anisotropic type II superconductor in a magnetic field

Up until now our analysis was confined to isotropic superconductors. Since however the new high-temperature superconductors are highly anisotropic we shall consider here some properties of such substances. We shall limit ourselves to the case of uniaxial symmetry, because the new substances have layered structures of either
tetragonal or orthorhombic symmetry. However even in the latter case the anisotropy in the basal plane is small.

In the GL free energy (17.5) one has instead of the electron mass m the mass tensor

$$m_{ik} = m_t \delta_{ik} + (m_l - m_t)\, n_i n_k, \tag{18.135}$$

where n is the unit vector along the main axis (it is normal to the basal plane or to the conducting layers). The principal values of m_{ik} are m_t and m_l. The corresponding term in (17.5) takes the form

$$\frac{1}{4}\left(\hat{m}^{-1}\right)_{ik}\left(\mathrm{i}\hbar\frac{\partial}{\partial x_i}-\frac{2e}{c}A_i\right)\Psi^*\left(-\mathrm{i}\hbar\frac{\partial}{\partial x_k}-\frac{2e}{c}A_k\right)\Psi$$

In accordance with this the first term in the GL equation (17.6) is replaced by

$$\frac{1}{4}\left(\hat{m}^{-1}\right)_{ik}\left(-\mathrm{i}\hbar\frac{\partial}{\partial x_i}-\frac{2e}{c}A_i\right)\left(-\mathrm{i}\hbar\frac{\partial}{\partial x_k}-\frac{2e}{c}A_k\right)\Psi$$

and the current instead of (17.9) becomes

$$j_i = e\left(\hat{m}^{-1}\right)_{ik}\left[-\frac{i\hbar}{2}\left(\Psi^*\frac{\partial}{\partial x_k}\Psi-\Psi\frac{\partial}{\partial x_k}\Psi^*\right)-\frac{2e}{c}A_k|\Psi|^2\right]. \tag{18.136}$$

We start with the field H_{c2}. In this case Ψ is small and we must write eq. (17.6) for Ψ in the linear approximation. We can take the field to be uniform. We choose the z-axis along the magnetic field and we place the main crystal axis in the xz-plane. As before, we take the vector potential $A_y = Hx$. Assuming that Ψ depends only on x we obtain

$$-\frac{1}{4}\hbar^2\left(\frac{n_z^2}{m_t}+\frac{n_x^2}{m_l}\right)\frac{\mathrm{d}^2\Psi}{\mathrm{d}x^2}+\frac{e^2H^2}{c^2m_t}x^2\Psi=\alpha|\tau|\Psi$$

Similarly to section 18.2 we find the critical field $\boldsymbol{H_{c2}}$ (Morris et al. 1972):

$$H_{c2}=\frac{\Phi_0}{2\pi\xi_t^2}\left(\cos^2\theta+\varepsilon^2\sin^2\theta\right)^{-1/2}, \tag{18.137}$$

where

$$\xi_t=\frac{\hbar}{\sqrt{4m_t\alpha|\tau|}},\quad \xi_l=\frac{\hbar}{\sqrt{4m_l\alpha|\tau|}}$$

are the correlation lengths,

$$\varepsilon=\sqrt{\frac{m_t}{m_l}}=\frac{\xi_l}{\xi_t},$$

θ is the angle between the main axis and the magnetic field. The limiting values of $\boldsymbol{H}_{c2}$ are $\boldsymbol{\Phi}_0/\left(2\pi\xi_t^2\right)$ for $\boldsymbol{n}\|\boldsymbol{H}$ and $\boldsymbol{\Phi}_0/\left(2\pi\xi_t\xi_l\right)$ for $\boldsymbol{n}\perp\boldsymbol{H}$. Although these formulae were derived for the vicinity of T_c they reflect also the situation at low temperatures.

Now we pass to the first critical field. Assuming $x>1$ and limiting ourselves to logarithmic accuracy we can make calculations for arbitrary temperatures, like in section 18.5. We can put $\Psi=\sqrt{\left(\frac{1}{2}n_s\right)}\mathrm{e}^{\mathrm{i}\chi}$ where $n_s=\mathrm{const}$. We introduce also the penetration depths

$$\delta_t=\sqrt{\frac{m_tc^2}{4\pi n_se^2}},\quad \delta_l=\sqrt{\frac{m_lc^2}{4\pi n_se^2}}.$$

Inserting into eq. (18.136) expression (18.135) for m_{ik}, taking rot from the Maxwell equation $\mathrm{rot}\,\boldsymbol{H}=(4\pi/c)\boldsymbol{j}$ and assuming one vortex line along l we obtain the generalisation of eq. (18.91):

$$H+\delta_t^2\,\mathrm{rot}\,\mathrm{rot}\,H+\left(\delta_l^2-\delta_t^2\right)\mathrm{rot}(n(n\,\mathrm{rot}\,H))=l\Phi_0\delta(\rho), \tag{18.138}$$

where ρ is the radius vector in the plane perpendicular to l. From eq. (18.138) it follows that $\mathrm{div}\,\boldsymbol{H}=0$.

The important part of the free energy has the form

$$\varepsilon_0 = \int \left[\frac{H^2}{8\pi} + \frac{1}{8}\left(\hat{m}^{-1}\right)_{ik} n_\mathrm{s}\left(\hbar\frac{\partial\chi}{\partial x_i} - \frac{2e}{c}A_i\right)\left(\hbar\frac{\partial\chi}{\partial x_k} - \frac{2e}{c}A_k\right)\right]\mathrm{d}V$$
$$= \frac{1}{8\pi}\int \left[H^2 + \delta_t^2(\mathrm{rot}\, H)^2 + \left(\delta_l^2 - \delta_t^2\right)(n\,\mathrm{rot}\, H)^2\right]\mathrm{d}V.$$

Integrating by parts and using eq. (18.138) we get

$$\varepsilon_0 = \frac{1}{8\pi}\Phi_0 H(0) l \tag{18.139}$$

The first critical field is determined by the condition

$$n\varepsilon_0 - \frac{BH_{\mathrm{c}1}}{4\pi} = n\varepsilon_0 - \frac{n\Phi_0 l H_{\mathrm{c}1}}{4\pi} = 0, \tag{18.140}$$

where n is the number of vortices per cm^2 of the cross-sectional plane (actually we consider only one vortex; n is introduced only for convenience of presentation).

Due to axial symmetry the vortex l will be oriented in the plane of the vector n and the external field $\boldsymbol{H}_{\mathrm{cl}}$ but in general will coincide with neither of them. We denote this plane by xz and we direct the z-axis along l. Performing the Fourier transformation

$$H = \int H_k \mathrm{e}^{\mathrm{i}k\rho}\frac{\mathrm{d}^2k}{(2\pi)^2}$$

with $k = (k_x, k_y)$ we get from eq. (18.138)

$$\left(1 + k^2\delta_t^2\right)H_k + \left(\delta_l^2 - \delta_t^2\right)[n\times k]\,(H_k[n\times k]) = l\Phi_0.$$

Now we pass to the first critical field. Assuming $x \gg 1$ and limiting ourselves to logarithmic accuracy we can make calculations for arbitrary temperatures, like in section 18.5. We can put $\Psi = \sqrt{\left(\frac{1}{2}n_s\right)}\mathrm{e}^{\mathrm{i}\chi}$ where $n_s = \mathrm{const}$. We introduce also the penetration depths

$$\delta_t = \sqrt{\frac{m_t c^2}{4\pi n_s e^2}}, \quad \delta_l = \sqrt{\frac{m_l c^2}{4\pi n_s e^2}}.$$

Inserting into eq. (18.136) expression (18.135) for m_{ik}, taking rot from the Maxwell equation $\mathrm{rot}\,\boldsymbol{H} = (4\pi/c)\boldsymbol{j}$ and assuming one vortex line along l we obtain the generalisation of eq. (18.91):

$$H + \delta_t^2\,\mathrm{rot}\,\mathrm{rot}\,H + \left(\delta_l^2 - \delta_t^2\right)\mathrm{rot}(n(n\,\mathrm{rot}\,H)) = l\Phi_0\delta(\rho), \tag{18.138}$$

where ρ is the radius vector in the plane perpendicular to l. From eq. (18.138) it follows that $\mathrm{div}\,\boldsymbol{H} = 0$.

The important part of the free energy has the form

$$\varepsilon_0 = \int \left[\frac{H^2}{8\pi} + \frac{1}{8}\left(\hat{m}^{-1}\right)_{ik} n_\mathrm{s}\left(\hbar\frac{\partial\chi}{\partial x_i} - \frac{2e}{c}A_i\right)\left(\hbar\frac{\partial\chi}{\partial x_k} - \frac{2e}{c}A_k\right)\right]\mathrm{d}V$$
$$= \frac{1}{8\pi}\int \left[H^2 + \delta_t^2(\mathrm{rot}\, H)^2 + \left(\delta_l^2 - \delta_t^2\right)(n\,\mathrm{rot}\, H)^2\right]\mathrm{d}V.$$

Integrating by parts and using eq. (18.138) we get

$$\varepsilon_0 = \frac{1}{8\pi}\Phi_0 H(0) l \tag{18.139}$$

The first critical field is determined by the condition

$$n\varepsilon_0 - \frac{BH_{c1}}{4\pi} = n\varepsilon_0 - \frac{n\Phi_0 l H_{c1}}{4\pi} = 0, \tag{18.140}$$

where n is the number of vortices per cm^2 of the cross-sectional plane (actually we consider only one vortex; n is introduced only for convenience of presentation).

Due to axial symmetry the vortex l will be oriented in the plane of the vector n and the external field $\boldsymbol{H}_{\rm cl}$ but in general will coincide with neither of them. We denote this plane by xz and we direct the z-axis along l. Performing the Fourier transformation

$$H = \int H_k \mathrm{e}^{\mathrm{i}k\rho} \frac{\mathrm{d}^2 k}{(2\pi)^2}$$

with $k = (k_x, k_y)$ we get from eq. (18.138)

$$\left(1 + k^2\delta_t^2\right) H_k + \left(\delta_l^2 - \delta_t^2\right) [n \times k] \left(H_k [n \times k]\right) = l\Phi_0.$$

Multiplying by $[n \times k]$ and solving the resulting equation we find

$$\begin{aligned} H_k[n \times k] &= \frac{l[n \times k]\Phi_0}{1 + \delta_l^2 k^2 + [n \times k]^2 \left(\delta_l^2 - \delta_t^2\right)} \\ &= \frac{n_x k_y \varphi_0}{1 + \delta_l^2 k^2 + \left(\delta_t^2 - \delta_l^2\right) n_x^2 k_x^2} \end{aligned}$$

Multiplying eq. (18.141) by $\boldsymbol{l}$ and substituting $\boldsymbol{H_k}[\boldsymbol{n} \times \boldsymbol{k}]$ we get

$$lH_k = \frac{\Phi_0 \left[1 + \left(\delta_t^2 n_x^2 + \delta_l^2 n_z^2\right) k^2\right]}{\left(1 + \delta_t^2 k^2\right) \left[1 + \delta_l^2 k^2 + \left(\delta_t^2 - \delta_l^2\right) n_x^2 k_x^2\right]}. \tag{18.142}$$

Expression (18.139) for ε_0 contains $\boldsymbol{H}(0)\boldsymbol{l} = (2\pi)^{-2} \int \boldsymbol{H}_k \boldsymbol{l}\, \mathrm{d}^2\boldsymbol{k}$. According to eq. (18.142) this is a logarithmic integral. It must be limited from above by $k \sim \xi^{-1}$. Within logarithmic accuracy we obtain

$$\varepsilon_0 = \left(\frac{\Phi_0}{4\pi\delta_t}\right)^2 \ln x \frac{\sqrt{\delta_t^2 \sin^2\theta + \delta_l^2 \cos^2\theta}}{\delta_l} \tag{18.143}$$

where θ is the angle between n and l ($n_z = \cos\theta, n_x = \sin\theta$). Denoting the angle between $\boldsymbol{H}_{\rm cl}$ and $\boldsymbol{n}$ by $\boldsymbol{\theta}_1$ we get from eq. (18.140)

$$H_{c1}(\theta_1, \theta) = \frac{\Phi_0 \ln \varkappa}{4\pi\delta_t^2} \frac{\left(\varepsilon^2 \sin^2\theta + \cos^2\theta\right)^{1/2}}{\cos(\theta_1 - \theta)} \tag{18.144}$$

where as before $\varepsilon = (m_t/m_l)^{1/2} = \delta_t/\delta_l$. The true value of $\boldsymbol{H}_{c1}$ is obtained by minimization over $\boldsymbol{\theta}$. We find (Balatskii et al. 1986)

$$\tan\theta_0 = \frac{1}{\varepsilon}\tan\theta_1 \tag{18.145}$$

$$H_{c1} = \frac{\Phi_0 \ln x}{4\pi\delta_t^2} \frac{1}{\sqrt{\cos^2\theta_1 + \varepsilon^{-2}\sin^2\theta_1}} \tag{18.146}$$

Consider the limiting cases. The case $\varepsilon \ll 1$ corresponds to a layered structure with $m_l > m_t$. The electrons in this case rarely jump from one layer to another. Therefore the field normal to the layers is easily screened while a field having a component within the layer plane is screened with much greater difficulty. Hence the vortices corresponding to field penetration exhibit a trend towards lying in the layer plane and at $\boldsymbol{H}_{\rm cl} \perp \boldsymbol{n}$ they are formed at relatively small

fields (at $\theta_1 = \frac{1}{2}\pi$ one has $H_{\rm cl} = \Phi_0 \ln x/4\pi\delta_l\delta_t$). The opposite case $\varepsilon > 1$ corresponds to a quasi-onedimensional structure. Here the field directed along the main axis is poorly screened. Therefore the vortices appear preferably in this direction ($\theta_0 \to 0$) even if the external field makes a large angle with the axis.

We shall not analyse here the whole structure of the mixed state at $H_{\rm c1} < H < H_{\rm c2}$. Physically it is clear that with increasing vortex density their orientation will approach that of the external field.

Multiplying by $[n \times k]$ and solving the resulting equation we find

$$H_k[n \times k] = \frac{l[n \times k]\Phi_0}{1 + \delta_t^2 k^2 + [n \times k]^2 (\delta_l^2 - \delta_t^2)} = \frac{n_x k_y \varphi_0}{1 + \delta_l^2 k^2 + (\delta_t^2 - \delta_l^2) n_x^2 k_x^2}$$

Multiplying eq. (18.141) by l and substituting $\boldsymbol{H}_k[\boldsymbol{n} \times \boldsymbol{k}]$ we get

$$lH_k = \frac{\Phi_0 \left[1 + (\delta_t^2 n_x^2 + \delta_l^2 n_z^2) k^2\right]}{(1 + \delta_t^2 k^2)\left[1 + \delta_l^2 k^2 + (\delta_t^2 - \delta_l^2) n_x^2 k_x^2\right]} \tag{18.142}$$

Expression (18.139) for ε_0 contains $\boldsymbol{H}(0)\boldsymbol{l} = (2\pi)^{-2} \int \boldsymbol{H}_k \boldsymbol{l}\, \mathrm{d}^2\boldsymbol{k}$. According to eq. (18.142) this is a logarithmic integral. It must be limited from above by $k \sim \xi^{-1}$. Within logarithmic accuracy we obtain

$$\varepsilon_0 = \left(\frac{\Phi_0}{4\pi\delta_t}\right)^2 \ln x \frac{\sqrt{\delta_t^2 \sin^2\theta + \delta_l^2 \cos^2\theta}}{\delta_l} \tag{18.143}$$

where θ is the angle between n and l ($n_z = \cos\theta, n_x = \sin\theta$). Denoting the angle between $\boldsymbol{H}_{\rm c1}$ and $\boldsymbol{n}$ by $\boldsymbol{\theta}_1$ we get from eq. (18.140)

$$H_{\rm c1}(\theta_1, \theta) = \frac{\Phi_0 \ln x}{4\pi\delta_t^2} \frac{\left(\varepsilon^2 \sin^2\theta + \cos^2\theta\right)^{1/2}}{\cos(\theta_1 - \theta)} \tag{18.144}$$

where as before $\varepsilon = (m_t/m_l)^{1/2} = \delta_t/\delta_l$. The true value of $H_{\rm c1}$ is obtained by minimization over θ. We find (Balatskii et al. 1986)

$$\tan\theta_0 = \frac{1}{\varepsilon^2} \tan\theta_1 \tag{18.145}$$

$$H_{\rm cl} = \frac{\Phi_0 \ln \varkappa}{4\pi\delta_t^2} \frac{1}{\sqrt{\cos^2\theta_1 + \varepsilon^{-2}\sin^2\theta_1}} \tag{18.146}$$

Consider the limiting cases. The case $\varepsilon \ll 1$ corresponds to a layered structure with $m_l > m_t$. The electrons in this case rarely jump from one layer to another. Therefore the field normal to the layers is easily screened while a field having a component within the layer plane is screened with much greater difficulty. Hence the vortices corresponding to field penetration exhibit a trend towards lying in the layer plane and at $\boldsymbol{H}_{\rm c1} \perp \boldsymbol{n}$ they are formed at relatively small fields (at $\theta_1 = \frac{1}{2}\pi$ one has $H_{\rm c1} = \Phi_0 \ln x/4\pi\delta_l\delta_t$). The opposite case $\varepsilon > 1$ corresponds to a quasi-onedimensional structure. Here the field directed along the main axis is poorly screened. Therefore the vortices appear preferably in this direction ($\theta_0 \to 0$) even if the external field makes a large angle with the axis.

We shall not analyse here the whole structure of the mixed state at $\boldsymbol{H}_{\rm c1} < \boldsymbol{H} < \boldsymbol{H}_{\rm c2}$. Physically it is clear that with increasing vortex density their orientation will approach that of the external field.

In conclusion we consider the anisotropy of the penetration depth of a weak magnetic field. To this purpose we must use the reduced eq. (18.138) or eq. (18.141) without the right-hand side. This time we direct k along the z-axis (this is the normal to the surface of the superconducting half-space) and we choose n in the xz-plane. One can easily prove that the components H_y and H_x have different penetration depths, namely

$$\delta(H_x) = \delta_t, \quad \delta(H_y) = \delta_t \sqrt{\cos^2\theta + \varepsilon^{-2}\sin^2\theta}. \tag{18.147}$$

This behaviour is again easily understood from the viewpoint of the anisotropy of electron hopping. For $\varepsilon \to 0$, i.e. for the layered structure, the field is poorly screened by currents demanding electron hopping between the layers, and the corresponding penetration depth increases.

8.4.9 18.8. Superconducting magnets. Pinning

The idea of the application of superconductors instead of ordinary metals with the purpose of eliminating ohmic losses has been put forward since the discovery of superconductivity. The obstacle is the necessity of attaining low temperatures. The high cost of the equipment and of the operation of superconducting cables with helium cooling makes the use of superconductivity for the transmission of electric power economically inefficient*.

The situation is different as far as the cooling of a limited volume is concerned. It is for this reason that at present the use of superconductors for the production of powerful magnets is rapidly expanding. A conventional electromagnet, which is a coil made of copper or aluminum wire, consumes a power which increases proportionately to H^2, where H is the magnetic field it produces. Maintaining a field of 100 kOe in an aperture of diameter 2.5 cm thus require a power of the order of a megawatt. This energy is almost completely released in the form of Joule heat, and in order to remove this heat, a huge and expensive water cooling system is needed**.

If the coil (solenoid) is made of a superconductor, energy is required only for maintaining the helium temperature. This may be several orders of magnitude smaller than the energy consumed by the corresponding electromagnet; besides, the entire installation is much more compact. It should be noted that the superconducting coil can be short-circuited and in this case it is converted to a permanent magnet. As we know, the field flux through a hollow superconductor does not vary with time because any change in the external conditions is compensated for by supercurrents. Therefore, a superconducting permanent magnet is characterized by unique constancy of the magnetic field produced.

The idea of superconducting magnets was first advanced by H. Kamerlingh Onnes. But the superconductors known at that time had low critical fields, of the order of hundreds of oersteds. The situation changed in the 1960s, when superconductors appeared with critical fields above 100 kOe ; also, cryostats, i.e., devices for maintaining helium temperatures, were highly improved and became less expensive. The subsequent investigations showed that the new materials exhibiting high critical fields are type II superconductors, which are well described by the theory presented in the preceding sections.

The highest critical fields known have been produced in the so-called Chevrel phases: compounds of the type $\mathrm{Me}_x\,(\mathrm{Mo}_6\,\mathrm{S}_8)_y$ (Me = metals: Pb, Li, and others). They reach 600 kOe . There are predictions that superconducting ceramics may have even higher critical fields, up to 2 MO . However, good mechanical properties of alloys are required for practical needs and

*This conclusion will probably change if ways are found for the technology of application of ceramics which are superconducting at liquid nitrogen temperatures.

** It must be noted that water pumps generate vibrations which are very detrimental in most cases.

therefore at present use is made of $\mathrm{Nb-Zr-Ti}$ alloys with critical fields of up to $110-120$kOe and Nb_3Sn with a critical field up to 230 kOe .

Nevertheless, the possibility of using type II superconductors to produce high fields is not quite evident. In fact, as has been established in the preceding sections, at $x \gg 1$ there is a large region of the mixed state, starting with the field $H_{c1} \sim H_{cm}/x$ and ending with $H_{c2} \sim H_{cm}\varkappa$. Hence, if there is a high field, the superconductor is certainly in the mixed state and is threaded by vortices. The current that creates a field in the solenoid flows perpendicular to the vortices. But in this case, the vortices are acted on by a Lorentz force in a direction perpendicular to $\boldsymbol{H}$ and $\boldsymbol{j}$.

This force can be found as follows. Suppose there is a single vortex with current $\boldsymbol{j}$ in the superconductor and that an external current $\boldsymbol{j}^{\text{ext}}$ is passed through it. The total current will then be $\boldsymbol{j}+\boldsymbol{j}^{\text{ext}}$. Substituting into eq. (18.93), we obtain the current interaction energy:

$$\Lambda \int j^{ext} j dV$$

(the interaction energy for magnetic fields is relatively small). In this particular case, $\boldsymbol{j}$ depends on $\boldsymbol{\rho}-\boldsymbol{\rho}_0$, where $\boldsymbol{\rho}_0$ is the coordinate of the vortex axis. The component of the force that acts on the vortex axis is a derivative of the potential energy with respect to its coordinate with a minus sign:

$$\begin{aligned}
-\frac{\partial}{\partial x_{0k}}\Lambda \int j^{\text{ext}} j \, \mathrm{d}V &= -\Lambda \sum_{i=1,2} \int j_i^{\text{ext}} \frac{\partial}{\partial x_{0k}} j_i \, \mathrm{d}V \\
&= \Lambda \sum_{i=1,2} \int j_i^{\text{ext}} \frac{\partial}{\partial x_k} j_i \, \mathrm{d}V \\
&= \Lambda \sum_{i=1,2} \int j_i^{\text{ext}} \left(\frac{\partial}{\partial x_k} j_i - \frac{\partial}{\partial x_i} j_k \right) \mathrm{d}V + \Lambda \sum_{i=1,2} \int j_i^{\text{ext}} \frac{\partial}{\partial x_i} j_k \, \mathrm{d}V
\end{aligned}$$

(we have used the fact that j depends on $\rho-\rho_0$).

The last term is equal to zero, because integrating by parts we obtain $-\Lambda \int j_k \operatorname{div} j^{\text{ext}} \, \mathrm{d}V = 0 \, (\operatorname{div} j^{\text{ext}} = 0)$. The factor in parentheses in the first term is equal to zero at $i=k$, and at $i \neq k$ it is the component of rot j along the z axis (because $i,k = x,y$). It is not difficult to see that on the whole the integral is equal to

$$\Lambda \int \left[j^{\text{ext}} \operatorname{rot} j \right] \mathrm{d}V.$$

But for the vortex

$$\begin{aligned}
\operatorname{rot} j &= -\frac{1}{\Lambda c} \operatorname{rot} \left(A - \frac{\hbar c}{2e} \nabla \chi \right) \\
&= \frac{1}{\Lambda c} \frac{\hbar c}{2e} 2\pi \delta \left(\rho - \rho_0 \right)
\end{aligned}$$

(see formulae 18.90 and 18.40).
Hence, the force that acts on a unit length of the vortex is

$$f_{\text{L}} = \frac{\Phi_0}{c} \left[j^{\text{ext}} \cdot b \right], \tag{18.148}$$

where $\Phi_0 = \pi\hbar c/e$ is the flux quantum and b is the unit vector along the vortex axis. Multiplying by the number of vortices per unit cross-sectional area, $n = B/\Phi_0$, we obtain the Lorentz force per unit volume ($nb = B/\Phi_0$):

$$F_L = \frac{1}{c}\left[j^{\text{ext}}\, B\right]. \tag{18.149}$$

Under the action of this force the vortex lattice must begin to move. Suppose that this motion is opposed by a viscous force, which is proportional to the velocity. Let us assume that for one vortex

$$f_{\text{v}} = -\eta v_{\text{L}}, \tag{18.150}$$

where v_L is the velocity of vortex motion and η is a certain "viscosity coefficient". At equilibrium $f_{\text{L}} + f_{\text{v}} = 0$, i.e.,

$$v_{\text{L}} = \frac{\Phi_0}{\eta \text{c}}\left[j^{\text{ext}}\, b\right]. \tag{18.151}$$

Hence, the vortices move perpendicular to $\boldsymbol{B}$ and $\boldsymbol{j}^{\text{ext}}$. This motion of the vortex lattice leads to the generation of an electric field. Indeed, if in the coordinate system moving together with the lattice with a velocity v_{L} there is an average magnetic field (induction) $\boldsymbol{B}$, then in accordance with the rules of electrodynamics an extra electric field arises upon transformation to the laboratory coordinate system:

$$E = \frac{1}{c}\left[B v_{\text{L}}\right]. \tag{18.152}$$

Substituting eq. (18.138) and taking into account that $\boldsymbol{b} = \boldsymbol{B}/\boldsymbol{B}$ and $\boldsymbol{B} \perp \mathbf{j}^{\text{ext}}$, we obtain

$$E = \frac{\Phi_0 B}{\eta c^2} j^{\text{ext}} \tag{18.153}$$

But the generation of an electric field along $\boldsymbol{j^{ext}}$ implies the appearance of electrical resistance:

$$\rho = \frac{E}{j^{\text{ext}}} = \frac{\Phi_0 B}{\eta c^2} \tag{18.154}$$

If the superconductor is completely homogeneous, then upon attainment of the field H_{c2} the resistance ρ must be equal to ρ_{n}, the resistance of a normal metal. From this it follows that

$$\rho_{\text{n}} = \frac{\Phi_0 H_{\text{c2}}}{\eta c^2}$$

and therefore we find that

$$\eta = \frac{\Phi_0 H_{\text{c2}}}{\rho_n c^2} \tag{18.155}$$

and

$$\rho = \rho_{\text{n}} \frac{B}{H_{\text{c2}}}. \tag{18.156}$$

The last formula is very simple and resembles the formula for the heat capacity (18.106). It could also be interpreted as arising from the fact that the vortex cores with a diameter of the order of ξ are in the normal state. However, if the vortex lattice were at rest, the supercurrent would easily go around the normal cores and no resistance would arise. The appearance of resistance is the result of the motion of the vortices under the action of the Lorentz force.

In fact, however, formulae (18.155) and (18.156) are valid only by order of magnitude, mostly far from T_{c} and H_{c2}. The true viscosity η depends on many mechanisms and not only on the

energy dissipation in the normal cores, and is a complex function of field and temperature. Besides, the simple linear relation (18.150) does not always hold.

Thus, we come to the conclusion that superconductivity is destroyed as soon as vortices appear, i.e., at a field equal to $H_{c1} \sim H_{cm}/x$. This means that not only we gain nothing with increasing x but, on the contrary, we strongly lose in the critical field. However, there is a way for coping with this shortcoming. To do this, the motion of the vortex lattice must be stopped, in which case, in accordance with formula (18.152), $E = 0$ and, hence, $\rho = 0$ too. To this end, we have to fasten the vortices at certain points in the sample. This phenomenon is known as pinning.

We have already dealt in section 18.5 with the surface barrier that hinders the entry of vortices into the sample and their escape from it. From this example it is
seen that irregularities may be responsible for the formation of barriers impeding the motion of vortices. It is clear that irregularities with a size larger than ξ will be very effective for pinning*.

Consider, as an example, a pore in a superconductor with a size of $d \gg$. We know that the core energy per unit length of the vortex is of order $(\Phi_0/\delta)^2$ (see eq. 18.95). This may be put in a different way. As soon as the core is in the normal state there is an excess energy $\boldsymbol{H}_{cm}^2/8\pi$ per cm^3 and an excess energy $\boldsymbol{H}_{cm}^2 \cdot \boldsymbol{\xi}^2$ per unit length. The identity of these expressions follows from (18.97).

If the vortex passes through the pore, the corresponding part of the core energy is absent. This means that the total energy is lower, i.e., the vortex is attracted to the pore. The force of this attraction can be found if one takes into account that the vortex disappears, merging with its image at a distance of order ξ from the edge of the pore (section 18.5). Hence, the force equal to the energy gradient will be of the order of the energy itself divided by ξ. For a pore with a size d,

$$f_p \sim H_{cm}^2 d\xi. \tag{18.157}$$

When the current is passing, the vortex is acted on by the Lorentz force, which, in accordance with (18.148), after being multiplied by the length d is of the order of ($H_{cm} \sim \Phi_0/\delta\xi$):

$$f_L d \sim \Phi_0 j^{ext} \frac{d}{c} \sim H_{cm} j^{ext} \delta\xi \frac{d}{c}.$$

Equating these forces, we find the critical current density capable of unpinning the vortex from the pore:

$$j^{ext} \sim H_{cm} \frac{c}{\delta}. \tag{18.158}$$

Comparing with formula (17.62), we see that this value is comparable with the current density required to break up Cooper pairs.

In fact, of course, we must take into account that the pinning force acts on a limited portion of the vortex line, whereas the Lorentz force pulls the entire vortex. Moreover, in real cases there are many interacting vortices that form a lattice, and therefore in calculations of the critical current density one has to take account of the lattice distortion and of the elastic forces that arise in this case. We shall not discuss particular models and the results obtained, especially as the nature of the pinning centers in superconductors employed in technology has not been studied in detail.

Moreover, it is not always clear how the current is actually distributed throughout the superconductors in the mixed state with pinning. Although we know, for example, that in the absence of a magnetic field the current flows only in a surface layer of

thickness δ, experiment shows that in the case under consideration the situation is different, and a considerable part of the current flows through the inner portion of the superconductor. This is associated with the fact that the current is a function of the field: $j_c(B)$. The passage of the current leads to the formation of a "critical profile" of the current, such that the induction and current at each point of the cross section of the conductor corresponds to $j_c(B)$. At $x > 1$ and a high defect density the current is distributed almost uniformly along the cross section. In a general case, we may speak only of the "current-carrying capacity", which is conventionally expressed in terms of the average current density. So far, critical values have been attained of the order of 10^6 A/cm^2 (for ceramics much less, $< 10^3$ A/cm^2).

Thus, according to what has been said above, we get the impression that before the critical current is attained the resistance is equal to zero, and then resistance arises in a jumpwise manner. It is easy, however, to see that this occurs only at $T = 0$. In fact, the pinning centers create for the vortex lattice a potential relief consisting of "valleys" separated by "mountain chains" - potential barriers. At finite temperature a transition from one valley to another is possible due to thermal fluctuations. The result is that even before the true critical current density is achieved there arises a "creep": the fluctuational jumpwise displacement of the vortex lattice. This gives rise to resistance. It should be emphasized that this occurs at any finite temperature, and therefore in the strict sense of the word the critical current in the mixed state at $T > 0$ is equal to zero.

However, in reality the situation is not that hopeless. Suppose we have a superconducting permanent magnet - a short-circuited solenoid. It is used under operating conditions for a limited period of time, because during all this time the energy has to be consumed on cooling. The resistance associated with the creep of vortices is so small that the current flowing through the solenoid does not change appreciably during, say 100 years; from a practical viewpoint the resistance is equal to zero.

We shall not describe here the creep theory (see Anderson 1962; Anderson and Kim 1964). We note only that according to this theory the field in the hole of the solenoid falls off by a very slow law:

$$B(t) = B(0)(1 - \alpha \ln t)$$

with the coefficient $\alpha \sim 10^{-3}$. Hence, the decrease of the current in the solenoid and of the magnetic field created by it takes enormous periods of time.

We may conclude that the creep is not dangerous and that it may be neglected, i.e., we may presume that from the practical standpoint the situation is the same as at $T = 0$, and unless the critical current is not attained the sample is superconducting. As a matter of fact, the creep may cause another hazard. If a bundle of vortices slips at some point, heat is released. This leads to a sharp decrease in the values of the critical field and current and may drive a portion of the magnet normal. In such a case, the heat release increases drastically and, as a result, an instability arises, which may destroy the magnet.

In order to avoid these processes, superconducting cables or ribbons for magnets are made multicore, and a normal metal (usually copper) is used as an insulator. [In comparison with a superconductor, any substance with finite resistance is an insulator.] However, while the superconductor exhibits low thermal conductivity, because the heat can be transferred only by quasiparticles, whose number at low temperatures is exponentially small (section 19.1), a normal metal is a good heat conductor. It is the normal metal that removes heat in the case

---

- A detailed investigation shows that smaller-scale irregularities can exert a collective action on the entire vortex lattice and also lead to pinning.

of sudden heating. Moreover, if current ceases to flow through the superconductor, the thick normal conductor connected in parallel will play the role of a shunt.

8.5 19 Kinetics of superconductors

Up until now we have been concerned only with equilibrium phenomena taking place in superconductors, i.e., with their behavior upon variation of temperature and of the external static magnetic field. The only exception was section 18.8, where we considered qualitatively the kinetics of the vortex structure upon passage of current.

A rigorous treatment of the kinetics of superconductors calls for the application of detailed equations of the BCS microscopic theory, which requires very complicated calculations. In most cases the answer cannot be found in analytical form. A certain simplification can be achieved for fields that vary gradually in space and in time: $\omega < \Delta/h, k < \xi_0^{-1}$, where ω and k are the frequency and the wave vector of the field.

Nevertheless, even in this case the resultant "kinetic equation" (see Aronov et al. 1981) is rather complicated and does not cover all the interesting phenomena. For this reason, we will confine ourselves in some cases to a qualitative description and try, where possible, to give estimates on the basis of simple physical considerations. We begin with phenomena that occur in weak fields or with a low temperature gradient, when the state of the superconductor deviates little from equilibrium; then we will discuss certain effects associated with strong nonequilibrium.

8.5.1 19.1. Electronic thermal conductivity

The transport of heat in superconductors is accomplished, just as in normal metals, by quasiparticles of the electron liquid and by phonons. At not too low temperatures the major contribution comes from electrons. As for the lowest temperatures, in this case too the electron contribution can be separated from the phonon contribution. For example, in a magnetic field above H_c the electrons become normal and thus we can find the difference in thermal conductivity between the superconducting and the normal state. As regards the electronic thermal conductivity of a normal metal, this can be either extrapolated from the region of $T > T_c$ or separated with the aid of a strong magnetic field, as described in Part I. Thus, the electronic thermal conductivity of a superconductor can be deduced from experimental data.

In calculating the thermal conductivity of a normal metal we were faced with the fact that the temperature gradient leads to the generation of an electric field, which
is determined from the condition of the absence of current. However, this effect introduces only a small correction, of the order of $(T/\mu)^2$ (see section 6.1). In superconductors there is no electric field, but the current of quasiparticles is balanced by a countercurrent of Cooper pairs (this point will be discussed in detail in section 19.2). In calculating thermal conductivity one may neglect the motion of Cooper pairs since it makes only a correction of order $(T/\mu)^2$.

At temperatures below T_c the dominant mechanism of electron scattering is the scattering from impurities. Therefore we will be concerned only with this mechanism here. The kinetic equation for quasiparticles has the usual form

$$\frac{\partial \varepsilon}{\partial p}\frac{\partial n}{\partial r} - \frac{\partial \varepsilon}{\partial r}\frac{\partial n}{\partial p} = I(n), \tag{19.1}$$

where ε is the energy of quasiparticles and $-\partial\varepsilon/\partial r$ is the force that acts on quasiparticles.

The form of the collision integral is determined as follows. Suppose that the impurities have no spin. In this case, the electrons conserve their spin on scattering. Moreover, the collisions

with impurities are elastic, i.e., the energy of quasi-particles is conserved. In view of this, the scattering of electrons from impurities may be described by the term in the Hamiltonian:

$$\mathscr{H}_{\text{imp}} = \sum_{\sigma,p,p'} a^{+}_{p',\sigma} a_{p,\sigma} V_{p'p}, \tag{19.2}$$

where $V_{p'p}$ is the interaction matrix element, which is a function only of $\theta = \left(\widehat{p,p'}\right)$. Expression (19.2) corresponds to the disappearance of an electron of momentum $\boldsymbol{p}$ and to the creation, in place of it, of another electron of momentum $\boldsymbol{p}'$.

In order to pass to quasiparticles, we substitute the Bogoliubov transformation (16.14). Here only those terms are retained which are not associated with a change in energy, i.e., the terms describing the creation or annihilation of two quasiparticles are omitted. As a result, we find

$$\mathscr{H}_{\text{imp}} = \sum_{\sigma,p'p'} \alpha^{+}_{p'\sigma} \alpha_{p\sigma} V_{p'p} \left(u_p u_{p'} - v_p v_{p'}\right). \tag{19.3}$$

The energy of quasiparticles is conserved upon scattering from impurities. Hence, $\varepsilon_p = \varepsilon_{p'}$. From this it follows that $\xi_p = \pm\xi_{p'}$. If $\xi_{p'} = \xi_p$, then $u_{p'} = u_p, v_{p'} = v_p, u_p^2 - v_p^2 = \xi_p/\varepsilon_p$. But if $\xi_{p'} = -\xi_p$, then $v_{p'} = u_p$ and $u_{p'} = v_p$ and expression (19.3) vanishes.

Let us now find the scattering probability per unit time, in other words, the function that replaces τ^{-1} in section 3.2*. So, we have

$$\begin{aligned}\tau_{\text{str}}^{-1} =& \frac{2\pi}{\hbar} \int |V_{p'p}|^2 \left(1 - \cos\theta\right) \left(u_p u_{p'} - v_p v_{p'}\right)^2 \\ & \times \delta\left(\tau_p \cdot \varepsilon_{r'}\right) \frac{d^3 p'}{(2\pi\hbar)^3}\end{aligned}$$

$$\begin{aligned}=& \frac{\pi}{\hbar} \nu(\mu) \left(\frac{\xi_p}{\varepsilon_p}\right)^2 \\ & \times \left|\frac{d\xi_p}{d\varepsilon_p}\right| \int |V(\theta)|^2 (1 - \cos\theta) \frac{d\Omega}{4\pi} \\ =& \tau_{\text{tr}}^{-1} \frac{|\xi_p|}{\varepsilon_p}\end{aligned} \tag{19.4}$$

we have made the replacements

$$\begin{aligned}& \mathrm{d}^3 p' \to p_0^2 \, \mathrm{d}p' \mathrm{d}\Omega \to p_0^2 \left(\frac{\mathrm{d}\xi'}{v}\right) \mathrm{d}\Omega \\ & \delta\left(\varepsilon - \varepsilon'\right) = \left|\frac{\mathrm{d}\xi}{\mathrm{d}\varepsilon}\right| \delta\left(|\xi| - |\xi'|\right) \to \left|\frac{\mathrm{d}\xi}{\mathrm{d}\varepsilon}\right| \delta\left(\xi - \xi'\right)\end{aligned}$$

since for $\xi' = -\xi$ we have $\tau_{\text{str}}^{-1} = 0$. From eq. (19.4) it follows that the collision integral is given by

$$I(n) = -\frac{|\xi_p|}{\varepsilon_p} \frac{n - n_{\text{F}}}{\tau_{\text{tr}}}. \tag{19.5}$$

- Recall that in Part II we use the notation τ_{tr} instead of τ.

Substituting into the left-hand side of the kinetic equation the equilibrium function

$$n_F = \frac{1}{\exp(\varepsilon/T)+1} \tag{19.6}$$

and using the fact that

$$\frac{\partial n_{\mathrm{F}}}{\partial r} = -\frac{\varepsilon}{T}\frac{\partial n_{\mathrm{F}}}{\partial \varepsilon}\nabla T, \tag{19.7}$$

$$\frac{\partial \varepsilon}{\partial p} = \frac{\partial \varepsilon}{\partial \xi}\frac{\mathrm{d}\xi}{\mathrm{d}p} = v\left(\frac{\xi}{\varepsilon}\right), \tag{19.8}$$

where $v = p/m$, we find*:

$$-\frac{\xi}{T}\frac{\partial n_{\mathrm{F}}}{\partial \varepsilon} v\nabla T = -\left(n - n_{\mathrm{F}}\right)\left(\frac{|\xi|}{\varepsilon}\right)\frac{1}{\tau_{\mathrm{tr}}}, \tag{19.9}$$

from which it follows that the nonequilibrium correction is

$$n^{(1)} = n - n_{\mathrm{F}} = \frac{\varepsilon}{T}\frac{\partial n_{\mathrm{F}}}{\partial \varepsilon}\tau_{\mathrm{tr}}\operatorname{sign}\xi v\nabla T \tag{19.10}$$

$$\operatorname{sign}\xi = \frac{\xi}{|\xi|}$$

The heat flux is expressed by

$$q = 2\int \varepsilon\frac{\partial \varepsilon}{\partial p} n\frac{\mathrm{d}^3 p}{(2\pi\hbar)^3}. \tag{19.11}$$

The factor 2 arises as a result of summation over the spin projections. Since n_F depends only on ε, the only contribution here comes from $n^{(1)}$. Substituting (19.10) and (19.8) and passing to the integration over ε, we obtain

$$\begin{aligned} q &= \frac{2\nu}{T}\int_{\Delta}^{\infty}\mathrm{d}\varepsilon\int\frac{\mathrm{d}\Omega}{4\pi}\varepsilon^2\tau_{\mathrm{tr}} v(v\nabla T)\frac{\partial n_{\mathrm{F}}}{\partial \varepsilon} \\ &= \frac{2\nu\nabla T}{3T}v^2\tau_{\mathrm{tr}}\int_{\Delta}^{\infty}\mathrm{d}\varepsilon\varepsilon^2\frac{\partial n_{\mathrm{F}}}{\partial \varepsilon} \\ &= -\left(n_{\mathrm{e}}\frac{\tau_{\mathrm{tr}}}{2mT^2}\right)\int_{\Delta}^{\infty}\mathrm{d}\varepsilon\frac{\varepsilon^2}{\cosh^2(\varepsilon/2T)}\nabla T \end{aligned} \tag{19.12}$$

(here the 2 arises from the integration over the regions $\xi > 0$ and $\xi < 0; n_{\mathrm{e}} = p_0^3/3\pi^2\hbar^3$). Hence, we have (Geilikman 1958)*:

$$x = \frac{n_{\mathrm{e}}\tau_{\mathrm{tr}}T}{2m}\int_{\Delta/T}^{\infty}\frac{x^2}{\cosh^2\left(\frac{1}{2}x\right)}\mathrm{d}x.$$

With $T \to T_{\mathrm{c}}$, from the above equation we obtain expression (3.28) for a normal metal. But if $T \to 0$, then $\cosh\left(\frac{1}{2}x\right) \approx \frac{1}{2}\exp\left(\frac{1}{2}x\right)$ and

---

- While substituting the equilibrium function n_{F} into the left-hand side of eq. (19.1), we must, strictly speaking, take into account that $\varepsilon = \left(\xi^2 + \Delta^2\right)^{1/2}$, where Δ depends on T and, hence, on r. However, the corresponding contributions from the two terms on the left-hand side of eq. (19.1) cancel.

$$\varkappa \approx \frac{2n_{\mathrm{e}}\tau_{\mathrm{tr}}T}{m}\left(\frac{\Delta(0)}{T}\right)^{2}\exp\left(\frac{-\Delta(0)}{T}\right). \tag{19.13}$$

The graph of x/x_{n} against T/T_{c} is given in fig. 122 .

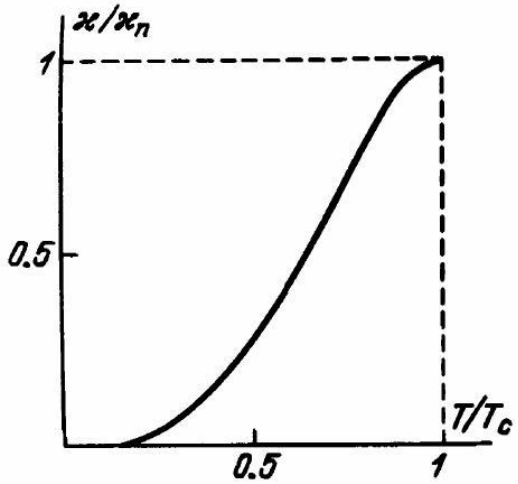


Fig. 122.

8.5.2 19.2. Thermoelectric phenomena

As has been pointed out in the preceding section, a temperature gradient leads to the appearance not only of a heat flux but also of a flux of quasiparticles, i.e., a "normal current". However, it is balanced by a superconducting current which flows in the opposite direction, because in the bulk of the superconductor the current must be equal to zero (otherwise the Meissner effect would not have occurred). Therefore, it has long been thought that there are no thermoelectric phenomena in a super-conductor. It has turned out, in fact, that the appearance of a supercurrent is amenable to detection.

The presence of a supercurrent implies that the momentum of Cooper pairs is no longer equal to zero, i.e., the Bose condensate of Cooper pairs comes into motion. In this case, the Bogoliubov transformation formulae (16.14) must be replaced by the following:

$$\begin{aligned} a_{p,+} &= u_p\alpha_{p,+} + v_p\alpha^{+}_{-p+q,-} \\ a_{p,-} &= u_{-p+q}\alpha_{p,-} - v_{-p+q}\alpha^{+}_{-p+q,+} \end{aligned} \tag{19.14}$$

The meaning of these transformations is as follows: the term with v in each of the formulae corresponds to the binding of electrons into a Cooper pair with momentum q and to its escape into the condensate (evidently $q = 2mv_{\mathrm{s}}$). Instead, an electron appears with momentum $-p+q$ and opposite spin projection.

The subscripts for u and v in the second formula are chosen such that the following condition is satisfied:

- In this and subsequent sections x is the coefficient of thermal conductivity.

$$\{a_{p,+}, a_{-p+q,-}\} = -u_p v_p + u_p v_p = 0$$

The coefficients u and v are connected by the same relation as before:

$$|u_p|^2 + |v_p|^2 = 1. \tag{19.15}$$

Substituting formulae (19.14) into the Hamiltonian (16.13) and averaging, we obtain

$$\begin{aligned}\langle \mathscr{H} - \mu N \rangle = \sum_p \big\{ & \xi \left[n_{p,+} + |v_p|^2 \left(1 - n_{p,+} - n_{-p+q,-}\right)\right] \\ & + \xi' \left[n_{-p+q,-} + |v_p|^2 \left(1 - n_{p,+} - n_{-p+,q-}\right)\right] \big\} - \frac{|\Delta|^2}{g},\end{aligned} \tag{19.16}$$

where

$$\Delta = g \sum_p u_p v_p \left(1 - n_{p,+} - n_{-p+q,-}\right), \tag{19.17}$$

$$\xi' = \xi(-p+q). \tag{19.18}$$

We will find the real solution for u and v (this does not alter the result but simplifies the computations). In this case, Δ is also real. Minimizing with respect to v_p and using (19.15), we get

$$u^2 = u^2_{-p+q} = \frac{1}{2}\left(1 + \frac{\xi + \xi'}{2\varepsilon}\right), \tag{19.19}$$

$$v_p^2 = v^2_{-p+q} = \frac{1}{2}\left(1 - \frac{\xi + \xi'}{2\varepsilon}\right), \tag{19.20}$$

$$\varepsilon = \left[\frac{1}{4}\left(\xi + \xi'\right)^2 + \Delta^2\right]^{1/2}. \tag{19.21}$$

Varying eq. (19.16) with respect to $n_{p,+}$ and $n_{p,-}$, we find the value of energy in the Fermi distribution functions (19.17):

$$\varepsilon_{p,+} = \varepsilon + \frac{1}{2}\left(\xi - \xi'\right), \quad \varepsilon_{-p+q,-} = \varepsilon - \frac{1}{2}\left(\xi - \xi'\right). \tag{19.22}$$

Let us calculate the electric current. Here we must take into account the difference between charge transfer and energy transfer. Whereas the energy is transferred by quasi-particles, which have an energy $\varepsilon = (\xi^2 + \Delta^2)^{1/2}$ and velocity $\partial\varepsilon/\partial p$, the charge is transferred by initial electrons with velocity p/m (the corresponding operators are a and $a^+$and not α and α^+). Thus, the current operator has the form

$$j = \frac{e}{m} \sum_{p,\sigma} p a^+_{p,\sigma} a_{p,\sigma}. \tag{19.23}$$

The same result has been obtained earlier (see formulae 16.59′ and 16.62 at $\boldsymbol{A} = 0$ and $\boldsymbol{q} = 0$).

Substituting here the transforms (19.14) and averaging gives

$$j = \sum_p p \left[u_p^2 n_{p,+} + v_p^2 \left(1 - n_{-p+q,-}\right) + u_n^2 n_{p,-} + v_p^2 \left(1 - n_{-p+q,+}\right)\right]$$

(here we have used qualities 19.20,19.21). We pass now to a new variable: $\boldsymbol{p} \to \boldsymbol{p} + \frac{1}{2}\boldsymbol{q}$. Assuming that $|\boldsymbol{q}| < p_0$, we obtain

$$\begin{array}{lll} \xi \to \xi + \frac{1}{2}vq, & \xi' \to \xi - \frac{1}{2}vq, & \frac{1}{2}(\xi + \xi') \to \xi \\ \varepsilon \to (\xi^2 + \Delta^2)^{1/2}, & \varepsilon_p \to \varepsilon + \frac{1}{2}vq/2, & \varepsilon_{-p+q} \to \varepsilon - \frac{1}{2}vq. \end{array} \tag{19.24}$$

The expression for the current takes the form

$$j = 2\sum_p \left(p + \frac{1}{2}q\right)\left[u_p^2 n_p + v_p^2(1 - n_{-p+q})\right] \tag{19.25}$$

The momentum of the pairs is connected with the velocity of the condensate by the relation $q = 2mv_\mathrm{s}$. Since $v = p/m$, we have

$$\frac{1}{2}vq = pv_\mathrm{s}. \tag{19.26}$$

The result obtained may be interpreted as follows. In the coordinate system associated with the moving condensate the energy of quasiparticles is ε and the momentum of electrons is $\boldsymbol{p}$. But if we pass to the laboratory coordinate system, the energy of quasiparticles becomes equal to $\varepsilon + pv_\mathrm{s}$ and the electron momentum to $p + mv_\mathrm{s}$.

In the preceding section, while calculating the thermal conductivity we should have replaced, strictly speaking, ε in expression (19.11) by $\varepsilon + pv_\mathrm{s}$ and $\partial\varepsilon/\partial p$ by $\partial\varepsilon/\partial p + v_\mathrm{s}$. But here one must take into account that the superconducting current arises only as a result of the appearance of a temperature gradient, i.e., $v_\mathrm{s} \propto \nabla\mathrm{T}$. Substitution into eq. (19.11) of the equilibrium distribution function n_F instead of n under the integral yields the gradient in momentum space of a certain function $f(\varepsilon + pv_\mathrm{s})$. The integral over d^3p is transformed to a surface integral and is equal to zero because $n_F(\infty) = 0$. Therefore, only the integral of the nonequilibrium contribution $n^{(1)}$ is left, which itself is proportional to ∇T. Hence, in this integral we may put $v_\mathrm{s} = 0$.

Let us return to formula (19.25). We substitute into it $n = n_\mathrm{F} + n^{(1)}$, where $n^{(1)} < n_\mathrm{F}$, and limit ourselves to the terms of first order in $n^{(1)}$ and v_s (of order ∇T). This gives

$$\begin{aligned} j =& 2ev_\mathrm{s}\sum_p \left[u_p^2 n_\mathrm{F} + v_p^2(1 - n_\mathrm{F})\right] \\ &+ 2\frac{e}{m}\sum_p p(pv_\mathrm{s})\frac{\partial n_\mathrm{F}}{\partial\varepsilon} + 2\frac{e}{m}\sum_p pn^{(1)} \end{aligned} \tag{19.27}$$

In the last term it is taken into account that $n_{-p}^{(1)} = -n_p^{(1)}$ (see 19.10). We have also used the condition (19.15).

If we perform the Bogoliubov transformation (16.14) in the electron density operator

$$n_\mathrm{e} = \sum_p a_{p,\sigma}^+ a_{p,\sigma}$$

and average, we obtain

$$n_\mathrm{e} = 2\sum_p \left[u_p^2 n_\mathrm{F} + v_p^2(1 - n_\mathrm{F})\right].$$

Thus, the first term in (19.27) is equal to $n_e v_s e$. We compare the second term in (19.27) with formula (16.83) for the momentum of quasiparticles moving with velocity $\boldsymbol{u}$ (in our case

the role of $\boldsymbol{u}$ is played by $-\boldsymbol{v}_\mathrm{s}$). The proportionality factor between $\boldsymbol{P}$ and $\boldsymbol{mu}$ is the "number of normal electrons" $\boldsymbol{n}_\mathrm{n}$. Hence, the first two terms in (19.27) give

$$(n_\mathrm{e} - n_\mathrm{n})\, ev_\mathrm{s} = n_\mathrm{s} ev_\mathrm{s} = j_\mathrm{s}$$

This is just the superconducting current.
The last term in eq. (19.27) is the current of quasiparticles, which arises under the action of the temperature gradient. Substituting (19.10) and passing to integration over ξ, we get

$$j_\mathrm{n} = \mathrm{e} \int \frac{\varepsilon}{T} \frac{\partial n_\mathrm{F}}{\partial \varepsilon} \tau_\mathrm{tr} \operatorname{sign} \xi v (v \nabla T) \nu \mathrm{d}\xi \frac{\mathrm{d}\Omega}{4\pi}$$

This integral vanishes in the first approximation in ξ because of the presence of the factor sign ξ. Therefore, just as in a normal metal, we must expand the factor $\tau_\mathrm{tr} v^2 \nu$ in the integrand in ξ :

$$\tau_\mathrm{tr} v^2 \nu = \left(\tau_\mathrm{tr} v^2 \nu\right)_\mu + \xi \frac{\partial}{\partial \mu} \left(\tau_\mathrm{tr} v^2 \nu\right)_\mu$$

The second term gives a nonzero result. Here

$$\int_{-\infty}^{\infty} \xi \operatorname{sign} \xi \mathrm{d}\xi \to \int_{-\infty}^{\infty} |\xi| \mathrm{d}\xi \to 2 \int_0^{\infty} |\xi| \mathrm{d}|\xi| \to 2 \int_\Delta^{\infty} \varepsilon \mathrm{d}\varepsilon$$

The result is given by (Gal'perin et al. 1973, 1974)

$$\begin{aligned} j_\mathrm{n} &= \frac{2}{3} e \left[\frac{\partial}{\partial \mu} \left(\tau_\mathrm{tr} v^2 \nu\right)_\mu\right] \frac{\nabla T}{T} \int_\Delta^{\infty} \varepsilon^2 \frac{\partial n}{\partial \varepsilon}\, \mathrm{d}\varepsilon \\ &= -\frac{2}{3} e \left(\frac{\partial}{\partial \mu} \left(\tau_\mathrm{tr} v^2 \nu\right)_\mu\right) T \nabla T \int_{\Delta/T}^{\infty} \frac{x^2}{\cosh^2\left(\frac{1}{2}x\right)} \mathrm{d}x \\ &= -e \left(\frac{\partial}{\partial \mu} \ln \left(\tau_\mathrm{tr} v^2 \nu\right)_\mu\right) x \nabla T \end{aligned} \tag{19.28}$$

where x is the thermal conductivity coefficient. Taking into account that in a normal metal $j_\mathrm{n} = -\beta \nabla T$ and comparing formulas (3.24) and (6.19), we see that the expression for j_n written in terms of x does not differ from a normal metal. Since $T \to T_\mathrm{c}$ and $x \to x_\mathrm{n}$, the same is valid for j_n. Taking into account that for impurity scattering $\tau_\mathrm{tr} = l/v \propto \mu^{-1/2}, v^2 \propto \mu$ and $\nu \propto p_0 \propto \mu^{1/2}$, we finally obtain

$$j_\mathrm{s} = -j_\mathrm{n} = \frac{e}{\mu} \varkappa \nabla T \tag{19.29}$$

The asymptotics are found with the aid of the formulas for x : (3.24) with $T \to T_\mathrm{c}$ and (19.13) with $T \to 0$.

A question now arises as to whether we can determine experimentally the presence of a supercurrent. To this end, we use the expression for the supercurrent in terms of the phase of the order parameter (17.75):

$$j_\mathrm{s} = \frac{\hbar e n_\mathrm{s}}{2m} \left(\nabla \chi - \frac{2e}{\hbar c} A\right) \tag{19.30}$$

(here we have substituted $|\Psi|^2 = n_\mathrm{s}/2$, the number of Cooper pairs). Comparing expressions (19.30) and (19.29), we find

$$\nabla \chi = \frac{2m}{\hbar e n_\mathrm{s}} \frac{e\chi}{\mu} \nabla T + \frac{2e}{\hbar c} A. \tag{19.31}$$

Suppose now that we have a ring consisting of two different superconductors (fig. 123). We assume that the junctions are at different temperatures, T_1 and T_2. We integrate expression (19.31) over a closed loop C , which passes through the bulk

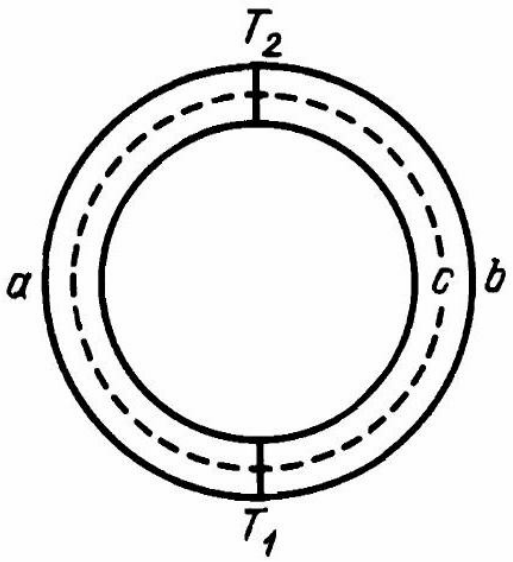


Fig. 123.

of superconductors. The change of the phase along the closed loop must be equal to $2\pi n$, where n is an integer. Hence, we have

$$2\pi n = \frac{2m}{\hbar}\oint_C \frac{x}{\mu n_\mathrm{s}}\nabla T\ \mathrm{d}l + \frac{2e}{\hbar c}\oint_\mathrm{C} A\ \mathrm{d}l$$
$$= \frac{2m}{\hbar}\int_{T_1}^{T_2}\left[\left(\frac{x}{\mu n_\mathrm{s}}\right)_\mathrm{b} - \left(\frac{x}{\mu n_\mathrm{s}}\right)_\mathrm{a}\right]\mathrm{d}T + 2\pi\frac{\Phi}{\Phi_0}$$

or

$$\frac{\Phi}{\Phi_0} = n + \frac{m}{\pi\hbar}\cdot\int_{T_1}^{T_2}\left[\left(\frac{x}{\mu n_\mathrm{s}}\right)_\mathrm{a} - \left(\frac{x}{\mu n_\mathrm{s}}\right)_\mathrm{b}\right]\mathrm{d}T. \tag{19.32}$$

From this formula it follows that the magnetic flux passing through the loop is not equal to an integer number of flux quanta and has a correction which depends on temperature. This correction is a manifestation of thermoelectricity in superconductors.

At first glance it seems paradoxical that a magnetic flux can pass through the ring in the absence of current. In fact, the statement that $\boldsymbol{j} = \mathbf{0}$ refers only to the bulk of the superconductor. A superconducting current is circulating along the inner surface of the ring and it is this supercurrent that produces the magnetic flux.

Let us estimate the magnitude of the correction to the magnetic flux. We assume that $T \sim T_\mathrm{c}$ and, hence, $n_\mathrm{s} \sim n_\mathrm{e}$ and $x \sim x\,(T_\mathrm{c})$. The expression for $x(T)$ is derived from formula (3.28). We have

$$\frac{\Delta\Phi}{\Phi_0\Delta T} \sim \frac{m}{\hbar}\frac{x}{\mu n_\mathrm{e}} \sim \frac{m}{\hbar}\frac{n_\mathrm{e}\tau_\mathrm{tr}}{m\mu n_\mathrm{e}}T_\mathrm{c}$$
$$\sim \frac{T_\mathrm{c}}{\mu}\frac{\tau_\mathrm{tr}}{\hbar} \sim 10^{-4}\frac{l}{v\hbar} \sim 10^{12}\mathrm{erg}^{-1} \sim 10^{-4}\ \mathrm{K}^{-1}$$

(we assume here that the mean free path $l \sim 10^{-3}$ cm and $T_\mathrm{c}/\mu \sim 10^{-4}$). Thus, the temperature contribution is very small (10^{-4} flux quantum per 1 K). Its measurement

is hindered also by the fact that it is difficult to protect the superconducting ring against a small trapped magnetic flux. Therefore, in practice one has to measure the difference effect with $T_1 \rightleftharpoons T_2$. The corresponding measurement has been carried out (Zavaritskii 1974) with the aid of a SQUID (section 22.8) and has qualitatively confirmed the theory. However, other results exceed the theoretical predictions*.

8.5.3 19.3. The behavior of superconductors in a weak high-frequency field

The behavior of superconductors in a weak, time-independent field has been considered in sections 16.7 and 16.8. In principle, the same method can be used to find the relationship between the current and a field of finite frequency. We do not give the relevant calculations here because they are very cumbersome (see, for example, Abrikosov and Khalatnikov 1958). Instead, we present some of the fundamental results (Abrikosov et al. 1958, 1959, Mattis and Bardeen 1958).

First of all let us consider the case $T = 0$. In this case the superconductor does not contain quasiparticles that could have absorbed quanta of any energy. The absorption of electromagnetic waves begins only when

$$\hbar\omega = 2\Delta(0). \tag{19.33}$$

This is the energy required for the breakdown of Cooper pairs. In the limit, when $\hbar\omega > 2\Delta$ the difference between a super-conductor and a normal metal disappears, i.e., the relationship between the current and the field tends to that existing in a normal metal.

The absorption of electromagnetic energy is proportional to the real part of the impedance. For a pure superconductor in the limiting Pippard case the following relation holds:

$$\frac{Z_\mathrm{s}}{R_\mathrm{n}} = -2\mathrm{i}\left[\frac{\pi\hbar\omega}{\Delta Q_1(\omega)}\right]^{1/3}, \tag{19.34}$$

where $Q_1(\omega)$ enters into the proportionality factor between the current and the field:

$$j = -Q(q,\omega)A(q,\omega), \quad Q(q,\omega) = \frac{3}{4}\frac{n_\mathrm{e}e^2}{mc}\frac{\Delta}{\hbar vq}Q_1(\omega), \tag{19.35}$$

and R_n is the value of R for a normal metal.

The real part of the impedance manifests itself only if the imaginary part Q_1 is nonzero. A plot of $\operatorname{Im} Q_1(\omega)$ at $T = 0$ is shown in fig. 124. The $R_\mathrm{s}(\omega)/R_\mathrm{n}$ plot has

is hindered also by the fact that it is difficult to protect the superconducting ring against a small trapped magnetic flux. Therefore, in practice one has to measure the difference effect with $T_1 \rightleftharpoons T_2$. The corresponding measurement has been carried out (Zavaritskii 1974) with the aid of a SQUID (section 22.8) and has qualitatively confirmed the theory. However, other results exceed the theoretical predictions*.

- V. I. Kozub (1985) proposed the following explanation. In order to enhance the effect, the superconductors making up the ring are usually chosen such that they differ in their parameters, particularly in T_c. For one of the superconductors the temperature is very low and the energy transport is mainly realized by phonons. These phonons are irradiated into the other superconductor and produce a phonon wind, which drags the quasiparticles. An estimate shows that this effect can increase the observed magnetic flux by two orders of magnitude.

8.5.4 19.3. The behavior of superconductors in a weak high-frequency field

The behavior of superconductors in a weak, time-independent field has been considered in sections 16.7 and 16.8. In principle, the same method can be used to find the relationship between the current and a field of finite frequency. We do not give the relevant calculations here because they are very cumbersome (see, for example, Abrikosov and Khalatnikov 1958). Instead, we present some of the fundamental results (Abrikosov et al. 1958, 1959, Mattis and Bardeen 1958).

First of all let us consider the case $\boldsymbol{T} = 0$. In this case the superconductor does not contain quasiparticles that could have absorbed quanta of any energy. The absorption of electromagnetic waves begins only when

$$\hbar\omega = 2\Delta(0). \tag{19.33}$$

This is the energy required for the breakdown of Cooper pairs. In the limit, when $\hbar\omega > 2\Delta$ the difference between a super-conductor and a normal metal disappears, i.e., the relationship between the current and the field tends to that existing in a normal metal.

The absorption of electromagnetic energy is proportional to the real part of the impedance. For a pure superconductor in the limiting Pippard case the following relation holds:

$$\frac{Z_\mathrm{s}}{R_\mathrm{n}} = -2\mathrm{i}\left[\frac{\pi\hbar\omega}{\Delta Q_1(\omega)}\right]^{1/3}, \tag{19.34}$$

where $Q_1(\omega)$ enters into the proportionality factor between the current and the field:

$$j = -Q(q,\omega)A(q,\omega), \quad Q(q,\omega) = \frac{3}{4}\frac{n_\mathrm{e}e^2}{mc}\frac{\Delta}{\hbar vq}Q_1(\omega), \tag{19.35}$$

and R_n is the value of R for a normal metal.

The real part of the impedance manifests itself only if the imaginary part Q_1 is nonzero. A plot of $\mathrm{Im}\, Q_1(\omega)$ at $T = 0$ is shown in fig. 124. The $R_\mathrm{s}(\omega)/R_\mathrm{n}$ plot has

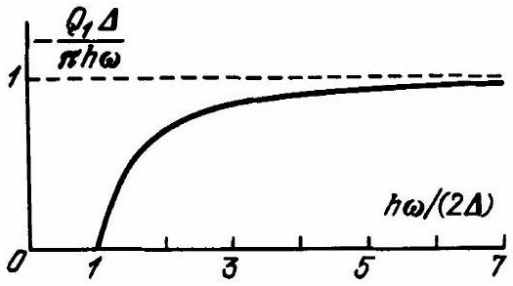


Fig. 124.

- V. I. Kozub (1985) proposed the following explanation. In order to enhance the effect, the superconductors making up the ring are usually chosen such that they differ in their parameters, particularly in T_c. For one of the superconductors the temperature is very low and the energy transport is mainly realized by phonons. These phonons are irradiated into the other superconductor and produce a phonon wind, which drags the quasiparticles. An estimate shows that this effect can increase the observed magnetic flux by two orders of magnitude.

qualitatively the same form. Near the absorption threshold

$$\operatorname{Im} Q_1 \approx -\pi^2 \left(\frac{\hbar\omega}{2\Delta} - 1 \right). \tag{19.35'}$$

The ratio $R_s(\omega)/R_n$ is also proportional to this quantity.
At $T > 0$ there are quasiparticles in the superconductor which can absorb electromagnetic quanta of any frequency. If $T < T_c$, the number of quasiparticles is exponentially small ($\sim \exp[-\Delta(0)/T]$). In the case $\omega < \Delta$ the same exponential is contained in the imaginary part of $Q_1(\omega)$ and in the real part of the impedance. The expression for $\operatorname{Im} Q_1$ for $\omega, T \ll \Delta$ reads

$$\operatorname{Im} Q_1 \approx -4\pi \sinh\left(\frac{\omega}{2T}\right) K_0\left(\frac{\omega}{2T}\right) \exp\left(\frac{-\Delta(0)}{T}\right), \tag{19.35"}$$

where K_0 is the MacDonald function.
Starting with $\hbar\omega = 2\Delta(0) = 3.52T_c$ a finite absorption also occurs at $T = 0$. This is clearly seen in the experimental plots obtained for aluminum at various frequencies and temperatures (fig. 125) (Biondi and Garfunkel 1959). Note that with $\omega \to 0$ the dependence $R_s(T)$ assumes the same form as the resistivity curve at constant current: $R = 0$ at $T < T_c$ and $R_s = R_n$ at $T > T_c$.

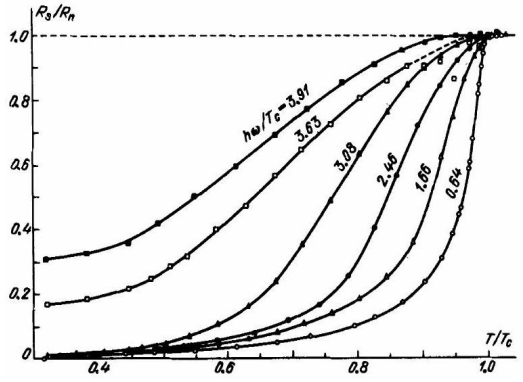


Fig. 125.

The characteristic wavelengths corresponding to the condition (19.33) lie within a range of the order of $1 - 0.1$ mm and the corresponding frequencies are of the order of $\nu = \omega/2\pi \sim 10^{11} - 10^{12}$ Hz. Note that in the optical range $\nu \sim 10^{15}$ Hz. For these frequencies the impedance of superconductors does not differ from that of normal metals.

However, in principle, apart from elastic reflection at an unshifted frequency, one can also observe Raman light scattering when part of the quantum energy is transferred to the electronic system. In this case (Abrikosov and Fal'kovsii 1961, 1987, Abrikosov and Genkin 1973) the spectral dispersion of the reflected light contains "satellites", i.e., quanta with an altered frequency. In this case, we are speaking of the breakup of the pairs and therefore at low temperatures a "Stokes satellite" appears, with a continuous frequency distribution $\hbar\omega \leqslant \hbar\omega_0 - 2\Delta$ (ω_0 is the frequency of the incident light). The intensity of the satellite is rather low because the interaction of light with the electronic system occurs only in a thin skin layer. Here, special care must be taken in order for the line of the incident light to be narrow (in the sense of the spectral width) and the intensity not to be very high, otherwise the specimen will be heated. The value of Δ is also important. For substances with large Δ the line needs not be so narrow. Thus Raman scattering was first definitely observed in the high- T_c ceramic $YBa_2Cu_3O_{7-\delta}$ (Bazhenov et al: 1987, Lyons et al. 1987). In an anisotropic superconductor $\Delta_{\min}$ is established in this way (Abrikosov and Fal'kovskii 1987).

In conclusion, we give one more relation between the current and the field for a dirty superconductor in the London limit ($q = 0$) in the vicinity of the critical temperature and also for a low frequency: $\omega \lll T_c$ (this case is of interest for what follows). We have

$$j = \left(\frac{-c}{4\pi\delta^2} + \frac{i\omega\sigma}{c} \right) A,$$

where $\sigma = n_e e^2 \tau_{tr}/m$ is the conductivity of a normal metal; δ depends on the ratio of ξ_0 to l, but in all cases it corresponds to the static penetration depth (sections 16.9 and 16.10). In other words, for the case under consideration

$$\boldsymbol{j} = \boldsymbol{j}_s + \boldsymbol{j}_n$$

where j_s is expressed by the formula for constant field and $j_n = \boldsymbol{\sigma E}\,(\boldsymbol{E} = -\boldsymbol{c^{-1}}\partial \boldsymbol{A}/\partial t = (\mathrm{i}\omega/c)\boldsymbol{A}$. This is consistent with the concepts of London electrodynamics. However, with other relationships between ω, Δ and T there is no such agreement.

8.5.5 19.4. Absorption of ultrasound

In accordance with section 12.1, the variation of the electron energy in a field of sound waves may be considered to be equal to $\Lambda_{ik}(p)u_{ik}(r,t)$, where u_{ik} is the strain tensor and Λ_{ik} is the deformation potential. This quantity plays the role of the potential energy. The relevant operator may be written similarly to eq. (19.2). The frequency of the sound that can actually be generated does not exceed 10^9 Hz, whereas $\Delta/(2\pi\hbar) \sim 10^{11}$ Hz. Hence, $\hbar\omega < \Delta$. In view of this, in transformating to operators of quasiparticles we have again to drop the terms corresponding to creation and annihilation of two quasiparticles. As regards the terms corresponding to scattering, one has to take account of the fact that the electron energy upon absorption of a phonon increases by an amount $\hbar\omega$. Therefore, $\varepsilon \neq \varepsilon'$ in formula (19.3).

We assume that $\omega\tau_{tr} > 1$ and apply the quantum approach described in section 12.2. The only difference from formula (12.20) lies in the appearance of the factor $(uu' - vv')^2$. Inserting the expressions for u and v, we obtain (assuming that the normalization volume $V = 1$):

$$Q = -\pi\omega^2 \sum_{p,p'} |U_{p'p}|^2\, \delta\left(\omega_{p'p} - \omega\right) \frac{\partial n_F}{\partial \varepsilon} \frac{1}{2} \left(1 + \frac{\xi_p \xi_{p'} - \Delta^2}{\varepsilon_p \varepsilon_{p'}} \right). \tag{19.36}$$

The matrix element $U_{p'p}$ is given by (at $k < p_0$)

$$U_{p'p} = \Lambda_{ik}(p) u^0_{ik} \delta_{p',p+\hbar k}, \tag{19.37}$$

where $u^0_{ik} = \frac{1}{2}\mathrm{i}\left(k_i u^0_k - k_k u^0_i\right)$ and u^0 is the amplitude of the sound wave. Passing from the sums over momenta to integrals $\sum_p = (2\pi\hbar)^{-3} \int \mathrm{d}^3 p$ and considering that

$$\delta^2_{p'p} = \delta_{p'p} \to (2\pi\hbar)^3 \left(\delta\left(p' - p\right)\right.,$$

we get

$$Q = -\pi\omega^2\hbar \int \frac{\mathrm{d}^3 p}{(2\pi\hbar)^3} \left|\Lambda_{ik}(p) u^0_{ik}\right|^2 \delta\left(\varepsilon_{p'} - \varepsilon_p - \hbar\omega\right) \frac{\partial n_F}{\partial \varepsilon} \frac{1}{2} \left(1 + \frac{\xi_p \xi_{p'} - \Delta^2}{\varepsilon_p \varepsilon_{p'}} \right), \tag{19.38}$$

where $\boldsymbol{p'} = \boldsymbol{p} + \boldsymbol{\hbar k}$.

In formula (19.38) $\int \mathrm{d}^3 p (2\pi\hbar)^{-3}$ corresponds to $\frac{1}{4}\nu \int \mathrm{d}\xi\, \mathrm{d}\cos\frac{1}{2}\theta$, where $\theta = \widehat{(v,k)}$. Taking into

account that $\xi' = \xi + vk\cos\theta$ and $vk \gg \omega$ (because $v \gg s$; s is the sound velocity), we can pass to the integration over $\boldsymbol{\xi}$ and $\boldsymbol{\xi}'$ and write

$$\int \frac{d^3p}{(2\pi\hbar)^3} \to \frac{\nu}{4\hbar vk} \int_{-\infty}^{\infty} d\xi \int_{-\infty}^{\infty} d\xi'$$

(instead of $|\Lambda_{ik}(p)|^2$ we must take $\overline{|\Lambda_{ik}(p)|^2}$, which signifies the average over the line on the Fermi surface, where $\cos\theta = 0$ or $v \perp k$). The integration over ξ and ξ' leads to the cancellation of the odd terms with respect to ξ and ξ' in eq. (19.38). After this we may pass over to the integration over ε, taking account of the two possible signs of ξ : $\int_{-\infty}^{\infty} \mathrm{d}\xi \to 2\int_{\Delta}^{\infty} \varepsilon \left(\varepsilon^2 - \Delta^2\right)^{-1/2} \mathrm{d}\varepsilon$. As a result, we obtain

$$Q = -\frac{\pi\omega^2\nu}{vk} \int_{\Delta}^{\infty} \left|\Lambda_{ik} u_{ik}^0\right|^2 \left[\varepsilon(\varepsilon + \hbar\omega) - \Delta^2\right] \times \left(\varepsilon^2 - \Delta^2\right)^{-1/2} \left[(\varepsilon + \hbar\omega)^2 - \Delta^2\right]^{-1/2} \frac{\partial n_{\mathrm{F}}}{\partial \varepsilon}\, \mathrm{d}\varepsilon. \tag{19.39}$$

tensor and Λ_{ik} is the deformation potential. This quantity plays the role of the potential energy. The relevant operator may be written similarly to eq. (19.2). The frequency of the sound that can actually be generated does not exceed 10^9 Hz, whereas $\Delta/(2\pi\hbar) \sim 10^{11}$ Hz. Hence, $\hbar\omega < \Delta$. In view of this, in transformating to operators of quasiparticles we have again to drop the terms corresponding to creation and annihilation of two quasiparticles. As regards the terms corresponding to scattering, one has to take account of the fact that the electron energy upon absorption of a phonon increases by an amount $\hbar\omega$. Therefore, $\varepsilon \neq \varepsilon'$ in formula (19.3).

We assume that $\omega\tau_{\mathrm{tr}} > 1$ and apply the quantum approach described in section 12.2. The only difference from formula (12.20) lies in the appearance of the factor $(uu' - vv')^2$. Inserting the expressions for u and v, we obtain (assuming that the normalization volume $\boldsymbol{V} = \mathbf{1}$):

$$Q = -\pi\omega^2 \sum_{p,p'} |U_{p'p}|^2\, \delta\left(\omega_{p'p} - \omega\right) \frac{\partial n_{\mathrm{F}}}{\partial \varepsilon} \frac{1}{2} \left(1 + \frac{\xi_p \xi_{p'} - \Delta^2}{\varepsilon_p \varepsilon_{p'}}\right). \tag{19.36}$$

The matrix element $U_{p'p}$ is given by (at $k < p_0$)

$$U_{p'p} = \Lambda_{ik}(p) u_{ik}^0 \delta_{p',p+hk}, \tag{19.37}$$

where $u_{ik}^0 = \frac{1}{2}\mathrm{i}\left(k_i u_k^0 - k_k u_i^0\right)$ and u^0 is the amplitude of the sound wave. Passing from the sums over momenta to integrals $\sum_p = (2\pi\hbar)^{-3} \int \mathrm{d}^3p$ and considering that

$$\delta_{p'p}^2 = \delta_{p'p} \to (2\pi\hbar)^3 \left(\delta\left(p' - p\right)\right.,$$

we get

$$Q = -\pi\omega^2\hbar \int \frac{\mathrm{d}^3p}{(2\pi\hbar)^3} \left|\Lambda_{ik}(p) u_{ik}^0\right|^2 \delta\left(\varepsilon_{p'} - \varepsilon_p - \hbar\omega\right) \frac{\partial n_{\mathrm{F}}}{\partial \varepsilon} \frac{1}{2} \left(1 + \frac{\xi_p \xi_{p'} - \Delta^2}{\varepsilon_p \varepsilon_{p'}}\right), \tag{19.38}$$

where $\boldsymbol{p}' = \boldsymbol{p} + \boldsymbol{\hbar k}$.

In formula (19.38) $\int \mathrm{d}^3p(2\pi\hbar)^{-3}$ corresponds to $\frac{1}{4}\nu \int \mathrm{d}\xi\ \mathrm{d}\cos\frac{1}{2}\theta$, where $\theta = \widehat{(v,k)}$. Taking into account that $\xi' = \xi + vk\cos\theta$ and $vk \gg \omega$ (because $v \gg s$; s is the sound velocity), we can pass to the integration over $\boldsymbol{\xi}$ and $\boldsymbol{\xi}'$ and write

$$\int \frac{d^3p}{(2\pi\hbar)^3} \to \frac{\nu}{4\hbar vk} \int_{-\infty}^{\infty} d\xi \int_{-\infty}^{\infty} d\xi'$$

(instead of $|\Lambda_{ik}(p)|^2$ we must take $\overline{|\Lambda_{ik}(p)|^2}$, which signifies the average over the line on the Fermi surface, where $\cos\theta = 0$ or $v \perp k$). The integration over ξ and ξ' leads to the cancellation of the odd terms with respect to ξ and ξ' in eq. (19.38). After this we may pass over to the integration over ε, taking account of the two possible signs of ξ : $\int_{-\infty}^{\infty} \mathrm{d}\xi \to 2\int_{\Delta}^{\infty} \varepsilon\,(\varepsilon^2-\Delta^2)^{-1/2}\ \mathrm{d}\varepsilon$. As a result, we obtain

$$Q = -\frac{\pi\omega^2\nu}{vk}\int_{\Delta}^{\infty} \left|\Lambda_{ik}u_{ik}^0\right|^2 \left[\varepsilon(\varepsilon+\hbar\omega)-\Delta^2\right] \times \left(\varepsilon^2-\Delta^2\right)^{-1/2}\left[(\varepsilon+\hbar\omega)^2-\Delta^2\right]^{-1/2}\frac{\partial n_{\mathrm{F}}}{\partial\varepsilon}\,\mathrm{d}\varepsilon. \tag{19.39}$$

Since $\hbar\omega < \Delta$, all the brackets under the integral sign give unity. Comparing with the expression for a normal metal (at $\Delta = 0$) and taking into account that for the absorption coefficient to be obtained the quantity Q is divided in both cases by the same sound energy flux I, we obtain (Bardeen et al. 1957):

$$\frac{\Gamma_{\mathrm{s}}}{\Gamma_{\mathrm{n}}} = -2\int_{\Delta}^{\infty}\frac{\partial n_{\mathrm{F}}}{\partial\varepsilon}\,\mathrm{d}\varepsilon = 2n_{\mathrm{F}}(\Delta) = \frac{2}{\mathrm{e}^{\Delta/T}+1}. \tag{19.40}$$

As $T \to T_{\mathrm{c}}$ this ratio tends to unity and at low temperatures it falls off as $\exp(-\Delta/T)$, i.e., proportionally to the number of quasiparticles. The curve showing the dependence of $\Gamma_{\mathrm{s}}/\Gamma_{\mathrm{n}}$ on T/T_{c} is given in fig. 126.

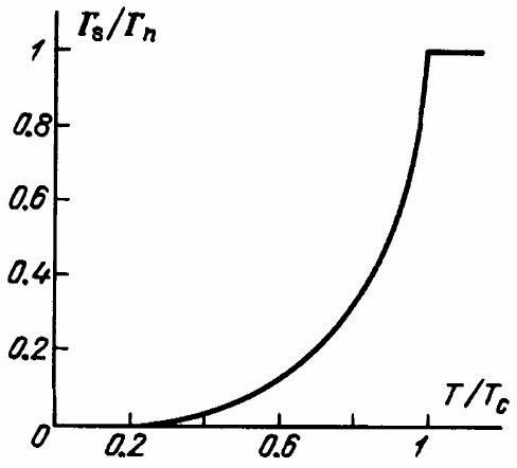


Fig. 126.

8.5.6 19.5. Stimulation of superconductivity by high-frequency, high-intensity field and sound

Up until now, while dealing with the behavior of superconductors under the influence of various external factors, we have limited our treatment to linear problems. Examples are the calculation of the current under the action of a small external field, and heat flux and electric current in the presence of a small temperature gradient. Such calculations are called calculations of the linear response of the system.

However, as the amplitude of external perturbations increases the nonlinear response may also become significant. In particular, under the action of a varying electromagnetic field a current with a frequency twice as high may be generated, which will lead to the emission of an electromagnetic wave at a doubled frequency. Hence, when an electromagnetic wave falls on

the metal surface, a reflected wave of doubled frequency may appear. Other nonlinear effects may also arise.

Since $\hbar\omega < \Delta$, all the brackets under the integral sign give unity. Comparing with the expression for a normal metal (at $\Delta = 0$) and taking into account that for the absorption coefficient to be obtained the quantity Q is divided in both cases by the same sound energy flux I, we obtain (Bardeen et al. 1957):

$$\frac{\Gamma_{\mathrm{s}}}{\Gamma_{\mathrm{n}}} = -2\int_{\Delta}^{\infty} \frac{\partial n_{\mathrm{F}}}{\partial \varepsilon}\, \mathrm{d}\varepsilon = 2n_{\mathrm{F}}(\Delta) = \frac{2}{\mathrm{e}^{\Delta/T}+1}. \tag{19.40}$$

As $T \to T_{\mathrm{c}}$ this ratio tends to unity and at low temperatures it falls off as $\exp(-\Delta/T)$, i.e., proportionally to the number of quasiparticles. The curve showing the dependence of $\Gamma_{\mathrm{s}}/\Gamma_{\mathrm{n}}$ on T/T_{c} is given in fig. 126.

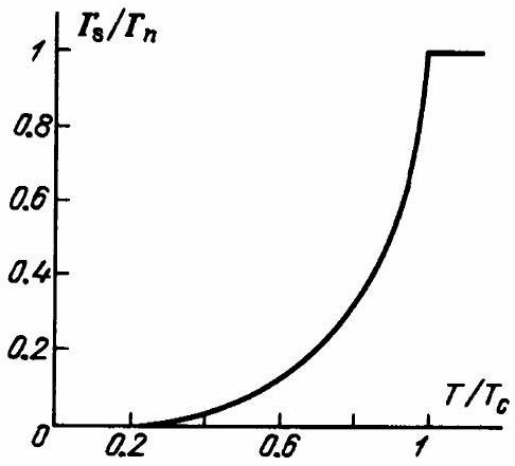


Fig. 126.

8.5.7 19.5. Stimulation of superconductivity by high-frequency, high-intensity field and sound

Up until now, while dealing with the behavior of superconductors under the influence of various external factors, we have limited our treatment to linear problems. Examples are the calculation of the current under the action of a small external field, and heat flux and electric current in the presence of a small temperature gradient. Such calculations are called calculations of the linear response of the system.

However, as the amplitude of external perturbations increases the nonlinear response may also become significant. In particular, under the action of a varying electromagnetic field a current with a frequency twice as high may be generated, which will lead to the emission of an electromagnetic wave at a doubled frequency. Hence, when an electromagnetic wave falls on the metal surface, a reflected wave of doubled frequency may appear. Other nonlinear effects may also arise.

We shall consider a specific nonlinear action of a high-frequency field (electromagnetic wave or sound), on superconductors which leads to a qualitatively new effect - an increase in the critical temperature of the superconducting transition, or, stimulation of superconductivity (Eliashberg 1970, Ivlev and Eliashberg 1971).

In sections 16.4 and 16.5 we have found the energy spectrum of quasiparticles in a superconductor and the equation for Δ. Formula (16.21), which relates Δ to the distribution function,

is valid for an arbitrary distribution and not only for the equilibrium distribution expressed by the Fermi function. Thus, we have

$$1 = \frac{1}{2} g \int \frac{d^3p}{(2\pi\hbar)^3} \frac{1-2n}{\varepsilon} \tag{19.41}$$

where $\varepsilon = (\xi^2 + \Delta^2)^{1/2}$.
With an equilibrium distribution we have seen that in the case $T = 0$, when no quasiparticles are present, Δ is at a maximum. At finite temperatures the appearance of quasiparticles leads to a decrease in Δ. Here, in the integral (19.41) quasi-particles with an energy of the order of Δ were the most important.

Suppose now that the electronic system absorbs quanta of energy $\hbar\omega$. If $\hbar\omega > 2\Delta$, new quasiparticles will be created and, hence, Δ will decrease. However, if $\hbar\omega < \Delta$, new quasiparticles cannot be created and the quanta are absorbed by the quasiparticles already present. This leads to their redistribution over the energies. If an appreciable number of quasiparticles receive an extra energy larger than Δ, it means that they move into another energy region. Hence, they leave the region which is relevant in the integral (19.41), and in this sense the situation begins to resemble that observed at $T = 0$. As a result, Δ increases.

To simplify the calculation, we assume that the temperature is close to T_c, i.e., $\Delta < T_c$ but still $\omega < \Delta$. Besides, we presume that the intensity of the external field is not too high, so the relative change of Δ is small.

We substitute $n = n_F(\varepsilon) + n - n_F$ into eq. (19.41). The integral with n_F is expanded in Δ, as was done in section 16.5 (formula 16.32). So, we obtain

$$\ln\left(\frac{T_c}{T}\right) - \frac{7}{8}\zeta(3)\frac{\Delta^2}{\pi^2 T_c^2} - 2\int_\Delta^\infty \mathrm{d}\varepsilon \left(\varepsilon^2 - \Delta^2\right)^{-1/2} \overline{(n - n_F)} = 0, \tag{19.42}$$

where the overbar in the last integral signifies averaging over the angles. We used here formula (16.25) for T_c; in the integral of $n - n_F$ we passed to the variable ε and took into account two signs of ξ. With our assumptions $\ln(T_c/T) \approx (T_c - T)/T_c$. If the distribution function depends on time, then in the integral we have to take the time-averaged quantity.

The distribution function n can be determined from the kinetic equation.
The calculations based on the detailed microscopic (BCS) theory, which takes account of the dependence of the quantities on time, involve very complicated kinetic equations, which are different, depending on the character of the external force. The difficulty is aggravated by the fact that the scattering from impurities, while being elastic, does not give rise to the relaxation of quasiparticles with respect
to energy, and therefore we must take into account the interaction with phonons. The latter circumstance leads to complication of the collision integral. Therefore, instead of detailed calculations, we shall make a simple estimate*.

Suppose we have a thin specimen, which is smaller than the penetration depth, onto which a high-frequency electromagnetic wave falls. As has been noted at the end of section 19.3, a normal current $j_n = \sigma E$ arises in it, which gives rise to ohmic losses. The energy received by the electronic system per unit time is given by

$$\frac{\partial Q}{\partial t} = \sigma\overline{E^2} = \frac{1}{2}\sigma E_0^2, \tag{19.43}$$

where $E = E_0 \cos\omega t$. Near T_c the quantity σ is equal to the conductivity of a normal metal, i.e., $\sigma = n_e e^2 \tau_{tr}/m$. This includes the time of scattering from impurities, because this process is the dominant one.

The electronic system transfers the received energy to the lattice in the form of phonons. However, this process is slow, taking a time $\tau_{\rm ph}$. Therefore, the effective temperature of the electronic system increases. It is rather obvious that

$$\tau_{\rm ph}\frac{\partial Q}{\partial t}\sim C_{\rm e}\delta T, \tag{19.44}$$

where $C_{\rm e}$ is the electronic heat capacity, which has the same order of magnitude as that in a normal metal, i.e., $C_{\rm e}\sim p_0 mT/\hbar^3$.

From formulae (1943) and (19.44) we find

$$\delta T\sim\frac{\tau_{\rm ph}\sigma E_0^2}{C_{\rm e}}\sim\frac{\tau_{\rm ph}n_{\rm e}e^2\tau_{\rm tr}E_0^2\hbar^3}{m\cdot mp_0T}\sim\frac{\left(evE_0\right)^2\tau_{\rm ph}\tau_{\rm tr}}{T}. \tag{19.45}$$

When the quasiparticles are heated by the field, their number is not changed because $\omega\ll\Delta$. This may be taken into account if we introduce the effective chemical potential. The new distribution will have the form

$$n=\frac{1}{\exp\left(\frac{\varepsilon-\delta\mu}{T+\delta T}\right)+1}$$

From the condition

$$\int_0^\infty n\,{\rm d}\xi=\int_\Delta^\infty\frac{n\varepsilon}{\left(\varepsilon^2-\Delta^2\right)^{1/2}}\,{\rm d}\varepsilon=\int_\Delta^\infty\frac{n_{\rm F}\varepsilon}{\left(\varepsilon^2-\Delta^2\right)^{1/2}}\,{\rm d}\varepsilon=\ {\rm const}$$

we find, by expanding in $\delta\mu$ and δT,

$$-\delta\mu\int_\Delta^\infty\frac{\partial n_{\rm F}}{\partial\varepsilon}\frac{\varepsilon}{\left(\varepsilon^2-\Delta^2\right)^{1/2}}\,{\rm d}\varepsilon-\frac{\delta T}{T}\int_\Delta^\infty\frac{\partial n_{\rm F}}{\partial\varepsilon}\frac{\varepsilon^2}{\left(\varepsilon^2-\Delta^2\right)^{1/2}}=0.$$

Since $\Delta<T$, we may put $\Delta=0$ everywhere. So, we obtain

$$\delta\mu=-2\delta T\ln 2.$$

Substituting

$$n\approx n_{\rm F}-\frac{\partial n_{\rm F}}{\partial\varepsilon}\left(\delta\mu+\frac{\varepsilon}{T}\delta T\right)$$

into the last term of eq. (19.42), we find

$$\begin{aligned}\int_\Delta^\infty{\rm d}\varepsilon\frac{1}{\left(\varepsilon^2-\Delta^2\right)^{1/2}}\frac{-\partial n_{\rm F}}{\partial\varepsilon}\left(\delta\mu+\frac{\varepsilon}{T_{\rm c}}\delta T\right)\\ \approx\frac{\delta\mu}{4T_{\rm c}}\ln\left(\frac{T_{\rm c}}{\Delta}\right)+\frac{\delta T_{\rm c}}{2T_{\rm c}}\approx-\frac{\delta T}{2T_{\rm c}}\ln 2\ln\left(\frac{T_{\rm c}}{\Delta}\right).\end{aligned}$$

We have confined ourselves to logarithmic accuracy with respect to $\ln\left(T_{\rm c}/\Delta\right)$. It is important that the integral is negative. Equation (19.42) is now written in the form

$$\frac{T-T_{\rm c}}{T_{\rm c}}=a\tau_{\rm ph}\tau_{\rm tr}\frac{\left(evE_0\right)^2}{T_{\rm c}^2}-\left[\frac{7}{8}\zeta(3)\right]\frac{\Delta^2}{\pi^2T_{\rm c}^2}, \tag{19.46}$$

where a is a coefficient of the order of unity (we assume that $\ln\left(T_{\rm c}/\Delta\right)$ is not large). A plot of $\left(T-T_{\rm c}\right)/T_{\rm c}$ against Δ is given in fig. 127. The lower curve corresponds to the equilibrium case $E_0=0$. In the presence of a wave, i.e. at $E_0\neq 0$, we obtain the upper curve, which

*The reasoning given here stems from B. I. Ivlev.

reaches a certain positive value with decreasing Δ. However, the theory outlined here may be applied only for $\Delta > \frac{1}{2}\omega$. At lower Δ the creation of new quasiparticles begins. The coefficient of Δ^2 in eq. (19.46) decreases and may even change sign (the dashed curve).

Thus, we come to the conclusion that the curve in fig. 127 exhibits a maximum at $\Delta \neq 0$ corresponding to $T - T_c > 0$. This means that if the film is kept at a temperature above T_c and irradiated, it can pass in a jumpwise manner to the superconducting state with a finite Δ. Of course, this effect may occur only at temperatures not too far from T_c.

The results obtained can be extended without any difficulty to the case where the excitation is accomplished by a sound wave. Comparing the two terms on the

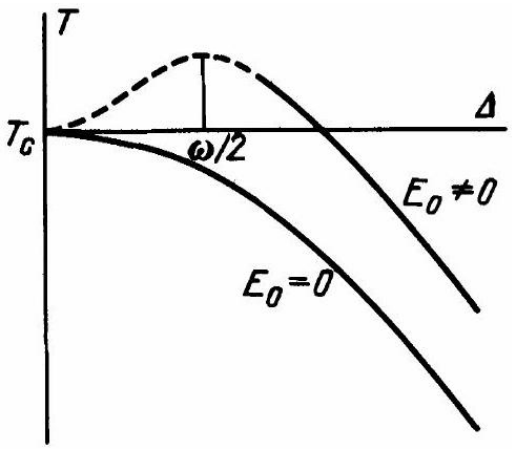


Fig. 127.

right-hand side of the kinetic equation (12.6), we arrive at the conclusion that in this case evE_0 in (19.46) must be replaced by $\Lambda_{ik}\dot{u}_{ik} \sim \omega\varepsilon_F k u^0 = \omega^2\varepsilon_F u^0/s$, where u^0 is the wave amplitude and s is the sound velocity.

The ideas presented here are in qualitative agreement with experiment (Wyatt et al. 1966). The measurement of the critical current of a film subjected to electromagnetic irradiation has shown that the current increases, depending on the irradiation dose. The effect has been observed near T_c and at not too high intensities.

It should, however, be noted that the experiments have been carried out on so-called bridges, i.e., films with a constriction. In this case, apart from the mechanism described, there is another mechanism of stimulation of superconductivity (Aslamazov and Larkin 1978), which will not be described here.

8.5.8 19.6. Paraconductivity

In section 17.1 we have given an estimate of the fluctuational region near T_c. According to formulae (17.21) and (17.22), it proved to be extremely small. As has already been said, this is caused by a large correlation length. The estimate made was based on a fluctuational correction to the heat capacity of a bulk metal. However, relative fluctuations are always larger for systems of smaller dimensions, i.e., filaments and films having a thickness smaller than δ and ξ. Actually, in such specimens it is not convenient to determine the heat capacity and it is much simpler to measure the conductivity. As will be shown below, the fluctuational correction to the conductivity of thin films is found to be so high that it can be measured. The physical cause for extra conductivity lies in the possibility of fluctuational creation of Cooper pairs, which produces an additional "channel" for current. This effect has become known as paraconductivity (Aslamazov and Larkin 1968).

In order to find the value of paraconductivity, a time-dependent generalization of the Ginzburg-Landau equations is required. This is associated with the fact that the electric field can be defined as $\boldsymbol{E} = -\boldsymbol{c}^{-1}\partial\boldsymbol{A}/\partial t$, where $\boldsymbol{A}$ is the vector potential; but in this case, $\boldsymbol{A}$ has to be regarded as being dependent on time. It may also be assumed that $\boldsymbol{E} = -\Delta\varphi$ and $\boldsymbol{A} = 0$, but, as will be shown below, the scalar potential φ is contained in the equation for Ψ in combination with $\partial\Psi/\partial t$. In other words, the electric field in superconductors leads necessarily to nonstationary phenomena. The London equation $\partial(\Lambda\boldsymbol{j})/\partial t = \boldsymbol{E}$ also corresponds to this.

The general nonstationary BCS equations are very complicated, even in the limit of slow time and space variations of the field and order parameter. It is for this reason that we shall not give their derivation here; instead, we write the model equation for the vicinity of T_c, which in general correctly reflects the qualitative aspects of the behavior of the order parameter and in some cases is exact.

If a departure from equilibrium is assumed, then $\delta\int\Omega_{\mathrm{s}}\mathrm{d}V/\delta\Psi^*$ is no longer equal to zero (in ch. 17 we derived the Ginzburg-Landau equation for Ψ on the condition that this variational derivative be zero). At the same time, in the absence
of equilibrium Ψ begins to depend on time. At small deviations from equilibrium it is natural to assume that $\partial\Psi/\partial t$ is proportional to $\delta\int\Omega_{\mathrm{s}}\mathrm{d}V/\delta\Psi^*$.

However, gauge invariance requires that $\partial\Psi/\partial t$ should be included in the equation in the following combination:

$$\frac{\partial\Psi}{\partial t} + 2\mathrm{i}\frac{e}{\hbar}\varphi\Psi,$$

where φ is the scalar potential of the electric field. The complete condition of gauge invariance requires, in fact, the invariance of the electric and magnetic fields:

$$E = -\frac{1}{c}\frac{\partial A}{\partial t} - \nabla\varphi, \quad H = \operatorname{rot} A$$

upon variation of the potentials $A \to A + \nabla\eta$, and $\varphi \to \varphi - c^{-1}\partial\eta/\partial t$, where η is a scalar. It is not difficult to see that in a case where $\boldsymbol{A}$ is included in the equation in the combination $[-\mathrm{i}\hbar\nabla - (2e/c)A]\Psi$ and φ in the combination $[\partial/\partial t + 2\mathrm{i}(e/\hbar)\varphi]\Psi$, the guage transformation is compensated by the variation of the phase of the function Ψ. Thus, we have

$$-\gamma\left(\frac{\partial\Psi}{\partial t} + 2\mathrm{i}\frac{e}{\hbar}\varphi\Psi\right) = \frac{\delta\int\Omega_{\mathrm{s}}\,\mathrm{d}V}{\sigma\Psi^*}. \tag{19.47}$$

The microscopic derivation shows that in the paraconductivity problem eq. (19.47) gives an exact answer if the correct choice of the constant γ is made.

The constant γ can be determined from the following considerations. On the right-hand side of eq. (19.47) there is a term $-(\hbar^2/4m)\,\Delta\Psi$. On the whole this equation resembles the diffusion equation (see section 3.5):

$$\frac{\partial n}{\partial t} = D\Delta n.$$

The role of the diffusion coefficient D is played by $\hbar^2/(4m\gamma)$. On the other hand, in the presence of impurities the Ginzburg-Landau equation may be written in the form (17.6″). It is easy to see that in this equation the coefficient $\pi D\hbar/8T_{\mathrm{c}}$ plays the same role as the coefficient $\hbar^2/4m\alpha$ in a pure superconductor. Writing

$$\frac{\hbar^2}{4m} = \frac{\pi D\hbar\alpha}{8T_c} = D\gamma$$

we have

$$\gamma = \frac{\pi\hbar\alpha}{8T_{\rm c}}. \tag{19.48}$$

This value coincides with the value obtained in the BCS microscopic theory.
We are interested in the fluctuational correction to Ψ that arises under the action of a constant electric field. It is assumed to be small and therefore to first order the
correction we look for will be proportional to $\boldsymbol{E}$. But since $\boldsymbol{E}$ does not depend on time, the same will also refer to the correction to Ψ. In view of this, the derivative $\partial\Psi/\partial t$ may be omitted from (19.47). Assuming Ψ to be small, we retain the terms linear in Ψ. Substituting the Ginzburg-Landau functional into (19.47) yields

$$2\gamma \mathrm{i}\frac{e}{\hbar}\varphi\Psi + \alpha\tau\Psi - \frac{\hbar^2}{4m}\Delta\Psi = 0 \tag{19.49}$$

We have chosen the gauge at which $\boldsymbol{A} = 0$ and $\boldsymbol{E} = -\nabla\varphi$. Since $\boldsymbol{E}$ is homogeneous, it follows that $\varphi = -Er$. Recall that $\tau = (T - T_{\rm c})\,T_{\rm c}$.

In the absence of an electric field Ψ undergoes equilibrium fluctuations. The probability of fluctuations is proportional to (see Appendix II)

$$\begin{aligned} W &\propto \exp\left(-\frac{1}{T}\int \Omega_{\rm s}\ \mathrm{d}V\right) \\ &\propto \exp\left[-\frac{1}{T}\sum_p \left(\alpha\tau + p^2/4m\right)|\Psi_p|^2\right] \end{aligned} \tag{19.50}$$

where $\Psi_p = \int \Psi(r)\mathrm{e}^{-\mathrm{i}pr/\hbar}\mathrm{d}V$. Hence, the average equilibrium fluctuation $\left|\Psi_p^{(0)}\right|^2$ is given by

$$\begin{aligned} \left\langle\left|\Psi_p^{(0)}\right|^2\right\rangle &= \frac{\int |\Psi_p|^2 \exp\left[-\frac{1}{T}\left(\alpha\tau + \frac{p^2}{4m}\right)|\Psi_p|^2\right] \mathrm{d}\,|\Psi_p|^2}{\int \exp\left[-\frac{1}{T}\left(\alpha\tau + \frac{p^2}{4m}\right)|\Psi_p|^2\right] \mathrm{d}\,|\Psi_p|^2} \\ &= \frac{T}{\alpha\tau + p^2/4m} \end{aligned} \tag{19.51}$$

where $\langle\cdots\rangle$ signifies the statistical average.
In the presence of a weak electric field we have $\Psi_p = \Psi_p^{(0)} + \Psi_p^{(1)}$. Since the momentum representation of the quantity $\boldsymbol{r}\boldsymbol{\Psi}(\boldsymbol{r})$ is $\mathrm{i}\hbar(\partial/\partial\boldsymbol{p})\Psi_p$, we obtain in the first approximation in E :

$$2\gamma eE\frac{\partial\Psi_p^{(0)}}{\partial p} + \left(\alpha\tau + \frac{p^2}{4m}\right)\Psi_p^{(1)} = 0$$

from which it follows that

$$\Psi_p^{(1)} = -2\frac{\gamma e}{\alpha\tau + p^2/4m}E\frac{\partial\Psi(0)}{\partial p} \tag{19.52}$$

The average electric current in the Ginzburg-Landau theory is

$$\begin{aligned} j &= -\mathrm{i}\frac{e\hbar}{2m}\left\langle\Psi^*\nabla\Psi - \Psi\nabla\Psi^*\right\rangle \\ &= \sum_p \frac{ep}{m}\left\langle|\Psi_p\right|^2\right\rangle \end{aligned} \tag{19.53}$$

If we substitute $\left\langle \left|\Psi_p^{(0)}\right|^2 \right\rangle$ into this formula in accoradance with (19.51), we obtain zero. In the next approximation we have

$$\begin{aligned} j &= \sum_p \frac{ep}{m} \left\langle \Psi_p^{(0)} \Psi_p^{(1)*} + \Psi_p^{(1)} \Psi_p^{(0)*} \right\rangle \\ &= -2\frac{\gamma e^2}{m} \sum_p \frac{p}{\alpha\tau + p^2/4m} \left\langle E \frac{\partial \Psi_p^{(0)*}}{\partial p} \Psi_p^{(0)} + E \frac{\partial \Psi_p^{(0)}}{\partial p} \Psi_p^{(0)*} \right\rangle \\ &= -2\frac{\gamma e^2}{m} \sum_p \frac{p}{\alpha\tau + p^2/4m} \left(E \frac{\partial}{\partial p} \right) \left\langle \left|\Psi_p^{(0)}\right|^2 \right\rangle . \end{aligned}$$

Substituting eq. (19.51) into the last formula, we find

$$j = \frac{T\gamma e^2}{m^2} \sum_p p \frac{(pE)}{(\alpha\tau + p^2/4m)^3}. \tag{19.54}$$

The change from summation to integration is carried out according to the following rules*:

$$\sum_p \to \begin{cases} \int \frac{\mathrm{d}^3 p}{(2\pi\hbar)^3} & \text{three-dimensional case ,} \\ \frac{1}{d} \int \frac{\mathrm{d}^2 p}{(2\pi\hbar)^2} & \text{thin film, thickness } d < \frac{\hbar}{(4m\alpha\tau)^{1/2}} \sim \xi, \\ \frac{1}{S} \int \frac{\mathrm{d}p}{2\pi\hbar} & \text{thin wire, cross section } S < \xi^2. \end{cases}$$

*These rules are established as follows. We have the sum over the momenta, which converges at $p^2 \sim (\hbar/\xi)^2$. In a specimen with dimensions L_1, L_2 and L_3 the components of the momentum take on the values

$$p_x = 2\pi \frac{\hbar n_x}{L_1}, \quad p_y = 2\pi \frac{h n_y}{L_2}, \quad p_z = 2\pi \frac{\hbar n_z}{L_3},$$

where n_x, n_y and n_z are integers. If one of the dimensions (say $L_z = d$) is found to be smaller than ξ, then in the sum over the corresponding n a substantial contribution comes only from $n_z = 0$. Therefore, the sum over momenta, divided by the volume, assumes the form

$$\frac{1}{V} \sum_p \to \frac{1}{dL_1 L_2} \int \mathrm{d}^2 p \frac{L_1 L_2}{(2\pi\hbar)^2}$$

We have an analogous situation with a wire. This must be taken into account because we do not explicitly write out the normalization volume, assuming it to be unity in the ordinary three-dimensional case.

If we substitute $\left\langle \left|\Psi_p^{(0)}\right|^2 \right\rangle$ into this formula in accoradance with (19.51), we obtain zero. In the next approximation we have

$$\begin{aligned} j &= \sum_p \frac{ep}{m} \left\langle \Psi_p^{(0)} \Psi_p^{(1)*} + \Psi_p^{(1)} \Psi_p^{(0)*} \right\rangle \\ &= -2\frac{\gamma e^2}{m} \sum_p \frac{p}{\alpha\tau + p^2/4m} \left\langle E \frac{\partial \Psi_p^{(0)*}}{\partial p} \Psi_p^{(0)} + E \frac{\partial \Psi_p^{(0)}}{\partial p} \Psi_p^{(0)*} \right\rangle \\ &= -2\frac{\gamma e^2}{m} \sum_p \frac{p}{\alpha\tau + p^2/4m} \left(E \frac{\partial}{\partial p} \right) \left\langle \left|\Psi_p^{(0)}\right|^2 \right\rangle . \end{aligned}$$

Substituting eq. (19.51) into the last formula, we find

$$j = \frac{T\gamma e^2}{m^2} \sum_p p \frac{(pE)}{(\alpha\tau + p^2/4m)^3} \tag{19.54}$$

The change from summation to integration is carried out according to the following rules*:

$$\sum_p \to \begin{cases} \int \frac{d^3p}{(2\pi\hbar)^3} & \text{three-dimensional case,} \\ \frac{1}{d}\int \frac{d^2p}{(2\pi\hbar)^2} & \text{thin film, thickness } d < \frac{\hbar}{(4m\alpha\tau)^{1/2}} \sim \xi \\ \frac{1}{S}\int \frac{dp}{2\pi\hbar} & \text{thin wire, cross section } S < \xi^2 \end{cases}$$

*These rules are established as follows. We have the sum over the momenta, which converges at $p^2 \sim (\hbar/\xi)^2$. In a specimen with dimensions L_1, L_2 and L_3 the components of the momentum take on the values

$$p_x = 2\pi\frac{\hbar n_x}{L_1}, \quad p_y = 2\pi\frac{hn_y}{L_2}, \quad p_z = 2\pi\frac{\hbar n_z}{L_3}$$

where n_x, n_y and n_z are integers. If one of the dimensions (say $L_z = d$) is found to be smaller than ξ, then in the sum over the corresponding n a substantial contribution comes only from $n_2 = 0$. Therefore, the sum over momenta, divided by the volume, assumes the form

$$\frac{1}{V}\sum_p \to \frac{1}{dL_1L_2}\int \mathrm{d}^2p \frac{L_1L_2}{(2\pi\hbar)^2}$$

We have an analogous situation with a wire. This must be taken into account because we do not explicitly write out the normalization volume, assuming it to be unity in the ordinary three-dimensional case.

Taking the integrals in (19.54) for all three cases and substituting γ according to (19.48), we obtain the values of paraconductivity:

$$\sigma' = \begin{cases} \frac{1}{8\pi}\left(\frac{e}{\hbar}\right)^2\left(\frac{\alpha m}{\tau}\right)^{1/2} & \text{three-dimensional case ,} \\ \frac{1}{16}\frac{e^2}{\hbar\ \mathrm{d}\tau} & \text{film, thickness } d < \xi, \\ \frac{\pi}{32}\frac{e^2}{\alpha^{1/2}\tau^{3/2}Sm^{1/2}} & \text{wire, cross section } S < \xi^2. \end{cases} \tag{19.55}$$

We can substitute here the formulae for α in accordance with eq. (17.14) for a pure superconductor ($\xi_0 < l$) and eq. (17.18) for an alloy ($\xi_0 > l$). To order of magnitude we have: $\sigma' \sim (e^2/\xi_0\hbar)\,\tau^{-1/2}$ for the three-dimensional case, $\sigma' \sim (e^2/d\hbar)\,\tau^{-1}$ for the two-dimensional case, and $(e^2\xi_0/S\hbar)\,\tau^{-3/2}$ for the onedimensional case.

The two-dimensional case is the most interesting since formula (19.55) for this case contains no characteristics of the film, except its thickness and T_c. Moreover, as has already been pointed out, the fluctuations in a film are stronger than in a three-dimensional specimen; this is also seen from formulae (19.55). Finally, such a film is easy to prepare. Experimental data (Glover 1967) have completely confirmed the formula (19.55) for this case.

Formulae (19.55) turn to infinity as $T \to T_c$, which is evidence that they are not valid in the immediate vicinity of T_c. The range of validity is set up by the requirement that the fluctuational correction be much less than the normal conductivity $\sigma = n_e e^2\tau_{tr}/m$.

Another source of error is the neglect of the interaction of electrons with fluctuating Cooper pairs. This effect also enhances the conductivity, but it cannot be interpreted so simply as in the above-described paraconductivity of fluctuational Cooper pairs. The corresponding "anomalous Maki-Thompson conductivity" (Maki 1968, Thompson 1970) proves to be small in many cases*, in particular under experimental conditions (Glover 1967), which makes it possible to obtain a confirmation of formulae (19.55).

Taking the integrals in (19.54) for all three cases and substituting γ according to (19.48), we obtain the values of paraconductivity:

$$\sigma' = \begin{cases} \frac{1}{8\pi}\left(\frac{e}{\hbar}\right)^2\left(\frac{\alpha m}{\tau}\right)^{1/2} & \text{three-dimensional case,} \\ \frac{1}{16}\frac{e^2}{\hbar\ \mathrm{d}\tau} & \text{film, thickness } d < \xi, \\ \frac{\pi}{32}\frac{e^2}{\alpha^{1/2}\tau^{3/2}Sm^{1/2}} & \text{wire, cross section } S < \xi^2. \end{cases} \tag{19.55}$$

We can substitute here the formulae for α in accordance with eq. (17.14) for a pure superconductor ($\xi_0 < l$) and eq. (17.18) for an alloy ($\xi_0 > l$). To order of magnitude we have: $\sigma' \sim (e^2/\xi_0\hbar)\,\tau^{-1/2}$ for the three-dimensional case, $\sigma' \sim (e^2/d\hbar)\,\tau^{-1}$ for the two-dimensional case, and $(e^2\xi_0/S\hbar)\,\tau^{-3/2}$ for the onedimensional case.

The two-dimensional case is the most interesting since formula (19.55) for this case contains no characteristics of the film, except its thickness and T_c. Moreover, as has already been pointed out, the fluctuations in a film are stronger than in a three-dimensional specimen; this is also seen from formulae (19.55). Finally, such a film is easy to prepare. Experimental data (Glover 1967) have completely confirmed the formula (19.55) for this case.

Formulae (19.55) turn to infinity as $T \to T_c$, which is evidence that they are not valid in the immediate vicinity of T_c. The range of validity is set up by the requirement that the fluctuational correction be much less than the normal conductivity $\sigma = n_e e^2 \tau_{tr}/m$.

Another source of error is the neglect of the interaction of electrons with fluctuating Cooper pairs. This effect also enhances the conductivity, but it cannot be interpreted so simply as in the above-described paraconductivity of fluctuational Cooper pairs. The corresponding "anomalous Maki-Thompson conductivity" (Maki 1968, Thompson 1970) proves to be small in many cases*, in particular under experimental conditions (Glover 1967), which makes it possible to obtain a confirmation of formulae (19.55).

Taking the integrals in (19.54) for all three cases and substituting γ according to (19.48), we obtain the values of paraconductivity:

$$\sigma' = \begin{cases} \frac{1}{8\pi}\left(\frac{e}{\hbar}\right)^2\left(\frac{\alpha m}{\tau}\right)^{1/2} & \text{three-dimensional case ,} \\ \frac{1}{16}\frac{e^2}{\hbar\ \mathrm{d}\tau} & \text{film, thickness } d < \xi, \\ \frac{\pi}{32}\frac{e^2}{\alpha^{1/2}\tau^{3/2}Sm^{1/2}} & \text{wire, cross section } S < \xi^2. \end{cases} \tag{19.55}$$

We can substitute here the formulae for α in accordance with eq. (17.14) for a pure superconductor ($\xi_0 < l$) and eq. (17.18) for an alloy ($\xi_0 > l$). To order of magnitude we have: $\sigma' \sim (e^2/\xi_0\hbar)\,\tau^{-1/2}$ for the three-dimensional case, $\sigma' \sim (e^2/d\hbar)\,\tau^{-1}$ for the two-dimensional case, and $(e^2\xi_0/S\hbar)\,\tau^{-3/2}$ for the onedimensional case.

The two-dimensional case is the most interesting since formula (19.55) for this case contains no characteristics of the film, except its thickness and T_c. Moreover, as has already been pointed out, the fluctuations in a film are stronger than in a three-dimensional specimen; this is also seen from formulae (19.55). Finally, such a film is easy to prepare. Experimental data (Glover 1967) have completely confirmed the formula (19.55) for this case.

Formulae (19.55) turn to infinity as $T \to T_c$, which is evidence that they are not valid in the immediate vicinity of T_c. The range of validity is set up by the requirement that the fluctuational correction be much less than the normal conductivity $\sigma = n_e e^2 \tau_{tr}/m$.

- The Maki-Thompson conductivity disappears if, for example, the superconductor contains magnetic impurities.

*The Maki-Thompson conductivity disappears if, for example, the superconductor contains magnetic impurities.

Another source of error is the neglect of the interaction of electrons with fluctuating Cooper pairs. This effect also enhances the conductivity, but it cannot be interpreted so simply as in the above-described paraconductivity of fluctuational Cooper pairs. The corresponding "anomalous Maki-Thompson conductivity" (Maki 1968, Thompson 1970) proves to be small in many cases*, in particular under experimental conditions (Glover 1967), which makes it possible to obtain a confirmation of formulae (19.55).

8.6 20 The interface between a superconductor and a normal metal

8.6.1 20.1. The proximity effect

The superconducting correlation manifests itself not only in a superconductor but also at the interface between a superconductor and a normal metal. It is rather natural to guess that the normal metal has an effect on the superconductor, bringing about a decrease in Δ at a distance of order ξ. In particular, if the thickness of the superconductor is less than ξ, it ceases to be superconductive altogether. On the other hand, the superconductor must be expected to exert an effect on the normal metal. A thin film of a normal metal deposited onto a bulk superconductor must be superconducting. These phenomena have been detected experimentally (Meissner 1958, 1959) and have come to be known as proximity effects.

We shall consider the proximity effects using the Ginzburg-Landau equations. In order not to go beyond the framework of the Ginzburg-Landau theory, we deal with two models. In the first model we consider a superconductor at a temperature close to T_c, which has an interface with a normal metal that either does not become a superconductor at all or has a critical temperature far below T_c. The second model is the interface between two superconductors with close critical temperatures, T_{c1} and T_{c2}; it is assumed that $T_{c1} < T < T_{c2}$, i.e., one metal is in the superconducting state and the other in the normal state.

Let us consider the first model. We assume first that we have two bulk metals. In section 17.1 we obtained the boundary condition (17.7) on the surface of the superconductor, assuming the variation of $\delta\Psi$ at the interface to be arbitrary. This condition makes sense at the interface with a vacuum or a dielectric, since the influence of such an interface on electrons in the superconductor is extended over distances of the order of interatomic spacings. From the boundary condition (17.7), it follows, in particular, that the normal component of the supercurrent vanishes at the interface:

$$jn\big|_{\mathrm{b}} = 0. \tag{20.1}$$

Condition (20.1) must also be fulfilled at the interface with a normal metal, because no nondissipative current can flow in a normal metal. However, the mutual effect of the electrons of the two metals can be extended much farther than the
interatomic distances. In view of this we apply, instead of eq. (17.7), a different boundary condition:

$$n\left[\nabla - \frac{2\mathrm{i}e}{c\hbar}A\right]\Psi\Big|_{\mathrm{b}} = \frac{1}{t}\Psi\Big|_{\mathrm{b}}. \tag{20.2}$$

- The Maki-Thompson conductivity disappears if, for example, the superconductor contains magnetic impurities.

This condition is also consistent with (20.1). The coefficient t must be of the order of ξ, but its exact value can be determined only with the aid of the BCS theory. The result proves to be (Zaitsev 1965):

$$t = \begin{cases} 0.6\xi_{0\mathrm{n}} & \text{pure superconductor,} \\ 0.3\,(\xi_{0\mathrm{n}} l)^{1/2} & \text{superconductor with } \xi_0 > l, \end{cases} \tag{20.2'}$$

where $\xi_{0\mathrm{n}} = (\gamma/\pi^2)\,(\hbar v_n/T_\mathrm{c}) = 0.18\hbar v_\mathrm{n}/T_\mathrm{c}$ (formula 16.82) and v_n is the Fermi velocity in a normal metal.

Consider a planar interface. In this case, the boundary condition (20.2) assumes the following form:

$$\left.\frac{\mathrm{d}\Psi}{\mathrm{d}x}\right|_{x=0} = \frac{1}{t}\Psi(0). \tag{20.3}$$

Instead of the Ginzburg-Landau equation for Ψ we may take its integral (17.27), which in the absence of a magnetic field ($A = 0$) is given by

$$\xi^2\left(\frac{\mathrm{d}\Psi}{\mathrm{d}x}\right)^2 + \Psi^2 - \frac{\mathrm{t}}{2}\Psi^4 = \frac{1}{2} \tag{20.4}$$

[here we have expressed Ψ in units of $\Psi_0 = (\alpha|\tau|/b)^{1/2}$ and introduced the notation $\xi^2 = \hbar^2/(4m\alpha|\tau|)$]; the constant on the right-hand side is determined from the condition that in the bulk of the superconductor $\Psi = 1,\ \mathrm{d}\Psi/\mathrm{d}x = 0$.

Equation (20.4) has been solved in section 17.2 in calculations of the surface energy at the interface between a superconductor and a normal metal. The solution has the form

$$\Psi = \tanh\left(\frac{x - x_0}{\sqrt{2}\xi}\right). \tag{20.5}$$

The value of x_0 is determined from the boundary condition (20.3). This gives

$$\sinh\left(\frac{x_0\sqrt{2}}{\xi}\right) = -\frac{2t}{\xi}. \tag{20.6}$$

According to eq. (20.5), the characteristic scale of variation of Ψ is the length $\xi(T)$, which increases upon approach to T_c as $(T_\mathrm{c} - T)^{-1/2}$. At the same time, the quantity t does not depend on temperature. According to formulae (17.14) and (17.18) for α and formulae (20.2') for t, the ratio t/ξ is of order $\tau^{1/2}$ in all cases. In accordance with eq. (20.6), this means that upon approach to T_c, the relation x_0/ξ falls off. This implies that the value of the function Ψ at the interface decreases with increasing ξ. It should be noted that the Ginzburg-Landau theory can actually
be applied only to a case where all the quantities involved vary over distances much larger than ξ_0 or $(\xi_0 l)^{1/2}$, i.e., we necessarily have $\xi > t$ and $x_0 \approx 0$ (the Fermi velocities are all of the same order of magnitude in all good metals, which is why $\xi_{0n} \sim \xi_{0s}$). This means that, strictly speaking, within the range of validity of the GinzburgLandau theory the boundary condition is $\Psi(0) = 0$ rather than (20.3).

Let us now consider the problem of a superconducting film deposited onto the surface of a bulk metal. The ordinary boundary condition $\mathrm{d}\Psi/\mathrm{d}x = 0$ is fulfilled at the interface with vacuum. It is not difficult to see that the thin-film problem is equivalent to the problem of a sandwich, i.e., a superconducting layer between two bulk layers of the same normal metal. Evidently, the function Ψ must be symmetrical, i.e., $\mathrm{d}\Psi/\mathrm{d}x = 0$ in the middle of the film. A deposited film of thickness d is thus equivalent to a sandwiched film of thickness $2d$.

We introduce a new variable, $u = x/(\xi\sqrt{2})$ and write the integral of the GinzburgLandau equation for Ψ. In a specimen of finite thickness we can no longer assume that the constant on the right-hand side of (20.4) is $\frac{1}{2}$. We designate it by $\frac{1}{2}(1-s^2)$. So, we obtain

$$\left(\frac{\mathrm{d}\Psi}{\mathrm{d}u}\right)^2 = \left(1-\Psi^2\right)^2 - s^2 \tag{20.7}$$

Let the interface with the metal lie at $x = 0$ and that with the vacuum at $x = d$. From the foregoing it is clear that near the interface with the metal Ψ is small and in moving away from it Ψ increases. On this basis we find from eq. (20.7) that

$$\frac{\mathrm{d}\Psi}{\mathrm{d}u} = \left[\left(1-\Psi^2\right)^2 - s^2\right]^{1/2} \tag{20.8}$$

$$\int_0^{\Psi} \frac{1}{(1-s-\Psi_1^2)^{1/2}} \frac{1}{(1+s-\Psi_1^2)^{1/2}}\, \mathrm{d}\Psi_1 = u \tag{20.9}$$

Here it is taken into account that $\Psi \approx 0$ at $u = 0$. At $u = d/(\xi\sqrt{2}), \mathrm{d}\Psi/\mathrm{d}u = 0$, i.e., according to eq. (20.8),

$$\Psi \frac{d}{\xi\sqrt{2}} = (1-s)^{1/2} \tag{20.10}$$

Substitution into eq. (20.9) gives

$$\int_0^{(1-s)^{1/2}} \frac{1}{(1-s-\Psi_1^2)^{1/2}} \frac{1}{(1+s-\Psi_1^2)^{1/2}}\, \mathrm{d}\Psi_1 = \frac{d}{\xi\sqrt{2}} \tag{20.11}$$

We make the replacement of the integration variable $\Psi_1 = (1-s)^{1/2}\sin\varphi$. The last formula then becomes

$$(1+s)^{-1/2} \int_0^{\frac{1}{2}\pi} \mathrm{d}\varphi \frac{1}{(1-k^2\sin\varphi)^{1/2}} = \frac{1}{(1+s)^{1/2}} K(k) = \frac{d}{\xi\sqrt{2}} \tag{20.12}$$

where $k^2 = (1-s)/(1+s)$ and $K(k)$ is the complete elliptic integral of the first kind. Let d be fixed. Upon approach to T_c the value of ξ increases, i.e., the right-hand side in eq. (20.12) decreases. The lowest value of the elliptic integral is obtained at $k = 0$, i.e., at $s = 1$, and is equal to $\frac{1}{2}\pi$. Hence, ξ cannot increase indefinitely and the permissible maximum value is

$$\xi_{\max} = \frac{2}{\pi} d \tag{20.13}$$

But this means that superconductivity cannot be preserved up to T_c. In other words, the critical temperature must decrease. In accord with the definition of $\boldsymbol{\xi}$ we obtain (Werthamer 1963):

$$\frac{T_\mathrm{c} - T_\mathrm{c}(d)}{T_\mathrm{c}} = \frac{1}{16}\pi^2 \frac{\hbar^2}{m\alpha} \frac{1}{\mathrm{d}^2}. \tag{20.14}$$

On the other hand, with $k \to 1$, i.e., $s \to 0$, the elliptic integral increases indefinitely, which corresponds to large values of d. Putting $s = 0$ in formula (20.9), we arrive at the dependence (20.5) with $x_0 = 0$.

Let us examine the behavior of Ψ near T_c. To do this, we assume that $1 - s = r < 1$. Then, $k^2 \approx \frac{1}{2}r < 1$ and $K(k) \approx \frac{1}{2}\pi\left(1 + \frac{1}{4}k^2\right) \approx \frac{1}{2}\pi\left(1 + \frac{1}{8}r\right)$. Hence, according to eq. (20.12),

$$r \approx \frac{16}{\pi}\left(\frac{d}{\xi} - \frac{d}{\xi_{\max}}\right)$$

From (20.9) we obtain in this case

$$\Psi \approx \sqrt{r}\sin(u\sqrt{2}) = \frac{4}{\sqrt{\pi}}\left(\frac{\mathrm{d}}{\xi} - \frac{\mathrm{d}}{\xi_{\max}}\right)^{1/2}\sin\left(\frac{x}{\xi_{\max}}\right). \tag{20.15}$$

This formula can naturally be applied only for $r < 1$. It enables one to assert that the transition to the normal state is still a second-order phase transition. If we express formula (20.15) in the form of a temperature dependence and assume that $T_{\mathrm{c}}(d) - T < T_{\mathrm{c}} - T_{\mathrm{c}}(d)$, the result will be

$$\Psi \approx 2\left(\frac{T_{\mathrm{c}}(d) - T}{T_{\mathrm{c}} - T_{\mathrm{c}}(\ \mathrm{d})}\right)^{1/2}\sin\left(\frac{\pi x}{2d}\right). \tag{20.16}$$

Although the derivation made is valid only for the neighborhood of T_{c}, we can draw a qualitative conclusion concerning what will occur at lower temperatures. Evidently, as $T \to 0, \xi \to \xi_0$ (or $(\xi_0 l)^{1/2}$ for a dirty superconductor). From eq. (20.13) (which may be written in the form $d_{\min} = \frac{1}{2}\pi\xi$) it follows that at thicknesses smaller than ξ_0 the superconductivity of the deposited film will be absent at any temperatures.

In order to trace out the behavior of a thin film of a normal metal on the surface of a bulk superconductor, one has to use the second of the models described at the beginning of this section. Suppose that two superconductors with slightly different
where $k^2 = (1-s)/(1+s)$ and $K(k)$ is the complete elliptic integral of the first kind. Let d be fixed. Upon approach to T_{c} the value of ξ increases, i.e., the right-hand side in eq. (20.12) decreases. The lowest value of the elliptic integral is obtained at $k = 0$, i.e., at $s = 1$, and is equal to $\frac{1}{2}\pi$. Hence, ξ cannot increase indefinitely and the permissible maximum value is

$$\xi_{\max} = \frac{2}{\pi}d \tag{20.13}$$

But this means that superconductivity cannot be preserved up to T_{c}. In other words, the critical temperature must decrease. In accord with the definition of $\boldsymbol{\xi}$ we obtain (Werthamer 1963):

$$\frac{T_{\mathrm{c}} - T_{\mathrm{c}}(d)}{T_{\mathrm{c}}} = \frac{1}{16}\pi^2\frac{\hbar^2}{m\alpha}\frac{1}{\mathrm{d}^2}. \tag{20.14}$$

On the other hand, with $k \to 1$, i.e., $s \to 0$, the elliptic integral increases indefinitely, which corresponds to large values of d. Putting $s = 0$ in formula (20.9), we arrive at the dependence (20.5) with $x_0 = 0$.

Let us examine the behavior of Ψ near T_c. To do this, we assume that $1 - s = r < 1$. Then, $k^2 \approx \frac{1}{2}r < 1$ and $K(k) \approx \frac{1}{2}\pi\left(1 + \frac{1}{4}k^2\right) \approx \frac{1}{2}\pi\left(1 + \frac{1}{8}r\right)$. Hence, according to eq. (20.12),

$$r \approx \frac{16}{\pi}\left(\frac{d}{\xi} - \frac{d}{\xi_{\max}}\right)$$

From (20.9) we obtain in this case

$$\Psi \approx \sqrt{r}\sin(u\sqrt{2}) = \frac{4}{\sqrt{\pi}}\left(\frac{\mathrm{d}}{\xi} - \frac{\mathrm{d}}{\xi_{\max}}\right)^{1/2}\sin\left(\frac{x}{\xi_{\max}}\right). \tag{20.15}$$

This formula can naturally be applied only for $r < 1$. It enables one to assert that the transition to the normal state is still a second-order phase transition. If we express formula

(20.15) in the form of a temperature dependence and assume that $T_c(d) - T < T_c - T_c(d)$, the result will be

$$\Psi \approx 2\left(\frac{T_{\mathrm{c}}(d) - T}{T_{\mathrm{c}} - T_{\mathrm{c}}(\ \mathrm{d})}\right)^{1/2} \sin\left(\frac{\pi x}{2d}\right) \tag{20.16}$$

Although the derivation made is valid only for the neighborhood of T_c, we can draw a qualitative conclusion concerning what will occur at lower temperatures. Evidently, as $T \to 0, \xi \to \xi_0$ (or $(\xi_0 l)^{1/2}$ for a dirty superconductor). From eq. (20.13) (which may be written in the form $d_{\min} = \frac{1}{2}\pi\xi$) it follows that at thicknesses smaller than ξ_0 the superconductivity of the deposited film will be absent at any temperatures.

In order to trace out the behavior of a thin film of a normal metal on the surface of a bulk superconductor, one has to use the second of the models described at the beginning of this section. Suppose that two superconductors with slightly different
critical temperatures ($T_{c2} - T_{c1} < T_{c1}$) are in contact with each other and let us assume that $T_{c1} < T < T_{c2}$. In such a case, metal (1) will be normal and metal (2) will be a superconductor. According to Zaitsev (1965), in the case of slightly different parameters of the metals, the boundary conditions reduce to the continuity of Ψ and $\mathrm{d}\Psi/\mathrm{d}x$:

$$\Psi_1(0) = \Psi_2(0), \quad \left.\frac{\mathrm{d}\Psi_1}{\mathrm{d}x}\right|_{x=0} = \left.\frac{\mathrm{d}\Psi_2}{\mathrm{d}x}\right|_{x=0}, \tag{20.17}$$

where the interface is assumed at $x = 0$.
First, just as in the first model, we assume that the two metals are bulk metals. Let the normal metal occupy the half-plane $x > 0$ and the superconductor the half-plane $x < 0$. Then, at $x < 0$ eq. (20.4) is satisfied. The solution of this equation is

$$\Psi_2 = \tanh\left[\frac{x_0 - x}{\sqrt{2}\xi_2}\right], \quad x < 0. \tag{20.18}$$

At $x > 0$ in the Ginzburg-Landau equation $\tau > 0$. Therefore, in passing to dimensionless variables the term with Ψ^2 in (20.4) will have a different sign. Moreover, the constant on the right-hand side will be equal to zero and not to $\frac{1}{2}$, since $\Psi \to 0$ and $\mathrm{d}\Psi/\mathrm{d}x \to 0$ as $x \to \infty$. Thus, we obtain

$$\xi_1^2\left(\frac{\mathrm{d}\Psi_1}{\mathrm{d}x}\right)^2 = \Psi_1^2 + \frac{1}{2}\Psi_1^4, \quad x > 0 \tag{20.19}$$

Suppose that $x_0 < \xi_2$ in formula (20.18). Then, $\Psi_2(0) < 1$ at $x = 0$ and, hence, according to (20.17) $\Psi_1(0)$ is also much less than unity, but since according to (20.19) Ψ_1 decreases monotonically as $x \to \infty$, it follows that everywhere $\Psi_1(x) < 1$. Solving eq. (20.19) under this assumption, we obtain

$$\Psi_1 = C\exp\left(-\frac{x}{\xi_1}\right).$$

From the boundary conditions (20.17) we find $C = x_0\left(\sqrt{2}\xi_2\right), x_0 \approx \xi_1$ and, hence,

$$\begin{aligned} \Psi_1 &= \tfrac{\xi_1}{\sqrt{2}}\xi_2 \exp\left(-\tfrac{x}{\xi_1}\right), \quad x > 0, \\ \Psi_2 &= \tanh\left(\tfrac{\xi_1 + |x|}{\sqrt{2}\xi_2}\right), \qquad x < 0. \end{aligned} \tag{20.20}$$

From formulae (20.19) it follows that Ψ falls off rapidly in the bulk of the normal metal but also that it decreases significantly in the superconductor near the interface.

Let us now assume that the normal plate has a finite thickness d, i.e., $\mathrm{d}\Psi/\mathrm{d}x = 0$ at $x = d$. In this case eq. (20.19) will contain an unknown constant and we write it in the form

$$2\xi_1^2 \left(\frac{\mathrm{d}\Psi_1}{\mathrm{d}x}\right)^2 = \left(1 + \Psi_1^2\right)^2 - s^2$$

critical temperatures ($T_{c2} - T_{c1} < T_{c1}$) are in contact with each other and let us assume that $T_{c1} < T < T_{c2}$. In such a case, metal (1) will be normal and metal (2) will be a superconductor. According to Zaitsev (1965), in the case of slightly different parameters of the metals, the boundary conditions reduce to the continuity of Ψ and $\mathrm{d}\Psi/\mathrm{d}x$:

$$\Psi_1(0) = \Psi_2(0), \quad \left.\frac{\mathrm{d}\Psi_1}{\mathrm{d}x}\right|_{x=0} = \left.\frac{\mathrm{d}\Psi_2}{\mathrm{d}x}\right|_{x=0}, \tag{20.17}$$

where the interface is assumed at $x = 0$.
First, just as in the first model, we assume that the two metals are bulk metals. Let the normal metal occupy the half-plane $x > 0$ and the superconductor the half-plane $x < 0$. Then, at $x < 0$ eq. (20.4) is satisfied. The solution of this equation is

$$\Psi_2 = \tanh\left[\frac{x_0 - x}{\sqrt{2}\xi_2}\right], \quad x < 0. \tag{20.18}$$

At $x > 0$ in the Ginzburg-Landau equation $\tau > 0$. Therefore, in passing to dimensionless variables the term with Ψ^2 in (20.4) will have a different sign. Moreover, the constant on the right-hand side will be equal to zero and not to $\frac{1}{2}$, since $\Psi \to 0$ and $\mathrm{d}\Psi/\mathrm{d}x \to 0$ as $x \to \infty$. Thus, we obtain

$$\xi_1^2 \left(\frac{\mathrm{d}\Psi_1}{\mathrm{d}x}\right)^2 = \Psi_1^2 + \frac{1}{2}\Psi_1^4, \quad x > 0 \tag{20.19}$$

Suppose that $x_0 < \xi_2$ in formula (20.18). Then, $\Psi_2(0) < 1$ at $x = 0$ and, hence, according to (20.17) $\Psi_1(0)$ is also much less than unity, but since according to (20.19) Ψ_1 decreases monotonically as $x \to \infty$, it follows that everywhere $\Psi_1(x) < 1$. Solving eq. (20.19) under this assumption, we obtain

$$\Psi_1 = C \exp\left(-\frac{x}{\xi_1}\right).$$

From the boundary conditions (20.17) we find $C = x_0\left(\sqrt{2}\xi_2\right), x_0 \approx \xi_1$ and, hence,

$$\begin{aligned} \Psi_1 &= \tfrac{\xi_1}{\sqrt{2}}\xi_2 \exp\left(-\tfrac{x}{\xi_1}\right), \quad x > 0, \\ \Psi_2 &= \tanh\left(\tfrac{\xi_1 + |x|}{\sqrt{2}\xi_2}\right), \qquad x < 0. \end{aligned} \tag{20.20}$$

From formulae (20.19) it follows that Ψ falls off rapidly in the bulk of the normal metal but also that it decreases significantly in the superconductor near the interface.

Let us now assume that the normal plate has a finite thickness d, i.e., $\mathrm{d}\Psi/\mathrm{d}x = 0$ at $x = d$. In this case eq. (20.19) will contain an unknown constant and we write it in the form

$$2\xi_1^2 \left(\frac{\mathrm{d}\Psi_1}{\mathrm{d}x}\right)^2 = \left(1 + \Psi_1^2\right)^2 - s^2$$

which leads to

$$\frac{\mathrm{d}\Psi_1}{\mathrm{d}x} = -\frac{1}{\sqrt{2}\xi_1}\left[\Psi_1^2 - (s-1)\right]^{1/2}\left[\Psi_1^2 + s + 1\right]^{1/2} \tag{20.21}$$

and

$$\int_{(s-1)^{1/2}}^{\Psi_1} \mathrm{d}\Psi_3 \frac{1}{\left[\Psi_3^2-(s-1)\right]^{1/2}} \frac{1}{\left(\Psi_3^2+s+1\right)^{1/2}} = \frac{d-x}{\sqrt{2}\xi_1} \tag{20.22}$$

(here we have already taken into account that $\mathrm{d}\Psi_1/\mathrm{d}x = 0$ at $x = d$, i.e., $\Psi_1 = (s-1)^{1/2}$).

Suppose, as before, that the condition (20.20) is satisfied. It is clear that as long as the thickness of the normal film is not too small we still have $x_0 < \xi_2$ in (20.18), i.e.,

$$\Psi_2(0) \approx \frac{x_0}{\sqrt{2}\xi_2}, \quad \left.\frac{\mathrm{d}\Psi_2}{\mathrm{d}x}\right|_{x=0} \approx -\frac{1}{\sqrt{2}\xi_2}.$$

From the boundary conditions (20.17) we determine s and x_0. Since $\Psi_1(0) = \Psi_2(0) < 1$, it follows that, as before, $\Psi_1(x) < 1$. Hence, in the second factor of the integrand in eq. (20.22) we may put $\Psi_3 \approx 0$. The integral is then taken and we obtain

$$\operatorname{arccosh}\left(\frac{\Psi_1}{(s-1)^{1/2}}\right) = \frac{d-x}{\xi_1}. \tag{20.23}$$

It is obvious that s is close to unity. This has been taken into account in eq. (20.23). Substituting $\Psi_1(0)$ and $x = 0$, we have

$$\operatorname{arccosh}\left(\frac{x_0}{\sqrt{2}\xi_2(s-1)^{1/2}}\right) = \frac{d}{\xi_1}. \tag{20.24}$$

Taking into account that Ψ_1^2 is small and that s is close to unity, we obtain from the equality of the derivatives at $x = 0$ and formula (20.21)

$$\left[\left(\frac{x_0}{\sqrt{2}\xi_2}\right)^2-(s-1)\right]^{1/2} = \frac{\xi_1}{\sqrt{2}\xi_2}. \tag{20.25}$$

First, let $d \gg \xi_1$. Then, according to eq. (20.24), $x_0/\xi_2 \gg (s-1)^{1/2}$. From eq. (20.25) we obtain $x_0 = \xi_1$. Substituting into eq. (20.24), we find $(s-1)^{1/2} = \left(\sqrt{2}\xi_1/\xi_2\right)\exp\left(-d/\xi_1\right)$. Substitution into eq. (20.23) yields

$$\Psi_1 = \frac{\xi_1}{\sqrt{2}\xi_2}\left[\exp\left(-\frac{x}{\xi_1}\right)+\exp\left(\frac{x-2d}{\xi_1}\right)\right]. \tag{20.26}$$

But if $d < \xi_1$, then the argument of arccosh in (20.24) must be close to unity. Expanding in d/ξ_1, we obtain

$$(s-1)^{1/2} = \left(\frac{x_0}{\sqrt{2}\xi_2}\right)\left(1-\frac{d^2}{2\xi_1^2}\right).$$

We insert this expression into eq. (20.25) and find

$$x_0 = \frac{\xi_1^2}{d}$$

Finally, from eq. (20.23) we obtain Ψ_1 :

$$\Psi_1 = \frac{\xi_1^2}{\sqrt{2}\xi_2 d}\left(1-\frac{dx}{\xi_1^2}-\frac{x^2}{2\xi_1^2}\right) \tag{20.27}$$

In order that the condition $x_0 < \xi_2$ be satisfied, it is necessary that

$$\xi_1 > d > \frac{\xi_1^2}{\xi_2}. \tag{20.28}$$

Thus, it turns out that even with the thickness of the normal film being smaller than ξ_1 the function Ψ_1 in it will still be small. Only at still smaller thicknesses does Ψ_1 begin to approach unity. Under the assumption $x_0 > \xi_2$, which corresponds to $d < \xi_1^2/\xi_2$, we obtain, just as in the preceding case,

$$\Psi_1 = 1 - \sqrt{2}\frac{d\xi_2}{\xi_1^2} - \frac{2dx}{\xi_1^2} + \frac{x^2}{\xi_1^2} \tag{20.29}$$

Within the framework of the Ginzburg-Landau theory we cannot consider the behavior of a normal film with the critical temperature being much lower than in a superconductor or in a nonsuperconducting film. However, from the foregoing it is sufficiently clear that due to the proximity effect it will be superconductive if its thickness is sufficiently small, and that with a large thickness it will remain normal.

8.6.2 20.2. Superconductivity of twinning planes

As was already mentioned in section 16.11, in several metals an increase of T_c at twinning planes of crystals has been reported (Khaikin and Khlyustikov 1981; see also Khlyustikov and Buzdin 1987). When a "bicrystal" was prepared, i.e., two single crystals of different orientation were grown approaching each other, a contact plane appeared. In the general case of arbitrary relative orientation such a boundary behaves by no means extraordinarily. However, if the relative orientation is especially chosen so that the boundary is a crystallographic plane (a plane filled by crystalline atoms) for both crystals then they are called "twins". The appearance of such a plane means a new symmetry element which was absent in the crystallographic group (see e.g. fig. 128).

It appeared that, in the vicinity of the twinning boundary thus created in tin, niobium, rhenium and thallium, superconductivity prevails up to a temperature slightly higher than T_{c0} - the critical temperature of the sample without such a boundary. For tin this increase was 0.04 K ($T_{c0} = 3.7$ K), for niobium it was 0.11 K

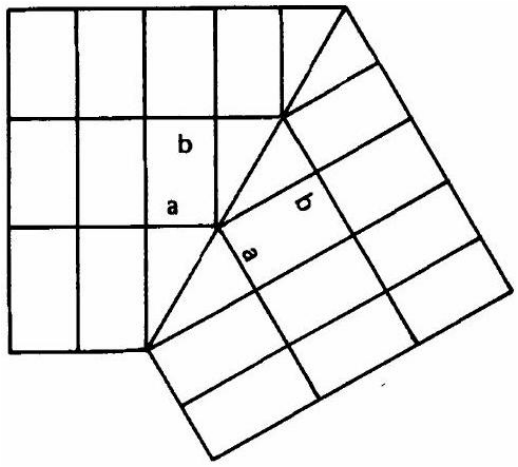


Fig. 128.

($T_{c0} = 9.3$ K). Of course this increase is not large. However, it should be kept in mind that the superconducting region is surrounded by the normal metal, which suppresses

its superconductivity due to the proximity effect. To reduce this effect, samples were prepared consisting of small particles with sizes less than ξ or pellets of powders consisting of small particles, which were pressed so that one could expect twin boundaries with a small spacing. In such a way it was possible to detect signs of superconductivity (diamagnetism) in tin up to 12 K , i.e. to a temperature exceeding $T_{\rm co}$ by more than a factor of 3 .

The properties of twinning planes became of special interest recently because they appear spontaneously in the high-temperature superconductor $YBa_2Cu_3O_{7-\delta}$. The reason is that such samples must be prepared at high temperature, over 900°C. This is necessary either for sintering of the ceramic or for growing single crystals. When the temperature is lowered a phase transition takes place (at $\sim$ 750°C) from a tetragonal to an orthorhombic phase: $a = 3.823\mathring{\rm A}, b = 3.884\mathring{\rm A}, c = 11.674\mathring{\rm A}$. An abrupt reduction of the volume takes place and the crystal is split into flat domains with different orientation of the a and b axes. The domains are separated by twin boundaries parallel to the c-axis and dividing the basal rectangular face along the diagonal (see fig. 128)*. The spacing between these boundaries depends on the preparation method and varies between 500 and 1500Å. Since the correlation length in this substance is small (in the basal plane $\xi_0 \approx 16\mathring{\rm A}$), one can practically assume these planes to be isolated. As will be shown below the spontaneous appearance of twinning planes leads to several interesting phenomena near $T_{\rm c0}$.

The increase of $T_{\rm c}$ in the vicinity of the twin boundary can be explained in various ways. First of all special types of lattice vibrations may exist which are connected particularly with the twinning planes, similar to the Rayleigh waves at the surface. The exchange by these phonons can enhance the electron attraction. Secondly a weakening of Coulomb repulsion close to the boundary is possible. Finally special electronic states are possible in which the electrons move freely along the boundary

but cannot leave it due to the rapid damping of the wave function. Such states are called Tamm states. Superconductivity can be associated with such electrons. If the boundary is not a twinning plane then it contains a large concentration of dislocations or other defects which can destroy the singular electronic or phonon states. This can explain why T_c does not increase at an arbitrary boundary.

In what follows we shall assume that the reason of the increase of $T_{\rm c}$ is the local increase of interaction between electrons due either to new types of phonons or to the reduction of Coulomb repulsion. Let us assume that the dimensionless constant of Cooper pairing entering eq. (16.23) for $\Delta, \lambda = \frac{1}{2}g\nu$, has a sharp peak near the twinning plane: $\lambda = \lambda_0 + \delta\lambda(x)$, where x is directed along the normal to the boundary plane. Let us denote the relative increase of the critical temperature by τ_0 :

$$\tau_0 = \frac{T_{\rm c} - T_{\rm c0}}{T_{\rm c0}}. \tag{20.30}$$

This quantity can be estimated from the following argument. In the vicinity of the boundary local superconductivity appears in a layer of the order of $\xi_{\rm c} \approx \xi_0 \tau_0^{-1/2}$, where ξ_0 is defined by formula (16.82). If the peak of λ has a width d ($d < \xi_0 < \xi_c$; actually, d should be of the order of interatomic distances) then due to the proximity effect the effective increase of λ will be of the order of $\delta\lambda d/\xi_{\rm c}$. But since T_c is proportional to $\exp(-1/\lambda)$ we get the estimate

$$\frac{\delta T_{\rm c}}{T_{\rm c}} = \tau_0 \approx \frac{\delta\lambda}{\lambda_0^2}\frac{d}{\xi_{\rm c}}.$$

- Recently it has become clear that domain boundaries in YBaCuO can be of several kinds, and that some of these suppress superconductivity. Here we consider only true twinning planes.

Substituting ξ_c we get

$$\tau_0 \sim \left(\frac{\delta\lambda}{\lambda_0^2}\frac{d}{\xi_0}\right)^2. \tag{20.31}$$

Now we consider this question in greater detail. The order parameter for a uniform superconductor was obtained from eq. (16.21). Particularly, at $\Delta \to 0$ the expression for T_c was derived. In the inhomogeneous case, assuming g to depend on x, one can obtain a generalisation of (16.21) for the nonuniform case (limit $\Delta \to 0$):

$$\begin{aligned}\Delta(x) &= \int \lambda(x) K\left(r-r'\right)\Delta\left(x'\right)\mathrm{d}V' \\ &= \lambda_0 \int K\left(r-r'\right)\Delta\left(x'\right)\mathrm{d}V' + \int \delta\lambda(x) K\left(r-r'\right)\Delta\left(x'\right)\mathrm{d}V'\end{aligned} \tag{20.32}$$

Here we suppose that $\lambda = \lambda_0 + \delta\lambda(x)$ where $\delta\lambda(x)$ is finite in an interval of the order of d. Since the kernel $K\left(r-r'\right)$ varies on a scale of order of ξ_0 (see section 16.9) and $\Delta(x)$ varies on a scale ξ_c, both of these distances being much larger than d, it is possible to substitute in the second term of (20.32) x' entering $K\left(r-r'\right)\Delta\left(x'\right)$ by
zero. Denoting

$$\Lambda = \int \delta\lambda(x)\mathrm{d}x \sim \delta\lambda d$$

one arrives at

$$\Delta(x) = \lambda_0 \int K\left(x-x',\rho\right)\Delta\left(x'\right)\mathrm{d}x'\mathrm{d}\rho + \Lambda\Delta(0)\int K(x,\rho)\mathrm{d}\rho \tag{20.33}$$

We have now separated the dependences on x and on $\rho = y, z$.
To solve eq. (20.33) we pass to the Fourier transform,

$$\Delta(p) = \lambda_0 K\left(p, q_\perp = 0\right)\Delta(p) + \Lambda\Delta(x=0)K\left(p, q_\perp = 0\right).$$

The solution is

$$\Delta(p) = \frac{\Lambda\Delta(x=0)K(p,0)}{1-\lambda_0 K(p,0)}. \tag{20.34}$$

Here p is the momentum along x and $q_\perp$ is the momentum in the transverse direction. Taking into account that

$$\Delta(x=0) = \int \Delta(p)\frac{\mathrm{d}p}{2\pi}$$

we get the self-consistency relation, defining the critical temperature,

$$1 = \Lambda \int \frac{K(p)}{1-\lambda_0 K(p)}\frac{\mathrm{d}p}{2\pi}. \tag{20.35}$$

It is easy to see that the critical temperature for a bulk superconductor is obtained from the condition

$$1 - \lambda_0 K\left(T_{co}, p=0\right) = 0. \tag{20.36}$$

We transform the denominator of formula (20.35) accordingly:

$$1-\lambda_0 K\left(T_{\mathrm{c}}, p\right)=\lambda_0\left[K\left(T_{\mathrm{c} 0}, 0\right)-K\left(T_{\mathrm{c}}, 0\right)\right]+\lambda_0\left[K\left(T_{\mathrm{c}}, 0\right)-K\left(T_{\mathrm{c}}, p\right)\right]$$
$$=\lambda_0\left[\ln\left(\frac{T_{\mathrm{c}}}{T_{\mathrm{c} 0}}\right)+\frac{7\zeta(3)}{48\pi^2}\left(\frac{vp}{T_{\mathrm{c}}}\right)^2\right]. \tag{20.37}$$

In the last formula the first term corresponds to the first bracket and it is obtained just as in the derivation of formula (16.25) for T_{c}. In order to find the second term, it is necessary to know K for a finite p, which corresponds to a moving Bosecondensate of Conper pairs. The corresponding derivation is done in section 21.2 and the expression for $K(p)$ corresponds to the rignt-nand side of formula (21.24), divided by $\lambda_0=\frac{1}{2}g\nu$, with $I=0$ and $|q|=p$. Expanding in powers of p, we get the
zero. Denoting

$$\Lambda=\int\delta\lambda(x)\mathrm{d}x\sim\delta\lambda d$$

one arrives at

$$\Delta(x)=\lambda_0\int K\left(x-x',\rho\right)\Delta\left(x'\right)\mathrm{d}x'\mathrm{d}\rho+\Lambda\Delta(0)\int K(x,\rho)\mathrm{d}\rho \tag{20.33}$$

We have now separated the dependences on x and on $\rho=y,z$.
To solve eq. (20.33) we pass to the Fourier transform,

$$\Delta(p)=\lambda_0 K\left(p,q_\perp=0\right)\Delta(p)+\Lambda\Delta(x=0)K\left(p,q_\perp=0\right).$$

The solution is

$$\Delta(p)=\frac{\Lambda\Delta(x=0)K(p,0)}{1-\lambda_0 K(p,0)} \tag{20.34}$$

Here p is the momentum along x and $q_\perp$ is the momentum in the transverse direction. Taking into account that

$$\Delta(x=0)=\int\Delta(p)\frac{\mathrm{d}p}{2\pi}$$

we get the self-consistency relation, defining the critical temperature,

$$1=\Lambda\int\frac{K(p)}{1-\lambda_0 K(p)}\frac{\mathrm{d}p}{2\pi} \tag{20.35}$$

It is easy to see that the critical temperature for a bulk superconductor is obtained from the condition

$$1-\lambda_0 K\left(T_{c0},p=0\right)=0 \tag{20.36}$$

We transform the denominator of formula (20.35) accordingly:

$$1-\lambda_0 K\left(T_c,p\right)=\lambda_0\left[K\left(T_{c0},0\right)-K\left(T_c,0\right)\right]+\lambda_0\left[K\left(T_c,0\right)-K\left(T_c,p\right)\right]$$
$$=\lambda_0\left[\ln\left(\frac{T_c}{T_{c0}}\right)+\frac{7\zeta(3)}{48\pi^2}\left(\frac{vp}{T_c}\right)^2\right]. \tag{20.37}$$

In the last formula the first term corresponds to the first bracket and it is obtained just as in the derivation of formula (16.25) for T_c. In order to find the second term, it is necessary to know K for a finite p, which corresponds to a moving Bosecondensate of Conper pairs. The corresponding derivation is done in section 21.2 and the expression for $K(p)$ corresponds to the rignt-nand side of formula (21.24), divided by $\lambda_0 = \frac{1}{2}g\nu$, with $I = 0$ and $|q| = p$. Expanding in powers of p, we get the
expression in (20.37). Since in the integral (20.35) only small p 's are essential, we can put in the numerator $K(p) \approx K(0) \approx \lambda_0^{-1}$, after which the integral takes the form

$$1 = \frac{\Lambda}{\lambda_0^2} \int \frac{\mathrm{d}p}{2\pi} \left[\tau_0 + \frac{7\zeta(3)}{48\pi^2} \frac{v^2 p^2}{T_c^2} \right]^{-1} \tag{20.38}$$

(here, as before, $\tau_0 = (T_c - T_{c0})/T_{c0}$). Calculating the integral and expressing τ_0 we obtain

$$\tau_0 = 0.45 \left(\frac{\Lambda}{\lambda_0^2 \xi_0} \right)^2, \tag{20.39}$$

which corresponds to the estimate (20.31).
A similar derivation can be performed for a superconductor containing impurities with $l < \xi_0$. In this case in (20.31) $\xi_0^2 \to \xi_0 l$. For pure tin $\xi_0 = 3.1 \times 10^{-5}$ cm, $\lambda \approx 0.3$. In order to have $\Delta T_c = 0.04$ K, i.e. $\tau_0 = 0.011$, one should have $\Lambda \approx 4 \times 10^{-7}$. Even if we put $d \sim 40\mathring{\mathrm{A}}$ we get $\delta\lambda \approx 1$; but d is probably even smaller. Thus, a seemingly small displacement of the critical temperature leads to a considerable value of the interaction constant.

Since we consider a narrow vicinity of T_{c0} we may apply Ginzburg-Landau theory. As we shall see below, this will be insufficient for calculating the critical magnetic field of the twinning plane superconductivity at $T < T_{co}$, but we shall not consider this case. The appearance of a twinning plane with a larger critical temperature can be naturally taken into account by adding a term $-\frac{1}{2}\gamma\delta(x)|\Psi|^2$ to the GL free energy. After that the GL functional in a given external field H_0 takes the form

$$\begin{aligned} \int \Omega_{\mathrm{sH}}\, \mathrm{d}V = &\int \Omega_{\mathrm{nH}}\, \mathrm{d}V \\ &+ \int \left\{ \frac{(H - H_0)^2}{8\pi} + \frac{1}{4m} \left| \left(-i\hbar\nabla - \left(\frac{2e}{c} \right) A \right) \Psi \right|^2 + \alpha\tau|\Psi|^2 + \frac{1}{2} b|\Psi|^4 \right. \\ &\left. -\gamma\delta(x)|\Psi|^2 \right\} \mathrm{d}V \end{aligned} \tag{20.40}$$

Variation over Ψ^* yields

$$\frac{1}{4m} \left[-i\hbar\nabla - \left(\frac{2e}{c} \right) A \right]^2 \Psi + \alpha\tau\Psi + b|\Psi|^2\Psi = \gamma\delta(x)\Psi. \tag{20.41}$$

First let us consider the case where there is no magnetic field. It is natural to assume in this case that Ψ depends only on x and that it is real. Then we find

$$-\frac{\hbar^2}{4m} \frac{d^2\Psi}{dx^2} + \alpha\tau\Psi + b\Psi^3 = \gamma\delta(x)\Psi. \tag{20.42}$$

The right-hand side of this equation corresponds to a discontinuity of $\mathrm{d}\Psi/\mathrm{d}x$.
Therefore, instead of the δ-function term we can write a boundary condition

$$\left. \frac{\mathrm{d}\Psi}{\mathrm{d}x} \right|_0 = -\frac{2m\gamma}{\hbar^2} \gamma\Psi(0) \tag{20.43}$$

Actually, instead of adding the δ-function term to the free energy we could write the "surface invariant" (Andreev 1987):

$$\int \mathrm{d}S \left[A\left|\Psi_+\right|^2 + B\left|\Psi_-\right|^2 + C\left(\Psi_+^*\Psi_- + \Psi_-^*\Psi_+\right)\right]$$

where

$$\Psi_+ = \Psi(x+0), \quad \Psi_- = \Psi(x-0)$$

After that variation of Ψ on both sides of the surface would yield more general boundary conditions than (20.43). However, it should be remembered that the twinning plane is necessarily connected with the appearance of a new symmetry element, e.g. a mirror reflection plane. In the corresponding transformation $|\Psi_+|^2 \rightleftarrows |\Psi_-|^2$. Thus, for $\Psi_+$and Ψ_-themselves a symmetrical transformation is possible, namely $\Psi_+ = \Psi_-$, as well as an antisymmetrical one: $\Psi_+ = -\Psi_-$. In the last case Ψ must turn to zero at interatomic distances from the twinning plane. This would lead to an energy increase, but there is no necessity for such a phase jump (such as an increasing vector potential, ch. 18, or a phase slip center, ch. 22). The symmetrical case coincides completely with the addition of the $\delta(x)$ term, and only this case are we going to consider.

First of all we show that the new parameter γ in (20.41) is uniquely connected with the increase of the critical temperature at the twinning plane. To this purpose consider eq. (20.42) in the linear approximation,

$$-\frac{h^2}{4m}\frac{d^2\Psi}{\mathrm{d}x^2} + \alpha\tau\Psi = 0$$

The solution of this equation, descending at $x \to \pm\infty$, is proportional to $\exp(-q|x|)$, where $q = \sqrt{4m\alpha\tau}/\hbar$. From the boundary condition (20.43) we find $q = 2m\gamma/\hbar^2$ and hence

$$\tau_0 = \frac{T_\mathrm{c} - T_{\mathrm{c}0}}{T_{\mathrm{c}0}} = \frac{m\gamma^2}{\hbar^2\alpha}. \tag{20.44}$$

Now we introduce new dimensionless variables:

$$\varphi = \frac{\Psi}{\Psi_0}, \quad t = \frac{T - T_{\mathrm{c}0}}{T_\mathrm{c} - T_{\mathrm{c}0}}, \quad x' = \frac{x}{\xi_\mathrm{c}},$$

where

$$\xi_\mathrm{c} = \frac{1}{q\left(T_\mathrm{c}\right)} = \frac{h}{\sqrt{4m\alpha\tau_0}}, \quad \Psi_0 = \sqrt{\frac{\alpha\tau_0}{b}} = \Psi\left(-\tau_0\right).$$

With these variables equation (20.42) does not contain any characteristics of the superconductor:

$$-\frac{d^2\varphi}{dx^2} + t\varphi + \varphi^3 = 2\delta(x)\varphi \tag{20.45}$$

(we omit the prime on $\boldsymbol{x}$). The right-hand side is equivalent to the boundary condition

$$\varphi'(0) = -\varphi(0) \tag{20.46}$$

Equation (20.45) (without the right-hand side) has a first integral. Multiplying by $\mathrm{d}\varphi/\mathrm{d}x$ and integrating with respect to x we get

$$-\left(\frac{\mathrm{d}\varphi}{dx}\right)^2 + t\varphi^2 + \frac{1}{2}\varphi^4 = \text{ const.} \tag{20.47}$$

Since at $x = \pm\infty$ we have $\varphi = 0$, it follows that const. $= 0$. Solving the equation thus obtained we have

$$\varphi = \frac{\sqrt{2t}}{\sinh(|x|\sqrt{t} + p)}. \tag{20.48}$$

The constant p is found from the boundary condition (20.46)

$$p = \frac{1}{2} \ln \left(\frac{1 + \sqrt{t}}{1 - \sqrt{t}} \right). \tag{20.49}$$

So the function φ in the general case decays exponentially while departing from the twinning plane, with a characteristic distance $\xi_c/\sqrt{t} = \xi(T)$, as expected. However, this happens only far from T_{co}, the critical temperature of the bulk specimen. Close to T_{c0} we have $t \to 0, p \approx \sqrt{t}, \varphi \approx \sqrt{2}/(|x| + 1)$, i.e. the exponential decay is replaced by a power law.

Now we shall consider the thermodynamics of twinning-plane superconductivity. It is evident that a single plane makes a negligible contribution to the thermodynamic functions, of the order of ξ_c/L, where L is the size of the sample. However, as mentioned above, in the high-temperature oxide $YBa_2Cu_3O_{7-\delta}$ a whole system of parallel twinning planes appears spontaneously. Therefore the corresponding contribution will not be negligible, particularly close to T_{c0}.

So we assume that there exists a system of parallel periodic twinning planes perpendicular to the x-axis, with a spacing L. Let us put the origin in the middle between two planes (fig. 129). Evidently φ will have a minimum at this point which we denote as φ_1. At this point $\mathrm{d}\varphi/\mathrm{d}x = 0$. Therefore in the first integral (20.47)

$$\text{const.} \;= t\varphi_1^2 + \frac{1}{2}\varphi_1^4. \tag{20.50}$$

At the twinning plane φ reaches a maximal value, which we denote by φ_0. According to the boundary condition (20.46) $(\varphi')^2 = \varphi_0^2$. Inserting this into (20.47) we find

$$\text{const.} \;= (t-1)\varphi_0^2 + \frac{1}{2}\varphi_0^4. \tag{20.51}$$

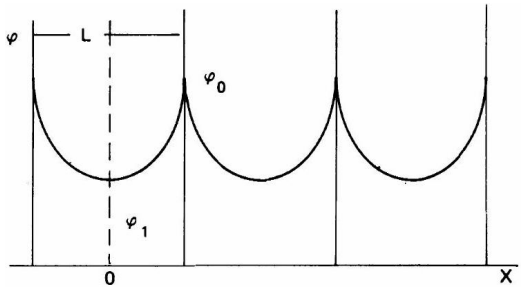


Fig. 129.

Comparing eqs. (20.50) and (20.51) we get the first relation

$$2t\varphi_1^2 + \varphi_1^4 = 2(t-1)\varphi_0^2 + \varphi_0^4. \tag{20.52}$$

Substituting (20.50) into (20.47) and expressing $\mathrm{d}x$ in terms of $\mathrm{d}\varphi$ we find

$$\mathrm{d}x = \frac{\sqrt{2}\;\mathrm{d}\varphi}{\left[(\varphi^2 - \varphi_1^2)\,(2t + \varphi^2 + \varphi_1^2)\right]^{1/2}}.$$

Integrating from $x = 0$ to $x = \frac{1}{2}L$ (i.e. $x = L/2\xi_c$ in dimensionless units) we find

$$\frac{L}{2\xi\,(T_c)} = \int_{\varphi_1}^{\varphi_0} \frac{\sqrt{2}\;\mathrm{d}\varphi}{\left[(\varphi^2 - \varphi_1^2)\,(2t + \varphi^2 + \varphi_1^2)\right]^{1/2}}. \tag{20.53}$$

Relations (20.52) and (20.53) are implicit formulae defining φ_1 and φ_0 as functions of t for a given spacing between the planes L.

The entropy is equal to

$$\begin{aligned}\int S_\mathrm{s}\;\mathrm{d}V &= -\frac{\partial}{\partial T}\int \Omega_\mathrm{s}\;\mathrm{d}V \\ &= -\int \left(\frac{\partial \Omega_\mathrm{s}}{\partial T}\right)_\Psi \mathrm{d}V - \int \frac{\partial \Psi}{\partial t}\left(\frac{\partial \Omega_\mathrm{s}}{\partial \Psi}\right)_T \mathrm{d}V\end{aligned}$$

But the latter term turns to zero since the condition $\partial\Omega_\mathrm{s}/\partial\Psi$ defined the GL equation. So only the first term remains and we get per unit volume

$$S = -\frac{\alpha}{T_{c0}}\int_0^{L/2} |\Psi|^2 \frac{\mathrm{d}x}{\frac{1}{2}L}.$$

Transforming to dimensionless variables, we get

$$\begin{aligned}S &= -\frac{2\alpha\xi_c\,|\Psi_0|^2}{LT_{c0}}\int_0^{L/2\xi_c} \varphi^2\;\mathrm{d}x \\ &= -\frac{2\xi_c\alpha^2\tau_0}{LT_{c0}b}\int_{\varphi_1}^{\varphi_0} \frac{\sqrt{2}\varphi^2\;\mathrm{d}\varphi}{\left[(\varphi^2 - \varphi_1^2)\,(2t + \varphi^2 + \varphi_1^2)\right]^{1/2}}.\end{aligned} \tag{20.54}$$

According to Landau phase transition theory (see Appendix II) the jump of the heat capacity of the bulk specimen at the transition point is

$$\Delta C_0 = \frac{\alpha^2}{bT_{c0}}$$

(this formula can also be obtained from relations 15.8 and 12.3). Differentiating S with respect to temperature and dividing by ΔC_0 we get (Abrikosov and Buzdin 1988)

$$\frac{C}{\Delta C_0} = -\frac{2\xi_\mathrm{c}}{L}\frac{T}{T_{c0}}\frac{\partial}{\partial T}\left\{\int_{\varphi_1}^{\varphi_0} \frac{\sqrt{2}\varphi^2\;\mathrm{d}\varphi}{\left[(\varphi^2 - \varphi_1^2)\,(2t + \varphi^2 + \varphi_1^2)\right]^{1/2}}\right\}. \tag{20.55}$$

Hence formulae (20.52), (20.53) and (20.55) present the temperature dependence of the heat capacity and depend on the parameter L/ξ_c. Figure 130 presents the experimental data on the temperature dependence of the heat capacity of a single crystal $YBa_2Cu_3O_{7-\delta}$ (Inderhees et al. 1987) together with the theoretical curve for $L/\xi_\mathrm{c} = 12$ giving the best fit. Excluding the small peak in the vicinity of T_{c0}, which

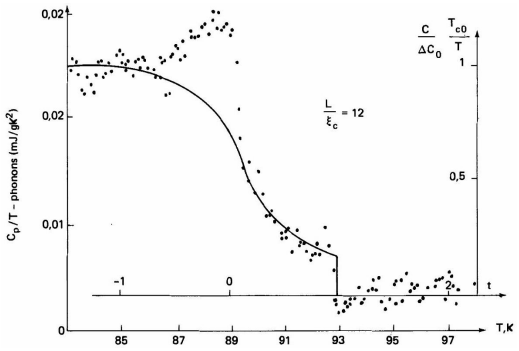


Fig. 130.

can be ascribed to fluctuations not taken into account in GL theory, the fitting is good. So one may conclude that 93 K corresponds to T_c i.e. to the critical temperature of the twinning plane superconductivity, whereas the bulk critical temperature T_{c0} is 89 K . Since $\xi_c \sim \xi_0 \tau_0^{-1/2}$, we have, with $\xi_0 \approx 16\text{Å}, \xi_c \approx 75.5\text{Å}$. So $L \approx 900\text{Å}$, which is reasonable.

According to Landau phase transition theory (see Appendix II) the jump of the heat capacity of the bulk specimen at the transition point is

$$\Delta C_0 = \frac{\alpha^2}{bT_{c0}}$$

(this formula can also be obtained from relations 15.8 and 12.3). Differentiating S with respect to temperature and dividing by ΔC_0 we get (Abrikosov and Buzdin 1988)

$$\frac{C}{\Delta C_0} = -\frac{2\xi_c}{L}\frac{T}{T_{c0}}\frac{\partial}{\partial T}\left\{\int_{\varphi_1}^{\varphi_0} \frac{\sqrt{2}\varphi^2 \, \mathrm{d}\varphi}{\left[(\varphi^2 - \varphi_1^2)\,(2t + \varphi^2 + \varphi_1^2)\right]^{1/2}}\right\}. \tag{20.55}$$

Hence formulae (20.52), (20.53) and (20.55) present the temperature dependence of the heat capacity and depend on the parameter L/ξ_c. Figure 130 presents the experimental data on the temperature dependence of the heat capacity of a single crystal $YBa_2Cu_3O_{7-8}$ (Inderhees et al. 1987) together with the theoretical curve for $L/\xi_c = 12$ giving the best fit. Excluding the small peak in the vicinity of T_{c0}, which

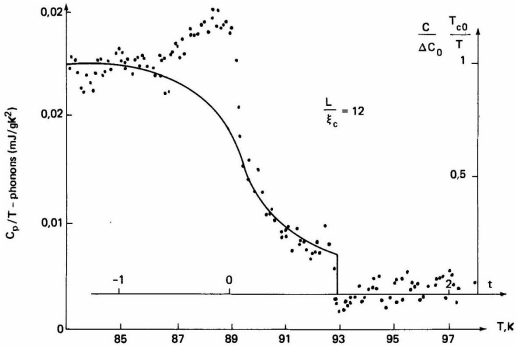


Fig. 130.

can be ascribed to fluctuations not taken into account in GL theory, the fitting is good. So one may conclude that 93 K corresponds to T_c i.e. to the critical temperature of the twinning plane superconductivity, whereas the bulk critical temperature T_{c0} is 89 K . Since $\xi_c \sim \xi_0 \tau_0^{-1/2}$, we have, with $\xi_0 \approx 16\text{Å}, \xi_c \approx 75.5\text{Å}$. So $L \approx 900\text{Å}$, which is reasonable.

According to Landau phase transition theory (see Appendix II) the jump of the heat capacity of the bulk specimen at the transition point is

$$\Delta C_0 = \frac{\alpha^2}{bT_{c0}}$$

(this formula can also be obtained from relations 15.8 and 12.3). Differentiating S with respect to temperature and dividing by ΔC_0 we get (Abrikosov and Buzdin 1988)

$$\frac{C}{\Delta C_0} = -\frac{2\xi_c}{L}\frac{T}{T_{c0}}\frac{\partial}{\partial T}\left\{\int_{\varphi_1}^{\varphi_0}\frac{\sqrt{2}\varphi^2\,\mathrm{d}\varphi}{\left[(\varphi^2-\varphi_1^2)\,(2t+\varphi^2+\varphi_1^2)\right]^{1/2}}\right\}. \tag{20.55}$$

Hence formulae (20.52), (20.53) and (20.55) present the temperature dependence of the heat capacity and depend on the parameter L/ξ_c. Figure 130 presents the experimental data on the temperature dependence of the heat capacity of a single crystal $YBa_2Cu_3O_{7-\delta}$ (Inderhees et al. 1987) together with the theoretical curve for $L/\xi_c = 12$ giving the best fit. Excluding the small peak in the vicinity of T_{c0}, which

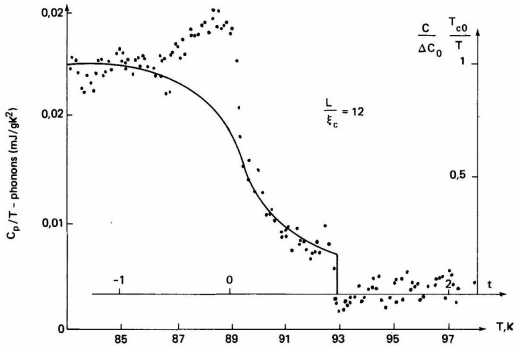


Fig. 130.

can be ascribed to fluctuations not taken into account in GL theory, the fitting is good. So one may conclude that 93 K corresponds to T_c i.e. to the critical temperature of the twinning plane superconductivity, whereas the bulk critical temperature T_{c0} is 89 K . Since $\xi_c \sim \xi_0\tau_0^{-1/2}$, we have, with $\xi_0 \approx 16\text{Å}, \xi_c \approx 75.5\text{Å}$. So $L \approx 900\text{Å}$, which is reasonable.

We now proceed to the calculation of the critical magnetic field. Let us consider only the case when the magnetic field is parallel to the twinning plane. Obviously, if the superconductor is of type II the disappearance of twinning plane superconductivity will proceed as a second-order transition. Let us assume H along the z-axis and choose the vector potential as $A_y(x)$. Then we should add a term e^2A^2/mc^2 to the left-hand side of (2.41). Let us introduce some quantities:

- the penetration depth

$$\delta = \sqrt{\frac{2mc^2}{4\pi\psi_0^2(2e)^2}}$$

$$\kappa = \frac{\delta}{\xi_c} = \frac{mc}{e}\sqrt{\frac{b}{2\pi}}$$

- the Ginzburg-Landau parameter

$$H_{\mathrm{cm}}\left(-\tau_0\right)=2\alpha\tau_0\sqrt{\frac{\pi}{b}}$$

- the scale for the critical field

$$H_{\mathrm{c2}}\left(-\tau_0\right)=\kappa\sqrt{2}H_{\mathrm{cm}}\left(-\tau_0\right)=2\alpha\tau_0\frac{mc}{e}.$$

Close to the critical field we can assume $A_y(x)=H_0x$. With dimensionless variables we get

$$-\varphi''(x)+h^2x^2\varphi(x)+t\varphi(x)-2\delta(x)\varphi(x)=0 \tag{20.56}$$

where $h=H_0/H_{\mathrm{c2}}\left(-\tau_0\right)$. We first find the solutions of eq. (20.56) in the limiting cases. First we consider the vicinity of T_c, i.e. $t\to 1$. In this case h will be small and therefore the corresponding term can be treated as a perturbation. Let us rewrite eq. (20.56) in the following form:

$$-\varphi''(x)+\varphi(x)+h^2x^2\varphi(x)=(1-t)\varphi(x)$$

with the boundary condition $\varphi'(0)=-\varphi(0)$. In the case under consideration $1-t$ plays the role of energy. In the zeroth approximation $1-t=0$ and the eigenfunction is

$$\varphi\propto \mathrm{e}^{-|x|}.$$

In the first approximation the perturbation has to be averaged over the unperturbed state. So we get

$$1-t=\frac{\int_{-\infty}^{\infty}h^2x^2\mathrm{e}^{-2|x|}\mathrm{d}x}{\int_{-\infty}^{\infty}\mathrm{e}^{-2|x|}\mathrm{d}x}$$

We find therefrom

$$1-t=\frac{1}{2}h^2$$

i.e.

$$h=[2(1-t)]^{1/2} \tag{20.57}$$

We now proceed to the calculation of the critical magnetic field. Let us consider only the case when the magnetic field is parallel to the twinning plane. Obviously, if the superconductor is of type II the disappearance of twinning plane superconductivity will proceed as a second-order transition. Let us assume H along the z-axis and choose the vector potential as $A_y(x)$. Then we should add a term e^2A^2/mc^2 to the left-hand side of (2.41). Let us introduce some quantities:

- the penetration depth

$$\delta=\sqrt{\frac{2mc^2}{4\pi\psi_0^2(2e)^2}}$$

$$\kappa=\frac{\delta}{\xi_c}=\frac{mc}{e}\sqrt{\frac{b}{2\pi}}$$

- the Ginzburg-Landau parameter

$$H_{\mathrm{cm}}\left(-\tau_0\right) = 2\alpha\tau_0\sqrt{\frac{\pi}{b}}$$

- the scale for the critical field

$$H_{\mathrm{c2}}\left(-\tau_0\right) = \kappa\sqrt{2}H_{\mathrm{cm}}\left(-\tau_0\right) = 2\alpha\tau_0\frac{mc}{e}.$$

Close to the critical field we can assume $A_y(x) = H_0 x$. With dimensionless variables we get

$$-\varphi''(x) + h^2x^2\varphi(x) + t\varphi(x) - 2\delta(x)\varphi(x) = 0, \tag{20.56}$$

where $h = H_0/H_{\mathrm{c2}}\left(-\tau_0\right)$. We first find the solutions of eq. (20.56) in the limiting cases. First we consider the vicinity of T_c, i.e. $t \to 1$. In this case h will be small and therefore the corresponding term can be treated as a perturbation. Let us rewrite eq. (20.56) in the following form:

$$-\varphi''(x) + \varphi(x) + h^2x^2\varphi(x) = (1-t)\varphi(x)$$

with the boundary condition $\varphi'(0) = -\varphi(0)$. In the case under consideration $1-t$ plays the role of energy. In the zeroth approximation $1 - t = 0$ and the eigenfunction is

$$\varphi \propto \mathrm{e}^{-|x|}.$$

In the first approximation the perturbation has to be averaged over the unperturbed state. So we get

$$1 - t = \frac{\int_{-\infty}^{\infty} h^2x^2\mathrm{e}^{-2|x|}\mathrm{d}x}{\int_{-\infty}^{\infty}\mathrm{e}^{-2|x|}\mathrm{d}x}$$

We find therefrom

$$1 - t = \frac{1}{2}h^2$$

i.e.

$$h = [2(1-t)]^{1/2}. \tag{20.57}$$

Now we pass to conventional units. Since H_{c2} varies linearly with temperature close to T_{co} we can write

$$H_{\mathrm{c2}}\left(-\tau_0\right) = \left.\frac{\mathrm{d}H_{\mathrm{c2}}}{\mathrm{d}T}\right|_{T_{\mathrm{c0}}}\left(T_{\mathrm{c}} - T_{\mathrm{c0}}\right).$$

Keeping in mind that $t = \left(T - T_{\mathrm{c0}}\right)/\left(T_{\mathrm{c}} - T_{\mathrm{c0}}\right)$ we find:

$$1 - t = \frac{T_c - T}{T_c - T_{c0}}.$$

Hence the critical field of the twinning plane is

$$H^{\mathrm{t}}_{\mathrm{c2}}(T) = \left|\frac{\mathrm{d}H_{\mathrm{c2}}}{\mathrm{d}T}\right|\left[2\left(T_{\mathrm{c}} - T\right)\left(T_{\mathrm{c}} - T_{\mathrm{c0}}\right)\right]^{1/2}. \tag{20.58}$$

One sees that $H_{c2}^{t} \sim (T_c - T)^{1/2}$. This behaviour corresponds to a thin film having a thickness ξ_c (see 17.48′).

Another limiting case is the field at temperature $t < 0, |t| > 1$ i.e. on the scale $T_c - T_{c0}$ deep in the superconducting region, not so far however from T_{c0} as to violate the applicability condition of GL theory: $T_{c0} - T < T_{c0}$. Under these conditions the twinning plane itself is a perturbation. Let us rewrite eq. (20.56) in the form

$$-\varphi''(x) + h^2x^2\varphi(x) - 2\delta(x)\varphi(x) = -t\varphi(x) \qquad (\prime)$$

Neglecting the term with $\delta(x)$ we have solutions of (20.56′) descending with $x \to \pm\infty$ if $-t = h(2n+1)$. The smallest eigenvalue is $-t = h$. The corresponding eigenfunction is $\varphi_0 = (h/\pi)^{1/4} \exp\left(-\frac{1}{2}hx^2\right)$. Considering the term with $\delta(x)$ as a perturbation we obtain the first approximation,

$$-t = h + \int \varphi^2[-2\delta(x)]\mathrm{d}x = h - 2\sqrt{\frac{h}{\pi}}.$$

Since h is large in this case the second term is in fact a correction. Solving with respect to h we find

$$h = -t + \sqrt{\frac{2|t|}{\pi}} \qquad (20.59)$$

Multiplying by $H_{c2}(-\tau_0) = |\mathrm{d}H_{c2}/\mathrm{d}T|_{T_{c0}}(T_c - T_{c0})$ we see that $h = -t$ corresponds to $H_{c2}^{t}(T) = |\mathrm{d}H_{c2}/\mathrm{d}T|(T_{c0} - T) = H_{c2}$. Hence

$$\frac{H_{c2}^{t}(T) - H_{c2}(T)}{H_{c2}(T)} = \frac{2}{\sqrt{\pi|t|}}. \qquad (20.60)$$

It follows that $H_{c2}^{t}(T) > H_{c2}(T)$ at any temperature (fig. 131) and hence in type-II superconductors twinning plane superconductivity can exist in the absence of bulk superconductivity in the proper interval of magnetic fields up to $T = 0$. Of course the critical field H_{c2}^{t} at low temperature cannot be calculated from the GL equations and demands a more complete microscopic theory.

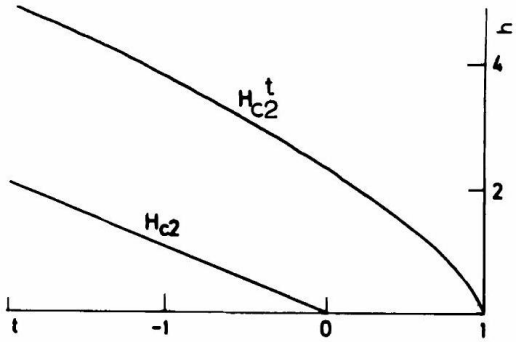


Fig. 131.

We have considered until now the limiting cases. An expression for h which is valid for any t (within the applicability region of GL-theory) can be obtained in the following way. We assume for the general solution of eq. (20.56') the following form:

$$\varphi(x) = \sum_n c_n\varphi_n(x), \qquad (20.61)$$

where φ_n are eigenfunctions, corresponding to the eigenvalues of the parameter $t : \varepsilon_n = h(2n+1)$; substituting into (20.56'), multiplying by $\varphi_n(x)$ and integrating with respect to x we find

$$c_n = \frac{2\varphi(0)\varphi_n(0)}{t+\varepsilon_n}. \tag{20.62}$$

Taking into account the self-consistency condition

$$\varphi(0) = \sum_n c_n \varphi_n(0)$$

we find

$$1 = \sum_n \frac{2\varphi_n^2(0)}{t+\varepsilon_n}. \tag{20.63}$$

The normalized eigenfunctions of eq. (20.56) (without the δ-term) are expressed by (see Landau and Lifshitz 1974)

$$\varphi_n = \left(\frac{h}{\pi}\right)^{1/4} (2^n n!)^{-1/2} \exp\left(-\frac{1}{2}hx^2\right) \mathrm{H}_n(x\sqrt{h}), \tag{20.64}$$

where H_n are the Hermite polynomials

$$\mathrm{H}_n(x) = (-1)^n \mathrm{e}^{x^2} \frac{\mathrm{d}^n}{\mathrm{d}x^n} \mathrm{e}^{-x^2}. \tag{20.65}$$

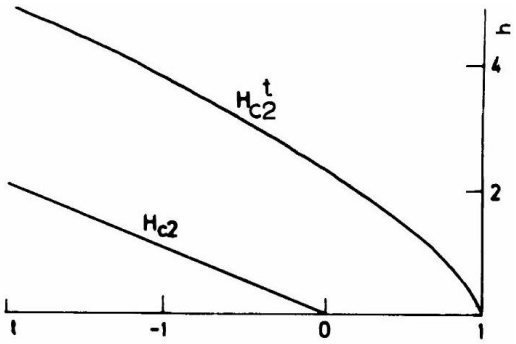


Fig. 131.

We have considered until now the limiting cases. An expression for h which is valid for any t (within the applicability region of GL-theory) can be obtained in the following way. We assume for the general solution of eq. (20.56') the following form:

$$\varphi(x) = \sum_n c_n \varphi_n(x), \tag{20.61}$$

where φ_n are eigenfunctions, corresponding to the eigenvalues of the parameter $t : \varepsilon_n = h(2n+1)$; substituting into (20.56'), multiplying by $\varphi_n(x)$ and integrating with respect to x we find

$$c_n = \frac{2\varphi(0)\varphi_n(0)}{t+\varepsilon_n}. \tag{20.62}$$

Taking into account the self-consistency condition

$$\varphi(0) = \sum_n c_n \varphi_n(0)$$

we find

$$1 = \sum_n \frac{2\varphi_n^2(0)}{t + \varepsilon_n}. \tag{20.63}$$

The normalized eigenfunctions of eq. (20.56) (without the δ-term) are expressed by (see Landau and Lifshitz 1974)

$$\varphi_n = \left(\frac{h}{\pi}\right)^{1/4} (2^n n!)^{-1/2} \exp\left(-\frac{1}{2}hx^2\right) \mathrm{H}_n(x\sqrt{h}), \tag{20.64}$$

where $\mathbf{H_n}$ are the Hermite polynomials

$$\mathrm{H}_n(x) = (-1)^n \mathrm{e}^{x^2} \frac{\mathrm{d}^n}{\mathrm{d}x^n} \mathrm{e}^{-x^2}. \tag{20.65}$$

Putting $x = 0$ we have

$$\mathrm{H}_{2n}(0) = (-1)^n 2^n (2n-1)!!, \quad \mathrm{H}_{2n+1}(0) = 0.$$

Substituting into eq. (20.63) we get an equation for h :

$$\begin{aligned} h^{1/2} &= \frac{2}{\pi^{1/2}} \sum_{k=0}^{\infty} \frac{(2k)!}{(k!)^2 2^{2k}(t/h + 4k + 1)} \\ &= \frac{1}{2\sqrt{\pi}} B\left(\frac{1}{2}, \frac{1}{4}\left(1 + \frac{t}{h}\right)\right) \end{aligned} \tag{20.66}$$

where $\mathrm{B}(x, y) = \Gamma(x)\Gamma(y)/\Gamma(x + y)$ is the beta-function. From the general expression the limiting cases (20.52) and (20.59) can also be obtained.

With respect to the high-temperature oxide $\mathrm{Y - Ba - Cu - O}$, the formula (20.58) is of the main interest. Experiments with samples having parallel c-axes of the crystallites and the magnetic field also in the same direction (Fang et al. 1987) showed that around the critical temperature the critical field is proportional to $(T_c - T)^{1/2}$ rather than to $T_\mathrm{c} - T$. Hence it can be concluded that this is due to twinning plane superconductivity. If we use the value $|\mathrm{d}H_{\mathrm{c}2}/\mathrm{d}T| \sim 10\mathrm{kOe/K}$ which is known from other sources then we obtain $T_c - T_{c0} \approx 5 - 6$ K, which fits the result for the specific heat.

Now let us consider the case when the twinning boundary is formed in a type-I superconductor. First of all it should be mentioned that there exists an effective GL parameter for twinning plane superconductivity, namely

$$\kappa_{\mathrm{eff}} \sim \frac{\lambda_{\mathrm{L}}[\psi]}{\xi_{\mathrm{c}}} \sim \frac{\lambda_{\mathrm{L}0}}{\psi\xi_{\mathrm{c}}} \sim \frac{\lambda_{\mathrm{L}0}}{\xi_{\mathrm{c}}\left[\left(T_{\mathrm{c}} - T\right)/T_{\mathrm{c}0}\right]^{1/2}}. \tag{20.67}$$

Hence close to T_c we have $\kappa_{\mathrm{eff}} > 1$ and there is a second-order phase transition which is described by the preceding formulae. At some temperature where $\kappa_{\mathrm{eff}} \approx 1$ a "tricritical point" occurs and the transition becomes first-order.

In order to calculate the first-order transition critical field we apply a method similar to the one we used for the calculation of the surface energy (section 17.2). Let us assume $\kappa < 1$, i.e., $\xi > \delta$. Then the field practically does not penetrate into the superconducting region. We shall suppose this region to be $-L < x < L$ (its size is still to be determined). So we arrive at eq.

(20.42) or (20.45) but with another boundary condition: $\varphi(\pm L/\xi_c) = 0$. We have to calculate the free energy of this region which is equal to (see 20.40 ; we have passed to reduced variables)

$$\begin{aligned}\Omega &\equiv \int \Omega_{\mathrm{sH}}\,\mathrm{d}x - \int \Omega_{\mathrm{nH}}\,\mathrm{d}x \\ &= \frac{H_{\mathrm{c}}^2}{4\pi}\xi_{\mathrm{c}}\left\{\int_{-L/\xi_{\mathrm{c}}}^{L/\xi_0}\left[\varphi'^2 + t\varphi^2 + \frac{1}{2}\varphi^4 + \frac{1}{2}h_0^2\right]\mathrm{d}x - 2\varphi^2(0)\right\}\end{aligned} \tag{20.68}$$

where $h_0 = H_0/H_{\mathrm{cm}}\,(-\tau_0)$.
Putting $x = 0$ we have

$$\mathrm{H}_{2n}(0) = (-1)^n 2^n (2n-1)!!, \quad \mathrm{H}_{2n+1}(0) = 0.$$

Substituting into eq. (20.63) we get an equation for h :

$$\begin{aligned}h^{1/2} &= \frac{2}{\pi^{1/2}}\sum_{k=0}^{\infty}\frac{(2k)!}{(k!)^2 2^{2k}(t/h + 4k + 1)} \\ &= \frac{1}{2\sqrt{\pi}}B\left(\frac{1}{2}, \frac{1}{4}\left(1 + \frac{t}{h}\right)\right)\end{aligned} \tag{20.66}$$

where $\mathrm{B}(x,y) = \Gamma(x)\Gamma(y)/\Gamma(x+y)$ is the beta-function. From the general expression the limiting cases (20.52) and (20.59) can also be obtained.

With respect to the high-temperature oxide $\mathrm{Y-Ba-Cu-O}$, the formula (20.58) is of the main interest. Experiments with samples having parallel c-axes of the crystallites and the magnetic field also in the same direction (Fang et al. 1987) showed that around the critical temperature the critical field is proportional to $(T_c - T)^{1/2}$ rather than to $\boldsymbol{T_{\mathrm{c}}} - \boldsymbol{T}$. Hence it can be concluded that this is due to twinning plane superconductivity. If we use the value $|\mathrm{d}H_{c2}/\mathrm{d}T| \sim 10\mathrm{kOe/K}$ which is known from other sources then we obtain $T_c - T_{c0} \approx 5 - 6$ K, which fits the result for the specific heat.

Now let us consider the case when the twinning boundary is formed in a type-I superconductor. First of all it should be mentioned that there exists an effective GL parameter for twinning plane superconductivity, namely

$$\kappa_{\mathrm{eff}} \sim \frac{\lambda_{\mathrm{L}}[\psi]}{\xi_{\mathrm{c}}} \sim \frac{\lambda_{\mathrm{L0}}}{\psi\xi_{\mathrm{c}}} \sim \frac{\lambda_{\mathrm{L0}}}{\xi_{\mathrm{c}}\left[\left(T_{\mathrm{c}} - T\right)/T_{\mathrm{c0}}\right]^{1/2}}. \tag{20.67}$$

Hence close to T_{c} we have $\kappa_{\mathrm{eff}} \gg 1$ and there is a second-order phase transition which is described by the preceding formulae. At some temperature where $\kappa_{\mathrm{eff}} \approx 1$ a "tricritical point" occurs and the transition becomes first-order.

In order to calculate the first-order transition critical field we apply a method similar to the one we used for the calculation of the surface energy (section 17.2). Let us assume $\kappa < 1$, i.e., $\xi > \delta$. Then the field practically does not penetrate into the superconducting region. We shall suppose this region to be $-L < x < L$ (its size is still to be determined). So we arrive at eq. (20.42) or (20.45) but with another boundary condition: $\varphi(\pm L/\xi_c) = 0$. We have to calculate the free energy of this region which is equal to (see 20.40; we have passed to reduced variables)

$$\begin{aligned}\Omega &\equiv \int \Omega_{\mathrm{sH}}\,\mathrm{d}x - \int \Omega_{\mathrm{nH}}\,\mathrm{d}x \\ &= \frac{H_{\mathrm{c}}^2}{4\pi}\xi_{\mathrm{c}}\left\{\int_{-L/\xi_{\mathrm{c}}}^{L/\xi_0}\left[\varphi'^2 + t\varphi^2 + \frac{1}{2}\varphi^4 + \frac{1}{2}h_0^2\right]\mathrm{d}x - 2\varphi^2(0)\right\}\end{aligned} \tag{20.68}$$

where $h_0 = H_0/H_{\mathrm{cm}}\,(-\tau_0)$.

This time we shall use the full equations containing the field. Choosing the vector potential as $A_y(x)$ we get

$$-\frac{\hbar^2}{4m}\frac{\mathrm{d}^2\Psi}{\mathrm{d}x^2}+\frac{e^2}{mc^2}A^2\Psi+\alpha\tau\Psi+\frac{1}{2}b\Psi^3=\gamma\delta(x)\Psi \tag{20.69}$$

$$\frac{\mathrm{d}^2A}{\mathrm{d}x^2}=\frac{8\pi e^2}{mc^2}\Psi^2A \tag{20.70}$$

We introduce a new scale for $\boldsymbol{A}$:

$$A_0=H_{\mathrm{c}}\,(-\tau_0)\,\delta\,(-\tau_0)=\left(\alpha\tau_0\frac{mc^2}{2e^2}\right)^{1/2}$$

Multiplying eq. (20.69) without the right-hand side by $\mathrm{d}\Psi/\mathrm{d}x$ and eq. (20.70) by $(8\pi)^{-1}\,\mathrm{d}\boldsymbol{A}/\mathrm{d}x$, adding them up and integrating with respect to x we obtain in dimensionless variables the first integral

$$-2\varphi'^2+(2t+A)^2\varphi^2+\varphi^4-\left(A'\right)^2x^2=-h_0^2 \tag{20.71}$$

The constant is chosen from the condition at the boundary of the superconducting region $\varphi=0, H=H_0$.

From this integral we have inisde the region under consideration at $x<0$

$$\frac{\mathrm{d}\varphi}{\mathrm{d}x}=-\left(t\varphi^2+\frac{1}{2}\varphi^4+\frac{1}{2}h_0^2\right)^{1/2} \tag{20.72}$$

(we have put $\boldsymbol{A}=\boldsymbol{A}'=0$). On the other hand, using the boundary condition at the twinning plane we get from eq. (20.72):

$$h_Q^2=2(1-t)\varphi^2(0)-\varphi^4(0) \tag{20.73}$$

Using the first integral (20.72) we get from eq. (20.68)

$$\Omega=\frac{H_{\mathrm{cm}}^2\,(-\tau_0)}{4\pi}\xi_{\mathrm{c}}\left\{\int_{-L/\xi_{\mathrm{c}}}^{L/\xi_{\mathrm{c}}}2\left(\varphi'\right)^2\,\mathrm{d}x-2\varphi^2(0)\right\}$$

With the aid of eq. (20.72) we pass over to the integration over φ and introduce the new variable $y=\varphi/\varphi(0)$; we apply also eq. (20.73):

$$\Omega=\frac{1}{\pi}H_{\mathrm{cm}}^2\,(-\tau_0)\,\varphi^2(0)\xi_{\mathrm{c}}\left\{\int_0^1\left[1-t\left(1-y^2\right)+\frac{1}{2}\left(y^4-1\right)\varphi^2(0)\right]^{1/2}\,\mathrm{d}y-\frac{1}{2}\right\}$$

The first-order transition is defined by the condition $\Omega=0$. This gives an implicit definition of $\varphi(0)$:

$$\int_0^1\left[1-t\left(1-y^2\right)+\frac{1}{2}\left(y^4-1\right)\varphi^2(0)\right]^{1/2}\,\mathrm{d}y=\frac{1}{2} \tag{20.74}$$

Having obtained $\varphi(0)$ we can find the critical field from eq. (20.73). Actually this can be done only numerically. It appears that the transition curve crosses the curve

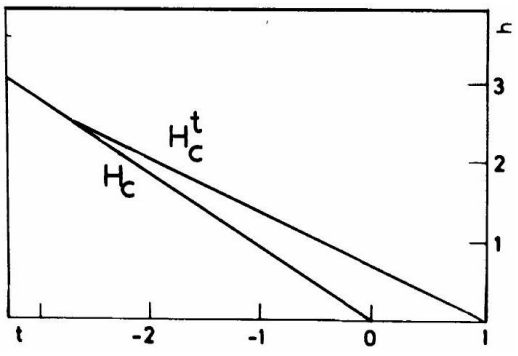


Fig. 132.

for the transition of the bulk material (fig. 132), i.e., the region of twinning plane superconductivity is thus limited to the vicinity of T_{c0}.

The width of the superconducting region is of the order of ξ_c; it can be found easily from the integral (20.72)

$$\frac{2L}{\xi_c} = \int_0^{\varphi(0)} \frac{\mathrm{d}\varphi}{\left(t\varphi^2 + \frac{1}{2}\varphi^4 + \frac{1}{2}h_0^2\right)^{1/2}}. \tag{20.75}$$

Since the field is completely expelled from a region of width $2L$, the magnetic moment of such a plane per unit area is equal to

$$\mu_d = -\frac{1}{2\pi} HL(H). \tag{20.76}$$

The calculation performed here is valid for $\kappa = 0$. However it can be generalized to finite κ 's. Since nothing is used here apart from the constants of the bulk superconductor the results are universal. A numerical calculation for $\kappa = 0.13$ (tin) gives excellent agreement with experiment (fig. 133).

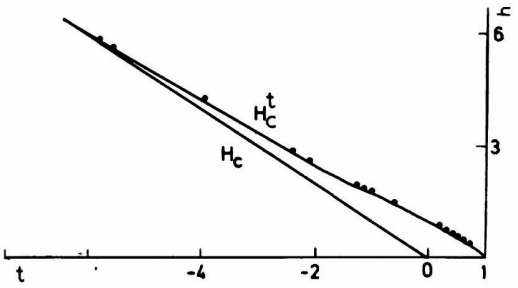


Fig. 133.

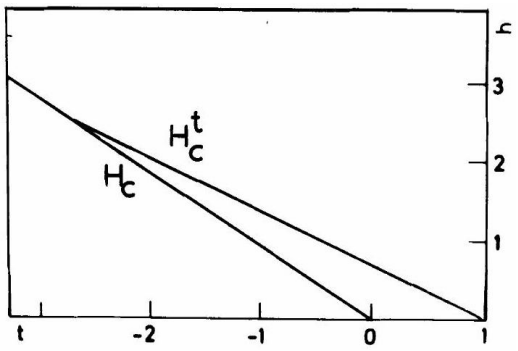


Fig. 132.

for the transition of the bulk material (fig. 132), i.e., the region of twinning plane superconductivity is thus limited to the vicinity of T_{c0}.

The width of the superconducting region is of the order of ξ_c; it can be found easily from the integral (20.72)

$$\frac{2L}{\xi_c} = \int_0^{\varphi(0)} \frac{\mathrm{d}\varphi}{\left(t\varphi^2 + \frac{1}{2}\varphi^4 + \frac{1}{2}h_0^2\right)^{1/2}}. \tag{20.75}$$

Since the field is completely expelled from a region of width $2L$, the magnetic moment of such a plane per unit area is equal to

$$\mu_d = -\frac{1}{2\pi} HL(H). \tag{20.76}$$

The calculation performed here is valid for $\kappa = 0$. However it can be generalized to finite κ 's. Since nothing is used here apart from the constants of the bulk superconductor the results are universal. A numerical calculation for $\kappa = 0.13$ (tin) gives excellent agreement with experiment (fig. 133).

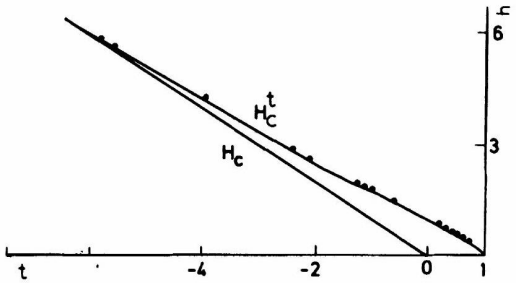


Fig. 133.

The existence of twinning planes can explain some other properties of the superconducting oxide Y − Ba − Cu − O. For example, films which are prepared by another technology contain no twinning planes and their critical temperature does not exceed 89 K . Furthermore, as already mentioned the superconductivity of an isolated twinning plane is suppressed by its normal surroundings due to the proximity effect. Hence the critical temperature could be raised if the twinning planes could be placed at distances less than ξ_c or if they were formed in granules of the proper size. As was mentioned already, Khaikin and Khlyustikov (1981) in pressing samples from a powder of pure tin managed to discover traces of superconductivity up to 12 K , i.e. at temperatures higher than $3T_{c0}$. It is not excluded that communications about signs of

superconductivity in $Y-Ba-Cu-O$ up to 500 K appearing from time to time, are connected with the existance of regions with dense arrays of twinning planes.

For more details about twinning-plane superconductivity see the review by Khlyustikov and Buzdin (1987).

8.6.3 20.3. Andreev reflection

In section 20.1 we have been concerned with the behavior of the superconducting order parameter in the vicinity of the contact between a superconductor and a normal metal. Let us now consider another aspect of such a contact.

As has been said in Part I, the chemical potentials of electrons in both metals must be equal. But the electrons in the ground state of a superconductor are bound into Cooper pairs, and in a normal metal they exist one by one. Hence, the chemical potentials of two separate electrons in a normal metal and of a Cooper pair in a superconductor must be equal. Suppose an electron has been transferred from the normal metal to the superconductor. In this case, it will have no partner, with which it could have been bound into a Cooper pair, which means that its energy will be higher by half the binding energy, i.e., by an amount Δ. Hence, for an individual electron the energy levels in the superconductor begin by Δ higher than in the normal metal. Thus, if its excitation energy above the Fermi level is less than Δ, it must be reflected from the interface.

Such reflection occurs in a rather peculiar manner. In order to ascertain this, it will be better to use the language of the quasiparticle concept. Suppose, for the sake of simplicity, that we deal with the interface between the normal and superconducting layers in the intermediate state of a superconductor. In this case the metals are identical, in principle, and Δ varies from zero to an equilibrium value in the bulk superconductor at a distance $\xi \sim \hbar v/\Delta$. The energy spectrum of quasiparticles expressed by the formula $\varepsilon = (\xi^2 + \Delta^2)^{1/2}$ varies in the manner shown in fig. 134. Quasiparticles with an energy less than Δ in the bulk superconductor must be reflected back into the normal metal. Upon such reflection the energy must be conserved.

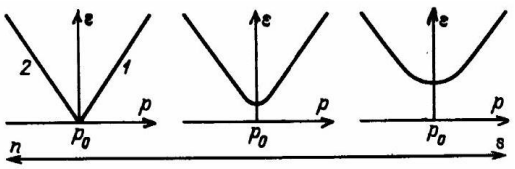


Fig. 134.

As for the variation of the quasimomentum δp, it can be evaluated in the following way. The quantity δp is of order $\mathrm{d}p/\mathrm{d}t$ multiplied by the time passed in the interface region, i.e., ξ/v. As regards $\mathrm{d}p/\mathrm{d}t$, it is equal to the acting force: $-\mathrm{d}V/\mathrm{d}x \sim \Delta/\xi$. This gives

$$\delta p \sim \frac{\xi}{v}\frac{\Delta}{\xi} \sim \frac{\Delta}{v} \sim p_0\frac{\Delta}{p_0 v} \sim p_0\frac{\Delta}{\varepsilon_\mathrm{F}} < p_0.$$

This means that the variation of the quasimomentum is smaller than the quasimomentum itself. But the motion of the electron after reflection must be directed away from the interface.

All these conditions can be fulfilled only in a single way, namely, if the quasiparticle is transferred, say, from branch 1 of the energy spectrum to branch 2 (fig. 134), i.e., is converted from a "particle" to an "antiparticle" with a close quasimomentum. The energy and the quasimomentum do not change. As regards the velocity, it will be equal after reflection to

$$v_{\text{ref}} = \frac{\partial \left[v \left(p_0 - p \right) \right]}{\partial p} = -\frac{vp}{p} = -v_{\text{inc}}$$

Thus, upon such reflection the "particle" is converted to an "antiparticle". The quasimomentum and energy are conserved and the velocity changes sign. Such reflection is radically different from the specular reflection of electrons, where only the normal component of the electron velocity changes sign with respect to the interface. The specificity of this reflection, called Andreev reflection (Andreev 1964), is associated with the slowness of the variation of the potential, the role of which is played by Δ.

A question may arise as to the conservation of charge. The answer is: an electron residing at the Fermi boundary slightly above it picks up another electron with an opposite quasimomentum, which lies slightly below the Fermi boundary, and forms with it a Cooper pair, which goes into the superconductor condensate. An "antiparticle" is left, with a momentum opposite to the momentum of the picked-up electron, i.e., a momentum coinciding with the momentum of the original electron.

Evidently, upon Andreev reflection the transfer from branch 2 to branch 1 of the energy spectrum is also possible, i.e., the antiparticle may be converted to a particle with the opposite velocity. Moreover, it is clear that due to the proximity effect the slowness of variation of the potential will also be conserved for quasiparticles upon contact of the normal metal with a completely foreign superconductor, which means that the reflection law will remain valid.

Direct observation of Andreev reflection is possible by means of the nonresonant size effect described in section 8.3. The effect consist in the following: as soon as the extremal diameter of the trajectory in the magnetic field (or an integer number of such diameters) fits into the plate thickness, a singularity of surface impedance arises. Figure 135 sketches the situation in a case where half the extremal trajectory fits into a layer of a normal metal applied onto a superconductor surface. An electron approaching the interface is converted to an antiparticle with an opposite velocity. This antiparticle travels the same electron trajectory in the opposite direction and eventually approaches the interface. The antiparticle is then converted to an electron and the process repeats itself.

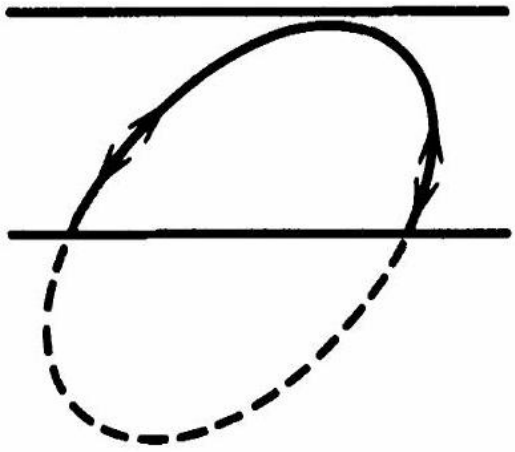


Fig. 135.

Thus, the singularities of the impedance will arise not only in those fields where an integer number of diameters fit into the thickness of the normal plate but also when their number is half-integral. In other words, extra singularities of $Z(H)$ will arise in the middle between the original ones. This is actually observed in experiments (Krylov and Sharvin 1970, 1973).

Note that if the extremal cross section is not the central one, then in an ordinary experiment on the size effect a spiral trajectory corresponds to it in coordinate space, i.e., the electron is displaced along the field. But if the trajectory corresponds to an extra resonance, the velocity component along the field will also change sign upon reflection and the antiparticle will pass its half of the turn of the coil in the opposite direction. Hence, each quasiparticle stays within one half of the turn of the helix, and on the average, no displacement occurs along the field.

8.6.4 20.4. Low-temperature heat capacity of the intermediate state

In the previous section we have already considered the case where the reflection from the n − s (normal-superconducting) interface leads to the replacement of translational motion by periodic motion. Let us now consider another case of the same kind: the intermediate state. We assume that the layers are plane-parallel. For microscopic samples the layer thickness is usually of the order of 10^{-3} cm, i.e., much
larger than ξ, and the n − s interfaces may be taken into account by using the boundary condition. We obtain a periodic picture of the motion of quasiparticles in a normal layer: a quasiparticle of particle-type reaches the interface and is converted to an antiparticle; It then flies back to another interface and is converted to a particle, and the entire process is repeated.

The presence of a magnetic field in the normal layers does not alter the situation because the curved trajectory of the antiparticle exactly repeats the trajectory of the particle that has travelled in the opposite direction. As a matter of fact, in real type I superconductors the Larmor radius in the critical field ($\sim 100 - 1000$ Oe) is not less than 10^{-2} cm and this implies that the trajectories may be assumed to be straight (fig. 136).

The periodic motion is quantized according to the Bohr rule:

$$\oint p \, \mathrm{d}l = 2\pi\hbar[n + \gamma(n)], \tag{20.77}$$

where $\gamma(n) < 1$. Since for the particle $\varepsilon = \xi = v\,(p_\mathrm{p} - p_0)$, it follows that its quasimomentum is given by (here we use the symbol ε in place of ε_qp):

$$p_\mathrm{p} = p_0 + \frac{\varepsilon}{v}.$$

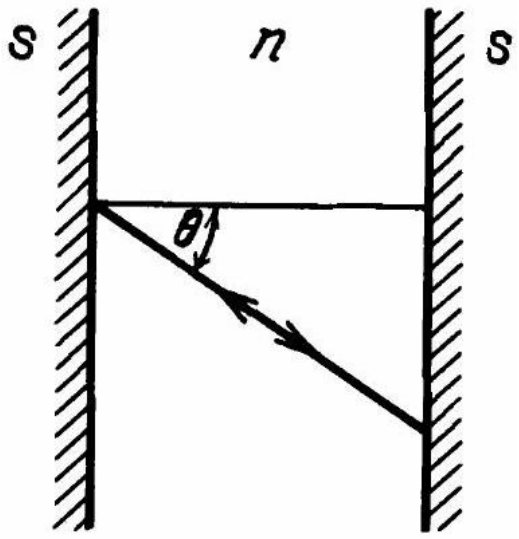


Fig. 136.

The reflected antiparticle has an energy $\varepsilon = -\xi = v\,(p_0 - p_\mathrm{a})$ and, hence, its quasimomentum is

$$p_\mathrm{a} = p_0 - \frac{\varepsilon}{v}.$$

In the integral (20.77) p is the same on both halves of the trajectory, but $\mathrm{d}l$ changes sign. If the width of the layer is a, then the pathlength in one direction is $a/|\cos\theta|$, where θ is the angle between the trajectory and the normal to the interface (fig. 136). As a result, we obtain from eq. (20.77)

$$(p_\mathrm{p} - p_\mathrm{a}) \cdot \frac{a}{|\cos\theta|} = 2\pi(n+\gamma).$$

Substituting the expressions for p_p and p_a, we obtain (Andreev 1965):

$$\varepsilon(n,\theta) = \pi\hbar(n+\gamma)v\frac{|\cos\theta|}{a} \tag{20.78}$$

This is the formula for the energy spectrum of quasiparticles in the intermediate state. The energy depends on the discrete variable n and the continuous angle variable θ.

Let us now find the density of states. The vector $n = p/p$ is uniquely determined by its projections onto the plane of the layer boundary. The number of states is expressed by the formula

$$2S\ \mathrm{d}p_x\frac{\mathrm{d}p_y}{(2\pi\hbar)^2}$$

where S is the area of the interface and the factor 2 stems from two spin projections. We introduce the angle φ in the p_x, p_y plane. In such a case, for the number of states we have

$$2Sp_\perp dp_\perp\frac{d\varphi}{(2\pi\hbar)^2}$$

where $p_\perp = \left(p_x^2 + p_y^2\right)^{1/2}$. But since $p_\perp^2 + p_z^2 = p_0^2$, it follows that $p_\perp \mathrm{d}p_\perp \to |p_z|\,\mathrm{d}p_z = p_0^2|\cos\theta|\mathrm{d}(\cos\theta)$. Thus, we find that the number of states per quantum number n in eq. (20.78) is

$$2Sp_0^2|\cos\theta|\mathrm{d}(\cos\theta)\frac{\mathrm{d}\varphi}{(2\pi\hbar)^2} = 2Sp_0^2|\cos\theta|\frac{\mathrm{d}\Omega}{(2\pi\hbar)^2} \tag{20.79}$$

where $\mathrm{d}\Omega$ is an element of the solid angle for the directions of the vector p.
For the free energy per unit volume of the normal layer we obtain (see eq. 10.11):

$$\Omega(T) = -\frac{T}{a}\sum_n \int\ \mathrm{d}\Omega 2p_0^2\frac{|\cos\theta|}{(2\pi h)^2}\ln\left[1+\exp\left(-\frac{\varepsilon(n,\theta)}{T}\right)\right].$$

Since ε depends only on $|\cos\theta|$, the integral $\int \mathrm{d}\Omega = \int_{-1}^{1}\mathrm{d}\cos\theta\int\ \mathrm{d}\varphi$ may be replaced by $4\pi\int_0^1\ \mathrm{d}\cos\theta$. Here we find

$$\Omega(T) = -\frac{2p_0^2T}{a\pi\hbar^2}\sum_n\int_0^1 x\ \mathrm{d}x\ln\left[1+\exp\left(-\frac{\varepsilon(n,x)}{T}\right)\right] \tag{20.80}$$

Further we consider two temperature regions. If $T > \hbar v/a$, the summation over n may be replaced by an integration. In this case, introducing the variable ε in place n, we have in accordance with (20.78):

$$\Omega(T) = -\frac{2p_0^2 T}{v\pi^2\hbar^3}\int_0^\infty \mathrm{d}\varepsilon \ln\left(1+\mathrm{e}^{-\varepsilon/T}\right)$$
$$= -\frac{p_0^2 T}{v\pi^2\hbar^3}\int_{-\infty}^\infty \mathrm{d}\varepsilon \ln\left(1+\mathrm{e}^{-|\varepsilon|/T}\right)$$

This is the usual expression for a normal metal. Evaluation of the integral gives

$$\Omega(T) = -\frac{1}{6}\frac{p_0^2}{v\pi^2\hbar^3}\pi^2 T^2$$

This yields the usual formula for the electronic heat capacity of a normal metal (see eq. 2.29):

$$C = -T\frac{\partial^2\Omega}{\partial T^2} = \frac{p_0 m}{3\hbar^3}T$$

But if $T < \hbar v/a$, the procedure is different. In the integral (20.79), instead of the variable x we introduce, using formula (20.78), the variable $y = \varepsilon/T$. So, we obtain

$$\Omega(T) = -\frac{2p_0^2T^3a}{\pi^3\hbar^4v^2}\sum_n \frac{1}{(n+\gamma)^2}\int_0^{\pi\hbar(n+\gamma)v/aT} y\ \mathrm{d}y \ln\left(1+\mathrm{e}^{-y}\right)$$

The limit of integration over y may be put equal to infinity because of the rapid convergence of the integral. The sum over n converges and gives a number of the order of unity, which we designate by α. On the whole, after taking the integral over y we obtain

$$\Omega(T) = -3\zeta(3)\frac{\alpha p_0^2 T^3 a}{2\pi^3\hbar^4 v^2}$$

from which we have

$$C = -T\frac{\partial^2\Omega}{\partial T^2} = \beta\frac{p_0^2T^2a}{\hbar^4v^2}$$

where

$$\beta = 9\frac{\zeta(3)}{\pi^3}\sum_n (n+\gamma)^{-2}$$

Taking into account that the fraction of normal layers is always equal to $x_n = B/H_{\mathrm{cm}}$ (the dependence of B on the external field being determined by the geometry of the experiment), we find for the heat capacity of the entire sample (Andreev 1965):

$$C = \begin{cases} \frac{p_0 mB}{3\hbar^3 H_{\mathrm{cm}}}T, & T > \frac{\hbar v}{a}, \\ \beta\frac{m^2aB}{\hbar^4 H_{\mathrm{cm}}}T^2, & T < \frac{\hbar v}{a}. \end{cases} \tag{20.81}$$

Experimental measurements of the heat capacity of superconductors in the intermediate state (Zavaritskii 1965) have confirmed formulae (20.81).

8.7 21 Superconductivity and magnetism

8.7.1 21.1. Superconductors containing magnetic impurities. Gapless superconductivity

As has been pointed out in section 16.9, impurities in a small concentration exert only a slight effect on the thermodynamic properties of superconductors. The variation of these

properties is of the relative order of $a/l \sim c_\mathrm{i}$, where a is the atomic dimension, l is the mean free path, and c_i the atomic concentration. The behavior of the magnetic impurities described in sections 4.6 and 13.7 is completely different. The action of these impurities is measured by the quantity ξ/l_s, where l_s is the mean free path relative to the spin flip associated with these impurities. The same may be written in the form $\hbar/(\tau_\mathrm{s}T_\mathrm{c})$, where $\tau_\mathrm{s} = l_\mathrm{s}/v$ is the corresponding mean free time. This is associated with the completely different action of ordinary nonmagnetic (potential) impurities and magnetic atoms on Cooper pairs.

Usually, impurities act only on the electric charge and, hence, scatter both electrons of a Cooper pair identically, and this does not lead to its collapse. As for magnetic impurities, they are capable of flipping the electron spin. Hence, upon scattering from such an impurity the pair can pass to a state with parallel spins (triplet state), where the Pauli principle requires that the electrons comprising the pair be not at a single point and be described by an antisymmetric coordinate wave function. The pair is thus broken up.

It has been shown in section 4.6 that to first order the probability of scattering of an electron from a magnetic impurity is proportional to $(J/n)^2 S(S+1)$. This quantity replaces $|V_{p'p}|^2$ in the probability of scattering from an ordinary impurity. In fact, the interaction of an electron with each impurity contains both the potential part (V) and the exchange part ($-(J/n)(\sigma S)$); the former is, as a rule, larger than the latter; however, in the effect of interest to us the potential part does not play a role and will be neglected here. The scattering time associated only with the exchange interaction will be denoted as τ_s.

The theory that provides an accurate description of the action of magnetic impurities (Abrikosov and Gor'kov 1960a) is based on the application of the methods of quantum field theory and it is too complicated to be described here. Therefore, we shall make an attempt to present the basic features of such objects with the aid of simple reasonings.

We begin with the critical temperature. The general formula for the dependence $\Delta(T)$ for pure superconductors is given in section 16.5 (formula 16.23). It may be rewritten in a different form by using the property of the hyperbolic tangent

$$\tanh\left(\frac{1}{2}\pi x\right) = \frac{4x}{\pi}\sum_{k=1}^{\infty}\frac{1}{(2k-1)^2+x^2} \tag{21.1}$$

On the basis of this formula we obtain from eq. (16.23):

$$1 = 2g\nu(\mu)T\sum_{\omega_k=\pi T}^{\hbar\omega_\mathrm{D}}\int_0^\infty \frac{\mathrm{d}\xi}{\omega_k^2+\xi^2+\Delta^2}, \tag{21.2}$$

where $\omega_k = \pi T(2k-1)$. Here we have transferred the summation in finite limits to ω_k, which will be convenient in what follows and, strictly speaking, is more correct than the limitation on ξ.

If the integrand is treated formally, it has imaginary poles at $\omega_k = \pm\mathrm{i}\left(\xi^2+\Delta^2\right)^{1/2} = \pm\mathrm{i}\varepsilon$. The possibility of the breakup of pairs under the action of magnetic impurities leads to a finite lifetime. This point has already been discussed in section 2.2. The wave function of the state $\exp(-\mathrm{i}\xi t/\hbar)$ takes on a damping factor $\exp(-\gamma t/\hbar)$. This may be interpreted as if the energy of quasiparticles acquires an imaginary correction $-\mathrm{i}\gamma$. In view of this, it becomes clear why in the exact theory ω_k is replaced by $\omega_k + \hbar\tau_\mathrm{s}^{-1}$ in expression (21.2). In fact, the new integrand has poles at points $\omega_k = \pm\mathrm{i}\left(\varepsilon \pm \mathrm{i}\hbar\tau_\mathrm{s}^{-1}\right)$.

In order to obtain $\boldsymbol{T}_\mathrm{c}$, we put $\boldsymbol{\Delta} = \mathbf{0}$. So, we have

$$1 = 2g\nu T\sum_{\omega_k=\pi T}^{\hbar\omega_0}\int_0^\infty \frac{\mathrm{d}\xi}{\left(\omega_k+\hbar\tau_\mathrm{s}^{-1}\right)^2+\xi^2}$$

The integral over $\boldsymbol{\xi}$ gives

$$1 = g\nu\pi T \sum_{\omega_k=\pi T}^{\hbar\omega_\mathrm{D}} \frac{1}{\omega_k + \hbar\tau_\mathrm{s}^{-1}} = g\nu \sum_{k=1}^{\hbar\omega_\mathrm{D}/2\pi T} \frac{1}{2k-1+\rho},$$

where we have substituted $\omega_k = \pi T(2k-1)$ and introduced the dimensionless parameter $\rho = \hbar/(\tau_\mathrm{s}\pi T)$.

We subtract and add to the last sum a similar sum with $\rho = 0$. The difference rapidly converges, and therefore the limit of the sum over k may be extended to infinity. Substituting the value of the sum of $(2k-1)^{-1}$, we have

$$\begin{aligned} 1 =& \frac{1}{2} g\nu \ln\left(\frac{2\gamma\omega_\mathrm{D}\hbar}{\pi T_\mathrm{c}}\right) \\ &+ g\nu \sum_{k=1}^{\infty} \left(\frac{1}{2k-1+\rho} - \frac{1}{2k-1}\right), \quad \gamma = 1.78 \end{aligned}$$

Let us use the following property of the Γ-functions:

$$\psi(x) - \psi(y) = \sum_{k=0}^{\infty} \left(\frac{1}{y+k} - \frac{1}{x+k}\right), \tag{21.3}$$

where $\psi(x) = \Gamma'(x)/\Gamma(x)$ is the logarithmic derivative of the Γ-function; the latter is determined as follows: $\Gamma(n) = (n-1)\,!$ for integer values of $x = n$, and for noninteger values we have

$$\Gamma(x) = \int_0^\infty \mathrm{e}^{-t} t^{x-1}\, \mathrm{d}t \tag{21.4}$$

Dividing by $\frac{1}{2}g\nu$, rearranging the terms and using formula (16.25), we obtain

$$\ln\left(\frac{T_{\mathrm{c}0}}{T_\mathrm{c}}\right) = \psi\left(\frac{1}{2} + \frac{1}{2}\rho\right) - \psi\left(\frac{1}{2}\right), \tag{21.5}$$

where $T_{\mathrm{c}0}$ is the critical temperature of a pure superconductor. This formula is exact and holds for any $\rho = \hbar/(\pi T_\mathrm{c}\tau_\mathrm{s})$. As for τ_s itself, from the foregoing it is clear that τ_s^{-1} is proportional to $\pi\nu(\mu)(J/n)^2 S(S+1)n_\mathrm{m}$ and the exact value of the quantity appearing in eq. (21.5) is

$$\frac{\hbar}{\tau_\mathrm{s}^{-1}} = \frac{7}{24}\pi\nu(\mu)\frac{J}{n}S(S+1)n_\mathrm{m}, \tag{21.6}$$

where n_m is the concentration of magnetic atoms.

Let us now consider the asymptotic values of formula (21.5). At $\rho < 1$ we use the following expansion:

$$\psi\left(\frac{1}{2} + \frac{1}{2}\rho\right) \approx \psi\left(\frac{1}{2}\right) + \frac{1}{2}\psi'\left(\frac{1}{2}\right)\rho = \psi\left(\frac{1}{2}\right) + \frac{1}{4}\pi^2\rho.$$

Expanding $\ln(T_{\mathrm{c}0}/T_\mathrm{c}) \approx (T_{\mathrm{c}0} - T_\mathrm{c})/T_{\mathrm{c}0}$, we obtain

$$T_\mathrm{c} \approx T_{\mathrm{c}0} - \frac{\pi\hbar}{4\tau_\mathrm{s}}. \tag{21.7}$$

From this we see that, in contrast to ordinary impurities, magnetic impurities lower T_c significantly.

Obviously, at $\hbar\tau_s^{-1} \sim T_{c0}$ the superconductivity must disappear altogether, i.e., T_c must vanish. In the vicinity of this point in formula (21.5) $\rho \gg 1$. Consider the corresponding asymptotics. At large x

$$\psi(x) \approx \ln x - \frac{1}{2x} - \frac{1}{12x^2}$$

and $\psi\left(\frac{1}{2}\right) = -\ln(4\gamma)$. Expanding in ρ^{-1}, we have

$$\ln\left(\frac{T_{co}\pi\tau_s}{2\gamma\hbar}\right) \approx \frac{1}{6}\left(\frac{\pi T_c\tau_s}{\hbar}\right)^2. \tag{21.8}$$

From this it follows that the critical concentration at which $T_c = 0$ corresponds to

$$\frac{\hbar}{\tau_{sc}^{-1}} = \frac{\pi T_{co}}{2\gamma}. \tag{21.9}$$

In the vicinity of the critical concentration the critical temperature is given by

$$T_c \approx \sqrt{6}\frac{\hbar}{\pi}\frac{(\tau_s - \tau_{sc})^{1/2}}{\tau_{sc}^{3/2}} \tag{21.10}$$

A further fundamental consequence of the presence of magnetic impurities is gapless superconductivity. The point is that magnetic impurities not only reduce the binding energy of Cooper pairs but, as exact calculations show (Abrikosov and Gor'kov 1960a), the result is that not all pairs have the same binding energy. In this sense, the situation is similar to a weakly nonideal Bose gas (see, for example, Abrikosov et al. 1962). Whereas in an ideal Bose gas at $T = 0$ all the particles are present in the condensate, i.e., have $\boldsymbol{p}$ and ε equal to zero and are described by a coherent wave function $\Psi = \text{const.}$, in a nonideal gas at $T = 0$ only a certain part of the particles are present in the condensate, and the remaining particles have an energy and momentum different from zero. However, in this case too the order parameter is the coherent wave function of the condensate particle.

In superconductors containing magnetic impurities the situation is the same. The Bose condensate of Cooper pairs does not contain all the pairs: some of these have smaller binding energies. Evidently, for such pairs to be broken up it is necessary to consume a smaller energy than that required for the collapse of the pairs present in the condensate. Up until now the quantity Δ alone has described both the number of pairs in the condensate and the binding energy. However, in application to superconductors with magnetic impurities this statement becomes invalid. Whereas one quantity described the order parameter (we still denote it as Δ), i.e., the wave function of the condensate, a completely different quantity characterizes the minimum binding energy of the pairs or the energy gap, which manifests itself in the low-temperature heat capacity, thermal conductivity, absorption of electromagnetic radiation and ultrasound, etc.

It is exactly the order parameter that determines the basic specific features of superconductors: the Meissner effect and the absence of electrical resistance. As long as Δ is finite all these properties are operative. At the same time, the energy gap may vanish; this is actually observed in superconductors containing magnetic impurities in a given concentration range (n_{mc} corresponds to τ_{sc} according to formulas 21.9 and 21.6):

$$0.91 n_{mc} < n_m < n_{mc}.$$

A natural question may arise: How does this agree with the Landau criterion? According to this criterion superconductivity is impossible in the absence of a gap in the energy spectrum. However, the Landau criterion has been deduced for pure systems, in which spatial homogeneity

exists and the momentum is conserved. For systems containing impurities this criterion cannot be applied.

We give here, without derivation, the formula for the energy gap,

$$\hbar\omega_0 = \left[\Delta_0^{2/3} - \left(\frac{\hbar}{\tau_\mathrm{s}}\right)^{2/3}\right]^{3/2} \tag{21.11}$$

In the vicinity of the critical concentration the critical temperature is given by

$$T_\mathrm{c} \approx \sqrt{6}\frac{\hbar}{\pi}\frac{(\tau_\mathrm{s} - \tau_\mathrm{sc})^{1/2}}{\tau_\mathrm{sc}^{3/2}}. \tag{21.10}$$

A further fundamental consequence of the presence of magnetic impurities is gapless superconductivity. The point is that magnetic impurities not only reduce the binding energy of Cooper pairs but, as exact calculations show (Abrikosov and Gor'kov 1960a), the result is that not all pairs have the same binding energy. In this sense, the situation is similar to a weakly nonideal Bose gas (see, for example, Abrikosov et al. 1962). Whereas in an ideal Bose gas at $T = 0$ all the particles are present in the condensate, i.e., have $\boldsymbol{p}$ and ε equal to zero and are described by a coherent wave function $\Psi = \mathrm{const.}$, in a nonideal gas at $T = 0$ only a certain part of the particles are present in the condensate, and the remaining particles have an energy and momentum different from zero. However, in this case too the order parameter is the coherent wave function of the condensate particle.

In superconductors containing magnetic impurities the situation is the same. The Bose condensate of Cooper pairs does not contain all the pairs: some of these have smaller binding energies. Evidently, for such pairs to be broken up it is necessary to consume a smaller energy than that required for the collapse of the pairs present in the condensate. Up until now the quantity Δ alone has described both the number of pairs in the condensate and the binding energy. However, in application to superconductors with magnetic impurities this statement becomes invalid. Whereas one quantity described the order parameter (we still denote it as Δ), i.e., the wave function of the condensate, a completely different quantity characterizes the minimum binding energy of the pairs or the energy gap, which manifests itself in the low-temperature heat capacity, thermal conductivity, absorption of electromagnetic radiation and ultrasound, etc.

It is exactly the order parameter that determines the basic specific features of superconductors: the Meissner effect and the absence of electrical resistance. As long as Δ is finite all these properties are operative. At the same time, the energy gap may vanish; this is actually observed in superconductors containing magnetic impurities in a given concentration range (n_mc corresponds to τ_sc according to formulas 21.9 and 21.6):

$$0.91 n_\mathrm{mc} < n_\mathrm{m} < n_\mathrm{mc}.$$

A natural question may arise: How does this agree with the Landau criterion? According to this criterion superconductivity is impossible in the absence of a gap in the energy spectrum. However, the Landau criterion has been deduced for pure systems, in which spatial homogeneity exists and the momentum is conserved. For systems containing impurities this criterion cannot be applied.

We give here, without derivation, the formula for the energy gap,

$$\hbar\omega_0 = \left[\Delta_0^{2/3} - \left(\frac{\hbar}{\tau_\mathrm{s}}\right)^{2/3}\right]^{3/2} \tag{21.11}$$

and the formula for the electronic heat capacity in the gapless region:

$$C = \frac{1}{3}\pi^2\nu(\mu)\left[1 - \left(\frac{\tau_s\Delta_0}{\hbar}\right)^2\right]^{1/2} T, \tag{21.12}$$

where Δ_0 is the order parameter at $T = 0$, which depends in a complicated way on τ_s. At the boundary of the gapless region $\Delta_0(\tau_s) = \hbar/\tau_s$.

The disappearance of the gap can conveniently be traced out from the density of states. For a normal metal $\nu_n = p_0 m/(\pi^2\hbar^3) = \text{const}$. For a pure superconductor

$$\nu(\varepsilon) = \frac{1}{\pi^2\hbar^3} p_0 m \frac{d\xi}{d\varepsilon} = \nu_n \varepsilon \left(\varepsilon^2 - \Delta^2\right)^{-1/2}$$

at $\varepsilon > \Delta$ and 0 at $\varepsilon < \Delta$. Note that $\nu(\varepsilon)$ has a square root singularity for $\varepsilon \to \Delta$. The density of states $\nu(\varepsilon)$ is given in fig. 137 at various values of τ_s. The ordinate represents $\nu(\varepsilon)/\nu_n$ and the abscissa represents $\varepsilon/\Delta_0(\tau_s)$. The curves are labeled with the corresponding values of

$$\hbar/\tau_s\Delta_0.$$

It should be noted that magnetic impurities do not provide the only pair-breaking mechanism. It was later found that the same effect is exhibited by any perturbations giving rise to terms in the Hamiltonian that are noninvariant under change of the sign of time (see Maki 1969).

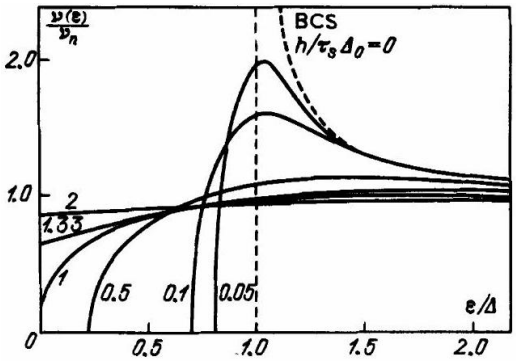


Fig. 137.

Cooper pairs constitute a superposition of the states of electrons with opposite momenta and spins. These states result from one another by inversion of the sign of time (the momentum and spin change sign with $t \to -t$). A perturbation which is noninvariant under the change of the sign of time acts differently on the electrons contained in a Cooper pair and, as it were, pulls it apart.

An example is an external magnetic field. Of course, the field does not penetrate a bulk superconductor, and therefore we assume that we are dealing here with a
thin film with a thickness smaller than δ and ξ. The main perturbation from the magnetic field is $-(e/mc)pA$. The wave function of the electron is proportional to $\exp(-i\varepsilon t/\hbar)$. From this we see that in the presence of a magnetic field between the electrons that form a pair, i.e., have momenta p and $-p$, there arises a phase difference, which varies with time according to the law

$$\frac{d\theta}{dt} = \frac{2e}{\hbar c} vA, \qquad \text{with} \qquad v = p_0/m. \tag{21.13}$$

However, the electrons are scattered by impurities or at the boundaries of the sample. Therefore, they execute a Brownian diffusive motion with, according to sections 3.5 and 5.5,

$$\overline{x^2} \sim Dt \sim lvt \sim v^2 t\tau_{\rm tr},$$

where $D \sim lv \sim v^2\tau_{\rm tr}$ is the diffusion coefficient. This relation may be extended to any quantity: the mean square of the sought-for quantity is of the order of the square of the instantaneous rate of its change multiplied by $t\tau_{\rm tr}$. In our case,

$$\overline{\theta^2} \sim \left(\frac{{\rm d}\theta}{{\rm d}t}\right)^2 t\tau_{\rm tr}.$$

Hence, for θ to be of the order of 2π, a time τ_H is needed, with

$$\frac{1}{\tau_{\rm H}} \sim \left(\frac{{\rm d}\theta}{{\rm d}t}\right)^2 \tau_{\rm tr},$$

where $({\rm d}\theta/{\rm d}t)^2$ is the mean square value of eq. (21.13). Thus, we have ($A \sim Hd$)

$$\frac{1}{\tau_{\rm H}} \sim v^2\tau_{\rm tr}\left(\frac{e}{\hbar c}\right)^2 H^2 d^2 \sim D\left(\frac{e}{\hbar c}\right)^2 H^2 d^2. \tag{21.14}$$

Other examples could also be given, namely the mixed state in a bulk type II superconductor and in a film in a perpendicular magnetic field, small particles, etc. It can be shown (see Maki 1969) that all the formulas derived for magnetic impurities remain to be valid for all pair-breaking mechanisms. Only the physical meaning of the constant ρ is changed.

8.7.2 21.2. The inhomogeneous superconducting state

In the preceding section we have said that magnetic impurities destroy superconductivity. The situation is even worse in a case where there is ferromagnetic ordering. In such a case, the number of electrons with different orientations of the spin is different, which means that the corresponding Fermi surfaces are also different. If ferromagnetism is strong, i.e., the Curie temperature is of the order of hundreds of degrees, as is the case with ordinary ferromagnets based on transition metals, superconductivity is impossible.

However, with rare-earth metals or actinides the situation may be different. The magnetism of such atoms is associated with the unfilled 4 f and 5 f shells. These are inner shells with a small radius. In neighboring atoms they practically do not overlap. In view of this, the exchange interaction of the spins is realized by way of an indirect exchange through conduction electrons. In other words, one may proceed from the picture of localized spins which interact with conduction electrons by the mechanism discussed in section 4.1.

In the next section we shall consider in more detail the interaction between two localized spins, which is transmitted by conduction electrons (RKKY). Of importance at this point is only the circumstance that the resultant magnetism is "weak" with a Curie temperature of the order of a few degrees. It is for this reason that the question arises as to the mutual effect of ferromagnetism and superconductivity.

Two extreme situations may be encountered. If the Curie temperature of the ferromagnetic transition θ is somewhat higher than the critical temperature of the superconducting transition $T_{\rm c}$ (not much higher), superconductivity may arise against the background of existing ferromagnetism. But if the temperature of the superconducting transition is higher than the Curie temperature, ferromagnetism arises against the background of superconductivity. It is possible that the phases that will be considered in this and subsequent sections do not cover the entire variety of existing possibilities, but they give an idea of the specific features of the mutual effect of such antagonistic phenomena, as ferromagnetism and superconductivity.

We begin with the case where superconductivity appears against the background of ferromagnetism. Instead of eq. (16.13), we write the Hamiltonian

$$\mathscr{H} - \mu N = \sum_{p,\sigma} (\xi_p - \sigma_z I)\, a^+_{p,\sigma} a_{p,\sigma} - g \sum a^+_{p'_1,+} a^+_{p'_2,-} - a_{p_2,-} a_{p_1,+}, \tag{21.15}$$

where I is the self-consistent "molecular field", under the action of which the electron energy begins to depend on the projection spins ($\sigma_z = \pm 1$). Further, we introduce the operators $\alpha_{p,+}$ and $\alpha_{p,-}$ in accordance with formulas (16.14) and repeat the entire derivation given in section 16.4 taking account of the altered Hamiltonian. In such a case we obtain the same formulas for the coefficients u and v and formula (16.21) for Δ, but the energies included in the Fermi distributions $n_{p,+}$ and $n_{p,-}$ have the form

$$\varepsilon_{p,+} = \varepsilon_p - I, \quad \varepsilon_{p,-} = \varepsilon_p + I,$$

as before,

$$\varepsilon_p = \left(\xi_p^2 + \Delta^2\right)^{1/2}.$$

Let us consider only the case $T = 0$. Since $\varepsilon_p > 0$, it follows that $n_{p,-} = 0$. Therefore, the sum over p in (16.21) is bounded from below by the condition $\varepsilon_{p,+} > 0$ or $\varepsilon_p > I$. Two cases are possible. If $\Delta > I$, the condition $\varepsilon_{p,+} > I$ does not impose restrictions on the domain of integration over p and we obtain $\Delta = \Delta_0$. But if $\Delta < I$, then, passing
to the integral, we have

$$\frac{2}{g\nu} = \ln \frac{2\hbar\omega_{\mathrm{D}}}{\Delta_0} = \int_{(I^2-\Delta^2)^{1/2}}^{\hbar\omega_{\mathrm{D}}} \frac{\mathrm{d}\xi}{\varepsilon} = \ln \frac{2\hbar\omega_{\mathrm{D}}}{I + (I^2 - \Delta^2)^{1/2}}. \tag{21.16}$$

From this we see that $I + (I^2 - \Delta^2)^{1/2} = \Delta_0$ or

$$\Delta = \left[\Delta_0 (2I - \Delta_0)\right]^{1/2}. \tag{21.17}$$

Thus, we obtain two branches of the solution of eq. (21.16), which are shown in fig. 138. However, the nonzero solution for Δ implies only the local minimum of the free energy; this may correspond to a metastable rather than to the equilibrium state. In order to find out whether the transition to the superconducting state really occurs, we must find the free-energy difference $\Omega_{\mathrm{s}} - \Omega_{\mathrm{n}}$. For this purpose we use formula (16.38).

In the region where $\Delta_1 > I$ we have, as before,

$$\frac{\partial g^{-1}(\Delta_1)}{\partial \Delta_1} = -\frac{\nu}{2\Delta_1}. \tag{21.18}$$

In the region where $\Delta_1 < I$ we obtain from (21.16)

$$\begin{aligned} \frac{\partial g^{-1}(\Delta_1)}{\partial \Delta_1} &= \frac{1}{2}\nu \frac{\Delta_1}{I + (I^2 - \Delta_1^2)^{1/2}} \frac{1}{(I^2 - \Delta_1^2)^{1/2}} \\ &= \frac{\nu}{2\Delta_1} \frac{\left[I - (I^2 - \Delta_1^2)^{1/2}\right]}{(I^2 - \Delta_1^2)^{1/2}} \end{aligned} \tag{21.19}$$

On the lower branch of fig. 138, formula (21.19) holds for all Δ_1; substituting it into (16.38), we find

$$\begin{aligned} \Omega_{\mathrm{s}} - \Omega_{\mathrm{n}} &= \frac{1}{4}\nu \left[I - \left(I^2 - \Delta^2\right)^{1/2}\right]^2 \\ &= \frac{1}{4}\nu (2I - \Delta_0)^2 \end{aligned} \tag{21.20}$$

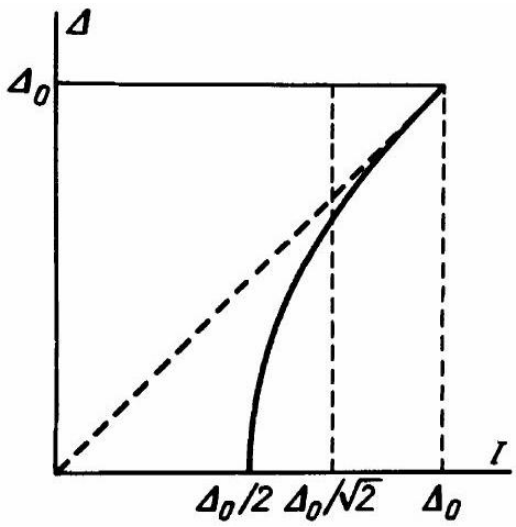


Fig. 138.

to the integral, we have

$$\frac{2}{g\nu} = \ln\frac{2\hbar\omega_{\mathrm{D}}}{\Delta_0} = \int_{(I^2-\Delta^2)^{1/2}}^{\hbar\omega_{\mathrm{D}}} \frac{\mathrm{d}\xi}{\varepsilon} = \ln\frac{2\hbar\omega_{\mathrm{D}}}{I+(I^2-\Delta^2)^{1/2}}. \tag{21.16}$$

From this we see that $I + (I^2 - \Delta^2)^{1/2} = \Delta_0$ or

$$\Delta = \left[\Delta_0\,(2I - \Delta_0)\right]^{1/2}. \tag{21.17}$$

Thus, we obtain two branches of the solution of eq. (21.16), which are shown in fig. 138. However, the nonzero solution for Δ implies only the local minimum of the free energy; this may correspond to a metastable rather than to the equilibrium state. In order to find out whether the transition to the superconducting state really occurs, we must find the free-energy difference $\Omega_{\mathrm{s}} - \Omega_{\mathrm{n}}$. For this purpose we use formula (16.38).

In the region where $\Delta_1 > I$ we have, as before,

$$\frac{\partial g^{-1}(\Delta_1)}{\partial\Delta_1} = -\frac{\nu}{2\Delta_1}. \tag{21.18}$$

In the region where $\Delta_1 < I$ we obtain from (21.16)

$$\begin{aligned}\frac{\partial g^{-1}(\Delta_1)}{\partial\Delta_1} &= \frac{1}{2}\nu\frac{\Delta_1}{I+(I^2-\Delta_1^2)^{1/2}}\frac{1}{(I^2-\Delta_1^2)^{1/2}}\\ &= \frac{\nu}{2\Delta_1}\frac{\left[I-(I^2-\Delta_1^2)^{1/2}\right]}{(I^2-\Delta_1^2)^{1/2}}\end{aligned} \tag{21.19}$$

On the lower branch of fig. 138, formula (21.19) holds for all Δ_1; substituting it into (16.38), we find

$$\begin{aligned}\Omega_{\mathrm{s}} - \Omega_{\mathrm{n}} &= \frac{1}{4}\nu\left[I - \left(I^2-\Delta^2\right)^{1/2}\right]^2\\ &= \frac{1}{4}\nu\,(2I-\Delta_0)^2,\end{aligned} \tag{21.20}$$

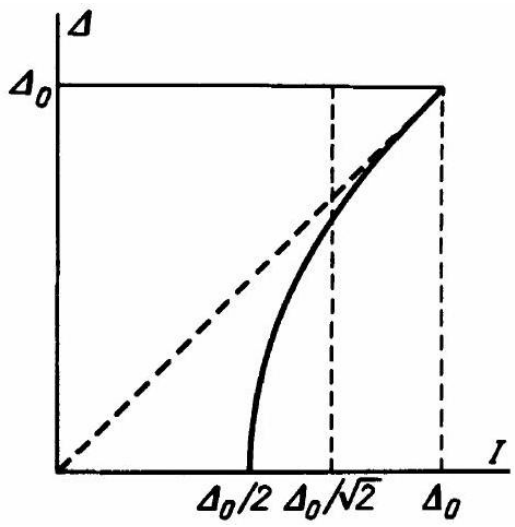


Fig. 138.

where we have substituted (21.17) and have taken into account that $I < \Delta_0$. So, in this case $\Omega_s - \Omega_n > 0$, i.e., the superconducting transition does not occur.

On the upper branch of fig. 132, $\Delta = \Delta_0 > I$. Therefore, there are two domains of integration: $\Delta_1 < I$ and $\Delta_1 > I$. Inserting formulas (21.18) and (21.19) into (16.38), we obtain

$$\Omega_s - \Omega_n = \frac{1}{4}\nu\left(2I^2 - \Delta_0^2\right), \tag{21.21}$$

from which follows that the upper branch in fig. 138, i.e. $\Delta = \Delta_0$, corresponds to equilibrium superconductivity at

$$I < \frac{\Delta_0}{\sqrt{2}} = 0.707\Delta_0. \tag{21.22}$$

Thus, in the model under discussion, as I increases at the point $I = \Delta_0/\sqrt{2}$ a first-order phase transition occurs from the superconducting phase with $\Delta = \Delta_0$ to the normal phase with $\Delta = 0$. The remaining portions of the solid curves in fig. 138 correspond to the metastable phases.

However, a more detailed investigation shows that the real situation is more complicated. In the preceding treatment we were concerned only with the possibility of the appearance of superconductivity with $\Delta = \text{const}$. It turns out that at values of I larger than the critical value (21.22) there may appear a superconducting phase with an inhomogeneous order parameter $\Delta(r)$ by way of a second-order phase transition (Larkin and Ovchinnikov 1964, Fulde and Ferrell 1964). This new phase is sometimes called the LOFF phase.

In order to demonstrate this transition, we make use of the fact that near the transition point, Δ is small and the equation for Δ will necessarily be linear. This will permit us to use a Fourier expansion and raise the question of the generation of a single Fourier harmonic, i.e.

$$\Delta(r) = \Delta \exp(\mathrm{i}qr/\hbar). \tag{21.23}$$

If we recall that $\Delta(r)$ plays the role of the coherent wave function of the condensate of Cooper pairs, then formula (21.23) corresponds to the moving condensate, in which the pairs have a momentum $\boldsymbol{q}$, i.e., the velocity $\boldsymbol{v}_s = \boldsymbol{q}/2\boldsymbol{m}$.

The problem of the moving condensate has been considered in section 19.2. We substitute formulae (19.19)-(19.21) into the equation for Δ derived in section 19.2, following which we make the transformation of the momentum variable $p \to p + \frac{1}{2}q$ and use formulas (19.24).

Taking into account that for quasiparticles with spin $+\frac{1}{2}$ the energy contains a term with $-I$, and in the opposite case a term with $+I$, we finally obtain

$$1 = \frac{1}{2} g \sum_p \frac{1 - n_+ - n_-}{\varepsilon}, \tag{21.24}$$

where $n_+$and $n_-$are the equilibrium Fermi functions with energies given by

$$\varepsilon_+ = \varepsilon + \frac{1}{2} vqx - I, \quad \varepsilon_- = \varepsilon - \frac{1}{2} vqx + I, \tag{21.25}$$

where $\varepsilon = (\xi^2 + \Delta^2)^{1/2}$ and $x = \cos(p, q)$. We assumed that $vq > 2I$ (this is confirmed by subsequent calculations). Since we are interested in the transition region, we assume that $\Delta < I$. Just as before, we set $T = 0$.

The integral on the right-hand side of eq. (21.24) is different from zero if $n_+ = n_- = 1$, i.e. $\varepsilon_+, \varepsilon_- < 0$, or $n_+ = n_- = 0$, i.e., $\varepsilon_+, \varepsilon_- > 0$; the latter condition, which gives $2(I + \varepsilon)/vq > x > 2(I - \varepsilon)/vq$, is realized. Taking into account that x varies in the region $-1 \leqslant x \leqslant 1$, and $0 < |\xi| \leqslant \hbar\omega_D$, we obtain from (21.24):

$$\begin{aligned}
\frac{2}{g\nu} &= \ln \frac{2\hbar\omega_{\mathrm{D}}}{\Delta_0} + \frac{1}{2} \ln \frac{2\hbar\omega_{\mathrm{D}}}{\frac{1}{2}vq - I + \left[\left(\frac{1}{2}vq - I\right)^2 - \Delta^2\right]^{1/2}} \\
&+ \frac{1}{2} \ln \frac{2\hbar\omega_{\mathrm{D}}}{\frac{1}{2}vq + I + \left[\left(\frac{1}{2}vq + I\right)^2 - \Delta^2\right]^{1/2}} \\
&- \frac{I}{vq} \ln \frac{1}{\frac{1}{2}vq + I + \left[\left(\frac{1}{2}vq + I\right)^2 - \Delta^2\right]^{1/2}} \\
&+ \frac{1}{vq} \left\{ \left[\left(\frac{1}{2}vq - I\right)^2 - \Delta^2\right]^{1/2} + \left[\left(\frac{1}{2}vq - I\right)^2 - \Delta^2\right]^{1/2} \right\}
\end{aligned} \tag{21.26}$$

Transposing terms and introducing new variables $z = I/\Delta_0, y = vq/2I$ and $s = \Delta/I$, we see that

$$\begin{aligned}
\ln(1/z) = &\Big\{ (y-1) \ln \left[y - 1 + \left((y-1)^2 - s^2\right)^{1/2} \right] \\
&+ (y+1) \ln \left[y + 1 + \left((y+1)^2 - s^2\right)^{1/2} \right] \Big\} (2y)^{-1} \\
&+ \left\{ \left((y-1)^2 - s^2\right)^{1/2} + \left((y+1)^2 - s^2\right)^{1/2} \right\} (2y)^{-1}
\end{aligned} \tag{21.27}$$

At the transition point $s = 0$, so we have

$$\ln(1/z) + 1 - \ln 2 = [(y-1)\ln(y-1) + (y+1)\ln(y+1)](2y)^{-1}. \tag{21.28}$$

The right-hand side has the asymptotics of $\ln y$ with $y \to \infty$ and $-(y-1)\ln[1/(y-1)]$ with $y \to 1$. From this it can be seen that at a certain y it has a minimum. Evidently, it has a corresponding maximum value of $z = I/\Delta_0$ at which $\Delta \neq 0$ appears for the first time. If the minimum of the right-hand side is found numerically, we obtain $y_{\mathrm{c}} = 1.19$ and $z_{\mathrm{c}} = 0.754$. Thus, it turns out that $\Delta \neq 0$ appears for the first time at

$$I_c = 0.754\Delta_0, \tag{21.29}$$

$$(vq)_c = 2.38 I_c. \tag{21.30}$$

The quantity $\boldsymbol{I_c}$ is larger than the values obtained earlier, (eq. 21.22), for an immobile condensate at rest (i.e. $\Delta(r) = \text{const.}$).

Now we have to check whether the appearance of a finite Δ corresponds to a decrease in free energy. Here, however, we should make a remark. When we were concerned with the problem of solving the equation for Δ in the limit $\Delta \to 0$, we could use the linearity of this equation and consider a single Fourier harmonic. We found out that a harmonic with a definite $q_c = 2.38 I/v$ appears for the first time.

But the isotropy and linearity of the problem implies that any linear combination of harmonics with different q equal in magnitude to q_c may also appear equally well.

The question of the choice of a particular combination is solved by comparing their free energies, where Δ is expressed as a function of $I_c - I$. However, this requires the solution of a nonlinear problem, for which the method used here is inapplicable. Of course, we can generalize the Bogoliubov transformation, just as has been done in the literature (De Gennes 1966). However, we shall not give the cumbersome calculations here; we shall only show that even in the simplest case of a single Fourier harmonic, which has been considered above, the free energy decreases as a result of superconducting pairing. We also note that a detailed analysis of the problem of the most favorable structure of $\Delta(r)$ has not yet been carried out, which to a certain extent is accounted for by the lack of experimental observations of the LOFF phase.

Thus, we are to find the free energy. Using formula (21.26), we obtain

$$\begin{aligned} \frac{\partial g^{-1}}{\partial \Delta} = \frac{\nu}{2\Delta} \Bigg\{ -1 + \frac{1}{vq} \left[\left(\tfrac{1}{2} vq - I \right)^2 - \Delta^2 \right]^{1/2} \\ + \frac{1}{vq} \left[\left(\tfrac{1}{2} vq + I \right)^2 - \Delta^2 \right]^{1/2} \Bigg\}. \end{aligned} \tag{21.31}$$

Expanding in Δ and substituting into (16.38) lead to

$$\Omega_s - \Omega_n = -\frac{\omega \Delta^4}{16 I_c^2 \left(y_c^2 - 1 \right)}. \tag{21.32}$$

In order to express Δ in terms of $I_c - I$, we expand eq. (21.27) in $s = \Delta / I$. The result is

$$\frac{I_c - I}{I_c} = \frac{1}{4 \left(y_c^2 - 1 \right)} \left(\frac{\Delta}{I_c} \right)^2.$$

Substituting $y_c = 1.19$, we find

$$\Delta \approx 1.3 \left[\left(I_c - I \right) I_c \right]^{1/2}. \tag{21.33}$$

Using this value and $I_c = 0.754\Delta_0$, we obtain

$$\Omega_s - \Omega_n = -0.42 \nu \left(I_c - I \right)^2. \tag{21.34}$$

Thus, as a result of the formation of an inhomogeneous superconducting condensate, the free energy is really lowered.

As has been said above, the structure considered is only the simplest example. As a matter of fact, one should expect the generation of a three-dimensional structure (for example, with a set of $\boldsymbol{q}$ directed along the principal axes of the tetrahedron) with periods of the order of $\hbar v / \Delta_0 \sim \xi(0)$. The possibility is not excluded that in such a case $\Delta(r) = 0$ at certain points, i.e.,

the superconductivity will appear to be gapless. This will lead to a non-exponential temperature dependence of the heat capacity. For instance, $C \propto \ln^{-3}(\Delta/T)$ for $\Delta(r) \propto \cos(qr/\hbar)$ (Larkin and Ovchinnikov 1964).

Since under actual conditions it is difficult to avoid the generation of structural defects, the question arises as to the stability of the inhomogeneous superconducting phase towards defects. Analysis shows (Aslamazov and Larkin 1968) that, in principle, the LOFF phase persists in the presence of any defect concentration, i.e., the free energy decreases with the appearance of $\Delta(r)$. However, the corresponding value of I_c decreases with defect concentration, and at a concentration corresponding to the mean free path $l < \xi(0), I_c$ becomes less than the value determined by formula (21.22). Here the equilibrium phase will be the homogeneous superconducting phase with $\Delta = \Delta_0$; it is formed by way of a transition of first order in I. The quantity I_c in this case plays the role of the supercooling limit for the normal phase. When I_c further decreases, the inhomogeneous superconductivity of the LOFF phase may appear as a metastable phase.

The LOFF phase has so far not been observed experimentally and it would be rather difficult to create the necessary conditions (see section 21.3).

8.7.3 21.3. Ferromagnetic superconductors

Let us now consider another possibility, namely the case $\theta < T_c$ (θ is the Curie temperature), where ferromagnetism appears against the background of superconductivity (see the review article by Bulaevskii et al. 1985). This situation occurs, for example, in the compounds $HoMo_6\ S_8$ and $ErRh_4\ B_4$. In compounds of this type, as the temperature decreases a superconducting transition occurs first (at temperature T_{c1}).

As the temperature decreases further, a magnetic transition arises against the superconductivity background, which leads to a very peculiar lamellar or domain magnetic structure, in which the magnetization in neighboring layers has an opposite direction (temperature T_M). Since the superconducting current screens off the magnetic field, this magnetic structure can be recognized only with the aid of neutron diffraction. Neutrons, which have a magnetic moment, "feel" the magnetic structure and are diffracted on it, just as light on a diffraction grid or X-radiation in a crystal.

Finally, when the temperature continues to decrease, a first-order phase transition to a non-superconducting ferromagnetic state (temperature T_{c2}) occurs. The values of these temperatures are $T_{c1} = 1.8$ K, $T_M = 0.7$ K, $T_{c2} = 0.65$ K for $HoMo_6\ S_8$; $T_{c1} = 8.7$ K, $T_M = 0.8$ K, $T_{c2} = 0.75$ K for $ErRh_4\ B_4$. In order to understand the sequence of these transitions, let us examine, first of all, the mechanism of an indirect exchange interaction of spins via conduction electrons.

We begin with the Hamiltonian of the interaction of spins with conduction electrons (eq. 4.39), which is written in terms of the operators a and a^+:

$$\mathscr{H}_{eS} = -\frac{J}{n} \sum_{\substack{p,p' \\ \sigma,\sigma'}} a^+_{p',\sigma'}, \sigma_{\sigma',\sigma} a_{p,\sigma} \exp\left[\frac{i}{\hbar}(p - p')\, r_i\right] S_i, \tag{21.35}$$

where σ are the Pauli matrices; S_i are the spin operators of magnetic atoms*; σ, σ' are the projections of the electron spin; r_i are the positions of the atoms.

Expression (21.35) describes the interaction of an electron with spins, in which the electron's momentum is $\boldsymbol{p}$ in the initial state and $\boldsymbol{p}'$ in the final state, σ and σ' being the initial and final spin projections, respectively.

As for the factor that depends on $\boldsymbol{r}_i$, the replacement of the sum over $\boldsymbol{r}_i$ by an integral over the volume would have led to the appearance of the Fourier component of the function $\boldsymbol{S}(\boldsymbol{r})$. In this case, the resultant expression obtained would be analogous to the Hamiltonian (16.60),

which describes the interaction of electrons with an electromagnetic field. It may be treated as the change of the momentum and spin of the electron upon absorption of a quantum of the external field. The presence of the sum over r_i in (21.35) takes into account the discreteness in the position of the spins.

Let us first consider a nonsuperconducting metal. Taking the second order of perturbation theory and separating in it the terms with $\boldsymbol{r}_i \neq \boldsymbol{r}_k$, which describe the interaction of the spins, we obtain

$$\begin{aligned} E_{\mathrm{SS}} =& \sum_{m\neq 0} \frac{\left|\left(\mathscr{H}_{\mathrm{eS}}\right)_{m0}\right|^2}{E_0 - E_m} \\ =& \left(\frac{J}{n}\right)^2 \sum_{\substack{p,p';\sigma,\sigma' \\ i\neq k}} \frac{n_p\left(1-n_{p'}\right)}{\xi_p - \xi_{p'}} \\ & \times \exp\left(\frac{\mathrm{i}}{\hbar}\left(p-p'\right)\left(r_i - r_k\right)\right) \sigma^l_{\sigma',\sigma}\sigma^m_{\sigma,\sigma'} S^l_i S^m_k \\ =& 2\left(\frac{J}{n}\right)^2 \sum_{\substack{p,p' \\ i\neq k}} \frac{n_p\left(1-n_{p'}\right)}{\xi_p - \xi_{p'}} \\ & \times \exp\left(\frac{\mathrm{i}}{\hbar}\left(p-p'\right) r_{ik}\right) S_i S_k \end{aligned}$$

where $\boldsymbol{r}_{ik} = \boldsymbol{r}_i - \boldsymbol{r}_k$ and the factor $\boldsymbol{n}_p\left(1-\boldsymbol{n}_{p'}\right)$ takes account of the presence of electrons in the initial state and their absence in the final state. We introduce new variables $p \to p + \frac{1}{2}q, p' = p - \frac{1}{2}q$.

We take into account the fact that finite temperature leads only to corrections of order $(T/\mu)^2$ and we therefore set $T = 0$. Then $\xi_p < 0$ and $\xi_{p'} > 0$. The expression obtained may be written in the form

$$E_{\mathrm{SS}} = -2\left(\frac{J}{n}\right)^2 \sum_{i\neq k} \int \frac{\mathrm{d}^3 q}{(2\pi\hbar)^3} F(q) \exp\left(\frac{\mathrm{i}qr_{ik}}{\hbar}\right) S_i S_k, \tag{21.36}$$

where

$$F(q) = \int \frac{\mathrm{d}^3 p}{(2\pi\hbar)^3} \frac{1}{\xi' - \xi} \theta\left(\xi'\right)\theta(-\xi), \tag{21.37}$$

and $\theta(x) = 1$ at $x > 0$ and $\theta(x) = 0$ at $x < 0, \xi = \xi\left(p + \frac{1}{2}q\right) = (2m)^{-1}\left[\left(p + \frac{1}{2}q\right)^2 - p_0^2\right]$, $\xi' = \xi\left(p - \frac{1}{2}q\right)$. Integration gives

$$F(q) = \frac{1}{4}\nu f\left(q/2p_0\right), \tag{21.38}$$

where $\nu = p_0 m/\left(\pi^2\hbar^3\right)$ is the density of states and

$$f(x) = \frac{1}{2}\left(1 + \frac{1-x^2}{2x}\ln\left|\frac{1+x}{1-x}\right|\right) \tag{21.39}$$

is the so-called Lindhard function.
Substitution of eqs. (21.38) and (21.39) into (21.36) and integration over $\boldsymbol{q}$ leads to

---

- Here we do not consider the Kondo effect and therefore we assume that S_i are classical vectors.

$$E_{\mathrm{SS}} = \left(\frac{J}{n}\right)^2 \nu \frac{p_0^3}{\pi\hbar^3} \times \sum_{i\neq k} \left[\cos\left(\frac{2p_0 r_{ik}}{\hbar}\right)\left(\frac{2p_0 r_{ik}}{\hbar}\right)^{-3} - \sin\left(\frac{2p_0 r_{ik}}{\hbar}\right)\left(\frac{2p_0 r_{ik}}{\hbar}\right)^{-4}\right] S_i S_k, \tag{21.40}$$

which is called the RKKY interaction after the authors (Ruderman and Kittel 1954, Kasuya 1956 and Yosida 1957).

Suppose that the interaction of the spins (eq. 21.40), leads to the formation of a helicoidal magnetic structure, for which $\boldsymbol{S} = \boldsymbol{S}(\boldsymbol{r})$, with

$$\begin{aligned} S_x &= S\cos(qz/\hbar), \\ S_y &= S\sin(qz/\hbar), \\ S_z &= 0. \end{aligned} \tag{21.41}$$

This means that the end of the vector $\boldsymbol{S}$ describes in space a spiral line around the z axis. Upon substitution into (21.36) we pass from the summation over i, k to integration according to the formula $\sum_i \to n\int \mathrm{d}V$, where n is the number of spins per unit volume. As a result, we have per unit volume

$$E_{\mathrm{SS}} = -2J^2S^2F(q) = -\frac{1}{2}J^2\nu S^2 f\left(q/2p_0\right). \tag{21.42}$$

A maximum of $f(q)$ corresponds to the lowest energy. The Lindhard function (21.39) is equal to unity at $q = 0$ and decreases monotonically with increasing x [the asymptotic with $x \to \infty$ is $f(x) \approx 2/(3x^2)$]. Hence, for the energy minimum we have $q = 0$, i.e. ferromagnetic ordering.

This conclusion is not general, as a matter of fact. If we take into account that the spins occupy certain positions in space, we cannot pass from the summation over r_i to the integration over the volume. For certain lattices, other types of spin ordering are more favorable, namely antiferromagnetic or helicoidal ordering with $\boldsymbol{q} \neq 0$. But here we confine ourselves to the simplest case.

How does the situation change in a superconductor? In order to find the answer to this question, we must express in the Hamiltonian (21.35) the operators a and a^+in terms of α and α^+in accordance with the Bogoliubov formulas (16.14). We assume from the start that spin ordering is helocoidal and is described by formulas (21.41). In this case, we obtain

$$\begin{aligned} \mathscr{H}_{eS} = -\frac{J}{n}\sum_{p,p',i} &\left(S_i^x - \mathrm{i}S_i^y\right)\left(u_{p'}\alpha^+_{p',+} + v_{p'}\alpha_{-p',-}\right)\left(u_p\alpha_{p,-} - v_p\alpha^+_{-p,+}\right) \\ &+ \left(S_i^x + \mathrm{i}S_i^y\right)\left(u_{p'}\alpha^+_{p',-} - v_{p'}\alpha_{-p',+}\right)\left(u_p\alpha_{p,+} + v_p\alpha^+_{-p,-}\right) \end{aligned}$$

Let us find, as before, the second order of perturbation theory and retain the terms with $i \neq k$. We assume that $T = 0$. This means that all the numbers $n_{p,+}$ and $n_{p,-}$ for quasiparticles are taken to be equal to zero. Of course, strictly speaking, this is justifiable only for the limiting case, when the temperature of magnetic ordering T_{M} is much lower than T_{cl}. As a result, we obtain

$$E_{\rm SS} = -\sum_{\substack{p,p'\\ i\neq k}} \frac{\left(u_p v_{p'} - u_{p'} v_p\right)^2}{\varepsilon + \varepsilon'} \exp\left[\frac{\mathrm{i}}{\hbar}\left(p - p'\right) r_{ik}\right] S_i S_k.$$

Substituting formulas (16.19) for u and v yields

$$E_{\rm SS} = -\frac{1}{2}\left(\frac{J}{n}\right)^2 \sum_{p,p';i\neq k} \left(1 - \frac{\xi\xi' + \Delta^2}{\varepsilon\varepsilon'}\right) \times \frac{1}{\varepsilon + \varepsilon'} \exp\left[\frac{\mathrm{i}}{\hbar}\left(p - p'\right) r_{ik}\right] S_i S_k \tag{21.43}$$

We introduce the same variables as before. Then, instead of formula (21.36), we obtain a formula of the same type, which however, will contain $F_1(q)$:

$$F_1(q) = \frac{1}{4}\int \frac{\mathrm{d}^3 p}{(2\pi\hbar)^3}\left(1 - \frac{\xi\xi' + \Delta^2}{\varepsilon\varepsilon'}\right)\frac{1}{\varepsilon + \varepsilon'}. \tag{21.44}$$

First of all, note that $F_1(q) = 0$ at $q = 0$. In fact, here $\xi = \xi'$ and $\xi^2 + \Delta^2 = \varepsilon^2$. The physical explanation of this circumstance consists in the following. An indirect exchange interaction between the spins arises from the fact that the spin S_i at point $\boldsymbol{r}_i$ polarizes the surrounding electrons and they in turn polarize the other spin S_k. But if we are dealing with a superconductor, the electrons in the ground state are not polarized, and the excited state is separated from the ground state by an energy gap. The static spin cannot change the energy of the electronic system and, hence, cannot polarize it. From this it follows that while ferromagnetism hinders superconductivity, the latter in turn impedes the generation of ferromagnetism.

In what follows, we need, as before, the maximum of function $F_1(q)$. It will be seen that this maximum corresponds to $\Delta/v \sim \hbar/\xi < q < 2p_0$. Therefore, instead of a detailed calculation of function F_1, we can find its asymptotics, assuming that $\Delta < vq < 2p_0 v$. To this end, we add and subtract in eq. (21.44) the corresponding expression with $\Delta = 0$. The difference converges at $p \sim \Delta/v, vq \sim \Delta$. In view of this, we may differentiate the difference with respect to Δ and then, introducing the variables ξ and ξ' in place of p and $\theta = (p, q)$, we assume the limits of integration over these variables to be infinite. As a result, we find

$$\begin{aligned}\frac{\partial}{\partial\Delta^2}[F_1(q) - F(q)] &= \frac{\nu}{4vq}\int_0^\infty \mathrm{d}\xi \int_0^\infty \mathrm{d}\xi' \\ &\times \frac{-3 + \frac{1}{\varepsilon^2} + \frac{1}{\varepsilon'^2} + \frac{1}{\varepsilon\varepsilon'}}{2\varepsilon\varepsilon'\left(\varepsilon + \varepsilon'\right)} \\ &= \frac{\nu}{8vq\Delta}\int_0^\infty \mathrm{d}\varphi_1 \int_0^\infty \mathrm{d}\varphi_2 \\ &\times \frac{-3 + \frac{1}{\cosh^2\varphi_1} + \frac{1}{\cosh^2\varphi_2} + \frac{1}{\cosh\varphi_1\cosh\varphi_2}}{\cosh\varphi_1 + \cosh\varphi_2}\end{aligned}$$

where we have introduced the variables $\xi = \Delta\sinh\varphi_1, \xi' = \Delta\sinh\varphi_2$. The resultant dimensionless integral over φ_1 and φ_2 is found to be equal to $-\frac{1}{2}\pi^2$.

Integrating over Δ, we obtain

$$F_1(q) - F(q) = -\frac{\nu\pi^2\Delta}{8vq} = -\frac{\nu\pi\hbar}{8\xi_0 q}$$

where we have introduced the notation $\xi_0 = \hbar v/\pi\Delta$, which has already been used before. The remaining part equal to $F(q)$ may be expanded in a series in q because of the smallness of q. Using expressions (21.38) and (21.39), we have

$$F_1(q) \approx \frac{\nu}{4}\left(1 - \frac{q^2}{12p_0^2} - \frac{\pi\hbar}{2\xi_0 q}\right). \tag{21.45}$$

In order to avoid confusion, we should remark that this formula cannot be applied for both too small and too large values of q.

Analogously to eq. (21.42), the energy per unit volume is given by

$$E_{\mathrm{SS}} = -2J^2S^2F_1(q) \tag{21.46}$$

The maximum of function $F_1(q)$ is attained at

$$q = \left(\frac{2\pi\hbar p_0^2}{\xi_0}\right)^{1/3}. \tag{21.47}$$

This means that magnetic ordering has a helicoidal structure with a period given by

$$d = \frac{2\pi\hbar}{q} = \frac{2}{3^{1/2}}\left(\frac{\pi\hbar}{p_0}\right)^{2/3}\xi_0^{1/3} \sim a^{2/3}\xi_0^{1/3}, \tag{21.48}$$

where $a \sim \hbar/p_0$ is of the order of atomic dimensions (Anderson and Suhl 1959).
The resultant period is large compared to atomic dimensions but it is small compared to ξ_0. Since the events that occur at distances of order ξ_0 are important in superconductors, it may be said that magnetization changes so rapidly that it averages out at distances of order ξ_0 and therefore may exist together with superconductivity.

In fact, apart from the exchange interaction of the spins, there also occurs a spin-orbit interaction, which is very strong in rare-earth elements because of their large atomic number. In contrast to the exchange interaction, this interaction depends on the spin orientation relative to the crystallographic axes. This gives rise to a so-called anisotropy field. The latter selects, among the spin directions, the so-called easy directions of magnetization. The simplest case is a uniaxial crystal with an easy direction of magnetization along the axis. In such a crystal, the orientations of the spin along the axis in the forward and reverse directions are energetically the most favorable. The presence of such an anisotropy field "remodels" the helicoidal magnetic structure into a domain structure composed of planar layers (domains) with opposite magnetization of the successive layers.

Since the magnetization in each domain is homogeneous, it follows that in formula (21.45), in place of the second term, we must write the energy of the interdomain boundary. In each such wall there occurs a gradual spin flip from one easy direction of magnetization to another. This can happen by gradual rotation of the magnetic moment with conservation of its magnitude as well as by a gradual change of its magnitude with the direction staying parallel to the easy magnetization axis. In the substances under consideration a change of direction of the moment is unfavourable due to the large anisotropy energy; therefore walls of the second type actually occur (they are called "linear walls"). Since the exchange energy is minimal if the moment does not vary in space, the wall has an additional exchange energy $J^2S^2\nu\,(a/\delta_{\mathrm{w}})^2\,\delta_{\mathrm{w}}$, where δ_{w} is the thickness of the wall and a is the interatomic distance [this energy corresponds to the term $\int c(\nabla\varphi)^2\,\mathrm{d}V$ in formula (AII.15)]. On the other hand the value of the order parameter in the wall is less than the bulk value and this contributes an additional energy of the order of $J^2S^2|\tau|\nu\delta_{\mathrm{w}}$, where $\tau = (T - T_{\mathrm{m}})/T_{\mathrm{m}}$ [this corresponds to $\int \alpha\tau\varphi^2\,\mathrm{d}V$ in (AII.15)]. Minimizing the total energy with respect to δ_{w},

$$E_{\rm w} = J^2 S^2 \nu \left(\frac{a^2}{\delta_{\rm w}} + \delta_{\rm w} |\tau| \right)$$

we get

$$\delta_{\rm w} \sim \frac{a}{|\tau|^{1/2}}, \quad E_{\rm w} \sim J^2 S^2 \nu a |\tau|^{1/2}$$

Strictly speaking this is true for $|\tau| < 1$, but in fact it gives a correct estimate even for $|\tau| \sim 1$.

If the period of the domain structure is d, then, on the average, we have $E_{\rm w}/d \sim J^2 S^2 \nu a/d$ per unit volume. Moreover, we have to add the exchange energy that arises from the superconductivity, represented by the third term in eq. (21.45). Taking into account that $q \sim \hbar/d$, we obtain the total extra energy dependent on d :

$$\Delta E(d) \sim J^2 S^2 \nu \left(\frac{a}{d} + \frac{d}{\xi_0} \right)$$

Minimizing with respect to d, we find

$$d \sim (a \xi_0)^{1/2} \tag{21.49}$$

$$\Delta E(d) \sim J^2 S^2 \nu \left(\frac{a}{\xi_0} \right)^{1/2}. \tag{21.50}$$

Again, the period of the structure is found to be smaller than ξ_0, and therefore the magnetization has a slight effect on superconductivity.

In order to solve the problem of the transition to a normal ferromagnetic material, let us compare the corresponding energies at $T = 0$. From formula (21.42) at $q = 0$ we obtain $E_{\rm n} = \frac{1}{2} J^2 S^2 \nu$. The excess energy associated with the domain walls is expressed by formula (21.50). However, the onset of superconductivity gives rise to an extra negative energy given by formula (16.41). If

$$J^2 S^2 \nu \left(\frac{a}{\xi_0} \right)^{1/2} < \nu \Delta^2(0) \tag{21.51}$$

the superconductivity with the domain magnetic structure will persist up to $T = 0$. This is what happens in $HoMo_6Se_8$. If the opposite inequality is fulfilled, then at some finite temperature T_{c2} a first-order phase transition takes place from the domain superconducting structure to a normal ferromagnetic substance. This is observed in $HoMo_6\ S_8$ and $ErRh_4\ B_4$. The criterion (21.51) may be rewritten by taking advantage of the fact that

$$\Delta(0) \sim T_{\rm cl1}, \quad \xi_0 \sim \frac{\hbar v}{T_{\rm cl}}, \quad a \sim \frac{\hbar}{p_0}, \quad p_0 v \sim \varepsilon_{\rm F}, \quad \frac{J^2 S^2}{\varepsilon_{\rm F}} \sim \theta$$

(θ is the Curie point) (see below):

$$\theta \frac{\varepsilon_{\rm F}^{1/2}}{T_{\rm c1}^{3/2}} < 1. \tag{21.51'}$$

In superconductors that pass to the normal ferromagnetic phase below T_{c2} the following interesting phenomenon can be observed. If a current is passed through such a superconductor at a temperature below T_{c2}, then due to finite resistance it will heat the sample and the temperature will become higher than T_{c2}. But in this

case the heating will stop and the temperature will fall below T_{c2} and the process will repeat itself. This may result in the following: alternating domains of the normal and the superconducting phase will move throughout the sample with the current; such domains are called autowaves (Buzdin and Mikhailov 1986).

Let us now consider the lower boundary of the domain phase. Since the energy of domain walls is only a small correction to the main exchange energy of the spin-spin interaction, the Curie temperature θ will differ little from the value for a normal ferromagnetic material. To find the latter value, we employ the self-consistent field method (Abrikosov and Gor'kov 1962b). Suppose a ferromagnetic state has been formed and, as a result, the electron spin has been polarized, i.e., $\langle\sigma\rangle$, where $\langle\cdots\rangle$ signifies the equilibrium average at a given temperature referred to unit volume. In accordance with the Hamiltonian (4.39), this is equivalent to the action of an effective magnetic field on each spin of a rare-earth ion, in which case the role of $g\beta H$ is played by $(J/n)\langle\sigma\rangle$ ($g\beta S$ is the magnetic moment of the ion, g is the gyromagnetic ratio and β is the Bohr magneton). The free energy of the entire system of ionic spins per unit volume is ($n_{\mathrm{m}} = n$):

$$\begin{aligned} F_{\mathrm{i}} &= -nT \ln \sum_{M=-S}^{S} \exp\left(\frac{J}{n}\langle\sigma\rangle\frac{M}{T}\right) \\ &= -nT\left[\ln\sinh\left(\frac{J}{n}\langle\sigma\rangle\frac{S+\frac{1}{2}}{T}\right) - \ln\sinh\left(\frac{J}{n}\frac{\langle\sigma\rangle}{2T}\right)\right]. \end{aligned} \tag{21.52}$$

On the other hand, the polarization of electron spins implies their redistribution among the energy levels, i.e., the generation of different Fermi surfaces for $\sigma = +1$ and -1 , which is also equivalent to the action of a certain magnetic field. According to section 10.1, under the action of the magnetic field H a paramagnetic moment arises in the electronic system ($s = \frac{1}{2}\sigma$):

$$M = \beta\langle\sigma\rangle = \beta^2\nu H = \chi H,$$

where χ is the magnetic susceptibility. On the other hand, the change in free energy for a given moment M is (see eq. 10.2):

$$F_{\mathrm{e}} = \int H\ \mathrm{d}M = \frac{1}{2}\chi H^2 = \beta^2\frac{\langle\sigma\rangle^2}{2\chi} = \frac{\langle\sigma\rangle^2}{2\nu}. \tag{21.53}$$

Let us find the minimum of $F_{\mathrm{e}} + F_{\mathrm{i}}$. Differentiating with respect to $\langle\sigma\rangle$, we get

$$\frac{\langle\sigma\rangle}{\nu} - JSB_{\mathrm{s}}\left(\frac{J}{n}\frac{\langle\sigma\rangle}{T}\right) = 0, \tag{21.54}$$

where $\mathbf{B}_{\boldsymbol{S}}(\boldsymbol{x})$ is the Brillouin function defined by

$$\mathrm{B}_S(x) = \left(\frac{S+\frac{1}{2}}{S}\right)\coth\left[\left(S+\frac{1}{2}\right)x\right] - \frac{1}{2S}\coth\left(\frac{1}{2}x\right). \tag{21.55}$$

In order to find the Curie temperature θ, we assume that $\langle\sigma\rangle \to 0$. Taking into account that at $x \ll 1$

$$\mathrm{B}_S(x) \approx \frac{1}{3}(S+1)x$$

we obtain from (21.52)

$$\theta = J^2\nu S\frac{(S+1)}{3n}. \tag{21.56}$$

Taking into account that $\nu \sim n_e/\varepsilon_F$ and $n_e \sim n$, we find

$$\theta \sim \frac{J^2 S^2}{\varepsilon_F}. \qquad (\prime)$$

Two situations are possible. If ε_F is of the same order as in ordinary metals, then at $\theta \sim 1$ K we have $JS \sim 10^2$ K, i.e. $JS > \Delta(0)$ (cf., with 21.22, $JS = I$). In this case, the coexistence of superconductivity and ferromagnetism is possible only at $\theta < T_{cl}$, and the change of the phases with decreasing temperature will occur in the sequence described in the present section. But if $\theta > T_c$, then superconductivity will not appear at all.

However, there is still another possibility, in principle. As has already been said in section 16.10, a sharp peak may appear in the density of states at the Fermi boundary; this peak, known as the Abrikosov-Suhl resonance, manifests itself in various properties at low temperatures. It may be interpreted as an increase in the effective mass - "heavy fermions". Evidently, in such a case in formula (21.56) ν will be anomalously high and, hence, JS may be found to be of order Δ. In this case, superconductivity may arise at $\theta \geqslant T_c$ and also the inhomogeneous superconducting LOFF phase described in the preceding section may appear. Actually, for this to occur it is necessary that $m^* > 10^3 m, \theta, T_c > 10$ K, which has never been observed.

The exchange interaction of electrons with ions (4.39) in the case of a large negative J may give rise to the unusual effect of reentrant superconductivity (Jaccarino and Peter 1962). We are speaking here of antiferromagnetic superconductors or of ferromagnetic superconductors at a temperature above the Curie point. Under the action of an external field an average polarization of the nuclear spin $\langle \boldsymbol{S} \rangle$ appears. Because of this, the electron spins will be acted on by an effective field given by

$$I = \frac{J}{n}\langle S \rangle + \beta H \qquad (21.57)$$

If J is sufficiently large in absolute magnitude, then the first term in this formula is larger than the second. Under the influence of the field the superconductivity is destroyed by a paramagnetic mechanism. As H increases further the first term tends towards saturation because $|\langle \boldsymbol{S} \rangle|$ cannot exceed $n\boldsymbol{S}$, where $\boldsymbol{S}$ is the spin of an individual ion. If $J < 0$, this may lead to a decrease in the magnitude of I and to

In order to find the Curie temperature θ, we assume that $\langle \sigma \rangle \to 0$. Taking into account that at $x \ll 1$

$$\mathrm{B}_S(x) \approx \frac{1}{3}(S+1)x$$

we obtain from (21.52)

$$\theta = J^2 \nu S \frac{(S+1)}{3n}. \qquad (21.56)$$

Taking into account that $\nu \sim n_e/\varepsilon_F$ and $n_e \sim n$, we find

$$\theta \sim \frac{J^2 S^2}{\varepsilon_F}. \qquad (21.56')$$

Two situations are possible. If ε_F is of the same order as in ordinary metals, then at $\theta \sim 1$ K we have $JS \sim 10^2$ K, i.e. $JS > \Delta(0)$ (cf., with 21.22, $JS = I$). In this case, the coexistence of superconductivity and ferromagnetism is possible only at $\theta < T_{cl}$, and the change of the phases with decreasing temperature will occur in the sequence described in the present section. But if $\theta > T_c$, then superconductivity will not appear at all.

However, there is still another possibility, in principle. As has already been said in section 16.10, a sharp peak may appear in the density of states at the Fermi boundary; this peak, known

as the Abrikosov-Suhl resonance, manifests itself in various properties at low temperatures. It may be interpreted as an increase in the effective mass - "heavy fermions". Evidently, in such a case in formula (21.56) ν will be anomalously high and, hence, JS may be found to be of order Δ. In this case, superconductivity may arise at $\theta \geqslant T_c$ and also the inhomogeneous superconducting LOFF phase described in the preceding section may appear. Actually, for this to occur it is necessary that $m^* > 10^3 m, \theta, T_c > 10$ K, which has never been observed.

The exchange interaction of electrons with ions (4.39) in the case of a large negative J may give rise to the unusual effect of reentrant superconductivity (Jaccarino and Peter 1962). We are speaking here of antiferromagnetic superconductors or of ferromagnetic superconductors at a temperature above the Curie point. Under the action of an external field an average polarization of the nuclear spin $\langle \boldsymbol{S} \rangle$ appears. Because of this, the electron spins will be acted on by an effective field given by

$$I = \frac{J}{n}\langle S \rangle + \beta H \tag{21.57}$$

If J is sufficiently large in absolute magnitude, then the first term in this formula is larger than the second. Under the influence of the field the superconductivity is destroyed by a paramagnetic mechanism. As H increases further the first term tends towards saturation because $|\langle \boldsymbol{S} \rangle|$ cannot exceed $n\boldsymbol{S}$, where $\boldsymbol{S}$ is the spin of an individual ion. If $J < 0$, this may lead to a decrease in the magnitude of I and to
the onset of superconductivity. In still larger fields the superconductivity is completely destroyed, due mainly to the second term in eq. (21.57) with the aid of the paramagnetic mechanism or due to the orbital effect of pair rotation. An example is the compound $Eu_{0.75}Sn_{0.25}Mo_6\ S_{7.2}Se_{0.8}$.

More detailed information about ferromagnetic and antiferromagnetic superconductors can be found in the literature (Bulaevskii et al. 1985, Buzdin and Bulaevskii 1986).

8.7.4 21.4. The Knight shift

One of the highly sensitive methods of determination of internal magnetic fields in a solid, which is also frequently used to determine structural details is the nuclear magnetic resonance (NMR) method. If the nucleus has a spin, it also has a magnetic moment.

$$\mu_{\mathrm{n}} = \gamma \hbar S_{\mathrm{n}}. \tag{21.58}$$

Nuclear magnetic moments are thousands of times lower than the electronic moments:

$$\gamma\hbar \sim \frac{e\hbar}{M_{\mathrm{p}}c} \sim \frac{\beta m}{M_{\mathrm{p}}},$$

where m is the mass of the electron and M_{p} is the mass of the proton. If the nuclear moment is placed in a magnetic field, its energy has the usual form

$$\varepsilon = -\mu_{\mathrm{n}}\boldsymbol{H} = -\gamma\hbar M H, \tag{21.59}$$

where M is the magnetic quantum number (the projection of the nuclear spin onto $\boldsymbol{H}$). This system with equidistant levels is capable of absorbing electromagnetic quanta with an energy $\gamma\hbar H$. Considering that $\beta \sim 10^{-20}$ and $\gamma\hbar \sim 10^{-23}$, we obtain $\omega \sim \gamma H$, i.e., $\omega \sim 10^8$ s^{-1} in a field of the order of 10^4Oe. This makes nuclear magnetic resonance a convenient tool for the various investigations.

The nuclear spin interacts with electrons when the electrons create a magnetic field. In a nonmagnetic metal in the absence of a magnetic field the electronic system has no magnetic moment and the nuclear spin does not interact with the electrons. If an external magnetic

field is turned on, it is capable not only of directly acting on the nuclear spin but, through the orientation of the electron spin, it can also produce a nonzero electronic field in the region of the nucleus. However, in practice only the field created by the spin of s-electrons is important because only these electrons have a finite wave function at the point of location of the nucleus (according to quantum mechanics, $\psi(r) \propto r^l$, where l is the orbital moment).

In metals, the electron spins are polarized under the action of a magnetic field. Since among the valence electrons there are always electrons for which the wave function in the vicinity of the nucleus is close to the atomic s-function, their
polarization generates an extra field, which acts on the nuclear spin. This leads to a shift of the NMR frequency; this shift is known as the Knight shift (Knight 1949).

The magnitude of the Knight shift can be calculated as follows. The Hamiltonian of the magnetic dipolar interaction of electrons with a nucleus may be written in the form

$$\mathscr{H}_{\text{en}} = -2\beta \left[3(sr)\frac{\mu_{\text{n}} r}{r^5} - \frac{s\mu_{\text{n}}}{r^3}\right] = -2\beta s \operatorname{rot} A, \tag{21.60}$$

where $\boldsymbol{A}$ is the vector potential of the field created by the spin:

$$A = \frac{[\mu_{\text{n}} r]}{r^3} = \operatorname{rot}\left(\frac{\mu_{\text{n}}}{r}\right). \tag{21.61}$$

Substituting into (21.60), we obtain

$$\begin{aligned}\mathscr{H}_{\text{en}} &= -2\beta s \operatorname{rot}\operatorname{rot}\left(\frac{\mu_{\text{n}}}{r}\right) = -2\beta s \left(\operatorname{grad}\operatorname{div} - \nabla^2\right)\frac{\mu_{\text{n}}}{r} \\ &= -2\beta\left[(s\nabla)(\mu_{\text{n}}\nabla) - (s\mu_{\text{n}})\nabla^2\right]\frac{1}{r} \\ &= -2\beta\left[(s\nabla)(\mu_{\text{n}}\nabla) - \frac{1}{3}(s\mu_{\text{n}})\nabla^2\right]\frac{1}{r} + \frac{4}{3}\beta(s\mu_{\text{n}})\nabla^2\frac{1}{r}.\end{aligned} \tag{21.62}$$

The Hamiltonian obtained must be averaged over the electronic wave function. Here the first term in (21.62) gives a nonzero result only with wave functions that behave in the vicinity of the nucleus as atomic states with $l \neq 0$; therefore, it makes a small contribution. The second term, by virtue of Coulomb's law

$$\nabla^2\frac{1}{r} = -4\pi\delta(r)$$

is equal to

$$\mathscr{H}_{\text{en}} = -\frac{16}{3}\pi\beta s\mu_{\text{n}}\delta(r).$$

On averaging this gives*

$$E_{\text{en}} = -\frac{16}{3}\pi\beta\langle s\rangle\mu_{\text{n}}\frac{|\psi_{\text{s}}(0)|^2}{n}, \tag{21.63}$$

where n is the density of atoms.
In a magnetic field the average electron spin of unit volume is equal to

$$\langle s\rangle = \frac{\chi H}{2\beta},$$

polarization generates an extra field, which acts on the nuclear spin. This leads to a shift of the NMR frequency; this shift is known as the Knight shift (Knight 1949).

The magnitude of the Knight shift can be calculated as follows. The Hamiltonian of the magnetic dipolar interaction of electrons with a nucleus may be written in the form

$$\mathscr{H}_{\text{en}} = -2\beta \left[3(sr)\frac{\mu_{\text{n}} r}{r^5} - \frac{s\mu_{\text{n}}}{r^3}\right] = -2\beta s \operatorname{rot} A, \tag{21.60}$$

where $\boldsymbol{A}$ is the vector potential of the field created by the spin:

$$A = \frac{[\mu_{\text{n}} r]}{r^3} = \operatorname{rot}\left(\frac{\mu_{\text{n}}}{r}\right). \tag{21.61}$$

Substituting into (21.60), we obtain

$$\begin{aligned}\mathscr{H}_{\text{en}} &= -2\beta s \operatorname{rot}\operatorname{rot}\left(\frac{\mu_{\text{n}}}{r}\right) = -2\beta s \left(\operatorname{grad}\operatorname{div} - \nabla^2\right)\frac{\mu_{\text{n}}}{r} \\ &= -2\beta\left[(s\nabla)(\mu_{\text{n}}\nabla) - (s\mu_{\text{n}})\nabla^2\right]\frac{1}{r} \\ &= -2\beta\left[(s\nabla)(\mu_{\text{n}}\nabla) - \frac{1}{3}(s\mu_{\text{n}})\nabla^2\right]\frac{1}{r} + \frac{4}{3}\beta(s\mu_{\text{n}})\nabla^2\frac{1}{r}\end{aligned} \tag{21.62}$$

The Hamiltonian obtained must be averaged over the electronic wave function. Here the first term in (21.62) gives a nonzero result only with wave functions that behave in the vicinity of the nucleus as atomic states with $l \neq 0$; therefore, it makes a small contribution. The second term, by virtue of Coulomb's law

$$\nabla^2\frac{1}{r} = -4\pi\delta(r)$$

is equal to

$$\mathscr{H}_{\text{en}} = -\frac{16}{3}\pi\beta s\mu_{\text{n}}\delta(r).$$

On averaging this gives*

$$E_{\text{en}} = -\frac{16}{3}\pi\beta\langle s\rangle\mu_{\text{n}}\frac{|\psi_{\text{s}}(0)|^2}{n}, \tag{21.63}$$

where n is the density of atoms.
In a magnetic field the average electron spin of unit volume is equal to

$$\langle s\rangle = \frac{\chi H}{2\beta},$$

from which we have

$$E_{\text{en}} = -\frac{8}{3}\pi\chi\frac{|\psi_{\text{s}}(0)|^2}{n}(\mu_{\text{n}}\boldsymbol{H}).$$

Thus, the nuclear spin is acted on by an extra magnetic field:

- In order to derive formula (21.63), use may be made of the electron wave function written in terms of the Wannier function (1.22) and account may be taken of the fact that $w_n(r) \approx \psi_s(r - a_n)$ falls off rapidly as r moves away from a_n.

- In order to derive formula (21.63), use may be made of the electron wave function written in terms of the Wannier function (1.22) and account may be taken of the fact that $w_n(r) \approx \psi_s(r - a_n)$ falls off rapidly as r moves away from a_n.

$$\Delta H = \frac{8}{3}\pi\chi\frac{|\psi_{\rm s}(0)|^2}{n}H. \tag{21.64}$$

Experimental determination of the NMR frequency and, hence, of the Knight shift, makes it possible to measure the spin magnetic susceptibility χ directly. Of course, for a normal metal this method becomes less valuable because the magnitude of $|\psi_s(0)|^2$, the probability density of finding electrons at the nucleus, cannot be calculated exactly. But if the metal passes to the superconducting state, the ratio $\chi_{\rm s}(T)/\chi_{\rm n}$ can be studied.

Of the greatest interest is $\chi_{\rm s}(0)$. At first sight it must be equal to zero. Indeed, in the ground state the electrons are bound into Cooper pairs with zero spin and the excited states are separated from the ground state by an energy gap. Hence, a small magnetic field is not capable of generating magnetization, i.e., $\chi_{\rm s}(0) = 0$. However, in practice $\chi_{\rm s}(0)$ is always found not only to be finite but often even to be close to $\chi_{\rm n}$ (recall that at low temperatures $\chi_{\rm n}$ is practically independent of temperature).

Attempts have been made to explain this paradox by the assumption of triplet pairing, i.e., Cooper pairs with parallel spins and $l = 1, 3\ldots$ (the oddness of l is the result of the symmetry of the wave function of Fermi particles: if it is symmetric with respect to spin transposition, then it must be antisymmetric with respect to the coordinates), but this idea has not been confirmed.

In order to understand the origin of finite $\chi_{\rm s}(0)$, we must take into account that NMR experiments with a superconductor must be carried out on small particles (or very thin films) with a size less than the penetration depth. Otherwise, the magnetic field will not penetrate the superconductor or will be strongly inhomogeneous, which will not make it possible to observe the resonance. In small particles, even if they are single-crystalline, the electrons are inevitably scattered from the boundaries, i.e., we certainly have $l < \delta$. It can be shown that ordinary potential scattering does not give rise to $\chi_{\rm s}(0)$.

However, apart from this there necessarily is spin-orbit scattering, which has already been considered in section 11.4. The Hamiltonian of the spin-orbital part of the electron-impurity interaction is proportional to $(mc)^{-1}[-{\rm i}\hbar\nabla V, p]s$, where V is the potential of the impurity*; this Hamiltonian gives a correction to the scattering amplitude proportional to $[pp']\,s$, where p and p' are the electron momentum before and after scattering. Since the correction in the Hamiltonian is symmetric with respect to a change in sign of time (with $t \to -t, p \rightleftharpoons -p'$ and $s \to -s$), it does not

lead to a noticeable change in the thermodynamic quantities of superconductors (section 21.1).

However, in the presence of this interaction the electron spin is not conserved. Hence, the states cannot be classified in accordance with the total spin of the electronic system S, and in the ground state of the superconductor there is an admixture of states with $S \neq 0$. In view of this, polarization in a weak field is also possible.

The results of calculation of this effect (Abrikosov and Gor'kov 1960b, 1962a) are as follows. The ratio $\chi_{\rm s}/\chi_{\rm n}$ depends on temperature and on the parameter $l_{\rm s0}/\xi_0$, where $l_{\rm s0}$ is the spin-orbital mean free path associated with the corresponding contribution to the scattering amplitude:

$$f\,(p,p') = a + \frac{{\rm i}b}{p_0^2}\,([pp']\,\sigma)\,, \quad l_{\rm s0} = v\tau_{\rm s0}$$
$$\frac{1}{\tau_{\rm s0}} = n_{\rm i}\nu\frac{\pi}{\hbar}\int |b|^2\sin^2\theta\frac{{\rm d}\Omega}{4\pi} \tag{21.65}$$

*The explanation of the physical origin of the spin-orbit interaction and its estimate are given at the beginning of section 10.7.

where n_i is the impurity concentration.
At $T = 0$ we obtain

$$\frac{\chi_\mathrm{s}(0)}{\chi_\mathrm{n}} \approx \frac{1}{6}\pi^2\frac{\xi_0}{l_{\mathrm{s}0}},$$
$$\frac{\chi_\mathrm{s}(0)}{\chi_\mathrm{n}} \approx 1 - \frac{3}{4}\frac{l_{\mathrm{s}0}}{\xi_0}, \quad \xi_0 < l_{\mathrm{s}0} \tag{21.66}$$

(recall that $\xi_0 = \hbar v/(\pi\Delta(0))$. From formulae (21.63) it follows that with a weak spin-orbital scattering $\chi_\mathrm{s}(0)$ is small and with a strong scattering $\chi_\mathrm{s}(0)$ approaches unity. This result is in agreement with experiment.
lead to a noticeable change in the thermodynamic quantities of superconductors (section 21.1).

However, in the presence of this interaction the electron spin is not conserved. Hence, the states cannot be classified in accordance with the total spin of the electronic system S, and in the ground state of the superconductor there is an admixture of states with $S \neq 0$. In view of this, polarization in a weak field is also possible.

The results of calculation of this effect (Abrikosov and Gor'kov 1960b, 1962a) are as follows. The ratio $\chi_\mathrm{s}/\chi_\mathrm{n}$ depends on temperature and on the parameter $l_{\mathrm{s}0}/\xi_0$, where $l_{\mathrm{s}0}$ is the spin-orbital mean free path associated with the corresponding contribution to the scattering amplitude:

$$f\,(p, p') = a + \frac{\mathrm{i}b}{p_0^2}\,([pp']\,\sigma)\,, \quad l_{\mathrm{s}0} = v\tau_{\mathrm{s}0} \tag{21.65}$$
$$\frac{1}{\tau_{\mathrm{s}0}} = n_\mathrm{i}\nu\frac{\pi}{\hbar}\int |b|^2 \sin^2\theta \frac{\mathrm{d}\Omega}{4\pi}$$

where n_i is the impurity concentration.
At $T = 0$ we obtain

$$\frac{\chi_\mathrm{s}(0)}{\chi_\mathrm{n}} \approx \frac{1}{6}\pi^2\frac{\xi_0}{l_{\mathrm{s}0}}, \quad \xi_0 < l_{\mathrm{s}0},\ \xi_\mathrm{s}, l_{\mathrm{s}0} \geqslant 1 - \frac{3}{4}\frac{l_{\mathrm{s}0}}{\xi_0}, \quad \xi_\mathrm{n} \geqslant l \tag{21.66}$$

(recall that $\xi_0 = \hbar v/(\pi\Delta(0))$. From formulae (21.63) it follows that with a weak spin-orbital scattering $\chi_\mathrm{s}(0)$ is small and with a strong scattering $\chi_\mathrm{s}(0)$ approaches unity. This result is in agreement with experiment.

8.8 22 Tunnel junctions. The Josephson effect

8.8.1 22.1. Single-particle tunnel current

The tunneling effect is one of the most familiar phenomena of quantum mechanics, since it demonstrates clearly the difference between quantum mechanics and classical mechanics. According to quantum mechanics, a particle can pass through a potential barrier even in those cases where the barrier height exceeds its energy. This phenomenon has already been considered in section 10.7 in connection with the discussion of magnetic breakdown.

The probability of passing through the barrier is primarily determined by an exponential factor:

$$W \sim \exp\left(-\frac{2}{\hbar}\int \mathrm{Im}\,(p_x)\,\mathrm{d}x\right)$$
$$= \exp\left\{-\frac{2(2m)^{1/2}}{\hbar}\int_{x_1}^{x_2}[U(x)-E]^{1/2}\,\mathrm{d}x\right\}. \qquad (22.1)$$

The integration is carried out over the region where $U(x) > E$ (see fig. 139). From the above formula it follows that the probability of passing through the barrier falls off with increasing barrier height ($U_{\max} - E$) and width ($x_2 - x_1$) and also with increasing mass of the particle.

We may actually speak of electrons and if the barrier is a layer of an insulator, then its thickness must not exceed a few interatomic distances. It is simpler to use a natural oxide layer which is formed at the surface of many metals: aluminum,

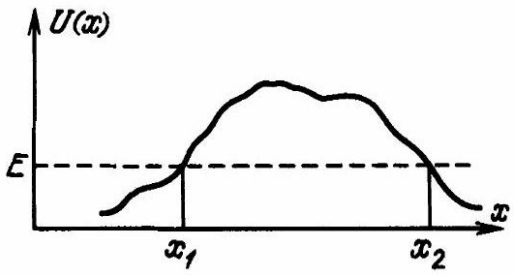


Fig. 139.

tin, lead, etc. Vaporization of a layer of the same or another metal gives rise to a so-called tunnel junction or contact (Giaever 1960a); this simple electronic device is an exceedingly valuable tool for the investigation of superconductivity.

We begin the study of the tunnel junction with two normal metals. At equilibrium the chemical potentials are equal (fig. 140a). If we apply a potential difference, this will fall entirely over the high-resistance dielectric layer. The chemical potentials of the two metals will then be at different heights (the level difference eV, fig. 140b). Assuming the barrier height to be much larger than eV, we find that the number of electrons that can be transferred to the free levels of another metal is proportional to eV and that all of them pass through the barrier with equal probability. From this it follows that the current will be proportional to V, and this is consistent with Ohm's law (fig. 141, curve 1).

Now let one of the metals be normal and the other a superconductor. We assume that $T = 0$. At equilibrium in the absence of a potential difference the chemical potentials must be equal. But the electrons in the superconductor are bound into Cooper pairs, and these are in the Bose condensate. This energy level is just the chemical potential of the pair. From the side of the normal metal, this pair corresponds to two free quasiparticles of the gas model at the Fermi level. Suppose that an electron has been transferred from the normal metal into the superconductor. But, as a matter of fact, it does not enter into the composition of the pair. If the binding energy is 2Δ, then the energy of one unpaired electron exceeds by Δ the energy of an electron in a Cooper pair. Hence, in order to transport an electron from a normal metal into a superconductor, it must receive extra energy.



Fig. 140.

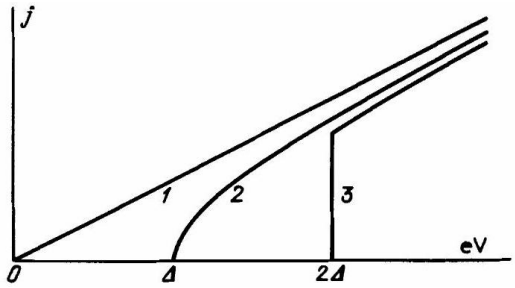


Fig. 141.

The same must be done in order to transport an electron from a superconductor to a normal metal. First we must break up a pair, which requires an energy Δ per electron, following which the electron can pass into the normal metal.

A natural question arises here: Why cannot the pairs be transferred as a whole? Within the framework of the concepts outlined above this is associated with the fact that the pair has a double charge (this increases U in formula 22.1) and a double mass as compared to an individual electron, and therefore the probability of passing through the barrier is vanishingly small for it.

The situation just described may be sketched by an electron level diagram (fig. 142). The superconductor is on the left and the normal metal on the right. The hatched regions correspond to filled levels. The band $\pm\Delta$ on the left around the dashed line is the forbidden band. Above it are the allowed states. The diagram in fig. 142 reflects the fact that for one electron to be transported through the barrier in any direction, so being transferred from a filled state to a free state, it must acquire an energy Δ. With this diagram we need not think of its origin (i.e., of the pairs); we are to deal only with quasiparticles.

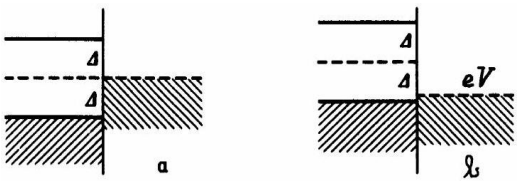


Fig. 142.

When a potential difference is applied, one side of the diagram begins to shift relative to the other and when the filled levels are found to be opposite the empty levels, an electric current will flow. Hence, the condition for the flow of current is

$$eV = \Delta. \tag{22.2}$$

Let us now find the complete dependence $j(V)$. In order to be able to integrate over the energy, we must know the density of states. For the electrons of a normal metal it is given by

$$\nu_{\mathrm{n}} = \frac{p_0 m}{\pi^2 \hbar^3} = \text{ const } .$$

For the quasiparticles of a superconductor we have

$$\nu_{\mathrm{s}} = 8\pi p^2 \frac{\mathrm{d}p}{(2\pi\hbar)^3 \, \mathrm{d}\varepsilon} = \frac{p_0^2 \, \mathrm{d}\xi}{v\pi^2\hbar^3 \, \mathrm{d}\varepsilon} = \frac{p_0 m}{\pi^2\hbar^3} \frac{\mathrm{d}\xi}{\mathrm{d}\varepsilon}$$

The same must be done in order to transport an electron from a superconductor to a normal metal. First we must break up a pair, which requires an energy Δ per electron, following which the electron can pass into the normal metal.

A natural question arises here: Why cannot the pairs be transferred as a whole? Within the framework of the concepts outlined above this is associated with the fact that the pair has a double charge (this increases U in formula 22.1) and a double mass as compared to an individual electron, and therefore the probability of passing through the barrier is vanishingly small for it.

The situation just described may be sketched by an electron level diagram (fig. 142). The superconductor is on the left and the normal metal on the right. The hatched regions correspond to filled levels. The band $\pm\Delta$ on the left around the dashed line is the forbidden band. Above it are the allowed states. The diagram in fig. 142 reflects the fact that for one electron to be transported through the barrier in any direction, so being transferred from a filled state to a free state, it must acquire an energy Δ. With this diagram we need not think of its origin (i.e., of the pairs); we are to deal only with quasiparticles.

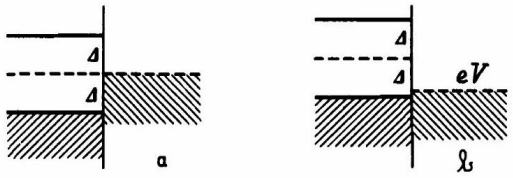


Fig. 142.

When a potential difference is applied, one side of the diagram begins to shift relative to the other and when the filled levels are found to be opposite the empty levels, an electric current will flow. Hence, the condition for the flow of current is

$$eV = \Delta. \tag{22.2}$$

Let us now find the complete dependence $j(V)$. In order to be able to integrate over the energy, we must know the density of states. For the electrons of a normal metal it is given by

$$\nu_{\mathrm{n}} = \frac{p_0 m}{\pi^2 \hbar^3} = \text{ const } .$$

For the quasiparticles of a superconductor we have

$$\nu_{\mathrm{s}} = 8\pi p^2 \frac{\mathrm{d}p}{(2\pi\hbar)^3 \, \mathrm{d}\varepsilon} = \frac{p_0^2 \, \mathrm{d}\xi}{v\pi^2\hbar^3 \, \mathrm{d}\varepsilon} = \frac{p_0 m}{\pi^2\hbar^3} \frac{\mathrm{d}\xi}{\mathrm{d}\varepsilon}$$

$$= \frac{\nu_n \varepsilon}{(\varepsilon^2 - \Delta^2)^{1/2}}, \quad \varepsilon > \Delta$$

(this formula has already been given in section 21.1).
This is the true density of states. However, if we wish to use the level diagram given in fig. 136, we have to assume that ε may be negative and

$$\nu_s = \begin{cases} \nu_n |\varepsilon| / (\varepsilon^2 - \Delta)^{1/2}, & |\varepsilon| > \Delta \\ 0, & |\varepsilon| < \Delta \end{cases} \tag{22.3}$$

Here $\varepsilon > 0$ corresponds to the generation of quasiparticles in a superconductor upon transport of electrons from the normal metal and $\varepsilon < 0$ corresponds to the breakup of the pairs and to the transport of the electrons in the opposite direction*. Of importance is the fact that $\nu_s(|\varepsilon| \to \Delta) \to \infty$, although this infinity is integrable, i.e., the total number of states within an infinitesimal energy interval near $|\varepsilon| = \Delta$ is an infinitesimal quantity.

The current that flows from one metal to another must be proportional to the tunneling probability, the number of occupied states in the first metal, the number of empty states in the second, and also to the densities of states in both metals.

Suppose a potential difference is applied as in fig. 142. Let us find the total current flowing from the superconductor to the normal metal in the forward and reverse directions. In accordance with what has been said above, we have

$$\begin{aligned} j &\propto \int W \nu_1(\varepsilon - eV) \nu_2(\varepsilon) \{ n_1(\varepsilon - eV) [1 - n_2(\varepsilon)] - n_2(\varepsilon) [1 - n_1(\varepsilon - eV)] \} \, \mathrm{d}\varepsilon \\ &= \int W \nu_1(\varepsilon - eV) \nu_2(\varepsilon) [n_1(\varepsilon - eV) - n_2(\varepsilon)] \, \mathrm{d}\varepsilon \\ &= W \nu_{1n} \nu_{2n} \int |\varepsilon - eV| \left[(\varepsilon - eV)^2 - \Delta^2 \right]^{-1/2} [n_1(\varepsilon - eV) - n_2(\varepsilon)] \, \mathrm{d}\varepsilon \end{aligned} \tag{22.4}$$

Since $T = 0$, it follows that $n(\varepsilon) = 0$ at $\varepsilon > 0$ and $n(\varepsilon) = 1$ at $\varepsilon < 0$. Hence, the difference $n_1 - n_2$ gives unity in the interval $0 < \varepsilon < eV$ and zero outside. The density of states under the integral is different from zero at $|\varepsilon - eV| > \Delta$, i.e., in this case $\varepsilon < eV - \Delta$. From this it follows that there is no current at $eV < \Delta$. At $eV > \Delta$ we have

$$\begin{aligned} j &\propto W \nu_{1n} \nu_{2n} \int_0^{eV - \Delta} (eV - \varepsilon) \left[(eV - \varepsilon)^2 - \Delta^2 \right]^{-1/2} \, \mathrm{d}\varepsilon \\ &= W \nu_{1n} \nu_{2n} \left[(eV)^2 - \Delta^2 \right]^{1/2} \end{aligned} \tag{22.5}$$

At $eV > \Delta$ the difference between the normal metal and the superconductor must disappear, i.e., the current must be the same as in the tunnel junction between two
normal metals, in which case we have

$$\frac{j}{j_n} = \frac{\left[(eV)^2 - \Delta^2 \right]^{1/2}}{eV} \tag{22.6}$$

- The introduction of negative ε is analogous to the transition in a normal metal from $|\xi|$ to ξ, i.e., from quasiparticles of particle- and antiparticle-type to the gas model.

The result is given in fig. 141 (curve 2).
Let us now consider the tunnel junction between two superconductors, which are assumed here, for simplicity, to be identical. Analogously to the foregoing, we find

$$j \propto W\nu_{\mathrm{n}}^2 \int_{\Delta}^{eV-\Delta} (eV-\varepsilon)\left[(eV-\varepsilon)^2-\Delta^2\right]^{-1/2} \varepsilon\left(\varepsilon^2-\Delta^2\right)^{-1/2}\ \mathrm{d}\varepsilon \tag{22.7}$$

The current is different from zero at $eV > 2\Delta$. Evaluation of the integral yields the following result:

$$\frac{j}{j_{\mathrm{n}}} = \mathrm{E}\left(\frac{\left[(eV)^2-(2\Delta)^2\right]^{1/2}}{eV}\right) - 2\left(\frac{\Delta}{eV}\right)^2\ \mathrm{K}\left(\frac{\left[(eV)^2-(2\Delta)^2\right]^{1/2}}{eV}\right), \tag{22.8}$$

where K and E are complete elliptic integrals of the first and second kind:
$K(k) = \int_0^{\pi/2}\ \mathrm{d}\varphi\left(1-k^2\sin^2\varphi\right)^{-1/2}$, $\mathrm{E}(k) = \int_0^{\pi/2}\ \mathrm{d}\varphi\left(1-k^2\sin^2\varphi\right)^{1/2}$.

As must be the case, $j/j_{\mathrm{n}} \to 1$ as $eV \to \infty$. However, in contrast to the junction between a superconductor and a normal metal, the threshold for the generation of current is at $eV = 2\Delta$ and at the threshold the current remains finite, i.e., as eV increases gradually, at the point $eV = 2\Delta$ a jump occurs in current from zero to a finite value. According to eq. (22.8), at $eV = 2\Delta$

$$\frac{j}{j_{\mathrm{n}}} = \frac{1}{4}\pi \tag{22.10}$$

The results are shown in fig. 141 (curve 3).
In principle, one can easily find the expressions for the tunnel current at $T \neq 0$. To this end, one must substitute into the general formula (22.4) the corresponding densities of states (with $\Delta(T)$) and the distribution functions at finite temperatures. We will not perform this calculation, because it involves cumbersome formulae with complex integrals; instead, we will describe the physical picture.

In the case of the $s-n$ junction at finite temperature in a superconductor there is a certain number of broken Cooper pairs. Therefore, individual electrons can pass through the barrier into the normal metal without an extra energy Δ. On the other hand, the electrons of the normal metal can pass into the superconductor, where there are partners with which they can form pairs. From this it is seen that electric current is generated at an arbitrary small potential difference and increases with increasing V. If the temperature is not close to T_{c}, the current increases especially
noticeably at $eV = \Delta(T)$, since the pair-breaking mechanism comes into play. In view of this, $\Delta(T)$ can be found experimentally directly from the maximum of the derivative $\mathrm{d}j/\mathrm{d}V$. It is even better to use for this purpose the junction between two identical superconductors, in which the current increases more drastically in the vicinity of $V = 2\Delta(T)/e$.

Consider now the characteristic of the tunnel junction of two different superconductors. It is easy to see that at $T = 0$ it will have a form similar to curve 3 in fig. 141 , with a discontinuity in the current at $V = (\Delta_1 + \Delta_2)/e$. The characteristic at finite temperature is more interesting. We shall assume that $T_{\mathrm{c}2} > T_{\mathrm{c}1}$ and $T \leqslant T_{\mathrm{c}1}$. Instead of the level diagram shown in fig. 142, we plot the density of states along the horizontal axis; for the left metal it will be plotted to the left and for the right metal to the right (fig. 137). Thermal excitation is represented conventionally as a certain number of carriers in the left upper band and a certain

number of empty states in the left lower band (in the superconductor on the right the excitation is small because of $T \ll T_{c2}$).

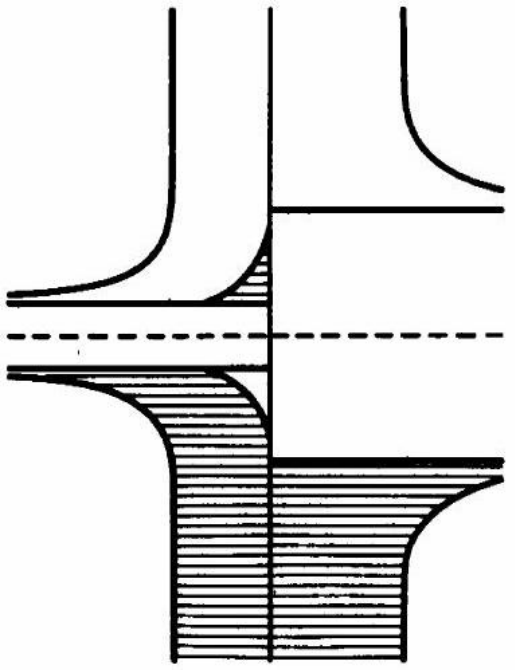


Fig. 143.

As the potential difference increases the left part of fig. 143 is shifted upwards relative to the right part. The current increases due to an increase in the number of thermally excited electrons which reside opposite the empty states in the right upper band. This will continue until the edge of the left upper band coincides with the edge of the right one, i.e., up to $V = (\Delta_2 - \Delta_1)/e$. Following this, the number of electrons capable of passing from left to right will remain constant and the number of empty states, which is proportional to the density of states, will decrease. Hence, the current-voltage characteristic $j(V)$ will bend downwards. This will continue until the upper edge of the lower left band is opposite the lower edge of the upper right band, i.e., up to $V = (\Delta_1 + \Delta_2)/e$, following which $j(V)$ will begin to increase. So, in the case under consideration the current-voltage characteristic will be nonmonotonic (fig. 144) (Giaever 1960b, Nicol et al. 1960).
noticeably at $eV = \Delta(T)$, since the pair-breaking mechanism comes into play. In view of this, $\Delta(T)$ can be found experimentally directly from the maximum of the derivative $\mathrm{d}j/\mathrm{d}V$. It is even better to use for this purpose the junction between two identical superconductors, in which the current increases more drastically in the vicinity of $V = 2\Delta(T)/e$.

Consider now the characteristic of the tunnel junction of two different superconductors. It is easy to see that at $T = 0$ it will have a form similar to curve 3 in fig. 141 , with a discontinuity in the current at $V = (\Delta_1 + \Delta_2)/e$. The characteristic at finite temperature is more interesting. We shall assume that $T_{c2} > T_{c1}$ and $T \leqslant T_{c1}$. Instead of the level diagram shown in fig. 142, we plot the density of states along the horizontal axis; for the left metal it will be plotted to the left and for the right metal to the right (fig. 137). Thermal excitation is represented conventionally as a certain number of carriers in the left upper band and a certain number of empty states in the left lower band (in the superconductor on the right the excitation is small because of $T \ll T_{c2}$).

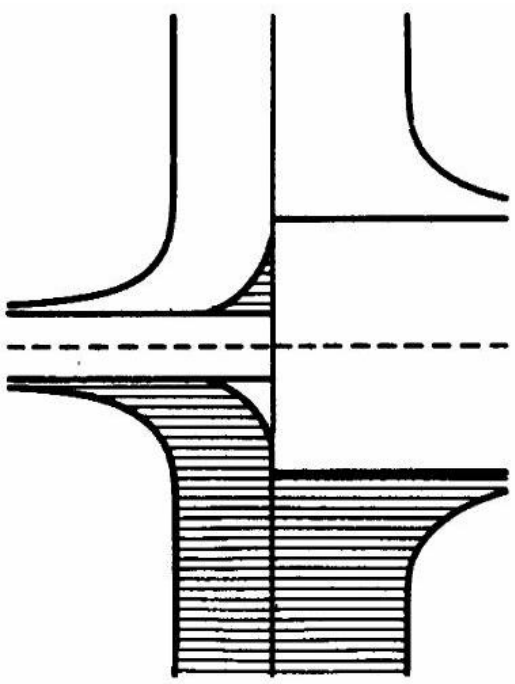


Fig. 143.

As the potential difference increases the left part of fig. 143 is shifted upwards relative to the right part. The current increases due to an increase in the number of thermally excited electrons which reside opposite the empty states in the right upper band. This will continue until the edge of the left upper band coincides with the edge of the right one, i.e., up to $V = (\Delta_2 - \Delta_1)/e$. Following this, the number of electrons capable of passing from left to right will remain constant and the number of empty states, which is proportional to the density of states, will decrease. Hence, the current-voltage characteristic $j(V)$ will bend downwards. This will continue until the upper edge of the lower left band is opposite the lower edge of the upper right band, i.e., up to $V = (\Delta_1 + \Delta_2)/e$, following which $j(V)$ will begin to increase. So, in the case under consideration the current-voltage characteristic will be nonmonotonic (fig. 144) (Giaever 1960b, Nicol et al. 1960).

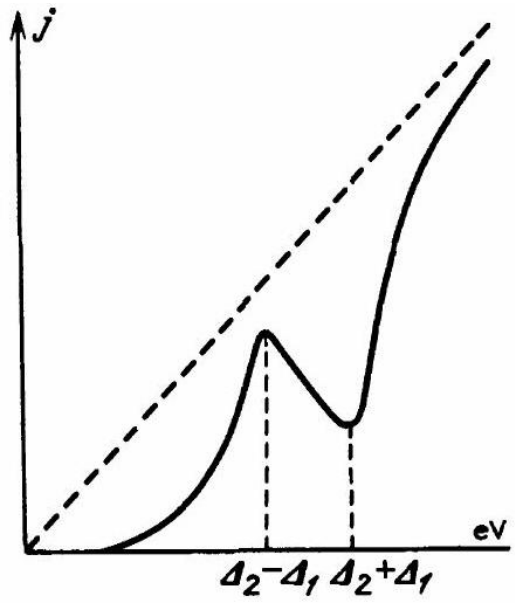


Fig. 144.

Tunnel junctions have played an important role in the direct determination of the energy gap Δ and the density of states and of their temperature dependence. In particular, with the aid of tunneling measurements it has been proved that gapless superconductivity is possible and the theory (Abrikosov and Gor'kov 1960a) has been confirmed quantitatively. Moreover, it has turned out that in the more exact theory, which takes account of the phonon spectrum and the energy dependence of the electron-phonon interaction, the tunneling characteristic makes it possible to determine the parameter $\alpha^2(\omega)\rho(\omega)$, where α is the electron-phonon interaction constant and $\rho(\omega)$ is the density of states of phonons. Since $\rho(\omega)$ can be determined independently, one can find $\alpha(\omega)$.

In concluding this section, we note that, apart from the tunnel current considered here, which is associated with the transfer of quasiparticles from one metal to another and which arises in the presence of a finite potential difference (a singleparticle current), there also exists a superconducting current flowing through the junction. The latter current will be considered in the sections that follow. There is no superconducting current in experiments if the insulating layer is rather thick (though in any case we may speak only of a few interatomic distances). In the case of a very thin insulating layer the two types of current are both generated, which manifest themselves in a peculiar manner in different circumstances. This point will be discussed below.

8.8.2 22.2. The Josephson effect

Up until now we have considered the metals on both sides of the junction separately, assuming that the coherent electronic states are formed on both sides independently. In fact, the passage of electrons through the barrier is the result of penetration of the electron wave function through the junction, and therefore a consistent theory
must deal with the formation of a coherent state in the electronic system as a whole. It may be said that at the junction between two superconductors the formation of Cooper pairs of electrons belonging to different metals is possible.

This circumstance leads to the possibility of pair tunneling with a probability comparable with the probability of tunneling of one electron and of the formation of a general condensate. Hence, at $V = 0$ a finite supercurrent can flow across the junction. This phenomenon was

predicted by Josephson (1962, 1964).

The magnitude of the Josephson superconducting current can be found from the following considerations (Josephson 1962, 1964). Let us find the excess energy associated with the existence of a tunnel junction and the presence of superconductivity. We shall evidently obtain an expression proportional to Δ_1 and Δ_2 and symmetrical with respect to these quantities. The simplest form is

$$\begin{aligned} E &= C \int \left[|\Delta_1 \Delta_2| - \frac{1}{2} \left(\Delta_1 \Delta_2^* + \Delta_1^* \Delta_2 \right) \right] \mathrm{d}y \ \mathrm{d}z \\ &= 2C \int |\Delta_1 \Delta_2| \left[1 - \cos \left(\chi_2 - \chi_1 \right) \right] \mathrm{d}y \ \mathrm{d}z \end{aligned}$$

(C is a constant and yz is the junction plane). We have assumed that $\Delta_{1,2}$ are complex and that the energy is normalized to zero at $\chi_1 - \chi_2 = 0$ (see below).

The dependence of the energy on the phase difference can be understood as follows. Suppose that a magnetic field parallel to the junction plane is applied; it is described by a vector potential $\boldsymbol{A}$. From the condition of gauge invariance it follows that the phase enters into the following combination with the vector potential:

$$\nabla \chi - \frac{2e}{\hbar c} A$$

We choose the vector potential to be normal to the junction plane (the x axis) and integrate the above-given combination over x from point 2 in the bulk of the left superconductor to point 1 in the bulk of the right one. As a result, we obtain

$$\chi_1 - \chi_2 - \frac{2e}{\hbar \dot{c}} \int_2^1 A_x \ \mathrm{d}x$$

Thus, in the presence of a magnetic field at the junction the energy is

$$E = C \int |\Delta_1 \Delta_2| \left[1 - \cos \left(\chi_1 - \chi_2 - \frac{2e}{ch} \int_2^1 A_x \ \mathrm{d}x \right) \right] \mathrm{d}y \ \mathrm{d}z \tag{22.11}$$

By varying with respect to $\boldsymbol{A_x}$ we have

$$\delta E = -\frac{2e}{c\hbar} C \int |\Delta_1 \Delta_2| \sin \left(\chi_1 - \chi_2 - \frac{2e}{c\hbar} \int_2^1 A_x \ \mathrm{d}x \right) \delta A_x \ \mathrm{d}V$$

However, according to the general formula of electrodynamics, the change in energy upon variation of the vector potential is given by

$$\delta E = -\frac{1}{c} \int j \delta A \ \mathrm{d}V$$

where $\boldsymbol{j}$ is the current density. Comparing the last two formulas, we obtain (we have changed the sign of the argument):

$$j = 2 \frac{e}{\hbar} C \left| \Delta_1 \Delta_2 \right| \sin \left(\chi_1 - \chi_2 - \frac{2e}{c\hbar} \int_2^1 A_x \ \mathrm{d}x \right).$$

The maximum magnitude of the sine is unity. Therefore we may write the following expression for the current:

$$j = j_c \sin \left(\chi_1 - \chi_2 - \frac{2e}{c\hbar} \int_2^1 A_x \ \mathrm{d}x \right), \tag{22.12}$$

where j_c is the critical current across the junction. In particular, in the absence of a field

$$j = j_c \sin(\chi_1 - \chi_2). \tag{22.13}$$

Thus, a phase difference for the functions Δ_1 and Δ_2 corresponds to the presence of a superconducting current.

According to the above derivation, j_c must be proportional to Δ_1 and Δ_2; it must also be proportional to the probability of electron tunneling through the junction. But the conductivity of the junction in the normal state, or R^{-1}, where R is the junction resistance, is proportional to the same quantity. In contrast to ordinary conductivity, it will be reasonable to write here $j = R^{-1}V$ (V is the potential difference) instead of $j = \sigma E$. The quantity R corresponds to the total resistance of 1 cm^2 of the junction area and has the dimensions of s $\cdot$ cm (or ohm $\cdot$cm^2).

The complete formula for two different superconductors at $T = 0$ has the form (Ambegoakar and Baratoff 1963)

$$j_c = \frac{2}{eR}\frac{\Delta_1\Delta_2}{\Delta_1 + \Delta_2}\,\mathrm{K}\left(\frac{|\Delta_1 - \Delta_2|}{\Delta_1 + \Delta_2}\right), \tag{22.14}$$

where K is a complete elliptic integral of the first kind (see formula 22.9). For two identical superconductors, we substitute $K(0) = \frac{1}{2}\pi$ and obtain

$$j_c = \frac{\pi\Delta}{2eR}. \tag{22.15}$$

At a finite temperature, instead of (22.15) we have (Ambegoakar and Baratoff 1963)

$$j_c = \frac{\pi\Delta(T)}{2eR}\tanh\left(\frac{\Delta(T)}{2T}\right). \tag{22.16}$$

In particular, near T_c,

$$j_c \approx \frac{\pi\Delta^2(T)}{4eRT_c}. \tag{22.17}$$

The microscopic derivation of formulas (22.14), (22.15) and (22.16) will be given in the next section.

For the Josephson effect to be observed in experiments, junctions with a resistivity of 0.1ohm $\cdot$ mm^2 are required. Actually, it is possible to attain even lower resistivities: 10^{-4}ohm $\cdot$ mm^2 and lower. The corresponding critical current density can reach $10^2 - 10^3$ A/cm^2. If we compare this value with the current density corresponding to the breakup of the pairs in a bulk superconductor (17.63), which is of the order of 10^8 A/cm^2, then the maximum Josephson effect appears to be much lower. Therefore, the Josephson effect and the associated phenomena are sometimes called weak superconductivity.

Thus, apart from the single-particle current found in the preceding section, a superconducting current not exceeding j_c may also flow across the tunnel junction. The Josephson effect is actually observed as follows. The current across the junction is varied and the potential difference is measured. At low magnitudes of the current V remains equal to zero. When the current exceeds j_c, there occurs a switching to the single-particle characteristic and when the current continues to increase the $V(j)$ follows the single-particle curve. However, when the current falls off, a hysteresis occurs rather commonly, namely the single-particle characteristic continues down to the point $j = 0, V = 2\Delta/e$ as V decreases, following which V vanishes in a jumpwise manner (see the oscillogram in fig. 145 for the two directions of the current).

Even in this simple example we see that the theoretical dependence of the current on the potential difference and the experimental determination of $V(j)$ give, in fact, different results,

which are accounted for by an abrupt jump of the characteristics measured from one regime to another and by the appearance of "steps", i.e., by a



Fig. 145.

In particular, near T_c,

$$j_c \approx \frac{\pi\Delta^2(T)}{4eRT_c}. \tag{22.17}$$

The microscopic derivation of formulas (22.14), (22.15) and (22.16) will be given in the next section.

For the Josephson effect to be observed in experiments, junctions with a resistivity of $0.1\text{ohm} \cdot \text{mm}^2$ are required. Actually, it is possible to attain even lower resistivities: 10^{-4} ohm $\cdot\text{mm}^2$ and lower. The corresponding critical current density can reach $10^2 - 10^3$ A/cm^2. If we compare this value with the current density corresponding to the breakup of the pairs in a bulk superconductor (17.63), which is of the order of 10^8 A/cm^2, then the maximum Josephson effect appears to be much lower. Therefore, the Josephson effect and the associated phenomena are sometimes called weak superconductivity.

Thus, apart from the single-particle current found in the preceding section, a superconducting current not exceeding j_c may also flow across the tunnel junction. The Josephson effect is actually observed as follows. The current across the junction is varied and the potential difference is measured. At low magnitudes of the current V remains equal to zero. When the current exceeds j_c, there occurs a switching to the single-particle characteristic and when the current continues to increase the $V(j)$ follows the single-particle curve. However, when the current falls off, a hysteresis occurs rather commonly, namely the single-particle characteristic continues down to the point $j = 0, V = 2\Delta/e$ as V decreases, following which V vanishes in a jumpwise manner (see the oscillogram in fig. 145 for the two directions of the current).

Even in this simple example we see that the theoretical dependence of the current on the potential difference and the experimental determination of $V(j)$ give, in fact, different results, which are accounted for by an abrupt jump of the characteristics measured from one regime to another and by the appearance of "steps", i.e., by a

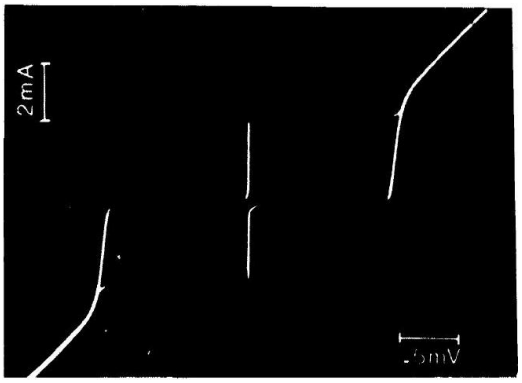


Fig. 145.

In particular, near T_c,

$$j_c \approx \frac{\pi \Delta^2(T)}{4eRT_c}. \tag{22.17}$$

The microscopic derivation of formulas (22.14), (22.15) and (22.16) will be given in the next section.

For the Josephson effect to be observed in experiments, junctions with a resistivity of 0.1ohm $\cdot$ mm^2 are required. Actually, it is possible to attain even lower resistivities: 10^{-4} ohm $\cdot$mm^2 and lower. The corresponding critical current density can reach $10^2 - 10^3$ A/cm^2. If we compare this value with the current density corresponding to the breakup of the pairs in a bulk superconductor (17.63), which is of the order of 10^8 A/cm^2, then the maximum Josephson effect appears to be much lower. Therefore, the Josephson effect and the associated phenomena are sometimes called weak superconductivity.

Thus, apart from the single-particle current found in the preceding section, a superconducting current not exceeding j_c may also flow across the tunnel junction. The Josephson effect is actually observed as follows. The current across the junction is varied and the potential difference is measured. At low magnitudes of the current V remains equal to zero. When the current exceeds j_c, there occurs a switching to the single-particle characteristic and when the current continues to increase the $V(j)$ follows the single-particle curve. However, when the current falls off, a hysteresis occurs rather commonly, namely the single-particle characteristic continues down to the point $j = 0, V = 2\Delta/e$ as V decreases, following which V vanishes in a jumpwise manner (see the oscillogram in fig. 145 for the two directions of the current).

Even in this simple example we see that the theoretical dependence of the current on the potential difference and the experimental determination of $V(j)$ give, in fact, different results, which are accounted for by an abrupt jump of the characteristics measured from one regime to another and by the appearance of "steps", i.e., by a

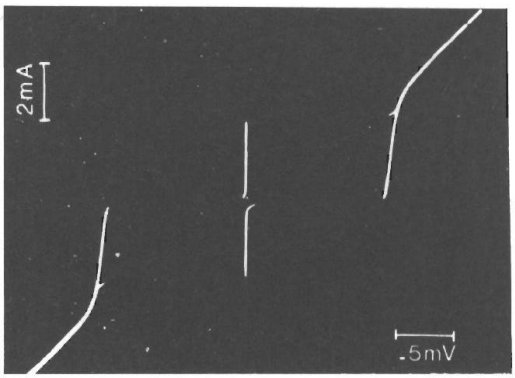


Fig. 145.

discontinuous variation of V at a given current. Since our purpose is to describe the fundamental aspect of the main physical phenomena, we will be concerned, as a rule, with the dependence $j(V)$, making qualitative reservations regarding the events that occur in actual measurements of $V(j)$.

Let us now examine the following problem. At first sight it seems that since the Josephson current and the single-particle current are proportional to the same quantity, namely R^{-1}, they must be observed under identical conditions. However, as has already been pointed out, in practice the Josephson effect disappears much earlier than the single-particle current with increasing $\boldsymbol{R}$. The cause is the fluctuational potential difference in the junction. This potential difference destroys the Josephson superconducting current but it has little effect on the single-particle current. This is associated with the fact that the single-particle current is generated at a finite potential difference and therefore small fluctuations are not important, whereas the Josephson current occurs at $V = 0$. According to the Nyquist theorem, the fluctuations in V increase proportionately to R (see Lifshitz and Pitaevskii 1978), which just accounts for the difference in behavior of the Josephson and single-particle currents. We shall confine ourselves to this qualitative explanation without describing the theory of fluctuations in the Josephson junctions (see Barone and Paterno 1982).

In concluding this section, we give a simple quantitative derivation of the Josephson current based on the Ginzburg-Landau theory (Aslamazov and Larkin 1969). The Josephson effect can be observed not only in a tunnel junction but also in any superconductor with a "weak link". One example is a film with a constriction (fig. 146) called a bridge. Upon passage of the current its density in the bridge may exceed the critical value (section 17.4). As a result, the bridge begins to play the same role with respect to the wider portions of the film as does the insulating layer in the tunnel junction between two superconductors. In particular, a Josephson current can flow across the bridge.

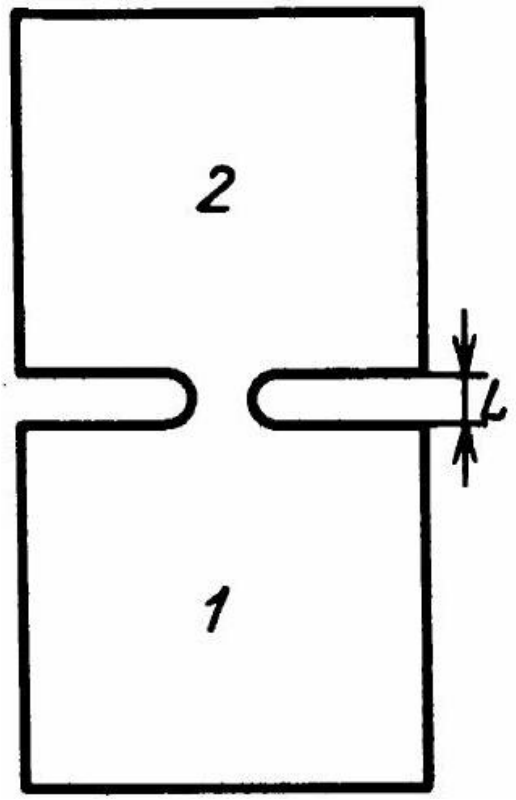


Fig. 146.

Because of the weakness of the Josephson current we may ignore the magnetic field generated by it. Let us write the first Ginzburg-Landau equation (17.6') in the absence of the field:

$$-\frac{1}{\chi^2}\Delta\Psi - \Psi + |\Psi|^2\Psi = 0. \tag{22.18}$$

Suppose that the bridge length L is much smaller than ξ (or, in reduced units, $L/\delta < x^{-1}$). In such a case the first term in eq. (22.18), which is of order $(\delta/xL)^{-2}$, is considerably larger than the remaining ones and we may retain only this term in eq. (22.18). So we obtain

$$\Delta\Psi = 0. \tag{22.19}$$

Far from the constriction $\Psi \to$ const. We assume that the constant is equal to $\exp(\mathrm{i}\chi_1)$ in the lower part and to $\exp(\mathrm{i}\chi_2)$ in the upper one (since in the bulk the current density is low and $|\Psi| = 1$). The solution of eq. (22.19) will be sought for in the form

$$\Psi = f(r)\exp(\mathrm{i}\chi_1) + [1 - f(r)]\exp(\mathrm{i}\chi_2)\,. \tag{22.20}$$

Evidently, the function $f(r)$ tends to unity in the bulk of film 1 and to zero in the bulk of film 2. Substituting into eq. (22.19) gives

$$\Delta f = 0.$$

The solution of this equation depends on the particular assumptions concerning the shape of the bridge.

Since we are interested only in the fundamental aspect of the problem, we will not consider the particular models; we substitute Ψ in the form (22.20) into the expression for the current (17.9) (with $\boldsymbol{A} = 0$) and use the ordinary units (here eq. 22.20 is multiplied by Ψ_0). As a result, we have

$$j = \frac{e\hbar}{m}\Psi_0^2 \nabla f \sin(\chi_1 - \chi_2) \tag{22.21}$$

This expression corresponds in form to (22.13) ($\nabla f \sim L^{-1}$), with $j_c \propto \Psi_0^2(T) \propto \Delta^2(T)$, just as in formula (22.17) for the tunnel junction in the neighborhood of T_c.

8.8.3 22.3. Microscopic derivation of the Josephson current

We shall employ the method of the so-called tunneling Hamiltonian. We assume that the creation and annihilation of electrons in the left superconductor is described by the operators $a^+_{p,\sigma}$and $a_{p,\sigma}$ and in the right one, accordingly, by $b^+_{p,\sigma}$and $b_{p,\sigma}$ and introduce an additional term into the Hamiltonian:

$$\mathscr{H}_T = \sum_{p,q,\sigma} T_{pq} a^+_{p,\sigma} b_{q,\sigma} + T^*_{pq} b^+_{q,\sigma} a_{p,\sigma}. \tag{22.22}$$

Because of the weakness of the Josephson current we may ignore the magnetic field generated by it. Let us write the first Ginzburg-Landau equation (17.6') in the absence of the field:

$$-\frac{1}{\chi^2}\Delta\Psi - \Psi + |\Psi|^2\Psi = 0. \tag{22.18}$$

Suppose that the bridge length L is much smaller than ξ (or, in reduced units, $L/\delta < x^{-1}$). In such a case the first term in eq. (22.18), which is of order $(\delta/xL)^{-2}$, is considerably larger than the remaining ones and we may retain only this term in eq. (22.18). So we obtain

$$\Delta\Psi = 0. \tag{22.19}$$

Far from the constriction $\Psi \to$ const. We assume that the constant is equal to $\exp(i\chi_1)$ in the lower part and to $\exp(i\chi_2)$ in the upper one (since in the bulk the current density is low and $|\Psi| = 1$). The solution of eq. (22.19) will be sought for in the form

$$\Psi = f(r)\exp(i\chi_1) + [1 - f(r)]\exp(i\chi_2). \tag{22.20}$$

Evidently, the function $f(r)$ tends to unity in the bulk of film 1 and to zero in the bulk of film 2. Substituting into eq. (22.19) gives

$$\Delta f = 0$$

The solution of this equation depends on the particular assumptions concerning the shape of the bridge.

Since we are interested only in the fundamental aspect of the problem, we will not consider the particular models; we substitute Ψ in the form (22.20) into the expression for the current (17.9) (with $\boldsymbol{A} = 0$) and use the ordinary units (here eq. 22.20 is multiplied by Ψ_0). As a result, we have

$$j = \frac{e\hbar}{m}\Psi_0^2 \nabla f \sin(\chi_1 - \chi_2) \tag{22.21}$$

This expression corresponds in form to (22.13) ($\nabla f \sim L^{-1}$), with $j_c \propto \Psi_0^2(T) \propto \Delta^2(T)$, just as in formula (22.17) for the tunnel junction in the neighborhood of T_c.

8.8.4 22.3. Microscopic derivation of the Josephson current

We shall employ the method of the so-called tunneling Hamiltonian. We assume that the creation and annihilation of electrons in the left superconductor is described by the operators $a^+_{p,\sigma}$and $a_{p,\sigma}$ and in the right one, accordingly, by $b^+_{p,\sigma}$and $b_{p,\sigma}$ and introduce an additional term into the Hamiltonian:

$$\mathscr{H}_{\mathrm{T}} = \sum_{p,q,\sigma} T_{pq} a^+_{p,\sigma} b_{q,\sigma} + T^*_{pq} b^+_{q,\sigma} a_{p,\sigma}. \tag{22.22}$$

Because of the weakness of the Josephson current we may ignore the magnetic field generated by it. Let us write the first Ginzburg-Landau equation (17.6') in the absence of the field:

$$-\frac{1}{\chi^2}\Delta\Psi - \Psi + |\Psi|^2\Psi = 0 \tag{22.18}$$

Suppose that the bridge length L is much smaller than ξ (or, in reduced units, $L/\delta < x^{-1}$). In such a case the first term in eq. (22.18), which is of order $(\delta/xL)^{-2}$, is considerably larger than the remaining ones and we may retain only this term in eq. (22.18). So we obtain

$$\Delta\Psi = 0. \tag{22.19}$$

Far from the constriction $\Psi \to$ const. We assume that the constant is equal to $\exp(\mathrm{i}\chi_1)$ in the lower part and to $\exp(\mathrm{i}\chi_2)$ in the upper one (since in the bulk the current density is low and $|\Psi| = 1$). The solution of eq. (22.19) will be sought for in the form

$$\Psi = f(r)\exp(\mathrm{i}\chi_1) + [1 - f(r)]\exp(\mathrm{i}\chi_2). \tag{22.20}$$

Evidently, the function $f(r)$ tends to unity in the bulk of film 1 and to zero in the bulk of film 2. Substituting into eq. (22.19) gives

$$\Delta f = 0.$$

The solution of this equation depends on the particular assumptions concerning the shape of the bridge.

Since we are interested only in the fundamental aspect of the problem, we will not consider the particular models; we substitute Ψ in the form (22.20) into the expression for the current (17.9) (with $\boldsymbol{A} = 0$) and use the ordinary units (here eq. 22.20 is multiplied by Ψ_0). As a result, we have

$$j = \frac{e\hbar}{m}\Psi_0^2 \nabla f \sin(\chi_1 - \chi_2) \tag{22.21}$$

This expression corresponds in form to (22.13) ($\nabla f \sim L^{-1}$), with $j_{\mathrm{c}} \propto \Psi_0^2(T) \propto \Delta^2(T)$, just as in formula (22.17) for the tunnel junction in the neighborhood of T_{c}.

8.8.5 22.3. Microscopic derivation of the Josephson current

We shall employ the method of the so-called tunneling Hamiltonian. We assume that the creation and annihilation of electrons in the left superconductor is described by the operators $a^+_{p,\sigma}$and $a_{p,\sigma}$ and in the right one, accordingly, by $b^+_{p,\sigma}$and $b_{p,\sigma}$ and introduce an additional term into the Hamiltonian:

$$\mathscr{H}_{\mathrm{T}} = \sum_{p,q,\sigma} T_{pq} a^+_{p,\sigma} b_{q,\sigma} + T^*_{pq} b^+_{q,\sigma} a_{p,\sigma}. \tag{22.22}$$

This additional term describes the transport of electrons from one metal to the other. Such a Hamiltonian, in fact, does not completely correspond to the problem under consideration because instead of the real potential barrier (22.22) it actually implies the transfer of free electrons from one phase space to another. However, with correct normalization of the transition matrix T_{pq} it is equivalent to the physical problem under consideration and therefore makes it possible to express the super-current in terms of the junction resistance in the normal state. It is this problem that we shall begin with.

The total current $\langle I \rangle$ from left to right is evidently equal to the rate of decrease of the number of electrons in the left metal multiplied by the electron charge. In accordance with quantum mechanics (see Landau and Lifshitz 1974), the current operator is given by

$$J = -e\dot{N}_{\mathrm{L}} = -\frac{ie}{\hbar}\left[\mathscr{K} N_{\mathrm{L}}\right] = -\frac{ie}{\hbar}\left[\mathscr{H}_{\mathrm{T}} N_{\mathrm{L}}\right], \tag{22.23}$$

where only the part $\mathscr{H}_T$ of the total Hamiltonian is left because it is only this part of the Hamiltonian that leads to nonconservation of the numbers of electrons in the left and the right metal separately, i.e., it does not commute with N_{L} and N_{R}. Substituting expression (22.22) for $\mathscr{H}_T$ into eq. (22.23) and

$$N_L = \sum_{p,\sigma} a^+_{p,\sigma} a_{p,\sigma} \tag{22.24}$$

(section 16.4), we obtain

$$J = \frac{ie}{\hbar}\left(\sum_{p,q,\sigma} T_{pq} a^+_{p,\sigma} b_{q,\sigma} - \sum_{p,q,\sigma} T^*_{pq} b^+_{q,\sigma} a_{p,\sigma}\right). \tag{22.25}$$

The above expression is the operator which is to be averaged over the state of the system. For a normal metal, to within the terms of order $(T/\mu)^2$ we can average over the state at $T = 0$. Thus,

$$\langle J \rangle = \langle \psi_0^* J \psi_0 \rangle . \tag{22.26}$$

Because of the smallness of the electron tunneling probability, we could have taken ψ_0 in a first approximation for the principal part of the Hamiltonian without $\mathscr{H}_T$. However, such an average is equal to zero. In view of this, we find the first approximation to the function ψ_0.

According to perturbation theory (see Landau and Lifshitz 1974),

$$\psi_0 \approx \psi_0^{(0)} + \psi_0^{(1)} = \psi_0^{(0)} + \sum_m \frac{(\mathscr{H}_{\mathrm{T}})_{m0}}{E_0^{(0)} - E_m^{(0)} + \mathrm{i}\delta} \psi_m^{(0)}, \tag{22.27}$$

where the sum runs over the excited states of the system and the superscript (0) signifies that we are dealing with the eigenstates and functions of the Hamiltonian without $\mathscr{H}_{\mathbf{T}}$. The correction i δ in the denominator takes account of the circumstance

This additional term describes the transport of electrons from one metal to the other. Such a Hamiltonian, in fact, does not completely correspond to the problem under consideration because instead of the real potential barrier (22.22) it actually implies the transfer of free electrons from one phase space to another. However, with correct normalization of the transition matrix T_{pq} it is equivalent to the physical problem under consideration and therefore makes it possible to express the super-current in terms of the junction resistance in the normal state. It is this problem that we shall begin with.

The total current $\langle I \rangle$ from left to right is evidently equal to the rate of decrease of the number of electrons in the left metal multiplied by the electron charge. In accordance with quantum mechanics (see Landau and Lifshitz 1974), the current operator is given by

$$J = -e\dot{N}_{\mathrm{L}} = -\frac{ie}{\hbar}\left[\mathscr{K} N_{\mathrm{L}}\right] = -\frac{ie}{\hbar}\left[\mathscr{H}_{\mathrm{T}} N_{\mathrm{L}}\right], \tag{22.23}$$

where only the part $\mathscr{H}_{\mathrm{T}}$ of the total Hamiltonian is left because it is only this part of the Hamiltonian that leads to nonconservation of the numbers of electrons in the left and the right metal separately, i.e., it does not commute with N_{L} and N_{R}. Substituting expression (22.22) for $\mathscr{H}_T$ into eq. (22.23) and

$$N_L = \sum_{p,\sigma} a^+_{p,\sigma} a_{p,\sigma} \tag{22.24}$$

(section 16.4), we obtain

$$J = \frac{ie}{\hbar}\left(\sum_{p,q,\sigma} T_{pq} a^+_{p,\sigma} b_{q,\sigma} - \sum_{p,q,\sigma} T^*_{pq} b^+_{q,\sigma} a_{p,\sigma}\right). \tag{22.25}$$

The above expression is the operator which is to be averaged over the state of the system. For a normal metal, to within the terms of order $(T/\mu)^2$ we can average over the state at $T = 0$. Thus,

$$\langle J\rangle = \langle \psi_0^* J \psi_0\rangle .$$

Because of the smallness of the electron tunneling probability, we could have taken ψ_0 in a first approximation for the principal part of the Hamiltonian without $\mathscr{H}_{\mathrm{T}}$. However, such an average is equal to zero. In view of this, we find the first approximation to the function ψ_0.

According to perturbation theory (see Landau and Lifshitz 1974),

$$\psi_0 \approx \psi_0^{(0)} + \psi_0^{(1)} = \psi_0^{(0)} + \sum_m \frac{(\mathscr{H}_{\mathrm{T}})_{m0}}{E_0^{(0)} - E_m^{(0)} + \mathrm{i}\delta}\psi_m^{(0)}, \tag{22.27}$$

where the sum runs over the excited states of the system and the superscript (0) signifies that we are dealing with the eigenstates and functions of the Hamiltonian without $\mathscr{H}_{\boldsymbol{T}}$. The correction i δ in the denominator takes account of the circumstance
that the spectrum is, in fact, continuous (see Landau and Lifshitz 1974). Substitution into (22.26) yields

$$\langle J\rangle = \left\langle \psi_0^{(1)*} J \psi_0^{(0)}\right\rangle + \left\langle \psi_0^{(0)*} J \psi_0^{(1)}\right\rangle . \tag{22.28}$$

Using formulae (22.25), (22.27) and (22.22), we easily find that only those terms are nonzero which enter into the products $T_{pq}T^*_{pq} = |T_{pq}|^2$. The resultant expression contains the differences

$$\frac{1}{E_0^{(0)} - E_m^{(0)} + \mathrm{i}\delta} - \frac{1}{E_0^{(0)} - E_m^{(0)} - \mathrm{i}\delta} = -2\pi\mathrm{i}\delta\left(E_0^{(0)} - E_m^{(0)}\right),$$

because the principal values of such denominators cancel and only the residue in the pole is retained. The final result is

$$\begin{aligned}\langle J\rangle =& \frac{2\pi e}{\hbar}\sum_{m,p,q,\sigma} |T_{pq}|^2\,\delta\left(E_0^{(0)} - E_m^{(0)}\right)\\ &\times\left[\left(a^+_{p,\sigma}b_{q,\sigma}\right)_{0m}\left(b^+_{q,\sigma}a_{p,\sigma}\right)_{m0} - \left(b^+_{q,\sigma}a_{p,\sigma}\right)_{0m}\left(a^+_{p,\sigma}b_{q,\sigma}\right)_{m0}\right].\end{aligned} \tag{22.29}$$

The expression in brackets gives

$$n_{p,\sigma}\left(1-n_{q,\sigma}\right)-n_{q,\sigma}\left(1-n_{p,\sigma}\right)=n_{p,\sigma}-n_{q,\sigma}$$
$$=n_{\mathrm{F}}\left(\xi_p-eV\right)-n_{\mathrm{F}}\left(\xi_q\right)$$

where n_{F} are the Fermi functions and their arguments correspond to the fact that a potential difference is applied to the junction. Passing from the summation over the momenta to integration and taking into account that only the electrons in the vicinity of the Fermi boundary are involved in the current, we obtain

$$\sum_p \to V_1\left(\frac{1}{2}\nu_1\right)\int \mathrm{d}\xi_p$$

where V_1 is the volume of the left metal and ν_1 is the density of states; then

$$\langle J\rangle = \frac{4\pi e}{\hbar}V_1V_2\left(\frac{1}{2}\nu_1\right)\left(\frac{1}{2}\nu_2\right)\overline{|T_{pq}|^2}$$
$$\times\int \mathrm{d}\xi_p\int \mathrm{d}\xi_q\delta\left(\xi_p-\xi_q\right)\left[n_{\mathrm{F}}\left(\xi_p-eV\right)-n_{\mathrm{F}}\left(\xi_q\right)\right]$$

where $\overline{|T_{pq}|^2}$ signifies the average over both Fermi surfaces. Taking the integral and dividing by the junction area, we obtain the current density

$$j=\frac{\pi e}{\hbar}eV\nu_1\nu_2\overline{|T_{pq}|^2}\frac{V_1V_2}{S}.$$

Writing this expression in the form $j=V/R$, we have

$$\frac{1}{R}=\frac{\pi e^2}{\hbar}\nu_1\nu_2\left|\overline{T_{pq}|^2}\frac{V_1V_2}{S}.\right. \tag{22.30}$$

It is not difficult to see that since T_{pq} has the dimensions of the energy R has the correct dimensions cm.s. At the same time it is clear that the correct normalization of T_{pq} must include the factor $\left(V_1V_2/S\right)^{-1/2}$.

Let us now find the Josephson current for two superconductors, expressing it first in terms of $|T_{pq}|^2$ and then with the aid of formula (22.30) in terms of R. To do this, we return to formulas (22.28), (22.27) and (22.25). The expressions thus obtained contain terms of two types: terms that contain a^+a and b^+b and those which include the combination a^+a^+bb or aab^+b^+. We have used terms of the first type in the derivative of the current flowing across the normal junction and they vanish at $V=0$. In a superconductor they give a single-particle current, which we derived with the aid of a more concise method in section 22.1, and they are also equal to zero in the absence of a potential difference.

The remaining terms have the form

$$\mathrm{i}\frac{e}{\hbar}\sum_{p,q,\sigma,m}\left[T_{pq}T_{p_1q_1}\left(a^+_{p,\sigma}b_{q,\sigma}\right)_{0m}\left(a^+_{p_1,\sigma_1}b_{q_1,\sigma_1}\right)_{m0}\right.$$
$$\times\left(\frac{1}{E_0^{(0)}-E_m^{(0)}+\mathrm{i}\delta}+\frac{1}{E_0^{(0)}-E_m^{(0)}-\mathrm{i}\delta}\right)$$
$$-T^*_{pq}T^*_{p_1q_1}\left(b_{q,\sigma}a_{p,\sigma}\right)_{0m}\left(b^+_{q_1,\sigma_1}a^+_{p_1,\sigma_1}\right)_{m0}$$
$$\left.\times\left(\frac{1}{E_0^{(0)}-E_m^{(0)}+\mathrm{i}\delta}+\frac{1}{\left(E_0^{(0)}+E_m^{(0)}+\mathrm{i}\delta\right.}\right)\right]$$

We transform the operators $a_{p,\sigma}$ and $b_{q,\sigma}$ using the Bogoliubov formulas (16.14). However, in this particular case, there is no ground for considering the coefficients u_p and v_p to be real since, in contrast to the thermodynamic quantities, the Josephson current depends not only on the moduli but also on the phases of these quantities. In view of this, we write the Bogoliubov transformation in a somewhat modified form:

$$a_{p,+} = u_p \alpha_{p,+} + v_p^* \alpha_{-p,-}^+, \quad a_{p,-} = u_p \alpha_{p,-} - v_p^* \alpha_{-p,+}^+, \tag{22.31}$$

where $|u_p|^2 + |v_p|^2 = 1$. Here, having performed all the calculations of section 16.4, we get

$$\begin{aligned} &|u_p|^2 = \tfrac{1}{2}\left(1 + \tfrac{\xi_p}{\varepsilon_p}\right), \quad |v_p|^2 = \tfrac{1}{2}\left(1 - \tfrac{\xi_p}{\varepsilon_p}\right), \\ &\varepsilon_p = \left(\xi_p^2 + |\Delta|^2\right)^{1/2}, \quad \Delta = g \textstyle\sum_p u_p v_p^* \left(1 - n_{p,+} - n_{p,-}\right). \end{aligned} \tag{22.32}$$

Averaging of the operator at $T \neq 0$ must be carried out, strictly speaking, in two stages: first over the given quantum states and then over the Gibbs distribution. However, we can use the fact that the entire system composed of a large number of particles is in a certain quantum state with an accuracy of up to small fluctuations, this state being characterized by the equilibrium occupation numbers $n_F(\varepsilon)$.

One more property of the matrix T_{pq} will be required here. As has been noted in section 1.1, the Schrödinger equation is invariant under the transformation $t \to -t$ and $\psi \to \psi^*$. With this transformation the momenta p and q change sign [$\exp(\mathrm{i}pr/\hbar) \to \exp(-\mathrm{i}pr/\hbar)$] and there also occurs the inversion of the tunneling transition, i.e., $b_q \rightleftharpoons a_{-p}$. This means that T_{pq} has the following property:

$$T_{pq} = T_{-p-q}^* \tag{22.33}$$

After performing rather simple but time-consuming calculations we obtain an expression proportional to $u_p^* v_p u_q v_q^* - u_p v_p^* u_q^* v_q$. If we assume that $u_p^* v_p = |u_p|\,|v_p| \exp(\mathrm{i}\chi_1)$, $u_q^* v_q = |u_q|\,|v_q| \exp(\mathrm{i}\chi_2)$, then this difference is equal to $|u_p v_p u_q v_q|\, 2\mathrm{i} \sin(\chi_1 - \chi_2)$. As regards the energy denominators, it follows that, in contrast to a normal metal, the terms with $+\mathrm{i}\delta$ and $-\mathrm{i}\delta$ add up, i.e., the doubled principal value of the integral is retained. On the whole, we obtain

$$\begin{aligned} \langle J \rangle =& 8\frac{e}{\hbar} \sum_{p,q} |u_p v_p u_q v_q|\, |T_{pq}|^2 \sin(\chi_1 - \chi_2) \\ &\times \left[\frac{n_p (1 - n_q)}{\varepsilon_p - \varepsilon_q} - \frac{n_p n_q}{\varepsilon_p + \varepsilon_q} + \frac{(1 - n_p)(1 - n_q)}{\varepsilon_p + \varepsilon_q} - \frac{(1 - n_p) n_q}{\varepsilon_p - \varepsilon_q} \right]. \end{aligned}$$

Collecting terms with identical denominators, using the formula

$$|u_p v_p| = \frac{|\Delta|}{2\varepsilon_p} \tag{22.34}$$

and passing over from summation to integration first over ξ_p and ξ_q and then over ε_p and ε_q (with account taken of two possible signs of ξ), and, finally, expressing the Fermi functions via the hyperbolic tangents, we obtain

$$\begin{aligned} j =& -\frac{2e}{\hbar} \overline{|T_{pq}|^2} \frac{V_1 V_2}{S} \sin(\chi_1 - \chi_2)\, \nu_1 \nu_2 \Delta_1 \Delta_2 \\ &\times \int_{\Delta_1}^{\infty} \mathrm{d}\varepsilon_1 \int_{\Delta_2}^{\infty} \mathrm{d}\varepsilon_2 \frac{\left[\varepsilon_1 \tanh\left(\frac{\varepsilon_2}{2T}\right) - \varepsilon_2 \tanh\left(\frac{\varepsilon_1}{2T}\right)\right]}{\left(\varepsilon_1^2 - \varepsilon_2^2\right) \xi_1 \xi_2} \end{aligned}$$

where $\xi_{1,2} = \left(\varepsilon_{1,2}^2 - \Delta_{1,2}^2\right)^{1/2}$.

Let us first consider the integral over ε_1. It may be written in the form of a contour integral in

a complex plane with branch cuts along the real axis from Δ to ∞ and from $-\infty$ to $-\Delta$ (fig. 147a). Following this, the contour of integration can may be "straightened up" (fig. 147b) and, as a result, we obtain the sum of residues from

One more property of the matrix T_{pq} will be required here. As has been noted in section 1.1, the Schrödinger equation is invariant under the transformation $t \to -t$ and $\psi \to \psi^*$. With this transformation the momenta p and q change sign [$\exp(ipr/\hbar) \to \exp(-ipr/\hbar)$] and there also occurs the inversion of the tunneling transition, i.e., $b_q \rightleftharpoons a_{-p}$. This means that T_{pq} has the following property:

$$T_{pq} = T^*_{-p-q}. \tag{22.33}$$

After performing rather simple but time-consuming calculations we obtain an expression proportional to $u_p^* v_p u_q v_q^* - u_p v_p^* u_q^* v_q$. If we assume that $u_p^* v_p = |u_p|\,|v_p| \exp(i\chi_1)$, $u_q^* v_q = |u_q|\,|v_q| \exp(i\chi_2)$, then this difference is equal to $|u_p v_p u_q v_q|\, 2i \sin(\chi_1 - \chi_2)$. As regards the energy denominators, it follows that, in contrast to a normal metal, the terms with $+i\delta$ and $-i\delta$ add up, i.e., the doubled principal value of the integral is retained. On the whole, we obtain

$$\begin{aligned}\langle J \rangle =& 8\frac{e}{\hbar} \sum_{p,q} |u_p v_p u_q v_q|\, |T_{pq}|^2 \sin(\chi_1 - \chi_2) \\ &\times \left[\frac{n_p (1 - n_q)}{\varepsilon_p - \varepsilon_q} - \frac{n_p n_q}{\varepsilon_p + \varepsilon_q} + \frac{(1 - n_p)(1 - n_q)}{\varepsilon_p + \varepsilon_q} - \frac{(1 - n_p) n_q}{\varepsilon_p - \varepsilon_q} \right].\end{aligned}$$

Collecting terms with identical denominators, using the formula

$$|u_p v_p| = \frac{|\Delta|}{2\varepsilon_p} \tag{22.34}$$

and passing over from summation to integration first over ξ_p and ξ_q and then over ε_p and ε_q (with account taken of two possible signs of ξ), and, finally, expressing the Fermi functions via the hyperbolic tangents, we obtain

$$\begin{aligned} j =& -\frac{2e}{\hbar} \overline{|T_{pq}|^2} \frac{V_1 V_2}{S} \sin(\chi_1 - \chi_2)\, \nu_1 \nu_2 \Delta_1 \Delta_2 \\ &\times \int_{\Delta_1}^{\infty} d\varepsilon_1 \int_{\Delta_2}^{\infty} d\varepsilon_2 \frac{\left[\varepsilon_1 \tanh\left(\frac{\varepsilon_2}{2T}\right) - \varepsilon_2 \tanh\left(\frac{\varepsilon_1}{2T}\right)\right]}{(\varepsilon_1^2 - \varepsilon_2^2)\, \xi_1 \xi_2} \end{aligned}$$

where $\xi_{1,2} = \left(\varepsilon_{1,2}^2 - \Delta_{1,2}^2\right)^{1/2}$.

Let us first consider the integral over ε_1. It may be written in the form of a contour integral in a complex plane with branch cuts along the real axis from Δ to ∞ and from $-\infty$ to $-\Delta$ (fig. 147a). Following this, the contour of integration can may be "straightened up" (fig. 147b) and, as a result, we obtain the sum of residues from

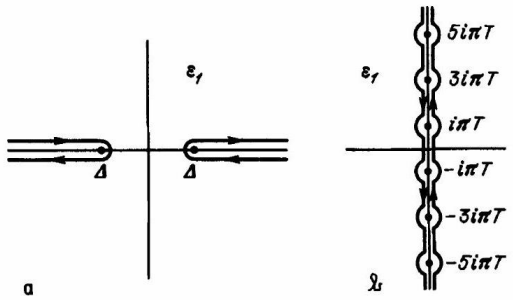


Fig. 147.

$\tanh(\varepsilon_1/2T)$, which are located at the points $\mathrm{i}\pi T(2n+1)$:

$$\int_\Delta^\infty \mathrm{d}\varepsilon_1 \cdots = \frac{1}{4}\int_C \mathrm{d}\varepsilon_1 \cdots$$
$$= \frac{1}{4}\cdot 2T\cdot 2\pi \sum_{n=-\infty}^{\infty} \varepsilon_2 \frac{1}{[\pi^2T^2(2n+1)^2+\varepsilon_2^2]\,[\pi^2T^2(2n+1)^2+\Delta_1^2]^{1/2}\,(\varepsilon_2^2-\Delta_2^2)^{1/2}}$$

Now the same procedure will be used for the integral over ε_2. In each of the terms of the sum over n there are two residues with respect to ε_2 at $\pm\mathrm{i}\pi T(2n+1)$. As a result, we get $j = j_\mathrm{c}\sin(\chi_1-\chi_2)$, where

$$j_\mathrm{c} = \frac{2}{eR}\pi T\Delta_1\Delta_2 \sum_{n=0}^{\infty} \frac{1}{[\pi^2T^2(2n+1)^2+\Delta_1^2]^{1/2}} \frac{1}{[\pi^2T^2(2n+1)^2+\Delta_2^2]^{1/2}}.$$

Let us consider two cases. Suppose the metals are identical. In this case, using relation (21.1),

$$\sum_{n=1}^{\infty} \frac{1}{(2n-1)^2+x^2} = \frac{\pi}{4x}\tanh\left(\frac{1}{2}\pi x\right),$$

we have

$$j_\mathrm{c} = \frac{\pi}{2eR}\Delta\tanh\left(\frac{\Delta}{2T}\right),$$

which corresponds to formulae (22.13) and (22.16).
Suppose now that the metals are different but $T\to 0$. Here the intervals between the values of $\pi T(2n+1)$ are small as compared with Δ and we may replace the sum by an integral. As a result, we have

$$j_\mathrm{c} = \frac{1}{eR}\Delta_1\Delta_2\int_0^\infty \frac{\mathrm{d}\omega}{(\omega^2+\Delta_1^2)^{1/2}\,(\omega^2+\Delta_2^2)^{1/2}}$$
$$= \frac{2}{eR}\frac{\Delta_1\Delta_2}{\Delta_1+\Delta_2}K\left(\frac{|\Delta_1-\Delta_2|}{\Delta_1+\Delta_2}\right)$$

that is, formula (22.14).

8.8.6 22.4. The Josephson effect in a magnetic field

Suppose that a magnetic field is applied parallel to the plane of the tunnel junction (yz). Let, for example, H be directed along z. In this case, we may introduce a vector potential:

$$A_x = H_z(x)y. \tag{22.35}$$

The area of the junction is assumed to be so small that the effect of the field created by the current may be neglected. The relevant condition will be derived later. In the presence of the field the current density has the form of (22.12). Taking into account that H_z does not depend on x in the insulating layer (d') and falls off in the superconductor by the law $\exp(-x/\delta)$, we get

$$\int_2^1 A_x\,\mathrm{d}x = H_{z0}yd \tag{22.36}$$

where

$$d = 2\delta(T) + d' \approx 2\delta(T). \tag{22.37}$$

Here we have taken into account that $d' \sim 10^{-7} - 10^{-8}$ cm and $\delta(T) \sim 10^{-5} - 10^{-6}$ cm. Hence, the current density in the presence of a steady field has the form ($H \equiv H_{z0}$)

$$j = j_c \sin\left(\chi_1 - \chi_2 + \frac{2eHdy}{c\hbar}\right). \tag{22.38}$$

Thus, the current density in the presence of a field varies in a direction perpendicular to the field and even changes sign.

In practice, naturally it is the total current that is measured or, what is the same thing, the average current density. Since in the direction of the field the current is homogeneous, the average current density is given by

$$\begin{aligned}\bar{j} &= \frac{1}{L}\int_0^L j(y)\mathrm{d}y \\ &= j_c \frac{c\hbar}{2eHLd}\left[-\cos\left(\chi_1 - \chi_2 + \frac{2e}{c\hbar}HLd\right) + \cos\left(\chi_1 - \chi_2\right)\right]\end{aligned} \tag{22.38'}$$

where L is the length of the junction along y. It is not difficult to see that $HLd = \Phi$ is the field flux across the junction. Introducing the flux quantum $\Phi_0 = \pi\hbar c/e$, we may write expression (22.38) in the form

$$\bar{j} = j_c \frac{\Phi_0}{\pi\Phi}\sin\left(\frac{\pi\Phi}{\Phi_0}\right)\sin\left(\theta_0 + \frac{\pi\Phi}{\Phi_0}\right), \tag{23.39}$$

where $\theta_0 = \chi_1 - \chi_2$.

From eq. (22.39) it follows that $\bar{j}$ vanishes at $\Phi = n\Phi_0$, i.e., when the field flux across the junction is equal to an integer number of quanta. The maximum value of current in the intervals between these values is obtained by the choice of the phase difference and evidently corresponds to $\sin\left[\theta_0 - (\pi\Phi/\Phi_0)\right] = \pm 1$. As a result, it turns out that (Rowell 1963)

$$\bar{j}_{\max} = j_c \left|\frac{\sin\left(\pi\Phi/\Phi_0\right)}{\pi\Phi/\Phi_0}\right|. \tag{22.40}$$

The graph of this function is given in fig. 148. The importance of the dependence (22.40) lies in the fact that it allows one to measure the value of d, i.e., $\delta(T)$ from the points in which $\bar{j}_{\max} = 0$. In principle, one could also use this dependence for measuring the magnetic field, but in practice Josephson interferometers are used for this purpose (section 22.8).

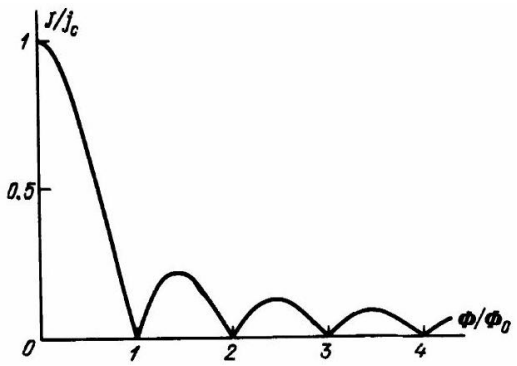


Fig. 148.

Now we shall be concerned with the study of a wide junction, in which case we cannot neglect the field generated by the Josephson current. Here, even in the absence of the external field the distribution of current along the junction becomes nonuniform. Let θ denote the complete argument in formula (22.12). Although the inhomogeneity of the field along y no longer permits us to take the vector potential in the form (22.35), the difference $\theta(y+dy)-\theta(y)$ may still be written as

$$\theta(y+\mathrm{d}y)-\theta(y)=\frac{2e}{\hbar c}H(y)d\cdot\ \mathrm{d}y=\frac{2\pi}{\Phi_0}H(y)d\cdot\ \mathrm{d}y$$

(we assume that H has only one component, H_z). From this we see that

$$H(y)=\frac{\Phi_0}{2\pi d}\frac{\mathrm{d}\theta}{\mathrm{d}y}. \tag{22.41}$$

According to Maxwell's equation

$$j=\frac{c}{4\pi}\frac{\mathrm{d}H}{\mathrm{d}y}. \tag{22.42}$$

At the same time, $j=j_\mathrm{c}\sin\theta$. Substituting this into eq. (22.42) and using eq. (22.41), we arrive at the equation for $\boldsymbol{\theta}$ (Ferrell and Prange 1963)

$$\frac{\mathrm{d}^2\theta}{\mathrm{d}y^2}=\frac{\sin\theta}{\delta_\mathrm{J}^2}, \tag{22.43}$$

where

$$\delta_\mathrm{J}=\left(\frac{c\Phi_0}{8\pi^2 j_\mathrm{c}d}\right)^{1/2} \tag{22.44}$$

Let us consider a case where there is a field $H_y=H$ but there is no net current across the junction. If the field is low, the quantity θ may be assumed to be small. Replacing $\sin\theta$ by θ, we obtain

$$\frac{\mathrm{d}^2\theta}{\mathrm{d}y^2}=\frac{\theta}{\delta_\mathrm{J}^2}, \tag{22.45}$$

the solution of which is

$$\theta=\theta_0\exp\left(\frac{-y}{\delta_\mathrm{J}}\right).$$

Inserting this into eq. (22.41) gives

$$H(y)=H_0\exp\left(\frac{-y}{\delta_\mathrm{J}}\right). \tag{22.46}$$

The result obtained is easy to interpret. If the super-conducting current can flow across the junction, it can screen out the applied field. The corresponding penetration depth δ_J is given by formula (22.44). If we substitute into it the orders of magnitudes of the parameters, then for $j_\mathrm{c}\sim 10^2$ A/cm^2 we obtain $\delta_\mathrm{J}\sim 10^{-2}$ cm, which is much larger than the ordinary penetration depth. The junction may be regarded as narrow if its width $L<\delta_\mathrm{J}$. In this case, the field of the current may be neglected and no screening of the external magnetic field takes place. But if $L>\delta_\mathrm{J}$, the junction is wide and the screening must be taken into account.

Thus, the Josephson junction is, to a certain extent, a two-dimensional superconductor with the corresponding Meissner effect. As a matter of fact, of course, the current lines are closed

in the three-dimensional space: the current flows in both superconductors perpendicular to the field in a layer of thickness δ (fig. 149a).

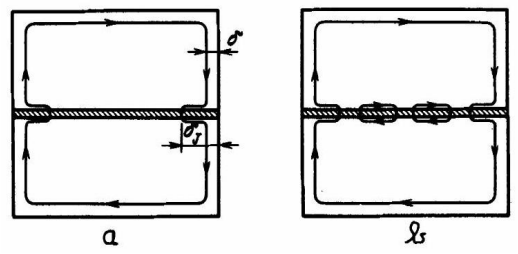


Fig. 149.

So far we have considered the field to be weak and made the replacement $\sin\theta \approx \theta$. In the case of a strong field this cannot be done. Let us return to eq. (22.43); we multiply both sides by $\mathrm{d}\theta/\mathrm{d}y$ and integrate over y. As a result, we get

$$\left(\frac{\mathrm{d}\theta}{\mathrm{d}y}\right)^2 = -2\frac{\cos\theta}{\delta_\mathrm{J}^2} + C \tag{22.47}$$

(C is a constant). This gives (it is convenient here to fix the point where $\theta = \pi$)

$$y - y_0 = \int_\pi^\theta \mathrm{d}\theta_1 \left(C - 2\frac{\cos\theta_1}{\delta_\mathrm{J}^2}\right)^{-1/2}. \tag{22.48}$$

Let us find a solution of the "soliton" type, in which the current is nonzero in a narrow vicinity of some point and is equal to zero far from it. Then, $\mathrm{d}\theta/\mathrm{d}y \to 0$ as $y \to \pm\infty$. This can be attained by assuming that $\theta \to 0$ with $y \to -\infty$ and $\theta \to 2\pi$ with $y \to \infty$. In this case $C = 2\delta_\mathrm{J}^{-2}$ in eq. (22.47). The integral (22.48) is easily evaluated in such a case; as a result, we obtain

$$\theta(y) = 4\arctan\left[\exp\left(\frac{y - y_0}{\delta_\mathrm{J}}\right)\right]. \tag{22.49}$$

The plots for $\theta(y)$, the field and current are given in fig. 150. From these plots it is seen that the solution obtained corresponds to a vortex with the center at y_0*. The picture of current lines (for two vortices) is shown in fig. 149b.

Let us find the field flux in a single vortex. According to (22.41),

$$\Phi = d\int_{-\infty}^{\infty} H\ \mathrm{d}y = \frac{\Phi_0}{2\pi d} d[\theta(\infty) - \theta(-\infty)] = \Phi_0.$$

Thus, the vortex carries a magnetic flux quantum. We come to the conclusion that the Josephson junction in the external field is the two-dimensional analog of a type II superconductor.

*The idea of the appearance of such vortices was advanced by Josephson (Josephson 1965).

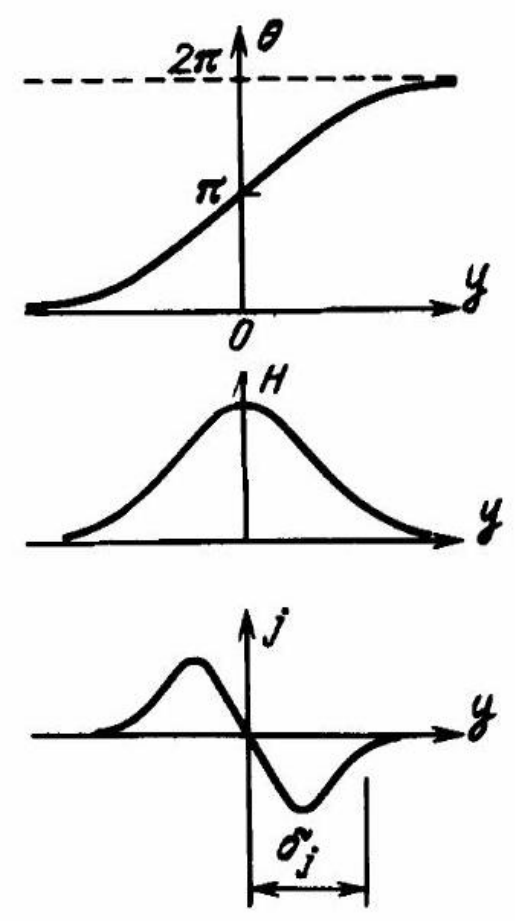


Fig. 150.

Vortices begin to be formed in an external field $H = H_{c1}$, which is of the order of the average field in the vortex, i.e., $H_{c1} \sim \Phi_0/(d\delta_J)$. The exact formula reads (Josephson 1965):

$$H_{c1} = \frac{2\Phi_0}{\pi^2 \delta_J d}. \tag{22.50}$$

The vortex concentration increases with increasing field, but since the Josephson vortex has no "normal core", in which the order parameter decreases strongly, it follows that no transition occurs to the normal state at any field H_{c2}.

In the limiting case at high fields the vortices overlap and the field in the junction is almost homogeneous*. From (22.41) it follows that mainly $\theta \approx H(2\pi d/\Phi_0)(y - y_0)$, i.e., $\mathrm{d}\theta/\mathrm{d}y = \text{const}$. According to eqs. (22.47) and (22.48), the second term in parentheses of the integrand (22.48) is much smaller than the first and we can carry out an expansion. Finally, we find

$$\theta \approx H\frac{2\pi d}{\Phi_0}(y - y_0) - \left(\frac{H_{c1}\pi}{4H}\right)^2 \sin\left(2\pi d H \frac{y - y_0}{\Phi_0}\right), \tag{22.51}$$

where we have used formula (22.50). Thus, in addition to the regular increase of the phase in the junction plane in a direction perpendicular to the field there occur small oscillations of the phase, which fall off rapidly in amplitude with increasing field.

*In this sense, a strong field leads to the same situation that occurs in a narrow junction. This is natural: in both cases the Josephson current cannot screen out the field.

8.8.7 22.5. The ac Josephson effect

Suppose that the current passing through the Josephson junction becomes larger than the critical current. In this case, superconductivity is destroyed and a potential difference appears. From the condition of gauge invariance it follows that in the equations the potential always appears together with the derivative of the phase with respect to time in the combination (section 19.6)

$$2e\varphi + \hbar\frac{\partial\chi}{\partial t}$$

that is, $(2e/\hbar)\int^t \varphi(t_1)\,\mathrm{d}t_1$ is added to the phase χ. This means that in the presence of the potential difference the phase difference satisfies the equation

$$\frac{\partial\theta}{\partial t} = \frac{2e}{\hbar}V \tag{22.52}$$

where $V = \varphi_1 - \varphi_2$. If $V = \text{const.}$, then the phase difference is given by

$$\theta = \theta_0 + \frac{2eV}{\hbar}t. \tag{22.53}$$

This relation was first derived by Josephson (Josephson 1962, 1964) for the tunnel junction, but, as was found out later, it describes the so-called resistive state of superconductors in various cases (for example, see formula 22.91, section 22.9). Thus, if a constant potential difference is maintained at the junction, an alternating current will flow across the junction:

$$j = j_\mathrm{c}\sin\left(\theta_0 + \frac{2eV}{\hbar}t\right). \tag{22.54}$$

The frequency

$$\omega = 2eV/\hbar \tag{22.55}$$

corresponds to 10^{11} s^{-1} for $V \sim 10^{-4}V$.
As has been noted in section 22.2, the potential difference is measured experimentally at a given current. The current is made up of a normal (single-particle) and a superconducting current. The normal current is V/R (we are considering a case where V is not too close to $2\Delta/e$) or, according to eq. (22.52), $(\hbar/2eR)\partial\theta/\partial t$. Thus, we have

$$j = j_\mathrm{c}\sin\theta + \frac{\hbar}{2eR}\frac{\partial\theta}{\partial t}. \tag{22.56}$$

Integration of this equation gives

$$\theta = 2\arctan\left\{\left[1 - \left(\frac{j_c}{j}\right)^2\right]^{1/2}\tan\left[eRt\frac{(j^2 - j_c^2)^{1/2}}{\hbar}\right] + \frac{j_c}{j}\right\}. \tag{22.57}$$

8.8.8 22.5. The ac Josephson effect

Suppose that the current passing through the Josephson junction becomes larger than the critical current. In this case, superconductivity is destroyed and a potential difference appears. From the condition of gauge invariance it follows that in the equations the potential always appears together with the derivative of the phase with respect to time in the combination (section 19.6)

$$2e\varphi + \hbar\frac{\partial\chi}{\partial t}$$

that is, $(2e/\hbar)\int^t \varphi(t_1)\,\mathrm{d}t_1$ is added to the phase χ. This means that in the presence of the potential difference the phase difference satisfies the equation

$$\frac{\partial\theta}{\partial t} = \frac{2e}{\hbar}V \tag{22.52}$$

where $V = \varphi_1 - \varphi_2$. If $V = \text{const.}$, then the phase difference is given by

$$\theta = \theta_0 + \frac{2eV}{\hbar}t. \tag{22.53}$$

This relation was first derived by Josephson (Josephson 1962, 1964) for the tunnel junction, but, as was found out later, it describes the so-called resistive state of superconductors in various cases (for example, see formula 22.91, section 22.9). Thus, if a constant potential difference is maintained at the junction, an alternating current will flow across the junction:

$$j = j_\mathrm{c}\sin\left(\theta_0 + \frac{2eV}{\hbar}t\right). \tag{22.54}$$

The frequency

$$\omega = 2eV/\hbar \tag{22.55}$$

corresponds to $10^{11}\ \mathrm{s}^{-1}$ for $V \sim 10^{-4}V$.
As has been noted in section 22.2, the potential difference is measured experimentally at a given current. The current is made up of a normal (single-particle) and a superconducting current. The normal current is V/R (we are considering a case where V is not too close to $2\Delta/e$) or, according to eq. (22.52), $(\hbar/2eR)\partial\theta/\partial t$. Thus, we have

$$j = j_\mathrm{c}\sin\theta + \frac{\hbar}{2eR}\frac{\partial\theta}{\partial t}. \tag{22.56}$$

Integration of this equation gives

$$\theta = 2\arctan\left\{\left[1 - \left(\frac{j_c}{j}\right)^2\right]^{1/2}\tan\left[eRt\frac{(j^2 - j_c^2)^{1/2}}{\hbar}\right] + \frac{j_c}{j}\right\}. \tag{22.57}$$

From this, using $V = (\hbar/2e)\mathrm{d}\theta/\mathrm{d}t$, we find (Aslamazov and Larkin 1969)

$$V(t) = \frac{Rj\,(j^2 - j_\mathrm{c}^2)}{\left[j^2 + j_\mathrm{c}^2\cos\omega t + j_\mathrm{c}\,(j^2 - j_\mathrm{c}^2)^{1/2}\sin\omega t\right]}, \tag{22.58}$$

where

$$\omega = \frac{2eR}{\hbar}\left(j^2 - j_\mathrm{c}^2\right)^{1/2}. \tag{22.59}$$

This formula may be rewritten in the form

$$V(t) = R\frac{(j^2 - j_\mathrm{c}^2)}{j + j_\mathrm{c}\cos(\omega t - \theta_1)}, \tag{/}$$

where $\theta_1 = \arccos(j_\mathrm{c}/j)$. As $j \to \infty, V \to Rj$, i.e., tends to the value for a normal metal. The plot of V/Rj_c against ωt is given in fig. 151 for several values of j_c/j.

Averaging of formula (22.58) over time gives

$$\bar{V} = \frac{1}{2\pi}\int_0^{2\pi} V(t)\mathrm{d}(\omega t) = R\left(j^2 - j_\mathrm{c}^2\right)^{1/2} = \frac{\omega\hbar}{2e}. \tag{22.60}$$

This dependence $\bar{V}(j)$ has been confirmed experimentally. Note also that when a steady current is maintained the average voltage and the frequency ω (22.59) are connected by the Josephson relation (22.55). The average values $\bar{V}/(Rj_\mathrm{c})$ are marked by dashed lines in fig. 151.

Since the tunnel junction is simultaneously a planar capacitor, it has a certain capacitance, i.e., there is a charge on the capacitor plates equal to $Q = CV$, the capacitance being given by $C = \varepsilon/(4\pi d')$, where d' is the thickness of the insulator

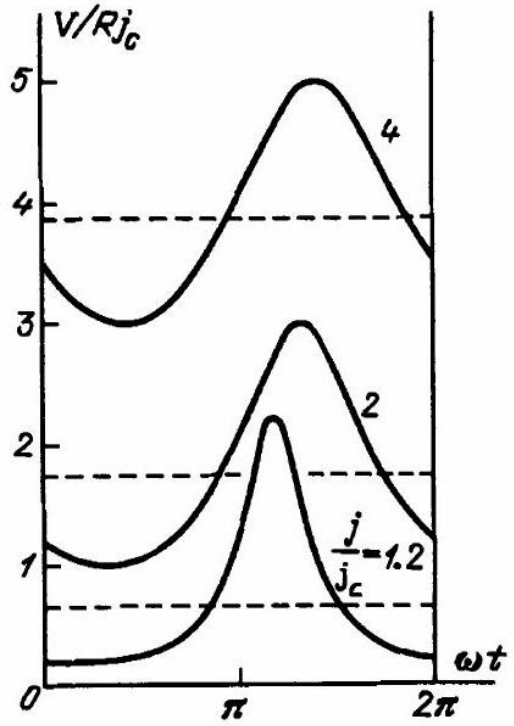


Fig. 151.

layer and ε is its dielectric constant. The change of this charge Q with time also makes a contribution to the current, which is equal to $\partial Q/\partial t = C\partial V/\partial t = (C\hbar/2e)\partial^2\theta/\partial t^2$, so that the complete equation is written, instead of (22.56), in the form (McCumber 1968, Stewart 1968, Johnson 1968)

$$j = j_\mathrm{c}\sin\theta + \frac{\hbar}{2eR}\frac{\partial\theta}{\partial t} + \frac{C\hbar}{2e}\frac{\partial^2\theta}{\partial t^2}. \tag{22.61}$$

We shall not consider her all the possible limiting cases. The limit considered above corresponds to a small capacitance or, more exactly, to a case where the third term in (22.61) is small compared to the second term, i.e., $\omega C/R \sim CeR^2 j/\hbar < 1$.

Associated with the ac Josephson effect is also another peculiar phenomenon: the appearance of steps in the voltage-current characteristic when a varying external field is applied (Josephson 1962, 1964, Shapiro 1963, Shapiro et al. 1964)*. The experiment is carried out as follows. A steady current j is passed across the Josephson junction and, besides, a varying potential difference $v\cos\Omega t$ is applied. The timeaveraged current-voltage characteristic, i.e., $\overline{V(t)}$, is taken as a function of j. Here, for the sake of simplicity, we state the problem in a different manner; we assume that the following potential difference is applied to the junction:

$$V(t) = V_0 + v\cos\Omega t, \tag{22.62}$$

and we find the current.
From (22.52) we have

$$\theta(t) = \frac{2e}{\hbar}\left(V_0 t + \frac{v}{\Omega}\sin\Omega t + \theta_0\right). \tag{22.63}$$

The Josephson current is equal to

$$\begin{aligned} j =& j_\mathrm{c}\sin\theta(t) = j_\mathrm{c}\sin\left[\frac{2e}{\hbar}\left(V_0 t + \theta_0\right)\right]\cos\left(\frac{2ev}{\hbar\Omega}\sin\Omega t\right) \\ &+ j_\mathrm{c}\cos\left[\frac{2e}{\hbar}\left(V_0 t + \theta_0\right)\right]\sin\left(\frac{2ev}{\hbar\Omega}\sin\Omega t\right) \end{aligned} \tag{22.64}$$

The anharmonic factor appearing in this expression may be expanded in Fourier series:

$$\begin{aligned} \cos(a\sin\Omega t) &= \sum_{n=-\infty}^{\infty} A_n \exp(\mathrm{i}n\Omega t), \\ \sin(a\sin\Omega t) &= \sum_{n=-\infty}^{\infty} B_n \exp(\mathrm{i}n\Omega t), \end{aligned}$$

where

$$\begin{aligned} A_n &= \frac{1}{2\pi}\int^{2\pi} \cos(a\sin x)\exp(-\mathrm{i}nx)\mathrm{d}x = \mathrm{J}_{2k}(a), \quad n = 2k \\ B_n &= \frac{1}{2\pi}\int_0^{2\pi} \sin(a\sin x)\exp(-\mathrm{i}nx)\mathrm{d}x \\ &= -\mathrm{i}\mathrm{J}_{2k+1}(a), \quad n = 2k+1 \end{aligned}$$

where J_n are Bessel functions. Substituting into formula (22.64) and using the rule $\mathrm{J}_n(x) = (-1)^n\ \mathrm{J}_{-n}(x)$, we obtain

$$\begin{aligned} j = j_\mathrm{c}\sin&\left[\frac{2e}{\hbar}\left(V_0 t + \theta_0\right)\right]\left[\mathrm{J}_0\left(\frac{2ev}{\hbar\Omega}\right) + 2\sum_{k=1}^{\infty}\mathrm{J}_{2k}\left(\frac{2ev}{\hbar\Omega}\right)\cos(2k\Omega t)\right] \\ &+ j_\mathrm{c}\cos\left[\frac{2e}{\hbar}\left(V_0 t + \theta_0\right)\right]\left[2\sum_{k=1}^{\infty}\mathrm{J}_{2k-1}\left(\frac{2ev}{\hbar\Omega}\right)\sin[(2k-1)\Omega]\right]. \end{aligned} \tag{22.65}$$

Separating some particular term of the first sum, we get

$$\begin{aligned} j_\mathrm{c}\sin&\left[\frac{2e}{\hbar}\left(V_0 t + \theta_0\right)\cdot 2\ \mathrm{J}_{2k}\left(\frac{2ev}{\hbar\Omega}\right)\cos(2k\Omega t)\right] \\ &= j_\mathrm{c}\ \mathrm{J}_{2k}\left(\frac{2ev}{\hbar\Omega}\right)\left\{\sin\left[\left(\frac{2ev_0}{\hbar} + 2k\Omega\right)t + \theta_0\right]\right. \\ &\qquad \left. + \sin\left[\left(\frac{2eV_0}{\hbar} - 2k\Omega\right)t + \theta_0\right]\right\}. \end{aligned}$$

Any term of the second sum transforms to the following form in an analogous way:

*They are usually called Shapiro steps after the author of the experimental discovery.

$$j_c\ \mathrm{J}_{2k-1}\left(\frac{2ev}{\hbar\Omega}\right)\left\{\sin\left[\left(\frac{2eV_0}{\hbar}+(2k-1)\Omega\right)t+\theta_0\right]\right.$$
$$\left.-\sin\left[\left(\frac{2eV_0}{\hbar}-(2k-1)\Omega\right)t+\theta_0\right]\right\}.$$

Thus, we see that in a case where

$$\frac{2eV_0}{\hbar}=n\Omega, \tag{22.66}$$

where n is an integer, a time-independent term appears in the current, which is proportional to

$$\bar{j}_n=(-1)^n j_c\ \mathrm{J}_n\left(\frac{2ev}{\hbar\Omega}\right)\sin\theta_0. \tag{22.67}$$

This means that in the $\bar{j}_n(V_0)$ curve resonance peaks add up to the single-particle current (section 22.1) at values of V_0 given by formula (22.66).

As has already been said, in experiments actually the potential difference is measured at a given current. In order to obtain an exact answer, we have to solve the equation for the phase, as has been done in the absence of a high-frequency field. However, if resonance corrections are not too large, we may use the following procedure. We plot the $\bar{j}(V_0)$ curve by adding to the single-particle characteristic vertical portions corresponding to the maximum values of resonance corrections, i.e., $\max\bar{j}_n = j_c\,|J_n(2eV/\hbar\Omega)|$ at $V_0 = V_{0n} = n\hbar\Omega/2e$. An increase in the current leads to a jumpwise change in regime, from purely superconducting ($V_0 = 0$) to the case with a finite V_0; this occurs whenever the current reaches the end of the corresponding vertical portion. This gives rise to a stepped curve (fig. 152)*. Actually, this was the first experimental demonstration of the ac Josephson effect (Shapiro 1963, Shapiro et al. 1964).

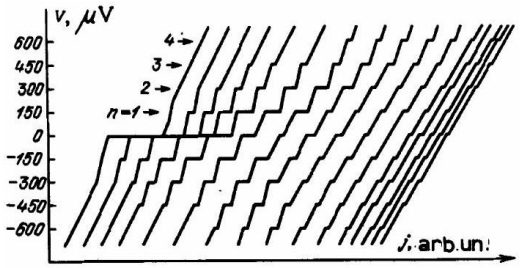


Fig. 152.

In concluding this section, we give a physical interpretation of relations (22.55) and (22.66). While passing the static potential difference, the Cooper pair receives an excess energy and can emit it in the form of a quantum with $\hbar\omega = 2eV$. But if the junction is in an external field, there occurs an exchange of energy with the external field, in which emission and absorption of many quanta of the external field are possible. This is described by formula (22.66).

8.8.9 22.6. Waves in the Josephson junction

Suppose that the Josephson junction is simultaneously subjected to the action of a steady magnetic field and a steady potential difference. In such a case, the phase

difference has simultaneously space and time components. In accordance with formulas (22.38) and (22.54) we find

$$j = j_c \sin\left[\theta_0 + \frac{2eV}{\hbar}t + \frac{2eHd}{\hbar c}y\right]. \tag{22.68}$$

But this is nothing but the moving wave formula. The frequency of this wave is $\omega = 2eV/\hbar$ and the wave vector $k = 2eHd/\hbar c$. Hence, the phase velocity is given by

$$v_0 = \frac{\omega}{k} = \frac{cV}{Hd}. \tag{22.69}$$

The physical meaning of this formula consists in that upon application of the potential difference the sinusoidal current density (22.38) begins to shift along the junction with a constant velocity (22.69) (Eck et al. 1964).

The result (22.68) refers to a case where a steady potential difference and a steady magnetic field are maintained in the junction. Let us now find the waves that propagate spontaneously along the junction. To this end, we make use of the formula for the current (22.61) and substitute into it the Maxwell equation (22.42), expressing H with the aid of formula (22.41). As a result, we obtain the equation

$$\frac{\partial^2\theta}{\partial y^2} - \frac{1}{c_0^2}\left(\frac{\partial^2\theta}{\partial t^2} + \gamma\frac{\partial\theta}{\partial t}\right) = \frac{\sin\theta}{\delta_J^2}, \tag{22.70}$$

where

$$c_0 = \left(\frac{ec}{4\pi^2 dC\hbar\Phi_0}\right)^{1/2} = c\left(\frac{d'}{\varepsilon d}\right)^{1/2}, \tag{22.71}$$

$$\gamma = \tau^{-1} = \frac{1}{RC}. \tag{22.72}$$

The penetration depth δ_J is expressed by formula (22.44) and the capacitance is given by $C = \varepsilon/(4\pi d')$.

If we assume that there is no Josephson current i.e., if we put $j_c = 0$, then $\delta_J = \infty$ and the right-hand side of eq. (22.70) vanishes. If we also neglect damping, i.e., if we set $\gamma = 0$, we will obtain the equation for the propagation of waves with a velocity c_0. From formula (22.71) it follows that this velocity is much less than the velocity of light. Although the equation is written for a somewhat unusual quantity - the phase difference - we may rewrite it in the form of an equation for H by differentiating with respect to z, and in the form of the an equation for E by differentiating with respect to t. Thus, we see that in the absence of a Josephson current along the junction between two superconductors separated by an insulating barrier, waves can propagate with the velocity c_0. Such waves are called Swihart waves (Swihart 1961).

Let us now consider eq. (22.70) in detail, i.e., we assume that a Josephson current is possible. Without damping (i.e., at $\gamma = 0$) this equation is usually called the sine-Gordon equation (upon replacement of $\sin\theta$ by θ it corresponds to the Klein-Gordon-Fock equation for elementary particles with zero spin). It is rather evident
that in the presence of a potential difference and magnetic field a peculiar resonance may arise when the phase velocity of Josephson waves v_0 coincides with the velocity c_0(22.71) (Eck et al.

- Figure 146 shows the experimental characteristics of a point Nb – Nb junction (Grimes and Shapiro 1968). The abscissa is the current and the ordinate represents the potential difference. Each of the curves corresponds to both directions of the current. The different curves correspond to different amplitudes of the high-frequency field and are shifted relative to one another along the abscissa (the null current is taken as the center of symmetry of a given curve). Actually, in the problem with a given current the steps are not exactly rectangular: instead of a jump at some critical j there is a variation $V(j)$.

1964). In order to find the result, we assume that the right-hand side of (22.70) is small and look for a solution in the form (Kulik 1965)

$$\theta = \theta^{(0)} + \theta^{(1)},$$

where $\theta^{(1)} < \theta^{(0)}$ and

$$\theta^{(0)} = \theta_0 + \frac{2eV}{\hbar}t + \frac{2eHd}{\hbar}y = \theta_0 + \omega t + ky.$$

To first order we obtain from eq. (22.70)

$$\frac{\partial^2\theta^{(1)}}{\partial y^2} - \frac{1}{c_0^2}\left(\frac{\partial^2\theta^{(1)}}{\partial t^2} + \gamma\frac{\partial\theta^{(1)}}{\partial t}\right) = \frac{\sin\left(\theta_0 + \omega t + ky\right)}{\delta_\mathrm{J}^2}. \tag{22.73}$$

From this we find

$$\theta^{(1)} = \frac{c_0^2}{\delta_\mathrm{J}^2}\,\mathrm{Im}\left\{\frac{\exp\left[\mathrm{i}\left(\theta_0 + \omega t + ky\right)\right]}{\omega^2 - c_0^2k^2 - \mathrm{i}\omega\gamma}\right\}. \tag{22.74}$$

We substitute expression (22.74) into the complete formula for the Josephson current $j = j_\mathrm{c}\sin\theta$ and average it over time and coordinate*:

$$\begin{aligned}\bar{j} &= \lim_{\substack{T\to\infty\\L\to\infty}}\frac{1}{T}\int_0^T \mathrm{d}t\frac{1}{L}\int_0^L \mathrm{d}y j_\mathrm{c}\sin\theta(y,t)\\ &\approx \lim_{\substack{T\to\infty\\L\to\infty}}\frac{1}{T}\int_0^T \mathrm{d}t\frac{1}{L}\int_0^L \mathrm{d}y j_\mathrm{c}\cos\theta^{(0)}(y,t)\theta^{(1)}(y,t)\\ &= j_\mathrm{c}\frac{\omega c_0^2\gamma}{2\delta_\mathrm{J}^2}\frac{1}{\left(\omega^2 - c_0^2k^2\right)^2 + \omega^2\gamma^2}\end{aligned} \tag{22.75}$$

Thus, we obtain a sharp maximum of the average current at $\omega = c_0k$ or $v_0 = c_0$, i.e., according to eq. (22.69),

$$v_0 = \left(\frac{c_0}{c}\right)Hd \tag{22.76}$$

(fig. 153). In this case, there is a resonance with respect to the phase velocities of Josephson and Swihart waves. The condition for the applicability of the result obtained is the smallness of $\bar{j}$ as compared with j_c. Taking $\bar{j}$ in the maximum, we find

$$\frac{c_0^2}{\delta_\mathrm{J}^2} < \omega\gamma, \tag{22.77}$$

that is, the damping γ must not be too small.

*The remaining current components (the single-particle current and the capacitive current) are proportional to the time derivatives of θ and upon averaging they give zero.

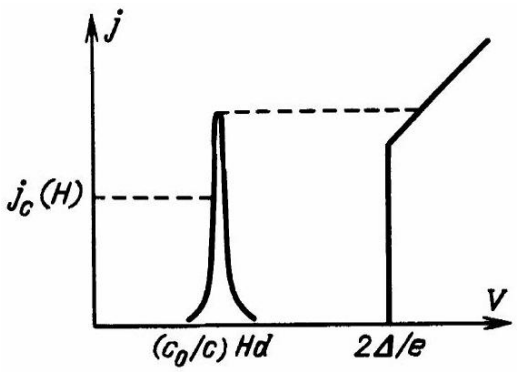


Fig. 153.

As has been repeatedly noted, in practice a steady current across the junction is specified and the steady part of the arising potential difference is recorded. Just as upon application of a varying field, in the case under consideration the current increases up to a limiting value at a given voltage, which is followed by a discontinuous switch to a different regime with a different voltage, i.e., steps appear in the characteristic (see fig. 153).

In order for the above-described resonance effect $v_0 = c_0$ to be observed, it is necessary that the principal Josephson maximum at $V = 0$ be not greater than the resonance maximum with the condition (22.76). Otherwise, a switch will occur of the characteristics with $V = 0$ to the single-particle branch. In view of this, one has to choose the value of the magnetic field close to the value that makes the principal Josephson current vanish (see formula (22.40).

Up until now we have considered the junction to be infinite. A finite junction of width L permits the generation of standing electromagnetic waves if there is an integer number of half-waves within a distance L, i.e., $L = \frac{1}{2}n\lambda$ or $k_n = n\pi/L$. The corresponding frequencies are

$$\omega_n = \frac{c_0 n\pi}{L}. \tag{22.78}$$

Such frequencies correspond to potential differences $V_n = \hbar\omega_n/2e$, i.e.,

$$V_n = \frac{\hbar c_0}{2e}\frac{n\pi}{L}. \tag{22.79}$$

Therefore, instead of a single resonance for an infinite junction, we obtain a set of discrete resonances. We shall not give here a detailed derivation; we confine ourselves to a description of the qualitative picture.

Calculation (Kulik 1965, Dmitrenko et al. 1965) shows that at V_n defined by condition (22.79) sharp maxima of the average current $\bar{j}$ appear at $V = V_n$. The height of these maxima depends on n in such a manner that the highest maximum
is that which most closely corresponds to the resonance condition for phase velocities, (22.76), i.e., that for which

$$\left|V_{n_0} - \frac{c_0}{c}Hd\right| = \min. \tag{22.80}$$

Hence, by varying H we can shift the modulation of the "fence" of the maxima (22.79). Since in actual experiments one is concerned with the measurement of $\bar{V}(j)$ instead of $\bar{j}(V)$, a stepped characteristic is obtained (fig. 154), whose shape is essentially governed by the magnetic field H (the term adopted in the literature is "Fiske steps" after the author who discovered them (Fiske 1964).

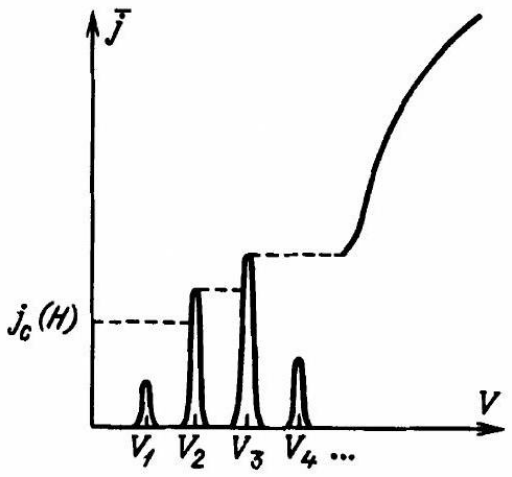


Fig. 154.

As the width of the junction increases the spacing between the adjacent maxima decreases in accordance with formula (22.79). The maxima begin to overlap, and in the limit $L \to \infty$ the curve (22.75) is obtained (cf. figs. 154 and 153).

These properties of the characteristic of finite junctions have been used for the generation of electromagnetic waves with the aid of Josephson junctions (Yanson et al. 1965; Langenberg et al. 1965). One of the resonances (22.79) was used; its amplitude was increased by choosing the magnetic field in accordance with condition (22.80).

8.8.10 22.7. Josephson junctions with a normal metal or a semiconductor layer

In the section that follows we will consider various methods used to prepare Josephson junctions. One of the most widespread is still a tunnel junction with an insulating barrier. However, it is rather difficult to prepare such a junction in a controlled manner. As has already been said, the insulator barrier must be very thin and have no short-circuited portions. The usual procedure is the oxidation of a
is that which most closely corresponds to the resonance condition for phase velocities, (22.76), i.e., that for which

$$\left| V_{n_0} - \frac{c_0}{c} Hd \right| = \min . \tag{22.80}$$

Hence, by varying H we can shift the modulation of the "fence" of the maxima (22.79). Since in actual experiments one is concerned with the measurement of $\bar{V}(j)$ instead of $\bar{j}(V)$, a stepped characteristic is obtained (fig. 154), whose shape is essentially governed by the magnetic field H (the term adopted in the literature is "Fiske steps" after the author who discovered them (Fiske 1964).

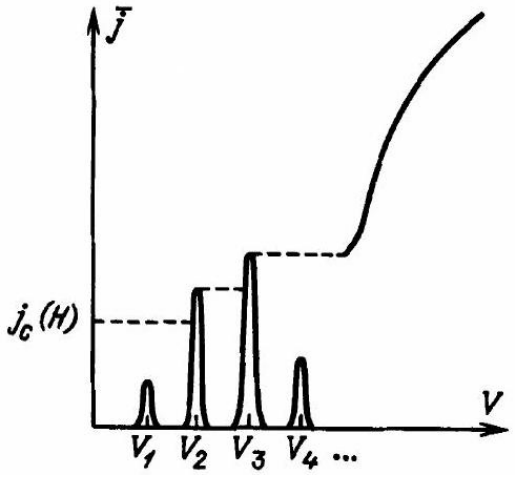


Fig. 154.

As the width of the junction increases the spacing between the adjacent maxima decreases in accordance with formula (22.79). The maxima begin to overlap, and in the limit $L \to \infty$ the curve (22.75) is obtained (cf. figs. 154 and 153).

These properties of the characteristic of finite junctions have been used for the generation of electromagnetic waves with the aid of Josephson junctions (Yanson et al. 1965; Langenberg et al. 1965). One of the resonances (22.79) was used; its amplitude was increased by choosing the magnetic field in accordance with condition (22.80).

8.8.11 22.7. Josephson junctions with a normal metal or a semiconductor layer

In the section that follows we will consider various methods used to prepare Josephson junctions. One of the most widespread is still a tunnel junction with an insulating barrier. However, it is rather difficult to prepare such a junction in a controlled manner. As has already been said, the insulator barrier must be very thin and have no short-circuited portions. The usual procedure is the oxidation of a
metal followed by sputtering a film of another superconducting metal. But here gaps may appear in the oxide layer and, hence, short-circuited regions. But if the oxide layer is made too thick, no Josephson current will flow.

In view of this, attempts are being made to use a normal metal or semiconductor layer instead of an insulator. The transparency of such a layer, as will be seen below, is much larger than that of an insulator and, hence, it may be made thicker. In such a case it is easier to control the barrier transparency and, hence, to prepare junctions with required properties.

We begin with a normal layer ($s-n-s$ junctions). We use the model described in section. 20.1: the junction between two metals with slightly differing critical temperatures. We assume that $T_{c2} - T_{c1} < T_{c1}$ and $T_{c1} < T < T_{c2}$. Suppose that the metals form a sandwich, in which the first, normal metal forms a layer of thickness d between two superconducting plates of the second metal. We assume, as before, that $\xi_2 > \xi_1$ and put $d > \xi_1$. In this case, the critical current flowing across the junction [which will evidently turn out to be proportional to $\exp(-d/\xi_1)$] will be so small that it will not affect the Ψ functions in both superconductors. Therefore, they may be taken in the form (20.18) with some phase factor. Thus, for the metals on the right and left sides we have respectively:

$$\begin{aligned}\Psi_{\mathrm{r}} &= \tanh\left(\frac{x-\frac{1}{2}d+x_{0\mathrm{r}}}{\sqrt{2}\xi_2}\right)\exp\left(\mathrm{i}\chi_1\right), \quad x > \tfrac{1}{2}d \\ \Psi_1 &= \tanh\left(\frac{\frac{1}{2}d+x_{01}-x}{\sqrt{2}\xi_2}\right)\exp\left(\mathrm{i}\chi_2\right), \quad x < -\tfrac{1}{2}d\end{aligned} \tag{22.81}$$

In the normal metal which forms the strip $-\frac{1}{2}d < x < \frac{1}{2}d$, use may be made of the linearized Ginzburg-Landau equation

$$\xi_1^2 \frac{\mathrm{d}^2\Psi}{\mathrm{d}x^2} = \Psi$$

of which the solution is

$$\Psi = A\exp\left(\frac{x}{\xi_1}\right) + B\exp\left(\frac{-x}{\xi_1}\right). \tag{22.82}$$

Using the continuity condition $\mathrm{d}\Psi/\mathrm{d}x$ at the boundaries (the continuity of Ψ is determined by $x_{0\mathrm{r}}$ and x_{01}, which are of no interest in this particular problem) and taking into account that $x_{0\mathrm{r}}, x_{01} < \xi_2$ (section 20.1), we find

$$\begin{aligned}A &\approx \frac{\xi_1}{\sqrt{2}\xi_2}\exp\left(\mathrm{i}\chi_1 - \frac{d}{2\xi_1}\right) \\ B &\approx \frac{\xi_1}{\sqrt{2}\xi_2}\exp\left(\mathrm{i}\chi_2 - \frac{d}{2\xi_1}\right)\end{aligned} \tag{22.83}$$

The current is given by

$$j = -\frac{ie\hbar}{2m}\Psi_0^2\left(\Psi^*\nabla\Psi - \Psi\nabla\Psi^*\right),$$

where $\Psi_0^2 = \alpha|\tau|/b$. Substituting eqs. (22.82) and (22.83), we see that the current does not depend on x and is equal to

$$\begin{aligned}j &= -\frac{\mathrm{i}e\hbar\alpha|\tau|}{2mb}\left(B^*A - A^*B\right) \\ &= \frac{e\hbar\alpha|\tau|}{2mb}\frac{\xi_1}{\xi_2^2}\exp\left(-\frac{d}{\xi_1}\right)\sin\left(\chi_1 - \chi_2\right).\end{aligned} \tag{22.84}$$

Considering that Ψ^2 at the boundary is equal to $(\alpha|\tau|/b)\,(\xi_1^2/2\xi_2^2)$ (see eq. 20.19), we may write

$$j = \frac{e\hbar}{m\xi_1}\left|\Psi\left(\frac{1}{2}d\right)\right|^2\exp\left(-\frac{d}{\xi_1}\right)\sin\left(\chi_1 - \chi_2\right), \tag{22.85}$$

which is strongly reminiscent of formula (22.21).
In this case, the smallness of the Josephson current is due primarily to the violation of the superconducting correlation in the normal metal, this being responsible for the appearance of the factor $\exp\left(-d/\xi_1\right)$. Although the derivation given refers to a very special model, the basic qualitative inference about the critical current being proportional to $\exp\left(-d/\xi_1\right)$, where ξ_1 is the correlation length in the normal metal, is valid in all cases. Note that, in contrast to an ordinary tunnel junction with an insulating layer, where the smallness of the Josephson current is due to the small permeability of the potential barrier to electrons, here it is due to the loss of the coherence of the Cooper pairs in the normal metal.
$\mathrm{s}-\mathrm{n}-\mathrm{s}$ junctions have not found wide application in practice. This is due to the low resistance

of the metal to normal current, which proves to be inconveient for instruments that make use of Josephson elements. This explains why Josephson elements with a semiconductor barrier s-sm-s have lately been studied intensively (see Alfeev 1979; Aslamazov and Fistul' 1979, 1981, 1982, 1984).

As is known, the electric properties of semiconductors are determined to a considerable extent by the presence of impurities. The impurities in semiconductors create additional electron energy levels in the forbidden region between the last filled band (valence band) and the first empty band (conduction band). The levels may be shallow, i.e., they may lie close to the edge of the valence band (acceptors) or of the conduction band (donors), or deep, i.e., they may lie in the bulk of the forbidden region. If the impurity concentration that creates shallow levels is high, the impurity levels extend into the band that "creeps" on the conduction or valence band. Here, the semiconductor becomes "degenerate", i.e., a finite number of current carriers arises in a band at $T = 0$. Such a semiconductor is, in fact, a semimetal, i.e., in this case the s-sm-s junction becomes a s-n-s junction.

At lower impurity concentrations the electrons or holes in the bands are generated only by way of thermal excitation. However, since the critical temperatures of superconductors are low as compared with the excitation energy, the presence of thermally activated carriers may be neglected. In such a case, the semiconductor is,
in fact, an insulator and the height of the potential barrier is equal to the lowest energy required for the generation of electrons in the valence band or of holes in the conduction band or, in other words, to the energy gap. Comparing the exponents of the temperature excitation (V/T) and of the tunneling probabilities ($d\sqrt{mV}/\hbar$) (see section 22.1), where V corresponds to $U(x) - \mu$, we see that for $V > 10^{-2}$eV and $d < 10^{-3}$ cm the thermal excitation may really be ignored.

In real determinations of the tunneling probability (Aslamazov and Fistul' 1979, 1981, 1982, 1984) one must take into account the effects that arise at the metalsemiconductor interface. In section 6.1 we have considered the contact between two metals. It has been pointed out that part of the electrons are transferred from one metal to the other, as a result of which an electrical double layer is formed in the vicinity of the interface; at this double layer there is a jump in the potential - a contact potential difference. The thickness of the double layer is of the order of interatomic distance because it is at such distances that the electric field is screened.

The situation is different in semiconductors, where the screening is much weaker. If the semiconductor layer is very thin, it may happen that all the electrons residing at the impurity levels will move into the metal and, as a result, the potential barrier will increase almost up to the spacing between the valence band and the conduction band. On the other hand, with the escape of electrons the semiconductor will acquire an electric charge, which in turn will reduce the effective barrier to a certain extent.

In the thicker layers of the semiconductor the electrons will pass into the metals from the boundary regions. In such a case the potential barrier in the middle will be determined by the energy gap for the impurity levels, and at the edges high but narrow "Schottky barriers" will be generated.

Besides, there exist other effects which exert an influence on the tunneling probability. They include fluctuations in the impurity concentration, leading to the formation of narrow channels with lowered barriers (Aslamazov and Fistul' 1982), the formation of "resonance" trajectories along the periodic arrays of impurity states in a semiconductor (Aslamazov and Fistul' 1984) and, finally, the illumination effects. It has been found experimentally that some s-sm-s junctions, in which no Josephson effect has been observed, exhibit the effect as a result of illumination and retain it when the illumination is turned off (see Barone and Paterno 1982). This is presumably associated with the formation of long-lived metastable electronic states on impurities.

8.8.12 22.8. Practical applications of the Josephson effect

It has been shown in section 22.4 that the critical Josephson current depends strongly on the magnetic field. This property can be used for the measurement of small magnetic fields. In fact, for this purpose use is made not of Josephson elements but of so-called Josephson interferometers of SQUIDs (superconducting quantum interference devices).

One of the schemes of such an interferometer is given in fig. 155. It shows two Josephson elements connected in parallel. The total current across the first element is equal to $I_{c1} \sin \theta_1$ and that flowing across the second is $I_{c2} \sin \theta_2$. The overall current across both junctions is given by

$$I = I_{c1} \sin \theta_1 + I_{c2} \sin \theta_2. \tag{22.86}$$

Suppose that a magnetic field is applied normal to the junction plane. Let us carry out a derivation analogous to that made in section 17.6, where magnetic flux quantization was discussed. From the fact that $\mathbf{j} = \mathbf{0}$ in the bulk of a superconductor it may be concluded that the order-parameter phase satisfies the condition

$$\nabla \chi = \frac{2e}{c\hbar} A$$

Integrating along the dashed contour, we see that the variation of the phase along the entire contour is

$$\theta_1 - \theta_2 + \frac{2d}{ch} \Phi,$$

where Φ is the field flux across the contour and θ_1 and θ_2 are the jumps in the phase at the Josephson junctions.

For the order parameter to be single-valued, it is necessary that the total change in the phase be equal to $2\pi n$, where n is an integer, i.e.,

$$\theta_1 - \theta_2 + \frac{2\pi\Phi}{\Phi_0} = 2\pi n$$

(we have substituted $\Phi_0 = \pi c\hbar/e$, the magnetic flux quantum). We may introduce a certain quantity θ and write

$$\theta_1 = \theta - \frac{\pi\Phi}{\Phi_0} + 2\pi n, \quad \theta_2 = \theta + \frac{\pi\Phi}{\Phi_0}.$$

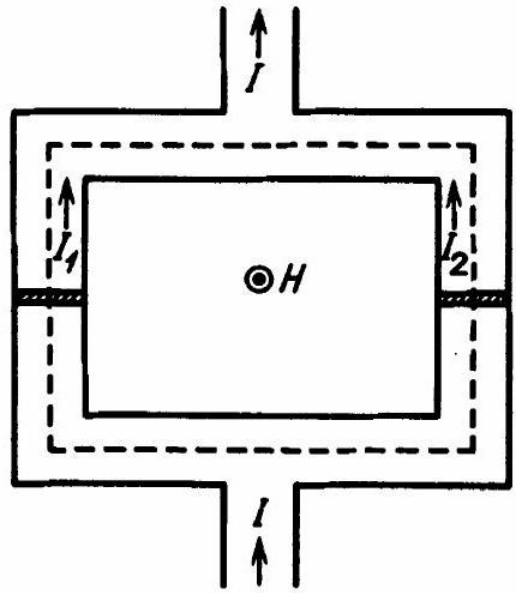


Fig. 155.

Substituting this into formula (22.86) (we assume the magnetic field to be so small that it has no effect on I_{c1} and I_{c2}), we have

$$I = I_{c1} \sin\left(\theta - \frac{\pi\Phi}{\Phi_0}\right) + I_{c2} \sin\left(\theta + \frac{\pi\Phi}{\Phi_0}\right).$$

If both junctions are identical, i.e., $I_{c1} = I_{c2} = I_c$, then

$$I_{\max} = \max\left[2I_c \sin\theta \cos\left(\frac{\pi\Phi}{\Phi_0}\right)\right] = 2I_c \left|\cos\left(\frac{\pi\Phi}{\Phi_0}\right)\right|. \tag{22.87}$$

It follows from this that the total critical current vanishes at

$$\Phi = \left(n + \frac{1}{2}\right)\Phi_0. \tag{22.88}$$

But in this case we are dealing not with the magnetic flux across an isolated junction, HLd, but with the flux through a large cavity, $\Phi = HS$ (S is the area of the cavity). Since the magnetic flux quantum is a very small quantity, $\Phi_0 = 2 \times 10^{-7}\text{Oe}\cdot\text{cm}^2$, it follows that with the aid of the Josephson interferometer we can measure a field as small as 10^{-10}Oe (recall that the magnetic field of the Earth is 0.5 Oe).

The scheme described above is not the only one possible. There are others, which are more convenient in some cases.

One of the important problems in measuring such small fields is the protection against numerous noises, i.e., random fields that result from various sources, especially in cities. Of course, the creation of such protection would have limited the application of SQUIDs considerably. However, it has been possible to avoid this in practice. The point is that noise sources are usually at a large distance from the object studied and the fields resulting from such sources vary very little in space. Circuits have been developed, which record only the magnetic field gradient or even its second derivative. Although the sensitivity is reduced to a certain extent, the protection may be dispensed with.

Apart from applications for physical investigations, SQUIDs have been employed in biology and medicine. The weak currents that flow in organisms produce, in space, magnetic

fields that can be measured. Thus, it is possible to obtain magnetocardiograms and magnetoencephalograms (records of the variation with time of magnetic fields associated with the electrical activity of the heart and the brain). These methods of investigation provide much more details than do the ordinary measurements of the electric potentials (electrocardiography and electroencephalography) and are carried out by a contactless method. Moreover, by recording the magnetic fields at various points of space relative to the object under examination one can calculate the distribution of currents producing these fields with the aid of computers. Although these investigations have been started only recently, it is clear even today that SQUIDs have provided biology and medicine with unique methods of investigation and diagnostics.

The extraordinary sensitivity of SQUIDs to magnetic fields makes it possible to use them for developing supersensitive galvanometers and voltmeters. It has become
possible to measure alternating currents of down to 10^{-14} A and potential differences of down to 10^{-15} V.

The capability of closed superconducting circuits to retain undamped current and also the possibility of destroying the superconductivity by magnetic field are used to develop superconducting memory elements for computers - cryotrons. Some of these devices make use of Josephson elements. Two circumstances are important here: miniaturization and high-speed response. For miniaturization use is made of sputtered superconducting films. The smallest contact area produced in this way is 10^{-9} cm^2 (edge contact, fig. 156a). As regards the high-speed response, the switch of the tunnel junction from the Josephson mode, $j < j_c, V = 0$, to the single-particle mode, $j > j_c, V > 2\Delta/e$, is accomplished during a time less than 10^{-10} s.

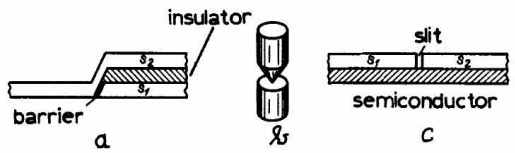


Fig. 156.

One of the key problems in the development of increasingly compact microcircuits, i.e., containing an ever increasing number of elements in a given volume, is the removal of heat released inside such a microcircuit during its operation. The contact with the cooling liquid or gas occurs only along the surface, and heat conduction cannot provide efficient heat removal from the volume. And an increase in temperature can lead to the destruction of the entire structure. In this sense, Josephson elements possess an important advantage because the heat release upon their switching is negligible.

We have so far been concerned with the use of the dc Josephson effect. As regards the ac Josephson effect, in spite of the existence of many ideas, it is still used in rare cases. It would be most natural to use Josephson elements for the generation of electromagnetic oscillations with a retunable frequency. The main difficulty is bringing the waves outside the junction. The use of the resonance of Josephson waves with Swihart waves (section 22.6) has made it possible to obtain a radiation power of up to 10^{-10} W with an efficiency of 2%. Of course, this figure is very low, and at present there exist other devices which enable one to obtain a much higher power at the same frequencies.

In principle, the following two applications of Josephson generation are possible: (a) in low-temperature low-noise devices that do not require a high power; and (b) for measurement of potential differences smaller than 10^{-15} V using the relation $\omega = 2eV/\hbar$, since frequency determinations are carried out with a high accuracy and allow one to bring the measured voltage down to 10^{-17} V.

A further application of the ac Josephson effect is the detection of external radiation. The simplest application is to use the decrease of the critical Josephson current in the presence of an external electromagnetic field. According to formula (22.67),

$$j_{0c} = j_c \left| J_0 \left(\frac{2eV}{\hbar\Omega} \right) \right|, \tag{22.89}$$

where J_0 is the Bessel function. In principle, one can also use the other steps of the characteristic (at $V_n = n\hbar\Omega/2e$).

In conclusion, let us consider various methods for the preparation of Josephson elements. We have already considered two types: the tunnel junction and the bridge. In the first case, the surface of a superconductor is subjected to oxidation or a layer of a normal metal or a semiconductor is deposited onto it by sputtering. This is followed by sputtering a film of a second superconductor over the first one. One of the versions of the tunnel junction is the edge, in which the junction is made along the edge of a thin film (fig. 156a).

As for the bridge, it can be prepared in the form of a film with a constriction (fig. 146) or a film of varying thickness. A further type of bridge is a point junction (fig. 156b).

Finally, the use of a normal metal or semiconductor as the barrier makes it possible to produce so-called palanar elements (fig. 156c), in which a superconductor film with a very narrow slit is sputtered onto a semiconductor substrate. Here, the substrate serves as the barrier. In planar elements it is easier to control the properties of the barrier mateirial; this may be an ordinary bulk single-crystalline sample with a certain amount of dopant (if we deal with a semiconductor).

8.8.13 22.9. The dynamical resistive state of a thin superconductor at supercritical currents

It has been shown in section 17.5 that for a very thin superconductor there exists a critical current density above which the superconductivity is destroyed. On the basis of this result one could come to the conclusion that when the current increases up to this value there occurs a transition to the normal phase and the characteristic changes to the linear dependence $\boldsymbol{j} = \sigma \boldsymbol{E}$ (fig. 157). In fact, the experimental findings are dependences of the type shown in fig. 158 (Meyer and Minnigerode 1972), i.e., a gradual approach to the normal resistance, and jumps in the electric field. This strongly resembles the picture considered in section 22.5 for the Josephson junction, and shows that superconductivity is retained in some form in the presence of the electric field as well.

At first sight this conclusion seems paradoxical. As a matter of fact, from the London equation $\partial(\Lambda \boldsymbol{j})/\partial t = \boldsymbol{E}$ it follows that in the presence of an electric field the current must increase with time. Hence, it will certainly exceed the critical value,

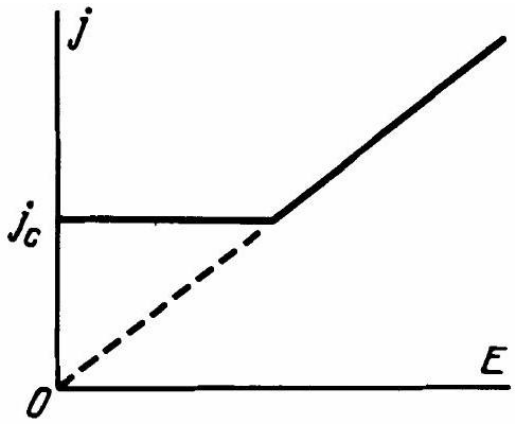


Fig. 157.

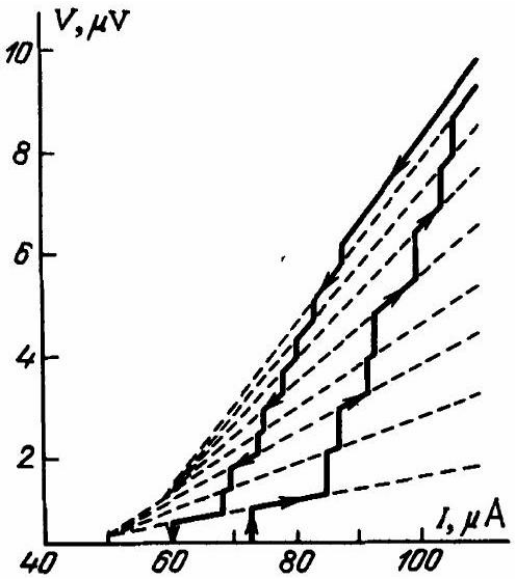


Fig. 158.

which will lead to the destruction of superconductivity. On the other hand, we have already encountered a similar phenomenon: the motion of the vortex lattice in a type II superconductor under the action of a magnetic field and a current perpendicular to it leads to the generation of an electric field with the superconducting order parameter being retained. Another example is the Josephson junction at $j > j_c$.

The appearance of an electric field certainly leads to nonstationarity, i.e., time dependence of the quantities. As has already been noted, the nonstationary equations of the theory of superconductivity are very complicated, even in the limit of slow time and space variations. Therefore, we use the model equation (19.47) for the vicinity of T_c.

However, in this case we have to overcome the following difficulty. Suppose we have an infinite superconducting wire. It is clear that the electric field that arises in it must be, on an average, homogeneous along the wire. But in this case Ψ must also be homogeneous on an average. At the same time, the potential φ appearing in eq. (19.47) must increase in magnitude.

A difficulty of the same kind has been enountered in ch. 18, where we dealt with type II superconductors in a magnetic field. It has been shown that the rise of the vector potential is compensated by the appearance of vortices. They give rise to jumps in the phase gradient at the cut lines that pass through the vortex centers (see fig. 113).

We shall now consider a superconducting wire (a whisker) having a diameter much smaller than both δ and ξ. Here all the quantities will depend only on the coordinate along the wire and on time. Thus, instead of the (x, y) plane in this case we have the (x, t) plane. Since the magnetic field of the current in the whisker is small, we may choose $\boldsymbol{A} = 0$ and $\boldsymbol{E} = -\nabla\varphi$. In this case we can establish the similarity with the vortex picture:

$$-\mathrm{i}\frac{\partial}{\partial x} \to -\mathrm{i}\frac{\partial}{\partial x}, \quad -\mathrm{i}\frac{\partial}{\partial y} - \frac{2e}{\hbar c}A_y \to -\mathrm{i}\frac{\partial}{\partial t} + \frac{2e}{\hbar}\varphi. \tag{22.90}$$

Comparing with fig. 113 and the reasonings given in section 18.2, we come to the conclusion that a vortex lattice appears in the (x, t) plane (Ivlev and Kopnin 1978). On encircling each vortex the phase must vary by an amount 2π. The compensation of the increase of the scalar potential will occur due to the jumps in the phase derivative at the cut line along the t axis. The compensation condition reads

$$\frac{2\pi}{t_0} = \frac{2e}{\hbar}\langle E\rangle a, \tag{22.91}$$

where t_0 is the time period, a is the space period and $\langle E\rangle$ is the average electric field (with respect to the coordinate and time). Solving condition (22.91) for the electric field, we obtain

$$\langle E\rangle = \frac{\Phi_0}{ct_0}\frac{n}{L}, \tag{22.92}$$

where $\boldsymbol{\Phi}_0$ is the flux quantum, L is the length of the conductor and n is the number of "vortex" centers ($n = L/a$).

The physical interpretation of the resultant picture is different from that observed with magnetic vortices. At certain points along the conductor there a jump occurs in the time derivative of the phase $\partial\chi/\partial t$, i.e., the rate of variation of the phase with time. This process is periodic. During the larger part of the period the rate of change of the phase on two sides of the points on the conductor is the same. However, at certain moments the phase changes more sharply, and this occurs differently on the two sides from this point, so that a phase difference equal to 2π results. Therefore, such points are called "phase slip centers"*. Since the function $\Psi = |\Psi|\exp(\mathrm{i}\chi)$ must be single-valued, it follows that at the center itself $|\Psi| = 0$ at the moment of phase slip.

Note that fig. 113 shows a rectangular lattice corresponding to the time-independent location of the phase slip centers along the superconductor. However, generally speaking, the lattice may also be oblique, which would correspond to the motion of the entire structure along the superconductor with a constant velocity. This is possible, in principle, for a finite superconductor if there is a mechanism of creation and destruction of the phase slip centers at the edges.

Let us now consider the events that occur in a thin superconductor of finite length. At $\boldsymbol{A} = 0$ the expression for the current has the form

$$j = |\Psi|^2\frac{\hbar e}{m}\frac{\partial\chi}{\partial x}. \tag{22.93}$$

If we plot a three-dimensional graph in which x is the coordinate along the superconductor, z corresponds to $\mathrm{Re}\,\Psi$, and y corresponds to $\mathrm{Im}\,\Psi$, then the spiral curve will correspond to a state with current (fig. 159a). However, in the presence of an electric field the current increases with time; this means that the spiral is "compressed", i.e., the density of its turns increases. But this process cannot continue for an indefinitely long time because the current reaches a

*The idea of the phase slip centers was first put forward by Anderson (1966) and Little (1967) and described in detail by Langer and Ambegoakar (1967).

value j_c. There is only one possibility: to dispose of one of the turns of the spiral. But to do this, we have to "straighten out" the spiral at some place. This exactly corresponds to the appearance of a phase slip center and, in particular, $|\Psi| = 0$ (fig. 159b).

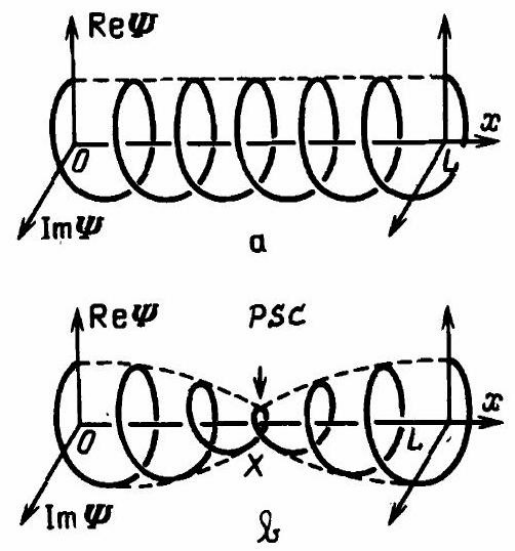


Fig. 159.

Let us consider a simple model (Skocpol et al. 1974), which explains the characteristic curve in fig. 158 with jumps in the potential difference. Suppose that the thin superconductor under study is connected on both sides to bulk specimens of the same metal. Such a construction is called a bridge and we have already described it as a possible realization of the Josephson junction. In this particular case, the constricted portion is assumed to be long. For bulk superconductors the flowing
current is weak and they are in a state of equilibrium. If the temperature is close to T_c and eq. (19.47) is applicable, then in the junctions its right-hand side must equal zero and, hence, the left-hand side must also vanish. Substituting $\Psi = |\Psi| e^{ix}$, we obtain

$$\frac{\partial |\Psi|}{\partial t} + i \left(\frac{\partial \chi}{\partial t} + \frac{2e}{\hbar} \varphi \right) |\Psi| = 0.$$

Separating the real and imaginary parts, we have

$$\frac{\partial |\Psi|}{\partial t} = 0, \tag{22.94}$$

$$\frac{\partial \chi}{\partial t} + \frac{2e}{\hbar} \varphi = 0. \tag{22.95}$$

These equation are the boundary conditions for the thin superconductor under study. Condition (22.95) is also realized at temperatures far from T_c. It may be interpreted as the equality of the chemical potentials of "normal electrons" ($\mu_n = e\varphi$) and of electrons constituting the Cooper pairs ($\mu_s = -\frac{1}{2}\hbar \partial \chi / \partial t$). We introduce the notation

$$\eta = \mu_n - \mu_s = e\varphi + \frac{1}{2}\hbar \frac{\partial \chi}{\partial t}. \tag{22.96}$$

According to (22.95), $\eta = 0$ in a bulk superconductor. However, just as in the case of a magnetic field, this quantity cannot vanish abruptly and has a finite penetration depth.

Indeed, let us visualize the interface between a superconductor and a normal metal. If an electron is "injected" into the superconductor, then in order to assume an equilibrium state it has to lose an energy Δ because the equilibrium electrons are bound into pairs with a binding energy 2Δ (per two particles).

The electron loses its energy in collisions. However, collisions with impurities are inefficient because they are elastic, and collisions with quasiparticles are rare ($\propto \mathrm{e}^{-\Delta/T}$). Therefore, the only process that provides energy relaxation is the emission of phonons. At low temperatures the characteristic time of such a process, τ_{ph}, is large. As a result of this, the penetration depth for the quantity η is large compared to the correlation length ξ (of order $\xi\,(T_{\mathrm{c}}\tau_{\mathrm{ph}}/\hbar)^{1/2}$ for a pure superconductor). We label this quantity by δ_E, since it also determines the spatial variation of the electric field in the superconductor.

By analogy with the London equation we write

$$\frac{\partial^2\eta}{\partial x^2} - \delta_E^{-2}\eta = 0 \tag{22.97}$$

(the exact theory confirms this equation; see Ivlev and Kopnin 1984). Suppose the junctions of the superconductor are located at points 0 and L. Solving eq. (22.97)
with the boundary condition $\eta = 0$ at $x = 0$, we get

$$\eta = C_1 \sinh\left(\frac{x}{\delta_E}\right) \tag{22.98}$$

On the other hand, we can solve eq. (22.97) by using the boundary condtion $\boldsymbol{\eta} = \mathbf{0}$ at $x = L$. This gives

$$\eta = C_2 \sinh\left(\frac{x-L}{\delta_E}\right) \tag{22.99}$$

If there are no phase slip centers in the superconductor, the general solution is $\eta = 0$. This is possible only as long as the current is less than j_{c}.

When the current exceeds j_c, a phase slip center appears. Let it be located at point X. Here we obtain

$$\eta(X-0) = C_1 \sinh\left(\frac{X}{\delta_E}\right), \quad \eta(X+0) = C_2 \sinh\left(\frac{X-L}{\delta_E}\right).$$

But at the phase slip center the phase derivative $\partial\chi/\partial t$ undergoes a discontinuity: $\Delta(\partial\chi/\partial t) = 2\pi/t_0$. In accordance with (22.96), it follows that

$$C_2 \sinh\left(\frac{X-L}{\delta_E}\right) - C_1 \sinh\left(\frac{X}{\delta_E}\right) = \frac{\pi\hbar}{t_0}. \tag{22.100}$$

Due to the phase slip all the quantities depend periodically on time with a period t_0. In experiments the time-averaged current and potential difference are measured (such averages are designated by a bar). According to (22.96), $\eta = e\bar{\varphi}$ (since $\overline{\partial\chi}/\partial t = 0$). The average electric field on the left from the point of phase slip ($0 < x < X$) is deduced from formula (22.98):

$$\bar{E} = -\frac{\partial\varphi}{\partial x} = -\frac{1}{e}\frac{\partial\eta}{\partial x} = -\frac{C_1}{e\delta_E}\cosh\left(\frac{x}{\delta_E}\right). \tag{22.101}$$

On the right of $X (X < x < L)$ we have

$$\bar{E} = -\frac{C_2}{e\delta_E}\cosh\left(\frac{x-L}{\delta_E}\right) \tag{22.102}$$

The constants C_1 and C_2 are found on the basis of the following considerations.
In experiments the total current j is specified most easily. It consists of the superconducting and normal parts:

$$j = j_\mathrm{s} + j_\mathrm{n}$$

This formula is exact near T_c (see the end of section 19.3); j_s was determined in section 16.8 ($j_\mathrm{s} = -QA$, where Q is expressed by formulae 16.88 and 16.92) and $j_\mathrm{n} = \sigma E$, where σ is the normal conductivity. However, in principle, an analogous formula may be written at any temperatures. To do this, one must use the relation
$j = -QA$ in the limit $q = 0, \omega < \Delta$ (here we mean the gauge $\varphi = 0, E = -c^{-1}\partial A/\partial t$) and expand in ω :

$$j = -Q(0)A + \frac{i\omega}{c}\sigma A,$$

where σ is a certain constant, which depends on Δ. The second term plays the role of j_n since $(\mathrm{i}\omega/c)A = -c^{-1}\partial A/\partial t = E$.

According to fig. 153, at the phase slip center the supercurrent fluctuates from the maximum value to zero. The maximum value must not exceed j_c. In view of this, in such a center $\bar{j}_\mathrm{s} = \alpha j_\mathrm{c}$, where $\alpha < 1$. We assume that even in the presence of several centers in each of them $\bar{j}_\mathrm{s} = \alpha j_\mathrm{c}$ with the same α, which is independent of the number of centers. Of course, this is a model assumption but, as will be seen below, it enables one to account for the stepped characteristic in fig. 158. At this point we will consider a single center. Thus, we have

$$\bar{j}_\mathrm{s}(X) = j - \bar{j}_\mathrm{n}(X) = \alpha j_\mathrm{c}. \tag{22.103}$$

Substituting $j_\mathrm{n} = \sigma E$ and E into eq. (22.103) in accordance with eqs. (22.101) and (22.102), we find

$$C_1 = -\frac{(j - \alpha j_c)\, e\delta_E}{\sigma \cosh\left(X/\delta_E\right)}, \quad C_2 = -\frac{(j - \alpha j_c)\, e\delta_E}{\sigma \cosh\left[(L - X)/\delta_E\right]}. \tag{22.104}$$

The period t_0 is associated with the potential difference. Inserting the length of the conductor L as a space period into formula (22.91) gives

$$\frac{2\pi}{t_0} = \frac{2e}{\hbar}\langle E\rangle L = \frac{2e}{\hbar}\int_0^L \bar{E}\ \mathrm{d}x = \frac{2e}{\hbar}[\varphi(0) - \bar{\varphi}(L)] = \frac{2eV}{\hbar}. \tag{22.105}$$

This is none other than the Josephson relation (22.55).
Formula (22.105) can also be derived directly from the problem under examination. Since at the ends of the conductor $\boldsymbol{\eta} = 0$, it follows that

$$\varphi(0) - \varphi(L) = \frac{\hbar}{2e}\left[\left(\frac{\partial\chi}{\partial t}\right)_L - \left(\frac{\partial\chi}{\partial t}\right)_0\right].$$

If we take the time average, then the regular part of the derivative $\partial\chi/\partial t$ gives zero and there will remain only a jump equal to $2\pi/t_0$, i.e., $\bar{\varphi}(0) - \bar{\varphi}(L) = \hbar\pi/et_0$, which is consistent with formula (22.105).

Inserting the expressions for C_1 and C_2 into eq. (22.100) and expressing the right-hand side in terms of V, we obtain

$$V = (j - \alpha j_\mathrm{c})\,\frac{\delta_E}{\sigma}\left[\tanh\left(\frac{X}{\delta_E}\right) + \tanh\left(\frac{L - X}{\delta_E}\right)\right].$$

From symmetry considerations it may be presumed that the phase slip center is located in the middle of the conductor, i.e., $X = \frac{1}{2}L$. Here we have

$$V = 2\left(j - \alpha j_{\rm c}\right)\frac{\delta_E}{\sigma}\tanh\left(\frac{L}{2\delta_E}\right). \tag{22.106}$$

In accord with eqs. (22.101) and (22.102) $\bar{E}$ and also the normal current increase from the edges to the middle portion of the conductor. Hence, the supercurrent is at a maximum at the edges. Here it cannot exceed j_c. This leads to the following condition:

$$j_{\rm s}(0) = j - \frac{(j - \alpha j_{\rm c})}{\cosh\left(L/2\delta_E\right)} \leqslant j_{\rm c}$$

At the same time, we must have $j \geqslant j_c$. From this we obtain the interval of values of the current j within which formula (22.106) applies:

$$j_{\rm c} \leqslant j \leqslant j_{\rm c}\frac{1 - \alpha\,\mathrm{sech}\left(L/2\delta_E\right)}{1 - \mathrm{sech}\left(L/2\delta_E\right)} \tag{22.107}$$

At $j = j_c$ there is a jump in the potential from zero to

$$V_1 = 2(1-\alpha)j_{\rm c}\frac{\delta_E}{\sigma}\tanh\left(\frac{L}{2\delta_E}\right) \tag{22.108}$$

This is followed by a linear portion of the characteristic up to the upper limit of the current given by formula (22.107). Here we have

$$V_1' = \frac{2(1-\alpha)j_{\rm c}\left(\delta_E/\sigma\right)\tanh\left(L/2\delta_E\right)}{1 - \mathrm{sech}\left(L/2\delta_E\right)}. \tag{22.109}$$

At a current j exceeding the upper limit in (22.107) two phase slip centers appear. It is rather natural to assume that they will be located so that the current $j_{\rm n}$ is symmetric with respect to either of them. This is possible if they are located at $X_1 = \frac{1}{4}L, X_2 = \frac{3}{4}L$. In such a case,

$$\begin{aligned}
\eta &= C_1 \sinh\left(\tfrac{x}{\delta_E}\right), && 0 < x < X_1,\\
\eta &= C_2 \sinh\left(\tfrac{x-\frac{1}{2}L}{\delta_E}\right), && X_1 < x < X_2,\\
\eta &= C_3 \sinh\left(\tfrac{x-L}{\delta_E}\right), && X_2 < x < L.
\end{aligned}$$

Let us define the coefficients C_1, C_2 and C_3, from the condition requiring that in the phase slip centers $\bar{j}_{\rm s} = j - \bar{j}_{\rm n}$ be equal to $\alpha j_{\rm c}$. This gives

$$C_1 = C_2 = C_3 = -\left(j - \alpha j_c\right)\frac{\left(e\delta_E/\sigma\right)}{\cosh\left(L/4\delta_E\right)}.$$

From the condition of the jump in η in the phase slip center we obtain the relation between the coefficients C_i and the period t_0, and from a formula analogous to

In accord with eqs. (22.101) and (22.102) $\bar{E}$ and also the normal current increase from the edges to the middle portion of the conductor. Hence, the supercurrent is at a maximum at the edges. Here it cannot exceed j_c. This leads to the following condition:

$$j_{\rm s}(0) = j - \frac{(j - \alpha j_{\rm c})}{\cosh\left(L/2\delta_E\right)} \leqslant j_{\rm c}$$

At the same time, we must have $j \geqslant j_c$. From this we obtain the interval of values of the current j within which formula (22.106) applies:

$$j_c \leqslant j \leqslant j_c \frac{1-\alpha \operatorname{sech}(L/2\delta_E)}{1-\operatorname{sech}(L/2\delta_E)}. \tag{22.107}$$

At $j = j_c$ there is a jump in the potential from zero to

$$V_1 = 2(1-\alpha) j_c \frac{\delta_E}{\sigma} \tanh\left(\frac{L}{2\delta_E}\right) \tag{22.108}$$

This is followed by a linear portion of the characteristic up to the upper limit of the current given by formula (22.107). Here we have

$$V_1' = \frac{2(1-\alpha) j_c (\delta_E/\sigma) \tanh(L/2\delta_E)}{1-\operatorname{sech}(L/2\delta_E)}. \tag{22.109}$$

At a current j exceeding the upper limit in (22.107) two phase slip centers appear. It is rather natural to assume that they will be located so that the current j_n is symmetric with respect to either of them. This is possible if they are located at $X_1 = \frac{1}{4}L, X_2 = \frac{3}{4}L$. In such a case,

$$\begin{aligned}
\eta &= C_1 \sinh\left(\tfrac{x}{\delta_E}\right), && 0 < x < X_1, \\
\eta &= C_2 \sinh\left(\tfrac{x-\frac{1}{2}L}{\delta_E}\right), && X_1 < x < X_2, \\
\eta &= C_3 \sinh\left(\tfrac{x-L}{\delta_E}\right), && X_2 < x < L.
\end{aligned}$$

Let us define the coefficients C_1, C_2 and C_3, from the condition requiring that in the phase slip centers $\bar{j}_s = j - \bar{j}_n$ be equal to $\alpha \bar{j}_c$. This gives

$$C_1 = C_2 = C_3 = -(j - \alpha j_c) \frac{(e\delta_E/\sigma)}{\cosh(L/4\delta_E)}.$$

From the condition of the jump in η in the phase slip center we obtain the relation between the coefficients C_i and the period t_0, and from a formula analogous to (22.105) (but this time we have $4\pi/t_0$ on the left-hand side) we deduce the relation between t_0 and V. This gives the following portion of the characteristic:

$$V = 4(j - \alpha j_c) \frac{\delta_E}{\sigma} \tanh\left(\frac{L}{4\delta_E}\right). \tag{22.110}$$

Formula (22.110) holds at currents starting from the upper limit (22.107) up to the point where the maximum of the supercurrent reaches the value j_c. Such a maximum is attained at $x = 0, \frac{1}{2}L$ and L. This yields

$$j_c \frac{1-\alpha \operatorname{sech}(L/2\delta_E)}{1-\operatorname{sech}(L/2\delta_E)} \leqslant j \leqslant \frac{1-\alpha \operatorname{sech}(L/4\delta_E)}{1-\operatorname{sech}(L/4\delta_E)}. \tag{22.111}$$

At the lower edge of this interval there occurs a jump in the voltage from the value V_1'(22.109) to

$$V_2 = \frac{4(1-\alpha) j_c (\delta_E/\sigma) \tanh(L/4\delta_E)}{1-\operatorname{sech}(L/2\delta_E)} \tag{22.112}$$

(it is not difficult to see that $\boldsymbol{V_2} > \boldsymbol{V_1'}$). This is followed by a linear portion of the characteristic in accordance with formula (22.110), which continues up to the upper limit of the interval (22.111), on which the voltage becomes equal to

$$V_2' = \frac{4(1-\alpha) j_c (\delta_E/\sigma) \tanh(L/4\delta_E)}{1-\operatorname{sech}(L/4\delta_E)}. \tag{22.113}$$

A further increase in the current leads to the appearance of a large number of phase slip centers and to the analogous dependences $V(j)$. A plot of $\sigma E/j_c$ against $j/j_c (E = V/L)$ for $L/\delta_E = 16$ is given in fig. 160. Here we take $\alpha = 0.09$ (see below).

Thus, it turns out that the characteristic consists of jumps in voltage and portions with a linear dependence $V(j)$. This is in agreement with experiment. As L increases

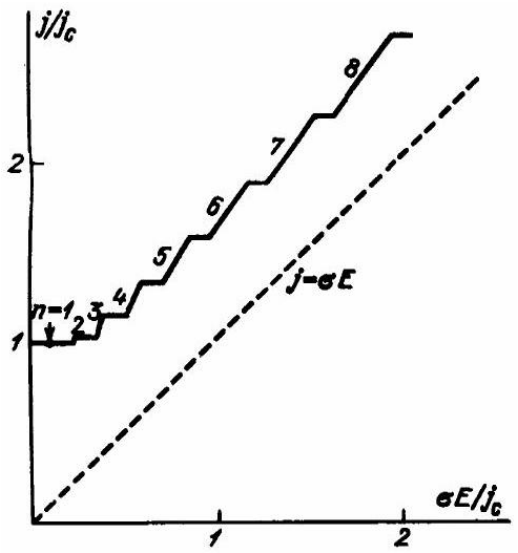


Fig. 160.

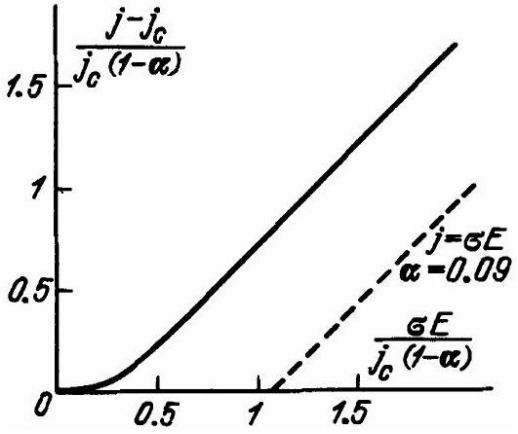


Fig. 161.

the intervals (22.107) and (22.111) and all the subsequent ones decrease and the characteristic approaches a continuous $V(j)$ curve. This dependence is not difficult to find by generalizing the preceding derivation to n phase slip centers. The linear portion of the characteristic of the number n has the form

$$V_n(j) = 2n \tanh\left(\frac{L}{2n\delta_E}\right)(j - \alpha j_c)\frac{\delta_E}{\sigma}. \tag{22.114}$$

The magnitude of the total current at which the maximum supercurrent reaches the critical value is given by

$$j_n = j_c \frac{1 - \alpha \operatorname{sech}(L/2n\delta_E)}{1 - \operatorname{sech}(L/2n\delta_E)}. \tag{22.115}$$

Inserting (22.115) into (22.114) yields

$$V_n\left(j_n\right)=\frac{2nj_c(1-\alpha)\left(\delta_E/\sigma\right)\sinh\left(L/2n\delta_E\right)}{\cosh\left(L/2n\delta_E\right)-1}. \tag{22.116}$$

With $n\to\infty$ the number n may be treated as a continuous variable. It is even more convenient to introduce the variable $z=L/\left(2n\delta_E\right)$. From eqs. (22.115) and (22.116) we obtain

$$\frac{(j-j_c)}{j_c(1-\alpha)}=\frac{1}{\cosh z-1}, \tag{22.117}$$

$$\frac{\sigma E}{j_c(1-\alpha)}=\frac{\sinh z}{z}\frac{1}{\cosh z-1}, \tag{22.118}$$

where $E=V/L$. This is a parametric representation of the dependence $E(j)$ in the limit $L>\delta_E$.

With a large current $j>j_{\rm c}$ we have $z\ll 1$. In such a case we find from eqs. (22.117) and (22.118)

$$j=\sigma E+\frac{1}{3}(2+\alpha)j_c, \tag{22.119}$$

that is, the characteristic is a straight line parallel to Ohm's law. Conversely, large z values correspond to the vicinity of $j_{\rm c}$. From eqs. (22.117) and (22.118) we obtain in this case

$$\frac{j-j_{\rm c}}{j_{\rm c}}\approx 2(1-\alpha)\exp\left(-\frac{j_{\rm c}(1-\alpha)}{\sigma E}\right). \tag{22.120}$$

The $j(V)$ curve with $V\to 0$ and $j\to j_{\rm c}$ has a horizontal tangent. The plot of the curve (22.117) and (22.118) is given in fig. 161.

The results of the phenomenological model described above are in good agreement with the results of the exact theory (Ivlev and Kopnin 1984)*. Comparing the formulae derived by both methods, we may conclude that $\alpha\leqslant 0.09$.

that is, the characteristic is a straight line parallel to Ohm's law. Conversely, large z values correspond to the vicinity of j_c. From eqs. (22.117) and (22.118) we obtain in this case

$$\frac{j-j_{\rm c}}{j_{\rm c}}\approx 2(1-\alpha)\exp\left(-\frac{j_{\rm c}(1-\alpha)}{\sigma E}\right). \tag{22.120}$$

The $j(V)$ curve with $V\to 0$ and $j\to j_{\rm c}$ has a horizontal tangent. The plot of the curve (22.117) and (22.118) is given in fig. 161.

The results of the phenomenological model described above are in good agreement with the results of the exact theory (Ivlev and Kopnin 1984)*. Comparing the formulae derived by both methods, we may conclude that $\alpha\leqslant 0.09$.

- The exact theory is not free from some arbitrariness either, but many of the data provide evidence in favor of the principle of "minimum entropy production". If this principle is used, in the exponential law (22.119) we obtain the coefficient 0.91 (as $1-\alpha$) and in the formula for $j>j_c$ we obtain an extra current $\Delta j=0.68j_c$. If $\alpha=0.09$ is inserted into formula (22.119), we obtain $\Delta j=0.696j_c$.

*The exact theory is not free from some arbitrariness either, but many of the data provide evidence in favor of the principle of "minimum entropy production". If this principle is used, in the exponential law (22.119) we obtain the coefficient 0.91 (as $1-\alpha$) and in the formula for $j>j_{\rm c}$ we obtain an extra current $\Delta j=0.68j_{\rm c}$. If $\alpha=0.09$ is inserted into formula (22.119), we obtain $\Delta j=0.696j_{\rm c}$.

Part IV
Junctions, tunneling

9 Typical Methods for Junctions with Examples

9.1 Reminder of Tunneling in Mesoscopic Physics and in Semiconductors

(a brief review of mesoscopic physics, since it is used here. just paragraphs with main ideas, details - in the note on mesoscopic physics)

9.2 Josephson Junction: Basic Models and Effects

9.2.1 4.1 Phase Coherence and Types of Weak Links

In 1962 B. Josephson published a theoretical paper [10] predicting the existence of two fascinating effects. One was supposed to find them in superconducting tunnel junctions. The basic idea of the first effect was that a tunnel junction [1] should be able to sustain a zero-voltage (superconducting) current. The critical value of this current was predicted to depend on the external magnetic field in a very unusual way: If the current exceeds its critical value, which is a characteristic of a particular junction, the junction begins to generate high-frequency electromagnetic waves. This is the second Josephson effect.

Both effects were thoroughly verified by experiment [11, 30] shortly after [10] was published. Moreover, it soon became clear that the Josephson effects exist not only in tunnel junctions, but also in other kinds of the so-called weak links, that is, short sections of superconducting circuits where the critical current is substantially suppressed [20, 31, 32].

The effects of weak superconductivity have their origin in the quantum nature of the superconducting state. We already know that the foundation of the superconducting state is the existence of the Bose condensate. That is to say, all electron pairs in the superconducting state occupy the same quantum level and are described by a single wavefunction, common to all of them. Their behavior is mutually conditioned, they are coherent.

Imagine two bulk pieces of a superconductor at the same temperature, completely isolated from each other. When both pieces are in the superconducting state, the superconducting electrons in each of them have their own superconducting wavefunction. Furthermore, since the temperatures and the materials of the superconductors are identical, the amplitudes of the wavefunctions must also be the same. This does not hold for the phases, however, which are arbitrary. This situation remains as long as the superconductors are isolated from each other. Let us now establish a weak contact between them, i.e., a contact that is weak enough so as not to change radically the electron states of the two pieces but sufficient to play the role of a perturbation. A new wavefunction will then emerge for the superconductor as a whole, which can be considered as a result of interference between the wavefunctions from the two pieces. As mentioned above, the amplitudes of the two wavefunctions had been equal even before the weak link was established. But not their phases: the phase coherence is a direct result of establishing the weak link. It is therefore often said that phase coherence sets up in weakly-coupled superconductors.

High-quality tunnel Josephson junctions, typically made of niobium with a barrier of aluminum oxide, presently serve as basic elements for low-temperature superconducting electronics.

Here it should be noted that a weak link between two superconductors is merely a convenient place for letting interference effects become visible. As to the interference effects in superconductors themselves, they were known long before the discovery of the Josephson effects. The most famous example is the magnetic flux quantization in a superconducting ring: the magnetic flux frozen in such a ring can assume only quantized values because the supercurrent, circulating in the ring and generating this magnetic flux, is quantized. And the quantization of the supercurrent is a typical interference effect. The current can assume only those values that yield an integral number of wavelengths of the superconducting wavefunction over the length of the ring. This situation is exactly analogous to the quantization of electron orbits in the Bohr atom.

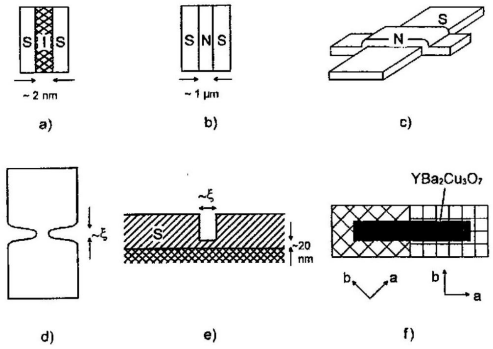


Fig. 4.1. Different types of weak links: (a) tunnel junction (SIS); (b) sandwich (SNS): (c) normal film N causes local suppression of the order parameter of a superconducting film S; (d) Dayem bridge, top view; (e) bridge of variable thickness, longitudinal cross-section; (f) grain-boundary junction (??? why is is grain? The pic. is different from rus book).

Let us now consider different types of weak links. First, there are devices without a concentration of a current (see Fig. 4.1. a)) (????). The thickness of an insulating layer is typically about $1-2$ nm and the critical current density is in the range $10-10^4$ A cm^{-2}, i.e., much less than the critical current density of the bulk superconductors. [2]

In superconductor-normal metal-superconductor (SNS) sandwiches, the normal layer can be as thick as 10^{-4} cm (Fig. 4.1 (b)). The wavefunctions of the superconducting electrons penetrate the normal metal due to the proximity effect. In the region of their overlap, the wavefunctions interfere, with the consequence that phase coherence is established between the bulk superconductors. If the amplitude of the superconducting wavefunction in the weak link is small, the critical current is also small.

The same effect can be achieved if the normal layer between the two superconductors is replaced by a doped semiconductor or another superconductor with a small critical current density. For example, if a narrow superconducting film is covered with a narrow film of a normal metal (Fig. 4.1 (c)), the amplitude of the superconducting electron wavefunction in the film is reduced where the film is in contact with the normal metal, due to the proximity effect. This causes a local decrease of the critical current density, that is, a weak link is established.

In devices with concentration of current, the critical current density in the weak link is the same as in the bulk, but the absolute value of the critical current is much less. A superconducting film with a short narrow constriction (Dayem bridge) falls into this category, provided the size of the constriction is of the order of the coherence length ξ (see Fig. 4.1 (d)). Another example is a bridge of variable thickness, such that the thickness of the main film is hundreds of nm while the thickness of the bridge itself is only several dozen nm (Fig. 4.1 (e)).

Finally, a weak link typical of high-temperature superconductors is shown in Fig. 4.1 (f). It

is called a grain boundary (or bi-crystal) junction. Due to the extremely short coherence length in high- T_c materials ($\xi \sim 1$ nm), defects in their crystal structure can act as weak links. The best-controlled defects can be produced between two regions of an epitaxially grown high- T_c film with different crystal orientations (grain boundary). The critical current density of such a weak link can be varied by changing the misorientation angle between the two crystallites.

Different types of weak links based on conventional low- T_c superconductors are described in a classic review by Likharev [31]. Various weak links and SNS structures made of high- T_c superconducting materials have been recently reviewed by Gross [33].

9.2.2 4.2 The DC Josephson Effect

Background for Derivation of Josephson Effect

Let us start with the first Josephson effect which is a dc effect. The physics behind it is essentially as follows. A sufficiently small current can pass through a weak link (Josephson junction) without dissipation. In other words, when such a current passes through the weak link, no voltage is generated across the junction. Since the current is always small, the magnetic field generated by it can be neglected and, following the Ginzburg-Landau theory, we can argue that the density of the current is determined by the phase gradient $\nabla\theta$ of the superconducting electron wavefunction.

An important characteristic of the weak link is that the phase gradient $\nabla\theta$ is very large compared to the phase gradients inside the bulk superconductors (in the following we shall refer to them as 'electrodes'). For a tunnel junction, strictly speaking, the expression 'phase gradient' is inappropriate and one should rather speak of a discontinuous phase jump across the junction. Therefore, from now on we shall always analyze the phase difference across the weak link:

$$\varphi = \theta_2 - \theta_1$$

where θ_1 and θ_2 are the phases of the superconducting electron wavefunctions in the first and second electrodes, respectively.

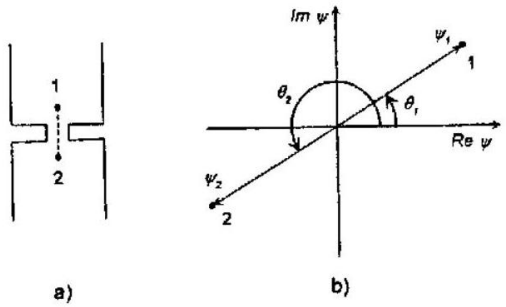


Fig. 4.2. (a) Example of weak link (Dayem bridge). The phase gradient $\nabla\theta$ is taken along the dashed line from point 1 to point 2; (b) representation of the order parameter in the complex plane. Passing from point 1 to point 2 in the weak link corresponds to passing from ψ_1 to ψ_2 in the complex plane, along the line $1-2$.

General relation

(????????? I don't understand that this is obvious????)

Now our task is to find the relation between the current through the weak link, I_s, and the phase difference φ. Let us first establish some general and almost self-evident relations.

(1) If the current through the junction is $I_8 = 0$, the phase difference is also $\varphi = 0$.

(2) Since the variation of the phase θ by 2π in one of the electrodes does not change anything physically, it is evident that $I_s(\varphi)$ is a periodic function with period 2π, that is, $I_s(\varphi) = I_s(\varphi + 2\pi)$.

(3) Changing the sign of the current must cause a change of the sign of the phase difference; therefore, $I_\mathrm{s}(\varphi) = -I_\mathrm{s}(-\varphi)$.

(4) The last relation, $I_\mathrm{a}(\pi) = 0$, is somewhat less obvious. Let us assume [3] that the length of the weak link is small but finite so that we can introduce a phase gradient $\nabla\theta$ across it. On going along the dashed line (Fig. 4.2 (a)) from point 1 to point 2, the complex order parameter runs through values varying from ψ_1 to ψ_2 along the straight line $1-2$ in the complex plane of ψ (see Fig. 4.2 (b)).

It is obvious that $\nabla\theta$ along the line is zero, resulting in $I_\mathrm{s} = 0$. At this point one can raise an objection. What happens if we go from ψ_1 to ψ_2 not along the straight line but along, say, a semicircle of radius $|\psi|$? The answer is $\nabla\theta \neq 0$ and $I_\mathrm{s} \neq 0$. Such a situation indeed occurs in long thin superconducting filaments. In that case, however, two paths are possible to go from ψ_1 to ψ_2: anticlockwise and clockwise, so that the corresponding gradients $\nabla\theta$ will be of opposite signs. This means that $I_8(\varphi)$ will become a multiple-valued function. However, by definition, such junctions can no longer be regarded as Josephson junctions.

Now let us ask: what is the simplest representation of $I_s(\varphi)$ having all four of the above properties? The function $\sin\varphi$ is an obvious satisfactory answer, and we can propose

$$I_\mathrm{s}(\varphi) = I_\mathrm{c}\sin\varphi, \tag{4.1}$$

where I_c is the maximum dissipation-free current through the junction often referred to as the critical current.

Derivation of Josephson Equations by Quantum Mechanics

Let us prove that our proposal is indeed appropriate. Two derivations of (4.1) will be given. The first, applicable to tunnel Josephson junctions, is due to Feynman [34] and the second, relevant to the case of short narrow constrictions, is by Aslamazov and Larkin [35].

But first a short foray into quantum mechanics.
The evolution of a quantum-mechanical system with time is described by a wavefunction $\Psi(t)$ which is the solution of the Schrdinger equation:

$$\mathrm{i}\hbar\frac{\partial\Psi}{\partial t} = \hat{H}\Psi \tag{4.2}$$

where $\hat{H}$ is the Hamilton operator of the system. If the system is allowed only discrete states ψ_α (where α is a series of indices each characterizing a given state), its wavefunction can be expanded in a series

$$\Psi(t) = \sum_\alpha C_\alpha(t)\psi_\alpha \tag{4.3}$$

Substitution of this in (4.2) gives

$$\mathrm{i}\hbar\frac{\mathrm{d}C_\beta}{\mathrm{d}t} = \sum_\alpha H_{\beta\alpha}C_\alpha(t) \tag{4.4}$$

Here

$$H_{\beta\alpha} = \int \psi_\beta^*\hat{H}\psi_\alpha \mathrm{d}V$$

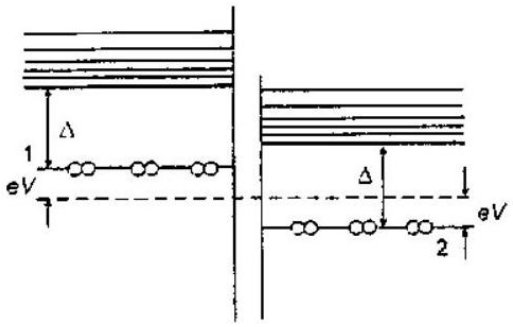


Fig. 4.3. Energy-level diagram for a tunnel Josephson junction with a finite voltage V applied to it. Levels 1 and 2 are separated by $2e$ V

One can see that $H_{\beta\beta}$ is the energy of the system in the state ψ_β, and $H_{\beta\alpha}$ is the matrix element characterizing the probability of a transition from the state ψ_α to the state ψ_β. The function $C_\alpha(t)$ represents the amplitude of the state ψ_α, and $|C_\alpha|^2$ gives the probability of finding the system in the state ψ_α.

Let us now go back to a tunnel Josephson junction. Assume that, in the general case, the current through the junction is so large ($I_8 > I_C$) that a voltage V appears across the junction. The corresponding energy diagram is shown in Fig. 4.3. Following Feynman [34], we consider a system of superconducting electrons, or Cooper pairs, as a two-level quantum-mechanical system. That is, we suppose that an electron pair with charge $2e$ can occupy either level 1 or level 2 . Then its energy will be either H_{11} or H_{22}, respectively, where $H_{11} = eV$ and $H_{22} = -eV$. The transition from level 1 to level 2 is governed by the matrix element $H_{12} = H_{21} = K$. Then (4.4) becomes

$$\begin{aligned} \mathrm{i}\hbar\frac{\mathrm{d}C_1}{\mathrm{d}t} &= eVC_1(t) + KC_2(t) \\ \mathrm{i}\hbar\frac{\mathrm{d}C_2}{\mathrm{d}t} &= KC_1(t) - eVC_2(t) \end{aligned} \tag{4.5}$$

Here C_1 is the amplitude of the pair state at level t and $|C_1|^2$ is normalized in such a way that $|C_1|^2 = n_5$, where n_5 is the superconducting electron density in the junction electrodes. For the sake of simplicity, we assume that both electrodes are made of the same material. Expressing the amplitudes C_1 and C_2 as

$$C_1 = \sqrt{n_\mathrm{R}}\mathrm{e}^{\mathrm{i}\theta_1}, \quad C_2 = \sqrt{n_\mathrm{R}}\mathrm{e}^{\mathrm{i}\theta_2}$$

substituting these in (4.5), and separating real and imaginary parts, we obtain
(!!! here I'll add a detailed derivation, see wiki about it for now!!!)

$$\frac{\mathrm{d}n_\mathrm{s}}{\mathrm{d}t} = \frac{2Kn_\mathrm{s}}{\hbar}\sin\varphi \tag{4.6}$$

$$\frac{\mathrm{d}\theta_1}{\mathrm{d}t} = -\frac{K}{\hbar}\cos\varphi - \frac{eV}{\hbar} \tag{4.7}$$

$$\frac{\mathrm{d}\theta_2}{\mathrm{d}t} = -\frac{K}{\hbar}\cos\varphi + \frac{eV}{\hbar} \tag{4.8}$$

The current through the tunnel junction is proportional to $\mathrm{d}n_5/\mathrm{d}t$. Indeed, when the current is switched on, the superconducting electron density starts to vary at the rate $\mathrm{d}n_5/\mathrm{d}t$ thereby giving rise to a current $I_5 = \mathrm{d}n_5/\mathrm{d}t$. This means that electrons start to leave the superconducting electrode. But this process is immediately compensated by the arrival of new

electrons from an external current source, because the junction is a part of a closed electric circuit. Therefore, the density n_s remains constant due to electroneutrality of the system as a whole. However, for defining the supercurrent, it is sufficient to assume $I_6 \propto \mathrm{d}n_5/\mathrm{d}t$. Then from (4.6) we immediately obtain the equation for the dc Josephson effect

$$I_s = I_c \sin\varphi \tag{4.9}$$

Derivation from Ginzburg-Landau Equations

(????)

Another way to derive the same equation, as applied to a weak link formed by a short narrow constriction, has been proposed by Aslamazov and Larkin [35]. Assume that a bridge, as in Fig. 4.4, is so short that its length is $L \ll \xi$.

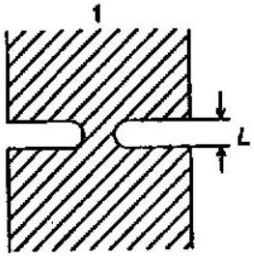


Fig. 4.4. Short narrow constriction (bridge) of length $L \ll \xi$ links together two wide films 1 and 2

In the absence of external magnetic field, the first Ginzburg-Landau equation (3.12) for such a bridge takes the form

$$-\xi^2\nabla^2\psi - \psi + \psi|\psi|^2 = 0. \tag{4.10}$$

The order parameter in a short bridge varies substantially over the length of the bridge, L. In this case, $\nabla^2\psi$ can be estimated as

$$\nabla^2\psi \sim \psi/L^2.$$

On the other hand, the amplitude of the order parameter is $|\psi| \sim 1$. It follows that the dominant term in (4.10) is the first one, since

$$\xi^2/L^2 \gg 1,$$

while all other terms are of the order 1 . This allows us to simplify (4.10):

$$\nabla^2\psi = 0 \tag{4.11}$$

Now assume that, far away from the constriction, the order parameter ψ in film 1 is

$$\psi = \psi_1 \mathrm{e}^{\mathrm{i}\theta_1}$$

and in film 2 it is

Here ψ_1, ψ_2, θ_1, and θ_2 are constants independent of the coordinates. Within the area of the constriction, the two wavefunctions interfere and we therefore seek the solution of (4.11) in the form

$$\psi = \psi_1 \mathrm{e}^{\mathrm{i}\theta_1} f(r) + \psi_2 \mathrm{e}^{\mathrm{i}\theta_2}[1 - f(r)] \tag{4.12}$$

subject to the conditions $f(r) \to 1$ in the interior of film 1 and $f(r) \to 0$ in the interior of film 2.

Substituting (4.12) into (4.11), we obtain the equation for $f(r)$:

$$\nabla^2 f(r) = 0$$

However, there is no need to solve this equation here. It suffices to know that the solution exists, and we can immediately go over to calculating the supercurrent which, by the second Ginzburg-Landau equation (3.17), is

$$j_{\rm s} = \frac{|\alpha|\hbar e}{\beta m} \operatorname{Im}(\psi^* \nabla \psi)$$

Substituting here (4.12) and applying simple algebra, we obtain for the supercurrent density through the bridge:

$$j_s = j_c \sin\varphi, \tag{4.13}$$

(??? this j_c is not a critical current of the SC, it is just a maximal current that can flow through the link, right??)

where again $\varphi = \theta_2 - \theta_1$.

Thus we have arrived at the same simple relation between the supercurrent and the phase difference of the superconducting wavefunctions in the junction electrodes as before. In the following we shall always assume that this relation holds.

Derivation of Josephson equations from GL: Second Way (???)

(still, I am not sure, how to do it)

Proof from GL eq:

$$\mathbf{n} \cdot \left(\nabla_{\mathbf{r}} - i\frac{2e}{\hbar c}\mathbf{A} \right) \Delta = 0$$

$$\mathbf{n} \cdot \left(\nabla_{\mathbf{r}} - i\frac{2e}{\hbar c}\mathbf{A} \right) \Delta_1 = \mathbf{n} \cdot \left(\nabla_{\mathbf{r}} - i\frac{2e}{\hbar c}\mathbf{A} \right) \Delta_2 = \frac{\Delta_2 - \Delta_1}{\Lambda}.$$

Вид правой части можно было бы угадать, исходя из требования линейности по Δ_1 и Δ_2 (так как параметр порядка мал), а также из того, что при перестановке местами полупространств 1 и 2 ток должен менять направление - поэтому должна войти разность Δ_1 и Δ_2. Параметр Λ имеет размерность длины и равен $\Lambda = \sigma R \mathcal{A} \sim l/\mathcal{T}$, $\sigma = 2e^2\nu D$ - проводимость сверхпроводника в нормальном состоянии (при нагревании выше T_c), R и $\mathcal{A}$ - сопротивление и площадь границы, l - длина свободного пробега, а $\mathcal{T} < 1$ - вероятность туннелирования электрона с энергией порядка энергии Ферми через границу между сверхпроводниками при $T > T_c$. Из $\mathbf{j}_s = 4eaD \operatorname{Im}\Delta^* \left(\nabla_{\mathbf{r}} - i\frac{2e}{\hbar c}\mathbf{A} \right) \Delta$

$$\mathbf{n} \cdot \mathbf{j_{s1}} = \mathbf{n} \cdot \mathbf{j_{s2}} = \frac{\pi}{4eT_c R\mathcal{A}} \operatorname{Im}(\Delta_1^* \Delta_2)$$

Если граница малопрозрачна, то модули параметров порядка с двух сторон от границы совпадают со своими значениями в объёме, и параметры порядка отличаются только фазами: $\Delta_{1(2)} = \Delta_0 e^{i\varphi_{1(2)}}$. Поэтому

$$j_s = \frac{\pi\Delta_0^2}{4eT_c R\mathcal{A}} \sin(\varphi_2 - \varphi_1)$$

$$I_s = I_c \sin(\varphi_2 - \varphi_1), \quad I_c = \frac{\pi\Delta_0^2}{4eT_c R}$$

$$I_c(T) = C\frac{T_c - T}{R_N}, \quad C := \frac{2\pi^3}{7\zeta(3)e} \approx 635\frac{\text{mKB}}{\text{K}},$$

ибо $|\Delta| \equiv \Delta_0 = \sqrt{-\frac{\hbar T_c}{\tau_{\text{GL}} b}} = \sqrt{\frac{\alpha T_c (T_c - T)}{b}}$.

9.2.3 4.3 The AC Josephson Effect

Relation of the voltage on the junction and the phase

So far we have considered the case of a small current $I < I_c$ through a weak link. If the current supplied by an external source exceeds the critical value I_c, it causes a voltage V to appear across the junction. What consequences should then be expected?

The behavior of a quantum-mechanical system is described by the Schrdinger equation

$$\mathrm{i}\hbar\frac{\partial\psi}{\partial t} = \hat{H}\psi \tag{4.14}$$

where $\hat{H}$ is the system's Hamiltonian.

The wavefunction of a stationary state ψ_1 satisfies the equation

$$\hat{H}\psi_1 = E\psi_1$$

where E is the energy of the state and $\psi_1 = |\psi_1|\, e^{\mathrm{i}\theta(t)}$, with $|\psi_1|$ being independent of time. On substitution of this wavefunction into (4.14) we get

$$-\hbar\frac{\partial\theta}{\partial t} = E \tag{4.15}$$

The presence of the voltage V across the weak link suggests that the Cooper pair energies in superconductors on either side of the junction, E_1 and E_2, are related to each other by

$$E_1 - E_2 = 2eV \tag{4.16}$$

because the charge of a pair is $2e$.

Substituting (4.16) into (4.15), we obtain the second fundamental Josephson relation:

$$2eV = \hbar\frac{\partial\varphi}{\partial t} \tag{4.17}$$

The same relation can be obtained by subtracting (4.7) from (4.6).

Current, which is more then I_c (RSJ model)

Now, what happens to a Josephson junction if we apply a constant current $I > I_c$ to it? Since the supercurrent cannot exceed I_c, now a current of normal electrons I_n must start flowing through the junction, in addition to the supercurrent. This conclusion leads us directly to the so-called resistively shunted model of the Josephson junction (RSJ) in which the latter is considered as a circuit made up of the Josephson junction itself and a normal resistance connected in parallel (Fig. 4.5).

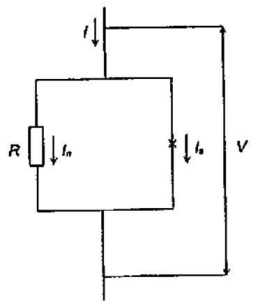


Fig. 4.5. Resistively shunted model of a Josephson junction. The supercurrent through the junction is $I_g = I_c \sin\varphi$

The total current I is then a sum of the normal current V/R and the supercurrent $I_s = I_c \sin\varphi$:

$$I = I_c \sin\varphi + \frac{\hbar}{2eR}\frac{\partial\varphi}{\partial t} \tag{4.18}$$

where R is the normal-state resistance of the junction. This differential equation can be easily integrated. Substituting the solution into (4.17), we obtain the voltage across the junction as

$$V(t) = R\frac{I^2 - I_c^2}{I + I_c \cos\omega t} \tag{4.19}$$

$$\omega = \frac{2e}{\hbar}R\sqrt{I^2 - I_c^2} \tag{4.20}$$

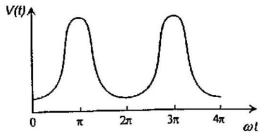


Fig. 4.6. Voltage across the Josephson junction at $I \geq I_c$

Thus we have found a fascinating property of the Josephson junction. If an external dc current I through the junction exceeds the critical current I_c, it causes a voltage V to appear across the junction, which oscillates periodically with time. This phenomenon is often referred to as Josephson radiation. (??? why?? currently, we said nothing about radiation, however, maybe it is a consequence of this formula???)

The time dependence of V is sketched in Fig. 4.6. The frequency of the ac voltage depends on the amount by which the current through the junction, I, exceeds the critical value I_c (see (4.20)).

If we now connect the junction to a dc voltmeter, the latter will register the average value over one period, $\bar{V}$. Averaging of (4.19) over time gives (???? how???)

$$2e\bar{V} = \hbar\omega \tag{4.21}$$

This formula has a very clear physical interpretation. If the average separation between the energy levels of the Cooper pairs in the superconducting electrodes is $2e\bar{V}$, then, as a result of the transfer of one pair through the weak link, this energy is released by the junction in the form of one quantum of electromagnetic radiation.

The current-voltage characteristic of the junction predicted by (4.20) and (4.21) is shown in Fig. 4.7.

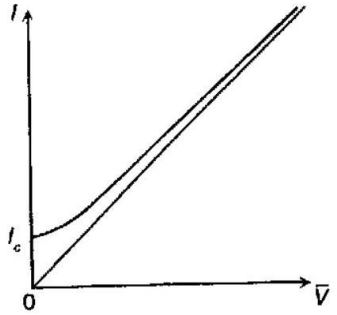


Fig. 4.7. Current-voltage characteristic of a Josephson junction

Note that the relations (4.17) and (4.21) are absolutely precise and fundamental and exact. They have been confirmed by numerous experiments. The first experimental observation of the Josephson radiation was reported in 1964 by Yanson, Svistunov and Dmitrenko [11].

9.2.4 1001 Questions about what exactly happens in JJ?

What is the most exact CPR in JJ?

(??? I don't know, this theory predicts that there is these features, another - that there are another and so on. I'll answer later)

(actually, there is a big article about it Current-phase relation in Josephson junctions by Golubov, Kupriyanov, Il'ichev, so I'll write main statements from it here)

What was approximated?

(discuss all these approximations)

Was self-consistency taken into account in Josephson relations?

(??????discussion of it. see de gennes book)

9.2.5 Experimental Confirmation of CPR in JJ

(!!! write this! for which experiments which results?)

9.2.6 Shapiro Steps

(about them)

9.2.7 Josephson Junction in an External Magnetic Field

Model of Josephson Junction in a Weak External Magnetic Field

In this section we shall restrict our attention to Josephson junctions without concentration of current, that is, to sandwiches and tunnel junctions. Suppose, for example, that such a junction consists of two bulk superconducting slabs separated by a thin insulating layer, as in Fig. 4.8.

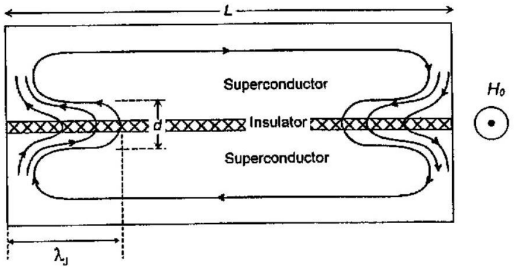


Fig. 4.8. Tunnel Josephson junction in a magnetic field H_0. The distribution of the screening (Meissner) supercurrent is shown by lines with arrows

If this system is placed in an external magnetic field parallel to the plane of the junction, a screening supercurrent will be generated at the outer surfaces of the slabs. This current circulates within a surface layer of thickness λ and, in doing so, has to cross the weak link, where the critical current density is very small. Therefore, in order to maintain its dissipation-free flow, the current must spread over a rather wide area protruding into the junction. This situation is illustrated in Fig. 4.8. Let us try to describe it in mathematical terms.

Consider a Josephson junction in an external magnetic field. The plane of the junction coincides with the x axis and the magnetic field is directed along the z axis. The length along the y axis of the region penetrated by the current and the magnetic field is $d = 2\lambda + t$ (see Fig. 4.8). Here t is the thickness of the insulating layer. Consider two closely spaced pairs of points in the vicinity of the junction: 1, 2 and 3, 4, as in Fig. 4.9. All the points are chosen outside the area penetrated by the magnetic field and the distance between them is

The generalized momentum of a Cooper pair has the form

$$\hbar\nabla\theta = 2mv_\mathrm{s} + \frac{2e}{c}\boldsymbol{A} \tag{4.22}$$

where θ is the phase of the wavefunction, v_s the pair velocity, m the electron mass, e the electron charge, and $\boldsymbol{A}$ the vector potential. Let us integrate this equation along the dashed curves shown in Fig. 4.9.

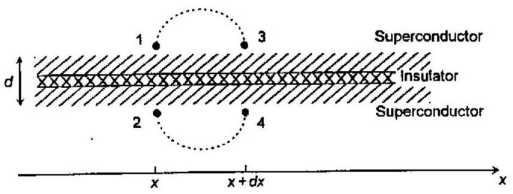


Fig. 4.9. Section near the edge of the Josephson junction. The dashed area is the region penetrated by the magnetic field

Since both curves are outside the area penetrated by the supercurrent, we have $v_\mathrm{s} = 0$:

$$\hbar\left[\int_1^3 \nabla\theta\cdot\,\mathrm{d}\boldsymbol{l} + \int_4^2 \nabla\theta\cdot\,\mathrm{d}\boldsymbol{l}\right] = \frac{2e}{c}\left[\int_1^3 \boldsymbol{A}\cdot\,\mathrm{d}\boldsymbol{l} + \int_4^2 \boldsymbol{A}\cdot\,\mathrm{d}\boldsymbol{l}\right]. \tag{4.23}$$

The distance d is assumed to be negligibly small. Then the right-hand side of (4.23) can be approximated by

$$\frac{2e}{c}\oint A\cdot\,\mathrm{d}l = \frac{2e}{c}\,\mathrm{d}\Phi, \tag{4.24}$$

where $\mathrm{d}\Phi$ is the magnetic flux enclosed by the contour comprising the dashed curves $1-3$ and $4-2$ which are supplemented with missing sections $3-4$ and 2-1. Carrying out the integration on the left-hand side we get

$$\hbar\left(\theta_3-\theta_1+\theta_2-\theta_4\right)=\frac{2e}{c}\,\mathrm{d}\Phi$$

Taking into account that $\theta_3-\theta_4=\varphi(x+\mathrm{d}x)$ and $\theta_1-\theta_2=\varphi(x)$, we have

$$\varphi(x+\mathrm{d}x)-\varphi(x)=\frac{2e}{\hbar c}\,\mathrm{d}\Phi,$$

or, recalling that $\Phi_0=\pi\hbar c/e$,

$$\frac{\mathrm{d}\varphi}{\mathrm{d}x}=\frac{2\pi}{\Phi_0}\frac{\mathrm{d}\Phi}{\mathrm{d}x}. \tag{4.25}$$

Noting that $(1/d)\mathrm{d}\Phi/\mathrm{d}x$ is the magnetic field H at the point x of the junction, we can write

$$H=\frac{\Phi_0}{2\pi d}\frac{\mathrm{d}\varphi}{\mathrm{d}x}. \tag{4.26}$$

This magnetic field H is directed along the z axis. By Maxwell's equations, the supercurrent through the junction in the direction of the y axis is

$$j_\mathrm{s}=\frac{c}{4\pi}\frac{\mathrm{d}H}{\mathrm{d}x}.$$

Inserting (4.26) and recalling the fundamental Josephson relation between the current and the phase difference, $j_\mathrm{s}=j_\mathrm{c}\sin\varphi$, we arrive at the so-called Ferrell-Prange equation [36]:

$$\frac{\mathrm{d}^2\varphi}{\mathrm{d}x^2}=\frac{1}{{\lambda_\mathrm{J}}^2}\sin\varphi, \tag{4.27}$$

where λ_J is

$$\lambda_\mathrm{J}=\left(\frac{c\Phi_0}{8\pi^2 j_\mathrm{c} d}\right)^{1/2}. \tag{4.28}$$

But, actually, nearly no one knows, what is the Ferrell-Prange equation, so it is better to name it "equation of phase when magnetic field is present".

The solution of (4.27), $\varphi(x)$, gives the phase difference distribution over the junction. Consider the case of a very weak external field $H_0\ll\Phi_0/\left(2\pi\lambda_\mathrm{J}d\right)$. Both the currents through the junction and the phase difference φ are then small. Hence we can rewrite (4.27) as

$$\frac{\mathrm{d}^2\varphi}{\mathrm{d}x^2}=\frac{1}{\lambda_\mathrm{J}^2}\varphi.$$

This equation can be easily solved to give

$$\varphi(x)=\varphi(0)\exp\left(-x/\lambda_\mathrm{J}\right). \tag{4.29}$$

Substituting this solution into (4.26), we find the magnetic field in the junction:

$$H(x)=H_0\exp\left(-x/\lambda_\mathrm{J}\right).$$

(!!! add some plot about it here!!!)

One can see that the quantity λ_J, which has the dimensions of length, represents the depth of magnetic field penetration into the Josephson junction. λ_J is usually referred to as the Josephson penetration depth.

In the International System of Units (SI), equation (4.28) takes the form:

$$\lambda_{\mathrm{J}} = \left(\frac{\Phi_0}{2\pi\mu_0 j_{\mathrm{c}} d} \right)^{1/2}$$

where $\mu_0 = 4\pi \times 10^{-7}\mathrm{Hm}^{-1}, \Phi_0 = 2.07 \times 10^{-15}$ Wb, j_{c} is the density of the critical current through the junction in Am^{-2}, and d is taken in m . Taking parameters typical of a tunnel Josephson junctions $d \sim 10^{-5}$ cm, $j_{\mathrm{c}} \sim 10^2 \mathrm{Acm}^{-2}$, we obtain $\lambda_{\mathrm{J}} \sim 0.1$ mm, i.e., it is a macroscopic length.

Not Weak Magnetic Field Penetration into a Josephson Junction. Josephson Vortices

What happens if the external field in JJ becomes not weak? It turned out that the behavior of a Josephson junction in an external magnetic field is reminiscent of the behavior of a type-II superconductor. Just as with type-II superconductors, when the external field exceeds a certain critical value H_{cl}, which is a characteristic of the junction, the field starts to penetrate into the junction in the form of superconducting vortices, each carrying one magnetic flux quantum Φ_0. In the case of a Josephson junction, they are called Josephson vortices.

Indeed, one of the solutions of the Ferrell-Prange equation (4.27) has the form

$$\varphi_0(x) = 4 \arctan \left\{ \exp \left(x/\lambda_{\mathrm{J}} \right) \right\}. \tag{4.30}$$

One can easily verify that this solution satisfies (4.27). The functions $\varphi_0(x)$, $\mathrm{d}\varphi_0/\mathrm{d}x \sim H$, and $\mathrm{d}^2\varphi_0/\mathrm{d}x^2 \sim j_{\mathrm{s}}$ are shown in Fig. 4.10.

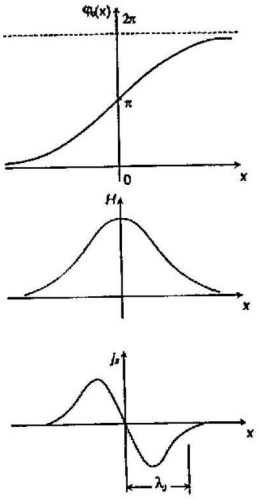


Fig. 4.10. Phase difference $\varphi_0(x)$, magnetic field $H(x)$, and supercurrent $j_s(x)$ for a Josephson vortex

A Josephson vortex represents a so-called soliton, that is, it is a localized solitary excitation of an extended Josephson junction.

These are the static properties of Josephson vortices, also known as Josephson fluxons. When a dc bias current is applied to a Josephson junction, the vortices can move along the junction and their motion leads to the appearance of a dc voltage accompanied by Josephson radiation, according to (4.21). This dynamic state is described by the so-called perturbed sine-Gordon equation [37], which is a more general case of (4.27) for the spaceand time-dependent φ. Moving Josephson fluxons exhibit relativistic properties of solitons (nonlinear solitary electromagnetic waves) and have been extensively studied both theoretically and experimentally. (!!! I'll add this to the theory later!!!)

The size of a static vortex along the x axis of the junction is $\sim 2\lambda_{\mathrm{J}}$ and along the y axis $\sim d \ll 2\lambda_{\mathrm{J}}$.

Thus, beginning at the field $H_{\rm cl}$, penetration of Josephson vortices into the junction becomes energetically favorable. Having penetrated into the junction, the vortices form a linear chain and the junction goes into the mixed state. So far we have a complete analogy with a type-II superconductor. But is the analogy really complete? The answer is 'no'.

The thing is that, unlike an Abrikosov vortex (see Chap.5), a Josephson vortex does not have a normal core. The existence of the normal core in typeII superconductors relates to the second critical field H_{c2}: Superconductivity disappears when an external magnetic field presses the vortices so close together that their normal cores come into contact. The absence of a normal core for Josephson vortices implies that there is no upper critical field for a Josephson junction. Nevertheless, as we shall soon find out, the dependence of the maximum current through the junction on magnetic field can be rather curious.

Let us find the lower critical field of the junction, $H_{\rm cl}$. In order to do that, we shall analyze the free energy of the junction.

As the current through the junction increases from zero to a certain value $j_{\rm s}$ over a time t, a certain amount of energy is being stored by the junction. Per unit area of the junction, this energy is

$$w_{\rm J} = \int_0^t j_{\rm s} V \, {\rm d}t$$

Here V is the voltage across the junction, which appears during the process of increasing the current and obeys the general relation (4.17). Substituting here $j_{\rm s} = j_{\rm c} \sin\varphi$ and (4.17), we obtain, after carrying out elementary integration,

$$w_{\rm J} = \frac{\hbar}{2e} j_{\rm c} (1 - \cos\varphi) \tag{4.32}$$

One notices that the Josephson junction plays the role of a nonlinear inductance which stores the energy. In addition to this energy, there is also a magnetic energy, which, per unit area of the junction, is given by

$$w_H = \frac{H^2}{8\pi} d \tag{4.33}$$

Taking the sum of (4.32) and (4.33) and carrying out integration over the length of the junction L (see Fig. 4.8), we obtain the total free energy of the junction, per unit length along the direction of the magnetic field (i.e., the z direction):

$$W = \int_0^L {\rm d}x \left[\frac{H^2}{8\pi} d + \frac{\hbar}{2e} j_{\rm c} (1 - \cos\varphi) \right]$$

Substituting (4.26) into this equation, we can modify the expression for W to

$$W = \int_0^L {\rm d}x \left[\frac{\Phi_0^2}{32\pi^3 d} \left(\frac{{\rm d}\varphi}{{\rm d}x} \right)^2 + \frac{\hbar}{2e} j_{\rm c} (1 - \cos\varphi) \right] \tag{4.34}$$

Using the variational method to minimize W, we arrive once again at the Ferrell-Prange equation (4.27).

From (4.34), one can easily derive the free energy W_0 of an individual Josephson vortex in an infinite junction. To do so, the expression for $\varphi_0(x)$ (4.30) should be substituted into (4.34) and the integration carried out. As a result we get

$$W_0 = \frac{4\Phi_0 j_c}{\pi c}\lambda_J \tag{4.35}$$

If the junction is placed in an external magnetic field H_0, the Gibbs free energy of a Josephson vortex becomes, by (1.22),

$$\mathcal{G}_0 = W_0 - \Phi_0 H_0/4\pi \tag{4.36}$$

Thus, if the external field is sufficiently weak, the energy is $\mathcal{G}_0 > 0$ and the existence of a Josephson vortex in the interior of the junction is energetically unfavorable. Penetration of a vortex into the junction becomes favorable beginning at a certain value of the external field H_0 which corresponds to $\mathcal{G} = 0$. This field is called the lower critical field H_{c1}:

(???? this is not the lower cr field in type 2 SC, right???)

$$H_{c1} = \frac{2}{\pi^2}\frac{\Phi_0}{\lambda_J d} \tag{4.37}$$

The field H_{c1} is obviously less than the field at the center of the vortex, $H(0)$. The latter, from (4.30) and (4.26), is

$$H(0) = \frac{\Phi_0}{\pi\lambda_J d} \tag{4.38}$$

The field $H(0)$ is effectively the superheating field for the Meissner state of the junction.

4.4.3 Maximum Zero-Voltage Current of a Josephson Junction. High Magnetic Fields

Let us turn to high magnetic fields:

$$H_0 \gg \frac{\Phi_0}{2\pi\lambda_J d} \tag{4.39}$$

We assume that the size of the junction is $L \ll 2\lambda_J$. Thus we can ignore the self-induced field due to the current passing through the junction, because it is much less than H_0. The inequality (4.39) can be interpreted as a condition on the distance between the neighboring Josephson vortices in the chain: their distance must be much less than λ_J. Then it follows from (4.26) that

$$\frac{\mathrm{d}\varphi}{\mathrm{d}x} = \frac{2\pi d}{\Phi_0}H_0$$

and, carrying out integration, we get

$$\varphi(x) = \frac{2\pi d}{\Phi_0}H_0 x + C \tag{4.40}$$

where C is an arbitrary integration constant. Substituting (4.40) into the first Josephson relation (4.13) we obtain

$$j_s = j_c \sin\left(\frac{2\pi x}{a} + C\right) \tag{4.41}$$

where we use the notation

$$a = \Phi_0/H_0 d \tag{4.42}$$

It follows from (4.41) that the chain of Josephson vortices in this limit is indeed very dense. It is sketched in Fig. 4.11, together with the corresponding distribution of the tunneling supercurrent.

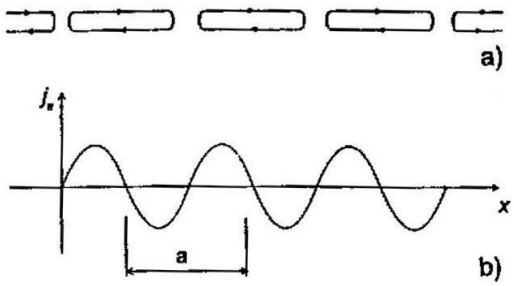


Fig. 4.11. (a) Densely packed chain of vortices representing the mixed state in a tunnel Josephson junction; (b) corresponding distribution of the tunneling supercurrent through the junction

The total current through the junction can be found by integration of j_s in (4.41) over the entire length of the junction:

$$I_{\mathrm{B}} = j_{\mathrm{c}} \int_{-L/2}^{L/2} \sin(2\pi x/a + C)\mathrm{d}x.$$

As a result we have:

$$I_{\mathrm{s}} = j_{\mathrm{c}} L \frac{\sin(\pi L/a)}{\pi L/a} \sin C \tag{4.43}$$

It follows from (4.43) that, in a fixed magnetic field, a change of the total current through the junction, I_s (which is supplied by an external source) causes a subsequent change of the constant C. The latter adjusts itself to each value of I_s. Then the maximum total current, $I_{\max}$, which can pass through the junction without dissipation is simply the amplitude of the quantity written in (4.43) before $\sin C$:

$$I_{\max} = I_{\mathrm{c}} \left| \frac{\sin(\pi L/a)}{\pi L/a} \right| \tag{4.44}$$

$$I_{\mathrm{c}} = j_{\mathrm{c}} L$$

The expression for $I_{\max}$, equation (4.44), can be written in a more convenient form if we note that, according to (4.42),

$$\pi L/a = \pi \Phi/\Phi_0 \tag{4.45}$$

where Φ is the total magnetic flux through the Josephson junction:

$$\Phi = H_0 L d.$$

On substitution of (4.45) into (4.44), we obtain the final result:

$$I_{\max} = I_{\mathrm{c}} \left| \frac{\sin\left(\pi\Phi \frac{\Phi/\Phi_0)}{\pi\Phi}\right.}{\pi/\Phi_0} \right|. \tag{4.46}$$

The dependence of $I_{\max}$ on the external magnetic field $H_0 = \Phi/(Ld)$ is shown in Fig. 4.12.

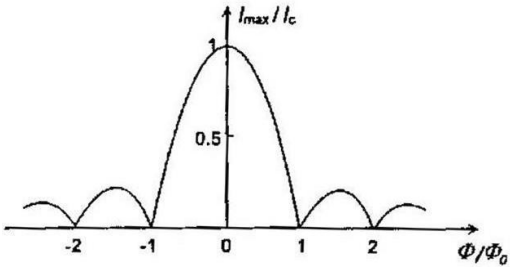


Fig. 4.12. Maximum supercurrent through a Josephson junction versus the external magnetic field parallel to the plane of the junction

As one can conclude from the plot and from (4.46), the mixed state in the junction is absolutely unstable (that is, a negligibly small current suffices to destroy it) when the total magnetic flux Φ is equal to an integral number of Φ_0. In contrast, it is most stable whenever there are a half-integral number of flux quanta enclosed in the junction. Experiment [40] has given a spectacular verification of (4.46), as one can see from Fig. 4.13.

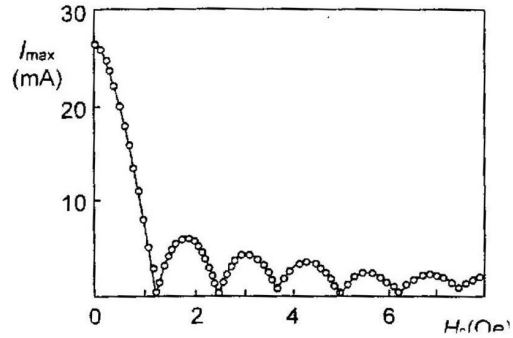


Fig. 4.13. Experimentally observed dependence of the maximum supercurrent through a $Sn - SnO_x$-Sn junction on magnetic field [40]

9.2.8 SQUIDs (Superconducting Quantum Interferometers): Basic Concepts

This section is concerned with the basic principles underlying the devices known as superconducting quantum interference devices (SQUIDs). These devices, though very simple in design, have opened new horizons in lowtemperature measurement techniques. Many SQUID-based instruments are unique in their sensitivity. The most celebrated examples are SQUID magnetometers, which are able to resolve flux increments of $\sim 10^{-10}$G, and precision voltmeters with the sensitivity of $\sim 10^{-15}$ V.

So, what is SQUID? There are two basic types of SQUIDs to distinguish: a two-junction dc SQUID and a single-junction rf SQUID.

4.5.1 The Two-Junction SQUID (DC SQUID)

This device consists of two Josephson junctions connected in parallel. In practice, the circuit consists of two bulk superconductors which, together with the Josephson junctions a and b, form a ring as in Fig. 4.14. The flux through the loop of the SQUID is generated by a magnetic coil placed in the interior of the ring. To understand how this type of SQUID operates, we need to know how the maximum zero-voltage current $I_{\max}$ through the device depends on the total magnetic flux Φ enclosed in the SQUID loop.

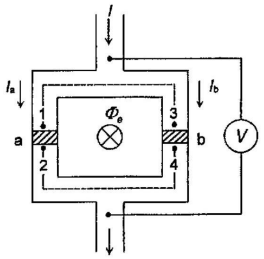


Fig. 4.14. Superconducting interferometer: two Josephson junctions, a and b, are connected in parallel. The interior of the SQUID loop is threaded by a magnetic flux Φ

Consider two pairs of points in the interiors of the superconductors: (1,2) and (3.) all of which are rigse to the iunctions a and h as illustrated in

Fig. 4.14. Carrying out integration of (4.22) along the dashed contour from point 1 to point 3 and from point 4 to point 2, we obtain [5]

$$\theta_3 - \theta_1 + \theta_2 - \theta_4 = \frac{2e}{\hbar}\left(\int_1^3 \boldsymbol{A}\cdot\ \mathrm{d}\boldsymbol{l} + \int_4^2 \boldsymbol{A}\cdot\ \mathrm{d}\boldsymbol{l}\right) \tag{4.47}$$

The term $2mv_\mathrm{s}$ has been omitted because the contour passes everywhere through the interior of the superconductor, well away from the edges. There is no supercurrent there and $v_\mathrm{s} = 0$. The distance between points 1 and 2, as well as between 3 and 4, is small compared to the length of the dashed contour. In addition, the vector potential $\boldsymbol{A}$ does not have any special features near the junctions. Therefore, the right-hand side of (4.47) can be supplemented by an integral along the sections $3-4$ and 1-2. As a result we get

$$\varphi_\mathrm{a} - \varphi_\mathrm{b} = \frac{2e}{\hbar}\oint A\cdot\ \mathrm{d}l$$

or

$$\varphi_\mathrm{a} - \varphi_\mathrm{b} = 2\pi\Phi/\Phi_0 \tag{4.48}$$

where Φ is the total magnetic flux enclosed in the loop of the interferometer, $\varphi_\mathrm{a} = \theta_2 - \theta_1, \varphi_\mathrm{b} = \theta_4 - \theta_3$, and $\Phi_0 = \pi\hbar c/e$ is the magnetic flux quantum.

The current through the junction a is, from (4.1),

$$I_\mathrm{a} = I_\mathrm{c}\sin\varphi_\mathrm{a},$$

and through the junction b,

$$I_\mathrm{b} = I_c\sin\varphi_\mathrm{b}$$

(the junctions are assumed to be identical and characterized by the same value of the critical current, I_c). The total current through the interferometer is then the sum of I_a and I_b:

$$I = I_\mathrm{c}\left(\sin\varphi_\mathrm{a} + \sin\varphi_\mathrm{b}\right) \tag{4.49}$$

Noting that $\sin\varphi_\mathrm{a} + \sin\varphi_\mathrm{b} = 2\sin\left[\left(\varphi_\mathrm{a} + \varphi_\mathrm{b}\right)/2\right]\cos\left[\left(\varphi_\mathrm{a} - \varphi_\mathrm{b}\right)/2\right]$ and using (4.48), we can modify (4.49) to the form

$$I = 2I_\mathrm{c}\cos\frac{\pi\Phi}{\Phi_0}\sin\left(\varphi_\mathrm{b} + \frac{\pi\Phi}{\Phi_0}\right). \tag{4.50}$$

If the total flux enclosed in the loop of the SQUID is fixed, the only parameter which adjusts itself to a given total current I is, from (4.50), φ_b. It follows (just as in the preceding section when (4.44) was being derived) that the maximum dissipation-free current of the device is

$$I_{\max} = 2I_c \left|\cos\left(\pi\Phi/\Phi_0\right)\right| \tag{4.51}$$

The dependence of $I_{\max}$ on Φ is illustrated in Fig. 4.15. The superconducting state of the ring is most stable with respect to the external current I when an

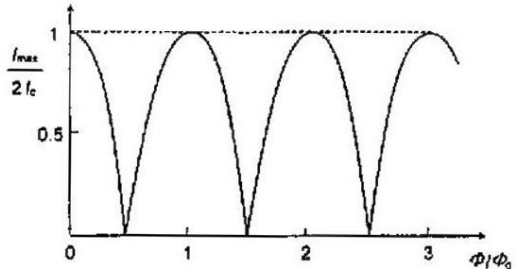


Fig. 4.15. Dependence of the maximum supercurrent through the two-junction interferometer on the total magnetic flux through its interior

integral number of flux quanta are enclosed in the interferometer. In contrast, a half-integral number of flux quanta in the loop corresponds to an unstable superconducting state. That is to say, a negligibly small current I suffices in the latter case to drive the device to the resistive state, with a finite voltage across the junction (see Fig. 4.14).

We would like to emphasize that Φ is the total flux through the loop of the interferometer. The flux supplied externally by the magnetic coil, Φ_e, is related to Φ by

$$\Phi = \Phi_{\mathrm{e}} - LI_{\mathrm{sc}},$$

where L is the inductance of the interferometer and I_{BC} is the screening current circulating in it. The critical current of the SQUID is periodic in Φ_e, too, with period Φ_0. This dependence is illustrated in Fig. 4.16.

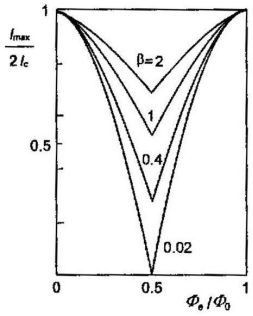


Fig. 4.16. Critical current of the two-junction SQUID versus external magnetic flux, for several values of the parameter $\beta = 2LI_{\mathrm{c}}/\Phi_0$[41]

A detailed analysis of the two-junction SQUID operation is given by Clarke in [41].

The unique sensitivity of dc SQUIDs can be employed in many situations where a variation of the quantity of interest can be converted into a variation of magnetic flux. The only limit on it is set by thermal noise in Josephson junctions which is estimated as several units per $10^{-5}\Phi_0$, provided the time of the measurements is longer than 1 s . Therefore, in principle, it is possible to resolve increments of magnetic field of the order of $10^{-10} - 10^{-11}$G. For comparison, the Earth's magnetic field is about 0.5 G .

After the discovery of high- T_{c} superconductors, SQUIDs made of these materials were shown to operate well at the temperature of liquid nitrogen (77 K). Since this temperature range is much easier to attain than liquid helium temperature (4.2 K), the high- T_{c} SQUIDs have the potential to fill a broad range of applications. These include biomagnetic measurements, nondestructive evaluation, and geomagnetic probing. The present status of highT_{c} SQUIDs is described in a recent review [42].

4.5.2 The Single-Junction SQUID (RF SQUID)

The basic element of a single-junction SQUID is a superconducting ring containing a Josephson junction. Consider two points, 1 and 2, in the vicinity of the junction, as shown in Fig. 4.17. The dashed contour 1-2 passes through the interior of the superconductor in such a way that its distance from the edges is everywhere larger than λ. Therefore, there is no supercurrent at any point of the contour and $v_6 = 0$.

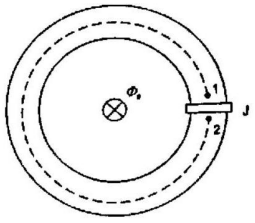


Fig. 4.17. Single-junction SQUID: a single junction J closes a superconducting ring. An external flux Φ_e is generated by a magnetic coil inserted in the ring

Let us go back to the general equation (4.22) and integrate along the dashed contour from point 1 to point 2 . Taking into account that $v_s = 0$, we have

$$\hbar\,(\theta_2 - \theta_1) = 2e \int_1^2 \boldsymbol{A} \cdot \, \mathrm{d}\boldsymbol{l} \tag{4.52}$$

The distance between points 1 and 2 across the junction is much shorter than their distance along the dashed contour, and the vector potential does not have peculiarities in the vicinity of the junction. Therefore, the variation of the right-hand side of (4.52) will be negligible if we supplement it with an integral $\int_2^1 \boldsymbol{A} \cdot \, \mathrm{d}l$ across the junction. Then (4.52) can be rewritten as

$$\sin = 2\rho \oint A \cdot \, \mathrm{d}I \tag{4.53}$$

where φ is the phase difference across the junction J. Equation (4.53) can be further reduced to

$$\varphi = 2\pi\Phi/\Phi_0, \tag{4.54}$$

where Φ is the total magnetic flux enclosed in the SQUID loop. In general, this flux Φ is not equal to the externally supplied flux Φ_e. Their difference is due to the screening current circulating in the superconducting ring:

$$\Phi = \Phi_e - LI_{sc}, \tag{4.55}$$

where L is the inductance of the ring. Since the current I_{sc} passes through both the ring and the junction, its relation to the phase difference of the superconducting electron wavefunction is given by the well-known expression (4.1). Together with (4.54) and (4.55), this yields

$$\Phi_e = \Phi + LI_c \sin\,(2\pi\Phi/\Phi_0) \tag{4.56}$$

This formula can be considered as an implicit relation between Φ and Φ_e. It is illustrated graphically in Fig. 4.18.

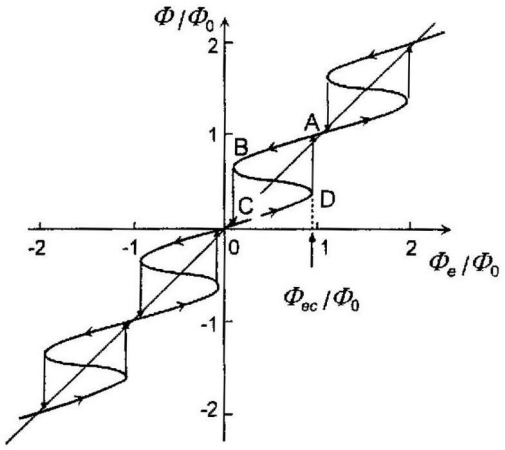
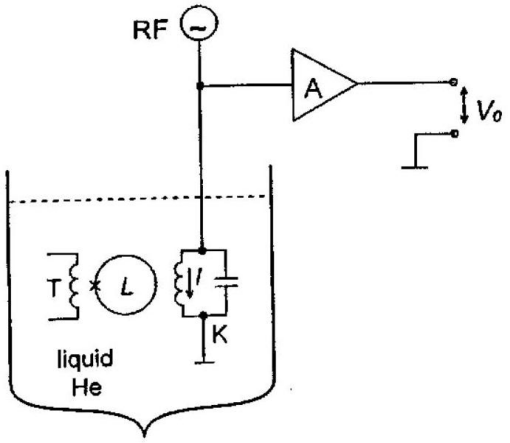


Fig. 4.18. Total magnetic flux Φ enclosed in the loop of a single-junction interferometer versus the external flux Φ_e through the loop

Let us now analyze the physics of SQUID operation. First we increase the external flux Φ_e (that is, we increase the current through the magnetic coil inserted in the SQUID loop). As an immediate response, a screening current I_{sc} starts to flow in the ring and generates its own magnetic flux which partially cancels the external flux Φ_e. Therefore, the total flux is less than Φ_e. Why is the cancellation only partial? If the ring were solid, without the weak link, the cancellation would be complete and the total flux would be $\Phi = 0$.



Fig, 4.19. Block-diagram of an rf SQUID. RF is a high-frequency current supply (of large internal resistance), A a high-frequency amplifier, L a single-junction interferometer, T a secondary coil of a flux transformer, and K a highfrequency resonant circuit

This situation can also be described in a different way. In order to supply the external flux Φ_e, it is not always necessary to place a magnetic coil in the loop of the device; it is merely convenient in practice. Alternatively, the loop can be placed in a homogeneous external field. Then Φ_e is simply the product of the induction of the external field and the area of the loop (here we assume that the plane of the loop is perpendicular to the external magnetic field). Then it is easy to see that, if the superconducting ring were solid, that is, without a weak link, the total flux Φ through it would be zero. On the other hand, when the weak link is present, it can be identified with a region where the external magnetic field can penetrate into the ring's interior. As a result, the screening is not perfect.

As the external flux Φ_e is increased further, the screening current increases, too, until it reaches its critical value at $\Phi_e = \Phi_{ec}$, as illustrated in Fig. 4.18. At this moment (point D in Fig. 4.18) the system becomes unstable and jumps to the next quantum state (point A in Fig. 4.18). As a result, the total magnetic flux through the loop exceeds the external flux and the screening current changes its direction. However, as the external flux continues to increase and at some moment reaches the value of the flux quantum Φ_0, the total flux also becomes equal

to Φ_0 and the screening current vanishes, which is effectively equivalent to $\Phi_e = 0$ (see Fig. 4.18). With further increase of Φ_e, this switching process repeats itself with period Φ_0. If Φ_e is decreased, the jumps will start from points analogous to point B. Thus, a cyclic variation of the external flux Φ_e is accompanied by a hysteresis loop CDABC. The area of the loop is proportional to the energy dissipated in the junction.

Now our knowledge of the properties of a superconducting ring with a single Josephson junction is sufficient to understand how the rf SQUID operates. Its block-diagram is shown in Fig. 4.19. A current of frequency ν is supplied by a high-impedance ac current source to the resonant circuit K .
(Frequencies $\nu \approx 10 - 20$MHz are used most often. However, there are also SQUIDs operating at higher frequencies such as several GHz). The coil of the resonant circuit is coupled to the loop of the interferometer I. The rf voltage across the circuit K is amplified by the amplifier A . This voltage, V_0, is the output of the device. The device input is the coil T inductively coupled to the SQUID loop L.

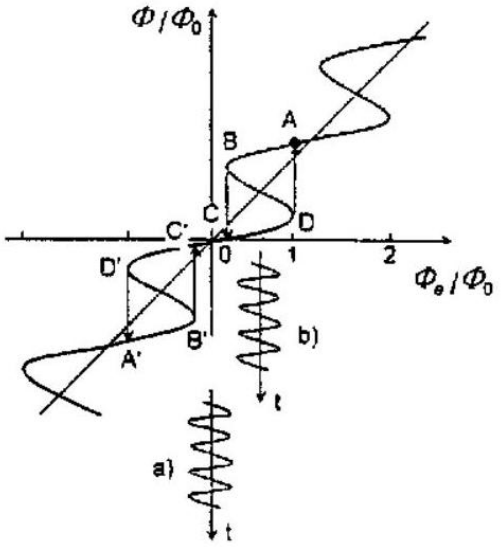
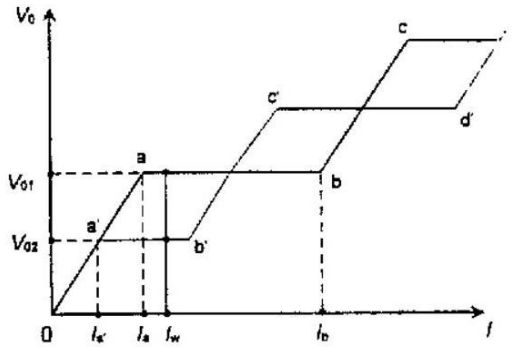


Fig. 4.20. Variation of the external flux with time: (a) when zero flux is generated by the input coil T ($\Phi_T = 0$); (b) when $\Phi_T = \Phi_0/2$



Now let us work out how the output V_0 relates to the value of the current I through the resonant circuit K. Assume that the current through the input coil T is zero. Then the external flux Φ_e is generated entirely by the circuit K and has the frequency ν, as in Fig. 4.20 (a). In turn, the sinusoidal variation of Φ_e causes a sinusoidal variation of the total flux Φ (see Fig. 4.20) resulting in an rf voltage V_0 at the output. An increase of the bias current I causes a proportional increase of the amplitude of Φ_e and, as a consequence, of Φ and V_0. Thus the dependence of V_0 on I is linear (at the initial part 0a of the rf current-voltage characteristic in Fig. 4.21) until the current reaches a value such that $\Phi_e = \Phi_{ec}$ (see Fig. 4.18). At this moment, a discontinuous jump of the total flux occurs, corresponding to closing a hysteresis loop on the $\Phi(\Phi_e)$ curve, and an amount of heat proportional to the area of the loop is

Fig. 4.21. RF current-voltage characteristic of the SQUID; bold line (Oabc...) corresponds to the input flux $\Phi_T = 0$, thin line (0a′b′c′d′ . . .) - to $\Phi_T = \Phi_0/2$

dissipated. The necessary amount of energy, which is quite large, is borrowed from the resonant circuit K . As a result, the amplitude of the current I sharply decreases and it takes a long time (a large number of rf oscillation periods) for the current to recover its initial value. A further increase of the amplitude of current supplied by the generator will not result in an increase of the output voltage V_0 because the above process will repeat itself again and again. The only difference will be that the time required for the current I to recover will steadily decrease, that is, a smaller number of rf periods will be needed. This means that we arrive at the horizontal part ab of the current-voltage characteristic in Fig. 4.21. Finally, at a certain value of the bias current, the current I will reach a value (I_b) such that the time of one period will be sufficient for the rf current supply to replenish the energy of the circuit K that has been absorbed by the interferometer during two hysteresis cycles DABC and D′A′B′C′ shown in Fig. 4.20. At $I > I_\mathrm{b}$, the total magnetic flux Φ and the output voltage V_0 will start to increase again and their increase will continue until Φ_e reaches the second critical value. At that point, hysteretic energy losses will occur again and the whole process will repeat itself resulting in the second plateau on the current-voltage characteristic.

Let us now turn to the case when there is a finite current through the input coil T generating a dc flux $\Phi_T = \Phi_0/2$. The time dependence of Φ_e in this case is illustrated in Fig. 4.20 (b). Clearly, the critical value Φ_{ec} is now reached at a significantly smaller current $I_{a'} < I_a$ through the resonant circuit. In addition, the length of the first plateau is only half as long because the current supply now has to compensate for the energy loss during just one hysteresis cycle. However, all subsequent plateaus on the current-voltage characteristic are of normal length again, since the energy to be recovered is dissipated during pairs of hysteresis cycles.

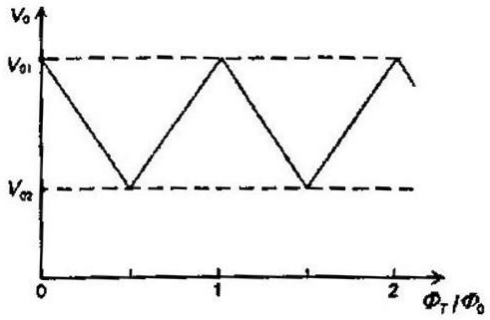


Fig. 4.22. Dependence of the output rf voltage V_0 on the external flux Φ_T generated by the input coil T

As the final stage of our analysis of SQUID operation, let us supply the device with some bias ac current I_w, as in Fig. 4.21. If $\Phi_T = 0$, the output voltage will be V_{01}; if $\Phi_T = \Phi_0/2$, the output voltage will be V_{02}. The question is: how will the voltage V_0 change if we increase the input flux Φ_T from 0 to $\Phi_0/2$? Obviously, it will gradually decrease from V_{01} to V_{02}. However, if $\Phi_T = \Phi_0$, the situation is analogous to the case $\Phi_T = 0$, as one can see

so-called 'triangular' dependence of the output voltage V_0 on the input flux (Fig. 4.22). It follows from this figure that the device is sensitive to variations of the magnetic flux Φ_T, with sensitivity much better than one flux quantum. Theoretical analysis of the sensitivity of rf SQUIDs has demonstrated that devices with sensitivity of the order of $10^{-5}\Phi_0$ are feasible, provided the measuring time is not less than 1 s .

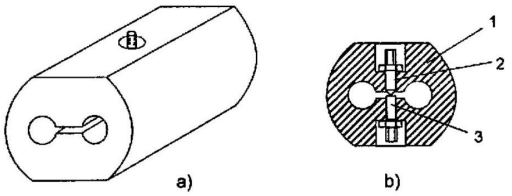


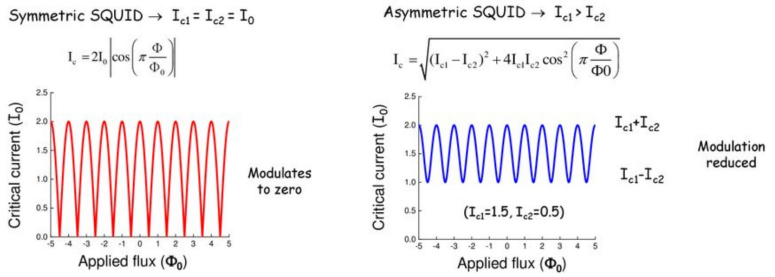
Fig. 4.23. Single-contact SQUID proposed by Zimmerman: (a) general view; (b) cross-section along the central plane: 1 - solid niobium frame, 2 - pointed niobium screw, 3 - flat niobium screw

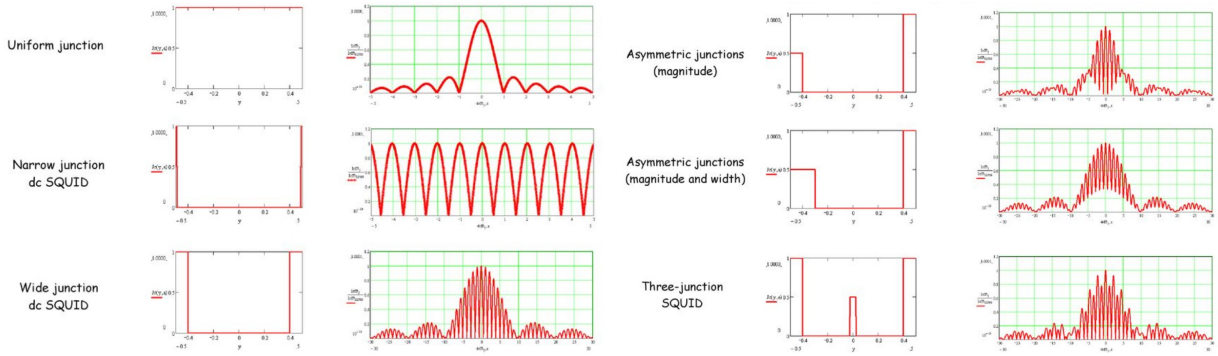
A classic bulk SQUID design which has proved to be very useful in practice is the symmetric single-weak-link device proposed by Zimmerman (Fig. 4.23). Here the Josephson junction is implemented as a point contact. The input coil T and the coil of the resonant circuit K (see Fig. 4.19) are inserted in the two holes of the device. Nowadays, the best low- and high- T_c SQUIDs are made using the planar multilayer thin film technology [42].

9.2.9 SQUIDs: Typical Modifications

Overview of Modifications

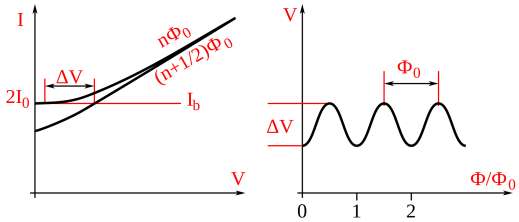
Asymmetric SQUID will shift current up:





(???)

(??)

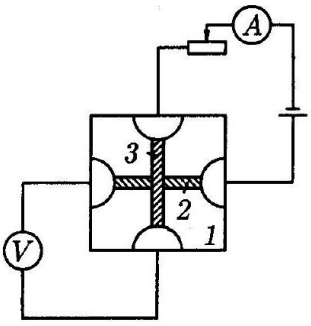


Overview of Methods to Describe Modifications in SQUID

(??? had a long time this question)

9.2.10 46. Tunneling Effects by Shmidt

Наиболее прямое измерение энергетической щели в сверхпронодниках может быть проведено с помощью туннельных экспериментов. Эту методику разработал Гевер в 1960 г. [133]. В принцине она очень проста (рис. 46.1). На стеклянную пластинку с заранее подготовленными контактами наносится узкая полоска пленки первого металла. Затем эта полоска окисляется так, чтобы пленка оказалась покрытой слоем изолирующего окисла толщиной в несколько десятков ангстрем (барьерный слой). После этого в поперечном направлении наносится узкая полоска пленки второго металла. Место пересечения этих двух полосок (площадью порядка 1m^2) и представляет собой туннельный переход. Исследование заключается в изучении вольт-амперной характеристики такого перехода. Физика дела заключается в том, что здесь испольэуется специфическое квантовомеханическое свойство электрона проходить тонкие потенциальные барьеры (в данном случае - слой окисла) посредством так называемого туннельного перехода.



46.1. Туннельные характеристики.

Обсудим теперь, какой вид будут иметь вольт-амперные характеристики для разных случаев туннельных переходов.

Простейший случай - когда и первый, и второй металлы нормальные металлы. При установлении контакта между металлами их уровни Ферми уравниваются за счет возникновения контактной разности потенциалов. Энергетическая диаграмма изображена на рис. 46.2, а. Если теперь на туннельный переход подать разность потенциалов V (рис. 46.2, б), то уровни Ферми металлов разойдутся на величину eV, и возникнет туннельный ток. Если предположить, что плотность состояний в интересующей нас области энергий остается постоянной ($N(0)$), то из рис. 46.2, б ясно, что сила тока будет пропорциональна eV, т. е. будет выполняться закон Ома.

Рассмотрим теперь случай, когда первый металл - нормальный, а второй - сверхпроводник. Мы уже знаем, какой вид имеет спектр элементарных возбуждений сверхпроводника (рис. 45.1 и 45.2). Энергия элементарных возбуждений отсчитывается от уровня основного состояния сверхпроводника. В нормальном металле энергия элементарного возбуждения отсчитывается от уровня Ферми. Поэтому при создании туннельного контакта между нормальным металлом и сверхпроводником за счет контактной разности потенциалов должны уравняться уровень Ферми нормального металла и уровень основного состояния сверхпроводника. Именно это состояние изображено на рис. 46.3, *а*.

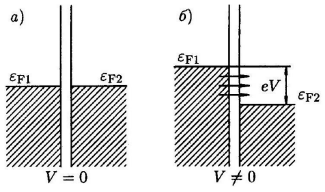
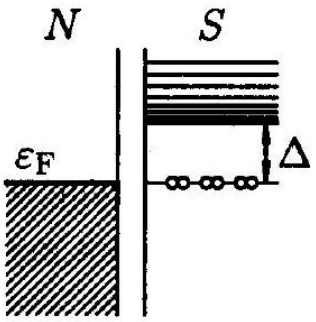


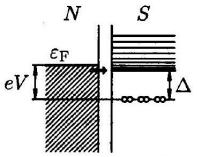
Рис. 46.2. Энергетическая диаграмма для случая контакта двух нормальных металлов: $a)V = 0$; б) $V \neq 0$, идет туннельный ток, пропорциональный eV.

Рассмотрим сперва случай, когда $T = 0$.

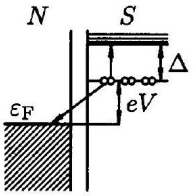
Приложим к туннельному переходу некоторую разность потенциалов V. Пусть в результате этого уровень Ферми нормального металла поднялся над уровнем основного состояния сверхцроводника на величину eV. Из рис. 46.3, б ясно, что туннельный ток электронов из N в S может начаться только тогда, ко'да величина eV станет равной энергетической щели Δ в S или «ревзойдет ее. Тот же результат получится, если поменять по лярность приложенного к переходу напряжения. Теперь туннелирование электрона из S в N будет происходить тогда, когда окажется энергетически допустимым разрыв электронной пары в S, т. е. когда энергия, выделившаяся при туннелировании одного электрона пары, окажется достаточной, чтобы закинуть второй электрон этой пары в область разрешенных энергий для одиночных электронов, т.е. выше щели (см. рис. 46.3, в).



а)



б)



в)

Рис. 46.3. Энергетическал диаграмма для туннельного NS-перехода: а) $V = 0$, уровень ε_F противостоит уровню основного состояния сверхпроводника; б) $V \neq 0, |eV| > \Delta$, идет туннельный ток электронов из N в S; в $)V \neq 0, |eV| > \Delta$, идет туннельный ток электронов из S в N.

Таким образом, вольт-амперная характеристика такого туннельного перехода будет нечетной функцией V. Она изображена на рис. 46.4.

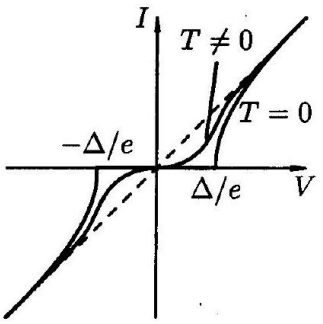


Рис. 46.4. Вольт-амперная характеристика туннельного NIS-перехода.

В случае, если $T \neq 0$, как нетрудно сообразить, вольт-амперная характеристика будет несколько размазанной.

Переходим к рассмотрению туннельных эффектов в S_1IS_2 переходах, когда оба металла (S_1 и S_2), разделенные туннельным слоем изолятора (I), являются сверхпроводниками.

Сперва рассмотрим случай $T = 0$. Согласно рис. 46.5, туннельный ток может возникнуть только тогда, когда к туннельному переходу будет приложено напряжение $V > (\Delta_1 + \Delta_2)/e$. Действительно, только в этом случае возможен процесс, изображенный на этом рисунке: электронная пара в S_1 разрывается, один из электронов этой пары туннелирует в S_2 с выделением энергии, равной или большей, чем Δ_1. При этом второй электрон разорванной пары, поглощая эту энергию, возбуждается в состояния спектра квазичастиц S_1.

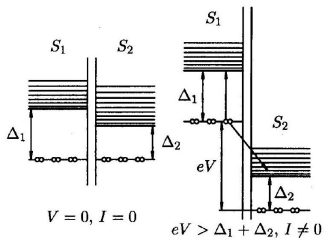
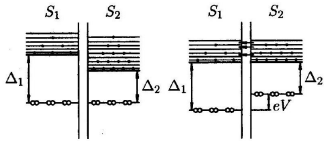


Рис. 46.5. Энергетические диаграммы для туннельного перехода S_1IS_2, $T = 0$.

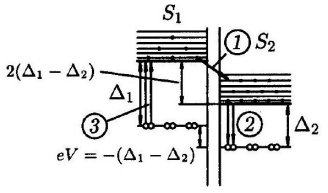
Для реального случая, когда $T \neq 0$, картина будет несколько более сложной. Теперь в каждом из сверхпроводников имеется какое-то количество возбужденных одиночных электронов, равновесное количество которых определяется температурой.

Энергетические диаграммы туннельного перехода в этом 'лучае изображены на рис.46.6. Количество возбуждений в данний области спектра схематично изображается количеством то'лек на данном энергетическом уровне. Видно, что если $V = 0$



а)

б)



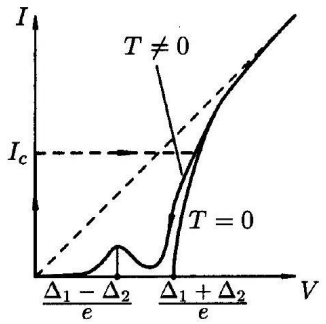
в)

Рис. 46.6. Туннелирование между двумя сверхпроводниками при $T \neq 0$: а) $V = 0$, концентрация возбуждений с одинаковой энергией в S_1 и S_2 одинакова, поэтому ток равен нулю; б) $eV = \Delta_1 - \Delta_2$, ток обусловлен переходом возбужденных частиц из S_2 в S_1; в) $eV = -(\Delta_1 - \Delta_2)$, возбужденная частица переходит из S_1 в S_2, (процесс 1), объединившись с электронами в S_2, она образует пару и попадает на основной уровень (процесс 2), выделившейся энергии $2\Delta_1$ достаточно для разрыва пары в S_1 (процесс 3).

(рис. 46.6, a), то несмотря на то, что щели в S_1 и S_2 разные, количество возбуждений на противостоящих друг другу уровнях в S_1 и S_2 будет одинаково. Поэтому количество частиц, туннелирующих из S_1 в S_2, будет равно тому же числу частиц, туннелирующих из S_2 в S_1, т.е. как это и должно быть, в равновесных условиях полный туннельный ток $I = 0$.

Если теперь приложить даже небольшое напряжение V, то равновесие нарушится и возникнет ток квазичастиц из одного сверхпроводника в другой. Не будем, однако, забывать, что плотность состоянии квазичастиц в сверхпроводнике имеет особен-

Рис. 46.7. Сверхпроводящие и квазичастичные ветви вольтамперных характеристик туннельного S_1IS_2-перехода для $T = 0$ и $T \neq 0$.

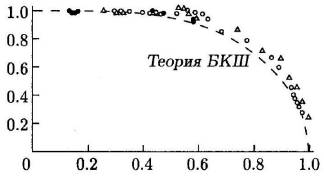


ность при $E = \Delta$ (см. (45.5) и рис. 45.2). Поэтому если приложить к переходу разность потенциалов V такую, что $eV = \Delta_1 - \Delta_2$ (рис. 46.6,), то друг против друга окажутся области с. плотностью состояний $\rho = \infty$ и в S_1, и в S_2. Естественно, это зызовет большой всплеск туннельного тока. Дальнейшее увеличение V приведет к тому, что уровни с $\rho = \infty$ разойдутся и полный туннельный ток уменьшится. Отсюда можно сделать вывод, что при $V = (\Delta_1 - \Delta_2)/e$ на вольт-амперной характеристике должен наблюдаться максимум тока (рис. 46.7). При изменении знака V возникнет диаграмма, изображенная на рис. 46.6, в. Здесь тоже возникнет всплеск тока при $|V| = (\Delta_1 - \Delta_2)/$. Таким образом, и в случае контакта двух сверхпроводников вольт-амперная характеристика будет нечетной функцией напряжения V.

В заключение приведем результат туннельного эксперимента Гевера и Мегерле [134] по изучению величины энергетической цели в различных сверхпроводниках и ее зависимости от температуры (рис. 46.8). Штриховой линией показана зависимость, 'ледующая из теории Бардина-Купера-Шриффера.

46.2*. Энергия связи SIS-перехода и температурная зависимость критического тока.

Прежде чем приступить к исследованию SIS-перехода мы приведем вычисление проводимости туннельного перехода в нормальном состоянии. Это окажется полезно для дальнейшего, т.к. мы будем сейчас использовать в более простой ситуации тот же самый метод "туннельного$\Delta(T)/\Delta(0)$



T/T_c

Рис. 46.8. Экспериментальные результаты изучения температурной зависимости энергетической щели в индии (светлые кружки), олове (треугольники) и свинце (черные кружки). Штриховая линия - зависимость $\Delta(T)$ согласно теории БКШ.

гамильтониана", который нам понадобится для решения основной задачи. Рассмотрим два куска нормального металла, разделенных потенциальным барьером из изолятора. Электрон с импульсом $\hbar\mathbf{k}$ в 1 -м куске металла, подлетающий к барьеру, может протуннелировать под барьером и оказаться во 2 -м куске уже с импульсом $\hbar\mathbf{q}$. Заметим, что как правило $\mathbf{q} \neq \mathbf{k}$, поскольку туннельный барьер вовсе не обязан быть однородным. Квантовомеханическую амплитуду этого процесса мы обозначим через $t_{\mathbf{k},\mathbf{q}}$. Будем теперь считать, что к 1-му куску металла приложено напряжение V относительно 2-го, и вычислим вероятность перехода электрона в единицу времени из любого занятого состояния 1 -го металла в любое свободное состояние 2-го. Для этого мы используем "золотое правило Ферми» для вероятности переходов (в единицу времени) в непрерывном спектре [49]:

$$\Gamma^{\rightarrow}(V) = \frac{2\pi}{\hbar}\frac{1}{\mathcal{V}_1\mathcal{V}_2}\sum_{\mathbf{k},\mathbf{q},\sigma}\left|t_{\mathbf{k},\mathbf{q}}\right|^2\delta\left(\varepsilon_k - \varepsilon_q - eV\right)f\left(\varepsilon_k\right)\left(1 - f\left(\varepsilon_q\right)\right) \tag{46.1}$$

где $\mathcal{V}_{1,2}$-объемы двух металлов, $f(\varepsilon) = \left(e^{\varepsilon/k_{\mathrm{B}}T} + 1\right)^{-1}$ - фермиевская функция заполнения для электрона с энергией ε, а σ проекция электронного спина (подразумевается, что переворота спина при туннелировании не происходит). Переходя от суммирования по импульсам к интегрированию по энергиям электрона в начальном и конечном состояниях и считая туннельные матричные элементы и плотности состояний $N_{1,2}(\varepsilon)$ металлов не зависящими от энергии вблизи ферми-поверхности, получим (суммирование по спину дает лишнюю двойку):

$$\Gamma^{\rightarrow}(V) = \frac{4\pi}{\hbar}N_1(0)N_2(0)\left\langle\left|t_{\mathbf{k},\mathbf{q}}\right|^2\right\rangle\int d\varepsilon f(\varepsilon)(1 - f(\varepsilon + eV)), \tag{46.2}$$

где $\left\langle\left|t_{\mathbf{k},\mathbf{q}}\right|^2\right\rangle$ - усредненные по Ферми-поверхности матричные элементы. Для вычисления среднего тока при $T > 0$ надо также написать аналогичное выражение для вероятности перехода $\Gamma^{\leftarrow}(V)$ в обратную сторону, однако в уже сделанном приближении $N(\varepsilon) = N(0)$ результат для туннельной проводимости от гемпературы не зависит, так что можно ограничиться вычислением интеграла (46.2) при $T = 0$, дающего $I(V) = e\Gamma^{\rightarrow}(V)$. В результате

$$\frac{I(V)}{V} = \frac{1}{R_n} = \frac{4\pi e^2}{\hbar}N_1(0)N_2(0)\left\langle\left|t_{\mathbf{k},\mathbf{q}}\right|^2\right\rangle \tag{46.3}$$

ЗЗаметим, что мы определили плотности состояний $N(\varepsilon)$ в расчете на одну проекцию спина.

Вернемся к сверхпроводящему туннельному S_1IS_2-контакту и нокажем, что энергетические щели сверхпроводников и значение нормального сопротивления R_n определяют не только поведение квазичастичной (возвратной) ветви вольтамперной характеристики, но и величину ее прямой ветви, т. е. величину критического

сверхпроводящего тока I_c (рис. 46.7). Для этого рассмотрим детально процесс парного туннелирования в S_1IS_2-переходе.

Наличие туннельного взаимодействия между сверхпроводниками S_1 и S_2 приводит к тому, что полная энергия системы оказывается меньше суммы энергий отдельных сверхпроводников на величину энергии связи $E_{\text{св}}$. Мы подробно обсудим вычисление этой величины при $T = 0$. Как и ранее, туннельный барьер можно
рассматривать как источник упругого рассеяния, который переводит электрон из состояния с импульсом $\mathbf{k}$ в сверхпроводнике S_1 в состояние с импульсом q в сверхпроводнике S_2. Однако теперь нам удобнее вычислять поправку к энергии системы, связанную с такими переходами, которая может быть определена с помощью второго порядка квантовомеханической теории возмущений [49]:

$$E_{\text{cB}} = \sum_{\mathbf{k},\mathbf{q}} \frac{|H_t|^2_{\mathbf{kq}}}{E_0 - E_{\mathbf{kq}}} \tag{46.4}$$

Здесь H_t - туннельный гамильтониан, описывающий (точно так же, как и в нормальном состоянии) переход $(1,\mathbf{k}) \rightarrow (2,\mathbf{q})$ электрона с импульсом $\hbar\mathbf{k}$ из сверхпроводника S_1 в состояние с импульсом $\hbar\mathbf{q}$ в сверхпроводнике S_2, а также обратный процесс $(2,\mathbf{q}) \rightarrow (1,\mathbf{k})$; через E_0 и E_{kq} обозначены соответственно энергии основного и возбужденного состояний системы. Возбужденное состояние возникает в связи с переходом одного электрона из состояния $\mathbf{k}$ (или $-\mathbf{k}$) в S_1 в состояние $\mathbf{q}(-\mathbf{q})$ в S_2, т. е. с возникновением возбуждений, по одному в каждом сверхпроводнике. Нужно отметить, что процесс парного туннелирования, по существу, не является двухчастичным, поскольку туннелирование электронов из состояний $\mathbf{k}$ и $-\mathbf{k}$ происходит по одному и определяется одночастичными туннельными матричными элементами, а возбуждения в сверхпроводниках S_1 и S_2 являются виртуальными, т.е. существующим в течение короткого периода между туннелированием первого и второго электронов пары. Следуя [64] (см. также [112]), представим энергию связи (46.4) через матричные элементы одночастичного туннелирования $t_{\text{k,q}}$ и факторы когерентности $u_{\mathbf{k}}, v_{\mathbf{k}}, u_{\mathbf{q}}, v_{\mathbf{q}}$, смысл которых был подробно рассмотрен в 44:

$$E_{\text{CB}} = -2\sum_{k,q} |t_{\mathbf{k},\mathbf{q}}|^2 \frac{|v_{\mathbf{k}}u_{\mathbf{q}} + v_{\mathbf{q}}u_{\mathbf{k}}|^2}{E_k + E_q} \tag{46.5}$$

В (46.5) величина $v_{\mathbf{k}}u_{\mathbf{q}} + v_{\mathbf{q}}u_{\mathbf{k}}$ - амплитуда вероятности того, что при $T = 0$ состояния $(\mathbf{k}, -\mathbf{k})$ в S_1 заняты, а состояния $(\mathbf{q}, -\mathbf{q})$
в S_2 - свободны или наоборот, а множитель 2 учитывает вырождение виртуальных состояний по спину; наконец, $E_k + E_q$ - суммарная энергия двух виртуальных возбуждений, возникающих в процессе парного туннелирования. Используя формулу (45.13) и следующие из нее соотношения

$$\begin{aligned} 2u_{\mathbf{k}}v^*_{\mathbf{k}} &= \tfrac{\widetilde{\Delta}_1}{E_k}, \qquad 2u_{\mathbf{q}}{v_{\mathbf{q}}}^* = \tfrac{\widetilde{\Delta}_2}{E_q} \\ |u_{\mathbf{k}}|^2 - |v_{\mathbf{k}}|^2 &= \tfrac{\varepsilon_k}{E_k}, \qquad |u_{\mathbf{q}}|^2 - |v_{\mathbf{q}}|^2 = \tfrac{\varepsilon_q}{E_q} \end{aligned} \tag{46.7}$$

преобразуем (46.5) к виду

$$E_{\text{CB}} = -\sum_{k,q} \frac{|t_{\text{k},\mathbf{q}}|^2}{E_k + E_q}\left[1 - \frac{\varepsilon_k\varepsilon_q}{E_kE_q} + \text{Re}\,\frac{\widetilde{\Delta}_1\widetilde{\Delta}^*_2}{E_kE_q}\right] \tag{46.8}$$

Здесь Re - действительная часть. При записи соотношений (46.6) и (46.8) учитывалось, что $\widetilde{\Delta}_{1,2}$ - комплексные функции, которые, по существу, представляют собой комплексные

параметры порядка в сверхпроводниках S_1 и S_2 и могут быть выражены (аналогично тому, как это сделано в 21 при выводе джозефсоновского соотношения для мостика Асламазова - Ларкина) через амплитуду и фазу параметра порядка:

$$\tilde{\Delta}_1 = \Delta_1 e^{i\theta_1}, \quad \tilde{\Delta}_2 = \Delta_2 e^{i\theta_2}, \quad \tilde{\Delta}_2^* = \Delta_2 e^{-i\theta_2} \tag{46.9}$$

Здесь $\Delta_{1,2}$ - действительные величины, представляющие собой щели в берегах S_1IS_2-перехода.

Рассмотрим сначала последний член в квадратных скобках в (46.8) - единственный, который зависит от разности фаз $\varphi = \theta_1 - \theta_2$ - и обозначим его через $-E_J \cos\varphi$. Переходя от суммирования по k и q к интегрированию по энергиям электронного спектра в S_1 и S_2, с учетом (46.3) и (46.9) получим для E_J при $T = 0$:

$$E_J(T=0) = \frac{\hbar}{4\pi e^2 R_n} \Delta_1 \Delta_2 \int\limits_{-\infty}^{\infty} \int\limits_{-\infty}^{\infty} \frac{d\varepsilon_1 d\varepsilon_2}{E_1 E_2 (E_1 + E_2)} \tag{46.10}$$

Расширение пределов интегрирования в (46.10) до $\pm\infty$ допустимо, поскольку интегралы быстро сходятся при $\varepsilon_{1,2} \sim |\Delta|$. Заменой переменных $\varepsilon_{1,2} = \Delta_{1,2} \operatorname{sh} x_{1,2}$ и несложными выкладками интеграл в выражении (46.10) приводится к эллиптическому, и в результате получаем

$$E_J(T=0) = \frac{\hbar}{e^2 R_n} \frac{\Delta_1 \Delta_2}{\Delta_1 + \Delta_2} K\left(\frac{|\Delta_1 - \Delta_2|}{\Delta_1 + \Delta_2}\right) \simeq \frac{\pi\hbar}{2e^2 R_n} \frac{\Delta_1 \Delta_2}{\Delta_1 + \Delta_2}, \tag{46.11}$$

где последнее равенство приближенно верно, когда Δ_1 и Δ_2 отличаются не более чем в $2-3$ раза, и является точным при $\Delta_1 = \Delta_2$.

Второй член в квадратных скобках в уравнении (46.8) обращается в нуль (ввиду нечетности) при интегрирования по $\varepsilon_k, \varepsilon_q$, в то время как первый член формально расходится при $|\varepsilon_{k,q}| \to \to \infty$. Однако нас интересует только вклад в энергию, связанный с наличием сверхпроводимости в берегах контакта, поэтому мы вычтем из этого расходящегося интеграла его аналог, вычисленный для нормального состояния берегов. Обозначая полученное выражение через $E_1(T=0)$, получаем

$$E_1(T=0) = \frac{\hbar}{4\pi e^2 R_n} \Delta_1 \Delta_2 \int\limits_{-\infty}^{\infty} \int\limits_{-\infty}^{\infty} d\varepsilon_1 d\varepsilon_2 \left(\frac{1}{|\varepsilon_1| + |\varepsilon_2|} - \frac{1}{E_1 + E_2}\right) \tag{46.12}$$

Легко проверить, [1)] что значение интеграла (46.12) совпадает со значением $E_J(T=0)$, определенным в (46.10). Поэтому

1)Рассмотрим для примера случай одинаковых сверхпроводников, $\Delta_1 = \Delta_2$. Разность $E_1 - E_J$ приводится заменой переменных $\varepsilon_1 = \Delta x, \varepsilon_2 = \Delta y$ к выражению, пропорциональному интегралу

$$\int\limits_0^{\infty} dxdy \left[\frac{1}{x+y} - \left(1 + \frac{1}{\sqrt{1+x^2}\sqrt{1+y^2}}\right) \frac{1}{\sqrt{1+x^2} + \sqrt{1+y^2}}\right],$$

который равен нулю.

полное выражение для энергии SIS-контакта $E_{\text{св}}(\varphi)$ совпадает с (22.11). Соответственно, величина критического тока туннельного S_1IS_2-перехода связана со значениями энергетической щели в S_1 и S_2 следующим выражением:

$$I_c(T=0) \simeq \frac{\pi}{e}\frac{\Delta_1\Delta_2}{R_n\left(\Delta_1+\Delta_2\right)} \tag{46.13}$$

При отличных от нуля температурах вычисление $E_J(T)$ изложенным методом весьма усложняется, т.к. приходится учитывать фермиевскую функцию распределения квазичастиц, а также процессы их туннелирования между берегами S_1 и S_2. Температурная зависимость критического тока SIS-перехода может быть вычислена аналитически для случая одинаковых сверхпроводящих берегов ($\Delta_1 = \Delta_2 = \Delta$). Эта зависимость получена Амбегаокаром и Баратовым [135] (см. [112, 136, 137]):

$$I_c(T) = \frac{\pi\Delta(T)}{2eR_n}\,\mathrm{th}\left(\frac{\Delta(T)}{2k_{\mathrm{B}}T}\right) \tag{46.14}$$

При стремлении T к нулю выражение (46.14) переходит в (46.13) (с $\Delta_1 = \Delta_2 = \Delta$).

При $T \to T_c$ критический ток джозефсоновского перехода пропорционален $\Delta^2(T) \propto (T_c - T)$. Вывод о том, что вблизи точки перехода энергия связи симметричного перехода $E_J(T) \propto (T_c- \ -T)$, можно было сделать и с помощью свободной энергии Гинзбурга-Ландау: вклад в энергию, связанный с наличием туннелирования между двумя сверхпроводниками, должен быть пропорционален произведению обоих параметров порядка, $E_J(T) \propto \psi_1(T)\psi_2(T)$. В случае одинаковых сверхпроводников получаем, как и выше, $E_J(T) \propto \psi^2(T) \propto (T_c - T)$. В то же время, если берега контакта имеют различные температуры сверхпроводящего перехода T_c, джозефсоновская энергия и критический ток стремятся к нулю пропорционально $\left(T_c^{\min} - T\right)^{1/2}$. Все эти выводы о поведении вблизи T_c сделаны для случая SIS-перехода, когда туннелирование слабое, и потому мало влияет на параметры порядка обоих сверхпроводников. Иначе дело обстоит с SNS-пере ходами, когда параметр порядка вблизи NS-границы может быть сильно подавлен из-за эффекта близости (подробнее см. [136]).

Формулу (23.8) для случая SIS-перехода с одинаковыми сверхпроводящими берегами удобно также записать, используя определение квантового сопротивления, введенное в (23.8),

$$\frac{E_J}{\Delta} = \frac{1}{2}\frac{R_Q}{R_n} \tag{46.15}$$

9.2.11 7.4 Andreev Reflection

Theory by Schmidt

Let us examine the process in which the normal current converts into superconducting current. We shall try to understand what happens at the normal metal-superconductor interface and how far from the interface the conversion of the normal current into supercurrent takes place.

Before beginning our analysis, let us agree on what the term 'interface' means exactly. In its most pure form, it is the interface between a normal and a superconducting domain in the intermediate state of a superconductor, In this case, the order parameter (energy gap) has its maximum value $\Delta(T)$ deep inside the superconducting domain and is zero deep inside the normal region. The transition from one value to the other occurs over the coherence length $\xi(T)$. It is this transitional region to which we shall refer as the NS interface. In the case of mechanical contact between two metals - normal and superconducting - the situation remains the same, at least qualitatively. At $T \approx T_c$, the width of the interface, $\xi(T)$, is rather large and we can apply to it the following analysis. We are interested in what happens to an electron in the normal metal when, while moving towards the superconductor, it encounters the NS interface. We

assume that the electron's energy is less than the energy gap of the superconductor. This process is illustrated in Fig. 7.3. At some moment of time while approaching the superconducting region, the normal electron reaches a point x which already belongs to the superconducting region but where the value of the gap $\Delta(x)$ is still small. At this moment it converts into an electron-like quasiparticle of the superconductor and, in momentum space, fills an appropriate $\boldsymbol{k}$ state, in accordance with the value of its energy E_k. At the next moment, as the quasiparticle moves closer to the superconducting region, it reaches the area with a larger value of the gap thereby moving, in momentum space, to another $\boldsymbol{k}$ state, closer to k_{F}. This results in an increase of the quasiparticle charge.

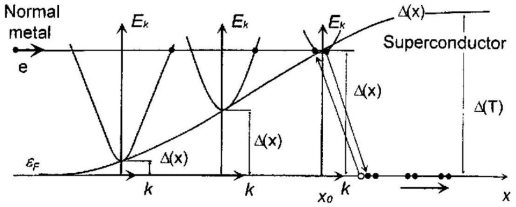


Fig. 7.3. Schematic diagram of Andreev reflection. Once in the vicinity of an NS interface, a quasiparticle (electron) moves from one $\boldsymbol{k}$ state to another, gradually changing its charge as it moves closer to the superconducting region

Thus, as an electron-like excitation moves from the normal metal towards the NS interface, it gradually reduces its charge. Finally, as one can see from the sketch in Fig. 7.3, the momentum of the quasiparticle becomes k_F, its group velocity zero and, according to (7.6), its charge reduces to zero ($q_{k_{\mathrm{F}}} = 0$). This happens when the quasiparticle reaches the point x_0, where its energy is equal to the energy gap. At this point, the quasiparticle is reflected back from the interface and, in momentum space, moves to the left-hand branch of the energy spectrum, which is populated by holes. Now its group velocity is directed to the left, that is, in the direction from the superconductor towards the normal metal, and its charge becomes negative. But propagation of a negative charge to the left is equivalent to propagation of a positive charge to the right. Therefore, the process of reflection we have just analyzed gives rise to a charge transfer from the normal metal to the superconductor, i.e., to an electric current.

This process was first proposed theoretically by Andreev [70] and is called Andreev reflection.

The decrease of the quasiparticle charge, as it approaches the superconducting region, gives a clear indication that the condensate is also involved in the process of Andreev reflection. The quasiparticle charge does not disappear, it is transferred to the condensate! Physically, this means that: having reached the interface, the quasiparticle finds itself a partner and together they enter the condensate, while the newly formed hole goes back to the normal metal. This process accounts for the transfer through the NS interface of the part of the current that is carried by excitations with energies below the energy gap $\Delta(T)$. The process of normal current conversion into the supercurrent takes place within the region $\sim \xi(T')$. The behavior of excitations with energies $E_k > \Delta(T)$ is entirely different. As we are soon to find out, they can penetrate the interior of the superconductor to distances well in excess of the coherence length $\xi(T)$.

9.2.12 Andreev Reflection: Experimental Consequences

(here is preparation to experiments, what and how can be detected?)

9.3 Overview and Comparison of Methods for different JJ

Overview of well-known methods for describing tunneling

(write that there is BdG method and key formulas)

Different forms of Josephson relation for different junctions

(write that the formula below is a more general case)
After approximation of small area:

$$J_1(\varphi) = \frac{DE_J\pi}{2\Phi_0}\tanh\left(\beta E_J\sqrt{1-D\sin^2\frac{\varphi}{2}}/2\right)\frac{\sin\varphi}{\sqrt{1-D\sin^2\frac{\varphi}{2}}}$$

Overview of well-known methods for evaluation of a current

$$J_Q(x) = e\sum_n f_n\left\{J_{u_n}(x) + J_{v_n}(x)\right\}$$

$$f_n = f\left(E_n\right) = \frac{1}{1+e^{E_n/k_BT}} \qquad J_{u_n}(x) = \frac{\hbar}{m}\operatorname{Im}\left\{u_n^*(x)\left[\nabla u_n(x)\right]\right\} \qquad J_{v_n}(x) = \frac{\hbar}{m}\operatorname{Im}\left\{v_n^*(x)\left[\nabla v_n(x)\right]\right\}$$

(this is from Chang, Bagwell. write this method below!!!!)
Then, there are complicated formulas for the total current.
(I'll derive them in separate note, then I'll write something here about them)

Overview of exotic methods for evaluation of a current

Here, I'll collect not tasted methods, which may produce a correct result, but also may not.
(Piasotski's strange method)

Which method to chose to describe some typical JJ?

(!!!!! a very important question, I'll answer later!!!)

there is a GL method. Maybe it is a good one?

there is a GF in TB model method. Maybe it is a good one? A lot of people are using it...

there is a Beenakker's method. Maybe it is a good one?

there is a GF in continual model method. Maybe it is a good one? I have no idea how to use it.

Which method to chose to describe some JJ with disorder?

(I'LL WRITE LATER METHODS FOR OTHER EFFECTS IN JJ)

9.4 Special properties and Deeper Understanding of SC Contacts

9.4.1 22. Nonstationary Josephson Effect, Resistive Characteristics

Если ток, задаваемый внешним источником, превысит критическое значение I_c, на слабой связи появится напряжение V. К каким это приведет последствиям?

22.1. Джозефсоновская генерация.

Поведение квантовомеханической системы определяется решением уравнения Шредингера

$$i\hbar\frac{\partial\psi}{\partial t} = \widehat{H}\psi \tag{22.1}$$

где $\widehat{H}$ - гамильтониан системы.

Волновая функция стационарного состояния ψ_1 удовлетворяет уравнению

$$\widehat{H}\psi_1 = E\psi_1$$

где E-энергия этого стационарного состояния, $\psi = \psi_1 e^{i\theta(t)}$, причем ψ_1 не зависит от времени. Подставляя эту волновую функцию в (22.1), получим

$$-\hbar\frac{\partial\theta}{\partial t} = E \tag{22.2}$$

Если на слабой связи установилась разность потенциалов V, то это означает, что энергии куперовских пар в берегах перехода E_1 и E_2 связаны соотношением

$$E_1 - E_2 = 2eV \tag{22.3}$$

так как заряд одной пары равен $2e$.

Подставляя (22.3) в (22.2), получим второе фундаментальное соотношение Джозефсона

$$2eV = \hbar\frac{\partial\varphi}{\partial t} \tag{22.4}$$

Точно то же самое соотношение получится, если из формулы (21.8) вычесть формулу (21.7).

Что же происходит с джозефсоновским переходом, когда по нему течет заданный извне постоянный ток $I > I_c$? Поскольку сверхток не может быть больше I_c, ясно, что теперь, кроме сверхтока, возникнет ток нормальной компоненты, т.е. возникнет ток одиночных электронов. Это утверждение сразу приводит нас к так называемой резистивной модели, т.е. рассматрению джозефсоновского перехода как параллельного включения собственно джозефсоновского контакта, пропускающего только сверхток, и нормального участка (рис. 22.1). Полный ток I равен сумме нормального тока V/R и сверхтока $I_s = I_c \sin\varphi$:

$$I = I_c \sin\varphi + \frac{\hbar}{2eR}\frac{\partial\varphi}{\partial t} \tag{22.5}$$

где R-сопротивление перехода в нормальном состоянии. Это дифференциальное уравнение относительно функции $\varphi(t)$ элементарно интегрируется. Подставляя решение в (22.4), получим напряжение на переходе в виде

$$V(t) = R\frac{I^2 - I_c^2}{I + I_c\cos\omega t} \tag{22.6}$$

$$\omega = \frac{2e}{\hbar}R\sqrt{I^2 - I_c^2} \tag{22.7}$$

Так мы обнаруживаем удивительное свойство джозефсоновского перехода. Если заданный извне постоянный ток I больше критического тока перехода, на нем возникает напряжение V, периодически зависящее от времени. Это явление получило название

джозефсоновской генерации. Схематическая зависимость $V(t)$ от времени дана на рис. 22.2. Частота колебаний напряжения зависит от того, насколько превышает ток через переход I его критическое значение I_c (см. (22.7)).

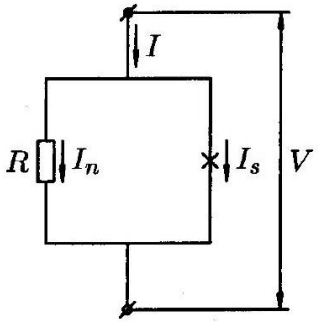


Рис. 22.1. Резистивная модель джозефсоновского перехода. Сверхток через собственно джозефсоновский переход равен $I_s = I_c \sin\varphi$.

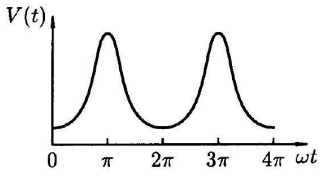


Рис. 22.2. Напряжение на переходе (джозефсоновская генерация).

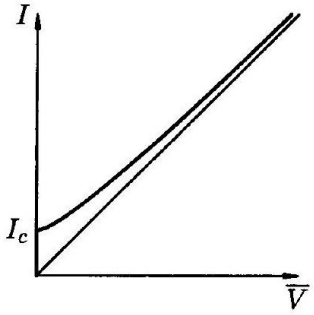
Вольтметр постоянного тока, подключенный к переходу, покажет, конечно, среднее по периоду значение $\bar{V}$. Усреднение по
времени формулы (22.6) дает

$$2e\bar{V} = \hbar\omega. \tag{22.8}$$

Эта формула имеет совершенно ясную интерпретацию. Если среднее расстояние по энергиям между уровнями куперовских пар в двух половинках перехода равно $2e\bar{V}$, то при переходе одной пары через область слабой связи такая энергия выделяется в виде кванта электромагнитного излучения.

Вольт-амперная характеристика перехода, которая следует из формул (22.7) и (22.8), показана на рис. 22.3.

Рис. 22.3. Вольт-амперная характеристика джозефсоновского перехода.



При токе через переход $I = I_s + I_n$, достаточно близком к I_c, значительная его доля протекает в виде сверхпроводящего тока I_s через джозефсоновский элемент на эквивалентной схеме рис.22.1. При $I \gg I_c$ практически весь постоянный ток течет через резистивный элемент ($I \simeq I_n$), и вольт-амперналл характеристика на этом участке выходит на характеристику перехода в нормальном состоянии. Чтобы подробнее

пояснить такое поведение, представим скорость изменения разности фаз на переходе в таком виде:

$$\frac{d\varphi}{dt} = \frac{2e}{\hbar}V = \frac{2e}{\hbar}R\,(I - I_s) = \frac{2e}{\hbar}R\,(I - I_c \sin\varphi) \tag{22.9}$$

Можно заметить, что в течение первого полупериода джозефсоновского тока, когда $I_s = I_c \sin\varphi$ совпадает по направлению с полным током I через переход ($\sin\varphi > 0$), скорость иэменения
разности фаз меньше, чем в течение второго полупериода, когда сверхпроводящий ток имеет обратное направление ($\sin\varphi < 0$). Усреднение по полному периоду даст сверхпроводящую компоненту, совпадающую по направлению с I, что обеспечит уменьшение доли нормальной компоненты I_n в полном токе. С увеличением I доля I_s в (22.9), ограниченная I_c, будет уменьшаться, и скорости изменения разности фаз на положительном и отрицательном полупериодах в конце концов сравняются. Это приведет к исчезновению сверхпроводящей компоненты в среднем по времени токе и выходу вольт-амперной характеристики на линейную зависимость $V = RI$.

Здесь необходимо отметить, что соотношения (22.4) и (22.8) являются совершенно фундаментальными и точными. Многочисленные эксперименты подтвердили их с громадной точностью.

Впервые джозефсоновская генерация наблюдалась советскими физиками И. К. Янсоном, В. М. Свистуновым и И. Д. Дмитренко [14] в 1964 г.

При нарастании тока через переход от нуля до величины I_s за время t в переходе запасается некоторая энергия:

$$E_{\text{сВ}} = \int_0^t I_s V dt \tag{22.10}$$

Здесь V-это напряжение, возникающее на переходе в процессе нарастания тока согласно общей формуле (22.4). Подставляя сюда $I_s = I_c \sin\varphi$ и (22.4), после элементарного интегрирования получим

$$E_{\text{СВ}} = E_{\text{J}}(1 - \cos\varphi), \tag{22.11}$$

где

$$E_J = \hbar I_c/2e = \Phi_0 I_c/2\pi \tag{22.12}$$

есть максимальная величина понижения энергии перехода за счет наличия слабой связи между сверхпроводящими берегами. Энер гию (22.12) мы в дальнейшем будем называть просто джозефсоновской энергией. Джозефсоновский переход является фактически нелинейной индуктивностью, запасающей энергию при изменении тока через него.

При вычислении полной свободной энергии замкнутой системы, в которую включен джозефсоновский переход, нужно учитывать также энергию, затрачиваемую источником тока:

$$E_{\text{ист}} = \int_0^t IV dt = \frac{\hbar I}{2e}\varphi = \frac{\Phi_0}{2\pi} I\varphi \tag{22.13}$$

Таким образом, свободная энергия для рассматриваемого случая перехода с заданным током (т.е. потенциальный "рельеф" вдоль угловой координаты φ) определяется соотношением

$$E = E_{\mathrm{J}}(1 - \cos\varphi) - \frac{\Phi_0}{2\pi} I\varphi \tag{22.14}$$

которое графически изображено на рис. 22.4. С увеличением тока через переход средний наклон изображенного рельефа (часто называемого "стиральной доской») возрастает, а глубина локальных минимумов, расположенных в точках $\varphi_0 = \arcsin(I/I_c) + +2\pi n$, уменьшается. При $I = I_c$ потенциальные барьеры U_0 на кривой (22.14) исчезают, что соответствует непрерывному изменению фазы и появлению напряжения на переходе.

22.2*. Критический ток и “ток возврата” джозефсоновского перехода с емкостью.

Механизмы токопереноса в туннельных сверхпроводящих переходах будут подробно рассмотрены в 46. Покажем здесь, что поведение туннельного джозефсоновского перехода, в котором два сверхпроводящих берега разделены тонкой прослойкой изолятора, как это изображено на рис. 20.1, а, сходно с поведением массивной частицы в потенциале, изображенном на рис. 22.4. Для описания туннельного перехода в рамках резистивной модели необходимо дополнить эквивалентную схему (рис. 22.1) параллельно включенной емкостью C. Ток

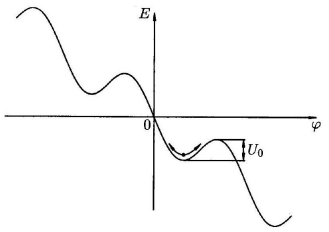


Рис. 22.4. Потенциальный рельеф $E(\varphi)$ джозефсоновского перехода с заданным током.

смещения через емкостной элемент

$$I_D = C\frac{dV}{dt} = \frac{\hbar C}{2e}\frac{d^2\varphi}{dt^2} \tag{22.15}$$

должен быть добавлен в соотношение (22.5), которое примет вид

$$\frac{\hbar C}{2e}\ddot{\varphi} + \frac{\hbar}{2eR}\dot{\varphi} + I_c \sin\varphi = I \tag{22.16}$$

или

$$\left(\frac{\hbar}{2e}\right)^2 C\ddot{\varphi} + \left(\frac{\hbar}{2e}\right)^2 R^{-1}\dot{\varphi} + E_{\mathrm{J}} \sin\varphi = E_{\mathrm{J}}\frac{I}{I_c} \tag{22.17}$$

где $\ddot{\varphi}$ и $\dot{\varphi}$ означает производные φ по времени второго и первого порядка. Уравнение (22.17) - фактически уравнение движения малтника с моментом инерции $J = \left(\frac{\hbar}{2e}\right)^2 C$, коэффициентом вязкости $\eta = \left(\frac{\hbar}{2e}\right)^2 R^{-1}$, максимальным гравитационным моментом $mgl = E_{\mathrm{J}}$ и приложенным вращающим моментом $E_{\mathrm{J}}(I/I_c)\,;\ddot{\varphi}$ и $\dot{\varphi}$ - угловое ускорение и угловая скорость маятника. Легко видеть, что собственная частота малых колебаний $(\mathrm{mgl/J})^{1/2}$, на зываемая в джозефсоновском случае плазменной частотой перехода, выражается соотношением

$$\omega_p = \left(\frac{E_{\mathrm{J}}}{J}\right)^{1/2} = \left(\frac{2\pi I_c}{C\Phi_0}\right)^{1/2} \tag{22.18}$$

Плазменная частота может рассматриваться также как резонансная частота

$$\omega_p = (L_\mathrm{J} C)^{-1/2} \tag{22.19}$$

высокочастотного контура с емкостью C и индуктивностью L_J. Сравнение (22.19) и (22.18) дает для собственной индуктивности джозефсоновского перехода следующее значение (для малых изменений φ!):

$$L_\mathrm{J} = \frac{\Phi_0}{2\pi I_c} \tag{22.20}$$

Выражение (22.17) часто бывает удобно представлять также как уравнение движения массивной частицы в периодическом потенциале, представленном на рис. 22.4. В этом случае величина $\left(\frac{\hbar}{2e}\right)^2 C$ играет роль массы m частицы. С точностью до замены φ на линейную координату x мы получаем уравнение движения частицы в вязкой среде с $\eta = \left(\frac{\hbar}{2e}\right)^2 R^{-1}$ в одномерном периодическом потенциале $E_\mathrm{J}(1 - \cos x)$ под действием приложенной силы $E_\mathrm{J}\,(I/I_c)$. «Масса», определяющая «инерционное» поведение перехода при изменении φ, связана с величиной емкости C. «Кинетическая энергия" $mv^2/2$ такой частицы, пропорциональная m и $\dot{\varphi}^2$, в точности равна электрической энергии $CV^2/2$, запасаемой в переходе при возникновении напряжения $V = \frac{\hbar}{2e}\dot{\varphi}$, пропорционального скорости изменения разности фаз φ на переходе.

Выше мы показали, что массивная частица начинает непрерывно двигаться при наклоне "стиральной доски», соответствующем $I = I_c$. Однако в связи с инерцией частицы остановить ее можно только несколько уменьшив угол наклона по сравнению с критическим, т. е. при некотором «токе возврата» $I_r < I_c$.

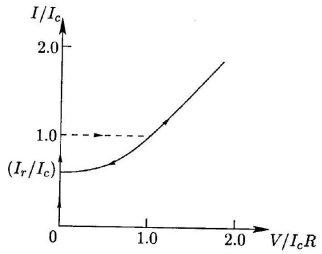


Рис. 22.5. Вольт-амперная характеристика перехода с $\beta_\mathrm{C} = 4$.

Ток возврата (или «ток захвата») тем меньше, чем выше емкость («масса») и чем меньше вязкость, т.е. выше сопротивление туннельного перехода. Гистерезисное поведение вольт-амперной характеристики туннельного перехода показано на рис. 22.5. Количественно ток возврата и необратимость резистивных свойств определяются величиной параметра Маккамбера [52]:

$$\beta_\mathrm{C} = (2e/\hbar) I_c C R^2 \tag{22.21}$$

Использование параметра β_C и характержой джозефсоновской частоты $\omega_c = (2e/\hbar) I_c R$ позволяет упростить (22.17):

$$I/I_c = \beta_\mathrm{C} \omega_c^{-2} \ddot{\varphi} + \omega_c^{-1} \dot{\varphi} + \sin\varphi \tag{22.22}$$

При $\beta_\mathrm{C} \leqslant 1$ можно пренебречь «емкостным» членом в (22.22) и получить снова (22.5). В этом случае вольт-амперная характеристика однозначна и описывается соотношением (22.7) для переходов с непосредственной проводимостью:

$$V = R\sqrt{I^2 - I_c^2} \tag{22.23}$$

При $\beta_C > 1$ вольт-амперные характеристики приобретают гистерезисный вид, показанный на рис. 22.5. Прямая ветвь представляет собой вертикальную ступеньку тока от 0 до I_c при нулевом
напряжении, после которой следует срыв на возвратную ветвь (называемую также часто «квазичастичной ветвью). Численные расчеты [52, 53] дают зависимость тока возврата I_r от β_C, показанную на рис. 22.6. Для $\beta_C \to \infty$ имеем $I_r \to 0$. Это означает, что возвратная часть вольт-амперной характеристики линейна [1)] ($V = RI$), как показано на рис. 22.7, т.е. в эквивалентной схеме резистивной модели, которая представляет собой параллельное включение R, C и собственно джозефсоновского элемента (переносящего сверхпроводящий ток $I_c \sin\varphi$), транспортный ток течет только через нормальное сопротивление. Чтобы объяснить физическую природу изменения поведения обратного хода характеристики при увеличении емкости перехода, представим β_C (см. (22.21)) через проводимость $\omega_c C$ емкостного элемента эквивалентной схемы на характерной джозефсоновской частоте ω_c и проводимости резистивного элемента $G = 1/R$:

$$\beta_C = \omega_c C/G \tag{22.24}$$

Легко видеть, что при $\beta_C \gg 1$ емкостной элемент полностью шунтирует переменный джозефсоновский ток, зануляя сверхпроводящую часть в полном транспортном токе через джозефсоновский контакт. При малых C среднее по времени значение сверхпроводящей компоненты не равно нулю, поэтому напряжения в интервале от нуля до нескольких $V_c = I_c R$ понижаются по сравнению со случаем нормального туннельного контакта.

Ш-з.

22.1. Два джозефсоновских перехода с критическими токами $I_{c1} = 500$ мкА и $I_{c2} = 700$ мкА включены параллельно в сверхпроводящую цепь. Полный ток через оба перехода равен 1 мА. Чему равны токи в каждом из переходов?

Solution

Поскольку переходы включены параллельно, разности фаз φ_1 и φ_2 на переходах будут равны. Поэтому токи по переходам распределяются пропорционально их критическим токам: $I_1 = 0.417\text{MA}, I_2 = 0.583\text{MA}$.

• Мы пренебрегаем здесь для простоты щелью в энергетическом спектре нормальных носителей в сверхпроводнике и особенностью в плотности их состояний, которые будут обсуждаться в §$45 – 46. Вольт-амперные характеристики с квазичастичными (возвратными) ветвями, рассчитанные с учетом этих особенностей, приведены на рис. 46.7.

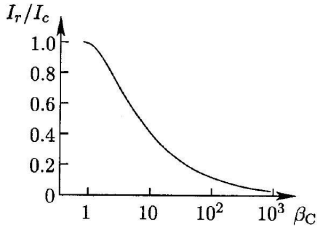


Рис. 22.6. Зависимость тока возврата от величины β_C [52].

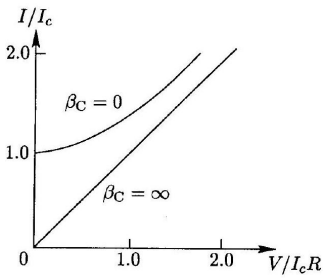


Рис. 22.7. Вольт-амперные характеристики джозефсоновских переходов, рассчитанные в рамках резистивной модели (см. примечание на с. 131) для случаев незначительной ($\beta_C = 0$) и доминирующей ($\beta_C = \infty$) емкостей.

Ш-з.

22.2. Найти разность между максимальным и минимальным значениями V на графике рис. 22.2.

Ответ. $V_{\max} - V_{\min} = 2I_cR$.

Ш-з.

22.3. Точечный контакт имеет критический ток $I_c = 1$ мА и сопротивление в нормальном состоянии $R = 2$ Ом. Найти величину постоянного напряжения на контакте $\bar{V}$ и частоту джозефсоновской генерации ν, если через контакт течет ток $I = 1.2$ mA.

Ответ. $\bar{V} = 1.33$МВ; $\nu = 641$ ГГц.

Ш-з.

22.4. Критический ток джозефсоновского перехода равен $I_c = 100$ мкА. Через переход пропускается постоянный ток $I_0 = 70$ мкА и слабый переменный ток с амплитудой $I_1 =$ 2МКА и частотой $\nu = 10$М ц, т.е. $I = I_0 + I_1 \sin 2\pi\nu t$. Найти напряжение на переходе, пользуясь СИ.

Solution

Разность фаз на переходе ищем в виде $\varphi = \varphi_0 + \varphi_1$, где φ_0 - разность фаз, создаваемая постоянным током I_0. Напряжение на переходе $V = (\Phi_0/2\pi)\, d\varphi/dt = (\Phi_0/2\pi)\, d\varphi_1/dt$, но $d\varphi_1/dt = (dI/dt)\,(dI/d\varphi_1)^{-1}$. Подставляя это выражение в выражение для V, получим

$$V = \frac{\Phi_0}{I_c \cos\varphi_0} \nu I_1 \sin(2\pi\nu t + \pi/2)$$

При условиях задачи амплитуда переменного напряжения будет 0.58 нВ.

Замечание. Из решения задачи следует, что напрлжение V опережает по фазе ток через переход на угол $\pi/2$. Это значит, что переход ведет себя как индуктивность $L = \Phi_0/\left(2\pi I_c \cos\varphi_0\right)$.

9.4.2 23*. Fluctuations of Critical Current, Macroscopic Tunneling

23.1. Тепловые флуктуации критического тока в джозефсоновском переходе.

Величина I_c является фундаментальной характеристикой джозефсоновского перехода, определяемой энергией связи E_J (22.12). Мы видели выше, что при токе через переход $I = I_c$ исчезают барьеры (U_0) в потенциальном рельефе $E(\varphi)$. Однако и при

несколько более низких токах возможен распад метастабильных состояний джозефсоновского перехода путем преодоления потенциальных барьеров за счет шума в измерительных цепях, за счет тепловых и квантовых флуктуаций фазы. Таким образом, реально наблюдаемый критический ток, выше которого начинается непрерывное изменение фазы во времени и возникает напряжение на переходе, несколько меньше, чем $I_c = \frac{2e}{\hbar} E_J = \frac{2\pi}{\Phi_0} E_\mathrm{J}$. Здесь нужно оговориться, что если затухание велико (т.е. величина параметра Маккамбера β_C достаточно мала), то единичная флуктуация «перебросит" переход в состояние, соответствующее следующему локальному минимуму; возникающий короткий импульс напряжения, соответствующий отдельному флуктуационному процессу, зафиксировать практически невозможно. В переходах с малым затуханием ($\beta_\mathrm{C} \gg 1$) из за большой инерции система не задержится в соседнем минимуме, а будет разгоняться пока $\dot{\varphi}$ (т. е. V) не достигнет стационарного значения за счет возрастания диссипативного члена в (22.17). Этому процессу соответствует скачок на вольт-амперной характеристике, показанный на рис. 22.5.

Рассмотрим термоактивационный распад метастабильного состояния джозефсоновского перехода с током, т.е. термоактивационное преодоление барьера U_0, изображенного на рис.22.4. Высота этого барьера при токах чуть ниже критического ($|I - I_c| \ll I_c$) невелика и определяется выражением [54, 55]

$$U_0(I) = \frac{4\sqrt{2}}{3} E_\mathrm{J} \left(1 - I/I_c\right)^{3/2} \tag{23.1}$$

Частота собственных колебаний перехода на дне потенциальной ямы есть

$$\omega(I) = \omega_p \left[1 - (I/I_c)^2\right]^{1/4} \tag{23.2}$$

где ω_p - плазменная частота (22.18). Скорость распада состояния пропорциональна частоте попыток (23.2) и больцмановскому фактору $\exp\left(-U_0/k_\mathrm{B}T\right)$. Вероятность распада при конечных температурах сильно возрастает с приближением I к $I_c\,(U_0 \to 0)$. Дополнительные предэкспоненциальные множители, полученные из точных количественных расчетов, подробно обсуждались в работах [56, 57, 55]. На рис. 23.1 представлены расчеты [58] вольтамперных характеристик для переходов с $\beta_\mathrm{C} \geqslant 1$, учитывающие тепловые флуктуации. (Параметр $\gamma = 2E_\mathrm{J}/\left(k_\mathrm{B}T\right)$.) Эксперименты, проведенные как на переходах со слабым затуханием [54], так и на переходах с сильным затуханием [59], показали хорошее согласие с расчетами. В последней работе переход с сильным затуханием включался в сверхпроводящее кольцо, ток I через переход задавался путем приложения внешнего магнитного поля, а распад метастабильного состояния фиксировался по проникновению магнитного потока в кольцо. Для измерения магнитного потока использовался чувствительный сквид-магнитометр, описапио работы которого посвящены последние разделы данной главы.

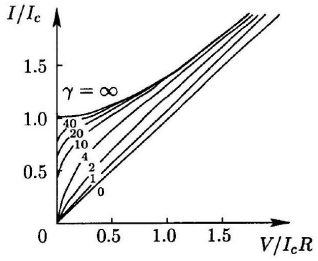


Рис. 23.1. Влияние тепловых флуктуаций на вольт-амперные характеристики джозефсоновских переходов с $\beta_\mathrm{C} \geqslant 1\,(\gamma = 2E_\mathrm{J}/\left(k_\mathrm{B}T\right))$. Расчеты взяты из работы [58].

23.2. Макроскопические квантовые эффекты.

Прежде чем обратиться к процессам квантового распада метастабильных состояний джозефсоновского перехода, рассмотрим условия, при которых джозефсоновский контакт становится по-настоящему квантовым макроскопическим объектом, т.е. одна из макроскопических степеней свободы (сверхпроводящая фаза) становится настоящей квантовомеханической переменной.

Явление сверхпроводимости в целом невозможно описать без привлечения квантовой механики. Эффекты Джозефсона - наиболее яркий пример установления когерентных волновых свойств между двумя массивными слабосвязанными сверхпроводниками. Движение сверхпроводящих электронов является существенно квантовым, и фаза сверхпроводящей волновой функции явно проявляется в различных интерференционных эффектах. Тем не менее, в большинстве случаев изменение фазы во времени может быть достаточно точно описано классической механикой. Мы видели это в предыдущем разделе в случае динамики разности фаз в одиночном туннельном джозефсоновском переходе. При выводе другого важного квантовомеханического эффекта, квантования магнитного потока, мы также фактически пользовались квази классическими выражениями и правилами квантования. Главной особенностью квазиклассического приближения, справедливого для макроскопических объектов с огромным числом степеней свободы, является то, что канонически сопряженные переменные могут иметь одновременно точные значения. Однако существуют условия, при которых фаза параметра порядка становится настоящей квантовомеханической переменной. Это приводит к т. наз. макроскопическим квантовым эффектам [55].

Вернемся к случаю малтника, уравнение движения которого аналогично уравнению (22.17) для разности фаз в одиночном джозефсоновском туннельном переходе. В случае маятника канонически сопряженными переменными (аналогичными координате и импульсу) являются угловая координата φ и момент импульса M. Если масса маятника стремится к нулю, необходимо учитывать квантовые эффекты в динамике, вообще говоря, макроскопической степени свободы φ. Из соотношения неопределенности

$$\Delta\varphi\Delta M \sim \hbar \tag{23.3}$$

следует, что величины φ и M не могут быть определены точно одновременно. Даже при нулевой температуре центр масс маятника не может находится в состоянии покоя, поскольку это означало бы, что и φ, и M точно определены ($\varphi = 0, M = 0$). Следовательно, в квантовом пределе центр масс маятника должен испытывать, кроме тепловых флуктуаций, флуктуации квантовой природы. Таким образом, если обычные когерентные эффекты - это квантовое когерентное движение микрочастиц (например, электронов в сверхпроводнике), то в макроскопических квантовых эффектах проявляется квантовое поведение макрообъекта в целом [60, 61].

Для перехода к квантовому пределу в джзефсоновском случае к нулю должна стремиться емкость C туннельного контакта, играющая роль массы. Квантовые флуктуации становятся значительными при приближении электрической («кулоновской») энергии перехода

$$E_{\mathrm{C}} = e^2/2C \tag{23.4}$$

к джозефсоновской энергии E_{J} (22.12). Для экспериментального наблюдения квантовых эффектов важно, чтобы тепловые флуктуации были малы, т.е. выполнялось неравенство $k_{\mathrm{B}}T < E_{\mathrm{C}}, E_{\mathrm{J}}$. Необходимые условия достигаются в джозефсоновских туннельных переходах с субмикронными размерами и емкостью, меньшей примерно 10^{-15}Ф, при температурах ниже 0.1 К. Напряжению $V \sim 100$ мкВ в таких переходах соответствует разность зарядов на обкладках $Q = CV \sim 10^{-19}$К, т.е. порядка одного заряда электрона.

В нормальном состоянии высокая электрическая энергия e^2/C, возникающая в туннельном переходе в связи с туннелированием одного электрона, приводит к "кулоновской блокаде» туннелирования при напряжениях $V \leqslant e/C$[62, 63]. Появление дополнительного кулоновского члена $Q^2/2C$ в энергии джозефсоновского перехода (22.14) также сильно изменяет динамику туннелирования сверхпроводящих пар [64, 65]. На рис. 23.2 приведена экспериментальная вольт-амперная характеристика из [66], полученная при $T < 0.1$ K для джозефсоновского туннельного перехода с площадью 0.01 мкм ^{2}, емкостью $5 \cdot 10^{-16}$Ф, джозефсоновской энергией $E_\text{J} \simeq 10^{-4}$ эВ и кулоновской энергией $E_\text{C} \simeq \simeq 1.6 \cdot 10^{-4}$ эВ. Легко видеть, что «зарядовые эффекты" приводят к исчезновению джозефсоновского критического тока и появлению области кулоновской блокады туннелирования куперовских пар при напряжениях, близких к нулю (от нуля до V_b).

Рассмотрим подробнее, с какими канонически сопряженными макроскопическими квантовыми переменными мы имеем дело в случае джозефсоновского перехода. "Момент импульса" перехода $M = J\dot{\varphi}$ с учетом того, что $J = (\hbar/2e)^2 C$ (см. обсуждение (22.17)), равен

$$M = J\dot{\varphi} = \left(\frac{\hbar}{2e}\right)^2 C\dot{\varphi} = \frac{\hbar}{2e} CV = \frac{Q\hbar}{2e} \tag{23.5}$$

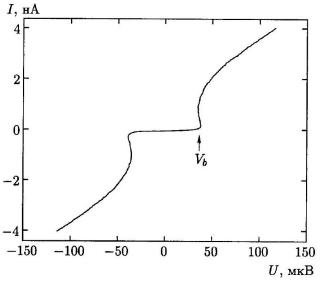


Рис. 23.2. Вольт-амперная характеристика джозефсоновского туннельного перехода с субмикронными размерами [66]; V_b - критическое напряжение «кулоновской блокады».

где Q-электрический заряд на «обкладках» туннельного перехода, индуцированный напряжением V (пропорциональным $\dot{\varphi}$) на переходе. Таким образом, соотношение (23.3) принимает вид

$$\Delta\varphi\Delta Q \sim 2e \tag{23.6}$$

или

$$\Delta\varphi\Delta n \sim 1 \tag{23.7}$$

где $n = Q/2e$ - разбаланс количества сверхпроводящих пар, создающих заряд на обкладках туннельного перехода. В области величин токов и напряжений, где проявляются квантовые эффекты (рис. 23.2), через туннельный переход с $E_\text{J} \sim E_\text{C}$ проходят единицы электронов, т. е. величина n хорошо определена. Это означает, что разность фаз φ должна быть сильно размыта квантовыми флуктуациями, что и приводит к почти полному исчезновению критического тока. Подробнее этот вопрос мы рассмотрим в следующем параграфе.

Сильные флуктуации сверхпроводящей фазы могут возникать не только в туннельных переходах с кулоновской блокадой носителей. Локализация заряда возникает и в сверхпроводящих структурах с непосредственной проводимостью с увеличением беспорядка в области слабых связей и при приближении их нормального сопротивления к "квантовому сопротивлению"

$$R_Q \equiv \frac{h}{(2e)^2} \simeq 6.5\text{КОМ} \tag{23.8}$$

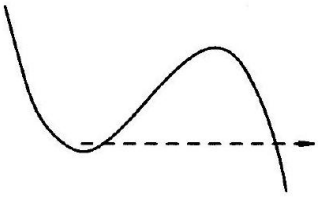
В этом случае уменьшение подвижности носителей заряда, приводящее к затруднению переноса пар через высокоомную слабую связь, также должно сопровождаться увеличением квантовых флуктуаций сверхпроводящей фазы [67, 68].

23.3. Макроскопическое квантовое туннелирование и когерентность.

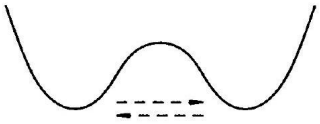
Если понижать температуру, скорость распада метастабильного состояния в потенциале, изображенном на рис. 22.4, выйдет на константу, которая определяется квантовыми флуктуациями. При таком распаде система в целом (как квантовая частица!) туннелирует под барьером U_0 (рис. 23.3, а). Впервые влияние квантовых флуктуаций на наблюдаемый критический ток туннельных джозефсоновских переходов малых размеров было вычислено в работе [69]. Скорость квантового распада при $T = 0$ можно оценить, полагая, что теперь в роли $k_\text{B}T$ в «больцмановском факторе» (ср. с обсуждением после (23.2)) выступает энергия нулевых колебаний, равная по порядку величины $\hbar\omega(I)$:

$$\tau_Q^{-1} = a_q \frac{\omega(I)}{2\pi} \exp\left(-\alpha \frac{U_0}{\hbar\omega(I)}\right) \tag{23.9}$$

Точные вычисления α и предэкспоненциального множителя a_q проведены в [55, 70, 71]. Наличие затухания в системе, $\eta = (\hbar/2e)^2 R^{-1}$, приводит к появлению в (23.9) дополнительного
множителя [72] $\exp\left(-2\pi U_0/\left(2eI_c R\right)\right)$. Таким образом, вероятность квантовых процессов распада действительно должна возрастать с уменьшением емкости джозефсоновского перехода (в связи с возрастанием плазменной частоты перехода) и увеличением его сопротивления (в связи с уменьшением затухания), как это указывалось в предыдущем разделе.



а)



б)

Рис. 23.3. Макроскопическое квантовое туннелирование (а) и макроскопическая квантовая когерентность (б) в джозефсоновских системах.

Первые же эксперименты [73, 74] по измерению времени жизни метастабильного сверхпроводящего состояния малых джозефсоновских туннельных контактов подтвердили теоретические предсказания того, что ширина распределения плотности вероятности перехода в резистивное состояние таких контактов не зависит от температуры при достаточно низких ее значениях, причем температура выхода на квантовый режим преодоления барьера определяется величиной плазменной частоты контакта. Еще одним фактором, влияющим на время жизни метастабильного состояния туннельного перехода с током, является наличие квантованных уровней энергии

джозефсоновского перехода [75] в ямах потенциала «стиральной доски» (рис. 23.4). Скорость распада с уровня E_i определяется как вероятностью заселенности данного уровня при конечной температуре, так и шириной потенциального барьера на этом уровне. Скорость распада можно увеличить, прикладывая к образцу высокочастотное электромагнитное поле $\hbar\Omega$, соответствующее расстоянию между уровнями, и, таким образом, увеличивая заселенность вышележащих уровней. Эксперименты [76] прекрасно подтвердили резонансное увеличение скорости распада при совпадении частоты приложен ного высокочастотного поля и расстояния между квантованными уровнями энергии в джозефсоновских переходах с малой емкостью.

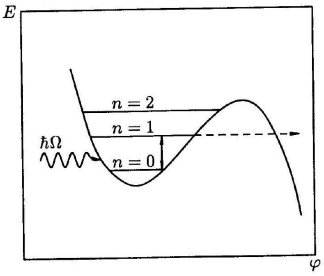


Рис. 23.4. Дискретные энергетические состояния в субмикронных туннельных джозефсоновских контактах и переходы между ними под действием высокочастотного электромагнитного поля.

Систематические экспериментальные исследования зависимости квантовых процессов в туннельных контактах от величины их сопротивления выполнены в работах [77, 78, 79]. Обнаружен фазовый переход из сверхпроводящего в диэлектрическое состояние при приближении сопротивления туннельного контакта к квантовому сопротивлению (23.8), который связывается с резким возрастанием флуктуаций сверхпроводящей фазы в контакте за счет макроскопического квантового туннелирования.

Еще одно важное понятие, которое возникло при исследовании структур с джозефсоновскими контактами, находящимися в "квантовом пределе", это понятие о макроскопической квантовой когерентности. В таких системах (например, сверхпроводящем кольце с тремя джозефсоновскими переходами во внешнем магнитном поле, равном половине кванта магнитного потока) джозефсоновская энергия может иметь два почти вырожденных
минимума при значениях фазы φ_1 и φ_2, разделенных потенциальным барьером (рис. 23.3, б).

Если диссипацию в контактах удается сделать очень слабой, становится возможным квантовомеханическое туннельное проникновение фазы из одного минимума в другой (обозначим амплитуду такого процесса $\mathcal{T}$), и правильными собственными состояниями системы являются смеси состояний, локализованных в первой и второй ямах. Иначе говоря, весь джозефсоновский контакт описывается волновой функцией $\Psi(\varphi)$, зависящей от фазы φ : $\Psi(\varphi) = a_1\Psi_1(\varphi) + a_2\Psi_2(\varphi)$, где волновые функции $\Psi_{1,2}(\varphi)$ соответствуют состояниям, локализованным в первой и второй ямах. Состояние с волновой функцией $\Psi(\varphi)$, в котором обе амплитуды $a_{1,2}$ отличны от нуля, является когерентной смесью исходных (локализованных) состояний. Так, если энергии $E_{1,2}$ локализованных состояний 1,2 точно равны, то правильными собственными состояниями будут симметричное (основное) с $a_1 = a_2$ и возбужденное антисимметричное, $a_1 = -a_2$, а расщепление их энергетических уровней равно $2\mathcal{T}$. При увеличении исходного расщепления уровней $|E_1 - E_2|$ до величин, больших $\mathcal{T}$, роль туннелирования падает, а когерентные состояния становятся все более близкими к исходным локализованным. Экспериментальное подтверждение существования макроскопически когерентных

состояний в системах джозефсоновских контактов было получено совсем недавно в работах [80, 81].

9.4.3 Ambegoakar-Baratoff formula

(see LS for now, later I'll read something related)

Derivation of Ambegoakar-Baratoff formula

(I'll write later)

О большом токе через контакт

Что произойдет, если пропустить через контакт ток, больший чем I_0? Детальный ответ на этот вопрос зависит от свойств цепи, в которую включен контакт. Однако джозефсоновский контакт используемый в таком режиме обладает одним весьма общим свойством. При токе превосходящем I_0 на контакте появится конечное напряжение $V(t)$, в общем случае зависящее от времени. Это напряжение приводит к изменению фазы $\varphi = \varphi_b - \varphi_a$ согласно соотношению Джозефсона для фазы

$$\hbar \frac{d\varphi}{dt} = 2eV(t)$$

которое следует из калибровочной инвариантности. Таким образом, фаза и ток оказываются зависящими от времени. Зная свойства внешней цепи, можно самосогласованно связать напряжение на контакте $V(t)$ и туннельный ток $I(t)$, и таким образом определить динамику системы.

9.4.4 Superconducting weak links by Likharev: Main Statements

(more details in special note)

9.4.5 Current-phase relation in JJ by Golubov et al.: Main Statements

(more details in special note)

9.4.6 Other basic features of Josephson junctions

How to fix phases on contacts?

(???? как вообще можно зафиксировать разность фаз в SNS контакте???? пока не думал про это, не очевидный вопрос, мб магнитным полем в сквиде, но тогда ведь не будет работать модель просто контакта?)

Dynamics after connection of two contacts (??)

??? тут обсуждение, что будет, если соединить два сверхпроводника? правильно понимаю, что их фаза начнет как-то меняться и в итоге перейдет к равновесию фаз и нулевому току в контакте???)

(вопрос оставлен, наверняка, кто-то уже это изучил, пока просто не до этого, такое пока не моделировал.)

9.4.7 Inelastic tunneling: Main Concepts

(??? I don't understand, where was elastic and why here there is an inelastic tunneling, but maybe I'll think more about arxiv.org/pdf/2403.04441v2 and write it later here. Anyway, I need to discuss, what if the tunneling is nonelastic and what is meant by it?)

9.4.8 Josephson radiation

(про это есть статьи, вроде она тоже есть, но я пока это не понимаю. видимо, с какой-то частотой действительно фотоны вылетают. потом добавлю статьи и подумаю про это, не актуально пока)

Experimental Observation of the Tunnel Effect for Cooper Pairs with the Emission of Photons by I.K. Yanson, V.M. Svistunov, I.M. Dmitrenko 1964

First observation of Josephson radiation (info from Shmidt's book).
(??? read their article and tell what happened?? maybe it is a task for 2 hours)

9.4.9 Junctions by de Gennes book

(???? I'll write here what he wrote there, there are nontrivial statements!)

9.5 Bogliubov-de Gennes Equations for Superconductors in the Continuum Model

9.5.1 1.2 Hopping in a Quantum Many-Body Hamiltonian

Theory

A typical solid consists of the order of 10^{23} atoms. Each atom has the atomic number of electrons. In addition to interacting with nuclei, these electrons are interacting among themselves. In principle, one can start with a Hamiltonian to describe the motions of both electrons and nuclei:

$$\mathscr{H} = \sum_i \frac{\mathbf{p}_i^2}{2m_e} - \sum_{i,I} \frac{Z_I e^2}{|\mathbf{r}_i - \mathbf{R}_I|} + \frac{1}{2}\sum_{i,j} \frac{e^2}{|\mathbf{r}_i - \mathbf{r}_j|} + \sum_I \frac{\mathbf{P}_I^2}{2M_I} + \frac{1}{2}\sum_{I,J} \frac{Z_I Z_J e^2}{|\mathbf{R}_I - \mathbf{R}_J|} \tag{1.1}$$

Here the first and the fourth terms are the kinetic energy of the electrons and nuclei while the second, third, fifth terms represent the potential energy due to the Coulomb interaction between electrons and nuclei and among the electronic and nuclear degrees of freedom themselves. The variables $\mathbf{p}_i$ and $\mathbf{P}_I$ denote the momentum of each individual electron and nucleus, while the coordinates $\mathbf{r}_i$ and $\mathbf{R}_I$ are the variables conjugate to $\mathbf{p}_i$ and $\mathbf{P}_I$. The quantities m_e, M_I, and Z_I are the mass of electron and nucleus, and the atomic number, respectively. Note that each electron carries a negative charge $-e(e > 0)$ and each nucleus carries a positive charge $Z_I e$. Therefore, the interaction between electrons and nuclei is attractive while that among electrons or nuclei themselves is repulsive. A schematic drawing of this many-particle problem for a frozen lattice of nuclei is shown in Fig. 1.1.

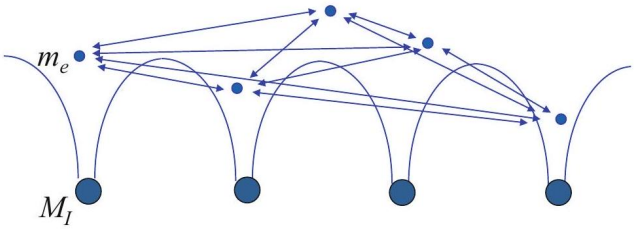


Fig. 1.1 Many-particle Hamiltonian of a solid consisting of electrons in a frozen lattice of nuclei

Classically, the equations of motion of the whole system are given by the Hamilton's equations

$$\dot{r}_{i,\alpha} = \frac{\partial \mathscr{H}}{\partial p_{i,\alpha}}, \quad \dot{p}_{i,\alpha} = -\frac{\partial \mathscr{H}}{\partial r_{i,\alpha}}, \tag{1.2}$$

for the electronic degrees of freedom, and

$$\dot{R}_{I,\alpha} = \frac{\partial \mathscr{H}}{\partial P_{I,\alpha}}, \quad \dot{P}_{I,\alpha} = -\frac{\partial \mathscr{H}}{\partial R_{I,\alpha}}, \tag{1.3}$$

for the nuclear degrees of freedom. These equations are precisely equivalent to the Newton's laws of motion. Here $\alpha(= x, y, z)$ denotes the three components of a vector in the cartesian coordinate system. Unfortunately, many important physical properties of electronic phenomena in solids cannot be captured by the classical mechanics and require a description within the quantum mechanics. There the coordinates and momenta no longer commutate with each other. Instead they should follow the Heisenberg uncertainty principles as represented by the commutators:

$$[r_{i,\alpha}, p_{j,\beta}]_- = i\hbar\delta_{ij}\delta_{\alpha\beta} \text{ and } [R_{I,\alpha}, P_{J,\beta}]_- = i\hbar\delta_{IJ}\delta_{\alpha\beta} \tag{1.4}$$

Here $\hbar$ is the reduced Planck's constant. The commutators by Eq. (1.4) indicate the coordinates and momenta are now quantum mechanical operators. In the coordinate representation, the momentum operator can be written as

$$\mathbf{p}_i = \frac{\hbar}{i}\nabla_i \text{ and } \mathbf{P}_I = \frac{\hbar}{i}\nabla_I. \tag{1.5}$$

Correspondingly, the operator form of the Hamiltonian (1.1) becomes

$$\mathscr{H} = -\sum_i \frac{\hbar^2}{2m_e}\nabla_i^2 - \sum_{i,I} \frac{Z_I e^2}{|\mathbf{r}_i - \mathbf{R}_I|} + \frac{1}{2}\sum_{i,j} \frac{e^2}{|\mathbf{r}_i - \mathbf{r}_j|} - \sum_I \frac{\hbar^2}{2M_I}\nabla_I^2 + \frac{1}{2}\sum_{I,J} \frac{Z_I Z_J e^2}{|\mathbf{R}_I - \mathbf{R}_J|}. \tag{1.6}$$

As such, the evolution of a state of the whole system is described by a quantum many-body wave-function, described by the Schrödinger equation [1]:

$$i\hbar\frac{\partial \Psi}{\partial t} = \mathscr{H}\Psi \tag{1.7}$$

where the many-body wave-function is the function of the variables $(\{\mathbf{r}_i\}, \{\mathbf{R}_I\}; t)$. When there are no external potentials or when they are time independent, the wave function can take the form

$$\Psi(\{\mathbf{r}_i\}, \{\mathbf{R}_I\}; t) = \Phi(\{\mathbf{r}_i\}, \{\mathbf{R}_I\})\, e^{-iEt/\hbar} \tag{1.8}$$

with the $\Phi(\{\mathbf{r}_i\}, \{\mathbf{R}_I\})$ satisfying the steady-state Schrödinger equation:

$$\mathscr{H}\Phi\left(\{\mathbf{r}_i\},\{\mathbf{R}_I\}\right)=E\Phi\left(\{\mathbf{r}_i\},\{\mathbf{R}_I\}\right). \tag{1.9}$$

Here E is the total energy of the many-particle system. Theoretically, the wavefunctions $\Phi\left(\{\mathbf{r}_i\},\{\mathbf{R}_I\}\right)$ contain all information needed to describe every property of the system. In practice, a direct solution of Eq. (1.9) is prohibitively difficult and a hierarchy of theoretical approximations are in order. Notice that the only small term in Eq. (1.6) is the kinetic energy of nuclear motion, which is smaller than that of electronic motion by a factor of m_e/M_I. Therefore, within the Born-Oppenheimer approximation [10], the wave function for the entire system can be written as

$$\Phi_{\alpha n}\left(\{\mathbf{r}_i\},\{\mathbf{R}_I\}\right)=\Psi_\alpha\left(\{\mathbf{r}_i\}:\{\mathbf{R}_I\}\right)u_{n\alpha}\left(\{\mathbf{R}_I\}\right). \tag{1.10}$$

Here $\Psi_\alpha\left(\{\mathbf{r}_i\}:\{\mathbf{R}_I\}\right)$ are the wave-functions for the electrons with the nuclei positions $\{\mathbf{R}_I\}$ as a fixed set of parameters and satisfying the equation

$$\begin{aligned}&\left[-\sum_i\frac{\hbar^2}{2m_e}\nabla_i^2-\sum_{i,I}\frac{Z_Ie^2}{|\mathbf{r}_i-\mathbf{R}_I|}+\frac{1}{2}\sum_{i,j}\frac{e^2}{|\mathbf{r}_i-\mathbf{r}_j|}+\frac{1}{2}\sum_{I,J}\frac{Z_IZ_Je^2}{|\mathbf{R}_I-\mathbf{R}_J|}\right]\Psi_\alpha\left(\{\mathbf{r}_i\}:\{\mathbf{R}_I\}\right)\\&=W_\alpha\left(\{\mathbf{R}_I\}\right)\Psi_\alpha\left(\{\mathbf{r}_i\}:\{\mathbf{R}_I\}\right)\end{aligned} \tag{1.11}$$

while $u_{n\alpha}\left(\{\mathbf{R}_I\}\right)$ are the wave-functions for the nuclear motion, and they satisfy the equation

$$\left[-\sum_I\frac{\hbar^2}{2M_I}\nabla_I^2+W_\alpha\left(\{\mathbf{R}_I\}\right)-E\right]u_{n\alpha}\left(\{\mathbf{R}_I\}\right)=0, \tag{1.12}$$

within the so-called "frozen phonon" approximation. By going beyond the Born-Oppenheimer approximation, a perturbation theory can be developed for the electron-phonon interactions, which are responsible for the inelastic scattering of electrons in metals, polaron formation in ionic crystals, and pairing of electrons in some metals and compounds. As such, it is important to focus on the electronic dynamics as described by Eq. (1.11) with the nuclear positions $\{\mathbf{R}_I\}$ as parameters. It has no effect whether we solve for W including nucleus-nucleus repulsive interaction or solve the following equation

$$\left[-\sum_i\frac{\hbar^2}{2m_e}\nabla_i^2-\sum_{i,I}\frac{Z_Ie^2}{|\mathbf{r}_i-\mathbf{R}_I|}+\frac{1}{2}\sum_{i,j}\frac{e^2}{|\mathbf{r}_i-\mathbf{r}_j|}\right]\Psi_\alpha\left(\{\mathbf{r}_i\}:\{\mathbf{R}_I\}\right)=E_\alpha\left(\{\mathbf{R}_I\}\right)\Psi_\alpha\left(\{\mathbf{r}_i\}:\{\mathbf{R}_I\}\right) \tag{1.13}$$

and add the nucleus-nucleus repulsive interaction afterwards. Equation (1.13) must be solved with the appropriate boundary conditions for the wave-functions. For example, $\Psi_\alpha\left(\{\mathbf{r}_i\}:\{\mathbf{R}_I\}\right)$ must be vanishing when the electrons are infinitely far away from an isolated atom or molecule, or must be satisfying the periodic boundary condition for crystalline solids. Also since electrons are spin- $\frac{1}{2}$ fermions, the wavefunctions Ψ_α must be antisymmetric with the interexchange of two electrons. Even so, due to the inter-electron Coulomb repulsion, Eq.(1.13) cannot be solved directly except for problems with few number of electrons. The difficulty in solving it numerically grows exponentially with the increase in the number of correlated electrons. This exponential problem will not be overcome for the cases involving many correlated electrons, which are typical in solids, regardless of the fact that the computational power is continuing to grow rapidly.

[1] For simplicity, the discussion is restricted to the non-relativistic limit. For a fully relativistic description, the kinetic energy at least for the electronic degrees of freedom should be replaced by the Dirac Hamiltonian.

To approach this problem, two strategies are mostly taken. One is to directly deal with Eq. (1.13) and map it onto a single-particle Hamiltonian while the other is to dramatically reduce Eq. (1.13) to an effective quantum many-body Hamiltonian so that electronic correlation effects can be qualitatively understood. The former is borne out within density functional theory (DFT) [11], in which the problem is made equivalent to solving the single-particle Kohn-Sham equations [12]:

$$\left[-\frac{\hbar^2}{2m_e}\nabla^2 + V_{\mathrm{KS},s}(\mathbf{r})\right]\psi_{s,\alpha}(\mathbf{r}) = E_{s,\alpha}\psi_{s,\alpha}(\mathbf{r}) \tag{1.14}$$

with

$$V_{\mathrm{KS},s}(\mathbf{r}) = -\sum_I \frac{Z_I e^2}{|\mathbf{r}-\mathbf{R}_I|} + \int d^3r' \frac{e^2 n(\mathbf{r}')}{|\mathbf{r}-\mathbf{r}'|} + V_{\mathrm{xc},s}(\mathbf{r}) \tag{1.15}$$

In Eq. (1.14), $\psi_{s,\alpha}$ and $E_{s,\alpha}$ are the Kohn-Sham eigenfunctions and the corresponding eigenvalues for spin projection s. In the DFT framework, the electronic correlation effects are encoded in the exchange-correlation potential $V_{\mathrm{xc},s}(\mathbf{r})$.[2] A schematic drawing of this single-particle problem is shown in Fig. 1.2.

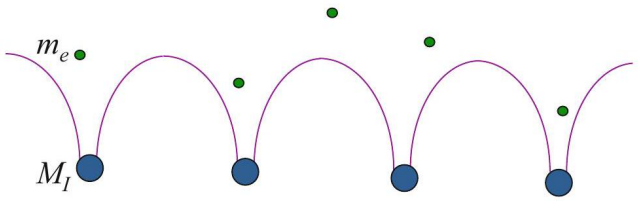


Fig. 1.2 Single-particle Hamiltonian of a solid consisting of electrons in a frozen lattice of nuclei

Since the single-particle Kohn-Sham potential $V_{\mathrm{KS},s}$ is in turn determined by the Kohn-Sham eigenfunctions via the local electron density $n(\mathbf{r}) = \sum_s \sum_{\alpha=1}^{N_s} |\psi_{s,\alpha}(\mathbf{r})|^2$ with the total number of $N_e = N_\uparrow + N_\downarrow$ electrons occupying N_e lowest-lying spin-orbitals, the KohnSham equations (1.14) should be solved self-consistently. Although the mapping from Eq.(1.13) to Eq.(1.14) is exact under the Hohenberg-Kohn theorem [13] for the ground state, the construction of the functional itself is nontrivial. So far the local density approximation (LDA) and its variants like generalized-gradient approximation (GGA) are the most often used. The LDA- or GGA-based DFT theory has been very successful in describing many materials for both groundstate energies and band structures, suggesting weak electronic correlations in these materials. However, the LDA-based DFT is not successful in describing other important classes of materials with open d - and f-shell orbitals (i.e., with partially occupied valence electrons occupying these orbitals). For example, LDA-based DFT predicts such transition metal oxides as La_2CuO_4, MnO, and NiO to be metals but they are insulators in reality. Similarly, for intermetallic f-electron systems like lanthanides and actinides, the LDA-based DFT usually gives effective mass of quasiparticles around the Fermi energy one or two orders of magnitude smaller than the experimental values. This failure demonstrates that the LDA-based DFT does not adequately address the electronic correlations in these materials, where the electrons experience very strong Coulomb repulsion when they occupy these narrow orbitals. The construction of more powerful exchange-correlation functionals for these narrow band materials remains a challenge in the DFT community [14].

Instead in the latter strategic approach, the electronic correlations are addressed directly by treating the competition between electron kinetic energy and interelectron potential energy in a quantum many-body manner but within a much simplified low-energy model Hamiltonian

[15, 16]. Some representative low-energy models will be presented after we introduce the second quantization in the next section.

9.5.2 1.3 Second Quantization of Hopping Hamiltonians

Theory

The direct treatment of the quantum many-body systems through the Schrödinger wave-function method is cumbersome and is not practical. It is convenient to use the second quantization to discuss the many identical interacting particles. As we recall, in the first quantization, the physical observables become quantum mechanical operators and the total energy is the expectation value of the Hamiltonian operator against the many-particle wave-function, which is the summation of the contributions for the single-particle kinetic energy and two-particle potential energy. In the second quantization, the wave-function itself becomes field operators, which can be expressed in the particle occupation number representation. In this representation, the many-particle state can be described by the occupation of identical particles in each single-particle state and the statistics symmetry regarding the particle being of Bose or Fermi character is protected in each step. This field quantization method is not only essential for the description of particle creation and destruction in the relativistic quantum field theory, but also powerful to describe the strongly correlated electronic systems.

For the correlated electrons as described by the Schrödinger equation (1.13), the Hamiltonian can be rewritten as

$$\mathscr{H}_e = \sum_i h\left(\mathbf{r}_i\right) + \frac{1}{2}\sum_{ij} v_{ee}\left(|\mathbf{r}_i - \mathbf{r}_j|\right), \tag{1.16}$$

where the single-particle operator

$$h\left(\mathbf{r}_i\right) = -\frac{\hbar^2}{2m_e}\nabla_i^2 - \sum_I \frac{Z_I e^2}{|\mathbf{r}_i - \mathbf{R}_I|} \tag{1.17}$$

and the two particle operator

$$v_{ee}\left(|\mathbf{r}_i - \mathbf{r}_j|\right) = \frac{e^2}{|\mathbf{r}_i - \mathbf{r}_j|} \tag{1.18}$$

Since electrons are fermions, the Hamiltonian (1.16) in the second quantized form is given by Fetter and Walecka [17], Mahan [18]

$$\hat{\mathscr{H}_e} = \int d\mathbf{x}\hat{\psi}^\dagger(\mathbf{x})h(\mathbf{x})\hat{\psi}(\mathbf{x}) + \frac{1}{2}\iint d\mathbf{x}d\mathbf{x}'\hat{\psi}^\dagger(\mathbf{x})\hat{\psi}^\dagger\left(\mathbf{x}'\right)v_{ee}\left(\mathbf{x},\mathbf{x}'\right)\hat{\psi}\left(\mathbf{x}'\right)\hat{\psi}(\mathbf{x}) \tag{1.19}$$

The first term on the right-hand side describes the non-interacting (also called single-particle) part of electrons while the second term the electron-electron interaction. Here the variable $\mathbf{x}$ denotes both the real-space coordinates $\mathbf{r}$ and the spin projection (usually along the z-axis) s, that is, $\mathbf{x} \equiv (\mathbf{r}, s)$. Different from the continuous variable $\mathbf{r}$, the spin projection can only take the discretized values,
$s = \pm\hbar/2$.[3] Therefore, a summation is implied in the integral over the spin index in $\mathbf{x}$. In Eq. (1.19), the field operator $\hat{\psi}^\dagger(\mathbf{x})(\hat{\psi}(\mathbf{x}))$ creates (annihilates) an electron at a coordinate $\mathbf{x}$, and they satisfy the anticommutation rules as

[2] A spin index is introduced to allow for possible magnetic states. However, for simplicity of the discussion, the spin-orbit coupling effect is neglected.

$$\left\{\hat{\psi}(\mathbf{x}), \hat{\psi}\left(\mathbf{x}'\right)\right\} = 0 \tag{1.20a}$$

$$\left\{\hat{\psi}^{\dagger}(\mathbf{x}), \hat{\psi}^{\dagger}\left(\mathbf{x}'\right)\right\} = 0 \tag{1.20b}$$

$$\left\{\hat{\psi}(\mathbf{x}), \hat{\psi}^{\dagger}\left(\mathbf{x}'\right)\right\} = \delta\left(\mathbf{x}-\mathbf{x}'\right) \tag{1.20c}$$

We note that the field operator $\hat{\psi}^{\dagger}(\mathbf{x})$ is the hermitian conjugate of $\hat{\psi}(\mathbf{x})$. Here the curly brackets represent the anticommutator, i.e., for two operators $\hat{A}$ and $\hat{B}$,

$$\{\hat{A}, \hat{B}\} = \hat{A}\hat{B} + \hat{B}\hat{A} \tag{1.21}$$

The δ-function is understood as Dirac-type for the continuous spatial coordinates while as Kronecker-type for the discrete variables, that is,

$$\delta\left(\mathbf{x}-\mathbf{x}'\right) = \delta\left(\mathbf{r}-\mathbf{r}'\right)\delta_{ss'} \tag{1.22}$$

More generally, if the single-particle Hamiltonian is non-local in the $\mathbf{x}$ coordinate space, which is especially true when the spin-orbit coupling due to the relativistic effect is included, the single-particle Hamiltonian takes the form of $h\left(\mathbf{x}, \mathbf{x}'\right)$. The system Hamiltonian of correlated electrons is then written as

$$\hat{\mathscr{H}_e} = \iint d\mathbf{x}d\mathbf{x}'\hat{\psi}^{\dagger}(\mathbf{x})h\left(\mathbf{x}, \mathbf{x}'\right)\hat{\psi}\left(\mathbf{x}'\right) + \frac{1}{2}\iint d\mathbf{x}d\mathbf{x}'\hat{\psi}^{\dagger}(\mathbf{x})\hat{\psi}^{\dagger}\left(\mathbf{x}'\right)v_{ee}\left(\mathbf{x}, \mathbf{x}'\right)\hat{\psi}\left(\mathbf{x}'\right)\hat{\psi}(\mathbf{x}). \tag{1.23}$$

Similarly, for any single-particle operator having

$$\mathscr{O} = \sum_i O\left(\mathbf{r}_i\right) \tag{1.24}$$

in the first quantization, its second quantized form is given by

$$\mathscr{O} = \int d\mathbf{x}\hat{\psi}^{\dagger}(\mathbf{x})O(\mathbf{x})\hat{\psi}(\mathbf{x}) \tag{1.25}$$

or

$$\mathscr{O} = \iint d\mathbf{x}d\mathbf{x}'\hat{\psi}^{\dagger}(\mathbf{x})O\left(\mathbf{x}, \mathbf{x}'\right)\hat{\psi}\left(\mathbf{x}'\right) \tag{1.26}$$

for the non-local case. In addition, although the original electron-electron interaction v_{ee} is repulsive, the second quantized Hamiltonian for the low-energy modeling remains to have the similar form even if inter-particle interaction is attractive.

Depending on the specific form of the Hamiltonian to be studied, the field operators can be expanded in terms of a complete set of basis functions, which are usually the eigenstates of the single-particle part of the Hamiltonian.

In the jellium model, where an interacting electron gas is placed in a background of the uniformly distributed positive charges, it is convenient to write the field operators as a linear combination of creation and annihilation operators corresponding to plane waves

$$\psi_{\sigma}(\mathbf{r}) = \frac{1}{\sqrt{\mathscr{V}}}\sum_{\mathbf{k}} e^{i\mathbf{k}\cdot\mathbf{r}}c_{\mathbf{k}\sigma}, \tag{1.27a}$$

$$\psi_{\sigma}^{\dagger}(\mathbf{r}) = \frac{1}{\sqrt{\mathscr{V}}}\sum_{\mathbf{k}} e^{-i\mathbf{k}\cdot\mathbf{r}}c_{\mathbf{k}\sigma}^{\dagger}, \tag{1.27b}$$

[3] Later on, we will also interchangeably use the symbol $\sigma = \pm 1$ for the spin variables, $s = (\hbar/2)\sigma$.

where $\mathscr{V}$ denotes the volume of the gas, and the annihilation and creation operators $c_{i\sigma}$ and $c_{i\sigma}^{\dagger}$ satisfy the anticommutation relation for fermions

$$\left\{c_{\mathbf{k}\sigma}, c_{\mathbf{k}'\sigma'}^{\dagger}\right\} = \delta_{\mathbf{k}\mathbf{k}'}\delta_{\sigma\sigma'} \tag{1.28a}$$

$$\{c_{\mathbf{k}\sigma}, c_{\mathbf{k}'\sigma'}\} = \left\{c_{\mathbf{k}\sigma}^{\dagger}, c_{\mathbf{k}'\sigma'}^{\dagger}\right\} = 0. \tag{1.28b}$$

Accordingly, the second quantized Hamiltonian for the interacting electron gas is given by

$$\mathscr{H} = \sum_{\mathbf{k}\sigma} \varepsilon_{\mathbf{k}} c_{\mathbf{k}\sigma}^{\dagger} c_{\mathbf{k}\sigma} + \frac{1}{2\mathscr{V}} \sum_{\mathbf{q}\neq 0} \sum_{\mathbf{k}\mathbf{k}'} \sum_{\sigma\sigma'} v_{ee}(\mathbf{q}) c_{\mathbf{k}+\mathbf{q},\sigma}^{\dagger} c_{\mathbf{k}'-\mathbf{q},\sigma'}^{\dagger} c_{\mathbf{k}'\sigma'} c_{\mathbf{k}\sigma} \tag{1.29}$$

where

$$\varepsilon_{\mathbf{k}} = \frac{\hbar^2 k^2}{2m_e} \tag{1.30}$$

is the single-particle energy dispersion and

$$v_{ee}(\mathbf{q}) = \frac{4\pi e^2}{q^2} \tag{1.31}$$

is the Fourier transform of the long-ranged Coulomb repulsion.

For the narrow band materials, the electronic correlations are significant. It is convenient to represent the field operators in terms of local orbitals. Representative examples of these local orbitals are Wannier orbitals or local atomic orbitals within the tight-binding approximation (TBA) to the systems with large atomic distances. If we consider only a single narrow band to be partially filled in a solid, the field operators can be represented as

$$\psi_{\sigma}(\mathbf{r}) = \sum_{i} \phi\left(\mathbf{r} - \mathbf{R}_i\right) c_{i\sigma} \tag{1.32a}$$

$$\psi_{\sigma}^{\dagger}(\mathbf{r}) = \sum_{i} \phi^{*}\left(\mathbf{r} - \mathbf{R}_i\right) c_{i\sigma}^{\dagger} \tag{1.32b}$$

where $\phi\left(\mathbf{r} - \mathbf{R}_i\right)$ is the localized orbital at atomic site $\mathbf{R}_i$, and the annihilation and creation operators $c_{i\sigma}$ and $c_{i\sigma}^{\dagger}$ satisfy the anticommutation relation for fermions

$$\left\{c_{i\sigma}, c_{j\sigma'}^{\dagger}\right\} = \delta_{ij}\delta_{\sigma\sigma'}, \tag{1.33a}$$

$$\{c_{i\sigma}, c_{j\sigma'}\} = \left\{c_{i\sigma}^{\dagger}, c_{j\sigma'}^{\dagger}\right\} = 0. \tag{1.33b}$$

The Hamiltonian for the single-orbital Hubbard model is given by Hubbard [1]

$$\mathscr{H} = -\sum_{ij} t_{ij} c_{i\sigma}^{\dagger} c_{j\sigma} + \frac{U}{2} \sum_{i\sigma} n_{i\sigma} n_{i\bar{\sigma}} \tag{1.34}$$

where $\bar{\sigma} = -\sigma$ with $\sigma = +1$ or $\uparrow$ for spin up and $\sigma = -1$ or $\downarrow$ for spin down,

$$t_{ij} = -\int d\mathbf{r} \phi^{*}\left(\mathbf{r} - \mathbf{R}_i\right) h(\mathbf{r}) \phi\left(\mathbf{r} - \mathbf{R}_j\right) \tag{1.35}$$

is the hopping integral between two atomic sites,

$$U = e^2 \iint d\mathbf{r} d\mathbf{r}' \frac{|\phi(\mathbf{r} - \mathbf{R}_i)|^2 |\phi(\mathbf{r}' - \mathbf{R}_i)|^2}{|\mathbf{r} - \mathbf{r}'|} \tag{1.36}$$

To derive this Hubbard model, the multi-center integral for the Coulomb interaction has been neglected.

Similarly, within the TBA, the Anderson lattice model is defined as [19]

$$\mathscr{H} = -\sum_{i,\sigma} t_{ij} c_{i\sigma}^{\dagger} c_{j\sigma} + \sum_{ij,\sigma\alpha} \left(V_{i\sigma,j\alpha} c_{i\sigma}^{\dagger} f_{j\alpha} + \text{ H.c. } \right) + \sum_{i,\alpha} \varepsilon_i^f f_{i\alpha}^{\dagger} f_{i\alpha} + \frac{U_f}{2} \sum_i n_{i\alpha}^f n_{i\bar{\alpha}}^f \tag{1.37}$$

Here the localized f-orbitals with energy level ε_i^f is hybridized with the conduction band while the electrons within the localized f-orbital electrons experience Hubbard- U repulsion. The quantity $V_{i\sigma,j\alpha}$ is the hybridization strength and the index α represents a two-component quantum state of the f-orbital.

These minimal models have been intensively used for understanding such emergent phenomena as localization-delocalization, heavy fermion, magnetism and superconductivity in transition metal oxides and intermetallic f-electron systems in condensed matter physics community. The creation and annihilation operators in the second quantization are also the central elements in the definition of Green's functions, which are used in quantum many-body theory. In particular, the Green's functions have been used as convenient quantities to evaluate the dynamic self-energies within the dynamical mean-field theory (DMFT) [20] for strongly correlated electronic systems, which maps the quantum lattice manybody problem to an effective quantum impurity one (still strongly correlated!). Recently, the LDA+DMFT approach [21-23] has been developed to investigate strongly correlated electronic materials. The approach incorporates the merits from both LDA and DMFT, and has been successful in giving a unified description of electronic states from weak to strong coupling limits, on the aspects of quasiparticle renormalization and magnetism. As for the phenomenology of superconductivity and related ordering states, the above quantum many-body approaches also lay down the foundations for the effective modeling description covered in the following chapters.

9.5.3 1.5 Derivation of the BdG Equations in the Continuum Model

The BdG [9] approach relies on the assumption that there exist well-defined quasiparticles in the superconductor. It has the advantage of providing information about the one-particle excitations of the system. The quasiparticle excitation spectrum can be obtained, together with the corresponding quasiparticle amplitudes. The BdG formalism is essentially correct in the weak-coupling regime, but also yields qualitative results in situations of very strong coupling, as was pointed out by Bishop et al. [24]. The interest in microscopic electronic structure calculations of this type was revived by low-temperature scanning-tunneling-microscopy (STM) experiments which provided extremely detailed, spatially resolved, excitation spectra around a single impurity, near the interface/surface, and around a vortex core in the presence of an Abrikosov flux lattice. An explanation of these results requires the knowledge of the one-particle local density of states of the system, which is best described in the framework of the BdG theory.

1.5.1 Derivation

We start with the second-quantized Hamiltonian for electrons experiencing an effective two-particle attractive interaction:

$$\mathscr{H} = \int d\mathbf{r}\psi_\alpha^\dagger(\mathbf{r})h_\alpha(\mathbf{r})\psi_\alpha(\mathbf{r}) - \frac{1}{2}\iint d\mathbf{r}d\mathbf{r}' V_{\text{eff}}\left(\mathbf{r},\mathbf{r}'\right)\psi_\alpha^\dagger(\mathbf{r})\psi_\beta^\dagger\left(\mathbf{r}'\right)\psi_\beta\left(\mathbf{r}'\right)\psi_\alpha(\mathbf{r}) \tag{1.38}$$

Here $\psi_\alpha^\dagger(\mathbf{r})$ and $\psi_\alpha(\mathbf{r})$ are creation and annihilation field operators of an electron with spin α at position $\mathbf{r}$. They obey the anti-commutation relation

$$\left\{\psi_\alpha(\mathbf{r}), \psi_\beta^\dagger\left(\mathbf{r}'\right)\right\} = \delta\left(\mathbf{r}-\mathbf{r}'\right)\delta_{\alpha\beta}, \tag{1.39}$$

$$\left\{\psi_\alpha(\mathbf{r}), \psi_\beta\left(\mathbf{r}'\right)\right\} = \left\{\psi_\alpha^\dagger(\mathbf{r}), \psi_\beta^\dagger\left(\mathbf{r}'\right)\right\} = 0. \tag{1.40}$$

The single particle Hamiltonian is given by

$$h_\alpha(\mathbf{r}) = \frac{\left[\frac{\hbar}{i}\nabla_{\mathbf{r}} + \frac{e}{c}\mathbf{A}(\mathbf{r})\right]^2}{2m_e} - e\phi(\mathbf{r}) + \alpha\mu_B H(\mathbf{r}) - E_F, \tag{1.41}$$

with $\mathbf{A}(\mathbf{r})$ and $\phi(\mathbf{r})$ the vector and scalar potentials. The magnetic field $H(\mathbf{r})$ has assumed to be along the z direction. The single particle energy is measured relative to the Fermi energy E_F. We have also chosen $V_{\text{eff}}\ (\mathbf{r},\mathbf{r}')$ to be positive while introduced a prefactor "-" to denote the attractive interaction in the second term of Eq. (1.38). Of course, the symmetry relation $V_{\text{eff}}\ (\mathbf{r}',\mathbf{r}) = V_{\text{eff}}\ (\mathbf{r},\mathbf{r}')$ still holds. The repeated spin index means the summation. Since we are most interested in the electron pairing in a superconductor, we can perform a Hartree-Fock-like meanfield approximation to the second term of Eq.(1.38) but in the particle-particle pairing channel. [4] A caution should be taken that this assumption is reasonable at low temperatures when the system is deep into the superconducting state, and the superconducting phase fluctuation, which is important near the transition temperature, is neglected. The mean-field Hamiltonian can then be written as follows:

$$\mathscr{H}_{eff} = \int d\mathbf{r}\psi_\alpha^\dagger(\mathbf{r})h_\alpha(\mathbf{r})\psi_\alpha(\mathbf{r}) + \iint d\mathbf{r}d\mathbf{r}'\left[\Delta\left(\mathbf{r},\mathbf{r}'\right)\psi_\uparrow^\dagger(\mathbf{r})\psi_\downarrow^\dagger\left(\mathbf{r}'\right) + \text{ H.c. }\right] + \iint d\mathbf{r}d\mathbf{r}'\frac{\left|\Delta\left(\mathbf{r},\mathbf{r}'\right)\right|^2}{V_{\text{eff}}\ (\mathbf{r},\mathbf{r}')} \tag{1.42}$$

where the pair potential is given by

$$\Delta\left(\mathbf{r},\mathbf{r}'\right) = -V_{\text{eff}}\ \left(\mathbf{r}-\mathbf{r}'\right)\left\langle\psi_\downarrow\left(\mathbf{r}'\right)\psi_\uparrow(\mathbf{r})\right\rangle = V_{\text{eff}}\ \left(\mathbf{r}-\mathbf{r}'\right)\left\langle\psi_\uparrow(\mathbf{r})\psi_\downarrow\left(\mathbf{r}'\right)\right\rangle, \tag{1.43}$$

$$\Delta^*\left(\mathbf{r},\mathbf{r}'\right) = -V_{\text{eff}}\ \left(\mathbf{r}-\mathbf{r}'\right)\left\langle\psi_\uparrow^\dagger(\mathbf{r})\psi_\downarrow^\dagger\left(\mathbf{r}'\right)\right\rangle = V_{\text{eff}}\ \left(\mathbf{r}-\mathbf{r}'\right)\left\langle\psi_\downarrow^\dagger\left(\mathbf{r}'\right)\psi_\uparrow^\dagger(\mathbf{r})\right\rangle. \tag{1.44}$$

The effective Hamiltonian equation (1.42) is in a bi-linear form and can be diagonalized exactly. By using the commutation relation for fermionic operators $\hat{A},\hat{B},\hat{C}$

$$[A,BC]_- = \{A,B\}C - B\{A,C\}, \tag{1.45}$$

and the function property

$$\int dx' f\left(x'\right)\frac{d\delta\left(x-x'\right)}{dx'} = -\frac{df(x)}{dx} \tag{1.46}$$

we obtain the following relations

$$[\psi_\uparrow(\mathbf{r}), \mathscr{H}_{eff}]_- = h_\uparrow(\mathbf{r})\psi_\uparrow(\mathbf{r}) + \int d\mathbf{r}'\Delta(\mathbf{r},\mathbf{r}')\,\psi_\downarrow^\dagger(\mathbf{r}'), \tag{1.47a}$$

$$\left[\psi_\uparrow^\dagger(\mathbf{r}), \mathscr{H}_{eff}\right]_- = -h_\uparrow^*(\mathbf{r})\psi_\uparrow^\dagger(\mathbf{r}) - \int d\mathbf{r}'\Delta^*(\mathbf{r},\mathbf{r}')\,\psi_\downarrow(\mathbf{r}'), \tag{1.47b}$$

$$[\psi_\downarrow(\mathbf{r}), \mathscr{H}_{eff}]_- = h_\downarrow(\mathbf{r})\psi_\downarrow(\mathbf{r}) - \int d\mathbf{r}'\Delta(\mathbf{r}',\mathbf{r})\,\psi_\uparrow^\dagger(\mathbf{r}'), \tag{1.47c}$$

$$\left[\psi_\downarrow^\dagger(\mathbf{r}), \mathscr{H}_{eff}\right]_- = -h_\downarrow^*(\mathbf{r})\psi_\downarrow(\mathbf{r}) + \int d\mathbf{r}'\Delta^*(\mathbf{r}',\mathbf{r})\,\psi_\uparrow(\mathbf{r}'). \tag{1.47d}$$

Note that $h^*(\mathbf{r}) \neq h(\mathbf{r})$. Equations (1.47)(a)-(d) show that the electron field operator can be expressed as a linear combination of electron- and hole-like quasiparticle excitations, which enables us to perform a Bogoliubov canonical transformation [25, 26]:

$$\psi_\sigma(\mathbf{r}) = \sum_n \left[u_{n\sigma}(\mathbf{r})\gamma_n - \sigma v_{n\sigma}^*(\mathbf{r})\gamma_n^\dagger\right]. \tag{1.48}$$

Be reminded the summation is over the excitation states with positive energy. In the expanded form for each individual spin projection, the transformation becomes

$$\psi_\uparrow(\mathbf{r}) = \sum_n \left[u_\uparrow^n(\mathbf{r})\gamma_n - v_\uparrow^{n*}(\mathbf{r})\gamma_n^\dagger\right], \qquad \psi_\uparrow^\dagger(\mathbf{r}) = \sum_n \left[u_\uparrow^{n*}(\mathbf{r})\gamma_n^\dagger - v_\uparrow^n(\mathbf{r})\gamma_n\right], \tag{1.49}$$

$$\psi_\downarrow(\mathbf{r}) = \sum_n \left[u_\downarrow^n(\mathbf{r})\gamma_n + v_\downarrow^{n*}(\mathbf{r})\gamma_n^\dagger\right], \qquad \psi_\downarrow^\dagger(\mathbf{r}) = \sum_n \left[u_\downarrow^{n*}(\mathbf{r})\gamma_n^\dagger + v_\downarrow^n(\mathbf{r})\gamma_n\right]. \tag{1.50}$$

In the above transformation, the quasiparticle operators γ_n and $\gamma_n^\dagger$ are also fermionic operators obeying the anti-commutation relation

$$\left\{\gamma_n, \gamma_m^\dagger\right\} = \delta_{nm}, \tag{1.51}$$

$$\{\gamma_n, \gamma_m\} = \left\{\gamma_n^\dagger, \gamma_m^\dagger\right\} = 0. \tag{1.52}$$

The anti-communication relation between the quasiparticle operators also ensures the anti-communication relation for the original electron field operators given in Eqs. (1.39) and (1.40).

The remaining task is to establish the eigen-equation for the quasiparticle wave functions $(u_\sigma(\mathbf{r}), v_\sigma(\mathbf{r}))^{\mathrm{T}}$. Assume the diagonalized Hamiltonian to be

$$\mathscr{H}_{eff} = E_g + \sum_n E_n\gamma_n^\dagger\gamma_n \tag{1.53}$$

where the excitation energy is positive and E_g is the ground state energy. We first observe the following commutation relations

$$\left[\gamma_n^\dagger, \mathscr{H}_{eff}\right]_- = -E_n\gamma_n^\dagger, \tag{1.54}$$

$$[\gamma_n, \mathscr{H}_{eff}]_- = E_n\gamma_n. \tag{1.55}$$

[4] We notice that the normal-state Hartree-Fock term can be absorbed into the chemical potential, which will not modify the results qualitatively.

[5] Here we only consider the spin-singlet pairing, in which a spin-up electron is paired with a spin-down electron. The spin-triplet pairing, in which electrons are paired with equal spin, can be discussed similarly.

(add the derivation of them here!!!)

Upon the substitution of Eqs. (1.49) and (1.50), and with the aid of Eqs. (1.54) and (1.55), we can compare the coefficients of these terms with γ_n and $\gamma_n^\dagger$ and arrive at the following set of equations:

$$\begin{cases} h_\uparrow(\mathbf{r})u_\uparrow^n(\mathbf{r}) + \int d\mathbf{r}'\Delta\left(\mathbf{r},\mathbf{r}'\right)v_\downarrow^n\left(\mathbf{r}'\right) = E_n u_\uparrow^n(\mathbf{r}), \\ h_\downarrow(\mathbf{r})u_\downarrow^n(\mathbf{r}) + \int d\mathbf{r}'\Delta\left(\mathbf{r}',\mathbf{r}\right)v_\uparrow^n\left(\mathbf{r}'\right) = E_n u_\downarrow^n(\mathbf{r}), \\ \int d\mathbf{r}'\Delta^*\left(\mathbf{r},\mathbf{r}'\right)u_\downarrow^n\left(\mathbf{r}'\right) - h_\uparrow^*(\mathbf{r})v_\uparrow^n(\mathbf{r}) = E_n v_\uparrow^n(\mathbf{r}), \\ \int d\mathbf{r}'\Delta^*\left(\mathbf{r}',\mathbf{r}\right)u_\uparrow^n\left(\mathbf{r}'\right) - h_\downarrow^*(\mathbf{r})v_\downarrow^n(\mathbf{r}) = E_n v_\downarrow^n(\mathbf{r}). \end{cases} \tag{1.56}$$

To see the structure of the above set of equations more clearly, we can write it into a compact matrix form:

$$\int d\mathbf{r}'\hat{M}\left(\mathbf{r},\mathbf{r}'\right)\hat{\phi}\left(\mathbf{r}'\right) = E_n\hat{\phi}(\mathbf{r}) \tag{1.57}$$

where

$$\hat{M}\left(\mathbf{r},\mathbf{r}'\right) = \begin{bmatrix} h_\uparrow(\mathbf{r})\delta\left(\mathbf{r}-\mathbf{r}'\right) & 0 & 0 & \Delta\left(\mathbf{r},\mathbf{r}'\right) \\ 0 & h_\downarrow(\mathbf{r})\delta\left(\mathbf{r}-\mathbf{r}'\right) & \Delta\left(\mathbf{r}',\mathbf{r}\right) & 0 \\ 0 & \Delta^*\left(\mathbf{r},\mathbf{r}'\right) & -h_\uparrow^*(\mathbf{r})\delta\left(\mathbf{r}-\mathbf{r}'\right) & 0 \\ \Delta^*\left(\mathbf{r}',\mathbf{r}\right) & 0 & 0 & -h_\downarrow^*(\mathbf{r})\delta\left(\mathbf{r}-\mathbf{r}'\right) \end{bmatrix} \tag{1.58}$$

and

$$\hat{\phi}\left(\mathbf{r}'\right) = \begin{pmatrix} u_\uparrow^n(\mathbf{r}) \\ u_\downarrow^n(\mathbf{r}) \\ v_\uparrow^n(\mathbf{r}) \\ v_\downarrow^n(\mathbf{r}) \end{pmatrix}. \tag{1.59}$$

From Eq. (1.58), we can see that in the absence of spin-orbit coupling and other spin-flip scattering interactions, the set of equations as given by Eq. (1.58) is blocked diagonalized into two subsets of equations:

$$\begin{cases} h_\uparrow(\mathbf{r})u_\uparrow^{\tilde{n}1}(\mathbf{r}) + \int d\mathbf{r}'\Delta\left(\mathbf{r},\mathbf{r}'\right)v_\downarrow^{\tilde{n}1}\left(\mathbf{r}'\right) = E_{\tilde{n}1}u_\uparrow^{\tilde{n}1}(\mathbf{r}), \\ \int d\mathbf{r}'\Delta^*\left(\mathbf{r}',\mathbf{r}\right)u_\uparrow^{\tilde{n}1}\left(\mathbf{r}'\right) - h_\downarrow^*(\mathbf{r})v_\downarrow^{\tilde{n}1}(\mathbf{r}) = E_{\tilde{n}1}v_\downarrow^{\tilde{n}1}(\mathbf{r}), \end{cases} \tag{1.60}$$

and

$$\begin{cases} h_\downarrow(\mathbf{r})u_\downarrow^{\tilde{n}2}(\mathbf{r}) + \int d\mathbf{r}'\Delta\left(\mathbf{r}',\mathbf{r}\right)v_\uparrow^{\tilde{n}2}\left(\mathbf{r}'\right) = E_{\tilde{n}2}u_\downarrow^{\tilde{n}2}(\mathbf{r}), \\ \int d\mathbf{r}'\Delta^*\left(\mathbf{r},\mathbf{r}'\right)u_\downarrow^{\tilde{n}2}\left(\mathbf{r}'\right) - h_\uparrow^*(\mathbf{r})v_\uparrow^{\tilde{n}2}(\mathbf{r}) = E_{\tilde{n}2}v_\uparrow^{\tilde{n}2}(\mathbf{r}). \end{cases}$$

That is, the spin-up electron-like component of wave function $u_\uparrow(\mathbf{r})$ is coupled only to the spin-down hole-like component of wave function $v_\downarrow(\mathbf{r})$ while the spin-down electron-like component of wave function $u_\downarrow(\mathbf{r})$ is coupled only to the spin-up holelike component of wave function $v_\uparrow(\mathbf{r})$. Each of these two subsets of equations are now a 2 by 2 matrix equation in the Nambu space. By breaking the $U(1)$ gauge symmetry, this unusual space allows the emergence

of superconducting pairing state. The mathematical structure of these equations looks similar to those describing the coupling between particles in conduction band and holes in the valence band in semiconductor physics. However, we should be cautioned that the origin of these equations in superconductors is really due to an effective electronelectron pairing. To be clear, we have redefined the number of eigenstate index. If the original set of eigen-equations as given in Eq. (1.56) has N number of eigenvalues, each subset of eigen-equations will have $N/2$ number of eigenvalues. In this decoupling, the diagonalized Hamiltonian as given in Eq.(1.53) can be written as:

$$\mathscr{H}_{eff} = E_g + \sum_{\tilde{n}\mu} E_{\tilde{n}\mu}\gamma^{\dagger}_{\tilde{n}\mu}\gamma_{\tilde{n}\mu} \tag{1.62}$$

with $\mu = 1, 2$. Correspondingly, the canonical transform can also be re-written as:

$$\begin{aligned}
\psi_{\uparrow}(\mathbf{r}) &= \sum_{\tilde{n}} \left[u^{\tilde{n}1}_{\uparrow}(\mathbf{r})\gamma_{\tilde{n}1} - v^{\tilde{n}2*}_{\uparrow}(\mathbf{r})\gamma^{\dagger}_{\tilde{n}2} \right], \qquad \psi^{\dagger}_{\uparrow}(\mathbf{r}) = \sum_{\tilde{n}} \left[u^{\tilde{n}1*}_{\uparrow}(\mathbf{r})\gamma^{\dagger}_{\tilde{n}1} - v^{\tilde{n}2}_{\uparrow}(\mathbf{r})\gamma_{\tilde{n}2} \right], \\
\psi_{\downarrow}(\mathbf{r}) &= \sum_{\tilde{n}} \left[u^{\tilde{n}2}_{\downarrow}(\mathbf{r})\gamma_{\tilde{n}2} + v^{\tilde{n}1*}_{\downarrow}(\mathbf{r})\gamma^{\dagger}_{\tilde{n}1} \right], \qquad \psi^{\dagger}_{\downarrow}(\mathbf{r}) = \sum_{\tilde{n}} \left[u^{\tilde{n}2*}_{\downarrow}(\mathbf{r})\gamma^{\dagger}_{\tilde{n}2} + v^{\tilde{n}1}_{\downarrow}(\mathbf{r})\gamma_{\tilde{n}1} \right].
\end{aligned} \tag{1.63}$$

We now prove that the set of equations given by Eqs. (1.60) and (1.61) has the following symmetry property: If $\left(u^{\tilde{n}1}_{\uparrow}, v^{\tilde{n}1}_{\downarrow}\right)^{\mathrm{T}}$ is the eigenfunction of Eq. (1.60) with eigenvalue $E_{\tilde{n}1}$, then $\left(v^{\tilde{n}1*}_{\downarrow}, -u^{\tilde{n}1*}_{\uparrow}\right)^{\mathrm{T}}$ is also the eigensolution to Eq. (1.61) with eigenvalue $-E_{\tilde{n}1}$. We take the complex conjugation to Eq.(1.60), which yields to

$$\begin{cases} h^{*}_{\uparrow}(\mathbf{r})u^{\tilde{n}1*}_{\uparrow}(\mathbf{r}) + \int d\mathbf{r}'\Delta^{*}(\mathbf{r},\mathbf{r}')\, v^{\tilde{n}1*}_{\downarrow}(\mathbf{r}') = E_{\tilde{n}1}u^{\tilde{1}1*}_{\uparrow}(\mathbf{r}), \\ \int d\mathbf{r}'\Delta(\mathbf{r}',\mathbf{r})\, u^{\tilde{n}1*}_{\uparrow}(\mathbf{r}') - h_{\downarrow}(\mathbf{r})v^{\tilde{n}1*}_{\downarrow}(\mathbf{r}) = E_{\tilde{n}1}v^{\tilde{n}}_{\downarrow}(\mathbf{r}) \end{cases} \tag{1.65}$$

Multiplying the second expression in the above set of equations by a minus sign on both sides, we re-arrange the whole set of equations into

$$\begin{cases} h_{\downarrow}(\mathbf{r})v^{\tilde{n}1*}_{\downarrow}(\mathbf{r}) + \int d\mathbf{r}'\Delta(\mathbf{r}',\mathbf{r})\left(-u^{\tilde{n}1*}_{\uparrow}(\mathbf{r}')\right) = -E_{\tilde{n}1}v^{\tilde{n}1*}_{\downarrow}(\mathbf{r}), \\ \int d\mathbf{r}'\Delta^{*}(\mathbf{r},\mathbf{r}')\, v^{\tilde{n}1*}_{\downarrow}(\mathbf{r}') - h^{*}_{\uparrow}(\mathbf{r})\left(-u^{\tilde{n}1*}_{\uparrow}(\mathbf{r})\right) = -E_{\tilde{n}1}\left(-u^{\tilde{N}1*}_{\uparrow}(\mathbf{r})\right). \end{cases} \tag{1.66}$$

Equation (1.66) is just identical to Eq. (1.61) with the equivalence:

$$\begin{pmatrix} u^{\tilde{n}2}_{\downarrow}(\mathbf{r}) \\ v^{\tilde{n}_2}_{\uparrow}(\mathbf{r}) \end{pmatrix} \equiv \begin{pmatrix} v^{\tilde{n}1*}_{\downarrow}(\mathbf{r}) \\ -u^{\tilde{n}1}_{\uparrow}(\mathbf{r}) \end{pmatrix}, \tag{1.67}$$

and $E_{\tilde{n}2} \equiv -E_{\tilde{n}1}$. This property has a significant consequence. It suggests that we merely need to solve one set of equations, e.g., Eq.(1.60), instead of both Eqs. (1.60) and (1.61), and obtain all information essential for the measurable. It saves the computational time significantly, which is desirable for the real-space inhomogeneous or disordered problems, even in a collinear spin-polarization. Note again here that this simplification exists in the absence of the spin-orbit coupling and other spin-flip scattering terms in the Hamiltonian. However, a more general symmetry property, as will be shown in the next chapter, can be derived even in the presence of these terms. We note that Eqs. (1.60) and (1.61) involve the pair potential $\Delta(\mathbf{r},\mathbf{r}')$. Substituting Eqs. (1.49) and (1.50) into Eq. (1.43), we arrive at

$$\begin{aligned}\Delta(\mathbf{r},\mathbf{r}') &= V(\mathbf{r}-\mathbf{r}')\langle\psi_\uparrow(\mathbf{r})\psi_\downarrow(\mathbf{r}')\rangle \\ &= V(\mathbf{r}-\mathbf{r}')\sum_{\tilde{n}}{}'\left[u_\uparrow^{\tilde{n}1}(\mathbf{r})v_\downarrow^{\tilde{\tilde{1}}*}(\mathbf{r}')f(-E_{\tilde{n}1})-v_\uparrow^{\tilde{n}2*}(\mathbf{r})u_\downarrow^{\tilde{\tilde{2}}2}(\mathbf{r}')f(E_{\tilde{n}2})\right] \\ &= V(\mathbf{r}-\mathbf{r}')\sum_{\tilde{n}}u_\uparrow^{\tilde{n}1}(\mathbf{r})v_\downarrow^{\tilde{n}1*}(\mathbf{r}')f(-E_{\tilde{n}1}) \qquad (1.68)\end{aligned}$$

On the other hand,

$$\begin{aligned}\Delta(\mathbf{r},\mathbf{r}') &= -V(\mathbf{r}-\mathbf{r}')\langle\psi_\downarrow(\mathbf{r}')\psi_\uparrow(\mathbf{r})\rangle \\ &= -V(\mathbf{r}-\mathbf{r}')\sum_{\tilde{n}}{}'\left[-u_\downarrow^{\tilde{n}2}(\mathbf{r}')v_\uparrow^{\tilde{n}2*}(\mathbf{r}')f(-E_{\tilde{n}2})+v_\downarrow^{\tilde{n}1*}(\mathbf{r}')u_\uparrow^{\tilde{n}1}(\mathbf{r}')f(E_{\tilde{n}1})\right] \\ &= -V(\mathbf{r}-\mathbf{r}')\sum_{\tilde{n}}u_\uparrow^{\tilde{n}1}(\mathbf{r})v_\downarrow^{\tilde{n}1*}(\mathbf{r}')f(E_{\tilde{n}1}) \qquad (1.69)\end{aligned}$$

Here we have used the symmetry property in the derivation, and the statistical average

$$\left\langle\gamma_{\tilde{n}\mu}^\dagger\gamma_{\tilde{m}\nu}\right\rangle=\delta_{\tilde{n}\tilde{m}}\delta_{\mu\nu}f(E_{\tilde{n}\mu}), \qquad (1.70)$$

and

$$\langle\gamma_{\tilde{n}\mu}\gamma_{\tilde{m}\nu}\rangle=\left\langle\gamma_{\tilde{n}\mu}^\dagger\gamma_{\tilde{m}\nu}^\dagger\right\rangle=0, \qquad (1.71)$$

where the Fermi distribution function

$$f(E_{\tilde{n}\mu})=\frac{1}{\exp(E_{\tilde{n}\mu}/k_BT)+1}, \qquad (1.72)$$

with k_B the Boltzmann constant and T the temperature. Notice the disappearance of "$'$" above the summation symbol, meaning the summation is over both positive and negative eigenvalues. Combination of Eqs. (1.68) and (1.69) gives

$$\Delta(\mathbf{r},\mathbf{r}')=\frac{V(\mathbf{r}-\mathbf{r}')}{2}\sum_{\tilde{n}}u_\uparrow^{\tilde{n}1}(\mathbf{r})v_\downarrow^{\tilde{n}1*}(\mathbf{r}')\tanh\left(\frac{E_{\tilde{n}1}}{2k_BT}\right). \qquad (1.73)$$

For spin-singlet pairing, $\Delta(\mathbf{r},\mathbf{r}')=\Delta(\mathbf{r}',\mathbf{r})$, and we can have a more symmetric form of the expression

$$\Delta(\mathbf{r},\mathbf{r}')=\frac{V(\mathbf{r}-\mathbf{r}')}{4}\sum_{\tilde{n}}\left[u_\uparrow^{\tilde{n}1}(\mathbf{r})v_\downarrow^{\tilde{n}1*}(\mathbf{r}')+u_\uparrow^{\tilde{n}1}(\mathbf{r}')v_\downarrow^{\tilde{n}1*}(\mathbf{r})\right]\tanh\left(\frac{E_{\tilde{n}1}}{2k_BT}\right) \qquad (1.74)$$

When there is no spin-polarization effect, Eqs. (1.60) and (1.61) are identical and they recover the original formalism proposed by de-Gennes [9] for an s-wave superconductor and that for an anisotropic superconductor [27]. Since a Bogoliubov canonical transformation is involved in the development of the formalism, these sets of equations are called the Bogoliubov-de Gennes equations.

1.5.2 Local Density of States

Once the solution to the BdG equations is obtained, the local density of states can be evaluated according to

$$\rho(\mathbf{r}, E) = \sum_{n,\sigma}{}' \left\{ \left|u_\sigma^n(\mathbf{r})\right|^2 \delta\left(E - E_n\right) + \left|v_{\bar{\sigma}}^n(\mathbf{r})\right|^2 \delta\left(E + E_n\right) \right\}, \tag{1.75}$$

where $\delta(x)$ is the Dirac delta function and can approximated numerically as

$$\delta(x) = \frac{1}{\pi} \frac{\Gamma}{x^2 + \Gamma^2}, \tag{1.76}$$

with Γ a lifetime broadening parameter. In the absence of the spin-orbit coupling and spin-flip scattering, Eq.(1.75) becomes

$$\rho(\mathbf{r}, E) = \sum_n \left\{ \left|u_\uparrow^n(\mathbf{r})\right|^2 \delta\left(E - E_n\right) + \left|v_\downarrow^n(\mathbf{r})\right|^2 \delta\left(E + E_n\right) \right\}. \tag{1.77}$$

Equivalently, the thermalized local density of states can be written as

$$\rho(\mathbf{r}, E) = \sum_n \left\{ \left|u_\uparrow^n(\mathbf{r})\right|^2 \left(-\frac{\partial f\left(E - E_n\right)}{\partial E} \right) + \left|v_\downarrow^n(\mathbf{r})\right|^2 \left(-\frac{\partial f\left(E + E_n\right)}{\partial E} \right) \right\}. \tag{1.78}$$

The local density of states is proportional to the local tunneling conductance as measured by the scanning tunneling microscopy.

In the following discussion, unless specified otherwise the BdG equation (1.60) will be mainly used. We will drop the spin subscript to u and v, and the quasiparticle branch index, as well as the symbol tilde on the eigenstate index. We keep only the spin index for the single-particle Hamiltonian itself.

1.5.3 Gauge Invariance

The choice of the vector potential $\mathbf{A}$ is not unique, since $\mathbf{A}'(\mathbf{r}) = \mathbf{A}(\mathbf{r}) + \nabla\chi(\mathbf{r})$, with χ an arbitrary function, will give the same magnetic field as that determined from $\mathbf{A}$, that is, $\nabla \times \mathbf{A}'(\mathbf{r}) = \nabla \times \mathbf{A}(\mathbf{r}) = \mathbf{H}(\mathbf{r})$. Thus $\mathbf{A}$ and $\mathbf{A}'$ are equally acceptable to describe the field $\mathbf{H}(\mathbf{r})$. All physically measurable quantities will have the same expectation values when calculated with $\mathbf{A}$ and $\mathbf{A}'$.

Suppose that the eigenfunctions (u, v) of the BdG equation with the vector potential $\mathbf{A}$ are known. It can be easily proved that the eigenfunctions (u', v') with the vector potential $\mathbf{A}' = \mathbf{A} + \nabla\chi(\mathbf{r})$ differs from (u, v) as

$$\begin{pmatrix} u'(\mathbf{r}) \\ v'(\mathbf{r}) \end{pmatrix} = \begin{pmatrix} e^{-ie\chi(\mathbf{r})/\hbar c} & 0 \\ 0 & e^{ie\chi(\mathbf{r})/\hbar c} \end{pmatrix} \begin{pmatrix} u(\mathbf{r}) \\ v(\mathbf{r}) \end{pmatrix}, \tag{1.79}$$

while the pair potential is modified as

$$\Delta'\left(\mathbf{r}, \mathbf{r}'\right) = \Delta\left(\mathbf{r}, \mathbf{r}'\right) e^{-ie[\chi(\mathbf{r}) + \chi(\mathbf{r}')]/\hbar c} \tag{1.80}$$

9.5.4 1.7 Solution to the BdG Equations in Homogeneous Systems

Theory

Let us start with the non-spin-polarization situation. In homogeneous systems, there exists the translational symmetry. In the limit of homogeneous electron gas, the translation symmetry

itself is continuous. Therefore, it would be convenient to expand the BdG wave function in terms of plane waves:

$$\begin{pmatrix} u(\mathbf{r}) \\ v(\mathbf{r}) \end{pmatrix} = \frac{1}{\sqrt{\Omega}} \begin{pmatrix} u_{\mathbf{k}} \\ v_{\mathbf{k}} \end{pmatrix} e^{i\mathbf{k}\cdot\mathbf{r}}, \tag{1.98}$$

where Ω is the volume of the entire system. Substitution of Eq.(1.98) into Eq. (1.60) leads to

$$\xi_{\mathbf{k}} u_{\mathbf{k}} + \Delta_{\mathbf{k}} v_{\mathbf{k}} = E_{\mathbf{k}} u_{\mathbf{k}}, \tag{1.99a}$$
$$\Delta^*_{\mathbf{k}} u_{\mathbf{k}} - \xi_{\mathbf{k}} v_{\mathbf{k}} = E_{\mathbf{k}} u_{\mathbf{k}}, \tag{1.99b}$$

where

$$\xi_{\mathbf{k}} = \frac{\hbar k^2}{2m_e} - E_F \tag{1.100}$$

is the single-particle energy dispersion, while

$$\Delta_{\mathbf{k}} = \int d\mathbf{r}' \Delta(\mathbf{r}, \mathbf{r}') \, e^{-i\mathbf{k}\cdot(\mathbf{r}-\mathbf{r}')}, \tag{1.101}$$

is the Fourier transform of the real-space superconducting pair potential. Using the definition of the pair potential $\Delta(\mathbf{r}, \mathbf{r}')$ given by Eq. (1.74) into Eq. (1.101), we obtain

$$\Delta_{\mathbf{k}} = \frac{1}{2\Omega} \sum_{\mathbf{k}'} V_{\mathbf{k}\mathbf{k}'} u_{\mathbf{k}} v^*_{\mathbf{k}'} \tanh\left(\frac{E_{\mathbf{k}'}}{2k_B T}\right) \tag{1.102}$$

with the term

$$V_{\mathbf{k}\mathbf{k}'} = \int d\mathbf{r}' V(\mathbf{r}, \mathbf{r}') \, e^{-i\mathbf{k}\cdot(\mathbf{r}-\mathbf{r}')} \cos(\mathbf{k}\cdot(\mathbf{r}-\mathbf{r}')) \tag{1.103}$$

retaining only the pairing interaction of allowed orbital harmonics. For an isotropic s-wave pairing symmetry, we use the ansatz

$$V_{\mathbf{k}\mathbf{k}'} = V_s, \tag{1.104}$$

and correspondingly

$$\Delta_{\mathbf{k}} = \Delta_s \tag{1.105}$$

which has no momentum dependence. For a d-wave pairing symmetry in a two-dimensional system, we have the ansatz

$$V_{\mathbf{k}\mathbf{k}'} = V_d \cos(2\phi_{\mathbf{k}}) \cos(2\phi_{\mathbf{k}'}), \tag{1.106}$$

and correspondingly

$$\Delta_{\mathbf{k}} = \Delta_d \cos(2\phi_{\mathbf{k}}) \tag{1.107}$$

with $\phi_{\mathbf{k}}$ being the azimuthal angle of $\mathbf{k}$ around the Fermi energy. We note that in the summation on the right-hand-side of Eq.(1.102), both positive and negative energy eigenvalues are still taken into account. The profile of the energy gap around the Fermi surface for these two types of pairing symmetry is depicted in Fig. 1.4.

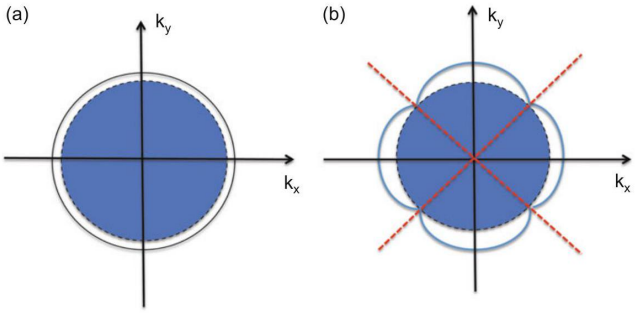


Fig. 1.4 A schematic drawing of quasiparticle excitation gap for an s-wave (a) and a $d_{x^2-y^2}$-wave pairing superconductor (b)

For the isotropic s-wave superconductors, the quasiparticle gap is uniform along the Fermi surface. For the $d_{x^2-y^2}$-wave superconductors, the quasiparticle gap is closed at some special momentum directions $\varphi = \frac{\pi}{4}, \frac{3\pi}{4}, \frac{5\pi}{4}, \frac{7\pi}{4}$. These gapless quasiparticles are called nodal quasiparticles.

A little algebra yields the eigensolutions

$$\begin{pmatrix} u_{\mathbf{k}} \\ v_{\mathbf{k}} \end{pmatrix} = \begin{pmatrix} u_{\mathbf{k}}^{(0)} e^{i\varphi_{\mathbf{k}}} \\ v_{\mathbf{k}}^{(0)} \end{pmatrix} \tag{1.108}$$

corresponding to the eigenvalue

$$E_{\mathbf{k}} = \sqrt{\xi_{\mathbf{k}}^2 + |\Delta_{\mathbf{k}}|^2} \tag{1.109}$$

and

$$\begin{pmatrix} u_{\mathbf{k}} \\ v_{\mathbf{k}} \end{pmatrix} = \begin{pmatrix} -v_{\mathbf{k}}^{(0)} e^{i\varphi_{\mathbf{k}}} \\ u_{\mathbf{k}}^{(0)} \end{pmatrix} \tag{1.110}$$

corresponding to the eigenvalue $-E_{\mathbf{k}}$. Here the BdG wave function amplitude is given by

$$\begin{pmatrix} u_{\mathbf{k}}^{(0)} \\ v_{\mathbf{k}}^{(0)} \end{pmatrix} = \begin{pmatrix} \sqrt{\frac{1}{2}\left(1 + \frac{\xi_k}{E_k}\right)} \\ \sqrt{\frac{1}{2}\left(1 - \frac{\xi_k}{E_k}\right)} \end{pmatrix} \tag{1.111}$$

and $\varphi_{\mathbf{k}}$ is the phase angle of $\Delta_{\mathbf{k}}$. Therefore, we obtain the self-consistency equation for the pair potential

$$\Delta_s = \frac{1}{(2\pi)^3} \int d\mathbf{k} V_s \frac{\Delta_s}{2E_{\mathbf{k}}} \tanh\left(\frac{E_{\mathbf{k}}}{2k_B T}\right), \tag{1.112}$$

for a three-dimensional s-wave superconductor with the quasiparticle excitation energy $E_{\mathbf{k}} = \sqrt{\xi_{\mathbf{k}}^2 + \Delta_s^2}$; and

$$\Delta_d = \frac{1}{(2\pi)^2} \int d\mathbf{k} V_d \cos^2(2\varphi) \frac{\Delta_d}{2E_{\mathbf{k}}} \tanh\left(\frac{E_{\mathbf{k}}}{2k_B T}\right), \tag{1.113}$$

for a two-dimensional $d_{x^2-y^2}$-wave superconductor with the quasiparticle excitation energy $E_{\mathbf{k}} = \sqrt{\xi_{\mathbf{k}}^2 + (\Delta_d \cos(2\varphi))^2}$.

We can convert the three-dimensional integral into

$$\int d\mathbf{k} \to \int_0^{2\pi} d\phi \int_0^{\pi} \sin\theta d\theta \int_0^{\infty} k^2 dk \to 4\pi \int_0^{\infty} k^2 dk$$

when the integrand has the spherical symmetry;
while we can convert the two-dimensional integral into

$$\int d\mathbf{k} \to \int_0^{2\pi} d\phi \int_0^{\infty} kdk \to 2\pi \int_0^{\infty} kdk,$$

when the integrand has the cylindrical symmetry. Therefore, for a parabolic normalstate single-particle energy dispersion, $\xi_{\mathbf{k}} = \frac{\hbar^2 k^2}{2m_e} - E_F$, the integral over momentum amplitude k can be changed to the integral over the energy as

$$\frac{1}{(2\pi)^D} \int d\mathbf{k} \to \int g(\epsilon) d\epsilon, \tag{1.114}$$

where $D = 2$ and 3 and $g(\epsilon)$ denotes the density of states for electrons of one spin orientation, and is given by

$$g(\epsilon) = \frac{1}{4\pi^2} \left(\frac{2m_e}{\hbar^2} \right)^{3/2} \epsilon^{1/2} \tag{1.115}$$

for the three-dimensional system, while

$$g(\epsilon) = \frac{m_e}{2\pi\hbar^2} \epsilon \tag{1.116}$$

for the two-dimensional system.

These expressions of density of states are shown in Fig. 1.5.

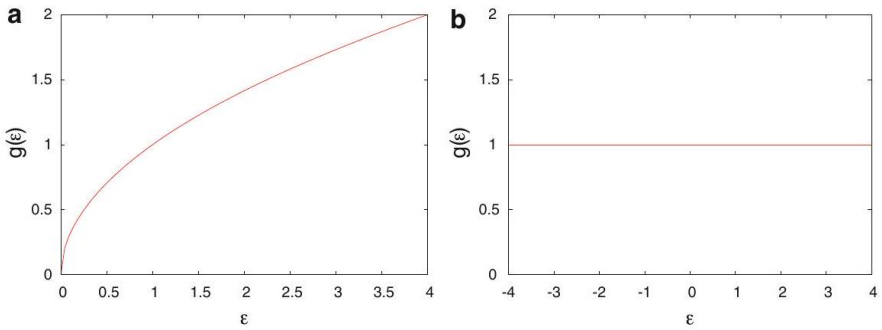


Fig. 1.5 Density of states for a three-dimensional (a) and a two-dimensional (b) electron gas

In the BCS-type weak-coupling theory for superconductivity, the pairing interaction is limited to a range of $[-\hbar\omega_c, \hbar\omega_c]$ around the Fermi surface. The cutoff ω_c is the Debye frequency of phonons in conventional superconductors. In most strongly correlated superconductors, ω_c is the energy scale characterizing spin, charge, or orbital fluctuations and is approximated by the width of a renormalized narrow band. One should be cautioned that for the strongly correlated superconductivity, the description of retardation effect is beyond the scope of BCS-based BdG theory.

Now the self-consistency equations (1.112) and (1.113), for the non-trivial $\Delta_s \neq 0$ and $\Delta_d \neq 0$, become

$$1 = \int_{-\hbar\omega_c}^{\hbar\omega_c} d\epsilon g(\epsilon) V_s \frac{1}{2E} \tanh\left(\frac{E}{2k_B T} \right) \approx g(0) V_s \int_0^{\hbar\omega_c} d\epsilon \frac{1}{E} \tanh\left(\frac{E}{2k_B T} \right), \tag{1.117}$$

for the s-wave superconductivity; and

$$\begin{aligned} 1 &= \frac{1}{2\pi}\int_{-\hbar\omega_c}^{\hbar\omega_c}\int_0^{2\pi} d\epsilon d\varphi g(\epsilon) V_d \cos^2(2\varphi)\frac{1}{2E}\tanh\left(\frac{E}{2k_BT}\right) \\ &= \frac{g(0)V_d}{2\pi}\int_0^{\hbar\omega_c}\int_0^{2\pi} d\epsilon d\varphi \cos^2(2\varphi)\frac{1}{E}\tanh\left(\frac{E}{2k_BT}\right), \end{aligned} \tag{1.118}$$

for the d-wave superconductivity. To derive the second line in each of the above two equations, we use the assumption that the density of states changes slightly in the range of $[-\hbar\omega_c, \hbar\omega_c]$ around the Fermi surface and can be approximated by that at the Fermi energy, i.e., $g(0)$. For the temperature $T = 0$ K, an analytical expression for the s-wave superconductors can be obtained

$$\Delta_s(T=0) = \hbar\omega_c \sinh^{-1}\left[\frac{1}{g(0)V_s}\right] \approx 2\hbar\omega_c \exp\left[-\frac{1}{g(0)V_s}\right], \tag{1.119}$$

for $g(0)V_s \ll 1$; while for the d-wave superconductivity, the following numerical solution needs to be found

$$1 = \frac{g(0)V_d}{2\pi}\int_0^{\hbar\omega_c}\int_0^{2\pi} d\epsilon d\varphi \frac{\cos^2(2\varphi)}{\sqrt{\epsilon^2 + \Delta_d^2(T=0)\cos^2(2\varphi)}} \tag{1.120}$$

The condition for the superconducting transition temperature is $\Delta_s = 0$ for s-wave superconductors while $\Delta_d = 0$ for the d-wave superconductors, which leads to

$$1 = g(0)V_s\int_0^{\hbar\omega_c} d\epsilon \frac{1}{\epsilon}\tanh\left(\frac{\epsilon}{2k_BT}\right), \tag{1.121}$$

and

$$1 = \frac{g(0)V_d}{2}\int_0^{\hbar\omega_c} d\epsilon \frac{1}{\epsilon}\tanh\left(\frac{\epsilon}{2k_BT}\right). \tag{1.122}$$

In the condition of $\hbar\omega_c/k_BT_c \gg 1$, we have

$$\begin{aligned} T_c &= \frac{2e^\gamma}{k_B\pi}\hbar\omega_c \exp\left[-\frac{1}{g(0)V_s}\right] \\ &= 1.13\hbar\omega_c \exp\left[-\frac{1}{g(0)V_s}\right] \end{aligned} \tag{1.123}$$

and

$$\begin{aligned} T_c &= \frac{2e^\gamma}{k_B\pi}\hbar\omega_c \exp\left[-\frac{1}{2g(0)V_d}\right] \\ &= 1.13\hbar\omega_c \exp\left[-\frac{1}{2g(0)V_d}\right]. \end{aligned} \tag{1.124}$$

Here the Euler constant $\gamma \approx 0.5772$ is used.
With the BdG solutions as given by Eqs. (1.108) and (1.110), we can find the bulk density of states

$$\frac{\rho_s(E)}{g(0)} = \begin{cases} \frac{E}{\sqrt{E^2-\Delta_s^2}}, & E > \Delta_s \\ 0, & E < \Delta_s \end{cases} \tag{1.125}$$

for the uniform s-wave superconductors, and

$$\frac{\rho_d(E)}{g(0)} = \begin{cases} \int_0^{2\pi} \frac{d\varphi}{2\pi} \frac{E}{\sqrt{E^2-\Delta_d^2\cos^2(2\varphi)}}, & E > |\Delta_d \cos(2\varphi)| \\ 0, & E < |\Delta_d \cos(2\varphi)| \end{cases} \tag{1.126}$$

for the uniform d-wave superconductors. A schematic density of states for both s-wave and d-wave superconductors is shown in Fig. 1.6.

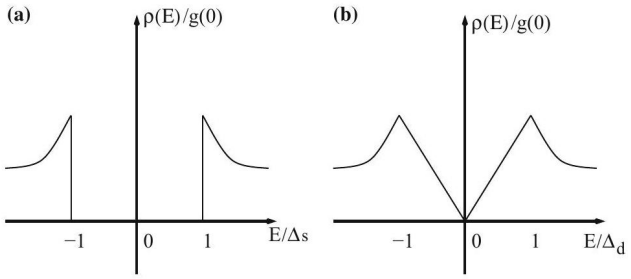


Fig. 1.6 Quasiparticle density of states for a uniform three-dimensional s-wave (a) and a uniform two-dimensional d-wave (b) superconductor

For the s-wave superconductors, a sharp gap feature is seen with vanishing density of states inside the energy range of $[-\Delta_s, \Delta_s]$, while for the d-wave superconductors, the density of states is linear in energy inside $[-\Delta_d, \Delta_d]$, due to the existence of nodal quasiparticles.

All the above discussions demonstrate that, in the homogeneous superconductors, the BdG equations can reproduce all the known results obtained through the Bogoliubov-Valatin canonical transformation. However, as will be demonstrated in later chapters, the BdG equations are more convenient to study the properties of inhomogeneous superconductors.

9.5.5 1.8 Relation of BdG Method to the Abrikosov-Gor'kov Equations

(??? this is what I don't understand now. I'll first write about Abrikosov equation explicitly, then thin about their connection)

Derivation of Abrikosov equations in a new formalism

We should also be aware that the Hamiltonian (1.42) can also be solved via the Green's function technique. We first define a two-component field operator in the Nambu space [44, 45]:

$$\hat{\Psi}(\mathbf{r},\tau) = \begin{pmatrix} \psi_\uparrow(\mathbf{r},\tau) \\ \psi_\downarrow^\dagger(\mathbf{r},\tau) \end{pmatrix}, \tag{1.127}$$

where

$$\psi_\sigma(\mathbf{r},\tau) = e^{\mathscr{H}_{eff}\tau/\hbar}\psi_\sigma(\mathbf{r})e^{-\mathscr{H}_{eff}\tau/\hbar} \tag{1.128}$$

$$\psi_\sigma^\dagger(\mathbf{r},\tau) = e^{eff\tau/\hbar}\psi_\sigma^\dagger(\mathbf{r})e^{-\mathscr{H}_{eff}\tau/\hbar}. \tag{1.129}$$

are the field operators defined in the Heisenberg picture. Note that $\psi_\sigma^\dagger(\mathbf{r},\tau) \neq [\psi_\sigma(\mathbf{r},\tau)]^\dagger$. We can then introduce the Green's function

$$\begin{aligned}\mathscr{G}\left(\mathbf{r}\tau;\mathbf{r}'\tau'\right) &= -\left\langle T_\tau\left[\hat{\Psi}(\mathbf{r},\tau)\otimes\hat{\Psi}^\dagger\left(\mathbf{r}',\tau'\right)\right]\right\rangle \\ &= -\theta\left(\tau-\tau'\right)\left\langle\hat{\Psi}(\mathbf{r},\tau)\otimes\hat{\Psi}^\dagger\left(\mathbf{r}',\tau'\right)\right\rangle+\theta\left(\tau'-\tau\right)\left\langle\hat{\Psi}^\dagger\left(\mathbf{r}',\tau'\right)\otimes\hat{\Psi}(\mathbf{r},\tau)\right\rangle \end{aligned} \tag{1.130}$$

Here $\otimes$ means the direct product of two vector fields. The bracket $\langle\ldots\rangle$ means the statistic average

$$\langle\hat{O}\rangle = \mathrm{Tr}\left[e^{-\beta\left(\mathscr{H}_{eff}-\Omega\right)}\hat{O}\right] \tag{1.131}$$

with the thermodynamic potential Ω given by

$$e^{-\beta\Omega} = \mathrm{Tr}\left[e^{-\beta\mathscr{H}_{eff}}\right] \tag{1.132}$$

The factor T_τ is a τ-ordering operator, which arranges operators with earliest time τ to the right. The subscript τ is affixed to T to distinguish T_τ from the temperature. In expanded form, the Green's function becomes

$$\mathscr{G}(\mathbf{r}\tau;\mathbf{r}'\tau') = \begin{pmatrix} -\langle T_\tau[\psi_\uparrow(\mathbf{r},\tau)\psi_\uparrow^\dagger(\mathbf{r}',\tau')]\rangle - \langle T_\tau[\psi_\uparrow(\mathbf{r},\tau)\psi_\downarrow(\mathbf{r}',\tau')]\rangle \\ -\langle T_\tau[\psi_\downarrow^\dagger(\mathbf{r},\tau)\psi_\uparrow^\dagger(\mathbf{r}',\tau')]\rangle - \langle T_\tau[\psi_\downarrow^\dagger(\mathbf{r},\tau)\psi_\downarrow(\mathbf{r}',\tau')]\rangle \end{pmatrix}, \tag{1.133}$$

(?? this is 4x4 matrix, right?)

Since the trace is unchanged upon a cyclic variation of operators, we can easily prove that the Green's function is a function of the difference $\tau-\tau'$, that is,

$$\mathscr{G}\left(\mathbf{r}\tau;\mathbf{r}'\tau'\right) = \mathscr{G}\left(\mathbf{r},\mathbf{r}';\tau-\tau'\right), \tag{1.134}$$

with $\tau-\tau'$ restricted in the range of $[-\beta,\beta]$ and the factor $\beta = 1/k_BT$. Therefore, the Fourier transform is given by

$$\mathscr{G}\left(\mathbf{r},\mathbf{r}';i\omega_n\right) = \int_0^{\beta\hbar} d\tau e^{i\omega_n\tau}\mathscr{G}\left(\mathbf{r},\mathbf{r}';\tau\right) \tag{1.135}$$

$$\mathscr{G}\left(\mathbf{r},\mathbf{r}';\tau\right) = \frac{1}{\beta}\sum_n e^{-i\omega_n\tau}\mathscr{G}\left(\mathbf{r},\mathbf{r}';i\omega_n\right) \tag{1.136}$$

where the Matsubara frequency $\omega_n = (2n+1)\pi k_BT/\hbar$ with $n=-\infty,\ldots,-1,0,1,\ldots,\infty$. Using the equation of motion for $\psi_\sigma(\mathbf{r},\tau)$ and $\psi_\sigma^\dagger(\mathbf{r},\tau)$:

$$\begin{aligned} -\hbar\tfrac{\partial\psi_\sigma(\mathbf{r},\tau)}{\partial\tau} &= \left[\psi_\sigma(\mathbf{r},\tau),\mathscr{H}_{eff}\right]_-, \\ -\hbar\tfrac{\partial\psi_\sigma^\dagger(\mathbf{r},\tau)}{\partial\tau} &= \left[\psi_\sigma^\dagger(\mathbf{r},\tau),\mathscr{H}_{eff}\right]_-, \end{aligned} \tag{1.138}$$

and Eq.(1.47), we can obtain the equation of motion for the Green's function

$$\int d\mathbf{r}''\hat{M}\left(\mathbf{r},\mathbf{r}'';\tau\right)\mathscr{G}\left(\mathbf{r}''\tau;\mathbf{r}'\tau'\right) = \delta\left(\mathbf{r}-\mathbf{r}'\right)\delta\left(\tau-\tau'\right)\hat{1} \tag{1.139}$$

with

$$\hat{M}\left(\mathbf{r},\mathbf{r}',\tau\right) = \begin{pmatrix} \left(-\frac{\partial}{\partial\tau}-h_\uparrow(\mathbf{r})\right)\delta\left(\mathbf{r}-\mathbf{r}'\right) & -\Delta\left(\mathbf{r},\mathbf{r}'\right) \\ -\Delta^*\left(\mathbf{r}',\mathbf{r}\right) & \left(-\frac{\partial}{\partial\tau}+h_\downarrow^*(\mathbf{r})\right)\delta_{ij} \end{pmatrix}. \tag{1.140}$$

for the spin-single pairing case, and subject to the self-consistency condition:

$$\Delta(\mathbf{r},\mathbf{r}') = -V(\mathbf{r},\mathbf{r}')\mathscr{G}_{12}\left(\mathbf{r}\tau \to \tau' + 0^+, \mathbf{r}'\tau'\right) \tag{1.141}$$

$$\Delta^*(\mathbf{r},\mathbf{r}') = -V(\mathbf{r},\mathbf{r}')\mathscr{G}_{21}\left(\mathbf{r}'\tau \to \tau' + 0^+, \mathbf{r}\tau'\right) \tag{1.142}$$

Equation (1.139) is the famous Abrisokov-Gorkov equations [46] for superconductivity in the continuum model.

(????? why?????)

This set of equations is also the starting point for the derivation of Ginzburg-Landau theory. When the order parameter varies slowly in space, the approximate Ginzburg-Landau theory is simpler to solve than the original Abrisokov-Gorkov theory.

Relation between BdG and AG equations

The Abrikosov-Gorkov theory is closely related to the BdG theory. With the time dependence of the quasiparticle operators:

$$\gamma_n(\tau) = \gamma_n e^{-E_n\tau/\hbar} \tag{1.143}$$

$$\gamma_n^\dagger(\tau) = \gamma_n^\dagger e^{E_n\tau/\hbar}. \tag{1.144}$$

and the canonical transformation, we can obtain for example:

$$\begin{aligned}\mathscr{G}_{11}(\mathbf{r},\mathbf{r}';\tau) =& -\theta(\tau)\sum_{\tilde{n}}\left[u_\uparrow^{\tilde{n}1}(\mathbf{r})u_\uparrow^{\tilde{n}1*}(\mathbf{r}')f(-E_{\tilde{n}1})e^{-E_{\tilde{n}1}\tau/\hbar} + v_\uparrow^{\tilde{n}2*}(\mathbf{r})v_\uparrow^{\tilde{n}_2}(\mathbf{r}')f(E_{\tilde{n}2})e^{E_{\tilde{n}2}\tau/\hbar}\right]\\ &+\theta(-\tau)\sum_{\tilde{n}}\left[u_\uparrow^{\tilde{n}1*}(\mathbf{r}')u_\uparrow^{\tilde{n}1}(\mathbf{r})f\left(E_{\tilde{n}1}e^{-E_{\tilde{n}1}\tau/\hbar} + v_\uparrow^{\tilde{n}2*}(\mathbf{r}')v_\uparrow^{\tilde{n}2}(\mathbf{r})f(-E_{\tilde{n}2})e^{E_{\tilde{n}2}\tau/\hbar}\right],\end{aligned} \tag{1.145}$$

and

$$\begin{aligned}\mathscr{G}_{22}(\mathbf{r},\mathbf{r}';\tau) =& -\theta(\tau)\sum_{\tilde{n}}\left[u_\downarrow^{\tilde{n}2*}(\mathbf{r})u_\downarrow^{\tilde{n}2}(\mathbf{r}')f(E_{\tilde{n}2})e^{E_{\tilde{n}2}\tau/\hbar} + v_\downarrow^{\tilde{n}1}(\mathbf{r})v_\downarrow^{\tilde{n}1*}(\mathbf{r}')f(-E_{\tilde{n}1})e^{-E_{\tilde{n}1}\tau/\hbar}\right]\\ &+\theta(-\tau)\sum_{n}\left[u_\downarrow^{\tilde{n}2}(\mathbf{r}')u_\downarrow^{\tilde{n}_2}(\mathbf{r})f(-E_{\tilde{n}2})e^{E_{\tilde{n}2}\tau/\hbar} + v_\downarrow^{\tilde{n}1*}(\mathbf{r}')v_\downarrow^{\tilde{1}1}(\mathbf{r})f(E_{\tilde{n}1})e^{-E_{\tilde{n}1}\tau/\hbar}\right].\end{aligned} \tag{1.146}$$

It is straightforward to obtain the Green's function in the frequency domain

$$\begin{aligned}&\mathscr{G}_{11}(\mathbf{r},\mathbf{r}';i\omega_n) = \int_0^{\beta\hbar} d\tau e^{i\omega_n\tau}\mathscr{G}_{11}(\mathbf{r},\mathbf{r}';\tau)\\ =& -{\sum_{\tilde{n}}}'\left[u_\uparrow^{\tilde{n}1}(\mathbf{r})u_\uparrow^{\tilde{n}1*}(\mathbf{r}')f(-E_{\tilde{n}1})\int_0^{\beta\hbar}d\tau e^{(i\omega_n - E_{\tilde{n}1}/\hbar)\tau} + v_\uparrow^{\tilde{n}2*}(\mathbf{r})v_\uparrow^{\tilde{n}2}(\mathbf{r}')f(E_{\tilde{n}2})\int_0^{\beta\hbar}d\tau e^{(i\omega_n + E_{\tilde{n}2}/\hbar)\tau}\right]\\ =& -{\sum_{\tilde{n}}}'\left\{\frac{u_\uparrow^{\tilde{n}1}(\mathbf{r})u_\uparrow^{\tilde{n}1*}(\mathbf{r}')}{i\omega_n - E_{\tilde{n}1}/\hbar}f(-E_{\tilde{n}1})\left(e^{\beta\hbar(i\omega_n - E_{\tilde{n}1}/\hbar)} - 1\right) + \frac{v_\uparrow^{\tilde{n}2*}\left((\mathbf{r})v_\uparrow^{\tilde{n}2}(\mathbf{r}')\right.}{i\omega_n + E_{\tilde{n}2}/\hbar}f(E_{\tilde{n}2})\left(e^{\beta\hbar(i\omega_n + E_{\tilde{n}2}/\hbar)} - 1\right)\right\}\\ =& {\sum_{\tilde{n}}}'\left[\frac{u_\uparrow^{\tilde{n}1}(\mathbf{r})u_\uparrow^{\tilde{n}1*}(\mathbf{r}')}{i\omega_n - E_{\tilde{n}1}/\hbar} + \frac{v_\uparrow^{\tilde{n}2*}(\mathbf{r})v_\uparrow^{\tilde{n}2}(\mathbf{r}')}{i\omega_n + E_{\tilde{n}2}/\hbar}\right],\end{aligned} \tag{1.147}$$

and

$$
\begin{aligned}
&\mathscr{G}_{22}(\mathbf{r},\mathbf{r}';i\omega_n)=\int_0^{\beta\hbar}d\tau e^{i\omega_n\tau}\mathscr{G}_{22}\left(\mathbf{r},\mathbf{r}';\tau\right)\\
&=-\sum_{\tilde{n}}{}'\left[u_{\downarrow}^{\tilde{n}2*}(\mathbf{r})u_{\downarrow}^{\tilde{n}2}\left(\mathbf{r}'\right)f\left(E_{\tilde{n}2}\right)\int_0^{\beta\hbar}d\tau e^{(i\omega_n+E_{\tilde{n}2}/\hbar)\tau}+v_{\downarrow}^{\tilde{n}1}(\mathbf{r})v_{\downarrow}^{\tilde{n}1*}\left(\mathbf{r}'\right)f\left(-E_{\tilde{n}1}\right)\int_0^{\beta\hbar}d\tau e^{(i\omega_n+E_{\tilde{n}1}/\hbar)\tau}\right]\\
&=-\sum_{\tilde{n}}{}'\left\{\frac{u_{\downarrow}^{\tilde{n}2*}(\mathbf{r})u_{\downarrow}^{\tilde{n}2}\left(\mathbf{r}'\right)}{i\omega_n+E_{\tilde{n}2}/\hbar}f\left(E_{\tilde{n}2}\right)\left(e^{\beta\hbar(i\omega_n+E_{\tilde{n}2}/\hbar)}-1\right)+\frac{v_{\downarrow}^{\tilde{n}1}(\mathbf{r})v_{\downarrow}^{\tilde{n}1*}\left(\mathbf{r}'\right)}{i\omega_n-E_{\tilde{n}1}/\hbar}f\left(E_{\tilde{n}1}\right)\left(e^{\beta\hbar(i\omega_n-E_{\tilde{n}1}/\hbar)}-1\right)\right\}\\
&=\sum_{\tilde{n}}{}'\left[\frac{u_{\downarrow}^{\tilde{n}2*}(\mathbf{r})u_{\downarrow}^{\tilde{n}}\left(\mathbf{r}'\right)}{i\omega_n+E_{\tilde{n}2}/\hbar}+\frac{v_{\downarrow}^{\tilde{n}1}(\mathbf{r})v_{\downarrow}^{\tilde{n}1*}\left(\mathbf{r}'\right)}{i\omega_n-E_{\tilde{n}1}/\hbar}\right].
\end{aligned}
\tag{1.148}
$$

Here we have used the fact that

$$
e^{i\omega_n\beta\hbar}=-1 \tag{1.149}
$$

In addition, if we know the solution to the Abrikosov-Gorkov equations of motion for the Green's functions, the local density of states can be calculated as

$$
\begin{aligned}
\rho_{\uparrow}(\mathbf{r},E)&=-\frac{1}{\hbar\pi}\operatorname{Im}\left[\mathscr{G}_{11}\left(\mathbf{r},\mathbf{r};i\omega_n\rightarrow E/\hbar+i0^{+}\right)\right]\\
&=\sum_{\tilde{n}}{}'\left[\left|u_{\uparrow}^{\tilde{n}1}(\mathbf{r})\right|^2\delta\left(E-E_{\tilde{n}1}\right)+\left|v_{\uparrow}^{\tilde{n}2}(\mathbf{r})\right|^2\delta\left(E+E_{\tilde{n}2}\right)\right],
\end{aligned}
\tag{1.150}
$$

and

$$
\begin{aligned}
\rho_{\downarrow}(\mathbf{r},E)&=\frac{1}{\hbar\pi}\operatorname{Im}\left[\mathscr{G}_{22}\left(\mathbf{r},\mathbf{r};-i\omega_n\rightarrow-\left(E/\hbar+i0^{+}\right)\right)\right]\\
&=\sum_{\tilde{n}}{}'\left[\left|u_{\downarrow}^{\tilde{\tilde{2}}2}(\mathbf{r})\right|^2\delta\left(E-E_{\tilde{n}2}\right)+\left|v_{\downarrow}^{\tilde{n}1}(\mathbf{r})\right|^2\delta\left(E+E_{\tilde{n}2}\right)\right].
\end{aligned}
\tag{1.151}
$$

Here we have used the following identity for the real frequency ω

$$
\frac{1}{\omega\pm i0^{+}}=\mathscr{P}\frac{1}{\omega}\mp i\pi\delta(\omega) \tag{1.152}
$$

with $\mathscr{P}$ denotes a Cauchy principal value. Therefore, we have demonstrated an exact relation between the BdG theory and the Abrikosov-Gorkov theory.

(????? what is it???)

9.6 Transport Across Normal-Metal/Superconductor Junctions

I'LL ADD THEORY BELOW FROM ORIGINAL PAPERS TO THIS SECTION!!!

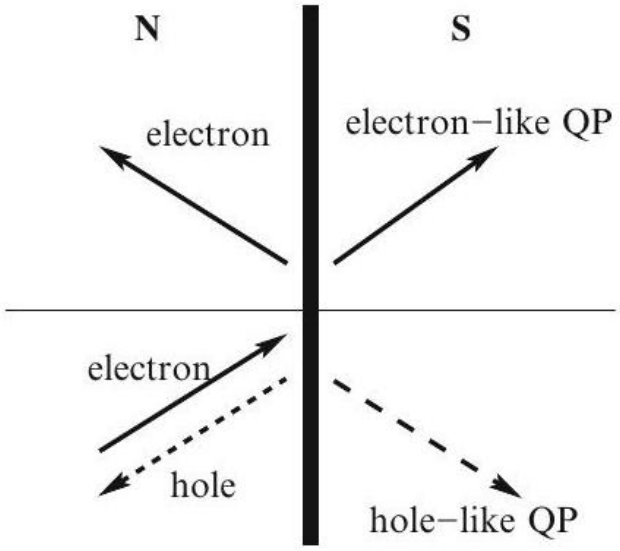
9.6.1 6.1 Blonder-Tinkham-Klapwijk Scattering Formalism

(!!! I'll later WRITE WHAT IS BTK FORMALISM IN ONE LINE!!!! TO MAKE SURE THAT I UNDERSTAND IT.)

Theory

In a phase-coherent normal-superconducting hybrid structure, electrons are not only intrinsically coherent in the superconducting part but also retain phase memory all through the normal conducting region. Therefore, the transport properties are determined in detail by the quasiparticle states produced by elastic scattering from inhomogeneities and boundaries. In the presence of superconductivity, a scattering process known as the Andreev reflection [1] occurs: As shown schematically in Fig.6.1, an electron incident from the normal conductor with an energy below the superconducting quasiparticle energy gap cannot drain off individually into the superconductor. It is instead coherently reflected from the normal-metal/superconductor (NS) interface as a hole by transferring a charge $-2e$ to the superconductor. This process goes beyond the lowest-order description within the tunneling Hamiltonian model for the NS junction, which predicts that the tunneling conductance is proportional to the density of states. In 1982, Blonder, Tinkham, and Klapwijk [2] (BTK) pointed out that the contribution to the subgap conductance from the Andreev reflection can be significant, and further developed a scattering theory of transport through an NS interface with the arbitrary barrier strength.

Fig. 6.1 Schematic drawing of the scattering process for an incident electron beam impinged upon a normal-metal superconductor interface



We now discuss the derivation of the BTK formula. The time-dependent BdG equations can be directly generalized from Eq.(1.60)

$$h_{\uparrow}(\mathbf{r})f(\mathbf{r},t)+\int d\mathbf{r}'\Delta\left(\mathbf{r},\mathbf{r}'\right)g\left(\mathbf{r}',t\right)=i\hbar\frac{\partial f(\mathbf{r},t)}{\partial t} \tag{6.1a}$$

$$\int d\mathbf{r}'\Delta^{*}\left(\mathbf{r}',\mathbf{r}\right)f\left(\mathbf{r}',t\right)-h_{\downarrow}^{*}(\mathbf{r})g(\mathbf{r},t)=i\hbar\frac{\partial g(\mathbf{r},t)}{\partial t} \tag{6.1b}$$

Now the time dependence of the potentials is included implicitly. From the above equation, we derive the continuity equation for BdG quasiparticles. We multiply Eq. (6.1a) on both sides from the left by $f^{*}(\mathbf{r},t)$ while Eq. (6.1b) by $g^{*}(\mathbf{r},t)$ such that

$$f^{*}(\mathbf{r},t)h_{\uparrow}(\mathbf{r})f(\mathbf{r},t)+\int d\mathbf{r}'f^{*}(\mathbf{r},t)\Delta\left(\mathbf{r},\mathbf{r}'\right)g\left(\mathbf{r}',t\right)=i\hbar f^{*}(\mathbf{r},t)\frac{\partial f(\mathbf{r},t)}{\partial t}$$

$$\int d\mathbf{r}'g^{*}(\mathbf{r},t)\Delta^{*}\left(\mathbf{r}',\mathbf{r}\right)f\left(\mathbf{r}',t\right)-g^{*}(\mathbf{r},t)h_{\downarrow}^{*}(\mathbf{r})g(\mathbf{r},t)=i\hbar g^{*}(\mathbf{r},t)\frac{\partial g(\mathbf{r},t)}{\partial t}$$

We then take the complex conjugation to the above two expressions

$$-f(\mathbf{r},t)h_{\uparrow}^{*}(\mathbf{r})f^{*}(\mathbf{r},t)-\int d\mathbf{r}'f(\mathbf{r},t)\Delta^{*}\left(\mathbf{r},\mathbf{r}'\right)g^{*}\left(\mathbf{r}',t\right)=i\hbar f(\mathbf{r},t)\frac{\partial f^{*}(\mathbf{r},t)}{\partial t}$$
$$-\int d\mathbf{r}'g(\mathbf{r},t)\Delta\left(\mathbf{r}',\mathbf{r}\right)f^{*}\left(\mathbf{r}',t\right)+g(\mathbf{r},t)h_{\downarrow}(\mathbf{r})g^{*}(\mathbf{r},t)=i\hbar g(\mathbf{r},t)\frac{\partial g^{*}(\mathbf{r},t)}{\partial t}$$

Combine the above two sets of equations together, we arrive at

$$\frac{\partial|f(\mathbf{r},t)|^{2}}{\partial t}+\nabla\cdot\mathbf{J}_{1}=S_{1}, \tag{6.4}$$
$$\frac{\partial|g(\mathbf{r},t)|^{2}}{\partial t}+\nabla\cdot\mathbf{J}_{2}=S_{2} \tag{6.5}$$

where

$$\mathbf{J}_{1}=\mathrm{Re}\left[f^{*}(\mathbf{r},t)\mathbf{v}_{e}f(\mathbf{r},t)\right] \tag{6.6}$$
$$\mathbf{J}_{2}=-\mathrm{Re}\left[g^{*}(\mathbf{r},t)\mathbf{v}_{h}g(\mathbf{r},t)\right] \tag{6.7}$$

with the mechanical velocity of electron and hole as

$$\mathbf{v}_{e}=(\mathbf{p}+e\mathbf{A})/m_{e},\quad \mathbf{v}_{h}=(\mathbf{p}-e\mathbf{A})/m_{e} \tag{6.8}$$

The source term are respectively given by

$$S_{1}=\frac{2}{\hbar}\,\mathrm{Im}\left[f^{*}(\mathbf{r},t)\Delta\left(\mathbf{r},\mathbf{r}'\right)g\left(\mathbf{r}',t\right)\right] \tag{6.9}$$

and

$$S_{2}=\frac{2}{\hbar}\,\mathrm{Im}\left[g^{*}(\mathbf{r},t)\Delta^{*}\left(\mathbf{r}',\mathbf{r}\right)f\left(\mathbf{r}',t\right)\right] \tag{6.10}$$

The total particle density is defined as the probability density for finding an electron or a hole at a particular time t and position $\mathbf{r}$,

$$P(\mathbf{r},t)=2\sum_{n}f\left(E_{n}\right)\left[|f^{n}(\mathbf{r},t)|^{2}+|g^{n}(\mathbf{r},t)|^{2}\right]. \tag{6.11}$$

Correspondingly, the quasiparticle current density is given by

$$\mathbf{J}_{P}=2\sum_{n}f\left(E_{n}\right)\left[\mathbf{J}_{1}^{n}+\mathbf{J}_{2}^{n}\right], \tag{6.12}$$

and the source term

$$S_{P}=2\sum_{n}f\left(E_{n}\right)\left[S_{1}^{n}+S_{2}^{n}\right] \tag{6.13}$$

The charge density is defined as follows

$$Q(\mathbf{r},t)=-2e\sum_{n}\left\{f\left(E_{n}\right)|f^{n}(\mathbf{r},t)|^{2}+\left[1-f\left(E_{n}\right)\right]|g^{n}(\mathbf{r},t)|^{2}\right\} \tag{6.14}$$

Correspondingly, the electrical current density should be

$$\begin{aligned}\mathbf{J}_Q &= -2e\sum_n \left\{f\left(E_n\right)\mathbf{J}_1^n + \left[1-f\left(E_n\right)\right]\mathbf{J}_2^n\right\} \\ &= -2e\sum_n \left\{f\left(E_n\right)\mathrm{Re}\left[f^{n*}(\mathbf{r},t)\mathbf{v}_e f^n(\mathbf{r},t)\right]\right. \\ &\quad \left.-\left[1-f\left(E_n\right)\right]\mathrm{Re}\left[g^{n*}(\mathbf{r},t)\mathbf{v}_h g^n(\mathbf{r},t)\right]\right\}, \\ &= \frac{-2e\hbar}{m}\sum_n \left\{f\left(E_n\right)\mathrm{Im}\left[f^{n*}(\mathbf{r},t)(\nabla + ie\mathbf{A}/\hbar c)f^n(\mathbf{r},t)\right]\right. \\ &\quad \left.-\left[1-f\left(E_n\right)\right]\mathrm{Im}\left[g^{n*}(\mathbf{r},t)(\nabla - ie\mathbf{A}/\hbar c)g^n(\mathbf{r},t)\right]\right\}, \end{aligned} \tag{6.15}$$

and the source term is

$$S_Q = -2e\sum_n \left\{f\left(E_n\right)S_1^n + \left[1-f\left(E_n\right)\right]S_2^n\right] \tag{6.16}$$

The vector potential $\mathbf{A}(\mathbf{r})$ entering the BdG equations is in turn related to the electrical current distribution $\mathbf{J}_Q(\mathbf{r})$ by Maxwell's equation

$$\nabla \times (\nabla \times \mathbf{A}) = \frac{4\pi}{c}\mathbf{J}_Q \tag{6.17}$$

It should be pointed out that the two-fold spin degeneracy has been included explicitly. At a first glance, the current are not conserved. However, if we take into account the self-consistency condition about the pair potential, we can check that the source term S_Q is zero. For this reason, in non-self-consistent theory the current is evaluated in the normal region (where the current is conserved since the pair potential is zero) and the current in the superconducting region is inferred indirectly. Obviously, the source term S_P can never become zero, which is allowed by the mother nature itself in the superconductivity. We refer to [2-4] for more discussion of these definitions. The present current expression has been used to study the transport properties through a superconducting point contact [5].

The BTK transport theory is based on the assumption that the electrons are ballistically accelerated without scattering before they hit the NS interface. In addition, one assumes that the distribution functions of all incoming particles are given by equilibrium Fermi-Dirac functions, apart from the energy shift due to the voltage bias. It is convenient to choose the electrochemical potential of the electrons in the superconductor as the reference since it remains a well-defined quantity even when the quasiparticle populations are far from equilibrium. With this convention, all incoming electrons from the superconductor side have the distribution function $f_{FD}(E)$, while those coming in from the normal-metal side have the distribution function $f_{FD}(E-eV)$. Since the current must be conserved, we can evaluate it in any plane for an actual two-dimensional or three-dimensional geometry. For a planar junction, we can always first calculate the current for a given incident direction of electron beams, with angle θ, as shown in Fig. 6.1, from which the total current can be obtained by integrating over the transverse momentum. Assuming the current flow along the x-direction, which is perpendicular the NS junction, we can write the current as

$$I(\theta, V) = 2N(0)ev_{F,x}\mathscr{A}\int_{-\infty}^{\infty}\left[f_{\rightarrow}(E) - f_{\leftarrow}(E)\right]dE. \tag{6.18}$$

Here $\mathscr{A}$ is the cross-sectional area of the interface, $N(0)$ is the one-spin density of states at the Fermi energy at ϵ_F, and $v_{F,x} = v_F\cos\theta$. With the assumption about the incoming populations, it follows that

$$f_{\rightarrow}(E) = f_{FD}(E - eV), \tag{6.19}$$

while

$$f_{\leftarrow}(E) = A(E)\left[1 - f_{\rightarrow}(E)\right] + B(E)f_{\rightarrow}(E) + [C(E) + D(E)]f_{FD}(E). \tag{6.20}$$

Here the probabilities $A(E), B(E), C(E)$, and $D(E)$ are for normal reflection, Andreev reflection, transmission through the interface with a wave vector on the same side of the Fermi surface and that crossing the Fermi surface. We have represented the current incident from the superconducting side in terms of the summation of $C(E)$ and $D(E)$. Substituting Eqs. (6.19) and (6.20) into Eq. (6.18), we arrive at

$$I(\theta, V) = 2N(0)ev_{F,x}\mathscr{A}\int_{-\infty}^{\infty}\left[f_{FD}(E - eV) - f_{FD}(E)\right]\left[1 + A(E) - B(E)\right]dE. \tag{6.21}$$

Here we have used the symmetry that the probabilities $A(E), B(E), C(E)$, and $D(E)$ are even functions of E, and $f_{FD}(-E) = 1 - f_{FD}(E)$. The quantity $1 + A(E) - B(E)$ can be referred as the transmission coefficient for electrical current. It shows that while the ordinary reflection (described by $B(E)$) reduces the current, the Andreev reflection (described by $A(E)$) increases the current by giving one electron to form a Cooper pair together with the incident electron. From Eq. (6.21), we can also obtain the differential conductance for a given incident direction of electrons as:

$$G_{NS}(\theta, V) = \frac{\partial I(\theta)}{\partial V} = 2N(0)e^2v_{F,x}\mathscr{A}\int_{-\infty}^{\infty}\left[-\frac{f_{FD}(E - eV)}{\partial E}\right]\left[1 + A(E) - B(E)\right]dE. \tag{6.22}$$

At zero temperature, we have

$$-\frac{\partial f_{FD}(E - eV)}{\partial E} = \delta(E - eV), \tag{6.23}$$

which leads to

$$G_{NS}(\theta, V) = 2N(0)e^2v_{F,x}\mathscr{A}[1 + A(eV) - B(eV)] \tag{6.24}$$

Equations (6.22) and (6.24) represent the BTK scattering formalization for the transport across the NS junction, while the BdG equations provide a framework to evaluate the reflection probability quantitatively. Interestingly, the BTK formula can also be considered as the revised version of the Landauer-Büttiker formula [6, 7] for an NS junction. The latter has been extensively used to describe the quantum coherent transport in mesoscopic normal conductors. We first point out that the original BTK theory is applicable to a junction with translational invariance along the NS interface. A more general Landauer-Büttiker-like theory has been developed [8-12] to describe the quantum phase-coherence transport through normalmetal superconductor hybrid structures. With this generalized theory, the zero-bias conductance anomaly observed in the differential conductance of a semiconductor in contact with a conventional s-wave superconductor [13-15] has been interpreted as a combined consequence of multiple impurity scattering inside the semiconductor and the Andreev reflection at the interface [11, 16]. The generalized scattering formalism can also be cast into the random matrix theory [17] to study the excess conductance of semiconductor-superconductor junctions, where the elastic impurity scattering in the normal region is important.

In this chapter, we consider no impurity scattering at the NS interface and instead focus on the consequence of superconducting pairing symmetry on the conductance. Part of the

motivation comes from the observation of zero-bias conductance peak (ZBCP) when electrons are tunneling into the *ab*-oriented thin films of high-temperature superconductors [18-21]. This ZBCP cannot be explained by conventional tunneling theories. Although the feature was originally analyzed based on the conventional *s*-wave tunneling model by introducing the spin-flip scattering of the tunnel electrons from magnetic impurities speculated to exist in the insulating barrier, the mechanism is inconsistent with the experimentally observed nonlinear splitting of the ZBCP with the magnetic field and the absence of the ZBCP in the tunneling conductance of *c*-axis-oriented YBaCuO/Pb junctions. Now it has become clear [22-25] that the ZBCP observed in high-temperature cuprates originates instead from the *d*-wave pairing symmetry.

9.6.2 6.2 Tunneling Conductance Through a NS Junction

Theory

Without loss of generality, we consider a two-dimensional normal-metal /superconductor junction. The setup is relevant to the high-temperature cuprates, where the superconductivity emerges mainly in the two-dimensional copper-oxide plane. As we have derived in Chap. 1, the motion of quasiparticles in a normal-metal superconductor junction can be described by the BdG equation (1.60)

$$\mathscr{H}_e(\mathbf{r})u(\mathbf{r}) + \int d\mathbf{r}'\Delta\left(\mathbf{r},\mathbf{r}'\right)v\left(\mathbf{r}'\right) = Eu(\mathbf{r}) \tag{6.25a}$$

$$-\mathscr{H}_e^*(\mathbf{r})v(\mathbf{r}) + \int d\mathbf{r}'\Delta^*\left(\mathbf{r}',\mathbf{r}\right)u\left(\mathbf{r}'\right) = Ev(\mathbf{r}) \tag{6.25b}$$

Here $(u(\mathbf{r}), v(\mathbf{r}))$ is the quasiparticle wave function of the BdG equations. $\mathscr{H}_e(\mathbf{r}) = -\hbar^2\nabla_{\mathbf{r}}^2/2m_e + V(\mathbf{r}) - E_F$ is the single-particle Hamiltonian, where $V(\mathbf{r})$ is the usual static potential, and E_F is the Fermi energy. Therefore, the excitation energy is
measured with respect to the Fermi energy E_F. Again we have dropped the spin indices to the quasiparticle wave function for the case without spin-polarization and spin-flip scattering. $\Delta\left(\mathbf{r},\mathbf{r}'\right)$ is the pair potential, the dependence of which on $\mathbf{r}$ and $\mathbf{r}'$ cannot be reduced to a dependence on the difference of the two coordinates, that is, $\mathbf{r}-\mathbf{r}'$, for an inhomogeneous case. By introducing the center-of-mass coordinates $\mathbf{R} = \left(\mathbf{r}+\mathbf{r}'\right)/2$ and the relative coordinates $\mathbf{s} = \mathbf{r}-\mathbf{r}'$, we can write the pair potential in terms of $\mathbf{R}$ and $\mathbf{r}$

$$\tilde{\Delta}(\mathbf{R},\mathbf{s}) \equiv \Delta\left(\mathbf{r},\mathbf{r}'\right) \tag{6.26}$$

By performing the Fourier transform with respect to the relative coordinate s, we can write the pair potential in the mixed representation

$$\tilde{\Delta}(\mathbf{R},\mathbf{k}) = \int d\mathbf{s}\tilde{\Delta}\left(\mathbf{R}+\frac{\mathbf{s}}{2},\mathbf{R}-\frac{\mathbf{s}}{2}\right)e^{-i\mathbf{k}\cdot\mathbf{s}} \tag{6.27}$$

This shows clearly that for an unconventional superconductor like that with d wave pairing symmetry, the pair potential depends not only on the center-of-mass coordinate $\mathbf{R}$ but also on the relative wave vector $\mathbf{k}$, which in the weak-coupling theory is fixed on the Fermi surface such that only its direction $\hat{\mathbf{k}}_F = \mathbf{k}_F/k_F$ is a variable, where k_F is the magnitude of the Fermi wave vector.

An investigation of the BdG equations shows that $u(\mathbf{r})$ and $v(\mathbf{r})$ oscillate on the scale of the superconducting coherence length $\xi_0 = \hbar v_F/2\Delta_0$, which is much larger than the inverse Fermi wave vector k_F^{-1}. Here v_F is the Fermi velocity and Δ_0 is the maximum value of the pair potential in the bulk region of the superconductor. Therefore, we can introduce a new set of wave functions

$$\begin{pmatrix}\bar{u}(\mathbf{r})\\ \bar{v}(\mathbf{r})\end{pmatrix} = e^{-i\mathbf{k}_F\cdot\mathbf{r}}\begin{pmatrix}u(\mathbf{r})\\ v(\mathbf{r})\end{pmatrix}, \tag{6.28}$$

to divide out the fast oscillation. The substitution of Eq. (6.28) into Eq. (6.25) leads to the Andreev equations [1, 26]:

$$E\bar{u}(\mathbf{r}) = -i\left(\hbar^2/m_e\right)\mathbf{k}_F\cdot\nabla\bar{u}(\mathbf{r}) + \tilde{\Delta}\left(\mathbf{r},\hat{\mathbf{k}}_F\right)\bar{v}(\mathbf{r}) \tag{6.29a}$$

$$E\bar{v}(\mathbf{r}) = i\left(\hbar^2/m_e\right)\mathbf{k}_F\cdot\nabla\bar{v}(\mathbf{r}) + \tilde{\Delta}^*\left(\mathbf{r},\hat{\mathbf{k}}_F\right)\bar{u}(\mathbf{r}) \tag{6.29b}$$

when we retain only terms of the lowest order in $(k_F\xi_0)^{-1}$. We show this by looking at

$$\int d\mathbf{r}'\Delta\left(\mathbf{r},\mathbf{r}'\right)\bar{v}\left(\mathbf{r}'\right)e^{-i\mathbf{k}\cdot(\mathbf{r}-\mathbf{r}')} = \int d\mathbf{s}\tilde{\Delta}(\mathbf{r}-\mathbf{s}/2,\mathbf{s})\bar{v}(\mathbf{r}-\mathbf{s})e^{-i\mathbf{k}\cdot\mathbf{s}} \tag{6.30}$$

Assuming that $\bar{v}(\mathbf{r})$ is a slowly varying function as is $\tilde{\Delta}(\mathbf{R},\mathbf{s})$ in the first argument

$$\begin{aligned}\tilde{\Delta}(\mathbf{r}-\mathbf{s}/2,\mathbf{s}) &\approx \tilde{\Delta}(\mathbf{r},\mathbf{s}) - \mathbf{s}\cdot\nabla_{\mathbf{r}}\tilde{\Delta}(\mathbf{r},\mathbf{s})/2,\\ \bar{v}(\mathbf{r}-\mathbf{s}) &\approx \bar{v}(\mathbf{r}) - \mathbf{s}\cdot\nabla_{\mathbf{r}}\bar{v}(\mathbf{r}),\end{aligned}$$

we have

$$\begin{aligned}&\int d\mathbf{s}\tilde{\Delta}(\mathbf{r}-\mathbf{s}/2,\mathbf{s})\bar{v}(\mathbf{r}-\mathbf{s})e^{-i\mathbf{k}\cdot\mathbf{s}} = \int d\mathbf{s}\left[\tilde{\Delta}(\mathbf{r},\mathbf{s}) - \mathbf{s}\cdot\nabla_{\mathbf{r}}\tilde{\Delta}(\mathbf{r},\mathbf{s})/2\right]\left[\bar{v}(\mathbf{r}) - \mathbf{s}\cdot\nabla_{\mathbf{r}}\bar{v}(\mathbf{r})\right]\\ \approx&\int d\mathbf{s}\tilde{\delta}(\mathbf{r},\mathbf{s})\bar{v}(\mathbf{r})e^{-i\mathbf{k}\cdot\mathbf{s}} - \int d\mathbf{s}\frac{\mathbf{s}}{2}\cdot\nabla_{\mathbf{r}}\tilde{\Delta}(\mathbf{r},\mathbf{s})e^{-i\mathbf{k}\cdot\mathbf{s}} - \int d\mathbf{s}\tilde{\Delta}(\mathbf{r},\mathbf{s})\mathbf{s}\cdot\nabla_{\mathbf{r}}\bar{v}(\mathbf{r})e^{-i\mathbf{k}\cdot\mathbf{s}}\\ =&\tilde{\Delta}(\mathbf{r},\mathbf{k}) - i\left[\nabla_{\mathbf{r}}\bar{v}(\mathbf{r}) + \frac{\bar{v}(\mathbf{r})}{2}\nabla_{\mathbf{r}}\right]\cdot\nabla_{\mathbf{k}}\tilde{\Delta}(\mathbf{r},\mathbf{k})\end{aligned} \tag{6.31}$$

Here we have used the identities

$$\begin{aligned}\int d\mathbf{s}\nabla_{\mathbf{r}}\frac{\mathbf{s}}{2}\cdot\tilde{\Delta}(\mathbf{r},\mathbf{s})\bar{v}(\mathbf{r})e^{-i\mathbf{k}\cdot\mathbf{s}} &= \frac{\bar{v}(\mathbf{r})}{2}\nabla_{\mathbf{r}}\cdot\int d\mathbf{s}\tilde{\Delta}(\mathbf{r},\mathbf{s})\mathbf{s}e^{-i\mathbf{k}\cdot\mathbf{s}}\\ &= \frac{\bar{v}(\mathbf{r})}{2}\nabla_{\mathbf{r}}\cdot\int d\mathbf{s}i\nabla_{\mathbf{k}}e^{-i\mathbf{k}\cdot\mathbf{s}}\tilde{\Delta}(\mathbf{r},\mathbf{s})\\ &= i\frac{\bar{v}(\mathbf{r})}{2}\nabla_{\mathbf{r}}\cdot\nabla_{\mathbf{k}}\tilde{\Delta}(\mathbf{r},\mathbf{k}),\end{aligned}$$

and similarly

$$\begin{aligned}\int d\mathbf{s}\tilde{\Delta}(\mathbf{r},\mathbf{s})\mathbf{s}\cdot\nabla_{\mathbf{r}}\bar{v}(\mathbf{r})e^{-i\mathbf{k}\cdot\mathbf{s}} &= \nabla_{\mathbf{r}}\bar{v}(\mathbf{r})\cdot\int d\mathbf{s}\tilde{\Delta}(\mathbf{r},\mathbf{s})\mathbf{s}e^{-i\mathbf{k}\cdot\mathbf{s}}\\ &= i\nabla_{\mathbf{r}}\bar{v}(\mathbf{r})\cdot\int d\mathbf{s}i\nabla_{\mathbf{k}}e^{-i\mathbf{k}\cdot\mathbf{s}}\tilde{\Delta}(\mathbf{r},\mathbf{s})\\ &= i\nabla_{\mathbf{r}}\bar{v}(\mathbf{r})\cdot\nabla_{\mathbf{k}}\tilde{\Delta}(\mathbf{r},\mathbf{k})\end{aligned}$$

Therefore, it is clear that the second term of the sum in Eq.(6.31) is down by a factor of $(k_F\xi_0)^{-1}$ as compared with the first term. If we restrict ourselves to the terms in lowest order of the small parameters, we are left with Eq.(6.29), a firstorder differential equation in which $\mathbf{k}$ is treated as a parameter. Since $\tilde{\Delta}(\mathbf{r},\mathbf{k})$ is defined only for $\mathbf{k}$ around the Fermi wave vector, we can replace the $\mathbf{k}$-dependence of $\tilde{\Delta}(\mathbf{r},\mathbf{k})$ by one on the direction $\hat{\mathbf{k}}_F$.

From now on we assume that the edge interface is specular, runs along the y direction, and the transport direction is normal to the interface (i.e., along the x-axis) (see Fig. 6.1 for the setup). In this case, $\bar{u}, \bar{v}$, and $\tilde{\Delta}$ spatially depend only on the variable x since the system is translational invariant along the interface. The Andreev equations then reduce to the form:

$$E\bar{u}(x) = -i\left(\hbar^2/m_e\right) k_{Fx} \frac{d\bar{u}(x)}{dx} + \tilde{\Delta}\left(\hat{\mathbf{k}}_F, x\right) \bar{v}(x) \tag{6.32a}$$

$$E\bar{v}(x) = i\left(\hbar^2/m_e\right) k_{Fx} \frac{d\bar{v}(x)}{dx} + \tilde{\Delta}\left(\hat{\mathbf{k}}_F, x\right) \bar{u}(x) \tag{6.32b}$$

Here we have assumed the superconducting pair potential to be real. We further choose the interface at $x = 0$. The region $x < 0$ is occupied by the normal conductor while the region $x > 0$ is occupied by the superconductor. At the NS interface, quasiparticles (e.g., electron like excitations) are partially reflected as electron-like and hole-like excitations due to the non-zero pair potential in the superconductor. When the wave vectors of electron-like and hole-like excitations are different, the pair potentials experienced by electron-like and hole-like excitations should be different for an unconventional superconductor. We denote the incident and reflected wave vectors by $\mathbf{k}_+ = (k_x, k_y)$ and $\mathbf{k}_- = (-k_x, k_y)$, respectively. The pair potential then takes the form

$$\tilde{\Delta}\left(\mathbf{k}_\pm, x\right) = \begin{cases} 0, & x < 0 \\ \Delta_0, & 0 \le x \end{cases} \tag{6.33}$$

for the s-wave superconductor, while

$$\tilde{\Delta}\left(\mathbf{k}_\pm, x\right) = \begin{cases} 0, & x < 0 \\ \Delta_0 \cos\left(2\theta_\pm\right), & 0 \le x \end{cases} \tag{6.34}$$

for the $d_{x^2-y^2}$-wave superconductor. Here $\theta_\pm = \theta \mp \alpha$ with θ the incident angle of electron excitations injected from the normal conductor and α the disorientation angle of the crystalline axis along which the $d_{x^2-y^2}$-wave superconducting pair potential reaches the maximum. Both θ and α are measured relative to the positive x-axis. In addition, to capture the essential interfacial scattering at the interface, we include a δ-function potential

$$V(x) = H\delta(x) \tag{6.35}$$

The metallic contact and the tunnel junction correspond to the two limiting cases of the barrier strength $H = 0$ and $H \to \infty$.

In the condition of an electron beam incident from the normal conductor at an angle θ, the solution to the Andreev equations (6.29),

$$\Psi(x) = \begin{pmatrix} \bar{u}(x) \\ \bar{v}(x) \end{pmatrix}$$

is given by

$$\Psi_{\mathrm{I}}(x) = \begin{pmatrix} 1 \\ 0 \end{pmatrix} e^{iq_e x} + a \begin{pmatrix} 0 \\ 1 \end{pmatrix} e^{iq_h x} + b \begin{pmatrix} 1 \\ 0 \end{pmatrix} e^{-iq_e x} \tag{6.36}$$

for $x < 0$, and

$$\Psi_{\mathrm{II}}(x) = c \begin{pmatrix} u_+ e^{i\phi_+} \\ v_+ \end{pmatrix} e^{ik_{e,+}x} + d \begin{pmatrix} v_- e^{i\phi_-} \\ u_- \end{pmatrix} e^{-ik_{h,-}x} \tag{6.37}$$

for $x \geq 0$. Here the wave vectors are determined from the energy dispersion:

$$q_{e,h} = k_{fx} \pm \frac{m_e E}{\hbar^2 k_{Fx}} \tag{6.38}$$

$$k_{e(h),+} = k_{Fx} \pm \frac{m_e \sqrt{E^2 - \left|\tilde{\Delta}\left(\mathbf{k}_+\right)\right|^2}}{\hbar^2 k_{Fx}} \tag{6.39}$$

$$k_{e(h),-} = k_{Fx} \pm \frac{m_e \sqrt{E^2 - \left|\tilde{\Delta}\left(\mathbf{k}_-\right)\right|^2}}{\hbar^2 k_{Fx}} \tag{6.40}$$

For a given pair potential, these wave vectors are schematically described in Fig. 6.2. The coherence factors in the superconducting regions are

$$u_\pm^2 = \frac{1}{2}\left(1 + \frac{\sqrt{E^2 - \left|\tilde{\Delta}\left(\mathbf{k}_\pm\right)\right|^2}}{E}\right), \tag{6.41}$$

$$v_\pm^2 = \frac{1}{2}\left(1 - \frac{\sqrt{E^2 - \left|\tilde{\Delta}\left(\mathbf{k}_\pm\right)\right|^2}}{E}\right) \tag{6.42}$$

respectively. The characteristic phases are given by

$$\phi_\pm = \cos^{-1}\left(\frac{\cos 2(\theta \mp \alpha)}{|\cos 2(\theta \mp \alpha)|}\right). \tag{6.43}$$

Imposing the boundary conditions at the interface

$$\Psi_{\mathrm{II}}(0) = \Psi_{\mathrm{I}}(0), \tag{6.44a}$$

$$\Psi'_{\mathrm{II}}(0) - \Psi'_{\mathrm{I}}(0) = \left(\frac{2m_e H}{\hbar^2}\right)\Psi'_{\mathrm{I}}(0), \tag{6.44b}$$

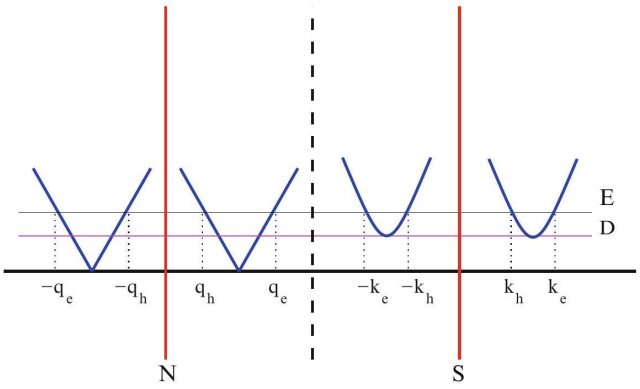


Fig. 6.2 Schematic diagram of energy versus momentum at the normal-metal/superconductor interface

and carrying out the algebraic reduction, we obtain

$$a = \frac{u_- v_+}{(1+Z^2)\, u_+ u_- e^{i\phi_+} - Z^2 v_+ v_- e^{i\phi_-}}, \tag{6.45}$$

and

$$b = -\frac{(iZ+Z^2)\left(u_+ u_- e^{i\phi_+} - v_+ v_- e^{i\phi_-}\right)}{(1+Z^2)\, u_+ u_- e^{i\phi_+} - Z^2 v_+ v_- e^{i\phi_-}} \tag{6.46}$$

where $Z = m_e H/\hbar^2 k_F \cos\theta = Z_0/\cos\theta$ with $Z_0 = m_e H/\hbar^2 k_F$. The corresponding normal and Andreev reflection probabilities are then given by $B(E,\theta) = |b(E,\theta)|^2$, and $A(E,\theta) = |a(E,\theta)|^2$, respectively. Therefore, the differential conductance can be determined upon the substitution of Eqs. (6.45) and (6.46) into Eq. (6.24). For the normal-metal/normal-metal junction, that is, the superconductor in the region $x \geq 0$ replaced by the normal metal, the Andreev and normal reflection amplitudes are given by

$$a = 0 \tag{6.47}$$

and

$$b(E,\theta) = -\frac{Z(1+iZ)}{1+Z^2} \tag{6.48}$$

which leads to the differential conductance

$$G_{NN}(E,\theta) = 2N(0)e^2 \mathscr{A} \frac{v_{F,x}}{1+Z^2} \tag{6.49}$$

For the 2D model we are considering, we shall take an average over the incident angle

$$\begin{aligned}\bar{G}_{NS}(E) &= \frac{1}{\pi}\int_{-\pi/2}^{\pi/2} d\theta G_{NS}(E,\theta) \\ &= \frac{2N(0)e^2\mathscr{A}v_F}{\pi}\int_{-\pi/2}^{\pi/2} d\theta \cos\theta [1 + A(E,\theta) - B(E,\theta)],\end{aligned} \tag{6.50}$$

for the NS junction, and

$$\begin{aligned}\bar{G}_{NN}(E) &= \frac{1}{\pi}\int_{-\pi/2}^{\pi/2} d\theta G_{NN}(E,\theta) \\ &= \frac{2N(0)e^2\mathscr{A}v_F}{\pi}\int_{-\pi/2}^{\pi/2} d\theta \frac{\cos\theta}{1+Z^2} \\ &= \frac{2N(0)e^2\mathscr{A}v_F}{\pi}\left[2 - \frac{Z_0^2}{\sqrt{1+Z_0^2}}\ln\frac{\sqrt{1+Z_0^2}+1}{\sqrt{1+Z_0^2}-1}\right],\end{aligned} \tag{6.51}$$

for the NN junction. Therefore, we can define a normalized differential conductance

$$\begin{aligned} g_{NS}(E) &= \frac{\bar{G}_{NS}(E)}{\bar{G}_{NN}(E)} \\ &= \frac{1}{\mathscr{N}}\int_{-\pi/2}^{\pi/2} d\theta \cos\theta [1 + A(E,\theta) - B(E,\theta)],\end{aligned} \tag{6.52}$$

where

$$\mathscr{N} = 2 - \frac{Z_0^2}{\sqrt{1+Z_0^2}} \ln \frac{\sqrt{1+Z_0^2}+1}{\sqrt{1+Z_0^2}-1}. \tag{6.53}$$

This normalized conductance is useful to the comparison with the standard transport measurement across the NS junction. For the orifice model of the point contact spectroscopy, we can set a specific incident angle and do not perform an average. In this case, we can still define a normalized conductance but now for a given incident angle θ.

$$g_{NS,PCS}(E,\theta) = \left(1+Z^2\right)\left[1 + A(E,\theta) - B(E,\theta)\right] \tag{6.54}$$

In the following, we discuss a few representative cases of the transport across the NS junction.

s-Wave NS Junction For the s-wave NS junction, the superconducting pair potential has no momentum dependence and as such is independent of the incident angle. Therefore, we have

$$u_\pm^2 = u_0^2 = \frac{1}{2}\left(1 + \frac{\sqrt{E^2 - \left|\tilde{\Delta}_0\right|^2}}{E}\right) \tag{6.55}$$

and

$$v_\pm^2 = v_0^2 = \frac{1}{2}\left(1 - \frac{\sqrt{E^2 - \left|\tilde{\Delta}_0\right|^2}}{E}\right) \tag{6.56}$$

In addition, $\phi_\pm = 0$. The Andreev reflection and normal reflection amplitudes are given by

$$a = \frac{u_0 v_0}{u_0^2 + \left(u_0^2 - v_0^2\right) Z^2}, \tag{6.57}$$

and

$$b = \frac{-\left(Z^2 + iZ\right)\left(u_0^2 - v_0^2\right)}{u_0^2 + \left(u_0^2 - v_0^2\right) Z^2} \tag{6.58}$$

respectively. These expressions suggest that, for the contact case $Z_0 = 0$, when the energy E is smaller than the superconducting gap $\tilde{\Delta}_0$, $A(E) = |a|^2 = 1$ and $B(E) = |b|^2 = 0$, explaining the double of the conductance as compared with that for the NN junction. In the tunneling limit $Z_0 \to \infty$, we have $A(E) = 0$ and $B(E) = 1$ so that the conductance is zero for $E < \tilde{\Delta}_0$. The numerical results of the differential conductance for the NS junction with s-wave pairing symmetry are shown in Fig. 6.3. The Andreev reflection is suppressed with increased interface barrier strength in the s-wave NS junction and the resulting differential conductance has the profile of the s-wave density of states in the tunneling limit.

d-Wave NS Junction As we have mentioned before, for the NS junction with an unconventional pairing symmetry, the energy experienced by electronic-like and hole-like excitations are sensitive to both the relative crystalline orientation between the normal metal and the superconductor and the incident angle. To demonstrate this, we consider the $d_{x^2-y^2}$-wave pairing symmetry of the superconductor, choosing $\alpha = \pi/4$ and $\theta = \pi/4$.[1] This angle of the relative crystalline orientation

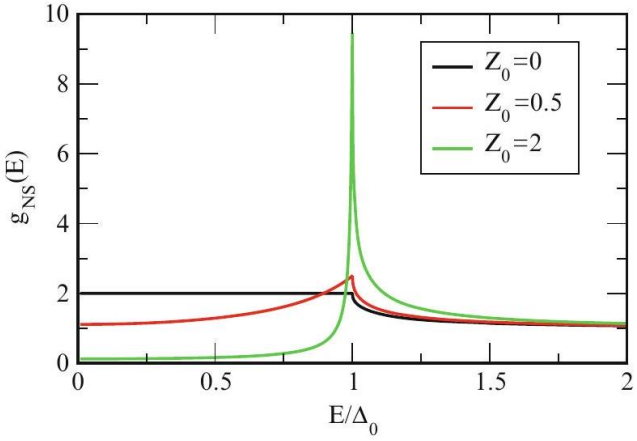


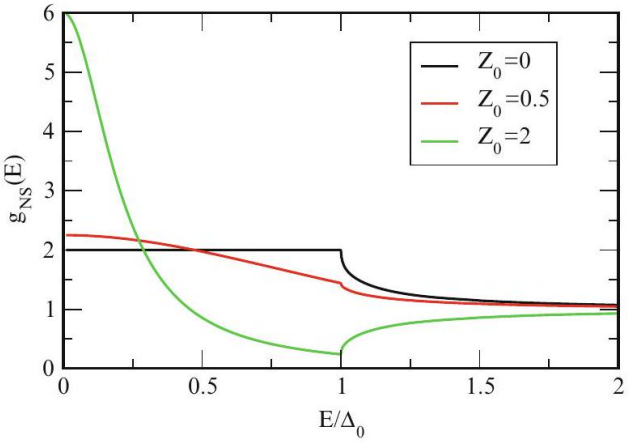
Fig. 6.3 Differential conductance for a normal-metal/s-wave superconductor junction for various values of interface barrier strength. The energy is measured in units of the superconducting pair potential. The incident angle is chosen to be $\theta = 0$ corresponds to the square lattice of copper-oxide plane of high-temperature cuprates interfaced with the normal metal along the [110] direction. These angles determine $\tilde{\Delta}(\mathbf{k}_+) = \tilde{\Delta}_0$ while $\tilde{\Delta}(\mathbf{k}_-) = -\tilde{\Delta}_0$. The BdG wave function amplitudes $u_\pm$and $v_\pm$ are still given by the formula similar to the s-wave case presented above. However, we have now the characteristic phase $\phi_+ = 0$ while $\phi_- = \pi$ due to the sign change of the pair potential experienced by electron-like and hole-like excitations. In this case, the Andreev and normal-state reflection amplitudes are found as

$$a = \frac{u_0 v_0}{u_0^2 + Z^2} \tag{6.59}$$

and

$$b = -\frac{iZ + Z^2}{u_0^2 + Z^2} \tag{6.60}$$

These expressions suggest that for the perfect contact $Z_0 = 0$, the Andreev reflection is still complete with $A(E) = 1$ and $B(E) = 0$ for $E < \Delta_0$. Even more interestingly, for the tunneling limit $Z_0 \to \infty$, as $E \to 0, A(E) \to 1$ while $B(E) \to 0$, indicating a conductance anomaly. The numerical results on the differential conductance for the d-wave NS junction are shown in Fig. 6.4 for $\alpha = \theta = \pi/4$. It shows clearly that the zero-energy conductance peak appears in the limiting case of tunneling barrier. This anomaly is solely due to the sign change of $d_{x^2-y^2}$-wave superconducting order parameter under the above condition. This existence of the zero-bias conductance peak has been used to identify the $d_{x^2-y^2}$-wave pairing symmetry in the hightemperature cuprates.



[1] The results for $\alpha = \theta = 0$ are very similar to the s-wave NS junction.

Fig. 6.4 Differential conductance for a normal-metal/d-wave superconductor junction for various values of interface barrier strength. The energy is measured in units of the superconducting pair potential. The crystalline orientation between the normal metal and the d-wave superconductor and the incident angle is chosen to be $\alpha = \pi/4$ and $\theta = \pi/4$, respectively

9.6.3 6.3 Suppression of Andreev Reflection in a FS Junction

Theory

In the Andreev reflection process, the incoming electron and the Andreev reflected hole occupy energy bands with opposite spins. For the case of normal metals, due to the spin degeneracy of the energy levels, no spin effects occur with the Andreev reflection. However, in a metallic ferromagnet, the energy band is split. The interplay of superconductivity and ferromagnetism in hybrid structures has been a very interesting topic. A lot of works have focused on the changes of the critical temperature of the superconductor in s-wave superconductor/ferromagnet multilayers [27-34], the Josephson critical current in superconductor/ferromagnet/superconductor junctions [35-38], and the magnetic coupling in ferromagnet/superconductor/ferromagnet multilayers [39, 40]. In tunneling regime, the Andreev reflection is unimportant [41]. However, in the contact regime, the spin splitting effect on the Andreev reflection in ferromagnet/superconductor cannot be ignored [42-44]. To model the spin splitting effect on the Andreev reflection in a ferromagnet/s-wave superconductor junction, we consider the Stoner model, in which the motion of conduction electrons inside the ferromagnet can be described by an effective single-particle Hamiltonian with an exchange interaction while the influence of the magnetization of the ferromagnet on the orbital motion of conduction electrons is neglected. As we have discussed in previous chapters, in the absence of spin-flip scattering, the spin-dependent (four-component) BdG equations are decoupled into two sets of (two-component) equations, one for the spin-up electron and spin-down hole quasiparticle wave functions $(u_\uparrow, v_\downarrow)^T$, while the other for spin-down electron and spin-up hole quasiparticle wave functions $(u_\downarrow, v_\uparrow)^T$. The set of BdG equations for $(u_\uparrow, v_\downarrow)^T$ can be written as:

$$[\mathscr{H}_e(\mathbf{r}) - h(\mathbf{r})]\, u_\uparrow(\mathbf{r}) + \int d\mathbf{r}' \Delta(\mathbf{r}, \mathbf{r}')\, v_\downarrow(\mathbf{r}') = E u_\uparrow(\mathbf{r}) \tag{6.61a}$$

$$-[\mathscr{H}_e^*(\mathbf{r}) + h(\mathbf{r})]\, v_\downarrow(\mathbf{r}) + \int d\mathbf{r}' \Delta^*(\mathbf{r}', \mathbf{r})\, u_\uparrow(\mathbf{r}') = E v_\downarrow(\mathbf{r}) \tag{6.61b}$$

Compared with the case of a NS junction considered in the previous section [cf. Eq.(6.25)], an exchange field $h(\mathbf{r}) = h_0\Theta(-x)$ in the ferromagnet is now introduced. The set of BdG equations for $(u_\downarrow, v_\uparrow)^T$ is obtained by simply changing the sign before $h(\mathbf{r})$ in Eq. (6.61). Following the same procedure as given in the previous section, we have the solution to the Andreev equations as:

$$\Psi_{\mathrm{I}}(x) = \begin{pmatrix}1\\0\end{pmatrix} e^{iq_e x} + r_{\downarrow\uparrow}\begin{pmatrix}0\\1\end{pmatrix} e^{iq_h x} + r_{\uparrow\uparrow}\begin{pmatrix}1\\0\end{pmatrix} e^{-iq_e x} \tag{6.62}$$

for $x < 0$, and

$$\Psi_{\mathrm{II}}(x) = c\begin{pmatrix}u_+ e^{i\phi_+}\\ v_+\end{pmatrix} e^{ik_{e,+}x} + \begin{pmatrix}v_- e^{i\phi_-}\\ u_-\end{pmatrix} e^{-ik_{h,-}x} \tag{6.63}$$

for $x \geq 0$. Here the wave vectors are determined from the energy dispersion:

$$q_{e\uparrow,h\downarrow} = \sqrt{k_{Fx}^2 \pm \frac{2m_e}{\hbar^2}(E + h_0)}, \tag{6.64}$$

$$k_{e(h),+} = k_{Fx} \pm \frac{m_e\sqrt{E^2 - \left|\tilde{\Delta}(\mathbf{k}_+)\right|^2}}{\hbar^2 k_{Fx}} \tag{6.65}$$

$$k_{e(h),-} = k_{Fx} \pm \frac{m_e\sqrt{E^2 - \left|\tilde{\Delta}(\mathbf{k}_-)\right|^2}}{\hbar^2 k_{Fx}} \tag{6.66}$$

Since the Andreev reflection for the s-wave NS junction is most pronounced in the contact case, we consider the barrier strength $H = 0$. Therefore, the boundary conditions now become:

$$\Psi_{\mathrm{II}}(0) = \Psi_{\mathrm{I}}(0) \tag{6.67a}$$

$$\Psi'_{\mathrm{II}}(0) = \Psi'_{\mathrm{I}}(0) \tag{6.67b}$$

The important difference between the NS and FS junctions are now revealed by the momentum difference in the ferromagnet. To show this, we expand the boundary conditions:

$$\begin{pmatrix} u_+ e^{i\phi_+} c + v_- e^{i\phi_-} d \\ v_+ c + u_- d \end{pmatrix} = \begin{pmatrix} 1 + r_{\uparrow\uparrow} \\ r_{\downarrow\uparrow} \end{pmatrix}, \tag{6.68a}$$

and

$$\begin{pmatrix} u_+ e^{i\phi_+} c - v_- e^{i\phi_-} d \\ v_+ c - u_- d \end{pmatrix} = \begin{pmatrix} \frac{q_{e\uparrow}}{k_{Fx}}(1 - r_{\uparrow\uparrow}) \\ \frac{q_{\downarrow\downarrow}}{k_{Fx}} r_{\downarrow\uparrow} \end{pmatrix}, \tag{6.68b}$$

which gives

$$r_{\downarrow\uparrow} = \frac{4u_- v_+ \bar{q}_e \uparrow}{(1 + \bar{q}_{e\uparrow})(1 + \bar{q}_{h\downarrow}) u_+ u_- e^{i\phi_+} - (1 - \bar{q}_e \uparrow)(1 - \bar{q}_{h\downarrow}) v_+ v_- e^{i\phi_-}}, \tag{6.69}$$

and

$$r_{\uparrow\uparrow} = \frac{-(1 - \bar{q}_{e\uparrow})(1 + \bar{q}_{h\downarrow}) u_+ u_- e^{i\phi_+} + (1 + \bar{q}_{e\uparrow})(1 - \bar{q}_{h\downarrow}) v_+ v_- e^{i\phi_-}}{(1 + \bar{q}_{e\uparrow})(1 + \bar{q}_{h\downarrow}) u_+ u_- e^{i\phi_+} - (1 - \bar{q}_{e\uparrow})(1 - \bar{q}_{h\downarrow}) v_+ v_- e^{i\phi_-}} \tag{6.70}$$

Here the normalized wave vectors in the ferromagnet are given by

$$\bar{q}_{e\uparrow(h\downarrow)} = \sqrt{1 \pm \bar{h}}, \tag{6.71}$$

with $\bar{h} = 2m_e h_0/\hbar^2 k_{Fx} = \bar{h}_0/\cos\theta$.
We can follow the similar discussion on the NS junction and write down the differential conductance for the FS junction, for a given incident angle, as:

$$g_{FS,PCS} = \frac{1}{2}\Sigma_\sigma \left[1 + (\bar{q}_{h\bar{\sigma}}/\bar{q}_{e\sigma})\left|r_{\bar{\sigma}\sigma}\right|^2 - \left|r_{\sigma\sigma}\right|^2\right], \tag{6.72}$$

which has been normalized to the conductance for the NN junction. The prefactor $\bar{q}_{h\bar{\sigma}}/\bar{q}_{e\sigma}$ before the Andreev reflection amplitude takes care of the fact that the electron and hole have different velocity in the ferromagnet. In Fig. 6.5, the differential conductance is shown for a ferromagnet/s-wave superconductor junction for various values of the exchange interaction

strength in the ferromagnet. The suppression of subgap conductance is seen clearly with the increase of exchange coupling strength. Experimental study has also been extended to ferromagnet/highT_c superconductor junctions [45]. The corresponding theory with a $d_{x^2-y^2}$-wave pairing symmetry has also been developed along the same line discussed above but with an emphasis on the zero-bias conductance [46] and the Fermi wave vector mismatch between the ferromagnet and superconductor [47].

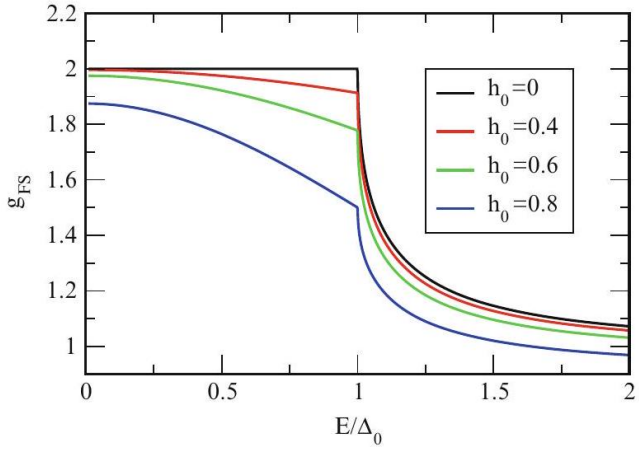


Fig. 6.5 Differential conductance for a ferromagnet/s-wave superconductor junction for various values of exchange interaction strength in the ferromagnet. The energy is measured in units of the superconducting pair potential. The crystalline orientation between the normal metal and the s-wave superconductor and the incident angle is chosen to be $\alpha = 0$ and $\theta = 0$, respectively

9.6.4 Transport Properties Through a Topological-Insulator/Superconductor Junction

Theory

So far, we have discussed the transport properties across the junctions involving conventional metals and ferromagnets. There is another class of quantum materials, so-called topological insulators (TI). They are insulating in bulk but host a gapless surface states with a Dirac-like linear dispersion [48, 49]. Like in graphene, the Dirac-like linear dispersion has a fundamental implication to various new phenomena. In TI, the surface states are topologically protected by time-reversal symmetry, and are robust against nonmagnetic disorder and perturbations. More interestingly, topological superconductivity can be induced in TIs through chemical doping [50] or proximately induced at the TI/superconductor interfaces [51-53]. Therefore, the transport through the topological superconductor junctions should be very interesting. Especially, the possible existence of Majorana fermions in the condensed matter systems is of significant implication to the technology like quantum computers and other electronic devices [54-58]. The property of the antiparticle of an Majorana fermion being itself holds a key to quantum coherence protection.

Here we consider a Dirac-normal-metal/ferromagnet insulator/s-wave topological superconductor junction. The Dirac-BdG equations can be written as:

$$\begin{pmatrix} H_{\uparrow\uparrow}(\mathbf{r}) & H_{\uparrow\downarrow} & 0 & \Delta(\mathbf{r}) \\ H_{\downarrow\uparrow}(\mathbf{r}) & H_{\downarrow\downarrow}(\mathbf{r}) & \Delta(\mathbf{r}) & 0 \\ 0 & \Delta^*(\mathbf{r}) & -H^*_{\uparrow\uparrow}(\mathbf{r}) & H^*_{\uparrow\downarrow}(\mathbf{r}) \\ \Delta^*(\mathbf{r}) & 0 & H^*_{\downarrow\uparrow}(\mathbf{r}) & -H^*_{\downarrow\downarrow}(\mathbf{r}) \end{pmatrix} \begin{pmatrix} u_\uparrow(\mathbf{r}) \\ u_\downarrow(\mathbf{r}) \\ v_\uparrow(\mathbf{r}) \\ v_\downarrow(\mathbf{r}) \end{pmatrix} = E \begin{pmatrix} u_\uparrow(\mathbf{r}) \\ u_\downarrow(\mathbf{r}) \\ v_\uparrow(\mathbf{r}) \\ v_\downarrow(\mathbf{r}) \end{pmatrix}. \tag{6.73}$$

Here the single-particle Hamiltonian matrix in the spin-space is given by

$$\hat{H} = \hat{h}(\mathbf{r}) + \hat{M}(\mathbf{r}), \tag{6.74}$$

where the Dirac-like Hamiltonian for the topological surface state is

$$\hat{h}(\mathbf{r}) = v_F \left(p_x\sigma_y - p_y\sigma_x\right) - E_F[\Theta(-x) + \Theta(x-d)] \tag{6.75}$$

with E_F is the Fermi energy, the potential for the ferromagnetic insulator is

$$\begin{aligned}\hat{M} &= \mathbf{m}\cdot\sigma\Theta(x)\Theta(d-x),\\ &= \begin{pmatrix} m_z & m_x - im_y \\ m_x + im_y & -m_z \end{pmatrix}.\end{aligned} \tag{6.76}$$

with $\mathbf{m}$ being the magnetization vector and the σ the Pauli matrices. The pair potential for the s-wave superconductor is given by

$$\Delta(\mathbf{r}) = \Delta\Theta(x-d) \tag{6.77}$$

The quasiparticle energy is measured with respect to the Fermi energy $E_F = \hbar v_F k_F$ with v_F and k_F being the Fermi velocity and wave vector.

When a beam of electrons is incident from the Dirac-like normal metal with an angle θ, the wave function is given by

$$\Psi_{\mathrm{I}}(x) = \begin{pmatrix} 1 \\ ie^{i\theta} \\ 0 \\ 0 \end{pmatrix} e^{ik_x x} + a \begin{pmatrix} 0 \\ 0 \\ 1 \\ -ie^{-i\theta} \end{pmatrix} e^{ik_x x} + b \begin{pmatrix} 1 \\ -ie^{-i\theta} \\ 0 \\ 0 \end{pmatrix} e^{-ik_x x} \tag{6.78}$$

for $x < 0$;

$$\begin{aligned}\Psi_{\mathrm{II}}(x) =& c_{e,+} \begin{pmatrix} 1 \\ \Gamma_{e,+} \\ 0 \\ 0 \end{pmatrix} e^{ik^+_{e,x}x} + c_{e,-} \begin{pmatrix} 1 \\ \Gamma_{e,-} \\ 0 \\ 0 \end{pmatrix} e^{ik^-_{e,-}x} \\ &+ c_{h,+} \begin{pmatrix} 0 \\ 0 \\ 1 \\ \Gamma_{h,+} \end{pmatrix} e^{ik_{h,+}x} + c_{h,-} \begin{pmatrix} 0 \\ 0 \\ 1 \\ \Gamma_{h,-} \end{pmatrix} e^{ik_{h,-}x},\end{aligned} \tag{6.79}$$

for $0 \le x \le d$. Here

$$k_x = k_F \cos\theta \tag{6.80}$$

$$k_y = k_F \sin\theta \tag{6.81}$$

$$k_{e,\pm} = -\frac{m_y}{\hbar k_F} \pm \frac{i}{\hbar k_F}\sqrt{m_z^2 + \left(\hbar v_F k_y - m_x\right)^2}, \tag{6.82}$$

$$k_{h,\pm} = \frac{m_y}{\hbar k_F} \mp \frac{i}{\hbar k_F}\sqrt{m_z^2 + \left(\hbar v_F k_y + m_x\right)^2} \tag{6.83}$$

$$\Gamma_{e,\pm} = -\frac{m_z}{-\hbar v_F\left(ik_{e,\pm} + k_y\right) + \left(m_x - im_y\right)} \tag{6.84}$$

$$\Gamma_{h,\pm} = -\frac{m_z}{\hbar v_F\left(ik_{h,\pm} - k_y\right) + \left(m_x + im_y\right)} \tag{6.85}$$

For the wave function in the topological superconducting region, we would like to give a more expanded discussion because the BdG equations become a set of 4×4 coupled matrix equations. We first write the wave function in the form

$$\begin{aligned}\Psi(x,y) &= \Psi(x)e^{ik_y y} \\ &= \begin{pmatrix} u_{0,\uparrow} \\ u_{0,\downarrow} \\ v_{0,\uparrow} \\ v_{0,\downarrow} \end{pmatrix} e^{iq_x x + ik_y y}. \end{aligned} \tag{6.86}$$

On substitution of Eq. (6.86) into Eq. (6.73), we arrive at the matrix equations

$$\begin{pmatrix} E+E_F & -\hbar v_F(-iq_x - k_y) & 0 & -\Delta \\ -\hbar v_F(iq_x - k_y) & E+E_F & -\Delta & 0 \\ 0 & -\Delta & E-E_F & \hbar v_F(iq_x - k_y) \\ -\Delta & 0 & \hbar v_F(-iq_x - k_y) & E-E_F \end{pmatrix} \begin{pmatrix} u_{0,\uparrow} \\ u_{0,\downarrow} \\ v_{0,\uparrow} \\ v_{0,\downarrow} \end{pmatrix} = 0 \tag{6.87}$$

which leads to the eigenvalue equation
$[(E+|\Pi|+E_F)(E-|\Pi|-E_F)-\Delta^2][(E-|\Pi|+E_F)(E+|\Pi|-E_F)-\Delta^2]=0.$
In the above equation, we have denoted

$$\Pi = i\hbar v_F(q_x - ik_y) = i|\Pi|e^{-i\gamma} \tag{6.89}$$

with $\gamma = \tan^{-1}(q_x/k_y)$. Equation (6.88) can be decoupled as

$$(E+|\Pi|+E_F)(E-|\Pi|-E_F)-\Delta^2 = 0 \tag{6.90}$$

and

$$(E-|\Pi|+E_F)(E+|\Pi|-E_F)-\Delta^2 = 0, \tag{6.91}$$

which gives four eigenvalues

$$E_{1,2} = \pm\sqrt{(-|\Pi|-E_F)^2+\Delta^2}, \tag{6.92}$$

$$E_{3,4} = \pm\sqrt{(|\Pi|-E_F)^2+\Delta^2}, \tag{6.93}$$

respectively.
We now derive the eigenfunctions corresponding to the above eigenvalues. We first write Eq. (6.87) in an expanded form

$$(E+E_F)u_{0,\uparrow} + \Pi u_{0,\downarrow} - \Delta v_{0,\downarrow} = 0 \tag{6.94a}$$

$$\Pi^* u_{0,\uparrow} + (E+E_F)u_{0,\downarrow} - \Delta v_{0,\uparrow} = 0 \tag{6.94b}$$

$$-\Delta u_{0,\downarrow} + (E-E_F)v_{0,\uparrow} - \Pi^* v_{0,\downarrow} = 0 \tag{6.94c}$$

$$-\Delta u_{0,\uparrow} - \Pi v_{0,\uparrow} + (E-E_F)v_{0,\downarrow} = 0. \tag{6.94d}$$

These wavefunctions are also subjected to the normalization condition:

$$|u_{0,\uparrow}|^2 + |u_{0,\downarrow}|^2 + |v_{0,\uparrow}|^2 + |v_{0,\downarrow}|^2 = 2. \tag{6.95}$$

Here we have used an unusual normalization factor "2" to be consistent with the intensity of the incident beam. Since there are four unknowns but five equations, we use only Eqs. (6.94a)-(6.94c) together with the normalization condition. From Eqs. (6.94a) and (6.94b), we can express $u_{0,\uparrow}$ and $u_{0,\downarrow}$ in terms of $v_{0,\uparrow}$ and $v_{0,\downarrow}$. A little algebra yields:

$$u_{0,\uparrow} = \frac{\Delta}{\left(E+E_F\right)^2 - |\Pi|^2}\left[\left(E+E_F\right)v_{0,\downarrow} - \Pi v_{0,\uparrow}\right] \tag{6.96a}$$

$$u_{0,\downarrow} = \frac{\Delta}{\left(E+E_F\right)^2 - |\Pi|^2}\left[\left(E+E_F\right)v_{0,\uparrow} - \Pi^* v_{0,\downarrow}\right] \tag{6.96b}$$

Substitution of Eqs. (6.96a) and (6.96b) into Eq. (6.94c) gives

$$\begin{aligned} v_{0,\uparrow} &= -\frac{i|\Pi|e^{i\gamma}\left[-\Delta^2 + \left(E+E_F\right)^2 - |\Gamma|^2\right]}{-\Delta^2\left(E+E_F\right) + \left(E-E_F\right)\left[\left(E+E_F\right)^2 - |\Pi|^2\right]} v_{0,\downarrow} \\ &= \begin{cases} ie^{i\gamma}v_{0,\downarrow}, \text{ for } E_{3,4} \\ -ie^{i\gamma}v_{0,\downarrow}, \text{ for } E_{1,2} \end{cases} \end{aligned} \tag{6.97}$$

which in turn gives

$$u_{0,\downarrow} = \begin{cases} ie^{i\gamma}u_{0,\uparrow}, & \text{for } E_{3,4}, \\ -ie^{i\gamma}u_{0,\uparrow}, & \text{for } E_{1,2}, \end{cases} \tag{6.98}$$

We can then substitute Eqs. (6.97) and (6.98) back into Eq. (6.96a) and obtain:

$$u_{0,\uparrow} = \frac{\Delta}{\left(E+E_F\right) - |\Pi|}v_{0,\downarrow}, \tag{6.99}$$

for $E_{3,4}$, while

$$u_{0,\uparrow} = \frac{\Delta}{\left(E+E_F\right) + |\Pi|}v_{0,\downarrow} \tag{6.100}$$

for $E_{1,2}$. Substituting these relations into the normalization condition Eq. (6.95), we are able to arrive at

$$\left(u_{0,\uparrow}^{(3,4)}\right)^2 = \frac{1}{2}\left(1 + \frac{|\Pi| - E_F}{E_{3,4}}\right), \tag{6.101a}$$

$$\left(v_{0,\downarrow}^{(3,4)}\right)^2 = \frac{1}{2}\left(1 - \frac{|\Pi| - E_F}{E_{3,4}}\right), \tag{6.101b}$$

and

$$\left(u_{0,\uparrow}^{(1,2)}\right)^2 = \frac{1}{2}\left(1 - \frac{|\Pi| - E_F}{E_{1,2}}\right) \tag{6.101c}$$

$$\left(v_{0,\downarrow}^{(1,2)}\right)^2 = \frac{1}{2}\left(1 + \frac{|\Pi| - E_F}{E_{1,2}}\right) \tag{6.101d}$$

Eigenfunctions as given by Eq. (6.101) suggest that for an incident wave from the normal metal with energy E, the transmitted wave function should have the form

$$\Psi_{\rm III}(x) = t_e \begin{pmatrix} u_0 \\ iu_0 e^{i\theta} \\ iv_0 e^{i\theta} \\ v_0 \end{pmatrix} e^{ik_x x} + t_h \begin{pmatrix} v_0 \\ -iv_0 e^{i\theta} \\ -iu_0 e^{i\theta} \\ u_0 \end{pmatrix} e^{-ik_x x} \tag{6.102}$$

for $x \geq d$, where the coherence factors

$$u_0 = \sqrt{\frac{1}{2}\left(1 + \frac{\sqrt{E^2 - \Delta^2}}{E}\right)}, \tag{6.103a}$$

$$v_0 = \sqrt{\frac{1}{2}\left(1 - \frac{\sqrt{E^2 - \Delta^2}}{E}\right)}. \tag{6.103b}$$

Here we have used the Andreev approximation to take the x-component of the wave vector to be the same as that projected from $\mathbf{k}_F$, that is, $q_x = k_x = k_F \cos\theta$ with $\gamma \approx \theta$.

We can now impose the boundary conditions

$$\Psi_{\rm I}(x = 0) = \Psi_{\rm II}(x = 0), \tag{6.104}$$

at $x = 0$, and

$$\Psi_{\rm II}(x = d) = \Psi_{\rm III}(x = d), \tag{6.105}$$

at $x = d$. A straightforward but tedious algebra yields the reflection amplitudes

$$a = \frac{1 + e^{2i\theta}}{(\mathscr{M}_{11} - ie^{-i\theta}\mathscr{M}_{12}) - (ie^{i\theta}\mathscr{M}_{21} + \mathscr{M}_{22})} \tag{6.106a}$$

$$b = \frac{\left(\mathscr{M}_{11} - ie^{-i\theta}\mathscr{M}_{12}\right) e^{i2\theta} + \left(ie^{i\theta}\mathscr{M}_{21} + \mathscr{M}_{22}\right)}{(\mathscr{M}_{11} - ie^{-i\theta}\mathscr{M}_{12}) - (ie^{i\theta}\mathscr{M}_{21} + \mathscr{M}_{22})} \tag{6.106b}$$

where

$$\begin{aligned}
\mathscr{M}_{11} =& \mathscr{D}^{-1}\Big[-ie^{i\theta}e^{i\left(k_{h,+}+k_{e,+}\right)d}\left(1+\Gamma_{h,+}\right)\left(\Gamma_{h,+}+\Gamma_{h,-}-\Gamma_{e,+}\right) \\
&+\left(u_0^2-v_0^2\right)e^{i\left(k_{h,+}+k_{e,-}\right)d}\left(1+\Gamma_{h,+}\right)\left(\Gamma_{h,+}+\Gamma_{h,-}-\Gamma_{e,-}\right) \\
&+\left(u_0^2-v_0^2\right)e^{2i\theta}e^{i\left(k_{h,-}+k_{e,-}\right)d}\left(1+\Gamma_{-}\right)\left(\Gamma_{h,+}+\Gamma_{h,-}-\Gamma_{e,+}\right) \\
&+ie^{i\theta}e^{i\left(k_{h,-}+k_{e,-}\right)d}\left(1+\Gamma_{h,-}\right)\left(\Gamma_{h,+}+\Gamma_{h,-}-\Gamma_{e,-}\right)\Big]
\end{aligned} \tag{6.107a}$$

$$\begin{aligned}
\mathscr{M}_{12} =& \mathscr{D}^{-1}\Big[ie^{i\theta}e^{i\left(k_{h,-}+k_{e,+}\right)d}\left(1+\Gamma_{h,+}\right)\left(1+\Gamma_{e,+}\right) \\
&-\left(u_0^2-v_0^2\right)e^{i\left(k_{h,-}+k_{e,-}\right)d}\left(1+\Gamma_{h,+}\right)\left(1+\Gamma_{e,-}\right) \\
&-\left(u_0^2-v_0^2\right)e^{2i\theta}e^{i\left(k_{h,-}+k_{e,-}\right)d}\left(1+\Gamma_{h,-}\right)\left(1+\Gamma_{e,+}\right) \\
&-ie^{i\theta}e^{i\left(k_{h,-}+k_{e,-}\right)d}\left(1+\Gamma_{h,-}\right)\left(1+\Gamma_{e,-}\right)
\end{aligned} \tag{6.107b}$$

$$\begin{aligned}
\mathscr{M}_{21} =& \mathscr{D}^{-1}\Big[-ie^{i\theta}e^{i\left(k_{h,+}+k_{e,+}\right)d}\left(\Gamma_{e,+}+\Gamma_{e,-}\Gamma_{h,-}\right)\left(\Gamma_{h,+}+\Gamma_{h,-}\Gamma_{e,-}\right) \\
&+\left(u_0^2-v_0^2\right)e^{i\left(k_{h,+}+k_{e,-}\right)d}\left(\Gamma_{e,+}+\Gamma_{e,-}\Gamma_{h,+}\right)\left(\Gamma_{h,+}+\Gamma_{h,-}\Gamma_{e,-}\right)
\end{aligned}$$

$$+\left(u_0^2-v_0^2\right)e^{2i\theta}e^{i\left(k_{h,-}+k_{e,+}\right)d}\left(\Gamma_{e,+}+\Gamma_{e,-}\Gamma_{h,-}\right)\left(\Gamma_{h,+}+\Gamma_{h,-}\Gamma_{e,+}\right)$$
$$+ie^{i\theta}e^{i\left(k_{h,-}+k_{e,-}\right)d}\left(\Gamma_{e,+}+\Gamma_{e,-}\Gamma_{h,-}\right)\left(\Gamma_{h,+}+\Gamma_{h,-}\Gamma_{e,-}\right)\Big] \tag{6.107c}$$

$$\begin{aligned}\mathscr{M}_{22}=&\mathscr{D}^{-1}\Big[ie^{i\theta}e^{i\left(k_{h,+}+k_{e,-}\right)d}\left(\Gamma_{e,+}+\Gamma_{e,-}\Gamma_{h,+}\right)\left(1+\Gamma_{e,+}\right)\\&-\left(u_0^2-v_0^2\right)e^{i\left(k_{h,-}+k_{e,-}\right)d}\left(\Gamma_{e,+}+\Gamma_{e,-}\Gamma_{h,+}\right)\left(1+\Gamma_{e,-}\right)\\&-\left(u_0^2-v_0^2\right)e^{2i\theta}e^{i\left(k_{h,-}+k_{e,-}\right)d}\left(\Gamma_{e,+}+\Gamma_{e,-}\Gamma_{h,-}\right)\left(1+\Gamma_{e,+}\right)\\&-ie^{i\theta}e^{i\left(k_{h,-}+k_{e,-}\right)d}\left(\Gamma_{e,+}+\Gamma_{e,-}\Gamma_{h,-}\right)\left(1+\Gamma_{e,-}\right)\Big]\end{aligned} \tag{6.107d}$$

with

$$\mathscr{D}=\frac{2iu_0v_0e^{i\theta}e^{i(k_{e,+}+k_{e,-})d}}{\left(\Gamma_{e,+}-\Gamma_{e,-}\right)\left(\Gamma_{h,+}-\Gamma_{h,-}\right)}. \tag{6.108}$$

With these coefficients, the differential conductance can be calculated as $G_S(\theta)=1+|a|^2-|b|^2$. Also we can evaluate the differential conductance when the superconductor is set into the normal state, which has the expression

$$G_N(\theta)=\frac{1}{\cosh^2\left(\kappa_e d\right)+\tan^2\theta\sinh^2\left(\kappa_e d\right)\left(k_y-m_x/\hbar v_F\right)^2/\kappa_e^2} \tag{6.109}$$

where

$$\kappa_e=\sqrt{m_z^2+\left(\hbar v_F k_y-m_x\right)^2}/\hbar v_F \tag{6.110}$$

The normalized differential conductance can be calculated according to

$$\sigma=\frac{\int_{-\pi/2}^{\pi/2}G_S(\theta)\cos\theta d\theta}{\int_{-\pi/2}^{\pi/2}G_N(\theta)\cos\theta d\theta} \tag{6.111}$$

When $m_x=0$, the differential conductance is reduced to [55]:

$$G_S(\theta)=\frac{G_N\left[1+G_N|\Gamma|^2-\left(1-G_N\right)|\Gamma|^4\right]}{\left|1+\left(1-G_N\right)e^{i\varphi}\Gamma^2\right|^2} \tag{6.112}$$

where

$$e^{i\varphi}=\frac{m_z\cos\theta+iE_F\sin\theta}{m_z\cos\theta-iE_F\sin\theta]}, \tag{6.113}$$

and

$$\Gamma=\frac{\Delta}{E+\sqrt{E^2-\Delta^2}}. \tag{6.114}$$

In the insulating limit, $G_N\to 0$, the pole of Eq. (6.112) leads to the bound state energy

$$E_b=-\frac{\Delta E_F\sin\theta\,\mathrm{sgn}\left(m_z\right)}{\sqrt{E_F^2\sin^2\theta+m_z^2\cos^2\theta}}. \tag{6.115}$$

These states are the manifestation of chiral Majorana mode (CMM) [51], which has a dispersion along the interface between the ferromagnetic insulator and conventional s-wave superconductor. However, these states are localized in the direction perpendicular to the interface.

Equation (6.115) suggests that the conductance is contributed mainly by these bound states in the tunneling limit. The representative results of the conductance are reported by Tanaka and co-workers [55]. As shown in Fig. 6.6, the bound state energy is dispersive as a function of the incident angle. In addition, the slope in the energy near the vertical incident angle $\theta = 0$ becomes more flat when the ferromagnetic exchange interaction increases (see Fig. 6.6a). The flatted band of bound states near $\theta = 0$ will then make dominant contribution to the integrated conductance. Therefore, the zero-bias conductance peak is enhanced with increased m_z (see Fig. 6.6b). These results are remarkable in view of the fact that the ferromagnetic exchange interaction in ferromagnet/conventional superconductor junctions suppresses the zero-bias differential conductance. Interesting results from the topological nature of the superconductor have also been found in thermal transport properties [59].

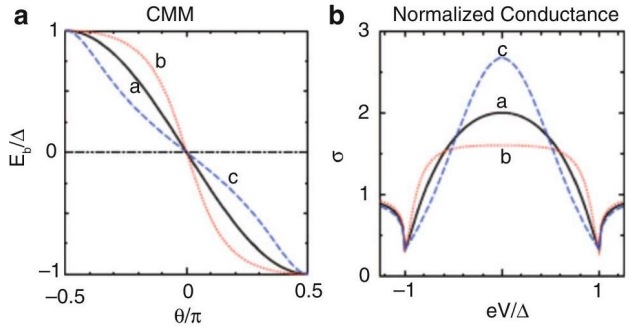


Fig. 6.6 Chiral Majorana mode energy dispersion E_b as a function of the incident angle θ (a) and integrated tunneling conductance σ in N/FI/S junctions (b). The parameter $(m_z/E_F)\, k_F d = 1$ is fixed and $m_x = m_y = 0$. The other variation parameter $m_z/E_F = 1, 0.5, 2$ for curves a, b, and c, respectively. From [55]

9.7 BdG Equations in Tight-Binding Model

9.7.1 2.1 Derivation of BdG Equations in a Tight-Bind Model

Theory

In the previous chapter, we have derived the BdG equations in the continuum model. The continuum model is reasonable to describe weak-coupling superconductors, especially when they have a wide-band metallic normal state. For the superconductors like high-temperature cuprates, the electronic band is quite narrow. Therefore, as we are encountered in solid state physics [1], the tight-binding model, either constructed from atomic orbitals or from Wannier orbitals, is appropriate to be used for studying narrow band behaviors arising from electronic correlation effects.

We generalize the second-quantized Hamiltonian given by Eq. (1.38) to include the spin-orbit coupling and spin-flip scattering interactions, in addition to the regular potential scattering. The single-particle part of the Hamiltonian is of the form:

$$H_0 = \iint d\mathbf{r} d\mathbf{r}' \psi_\alpha^\dagger(\mathbf{r}) h_{\alpha\beta}(\mathbf{r}, \mathbf{r}')\, \psi_\beta(\mathbf{r}') \tag{2.1}$$

where $h_{\alpha\beta}(\mathbf{r}, \mathbf{r}')$ is general enough to include the non-local and spin-flip effects. The field operators are now expressed in the localized-state basis as

$$\psi_\alpha(\mathbf{r}) = \sum_i w(\mathbf{r} - \mathbf{R}_i)\, c_{i\alpha} \tag{2.2a}$$

$$\psi_\alpha^\dagger(\mathbf{r}) = \sum_i w^*(\mathbf{r} - \mathbf{R}_i)\, c_{i\alpha}^\dagger \tag{2.2b}$$

where $c_{i\alpha}^{\dagger}\left(c_{i\alpha}\right)$ creates (annihilates) an electron of spin α at site i, and $w\left(\mathbf{r}-\mathbf{R}_i\right)$ is a localized orbital around the atomic site $\mathbf{R}_i$. The atomic orbitals or maximally localized Wannier orbitals are most amenable to have a physical interpretation. Substitution of these expressions into Eq. (2.1) gives

$$\begin{aligned} H_0 &= \sum_{ij,\sigma\sigma'} c_{i\sigma}^{\dagger} h_{i\sigma,j\sigma'} c_{j\sigma} \\ &= -\sum_{i\neq j,\sigma\sigma'} t_{i\sigma,j\sigma'} c_{i\sigma}^{\dagger} c_{j\sigma'} + \sum_{i\sigma} \epsilon_i c_{i\sigma}^{\dagger} c_{i\sigma} + \sum_{i,\sigma\sigma'} \Omega_{i,\sigma\sigma'} c_{i\sigma}^{\dagger} c_{i\sigma'} \end{aligned} \tag{2.3}$$

Here the summation over the site indices ij in the kinetic energy (and also the nearest-neighbor interaction in Eq. 2.4 below) excludes those term with $i=j$. In the kinetic energy, the spin-orbit term has also been included by identifying the spin flip when an electron hops from one site to its nearest neighbor. The on-site single particle energy is introduced to consider the disorder or such inhomogeneity problems as those with a (non-magnetic) single impurity; while the third term accounts for the magnetic impurity effects (with the internal dynamics of the magnetic impurity neglected here).

We then follow the same ansatz for the extended Hubbard model [2], and write down an effective model Hamiltonian for superconductivity:

$$\begin{aligned} \mathscr{H} &= H_0 - \mu \sum_{i\sigma} c_{i\sigma}^{\dagger} c_{i\sigma} + U \sum_i \left(n_{i\uparrow} - \frac{1}{2}\right)\left(n_{i\downarrow} - \frac{1}{2}\right) - \frac{V}{2} \sum_{i\neq j} n_i n_j = \\ &= \sum_{ij,\sigma\sigma'} c_{i\sigma}^{\dagger} \left[h_{i\sigma,j\sigma'} - \left(\mu + \frac{U}{2}\right)\delta_{ij}\delta_{\sigma\sigma'}\right] c_{j\sigma'} + U \sum_i n_{i\uparrow} n_{i\downarrow} - \frac{V}{2} \sum_{i\neq j} n_i n_j. \end{aligned} \tag{2.4}$$

Here $n_i = \sum_{\sigma} n_{i\sigma}$ with $n_{i\sigma} = c_{i\sigma}^{\dagger} c_{i\sigma}$ is the particle number operator on site i. The on-site and nearest-neighbor electron-electron interaction strengths are, respectively, U and V. Positive values of U and negative values of V represent the repulsive interaction while negative values of U and positive values of V represent the attractive interaction since we have assigned a minus sign before the nearestneighbor interaction term. Note that the single particle energy is measured with respect to the chemical potential μ.

The derivation of the BdG equations for the on-site and nearest-neighbor pairing interaction is similar to that for the continuum model in Chap. 1. To be distinct, the above extended Hubbard model enables a description of possible competing orders. We show one example here by considering on-site repulsion ($U>0$), which drives magnetic instability, and nearest-neighbor attraction ($V>0$) for the d-wave pairing superconductivity. Therefore, we retain the standard Hartree-Fock term for the onsite repulsion and the anomalous Hartree-Fock terms for nearest-neighbor attraction. The inclusion of an onsite repulsion in the mean-field approximation helps stabilize the d-wave pairing state, which comes from the nearest-neighbor pairing interaction. The effective mean-field Hamiltonian with a singlet pairing symmetry is now given by:

$$\mathscr{H}_{eff} = \sum_{ij,\sigma\sigma'} c_{i\sigma}^{\dagger} \tilde{h}_{i\sigma,j\sigma'} c_{j\sigma'} + \sum_{ij} \left[\Delta_{ij} c_{i\uparrow}^{\dagger} c_{j\downarrow}^{\dagger} + \Delta_{ij}^{*} c_{j\downarrow} c_{i\uparrow}\right] + E_{const} \tag{2.5}$$

Here the effective single-particle Hamiltonian is given by

$$\tilde{h}_{i\sigma,j\sigma'} = h_{i\sigma,j\sigma'} - \left(\mu + \frac{U}{2} - U\left\langle n_{i\bar{\sigma}}\right\rangle\right)\delta_{ij}\delta_{\sigma\sigma'}, \tag{2.6}$$

the singlet-pairing potential

$$\Delta_{ij} = \frac{V}{2}\left(\langle c_{i\uparrow}c_{j\downarrow}\rangle - \langle c_{i\downarrow}c_{j\uparrow}\rangle\right), \tag{2.7}$$

$$\Delta_{ij}^{*} = \frac{V}{2}\left(\left\langle c_{j\downarrow}^{\dagger}c_{i\uparrow}^{\dagger}\right\rangle - \left\langle c_{j\uparrow}^{\dagger}c_{i\downarrow}^{\dagger}\right\rangle\right), \tag{2.8}$$

and the constant energy term is given by

$$E_{\text{const}} = -U\langle n_{i\uparrow}\rangle\langle n_{i\downarrow}\rangle + \sum_{ij}\frac{|\Delta_{ij}|^2}{V} \tag{2.9}$$

It is evident that the singlet pairing potential satisfies the symmetry properties: $\Delta_{ji} = \Delta_{ij}$. Also we note again that the single particle energy is measured with respect to the chemical potential μ.

We then obtain the following commutation relations:

$$[c_{i\uparrow}, \mathscr{H}_{eff}]_{-} = \sum_{j\sigma'}\tilde{h}_{i\uparrow,j\sigma'}c_{j\sigma'} + \sum_{j}\Delta_{ij}c_{j\downarrow}^{\dagger}, \tag{2.10a}$$

$$\left[c_{i\uparrow}^{\dagger}, \mathscr{H}_{eff}\right]_{-} = -\sum_{j\sigma'}\tilde{h}_{j\sigma',i\uparrow}c_{j\sigma'}^{\dagger} - \sum_{j}\Delta_{ij}^{*}c_{j\downarrow}, \tag{2.10b}$$

$$[c_{i\downarrow}, \mathscr{H}_{eff}]_{-} = \sum_{j\sigma'}\tilde{h}_{i\downarrow,j\sigma'}c_{j\sigma'} - \sum_{j}\Delta_{ji}c_{j\uparrow}^{\dagger}, \tag{2.10c}$$

$$\left[c_{i\downarrow}^{\dagger}, \mathscr{H}_{eff}\right]_{-} = -\sum_{j\sigma'}\tilde{h}_{j\sigma',i\downarrow}c_{j\sigma'}^{\dagger} + \sum_{j}\Delta_{ji}^{*}c_{j\uparrow}. \tag{2.10d}$$

Equations (2.10)(a)-(d) show that the electron field operator can be expressed as a linear combination of electron- and hole-like quasiparticle excitations, which
enables us to perform a Bogoliubov canonical transformation:

$$c_{i\sigma} = \sum_{n}{}'\left(u_{i\sigma}^{n}\gamma_n - \sigma v_{i\sigma}^{n*}\gamma_n^{\dagger}\right), \quad c_{i\sigma}^{\dagger} = \sum_{n}{}'\left(u_{i\sigma}^{n*}\gamma_n^{\dagger} - \sigma v_{i\sigma}^{n}\gamma_n\right), \tag{2.11}$$

where $\sigma = \pm 1$ denotes the up and down spin orientations. The operators $\gamma_n^{\dagger}(\gamma_n)$ create (annihilate) a Bogoliubov quasiparticle at state n. The prime sign above the summation in the transformation means only those states with positive energy are counted. The quasiparticle operators satisfy the anti-commutation relations:

$$\left\{\gamma_n, \gamma_m^{\dagger}\right\} = \delta_{nm}, \tag{2.12}$$

$$\{\gamma_n, \gamma_m\} = \left\{\gamma_n^{\dagger}, \gamma_m^{\dagger}\right\} = 0 \tag{2.13}$$

These relations also guarantee the anti-commutation relations among the original electronic field operators.

With the above canonical transformation, the Hamiltonian is diagonalized in the following form:

$$H_{eff} = \sum_{n}E_n\gamma_n^{\dagger}\gamma_n + E'_{\text{const}}, \tag{2.14}$$

where the index n also includes the pseudo-spin state index. Upon substitution of Eq. (2.11) into Eq. (2.10), and with the aid of the following commutation relations,

$$\left[\gamma_n^\dagger, H_{eff}\right]_- = -E_n\gamma_n^\dagger, \tag{2.15}$$

$$\left[\gamma_n, H_{eff}\right]_- = E_n\gamma_n, \tag{2.16}$$

we compare the coefficients of the terms with γ_n and $\gamma_n^\dagger$ and arrive at

$$E_n u_{i\uparrow}^n = \sum_{j\sigma'} \tilde{h}_{i\uparrow,j\sigma'} u_{j\sigma'} + \sum_j \Delta_{ij} v_{j\downarrow}^n, \tag{2.17}$$

$$E_n u_{i\downarrow}^n = \sum_{j\sigma'} \tilde{h}_{i\downarrow,j\sigma'} u_{j\sigma'}^n + \sum_j \Delta_{ji} v_{j\uparrow}^n, \tag{2.18}$$

$$E_n v_{i\uparrow}^n = -\sum_{j\sigma'} \sigma' \tilde{h}_{i\uparrow,j\sigma'}^* v_{j\sigma'}^n + \sum_j \Delta_{ij}^* u_{j\downarrow}^n, \tag{2.19}$$

$$E_n v_{i\downarrow}^n = \sum_{j\sigma'} \sigma' \tilde{h}_{i\downarrow,j\sigma'}^* v_{j\sigma'}^n + \sum_j \Delta_{ji}^* u_{j\uparrow}^n. \tag{2.20}$$

This set of BdG equations can be cast into a matrix form:

$$\sum_j \hat{M}_{ij}\hat{\phi}_j = E_n\hat{\phi}_i \tag{2.21}$$

where

$$\hat{M}_{ij} = \begin{bmatrix} \tilde{h}_{i\uparrow,j\uparrow} & \tilde{h}_{i\uparrow,j\downarrow} & 0 & \Delta_{ij} \\ \tilde{h}_{i\downarrow,j\uparrow} & \tilde{h}_{i\downarrow,j\downarrow} & \Delta_{ji} & 0 \\ 0 & \Delta_{ij}^* & -\tilde{h}_{i\uparrow,j\uparrow}^* & \tilde{h}_{i\uparrow,j\downarrow}^* \\ \Delta_{ji}^* & 0 & \tilde{h}_{i\downarrow,j\uparrow}^* & -\tilde{h}_{i\downarrow,j\downarrow}^* \end{bmatrix}, \tag{2.22}$$

and

$$\hat{\phi}_i = \begin{pmatrix} u_{i\uparrow} \\ u_{i\downarrow} \\ v_{i\uparrow} \\ v_{i\downarrow} \end{pmatrix} \tag{2.23}$$

This set of BdG equations is subjected to the self-consistency conditions:

$$n_{i\uparrow} = \sum_n{}' \left[\left|u_{i\uparrow}^n\right|^2 f\left(E_n\right) + \left|v_{i\uparrow}^n\right|^2 f\left(-E_n\right)\right], \tag{2.24}$$

$$n_{i\downarrow} = \sum_n{}' \left[\left|u_{i\downarrow}^n\right|^2 f\left(E_n\right) + \left|v_{i\downarrow}^n\right|^2 f\left(-E_n\right)\right], \tag{2.25}$$

and

$$\Delta_{ij} = \frac{V}{4}\sum_n{}' \left[\left(u_{i\uparrow}^n v_{j\downarrow}^{n*} + u_{j\downarrow}^n v_{i\uparrow}^{n*}\right) + \left(u_{i\downarrow}^n v_{j\uparrow}^{n*} + u_{j\uparrow}^n v_{i\downarrow}^*\right)\right] \tanh\left(\frac{E_n}{2k_BT}\right), \tag{2.26}$$

where $f(E)$ is the Fermi-Dirac distribution function defined in Eq. (1.72).

From Eqs. (2.17)-(2.20), it is not difficult to prove the following theorem:
If $\left(u_{i\uparrow}^{n}, v_{i\downarrow}^{n}, u_{i\downarrow}^{n}, v_{i\uparrow}^{n}\right)$ is the solution to the BdG equations with eigenvalue E_n, then $\left(-v_{i\uparrow}^{n*}, u_{i\downarrow}^{n*}, v_{i\downarrow}^{n*}, -u_{i\uparrow}^{n*}\right)$ is the solution to the same equations with eigenvalue $-E_n$. Using this symmetry property, we can also rewrite Eqs. (2.24)-(2.26) as

$$n_{i\uparrow} = \sum_{n} \left|u_{i\uparrow}^{n}\right|^{2} f\left(E_n\right), \tag{2.27}$$

$$n_{i\downarrow} = \sum_{n} \left|v_{i\downarrow}^{n}\right|^{2} f\left(-E_n\right), \tag{2.28}$$

and

$$\Delta_{ij} = \frac{V}{4} \sum_{n} \left[u_{i\uparrow}^{n} v_{j\downarrow}^{n*} + u_{j\uparrow}^{n} v_{i\downarrow}^{*}\right] \tanh\left(\frac{E_n}{2k_B T}\right). \tag{2.29}$$

In the absence of spin-orbit coupling and other spin-flip scattering terms, that is $\tilde{h}_{i\uparrow,j\downarrow} = \tilde{h}_{i\downarrow,j\uparrow} = 0$, the BdG equations become block-diagonalized into two sets of equations:

$$\begin{cases} E_{\tilde{n}1} u_{i\uparrow}^{\tilde{n}1} = \sum_j \tilde{h}_{i\uparrow,j\uparrow} u_{j\uparrow}^{\tilde{n}1} + \sum_j \Delta_{ij} v_{j\downarrow}^{\tilde{n}1}, \\ E_{\tilde{n}1} v_{i\downarrow}^{\tilde{n}1} = -\sum_j \tilde{h}_{i\downarrow,j\downarrow}^{*} v_{j\downarrow}^{\tilde{n}1} + \sum_j \Delta_{ji}^{*} u_{j\uparrow}^{\tilde{n}1}, \end{cases} \tag{2.30}$$

and

$$\begin{cases} E_{\tilde{n}2} u_{i\downarrow}^{\tilde{n}2} = \sum_j \tilde{h}_{i\downarrow,j\downarrow} u_{j\downarrow}^{\tilde{n}2} + \sum_j \Delta_{ji} v_{j\uparrow}^{\tilde{n}}, \\ E_{\tilde{n}2} v_{i\uparrow}^{\tilde{n}2} = -\sum_j \tilde{h}_{i\uparrow,j\uparrow}^{*} v_{j\uparrow}^{n} + \sum_j \Delta_{ij}^{*} u_{j\downarrow}^{n}. \end{cases} \tag{2.31}$$

This block-diagonalization structure leads to a distinct nature of the canonical transformation:

$$c_{i\uparrow} = \sum_{\tilde{n}}{}' \left(u_{i\uparrow}^{\tilde{n}1} \gamma_{\tilde{n}1} - v_{i\uparrow}^{\tilde{n}2*} \gamma_{\tilde{n}2}^{\dagger}\right), \qquad c_{i\uparrow}^{\dagger} = \sum_{\tilde{n}}{}' \left(u_{i\uparrow}^{\tilde{n}1} * \gamma_{\tilde{n}1}^{\dagger} - v_{i\uparrow}^{\tilde{n}2} \gamma_{\tilde{n}2}\right), \tag{2.32}$$

$$c_{i\downarrow} = \sum_{\tilde{n}}{}' \left(u_{i\downarrow}^{\tilde{n}2} \gamma_{\tilde{n}2} + v_{i\downarrow}^{\tilde{n}1*} \gamma_{\tilde{n}1}^{\dagger}\right), \qquad c_{i\downarrow}^{\dagger} = \sum_{\tilde{n}}{}' \left(u_{i\downarrow}^{\tilde{n}2*} \gamma_{\tilde{n}2}^{\dagger} + v_{i\downarrow}^{\tilde{n}1} \gamma_{\tilde{n}1}\right). \tag{2.33}$$

The block diagonalization and the symmetry property suggest that we merely need to solve Eq. (2.30) subject to the self-consistency condition:

$$n_{i\uparrow} = \sum_{\tilde{n}} \left|u_{i\uparrow}^{\tilde{n}1}\right|^{2} f\left(E_{\tilde{n}1}\right), \tag{2.34}$$

$$n_{i\downarrow} = \sum_{\tilde{n}} \left|v_{i\downarrow}^{\tilde{n}1}\right|^{2} f\left(-E_{\tilde{n}1}\right), \tag{2.35}$$

and

$$\Delta_{ij} = \frac{V}{4} \sum_{\tilde{n}} \left[u_{i\uparrow}^{\tilde{n}1} \tilde{p}_{j\downarrow}^{\tilde{n}1*} + u_{j\uparrow}^{\tilde{n}1} v_{i\downarrow}^{\tilde{1}1*}\right] \tanh\left(\frac{E_{\tilde{n}1}}{2k_B T}\right). \tag{2.36}$$

Therefore, by reducing the diagonalization of a $4N$ by $4N$ matrix down to that of a $2N$ by $2N$ matrix, the computational efficiency is improved significantly. Here N would be $N_x N_y$ for

a two-dimensional lattice while $N_xN_yN_z$ for a three-dimensional lattice with N_x, N_y, and N_z being the linear dimension of the system. When it is obvious that no spin-flip effect occurs, the reduced set of BdG equations, Eq. (2.30), will be used with the hat symbol on the energy eigenvalue index and the set index dropped. It will be encountered frequently in the later discussions.

It is straightforward for us to obtain the BdG equations for an s-wave superconductor in the lattice model. There we first replace U by $-U(U > 0)$ so that the Hamiltonian becomes

$$\mathscr{H} = \sum_{ij,\sigma\sigma'} c^{\dagger}_{i\sigma} \left[h_{i\sigma,j\sigma'} - \mu\delta_{ij}\delta_{\sigma\sigma'} \right] c_{j\sigma'} - U \sum_{i} n_{i\uparrow} n_{i\downarrow} \tag{2.37}$$

which leads to the BdG equations:

$$E_n u^n_{i\uparrow} = \sum_{j\sigma'} \tilde{h}_{i\uparrow.j\sigma'} u_{j\sigma'} + \Delta_{ii} v^n_{i\downarrow}, \tag{2.38}$$

$$E_n u^n_{i\downarrow} = \sum_{j\sigma'} \tilde{h}_{i\downarrow,j\sigma'} u^n_{j\sigma'} + \Delta_{ii} v^n_{i\uparrow}, \tag{2.39}$$

$$E_n v^n_{i\uparrow} = -\sum_{j\sigma'} \sigma' \tilde{h}^*_{i\uparrow.j\sigma'} v^n_{j\sigma'} + \Delta^*_{ii} u^n_{j\downarrow}, \tag{2.40}$$

$$E_n v^n_{i\downarrow} = \sum_{j\sigma'} \sigma' \tilde{h}^*_{i\downarrow,j\sigma'} v^n_{j\sigma'} + \Delta^*_{ii} u^n_{i\uparrow}. \tag{2.41}$$

Here

$$\tilde{h}_{i\sigma,j\sigma'} = h_{i\sigma,j\sigma'} - \mu\delta_{ij}\delta_{\sigma\sigma'}, \tag{2.42}$$

and the self-consistency condition

$$\Delta_{ii} = \frac{U}{2} \sum_{n}{}' \left[u^n_{i\uparrow} v^{n*}_{i\downarrow} + u^n_{i\downarrow} v^{n*}_{i\uparrow} \right] \tanh\left(\frac{E_n}{2k_BT} \right). \tag{2.43}$$

In the absence of spin-orbit coupling and spin-flip scattering, the BdG equations become

$$\begin{cases} E_{\tilde{n}1} u^{\tilde{n}1}_{i\uparrow} = \sum_j \tilde{h}_{i\uparrow,j\uparrow} u^{\tilde{n}1}_{j\uparrow} + \Delta_{ii} v^{\tilde{n}1}_{i\downarrow}, \\ E_{\tilde{n}1} v^{\tilde{n}1}_{i\downarrow} = -\sum_j \tilde{h}^*_{i\downarrow,j\downarrow} v^{\tilde{n}1}_{j\downarrow} + \Delta^*_{ii} u^{\tilde{n}1}_{i\uparrow}, \end{cases} \tag{2.44}$$

and

$$\begin{cases} E_{\tilde{n}2} u^{\tilde{n}2}_{i\downarrow} = \sum_j \tilde{h}_{i\downarrow,j\downarrow} \tilde{u}^{\tilde{2}}_{j\downarrow} + \Delta_{ii} v^{\tilde{n}2}_{i\uparrow}, \\ E_{\tilde{n}2} v^{\tilde{n}2}_{i\uparrow} = -\sum_j \tilde{h}^*_{i\uparrow,j\uparrow} v^n_{j\uparrow} + \Delta^*_{ii} u^*_{i\downarrow} \end{cases} \tag{2.45}$$

with

$$\Delta_{ii} = \frac{U}{2} \sum_{\tilde{n}} u^{\tilde{n}1}_{i\uparrow} v^{\tilde{n}1*}_{j\downarrow} \tanh\left(\frac{E_{\tilde{n}1}}{2k_BT} \right). \tag{2.46}$$

Unless explicitly specified, we will focus on Eq. (2.44) with the tilde on the eigenenergy index and set index dropped.

The tight-binding model, from which the BdG equations are derived, has the origin from such strongly correlated models as the $t - J$ model [3] for hightemperature cuprates. The derived BdG equations in the tight-binding model have been used not only for unconventional superconductors with narrow electron band [4-9] but also for s-wave superconductors [10]. The calculated quantities range from the local density states to the superfluid density, which will be discussed in more details in later chapters.

9.7.2 Local Density of States and Bond Current in the Lattice Model

Theory

From Eqs. (2.24), (2.25), we extract the expression for the local density of states:

$$\rho_{i\sigma}(E) = \sum_{n}{}' \left[\left| u_{i\sigma}^{n} \right|^2 \delta \left(E_n - E \right) + \left| v_{i\sigma} \right|^2 \delta \left(E_n + E \right) \right] \tag{2.47}$$

and the corresponding thermalized density of states

$$\rho_{i\sigma}(E) = -\sum_{n}{}' \left[\left| u_{i\sigma}^{n} \right|^2 f' \left(E_n - E \right) + \left| v_{i\sigma} \right|^2 f' \left(E_n + E \right) \right]. \tag{2.48}$$

The bond current can be derived in the following way. The Heisenberg equation of motion for $\langle n_i \rangle = \langle n_{i\uparrow} \rangle + \langle n_{i\downarrow} \rangle$ is:

$$\begin{aligned} i\hbar \frac{\partial \langle n_i \rangle}{\partial t} &= \left\langle \left[n_i, H \right]_- \right\rangle \\ &= \left\langle \left\{ - \sum_{j \neq i, \sigma, \sigma'} \left[-t \left(j\sigma', i\sigma \right) c_{j\sigma'}^{\dagger} c_{i\sigma} + t \left(i\sigma, j\sigma' \right) c_{i\sigma}^{\dagger} c_{j\sigma'} \right] \right\} \right\rangle \end{aligned} \tag{2.49}$$

where H is the system Hamiltonian given by Eq. (2.4). The electrical current operator from site j to site i is then found to be:

$$\hat{J}_{ij} = \frac{e}{i\hbar} \sum_{\sigma, \sigma'} \left[t \left(i\sigma, j\sigma' \right) c_{i\sigma}^{\dagger} c_{j\sigma'} - t \left(j\sigma', i\sigma \right) c_{j\sigma'}^{\dagger} c_{i\sigma} \right], \tag{2.50}$$

and the average bond current is given by:

$$J_{ij} = \frac{e}{i\hbar} \sum_{\sigma, \sigma'} \sum_{n}{}' \left\{ t \left(i\sigma, j\sigma' \right) \left[u_{i\sigma}^{n*} u_{j\sigma'}^{n} f \left(E_n \right) + \sigma\sigma' v_{i\sigma}^{n} v_{j\sigma'}^{n*} \left(1 - f \left(E_n \right) \right) \right] - \text{ c.c. } \right\} \tag{2.51}$$

Using the symmetry property of the BdG equations, we can also write the physical quantities in the following form:

$$n_{i\sigma} = \sum_{n} \left| u_{i\sigma}^{n} \right|^2 f \left(E_n \right) = \sum_{n} \left| v_{i\sigma}^{n} \right|^2 \left[1 - f \left(E_n \right) \right], \tag{2.52}$$

$$\begin{aligned} J_{ij} &= \frac{e}{i\hbar} \sum_{\sigma, \sigma'} \sum_{n} \left\{ t \left(i\sigma, j\sigma' \right) u_{i\sigma}^{n*} u_{j\sigma'}^{n} f \left(E_n \right) - \text{ c.c. } \right\} \\ &= \frac{e}{i\hbar} \sum_{\sigma, \sigma'} \sum_{n} \left\{ t \left(i\sigma, j\sigma' \right) \sigma\sigma' v_{i\sigma}^{n} v_{j\sigma'}^{n*} \left(1 - f \left(E_n \right) \right) - \text{ c.c. } \right\}, \end{aligned} \tag{2.53}$$

and

$$\rho_{i\sigma}(E) = -\sum_{n} \left| u_{i\sigma}^{n} \right|^2 f' \left(E_n - E \right) = -\sum_{n} \left| v_{i\sigma}^{n} \right|^2 f' \left(E_n + E \right). \tag{2.54}$$

These new formulations are especially useful when we study the ferromagnetic impurity or Zeeman effect because the wavefunction of quasiparticles can be solved in a 2×2 spin space.

9.7.3 Nambu Notation for SC Junctions

(??? see my thesis, I'll write here it later)

Theory

9.7.4 Optical Conductivity and Superfluid Density in the Lattice Model

(??? what is the meaning of both values??)

Derivation by (???)

The BdG solutions can not only describe the local density of states, which is a direct measure of single particle properties, but also the eigenfunctions can be used to study the two-particle correlations. In particular, the optical superconductivity reveals the information about the coherent peak [11], while the superfluid stiffness [12] and its temperature dependence set a criterion for superconductivity. Both quantities are directly measurable in experiments. Theoretically, the formulae for these quantities, as derived from the BdG method, are also valid for inhomogeneous superconductors.

The formula of the superfluid density in a lattice model was first derived by Scalapino et al. [12, 13] in a Hubbard model. It was then used for calculations in other models. In the following, we give the derivation for the model with the Hamiltonian defined by Eq. (2.4) in the absence of spin-orbit coupling and other spin-flip scattering, that is,

$$\mathscr{H} = \sum_{ij,\sigma} c_{i\sigma}^{\dagger} \left[-t_{ij} - \left(\mu + \frac{U}{2} - U_i^{\mathrm{imp}} \right) \delta_{ij} \right] c_{j\sigma} + U \sum_i n_{i\uparrow} n_{i\downarrow} - \frac{V}{2} \sum_{i \neq j} n_i n_j$$

Here the impurity potential is represented by U_i^{imp} .
In the presence of an electric field pointing to the x-direction,

$$E_x \left(\mathbf{r}_i, t \right) = \Xi_x e^{i(\mathbf{q} \cdot \mathbf{r}_i - \omega t)} \tag{2.56}$$

The current density along the x-direction is defined as

$$J_x \left(\mathbf{r}_i, t \right) = \sigma_{xx} \left(\mathbf{r}_i, \omega \right) E_x \left(\mathbf{r}_i, t \right) \tag{2.57}$$

where $\sigma_{xx} \left(\mathbf{r}_i, \omega \right)$ is the local conductivity. In the Coulomb gauge, which dictates $\nabla \cdot \mathbf{A} = 0$ and the scalar potential $\phi = 0$, the electric field can be expressed in terms of a vector potential

$$A_x \left(\mathbf{r}_i, t \right) = -\frac{i}{\omega} E_x \left(\mathbf{r}_i, t \right) \tag{2.58}$$

Therefore, the total Hamiltonian becomes

$$H_{\mathrm{t}} = -\sum_{ij,\sigma} \tilde{t}_{ij} c_{i\sigma}^{\dagger} c_{j\sigma} + \sum_{i\sigma} \left(U_i^{\mathrm{imp}} - \frac{U}{2} - \mu \right) c_{i\sigma}^{\dagger} c_{i\sigma} + U \sum_i n_{i\uparrow} n_{i\downarrow} - \frac{V}{2} \sum_{ij} n_i n_j \tag{2.59}$$

where

$$\tilde{t}_{ij} = t_{ij} e^{i\phi_{ij}(t)} \tag{2.60}$$

with the gauge phase $\phi_{ij}(t) = eA_{ij} = eA_x \left(\mathbf{r}_i, t \right) (x_i - x_j)$. Hereafter the charge e for electrons includes the sign. In the linear response limit, we expand this hopping term up to the second order of $A_x \left(\mathbf{r}_i, t \right)$:

$$\tilde{t}_{ij} \approx t\left[1 + i\phi_{ij} + \frac{1}{2!}\left(i\phi_{ij}\right)^2\right]. \tag{2.61}$$

The total Hamiltonian can then be rewritten as:

$$H_{\mathrm{t}} = H - i\sum_{ij,\sigma}\phi_{ij}(t)t_{ij}c_{i\sigma}^{\dagger}c_{j\sigma} + \frac{1}{2}\sum_{ij,\sigma}\phi_{ij}^2(t)t_{ij}c_{i\sigma}^{\dagger}c_{j\sigma} \tag{2.62}$$

If we limit the hopping integral only between the nearest neighbors, we have

$$\begin{aligned}
H_{\mathrm{t}} =& H - iea\sum_{i,\sigma}\left[-A_x\left(\mathbf{r}_i,t\right)t_{i,i+\hat{x}}c_{i\sigma}^{\dagger}c_{i+\hat{x},\sigma} + A_x\left(\mathbf{r}_{i+\hat{x}},t\right)t_{i+\hat{x},i}c_{i+\hat{x},\sigma}^{\dagger}c_{i\sigma}\right] \\
&+ \frac{e^2a^2}{2}\sum_{i,\sigma}\left[A_x^2\left(\mathbf{r}_i,t\right)t_{i,i+\hat{x}}c_{i\sigma}^{\dagger}c_{i+\hat{x},\sigma} + A_x^2\left(\mathbf{r}_{i+\hat{x}},t\right)t_{i+\hat{x},i}c_{i+\hat{x},\sigma}^{\dagger}c_{i\sigma}\right] \\
\approx& H - iea\sum_{i,\sigma}A_x\left(\mathbf{r}_i,t\right)\left[-t_{i,i+\hat{x}}c_{i\sigma}^{\dagger}c_{i+\hat{x},\sigma} + t_{i+\hat{x},i}c_{i+\hat{x},\sigma}^{\dagger}c_{i\sigma}\right] \\
&+ \frac{e^2a^2}{2}\sum_{i,\sigma}A_x^2\left(\mathbf{r}_i,t\right)\left[t_{i,i+\hat{x}}c_{i\sigma}^{\dagger}c_{i+\hat{x},\sigma} + t_{i+\hat{x},i}c_{i+\hat{x},\sigma}^{\dagger}c_{i\sigma}\right] \\
\approx& H - ea\sum_{i}A_x\left(\mathbf{r}_i,t\right)J_x^P\left(\mathbf{r}_i\right) - \frac{e^2a^2}{2}\sum_{i}A_x^2\left(\mathbf{r}_i,t\right)K_x\left(\mathbf{r}_i\right) \\
=& H + H'(t)
\end{aligned} \tag{2.63}$$

where the particle current and the local kinetic energy associated with the x-oriented links are defined as

$$\begin{aligned}
J_x^P\left(\mathbf{r}_i\right) &= i\sum_{\sigma}\left[t_{i+\hat{x},i}c_{i+\hat{x},\sigma}^{\dagger}c_{i\sigma} - t_{i,i+\hat{x}}c_{i\sigma}^{\dagger}c_{i+\hat{x},\sigma}\right] \\
&= it\sum_{\sigma}\left[c_{i+\hat{x},\sigma}^{\dagger}c_{i\sigma} - c_{i\sigma}^{\dagger}c_{i+\hat{x},\sigma}\right]
\end{aligned} \tag{2.64}$$

and

$$\begin{aligned}
K_x\left(\mathbf{r}_i\right) &= -\sum_{\sigma}\left[t_{i,i+\hat{x}}c_{i\sigma}^{\dagger}c_{i+\hat{x},\sigma} + t_{i+\hat{x},i}c_{i+\hat{x},\sigma}^{\dagger}c_{i\sigma}\right] \\
&= -t\sum_{\sigma}\left[c_{i\sigma}^{\dagger}c_{i+\hat{x},\sigma} + c_{i+\hat{x},\sigma}^{\dagger}c_{i\sigma}\right]
\end{aligned} \tag{2.65}$$

The x-oriented current density operator is then found to be

$$J_x^Q\left(\mathbf{r}_i\right) = -\frac{\delta H'(t)}{\delta A_x\left(\mathbf{r}_i,t\right)} = eJ_x^P\left(\mathbf{r}_i\right) + e^2K_x\left(\mathbf{r}_i\right)A_x\left(\mathbf{r}_i,t\right). \tag{2.66}$$

Here we have set the lattice constant $a = 1$.
An alternative derivation of the current density operator is to start with the electric polarization operator:

$$\mathbf{P} = e\sum_{i}\mathbf{r}_i n_i \tag{2.67}$$

with its x-component

$$P_x = e\sum_i x_i n_i \tag{2.68}$$

The time-derivative is

$$\begin{aligned} J_x^Q(\mathbf{r}_i) &= i\left[H_{\mathrm{t}}, P_x\right] \\ &= ie\sum_{ij,\sigma} x_i\left[\tilde{t}_{ij}c_{i\sigma}^\dagger c_{j\sigma} - \tilde{t}_{ji}c_{j\sigma}^\dagger c_{i\sigma}\right] \\ &= ie\sum_{ij,\sigma}\left(x_i - x_j\right)\tilde{t}_{ij}c_{i\sigma}^\dagger c_{j\sigma} \\ &= ie\sum_{ij,\sigma}\left(x_i - x_j\right)t_{ij}\left(1 + i\phi_{ij}\right)c_{i\sigma}^\dagger c_{j\sigma} \\ &= eJ_x^P(\mathbf{r}_i) + e^2K_x(\mathbf{r}_i)A_x(\mathbf{r}_i,t) \end{aligned} \tag{2.69}$$

Now let us calculate the expectation value of the current density operator. In the linear response theory, the statistical operator in the interaction picture is given by:

$$\hat{\rho}_I(t) = \hat{\rho}_I(-\infty) - \frac{i}{\hbar}\int_{-\infty}^{t}\left[H_I'(t'), \hat{\rho}_I(-\infty)\right] - dt' \tag{2.70}$$

The expectation of a physical variable is found to be:

$$\langle\hat{O}\rangle = \mathrm{Tr}\left[\hat{\rho}_I(-\infty)\hat{O}_I\right] - \frac{i}{\hbar}\int_{-\infty}^{t}\mathrm{Tr}\left\{\hat{\rho}_I(-\infty)\left[\hat{O}_I(t), H_I'(t')\right]_-\right\}dt' \tag{2.71}$$

$$= \left\langle\hat{O}_I\right\rangle_0 - \frac{i}{\hbar}\int_{-\infty}^{t}\left\langle\left[\hat{O}_I(t), H_I'(t')\right]_-\right\rangle_0 dt' \tag{2.72}$$

where

$$\hat{O}_I = e^{iHt}\hat{O}e^{-iHt} \tag{2.73}$$

and

$$H_I'(t) = e^{iHt}H'(t)e^{-iHt} \tag{2.74}$$

with the term proportional to $A^2(t)$ in $H'(t)$ neglected. The particle current density is then given by

$$\left\langle J_x^P(\mathbf{r}_i)\right\rangle = -i\int_{-\infty}^{t}\left\langle\left[J_x^P(\mathbf{r}_i,t), H_I'(t)\right]\right\rangle, \tag{2.75}$$

where the particle operator and the perturbation term in the Heisenberg picture with respect to the unperturbed Hamiltonian H are given by, respectively,

$$J_x^P(\mathbf{r}_i,t) = e^{iHt}J_x^P(\mathbf{r}_i)e^{-iHt} \tag{2.76}$$

We notice that the first term in $H'(t)$ can be rewritten as

$$-e\sum_{i,\sigma}A_x(\mathbf{r}_i,t)J_x^P(\mathbf{r}_i) = \frac{ie}{\omega}J_x^P(-\mathbf{q})\Xi_x e^{-i\omega t} \tag{2.77}$$

where the Fourier transform of the particle density operator is given by

$$J_x^P(\mathbf{q}) = \sum_i e^{-i\mathbf{q}\cdot\mathbf{r}_i} J_x^P(\mathbf{r}_i) \tag{2.78}$$

We then obtain

$$\left\langle J_x^P(\mathbf{r}_i)\right\rangle = \frac{e}{\omega} E_x(\mathbf{r}_i,t)\, e^{-i\mathbf{q}\cdot\mathbf{r}_i} \int_{-\infty}^{t} dt' e^{i\omega(t-t')} \left\langle \left[J_x^P(\mathbf{r}_i,t), J_x^P(-\mathbf{q},t')\right]\right\rangle. \tag{2.79}$$

Finally, the current density is found to be

$$\begin{aligned}\left\langle J_x^Q(\mathbf{r}_i)\right\rangle =& \frac{e^2}{\omega} E_x(\mathbf{r}_i,t)\, e^{-i\mathbf{q}\cdot\mathbf{r}_i} \int_{-\infty}^{t} dt' e^{i\omega(t-t')} \left\langle \left[J_x^P(\mathbf{r}_i,t), J_x^P(-\mathbf{q},t')\right]\right\rangle \\ & - \frac{ie^2}{\omega} \left\langle K_x(\mathbf{r}_i)\right\rangle E_x(\mathbf{r}_i,t)\end{aligned} \tag{2.80}$$

The local conductivity is then given by

$$\begin{aligned}\sigma_{xx}(\mathbf{r}_i,\omega) =& \frac{\left\langle J_x^Q(\mathbf{r}_i)\right\rangle}{E_x(\mathbf{r}_i,t)} \\ =& \frac{e^2}{\omega} e^{-i\mathbf{q}\mathbf{r}_i} \int_{-\infty}^{t} dt' e^{i\omega(t-t')} \left\langle \left[J_x^P(\mathbf{r}_i,t), J_x^P(-\mathbf{q},t')\right]\right\rangle - \frac{ie^2}{\omega}\left\langle K_x(\mathbf{r}_i)\right\rangle\end{aligned} \tag{2.81}$$

To eliminate the atomic fluctuations, we take an average over the spatial variable $\mathbf{r}_i$ and obtain the conductivity

$$\sigma_{xx}(\mathbf{q},\omega) = \frac{e^2}{N\omega} \int_{-\infty}^{t} dt' e^{i\omega(t-t')} \left\langle \left[J_x^P(\mathbf{q},t), J_x^P(-\mathbf{q},t')\right]\right\rangle - \frac{ie^2}{\omega}\left\langle K_x\right\rangle.$$

where

$$\left\langle K_x\right\rangle = \frac{1}{N}\sum_i \left\langle K_x(\mathbf{r}_i)\right\rangle \tag{2.82}$$

Since the correlation function in Eq. (2.82) is only a function of the time difference $t-t'$, we can express the conductivity as

$$\begin{aligned}\sigma_{xx}(\mathbf{q},\omega) &= \frac{e^2}{N\omega}\int_0^{\infty} dt e^{i\omega t} \left\langle \left[J_x^P(\mathbf{q},t), J_x^P(-\mathbf{q},0)\right]\right\rangle - \frac{ie^2}{\omega}\left\langle K_x\right\rangle \\ &= \frac{e^2}{i\omega}\left[\frac{i}{N}\int_{-\infty}^{\infty} dt\theta(t) e^{i\omega t} \left\langle \left[J_x^P(\mathbf{q},t), J_x^P(-\mathbf{q},0)\right]\right\rangle + \left\langle K_x\right\rangle\right] \\ &= \frac{e^2}{i\omega}\left[-\Pi_{xx}(\mathbf{q},\omega) + \left\langle K_x\right\rangle\right],\end{aligned} \tag{2.83}$$

where we define the retarded correlation function of the particle current operator as

$$\Pi_{xx}(\mathbf{q},t) = -\frac{i}{N}\theta(t)\left\langle \left[J_x^P(\mathbf{q},t), J_x^P(-\mathbf{q},0)\right]\right\rangle, \tag{2.84}$$

with its Fourier transform

$$\Pi_{xx}(\mathbf{q},\omega) = \int_{-\infty}^{\infty} dt e^{i\omega t}\Pi_{xx}(\mathbf{q},t) \tag{2.85}$$

The frequency-dependent, uniform electrical conductivity is given by taking the limit $\mathbf{q} \to 0$:

$$\sigma_{xx}(\omega) = \frac{e^2}{i\omega} \left[-\Pi_{xx}(\mathbf{q} = 0, \omega) + \langle K_x \rangle \right]. \tag{2.86}$$

The dc conductivity is obtained by taking first the limit $\mathbf{q} \to 0$ and then the limit $\omega \to 0$.

$$\sigma_{xx} = -\lim_{\omega \to 0} \frac{e^2}{i\omega} \left[-\Pi_{xx}(\mathbf{q} = 0, \omega) + \langle K_x \rangle \right]. \tag{2.87}$$

Be reminded that the order of these limits cannot be reversed.
Similarly the transverse conductivity can also be derived as:

$$\sigma_{xy}(\mathbf{q}, \omega) = \frac{e^2}{i\omega} \left[-\Pi_{xy}(\mathbf{q}, \omega) \right]. \tag{2.88}$$

It is convenient to calculate the retarded correlation function in the Matsubara formalism. First define the equivalent current-current correlation function in the Matsubara formalism:

$$\Pi_{xx}(\mathbf{q}, \tau) = -\frac{1}{N} \left\langle T_\tau \left[J_x^P(\mathbf{q}, \tau) J_x^P(-\mathbf{q}, 0) \right] \right\rangle, \tag{2.89}$$

$$\Pi_{xx}\left(\mathbf{q}, i\omega_n\right) = \int_0^\beta d\tau e^{i\omega_n \tau} \Pi_{xx}(\mathbf{q}, \tau), \tag{2.90}$$

where $\omega_n = 2n\pi T$ since the current density operator is regarded as a bosonic operator acting as a composite particle. The Matsubara function is evaluated as best one can. Then the desired retarded function is obtained by performing the analytical continuation $i\omega_n \to \omega + i\delta$:

$$\Pi_{xx}(\mathbf{q}, \omega) = \Pi_{xx}\left(\mathbf{q}, i\omega_n \to \omega + i\delta\right). \tag{2.91}$$

Technically, we always write the conductivity formula as:

$$\sigma_{xx}(\mathbf{q}, \omega) = \frac{e^2}{i(\omega + i\delta)} \left[-\Pi_{xx}(\mathbf{q}, \omega) + \langle K_x \rangle \right], \tag{2.92}$$

and its uniform counterpart

$$\sigma_{xx}(\omega) = \frac{e^2}{i(\omega + i\delta)} \left[-\Pi_{xx}(\mathbf{q} = 0, \omega) + \langle K_x \rangle \right] \tag{2.93}$$

If the numerator approaches a finite limit as $\omega \to 0$, the real part of $\sigma_{xx}(\omega)$ will contain a delta function contribution $D\delta(\omega)$ with the "Drude weight" given by

$$\frac{D}{\pi e^2} \equiv \frac{\rho^*}{4\pi} = -\langle K_x \rangle + \Pi_{xx}(\mathbf{q} = 0, \omega \to 0) \tag{2.94}$$

with ρ^* an effective density of the mobile charge carriers in units of their mass. This implies a zero resistance state.

In a superconductor, the Meissner effect is the current response to a static, i.e., $\omega = 0$ and transverse gauge potential $\mathbf{q} \cdot \mathbf{A}(\mathbf{q}, \omega = 0) = 0$. In this case, the electric field $\mathbf{E} = 0$. When we only apply a transverse electric field along the x direction, we should have $q_x A_x(\mathbf{q}, \omega = 0) = 0$, which requires $q_x = 0$. Following the same procedure as before, we can find the expectation value of the electrical current operator

$$\left\langle J_x^Q\left(\mathbf{r}_i\right) \right\rangle = ie^2 A_x\left(\mathbf{r}_i\right) e^{-i\mathbf{q}\cdot\mathbf{r}_i} \int_{-\infty}^{t} dt' \left\langle \left[J_x^P\left(\mathbf{r}_i, t\right), J_x^P\left(-\mathbf{q}, t'\right) \right] \right\rangle + e^2 \left\langle K_x\left(\mathbf{r}_i\right) \right\rangle A_x\left(\mathbf{r}_i\right) \tag{2.95}$$

We then have

$$\frac{\left\langle J_x^Q\left(\mathbf{r}_i\right)\right\rangle}{e^2 A_x\left(\mathbf{r}_i\right)}=ie^{-i\mathbf{q}\cdot\mathbf{r}_i}\int_{-\infty}^{t}dt'\left\langle\left[J_x^P\left(\mathbf{r}_i,t\right),J_x^P\left(-\mathbf{q},t'\right)\right]\right\rangle+\left\langle K_x\left(\mathbf{r}_i\right)\right\rangle. \tag{2.96}$$

By performing an average over the spatial variable $\mathbf{r}_i$ to eliminate the atomic fluctuations, we define an effective "Drude weight" as

$$\frac{D_s}{\pi e^2}=\frac{\rho_s^*}{4\pi}=-\left\langle K_x\right\rangle+\Pi_{xx}\left(q_x=0,q_y\to 0,\omega=0\right). \tag{2.97}$$

The quantity D_s measures the superfluid density in units of the mass. The crucial difference between ρ^* and ρ_s^* is the order in which the momentum and frequency approach zero.

For a superconductor, we perform the BdG transformation:

$$c_{i\sigma}=\sum_{n(E_n\geq 0)}\left(u_{i\sigma}^n\gamma_n-\sigma v_{i\sigma}^{n*}\gamma_n^\dagger\right) \tag{2.98}$$

The kinetic energy can be found readily:

$$\left\langle K_x\right\rangle=-\frac{t}{N}\sum_{i,n,\sigma}\left\{f\left(E_n\right)\left[u_{i+x,\sigma}^{n*}u_{i\sigma}^n+\text{ c.c. }\right]+\left(1-f\left(E_n\right)\right)\left[v_{i+x,\sigma}^n v_{i\sigma}^{n*}+\text{ c.c }\right]\right\} \tag{2.99}$$

However, the re-expression of the current-current correlation function is much more tedious. In the expansion form, the commutator:

$$\left[J_x^P(\mathbf{q},t),J_x^P(-\mathbf{q},0)\right]=(it)^2\sum_{i\sigma}\sum_{i'\sigma'}e^{-i\mathbf{q}\cdot\left(\mathbf{r}_i-\mathbf{r}_i\right)}[\hat{A}+\hat{B}+\hat{C}+\hat{D}], \tag{2.100}$$

where

$$\hat{A}=\left[c_{i+\hat{x},\sigma}^\dagger(t)c_{i\sigma}(t),c_{i'+\hat{x},\sigma'}^\dagger c_{i'\sigma'}\right], \tag{2.101}$$

$$\hat{B}=-\left[c_{i+\hat{x},\sigma}^\dagger(t)c_{i\sigma}(t),c_{i'\sigma'}^\dagger c_{i'+\hat{x},\sigma'}\right], \tag{2.102}$$

$$\hat{C}=-\left[c_{i\sigma}^\dagger(t)c_{i+\hat{x},\sigma}(t),c_{i'+\hat{x},\sigma'}^\dagger c_{i'\sigma'}\right], \tag{2.103}$$

$$\hat{D}=\left[c_{i\sigma}^\dagger(t)c_{i+\hat{x},\sigma}(t),c_{i'\sigma'}^\dagger c_{i'+\hat{x},\sigma'}\right], \tag{2.104}$$

with

$$\begin{aligned}c_{i+\hat{x},\sigma}^\dagger(t)c_{i\sigma}(t)&=\sum_{n_1,n_2}\left[\left(u_{i+\hat{x},\sigma}^{n_1*}\gamma_{n_1}^\dagger(t)-\sigma v_{i+\hat{x},\sigma}^{n_1}\gamma_{n_1}(t)\right)\left(u_{i\sigma}^{n_2}\gamma_{n_2}(t)-\sigma v_{i\sigma}^{n_2*}\gamma_{n_2}^\dagger(t)\right)\right]\\&=\sum_{n_1n_2}\Big[u_{i+\hat{x},\sigma}^{n_1*}u_{i\sigma}^{n_2}e^{i\left(E_{n_1}-E_{n_2}\right)t}\gamma_{n_1}^\dagger\gamma_{n_2}-\sigma u_{i+\hat{x},\sigma}^{n_1*}v_{i\sigma}^{n_2*}e^{i\left(E_{n_1}+E_{n_2}\right)t}\gamma_{n_1}^\dagger\gamma_{n_2}^\dagger\\&\quad-\sigma v_{i+\hat{x},\sigma}^{n_1}u_{i\sigma}^{n_2}e^{-i\left(E_{n_1}+E_{n_2}\right)t}\gamma_{n_1}\gamma_{n_2}+v_{i+\hat{x},\sigma}^{n_1}v_{i\sigma}^{n_2*}e^{-i\left(E_{n_1}-E_{n_2}\right)t}\gamma_{n_1}\gamma_{n_2}^\dagger\Big],\end{aligned} \tag{2.105}$$

and

$$
\begin{aligned}
c^{\dagger}_{i\sigma}(t)c_{i+\hat{x},\sigma}(t) &= \sum_{n_1,n_2}\left[\left(u^{n_1*}_{i\sigma}\gamma^{\dagger}_{n_1}(t)-\sigma v^{n_1}_{i\sigma}\gamma_{n_1}(t)\right)\left(u^{n_2}_{i+\hat{x},\sigma}\gamma_{n_2}(t)-\sigma v^{n_2*}_{i+\hat{x},\sigma}\gamma^{\dagger}_{n_2}(t)\right)\right] \\
&= \sum_{n_1 n_2}\Big[u^{n_1*}_{i\sigma}u^{n_2}_{i+\hat{x},\sigma}e^{i\left(E_{n_1}-E_{n_2}\right)t}\gamma^{\dagger}_{n_1}\gamma_{n_2}-\sigma u^{n_1*}_{i\sigma}v^{n_2*}_{i+\hat{x},\sigma}e^{i\left(E_{n_1}+E_{n_2}\right)t}\gamma^{\dagger}_{n_1}\gamma^{\dagger}_{n_2} \\
&\quad -\sigma v^{n_1}_{i\sigma}u^{n_2}_{i+\hat{x},\sigma}e^{-i\left(E_{n_1}+E_{n_2}\right)t}\gamma_{n_1}\gamma_{n_2}+v^{n_1}_{i\sigma}v^{n_2*}_{i+\hat{x},\sigma}e^{-i\left(E_{n_1}-E_{n_2}\right)t}\gamma_{n_1}\gamma^{\dagger}_{n_2}\Big] \qquad (2.106)
\end{aligned}
$$

Using the following relations

$$
\begin{aligned}
\left\langle\left[\gamma^{\dagger}_{n_1}\gamma_{n_2},\gamma^{\dagger}_{n_3}\gamma_{n_4}\right]\right\rangle &= \left(\left\langle\gamma^{\dagger}_{n_1}\gamma_{n_1}\right\rangle-\left\langle\gamma^{\dagger}_{n_2}\gamma_{n_2}\right\rangle\right)\delta_{n_1n_4}\delta_{n_2n_3}, \qquad (2.107)\\
\left\langle\left[\gamma^{\dagger}_{n_1}\gamma_{n_2},\gamma_{n_3}\gamma^{\dagger}_{n_4}\right]\right\rangle &= -\left(\left\langle\gamma^{\dagger}_{n_1}\gamma_{n_1}\right\rangle-\left\langle\gamma^{\dagger}_{n_2}\gamma_{n_2}\right\rangle\right)\delta_{n_1n_3}\delta_{n_2n_4}, \qquad (2.108)\\
\left\langle\left[\gamma^{\dagger}_{n_1}\gamma^{\dagger}_{n_2},\gamma_{n_3}\gamma_{n_4}\right]\right\rangle &= \left(\delta_{n_1n_4}\delta_{n_2n_3}-\delta_{n_1n_3}\delta_{n_2n_4}\right)\left(\left\langle\gamma^{\dagger}_{n_1}\gamma_{n_1}\right\rangle-\left\langle\gamma^{\dagger}_{n_2}\gamma^{\dagger}_{n_2}\right\rangle\right), \qquad (2.109)\\
\left\langle\left[\gamma_{n_1}\gamma_{n_2},\gamma^{\dagger}_{n_3}\gamma^{\dagger}_{n_4}\right]\right\rangle &= \left(\delta_{n_1n_4}\delta_{n_2n_3}-\delta_{n_1n_3}\delta_{n_2n_4}\right)\left(\left\langle\gamma_{n_1}\gamma^{\dagger}_{n_1}\right\rangle-\left\langle\gamma^{\dagger}_{n_2}\gamma_{n_2}\right\rangle\right), \qquad (2.110)\\
\left\langle\left[\gamma_{n_1}\gamma^{\dagger}_{n_2},\gamma^{\dagger}_{n_3}\gamma_{n_4}\right]\right\rangle &= -\left(\left\langle\gamma_{n_1}\gamma^{\dagger}_{n_1}\right\rangle-\left\langle\gamma_{n_2}\gamma^{\dagger}_{n_2}\right\rangle\right)\delta_{n_1n_3}\delta_{n_2n_4}, \qquad (2.111)\\
\left\langle\left[\gamma_{n_1}\gamma^{\dagger}_{n_2},\gamma_{n_3}\gamma^{\dagger}_{n_4}\right]\right\rangle &= \left(\left\langle\gamma_{n_1}\gamma^{\dagger}_{n_1}\right\rangle-\left\langle\gamma_{n_2}\gamma^{\dagger}_{n_2}\right\rangle\right)\delta_{n_1n_4}\delta_{n_2n_3}, \qquad (2.112)
\end{aligned}
$$

we obtain

$$
\begin{aligned}
\langle\hat{A}\rangle = \sum_{n_1n_2}\Big[&u^{n_1*}_{i+\hat{x},\sigma}u^{n_2}_{i\sigma}e^{i\left(E_{n_1}-E_{n_2}\right)t}u^{n_2*}_{i'+\hat{x},\sigma'}u^{n_1}_{i'\sigma'}\left(\left\langle\gamma^{\dagger}_{n_1}\gamma_{n_1}\right\rangle-\left\langle\gamma^{\dagger}_{n_2}\gamma_{n_2}\right\rangle\right)\\
&-u^{n_1*}_{i+\hat{x},\sigma}u^{n_2}_{i\sigma}e^{i\left(E_{n_1}-E_{n_2}\right)t}v^{n_1}_{i'+\hat{x},\sigma'}v^{n_2*}_{i'\sigma'}\left(\left\langle\gamma^{\dagger}_{n_1}\gamma_{n_1}\right\rangle-\left\langle\gamma^{\dagger}_{n_2}\gamma_{n_2}\right\rangle\right)\\
&+\sigma\sigma' u^{n_1*}_{i+\hat{x},\sigma}v^{n_2*}_{i\sigma}e^{i\left(E_{n_1}+E_{n_2}\right)t}v^{n_2}_{i'+\hat{x},\sigma'}u^{n_1}_{i'\sigma'}\left(\left\langle\gamma^{\dagger}_{n_1}\gamma_{n_1}\right\rangle-\left\langle\gamma_{n_2}\gamma^{\dagger}_{n_2}\right\rangle\right)\\
&-\sigma\sigma' u^{n_1*}_{i+\hat{x},\sigma}v^{n_2*}_{i\sigma}e^{i\left(E_{n_1}+E_{n_2}\right)t}v^{n_1}_{i'+\hat{x},\sigma'}u^{n_2}_{i'\sigma'}\left(\left\langle\gamma^{\dagger}_{n_1}\gamma_{n_1}\right\rangle-\left\langle\gamma_{n_2}\gamma^{\dagger}_{n_2}\right\rangle\right)\\
&+\sigma\sigma' v^{n_1}_{i+\hat{x},\sigma}u^{n_2}_{i\sigma}e^{-i\left(E_{n_1}+E_{n_2}\right)t}u^{n_2*}_{i'+\hat{x},\sigma'}v^{n_1*}_{i'\sigma'}\left(\left\langle\gamma_{n_1}\gamma^{\dagger}_{n_1}\right\rangle-\left\langle\gamma^{\dagger}_{n_2}\gamma_{n_2}\right\rangle\right)\\
&-\sigma\sigma' v^{n_1}_{i+\hat{x},\sigma}u^{n_2}_{i\sigma}e^{-i\left(E_{n_1}+E_{n_2}\right)t}u^{n_1*}_{i'+\hat{x},\sigma'}v^{n_2*}_{i'\sigma'}\left(\left\langle\gamma_{n_1}\gamma^{\dagger}_{n_1}\right\rangle-\left\langle\gamma^{\dagger}_{n_2}\gamma_{n_2}\right\rangle\right)\\
&-v^{n_1}_{i+\hat{x},\sigma}v^{n_2*}_{i\sigma}e^{-i\left(E_{n_1}-E_{n_2}\right)t}u^{n_1*}_{i'+\hat{x},\sigma'}u^{n_2}_{i'\sigma'}\left(\left\langle\gamma_{n_1}\gamma^{\dagger}_{n_1}\right\rangle-\left\langle\gamma_{n_2}\gamma^{\dagger}_{n_2}\right\rangle\right)\\
&+v^{n_1}_{i+\hat{x},\sigma}v^{n_2*}_{i\sigma}e^{-i\left(E_{n_1}-E_{n_2}\right)t}v^{n_2}_{i'+\hat{x},\sigma'}v^{n_1*}_{i'\sigma'}\left(\left\langle\gamma_{n_1}\gamma^{\dagger}_{n_1}\right\rangle-\left\langle\gamma_{n_2}\gamma^{\dagger}_{n_2}\right\rangle\right)\Big], \qquad (2.113)
\end{aligned}
$$

$$
\begin{aligned}
\langle\hat{B}\rangle = \sum_{n_1n_2}\Big[&-u^{n_1*}_{i+\hat{x},\sigma}u^{n_2}_{i\sigma}e^{i\left(E_{n_1}-E_{n_2}\right)t}u^{n_2*}_{i',\sigma'}u^{n_1}_{i'+\hat{x},\sigma'}\left(\left\langle\gamma^{\dagger}_{n_1}\gamma_{n_1}\right\rangle-\left\langle\gamma^{\dagger}_{n_2}\gamma_{n_2}\right\rangle\right)\\
&+u^{n_1*}_{i+\hat{x},\sigma}u^{n_2}_{i\sigma}e^{i\left(E_{n_1}-E_{n_2}\right)t}v^{n_1}_{i',\sigma'}v^{n_2*}_{i'+\hat{x},\sigma'}\left(\left\langle\gamma^{\dagger}_{n_1}\gamma_{n_1}\right\rangle-\left\langle\gamma^{\dagger}_{n_2}\gamma_{n_2}\right\rangle\right)\\
&-\sigma\sigma' u^{n_1*}_{i+\hat{x}\sigma}v^{n_2*}_{i\sigma}e^{i\left(E_{n_1}+E_{n_2}\right)t}v^{n_2}_{i',\sigma'}u^{n_1}_{i'+\hat{x},\sigma'}\left(\left\langle\gamma^{\dagger}_{n_1}\gamma_{n_1}\right\rangle-\left\langle\gamma_{n_2}\gamma^{\dagger}_{n_2}\right\rangle\right)\\
&+\sigma\sigma' u^{n_1*}_{i+\hat{x}\sigma}v^{n_2*}_{i\sigma}e^{i\left(E_{n_1}+E_{n_2}\right)t}v^{n_1}_{i',\sigma'}u^{n_2}_{i'+\hat{x},\sigma'}\left(\left\langle\gamma^{\dagger}_{n_1}\gamma_{n_1}\right\rangle-\left\langle\gamma_{n_2}\gamma^{\dagger}_{n_2}\right\rangle\right)\\
&-\sigma\sigma' v^{n_1}_{i+\hat{x},\sigma}u^{n_2}_{i\sigma}e^{-i\left(E_{n_1}+E_{n_2}\right)t}u^{n_2*}_{i'\sigma'}v^{n_1*}_{i'+\hat{x},\sigma'}\left(\left\langle\gamma_{n_1}\gamma^{\dagger}_{n_1}\right\rangle-\left\langle\gamma^{\dagger}_{n_2}\gamma_{n_2}\right\rangle\right)\\
&+\sigma\sigma' v^{n_1}_{i+\hat{x},\sigma}u^{n_2}_{i\sigma}e^{-i\left(E_{n_1}+E_{n_2}\right)t}u^{n_1*}_{i'\sigma'}v^{n_2*}_{i'+\hat{x},\sigma'}\left(\left\langle\gamma_{n_1}\gamma^{\dagger}_{n_1}\right\rangle-\left\langle\gamma^{\dagger}_{n_2}\gamma_{n_2}\right\rangle\right)\\
&+v^{n_1}_{i+\hat{x},\sigma}v^{n_2*}_{i\sigma}e^{-i\left(E_{n_1}-E_{n_2}\right)t}u^{n_1*}_{i'\sigma'}u^{n_2}_{i'+\hat{x},\sigma'}\left(\left\langle\gamma_{n_1}\gamma^{\dagger}_{n_1}\right\rangle-\left\langle\gamma_{n_2}\gamma^{\dagger}_{n_2}\right\rangle\right)\\
&-v^{n_1}_{i+\hat{x},\sigma}v^{n_2*}_{i\sigma}e^{-i\left(E_{n_1}-E_{n_2}\right)t}v^{n_2}_{i'\sigma'}v^{n_1*}_{i'+\hat{x},\sigma'}\left(\left\langle\gamma_{n_1}\gamma^{\dagger}_{n_1}\right\rangle-\left\langle\gamma_{n_2}\gamma^{\dagger}_{n_2}\right\rangle\right)\Big], \qquad (2.114)
\end{aligned}
$$

$$\begin{aligned}\langle C\rangle = \sum_{n_1 n_2}\Big[&-u^{n_1*}_{i\sigma}u^{n_2}_{i+\hat{x},\sigma}e^{i\left(E_{n_1}-E_{n_2}\right)t}u^{n_2*}_{i'+\hat{x},\sigma'}u^{n_1}_{i'\sigma'}\left(\left\langle\gamma^\dagger_{n_1}\gamma_{n_1}\right\rangle-\left\langle\gamma^\dagger_{n_2}\gamma_{n_2}\right\rangle\right)\\
&+u^{n_1*}_{i\sigma}u^{n_2}_{i+\hat{x},\sigma}e^{i\left(E_{n_1}-E_{n_2}\right)t}v^{n_1}_{i'+\hat{x},\sigma'}v^{n_2*}_{i'\sigma'}\left(\left\langle\gamma^\dagger_{n_1}\gamma_{n_1}\right\rangle-\left\langle\gamma^\dagger_{n_2}\gamma_{n_2}\right\rangle\right)\\
&-\sigma\sigma' u^{n_1*}_{i\sigma}v^{n_2*}_{i+\hat{x},\sigma}e^{i\left(E_{n_1}+E_{n_2}\right)t}v^{n_2}_{i'+\hat{x},\sigma'}u^{n_1}_{i'\sigma'}\left(\left\langle\gamma^\dagger_{n_1}\gamma_{n_1}\right\rangle-\left\langle\gamma_{n_2}\gamma^\dagger_{n_2}\right\rangle\right)\\
&+\sigma\sigma' u^{n_1*}_{i\sigma}v^{n_2*}_{i+\hat{x},\sigma}e^{i\left(E_{n_1}+E_{n_2}\right)t}v^{n_1}_{i'+\hat{x},\sigma'}u^{n_2}_{i'\sigma'}\left(\left\langle\gamma^\dagger_{n_1}\gamma_{n_1}\right\rangle-\left\langle\gamma_{n_2}\gamma^\dagger_{n_2}\right\rangle\right)\\
&-\sigma\sigma' v^{n_1}_{i\sigma}u^{n_2}_{i+\hat{x},\sigma}e^{-i\left(E_{n_1}+E_{n_2}\right)t}u^{n_2*}_{i'+\hat{x},\sigma'}v^{n_1*}_{i'\sigma'}\left(\left\langle\gamma_{n_1}\gamma^\dagger_{n_1}\right\rangle-\left\langle\gamma^\dagger_{n_2}\gamma_{n_2}\right\rangle\right)\\
&+\sigma\sigma' v^{n_1}_{i\sigma}u^{n_2}_{i+\hat{x},\sigma}e^{-i\left(E_{n_1}+E_{n_2}\right)t}u^{n_1}_{i'+\hat{x},\sigma'}v^{n_2*}_{i'\sigma'}\left(\left\langle\gamma_{n_1}\gamma^\dagger_{n_1}\right\rangle-\left\langle\gamma^\dagger_{n_2}\gamma_{n_2}\right\rangle\right)\\
&+v^{n_1}_{i\sigma}v^{n_2*}_{i+\hat{x},\sigma}e^{-i\left(E_{n_1}-E_{n_2}\right)t}u^{n_1*}_{i'+\hat{x},\sigma'}u^{n_2}_{i'\sigma'}\left(\left\langle\gamma_{n_1}\gamma^\dagger_{n_1}\right\rangle-\left\langle\gamma_{n_2}\gamma^\dagger_{n_2}\right\rangle\right)\\
&-v^{n_1}_{i\sigma}v^{n_2*}_{i+\hat{x},\sigma}e^{-i\left(E_{n_1}-E_{n_2}\right)t}v^{n_2}_{i'+\hat{x},\sigma'}v^{n_1*}_{i'\sigma'}\left(\left\langle\gamma_{n_1}\gamma^\dagger_{n_1}\right\rangle-\left\langle\gamma_{n_2}\gamma^\dagger_{n_2}\right\rangle\right)\Big],\end{aligned}\tag{2.115}$$

and

$$\begin{aligned}\langle\hat{D}\rangle = \sum_{n_1 n_2}\Big[&u^{n_1*}_{i\sigma}u^{n_2}_{i+\hat{x},\sigma}e^{i\left(E_{n_1}-E_{n_2}\right)t}u^{n_2*}_{i'\sigma'}u^{n_1}_{i'+\hat{x},\sigma'}\left(\left\langle\gamma^\dagger_{n_1}\gamma_{n_1}\right\rangle-\left\langle\gamma^\dagger_{n_2}\gamma_{n_2}\right\rangle\right)\\
&-u^{n_1*}_{i\sigma}u^{n_2}_{i+\hat{x},\sigma}e^{i\left(E_{n_1}-E_{n_2}\right)t}v^{n_1}_{i'\sigma'}v^{n_2*}_{i'+\hat{x}\sigma'}\left(\left\langle\gamma^\dagger_{n_1}\gamma_{n_1}\right\rangle-\left\langle\gamma^\dagger_{n_2}\gamma_{n_2}\right\rangle\right)\\
&+\sigma\sigma' u^{n_1*}_{i\sigma}v^{n_2*}_{i+\hat{x},\sigma}e^{i\left(E_{n_1}+E_{n_2}\right)tt}v^{n_2}_{i'\sigma'}u^{n_1}_{i'+\hat{x},\sigma'}\left(\left\langle\gamma^\dagger_{n_1}\gamma_{n_1}\right\rangle-\left\langle\gamma_{n_2}\gamma^\dagger_{n_2}\right\rangle\right)\\
&-\sigma\sigma' u^{n_1*}_{i\sigma}v^{n_2*}_{i+\hat{x},\sigma}e^{i\left(E_{n_1}+E_{n_2}\right)t}v^{n_1}_{i'\sigma'},u^{n_2}_{i'+\hat{x},\sigma'}\left(\left\langle\gamma^\dagger_{n_1}\gamma_{n_1}\right\rangle-\left\langle\gamma_{n_2}\gamma^\dagger_{n_2}\right\rangle\right)\\
&+\sigma\sigma' v^{n_1}_{i\sigma}u^{n_2}_{i+\hat{x},\sigma}e^{-i\left(E_{n_1}+E_{n_2}\right)t}u^{n_2}_{i'\sigma'}v^{n_1}_{i'+\hat{x},\sigma'}\left(\left\langle\gamma_{n_1}\gamma^\dagger_{n_1}\right\rangle-\left\langle\gamma^\dagger_{n_2}\gamma_{n_2}\right\rangle\right)\\
&-\sigma\sigma' v^{n_1}_{i\sigma}u^{n_2}_{i+\hat{x},\sigma}e^{-i\left(E_{n_1}+E_{n_2}\right)t}u^{n_1*}_{i'\sigma'}v^{n_2}_{i'+\hat{x},\sigma'}\left(\left\langle\gamma_{n_1}\gamma^\dagger_{n_1}\right\rangle-\left\langle\gamma^\dagger_{n_2}\gamma_{n_2}\right\rangle\right)\\
&-v^{n_1}_{i\sigma}v^{n_2*}_{i+\hat{x},\sigma}e^{-i\left(E_{n_1}-E_{n_2}\right)t}u^{n_1*}_{i'\sigma'}u^{n_2}_{i'+\hat{x},\sigma'}\left(\left\langle\gamma_{n_1}\gamma^\dagger_{n_1}\right\rangle-\left\langle\gamma_{n_2}\gamma^\dagger_{n_2}\right\rangle\right)\\
&+v^{n_1}_{i\sigma}v^{n_2*}_{i+\hat{x},\sigma}e^{-i\left(E_{n_1}-E_{n_2}\right)t}v^{n_2}_{i'\sigma'}v^{n_1*}_{i'+\hat{x},\sigma'}\left(\left\langle\gamma_{n_1}\gamma^\dagger_{n_1}\right\rangle-\left\langle\gamma_{n_2}\gamma^\dagger_{n_2}\right\rangle\right)\Big].\end{aligned}\tag{2.116}$$

By defining

$$A_{n_1,n_2}(\mathbf{q}) = \sum_{i\sigma}e^{-i\mathbf{q}\cdot\mathbf{r}_i}\left[u^{n_1*}_{i+\hat{x},\sigma}u^{n_2}_{i\sigma}-u^{n_1*}_{i\sigma}u^{n_2}_{i+\hat{x},\sigma}\right],\tag{2.117}$$

$$B_{n_1,n_2}(\mathbf{q}) = \sum_{i\sigma}\sigma e^{-i\mathbf{q}\cdot\mathbf{r}}\left[u^{n_1*}_{i+\hat{x},\sigma}v^{n_2*}_{i\sigma}-u^{n_1*}_{i\sigma}v^{n_2*}_{i+\hat{x},\sigma}\right]\tag{2.118}$$

$$C_{n_1,n_2}(\mathbf{q}) = \sum_{i\sigma}\sigma e^{-i\mathbf{q}\cdot\mathbf{r}}\left[v^{n_1}_{i+\hat{x},\sigma}u^{n_2}_{i\sigma}-v^{n_1}_{i\sigma}u^{n_2}_{i+\hat{x},\sigma}\right]\tag{2.119}$$

$$D_{n_1,n_2}(\mathbf{q}) = \sum_{i\sigma}e^{-i\mathbf{q}\cdot\mathbf{r}_i}\left[v^{n_1}_{i+\hat{x},\sigma}v^{n_2*}_{i\sigma}-v^{n_1}_{i\sigma}v^{n_2*}_{i+\hat{x},\sigma}\right]\tag{2.120}$$

we find the current-current correlation function

$$
\begin{aligned}
\Pi_{xx}(\mathbf{q},\omega) =& -\frac{1}{N}\sum_{n_1,n_2}\left\{\frac{A_{n_1,n_2}(\mathbf{q})\left[-A^*_{n_1,n_2}(\mathbf{q})-D_{n_1,n_2}(-\mathbf{q})\right]}{\omega+(E_{n_1}-E_{n_2})+i\delta}\left(\left\langle\gamma^\dagger_{n_1}\gamma_{n_1}\right\rangle-\left\langle\gamma^\dagger_{n_2}\gamma_{n_2}\right\rangle\right)\right.\\
&+\frac{B_{n_1,n_2}(\mathbf{q})\left[-B^*_{n_1,n_2}(\mathbf{q})-C_{n_1,n_2}(-\mathbf{q})\right]}{\omega+(E_{n_1}+E_{n_2})+i\delta}\left(\left\langle\gamma^\dagger_{n_1}\gamma_{n_1}\right\rangle-\left\langle\gamma_{n_2}\gamma^\dagger_{n_2}\right\rangle\right)\\
&+\frac{C_{n_1,n_2}(\mathbf{q})\left[-C^*_{n_1,n_2}(\mathbf{q})-B_{n_1,n_2}(-\mathbf{q})\right]}{\omega-(E_{n_1}+E_{n_2})+i\delta}\left(\left\langle\gamma_{n_1}\gamma^\dagger_{n_1}\right\rangle-\left\langle\gamma^\dagger_{n_2}\gamma_{n_2}\right\rangle\right)\\
&\left.+\frac{D_{n_1,n_2}(\mathbf{q})\left[-D^*_{n_1,n_2}(\mathbf{q})-A_{n_1,n_2}(-\mathbf{q})\right]}{\omega-(E_{n_1}-E_{n_2})+i\delta}\left(\left\langle\gamma_{n_1}\gamma^\dagger_{n_1}\right\rangle-\left\langle\gamma_{n_2}\gamma^\dagger_{n_2}\right\rangle\right)\right\}\\
=&\frac{1}{N}\sum_{n_1,n_2}\left\{\frac{A_{n_1,n_2}(\mathbf{q})\left[A^*_{n_1,n_2}(\mathbf{q})+D_{n_1,n_2}(-\mathbf{q})\right]}{\omega+(E_{n_1}-E_{n_2})+i\delta}\left[f\left(E_{n_1}\right)-f\left(E_{n_2}\right)\right]\right.\\
&+\frac{B_{n_1,n_2}(\mathbf{q})\left[B^*_{n_1,n_2}(\mathbf{q})+C_{n_1,n_2}(-\mathbf{q})\right]}{\omega+(E_{n_1}+E_{n_2})+i\delta}\left[f\left(E_{n_1}\right)-f\left(-E_{n_2}\right)\right]\\
&+\frac{C_{n_1,n_2}(\mathbf{q})\left[C^*_{n_1,n_2}(\mathbf{q})+B_{n_1,n_2}(-\mathbf{q})\right]}{\omega-(E_{n_1}+E_{n_2})+i\delta}\left[f\left(-E_{n_1}\right)-f\left(E_{n_2}\right)\right]\\
&\left.+\frac{D_{n_1,n_2}(\mathbf{q})\left[D^*_{n_1,n_2}(\mathbf{q})+A_{n_1,n_2}(-\mathbf{q})\right]}{\omega-(E_{n_1}-E_{n_2})+i\delta}\left[f\left(-E_{n_1}\right)-f\left(-E_{n_2}\right)\right]\right\}. \qquad (2.121)
\end{aligned}
$$

Using the symmetry relation of eigenstates for positive and negative eigenvalues in the BdG equation, we can write the Π_{xx} in a simplified form:

$$
\Pi_{xx}(\mathbf{q},\omega)=\frac{1}{N}\sum_{n_1,n_2}\left\{\frac{A_{n_1,n_2}(\mathbf{q})\left[A^*_{n_1,n_2}(\mathbf{q})+D_{n_1,n_2}(-\mathbf{q})\right]}{\omega+(E_{n_1}-E_{n_2})+i\delta}\left[f\left(E_{n_1}\right)-f\left(E_{n_2}\right)\right]\right\}, \qquad (2.122)
$$

where E_n cover all eigenvalues from the BdG equation.
For the optical conductivity and charge stiffness, we set $\mathbf{q}=0$ and obtain:

$$
\Pi_{xx}(\omega)=\frac{1}{N}\sum_{n_1,n_2}\left\{\frac{A_{n_1,n_2}\left[A^*_{n_1,n_2}+D_{n_1,n_2}\right]}{\omega+(E_{n_1}-E_{n_2})+i\delta}\left[f\left(E_{n_1}\right)-f\left(E_{n_2}\right)\right]\right\}, \qquad (2.123)
$$

where $A=A(\mathbf{q}=0)$ and $D=D(\mathbf{q}=0)$.
For the superfluid density, we first set $\omega=0$ and obtain

$$
\Pi_{xx}(\mathbf{q}\to 0)=\frac{1}{N}\sum_{n_1,n_2}\left\{\frac{A_{n_1,n_2}(\mathbf{q}\to 0)\left[A^*_{n_1,n_2}(\mathbf{q}\to 0)+D_{n_1,n_2}(-\mathbf{q}\to 0)\right]}{E_{n_1}-E_{n_2}}\left[f\left(E_{n_1}\right)-f\left(E_{n_2}\right)\right]\right\}. \qquad (2.124)
$$

Alternative derivation

An alternative derivation of the optical conductivity and superfluid can be carried out within the Green function method, which is left for the readers to explore as an exercise. The above formulae for optical conductivity and superfluid density are particularly useful for the study of inhomogeneous superconductors.

9.7.5 2.2 Solution to the Lattice BdG Equations for a Uniform Superconductor

Theory

We consider the case in the absence of spin-orbit coupling and other spin-flip scattering effect, and assume only a superconducting order is present in the system. In the nearest-neighbor hopping approximation for the tight-binding model of a cubic system, the normal-state single-particle energy dispersion is given by

$$\epsilon_{\mathbf{k}} = -2t\left(\cos k_x a + \cos k_y a + \cos k_z a\right) \tag{2.125}$$

for a three-dimensional cubic lattice, while

$$\epsilon_{\mathbf{k}} = -2t\left(\cos k_x a + \cos k_y a\right), \tag{2.126}$$

for a two-dimensional square lattice. Here a is the lattice constant and t is the nearest-neighbor hopping integral. From these dispersions, the normal-state density of states can be numerically evaluated. The results of normal-state density of states are shown in Fig.2.1.

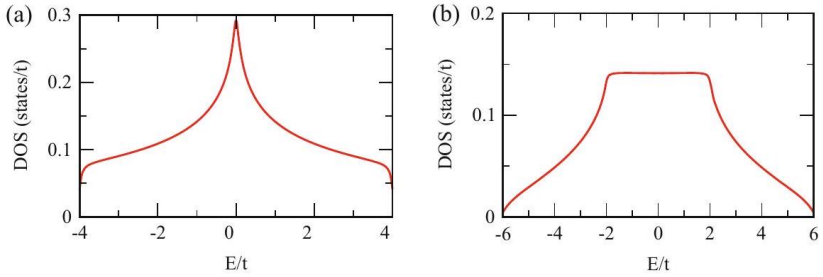


Fig. 2.1 Normal-state single-particle density of states for a two-dimensional (a) and threedimensional (b) system. Lattice size is chosen to be 400×400 for the 2D system and $200 \times 200 \times 200$ for the 3D system. The intrinsic lifetime broadening $\Gamma = 0.05$ is used for the calculation

As one can see, for the 2D system, the DOS exhibits the van Hove singularity. The strong energy dependence of this DOS will influence the magnitude of the superconducting order parameter. For high-temperature cuprate superconductors, the electrons are mostly confined into a two-dimensional Cu square lattice and the energy dispersion for the low-energy $\mathrm{Cu}-3d$ electrons usually includes the next-nearest-neighbor hopping

$$\epsilon_{\mathbf{k}} = -2t\left(\cos k_x a + \cos k_y a\right) - 4t' \cos k_x a \cos k_y a \tag{2.127}$$

We consider a pristine 2D superconductor with an s-wave or $d_{x^2-y^2}$-wave pairing symmetry. In this case, the system is invariant under a translation with a lattice constant a of the square lattice, and the BdG wave functions take the Bloch wavelike:

$$u_i = \frac{1}{\sqrt{N_L}} u_{\mathbf{k}} e^{i\mathbf{k}\cdot\mathbf{r}_i}, \tag{2.128}$$

$$v_i = \frac{1}{\sqrt{N_L}} v_{\mathbf{k}} e^{i\mathbf{k}\cdot\mathbf{r}_i} \tag{2.129}$$

which gives rise to

$$E_{\mathbf{k}} u_{\mathbf{k}} = \xi_{\mathbf{k}} u_{\mathbf{k}} + \Delta_{\mathbf{k}} v_{\mathbf{k}} \tag{2.130a}$$

$$E_{\mathbf{k}} v_{\mathbf{k}} = -\xi_{\mathbf{k}} v_{\mathbf{k}} + \Delta_{\mathbf{k}}^* u_{\mathbf{k}} \tag{2.130b}$$

Here

$$\xi_{\mathbf{k}} = \epsilon_{\mathbf{k}} - \mu \tag{2.131}$$

and

$$\Delta_{\mathbf{k}} = \Delta_s \tag{2.132}$$

for the s-wave pairing symmetry while

$$\Delta_{\mathbf{k}} = (\Delta_d/2)\left(\cos k_x a - \cos k_y a\right) \tag{2.133}$$

for the d-wave pairing symmetry.
A little algebra yields to the eigensolutions

$$\begin{pmatrix} u_{\mathbf{k}} \\ v_{\mathbf{k}} \end{pmatrix} = \begin{pmatrix} u_{\mathbf{k}}^{(0)} e^{i\varphi_{\mathbf{k}}} \\ v_{\mathbf{k}}^{(0)} \end{pmatrix} \tag{2.134}$$

corresponding to the eigenvalue

$$E_{\mathbf{k}} = \sqrt{\xi_{\mathbf{k}}^2 + \left|\Delta_{\mathbf{k}}\right|^2} \tag{2.135}$$

and

$$\begin{pmatrix} u_{\mathbf{k}} \\ v_{\mathbf{k}} \end{pmatrix} = \begin{pmatrix} -v_{\mathbf{k}}^{(0)} e^{i\varphi_{\mathbf{k}}} \\ u_{\mathbf{k}}^{(0)} \end{pmatrix} \tag{2.136}$$

corresponding to the eigenvalue $-E_{\mathbf{k}}$. Here the BdG wave function amplitude is given by

$$\begin{pmatrix} u_{\mathbf{k}}^{(0)} \\ v_{\mathbf{k}}^{(0)} \end{pmatrix} = \begin{pmatrix} \sqrt{\frac{1}{2}\left(1 + \frac{\xi_k}{E_k}\right)} \\ \sqrt{\frac{1}{2}\left(1 - \frac{\xi_k}{E_k}\right)} \end{pmatrix} \tag{2.137}$$

and $\varphi_{\mathbf{k}}$ is the phase angle of $\Delta_{\mathbf{k}}$. Therefore, we obtain the self-consistency equation for the pair potential

$$\Delta_s = \frac{1}{N_L} \sum_{\mathbf{k}} V_s \frac{\Delta_s}{2E_{\mathbf{k}}} \tanh\left(\frac{E_{\mathbf{k}}}{2k_B T}\right), \tag{2.138}$$

for a three-dimensional s-wave superconductor with the quasiparticle excitation energy $E_{\mathbf{k}} = \sqrt{\xi_{\mathbf{k}}^2 + \Delta_s^2}$; and

$$\Delta_d = \frac{1}{N_L} \sum_{\mathbf{k}} V_d \left(\cos k_x a - \cos k_y a\right)^2 \frac{\Delta_d}{2E_{\mathbf{k}}} \tanh\left(\frac{E_{\mathbf{k}}}{2k_B T}\right) \tag{2.139}$$

for a two-dimensional $d_{x^2-y^2}$-wave superconductor with the quasiparticle excitation energy $E_{\mathbf{k}} = \sqrt{\xi_{\mathbf{k}}^2 + \left[\frac{\Delta_d}{2}\left(\cos k_x a - \cos k_y a\right)\right]^2}$. In Fig. 2.2, the temperature dependence of superconducting order parameter for various values of chemical potential is shown.

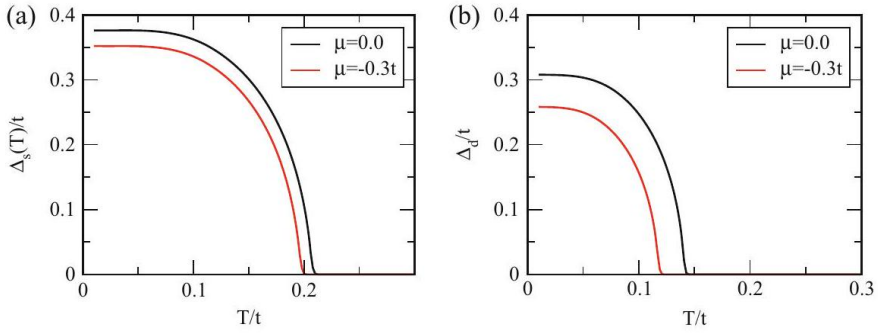


Fig. 2.2 Temperature dependence of the superconducting order parameter for an s-wave (a) and $d_{x^2-y^2}$-wave (b) pairing symmetry for various values of chemical potential in a 2 D tight-binding lattice model with nearest-neighbor hopping. Lattice size is chosen to be 400×400 for the calculations. The energy and temperature (k_BT and k_B is set to 1) are measured in units of t

The results show that the zero-temperature superconducting pair potential and transition temperature are dependent on the location of the chemical potential, at which the intensity of density of states is tuned. In the 2D tight-binding model with nearest-neighbor hopping, the van Hove singularity occurs at the normal state energy $\epsilon = 0$. In Fig. 2.3, we show the typical feature of density of states for a 2D superconductor described by a square-lattice tight-binding model.

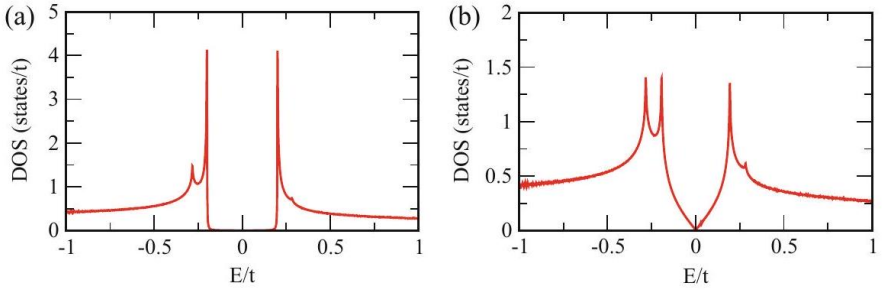


Fig. 2.3 Density of states for a pristine 2D superconductor with s-wave (a) and $d_{x^2-y^2}$-wave (b) pairing symmetry. A square-lattice tight-binding model with normal-state single-particle energy dispersion given by Eq. (2.127) is used. The parameter $t = -0.3t$ and $\mu = -t$, and $\Delta_s = \Delta_d = 0.2t$ are taken. Lattice size is chosen to be 4096×4096 and $\Gamma = 0.001t$ is used for the calculations

The normalstate single-particle energy dispersion given by Eq. (2.127) with $t' = -0.3$t and a chemical potential $\mu = -t$ are considered. For the s-wave pairing symmetry, a well-shape characteristic as marked by the superconducting coherent peaks around the Fermi energy at $E = 0$ is exhibited in the density of states. Instead, for the $d_{x^2-y^2}$-wave pairing symmetry, a V-shape characteristic is exhibited in the density of states around the Fermi energy, which arises from the gapless nodal quasiparticles. In addition, the normal-state van Hove singularity peak is shifted by the superconducting gap opening.

9.7.6 2.3 Lattice Abrikosov-Gorkov Equations

Theory

Similar to the continuum model, we can also establish the Abrikosov-Gorkov theory in the lattice model. Here we generalize it to include the effects of spin-orbit coupling and spin-flip scattering. We first define a 4 -component spinor field operator in the Nambu space

$$\hat{\Psi}_i(\tau) = \begin{pmatrix} c_{i\uparrow}(\tau) \\ c_{i\downarrow}(\tau) \\ c^\dagger_{i\uparrow}(\tau) \\ c^\dagger_{i\downarrow}(\tau) \end{pmatrix}, \tag{2.140}$$

and

$$\hat{\Psi}^\dagger_i(\tau) = \left(c^\dagger_{i\uparrow}(\tau) c^\dagger_{i\downarrow}(\tau) c_{i\uparrow}(\tau) c_{i\downarrow}(\tau) \right), \tag{2.141}$$

where the electronic operators

$$c_{i\sigma}(\tau) = e^{\mathscr{H}_{eff}\tau/\hbar} c_{i\sigma} e^{-\mathscr{H}_{eff}\tau/\hbar}, \tag{2.142}$$

$$c^\dagger_{i\sigma}(\tau) = e^{\mathscr{H}_{eff}\tau/\hbar} c^\dagger_{i\sigma} e^{-\mathscr{H}_{eff}\tau/\hbar}, \tag{2.143}$$

are defined in the imaginary-time space and $\mathscr{H}_{\text{eff}}$ is given by Eq.(2.5).

Why do we use this notation and not other Nambu notation? Because this works. Other notation also works. Right?

Note that $c^\dagger_{i\sigma}(\tau) \neq [c_{i\sigma}(\tau)]^\dagger$. We then introduce the real-space Green's function in the lattice model as

$$\begin{aligned} \mathscr{G}(i\tau; j\tau') &= -\left\langle T_\tau \left(\hat{\Psi}_i(\tau) \otimes \hat{\Psi}^\dagger_j(\tau') \right\rangle \right. \\ &= -\theta(\tau - \tau') \left\langle \hat{\Psi}_i(\tau) \otimes \hat{\Psi}^\dagger_j(\tau') \right\rangle + \theta(\tau' - \tau) \left\langle \hat{\Psi}^\dagger_j(\tau') \otimes \hat{\Psi}_i(\tau) \right\rangle \end{aligned} \tag{2.144}$$

Therefore, in an expanded form, it becomes

$$\mathscr{G}(i\tau; j\tau') = \begin{pmatrix} -\langle T_\tau(c_{i\uparrow}(\tau)c^\dagger_{j\uparrow}(\tau')\rangle - \langle T_\tau(c_{i\uparrow}(\tau)c^\dagger_{j\downarrow}(\tau')\rangle - \langle T_\tau(c_{i\uparrow}(\tau)c_{j\uparrow}(\tau')\rangle - \langle T_\tau(c_{i\uparrow}(\tau)c_{j\downarrow}(\tau')\rangle .... \\ -\langle T_\tau(c_{i\downarrow}(\tau)c^\dagger_{j\uparrow}(\tau')\rangle - \langle T_\tau(c_{i\downarrow}(\tau)c^\dagger_{j\downarrow}(\tau')\rangle - \langle T_\tau(c_{i\downarrow}(\tau)c_{j\uparrow}(\tau')\rangle - \langle T_\tau(c_{i\uparrow}(\tau)c_{j\downarrow}(\tau')\rangle .... \\ -\langle T_\tau(c^\dagger_{i\uparrow}(\tau)c^\dagger_{j\uparrow}(\tau')\rangle - \langle T_\tau(c^\dagger_{i\uparrow}(\tau)c^\dagger_{j\downarrow}(\tau')\rangle - \langle T_\tau(c^\dagger_{i\uparrow}(\tau)c_{j\uparrow}(\tau')\rangle - \langle T_\tau(c^\dagger_{i\uparrow}(\tau)c_{j\downarrow}(\tau')\rangle .... \\ -\langle T_\tau(c^\dagger_{i\downarrow}(\tau)c^\dagger_{j\uparrow}(\tau')\rangle - \langle T_\tau(c^\dagger_{i\downarrow}(\tau)c^\dagger_{j\downarrow}(\tau')\rangle - \langle T_\tau(c^\dagger_{i\downarrow}(\tau)c_{j\uparrow}\tau')\rangle - \langle \tau_\tau(c^\dagger_{i\downarrow}(\tau)c_{j\downarrow}(\tau')\rangle ... \end{pmatrix}. \tag{2.145}$$

(???? how to understand it???)

Since the trace is unchanged upon a cyclic variation of operators, we can easily prove that the Green's function is a function of the difference $\tau - \tau'$, that is,

$$\mathscr{G}(i\tau; j\tau') = \mathscr{G}(i, j; \tau - \tau'), \tag{2.146}$$

with $\tau - \tau'$ restricted in the range of $[-\beta, \beta]$ and the factor $\beta = 1/k_B T$. Therefore, the Fourier transform is given by

$$\mathscr{G}(i, j; i\omega_n) = \int_0^\beta d\tau e^{i\omega_n \tau} \mathscr{G}(i, j; \tau), \tag{2.147}$$

$$\mathscr{G}(i, j; \tau) = \frac{1}{\beta} \sum_n e^{-i\omega_n \tau} \mathscr{G}(i, j; i\omega_n), \tag{2.148}$$

where the Matsubara frequency $\omega_n = (2n+1)\pi k_B T/\hbar$ with $n = -\infty, \ldots, -1, 0, 1, \ldots, \infty$.

Using the equation of motion for $c_{i\sigma}(\tau)$ and $c^\dagger_{i\sigma}(\tau)$:

$$-\hbar\frac{\partial c_{i\sigma}(\tau)}{\partial\tau}=\left[c_{i\sigma}(\tau),\mathscr{H}_{eff}\right]_{-}, \tag{2.149}$$

$$-\hbar\frac{\partial c_{i\sigma}^{\dagger}(\tau)}{\partial\tau}=\left[c_{i\sigma}^{\dagger}(\tau),\mathscr{H}_{eff}\right]_{-}, \tag{2.150}$$

and Eq. (2.10), we can obtain the equation of motion for the Green's function

$$\sum_{j'}\hat{M}_{ij'}(\tau)\mathscr{G}\left(j'\tau;j\tau'\right)=\delta_{ij}\delta\left(\tau-\tau'\right)\hat{1}, \tag{2.151}$$

with

$$\hat{M}_{ij}(\tau)=\begin{pmatrix}-\frac{\partial}{\partial\tau}\delta_{ij}-\tilde{h}_{i\uparrow,j\uparrow} & -\tilde{h}_{i\uparrow,j\downarrow} & 0 & -\Delta_{ij}\\ -\tilde{h}_{i\downarrow,j\uparrow} & -\frac{\partial}{\partial\tau}\delta_{ij}-\tilde{h}_{i\downarrow,j\downarrow} & -\Delta_{ji} & 0\\ 0 & -\Delta_{ij}^{*} & -\frac{\partial}{\partial\tau}\delta_{ij}+\tilde{h}_{i\uparrow,j\uparrow}^{*} & -\tilde{h}_{i\uparrow,j\downarrow}^{*}\\ -\Delta_{ji}^{*} & 0 & -\tilde{h}_{i\uparrow,j\downarrow}^{*} & -\frac{\partial}{\partial\tau}\delta_{ij}+\tilde{h}_{i\downarrow,j\downarrow}^{*}\end{pmatrix} \tag{2.152}$$

for the spin-singlet pairing case, and subject to the self-consistency condition:

$$\Delta_{ij}=-\frac{V}{2}\left[\mathscr{G}_{14}\left(i\tau\rightarrow\tau'+0^{+},j\tau'\right)-\mathscr{G}_{23}\left(i\tau\rightarrow\tau'+0^{+},j\tau'\right)\right], \tag{2.153}$$

$$\Delta_{ij}^{*}=-\frac{V}{2}\left[\mathscr{G}_{41}\left(i\tau\rightarrow\tau'+0^{+},j\tau'\right)-\mathscr{G}_{32}\left(i\tau\rightarrow\tau'+0^{+},j\tau'\right)\right]. \tag{2.154}$$

In the absence of the spin-orbit coupling and spin-flip scattering, we can decouple the equation of motion for the Green's function into two sets:

$$\sum_{j'}\begin{pmatrix}-\frac{\partial}{\partial\tau}\delta_{ij'}-\tilde{h}_{i\uparrow,j'\uparrow} & -\Delta_{ij'}\\ -\Delta_{j'i}^{*} & -\frac{\partial}{\partial\tau}\delta_{ij'}+\tilde{h}_{i\downarrow,j'\downarrow}^{*}\end{pmatrix}\begin{pmatrix}\mathscr{G}_{11}\left(j'\tau;j\tau'\right)\mathscr{G}_{14}\left(j'\tau;j\tau'\right)\\ \mathscr{G}_{41}\left(j'\tau;j\tau'\right)\mathscr{G}_{44}\left(j'\tau;j\tau'\right)\end{pmatrix}=\delta_{ij}\delta\left(\tau-\tau'\right)\hat{1}, \tag{2.155}$$

and

$$\sum_{j'}\begin{pmatrix}-\frac{\partial}{\partial\tau}\delta_{ij'}-\tilde{h}_{i\downarrow\cdot j'\downarrow} & -\Delta_{j'i}\\ -\Delta_{ij'}^{*} & -\frac{\partial}{\partial\tau}\delta_{ij'}+\tilde{h}_{i\uparrow,j'\uparrow}^{*}\end{pmatrix}\begin{pmatrix}\mathscr{G}_{22}\left(j'\tau;j\tau'\right)\mathscr{G}_{23}\left(j'\tau;j\tau'\right)\\ \mathscr{G}_{32}\left(j'\tau;j\tau'\right)\mathscr{G}_{33}\left(j'\tau;j\tau'\right)\end{pmatrix}=\delta_{ij}\delta\left(\tau-\tau'\right)\hat{1}. \tag{2.156}$$

In this case, either one of the above two sets of equations of motion is sufficient to solve the whole problem. More interestingly, there exists a close relation between the Green's function and the BdG eigenfunctions. Specifically, with the time dependence of the quasiparticle operators:

$$\gamma_{n}(\tau)=\gamma_{n}e^{-E_{n}\tau/\hbar} \tag{2.157}$$

$$\gamma_{n}^{\dagger}(\tau)=\gamma_{n}^{\dagger}e^{E_{n}\tau/\hbar} \tag{2.158}$$

and the canonical transformation, we can obtain for the most general case the following matrix elements of the Green's function

$$\begin{aligned}\mathscr{G}_{11}(i,j;\tau) =& -\theta(\tau)\sum_n \left[u_{i\uparrow}^n u_{j\uparrow}^{n*} f\left(-E_n\right) e^{-E_n\tau/\hbar} + v_{i\uparrow}^{n*} v_{j\uparrow}^n f\left(E_n\right) e^{E_n\tau/\hbar}\right] \\ &+\theta(-\tau)\sum_n \left[u_{j\uparrow}^{n*} u_{i\uparrow}^n f\left(E_n\right) e^{-E_n\tau/\hbar} + v_{j\uparrow}^n v_{i\uparrow}^{n*} f\left(-E_n\right) e^{E_n\tau/\hbar}\right] \end{aligned} \tag{2.159}$$

and

$$\begin{aligned}\mathscr{G}_{44}(i,j;\tau) =& -\theta(\tau)\sum_n \left[u_{i\downarrow}^{n*} u_{j\downarrow}^n f\left(E_n\right) e^{E_n\tau/\hbar} + v_{i\downarrow}^n v_{j\downarrow}^{n*} f\left(-E_n\right) e^{-E_n\tau/\hbar}\right] \\ &+\theta(-\tau)\sum_n \left[u_{j\downarrow}^n u_{i\downarrow}^{n*} f\left(-E_n\right) e^{E_n\tau/\hbar} + v_{j\downarrow}^{n*} v_{i\downarrow}^n f\left(E_n\right) e^{-E_n\tau/\hbar}\right]. \end{aligned} \tag{2.160}$$

It is straightforward to obtain the Green's function in the frequency domain

$$\begin{aligned}&\mathscr{G}_{11}\left(i,j;i\omega_n\right) = \int_0^{\beta\hbar} d\tau e^{i\omega_n\tau}\mathscr{G}_{11}(i,j;\tau) \\ =& -\sum_n{}' \left[u_{i\uparrow}^n u_{j\uparrow}^{n*} f\left(-E_n\right)\int_0^{\beta\hbar} d\tau e^{(i\omega_n - E_n/\hbar)\tau} + v_{i\uparrow}^{n*} v_{j\uparrow}^n f\left(E_n\right)\int_0^{\beta\hbar} d\tau e^{(i\omega_n + E_n/\hbar)\tau}\right] \\ =& -\sum_n{}' \left\{\frac{u_{i\uparrow}^n u_{j\uparrow}^{n*}}{i\omega_n - E_n/\hbar} f\left(-E_n\right)\left(e^{\beta\hbar(i\omega_n - E_n/\hbar)} - 1\right) + \frac{v_{i\uparrow}^{n*} v_{j\uparrow}^n}{i\omega_n + E_n/\hbar} f\left(E_n\right)\left(e^{\beta\hbar(i\omega_n + E_n/\hbar)} - 1\right)\right\} \\ =& \sum_n{}' \left[\frac{u_{i\uparrow}^n u_{j\uparrow}^{n*}}{i\omega_n - E_n/\hbar} + \frac{v_{i\uparrow}^{n*} v_{j\uparrow}^n}{i\omega_n + E_n/\hbar}\right] \end{aligned} \tag{2.161}$$

and

$$\begin{aligned}\mathscr{G}_{44}\left(i,j;i\omega_n\right) =& \int_0^{\beta\hbar} d\tau e^{i\omega_n\tau}\mathscr{G}_{44}(i,j;\tau) \\ =& -\sum_n{}' \left[u_{i\downarrow}^{n*} u_{j\downarrow}^n f\left(E_n\right)\int_0^{\beta\hbar} d\tau e^{(i\omega_n + E_n/\hbar)\tau}\right. \\ &\left. + v_{i\downarrow}^n v_{j\downarrow}^{n*} f\left(-E_n\right)\int_0^{\beta\hbar} d\tau e^{(i\omega_n + E_n/\hbar)\tau}\right] \\ =& -\sum_n{}' \left\{\frac{u_{i\downarrow}^{n*} u_{j\downarrow}^n}{i\omega_n + E_n/\hbar} f\left(E_n\right)\left(e^{\beta\hbar(i\omega_n + E_n/\hbar)} - 1\right)\right. \\ &\left. + \frac{v_{i\downarrow}^n v_{j\downarrow}^{n*}}{i\omega_n - E_n/\hbar} f\left(E_n\right)\left(e^{\beta\hbar(i\omega_n - E_n/\hbar)} - 1\right)\right\} \\ =& \sum_n{}' \left[\frac{u_{i\downarrow}^{n*} u_{j\downarrow}^n}{i\omega_n + E_n/\hbar} + \frac{v_{i\downarrow}^n v_{j\downarrow}^{n*}}{i\omega_n - E_n/\hbar}\right] \end{aligned} \tag{2.162}$$

Other matrix elements of the Green's function can be evaluated in the same way, which are left for exercise.

In the absence of the spin-orbit coupling and spin-flip scattering, we can rewrite the Green's matrix elements as

$$\mathscr{G}_{11}\left(i,j;i\omega_n\right)=\sum_{\tilde{n}}{}'\left[\frac{u_{i\uparrow}^{\tilde{n}1}u_{j\uparrow}^{\tilde{n}1*}}{i\omega_n-E_{\tilde{n}1}/\hbar}+\frac{v_{i\uparrow}^{\tilde{n}2*}v_{j\uparrow}^{\tilde{n}2}}{i\omega_n+E_{\tilde{n}2}/\hbar}\right], \tag{2.163}$$

and

$$\mathscr{G}_{44}\left(i,j;i\omega_n\right)=\sum_{\tilde{n}}{}'\left[\frac{u_{i\downarrow}^{\tilde{n}2*}u_{j\downarrow}^{\tilde{n}2}}{i\omega_n+E_{\tilde{n}2}/\hbar}+\frac{v_{i\downarrow}^{\tilde{n}1}\nu_{j\downarrow}^{\tilde{n}1*}}{i\omega_n-E_{\tilde{n}1}/\hbar}\right]. \tag{2.164}$$

In summary, we have demonstrated that once we know the eigensolution of the BdG equations, the Abrikosov-Gorkov Green's function can be expressed rigorously. Conversely, if we know the solution to the Abrikosov-Gorkov equations of motion for the Green's functions, the local density of states can be calculated as

$$\begin{aligned}\rho_{i,\uparrow}(E)&=-\frac{1}{\hbar\pi}\operatorname{Im}\left[\mathscr{G}_{11}\left(i,i;i\omega_n\rightarrow E/\hbar+i0^+\right)\right]\\&=\sum_{\tilde{n}}{}'\left[\left|u_{i\uparrow}^{\tilde{n}1}\right|^2\delta\left(E-E_{\tilde{n}1}\right)+\left|v_{i\uparrow}^{\tilde{n}2}\right|^2\delta\left(E+E_{\tilde{n}2}\right)\right],\end{aligned} \tag{2.165}$$

and

$$\begin{aligned}\rho_{i,\downarrow}(E)&=\frac{1}{\hbar\pi}\operatorname{Im}\left[\mathscr{G}_{44}\left(i,i;-i\omega_n\rightarrow-\left(E/\hbar+i0^+\right)\right)\right]\\&=\sum_{\tilde{n}}{}'\left[\left|u_{i\downarrow}^{\tilde{n}2}\right|^2\delta\left(E-E_{\tilde{n}2}\right)+\left|v_{i\downarrow}^{\tilde{n}1}\right|^2\delta\left(E+E_{\tilde{n}2}\right)\right].\end{aligned} \tag{2.166}$$

The above expressions for the local density of states are the same as those given in terms of the eigensolution to the BdG equations (2.47). As we will show in later chapters, the Green's function technique is very useful and convenient for some situations.

9.8 Junctions in Microscopic Framework: Basics

(it is a hard method, I'll add soon it, see Abrikosov's book and LSh problems.)

9.9 Junctions in Microscopic Framework: Other Features

(it is a hard method)

9.10 GF method for JJ

(write what are we using)

9.10.1 Caroli's GF Method

(???)

9.10.2 GF method for JJ: Examples

(collect from articles results of this method, there are a lot of them)

9.11 Beeankker's Determinant Framework: Basics

(I'll learn it later)

9.12 Beeankker's Determinant Framework: Other Features

(I'll learn it later)

9.13 Green's function for SC Junctions: Other Working Methods

(I'll write most useful methods from my special note about it here later)

9.14 "Classic" theoretical results of Josephson Junctions: An Overview

(there are a lot of great forgotten articles, I'll write idea of many of them here. Detailed analysis of them will be in another note)

Methods of Kulik

(??? think about his article and write it here!)

10 Well-Known Models of Junctions

10.1 Very Famous Models

10.1.1 Blonder Tinkham Klapwijk Original Model 1: Basics

This article teaches us how to work with BdG equation and how to write basic formulas for the current.
(??? how????)

[MOVE TO THE SECTION BEFORE]

The Model

We propose a simple theory for the $I-V$ curves of normal-superconducting microconstriction contacts which describes the crossover from metallic to tunnel junction behavior. The detailed calculations are performed within a generalized semiconductor model, with the use of the Bogoliubov equations to treat the transmission and reflection of particles at the $N-S$ interface. By including a barrier of arbitrary strength at the interface, we have computed a family of $I-V$ curves ranging from the tunnel junction to the metallic limit. Excess current, generated by Andreev reflection, is found to vary smoothly from $4\Delta/3eR_N$ in the metallic case to zero for the tunnel junction. Charge-imbalance generation, previously calculated only for tunnel barriers, has been recalculated for an arbitrary barrier strength, and detailed insight into the conversion of normal current to supercurrent at the interface is obtained. We emphasize that the calculated differential conductance offers a particularly direct experimental test of the predictions of the model.

I. Introduction, conclusion

In recent years there has been much experimental and theoretical work on small-area highcurrent-density superconducting junctions, since such junctions have advantages for certain practical applications. Although the properties (I-V curves, etc.) of classic (high-barrier) tunnel junctions have long been understood in great detail, [1] the properties of metallic (no-barrier) junctions have been studied only more recently [2–4] and in less detail, and the transitional case (small barrier) has received practically no attention at all. Here, we present a new unified treatment which is sufficiently general to embrace both limits, as well as the intermediate regime.

In this paper, we confine our attention primarily to the $N - S$ interface in the context of a generalized Andreev reflection model. This avoids the complications of the Josephson effect, while allowing complete delineation of I - V curves including the so-called "excess currrent" at high voltage, as it increases from zero in tunnel junctions to its limiting value in clean metallic contacts.

The paper begins with a careful clarification of the relation between a general semiconductor model of the superconducting energy levels and the excitations of the BCS model and the Bogoliubov equations. With this in hand, we are quickly led to complete $I - V$ curves for the case of arbitrary barrier strength. We also compute the generalization of the tunnel-injection results for the generation of charge imbalance in the superconductor, and give new insight into the detailed processes involved in the conversion from normal to supercurrent at an N-S interface. Some of the results which we obtain by our simple technique have been obtained earlier by other more mathematically complex theories, but our method gives greater physical insight. Moreover, the simplicity of our method has allowed us to treat a broader range of problems having direct experimental implications. We have also used this model in a previous publication [5] to explain the origin of the excess current and of the subharmonic gap structure which is observed in metallic S-S contacts.

IX. CONCLUSION

We have proposed a simple theory for the $N - S$ microconstriction or point contact that is general enough to describe the complete crossover from metallic to small-area tunnel-junction behavior. From this model, a deeper understanding of the semiconductor picture, excess currents, current conversion, and charge-imbalance processes have emerged, in addition to calculation of $I - V$ curves for arbitrary barrier strength. The latter results are directly accessible to experiment, and should be helpful in interpreting the wide variety of $I - V$ curve shapes observed in the laboratory. The application of this model to the $S - N - S$ case has been presented elsewhere, [5] where it has been shown to offer an explanation of the SGS observed in metallic weak links.

ii. Generalized semiconductor scheme

It has long been conventional to simplify the calculation of tunnel currents by taking advantage of the fact that the BCS coherence factors u_k and v_k drop out of the computation if excitations with the same energy E_k, but with $k < k_F$ and $k > k_F$, are grouped together.

Then a very simple "semiconductor model" can be established, in which only the superconducting density of states $N_s(E)$ distinguishes the superconductor from the situation in the normal state. However, in combining $k_<$and $k_>$for each E_k, information is lost. For instance, the quasiparticle charge imbalance Q^* refers specifically to the imbalance between the two branches $k > k_F$ and $k < k_F$ of the quasiparticle spectrum, a distinction which is completely suppressed in the simplest semiconductor model. Another shortcoming of the elementary semiconductor model is that the density-of-states factor makes no reference to the microscopic nature of the

states. For example, it is clear that the current must be carried toward and away from the junction by waves traveling in the appropriate directions, yet this physical fact is obscured in the usual tunnel-Hamiltonian model.

Here, we describe a generalized semiconductor model specifically designed to avoid this loss of information. The key innovation is the use of the Bogoliubov equations [6] to handle the interface; this treats all cases from a clean metallic interface to a tunnel junction in the same formal way by matching wave functions at the boundary. These results determine the probability current carried by the various excitations characterized by the semiconductor diagram. For simplicity, we restrict attention to metal clean enough to allow use of momentum as a good quantum number for labeling the various waves.

If one considers only energies $E > \Delta$, the Bogoliubov equation solutions (see Appendix for details) for the incident, transmitted, and reflected particles can be identified with the conventional BCS quasiparticle excitations with energy

$$E_k = \left(\Delta^2 + \epsilon_k^2\right)^{1/2} \tag{1}$$

with respect to the electrochemical potential for condensed pairs, where

$$\epsilon_k = \frac{\hbar^2 k^2}{2m} - \epsilon_F \tag{2}$$

Because only the square of ϵ_k enters the expression for E_k, there will be a pair of magnitudes of k associated with each energy, namely,

$$\hbar k^{\pm} = (2m)^{1/2} \left[\epsilon_F \pm \left(E_k^2 - \Delta^2\right)^{1/2}\right]^{1/2} \tag{3}$$

Moreover, because of the BCS pairing of k and $-k$, one must consider both signs of k together, so that there is a fourfold degeneracy of relevant states for each E, as sketched in Fig. 1. Of course there is an additional twofold spin degeneracy, but in the absense of spin-flip processes this affects only normalizations, and it need not concern us here.

The nature of one type of these BCS quasiparticle states is given by the usual Bogoliubov transformation [7] as

$$\gamma_{k0}^* = u_k c_{k\uparrow}^* - v_k c_{-k\downarrow} \tag{4}$$

where the BCS coherence factors are given by

$$u_k^2 = 1 - v_k^2 = \frac{1}{2}\left(1 + \epsilon_k / E_k\right) \tag{5}$$

Although, in general, Eq. (5) determines the magnitudes of u_k and v_k (which can have phase factors), for simplicity we take them to be real and positive. For the $N - S$ case treated here, this involves no loss of generality; only in S - S devices does phase play a role. The excitations described in Eq. (4) consist partly of electrons created at $+k$ (i.e., $u_k c_{k\uparrow}^*$) and partly of holes created at $-k$ (i.e., $v_k c_{-k\downarrow}$, the destruction of an electron at $-k$). Since either term increases the system momentum by $+k$, the subscript k in γ_{k0}^* is a well-defined momentum index suitable for labeling. From Eq. (5) we see that the excitations at $\pm k^+$are predominantly electronlike, while these at $\pm k^-$are predominantly holelike. The other members of the degenerate set are described by including the complementary BCS operator γ_{k1} and also including both senses of k.

In preparation for the application of boundary conditions, we note that the excitation described by Eq. (4) is described in the Bogoliubov-equation formalism (see Appendix for details) as a two-element column vector,

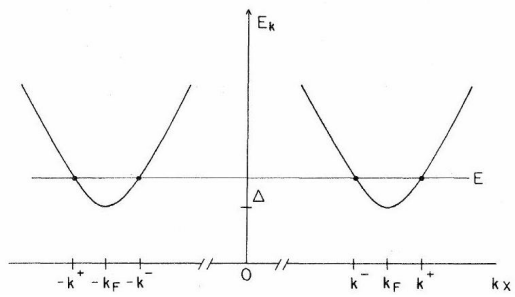


FIG. 1. Schematic plot of excitation energies E_k vs k along an axis passing through the center of the Fermi sphere in the superconducting state. The scale has been greatly expanded near $\pm k_F$.

$$\psi_{k0} = \begin{bmatrix} f_k(x,t) \\ g_k(x,t) \end{bmatrix} \tag{6}$$

Here f_k and g_k satisfy the differential equations

$$\begin{aligned} \left[-\frac{\hbar^2}{2m}\nabla^2 - \mu(x) + V(x)\right] f + \Delta g &= i\hbar\frac{\partial f}{\partial t} \to Ef \\ -\left[-\frac{\hbar^2}{2m}\nabla^2 - \mu(x) + V(x)\right] g + \Delta f &= i\hbar\frac{\partial g}{\partial t} \to Eg \end{aligned} \tag{7}$$

and they are proportional to u_k and v_k, respectively, when $V(x)$ is constant. The time derivatives may be replaced as indicated in solutions for stationary states of energy E.

As written in Eq. (4), the excitations γ^*_{k0} change the charge of the superconductor by the fractional electronic charge $q_k = u_k^2 - v_k^2 = \epsilon_k/E_k = \pm N_s(E)^{-1}$. Since physically allowable operators must conserve charge exactly, it is convenient [7] to introduce operators of the form

$$\gamma^*_{ek0} = u_k c^*_{k\uparrow} - v_k S^* c_{-k\downarrow}, \tag{8a}$$

$$\gamma^*_{hk0} = u_k S c^*_{k\uparrow} - v_k c_{-k\downarrow} = S\gamma^*_{ek0} \tag{8b}$$

where S^* adds a pair to the condensate and S destroys one. These operators create excitations while changing the charge by exactly $\pm e$, corresponding to the subscripts e and h for electron and hole, respectively. Accordingly, they are better adapted to describe the energy levels analogous to those of ordinary electrons. The excitations described by Eqs. (8a) and (8b) are identical, and in no sense cancel as one might suppose for electron and hole operators. The systems resulting from (8a) and (8b) differ only by one condensed pair from the reservoir at the chemical potential.

Now for any system with fermion excitations such as these, the total system energy can be written as

$$E = E_G + \sum_k E_k \gamma^*_k \gamma_k + \mu N \tag{9}$$

where E_G is the ground-state energy, and the sum runs over all the excitations, which have $E_k \geq 0$. The electrochemical potential μ must be introduced explicitly since we are interested in treating processes which change the number N of electrons in a subsystem at given μ by ± 1. In fact, the energy required to make an excitation with charge e is

$$E_{ek} = \mu + E_k, \tag{10a}$$

while that to make an excitation with charge $-e$ differs by 2μ and is

$$E_{hk} = -\mu + E_k = -(\mu - E_k) \tag{10b}$$

We can now tabulate (see Table I) the possible charge-conserving processes involving subsystems 1 and 2, and write down the corresponding condition set by the conservation of energy. There are four distinct cases, each of which conserves energy equally well in reverse, making eight cases in all. As is evident from Table I, all these energetically allowed transitions occur as "horizontal" ones only if we plot both $\pm E_{ki}$ symmetrically about each μ_i, as is motivated by recalling that $\mu - E_k = -E_{hk}$ (see Fig. 2). Further, the four cases of Table I include all the combinations of $\pm E_k$, so that all horizontal transitions in such a "reflected" or semiconductor-model diagram are energetically allowed.

There is, however, another constraint on the system; namely, a particle incident from the left can only produce transmitted particles with positive group velocity ($dE/d\hbar k$) and reflected ones with negative group velocities. In general, there is a finite probability of all the transfers allowed by these considerations to occur, but in the special case of zero barrier and no discontinuity in electronic-band parameters across the $N - S$ interface, it turns out that there is essentially zero crossover between channels inside and outside the Fermi surface, even near the gap edge. It is here that the Bogoliubov equations prove most useful: The semiconductor diagram shows which transitions are energetically allowed; the Bogoliubov equations provide the

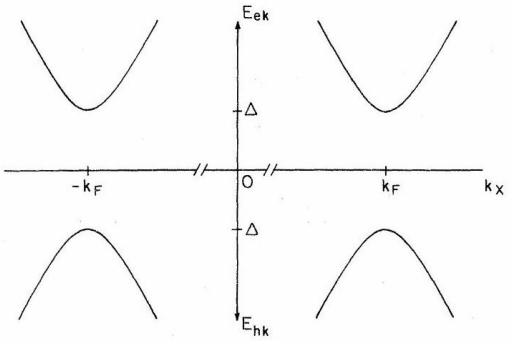


FIG. 2. Semiconductor version of Fig. 1. Inclusion of the quasiparticle branches in the lower half plane allows all the transitions in Table I to be "horizontal."

TABLE I. Processes involving transfer of a single electronic charge.

Process	Energy condition
1. Electron from $1 \to 2$ (or reverse)	$\mu_1 + E_{k1} = \mu_2 + E_{k2}$
2. Hole from $1 \to 2$ (or reverse)	$\mu_1 - E_{k1} = \mu_2 - E_{k2}$
3. Create electron in 1 and hole in 2 (or destroy both)	$\mu_1 + E_{k1} = \mu_2 - E_{k2}$
4. Create hole in 1 and electron in 2 (or destroy both)	$\mu_1 - E_{k1} = \mu_2 + E_{k2}$

quantitative probability that each will occur.

As a final preliminary, we consider the special case of the normal metal, obtained by letting $\Delta \to 0$ in the expressions for the superconducting case. Here the situation simplifies from the superconducting case shown in Fig. 2 because electronlike excitations cannot be made inside the Fermi sphere, since the states there are fully occupied in the ground state, and excitations must be orthogonal to the ground state. Similarly, hole excitations are possible only outside the Fermi sphere. As a result, in the normal metal only the branches shown in Fig. 3 exist.

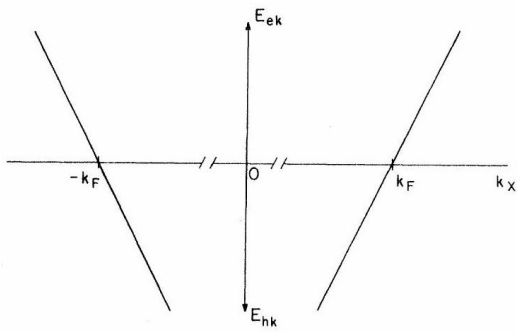


FIG. 3. E_k vs k for the normal state.

iii. The n-s boundary in equilibrium

We start by considering the dynamic equilibrium which exists at an N-S interface with no applied voltage, as sketched in Fig. 4. In this equilibrium situation, all relevant quaisparticle states (such as those labeled $0, 1, 2, 3, 4$, and 5 in the figure) are occupied with the same probability $f_0(E)$, which also gives the probability of a hole in the state 6 at $-E$. Viewed kinematically in a semiclassical approximation, however, particles approach the interface and are transmitted and reflected with certain probabilities, which are given by the products of squared amplitudes of Bogoliubov-equation solutions times their appropriate group velocities. The self-consistency of the equilibrium state provides a useful check on the computed probability coefficients.

To be concrete, consider an electron incident on the interface from the normal state with energy $E > \Delta$, as indicated by the arrow at the state labeled 0 in Fig. 4.

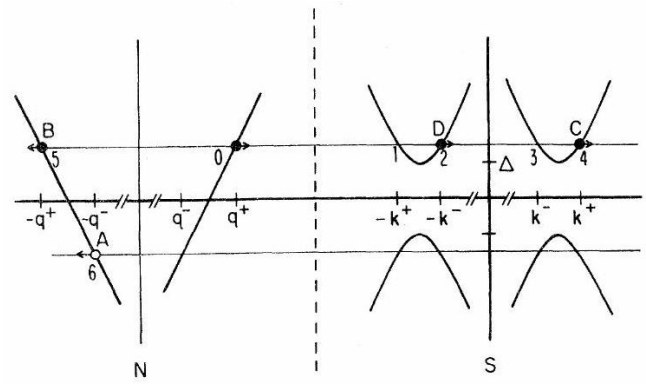


FIG. 4. Schematic diagram of energy vs momentum at $N - S$ interface. The open circles denote holes, the closed circles electrons, and the arrows point in the direction of the group velocity. This figure describes an incident electron at)0), along with the resulting transmitted $(2, 4)$ and reflected $(5, 6)$ particles.

By matching slope and value of the wave function across the interface, one finds the probabilities $A(E), B(E), C(E)$, and $D(E)$ for the four processes indicated by those labels in Fig. 4, i.e., outgoing particles at points $6, 5, 4$, and 2, respectively. In words, $C(E)$ is the probability of transmission through the interface with a wave vector on the same side of the Fermi surface (i.e., $q^+ \to k^+$, not $-k^-$, while $D(E)$ gives the probability of transmission with crossing through the Fermi surface (i.e., $q^+ \to -k^-$). $B(E)$ is the probability of ordinary reflection, while $A(E)$ is the probability of Andreev [8] reflection as a hole on the other side of the Fermi surface. The latter process is not included in Table I, since it involves a transfer of a pair carrying $2e$ across the interface, while the processes in Table I transfer only a single electronic charge. The energy conservation condition appropriate for Andreev reflection is found by equating the energy of the initial electronlike excitation with that of the final holelike excitation plus a Cooper pair at the chemical potential. That is, $E_{ek} = E_{hk} + 2\mu$, from which it follows that

$$|E_e| = |E_h| \tag{11}$$

In other words, the hole is generated as far below μ as the electron was above, as drawn in Fig. 4. Of course, this result is obvious in the excitation representation.

It should be clearly understood that the probabilities A, B, C, and D (and the similar set A', B', C', and D' for quasiparticles incident from the superconducting side) are those appropriate for probability current, taking account of the cancelling effects of state density and group velocity. For example, consider the flow of particles across the interface in the energy range E to $E + dE$, and including only states outside the Fermi surface. From left to right, the current from states at 0 to those at 4 in Fig. 4 is proportional to $v_F C(E) f_0(E) dE$; the balancing current from right to left, i.e., from states at 1 to those at 5, is proportional to $v_F C'(E) f_0(E) N_s(E) dE$, where $N_s(E)$ is the normalized density of states in the superconductor. In equilibrium these flows are exactly equal, so that

$$C'(E) N_s(E) = C(E) \tag{12a}$$

and similarly

$$D'(E) N_s(E) = D(E) \tag{12b}$$

governs the branch-crossing transfers. The results of Eqs. (12) can be derived by direct computation, or by appeal to time-reversal symmetry. For simplicity, in the remainder of the paper we write all expressions in terms of $C(E)$ and $D(E)$, avoiding the need for explicit inclusion of the density-ofstates factor $N_s(E)$ or the quasiparticle group velocity $v_g = N_s^{-1} v_F$ in integrations over energy.

Recognizing the symmetry of the problem about μ, we see that $A(E)$ and $B(E)$ are even functions of E. Similarly, $C(E)$ and $D(E)$ are also even functions of E, provided one uses the convention that $D(E)$ describes processes in which the transmission involves branch crossing, while $C(E)$ governs transmission processes in which the particle stays on the same branch.
It is important to note that the conservation of probability requires that

$$A(E) + B(E) + C(E) + D(E) = 1 \tag{13}$$

This result is particularly useful in simplifying expressions for energies below the gap, $|E| < \Delta$, where there can be no transmitted quasiparticles, so that $C = D = 0$. Then, Eq. (13) reduces simply to $A(E) = 1 - B(E)$, so that a single function of energy is all that is needed.

Now, in general, A, B, C, and D depend on the angle of incidence of the trajectory and on the detailed shape of the scattering potential. For simplicity, we restrict ourselves to a one-dimensional (1D) geometry. For the purposes of this paper, the actual three-dimensional (3D) geometry is invoked only to enforce three boundary conditions on the 1D model: that the junction is well-cooled, and that the energy gap and the electric potential both rise to their full asymptotic values on a scale shorter than ξ on either side of the neck.

To capture the essential effect of any interfacial scattering with a single parameter, we model it by a repulsive potential $H\delta(x)$ located at the interface. This is meant to represent the effect of the typical oxide layer in a point contact, the localized disorder in the neck of a short microbridge, or the intentional oxide barrier in a high-current-density tunnel junction. The calculations with the Bogoliubov equations are quite straighforward, but are given in the Appendix to avoid a digression at this point. The results of the calculations are values of the four coefficients A, B, C, and D as functions of energy and barrier strength. To simplify the formulas, we have introduced a dimensionless barrier strength $Z = k_F H / 2\epsilon_F = H/\hbar v_F$. The significance of this Z is illuminated by noting that the transmission coefficient in the normal state is simply $(1 + Z^2)^{-1}$, and the corresponding reflection coefficient is $Z^2/(1 + Z^2)$.

The expressions for the energy dependences of A, B, C, and D for $E > \Delta$ can be conveniently written in terms of u_0 and v_0, the BCS parameters u and v evaluated on the branch outside the Fermi surface. The results are as given in Table II. For convenience, in addition to the general results we also list the limiting forms of the results for zero barrier ($Z = 0$) and for a strong barrier [$Z^2 (u^2 - v^2) \gg 1$], as well as for $\Delta = 0$ (the normal-metal case). Curves computed using the general results are plotted in Fig. 5 for $Z = 0, 0.3, 1$, and 3. In the special case of $E = \Delta$, one notes from Table II that $A = 1$ and $B = C = D = 0$, independent of Z.

TABLE II. Transmission and reflection coefficients. A gives the probability of Andreev reflection (i.e., reflection with branch crossing), B of ordinary reflection, C of transmission without branch crossing, and D of transmission with branch crossing (see text). $\left(\gamma^2 = \left[u_0^2 + Z^2 (u_0^2 - v_0^2)\right]^2, u_0^2 = 1 - v_0^2 = \frac{1}{2}\left\{1 + \left[(E^2 - \Delta^2)/E^2\right]^{1/2}\right\},$ and $N_s(E) = (u_0^2 - v_0^2)^{-1}$.)

	A	B	C	D
Normal state	0	$\frac{Z^2}{1+Z^2}$	$\frac{1}{1+Z^2}$	0
General form				
$E<\Delta$	$\frac{\Delta^2}{E^2+(\Delta^2-E^2)(1+2Z^2)^2}$	$1-A$	0	0
$E>\Delta$	$\frac{u_0^2 v_0^2}{\gamma^2}$	$\frac{(u_0^2-v_0^2)^2 Z^2(1+Z^2)}{\gamma^2}$	$\frac{u_0^2(u_0^2-v_0^2)(1+Z^2)}{\gamma^2}$	$\frac{v_0^2(u_0^2-v_0^2)Z^2}{\gamma^2}$
No barrier ($Z=0$)				
$E<\Delta$	1	0	0	0
$E>\Delta$	v_0^2/u_0^2	0	$1-A$	0
Strong barrier [$Z^2(u^2-v^2)>>1$]				
$E<\Delta$	$\frac{\Delta^2}{4Z^2(\Delta^2-E^2)}$	$1-A$	0	0
$E>\Delta$	$\frac{u_0^2 v_0^2}{Z^4(u_0^2-v_0^2)^2}$	$1-\frac{1}{Z^2(u_0^2-v_0^2)}$	$\frac{u_0^2}{Z^2(u_0^2-v_0^2)}$	$\frac{v_0^2}{Z^2(u_0^2-v_0^2)}$

Accordingly, except for $Z = 0$, $A(E)$ has a sharp peak at the gap edge, although this peak becomes unobservably narrow for large values of Z.

Although we have developed this technique quite independently, other workers have also employed the Bogoliubov equations, and along similar lines. Andreev [8] in 1964 used them to calculate the thermal-boundary resistance at an $N - S$ interface. Thus, he was essentially concerned with the restriction of quasiparticle flow from N to S caused by the gap. Kümmel [9] expanded the equations to include the condensate phase, and then used them to calculate the momentum balance of electricalcurrent flow near a vortex core. He emphasized the interchange of current between quasiparticles and the pairs in geometries where the gap varied with position. Then, in 1971 Demers and Griffin [10] and Griffin and Demers, [11] calculated the transmission coefficients in $N - S - N$ and $S - N - S$ geometries and made the extension to a δ-function barrier at the interface. Surprisingly, this important work remained essentially unnoticed for a number of years but recently (1977) Entin-Wohlman [12] has drawn on it to develop boundary conditions that she used in solving the Gor'kov gap equation at an N-S interface. Thus, use of the Bogoliubov equations to determine the fraction and type of reflected particles is not new, though perhaps the technique remains underutilized. What is new is our extension of the method to calculations at finite bias voltage (as described in the next section) and our development of a framework that allows the physical consequences of these processes to emerge more clearly.

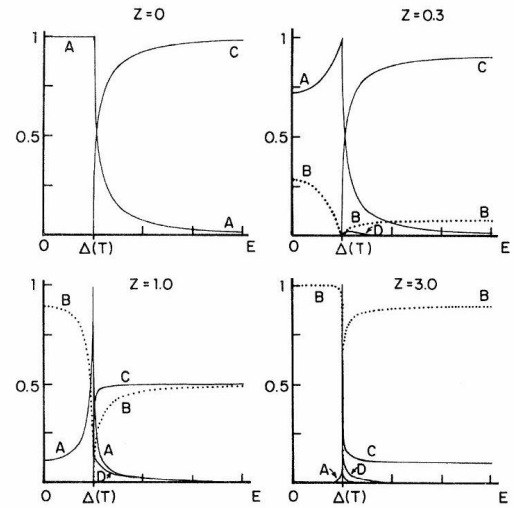


FIG. 5. Plots of transmission and reflection coefficients at N-S interface. A gives probability of Andreev reflection, B gives probability of ordinary reflection, C gives transmission probability without branch crossing, and D gives probability of transmission with branch crossing. The parameter Z measures the barrier strength at the interface.

iv. The n-s boundary at finite voltage: $I - v$ curves

When a voltage is applied, nonequilibrium quasiparticle populations will be generated, which can in general be found only by obtaining a self-consistent solution to a suitable Boltzmann equation. This solution is greatly simplified if one can assume ballistic acceleration of the particles without scattering. This is a good approximation for our case of a small orifice connecting massive electrodes, so long as the diameter of the orifice is small compared to a mean-free path. Moreover, in this regime, Bogoliubov-equation solutions neglecting scattering potentials except at the interface should also be usable. [13] The physical assumption which we use to define the problem is then that the distribution functions of all incoming particles are given by equilibrium Fermi functions, apart from the energy shift due to the accelerating potential. It is convenient to choose the electrochemical potential of the pairs in the superconductor as our reference level, since that remains a welldefined quantity even when the quasiparticle populations are far from equilibrium. Moreover, it is the quantity which defines the location of the "mirror plane" of the semiconductor diagram. With this convention, all incoming electrons from the S side have the distribution function $f_0(E)$, while those coming in from the N side are described by $f_0(E - eV)$.
Since the current must be conserved, it can be calculated in any plane. It is particularly convenient to do so on the N side of the interface, where all current is carried by single particles, and none as a supercurrent. To find the current in our 1D model, we take the difference between $f_{\rightarrow}(E)$ and $f_{\leftarrow}(E)$, the distribution functions at points such as 0 and 5 on Fig. 4, and integrate over E. That is,

$$\begin{aligned} I &= \mathscr{A} J \\ &= 2N(0)ev_F\mathscr{A} \int_{-\infty}^{\infty} [f_{\rightarrow}(E) - f_{\leftarrow}(E)]\, dE \end{aligned} \tag{14}$$

where $\mathscr{A}$ is an effective-neck cross-sectional area, including a numerical factor for angular averaging which will depend on the actual 3D geometry. For example, in the orifice model of a

point contact, $\mathscr{A} = \pi a^2/4$, where a is the radius of the orifice. [14] As usual, $N(0)$ refers to the one-spin density of states at ϵ_F.

With our assumption about incoming populations, it follows that

$$f_{\rightarrow}(E) = f_0(E - eV) \tag{15}$$

while

$$f_{\leftarrow}(E) = A(E)\left[1 - f_{\rightarrow}(-E)\right] + B(E)f_{\rightarrow}(E) + [C(E) + D(E)]f_0(E) \tag{16}$$

In writing Eq. (16), we have chosen to write $f_{\rightarrow}(E)$ instead of $f_0(E - eV)$ in anticipation of later dealing with more complicated problems where $f_{\rightarrow}(E)$ and $f_{\leftarrow}(E)$ must be found self-consistently. Even in such cases, Eq. (16) remains valid as it stands, and serves as a boundary condition for a Boltzmann equation, whose solution would be inserted into the general expression (14) to find the current. However, in the present simple case, we can simply substitute Eqs. (15) and (16) into Eq. (14), obtaining

$$\begin{aligned} I_{NS} &= 2N(0)ev_F\mathscr{A}\int_{-\infty}^{\infty}(f_0(E - eV) - \{\, A(E)f_0(E + eV) + B(E)f_0(E - eV) \\ &\quad + [1 - A(E) - B(E)]f_0(E)\})\, dE \\ &= 2N(0)ev_F\mathscr{A}\int_{-\infty}^{\infty}\left[f_0(E - ev) - f_0(E)\right]\left[1 + A(E) - B(E)\right]dE \end{aligned} \tag{17}$$

In obtaining the final form, we have used the properties that $A + B + C + D = 1, A(E) = A(-E)$, and $f_0(-E) = 1 - f_0(E)$. The quantity $[1 + A(E) - B(E)]$ in Eq. (17) can be referred to as the "transmission coefficient for electrical current." Its form shows that while ordinary reflection [described by $B(E)$] reduces the current, Andreev reflection [described by $A(E)$] increases it by giving up to two transferred electrons (a Cooper pair) for one incident one.

If both sides of the interface are normal metal, $A = 0$ since there is no Andreev reflection, and $1 - B = C = (1 + Z^2)^{-1}$ as noted above, so that Eq. (17) reduces to the simple form

$$I_{NN} = \frac{2N(0)e^2v_F\mathscr{A}}{1 + Z^2}V \equiv \frac{V}{R_N} \tag{18}$$

Note that even in the absence of a barrier ($Z = 0$), there is still a nonzero normal-state resistance. This is the spreading resistance typical of a two-dimensional (2D) or 3D geometry, often referred to as the Sharvin resistance [14] in the present case of a point-contact geometry with infinite mean free path relative to orifice size.

For the more interesting N - S case, we have integrated (17) numerically to obtain $I - V$ curves for a number of barrier strengths at $T = 0$. The results are shown in Fig. 6. The effect of changing the barrier strength is even more dramatic in the differential conductance dI/dV, plotted versus V in Fig. 7, again at $T = 0$. From Figs. 6 and 7, it is clear that barrier strengths $Z \gtrsim 10$ give results essentially indistinguishable from those for classical tunnel junctions, although, as our model demonstrates, there is a continuous variation from the metallic to the tunneling limit. To facilitate the interpretation of experimental dI/dV curves, it is useful to note at $T = 0$, Eq. (17) implies that dI/dV is proportional to the transmission coefficient for electrical current, $1 + A(eV) - B(eV)$, while at $T \neq 0, dI/dV$ is proportional to a thermally smeared version of the same quantity.

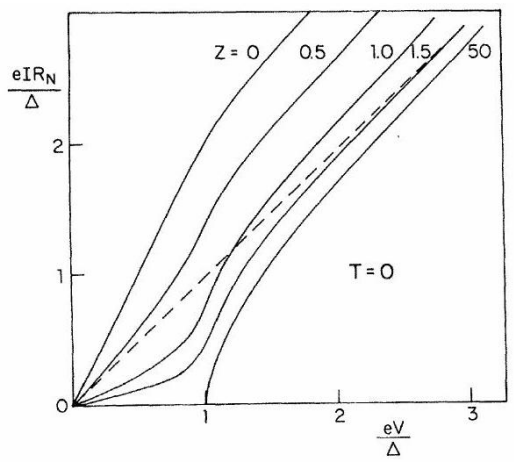


FIG. 6. Current vs voltage for various barrier strengths Z at $T = 0$. These curves attain their asympototic limits only for very high voltages. For example, the tunnel junction ($Z = 50$) curve will be within 1% of the normal-state curve (dotted line) only when $eV \geq 7\Delta$.

10.1.2 Blonder Tinkham Klapwijk Original Model 1: Advanced Sratements

[MOVE TO THE SECTION BEFORE]

v. Relation to transfer Hamiltonian approach

With the arbitrary barrier case well in hand, we are in a position to contrast our technique with the more conventional transfer Hamiltonian approach. If one assumes a thick oxide between two banks, to lowest order one can consider the two sides as noninteracting systems, containing electrons in standing-wave states labeled by quantum numbers k_L or k_R. Of course, they are not truly unconnected and there is a small probability that an electron from one side can tunnel to the other side; thus the wave function must actually penetrate through the barrier. Since this penetration will change the energy of the system, many workers have tried to model the resulting change by adding a "transfer" term to the Hamiltonian, although this phenomenological model has never been fully justified. [15] The tunneling transfer matrix element T is tricky to evaluate, since it is a function of the amplitude of the small tail on the penetrating wave and requires some microscopic knowledge of the system. Nonetheless, many workers have calculated T, and the result, for eV much smaller than the barrier height, is an essentially featureless matrix element much like that for an $N - N$ contact.

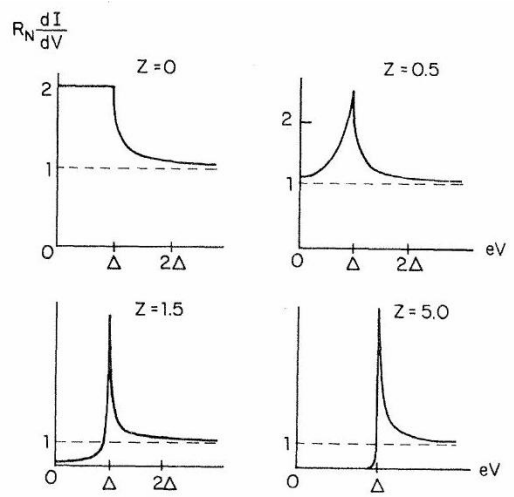


FIG. 7. Differential conductance vs voltage for various barrier strengths Z at $T = 0$. This quantity is proportional to the transmission coefficient for electric current for particles at $E = eV$.

By treating the tunneling as a perturbation, one can calculate the current by using the Golden Rule, and find the electron-transfer rate proportional to a squared matrix element times the number density of unoccupied final states. This is in the origin of the BCS density-of-states factor times the thermal weighting factor $[1-f(E-eV)]$ which appears in the tunneling current, for particles from L to R. When we integrate over all states on the left, an additional $N_L(E)f(E)$ appears, for a total probability (per unit energy) of

$|T|^2 N_L(E)N_R(E-eV)f(E)[1-f(E-eV)]$.

The latter two factors reflect the view that this is a stochastic process involving two independent banks, so that the joint probability for tunneling is proportional to the probability of the initial states being occupied times the probability of final states being unoccupied (i.e., unblocked). When we combine currents in both directions, the cross terms involving products of Fermi functions cancel, and we are left with the usual tunneling result in which the current is proportional to an integral over

$$N_L(E)N_R(E-eV)[f(E-eV)-f(E)]$$

The Bogoliubov equation approach is quite different in spirit. As we saw above, the current transmission coefficient (in contrast to the matrix element squared in the tunnel calculation) varies rapidly for $|E| \approx \Delta$. This is the origin of the density-of-states factor in the final result. In no sense are the two banks decoupled; we associate a given set of wave vectors on the left $(q^+, -q^+, q^-)$ with a specific set on the right (k^+, k^-), regardless of the barrier height. $q^+$is not an "initial" state from which transfer can be blocked by an occupied "final" state k^+. Rather, a wave packet describing an incident particle in q^+evolves continuously into transmitted and reflected wave packets in the completely deterministic way described by Liouville's theorem without scattering. Thus, we associate one distribution function with this entire set of wave vectors. Combining currents originating from both sides gives a difference in Fermi functions just as the transfer Hamiltonian did (after cancellation of cross terms), but the rationale is entirely different in detail. Since we can achieve the same result with a model that has a larger range of validity and usefulness, we have chosen this latter point of view.

vi. Excess current

Although the high-voltage ($eV \gg \Delta$) portion of each $I-V$ characteristic in Fig. 6 is linear with slope R_N, it does not in general fall on the normal-state curve $V = IR_N$ (as it does in a tunnel junction). Rather, it is displaced by a constant amount referred to as the excess current, $I_{\rm exc}$, which can be found by extrapolation back to the $V = 0$ axis. By manipulation of Eqs. (16) and (17), this $I_{\rm exc}$ can be written as

$$I_{\rm exc} \equiv (I_{NS} - I_{NN})|_{eV\gg\Delta} = \frac{1}{eR_N[1-B(\infty)]}\int_0^\infty [A(E) - B(E) + B(\infty)]dE \qquad (19)$$

where from Table II, $B(\infty) = Z^2/(1+Z^2)$ is the reflection coefficient at high energy or in the normal state. Using this expression and those in Table II, we have computed numerically the dependence of $I_{\rm exc}R_N$ (the "insufficient voltage" referred to by Likharev [2]) upon barrier strength Z. Since this high-voltage limit depends on T only through the magnitude of Δ, the normalized quantity $I_{\rm exc}\, R_N/\Delta$ is a function only of barrier strength. This dependence is plotted in Fig. 8. Note the rapid falloff with increasing Z; clearly, excess current will be seen only in relatively barrier-free contacts.

More generally, one can define a voltage-dependent excess current,

$$I_{\rm exc}(V) = I_{NS}(V) - I_{NN}(V) \tag{20}$$

which simply gives the extra current due to the superconductivity. Since $I_{NN}(V)$ is simply V/R_N, finding $I_{\rm exc}\,(V)$ is equivalent to giving the entire I V curve, as was done in Fig. 6. However, it is worth noting that for $Z = 0$ and $\Delta << kT$, the calculation can be carried out analytically, with the result,

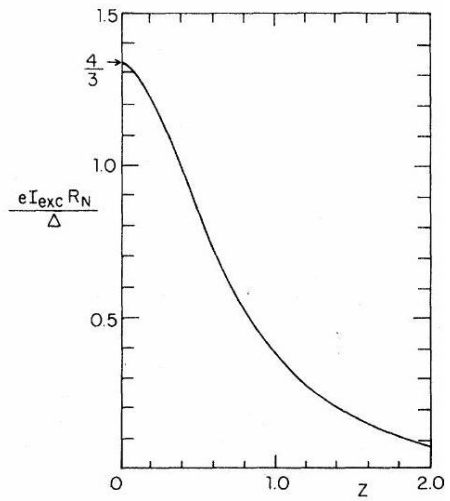


FIG. 8. Excess current (in units of Δ/eR_N) as a function of barrier strength Z. The temperature dependence of the curve is entirely contained within $\Delta(T)$.

$$I_{\rm exc}(V) = (4\Delta/3eR_N)\tanh(eV/2kT), \quad \Delta << kT \tag{21}$$

As noted in our previous work, this result agrees in detail with that obtained by Zaitsev [4] for a clean metallic NS contact, after correcting a factor of 2 in his result.

We can also calculate the excess current for an $S - S'$ contact, by using the $N - S$ result above. As we explained in a previous publication, [5] in the highvoltage limit, the $S - S'$ device can be thought of as a series combination of an $S - N$ and a $N - S'$ microconstriction. The "insufficient voltages" of the two simply add, so that the excess current is the sum of the contributions from the two sides. For example, in the clean contact with $Z = 0$, we find

$$I_{\rm exc} = 4\,(\Delta + \Delta')\,/3eR_N$$

While the excess current has a clear mathematical definition, it may be a difficult quantity to measure reliably, for at least two reasons. First, for voltages greater than the gap, heating will generally distort the $I - V$ curve away from its ideal isothermal shape. [16] There may, in fact, be no linear region at high voltages until heating has driven the contact fully normal. Secondly, even in the absence of heating, care must be taken to carry the measurement to sufficiently high voltages to obtain a true asymptote. For example, the tunnel junction curve in Fig. 6 (i.e., $Z = 50$) appears to have a significant negative (rather than zero) excess current, even at a voltage as high as $eV = 3\Delta$. Of course, if one assumes our computed I - V curves are correct and applicable to the contact at hand, one can determine a value of Z by fitting the measured curves at lower voltages.

vii. Analysis of currents and charge-imbalance generation

In this section we establish a formalism for separating the total current I_{NS} into parts differentiated according to the mechanism of charge transfer. In particular, we distinguish the

part of the current I^*_{NS} associated with the creation of quasiparticle charge imbalance Q^* in the superconductor from the part that is converted directly into supercurrent. We also define linear-response coefficients giving the normalized differential conductance Y and its counterpart Y^*, describing quasiparticle charge injection, and evaluate them as functions of Z and T.

For tunnel junctions, the rate of generation of quasiparticle charge branch imbalance has been discussed in some detail by Tinkham and Clarke [17] (TC), by Tinkham, [18] by Pethick and Smith [19] (PS), and by Clarke, et al. [20] (CESST). The latter authors reviewed carefully the interrelations of the definitions and conventions of the various treatments including the rather different conceptual approach of Schmid and Schön. [21] Using our present method, we can generalize the tunnel results to arbitrary barrier strength, providing a description which covers all cases from the tunnel limit to the ideal metallic contact, and which gives very detailed insight into the process.

To minimize repetition, we refer the reader to CESST for an index of the earlier work, and only summarize the essential points. Noting that quasiparticles at k have a charge

$$q_k = u_k^2 - v_k^2 = \epsilon_k / E_k = \pm N_s \left(E_k\right)^{-1} \tag{22}$$

the total quasiparticle charge (per unit volume, in units of e) is

$$Q^* = \sum_k q_k f_k \tag{23}$$

where f_k is the actual occupation number in a nonequilibrium system. To retain electrical neutrality, there must be an equal and opposite change in the condensate charge, produced by a shift in μ_s. [The quantity Q defined earlier by TC differs from Q^* by replacement of q_k in Eq. (23) by $\operatorname{sgn} q_k = \pm 1$, and represents the numerical population imbalance between the branches. Since Q^* appears to have more general physical significance, we confine our attention to it in this paper.]

To illuminate this problem, it is helpful to rewrite the expression (17) for the current in a form emphasizing the transmitted (rather than reflected) particles by using the sum rule (13) to replace $1 + A - B$ by $2A + C + D$. Thus, we write the total current as

$$I_{NS} = 2N(0)ev_F \mathscr{A} \int_{-\infty}^{\infty} [f_0(E - eV) - f_0(E)] \times [2A(E) + C(E) + D(E)]dE \tag{24}$$

This can be decomposed into two parts by recognizing that the term $2A(E)$ represents the current

$$I^A_{NS} = 2N(0)ev_F \mathscr{A} \int_{-\infty}^{\infty} [f_0(E - eV) - f_0(E)] \times [2A(E)]dE \tag{25}$$

due to Andreev reflection, in which the current in the superconductor is carried entirely by pairs. The remainder of I_{NS} is the current

$$I^{\mathrm{qp}}_{NS} = 2N(0)ev_F \mathscr{A} \int_{-\infty}^{\infty} [f_0(E - eV) - f_0(E)] \times [C(E) + D(E)]dE \tag{26}$$

due to quasiparticle transfer. But even $I_{NS}^{\rm qp}$ does not represent the rate of generation of quasiparticle charge at the interface, which we will call I_{NS}^{*}. To compute that, we must distinguish quasiparticles in the two channels, $k^{+}$and k^{-}, and also take account of their fractional charge $q_k = \pm N_s(E)^{-1}$. Thus,

$$I_{NS}^{*} = 2N(0)ev_F\mathscr{A}\int_{-\infty}^{\infty}[f_0(E-eV)-f_0(E)]\times[C(E)-D(E)]N_s^{-1}(E)dE \tag{27}$$

Finally, since experiments usually involve current bias rather than voltage bias, it has been useful to determine the ratio

$$F^{*} \equiv I^{*}/I \tag{28}$$

giving the charge imbalance generated as a fraction of the injected current. These quantities have been evaluated in the past for tunnel junctions, but now we can evaluate them for arbitrary barrier strength, as a function of V and T.

To make contact with the earlier work on tunnel injection, we note that for strong barriers the results in Table II show that $A \propto Z^{-4} << 1$, so I_{NS}^{A} is negligible and $I_{NS} \approx I_{NS}^{\rm qp}$ reproduces the form of the usual expression for tunnel current, namely,

$$I_{NS}^{\rm qp} = \frac{1}{eR_N}\int_{-\infty}^{\infty}[f_0(E-eV)-f_0(E)]N_s(E)dE, \quad Z^2 \gg 1 \tag{29}$$

The density-of-states factor $N_s(E)$ is not inserted arbitrarily at this point; rather, it arises from the limiting form of $C+D$ given in Table II, namely $Z^{-2}\left(u^2-v^2\right)^{-1}$. As is well known, Eq. (29) shows no excess current; the Andreev term is essential for that, but it is important only for weak barriers.

Again taking the strong barrier limit to evaluate I_{NS}^{*}, we note from Table II that $(C-D) = Z^{-2}$, so that Eq. (27) becomes

$$I_{NS}^{*} = \frac{1}{eR_N}\int_{-\infty}^{\infty}[f_0(E-eV)-f_0(E)]N_s^{-1}(E)dE, \quad Z^2 \gg 1 \tag{30}$$

again exactly equivalent to the standard tunneling result for $\dot{Q}_{\rm inj}^{*}$.

For comparison, we now consider the same quantities in the other limiting case of no barrier, $Z = 0$. Then, as noted in Table II, $B = D = 0$ and $C = 1 - A$. In this case, the total current is

$$I_{NS} = \frac{1}{eR_N}\int_{-\infty}^{\infty}[f_0(E-eV)-f_0(E)][1+A(E)]dE, \quad Z = 0$$

The Andreev portion of the current I_{NS}^{A} is still given by Eq. (25), but $I_{NS}^{\rm qp}$ can be rewritten in terms of $A(E)$ as

$$I_{NS}^{\rm qp} = \frac{1}{eR_N}\int_{-\infty}^{\infty}[f_0(E-eV)-f_0(E)][1-A(E)]dE, \quad Z = 0$$

while

$$I^*_{NS} = \frac{1}{eR_N}\int_{-\infty}^{\infty}[f_0(E-eV)-f_0(E)][1-A(E)]N_s^{-1}(E)dE, \quad Z=0 \tag{33}$$

Note that in Eqs. (32) and (33) there is no contribution to the integrals for $|E|<\Delta$, where $1-A=0$; but in Eq. (31), $1+A=2A=2$ in the gap, where there is a large current derived entirely from the Andreev-reflection process. By contrast, in the strong-barrier limit, there is no current at all in the gap, all current being carried by quasiparticles above the gap. Since Q^* is generated only by quasiparticles, the ratio $F^*=I^*/I$ will in general be smaller for metallic contacts than for tunnel junctions.

In the important special case of very low voltages across the contact ($eV << kT$), we can replace the difference of Fermi functions in the expressions (24) - (27) and (29) - (33) by $eV\,(-\partial f_0/\partial E)$ and define generalized linear-response functions analogous to the Y and Z of CESST. These two functions are the ratios of I_{NS} and I^*_{NS}, respective- ly, to the current I_{NN} at the same small voltage. We now generalize these quatities to include a dependence on barrier strength as well. In doing so, we also change the notation from Y and Z to Y and Y^* to gain in suggestiveness and to avoid confusion with the use of Z for normalized barrier strength in this paper. Specifically, we define

$$Y(Z,T) = \left.\frac{I_{NS}(Z,T)}{I_{NN}(Z)}\right|_{eV\to 0} = \left(1+Z^2\right)\int_{-\infty}^{\infty}\left(-\frac{\partial f_0}{\partial E}\right)[2A(E)+C(E)+D(E)]dE \tag{34}$$

and

$$Y^*(Z,T) = \left.\frac{I^*_{NS}(Z,T)}{I_{NN}(Z)}\right|_{eV\to 0} = \left(1+Z^2\right)\int_{-\infty}^{\infty}\left(-\frac{\partial f_0}{\partial E}\right)[C(E)-D(E)]N_s^{-1}(E)dE \tag{35}$$

In the strong barrier limit, $A\sim Z^{-4}\sim 0$, and using the limiting forms of C and D from Table II as above, we obtain

$$Y(Z\gg 1,T) = \int_{-\infty}^{\infty}\left(-\frac{\partial f_0}{\partial E}\right)N_s(E)dE \tag{36}$$

and

$$Y^*(Z\gg 1,T) = \int_{-\infty}^{\infty}\left[-\frac{\partial f_0}{\partial E}\right)N_s^{-1}(E)dE \tag{37}$$

which are exactly the standard tunneling results given by CESST and others. In the zero barrier limit, $Z=0, B=D=0, C=1-A$, and we have

$$Y(Z=0,T) = \int_{-\infty}^{\infty}\left(-\frac{\partial f_0}{\partial E}\right)[1+A(E)]dE \tag{38}$$

$$Y^*(Z=0,T) = \int_{-\infty}^{\infty}\left(-\frac{\partial f_0}{\partial E}\right)[1-A(E)]N_s^{-1}(E)dE \tag{39}$$

These coefficients Y and Y^*, and their ratio $F^* = Y^*/Y$, are plotted versus T for various values of Z in Figs. 9-11. Note that $Y^*(Z,T)$ is almost independent of the barrier strength Z.

viii. Applications and discussion

A direct application of our results is to fit the temperature dependence of the differential conductance of a point contact at zero voltage, which should be simply $Y(Z,T)/R_N$. This quantity is easily measured, and, unlike the excess current, it is not subject to problems with heating effects.

Although the parameter Z plays a fundamental role in our theory, it cannot be independently determined, and must be inferred from the I - V curve. However, since both $I_{\rm exc}$ and $Y(Z,T)$ depend on Z, we can test the model by comparing these two experimentally accessible quantities against each other. Figure 12 shows $Y(Z,T=0)$ vs $eR_N I_{\rm exc}/\Delta$. They exhibit an approximately linear relationship to each other, as might be expected physically, since both depend linearly on the Andreev-reflection probability.

In addition to our theoretical curve, two other points are displayed in Fig. 12. The point marked Zaitsev-clean is the result found by Zaitsev [4] for a microconstriction with no scattering in the bulk or in the neck, and it agrees exactly with our calculation for $Z = 0$. The point labeled AVZ-dirty is the the result of a calculation by Artemenko, Volkov, and Zaitsev [3] for a microconstriction in the dirty limit ($\tau kT << \hbar$) where the neck is short compared to the nonequilibrium length $\xi(T)(1-t)^{1/4}$. Although our model is not intended to describe diffusive transport in the presence of distributed bulk scattering, a suitable value ($Z \sim 0.55$) of the strength of our 1D δ-function barrier potential gives results very close to those obtained by their

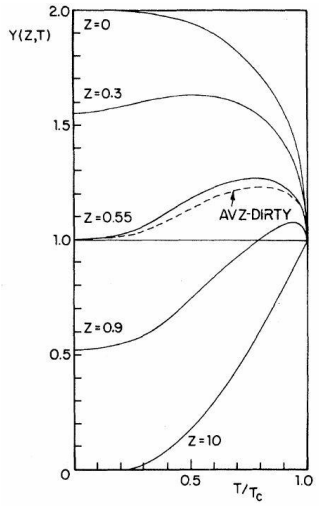


FIG. 9. Y, the zero-voltage differential conductance in units of the normal-state conductance, vs T, for various barrier strengths Z. The curve AVZ-dirty is described in the text.

Green's-function method.

(??? i think, there is no GF method here, just some discussion. Right???)

Our charge-imbalance results may also provide a useful perspective on the work of Hsiang and Clarke [22] on resistance due to charge-imbalance relaxation near an $N-S$ interface. By a physical argument, they reasoned that the appropriate F^* for a clean metallic interface could be approximated by what we call here $Y^*(Z \gg 1)$ as computed for a tunnel junction. Our calculation would instead give $F^* = Y^*(Z=0)/Y(Z=0)$. As just noted above, Y^* is almost independent of barrier strength Z, so $Y^*(Z \gg 1) \approx Y^*(Z=0)$. But the denomina-

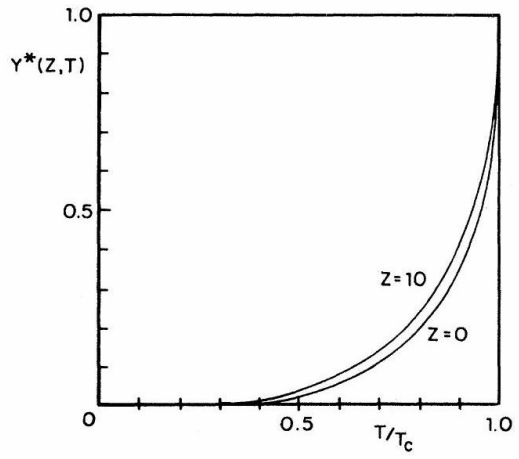


FIG. 10. Y^*, the normalized differential charge imbalance conductance at zero voltage, vs T, for various barrier strengths Z.

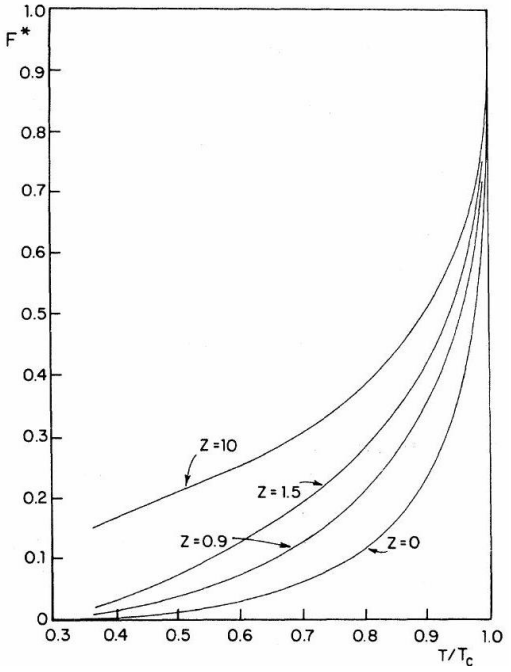


FIG. 11. F^*, the ratio of quasiparticle charge injected to total injected current, as a function of T for various barrier strengths Z.

tor factor $Y(Z = 0)$ varies from 1 at T_c to 2 at $T = 0$, so the resulting T dependence of our F^* is somewhat different from that used by Hsiang and Clarke, although it has the same qualitative shape. Because the interfaces studied by Hsiang and Clarke were not point contacts of the sort we have been treating, however, it is not clear that our results should be expected to describe their data in detail.

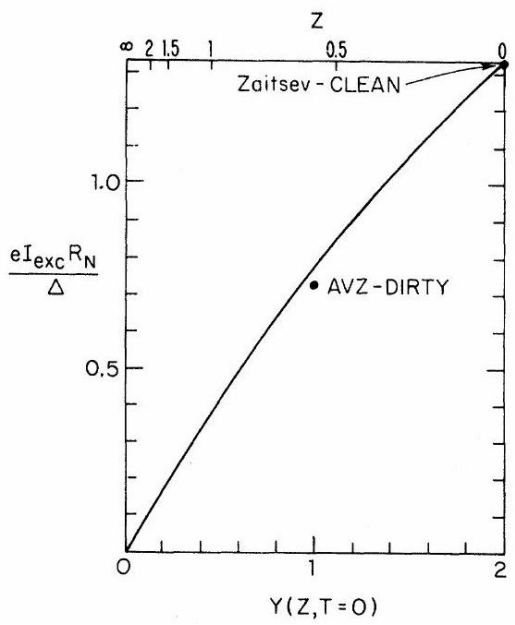


FIG. 12. $eI_{\rm exc}\, R_N/\Delta$ vs $Y(T=0)$ as the barrier strength parameter Z ranges from ∞ to 0. The points AVZ-dirty and Zaitsev-clean are discussed in Sec. VIII.

As noted above, the total current I_{NS} can be expressed as the sum of three terms: I^A_{NS}, the Andreev term with no quasiparticle transfer; I^*_{NS}, the injection rate of quasiparticle charge; and $(I^{\rm qp}_{NS} - I^*_{NS})$, the current carried by the pairs that must flow to compensate for the fractional charges of the quasiparticles. The current I^*_{NS} relaxes to supercurrent over a distance $\Lambda_{Q^*} = (D\tau_{Q^*})^{1/2}$, a diffusion length determined by τ_{Q^*}, the chargeimbalance relaxation time.

The picture described in the previous paragraph corresponds to the viewpoint of TC and PS, in which the current $(I - I^*)$ is viewed as being converted discontinuously to supercurrent at the interface. [23] If one examines the problem more deeply, however, one can obtain a more microscopic view of the conversion process. The key point is that there are solutions of the Bogoliubov equations even for $|E| < \Delta$, but they are evanescent waves which decay in a distance

$$\hbar v_F/2\left(\Delta^2 - E^2\right)^{1/2} \sim \xi(T).$$

(See the Appendix for details.) Thus, even the Andreev current I^A_{NS} is carried for $\sim \xi$ as a quasiparticle current before decaying into a pair current, and the interference of $k^+$and k^-waves causes a similar effect also for the current $I^{\rm qp}_{NS} - I^*_{NS}$ above the gap. This two-step conversion process is shown schematically in Fig. 13. This point of view is reminiscent of that of Schmid and Schön, who treat the entire injected current as a source of

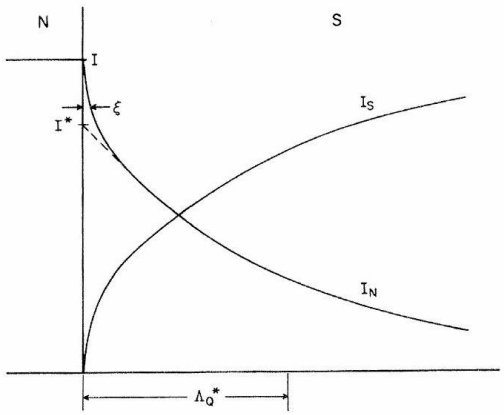


FIG. 13. Schematic diagram of conversion of normal current to supercurrent at $N - S$ interface. The evanescent waves due to Andreev reflection die out over a distance of order ξ,

while the injected quasiparticle charge imbalance relaxes over a charge diffusion length Λ_{Q^*}. charge imbalance, but combine "conversion" terms with τ_{Q^*} relaxation to find a shorter effective relaxation time $\tau_R < \tau_{Q^*}$, which reproduces the same steady-state Q^* as found by the two-step analysis of Tinkham and Clarke [17,18] and of Pethick and Smith. [19] There seems to be a gain in physical insight, however, in distinguishing the two types of processes.

Recognition of the existence of a penetration depth of order ξ for the evanescent quasiparticle waves in the gap also provides a more clear-cut explanation for one aspect of the observations of Octavio et al. [16] on subharmonic gap structure (SGS) in tin variable-thickness bridges (VTB's). They observed voltage-dependent shifts in the positions of the SGS which they attributed to heating. Using the gap shift as a thermometer, with $\Delta_{\rm BCS}(T)$ as the calibration curve, they could infer temperature rises. These temperature increases were roughly proportional to the dissipated power P, but much

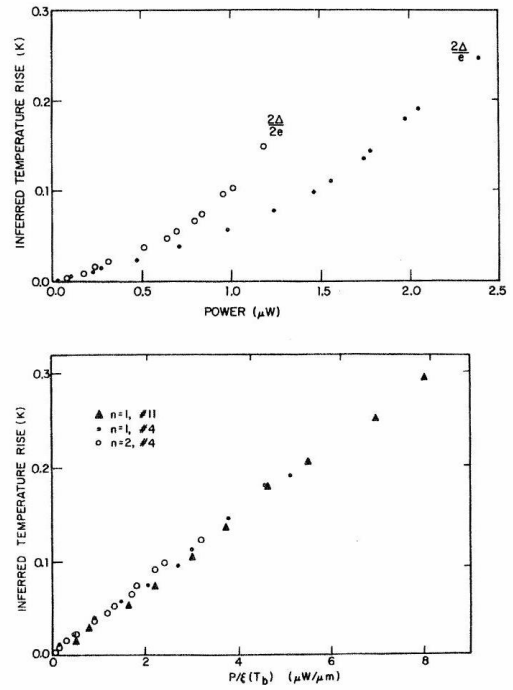


FIG. 14. Temperature rise in tin variable-thickness bridge inferred from depression of energy gap as found from subharmonic gap structure (after Octavio et al.). (a) depicts temperature rise vs power dissipated, P. (b) depicts temperature rise vs $P/\xi(T)$. The superior linear fit in (b) is consistent with observed gap being sensed at a distance $\sim \xi$ from center of bridge.

more precisely proportional to $P/\xi(T)$, as shown by the comparison of Fig. 14(a) and 14(b). Given the 3D cooling of these VTB's, in which the temperature rise is proportional to P/r (where r is the distance from the center of the contact), this observation was interpreted as showing that the energy gap giving the SGS was that in the superconductor at a distance $\sim \xi$ from the center. In a recent paper, [5] we have argued that the SGS arises from multiple Andreev reflections together with the sharp change in $A(E)$ at the gap edge. Given the penetration of the evanescent waves to a depth $\sim \xi(T)$, it is plausible that the gap reflected in the SGS should be that at a similar depth into the bank, as assumed by Octavio et al. on the basis of somewhat different reasoning.

Appendix

The Bogoliubov equations may be written

$$i\hbar\frac{\partial f}{\partial t} = \left[-\frac{\hbar^2\nabla^2}{2m} - \mu(x) + V(x)\right] f(x,t) + \Delta(x)g(x,t) \tag{A1a}$$

$$i\hbar\frac{\partial g}{\partial t} = -\left[\frac{-\hbar^2\nabla^2}{2m} - \mu(x) + V(x)\right] g(x,t) + \Delta(x)f(x,t) \tag{A1 b}$$

where $\Delta(x)$ is the energy gap and $\mu(x)$ is the chemical potential (specifically that of the condensate, in case of nonequilibrium conditions where μ is not uniquely defined). In the normal metal [$\Delta(x) = 0$], Eq. (A1a) is the Schrödinger equation for electrons, while Eq. (A1b) is the time-reversed Schrödinger equation for electrons. Since an electron satisfying the time-reversed Schrödinger equation behaves in many ways like a hole, we will adopt that terminology here.

For $\Delta \neq 0$, the electron and hole wave functions couple together, with two major consequences. First, a gap appears in the E vs k relation, just as it does in elementary BCS theory. To see this result more clearly, we solve Eq. (A1) for a specific geometry. The simplest example is one where $\mu(x), \Delta(x)$, and $V(x)$ are all constant, and the solutions to Eq. (A1) are time-independent plane waves. Taking as our trial solutions $f = \widetilde{u}e^{ikx-iEt/\hbar}$ and $g = \widetilde{v}e^{ikx-iEt/\hbar}$, we find for $V = 0$

$$E\tilde{u} = \left[\frac{\hbar^2k^2}{2m} - \mu\right]\tilde{u} + \Delta\widetilde{v} \tag{A2a}$$

$$E\widetilde{v} = -\left(\frac{\hbar^2k^2}{2m} - \mu\right)\widetilde{v} + \Delta\tilde{u} \tag{A2b}$$

Solving Eqs. (A2a) and (A2b) for E we obtain

$$E^2 = \left(\frac{\hbar^2k^2}{2m} - \mu\right)^2 + \Delta^2 \tag{A3}$$

There are two roots for E. We are concerned with excitations above the ground state ($E \geq 0$), and in this case

$$\widetilde{u}^2 = \frac{1}{2}\left[1 \pm \frac{(E^2 - \Delta^2)^{1/2}}{E}\right] = 1 - \widetilde{v}^2 \tag{A4}$$

$$\hbar k^{\pm} = \sqrt{2m}\left[\mu \pm \left(E^2 - \Delta^2\right)^{1/2}\right]^{1/2} \tag{A5}$$

We also define

$$1 - v_0^2 = u_0^2 = \frac{1}{2}\left(1 + \frac{(E^2 - \Delta^2)^{1/2}}{E}\right)$$

For $|E| < \Delta$, $\tilde{u}$ and $\widetilde{v}$ will be complex conjugates. This definition differs from the usual BCS convention in which u_k and v_k are not defined for $E < \Delta$. Using the notation

$$\psi = \begin{bmatrix} f(x) \\ g(x) \end{bmatrix}$$

the four types of quasiparticle waves for a given energy take the forms

$$\psi_{\pm k^+} = \begin{bmatrix} u_0 \\ v_0 \end{bmatrix} e^{\pm ik^+ x} \tag{A6a}$$

and

$$\psi_{\pm k^-} = \begin{bmatrix} v_0 \\ u_0 \end{bmatrix} e^{\pm ik^- x} \tag{A6b}$$

The ψ 's are the position space representation of the $\gamma^*_{k0} = u_k c^*_{k\uparrow} - v_k c_{-k\downarrow}$ since $c^*_{k\uparrow}$ produces the wave e^{ikx}, while $c_{-k\downarrow}$ destroys an electron at $-k$, leaving the system with a net positive momentum represented by the creation of a hole wave e^{ikx}.

A second consequence, which follows from the $E(k)$ relation (A3), is that the group velocity $v_g = dE/d\hbar k$ goes to zero at the gap edge, even while the phase velocity remains near the normalstate value. This has some interesting consequences, as can best be illustrated by deriving conservation laws for probability and charge.

We define $P(x)$ to be the probability density for finding either an electron or a hole at a particular time and place. Thus, for a solution to Eq. (A1), $P(x,t) = |f|^2 + |g|^2$. Using Eq. (A1) to evaluate $\partial P/\partial t$, we find

$$\frac{\partial P}{\partial t} + \vec{\nabla} \cdot \overrightarrow{\mathrm{J}}_P = 0 \tag{A7}$$

where

$$\overrightarrow{\mathbf{J}}_P = \frac{\hbar}{m} \left[\mathrm{Im}\left(f^* \nabla f\right) - \mathrm{Im}\left(g^* \nabla g\right) \right] \tag{A8}$$

Note that the hole current enters Eq. (A8) with a sign opposite to that of the electron part, just as one expects for a "time-reversed" particle. One can also show that $J_P \propto v_g = \partial E/\partial \hbar k$. Thus, at the gap edge, it is zero.

We can also derive a conservation law for quasiparticle charge. Assigning a unit charge $+e$ to the electron and $-e$ to the hole, the net quasiparticle charge density in one of these excitation waves is $Q = e\left(|f|^2 - |g|^2\right)$. Using Eq. (A1), it is easy to show that

$$\frac{\partial Q}{\partial t} + \vec{\nabla} \cdot \overrightarrow{\mathrm{J}}_Q = \frac{4e\Delta}{\hbar} \mathrm{Im}\left(f^* g\right) \tag{A9}$$

where

$$\overrightarrow{\mathbf{J}}_Q = \frac{e\hbar}{m} \left[\mathrm{Im}\left(f^* \nabla f\right) + \mathrm{Im}\left(g^* \nabla g\right) \right] \tag{A10}$$

The term on the right in Eq. (A9) is a source (or drain) term connecting the quasiparticles with the condensate, and we will see an explicit interchange of currents when treating the $N - S$ case below. However, for now we concentrate on Eq. (A10). Both the electron and hole contribution to the quasiparticle current enter with the same sign, and a moment's thought shows this to be reasonable. An electron ($f \propto e^{ik^+ x}$), moves in the positive direction and carries a positive current. A hole, ($g \propto e^{ik^+ x}$), moves in the negative direction, but also carries a positive current due to the sign of its charge. Thus, while $J_P \propto v_g = 0$ at the gap edge, $J_Q = e v_F$, so one can view the charge current as traveling with the Fermi velocity. Of course, for the normal metal nothing so dramatic occurs, and we always find simply $J_Q = e J_P$.

Starting from the basic Eq. (A1), it is a simple matter to work out the boundary conditions on steady-state plane-wave solutions at an N-S interface. To model the elastic scattering that usually occurs in the orifice, we include a δ-function potential in Eq. (A1), i.e., $V(x) = H\delta(x)$.

The appropriate boundary conditions, for particles traveling from N to S are as follows.

(i) Continuity of ψ at $x = 0$, so $\psi_S(0) = \psi_N(0) \equiv \psi(0)$.

(ii) $(\hbar/2m)\,(\psi'_S - \psi'_N) = H\psi(0)$, the derivative boundary condition appropriate for δ functions.

(iii) Incoming (incident), reflected, and transmitted wave directions are defined by their group velocities. We assume the incoming electron produces only outgoing particles.

Thus,

$$\psi_{\text{inc}} = \begin{bmatrix} 1 \\ 0 \end{bmatrix} e^{iq^+x}, \hbar q^{\pm} = \sqrt{2m}\sqrt{\mu \pm E}$$

$$\psi_{\text{refl}} = a \begin{bmatrix} 0 \\ 1 \end{bmatrix} e^{iq^-x} + b \begin{bmatrix} 1 \\ 0 \end{bmatrix} e^{-iq^+x}$$

$$\psi_{\text{trans}} = c \begin{bmatrix} u_0 \\ v_0 \end{bmatrix} e^{ik^+x} + d \begin{bmatrix} v_0 \\ u_0 \end{bmatrix} e^{-ik^-x}$$

Applying the boundary conditions, and carrying out an algebraic reduction, we find

$$a = \frac{u_0 v_0}{\gamma} \tag{A11a}$$

$$b = -\frac{(u_0^2 - v_0^2)\,(Z^2 + iZ)}{\gamma} \tag{A11b}$$

$$c = \frac{u_0(1 - iZ)}{\gamma} \tag{A11c}$$

$$d = \frac{iv_0 Z}{\gamma} \tag{A11d}$$

where

$$Z = \frac{mH}{\hbar^2 k_F} = H/\hbar v_F$$

and

$$\gamma = u_0^2 + \left(u_0^2 - v_0^2\right) Z^2$$

For simplicity, we have let $k^+ = k^- = q^+ = q^- = k_F$, whenever that substitution did not lead to a qualitative charge. Note that in the absence of a barrier (i.e., $Z = 0$), $b = d = 0$. Physically speaking, this means that all reflection is Andreev reflection and all transmission occurs without branch crossing.

The quantities $A(E), B(E), C(E)$, and $D(E)$ used in the main body of the paper are actually the probability currents, for the particle, measured in units of v_F. For example, $A = J_P^A/v_F = a^*a$, and $D = d^*d\,(u_0^2 - v_0^2)$. Since plane-wave currents are spatially uniform, we need not specify the position at which they are evaluated. However, for $E < \Delta$, $k^+$and k^-in the superconductor have small imaginary parts which lead to an exponential decay on a length scale λ, where

$$\lambda = \frac{\hbar v_F}{2\Delta}\left[1 - \left(\frac{E}{\Delta}\right)^2\right]^{1/2} \tag{A12}$$

Although right at the gap edge the length diverges, the characteristic length is $\hbar v_F/2\Delta = 1.22\xi(T)$. Thus, in order of magnitude terms, one can say that the particles penetrate a depth $\sim \xi(T)$ before the current is converted to a supercurrent carried by the condensate. For clarity,

we have defined $C(E)$ and $D(E)$ as the probability currents at $x > \lambda$, measured in units of v_F. The changeover from full to zero current is described next.

As a simple example of quasiparticle current being converted to condensate current, we consider the case $H = 0$. Then, $b = d = 0, a = u_0/v_0$, and $c = 1/u_0$. For $E < \Delta, a^* a = 1$, which means the incident electron is totally reflected as a hole. Thus, the total charge carried in the normal metal equals $2ev_F$, but in the superconductor J_Q is exponentially small for $x \gg 0$. Explicitly,

$$J_Q^C = (e\hbar/m)\,\mathrm{Im}\left[\left(ce^{ik^+x}\right)^* \nabla \left(ce^{ik^+x}\right)(u_0^* u_0 + v_0^* v_0)\right]$$

Letting $k^+ \approx k_F + i\eta/\hbar v_F$, where $\eta = (\Delta^2 - E^2)^{1/2}$, we have

$$J_Q^C = \frac{|u_0|^2 + |v_0|^2}{|u_0|^2} e v_F e^{-2\eta x/\pi v_F}$$

Below the gap, $|u_0|^2 = |v_0|^2$, so

$$J_Q^C = 2ev_F e^{-2\eta x/\hbar v_F}$$

The "disappearing current" reappears as current carried by the condensate. Rewriting the drain term in Eq. (A9) as

$$-\vec{\nabla} \cdot \overrightarrow{\mathrm{J}}_s \equiv (4e\Delta/\hbar)\,\mathrm{Im}\,(f^* g) \tag{A13}$$

then

$$\begin{aligned} J_s &= \frac{4e\Delta}{\hbar} \int_0^x \mathrm{Im}\left(c^* v_0^* e^{-ik'^*} c u_0 e^{ik+x'}\right) dx' \\ &= \frac{4e\Delta}{\hbar}\,\mathrm{Im}\left[\frac{v_0^* u_0}{u_0^* u_0}\right) \int_0^x e^{-2\eta x'/\hbar v_F} dx' \\ &= 2ev_F\left(1 - e^{-2\eta x/\pi u_F}\right) \end{aligned} \tag{A14}$$

This is the desired result, explicitly showing the supercurrent increasing to an asymptotic value as $x \to \infty$, at the same rate as the quasiparticle current dies away.

What BTK teaches us?

It teaches us how to use formulas for current from BdG.
(??? right?? I'll write later, which exactly formulas are new here?)

10.1.3 Suppression of the Josephson current through a narrow, mesoscopic, semiconductor channel by a single impurity by Bagwell

We study the Josephson current through a ballistic, normal, one-dimensional quantum channel in contact with two superconducting electrodes. A single point impurity having reflection coefficient R is placed in the normal conductor. The impurity couples the Andreev energy levels of forward and reverse moving electrons inside the junction, opening energy gaps in the quasiparticle level spectrum versus superconducting phase difference ϕ. These "Andreev" energy

gaps suppress the Josephson current in much the same way as disorder suppresses the magnetic flux driven currents in a normal mesoscopic ring. Finite temperature "energy averages" the contribution of Andreev levels above the Fermi energy with those below μ, further suppressing the Josephson current. The portion of the Josephson current carried by scattering states outside the superconducting gap is similarly suppressed by disorder and finite temperature.

This is basically a little problem for practice in methods, and it worth our attention, because it is simply formulated and nontrivial.

I Introduction and conclusion

Introduction

The Josephson effect in a clean superconductornormal-superconductor (SNS) junction is very different from the Josephson effect in a tunnel junction. Coherent Andreev reflection, [1] whereby an electron incident on a superconductor from a normal conductor is reflected as a hole, is the mechanism responsible for supercurrent flow in clean SNS junctions. [2] Quasiparticles incident from the normal region of an SNS junction are Andreev reflected off the pair-potential discontinuity at each SN interface, and their wave interference produces a set of resonant levels which carry the Josephson current. Such a description for the Josephson current assumes quasiparticles in the normal region can move without losing phase information, that is, it assumes the SNS junction is a mesoscopic system.

When the normal region of the SNS junction forms a quantum point contact, [3,4] the natural Josephson current scale is $I_c = e\Delta/\hbar$ (Refs. 5 and 6)(2Δ is the energy gap of the superconductor) and the current phase relation is $I(\phi) = I_c \sin(\phi/2)$.[6,7] If a tunnel barrier is then introduced into the normal region of the point contact, electrons often reflect simply as electrons, rather than as a hole. The current through such a dirty SNS point contact then evolves gradually [8–13] with decreasing barrier transmissivity T into the usual Josephson form [14] $I(\phi) = I_c \sin(\phi)$, where $I_c = e\Delta T/2\hbar$. In long and clean SNS junctions, where the extent of the normal region L is longer than the Bardeen-Cooper-Schrieffer (BCS) healing length ξ_0, the natural Josephson current scale is $I_c = ev_F/L$ (Refs. 2 and $15-18$) (v_F is the Fermi velocity) and the current phase relation assumes a triangular shape. These developments, and other calculations where different types of mesoscopic systems are embedded in the normal region of an SNS junction, [18–20] are reviewed in Refs. 21 and 22.

In this paper we apply the Bogoliubov-de Gennes equations [23,24] to describe the Josephson current in both clean SNS junctions and in SNS junctions containing a tunnel barrier. We obtain expressions for the Josephson current versus superconducting phase difference ϕ for both short ($L < \xi_0$) and long ($L > \xi_0$) SNS junctions, and which account for both the bound levels inside the superconducting energy gap and scattering states outside the gap. We show that introducing a tunnel barrier forces quasiparticles in the normal region to form standing waves at $\phi = \pm\pi$, so that the effect of disorder on the Josephson current can be interpreted in a manner very analogous to electrons confined to a normal mesoscopic ring [25,26] or to electrons in a spatially periodic potential. Many magnetic flux sensitive effects predicted for normal mesoscopic rings [27–29] therefore have analogs for the Josephson effect in SNS junctions.

CONCLUSIONS

Bulk supercurrents flow in response to gradients in the phase $\phi(x)$ of the order parameter $\Delta(x) = |\Delta(x)| \exp[i\phi(x)]$, and are maximum when the phase gradient $\nabla\phi(x)$ is large. From this perspective, the Josephson relation for a tunnel junction, $I = I_c \sin(\phi)$, is quite counterintuitive. The Josephson tunneling current $I = I_c \sin(\phi)$ decreases as the driving phase difference increases, and is smallest when the superconducting phase difference is a maximum. The cur-

rent phase relation $I = I_c \sin(\phi)$ is thus analogous to negative differential resistance in a normal conductor, where the normal current decreases as the driving voltage difference increases.

A more intuitive current phase relation exists for clean SNS junctions. For either long or short junctions, the Josephson current always increases as the superconducting phase difference increases, and is maximum when the superconducting phase difference is a maximum. Only when an impurity, tunnel barrier, or geometrical irregularity is present in the junction is the supercurrent zero when the superconducting phase difference is maximum at $\phi = \pm\pi$. The quasiparticle energy gap opening at $\phi = \pm\pi$ in the Andreev level spectrum versus superconducting phase difference when these imperfections are present, and the associated formation of "standing waves" with $dE_n^{\pm}/d\phi = 0$, explain the resulting suppression of the Josephson current. Finite temperature also mixes in a contribution to the Josephson current from the Andreev levels associated with reverse-moving electrons to those of the forward-moving ones, via thermal "energy averaging" instead of directly modifying the energy level spectrum, and therefore has a qualitatively similar effect as disorder on suppressing the Josephson current.

II. SNS junction with an impurity

We model the SNS junction [2] by a step change in the pair potential shown in Fig. 1, namely

$$\Delta(x) = \begin{cases} \Delta e^{i\phi_1}, & x < 0 \\ 0, & 0 < x < L \\ \Delta e^{i\phi_2}, & x > L \end{cases} \tag{1}$$

This model for the pair potential requires that the superconductor widen adiabatically to an infinite width. [6,17] The large superconducting banks can then be viewed as an "order parameter reservoir," where the supercurrent density is effectively zero. In that case, phase gradients of the superconducting order parameter in the contacts, required to support supercurrent flow, are negligible compared to phase gradients near the junction itself. The disorder we describe by a single point impurity placed in the junction

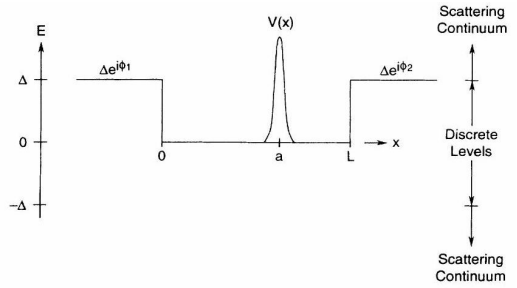


FIG. 1. Scattering potential which describes a mesoscopic Josephson junction. "Andreev" bound states form in the pair potential well. Both the bound levels and scattering states carry parts of the Josephson current.

$$V(x) = V_s \delta(x - a) \tag{2}$$

where $0 \leq a \leq L$.

The potentials $\Delta(x)$ and $V(x)$ enter the Bogoliubov-de Gennes equation of motion for the quasi-particles [23]

$$\begin{pmatrix} H(x) - \mu & \Delta(x) \\ \Delta^*(x) & -[H^*(x) - \mu] \end{pmatrix} \begin{pmatrix} u(x) \\ v(x) \end{pmatrix} = E \begin{pmatrix} u(x) \\ v(x) \end{pmatrix},$$

where the one-electron Hamiltonian $H(x)$ is

$$H(x) = \frac{1}{2m}\left(-i\hbar\frac{d}{dx} - eA(x)\right)^2 + V(x) \tag{4}$$

Equation (3) embodies the quasiparticle dispersion relation for a uniform superconductor,

$$E^2 = \left(\frac{\hbar^2 k^2}{2m} - \mu\right)^2 + \Delta^*\Delta \tag{5}$$

and does not depend on the specific form of the microscopic Hamiltonian giving rise to the pairing potential. We neglect the vector potential A, the electron spin, and the self-consistency condition for $\Delta(x)$. Neglecting the self-consistency condition for $\Delta(x)$ is equivalent to neglecting the proximity effect.

The Andreev levels [the discrete eigenvalues E from Eq. (3) occurring for $|E| < \Delta$] are determined by matching the solutions of Eq. (3) for a spatially uniform pair potential at $x = 0, x = a$, and $x = L$. Details of this procedure are given in Appendix A. For a clean SNS junction this was first done by Kulik, [2] who found the Andreev levels are determined from

$$2\cos^{-1}\left(\frac{E}{\Delta}\right) + \left(\frac{L}{\xi_0}\right)\left(\frac{E}{\Delta}\right) \pm \phi = 2\pi n \tag{6}$$

Here $\xi_0 = \hbar v_F/2\Delta$ is the BCS healing length, $\phi = \phi_2 - \phi_1$ the superconducting phase difference, and $n = 0, \pm 1, \pm 2, \ldots$.

Equation (6) can be interpreted in terms of BohrSommerfeld quantization of the periodic electron-hole orbits in the normal region. [30] The term $2\cos^{-1}(E/\Delta)$ is the phase shift acquired from the evanescent quasiparticle waves penetrating into the superconducting regions. The term $(EL/\Delta\xi_0)$ is the phase shift acquired from free electron and hole propagation in the normal region. Finally the superconducting phase difference ϕ enters Eq. (6) because, in Andreev reflection, the reflected electron and holes acquire an additional phase shift equal to the phase of the superconducting order parameter. Changing ϕ therefore affects the energy levels in a manner similar to changing the size of a confining potential well in ordinary quantum mechanics.

In the presence of a point impurity potential $V(x)$, Eq. (6) is modified to [31]

$$2\cos^{-1}\left(\frac{E}{\Delta}\right) + \left(\frac{L}{\xi_0}\right)\left(\frac{E}{\Delta}\right) \pm \alpha = 2\pi n \tag{7}$$

where the "effective phase" α is determined from

$$\cos(\alpha) = T\cos(\phi) + R\cos\left[\left(\frac{L-2a}{\xi_0}\right)\left(\frac{E}{\Delta}\right)\right] \tag{8}$$

This effective phase α depends on the the normal electron current transmission probability T, given in our point defect model by

$$T = 1 - R = \frac{1}{1 + \left(mV_s/\hbar^2 k_F\right)^2} \tag{9}$$

where $\hbar k_F = \sqrt{2m\mu}$ and μ is the Fermi energy. When $T \to 1$ we recover the Andreev levels for the clean junction, since $\alpha \to \phi$. In the opposite limit of small transmission, where $T \to 0, \alpha$ also becomes small and is nearly independent of the actual phase difference ϕ. If the junction is long compared to the healing length ($L > \xi_0$), and if an impurity is present ($T \neq 1$), α also depends on the particle's energy and the impurity position $|L - 2a|$.

To compute the Josephson current induced by the superconducting phase difference, one must compute both the electrical current $I_n^{\pm}(\phi)$ carried by quasiparticles occupying each Andreev level $E_n^{\pm}(\phi)$ ("discrete" levels with $|E_n^{\pm}| < \Delta$) and the imbalance $I(E, \phi)$ in the electrical

current per unit energy carried by quasiparticles flowing in the "continuum" levels (where $|E| > \Delta$). Once both $I_n^{\pm}(\phi)$ and $I(E,\phi)$ are known, the total current can be written down if one knows the occupation probabilty for these energy levels. Since the Josephson current flows near equilibrium, we assume that the single particle levels are thermally populated according to the Fermi distribution function $f(E)$. We therefore obtain the contribution $I_d(\phi)$ to the Josephson current from the discrete spectrum as

$$I_d(\phi) = \sum_n \left\{ I_n^+(\phi) f\left(E_n^+(\phi)\right) + I_n^-(\phi) f\left(E_n^-(\phi)\right) \right\} \tag{10}$$

and the contribution $I_c(\phi)$ to the Josephson current from the continuous spectrum as

$$I_c(\phi) = \left(\int_{-\infty}^{-\Delta} + \int_{\Delta}^{\infty} \right) I(E,\phi) f(E) dE \tag{11}$$

The total supercurrent $I(\phi)$ is then computed from

$$I(\phi) = I_d(\phi) + I_c(\phi) \tag{12}$$

In this viewpoint only energies below the Fermi energy ($E \leq 0$) contribute to the Josephson current flow at $T = 0$. An additional contribution to the Josephson current results if the pair potential itself changes with superconducting phase difference. 13, 21, 32

For a clean junction ($R = 0$), we obtain the electrical current [24] $I_n^{\pm}(\phi)$ carried by each occupied Andreev level from the normalized quasiparticle wave functions $u(x)$ and $v(x)$ as

$$I_n^{\pm}(\phi) = \mp \frac{e v_F}{L + 2\xi\left(E_n^{\pm}(\phi)\right)} \tag{13}$$

where $\xi(E)$ is the energy dependent healing length [24]

$$\xi(E) = \left(\frac{\hbar v_F}{2\Delta}\right)\left(\frac{\Delta}{\sqrt{\Delta^2 - E^2}}\right) = \xi_0 \left(\frac{\Delta}{\sqrt{\Delta^2 - E^2}}\right) \tag{14}$$

and $E_n^{\pm}(\phi)$ is found from Eq. (6). One could, in principle, perform the same calculation with the impurity present. Unfortunately, the analytical calculation proves intractable. However, if such a calculation could be done, it must yield

$$I_n^{\pm}(\phi) = \mp \frac{e v_F}{L + 2\xi\left(E_n^{\pm}(\phi)\right)} \frac{T \sin(\phi)}{\sin(\alpha)} \frac{1}{\gamma} \tag{15}$$

with $E_n^{\pm}(\phi)$ now found from Eqs. (7) and (8). Here γ is a "feedback" factor

$$\gamma = 1 \pm \left(\frac{\hbar}{2e\Delta}\right)\left(\frac{e v_F}{L + 2\xi\left(E_n^{\pm}(\phi)\right)}\right)\left(\frac{R}{\sin(\alpha)}\right)\left(\frac{L - 2a}{\xi_0}\right) \sin\left(\frac{(L-2a)E_n^{\pm}(\phi)}{\Delta \xi_0}\right) \tag{16}$$

Equations (15) and (16) follow from free energy considerations given below.

The continuous spectrum also contributes to the Josephson current flow in a long SNS junction having $L > \xi_0$. This "continuous spectrum" can be viewed as being composed of "leaky" Andreev levels. [17] When $|E| > \Delta$, it is possible for either the electron or hole composing the Andreev level to escape from the junction by simply transmitting over the pair potential. Although this leakage away from the junction leads to a finite lifetime for the Andreev levels, reducing the total contribution to $I(E,\phi)$ from the continuum Andreev level and spreading it out over a finite-energy range, [18] these broadened Andreev levels nonetheless exist and contribute significantly to the supercurrent flow in long SNS junctions.

We find it most convenient to calculate the continuum current $I_c(\phi)$ using the quasiparticle transmission formalism of van Wees, Lenssen, and Harmans. [18] The method of van Wees, Lenssen, and Harmans is closely analogous to the Landauer-Büttiker transmission formalism [4] for normal currents, and is mathematically equivalent to the transmission formalism of Furusaki, Takayanagi, and Tsukada. [20] Applying this formalism, we find (in Ap- pendix B) the continuum contribution $I_c(\phi)$ for a clean SNS junction to be

$$I_c(\phi) = \frac{2e}{h}\left(\int_{-\infty}^{-\Delta} + \int_{\Delta}^{\infty}\right)\left|u_0^2 - v_0^2\right|\left(\frac{1}{D(E,-\phi)} - \frac{1}{D(E,\phi)}\right)f(E)dE \tag{17}$$

where the function $D(E,\phi)$ is

$$D(E,\phi) = u_0^4 + v_0^4 - 2u_0^2v_0^2\cos\left[\left(\frac{E}{\Delta}\right)\left(\frac{L}{\xi_0}\right) + \phi\right] \tag{18}$$

Here u_0 and v_0 are the standard BCS "coherence" factors

$$2u_0^2 = 1 + \frac{\sqrt{E^2-\Delta^2}}{E} \tag{19}$$

and

$$2v_0^2 = 1 - \frac{\sqrt{E^2-\Delta^2}}{E} \tag{20}$$

The contribution $I_c(\phi)$ to the Josephson current in a clean SNS junction has been calculated previously. [2], 15 – 18, 20 We feel Eq. (17) is probably identical to the analytical results of Ishii, [15] Svidzinski, Antsygina, and Bratus, [16] and Furusaki, Takayanagi, and Tsukada. [20] In the presence of the point impurity, Eq. (17) is modified to

$$I_c(\phi) = \frac{2e}{h}T\left(\int_{-\infty}^{-\Delta} + \int_{\Delta}^{\infty}\right)\left|u_0^2 - v_0^2\right|\left(\frac{1}{D(E,-\alpha)} - \frac{1}{D(E,\alpha)}\right)\frac{\sin(\phi)}{\sin(\alpha)}f(E)dE \tag{21}$$

with the effective phase α defined in Eq. (8). A computation given in Appendix B yields Eq. (21).

Equations (17) and (21) show that the continuous spectrum makes no contribution to the Josephson current if $L \ll \xi_0$, since Eq. (18) gives $D(E,\alpha) = D(E,-\alpha)$ when $L \ll \xi_0$. Further, only energies within a few Δ of the Fermi level make any sizable contribution to $I_c(\phi)$, since the phase sensitive term in Eq. (18) for $D(E,\phi)$ is significant only within a few Δ of the Fermi energy. Thus, the Josephson current at $T = 0$ is not limited to flowing only at the Fermi energy (the case for normal currents at $T = 0$ and small bias voltages), or even limited to flow within an energy range Δ below the Fermi level (false only if $L \ll \xi_0$), but flows over an energy range extending several Δ below the Fermi energy when $L > \xi_0$. Equations (17) and (21) also show that the continuum contribution $I_c(\phi)$ is negligible near $\phi = \pm\pi$, and that $I_c(\phi = \pm\pi) = 0$.

An alternate method to compute Josephson currents requires the change in Helmholtz free energy F with superconducting phase difference [13,21,32,33]

$$I(\phi) = \frac{2e}{\hbar}\frac{dF(\phi)}{d\phi} \tag{22}$$

Equation (22) provides additional insight into the supercurrent formulas presented in this section. Since Eqs. (7)

and (8) hold for the SNS junction with an impurity, our results for the dirty SNS junction follow from those of the clean SNS junction plus the chain rule of differentiation

$$\frac{dF}{d\phi} = \frac{dF}{d\alpha}\frac{d\alpha}{d\phi} \tag{23}$$

where we have from Eq. (8)

$$\left.\frac{\partial\alpha}{\partial\phi}\right|_E = \frac{T\sin(\phi)}{\sin(\alpha)} \tag{24}$$

The factor (24) appears both in our expression (15) for the current $I_n^{\pm}(\phi)$ carried by each Andreev level and in the expression (21) for the continuum supercurrent $I_c(\phi)$. As we argue more precisely in Appendix C, Eq. (23) for the derivative of the free energy, together with Eqs. (7) and (8), implies that Eq. (15) for $I_n^{\pm}(\phi)$ in the dirty junction follows from Eq. (13) for the clean junction. By similar arguments, Eq. (21) for $I_c(\phi)$ in the dirty junction follows from Eq. (17) for the clean junction.

III. Junction shorter than the healing length

In the limit of a "point contact" or "short" junction, for which $L \ll \xi_0$, we immediately find from Eq. (8) that the Andreev level spectrum is determined as

$$E^{\pm} = \pm\Delta\cos(\alpha/2) = \pm\Delta\sqrt{1 - T\sin^2(\phi/2)} \tag{25}$$

where

$$\cos(\alpha) = T\cos(\phi) + R \tag{26}$$

Equation (25) is a special case of the more general expression derived by Beenakker [13] when multiple quantum channels are open.

We graph Eq. (25) in Fig. 2.[34] The dotted lines show

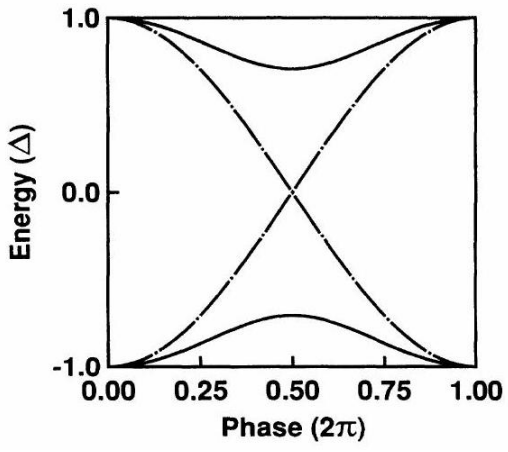


FIG. 2. Andreev levels $E^{\pm}(\phi)$ as a function of superconducting phase difference ϕ for a junction shorter than the healing length ($L \ll \xi_0$). The unperturbed levels in the clean junction (dotted), corresponding to a left-moving (E^+)and right-moving (E^-)electrons, become coupled by the impurity. As a result, the energy degeneracy at $\phi = \pm\pi$ is lifted and an energy gap of size $E_{\rm gap} = 2\Delta\sqrt{R}$ appears in the quasiparticle energy spectrum for the dirty SNS junction (solid). the position of the Andreev levels versus phase difference when no impurities are present. [6,35] The level $E^+(\phi)$ corresponds to an electron traveling in the negative- x direction, while the level $E^-(\phi)$ describes an electron moving along the positive- x direction. These two sets of

Andreev levels are independent when no impurity is present in the junction. However, since the impurity will reflect electrons, it will couple these unperturbed Andreev levels. This effect is most pronounced when the levels are degenerate in energy, i.e., at $\phi = \pm\pi$, so that the impurity opens an energy gap in the Andreev level spectrum versus superconducting phase difference having size

$$E_{\rm gap} = 2\Delta\sqrt{R} \tag{27}$$

Figure 2 is reminiscent of the effects of impurities on the energy level spectrum of a small normal metal ring subject to an Aharonov-Bohm flux, [25,26] and has also been previously suggested for a composite ring made of part normal and part superconducting material when the normal segment is disordered. [36] However, the motion of Andreev reflected electrons in the SNS junction is already periodic, so that a ring geometry (or other type of spatially periodic potential) is not required for $V(x)$ to open gaps in the quasiparticle energy spectrum. It is these "standing waves" forming in the energy level spectrum $E_n^{\pm}(\phi)$, due to the impurity, which suppress the Josephson current.

Using the properties $E^+ = -E^-$and $f\,(E^+) = 1$ - $f\,(E^-)$, we readily obtain from Eqs. (25), (15), and (10)

$$I(\phi) = \frac{e\Delta}{\hbar} T \sin(\alpha/2) \left(\frac{\sin(\phi)}{\sin(\alpha)}\right) \tanh\left(\frac{\Delta}{2kT}\cos(\alpha/2)\right).$$

Writing this in terms of the phase difference ϕ, we find

$$I(\phi) = \frac{e\Delta}{2\hbar} T \left(\frac{\sin(\phi)}{\sqrt{1 - T\sin^2(\phi/2)}}\right) \tanh\left(\frac{\Delta}{2kT}\sqrt{1 - T\sin^2(\phi/2)}\right) \tag{29}$$

again a limiting case of the multichannel formula from Ref. 13. The single-channel formula, Eq. (29), has also been obtained previously. [8–13]

We consider the zero-temperature limit of Eqs. (28) and (29) in Fig. 3, where we can set $\tanh\,(E^+/2kT) = 1$. In the $kT = 0$ case, Eq. (28) becomes

$$I(\phi) = \frac{e\Delta}{\hbar} T \sin(\alpha/2) \left(\frac{\sin(\phi)}{\sin(\alpha)}\right) \tag{30}$$

Equation (30) interpolates nicely between the point contact and tunnel junction, as discussed in Refs. 13 and 21. When the transmission is nearly one, so that the effective phase difference $\alpha \simeq \phi$, we obtain the result [7] for a point contact, $I(\phi) = (\pi G\Delta/e)\sin(\phi/2)$, where $G = 2e^2/h$. In the other limit, where the transmission T is small, the effective phase α is also small and is nearly independent of ϕ. We can then approximate $\sin(\alpha) \simeq \alpha$

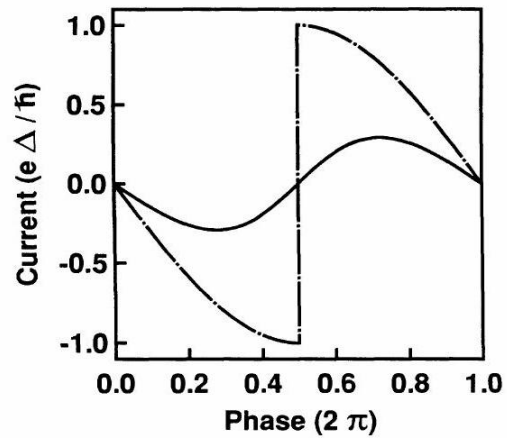


FIG. 3. The "discretized" Josephson current in a clean point contact (dotted) is suppressed by the presence of a tunnel barrier (solid). Regions analogous to "negative differential resistance" in a normal conductor, where the Josephson current decreases as the phase difference increases, are produced by the energy gap in Fig. 2.

so that we obtain the result for a tunnel junction [14] $I(\phi) = (\pi G\Delta/2e)\sin(\phi)$, where the normal conductance is given by a Landauer-type formula $G = 2e^2T/h$.[4]

The effect of finite temperature on the Josephson current is qualitatively similar to that of impurity scattering, since both introduce a mixture of Andreev levels associated with left- and right-moving electrons into the supercurrent. The temperature dependence of Eq. (28) arises from the combination of Fermi factors

$f(E^-) - f(E^+) = 1 - 2f(E^+) = \tanh\left(\frac{E^+}{2kT}\right)$,

so that the temperature dependence of the Josephson current can be viewed as thermally "energy averaging" [37] the contribution of some left-moving electrons above the Fermi energy with right-moving ones below μ. The hightemperature limit of Eq. (28) as $kT \to kT_c$ is [13]

$$I(\phi) = \frac{e\Delta^2}{4\hbar kT_c} T\sin(\phi) \tag{32}$$

which has the same $\sin(\phi)$ dependence as a tunnel junction, again illustrating the similar effects of disorder and finite temperature on the Josephson current. Equation (32) resembles the well-known result of Aslamazov and Larkin [38] for the Josephson current through a point contact calculated from Ginzburg-Landau theory. But since the Ginzburg-Landau theory is valid only near T_c, it will never produce the correct low-temperature form $\sin(\phi/2)$ for the clean point contact.

The sharp discontinuity at $\phi = \pm\pi$ for the clean junction at zero temperature arises from the sharp discontinuity in the Fermi function at $T = 0$.[17] When $\phi = \pi$ the Andreev level E^-(carrying a current $I^- = e\Delta/\hbar$) moves above the Fermi level, while the level E^+(carrying a current $I^+ = -e\Delta/\hbar$) passes below the Fermi level. Thus, the level E^-empties while E^+becomes populated. This change in Andreev level occupation produces a discontinuity in the supercurrent of $2e\Delta/\hbar$. On the other hand, when the transmission T is small, the levels $E^+$and E^- have combined to form a standing wave with $dE^\pm/d\phi = 0$ when $\phi = \pm\pi$, so that the Josephson current falls to zero near $\phi = \pm\pi$.

One would naively predict a critical "depairing current" 23, 39, 40 of order $e\Delta/\hbar$ for a one-dimensional (1D) superconductor. In the presence of a uniform superfluid flow having velocity v_s, the quasiparticle energies are shifted by an amount $\Delta E = p_F \cdot v_s$, where p_F is the Fermi momentum. Thus, the quasiparticle energy gap goes to zero when $\Delta = p_F v_c$, where v_c is the critical "depairing velocity," an argument originally advanced by Landau. [40] All the electrons below the Fermi energy then move at velocity v_c, giving a critical current I_c of

$$I_c = env_c = e\left(\frac{2k_F}{\pi}\right)\left(\frac{\Delta}{p_F}\right) = \left(\frac{e\Delta}{\hbar}\right)\left(\frac{2}{\pi}\right) \tag{33}$$

which is correct to within a numerical factor of order unity. A better treatment [41] would probably slightly increase the numerical value of this current. Thus, the "discretization of the Josephson current" in a superconducting quantum point contact, [6] which follows as a limiting case of Eq. (6), can be understood as simply the Landau depairing current of a 1D superconductor.

IV. Junction longer than the healing length

When the junction length L becomes comparable to the BCS healing length ξ_0, more Andreev levels become bound in the pair potential well and the continuum levels begin to carry a

supercurrent. Despite these differences in detail, the basic picture given in the preceding section is still qualitatively correct. Quasiparticles trapped in the normal region of the SNS junction set up standing waves near $\phi = \pm\pi$ when an impurity is present, suppressing the Josephson current.

Figure 4 shows the Andreev levels [from Eqs. (7) and (8)] in a clean SNS junction (dashed line) and when an impurity is placed in the normal region (solid line). [42] The discrete energy level spectrum is quite similar to the normal mesoscopic ring [26] and to electrons in a periodic lattice. The energy gap near $E = 0$ for $\phi = \pi, a \simeq L/2$, and small R can be found (Appendix D) as

$$E_{\rm gap} \simeq 2\sqrt{R}\,(\hbar v_F/L_{\rm eff}\,) \tag{34}$$

where $L_{\rm eff}^2 = (L+2\xi_0)^2 + R(L-2a)^2$. For both long and short SNS junctions, the Andreev gap therefore obeys

$$\pi E_{\rm gap} \simeq \sqrt{R} I_c \Phi_0 \tag{35}$$

where I_c is the critical current of the clean junction and $\Phi_0 = h/e$ is the normal metal flux quantum. The statement (35) is exact for a short junction.

We plot the Josephson current corresponding to Fig. 4 in Fig. 5. In Fig. 5(a) we recover the known result for the Josephson current (solid) in a long and clean SNS junction. [15–18] The current phase relation is triangular with a critical current $I_c = ev_F/\,(L+2\xi_0)$. The critical current I_c is a consequence solely of the current $I_d(\phi)$ carried by the Andreev levels (short dashes), since Eq. (21) shows the continuum current is zero at $\phi = \pi$. The crit-

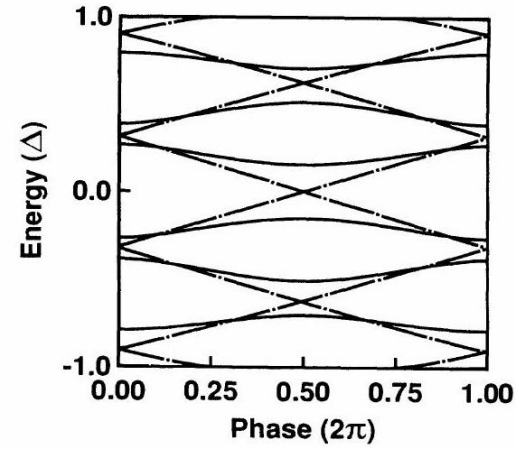


FIG. 4. Andreev levels in a long ($L > \xi_0$) junction with (solid) and without (dashed) an impurity present. As for the short junction, Andreev gaps open in the quasiparticle level spectrum. The analogy with "free electron" and "periodic potential" energy bands is evident in the figure.

ical current $I_c = ev_F/\,(L+2\xi_0)$ follows from Eq. (13) and holds for all values of L, even for $L \ll \xi_0$ when the current phase relation is not triangular. The discretized Josephson current from Sec. III also follows by taking $L \to 0$ in this formula, namely $I_c = ev_F/2\xi_0 = e\Delta/\hbar$.

To obtain the correct dependence of the supercurrent on the phase (triangular as $L \to \infty$), it is necessary to account for the current $I_c(\phi)$ carried in the continuum levels (long dashes). The continuum currents can be understood naively and qualitatively by extrapolating the energy levels from Fig. 4 into the continuum and, ignoring their broadening, treating these continuum Andreev levels "as if" they carried the current from Eqs. (10) and (C4). Thus, the continuum currents $I_c(\phi)$ augment the discrete level currents $I_d(\phi)$ before the first Andreev level moves into the continuum near $\phi \simeq \pi/4$. $I_c(\phi)$ opposes $I_d(\phi)$ after the Andreev level closest to $E = -\Delta$

becomes unbound. (The precise value of ϕ where the lowest Andreev level unbinds depends on the junction length L.) We note the continuum supercurrent $I_c(\phi)$ is not sinusoidal. [15] We also note that $I(\phi)$ is a "small" difference between many larger currents [15–17] carried in each discrete level, along with the larger continuum currents.

The Josephson current through a long and dirty junction is shown in Fig. 5(b). The triangular current phase relation for the clean junction has evolved into an approximately sinusoidal dependence (solid). Neither $I_c(\phi)$ (long dashes) or $I_d(\phi)$ (short dashes) appears to be sinusoidal, although their sum $I(\phi)$ is approximately sinusoidal. For a long and dirty SNS junction, the continuum contribution $I_c(\phi)$ is not only essential to obtain a sinusoidal $I(\phi)$, but is also required to obtain the correct magnitude of the critical current. The continuum levels now contribute to the critical current magnitude, since I_c no longer occurs at $\phi = \pm\pi$. The parameters chosen [42] for this calculation give a transmission probability $T \simeq \frac{1}{2}$, so that comparing Figs. 5(a) and 5(b) reveals (for this cal- culation) that the critical current in the dirty junction is less than $T/2$ times the critical current of the clean junction. For a more transparent impurity, these ratios would be limited by the transmission coefficient T.

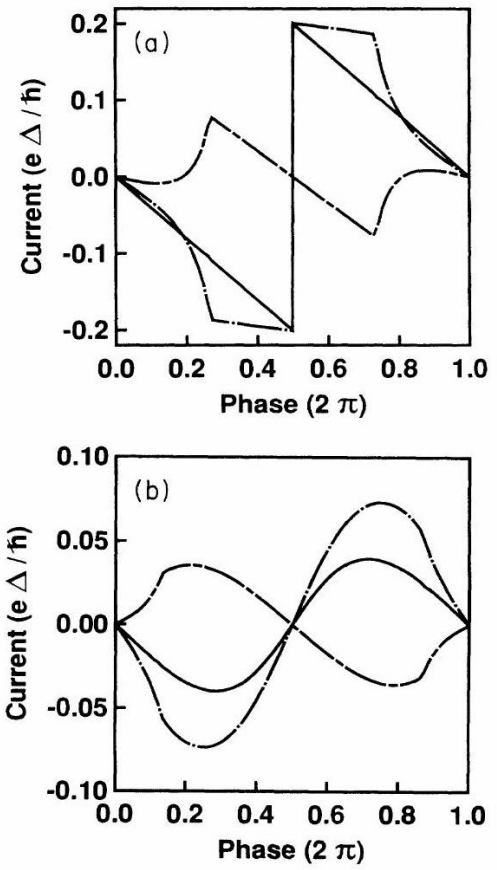


FIG. 5. Josephson current (solid) in a long junction that (a) is clean (b) has an impurity. The impurity rounds the triangular current versus phase relation into a sinusoidal shape, similar to its effect on the short SNS junction. Currents flowing in the scattering continuum (long dashes) and discrete levels (short dashes) combine to give the total Josephson current.

The continuum contribution $I_c(\phi)$ to the Josephson current is suppressed by finite temperature in the same way as the discrete contribution $I_d(\phi)$. Equation (21) can be written as an integral solely over the excitation spectrum as

$$I_c(\phi) = \frac{2e}{h} T \int_{\Delta}^{\infty} \left|u_0^2 - v_0^2\right| \left(\frac{1}{D(E,-\alpha)} - \frac{1}{D(E,\alpha)}\right) \frac{\sin(\phi)}{\sin(\alpha)} [2f(E) - 1] dE \tag{36}$$

The temperature-dependent factor in Eq. (36) is 1 $2f(E) = \tanh(E/2kT)$, implying the same physics of thermal "energy averaging" [37] for currents carried in the continuum levels as that discussed for the discrete levels in Sec. III. Thus, in this viewpoint, all the Josephson current flowing in the continuum at $T = 0$ is carried below the superconducting gap at $E \leq -\Delta$.

One could plausibly argue that moving the single impurity inside the normal region would produce mesoscopic fluctuations [13,43] in the critical current I_c. Equations (7) and (8) show that moving the single impurity will change the Andreev energy levels $E_n^{\pm}$in a long junction ($L \gg \xi_0$). However, it is not obvious that these fluctuating energy levels will cause the Josephson current to fluctuate. For example, it was originally believed from an analogous argument that the critical current would oscillate by varying L even in a clean SNS junction. [2] Later it was realized [15–17] that the critical current does not oscillate, but instead decreases monotonically with L as $I_c = ev_F/(L + 2\xi_0)$. This is because, as the various Andreev levels are forced into the continuum by reducing L, they do not immediately stop carrying a supercurrent. Instead, their contribution to I_c gradually decreases as they move farther outside the superconducting gap. A similar situation holds when moving the single impurity inside the SNS junction.

Moving the impurity away from the center of the junction ($a = L/2$) monotonically reduces the critical current I_c in Fig. 6, [44] showing that I_c does not fluctuate or oscillate with a. As the Andreev levels are forced farther away from the Fermi level by moving the impurity away from the center of the SNS junction, their contribution to I_c gradually decreases. The approximate analysis given in Appendix D agrees with this numerical result. If the impurity is moved a few healing lengths inside one of the superconducting contacts, the critical current should recover its full ballistic value ($I_c^{\text{clean}} = 0.2e\Delta/\hbar$ for the parameters used in Fig. 6), though we have not performed this calculation. In contrast, when the contacts are in their normal state, moving the impurity has no effect on the conductance. The normal state conductance [4] $G = 2e^2T/h$ does not fluctuate as a function of impurity position a, since the transmission coefficient T from Eq. (9) is independent of the impurity position. Therefore, the changing I_c as a function of impurity position a in Fig. 6 is a mesoscopic effect due to the interference of electron waves with the pair potential discontinuities at each SN interface. Mesoscopic fluctuations of the critical current studied in Refs. 13 and 43 have a different origin, arising from the wave interference between multiple impurity scattering events inside the normal region.

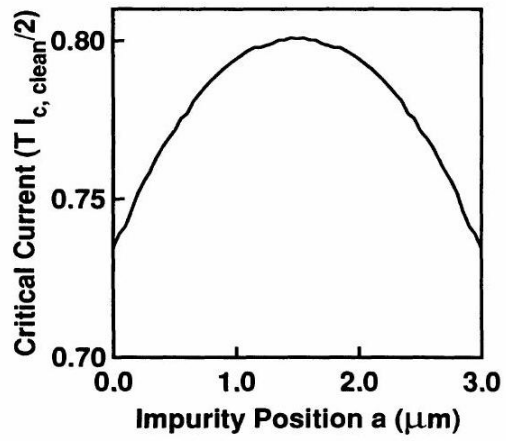


FIG. 6. Moving the lone impurity away from the center of the normal region suppresses the Josephson current in a long SNS junction, even though the normal state conductance of the junction remains unchanged. This mesoscopic effect is due to wave interference of the quasiparticles with the discontinuity in the pairing potential.

10.1.4 Suppression of the Josephson current through a narrow, mesoscopic, semiconductor channel by a single impurity by Bagwell: Calculations

Appendix A: Scattering from the SNS potential

In this appendix we obtain the electrical current [24] transmission amplitude for the scattering of an electronlike excitation incident from the left contact on the potentials $\Delta(x)$ and $V(x)$, shown schematically in Fig. 7.

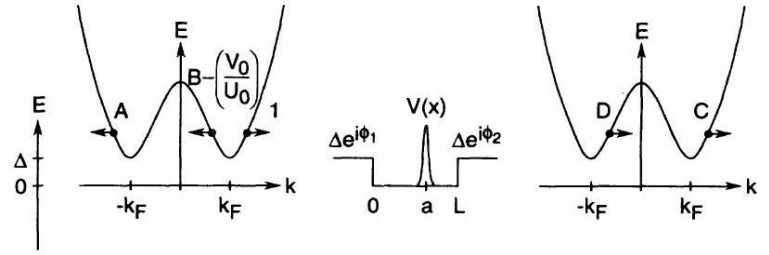


FIG. 7. An electronlike excitation incident from the left contact generates both reflected and transmitted quasiparticles. The transmission amplitudes C and D as a function of the superconducting phase difference $\phi_2 - \phi_1$ determine the Josephson current.

To do this, we match the solutions of Eq. (3) in the regions of uniform pair potential shown in Fig. 1. The poles of this transmission amplitude [45] yield Eqs. (7) and (8) for the discrete Andreev levels, and therefore the electrical current $I_n^{\pm}(\phi)$ carried by the discrete levels. Appendix B shows how the transmission coefficient found in this appendix can be used to obtain Eq. (21) for the continuum current $I_c(\phi)$.

The energy dispersion curve from Eq. (5) can be described by the wave vectors k_e and k_h, where

$$\frac{\hbar^2 k_e^2}{2m} - \mu = \sqrt{E^2 - \Delta^2} \tag{A1}$$

and

$$\frac{\hbar^2 k_h^2}{2m} - \mu = -\sqrt{E^2 - \Delta^2} \tag{A2}$$

with $|k_e| > k_F$ and $|k_h| < k_F$. The "excitation spectrum" of this dispersion law, which includes only the states having $E > 0$, is plotted in Fig. 7.

For a homogeneous superconductor having a pair potential $\Delta(x) = \Delta e^{i\phi_1}$, Eq. (3) has both electronlike solutions for $E > 0$,

$$\begin{pmatrix} u(x) \\ v(x) \end{pmatrix} = \begin{pmatrix} u_0 e^{i\phi_1} \\ v_0 \end{pmatrix} e^{\pm i k_e x} \tag{A3}$$

and holelike solutions for $E > 0$,

$$\begin{pmatrix} u(x) \\ v(x) \end{pmatrix} = \begin{pmatrix} v_0 e^{i\phi_1} \\ u_0 \end{pmatrix} e^{\pm i k_h x} \tag{A4}$$

The "coherence" factors u_0 and v_0 are given by Eqs. (19) and (20). For $E^2 \leq \Delta^2$, $u(x)$ and $v(x)$ decay inside the superconductor [24] with an energy dependent healing length $\xi(E)$ given in Eq. (14). The current carried by normal electrons in the N region (for $E^2 < \Delta^2$) is then converted to a supercurrent within a length $\xi(E)$ inside the superconductor. [24]

We consider now an electronlike excitation incident from the left contact above the superconducting gap, as shown in Fig. 7. The waves generated by this incident electron can be

grouped into four sets (denoted by coefficients A, B, C, and D) which properly include the Andreev reflections. For the electronlike excitations transmitted into right contact we have

$$C\begin{pmatrix} u_0 e^{i\phi_2} \\ v_0 \end{pmatrix} e^{ik_e(x-L)} (x > L) \tag{A5}$$

supported by electrons in the normal region

$$C\begin{pmatrix} u_0 e^{i\phi_2} \\ 0 \end{pmatrix} e^{i\tilde{k}_e(x-L)} (a < x < L) \tag{A6}$$

and holes in the normal region

$$C\begin{pmatrix} 0 \\ v_0 \end{pmatrix} e^{i\tilde{k}_h(x-L)} \quad (a < x < L) \tag{A7}$$

Similarly, for holelike excitations transmitted into the right contact, the waves

$$D\begin{pmatrix} v_0 e^{i\phi_2} \\ u_0 \end{pmatrix} e^{-ik_h(x-L)} \quad (x > L) \tag{A8}$$

$$D\begin{pmatrix} v_0 e^{i\phi_2} \\ 0 \end{pmatrix} e^{-i\tilde{k}_e(x-L)} \quad (a < x < L) \tag{A9}$$

and

$$D\begin{pmatrix} 0 \\ u_0 \end{pmatrix} e^{-i\tilde{k}_h(x-L)} \quad (a < x < L) \tag{A10}$$

are required. I use the notation $\tilde{k}_e$ and $\tilde{k}_h$ to denote the wave vectors in Eqs. (A1) and (A2) when $\Delta = 0$.

A similar procedure applied to the left SN interface is only slightly complicated by the presence of an incident electronlike wave (source term). This source term, which carries an electrical current [24] of $e\hbar k_e/m$, is

$$\begin{pmatrix} u_0 e^{i\phi_1} \\ v_0 \end{pmatrix} e^{ik_e x} \quad (x < 0) \tag{A11}$$

The Andreev reflected holelike excitation is

$$\left(B - \frac{v_0}{u_0}\right)\begin{pmatrix} v_0 e^{i\phi_1} \\ u_0 \end{pmatrix} e^{ik_h x} \quad (x < 0) \tag{A12}$$

The resulting electrons in the normal region are

$$\left(B - \frac{v_0}{u_0} + \frac{u_0}{v_0}\right)\begin{pmatrix} v_0 e^{i\phi_1} \\ 0 \end{pmatrix} e^{i\tilde{k}_e x} \quad (0 < x < a) \tag{A13}$$

and holes

$$B\begin{pmatrix} 0 \\ u_0 \end{pmatrix} e^{i\tilde{k}_h x} \quad (0 < x < a) \tag{A14}$$

The electronlike excitations reflected into the left contact are

$$A\begin{pmatrix} u_0 e^{i\phi_1} \\ v_0 \end{pmatrix} e^{-ik_e x} \quad (x < 0) \tag{A15}$$

supporting electrons in the normal region

$$A\begin{pmatrix} u_0 e^{i\phi_1} \\ 0 \end{pmatrix} e^{-i\tilde{k}_e x} \quad (0 < x < a) \tag{A16}$$

and holes

$$A\begin{pmatrix} 0 \\ v_0 \end{pmatrix} e^{-i\tilde{k}_h x} \quad (0 < x < a) \tag{A17}$$

The scattered waves written above assume $\mu \gg \Delta$, so that we can neglect the difference $(k_e - k_h)$ except when it appears in an exponent. This "Andreev approximation" is usually made in most works on the Josephson effect in SNS junctions.

The scattering matrix [46] (for both electrons and holes) connects the current amplitudes of incoming and outgoing waves at the impurity ($x = a$). The scattering matrix for electrons at $x = a$ gives

$$\begin{pmatrix} C u_0 e^{i\phi_2} e^{i\tilde{k}_e(a-L)} \\ A u_0 e^{i\phi_1} e^{-i\tilde{k}_e a} \end{pmatrix} = \begin{pmatrix} t\left(\tilde{k}_e\right) r\left(\tilde{k}_e\right) \\ r\left(\tilde{k}_e\right) t\left(\tilde{k}_e\right) \end{pmatrix} \begin{pmatrix} \left(B - \frac{v_0}{u_0} + \frac{u_0}{v_0}\right) v_0 e^{i\phi_1} e^{i\tilde{k}_e a} \\ D v_0 e^{i\phi_2} e^{-i\tilde{k}_e(a-L)} \end{pmatrix} \tag{A18}$$

Equation (A18) contains the source term. A similar scattering matrix connects the the hole current amplitudes

$$\begin{pmatrix} D u_0 e^{-i\tilde{k}_h(a-L)} \\ B u_0 e^{i\tilde{k}_h a} \end{pmatrix} = \begin{pmatrix} t^*\left(\tilde{k}_h\right) r^*\left(\tilde{k}_h\right) \\ r^*\left(\tilde{k}_h\right) t^*\left(\tilde{k}_h\right) \end{pmatrix} \begin{pmatrix} A v_0 e^{-i\tilde{k}_h a} \\ C v_0 e^{i\tilde{k}_h}(a - L) \end{pmatrix} \tag{A19}$$

where, for our point scatterer model, the current transmission and reflection amplitudes are

$$t(k) = \frac{1}{1 + i\left(m V_s / \hbar^2 k\right)} \tag{A20}$$

and

$$r(k) = \frac{-i\left(m V_s / \hbar^2 k\right)}{1 + i\left(m V_s / \hbar^2 k\right)} \tag{A21}$$

The electrical current [24] flowing into the right contact, due to the electrical current imposed from the left contact, is

$$J_Q \simeq \frac{e\hbar}{m} \tilde{k}_e \left(|C|^2 - |D|^2\right) \tag{A22}$$

Hence, we must compute the coefficients C and D to obtain the electrical current. The matrix equation for C is

$$\left(\frac{v_0}{u_0}\right)^2 \begin{pmatrix} t\left(\tilde{k}_e\right) r\left(\tilde{k}_e\right) \\ r\left(\tilde{k}_e\right) t\left(\tilde{k}_e\right) \end{pmatrix} \begin{pmatrix} e^{i\left(\tilde{k}_e-\tilde{k}_h\right)a} & 0 \\ 0 & e^{i\phi_e} e^{-i\left(\tilde{k}_e-\tilde{k}_h\right)(a-L)} \end{pmatrix}$$
$$\times \begin{pmatrix} t^*\left(\tilde{k}_h\right) r^*\left(\tilde{k}_h\right) \\ r^*\left(\tilde{k}_h\right) t^*\left(\tilde{k}_h\right) \end{pmatrix} \begin{pmatrix} e^{-i\left(\tilde{k}_e-\tilde{k}_h\right)(a-L)} e^{-i\phi} & 0 \\ 0 & e^{i\left(\tilde{k}_e-\tilde{k}_h\right)a} \end{pmatrix} \begin{pmatrix} C' \\ A' \end{pmatrix} +$$
$$+ \begin{pmatrix} t\left(\tilde{k}_e\right) r\left(\tilde{k}_e\right) \\ r\left(\tilde{k}_e\right) t\left(\tilde{k}_e\right) \end{pmatrix} \left(\begin{bmatrix} 1-\left(\frac{v_0}{u_0}\right)^2 \\ 0 \end{bmatrix} e^{i\tilde{k}_e a} \right)$$
$$= \begin{pmatrix} 10 \\ 0 \quad 1 \end{pmatrix} \begin{pmatrix} C' \\ A' \end{pmatrix}. \tag{A23}$$

Here C' and A' are the same as C and A up to a phase factor, so that $C' = C\exp(i\phi)\exp\left[i\tilde{k}_e(a-L)\right]$ and $A' = A\exp\left(-i\tilde{k}_e a\right)$. The analogous matrix equation for D is

$$\left(\frac{v_0}{u_0}\right)^2 \begin{pmatrix} t^*\left(\tilde{k}_h\right) r^*\left(\tilde{k}_h\right) \\ r^*\left(\tilde{k}_h\right) t^*\left(\tilde{k}_h\right) \end{pmatrix} \begin{pmatrix} e^{-i\left(\tilde{k}_e-\tilde{k}_h\right)(a-L)} e^{-i\phi} & 0 \\ 0 & e^{i\left(\tilde{k}_e-\tilde{k}_h\right)a} \end{pmatrix}$$
$$\times \begin{pmatrix} t\left(\tilde{k}_e\right) r\left(\tilde{k}_e\right) \\ r\left(\tilde{k}_e\right) t\left(\tilde{k}_e\right) \end{pmatrix} \begin{pmatrix} e^{i\left(\tilde{k}_e-\tilde{k}_h\right)a} & 0 \\ 0 & e^{i\phi} e^{-i\left(\tilde{k}_e-\tilde{k}_h\right)(a-L)} \end{pmatrix} \begin{pmatrix} B' \\ D' \end{pmatrix}$$

$$+\left(\tfrac{v_0}{u_0}\right)\begin{pmatrix} t^*(\tilde{k}_h)\, r^*(\tilde{k}_h) \\ r^*(\tilde{k}_h)\, t^*(\tilde{k}_h) \end{pmatrix}\begin{pmatrix} e^{-i(\tilde{k}_e-\tilde{k}_h)(a-L)}e^{-i\phi} & 0 \\ 0 & e^{i(\tilde{k}_e-\tilde{k}_h)a} \end{pmatrix}\begin{pmatrix} t(\tilde{k}_e)\, r(\tilde{k}_e) \\ r(\tilde{k}_e)\, t(\tilde{k}_e) \end{pmatrix}\begin{pmatrix} \left[1-\left(\frac{v_0}{u_0}\right)^2\right] e^{i\tilde{k}_e a} \\ 0 \end{pmatrix}$$

$$= \begin{pmatrix} 1 & 0 \\ 0 & 1 \end{pmatrix} \begin{pmatrix} B' \\ D' \end{pmatrix}. \tag{A24}$$

Here B' and D' are the same as B and D up to a phase factor, where $B' = B\exp\left(i\tilde{k}_h a\right)$ and $D' = D\exp\left[-i\tilde{k}_h(a-L)\right]$.

Equations (A23) and (A24) are in a form which can be easily generalized to arbitrary elastic scattering potentials and multiple-moded electron waveguides. Further, Eqs. (A23) and (A24) can be interpreted directly in terms of the phase shifts acquired by the electron and hole Feynman paths multiply reflected from the scatterer and multiply Andreev reflected from the SN boundaries. The remaining considerations here and in Appendix B now specialize to the case where the transmission amplitude is independent of energy.

We directly invert Eqs. (A23) and (A24) to find

$$C' = t\frac{\left[1-\left(\frac{v_0}{u_0}\right)^2 e^{i\phi} e^{i\left(\tilde{k}_e-\tilde{k}_h\right)L}\right]\left[1-\left(\frac{v_0}{u_0}\right)^2\right] e^{i\tilde{k}_e a}}{\left[1-\left(\frac{v_0}{u_0}\right)^2 e^{i\alpha} e^{i\left(\tilde{k}_e-\tilde{k}_h\right)L}\right]\left[1-\left(\frac{v_0}{u_0}\right)^2 e^{-i\alpha} e^{i\left(\tilde{k}_e-\tilde{k}_h\right)L}\right]} \tag{A25}$$

and

$$D' = \left(\frac{v_0}{u_0}\right) \frac{\left(tr^* e^{-i\phi} e^{i\left(\tilde{k}_e - \tilde{k}_h\right)(L-a)} + rt^* e^{i\left(\tilde{k}_e - \tilde{k}_h\right)a}\right)\left[1 - \left(\frac{v_0}{u_0}\right)^2\right] e^{i\tilde{k}_e a}}{\left[1 - \left(\frac{v_0}{u_0}\right)^2 e^{i\alpha} e^{i\left(\tilde{k}_e - \tilde{k}_h\right)L}\right]\left[1 - \left(\frac{v_0}{u_0}\right)^2 e^{-i\alpha} e^{i\left(\tilde{k}_e - \tilde{k}_h\right)L}\right]} \tag{A26}$$

The angle α in Eqs. (A25) and (A26) is determined from
$\cos(\alpha) = T\cos(\phi) + R\cos\left[\left(\tilde{k}_h - \tilde{k}_e\right)(L-2a)\right]$.

If we remove the tunnel barrier ($\alpha \to \phi$ and $t \to 1$) and set the phase difference ϕ to zero, Eq. (A25) gives the result of Demers and Griffin [47] for the transmission amplitude of an electronlike excitation between two superconductors.

The discrete levels in the SNS potential with a tunnel barrier are found [45] by computing the poles of the transmission amplitudes C' or D'. Therefore, the Andreev levels are determined from

$$1 = \left(\frac{v_0}{u_0}\right)^2 e^{\pm i\alpha} e^{i\left(\tilde{k}_e - \tilde{k}_h\right)L} \tag{A28}$$

Since $(v_0/u_0)^2 = \exp\left[2i\cos^{-1}(E/\Delta)\right]$ for $|E| < \Delta$, Eq. (A28) reduces to

$$2\cos^{-1}(E/\Delta) + \left(\tilde{k}_e - \tilde{k}_h\right)L \pm \alpha = 2\pi n \tag{A29}$$

Using $\tilde{k}_e - \tilde{k}_h \simeq k_F E/\mu = E/\Delta\xi_0$, Eqs. (A27) and (A29) reduce to Eqs. (7) and (8).

Equations (7) and (8) also determine the location of the "leaky" Andreev levels in the continuum. In the continuum, the solution of Eqs. (7) and (8) will occur at a complex energy $E = E_R + iE_I$. The imaginary part of this pole can then be interpreted as the lifetime $(\hbar/|E_I|)$ of the leaky Andreev level. The locations of both the discrete poles and the continuum poles of the transmission amplitude are shown in Fig. 8.

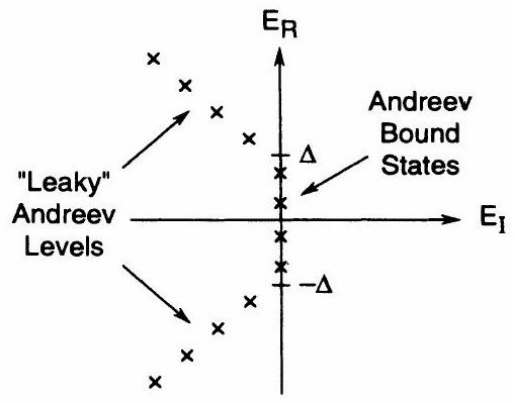


FIG. 8. Poles of the quasiparticle transmission amplitude determine the natural eigenergies of the SNS potential. Welldefined quantum levels exist inside the superconducting energy gap, while scattering resonances outside the gap have a finite lifetime $\hbar/|E_I|$.

Appendix B: Continuum supercurrents

Continuum supercurrents can only flow if there is an imbalance in the electrical currents carried by the quasiparticles incident from the left and right superconducting contacts. The imbalance $I(E,\phi)$ will be proportional to the difference in the transmission coefficients $T^e_{L\to R}(E,\phi) - T^e_{L\leftarrow R}(E,\phi)$ (transmission from left to right minus transmission from right to left) for electrical currents across the SNS junction. This conclusion follows because, near

equilibrium, quantum states in the left and right contacts are equally thermally populated according to the Fermi function $f(E)$ at each energy, and because there are no inelastic scattering processes in the junction.

To obtain the continuum currents we invoke the insights of van Wees, Lenssen, and Harmans. [18] Reference 18 notes that that the electrical current $I(E)$ carried by a single filled quantum state per unit energy is $I(E) = ev_p(E)N_s^+(E)$, where v_p is the phase velocity and $N_s^+(E)$ the superconducting density of states for quasiparticles moving in one direction. We can write this current as $I(E) = e\left(v_p(E)/v_g(E)\right)v_g(E)N_s^+(E)$, where v_g is the group velocity. (Reference 24 defines these phase and group velocities.) Just as in the normal metal, [4] the group velocity times the density of states cancels to $v_g(E)N_s^+(E) = 1/h$. The other factor,

$$v_p(E)/v_g(E) = 1/\left|u_0^2 - v_0^2\right| = N_s^+(E)/N_n^+(E)$$

is simply the ratio of the density of states in the superconductor to the density of states in the normal metal. [This factor $N_s^+(E)/N_n^+(E)$ appears prominently in the study of superconducting tunnel junctions.] The electrical current carried by electronlike excitations in the continuum is therefore

$$I_c^e(\phi) = \frac{2e}{h}\left(\int_{-\infty}^{-\Delta} + \int_{\Delta}^{\infty}\right)\frac{1}{|u_0^2 - v_0^2|}\left[T_{L\to R}^e(E,\phi) - T_{L\leftarrow R}^e(E,\phi)\right]f(E)dE \tag{B1}$$

The additional factor of 2 in Eq. (B1) comes from the electron spin.

We now evaluate the transmission coefficients appearing in Eq. (B1) for our model problem. The transmission coefficient for the electrical currents carried by electronlike excitations incident from the left contact is

$$T_{L\to R}^e(E,\phi) = |C'|^2 - |D'|^2 \tag{B2}$$

with C' and D' determined from Eqs. (A25) and (A26) in Appendix A. Computing these quantities, we find

$$|C'|^2 = T\left|u_0^2 - v_0^2\right|^2 \frac{D(E,\phi)}{D(E,\alpha)D(E,-\alpha)} \tag{B3}$$

and

$$\begin{aligned}|D'|^2 = &\left|u_0^2 - v_0^2\right|^2 \frac{2TRu_0^2v_0^2}{D(E,\alpha)D(E,-\alpha)} \\ &\times\left\{1 + \cos\left[\left(\tilde{k}_e - \tilde{k}_h\right)(L-2a) - \phi\right]\right\}\end{aligned} \tag{B4}$$

where $D(E,\alpha)$ is given by Eq. (18). $T_{L\leftarrow R}^e(E,\phi)$ is easily found from $T_{L\to R}^e(E,\phi)$ by the transformations $\phi \to -\phi$ and $a \to (L-a)$. Therefore,

$$\begin{aligned}T_{L\to R}^e(E,\phi) - &T_{L\leftarrow R}^e(E,\phi) \\ &= T\left|u_0^2 - v_0^2\right|^2 \frac{D(E,\phi) - D(E,-\phi)}{D(E,\alpha)D(E,-\alpha)}\end{aligned} \tag{B5}$$

Equation (B5) can be recast as

$$T^e_{L\to R}(E,\phi) - T^e_{L\leftarrow R}(E,\phi) = T\left|u_0^2 - v_0^2\right|^2 \frac{\sin(\phi)}{\sin(\alpha)} \frac{D(E,\alpha) - D(E,-\alpha)}{D(E,\alpha)D(E,-\alpha)} \tag{B6}$$

Combining Eqs. (B6) and (B1), we find

$$I_c^e(\phi)\big|_{E>\Delta} = \frac{2e}{h} T \int_{\Delta}^{\infty} \left|u_0^2 - v_0^2\right| \left(\frac{1}{D(E,-\alpha)} - \frac{1}{D(E,\alpha)}\right) \times \frac{\sin(\phi)}{\sin(\alpha)} f(E)dE \tag{B7}$$

One can now choose several alternate paths to Eq. (21). We have chosen what seems (to us) the most straightforward. Consider the full dispersion relation shown in Fig. 9. It can be separated into an electron branch (standard parabola) and hole branch (inverted parabola). These branches should all be populated according to a Fermi function $f(E)$ at finite temperatures, including

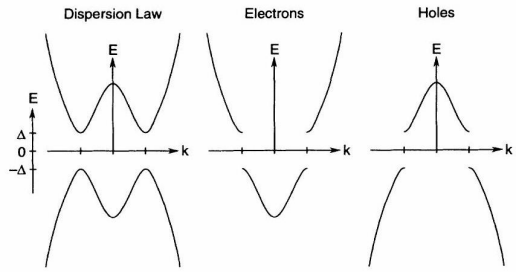
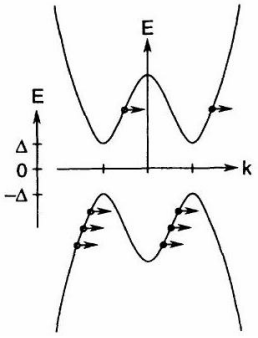


FIG. 9. The total dispersion law for a uniform superconductor can be decomposed into electronlike and holelike states.

Left Contact



Right Contact

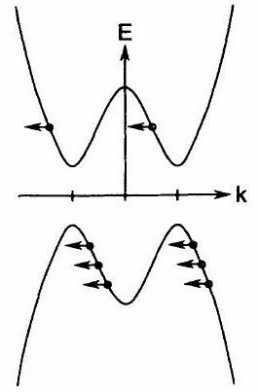


FIG. 10. Both electronlike and holelike states are incident on the SNS potential from all possible branches of the dispersion curve. These quantum levels are populated according to the Fermi function $f(E)$, even in the presence of supercurrent flow.

the hole branches. To compute the Josephson current, one must therefore work also with the negative energy ($E < 0$) solutions of the Bogoliubov-de Gennes equations. We consider quasiparticles incident in all possible branches of the dispersion curve, as shown pictorially in Fig. 10.

Calculating the currents implied from Fig. 10, the total electronlike currents are given by integrating Eq. (B7) over the entire continuum, which is the same as Eq. (21). The hole currents are found to be equal to the electron currents, thereby giving a continuum current too large by a factor of 2. This factor of 2 is easily understood when we note that the dispersion law shown in Fig. 9 contains twice the number of states as the normal metal. We therefore correct for this excess number of quasiparticle states by dividing a factor of 2 into the final result, namely,

$$2I_c(\phi) = I_c^e(\phi) + I_c^h(\phi) \tag{B8}$$

obtaining Eq. (21).

We feel that the physics of Josephson current flow may be less transparent when working solely with the excitation spectrum. Since the excitation spectrum will not be populated at $T = 0$, [18] it is unclear how it can carry the required zero-temperature Josephson current. It was even noted in Ref. 18 that "this seems to prevent the calculation" of the Josephson current at $T = 0$. However, a disadvantage of working with the full dispersion curve is that one must also use the negative energy solutions of Eq. (3). Further, one must compute twice the number of transmission coefficients. Alternatively, one could compute the currents carried by only the electron branch (or only by the hole branch) of the dispersion curve, and still use both positive and negative energies.

Appendix C: supercurrent from free energy

The free energy of a set of independent fermions in the grand canonical ensemble is

$$F = N\mu - kT \sum_E \ln\left(1 + e^{-E/kT}\right) \tag{C1}$$

The derivative of F with respect to the phase difference becomes a sum over the discrete energies $E_n(\phi)$ and integral over the continuum density of states $\rho(E, \phi)$

$$\frac{dF}{d\phi} = \sum_n \frac{dE_n}{d\phi} f\left(E_n\right) + \left(\int_{-\infty}^{-\Delta} + \int_{\Delta}^{\infty} \right) \left. \frac{d\rho(E,\phi)}{d\phi} \right|_E \times \ln\left(1 + e^{-E/kT}\right) dE \tag{C2}$$

The discrete spectrum therefore carries the Josephson current suggested in Sec. II, namely Eq. (10), where

$$I_d(\phi) = \frac{2e}{\hbar} \sum_n \{ \frac{dE_n^+(\phi)}{d\phi} f\left(E_n^+(\phi)\right) + \frac{dE_n^-(\phi)}{d\phi} f\left(E_n^-(\phi)\right) \Big\} \tag{C3}$$

letting us identify the current $I_n^{\pm}(\phi)$ carried by an Andreev level as

$$I_n^{\pm}(\phi) = \frac{2e}{\hbar}\frac{dE_n^{\pm}(\phi)}{d\phi} \tag{C4}$$

Equation (C3) is computationally much simpler than obtaining the current from the quasiparticle wave functions $u(x)$ and $v(x)$, and shows how to easily compute $I_d(\phi)$ when the transmission amplitudes depend on the energy. Further, Eq. (C3) is identical to the current carried by the discrete spectrum from Ref. 13.

We now show how Eq. (15) for the current $I_n^{\pm}(\phi)$ carried by an Andreev level follows from Eq. (C4) combined with Eqs. (7) and (8). We wish to compute

$$\frac{dE_n^{\pm}}{d\phi} = \frac{dE_n^{\pm}}{d\alpha}\frac{d\alpha}{d\phi} \tag{C5}$$

Equation (7) shows how the energy depends on the effective phase α. We find

$$\frac{dE_n^{\pm}}{d\alpha} = \frac{\partial E_n^{\pm}}{\partial \alpha} = \mp\frac{\hbar}{2e}\frac{ev_F}{L + 2\xi\left(E_n^{\pm}\right)} \tag{C6}$$

On the other hand, Eq. (8) shows that $\alpha(E,\phi)$ is a function of both the energy and the phase difference. Therefore

$$d\alpha = \left.\frac{\partial \alpha}{\partial E}\right|_{\phi} dE + \left.\frac{\partial \alpha}{\partial \phi}\right|_{E} d\phi \tag{C7}$$

Combining (C5), (C6), and (C7), we find

$$\frac{dE_n^{\pm}}{d\phi} = \frac{\partial E_n^{\pm}}{\partial \alpha}\left.\frac{\partial \alpha}{\partial \phi}\right|_{E}\frac{1}{\gamma} \tag{C8}$$

where γ is the feedback factor in Eq. (15), namely

$$\gamma = 1 - \left.\frac{\partial E_n^{\pm}}{\partial \alpha}\frac{\partial \alpha}{\partial E}\right|_{\phi} \tag{C9}$$

Equation (8) gives

$$\left.\frac{\partial \alpha}{\partial E}\right|_{\phi} = \left(\frac{R}{\Delta \sin(\alpha)}\right)\left(\frac{L-2a}{\xi_0}\right)\sin\left(\frac{L-2a}{\xi_0}\frac{E}{\Delta}\right) \tag{C10}$$

so that combining (C10) with (24), (C6), (C8), (C9), and (C4) yields Eq. (15).

The continuum contribution to the supercurrent in Eq. (C2) requires the derivative of the continuum density of states with respect to the phase difference

$$\left.\frac{d\rho(E,\phi)}{d\phi}\right|_{E} = \left.\frac{d\rho(E,\alpha)}{d\alpha}\right|_{E}\left.\frac{\partial \alpha}{\partial \phi}\right|_{E} \tag{C11}$$

Equation (C11) implies that we can take the result (17) for $I_c(\phi)$ in the clean junction, replace ϕ by α, then multiply the integrand by (24) to obtain Eq. (21) for $I_c(\phi)$ in the dirty junction. Even though we exploit the continuum contribution of Eq. (C2) to better understand the formulas presented in Sec. II, we do not immediately see the full correspondence between the continuum contribution [13] in Eq. (C2) and the transmission formalism [18] for computing supercurrents carried in the continuum. However, we feel the two methods can probably be shown to be identical.

Appendix D: approximate Andreev levels in a long junction

In this appendix we obtain approximate expressions for the Andreev levels in a long SNS junction with an impurity. Equation (8) can be recast as
$\cos^2(\alpha/2) = 1 - T\sin^2(\phi/2) - R\sin^2[(L-2a)E/2\Delta\xi_0]$.
For $E \ll \Delta$, Eq. (7) becomes

$$E^{\pm} \simeq \left(\frac{\hbar v_F}{2L^*}\right)(2\pi n - \pi \mp \alpha) \tag{D2}$$

with $L^* = L + 2\xi_0$. Taking the impurity exactly in the center of the junction, $a = L/2$, we immediately obtain from Eqs. (D1) and (D2)

$$E^{\pm} \simeq \pi\left(\frac{\hbar v_F}{2L^*}\right)\{2n - 1 \mp \frac{2}{\pi}\cos^{-1}\left[\sqrt{1 - T\sin^2(\phi/2)}\right] \tag{D3}$$

We therefore find the Andreev energy gap near $E = 0$ and $\phi = \pi$ as

$$E_{\rm gap} \simeq 2\pi\left(\frac{\hbar v_F}{2L^*}\right)\left(1 - \frac{2}{\pi}\cos^{-1}\sqrt{R}\right) \tag{D4}$$

which becomes $E_{\rm gap} \simeq (2\sqrt{R})\,(\hbar v_F/L^*)$ for small R. For $T \to 1, E \simeq 0$, and near $\phi \simeq \pi$, we can expand Eq. (D3) as

$$E^{\pm} \simeq \pm 2\left(\frac{\hbar v_F}{2L^*}\right)\sqrt{1 - T\sin^2(\phi/2)} \tag{D5}$$

The slope of the Jospehson current versus phase at $\phi = \pi$ is then approximately

$$\left.\frac{dI}{d\phi}\right|_{\phi=\pi} \simeq \left(\frac{ev_F}{L^*}\right)\left(\frac{T}{2\sqrt{R}}\right).$$

For an impurity which is not centered in the junction, and taking $E \ll \Delta$ and $L - 2a \ll \xi_0$, we can approximate Eq. (D1) as

$$\cos^2(\alpha/2) \simeq 1 - T\sin^2(\phi/2) - R\left((L-2a)E/2\Delta\xi_0\right)^2.$$

Solving Eq. (D7) together with Eq. (D2) for $E^{\pm}$merely replaces $L^* \to L_{\rm eff}$ in Eqs. (D5) and (D6), where $L_{\rm eff}^2 = (L + 2\xi_0)^2 + R(L-2a)^2$. This very approximate analysis confirms Eqs. (34) and (35) in Sec. IV.

10.1.5 Ballistic JC through an asymmetric SNS by Chang, Bagwell

(here will be main method and statement, details will be in the special note)

10.1.6 Josephson and Andreev transport through quantum dots

(see special note about it for now, a very good topic for practice! Later I'll write main statements about it also here)

10.1.7 JJ through a Semiconductor Nanowire

(also, first I'll write it in special note, then - here. There are many articles about it, so I'll select most important ones)

11 Specific Junctions, Applications

11.1 SFS Junction (Junction Through a Ferromagnet)

11.1.1 47*. SFS junction by Shmidt

В разд. 15.2 было показано, что сверхпроводящие пары могут проникать через SN-границу в нормальный металл на глубину ξ_N. Более подробно процесс электропереноса в SNS-переходах будет рассмотрен в 55. Сейчас мы рассмотрим эффект близости в системе сверхпроводник - ферромагнетик (SF) и необычные свойства джозефсоновских SFS-переходов. Но сначала вернемся к эффекту близости в SN-системе и покажем, как оценка длины когерентности ξ_N может быть получена из простых физических соображений. Очевидно, что время жизни τ_p сверхпроводящей пары в несверхпроводящем металле тем меньше, чем больше характерная энергия ΔE процессов, разрушающих пары. Величина τ_p может быть оценена с помощью соотношения неопределенностей:

$$\tau_p \Delta E \sim \hbar \tag{47.1}$$

В нормальном немагнитном металле распаривание происходит за счет тепловых флуктуаций (характерная энергия $\Delta E = k_{\mathrm{B}}T$), т.е. $\tau_p \sim \hbar/k_{\mathrm{B}}T$. В чистый металл пары могут распространяться на глубину порядка $v_{\mathrm{F}}\tau_p \sim \hbar v_{\mathrm{F}}/k_{\mathrm{B}}T$ (ср. с формулой (15.13) для длины затухания параметра порядка в чистом металле). В "грязный» металл пары проникают на длину диффузии за время τ_p, т.е. длина затухания равна $\xi_N \sim \sqrt{D\tau_p} \sim (\hbar D/k_{\mathrm{B}}T)^{1/2}$ (где $D = l_n v_{\mathrm{F}}/3$), что с точностью до $\sqrt{2\pi}$ совпадает с (15.14). В случае SF-контакта в ферромагнетике появляется еще один распаривающий фактор - обменное взаимодействие, которое
пытается выстроить спины электроны в одном направлении, т.е. разрушить пару, которая образована из электронов с противоположно направленными спинами. Если температура Кюри ферромагнетика T_{C} много больше критической температуры T_c сверхпроводника, то средняя обменная энергия в ферромагнетике $E_{ex} \gg k_{\mathrm{B}}T$, и обменное взаимодействие можно считать единственным распаривающим фактором, т.е. $\Delta E \sim E_{\mathrm{ex}}$ в (47.1). В этом случае длина эатухания параметра порядка в "грязном" ферромагнетике $\sqrt{D\tau_p}$ равна

$$\xi_{F1} = \left(\frac{\hbar D}{E_{ex}}\right)^{1/2}, \quad E_{ex} \gg k_{\mathrm{B}}T \tag{47.2}$$

Мы присвоили величине ξ_{F1} дополнительный индекс «1», поскольку длина затухания, как будет показано ниже, - только реальная часть комплексной длины когерентности ξ_F куперовских пар в ферромагнетике. Если наведенный в нормальном металле вблизи SN-границы параметр порядка описывается затухающей экспонентой $\Psi_N(x) = \Psi_{N0}e^{-k_N x}$, где $k_N = 1/\xi_N$, то в SF-случае наведенный параметр порядка не только затухает, но и осциллирует:

$$\Psi_F(x) = \Psi_{F0}e^{-k_F x} = \Psi_{F0}e^{-k_{F1}x}e^{-ik_{F2}x} \tag{47.3}$$

Здесь Ψ_{F0} - параметр порядка в ферромагнетике на SF-границе, а комплексная величина $k_F = 1/\xi_F = k_{F1} + ik_{F2}$. Ее вещественная часть $k_{F1} = 1/\xi_{F1}$, где ξ_{F1} - введенная ранее длина затухания. Мнимая же часть $k_{F2} = 1/\xi_{F2}$ определяет собой длину волны $2\pi\xi_{F2}$ осцилляций параметра порядка в ферромагнетике, см. рис. 47.1. Можно показать, что в случае "грязного» ферромагнетика без спин-орбитального рассеяния и с

$E_{ex} \gg k_{\mathrm{B}}T$ величины ξ_{F1} и ξ_{F2} равны и описываются формулой (47.2). Комплексную длину когерентности можно тогда записать в виде

$$\xi_F = \left(\frac{\hbar D}{2iE_{ex}}\right)^{1/2} \tag{47.4}$$

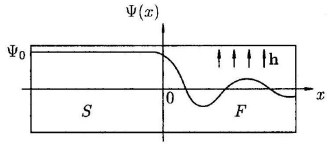
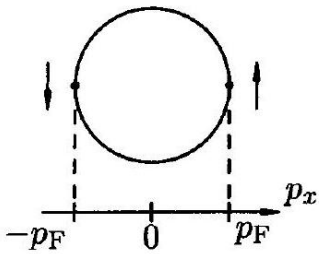


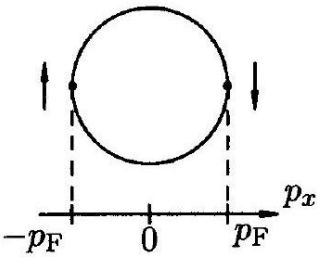
Рис. 47.1. Схематическое изображение поведения параметра порядка вблизи SF-границы; h - обменное поле в ферромагнетике.

S

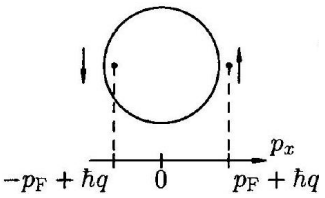
а)



б)



ψ



ψ

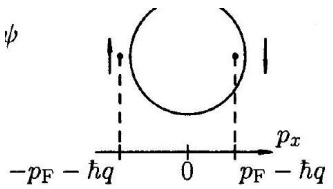


Рис. 47.2. Возникновение ненулевого суммарного импульса пары в ферромагнетике вблизи SF-границы в присутствии обменного поля h. Части а) и б) рисунка соответствуют различным направлениям спинов электронов с положительным и отрицательным импульсами относительно направления обменного поля.

Прежде чем перейти к случаю относительно малых обменных энергий $E_{ex} \geqslant k_{\rm B}T$, попробуем понять физические причины возникновения в ферромагнетике знакопеременного параметра порядка $\Psi_F(x)$. В основе этого явления лежит возможность появления пар с ненулевым суммарным импульсом в присутствии обменного поля, предсказанная для магнитных сверхпроводников в 1964 г. в работах Ларкина и Овчинникова [138], а также Фульде и Феррела [139]. Объемные сверхпроводники с таким состоянием параметра порядка (обозначаемым обычно как LOFF-состояние) пока не обнаружены. Однако вполне реализуемой модификацией LOFF-состояния является осциллирующий параметр порядка вблизи SF-границы, предсказанный позднее в работах [140, 141]. Простая физическая картина появления ненулевого суммарного импульса пары в ферромагнетике, предложенная в работе [142], показана на рис. 47.2. Обсудим здесь слу'ай чистых металлов - сверхпроводника и ферромагнетика. Тог'да пара образована электронами с противоположными (лежащими на ферми-поверхности) импульсами $\hbar\mathbf{k}$ и - $\hbar\mathbf{k}$, так что суммарный импульс пары $\hbar\mathbf{q} = 0$. В ферромагнитной области произойдет изменение энергий электронов пары за счет обменного взаимодействия: тот электрон (назовем его 1 -м), спин которого направлен параллельно обменному полю ферромагнетика, уменьшит свою энергию на E_{ex}, а второй электрон той же пары увеличит свою энергию на E_{ex}. Но энергии электронов, образующих куперовскую пару должны быть равны - казалось бы, это озна'гает немедленное разрушение пары обменным полем! Однако эту проблему можно обойти: увеличим импульс 1 -го электрона до величины $\hbar k_1$ такой, что $\hbar^2 k_1^2/2m - \hbar^2 k^2/2m = E_{ex}$, т.е. $k_1 - k = q_1 \sim E_{ex}/\hbar v_{\rm F}$, а импульс 2-го электрона уменьшим (по абсолютной величине) на такую же величину, - до $\hbar k_2 = \hbar k - \hbar q_1$. 'Тогда противоположные по знаку изменения обменной энергии двух электронов будут скомпенсированы иэменениями их кинетических энергий, а полные энергии останутся одинаковыми, и гара не будет разрушаться. Но такая пара будет теперь иметь ченулевой полный импульс $\hbar q = 2\hbar q_1$, так что ее вклад в параметр порядка будет пропорционален e^{iqx}. Кроме рассмотренной конфигурации спинов в паре возможна и такая, где 1-й электрон (со спином вдоль обменного поля) имеет импульс $-\hbar k$, а 2 -й импульс $\hbar k$. Такая пара приобретет полный импульс $-\hbar q$, и полный параметр порядка будет вести себя как

$$\Psi_F(x) = \Psi_{F0}\left(e^{iqx} + e^{-iqx}\right)/2 = \Psi_{F0}\cos(qx), \tag{47.5}$$

так что длина волны $2\pi\xi_{F2}$ осцилляций параметра порядка равна $2\pi/q \sim \hbar v_F/E_{ex}$. В грязном металле направление импульсов электронов быстро меняется из-за рассеяния на примесях, поэтому зависимость типа (47.5) должна быть усреднена по направлениям вектора q. Аккуратное вычисление [142] показывает, как упоминалось выше, что наряду с осцилляциями параметра порядка появляется и их затухание, причем в грязном пределе $\xi_{F1} = \xi_{F2} = \sqrt{\hbar D/E_{ex}}$.

В связи со знакопеременностью параметра порядка (47.5) естественно ожидать, что в SFS-переходе с толщиной ферромагнетика $d_F \simeq \pi\xi_{F2}$ знаки параметра порядка на сверхпроводящих берегах будут разными, т. е. разность фаз на переходе будет равна π в отсутствие внешнего поля и тока (что не противоречит стационарному уравнению Джозефсона (21.1)). Такой джозефсоновский «л-контакт" был впервые предложен в работе [143] и подробно рассмотрен для SFS-случая в работе [144]. Другой тип π-контакта, возникающего из-за нетривиальной d-волновой симметрии параметра порядка в ВТСП, будет обсуждаться в 49.

На рис. 47.3 представлен результат расчета [145] распределения параметра порядка в грязной ферромагнитной прослойке для различных соотношений толщины слоя d_F и периода осцилляций параметра порядка $2\pi\xi_{F2}$. На следующем рисунке 47.4 изображены зависимости свободных энергий Гинзбурга-Ландау для состояний SFS-перехода с разностями фаз на берегах, равными 0 и π (будем их для краткости называть 0 -состояние и π-состояние). Видно, что π-состояние действительно становится более устойчивым при $d_F \simeq \pi\xi_{F2}$, а затем вновь сменяется обычным 0 -состоянием при дальнейшем увеличении d_F. На рис. 47.3 показано также (штриховой линией) распределение параметра порядка

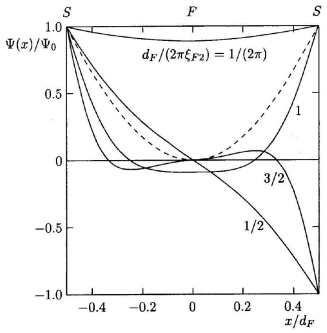


Рис. 47.3. Пространственное распределение параметра порядка в F слое SFS-перехода, вычисленное [145] для различных значений отношения $d_F/2\pi\xi_{F2}$; для отношений, равных $1/2\pi$ и 1, наинизшая энергия достигается в 0 -состоянии, а для отношений $1/2$ и $3/2$ более выгодным оказывается π-состояние.

для 0 -состояния при $d_F = \pi\xi_{F2}$, когда оно имеет более высокую энергию, чем π-состояние (как видно из рисунка, средний квадрат градиента параметра порядка в 0-состоянии выше, чем в π состоянии, что и повышает энергию первого).

Рассмотрим теперь случай относительно малых обменных энергий $E_{ex} \geqslant k_{\mathrm{B}}T$, когда в распаривание дают сравнимый вклад как тепловая энергия, так и обменное поле. Из сравнения выражений (15.14) и (47.4) довольно очевидно (и это можно строго показать), что общее выражение для комплексной длины
F_Γ, отн. ед.

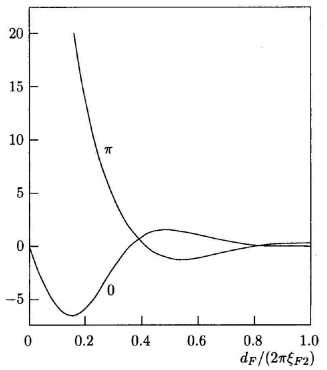


Рис. 47.4. Результат вычислений [145] свободной энергии Гинзбурга Ландау в F-слое для 0 - и π-состояний.

когерентности будет теперь иметь вид

$$\xi_F = \left(\frac{\hbar D}{2\left(\pi k_{\mathrm{B}}T + iE_{ex}\right)}\right)^{1/2} \tag{47.6}$$

Выделяя из этого выражения вещественную и мнимую части для чего удобно записать

$$\pi k_{\mathrm{B}}T + iE_{ex} = \sqrt{(\pi k_{\mathrm{B}}T)^2 + E_{ex}^2}\exp\left(i\,\mathrm{arctg}\left(E_{ex}/\pi k_{\mathrm{B}}T\right)\right)$$

— получим окончательно

$$\xi_{F1,2} = \sqrt{\frac{\hbar D}{\left((\pi k_{\mathrm{B}}T)^2 + E_{ex}^2\right)^{1/2} \pm \pi k_{\mathrm{B}}T}}. \tag{47.7}$$

Это выражение переходит в (47.2) при $E_{ex} \gg k_{\mathrm{B}}T$ и в (15.14) при $E_{ex} = 0$. Важно заметить, что в то время как длина затухания ξ_{F1} растет с понижением температуры (как и для SN контакта), длина волны осцилляций $2\pi\xi_{F2}$ уменьшается. Это дает возможность наблюдать переход SFS-контакта в π-состояние при понижении температуры. Такой эксперимент представлен в работе [145], где в качестве ферромагнитной прослойки был использован сплав CuNi с температурой Кюри около 20 К. На рис. 47.5 представлено семейство измеренных температурных зависимостей критического тока SFS-переходов $\mathrm{Nb-CuNi-Nb}$ с толщиной F-слоя d_F, близкой к $\pi\xi_{F2}$. При наименьшей толщине в 23 нм зависимость $I_c(T)$ не отличается качественно от обычной для SNS-переходов, $I_c \propto e^{-\alpha\sqrt{T}}$. При небольшом увеличении d_F наблюдается насыщение при низких температурах, а потом и немонотонная зависимость $I_c(T)$. Наконец, при толщине $d_F = 27$ нм наблюдается возвратное осциллирующее поведение $I_c(T)$ с обращением в нуль при $T = T_{\text{пер}} \simeq 2$ К. Такое поведение может являться только следствием перехода в π-состояние при $T < T_{\text{пер}}$. В точке этого перехода формальное выражение для $I_c(T)$ проходит через нуль и уходит в отрицательную область. Поскольку в эксперименте измеряется положительно определенная величина критического тока, на зависимости $I_c(T)$ возникает излом в точке $T = T_{\text{пер}}$.

Прямым доказательством перехода SFS-контактов в π-состояние явилось измерение [146] критического тока интерферометра из пяти SFS-контактов, изображенного на рис. 47.6, в зависимости от приложенного магнитного поля. При переходе контактов в π-состояние в каждой ячейке сетки должен возникнуть набег фазы 3π, что в соответствии с (25.2) эквивалентно приложению к сетке магнитного поля с полуцелым потоком на ячейку. Как и в случае двухконтактного интерферометра, описанного

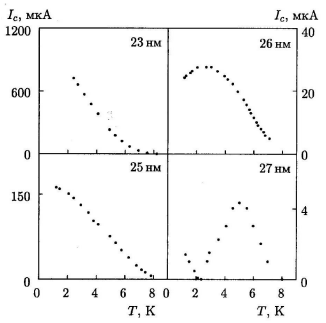


Рис. 47.5. Температурные зависимости критического тока SFS-переходов $\mathrm{Nb-Cu_{0.48}Ni_{0.52}-Nb}$ с толщинами ферромагнитного слоя Cu/Ni от 23 до 27 нм [145].

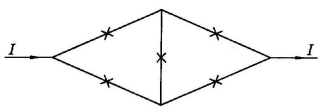


Рис. 47.6. Схематическое изображение треугольной сетки SFS-контактов, состоящей из двух ячеек.

в разд. 25.1, это приведет к смещению зависимости $I_c(H)$ на полпериода. Такой сдвиг, экспериментально обнаруженный при понижении температуры в работе [146], представлен на рис. 47.7.

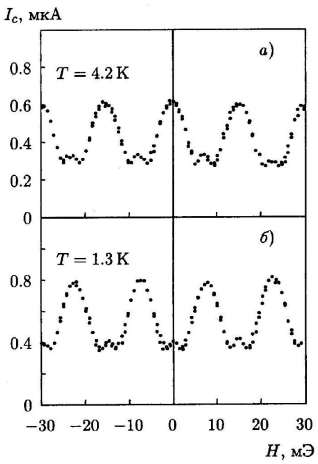


Рис. 47.7. Зависимости $I_c(H)$ двухячеистой сетки SFS-контактов до перехода контактов в π-состояние и после такого перехода ($T_{\text{пер}} = 2.2$ K). Ниже температуры перехода зависимости сдвигаются на полпериода.

11.2 Multiterminal junctions

(first, I'll write this in a separate note)

11.3 Very exotic models and properties of junctions

11.3.1 Casimir froce in Josephson Junctions

(see articles or my special note about it for now)

Casimir-Josephson force in a nutshell

$$F = -\frac{g\hbar v_{\text{F}}}{24\pi L^2}\left(\pi^2 - 3\phi^2\right), \quad |\phi| < \pi$$

$F = -d\Omega/dL$, Ω - free energy.

Why Casimir-Josephson force can be interesting?

- To test some method.
(?? if it give the obtained result by Beenakker. Good theoretical practice!)

Casimir-Josephson force theory

(пока не пишу, потому что тема бесполезная, для прикола вообще ее обсуждать только можно. мб когда-то посмотрю, пока нет в планах)

11.4 Application of Junctions: Main Ideas

11.4.1 4.6 Applications of Weak Superconductivity

The phenomenon of weak superconductivity - renowned for its beautiful physics - is also the basis of a large number of applications. Some of them are outlined below.

We already know that, if the current through a Josephson junction exceeds a critical value, the voltage across the junction has an ac component. The frequency of this component is

defined by (4.21). It is easy to see that, if the junction is exposed to an external rf field and the frequency of the field coincides with the frequency of the Josephson radiation, some sort of resonance must appear. Indeed, in this case, the current-voltage characteristic showing the average values of the current and voltage has the form of a staircase, as in Fig. 4.24. The spacing of the constant voltage steps is exactly $\hbar\omega/2e$. Historically, these steps are called Shapiro steps [30]. Since the frequency can be measured very accurately and the quantities $\hbar$ and e are universal constants, the spacing of the voltage steps on the current-voltage

Josephson junction can be used as a voltage standard [44]. Conversely, the ac Josephson effect can be used to build high-frequency oscillators. Due to the limited radiation power of a single Josephson junction, various types of junction arrays have been proposed in order to increase the output power and to achieve coherent emission of radiation [45].

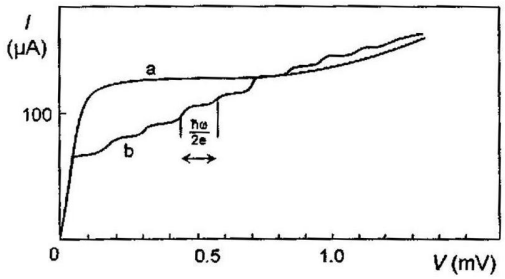


Fig. 4.24. Current-voltage characteristic of a Josephson junction: (a) without external rf electromagnetic field; (b) in the presence of an external of field. The finite slope of the superconducting part is due to a normal film connected in series with the junction [43]

The most celebrated use of SQUIDs is as high-sensitivity magnetometers which are able to register increments of magnetic field of the order of 10^{-10}G in 1 Hz bandwidth. For comparison, recall that the Earth's magnetic field is about 0.5 G . Obviously, the availability of such sensitive devices opens new horizons in various fields of science: geology, geophysics, biophysics, and others. An example is the use of SQUIDs in pioneering studies of the magnetic fields associated with the human heart, the so-called magneto-cardiograms. It turned out that they provide a lot more information about heart problems than the usual electro-cardiograms and therefore promise to become a tool for better diagnostics in this field.

If a SQUID is used as a zero-current device incorporated in an ordinary bridge circuit, it behaves as a voltmeter with sensitivity of about 10^{-15} V. Such voltmeters are already being used in physics laboratories. In addition, Josephson junctions are used in various high-frequency detectors and sensors, in particular, as sensitive elements for detection of millimeter and submillimeter electromagnetic waves in radiotelescopes.

Finally, it is important to mention the use of Josephson junctions as logic and memory elements in digital electronics. They allow much higher operation frequencies (up to hundreds of GHz) than conventional semiconductor-based elements. Another key factor in favor of superconducting digital electronics is the reduced energy consumption as compared to semiconductors. The most ..... –... t.... of lorin is the en.ralled RSFO (ranid single flux quantum) logic which is presently under development in many research laboratories [46].

The sphere of SQUID applications is bound to widen rapidly in the near future and at this particular moment it is impossible to foretell what wonderful results may follow.

Problems

Problem 4.1. Two Josephson junctions with critical currents $I_{c1} = 5 \times 10^{-4}$ A and $I_{c2} = 7 \times 10^{-4}$ A are connected in parallel. The total current through both junctions is 1×10^{-3} A. Find the current through each junction.

Problem 4.2. Find the difference between the maximum and minimum values of V in the plot of Fig. 4.6.

Problem 4.3. Consider a point contact having the critical current $I_c = 10^{-3}$ A and the normal state resistance $R = 2\Omega$. Find the value of the constant voltage across the junction, $\bar{V}$, and the frequency of Josephson radiation, ν, if the current through the contact is $I = 1.2 \times 10^{-3}$ A.
Problem 4.4. Consider a Josephson junction to which a dc current $I_0 = 7 \times 10^{-5}$ A and an ac current of amplitude $I_1 = 2 \times 10^{-6}$ A and frequency $\nu = 10$MHz are applied. That is, the total current applied to the junction is $I = I_0 + I_1 \sin 2\pi\nu t$. The critical current of the junction is $I_c = 10^{-4}$ A. Find the voltage across the junction (in SI units).
Problem 4.5. Consider a tunnel Josephson junction formed by two Pb films. Find the critical field for penetration of a vortex into the junction, H_{cl}, and the field at the center of the vortex. The London magnetic penetration depth for Pb is $\lambda = 400$Å and the critical current density of the junction is $j_c = 10$ A cm^{-2}.
Problem 4.6. Assume that the length of the tunnel junction in Problem 4.5 is $L = 0.2$ mm. Find the external fields corresponding to the first two maxima of the critical current.
Problem 4.7. Consider a single-junction interferometer of inductance 2×10^{-9}H. If the critical current of the junction decreases, the hysteresis in the dependence $\Phi(\Phi_e)$ will disappear at a certain value of the critical current. Find this value.

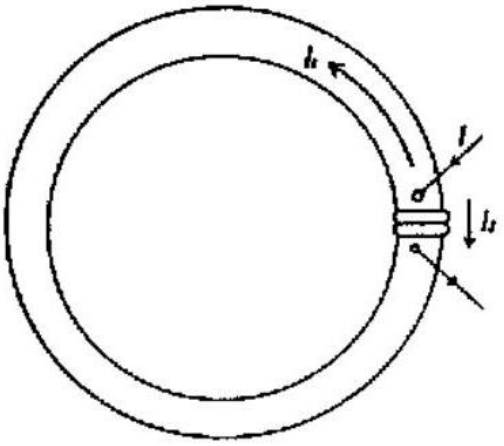


Fig. 4.25. See Problem 4.8. An external source supplies a current I, a part of which, I_r, passes through the ring and the other part, I_J, through the Josephson junction
I, a part of which (I_r) passes through the ring and the other part (I_s) through the Josephson junction, as illustrated in Fig. 4.25. The critical current of the junction is $I_c = 10^{-6}$ A. Find the total current I.

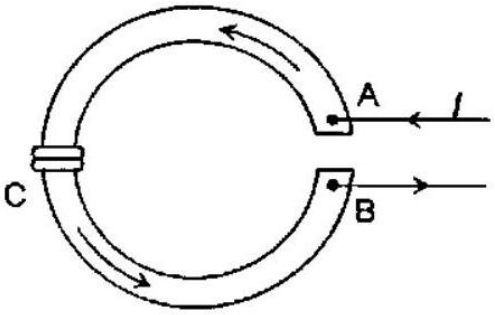


Fig. 4.26. See problem 4.9
Problem 4.9. Consider an SNS Josephson junction with the critical current $I_c = 10^{-6}$ A incorporated in a superconducting ring of inductance $L = 10^{-9}$H. From the side opposite to the junction, a small piece of the ring is cut out, as shown in Fig. 4.26. An external current source connected to the cut supplies a current $I = 0.4 \times 10^{-6}$ A. Find the difference in the phase of the wavefunction between the points A and B, φ_{AB}. Make a plot of the current as a function of the phase difference φ_{AB}.

Part V
Very Useful Methods

12 Methods for BCS SC

12.1 Transformations

12.1.1 Selected GF methods for superconductivity

Assumed formulas for the main derivation of bare Green's function $g^j_{1,1}$ for the discrete model

In quantum mechanics, we can set any set of basis vectors. For the case of a boundary the following set of functions is sufficient

$$\psi_k(n) = \sqrt{\frac{2}{\pi}}\sin(kn), \quad k \in [0,\pi], \quad n \in \mathbb{N}. \tag{12.1}$$

These satisfy

$$\sum_{n=1}^{\infty}\psi_k(n)\psi^\dagger_{k'}(n) = \delta(k-k'), \qquad \int_0^\pi dk\psi^\dagger_k(n)\psi_k(n') = \delta_{n,n'}. \tag{12.2}$$

These are the completeness and the orthogonality relations. After acting with the Hamiltonian $h^{n,n'}_{SC,j} := -\tau_z(t_j\delta_{n',n+1} + t_j\delta_{n',n-1} + \mu\delta_{n',n}) + (\Delta_j e^{i\varphi_j}\tau_+ + \Delta_j e^{-i\varphi_j}\tau_-)\delta_{n',n}$ on these vectors, with help of $\sin x + \sin y = 2\sin\frac{x+y}{2}\cos\frac{x-y}{2}$ one has:

$$\begin{aligned}
\sum_{n'=1}^{\infty} h^{n,n'}_{SC,j}\psi_k(n') &= \sqrt{\frac{2}{\pi}}\sum_{n'=1}^{\infty}\Big[-\tau_z(t_j\delta_{n',n+1} + t_j\delta_{n',n-1} + \mu\delta_{n',n})\sin(kn') + \\
&\qquad + (\Delta_j e^{i\varphi_j}\tau_+ + \Delta_j e^{-i\varphi_j}\tau_-)\delta_{n',n}\sin(kn')\Big] = \\
&= \sqrt{\frac{2}{\pi}}\Big[-\tau_z t_j(\sin(k(n+1)) + \sin(k(n-1))) + \mu\sin(kn) + (\Delta_j e^{i\varphi_j}\tau_+ + \Delta_j e^{-i\varphi_j}\tau_-)\sin(kn)\Big] = \\
&= \sqrt{\frac{2}{\pi}}\Big[-\tau_z t_j\cdot 2\sin(kn)\cos(k) + \mu\sin(kn) + (\Delta_j e^{i\varphi_j}\tau_+ + \Delta_j e^{-i\varphi_j}\tau_-)\sin(kn)\Big] = \\
&= h^j_k\psi_k(n), \qquad\qquad h^j_k := -\tau_z\left(2t_j\cos(k) + \mu\right) + (\Delta_j e^{i\varphi_j}\tau_+ + \Delta_j e^{-i\varphi_j}\tau_-).
\end{aligned}$$

Now, we obtain the expression of the Green's function, that is defined as a solution of

$$zG_{n,n'} - \sum_{n=1}^{\infty} h_{n-n''}G_{n'',n'} = \delta_{n,n'}. \tag{12.3}$$

If we decompose as

$$G_{n,n'} = \int_0^\pi dk\psi_k(n)G_k(n'), \tag{12.4}$$

we will have

$$zG_k(n') - h^j_k G_k(n') = \psi_k(n'), \tag{12.5}$$

$$G_k(n') = \frac{\psi_k(n')}{z - h^j_k}, \tag{12.6}$$

hence

$$G_{n,n'} = \int_0^{\pi} dk \frac{\psi_k(n)\psi_k(n')}{z - h_k^j}. \tag{12.7}$$

This is called Lehmann's representation. This is how the (**??**) was obtained.

12.1.2 Matrix transformations for BCS

Tips for working with matrices in superconductivity

Use Pauli's formula with denominators squared!
(I'll write it later!)

Don't do it by elements of a matrix, it is nonsense!

(write a little example here)

Don't do it by Wolram, it is not working!

(??? why??? but expressions are big and it is a problem. still, it is a question, why he can't compute it???)

Below there is an expression that I tried. (??? why it doesn't work???)

```
A = Inverse[
  z PauliMatrix[0] - (2 t Cos[k] - mu)  PauliMatrix[3] -
   del {{0, Exp[I ph]}, {Exp[-I ph], 0}}]
2/Pi Integrate[Sin[k]^2 A, {k, 0, Pi}]

2/Pi Integrate[
  Sin[k]^2  (-mu + z + 2 t Cos[k])/(-del^2 - mu^2 + z^2 +
    4 mu t Cos[k] - 4 t^2 Cos[k]^2), {k, 0, Pi}]
```

Examples

(I'll add a lot of them here and in the section of problems!)

Derivation of BCS Green's function

12.2 Numerical methods

12.2.1 Typical examples of numerical methods

Numerical Calculation of $\Delta(T)$

[WRITE IT IN WORDS AND GENERAL IDEA, THE EXACTLY CODE IS IN THE SECTION OF PROBLEMS!!!]

Approach 1, by Python

We start from the gap equation and some introduced variables:

$$\eta := \frac{1}{N(0)V}; \quad \eta = \int_0^{\hbar\omega_D} \tanh\frac{\sqrt{\Delta^2+\xi^2}}{2k_BT}\frac{d\xi}{\sqrt{\Delta^2+\xi^2}}; \qquad \Delta_0 \approx 1.76 k_B T_c; \qquad \frac{\hbar\omega_D}{\Delta_0} = \sinh\eta;$$

We transform it as follows:

$$\eta = \int_0^{\hbar\omega_D} \tanh\left(\frac{\Delta_0}{2k_BT_c}\frac{1}{T/T_c}\frac{\Delta}{\Delta_0}\sqrt{1+\xi^2/\Delta^2}\right)\frac{d\xi/\Delta}{\sqrt{1+\xi^2/\Delta^2}}$$
$$\approx \int_0^{\delta^{-1}\sinh\eta} \tanh\left(0.882\frac{\delta}{\tau}\sqrt{1+z^2}\right)\frac{dz}{\sqrt{1+z^2}} \qquad \delta := \Delta(T)/\Delta_0, \qquad \tau := T/T_c$$

here $\hbar\omega_D/\Delta = \Delta_0\hbar\omega_D/(\Delta_0\Delta) = \sinh\eta/\delta$. The number 0.882 is more precise than 1.76/2 for the computer.

The numerical strategy is as follows. We fix δ and find τ, change δ and solve for $\tau, \ldots$ up to obtain $\delta(\tau)$.

```
import numpy as np
import matplotlib.pyplot as plt
from scipy.integrate import quad
from scipy.optimize import fsolve
from matplotlib.ticker import FormatStrFormatter, MultipleLocator

eta = 1 / 0.35

def bcs_gap_equation(d, t):
    integral, _ = quad(lambda z: np.tanh(0.882 * d * np.sqrt(1 + z**2) / t) / np.sqrt(1 +
    z**2), 0, np.sinh(eta) / d)
    return eta - integral

d_vals = np.linspace(0.1, 0.9999, 70)  # don't set zero here, since we are deviding by d.

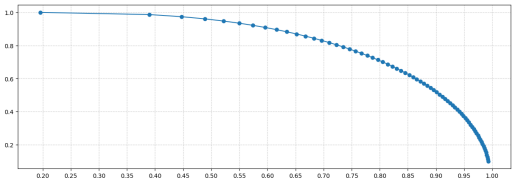
t0 = 0.1
t_vals = [fsolve(lambda t: bcs_gap_equation(d, t), t0)[0] for d in d_vals]

plt.figure(figsize=(15, 5))
plt.plot(t_vals, d_vals, marker='o', linestyle='-')
plt.grid(True, linestyle='--', alpha=0.6)

# Set x-axis grid step to 0.05
plt.gca().xaxis.set_major_locator(MultipleLocator(0.05))

plt.gca().xaxis.set_major_formatter(FormatStrFormatter('%.2f'))
plt.show()
```

We get what we expected:



The disadvantage of this approach is that there are no homogeneous points on temperature axes, only on gap axes. But still, it is fine.

(????) This is simpler than first fixing τ to solve for δ, because of the $1/\delta$ in the boundary, but maybe Im wrong on this point. (??? I'll maybe try later it and write here code for this way)

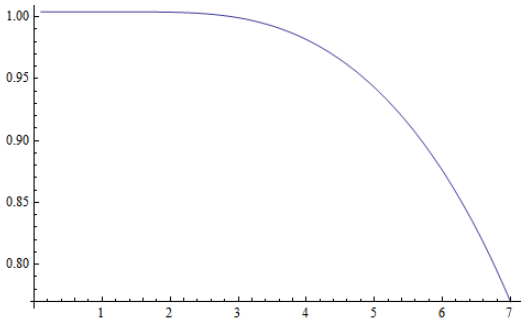
Approach 2, by Wolfram

(????)

```
kb = 1.38 10^(-23);
h = 6.62 10^-34;
hbar = h/2/Pi;
Tc = 9.2;
```

```
Delta0 = 3.528/2*Tc*kb;
omegad = 296*kb/hbar;
Delta[T_]:=
  Block[{a = Log[1.13*hbar*omegad/kb/Tc], b = hbar *omegad/2/kb},
   Return[     FindRoot[     NIntegrate[
         Tanh[b/T*Sqrt[\[Epsilon]^2 + x^2]]/
          Sqrt[\[Epsilon]^2 + x^2], {\[Epsilon], 0, 1},  AccuracyGoal -> 2] - a, {x, 0.01,
    0.1}][[1, 2]]*hbar* omegad]];
Plot[Delta[x]/Delta0, {x, 0.1, 7}]
```

We get what we expected:



(??? there are warnings and the T axes is not normalized. so maybe it is a bad code, but still, it can teach us about using wolfram for superconductivity, so I'll keep it for now.)

13 Bogliubov-de Gennes Equations: Methods and Applications by Jian-Xin Zhu

13.1 3 Local Electronic Structure Around a Single Impurity in Superconductors

Abstract

In this chapter, I am going to discuss the local electronic structure around a single impurity. Both the nonmagnetic and magnetic impurity scattering in conventional s-wave and unconventional d-wave superconductors will be considered. The local electron density of states and the existence of impurity bound or virtual bound states will be explored. The possible realization of Majorana zero-energy modes is discussed for the case of electrons coupled to a spin chain in an s-wave superconductor. These results have a direct relevance to the STM measurements. The results will also be compared with the T-matrix method.

13.1.1 3.1 Introduction

The local electronic structure around a single impurity in a superconductor can provide unique information about the superconducting pairing symmetry [1]. The obtained local density of states can be directly measured by the scanning tunneling microscopy (STM) nowadays. The STM technique has made a significant stride in understanding the pairing symmetry of unconventional superconductors. Theoretically, the study of local electronic structure around a single impurity is also a very important step toward understanding the disorder effect on the bulk superconductivity. The impurity scattering can be either static, which we usually treat as the potential scattering, or dynamic like magnetic impurity or electronic scattering off a local vibrational mode, both of which has internal degrees of freedom. The dynamic scatters cause the inelastic scattering effect of electrons. Here we limit the discussions on the elastic scattering off potential scatters and without loss of generality, consider two-dimensional superconductors, which are described by a tight-binding model on a square lattice.

13.1.2 3.2 Yu-Shiba-Rusinov Impurity States in an s-Wave Superconductor

The condition for the existence of bound state and the spatial oscillations of order parameter and electron density was first studied by Fetter [2] around a spherical impurity in an s-wave superconductor. The existence of bound states due
to resonance scattering in an s-wave superconductor was also considered in an Anderson impurity model by Machida and Shibata [3], Shiba [4], and Machida [5]. For these cases of nonmagnetic impurity scattering, because the product of the bulk superconducting order parameter and the density of states at the Fermi energy is too small (of the order of 10^{-3}), the bound state energy is essentially located near the gap edge. However, the situation becomes very different in the presence of a single magnetic impurity. The quasiparticle scattering off a classical spin was first studied by Yu [6], Shiba [7], and Rusinov [8, 9], who predicted the existence of in-gap bound states, with the energy depending on the exchange coupling between the classical spin and conduction electrons.

The Hamiltonian for an s-wave superconductor with a single-site impurity can be written as

$$\mathscr{H} = \sum_{ij,\sigma} \left[-t_{ij} - \mu\delta_{ij}\right] c^{\dagger}_{i\sigma} c_{j\sigma} + \sum_{i} \left[\Delta_i c^{\dagger}_{i\uparrow} c^{\dagger}_{j\downarrow} + \text{ H.c. } \right] + \sum_{\sigma} \left(\epsilon_I + J\sigma\right) c^{\dagger}_{0\sigma} c_{0\sigma}. \tag{3.1}$$

In principle, as we discussed in earlier chapters, the pair potential Δ_i should be determined self-consistently. However, at this moment, we neglect this selfconsistency and approximate this pair potential by that for the pristine system. As such,

$$\begin{aligned} \mathscr{H}_0 &= \sum_{ij,\sigma} \left[-t_{ij} - \mu\delta_{ij}\right] c^{\dagger}_{i\sigma} c_{j\sigma} + \sum_{i} \left[\Delta_i c^{\dagger}_{i\uparrow} c^{\dagger}_{j\downarrow} + \text{ H.c. } \right] \\ &= \sum_{\mathbf{k}\sigma} \xi_{\mathbf{k}} c^{\dagger}_{\mathbf{k}\sigma} c_{\mathbf{k}\sigma} + \Delta_s \sum_{\mathbf{k}} \left[c^{\dagger}_{\mathbf{k}\uparrow} c^{\dagger}_{-\mathbf{k}\downarrow} + \text{ H.c. } \right] \end{aligned} \tag{3.2}$$

and

$$\mathscr{H}_{imp} = \sum_{\sigma} \left(\epsilon_I + J\sigma\right) c^{\dagger}_{0\sigma} c_{0\sigma} \tag{3.3}$$

Here ϵ_I and J are the strength of the nonmagnetic and ferromagnetic impurity scattering, respectively. Figure 3.1 shows the relative strength of potential in spin up and down channels. In this case, it is particularly convenient to solve the problem in the T-matrix method. By following procedure given in the previous chapter, the

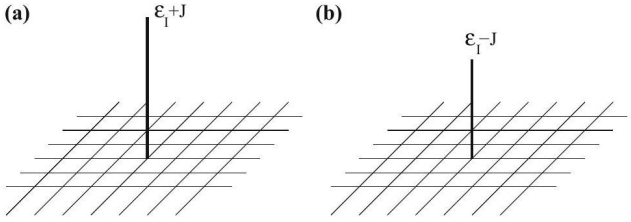


Fig. 3.1 Relative strength of the impurity potential in spin up (a) and spin down (b) channels

Abrikosov-Gorkov equations of motion for the Green's function corresponding to the Hamiltonian equation (3.1) is found to be:

$$\sum_{j'}\left[i\omega_n\delta_{ij'}\hat{\sigma}_0-\hat{h}_{ij'}\right]\mathscr{G}\left(j',j;i\omega_n\right)=\delta_{ij}\hat{\sigma}_0+\hat{V}_{imp}\delta_{i0}\mathscr{G}\left(0,j;i\omega_n\right), \tag{3.4}$$

Because of the non-spin-flip scattering considered here, the Green's function has been redefined from Eq. (2.155) as

$$\mathscr{G}(i,j;\tau)=\begin{pmatrix} -\left\langle T_\tau\left(c_{i\uparrow}(\tau)c_{j\uparrow}^\dagger\right)\right\rangle & -\left\langle T_\tau\left(c_{i\uparrow}(\tau)c_{j\downarrow}\right)\right\rangle \\ -\left\langle T_\tau\left(c_{i\downarrow}^\dagger(\tau)c_{i\uparrow}^\dagger\right)\right\rangle & -\left\langle T_\tau\left(c_{i\downarrow}^\dagger(\tau)c_{j\downarrow}\right)\right\rangle \end{pmatrix}, \tag{3.5}$$

which is a 2×2 matrix in the Nambu space. In Eq. (3.4), the impurity scattering matrix is written as

$$\hat{V}_{imp}=\epsilon_I\hat{\sigma}_3+J\hat{\sigma}_0 \tag{3.6}$$

with the identify matrix

$$\hat{\sigma}_0=\begin{pmatrix}1&0\\0&1\end{pmatrix}, \tag{3.7}$$

and the third component of the Pauli matrix

$$\hat{\sigma}_3=\begin{pmatrix}1&0\\0&-1\end{pmatrix}. \tag{3.8}$$

The single particle Hamiltonian is also a 2×2 matrix

$$\hat{h}_{ij}=\begin{pmatrix}-t_{ij}-\mu\delta_{ij} & \Delta_s\\ \Delta_s & t_{ij}+\mu\delta_{ij}\end{pmatrix}. \tag{3.9}$$

On the other hand, we can also have the Abrikosov-Gorkov equations of motion for the Green's function corresponding to the Hamiltonian equation (3.2):

$$\sum_{j'}\left[i\omega_n\delta_{ij'}\hat{\sigma}_0-\hat{h}_{ij'}\right]G_0\left(j',j;i\omega_n\right)=\delta_{ij}\hat{\sigma}_0, \tag{3.10}$$

where $\mathscr{G}_0\left(i,j';i\omega_n\right)$ is the Fourier transform of

$$\mathscr{G}_0(i,j;\tau)=\begin{pmatrix} -\left\langle T_\tau\left(c_{i\uparrow}(\tau)c_{j\uparrow}^\dagger\right)\right\rangle_0 & -\left\langle T_\tau\left(c_{i\uparrow}(\tau)c_{j\downarrow}\right)\right\rangle_0 \\ -\left\langle T_\tau\left(c_{i\downarrow}^\dagger(\tau)c_{i\uparrow}^\dagger\right)\right\rangle_0 & -\left\langle T_\tau\left(c_{i\downarrow}^\dagger(\tau)c_{j\downarrow}\right)\right\rangle_0 \end{pmatrix}, \tag{3.11}$$

with subscript " 0 " for the statistical average and Heisenberg field operator $c_{i\sigma}(\tau)$ with respect to Eq. (3.2). Since the Hamiltonian equation (3.2) holds the spatial translational invariance, we can find

$$\mathscr{G}_0\left(i,j;i\omega_n\right)=\frac{1}{N_L}\sum_{\mathbf{k}}\mathscr{G}_0\left(\mathbf{k};i\omega_n\right)e^{i\mathbf{k}\cdot\left(\mathbf{r}_i-\mathbf{r}_j\right)} \tag{3.12}$$

with

$$\begin{aligned}\mathscr{G}_0\left(\mathbf{k};i\omega_n\right)&=\begin{bmatrix} i\omega_n-\xi_{\mathbf{k}} & -\Delta_s\\ -\Delta_s & i\omega_n+\xi_{\mathbf{k}}\end{bmatrix}^{-1}\\ &=\frac{1}{\left(i\omega_n-\xi_{\mathbf{k}}\right)\left(i\omega_n+\xi_{\mathbf{k}}\right)-\Delta_s^2}\begin{pmatrix} i\omega_n+\xi_{\mathbf{k}} & \Delta_s\\ \Delta_s & i\omega_n-\xi_{\mathbf{k}}\end{pmatrix}.\end{aligned} \tag{3.13}$$

In a tight-binding model up to the next-nearest-neighbor hopping, the single particle energy dispersion is given by Eq. (2.127) and

$$\xi_{\mathbf{k}} = \epsilon_{\mathbf{k}} - \mu \tag{3.14}$$

The wave vector in the square lattice is given by $\mathbf{k} = k_x \mathbf{e}_x + k_y \mathbf{e}_y$ with $k_{x,y} = \frac{2\pi}{N_L} n_{x,y}$ and $n_{x,y}$ running from $-N_{x,y}/2$ to $N_{x,y}/2 - 1$, the lattice vector in the direct space is given by $\mathbf{r}_i = i_x a \mathbf{e}_x + i_y a \mathbf{e}_y$ with the integers $i_{x,y}$ running from $-N_{x,y}/2$ to $N_{x,y}/2 - 1$. The unit vectors $\mathbf{e}_{x,y}$ are along the bond direction of the square lattice and the $N_L = N_x N_y$.

From Eqs. (3.4) and (3.10), we can obtain the recursion relation:

$$\begin{aligned} \mathscr{G}(i,j;i\omega_n) &= \mathscr{G}_0(i,j;i\omega_n) + \sum_{j'} \mathscr{G}_0(i,j';i\omega_n) \hat{V}_{imp} \delta_{j'0} \mathscr{G}(j',j;i\omega_n) \\ &= \mathscr{G}_0(i,j;i\omega_n) + \mathscr{G}_0(i,0;i\omega_n) \hat{V}_{imp} \mathscr{G}(0,j;i\omega_n) . \end{aligned} \tag{3.15}$$

From Eq. (3.15), we can evaluate the Green's function with site i at the impurity site

$$\mathscr{G}(0,j;i\omega_n) = \mathscr{G}_0(0,j;i\omega_n) + \mathscr{G}_0(0,0;i\omega_n) \hat{V}_{imp} \mathscr{G}(0,j;i\omega_n) , \tag{3.16}$$

which leads to

$$\mathscr{G}(0,j;i\omega_n) = \left[\hat{\sigma}_0 - \mathscr{G}_0(0,0;i\omega_n) \hat{V}_{imp}\right] \mathscr{G}_0(0,j;i\omega_n) . \tag{3.17}$$

We then substitute Eq. (3.17) into Eq. (3.15) and arrive at

$$\mathscr{G}(i,j;i\omega_n) = \mathscr{G}_0(i,j;i\omega_n) + \mathscr{G}_0(i,0;i\omega_n) \hat{T}_{imp}(i\omega_n) \mathscr{G}_0(0,j;i\omega_n) , \tag{3.18}$$

where the T-matrix is given by

$$\hat{T}_{imp}^{-1}(i\omega_n) = \left[\hat{V}_{imp}^{-1} - \mathscr{G}_0(0,0;i\omega_n)\right]^{-1} . \tag{3.19}$$

With the matrix $\hat{V}_{imp}$ given by Eq. (3.6), we can determine the T-matrix to be

$$\hat{T}_{imp}(i\omega_n) = \frac{1}{\Pi(i\omega_n)} \begin{pmatrix} \frac{1}{-\epsilon_I + J} - \mathscr{G}_{22}^0(i\omega_n) & \mathscr{G}_{12}^0(i\omega_n) \\ \mathscr{G}_{21}^0(i\omega_n) & \frac{1}{\epsilon_I + J} - \mathscr{G}_{11}^0(i\omega_n) \end{pmatrix} , \tag{3.20}$$

where

$$\Pi(i\omega_n) = \left(\frac{1}{\epsilon_I + J} - \mathscr{G}_{11}^0(i\omega_n)\right)\left(\frac{1}{-\epsilon_I + J} - \mathscr{G}_{22}^0(i\omega_n)\right) - \mathscr{G}_{12}^0(i\omega_n)\mathscr{G}_{21}^0(i\omega_n) . \tag{3.21}$$

Here we have abbreviated the Green's function $\mathscr{G}_0(0,0;i\omega_n)$ as $\mathscr{G}^0(i\omega_n)$. The pole of the T-matrix with

$$\Pi(i\omega_n \to \omega_c) = 0 \tag{3.22}$$

determines a true or virtual bound state induced by the impurity scattering. Physically, the most direct measure of the possible existence of this kind of states is through the calculation of local density of states (LDOS):

$$\begin{aligned} \rho_i(E) &= \rho_{i\uparrow}(E) + \rho_{i\downarrow}(E) \\ &= -\frac{1}{\pi} \mathrm{Im}\left[\mathscr{G}_{11}\left(i,i;i\omega_n \to E + i0^+\right) - \mathscr{G}_{22}\left(i,i;-i\omega_n \to -\left(E + i0^+\right)\right)\right] \end{aligned} \tag{3.23}$$

which follows from the discussion in Chap. 2.
In Fig. 3.2, we show the energy dependence of LDOS around a single zero-ranged potential scatter in an s-wave superconductor defined on a two-dimensional lattice. The results are obtained within the T-matrix theory, where the self-consistency on the superconducting pair potential is neglected. The lattice is described by a tight-binding model with the hopping parameter included up to the next-nearestneighbors. As is shown, the shape of LDOS for the nonmagnetic impurity remains similar to that for the pristine case (i.e., no impurity scattering). Its intensity on the impurity site (see Fig. 3.2a) suppressed significantly while the LDOS intensity on the nearest-neighboring site to the impurity shows almost no change compared to the pristine case. However, in the presence of a ferromagnetic potential scatter, in-gap quasiparticle states are induced. They are revealed as peaks in the LDOS inside the superconducting gap (see Fig. 3.2b). The location of these in-gap states is dependent on the exchange coupling strength. It first moves toward the Fermi energy with the increased coupling strength and then crosses the Fermi energy when the coupling

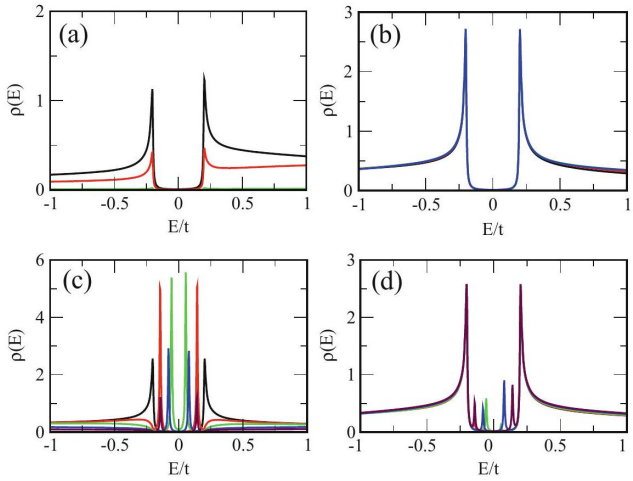


Fig. 3.2 Local density of states around a zero-ranged nonmagnetic ((a)-(b)) and magnetic ((c)(d)) potential scatter in an s-wave superconductor defined on a two-dimensional square lattice. The left column is for the LDOS calculated at the impurity site while the right column is for the LDOS calculated at a site nearest-neighboring to the impurity site. For the nonmagnetic potential scatter $((\mathbf{a})-(\mathbf{b}))$, we take $\varepsilon_I = 1t$ (black), $2t$ (red), $10t$ (green), and 100t (blue) with J fixed at 0 . For the magnetic potential scatter $((\mathbf{c})-(\mathbf{d}))$, we take $J = 0.01$ (black), $0.5t$ (red), $1t$ (green), $2t$ (blue), and $3t$ (maroon) with ε_I fixed at 0 . Here we have used a tight-binding model up to next-nearest neighbor hopping with $t' = -0.2t$ and $\mu = -0.8t$. The pair potential is taken as $\Delta_0 = 0.2t$. The broadening parameter is $\gamma = 0.005t$

strength is further increased. In addition, the spectral weight of the particle and hole in-gap states on the impurity site is nearly symmetric while noticeably asymmetric on the nearest-neighboring sites.

As we have shown above, the T-matrix theory is quite convenient for the study of local quasiparticle properties around a single-site impurity in a uniform background of superconducting order parameter. Rigorously, the superconducting order parameter can be modified near the impurity. In this case, one needs to solve the BdG equations self-consistently. Since a single-site impurity breaks the transitional invariance in space, a very large system size should be considered at a first glance, which presents the computational challenge for diagonalization of the system Hamiltonian. In practice, since the superconducting order parameter around a single impurity varies at a length scale of the superconducting coherence

length ξ, which is inversely proportional to the superconducting energy gap, we can consider a finite area around the impurity. However, this is not generically true for the quasiparticle states, which can be extended into a region further away from the impurity site. To accommo-

date these conditions, one can use a supercell technique. We now consider the single impurity problem as an example of how to use the technique. Consider the supercell containing a single impurity located at the center on a two-dimensional lattice. The cell size is $N_x \times N_y$. Therefore, the entire system now consists of a repeated stacking of these supercells. When the supercell size is sufficiently large that the quasiparticle states induced by the single impurity do not overlap between two nearest-neighboring supercells, the physics from this superlattice should mimick the problem of a single impurity in an otherwise pristine system. For the superlattice, we can apply Bloch theorem to write the BdG wavefunction as

$$\begin{cases} u_{i\sigma} = \frac{1}{\sqrt{M}} \bar{u}_{\tilde{i}\sigma} e^{i\mathbf{K}\cdot\left(\mathbf{R}+\mathbf{r}_{\tilde{i}}\right)}, \\ v_{i\sigma} = \frac{1}{\sqrt{M}} \bar{v}_{i\sigma} e^{i\mathbf{K}\cdot\left(\mathbf{R}+\mathbf{r}_{\tilde{i}}\right)}, \end{cases} \tag{3.24}$$

Here $M = M_x \times M_y$ with $M_x N_x$ and $M_y N_y$ the linear dimension of the entire system. The symbol $\tilde{i}$ labels the sites in a given unit cell. The Bravais lattice $\mathbf{R} = I_x N_x \mathbf{e}_x + I_y N_y \mathbf{e}_y$ with $I_{x(y)}$ integers and $\mathbf{e}_{x(y)}$ unit vectors along the x and y-bond directions. To simplify the discussion, we have taken the unit length $a = 1$. Subjecting the above Block wave function to the periodic boundary condition leads to the wave vectors corresponding to the supercell

$$\mathbf{K} = K_x \mathbf{e}_x + K_y \mathbf{e}_y, \tag{3.25}$$

where $K_x = 2\pi n_x / M_x N_x$ and $K_y = 2\pi n_y / M_y N_y$ with $n_x = -M_x/2, -M_x/2+1, \ldots, M_x/2-2, M_x/2-1$ and $n_y = -M_y/2, -M_y/2+1, \ldots, M_y/2-2, M_y/2-1$ for M_x and M_y even integers. Upon substitution of Eq. (3.24) into Eq. (2.44), we obtain the BdG equations in a tight-binding model with hopping integrals up to the next-nearest neighbors:

$$E_n(\mathbf{K}) u^n_{\tilde{i}\uparrow}(\mathbf{K}) = \sum_{\delta} \tilde{h}_{\tilde{i}\uparrow, i+\delta\uparrow} e^{i\mathbf{K}\cdot\mathbf{r}_\delta} u^n_{i+\delta\uparrow}(\mathbf{K}) + \Delta_{\tilde{i}\tilde{i}} v^n_{\tilde{i}\downarrow}(\mathbf{K}), \tag{3.26}$$

$$E_n(\mathbf{K}) v^n_{\tilde{i}\downarrow}(\mathbf{K}) = -\sum_{\delta} \tilde{h}^*_{\tilde{i}\downarrow, i+\delta\downarrow} e^{i\mathbf{K}\cdot\mathbf{r}_\delta} v^n_{i+\delta\uparrow}(\mathbf{K}) + \Delta^*_{\tilde{i}\tilde{i}\uparrow} u^n_{\tilde{i}}(\mathbf{K}), \tag{3.27}$$

subject to the self-consistency condition:

$$\Delta_{\tilde{i}\tilde{i}} = \frac{U}{2M} \sum_{\mathbf{K},n} u^n_{i\uparrow}(\mathbf{K}) v^{n*}_{\tilde{i}\downarrow}(\mathbf{K}) \tanh\left(\frac{E_n(\mathbf{K})}{2k_B T}\right) \tag{3.28}$$

Once the self-consistent solution is obtained, the local density of states in a given supercell is then evaluated according to

$$\rho_{\tilde{i}}(E) = \frac{1}{M} \sum_{\mathbf{K},n} \left[\left| u^n_{i\uparrow}(\mathbf{K}) \right|^2 \delta\left(E - E_n(\mathbf{K})\right) + \left| v^n_{\tilde{i}\downarrow}(\mathbf{K}) \right|^2 \delta\left(E + E_n(\mathbf{K})\right] . \right) \tag{3.29}$$

Figure 3.3 shows the self-consistent solution of a single impurity in an s-wave superconductor. As we can see, in the presence of a unitary non-magnetic impurity, the superconducting order parameter is indeed strongly suppressed at the impurity site. However, no impurity bound states exist. Instead, in the presence of a ferromagnetic impurity, the superconducting order parameter is suppressed even with an intermediate exchange coupling. In this case, the quasiparticle peaks with energies inside the gap are exhibited in the local density of states. The results are qualitatively consistent with those obtained within the T-matrix theory, suggesting the in-gap states are of Yu-Shiba-Rusinov origin. Therefore, this example demonstrates that

the

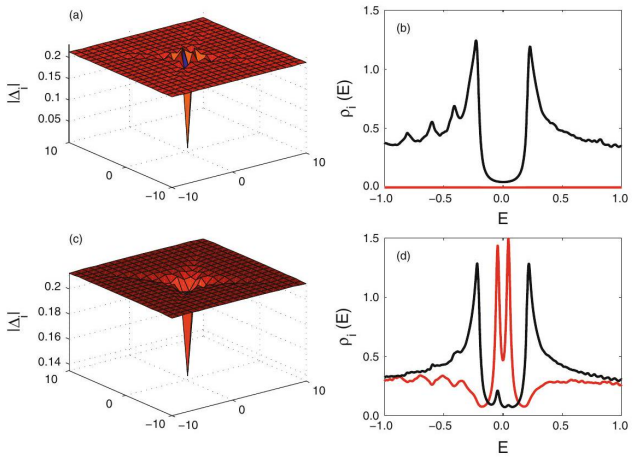


Fig. 3.3 Self-consistent solution to a single impurity in an s-wave superconductor. The top row displays the results of the spatial variation of the superconducting order parameter and the local density of states for a nonmagnetic impurity. The bottom row displays those for a ferromagnetic impurity. For the local density of states, only the results on the impurity site (red line) and on the site nearest neighbor to the impurity site (black line) are plotted. The calculations are carried out for an s-wave superconductor defined on a two-dimensional square lattice. The pairing interaction is taken to be $U = 1.5t$ and the temperature $T = 0.01t$. The supercell size has the dimension of 21 by 21 . The nonmagnetic impurity potential strength $\epsilon_I = 100t$ while the ferromagnetic impurity potential $J = 1t$. Here we have used a tight-binding model up to next-nearest neighbor hopping with $t' = -0.2t$ and $\mu = -0.8t$. The broadening parameter is $\gamma = 0.01t$
fully self-consistent BdG approach can provide more insight into the local electronic structure of a superconductor.

13.1.3 3.3 Majorana Fermion in an s-Wave SC with a Chain of Localized Spins

As we know, the conventional fermions come with a pair of the creation and annihilation operators, $\left(c^\dagger, c\right)$, satisfying the Fermi-Dirac anti-commutation relations $\left\{c, c^\dagger\right\} = 1$. The operators c and $c^\dagger$ are not self-adjoint but they are the adjoint of each other. In contrast to these complex fermions, Majorana fermions are real-valued fermions, that is, they are their own anti-particles and self-adjoint with the property of $c^\dagger = c$. Although these particles may or may not exist in nature as elementary particles, there is intensive interest in their realization in solid state systems [10-13]. In particular, it is proposed that the Majorana fermions can perform better than the complex fermions in keeping the quantum coherence and are proposed as basic building units for quantum computation [14]. For the realization of Majorana fermions in superconductors, a natural strategy is to use the zero-energy or midgap Bogoliubov excitation modes. This observation follows from the particlehole symmetry of Bogoliubov quasiparticles as evident from the BdG equations: The quasiparticle operators $\gamma(E)$ and $\gamma^\dagger(E)$ are related by

$$\gamma(E) = \gamma^\dagger(-E). \tag{3.30}$$

When the quasiparticle excitation energy is zero, we obtain $\gamma = \gamma^\dagger$, suggesting that the particle is its own antiparticle. The search of midgap excitations with the character of Majorana fermions has been made in chiral p-wave superconductors in early years [15, 16] and more recently revived with new proposals [17]. A specific system of interest is that a chain of magnetic atoms on surface of a conventional s-wave superconductor. It has been shown [18-20] that when

the magnetic atoms in the chain form a spiral with the correct pitch, the Yu-Shiba-Rusinov states discussed in previous section can give rise to an effective one-dimensional topological superconductor with Majorana fermions bound to its ends. A schematic setup is shown in Fig. 3.4. The model Hamiltonian is given by

$$\begin{aligned}\mathscr{H} = &\sum_{ij\sigma} \left(-t_{ij} - \delta_{ij}\mu\right) c^\dagger_{i\sigma} c_{j\sigma} + J \sum_{i\in I} \mathbf{S}_i \cdot \left(c^\dagger_{i\sigma} \sigma_{\sigma\sigma'} c_{i\sigma'}\right) \\ &+ \sum_i \left[\Delta_i c^\dagger_{i\uparrow} c^\dagger_{i\downarrow} + \text{ H.c. }\right]. \end{aligned} \tag{3.31}$$

Here the s-wave superconducting pair potential is defined in the BCS mean-field approximation

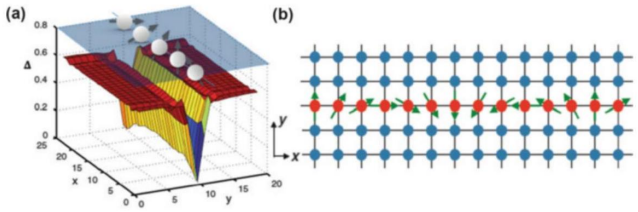


Fig. 3.4 (a) Schematic picture of a chain of magnetic impurities adsorbed on the surface of an s-wave superconductor. Suppression of the superconducting order parameter Δ_i from the selfconsistent BdG solution is also shown. (b) The tight-binding lattice with a row of magnetic atoms. From [21]

$$\Delta_i = U \left\langle c_{i\uparrow} c_{i\downarrow} \right\rangle \tag{3.32}$$

where U is an effective pairing interaction. The third term in the Hamiltonian describes the exchange coupling with strength J of a chain of magnetic spins with the superconducting electrons. We consider a two-dimensional lattice of the dimension $N_L = N_x \times N_y$ for the s-wave superconductor, which lies in the xy plane, and choose the chain of the magnetic atoms aligned along the x-direction. For the case that the magnetic moments form a coplanar spiral at wave vector G, the classical spin can be written as

$$\mathbf{S}_i = S\left(\cos Gx_i, -\sin Gx_i, 0\right) \tag{3.33}$$

where (x_i, y_i) are the coordinate of site i. It represents the spin rotating in the $x-y$ plane. With a periodic condition along the x-direction, it is convenient to perform a spin-dependent gauge transformation to superconducting electron operators:

$$c_{i\sigma} \to c_{i\sigma} = \tilde{c}_{i\sigma} \exp\left[\frac{i}{2}\sigma G x_i\right], \tag{3.34}$$

which effectively aligns the local spin quantization axis for the conduction electrons along the classical spin $\mathbf{S}_i$ and leads to the Hamiltonian

$$\begin{aligned}\mathscr{H} = &\sum_{ij\sigma} \left(-t_{ij} e^{-\frac{i}{2}\sigma G(x_i - x_j)} - \delta_{ij}\mu\right) \tilde{c}^\dagger_{i\sigma} \tilde{c}_{j\sigma} + JS \sum_{i\in I} \tilde{c}^\dagger_{i\sigma} \sigma^x_{\sigma\sigma'} \tilde{c}_{i\sigma'} \Bigg) \\ &+ \sum_i \left[\Delta_i \tilde{c}^\dagger_{i\uparrow} \tilde{c}^\dagger_{i\downarrow} + \text{ H.c. }\right] - \frac{1}{U} \sum_i |\Delta_i|^2 . \end{aligned} \tag{3.35}$$

In the spin reference frame with spin quantized along the x-direction, the effective hopping term becomes spin-dependent $-t_{ij} e^{-\frac{i}{2}\sigma G(x_i - x_j)}$ and can be interpreted as the

hopping with an effective spin-orbit coupling; while the last term in the first line of the above Hamiltonian represents a uniform Zeeman field of the strength JS.

In the one-dimensional limit $N_y = 1$, the entire system is translationally invariant and the pair potential Δ is a constant. We can perform a canonical transformation

$$\tilde{c}_{i\sigma} = \frac{1}{\sqrt{N_L}} \sum_k \tilde{c}_{k\sigma} e^{ikx_i} \tag{3.36}$$

into the Block representation, where k is the wave vector in the first Brillouin zone of the one-dimensional system. The Hamiltonian is then found as

$$\begin{aligned} \mathscr{H} = & \sum_{k\sigma} \xi_{k\sigma} \tilde{c}^\dagger_{k\sigma} \tilde{c}_{k\sigma} + JS \sum_{k\sigma\sigma'} \tilde{c}^\dagger_{k\sigma} \sigma^x_{\sigma\sigma'} \tilde{c}_{k\sigma'} \\ & + \sum_k \left[\Delta \tilde{c}^\dagger_{k\uparrow} \tilde{c}^\dagger_{-k\downarrow} + \text{ H.c. } \right] - \frac{N_x}{U} \Delta^2 \end{aligned} \tag{3.37}$$

where the spin-dependent energy dispersion in nearest-neighbor hopping model is given by

$$\xi_{k\sigma} = -2t \cos[(k + \sigma G/2)a] - \mu \tag{3.38}$$

with a being the lattice constant. In the normal state ($\Delta = 0$), the single-particle energy dispersion of the system becomes

$$E_k = \xi_{k,+} \pm \sqrt{\xi_{k,-} + J^2 S^2} \tag{3.39}$$

where

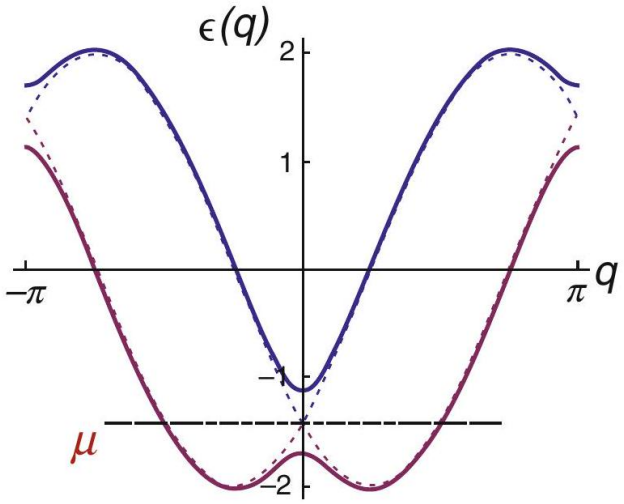
$$\xi_{k,\pm} = \frac{1}{2} \left[\xi_{k\uparrow} \pm \xi_{k\downarrow} \right] \tag{3.40}$$

For $k = 0, \pi$ so that $\xi_{k,-} = 0$, the quasiparticle has an excitation gap of JS, as shown in Fig. 3.5. It implies that when the chemical potential lies inside the gap by satisfying the condition

$$|\mu + 2t \cos(Ga/2)| \leq JS, \tag{3.41}$$

there exists a single non-degenerate Fermi point in the right half of the Brillouin zone. The Kitaev criterion [22] then tells that the system is a one-dimensional topological superconductor upon turning on the small superconducting pair potential ($\Delta \neq 0$). It turns out [23-25] that in the one-dimensional system, for an optimized spin spiral pitch G, which minimizes the ground-state energy, the condition Eq. (3.41) is always satisfied.

Fig. 3.5 Normal-state energy dispersion in the one-dimensional electron system coupled to the one-dimensional spin chain. From [21]



For the two-dimensional superconductor, the translation invariance is broken along the y-direction, that is, perpendicular to the spin chain, we can only rely on the numerical simulations to solve the BdG equations

$$\sum_j \tilde{H}_{ij}\Psi_j^n = E_n\Psi_i^n \tag{3.42}$$

where the matrix

$$\tilde{H}_{ij} = \begin{bmatrix} \tilde{h}_{i\uparrow,j\uparrow} & \tilde{h}_{i\uparrow,j\downarrow} & 0 & \delta_{ij}\Delta_i \\ \tilde{h}_{i\downarrow,j\uparrow} & \tilde{h}_{i\downarrow,j\downarrow} & \delta_{ij}\Delta_i & 0 \\ 0 & \delta_{ij}\Delta_i^* & -\tilde{h}^*_{i\uparrow,j\uparrow} & \tilde{h}^*_{i\uparrow,j\downarrow} \\ \delta_{ij}\Delta_i^* & 0 & \tilde{h}^*_{i\downarrow,j\uparrow} & -\tilde{h}^*_{i\downarrow,j\downarrow} \end{bmatrix}, \tag{3.43}$$

and the eigenvector $\Psi_i^n = \left(u_{i\uparrow}^n, u_{i\downarrow}^n, v_{i\uparrow}^n, v_{i\downarrow}^n\right)^{\text{Transpose}}$. Here the matrix normal-state single-particle Hamiltonian matrix is given by

$$\tilde{h}_{ij} = \begin{pmatrix} -t_{ij}e^{-\frac{i}{2}G(x_i-x_j)} - \delta_{ij}\mu & JS\delta_{ij} \\ JS\delta_{ij} & -t_{ij}e^{\frac{i}{2}G(x_i-x_j)} - \delta_{ij}\mu \end{pmatrix}. \tag{3.44}$$

For the bulk system, the closed boundary condition is applicable and the system is still translationally invariant along the x-direction, which allows us to introduce a mixed representation through the transformation

$$\Psi_i^n = \frac{1}{\sqrt{N_x}}\sum_{k_x}\Psi_{i_y}^{\tilde{n}}\left(k_x\right)e^{ik_x i_x a} \tag{3.45}$$

The BdG equations can be block-diagonalized as
with

$$\begin{aligned}&\tilde{h}_{i,j,j_y}\left(k_x\right)\\ &= \begin{pmatrix} -t_{i,j_y} + \left(-2t\cos\left[\left(k_x + G/2\right)a\right] - \mu\right)\delta_{i,j_y} & JS\delta_{i,j_y} \\ JS\delta_{i,j_y} & -t_{i,j_y} + \left(-2t\cos\left[\left(k_x - G/2\right)a\right] - \mu\right)\delta_{i,j_y} \end{pmatrix}.\end{aligned} \tag{3.47}$$

With the aid of these eigensolutions, the ground-state energy can be calculated as a function of the free-parameter G, that is $E_g(G)$, for a given chemical potential, from which the spin spiral pitch G^* can be determined. The typical results are shown in Fig. 3.6 [21]. The strong

suppression of the s-wave superconducting order parameter

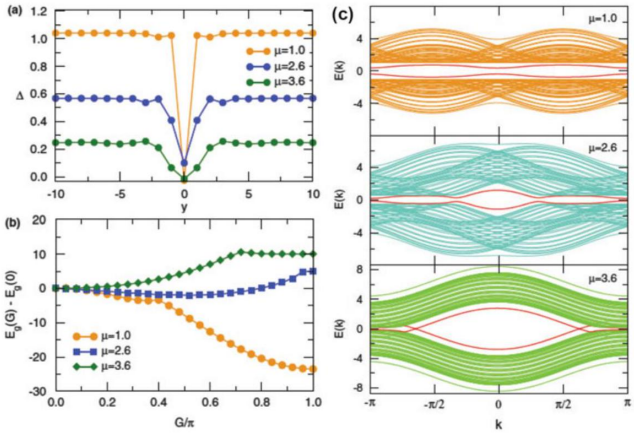


Fig. 3.6 Spatial variation of the superconducting order parameter Δ_{i_y} obtained through the selfconsistent solution to the BdG equations (3.42) (a), the dependence of the ground-state energy on the spiral pitch (b), and band structure on the longitudinal wave vector k_x (c) for various values of the chemical potential $\mu = 1.0, 2.6, 3.6$. The system size is taken to be $N_L = N_x \times N_y = 100 \times 20$. The other parameter values are chosen as $U = 3.6, JS = 2$. The energies are measured in units of nearest neighbor hopping parameter $t = 1$. From [21]
(see Fig. 3.6a) is seen along the spin chain. This superconducting potential quantum well can trap low-energy quasiparticle states. For the chosen chemical potential values, the optimized spiral pitch G_* has the values of $\pi, 0$ and in between (see Fig. 3.6c), corresponding to the antiferromagnetic, ferromagnetic, and topological spiral phases. In all these phases, distinctive Shiba states are obtained (see Fig. 3.6c). These are described by the effective one-dimensional model and the Majorana zeroenergy edge modes can be induced in the system with open boundaries (i.e., at the both ends of the spin chain).

13.1.4 3.4 Impurity Resonance State in a d-Wave Superconductor

The d-wave pairing symmetry, especially, $d_{x^2-y^2}$-wave pairing symmetry, has been observed in high-temperature cuprate superconductors [26, 27]. As we have discussed above, the s-wave superconductivity is not so sensitive to non-magnetic impurity potential scattering, by showing no existence of in-gap states. However, for a d-wave pairing symmetry, the local electronic structure can be quite distinct in the immediate vicinity of an isolated non magnetic impurity [28-40]. It has been theoretically predicted by Balatsky, Salkola and co-workers [31, 32] that, in a d-wave superconductor, a single nonmagnetic impurity can generate quasiparticle resonance states at subgap energies. This prediction has been confirmed by scanning tunneling microscopy experiments [41].

To demonstrate this local properties, we can again employ the T-matrix theory as explained in Sect. 4.2 except that the pair potential is now of the form

$$\Delta_{\mathbf{k}} = \frac{\Delta_0}{2} (\cos k_x - \cos k_y) \tag{3.48}$$

defined in a tight-binding model for a square lattice.
In Fig. 3.7, we show the energy dependence of LDOS around a single zero-ranged potential scatter in a $d_{x^2-y^2}$-wave superconductor defined on a two-dimensional lattice. The results are obtained within the T-matrix theory, where the self-consistency on the superconducting pair potential is neglected. The lattice is described by a tight-binding model with the hopping parameter included up to the next-nearestneighbors. As is shown, the shape of LDOS for the nonmagnetic impurity can change dramatically with the strength of the scattering potential. In particular, due to the locally breaking of the particle-hole symmetry of the electronic states,

the spectral weight for the electron and hole component of quasiparticle resonance peaks is biased. For the repulsive potential scatter, the LDOS resonance state has a dominant hole component on the impurity site (see Fig. 3.7a) while a dominant electron component on the nearest-neighboring site to the impurity (see Fig.3.7b). In contrast, for the attractive potential scatter, the LDOS resonance has a dominant electron component on the impurity site (Fig. 3.7c) but a dominant hole contribution on the nearest-neighboring sites (Fig. 3.7d).

To take into account the full self-consistency of the superconducting order parameter, we use the supercell technique as discussed in Sect.4.2. Now for

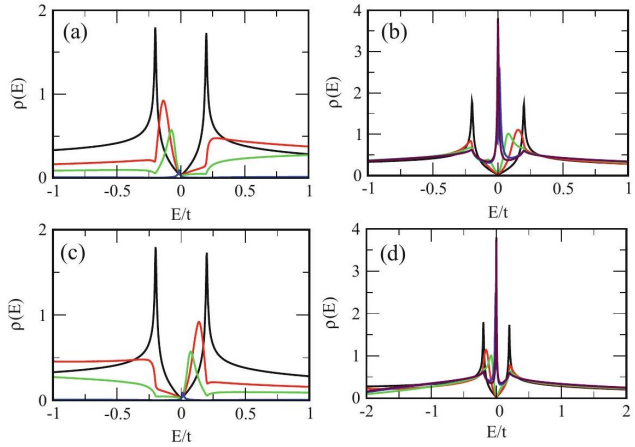


Fig. 3.7 Local density of states around a zero-ranged nonmagnetic potential scatter in a d-wave superconductor defined on a two-dimensional square lattice. The left column is for the LDOS calculated at the impurity site while the right column is for the LDOS calculated at a site nearestneighboring to the impurity site. For the repulsive potential scatter ($(\mathbf{a})-(\mathbf{b})$), we take $\varepsilon_I = 1t$ (red), $2t$ (green), $10t$ (blue), and 100t (maroon). For the attractive potential scatter ((c)-(d)), we take $\varepsilon_I = -1t$ (red), $-2t$ (green), $-10t$ (blue), $-100t$ (maroon). The DOS for the pristine system ($\varepsilon_I = 0$ with black lines) is also shown. Here we have used a tight-binding model up to next-nearest neighbor hopping with $t' = -0.2t$ and $\mu = -0.8t$. The pair potential is taken as $\Delta_0 = 0.2t$. The broadening parameter is $\gamma = 0.005t$

the d-wave superconducting order parameter, the pairing interaction should be of nearest-neighbor type on a square lattice. In the supercell technique, the BdG equations [c.f. Eq. (2.30)] become:

$$E_n(\mathbf{K})u^n_{i\uparrow}(\mathbf{K}) = \sum_{\delta} e^{i\mathbf{K}\cdot\mathbf{r}_\delta}\left[\tilde{h}_{\tilde{i}\uparrow,i+\delta\uparrow}u^n_{\tilde{i}+\delta\uparrow}(\mathbf{K}) + \Delta_{\tilde{i},\tilde{i}+\delta}v^n_{\tilde{i}+\delta\downarrow}(\mathbf{K})\right], \tag{3.49}$$

$$E_n(\mathbf{K})v^n_{i\downarrow}(\mathbf{K}) = \sum_{\delta} e^{i\mathbf{K}\cdot\mathbf{r}_\delta}\left[-\tilde{h}^*_{i\downarrow,i+\delta\downarrow}v^n_{\tilde{i}+\delta\uparrow}(\mathbf{K}) + \Delta^*_{\tilde{i}+\delta,\tilde{i}}u^n_{i+\delta\uparrow}(\mathbf{K})\right], \tag{3.50}$$

subject to the self-consistency condition:

$$\Delta_{\tilde{i}\tilde{i}+\delta} = \frac{V}{4M}\sum_{\mathbf{K},n}\left[u^n_{i\uparrow}(\mathbf{K})v^{n*}_{\tilde{i}+\delta\downarrow}(\mathbf{K})e^{-i\mathbf{K}\cdot\mathbf{r}_\delta} + u^n_{i+\delta,\uparrow}(\mathbf{K})v^{n*}_{i\downarrow}(\mathbf{K})e^{i\mathbf{K}\cdot\mathbf{r}_\delta}\right]\tanh\left(\frac{E_n(\mathbf{K})}{2k_BT}\right). \tag{3.51}$$

The d-wave and the induced extended-s-wave OP components are then defined as

$$\Delta_d(\mathbf{i}) = \frac{1}{4}\left[\Delta_{\hat{x}}(\mathbf{i}) + \Delta_{-\hat{x}}(\mathbf{i}) - \Delta_{\hat{y}}(\mathbf{i}) - \Delta_{-\hat{y}}(\mathbf{i})\right] \tag{3.52}$$

$$\Delta_s(\mathbf{i}) = \frac{1}{4}\left[\Delta_{\hat{x}}(\mathbf{i}) + \Delta_{-\hat{x}}(\mathbf{i}) + \Delta_{\hat{y}}(\mathbf{i}) + \Delta_{-\hat{y}}(\mathbf{i})\right] \tag{3.53}$$

Here $\hat{x}$ and $\hat{y}$ are the unit vectors along x - and y-bond direction of the square lattice. We note that the expression for the LDOS is still the same as that given by Eq. (3.29). In Fig. 3.8, the typical results are shown for a repulsive impurity with the scattering strength in the unitary limit. The d-wave superconducting order parameter is strongly suppressed near the impurity site while a subdominant (extended) s-wave superconducting order parameter is induced around the impurity. In addition, the LDOS near the impurity site exhibits a resonance peak close to the Fermi energy and the spatial dependence of the LDOS at this resonance energy shows tails along the

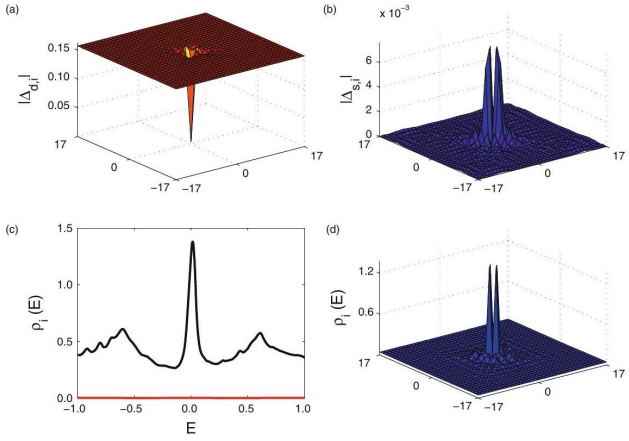


Fig. 3.8 Self-consistent solution to the BdG equations for a single impurity in a d-wave superconductor. The top row displays the spatial variation of the d-wave (a) and induced s-wave (b) components of the superconducting order parameter. The bottom row displays the local density of states on the site nearest neighbor to the impurity site (c) and the spatial dependence of the LDOS at the resonance energy $E_r = 0.014t(\mathbf{d})$. The calculations are carried out for the $d_{x^2-y^2}$ - wave superconductor defined on a two-dimensional square lattice. The pairing interaction is taken to be $V = 1.5t$ and the temperature $T = 0.01t$. The supercell size has the dimension of 35 by 35 . The nonmagnetic impurity potential strength $\epsilon_I = 100t$. Here we have used a tight-binding model up to next-nearest neighbor hopping with $t' = -0.2t$ and $\mu = -0.8t$. The broadening parameter is $\gamma = 0.02t$
nodal direction of the $d_{x^2-y^2}$-wave order parameter. These results are fully consistent with those obtained from the T-matrix theory.

Before closing this chapter, one remark is in order. All of the BdG equations presented so far are derived within an effective BCS theory, which is believed to describe reasonably well the quasiparticles in the superconducting dome even for high-temperature cuprates. Actually, the phase diagram of high-temperature cuprate superconductors is much more complicated with an antiferromagnetic Neel order in its parent compound. These features are mostly discussed in the $t-J$ model, which is a low-energy model derived from the one-band Hubbard model in the localized moment limit. Therefore, it should be appropriate to discuss the superconducting phase within this model. The $t-J$ model Hamiltonian defined on a two-dimensional square lattice can be written as:

$$\begin{aligned}\mathscr{H} = &-\sum_{\langle \mathbf{i}\rangle\sigma} t_{\mathbf{i}j} c^{\dagger}_{\mathbf{i}\sigma} c_{\mathbf{j}\sigma} + \sum_{\mathbf{i}\in I} \varepsilon_{\mathbf{i}} n_{\mathbf{i}} - \mu \sum_{\mathbf{i}} n_{\mathbf{i}} \\ &+ \frac{J}{2} \sum_{\langle \mathbf{ij}\rangle} \left[\mathbf{S}_{\mathbf{i}} \cdot \mathbf{S}_{\mathbf{j}} - \frac{1}{4} n_{\mathbf{i}} n_{\mathbf{j}} \right] + \frac{W}{2} \sum_{\langle \mathbf{ij}\rangle} n_{\mathbf{i}} n_{\mathbf{j}}. \end{aligned} \tag{3.54}$$

Here the electrons are subjected to single occupancy constraint with $\mathbf{S}_{\mathbf{i}}$ the spin- $\frac{1}{2}$ operator on site $\mathbf{i}$. The quantity $n_{\mathbf{i}} = \sum_{\sigma} c^{\dagger}_{\mathbf{i}\sigma} c_{\mathbf{i}\sigma}$ is the electron number operator on site $\mathbf{i}$ and ε_i is the

on-site single-particle potential introduced to describe the impurity scattering or more generally disorder effect. The superexchange interaction $J > 0$ ensures an antiferromagnetic state at zero doping. We have also included a direct nearest-neighbor interaction term so that $W = 0$ and $J/4$ correspond to two versions of the standard $t - J$ model. This term will also adjust the magnitude of the resultant d-wave OP, as will be shown below. Upon doping, the model can be solved within the slave-boson mean-field (SBMF) method [42]. The electron operator as

$$c_{\mathbf{i}\sigma} = b_{\mathbf{i}}^{\dagger} f_{\mathbf{i}\sigma}, \tag{3.55}$$

where $f_{\mathbf{i}\sigma}$ and $b_{\mathbf{i}}$ are the operators for a spinon (a neutral spin- $\frac{1}{2}$ fermion) and a holon (a spinless charged boson). These auxiliary degrees of freedom are subjected to the constraint

$$b_i^{\dagger} b_i + \sum_{\sigma} f_{i\sigma}^{\dagger} f_{i\sigma} \leq 1, \tag{3.56}$$

arising from the single occupancy of electrons $\sum_{\sigma} c_{i\sigma}^{\dagger} c_{i\sigma} \leq 1$. In the SBMF method, this constraint is enforced by introducing a term into the Hamiltonian

$$\sum_i \lambda_i \left[1 - b_i^{\dagger} b_i - \sum_{\sigma} f_{i\sigma}^{\dagger} f_{i\sigma} \right], \tag{3.57}$$

where λ_i is the site-dependent Lagrange multiplier in the presence of impurity scattering potential. In addition, the spin and electron density operators are given
by

$$\mathbf{S}_i = \frac{1}{2} \sum_{\sigma\sigma'} f_{i\sigma}^{\dagger} \boldsymbol{\sigma}_{\sigma\sigma'} f_{i\sigma'} \tag{3.58}$$

with σ being the Pauli matrix, and

$$n_{i\sigma} = f_{i\sigma}^{\dagger} f_{i\sigma} \tag{3.59}$$

By applying the Wick theorem to the interaction terms, we derive a mean-field Hamiltonian

$$\mathscr{H}_{\mathrm{MF}} = \sum_{ij,\sigma} \tilde{h}_{ij} f_{i\sigma}^{\dagger} f_{j\sigma} + \sum_{ij} \left[\Delta_{ij} f_{i\uparrow}^{\dagger} \uparrow_{j\downarrow}^{\dagger} + \text{H.c.} \right] + \sum_i \lambda_i \left(1 - b_i^* b_i \right) \tag{3.60}$$

Here the single-particle Hamiltonian is given by

$$\tilde{h}_{ij} = -t_{ij} b_i b_j^* - \left(\frac{J}{2} + W \right) \chi_{ij} + \left(\varepsilon_i - \mu - \lambda_i \right) \delta_{ij} \tag{3.61}$$

with the resonance valence bond order

$$\chi_{ij} = \frac{1}{4} \sum_{\sigma} \left[\left\langle f_{i\sigma}^{\dagger} f_{j\sigma} \right\rangle + \text{ccc.} \right] \tag{3.62}$$

and the pair potential

$$\Delta_{ij} = \frac{J - W}{2} \left[\langle f_{i\uparrow} f_{i\downarrow} \rangle - \langle f_{i\downarrow} \downarrow f_{j\uparrow} \rangle \right]. \tag{3.63}$$

Due to the holon Bose condensation, which is now treated as a c-number, at low temperatures, the quasiparticles are determined by the spinon degree of freedom only. Without loss of generality, when we take the holon operator as a real number, the application of the Hellmann-Feynman theorem gives rise to the constraints

$$b_i^2 + \sum_\sigma \left\langle f_{i\sigma}^\dagger f_{i\sigma} \right\rangle = 1 \tag{3.64}$$

and

$$\lambda_i = -\sum_j t_{ij}\chi_{ij} b_j / b_i \tag{3.65}$$

Within these mean-field approximations, the BdG equations are derived to be

$$\sum_{\mathbf{j}} \begin{pmatrix} \tilde{h}_{\mathbf{ij}} & \Delta_{\mathrm{ij}} \\ \Delta_{\mathrm{ij}}^\dagger & -\tilde{h}_{\mathbf{ij}}^* \end{pmatrix} \begin{pmatrix} u_{\mathbf{j}}^n \\ v_{\mathbf{j}}^n \end{pmatrix} = E_n \begin{pmatrix} u_{\mathrm{i}}^n \\ v_{\mathbf{i}}^n \end{pmatrix}. \tag{3.66}$$

The local electronic structure around a single nonmagnetic impurity in the $t-J$ model has been studied in the further simplification with a uniform b_i[40, 43]. The results from these studies are qualitatively consistent with those obtained from the above phenomenological BCS model for d-wave superconductors. The full self-consistent solution to the above BdG equations is left for readers to practise.

13.2 4 Disorder Effects on Electronic and Transport Properties in Superconductors

Abstract

In this chapter, we discuss the disorder effects. The disorder comprises of a distribution of nonmagnetic impurities. As such, ensemble averaged effects will be relevant. We focus on the suppression of superconductivity by considering the response of superconducting order parameter, transition temperature, and superfluid density in both s-wave and d-wave superconductors. Finally, we also discuss the localization/delocalization of gapless quasiparticles in a disordered d-wave superconductor within a single-parameter scaling approach.

13.2.1 4.1 Anderson Theorem for Disordered s-Wave Superconductor

A remarkable feature of the isotropic s-wave superconductors is the insensitivity of the superconductivity to the diluted nonmagnetic impurities. This robustness is demonstrated by the Anderson theorem [1]. The theorem states that because the superconductivity arises from the instability of the Fermi surface upon the pairing of time-reversed electronic states, any perturbation should not affect the mean-field superconducting order parameter and transition temperature as long as it does not lift the Kramers degeneracy. We first discuss this theorem within the AbrikosovGorkov theory [2]. For simplicity, we consider the zero-ranged interactions between the conduction electrons and nonmagnetic impurities

$$U(\mathbf{r}) = u_0 \sum_{i\in I} \delta\left(\mathbf{r} - \mathbf{R}_i\right) \tag{4.1}$$

where u_0 is the strength of the scattering potential while $\mathbf{R}_i$ is the position of individual impurities. The Abrikosov-Gorkov equations are derived in Chap. 1 and written as in the continuum limit

$$\begin{aligned} &\left[i\omega_n + \tfrac{\nabla^2}{2m_e} + E_F - U(\mathbf{r})\right] \mathscr{G}\left(\mathbf{r}, \mathbf{r}'; i\omega_n\right) \\ &+ \int d\mathbf{r}'' \Delta\left(\mathbf{r}, \mathbf{r}''\right) \mathscr{F}^\dagger\left(\mathbf{r}'', \mathbf{r}'; i\omega_n\right) = \delta\left(\mathbf{r} - \mathbf{r}'\right) \end{aligned} \tag{4.2a}$$

$$\left[-i\omega_n + \frac{\nabla^2}{2m_e} + E_F - U(\mathbf{r})\right] \mathscr{F}^\dagger(\mathbf{r}, \mathbf{r}'; i\omega_n) + \int d\mathbf{r}'' \Delta^*(\mathbf{r}, \mathbf{r}'') \mathscr{G}(\mathbf{r}'', \mathbf{r}'; i\omega_n) = 0 \tag{4.2b}$$

Here $\omega_n = (2n+1)\pi T$ with n any integer is the Matsubara frequency for electrons, E_F is the Fermi energy, and $\mathscr{G}$ and $\mathscr{F}^\dagger$ are the normal and anomalous Green's functions. The pair potential is given by

$$\Delta^*(\mathbf{r}, \mathbf{r}') = V(\mathbf{r} - \mathbf{r}') T \sum_{\omega_n} \mathscr{F}^\dagger(\mathbf{r}, \mathbf{r}'; i\omega_n), \tag{4.3}$$

where $-V(\mathbf{r} - \mathbf{r}')$ is the pairing interaction. After averaging over the impurity configurations, the transitional invariance is restored so that we can write the above system of equations in the momentum space

$$[i\omega_n - \xi_{\mathbf{p}} - \mathscr{G}_{\omega_n}] \mathscr{G}(\mathbf{p}; i\omega_n) + [\Delta(\mathbf{p}) + \mathscr{F}_{\omega_n}] \mathscr{F}^\dagger(\mathbf{p}; i\omega_n) = 1, \tag{4.4a}$$

$$[i\omega_n + \xi_{\mathbf{p}} + \mathscr{G}_{-\omega_n}] \mathscr{F}^\dagger(\mathbf{p}; i\omega_n) + \left[\Delta^*(\mathbf{p}) + \mathscr{F}^\dagger_{\omega_n}\right] \mathscr{G}(\mathbf{p}; i\omega_n) = 0, \tag{4.4b}$$

where

$$\xi_{\mathbf{p}} = \frac{\mathbf{p}^2}{2m_e} - E_F \tag{4.5}$$

and

$$\mathscr{G}_{\omega_n} = \frac{n_i u_0^2}{(2\pi)^2} \int \mathscr{G}(\mathbf{p}'; i\omega_n) \, d\mathbf{p}' \tag{4.6a}$$

$$\mathscr{F}^\dagger_{\omega_n} = \frac{n_i u_0^2}{(2\pi)^2} \int \mathscr{F}^\dagger(\mathbf{p}'; i\omega_n) \, d\mathbf{p}' \tag{4.6b}$$

with n_i as the density of nonmagnetic impurities. We note that $\mathscr{F}^\dagger_{\omega_n} = (\mathscr{F}_{\omega_n})^*$. We can solve Eq. (4.4) to obtain

$$\mathscr{G}(\mathbf{p}; i\omega_n) = -\frac{i\omega_n - \mathscr{G}_{\omega_n} + \xi_{\mathbf{p}}}{-(i\omega_n - \mathscr{G}_{\omega_n})^2 + \xi_{\mathbf{p}}^2 + \left|\Delta^*(\mathbf{p}) + \mathscr{F}^\dagger_{\omega_n}\right|^2} \tag{4.7a}$$

$$\mathscr{F}^\dagger(\mathbf{p}; i\omega_n) = \frac{\Delta^*(\mathbf{p}) + \mathscr{F}^\dagger_{\omega_n}}{-(i\omega_n - \mathscr{G}_{\omega_n})^2 + \xi_{\mathbf{p}}^2 + \left|\Delta^*(\mathbf{p}) + \mathscr{F}^\dagger_{\omega_n}\right|^2} \tag{4.7b}$$

On substitution of Eq.(4.7) into Eq. (4.6), we find

$$\mathscr{G}_{\omega_n} = \frac{n_i u_0^2}{(2\pi)^2} \int \frac{-(i\omega_n - \mathscr{G}_{\omega_n})}{-(i\omega_n - \mathscr{G}_{\omega_n})^2 + \xi_{\mathbf{p}'}^2 + \left|\Delta^*(\mathbf{p}') + \mathscr{F}^\dagger_{\omega_n}\right|^2} d\mathbf{p}' \tag{4.8a}$$

$$\mathscr{F}^\dagger_{\omega_n} = \frac{n_i u_0^2}{(2\pi)^2} \int \frac{\Delta^*(\mathbf{p}') + \mathscr{F}^\dagger_{\omega_n}}{-(i\omega_n - \mathscr{G}_{\omega_n})^2 + \xi_{\mathbf{p}'}^2 + \left|\Delta^*(\mathbf{p}') + \mathscr{F}^\dagger_{\omega_n}\right|^2} d\mathbf{p}' \tag{4.8b}$$

Here we have dropped the contribution to the integral from the term linear in $\xi_{\mathbf{p}}$ in the numerator of $\mathscr{G}(\mathbf{p}; i\omega_n)$. The pair potential is subjected to the self-consistency:

$$\Delta^*(\mathbf{k}) = T\sum_{i\omega_n}\int \frac{d\mathbf{p}}{(2\pi)^2} V(\mathbf{k}-\mathbf{p})\mathscr{F}^\dagger(\mathbf{p}; i\omega_n) \tag{4.9}$$

In the weak-coupling limit, the pairing interaction is limited to a small range near the Fermi surface. As we discussed in the early chapter, for the s-wave pairing symmetry, the pairing interaction is approximated as

$$V(\mathbf{k}-\mathbf{p}) = V_s. \tag{4.10}$$

From the structure of Eq. (4.8), we can write that for the s-wave pairing symmetry

$$\mathscr{G}_{\omega_n} = -i\omega_n\eta_{\omega_n}, \tag{4.11}$$

and

$$\mathscr{F}_{\omega_n} = \Delta_s\eta_{\omega_n}. \tag{4.12}$$

This gives rise to

$$\begin{aligned}
\eta_{\omega_n} &= \frac{n_i u_0^2}{(2\pi)^2}\int \frac{1+\eta_{\omega_n}}{(\omega_n^2+\Delta_s^2)(1+\eta_{\omega_n})^2+\xi_{\mathbf{p}}^2} d\mathbf{p} \\
&= n_i u_0^2 N(0)\int\frac{d\phi}{2\pi}\int \frac{1+\eta_{\omega_n}}{(\omega_n^2+\Delta_s^2)(1+\eta_{\omega_n})^2+\xi^2} d\xi \qquad (4.13)\\
&= n_i u_0^2 N(0)\int\frac{d\phi}{2\pi}\frac{\pi(1+\eta_{\omega_n})}{\sqrt{(\omega_n^2+\Delta_s^2)(1+\eta_{\omega_n})^2}} \qquad (4.14)\\
&= \frac{1}{2\tau}\frac{1}{\sqrt{\omega_n^2+\Delta_s^2}} \qquad (4.15)
\end{aligned}$$

where $\tau^{-1} = 2\pi n_i u_0^2 N(0)$ with $N(0)$ the density of states per electron spin at the Fermi energy is the impurity scattering rate. Here we have used the integral

$$\int \frac{dx}{1+x^2} = \tan^{-1}(x)$$

The self-consistency solution in the presence of impurity scattering can then be found as

$$\Delta_s = 2g_s\pi T\sum_{i\omega_n}\frac{\Delta_s}{\sqrt{\omega_n^2+\Delta_s^2}} \tag{4.16}$$

where $g_s = N(0)V_s/2$. We note that when the summation over the Matsubara frequency is performed, the cutoff frequency ω_c, which is related to the pairing mechanism, should be introduced. Equation (4.16) indicates that the s-wave superconducting order parameter does not depend on the impurity scattering rate.

The Anderson theorem can also be shown through the BdG equations [3]. As discussed in Chap. 1, the s-wave order parameter is given as

$$\Delta(\mathbf{r}) = V_s\sum_{n(E_n\geq 0)} u_n(\mathbf{r})v_n^*(\mathbf{r})\tanh\left(\frac{E_n}{2k_BT}\right) \tag{4.17}$$

At zero temperature, it is further simplified as

$$\Delta(\mathbf{r}) = V_s \sum_{n(E_n \geq 0)} u_n(\mathbf{r}) v_n^*(\mathbf{r}) \tag{4.18}$$

On the other hand, the BCS variational wave function that pairs electrons in timereversed states is given by

$$\Psi_{\rm BCS}\rangle = \prod_n \left(a_n + b_n c_{n\uparrow}^\dagger c_{\bar{n}\downarrow}^\dagger\right)|0\rangle \tag{4.19}$$

Here $|0\rangle$ stands for the filling Fermi sea, and $c_{n\uparrow}^\dagger$ creates an up-spin electron with wave function $\phi_n(\mathbf{r})$, and $c_{\bar{n}\downarrow}^\dagger$ creates a down-spin electron in $\phi_n(\mathbf{r})^*$, where $\phi_n(\mathbf{r})$ is an eigenfunction of the single-particle Hamiltonian. It thus restricts the trial wave function to the subspace of either doubly occupied or empty levels. The coefficients a_n and b_n are subjected to the normalization condition $|a_n|^2 + |b_n|^2 = 1$. When $\Delta(\mathbf{r})$ is independent of $\mathbf{r}$, we have

$$u_n(\mathbf{r}) = a_n \phi_n(\mathbf{r}) \tag{4.20a}$$
$$v_n(\mathbf{r}) = b_n \phi_n(\mathbf{r}) \tag{4.20b}$$

which leads to

$$\Delta(\mathbf{r}) = V_s \sum_n a_n b_n^* |\phi_n(\mathbf{r})|^2 \tag{4.21}$$

In the absence of a magnetic field, a_n, b_n, and $\phi_n(\mathbf{r})$ can be taken to be real. With the above variational wave function, the energy is given by

$$\begin{aligned} E_G &= \langle \Psi_{\rm BCS}| \mathscr{H} |\Psi_{\rm BCS}\rangle \\ &= \sum_n 2\xi_n - V_s \sum_{n\neq m} a_n a_m b_n b_m \int \phi_n^2(\mathbf{r}) \phi_m^2(\mathbf{r}) d\mathbf{r} \end{aligned} \tag{4.22}$$

subject to the normalization condition for a_n and b_n, where ξ_n is the eigenvalue of the state $\phi_n(\mathbf{r})$. The a_n and b_n can be written as $a_n = \sin\theta_n$ and $b_n = \cos\theta_n$. The variational principle leads to the equation

$$\xi_n \tan(2\theta_n) = \frac{V_s}{2} \sum_{n\neq m} \sin(2\theta_m) \int \phi_n^2(\mathbf{r}) \phi_m^2(\mathbf{r}) d\mathbf{r} \tag{4.23}$$

We now define

$$\tan(2\theta_n) = \frac{\Delta_n}{\xi_n}, \tag{4.24}$$

which implies

$$\sin(2\theta_n) = \frac{\Delta_n}{\sqrt{\xi_n^2 + \Delta_n^2}} = 2a_n b_n \tag{4.25}$$

Equation (4.23) now becomes

$$\Delta_n = V_s \sum_{m\neq n} \frac{\Delta_m}{2\sqrt{\xi_m^2 + \Delta_m^2}} \int \phi_n^2(\mathbf{r}) \phi_m^2(\mathbf{r}) d\mathbf{r} \tag{4.26}$$

Using Eq. (4.21), we obtain

$$\Delta_n = \int \Delta(\mathbf{r})\phi_n^2(\mathbf{r})d\mathbf{r} \tag{4.27}$$

once the condition $m \neq n$ is relaxed.
For a pristine system, $\Delta_n = \Delta(\mathbf{r}) = \Delta_0$. For disordered systems, $\phi_n(\mathbf{r})$ is a complicated wave function. However, if we assume $\Delta(\mathbf{r}) = \tilde{\Delta}$, then the normalization condition $\int \phi_n(\mathbf{r})^2 d\mathbf{r} = 1$ gives rise to $\Delta_n = \tilde{\Delta}$, which is independent
of n. With this condition, the gap equation (4.26) gives

$$\tilde{\Delta} = \int V_s \frac{\tilde{\Delta} N(\epsilon, \mathbf{r})}{\sqrt{\epsilon^2 + \tilde{\Delta}^2}} \phi_n^2(\mathbf{r}) d\mathbf{r} \tag{4.28}$$

where we introduce the normal-state single-particle density of states for the disordered system

$$N(\epsilon, \mathbf{r}) = \sum_m \phi_m^2(\mathbf{r}) \delta(\epsilon - \xi_m) \tag{4.29}$$

In weakly disordered system, $N(\epsilon, \mathbf{r}) \approx N(0)$, the gap equation (4.28) gives $\tilde{\Delta} = \Delta_0$. As such, the transition temperature is also insensitive to the disorder effect. This is the Anderson theorem.

13.2.2 4.2 Suppression of Superconductivity in a Disordered d-Wave Superconductor

For the $d_{x^2-y^2}$-wave pairing symmetry, the pairing interaction can be written as

$$V(\mathbf{k} - \mathbf{p}) = V_d \cos 2\phi \cos 2\phi' \tag{4.30}$$

where the angle $\phi = \tan^{-1}(k_{F,y}/k_{F,x})$ with $k_{F,x(y)}$ the two components of the Fermi wave vector. Correspondingly, the superconducting pair potential is of the form

$$\Delta(\mathbf{k}) = \Delta_d \cos 2\phi \tag{4.31}$$

This special form of the d-wave pairing symmetry leads to the breaking of the scaling law for $\mathscr{F}_{\omega_n}$ and in particular $\mathscr{F}_{\omega_n} = 0$. The self-consistency equation for the d-wave pair potential then becomes

$$\Delta_d = 2g_d \pi T \sum_{i\omega_n} \int \frac{d\phi'}{2\pi} \frac{\Delta_d \cos^2(2\phi')}{\sqrt{\omega_n^2 (1 + \eta_{\omega_n})^2 + (\Delta_d \cos(2\phi'))^2}} \tag{4.32}$$

where $g_d = N(0)V_s/2$ and

$$\eta_{\omega_n} = \frac{1}{2\tau} \int \frac{d\phi'}{2\pi} \frac{1 + \eta_{\omega_n}}{\sqrt{\omega_n^2 (1 + \eta_{\omega_n})^2 + (\Delta_d \cos(2\phi'))^2}} \tag{4.33}$$

Equation (4.32) suggests that the nonmagnetic impurity scattering is pairing breaking and can suppress the transition temperature of the d-wave superconductivity.
The transition temperature from the AG theory is then found [4-7] to be

$$\ln\left(\frac{T_c}{T_{c0}}\right) = \Psi\left(\frac{1}{2}\right) - \Psi\left(\frac{1}{2} + \frac{1}{4\pi\tau T_c}\right). \tag{4.34}$$

Here $\Psi(x)$ is the digamma function and T_{c0} is the transition temperature of a pure system.

The impurity scattering also influences the superfluid density and the penetration depth in a d-wave superconductor. For these quantities, one calculates the electromagnetic response tensor $\mathscr{K}$, relating the current density $\mathbf{j}$ to an applied vector potential $\mathbf{A}$:

$$\mathbf{j} = -\mathscr{K}\,\mathbf{A} \tag{4.35}$$

If the electromagnetic tensor is diagonal $\mathscr{K}_{ij} = \mathscr{K}_{ii}\delta_{ij}$, the penetration depth λ_i for the current flowing in the direction i is given by

$$\lambda_i^{-2} = (4\pi/c)\mathscr{K}_{ii} \tag{4.36}$$

where c is the velocity of light. The AG theory for a disordered BCS d-wave superconductivity then gives the response tensor [4]:

$$\mathscr{K}_{ij} = \frac{e^2}{c}\left\langle v_i(\mathbf{k})v_j(\mathbf{k})\int_0^\infty d\omega \tanh\left(\frac{\omega}{2k_BT}\right)\mathrm{Re}\,\frac{\Delta_k^2}{(\tilde{\omega}^2-\Delta_k^2)^{3/2}}\right\rangle. \tag{4.37}$$

Here $\langle\cdots\rangle \equiv 2(2\pi)^{-2}\int dS_F/|\mathbf{v}(\mathbf{k})|\cdots$ represents an angular average over an arbitrary Fermi surface in a two-dimensional metal, and $\mathbf{v}(\mathbf{k})$ is the Fermi velocity. The renormalized frequency $\tilde{\omega} = \omega - \Sigma_0$ with the impurity self-energy obtained from the T-matrix approximation [8-13]

$$\Sigma_0 = \frac{\Gamma G_0}{(u_0N(0))^{-1} - G_0^2}, \tag{4.38}$$

where $\Gamma = n_i/\pi N(0) = 1/2\tau$ is the scattering rate with n_i being the impurity concentration, and G_0 is the integrated diagonal Green's function averaged over the impurity configuration

$$G_0 = -i\left\langle\frac{\tilde{\omega}}{(\tilde{\omega}^2-\Delta_k^2)^{1/2}}\right\rangle. \tag{4.39}$$

Equation (4.37) can be decomposed into two parts

$$\mathscr{K}_{ij}(T) = \mathscr{K}_{ij}(T=0) + \delta\mathscr{K}_{ij}(T) \tag{4.40}$$

where

$$\mathscr{K}_{ij}(T=0) = \frac{e^2}{c}\left\langle v_i(\mathbf{k})v_j(\mathbf{k})\int_0^\infty d\omega\,\mathrm{Re}\,\frac{\Delta_k^2}{(\tilde{\omega}^2-\Delta_k^2)^{3/2}}\right\rangle, \tag{4.41}$$

and

$$\delta\mathscr{K}_{ij}(T) = \frac{-2e^2}{c}\left\langle v_i(\mathbf{k})v_j(\mathbf{k})\int_0^\infty d\omega f_{\mathrm{FD}}(\omega)\,\mathrm{Re}\,\frac{\Delta_k^2}{(\tilde{\omega}^2-\Delta_k^2)^{3/2}}\right\rangle \tag{4.42}$$

In the impurity-dominated gapless regime, the renormalized frequency takes the form [4] $\tilde{\omega} \to i\gamma + a\omega$, where γ is a constant dependent on the impurity concentration and scattering strength, while the constant $a \sim O(1)$. At low temperatures, it allows us to replace $\tilde{\omega}$ by this limiting form, which gives rise to

$$\delta\mathscr{K}_{ij}(T) = \frac{-e^2}{c}\frac{\pi^2}{2}\gamma a T^2\left\langle v_i(\mathbf{k})v_j(\mathbf{k})\frac{\Delta_k^2}{(\gamma^2+\Delta_k^2)^{5/2}}\right\rangle. \tag{4.43}$$

For the $d_{x^2-y^2}$-wave pairing symmetry, the angular average in the above equation varies as γ^{-2}. It suggests that the coefficient of the T^2-dependence in the penetration depth is proportional to the inverse γ but the T^2 behavior is valid in a very narrow temperature range $\sim \gamma$.

The impurity scattering also affects the zero-temperature tensor $\mathscr{K}_{ij}(T=0)$, which is given by

$$\mathscr{K}_{ij}(T=0) = \mathscr{K}_{ij}(T=0,\Gamma=0) + \frac{e^2}{c}\left\langle v_i(\mathbf{k})v_j(\mathbf{k})\frac{\Delta_k^2}{(\gamma^2+\Delta_k^2)^{1/2}}\right\rangle. \tag{4.44}$$

The scaling relation between the zero-temperature superfluid density $\rho_s \propto \mathscr{K}_{ii}$ and the superconducting transition temperature based on the AG theory for a disordered d-wave superconductor is shown in Fig.4.1. It has been found that for hightemperature cuprate superconductors, the experimentally observed T_c is much more robust than one would expect from the AG theory, when it is measured against the corresponding zero-temperature superfluid density. Originally, the failure has also been ascribed to the mean-field nature of the BCS-type theory in view of the fact that the normal state is a non-Fermi liquid in the optimally doped high-temperature cuprates [15]. It turns out [14] that the discrepancy between the theory and the experiment comes mainly from the inadequacy of the AG theory itself to determine the suppression of the superconducting transition temperature for high-temperature d-wave superconductors. In the AG theory, one crucial assumption in the derivation of the transition temperature is that the spatial dependence of the superconducting order is replaced by an averaged value, as shown in Fig.4.2. This assumption is only valid when the superconducting coherence ξ is much larger than the average distance between impurities l_i. The superconducting coherence length is inversely proportional to the maximal amplitude of the order parameter in the momentum

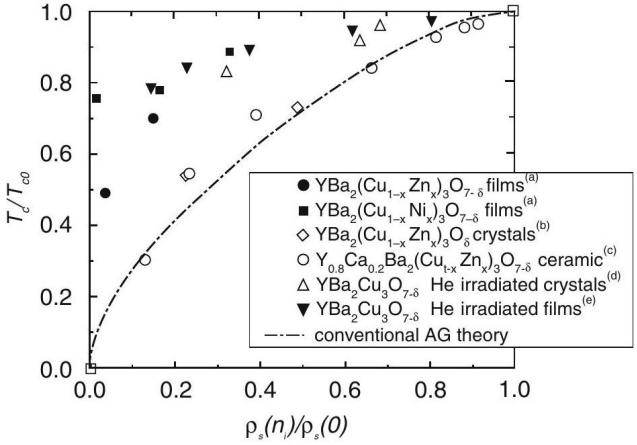


Fig. 4.1 Normalized critical temperature versus the normalized zero-temperature superfluid density. The dashed line denotes the results from the AG theory while the experimental data are represented by symbols. From [14]

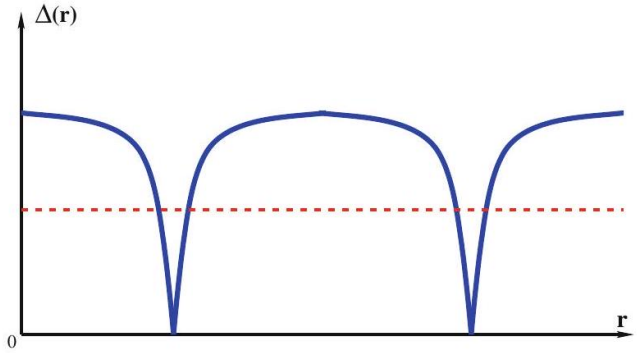


Fig. 4.2 Schematic drawing of the spatial dependence of the superconducting order param-

eter around impurities in a superconductor with a short coherence length (solid blue line). In the AG theory, it is replaced with an averaged value (dashed red line)
space and has the following form:

$$\xi(T) \approx \xi_0 \left(1 - T/T_{c0}\right)^{-1/2} \tag{4.45}$$

For a superconductor with a short coherence length, the superconducting order parameter can be recovered to the bulk value within a distance much shorter than l_i (see solid blue line in Fig. 4.2). As such, the areas of the depressed order parameter around impurities do not overlap, and the superconducting order parameter in most areas of the system is not affected at all. Only when the depressed areas begin to
overlap ($\xi(T) \gg l_i$), the entire system can be affected as if the order parameter is suppressed everywhere. This weakness of the AG theory can be fully overcome by solving the BdG equations self-consistently, in which the inhomogeneity of the superconducting order parameter is fully taken care of.

To be complete, let us re-derive the superfluid density within the lattice model. The derivation follows closely that for the optical properties discussed in Chap. 2. Again we calculate the superfluid stiffness for a current response to a vector potential of wave vector $\mathbf{q}$ and frequency ω along the x-direction in a two-dimensional square lattice through the Kubo formula. By expanding the Hamiltonian to include the interaction between electrons and an electromagnetic field, the time-dependent Hamiltonian is given by

$$\mathscr{H}_t = \mathscr{H}_{BCS} + \mathscr{H}'(t) \tag{4.46}$$

where the BCS Hamiltonian in the tight-binding model has already been discussed in Chap. 2, and $\mathscr{H}'(t)$ describes the coupling of electrons to the external electromagnetic field up to the second order

$$\mathscr{H}'(t) = -ea \sum_i A_x\left(\mathbf{r}_i, t\right) \left(J_x^P\left(\mathbf{r}_i\right) + \frac{ea}{2} A_x\left(\mathbf{r}_i, t\right) K_x\left(\mathbf{r}_i\right) \right), \tag{4.47}$$

where a is the lattice constant, A_x is the vector potential along the x-axis, and the particle current density operator

$$J_x^P\left(\mathbf{r}_i\right) = -i \sum_{\sigma,\delta} \left[t_{i,i+\delta} c_{i\sigma}^\dagger c_{i+\delta,\sigma} - \text{ H.c. } \right], \tag{4.48}$$

and the kinetic energy density operator

$$K_x\left(\mathbf{r}_i\right) = -\sum_{\sigma,\delta} \left[t_{i,i+\delta} c_{i\sigma}^\dagger c_{i+\delta,\sigma} + \text{ H.c } \right] \tag{4.49}$$

The variable $\delta = \hat{x}$ for the nearest-neighbor hopping model and $\delta = \hat{x}, \hat{x} \pm \hat{y}$ for next-nearest-hopping model. The charge current density operator along the x-axis is then found to be

$$J_x^Q\left(\mathbf{r}_i\right) \equiv -\frac{\delta \mathscr{H}'(t)}{\delta A_x\left(\mathbf{r}_i, t\right)} = e J_x^P\left(\mathbf{r}_i\right) + e^2 K_x\left(\mathbf{r}_i\right) A_x\left(\mathbf{r}_i, t\right) \tag{4.50}$$

We then calculate the paramagnetic component of the electric current density to the first order in A_x:

$$\left\langle J_x^P \left(\mathbf{r}_i \langle \right) = -i \int_{-\infty}^{t} \left\langle J_x^P(t), \mathscr{H}'\left(t'\right) \right]_- \right\rangle_0 dt' \tag{4.51}$$

while the diamagnetic part only to the zeroth order, that is, $\langle K_x \rangle_0$. Here $\langle \cdots \rangle_0$ stands for the thermodynamic average with respect to the non-perturbed $\mathscr{H}_{\rm BCS}$. The current response is then obtained as

$$-\frac{J_x^Q(\mathbf{r}_i)}{e^2 A_x(\mathbf{r}_i)} = -ie^{-\mathbf{q}\cdot\mathbf{r}_i}\int_{-\infty}^{t} dt' \left\langle \left[J_x^P(\mathbf{q},t), J_x^P(-\mathbf{q},t')\right]_- \right\rangle_0 - \langle K_x(\mathbf{r}_i)\rangle_0 \tag{4.52}$$

Please keep in mind that the variables t and t' in the vector potential and the integral boundary are the time.

We then perform a lattice average over the spatial variable $\mathbf{r}_i$ to eliminate the atomic-scale fluctuations, and define an effective "Drude weight" as a measure of the superfluid density

$$\rho_s \equiv \frac{D_s}{\pi e^2} = -\langle K_x \rangle_0 + \Pi_{xx}(\mathbf{q}\to 0, \omega = 0) \tag{4.53}$$

Here the first term

$$K_x\rangle_0 = \frac{1}{N_L}\sum_i K_{x,i} \tag{4.54}$$

with the local kinetic energy

$$K_{x,i} = -2t \sum_{n(E_n\geq 0)} \left(f(E_n)\left[u_{i+\hat{x}}^{n*}u_i^n + \text{c.c}\right] + f(-E_n)\left[v_{i+\hat{x}}^n n_i^{n*} + \text{c.c}\right]\right). \tag{4.55}$$

The second term is the current-current correlation function with a double sum over lattice sites

$$\Pi_{xx}(\mathbf{q}\to 0;\omega = 0) = \frac{1}{N_L}\sum_{i,j}\Pi_{xx}^{ij}(\omega = 0), \tag{4.56}$$

where

$$\Pi_{xx}^{ij}(\omega = 0) = \sum_{n_1\left(E_{n_1}\geq 0\right), n_2\left(E_{n_2}\geq 0\right)} A_{n_1,n_2}^i \left[A_{n-1,n_2}^{j*} + D_{n_1,n_2}^j\right] \frac{f(E_{n_1}) - f(E_{n_2})}{E_{n_1} - E_{n_2}} \tag{4.57}$$

with

$$A_{n_1,n_2}^i = 2\left[u_{i+\hat{x}}^{n_1*}u_i^{n_2} - u_i^{n_1*}u_{i+\hat{x}}^{n_2}\right], \tag{4.58a}$$

$$D_{n_1,n_2}^i = 2\left[v_{i+\hat{x}}^{n_1}v_i^{n_2*} - v_i^{n_1}v_{i+\hat{x}}^{n_2*}\right]. \tag{4.58b}$$

Typical results from the solution to the BdG equations are shown in Fig.4.3. As the superconducting coherence length increases, the discrepancy between the

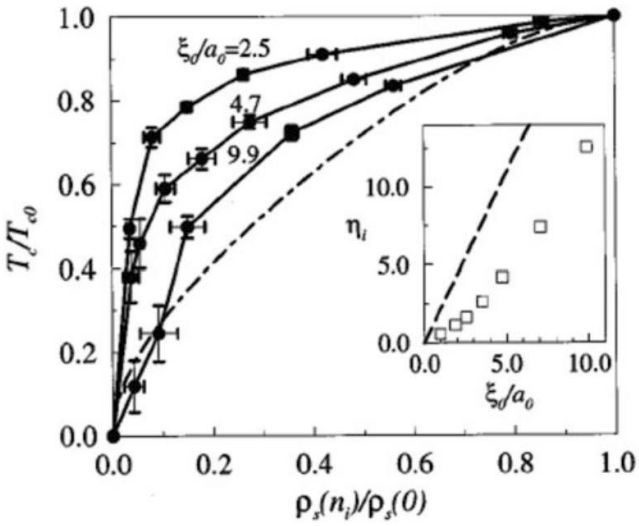


Fig. 4.3 Normalized critical temperature versus the normalized zero-temperature superfluid density obtained from a fully self-consistent solution to the BdG equations in a tight-binding model. The dashed line denotes the results from the AG theory. From [14]

rigorous critical temperature and that from the AG theory diminishes. However, at a very short coherence, the result from the AG theory deviates significantly from the true T_c. In addition, the typical temperature-dependence of the superfluid stiffness is shown in Fig. 4.4. The pileup of the impurity resonance states near the Fermi energy in a disordered d-wave superconductor gives rise to the T^2-dependence of the superfluid stiffness at low temperatures. Increase of the impurity concentration expands the temperature range for the T^2 behavior of ρ_s before it turns into a T linear behavior.

13.2.3 4.3 Quasiparticle Localization in a Disordered d-Wave Superconductor

In Sect. 3.4, we have shown that a single impurity in the unitary scattering limit can produce a zero-energy quasiparticle resonance states. These states have a long decay distance away from the impurity site. A natural question arises as to whether the possible overlap of these states in an ensemble of unitary impurities can create extended low-energy quasiparticle states. We consider this question by using the one-parameter scaling analysis. The one-parameter scaling analysis [17, 18] has been a popular method to study the electronic localization/delocalization in Anderson disordered metals. Our discussion is based on the transfer matrix method and follows that of MacKinnon and Kramer [19] for the disordered solids. To discuss the two-dimensional d-wave disordered superconductors, we first consider a system

Fig. 4.4 Temperature dependence of the normalized superfluid density calculated from a full self-consistent solution to the BdG equations in a two-dimensional lattice model with nearest-neighbor hopping approximation. From [16]

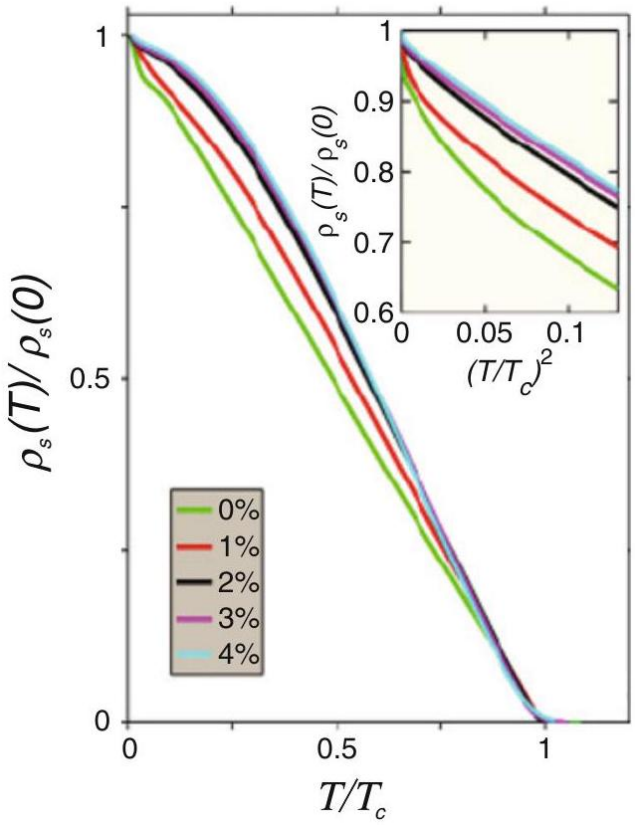
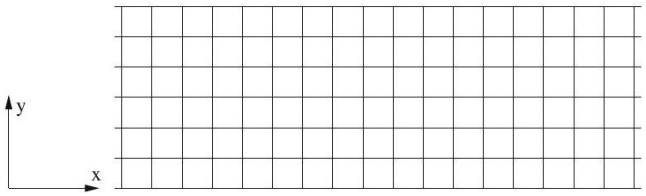


Fig. 4.5 Schematic drawing of a quasi-one-dimensional strip



of electrons defined on a quasi-one-dimensional strip. When the strip width goes to infinity, the strip is expanded into a two-dimensional lattice. The geometry is shown in Fig. 4.5.

We write down the Anderson Hamiltonian as

$$\mathscr{H} = -\sum_{ij} t_{ij} c_i^\dagger c_j + \sum_i \epsilon_i c_i^\dagger c_i \tag{4.59}$$

Here the site index $i = (i_x, i_y)$ with the two components defined in the coordinate system shown in Fig. 4.5 and the variable ϵ_i is on-site potential for the disorder effect. For simplicity of discussion, we have neglected the spin index for electrons. By performing a canonical transformation,

$$c_i = \sum_n \phi_i^n \gamma_n, \tag{4.60}$$

with γ_n is the quasiparticle operator, the problem becomes to solve the Schrödinger equation

$$\sum_j H_{ij}\phi_j = E\phi_i \tag{4.61}$$

In the nearest-neighbor hopping approximation, the expanded form of the above equation is

$$\phi_{i_x+1,i_y} = -E\phi_{i_x,i_y} + \epsilon_{i_x,i_y}\phi_{i_x,i_y} - \phi_{i_x,i_y+1} - \phi_{i_x,i_y-1} - \phi_{i_x-1,i_y}. \tag{4.62}$$

Here we have used the nearest-neighbor hopping parameter $t = 1$ and measured the energy in units of t. We introduce a column vector to denote the coefficients of the i_x-th one-dimensional slice (along the y-direction),

$$\hat{\phi}_{i_x} = \begin{pmatrix} \phi_{i_x,1} \\ \phi_{i_x,2} \\ \cdots \\ \phi_{i_x,M} \end{pmatrix} \tag{4.63}$$

where M is the width of the strip. Equation (4.62) can then be cast into a matrix form

$$\begin{pmatrix} \hat{\phi}_{i_x+1} \\ \hat{\phi}_{i_x} \end{pmatrix} = T_{i_x} \begin{pmatrix} \hat{\phi}_{i_x} \\ \hat{\phi}_{i_x-1} \end{pmatrix}. \tag{4.64}$$

Here the transfer matrix is given by

$$T_{i_x} = \begin{pmatrix} -\left(E\hat{1} - \hat{H}_{i_x}\right) - \hat{1} & \\ \hat{1} & \hat{0} \end{pmatrix} \tag{4.65}$$

where the $\hat{H}_{i_x}$ is the Hamiltonian for the i_x-th slice of the quasi-one-dimensional strip when it is not coupled to the rest. Equation (4.64) gives us a recursion formula for the coefficients $\hat{\phi}_{i_x}$. That is, if we are given the initial coefficients $\hat{\phi}_0$ and $\hat{\phi}_1$, the coefficient $\hat{\phi}_n$ can be obtained through the accumulated transfer matrix

$$P_n = \prod_{i_x=1}^{n} T_{i_x} \tag{4.66}$$

That is,

$$\begin{pmatrix} \hat{\phi}_{n+1} \\ \hat{\phi}_n \end{pmatrix} = P_n \begin{pmatrix} \hat{\phi}_1 \\ \hat{\phi}_0 \end{pmatrix}. \tag{4.67}$$

The matrix P_n satisfies the Oseledec's multiplicative ergodic theorem [20, 21]: For any initial vector

$$\begin{pmatrix} \hat{\phi}_1 \\ \hat{\phi}_0 \end{pmatrix}, \tag{4.68}$$

there exits an orthonormal set of vectors $v_i (1 \leq i \leq 2M)$ such that

$$\gamma_i = \lim_{n\to\infty} \frac{1}{n} \ln \|P_n v_i\| \tag{4.69}$$

exists. Due to the ergodicity of the system, the set of values $\{\gamma_i\}$ are independent on the initial values of the coefficients $\left(\hat{\phi}_1, \hat{\phi}_0\right)^{\text{Transpose}}$, and thus they describe the global properties of the system. The γ_i can be calculated as the log of the eigenvalues of

$$\left[P_n P_n^{\dagger}\right]^{\frac{1}{2n}} \tag{4.70}$$

The vector v_i are now the eigenvectors of $P_n P_n^{\dagger}$ and are indecent of n for large n. In another word, the matrix $\left[P_n P_n^{\dagger}\right]^{\frac{1}{2n}}$ converges to a limiting matrix when $n \to \infty$, which determines the modulus of the eigenvalues of P_n and the corresponding eigenvectors. We note that the matrix P_n is not hermitian and the eigenvalues are in general complex. The eigenvectors v_i can also be called Lyapunov eigenvectors, which determine the properties of electronic states of disordered systems.

With the above introduction, let us turn to the case of disordered d-wave superconductors, where further technical details will be discussed on the calculation of the localization length. In the presence of disorder, the BdG equations (2.30) become

$$\begin{cases} E_n u_i^n = \sum_j h_{ij} u_j^n + \sum_j \Delta_{ij} v_j^n, \\ E_n v_i^n = -\sum_j h_{ij}^* v_j^n + \sum_j \Delta_{ji}^* u_j^n \end{cases} \tag{4.71}$$

where the single particle Hamiltonian

$$h_{ij} = -t_{ij} + (\epsilon_i - \mu)\,\delta_{ij} \tag{4.72}$$

with ϵ_i the on-site potential and μ the chemical potential. We assume the bond pair potential Δ_{ij}^* to be real and neglect the depression effect of the impurity scattering to take $\Delta_{ij} = \Delta$. The above equation in the nearest-neighbor hopping approximation is expanded as:

$$\begin{aligned} \left(E - \left(\epsilon_{i_x,i_y} - \mu\right)\right) u_{i_x,i_y} =& - t u_{i_x+1,iy} - t u_{i_x-1,iy} - t u_{i_x,i_y+1} - t u_{i_x,i_y-1} \\ &+ \Delta v_{i_x+1,iy} + \Delta v_{i_x-1,i_y} + \Delta v_{i_x,i_y+1} \\ &+ \Delta v_{i_x,i_y-1} \end{aligned} \tag{4.73a}$$

$$\begin{aligned} \left(E + \left(\epsilon_{i_x,i_y} - \mu\right)\right) v_{i_x,i_y} =& t v_{i_x+1,iy} + t v_{i_x-1,iy} + t v_{i_x,i_y+1} + t v_{i_x,i_y-1} \\ &+ \Delta u_{i_x+1,i_y} + \Delta u_{i_x-1,i_y} + \Delta u_{i_x,i_y+1} \\ &+ \Delta u_{i_x,i_y-1} \end{aligned} \tag{4.73b}$$

As for the normal state case ($\Delta = 0$), we introduce a column vector

$$\hat{\phi}_{i_x} = \begin{pmatrix} u_{i_x,1} \\ u_{i_x,2} \\ \cdots \\ u_{i_x,M} \\ v_{i_x,1} \\ v_{i_x,2} \\ \cdots \\ v_{i_x,M} \end{pmatrix}. \tag{4.74}$$

Now this vector has a dimension of $2M$. Equations (4.73) can be recast into a matrix form:

$$\begin{pmatrix} \hat{\phi}_{i_x+1} \\ \hat{\phi}_{i_x} \end{pmatrix} = T_{i_x} \begin{pmatrix} \hat{\phi}_{i_x} \\ \hat{\phi}_{i_x-1} \end{pmatrix} \tag{4.75}$$

Here the transfer matrix is

$$T_{i_x} = \begin{pmatrix} -\left(E\hat{1} - \hat{H}_{i_x}\right) - \hat{1} & \\ \hat{1} & 0 \end{pmatrix} \tag{4.76}$$

where

$$\hat{H}_{i_x} = \sum_{j_y} \begin{pmatrix} -t\delta_{j_y,i_y\pm1} + \left(\epsilon_{i_x,i_y} - \mu\right)\delta_{j_y,i_y} & \Delta\delta_{j_y,i_y\pm1} \\ \Delta\delta_{j_y,i_y\pm1} & t\delta_{j_y,i_y\pm1} - \left(\epsilon_{i_x,i_y} - \mu\right)\delta_{j_y,i_y} \end{pmatrix}. \tag{4.77}$$

is the BdG Hamiltonian for the i_x-slice when it is decoupled from the rest. The transfer matrix for the entire strip is given by

$$P_n = \prod_{i_x=1}^{n} T_{i_x} \tag{4.78}$$

connecting the coefficients at the left and right end of the strips

$$\begin{pmatrix} \hat{\phi}_{n+1} \\ \hat{\phi}_n \end{pmatrix} = P_n \begin{pmatrix} \hat{\phi}_1 \\ \hat{\phi}_0 \end{pmatrix}. \tag{4.79}$$

The system transfer matrix satisfies the Oseledec's multiplicative ergodic theorem. It allows to determine the localization length through the eigenvalues of $\left[P_n P_n^\dagger\right]^{1/2n}$ in the limit of $n \to \infty$. Specifically, the matrix

$$\Omega = \ln\left(P_n P_n^\dagger\right), \tag{4.80}$$

leads to $4M$ eigenvalues $\lambda_i (1 \le i \le 4M)$. Lyapunov exponents can then be defined as

$$\gamma_i = \lim_{n\to\infty} \frac{\lambda_i}{2n} \tag{4.81}$$

$$= \lim_{n\to\infty} \tilde{\lambda}_i \tag{4.82}$$

where $\tilde{\lambda}_i$ are the eigenvalues of the matrix $\ln\left(P_n P_n^\dagger\right)^{1/2n}$. Since the matrix P_n is symplectic, the eigenvalues of Ω occur in pairs, which are of opposite sign. The smallest positive Lyapunov exponent is the inverse of the quasi-one dimensional localization length

$$\lambda = \frac{1}{\gamma_{2M}}, \tag{4.83}$$

when we label the exponents in a decreasing order. In practical calculations, the eigenvalues of the matrix $e^\Omega = P_n P_n^\dagger \sim e^{2\gamma_i n}$ rises exponentially with the length of the strip. When the ratio of the eigenvalue closest to the unity from above and the largest eigenvalue becomes comparable to the machine accuracy, this closest to unity eigenvalue is lost. However, it is this eigenvalue that determines the localization length. This difficulty can be overcome by following the GrammSchmidt orthonormalization procedure, which is carried out for each column $B_{n,i}$ of the matrix P_n in succession:

$$\bar{B}_{n,i} = \left(B_{n,i} - \sum_{j<i} \left(\bar{B}_{n,j} \cdot B_{n,i}\right) \bar{B}_{n,j} \right) / b_n^{(i)}, \tag{4.84a}$$

$$b_n^{(i)} = \left| B_{n,i} - \sum_{j<i} \left(\bar{B}_{n,j} \cdot B_{n,i}\right) \bar{B}_{n,j} \right|, \tag{4.84b}$$

for $1 \le i \le 4M$. Through this procedure, each column is orthonormalized to the previous columns. The first column converges to the eigenvector corresponding to the largest eigenvalue, the second column to the second largest and so on. The Gramm-Schmidt transformation can be performed regularly (e.g., every fifth step) but not necessarily at every stage of iteration.

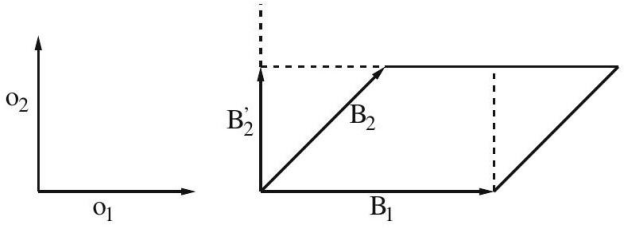


Fig. 4.6 The action of the system transfer matrix on an arbitrary set of orthonormal vectors o_1 and o_2 generates a new set of vectors of B_1 and B_2, which are orthogonalized by the Gramm-Schmidt procedure. However, the area of the parallelogram formed by B_1 and B_2 vectors is preserved

Pictorially, we can think of having P_n acting on a set of orthonormal unit vectors $o_i (1 \leq i \leq 4M)$ to generate a new set of vectors

$$B_i = P_n o^i \tag{4.85}$$

as shown in Fig. 4.6. They are just the columns of the transfer matrix itself. Notice that $B_1 \times B_2' = B_1 \times B_2$ with $B_2' = \bar{B}_2 * b^{(2)}$, and so on. The Gramm-Schmidt orthogonalization procedure preserves the area of a parallelogram formed by two vectors B_i and B_j. This process can be iterated successively through the entire strip, and the eigenvalues are given by

$$e^{n\gamma_1} = b^{(1)}(n_1)\, b^{(1)}(n_2) \ldots, \tag{4.86a}$$
$$e^{n\gamma_2} = b^{(2)}(n_1)\, b^{(2)}(n_2) \ldots, \tag{4.86b}$$
$$\cdots = \cdots, \tag{4.86c}$$
$$e^{n\gamma_{2M}} = b^{(2M)}(n_1)\, b^{(2M)}(n_2) \ldots, \tag{4.86d}$$
$$e^{n\gamma_{2M+1}} = b^{(2M+1)}(n_1)\, b^{(2M)}(n_2) \ldots, \tag{4.86e}$$
$$\cdots = \cdots \tag{4.86f}$$
$$e^{n\gamma_{4M-1}} = b^{(4M-1)}(n_1)\, b^{(4M-1)}(n_2) \ldots, \tag{4.86 g}$$
$$e^{n\gamma_{4M}} = b^{(4M)}(n_1)\, b^{(4M)}(n_2) \ldots, \tag{4.86h}$$

where $n = n_1 + n_2 + \ldots$. For the symplectic matrix P_n, the eigenvalues occur in pairs,

$$n\gamma_1, n\gamma_2, \cdots, n\gamma_{2M}, \frac{1}{n\gamma_{2M}}, \cdots, \frac{1}{n\gamma_2}, \frac{1}{n\gamma_1}, \tag{4.87}$$

where we have arranged them in descending order. As such, we have the following relation

$$n\gamma_{2M} = \frac{n}{\lambda} = \ln b_{n_1}^{(2M)} + \ln b_{n_2}^{(2M)} + \ldots \tag{4.88}$$

from which the localization length can be calculated iteratively

$$\lambda = \frac{n}{c_n^{(2M)}} \tag{4.89}$$

with

$$c_n^{(2M)} = \ln b_n^{(2M)} + c_{n-1}^{(2M)}. \tag{4.90}$$

More generally, we can define a channel dependent localization length

$$\lambda_i = \frac{n}{c_n^{(i)}}, \tag{4.91}$$

with

$$c_n^{(i)} = \ln b_n^{(i)} + c_{n-1}^{(i)}, \tag{4.92}$$

for $1 \leq i \leq 2M$. Since the spin carried by a quasiparticle in a superconductor is conserved [23], these localization lengths can then be used to determine the spin conductance for the strip with width M [24]:

$$g_s(M, n_i) = \sum_{j=1}^{2M} \cosh^{-2} \Lambda_j, \tag{4.93}$$

where $\Lambda_j = \lambda_j / M$ is the localization length in units of the strip width. In Fig. 4.7a, g_s is shown as a function of M and it monotonically decreases with the increase of M at $E = 0$ for each selected impurity density, indicative of a localization in the large M limit. In addition, as shown in Fig. 4.7b, all the data for various values of M at different n_i can be collapsed onto a single curve:

$$g_s(M, n_i) = f\left(\frac{\xi(n_i)}{M}\right) \tag{4.94}$$

so that the one-parameter scaling law is obeyed. The quantity $\xi(n_i)$ is the thermodynamic localization length which only depends on n_i as shown in the inset of Fig. 4.7b, and remains finite for all the disorder density n_i, suggesting that all the

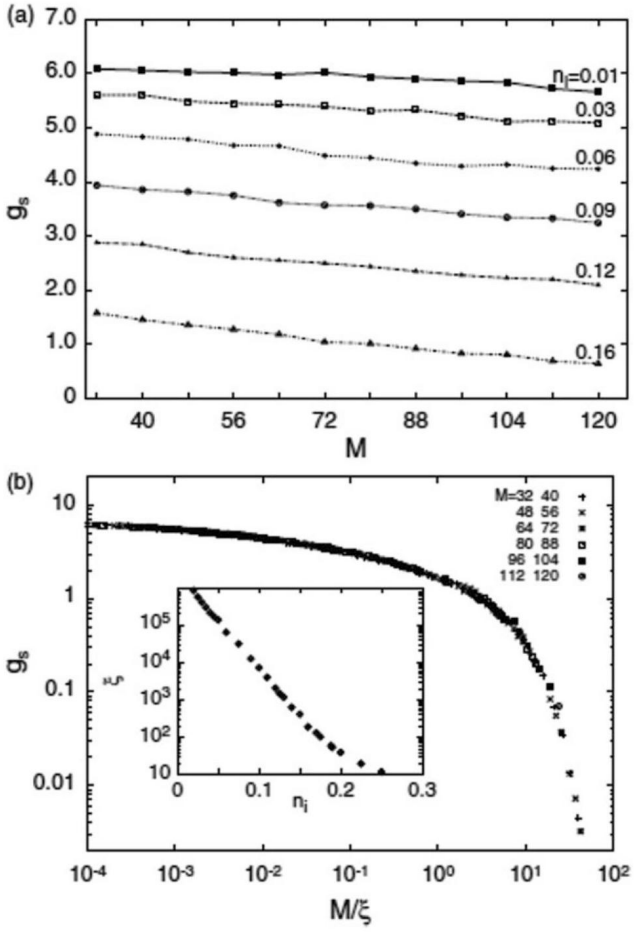


Fig. 4.7 Spin conductance as a function of the strip width M for various values of impurity concentration (a) and as a scaling function of M/ξ (b). Inset of (b): The thermodynamic localization length as a function of impurity concentration n_i. The energy of the quasiparticle state is $E = 0$. From [22]

states are localized even in the unitary limit with the presence of the zero energy resonance peak.

We remark that this scaling approach can also be applied to study the localization and delocalization in disordered topological superconductors.

13.3 5 Local Electronic Structure in Superconductors Under a Magnetic Field

Abstract

In this chapter, the calculation of local electronic structure in the presence of magnetic field is discussed. It starts with the continuum theory for a single vortex and proceeds to the lattice version for the vortex lattices in both conventional s-wave and unconventional d-wave superconductors. A generalization of the BdG formulation for a topological superconductor will be briefly explored. For high- T_c cuprates, the local induction of competing order around a magnetic vortex core is examined. Finally, the Zeeman-field induced FFLO superconducting state is also analyzed in depth.

13.3.1 5.1 Effect of the Magnetic Field

In Chap. 1, we have addressed the non-interacting electron part of the Hamiltonian in the absence of static electric and magnetic field. Since the magnetic field effect on the superconducting properties is unique, we give it an in-depth discussion here. The second quantized Hamiltonian for electrons in the presence of a static magnetic filed is

$$\mathscr{H}_0 = \int d\mathbf{r}\psi_\alpha^\dagger(\mathbf{r})h_\alpha(\mathbf{r})\psi_\alpha(\mathbf{r}) \tag{5.1}$$

Here the single-particle Hamiltonian

$$h_\alpha(\mathbf{r}) = \frac{\left[\frac{\hbar}{i}\nabla_\mathbf{r} + \frac{e}{c}\mathbf{A}(\mathbf{r})\right]^2}{2m_e} + V(\mathbf{r}) + \alpha\mu_B H(\mathbf{r}) - E_F, \tag{5.2}$$

where $\mathbf{A}(\mathbf{r})$ is the vector potential giving rise to the magnetic field $\mathbf{H}(\mathbf{r})$ (assumed to be along the z-direction of the spin axis)

$$\nabla \times \mathbf{A}(\mathbf{r}) = \mathbf{H}(\mathbf{r}) \tag{5.3}$$

$V(\mathbf{r})$ is the Coulomb potential contributed from the nuclear ions, and the third term in Eq. (5.2) describes the coupling of electron spin moment to the magnetic field.

The magnetic field has effects through both electron orbital and spin degrees of freedom. For the purpose of this chapter, we neglect the effect of spin-orbit coupling.

In wide-band systems, where $V(\mathbf{r})$ varies slowly, the free-electron gas approximation is usually made and the continuum model is a choice to study the magnetic field effect. For narrow-band systems, where the band structure effect is important, the tight-binding model is more convenient. Therefore, it is helpful to obtain the single-particle tight-binding Hamiltonian for the orbital effect of the magnetic field. The derivation follows that by Luttinger [1]. In the presence of a magnetic field, we expand the field operators as

$$\psi_\sigma(\mathbf{r}) = \sum_{\mathbf{R}_i} a\left(\mathbf{r} - \mathbf{R}_i\right) e^{-ie\Lambda_i/\hbar c} c_{i\sigma} \tag{5.4}$$

Here $a\left(\mathbf{r} - \mathbf{R}_i\right)$ are either maximally localized Wannier functions or atomic orbitals. They are localized about the lattice site $\mathbf{R}_i$ and drop off rapidly as $\mathbf{r}$ goes away from $\mathbf{R}_i$. The operator $c_{i\sigma}$ annihilates one electron of spin σ at site i. The integral

$$\Lambda_i = \int_{\mathbf{R}_i}^{\mathbf{r}} \mathbf{A}(\boldsymbol{\xi}) \cdot d\boldsymbol{\xi} \tag{5.5a}$$

$$\equiv \int_0^1 \left(\mathbf{r} - \mathbf{R}_i\right) \cdot \mathbf{A}\left(\mathbf{R}_i + \lambda\left(\mathbf{r} - \mathbf{R}_i\right)\right) d\lambda, \tag{5.5b}$$

is taken along the straight line path joining $\mathbf{R}_i$ to $\mathbf{r}$. The exponential factor in Eq. (5.4) has the effect of approximately removing the troublesome $\mathbf{A}\cdot\mathbf{P}$ and $\mathbf{P}\cdot\mathbf{A}$ terms. We consider

$$\left(\mathbf{P}+\frac{e\mathbf{A}(\mathbf{r})}{c}\right)a\left(\mathbf{r}-\mathbf{R}_i\right)e^{-ie\Lambda_i/\hbar c}=e^{-ie\Lambda_i/\hbar c}\left[\mathbf{P}-\frac{e\nabla\Lambda_i}{c}+\frac{e\mathbf{A}(\mathbf{r})}{c}\right]a\left(\mathbf{r}-\mathbf{R}_i\right), \tag{5.6}$$

which leads to

$$\left(\mathbf{P}+\frac{e\mathbf{A}(\mathbf{r})}{c}\right)^2 a\left(\mathbf{r}-\mathbf{R}_i\right)e^{-ie\Lambda_i/\hbar c}=e^{-ie\Lambda_i/\hbar c}\left[\mathbf{P}-\frac{e\nabla\Lambda_i}{c}+\frac{e\mathbf{A}(\mathbf{r})}{c}\right]^2 a\left(\mathbf{r}-\mathbf{R}_i\right) \tag{5.7}$$

We then use the identities

$$\nabla\times\mathbf{r}=0,\quad(\mathbf{A}\cdot\nabla)\mathbf{r}=\mathbf{A} \tag{5.8}$$

$$\nabla\times\mathbf{A}\left(\mathbf{R}_i+\lambda\left(\mathbf{r}-\mathbf{R}_i\right)\right)=\lambda\mathbf{H}\left(\mathbf{R}_i+\lambda\left(\mathbf{r}-\mathbf{R}_i\right)\right), \tag{5.9}$$

while

$$\begin{aligned}\int_0^1\mathbf{A}\left(\mathbf{R}+\lambda\left(\mathbf{r}-\mathbf{R}_i\right)\right)=&\ \lambda\mathbf{A}\left(\mathbf{R}_i+\lambda\left(\mathbf{r}-\mathbf{R}_i\right)\right)\big|_0^1-\int_0^1 d\lambda\lambda\frac{d\mathbf{A}\left(\mathbf{R}_i+\lambda\left(\mathbf{r}-\mathbf{R}_i\right)\right)}{d\lambda}\\&=\mathbf{A}(\mathbf{r})-\int_0^1 d\lambda\left(\left(\mathbf{r}-\mathbf{R}_i\right)\cdot\nabla\right)\mathbf{A}\end{aligned} \tag{5.10}$$

and prove that

$$\nabla\Lambda_i=\mathbf{A}(\mathbf{r})+\int_0^1 d\lambda\lambda\left(\mathbf{r}-\mathbf{R}_i\right)\times\mathbf{H}\left(\mathbf{R}_i+\lambda\left(\mathbf{r}-\mathbf{R}_i\right)\right) \tag{5.11}$$

By substituting Eq.(5.4) into Eq.(5.1), and using the expressions Eq.(5.7) and Eq. (5.11), one arrives at

$$\mathscr{H}_0=\sum_{ij,\sigma}\tilde{h}_{ij}c_{i\sigma}^{\dagger}c_{j\sigma} \tag{5.12}$$

where the field-modified one-electron Hamiltonian is given by

$$\begin{aligned}\tilde{h}_{ij}=\int d\mathbf{r}a^*\left(\mathbf{r}-\mathbf{R}_i\right)e^{ie(\Lambda_i-\Lambda_j)/\hbar c}\Bigg\{\frac{1}{2m_e}\Bigg(\mathbf{P}-\frac{e}{c}\int_0^1 d\lambda\lambda\left(\mathbf{r}-\mathbf{R}_i\right)\times\mathbf{H}\left(\mathbf{R}_j+\lambda\left(\mathbf{r}-\mathbf{R}_j\right)\right)^2\\+V(\mathbf{r})-E_F\Bigg\}a\left(\mathbf{r}-\mathbf{R}_j\right).\end{aligned} \tag{5.13}$$

We may now invoke the fact that the function a_i is localized, which allows us to approximate $\mathbf{r}\approx\mathbf{R}_j$ in the integral over λ in the above integral, as long as the magnetic fields are not varying too rapidly. This approximation leads to

$$\tilde{h}_{ij}=-t_{i\neq j}e^{i\varphi_{ij}}+\left(\epsilon_i-E_F\right)\delta_{ij} \tag{5.14}$$

where

$$t_{ij}=-\int d\mathbf{r}a^*\left(\mathbf{r}-\mathbf{R}_i\right)\left(\frac{\mathbf{p}^2}{2m_e}+V(\mathbf{r})\right)a\left(\mathbf{r}-\mathbf{R}_j\right) \tag{5.15}$$

is the hopping integral in the absence of magnetic field, and the Peierls phase is given by

$$\begin{aligned}\varphi_{ij} &= -\frac{e}{\hbar c}\int_{\mathbf{R}_j}^{\mathbf{R}_i}\mathbf{A}(\boldsymbol{\xi})\cdot\boldsymbol{\xi} \\ &= -\frac{2\pi}{\Phi_0}\int_{\mathbf{R}_j}^{\mathbf{R}_i}\mathbf{A}(\boldsymbol{\xi})\cdot\boldsymbol{\xi}\end{aligned} \tag{5.16}$$

Here the single-electron flux quantum is

$$\Phi_0 = \frac{hc}{e} \tag{5.17}$$

with h the Planck constant. The phase factor modifying the hopping integral is called as the Peierls substitution [2].

The spin Zeeman exchange interaction term can be easily found as

$$\sum_{i\sigma}\sigma\mu_B H_i c_{i\sigma}^{\dagger}c_{i\sigma} \tag{5.18}$$

in the tight-binding model, where H_i is an effective magnetic field at site i.
We conclude this section by summarizing the BdG equations in the presence of magnetic field:

$$\begin{cases} \tilde{h}_{\sigma}(\mathbf{r})u_{\sigma}^{n}(\mathbf{r}) + \int d\mathbf{r}'\Delta\left(\mathbf{r},\mathbf{r}'\right)v_{\bar{\sigma}}^{n}\left(\mathbf{r}'\right) = E_n u_{\sigma}^{n}(\mathbf{r}) \\ \int d\mathbf{r}'\Delta^{*}\left(\mathbf{r}',\mathbf{r}\right)u_{\sigma}^{n}\left(\mathbf{r}'\right) - \tilde{h}_{\bar{\sigma}}^{*}(\mathbf{r})v_{\bar{\sigma}}^{n}(\mathbf{r}) = E_n v_{\bar{\sigma}}^{n}(\mathbf{r}) \end{cases} \tag{5.19}$$

in the continuum limit, and

$$\begin{cases} E_n u_{i\sigma}^{n} = \sum_j \tilde{h}_{ij,\sigma}u_{j\sigma}^{n} + \sum_j \Delta_{ij}v_{j\bar{\sigma}}^{n}, \\ E_n v_{i\bar{\sigma}}^{n} = -\sum_j \tilde{h}_{ij,\bar{\sigma}}^{*}v_{j\bar{\sigma}}^{n} + \sum_j \Delta_{ji}^{*}u_{j\sigma}^{n}, \end{cases} \tag{5.20}$$

in the tight-binding model.

13.3.2 5.2 Vortex Core State in an s-Wave Superconductor

13.3.3 5.2.1 Single Isolated Vortex

The study of the single vortex line of an s-wave superconductor based on the BdG theory has been initiated with the seminal work by Caroli, de Gennes, and Matricon [3-5] and later by Bardeen et al. [6], in which various approximations were used. Later on, Shore et al. [7] and Gygi and Schlüter [8] obtained numerical solutions for quasiparticle amplitudes in a vortex core starting with approximate forms for the pair potential. It is important to note that, in these two calculations, the pair potential used as input was modeled from the experimentally inferred coherence length. The effect of the spatial dependence of the magnetic field was neglected, which seems to be justified when the GL parameter $\kappa \equiv \lambda/\xi$ is large, where λ and ξ are the penetration depth and coherence length, respectively.

Here we consider a single vortex in a two-dimensional s-wave superconductor. When the magnetic field is applied perpendicular to the 2D plane, the orbital effect is dominant over the spin Zeeman effect. By introducing the polar coordinate system
$\mathbf{r} = (r,\theta)$, the pair potential should have the form

$$\Delta(\mathbf{r}) = \Delta(r)e^{-i\theta} \tag{5.21}$$

It suggests that we can write the eigenfunctions as

$$\begin{pmatrix} u_n(\mathbf{r}) \\ v_n(\mathbf{r}) \end{pmatrix} = \begin{pmatrix} u_{j\mu} e^{i(\mu-1/2)\theta} \\ v_{j\mu} e^{i(\mu+1/2)\theta} \end{pmatrix},$$

which leads to the BdG equations

$$\begin{aligned} E_{j\mu} u_{j\mu}(r) =& \frac{\hbar^2}{2m_e} \left(-\frac{d^2 u_{j\mu}(r)}{dr^2} - \frac{1}{r}\frac{du_{j\mu}(r)}{dr} + \frac{(\mu-1/2)^2 u_{j\mu}(r)}{r^2} \right) - E_F u_{j\mu}(r) \\ &+ \Delta(r) v_{j\mu}(r) \qquad (5.22a) \\ E_{j\mu} v_{j\mu}(r) =& -\frac{\hbar^2}{2m_e} \left(-\frac{d^2 v_{j\mu}(r)}{dr^2} - \frac{1}{r}\frac{dv_{j\mu}(r)}{dr} + \frac{(\mu+1/2)^2 v_{j\mu}(r)}{r^2} \right) + E_F v_{j\mu}(r) \\ &+ \Delta(r) u_{j\mu}(r). \qquad (5.22b) \end{aligned}$$

Here the pair potential amplitude

$$\Delta(r) = \frac{U}{2} \sum_{j\mu(|E_{j\mu}| \le \omega_D)} u_{j\mu}(r) v_{j\mu}(r) \tanh\left(\frac{E_{j\mu}}{2k_{BT}} \right) \qquad (5.23)$$

is determined self-consistently, where U is an effective pairing interaction and ω_D is the cutoff. The azimuthal quantum number $|\mu| = \frac{1}{2}, \frac{3}{2}, \frac{5}{2}, \ldots$.

We first focus on solutions to the BdG equations (5.22) by following the original work by Caroli, de Gennes, and Matricon [3] and that in [9] in the assumption that the pair potential is known with a shape schematically drawn in Fig.5.1. Equations (5.22) can be rewritten as:

$$\begin{aligned} &\frac{\hbar^2}{2m_e} \left(-\frac{d^2 u_{j\mu}(r)}{dr^2} - \frac{1}{r}\frac{du_{j\mu}(r)}{dr} + \frac{(\mu^2+1/4)\, u_{j\mu}(r)}{r^2} \right) - E_F u_{j\mu}(r) + \Delta(r) v_{j\mu}(r) \\ &= \left(E_{j\mu} + \frac{\mu\hbar^2}{2m_e r^2} \right) u_{j\mu}(r) \qquad (5.24a) \\ &-\frac{\hbar^2}{2m_e} \left(-\frac{d^2 v_{j\mu}(r)}{dr^2} - \frac{1}{r}\frac{dv_{j\mu}(r)}{dr} + \frac{(\mu^2+1/4)\, v_{j\mu}(r)}{r^2} \right) + E_F v_{j\mu}(r) + \Delta(r) u_{j\mu}(r) \\ &= \left(E_{j\mu} + \frac{\mu\hbar^2}{2m_e r^2} \right) v_{j\mu}(r) \qquad (5.24b) \end{aligned}$$

We now introduce a radius r_c very close to the vortex core center, that is,

$$(\mu + 1/2) k_F^{-1} \ll r_c \ll \xi$$

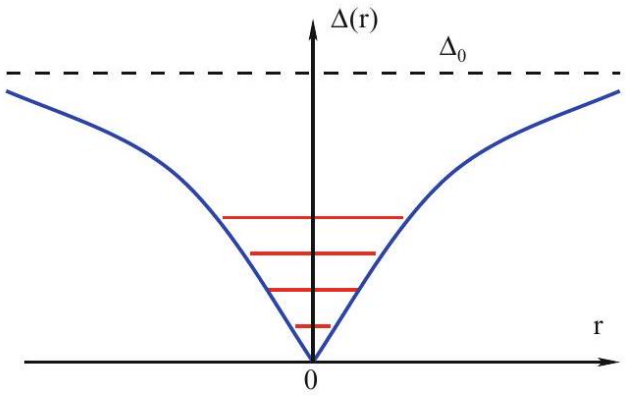


Fig. 5.1 The amplitude of superconducting order parameter $\Delta(r)$ around a single vortex core line. It vanishes at the core center $r = 0$ while rises to the bulk magnitude Δ_0 over a characteristic length ξ. The quasiparticle states with energies (red lines) smaller than the superconducting gap Δ_0 are bound near the vortex core center

For $r < r_c, \Delta(r)$ approaches to zero and we can neglect it in Eqs. (5.24), and obtain the solution as

$$\begin{pmatrix} u_\mu(r) \\ v_\mu(r) \end{pmatrix} = \begin{pmatrix} A_+ J_{\mu-\frac{1}{2}}\left[(k_F+q)\,r\right] \\ A_- J_{\mu+\frac{1}{2}}\left[(k_F-q)\,r\right] \end{pmatrix} \tag{5.25}$$

where k_F is the Fermi wave number, $q = E/\hbar v_F$ with $v_F = \hbar k_F/m_e$, and J_μ is the Bessel function. Here we have used the approximation

$$\left(k_F^2 \pm \frac{2m_e E}{\hbar^2}\right)^{1/2} \approx k_F \pm q \tag{5.26}$$

For $r > r_c$, we use the fact that the Hankel function $H_\mu(k_F r)$ satisfies the Bessel ordinary differential equation:

$$\frac{d^2 H_\mu(k_F r)}{dr^2} + \frac{1}{r}\frac{dH_\mu(k_F r)}{dr} + \left(k_F^2 - \frac{\mu^2}{r^2}\right) H_\mu(k_F r) = 0 \tag{5.27}$$

to separate this fast oscillating component out of the wave function and write in the form

$$\begin{pmatrix} u_\mu(r) \\ v_\mu(r) \end{pmatrix} = \begin{pmatrix} R_+(r) H_{\tilde{\mu}}(k_F r) + \text{ c.c} \\ R_-(r) H_{\tilde{\mu}}(k_F r) + \text{ c.c.} \end{pmatrix} \tag{5.28}$$

where the functions $R_\pm(r)$ are varying slowly in space, and the quantum number $\tilde{\mu} = \sqrt{\mu^2 + 1/4}$. Substituting Eq. (5.28) into Eq. (5.24), we obtain

$$\frac{\hbar^2}{2m_e}\left[-H_{\tilde{\mu}}\frac{d^2R_+(r)}{dr^2} - \left(2H'_{\tilde{\mu}} + \frac{H_{\tilde{\mu}}}{r}\right)\frac{dR_+(r)}{dr}\right] + \Delta(r) H_{\tilde{\mu}} R_-(r)$$

$$= \left(E + \frac{\mu\hbar^2}{2m_e r^2}\right) H_{\tilde{\mu}} R_+(r), \tag{5.29a}$$

$$-\frac{\hbar^2}{2m_e}\left[-H_{\tilde{\mu}}\frac{d^2R_-(r)}{dr^2} - \left(2H'_{\tilde{\mu}} + \frac{H_{\tilde{\mu}}}{r}\right)\frac{dR_-(r)}{dr}\right] + \Delta(r) H_{\tilde{\mu}} R_+(r)$$

$$= \left(E + \frac{\mu\hbar^2}{2m_e r^2}\right) H_{\tilde{\mu}} R_-(r) \tag{5.29b}$$

In the limit that $k_F r \gg 1$, we neglect the terms $HR''_\pm$ and $HR'_\pm/r$, and approximate $H'(k_F r) \approx i k_F H$ from the asymptotic form of the Hankel function

$$H_\mu(x) = \left(\frac{2}{\pi x}\right)^{1/2} \exp\left[i\left(x + \frac{\mu^2}{2x} - \frac{\mu\pi}{2} - \frac{\pi}{4}\right)\right] \tag{5.30}$$

for the limit $r \to \infty$. Equation (5.29) then becomes

$$-i\frac{\hbar^2 k_F}{m_e}\frac{dR_+(r)}{dr} + \Delta(r) R_-(r) = \left(E + \frac{\mu\hbar^2}{2m_e r^2}\right) R_+(r) \tag{5.31a}$$

$$i\frac{\hbar^2 k_F}{m_e}\frac{dR_-(r)}{dr} + \Delta(r) R_+(r) = \left(E + \frac{\mu\hbar^2}{2m_e r^2}\right) R_-(r) \tag{5.31b}$$

For $E \ll \Delta_0$ and $k_F r \gg \mu$, we can treat the right-hand-side of Eq.(5.31) perturbatively. To proceed, we write the envelope functions in the form

$$\begin{pmatrix} R_+(r) \\ R_-(r) \end{pmatrix} = \begin{pmatrix} e^{i\varphi} \\ e^{-i\varphi} \end{pmatrix} e^{-K} \tag{5.32}$$

Substitution of Eq. (5.32) into Eq. (5.31) gives

$$\hbar v_F \left(\frac{1}{2} \frac{d\varphi}{dr} + i \frac{dK}{dr} \right) + \Delta(r) e^{-i\varphi} = E + \frac{\mu \hbar^2}{2 m_e r^2} \tag{5.33a}$$

$$\hbar v_F \left(\frac{1}{2} \frac{d\varphi}{dr} - i \frac{dK}{dr} \right) + \Delta(r) e^{i\varphi} = E + \frac{\mu \hbar^2}{2 m_e r^2} \tag{5.33b}$$

Through addition and subtraction of Eqs. (5.33a) and (5.33b), we find

$$\frac{\hbar v_F}{2} \frac{d\varphi}{dr} + \Delta(r) \cos\varphi = E + \frac{\mu \hbar^2}{2 m_e r^2} \tag{5.34a}$$

$$\hbar v_F \frac{dK}{dr} - \Delta(r) \sin\varphi \tag{5.34b}$$

We further write the solution for φ and K up to the leading order of $E + \frac{\mu \hbar^2}{2 m_e r^2}$:

$$\varphi = \varphi_0 + \varphi_1 \tag{5.35a}$$

$$K = K_0 + K_1 \tag{5.35b}$$

It can be easily found that

$$\varphi_0 = \frac{\pi}{2} \tag{5.36a}$$

$$K_0 = (\hbar v_F)^{-1} \int_0^r \Delta(r')\, dr' \tag{5.36b}$$

Upon substitution of Eq. (5.35) together with Eq. (5.36) into Eq. (5.34), we arrive at

$$\frac{\hbar v_F}{2} \frac{d\varphi_1}{dr} - \Delta(r) \varphi_1 = E + \frac{\mu \hbar^2}{2 m_e r^2} \tag{5.37a}$$

$$K_1 = 0 \tag{5.37b}$$

where we have used the approximation $\sin\varphi_1 \approx \varphi_1$. Equation (5.37a) has the solution

$$\begin{aligned} \varphi_1(r) &= -\int_r^\infty e^{\frac{2}{\hbar v_F}\left[\int_0^r \Delta(r')dr' - \int_0^{r'} \Delta(r'')dr''\right]} \left(2q + \frac{\mu}{k_F r'^2} \right) dr' \\ &= -\int_r^\infty e^{2K_0(r) - 2K_0(r')} \left(2q + \frac{\mu}{k_F r'^2} \right) dr' \end{aligned} \tag{5.38}$$

On the other hand, for $r < r_c$, we can write

$$\varphi_1(r) = a_{-1}/r + a_0 + a_1 r + \dots$$

and

$$\Delta(r) = \left.\frac{d\Delta(r)}{dr}\right|_{r=0} r + \dots$$

and substitute them into Eq. (5.37a). By comparing the coefficients for the r^{-2} term, we have

$$a_{-1} = -\frac{\mu}{k_F}$$

so that

$$\frac{d\varphi_1}{dr} = 2q + \frac{\mu}{k_F r^2} - \frac{2\mu\Delta(r)}{\hbar k_F v_F r} \tag{5.39}$$

for $r < r_c$. We can then obtain

$$\begin{aligned}
\varphi_1(r_c) &= -\int_{r_c}^{\infty} e^{2K_0(r)-2K_0(r')}\left(2q + \frac{\mu}{k_F r'^2}\right) dr' \\
&\approx -\int_0^{\infty} e^{-2K_0(r')}\left(2q + \frac{\mu}{k_F r'^2}\right) dr' - \int_0^{r_c} \frac{d\varphi_1}{dr'} dr' \\
&\approx 2qr_c - \frac{\mu}{k_F r_c} - 2\int_0^{\infty} e^{-2K_0(r')}\left(q - \frac{\mu\Delta(r')}{\hbar k_F v_F r'}\right) dr'.
\end{aligned} \tag{5.40}$$

The final form of the wave function for $r > r_c$ is then

$$\begin{pmatrix} u_\mu(r) \\ v_\mu(r) \end{pmatrix} = \tilde{A} e^{-K_0(r)} \begin{pmatrix} e^{i\frac{\pi}{4}+i\frac{\varphi_1}{2}} H_{\tilde{\mu}}(k_F r) + \text{ c.c} \\ e^{-i\frac{\pi}{4}-i\frac{\varphi_1}{2}} H_{\tilde{\mu}}(k_F r) + \text{ c.c.} \end{pmatrix} \tag{5.41}$$

This wave function must be joined smoothly at $r = r_c$ with that from the region $r < r_c$ given by Eq. (5.25). Using the asymptotic form of the Bessel function

$$J_\mu(x) = \left(\frac{2}{\pi x}\right)^{1/2} \exp\left[x + \frac{\mu^2}{2x} - \frac{\mu\pi}{2} + \frac{\pi}{4}\right] \tag{5.42}$$

for $x \gg 1$ together with that of the Hankel function, Eq. (5.30), we obtain

$$\varphi_1(r_c) = 2qr_c - \frac{\mu}{k_F r_c} \tag{5.43}$$

Comparison of Eq. (5.43) with Eq. (5.40) leads to

$$\int_0^{\infty} e^{-2K_0(r')}\left(q - \frac{\mu\Delta(r')}{\hbar k_F v_F r'}\right) dr' = 0 \tag{5.44}$$

That is,

$$\begin{aligned}
E_\mu &= \frac{\mu}{k_F} \frac{\int_0^{\infty} e^{-2K_0(r')} \frac{\Delta(r')}{r'} dr'}{\int_0^{\infty} e^{-2K_0(r')} dr'} \\
&= \frac{\mu}{k_F} \left.\frac{d\Delta(r)}{dr}\right|_{r=0} g(k_F)
\end{aligned} \tag{5.45}$$

where the dimensionless function $g(k_F)$ depends on the shape of $\Delta(r)$ and is close to one. Using the approximation $\left.\frac{d\Delta(r)}{dr}\right|_{r=0} \approx \frac{\Delta_0}{\xi}$ with the coherence length $\xi = \hbar v_F / 2\Delta_0$, the energies of the vortex core bound states are given by

$$E_\mu = \mu \frac{\Delta_0^2}{E_F} \tag{5.46}$$

These are the Caroli-de Gennes-Matricon vortex core levels. The lowest bound state energy corresponds to $|\mu| = \frac{1}{2}$.

More rigorous solution to the BdG equations can only be obtained through numerical solution, which also determines the pair potential self-consistently [10, 11]. The radial functions are expanded in terms of the set of Bessel functions normalized in a disc of radius R:

$$\begin{pmatrix} u_{j\mu}(r) \\ v_{j\mu}(r) \end{pmatrix} = \sum_i \begin{pmatrix} c_{ji}\phi_{i\mu-\frac{1}{2}}(r) \\ d_{ji}\phi_{i\mu+\frac{1}{2}}(r) \end{pmatrix}, \tag{5.47}$$

where

$$\phi_{im}(r) = \frac{\sqrt{2}}{RJ_m(\alpha_{im})} J_m(\alpha_{im} r/R), \quad i = 1, 2, \ldots, N \tag{5.48}$$

with $m = \mu \mp \frac{1}{2}$ and α_{im} is the i th zero of $J_m(x)$. The BdG equations are now solved separately in each subspace of fixed angular momentum μ, which amounts to solve a $2N \times 2N$ matrix eigenvalue problem. Once the self-consistency solution is obtained, the local density of states as derived in Chap. 1 can be computed.

Typical results are shown in Figs. 5.2 and 5.3. As the temperature decreases, the vortex core size, as defined by $\left.\frac{d\Delta(r)}{dr}\right|_{r\to 0}$, shrinks, as originally predicted by Kramer and Pesch [13]. In addition, at very low-temperatures, the pair potential also exhibits Friedel-like oscillation, which is mainly contributed from the vortex core states. These vortex core states are displayed clearly in the local density of states probed near the core center. For a large zero-temperature coherence length, these core levels

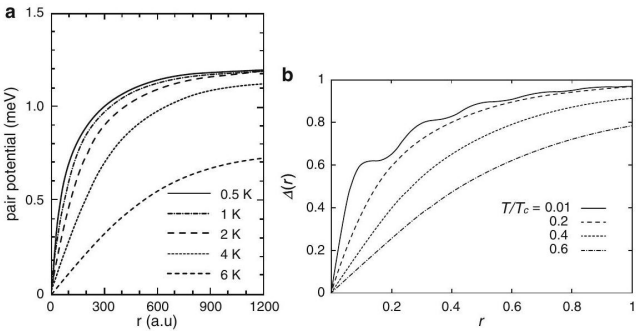


Fig. 5.2 Spatial variation of the pair potential $\Delta(r)$ as a function of distance away from the vortex core center, determined self-consistently, for $k_F\xi = 70$ (a) and 16 (b) for various temperatures. From [11] for (a) and [12] for (b)

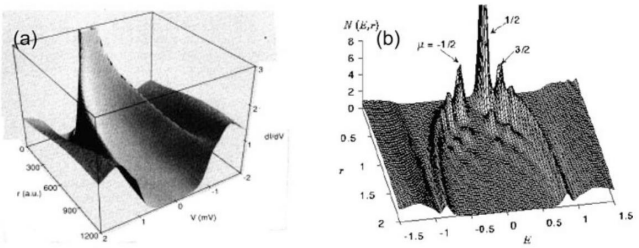


Fig. 5.3 Local density of states as a function of energy and distance from the vortex core center at $T = 0.13T_c$ and $k_F\xi = 70(\mathbf{a})$, and $T = 0.05T_c$ and $k_F\xi = 8(\mathbf{b})$. From [11] for (a) and [12] for (b)

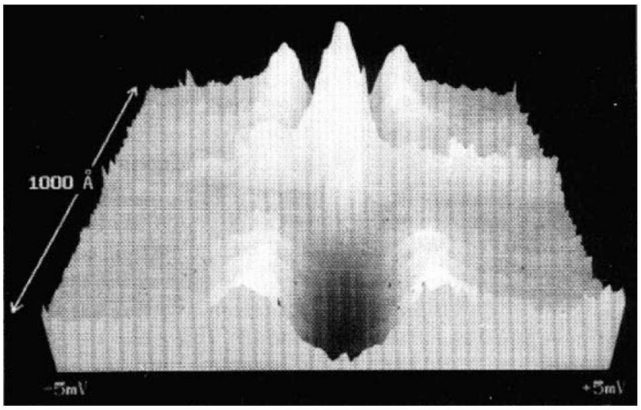


Fig. 5.4 Image of dI/dV on $2H-NbSe_2$ as a function of voltage bias (horizontal axis) and position along a line that intersects a vortex (vertical axis). From [14]

are close in energy and the discretization is thermally smeared, while for a short coherence length, the discretization of the levels is evident. The first experimental evidence for the Caroli-de Gennes-Matricon vortex core states comes from a series of scanning tunneling experiments on a layered hexagonal compound $2H-NbSe_2$ at low temperatures [14-16]. A spatial image of tunneling conductance across a vortex is shown in Fig. 5.4. There a tunneling conductance peak is observed at the vortex core center.

Recently, the STM experiments have also been carried out in a vortex core of a proximity-induced s-wave superconductor in Bi_2Te_3 thin films [17, 18]. The evolution of local tunneling conductance spectra with film thickness has led to a conjecture [18] that the zero-bias conductance peak observed at the core center reveals the existence of Majorana bound states. This conjecture has been supported by a very recent theoretical study [19] by solving a generalized set of BdG equations [20, 21]:

$$\begin{pmatrix} \hat{\mathscr{H}}_{\rm TI}(\mathbf{r}) & \hat{\Delta}(\mathbf{r}) \\ \hat{\Delta}^{\dagger}(\mathbf{r} & -\hat{\mathscr{H}}^{*}_{\rm TI}(\mathbf{r}) \end{pmatrix} \begin{pmatrix} \hat{u}(\mathbf{r}) \\ \hat{v}(\mathbf{r}) \end{pmatrix} = E \begin{pmatrix} \hat{u}(\mathbf{r}) \\ \hat{v}(\mathbf{r}) \end{pmatrix}. \tag{5.49}$$

Here the normal-state effective Hamiltonian of the TI

$$\hat{\mathscr{H}}_{\rm TI} = \epsilon \hat{\sigma}_z - iv_F \left[e^{-i\phi \hat{s}_z} \left(\partial_r \hat{s}_x + \frac{1}{r} \partial_\phi \hat{s}_y \right) + \partial_z \hat{s}_z \right] \hat{\sigma}_x - E_F, \tag{5.50}$$

with $\hat{s}_i$ and $\hat{\sigma}_i$ the Pauli matrices for spin and orbital degrees of freedom, and the Dirac mass

$$\epsilon = -\epsilon_0 - \frac{1}{2m_e} \left(\partial_r^2 + \frac{1}{r} \partial_r + \frac{1}{r^2} \partial_\phi^2 + \partial_z^2 \right), \tag{5.51}$$

in the cylindrical coordinates with the quantity $2\epsilon_0$ describing the bulk gap of the topological insulator. The proximity-induced superconducting gap has the form

$$\hat{\Delta} = e^{i\phi} \Delta_0 \hat{s}_x \tag{5.52}$$

where the superconducting gap Δ_0 is kept as a constant. We note that the BdG wave function $\left[\hat{u}(\mathbf{r}), \hat{v}(\mathbf{r}\right]^{\rm Transpose}$ is a total eight-component vector spanned in a spin-orbital-Nambu space. The BdG quasiparticle wave function around an isolated vortex takes the form

$$\begin{pmatrix} u_j^{s\sigma}(\mathbf{r}) \\ v_j^{s\sigma}(\mathbf{r}) \end{pmatrix} = \begin{pmatrix} e^{i(j-s/2+1/2)} \overline{u^{s\sigma}}(\mathbf{r}) \\ e^{i(j+s/2-1/2)} \bar{v}^{s\sigma}(\mathbf{r}) \end{pmatrix}, \tag{5.53}$$

where the superscripts $s(\pm 1)$ and $\sigma(=1,2)$ on u and v are spin and orbital indices. The coefficients $(\bar{u}^{s\sigma}(\mathbf{r}), \bar{v}^{s\sigma}(\mathbf{r}))$ can be expanded in terms of the Bessel orthonormal functions in

the radial direction [11] while the Gauss-Lobatto functions in the z direction [22]. Numerically, the authors of [19] has used a varying Fermi energy to simulate the thickness dependence of the local density of states around the vortex core. It was found that the local density of states profile evolves from a V-shape to a Y-shape as the Fermi energy level is tuned toward the bulk gap center, in a good agreement with the experimental results.

13.3.4 5.2.2 High Field Limit

The quasiparticle states of a superconductor in the low field limit can be sufficiently described by considering a single isolated vortex. In the high field limit, a vortex lattice is formed as a regular array [23], in which vortices are closely packed. In this limit, the single isolated vortex description is not adequate. Quasiparticle excitations of a superconductor in the high field limit are interesting in the possibility of Landau level quantization, which plays an important role in quantum Hall effect in a semiconductor two-dimensional electron gas.

Different from the single isolated vortex case, in the high magnetic field limit, the vector potential must be treated explicitly in the BdG equations (5.19) with $h(\mathbf{r})$ given by Eq. (5.1). For the extreme type-II superconductors, we can assume the vector potential is entirely determined by the external magnetic field. In the Landau gauge with the vector potential

$$\mathbf{A} = H(-y, 0, 0), \tag{5.54}$$

the pair potential for a triangular Abrikosov lattice has the form

$$\Delta(\mathbf{r}) = \Delta(T, H) \sum_n e^{i\pi a_{2,x} n^2/a_\Delta} e^{i2\pi n x/a_\Delta - (y/l_B + \pi n l_B/a_\Delta)^2}, \tag{5.55}$$

where the position vector $\mathbf{r} = (x, y)$. The unit vectors in the direct space of a triangular vortex lattice are

$$\mathbf{a}_1 = (a_{1,x}, a_{1,y}) = a_\Delta(1, 0), \quad \mathbf{a}_2 = (a_{2,x}, a_{2,y}) = a_\Delta \left(\frac{1}{2}, \frac{\sqrt{3}}{2} \right). \tag{5.56}$$

The magnetic length $l_B = \sqrt{\hbar c/eH}$. This form of the pair potential and the explicit appearance of the vector potential in the BdG equations break the rotational symmetry existing for the single isolated vortex. The BdG wave functions can be expanded as

$$\begin{pmatrix} u_{(\mathbf{r})} \\ v_{(\mathbf{r})} \end{pmatrix} = \sum_{n,\mathbf{q}} \begin{pmatrix} u_{n\mathbf{q}} \\ v_{n\mathbf{q}} \end{pmatrix} \phi_{n,\mathbf{q}}(\mathbf{r}). \tag{5.57}$$

Here $\phi_{n,\mathbf{q}}$ are the eigenfunctions to the single-particle Hamiltonian Eq. (5.1) in the magnetic sublattice representation for a vector potential chosen in the Landau gauge [24]:

$$\begin{aligned} \phi_{n,\mathbf{q}} =& \frac{1}{\sqrt{2^n n! \sqrt{\pi} l_B}} \sqrt{\frac{a_{2,y}}{L_x L_y}} \sum_m e^{i\frac{\pi a_{2,x}}{2a_\Delta} - imq_y a_{2,y}} e^{i(q_x + \pi m/a_\Delta)x - (y/l_B + q_x l_B + \pi m l_B/a_\Delta)^2/2} \\ & \times H_m\left(y/l_B + q_x l_B + \pi m l_B/a_\Delta\right) \end{aligned} \tag{5.58}$$

where $\mathbf{q} = (q_x, q_y)$ is the quasimomenta in the first magnetic Brillouin zone defined by the reciprocal vectors

$$\mathbf{Q}_1 = \left(a_{2,y}, -a_{2.x}\right)/l_B^2, \quad \mathbf{Q}_2 = \left(0, 2a_\Delta\right)/l_B^2 \tag{5.59}$$

L_x and L_y are the linear dimensions of the system, and $H_n(x)$ is the Hermite polynomial of order n. Substitution of Eq. (5.57) into Eq. (5.19) yields

$$\epsilon_n u_{n,\mathbf{q}} + \sum_m \Delta_{nm}(\mathbf{q}) v_{m,\mathbf{q}} = E_{n,\mathbf{q}} u_{n,\mathbf{q}} \tag{5.60a}$$

$$-\epsilon_n v_{n,\mathbf{q}} + \sum_m \Delta^*_{mn}(\mathbf{q}) u_{m,\mathbf{q}} = E_{n,\mathbf{q}} v_{n,\mathbf{q}} \tag{5.60b}$$

Here the normal-state Landau levels are given by

$$\epsilon_n = \left(n + \frac{1}{2}\right)\hbar\omega_c - E_F \tag{5.61}$$

with the cyclotron frequency $\omega_c = eH/m_e c$, and the matrix element for the pair potential is

$$\begin{aligned}\Delta_{nm}(\mathbf{q}) =& \frac{\Delta(T,H)}{\sqrt{2}} \frac{(-1)^m}{2^{n+m}\sqrt{n!m!}} \sum_k e^{i\pi a_{2,x} k^2/a_\Delta + 2ikq_y a_{2,y} - (q_x l_B + \pi k l_B/a_\Delta)^2} \\ & \times H_{n+m}\left[\sqrt{2}\left(q_x + \pi k/a_\Delta\right) l_B\right]\end{aligned} \tag{5.62}$$

Therefore, the BdG equations are now solved in a $2N_c \times 2N_c$ subspace for separate values of quasi momentum q. Due to the complex structure of the pair potential matrix elements, accurate solutions can only be obtained through numerical simulations [25-30]. The numerical results show that when the magnetic field is close to the upper critical field H_{c2}, gapless quasiparticle states can occur at discrete locations of the Fermi surface. We note that the gapless quasiparticle states in the s-wave superconductors are induced from the Cooper pair motion in the high magnetic field. Their existence can be detected by the de Haas-van Alphen oscillations at high magnetic field and low temperatures [31-34].

13.3.5 5.3 Vortex Core States in a d-Wave Superconductor

The study of vortex cores states in a d-wave superconductor finds its immediate relevance when high-temperature cuprates are found to have a d-wave pairing symmetry. A novel feature from a d-wave pairing symmetry is that the superconducting gap function experiences a continuous sign change at some special points of the Fermi energy, showing the existence of nodal quasiparticles. Similar to the previous section, here we first consider the quasiparticle core states in a single isolated vortex in the continuum model and for a vortex lattice in the tight-binding model.

13.3.6 5.3.1 Single Isolated Vortex

We begin with the BdG equations (5.19). The non-local nature of d-wave pairing introduces further complications. We introduce the center-of-mass coordinate system

$$\overline{\mathbf{R}} = \frac{\mathbf{r} + \mathbf{r}'}{2}, \quad \mathbf{s} = \mathbf{r} - \mathbf{r}' \tag{5.63}$$

to rewrite the equations as

$$h_{\mathbf{R}} u(\mathbf{R}) + \int \Delta(\mathbf{R} - \mathbf{s}/2, \mathbf{s}) v(\mathbf{R} - \mathbf{s}) d\mathbf{s} = E u(\mathbf{R}) \tag{5.64a}$$

$$-h^*_{\mathbf{R}} v(\mathbf{R}) + \int \Delta^*(\mathbf{R} - \mathbf{s}/2, \mathbf{s}) u(\mathbf{R} - \mathbf{s}) d\mathbf{s} = E u(\mathbf{R}) \tag{5.64b}$$

Here we have used a new label $\mathbf{R} = \mathbf{r}$ so that the single-particle Hamiltonian becomes

$$h_{\mathbf{R}} = \frac{\hbar^2}{2m_e}\left(\mathbf{p}_{\mathbf{R}} + \frac{e\mathbf{A}(\mathbf{R})}{c}\right) - E_F, \tag{5.65}$$

and

$$\overline{\mathbf{R}} = \mathbf{R} - \frac{\mathbf{s}}{2}, \quad \mathbf{s} = \mathbf{r} - \mathbf{r}' \tag{5.66}$$

The pair potential in the center-of-mass coordinate system is given by

$$\Delta(\overline{\mathbf{R}}, \mathbf{s}) = V(\mathbf{s}) \sum_n \left[u_n(\overline{\mathbf{R}} + \mathbf{s}/2) v_n^*(\overline{\mathbf{R}} - \mathbf{s}/2) + u_n(\overline{\mathbf{R}} - \mathbf{s}/2) v_n^*(\overline{\mathbf{R}} + \mathbf{s}/2) \tanh\left(\frac{E_n}{2k_B T}\right), \right. \tag{5.67}$$

with the energy summation subjected to a cutoff Ω_c in the continuum limit. The pairing interaction is parametrized as

$$V(\mathbf{s}) = V_d g(\varphi) \delta(s - a)/a, \tag{5.68}$$

with $\mathbf{s} = (s, \varphi)$ in the polar coordinates and a as a length scale for nonlocal pairing interaction. For the $d_{x^2-y^2}$-wave pairing symmetry, the angular dependent function

$$g(\varphi) = \cos^2(2\varphi). \tag{5.69}$$

This form of the pair interaction suggests that the d-wave order parameter depends on the relative coordinate s only through its polar angle. Therefore, we can expand it as

$$\Delta(\overline{\mathbf{R}}, \mathbf{s}) = \Delta(\overline{\mathbf{R}}, \theta; \varphi) = \sum_{p,l} e^{ip\theta} e^{il\varphi} \Delta_{pl}(R), \tag{5.70}$$

where $\overline{\mathbf{R}} = (\bar{R}, \theta)$. In this representation, p represents the winding number of the superconducting phase around the vortex and l represents the orbital angular momentum of the relative motion of two paired electrons. For the $d_{x^2-y^2}$-wave pairing symmetry, the order parameter near the single vortex should be contributed dominantly from a linear combination of components with $p = 1$, and $l = \pm 2$ at equal weight $\Delta(\bar{R}, \theta; \varphi) = e^{i\theta}\left[e^{i2\varphi}\Delta_{1,2}(\bar{R}) + e^{-i2\varphi}\Delta_{1,-2}(\bar{R})\right]$.

For the case of singe isolated d-wave vortex, we neglect the vector potential A, which is reasonable for extreme type-II superconductors. We can then follow the same procedure used for the single isolated s-wave vortex to solve the BdG equations (5.64) through the expansion of the wave function as

$$\begin{pmatrix} u_{j\mu}(R) \\ v_{j\mu}(R) \end{pmatrix} = \sum_i \begin{pmatrix} c_{ji}\phi_{i\mu-\frac{1}{2}}(R) \\ d_{ji}\phi_{i\mu+\frac{1}{2}}(R) \end{pmatrix}, \tag{5.71}$$

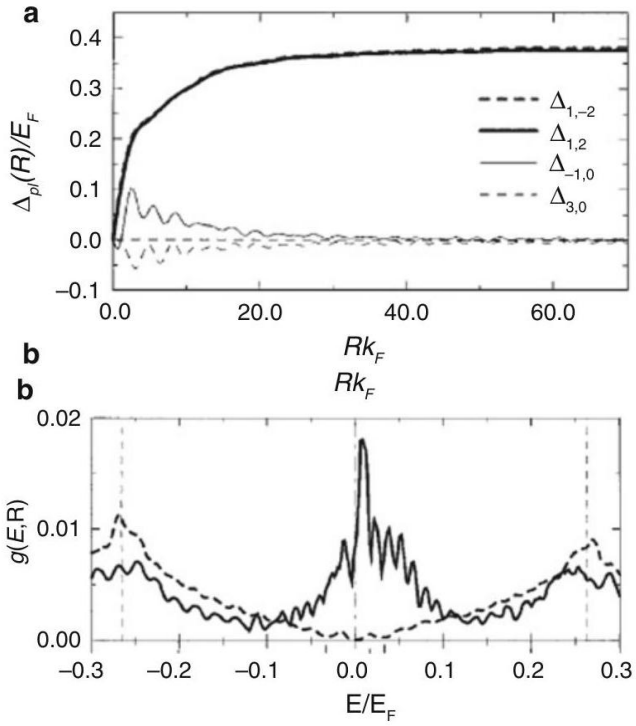
where

$$\phi_{im}(R) = \frac{\sqrt{2}}{R_0 J_m(\alpha_{im})} J_m(\alpha_{im} R/R_0), \quad i = 1, 2, \ldots, N \tag{5.72}$$

with $m = \mu \mp \frac{1}{2}$ and α_{im} is the i th zero of $J_m(x)$, and R_0 is the radius of a disk. The resultant equations can be solved via exact diagonalization with the order parameter obtained through an iteration procedure. Figure 5.5 shows the variation of the dominant component of the superconducting order parameter and the local tunneling conductance at the vortex center [35]. Due to the spatial anisotropy of the dominant $d_{x^2-y^2}$-wave component, other subdominant order parameter components are also induced near the vortex core (see Fig. 5.5a). The calculations

[35] also show that for a short coherence length $k_F\xi_0$ with $\xi_0 = \hbar v_F/\pi\Delta_0$ (Δ_0 is controlled by the pairing interaction strength V_d), the profile for the $d_{x^2-y^2}$-wave order parameter is quite universal and it follows the form $1/R^2$ instead of $\tanh(R/\xi')$ with ξ' a fitting parameter. In addition, a broad peak shows up near the Fermi energy in the local tunneling conductance at the vortex core center (see Fig. 5.5b). For the $d_{x^2-y^2}$-wave vortex core, even for a very short coherence (e.g., $k_F\xi_0 = 2.5$ for Fig. 5.5a), no clear splitting of the core level is obtained, which is in sharp contrast with the case of the s-wave vortex core. This is a clear indication that the nodal quasiparticles preexisting for the $d_{x^2-y^2}$-wave pairing even at zero field play an important role in the nature of vortex core states.

Fig. 5.5 Dominant order parameter component around a d-wave vortex (a) and the theoretically obtained tunneling conductance at the vortex core center. The system size is $k_F R_0 = 120$. The other parameter values are $k_F a = 2, \Omega_c/E_F = 0.3$, $V_d/E_F = 1.6$, and $T = 0$. From [35]



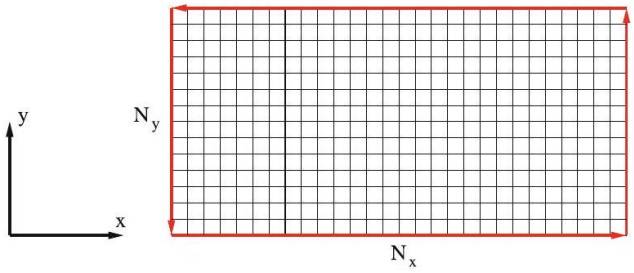
13.3.7 5.3.2 Quasiparticle States in a Mixed-State of d-Wave Superconductors

The order parameter profile for a single $d_{x^2-y^2}$-wave vortex core has also been studied by solving the BdG equations within the tight-binding model [36]. The use of tight-bind model enables one to incorporate band structure of normal-state superconductors, which is especially appropriate for high- T_c cuprates. As in the case of s-wave superconductors, when the magnetic field is much larger than the lower critical field H_{c1}, a vortex lattice is formed also in the d-wave superconductors. The quasiparticle spectrum in the mixed-state within the tight-binding model has been first studied by Wang and MacDonald [37] for a pure $d_{x^2-y^2}$-wave superconductor. It was shown that the local density of states at the d-wave vortex core exhibits a single broad peak at zero energy. The results are supported by the study of the single $d_{x^2-y^2}$-wave vortex line discussed above in the continuum model.

In this high-field limit, we again need to treat the magnetic field effect explicitly, which is described in the BdG equations (5.20). In the mixed state, the magnetic field effect is included through the Peierls phase factor $\varphi_{\mathbf{ij}} = -\frac{2\pi}{\Phi_0}\int_{\mathbf{r_j}}^{\mathbf{r_i}} \mathbf{A}(\mathbf{r})\cdot d\mathbf{r}$, where $\Phi_0 = hc/e(e>0)$ is the single-electron flux quantum. We still assume the superconductor under consideration is in the extreme type-II limit where the Ginzburg-Landau parameter $\kappa = \lambda/\xi$ goes to infinity so

that the screening effect from the supercurrent is negligible. Therefore, the vector potential $\mathbf{A}$ can be approximated by the solution

Fig. 5.6 Schematic drawing of a magnetic unit cell with linear dimensions of N_x and N_y. The red lines form a closed path around the unit cell



$\nabla \times \mathbf{A} = H\hat{\mathbf{z}}$, where H is the magnetic field externally applied along the c axis. The enclosed flux density within each plaquette is given by $\sum_{\square} \varphi_{\mathbf{ij}} = -\frac{2\pi H a^2}{\Phi_0}$.

We choose a Landau gauge to write the vector potential as $\mathbf{A} = (-Hy, 0, 0)$, where y is the y-component of the position vector $\mathbf{r}$. By considering a rectangular lattice, we introduce the magnetic translation operator $\mathscr{T}_{mn}\mathbf{r} = \mathbf{r} + \mathbf{R}$, where the translation vector $\mathbf{R} = mN_x a\hat{\mathbf{e}}_x + nN_y a\hat{\mathbf{e}}_y$ with N_x and N_y the linear dimension of the unit cell of the vortex lattice, as shown in Fig. 5.6. Note that the original crystal lattice is a. To ensure different $\mathscr{T}_{mn}$ to be commutable with each other, we have to take the strength of magnetic field so that the flux enclosed by each unit cell has a single-particle flux quantum, i.e, Φ_0, which is equivalent of two superconducting flux quanta each with $hc/2e$.

Under this condition, we can decouple the translation operator $\mathscr{T}_{mn}$ into two consecutive operations

$$\mathscr{T}_{mn} = \mathscr{T}_{0n}\mathscr{T}_{m0} \tag{5.73}$$

As such, we have

$$\mathbf{A}\left(\mathscr{T}_{m0}\mathbf{r}\right) = \mathbf{A}(\mathbf{r}) = \mathbf{A}(\mathbf{r}) + \nabla\phi_1 \tag{5.74}$$

which gives

$$\phi_1 = 0 \tag{5.75}$$

and

$$\mathbf{A}\left(\mathscr{T}_{0n}\mathbf{r}\right) = -Hy\hat{\mathbf{e}}_x - H\left(nN_y a\right)\hat{\mathbf{e}}_x = \mathbf{A}(\mathbf{r}) + \nabla\phi_2, \tag{5.76}$$

which gives

$$\phi_2 = -HnN_y ax \tag{5.77}$$

Therefore, the transformation $\mathscr{T}_{mn}$ leads to the transformation of the superconducting pair potential as:

$$\begin{aligned}\Delta\left(\mathscr{T}_{mn}\mathbf{r}\right) &= e^{-\frac{i4\pi}{\Phi_0}[-HnN_y a(x+mN_x a)]}e^{-\frac{i4\pi}{\Phi_0}\times 0}\Delta(\mathbf{r}) \\ &= e^{i\chi(\mathbf{r},\mathbf{R})}\Delta(\mathbf{r})\end{aligned} \tag{5.78}$$

where the phase accumulated by the order parameter upon the translation is

$$\chi(\mathbf{r},\mathbf{R}) = -\frac{4\pi}{\Phi_0}\left[-HnN_y a\left(x+mN_x a\right)\right]$$
$$= -\frac{4\pi}{\Phi_0}\mathbf{A}(\mathbf{R})\cdot\mathbf{r} + 4mn\pi \tag{5.79}$$

when $N_x N_y a^2 H = \Phi_0$. If we perform a successive application of four transformations along a closed path around the magnetic unit cell, as shown by the red lines in Fig. 5.6,

$$(0,0) \to (N_x a, 0) \to (N_x a, N_y a) \to (0, N_y a) \to (0,0) \tag{5.80}$$

the accumulated phase on the superconducting order parameter is 4π, which corresponds to two superconducting flux quanta.

From this property, we can obtain the magnetic Bloch theorem for the wavefunction of the BdG equations:

$$\begin{pmatrix} u_{\mathbf{k},\sigma}\left(\mathscr{T}_{mn}\tilde{\mathbf{r}}\right) \\ v_{\mathbf{k},\sigma}\left(\mathscr{T}_{mn}\tilde{\mathbf{r}}\right) \end{pmatrix} = e^{i\mathbf{k}\cdot\mathbf{R}} \begin{pmatrix} e^{i\chi(\mathbf{r},\mathbf{R})/2} u_{\mathbf{k},\sigma}(\tilde{\mathbf{r}}) \\ e^{-i\chi(\mathbf{r},\mathbf{R})/2} v_{\mathbf{k},\sigma}(\tilde{\mathbf{r}}) \end{pmatrix}. \tag{5.81}$$

Here $\tilde{\mathbf{r}}$ is the position vector defined within a given unit cell and $\mathbf{k} = \frac{2\pi l_x}{M_x N_x}\hat{\mathbf{e}}_x + \frac{2\pi l_y}{M_y N_y}\hat{\mathbf{e}}_y$ with $m_{x,y} = 0, 1, \ldots, M_{x,y} - 1$ are the wavevectors defined in the first Brillouin zone of the vortex lattice and $M_x N_x$ and $M_y N_y$ are the linear dimension of the whole system. The vortex carrying the flux quantum $hc/2e$ is the generic feature of the pairing theory for superconductivity. Comparing with the zero-field case but with the similar kind of supercell technique, we can see that the magnetic field also modifies the matching conditions between two neighboring unit cells. Similar type of the magnetic Bloch theorem can also be derived in the symmetry gauge for the vector potential. Typical numerical results are shown in Fig. 5.7 [37]: The d-wave order

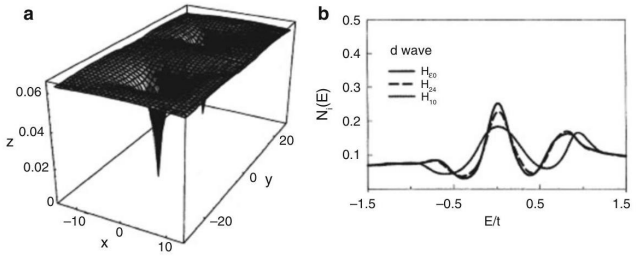


Fig. 5.7 Amplitude of a d-wave order parameter in a magnetic unit cell (a) and the local density of states at the vortex core center. From [37]

parameter as defined by

$$\Delta_d(i) = \frac{1}{4}\left[\Delta_{i,i+\hat{x}} + \Delta_{i,i-\hat{x}} - \Delta_{i,i+\hat{y}} - \Delta_{i,i-\hat{y}}\right], \tag{5.82}$$

is strongly suppressed at the vortex core. The local density of states at the vortex center exhibits a broad peak, which is clearly centered at the Fermi energy. No clear core level splitting is seen. These results are fully supported by the study of a single isolated d-wave vortex core in the continuum model discussed above.

The quasiparticle states near the vortex core can be probed by scanning tunneling microscopy. The unique feature of a pure d-wave pairing symmetry on the mixstate quasiparticles state can also be detected by nuclear magnetic resonance spectroscopy, which is essentially a site-selective probe. The correlation function between the two spin operators at equilibrium is

$$S_{ij}^{\alpha\beta}\left(t-t'\right) = \left\langle S_i^{\alpha}(t) S_j^{\beta}\left(t'\right)\right\rangle. \tag{5.83}$$

Its Fourier transform defines the dynamical structure factor

$$S_{ij}^{\alpha\beta} = \int_{-\infty}^{\infty} e^{i\omega t} S_{ij}^{\alpha\beta}(t) dt$$
$$= \frac{2\pi\hbar}{\mathscr{Z}} \sum_{\mu\nu} e^{-E_\mu/k_B T} \delta\left(E_\mu - E_v + \hbar\omega\right) \langle\mu|S_i^\alpha|v\rangle\langle v|S_j^\beta|\mu\rangle \tag{5.84}$$

where the partition function is given by

$$\mathscr{Z} = \sum_\mu e^{-E_\mu/k_B T} \tag{5.85}$$

If we define the response function

$$R_{ij}^{\alpha\beta}\left(t - t'\right) = -i\theta\left(t - t'\right) \left\langle \left[S_i^\alpha(t), S_j^\beta\left(t'\right) \right] \right\rangle \tag{5.86}$$

where $[A, B]$ denotes a commutator. Its Fourier transform is given by

$$R_{ij}^{\alpha\beta}(\omega + i\eta) = \int_{\infty}^{\infty} dt e^{i(\omega+i\eta)t} R_{ij}^{\alpha\beta}(t)$$
$$= \frac{1}{\mathscr{Z}} \sum_{\mu\nu} \frac{\left(e^{-E_\mu/k_B T} - e^{-E_v/k_B T}\right) \langle\mu|S_i^\alpha|v\rangle\langle v|S_j^\beta|\mu\rangle}{\left(E_\mu - E_v\right) + \hbar\omega + i\eta} \tag{5.87}$$

where η is an infinitesimal. Comparison of Eqs. (5.84) and (5.87) leads to the relation

$$S_{ij}^{\alpha\beta}(\omega) = -\frac{2}{1 - e^{-\hbar\omega/k_B T}} \operatorname{Im} R_{ij}^{\alpha\beta}(\omega). \tag{5.88}$$

In the limit of $\omega \to 0$, we have

$$S_{ij}^{\alpha\beta}(\omega \to 0) = -\frac{2}{\hbar\omega/k_B T} \operatorname{Im} R_{ij}^{\alpha\beta}(\omega \to 0). \tag{5.89}$$

This spin response function can be calculated conveniently in the Matsubara formalism. We are interested in the correlator between

$$S_i^+ = S_i^x + S_i^y = c_{i\uparrow}^\dagger c_{i\downarrow}$$

and

$$S_i^- = S_i^x - iS_i^y = c_{i\downarrow}^\dagger c_{i\uparrow}$$

and write down

$$\mathbf{R}_{ii}^{+-}(\tau) = -\left\langle T_\tau \left(S_i^+(\tau) S_i^-(0) \right) \right\rangle, \tag{5.90}$$

Using the Wick decoupling scheme and performing the Fourier transform, we obtain

$$\mathscr{R}_{ii}^{+-}\left(i\omega_n\right) = \sum_{nn'} u_i^n v_i^{n'} \left[u_i^{n*} v_i^{n'} - v_i^{n*} u_i^{n'} * \right] \frac{f\left(E_n\right) - f\left(-E_{n'}\right)}{i\omega_n + E_n + E_{n'}}, \tag{5.91}$$

from which we arrive at the spin-relaxation rate:

$$\begin{aligned}\frac{1}{T_1} =& \frac{J^2}{2\hbar^2}\mathscr{S}_{ii}^{+-}(\omega \to 0) \\ =& \frac{J^2\pi k_B T}{\hbar^2}\sum_{nn'}\mathrm{Re}\left\{u_i^n v_i^{n'}\left[u_i^{n*}v_i^{n'*} - v_i^{n*}u_i^{n'*}\right]\right\} \\ & \times\left(-\frac{\partial f(E)}{\partial E}\right)\Big|_{E=E_n}\delta\left(E_n + E_{n'}\right)\end{aligned} \tag{5.92}$$

where J is the strength of the coupling between the nuclear spin and the electron spin density on the lattice.

Figure 5.8 shows the temperature dependence of the spin relaxation rate on a few selected probing sites [38]. The results indicate that in the presence of vortices, $1/T_1$ follows $1/T_1 \sim T$ at low temperatures, which deviates from the T^3 behavior at zero field. This T-linear behavior arises from the low-energy states around the vortices. In addition, the temperature range for the T-linear behavior is expanded. This result is in sharp contrast with the $1/T_1 \propto e^{-\Delta_1/T}$ for the s-wave vortex lattice case at low temperature, where $\Delta_1 \sim \Delta_0^2/E_F$ [38]. Its magnitude of $1/T_1$ is also much larger than that for the zero-field case, suggesting a significant contribution from the gapless vortex-core states.

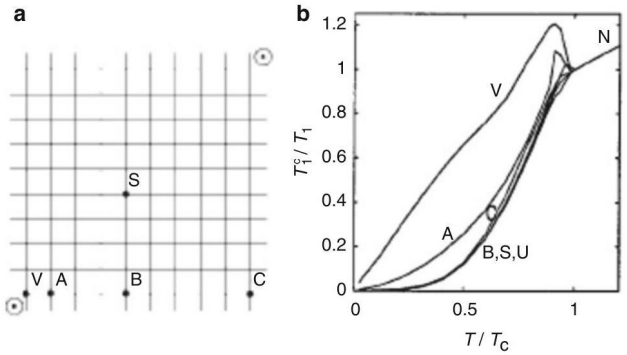


Fig. 5.8 Position of probing sites V, A, B, C, S in the square vortex lattice, where the nearestneighbor vortex is located in the 45° direction from the x-axis (due to the choice of symmetric gauge) (a), and the temperature dependence of spin relaxation rate. Line U shows the zero-field case. The line N is for the normal state at $T > T_c$. From [38]

For high-temperature cuprates, low temperature STM experiments observed a double-peak structure around zero bias in the local differential tunneling conductance at the vortex core center [40, 41]. The discrepancy between the theory and the experiment stimulated interesting theoretical proposals on the quasiparticles in the vortex core of high- T_c cuprates, including the mixed $d_{x^2-y^2} + id_{xy}$-wave pairing symmetry [35, 42], the Landau-level quantization [43], as well as competing order [39, 44-46]. Here we discuss the quasiparticle spectrum within a competing spin-density-wave scenario. Other competing scenarios [47] can be discussed within the same framework.

Beyond the tight-binding model with only a d-wave pairing term, we introduce a Hubbard on-site repulsion

$$H_U = U\sum_i \hat{n}_{i\uparrow}\hat{n}_{\downarrow} \tag{5.93}$$

where $\hat{n}_{i\sigma}$ is the local density operator and U is the strength of the on-site repulsion between two electrons with opposite spin polarization. By assuming that the on-site repulsion is solely responsible for the antiferromagnetism, we have a mean-field decoupling

$$H_{U,\mathrm{MF}} = \sum_{\sigma} m_{i\bar{\sigma}} \hat{n}_{i\sigma} \tag{5.94}$$

where $m_{i\sigma} = U n_{i\sigma}$ is the spin-dependent Hartree-Fock potential. The extended BdG equations can then be derived as:

$$\sum_{\mathbf{j}} \begin{pmatrix} \mathscr{H}_{\mathbf{ij},\sigma} & \Delta_{\mathrm{ij}} \\ \Delta^*_{\mathbf{ij}} & -\mathscr{H}^*_{\mathbf{ij},\bar{\sigma}} \end{pmatrix} \begin{pmatrix} u^n_{\mathbf{j}\sigma} \\ v^n_{\mathbf{j}\bar{\sigma}\bar{\sigma}} \end{pmatrix} = E_n \begin{pmatrix} u^n_{\mathbf{i}\sigma} \\ v^n_{\mathbf{i}\bar{\sigma}} \end{pmatrix}, \tag{5.95}$$

where $(u^n_{\mathbf{i}\sigma}, v^n_{\mathbf{i}\bar{\sigma}})$ is the quasiparticle wavefunction corresponding to the eigenvalue E_n, the single particle Hamiltonian $\mathscr{H}_{\mathbf{i},\sigma} = -t_{ij} e^{i\varphi_{\mathbf{ij}}} \delta_{\mathbf{i}+\delta,\mathbf{j}} + (m_{\mathbf{i},\bar{\sigma}} - \mu)\, \delta_{\mathbf{ij}}$. Notice that the quasiparticle energy is measured with respect to the Fermi energy. The selfconsistent conditions read:

$$m_{\mathbf{i}\sigma} = U \sum_{n} |u^n_{\mathbf{i}\sigma}|^2 f\left(E_n\right), \tag{5.96}$$

and

$$\Delta_{\mathbf{ij}} = \frac{V}{4} \sum_{n} \left(u^n_{\mathbf{i}\uparrow} v^{n*}_{\mathbf{j}\downarrow} + v^{n*}_{\mathbf{i}\downarrow} u^n_{\mathbf{j}\uparrow}\right) \tanh\left(\frac{E_n}{2k_B T}\right), \tag{5.97}$$

where V is the strength of d-wave pairing interaction and the Fermi distribution function $f(E) = 1/\left(e^{E/k_B T} + 1\right)$. Here the summation is also over those eigenstates with negative eigenvalues thanks to the symmetry property of the BdG equation: If $\left(u^n_{\mathbf{i}\uparrow}, u^n_{\mathbf{i}\downarrow}, v^n_{\mathbf{i}\uparrow}, v^n_{\mathbf{i}\downarrow}\right)^{\mathrm{Transpose}}$ is the eigenfunction of the 4×4 equation in the spin space with energy E_n, then $\left(v^{n\,*}_{\mathbf{i}\uparrow}, -v^{n\,*}_{\mathbf{i}\downarrow}, u^{n\,*}_{\mathbf{i}\uparrow}, -u^n_{\mathbf{i}\downarrow}\right)^*$ Transpose up to a global phase factor is the eigenfunction with energy $-E_n$.

For the optimally high- T_c cuprates, since there is no static spin-density-wave (SDW) order at zero field. One can choose the relative strength of Hubbard repulsion and the d-wave pairing interaction such that the antiferromagnetic SDW order is strongly suppressed while the system is only dominated by a pure d-wave superconducting order, which is uniform in real space. As such, the competing nature of the system will be uncovered by suppressing the superconducting order in the form of vortices when a magnetic field is applied. Representative results are shown in Fig. 5.9. With an appropriately chosen strength of the Hubbard repulsion, the SDW order is nucleated at the vortex core center, where the d-wave order parameter is depressed (see the left column of Fig. 5.9). More interestingly, with the SDW order localized at the vortex core center, the near-zero-energy broad peak in the local density of states for a pure d-wave vortex is suppressed with the amplitude of the SDW order (see the left column of Fig. 5.9). The exhibited double-peak structure in the LDOS is consistent with the STM tunneling conductance measured at the vortex core center.

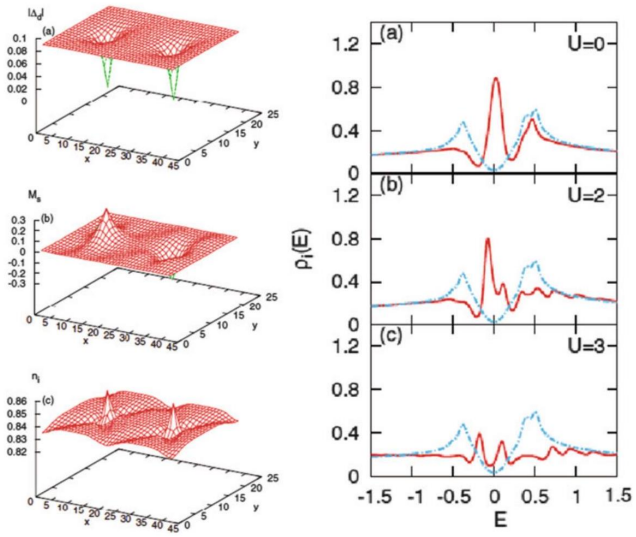


Fig. 5.9 Left column: Spatial variation of the d-wave order parameter (a), staggered spin-densitywave order $M_s = (-1)^i (n_{i\uparrow} - n_{i\downarrow})$ (**b**), and charge density $n_i = n_{i\uparrow} + n_{i\downarrow}$ (c) in a magnetic unit cell of size 42×21 for $V = 1.0$ and $U = 2$. Right column: The local density of states measured at the vortex core center for various values of Hubbard interaction $U = 0$ (a), 2 (b), and 3 (c). The filling factor defined as $\sum_i n_i / N_x N_y = 0.84$. From [39]

13.3.8 5.4 Fulde-Ferrell-Larkin-Ovchinikov State due to a Zeeman Magnetic Field

As we mentioned at the beginning of the chapter, the magnetic field also influences the superconductivity especially with the spin-singlet pairing through the spin Zeeman interaction. This effect is especially important for a low-dimensional system, where the orbital effect of magnetic field when aligned appropriately can be completely quenched. In this section, we will focus on the spin Zeeman effect by neglecting the orbital effect of the magnetic field.

The modification of superconductivity by the external magnetic field through the Zeeman coupling was first studied by Clogston and Chandrasekhar [48, 49]. It is concerned with the bound on the paramagnetic upper critical field by considering the Zeeman interaction alone, that is the Pauli limit, and the nature of the phase boundary. The paramagnetic pair-breaking effect comes from the Zeeman splitting
of the single electron energy bands. When a magnetic field is applied in the normal state, electron band is split into spin-up and spin-down sheets to gain the magnetic energy; while in the superconducting state, this paramagnetism is eliminated by the formation of spin-singlet Cooper pairs. Qualitatively, the destruction of the superconducting state by the Pauli paramagnetic pair breaking occurs when the normal-state paramagnetic energy

$$E_P = \frac{1}{2}\chi_n H_P^2 \tag{5.98}$$

takes over the superconducting condensation energy

$$E_c = \frac{1}{2}N(0)\Delta_{\mathrm{BCS}}^2(T). \tag{5.99}$$

Here the normal-spin susceptibility is given by

$$\chi_n = \frac{1}{2}g^2\mu_B^2 N(0), \tag{5.100}$$

with g being the gyromagnetic ratio, μ_B being the Bohr magneton, and N_0 the density of states at the Fermi energy per spin polarization. The quantity $\Delta_{\rm BCS}$ is the zerofield BCS energy gap. A little algebra yields

$$H_P(T) = \sqrt{2}\Delta_{\rm BCS}(T)/|g|\mu_B \tag{5.101}$$

On the other hand, if one assumes a second-order phase transition and the superconducting order parameter is always uniform in real space, the solution of the BdG equations (5.19) or (5.20) in the Pauli limit (that is, ignoring the orbital effect) will lead to an upper critical field, which will decrease with decreasing temperature below a critical temperature T^+. This transition line is metastable, which suggests that the transition below T^+(with the line defined by $H_P(T)$) becomes the first order. The phase diagram between the Zeeman field and the temperature is shown in Fig. 5.10.

A more unusual state was proposed by Fulde and Ferrell [50], and by Larkin and Ovchinnikov [51], where the pairing state is formed with a finite Cooper pair momentum at a larger Zeeman field. If the normal state is transitioned into this finitemomentum pairing (inhomogeneous in real space) state, the upper critical field can be enhanced. Specifically, the Cooper pairs are formed between electrons at $(\mathbf{k}, \uparrow)$ and those at $(-\mathbf{k}+\mathbf{q}, \downarrow)$, as shown in Fig. 5.11. The shifted momentum q due to the Zeeman field is estimated to be $q \sim 2\mu_B H/\hbar v_F$. The state originally proposed by Fulde and Ferrell has the form

$$\Delta(\mathbf{r}) = \Delta e^{i\mathbf{q}\cdot\mathbf{r}} \tag{5.102}$$

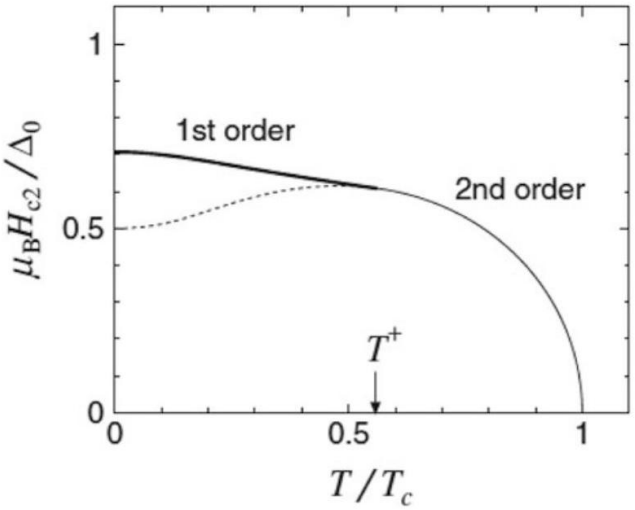


Fig. 5.10 The $H-T$ phase diagram of a two-dimensional superconductor in the pure Pauli limit, which can be realized by applying the field parallel to the plane. Below $T^+(\approx 0.56T_c)$, the transition becomes first order. The broken line represents the metastable transition line. From [52]

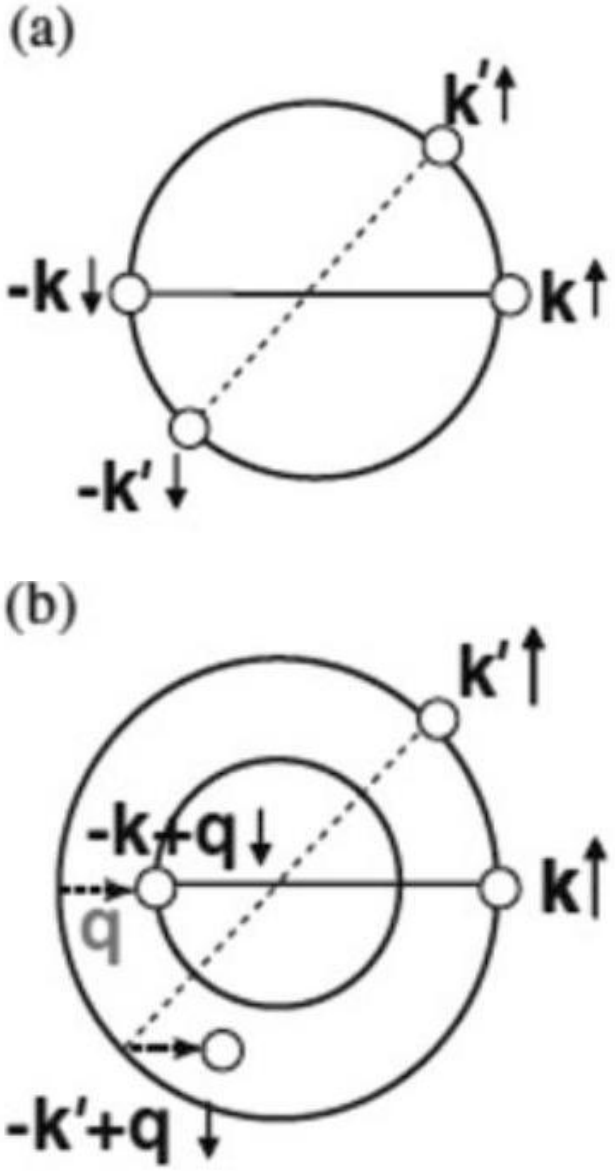


Fig. 5.11 Schematic picture of BCS pairing state ($\mathbf{q} = 0$)(**a**) and FFLO pairing state ($\mathbf{k} \uparrow, -\mathbf{k} + \mathbf{q} \downarrow$)(b). The inner and outer circles represent the Fermi surface of spin-up and spin-down electron bands. From [52]

with the amplitude of the order parameter remaining homogeneous. Note that the functionals $\Delta e^{i\mathbf{q}\cdot\mathbf{r}}$ and $\Delta e^{-i\mathbf{q}\cdot\mathbf{r}}$ are degenerate for a given $\mathbf{q}$, its equal weight linear combination can lift this degeneracy

$$\Delta(\mathbf{r}) = \Delta\left(e^{i\mathbf{q}\cdot\mathbf{r}} + e^{-i\mathbf{q}\cdot\mathbf{r}}\right) = 2\Delta\cos(\mathbf{q}\cdot\mathbf{r}) \tag{5.103}$$

Larkin and Ovchinnikov suggested this form of the order parameter can lead to an even more stable superconducting state in the presence of a larger Zeeman field. Nowadays, this finite-momentum pairing state is called FFLO state [52, 53].

The interest in the FFLO state is recently revived by the observation of a so-called "Q" phase in heavy-fermion $CeCoIn_5$ compound [54], which has a $d_{x^2-y^2}$-wave pairing symmetry at zero field. The problem has recently been numerically studied

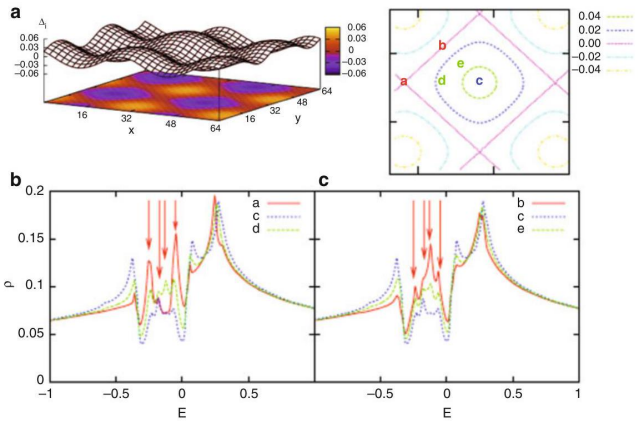


Fig. 5.12 Spatial variation of a d-wave order parameter in the Pauli limit of an external magnetic field (a) and the local density of states (b, c) at the sites marked on the contour plot (upper right panel) of equal magnitude of order parameter. The pairing interaction $V_d = 1.0$, the exchange field $h = H\mu_B = 0.15$, the chemical potential $\mu = -0.4$ in a nearest-neighbor hopping model. From [55]

by solving the BdG equations (5.20) with a d-wave pairing symmetry. Figure 5.12 shows the d-wave order parameter variation as well as the local density of states at several representative sites of the system [55]. The d-wave order parameter at lowtemperatures is stabilized into a square lattice in the form of $\Delta_0 [\cos q_x x + \cos q_y y]$ (see Fig. 5.12a). The spatial variation, especially the sign change of the d-wave order parameter in the real space gives rise to in-gap states exhibited in the local density of states (see Fig. 5.12b, c).

We note that just as interesting quasiparticle states in the mixed state of a superconductor arise from the vortex formation, novel quasiparticle states in the FFLO state through a large external Zeeman field are also due to the variation of order parameter, that is, the collective motion of Cooper pairs. In addition, the BdG formalism is also very powerful in studying the interplay between the Zeeman field and impurities.

13.4 7 Topological and Quantum Size Effects in SC at Reduced Length Scale

Abstract

The periodicity of persistent currents in multiply connected geometries arising from the Aharonov and Bohm effect is studied for both s-wave superconducting ring and d-wave superconducting cylinder. The loop geometry of a d-wave superconductor is also considered. The solutions of the BdG equations suggest that the hc/e-periodicity is a generic property in s-wave superconductor ring at the mesoscale and in unconventional superconductors. Finally, the theoretical approach to solving the BdG equations is also provided for nanoscale superconductors. The quantum size effects are showcased with the oscillation of transition temperature.

13.4.1 7.1 Persistent Current in a Mesoscopic s-Wave SC Ring

In classical electrodynamics, the Maxwell equations determine directly the behavior of electromagnetic fields $\mathbf{E}$ and $\mathbf{B}$, while the scalar and vector potentials merely play an auxiliary role through the relation

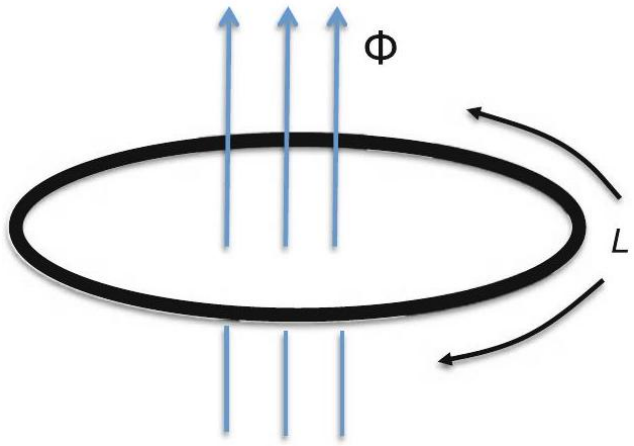
$$\mathbf{E} = -\nabla\varphi(\mathbf{r}), \quad \mathbf{B}(\mathbf{r}) = \nabla \times \mathbf{A}(\mathbf{r}),$$

in the static case. Therefore, the equation of motion of an electron is determined through the Lorentz force

$$\mathbf{F} = -e\left(\mathbf{E} + \frac{\mathbf{v}}{c} \times \mathbf{B}\right),$$

where $\mathbf{v}$ is the electron velocity. However, in quantum mechanics, the scalar and vector potentials enter the Schrödinger equation explicitly and have a direct consequence. In 1959, Aharonov and Bohm (AB) [1] showed that a charged particle can be deflected even when the classical force is absent. This AB effect has now been very well demonstrated by a persistent equilibrium current circulating in an isolated mesoscopic normal-metal ring pierced by an AB flux $\Phi = \oint \mathbf{A} \cdot \mathbf{l}$[2, 3]. This current always has a periodicity of $\Phi_0 = hc/e$, where Φ_0 is the single electron flux quantum. In a superconductor, electrons form Cooper pairs from an effective pairing interaction near the Fermi surface. The flux quantization with $\Phi_0/2$ has been used

Fig. 7.1 Schematic drawing of a one-dimensional superconducting ring of circumference L threaded by a magnetic flux Φ



as a powerful proof for the formation of electron pairs in a macroscopic multiply connected geometries [4-8]. However, we must keep in mind that the Cooper pairs are well defined in momentum space rather than in real space, which makes them distinct from particles with a charge $-2e$. Therefore, there is no reason for one to expect that the persistent current in a superconducting ring should have a periodicity of $\Phi_s = \Phi_0/2$, in particular, when the system is at a mesoscale.

We study this problem by considering a one-dimensional mesoscopic s-wave superconductor ring pierced by a magnetic flux, as shown in Fig. 7.1. Since the flux is restricted to the central hollow region, no magnetic field is experienced by the electrons. The BdG equations are still given by Eq. (5.19) but with no spin Zeeman term and $\nabla \times \mathbf{A} = 0$ on the ring arm. That is, the single-particle Hamiltonian in 1D has the form

$$\tilde{h}(x) = \frac{1}{2m_e}\left(\frac{\hbar}{i}\frac{d}{dx} + \frac{eA(x)}{c}\right)^2 - E_F. \tag{7.1}$$

Here we have used the spatial coordinate $x = 2\pi\theta/L$, where θ is the azimuthal angle, varying between 0 and L. In general, the detailed shape of the ring does not matter. Before we discuss the BdG equations, we first take a look at the wave function to the single-particle Hamiltonian with the Schrödinger equation

$$\tilde{h}(x)\tilde{\varphi}(x) = \epsilon\tilde{\varphi}(x) \tag{7.2}$$

The eigenfunction $\tilde{\varphi}(x)$ satisfies a periodic boundary condition

$$\tilde{\varphi}(x + L) = \tilde{\varphi}(x). \tag{7.3}$$

We introduce a singular gauge transformation

$$\tilde{\varphi}(x) = e^{-ie\chi(x)/\hbar c}\varphi(x) \tag{7.4}$$

Using the identity

$$\left(\frac{\hbar}{i}\frac{d}{dx} + \frac{eA(x)}{c}\right)\tilde{\varphi}(x) = e^{-ie\chi(x)/\hbar c}\left(\frac{\hbar}{i}\frac{d}{dx} + \frac{e}{c}\left(A(x) - \chi'(x)\right)\right)\varphi(x), \tag{7.5}$$

and

$$\left(\frac{\hbar}{i}\frac{d}{dx} + \frac{eA(x)}{c}\right)^2\tilde{\varphi}(x) = e^{-ie\chi(x)/\hbar c}\left(\frac{\hbar}{i}\frac{d}{dx} + \frac{e}{c}\left(A(x) - \chi'(x)\right)\right)^2\varphi(x), \tag{7.6}$$

we obtain

$$\left(\frac{\hbar}{i}\frac{d}{dx} + \frac{e}{c}\left(A(x) - \chi'(x)\right)\right)^2\varphi(x) = \epsilon\varphi(x) \tag{7.7}$$

The choice of the gauge

$$\chi'(x) = A(x), \tag{7.8}$$

leads to

$$-\frac{\hbar^2}{2m_e}\frac{d^2\varphi(x)}{dx^2} = \epsilon\varphi(x). \tag{7.9}$$

Solving Eq. (7.8) yields

$$\chi(x) = \int_0^x A\left(x'\right)dx' \tag{7.10}$$

Therefore, the boundary condition for the new wave function becomes

$$\begin{aligned}\varphi(x+L) &= e^{ie\chi(x+L)/\hbar c}\varphi(x+L)\\ &= e^{\frac{ie}{\hbar c}\int_x^{x+L}A(x')dx'}e^{\frac{ie}{\hbar c}\int_0^x A(x')dx'}\varphi(x)\\ &= e^{i2\pi\Phi/\Phi_0}\varphi(x).\end{aligned} \tag{7.11}$$

Here we have used the identity

$$\int_x^{x+L} A\left(x'\right)dx' = \Phi \tag{7.12}$$

This obervation enables us to apply a singular gauge transformation also to the BdG equations and obtain

$$\begin{pmatrix} h(x) & \Delta(x) \\ \Delta^*(x) & -h^*(x) \end{pmatrix}\begin{pmatrix}u(x)\\ v(x)\end{pmatrix} = E\begin{pmatrix}u(x)\\ v(x)\end{pmatrix}, \tag{7.13}$$

with the periodic boundary condition

$$u(x+L) = e^{i2\pi\Phi/\Phi_0}u(x) \tag{7.14a}$$

$$v(x+L) = e^{-i2\pi\Phi/\Phi_0}v(x) \tag{7.14b}$$

$$\Delta(x+L) = e^{i4\pi\Phi/\Phi_0}\Delta(x) \tag{7.14c}$$

Here the single-particle Hamiltonian is

$$h(x) = -\frac{\hbar^2}{2m_e}\frac{d^2}{dx^2} - E_F. \tag{7.15}$$

If the electron wave vector is k and the wave vector for the collective drift motion (superfluid motion) of the paired electrons is q, the initial Cooper pairing $(k\uparrow, -k\downarrow)$ will occur between electron states $(k+q\uparrow, -k+q\downarrow)$. This allows us to write the wave function and pair potential as

$$\Delta(x) = \Delta e^{2iqx} \tag{7.16a}$$
$$u(x) = u_{k,q}e^{i(k+q)x}, \tag{7.16b}$$
$$v(x) = v_{k,q}e^{i(k-q)x}, \tag{7.16c}$$

A little algebra yields the solution to the BdG equation (7.13) [9]:

$$E^{\pm}_{k,q} = (\hbar k)\frac{\hbar q}{m_e} \pm \sqrt{E_A^2 + \Delta^2} = (\hbar k)\frac{\hbar q}{m_e} \pm E^{(0)}_{k,q} \tag{7.17}$$

with the corresponding eigenfunctions $\left(u^+_{k,q}, v^+_{k,q}\right) = \left(u^{(0)}_{k,q}, v^0_{k,q}\right)$ while $\left(u^-_{k,q}, v^-_{k,q}\right) = \left(v^{(0)}_{k,q}, -u^0_{k,q}\right)$. Here

$$E^{(0)}_{k,q} = \sqrt{E_A^2 + \Delta^2}, \tag{7.18}$$
$$E_A = \frac{\hbar^2}{2m_e}\left(k^2 + q^2\right) - E_F, \tag{7.19}$$

and

$$\begin{pmatrix} u^{(0)}_{k,q} \\ v^{(0)}_{k,q} \end{pmatrix} = \begin{pmatrix} \sqrt{\frac{1}{2}\left(1 + \frac{E_A}{E^{(0)}_{k,q}}\right)} \\ \sqrt{\frac{1}{2}\left(1 - \frac{E_A}{E^{(0)}_{k,q}}\right)} \end{pmatrix} \tag{7.20}$$

The order parameter is then determined by

$$\Delta = \frac{g}{4}\sum_k \frac{\Delta}{E^{(0)}_{k,q}}\left[\tanh\left(\frac{E^{(0)}_{k,q} + \hbar^2 kq/m_e}{2k_BT}\right) + \tanh\left(\frac{E^{(0)}_{k,q} - \hbar^2 kq/m_e}{2k_BT}\right)\right] \tag{7.21}$$

Here the energy cutoff $|E_A| \leq \hbar\omega_D$ is implied in the summation. The boundary condition (7.14) on the wave functions gives

$$k = \frac{\pi}{L}n_k \tag{7.22}$$

and

$$q = \frac{\pi}{L}\left(n_q + \frac{\Phi}{\Phi_s}\right) \tag{7.23}$$

subject to the constraint that $n_k + n_q$ is an even integer and the superconducting flux quantum $\Phi_s = \Phi_0/2$. In addition, from Eq. (6.15), the charge current is now given by

$$I_Q = \frac{2\hbar e}{m_e}\sum_k (k+q)\left[f\left(E^+_{k,q}\right)u^{(0)^2}_{k,q} + f\left(E^{(-)}_{k,q}\right)v^{(0)^2}_{k,q}\right] \tag{7.24}$$

where $f(E)$ is the Fermi-Dirac distribution function.
The drift momentum q defines a superfluid velocity $v_s = \hbar q/m_e$. Equation (7.17) suggests that when the superfluid velocity $v_s = v_d$ with $v_d = \Delta/\hbar v_F$ being the Landau depairing velocity, the gap in the excitation spectrum is closed. The quantity also defines a depairing flux $\Phi_d/\Phi_s = (k_F L/2\pi)(\Delta/E_F)$. This tells us that even if the superconducting gap is not depressed, a gapless quasiparticle state can be induced by the magnetic flux. The numerical results do confirm this intuitive analysis. As shown in Fig. 7.2 (left panel), for a fixed value of ring circumference, when the ration of Δ/E_F is tuned such that $\Phi_d/\Phi_s < 1$, the supercurrent is only a function of magnetic flux with a normal-state period Φ_0. In addition, the selfconsistency solution also shows that the order parameter can be suppressed by an application of the magnetic flux (see Fig. 7.2 (right panel)).

Before we turn to the discussion on the case with a d-wave pairing symmetry, we show a derivation of flux-modified boundary condition for electrons in the 1 D ring

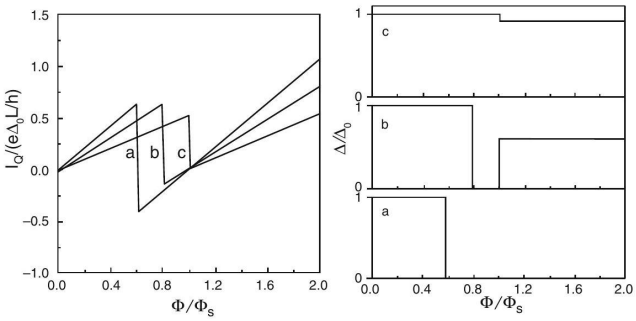


Fig. 7.2 Supercurrent at a fixed amplitude of s-wave order parameter (left panel) and the selfconsistently obtained order parameter as a function of magnetic flux Φ/Φ_S in a mesoscopic ring at $T = 0$ K. For the left panel, the values of $\Delta_0/E_F = 3.0 \times 10^{-3}(a); 4.0 \times 10^{-3}(b); 6 \times 10^{-3}(c)$. For the right panel, the pairing interaction strength is first tuned to give the zero-flux gap value as used for the left panel before it is used for the self-consistent calculations for the flux dependence. The other parameters used are $L = 1000$ nm, and $k_F = 400\pi/L, \hbar\omega_D = 300$ K. Adapted from [9]

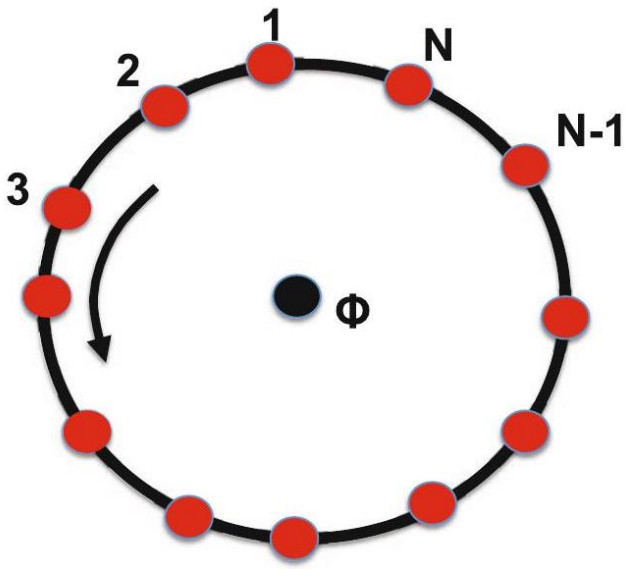


Fig. 7.3 Schematic drawing of a one-dimensional superconducting ring of circumference L threaded by a magnetic flux Φ in a tight-binding model

within a tight-binding model, as shown in Fig. 7.3. The single-particle Hamiltonian is given

by:

$$H = -\sum_{i \neq j} t_{ij} e^{i\theta_{ij}} c_i^\dagger c_j + \sum_i \epsilon_i c_i^\dagger c_i \tag{7.25}$$

where $\theta_{ij} = -\frac{2\pi}{\Phi_0}\int_j^i A(x)dx$ and ϵ is the on-site energy level. Here we have dropped the spin degrees of freedom. Introducing a canonical transformation

$$c_i = \sum_n \varphi_i^n \gamma_n, \tag{7.26}$$

with γ_n being the quasiparticle operator, and within the nearest-neighbor hopping approximation, the Hamiltonian can be diagonalized as

$$\underline{H}\underline{\varphi} = E\underline{\varphi}, \tag{7.27}$$

where

$$\underline{H} = \begin{pmatrix} \epsilon_1 & -te^{i\phi_1} & 0 & 0 & \dots & 0 & -te^{-i\phi_N} \\ -te^{-i\phi_1} & \epsilon_2 & -te^{-i\phi_2} & 0 & \dots & 0 & 0 \\ 0 & -te^{-i\phi_2} & \epsilon_3 & -te^{i\phi_3} & \dots & 0 & 0 \\ \dots & \dots & \dots & \dots & \dots & \dots & \dots \\ -te^{i\phi_N} & 0 & 0 & 0 & \dots & -t^{-i\phi_{N-1}} & \epsilon_N \end{pmatrix}, \tag{7.28}$$

and the eigenvectors $\varphi^{\text{Transpose}} = (\varphi_1, \varphi_2, \varphi_3, \dots \varphi_N)$. Here the accumulated phase for electrons hopping from site j to i has been abbreviated as $\theta_{i,i+1} = \phi_i$ and $\theta_{N,1} = \phi_N$. By performing a uniform transformation

$$\underline{U} = \begin{pmatrix} e^{i\sum_{i=1}^{N-1}\phi_i} & & & & \\ & e^{i\sum_{i=2}^{N-1}\phi_i} & & & \\ & & \dots & & \\ & & & e^{i\phi_{N-1}} & \\ & & & & 1 \end{pmatrix} \tag{7.29}$$

the eigenequation equation becomes

$$\underline{\tilde{H}}\underline{\bar{\varphi}} = E\underline{\bar{\varphi}}, \tag{7.30}$$

where

$$\underline{\hat{H}} = \begin{pmatrix} \epsilon_1 & -t & 0 & 0 & \dots & 0 & -te^{-i\sum_{i=1}^{N}\phi_i} \\ -t & \epsilon_2 & -t & 0 & \dots & 0 & 0 \\ 0 & -t & \epsilon_3 & -t & \dots & 0 & 0 \\ \dots & \dots & \dots & \dots & \dots & \dots & \dots \\ -te^{i\sum_{i=1}^{N}\phi_i} & 0 & 0 & 0 & \dots & -t & \epsilon_N \end{pmatrix}, \tag{7.31}$$

and

$$\overline{\bar{\varphi}} = \underline{U}^\dagger \underline{\varphi}. \tag{7.32}$$

Note that the total phase accumulated across the entire ring is $\sum_i^N \phi_i = 2\pi\Phi/\Phi_0$. Equation (7.31) suggests that the phase factors appearing in the Hamiltonian can be removed by using a modified periodic boundary condition:

$$\bar{\varphi}_{N+1} = \bar{\varphi}_1 \rightarrow \bar{\varphi}'_{N+1} = e^{i2\pi\Phi/\Phi_0}\bar{\varphi}'_1. \tag{7.33}$$

For the BdG equations in the tight-binding model, we can perform the unitary transformation

$$(\underline{U}_{\underline{U}^*})$$

to get the modified periodic boundary conditions for the eigenfunctions. The same procedure can also be applied to the cylindrical geometry, which can be regarded as a stacked array of rings of same radius).

13.4.2 7.2 Current in Multiply Connected Mesoscopic d-Wave SC Geometries

13.4.3 7.2.1 Cylindrical Geometry

For a $d_{x^2-y^2}$-wave pairing symmetry as appropriate to high-temperature cuprates, the pair potential experiences a sign change across the nodal directions and the gapless nodal quasiparticles exist even at zero magnetic field. The question on the periodicity of the supercurrent in a multiply connected geometry with the hollow threaded by a magnetic flux is also intriguing. We first consider the simpler case of a cylindrical geometry as shown in Fig. 7.4. We define the $x-y$ coordinate system

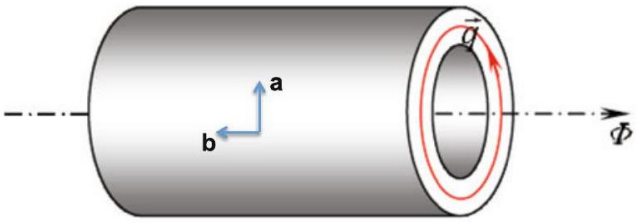


Fig. 7.4 Schematic drawing of a hollow d-wave superconducting cylinder. A magnetic flux Φ threads along the cylinder axis. The vectors **a** and **b** denotes the crystalline axes of an essentially two-dimensional system
to coincide with the crystalline axes, which are perpendicular and parallel to the cylinder axis, respectively. By following the same discussion as in the previous section but now in the tight-binding model, the BdG equations are given as

$$\sum_j \begin{pmatrix} \mathscr{H}_{ij} & \Delta_{ij} \\ \Delta_{ij}^* & -\mathscr{H}_{ij}^* \end{pmatrix} \begin{pmatrix} u_j^n \\ v_j^n \end{pmatrix} = E_n \begin{pmatrix} u_i^n \\ v_i^n \end{pmatrix}, \tag{7.34}$$

subject to the flux-modified boundary condition

$$\begin{pmatrix} u_{i_x+N_x,i_y}^n \\ v_{i_x+N_x,i_y}^n \end{pmatrix} = \begin{pmatrix} e^{i2\pi\Phi/\Phi_0} & 0 \\ 0 & e^{-i2\pi\Phi/\Phi_0} \end{pmatrix} \begin{pmatrix} u_{i_i,i_y}^n \\ v_{i_x,i_y}^n \end{pmatrix}. \tag{7.35}$$

Here (u_i^n, v_i^n) with i denoting the coordinates (i_x, i_y) are the eigenfunctions corresponding to eigenvalues E_n. The single particle Hamiltonian is given by

$$\mathscr{H}_{ij} = -t_{ij} - \mu\delta_{ij}, \tag{7.36}$$

where t_{ij} and μ are the hopping integral and chemical potential, respectively. We take a next-nearest-neighbor hopping approximation with t and t' representing the nearest neighbor and next-nearest neighbor hopping integrals, respectively. The BdG wave function has the form

$$\begin{pmatrix} u_i \\ v_i \end{pmatrix} = \begin{pmatrix} e^{i(\mathbf{k}+\mathbf{q})\cdot\mathbf{r}_i} & 0 \\ 0 & e^{i(\mathbf{k}-\mathbf{q})\cdot\mathbf{r}_i} \end{pmatrix} \begin{pmatrix} u_{\mathbf{k},\mathbf{q}} \\ v_{\mathbf{k},\mathbf{q}} \end{pmatrix}. \tag{7.37}$$

Corresponding to the energy eigenvalues

$$E^{(\pm)}_{\mathbf{k},\mathbf{q}} = Z_{\mathbf{k},\mathbf{q}} \pm E^{(0)}_{\mathbf{k},\mathbf{q}} \tag{7.38}$$

the electron and hole components of the quasiparticle amplitude are given by $(u_{\mathbf{k},\mathbf{q}}, v_{\mathbf{k},\mathbf{q}}) = \left(u^{(0)}_{\mathbf{k},\mathbf{q}}, v^{(0)}_{\mathbf{k},\mathbf{q}}\right)$ and $\left(v^{(0)}_{\mathbf{k},\mathbf{q}}, -u^{(0)}_{\mathbf{k},\mathbf{q}}\right)$ with

$$\left|u^{(0)}_{\mathbf{k},\mathbf{q}}\right|^2 = \frac{1}{2}\left(1 + \frac{Q_{\mathbf{k},\mathbf{q}}}{E^{(0)}_{\mathbf{k},\mathbf{q}}}\right), \quad \left|v^{(0)}_{\mathbf{k},\mathbf{q}}\right|^2 = \frac{1}{2}\left(1 - \frac{Q_{\mathbf{k},\mathbf{q}}}{E^{(0)}_{\mathbf{k},\mathbf{q}}}\right). \tag{7.39}$$

The quantities $Q_{\mathbf{k},\mathbf{q}} = \left[\xi_{\mathbf{k}+\mathbf{q}} + \xi_{\mathbf{k}-\mathbf{q}}\right]/2, Z_{\mathbf{k},\mathbf{q}} = \left[\xi_{\mathbf{k}+\mathbf{q}} - \xi_{\mathbf{k}-\mathbf{q}}\right]/2$, and $E^{(0)}_{\mathbf{k},\mathbf{q}} = \left[Q^2_{\mathbf{k},\mathbf{q}} + |\Delta_{\mathbf{k}}|^2\right]^{1/2}$. In the tight-binding approximation, up to the next-nearest neighbor, the conduction electrons have the normal state dispersion,

$$\xi_{\mathbf{k}} = -2t\left(\cos k_x + \cos k_y\right) - 4t' \cos k_x \cos k_y - \mu \tag{7.40}$$

The d-wave superconducting gap dispersion is given by

$$\Delta_{\mathbf{k}} = 2\Delta_d \phi(\mathbf{k}) \tag{7.41}$$

where $\phi(\mathbf{k}) = \cos k_x - \cos k_y$, and Δ_d is determined self-consistently:

$$\Delta_d = \frac{V_d}{4N_L} \sum_{\mathbf{k}} \frac{\phi^2(\mathbf{k})\Delta_d}{E^{(0)}_{\mathbf{k},\mathbf{q}}} \times \left[\tanh\left(\frac{E^{(0)}_{\mathbf{k},\mathbf{q}} + Z_{\mathbf{k},\mathbf{q}}}{2k_B T}\right) + \tanh\left(\frac{E^{(0)}_{\mathbf{k},\mathbf{q}} - Z_{\mathbf{k},\mathbf{q}}}{2k_B T}\right)\right] \tag{7.42}$$

where $N_L = N \times N$. Rigorously, the bond order parameters along the x and y directions do not follow the relation $\Delta_x = -\Delta_y$ in the presence of magnetic flux. Here we have imposed the restriction of $\Delta_x = -\Delta_y$ to enforce a rigorous d-wave symmetry. Notice that Δ_d is now a function of Φ/Φ_0. From the boundary condition given by Eq. (7.35), we can find the components of wave vectors $k_x = 2\pi\left(n_x - m/2\right)/N_x, q_x = 2\pi\left(\Phi/\Phi_0 + m/2\right)/N_x$, while $k_y = 2\pi n_y/N_y$, and $q_y = 0$, where $n_{x(y)}$ and m are integers. In particular, m is determined by minimizing $|q_x|$ for a given value of magnetic flux Φ. The electron filling factor and the single nearestneighbor bond current flowing around the cylinder are computed via,

$$n_e = \frac{2}{N_L} \sum_{\mathbf{k}} \left[f\left(E^{(+)}_{\mathbf{k},\mathbf{q}}\right)\left|u^{(0)}_{\mathbf{k},\mathbf{q}}\right|^2 + f\left(E^{(-)}_{\mathbf{k},\mathbf{q}}\right)\left|v^{(0)}_{\mathbf{k},\mathbf{q}}\right|^2\right] \tag{7.43}$$

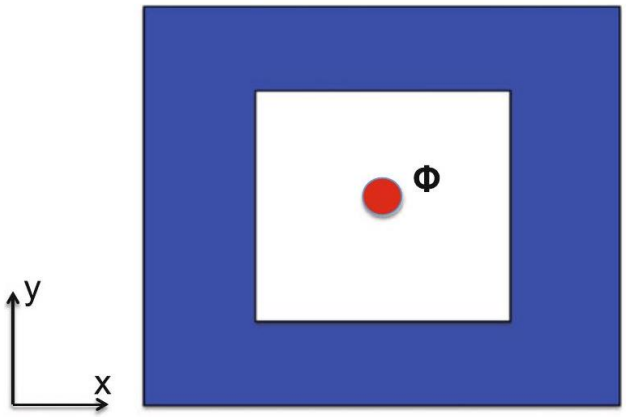
$$I = \frac{4te}{N_L} \sum_{\mathbf{k}} \left[f\left(E^{(+)}_{\mathbf{k},\mathbf{q}}\right)\left|u^{(0)}_{\mathbf{k},\mathbf{q}}\right|^2 + f\left(E^{(-)}_{\mathbf{k},\mathbf{q}}\right)\left|v^{(0)}_{\mathbf{k},\mathbf{q}}\right|^2\right] \times \left(1 + 2t' \cos k_y/t\right) \sin\left(k_x + q_x\right) \tag{7.44}$$

respectively. A factor of 2 has been included to account for the spin degeneracy. These physical quantities can be numerically evaluated and are reported in [10]. It is found that the order parameter and supercurrent are sensitive to both the system size and electron filling factor. We expect that the current profile should also be dependent on the crystalline orientation with respect to the magnetic flux direction. When the crystalline axes are mis-oriented by 45° away from the cylinder axis, the supercurrent flows along the quasiparticle nodal direction, the study of which is left to readers as an exercise.

13.4.4 7.2.2 Square Loop Geometry

For the smooth multiply geometries, the amplitude of the superconducting order parameter remains homogeneous and the breaking down of the $hc/2e$-periodicity in the supercurrent arises mainly from the competition between the linear dimension of

Fig. 7.5 Schematic drawing of a square loop carved out of a two-dimensional superconductor. A magnetic flux threads through the hole



the system and the superconducting coherence length, which is a typical mesoscopic effect. For unconventional superconductors, the sign change of the superconducting order can have more significant consequence in systems with sharp boundaries like surfaces and interfaces. Near these boundaries, zero-energy modes can be induced. Recently, the periodicity of supercurrent in a square loop has been investigated by solving the BdG equations in real-space within a tight-binding model. The geometry is schematically shown in Fig. 7.5. In this case, it is more convenient to treat directly the Peierls phase factor from the local hopping of electrons in the geometry. Specifically, the vector potential entering Peierls phase given by Eq. (5.16)

$$\varphi_{ij} = -\frac{2\pi}{\Phi_0}\int_j^i \mathbf{A}(\xi)\cdot\xi \tag{7.45}$$

can take the form

$$\mathbf{A}(\mathbf{r}) = \frac{\Phi}{2\pi\left(x^2+y^2\right)}(y,-x,0) \tag{7.46}$$

which ensures the electrons in the arms of the square loop experience only the AB effect.

Figure 7.6 display results from a representative study [11] by solving the BdG equations within a tight-binding model. Energy spectrum is symmetric with respect to the reversal $\Phi \to -\Phi$. Due to the low-energy quasiparticles within the superconducting gap maximum, there are bands inside the gap maximum and they are dispersive with the varying magnetic flux through the AB effect. In addition, the small gap open near the Fermi energy comes from the quantum size effect of the loop. Noticeably, the spectra in the flux region $\Phi \in [0, \Phi_0/4]$ are distinct from those in the region $\Phi \in [\Phi_0/4, \Phi_0/2]$, which leads to very different energy parabolas at $\Phi = 0$ and $\Phi = \Phi_0/2$. Consequently, the $\Phi_0/2$-periodicity is broken down in the supercurrent. Instead only the Φ_0-periodicity is generically satisfied, and should be regarded as a fundamental property of loops formed by unconventional

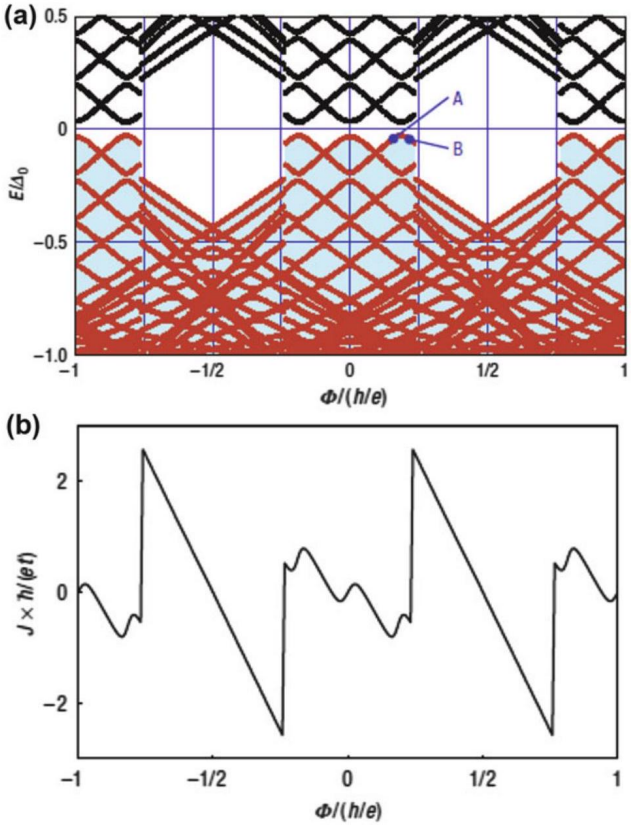


Fig. 7.6 Quasiparticle energy spectrum (a) and supercurrent (b) as a function of the magnetic flux in a square 40×40 loop with a hole of 14×14 unit cells of the original square lattice, obtained by solving the BdG equations self-consistently in a tight-binding model with a nearest-neighbor hopping approximation. The $d_{x^2-y^2}$-wave pairing interaction $0.3t$ is chosen, where t is the nearestneighbor hopping integral. Adapted from [11]

superconducting materials. This periodicity is also shown to survive against the impurity scattering and the change in the loop geometry. This example showcases further the power of the BdG theory when compared with the Ginzburg-Landau theory at a mesoscale.

13.4.5 7.3 Quantum Size Effects in Nanoscale Superconductors

Nanoscale metal and semiconductor systems like quantum dots and wires are interesting not only for their unique physical properties but also for their huge potential of technological applications. In these systems, the energy level discretization due to the quantize size effects is one of the key properties. For nanoscale superconductors, the quantum size effects not only set a quantum limit to superconductivity [12, 13], but also are responsible for many new phenomena such as shell effects [1417], which enhance the superconducting energy gap, as well as the oscillation of superconducting transition temperature [18, 19].

Theoretically, the BdG formalism is especially powerful in addressing these quantum size effects. The key idea is to expand the BdG eigenfunctions in terms of the complete set of normal-state single-particle eigenfunctions of the nanoscale systems themselves [20-25]. This approach has also been briefly discussed for the disorder effect and high-field effects in previous chapters. As examples, we consider the continuum model of BdG formalism for s-wave superconducting quantum wires and dots, as shown in Fig. 7.7. For convenience of the discussion, we write the BdG equations for an s-wave superconductor

$$\begin{pmatrix} h(\mathbf{r}) & \Delta(\mathbf{r}) \\ \Delta^*(\mathbf{r}) & -h^*(\mathbf{r}) \end{pmatrix} \begin{pmatrix} u_n(\mathbf{r}) \\ v_n(\mathbf{r}) \end{pmatrix} = E_n \begin{pmatrix} u_n(\mathbf{r}) \\ v_n(\mathbf{r}) \end{pmatrix}, \tag{7.47}$$

where the single-particle Hamiltonian is given by

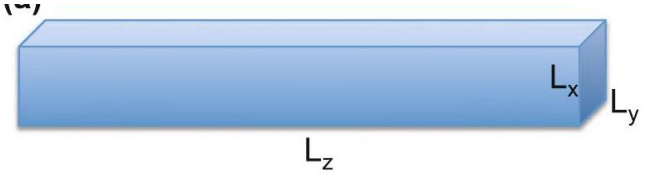
$$h(\mathbf{r}) = -\frac{\hbar^2\nabla^2}{2m_e} + V_c(\mathbf{r}) - E_F, \tag{7.48}$$

and the self-consistency condition is

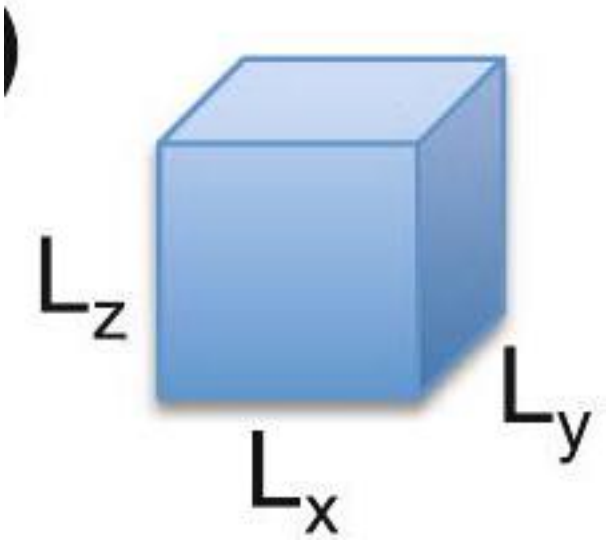
$$\Delta(\mathbf{r}) = g \sum_{n(E_n>0)} u_n(\mathbf{r}) v_n^*(\mathbf{r}) \tanh\left(\frac{E_n}{2k_BT}\right). \tag{7.49}$$

Fig. 7.7 Schematic drawing of a superconducting quantum wire (a) and a quantum dot(**b**). The variables L_x, L_y, and L_z are the linear dimension of these systems

(a)



(b)



For nanoscale superconductors, the confinement effect is described by the potential $V_c(\mathbf{r})$. For a superconducting quantum wire, the confinement is two-dimensional (e.g., in the $x-y$ plane shown in Fig. 7.7a); while for a superconducting quantum dot, it is three-dimensional (i.e., in all three directions shown in Fig. 7.7b). In the hard-wall approximation, $V(\mathbf{r})$ is

$$V(\mathbf{r}) = \begin{cases} 0, \text{ for } 0 \le x \le L_x, 0 \le |y| \le L_y, \\ \infty, \text{ otherwise} \end{cases} \tag{7.50}$$

for the wire; while

$$V(\mathbf{r}) = \begin{cases} 0, \text{ for } 0 \le x \le L_x, 0 \le |y| \le L_y, 0 \le |z| \le L_z, \\ \infty, \text{ otherwise,} \end{cases} \tag{7.51}$$

for the dot. The corresponding eigenfunctions and eigenvalues for the single-particle Hamiltonian are

$$w_\alpha(\mathbf{r}) = \frac{e^{ik_z z}}{\sqrt{2\pi}} \sqrt{\frac{2}{L_x}} \sqrt{\frac{2}{L_y}} \sin\left(\frac{n_x \pi x}{L_x}\right) \sin\left(\frac{n_y \pi y}{L_y}\right), \tag{7.52}$$

for

$$\epsilon_\alpha = \frac{\hbar^2}{2m_e}\left[\left(\frac{n_x\pi}{L_x}\right)^2 + \left(\frac{n_y\pi}{L_y}\right)^2 + k_z^2\right], \tag{7.53}$$

with α denoting the quantum numbers (n_x, n_y, k_z) for the quantum wire; while

$$w_\alpha(\mathbf{r}) = \sqrt{\frac{2}{L_x}}\sqrt{\frac{2}{L_y}}\sqrt{\frac{2}{L_z}}\sin\left(\frac{n_x\pi x}{L_x}\right)\sin\left(\frac{n_y\pi y}{L_y}\right)\sin\left(\frac{n_z\pi z}{L_z}\right), \tag{7.54}$$

for

$$\epsilon_\alpha = \frac{\hbar^2}{2m_e}\left[\left(\frac{n_x\pi}{L_x}\right)^2 + \left(\frac{n_y\pi}{L_y}\right)^2 + \left(\frac{n_z\pi}{L_z}\right)^2\right], \tag{7.55}$$

with α denoting the quantum numbers (n_x, n_y, n_z) for the quantum dot. We note that the eigenfunctions and eigenvalues for a harmonic potential confinement are also available analytically.

The BdG wavefunctions are then expanded as

$$u_n(\mathbf{r}) = \sum_\alpha u_{n,\alpha} w_\alpha(\mathbf{r}), \tag{7.56a}$$

$$v_n(\mathbf{r}) = \sum_\alpha v_{n,\alpha} w_\alpha(\mathbf{r}). \tag{7.56b}$$

Insertion of Eq. (7.56) into Eq. (7.47) leads to

$$\xi_\alpha u_{n,\alpha} + \sum_\beta \Delta_{\alpha\beta} v_{n,\beta} = E_n u_{n,\alpha}, \tag{7.57a}$$

$$\sum_\beta \Delta^*_{\alpha\beta} u_{n,\beta} - \xi_\alpha v_{n,\alpha} = E_n v_{n,\alpha}, \tag{7.57b}$$

where

$$\xi_\alpha = \epsilon_\alpha - E_F, \tag{7.58}$$

and

$$\Delta_{\alpha\beta} = \int w^*_\alpha(\mathbf{r})\Delta(\mathbf{r})w_\beta(\mathbf{r})d\mathbf{r} \tag{7.59}$$

We note that for a generally irregular wire or dot geometry, there are off-diagonal matrix elements for the single-particle Hamiltonian.

Figure 7.8 displays the numerical results on the superconducting transition temperature with the linear dimension of a square-cross-sectioned quantum wire of Pb, Sn, and Al [22]. It shows clearly the oscillation of transition temperature with the cross-section size. The pronounced resonance feature of the transition temperature is related to the tuning of the density of states in the confinement system. The relative T_c difference between the neighboring peak and valley values is increased with decreasing cross-section size. It also shows that the bulk transition temperature is approached when the linear dimension of the cross-section is several times longer than the bulk superconducting coherence. These results are qualitatively similar to those for cylindrical Al and Sn nano wires [26, 27], suggesting a robust nature of quantum confinement effects. In addition, the same method has also been applied to calculate the local electronic

structure in superconducting quantum wires, from which the quasiparticle interference due to the order parameter inhomogeneity is uncovered [25]. Furthermore, the interplay between the quantum confinement and magnetic field can also be studied in the same framework, which is left for readers as an exercise.

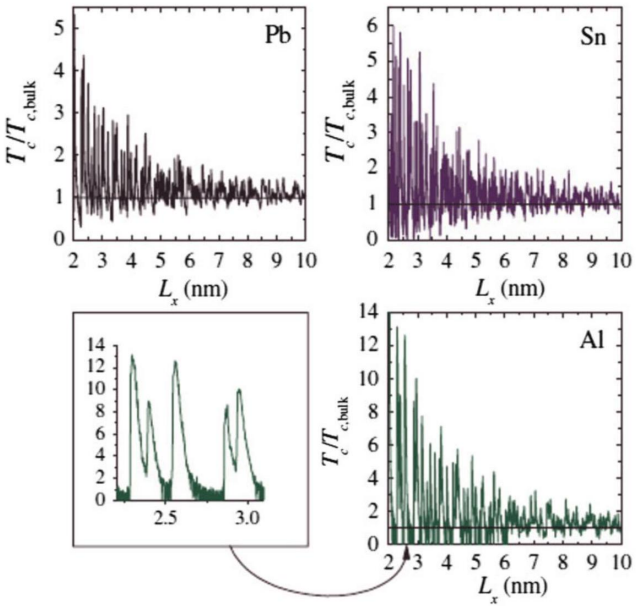


Fig. 7.8 The L_x dependent superconducting critical temperature for Pb, Sn, and Al square-cross-section nano wires. Calculations are with the Debye temperature 96, 195, 375 K and the dimensionless coupling strength $gN(0) = 0.39, 0.25, 0.18$ for Pb, Sn, and Al, respectively. The wire length $L_z = 500$ nm. From [22]

Part VI
Problems and Questions

14 Typical problems

(!!! скорее всего во многих задачах добавлю абзац с теорией, о которой идет речь, прежде чем задается задача! пока это не делаю и теорию продумываю в теор. частях)

14.1 Simplified problems about SC phenomena

(problems from the course of general physics)

14.1.1 Problems about superconductors in magnetic field

(currently, they are written in the note on electrodynamics, later I'll copy them also here)

14.1.2 Qualitative, basic problems about SC 1

O3-5.1 Superconducting ring with decreasing current

A ring with a diameter of $D = 5$cm was rolled from a superconducting wire with a radius of $r = 1$ mm, and the ends of the wire were connected by spot welding. The measurements showed that the contact was not very good, because in one hour the current in the ring decreased by 1% What is the resistance of the ring?

Solution.

(???? нужно подумать про индуктивность сверхпроводника.)
$R = \frac{L}{c^2 t} \ln \frac{\mathcal{J}_0}{\mathcal{J}(t)} \approx 4,4 \cdot 10^{-13}$Ом, где $L = 2\pi D \ln \frac{\pi D}{r}$.

O3-5.2 Superconducting cylinder with decreasing current

A long cylinder with a radius of $a = 1$ cm was rolled from a wide superconducting tape and the edges of the tape were welded along the generatrix. The measurements showed that the electrical contact at the welding site was not very good, because in one hour the current in the cylinder decreased by 1% What is the resistance R of the weld length unit?

Solution.

(аналогично прошлой (????))
$R = \frac{L}{c^2 t} \ln \frac{\mathcal{J}_0}{\mathcal{J}(t)} \approx 1,1 \cdot 10^{-13}$Om, где индуктивность единицы ленты $L \approx 4\pi^2 a^2$.

O3-5.3 Wire over superconductor

Find the distribution of surface currents on a flat surface of a superconductor if a rectilinear sufficiently long thin wire parallel to the plane of the superconductor is located at a distance of $h = 1$ cm from it. A current of $\mathcal{J} = 10$ A flows through the wire. Also find the force f acting on a unit length of wire.

Solution.

(????)
$i(x) = \frac{\mathcal{J}h}{\pi(h^2+x^2)}$; $f = \frac{\mathcal{J}^2}{c^2 h} = 1$ дин/см (рис. 236). Поверхностный ток направлен в соответствии с векторным произведением $\mathbf{i} = \frac{c}{4\pi}[\mathbf{nB}]$, т. е. от нас (перпендикулярно плоскости рисунка).

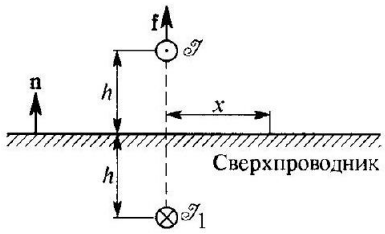
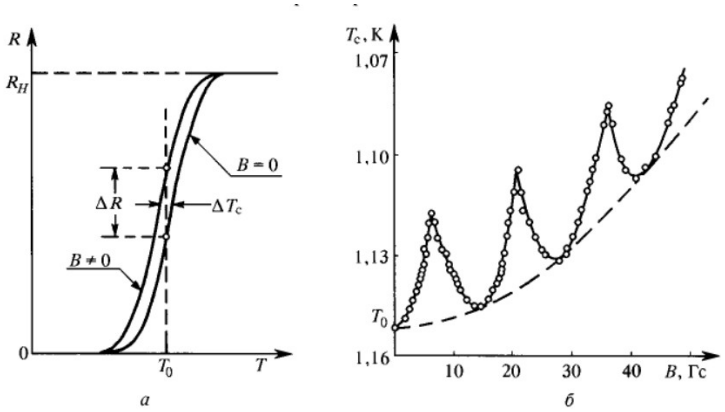


Рис. 236

ОЗ-5.14 Нить с нанесенной сверхпроводящей пленкой

В 1962 г. Литтлом и Парксом была обнаружена осцилляционная зависимость продольного сопротивления пленки сверхпроводника толщиной d, нанесенной на диэлектрическую нить диаметром $D \gg d$, от внешнего магнитного поля $\mathbf{B}$, направленного вдоль нити. Измерения проводились в области сверхпроводящего перехода при постоянной температуре пленки T_0. Зависимость сопротивления пленки от температуры в нулевом и конечном внешнем магнитном поле показана на рис. а). По результатам измерений была построена зависимость критической температуры пленки от магнитного поля (фазовая диаграмма), изображенная на рис. b)



Используя обобщенную формулу квантования Бора-Зоммерфельда $\oint (\mathbf{p}_\mathrm{s} d\mathbf{l}) = 2\pi n\hbar$, ($\mathbf{p}_\mathrm{s} = 2m\mathbf{v}_\mathrm{s} + \frac{2e}{c}\mathbf{A}$ - обобщенный импульс пары), объяснить полученную зависимость $T_\mathrm{c}(B)$ и вычислить диаметр нити. Учесть, что глубина проникновения $\Lambda(T_0) \gg d$, и поэтому эффектом квантования магнитного потока можно пренебречь.

Solution 5.14

(?????)

В силу условий $D \gg d$ и $\Lambda(T_0) \gg d$ можно пренебречь магнитным потоком через пленку и считать, что поле в диэлектрике равно внешнему. Тогда можно записать

$$\oint (\mathbf{p}_\mathrm{s} d\mathbf{l}) = \oint \left(2m\mathbf{v}_\mathrm{s} - \frac{2e}{c}\mathbf{A}\right) d\mathbf{l} = 2\pi n\hbar$$

откуда, используя теорему Стокса, получаем

$$v_\mathrm{s} = \frac{\hbar}{mD}\left(n + \frac{\Phi}{\Phi_0^{\mathrm{sc}}}\right), \qquad \Phi := \frac{\pi D^2}{4}B, \qquad \mathbf{B} := \operatorname{rot}\mathbf{A}, \qquad \Phi_0^{\mathrm{sc}} := \frac{\pi\hbar c}{e}$$

Дополнительная плотность полной энергии сверхпроводника при температуре T_0, обусловленная внешним полем B, равна

$$\Delta w = n_{\text{пар}}\ (T_0)\,\frac{2mv_\mathrm{s}^2}{2} + \frac{B^2}{8\pi}$$

где $n_{\text{пар}}$ - концентрация сверхпроводящих пар, равная $n_{\mathrm{sc}}/2$ (n_{sc} - концентрация сверхпроводящих электронов).

При заданном поле B квадрат скорости сверхпроводящих электронов v_s^2 должен быть минимальным, чтобы обеспечить минимум полной энергии. Таким образом, при увеличении B должна меняться и величина n в условии квантования Бора-Зоммерфельда. Это приводит к периодической зависимости v_s^2 от B (рис. 237).

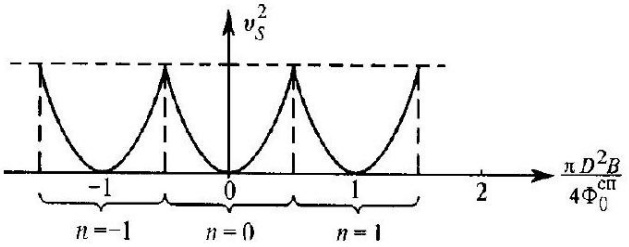


Рис. 237

Поскольку $|\Delta w| \propto k_{\mathbf{b}} \Delta T_{\mathrm{c}}(B)$, то периодическая зависимость v_{s}^2 приводит к периодической зависимости T_c, а член $B^2/(8\pi)$ приводит к монотонному изменению T_{c} (штриховая линия на рис. 82 к условию задачи). Как видно из рисунка, период осцилляций связан с «вхождением» (или «уходом») кванта магнитного потока $\frac{\Delta B \pi D^2}{4} = \Phi_0^{\mathrm{sc}}$, откуда $D = \sqrt{\frac{4\Phi_0^{\mathrm{sc}}}{\pi \Delta B}}$. Из графика находим $\Delta B \simeq 14$ Гс и, следовательно, $D \simeq 1,37 \cdot 10^{-4}$ см.

Сравнить с задачей 4.38 (эксперимент Шарвиных). (????)

O3-5.4 Levitation of the ring

Above the superconducting plane, on an insulating layer with a height of $h = 3$ mm, lies a thin wire ring with a radius of $r = 10$cm. The mass of the ring is $m = 1$ g. A constant current flows through the ring $\mathscr{J}$. Estimate at what value $\mathscr{J}$ the ring will begin to float in the air (levitate).

Solution.

(????)

$\mathcal{J} \geqslant c\sqrt{\frac{mgh}{2\pi r}} = 6,49 \cdot 10^{10}$ ед. СГСЭ $\approx 21,6$ А.

O3-5.5 Oscillations of a magnet over a superconductor

At a distance of a =9 cm above the surface of the superconductor, a thin permanent magnet hovers in the gravity field, the length of which is small compared to the distance of a. If one slightly move the magnet out of equilibrium, it would start to oscillate slowly in the vertical plane. Find the period of these oscillations.

Solution 5.5.

(???)

$T = \pi\sqrt{\frac{a}{g}} = 0,3$с.

O3-5.6 Rotation of a ball over a superconductor

A ball with a mass of $M = 10$ g and a radius of $R = 1$cm, made of a type I superconductor, rests in a magnetic field of $B = 1$ kGs, which is less than critical, at a temperature below the transition point. The temperature of the ball gradually rises such that the superconductivity disappears, and the ball begins to spin. Find the angular velocity ω of the ball's rotation.

Solution 5.6.

(????)

$\omega = \frac{5}{2}\frac{m_e c R B}{M e} = 1.42 \cdot 10^{-5} c^{-1}$.

Тут реально носителями тока являются куперовские пары, и для них гиромагнитное отношение $\gamma = \frac{2e}{2 \cdot 2mc} = \frac{e}{2mc}$ совпадает с γ для отдельного электрона.

O3-5.7 Rotation of a superconducting cylinder

In the experiment conducted by I. K. Kikoin, a cylinder made of a superconductor of the first kind with a mass of $M = 80$ g, height of $h = 20$ cm, radius of $R = 0.5$ cm at a temperature below the transition point is suspended vertically on an elastic thread in a magnetic field, which is less than critical one and directed along the axis of the cylinder. The suspension thread is not twisted in its original state. The temperature

is kept constant, and the magnitude of the magnetic field is gradually increased. At a field of $H = 1$ kOe, superconductivity disappears. As a result, the cylinder turns and the thread twists. Determine the maximum twisting angle if the thread's torsion modulus is $\alpha = 1$ erg/rad.

Solution

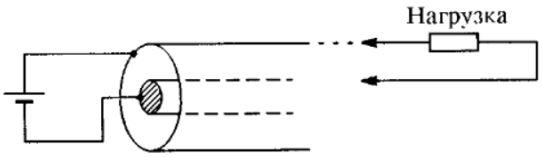
(????)
$\varphi = \frac{m_e c H R h}{e\sqrt{2\alpha M}} = 4,5 \cdot 10^{-5}$ рад.

Носителями тока являются куперовские пары, и для них гиромагнитное отношение $\gamma = \frac{2e}{2 \cdot 2mc} = \frac{e}{2mc}$ совпадает с γ для отдельного электрона.

(??? was there another experiment about it???)

O3-5.8 Using SC in ordinary wires?

Для исключения потерь электроэнергии на джоулево тепло в линиях передачи постоянного тока предложено использовать коаксиальный кабель, внутренняя жила и наружная оболочка которого выполнены из сверхпроводника. Кабель подключен к нагрузке, как это показано на рис. 89.



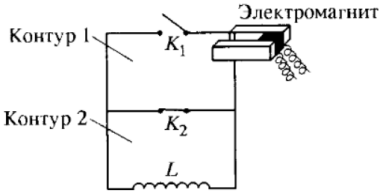
Максимально допустимые величины магнитной индукции на поверхности сверхпроводника $B = 500$ Гс и напряженности электрического поля изолирующей прослойки кабеля $E = 30$ кВ/см. При каком соотношении диаметров d/D жилы и оболочки можно передать наибольшую мощность W? Найти величину W, приняв диаметр наружной оболочки $D = 20$ см.

Solution 5.8.

$W = \frac{cD^2}{16l} BE = 1,4 \cdot 10^{16}$ эрг /с $= 1,4 \cdot 10^9$В при $\frac{D}{d} = \sqrt{e}$, где e - основание натурального логарифма.

O3-5.9 Магнитный насос (???)

На рис. 90 изображена схема магнитного насоса для «накачки» потока в соленоид.



Насос представляет собой два сверхпроводящих контура с ключами K_1 и K_2. Контур 2 включает в себя соленоид с большой самоиндукцией L, в то время как контур l обладает малой самоиндукцией $l \ll L$. Работа насоса заключается в том, что при закрытом ключе K_2 и открытом ключе K_1 в контуре I с помощью электромагнита создается мощью электромагнита создается магнитное поле. Ключ K_1 замыкается, магнит удаляется и после этого размыкается ключ K_2. Эта операция повторяется много раз. Какого увеличения потока можно достичь в такой системе?

Solution 5.9.

$\left(\frac{\Phi_n}{\Phi_1}\right)_{n\to\infty} = \frac{L}{l}$.

O3-5.10* The London Depth

Find the London penetration depth λ for a typical superconductor of the second kind with a concentration of superconducting electrons $n_{\text{sc}} = 10^{22}\text{cm}^{-3}$.

Solution 5.10*

The formula $\Lambda = \sqrt{\frac{m_e c^2}{4\pi n_{\rm sc} e}} = 0,53 \cdot 10^{-5}$ cm is known, but one can rederive the Meissner effect.

Уравнение движения электрона в сверхпроводнике

$$m\frac{\partial \mathbf{v}}{\partial t} = e\mathbf{E}.$$

Здесь мы заменили полную производную частной, что можно сделать, если пространственные изменения переменных малы ($\frac{d}{dt} = \frac{\partial}{\partial t} + (\mathbf{v}\nabla)$, $\frac{1}{t} \gg \frac{\langle v\rangle}{l}$ или $\omega_{\rm p} \gg \frac{v_{\rm F}}{\Lambda}$, откуда $\frac{v_{\rm F}}{c} \ll 1$).

Так как $\mathbf{E} = -\frac{1}{c}\frac{\partial \mathbf{A}}{\partial t}$ и $\mathbf{j} = en_{\rm sc}\mathbf{v}$, то

$$\mathbf{j} = -\frac{e^2 n_{\rm sc}}{m_{\rm e} c}\mathbf{A} = -\frac{c}{4\pi\Lambda^2}\mathbf{A}, \text{ где } \Lambda = \sqrt{\frac{m_e c^2}{4\pi n_{\rm sc} e^2}} = \frac{c}{\omega_{\rm p}}$$

Это уравнение заменяет закон Ома в сверхпроводниках.

$$\operatorname{rot}\mathbf{j} = -\frac{c}{4\pi\Lambda^2}\operatorname{rot}\mathbf{A} = -\frac{c}{4\pi\Lambda^2}\mathbf{B}$$

Используя уравнение Максвелла $\operatorname{rot}\mathbf{B} = \frac{4\pi}{c}\mathbf{j}$ (в сверхпроводниках $\mathbf{B} \approx \mathbf{H}$, а током смещения в металлах можно пренебречь), получаем

$$\operatorname{rot}\operatorname{rot}\mathbf{B} = \operatorname{grad}\operatorname{div}\mathbf{B} - \nabla^2\mathbf{B} = -\mathbf{B}/\Lambda^2$$

Поскольку $\operatorname{div}\mathbf{B} = 0$, то окончательно

$$\nabla^2\mathbf{B} = \frac{\mathbf{B}}{\Lambda^2}$$

Если однородное внешнее магнитное поле параллельно поверхности сверхпроводника, то уравнение переходит в $\frac{d^2B}{dx^2} = \frac{B}{\Lambda^2}$, где x - координата, направленная вглубь сверхпроводника по нормали к поверхности. Решение этого уравнения $B(x) \propto e^{-x/\Lambda}$, т. е. магнитное поле экспоненциально затухает вглубь сверхпроводника. Поскольку частота внешнего поля не входит в Λ, то результат в полной мере относится к постоянному магнитному полю. Искомая глубина $\Lambda = 5,3 \cdot 10^{-5}$ см.

О3-5.11 Сверхток в пластине

Найти распределение поля и тока в бесконечной пластине сверхпроводника толщиной d, помещенной в однородное параллельное пластине магнитное поле B_0.

Solution 5.11.

$B(x) = B_0\frac{\operatorname{ch}(x/\Lambda)}{\operatorname{ch}[d/(2\Lambda)]}$; $\quad j_{\rm s} = -\frac{cB_0}{4\pi\Lambda}\frac{\operatorname{sh}(x/\Lambda)}{\operatorname{ch}[d/(2\Lambda)]}$, где $\Lambda = \sqrt{\frac{m_e c^2}{4\pi n_{\rm sc} e^2}}$ - лондоновская глубина.

О3-5.12 Длина когерентности по щели

Исходя из соотношения неопределенностей, оценить характерный линейный размер (длину когерентности) электронной пары в сверхпроводнике с энергетической щелью $\Delta = 3$ мэВ в электронном спектре. Учесть, что в образовании пар участвуют электроны вблизи поверхности Ферми, скорость которых принять равной $v_{\rm F} \sim 10^8$ см/с.

Solution 5.12.

(?? this is basic topic in the theory)

$\xi \approx \frac{\hbar v_{\rm F}}{2\Delta} = 10^{-5}$ cm.
$\delta p = \Delta/v_F$ (???)
(in my theory there is no 1/2, but it does not matter)

О3-5.13 Разрушение куперовской пары

В сверхпроводнике электроны образуют пары с противоположно направленными спинами. В каком магнитном поле произойдет разрушение таких пар, сопровождаемое изменением направления спина одного из электронов пары, если в нулевом магнитном поле критическая температура сверхпроводника равна $T_c = 92$ K? Считать, что разрушение пары происходит при $T = 0$ K.

Solution 5.13.

(??? the solution is somewhat equating energy of spin spread and energy that holds together the pair, but I am not sure)
$B \approx \frac{k_B T_c}{\mu_B} \approx 1,4 \cdot 10^6$Гс.

О3-5.15 Maximal surface current

Какой максимальный ток течет по поверхности сверхпроводника I рода, находящегося во внешнем касательном магнитном поле, если величина критического магнитного поля $H_c = 400$ А/см, а лондоновская глубина проникновения $\Lambda = 0,5 \cdot 10^{-5}$ см?

Solution 5.15.

(???)
$j_{\max} = \frac{c}{4\pi}\left(\frac{\partial B}{\partial x}\right)_{\max} = -\frac{cH_c}{4\pi\Lambda} = 8 \cdot 10^7$ A/cm^2, т. е. ток затухает по тому же закону, что и поле.

О3-5.16 Current through a droplet

The current to be measured j flows through a niobium wire with a diameter of $2r_{\text{Nb}} = 0.1$ mm, forming point contacts A and B in a drop of superconducting metal solder Pb + Sn. Due to the presence of an oxide film on the niobium surface, the drop does not completely wet the wire, but only touches the niobium at certain points. Let there be only two such points, A and B, with a distance between them of $l_{AB} = 5$ mm (Fig. below). The thickness of the insulating film on the niobium surface can be considered small compared to the penetration depth.



Estimate the current strength at which one quantum of magnetic flux will pass through the droplet surface. The London lengths for niobium and solder are equal $\Lambda_{\text{Nb}} = 5 \cdot 10^{-6}$ см, $\Lambda_{\text{PbS}} = 10^{-5}$ см.

Solution 5.16*

(??? don't understand the statement. ???)
$\mathscr{E}_{\Phi_0} \approx 0,7$MA.
Решение. Магнитное поле проходит между двумя точечными контактами через поверхность, площадь которой практически равна произведению расстояния между контактами l_{AB} на сумму глубин проникновения в ниобий Λ_{Nb} и припой Λ_{PbSn}.

$$B = \frac{2\mathcal{J}}{cr_{\text{Nb}}}, \qquad \Phi = BS = \frac{2\mathcal{J}}{cr_{\text{Nb}}} l_{AB}\left[\Lambda_{\text{Nb}} + \Lambda_{\text{PbSn}}\right]$$
$$\mathcal{J}_{\Phi_0} = \Phi_0^{\text{sc}} \frac{cr_{\text{Nb}}}{2l_{AB}\left[\Lambda_{\text{Nb}} + \Lambda_{\text{PbSn}}\right]} = 6.9 \cdot 10^{-4} \text{ A} \approx 0,7 \text{ mA}.$$

О3-5.17* Thin film on a thread in a field

A thin film of a type I superconductor with a thickness of $d \ll \Lambda$ is considered, deposited on the surface of a dielectric filament, the radius of which is $R \gg d$. First, the thread is introduced into a longitudinal magnetic field at room temperature, and then the thread temperature drops below the critical temperature T_c. After that, the external magnetic field turns off. How is the magnetic flux captured by the filament and film quantized?
Hint. Use the Bohr-Sommerfeld quantization condition $\oint (\mathbf{p}_s d\mathbf{l}) = 2\pi n\hbar$, where $\mathbf{p}_s$ is the generalized momentum of the pair (see problems 5.14)

Solution 5.17*

Поскольку $d \ll \Lambda$, ток будет распределен по толщине пленки однородно. В силу условия $R \gg d$ магнитное поле в диэлектрике равно

$$B = \frac{4\pi}{c} j_{\text{s}} d$$

(как в соленоиде: $j_{\text{s}}d$ - линейная плотность тока). По определению $j_{\text{s}} = en_{\text{sc}}v_{\text{s}}$, где n_{sc} - плотность сверхпроводящих электронов, v_{s} - скорость центра масс пар. В магнитном поле обощенный импульс пары

$$\mathbf{p_s} = 2m\mathbf{v_s} - \frac{2e}{c}\mathbf{A}$$

Используя условие квантования Бора-Зоммерфельда

$$\oint (\mathbf{p}_{\text{s}} d\text{l}) = 2\pi n\hbar,$$

получаем

$$2\pi n\hbar = \frac{2m2\pi R}{n_{\text{sc}}e} j_{\text{s}} - \frac{2e}{c}\tilde{\Phi},$$

где $\tilde{\Phi} = \int(\text{rot}\,\mathbf{A}d\mathbf{s}) =$ вл R^2 - магнитный поток внутри цилиндра. Исключая j_s, находим:

$$\tilde{\Phi} = n\frac{\Phi_0^{\text{sc}}}{1 + 2\Lambda^2/(Rd)}.$$

Как видно из формулы, при $Rd \gg \Lambda^2$ квантование магнитного потока в тонкостенном цилиндре происходит так же, как и в массивном образце. Но, вообще говоря, «квант потока» всегда меньше Φ_0^{sc}.

Answer: $\Phi = n\Phi_0 \frac{1}{1+2\Lambda^2/(Rd)}$.

O3-5.18 Cryotron (????)

The cryotron is a control device invented by the Buck in 1953 (Fig. 93).
Control current of length $L = 2$ mm with number of turns $N = 20$. A superconducting tantalum wire AB with a diameter of $2a = 0.2$ mm is placed in the solenoid, through which current is passed $\mathscr{J}$. The critical field H_{c} for tantalum at 4.2 K is 100 Gs. By converting the wire from superconducting to normal by the field of the solenoid, the current flowing through the wire can be controlled, Therefore, the cryotron can be used in logic circuits as an active element, as well as as a storage element in computers.
What is the current gain $G = \mathscr{J}/\mathscr{J}'$ can be achieved in this device?

Solution 5.18.

$G = \frac{\mathscr{J}_c}{\mathscr{J}'_{\min}} = 2\pi N\frac{a}{L} \approx 6$, где $\mathscr{J}_c$ - предельный ток прямого провода, создающий разрушающее критическое поле $B_c = \frac{2}{cr}$, $\mathscr{J}'_{\min}$ - предельное (минимальное) значение управляющего тока, переводящего проволоку в нормальное состояние.

O3-5.19 Estimation of a critical field

Tantalum (Ta) crystallizes into a volume-centered cubic lattice with a constant $a = 3\mathring{\text{A}}$ and is a superconductor of the first kind ($T_{\text{c}} = 4,4$ K). Suppose that each Ta atom gives one electron to the conduction band and that the effective mass of it is equal to the mass of a free electron. Estimate from energy considerations the magnitude of the critical magnetic field H_{c} at $T \approx 0$ K, in which Cooper pairs are destroyed.

Solution 5.19.

$H_c \approx \frac{8\cdot 2^{2/3} k_{\text{B}} T_{\text{c}}}{\hbar(3\pi^2)^{1/3}}\sqrt{\frac{m\pi}{a}} \approx 730$Гс.
Плотность энергии сверхпроводника ниже плотности энергии нормального металла на величину плотности энергии связи куперовских пар.

Поскольку энергия связи одной пары равна 2Δ (по Δ на каждый электрон), то $\mathscr{E}_{\text{св}} = n_{\text{пар}}\, 2\Delta = \frac{n_{\text{sc}}}{2} 2\Delta$, где n_{sc} - плотность сверхпроводящих электронов. По аналогии с теплоемкостью металла $n_{\text{sc}} \simeq n\frac{2\Delta}{\varepsilon_{\mathbf{F}}}$

(«размытие распределения» примерно 2Δ), где $n = 2/a^3$ плотность электронов проводимости. Считая, что $\Delta \simeq 2k_{\mathrm{D}}T_{\mathrm{c}}$ (в теории сверхпроводимости Бардина-Купера-Шриффера: $\Delta = 1,76k_BT_c$), получаем

$$\mathscr{E}_{sc} \approx \frac{16\left(k_{\mathrm{B}}T_{\mathrm{c}}\right)^2}{a^3\varepsilon_{\mathrm{F}}} = \frac{32\left(k_{\mathrm{B}}T_{\mathrm{c}}\right)^2 m_{\mathrm{e}}}{a\hbar^2\left(3\pi^2\right)^{2/3}2^{2/3}}$$

Сверхпроводимость «разрушается», когда плотность энергии магнитного поля сравнивается с плотностью энергии связи

$$\frac{H_{\mathrm{c}}^2}{8\pi} = \mathscr{J}_{\mathrm{sc}}, \quad \text{откуда} \quad H_{\mathrm{c}} \approx \frac{8\cdot 2^{2/3}k_{\mathrm{L}}T_{\mathrm{c}}}{\hbar\left(3\pi^2\right)^{1/3}}\sqrt{\frac{m_{\mathrm{e}}\pi}{a}} \approx 730\text{Гс}$$

Отметим, что экспериментальное значение критического поля тантала составляет 830 Гс. Заметим также, что ответ можно выразить и в такой форме

$$H_{\mathrm{c}} \simeq \frac{\Phi_0^{\mathrm{c\Pi}}}{\pi\Lambda\xi}$$

О3-5.20 плотность критического тока распаривания j_{c} при $T = 0$ K для свинца (?????)

Оценить плотность критического тока распаривания j_{c} при $T = 0$ K для свинца, у которого $T_{\mathrm{c}} = 7,2$ K, $n_{\mathrm{sc}} \simeq 3\cdot 10^{22}$ см$^{-3}$, $v_{\mathrm{F}} \approx 10^8$ см/с.

Solution 5.20.

$j_{\mathrm{c}} \simeq \frac{2k_{\mathrm{B}}T_{\mathrm{c}}n_{\mathrm{sc}}e}{m_{\mathrm{e}}v_{\mathrm{F}}} \simeq 10^8$ A/cm^2.

О3-5.21 Расстояние между вихрями по намагниченности

Длинный цилиндр из сверхпроводника II рода, у которого нижнее критическое поле $H_{\mathrm{cl}} = 400$ Э, помещен в магнитное поле $H = 500$ Э, параллельно его образующей, при этом его намагниченность составила половину того значения, которое было при H_{cl}. Оценить среднее расстояние между вихрями магнитного потока в поле H.

Solution 5.21

* $d \approx \sqrt{\frac{\Phi_0^c}{B_2}} \approx 2,6\cdot 10^{-5}$с, где $B_2 = 300$ Гс.

Решение. В первом случае при внешнем поле $H = H_{\mathrm{c1}}$ $B_1 = H + 4\pi I_1 = 0$, откуда намагниченность $4\pi I_1 = -400$ Э. Во втором случае (см. графики на рис. 238) во внешнем поле $H = 500$ Э $B_2 = H + \frac{1}{2}(4\pi I_1) = 500 - 200 = 300$ Гс.

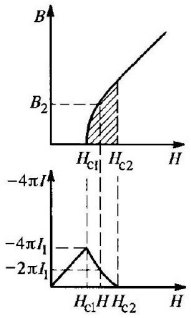


Рис. 238

Поскольку $H > H_{c1}$, то сверхпроводник находится в смешанном состоянии (полагаем, что $H < H_{c2}$). Плотность вихрей, т. е. их число, приходящееся на единицу площади оценим как

$$n = \frac{B_2}{\Phi_0^{\mathrm{cI^{II}}}}$$

Тогда расстояние между вихрями, магнитного потока, называемыми также вихрями Абрикосова,

$$d \approx \frac{1}{\sqrt{n}} = \sqrt{\frac{\Phi_0^{c\pi}}{B_2}} \approx 2,6\cdot 10^{-5}\ \text{cm}$$

Solution

При внешнем поле $H = H_{\text{c}\,1}$ $B_1 = H + 4\pi I_1 = 0$, откуда намагниченность $4\pi I_1 = -400$ Э. Во внешнем же поле $H = 500$ Э $B_2 = H + \frac{1}{2}(4\pi I_1) = 500 - 200 = 300$ Гс. Поскольку $H > H_{\text{c}1}$, то сверхпроводник находится в смешанном состоянии (полагаем, что $H < H_{\text{c}2}$). Плотность вихрей, т. е. их число, приходящееся на единицу площади оценим как

$$n = \frac{B_2}{\Phi_0^{c\pi}}$$

Тогда расстояние между вихрями

$$d \approx \frac{1}{\sqrt{n}} = \sqrt{\frac{\Phi_0^{\text{cT}}}{B_2}} \approx 2,6 \cdot 10^{-5} \text{ cm}$$

Ответ: $d \approx \sqrt{\frac{\Phi_0^{\text{cI}}}{B_2}} \approx 2,6 \cdot 10^{-5}$ cm, где $B_2 = 300$ Гс.

О3-5.22 Поле вихрей по рассеянию нейтронов

В 1964 г. Крибье с сотрудниками с помощью упругого рассеяния нейтронов на ниобии экспериментально подтвердил, что в сверхпроводниках II рода в магнитном поле $B > B_{\text{cI}}$ образуется треугольная вихревая решетка Абрикосова. В опытах наблюдался максимум первого порядка в отражении нейтронов с длиной волны $\lambda = 5$Å под углом $\theta = 20'$ по отношению к падающему пучку от плоскостей, разделенных расстоянием h (высота равностороннего треугольника структуры). В каком магнитном поле проводился эксперимент?

Solution 5.2

2. $B \approx \frac{\sqrt{3}}{2}\frac{\Phi_0^{c\pi}\theta^2}{\lambda^2} = 2430$ Гс, где $\Phi_0^c = \frac{hc}{2e} = 2,07 \cdot 10^{-7}$Гс $\cdot$ с^2 - квант магнитного потока в сверхпроводнике.

О3-5.23 Энергия электронов в вихре

Найти выражение для кинетической энергии $\mathcal{E}$ электронов на единицу длины вихря магнитного потока, проникшего в сверхпроводник II рода при $H > H_{c1}$, считая заданными плотность сверхпроводящих электронов n_{sc} , глубину проникновения Λ и длину когерентности $\xi \ll \Lambda$. Считать, что вихрь занимает по радиусу размер от ξ до Λ, а пары обладают минимально возможной проекцией углового момента.

Solution

По правилу квантования проекции момента импульса $2mv(r)r = \hbar(n = 1)$ находим распределение скоростей центров масс пар в вихре

$$v(r) = \frac{\hbar}{2mr}.$$

Это выражение справедливо при $\xi \ll r \ll \Lambda$, когда можно пренебречь вкладом интеграла $\oint \mathbf{A}d\mathbf{1}$ в правиле квантования Бора-Зоммерфельда (см. задачи 5.14 и 5.17). Если длина вихря равна L, то кинетическая энергия электронных пар в вихре

$$\mathscr{E}_L = \int \frac{2mv^2(r)}{2}\frac{n_{\text{sc}}}{2}dV = L\int_{\xi}^{\Lambda}\frac{\hbar^2}{8mr^2}n_{\text{sc}}2\pi r dr,$$

откуда и следует ответ задачи.

Ответ: 5.23* $\mathscr{E} = \frac{\pi n_{\text{sc}}\hbar^2}{4m}\ln\frac{\Lambda}{\xi}$.

О3-5.24

Найти магнитную энергию единицы длины вихря во внешнем поле $H > H_{\text{cl}}$, считая заданными плотность сверхпроводящих электронов n_{sc} и глубину проникновения $\Lambda \gg \xi$ (длины когерентности). Считать, что вихрь занимает по радиусу размер от ξ до Λ, а пары обладают минимально возможной проекцией углового момента. Получить выражение для H_{cl}, используя результат задачи 5.23.

Solution

$W_{\rm m} = -\mathfrak{M}H$, где $\mathfrak{M} = \mu_{\rm D}\int_{\xi}^{\Lambda}\frac{n_{\rm sc}}{2}2\pi r dr \simeq \frac{\pi n_{\rm sc}}{2}\Lambda^2$ - магнитный момент единицы длины вихря. Из условия $\mathscr{E} + \boldsymbol{W}_{\rm m} = 0$ находим $H_{\rm c1} = \frac{c\hbar}{e\Lambda^2}\ln\frac{\Lambda}{\xi} = \frac{\Phi_0^{\rm sc}}{2\pi\Lambda^2}\ln\frac{\Lambda}{\xi}$ (см. также задачу 5.25).

О3-5.25 Λ и ξ высокотемпературного сверхпроводника

Для высокотемпературного сверхпроводника $YBaCCu_3O_{7-\delta}$, где $\delta < 1$, критические поля $H_{\rm cl} = 10^3$ Э и $H_{\rm c2} = 10^6$ Э. Оценить глубину проникновения Λ и длину когерентности ξ при $T = 0$ К.

Solution

$\Lambda \approx \sqrt{\frac{\Phi_0^{\rm cП}}{\pi H_{\rm cl}}} \approx 0,8\cdot 10^{-5}$ cm; $\xi = \sqrt{\frac{\Phi_0^{\rm cГ}}{\pi H_{\rm c2}}} \approx 3\cdot 10^{-7}$ cm.

О3-5.26

Цилиндр из сверхпроводника II рода массой $M = 25$ г и длиной $l = 10$ см подвешен вдоль оси на тонкой нити. Вдоль оси цилиндра прикладывается такое магнитное поле $H = 10^4 \gg H_{\rm cl}$, что индукция $B \simeq H$. Вначале температура цилиндра $T < T_{\rm c}$, цилиндр покоился, а затем температура увеличилась выше критической. Найти установившуюся угловую частоту вращения цилиндра. Глубина проникновения магнитного поля $\Lambda = 10^{-5}$ см, плотность сверхпроводящих электронов $n_{\rm sc} = 10^{22}$ см$^{-3}$.

Solution

$\omega = \frac{\pi^2 n_{\rm sc}\Lambda^2 hlB}{\Phi_0^{c\pi}M} \approx 2\cdot 10^{-4}\text{c}^{-1}$.

14.1.3 Qualitative, basic problems about SC 2

О3-5.27 Сила на вихрь со стороны дефектов (??)

Плоская лента шириной $b = 0,5$ см из сверхпроводника II рода в смешанном состоянии помещена в магнитное поле $B = 10$ Тл, $H_{\rm cl} \ll B \ll H_{\rm c2}$, перпендикулярное поверхности ленты (рис. 94).

По ленте без диссипации течет ток $\mathcal{J} = 10$ А. При этом вихри неподвижны, удерживаемые структурными дефектами сверхпроводника. Вычислить силу F, действующую на отдельный вихрь со стороны дефектов кристалла. Считать, что ток однородно распределен по образцу, а вихревую структуру создают другие, независимые от (?) токи.

Solution

$F = \frac{1}{c}\frac{\mathcal{E}\Phi_0^{\rm sc}}{b} \approx 4\cdot 10^{-7}$ дин.

О3-5.28 Электрическое поле при вязком течении вихрей (???)

Пластинка из сверхпроводника II рода расположена в магнитном поле H (при этом $H > H_{\rm cl}$), перпендикулярном ее плоскости. Если вдоль пластины пропустить ток плотностью $\mathbf{j}$, то в результате взаимодействия с этим током вихри приходят в движение с конечной скоростью v, определяемой силой трения (приходящейся на единицу длины вихря) $F_{\rm тр} = \eta v$. Такое движение называется вязким течением вихрей. Какое электрическое поле появится в сверхпроводнике?

Solution 5.28

* $E = \frac{1}{c}vB = \frac{\Phi_0^{c\pi}jB}{\eta c^2}$.

Решение. Условием равномерного движения вихря является равенство сил $|\mathbf{F}_{\rm Tp}| = |\mathbf{F}_{\rm A}|$, где сила Ампера, действующая на единицу длины вихря

$$\mathbf{F_A} = \frac{1}{c}\left[\mathbf{j}\mathbf{\Phi}_0^{\text{cn}}\right], \quad \mathbf{\Phi}_0^{\text{cn}} = \frac{hc}{2e}\frac{\mathbf{B}}{B}.$$

Скорость вихря $\mathbf{v}$ образует правую тройку с векторами $\mathbf{j}$ и B. При этом $v = \frac{1}{c}\frac{j\Phi_0^{\text{sc}}}{\eta}$. В системе вихря, движущегося со скоростью $\mathbf{v}$, присутствует только магнитное поле B следовательно в лабараторной системе отсчета имеется также макроскопическое электрическое поле

$$\mathbf{E} = \frac{1}{c}[\mathbf{B}\mathbf{v}].$$

Легко увидеть, что $\mathbf{E}\|\mathrm{j}$ и поэтому $E = \frac{1}{c}vB = \frac{\Phi_0^{\text{sc}} jB}{\eta c^2}$.

О3-5.29* Проводимость при вязком течении вихрей (???)

Найти эффективную проводимость сверхпроводника II рода в режиме вязкого течения вихрей (См. задачу 5.28).

Solution 5.2

9*: $\sigma_{\text{eff}} = \sigma_{\text{n}}\frac{H_{c2}}{B}$, где σ_{n} - проводимость в сердцевине вихря, т. е. проводимость сверхпроводника в нормальном состоянии.

Решение. Как следует из предыдущей задачи (5.28*), $\mathbf{j} = \sigma_{\text{eff}}(B)\mathbf{E}$, где эффективная проводимость $\sigma_{\text{eff}}(B) = \Phi_0^{\text{sc}}/\left(\eta c^2\right)$.

Поскольку при $B = H_{\text{c2}}$ сверхпроводимость исчезает и материал становиться нормальным металлом, то

$$\sigma_{\text{eff}}(H_{\text{c2}}) = \frac{\Phi_0^{\text{cn}} H_{\text{c2}}}{\eta c^2} = \sigma_{\text{n}},$$

откуда $\frac{\Phi_0^{\text{sc}}}{\eta c^2} = \frac{\sigma_{\text{n}}}{H_{\text{c2}}}$ или $\sigma_{\text{eff}}(B) = \sigma_{\text{n}}\frac{B}{H_{\text{c2}}}$.

О3-5.30

В сверхпроводнике, содержащем примеси, электрон упруго рассеивается на примесных атомах без потери фазы. Если среднее расстояние между примесными атомами много меньше длины когерентности ξ, то электрон движется подобно броуновской частице. Исходя из этих соображений, оценить эффективную длину когерентности ξ в сверхпроводнике с постоянной решетки $a = 3$Å, средним расстоянием между примесями $b \simeq 30$Å и критической температурой $T_{\text{c}} = 25$ K.

Solution 5.30.

$\bar{\xi} = \sqrt{6D\tau_{\text{ког}}} \approx \sqrt{\frac{\hbar^2 b}{makT_{\text{c}}}} \approx 1,8 \cdot 10^{-6}$ см, где коэффициент диффузии $D = \frac{1}{3}v_{\text{F}}\lambda \approx \frac{1}{3}v_{\text{F}}b, \left(v_{\text{F}} \simeq \frac{\hbar}{ma}\right), \tau_{\text{ког}} \simeq \frac{\xi}{v_{\text{F}}}$ - время до того момента, когда сбивается фаза электронной волны.

Ш-з.45.2. Coupling constant

Определить константу связи $g = N(0)V$ для олова, если $t_c' = 3.74$ K, а дебаевская температура равна $\Theta_{\text{D}} = 195$ K.

Solution

Используя формулу $k_{\text{B}}T_c = 1.14\hbar\omega_{\text{D}}e^{-1/N(0)V}$, получим $g = \mathbf{0.245}$.

Ш-з.45.3. Critical Temperature of a similar material

Критическая температура смеси изотопов ртути со средним атомным весом 199.7 г равна 4.161 K. На сколько и в какую сторону изменится критическая температура для смеси со средним атомным весом 200.7 г?

Solution

(?? use isotope effect??)
Понизится на 0.01 K.

Ш-з.45.4. Critical Temperature

Туннельный эксперимент дал для индия значение энергетической щели $\Delta_0 = 5.3 \cdot 10^{-4}$ эВ. Какой должна быть согласно теории БКШ критическая температура индия? Сравнить с T_c индия 3.37 K.

Solution

(use that universal relation?)
$T_c = 2\Delta_0/\left(3.52 k_{\mathrm{B}}\right) = 3.49$ K.

О3-5.31

Величину верхнего критического поля H_{c2} для сверхпроводников II рода можно оценить из того условия, что разрушение куперовских пар происходит вследствие их закручивания в магнитном поле. Иначе говоря, пара может сохраняться лишь до тех пор, пока ларморовский радиус больше ее размера. Выразить H_{c2} через длину когерентности ξ и квант магнитного потока Φ_0^{CH}.

Solution 5.31.

$H_{\mathrm{c}2} = \frac{\hbar c}{2e\xi^2} = \frac{\Phi_0^{\mathrm{cП}}}{2\pi\xi^2}$.

О3-5.32

При каком напряжении начнет течь ток через туннельный переход нормальный металл-изолятор-сверхпроводник, если $T_{\mathrm{c}} = 92$ K, а измерения проводятся при $T \ll T_{\mathrm{c}}$?

Solution 5.32.

$V = \frac{\Delta}{e} \approx \frac{kT_{\mathrm{c}}}{e} \approx 0,008$ В. См. приложение II.

О3-5.33 ВАХ системы “алюминий-свинец”

В 1960 г. Гиавер измерил вольт-амперную характеристику сверхпроводящей системы алюминий-свинец при температуре, меньшей критических температур обоих металлов (рис. 95).
(вставлю скоро!)
Она имела максимум при $V_1 = 0,82$ мВ и минимум при $V_2 = 1,4$ мВ. Найти величины энергетических щелей (в эВ) и критические температуры свинца и алюминия.

Solution

Для SIS перехода:

$$eV_1 = eV_{\max} = \Delta_2 - \Delta_1$$
$$eV_2 = eV_{\min} = \Delta_2 + \Delta_1.$$

Мы принимаем минимум - началом возрастания тока при $T = 0$, что на самом деле не совсем так, потому что ток при чуть большем напряжении начнется. Откуда следует:

$$\Delta_2 = e\frac{V_1 + V_2}{2} = 1,11\mathrm{mB}.$$
$$\Delta_1 = e\frac{V_2 - V_1}{2} = 0,29\mathrm{mB}$$

Критическую температуру определяем из соотношения БКШ $k_{\mathrm{G}}T_{\mathrm{c}} = 0.57\Delta$, получаем $T_{\mathrm{c}1} \approx 1,9$ K; $T_{\mathrm{c}2} = 7,3$ K.

Solution 5.33*

Ответ задачи следует из уравнений

$$eV_1 = eV_{\max} = \Delta_2 - \Delta_1$$
$$eV_2 = eV_{\min} = \Delta_2 + \Delta_1.$$

Откуда следует:

$$\Delta_2 = e\frac{V_1 + V_2}{2} = 1,11 \text{ m B} .$$
$$\Delta_1 = e\frac{V_2 - V_1}{2} = 0,29 \text{ m B}$$

Критическую температуру определяем из соотношения $2\Delta = 3,52 k_{\mathrm{F}} T_c$, откуда $T_{\mathrm{c}1} \approx 1,9$ K; $T_{\mathrm{c}2} = 7,3$ K. Подробно эксперименты Гиавера рассмотрены в Приложении II.

O3-5.34

Оценить радиус эффективного взаимодействия сверхпроводящих электронов, исходя из следующих соображений: проходящий около иона электрон «толкает» его, создавая тем самым поляризацию решетки. Радиус взаимодействия соответствует расстоянию, на которое успел уйти этот электрон за время, равное полупериоду колебаний иона. Оценку провести для одновален-тного металла с простой кубической решеткой. Скорость звука $s = 3 \cdot 10^5$ см/с, эффективную массу электрона считать равной массе свободного электрона.

Solution 5.34.

$\xi = \frac{\hbar\pi}{m_e s} = 1,2 \cdot 10^{-5}$ cm $= 1200$Å.

O3-5.35 Penetration of field in metal

For a metal described by the free electron model, find the ratio of the maximum transparency length for electromagnetic waves in the normal state to the London penetration depth in the superconducting state.

Solution 5.35.

(??? what is длина прозрачности???)
5.35. $\lambda \leqslant \lambda_{\mathrm{p}} = 2\pi\sqrt{\frac{m_e c^2}{4\pi n_{\mathrm{se}} e^2}} = 2\pi\Lambda$, т. е. $\frac{\lambda}{\Lambda} \simeq 2\pi$.

O3-5.36 Heat capacity from vortices

In type II superconductors, which are located in an external magnetic field $H_{\mathrm{c}2} > H > H_{\mathrm{c}1}$, the electrons in the vortex crust are in a normal state. How does the contribution of these electrons to the heat capacity of a superconductor depend on the magnitude of the external field and temperature? Consider the correlation length independent of temperature.

Solution 5.36.

(???? need to learn type 2 sc better)
$\Delta C \propto BT$.

O3-5.37 Радиус сверхпроводящего вихря (????)

Решетка квантованных вихрей в сверхпроводниках II рода подобна системе вихревых нитей, возникающих во вращающемся сверхтекучем ^{4}He. Исходя из этой аналогии, оценить на основе критерия сверхтекучести Ландау радиус нормальной сердцевины (кора) магнитного вихря и соответствующую ему плотность тока. Величина энергетической щели сверхпроводника равна $\Delta(T)$, импульс Ферми p_{F}, концентрация сверхпроводящих электронов - $n_{\mathrm{sc}}(T)$.

Solution

Скорость движения центра масс куперовской пары при $r < \Lambda$ (лондоновской глубины) определим как (см. задачу 5.23)

$$v(r) = \frac{\hbar}{2mr}.$$

Если $v(r) \geqslant v_{\text{крит}} = \Delta(T)/p_{\text{F}}$, то сверхпроводимость «разрушается». Таким образом

$$\frac{\hbar}{2mr} \geqslant \frac{\Delta(T)}{p_{\mathbf{F}}}, \text{ откуда } r \leqslant \frac{\hbar v_{\mathbf{F}}}{2\Delta(T)} \simeq \xi(T).$$

Видно, что область нормальной фазы имеет размер порядка длины когерентности ξ. Плотность тока $j(r) = 2en_{\text{s}}v(r) = en_{\text{sc}}v(r)$. При $r = \xi$ получаем

$$j(\xi) = \frac{en_{\text{sc}}\hbar}{2m\xi} \simeq \frac{en_{\text{sc}}\Delta(T)}{\hbar p_{\text{F}}} \sim j_{\text{c}},$$

где j_{c} - ток распаривания (см. задачу 5.20).
Ответ: 5.37*. $r \ll \frac{\hbar v_{\text{F}}}{2\Delta(T)} \simeq \xi(T); j(\xi) \simeq \frac{en_{\text{sc}}\Delta(T)}{\hbar p_{\text{F}}}$.

О3-5.38 Магнитное поле в вихре

Используя полученное в предыдущей задаче выражение для радиальной зависимости плотности сверхпроводящего тока $j(r)$ в вихре (?? какое???), найти распределение магнитного поля $B(r)$ в вихре и оценить поле в его центре. Ответ выразить через квант магнитного потока Φ_0^c и характерные длины Λ и ξ.

Solution

5.38. $B(r) = \frac{\Phi_0^{\text{cm}}}{2\pi\Lambda^2}\ln\frac{\Lambda}{r}; B(0) = B(\xi) = \frac{\Phi_0^{\text{cm}}}{2\pi\Lambda^2}\ln\frac{\Lambda}{\xi} = H_{\text{c1}}$. По теории Абрикосова точное выражение $B(0) = 2H_{\text{c1}}$ (рассматривается область $\xi < r < \Lambda$).

Ш-з.45.1.

Во сколько раз плотность состояний в спектре элементарных возбущдении сверхпроводника больше плотности состояний электронов в вормальом металле около уровня Ферми для энергии возбуждений E, равных соответственно $1.01\Delta_0; 1.5\Delta_0; 2.0\Delta_0$?
(????)
Ответ. $\rho/N(0) = 7.12; 1.34; 1.15$.

14.2 Problems about Typical Methods, Effects

(добавлю из Белоусова и типичного статфиза задачи)

14.2.1 Framework of BCS: Problems about Basic Transformations

me. Mean field approximation of BCS Hamiltonian

Show that the Hamiltonian

$$\widehat{\mathcal{H}} = \sum_p \xi_p a_p^+ a_p - \frac{\lambda}{2}\sum_{pq} a_{p\alpha}^+ a_{-p\beta}^+ a_{q\beta} a_{-q\alpha}.$$

is approximately equivalent to the

$$\widehat{\mathcal{H}} = \sum_p \left(\xi_p\left(a_{p\uparrow}^+ a_{p\uparrow} + a_{p\downarrow}^+ a_{p\downarrow}\right) + \Delta a_{p\downarrow}^+ a_{-p\uparrow}^+ + \Delta^* a_{p\uparrow} a_{-p\downarrow}\right),$$

where Δ is an effective parameter, that is calculated from a operators.
Use Wick's theorem.

Solution by Wick's theorem

(these typical transformations (???))

me. Mean field approximation of BCS Hamiltonian

Show that the Hamiltonian

$$\widehat{\mathcal{H}} = \sum_p \xi_p a_p^+ a_p - \frac{\lambda}{2} \sum_{pq} a_{p\alpha}^+ a_{-p\beta}^+ a_{q\beta} a_{-q\alpha}.$$

is approximately equivalent to the

$$\widehat{\mathcal{H}} = \sum_p \left(\xi_p \left(a_{p\uparrow}^+ a_{p\uparrow} + a_{p\downarrow}^+ a_{p\downarrow} \right) + \Delta a_{p\downarrow}^+ a_{-p\uparrow}^+ + \Delta^* a_{p\uparrow} a_{-p\downarrow} \right),$$

where Δ is an effective parameter, that is calculated from a operators.
Use the path integral approach.

Solution by path integral

(habbard Stratonovich, etc.)

me. Green's function for BCS

For the BCS superconductor described by the $H_{\text{BCS}} = \sum_{\boldsymbol{k}} c_{\boldsymbol{k}\sigma}^\dagger \epsilon_{\boldsymbol{k}} c_{\boldsymbol{k}\sigma} + \Delta \left(c_{\boldsymbol{k}\uparrow} c_{-\boldsymbol{k}\downarrow} + \text{ h.c. } \right)$ where $\epsilon_{\boldsymbol{k}} := \boldsymbol{k}^2/(2m) - \mu$, prove that in the Nambu basis $\psi_{\boldsymbol{k}} = \left(c_{\boldsymbol{k}\uparrow}, c_{-\boldsymbol{k}\downarrow}^\dagger \right)$ the Hamiltonian has a form:

$$H_{\text{BCS}} = \sum_{\boldsymbol{k}} \psi_{\boldsymbol{k}}^\dagger h(\boldsymbol{k}) \psi_{\boldsymbol{k}}; \qquad h(\boldsymbol{k}) := \epsilon_{\boldsymbol{k}} \sigma^3 + \Delta \sigma^1$$

Then prove that the Green's function of the Nambu spinor is given by

$$G(\omega, \boldsymbol{k}) = (\omega - h(\boldsymbol{k}))^{-1} = \frac{\omega \sigma^0 + \epsilon_{\boldsymbol{k}} \sigma^3 + \Delta \sigma^1}{\omega^2 - \epsilon_{\boldsymbol{k}}^2 - \Delta^2}$$

Solution

(???? I'll write it later)

me. Inverse Bogoliubov transformations

In BCS theory, initially the Hamiltonian is written in terms of fermionic operators a and we introduce new operators b as

$$\begin{aligned} \hat{b}_{\mathbf{p}-} &= u_p \hat{a}_{\mathbf{p}-} + v_p \hat{a}_{-\mathbf{p},+}^\dagger, \\ \hat{b}_{\mathbf{p}+} &= u_p \hat{a}_{\mathbf{p}+} - v_p \hat{a}_{-\mathbf{p},-}^\dagger. \end{aligned} \qquad u^2 + v^2 = 1.$$

Find the expression of a operators in terms of b.

Solution

$$\begin{pmatrix} \hat{b}_{-\mathbf{p}-}^\dagger \\ \hat{b}_{\mathbf{p}+} \end{pmatrix} = \begin{pmatrix} u_p & v_p \\ -v_p & u_p \end{pmatrix} \begin{pmatrix} \hat{a}_{-\mathbf{p},-}^\dagger \\ \hat{a}_{\mathbf{p}+} \end{pmatrix} \qquad \Rightarrow \qquad \begin{pmatrix} \hat{a}_{-\mathbf{p},-}^\dagger \\ \hat{a}_{\mathbf{p}+} \end{pmatrix} = \begin{pmatrix} u_p & -v_p \\ v_p & u_p \end{pmatrix} \begin{pmatrix} \hat{b}_{-\mathbf{p}-}^\dagger \\ \hat{b}_{\mathbf{p}+} \end{pmatrix},$$

since $A = \begin{bmatrix} a & b \\ c & d \end{bmatrix} \Rightarrow A^{-1} = \frac{1}{|A|} \begin{bmatrix} d & -b \\ -c & a \end{bmatrix}$.
Result:

$$\begin{aligned} \hat{a}_{\mathbf{p}-} &= u_p \hat{b}_{\mathbf{p}-} - v_p \hat{b}_{-\mathbf{p},+}^\dagger, \\ \hat{a}_{\mathbf{p}+} &= u_p \hat{b}_{\mathbf{p}+} + v_p \hat{b}_{-\mathbf{p},-}^\dagger. \end{aligned}$$

me. Diagonalization of BCS Hamiltonian by basic transformations

Diagonalize the BCS Hamiltonian

$$\hat{H} = \sum_{\mathbf{p}\sigma} \varepsilon_{\mathbf{p}} \hat{a}^{\dagger}_{\mathbf{p}\sigma} \hat{a}_{\mathbf{p}\sigma} + \Delta \sum_{\mathbf{p}} \left[\hat{a}_{\mathbf{p}+} \hat{a}_{-\mathbf{p}-} + \hat{a}^{\dagger}_{-\mathbf{p}-} \hat{a}^{\dagger}_{\mathbf{p}+} \right]$$

by introduction of new fermionic operators b

$$\begin{aligned} \hat{b}_{\mathbf{p}-} &= u_p \hat{a}_{\mathbf{p}-} + v_p \hat{a}^{\dagger}_{-\mathbf{p},+}, \\ \hat{b}_{\mathbf{p}+} &= u_p \hat{a}_{\mathbf{p}+} - v_p \hat{a}^{\dagger}_{-\mathbf{p},-}; \end{aligned} \qquad u^2 + v^2 = 1.$$

Do it by plugging the new operators into the Hamiltonian, then by equating some terms to zero, obtain formulas for u and v.

Solution

We substitute $\hat{a}_{\mathbf{p}-} = u_p \hat{b}_{\mathbf{p}-} - v_p \hat{b}^{\dagger}_{-\mathbf{p},+}, \quad \hat{a}_{\mathbf{p}+} = u_p \hat{b}_{\mathbf{p}+} + v_p \hat{b}^{\dagger}_{-\mathbf{p},-},$

$$\begin{aligned} \varepsilon_{\mathbf{p}} \hat{a}^{\dagger}_{\mathbf{p}+} \hat{a}_{\mathbf{p}+} &= \varepsilon_{\mathbf{p}} (u_p \hat{b}^{\dagger}_{\mathbf{p}+} + v_p \hat{b}_{-\mathbf{p},-})(u_p \hat{b}_{\mathbf{p}+} + v_p \hat{b}^{\dagger}_{-\mathbf{p},-}) = \\ &= \varepsilon_{\mathbf{p}} \left[u_p^2 \hat{b}^{\dagger}_{\mathbf{p}+} \hat{b}_{\mathbf{p}+} + v_p^2 \hat{b}_{-\mathbf{p},-} \hat{b}^{\dagger}_{-\mathbf{p},-} + u_p v_p (\hat{b}_{-\mathbf{p},-} \hat{b}_{\mathbf{p},+} + \hat{b}^{\dagger}_{\mathbf{p},+} \hat{b}^{\dagger}_{-\mathbf{p},-}) \right]; \\ \varepsilon_{\mathbf{p}} \hat{a}^{\dagger}_{\mathbf{p}-} \hat{a}_{\mathbf{p}-} &= \varepsilon_{\mathbf{p}} (u_p \hat{b}^{\dagger}_{\mathbf{p}-} - v_p \hat{b}_{-\mathbf{p},+})(u_p \hat{b}_{\mathbf{p}-} - v_p \hat{b}^{\dagger}_{-\mathbf{p},+}) = \\ &= \varepsilon_{\mathbf{p}} \left[u_p^2 \hat{b}^{\dagger}_{\mathbf{p}-} \hat{b}_{\mathbf{p}-} + v_p^2 \hat{b}_{-\mathbf{p},+} \hat{b}^{\dagger}_{-\mathbf{p},+} - u_p v_p (\hat{b}_{-\mathbf{p},+} \hat{b}_{\mathbf{p}-} + \hat{b}^{\dagger}_{\mathbf{p}-} \hat{b}^{\dagger}_{-\mathbf{p},+}) \right]. \end{aligned}$$

Because of

$$-\sum_{\mathbf{p}} (\hat{b}_{-\mathbf{p},+} \hat{b}_{\mathbf{p}-} + \hat{b}^{\dagger}_{\mathbf{p}-} \hat{b}^{\dagger}_{-\mathbf{p},+}) \overset{\substack{\text{symm} \\ p \text{ region}}}{=} -\sum_{\mathbf{p}} (\hat{b}_{\mathbf{p},+} \hat{b}_{-\mathbf{p}-} + \hat{b}^{\dagger}_{-\mathbf{p}-} \hat{b}^{\dagger}_{\mathbf{p},+}) = \sum_{\mathbf{p}} (\hat{b}_{-\mathbf{p}-} \hat{b}_{\mathbf{p},+} + \hat{b}^{\dagger}_{\mathbf{p},+} \hat{b}^{\dagger}_{-\mathbf{p}-}),$$

the kinetic term is

$$\begin{aligned} &\sum_{\mathbf{p}} \varepsilon_{\mathbf{p}} (\hat{a}^{\dagger}_{\mathbf{p}-} \hat{a}_{\mathbf{p}-} + \hat{a}^{\dagger}_{\mathbf{p}+} \hat{a}_{\mathbf{p}+}) = \sum_{\mathbf{p}} \varepsilon_{\mathbf{p}} \Big[u_p^2 \hat{b}^{\dagger}_{\mathbf{p}+} \hat{b}_{\mathbf{p}+} + v_p^2 \hat{b}_{-\mathbf{p},-} \hat{b}^{\dagger}_{-\mathbf{p},-} + \\ &\qquad + u_p^2 \hat{b}^{\dagger}_{\mathbf{p}-} \hat{b}_{\mathbf{p}-} + v_p^2 \hat{b}_{-\mathbf{p},+} \hat{b}^{\dagger}_{-\mathbf{p},+} + 2u_p v_p (\hat{b}_{-\mathbf{p}-} \hat{b}_{\mathbf{p},+} + \hat{b}^{\dagger}_{\mathbf{p},+} \hat{b}^{\dagger}_{-\mathbf{p}-}) \Big] = \\ &= \sum_{\mathbf{p}} \varepsilon_{\mathbf{p}} \Big[u_p^2 \hat{b}^{\dagger}_{\mathbf{p}+} \hat{b}_{\mathbf{p}+} + v_p^2 (1 - \hat{b}^{\dagger}_{-\mathbf{p},+} \hat{b}_{-\mathbf{p},+}) + v_p^2 (1 - \hat{b}^{\dagger}_{-\mathbf{p},-} \hat{b}_{-\mathbf{p},-}) + u_p^2 \hat{b}^{\dagger}_{\mathbf{p}-} \hat{b}_{\mathbf{p}-} + \\ &\qquad + 2u_p v_p (\hat{b}_{-\mathbf{p}-} \hat{b}_{\mathbf{p},+} + \hat{b}^{\dagger}_{\mathbf{p},+} \hat{b}^{\dagger}_{-\mathbf{p}-}) \Big] = \\ &= \sum_{\mathbf{p}} 2\varepsilon_{\mathbf{p}} v_p^2 + \sum_{\mathbf{p}} \varepsilon_{\mathbf{p}} (u_p^2 - v_p^2)(\hat{b}^{\dagger}_{\mathbf{p}+} \hat{b}_{\mathbf{p}+} + \hat{b}^{\dagger}_{\mathbf{p}-} \hat{b}_{\mathbf{p}-}) + \sum_{\mathbf{p}} 2\varepsilon_{\mathbf{p}} u_p v_p (\hat{b}_{-\mathbf{p}-} \hat{b}_{\mathbf{p},+} + \hat{b}^{\dagger}_{\mathbf{p},+} \hat{b}^{\dagger}_{-\mathbf{p}-}). \end{aligned}$$

The interaction term has

$$\begin{aligned} \hat{a}_{\mathbf{p}+} \hat{a}_{-\mathbf{p}-} &= (u_p \hat{b}_{\mathbf{p}+} + v_p \hat{b}^{\dagger}_{-\mathbf{p},-})(u_p \hat{b}_{-\mathbf{p}-} - v_p \hat{b}^{\dagger}_{\mathbf{p},+}) = \\ &= u_p^2 \hat{b}_{\mathbf{p}+} \hat{b}_{-\mathbf{p}-} - v_p^2 \hat{b}^{\dagger}_{-\mathbf{p},-} \hat{b}^{\dagger}_{\mathbf{p},+} + u_p v_p (\hat{b}^{\dagger}_{-\mathbf{p},-} \hat{b}_{-\mathbf{p}-} - \hat{b}_{\mathbf{p}+} \hat{b}^{\dagger}_{\mathbf{p},+}); \\ \hat{a}^{\dagger}_{-\mathbf{p}-} \hat{a}^{\dagger}_{\mathbf{p}+} &= (u_p \hat{b}^{\dagger}_{-\mathbf{p}-} - v_p \hat{b}_{\mathbf{p},+})(u_p \hat{b}^{\dagger}_{\mathbf{p}+} + v_p \hat{b}_{-\mathbf{p},-}) = \\ &= u_p^2 \hat{b}^{\dagger}_{-\mathbf{p}-} \hat{b}^{\dagger}_{\mathbf{p}+} - v_p^2 \hat{b}_{\mathbf{p},+} \hat{b}_{-\mathbf{p},-} + u_p v_p (\hat{b}^{\dagger}_{-\mathbf{p}-} \hat{b}_{-\mathbf{p},-} - \hat{b}_{\mathbf{p},+} \hat{b}^{\dagger}_{\mathbf{p}+}). \end{aligned}$$

And it has the form

$$\begin{aligned} &\sum_{\mathbf{p}} \left[\Delta \hat{a}_{\mathbf{p}+} \hat{a}_{-\mathbf{p}-} + \Delta \hat{a}^{\dagger}_{-\mathbf{p}-} \hat{a}^{\dagger}_{\mathbf{p}+} \right] = \\ &= \sum_{\mathbf{p}} \left[(u_p^2 \Delta - v_p^2 \Delta) \hat{b}^{\dagger}_{-\mathbf{p}-} \hat{b}^{\dagger}_{\mathbf{p}+} + (u_p^2 \Delta - v_p^2 \Delta) \hat{b}_{\mathbf{p},+} \hat{b}_{-\mathbf{p},-} + u_p v_p (\Delta + \Delta)(\hat{b}^{\dagger}_{-\mathbf{p}-} \hat{b}_{-\mathbf{p},-} - \hat{b}_{\mathbf{p},+} \hat{b}^{\dagger}_{\mathbf{p}+}) \right] \end{aligned}$$

Totally, the Hamiltonian is diagonalized, if we take u_p, v_p such that for each $\mathbf{p}$

$$2\varepsilon_{\mathbf{p}} u_p v_p(\hat{b}_{-\mathbf{p}-}\hat{b}_{\mathbf{p},+} + \hat{b}^\dagger_{\mathbf{p},+}\hat{b}^\dagger_{-\mathbf{p}-}) + (u_p^2\Delta - v_p^2\Delta)\hat{b}^\dagger_{-\mathbf{p}-}\hat{b}^\dagger_{\mathbf{p}+} + (u_p^2\Delta - v_p^2\Delta)\hat{b}_{\mathbf{p},+}\hat{b}_{-\mathbf{p},-} = 0$$

$$\begin{aligned} \hat{b}_{-\mathbf{p}-}\hat{b}_{\mathbf{p},+}: &\qquad 2\varepsilon_{\mathbf{p}} u_p v_p + u_p^2\Delta - v_p^2\Delta = 0 \\ \hat{b}^\dagger_{\mathbf{p},+}\hat{b}^\dagger_{-\mathbf{p}-}: &\qquad 2\varepsilon_{\mathbf{p}} u_p v_p + u_p^2\Delta - v_p^2\Delta = 0 \end{aligned}$$

There are two solutions of the quadratic equation $\frac{u^2}{v^2} + 2\frac{\varepsilon_{\mathbf{p}}}{\Delta}\frac{u}{v} - 1 = 0$. There are two solutions, the first one is

$$\frac{u}{v} = \frac{-2\frac{\varepsilon}{\Delta} - \sqrt{\left(2\frac{\varepsilon}{\Delta}\right)^2 + 4}}{2} = -\frac{\varepsilon}{\Delta} - \sqrt{\frac{\varepsilon^2}{\Delta^2} + 1};$$

$$v^2 = \frac{1}{1 + \left(\frac{\varepsilon}{\Delta} + \sqrt{\frac{\varepsilon^2}{\Delta^2} + 1}\right)^2} = \frac{1}{1 + \frac{\varepsilon^2}{\Delta^2} + \frac{\varepsilon^2}{\Delta^2} + 1 + 2\frac{\varepsilon}{\Delta}\sqrt{\frac{\varepsilon^2}{\Delta^2} + 1}} =$$

$$= \frac{1}{2}\frac{\frac{\varepsilon^2}{\Delta^2} + 1 - \frac{\varepsilon}{\Delta}\sqrt{\frac{\varepsilon^2}{\Delta^2} + 1}}{\left(\frac{\varepsilon^2}{\Delta^2} + 1\right)^2 - \frac{\varepsilon^2}{\Delta^2}\left(\frac{\varepsilon^2}{\Delta^2} + 1\right)} = \frac{1}{2}\frac{\frac{\varepsilon^2}{\Delta^2} + 1 - \frac{\varepsilon}{\Delta}\sqrt{\frac{\varepsilon^2}{\Delta^2} + 1}}{\frac{\varepsilon^2}{\Delta^2} + 1} = \frac{1}{2}\left(1 - \frac{\varepsilon}{\Delta^2 + \varepsilon^2}\right);$$

$$u^2 = 1 - v^2 = \frac{1}{2}\left(1 + \frac{\varepsilon}{\sqrt{\Delta^2 + \varepsilon^2}}\right)$$

The second solution of the quadratic equation gives us the coefficients u, v vice versa. If we plug them into the Hamiltonian, the spectrum will be negative (since there is term $u^2 - v^2$), which is unphysical, so we don't consider this solution.

For real Δ, the Hamiltonian has the form:

$$\begin{aligned} \hat{H} &= \sum_{\mathbf{p}}\Big[2\varepsilon_{\mathbf{p}} v_p^2 + \varepsilon_{\mathbf{p}}(u_p^2 - v_p^2)(\hat{b}^\dagger_{\mathbf{p}+}\hat{b}_{\mathbf{p}+} + \hat{b}^\dagger_{\mathbf{p}-}\hat{b}_{\mathbf{p}-}) + 2u_p v_p\Delta(\hat{b}^\dagger_{-\mathbf{p}-}\hat{b}_{-\mathbf{p},-} + \hat{b}^\dagger_{\mathbf{p}+}\hat{b}_{\mathbf{p},+} - 1)\Big] \\ &= 2\sum_{\mathbf{p}}\Big[\varepsilon_{\mathbf{p}} v_p^2 - u_p v_p\Delta\Big] + \sum_{\mathbf{p}}(\varepsilon_{\mathbf{p}}(u_p^2 - v_p^2) + 2u_p v_p\Delta)\Big[\hat{b}^\dagger_{\mathbf{p}-}\hat{b}_{\mathbf{p},-} + \hat{b}^\dagger_{\mathbf{p}+}\hat{b}_{\mathbf{p},+}\Big] = \\ &= 2\sum_{\mathbf{p}}\Big[\varepsilon_{\mathbf{p}} v_p^2 - u_p v_p\Delta\Big] + \sum_{\mathbf{p}}\left(\varepsilon_{\mathbf{p}}\frac{\varepsilon}{\sqrt{\Delta^2 + \varepsilon^2}} + 2\frac{\Delta}{2\sqrt{\Delta^2 + \varepsilon^2}}\Delta\right)\Big[\hat{b}^\dagger_{\mathbf{p}-}\hat{b}_{\mathbf{p},-} + \hat{b}^\dagger_{\mathbf{p}+}\hat{b}_{\mathbf{p},+}\Big] = \\ &= 2\sum_{\mathbf{p}}\Big[\varepsilon_{\mathbf{p}} v_p^2 - u_p v_p\Delta\Big] + \sum_{\mathbf{p}}\sqrt{\Delta^2 + \varepsilon^2}\Big[\hat{b}^\dagger_{\mathbf{p}-}\hat{b}_{\mathbf{p},-} + \hat{b}^\dagger_{\mathbf{p}+}\hat{b}_{\mathbf{p},+}\Big]. \end{aligned}$$

me. Diagonalization of BCS Hamiltonian for complex Δ by basic transformations

Diagonalize the BCS Hamiltonian

$$\hat{H} = \sum_{\mathbf{p}\sigma}\varepsilon_{\mathbf{p}}\hat{a}^\dagger_{\mathbf{p}\sigma}\hat{a}_{\mathbf{p}\sigma} + \sum_{\mathbf{p}}\Big[\Delta^*\hat{a}_{\mathbf{p}+}\hat{a}_{-\mathbf{p}-} + \Delta\hat{a}^\dagger_{-\mathbf{p}-}\hat{a}^\dagger_{\mathbf{p}+}\Big]$$

by introduction of new fermionic operators b

$$\begin{aligned} \hat{b}_{\mathbf{p}-} &= u_p\hat{a}_{\mathbf{p}-} + v_p\hat{a}^\dagger_{-\mathbf{p},+}, \\ \hat{b}_{\mathbf{p}+} &= u_p\hat{a}_{\mathbf{p}+} - v_p\hat{a}^\dagger_{-\mathbf{p},-}; \end{aligned} \qquad u^2 + v^2 = 1.$$

Do it by plugging the new operators into the Hamiltonian, then by equating some terms to zero, obtain formulas for u and v. Don't assume that Δ is real-valued.

Solution

We substitute $\hat{a}_{\mathbf{p}-} = u_p\hat{b}_{\mathbf{p}-} - v_p\hat{b}^\dagger_{-\mathbf{p},+}, \quad \hat{a}_{\mathbf{p}+} = u_p\hat{b}_{\mathbf{p}+} + v_p\hat{b}^\dagger_{-\mathbf{p},-}$,

$$\begin{aligned} \varepsilon_{\mathbf{p}}\hat{a}^\dagger_{\mathbf{p}+}\hat{a}_{\mathbf{p}+} &= \varepsilon_{\mathbf{p}}(u_p\hat{b}^\dagger_{\mathbf{p}+} + v_p\hat{b}_{-\mathbf{p},-})(u_p\hat{b}_{\mathbf{p}+} + v_p\hat{b}^\dagger_{-\mathbf{p},-}) = \\ &= \varepsilon_{\mathbf{p}}\big[u_p^2\hat{b}^\dagger_{\mathbf{p}+}\hat{b}_{\mathbf{p}+} + v_p^2\hat{b}_{-\mathbf{p},-}\hat{b}^\dagger_{-\mathbf{p},-} + u_p v_p(\hat{b}_{-\mathbf{p},-}\hat{b}_{\mathbf{p},+} + \hat{b}^\dagger_{\mathbf{p},+}\hat{b}^\dagger_{-\mathbf{p},-})\big]; \end{aligned}$$

$$\varepsilon_{\mathbf{p}}\hat{a}^{\dagger}_{\mathbf{p}-}\hat{a}_{\mathbf{p}-} = \varepsilon_{\mathbf{p}}(u_p\hat{b}^{\dagger}_{\mathbf{p}-} - v_p\hat{b}_{-\mathbf{p},+})(u_p\hat{b}_{\mathbf{p}-} - v_p\hat{b}^{\dagger}_{-\mathbf{p},+}) =$$
$$= \varepsilon_{\mathbf{p}}\left[u_p^2\hat{b}^{\dagger}_{\mathbf{p}-}\hat{b}_{\mathbf{p}-} + v_p^2\hat{b}_{-\mathbf{p},+}\hat{b}^{\dagger}_{-\mathbf{p},+} - u_pv_p(\hat{b}_{-\mathbf{p},+}\hat{b}_{\mathbf{p}-} + \hat{b}^{\dagger}_{\mathbf{p}-}\hat{b}^{\dagger}_{-\mathbf{p},+})\right].$$

Because of

$$-\sum_{\mathbf{p}}(\hat{b}_{-\mathbf{p},+}\hat{b}_{\mathbf{p}-} + \hat{b}^{\dagger}_{\mathbf{p}-}\hat{b}^{\dagger}_{-\mathbf{p},+}) \overset{\substack{\text{symm}\\ p \text{ region}}}{=} -\sum_{\mathbf{p}}(\hat{b}_{\mathbf{p},+}\hat{b}_{-\mathbf{p}-} + \hat{b}^{\dagger}_{-\mathbf{p}-}\hat{b}^{\dagger}_{\mathbf{p},+}) = \sum_{\mathbf{p}}(\hat{b}_{-\mathbf{p}-}\hat{b}_{\mathbf{p},+} + \hat{b}^{\dagger}_{\mathbf{p},+}\hat{b}^{\dagger}_{-\mathbf{p}-}),$$

the kinetic term is

$$\sum_{\mathbf{p}}\varepsilon_{\mathbf{p}}(\hat{a}^{\dagger}_{\mathbf{p}-}\hat{a}_{\mathbf{p}-} + \hat{a}^{\dagger}_{\mathbf{p}+}\hat{a}_{\mathbf{p}+}) = \sum_{\mathbf{p}}\varepsilon_{\mathbf{p}}\Big[u_p^2\hat{b}^{\dagger}_{\mathbf{p}+}\hat{b}_{\mathbf{p}+} + v_p^2\hat{b}_{-\mathbf{p},-}\hat{b}^{\dagger}_{-\mathbf{p},-} +$$
$$+ u_p^2\hat{b}^{\dagger}_{\mathbf{p}-}\hat{b}_{\mathbf{p}-} + v_p^2\hat{b}_{-\mathbf{p},+}\hat{b}^{\dagger}_{-\mathbf{p},+} + 2u_pv_p(\hat{b}_{-\mathbf{p}-}\hat{b}_{\mathbf{p},+} + \hat{b}^{\dagger}_{\mathbf{p},+}\hat{b}^{\dagger}_{-\mathbf{p}-})\Big] =$$
$$= \sum_{\mathbf{p}}\varepsilon_{\mathbf{p}}\Big[u_p^2\hat{b}^{\dagger}_{\mathbf{p}+}\hat{b}_{\mathbf{p}+} + v_p^2(1 - \hat{b}^{\dagger}_{-\mathbf{p},+}\hat{b}_{-\mathbf{p},+}) + v_p^2(1 - \hat{b}^{\dagger}_{-\mathbf{p},-}\hat{b}_{-\mathbf{p},-}) + u_p^2\hat{b}^{\dagger}_{\mathbf{p}-}\hat{b}_{\mathbf{p}-} +$$
$$+ 2u_pv_p(\hat{b}_{-\mathbf{p}-}\hat{b}_{\mathbf{p},+} + \hat{b}^{\dagger}_{\mathbf{p},+}\hat{b}^{\dagger}_{-\mathbf{p}-})\Big] =$$
$$= \sum_{\mathbf{p}}2\varepsilon_{\mathbf{p}}v_p^2 + \sum_{\mathbf{p}}\varepsilon_{\mathbf{p}}(u_p^2 - v_p^2)(\hat{b}^{\dagger}_{\mathbf{p}+}\hat{b}_{\mathbf{p}+} + \hat{b}^{\dagger}_{\mathbf{p}-}\hat{b}_{\mathbf{p}-}) + \sum_{\mathbf{p}}2\varepsilon_{\mathbf{p}}u_pv_p(\hat{b}_{-\mathbf{p}-}\hat{b}_{\mathbf{p},+} + \hat{b}^{\dagger}_{\mathbf{p},+}\hat{b}^{\dagger}_{-\mathbf{p}-}).$$

The interaction term has

$$\hat{a}_{\mathbf{p}+}\hat{a}_{-\mathbf{p}-} = (u_p\hat{b}_{\mathbf{p}+} + v_p\hat{b}^{\dagger}_{-\mathbf{p},-})(u_p\hat{b}_{-\mathbf{p}-} - v_p\hat{b}^{\dagger}_{\mathbf{p},+}) =$$
$$= u_p^2\hat{b}_{\mathbf{p}+}\hat{b}_{-\mathbf{p}-} - v_p^2\hat{b}^{\dagger}_{-\mathbf{p},-}\hat{b}^{\dagger}_{\mathbf{p},+} + u_pv_p(\hat{b}^{\dagger}_{-\mathbf{p},-}\hat{b}_{-\mathbf{p}-} - \hat{b}_{\mathbf{p}+}\hat{b}^{\dagger}_{\mathbf{p},+});$$

$$\hat{a}^{\dagger}_{-\mathbf{p}-}\hat{a}^{\dagger}_{\mathbf{p}+} = (u_p\hat{b}^{\dagger}_{-\mathbf{p}-} - v_p\hat{b}_{\mathbf{p},+})(u_p\hat{b}^{\dagger}_{\mathbf{p}+} + v_p\hat{b}_{-\mathbf{p},-}) =$$
$$= u_p^2\hat{b}^{\dagger}_{-\mathbf{p}-}\hat{b}^{\dagger}_{\mathbf{p}+} - v_p^2\hat{b}_{\mathbf{p},+}\hat{b}_{-\mathbf{p},-} + u_pv_p(\hat{b}^{\dagger}_{-\mathbf{p}-}\hat{b}_{-\mathbf{p},-} - \hat{b}_{\mathbf{p},+}\hat{b}^{\dagger}_{\mathbf{p}+}).$$

And it has the form

$$\sum_{\mathbf{p}}\left[\Delta^*\hat{a}_{\mathbf{p}+}\hat{a}_{-\mathbf{p}-} + \Delta\hat{a}^{\dagger}_{-\mathbf{p}-}\hat{a}^{\dagger}_{\mathbf{p}+}\right] =$$
$$= \sum_{\mathbf{p}}\left[(u_p^2\Delta^* - v_p^2\Delta)\hat{b}^{\dagger}_{-\mathbf{p}-}\hat{b}^{\dagger}_{\mathbf{p}+} + (u_p^2\Delta - v_p^2\Delta^*)\hat{b}_{\mathbf{p},+}\hat{b}_{-\mathbf{p},-} + u_pv_p(\Delta + \Delta^*)(\hat{b}^{\dagger}_{-\mathbf{p}-}\hat{b}_{-\mathbf{p},-} - \hat{b}_{\mathbf{p},+}\hat{b}^{\dagger}_{\mathbf{p}+})\right]$$

Totally, the Hamiltonian is diagonalized, if we take u_p, v_p such that for each $\mathbf{p}$

$$2\varepsilon_{\mathbf{p}}u_pv_p(\hat{b}_{-\mathbf{p}-}\hat{b}_{\mathbf{p},+} + \hat{b}^{\dagger}_{\mathbf{p},+}\hat{b}^{\dagger}_{-\mathbf{p}-}) + (u_p^2\Delta^* - v_p^2\Delta)\hat{b}^{\dagger}_{-\mathbf{p}-}\hat{b}^{\dagger}_{\mathbf{p}+} + (u_p^2\Delta - v_p^2\Delta^*)\hat{b}_{\mathbf{p},+}\hat{b}_{-\mathbf{p},-} = 0$$

$$\hat{b}_{-\mathbf{p}-}\hat{b}_{\mathbf{p},+}: \qquad 2\varepsilon_{\mathbf{p}}u_pv_p + u_p^2\Delta - v_p^2\Delta^* = 0$$
$$\hat{b}^{\dagger}_{\mathbf{p},+}\hat{b}^{\dagger}_{-\mathbf{p}-}: \qquad 2\varepsilon_{\mathbf{p}}u_pv_p + u_p^2\Delta^* - v_p^2\Delta = 0$$

(??? now, I am not sure, how to proceed??? anyway, I'll think later, solution for a real Δ is fine)

Chalker,me. Diagonalization of BCS Hamiltonian by matrix notation

Diagonalize the following fermionic Hamiltonian,

$$\mathcal{H} = \epsilon\left(c_1^{\dagger}c_1 + c_2^{\dagger}c_2\right) + \lambda\left(c_1^{\dagger}c_2^{\dagger} + c_2c_1\right),$$

where ϵ and λ are real constants, by matrix notation. Note the opposite ordering of labels in the terms $c_1^{\dagger}c_2^{\dagger}$ and c_2c_1, which is also a requirement of Hermiticity.

Solution

The fermionic Bogoliubov transformation is

$$c_1^\dagger = ud_1^\dagger + vd_2$$
$$c_2^\dagger = ud_2^\dagger - vd_1,$$

where u and v are c-numbers, which we can in fact take to be real, because we have restricted ourselves to real λ. The transformation is useful only if fermionic anticommutation relations apply to both sets of operators. Let us suppose they apply to the operators d and $d^\dagger$, and check the properties of the operators c and $c^\dagger$. The coefficients of the transformation have been chosen to ensure that $\left\{c_1^\dagger, c_2^\dagger\right\} = 0$, while

$$\left\{c_1^\dagger, c_1\right\} = u^2\left\{d_1^\dagger, d_1\right\} + v^2\left\{d_2^\dagger, d_2\right\}$$

and so we must require $u^2 + v^2 = 1$, suggesting the parameterisation $u = \cos\theta, v = \sin\theta$. The remaining step is to substitute in $\mathcal{H}$ for $c^\dagger$ and c in terms of $d^\dagger$ and d, and pick θ so that terms in $d_1^\dagger d_2^\dagger + d_2 d_1$ have vanishing coefficient. The calculation is clearest when it is set out using matrix notation. First, we can write $\mathcal{H}$ as

$$\mathcal{H} = \frac{1}{2}\begin{pmatrix} c_1^\dagger & c_2 & c_2^\dagger & c_1 \end{pmatrix}\begin{pmatrix} \epsilon & \lambda & 0 & 0 \\ \lambda & -\epsilon & 0 & 0 \\ 0 & 0 & \epsilon & -\lambda \\ 0 & 0 & -\lambda & -\epsilon \end{pmatrix}\begin{pmatrix} c_1 \\ c_2^\dagger \\ c_2 \\ c_1^\dagger \end{pmatrix} + \epsilon$$

where we have used the anticommutator to make substitutions of the type $c^\dagger c = 1 - cc^\dagger$. For conciseness, consider just the upper block

$$\begin{pmatrix} c_1^\dagger & c_2 \end{pmatrix}\begin{pmatrix} \epsilon & \lambda \\ \lambda & -\epsilon \end{pmatrix}\begin{pmatrix} c_1 \\ c_2^\dagger \end{pmatrix}$$

and write the Bogoliubov transformation also in matrix form as

$$\begin{pmatrix} c_1 \\ c_2^\dagger \end{pmatrix} = \begin{pmatrix} \cos\theta & \sin\theta \\ -\sin\theta & \cos\theta \end{pmatrix}\begin{pmatrix} d_1 \\ d_2^\dagger \end{pmatrix}.$$

We pick θ so that

$$\begin{pmatrix} \cos\theta & -\sin\theta \\ \sin\theta & \cos\theta \end{pmatrix}\begin{pmatrix} \epsilon & \lambda \\ \lambda & -\epsilon \end{pmatrix}\begin{pmatrix} \cos\theta & \sin\theta \\ -\sin\theta & \cos\theta \end{pmatrix} = \begin{pmatrix} \bar{\epsilon} & 0 \\ 0 & -\bar{\epsilon} \end{pmatrix},$$

where $\tilde{\epsilon} = \sqrt{\epsilon^2 + \lambda^2}$.
(???? check it???)
Including the other 2×2 block of $\mathcal{H}$, we conclude that

$$\mathcal{H} = \bar{\epsilon}\left(d_1^\dagger d_1 + d_2^\dagger d_2\right) + \epsilon - \bar{\epsilon}.$$

(??? how to find the θ???)

Coleman,me. Diagonalization of BCS Hamiltonian by Nambu notation

Diagonalize the following fermionic Hamiltonian,

$$H_{\text{BCS}} = \sum_{\mathbf{k}\sigma}\epsilon_{\mathbf{k}} c_{\mathbf{k}\sigma}^\dagger c_{\mathbf{k}\sigma} + \sum_{\mathbf{k}}\left[\bar{\Delta} c_{-\mathbf{k}\downarrow} c_{\mathbf{k}\uparrow} + c_{\mathbf{k}\uparrow}^\dagger c_{-\mathbf{k}\downarrow}^\dagger \Delta\right]$$

by introduction of Nambu spinors $\psi_{\mathbf{k}} = \binom{c_{\mathbf{k}\uparrow}}{c_{-\mathbf{k}.\downarrow}^\dagger}$.

Solution

The kinetic energy can be written as

$$\sum_{\mathbf{k}} \epsilon_{\mathbf{k}} \left(c^\dagger_{\mathbf{k}\uparrow} c_{\mathbf{k}\uparrow} - c_{-\mathbf{k}\downarrow} c^\dagger_{-\mathbf{k}\downarrow} + 1 \right) = \left(c^\dagger_{\mathbf{k}\uparrow}, c_{-\mathbf{k}\downarrow} \right) \begin{bmatrix} \epsilon_{\mathbf{k}} & 0 \\ 0 & -\epsilon_{\mathbf{k}} \end{bmatrix} \begin{pmatrix} c_{\mathbf{k}\uparrow} \\ \bar{c}^\dagger_{-\mathbf{k}\downarrow} \end{pmatrix} + \sum_{\mathbf{k}} \epsilon_{\mathbf{k}}$$

where the sign reversal in the lower component derives from anticommuting the downspin electron operators. The energy $-\epsilon_{\mathbf{k}}$ is the energy to create a hole. We will drop the constant remainder term $\sum_{\mathbf{k}} \epsilon_{\mathbf{k}}$. We can now combine the kinetic and pairing terms into a single matrix:

$$\begin{aligned} \epsilon_{\mathbf{k}} \sum_{\sigma} c^\dagger_{\mathbf{k}\sigma} c_{\mathbf{k}\sigma} + \left[\bar{\Delta} c_{-\mathbf{k}\downarrow} c_{\mathbf{k}\uparrow} + c^\dagger_{\mathbf{k}\uparrow} c^\dagger_{-\mathbf{k}\downarrow} \Delta \right] &= \left(c^\dagger_{\mathbf{k}\uparrow}, c_{-\mathbf{k}\downarrow} \right) \begin{bmatrix} \epsilon_{\mathbf{k}} & \Delta \\ \bar{\Delta} & -\epsilon_{\mathbf{k}} \end{bmatrix} \begin{pmatrix} c_{\mathbf{k}\uparrow} \\ c^\dagger_{-\mathbf{k}\downarrow} \end{pmatrix} \\ &= \psi^\dagger_{\mathbf{k}} \begin{bmatrix} \epsilon_{\mathbf{k}} & \Delta_1 - i\Delta_2 \\ \Delta_1 + i\Delta_2 & -\epsilon_{\mathbf{k}} \end{bmatrix} \psi_{\mathbf{k}} \end{aligned}$$

And now by finding eigenvalues of a matrix, we get
(?? write it??)

$$E_{\mathbf{k}} \equiv \left| \vec{B}_{\mathbf{k}} \right| = \sqrt{\epsilon^2_{\mathbf{k}} + |\Delta|^2}$$

(??? I'll write it better later!)
So, at this point, one can ask, why we are doing something else, if this method is so compact? Yes, indeed, this is the best approach.

Shnirman.Piasotski.SC-intro.3.1 Diagonalization of BCS Hamiltonian by a ladder operators

Consider the following toy Hamiltonian with Fermionic field operators

$$H = \epsilon \left(c^\dagger_\uparrow c_\uparrow + c^\dagger_\downarrow c_\downarrow \right) + V \left(c^\dagger_\uparrow c^\dagger_\downarrow + c_\downarrow c_\uparrow \right) \qquad \begin{aligned} \{c_\sigma, c_{\sigma'}\} &= \left\{ c^\dagger_\sigma, c^\dagger_{\sigma'} \right\} = 0, \\ \left\{ c_\sigma, c^\dagger_{\sigma'} \right\} &= \delta_{\sigma,\sigma'} \end{aligned} \tag{13}$$

Defining the following objects

$$J_+ = c^\dagger_\uparrow c^\dagger_\downarrow, \quad J_- = c_\downarrow c_\uparrow, \quad J_z = \frac{1}{2}(N-1), \quad N = n_\uparrow + n_\downarrow, \quad n_\sigma = c^\dagger_\sigma c_\sigma \tag{15}$$

demonstrate the following relations hold:

$$[J_+, J_-] = 2J_z, \quad [J_\pm, J_z] = \mp J_\pm \tag{16}$$

Using $J_+ = J^\dagger_-$ we naturally obtain

$$[J_-, J_z] = J_-$$

In other words, we may assert that the operators $J_x = \frac{1}{2}(J_+ + J_-), J_y = \frac{1}{2i}(J_+ - J_-)$, and J_z form a representation of the $\mathfrak{su}(2)$ Lie algebra (note that the representation is reducible since the parity operator $e^{i\pi N}$ is conserved).
Using our definitions (15) we write the Hamiltonian in the language of J-s:

$$H = 2(\epsilon J_z + V J_x) + \epsilon = 2\sqrt{\epsilon^2 + V^2}\,(\cos\vartheta J_z + \sin\vartheta J_x) + \epsilon \tag{19}$$

$$\cos\vartheta = \frac{\epsilon}{\sqrt{\epsilon^2 + V^2}}, \quad \sin\vartheta = \frac{V}{\sqrt{\epsilon^2 + V^2}} \tag{20}$$

Show that the Hamiltonian (19) is diagonalised by the following unitary transformation $U = e^{i\vartheta J_y}$, that is

$$H_d = UHU^\dagger = 2\sqrt{\epsilon^2 + V^2} J_z + \epsilon \tag{21}$$

Next we define the Bogolubov operators

$$\gamma_\sigma = U^\dagger c_\sigma U, \quad \gamma^\dagger_\sigma = U^\dagger c^\dagger_\sigma U \equiv (\gamma_\sigma)^\dagger \tag{28}$$

By virtue of Eq. (21) we have

$$H = U^\dagger H_d U = 2\sqrt{\epsilon^2 + V^2} U^\dagger J_z U + \epsilon = \sqrt{\epsilon^2 + V^2} \left(\gamma^\dagger_\uparrow \gamma_\uparrow + \gamma^\dagger_\downarrow \gamma_\downarrow \right) + \epsilon - \sqrt{\epsilon^2 + V^2} \tag{29}$$

And what is left, is to show, how the new operators are related to the original c-operators. Using BCH formula, or by other way, show that

$$\gamma_\uparrow = \cos\frac{\vartheta}{2} c_\uparrow + \sin\frac{\vartheta}{2} c^\dagger_\downarrow, \qquad \gamma_\downarrow = \cos\frac{\vartheta}{2} c_\downarrow - \sin\frac{\vartheta}{2} c^\dagger_\uparrow. \tag{30}$$

Solution

One has

$$[J_+, J_-] = c_\uparrow^\dagger c_\downarrow^\dagger c_\downarrow c_\uparrow - c_\downarrow c_\uparrow c_\uparrow^\dagger c_\downarrow^\dagger = n_\uparrow n_\downarrow - (1-n_\uparrow)(1-n_\downarrow) = n_\uparrow + n_\downarrow - 1 = N - 1 \equiv 2J_z. \tag{17}$$

Next

$$[J_+, J_z] = \frac{1}{2} c_\uparrow^\dagger c_\downarrow^\dagger \left(c_\uparrow^\dagger c_\uparrow + c_\downarrow^\dagger c_\downarrow \right) - \frac{1}{2} \left(c_\uparrow^\dagger c_\uparrow + c_\downarrow^\dagger c_\downarrow \right) c_\uparrow^\dagger c_\downarrow^\dagger = -\frac{1}{2} \left(c_\uparrow^\dagger c_\downarrow^\dagger + c_\uparrow^\dagger c_\downarrow^\dagger \right) = -J_+. \tag{18}$$

Let us check the inverse transformation

$$U^\dagger J_z U = \cos\vartheta J_z + \sin\vartheta J_x \tag{22}$$

with the help of Baker-Campbell-Hausdor (BCH) formula

$$e^{-i\vartheta J_y} J_z e^{i\vartheta J_y} = \sum_{n=0}^{\infty} (-i\vartheta)^n \frac{[(J_y)^n, J_z]}{n!} \tag{23}$$

where the notation is such that

$$[(J_y)^n, J_z] = \left[J_y, \left[(J_y)^{n-1}, J_z \right] \right] \tag{24}$$

and evaluate

$$\left[(J_y)^{2m}, J_z \right] = \left[J_y, \left[(J_y)^{2m-1}, J_z \right] \right] = J_z \tag{25}$$

$$\left[(J_y)^{2m+1}, J_z \right] = \left[J_y, \left[(J_y)^{2m}, J_z \right] \right] = iJ_x \tag{26}$$

So that:

$$e^{-i\vartheta J_y} J_z e^{i\vartheta J_y} = J_z \sum_{n=0}^{\infty} \frac{(-1)^n \vartheta^{2n}}{(2n)!} + J_x \sum_{n=0}^{\infty} \frac{(-1)^n \vartheta^{2n+1}}{(2n+1)!} = \cos\vartheta J_z + \sin\vartheta J_x \tag{27}$$

In the same notations as before we have

$$\gamma_\sigma = U^\dagger c_\sigma U = \sum_{n=0}^{\infty} \left(-\frac{\theta}{2} \right)^n \frac{[(2iJ_y)^n, c_\sigma]}{n!} \tag{31}$$

First we establish

$$[2iJ_y, c_\uparrow] = -c_\downarrow^\dagger, \quad [2iJ_y, c_\downarrow] = c_\uparrow^\dagger, \tag{32}$$

$$\left[2iJ_y, c_\uparrow^\dagger \right] = -c_\downarrow, \quad \left[2iJ_y, c_\downarrow^\dagger \right] = c_\uparrow. \tag{33}$$

Or, introducing the secular notation, $\sigma = \uparrow \equiv +$ and $\sigma = \downarrow \equiv -$, we compactly write

$$[2iJ_y, c_\sigma] = -\sigma c_{-\sigma}^\dagger, \quad \left[2iJ_y, c_\sigma^\dagger \right] = -\sigma c_{-\sigma} \tag{34}$$

It follows that

$$\left[(2iJ_y)^{2m}, c_\sigma \right] = \left[2iJ_y, \left[(2iJ_y)^{2m-1}, c_\sigma \right] \right] = (-1)^m c_\sigma \tag{35}$$

$$\left[(2iJ_y)^{2m+1}, c_\sigma \right] = \left[2iJ_y, \left[(2iJ_y)^{2m}, c_\sigma \right] \right] = -(-1)^m \sigma c_{-\sigma}^\dagger \tag{36}$$

and hence

$$\gamma_\sigma = c_\sigma \sum_{m=0}^{\infty} \left(\frac{\vartheta}{2} \right)^{2m} \frac{(-1)^m}{(2m)!} + \sigma c_{-\sigma}^\dagger \sum_{m=0}^{\infty} \left(\frac{\vartheta}{2} \right)^{2m+1} \frac{(-1)^m}{(2m+1)!} = c_\sigma \cos\frac{\vartheta}{2} + \sigma c_{-\sigma}^\dagger \cos\frac{\vartheta}{2},$$

exactly what we wanted to show.

How does this relate to the "rotation of a combined particle operators" by the angle θ?

This is a good question, because this solution should be the same as just rotation, but it looks very different. (??????)

me. Obvious question about BCS Hamiltonian

The BCS Hamiltonian has the form:

$$\hat{H} = \int d^3 r \hat{\Psi}_\sigma^+(t,\mathbf{r}) \left(\frac{\left(\hat{\mathbf{p}} - \frac{e}{c}\mathbf{A}\right)^2}{2m} + e\varphi - \mu \right) \hat{\Psi}_\sigma(t,\mathbf{r}) + \\ + \frac{1}{2} \int d^3 r_1 d^3 r_2 \hat{\Psi}_\sigma^+(t,\mathbf{r}_1)\, \hat{\Psi}_{\sigma'}^+(t,\mathbf{r}_2)\, U(\mathbf{r}_1 - \mathbf{r}_2)\, \hat{\Psi}_{\sigma'}(t,\mathbf{r}_2)\, \hat{\Psi}_\sigma(t,\mathbf{r}_1)$$

where the $\hat{\Psi}_\sigma(t,\mathbf{r})$ is an operator of annihilation of an electron, $\hat{\mathbf{p}}$ - operator of the electron's momenta, A, φ - potential of a field.

But often in mathematics, one diagonalizes the Hamiltonian

$$H = \epsilon \left(c_\uparrow^\dagger c_\uparrow + c_\downarrow^\dagger c_\downarrow \right) + V \left(c_\uparrow^\dagger c_\downarrow^\dagger + c_\downarrow c_\uparrow \right) \tag{13}$$

and says that it is related to the BCS Hamiltonian. But how are they related?

Solution

One need to just go to the momenta space, change notation, then do the mean field approximation. Then, V will be the real gap and ϵ is the linearize spectrum.

(?? one can do here the derivation of second one from the first one, but it is rather obvious after going through basics of BCS, so I'll do it later)

me. Transformation of the gap equation

Show that the gap $\Delta = \lambda \cdot \sum_{\mathbf{p}'}' \langle \hat{a}_{-\mathbf{p}',-} \hat{a}_{\mathbf{p}',+} \rangle$ can be reexpressed in terms of the Fermi-Dirac distribution and itself after substituting the canonical transformation

$$\begin{aligned} \hat{a}_{\mathbf{p},-} &= u_p \hat{b}_{\mathbf{p}-} - v_p \hat{b}_{-\mathbf{p},+}^\dagger, \\ \hat{a}_{\mathbf{p},+} &= u_p \hat{b}_{\mathbf{p}+} + v_p \hat{b}_{-\mathbf{p},-}^\dagger, \end{aligned} \qquad u_{\mathrm{p}}^2, v_{\mathrm{p}}^2 = \frac{1}{2} \left(1 \pm \frac{\xi_{\mathrm{p}}}{\sqrt{\xi_{\mathrm{p}}^2 + \Delta^2}} \right);$$

Solution.

$$\begin{aligned} \Delta &= \lambda \sum_{\mathbf{p}'}' \left\langle (u_p \hat{b}_{-\mathbf{p}-} - v_p \hat{b}_{\mathbf{p},+}^\dagger)(u_p \hat{b}_{\mathbf{p}+} + v_p \hat{b}_{-\mathbf{p},-}^\dagger) \right\rangle = \\ &= \lambda \sum_{\mathbf{p}'}' \left\langle u_p^2 \hat{b}_{-\mathbf{p}-} \hat{b}_{\mathbf{p}+} - v_p u_p \hat{b}_{\mathbf{p},+}^\dagger \hat{b}_{\mathbf{p}+} - v_p^2 \hat{b}_{\mathbf{p},+}^\dagger \hat{b}_{-\mathbf{p},-}^\dagger + u_p v_p \hat{b}_{-\mathbf{p}-} \hat{b}_{-\mathbf{p},-}^\dagger \right\rangle = \\ &= \lambda \sum_{\mathbf{p}'}' u_p^2 \underbrace{\left\langle \hat{b}_{-\mathbf{p}-} \hat{b}_{\mathbf{p}+} \right\rangle}_{=0} - v_p u_p \underbrace{\left\langle \hat{b}_{\mathbf{p},+}^\dagger \hat{b}_{\mathbf{p}+} \right\rangle}_{=\bar{n}_{\mathbf{p}}} - v_p^2 \underbrace{\left\langle \hat{b}_{\mathbf{p},+}^\dagger \hat{b}_{-\mathbf{p},-}^\dagger \right\rangle}_{=0} + u_p v_p \underbrace{\left\langle \hat{b}_{-\mathbf{p}-} \hat{b}_{-\mathbf{p},-}^\dagger \right\rangle}_{1-\bar{n}_{\mathbf{p}}} \end{aligned}$$

$$\bar{n}_{\mathbf{p}} := \left\langle \hat{b}_{\mathbf{p}+}^\dagger \hat{b}_{\mathbf{p}+} \right\rangle = \left\langle \hat{b}_{\mathrm{p}-}^\dagger \hat{b}_{\mathbf{p}-} \right\rangle = [\exp(\varepsilon(p)/T) + 1]^{-1}$$

$$\Delta = \lambda \sum_{\mathbf{p}'}' u_p v_p (-\bar{n}_{\mathbf{p}} + 1 - \bar{n}_{\mathbf{p}}) = \lambda \sum_{\mathbf{p}'}' \frac{\Delta}{2\sqrt{\xi_p^2 + \Delta^2}} (1 - 2\bar{n}_{\mathbf{p}}).$$

$$\frac{1}{\lambda} = \frac{1}{2}\sum_{\mathbf{p}}{}' \frac{1-2\bar{n}_{\mathrm{p}}}{\sqrt{\xi_{\mathrm{p}}^2+\Delta^2}}$$

This is the well-known gap equation.

14.2.2 Framework of BCS: Basic, General Properties

Chalker-ex2.Q-2 Number of Particles, Free energy, gap

The BCS Hamiltonian is

$$H = \sum_{k\sigma}\epsilon(k)c_{k\sigma}^{\dagger}c_{k\sigma} - V\sum_{k,q}{}' c_{k\uparrow}^{\dagger}c_{-k\downarrow}^{\dagger}c_{-q\downarrow}c_{q\uparrow}$$

where $c_{k\sigma}^{\dagger}$ and $c_{k\sigma}$ denote fermion creation and annihilation operators for states labelled by wavevector, k, and spin, $\sigma =\uparrow,\downarrow$. The second summation, $\sum_{k,q}{}'$, is restricted to wavevectors k, q of states lying within the Debye energy, $\hbar\omega_D$, of the chemical potential, μ: $|\epsilon(k)$ - $\mu|, |\epsilon(q) - \mu| \leq \hbar\omega_D$. The BCS wavefunction is

$$|\mathrm{BCS}\rangle = \Pi_k\left(u_k + v_k c_{k\uparrow}^{\dagger}c_{-k\downarrow}^{\dagger}\right)|0\rangle,$$

where $|0\rangle$ is the vacuum state and $\{u_k, v_k\}$ are variational parameters, with $|u_k|^2 + |v_k|^2 = 1$. The number operator is

$$N = \sum_{k,\sigma} c_{k\sigma}^{\dagger}c_{k\sigma}$$

(i) Calculate the mean particle number, $\langle\mathrm{BCS}|N|\mathrm{BCS}\rangle$, and its variance,

$$\left\langle \mathrm{BCS}\left|N^2\right|BCS\right\rangle - \langle\mathrm{BCS}|N|\mathrm{BCS}\rangle^2$$

in the BCS wavefunction.

(ii) Show that the free energy of the system in the BCS state is

$$\langle\mathrm{BCS}|H-\mu N|\mathrm{BCS}\rangle = 2\sum_k(\epsilon(k)-\mu)\,|v_k|^2 - \frac{|\Delta|^2}{V}$$

where

$$\Delta = V\sum_k{}' u_k v_k^*$$

(iii) By minimising this free energy with respect to the variational parameters, u_k and v_k, derive the zero-temperature gap equation

$$1 = \frac{V}{2}\sum_k{}' \frac{1}{\left[|\Delta|^2+(\epsilon(k)-\mu)^2\right]^{1/2}}.$$

(iv) Show that, in the weak-coupling limit in which $|\Delta| \ll \hbar\omega_D$, the gap equation has the solution

$$|\Delta| = 2\hbar\omega_D\exp(-1/\nu V)$$

where ν is the density of states at the chemical potential.

Solution to (i)

(?? I'll think about it later. also, I'll write better theory about particle number in SC)

Solution to (ii)

Solution to (iii)

Solution to (iv)

me. Calculation of equation of the coupled two electrons

Two electrons near Fermi surface can be described by the following model:

$$\hat{H}_0(\mathbf{r}_1)\,\psi_{\mathbf{p}}(\mathbf{r}_1) = |\xi_{\mathbf{p}}|\,\psi_{\mathbf{p}}(\mathbf{r}_1), \qquad \psi_{\mathbf{p}}(\mathbf{r}) := V^{-\frac{1}{2}} e^{\frac{i\mathbf{p}\mathbf{r}}{\hbar}}, \qquad \xi_{\mathbf{p}} := v_F(p - p_F).$$

The wave function of two electrons $\psi_{\text{pair}}(\mathbf{r}_1, \mathbf{r}_2) := \sum_{\mathbf{p}} c_{\mathbf{p}} \psi_{\mathbf{p},+}(\mathbf{r}_1)\,\psi_{-\mathbf{p},-}(\mathbf{r}_2)$ obeys the following equation:

$$\left[\hat{H}_0(\mathbf{r}_1) + \hat{H}_0(\mathbf{r}_2) + \hat{V}(\mathbf{r}_1, \mathbf{r}_2)\right]\psi(\mathbf{r}_1, \mathbf{r}_2) = E\psi(\mathbf{r}_1, \mathbf{r}_2).$$

Show that it is equivalent to the following equation:

$$2|\xi_{\mathbf{p}}|\,c_{\mathbf{p}} + \sum_{\mathbf{p}'} V_{\mathbf{p}\mathbf{p}'} c_{\mathbf{p}'} = E c_{\mathbf{p}} \qquad V_{\mathbf{p}\mathbf{p}'} := \left\langle \mathbf{p}, +, -\mathbf{p}, - | \hat{V} | \mathbf{p}', +, -\mathbf{p}', - \right\rangle$$

Solution

One needs just to carefully substitute the ansatz, it is relatively easy, but neatness is still required.

$$\hat{H}_0(\mathbf{r}_1) \sum_{\mathbf{p}} c_{\mathbf{p}} \psi_{\mathbf{p},+}(\mathbf{r}_1)\,\psi_{-\mathbf{p},-}(\mathbf{r}_2) + \hat{H}_0(\mathbf{r}_2) \sum_{\mathbf{p}} c_{\mathbf{p}} \psi_{\mathbf{p},+}(\mathbf{r}_1)\,\psi_{-\mathbf{p},-}(\mathbf{r}_2) + \hat{V}(\mathbf{r}_1, \mathbf{r}_2) \sum_{\mathbf{p}'} c_{\mathbf{p}'} \psi_{\mathbf{p}',+}(\mathbf{r}_1)\,\psi_{-\mathbf{p}',-}(\mathbf{r}_2) =$$
$$= E \sum_{\mathbf{p}} c_{\mathbf{p}} \psi_{\mathbf{p},+}(\mathbf{r}_1)\,\psi_{-\mathbf{p},-}(\mathbf{r}_2).$$

$$|\xi_{\mathbf{p}}|(\mathbf{r}_1) \sum_{\mathbf{p}} c_{\mathbf{p}} \psi_{\mathbf{p},+}(\mathbf{r}_1)\,\psi_{-\mathbf{p},-}(\mathbf{r}_2) + |\xi_{\mathbf{p}}|(\mathbf{r}_2) \sum_{\mathbf{p}} c_{\mathbf{p}} \psi_{\mathbf{p},+}(\mathbf{r}_1)\,\psi_{-\mathbf{p},-}(\mathbf{r}_2) +$$
$$+ \sum_{\mathbf{p}} \psi_{\mathbf{p},+}(\mathbf{r}_1)\,\psi_{-\mathbf{p},-}(\mathbf{r}_2)\,\psi^{\dagger}_{\mathbf{p},+}(\mathbf{r}_1)\,\psi^{\dagger}_{-\mathbf{p},-}(\mathbf{r}_2)\,\hat{V}(\mathbf{r}_1, \mathbf{r}_2) \sum_{\mathbf{p}'} c_{\mathbf{p}'} \psi_{\mathbf{p}',+}(\mathbf{r}_1)\,\psi_{-\mathbf{p}',-}(\mathbf{r}_2) = E \sum_{\mathbf{p}} c_{\mathbf{p}} \psi_{\mathbf{p},+}(\mathbf{r}_1)\,\psi_{-\mathbf{p},-}(\mathbf{r}_2).$$

$$2|\xi_{\mathbf{p}}|\,c_{\mathbf{p}} + \sum_{\mathbf{p}'} V_{\mathbf{p}\mathbf{p}'} c_{\mathbf{p}'} = E c_{\mathbf{p}} \qquad V_{\mathbf{p}\mathbf{p}'} := \left\langle \mathbf{p}, +, -\mathbf{p}, - | \hat{V} | \mathbf{p}', +, -\mathbf{p}', - \right\rangle.$$

Done. Now, this equation can be used to show that indeed electrons are attracted. (??? add words, how exactly. it is already written in the theory)

Shnirman.Piasotski.SC-intro.2(m) Generalized Cooper problem

In the Cooper problem, there were two electrons on top of the full Fermi sea. Consider now a generalization. In this case the excited state is assumed to be a superposition of either of two electrons slightly above the Fermi level or of two holes slightly below the Fermi level (the total number of particles is, thus, not sharply defined). Note that in the grand-canonical description the energies of both electrons and holes are positive. Find the bound state wave function and the binding energy per particle Δ. Compare it with Δ of the BCS theory.

Solution

(????)
We assume the following Ansatz for the wave function

$$|\Psi\rangle = \sum_{-\hbar\omega_D < \xi_k < 0} \alpha(k)\chi(\sigma_1, \sigma_2)\, c_{-k,\sigma_2} c_{k,\sigma_1} |\Psi_0\rangle + \sum_{0 < \xi_k < \hbar\omega_D} \alpha(k)\chi(\sigma_1, \sigma_2)\, c^{\dagger}_{k,\sigma_1} c^{\dagger}_{-k,\sigma_2} |\Psi_0\rangle, \tag{5}$$

where $|\Psi_0\rangle = \prod_{k\leq k_F} c^\dagger_{k,\sigma}|0\rangle$ stands for the fully occupied Fermi sea, and $\xi_k \equiv \epsilon_k - \mu$.
In The wave function (5) includes the hole-like ($\xi_k < 0$) excitation as well as the electron-like ($\xi_k > 0$) ones.
The (BCS) Hamiltonian reads

$$H_{\rm BCS} = \sum_{k,\sigma} \epsilon_k c^\dagger_{k,\sigma} c_{k,\sigma} - \frac{1}{2}\frac{g}{V} \sum_{k,k',\sigma} c^\dagger_{k',\sigma} c^\dagger_{-k',-\sigma} c_{-k,-\sigma} c_{k,\sigma} \tag{6}$$

We will measure the energy of particles relative to the filled Fermi sphere $E_{\rm FS} = 2\sum\limits_{k\leq k_F} \epsilon_k$. Substituting the Ansatz (5) into the Schrödinger equation $(E + E_{\rm FS})\,|\Psi\rangle = H_{\rm BCS}|\Psi\rangle$, we obtain:

$$(2\,\mathrm{sign}\,(\xi_k)\,\epsilon_k - E)\,\alpha(k) = \frac{g}{V} \sum_{-\hbar\omega_D < \xi_{k_1} < \hbar\omega_D} \alpha\,(k_1) \tag{7}$$

Here $\alpha(k)$ for $\xi_k < 0$ describes hole-like excitations and for $\xi_k > 0$ it describes the particle-like excitations.
We introduce

$$C := \frac{1}{V} \sum_{-\hbar\omega_D < \xi_{k_1} < \hbar\omega_D} \alpha(k) \tag{8}$$

substitute it self-consistently and obtain the equation for E

$$\begin{aligned} 1 &= \frac{g}{2} \int\limits_{E_F}^{E_F+\hbar\omega_D} d\omega \frac{\rho(\omega)}{\omega - E/2} - \frac{g}{2} \int\limits_{E_F-\hbar\omega_D}^{E_F} d\omega \frac{\rho(\omega)}{\omega + E/2} \\ &= \frac{g\rho_F}{2} \log\left(\frac{E_F + (\hbar\omega_D - E/2)}{E_F - E/2}\right) + \frac{g\rho_F}{2} \log\left(\frac{E_F - (\hbar\omega_D - E/2)}{E_F + E/2}\right) \end{aligned} \tag{9}$$

Here we have used $1/V\sum\limits_k \to \int \rho(\omega)d\omega$. The density of states in the vicinity of the Fermi surface can be replaced by a constant one $\rho(\omega) \approx \rho_F$.

It follows that

$$\frac{2}{g\rho_F} = \log\left(\frac{E_F^2 - (\hbar\omega_D - E/2)^2}{E_F^2 - E^2/4}\right) \tag{10}$$

Thus for weak coupling $g\rho_F \ll 1$, under the usual condition $E_F \gg \hbar\omega_D$, we obtain

$$E \simeq 2E_F - 2\hbar\omega_D e^{-\frac{1}{g\rho_F}} \tag{11}$$

The binding energy per electron is then found from $E = 2E_F - 2\Delta$

$$\Delta = \hbar\omega_D e^{-\frac{1}{g\rho_F}} \tag{12}$$

(In the typical theory is was $\Delta = \hbar\omega_D e^{-\frac{2}{g\rho_F}}$)

(???? so, where this model is used??? I read something about something similar... I'll add later it here)

Shnirman.Piasotski.BCS.2 Density of states of the BCS quasiparticles

Calculate the density of states of the BCS quasiparticles.

Solution

The density of states (per spin projection) ai given by

$$\rho(E) = \sum_k \delta\,(E - E_k) \tag{7}$$

Here $E_k = \sqrt{\Delta^2 + \xi_k^2}$. We get
(??? what is ρ_0???)

$$\rho(E) = \rho_0 \int d\xi \delta\left(E - \sqrt{\Delta^2 + \xi^2}\right) \tag{8}$$

We define a new integration variable $x = \sqrt{\Delta^2 + \xi^2}$

$$\rho(E) = \rho_0 \int dx \left|\frac{d\xi}{dx}\right| \delta(E - x) \tag{9}$$

Since

$$\frac{dx}{d\xi} = \frac{\xi}{x} = \frac{\sqrt{x^2 - \Delta^2}}{x} \tag{10}$$

we obtain

$$\rho(E) = \frac{2\rho_0 E}{\sqrt{E^2 - \Delta^2}} \tag{11}$$

The factor 2 is due to the fact that ξ and $-\xi$ correspond to the same x. This is of course for $E > \Delta$. For $E < \Delta$ we get $\rho(E) = 0$.

Shnirman.Piasotski.SC-intro.3.2 BCS ground state

Here, we will use notation:

$$\gamma_\uparrow := \cos\frac{\vartheta}{2} c_\uparrow + \sin\frac{\vartheta}{2} c_\downarrow^\dagger, \qquad \gamma_\downarrow := \cos\frac{\vartheta}{2} c_\downarrow - \sin\frac{\vartheta}{2} c_\uparrow^\dagger. \tag{30}$$

$$U = e^{i\vartheta J_y}$$

$$J_+ = c_\uparrow^\dagger c_\downarrow^\dagger, \quad J_- = c_\downarrow c_\uparrow, \quad J_z = \frac{1}{2}(N-1), \quad N = n_\uparrow + n_\downarrow, \quad n_\sigma = c_\sigma^\dagger c_\sigma \tag{15}$$

The ground state is defined via the following condition $\gamma_\sigma|0\rangle_\gamma = 0$. Show that this implies the following relation $U|0\rangle_\gamma = |0\rangle$ where $|0\rangle$ is the vacuum state of original Fermions ($c_\sigma|0\rangle = 0$).
Consider the following representation

$$U^\dagger = e^{-i\vartheta J_y} = e^{a_+ J_+} e^{a_z J_z} e^{a_- J_-} \tag{42}$$

where $a_\pm, a_z$ are functions of the angle ϑ. By differentiating the Eq. (42) with respect to ϑ, establish the following system of non-linear differential equations

$$\frac{d}{d\vartheta} a_+ = -\frac{1}{2} e^{a_z}, \quad \frac{d}{d\vartheta} a_z = a_-, \quad \frac{d}{d\vartheta} a_- = \frac{1}{2}\left(1 + a_-^2\right), \tag{43}$$

$$a_+(0) = a_-(0) = a_z(0) = 0 \tag{44}$$

Show that these are solved by

$$a_\pm(\vartheta) = \mp \tan\frac{\vartheta}{2}, \quad a_z(\vartheta) = -2\log\cos\frac{\vartheta}{2} \tag{54}$$

Using the equation (40) along with the decomposition (42) and the result (54), prove that

$$|0\rangle_\gamma = (1 + a_+ J_+)\, e^{-\frac{1}{2}a_z}|0\rangle \equiv \left(\cos\frac{\vartheta}{2} - \sin\frac{\vartheta}{2} c_\uparrow^\dagger c_\downarrow^\dagger\right)|0\rangle \tag{59}$$

Solution

(????)
Applying the derivative we find

$$\begin{aligned}\frac{d}{d\vartheta} U^\dagger &= -iU^\dagger J_y = e^{a_+ J_+} e^{a_z J_z} e^{a_- J_-} \dot{a}_- J_- + e^{a_+ J_+} e^{a_z J_z} \dot{a}_z J_z e^{a_- J_-} + e^{a_+ J_+} \dot{a}_+ J_+ e^{a_z J_z} e^{a_- J_-} \\ &= U^\dagger J_- \dot{a}_- + U^\dagger e^{-a_- J_-} J_z e^{a_- J_-} \dot{a}_z + U^\dagger e^{-a_- J_-} e^{-a_z J_z} J_+ e^{a_z J_z} e^{a_- J_-} \dot{a}_+ \end{aligned} \tag{45}$$

It follows that

$$-iJ_y = J_- \dot{a}_- + e^{-a_- J_- J_z} e^{a_- J_-} \dot{a}_z + e^{-a_- J_-} e^{-a_z J_z} J_+ e^{a_z J_z} e^{a_- J_-} \dot{a}_+ \tag{46}$$

Now we consider

$$e^{-a_- J_-} J_z e^{a_- J_-} = J_z - a_- [J_-, J_z] = J_z - a_- J_-, \tag{47}$$
$$e^{-a_z J_z} J_+ e^{a_z J_z} = J_+ e^{-a_z} \tag{48}$$
$$e^{-a_- J_-} J_+ e^{a_- J_-} = J_+ + 2a_- J_z - a_-^2 J_- \tag{49}$$

The equality (46) is now

$$-\frac{1}{2}[J_+ - J_-] = J_- \dot{a}_- + (J_z - a_- J_-)\dot{a}_z + \left(J_+ + 2a_- J_z - a_-^2 J_-\right) e^{-a_z} \dot{a}_+ \tag{50}$$

Which yields the following system of ODEs

$$\frac{d}{d\vartheta} a_+ = -\frac{1}{2} e^{a_z}, \quad \frac{d}{d\vartheta} a_z = a_-, \quad \frac{d}{d\vartheta} a_- = \frac{1}{2}\left(1 + a_-^2\right) \tag{51}$$
$$a_+(0) = a_-(0) = a_z(0) = 0 \tag{52}$$

with the initial conditions deduced from the requirement

$$U^\dagger\big|_{\vartheta=0} = 1 \tag{53}$$

Equation (49) is solved by direct integration

$$\frac{da_-}{d\vartheta} = \frac{1}{2}\left(1 + a_-^2\right) \quad \Rightarrow \quad \int^{a_-} \frac{dy}{1+y^2} = \frac{1}{2}(\vartheta - \vartheta_0) \quad \Rightarrow \quad \arctan(a_-) = \frac{1}{2}(\vartheta - \vartheta_0) \quad \Rightarrow \quad a_-(\vartheta) = \tan\left(\frac{\vartheta}{2}\right), \tag{56}$$

where the integration constant is fixed by the initial conditions. Other equations yield

$$a_z(\vartheta) = \int_0^\vartheta d\vartheta' \tan\left(\frac{\vartheta'}{2}\right) = -2\ln\left(\cos\frac{\vartheta}{2}\right) \tag{57}$$

$$a_+(\vartheta) = -\frac{1}{2}\int_0^\vartheta d\vartheta' e^{-2\ln\left(\cos\frac{\vartheta'}{2}\right)} = -\tan\left(\frac{\vartheta}{2}\right) \tag{58}$$

To see this we consider

$$U^\dagger|0\rangle = e^{a_+ J_+} e^{a_z J_z} e^{a_- J_-}|0\rangle = e^{a_+ J_+} e^{a_z J_z}|0\rangle = e^{a_+ J_+} e^{\frac{1}{2}a_z(N-1)}|0\rangle = e^{-\frac{a_z}{2}} e^{a_+ J_+}|0\rangle = e^{-\frac{a_z}{2}}\left(1 + a_+ J_+\right)|0\rangle \tag{60}$$

where we used that $J_+^2|0\rangle = 0$. Now substituting the results of our previous consideration we find that

$$|0\rangle_\gamma = \left(\cos\frac{\vartheta}{2} - \sin\frac{\vartheta}{2} c_\uparrow^\dagger c_\downarrow^\dagger\right)|0\rangle \tag{61}$$

14.2.3 Problems about the Gap Equation

Shnirman.Piasotski.SC-intro.1 **Expectation value of operators in the BCS ground state:**

Following the dream team of Bardeen, Cooper, and Schrieffer, in the class we considered the following family of states as our variational ansatz for the ground state of the BCS Hamiltonian:

$$|\mathrm{BCS}\rangle = \prod_k \left(u_k + v_k c_{k,\uparrow}^\dagger c_{-k,\downarrow}^\dagger\right)|0\rangle \tag{1}$$

Here $|0\rangle$ is the Fermionic vacuum state $c_{k,\sigma}|0\rangle = 0, c_{k,\sigma}^\dagger$ and $c_{k,\sigma}$ are the Fermionic creation and annihilation operators obeying the standard canonical commutation relations

$$\{c_{k,\sigma}, c_{k',\sigma'}\} = \left\{c_{k,\sigma}^\dagger, c_{k',\sigma'}^\dagger\right\} = 0, \qquad \left\{c_{k,\sigma}, c_{k',\sigma'}^\dagger\right\} = \delta_{k,k'}\delta_{\sigma,\sigma'} \tag{2}$$

Prove the following result

$$\left\langle \mathrm{BCS}\left| c_{k',\uparrow}^\dagger c_{-k',\downarrow}^\dagger c_{-k,\downarrow} c_{k,\uparrow}\right|\mathrm{BCS}\right\rangle = u_k v_k u_{k'} v_{k'} \tag{3}$$

Solution

$$\left\langle \mathrm{BCS}\left| c^\dagger_{k',\uparrow} c^\dagger_{-k',\downarrow} c_{-k,\downarrow} c_{k,\uparrow} \right| \mathrm{BCS} \right\rangle =$$

$$= \langle 0| \prod_{k_2 \neq k} \left(u_{k_2} + v_{k_2} c_{k_2,\uparrow} c_{-k_2,\downarrow}\right) \left(u_k + v_k c_{k,\uparrow} c_{-k,\downarrow}\right) c^\dagger_{k',\uparrow} c^\dagger_{-k',\downarrow} c_{-k,\downarrow} c_{k,\uparrow}$$
$$\left(u_k + v_k c^\dagger_{k,\uparrow} c^\dagger_{-k,\downarrow}\right) \prod_{k_1 \neq k} \left(u_{k_1} + v_{k_1} c^\dagger_{k_1,\uparrow} c^\dagger_{-k_1,\downarrow}\right) |0\rangle =$$

$$= v_k \langle 0| \prod_{k_2 \neq k} \left(u_{k_2} + v_{k_2} c_{k_2,\uparrow} c_{-k_2,\downarrow}\right) \left(u_k c^\dagger_{k',\uparrow} c^\dagger_{-k',\downarrow} + v_k c_{k,\uparrow} c_{-k,\downarrow} c^\dagger_{k',\uparrow} c^\dagger_{-k',\downarrow}\right) \prod_{k_1 \neq k} \left(u_{k_1} + v_{k_1} c^\dagger_{k_1,\uparrow} c^\dagger_{-k_1,\downarrow}\right) |0\rangle$$

$$= v_k u_k \langle 0| \prod_{k_2 \neq k,k'} \left(u_{k_2} + v_{k_2} c_{k_2,\uparrow} c_{-k_2,\downarrow}\right) \left(u_{k'} + v_{k'} c_{k',\uparrow} c_{-k',\downarrow}\right) c^\dagger_{k',\uparrow} c^\dagger_{-k',\downarrow}$$
$$\left(u_{k'} + v_{k'} c^\dagger_{k',\uparrow} c^\dagger_{-k',\downarrow}\right) \prod_{k_1 \neq k} \left(u_{k_1} + v_{k_1} c^\dagger_{k_1,\uparrow} c^\dagger_{-k_1,\downarrow}\right) |0\rangle =$$

$$= v_k u_k u_{k'} v_{k'} \langle 0| \prod_{k_2 \neq k,k'} \left(u_{k_2} + v_{k_2} c_{k_2,\uparrow} c_{-k_2,\downarrow}\right) c_{k',\uparrow} c_{-k',\downarrow} c^\dagger_{k',\uparrow} c^\dagger_{-k',\downarrow} \prod_{k_1 \neq k,k'} \left(u_{k_1} + v_{k_1} c^\dagger_{k_1,\uparrow} c^\dagger_{-k_1,\downarrow}\right) |0\rangle =$$

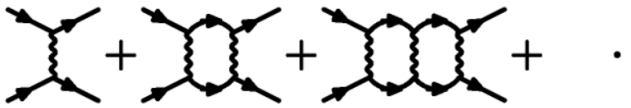
$$= v_k u_k u_{k'} v_{k'} \left\langle 0 \left| \prod_{k_2 \neq k,k'} \left(u_{k_2} + v_{k_2} c_{k_2,\uparrow} c_{-k_2,\downarrow}\right) \prod_{k_1 \neq k,k'} \left(u_{k_1} + v_{k_1} c^\dagger_{k_1,\uparrow}\, \uparrow^\dagger_{-k_1,\downarrow}\right) \right| 0 \right\rangle =$$

$$= v_k u_k u_{k'} v_{k'} \left\langle 0 \left| \prod_{k_1 \neq k,k'} \left(u^2_{k_1} + v^2_{k_1}\right) \right| 0 \right\rangle = v_k u_k u_{k'} v_{k'}$$

ЛШ-58. Scattering in Cooper channel, Bethe-Salpeter equation T_c, Δ_0

(??? write short reminder of the whole formalism)

Рассмотрим мацубаровскую амплитуду рассеяния в куперовском канале $\Gamma^C\left(i\varepsilon, i\varepsilon'\right)$) (энергии сталкивающихся частиц равны $\pm\varepsilon$, а разлетающихся равны $\pm\varepsilon'$). Она дается суммой лестничных графиков, изображенных на рис. ниже



Пусть каждой волнистой линии соответствует множитель $\Gamma^0\left(i\varepsilon, i\varepsilon'\right)$. Будем считать взаимодействие точечным и соответственно пренебрежем зависимостью Γ^C и Γ^0 от импульсов.

а) Суммируя куперовскую лестницу, выведите интегральное уравнение, определяющее $\Gamma^C\left(i\varepsilon, i\varepsilon'\right)$.

б) Рассмотрите модель, в которой $\Gamma^0\left(i\varepsilon, i\varepsilon'\right)$ факторизуется:

$$\Gamma^0\left(i\varepsilon, i\varepsilon'\right) = \lambda v(i\varepsilon) v\left(i\varepsilon'\right)$$

где λ - константа взаимодействия, а функция $v(i\varepsilon)$ - формфактор, определяющий масштаб энергий (спиновая структура опущена). Найдите температуру, при которой Γ^C обращается в бесконечность.

в) В случае, когда

$$v(i\varepsilon) = \frac{\omega_D}{\sqrt{\varepsilon^2 + \omega_D^2}},$$

найдите связь между T_c и ω_D.

Описанная здесь модель нефизична, поскольку настоящее электрон-фононное взаимодействие приводит к затравочной вершине Γ^0, зависящей от переданной энергии $\varepsilon - \varepsilon'$. Тем не менее, поскольку эта модель учитывает запаздывание притяжения между электронами на временах $\approx \omega_D^{-1}$, она дает качественно правильные предсказания.

Solution 58 а.

Выведем уравнение на $\Gamma^C(i\varepsilon, i\varepsilon')$, суммируя диаграммы на рис. из условия. Заметим, что в этих диаграммах сумма 4-импульсов $s = p_1 + p_2$ одинакова в каждой петле. Поэтому интегральное уравнение, соответствующее этим диаграммам, имеет вид

$$\Gamma^C(p, p'; s) = \Gamma^0(p, p') + \int \Gamma^0(p, k) G(k) G(s-k) \Gamma^C(k, p'; s) \frac{d^4k}{(2\pi)^4}$$

(конечно, по частотам следует брать не интеграл, а мацубаровскую сумму). Это уравнение отличается от аналогичного уравнения теории ферми-жидкости знаком перед интегральным членом. (Отличие возникает из-за того, что ферми-жидкостные диаграммы содержат фермионные петли, а куперовские диаграммы - нет.) (?????!!!!)

Положим $s = 0$, пренебрежем зависимостью Γ^0 и Γ^C от пространственного импульса, получим:

$$\Gamma^C(i\varepsilon, i\varepsilon') = \Gamma^0(i\varepsilon, i\varepsilon') + T \sum_{\varepsilon''} \int \frac{d^3p}{(2\pi)^3} \Gamma^0(i\varepsilon, i\varepsilon'') G(i\varepsilon'', \mathbf{p}) G(-i\varepsilon'', -\mathbf{p}) \Gamma^C(i\varepsilon'', i\varepsilon').$$

Интеграл по импульсам вычисляется переходом к интегрированию по ξ:

$$\int \frac{1}{(\varepsilon'')^2 + \xi_p^2} \frac{d^3p}{(2\pi)^3} = \frac{\pi\nu_0}{|\varepsilon''|}$$

(?? check it!)

Поэтому уравнение на куперовскую амплитуду принимает вид

$$\Gamma^C(i\varepsilon, i\varepsilon') = \Gamma^0(i\varepsilon, i\varepsilon') + \pi\nu_0 T \sum_{\varepsilon''} \Gamma^0(i\varepsilon, i\varepsilon'') \Gamma^C(i\varepsilon'', i\varepsilon') / |\varepsilon''|$$

Solution 58 б.

$$\Gamma^0(i\varepsilon, i\varepsilon') = \lambda v(i\varepsilon) v(i\varepsilon')$$

$$\Gamma^C(i\varepsilon, i\varepsilon') = \lambda v(i\varepsilon) \left(v(i\varepsilon') + \pi\nu_0 T \sum_{\varepsilon''} v(i\varepsilon'') \Gamma^C(i\varepsilon'', i\varepsilon') / |\varepsilon''| \right).$$

Из соображений симметрии (??? which???) следует, что

$$\Gamma^C(i\varepsilon, i\varepsilon') = \alpha v(i\varepsilon) v(i\varepsilon'),$$

thus

$$\alpha = \lambda + \pi\nu_0 \alpha\lambda T \sum_{\varepsilon''} v^2(i\varepsilon'') / |\varepsilon''|$$

$$\alpha = \lambda \left(1 - \pi\nu_0 \lambda T \sum_{\varepsilon''} v^2(i\varepsilon'') / |\varepsilon''| \right)^{-1}.$$

$$\alpha = \infty \qquad \Rightarrow \qquad \pi T \sum_{\varepsilon''} v^2(i\varepsilon'') / |\varepsilon''| = 1/\lambda\nu_0$$

Эта формула и определяет температуру перехода T_c.

Solution 58 в. с логарифмической точностью

By this point we know that the equation $\pi T_c \sum_{\varepsilon''} v^2(i\varepsilon'') / |\varepsilon''| = 1/\lambda\nu_0$ should hold.

We plug $v(i\varepsilon) := \omega_D / \left(\omega_D^2 + \varepsilon^2\right)^{1/2} \Rightarrow$ (?? meaning of it???) and fermionic frequencies: $\varepsilon = \omega = (2n+1)\pi T_c$, we have

$$2 \sum_{n=0}^{\infty} \frac{\omega_D^2}{(\omega_D^2 + \pi^2 T_c^2 (2n+1)^2)(2n+1)} = \frac{1}{\lambda\nu_0}.$$

Factor 2 originates from two sums (one from -∞ to 0 and another from 0 to ∞).

Множитель $v^2(i\varepsilon)$ обрезает сумму $\sum_{\varepsilon''} v^2\left(i\varepsilon''\right)/\left|\varepsilon''\right|$ при $n \approx n_{\max} = \omega_D/\pi T_c$. (???????)

Если считать $n_{\max} \gg 1$ и пренебречь множителем $v^2(i\varepsilon)$, заменив верхний предел суммы на $n_{\max}$, получим (то есть мы вообще выкидываем первую скобку из знаменателя, говоря, что она не особо повлияет)

$$\sum_{n=0}^{n_{\max}} \frac{1}{n+1/2} = \ln n_{\max} = \frac{1}{\nu_0 \lambda}$$

$$T_c \approx \frac{\omega_D}{\pi} e^{-1/\lambda\nu_0}$$

Значение коэффициента в этой формуле таким образом найти нельзя, да и, вообще, метод полезен только для быстрой оценки.

Solution 58 в. точно

The T_c comes out of the equation $2\sum_{n=0}^{\infty} \frac{\omega_D^2}{\left(\omega_D^2+\pi^2T_c^2(2n+1)^2\right)(2n+1)} = \frac{1}{\lambda\nu_0}$, so let us evaluate it exactly.

Here, we have два масштаба: T_c и ω_D, причем, $T_c \ll \omega_D$. Поэтому вклады этих масштабов можно разделить, используя следующий стандартный прием. Разобьем сумму на две части: по $n < n_0$ и по $n > n_0$, причем точку разбиения n_0 выберем так, что $n_0 \gg 1$, и одновременно $2\pi T_c n_0 \ll \omega_D$. Найдем сумму по каждой из областей, а затем сложим результаты. В области $n < n_0$ можно заменить функцию $v(i\varepsilon)$ на единицу, после чего эта часть суммы легко вычисляется с помощью тождеств

$$\sum_{k=1}^{\infty}(-1)^{k+1}/k = \ln 2, \quad \lim_{n\to\infty}\left(\sum_{k=1}^{n} 1/k - \ln n\right) = C$$

где $C = 0,577\ldots$ - постоянная Эйлера. Складывая эти два тождества, получаем вклад области $n < n_0$:

$$S\left(n < n_0\right) = \sum_{n=0}^{n_0} \frac{2}{2n+1} \approx \ln\left(2n_0\right)$$

В высокочастотной области $n > n_0$ можно пренебречь T_c по сравнению с ω_D и заменить сумму интегралом:

$$S\left(n > n_0\right) = \int\limits_{2\pi T n_0}^{\infty} \frac{\omega_D^2}{\varepsilon^2+\omega_D^2}\frac{d\varepsilon}{\varepsilon} = \frac{1}{2}\ln\frac{\varepsilon^2}{\varepsilon^2+\omega_D^2}\Big|_{2\pi T n_0}^{\infty}$$

$$S\left(n > n_0\right)|_{\omega_D \gg 2\pi n_0 T_c} = \ln\frac{\omega_D}{2\pi n_0 T_c}$$

В итоге, суммируя вклады от $n < n_0$ и $n \geqslant n_0$, получаем

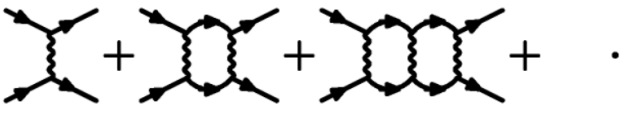
$$\frac{1}{\lambda\nu_0} = \ln\frac{\omega_D}{\pi T_c} + C$$

$$T_c = \frac{2\gamma}{\pi}\omega_D e^{-1/\lambda\nu_0}, \qquad \gamma := e^C$$

ЛШ-59. Temperature dependence of the gap $\Delta(T)$

(??? write short reminder of the whole formalism)

Рассмотрим мацубаровскую амплитуду рассеяния в куперовском канале $\Gamma^C\left(i\varepsilon, i\varepsilon'\right)$) (энергии сталкивающихся частиц равны $\pm\varepsilon$, а разлетающихся равны $\pm\varepsilon'$). Она дается суммой лестничных графиков, изображенных на рис. ниже



Пусть каждой волнистой линии соответствует множитель $\Gamma^0\left(i\varepsilon, i\varepsilon'\right)$. Будем считать взаимодействие точечным и соответственно пренебрежем зависимостью Γ^C и Γ^0 от импульсов.

Определите температурную зависимость $\Delta(T)$ для запаздывающего взаимодействия

$$\Gamma^0\left(i\varepsilon, i\varepsilon'\right) = \lambda v(i\varepsilon) v\left(i\varepsilon'\right), \qquad v(i\varepsilon) = \frac{\omega_D}{\sqrt{\varepsilon^2+\omega_D^2}}$$

Примите во внимание, что из-за запаздывания щель Δ становится функцией энергии ε спаривающихся частиц.

а) Соответственно рассмотрите величину $\tilde{\Delta}(\varepsilon)$ и, модифицируя уравнения

$$\Delta_{\alpha\beta} = \lambda \int F_{\alpha\beta}(\varepsilon, \mathbf{p}) \frac{d\varepsilon d^3p}{(2\pi)^4},$$

$$\Delta = \lambda T \sum_{\omega_n} \int F\left(i\omega_n, \mathbf{p}\right) \frac{d^3p}{(2\pi)^3} = \lambda T \sum_{\omega_n} \int \frac{\Delta}{\omega_n^2 + \xi_{\mathbf{p}}^2 + \Delta^2} \frac{d^3p}{(2\pi)^3},$$

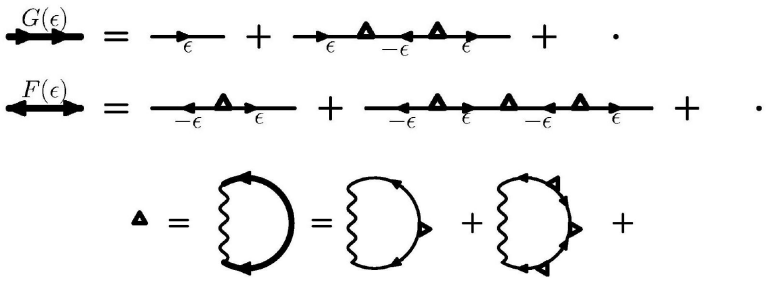
получите для $\tilde{\Delta}(\varepsilon)$ уравнение самосогласования.

б) В найденном уравнении вычислите интеграл по ξ. Изобразите качественное поведение решения уравнения $\Delta(T)$ на графике. Как $\Delta(T)$ ведет себя при $T \to 0$ и при $T \to T_c$?

в) Найдите сверхпроводящую щель $\Delta(T)$ в пределе низких температур ($T \to 0$) и вблизи точки перехода ($T \to T_c$).

Solution 59 a.

Диаграммы



показывают, что щель Δ возникает в результате свертки аномальной функции $F(i\varepsilon, \mathbf{p})$ и куперовской вершины $\Gamma^0\left(i\varepsilon, i\varepsilon'\right)$.

(???? what is their meaning exactly??? write these formulas. see theory about it for now)

Используем уравнение самосогласования:

$$\tilde{\Delta}(i\varepsilon) = T \sum_{\varepsilon'} \Gamma^0\left(i\varepsilon, i\varepsilon'\right) F\left(i\varepsilon', \mathbf{r}=\mathbf{r}'\right),$$

$$F\left(i\varepsilon, \mathbf{r}=\mathbf{r}'\right) := \int \frac{\tilde{\Delta}(i\varepsilon)}{\varepsilon^2 + \xi_p^2 + \tilde{\Delta}^2(i\varepsilon)} \frac{d^3p}{(2\pi)^3}. \qquad \Gamma^0\left(i\varepsilon, i\varepsilon'\right) = \lambda v(i\varepsilon) v\left(i\varepsilon'\right), \qquad \tilde{\Delta}(i\varepsilon) \equiv \Delta(T) v(i\varepsilon),$$

$$\Delta(T) = \lambda T \sum_{\varepsilon} \int \frac{v^2(i\varepsilon)\Delta(T)}{\varepsilon^2 + \xi_{\mathbf{p}}^2 + v^2(i\varepsilon)\Delta^2(T)} \frac{d^3p}{(2\pi)^3}.$$

Solution 59 б.

Вычисляя интеграл по ξ в $\Delta(T) = \lambda T \sum_{\varepsilon} \int \frac{v^2(i\varepsilon)\Delta(T)}{\varepsilon^2+\xi_{\mathbf{p}}^2+v^2(i\varepsilon)\Delta^2(T)} \frac{d^3p}{(2\pi)^3}$, (??? напишу тут 2 строчки этих преобразований, без слов?) получаем

$$\frac{1}{\lambda\nu_0} = \pi T \sum_{\varepsilon} \frac{v^2(i\varepsilon)}{\sqrt{\varepsilon^2 + \Delta^2(T) v^2(i\varepsilon)}}.$$

Рассмотрим качественно, как ведет себя решение этого уравнения. При $T \ll \Delta(T)$ сумму в правой части можно заменить интегралом. (??? why???)

Таким образом, в этом пределе зависимость от T исчезает, и $\Delta(T)$ стремится к постоянному пределу. Зависимость от T должна быть очень слабой, поскольку для гладкой функции сумма очень хорошо аппроксимирует значение интеграла. Ясно также, что при увеличении температуры величина щели $\Delta(T)$ будет уменьшаться. Формально это следует из того, что сумма в правой части (10.78) переоценивает значение интеграла тем больше, чем больше расстояние между мацубаровскими частотами. Поэтому для того, чтобы удержать правую часть постоянной, рост температуры следует компенсировать убыванием $\Delta(T)$.

Заметим, что при $\Delta = 0$ уравнение (10.78) совпадает с уравнением для определения температуры перехода (10.63), рассмотренным в предыдущей задаче. Это означает, что при $T = T_c$ щель $\Delta(T)$ обратится в нуль. Вблизи этой точки правая часть (10.78) зависит линейно от $T - T_c$ и квадратично от $\Delta(T)$. Поэтому $\Delta(T) \approx \sqrt{T_c - T}$. Из этих рассуждений также следует, что $\Delta(0) \approx T_c$. Полученная таким образом качественная зависимость $\Delta(T)$ согласуется с результатом численного решения уравнения Горькова, изображенном на рис. 10.11

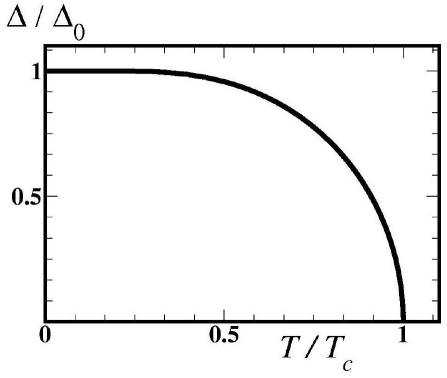


Рис. 10.11

Solution 59 в, Δ_0

Теперь вычислим $\Delta(T)$ при $T \to 0$. Вначале мы просто заменим сумму в $\frac{1}{\lambda\nu_0} = \pi T \sum\limits_{\varepsilon} \frac{v^2(i\varepsilon)}{\sqrt{\varepsilon^2+\Delta^2(T)v^2(i\varepsilon)}}$ интегралом и получим, что $\Delta_0 \equiv \Delta(T=0)$ удовлетворяет уравнению

$$\frac{1}{\nu_0\lambda} = \int\limits_0^\infty \frac{v^2(i\varepsilon)d\varepsilon}{\sqrt{\varepsilon^2 + \Delta_0^2 v^2(i\varepsilon)}}.$$

Найдем этот интеграл для $v(i\varepsilon) = \omega_D / \left(\varepsilon^2 + \omega_D^2\right)^{1/2}$:

$$\frac{1}{\nu_0\lambda} = \int\limits_0^\infty \frac{\omega_D^2 d\varepsilon}{\left(\varepsilon^2 + \omega_D^2\right)\sqrt{\varepsilon^2 + \Delta_0^2\omega_D^2/\left(\varepsilon^2 + \omega_D^2\right)}}.$$

Now, we note that $\Delta_0 \approx T_c \ll \omega_D$. We have a ε, which runs over all values. For $\varepsilon \leq \Delta_0$, we have $v^2(i\varepsilon) \approx 1$, but for $\varepsilon \geq \Delta_0$, we have $\varepsilon^2 \gg \Delta_0^2\omega_D^2/\left(\varepsilon^2 + \omega_D^2\right)$, thus we can just approximate under the square root $\Delta_0^2\omega_D^2/\left(\varepsilon^2 + \omega_D^2\right) \approx \Delta_0^2$:

$$\frac{1}{\nu_0\lambda} \approx \int\limits_0^\infty \frac{\omega_D^2 d\varepsilon}{\left(\varepsilon^2 + \omega_D^2\right)\sqrt{\varepsilon^2 + \Delta_0^2}}.$$

В этом интеграле имеется два существенно разных масштаба энергий: Δ_0 и ω_D. Поэтому можно introduce an energy ε_0, such that $\Delta_0 \ll \varepsilon_0 \ll \omega_D$ and integrate over two parts $\varepsilon < \varepsilon_0$ и $\varepsilon > \varepsilon_0$:

$$\int\limits_0^{\varepsilon_0} \frac{d\varepsilon}{\sqrt{\varepsilon^2 + \Delta_0^2}} + \int\limits_{\varepsilon_0}^\infty \frac{\omega_D^2 d\varepsilon}{\varepsilon\left(\varepsilon^2 + \omega_D^2\right)} = \ln\frac{2\varepsilon_0}{\Delta_0} + \ln\frac{\omega_D}{\varepsilon_0}.$$

Промежуточная энергия ε_0 выпадает. Окончательно получаем

$$\frac{1}{\lambda\nu_0} = \ln\frac{2\omega_D}{\Delta_0}.$$

That is how that complicated integral can be calculated with a little approximation!

Сравнивая это соотношение с выражением (10.73) для температуры перехода T_c, получаем соотношение

$$\Delta_0 = \frac{\gamma}{\pi} T_c$$

Заметим, что коэффициент в формуле (10.73) для T_c связан с конкретной формой обрезания по энергии. Что же касается соотношения (10.83) между Δ_0 и T_c, то при $T_c \ll \omega_D$ оно определяется только физикой низкоэнергетической области $\varepsilon \ll \omega_D$ и поэтому не зависит от выбора обрезающей функции $v(i\varepsilon)$. Кроме того, точно такое же соотношение между Δ_0 и T_c получается и при обрезании по ξ. Таким образом, соотношение (10.83) носит универсальный характер.

Solution 59 в, $\Delta(T)$ approximation at $T \ll T_c$

Now we know, how to evaluate the sum $\frac{1}{\lambda\nu_0} = \pi T \sum\limits_{\varepsilon} \frac{v^2(i\varepsilon)}{\sqrt{\varepsilon^2+\Delta^2(T)v^2(i\varepsilon)}}$, if we have $T = 0$ (because sum changes to the integral). But for low temperatures, we have a sum, so we need to do learn how to do the summation. (?????)

Это можно было бы сделать с помощью формулы суммирования Пуассона (10.47) (????). Однако гораздо проще получить ответ, заметив, что самым малым масштабом, на котором меняется правая часть, является Δ_0. Поэтому при расчете низкотемпературных поправок структурой правой части на масштабе ω_D можно пренебречь.

(???? why???) Тогда можно переписать (10.77) как

$$\frac{1}{\lambda\nu_0} = T \sum_{\varepsilon} \int\limits_{-\infty}^{\infty} \frac{d\xi}{\varepsilon^2 + \xi^2 + \Delta^2}$$

(?? check, maybe there should be π also here???)

$\sum\limits_{n=-\infty}^{\infty} \frac{1}{(2n+1)^2+a^2} = \frac{\pi}{2a} \operatorname{th} \frac{\pi a}{2}$,

$$\frac{1}{\lambda\nu_0} = \int\limits_{0}^{\infty} \operatorname{th} \frac{\sqrt{\xi^2+\Delta^2}}{2T} \frac{d\xi}{\sqrt{\xi^2+\Delta^2}}.$$

Этот интеграл логарифмически расходится, но его значение при $T = 0$ мы уже нашли, и сейчас нас интересуют поправки, возникающие при $T \neq 0$, которые, как мы сейчас увидим, описываются сходящимися интегралами. Минимальное значение аргумента гиперболического тангенса есть $\Delta/(2T) \gg 1$, поэтому $\operatorname{th} x \approx \operatorname{sign} x(1 - 2\exp(-|x|))$,

(??? I am not sure how first term came out, since there is no ω_D in the integral ????)

$$\frac{1}{\lambda\nu_0} = \ln\frac{2\omega_D}{\Delta} - 2\int\limits_{0}^{\infty} \frac{d\xi}{\sqrt{\xi^2+\Delta^2}} \exp\left(-\frac{\sqrt{\xi^2+\Delta^2}}{T}\right).$$

Так как при интегрировании второго члена вклад дают лишь $\xi \ll \Delta$, то $\sqrt{\xi^2+\Delta^2} \approx \Delta + \xi^2/(2\Delta)$,

$$\frac{1}{\nu_0\lambda} = \ln\frac{2\omega_D}{\Delta} - 2e^{-\Delta/T} \int\limits_{0}^{\infty} e^{-\xi^2/2\Delta T} \left(1 - \frac{\xi^2}{2\Delta^2}\right) \frac{d\xi}{\Delta}$$

$$\ln\frac{\Delta}{\Delta_0} = -\sqrt{\frac{2\pi T}{\Delta}} e^{-\Delta/T} \left(1 - \frac{T}{8\Delta}\right),$$

Δ_0 вставлено из замены $1/(\lambda\nu_0) = \ln(2\omega_D/\Delta_0)$.

$$\Delta\,(T \ll T_c) = \Delta_0 \left(1 - \sqrt{\frac{2\pi T}{\Delta_0}} e^{-\Delta_0/T} \left(1 - \frac{T}{8\Delta_0}\right)\right)$$

Выписанная поправка к Δ_0 понадобится нам при вычислении термодинамического потенциала в задаче 60 (???). (Точность выражения (10.88) может показаться чрезмерной, но оказывается, что главный член в выражении (10.88) не дает вклада в термодинамический потенциал, и нам придется учесть выписанную поправку.)

Solution 59 в, $\Delta(T)$ approximation at $T \approx T_c$

Теперь рассмотрим случай $T \to T_c$. В этом пределе $\Delta(T) \ll T$, поэтому правую часть (10.78) можно разложить по Δ:

$$\frac{1}{\lambda\nu_0} = \pi T \sum_{\varepsilon} \left(\frac{v^2(i\varepsilon)}{|\varepsilon|} - \frac{\Delta^2 v^4(i\varepsilon)}{2|\varepsilon|^3} \right)$$

Как показано в задаче 58, первый член в правой части логарифмически зависит от T и сравнивается с левой частью при $T = T_c$. Поэтому его можно объединить с левой частью, получив $\ln T_c/T$.
(??????????)
Что же касается второго члена, пропорционального Δ^2, то он определяется областью $\varepsilon \approx \pi T$, и в нем можно заменить $v^4(i\varepsilon)$ на единицу. Таким образом

$$\ln \frac{T}{T_c} = -\frac{\pi\Delta^2}{2} T \sum_{\varepsilon_n} \frac{1}{|\varepsilon_n|^3}$$

Сумма по мацубаровским частотам легко выражается через ζ-функцию:

$$\zeta(x) = \sum_{n=1}^{\infty} \frac{1}{n^x}, \quad \sum_{n=0}^{\infty} \frac{1}{(2n+1)^x} = \left(1 - \frac{1}{2^x}\right) \zeta(x).$$

(????? change of our sum to the template sum???)

$$\frac{T - T_c}{T_c} = -\frac{7\zeta(3)}{8\pi^2} \frac{\Delta^2}{T_c^2}$$

$$\Delta^2_{T \to T_c} = \frac{8\pi^2}{7\zeta(3)} T_c \left(T_c - T\right)$$

Таким образом, и в этом случае обрезка при $\omega \approx \omega_D$ оказалась несущественной для вычисления щели.

Подводя итог, можно сказать, что конкретный вид обрезания важен в основном для определения T_c. Все остальные физические величины сверхпроводника могут быть выражены через T_c с помощью универсальных соотношений, не зависящих от вида конкретной функции запаздывания $v(i\varepsilon)$. Это происходит потому, что физика сверхпроводника определяется масштабами энергий порядка $T_c \ll \omega_D$. Это оправдывает применение популярной модели, в которой запаздывание на временах порядка ω_D^{-1} учитывается с помощью обрезания интегралов по ξ, а не по ε (???? what is this ε physically????), т. е. запаздывающее взаимодействие заменяется на взаимодействие нелокальное в пространстве.

me. More intuition about BCS

Find $\mathrm{Tr} e^{-\beta H}$, where H is the BCS Hamiltonian

Solution

This is also a basic problem, but details are tricky, so it is a good one.
(Write it later)
(???) One should understand that constant in front of BCS Hamiltonian also has a contribution to the spectrum.

me. More intuition about the gap equation

The gap equation tells us that superconducting gap is obtained by

$$\frac{1}{\lambda} = \frac{1}{2} \sum_{\mathrm{p}}{}' \frac{1 - 2\langle \tilde{n}_p \rangle}{\sqrt{\xi_{\mathrm{p}}^2 + \Delta^2}},$$

where λ is just an input constant of the model; index $'$ indicates that we sum only near the Fermi surface and ξ_{p} is the dispersion, which tells us how kinetic energy of free electron looks like; and $\langle \tilde{n}_p \rangle$ is the averaged number of excitations over superconductive ground state.

Transform this equation to the form of equating averaging of an electron and hole annihilation operators. How this averaging is connected to the gap?

Reminder: $u_p^2 = \frac{1}{2}\left(1 + \frac{\xi_p}{\varepsilon_p}\right), v_p^2 = \frac{1}{2}\left(1 - \frac{\xi_p}{\varepsilon_p}\right)$.

Solution

This is a very easy question, since in the basic theory, there is a derivation from averaging of an electron and hole annihilation operators to the gap equation, so one needs to do just this basic steps to the opposite direction. And the meaning is exactly one, which was in the definition of the gap. However, going backwards is not trivial and it is a good problem for practice, if one don't look at any other theory and just use what is written in the problem statement.

(Write it later here)

14.2.4 Problems about Exotic Transformations in BCS Model

me. Evaluation of a trace

(write background that we work with typical notation in BCS)

For the averaging values, one often calculates traces of the operators. Consider the following transformation:

$$\begin{aligned}\mathrm{Tr}[e^{-\beta H_k}] &= \mathrm{Tr}\Big\{e^{-\beta(\xi_k-\varepsilon_k+\varepsilon_k\left[\hat{b}^\dagger_{\mathbf{k}-}\hat{b}_{\mathbf{k},-}+\hat{b}^\dagger_{\mathbf{k}+}\hat{b}_{\mathbf{k},+}\right])}\Big\} = \\ &= \mathrm{Tr}\Big\{e^{-\beta(\xi_k-\varepsilon_k)}\Big\}\mathrm{Tr}\Big\{e^{-\beta(\varepsilon_k\left[\hat{b}^\dagger_{\mathbf{k}-}\hat{b}_{\mathbf{k},-}+\hat{b}^\dagger_{\mathbf{k}+}\hat{b}_{\mathbf{k},+}\right])}\Big\} \\ &= 4e^{-\beta(\xi_k-\varepsilon_k)}(1+e^{-\beta\varepsilon_k}+e^{-\beta\varepsilon_k}+e^{-2\beta\varepsilon_k}) = \\ &= 4e^{-2\beta(\xi_k-\varepsilon_k)}(1+e^{-\beta\varepsilon_k})^2\end{aligned}$$

and 4 originates from four states: nothing is occupied, spin up is occupied, spin down is occupied and both spins are occupied.

Is it correct? If no, how to fix it?

Solution

No, it is not correct.

(???? I forgot the explanation, why. it was something about that if we have a constant, no states are for it, so trace does not produce 4. but I forgot, why exactly?)

(??? what to do with constant in front, it is maybe also not correct)

Zala,me. More intuition about constant term in the BCS

In the gap equation, one can do the following transformation:

$$\begin{aligned}&\mathrm{Tr}[\frac{\exp\Big[-\beta H\Big]}{\mathrm{Tr}[e^{-\beta H}]}c_{k,+}c_{-k,-}] = \\ &= \mathrm{Tr}[\frac{\exp\left[-\beta\sum_p\left\{-2\Big[\xi_p v_p^2-u_p v_p\Delta\Big]+\begin{pmatrix}c_{p\uparrow} & c^\dagger_{-p\downarrow}\end{pmatrix}\begin{bmatrix}\xi_p & \Delta(t)\\ \Delta(t) & -\xi_p\end{bmatrix}\begin{pmatrix}c_{p\uparrow}\\ c^\dagger_{-p\downarrow}\end{pmatrix}\right\}\right]}{\mathrm{Tr}[e^{-\beta H}]}c_{k,+}c_{-k,-}]\end{aligned}$$

Now, to evaluate this trace we need to work with the constant term, which $2\Big[\xi_p v_p^2-u_p v_p\Delta\Big]$.

(??? here, most likely the constant is wrong, I'll check later!!!)

One can say "this is just a constant, so I'll put it out exponent of it and it will be just a factor in front of the rest expression".

Another approach to the constant is by saying "this constant in matrix notation is actually the identity matrix", thus exponent of it will be an exponent of the constant times the identity matrix, so by taking the trace it will pop out ot the game at all".

Following one logic, constant plays role, following another - does not. What is the correct approach for the constant?

Solution

It is a good, but purely mathematical question.

(anyway, solution will be "the correct transformations will be such that the correct well-known equation is obtained at the end")

How to take properly constant term out: by just constant or by unit matrix?

(write formulas for both!)
These two approaches have a different outcome, since we take later 01 component. So, what is the correct one?

me. Checking trivial evolution of the density matrix

Write the equation of trivial evolution of superconductor's density matrix, if it is not perturbed by anything external. Show that even though time passes and density matrix evolves, the gap does not change.

Solution

This problem is good for application of the density matrix formalism, however, of course, it is useless and asks one about only understanding the formalism.

(write that first part about the formalism!!!!)

(does density matrix gather a trivial phase in its evolution????? write it in the theory of QM!!!)

For the case of the trivial evolution, we have:

$$\begin{aligned}\rho(t+\delta t) = \prod_p \exp\left[-\beta\Big(\epsilon_{\mathbf{k}} - 2\Big[\varepsilon_{\mathbf{p}} v_p^2 - u_p v_p \Delta\Big]\Big)\right]\cdot \\ \cdot \exp\left[-i \begin{pmatrix} c^\dagger_{p\uparrow}, c_{-p\downarrow}\end{pmatrix} \begin{bmatrix} \xi_p & \bar{\Delta} \\ \Delta & -\xi_p \end{bmatrix} \begin{pmatrix} c_{p\uparrow} \\ c^\dagger_{-p\downarrow}\end{pmatrix} \delta t\right]\cdot \\ \cdot \exp\left[-\beta \begin{pmatrix} c^\dagger_{\mathbf{k}\uparrow}, c_{-\mathbf{k}\downarrow}\end{pmatrix} \begin{bmatrix} \epsilon_{\mathbf{k}} & \bar{\Delta} \\ \Delta & -\epsilon_{\mathbf{k}} \end{bmatrix} \begin{pmatrix} c_{\mathbf{k}\uparrow} \\ c^\dagger_{-\mathbf{k}\downarrow}\end{pmatrix}\right]\cdot \\ \cdot \exp\left[i \begin{pmatrix} c^\dagger_{p\uparrow}, c_{-p\downarrow}\end{pmatrix} \begin{bmatrix} \xi_p & \bar{\Delta} \\ \Delta & -\xi_p \end{bmatrix} \begin{pmatrix} c_{p\uparrow} \\ c^\dagger_{-p\downarrow}\end{pmatrix} \delta t\right] / \mathrm{Tr}[e^{-\sum_{q\sigma'} \mu_q n_{p\sigma'}(t)}] \\ = \\ \prod_p \exp\left[-\beta\Big(\epsilon_{\mathbf{k}} - 2\Big[\varepsilon_{\mathbf{p}} v_p^2 - u_p v_p \Delta\Big]\Big)\right]\cdot \\ \cdot \exp\left[\begin{pmatrix} c^\dagger_{p\uparrow}, c_{-p\downarrow}\end{pmatrix} \Big(-i \begin{bmatrix} \xi_p & \bar{\Delta} \\ \Delta & -\xi_p \end{bmatrix} \delta t - \beta \begin{bmatrix} \epsilon_{\mathbf{k}} & \bar{\Delta} \\ \Delta & -\epsilon_{\mathbf{k}} \end{bmatrix} + i \begin{bmatrix} \xi_p & \Delta \\ \bar{\Delta} & -\xi_p \end{bmatrix} \delta t\Big) \begin{pmatrix} c_{p\uparrow} \\ c^\dagger_{-p\downarrow}\end{pmatrix} + \right. \\ \left. + \begin{pmatrix} c^\dagger_{p\uparrow}, c_{-p\downarrow}\end{pmatrix} \mathrm{Kommutators} \begin{pmatrix} c_{p\uparrow} \\ c^\dagger_{-p\downarrow}\end{pmatrix} + \cdots \right] / \mathrm{Tr}[e^{-\sum_{q\sigma'} \beta\varepsilon_{p\sigma'} n_{p\sigma'}(t)}]\end{aligned}$$

where here I defined

$$\begin{aligned}\mathrm{Kommutators} = \frac{1}{2}\left[-i \begin{bmatrix} \xi_p & \bar{\Delta} \\ \Delta & -\xi_p \end{bmatrix} \delta t, -\beta \begin{bmatrix} \epsilon_{\mathbf{k}} & \bar{\Delta} \\ \Delta & -\epsilon_{\mathbf{k}} \end{bmatrix}\right] + \\ + \frac{1}{2}\left[-i \begin{bmatrix} \xi_p & \bar{\Delta} \\ \Delta & -\xi_p \end{bmatrix} \delta t, i \begin{bmatrix} \xi_p & \bar{\Delta} \\ \Delta & -\xi_p \end{bmatrix} \delta t\right] + \\ + \frac{1}{2}\left[-\beta \begin{bmatrix} \epsilon_{\mathbf{k}} & \bar{\Delta} \\ \Delta & -\epsilon_{\mathbf{k}} \end{bmatrix}, i \begin{bmatrix} \xi_p & \bar{\Delta} \\ \Delta & -\xi_p \end{bmatrix} \delta t\right],\end{aligned}$$

where square brackets (with a comma inside) mean the commutator, not a matrix! And the "..." mean higher commutators, which will have a very long expression and I have no idea how to deal with them. Luckily, for the trivial evolution, we have

$$\mathrm{Kommutators} = 0,$$

because all operators under it are the same up to a constant (and also two commutators are zero together, because one is (-1) times another), so we will have

$$\rho(t+\delta t) = \prod_p \exp\left[-\beta\Big(\epsilon_{\mathbf{k}} - 2\Big[\varepsilon_{\mathbf{p}} v_p^2 - u_p v_p \Delta\Big]\Big)\right] \cdot$$
$$\cdot \exp\left[-\beta \begin{pmatrix} c^\dagger_{p\uparrow}, c_{-p\downarrow} \end{pmatrix} \begin{bmatrix} \epsilon_{\mathbf{k}} & \bar{\Delta} \\ \Delta & -\epsilon_{\mathbf{k}} \end{bmatrix} \begin{pmatrix} c_{p\uparrow} \\ c^\dagger_{-p\downarrow} \end{pmatrix}\right] / \mathrm{Tr}[e^{-\sum_{q\sigma'} \beta \varepsilon_{p\sigma'} n_{p\sigma'}(t)}] =$$
$$= \prod_p \exp\left[-\sum_{q\sigma'} \beta \varepsilon_{p\sigma'} n_{p\sigma'}(t)\right] / \mathrm{Tr}[e^{-\sum_{q\sigma'} \beta \varepsilon_{p\sigma'} n_{p\sigma'}(t)}].$$

The terms are combined back exactly as they combined into the initial expression. So, in other words, the density matrix does not evolve in the equilibrium.

Now, we can use our density matrix for getting the gap:
(I need to write that Denis's derivation in this notation)
(anyway, we have a one matrix in the numerator, so it is straightforward how to transform it)

14.2.5 Problems about Numerical Computations in BCS Model

Known,me. Numerical evaluation of gap equation by bisection method

Calculate the gap as a function of temperature numerically, using the bisection and sum terms without changing the sum to the integral.
(remind, what is the gap eq.)
(remind, what is the bisection method)

Solution

General input:

```
import numpy as np
import matplotlib.pyplot as plt
from scipy.optimize import bisect

# Parameters
tttt = 0.3        # hopping parameter
mu = 0.0          # chemical potential
lambd = 1.0       # coupling strength
cutoff = 0.1      # energy window near Fermi surface
N = 1000          # number of momentum points
p_vals = np.linspace(-np.pi, np.pi, N)

def disp(p):
    return -2 * tttt * np.cos(p)

def fermi(E, beta):
    x = beta * E
    x = np.clip(x, -700, 700)  # safe range to avoid overflow
    return 1 / (np.exp(x) + 1)


def gap_eq_func(Delta, T):
    beta = 1 / T
    sum_val = 0.0
    for p in p_vals:
        xi = disp(p) - mu
        if abs(xi) > cutoff:
            continue
        Ep = np.sqrt(xi**2 + Delta**2)
        f = fermi(Ep, beta)
        sum_val += (1 - 2 * f) / Ep
    return 0.5 * sum_val / N - 1 / lambd
```

Estimate critical temperature Tc (limit Delta -> 0):

```
def linearized_gap_eq(T):
    beta = 1 / T
    sum_val = 0.0
```

```
    for p in p_vals:
        xi = disp(p) - mu
        if abs(xi) > cutoff:
            continue
        Ep = abs(xi)
        f = fermi(Ep, beta)
        sum_val += (1 - 2 * f) / Ep
    return 0.5 * sum_val / N - 1 / lambd

from scipy.optimize import brentq
Tc = brentq(linearized_gap_eq, 0.001, 0.1)
```

Compute Delta(T) using bisection method:

```
T_vals = np.linspace(0.001, Tc, 200)
Delta_vals = []

for T in T_vals:
    try:
        Delta_T = bisect(gap_eq_func, 1e-6, 1.0, args=(T,), xtol=1e-6)
    except ValueError:
        Delta_T = 0.0  # Bisection failed; gap = 0
    Delta_vals.append(Delta_T)
```

Normalize:

```
Delta_vals = np.array(Delta_vals)
Delta_0 = Delta_vals[0]
T_norm = T_vals / Tc
Delta_norm = Delta_vals / Delta_0
```

Plot:

```
plt.figure(figsize=(8, 5))
plt.plot(T_norm, Delta_norm, label=r'$\Delta(T)/\Delta(0)$')
plt.xlabel(r'Normalized Temperature $T/T_c$')
plt.ylabel(r'Normalized Gap $\Delta(T)/\Delta(0)$')
plt.title('Superconducting Gap vs Temperature (Bisection Method)')
plt.grid(True)
plt.legend()
plt.tight_layout()
plt.show()
```

```
print(f"Estimated Tc = {Tc:.5f}, Delta(0) = {Delta_0:.5f}")
```

Known,me. Numerical evaluation of gap equation by iterations

Calculate the gap as a function of temperature numerically, using iterations and sum terms without changing the sum to the integral.
(remind, what is the gap eq.)
(remind, what is the iteration method)

Solution

(one needs to just multiply the gap eq. by the gap, such that the l.h.s. will be the updated gap. the rest is relatively trivial)

Known,me. Numerical evaluation of gap equation by changing to the integral

Calculate the gap as a function of temperature numerically by changing the sum to the integral and use the inbuilt commands of a popular programming language.
(remind, what is the gap eq.)
(remind, some function in python, for example)

Solution 1, by Python

We start from the gap equation and some introduced variables:

$$\eta := \frac{1}{N(0)V}; \quad \eta = \int_0^{\hbar\omega_D} \tanh \frac{\sqrt{\Delta^2+\xi^2}}{2k_BT} \frac{d\xi}{\sqrt{\Delta^2+\xi^2}}; \qquad \Delta_0 \approx 1.76 k_B T_c; \qquad \frac{\hbar\omega_D}{\Delta_0} = \sinh\eta;$$

We transform it as follows:

$$\eta = \int_0^{\hbar\omega_D} \tanh\left(\frac{\Delta_0}{2k_BT_c}\frac{1}{T/T_c}\frac{\Delta}{\Delta_0}\sqrt{1+\xi^2/\Delta^2}\right)\frac{d\xi/\Delta}{\sqrt{1+\xi^2/\Delta^2}}$$
$$\approx \int_0^{\delta^{-1}\sinh\eta} \tanh\left(0.882\frac{\delta}{\tau}\sqrt{1+z^2}\right)\frac{dz}{\sqrt{1+z^2}} \qquad \delta := \Delta(T)/\Delta_0, \qquad \tau := T/T_c$$

here $\hbar\omega_D/\Delta = \Delta_0\hbar\omega_D/(\Delta_0\Delta) = \sinh\eta/\delta$. The number 0.882 is more precise than 1.76/2 for the computer.

The numerical strategy is as follows. We fix δ and find τ, change δ and solve for $\tau, \ldots$ up to obtain $\delta(\tau)$.

```
import numpy as np
import matplotlib.pyplot as plt
from scipy.integrate import quad
from scipy.optimize import fsolve
from matplotlib.ticker import FormatStrFormatter, MultipleLocator

eta = 1 / 0.35

def bcs_gap_equation(d, t):
    integral, _ = quad(lambda z: np.tanh(0.882 * d * np.sqrt(1 + z**2) / t) / np.sqrt(1 +
    z**2), 0, np.sinh(eta) / d)
    return eta - integral

d_vals = np.linspace(0.1, 0.9999, 70)  # don't set zero here, since we are deviding by d.

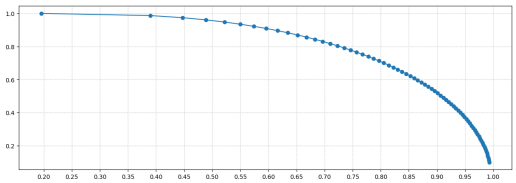
t0 = 0.1
t_vals = [fsolve(lambda t: bcs_gap_equation(d, t), t0)[0] for d in d_vals]

plt.figure(figsize=(15, 5))
plt.plot(t_vals, d_vals, marker='o', linestyle='-')
plt.grid(True, linestyle='--', alpha=0.6)

# Set x-axis grid step to 0.05
plt.gca().xaxis.set_major_locator(MultipleLocator(0.05))

plt.gca().xaxis.set_major_formatter(FormatStrFormatter('%.2f'))
plt.show()
```

We get what we expected:



The disadvantage of this approach is that there are no homogeneous points on temperature axes, only on gap axes. But still, it is fine.

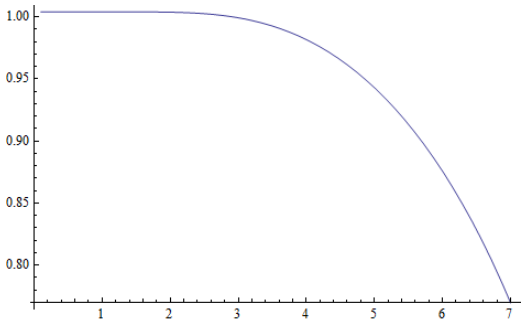
(????) This is simpler than first fixing τ to solve for δ, because of the $1/\delta$ in the boundary, but maybe Im wrong on this point. (??? I'll maybe try later it and write here code for this way)

Solution 2, by Wolfram

(???? write about FindRoot[] and NIntegrate[] commands, how do they work?)

```
kb = 1.38 10^(-23);
h = 6.62 10^-34;
hbar = h/2/Pi;
Tc = 9.2;
Delta0 = 3.528/2*Tc*kb;
omegad = 296*kb/hbar;
Delta[T_]:=
  Block[{a = Log[1.13*hbar*omegad/kb/Tc], b = hbar *omegad/2/kb},
   Return[     FindRoot[     NIntegrate[
         Tanh[b/T*Sqrt[\[Epsilon]^2 + x^2]]/
          Sqrt[\[Epsilon]^2 + x^2], {\[Epsilon], 0, 1},  AccuracyGoal -> 2] - a, {x, 0.01,
    0.1}][[1, 2]]*hbar* omegad]];
Plot[Delta[x]/Delta0, {x, 0.1, 7}]
```

We get what we expected:



(??? there are warnings and the T axes is not normalized. so maybe it is a bad code, but still, it can teach us about using wolfram for superconductivity, so I'll keep it for now.)

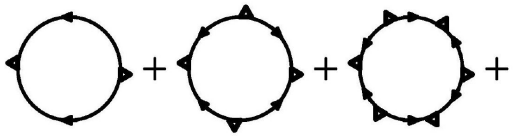
14.2.6 Questions about Applicability of Formulas

(here, there will be a questions like "I want to describe this phenomena, which formulas I should use?" Later I'll collect this from articles)

14.2.7 Problems about phenomena in the theoretical BCS 1

ЛШ-60. Heat capacity at $T < T_c$

(??? write short reminder of the whole formalism)
Покажите, что вклад электронов в термодинамический потенциал Ω сверхпроводящего металла дается диграммным рядом, показанным на рис. ниже.



Какие выражения сопоставляются различным диаграммам?
Выразите эту сумму графиков через функцию $\Delta(T)$, считая ее известной. Найдите температурную зависимость теплоемкости сверхпроводника:

а) при $T \ll T_c$

б) при $T \to T_c$. В этом случае достаточно взять первый график, показанный на рис. 10.9, поскольку вблизи T_c величина Δ мала. Сравните ответ с теплоемкостью нормального металла (см. [1], 36).

Hint: Вычисляя мацубаровскую сумму при низких температурах, удобно пользоваться формулой суммирования Пуассона $\sum_{n=-\infty}^{\infty} f(n) = \sum_{k=-\infty}^{\infty} \int_{-\infty}^{\infty} f(x) e^{2\pi i k x} dx$, оставляя в сумме по k лишь члены с $k = 0, \pm 1$. Напомним, что применять формулу Пуассона следует с осторожностью, поскольку она справедлива лишь для функций, аналитических на всей вещественной оси.

Solution 60. in general

Характерный масштаб энергий, дающих вклад в термодинамику, оказывается порядка $\max\{\Delta_0, T_c\}$, и следовательно эффектами запаздывания на временах порядка ω_D^{-1} можно пренебречь, выражая все величины через T_c или Δ_0.
Рассмотрим диаграммное разложение термодинамического потенциала, показанное на рис. 10.9. Как обычно, продифференцируем термодинамический потенциал по константе связи λ для того, чтобы убрать множитель $1/n$ перед диаграммами.
(????? why is it a typical approach????)
Как нетрудно заметить, если в каждой из диаграмм на рис. 10.9 перерезать одну из электронных линий, то получается одна из диаграмм на рис. 10.6, причем соответствие взаимнооднозначное. Поэтому

$$\frac{\lambda}{V}\frac{\partial\Omega}{\partial\lambda} = T\sum_{\omega_n}\int G_0^{-1}\left(i\omega_n,\mathbf{p}\right)\left(G\left(i\omega_n,\mathbf{p}\right)-G_0\left(i\omega_n,\mathbf{p}\right)\right)\frac{d^3p}{(2\pi)^3} =$$
$$= -T\sum_{\omega_n}\int \Delta^* F\left(i\omega_n,\mathbf{p}\right)\frac{d^3p}{(2\pi)^3} = -\frac{|\Delta|^2}{\lambda}.$$

Делая преобразование, мы воспользовались соотношениями $G_{\alpha\beta}(\varepsilon,\mathbf{p}) = G^0_{\alpha\beta}(\varepsilon,\mathbf{p}) + G^0_{\alpha\lambda}(\varepsilon,\mathbf{p})\Delta^*_{\lambda\mu}F_{\mu\beta}(\varepsilon,\mathbf{p})$ и $\Delta = \lambda T\sum_{\omega_n}\int\frac{\Delta}{\omega_n^2+\xi_{\mathbf{p}}^2+\Delta^2}\frac{d^3p}{(2\pi)^3}$.

Термодинамический потенциал получается интегрированием $\partial\Omega/\partial\lambda$ по λ от $\lambda = 0$ до истинного значения. Чтобы проинтегрировать по λ, выразим $d\lambda$ через $d\Delta$ с помощью $\Delta = \lambda T\sum_{\omega_n}\int\frac{\Delta}{\omega_n^2+\xi_{\mathbf{p}}^2+\Delta^2}\frac{d^3p}{(2\pi)^3}$:

$$\frac{d\lambda}{\lambda^2} = T\sum_{\omega_n}\int\frac{2\Delta d\Delta}{\left(\omega_n^2+\xi_{\mathbf{p}}+\Delta^2\right)^2}\frac{d^3p}{(2\pi)^3}$$

Поэтому

$$\frac{\Omega_s-\Omega_n}{V} = -2\int_0^{\Delta} T\sum_{\omega_n}\int\frac{\Delta^3 d\Delta}{\left(\omega_n^2+\xi_{\mathbf{p}}^2+\Delta^2\right)^2}\frac{d^3p}{(2\pi)^3}$$

Интегрируя по ξ и Δ, получим
(!??!?!??!!?!? a place for good calculations!!!!)

$$\frac{\Omega_s-\Omega_n}{V} = -\pi\nu_0 T\sum_{\omega_n}\left(\sqrt{\omega_n^2+\Delta^2}+\frac{\omega_n^2}{\sqrt{\omega_n^2+\Delta^2}}-2\left|\omega_n\right|\right).$$

Снова рассмотрим предельные случаи.

Approximation at $T\to 0$

$T\sum\limits_{\omega_n}\ldots \approx \int\ldots\frac{d\omega}{2\pi}$,

$$\sum_n f(n) \approx \int f(x)dx + \int e^{2\pi i x}f(x)dx + \int e^{-2\pi i x}f(x)dx + \ldots$$

$$f(x) := \sqrt{(2\pi Tx)^2+\Delta^2}+\frac{\Delta^2}{\sqrt{(2\pi Tx)^2+\Delta^2}} - 4\pi T|x|$$

Здесь неаналитичность $|x|$ не мешает использовать формулу Пуассона, поскольку для последнего слагаемого сумму в формуле Пуассона можно вычислить явно, не делая никаких приближений. (????)
(?????? a place for a calculation!!!!)
Вычислим сумму в (10.98) при $T\to 0$. Согласно формуле суммирования Пуассона,

$$\frac{\Omega_s-\Omega_n}{V} = -\pi\nu_0\sum_{k=-\infty}^{\infty}\int_{-\infty}^{\infty}\left(\sqrt{\omega^2+\Delta^2}+\frac{\omega_n^2}{\sqrt{\omega^2+\Delta^2}}-2|\omega|\right)ve^{ik\omega/T}\frac{d\omega}{2\pi}$$

Заметим, что первые два члена - плавные функции ω, поэтому интегралы от них экспоненциально малы. Поэтому нам достаточно удержать их лишь при $k = 0,\pm 1$. Что же касается последнего члена, то интеграл от него легко вычисляется и равен $-4T^2/k^2$. В результате выражение для термодинамического потенциала приводится к виду

$$\frac{\Omega_s-\Omega_n}{V} = -\nu_0\left[\int_0^{\infty}\left(\sqrt{\omega^2+\Delta^2}+\frac{\omega^2}{\sqrt{\omega^2+\Delta^2}}-2\omega\right)d\omega + \int_{-\infty}^{\infty}\left(\sqrt{\omega^2+\Delta^2}+\frac{\omega^2}{\sqrt{\omega^2+\Delta^2}}\right)\cos\frac{\omega}{T}d\omega - 2\sum_{k=1}^{\infty}\frac{T^2}{k^2}\right].$$

$$\int_0^{\infty}\left(\sqrt{\omega^2+\Delta^2}+\frac{\omega^2}{\sqrt{\omega^2+\Delta^2}}-2\omega\right)d\omega = \frac{\Delta^2}{2} \qquad\qquad \sum_{k=1}^{\infty}\frac{1}{k^2} = \frac{\pi^2}{6}$$

```
Integrate[(Sqrt[x^2 + d^2] + x^2/Sqrt[x^2 + d^2] - 2 x), {x, 0, Infinity}]
```

We are left with computation of $I := \int\limits_{-\infty}^{\infty} \left(\sqrt{\omega^2+\Delta^2} + \frac{\omega^2}{\sqrt{\omega^2+\Delta^2}}\right) \cos\frac{\omega}{T} d\omega$. Функция $\sqrt{\omega^2+\Delta^2}$ имеет скачок на разрезе от точки $i\Delta$ до бесконечности. В остальной же части верхней полуплоскости функция аналитична, поэтому контур интегрирования можно деформировать так, чтобы он огибал этот разрез (рис. 10.12)

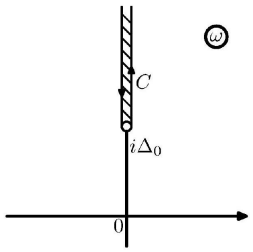


Рис. 10.12

$$\omega := i\Delta + iu,$$

(????? I don't know what happened???)

$$I = 2\int\limits_0^{\infty} \frac{\Delta^2 + 2u^2 + 4u\Delta}{\sqrt{2\Delta u + u^2}} e^{-(\Delta+u)/T} du$$

В этот интеграл дают вклад $u \approx T$, поэтому подынтегральное выражение можно разложить по u:

$$2\Delta^2 e^{-\Delta/T} \int\limits_0^{\infty} \left(1 + \frac{15}{4}\frac{u}{\Delta}\right) e^{-u/T} \frac{du}{\sqrt{2\Delta u}} = \sqrt{2\pi T\Delta^3} e^{-\Delta/T} \left(1 + \frac{15}{8}\frac{T}{\Delta}\right)$$

Finally:

$$\frac{\Omega_s - \Omega_n}{V} = -\frac{\nu_0\Delta^2}{2}\left(1 + 2\sqrt{\frac{2\pi T}{\Delta}} e^{-\Delta/T}\left(1 + \frac{15}{8}\frac{T}{\Delta}\right)\right) + \frac{\pi^2\nu_0 T^2}{3}.$$

Заметим, что последний член в этой формуле это взятый с обратным знаком термодинамический потенциал нормального металла. (???? why????)

Finally,

$$\Omega_s = -\frac{V\nu_0\Delta^2}{2}\left(1 + 2\sqrt{\frac{2\pi T}{\Delta}} e^{-\Delta/T}\left(1 + \frac{15}{8}\frac{T}{\Delta}\right)\right)$$

$\Delta\left(T \ll T_c\right) = \Delta_0\left(1 - \sqrt{\frac{2\pi T}{\Delta_0}} e^{-\Delta_0/T}\left(1 - \frac{T}{8\Delta_0}\right)\right)$,

$$\Omega_s = -\frac{\nu_0 V\Delta_0^2}{2}\left(1 + 4\sqrt{\frac{2\pi T^3}{\Delta_0^3}} e^{-\Delta_0/T}\right),$$

Обратим внимание на происходящее здесь сокращение главного температурнозависящего члена (??).

Then

(??? did we neglect other terms after second derivative wrt to T? why they are much less then one that survived???)

$$C_s = T\frac{\partial S_s}{\partial T} = -T\frac{\partial^2\Omega_s}{\partial T^2} = 2\nu_0 V\sqrt{\frac{2\pi\Delta_0^5}{T^3}} e^{-\Delta_0/T}.$$

Approximation at $T \to T_c$

Разложим $\frac{\Omega_s - \Omega_n}{V} = -\pi\nu_0 T\sum\limits_{\omega_n}\left(\sqrt{\omega_n^2+\Delta^2} + \frac{\omega_n^2}{\sqrt{\omega_n^2+\Delta^2}} - 2\left|\omega_n\right|\right)$ до четвертого порядка по Δ (член второго порядка обращается в нуль): (?? check!)

$$\frac{\Omega_s - \Omega_n}{V} = -\pi\nu_0\Delta^4 T\sum_{\omega_n}\frac{1}{\left|\omega_n\right|^3}$$

Сумма, как и в задаче 59, выражается через ζ-функцию: (?? check!)

$$\frac{\Omega_s - \Omega_n}{V} = -\frac{7\zeta(3)}{16\pi^2}\frac{\nu_0\Delta^4}{T_c^2}$$

Подставляя сюда Δ из (10.94), получим

$$\Omega_s - \Omega_n = -\frac{4\pi^2}{7\zeta(3)} V\nu_0 \left(T - T_c\right)^2$$

$$C_s - C_n = \frac{8\pi^2}{7\zeta(3)}\nu_0 T_c V,$$

$C_n := C_{\text{normal metal}} = \frac{2\pi^2}{3}\nu_0 VT$,

$$\frac{C_s - C_n}{C_n} = \frac{12}{7\zeta(3)}$$

Solution 2 (???)

Кстати, эту задачу можно решить, вычисляя термодинамический потенциал идеального газа квазичастиц со спектром (10.37). (?? попробую!)

ЛШ-61. The impact of the Coulomb interaction on superconductivity

Типично говорится, что влияние кулоновского взаимодействия на сверхпроводимость невелико благодаря сильному запаздыванию фононов. Рассмотрим вопрос об относительной важности электрон-электронного и электрон-фононного взаимодействий более подробно.

Оказывается удобным ввести упрощенную модель взаимодействия, в которой между электронами имеется мгновенное отталкивание и запаздывающее притяжение, причем как отталкивание, так и притяжение считаются точечными. При этом затравочная амплитуда рассеяния в куперовском канале имеет вид

$$\Gamma^0\left(i\varepsilon, i\varepsilon'\right) = \lambda v(i\varepsilon) v\left(i\varepsilon'\right) - \mu$$

где параметр μ характеризует величину отталкивания между электронами.

Найдите температуру, при которой амплитуда рассеяния в куперовском канале обращается в бесконечность. Покажите, что эффект отталкивания сводится к замене константы λ в выражении (10.30) для T_c на

$$\lambda_* = \lambda - \frac{\mu}{1 + \nu_0\mu \ln\left(\varepsilon_F/\omega_D\right)}.$$

Безразмерная величина кулоновского взаимодействия в металле есть $\nu_0\mu \approx e^2/\hbar v_F$ в пределе высокой электронной плотности и $\nu_0\mu \approx 1$ при обычных значениях плотности. Соответственно максимально возможная поправка к эффективной константе взаимодействия λ_*, согласно (10.49), имеет относительную малость $1/\ln\left(\varepsilon_F/\omega_D\right)$. Поэтому кулоновское взаимодействие в нормальном металле не может превратить притяжение в отталкивание и, следовательно, не подавляет сверхпроводимость.

Чтобы установить соответствие между моделью (10.48) и реальным кулоновским взаимодействием $V(\mathbf{q})$ в первом приближении достаточно подставить вместо μ среднее значение $V(\mathbf{q})$ в s-канале. Для случая экранированного кулоновского взаимодействия

$$V(\mathbf{q}) = \frac{4\pi e^2}{q^2 + \varkappa^2}; \quad \varkappa^2 = 8\pi\nu_0 e^2$$

(см. задачу 45) получаем следующее выражение:

$$\mu = \left\langle V_c\left(\mathbf{p} - \mathbf{p}'\right)\right\rangle = \frac{\pi e^2}{p_0^2}\ln\left(1 + \frac{4p_0^2}{\varkappa^2}\right),$$

где усреднение производится по положениям импульсов $\mathbf{p}$ и $\mathbf{p}'$ на ферми-поверхности.

Solution 61.

Рассмотрим уравнение (10.58) для куперовской амплитуды рассеяния, полученное в решении задачи 58. Если куперовская амплитуда $\Gamma^C(i\varepsilon, i\varepsilon')$ имеет полюс при $T \to T_c$, то в уравнении (10.58) можно пренебречь свободным членом:

$$\Gamma^C(i\varepsilon, i\varepsilon') = \pi\nu_0 T \sum_{\varepsilon''} \Gamma^0(i\varepsilon, i\varepsilon'')\,\Gamma^C(i\varepsilon'', i\varepsilon')\,/\,|\varepsilon''|$$

Зависимость от ε' в этом уравнении «сокращается». Поэтому можно считать, что решение факторизуется: (???? maybe it is vice versa, we want that ε' will not play role, thus we substitute: (??))

$$\Gamma^C(i\varepsilon, i\varepsilon') = \Phi(i\varepsilon)\Phi(i\varepsilon')$$

(Зависимость Γ^C от ε и ε' должна быть одинаковой ввиду симметрии куперовской лестницы.) Тогда функция $\Phi(\varepsilon)$ удовлетворяет уравнению

$$\Phi(i\varepsilon) = \pi\nu_0 T \sum_{\varepsilon'} \left(\Gamma^0(i\varepsilon, i\varepsilon')\,/\,|\varepsilon'|\right)\Phi(i\varepsilon')$$

Для Γ^0 из условия задачи это интегральное уравнение оказывается вырожденным и легко решается. Видно, что функция $\Phi(\varepsilon)$ содержит два члена: пропорциональный $v(i\varepsilon)$ и не зависящий от ε. Ищем решение в виде

$$\Phi(\varepsilon) = av(i\varepsilon) + b$$

Подставляя это выражение в (10.119) и приравнивая коэффициенты перед $v(i\varepsilon)$ и перед константой, получаем

$$a = \pi\lambda\nu_0 T \sum_{\varepsilon'} \left[av^2(i\varepsilon') + bv(i\varepsilon')\right]/\,|\varepsilon'|\,,$$
$$b = -\pi\mu\nu_0 T \sum_{\varepsilon'} [av(i\varepsilon) + b]/\,|\varepsilon'|\,.$$

На этот раз мы не будем заниматься точным вычислением сумм в этом выражении, а найдем их с логарифмической точностью, поскольку основной интерес будут представлять величины, стоящие перед логарифмами. Суммы, содержащие $v(i\varepsilon)$ и $v^2(i\varepsilon)$ следует обрезать сверху при $\varepsilon \approx \omega_D$. Сумму, не содержащую факторов запаздывания, мы обрежем сверху при $\varepsilon \approx \omega_p\,(\approx \varepsilon_F)$ - на плазменной частоте, которая играет в физике электрон-электронного взаимодействия роль, аналогичную ω_D для электрон-фононного взаимодействия. Таким образом, получаем

$$a = \nu_0\lambda \ln\frac{\omega_D}{T}(a+b)$$
$$b = -\mu\nu_0\left[a\ln\frac{\omega_D}{T} + b\left(\ln\frac{\omega_D}{T} + \ln\frac{\omega_p}{\omega_D}\right)\right].$$

Перенося во втором уравнении член с $\ln(\omega_p/\omega_D)$ в левую часть, можно переписать его в таком виде, что оно становится похоже на первое:

$$b = -\nu_0\mu_* \ln\frac{\omega_D}{T}(a+b); \quad \mu_* = \frac{\mu}{1+\nu_0\mu\ln(\omega_p/\omega_D)}$$

Мы ввели здесь эффективную куперовскую амплитуду μ_*, которая отличается от μ из-за запаздывания фононов.

Now, we sum similar equations for a and b and get the condition for their compatibility:

$$1 = (\lambda - \mu_*)\ln\frac{\omega_D}{T}$$

из которого находим температуру перехода:

$$T_c \approx \omega_D e^{-1/\lambda_*\nu_0}, \quad \lambda_* = \lambda - \mu_*$$

Таким образом, кулоновское взаимодействие действительно понижает температуру сверхпроводящего перехода, но не очень сильно. При $\nu_0\mu\ln\varepsilon_F/\omega_D \gg 1$ относительная поправка к λ мала как $1/\ln(\varepsilon_F/\omega_D)$.

(??? how many degrees is changed if one takes into account Coulomb???)

ЛШ-62. Response and susceptibility of electrons to the field

(??? write about задачу 51, what is going on there??? why the formalism is that we need to calculate the response for the susceptibility?? connection of χ and Q???)

При вычислении электромагнитного отклика сверхпроводника центральное место занимает рассмотренное в гл. 9 тождество Уорда

$$\Pi_{\alpha\beta}(\omega,\mathbf{k})|_{\mathbf{k}=0,\omega\to 0}=-\frac{ne^2}{m}\delta_{\alpha\beta},$$

где поляризационный оператор в частотно-импульсном представлении это $\Pi_{\alpha\beta}(\omega,\mathbf{k}) = \int \Pi_{\alpha\beta}(\omega,\mathbf{r})e^{-i\mathbf{kr}}d^3\mathbf{r}$, следующее из калибровочной инвариантности. Оно приводит к сокращению градиентного и диамагнитного вкладов в электрический ток, с которым мы уже сталкивались в задаче 51 при выводе формулы Друде. Прежде чем заниматься электродинамикой сверхпроводников, изучим тождество Уорда более подробно в случае нормального металла.

а) (Тождество Уорда в нормальном металле) Рассмотрим линейный отклик тока $\mathbf{j}$ в идеальном ферми-газе электронов на неоднородный статический векторный потенциал $\mathbf{A}$. В импульсном представлении линейное соотношение $\mathbf{j}$ и $\mathbf{A}$ записывается как

$$\mathbf{j}_\mathbf{k}=Q(\mathbf{k})\mathbf{A}_\mathbf{k}.$$

Калибровочная инвариантность требует, чтобы для ядра $Q(\mathbf{k})$ выполнялось свойство

$$Q(\mathbf{k})|_{k=0}=0.$$

Согласно тождеству Уорда, это равенство обеспечивается сокращением градиентной $\langle \mathbf{v}G\mathbf{v}G\rangle$ и диамагнитной частей тока $\mathbf{j}=-\frac{e}{mc}\left\langle\psi^+(\mathbf{r})\psi(\mathbf{r})\right\rangle\mathbf{A}(\mathbf{r})$ (см. задачу 51).

Проверьте это сокращение еще раз в более общем виде, не предполагая спектр электронов $\xi(\mathbf{p})$ квадратичным, а считая его произвольной функцией. Используйте соотношение $\mathbf{v}(\mathbf{p})=\nabla_\mathbf{p}\xi(\mathbf{p})$.

б) (Диамагнетизм Ландау.) С помощью тождества Уорда можно найти орбитальную магнитную восприимчивость χ_0 газа невзаимодействующих электронов. Согласно результату части а), разложение $Q(\mathbf{k})$ по $\mathbf{k}$ начинается с члена второй степени: $Q(\mathbf{k})=a\mathbf{k}^2+\mathrm{O}\left(\mathbf{k}^4\right)$.

Разложите петлю, показанную на рис. 10.10,

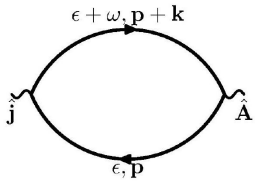


Рис. 10.10

по $\mathbf{k}$ и определите константу a. Как a связана с χ_0? Проверьте, что $\chi_0=-\frac{1}{3}\chi_{\text{пара}}$, где $\chi_{\text{пара}}$ - парамагнитная восприимчивость, найденная в задаче 23 (!?!???!?!?).

Если бы нас интересовало не сокращение $Q(0)$, а одно только вычисление χ_0, можно было бы действовать иначе. Рассмотрим оператор орбитального магнитного момента. $\mu=\frac{e}{mc}[\mathbf{r}\times\mathbf{p}]$ и найдем его среднее, используя функцию Грина в слабом магнитном поле: $G_H\left(E,\mathbf{r}_1,\mathbf{r}_2\right) = \exp\left(\frac{e}{\hbar c}\int\mathbf{A}\left(\mathbf{r}'\right)\mathbf{dr}'\right)G_0\left(E,\mathbf{r}_1,\mathbf{r}_2\right)$. (Интеграл берется по прямому пути, соединяющему $\mathbf{r}_1$ и $\mathbf{r}_2$.) Восприимчивость χ_0 получится, если выделить из G_H линейный по H член.

Solution 62 a.

Прежде чем вычислять $Q(0)$ для произвольного электронного спектра $\xi(\mathbf{p})$, уточним выражение для тока. Гамильтониан частиц со спектром $\xi(\mathbf{p})$ во внешнем магнитном поле $\mathbf{A}(\mathbf{r})$ есть

$$\widehat{\mathcal{H}}=\int\psi^+(\mathbf{r})\xi\left(\widehat{\mathbf{p}}-\frac{e}{c}\mathbf{A}\right)\psi(\mathbf{r})d^3\mathbf{r}$$

где $\widehat{\mathbf{p}}=-i\nabla_\mathbf{r}$. Ток, согласно общим принципам, получается варьированием гамильтониана по $\mathbf{A}$:

$$\widehat{\mathbf{j}}=e\psi^+(\mathbf{r})\nabla_\mathbf{p}\xi\left(\mathbf{p}-\frac{e}{c}\mathbf{A}\right)\psi(\mathbf{r})$$

(??? derive)

Выделим линейный по $\mathbf{A}$ член:

$$\widehat{\mathbf{j}} \approx e\psi^+(\mathbf{r})\nabla_{\mathbf{p}}\xi(\mathbf{p})\psi(\mathbf{r}) - \frac{e^2}{c}\psi^+(\mathbf{r})\nabla_{\mathbf{p}}\left[(\mathbf{A}\nabla_{\mathbf{p}})\,\xi(\mathbf{p})\right]\psi(\mathbf{r})$$

(??? i think, I was deriving it long time ago, I'll do it again)

При $\xi(\mathbf{p}) = \mathbf{p}^2/2m - E_F$ это выражение для тока переходит в обычную квантовомеханическую формулу. (??? check)

Проще всего вычисляется вклад в $Q(0)$ второго члена:

(???? why averaging is here???)

$$Q^{(2)}_{\alpha\beta}(\mathbf{k}) = -\frac{e^2}{c}\left\langle \psi^+ \frac{\partial^2\xi(\mathbf{p})}{\partial p_\alpha \partial p_\beta}\psi \right\rangle = -\frac{e^2}{c}\int \frac{\partial^2\xi(\mathbf{p})}{\partial p_\alpha \partial p_\beta} n_F(\xi(\mathbf{p}))\frac{2d^3p}{(2\pi)^3}$$

We are putting $\mathbf{A}$ outside the $\nabla_{\mathbf{p}}$, because it does not depend on coordinates. (??? right??)

Чтобы найти вклад первого члена, поступим стандартным образом:

$$\widehat{\mathcal{H}}_{\text{int}} \approx -\frac{1}{c}\int \widehat{\mathbf{j}}(\mathbf{r})\mathbf{A}(\mathbf{r})d^3r$$

Находя, как обычно, (??????????) поправку первого порядка к функции Грина и вычисляя с ее помощью $\langle\mathbf{j}\rangle$, получаем, что этот вклад дается петлей:

$$Q^{(1)}_{\alpha\beta}(i\Omega,\mathbf{k}) = -\frac{e^2}{c}\lim_{\tau\to+0} T\sum_{\omega_n}\int \frac{v_\alpha(\mathbf{p})v_\beta(\mathbf{p})}{i\omega_n - \xi(\mathbf{p})}\frac{e^{i\omega_n\tau}}{i\omega_n + i\Omega - \xi(\mathbf{p}+\mathbf{k})}\frac{2d^3p}{(2\pi)^3}$$

Мы ввели здесь множитель сходимости $e^{i\omega_n\tau}(\tau\to+0)$, который отвечает за правильный порядок ψ и ψ^+(ср. с задачей 35 (??????????????)).

$$\begin{aligned}
Q^{(1)}_{\alpha\beta}(\Omega=0,\mathbf{k}=0) &= -\frac{e^2}{c}\lim_{\tau\to+0} T\sum_{\omega_n} e^{i\omega_n\tau}\int \frac{v_\alpha(\mathbf{p})v_\beta(\mathbf{p})}{(i\omega_n - \xi(\mathbf{p}))^2}\frac{2d^3p}{(2\pi)^3} \overset{\mathbf{v}=\nabla_{\mathbf{p}}\xi(\mathbf{p})}{=} \\
&= -\frac{e^2}{c}\lim_{\tau\to+0} T\sum_{\omega_n} e^{i\omega_n\tau}\int v_\alpha(\mathbf{p})\nabla_\beta\frac{1}{i\omega_n - \xi(\mathbf{p})}\frac{2d^3p}{(2\pi)^3} \overset{\text{i b p}}{=} \\
&= +\frac{e^2}{c}\lim_{\tau\to+0} T\sum_{\omega_n} e^{i\omega_n\tau}\int \nabla_\beta v_\alpha(\mathbf{p})\frac{1}{i\omega_n - \xi(\mathbf{p})}\frac{2d^3p}{(2\pi)^3} = -Q^{(2)}_{\alpha\beta}
\end{aligned}$$

In the first transformation, we just noted that $\nabla_\beta\xi(\mathbf{p})/\left(i\omega_n - \xi(\mathbf{p})\right)^2 = \nabla_\beta\frac{1}{i\omega_n - \xi(\mathbf{p})}$.

(суммирование по мацубаровским частотам производится так же, как в выражении (7.59) в решении задачи 35). (!?!???! do the derivations?!? see problem 35!!????? I don't know, why formulas are the same?)

Итак, $Q_{\alpha\beta}(0) = 0$.

Solution 62 б. (????)

Чтобы найти диамагнитную восприимчивость ферми-газа χ_0, свяжем ее с константой a в разложении $Q(\mathbf{k}) = a\mathbf{k}^2 + \ldots$ По определению $Q(\mathbf{k})$,

$$\mathbf{j} = \widehat{Q}\mathbf{A} = -a\nabla^2\mathbf{A}$$

С другой стороны, ток связан с намагниченностью:

$$\mathbf{j} = c\,\mathrm{rot}\,\mathbf{M} = c\,\mathrm{rot}\,\chi_0\mathbf{B} = \chi_0 c\,\mathrm{rot}\,\mathrm{rot}\,\mathbf{A}.$$

Поскольку $\mathrm{div}\,\mathbf{A} = 0$, ток можно записать так:

$$\mathbf{j} = -\chi_0 c\nabla^2\mathbf{A}$$

Отсюда находим $\chi_0 = a/c$.

Теперь вычислим a. Предположим, что волновой вектор $\mathbf{k}$ направлен вдоль оси z, и найдем Q_{xx}:

$$Q_{xx} = -\lim_{\tau\to+0}\frac{e^2}{c}T\sum_{\omega_n} e^{i\omega_n\tau}\int \frac{v_x(\mathbf{p}+\mathbf{k})v_x(\mathbf{p})}{(i\omega_n - \xi_{\mathbf{p}+\mathbf{k}})\,(i\omega_n - \xi_{\mathbf{p}})}\frac{2d^3p}{(2\pi)^3}$$

В отличие от спиновой восприимчивости, орбитальная восприимчивость определяется не только окрестностью поверхности Ферми, но и всеми состояниями под ней, потому что квантование Ландау затрагивает все состояния с $E < E_F$, и конечная восприимчивость χ_0 возникает из-за отличия суммы квантованных энергий от интеграла по непрерывному спектру. Поэтому мы ограничимся случаем $\xi(\mathbf{p}) = \mathbf{p}^2/2m - E_F$. Разлагая $Q(k)$ по $k_z = k$, и имея в виду, что для квадратичного спектра $v_x(\mathbf{p}+\mathbf{k}) = v_x(\mathbf{p}) = p_x/m$, запишем

$$Q_{xx} = -\frac{e^2k^2}{c} T\sum_{\omega_n} e^{i\omega_n\tau} \int \frac{v_x^2}{i\omega_n - \xi_{\mathbf{p}}} \frac{\partial^2}{\partial p_z^2} \frac{1}{i\omega_n - \xi_{\mathbf{p}}} \frac{2d^3p}{(2\pi)^3}.$$

Проинтегрировав по частям, получим

$$\chi_0 = \frac{e^2}{c^2} T\sum_{\omega_n} e^{i\omega_n\tau} \int \frac{v_x^2 v_z^2}{\left(i\omega_n - \xi_{\mathbf{p}}\right)^4} \frac{2d^3p}{(2\pi)^3}.$$

Then, we average $\left\langle v_x^2 v_z^2 \right\rangle = v^4/15$ and get:

$$\chi_0 = \frac{e^2}{15c^2m^4} T\sum_{\omega_n} e^{i\omega_n\tau} \int \frac{p^4}{\left(i\omega_n - \xi_{\mathbf{p}}\right)^4} \frac{2d^3p}{(2\pi)^3}.$$

Here

$$\int_0^\infty \frac{p^6 dp}{\left(i\omega_n + E_F - p^2/2m\right)^4} \overset{\text{3x i b p}}{=} -\frac{5m^3}{2} \int_0^\infty \frac{dp}{i\omega_n + E_F - p^2/2m}$$

Proof. (I'll add formulas here, I did it long time ago) □

после чего суммирование по ω_n дает, как обычно, распределение Ферми (см. формулу (7.59) в з. 35) (???? do it???/):

$$\chi_0 = -\frac{e^2}{12\pi^2 mc^2} \int_0^\infty n_F\left(\xi_p\right) dp = -\frac{e^2 p_0}{12\pi^2 mc^2}$$

Используя выражение для спиновой восприимчивости, найденное в задаче 24 (??? comment, how we get it???)

$$\chi_{\text{para}} = 2\mu_B^2 \nu_0 = \frac{e^2}{4m^2c^2} \frac{mp_0}{\pi^2}$$

находим соотношение между орбитальной и спиновой восприимчивостью:

$$\chi_0 = -\frac{1}{3}\chi_{\text{para}}$$

Однако, это соотношение не универсально. Как видно из нашего вычисления, вклад в χ_0 дает весь спектр, а не только поверхность Ферми. Поэтому полученное соотношение между χ_0 и $\chi_{\text{пара}}$ верно лишь для квадратичного спектра. При более общем законе дисперсии $\xi(\mathbf{p})$ восприимчивость χ_0 по величине может оказаться даже больше, чем $\chi_{\text{пара}}$. В этом случае нормальный металл оказывается диамагнетиком.

ЛШ-63. London's equation from BCS

Найдите отклик тока в сверхпроводнике на статический векторный потенциал. Отличие от задачи 62 состоит в том, что теперь сокращения при $\mathbf{q} = 0$ нет. Положив $\mathbf{q} = 0$ в соотношении $\mathbf{j}_\mathbf{q} = Q(\mathbf{q})\mathbf{A}_\mathbf{q}$, получим так называемое уравнение Лондонов:

$$\mathbf{j}(\mathbf{r}) = -\frac{e^2}{mc} n_s \mathbf{A}(\mathbf{r}).$$

Величина n_s называется сверхтекучей плотностью. Как связаны n_s и Δ при $|T - T_c| \ll T_c$?

Физическая причина отсутствия сокращения вкладов в $Q(0)$ заключается в том, что калибровочная инвариантность в сверхпроводнике спонтанно нарушена. В нормальном металле сокращение $Q(0)$ обеспечивается тождеством Уорда (9.16), следующим из калибровочной инвариантности. А в сверхпроводнике калибровочная инвариантность отсутствует.

Определите глубину проникновения магнитного поля в сверхпроводник. Для этого с помощью уравнения Лондонов решите задачу о проникновении магнитного поля в объем сверхпроводника вблизи поверхности. Покажите, что магнитное поле затухает в глубину по экспоненциальному закону: $H(x) = H(0)\exp\left(-x/\delta_\Lambda\right), x > 0$, и найдите связь δ_Λ с n_S.

Покажите, что пренебрегать зависимостью ядра $Q(q)$ от q законно, если лондоновская глубина проникновения δ_Λ достаточно велика: $\delta_\Lambda \gg \xi_0 = \hbar v_F/\Delta_0$.

Solution 63.

(!! remind the formalism here!!!)
В этой задаче мы вычислим $Q(0)$ для сверхпроводника. При этом основное отличие от вычисления для нормального металла, проделанного в задаче 62, возникает из-за необходимости учесть как нормальные, так и аномальные средние.

Среднее от диамагнитного вклада в ток есть просто (?? why???)

$$Q^{(2)}(0) = -ne^2/mc$$

Градиентный вклад $Q^{(1)}_{\alpha\beta}(i\Omega, \mathbf{k})$ получается усреднением произведения токов и дается следующим выражением: (??? where does it originate????)

$$Q^{(1)}_{\alpha\beta}(i\Omega_s, \mathbf{k}) = \frac{1}{2c}\sum_{\sigma,\sigma'}\int_{-\beta}^{\beta} e^{i\Omega\tau}d\tau \int e^{i\mathbf{kr}}\left\langle \mathrm{T}_\tau \psi^+_\sigma(\mathbf{r},\tau)\hat{j}_\alpha\psi_\sigma(\mathbf{r},\tau)\psi^+_{\sigma'}(0,0)\widehat{j}_\beta\psi_{\sigma'}(0,0)\right\rangle d^3\mathbf{r}$$

где σ, σ' - спиновые индексы, а $\mathbf{j} = -i\frac{e}{m}\nabla_{\mathbf{r}}$.
For its computation, необходимо спарить ψ-операторы, учитывая как нормальные, так и аномальные средние. При этом теорема Вика по-прежнему справедлива, поскольку операторы ψ и ψ^+можно выразить линейным образом через операторы рождения и уничтожения квазичастиц сверхпроводника, для которых аномальные средние равны нулю. Таким образом,

$$\left\langle \mathrm{T}_\tau \psi^+_\sigma(\mathbf{r},\tau)\widehat{j}_\alpha\psi_\sigma(\mathbf{r},\tau)\psi^+_{\sigma'}(0,0)\widehat{j}_\beta\psi_{\sigma'}(0,0)\right\rangle = -\widehat{j}_\alpha G_{\sigma\sigma'}(\mathbf{r},\tau)\widehat{j}_\beta G_{\sigma'\sigma}(-\mathbf{r},-\tau) - \widehat{j}_\alpha F^+_{\sigma\sigma'}(\mathbf{r},\tau)\widehat{j}_\beta F_{\sigma'\sigma}(-\mathbf{r},-\tau)$$

Тогда $Q^{(1)}_{\alpha\beta}(i\Omega, \mathbf{k})$ принимает вид

$$Q^{(1)}_{\alpha\beta}(i\Omega, \mathbf{k}) = -\frac{1}{2c}\int_{-\beta}^{\beta} e^{i\Omega\tau}d\tau \int d^3r e^{i\mathbf{kr}}\left[2\widehat{j}_\alpha G(\mathbf{r},\tau)\widehat{j}_\beta G(-\mathbf{r},-\tau) + 2\widehat{j}_\alpha F(\mathbf{r},\tau)\widehat{j}_\beta F^*(-\mathbf{r},-\tau)\right]$$

Знаки петель, содержащих функции G и F, оказываются одинаковыми. Переписывая выражение (10.150) в импульсном представлении, получаем

$$Q^{(1)}_{\alpha\beta}(i\Omega, \mathbf{k}) = -\frac{Te^2}{c}\sum_{\omega_n}\int v_\alpha\left(\mathbf{p}-\frac{\mathbf{k}}{2}\right)v_\beta\left(\mathbf{p}+\frac{\mathbf{k}}{2}\right)\times$$
$$\times\left\{G\left(i\omega_n, \mathbf{p}-\frac{\mathbf{k}}{2}\right)G\left(i\omega_n+i\Omega, \mathbf{p}+\frac{\mathbf{k}}{2}\right) + F\left(i\omega_n, \mathbf{p}-\frac{\mathbf{k}}{2}\right)F^*\left(i\omega_n+i\Omega, \mathbf{p}+\frac{\mathbf{k}}{2}\right)\right\}\frac{2d^3p}{(2\pi)^3}.$$

thus

$$Q^{(1)}(\mathbf{k}=0) = \frac{1}{3}Q^{(1)}_{\alpha\alpha}(0) = -\frac{e^2T}{3m^2c}\sum_{\omega_n}\int \mathbf{p}^2\left(G^2(i\omega_n,\mathbf{p}) + |F(i\omega_n,\mathbf{p})|^2\right)\frac{2d^3p}{(2\pi)^3}.$$

Собирая вместе $Q^{(1)}$ и $Q^{(2)}$ и учитывая определение n_s, получим

$$n - n_s = -\frac{2T\nu_0 p_0^2}{3m}\sum_{\omega_n}\int_{-\infty}^{\infty}\frac{\Delta^2+\xi^2-\omega_n^2}{\left(\omega_n^2+\xi^2+\Delta^2\right)^2}d\xi$$

Here, при интегрировании по ω the integral обращается в нуль (??? why????), в то время как при интегрировании по ξ этого не происходит. Следовательно, оно не вполне корректно определено. Дело в том, что эта величина не «сидит» на поверхности Ферми, и для правильного учета состояний вдали от уровня Ферми следовало бы брать плотность состояний, зависящую от энергии. Однако сверхтекучая плотность, несомненно, определяется поверхностью Ферми, потому что только там и происходит перестройка электронных состояний. В глубине же фермиевского моря (т.е. при $\xi \sim E_F$) ничего не происходит.
(?????)
Поэтому можно поступить так: вычесть из этого выражения аналогичное с $\Delta = 0$, т. е. для нормального металла. Тогда вклад глубоких состояний выпадет. При этом, как мы знаем, для нормального металла $n_s = 0$. В результате

$$n_s = \frac{2\nu_0 p_0^2}{3m}T\sum_{\omega_n}\int_{-\infty}^{\infty}\left[\frac{\xi^2-\omega_n^2}{\left(\xi^2+\omega_n^2\right)^2} - \frac{\xi^2-\omega_n^2+\Delta^2}{\left(\xi^2+\omega_n^2+\Delta^2\right)^2}\right]d\xi.$$

Получившееся выражение можно интегрировать в любом порядке. Лучше всего сначала проинтегрировать по ξ. При этом оказываются полезными следующие соотношения:

$$\int\limits_{-\infty}^{\infty} \frac{dx}{\left(x^2+a^2\right)^2} = \frac{\pi}{2a^3}, \quad \int\limits_{-\infty}^{\infty} \frac{x^2 dx}{\left(x^2+a^2\right)^2} = \frac{\pi}{2a}$$

После интегрирования получаем ответ: (??? check???)

$$n_s = \frac{2\nu_0 p_0^2}{3m} T \sum_{\omega_n} \frac{\pi\Delta^2}{\left(\omega_n^2+\Delta^2\right)^{3/2}}.$$

Рассмотрим различные предельные случаи.

а) Case $T \to 0$.

Заменим сумму интегралом:

$$n_s = \frac{2\nu_0 p_0^2}{3m} \frac{\pi\Delta^2}{2\pi} \int\limits_{-\infty}^{\infty} \frac{d\omega}{\left(\omega^2+\Delta^2\right)^{3/2}} = \frac{2\nu_0 p_0^2}{3m} = \frac{p_0^3}{3\pi^2} = n.$$

Видим, что при $T = 0$ сверхтекучая плотность равна полной, как и должно быть в трансляционно-инвариантной системе.

б) Case $T \to T_c$.

В этом случае достаточно пренебречь Δ в знаменателе. Тогда сумма выражается через ζ-функцию (см. задачу 59), что дает

$$\frac{n_s}{n} = \frac{7\Delta^2}{4\pi^2 T_c^2} = 2\left(1 - \frac{T}{T_c}\right).$$

Таким образом, при $T \to T_c$ сверхтекучая плотность уменьшается до нуля.
Теперь свяжем n_s с глубиной проникновения. Запишем закон Ампера:

$$\operatorname{rot} \mathbf{H} = \frac{4\pi}{c}\mathbf{j} = -\frac{4\pi n_s e^2}{mc^2}\mathbf{A}$$

Поскольку $\mathbf{H} = \operatorname{rot} \mathbf{A}$, имеем

$$\nabla^2 \mathbf{A} = \frac{4\pi n_s e^2}{mc^2}\mathbf{A}$$

Пусть граница образца перпендикулярна оси x, а магнитное поле параллельно оси z. Тогда

$$A_y(x) = A_y(0) e^{-x/\delta_\Lambda}, \qquad \delta_\Lambda^2 := \frac{mc^2}{4\pi n_s e^2}$$

Отсюда получаем, что магнитное поле

$$H_z = -\frac{\partial A_y}{\partial x} = \frac{A_y(0)}{\delta_\Lambda} e^{-x/\delta_\Lambda} = H_z(0) e^{-x/\delta_\Lambda}$$

экспоненциально затухает в глубь сверхпроводника, причем глубина проникновения равна δ_Λ.
В нашем расчете мы пренебрегали дисперсией $Q(k)$. Выясним, при каких условиях это законно, или, иными словами, каков масштаб пространственной дисперсии в сверхпроводнике. Чтобы определить этот масштаб, следует сравнить kv (это и есть величина, которой мы пренебрегли) со всеми остальными величинами в знаменателях функций G и F в (10.151). Сравнивая ξ с Δ, получаем характерный волновой вектор $k_0 \approx \xi^{-1}(T) \approx \Delta(T)/(\hbar v_F)$. Заметим, однако, что при $T \to T_c \Delta(T) \to 0$ и основную роль в знаменателе играет $\omega_{n=0} = \pi T_c \approx \Delta_0$. Поэтому на самом деле характерный волновой вектор при любых температурах есть $k_0 \approx \xi_0^{-1} \approx \Delta_0/(\hbar v_F)$. Для того чтобы наш расчет был применим, должно быть $\delta_\Lambda \gg \xi_0$. В этом случае сверхпроводник называют лондоновским. Противоположный предельный случай называется пиппардовским.
Оказывается, что в сверхпроводниках есть два пространственных масштаба. Один из них, $\xi(T)$, - это масштаб корреляций параметра порядка Δ. Другой, ξ_0, это размер куперовской пары. При $T \to T_c$ различие между ними становится весьма ощутимым, поскольку при приближении T к T_c корреляционная длина $\xi(T)$ расходится, в то время как размер пары ξ_0 (он же масштаб пространственной дисперсии) при этом остается конечным.

Solution через матричную форму

Покажем, как производить подобные расчеты с помощью матричной функции Грина

$$\widehat{G} = \begin{bmatrix} G_{\uparrow\uparrow} & F_{\uparrow\downarrow} \\ F_{\downarrow\uparrow} & G_{\downarrow\downarrow} \end{bmatrix}$$

Она удовлетворяет такому уравнению:

$$(i\omega - \xi(\mathbf{p})\tau_z - \Delta_1\tau_x - \Delta_2\tau_y)\,\widehat{G} = \widehat{1}$$

($\Delta = \Delta_1 + i\Delta_2$).

$$\widehat{\mathbf{j}} = c\frac{\delta\widehat{G}^{-1}}{\delta\mathbf{A}} = e\mathbf{v}(\mathbf{p})\hat{1} - \frac{e^2}{mc}\mathbf{A}\tau_z, \qquad \widehat{G} := -\frac{1}{\omega_n^2 + \xi^2 + \Delta^2}\begin{pmatrix} i\omega_n + \xi & \Delta \\ \Delta^* & i\omega_n - \xi \end{pmatrix};$$

Вычисляя

$$\operatorname{Tr}\left(\widehat{j}_\alpha\hat{G}\,(i\omega_n, \mathbf{p})\,\hat{j}_\beta\hat{G}\,(i\omega_n, \mathbf{p})\right) = \frac{e^2 v_\alpha(\mathbf{p})v_\beta(\mathbf{p})}{\left(\omega_n^2 + \xi^2 + \Delta^2\right)^2}\operatorname{Tr}\left(\left(i\omega_n + \xi\tau_z + \Delta\tau_x\right)\left(i\omega_n + \xi\tau_z + \Delta\tau_x\right)\right) =$$
$$= 2e^2 v_\alpha(\mathbf{p})v_\beta(\mathbf{p})\frac{\Delta^2 + \xi^2 - \omega_n^2}{\left(\omega_n^2 + \xi^2 + \Delta^2\right)^2},$$

получим то же выражение, что и ранее (см. (10.156)).

14.2.8 Dirty Superconductors: Basic Problems 1

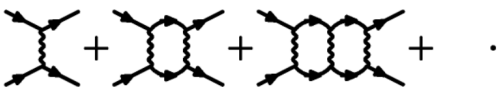
(I'll write here many problems about "how to describe this or that model")

ЛШ-64. Disorder doesn't change T_c

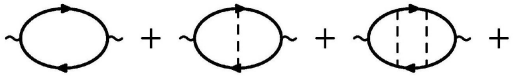
(?? remind the background!)

Обычно говорят, что куперовские пары образованы электронами с противоположными импульсами и спинами. Оказывается, беспорядок не разрушает куперовские пары, хоть импульс и становится плохим квантовым числом. Качественно это можно пояснить так. В присутствии примесей электроны двигаются по ломаным, от одной примеси к другой. За каждым электроном вдоль линии его движения остается деформация решетки, представляющая собой шлейф из виртуальных фононов, рассасывающийся за время порядка ω_D^{-1}. Этот «ароматический след» притягивает другие электроны, причем эффект притяжения максимален для электрона, движущегося в точности по той же траектории, но в обратном направлении. Такие состояния есть при любой степени беспорядка, поскольку увеличение концентрации примесей лишь делает траектории более изломанными, но не выделяет определенного направления движения на каждой из них (в отличие, скажем, от траекторий в магнитном поле). Из этого рассуждения видно, что чисто потенциальное рассеяние на примесях, оставляющее систему инвариантной по отношению к обращению времени, не подавляет сверхпроводимость. А магнитное поле, например, подавляет.

Рассмотрите куперовскую восприимчивость χ_C в присутствии примесей. Чтобы получить χ_C, усредните по беспорядку диаграммы куперовской лестницы



При этом каждый блок куперовской лестницы превращается в диффузионную лестницу, подобную



Покажите, что наличие примесей не меняет $\chi_C(\mathbf{k} = 0)$ и, следовательно, не приводит к изменению T_c.

Solution 64.

Для того чтобы изучить влияние примесей на T_c, рассмотрим диаграммы, образующие один блок куперовской лестницы, и усредним их по беспорядку:

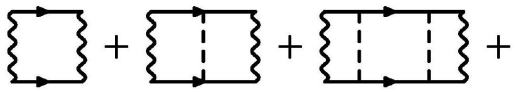
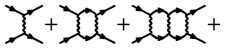
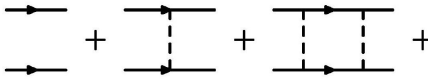


Рис. 10.13

Они имеют ту же структуру, что и диаграммы  . Отличие состоит в том, что куперовская петля теперь содержит примесную лестницу, описывающую рассеяние куперовской пары на примесях. Поэтому

$$\Gamma^C = -\frac{\lambda}{1+\lambda\Pi_c}, \qquad \Pi_c =$$



По сути дела, такая сумма уже была вычислена нами в задаче 54. Напомним, что усредненная по беспорядку функция Грина в грязном металле равна

$$G\left(i\omega_n, \mathbf{p}\right) = \frac{1}{i\omega_n - \xi_p + \frac{1}{2\tau}\operatorname{sign}\omega_n}.$$

Каждая ступенька куперовской лестницы, состоящая из двух функций Грина, взятая при $\Omega = 0, \mathbf{s} = 0$, есть

$$B_c\left(i\omega_n\right) = \int G\left(i\omega_n, \mathbf{p}\right) G\left(-i\omega_n, -\mathbf{p}\right) \frac{d^3p}{(2\pi)^3} = \int\limits_{-\infty}^{\infty} \frac{\nu_0 d\xi}{\left(\omega_n + \frac{1}{2\tau}\operatorname{sign}\omega_n\right)^2 + \xi^2} = \frac{2\pi\nu_0\tau}{1+2\tau\left|\omega_n\right|}$$

Суммировать B_c по ω_n не следует, поскольку столкновения с примесями - упругие. (????)

Теперь вычислим всю примесную лестницу. При этом полезно вспомнить, что примесная штриховая линия равна $nu_0^2 = \left(2\pi\nu_0\tau\right)^{-1}$ (см. гл. 9). (???????)
Суммируя геометрическую прогрессию, получаем

$$L\left(i\omega_n\right) = B_c\left(i\omega_n\right) + \frac{1}{2\pi\nu_0\tau}B_c^2\left(i\omega_n\right) + \ldots = \frac{B_c\left(i\omega_n\right)}{1 - B_c\left(i\omega_n\right)/\left(2\pi\nu_0\tau\right)} = \frac{\pi\nu_0}{\left|\omega_n\right|}$$

Как мы видим, τ полностью исчезло из этой формулы. Отметим, что выпадение τ из ответа формально обязано тому же сокращению, которое обеспечивает сохранение числа частиц при вычислении коррелятора плотность-плотность в ферми газе с примесями:

$$\langle n(\omega, \mathbf{q}) n(-\omega, -\mathbf{q})\rangle_{\mathbf{q}=0} = \pi\nu_0/(i\omega)$$

(см. задачу 52). Находим куперовскую петлю:

$$\Pi_c = -T\sum_{\omega_n} L\left(i\omega_n\right) = -2\pi\nu_0 T \sum_{\omega_n > 0} \frac{1}{\left|\omega_n\right|} = -\nu_0 \ln\frac{2\gamma\omega_D}{\pi T}$$

Поэтому

$$T_c = \frac{2\gamma}{\pi}\omega_D e^{-1/\lambda\nu_0}$$

как и в отсутствие примесей.

ЛШ-65*. London length in alloy

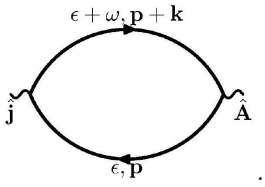
(?? remind the background!)
Рассеяние на примесях уменьшает сверхтекучую плотность n_s в формуле Лондонов (10.52). Чтобы найти зависимость n_s от концентрации примесей, определим ядро $Q(0)$ с учетом беспорядка. Процедура усреднения по беспорядку аналогична рассмотренной в задачах 50 и 51 (!?!?!?!??), с той только разницей, что вместо функций Грина свободных фермионов в сверхпроводнике надо использовать нормальную и аномальную функции (10.35) и (10.36).

a) Усредните по примесям матричную функцию Грина $\widehat{G}$. Используйте введенную в гл. 9 (???) модель δ-функционных примесей. Получите формулу

$$\langle\widehat{G}(i\omega, p)\rangle = \left(\widehat{G}_0(i\omega, \mathbf{p})^{-1} + \frac{i\omega - \Delta\tau_x}{2\tau\left(\omega^2 + \Delta^2\right)^{1/2}}\right)^{-1}$$

Не теряя общности, вычисления можно упростить, считая $\Delta^* = \Delta$. При этом в матричной записи $\widehat{G}_0^{-1}(i\omega, \mathbf{p}) = i\omega - \tau_z\xi(\mathbf{p}) - \Delta\tau_x$.

b) Усредните по беспорядку диаграмму для $Q(\mathbf{k})$, имеющую вид



Вычислив $\mathrm{Tr}(\widehat{j}\widehat{G}\widehat{j}\widehat{G})$ получите $Q(\mathbf{k})$, после чего по $Q(\mathbf{k}=0)$ определите сверхтекучую плотность.

Solution 65 a.

(!?!??!? все полностью опирается на задачи 50, 51)

Начнем с усреднения функций Грина сверхпроводника по примесям. Для этого мы вычислим матричную собственно-энергетическую часть



Рис. 10.15

При этом матричное выражение для примесной линии таково:

$$nu_0^2 \begin{pmatrix} 1 & 0 \\ 0 & 1 \end{pmatrix} = \frac{1}{2\pi\nu_0\tau}\widehat{1}$$

(примеси одинаково хорошо рассеивают как электроны, бегущие вперед, так и назад, и при этом не переводят одно из спаривающихся состояний в другое, поскольку у них разный спин). Вычисляем собственно-энергетическую часть в первом порядке по концентрации примесей, следуя методу задачи 50:

$$\widehat{\Sigma}\left(i\omega_n\right) = \frac{1}{2\pi\nu_0\tau}\int \widehat{G}\left(i\omega_n, \mathbf{p}\right)\frac{d^3p}{(2\pi)^3} = -\frac{1}{2\pi\nu_0\tau}\int \frac{i\omega_n\widehat{1} + \xi_{\mathbf{p}}\widehat{\tau}_z - \Delta\widehat{\tau}_x}{\omega_n^2 + \Delta^2 + \xi_{\mathbf{p}}^2}\frac{d^3p}{(2\pi)^3}$$

Интегрируя по ξ, (!!! do it!!) получаем

$$\widehat{\Sigma}\left(i\omega_n\right) = -\frac{1}{2\tau}\frac{i\omega_n\widehat{1} + \Delta\widehat{\tau}_x}{\sqrt{\omega_n^2+\Delta^2}}$$

Таким образом

$$\widehat{G}^{-1} = \widehat{G}_0^{-1} - \widehat{\Sigma} = i\tilde{\omega}_n\widehat{1} - \xi\widehat{\tau}_z - \tilde{\Delta}\widehat{\tau}_x,$$

$$\tilde{\omega}_n := \omega_n\left(1 + \frac{1}{2\tau\sqrt{\omega_n^2+\Delta^2}}\right), \qquad \tilde{\Delta} := \Delta\left(1 + \frac{1}{2\tau\sqrt{\omega_n^2+\Delta^2}}\right)$$

Обратим внимание, что

$$\tilde{\omega}_n/\tilde{\Delta} = \omega_n/\Delta$$

Как мы убедимся в дальнейшем, это свойство очень важно.

При вычислении $\widehat{\Sigma}$ мы использовали затравочные функции Грина G и F. Что произойдет, если теперь подставить исправленные функции Грина в выражение для $\widehat{\Sigma}$? Оказывается, $\widehat{\Sigma}$ при этом не изменится. Это легко видно из (10.178), поскольку при изменении в этом выражении ω_n и Δ в одно и то же число раз величина $\widehat{\Sigma}$ не меняется. Поэтому полученный нами ответ автоматически оказался решением интегрального уравнения для $\widehat{\Sigma}$, точно так же, как и для нормального металла (см. задачу 50).

В принципе, щель в грязном сверхпроводнике следует определять заново, решая уравнение самосогласования $\Delta_{\alpha\beta} = \lambda\int F_{\alpha\beta}(\varepsilon, \mathbf{p})\frac{d\varepsilon d^3p}{(2\pi)^4}$, принимающее вид

$$\Delta = \lambda T\sum_{\omega_n}\int_{-\infty}^{\infty}\frac{\nu_0 d\xi\tilde{\Delta}}{\tilde{\omega}_n^2 + \tilde{\Delta}^2 + \xi^2}$$

$$\Delta = \pi\lambda\nu_0 T\sum_{\omega_n}\frac{\tilde{\Delta}}{\sqrt{\tilde{\omega}_n^2+\tilde{\Delta}^2}} = \pi\lambda\nu_0 T\sum_{\omega_n}\frac{\Delta}{\sqrt{\omega_n^2+\Delta^2}}$$

не содержащему концентрации примесей. (Во втором равенстве мы использовали (10.181).) Таким образом, примеси не влияют не только на T_c, но и на термодинамику сверхпроводника вообще. Так происходит потому, что для термодинамических свойств существенна лишь полная плотность состояний (или, грубо говоря, сколько длин волн укладывается на каждой квазичастичной траектории) и совершенно не важно, как эти состояния устроены (т. е. по каким конкретно траекториям движутся квазичастицы, по прямым, или по ломаным, рассеиваясь на примесях).

Solution 65 б.

Теперь рассмотрим отклик сверхтекучего тока на внешнее магнитное поле. В отличие от T_c, эта величина гораздо более чувствительна к форме траекторий и сильно изменяется даже при малых концентрациях примесей. (Достаточно, чтобы длина свободного пробега стала меньше, чем размер куперовской пары ξ_0). Определим сверхтекучую плотность. Как и в задаче 51, для вычисления отклика достаточно провести вычисления с усредненными по примесям функциями Грина, потому что диаграмма с примесной линией, соединяющей разные функции Грина, равна нулю (из-за того, что вершина взаимодействия с электромагнитным полем векторная).

Усредненные же функции Грина отличаются от затравочных лишь заменой $\omega_n \to \tilde{\omega}_n, \Delta \to \tilde{\Delta}$. Поэтому можно сразу написать формулу для n_s по аналогии с задачей 50:

$$\frac{n-n_s}{n} = T\sum_{\omega_n} \int\limits_{-\infty}^{\infty} \frac{\xi^2 + \tilde{\Delta} - \tilde{\omega}_n^2}{\left(\xi^2 + \tilde{\Delta} + \tilde{\omega}_n^2\right)^2} d\xi$$

Исключим вклад ферми-моря, вычтя из этого выражения его значение при $\Delta = 0, \tau = \infty$, и проинтегрируем по ξ:

$$\frac{n_s}{n} = \pi T \sum_{\omega_n} \frac{\tilde{\Delta}^2}{\left(\tilde{\omega}^2 + \tilde{\Delta}^2\right)^{3/2}}$$

$$\frac{n_s}{n} = \pi T \sum_{\omega_n} \frac{\Delta^2}{\left(\omega_n^2 + \Delta^2\right)^{3/2}\left(1 + \frac{1}{2\tau\sqrt{\omega_n^2+\Delta^2}}\right)}.$$

$\tau\Delta_0 \gg 1 \quad \Rightarrow \quad$ результат задачи 63 (??),
$\tau\Delta_0 \ll 1 \quad \Rightarrow$

$$\frac{n_s}{n} = 2\pi\tau T \sum_{\omega_n} \frac{\Delta^2}{\left(\omega_n^2 + \Delta^2\right)^2} = \pi\tau\Delta \,\mathrm{th}\, \frac{\Delta}{2T}.$$

Интересно, что в грязном сверхпроводнике даже при $T \to 0$ сверхтекучая плотность много меньше полной:

$$\frac{n_s(T\to 0)}{n} = \pi\tau\Delta_0 \ll 1$$

Это связано с нарушением трансляционной инвариантности и «торможением» электронов примесями. Подставляя n_s в формулу для глубины проникновения δ_Λ (???), получаем

$$\delta_\Lambda = \frac{1}{2\pi}\sqrt{mc^2/\left[e^2\Delta\tau \,\mathrm{th}(\Delta/2T)\right]}$$

ЛШ-66*. Influence of magnetic impurities on superconductivity

(?? remind the background!)
Пусть кроме обычных примесей имеются также и магнитные:

$$H_{int} = \sum_{\mathbf{r}_a} J\psi^+(\mathbf{r}_a)\ \widehat{\sigma}^k\ \widehat{S}_a^k\ \psi(\mathbf{r}_a).$$

Здесь $\widehat{S}_a^k$ - оператор спина a-й примеси. Спины примесей будем считать некоррелированными. Такие примеси нарушают симметрию по отношению к обращению времени и поэтому легко подавляют сверхпроводимость. Найдите T_c как функцию концентрации примесей $n_{\text{маг.}}$ Покажите, что сверхпроводимость подавляется при относительно малой концентрации $n_{\text{маг}} \approx T_c/(v_F\sigma)$, где σ - сечение рассеяния на магнитной примеси.

Solution 66.

(!?!??!? суть решения напишу обязательно тут!!!)
Вначале найдем усредненную по парамагнитным примесям функцию Грина. Для того чтобы ее вычислить, мы используем модифицированную крестовую технику. Введем четырехкомпонентные функции Грина

$$\widehat{G} = -\begin{pmatrix} \langle \mathrm{T}_\tau \psi_\alpha^+(\mathbf{r},\tau)\psi_\beta(0,0)\rangle & \langle \mathrm{T}_\tau \psi_\alpha(\mathbf{r},\tau)\psi_\beta(0,0)\rangle \\ \left\langle \mathrm{T}_\tau \psi_\alpha^+(\mathbf{r},\tau)\psi_\beta^+(0,0)\right\rangle & \left\langle \mathrm{T}_\tau \psi_\alpha(\mathbf{r},\tau)\widehat{\psi}_\beta^+(0,0)\right\rangle \end{pmatrix}$$

(α и β - спиновые индексы). При этом функция Грина в отсутствие примесей равна

$$\widehat{G}_0 = -\frac{1}{\omega_n^2+\xi^2+\Delta^2}\begin{pmatrix} (i\omega_n+\xi)\,\delta_{\alpha\beta} & -\Delta_{\alpha\beta} \\ -\Delta_{\alpha\beta}^+ & (i\omega_n-\xi)\,\delta_{\alpha\beta} \end{pmatrix}$$

а $\Delta_{\alpha\beta} = i\Delta\sigma^y_{\alpha\beta}$ ($\sigma^i_{\alpha\beta}$– спиновые матрицы Паули). Как и в предыдущей задаче, найдем собственно-энергетическую часть из диаграммы на рис. 10.16:

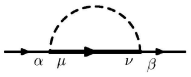


Рис. 10.16
В случае парамагнитных примесей штриховая линия имеет нетривиальную спиновую структуру. Ее можно найти, вычислив коррелятор флуктуаций примесного потенциала:

$$\left\langle \sum_a J\delta\left(\mathbf{r}-\mathbf{r}_a\right)\sigma^i_{\alpha\beta}S_i^a \sum_b J\delta\left(\mathbf{r}'-\mathbf{r}_b\right)\sigma^k_{\mu\nu}S_k^b \right\rangle = n_{\mathrm{mag}}J^2\delta\left(\mathbf{r}-\mathbf{r}'\right)\left\langle S^iS^k\right\rangle\sigma^i_{\alpha\beta}\sigma^k_{\mu\nu} =$$
$$= \frac{S(S+1)}{3}n_{\mathrm{mag}}J^2\delta\left(\mathbf{r}-\mathbf{r}'\right)\sigma^i_{\alpha\beta}\sigma^i_{\mu\nu}$$

Стоящее здесь скалярное произведение матриц Паули можно преобразовать, используя тождество Фирца: $\sigma^i_{\alpha\beta}\sigma^i_{\mu\nu} = 2\delta_{\alpha\nu}\delta_{\beta\mu} - \delta_{\alpha\beta}\delta_{\mu\nu}$. Получаем:

$$\widehat{\Sigma}_{\alpha\beta}\left(i\omega_n\right) = -\frac{n_{\mathrm{mag}}}{3}J^2S(S+1)\left(2\delta_{\alpha\beta}\delta_{\mu\nu}-\delta_{\alpha\mu}\delta_{\beta\nu}\right)\int\limits_{-\infty}^{\infty}\widehat{G}_{\mu\nu}\left(i\omega_n,\xi\right)\nu_0 d\xi$$

Подставим вначале в этот интеграл $\widehat{G}_0$. (?? why??)
Интегрирование производится довольно просто (?? do it!!), и мы получаем

$$\widehat{\Sigma}_{\alpha\beta}\left(i\omega_n\right) = -\frac{1}{2\pi\tau_s}\frac{i\omega_n\widehat{1}-2\delta_{\alpha\beta}\Delta_{\mu\nu}\delta_{\mu\nu}\widehat{\tau}_x+\Delta_{\alpha\beta}\widehat{\tau}_x}{\sqrt{\omega_n^2+\Delta^2}}$$

где $\tau_s = \frac{3}{\pi\nu_0 n_{\mathrm{mag}}J^2S(S+1)}$ - время релаксации спина на примесях. Поскольку $\Delta_{\mu\nu}\delta_{\mu\nu}=0$, то мы получаем таким образом, что $\widehat{G}^{-1} = \widehat{G}_0^{-1} - \widehat{\Sigma}$ отличается от $\widehat{G}_0$ заменой ω_n и Δ на

$$\tilde{\omega}_n = \omega_n\left(1+\frac{1}{2\tau_s\sqrt{\omega_n^2+\Delta^2}}\right), \qquad \tilde{\Delta} = \Delta\left(1-\frac{1}{2\tau_s\sqrt{\omega_n^2+\Delta^2}}\right)$$

Однако заметим, что теперь, в отличие от задачи 64,

$$\tilde{\omega}/\tilde{\Delta} \neq \omega/\Delta.$$

Поэтому если теперь подставить $\widehat{G}$ в (10.194), то получится другое значение $\widehat{\Sigma}$. Попробуем решить задачу самосогласованно, подставляя в (10.194) $\widehat{G}$ с неизвестными $\tilde{\omega}$ и $\tilde{\Delta}$. Тогда

$$\widehat{\Sigma}_{\alpha\beta}\left(i\omega_n\right) = -\frac{1}{2\pi\tau_s}\frac{i\tilde{\omega}_n\widehat{1}-\tilde{\Delta}_{\alpha\beta}\widehat{\tau}_x}{\sqrt{\tilde{\omega}_n^2+\tilde{\Delta}^2}}.$$

Уравнение Дайсона теперь приводит к условию самосогласования, определяющему $\tilde{\omega}$ и $\tilde{\Delta}$:

$$\tilde{\omega} = \omega + \frac{\tilde{\omega}}{2\tau_s\sqrt{\tilde{\omega}^2+\tilde{\Delta}^2}}, \qquad \tilde{\Delta} = \Delta - \frac{\tilde{\Delta}}{2\tau_s\sqrt{\tilde{\omega}^2+\tilde{\Delta}^2}}.$$

Теперь запишем уравнение Горькова, определяющее щель:

$$\Delta = \lambda T\sum_{\omega_n}\int\limits_{-\infty}^{\infty}\nu_0 d\xi F\left(i\omega_n,\xi\right) = \lambda T\sum_{\omega_n}\int\limits_{-\infty}^{\infty}\frac{\tilde{\Delta}\nu_0 d\xi}{\tilde{\omega}_n^2+\tilde{\Delta}^2+\xi^2} = \pi\lambda\nu_0 T\sum_{\omega_n}\frac{\tilde{\Delta}}{\sqrt{\tilde{\omega}_n{}^2+\tilde{\Delta}^2}}.$$

Из-за того, что $\tilde{\omega}/\tilde{\Delta} \neq \omega/\Delta$, это уравнение отличается от уравнения для чистого сверхпроводника.

Выведем отсюда уравнение, определяющее температуру перехода сверхпроводника с парамагнитными примесями T_c^*. Полагая $\Delta \to 0$, решим полученные уравнения $\tilde{\omega} = \omega + \frac{\tilde{\omega}}{2\tau_s\sqrt{\tilde{\omega}^2+\tilde{\Delta}^2}}$, и $\tilde{\Delta} = \Delta - \frac{\tilde{\Delta}}{2\tau_s\sqrt{\tilde{\omega}^2+\tilde{\Delta}^2}}$:

$$\tilde{\omega} = \omega + \frac{1}{2\tau_s}\operatorname{sign}\omega, \quad \tilde{\Delta}\left(1+\frac{1}{2\tau_s|\tilde{\omega}|}\right) = \Delta.$$

Тогда уравнение на T_c^* имеет вид:

$$1 = 2\pi\lambda\nu_0 T_c^*\sum_{\omega_n>0}\frac{\tilde{\Delta}}{\Delta\tilde{\omega}_n} = 2\pi\lambda\nu_0 T_c^*\sum_{\omega_n>0}\frac{1}{\tilde{\omega}_n+1/2\tau_s} = 2\pi\lambda\nu_0 T_c^*\sum_{\omega_n>0}\frac{1}{\omega_n+1/\tau_s}.$$

Остановимся на физическом смысле этой формулы. При рассеянии на парамагнитной примеси спин электрона может перевернуться, и τ_s есть среднее время между двумя переворотами спина, т.е. время жизни куперовской пары. Знаменатель в (10.204) описывает развал куперовских пар из-за рассеяния на магнитных примесях и уменьшение эффективного времени взаимодействия.

Если τ_s велико по сравнению с h/T_c^*, то парамагнитные примеси лишь слегка сдвигают T_c. Но при $\tau_s \approx \hbar/T_c^*$ сверхпроводимость полностью подавляется. Найдем критическое τ_s^*, полагая $T_c^* = 0$ и заменяя сумму на интеграл:

$$\frac{1}{\lambda\nu_0} = \ln\frac{2\gamma\omega_D}{\pi T_c} = \int\limits_0^{\omega_D}\frac{d\omega}{\omega+1/\tau_s^*} = \ln\left(\omega_D\tau_s^*\right)$$

откуда

$$\tau_s^* = 2\gamma\hbar/\left(\pi T_c\right)$$

Таким образом, парамагнитные примеси даже в малых концентрациях могут существенно повлиять на свойства сверхпроводника и даже полностью подавить сверхпроводимость. При этом оказывается, что в определенном интервале по концентрации примесей существует режим так называемой бесщелевой сверхпроводимости, в котором сопротивление металла равно нулю, но энергетическая щель отсутствует. Так получается из-за того, что примеси меняют энергию связи электронов в паре по-разному в разных частях образца. (???? add it to later parts of theory)

14.2.9 Dirty Superconductors: Basic Problems 2

ЛШ-67*. Верхнее критическое поле в грязном сверхпроводнике

Сверхпроводимость можно подавить магнитным полем, поскольку оно нарушает симметрию по отношению к обращению времени. Как именно происходит это подавление, зависит от характеристик сверхпроводника. Рассмотрим грязный сверхпроводник, в котором $l \ll \xi_0$, и, начиная с сильного поля H, в котором сверхпроводимость подавлена, будем постепенно уменьшать величину H и определим пороговое значение H, при котором сверхпроводимость восстанавливается. Оказывается, для Этого нужно изучить устойчивость системы по отношению к малым неоднородньим флуктуациям $\Delta(\mathbf{r})$. Формально, для этого надо рассмотреть куперовскую лестницу в слабом статическом поле $\mathbf{A}(\mathbf{r})$, таком что $\operatorname{rot}\mathbf{A} = \mathbf{H}$. Записав для этого случая уравнение самосогласования $\Delta_{\alpha\beta} = \lambda\int F_{\alpha\beta}(\varepsilon,\mathbf{p})\frac{d\varepsilon d^3p}{(2\pi)^4}$ в пределе $\Delta \to 0$, найдите, при каком поле существует нетривиальное решение этого уравнения. Это поле называется верхним критическим полем H_{c2}.

Solution 67.

(!?!??!? суть решения напишу обязательно тут!!!)

Как и в задаче 64, мы вначале найдем куперовскую примесную лестницу, а затем подставим ее в уравнение самосогласования. Вычисление куперовской лестницы во внешнем магнитном поле в общем случае довольно сложно. Однако если поле медленно меняется на длине свободного пробега, эта задача сильно упрощается. Заметим, что две ступеньки примесной лестницы находятся друг от друга на расстоянии порядка l. Это позволяет пренебречь изменением поля на одной ступеньке и рассмотреть ступеньку в постоянном поле. Изменение поля мы учтем, переходя к суммированию ступенек, каждая из которых чувствует магнитное поле на своем отрезке траектории.

Поскольку нас интересуют неоднородные решения уравнения самосогласования, мы вначале вычислим примесную лестницу при ненулевом суммарном импульсе $\mathbf{s}$ в нулевом магнитном поле. Это можно сделать так же, как и в задаче 54. Одна ступенька лестницы вычисляется точно так же:

$$B_c = \iint \frac{d\Omega}{4\pi} \frac{\nu_0 d\xi}{\left(i\omega - \xi + \frac{i}{2\tau}\operatorname{sign}\omega\right)\left(-i\omega - \xi + \mathbf{sv} - \frac{i}{2\tau}\operatorname{sign}\omega\right)} = \int \frac{d\Omega}{4\pi} \frac{2\pi\nu_0\tau}{1 + 2|\omega|\tau + i\tau\mathbf{sv}} = \frac{2\pi\nu_0\tau}{1 + 2|\omega|\tau + \tau D\mathbf{s}^2}$$

где D - коэффициент диффузии. Суммируя лестницу, получаем

$$C_\omega(\mathbf{s}) = \frac{B_c}{1 - B_c/2\pi\nu_0\tau} = \frac{2\pi\nu_0}{2|\omega| + D\mathbf{s}^2}$$

Теперь учтем магнитное поле. Пусть сначала его векторный потенциал $\mathbf{A}(\mathbf{r})$ постоянен. Тогда его учет сведется к сдвигу импульсов $\mathbf{p} \to \mathbf{p} - e\mathbf{A}/c$ в функциях Грина. Поэтому в примесной лестнице $\mathbf{s}$ заменится на $\mathbf{s} - 2e\mathbf{A}/c$:

$$\widehat{C}_\omega = \frac{2\pi\nu_0}{2|\omega| + D\left(\mathbf{s} - \frac{2e}{c}\mathbf{A}\right)^2}.$$

Удобно записать это выражение в координатном представлении. Будем считать $C_\omega(\mathbf{r}, \mathbf{r}')$ функцией начальной и конечной точек. Заменяя $\mathbf{s}$ на $-i\nabla_{\mathbf{r}}$, перепишем выражение для куперона в форме дифференциального уравнения:

$$\left[2|\omega| + D\left(-i\frac{\partial}{\partial\mathbf{r}} - \frac{2e}{c}\mathbf{A}\right)^2\right] C_\omega(\mathbf{r}, \mathbf{r}') = 2\pi\nu_0\delta(\mathbf{r} - \mathbf{r}').$$

Что изменится, если $\mathbf{A}(\mathbf{r})$ - медленно меняющаяся функция? Если мы намерены учитывать лишь первые два порядка по $\mathbf{A}$ в знаменателе (10.209), то легко понять, что все возможные усложнения связаны с появлением членов, зависящих от $\operatorname{div}\mathbf{A}$, поскольку это единственная вращательно инвариантная комбинация из производных A. (Иными словами, если $\mathbf{A}$ становится функцией $\mathbf{r}$, возникает вопрос о порядке операторов $\mathbf{A}(\mathbf{r})$ и ∇ в купероне.) Но выбирая калибровку, в которой $\operatorname{div}\mathbf{A} = 0$, мы всегда можем добиться исчезновения подобных поправок. Поэтому для того, чтобы вычислить примесную лестницу, достаточно решить уравнение

$$\left[2|\omega| + D\left(-i\frac{\partial}{\partial\mathbf{r}} - \frac{2e}{c}\mathbf{A}(\mathbf{r})\right)^2\right] C_\omega(\mathbf{r}, \mathbf{r}') = 2\pi\nu_0\delta(\mathbf{r} - \mathbf{r}').$$

Это уравнение можно вывести и напрямую. Для этого надо рассмотреть такие поправки к одной «ступеньке»:

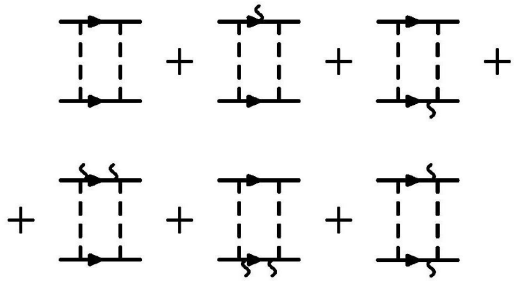


Рис. 10.17

(Волнистые линии на этом рисунке изображают взаимодействие с внешним магнитным полем.) После этого суммирование лестницы дает уравнение (10.211). Теперь запишем уравнение самосогласования, полагая $\Delta \to 0$. Вблизи H_{c2} состояние неоднородно, поэтому Δ зависит от $\mathbf{r}$. Уравнение Горькова имеет вид

$$\Delta(\mathbf{r}) = \lambda \int_{-\infty}^{\infty} F(\omega, \mathbf{r}, \mathbf{r}) \frac{d\omega}{2\pi}$$

Аномальная гриновская функция $F(\omega, \mathbf{r}, \mathbf{r})$ дается при $\Delta \to 0$ единственной диаграммой:



Рис. 10.18

Сравнивая ее с диаграммой для примесной лестницы, находим

$$F(\omega, \mathbf{r}, \mathbf{r}) = \int \Delta(\mathbf{r}')\, C_\omega(\mathbf{r}, \mathbf{r}')\, d^3 r'$$

Поэтому уравнение самосогласования записывается так:

$$\Delta(\mathbf{r}) = \lambda \int\limits_{-\infty}^{\infty} \frac{d\omega}{2\pi} \int C_\omega(\mathbf{r}, \mathbf{r}')\, \Delta(\mathbf{r}')\, d^3 r'$$

Чтобы найти его решения, удобно разложить $\Delta(\mathbf{r})$ по нормированным собственным функциям $\varphi_n(\mathbf{r})$ оператора в левой части (10.211). Эти функции обладают такими свойствами:

$$D\left(-i\frac{\partial}{\partial \mathbf{r}} - \frac{2e}{c}\mathbf{A}(\mathbf{r})\right)^2 \varphi_n(\mathbf{r}) = \mu_n \varphi_n(\mathbf{r}),$$

$$\int \varphi_n(\mathbf{r}) \varphi_m^*(\mathbf{r}) d^3 r = \delta_{nm}$$

($\mu_n - n$-е собственное значение). Запишем $\Delta(\mathbf{r})$ в виде

$$\Delta(\mathbf{r}) = \sum_n \Delta_n \varphi_n(\mathbf{r})$$

Куперон можно выразить через $\varphi_n(\mathbf{r})$:

$$C_\omega(\mathbf{r}, \mathbf{r}') = 2\pi\nu_0 \sum_n \frac{\varphi_n(\mathbf{r}) \varphi_n^*(\mathbf{r}')}{2|\omega| + \mu_n}$$

Это соотношение легко проверить, заметив, что эта функция в силу (10.215) удовлетворяет уравнению при $\mathbf{r} \neq \mathbf{r}'$, а при $\mathbf{r} \to \mathbf{r}'$ левая часть уравнения совпадает с δ-функцией, поскольку интеграл от нее по $\mathbf{r}$ равен 1 в силу (10.216). Тогда уравнение (10.214) перепишется так:

$$\Delta_n = \int\limits_{-\infty}^{\infty} \frac{2\pi\nu_0 \lambda \Delta_n}{2|\omega| + \mu_n} \frac{d\omega}{2\pi}.$$

Оно имеет нетривиальное решение при

$$\frac{1}{\nu_0 \lambda} = \int\limits_{-\infty}^{\infty} \frac{d\omega}{2|\omega| + \mu_n}$$

Интеграл следует обрезать сверху при $\omega = \omega_D$, как и ранее. В результате

$$\frac{1}{\nu_0 \lambda} = \ln \frac{2\omega_D}{\mu_n}.$$

Найдем собственные значения μ_n. Для этого нужно решить уравнение (10.215). Выберем калибровку $A_y = -Hx$. Тогда можно заметить, что уравнение (10.215) совпадает с уравнением Шредингера для частицы с массой $m = (2D)^{-1}$, зарядом $q = 2e$ и энергией μ_n в магнитном поле H. Из квантовой механики известно, что в этом случае собственные знвчения таковы:

$$E_n = \omega_H \left(n + \frac{1}{2}\right) + \frac{\hbar^2 k_z^2}{2m}; \quad \omega_H = \frac{qH}{mc}.$$

Это означает, что

$$\mu_n = \frac{4DeH}{c}\left(n + \frac{1}{2}\right) + Dk_z^2.$$

Поскольку собственные значения растут с ростом H, критическое магнитное поле определяется наименьшим собственным значением. Оно равно $\mu_0 = 2DeH/c$. Таким образом

$$\frac{1}{\nu_0 \lambda} = \ln \frac{\omega_D c}{DeH_{c2}}.$$

Выражая λ через T_c с помощью (10.73), получаем окончательно

$$H_{c2} = \frac{\pi}{2\gamma}\frac{T_c c}{De} = \frac{\pi}{\gamma}\frac{T_c}{\hbar D}\Phi_0$$

где $\Phi_0 = \hbar c/2e$ - квант потока.

Заметим, что собственные функции, отвечающие минимальному собственному значению, локализованы:

$$\varphi_{n,k_y}(x,y,z) = \frac{1}{\pi^{1/4} l_H^{1/2}} e^{ik_y y} e^{-(x-x_0)^2/2l_H^2},$$

Гπe

$$l_H = \sqrt{\hbar c/(qH)}, \quad x_0 = ck_y/(qH).$$

Таким образом, сверхпроводимость возникает в «нитях» толщины l_H. При понижении поля концентрация нитей быстро возрастает, пока они не заполнят собой весь объем.

В каких случаях переход от сверхпроводимости к нормальному металлу в магнитном поле устроен так, как описано в решении? Чтобы ответить на этот вопрос, надо сравнить магнитные поля, соответствующие различным сценариям разрушения сверхпроводимости. Мы вычислили магнитное поле, соответствующее разрушению сверхпроводимости неоднородным образом. Оценим поле, соответствующее разрушению сверхпроводимости сразу во всем объеме. Для этого надо сравнить энергию магнитного поля в объеме сверхпроводника с энергией конденсации. Энергия магнитного поля на единицу объема есть

$$E_{\text{mag}} = H^2/8\pi$$

Энергию конденсации легко оценить, считая, что частицы в интервале энергий Δ за счет конденсации понижают свою энергию на Δ. Число таких частиц в единице объема есть $\nu_0\Delta$, поэтому энергия конденсации равна

$$E_c \approx \nu_0\Delta^2 \approx \nu_0 T_c^2$$

Таким образом, магнитное поле, соответствующее однородному разрушению сверхпроводимости (термодинамическое критическое поле), есть

$$H_c \approx T_c\sqrt{\nu_0}$$

Сравним его с H_{c2}

$$\frac{H_c}{H_{c2}} \approx \sqrt{De\nu_0}c \approx \frac{v_F l\sqrt{mp_F/\hbar^3}}{c} \approx l\sqrt{\frac{e^2p_F^3}{mc^3\hbar^3}} \approx \frac{l}{\delta_\Lambda}$$

где δ_Λ - лондоновская глубина проникновения в чистом сверхпроводнике, определенная в (10.162). Таким образом, $H_{c2} \gg H_c$ при $l \ll \delta_\Lambda$. В этом случае H_{c2} действительно определяет границу сверхпроводящей фазы. Если же $H_{c2} \ll H_c$ (т. е. $\delta_\Lambda \ll l$), то переход происходит однородно по всему объему при поле H_c. В этом случае при $H = H_{c2} < H_c$ ничего особенного не происходит.

ЛШ-71. Плотность состояний в грязном металле

В неупорядоченном металле туннельная плотность состояний $\nu(\varepsilon)$ имеет особенность на уровне Ферми. Сингулярность $\nu(\varepsilon)$ при $\varepsilon \to E_F$ свидетельствует о том, что ферми-жидкостное состояние в металле в присутствии рассеяния на случайном потенциале весьма сильно модифицируется. Чтобы найти поправку к туннельной плотности состояний, возникающую из-за кулоновского взаимодействия, проделайте следующее.

а) Вычислите вершину взаимодействия электрона с электрическим полем с учетом беспорядка, используя мацубаровскую технику; просуммируйте для этого диаграммы на рис. 11.7.

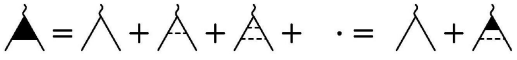


Рис. 11.7

Считайте, что переданный импульс $\mathbf{q}$ и переданная энергия ω_n удовлетворяют условиям $|\mathbf{q}| \ll 1, \omega_n\tau \ll 1$, где τ и l - время и длина свободного пробега. Покажите, что вершинная часть равна

$$\Gamma(\varepsilon_m, \omega_n, \mathbf{q}) = \begin{cases} 1/\left[\tau\left(|\omega_n| + D\mathbf{q}^2\right)\right] & \text{при } \varepsilon_m(\varepsilon_m - \omega_n) < 0 \\ 1 & \text{при } \varepsilon_m(\varepsilon_m - \omega_n) > 0 \end{cases}$$

где D - коэффициент диффузии. Диффузионный полюс выражения (11.35) описывает эффект усиления взаимодействия с внешним полем вследствие диффузии.

Изменение величины взаимодействия можно качественно объяснить тем, что изза диффузионного замедления динамики электроны проводят больше времени в области действия внешнего поля и поэтому

взаимодействуют с ним более сильно. То, насколько сильно диффузия замедляет динамику, зависит от размерности системы. Как мы знаем из задачи 9, критической размерностью является $D = 2$, поскольку при $D \leqslant 2$ число возвратов диффузионной траектории в исходную точку расходится, а при $D > 2$ - сходится. Поэтому эффекты усиления взаимодействия в грязном металле оказываются наиболее интересными в двумерном случае.

б) Найдите эффективное электрон-электронное взаимодействие $V(\omega_n, \mathbf{q})$ с учетом динамической экранировки. Для этого вычислите сумму диаграмм на рис. 8.3 и покажите, что заэкранированное взаимодействие есть

$$V(\omega_n, \mathbf{q}) = V_0(\mathbf{q}) \frac{|\omega_n| + D\mathbf{q}^2}{|\omega_n| + D\mathbf{q}^2 + \nu D\mathbf{q}^2 V_0(\mathbf{q})}$$

где $V_0(\mathbf{q})$ - затравочное взаимодействие. В качестве поляризационного оператора используйте мацубаровский коррелятор плотность-плотность, найденный в задаче 52.
(???? добавлю формулы!!!)

в) Найдите собственно-энергетическую поправку к функции Грина первого порядка по заэкранированному взаимодействию $V(\omega_n, \mathbf{q})$, соответствующую диаграмме на рис. 11.8.



Рис. 11.8
Используя найденное выражение, найдите поправку $\delta\nu(\varepsilon)$ к плотности состояний двумерного металла в случае кулоновского взаимодействия $V_0(\mathbf{r}) = e^2/|\mathbf{r}|$. Покажите, что в этом случае поправка к плотности состояний есть

$$\frac{\delta\nu(\varepsilon)}{\nu} = -\frac{e^2}{8\pi^2\hbar\sigma} \ln\frac{1}{|\varepsilon|\tau} \ln\frac{\tau D^2 \left(\nu e^2\right)^4}{|\varepsilon|},$$

где σ - двумерная проводимость. Расходимость $\delta\nu(\varepsilon)$ при $\varepsilon \to 0$ означает, что квазичастицы в двумерной неупорядоченной ферми-системе сильно отличаются от свободных фермионов. Усиление эффектов взаимодействия в плотности состояний (11.37) при малых ε свидетельствует о неприменимости теории возмущений в двумерном неупорядоченном металле при энергиях вблизи уровня Ферми.

(чуть лучше напишу условие! укажу, что у нас происходит, где появляется туннельная плотность!)

Solution 71 a.

Короче, знать нужно все, что выше, задача полностью опирается на пару ранее задач.

Рассмотрим вершинную часть взаимодействия электрона с внешним полем. Затравочная вершинная часть (в отсутствие примесей) равна единице. Вычислим вершинную часть, дающуюся диаграммами на рис. , используя усредненные по беспорядку мацубаровские функции Грина (см. (9.17)). Рассмотрим вначале поправку к вершине, соответствующую изображенной на рис. 11.9 диаграмме с одной примесной линией:

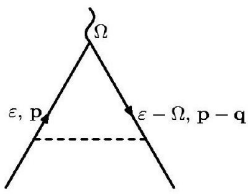


Рис. 11.9
Интересующее нас выражение

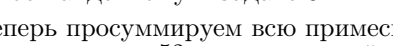
$$\Gamma^{(1)}(\varepsilon_m, \omega_n, \mathbf{q}) = \frac{1}{2\pi\nu_0\tau} \int \frac{1}{\left(i\varepsilon_m - \xi_{\mathbf{p}} + \frac{i}{2\tau}\operatorname{sign}\varepsilon_m\right)} \cdot \frac{1}{\left(i\varepsilon_m - i\omega_n - \xi_{\mathbf{p}-\mathbf{q}} + \frac{i}{2\tau}\operatorname{sign}(\varepsilon_m - \omega_n)\right)} \frac{d^2\mathbf{p}}{(2\pi)^2}$$

вычисляется таким же образом, как ступенька примесной лестницы в задаче 52. Заменяя интеграл по $d^2\mathbf{p}$ интегралом по ξ и вычисляя его методом вычетов, нетрудно показать, что выражение отлично от нуля только в том случае, когда знаки энергий ε_m и $\varepsilon_m - \omega_n$ различаются. (В противном случае оба вычета интегрируемого выражения попадают в одну и ту же полуплоскость комплексного ξ.)

В случае, когда знаки энергий различны и $\omega_n > 0$, получаем выражение

$$\Gamma^{(1)}(\varepsilon_m, \omega_n, \mathbf{q}) = \frac{1}{1 + \tau\omega_n + \tau D\mathbf{q}^2}$$

подобное найденному в задаче 52.

Теперь просуммируем всю примесную лестницу  .

Как и в задаче 52, интересующий нас лестничный ряд образует геометрическую прогрессию. Поэтому

$$\Gamma(\varepsilon_m, \omega_n, \mathbf{q}) = \frac{1}{1 - \Gamma^{(1)}} \approx \frac{1}{\tau(\omega_n + D\mathbf{q}^2)}$$

Рассматривая аналогично случай $\omega_n < 0$, можно убедиться в том, что ω_n в (11.76) следует заменить на $|\omega_n|$.

Если же знаки энергий ε_m и $\varepsilon_m - \omega_n$ в функциях Грина в (11.74) совпадают, то зануляется не только первая поправка $\Gamma^{(1)}$, но, как нетрудно видеть, и все остальные члены диаграммного ряда на рис.  .

Это является следствием общего правила, отмеченного в гл. 9 - примесная лестница отлична от нуля только если энергии в функциях Грина имеют разные знаки.

Solution 71 б.

Эффективное взаимодействие с учетом динамической экранировки вычисляется суммированием последовательности «пузырьковых» диаграмм (см. задачу 45):

$$V(\omega_n, \mathbf{q}) = \frac{V_0(\mathbf{q})}{1 - \Pi(\omega_n, \mathbf{q})\, V_0(\mathbf{q})}$$

где $\Pi(\omega_n, \mathbf{q})$ - поляризационный оператор, а $V_0(\mathbf{q})$ - затравочное взаимодействие. Подставляя поляризационный оператор $\Pi(\omega_n, \mathbf{q}) = -\nu D\mathbf{q}^2 / \left(|\omega_n| + D\mathbf{q}^2\right)$ из (9.23), получаем искомое выражение (11.36).

Для дальнейших вычислений нам понадобится двумерный фурье-образ кулоновского потенциала взаимодействия. Его проще всего найти, проинтегрировав известный фурье-образ трехмерного кулоновского потенциала по q_z:

$$V_0^{(2)}(\mathbf{q}) = V_0^{(3)}(q_x, q_y, z = 0) = \int\limits_{-\infty}^{\infty} \left(\frac{e^2}{|\mathbf{r}|}\right)_{\mathbf{q}} \frac{dq_z}{2\pi} = \int\limits_{-\infty}^{\infty} \frac{4\pi e^2}{\mathbf{q}^2 + q_z^2} \frac{dq_z}{2\pi} = \frac{2\pi e^2}{|\mathbf{q}|}$$

где $\mathbf{q} = (q_x, q_y)$

Solution 71 в.

Поправка к туннельной плотности состояний $\nu(\varepsilon)$ получается из поправки к функции Грина интегрированием по импульсам, которое можно заменить интегрированием по ξ:

$$\frac{\delta\nu(\varepsilon)}{\nu_0} = -\frac{1}{\pi} \int \delta G(\varepsilon, \xi) d\xi$$

Вычислим $\delta G(i\varepsilon, \mathbf{p})$ при $T = 0$, заменяя суммы по мацубаровским частотам интегралами. Будем для определенности считать, что $\varepsilon > 0$. Выражение, соответствующее диаграмме на рис. 11.8, есть

$$\delta G(i\varepsilon, \mathbf{p}) = G_0^2(i\varepsilon, \mathbf{p}) \iint \Gamma^2(\varepsilon, \omega, \mathbf{q}) V(\omega, \mathbf{q}) G(i\varepsilon - i\omega, \mathbf{p} - \mathbf{q}) \frac{d\omega d^2q}{(2\pi)^3}.$$

Наибольший вклад в интеграл по энергии возникает от области $\omega > \varepsilon$, так как в этой области вершинная часть $\Gamma(\varepsilon, \omega, \mathbf{q})$ имеет диффузионный полюс и поэтому велика - см. (11.35). Пренебрегая вкладом области $\omega < \varepsilon$, имеем

$$\delta G(i\varepsilon, \mathbf{p}) = \frac{1}{\left(i\varepsilon - \xi_{\mathbf{p}} + \frac{i}{2\tau}\right)^2} \int\limits_{\varepsilon}^{\infty} \frac{d\omega}{2\pi} \int \frac{1}{\left(i\varepsilon - i\omega - \xi - \mathbf{q}\mathbf{v}_{\mathbf{p}} - \frac{i}{2\tau}\right)} \frac{V_0(\mathbf{q})}{(\omega + D\mathbf{q}^2)\left(\omega + D\mathbf{q}^2 + \nu D\mathbf{q}^2 V_0(\mathbf{q})\right)} \frac{d^2\mathbf{q}}{(2\pi)^2}.$$

Удобно сразу проинтегрировать это выражение по ξ. При этом мы пренебрегаем членами ω и $\mathbf{qv}$ в знаменателе по сравнению с τ^{-1}, поскольку нас интересует вклад малых энергий и импульсов. (do this, it should be easy!!!)

Таким образом, получаем

$$\int \delta G(i\varepsilon,\xi)d\xi = 2\int\limits_{\varepsilon}^{\infty} d\omega \int \frac{V_0(\mathbf{q})}{(\omega+D\mathbf{q}^2)\left(\omega+D\mathbf{q}^2+\nu D\mathbf{q}^2V_0(\mathbf{q})\right)}\frac{d^2\mathbf{q}}{(2\pi)^2}.$$

Подставляя в это выражение фурье-образ затравочного взаимодействия (11.78), получаем

$$\int \delta G(i\varepsilon,\xi)d\xi = -2e^2\int\limits_{\varepsilon}^{\infty} d\omega \int\limits_{0}^{\infty} \frac{dq}{(\omega+Dq^2)\left(\omega+Dq^2+2\pi\nu e^2Dq\right)}$$

Проинтегрируем найденное выражение по q. Наибольший вклад в интеграл вносит область (??? why??)

$$\frac{\omega}{2\pi\nu De^2} \le q \le \sqrt{\frac{\omega}{D}}$$

в которой можно пренебречь Dq^2 по сравнению с ω, и ω - по сравнению с νe^2Dq. Обрезая логарифмически расходящийся интеграл на границах области (11.84), получаем

$$\int \delta G(i\varepsilon,\xi)d\xi = \frac{1}{4\pi\nu D}\int\limits_{\varepsilon}^{\infty} \ln\frac{\left(\nu e^2\right)^2}{D\omega}\frac{d\omega}{\omega}$$

Интеграл по частотам также логарифмически расходится на верхнем пределе. Чтобы получить вклад диффузионной области обрежем интеграл по ω на $\omega\tau \approx 1$, (При больших значениях ω электроны движутся баллистически, поэтому эта область описывается теорией ферми-жидкости и не приводит к сингулярности в плотности состояний.) Вычисляя интеграл по ω и удерживая при аналитическом продолжении с мнимых частот на вещественные лишь главный дважды логарифмический член, получаем поправку к туннельной плотности состояний:

$$\frac{\delta\nu(\varepsilon)}{\nu} = -\frac{1}{8\pi^2\nu D}\ln\frac{\left(\nu e^2\right)^4\tau D^2}{|\varepsilon|}\ln\frac{1}{|\varepsilon|\tau}.$$

Вклад (11.86) в плотность состояний имеет отрицательный знак и сингулярен на малых энергиях $\varepsilon \to 0$. С помощью соотношения Эйнштейна $\sigma = e^2\nu D$ произведение νD можно выразить через проводимость, что дает искомое выражение (11.37) для плотности состояний двумерного металла.

Discussion of the result

Остановимся на физическом смысле результата (11.86). Туннельная плотность состояний описывает реакцию электронной жидкости на добавление в нее электрона. Роль кулоновского взаимодействия в этом процессе состоит в следующем. Сразу после того, как электрон протуннелировал в металл, его заряд незаэкранирован и создает кулоновское поле. Под действием этого поля остальные электроны начинают двигаться так, чтобы заэкранировать вновь прибывший электрон. Макроскопически этот процесс приводит к максвелловской релаксации заряда. Таким образом, туннелирование одного электрона сопровождается коллективным растеканием заряда многих других электронов, что приводит к уменьшению вероятности туннелирования. В чистом металле максвелловская релаксация происходит почти мгновенно (за время порядка обратной плазменной частоты). Соответственно в этом случае поправки к $G(t-t')$ из-за взаимодействия достаточно быстро затухают на больших временах, и сингулярности в $G(\varepsilon)$ при $\varepsilon \to 0$ не возникает. В то же время в неупорядоченной системе, характеризующейся омической проводимостью, максвелловская релаксация происходит более медленно. Поэтому в этом случае влияние индуцированного туннелирующим электроном растекания заряда на амплитуду туннелирования оказывается существенным и соответствующая поправка к плотности состояний расходится на малых энергиях. Можно сказать, что плохо проводящая система сильнее «сопротивляется» попыткам добавить в нее электрон. Этот эффект и приводит к уменьшению одночастичной плотности состояний.

Поправка (11.86) приводит к специфической температурной зависимости туннельного тока, а также к его неомичности. Повторив проделанное выше вычисление $\delta\nu(\varepsilon)$ при конечной температуре, нетрудно убедиться в том, что результат (11.86) остается в силе с точностью до замены $\varepsilon \to \varepsilon_m = \pi T(2m+1)$. Соответствующая зависимость туннельного тока от T и V оказывается следующей:

$$G = \frac{dI}{dV} = G_0\left(1+\frac{\delta\nu\left(\varepsilon_{T,eV}\right)}{\nu}\right), \quad \varepsilon_{T,eV} = \max[T,eV]$$

Как видно из этого выражения, при уменьшении температуры и напряжения имеет место подавление туннельного тока, причем насыщения при $eV, T \to 0$ не происходит. Сингулярное поведение туннельного сопротивления при малых температурах или напряжениях, возникающее вследствие сингулярности $\nu(\varepsilon)$ при $\varepsilon \to E_F$, называется туннельной аномалией.

14.2.10 Problems about tunneling, junctions 1: Basic Models

me. Integral in the RSJ model

Find how much time is needed for the phase to change by 2π in the Josephson junction with resistance for the currents $I_c < I$.

Solution

One needs to remember the model and then compute a not so trivial integral.

$$I = \frac{V}{R} + I_c \sin(\phi) = \frac{\hbar}{2eR}\frac{\partial \phi}{\partial t} + I_c \sin(\phi)$$

(???)

$$\frac{\hbar}{2eR}\frac{d\phi}{I - I_c \sin(\phi)} = dt \qquad \Rightarrow \qquad \int_0^{t_0}, \int_0^{2\pi} \qquad \Rightarrow$$

```
Integrate[1/(A - Sin[x]), {x, 0, 2 Pi}]
```

(?? later maybe I'll solve it analytically, currently it is also fine to know how to get it with Wolfram)

$$t_0 = \frac{\hbar}{2eR}\frac{2\pi}{\sqrt{I^2 - I_c^2}}$$

ЛШ-68. Microscopic Framework of Tunneling

а) Выведите формулу для туннельного тока

$$I(V) = 4e\sum_{\mathbf{p},\mathbf{p}'} |T_{\mathbf{p}\mathbf{p}'}|^2 \int_{-\infty}^{\infty} \operatorname{Im} G_a^R(\mathbf{p}, \varepsilon + eV) \operatorname{Im} G_b^R(\mathbf{p}', \varepsilon) \left[n_F(\varepsilon) - n_F(\varepsilon + eV)\right] \frac{d\varepsilon}{\pi}$$

где $n_F(\varepsilon)$ - фермиевская функция распределения, а $G_a^R(\mathbf{p}, \varepsilon) = -i\int_0^{\infty} \left\langle \left[a_{\mathbf{p}}^+(t), a_{\mathbf{p}}(0)\right]\right\rangle e^{i\varepsilon t} dt$, используя мацубаровскую технику.

Для этого рассмотрите отклик туннельного тока $\widehat{I} = i\widehat{X}e^{ieVt} - i\widehat{X}^+ e^{-ieVt}$ на поле, пропорциональное туннельному оператору $X = \sum_{\mathbf{p},\mathbf{p}'} T_{\mathbf{p}\mathbf{p}'}\widehat{a}_{\mathbf{p}}^+ \widehat{b}_{\mathbf{p}'}$. Используя аналитические свойства мацубаровских функций Грина, перейдите от мнимых частот к вещественным и тем самым свяжите функцию отклика с величинами в реальном времени.

б) Рассмотрите туннелирование между двумя идеальными ферми-газами с постоянной плотностью состояний. Покажите, что при eV $\ll E_F$ вольт-амперная характеристика линейна, т. е. выполняется закон Ома $V = RI$, причем сопротивление контакта R не зависит от температуры и определяется соотношением

$$R^{-1} = 4\pi e^2 \nu_a \nu_b |T_0|^2$$

где ν_a и ν_b - плотности состояний берегов контакта.

в) Пусть в одном из ферми-газов имеется взаимодействие между частицами, так что собственно-энергетическая часть оказывается равной

$$\Sigma(\xi, \varepsilon) = a\xi - b\varepsilon$$

где ε - энергия частицы, а $\xi = v_F(p - p_0)$, причем $\xi, \varepsilon \ll E_F$. Найдите туннельное сопротивление.

Указание: Для электрон-фононного взаимодействия собственно-энергетическая часть есть функция ε, а от ξ не зависит (см. гл. 6). Поэтому в этом случае $a = 0$. Для электрон-электронного взаимодействия собственно-энергетическая часть зависит как от ξ, так и от ε, и поэтому $a \neq 0$ и $b \neq 0$. (????!??!)

Solution 68 a.

Согласно формуле Кубо, среднее от оператора туннельного тока (11.13) в низшем порядке теории возмущений по туннельному гамильтониану (11.11) равно

$$I(t) = i \int\limits_{-\infty}^{t} \left\langle \left[\widehat{H}_T\left(t'\right), \widehat{I}(t) \right] \right\rangle dt'.$$

Благодаря фазовым множителям $e^{\pm ieVt}$ операторы $\widehat{H}_T(t)$ и $\widehat{I}(t)$ явно зависят от времени. Чтобы свести задачу вычисления туннельного тока к стандартной задаче о нахождении функции отклика в равновесном состоянии, введем обобщенную воспри- имчивость $\chi(\omega)$

$$\chi(\omega) = i \int\limits_{0}^{\infty} \langle [\widehat{X}(t), \widehat{I}(0)] \rangle e^{i\omega t} dt$$

описывающую отклик туннельного тока на поле $\widehat{X}$, определенное соотношением (11.12). Нетрудно видеть, что туннельный ток как функция напряжения V на туннельном контакте связан с $\chi(\omega)$ следующим соотношением:

$$I(V) = 2 \operatorname{Re} \chi(\omega = eV)$$

Чтобы вычислить $\chi(\omega)$, найдем мацубаровскую восприимчивость

$$\chi_M\left(i\Omega_n\right) = \frac{1}{2} \int\limits_{-\beta}^{\beta} \left\langle \mathrm{T}_\tau \widehat{X}(\tau) \widehat{I}(0) \right\rangle e^{i\Omega_n \tau} d\tau$$

а затем продолжим ее на вещественные частоты. Раскроем среднее с помощью определений $\widehat{I} = \dot{\widehat{Q}}_a = ie \sum\limits_{\mathbf{p},\mathbf{p}'} T_{\mathbf{p}\mathbf{p}'} \widehat{a}^+_{\mathbf{p}} \widehat{b}_{\mathbf{p}'} +$ h.c., $X = \sum\limits_{\mathbf{p},\mathbf{p}'} T_{\mathbf{p}\mathbf{p}'} \widehat{a}^+_{\mathbf{p}} \widehat{b}_{\mathbf{p}'}$ получим

$$\left\langle \mathrm{T}_\tau \widehat{X}(\tau) \widehat{I}(0) \right\rangle = \sum_{\mathbf{p}_1,\mathbf{p}'_1,\mathbf{p}_2,\mathbf{p}'_2} T_{\mathbf{p}_1\mathbf{p}'_1} \left\langle \mathrm{T}_\tau \widehat{a}^+_{\mathbf{p}_1}(\tau) \widehat{b}_{\mathbf{p}'_1}(\tau) \left(T_{\mathbf{p}_2\mathbf{p}'_2} \widehat{a}^+_{\mathbf{p}_2}(0) \widehat{b}_{\mathbf{p}'_2}(0) - T^*_{\mathbf{p}_2\mathbf{p}'_2} \widehat{a}_{\mathbf{p}_2}(0) \widehat{b}^+_{\mathbf{p}'_2}(0) \right) \right\rangle.$$

В отсутствие сверхпроводящих корреляций в пробнике и образце средние вида $\left\langle \widehat{a}^+_{\mathbf{p}} \widehat{a}^+_{\mathbf{p}'} \right\rangle$ и $\left\langle \widehat{b}_{\mathbf{p}} \widehat{b}_{\mathbf{p}'} \right\rangle$ равны нулю. Поэтому только вклад второго члена в $\left\langle \mathrm{T}_\tau \widehat{X}(\tau) \widehat{I}(0) \right\rangle$ оказывается отличным от нуля. Далее, спаривая операторы, находим (????? почему минус в второй функции Грина?)

$$\left\langle \mathrm{T}_\tau \widehat{X}(\tau) \widehat{I}(0) \right\rangle = -ie \sum_{\mathbf{p}\mathbf{p}'} \left| T_{\mathbf{p}\mathbf{p}'} \right|^2 G_a(\tau, \mathbf{p}) G_b\left(-\tau, \mathbf{p}'\right)$$

где $G_a(\tau, \mathbf{p}) = -\left\langle \mathrm{T}_\tau \widehat{a}_{\mathbf{p}}(\tau) \widehat{a}^+_{\mathbf{p}}(0) \right\rangle$ и $G_b(\tau, \mathbf{p}) = -\left\langle \mathrm{T}_\tau \widehat{b}_{\mathbf{p}}(\tau) \widehat{b}^+_{\mathbf{p}}(0) \right\rangle$ - мацубаровские функции Грина соответственно пробника и образца. Записав функции Грина в частотном представлении (???) подставив в $\chi_M\left(i\Omega_n\right)$, получим

$$\chi_M\left(i\Omega_n\right) = -2ieT \sum_{\omega_m} \sum_{\mathbf{p}\mathbf{p}'} \left| T_{\mathbf{p}\mathbf{p}'} \right|^2 G_a\left(i\omega_m + i\Omega_n, \mathbf{p}\right) G_b\left(i\omega_m, \mathbf{p}'\right)$$

где множитель 2 учитывает суммирование по проекциям спина.

Теперь выполним аналитическое продолжение с помощью интегрального представления $G\left(i\varepsilon_n, \mathbf{r}_1, \mathbf{r}_2\right) = \frac{1}{\pi} \int\limits_{-\infty}^{\infty} \frac{\operatorname{Im} G^R(\varepsilon, \mathbf{r}_1, \mathbf{r}_2)}{\varepsilon - i\varepsilon_n} d\varepsilon$, с помощью которого мацубаровские функции Грина выражаются через мнимые части запаздывающих функций. В результате получим:

$$\chi_M\left(i\Omega_n\right) = -2ieT \sum_{\omega_m} \sum_{\mathbf{p}\mathbf{p}'} \left| T_{\mathbf{p}\mathbf{p}'} \right|^2 \int\limits_{-\infty}^{\infty} \int \frac{\operatorname{Im} G^R_a(\varepsilon, \mathbf{p}) \operatorname{Im} G^R_b\left(\varepsilon', \mathbf{p}'\right)}{\left(i\omega_m + i\Omega_n - \varepsilon\right)\left(i\omega_m - \varepsilon'\right)} \frac{d\varepsilon d\varepsilon'}{\pi^2}$$

$T\sum\limits_{\omega_m}\frac{1}{(i\omega_m+i\omega_n-\xi_{p+k})(i\omega_m-\xi_p)}=\frac{n_F(\xi_{p+k})-n_F(\xi_p)}{i\omega_n-\xi_{p+k}+\xi_p}\qquad\Rightarrow$

$$\chi_M\left(i\Omega_n\right)=-\frac{2ie}{\pi^2}\sum_{\mathbf{pp}'}\left|T_{\mathbf{pp}'}\right|^2\int\limits_{-\infty}^{\infty}\int\limits_{-\infty}^{\infty}\operatorname{Im}G_a^R(\varepsilon,\mathbf{p})\operatorname{Im}G_b^R\left(\varepsilon',\mathbf{p}'\right)\frac{n_F(\varepsilon)-n_F\left(\varepsilon'\right)}{\varepsilon'-\varepsilon+i\Omega_n}d\varepsilon d\varepsilon'.$$

Аналитическое продолжение (11.46) на вещественные частоты достигается заменой $i\Omega_n$ на $\omega+i0$. Вещественная часть полученного выражения дает туннельный ток

$$I(V)=\frac{4e}{\pi}\sum_{\mathbf{pp}'}\left|T_{\mathbf{pp}'}\right|^2\iint\limits_{-\infty}^{\infty}\delta\left(\varepsilon'-\varepsilon-eV\right)\operatorname{Im}G_a^R(\varepsilon,\mathbf{p})\operatorname{Im}G_b^R\left(\varepsilon',\mathbf{p}'\right)\left(n_F(\varepsilon)-n_F\left(\varepsilon'\right)\right)d\varepsilon d\varepsilon'=$$

$$=\frac{4e}{\pi}\sum_{\mathbf{pp}'}\left|T_{\mathbf{pp}'}\right|^2\int\limits_{-\infty}^{\infty}\operatorname{Im}G_a^R(\varepsilon+eV,\mathbf{p})\operatorname{Im}G_b^R\left(\varepsilon,\mathbf{p}'\right)\left(n_F(\varepsilon)-n_F(\varepsilon+eV)\right)d\varepsilon$$

Эта формула имеет совершенно общий характер, поскольку при её выводе не делалось никаких предположений о спектре и характере взаимодействия в пробнике и образце.

(???? or maybe it works only for noninteracting models?)

Solution 68 б.

Применим общую формулу

$$I(V)=\frac{4e}{\pi}\sum_{\mathbf{pp}'}\left|T_{\mathbf{pp}'}\right|^2\int\limits_{-\infty}^{\infty}\operatorname{Im}G_a^R(\varepsilon+eV,\mathbf{p})\operatorname{Im}G_b^R\left(\varepsilon,\mathbf{p}'\right)\left(n_F(\varepsilon)-n_F(\varepsilon+eV)\right)d\varepsilon$$

к задаче о туннельном контакте между двумя нормальными металлами. Мнимая часть запаздывающей функции Грина $G^R(\varepsilon,\mathbf{p})=\left(\varepsilon-\xi_{\mathbf{p}}+i0\right)^{-1}$ равна

$$\operatorname{Im}G^R(\varepsilon,\mathbf{p})=-\pi\delta\left(\varepsilon-\xi_{\mathbf{p}}\right)$$

(since $\lim_{\varepsilon\to0^+}\frac{1}{x\pm i\varepsilon}=\mp i\pi\delta(x)+\mathcal{P}\left(\frac{1}{x}\right)$).

Рассмотрим более простой случай шероховатого барьера, когда туннельный матричный элемент не зависит от импульсов: $T_{\mathbf{pp}'}=T_0$. Величина T_0 есть значение туннельного матричного элемента при энергии вблизи E_F. При этом каждая из двух функций Грина в общей формуле для тока через контакт интегрируется по импульсам отдельно (this is how we get rid of two sums, we just have two integrals) и соответственно вклад каждой из них есть

$$\int\operatorname{Im}G_{a(b)}^R(\varepsilon,\mathbf{p})\frac{d^3p}{(2\pi)^3}=-\pi\nu_{a(b)}$$

где $\nu_{a(b)}$ - плотность состояний с одной проекцией спина (??? why???).

Нетрудно проверить, что

$$\int\left(n_F(\varepsilon)-n_F(\varepsilon+eV)\right)d\varepsilon=eV$$

при произвольной температуре.

(???? no, I can't do it??? add this to the note on mathematics and typical methods of condensed matter.)

```
Integrate[(1/(Exp[ ve] + 1) - 1/(Exp[ ve + c] + 1)), {ve, -Infinity, Infinity}]
```

Yes, it gives the stated result, but why β disappears from the answer? Also, Wolfram counts with $4\pi i$, which might be not a problem (???).

For analytical calculation, there is a problem, because subtracted integrals at the negative axes are divergent themselves, so we need to work together with them. One can introduce a variable $a:=e^{\varepsilon}$, then come to

```
Integrate[(Exp[b]-1)/((a + 1) (a + Exp[b])), {a, 0, Infinity}]
```

and then neglect imaginary parts from Wolfram. (??? still, I don't understand it well)

Thus, the current can be expressed as

$$I(V)=V/R,\qquad R:=\left(4\pi e^2\left|T_0\right|^2\nu_a\nu_b\right)^{-1}.$$

R is сопротивление туннельного контакта. Таким образом, для контакта между нормальными металлами справедлив закон Ома, причем сопротивление при $T \ll E_F$ не зависит от температуры.

Нетрудно убедиться в том, что закон Ома с независящим от температуры сопротивлением получается и при произвольной зависимости туннельного матричного элемента $T_{\mathbf{pp}'}$ от импульсов $\mathbf{p}$ и $\mathbf{p}'$. Интересно, что даже в случае туннелирования через идеально гладкий барьер, при котором сохраняется параллельная барьеру компонента импульса, закон Ома по-прежнему имеет место при $T \ll E_F$. Эффект сохранения импульса при туннелировании существенно влияет на характер зависимости $I(V)$ при $eV, T \ll E_F$ только в тех случаях, когда и образец, и пробник представляют собой достаточно низкоразмерные системы.

Solution 68 в.

Одночастичная функция Грина с собственно-энергетической частью вида (11.31) имеет вид

$$G(\varepsilon, \mathbf{p}) = \frac{1}{G_0^{-1}(\varepsilon, \mathbf{p}) - \Sigma(\varepsilon, \mathbf{p})} = \frac{1}{\varepsilon(1+b) - \xi_{\mathbf{p}}(1+a) + i0}$$

При этом туннельная плотность состояний (??? check!)

$$\nu(\varepsilon) = -\frac{1}{\pi} \int \operatorname{Im} G(\varepsilon, \mathbf{p}) \frac{d^3\mathbf{p}}{(2\pi)^3} = \int \delta\left(\varepsilon(1+b) - \xi_{\mathbf{p}}(1+a)\right) \frac{d^3\mathbf{p}}{(2\pi)^3} = \frac{\nu_0}{1+a},$$

где ν_0 - плотность состояний без учета взаимодействия. Таким образом оказывается, что туннельная плотность состояний не зависит от константы b.

Полезно сравнить этот ответ с перенормировкой спектра квазичастиц. Функция Грина имеет полюс при

$$\varepsilon = \varepsilon_0(\mathbf{p}) = \frac{1+a}{1+b} v_F \left(|\mathbf{p}| - p_0\right)$$

Таким образом, константа b дает вклад в перенормировку спектра, не меняя при этом туннельный ток. Так происходит потому, что константа b определяет величину скачка в распределении частиц по импульсам на ферми-поверхности, равную вычету функции Грина в квазичастичном полюсе

$$Z = 1/(1+b)$$

Но поскольку перенормировка туннельной плотности состояний пропорциональна

$$\nu(\varepsilon) \approx Z(\partial\varepsilon/\partial\xi)^{-1}$$

вклады константы b в эффективную массу и в вычет Z взаимно сокращаются. Таким образом, туннельный ток зависит не только от перенормированного спектра квазичастиц $\varepsilon = \xi(p)$, но и от их структуры, описываемой величиной Z.

В случае электрон-фононного взаимодействия $a = 0$, и поэтому туннельный ток оказывается точно таким же, как и в отсутствие взаимодействия. Качественно это объясняется адиабатичностью фононов. Туннелирование электрона в металл происходит мгновенно, поэтому при туннелировании решетку можно считать неподвижной. Таким образом, вероятность туннелирования определяется свойствами свободных электронов. Фононы же затем за время порядка ω_D^{-1} подстраиваются под конечное состояние электронов после туннелирования, каким бы оно ни было.

Заметим, что наш вывод об отсутствии влияния электрон-фононного взаимодействия на туннельный ток имеет весьма общий характер. Как нетрудно видеть, туннельная плотность состояний (11.54) не меняется, если собственно-энергетическая часть $\Sigma(\varepsilon)$ зависит от энергии ε произвольным образом. Для полного сокращения эффектов взаимодействия требуется лишь отсутствие зависимости Σ от p, которое в случае электрон-фононного взаимодействия обеспечивается адиабатичностью фононов.

ЛШ-69. Туннельный ток в NS-контакте

Рассмотрим туннельный контакт между нормальным металлом и сверхпроводником, к которому приложено напряжение V. Выразите туннельный ток при $T < T_c$ через сопротивление контакта R в нормальном состоянии, т. е. при $T > T_c$. Покажите, что при нулевой температуре зависимость туннельного тока от V имеет порог:

$$I = \frac{1}{R}\sqrt{V^2 - (\Delta/e)^2}\,\operatorname{sign} V,$$

где Δ - сверхпроводящая щель при $T = 0$.

Найдите зависимость туннельного тока от температуры при $0 < T < T_c$?

Solution 69 в общем случае

Для нахождения туннельного тока между номальным металлом и сверхпроводником можно воспользоваться общим соотношением

$$\left\langle \mathrm{T}_\tau \widehat{X}(\tau)\widehat{I}(0)\right\rangle = \sum_{\mathbf{p}_1,\mathbf{p}_1',\mathbf{p}_2,\mathbf{p}_2'} T_{\mathbf{p}_1\mathbf{p}_1'} \left\langle \mathrm{T}_\tau \widehat{a}^+_{\mathbf{p}_1}(\tau)\widehat{b}_{\mathbf{p}_1'}(\tau)\left(T_{\mathbf{p}_2\mathbf{p}_2'}\widehat{a}^+_{\mathbf{p}_2}(0)\widehat{b}_{\mathbf{p}_2'}(0) - T^*_{\mathbf{p}_2\mathbf{p}_2'}\widehat{a}_{\mathbf{p}_2}(0)\widehat{b}^+_{\mathbf{p}_2'}(0)\right)\right\rangle.$$

При этом в сверхпроводнике аномальные средние вида $\left\langle \widehat{a}^+_{\mathbf{p}_1}\widehat{a}^+_{\mathbf{p}_2}\right\rangle$ отличны от нуля, и поэтому требуется заново проанализировать вклад двух членов под усреднением в туннельный ток. Однако, оказывается, что поскольку в номальном металле средние $\left\langle \widehat{b}_{\mathbf{p}_1'}\widehat{b}_{\mathbf{p}_2'}\right\rangle$ равны нулю, первый член в $\left\langle \mathrm{T}_\tau \widehat{X}(\tau)\widehat{I}(0)\right\rangle = \sum\limits_{\dots} T_{\mathbf{p}_1\mathbf{p}_1'}\langle\dots\rangle$ по-прежнему обращается в нуль при усреднении. Поэтому, как и в задаче 68, можно перейти от $\left\langle \mathrm{T}_\tau \widehat{X}(\tau)\widehat{I}(0)\right\rangle = \sum\limits_{\dots} T_{\mathbf{p}_1\mathbf{p}_1'}\langle\dots\rangle$ к выражению (11.48), в которое входят туннельные плотности состояний пробника и образца.

Туннельная плотность состояний дается мнимой частью функции Грина. Аналитическое продолжение функции Грина сверхпроводника (10.35) с положительных мацубаровских частот на вещественную ось дает

$$G^R(\varepsilon,\mathbf{p}) = \frac{\varepsilon+\xi_{\mathbf{p}}}{\varepsilon^2-\xi^2_{\mathbf{p}}-\Delta^2+i0\,\mathrm{sign}\,\varepsilon}$$

Следовательно туннельная плотность состояний есть

$$\nu(\varepsilon) = -\frac{1}{\pi}\int \mathrm{Im}\, G^R(\varepsilon,\mathbf{p})\frac{d^3p}{(2\pi)^3} = \nu_0\int\limits_{-\infty}^{\infty}(\varepsilon+\xi)\delta\left(\varepsilon^2-\xi^2-\Delta^2\right)\mathrm{sign}\,\varepsilon d\xi$$

Вычисляя интеграл от δ-функции, находим (shoul be easy, I'll check later)

$$\nu(\varepsilon) = \begin{cases} \nu_0|\varepsilon|/\left(\varepsilon^2-\Delta^2\right)^{1/2} & \text{при } |\varepsilon|>\Delta \\ 0 & \text{при } |\varepsilon|<\Delta \end{cases}$$

Этот результат может быть записан в виде $\pi\nu_0\partial\xi/\partial\varepsilon$, т.е. как плотность состояний квазичастиц с законом дисперсии $\varepsilon^2 = \Delta^2+\xi^2$. Хотя такой подход игнорирует различие между туннелирующими электронами и квазичастицами, в которые они превращаются в сверхпроводнике, результат в данном случае оказывается верным. Причина состоит в том, что квазичастицы теории БКШ состоят из двух электронов с одинаковой энергией. Их вклады в туннельную плотность состояний равны $|u_p|^2$ и $|v_p|^2$, где u_p и v_p - коэффициенты преобразования Боголюбова. Но поскольку $u_p^2+v_p^2=1$, суммарный вклад двух компонент квазичастицы в туннельный ток определяется только свойствами квазичастичного спектра. Так происходит потому, что эффекты взаимодействия в теории БКШ учитываются только в рамках теории среднего поля, и поэтому многочастичные эффекты оказываются относительно простыми.

Подставляем туннельную плотность состояний (11.60) в (11.48), находим туннельный ток:

$$I_{N-S}(V) = 4\pi e\nu_a\nu_b|T_0|^2\int\limits_{|\omega|>\Delta}(n_F(\omega)-n_F(\omega+eV))\frac{|\omega|d\omega}{\sqrt{\omega^2-\Delta^2}}.$$

Случай нулевой температуры.

Пусть eV > 0. Тогда интегрирование по энергиям производится в интервале $-eV<\varepsilon<0$ (??? why negative???). При eV < Δ интеграл (11.61) обращается в нуль, поскольку в этой области не выполнено условие $|\varepsilon|>\Delta$ (?? can we see it from formulas, or it is from common sense??). Для $eV>\Delta$ находим

$$I_{N-S}(V) = \frac{1}{eR}\int\limits_{-eV}^{-\Delta}\frac{|\varepsilon|d\varepsilon}{\sqrt{\varepsilon^2-\Delta^2}} = \frac{\sqrt{(eV)^2-\Delta^2}}{eR}$$

Таким образом, зависимость туннельного тока от напряжения имеет порог, равный Δ/e. Рассматривая аналогично случай $eV<0$, получаем искомую зависимость (11.32), обладающую свойством антисимметрии: $I_{N-S}(-V) = -I_{N-S}(V)$.

Случай малой температуры

Порог при $eV = \Delta$ является резким только при нулевой температуре. При конечной температуре в нормальном металле всегда имеются квазичастицы с энергией $\varepsilon > \Delta$, которые могут туннелировать в сверхпроводник. Поэтому естественно ожидать, что при $T > 0$ корневая особенность размывается и туннельный ток оказывается отличным от нуля при всех напряжениях.

Чтобы убедиться в том, что это действительно так, най дем туннельный ток под порогом при малых температурах $T \ll \Delta$. Интеграл в (11.61) при таких T определяется окрестностями точек $\varepsilon = \pm\Delta$. Введем обозначение $\varepsilon = \pm(\Delta + x)$ в каждой из областей. Как будет ясно из дальнейших вычислений, характерное значение x оказывается порядка T, поэтому можно разложить плотность состояний по x/Δ, then

$$I_{N-S}(V,T) = 4\pi e\nu_a\nu_b\,|T_0|^2 \int\limits_0^\infty \Big[n_F(\Delta + x) + n_F(-\Delta - x) - n_F(\Delta + eV + x) - n_F(-\Delta - x + eV)\Big]\frac{\Delta dx}{\sqrt{2\Delta x}}.$$

$n_F(-\varepsilon) = 1 - n_F(\varepsilon)$,

$$I_{N-S}(V,T) = \frac{1}{eR}\int\limits_0^\infty [n_F(\Delta - eV + x) - n_F(\Delta + x + eV)]\sqrt{\frac{\Delta}{2x}}dx.$$

(мы выразили туннельный матричный элемент T_0 через сопротивление контакта в нормальном состоянии, add this formla from the previous problem).

При больших положительных значениях энергии фермиевская функция распределения переходит в больцмановскую,

$$n_F(\varepsilon) \overset{\varepsilon \gg T}{\approx} e^{-\varepsilon/T}$$

и поэтому выражение для туннельного тока принимает следующий вид after a very trivial transformation:

$$I_{N-S}(V,T) = \frac{1}{eR}e^{-\Delta/T}\,\mathrm{sh}\,\frac{eV}{T}\cdot\int\limits_0^\infty \sqrt{\frac{2\Delta}{x}}e^{-x/T}dx$$

We trivially introduce $x' = x/T$, use $\Gamma(1/2) = \int x^{\frac{1}{2}-1}e^{-x}dx = \sqrt{\pi}$, and get

$$I_{N-S}(V,T) = \frac{\sqrt{2\pi\Delta T}}{eR}e^{-\Delta/T}\,\mathrm{sh}\,\frac{eV}{T}$$

Это выражение неприменимо в узкой окрестности порога при $(eV - \Delta) \sim T$, поскольку при таких напряжениях приближение $n_F(\varepsilon \gg T) \approx e^{-\varepsilon/T}$ нельзя применять к первому члену в (11.64).

Итак, при $0 < T \ll \Delta$ ток (11.61) при $eV < \Delta$ экспоненциально мал. По мере роста температуры ток под порогом $eV < \Delta$ возрастает, и когда температура достигает T_c, вольт-амперная характеристика становится омической, как для контакта между двумя нормальными металлами.

Помимо термоактивационного вклада в ток, описываемого $I_{N-S}(V,T) = \frac{\sqrt{2\pi\Delta T}}{eR}e^{-\Delta/T}\,\mathrm{sh}\,\frac{eV}{T}$, под порогом $eV = \Delta$ существует еще один весьма интересный вклад, не исчезающий при $T \to 0$. Он связан с когерентным туннелированием пары электронов с противоположными импульсами и спинами.

(??? add before that we don't consider two paericle tunnelings. why???)

Оказавшись в сверхпроводнике, такие два электрона могут образовать куперовскую пару. Туннелирование пары, в отличие от одночастичного туннелирования, не требует затраты энергии Δ на каждую частицу, и поэтому такой вклад не «вымерзает» при низких температурах. Когерентное туннелирование пар электронов часто называют андреевским отражением, поскольку описанный процесс перехода двух электронов из нормального металла в сверхпроводник можно рассматривать как превращение электрона в дырку при отражении от поверхности сверхпроводника. Вероятность двухчастичного туннелирования пропорциональна $|T_0|^4$, а не $|T_0|^2$, как для одночастичного туннелирования. Поэтому при $|T_0| \ll 1$ и не слишком низкой температуре двухчастичные процессы очень редки по сравнению с одночастичными. Вследствие этого андреевское отражение вносит существенный вклад в туннельный ток лишь при достаточно низких температурах.

ЛШ-70. Эффект Джозефсона.

В контакте двух сверхпроводников помимо одночастичного вклада в ток, рассмотренного в задачах 68 и 69 (! впишу формулы!), появляется дополнительный вклад, связанный с туннелированием куперовских пар. Формально этот вклад можно описать, заменив нормальные функции Грина в диаграмме на рис. 11.3 на аномальные - см. рис. 11.6.

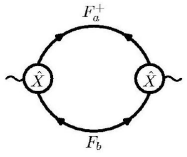


Рис. 11.6

Таким образом, туннельный эксперимент позволяет «измерить» аномальную функцию Грина в сверхпроводнике.

Покажите, что в равновесии, при $V = 0$, двухчастичный ток отличен от нуля и равен

$$I = I_0 \sin(\varphi_a - \varphi_b)$$

где $\varphi_{a(b)}$ - значения фазы сверхпроводящего параметра порядка $\Delta_{a(b)} = \left|\Delta_{a(b)}\right| e^{i\varphi_{a(b)}}$ на разных берегах контакта. Туннельный контакт между двумя сверхпроводниками, в котором имеет место эффект Джозефсона ($I = I_0 \sin(\varphi_a - \varphi_b)$), называется соответственно джозефсоновским контактом.

Рассмотрите случай, когда сверхпроводники по обе стороны контакта одинаковые, т.е. $\Delta_{a(b)} = \Delta e^{i\varphi_{a(b)}}$. Получите т.н. соотношение Амбегаокара-Баратова. для максимального тока в джозефсоновском контакте:

$$I_0(R) = \frac{\pi\Delta}{2eR} \operatorname{th} \frac{\Delta}{2T}$$

где R - сопротивление контакта при $T > T_c$.

Solution 70.

(??? remind background!!!)

Поскольку теперь у нас с обеих сторон контакта находятся сверхпроводники, первый член в выражении

$$\left\langle \mathrm{T}_\tau \widehat{X}(\tau)\widehat{I}(0)\right\rangle = \sum_{\mathbf{p}_1,\mathbf{p}_1',\mathbf{p}_2,\mathbf{p}_2'} T_{\mathbf{p}_1\mathbf{p}_1'} \left\langle \mathrm{T}_\tau \widehat{a}^+_{\mathbf{p}_1}(\tau)\widehat{b}_{\mathbf{p}_1'}(\tau)\left(T_{\mathbf{p}_2\mathbf{p}_2'}\widehat{a}^+_{\mathbf{p}_2}(0)\widehat{b}_{\mathbf{p}_2'}(0) - T^*_{\mathbf{p}_2\mathbf{p}_2'}\widehat{a}_{\mathbf{p}_2}(0)\widehat{b}^+_{\mathbf{p}_2'}(0)\right)\right\rangle.$$

оказывается отличным от нуля и усреднение необходимо выполнить заново. Как нетрудно видеть, первый член усредняется так же, как и раньше, с единственной разницей, состоящей в замене нормальных средних на аномальные.

Соответствующий вклад в восприимчивость χ_M выписывается по аналогии с задачей 68

(???? write here the derivation!!!)

и оказывается равным

$$\chi_{M,S-S}(i\Omega_n) = ieT\sum_{\omega_m}\sum_{\mathbf{pp}'} |T_{\mathbf{pp}'}|^2 F^+_{a,\mu\nu}(i\Omega_n + i\omega_m, \mathbf{p}) F_{b,\nu\mu}(i\omega_m, \mathbf{p}')$$

где $F_a(i\varepsilon_n, \mathbf{p})$ и $F_b(i\varepsilon_n, \mathbf{p})$ - аномальные функции Грина берегов контакта, а μ и ν - спиновые индексы. Суммируя по μ и ν с учетом спиновой структуры аномальных функций Грина, получаем выражение по виду сходное с (11.45) с точностью до замены нормальных функций Грина на аномальные:

$$\chi_{M,S-S}(i\Omega_n) = -2ieT\sum_{\omega_m}\sum_{\mathbf{pk}} |T_{\mathbf{pk}}|^2 F^+_a(i\Omega_n + i\omega_m, \mathbf{p}) F_b(i\omega_m, \mathbf{k})$$

Обратим внимание на то, что знаки выражений (11.45) и (11.69) совпадают. Это соответствует общему наблюдению о совпадении знаков «нормальных» ии «аномальных» петель, сделанному в решении задачи 63. (???? which????)

Поскольку, как мы увидим, джозефсоновский ток отличен от нуля в равновесии, т. е. при $V = 0$, нам будет достаточно вычислить $\chi_{M,S-S}(i\Omega_n)$ при $\Omega_n = 0$. Аналитическое продолжение оказывается ненужным, и можно сразу записать выражение для туннельного тока:

$$I_{S-S} = 4e|T_0|^2 T \operatorname{Im}\sum_{\omega_m}\int_{-\infty}^{\infty}\int_{-\infty}^{\infty} \frac{\Delta_a^*\nu_a d\xi_b}{\omega_m^2 + \xi_a^2 + |\Delta_a|^2}\frac{\Delta_b\nu_b d\xi_b}{\omega_m^2 + \xi_b^2 + |\Delta_b|^2} =$$

$$= 4\pi^2 e|T_0|^2 \nu_a\nu_b T \operatorname{Im}\sum_{\omega_m} \frac{\Delta_a^*\Delta_b}{\sqrt{\omega_m^2 + |\Delta_a|^2}\sqrt{\omega_m^2 + |\Delta_b|^2}}$$

Полученное выражение отлично от нуля когда фазы параметра порядка по разные стороны контакта различны. Пусть $\Delta_{a,b} = |\Delta_{a,b}| e^{i\varphi_{a,b}}$. Выражая туннельный матричный элемент T_0 через сопротивление контакта в нормальном состоянии, получаем соотношение Джозефсона:

$$I = I_0 \sin(\varphi_b - \varphi_a), \qquad I_0 = \frac{\pi}{eR} T \sum_{\omega_m} \frac{|\Delta_a| |\Delta_b|}{\sqrt{\omega_m^2 + |\Delta_a|^2}\sqrt{\omega_m^2 + |\Delta_b|^2}},$$

Отметим еще раз, что, в отличие от других разновидностей туннельного тока, джозефсоновский ток не связан с релаксацией к равновесному состоянию. Эффект Джозефсона ($I = I_0 \sin(\varphi_a - \varphi_b)$) имеет место в термодинамическом равновесии, и соответственно ток (11.71) между двумя сверхпроводниками с различающимися фазами параметра порядка может течь неограниченно долго.

Из-за того, что джозефсоновский ток отличен от нуля в равновесии также мы не рассматриваем вклад в туннельный ток $\left\langle \mathrm{T}_\tau \widehat{X}(\tau)\widehat{I}(0)\right\rangle = \sum_{...} T_{\mathbf{p}_1\mathbf{p}_1'} \langle ... \rangle$, содержащий нормальные средние. Как мы видели в задачах 68 и 69, такой вклад описывает некогерентное туннелирование отдельных электронов и приводит к току, исчезающему при $V = 0$ (???? why exactly, add formulas???).

Если $|\Delta_a| = |\Delta_b| \equiv \Delta$,

$$I_0 = \frac{\pi}{eR} T \sum_{\omega_m} \frac{\Delta^2}{\omega_m^2 + \Delta^2},$$

$\sum_{n=-\infty}^{\infty} \frac{1}{(2n+1)^2+a^2} = \frac{\pi}{2a} \operatorname{th} \frac{\pi a}{2}$ $\Rightarrow$

$$I_0(R) = \frac{\pi\Delta}{2eR} \operatorname{th} \frac{\Delta}{2T}$$

Фйг-7.1. Критический ток SNS перехода

Найти основную температурную зависимость критического тока SNS перехода при $T \to T_c$, используя теорию Гинзбурга-Ландау. Рассмотреть случая одинаковых и разных сверхпроводящих металлов.

Solution

(??? it is done before in BCS, but I don't know, how to do in in GL framework yet. it is interesting to see later, that if these results are the same? they should be...)

Фйг-7.2 Критический ток и ток захвата

Найти отношение критического тока I_c к току захвата I_r в джозефсоновском туннельном контакте с большим параметром Мак-Камбера $\beta_C \gg 1$.

Reminder: (??? what is this parameter?? what is the current of захват??)

Solution

(???)

14.2.11 Problems about tunneling, junctions 2: Basic Models

Фйг-7.3 Высота n-ой ступеньки Шапиро

Найти зависимость высоты n-ой ступеньки Шапиро от ее номера n для простейшей резистивной модели джожефсоновского контакта.

Reminder: (??? what is this ступенька??)

Solution

(???)

Фйг-7.4 Критический ток и поле для короткого SNS контакта

Вывести зависимость $I_c(B)$ критического тока от магнитного поля для короткого джозефсоновского перехода длины $L \leq \lambda_J$, где λ_J джозефсоновская глубина проникновения.

Solution

(??? maybe shmidt's theory is the best for it?? I have no idea, how to do it in BCS)

Фйг-7.5 Критический ток в двухконтактном СКВИДе

Для двухконтактного СКВИДа найти зависимость критического тока I_c от магнитного потока в катушке Φ_{ext} в двух предельных случаях: большого и малого параметра $\beta_L = 2\pi\mathcal{L}I_c/\Phi_0$, где $\mathcal{L}$ - индуктивность петли СКВИДа.

Solution

(??? maybe it is done in theory?)

Фйг-7.6* Джозефсоновский переход с флуктуациями сверхтока

Для длинного джозефсоновского перехода с длиной $L \gg \lambda_J$ плотность сверхтока в котором испытывает флуктуации по длине перехода, $j_c(x) = j_0 + \delta j(x)$, где среднее от $\delta j(x)$ равно 0, а коррелятор $\langle \delta j(x)\delta j(x')\rangle = D\delta(x-x')$, найти зависимость полного критического тока от магнитного поля B при больших полях, когда в области перехода находится много вихрей Джозефсона.

Solution

(??? if averaged now, then why there will be an impact?? I'll add a theory about such fluctuations later)

(?? is it a physical model???)

Фйг-13.2.Andreev level at $\phi = \pi$

Показать, что SNS контакт при разности фаз $\phi = \pi$ всегда содержит андреевский уровень с энергией $E = 0$.

Solution

(??? one can remember the CPR plot and it is always zero. so maybe basic derivation of Josephson relation is enough? anyway, I'll write an explicit answer later)

Фйг-13.3. Electronic heat capacity in the mixed state of type I SC

Найти электронную теплоемкость в смешанном состоянии сверхпроводника I рода, считая, что нормальные домены имеют плоскую форму и их толщина равна $d_N \gg \hbar v_F/\Delta$, а температура $T \ll T_c$.

Solution

(??? is there at all a mixed state of type I SC???? I'll listen to the lecture later. A. F. Andreev and P. Tekel wrote "Theory of a Surface "Mixed" State in Type I Superconductors", so there might be it.... I'll create a section in theory about it)

14.2.12 Problems about tunneling, junctions 3: Basic Models

Фйг-13.4. Эффективная масса возбуждений в вихре

Найти эффективную массу M_z возбуждений в коре абрикосовского вихря для произвольного отношения электронных масс $m_z/m_\perp$.
Reminder: (??? what is mass in the vortex)

Solution

(??? what is mass in the vortex)

Фйг-13.5. Mixed state, big field

Найти плотность электронных состояний в s-сверхпроводнике в смешанном состоянии с магнитным полем $B \ll H_{c2}$ при малых энергиях $E \ll \Delta$, и его теплоемкость при $T \ll T_c$.

Solution

(???)

Фйг-13.1. Андреевские уровни в SNS контакте

Найти низколежащие андреевские уровни в плоском SNS контакте в зависимости от разности фаз χ на сверхпроводящих берегах и при произвольном соотношении $\hbar v_F/\Delta$ и толщины нормальной области d.

Solution

(I think, there is a well-known formula, which should be in the beginning of my theory of Andreev reflection. Don't know it yet)

Shnirman, Piasotski.KIT.2024-5.1(m) ABS in an ideal long SNS

Consider a long SNS contact of length L. Provide a derivation for the Andreev reflection amplitude in the the left interface. Obtain the quantization condition and try to estimate the energies and the number of the Andreev bound states.

Solution

We need to just solve BdG equations. (??? need to write theory about it better!!)

We consider

$$H = \tau_z \left(\frac{p^2}{2m} - \mu \right) + (\Delta(x)\tau_+ + \text{h.c. }) \tag{1}$$

$$\Delta(x) = \Delta \left[\Theta(-x) + \Theta(x-L)e^{i\varphi} \right] \tag{2}$$

(???Why do they have v^*, not v?)
Left and right of the interface we have the following fundamental solutions

$$\psi_L(x) = \psi_k e^{ikx}, \quad \psi_R(x) = U\psi_k e^{ikx} \tag{3}$$

where

$$\psi_k = \begin{pmatrix} \Delta \\ \epsilon + \mu - \frac{k^2}{2m} \end{pmatrix}, \qquad \left(\frac{k^2}{2m} - \mu \right)^2 = -\Delta^2 + \epsilon^2, \qquad U := e^{i\varphi\tau_z/2} \tag{4}$$

We search for the bound state solutions, such that

$$\lim_{x\to-\infty} \psi_L(x) = \lim_{x\to\infty} \psi_R(x) = 0 \tag{5}$$

This forces us to choose

$$\psi_L(x) = c_+^L \psi_{-k_+} e^{-ik_+ x} + c_-^L \psi_{-k_-} e^{-ik_- x} = \begin{pmatrix} \psi_{-k_+} e^{-ik_+ x} & \psi_{-k_-} e^{-ik_- x} \end{pmatrix} \begin{pmatrix} c_+^L \\ c_-^L \end{pmatrix} \tag{6}$$

$$\psi_R(x) = c_+^R U \psi_{k_+} e^{ik_+(x-L)} + c_-^R U \psi_{k_-} e^{ik_-(x-L)} = U \begin{pmatrix} \psi_{k_+} e^{ik_+(x-L)} & \psi_{k_-} e^{ik_-(x-L)} \end{pmatrix} \begin{pmatrix} c_+^R \\ c_-^R \end{pmatrix} \tag{8}$$

$$k_\pm = \pm\sqrt{2m\mu \pm 2mi\sqrt{\Delta^2 - \epsilon^2}} \tag{9}$$

In the central section, all four fundamental solutions are admissible, so

$$\psi_C(x) = \left[c_{p+} e^{ik_N^p x} + c_{p-} e^{-ik_N^p x}\right] \begin{pmatrix} 1 \\ 0 \end{pmatrix} + \left[c_{h+} e^{ik_N^h x} + c_{h-} e^{-ik_N^h x}\right] \begin{pmatrix} 0 \\ 1 \end{pmatrix}, \tag{10}$$

$$k_N^p = \sqrt{2m(\mu + \epsilon)}, \quad k_N^h = \sqrt{2m(\mu - \epsilon).} \tag{11}$$

(!!! change what is below to true matrix notation!!!)
Now we apply the boundary conditions on the lhs

$$\begin{pmatrix} 0 & \begin{pmatrix} \psi_{-k_+} & \psi_{-k_-} \end{pmatrix} \\ 0 & -i \begin{pmatrix} k_+ \psi_{-k_+} & k_- \psi_{-k_-} \end{pmatrix} \end{pmatrix} \begin{pmatrix} c_+^R \\ c_-^R \\ c_+^L \\ c_-^L \end{pmatrix} = \begin{pmatrix} 1 & 1 & 0 & 0 \\ 0 & 0 & 1 & 1 \\ ik_N^p & -ik_N^p & 0 & 0 \\ 0 & 0 & ik_N^h & -ik_N^h \end{pmatrix} \begin{pmatrix} c_{p+} \\ c_{p-} \\ c_{h+} \\ c_{h-} \end{pmatrix}.$$

Now we apply the boundary conditions on the rhs

$$\begin{pmatrix} U \begin{pmatrix} \psi_{k_+} & \psi_{k_-} \end{pmatrix} & 0 \\ iU \begin{pmatrix} k_+ \psi_{k_+} & k_- \psi_{k_-} \end{pmatrix} & 0 \end{pmatrix} \begin{pmatrix} c_+^R \\ c_-^R \\ c_+^L \\ c_-^L \end{pmatrix} = \begin{pmatrix} e^{ik_N^p L} & e^{-ik_N^p L} & 0 & 0 \\ 0 & 0 & e^{ik_N^h L} & e^{-ik_N^h L} \\ ik_N^p e^{ik_N^p L} & -ik_N^p e^{-ik_N^p L} & 0 & 0 \\ 0 & 0 & ik_N^h e^{ik_N^h L} & -ik_N^h e^{-ik_N^h L} \end{pmatrix} \begin{pmatrix} c_{p+} \\ c_{p-} \\ c_{h+} \\ c_{h-} \end{pmatrix} \tag{14}$$

$$\begin{pmatrix} c_{p+} \\ c_{p-} \\ c_{h+} \\ c_{h-} \end{pmatrix} = \begin{pmatrix} 1 & 1 & 0 & 0 \\ 0 & 0 & 1 & 1 \\ ik_N^p & -ik_N^p & 0 & 0 \\ 0 & 0 & ik_N^h & -ik_N^h \end{pmatrix}^{-1} \begin{pmatrix} 0 & \begin{pmatrix} \psi_{-k_+} & \psi_{-k_-} \end{pmatrix} \\ 0 & -i \begin{pmatrix} k_+ \psi_{-k_+} & k_- \psi_{-k_-} \end{pmatrix} \end{pmatrix} \begin{pmatrix} c_+^R \\ c_-^R \\ c_+^L \\ c_-^L \end{pmatrix} \tag{15}$$

$$\begin{pmatrix} U \begin{pmatrix} \psi_{k_+} & \psi_{k_-} \end{pmatrix} & 0 \\ iU \begin{pmatrix} k_+ \psi_{k_+} & k_- \psi_{k_-} \end{pmatrix} & 0 \end{pmatrix} \begin{pmatrix} c_+^R \\ c_-^R \\ c_+^L \\ c_-^L \end{pmatrix} - M \begin{pmatrix} 0 & \begin{pmatrix} \psi_{-k_+} & \psi_{-k_-} \end{pmatrix} \\ 0 & -i \begin{pmatrix} k_+ \psi_{-k_+} & k_- \psi_{-k_-} \end{pmatrix} \end{pmatrix} \begin{pmatrix} c_+^R \\ c_-^R \\ c_+^L \\ c_-^L \end{pmatrix} = 0, \tag{16}$$

$$M := \begin{pmatrix} \cos\left(k_N^p L\right) & 0 & \sin\left(k_N^p L\right)/k_N^p & 0 \\ 0 & \cos\left(k_N^h L\right) & 0 & \sin\left(k_N^h L\right)/k_N^h \\ -k_N^p \sin\left(k_N^p L\right) & 0 & \cos\left(k_N^p L\right) & 0 \\ 0 & -k_N^h \sin\left(k_N^h L\right) & 0 & \cos\left(k_N^h L\right) \end{pmatrix} \tag{17}$$

It follows that we have the condition

$$\det \begin{pmatrix} UJ & -CJ + iSK^{-1}JK_S \\ iUJK_S & SKJ + iCJK_S \end{pmatrix} = 0 \tag{18}$$

where

$$C = \begin{pmatrix} \cos\left(k_N^p L\right) & 0 \\ 0 & \cos\left(k_N^h L\right) \end{pmatrix}, \quad S = \begin{pmatrix} \sin\left(k_N^p L\right) & 0 \\ 0 & \sin\left(k_N^h L\right) \end{pmatrix} \tag{19}$$

$$K = \begin{pmatrix} k_N^p & 0 \\ 0 & k_N^h \end{pmatrix}, \quad K_S = \begin{pmatrix} k_+ & 0 \\ 0 & k_- \end{pmatrix}, \tag{20}$$

$$J = \begin{pmatrix} \psi_{k_+} & \psi_{k_-} \end{pmatrix} = \begin{pmatrix} \Delta & \Delta \\ \epsilon - i\sqrt{\Delta^2 - \epsilon^2} & \epsilon + i\sqrt{\Delta^2 - \epsilon^2} \end{pmatrix}. \tag{21}$$

To obtain the desired result we approximate $k_N^p \approx k_N^h \approx k_+ \approx -k_- \approx k_F$ everywhere apart from the phases. In this connection, the secular equation (19) simplifies to
(!!!! this is the important point, how exactly it is done??? try to to it!!!)

$$\det\begin{pmatrix} UJ & -CJ+iSJ\tau_z \\ ik_F UJ\tau_z & k_F\left[SJ+iCJ\tau_z\right] \end{pmatrix} = \det\left[UJk_F\right]\det\left[SJ+iCJ\tau_z+iUJ\tau_z(J)^{-1}U^\dagger\left(CJ-iSJ\tau_z\right)\right]=0 \quad (23)$$

This yields the condition
(?? check!)

$$\left(\Delta^2-2\epsilon^2\right)\cos\left(\left[k_N^p-k_N^h\right]L\right)+\Delta^2\cos\varphi-2\epsilon\sqrt{\Delta^2-\epsilon^2}\sin\left(\left[k_N^p-k_N^h\right]L\right)=0. \quad (24)$$

If we parametrise the energies inside of the gap as $\epsilon=\Delta\cos\chi$, we find that

$$\cos\varphi=\cos\left(\left[k_N^p-k_N^h\right]L-2S_\chi\chi\right),\quad S_\chi=\frac{\sin(\chi)}{|\sin(\chi)|} \quad (25)$$

which is the condition discussed in the class

$$\varphi=\left[k_N^p-k_N^h\right]L-2S_\chi\chi \mod 2\pi \quad (26)$$

(??? what is the meaning of this formula???)

Shnirman, Piasotski.KIT.2024-5.2(m),BTK NS contact with δ-barrier

Consider NS contact with one transverse channel (effectively one-dimensional wire), where the superconducting order parameter vanishes for $x<0$ and is equal to $|\Delta|e^{i\phi}$ for $x>0$. Let us add a δ-potential barrier at $x=0$, namely $V(x)=H\delta(x)$. Write down the BdG equations for this case and find the scattering amplitudes in all possible scattering channels for an incoming (from the normal side) electron with energy E. Consider both cases $E<|\Delta|$ and $E>|\Delta|$.

Solution

The BdG equations read

$$\begin{pmatrix} -\frac{\hbar^2\nabla_x^2}{2m}+V(x)-\tilde{\mu} & \Delta(x) \\ \Delta^*(x) & \frac{\hbar^2\nabla_x^2}{2m}-V(x)+\tilde{\mu} \end{pmatrix}\begin{pmatrix} u \\ v^* \end{pmatrix}=E\begin{pmatrix} u \\ v^* \end{pmatrix} \quad (27)$$

This gives

$$\begin{pmatrix} -\frac{\hbar^2\nabla_x^2}{2m}+H\delta(x)-\tilde{\mu} & \Delta(x) \\ \Delta^*(x) & \frac{\hbar^2\nabla_x^2}{2m}-H\delta(x)+\tilde{\mu} \end{pmatrix}\begin{pmatrix} u \\ v^* \end{pmatrix}=E\begin{pmatrix} u \\ v^* \end{pmatrix} \quad (28)$$

The delta-function can only be compensated by a jump in the first derivative. Thus, instead of continuity of the first derivative we obtain a new boundary condition

$$\left.\frac{du}{dx}\right|_{x=+0}-\left.\frac{du}{dx}\right|_{x=-0}=\frac{2mH}{\hbar^2}u(x=0) \quad (29)$$

$$\left.\frac{dv^*}{dx}\right|_{x=+0}-\left.\frac{dv^*}{dx}\right|_{x=-0}=\frac{2mH}{\hbar^2}v^*(x=0) \quad (30)$$

These are in addition to the continuity of the wave functions themselves:

$$u(x=+0)=u(x=-0)\quad,\quad v^*(x=+0)=v^*(x=-0) \quad (31)$$

Case $E<|\Delta|$
As in the script the solution for $x<0$ reads

$$\Psi(x<0)=\frac{1}{\sqrt{v_F}}\begin{pmatrix}1\\0\end{pmatrix}e^{ik_e x}+\frac{r_N}{\sqrt{v_F}}\begin{pmatrix}1\\0\end{pmatrix}e^{-ik_e x}+\frac{r_A}{\sqrt{v_F}}\begin{pmatrix}0\\1\end{pmatrix}e^{ik_h x} \quad (32)$$

and the solution for $x>0$ reads

$$\Psi(x>0)=A\begin{pmatrix}U_g\\e^{-i\phi}U_g^*\end{pmatrix}e^{ik_1 x}+B\begin{pmatrix}U_g^*\\e^{-i\phi}U_g\end{pmatrix}e^{ik_2 x} \quad (33)$$

where

$$U_g \equiv \sqrt{\frac{E + i\sqrt{|\Delta|^2 - E^2}}{2E}} \tag{34}$$

$$k_1 = k_F \sqrt{1 + i\frac{\sqrt{|\Delta|^2 - E^2}}{\tilde{\mu}}} \tag{35}$$

$$k_2 = -k_F \sqrt{1 - i\frac{\sqrt{|\Delta|^2 - E^2}}{\tilde{\mu}}} \tag{36}$$

The continuity of the wave functions gives

$$\begin{aligned} \frac{1 + r_N}{\sqrt{v_F}} &= AU_g + BU_g^* \\ \frac{r_A}{\sqrt{v_F}} &= \left(AU_g^* + BU_g\right) e^{-i\phi} \end{aligned} \tag{37}$$

For the derivatives we approximately put $|k_e| \approx |k_h| \approx |k_1| \approx |k_2| \approx k_F$. Then

$$\begin{aligned} \frac{1 - r_N}{\sqrt{v_F}} + \frac{2mH}{ik_F\hbar^2}\left[\frac{1 + r_N}{\sqrt{v_F}}\right] &= AU_g - BU_g^* \\ \frac{r_A}{\sqrt{v_F}} + \frac{2mH}{ik_F\hbar^2}\left[\frac{r_A}{\sqrt{v_F}}\right] &= \left(AU_g^* - BU_g\right) e^{-i\phi} \end{aligned} \tag{38}$$

Adding and subtracting we obtain

$$AU_g = 1/\sqrt{v_F} + \frac{mH}{ik_F\hbar^2}\left[\frac{1 + r_N}{\sqrt{v_F}}\right] \tag{39}$$

$$AU_g^* e^{-i\phi} = r_A/\sqrt{v_F}\left[1 + \frac{mH}{ik_F\hbar^2}\right] \tag{40}$$

$$BU_g^* = r_N/\sqrt{v_F} - \frac{mH}{ik_F\hbar^2}\left[\frac{1 + r_N}{\sqrt{v_F}}\right] \tag{41}$$

$$BU_g e^{-i\phi} = -\frac{mH}{ik_F\hbar^2}\left[\frac{r_A}{\sqrt{v_F}}\right] \tag{42}$$

Excluding A from the first two equations we get

$$r_A\left[1 + \frac{mH}{ik_F\hbar^2}\right] = e^{-i\phi}e^{-i\gamma}\left[1 + \frac{mH}{ik_F\hbar^2}\left(1 + r_N\right)\right] \tag{43}$$

Here $\gamma(E) \equiv \arccos(E/|\Delta|)$ and $e^{-i\gamma} = U_g^*/U_g$. From the second pair of equations we exclude B and obtain

$$r_A\left[-\frac{mH}{ik_F\hbar^2}\right] = e^{-i\phi}e^{i\gamma}\left[r_N - \frac{mH}{ik_F\hbar^2}\left(1 + r_N\right)\right] \tag{44}$$

Let us introduce

$$Z = \frac{mH}{k_F\hbar^2} \tag{45}$$

Then the equations read

$$r_A[1 - iZ] = e^{-i\phi}e^{-i\gamma}\left[1 - iZ\left(1 + r_N\right)\right] \tag{46}$$

$$r_A iZ = e^{-i\phi}e^{i\gamma}\left[r_N + iZ\left(1 + r_N\right)\right] \tag{47}$$

Excluding r_N we obtain

$$r_A = \frac{e^{-i\phi}}{(1+Z^2)\,e^{i\gamma} - Z^2 e^{-i\gamma}} \tag{48}$$

The probability of Andreev reflection is equal to

$$|r_A|^2 = \frac{1}{\cos^2\gamma + (1+2Z^2)^2 \sin^2\gamma} \leq 1 \tag{49}$$

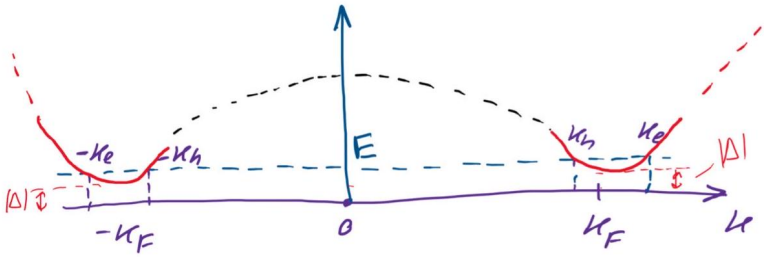
Of course one has $|r_N|^2 + |r_A|^2 = 1$.
Case $E > |\Delta|$
In this case the waves propagate further at $x > 0$. The possible solutions (propagating to the right) are the ones with $k = k_e$ and $k = -k_h$ in Fig. 1. The the solution for $x > 0$ reads

$$\Psi(x>0) = \frac{A}{\sqrt{v_g}} \begin{pmatrix} u_0 \\ e^{-i\phi} v_0 \end{pmatrix} e^{ik_e^{(s)} x} + \frac{B}{\sqrt{v_g}} \begin{pmatrix} v_0 \\ e^{-i\phi} u_0 \end{pmatrix} e^{-ik_h^{(s)} x} \tag{50}$$

where

$$u_0 \equiv \sqrt{\frac{E - \sqrt{E^2 - |\Delta|^2}}{2E}} \tag{51}$$

$$v_0 \equiv \sqrt{\frac{E + \sqrt{E^2 - |\Delta|^2}}{2E}} \tag{52}$$



Spectrum on the superconducting side of the NS contact.
The group velocity of these solutions reads (here $\xi_k > 0$)

$$v_g = \frac{1}{\hbar}\frac{\partial E_k}{\partial k} = \frac{1}{\hbar}\frac{\partial \sqrt{|\Delta|^2 + \xi_k^2}}{\partial k} = \frac{1}{\hbar}\frac{\xi_k}{E_k}\frac{\partial \xi_k}{\partial k} \approx \left(v_0^2 - u_0^2\right) v_F \tag{53}$$

The continuity of the wave functions at $x = 0$ gives

$$\begin{aligned} \frac{1 + r_N}{\sqrt{v_F}} &= \frac{A u_0 + B v_0}{\sqrt{v_g}} \\ \frac{r_A}{\sqrt{v_F}} &= \frac{A v_0 + B u_0}{\sqrt{v_g}} e^{-i\phi} \end{aligned} \tag{54}$$

For the derivatives we approximately put $|k_e| \approx |k_h| \approx \left|k_e^{(s)}\right| \approx \left|k_h^{(s)}\right| \approx k_F$. Then

$$\begin{aligned} \frac{1 - r_N}{\sqrt{v_F}} + \frac{2mH}{ik_F\hbar^2}\left[\frac{1 + r_N}{\sqrt{v_F}}\right] &= \frac{A u_0 - B v_0}{\sqrt{v_g}} \\ \frac{r_A}{\sqrt{v_F}} + \frac{2mH}{ik_F\hbar^2}\left[\frac{r_A}{\sqrt{v_F}}\right] &= \frac{A v_0 - B u_0}{\sqrt{v_g}} e^{-i\phi} \end{aligned} \tag{55}$$

```
expr = (1 + Z^2) Exp[I g] - Z^2 Exp[-I g];
Simplify[ComplexExpand@Abs@expr]
```

(??? Why do they have v^*, not v?)

S_1NS_2 Junction

Solution

(??? I'll add some question from Chang, Bagwell...)

Фйг-13.6. Maximal SC dot in normal metal

Рассмотреть гранулу очень малого размера a из сверхпроводящего металла. Найти (используя стандартную модель БКШ) оценку для величины a, при которой конечность размера гранулы начинает заметно влиять на условие для куперовской неустойчивости нормального металлического состояния.

Solution

(??? maybe it changes the Fermi energy? I have no idea, the whole BCS model does not take into account size of the material)

14.2.13 Ginzburg-Landau Formalism: Problems about phenomena [SEE COND MATT]

Б-3.4.5. Квантование потока

Комплексность сверхпроводящего параметра порядка $\psi = |\psi| \times \times \exp(i\theta)$ приводит к эффекту квантования магнитного потока в сверхпроводнике. Наряду с вектор-потенциалом $\mathbf{A}(\mathbf{r})$ градиент фазы $\nabla\theta$ также дает вклад в плотность сверхпроводящего тока:

$$\mathrm{j}_s = \frac{c}{4\pi\delta^2}\left(\frac{\hbar c}{2e}\nabla\theta - \mathbf{A}\right).$$

Доказать, что поток магнитного поля Φ через замкнутый контур C, на котором сверхпроводящий ток тождественно равен нулю $\mathbf{j}_s = 0$ и параметр порядка отличен от нуля $\psi \neq 0$, всегда кратен целому числу n квантов магнитного потока $\phi_0 = \pi\hbar c/e$. Найти пример простейшего вихревого состояния, несущего несколько квантов магнитного потока.

FOR PROBLEMS IN BELOUSOV SEE COND MATTER FOR NOW

Solution

(???)

Фйг-2.2. Квантование потока внутри тонкой пленки

Найти, как квантуется магнитный поток внутри тонкой ($d \ll \lambda$) сверхпроводящей пленки, нанесенной на поверхность цилиндрической нити радиуса $R \gg (d, \lambda)$.

Solution

(???)

Б-3.4.9. Тонкая пластина

Имеется тонкая пластина сверхпроводника первого рода с параметром Гинзбурга-Ландау $\varkappa \ll 1$ и толщиной D. Пластина находится во внешнем магнитном поле H_0, параллельном плоскостям пластины. Найти распределение сверхпроводящего тока и магнитного поля в пластине и определить критическое значение толщины пластины, при которой изменяется род фазового перехода в магнитном поле.

Solution

(???)

Б-3.4.10 Критический ток тонкой пленки

Определить критическую плотность сверхпроводящего тока j_s, который может протекать по тонкой пленке сверхпроводника толщиной d, много меньшей корреляционной длины ξ и глубины проникновения магнитного поля δ. Считать плотность сверхпроводящего тока однородной по сечению пленки.

Solution

(???)

FOR PROBLEMS IN BELOUSOV SEE COND MATTER FOR NOW

Б-3.4.6. Энергия в вихре и первое критическое поле

Для предельного сверхпроводника второго рода с параметром Гинзбурга-Ландау $\varkappa \gg 1$ найти:
а) энергию на единицу длины прямолинейного квантового вихря;
б) нижнее или первое критическое магнитное поле H_{c1}.

Solution

(???)

Б-3.4.7. Анизотропия верхнего критического поля

Коэффициент γ перед градиентным членом в разложении Гинзбурга-Ландау для свободной энергии сверхпроводящего кристалла должен отражать анизотропию направлений в кристалле и представляет собой тензор второго ранга $\gamma_{ij}(i,j = 1,2,3)$. В одноосном кристалле с тетрагональной или с гексагональной симметрией он равен

$$\gamma_{ij} = (\delta_{ij} - n_i n_j)\,\gamma_\perp + n_i n_j \gamma_\parallel,$$

где $\mathbf{n}$ - единичный вектор в направленин оси симметрин кристалла. (В кристаллах с кубической симметрией $\gamma_\perp = \gamma_\parallel$..) Рассмотреть анизотропию верхнего критического поля, т. е. зависимость поля H_{c2} от угла θ между осью симметрии кристалла $\mathbf{n}$ и направлением внешнего магнитного поля.

Solution

(???)

Б-3.4.8. Поверхностная сверхпроводимость

Параллельно плоской поверхности сверхпроводника приложено внешнее магнитное поле. Показать, что образование сверхпроводящей фазы начинается в приповерхностном слое сверхпроводника, и оценить соответствующее поверхностное критическое поле H_{c3}. Найти диапазон магнитных полей, в котором возможно явление поверхностной сверхпроводимости, заключающееся в наличии сверхпроводящей фазы в приповерхностном слое и ее отсутствии в объеме сверхпроводника.

FOR PROBLEMS IN BELOUSOV SEE COND MATTER FOR NOW

Б-3.4.11 эффект Литтла-Паркса

Определить период осцилляций температуры сверхпроводящего перехода тонкого полого цилиндра радиуса R и толщиной $d \ll \xi, \delta, R$ в зависимости от величины потока магнитного поля $\Phi = \pi R^2 H$, направленного вдоль оси цилиндра (эффект Литтла-Паркса).

Фйг-2.1. Эффект Литтла-Паркса

Найти зависимость T_c сверхпроводящего цилиндра с толщиной стенок d и радиусом $R \gg d \geq \xi_0$ от магнитного поля, направленного вдоль оси цилиндра (эффект Литтла-Паркса).

Б-3.4.12 Поверхностное натяжение in SN contact

Определить коэффициент поверхностного натяжения для границы между сверхпроводящей и нормальной фазами в сверхпроводнике первого рода с предельно малым параметром Гинзбурга-Ландау $\varkappa \ll 1$, когда можно пренебречь глубиной проникновения магнитного поля и считать, что магнитное поле не проникает в сверхпроводящую область.

Solution

(???)

FOR PROBLEMS IN BELOUSOV SEE COND MATTER FOR NOW

Б-3.4.13 Взаимодействие двух вихревых линий (!?!?!?!?)

Найти в сверхпроводнике второго рода с $\varkappa \gg 1$ энергию и силу взаимодействия двух параллельных вихревых линий, расположенных на расстоянии $r \gg \xi$ друг от друга. Показать, что квантованные вихри с одинаковым направлением циркуляции сверхпроводящего тока отталкиваются, а с противоположно направленными - притягиваются.

Б-3.4.14 Притяжение вихревой линии

Показать, что вихревая линия, параллельная поверхности сверхпроводника, притягивается к его поверхности. Определить силу притяжения.

Solution

(???)

Б-3.4.15. Фазовая диаграмма состояний в ферромагнитном сверхпроводнике

Металл с магнитными атомами, в котором могут сосуществовать и конкурировать два явления: сверхпроводимость и ферромагнетизм, можно назвать ферромагнитным сверхпроводником. Например, халькогениды $HoMo_6S_8, HoMo_6Se_8$ и борид $ErRh_4B_4$. Считая температуры сверхпроводящего перехода T_c и Кюри θ близкими, ферромагнитный сверхпроводник можно описать в рамках теории функционала Гинзбурга-Ландау с двумя взаимодействующими параметрами порядка: сверхпроводящим $\psi(\mathbf{r})$ и намагниченностью $\mathbf{M}(\mathbf{r})$, используя следующее разложение для плотности свободной энергии, отсчитанной от нормального состояния:

$$\Delta F = \alpha(T)|\psi|^2 + \frac{\beta}{2}|\psi|^4 + \frac{A(T)}{2}\mathbf{M}^2 + \frac{B}{4}\mathbf{M}^4 + G\mathbf{M}^2|\psi|^2$$

Константа взаимодействия $G > 0$, что соответствует подавлению сверхпроводимости при появлении ферромагнитного упорядочения. Коэффициенты разложения $\alpha(T) = \alpha_0\,(T - T_c)$ и $A(T) = A_0(T - \theta)$, а остальные не зависят от температуры. Для случая $T_c > \theta$ определить возможные фазы, найти род фазовых переходов и построить фазовую диаграмму состояний в зависимости от константы взаимодействия. Считать, что ферромагнитное состояние энергетически гораздо выгоднее, чем сверхпроводящее.

Solution

(???)

FOR PROBLEMS IN BELOUSOV SEE COND MATTER FOR NOW

Б-3.4.16 Антиферромагнитный геликоид

Пусть в изотропном ферромагнитном сверхпроводнике одновременно реализуются ферромагнитное и сверхпроводящее состояния. С учетом энергии магнитного поля величиной $\mathbf{h} = \operatorname{rot}\mathbf{A}$ и энергий

неоднородности функционал Гинзбурга-Ландау имеет вид

$$\Delta\mathcal{F} = \int d^3r \Delta F\left(\mathbf{M}(\mathbf{r}), \psi(\mathbf{r}), \psi^*(\mathbf{r}), \mathbf{A}(\mathbf{r})\right),$$

$$\Delta F = \frac{C_m}{2}(\nabla\mathbf{M})^2 + \frac{A(T)}{2}\mathbf{M}^2 + \frac{B}{4}\mathbf{M}^4 + \frac{(\mathbf{h}-4\pi\mathbf{M})^2}{8\pi} + \frac{\gamma}{2}\left|\left(-i\hbar\nabla - \frac{2e}{c}\mathbf{A}\right)\psi\right|^2 + \alpha(T)|\psi|^2 + \frac{\beta}{2}|\psi|^4 + G\mathbf{M}^2|\psi|^2.$$

При температурах заметно ниже точки Кюри θ и сверхпроводящего перехода T_c абсолютные величины вектора намагниченности $\mathbf{M}$ и сверхпроводящего параметра ψ можно считать фиксированными. Найти условие на коэффициент магнитной жесткости C_m, при котором однородное ферромагнитное упорядочение становится неустойчивым и возникает спин-спиральная фаза, в которой вектор намагниченности $\mathbf{M}$ равномерно поворачивается в плоскости, перпендикулярной выделенной оси при движении вдоль этой оси. Такая магнитная структура называется антиферромагнитным геликоидом. Определить период геликоида (шаг спирали) в зависимости от глубины проникновения магнитного поля δ. Возможность состояний с квантованными вихрями не рассматривать.

Solution

(???)

Б-3.4.17. Корреляции ψ

В нормальной фазе при температуре выше температуры сверхпроводящего перехода возможны флуктуации сверхпроводящего параметра порядка $\psi(\mathbf{r})$. Определить пространственную корреляционную функцию $\langle\psi(\mathbf{r})\psi^*(\mathbf{r}')\rangle$, пренебрегая членом четвертого порядка в функционале Гинзбурга-Ландау.

Solution

(???)

Б-3.4.18. Diamagnetic susceptibility of granules due to Cooper pairs

Возможность флуктуационного рождения сверхпроводящих куперовских пар в нормальной фазе при температуре выше температуры сверхпроводящего перехода T_c создает дополнительный вклад в диамагнитную восприимчивость металла. Вычислить флуктуационную поправку к диамагнитной восприимчивости во внешнем магнитном поле H при $T > T_c$ для нульмерного сверхпроводника (сферической гранулы малого радиуса: $R \ll \xi$ и $R \ll \delta$).

FOR PROBLEMS IN BELOUSOV SEE COND MATTER FOR NOW

Б-3.4.19. Размытие фазового перехода в 0D сверхпроводнике

В нульмерном сверхпроводнике - малой грануле с характерным размером $R \ll \xi(T)$ - найти поведение квадрата модуля сверхпроводящего параметра порядка $|\psi_0(T)|^2$ в области температур, близких к критической точке перехода T_c в объемном сверхпроводнике. Найти условие малости размытия фазового перехода, если объем гранулы V, а среднее расстояние между уровнями энергий вследствие размерного квантования равно $\delta\varepsilon$.

Фйг-2.3. Parallel critical field and thin film current

Найти параллельное критическое магнитное поле и критический ток для тонкой сверхпроводящей пленки (толщина $d \ll \lambda$).

Фйг-2.4. Change of transition temperature in a thin film

Пленка сверхпроводящего металла толщины d нанесена на толстый слой нормального металла. Граница S/N полностью прозрачна для электронов. Длина когерентности $\xi(T) = \xi_0\left(1 - T/T_{c0}\right)^{-1/2}$, причем $\xi_0 \ll d$. Найти сдвиг температуры перехода в зависимости от толщины d. Длину когерентости в нормальном металле ξ_n при $T \sim T_{c0}$ считать постоянной.

Фйг-2.5. Prove that $H_{c2}(T) > H_c(T)$

Показать, что при $\kappa > 1/\sqrt{2}$ неустойчивость нормального состояния по отношению к образованию сверхпроводящего параметра порядка наступает при поле $H_{c2}(T) > H_c(T)$.

14.2.14 Type II superconductors: Basic Problems 1

Фйг-3.1. Vortices in thin film

Найти зависимость плотности тока $j(r)$ на расстоянии r от центра вихря в тонкой пленке толщины $d \ll \lambda$, затем вычислить энергию такого вихря и энергию взаимодействия вихря и анти-вихря на расстоянии $r \gg \lambda$. Вычисления довести до конца в двух предельных случаях, $r \ll \lambda^2/d$ и $r \gg \lambda^2/d$.

Solution

(???)

Фйг-3.2. Surface barrier for vortices

Исследовать "поверхностный барьер" для входа вихрей в сверхпроводник II рода, используя лондоновское приближение; найти внешнее поле H^* при котором поверхностный барьер исчезает.

Solution

(???)

Фйг-3.3*

Выяснить, сохраняется ли поверхностный барьер (задача #1) для случая тонких пленок толщины $d \ll \lambda$.

Solution

(???)

Фйг-3.4.

Найти критическое поле H_{c3}, при котором с понижением поля возникают поверхностные сверхпроводящие состояния (выразить его значение через H_{c2}).

Solution

(???)

Фйг-3.5*. При $\kappa = 1/\sqrt{2}$ взаимодействие вихрей исчезает, и $H_c = H_{c1} = H_{c2}$

Показать, что при $\kappa = 1/\sqrt{2}$ взаимодействие вихрей исчезает, а все три критические поля H_c, H_{c1} и H_{c2} равны между собой.

Solution

(???)

Фйг-3.6.

Найти $B(H)$ при полях слегка больших H_{c1}, т.е. $H - H_{c1} \ll H_{c1}$.

Solution

(???)

Фйг-3.7. Уширение линии ЯМР

Определить уширение линии ЯМР из-за неоднородности магнитного поля в сверхпроводнике при $H_{c1} \ll B \ll H_{c2}$.

Solution

(???)

14.2.15 Other Problems by Shmidt's book

(I'll think about them later)

Problems

Problem 1.1. A Pb specimen with a flat surface is placed in a magnetic field parallel to this surface. The field is equal to the critical magnetic field, $H_{\rm cm}\,(T)$, and the temperature is 4.2 K. Find the surface current flowing within a 1 cm wide band

Problem 1.2. Find the free energy gain associated with the superconducting transition for 1 $\rm cm^3$ of Pb. The transition takes place at 4.2 K.

Problem 1.3. Under the conditions of Problem 1.2, find the amount of latent heat given up by 1 $\rm cm^3$ of Pb during the transition into the superconducting state.

Problem 1.4. Find the temperature at which the heat capacities of Pb in the normal and superconducting states are equal.

Problem 1.5. Find the value of the thermodynamic critical field of Sn at $T = 3$ K.

Problem 1.6. Find the value of the heat capacity jump at the critical temperature for 1 $\rm cm^3$ of Pb.

14.3 Questions about Checking Basic Knowledge

14.3.1 Questions about Understanding Basics 1

Какова глубина проникновения поля в сверхпроводник?

(про лондоновскую длину, все такое.)

I-motiv.3 Levitation of superconductor

(??? почему такое явление есть????)

KUL.2019.exam Overview of GL theory

a) Discuss in detail the Ginzburg-Landau (GL) theory. Explain how to arrive at the GL equations, discuss the physical meaning of the coefficients and parameters in the GL-equations.

b) Explain how the characteristic length scales appear from the GL theory and how to understand their physical meaning. Explain also their temperature dependence according to the GL theory.

c) Which characteristic length scale does not directly evolve from the GL theory? What is its physical meaning?

d) Compare the GL theory with other theories and models for superconductivity.

Answers:

(потом допишу, типичные хорошие вопросы)

1. Фазовым переходом какого рода является сверхпроводящий переход?

Answer:

2. Запишите выражение для спектра возбуждений $\varepsilon(p)$ в модели Бардина-Купера-Шриффера.

Answer:

3. Какова связь между энергетической щелью $\Delta(0)$ и критической температурой сверхпроводника T_c?

Answer:

4. Как зависит от константы взаимодействия λ энергетическая щель $\Delta(0)$ при нулевой температуре? Аналитична ли эта зависимость?

Answer:

5. Чему равна энергия связи куперовской пары при константе взаимодействия λ?

Answer:

6. Как связаны энергетическая щель Δ и концентрация сверхпроводящих электронов n_s?

Answer:

7. Как зависит от температуры энергетическая щель сверхпроводника $\Delta(T)$ вблизи точки перехода T_c?

Answer:

8. Как зависит от температуры T критический ток $j_c(T)$ сверхпроводника вблизи точки перехода T_c?

Answer:

9. Как зависит от температуры T критическое магнитное поле $\mathcal{H}_c(T)$ сверхпроводника вблизи точки перехода T_c?

Answer:

10. Как зависит от температуры T теплоемкость сверхпроводника $C_s(T)$ ниже точки перехода T_c?

Answer:

1. Запишите выражение для функционала Гинзбурга-Ландау Ω_s.

Answer:

2. Запишите уравнение Гинзбурга-Ландау для комплексного параметра порядка $\psi(\mathbf{r})$.

Answer:

3. Запишите уравнение Гинзбурга-Ландау для векторного потенциала $\mathcal{A}(\mathbf{r})$.

Answer:

4. Как зависит от температуры T корреляционная длина ξ вблизи точки перехода T_c? Чему равен размер куперовской пары?

Answer:

Как зависит от температуры T лондоновская глубина проникновения λ вблизи точки перехода T_c?

Answer:
(copy the well-known formulas)
(?? explain, why it is so by intuition and from what formulas this comes?)

6. Запишите выражение для плотности сверхпроводящего тока j_s.

Answer:

7. Запишите равенство, выражающее сущность эффекта Мейсснера.

Answer:

8. Запишите выражения для кванта магнитного потока Φ_0 и магнитного потока через полость сверхпроводника Ф.

Answer:

8. How many there are phonons at $T = 0$? Are they anough to couple all electrons near Fermi surface?

Answer:
There are zero phonons.
(??? why???)
They are not used for superconductivity because there, the virtual phonons are used.
(??? what are virtual phonons - I don't know, but there is paragraph about it in theory)

9. В каком соотношении находятся корреляционная длина ξ и лондоновская глубина проникновения магнитного поля λ для сверхпроводников II рода?

Answer:

10. Запишите оценочные выражения для верхнего $\mathcal{H}_{c2}$, нижнего $\mathcal{H}_{c1}$ и термодинамического $\mathcal{H}_c$ критических магнитных полей.

Answer:

11. Возможно ли проникновение в сверхпроводник нормального к поверхности магнитного поля?

Answer:
yes, this is the Meissner effect.

12. Возможно ли проникновение в сверхпроводник электрического поля?

Answer:
depends on dielectric properties (???)

14.3.2 Questions about Understanding Basics 2

(maybe I'll add reminders before answers for people not to look for some basics if they forgot the answer)

2. Какой эксперимент, основанный на использовании внешнего магнитного поля, позволяет отличить сверхпроводник от гипотетического идеального проводника (с $R = 0$)?

Answer:

3. Какие классы веществ, проявляющие SC свойства, известны на данный момент?

Answer:

4. Нарисуйте типичную для SC зависимость $R(T)$. Три способа определения критической T_c.

Answer:

5. Нарисуйте зависимости $H_c(T)$ и $n_s(T)$. Какими формулами они приближенно описываются?

Answer:

6. Переходом какого рода является переход в SC состояние?

Answer:

7. Каков физический смысл параметров сверхпроводящего состояния Δ_0 и ξ?

Answer:

Write the London equations. What is the physical meaning of λ_L? How are j_c and $H_c(0)$ related?

Answer:
(??? are these questions related?)

What is the radius of the core of the apricot vortex? What is the energy of a single apricot vortex and what does it consist of?

(maybe I'll add reminder here for people not to look for some basics if they forgot the answer)

Answer:

Question about basic properties of SC

10. В чём заключается и что однозначно доказывает изотопический эффект у SC?

Answer:

11. What is the energy ratio that describes the so-called "quasi-classical approximation" in BCS?

Answer:

ACTUALLY, IT IS A GOOD IDEA TO CREATE QUESTIONS LIKE "WHAT IS (SOMETHING)", and this something is not explained in the theory, but it is easily restored by the common sense, if one knows the theory!!!

I'll add some these questions later.

12. Как меняется вид зависимости плотности электронных состояний от энергии $N(E)$ и спектр возбуждений носителей $E(p)$ при переходе металл - SC (при $T \to 0$)? Какие формулы описывают их в рамках теории БКШ?

Answer:

13. Как вводятся константы электрон-фононного взаимодействия λ и кулоновского отталкивания μ^*? В чём заключается перенормировка λ в приближении сильной связи?

Answer:

14. Какое выражение для SC щели Δ_0 даёт теория БКШ (в пределе слабой связи)? Нарисуйте типичные зависимости $\Delta_0(\lambda)$ и $\Delta(T)$.

Answer:

15. Какое выражение для $T_\mathbf{c}$ даёт теория Элиашберга (в случае сильной эл.-фононной связи)?

Answer:

16. Как SC щель Δ_0 соотносится с такими физическими величинами как $T_\mathrm{c}, \xi_0, v_\mathrm{c}, j_\mathrm{c}, H_\mathrm{c}$?

Answer:

Question about zero gap

The gap equation $\Delta = \lambda \sum'_{\mathbf{p}'} u_p v_p \Big(-\bar{n}_\mathbf{p} + (1-\bar{n}_\mathbf{p}) \Big) = \lambda \sum'_{\mathbf{p}'} \frac{\Delta}{2\sqrt{\xi_p^2+\Delta^2}} (1-2\bar{n}_\mathbf{p})$ has two solutions, one is the $\Delta = 0$ and another is the well-known, which depends on the temperature. Why do we say that there is a superconductivity? Why the solution of $\Delta = 0$ is not good?

Answer:
The point is that the superconductor will be in a state with lower energy. Ans the ground state of $\Delta = 0$ has more energy then with $\Delta \neq 0$.
(I'll add later also formulas from the theory about the energy of the ground state)
Fun fact: In nonequilibrium this argument does not work since the energy of the superconductor is not conserved: it interacts with the external system creating the nonequilibrium.
(??? how to answer this question - see Stability of nonequilibrium Fermi distributions with respect to Cooper pairing by A. G. Aronov and V. L. Gurevich, I'll write later)

What is the energy density of Bose-Einstein condensation?

(maybe I'll add reminder here for people not to look for some basics if they forgot the answer)

Answer:
(??? I don't know. Is it related to SC?)

Question about basic properties of SC

Draw typical dependences of thermal conductivity $\varkappa$ and heat capacity C on temperature. What is the relative magnitude of the heat capacity jump?

Answer:
so, heat capacity has a jump and it is known.
thermal conductivity - (??? no, I should study it better)

Question about basic properties of theories of SC

What is a characteristic relation in BCS theory and the Ginzburg-Levanyuk criterion?

Answer:
characteristic relation
Ginzburg-Levanyuk - see theory, some relation, I'll write later

14.3.3 Questions about Understanding Basics 3

me. What is the analog between 2D potential well and BCS theory?

Answer:
(write here explicitly, what is in one case and what is in another and compare)

me. Why do we write BCS theory in Fourier space?

Answer:
(discuss second quantization, the same idea is everywhere, right? (????))

me. Averaging in BCS

Show that $\langle a_{q\downarrow} a_{-q\uparrow} \rangle$ is nonzero.

Solution

$$\langle a_{q\downarrow} a_{-q\uparrow} \rangle \sim \mathrm{tr} a_{q\downarrow} a_{-q\uparrow} e^{-\beta(\sum\limits_{\mathbf{p}\sigma} \xi_{\mathbf{p}} \hat{a}^\dagger_{\mathbf{p}\sigma} \hat{a}_{\mathbf{p}\sigma} + \frac{1}{\lambda}|\Delta|^2 + \sum\limits_{\mathbf{p}} [\Delta^* \hat{a}_{\mathbf{p}+} \hat{a}_{-\mathbf{p}-} + \Delta \hat{a}^\dagger_{-\mathbf{p}-} \hat{a}^\dagger_{\mathbf{p}+}])} \sim$$
$$\sim \mathrm{tr} a_{q\downarrow} a_{-q\uparrow} e^{-\beta \sum\limits_{\mathbf{p}} [\Delta^* \hat{a}_{\mathbf{p}+} \hat{a}_{-\mathbf{p}-}]} = ???$$

(????)

20. Как связаны параметры порядка теории БКШ и теории Гинзбурга - Ландау?

Answer:
(add that formula)

21. Как связаны λ_{GL} и H_{cl1} в теории Гинзбурга-Ландау? Как λ_{GL} зависит от длины свободного пробега и температуры?

Answer:

22. Как связаны $\xi_{\mathbf{gL}}$ и H_{c2} в теории Гинзбурга - Ландау? Как $\xi_{\mathbf{gL}}$ зависит от длины свободного пробега и температуры?

Answer:

23. Как связаны критические магнитные поля H_c, H_{cI} и H_{c2} друг с другом и с $\lambda_{\mathrm{GL}}, \xi_{\mathrm{GL}}$?

Answer:

24. Напишите уравнения Джозефсона, а также соотношение Амбегаокара и Баратова.

Answer:

25. Чему равен коэффициент пропорциональности между частотой и смещением в SISконтакте? Как предельная частота сверхтока зависит от величины SC щели Δ_0?

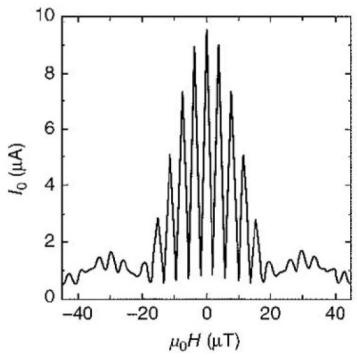
Answer:

14.3.4 Questions about Understanding Typical Phenomena 1

(discuss easy experiment and ask to explain it)

KUL-lect.joseph.eff Diffraction and interference in a YBaCuO SQUID structure (???)

We see results of (??? some experiment)



Can you explain the observed oscillations? Can you estimate the ratio ASQUID /AJJ?

Solution (????)

(don't know yet....)

14.3.5 Questions about Understanding Typical Phenomena 2

(discuss easy experiment and ask to explain it)

14.3.6 Questions about Understanding Special Models

(потом добавлю, книги по ним написаны, выделю хотя бы какие-то известные потом)

14.3.7 Problems about Understanding Special Effects

(есть куча статей, просто от туда беру графики, спрашиваю почему так? пока теор. части додумывать нужно, потом займусь сборкой этих задач.)

14.3.8 Hypothetical questions about сверхпроводниках

(из курса Фейгальмана скорее всего много вопросов можно найти.)

Когда могут быть кванты потока более чем 1? (????)

(хз, там какя-то умная теория на это.)

Когда могут быть решетки абрикосова не треугольные? (????)

(хз, там какя-то умная теория на это.)

Когда могут быть не s-спаривания? (????)

(хз, там какя-то умная теория на это.)

Когда могут быть? (????)

(хз, там какя-то умная теория на это.)

Когда могут быть? (????)

(хз, там какя-то умная теория на это.)

Когда могут быть? (????)

(хз, там какя-то умная теория на это.)

14.4 Other Questions about Superconductivity

14.4.1 Questions about what is exactly going on in BCS?

All these questions are discussed in detail in theory, but I'll collect them also here to have a nice "FAQ" section.

What is a Cooper pair operator?

Is, for example, is $c^\dagger_{p,+}c^\dagger_{-p,p}$ (where $c^\dagger$ is an electron creation operator) a Cooper pair operator?
Answer:
(?????)
This operator creates two excitations, however, a Cooper pair is in the ground state, so it is not an excitation, so my answer is that no, it is not a Cooper pair operator.
(??? TODO: write theory about it better, then write here how the real one looks like)

15 Problems about specific phenomena and properties

15.1 Problems about Special Useful Methods

15.1.1 Problems about GF Special Methods for SC 1

me. the Heisenberg equations for the discrete model

Here we will derive the Heisenberg equations for the Nambu fields $C_{n,j}$ and D.

Solution

We will use $i\frac{d}{dt}C_{n,ja}(t) = [C_{n,ja}(t), H_{\rm tot}]$ and we will change the names of inner indices $j \to p, n \to k, n' \to l$, we compute:

$$[C_{nja}, H_D] = \frac{1}{2}\left(C_{nja}D^\dagger_b h^{bc}_D D_c - D^\dagger_b h^{bc}_D D_c C_{nja} = C_{nja}D^\dagger_b h^{bc}_D D_c - (-1)^2 D^\dagger_b h^{bc}_D D_c C_{nja}\right) = 0;$$

$$[C_{n,ja}, H_{SC}] = \frac{1}{2}\left[C_{n,ja}\sum_{p,k,l} C^\dagger_{k,pb}\,[h^{k,l}_{SC,p}]^{bc}\,C_{l,pc} - \sum_{p,k,l} C^\dagger_{k,pb}\,[h^{k,l}_{SC,p}]^{bc}\,C_{l,pc}C_{n,ja}\right] =$$

$$= \tfrac{1}{2}\left[\textstyle\sum_{p,k,l}(-C^\dagger_{k,pb}C_{n,ja} + \delta_{kn}\delta_{pj}\delta_{ab})\,[h^{k,l}_{SC,p}]^{bc}\,C_{l,pc} - \sum_{p,k,l}\underbrace{C^\dagger_{k,pb}}_{=C_{k,pr}P_{rb}}\,[h^{k,l}_{SC,p}]^{bc}\,(P_{ac}\delta_{jp}\delta_{nl} - C_{n,ja}C_{l,pc})\right] =$$

$$= \tfrac{1}{2}\Big[-\sum_{p,k,l} C^\dagger_{k,pb}C_{n,ja}\,[h^{k,l}_{SC,p}]^{bc}\,C_{l,pc} + \sum_l [h^{n,l}_{SC,j}]^{ac}\,C_{l,jc} - \sum_k C_{k,jr}\underbrace{P_{rb}\,[h^{k,n}_{SC,j}]^{bc}\,P_{ac}}_{=-[h^{k,n}_{SC,j}]^{ra*}=-[h^{k,n}_{SC,j}]^{ar}} + \sum_{p,k,l} C^\dagger_{k,pb}\,[h^{k,l}_{SC,p}]^{bc}\,C_{n,ja}C_{l,pc}\Big] =$$

$$= \sum_l [h^{n,l}_{SC,j}]^{ac}\,C_{l,jc} = \Big[\sum_l [h^{n,l}_{SC,j}]\,C_{l,j}\Big]_a.$$

Let us remind, that here each $h^{k,l}_{SC,p}$ operator is a matrix of 4×4 dimensions, so two extra indices mean taking the row's and column's element. At the last step of the transformation we notice that the first and the fourth terms are the same but with different sign.

$$[C_{n,ja}, H_T] = -\tfrac{1}{2}\Big[C_{n,ja}\sum_{p=1} t'_p C^\dagger_{1,pb}\tau^{bc}_z D_c + C_{n,ja}\sum_{p=1} t'_p D^\dagger_b \tau^{bc}_z C_{1,pc} - \sum_{p=1} t'_p C^\dagger_{1,pb}\tau^{bc}_z D_c C_{n,ja} - \sum_{p=1} t'_p D^\dagger_b \tau^{bc}_z C_{1,pc}C_{n,ja}\Big] =$$

$$= -\frac{1}{2}\Big[\sum_{p=1} t'_p(-C^\dagger_{1,pb}C_{n,ja} + \delta_{n,1}\delta_{pj}\delta_{ab})\tau^{bc}_z D_c + \sum_{p=1} t'_p(-D^\dagger_b C_{n,ja})\tau^{bc}_z C_{1,pc} -$$

$$- \sum_{p=1} t'_p C^\dagger_{1,pb}\tau^{bc}_z \underbrace{D_c C_{n,ja}}_{=-C_{n,ja}D_c} - \sum_{p=1} t'_p \underbrace{D^\dagger_b}_{=D_d P_{db}}\tau^{bc}_z C_{1,pc}C_{n,ja}\Big] =$$

$$= -\frac{1}{2}\Big[t'_j\delta_{n,1}\tau^{ac}_z D_c - \sum_{p=1} t'_p D_d \underbrace{P_{db}\tau^{bc}_z P_{ca}}_{-\tau^{da}_z}\delta_{n1}\delta_{pj}\Big] =$$

$$= [-\delta_{n,1}\ t'_j\ \tau_z\ D]_a.$$

After restoring t-dependence and summing terms, we have

$$i\frac{d}{dt}C_{nj}(t) = \sum_l\ h^{n,l}_{SC,j}\ C_{l,j}(t) - \delta_{n,1}\ t'_j\ \tau_z\ D(t).$$

And this is the (**??**) The Eq. (**??**) is derived by exactly the same approach.

me. the Dyson equation for Green's functions for the discrete model

The Dyson equation for $[G^{0,0}_{0,0}(t)]_{a,b} := -i\Theta(t)\langle\{D_a(t),\ D^\dagger_b(0)\}\rangle$ is derived as follows.

Solution

We evaluate:

$$
\begin{aligned}
i\frac{d}{dt}[G^{0,0}_{0,0}(t)]_{a,b} = & \underbrace{\delta(t)\langle\{D_a(t),\ D^\dagger_b(0)\}\rangle}_{=\delta(t)\langle\{D_a(0),\ D^\dagger_b(0)\}\rangle=\delta_{ab}\delta(t)} - i\Theta(t)\langle\{i\frac{dD_a(t)}{dt},\ D^\dagger_b(0)\}\rangle \\
&= \delta(t)\delta_{ab} - i\Theta(t)\langle\{h^{ac}_D D_c(t),\ D^\dagger_b(0)\}\rangle - i\Theta(t)\langle\{\sum_{j=1}(-1)t'_j\tau^{ac}_z C_{1,jc}(t),\ D^\dagger_b(0)\}\rangle = \\
&= \delta(t)\delta_{ab} - i\Theta(t)h^{ac}_D\underbrace{\langle\{D_c(t),\ D^\dagger_b(0)\}\rangle}_{=[G^{0,0}_{0,0}(t)]_{a,b}} - \sum_{j=1}t'_j\tau^{ac}_z\underbrace{(-i)\Theta(t)\langle\{C_{1,jc}(t),\ D^\dagger_b(0)\}\rangle}_{=[G^{j,0}_{1,0}(t)]_{cb}}.
\end{aligned}
$$

Thus, in the matrix form we will get

$$
\left(i\frac{d}{dt} - h_D\right)G^{0,0}_{0,0}(t) + \sum_{j=1}t'_j\tau_z G^{j,0}_{1,0}(t) = \delta(t)
$$

Now, to use transformation $F[f](z) := \int_0^\infty dt e^{izt}f(t)$, the formulas below are used:

$$
\begin{aligned}
F[i\frac{d}{dt}[G^{0,0}_{0,0}(t)]_{a,b}](z) &= \int_0^\infty dt e^{izt} i\frac{d}{dt}[G^{0,0}_{0,0}(t)]_{a,b} = \\
&= ie^{izt}[G^{0,0}_{0,0}(t)]_{a,b}|^\infty_0 - i\cdot iz\int_0^\infty dt e^{izt}[G^{0,0}_{0,0}(t)]_{a,b} = z[G^{0,0}_{0,0}(z)]_{a,b}, \\
F[h_D[G^{0,0}_{0,0}(t)]_{a,b}](z) &= h_D[G^{0,0}_{0,0}(z)]_{a,b}, \\
F[\sum_{j=1}t'_j\tau_z[G^{j,0}_{1,0}(t)]_{ab}](z) &= \sum_{j=1}t'_j\tau_z[G^{j,0}_{1,0}(z)]_{ab}. \\
F[\delta(t)](z) &= 1,
\end{aligned}
$$

and we will have:

$$
[z - h_D]G^{0,0}_{0,0}(\omega) + \sum_{j=1}^{N}t'_j\tau_z G^{j,0}_{1,0}(\omega) = 1,
$$

Now, we will derive the Dyson eq. for $[G^{j,j'}_{n,n'}(t)]_{a,b} := -i\Theta(t)\langle\{C_{n,j,a}(t),\ C^\dagger_{n',j',b}(0)\}\rangle$, we evaluate:

$$
\begin{aligned}
i\frac{d}{dt}[G^{j,j'}_{n,n'}(t)]_{a,b} &= \delta(t)\underbrace{\langle\{C_{n,j,a}(t),\ C^\dagger_{n',j',b}(0)\}\rangle}_{=\delta_{nn'}\delta_{jj'}\delta_{ab}} - i\Theta(t)\langle\{i\frac{dC_{n,j,a}(t)}{dt},\ C^\dagger_{n',j',b}(0)\}\rangle = \\
&= \delta(t)\delta_{nn'}\delta_{jj'}\delta_{ab} + \textstyle\sum_l(-i\Theta(t))\langle\{[h^{n,l}_{SC,j}]^{ad}\ C_{l,jd}(t), C^\dagger_{n',j',b}(0)\}\rangle - (-i\Theta(t))\langle\{\delta_{n,1}t'_j\tau^{ad}_z D_d(t), C^\dagger_{n',j',b}(0)\}\rangle = \\
&= \delta(t)\delta_{nn'}\delta_{jj'}\delta_{ab} + \textstyle\sum_l[h^{n,l}_{SC,j}]^{ad}\ \underbrace{(-i\Theta(t))\langle\{C_{l,jd}(t), C^\dagger_{n',j',b}(0)\}\rangle}_{=[G^{j,j'}_{l,n'}]_{db}} - \delta_{n,1}t'_j\tau^{ad}_z\underbrace{(-i\Theta(t))\langle\{D_d(t), C^\dagger_{n',j',b}(0)\}\rangle}_{=[G^{0,j'}_{0,n'}]_{db}}.
\end{aligned}
$$

Also, $i\frac{d}{dt}[G^{j,j'}_{n,n'}(t)]_{a,b} \equiv \sum_l i\frac{d}{dt}[G^{j,j'}_{l,n'}(t)]_{a,b}\delta_{l,n}$, thus in matrix notation we will have:

$$
\sum_l i\frac{d}{dt}G^{j,j'}_{l,n'}(t)\delta_{l,n} = \delta(t)\delta_{nn'}\delta_{jj'}\delta_{ab} + \sum_l h^{n,l}_{SC,j}\ G^{j,j'}_{l,n'} - \delta_{n,1}t'_j\tau_z G^{0,j'}_{0,n'} \tag{15.1}
$$

$$
\sum_l\left[i\delta_{l,n}\frac{d}{dt} - h^{n,l}_{SC,j}\right]G^{j,j'}_{l,n'} + \delta_{n,1}t'_j\tau_z G^{0,j'}_{0,n'} = \delta(t)\delta_{nn'}\delta_{jj'}. \tag{15.2}
$$

The Fourier transform is done exactly as for the example above.

The other two Dyson equations (**??**) can be derived the same way.

me. $G^{j,0}_{n,0}(\omega)$ in terms of $-g^{j}_{n,1}(\omega)$

Solution

We define $g^{j}_{n'',n'}(\omega)$ as a solution of

$$\sum_{n''}[z\delta_{n,n''} - h^{n,n''}_{SC,j}]g^{j}_{n'',n'}(\omega) = \delta_{n,n'}. \tag{15.3}$$

To work with the it we need to understand this equation well. Here only n, n' are external indices, we can treat them as a matrix indices and imagine l.h.s. as a product of a matrix $[z - h_{SC,j}]$ and a vector-column $g^{j}(\omega)$, and the r.h.s. as the identity matrix. Thus, in this notation, $g^{j}(\omega) = [z - h_{SC,j}]^{-1}$ and has a type of a matrix (or in index notation $[g^{j}(\omega)]_{n,n''} = g^{j}_{n,n''}(\omega) = \left[[z - h_{SC,j}]^{-1}\right]_{n,n'}$). Another important feature of $g^{j}_{n'',n'}(\omega)$ is that it doesn't have same number of indices as $G^{j,j'}_{n'',n'}(\omega)$. This is because it describes only two pints (n and n') in j-th SC lead. Now, the Eq. (**??**) can be transformed as

$$\sum_{n''}[z\delta_{n,n''} - h^{n,n''}_{SC,j}]G^{j,0}_{n'',0}(\omega) = -\delta_{n,1}t'_j\tau_z G^{0,0}_{0,0}(\omega), \tag{15.4}$$

$$\sum_{n} g^{j}_{n',n}(\omega)\cdot\sum_{n''}\left[z\delta_{n,n''} - h^{n,n''}_{SC,j}\right]G^{j,0}_{n'',0}(\omega) = -\sum_{n} g^{j}_{n',n}(\omega)\ \delta_{n,1}\ t'_j\ \tau_z G^{0,0}_{0,0}(\omega) \tag{15.5}$$

$$\sum_{n''}\sum_{n}\left[z\delta_{n,n''} - h^{n,n''}_{SC,j}\right]g^{j}_{n',n}(\omega)G^{j,0}_{n'',0}(\omega) = -\sum_{n} g^{j}_{n',n}(\omega)\cdot\ \delta_{n,1}\ t'_j\ \tau_z G^{0,0}_{0,0}(\omega) \tag{15.6}$$

$$\sum_{n''}\delta_{n',n''}G^{j,0}_{n'',0}(\omega) = -\sum_{n} g^{j}_{n',n}(\omega)\ \delta_{n,1}\ t'_j\ \tau_z G^{0,0}_{0,0}(\omega) \tag{15.7}$$

$$G^{j,0}_{n',0}(\omega) = -g^{j}_{n',1}(\omega)t'_j\tau_z G^{0,0}_{0,0}(\omega) \tag{15.8}$$

$$G^{j,0}_{n,0}(\omega) = -g^{j}_{n,1}(\omega)t'_j\tau_z G^{0,0}_{0,0}(\omega), \quad j \neq 0. \tag{15.9}$$

At the second line we multiplied the whole sum (with fixed n) by $g^{j}_{n',n}(\omega)$ (with some unknown fixed n') and then summed all possible l.h.s. and r.h.s. over all n. Thus the (**??**) is proven.

me. Boundary Green's function $g^{j}_{1,1}$ for discrete model

The BGF approach proposes the calculation of the GF of 1D superconductor near its end by the following formula

$$G_{1,1} = G^{(0)}_0 - G^{(0)}_1[G^{(0)}_0]^{-1}G^{(0)}_{-1}, \tag{15.10}$$

where the translationally invariant SC GF is

$$G^{(0)}_{n-n'}(z) := \int_{-\pi}^{\pi}\frac{dk}{2\pi}\frac{e^{ik(n-n')}}{z - (-2t\cos k - \mu)\tau_z - \Delta_j\left[e^{i\varphi_j}\tau_+ + e^{-i\varphi_j}\tau_-\right]}. \tag{15.11}$$

Solution

(???? write what is going on???)

Here compared to main theory we have a basis of plane waves $|\psi\rangle = \frac{e^{ikn}}{\sqrt{2\pi}}$. For only this calculation we will introduce $\bar{\mathbf{\Delta}} := \Delta_j\left[e^{i\varphi_j}\tau_+ + e^{-i\varphi_j}\tau_-\right]$ to make formulas shorter. Considering this integral in the wide-band limit $t \gg \Delta_j$, we approximate it by linearizing near the Fermi points $\mu = 0$, $k = \pm\frac{\pi}{2}$:

$$G^{(0)}_{n-n'}(z) \approx e^{i\frac{\pi}{2}(n-n')}\int_{-\infty}^{\infty}\frac{dq}{2\pi}\frac{e^{iq(n-n')}}{z - 2tq\tau_z - \bar{\mathbf{\Delta}}} + e^{-i\frac{\pi}{2}(n-n')}\int_{-\infty}^{\infty}\frac{dq}{2\pi}\frac{e^{iq(n-n')}}{z + 2tq\tau_z - \bar{\mathbf{\Delta}}}. \tag{15.12}$$

We are interested in

$$G^{(0)}_0(z) \approx \frac{1}{t}\int_{-\infty}^{\infty}\frac{d\bar{q}}{2\pi}\frac{z + \bar{\mathbf{\Delta}}}{z^2 - \bar{q}^2 - \Delta_j^2} = -\frac{1}{t}\int_{-\infty}^{\infty}\frac{d\bar{q}}{2\pi}\frac{z + \bar{\mathbf{\Delta}}}{(\bar{q} - k_+)(\bar{q} - k_-)}; \qquad k_\pm(z) := \pm z\sqrt{1 - \frac{\Delta_0^2}{z^2}}. \tag{15.13}$$

The inversion is done the same way like in the main derivation. Closing the integration contour in the upper half-plane, we obtain

$$G_0^{(0)}(z) \approx -\frac{i}{2t}\frac{z+\bar{\mathbf{\Delta}}}{k_+} = -\frac{i}{2t}\frac{1+\frac{\bar{\mathbf{\Delta}}}{z}}{\sqrt{1-\frac{\Delta_j^2}{z^2}}}; \qquad [G_0^{(0)}(z)]^{-1} = 2ti\frac{1-\frac{\bar{\mathbf{\Delta}}}{z}}{\sqrt{1-\frac{\Delta_j^2}{z^2}}}. \tag{15.14}$$

Analogously,

$$G_1^{(0)}(z) \approx \frac{i\tau_z}{t}\int_{-\infty}^{\infty}\frac{d\bar{q}}{2\pi}\frac{\bar{q}e^{i\frac{\bar{q}}{2t}}}{z^2-\bar{q}^2-\Delta_j^2} = -\frac{i\tau_z}{t}\int_{-\infty}^{\infty}\frac{d\bar{q}}{2\pi}\frac{\bar{q}e^{i\frac{\bar{q}}{2t}}}{(\bar{q}-k_+)(\bar{q}-k_-)} \approx \frac{\tau_z}{2t}; \tag{15.15}$$

$$G_{-1}^{(0)}(z) \approx -\frac{i\tau_z}{t}\int_{-\infty}^{\infty}\frac{d\bar{q}}{2\pi}\frac{\bar{q}e^{-i\frac{\bar{q}}{2t}}}{z^2-\bar{q}^2-\Delta_j^2} = G_1^{(0)}(z), \tag{15.16}$$

where the last equality is obtained by re-defining the integration variable $\bar{q} \to -\bar{q}$. Collecting together all the contribution, we have

$$G_{1,1} = -\frac{i}{2t}\frac{1+\frac{\bar{\mathbf{\Delta}}}{z}}{\sqrt{1-\frac{\Delta_j^2}{z^2}}} - \frac{\tau_z}{2t}2ti\frac{1-\frac{\bar{\mathbf{\Delta}}}{z}}{\sqrt{1-\frac{\Delta_j^2}{z^2}}}\frac{\tau_z}{2t} = -\frac{i}{t}\frac{1+\frac{1}{z}\Delta_j\left[e^{i\varphi_j}\tau_+ + e^{-i\varphi_j}\tau_-\right]}{\sqrt{1-\frac{\Delta_j^2}{z^2}}}. \tag{15.17}$$

And this is the same result (**??**).

15.1.2 Problems about GF Special Methods for SC 1

me.* Density ABS for multiterminal QD junction

Here we will derive the DOS for the QD model (**??**).
(!!! write arguments, why one expects this formula!!!)
Hint:
(write useful math formulas for it!!)

Solution

(!!! more background is required for this derivation!!!!)
This is a complicated derivation.
The density of states $\rho(\omega) = \int \delta(\omega - E_s)$ can be obtained by the fundamental relation (**??**), which for our discrete model looks like:

$$\rho(\omega) = -\frac{1}{\pi}\sum_{\forall m}\text{Im tr}\,\widehat{G}_{m,m}(\omega+i\eta). \tag{15.18}$$

Here the trace is taken over the spin and particle-hole indices, and $\widehat{G}_{m,m'}(\omega+i\eta)$ is the full retarded ($z=\omega+i\eta$) Green's function of the system. In another words, in this notation we consider m and m' as all allowed points in our "sun-junction" **??**, so

$$\rho(\omega) = -\frac{1}{\pi}\text{Im tr}G_{0,0}^{0,0}(\omega+i\eta) - \frac{1}{\pi}\sum_{j=1}^{N}\sum_{n=1}^{\infty}\text{Im tr}G_{n,n}^{j,j}(\omega+i\eta). \tag{15.19}$$

To calculate it, we continue to exploit the Dyson equations (**??**), (**??**),(**??**) and (**??**). From them we have

$$G_{n,n'}^{j,j'}(\omega) = g_{n,n'}^{j}(\omega)\delta_{j,j'} - t'_j g_{n,1}^{j}(\omega)\tau_z G_{0,n'}^{0,j'}(\omega), \tag{15.20}$$

$$G_{0,n'}^{0,j'}(\omega) = -\,g_D(\omega)\sum_{j''=1}^{N} t'_{j''}\tau_z G_{1,n'}^{j'',j'}(\omega), \tag{15.21}$$

where the dot's GF is defined as a solution of

$$[z-h_D]g_D(\omega) = 1. \tag{15.22}$$

Derivation of (15.20) is easily done by looking at l.h.s. of (**??**) as on matrix equation and by inverting matrices. Together these equations give

$$G^{j,j'}_{n,n'}(\omega) = g^{j}_{n,n'}(\omega)\delta_{j,j'} + \sum_{j''=1}^{N} t'_j t'_{j''} g^{j}_{n,1}(\omega)\tau_z g_D(\omega)\tau_z G^{j'',j'}_{1,n'}(\omega). \tag{15.23}$$

From this, we find by setting $n = 1$ that

$$G^{j,j'}_{1,n'}(\omega) = g^{j}_{1,n'}(\omega)\delta_{j,j'} + \sum_{j''=1}^{N} g^{j}_{1,1}(\omega)\cdot t'_j t'_{j''}\tau_z g_D(\omega)\tau_z \cdot G^{j'',j'}_{1,n'}(\omega). \tag{15.24}$$

Now, we switch to the fully matrix notation. We define the block matrices

$$\hat{g}_{j,j'}(n,n') := g^{j}_{n,n'}(\omega)\delta_{j,j'}, \qquad \hat{t}_{j,j''} := t'_j t'_{j''}\tau_z g_D(\omega)\tau_z, \qquad \hat{G}_{j,j'}(n,n') := G^{j,j'}_{n,n'}(\omega). \tag{15.25}$$

We think about arguments in brackets as indices of the matrix, that is determined by each j and each j'. The sum in (15.24) is a tensor contraction by index j'', thus in matrix notation it is a multiplication of a matrix to the hatted $\hat{G}$. Thus we write a solution as

$$\hat{G}(1,n') = (1-\hat{g}(1,1)\hat{t})^{-1}\hat{g}(1,n'), \tag{15.26}$$

This formula in matrix notation gives the GF from (15.20) as

$$\hat{G}(n,n') = \hat{g}(n,n') + \hat{g}(n,1)\hat{t}(1-\hat{g}(1,1)\hat{t})^{-1}\hat{g}(1,n'). \tag{15.27}$$

Now we are ready to compute the DOS. We substitute the known already (**??**) and the $\hat{G}(n,n')$ and transform:

$$\begin{aligned}
\rho(\omega) =& -\frac{1}{\pi}\mathrm{Im}\,\mathrm{tr}[z - h_D - \Sigma(\omega)]^{-1} - \frac{1}{\pi}\sum_{n=1}^{\infty}\mathrm{Im}\,\mathrm{Tr}\hat{G}(n,n) = \\
=& \rho^{(0)}_{SC}(\omega) - \frac{1}{\pi}\mathrm{Im}\,\mathrm{tr}[z - h_D - \Sigma(\omega)]^{-1} - \frac{1}{\pi}\mathrm{Im}\,\mathrm{Tr}\left[\hat{t}(1-\hat{g}(1,1)\hat{t})^{-1}\sum_{n=1}^{\infty}\hat{g}(1,n)\hat{g}(n,1)\right] = \\
=& \rho^{(0)}_{SC}(\omega) - \frac{1}{\pi}\mathrm{Im}\,\mathrm{tr}[g_D^{-1}(\omega) - \Sigma(\omega)]^{-1} + \frac{1}{\pi}\mathrm{Im}\,\mathrm{Tr}\left[\hat{t}(1-\hat{g}(1,1)\hat{t})^{-1}\frac{\partial\hat{g}(1,1)}{\partial\omega}\right].
\end{aligned} \tag{15.28}$$

Here we have used the widely-known for GF specialists identity $\sum_{n=1}^{N} G_{1,n}G_{n,1} = -\frac{\partial G_{1,1}}{\partial\omega}$ (see[**?**]). Now we do the final transformation. We define $\mathcal{T}_j := t'_j\tau_z$ and rewrite

$$\hat{t} \equiv \mathcal{T} g_D(\omega)\mathcal{T}^T. \tag{15.29}$$

Now indices of $\hat{t}$ are distributed between $\mathcal{T}_j$ matrices. The sign "transpose" makes the column-vector $\mathcal{T}_j$ a row, such that by indices j, j'' we have a number (1×1 object). Now, by applying Woodbury matrix identity

$$(A+UCV)^{-1} = A^{-1} - A^{-1}U\left(C^{-1} + VA^{-1}U\right)^{-1}VA^{-1}$$

and identifying $\Sigma(\omega) := \mathcal{T}^T\hat{g}(1,1)\mathcal{T}$ (in the previous notation the definition looked like $\Sigma(\omega) := \sum_{j=1}^{N}\left(t'_j\right)^2\tau_z g^{j}_{1,1}(\omega)\tau_z$) the multiplier under trace will be

$$\begin{aligned}
(1-\hat{g}(1,1)\mathcal{T}g_D(\omega)\mathcal{T}^T)^{-1} &= (\hat{g}^{-1}(1,1) - \mathcal{T}g_D(\omega)\mathcal{T}^T)^{-1}\hat{g}^{-1}(1,1) = \\
&= 1 + \hat{g}(1,1)\mathcal{T}(g_D^{-1}(\omega) - \mathcal{T}^T\hat{g}(1,1)\mathcal{T})^{-1}\mathcal{T}^T = \\
&= 1 + \hat{g}(1,1)\mathcal{T}(g_D^{-1}(\omega) - \Sigma(\omega))^{-1}\mathcal{T}^T.
\end{aligned} \tag{15.30}$$

And we do the final step of the final transformation:

$$\rho(\omega) = \rho_{SC}^{(0)}(\omega) - \frac{1}{\pi}\mathrm{Im\,tr}[g_D^{-1}(\omega) - \Sigma(\omega)]^{-1} + \frac{1}{\pi}\mathrm{Im\,tr}\left[g_D(\omega)\Big(1 + \Sigma(\omega)(g_D^{-1}(\omega) - \Sigma(\omega))^{-1}\Big)\frac{\partial\Sigma(\omega)}{\partial\omega}\right] = \tag{15.31}$$

$$= \rho_{SC}^{(0)}(\omega) - \tfrac{1}{\pi}\mathrm{Im\,tr}\left[\left(g_D^{-1}(\omega) - \Sigma(\omega)\right)^{-1}\underbrace{\frac{\partial g_D^{-1}(\omega)}{\partial\omega}}_{\equiv 1}\right] + \tfrac{1}{\pi}\mathrm{Im\,tr}\left[\left(g_D^{-1}(\omega) - \Sigma(\omega)\right)^{-1}\tfrac{\partial\Sigma(\omega)}{\partial\omega}\right] =$$

$$= \rho_{SC}^{(0)}(\omega) - \frac{1}{\pi}\mathrm{Im\,tr}\left[\frac{\partial}{\partial\omega}\log\left(g_D^{-1}(\omega) - \Sigma(\omega)\right)\right] =$$

$$= \rho_{SC}^{(0)}(\omega) - \frac{1}{\pi}\mathrm{Im}\,\frac{\partial}{\partial\omega}\log\det\left[g_D^{-1}(\omega) - \Sigma(\omega)\right] =$$

$$= \underbrace{\rho_{SC}^{(0)}(\omega) + \rho_D^{(0)}(\omega)}_{\text{bare DOS}} + \underbrace{\left(-\frac{1}{\pi}\mathrm{Im}\,\frac{\partial}{\partial\omega}\log\det\left[1 - g_D(\omega)\Sigma(\omega)\right]\right)}_{\text{tunneling contribution}}. \tag{15.32}$$

Thus we have proven (**??**).

15.2 Problems about Special Effects

15.2.1 Problems about Nambu Notation for Applications

me. Nambu formalism

Show that

$$H_D := \sum_{\sigma=\pm}(V + \sigma\Delta_Z)d_\sigma^\dagger d_\sigma, \qquad \Leftrightarrow \qquad H_D = \frac{1}{2}D^\dagger\Big[V\tau_z + \Delta_Z\sigma_z\Big]D + \mathrm{const}; \quad D := \begin{pmatrix} d_+ \\ d_- \\ d_-^\dagger \\ -d_+^\dagger \end{pmatrix}.$$

Solution

Let us do it in the opposite direction.

$$H_D = \frac{1}{2}D^\dagger\Big[V\tau_z + \Delta_Z\sigma_z\Big]D =$$

$$= \frac{1}{2}\begin{pmatrix} d_+^\dagger & d_-^\dagger & d_- & -d_+ \end{pmatrix}\begin{pmatrix} \Delta_Z + V & 0 & 0 & 0 \\ 0 & V - \Delta_Z & 0 & 0 \\ 0 & 0 & \Delta_Z - V & 0 \\ 0 & 0 & 0 & -\Delta_Z - V \end{pmatrix}\begin{pmatrix} d_+ \\ d_- \\ d_-^\dagger \\ -d_+^\dagger \end{pmatrix} =$$

$$= \frac{1}{2}\Big((\Delta_Z + V)d_+^\dagger d_+ + (V - \Delta_Z)d_-^\dagger d_- + (\Delta_Z - V)d_- d_-^\dagger + (-\Delta_Z - V)(-d_+)(-d_+^\dagger)\Big) =$$

$$= \frac{1}{2}\Big((\Delta_Z + V)d_+^\dagger d_+ + (V - \Delta_Z)d_-^\dagger d_- + (\Delta_Z - V)(1 - d_- d_-^\dagger) + (-\Delta_Z - V)(1 - d_+ d_+^\dagger)\Big) =$$

$$= (\Delta_Z + V)d_+^\dagger d_+ + (V - \Delta_Z)d_-^\dagger d_- - V.$$

me. Nambu formalism

Show that

$$H_{SC} := \sum_{j=1}^{N}\left(-t_j\sum_{n=1}^{\infty}\sum_{\sigma=\pm}(c_{n,\sigma,j}^\dagger c_{n+1,\sigma,j} + c_{n+1,\sigma,j}^\dagger c_{n,\sigma,j}) + \Delta_j\sum_{n=1}^{\infty}(e^{i\varphi_j}c_{n,+,j}^\dagger c_{n,-,j}^\dagger + \mathrm{h.c.}) - \right.$$

$$\left. - \mu\sum_{\sigma=\pm}\sum_{n=1}^{\infty}c_{n,\sigma,j}^\dagger c_{n,\sigma,j}\right)$$

is equivalent to one in terms of $C_{n,j} := \begin{pmatrix} c_{n,+,j} & c_{n,-j} & c^\dagger_{n,-j} & -c^\dagger_{n,+j} \end{pmatrix}^T$:

$$H_{SC} = \frac{1}{2}\sum_{j=1}^{N}\left(-t_j\sum_{n=1}^{\infty}(C^\dagger_{n,j}\tau_z C_{n+1,j} + C^\dagger_{n+1,j}\tau_z C_{n,j}) + \Delta_j\sum_{n=1}^{\infty}(e^{i\varphi_j}C^\dagger_{n,j}\tau_+ C_{n,j} + \text{h.c.}) - \right.$$
$$\left. -\mu\sum_{n=1}^{\infty}C^\dagger_{n,j}\tau_z C_{n,j}\right) + \text{const.}$$

Solution

We will do in the opposite direction and by each part in the sum over j. The first part:

$$\frac{1}{2}(C^\dagger_{n,j}\tau_z C_{n+1,j} + C^\dagger_{n+1,j}\tau_z C_{n,j}) =$$
$$= \tfrac{1}{2}(c^\dagger_{n,+,j}\ c^\dagger_{n,-j}\ c_{n,-j}\ -c_{n,+j})\begin{pmatrix}1&0&0&0\\0&1&0&0\\0&0&-1&0\\0&0&0&-1\end{pmatrix}\begin{pmatrix}c_{n+1,+,j}\\c_{n+1,-j}\\c^\dagger_{n+1,-j}\\-c^\dagger_{n+1,+j}\end{pmatrix} + \tfrac{1}{2}(c^\dagger_{n+1,+,j}\ c^\dagger_{n+1,-j}\ c_{n+1,-j}\ -c_{n+1,+j})\begin{pmatrix}1&0&0&0\\0&1&0&0\\0&0&-1&0\\0&0&0&-1\end{pmatrix}\begin{pmatrix}c_{n,+,j}\\c_{n,-j}\\c^\dagger_{n,-j}\\-c^\dagger_{n,+j}\end{pmatrix} =$$
$$= \frac{1}{2}\Big(c^\dagger_{n,+,j}c_{n+1,+,j} + c^\dagger_{n,-j}c_{n+1,-j} - c_{n,-j}c^\dagger_{n+1,-j} - (-c_{n,+j})(-c^\dagger_{n+1,+j}) +$$
$$+ c^\dagger_{n+1,+,j}c_{n,+,j} + c^\dagger_{n+1,-j}c_{n,-j} - c_{n+1,-j}c^\dagger_{n,-j} - (-c_{n+1,+j})(-c^\dagger_{n,+j})\Big) =$$
$$= c^\dagger_{n+1,+,j}c_{n,+,j} + c^\dagger_{n+1,-j}c_{n,-j} - c_{n+1,-j}c^\dagger_{n,-j} - c_{n+1,+j}c^\dagger_{n,+j}.$$

This the exactly the term we needed. All was easy, since all operators in each term commute (the key transformation is the anticommutation relation). Now, the second part:

$$\frac{1}{2}(e^{i\varphi_j}C^\dagger_{n,j}\tau_+ C_{n,j} + \text{h.c.}) =$$
$$= \tfrac{1}{2}e^{i\varphi_j}(c^\dagger_{n,+,j}\ c^\dagger_{n,-j}\ c_{n,-j}\ -c_{n,+j})\begin{pmatrix}0&0&1&0\\0&0&0&1\\0&0&0&0\\0&0&0&0\end{pmatrix}\begin{pmatrix}c_{n,+,j}\\c_{n,-j}\\c^\dagger_{n,-j}\\-c^\dagger_{n,+j}\end{pmatrix} + \tfrac{1}{2}e^{-i\varphi_j}(c^\dagger_{n,+,j}\ c^\dagger_{n,-j}\ c_{n,-j}\ -c_{n,+j})\begin{pmatrix}0&0&0&0\\0&0&0&0\\1&0&0&0\\0&1&0&0\end{pmatrix}\begin{pmatrix}c_{n,+,j}\\c_{n,-j}\\c^\dagger_{n,-j}\\-c^\dagger_{n,+j}\end{pmatrix} =$$
$$= \frac{1}{2}e^{i\varphi_j}\left(c^\dagger_{n,+,j}c^\dagger_{n,-j} + c^\dagger_{n,-j}(-c^\dagger_{n,+j})\right) + \frac{1}{2}e^{-i\varphi_j}\left(c_{n,-j}c_{n,+,j} + (-c_{n,+j})c_{n,-j}\right) =$$
$$= \frac{1}{2}e^{i\varphi_j}\left(c^\dagger_{n,+,j}c^\dagger_{n,-j} + c^\dagger_{n,+,j}c^\dagger_{n,-j}\right) + \frac{1}{2}e^{-i\varphi_j}\left(c_{n,-j}c_{n,+,j} + c_{n,-j}c_{n,+,j}\right) =$$
$$= e^{i\varphi_j}c^\dagger_{n,+,j}c^\dagger_{n,-j} + e^{-i\varphi_j}c_{n,-j}c_{n,+,j}.$$

Another, slightly simpler way is to obtain only the first term and then to take h.c. of it to get the second term. Also, note that this is the place where we wee exactly, why there is a minus sign in the last component of the Nambu spinor, it generates the essential minus to obtain the required term. Finally, the last term:

$$\frac{1}{2}C^\dagger_{n,j}\tau_z C_{n,j} = \frac{1}{2}\begin{pmatrix}c^\dagger_{n,+,j} & c^\dagger_{n,-j} & c_{n,-j} & -c_{n,+j}\end{pmatrix}\begin{pmatrix}1&0&0&0\\0&1&0&0\\0&0&-1&0\\0&0&0&-1\end{pmatrix}\begin{pmatrix}c_{n,+,j}\\c_{n,-j}\\c^\dagger_{n,-j}\\-c^\dagger_{n,+j}\end{pmatrix} =$$
$$= \frac{1}{2}(c^\dagger_{n,+,j}c_{n,+,j} + c^\dagger_{n,-j}c_{n,-j} - c_{n,-j}c^\dagger_{n,-j} - (-c_{n,+j})(-c^\dagger_{n,+j})) =$$
$$= \frac{1}{2}(c^\dagger_{n,+,j}c_{n,+,j} - c_{n,+j}c^\dagger_{n,+j} + c^\dagger_{n,-j}c_{n,-j} - c_{n,-j}c^\dagger_{n,-j}) =$$
$$= \frac{1}{2}(c^\dagger_{n,+,j}c_{n,+,j} - (-c^\dagger_{n,+j}c_{n,+j} + 1) + c^\dagger_{n,-j}c_{n,-j} - (-c^\dagger_{n,-j}c_{n,-j} + 1)) =$$
$$= c^\dagger_{n,+,j}c_{n,+,j} + c^\dagger_{n,-j}c_{n,-j} - 1.$$

me. Nambu formalism

Prove that

$$H_T := -\sum_{j=1}^{N}t'_j\sum_{\sigma=\pm}(c^\dagger_{1,\sigma,j}d_\sigma + d^\dagger_\sigma c_{1,\sigma,j}). \qquad \Leftrightarrow \qquad H_T = -\frac{1}{2}\sum_{j=1}^{N}t'_j\sum_{\sigma=\pm}(C^\dagger_{1,j}\tau_z D + D^\dagger\tau_z C_{1,j}),$$

where $C_{n,j} := \begin{pmatrix} c_{n,+,j} & c_{n,-j} & c^\dagger_{n,-j} & -c^\dagger_{n,+j}\end{pmatrix}^T$ and $D := \begin{pmatrix} d_+ & d_- & d^\dagger_- & -d^\dagger_+\end{pmatrix}^T$.

Solution

We do it again from the opposite direction:

$$H_T = -\tfrac{1}{2}(c^\dagger_{1,+,j}\ c^\dagger_{1,-j}\ c_{1,-j}\ -c_{1,+j}) \begin{pmatrix} 1 & 0 & 0 & 0 \\ 0 & 1 & 0 & 0 \\ 0 & 0 & -1 & 0 \\ 0 & 0 & 0 & -1 \end{pmatrix} \begin{pmatrix} d_+ \\ d_- \\ d^\dagger_- \\ -d^\dagger_+ \end{pmatrix} - \tfrac{1}{2}(d^\dagger_+\ d^\dagger_-\ d_-\ -d_+) \begin{pmatrix} 1 & 0 & 0 & 0 \\ 0 & 1 & 0 & 0 \\ 0 & 0 & -1 & 0 \\ 0 & 0 & 0 & -1 \end{pmatrix} \begin{pmatrix} c_{1,+,j} \\ c_{1,-j} \\ c^\dagger_{1,-j} \\ -c^\dagger_{1,+j} \end{pmatrix} =$$

$$= -\frac{1}{2}(c^\dagger_{1,+,j}d_+ + c^\dagger_{1,-j}d_- - c_{1,-j}d^\dagger_- - c_{1,+j}d^\dagger_+ + d^\dagger_+ c_{1,+,j} + d^\dagger_- c_{1,-j} - d_- c^\dagger_{1,-j} - d_+ c^\dagger_{1,+j}) =$$

$$= -\frac{1}{2}(c^\dagger_{1,+,j}d_+ + c^\dagger_{1,-j}d_- - c_{1,-j}d^\dagger_- - c_{1,+j}d^\dagger_+).$$

This is the term in non-Nambu formalism (**??**).

me. normal Hamiltonian in Nambu space for the continuous model

(!! write better what is going on!!!???)
Prove that

$$H_{\mathrm{n}} = \sum_{\sigma,\sigma'=\pm} \int_\Omega dx \hat\psi^\dagger_\sigma(x) h_{\sigma,\sigma'}(p,x) \hat\psi_{\sigma'}(x) \qquad \Leftrightarrow \qquad H_{\mathrm{n}} \equiv \frac{1}{2}\int_\Omega dx\ \hat\Psi^\dagger(x) \mathcal{H}_{\mathrm{n}}(p,x) \hat\Psi(x),$$

where $\mathcal{H}_{\mathrm{n}}(p,x) := \begin{pmatrix} h(p,x) & 0 \\ 0 & -\sigma_y h^*(p,x)\sigma_y \end{pmatrix}$;
$h(p,x) := \sum\limits_{\sigma,\sigma'=\pm} h_{\sigma,\sigma'}(p,x)|\sigma\rangle\langle\sigma'|$;
$\hat\Psi(x) := \begin{pmatrix} \hat\psi(x) \\ i\sigma_y \left[\hat\psi^\dagger(x)\right]^T \end{pmatrix}$;
$\hat\psi(x) := \sum\limits_{\sigma=\pm} \hat\psi_\sigma(x)|\sigma\rangle$.

Solution

We will omit the arguments (p,x), (x) and prove to the other direction:

$$\hat\Psi^\dagger \mathcal{H}_{\mathrm{n}} \hat\Psi = (\hat\psi^\dagger_+ \quad \hat\psi^\dagger_- \quad \hat\psi_- \quad -\hat\psi_+) \begin{pmatrix} h_{++} & h_{+-} & 0 & 0 \\ h_{-+} & h_{--} & 0 & 0 \\ 0 & 0 & -h_{--} & h^*_{-+} \\ 0 & 0 & h^*_{+-} & -h_{++} \end{pmatrix} \begin{pmatrix} \hat\psi_+ \\ \hat\psi_- \\ \hat\psi^\dagger_- \\ -\hat\psi^\dagger_+ \end{pmatrix} =$$

$$= \begin{pmatrix} \hat\psi^\dagger_+ h_{++} + \hat\psi^\dagger_- h_{+-} & \hat\psi^\dagger_+ h_{-+} + \hat\psi^\dagger_- h_{--} & -\hat\psi_- h_{--} - \hat\psi_+ h^*_{-+} & \hat\psi_- h^*_{+-} - (-\hat\psi_+) h_{++} \end{pmatrix} \begin{pmatrix} \hat\psi_+ \\ \hat\psi_- \\ \hat\psi^\dagger_- \\ -\hat\psi^\dagger_+ \end{pmatrix} =$$

$$= \hat\psi^\dagger_+ h_{++} \hat\psi_+ + \hat\psi^\dagger_- h_{+-} \hat\psi_+ + \hat\psi^\dagger_+ h_{-+} \hat\psi_- + \hat\psi^\dagger_- h_{--} \hat\psi_- - \hat\psi_- h_{--} \hat\psi^\dagger_- - \hat\psi_+ h^*_{-+} \hat\psi^\dagger_- - \hat\psi_- h^*_{+-} \hat\psi^\dagger_+ - \hat\psi_+ h_{++} \hat\psi^\dagger_+ =$$

$$= 2\left(\hat\psi^\dagger_+ h_{++} \hat\psi_+ + \hat\psi^\dagger_- h_{+-} \hat\psi_+ + \hat\psi^\dagger_+ h_{-+} \hat\psi_- + \hat\psi^\dagger_- h_{--} \hat\psi_-\right) + \mathrm{const}\cdot\delta(0),$$

where at the last step we used anticommutative identities and the hermiticity of the Hamiltonian ($H = H^{*T}$) Because of which, for example, $h^*_{-+} = h_{+-}$. We remind that h-s are just complex functions, so ψ-s can go through it. Then, the factor 2 cancels with factor $1/2$ from the Nambu Hamiltonian and we get the exactly the term under the integral of non-Nambu Hamiltonian (**??**).

me. SC Hamiltonian in Nambu space for the continuous model

(!! write better what is going on!!!???)
Here we will prove that

$$H_{\mathrm{SC}} := \sum_{\sigma=\pm} \int_0^\infty dx \hat\chi^\dagger_\sigma(x) \left[\frac{p^2}{2m} - \mu\right] \hat\chi_\sigma(x) + \int_0^\infty dx \left[\Delta \hat\chi^\dagger_+(x) \hat\chi^\dagger_-(x) + \Delta^* \hat\chi_-(x) \hat\chi_+(x)\right]$$

is equivalent to

$$H_{\rm SC}=\frac{1}{2}\int_0^\infty dx\hat{\Upsilon}^\dagger(x)\mathcal{H}_{\rm SC}(p,x)\hat{\Upsilon}(x),\quad \mathcal{H}_{\rm SC}(p,x)=\begin{pmatrix}\left[\frac{p^2}{2m}-\mu\right] & i\Delta\sigma_y\\ -i\Delta^*\sigma_y & -\left[\frac{p^2}{2m}-\mu\right]\end{pmatrix},$$

where $\hat{\Upsilon}(x)=\begin{pmatrix}\hat{\chi}(x)\\ i\sigma_y\left[\hat{\chi}^\dagger(x)\right]^T\end{pmatrix}$, $\hat{\chi}(x)=\sum_{\sigma=\pm}\hat{\chi}_\sigma(x)|\sigma\rangle$.

Solution

We will omit dependence on $(p,x),(x)$ and do as before:

$$\hat{\Upsilon}^\dagger\mathcal{H}_{\rm SC}\hat{\Upsilon}=\begin{pmatrix}\hat{\chi}^\dagger & \hat{\chi}^T(-i\sigma_y)\end{pmatrix}\begin{pmatrix}\left[\frac{p^2}{2m}-\mu\right] & \Delta\\ \Delta^* & -\left[\frac{p^2}{2m}-\mu\right]\end{pmatrix}\begin{pmatrix}\hat{\chi}\\ i\sigma_y\hat{\chi}^{\dagger T}\end{pmatrix}=$$
$$=\begin{pmatrix}\hat{\chi}^\dagger\left[\frac{p^2}{2m}-\mu\right]+\hat{\chi}^T(-i\sigma_y)\Delta^* & \hat{\chi}^\dagger\Delta-(\hat{\chi}^T(-i\sigma_y))\left[\frac{p^2}{2m}-\mu\right]\end{pmatrix}\begin{pmatrix}\hat{\chi}\\ i\sigma_y\hat{\chi}^{\dagger T}\end{pmatrix}=$$
$$=\hat{\chi}^\dagger\left[\frac{p^2}{2m}-\mu\right]\hat{\chi}+\hat{\chi}^T(-i\sigma_y)\Delta^*\hat{\chi}+\hat{\chi}^\dagger\Delta(i\sigma_y\hat{\chi}^{\dagger T})-(\hat{\chi}^T(-i\sigma_y))\left[\frac{p^2}{2m}-\mu\right](i\sigma_y\hat{\chi}^{\dagger T})=$$
$$=\hat{\chi}^\dagger\left[\tfrac{p^2}{2m}-\mu\right]\hat{\chi}+\Delta^*\begin{pmatrix}\chi_+ & \chi_-\end{pmatrix}\begin{pmatrix}0 & -1\\ 1 & 0\end{pmatrix}\begin{pmatrix}\chi_+\\ \chi_-\end{pmatrix}+\Delta\begin{pmatrix}\chi_+^\dagger & \chi_-^\dagger\end{pmatrix}\begin{pmatrix}0 & 1\\ -1 & 0\end{pmatrix}\begin{pmatrix}\chi_+^\dagger\\ \chi_-^\dagger\end{pmatrix}-\left[\tfrac{p^2}{2m}-\mu\right]\begin{pmatrix}\chi_+ & \chi_-\end{pmatrix}\begin{pmatrix}\chi_+^\dagger\\ \chi_-^\dagger\end{pmatrix}=$$
$$=\left[\tfrac{p^2}{2m}-\mu\right](\chi_+^\dagger\chi_++\chi_-^\dagger\chi_-)+\Delta^*(\chi_-\chi_+-\chi_+\chi_-)+\Delta(-\chi_-^\dagger\chi_+^\dagger+\chi_+^\dagger\chi_-^\dagger)+\left[\tfrac{p^2}{2m}-\mu\right](-\chi_+\chi_+^\dagger-\chi_-\chi_-^\dagger)=$$
$$=2\left(\left[\frac{p^2}{2m}-\mu\right](\chi_+^\dagger\chi_++\chi_-^\dagger\chi_-)+\Delta\chi_+^\dagger\chi_-^\dagger+\Delta^*\chi_-\chi_+\right).$$

Now the equivalence with (**??**) is obvious. Also, this formula can also be found, for example, in [**?**] and the similar one in [**?**].

me. the Heisenberg equations for the continuous model

(!! write better what is going on!!!???)
Here we will derive the Heisenberg equations for the Nambu fields $\hat{\Psi}$ and $\hat{\Upsilon}$.

Solution

We will use $i\frac{d}{dt}\hat{\Upsilon}(x,t)=\left[\hat{\Upsilon}(x,t),H_{\rm tot}\right]$ and for it we compute:

$$\left[\hat{\Upsilon}_a(x),H_n\right]=\int_\Omega dx'\hat{\Upsilon}_a(x)\frac{1}{2}\hat{\Psi}_b^\dagger(x')\mathcal{H}_{\rm n}^{bc}(p',x')\hat{\Psi}_c(x')-\int_\Omega dx'\frac{1}{2}\hat{\Psi}_b^\dagger(x')\mathcal{H}_{\rm n}^{bc}(p',x')\hat{\Psi}_c(x')\hat{\Upsilon}_a(x)=$$
$$=\int_\Omega dx'\hat{\Upsilon}_a(x)\frac{1}{2}\hat{\Psi}_b^\dagger(x')\mathcal{H}_{\rm n}^{bc}(p',x')\hat{\Psi}_c(x')-\int_\Omega dx'(-1)^2\frac{1}{2}\hat{\Upsilon}_a(x)\hat{\Psi}_b^\dagger(x')\mathcal{H}_{\rm n}^{bc}(p',x')\hat{\Psi}_c(x')=0;$$

$$\left[\hat{\Upsilon}_a(x),H_{SC}\right]=\hat{\Upsilon}_a(x)\int dx'\frac{1}{2}\hat{\Upsilon}_b^\dagger(x')\mathcal{H}_{\rm SC}^{bc}(p',x')\hat{\Upsilon}_c(x')-\int dx'\frac{1}{2}\hat{\Upsilon}_b^\dagger(x')\mathcal{H}_{\rm SC}^{bc}(p',x')\hat{\Upsilon}_c(x')\hat{\Upsilon}_a(x)=$$
$$=\int dx'\frac{1}{2}(-\hat{\Upsilon}_b^\dagger(x')\hat{\Upsilon}_a(x)+\delta_{ab}\delta(x-x'))\mathcal{H}_{\rm SC}^{bc}(p',x')\hat{\Upsilon}_c(x')-$$
$$-\int dx'\frac{1}{2}\hat{\Upsilon}_b^\dagger(x')\mathcal{H}_{\rm SC}^{bc}(p',x')(-\hat{\Upsilon}_a(x)\hat{\Upsilon}_c(x')+\mathcal{C}_{ca}\delta(x-x'))=$$
$$=-\int dx'\frac{1}{2}\hat{\Upsilon}_b^\dagger(x')\hat{\Upsilon}_a(x)\mathcal{H}_{\rm SC}^{bc}(p',x')\hat{\Upsilon}_c(x')+\frac{1}{2}\mathcal{H}_{\rm SC}^{ac}(p,x)\hat{\Upsilon}_c(x)+$$
$$+\int dx'\frac{1}{2}\hat{\Upsilon}_b^\dagger(x')\mathcal{H}_{\rm SC}^{bc}(p',x')\hat{\Upsilon}_a(x)\hat{\Upsilon}_c(x')-\frac{1}{2}\hat{\Upsilon}_b^\dagger(x)\mathcal{H}_{\rm SC}^{bc}(p,x)\mathcal{C}_{ca}=$$

$$= -\int dx' \frac{1}{2}\hat{\Upsilon}_b^\dagger(x')\hat{\Upsilon}_a(x)\mathcal{H}_{\rm SC}^{bc}(p',x')\hat{\Upsilon}_c(x') + \int dx' \frac{1}{2}\hat{\Upsilon}_b^\dagger(x')\mathcal{H}_{\rm SC}^{bc}(p',x')\hat{\Upsilon}_a(x)\hat{\Upsilon}_c(x')$$
$$+ \frac{1}{2}\mathcal{H}_{\rm SC}^{ac}(p,x)\hat{\Upsilon}_c(x) - \frac{1}{2}\underbrace{\hat{\Upsilon}_b^\dagger(x)}_{=\hat{\Upsilon}_d C_{bd}}\mathcal{H}_{\rm SC}^{bc}(p,x)\mathcal{C}_{ca} =$$
$$= \int dx' \frac{1}{2}\hat{\Upsilon}_b^\dagger(x')\underbrace{[\mathcal{H}_{\rm SC}^{bc}(p',x'),\hat{\Upsilon}_a(x)]}_{=0}\hat{\Upsilon}_c(x') + \frac{1}{2}\mathcal{H}_{\rm SC}^{ac}(p,x)\hat{\Upsilon}_c(x) - \frac{1}{2}\hat{\Upsilon}_a\underbrace{\mathcal{C}_{bd}\mathcal{H}_{\rm SC}^{bc}(p,x)\mathcal{C}_{ca}}_{=-\mathcal{H}_{\rm SC}^{da*}=-\mathcal{H}_{\rm SC}^{ad}} =$$
$$= \mathcal{H}_{\rm SC}^{ac}(p,x)\hat{\Upsilon}_c(x) \equiv [\mathcal{H}_{\rm SC}(p,x)\hat{\Upsilon}(x)]_a.$$

Here we used the fact that each component $\mathcal{H}_{\rm SC}^{bc}$ is a scalar function, so it commutes with spinor $\hat{\Upsilon}_c(x)$ and that from charge-symmetry properties ($C_{ab}\hat{\Upsilon}_b^\dagger = \hat{\Upsilon}_a$) we have $\hat{\Upsilon}_b C_{ab} = \hat{\Upsilon}_b^\dagger$, since $C_{ab}^\dagger = C_{ab}$.

To be more mathematically strict, one can also agree about the positions of row and column indices of spinors (Ψ and Υ). We are not fixing much attention to it, since in case of doubt one can imagine matrices, rows, columns. Also, we omit upper-lower position of indices and agree that we sum over each repeated index despite its position.

Also, it is important to use the fact that that $\mathcal{H}_{\rm SC}$ is Hermitian, since this is the main property to use the transformations like $\mathcal{C}_{bd}\mathcal{H}_{\rm SC}^{bc}(p,x)\mathcal{C}_{ca} = -\mathcal{H}_{\rm SC}^{da*} = \mathcal{H}_{\rm SC}^{ad}$.

$$\left[\hat{\Upsilon}_a(x), H_T\right] = \frac{1}{2}\Big(\hat{\Upsilon}_a(x)\hat{\Upsilon}_b^\dagger(a)\mathcal{W}^{bc}\hat{\Psi}_c(\tilde{R}) + \underbrace{\hat{\Upsilon}_a(x)\hat{\Psi}_b^\dagger(\tilde{R})}_{=-\hat{\Psi}_b^\dagger(\tilde{R})\hat{\Upsilon}_a(x)}\mathcal{W}^{\dagger bc}\hat{\Upsilon}_c(a) -$$
$$- \hat{\Upsilon}_b^\dagger(a)\mathcal{W}^{bc}\underbrace{\hat{\Psi}_c(\tilde{R})\hat{\Upsilon}_a(x)}_{=-\hat{\Upsilon}_a(x)\hat{\Psi}_c(\tilde{R})} - \hat{\Psi}_b^\dagger(\tilde{R})\mathcal{W}^{\dagger bc}\hat{\Upsilon}_c(a)\hat{\Upsilon}_a(x)\Big) =$$
$$= \frac{1}{2}\Big(\delta_{ab}\delta(x-a)\mathcal{W}^{bc}\hat{\Psi}_c(\tilde{R}) - \hat{\Psi}_b^\dagger(\tilde{R})\mathcal{W}^{\dagger bc}\mathcal{C}_{ab}\delta(x-a)\Big) =$$
$$= \frac{1}{2}\Big(\delta_{ab}\delta(x-a)\mathcal{W}^{bc}\hat{\Psi}_c(\tilde{R}) - \hat{\Psi}_r(\tilde{R})\underbrace{\mathcal{C}_{br}\mathcal{W}^{\dagger bc}\mathcal{C}_{ab}}_{-\mathcal{W}^{ra*}=-\mathcal{W}^{ar}}\delta(x-a)\Big) =$$
$$= \delta(x-a)\mathcal{W}^{ac}\hat{\Psi}_c(\tilde{R}) \equiv [\delta(x-a)\mathcal{W}\hat{\Psi}(\tilde{R})]_a$$

After collecting terms and restoring t-dependence, we got

$$i\frac{d}{dt}\hat{\Upsilon}(x,t) = \mathcal{H}_{\rm SC}(p,x)\hat{\Upsilon}(x,t) + \delta(x-a)\mathcal{W}\hat{\Psi}(\tilde{R},t),$$

which is the Eq. (**??**). Analogous we get the Eq. (**??**). There is no value of writing the analogous derivation and as the one before, it is straightforward and bulky.

me. Derivative of the Dyson equations for the continuous model

(!! write better what is going on!!!???)

Here we will find the Dyson equation for $[G_{\rm NN}(x,x'|t)]_{ab} := -i\Theta(t)\langle\{\hat{\Psi}_a(x,t),\hat{\Psi}_b^\dagger(x',0)\}\rangle$.

Solution

We evaluate:

$$i\frac{d}{dt}[G_{\rm NN}(x,x'|t)]_{ab} = \underbrace{\delta(t)\langle\{\hat{\Psi}_a(x,t),\hat{\Psi}_b^\dagger(x',0)\}\rangle}_{=\delta(t)\langle\{\hat{\Psi}_a(x,0),\hat{\Psi}_b^\dagger(x',0)\}\rangle=\delta(t)\delta(x-x')\delta_{ab}} - i\Theta(t)\langle\{i\frac{d\hat{\Psi}_a(x,t)}{dt},\hat{\Psi}_b^\dagger(x',0)\}\rangle =$$
$$= \delta(t)\delta(x-x')\delta_{ab} - i\Theta(t)\langle\{\mathcal{H}_{\rm n}^{ac}(p,x)\hat{\Psi}_c(x,t),\hat{\Psi}_b^\dagger(x',0)\}\rangle - i\Theta(t)\langle\{\delta(x-\tilde{R})\mathcal{W}^{\dagger ac}\hat{\Upsilon}_c(a,t),\hat{\Psi}_b^\dagger(x',0)\}\rangle =$$
$$= \delta(t)\delta(x-x')\delta_{ab} + \mathcal{H}_{\rm n}^{ac}(p,x)\underbrace{(-i\Theta(t))\langle\{\hat{\Psi}_c(x,t),\hat{\Psi}_b^\dagger(x',0)\}\rangle}_{=[G_{NN}(x,x'|t)]_{cb}} + \delta(x-\tilde{R})\mathcal{W}^{\dagger ac}\underbrace{(-i\Theta(t))\langle\{\hat{\Upsilon}_c(a,t),\hat{\Psi}_b^\dagger(x',0)\}\rangle}_{=[G_{SN}(a,x'|t)]_{cb}}.$$

Note that purely the expression $\langle\{\hat{\Psi}_a(x,t),\hat{\Psi}_b^\dagger(x',0)\}\rangle$ is in general case complex to evaluate and the $\delta(t)$ and $\Theta(t)$ allow us to proceed. Also, we consider the Hamiltonian as a complex function, thus we can easily take it out of averaging. Thus in matrix form, we have

$$\left(i\frac{d}{dt} - \mathcal{H}_{\rm n}(p,x)\right)G_{\rm NN}(x,x'|t) = \delta(x-\tilde{R})\mathcal{W}^\dagger G_{SN}(a,x'|t) + \delta(t)\delta(x-x'). \tag{15.33}$$

Exactly the same way other Dyson Eq. (**??**) can be proven. To use transformation $F[f](z) := \int_0^\infty dt e^{izt} f(t)$, we prepare, for example, like

$$\begin{aligned} F[i\frac{d}{dt}G_{\rm NS}](z) &= \int_0^\infty dt e^{izt} i\frac{d}{dt}G_{\rm NS}(t) = ie^{izt}G_{\rm NS}(t)|_0^\infty - i\cdot iz\int_0^\infty dt e^{izt}G_{\rm NS} = zG_{\rm NS}(z), \\ F[\mathcal{H}_{\rm n}G_{\rm NS}](z) &= \mathcal{H}_{\rm n}G_{\rm NS}(z), \\ F[\delta(x-\tilde{R})\mathcal{W}^\dagger G_{\rm SS}](z) &= \delta(x-\tilde{R})\mathcal{W}^\dagger G_{\rm SS}(z). \end{aligned}$$

Now, the eq. $\left(i\frac{d}{dt} - \mathcal{H}_{\rm n}(p,x)\right) G_{\rm NS}(x,x'|t) = \delta(x-\tilde{R})\mathcal{W}^\dagger G_{\rm SS}(a,x'|t)$ will be transformed as

$$(z-\mathcal{H}_{\rm n})G_{\rm NS}(z) = \delta(x-\tilde{R})\mathcal{W}^\dagger G_{\rm SS}(z).$$

Other Dyson eq. (**??**) are transformed the same way.

15.2.2 Problems Transformations of SC Green's functions

me. spectral density for the continuous model

(!! write better what is going on!!!???)
Here we will find the formula for the $\rho_{\rm n}(\omega)$.

Solution

Fist, we notice that (we use $z := \omega + i\eta, \eta \to 0$)

$$\begin{aligned} \frac{\partial}{\partial z}\big[z-\mathcal{H}_{\rm n}(p,x)\big]m(x,x') &= \frac{\partial}{\partial z}\delta(x-x'), \\ m(x,x') + \big[z-\mathcal{H}_{\rm n}(p,x)\big]\frac{\partial m(x,x')}{\partial z} &= 0, \\ \frac{\partial m(x,x')}{\partial z} &= -\frac{1}{\big[z-\mathcal{H}_{\rm n}(p,x)\big]}m(x,x') \\ \frac{\partial m(x,x')}{\partial z}\delta(x'-x) &= -\frac{\delta(x'-x)}{\big[z-\mathcal{H}_{\rm n}(p,x)\big]}m(x,x') \\ \frac{\partial m(x,x')}{\partial z}\delta(x'-x) &= -m(x',x)m(x,x'). \end{aligned}$$

Here we see the importance of $m(x',x) \neq m(x,x')$ Analogously, the same formula for g is obtained. Now, with the help of $G_{\rm NN}(x,x') = m(x,x') + +m(x,\tilde{R})\mathcal{W}^\dagger g(a,a)\mathcal{W}D^{-1}m(\tilde{R},x')$ we will find the formula for $\rho_{\rm n}(\omega)$:

$$\begin{aligned} \rho_{\rm n}(\omega) =& -\frac{1}{\pi}{\rm Im}\int_\Omega dx {\rm tr} G_{\rm NN}(x,x) \\ =& \underbrace{-\frac{1}{\pi}{\rm Im}\int_\Omega dx {\rm tr} m(x,x)}_{=:\rho_{\rm n}^{(0)}(\omega)} - \frac{1}{\pi}{\rm Im}\,{\rm tr}\Big[m(x,\tilde{R})\mathcal{W}^\dagger g(a,a)\mathcal{W}D^{-1}\int_\Omega dx m(\tilde{R},x)\Big] \\ =& \rho_{\rm n}^{(0)}(\omega) - \frac{1}{\pi}{\rm Im}\,{\rm tr}\Big[m(x,\tilde{R})\mathcal{W}^\dagger g(a,a)\mathcal{W}D^{-1}\int_\Omega dx m(\tilde{R},x)\Big] = \\ =& \rho_{\rm n}^{(0)}(\omega) - \frac{1}{\pi}{\rm Im}\int_\Omega dx {\rm tr}\Big[\mathcal{W}^\dagger g(a,a)\mathcal{W}D^{-1}\int_\Omega dx m(\tilde{R},x)m(x,\tilde{R})\Big] = \\ =& \rho_{\rm n}^{(0)}(\omega) - \frac{1}{\pi}{\rm Im}\,{\rm tr}\Big[\mathcal{W}^\dagger g(a,a)\mathcal{W}D^{-1}\int_\Omega dx m(\tilde{R},x)m(x,\tilde{R})\Big] = \\ =& \rho_{\rm n}^{(0)}(\omega) + \frac{1}{\pi}{\rm Im}\,{\rm tr}\ \mathcal{W}^\dagger\ g(a,a)\ \mathcal{W}\ D^{-1}\ \frac{\partial m(\tilde{R},\tilde{R})}{\partial z}. \end{aligned}$$

Thus we have proven the (**??**).

Now, with the help of $G_{\rm SS}(x,x') = g(x,x') + g(x,a)\mathcal{M}[1-g(a,a)\mathcal{M}]^{-1}g(a,x')$ find a formula for the $\rho_{\rm SC}(\omega)$:

$$\begin{aligned}
\rho_{\rm SC}(\omega) &= -\frac{1}{\pi}{\rm Im}\int_0^\infty dx {\rm tr}\{G_{\rm SS}(x,x)\} = \\
&= \underbrace{-\frac{1}{\pi}{\rm Im}\int_0^\infty dx {\rm tr}\{g(x,x)\}}_{=:\rho^{(0)}_{\rm SC}(\omega)} - \frac{1}{\pi}{\rm Im}\int_0^\infty dx {\rm tr}\Big[g(x,a)\mathcal{M}[1-g(a,a)\mathcal{M}]^{-1}g(a,x)\Big] \\
&= \rho^{(0)}_{\rm SC}(\omega) - \frac{1}{\pi}{\rm Im}\ {\rm tr}\Big[\mathcal{M}[1-g(a,a)\mathcal{M}]^{-1}\int_0^\infty dx g(a,x)g(x,a)\Big] \\
&= \rho^{(0)}_{\rm SC}(\omega) + \frac{1}{\pi}{\rm Im}\ {\rm tr}\Big[\mathcal{M}[1-g(a,a)\mathcal{M}]^{-1}\frac{\partial g(a,a)}{\partial\omega}\Big] \\
&= \rho^{(0)}_{\rm SC}(\omega) + \frac{1}{\pi}{\rm Im}\ {\rm tr}\Big[\mathcal{W}m(\tilde{R},\tilde{R})\mathcal{W}^\dagger[1-g(a,a)\mathcal{W}m(\tilde{R},\tilde{R})\mathcal{W}^\dagger]^{-1}\frac{\partial g(a,a)}{\partial\omega}\Big].
\end{aligned}$$

Finally, one needs to use $(ABC)^{-1} = C^{-1}B^{-1}A^{-1}$ to simplify the expression under tr:

$$\begin{aligned}
&\mathcal{W}m(\tilde{R},\tilde{R})\mathcal{W}^\dagger[(m(\tilde{R},\tilde{R})\mathcal{W}^\dagger)^{-1}m(\tilde{R},\tilde{R})\mathcal{W}^\dagger - (m(\tilde{R},\tilde{R})\mathcal{W}^\dagger)^{-1}m(\tilde{R},\tilde{R})\mathcal{W}^\dagger g(a,a)\mathcal{W}m(\tilde{R},\tilde{R})\mathcal{W}^\dagger]^{-1}\tfrac{\partial g(a,a)}{\partial\omega}\Big] = \\
&= \mathcal{W}m(\tilde{R},\tilde{R})\mathcal{W}^\dagger(m(\tilde{R},\tilde{R})\mathcal{W}^\dagger)^{-1}[1-m(\tilde{R},\tilde{R})\mathcal{W}^\dagger g(a,a)\mathcal{W}]^{-1}(m(\tilde{R},\tilde{R})\mathcal{W}^\dagger)\frac{\partial g(a,a)}{\partial\omega} = \\
&= \mathcal{W}D^{-1}m(\tilde{R},\tilde{R})\mathcal{W}^\dagger\frac{\partial g(a,a)}{\partial\omega}
\end{aligned}$$

and finish our little proof:

$$\rho_{\rm SC}(\omega) = \rho^{(0)}_{\rm SC}(\omega) + \frac{1}{\pi}{\rm Im}\ {\rm tr}\Big[\mathcal{W}D^{-1}m(\tilde{R},\tilde{R})\mathcal{W}^\dagger\frac{\partial g(a,a)}{\partial\omega}\Big]. \tag{15.34}$$

$$= \rho^{(0)}_{\rm SC}(\omega) + \frac{1}{\pi}{\rm Im}\ {\rm tr}D^{-1}m(\tilde{R},\tilde{R})\frac{\partial\mathcal{W}^\dagger g(a,a)\mathcal{W}}{\partial\omega}. \tag{15.35}$$

We hope that by this point reader felt the whole beauty of the mathematical transformations.

15.2.3 Problems about флуктуационные эффекты в слабых контактах

Фйг-8.1. Напряжение при проскальзывании фазы

Найти среднее напряжение на джозефсоновском контакте с током $I < I_c$, возникающее из-за термически индуцированных процессов проскальзывания фазы (емкостью контакта пренебречь). Температуру считать малой по сравнению с E_J.

Solution

(???)

Фйг-8.2. $\bar{V}(I)$ в квантовом джозефсоновском контакте

Найти в квазиклассическом приближении при $T = 0$ зависимость среднего напряжения $\bar{V}(I)$ в квантовом джозефсоновском контакте с $E_J \gg E_C$ и $1/R = 0$, от тока в контакте I, при $I_c - I \ll I_c$.

Solution

(???)

Фйг-8.3. $\bar{V}(I)$ в квантовом джозефсоновском контакте

Найти в квазиклассическом приближении при $T = 0$ зависимость среднего напряжения $\bar{V}(I)$ в квантовом джозефсоновском контакте с $E_J \gg E_C$ и $1/R = 0$, от тока в контакте I, при условии $I \ll I_c$.

Solution

(???)

Фйг-8.4. Гамильтониан и ДУС из кольца с SNS котактом

Рассмотреть сверхпроводящее кольцо индуктивности L, замкнутое на квантовый джозефсоновский контакт энергии E_J и емкости C. Для случая, когда параметр $\beta_L = 2\pi L I_c/c\Phi_0$ слегка превышает 1, вывести эффективный гамильтониан двухуровневой квантовой системы. Найти условия на параметры задачи, при которых нижние 2 состояния будут заметно отделены по энергии от более высоких возбужденных состояний.

Solution

(???)

15.2.4 Problems about GF Special Methods for SC

me. Current in three-terminal junction

(!! rewrite it!!)
There are several ways to describe multiterminal junctions. For the mutlitermianl junction with a two-level system in the center (quantum dot), one way is to write density of states as

$$\rho(\omega) = \underbrace{\rho^{(0)}_{SC}(\omega) + \rho^{(0)}_{D}(\omega)}_{\text{bare DOS}} + \underbrace{\left(-\frac{1}{\pi} \mathrm{Im} \frac{\partial}{\partial \omega} \log\det\left[1 - g_D(\omega)\Sigma(\omega)\right] \right)}_{\text{tunneling contribution}}.$$

(?? where parameters mean??? also write the impostance of the self energy, since it will be used in the final formula)
Proof of this formula is complicated and requires some background of condensed matter. But we ca just use this formula and compute the current by calculation of free energy

$$F = -k_{\mathrm{B}}T \int_0^\infty d\varepsilon \rho(\varepsilon) \ln\left[2\cosh\left(\varepsilon/2k_{\mathrm{B}}T\right)\right]$$

and then the formula $I = \frac{2e}{\hbar}\frac{\partial F}{\partial \varphi}$. Do this calculation and obtain the current as a function of phase difference φ.
Hint: (write formula for the derivative of the log det)

Solution

One needs first to simplify the basic formula for the current, then take the derivative using formula from linear algebra, rewrite imaginary part as two terms and use the residue theorem to evaluate each (remembering, where are the poles of the Fermi function).
(!!! I need to redo it again!!!)

$$J_j(\varphi) = -\frac{2e}{h\beta} \int_0^\infty d\omega \ln\left(2\cosh\frac{\beta\omega}{2}\right) \frac{\partial}{\partial\varphi} \delta\rho(\omega,\varphi) \overset{[}{\Phi}_0 = \frac{h}{2e} \equiv \frac{\pi\hbar}{e}]\text{i b p} = \tag{15.36}$$

$$= -\frac{1}{\Phi_0} \mathrm{Im} \int_0^\infty d\omega \tanh\frac{\beta\omega}{2} \frac{\partial}{\partial\varphi} \ln\det d\left(\omega + i\eta, \varphi\right) \overset{f(\omega)=\frac{1}{e^{\beta\omega}+1}}{=} \tag{15.37}$$

$$= \frac{1}{\Phi_0} \mathrm{Im} \int_{-\infty}^{+\infty} d\omega f(\omega) \mathrm{tr} \frac{\partial}{\partial\varphi} \ln\det(\omega + i\eta - h_D - \Sigma(\omega + i\eta)) = \tag{15.38}$$

$$= \frac{1}{\Phi_0} \mathrm{Im} \int_{-\infty}^{+\infty} d\omega f(\omega) \mathrm{tr} \frac{1}{\omega + i\eta - h_D - \Sigma(\omega + i\eta)} \frac{\partial\Sigma(\omega + i\eta)}{\partial\varphi_j} = \tag{15.39}$$

$$= \frac{1}{2i\Phi_0} \int d\omega f(\omega) \,\mathrm{tr}\, \frac{1}{\omega + i\eta - h_D - \Sigma(\omega + i\eta)} \frac{\partial\Sigma(\omega + i\eta)}{\partial\varphi_j} - \tag{15.40}$$

$$- \frac{1}{2i\Phi_0} \int d\omega f(\omega) \,\mathrm{tr}\, \frac{1}{\omega - i\eta - h_D - \Sigma(\omega - i\eta)} \frac{\partial\Sigma(\omega - i\eta)}{\partial\varphi_j}. \tag{15.41}$$

The poles of the integrand allows one to make a simplification. The Fermi function produces fermionic poles. The first integral because of $\omega + i\eta$ has poles from the propagator in the lower-half of the complex plane, thus we need to close the contour to the upper-half. In this region we have only poles from Fermi's function (when $e^{\beta\omega} = -1$). It means, $\beta\omega = \pi + 2\pi n, n = 0, 1, 2, 3...$ The second integral should be closed in the lower part of the plane, where the poles are $\beta\omega = \pi + 2\pi n, n = -1, -2, -3..$, because of $\omega - i\eta$ in it. As a result,

$$J_j(\varphi) = \frac{1}{2i\Phi_0} \cdot 2\pi i \sum_{\omega_n \geq 0} \underbrace{\mathrm{res}(f(\omega))}_{-1/\beta} \mathrm{tr}\, \frac{1}{\omega + i\eta - h_D - \Sigma(\omega + i\eta)} \frac{\partial \Sigma(\omega + i\eta)}{\partial \varphi_j} - \tag{15.42}$$

$$- \frac{1}{2i\Phi_0} \cdot (-2\pi i) \sum_{\omega_n < 0} \underbrace{\mathrm{res}(f(\omega))}_{-1/\beta} \mathrm{tr}\, \frac{1}{\omega - i\eta - h_D - \Sigma(\omega - i\eta)} \frac{\partial \Sigma(\omega - i\eta)}{\partial \varphi_j} = \tag{15.43}$$

$$= -\frac{\pi}{\Phi_0} \frac{1}{\beta} \sum_{\omega_n} \mathrm{tr} \frac{1}{i\omega_n - h_D - \Sigma(i\omega_n)} \frac{\partial \Sigma(i\omega_n)}{\partial \varphi_j}. \tag{15.44}$$

At $T = 0$ the sum is changed to the integral:

$$J_j(\varphi, T = 0) = -\frac{1}{2\Phi_0} \int d\omega\ \mathrm{tr} \frac{1}{i\omega - h_D - \Sigma(i\omega)} \frac{\partial \Sigma(i\omega)}{\partial \varphi_j}. \tag{15.45}$$

From this equation, the Ambegoakar-Baratoff's formula can be obtained if one neglects $\Sigma(i\omega)$ in the denominator (this is the tunneling limit). This is because $\Sigma \sim \Gamma$, so after decomposition of the denominator into series, the terms from Σ from the denominator will be of the highest order in Γ.

me. the approximation of the current for two terminals

The general expression for the Josephson current (15.67) can be simplified for the case of two terminals by usage of the Sokhotski–Plemelj theorem as follows:

$$I_1 = \frac{1}{\Phi_0} \mathrm{Im} \int_{-\infty}^{+\infty} d\omega f(\omega) \mathrm{tr} \frac{1}{\omega + i\eta - h_D - \Sigma(\omega)} \frac{\partial \Sigma(\omega + i\eta)}{\partial \varphi_1} = \tag{15.46}$$

$$= -\frac{\pi}{\Phi_0} \sum_{\tau,\sigma=\pm} \int d\omega f(\omega) \delta\left(\omega - \tau\omega_A - \sigma E_Z\right) \frac{\partial}{\partial \varphi_1} \left(\Sigma(0) + \omega \left. \frac{d\Sigma(\omega)}{d\omega} \right|_{\omega=0} \right) = \tag{15.47}$$

$$= -\frac{\pi}{\Phi_0} \Big(f(\omega_A + E_Z) + f(\omega_A - E_Z) - f(-\omega_A + E_Z) - f(-\omega_A - E_Z) \Big) \frac{\partial}{\partial \varphi_1} \omega_A = \tag{15.48}$$

$$= -\frac{\pi}{\Phi_0} \Big(- \frac{2\mathrm{sh}(\beta\omega_A)}{\mathrm{ch}(\beta\omega_A) + \mathrm{ch}(\beta E_Z)} \Big) \frac{\partial}{\partial \varphi_1} \omega_A = \tag{15.49}$$

$$= \frac{2\pi E_J}{\Phi_0} \frac{\mathrm{sh}(\beta\omega_A)}{\mathrm{ch}(\beta\omega_A) + \mathrm{ch}(\beta E_Z)} \frac{\partial \sqrt{1 - D\sin^2 \frac{\varphi}{2}}}{\partial \varphi_1} \overset{\varphi := \varphi_2 - \varphi_1}{=} \tag{15.50}$$

$$= \frac{2\pi E_J}{\Phi_0} \frac{\mathrm{sh}(\beta\omega_A)}{\mathrm{ch}(\beta\omega_A) + \mathrm{ch}(\beta E_Z)} \frac{D \cdot 2 \sin \frac{\varphi}{2} \cos \frac{\varphi}{2}}{4\sqrt{1 - D\sin^2 \frac{\varphi}{2}}} = \tag{15.51}$$

$$= \frac{\pi D E_J}{2\Phi_0} \frac{\mathrm{sh}(\beta\omega_A)}{\mathrm{ch}(\beta\omega_A) + \mathrm{ch}(\beta E_Z)} \frac{\sin\varphi}{\sqrt{1 - D\sin^2 \frac{\varphi}{2}}}. \tag{15.52}$$

Thus we have (**??**).

me. spectrum in two terminals for the discrete model

Solution

$$E_{\tau,\sigma} = \tau\left[1+\frac{\Gamma_1}{\Delta_1}+\frac{\Gamma_2}{\Delta_2}\right]^{-1}\left(\sqrt{V^2+|\Gamma_1 e^{i\varphi_1}+\Gamma_2 e^{i\varphi_2}|^2}+\sigma\Delta_Z\right) = \tag{15.53}$$

$$= \frac{\tau}{1+\frac{\Gamma_1}{\Delta_1}+\frac{\Gamma_2}{\Delta_2}}\sqrt{V^2+\Gamma_1^2+\Gamma_2^2+2\Gamma_1\Gamma_2\cos(\varphi_1-\varphi_2)}+\sigma\frac{\Delta_Z}{1+\frac{\Gamma_1}{\Delta_1}+\frac{\Gamma_2}{\Delta_2}} \tag{15.54}$$

$$= \frac{\tau}{1+\frac{\Gamma_1}{\Delta_1}+\frac{\Gamma_2}{\Delta_2}}\sqrt{V^2+(\Gamma_1+\Gamma_2)^2-2\Gamma_1\Gamma_2+2\Gamma_1\Gamma_2\cos(\varphi_1-\varphi_2)}+\sigma E_Z, \tag{15.55}$$

$$= \frac{\sqrt{V^2+(\Gamma_1+\Gamma_2)^2}\tau}{1+\frac{\Gamma_1}{\Delta_1}+\frac{\Gamma_2}{\Delta_2}}\sqrt{1-2\Gamma_1\Gamma_2\frac{1}{V^2+(\Gamma_1+\Gamma_2)^2}\cdot 2\frac{1-\cos\varphi}{2}}+\sigma E_Z, \tag{15.56}$$

$$= \tau E_J\sqrt{1-D\sin^2\frac{\varphi}{2}}+\sigma E_Z, \tag{15.57}$$

where

$$E_J := \frac{\sqrt{V^2+(\Gamma_1+\Gamma_2)^2}}{1+\frac{\Gamma_1}{\Delta_1}+\frac{\Gamma_2}{\Delta_2}}, \qquad D := \frac{4\Gamma_2\Gamma_1}{V^2+(\Gamma_1+\Gamma_2)^2}, \qquad E_Z := \frac{\Delta_Z}{1+\frac{\Gamma_1}{\Delta_1}+\frac{\Gamma_2}{\Delta_2}}. \tag{15.58}$$

This is the (**??**).

me. spectrum in three terminals for the discrete model

Solution

$$E_{\tau,\sigma} = \tau\left[1+3\frac{\Gamma}{\Delta}\right]^{-1}\left(\sqrt{V^2+\Gamma^2(3+2\cos(\varphi-\chi)+2\cos\varphi+2\cos\chi)}+\sigma\Delta_Z\right) =$$

$$= \tau\left[1+3\frac{\Gamma}{\Delta}\right]^{-1}\left(\sqrt{V^2+3\Gamma^2-4\Gamma^2\left(-\frac{3}{2}+\frac{1-\cos(\varphi-\chi)}{2}+\frac{1-\cos\varphi}{2}+\frac{1-\cos\chi}{2}\right)}+\sigma\Delta_Z\right) =$$

$$= \tau\left[1+3\frac{\Gamma}{\Delta}\right]^{-1}\left(\sqrt{V^2+9\Gamma^2-4\Gamma^2\left(\sin^2\frac{(\varphi-\chi)}{2}+\sin^2\frac{\varphi}{2}+\sin^2\frac{\chi}{2}\right)}+\sigma\Delta_Z\right).$$

Thus

$$E_{\tau,\sigma} = \tau E_J\sqrt{1-D\Phi(\varphi,\chi)}+\sigma\tilde{\Delta}_Z, \tag{15.59}$$

where we introduce $\Phi(\varphi,\chi)$ and D with special coefficients, such that $D\in[0,1]$,

$$E_J := \left[1+3\frac{\Gamma}{\Delta}\right]^{-1}\sqrt{V^2+9\Gamma^2}, \tag{15.60}$$

$$D := \frac{9\Gamma^2}{V^2+9\Gamma^2}, \tag{15.61}$$

$$\Phi(\varphi,\chi) := \frac{4}{9}\left(\sin^2\varphi/2+\sin^2\chi/2+\sin^2(\varphi/2-\chi/2)\right), \tag{15.62}$$

$$\tilde{\Delta}_Z := \frac{\Delta_Z}{1+3\frac{\Gamma}{\Delta}}. \tag{15.63}$$

And we have (**??**). Note that with ore definition, the function $\Phi(\varphi,\chi)$ has a maximal value of 1, and the D is allowed to be from 0 to 1.

15.2.5 Problems about Majorana states in SC-s

(there are many articles about it, so there will be enough good question for like 10 pages... It is not important now)

15.2.6 Problems about vortices

(ADD LATER HERE PROBLEMS FROM BELOUSOV)

Фйг-5.1. Дрейф вихрей в пленке

Имеется пленка высокотемпературного сверхпроводника YBaCuO с $T_c = 93.5°\text{K}$. Толщина пленки 100 nm. В поперечном поле $B = 8T$ при температуре $T = 90.5°\text{K}$ измерено удельное сопротивление $0.5\mu\Omega \cdot \text{cm}$. Найти среднюю скорость дрейфа вихрей v_v, если через пленку течет транспортный ток с плотностью $j = 10^4$ A/cm^2. Найти также коэффициент диффузии вихрей D, размерность коего cm^2/s.

Solution

(???)

Фйг-5.2. $j_c(T)$ при пиннинге на цилиндрических отверстиях

Найти зависимость критического тока $j_c(T)$ от температуры вблизи критической, $T \to T_c - 0$, при наличии слабого магнитного поля, индуцирующего вихри, для случая пиннинга вихрей на цилиндрических отверстиях диаметра $d > \xi_0$.

Пояснение: учесть рост $\xi(T)$ вблизи T_c. Двумерную плотность отверстий n_2 считать самым малым параметром задачи.

Solution

(???)

Фйг-5.3. $j_c(T)$ при пинниге на изотропных слабых дефектах

Найти зависимость критического тока $j_c(T)$ от температуры вблизи критической, $T \to T_c - 0$, при наличии слабого магнитного поля, индуцирующего вихри. Пинниг вихрей возникает теперь из-за изотропных слабых дефектов. Объемная плотность дефектов n_3 велика, $n_3\xi_0^3 \gg 1$.

Solution

(???)

Фйг-5.4. Пленка с дыркой при тепловых изгибных флуктуациях

Один вихрь находится в сверхпроводящей пленке, поперечно ее плоскости,и зацепляется за одно цилиндрическое отверстие диаметра $d > \xi_0$, ось которого параллельна направлению магнитного поля. Толщину пленки считать сколь угодно большой. При достаточно высокой температуре T, близкой к T_c, тепловые изгибные флуктуации вихря становятся заметными, т.е. их типичная амплитуда $u_T = \left(\left\langle u^2 \right\rangle\right)^{1/2}$ превышает величину d. В такой ситуации сила пиннинга вихря резко падает, но остается ненулевой. Найти зависимость критического тока $j_c(T)$ в этом режиме от температуры.

Solution

(???)

Фйг-6.1. $B(H)$ при флуктуациях положений вихревых линий

К относительно тонкой пленке сверхпроводника (толщина $d \gg \xi$, но при этом $d \ll a_0 = \sqrt{\Phi_0/B}\Big)$ приложено слабое параллельное магнитное поле, создающее двумерную решетку из вихревых линий, расположенных в плоскости пленки, со средним расстоянием между вихрями $a_0 \gg \lambda$. Считать что все стандартные параметры сверхпроводника $-\xi, \lambda$ - известны. В пленке имеются точечные дефекты, приводящие к флуктуациям положения вихревых линий, в частности, поперечный "уход" $|u(z) - u(0)| \propto z^{2/3}$. Кроме того, дефекты приводят к ненулевой величине критического тока пленки j_c, которая много меньше тока распаривания j_0. Требуется найти, как меняется зависимость $B(H)$ в области $B \ll H_{c1}$ из-за наличия дефектов.

Solution

(???)

Фйг-6.2. Сопротивление по критическому току

Для сверхпроводника с $\xi \ll \lambda$ в магнитном поле B находящемся в интервале $H_{c1} \ll B \ll H_{c2}$ задан критический ток j_c малый по сравнению с током распаривания j_0. Величина j_c определяется пиннингом на слабых изотропных дефектах. Эти же дефекты приводят к разрушению дальнего порядка решетки вихрей на расстояниях $R_c \gg \lambda \gg a_0$. Оценить величину R_c, считая остальные параметры заданными.

Solution

(???)

Фйг-6.3. Температура плавления вихревой решетки

Для решетки точечных вихрей в тонкой пленке сверхпроводника, находящейся в поперечном поле $B \ll H_{c2}$, найти температуру плавления T_M вихревой решетки. Все параметры считать заданными, толщина $d \leq \xi \ll \lambda$.

Solution

(???)

Фйг-13.7. Уровни в вихре с p-спариванием

Найти уровни ϵ_μ в вихре в сверхпроводнике с p-спариванием типа $d_\pm(k) \propto k_x \pm i k_y$ (как в A-фазе ^{3}He), для случая магнитного поля направленного вдоль оси z.

Solution

(???)

15.2.7 Problems about fluctuation effects

Фйг-4.1. Параметр Гинзбурга Gi для типичных случаев

Получить по порядку величины параметра Гинзбурга Gi для сверхпроводников размерности d $= 1, 2, 3$, как в чистом так и в чистом и грязном пределах, выразив их через параметры металла (k_F и длина пробега l), поперечные размеры (для $d = 1, 2$) и температуру перехода T_c.

Solution

(У Варламова Ларкина решена, почитаю, додумаю, впишу!)

Фйг-4.2. Флуктуационная диамагнитная восприимчивость

Вычислить отношение χ_{fl}/χ_0 флуктуационной диамагнитной восприимчивости к восприимчивости металла для трехмерного сверхпроводника.

Solution

(???)

Фйг-4.3. Ширина флуктуационной области вблизи $H_{c2}(T)$

Оценить ширину $\mathrm{Gi}(B)$ флуктуационной области вблизи линии $H_{c2}(T)$ при достаточно сильных магнитных полях, $B \gg \mathrm{Gi}H_{c2}(0)$.

Solution

(???)

Фйг-4.4. $T_{c0} - T_{BKT}$ для слоистого ВТСП

Оценить величину температурного интервала $T_{c0} - T_{BKT}$ для слоистого ВТСП семейства BiCaSrCuO исходя из данных по сопротивлению вдоль слоев при температуре порядка $1.5T_c$.
(данные найти самостоятельно в литературе, например с помощью библиографии в книге В.В.Шмидта I'll change the formulation, add some data!!!)

Solution

(???)

Фйг-4.5. Сопротивление "пирловских" вихрей

Для тонкой пленки свепрохпроводника (толщина $d \ll \lambda$) оценить величину линейного сопротивления $(dV/dI)|_{I\to 0}$ при $T < T_c$, возникающего из-за ненулевой концентрации "пирловских" вихрей.
(??? add explanation, what are they???)

Solution

(???)

Фйг-4.6*. Ренормгруппа Костерлица для перехода распаривания вихрей

Вывести и решить уравнения ренормгруппы Костерлица для фазового перехода распаривания вихрей в пленке, найти зависимость $R_c(T)$ при $T \to T_c - 0$.

Solution

(???)

15.2.8 Problems about properties of unconventional superconductors

(see Mineev Samokhin for now, it is a big topic)

Green's function of topological SC

Find the Green's function of topological SC.
(??? cite something)

Solution:

(???)

15.2.9 Problems about models with unconventional superconductors

(see Mineev Samokhin for now, it is a big topic)

15.3 Creation of Special Models

15.3.1 Problems about Creation of a Model for Special Superconductors 1

(I'll summarize many things from articles here)

Create model for superconductor that is open to the surroundings

(just a framework for open SC)

Solution

Create model for superconductor that is in non-thermal state

(discuss that we want it to be not in thermal state, thus we introduce such openness. explain, what do we mean by this??)

Solution

Superconductor between two baths

Create model for superconductor that is between two baths with different temperatures.

Solution for 1D superconductor

(??? currently, it is a not really solved problem...)

First of all, the superconductor itself will be described by

$$H_0 = \sum_{k,\sigma} \Big(\xi_k c^\dagger_{k\sigma} c_{k\sigma} + \Delta \big(c_{k\uparrow} c_{-k\downarrow} + c^\dagger_{-k\downarrow} c^\dagger_{k\uparrow} \big) \Big);$$

To make it an open system, we will use the density matrix.
(??? did it act before on a wave function?? maybe... (???))
The Hamiltonian is nearly integrable
(??? write what it means???)
So we can use the GGE anzatz for it:

$$\rho_{\boldsymbol{\mu}}(t) = \frac{e^{-\sum_{q,\sigma} \mu_q(t) n_{q,\sigma}}}{\mathrm{Tr}[e^{-\sum_{q,\sigma} \mu_q(t) n_{q,\sigma}}]}$$

(??? write what the parameter here mean???)
By "can" we mean that the error from the exact computation will be little (??? how much??).
And as all open system the density matrix obey the following Lindblad equation:

$$\frac{d\rho}{dt} = -i[H_0, \rho] + \hat{\mathcal{D}}[\rho],$$

$$\hat{\mathcal{D}}[\rho] := \epsilon \sum_{\alpha} \left(L_\alpha \rho L_\alpha^\dagger - \frac{1}{2}\{L_\alpha^\dagger L_\alpha, \rho\} \right);$$

Here α is a multi-index, which is $\alpha = \{i, k_1, k_2\}$, where i means the type of Lindblad operator below, k is the momenta index (so we have sum over all the momenta).

The Lindblad operators will be

$$\begin{aligned} L_{1,k_1k_2} &= \sqrt{\gamma_{1,k_1k_2}}\, b^\dagger_{k_1,p_1} b_{k_2p_2}, & \gamma_{1,k_1k_2} &= e^{-(\varepsilon_{k_1,p_1} - \varepsilon_{k_2,p_2})/2T_b} \\ L_{2,k_1k_2} &= \sqrt{\gamma_{2,k_1k_2}}\, b^\dagger_{k_1,p_1} b^\dagger_{k_2p_2}, & \gamma_{2,k_1k_2} &= e^{-(\varepsilon_{k_1,p_1} + \varepsilon_{k_2,p_2})/2T_b} \\ L_{3,k_1k_2} &= \sqrt{\gamma_{3,k_1k_2}}\, b_{k_1,p_1} b_{k_2,p_2}, & \gamma_{3,k_1k_2} &= e^{+(\varepsilon_{k_1,p_1} + \varepsilon_{k_2,p_2})/2T_b} \end{aligned}$$

(???????????????? why there are so????????)

Note that the Lindblad operators depend on the spectrum ε, which depends on the gap Δ, which is changed in time. So, the Lindblad operators depend on time. (??? maybe it means that they can't be in this form??)

And here, the b operators are Bogoliubov ones:

$$\begin{aligned} \widehat{b}_{k,-} &= u_k \widehat{c}_{k,-} + v_k \widehat{c}^\dagger_{-k,+} & \widehat{c}_{k,+} &= u_k \widehat{b}_{k,+} + v_k \widehat{b}^\dagger_{-k,-} \\ \widehat{b}_{k,+} &= u_k \widehat{c}_{k,+} - v_k \widehat{c}^\dagger_{-k,-} & \widehat{c}_{k,-} &= u_k \widehat{b}_{k,-} - v_k \widehat{b}^\dagger_{-k,+} \end{aligned}$$

where the coefficients are

$$u_p^2 = \frac{1}{2}\left(1 + \frac{\xi_p}{\sqrt{\xi_p^2 + |\Delta|^2}}\right), \qquad v_p^2 = \frac{1}{2}\left(1 - \frac{\xi_p}{\sqrt{\xi_p^2 + |\Delta|^2}}\right)$$

in which there is the gap that obey self-consistency equation

$$\Delta := \lambda \sum_k \mathrm{Tr}\left(e^{-\sum_r \mu_r(\Delta) b_r^\dagger b_r} c_{k\uparrow} c_{-k\downarrow}\right); \qquad \widehat{\mathcal{H}} = E_0 + \sum_{k,\sigma} \varepsilon_{k,\sigma} b^\dagger_{k,\sigma} b_{k,\sigma}; \qquad \varepsilon_k = \sqrt{\xi_k^2 + |\Delta|^2}$$

(by which we mean that it is obtained from H, which also has Δ)

Now, what is left is to write, how one would solve the Liouville equation and how to obtain all physical parameters from the density matrix.

Solution for 1D superconductor (with another method (???))

(??? how to do it in another way?? read articles and write it here)

Solution for 3D superconductor

(??? I have no idea about it at all)

Create model for superconductor that has leakage of particles

(there is an article about it, so state their statement that some particles are lost, write model that takes it into account. explain, what do we mean by this??)

Solution

Create model for

Solution

15.3.2 Problems about Creation of a Model for Special Superconductors 2

(I'll summarize many things from articles here)

Create model for

Solution

Create model for

Solution

Create model for

Solution

15.4 Problems about Special Methods

15.4.1 Problems about numerical evaluation

me. Evaluate the gap equation

(??? still, I don't understand, how to compute it???)

15.5 Problems about Special Devices, Junctions

15.5.1 Problems about Creation of a Model for SC Devices 1

(I'll summarize many things from articles here)

Create model for open Josephson junction

Create a model of Josephson junction coupled to an electron reservoir. By reservoir, we mean that there is some probability of particles to escape from the central region.

Solution

(??? this is a really hard question for a professionals. I'll write this in the special note, then write it here)
(interesting that there are no Lindblad operators)
(see doi: 10.1063/5.0215522)

Create model for

Solution

Create model for

Solution

Model of S-TS junction

Create a model of a

Solution

(???)

Model of S-TS-S junction

Create a model of a

Solution

(???)

Model of S-QSHI-S Junction

Create a model of a

Solution

(???)

Model of N-QD-S junction

Create a model of a

Solution

(???)

15.5.2 Problems about Creation of a Model for SC Devices 2

(I'll summarize many things from articles here)

Create model for

Solution

Create model for

Solution

Create model for

(see note on SC devices for now)

Solution

15.5.3 Problems about special junctions with SC

Piasotski.et.al. Josephson junction by peculiar method

(write the main formula and the background)
Produce the well-known Josephson equation.

Solution

(I need to study that article again)

Piasotski.et.al. Majorana junction by peculiar method

(write the main formula and the background)
Produce the Josephson equation for the case of Majorana junction.
(write what is meant by Majorana junction!!!)

Solution

(I need to study that article again)

15.5.4 Problems about Creation of a Model of Special MTJJ

Zazunov.et.al. Model of S-QD-TS-TS

Create a model of a S-QD-TS-TS junction.
(add pictures)

Solution

(???)

Model of QD-S-S-S junction

Create a model of a QD-S-S-S junction

Solution by me

(???)

Solution by Matute-Ca˜nadas

(see that article again)

Model of multiterminal junctions with many s-wave superconductors

Create a model of a junction of a quantum dot (QD), that is couples to N conventional s-wave spin-singlet superconductors (S). The superconductors are not coupled to each other.

Solution

(???)

Model of S-QD-TS junction

Create a model of a junction of conventional s-wave spin-singlet superconductors (S), topological superconductor (TS) wires and a quantum dot (QD).
Consult if necessary the paper by Zazunov et al. https://arxiv.org/pdf/1801.10343

Solution

(???)

15.5.5 Problems about Special Junctions 1

(write from articles some transformations in their calculations. for now I write it in special note for them)

me. Calculation of Josephson current

(write that in MTJJ there is this and that formula for the current and density of states)
Find the current.
(point out that we have a GF in 4x4 matrix and the main point of the exercise is to understand how to work with it! delete or explain all that is related only to cond matter)

Solution

The current can be determined from the Gibbs free energy, which, in its turn, is derived from the density of states ρ (see review in Sec. **??**). More precisely, ρ is obtained from d matrix by $\rho(\omega,\varphi) = -\frac{1}{\pi}\operatorname{Im}\frac{\partial}{\partial\omega}\ln\det d\,(\omega,\varphi)$, and the d matrix is obtained from GF of the model by (**??**). Thus, the current in the j^{th} lead can be determined by some careful transformations:

$$J_j(\varphi) = -\frac{2e}{h\beta}\int_0^\infty d\omega \ln\left(2\cosh\frac{\beta\omega}{2}\right)\frac{\partial}{\partial\varphi}\delta\rho(\omega,\varphi) \overset{[}{\Phi_0}= \frac{h}{2e}\equiv\frac{\pi\hbar}{e}]\text{i b p}= \tag{15.64}$$

$$= -\frac{1}{\Phi_0}\operatorname{Im}\int_0^\infty d\omega\tanh\frac{\beta\omega}{2}\frac{\partial}{\partial\varphi}\ln\det d\,(\omega+i\eta,\varphi) \overset{f(\omega)=\frac{1}{e^{\beta\omega}+1}}{=} \tag{15.65}$$

$$= \frac{1}{\Phi_0}\operatorname{Im}\int_{-\infty}^{+\infty} d\omega f(\omega)\operatorname{tr}\frac{\partial}{\partial\varphi}\ln\det(\omega+i\eta-h_D-\Sigma(\omega+i\eta)) = \tag{15.66}$$

$$= \frac{1}{\Phi_0}\operatorname{Im}\int_{-\infty}^{+\infty} d\omega f(\omega)\operatorname{tr}\frac{1}{\omega+i\eta-h_D-\Sigma(\omega+i\eta)}\frac{\partial\Sigma(\omega+i\eta)}{\partial\varphi_j} = \tag{15.67}$$

$$= \frac{1}{2i\Phi_0}\int d\omega f(\omega)\operatorname{tr}\frac{1}{\omega+i\eta-h_D-\Sigma(\omega+i\eta)}\frac{\partial\Sigma(\omega+i\eta)}{\partial\varphi_j} - \tag{15.68}$$

$$- \frac{1}{2i\Phi_0}\int d\omega f(\omega)\operatorname{tr}\frac{1}{\omega-i\eta-h_D-\Sigma(\omega-i\eta)}\frac{\partial\Sigma(\omega-i\eta)}{\partial\varphi_j}. \tag{15.69}$$

The poles of the integrand allows one to make a simplification. The Fermi function produces fermionic poles. The first integral because of $\omega+i\eta$ has poles from the propagator in the lower-half of the complex plane, thus we need to close the contour to the upper-half. In this region we have only poles from Fermi's function (when $e^{\beta\omega}=-1$). It means, $\beta\omega=\pi+2\pi n, n=0,1,2,3...$ The second integral should be closed in the lower part of the plane, where the poles are $\beta\omega=\pi+2\pi n, n=-1,-2,-3..$, because of $\omega-i\eta$ in it. As a result,

$$J_j(\varphi) = \frac{1}{2i\Phi_0}\cdot 2\pi i\sum_{\omega_n\geq 0}\underbrace{\operatorname{res}(f(\omega))}_{-1/\beta}\operatorname{tr}\frac{1}{\omega+i\eta-h_D-\Sigma(\omega+i\eta)}\frac{\partial\Sigma(\omega+i\eta)}{\partial\varphi_j} - \tag{15.70}$$

$$- \frac{1}{2i\Phi_0}\cdot(-2\pi i)\sum_{\omega_n<0}\underbrace{\operatorname{res}(f(\omega))}_{-1/\beta}\operatorname{tr}\frac{1}{\omega-i\eta-h_D-\Sigma(\omega-i\eta)}\frac{\partial\Sigma(\omega-i\eta)}{\partial\varphi_j} = \tag{15.71}$$

$$= -\frac{\pi}{\Phi_0}\frac{1}{\beta}\sum_{\omega_n}\operatorname{tr}\frac{1}{i\omega_n-h_D-\Sigma(i\omega_n)}\frac{\partial\Sigma(i\omega_n)}{\partial\varphi_j}. \tag{15.72}$$

At $T=0$ the sum is changed to the integral[1]:

$$J_j(\varphi, T=0) = -\frac{1}{2\Phi_0}\int d\omega\ \operatorname{tr}\frac{1}{i\omega-h_D-\Sigma(i\omega)}\frac{\partial\Sigma(i\omega)}{\partial\varphi_j}. \tag{15.73}$$

From this equation, the Ambegoakar-Baratoff's formula can be obtained if one neglects $\Sigma(i\omega)$ in the denominator (this is the tunneling limit). This is because $\Sigma\sim\Gamma$, so after decomposition of the denominator into series, the terms from Σ from the denominator will be of the highest order in Γ.

To compute currents from j-th contact to j'-th we need to compute $J_j - J_{j'}$. Soon the results of this formula will be presented.

15.5.6 Problems about Special Junctions 2

(write from articles some transformations in their calculations. for now I write it in special note for them)

[1] See, for example, Eq. (89) in [**?**]

15.5.7 Problems about Special Junctions 3

(write from articles some transformations in their calculations. for now I write it in special note for them)

15.5.8 Problems about MTJJ

(I'll write it first in the note on MTJJ. that there is this or that setup, solve something in it. there are very many setup and it is a good challenge to derive something there)

Part VII
Specific Superconductivity in a Nutshell

16 Special also useful theories and properties

16.1 Details of general properties of superconductors

При нулевой температуре все электроны сверхпроводящие (????)

Вывод этого утверждения по Пухову следующий. Плотность электронов в сверхпроводнике n делится на нормальную n_n и сверхтекучую n_s части. Из теории ферми-жидкости (разложением и усреднением) $\mathbf{P} = -\mathbf{v}\frac{4\pi}{3(2\pi\hbar)^3}\int\limits_0^\infty dpp^4\frac{dn_B(\varepsilon)}{d\varepsilon}$, подставим фермиевское распределение и умножим на 2 (от спина), получаем

$$\rho_n = -\frac{8\pi}{3(2\pi\hbar)^3}\int\limits_0^\infty \frac{dn_F}{dp}p^4dp \overset{\text{around } p\approx p_F}{=} -\frac{p_F^4}{3\pi^2\hbar^3 v_F}\int\limits_{-\infty}^{+\infty}\frac{dn_F}{d\varepsilon}d\xi.$$

$\rho = mN/V = p_F^3 m/3\pi^2\hbar^3 \equiv \rho_n + \rho_s$,

$$\frac{\rho_n}{\rho} = -2\int\limits_0^{+\infty}\frac{dn_F}{d\varepsilon}d\xi.$$

Тут интеграл определяется температурной зависимостью щели $\Delta(T)$. Дифференцируем $\frac{1}{\lambda} = \frac{1}{2}\sum\limits_{\mathbf{p}}\cdot\frac{1+2\bar{n}_{\mathrm{p}}}{\sqrt{\xi_{\mathrm{p}}^2+\Delta^2}}$ по T и подставляем, получаем (!!! сделаю это уже очень скоро!!!)

$$\frac{\rho}{\rho_n} = 1 - \frac{d\ln T}{d\ln\Delta}.$$

Поэтому при $T\to 0$ плотность нормальной компоненты обращается в ноль $\rho_n \to 0$. Другими словами, при нулевой температуре все электроны становятся сверхпроводящими и $\frac{\rho_s}{\rho} = -\frac{d\ln T}{d\ln(\Delta/T)} \overset{x\to 0}{\to} 1$ 1.

(???? пока это вопрос, а то в другом месте написано, что нет, не все, ибо ферми сфера заполнена, рассеяние не может быть)

Общие важные вопросы про теории сверхпроводимости

Связи теорий сверхпроводимости друг с другом (????)

(??? оставшийся важный вопрос, потом пойму, пока прописать сами теории нужно еще)

Переходы между одними и другими типами сверхпроводников за счет изменения их параметров (????)

(укажу про эти задачи потом, что как доказать, что меняя такой-то параметр такие-то эффекты поменяются. пока тренируюсь в этом.)

Почему вообще классическая теория ГЛ работает для квантовых явлений? (????)

(тоже, стану умнее - допишу)

Как конкретно экспериментальные факты указывают на верную теорию сверхпроводимости?

1. Притяжение между электронами обеспечивается фононами решетки. Это взаимодействие не прямое, а опосредованное и не может выражаться потенциальной функцией $U(\mathbf{r}_1 - \mathbf{r}_2)$.

2. Для существования связанного состояния двух электронов нужна двумерность. Она обеспечивается тем, что движение электронов происходит на фоне заполненной ферми-сферы.

Эффективно взаимодействие выражается в рассеянии электрона на электроне. Чтобы электрон мог перейти из состояния $\mathbf{p}$ в состояние $\mathbf{p}'$, последнее, согласно принципу Паули, должно быть свободно. Это возможно лишь для состояний вблизи поверхности Ферми. Ширина области, в которой электроны могут притягиваться друг к другу $\sim \hbar\omega_D$, поскольку это максимальная энергия фононов, которую можно передать. Остальные электроны, находящиеся в глубине ферми-сферы, не могут изменить свой импульс.

В мелкой трёхмерной яме уровня, соответствующего связанному состоянию, нет. Он появляется только, если яма достаточно глубока и число Борна больше единицы. Откуда же появляется «низкоразмерность» движения, обеспечивающая существование пары? У нас не об изолированные частицы в 3D-пространстве, а о квазичастицы на фоне заполненной ферми-сферы. Испускание и поглощение фонона приводит лишь к повороту импульса электрона, его положение описывается только двумя углами на ферми-сфере, а величина импульса остаётся практически неизменной $p \approx p_F$. Наличие заполненной ферми-сферы делает задачу эффективно двумерной. Кроме того, мы заменяем плотность состояний вблизи поверхности Ферми на постоянную величину, что также соответствует двумерному случаю. В мелкой двумерной яме уровень, соответствующий связанному состоянию, есть всегда. Энергия связи экспоненциально мала по константе взаимодействия, что и объясняет малую величину температуры сверхпроводящего перехода (?? почему???).

Другие принципиальные свойства сверхпроводников

Вычисление сил, действующих на сверхпроводник в магнитном поле

(см ЛЛ8, еще додумать нужно. Вроде в общефизе тоже про это задачи были)

Самоиндукция сверхпроводников

(см ЛЛ8, еще додумать нужно. добавлю задачи про это в каталог)

Теоретическое доказательство, что проводимость сверхпроводника равна ровно бесконечности (?????)

(??? непонятно, почему все другие процессы дают ровно нулевой вклад в проводимость. а так- через переход к ур Лондонов это можно показать, допишу позже.)

16.2 Details of basic theories

16.2.1 Details of GL theory

Флуктуационная поправка к теплоемкости по ГЛ

(I'll summarize details about it here)

GL theory by Chelkatshev

(????)

$$F[\Delta(\mathbf{r})] = F_{n0} + \int d\mathbf{r}\frac{\mathbf{B}^2}{8\pi} + a\int d\mathbf{r}\Delta^*\left[\frac{\hbar}{\tau_{\mathrm{GL}}} - \hbar D\left(\nabla_{\mathbf{r}} - i\frac{2e}{\hbar c}\mathbf{A}\right)^2 + \frac{b}{2T_c}|\Delta|^2\right]\Delta,$$

τ_{GL} имеет размерность времени и меняет знак в точке сверхпроводящего перехода,

$$\frac{\hbar}{\tau_{\mathrm{GL}}} = \alpha\left(T - T_c\right),$$

Удобно нормировать параметр порядка так, чтобы его модуль совпадал с щелью в квазичастичной плотности состояний объёмного образца. Коэффициенты a, α, D и b слабо зависят от температуры, и их можно найти из БКШ. Для грязного предела (например, в сверхпроводящих сплавах с примесями), когда длина свободного пробега электрона l много меньше, чем $\xi_0 = \sqrt{\hbar D/T_c}$ (характерный размер куперовской пары при $T = 0$), D совпадает с коэффициентом диффузии электрона на уровне Ферми ($D = v_F l/3$),

$$a = \frac{\nu\pi}{8T_c}, \quad \alpha = \frac{8}{\pi}, \quad b = \frac{7\zeta(3)}{\pi^3}, \qquad \text{Kopnin N. B "Non-eq. SC"}$$

$\nu = mp_F/2\pi^2\hbar^3$, $\zeta(3) \approx 1.2$.

Условие применимости разложения $F[\Delta(\mathbf{r})]$ это $\Delta \ll \Delta(T \ll T_c) \equiv \Delta_0 \sim T_c$ и $\Delta \sim \sqrt{\hbar T_c/\tau_{\mathrm{GL}}} \sim \sqrt{(T_c - T)\,T_c}$, откуда следует условие $|T - T_c| \ll T_c$. Кроме того, Δ должна меняться в пространстве не слишком быстро (на расстояниях много больших ξ_0).

Для чистого случая:

$$a = 7\zeta(3)n/8\pi^2T_c^2, \qquad \alpha = 6\pi^2T_c/7\zeta(3)E_F, \qquad D = \hbar/4m, \qquad b = 3T_c/4E_F,$$

$n = p_F^3/3\pi^2\hbar^3$ - плотность электронов, $E_F = p_F^2/2m$ - энергия Ферми, m - масса электрона.

(??? тут у нас всегда обычная масса, не эффективная? этот вопрос не четко обсуждается в литературе, додумать нужно)

Микроскопический вывод функционала Гинзбурга Ландау по Враламову и Ларкину

6. 1. Функционал Гинзбурга — Ландау традиционного сверхпроводника

6. 2. Функционал Гинзбурга —Ландау для сверхпроводника с нетривиальной симметрией параметра порядка

О критерии Гинзбурга-Леванюка в разных случаях

(??? Когда-то доучу это!!!!)

$$Gi_{(D)} = \frac{1}{\alpha}\left[\frac{V_D}{V}\vartheta_D b(4m)^{\frac{D}{2}} T_{\mathrm{c}}^{\frac{D}{2}-1}\right]^{\frac{2}{4-D}}.$$

(???? верная ли формула эта???)

Подставим в эту формулу следующие из микроскопического рассмотрения значения параметров теории Гинзбурга - Ландау (2.6)(допишу их!!!), тогда

$$Gi_{(D)} = \left[\frac{7\zeta(3)\vartheta_D}{8\pi^2}\left(\frac{V_D}{V}\right)\frac{1}{\nu_D T_{\mathrm{c}}\xi^D}\right]^{\frac{2}{4-D}}$$

Так как $\nu_D T_{\mathrm{c}} \sim \nu_D v_F/\xi_c \sim p_F^{D-1}\xi_c^{-1} \sim \mathfrak{a}^{1-D}\xi_c^{-1}$, то

$$Gi_{(D)} \sim \left[\frac{7\zeta(3)\vartheta_D}{8\pi^2}\left(\frac{V_D}{V}\right)\frac{\xi_c \mathfrak{a}^{D-1}}{\xi^D}\right]^{\frac{2}{4-D}}$$

Также:

$$Gi_{(2)} = \frac{7\zeta(3)}{32\pi^3}\frac{1}{\nu_2 T_{\mathrm{c}}\xi^2}$$

$$Gi_{(3)} = \left[\frac{7\zeta(3)}{64\pi^3}\frac{1}{\nu_3 T_{\mathrm{c}}\xi^3}\right]^2$$

$\mathfrak{a}$ есть межатомное расстояние. Как уже упоминалось, в массивных традиционных сверхпроводниках ввиду большой величины корреляционной длины ($\xi_c \sim 10^{-6} \div 10^{-4}$ cm), которая намного превышает межатомное расстояние ($\mathfrak{a} \sim 10^{-8}$ см), флуктуационная поправка к теплоемкости оказывается чрезвычайно малой.

(!!!! нужно переписать таблицу, кривая получилась!!!)

$Gi_{(3)}$	$Gi_{(2)}$
$80\left(\frac{T_{\mathrm{c}}}{E_F}\right)^4, (c)$ $\frac{1{,}6}{(p_F l)^3}\left(\frac{T_{\mathrm{c}}}{E_F}\right), (d)$	$\left(\frac{T_{\mathrm{c}}}{E_F}\right), (d)$ $\frac{0{,}27}{p_F l}, (d)$
$Gi_{(1)}$	$\frac{1{,}3}{p_F^2 l d}, (d)$ film
$Gi_{(0)}$	
$0,5, (d)$ $1,3\left(p_F^2 S\right)^{-2/3}\left(T_{\mathrm{c}}\tau\right)^{-1/3}, (d)$ wire $2,3\left(p_F^2 S\right)^{-2/3}, (d)$ whisker	$\frac{\sqrt{7\zeta(3)}}{2\pi}\frac{1}{\sqrt{\nu T_{\mathrm{c}} V}} \approx$

Имеется связь между найденным числом Гинзбурга - Леванюка для грязного $2D$ случая $Gi_{(2)}^{(d)}$ и безразмерным кондактансом

$$G_\square = \frac{\hbar}{e^2 R_\square},$$

(???)

Другие определения

Уширение критической области магнитным полем

(потом когда-то дочитаю)

16.2.2 Details of BCS theory

Other forms of BCS hamiltonian

(write those from my master's thesis here!)

Size of a Cooper pair

$$\Delta \approx \left| \frac{p^2}{2m} - \frac{p_F^2}{2m} \right| \approx v_F \delta p.$$

Размер - это неопределенность координаты, из соотношения неопределённости:

$$\xi \approx \frac{\hbar v_F}{\Delta}.$$

Поскольку 2Δ есть энергия связи двух электронов,

$$\Delta \approx \left| \frac{p_2^2}{2m} - \frac{p_1^2}{2m} \right| \approx \frac{p_F \delta p}{m}, \quad (v_i \approx v_F)$$

Размер куперовской пары можно оценить также из щели в спектре: $\varepsilon(p) = \sqrt{\Delta^2 + v_F^2 (p - p_F)^2}$. Вдали от ферми-уровня $v_F |p - p_F| \gg \Delta$ спектр совпадает с случаем нормального металла: $\varepsilon(p) = v_F |p - p_F|$. Это значит, что эффект спаривания оказывает влияние только на электроны с импульсами в области шириной $\delta p \approx \Delta / v_F$. Соответственно, пространственный масштаб куперовской корреляции составляет $\xi \approx \hbar / \delta p \approx \hbar v_F / \Delta$.

$$\xi(v_F \approx 10^8 \text{ cm/c}, \Delta \approx 10K) \approx 2 \cdot 10^{-4}\text{см} \gg a = n^{-1/3} \approx 2 \cdot 10^{-8}\text{с}.$$

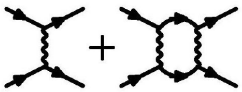
Пары проникают друг через друга, их нельзя представлять себе как классический газ частиц, расстояние между которыми больше их размеров.

Proof that all electrons are superconductive at $T = 0$

(see Pukhov, it is not so important)

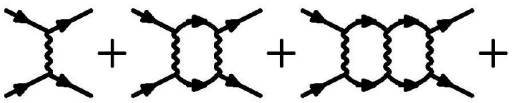
BCS by Abrikosov, Gorkov, Dzyaloshinski

О рассеянии в куперовском канале



$$\Gamma^0_{\alpha\alpha'\beta\beta'} = \frac{\lambda}{2} \left(\delta_{\alpha\alpha'} \delta_{\beta\beta'} - \delta_{\alpha\beta'} \delta_{\beta\alpha'} \right)$$

$$\lambda \nu_0 \ln \left(2\omega_D / \omega \right) \Gamma^0_{\alpha\alpha'\beta\beta'} \qquad \text{log div}$$

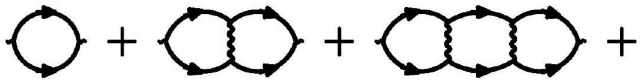


$$\left(-\lambda\nu_0 \ln\left(2\omega_D/\omega\right)\right)^{n-1} \Gamma^0_{\alpha\alpha'\beta\beta'}$$

$$\Gamma^C_{\alpha\alpha'\beta\beta'}(\omega) = \frac{1}{1-\lambda\nu_0 \ln 2\omega_D/\omega}\Gamma^0_{\alpha\alpha'\beta\beta'}$$

$$H_{\text{pert}} = \int \left\{\psi^+_\uparrow(\mathbf{r})\psi^+_\downarrow(\mathbf{r})\Delta(\mathbf{r}) + \psi_\downarrow(\mathbf{r})\psi_\uparrow(\mathbf{r})\Delta^*(\mathbf{r})\right\} d^3r$$

$$\chi_C = -\frac{\partial \left\langle \psi_\uparrow(\mathbf{r})\psi_\downarrow(\mathbf{r})\right\rangle}{\partial\Delta}$$



$$\chi_C\left(i\omega_n\right) = \Pi_C\left(i\omega_n\right) + \lambda\Pi^2_C\left(i\omega_n\right) + \ldots = \frac{\Pi_C\left(i\omega_n\right)}{1-\lambda\Pi_C\left(i\omega_n\right)},$$

$$\Pi_C\left(i\omega_n\right) = T\sum_m \int \frac{d^3p}{\left(i\varepsilon_m + i\omega_n - \xi_p\right)\left(-i\varepsilon_m - \xi_p\right)}.$$

$T\sum_{\omega_m} \frac{1}{\left(i\omega_m+i\omega_n-\xi_{p+k}\right)\left(i\omega_m-\xi_p\right)} = \frac{n_F\left(\xi_{p+k}\right)-n_F\left(\xi_p\right)}{i\omega_n-\xi_{p+k}+\xi_p}$, $\sum_{n=-\infty}^{\infty} \frac{1}{(2n+1)^2+a^2} = \frac{\pi}{2a}\,\text{th}\,\frac{\pi a}{2}$,

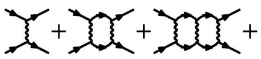
$$\Pi_C(0) = \frac{\nu_0}{2}\int\limits_{-\omega_D}^{\omega_D} \text{th}(\xi/2T)\frac{d\xi}{\xi}, \approx \nu_0 \ln \omega_D/T.$$

$$\lambda\Pi_C(0) = 1, \qquad \Rightarrow \qquad \lambda\nu_0 \ln\left(\frac{\omega_D}{T}\right) = 1$$

$$T_c = \frac{2\gamma}{\pi}\omega_D e^{-1/\lambda\nu_0} \sim \Delta = 2\omega_D e^{-1/\lambda\nu_0}$$

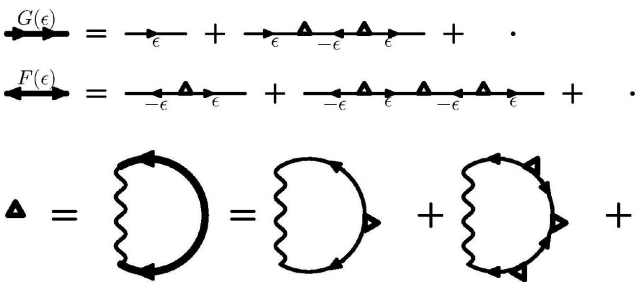
$\gamma = e^C$, $C = 0,577\ldots$

О функции Грина в сверхпроводнике

Последовательность диаграмм  $\sim$ eq. Бете-Солпитера $\Gamma_{ab}\left(p_i\right) = \Gamma^0_{ab}\left(p_i\right) + i\int \Gamma^0_{ab}\left(p'_i\right) G^{(1)}_a\left(p_{1+}\right) G^{(2)}_b\left(p_{2-}\right) \Gamma_{ab}\left(p''_i\right) \frac{d^4k}{(2\pi)^4}$

$$G_{\alpha\beta}\left(x,x'\right) := -i\left\langle\ \text{T}\psi_\alpha(x)\psi^+_\beta\left(x'\right)\right\rangle,$$
$$F_{\alpha\beta}\left(x,x'\right) := -i\left\langle\ \text{T}\psi_\alpha(x)\psi_\beta\left(x'\right)\right\rangle$$

Ужирнение (??????)



$$G_{\alpha\beta}(\varepsilon,\mathbf{p}) = G^0_{\alpha\beta}(\varepsilon,\mathbf{p}) + G^0_{\alpha\lambda}(\varepsilon,\mathbf{p})\Delta^*_{\lambda\mu}F_{\mu\beta}(\varepsilon,\mathbf{p}),$$
$$F_{\alpha\beta}(\varepsilon,\mathbf{p}) = G^0_{\alpha\lambda}(-\varepsilon,\mathbf{p})\Delta_{\lambda\mu}G_{\mu\beta}(\varepsilon,\mathbf{p})$$

$G_{\alpha\beta} = \delta_{\alpha\beta}G.$
$\Delta_{\alpha\beta} = \Delta(-i)\sigma^y_{\alpha\beta}.$

$$\Delta_{\alpha\beta} = \begin{pmatrix} 0 & -1 \\ 1 & 0 \end{pmatrix}\Delta, \qquad F_{\alpha\beta}(\varepsilon,\mathbf{p}) = \begin{pmatrix} 0 & -1 \\ 1 & 0 \end{pmatrix}F(\varepsilon,\mathbf{p}).$$

$$G_{\alpha\beta}(\varepsilon,\mathbf{p}) = \frac{\varepsilon+\xi_{\mathbf{p}}}{\varepsilon^2-\xi^2_{\mathbf{p}}-|\Delta|^2}\delta_{\alpha\beta}$$
$$F_{\alpha\beta}(\varepsilon,\mathbf{p}) = \frac{\Delta}{\varepsilon^2-\xi^2_{\mathbf{p}}-|\Delta|^2}i\sigma^y_{\alpha\beta}.$$

$$\varepsilon_{\mathbf{p}} = \sqrt{\xi^2_{\mathbf{p}}+\Delta^2}$$

$F_{\alpha\beta}(\varepsilon,\mathbf{p}) = \frac{\Delta}{\varepsilon^2-\xi^2_{\mathbf{p}}-|\Delta|^2}i\sigma^y_{\alpha\beta}$

$$\Delta_{\alpha\beta} = \lambda\int F_{\alpha\beta}(\varepsilon,\mathbf{p})\frac{d\varepsilon d^3p}{(2\pi)^4},$$

О термодинамике (???)

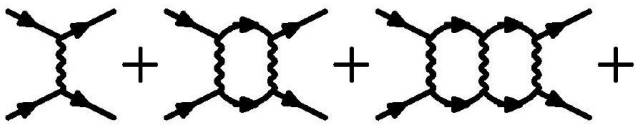
$$\Delta = \lambda T\sum_{\omega_n}\int F(i\omega_n,\mathbf{p})\frac{d^3p}{(2\pi)^3} = \lambda T\sum_{\omega_n}\int\frac{\Delta}{\omega_n^2+\xi^2_{\mathbf{p}}+\Delta^2}\frac{d^3p}{(2\pi)^3}.$$

(!?!??!?!)

16.2.3 BCS: examples of diagrammatic methods

Typical calculations in Gorkov's formalism

Finding T_c from Bethe-Salpeter equation



$$\Gamma^0(i\varepsilon,i\varepsilon') = \lambda v(i\varepsilon)v(i\varepsilon')$$

$$v(i\varepsilon) = \frac{\omega_D}{\sqrt{\varepsilon^2+\omega_D^2}},$$

$$\Gamma^C(p,p';s) = \Gamma^0(p,p') + \int\Gamma^0(p,k)G(k)G(s-k)\Gamma^C(k,p';s)\frac{d^4k}{(2\pi)^4}$$

$$\Gamma^C(i\varepsilon,i\varepsilon') = \Gamma^0(i\varepsilon,i\varepsilon') + T\sum_{\varepsilon''}\int\frac{d^3p}{(2\pi)^3}\Gamma^0(i\varepsilon,i\varepsilon'')G(i\varepsilon'',\mathbf{p})G(-i\varepsilon'',-\mathbf{p})\Gamma^C(i\varepsilon'',i\varepsilon').$$

$$\int \frac{1}{\left(\varepsilon''\right)^2+\xi_p^2}\frac{d^3p}{(2\pi)^3}=\frac{\pi\nu_0}{|\varepsilon''|}$$

$$\Gamma^C\left(i\varepsilon,i\varepsilon'\right)=\Gamma^0\left(i\varepsilon,i\varepsilon'\right)+\pi\nu_0 T\sum_{\varepsilon''}\Gamma^0\left(i\varepsilon,i\varepsilon''\right)\Gamma^C\left(i\varepsilon'',i\varepsilon'\right)/\left|\varepsilon''\right|$$

$$\Gamma^C\left(i\varepsilon,i\varepsilon'\right)=\lambda v(i\varepsilon)\left(v\left(i\varepsilon'\right)+\pi\nu_0 T\sum_{\varepsilon''}v\left(i\varepsilon''\right)\Gamma^C\left(i\varepsilon'',i\varepsilon'\right)/\left|\varepsilon''\right|\right).$$

$$\Gamma^C\left(i\varepsilon,i\varepsilon'\right)=\alpha v(i\varepsilon)v\left(i\varepsilon'\right)$$

$$\alpha=\lambda+\pi\nu_0\alpha\lambda T\sum_{\varepsilon''}v^2\left(i\varepsilon''\right)/\left|\varepsilon''\right|$$

$$\alpha=\lambda\left(1-\pi\nu_0\lambda T\sum_{\varepsilon''}v^2\left(i\varepsilon''\right)/\left|\varepsilon''\right|\right)^{-1}.$$

$$\pi T\sum_{\varepsilon''}v^2\left(i\varepsilon''\right)/\left|\varepsilon''\right|=1/\lambda\nu_0$$

$$v(i\varepsilon)=\omega_D/\left(\omega_D^2+\varepsilon^2\right)^{1/2}$$

$$2\sum_{n=0}^{\infty}\frac{\omega_D^2}{\left(\omega_D^2+\pi^2T_c^2(2n+1)^2\right)(2n+1)}=\frac{1}{\lambda\nu_0}.$$

$$\sum_{n=0}^{n_{\max}}\frac{1}{n+1/2}=\ln n_{\max}=\frac{1}{\nu_0\lambda}$$

$$T_c\approx\frac{\omega_D}{\pi}e^{-1/\lambda\nu_0}$$

$$2\sum_{n=0}^{\infty}\frac{\omega_D^2}{\left(\omega_D^2+\pi^2T_c^2(2n+1)^2\right)(2n+1)}=\frac{1}{\lambda\nu_0}.$$

$$\sum_{k=1}^{\infty}(-1)^{k+1}/k=\ln 2,\quad \lim_{n\to\infty}\left(\sum_{k=1}^{n}1/k-\ln n\right)=C=0.577$$

$$S\left(n<n_0\right)=\sum_{n=0}^{n_0}\frac{2}{2n+1}\approx\ln\left(2n_0\right)$$

$$S\left(n>n_0\right)=\int_{2\pi Tn_0}^{\infty}\frac{\omega_D^2}{\varepsilon^2+\omega_D^2}\frac{d\varepsilon}{\varepsilon}=\frac{1}{2}\ln\frac{\varepsilon^2}{\varepsilon^2+\omega_D^2}\Bigg|_{2\pi Tn_0}^{\infty}$$

$$S\left(n>n_0\right)=\ln\frac{\omega_D}{2\pi n_0T_c}$$

$$\frac{1}{\lambda\nu_0}=\ln\frac{\omega_D}{\pi T_c}+C$$

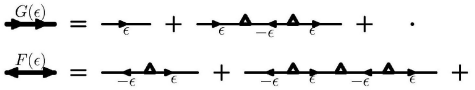
$$T_c=\frac{2\gamma}{\pi}\omega_De^{-1/\lambda\nu_0}\qquad\gamma=e^C$$

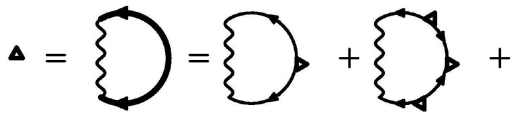
Determining $\Delta(T)$ in general case

$$\Gamma^0\left(i\varepsilon, i\varepsilon'\right) = \lambda v(i\varepsilon) v\left(i\varepsilon'\right), \qquad v(i\varepsilon) = \frac{\omega_D}{\sqrt{\varepsilon^2 + \omega_D^2}}$$

$$\Delta_{\alpha\beta} = \lambda \int F_{\alpha\beta}(\varepsilon, \mathbf{p}) \frac{d\varepsilon d^3p}{(2\pi)^4},$$

$$\Delta = \lambda T \sum_{\omega_n} \int F\left(i\omega_n, \mathbf{p}\right) \frac{d^3p}{(2\pi)^3} = \lambda T \sum_{\omega_n} \int \frac{\Delta}{\omega_n^2 + \xi_{\mathbf{p}}^2 + \Delta^2} \frac{d^3p}{(2\pi)^3},$$





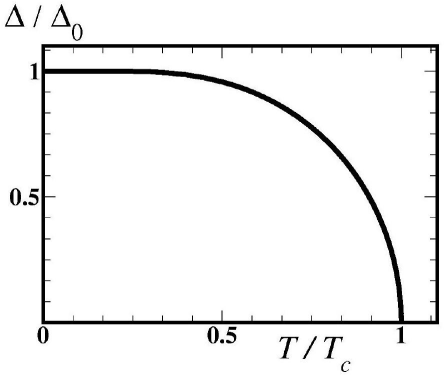
$$\tilde{\Delta}(i\varepsilon) = T \sum_{\varepsilon'} \Gamma^0\left(i\varepsilon, i\varepsilon'\right) F\left(i\varepsilon', \mathbf{r} = \mathbf{r}'\right),$$

$$F\left(i\varepsilon, \mathbf{r} = \mathbf{r}'\right) = \int \frac{\tilde{\Delta}(i\varepsilon)}{\varepsilon^2 + \xi_p^2 + \tilde{\Delta}^2(i\varepsilon)} \frac{d^3p}{(2\pi)^3}.$$

$$\tilde{\Delta}(i\varepsilon) = \Delta(T) v(i\varepsilon)$$

$$\Delta(T) = \lambda T \sum_{\varepsilon} \int \frac{v^2(i\varepsilon)\Delta(T)}{\varepsilon^2 + \xi_{\mathbf{p}}^2 + v^2(i\varepsilon)\Delta^2(T)} \frac{d^3p}{(2\pi)^3}.$$

$$\frac{1}{\lambda\nu_0} = \pi T \sum_{\varepsilon} \frac{v^2(i\varepsilon)}{\sqrt{\varepsilon^2 + \Delta^2(T) v^2(i\varepsilon)}}.$$



Determining Δ_0

$$\frac{1}{\nu_0\lambda} = \int_0^{\infty} \frac{v^2(i\varepsilon) d\varepsilon}{\sqrt{\varepsilon^2 + \Delta_0^2 v^2(i\varepsilon)}}. \qquad v(i\varepsilon) := \omega_D / \left(\varepsilon^2 + \omega_D^2\right)^{1/2}$$

$$\frac{1}{\nu_0\lambda} = \int\limits_0^\infty \frac{\omega_D^2 d\varepsilon}{(\varepsilon^2+\omega_D^2)\sqrt{\varepsilon^2+\Delta_0^2}}.$$

$$\int\limits_0^{\varepsilon_0} \frac{d\varepsilon}{\sqrt{\varepsilon^2+\Delta_0^2}} + \int\limits_{\varepsilon_0}^\infty \frac{\omega_D^2 d\varepsilon}{\varepsilon\,(\varepsilon^2+\omega_D^2)} = \ln\frac{2\varepsilon_0}{\Delta_0} + \ln\frac{\omega_D}{\varepsilon_0}.$$

$$\frac{1}{\lambda\nu_0} = \ln\frac{2\omega_D}{\Delta_0}.$$

$$\Delta_0 = \frac{\gamma}{\pi}T_c \qquad T_c = \frac{2\gamma}{\pi}\omega_D e^{-1/\lambda\nu_0}$$

Determining $\Delta(T)$ for $T \ll T_c$

$$\frac{1}{\lambda\nu_0} = T\sum_\varepsilon \int\limits_{-\infty}^\infty \frac{d\xi}{\varepsilon^2+\xi^2+\Delta^2} \qquad \sum_{n=-\infty}^{\infty} \frac{1}{(2n+1)^2+a^2} = \frac{\pi}{2a}\,\mathrm{th}\,\frac{\pi a}{2}$$

$$\frac{1}{\lambda\nu_0} = \int\limits_0^\infty \mathrm{th}\,\frac{\sqrt{\xi^2+\Delta^2}}{2T}\frac{d\xi}{\sqrt{\xi^2+\Delta^2}}.$$

$$\frac{1}{\lambda\nu_0} = \ln\frac{2\omega_D}{\Delta} - 2\int\limits_0^\infty \frac{d\xi}{\sqrt{\xi^2+\Delta^2}}\exp\left(-\frac{\sqrt{\xi^2+\Delta^2}}{T}\right).$$

$$\frac{1}{\nu_0\lambda} = \ln\frac{2\omega_D}{\Delta} - 2e^{-\Delta/T}\int\limits_0^\infty e^{-\xi^2/2\Delta T}\left(1-\frac{\xi^2}{2\Delta^2}\right)\frac{d\xi}{\Delta}$$

$$\ln\frac{\Delta}{\Delta_0} = -\sqrt{\frac{2\pi T}{\Delta}}e^{-\Delta/T}\left(1-\frac{T}{8\Delta}\right) \qquad \Delta_0 = \gamma T_c/\pi$$

$$\Delta\,(T\ll T_c) = \Delta_0\left(1-\sqrt{\frac{2\pi T}{\Delta_0}}e^{-\Delta_0/T}\left(1-\frac{T}{8\Delta_0}\right)\right)$$

Determining $\Delta(T)$ for $T \approx T_c$

$$\frac{1}{\lambda\nu_0} = \pi T\sum_\varepsilon \frac{v^2(i\varepsilon)}{\sqrt{\varepsilon^2+\Delta^2(T)v^2(i\varepsilon)}}.$$

$$\frac{1}{\lambda\nu_0} = \pi T\sum_\varepsilon\left(\frac{v^2(i\varepsilon)}{|\varepsilon|} - \frac{\Delta^2 v^4(i\varepsilon)}{2|\varepsilon|^3}\right)$$

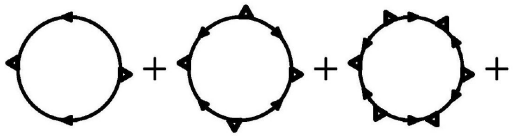
$$\ln\frac{T}{T_c} = -\frac{\pi\Delta^2}{2}T\sum_{\varepsilon_n}\frac{1}{|\varepsilon_n|^3}$$

$$\zeta(x) = \sum_{n=1}^\infty \frac{1}{n^x}, \quad \sum_{n=0}^\infty \frac{1}{(2n+1)^x} = \left(1-\frac{1}{2^x}\right)\zeta(x).$$

$$\frac{T-T_c}{T_c} = -\frac{7\zeta(3)}{8\pi^2}\frac{\Delta^2}{T_c^2}$$

$$\Delta^2_{T\to T_c} = \frac{8\pi^2}{7\zeta(3)} T_c \left(T_c - T\right)$$

Heat capacitance at $T < T_c$



$$\frac{\lambda}{V}\frac{\partial\Omega}{\partial\lambda} = T\sum_{\omega_n}\int G_0^{-1}\left(i\omega_n,\mathbf{p}\right)\left(G\left(i\omega_n,\mathbf{p}\right) - G_0\left(i\omega_n,\mathbf{p}\right)\right)\frac{d^3p}{(2\pi)^3} =$$

$$= -T\sum_{\omega_n}\int \Delta^* F\left(i\omega_n,\mathbf{p}\right)\frac{d^3p}{(2\pi)^3} = -\frac{|\Delta|^2}{\lambda}.$$

$$\frac{d\lambda}{\lambda^2} = T\sum_{\omega_n}\int \frac{2\Delta d\Delta}{\left(\omega_n^2 + \xi_{\mathbf{p}} + \Delta^2\right)^2}\frac{d^3p}{(2\pi)^3}$$

$$\frac{\Omega_s - \Omega_n}{V} = -2\int_0^{\Delta} T\sum_{\omega_n}\int \frac{\Delta^3 d\Delta}{\left(\omega_n^2 + \xi_{\mathbf{p}}^2 + \Delta^2\right)^2}\frac{d^3p}{(2\pi)^3}$$

$$\frac{\Omega_s - \Omega_n}{V} = -\pi\nu_0 T\sum_{\omega_n}\left(\sqrt{\omega_n^2+\Delta^2} + \frac{\omega_n^2}{\sqrt{\omega_n^2+\Delta^2}} - 2\left|\omega_n\right|\right).$$

а) $T \to 0$.

$\sum_n f(n) \approx \int f(x)dx + \int e^{2\pi i x} f(x)dx + \int e^{-2\pi i x} f(x)dx + \dots \qquad f(x) := \sqrt{(2\pi T x)^2 + \Delta^2} + \frac{\Delta^2}{\sqrt{(2\pi T x)^2+\Delta^2}} - 4\pi T|x|$

$$\Omega_s = -\frac{V\nu_0\Delta^2}{2}\left(1 + 2\sqrt{\frac{2\pi T}{\Delta}}e^{-\Delta/T}\left(1 + \frac{15}{8}\frac{T}{\Delta}\right)\right)$$

$$\Omega_s = -\frac{\nu_0 V\Delta_0^2}{2}\left(1 + 4\sqrt{\frac{2\pi T^3}{\Delta_0^3}}e^{-\Delta_0/T}\right)$$

$$C_s = T\frac{\partial S_s}{\partial T} = -T\frac{\partial^2\Omega_s}{\partial T^2} = 2\nu_0 V\sqrt{\frac{2\pi\Delta_0^5}{T^3}}e^{-\Delta_0/T}.$$

б) $T \to T_c$.

$$\frac{\Omega_s - \Omega_n}{V} = -\pi\nu_0\Delta^4 T\sum_{\omega_n}\frac{1}{\left|\omega_n\right|^3} \overset{\text{typ summ}}{=} -\frac{7\zeta(3)}{16\pi^2}\frac{\nu_0\Delta^4}{T_c^2}$$

$$\Omega_s - \Omega_n = -\frac{4\pi^2}{7\zeta(3)} V\nu_0\left(T - T_c\right)^2$$

$$C_s - C_n = \frac{8\pi^2}{7\zeta(3)}\nu_0 T_c V, \qquad C_n = \frac{2\pi^2}{3}\nu_0 VT$$

$$\frac{C_s - C_n}{C_n} = \frac{12}{7\zeta(3)}$$

Impact of Coulomb interaction on superconductivity

Кулоновское взаимодействие действительно понижает температуру сверхпроводящего перехода, но не очень сильно. При $\nu_0\mu \ln \varepsilon_F/\omega_D \gg 1$ относительная поправка к λ мала как $1/\ln(\varepsilon_F/\omega_D)$.

Proof:

$$\Gamma^0(i\varepsilon, i\varepsilon') = \lambda v(i\varepsilon) v(i\varepsilon') - \mu$$

$$\lambda_* = \lambda - \frac{\mu}{1 + \nu_0\mu \ln(\varepsilon_F/\omega_D)}.$$

$$V(\mathbf{q}) = \frac{4\pi e^2}{q^2 + \varkappa^2}; \quad \varkappa^2 = 8\pi\nu_0 e^2$$

$$\mu = \langle V_c(\mathbf{p} - \mathbf{p}')\rangle = \frac{\pi e^2}{p_0^2} \ln\left(1 + \frac{4p_0^2}{\varkappa^2}\right),$$

$$\Gamma^C(i\varepsilon, i\varepsilon') = \pi\nu_0 T \sum_{\varepsilon''} \Gamma^0(i\varepsilon, i\varepsilon'')\Gamma^C(i\varepsilon'', i\varepsilon')/|\varepsilon''|$$

$$\Gamma^C(i\varepsilon, i\varepsilon') = \Phi(i\varepsilon)\Phi(i\varepsilon')$$

$$\Phi(i\varepsilon) = \pi\nu_0 T \sum_{\varepsilon'} \left(\Gamma^0(i\varepsilon, i\varepsilon')/|\varepsilon'|\right)\Phi(i\varepsilon')$$

$$\Phi(\varepsilon) = av(i\varepsilon) + b$$

$$\begin{aligned} a &= \pi\lambda\nu_0 T \sum_{\varepsilon'} \left[av^2(i\varepsilon') + bv(i\varepsilon')\right]/|\varepsilon'|, \\ b &= -\pi\mu\nu_0 T \sum_{\varepsilon'} [av(i\varepsilon) + b]/|\varepsilon'|. \end{aligned} \quad \Rightarrow \quad \begin{aligned} a &= \nu_0\lambda \ln\frac{\omega_D}{T}(a+b) \\ b &= -\mu\nu_0\left[a\ln\frac{\omega_D}{T} + b\left(\ln\frac{\omega_D}{T} + \ln\frac{\omega_p}{\omega_D}\right)\right]. \end{aligned}$$

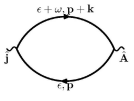
$$b = -\nu_0\mu_* \ln\frac{\omega_D}{T}(a+b); \quad \mu_* = \frac{\mu}{1 + \nu_0\mu\ln(\omega_p/\omega_D)}$$

$$1 = (\lambda - \mu_*)\ln\frac{\omega_D}{T}$$

$$T_c \approx \omega_D e^{-1/\lambda_*\nu_0}, \quad \lambda_* = \lambda - \mu_*$$

Тождество Уорда в нормальном метале.

$\Pi_{\alpha\beta}(\omega,\mathbf{k})|_{\mathbf{k}=0,\omega\to 0}=-\frac{ne^2}{m}\delta_{\alpha\beta}$,
$\Pi_{\alpha\beta}(\omega,\mathbf{k})=\int\Pi_{\alpha\beta}(\omega,\mathbf{r})e^{-i\mathbf{kr}}d^3\mathbf{r}$ -
$\mathbf{j}=-\frac{e}{mc}\langle\psi^+(\mathbf{r})\psi(\mathbf{r})\rangle\,\mathbf{A}(\mathbf{r})$
$\mathbf{v}(\mathbf{p})=\nabla_{\mathbf{p}}\xi(\mathbf{p})$.
$Q(\mathbf{k})=a\mathbf{k}^2+\mathrm{O}\left(\mathbf{k}^4\right)$.



$\chi_0=-\frac{1}{3}\chi_{\text{пара}}$,
$\mu=\frac{e}{mc}[\mathbf{r}\times\mathbf{p}]$
$G_H\left(E,\mathbf{r}_1,\mathbf{r}_2\right)=\exp\left(\frac{e}{\hbar c}\int\mathbf{A}\left(\mathbf{r}'\right)\mathbf{dr}'\right)G_0\left(E,\mathbf{r}_1,\mathbf{r}_2\right)$.

$$\widehat{\mathcal{H}}=\int\psi^+(\mathbf{r})\xi\left(\widehat{\mathbf{p}}-\frac{e}{c}\mathbf{A}\right)\psi(\mathbf{r})d^3\mathbf{r}$$

$$\widehat{\mathbf{j}}=e\psi^+(\mathbf{r})\nabla_{\mathbf{p}}\xi\left(\mathbf{p}-\frac{e}{c}\mathbf{A}\right)\psi(\mathbf{r})$$

$$\widehat{\mathbf{j}}=e\psi^+(\mathbf{r})\nabla_{\mathbf{p}}\xi(\mathbf{p})\psi(\mathbf{r})-\frac{e^2}{c}\psi^+(\mathbf{r})\nabla_{\mathbf{p}}\left[\left(\mathbf{A}\nabla_{\mathbf{p}}\right)\xi(\mathbf{p})\right]\psi(\mathbf{r})$$

$\xi(\mathbf{p})=\mathbf{p}^2/2m-E_F$

$$Q^{(2)}_{\alpha\beta}(\mathbf{k})=-\frac{e^2}{c}\left\langle\psi^+\frac{\partial^2\xi(\mathbf{p})}{\partial p_\alpha\partial p_\beta}\psi\right\rangle=-\frac{e^2}{c}\int\frac{\partial^2\xi(\mathbf{p})}{\partial p_\alpha\partial p_\beta}n_F(\xi(\mathbf{p}))\frac{2d^3p}{(2\pi)^3}$$

$$\widehat{\mathcal{H}}_{\text{int}}\ =-\frac{1}{c}\int\widehat{\mathbf{j}}(\mathbf{r})\mathbf{A}(\mathbf{r})d^3r$$

$$Q^{(1)}_{\alpha\beta}(i\Omega,\mathbf{k})=-\frac{e^2}{c}\lim_{\tau\to+0}T\sum_{\omega_n}\int\frac{v_\alpha(\mathbf{p})v_\beta(\mathbf{p})}{i\omega_n-\xi(\mathbf{p})}\frac{e^{i\omega_n\tau}}{i\omega_n+i\Omega-\xi(\mathbf{p}+\mathbf{k})}\frac{2d^3p}{(2\pi)^3}$$

$$Q^{(1)}_{\alpha\beta}(0)=-\frac{e^2}{c}\lim_{\tau\to+0}T\sum_{\omega_n}e^{i\omega_n\tau}\int\frac{v_\alpha(\mathbf{p})v_\beta(\mathbf{p})}{\left(i\omega_n-\xi(\mathbf{p})\right)^2}\frac{2d^3p}{(2\pi)^3}$$

$$Q^{(1)}_{\alpha\beta}(0)=-\frac{e^2}{c}\lim_{\tau\to+0}T\sum_{\omega_n}e^{i\omega_n\tau}\int v_\alpha(\mathbf{p})\nabla_\beta\frac{1}{i\omega_n-\xi(\mathbf{p})}\frac{2d^3p}{(2\pi)^3}$$

$$Q^{(1)}_{\alpha\beta}(0)=+\frac{e^2}{c}\lim_{\tau\to+0}T\sum_{\omega_n}e^{i\omega_n\tau}\int\nabla_\beta v_\alpha(\mathbf{p})\frac{1}{i\omega_n-\xi(\mathbf{p})}\frac{2d^3p}{(2\pi)^3}=-Q^{(2)}_{\alpha\beta}$$

$Q_{\alpha\beta}(0)=0$.

Диамагнитная восприимчивость

$Q(\mathbf{k}) = a\mathbf{k}^2 + \dots$

$$\mathbf{j} = \widehat{Q}\mathbf{A} = -a\nabla^2\mathbf{A}$$

$$\mathbf{j} = c\,\mathrm{rot}\,\mathbf{M} = c\,\mathrm{rot}\,\chi_0\mathbf{B} = \chi_0 c\,\mathrm{rot}\,\mathrm{rot}\,\mathbf{A}.$$

$$\mathbf{j} = -\chi_0 c\nabla^2\mathbf{A}$$

$$Q_{xx} = -\lim_{\tau\to+0}\frac{e^2}{c}T\sum_{\omega_n} e^{i\omega_n\tau}\int \frac{v_x(\mathbf{p}+\mathbf{k})v_x(\mathbf{p})}{(i\omega_n - \xi_{\mathbf{p}+\mathbf{k}})\,(i\omega_n - \xi_{\mathbf{p}})}\frac{2d^3p}{(2\pi)^3}$$

$\xi(\mathbf{p}) = \mathbf{p}^2/2m - E_F$.
$v_x(\mathbf{p}+\mathbf{k}) = v_x(\mathbf{p}) = p_x/m$,

$$Q_{xx} = -\frac{e^2k^2}{c}T\sum_{\omega_n} e^{i\omega_n\tau}\int \frac{v_x^2}{i\omega_n - \xi_{\mathbf{p}}}\frac{\partial^2}{\partial p_z^2}\frac{1}{i\omega_n - \xi_{\mathbf{p}}}\frac{2d^3p}{(2\pi)^3}.$$

$$\chi_0 = \frac{e^2}{c^2}T\sum_{\omega_n} e^{i\omega_n\tau}\int \frac{v_x^2v_z^2}{(i\omega_n - \xi_{\mathbf{p}})^4}\frac{2d^3p}{(2\pi)^3}.$$

($\langle v_x^2v_z^2\rangle = v^4/15$):

$$\chi_0 = \frac{e^2}{15c^2m^4}T\sum_{\omega_n} e^{i\omega_n\tau}\int \frac{p^4}{(i\omega_n - \xi_{\mathbf{p}})^4}\frac{2d^3p}{(2\pi)^3}.$$

$$\int_0^\infty \frac{p^6dp}{(i\omega_n + E_F - p^2/2m)^4} = -\frac{5m^3}{2}\int_0^\infty \frac{dp}{i\omega_n + E_F - p^2/2m}$$

$$\chi_0 = -\frac{e^2}{12\pi^2mc^2}\int_0^\infty n_F\left(\xi_p\right)dp = -\frac{e^2p_0}{12\pi^2mc^2}$$

$$\chi_{\text{para}} = 2\mu_B^2\nu_0 = \frac{e^2}{4m^2c^2}\frac{mp_0}{\pi^2}$$

$$\chi_0 = -\frac{1}{3}\chi_{\text{para}}$$

Уравнение Лондонов.

$$\mathbf{j}(\mathbf{r}) = -\frac{e^2}{mc}n_s\mathbf{A}(\mathbf{r}).$$

$$Q^{(2)}(0) = -ne^2/mc$$

$$Q^{(1)}_{\alpha\beta}\left(i\Omega_s,\mathbf{k}\right) = \frac{1}{2c}\sum_{\sigma,\sigma'}\int_{-\beta}^{\beta} e^{i\Omega\tau}d\tau\int e^{i\mathbf{kr}}\left\langle \mathrm{T}_\tau\psi^+_\sigma(\mathbf{r},\tau)\hat{j}_\alpha\psi_\sigma(\mathbf{r},\tau)\psi^+_{\sigma'}(0,0)\widehat{j}_\beta\psi_{\sigma'}(0,0)\right\rangle d^3\mathbf{r}$$

$\mathbf{j} = -i\frac{e}{m}\nabla_{\mathbf{r}}$.

$$\left\langle \mathrm{T}_\tau \psi^+_\sigma(\mathbf{r},\tau)\widehat{j}_\alpha\psi_\sigma(\mathbf{r},\tau)\psi^+_{\sigma'}(0,0)\widehat{j}_\beta\psi_{\sigma'}(0,0)\right\rangle = -\widehat{j}_\alpha G_{\sigma\sigma'}(\mathbf{r},\tau)\widehat{j}_\beta G_{\sigma'\sigma}(-\mathbf{r},-\tau) - \widehat{j}_\alpha F^+_{\sigma\sigma'}(\mathbf{r},\tau)\widehat{j}_\beta F_{\sigma'\sigma}(-\mathbf{r},-\tau)$$

$$Q^{(1)}_{\alpha\beta}(i\Omega,\mathbf{k}) = -\frac{1}{2c}\int\limits_{-\beta}^{\beta} e^{i\Omega\tau}d\tau\int d^3r e^{i\mathbf{kr}}\left[2\widehat{j}_\alpha G(\mathbf{r},\tau)\widehat{j}_\beta G(-\mathbf{r},-\tau) + 2\widehat{j}_\alpha F(\mathbf{r},\tau)\widehat{j}_\beta F^*(-\mathbf{r},-\tau)\right]$$

$$Q^{(1)}_{\alpha\beta}(i\Omega,\mathbf{k}) = -\frac{Te^2}{c}\sum_{\omega_n}\int v_\alpha\left(\mathbf{p}-\frac{\mathbf{k}}{2}\right)v_\beta\left(\mathbf{p}+\frac{\mathbf{k}}{2}\right)\times$$
$$\times\left\{G\left(i\omega_n,\mathbf{p}-\frac{\mathbf{k}}{2}\right)G\left(i\omega_n+i\Omega,\mathbf{p}+\frac{\mathbf{k}}{2}\right)+F\left(i\omega_n,\mathbf{p}-\frac{\mathbf{k}}{2}\right)F^*\left(i\omega_n+i\Omega,\mathbf{p}+\frac{\mathbf{k}}{2}\right)\right\}\frac{2d^3p}{(2\pi)^3}.$$

$$Q^{(1)}(0) = \frac{1}{3}Q^{(1)}_{\alpha\alpha}(0) = -\frac{e^2T}{3m^2c}\sum_{\omega_n}\int \mathbf{p}^2\left(G^2\left(i\omega_n,\mathbf{p}\right)+\left|F\left(i\omega_n,\mathbf{p}\right)\right|^2\right)\frac{2d^3p}{(2\pi)^3}$$

$$n-n_s = -\frac{2T\nu_0p_0^2}{3m}\sum_{\omega_n}\int\limits_{-\infty}^{\infty}\frac{\Delta^2+\xi^2-\omega_n^2}{\left(\omega_n^2+\xi^2+\Delta^2\right)^2}d\xi$$

$$n_s = \frac{2\nu_0p_0^2}{3m}T\sum_{\omega_n}\int\limits_{-\infty}^{\infty}\left[\frac{\xi^2-\omega_n^2}{\left(\xi^2+\omega_n^2\right)^2}-\frac{\xi^2-\omega_n^2+\Delta^2}{\left(\xi^2+\omega_n^2+\Delta^2\right)^2}\right]d\xi.$$

$$\int\limits_{-\infty}^{\infty}\frac{dx}{\left(x^2+a^2\right)^2} = \frac{\pi}{2a^3},\quad \int\limits_{-\infty}^{\infty}\frac{x^2dx}{\left(x^2+a^2\right)^2} = \frac{\pi}{2a}$$

$$n_s = \frac{2\nu_0p_0^2}{3m}T\sum_{\omega_n}\frac{\pi\Delta^2}{\left(\omega_n^2+\Delta^2\right)^{3/2}}.$$

а) $T\to 0$.

$$n_s = \frac{2\nu_0p_0^2}{3m}\frac{\pi\Delta^2}{2\pi}\int\limits_{-\infty}^{\infty}\frac{d\omega}{\left(\omega^2+\Delta^2\right)^{3/2}} = \frac{2\nu_0p_0^2}{3m} = \frac{p_0^3}{3\pi^2} = n.$$

б) $T\to T_c$.

$$\frac{n_s}{n} = \frac{7\Delta^2}{4\pi^2T_c^2} = 2\left(1-\frac{T}{T_c}\right).$$

$$\mathrm{rot}\,\mathbf{H} = \frac{4\pi}{c}\mathbf{j} = -\frac{4\pi n_se^2}{mc^2}\mathbf{A}$$

$$\nabla^2\mathbf{A} = \frac{4\pi n_se^2}{mc^2}\mathbf{A}$$

$$A_y(x) = A_y(0)e^{-x/\delta_\Lambda}$$

$$\delta_\Lambda^2 = \frac{mc^2}{4\pi n_s e^2}$$

$$H_z = -\frac{\partial A_y}{\partial x} = \frac{A_y(0)}{\delta_\Lambda} e^{-x/\delta_\Lambda} = H_z(0) e^{-x/\delta_\Lambda}$$

$k_0 \approx \xi^{-1}(T) \approx \Delta(T)/(\hbar v_F)$.

The same with matrix Green's function:

$$\widehat{G} = \begin{bmatrix} G_{\uparrow\uparrow} & F_{\uparrow\downarrow} \\ F_{\downarrow\uparrow} & G_{\downarrow\downarrow} \end{bmatrix}$$

$$(i\omega - \xi(\mathbf{p})\tau_z - \Delta_1\tau_x - \Delta_2\tau_y)\,\widehat{G} = \widehat{1}$$

($\Delta = \Delta_1 + i\Delta_2$).

$$\widehat{\mathbf{j}} = c\frac{\delta \widehat{G}^{-1}}{\delta \mathbf{A}} = e\mathbf{v}(\mathbf{p})\hat{1} - \frac{e^2}{mc}\mathbf{A}\tau_z, \qquad \widehat{G} := -\frac{1}{\omega_n^2 + \xi^2 + \Delta^2}\begin{pmatrix} i\omega_n + \xi & \Delta \\ \Delta^* & i\omega_n - \xi \end{pmatrix};$$

$$\begin{aligned}\mathrm{Tr}\left(\hat{j}_\alpha \hat{G}\left(i\omega_n, \mathbf{p}\right)\hat{j}_\beta \hat{G}\left(i\omega_n, \mathbf{p}\right)\right) &= \frac{e^2 v_\alpha(\mathbf{p}) v_\beta(\mathbf{p})}{\left(\omega_n^2 + \xi^2 + \Delta^2\right)^2}\,\mathrm{Tr}\left(\left(i\omega_n + \xi\tau_z + \Delta\tau_x\right)\left(i\omega_n + \xi\tau_z + \Delta\tau_x\right)\right) = \\ &= 2e^2 v_\alpha(\mathbf{p}) v_\beta(\mathbf{p})\frac{\Delta^2 + \xi^2 - \omega_n^2}{\left(\omega_n^2 + \xi^2 + \Delta^2\right)^2},\end{aligned}$$

16.2.4 Gorkov formalism

Уравнения Горькова по Минееву Самохину

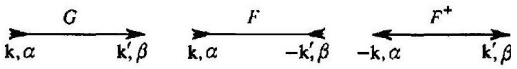
(??? строчка - в чем основная идея их???)

$$H = H_0 + H_{\text{int}} = \sum_{\mathbf{k},\mathbf{k}'} \left(\mathbf{k}\alpha\left|H_0\right|\mathbf{k}'\beta\right) a^+_{\mathbf{k}\alpha} a_{\mathbf{k}'\beta} + \frac{1}{2}\sum_{\mathbf{k},\mathbf{k}',\mathbf{q}} V_{\alpha\beta,\lambda\mu}\left(\mathbf{k},\mathbf{k}'\right) a^+_{-\mathbf{k}+\mathbf{q}/2,\alpha} a^+_{\mathbf{k}+\mathbf{q}/2,\beta} a_{\mathbf{k}'+\mathbf{q}/2,\lambda} a_{-\mathbf{k}'+\mathbf{q}/2,\mu} \tag{17.1}$$

$$H_0 = \frac{1}{2m}\left[-i\nabla + \frac{e}{c}\mathbf{A}(\mathbf{r})\right]^2 + U(\mathbf{r}) - \mu$$

$$G_{\alpha\beta}\left(\mathbf{k}, \tau_1; \mathbf{k}', \tau_2\right) = -\left\langle T_\tau a_{\mathbf{k}\alpha}\left(\tau_1\right) a^+_{\mathbf{k}'\beta}\left(\tau_2\right)\right\rangle \qquad a_{\mathbf{k}\alpha}(\tau) := \exp(\tau H) a_{\mathbf{k}\alpha} \exp(-\tau II) \tag{17.2}$$

$$\begin{aligned} F_{\alpha\beta}\left(\mathbf{k}, \tau_1; \mathbf{k}', \tau_2\right) &:= \left\langle T_\tau a_{\mathbf{k}\alpha}\left(\tau_1\right) a_{-\mathbf{k}'\beta}\left(\tau_2\right)\right\rangle \qquad \text{(an G f)} \\ F^+_{\alpha\beta}\left(\mathbf{k}, \tau_1; \mathbf{k}', \tau_2\right) &:= \left\langle T_\tau a^+_{-\mathbf{k}\alpha}\left(\tau_1\right) a^+_{\mathbf{k}'\beta}\left(\tau_2\right)\right\rangle \end{aligned} \tag{17.3}$$



(строчка про идею всего, что ниже, что по сути там делается?)

$$G_{\alpha\beta}\left(\mathbf{k},\mathbf{k}';\tau\right)=T\sum_{n}G_{\alpha\beta}\left(\mathbf{k},\mathbf{k}';\omega_n\right)e^{-i\omega_n\tau}\qquad \text{и т.д.}$$

$$\frac{\partial a_{\mathrm{k}\alpha}}{\partial\tau}=\left[H,a_{\mathrm{k}\alpha}\right]$$

$$\frac{\partial G_{\alpha\beta}\left(\mathbf{k},\mathbf{k}';\tau\right)}{\partial\tau}=-\left\langle T_\tau\left[H(\tau),a_{\mathbf{k}\alpha}(\tau)\right]a^+_{\mathbf{k}'\beta}(0)\right\rangle-\delta(\tau)\delta\left(\mathbf{k}-\mathbf{k}'\right)\delta_{\alpha\beta}$$

$$\frac{\partial G_{\alpha\beta}\left(\mathbf{k},\mathbf{k}';\tau\right)}{\partial\tau}=-\sum_{\mathbf{k}_1}\left(\mathbf{k}\alpha\left|H_0\right|\mathbf{k}_1\gamma\right)G_{\gamma\beta}\left(\mathbf{k}_1,\mathbf{k}'\right)-$$
$$-\sum_{\mathbf{k}_1,\mathbf{q}}V_{\gamma_1\alpha,\gamma_2\gamma_3}\left(\mathbf{k},\mathbf{k}_1\right)\left\langle T_\tau a^+_{-\mathbf{k}+\mathbf{q},\gamma_1}(\tau)a_{\mathbf{k}_1+\mathbf{q}/2,\gamma_2}(\tau)a_{-\mathbf{k}+\mathbf{q}/2,\gamma_3}(\tau)a^+_{\mathbf{k}'\beta}(0)\right\rangle-$$
$$-\delta(\tau)\delta\left(\mathbf{k}-\mathbf{k}'\right)\delta_{\alpha\beta}.$$

$$\left\langle T_\tau a^+_{-\mathbf{k}+\mathbf{q},\gamma_3}(\tau)a_{\mathbf{k}_1+\mathbf{q}/2,\gamma_2}(\tau)a_{-\mathbf{k}_1+\mathbf{q}/2,\gamma_3}(\tau)a^+_{\mathbf{k}'\beta}(0)\right\rangle\to\qquad\text{(m f appr)}$$
$$\to\left\langle T_\tau a^+_{-\mathbf{k}+\mathbf{q},\gamma_1}(\tau)a^+_{\mathbf{k}'\beta}(0)\right\rangle\left\langle T_\tau a_{\mathbf{k}_1+\mathbf{q}/2,\gamma_2}(\tau)a_{-\mathbf{k}_1+\mathbf{q}/2,\gamma_3}(\tau)\right\rangle$$

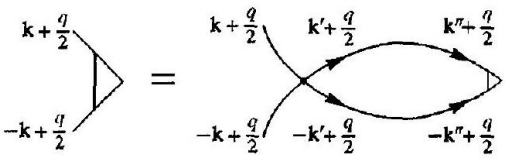
$$\Delta_{\alpha\beta}(\mathbf{k},\mathbf{q}):=-\sum_{\mathbf{k}'}V_{\beta\alpha,\lambda\mu}\left(\mathbf{k};\mathbf{k}'\right)F_{\lambda\mu}\left(\mathbf{k}'+\frac{\mathbf{q}}{2},\tau;\mathbf{k}'-\frac{\mathbf{q}}{2},\tau\right)=$$
$$=-T\sum_{n}\sum_{\mathbf{k}'}V_{\beta\alpha,\lambda\mu}\left(\mathbf{k},\mathbf{k}'\right)F_{\lambda\mu}\left(\mathbf{k}'+\frac{\mathbf{q}}{2},\mathbf{k}'-\frac{\mathrm{q}}{2};\omega_n\right)$$
$$\Delta^+_{\lambda,}(\mathbf{k},\mathbf{q}):=-T\sum_{n}\sum_{\mathbf{k}'}V_{\alpha\beta,\mu\lambda}\left(\mathbf{k}';\mathbf{k}\right)F^+_{\alpha\beta}\left(\mathbf{k}'-\frac{\mathbf{q}}{2},\mathbf{k}'+\frac{\mathbf{q}}{2};\omega_n\right)$$

$$\sum_{\mathbf{k}_1}\left(\mathbf{k}\alpha\left|i\omega_n-H_0\right|\mathbf{k}_1\gamma\right)G_{\gamma\beta}\left(\mathbf{k}_1,\mathbf{k}';\omega_n\right)+\sum_{\mathbf{q}}\Delta_{\alpha\gamma}(\mathbf{k},\mathbf{q})F^+_{\gamma\beta}\left(\mathbf{k}-\mathbf{q},\mathbf{k}';\omega_n\right)=\delta\left(\mathbf{k}-\mathbf{k}'\right)\delta_{\alpha\beta}\text{(Gor eq)}$$

$$\sum_{\mathbf{k}_1}\left\langle-\mathbf{k}_1\gamma\left|i\omega_n+H_0\right|-\mathbf{k}\alpha\right\rangle F^+_{\gamma\beta}\left(\mathbf{k}_1,\mathbf{k}';\omega_n\right)+\sum_{\mathbf{q}}\Delta^+_{\alpha\gamma}(\mathbf{k},\mathbf{q})G_{\gamma\beta}\left(\mathbf{k}+\mathbf{q},\mathbf{k}';\omega_{r_n}\right)=0\qquad\text{(Gor eq)}$$

$$\sum_{\mathbf{k}_1}\left\langle\mathbf{k}\alpha\left|i\omega_n-H_0\right|\mathbf{k}_1\gamma\right\rangle F_{\gamma\beta}\left(\mathbf{k}_1,\mathbf{k}';\omega_n\right)-\sum_{\mathbf{q}}\Delta_{\alpha\gamma}(\mathbf{k},\mathbf{q})G_{\beta\gamma}\left(-\mathbf{k}',-\mathbf{k}+\mathbf{q};-\omega_n\right)=0\qquad\text{(Gor eq)}$$

$F\approx\text{const}\cdot\Delta\Rightarrow$



- self-cons eq, or:

$$\Delta_{\alpha\beta}(\mathbf{k},\mathbf{q})\approx-T_{\mathrm{c}}\sum_{n}\sum_{\mathbf{k}',\mathbf{k}'',\mathbf{q}'}V_{\beta\alpha,\lambda\mu}\left(\mathbf{k},\mathbf{k}'\right)G^{(0)}_{\lambda\gamma}\left(\mathbf{k}'+\tfrac{\mathrm{q}}{2},\mathbf{k}''+\tfrac{\mathbf{q}'}{2};\omega_n\right)G^{(0)}_{\mu\delta}\left(-\mathbf{k}'+\tfrac{\mathrm{q}}{2},-\mathbf{k}''+\tfrac{\mathbf{q}'}{2};-\omega_n\right)\Delta_{\gamma\delta}\left(\mathbf{k}'',\mathbf{q}'\right)$$

$$\text{Homog-s} \Rightarrow \qquad G_{\alpha\beta}\left(\mathbf{k},\mathbf{k}';\omega_n\right)=G_{\alpha\beta}\left(\mathbf{k},\omega_n\right)\delta\left(\mathbf{k}-\mathbf{k}'\right) \qquad \text{и т. д.} \tag{17.10}$$

$$\Delta_{\alpha\beta}(\mathbf{k},\mathbf{q})=\Delta_{\alpha\beta}(\mathbf{k})\delta(\mathbf{q})$$

$$\Delta_{\alpha\beta}(k)=-\Delta_{\beta\alpha}(-k)$$

$$F_{\mathbf{k},\alpha\beta}=F_{\alpha\beta}(\mathbf{k},\tau;\mathbf{k},\tau)=T\sum_n F_{\alpha\beta}\left(\mathbf{k},\omega_n\right)$$

$$F^{+}_{\mathbf{k},\alpha\beta}=T\sum_n F^{+}_{\alpha\beta}\left(\mathbf{k},\omega_n\right)$$

$$\left\langle \mathbf{k}\alpha\left|H_0\right|\mathbf{k}'\beta\right\rangle=\xi_{\mathbf{k}}\delta\left(\mathbf{k}-\mathbf{k}'\right)\delta_{\alpha\beta}; \qquad \xi_{\mathbf{k}}=\xi_{-\mathbf{k}}$$

$$\begin{gathered}\left(i\omega_n-\xi_k\right)G_{\alpha\beta}\left(\mathbf{k},\omega_n\right)+\Delta_{\alpha\gamma}(\mathbf{k})F^{+}_{\gamma\beta}\left(\mathbf{k},\omega_n\right)=\delta_{\alpha\beta}\\ \left(i\omega_n+\xi_k\right)F^{+}_{\alpha\beta}\left(\mathbf{k},\omega_n\right)+\Delta^{+}_{\alpha\gamma}(\mathbf{k})G_{\gamma\beta}\left(\mathbf{k},\omega_n\right)=0\\ \left(i\omega_n-\xi_k\right)F_{\alpha\beta}\left(\mathbf{k},\omega_n\right)-\Delta_{\alpha\gamma}(\mathbf{k})G_{\beta\gamma}\left(-\mathbf{k},-\omega_n\right)=0\end{gathered} \tag{17.11}$$

singl, unit ph of triplet: $\left(\Delta\Delta^{+}\right)_{\alpha\beta}\propto\delta_{\alpha\beta}\Rightarrow$

$$\begin{gathered}G_{\alpha\beta}\left(\mathbf{k},\omega_n\right)=-\left(i\omega_n+\xi_k\right)\left[\omega_n^2+\xi_k^2+\Delta(\mathbf{k})\Delta^{+}(\mathbf{k})\right]^{-1}_{\alpha\beta}\\ F_{\alpha\beta}\left(\mathbf{k},\omega_n\right)=\Delta_{\alpha\gamma}(\mathbf{k})\left[\omega_n^2+\xi_k^2+\left(\Delta^{+}(\mathbf{k})\Delta(\mathbf{k})\right)\right]^{-1}_{\gamma\beta}\end{gathered} \tag{17.12}$$

$$G_{\alpha\beta}\left(\mathbf{k},\omega_n\right)=-\frac{i\omega_n+\xi_k}{\omega_n^2+\xi_k^2+\Delta_k^2}\delta_{\alpha\beta} \tag{17.13}$$

$$F_{\alpha\beta}\left(\mathbf{k},\omega_n\right)=\frac{\Delta_{\alpha\beta}(\mathbf{k})}{\omega_n^2+\xi_k^2+\Delta_k^2}$$

$$\Delta^2_{\mathbf{k}}:=\frac{1}{2}\operatorname{Sp}\Delta^{+}(\mathbf{k})\Delta(\mathbf{k})$$

$$G^{(0)}_{\alpha\beta}\left(\mathbf{k},\omega_n\right)=\frac{\delta_{\alpha\beta}}{i\omega_n-\xi_k} \qquad \text{(norm)} \tag{17.14}$$

Non-unit ph, tripl: $\left(\Delta\Delta^{+}\right)_{\alpha\beta}=\Delta^2\left(\mathrm{dd}^{*}\,\delta_{\alpha\beta}+\mathbf{m}\sigma_{\alpha\beta}\right)$; $\mathrm{m}(\mathbf{k})=i\,\mathrm{d}(\mathbf{k})\times\mathrm{d}^{*}(\mathbf{k})\neq 0$,

$$\begin{gathered}G_{\alpha\beta}\left(\mathbf{k},\omega_n\right)=-\left(i\omega_n+\xi_k\right)\frac{\left(\omega_n^2+\xi_k^2+\Delta^2|\,\mathrm{d}(\mathbf{k})|^2\right)\delta_{\alpha\beta}+\Delta^2\,\mathrm{m}(\mathbf{k})\sigma_{\alpha\beta}}{\left(\omega_n^2+E^2_{\mathrm{k},-}\right)\left(\omega_n^2+E^2_{k,-}\right)}\\ F_{\alpha\beta}\left(\mathbf{k},\omega_n\right)=\Delta\left(i\sigma\sigma_y\right)_{\alpha\beta}\frac{\left(\omega_n^2+\xi_k^2+\Delta^2|\,\mathrm{d}(\mathrm{k})|^2\right)\mathrm{d}(\mathbf{k})-i\Delta^2\,\mathrm{m}(\mathbf{k})\times\mathrm{d}(\mathbf{k})}{\left(\omega_n^2+E^2_{\mathbf{k},\mathrm{t}}\right)\left(\omega_n^2+E^2_{k,-}\right)}\end{gathered} \tag{17.15}$$

$$E_{\mathbf{k},\pm}:=\sqrt{\xi_k^2+\Delta^2\left(|\,\mathrm{d}(\mathbf{k})|^2\pm|\mathrm{m}(\mathbf{k})|\right)} \tag{17.16}$$

For tempr order par we use self-cons eq:

$$\Delta_{\alpha\beta}(\mathbf{k}) = -T\sum_{n}\sum_{k'} V_{\beta\alpha,\gamma\delta}\left(\mathbf{k},\mathbf{k}'\right)\frac{\Delta_{\gamma\delta}\left(\mathbf{k}'\right)}{\omega_n^2+\xi_{k'}^2+\Delta_{\mathbf{k}'}^2} \tag{17.17}$$

$\sum_{n=-\infty}^{\infty}\frac{1}{(2n+1)^2\pi^2+x^2} = \frac{1}{2x}\ln\frac{x}{2} \Rightarrow$

$$\Delta_{\alpha\beta}(\mathrm{k}) = -\sum_{\mathbf{k}'} V_{\beta\alpha,\gamma\delta}\left(\mathrm{k},\mathrm{k}'\right)\Delta_{\gamma\delta}\left(\mathrm{k}'\right)\frac{1}{2E_{\mathrm{k}'}}\,\mathrm{th}\left(\frac{E_{\mathrm{k}'}}{2T}\right) \tag{17.19}$$

Add eq. 6.5, 6.6 here!!!

Now, matrix form:

$$\hat{G}\left(\mathbf{k}_1,\mathbf{k}_2;\omega_n\right) = -\int_0^{1/T} d\tau e^{i\omega_n\tau}\left\langle T_\tau A_{\mathbf{k}_1}(\tau)A^+_{\mathbf{k}_2}(0)\right\rangle = \begin{pmatrix} G_{\alpha\beta}\left(\mathbf{k}_1,\mathbf{k}_2;\omega_n\right) & -F_{\alpha\beta}\left(\mathbf{k}_1,\mathbf{k}_2;\omega_n\right) \\ -F^+_{\alpha\beta}\left(\mathbf{k}_1,\mathbf{k}_2;\omega_n\right) & -G_{\beta\alpha}\left(-\mathbf{k}_2,-\mathbf{k}_1;-\omega_n\right)\end{pmatrix} \tag{17.20}$$

$$\hat{G}_0\left(\mathbf{k},\omega_n\right) = -\frac{1}{\omega_n^2+\xi_k^2+\Delta_k^2}\begin{pmatrix}\left(i\omega_n+\xi_k\right)\delta_{\alpha\beta} & \Delta_{\alpha\beta}(\mathbf{k}) \\ \Delta^+_{\alpha\beta}(\mathbf{k}) & \left(i\omega_n-\xi_k\right)\delta_{\alpha\beta}\end{pmatrix} = -\frac{i\omega_n\hat{\tau}_0+\xi_k\hat{\tau}_3+\dot{\Delta}(\mathbf{k})}{\omega_n^2+\xi_k^2+\Delta_k^2} \tag{17.21}$$

Now, spectral decomposition:

$$\hat{G}\left(\mathbf{k},\omega_n\right) = \int_{-\infty}^{+\infty}\frac{dz}{2\pi}\frac{\hat{\rho}(\mathbf{k},z)}{i\omega_n-z}$$

$$T\sum_n\frac{1}{i\omega_n-z} = \frac{1}{2}\,\mathrm{th}\,\frac{z}{2T} \tag{17.22}$$

$$\hat{\rho}(\mathbf{k},\omega) = -2\,\mathrm{Im}\,\hat{G}^R(\mathbf{k},\omega) = i\left(\hat{G}^R(\mathbf{k},\omega)-\hat{G}^A(\mathbf{k},\omega)\right)$$

$$\hat{G}^{R(\boldsymbol{A})}(\mathbf{k},\omega) = \hat{G}\left(\mathbf{k},\omega_n\right)\Big|_{i\omega_n\to\omega\pm i0} \tag{17.23}$$

$$\det\left\|E^2-\xi_k^2-\Delta(\mathbf{k})\Delta^+(\mathbf{k})\right\| = 0 \qquad \text{spectr} \tag{17.24}$$

$$E_{\mathbf{k}} = \sqrt{\xi_k^2+\Delta^2|g(\mathbf{k})|^2} \qquad \text{singl}$$

$$E_{\mathbf{k}} = \sqrt{\xi_k^2+\Delta^2|\,\mathrm{d}(\mathbf{k})|^2} \qquad \text{unit ph, tripl}$$

$$E_{\mathrm{k},\pm} = \sqrt{\xi_k^2+\Delta^2\left(|\,\mathrm{d}(\mathbf{k})|^2 \pm |\mathrm{d}^*(\mathbf{k})\times\mathrm{d}(\mathbf{k})|\right)} \qquad \text{non-unit ph, tripl} \tag{17.25}$$

T.e. нули спектра возбуждений для любых фаз триплетного спаривания определяется $\det \Delta(k) = 0$, то есть $\mathrm{d}^2(\mathbf{k}) = 0$.

Now, density of states:

$$N(E) := \sum_{\mathbf{k}\alpha} \delta\left(E - E_{\mathbf{k}}\right) \tag{17.26}$$

$$N(E) = \frac{1}{2\pi} \sum_{\mathbf{k}\alpha} \rho(\mathbf{k}, E) = -\frac{1}{\pi} \operatorname{Im} \sum_{\mathbf{k}\alpha} G\left(\mathbf{k}, \omega_n\right) \Big|_{i\omega_n \to E + i0} \tag{17.27}$$

(?? 5.29???)

$$\begin{aligned} N\left(E'\right) &= 2 \int \frac{d^3k}{(2\pi)^3} \delta\left(E - E_{\mathbf{k}}\right) = 2N_0 \int \frac{d\Omega}{4\pi} \int d\xi \delta\left(E - E_{\mathbf{k}}\right) = \\ &= 2N_0 \int \frac{d\Omega}{4\pi} \frac{dE'' E'}{\sqrt{E'^2 - \Delta_{\mathbf{k}}^2}} \delta\left(E' - E'\right) = 2N_0 \int \frac{d\Omega}{4\pi} \frac{E}{\sqrt{E^2 - \Delta_{\mathbf{k}}^2}} \end{aligned} \tag{17.28}$$

int over angles in $\Delta_{\mathbf{k}}^2 < E^2$.

(isotr, s-copl) $$N(E) = 2N_0 \begin{cases} 0, & E < \Delta \\ \frac{E}{\sqrt{E^2 - \Delta^2}}, & E > \Delta \end{cases}$$

And if there are zeros in spectrum:

$$N(E) = 2N_0 \int \frac{d\Omega}{4\pi} \frac{E}{\sqrt{E^2 - \Delta^2 \left(\hat{k}_x^2 + \hat{k}_y^2\right)}} = N_0 \int \sin\theta d\theta \frac{E}{\sqrt{E^2 - \Delta^2 \sin^2\theta}}$$

$$N(E) \approx N_0 \int_0^{E/\Delta} \theta d\theta \frac{E}{\sqrt{E^2 - \Delta^2\theta^2}} \sim N_0 \left(\frac{E}{\Delta}\right)^2 \tag{17.30}$$

(???)

Line of zeros $\Rightarrow$ $$N(E) \sim N_0 \frac{E}{\Delta}. \tag{17.31}$$

Подобные степенные зависимости плотности состояний квазичастиц от энергии приводят к степенному (а не экспоненциальному) температурному поведению термодинамических и кинетических характеристик необычных сверхпроводников.

16.2.5 General details of theories of SC

Connection of The Ginzburg-landau and BCS theories

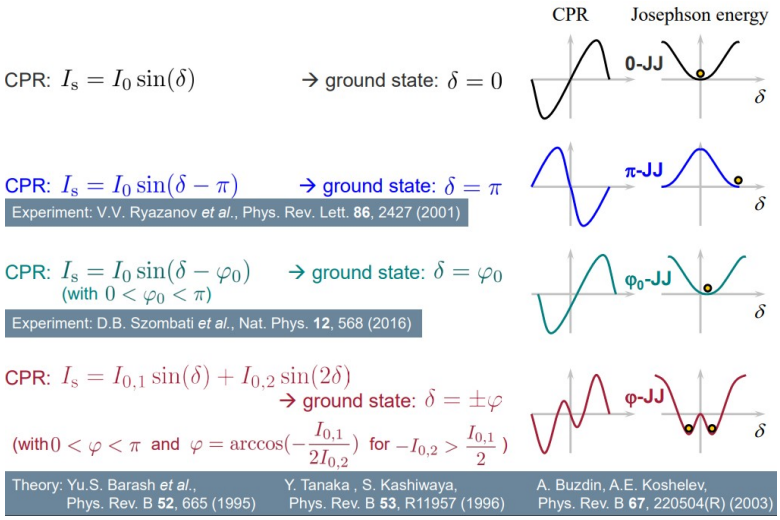
16.3 Details of well-known SC models

16.3.1 Josephson junctions: other methods and properties

Other proofs of JE

JE from Gorkov formalism

Overview of other JJ-s



(here I'll add comments, what is going on and why someone needs it)

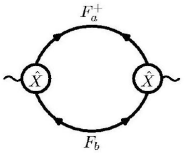
Description of some famous non-typical junctions

Теория Асламазова и Ларкина о геометрическом сужении в сверхпроводниках

(см Щелкочева, там хорошо написано, пока не до этого)

Двухчастичный эффект Джозефсона по ЛШ

(add formalism from Levitov Shitov about these calculations)
(??? idea of it???)



$$I = I_0 \sin(\varphi_a - \varphi_b)$$

(add here summary from LS)

On fabrication of Josephson Junctions

(not important)

Критический ток и «ток возврата» в JJ

(??? хз пока что)

Other basic properties of JJ s

(хз, что это, потом когда-то додумаю.)

(write about and Ferrell-Prange equation some words from Shmidt, no one knows this equation, but 4 lines for it is fine)

Josephson vertex by Shmidt (!??!)
(по идее тут ничего не должно быть нового, разве что так вот поле вихрями попадает, ну и окей. потом дочитаю.)

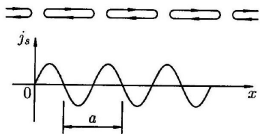


Рис. 24.4. а) Схематическое изображение смешанного состояния джозефсоновского туннельного перехода-плотно сжатая цепочка вихрей; б) распределение туннельного сверхтока через переход, которое при этом возникает.

Josephson radiation (???)

• DC bias current → AC response fd=3 GHz
• Power generated typically low & difficult to couple to external circuit (impedance mismatch)
• Nice recent experiment: direct detection of the emitted radiation.
(??? хз, что это такое, но есть статья про это, нужно будет - буду изучать, пока ничего такого не понимаю.)

16.3.2 RCSJ, SQUID: other methods and properties

Other properties of RCSJ model

Other about Shapiro steps

C. C. Grimes and S. Shapiro obtained such steps for different power of fields:

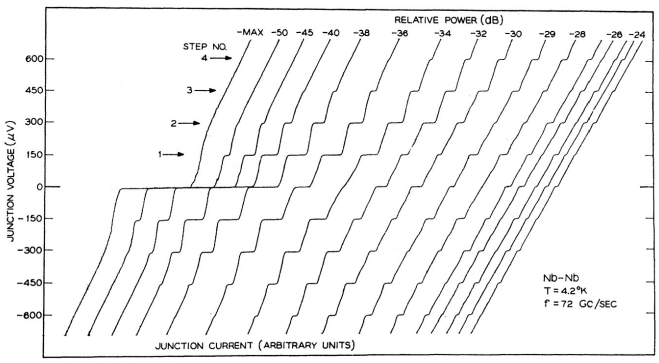


FIG. 1. Voltage-current curves for a Nb-Nb point-contact Josephson junction exposed to a 72-Gc/sec signal at various power levels.

Shapiro steps have been observed in nanotube Josephson junctions, superconducting nanowires and High-Temperature superconductors with additional interesting effects.

Fractional Shapiro steps have been observed in circuits with several Josephson junctions although all fractions can not be explained.

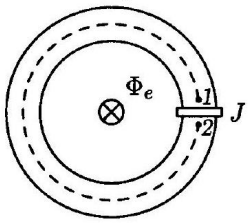
(??? maybe in later parts of this part I'll write about it, currently I don't need it)

Rf SQUID

(??? I have never needed it, so I'll just put it here)

ring. No d.c voltage may be established across rf squids.

We have properties as follows:

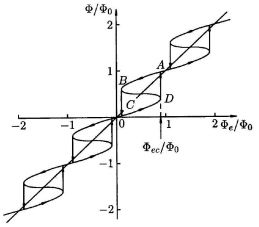


- non-linear inductance of Josephson junction gives a periodic modulation of the resonance frequency of the tank circuit

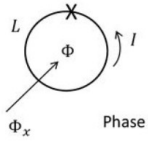
- these changes follow the amplitude of the rf current for a given working frequency response variies with $\Phi_o = h/2e = 2,0710^{-15}$Vs

- advantage: no electrical contacts

- disadvantage: noise of tank curcuit and amplifier large than intrinsic SQUID noise



rf SQUID (Superconducting Quantum interference Device) --- not a SQUID (no interference)



Phase coherence: $\phi + \frac{2\pi\Phi}{\Phi_0} = 0$

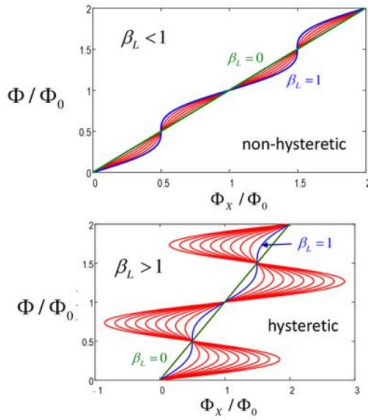
$$\Phi = \Phi_x + LI_c = \Phi_x + LI\sin\phi$$

$$\Phi = \Phi_x - LI\sin\left(\frac{2\pi\Phi}{\Phi_0}\right)$$

$$\frac{\Phi_x}{\Phi_0} = \frac{\Phi}{\Phi_0} + \left(\frac{LI_c}{\Phi_0}\right)\sin\left(\frac{2\pi\Phi}{\Phi_0}\right)$$

$$= \frac{\Phi}{\Phi_0} + \frac{1}{2\pi}\beta_L \sin\left(\frac{2\pi\Phi}{\Phi_0}\right)$$

Single-junction inductance parameter $\beta_L = \frac{2\pi LI_c}{\Phi}$

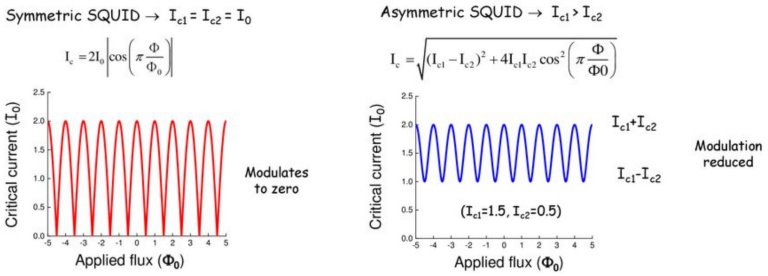


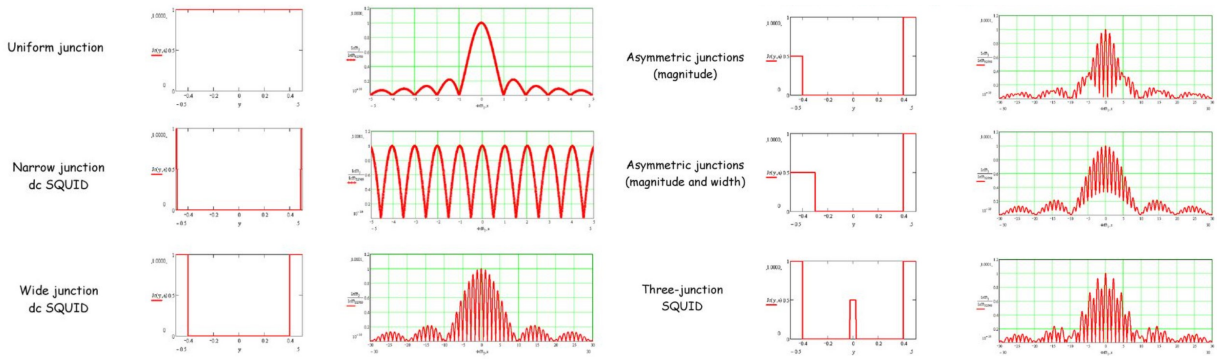
slope at half-integer Φ_0 $\frac{d\Phi}{d\Phi_x} = \frac{1}{1-\beta_L}$

Other about SQUID-s

Properties of modified SQUID-s

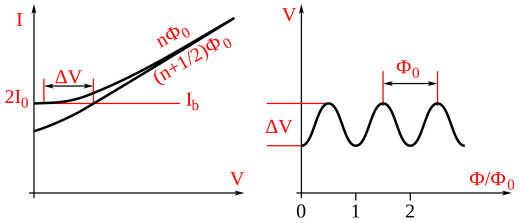
Asymmetric SQUID will shift current up:





(???)

(??)



Overview of applications of SQUID-s

(all applications will be reviewed in the end of this part, here there is a general summary, but with some meaningful information!)

16.3.3 Superconductors of II kind: other well-known properties

35* Анизотропные сверхпроводники II рода

(??)

36* Разрушение сверхпроводимости в тонкой пленке тепловыми вихрями, БКТ переход

Длина экранировки:

$$\lambda_{2d} = \frac{2\lambda^2}{d}.$$

$L^k_{\square} = 2\pi\lambda_{\text{eff}}$,
λ_{eff} равно либо λ, либо λ_{2d}.
$R \ll \lambda_{2d} \qquad \Rightarrow$
$U_2(R) = 2q_1q_2d\epsilon_0 \ln(R/\lambda_{2d})$,
$U_1 = d\epsilon_0 \ln(\lambda_{2d}/\xi)$,

$$U_{\text{pair}}(R) = 2\epsilon_0 d \ln\frac{R}{\xi} = \frac{\Phi_0^2}{4\pi^2\lambda_{2d}} \ln\frac{R}{\xi}.$$

В тонких пленках λ_{2d} может достигать макроскопических размеров. Так, при $\lambda = 3$ мкм (что легко достигается в близкой окрестности T_{c0}) и толщине пленки $d = 50$Å получим $\lambda_{2d} \simeq \simeq 3.6$ мм. При этом энергия кора вихря, $U_{\text{core}} = d\epsilon_0$, мала: $U_{\text{core}}/k_{\text{B}} \simeq 10$ K, в то время как полная энергия гораздо больше, $U_1/k_{\text{B}} \simeq 100$ K (мы выбрали здесь для оценки $\xi \simeq 0.1$ мкм).

$$n(L) \simeq (L/\xi)^2 \exp(-U_1(L)/T) = (L/\xi)^{2-\alpha},$$

$\alpha = \epsilon_0 d/k_{\text{B}}T = \Phi_0^2/(8\pi^2\lambda_{2d}k_{\text{B}}T)$.

$$\frac{1}{\lambda_{2d}(T_{\text{BKT}})} = \frac{d}{2\lambda_-^2(T_{\text{BKT}})} = \frac{16\pi^2 k_{\text{B}}T_{\text{BKT}}}{\Phi_0^2}.$$

$$n_s^{(2),\min} = \frac{8mk_{\text{B}}T_{\text{BKT}}}{\pi\hbar^2}$$

$$\ln\frac{R_c(T)}{\xi} = b\left(\frac{\text{Gi}^{(2D)}T}{T - T_{\text{BKT}}}\right)^{1/2},$$

(???)

37* Плавление решетки вихрей

$$B_m(T) \propto \frac{\Phi_0}{(k_{\text{B}}T)^2}\left(\frac{\Phi_0}{4\pi\lambda}\right)^4 \propto (1 - T/T_c)^2 \qquad \text{при} \qquad T \to T_c.$$

Поле плавления решетки убывает с повышением температуры быстрее, чем верхнее (и нижнее) критическое поле, которое ведет себя линейно вблизи температуры перехода, $H_{c2} \propto (1 - T/T_c)$.

$$\frac{B_m(T)}{H_{c2}(T)} = \alpha_m \frac{1 - T/T_c}{\text{Gi}}$$

α_m - number.

38 Критический ток в сверхпроводниках второго рода. Критическое состояние

39 Взаимодействие вихрей с центрами пиннинга

(??? допишу, если будет нужно)

$$F_{\text{возвр}} = \frac{2|M|\Phi_0}{\lambda a_0^2}\delta x.$$

$$F_{\text{возвр}} = \frac{2|M|B}{\lambda}\delta x.$$

$$\mathcal{F}_{\text{L}} = \frac{1}{c} I_{\text{Tp}} B,$$

$$I_c = \frac{2c|M|\sqrt{\Phi_0}}{\lambda\sqrt{B}}.$$

$$j_c = \frac{2c|M|\sqrt{\Phi_0}}{\lambda\sqrt{B}d}.$$

40 Резистивное состояние

(??? допишу, если будет нужно)

41* Коллективный пиннинг вихрей слабыми дефектами

(??? допишу, если будет нужно)

42* Крип магнитного потока и нелинейная проводимость в ВТСП.

(??? допишу, если будет нужно)

16.4 Other well-known methods for SC junctions

16.4.1 Tight-binding SC models

16.4.2 Overview of other tunneling properties

(collection of other famous results, but not so important ones)

Current and Ambeogakar-Baratoff's formula from Sauls

A Sharvin contact is a small constriction between two conductors where electron transport occurs ballistically without scattering, typically when the constriction size is smaller than the electron mean free path.

The total supercurrent at the point contact is obtained from Eq.

$$\mathbf{J}_e = 2N_f \int \frac{d\Omega_{\hat{\mathbf{p}}}}{4\pi} e\mathbf{v}_\mathbf{p} T \sum_n \frac{1}{4} \mathrm{Tr}\left\{\widehat{\tau}_3 \widehat{\mathfrak{G}}^{\mathrm{M}}\left(\mathbf{r}, \mathbf{p}; \varepsilon_n\right)\right\}$$

and the cross-section of the Sharvin contact,

$$I_s = \left(\pi a^2\right) 2N_f \int_{\hat{\mathbf{p}}\cdot\hat{\mathbf{n}}>0} \frac{d\Omega_\mathbf{p}}{4\pi} 2\hat{\mathbf{n}}\cdot\mathbf{v}_p \frac{\pi}{2} T \sum_n \frac{|\Delta|^2 \sin\vartheta}{\varepsilon_n^2 + |\Delta|^2 \cos^2(\vartheta/2)}$$

The normal-state Sharvin conductance, $G_\mathrm{N} = \frac{\pi a^2}{2} e^2 N_f v_f$, valid in the ballistic limit $\ell \gg a$, is determined by the area of the aperature, the density of states and Fermi velocity for quasiparticle charge transport. Thus, in terms of the contact resistance, $R_\mathrm{N} = 1/G_\mathrm{N}$,

$$I_s = \frac{\pi}{eR_\mathrm{N}} T \sum_n \frac{|\Delta|^2 \sin\vartheta}{\varepsilon_n^2 + |\Delta|^2 \cos^2(\vartheta/2)} = \frac{\pi|\Delta|}{eR_\mathrm{N}} \sin(\vartheta/2) \tanh\left(\frac{|\Delta|\cos(\vartheta/2)}{2T}\right)$$

where the last form is obtained using $\tanh(z) = 8z\sum_{k=1}^{\infty} \frac{1}{\pi^2(2k-1)^2+4z^2}$. This is the result for the current-phase relation originally obtained by K-O. It reduces to the current-phase relation for a Josephson tunnel junction, $I_s = I_c \sin\vartheta$, in the limit $T \to T_c$, where the critical current,

$$I_c = \frac{\pi|\Delta|^2}{4eR_\mathrm{N}T_c} \propto (1 - T/T_c), \quad |T - T_c| \ll T_c$$

is the result obtained by Ambegaokar and Baratoff, except that the tunnelling conductance is replaced by the Sharvin conductance. However, at low temperatures the current-phase becomes increasingly asymmetric near $\vartheta = \pi$ as shown in Fig. 2, and discontinuous at $T = 0$,

$$I_s(T=0) = \frac{\pi\Delta(0)}{eR_\mathrm{N}} \sin(\vartheta/2)\,\mathrm{sgn}(\cos(\vartheta/2))$$

In addition to the divergence of the slope $dI_s/\,d\vartheta|_{\vartheta=\pi}$ as $T \to 0$, the K-O result predicts a critical current that is twice that of the Ambegaokar-Baratoff result.

Heat conductance

$\varepsilon > \Delta$

$$\kappa_\mathrm{NS} = \frac{1}{2} N_f v_f \mathcal{A} \int_{|\Delta|}^{\infty} d\varepsilon \frac{\varepsilon^2/4T^2}{\cosh^2(\varepsilon/2T)} \left[1 - |r_\mathrm{A}(\varepsilon)|^2\right]$$

where $\mathcal{A}$ is an area of the contact (cf. For an N-N contact $\kappa_\mathrm{N} = \mathcal{A}\frac{\pi^2}{12} N_f v_f T\Big)$.

16.4.3 BTK Method

BTK Formalism and Basic Contacts

NS **Boundary**

$\psi_k = [u_k(x.t), v_k(x,t)]^T$ looks as follows:

$$\left[-\frac{\hbar^2}{2m}\nabla^2 + V(x) - \mu(x)\right] u_k(x,t) + \Delta(x) v_k(x,t) = i\hbar \frac{\partial u_k(x,t)}{\partial t} \tag{16.1}$$

$$-\left[-\frac{\hbar^2}{2m}\nabla^2 + V(x) - \mu(x)\right] v_k(x,t) + \Delta^*(x) u_k(x,t) = i\hbar \frac{\partial v_k(x,t)}{\partial t}, \tag{16.2}$$

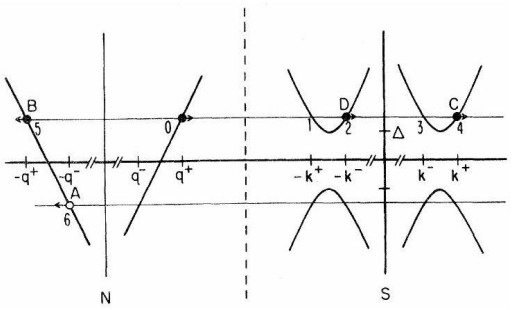
$u_k(x,t) \equiv u_k e^{ikx - iE_k t/\hbar}$
$v_k(x,t) \equiv v_k e^{ikx - iE_k t/\hbar}$
$\frac{\hbar^2 k_\pm^2}{2m} = \mu \pm \sqrt{E_k^2 - |\Delta|^2}.$

$$\psi_{\text{inc}}^N = \begin{bmatrix} 1 \\ 0 \end{bmatrix} e^{ik_+ x}, \tag{16.3}$$

$$\psi_{\text{refl}}^N = a \begin{bmatrix} 0 \\ 1 \end{bmatrix} e^{ik_- x} + b \begin{bmatrix} 1 \\ 0 \end{bmatrix} e^{-ik_+ x}, \tag{16.4}$$

$$\psi_{\text{trans}}^S = c \begin{bmatrix} u_0^2 \\ v_0^2 \end{bmatrix} e^{ik_+ x} + d \begin{bmatrix} v_0^2 \\ u_0^2 \end{bmatrix} e^{-ik_- x}, \tag{16.5}$$

$1 - v_0^2 = u_0^2 = \frac{1}{2}\left(1 + \frac{\left(E^2 - \Delta^2\right)^{1/2}}{E}\right)$



$\psi^N(0) = \psi^S(0) = \psi(0)$
$\frac{\hbar}{2m}\frac{d\psi^S(0)}{dx} - \frac{\hbar}{2m}\frac{d\psi^N(0)}{dx} = H\psi(0)$

$$A(E) = |a(E)|^2 = \frac{\Delta^2}{E^2 + \left(\Delta^2 - E^2\right)\left(1 + 2Z^2\right)^2}; \tag{16.6}$$

$$B(E) = |b(E)|^2 = 1 - A; \tag{16.7}$$

$Z := mH/\hbar^2 k_F$

$$I_{\text{NS}}(V) \propto \int_{-\infty}^{\infty} [f(E - eV) - f(E)] \left[1 + |a(E)|^2 - |b(E)|^2\right] dE, \tag{16.8}$$

Supercurrent Through a S_1NS_2 Junction

$$\begin{pmatrix} H(x) - \mu & \Delta(x) \\ \Delta^*(x) & -[H^*(x) - \mu] \end{pmatrix} \begin{pmatrix} u(x) \\ v(x) \end{pmatrix} = E \begin{pmatrix} u(x) \\ v(x) \end{pmatrix},$$

$$\Delta(x) = \begin{cases} \Delta_1 e^{i\phi_1}, & x < 0, \\ 0, & 0 < x < L, \\ \Delta_2 e^{i\phi_2}, & x > L; \end{cases}$$

$$H(x) := -\frac{\hbar^2}{2m}\frac{d^2}{dx^2}.$$

$$J_Q(x) = e \sum_n f_n \cdot \{J_{u_n}(x) + J_{v_n}(x)\} \tag{16.9}$$

$f_n := f(E_n) = \frac{1}{1 + e^{E_n/k_B T}}$,

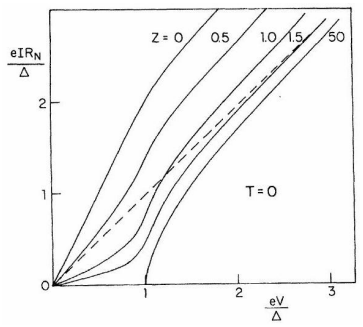


Figure 16.1: Current vs voltage for various barrier strengths $Z := mH/\hbar^2 k_F$ at $T = 0$. These curves attain their asympototic limits only for very high voltages. For example, the tunnel junction ($Z = 50$) curve will be within 1% of the normal-state curve (dotted line) only when $eV \geq 7\Delta$. Credit: [**?**].

$J_{u_n}(x) = \frac{\hbar}{m} \operatorname{Im}\{u_n^*(x)\,[\nabla u_n(x)]\}$; $J_{v_n}(x) = \frac{\hbar}{m} \operatorname{Im}\{v_n^*(x)\,[\nabla v_n(x)]\}$.

$$I(\phi) = \underbrace{I_1(\phi)}_{|E|<\Delta_1} + \underbrace{I_2(\phi)}_{E_1<|E|<\Delta_2} + \underbrace{I_3(\phi)}_{|E|>\Delta_2}. \tag{16.10}$$

$\phi =: \phi_2 - \phi_1$

$$-\arccos\left(\frac{E}{\Delta_1}\right) - \arccos\left(\frac{E}{\Delta_2}\right) + \frac{2LE}{\hbar v_F} \pm \phi = 2\pi n, \tag{16.11}$$

$$I_1(\phi) = \textstyle\sum_n \left\{I_n^+(\phi) f\left(E_n^+(\phi)\right) + I_n^-(\phi) f\left(E_n^-(\phi)\right)\right\}; \qquad I_n^\pm(\phi) = \mp \frac{ev_F}{L + \xi_1\left(E_n^\pm(\phi)\right) + \xi_2\left(E_n^\pm(\phi)\right)}, \tag{16.12}$$

$\xi_{1,2}(E) := \xi_{1,2} \frac{\Delta_{1,2}}{\sqrt{\Delta_{1,2}^2 - E^2}}$
$\xi_{1,2} := \hbar v_F / 2\,|\Delta_{1,2}|$.

$$I_2(\phi) = \frac{2e}{h}\left(\int_{\Delta_1}^{\Delta_2} - \int_{-\Delta_2}^{-\Delta_1}\right) \left|u_1^2 - v_1^2\right| \left(\frac{1}{D(E,-\phi)} - \frac{1}{D(E,\phi)}\right) f(E) dE; \tag{16.13}$$

$$I_3(\phi) = \frac{e}{h}\left(\int_{-\infty}^{-\Delta_2} + \int_{\Delta_2}^{\infty}\right) \left(\left|u_1^2 - v_1^2\right| + \left|u_2^2 - v_2^2\right|\right) \left(\frac{1}{D'(E,-\phi)} - \frac{1}{D'(E,\phi)}\right) f(E) dE; \tag{16.14}$$

$$D(E,\phi) := u_1^2 + v_1^2 - 2u_1 v_1 \cos\left[\frac{|E|}{\Delta_1}\frac{L}{\xi_1} + \phi - \arccos\left(\frac{|E|}{\Delta_2}\right)\right]; \tag{16.15}$$

$$D'(E,\phi) := u_1^2 u_2^2 + v_1^2 v_2^2 - 2u_1 u_2 v_1 v_2 \cos\left[\frac{|E|}{\Delta_1}\frac{L}{\xi_1} + \phi\right]; \tag{16.16}$$

$2u_{1,2}^2 = 1 + \frac{\sqrt{E^2 - \Delta_{1,2}^2}}{E}$; $2v_{1,2}^2 = 1 - \frac{\sqrt{E^2 - \Delta_{1,2}^2}}{E}$

$$E^\pm = \pm \frac{\Delta_1 \Delta_2 \sin(\phi)}{\sqrt{\Delta_1^2 + \Delta_2^2 - 2\Delta_1 \Delta_2 \cos(\phi)}} \tag{16.17}$$

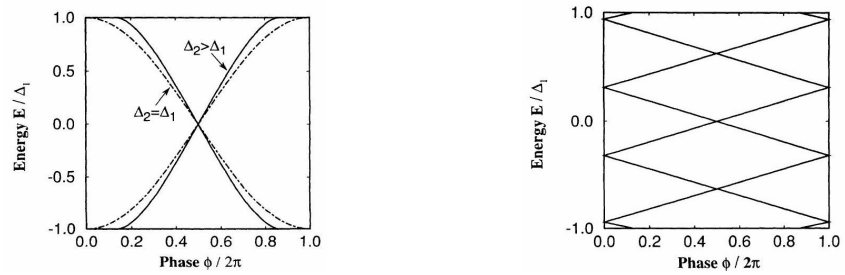


Figure 16.2: Left: ABS for point-contact junction with $\Delta_2/\Delta_1 = 1.5$ (solid) and $\Delta_2/\Delta_1 = 1.0$ (dashed). Right: ABS for a long SNS contact with $\Delta_2/\Delta_1 = 1.5$. Credit: [**?**].

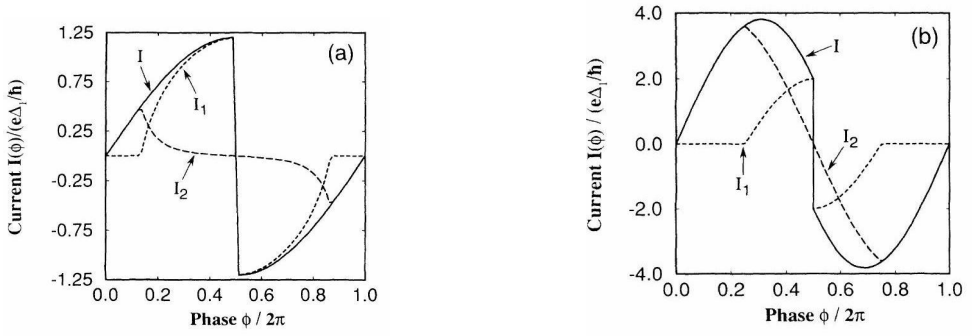


Figure 16.3: Total supercurrent $I(\phi)$ (solid) through a point-contact junction at $T = 0$ when the asymmetry is (a) $\Delta_2/\Delta_1 = 1.5$ and (b) $\Delta_2/\Delta_1 = 200$. The critical current in (b) is much bigger than in (a), and the CPR is changed. Credit: [**?**].

SNS Junction with Impurity

$$H(x) := \frac{1}{2m}\left(-i\hbar\frac{d}{dx} - eA(x)\right)^2 + V(x);$$

$$\begin{pmatrix} H(x)-\mu & \Delta(x) \\ \Delta^*(x) & -[H^*(x)-\mu] \end{pmatrix}\begin{pmatrix} u(x) \\ v(x) \end{pmatrix} = E\begin{pmatrix} u(x) \\ v(x) \end{pmatrix}, \qquad V(x) := V_s\delta(x-a), \qquad 0 \le a \le L;$$

$$\Delta(x) := \begin{cases} \Delta e^{i\phi_1}, & x < 0, \\ 0, & 0 < x < L, \\ \Delta e^{i\phi_2}, & x > L. \end{cases} \tag{16.18}$$

$$2\arccos\left(\frac{E}{\Delta}\right) + \frac{L}{\xi_0}\frac{E}{\Delta} \pm \alpha = 2\pi n, \tag{16.19}$$

$\xi_0 = \hbar v_F/2\Delta$
$\cos(\alpha) = T\cos(\phi) + R\cos\left[\left(\frac{L-2a}{\xi_0}\right)\left(\frac{E}{\Delta}\right)\right]$,
$\hbar k_F := \sqrt{2m\mu}$
$T = 1 - R = \frac{1}{1+(mV_s/\hbar^2 k_F)^2}$

$$E^{\pm} = \pm\Delta\cos(\alpha/2) = \pm\Delta\sqrt{1 - T\sin^2(\phi/2)}, \tag{16.20}$$

$\cos(\alpha) = T\cos(\phi) + R.$
$E_{\text{gap}} = 2\Delta\sqrt{R}$

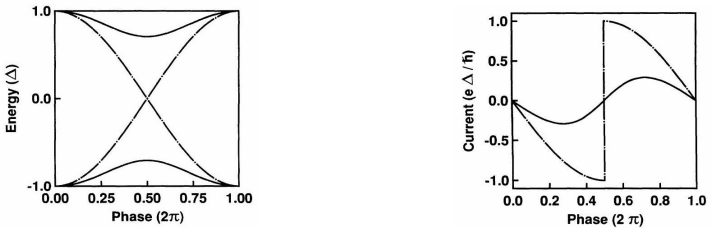


Figure 16.4: Left: ABS for a short junction. Right: Josephson current with impurity (solid) and unperturbed junction (dotted) Credit: [**?**].

$$I(\phi) = \frac{e\Delta}{\hbar} T \sin(\alpha/2) \frac{\sin(\phi)}{\sin(\alpha)}, \tag{16.21}$$

16.4.4 Beenakker's Determinant Method

$$\rho(\varepsilon) = -\frac{1}{\pi} \operatorname{Im} \frac{d}{d\varepsilon} \ln\det\left[1 - R_{\rm A}(\varepsilon + i0^+) S_{\rm N}(\varepsilon + i0^+)\right] + \rho_0(\varepsilon). \tag{16.22}$$

$$S_{\rm N}(\varepsilon) := \begin{pmatrix} s_0(\varepsilon) & 0 \\ 0 & s_0^*(-\varepsilon) \end{pmatrix}, \tag{16.23}$$

$$R_{\rm A}(\varepsilon) := i\alpha(\varepsilon) \begin{pmatrix} 0 & r_{\rm A} \\ r_{\rm A}^* & 0 \end{pmatrix}, \qquad r_{\rm A} := \begin{pmatrix} e^{i\phi/2}\sigma_y & 0 \\ 0 & e^{-i\phi/2}\sigma_y \end{pmatrix},$$
$$\alpha(\varepsilon) = e^{-i \arccos(\varepsilon/\Delta_0)} = \varepsilon/\Delta_0 - i\sqrt{1 - \varepsilon^2/\Delta_0^2}. \tag{16.24}$$

$$\rho(\varepsilon) = -\frac{1}{\pi} \operatorname{Im} \frac{d}{d\varepsilon} \ln\det\left[1 - M(\varepsilon + i0^+)\right] + \rho_0(\varepsilon), \qquad M(\varepsilon) := -\alpha(\varepsilon)^2 r_{\rm A}^* s_0^*(-\varepsilon) r_{\rm A} s_0(\varepsilon). \tag{16.25}$$

$F = -k_{\rm B}T \int_0^\infty d\varepsilon\, \rho(\varepsilon) \ln\left[2\cosh(\varepsilon/2k_{\rm B}T)\right],$

$$F = \frac{i}{4\pi} \int_{-\infty}^{\infty} d\varepsilon\, \tanh(\varepsilon/2k_{\rm B}T) \ln\det\left[1 - M(\varepsilon + i0^+)\right] + F_0, \tag{16.26}$$

$$F = -k_{\rm B}T \sum_{p=0}^{\infty} \ln\det\left[1 - M\left(i\omega_p + i\gamma\right)\right], \qquad \omega_p = (2p+1)\pi k_{\rm B}T. \tag{16.27}$$

$$\frac{E}{\Delta} = \pm\frac{1}{2}\sqrt{1 + \operatorname{Tr}\left(S\mathbf{e}^{i\phi}S^*\mathbf{e}^{-i\phi}\right)}, \tag{16.28}$$

$$E = \pm\frac{\Delta}{2}\sqrt{1 + \sum_{l,j} T_{lj} e^{-i(\phi_l - \phi_j)}}, \tag{16.29}$$

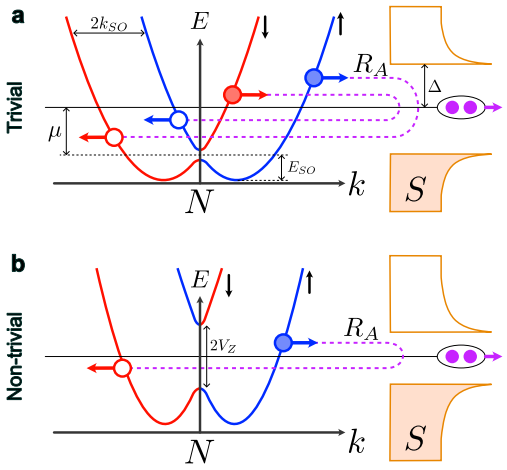
For example, for $H = \begin{pmatrix} -i\sigma_z\hat{v}\partial/\partial x & \Delta \\ \Delta^* & --i\sigma_z\hat{v}\partial/\partial x \end{pmatrix}$

$$I = -\frac{e}{\hbar}\frac{\partial}{\partial\varphi}T\sum_{\omega}\ln\det\left[1 - S_N S_A(\omega)\right],$$

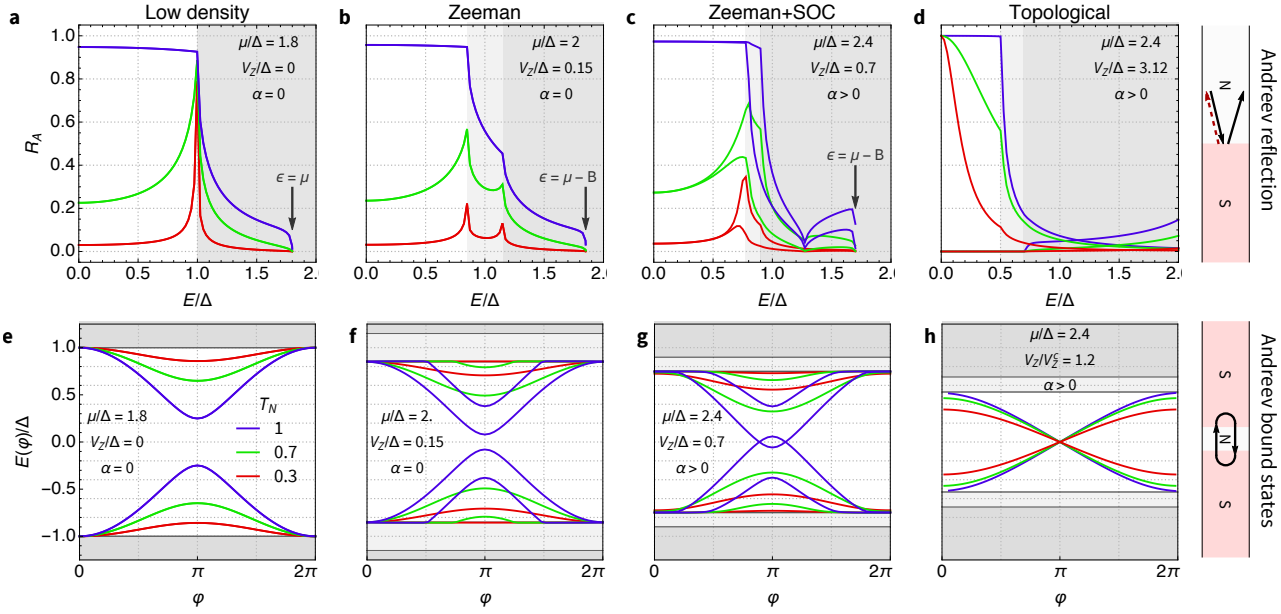
$S_N := \begin{pmatrix} S & 0 \\ 0 & -S^* \end{pmatrix}$, $S := \begin{pmatrix} r_L & t_{LR} \\ t_{RL} & r_R \end{pmatrix}$ $S_A = -i\begin{pmatrix} 0 & r_A \\ r_A^* & 0 \end{pmatrix}$ $r_A := \begin{pmatrix} e^{-\theta_L+i\varphi_L} & 0 \\ 0 & e^{-\theta_R+i\varphi_R} \end{pmatrix}$, $\theta := \operatorname{arcsinh}\frac{\omega}{\Delta}$.

16.4.5 Majorana wires and junctions

Main plots and formulas of Majorana wires



(???)
(write formulas for Hamiltonian, with which plot below is assumed)



Models of Majorana wires

(write Hamiltonians and show what is important about it)

$$H_w := \frac{1}{2}\int dx \Psi^\dagger(x)\mathcal{H}(x)\Psi(x), \qquad \mathcal{H}_w(x) := \left(-\frac{\hbar^2\partial_x^2}{2m^*} - \mu - i\alpha\partial_x\sigma_y\right)\tau_z + V_Z\sigma_x; \tag{16.30}$$

$$H_{\rm SC} = \int_{-\infty}^{\infty} dx \left(\Delta(x)\psi_\uparrow^\dagger(x)\psi_\downarrow^\dagger(x) + h.c.\right). \tag{16.31}$$

The SM Hamiltonian takes into account the so-called Rashba spinorbit (SO) interaction (term $i\alpha\partial_x\sigma_y$) and the existence of parallel to the nanowire axis magnetic field B (term $V_Z\sigma_x$, where $V_Z = \frac{1}{2}g\mu_B B$ is the usual Zeeman energy with effective g-factor). The usual Nambu notation is assumed (for example, the wave function $\Psi(x) = (\psi_\uparrow^\dagger, \psi_\downarrow^\dagger, \psi_\downarrow, -\psi_\uparrow)$ is a Nambu spinor).

Another model with Majoranas that will be used in our review and for which our method can be applicable is a model of topological superconductors They can be modeled, for example, as a low-energy limit of a Kitaev chain, and its Hamiltonian looks as follows:

$$H_{TS} = \int_0^\infty dx \Psi_{TS}^\dagger(x)\left(-iv_F\partial_x\sigma_z + \Delta\sigma_y\right)\Psi_{TS}(x). \tag{16.32}$$

Here the pairing gap Δ is induced by proximity effect and can be considered as real and positive; $\Psi_{TS}(x) = \left(c_r, c_l^\dagger\right)^T$ is the Nambu spinor, it contains right- and left-moving fermion operators $c_{r,l}(x)$. One can see that the difference between the conventional SC is the dispersion relation.

The model (16.30) has a discretized version, which looks as follows [**?**]:

$$H_{\rm wire} = \frac{1}{2}\sum_j \left[\Psi_j^\dagger\hat{h}\Psi_j + \left(\Psi_j^\dagger\hat{t}\Psi_{j+1} + \text{h.c.}\right)\right], \qquad \begin{aligned} \hat{h} &:= (2t-\mu)\sigma_z\tau_0 + V_x\sigma_0\tau_x + \Delta\sigma_x\tau_0, \\ \hat{t} &:= -t\sigma_z\tau_0 + i\alpha\sigma_z\tau_z, \\ \Psi_j^T &= \left(c_{j\uparrow}, c_{j\downarrow}, c_{j\downarrow}^\dagger, -c_{j\uparrow}^\dagger\right). \end{aligned}$$

Here $\hat{h}$ is responsible for a on-site energy and the $\hat{t}$ is a hopping matrix. Often the discretized models are analyzed more conveniently, and after one can take a continuous limit (as done in the main part of this thesis).

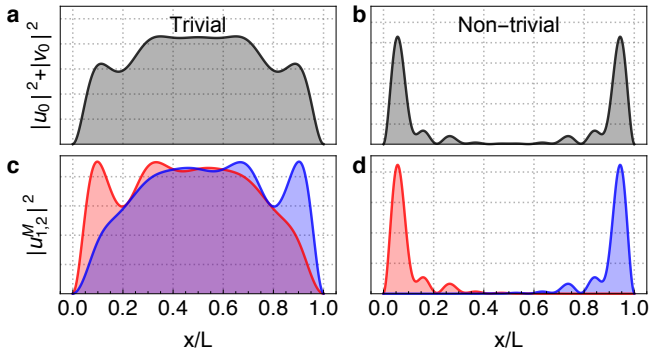


Figure 16.5: Wavefunction of the lowest energy state ψ_0 in a uniform $L = 1\mu$m Majorana nanowire for a trivial $V_Z = 0.5V_Z^c$ (a) and a non-trivial $V_Z = 1.4V_Z^c$ (b) cases. (c,d) Wavefunctions of the corresponding Majorana components $u_{1,2}^M(x)$ in the Majorana basis. In the trivial regime the left (red) and right (blue) Majorana components strongly overlap (c), whereas in the topological regime they move apart and concentrate at the ends of the nanowire (d). Credit: [**?**].

One can find a lot of physics from these Hamiltonians, was was reviewed in the introduction. The excitations of this model can be described by self-conjugation operators (which are known

from field theory as Majorana operators) $\gamma_1 := \gamma_1^\dagger$ and $\gamma_2 := \gamma_2^\dagger$. These can be obtained from unitary rotation $\gamma_1 := \psi_0^\dagger + \psi_0$, $\gamma_2 := i(\psi_0^\dagger - \psi_0)$, where the later operators are defined from the wave function in the model as $\psi_n := \int dx \sum_\sigma \left[u_{n\sigma}(x)\psi_\sigma(x) + v_{n\sigma}(x)\psi_\sigma^\dagger(x)\right]$. Here and $u_{n\sigma}(x), v_{n\sigma}(x)$ are the wavefunctions of electron and hole. The "big" value of V_Z is crucial for having the localization of the Majorana modes: if $V_Z > V_Z^c$ then we have a non-trivial topological regime and the wave-functions are localized. If $V_Z < V_Z^c$ then the regime is non-topological and the wave-functions are overlap strongly. This is illustrated in Fig. 16.5.

GF-s of Majorana wires

$$G(\tau) := -\langle \mathcal{T}_\tau \Psi_{\rm TS}(\tau)\Psi_{\rm TS}^\dagger(0)\rangle_0 = T\sum_\omega e^{-i\omega\tau}G_j(\omega); \qquad G(\omega) = \frac{1}{i\omega}\left(\sqrt{\omega^2+\Delta^2}\,\tau_0 + \Delta\tau_x\right).$$

Here $\Psi_{\rm TS} = (\psi\ \psi^\dagger)^T$ is a Nambu spinor and $\mathcal{T}_\tau$ is the time-ordering operator. The frequencies ω are the fermionic Matsubara frequencies ($\omega = 2\pi(n+1/2)/\beta$). This function can be used for description of multiterminal junctions with topological superconductors.

16.4.6 Fluctuation effects in weak contacts

Thermal fluctuations in the Josephson transition, phase slippage and I(V,T).

Macroscopic quantum effects: "phase tunneling" and transition to a resistive state.

Macroscopic quantum coherence in SQUIDS.

Aslamazov-Larkin increasement of cunductivity near T_c because of fluctuations

(write some main formulas)

(write something about experimental confirmation)

16.5 Other well-known theories and formalisms for typical SC

16.5.1 Superconductors with dissipation

(??? I'll study and write it soon)

SC in a Electromagnetic Field: Special Cases

(?? see AGD)

SC in a weak EM field by AGD

1. **Постоянное слабое магнитное поле (398).**
2. **Сверхпроводник в переменном поле (408).**

SC in an arbitrary field near T_c

(см. пока что Абрикосов, Горьков)

16.5.2 Theory of Superconducting Alloys by Abrikosov–Gorkov

1. Постановка вопроса (421).

2. Остаточное сопротивление нормального металла (423).

3. Электромагнитные свойства сверхпроводящих сплавов (432).

16.5.3 Other experimental hints for a true SC theory

(??? I'll write it very not soon, since it is not important)
Little–Parks oscillations, as a hit for BCS
(напишу тут, как из этого догадаться про BCS (???))

16.5.4 Effects of Temperature and Magnetic Field

Δ(T) при нетривиальном спаривании.
Теплоемкость и спиновая восприимчивость сверхпроводника.
Парамагнитный предел для синглетного сверхпроводника.
Диамагнитный отклик, глубина проникновения поля и ее температурная зависимость.

16.5.5 Eliashberg Theory of Electron–Phonon Interaction (???)

Обзор теории Элиашберга

Eliashberg theory is a theory of superconductivity that describes the role of phonons in providing the attractive interaction between two electrons. Phonon dynamics are taken into account, thus giving rise to retardation effects that impact the electrons, in the form of a frequency-dependent electron self-energy. Now the order parameter is frequency dependent (not static as in BCS).

Гамильтониан электрон-фононного взаимодействия и уравнения Дайсона.

(У Левитова Шитова же теория про это уже известна)

Формальное решение для функций Грина, спектральное представление и усреднение по ферми-поверхности.

(??)

Интегральное уравнение для параметра порядка $\Delta(\omega)$ и анализ его решения.

(У Левитова Шитова же уже это решалось, да?)

Роль кулоновского взаимодействия.

(задача Лев-в Шит-в)

Простое применение: изотопический эффект в сверхпроводимости.

(!!)

16.6 Unconventional Superconductivity in a Nutshell

(!!!!!! добавлю потом деление по типам тем!!!)

16.6.1 Overview of UC SC

(main all about it)

16.6.2 Fundamentals of UC SC

Formation of Cooper pair for UC SC

$$\Psi^l_{\text{pair}} = g_1(\mathbf{k})|\Pi\uparrow\rangle + g_2(\mathbf{k})(|\uparrow\downarrow\rangle + |\downarrow\uparrow\rangle) + g_3(\mathbf{k})|\downarrow\downarrow\rangle = \begin{pmatrix} g_1(\mathbf{k}) & g_2(\mathbf{k}) \\ g_2(\mathbf{k}) & g_3(\mathbf{k}) \end{pmatrix}.$$

$$g_\alpha(\mathbf{k}) = \sum_{m=-1}^{1} a^\alpha_{lm} Y_{lm}(\hat{\mathbf{k}})$$

- амплитуды состояний с $S_z = 1, 0$ и -1, соответственно.

Или через базиса симметричные матрицы $i\sigma\sigma_y = (i\sigma_x\sigma_y, i\sigma_y\sigma_y, i\sigma_z\sigma_y)$:

$$\Psi'_{\text{pair}} = i(\mathbf{d}(\mathbf{k})\boldsymbol{\sigma})\sigma_y = (d_x(\mathbf{k})\sigma_x + d_y(\mathbf{k})\sigma_y + d_z(\mathbf{k})\sigma_z)\, i\sigma_y = \\ = \begin{pmatrix} -d_x(\mathbf{k}) + id_y(\mathbf{k}) & d_z(\mathbf{k}) \\ d_z(\mathbf{k}) & d_x(\mathbf{k}) + id_y(\mathbf{k}) \end{pmatrix}$$

$$g_1 = -d_x + id_y, g_2 = d_z, g_3 = d_x + id_y$$

$$d_\alpha(\mathbf{k}) = \sum_{m=-l}^{1} b^\alpha_{lm} Y_{lm}(\hat{\mathbf{k}}).$$

Среднее значение спина пары:

$$\mathbf{S} = i\hbar \int \frac{d\Omega}{4\pi} \mathrm{d}^*(\mathbf{k}) \times \mathrm{d}(\mathbf{k});$$

Среднее значение орбитального момента пары:

$$\mathbf{L} = i\hbar \int \frac{d\Omega}{4\pi} \mathbf{d}^*(\mathbf{k}) \left[\mathbf{k} \times \frac{\partial}{\partial \mathbf{k}}\right] \mathbf{d}(\mathbf{k}).$$

Singlets, Triplets, other states

Operation	Singlet	Triplet
Fermion exchange	$\psi(\vec{k}) = \psi(-\vec{k})$	$\vec{d}(\vec{k}) = -\vec{d}(-\vec{k})$
Orbital rotation	$g\psi(\vec{k}) = \psi(R(g)\vec{k})$	$g\vec{d}(\vec{k}) = \vec{d}(R(g)\vec{k})$
Spin rotation	$g\psi(\vec{k}) = \psi(\vec{k})$	$g\vec{d}(\vec{k}) = \tilde{R}(g)\vec{d}(\vec{k})$
Time-reversal	$\widehat{K}\psi(\vec{k}) = \psi^*(-\vec{k})$	$\widehat{K}\vec{d}(\vec{k}) = -\vec{d}^*(-\vec{k})$
$U(1)$-gauge	$\widehat{\Phi}\psi(\vec{k}) = e^{i\phi}\psi(\vec{k})$	$\widehat{\Phi}\vec{d}(\vec{k}) = e^{i\phi}\vec{d}(\vec{k})$

2 Spin Structure of Paired States

(see Mineev)

3 Phases of Superfluid Helium-3

4 Superconducting States in Crystals

Energy of Elementary Excitations in Superconductors

$$V_{\alpha\beta,\lambda\mu}\left(\mathbf{k},\mathbf{k}'\right)=\frac{1}{2}V_{\Gamma}\left(k,k'\right)\sum_{i=1}^{d_{\Gamma}}\left(\psi_i(\hat{\mathbf{k}})\mathbf{g}_{\alpha\beta}\right)\left(\boldsymbol{\psi}_i^{*}\left(\hat{\mathbf{k}}'\right)\mathbf{g}_{\lambda\mu}^{+}\right)$$

$$\Psi=\prod_{\mathbf{k}}\left(u_{\mathbf{k}}+v_{\mathbf{k}}a_{\mathbf{k}\uparrow}^{+}a_{-\mathbf{k}\downarrow}^{+}\right)|\mathrm{vac}\rangle$$

$$T=0\quad\Rightarrow\quad\begin{array}{l}F_{\mathbf{k},\uparrow\downarrow}=\langle\Psi\left|a_{\mathbf{k}\uparrow}a_{-k\downarrow}\right|\Psi\rangle,\\ F_{\mathbf{k},\uparrow\downarrow}^{+}=\left\langle\Psi\left|a_{-k\uparrow}^{+}a_{k\downarrow}^{+}\right|\Psi\right\rangle.\end{array}\qquad T\neq 0\quad\Rightarrow\quad\begin{array}{l}F_{\mathbf{k},\alpha\beta}=\langle a_{\mathbf{k}\alpha}a_{-\mathbf{k}\beta}\rangle,\\ F_{\mathbf{k},\alpha\beta}^{+}=\left\langle a_{-k\alpha}^{+}a_{\mathbf{k}\beta}^{+}\right\rangle.\end{array}$$

Для нечетного потепциала взаимодействия $\Delta_{\mathbf{k},\alpha\beta}$ и $F_{\mathbf{k},\alpha\beta}$ также нечетны и описывают триплетное спаривание:

$$\Delta_{\mathbf{k},\alpha\beta}=\Delta\mathbf{d}(\mathbf{k})\left(i\sigma\sigma_y\right)_{\alpha,\beta}.$$

$$\mathbf{d}(\mathbf{k})=\mathbf{d}^{l}(\mathbf{k})=\sum_{m=-l}^{1}\mathbf{b}_{lm}(k)Y_{lm}(\dot{k})\qquad\int\frac{d\Omega}{4\pi}|\mathrm{d}(\mathbf{k})|^2=1$$

Для сверхпроводника с триплетным спариванием:

$$E_{\mathbf{k}}=\sqrt{\xi_k^2+\Delta^2|\mathbf{d}(\mathbf{k})|^2}$$

В B-фазе $\mathbf{d}=\hat{\mathbf{k}}$

$$E_k^B=\sqrt{\xi_k^2+|\Delta|^2}$$

то есть, как и в случае s-спаривания, на всей ферми-поверхности имеется щель, не зависящая от направления $\mathbf{k}$.

В A-фазе $\mathbf{d}=\sqrt{3/2}\left(\hat{k}_x+i\hat{k}_y,0,0\right)$

$$E_{\mathbf{k}}^A=\sqrt{\xi_k^2+\frac{3}{2}\Delta^2\left(\hat{k}_x^2+\hat{k}_y^2\right)}=\sqrt{\xi_k^2+\frac{3}{2}\Delta^2\sin^2\theta}$$

то есть щель в спектре обращается в нуль на северном и южном полюсах ($\theta=0,\pi$) ферми-сферы.

Gap in the Spectrum of Elementary Excitations and Critical Temperature

(??? основная идея???)

$$\Delta_{\mathbf{k},\alpha\beta}=-\sum_{\mathbf{k}'}V_{\beta\alpha,\lambda\mu}\left(\mathbf{k},\mathbf{k}'\right)F_{\mathbf{k}',\lambda\mu}\tag{6.1}$$

$$F_{\mathbf{k},\lambda\mu}=\langle a_{\mathbf{k}\lambda}a_{-\mathbf{k}\mu}\rangle=\left\langle\left(u_{\mathbf{k},\lambda\gamma}b_{\mathbf{k}\gamma}+v_{\mathbf{k},\lambda\gamma}b_{-\mathbf{k}\gamma}^{+}\right)\left(u_{-\mathbf{k},\mu\delta}b_{-\mathbf{k}\delta}+v_{-\mathbf{k}}\mu\delta b_{\mathbf{k}\delta}^{+}\right)\right\rangle$$

$$u_{\mathbf{k},\alpha\beta}=u_{\mathbf{k}}\delta_{\alpha\beta},\quad v_{\mathbf{k},\alpha\beta}=-v_{-\mathbf{k},\beta\alpha}$$

$$\langle b_{-\mathbf{k}\alpha}b_{\mathbf{k}\beta}\rangle=\left\langle b_{\mathbf{k}\alpha}^{+}b_{-\mathbf{k}\beta}^{+}\right\rangle=0$$

$$\left\langle b_{\mathbf{k}\alpha}^{+}b_{\mathbf{k}\beta}\right\rangle=\delta_{\alpha\beta}-\left\langle b_{\mathbf{k}\beta}b_{\mathbf{k}\alpha}^{+}\right\rangle=f_{\mathbf{k}}\delta_{\alpha\beta}\qquad f_{\mathrm{k}}=f\left(E_{\mathrm{k}}\right)=\frac{1}{\exp\left(E_{\mathrm{k}}/T\right)+1}$$

$$F_{\mathbf{k},\lambda\mu} = -u_{\mathbf{k}} v_{\mathbf{k},\lambda\mu} \left(1 - 2f_{\mathbf{k}}\right) = \frac{\Delta_{k,\lambda\mu}}{2E_{\mathbf{k}}} \left(1 - 2f_{\mathbf{k}}\right) \tag{6.3}$$

$$\Delta_{\mathbf{k},\alpha\beta} = -\sum_{\mathbf{k}'} V_{\beta\alpha,\lambda\mu}\left(\mathbf{k},\mathbf{k}'\right) \frac{1 - 2f_{\mathbf{k}'}}{2E_{\mathbf{k}'}} \Delta_{\mathbf{k}',\lambda\mu} \tag{6.4}$$

$$g(\mathbf{k}) = -\sum_{\mathbf{k}'} \frac{V\left(\mathbf{k},\mathbf{k}'\right)\left(1 - 2f_{\mathbf{k}'}\right)}{2\sqrt{\xi_{k'}^2 + \Delta^2 \left|g\left(\mathbf{k}'\right)\right|^2}} g\left(\mathbf{k}'\right) \qquad \text{singl} \tag{6.5}$$

$$\mathbf{d}(\mathbf{k}) = -\sum_{\mathbf{k}'} \frac{V\left(\mathbf{k},\mathbf{k}'\right)\left(1 - 2f_{\mathbf{k}'}\right)}{2\sqrt{\xi_{k'}^2 + \Delta^2 \left|\mathbf{d}\left(\mathbf{k}'\right)\right|^2}} \mathrm{d}\left(\mathbf{k}'\right) \qquad \text{tripl} \tag{6.6}$$

Solutions: (???????)

$$g(\mathbf{k}) = \sum_{m=-l}^{l} a_{lm} Y_{lm}(\hat{\mathbf{k}}) \tag{6.7}$$

$$\mathrm{d}(\mathbf{k}) = \sum_{m=-l}^{l} \mathrm{b}_{lm} Y_{lm}(\hat{\mathbf{k}}) \tag{6.8}$$

(??? how we come to temperature???)

$$1 = N_0 V_i \int_0^{\varepsilon_i} d\xi \frac{\mathrm{th}\left(|\xi|/2T_c\right)}{|\xi|} \tag{6.9}$$

$$1 = N_0 V_l \left(\ln \frac{\varepsilon_l}{2T_\mathrm{c}} - \int_0^{\infty} dx \frac{\ln x}{\mathrm{ch}^2\, x} \right)$$

$$T_\mathrm{C} = \frac{2\gamma}{\pi} \varepsilon_l \exp\left(-\frac{1}{N_0 V_l}\right) \tag{6.10}$$

$2\gamma/\pi \approx 1.14$, $\ln \gamma = C \approx 0.577$

$$a_{lm}(T) = N_0 V_i \int_0^{\varepsilon_1} d\xi \int \frac{d\Omega}{4\pi} \frac{\mathrm{th}\left(\sqrt{\xi^2 + \Delta^2(T)|g(\mathbf{k})|^2}/2T\right)}{\sqrt{\xi^2 + \Delta^2\left(T'\right)|g(\mathbf{k})|^2}} Y_{lm}^*(\hat{\mathbf{k}}) g(\mathbf{k}) \qquad \text{singl} \tag{6.11}$$

$$\mathbf{b}_{lm}(T) = N_0 V_l \int_0^{\varepsilon_1} d\xi \int \frac{d\Omega}{4\pi} \frac{\mathrm{th}\left(\sqrt{\xi^2 + \Delta^2(T)|\mathbf{d}(\mathbf{k})|^2}/2T\right)}{\sqrt{\xi^2 + \Delta^2(T)|\mathrm{d}(\mathbf{k})|^2}} Y_{im}^*(\hat{\mathbf{k}}) \mathrm{d}(\mathbf{k}) \qquad \text{tripl} \tag{6.12}$$

For s-coupl, $T = 0$:

$$\frac{1}{N_0 V_0} = \int_0^{\varepsilon_0} \frac{d\xi}{\sqrt{\xi^2 + \Delta_0^2}} \approx \ln \frac{2\varepsilon_0}{\Delta_0} \tag{6.13}$$

$$\Delta_0 = \Delta(T = 0) = 2\varepsilon_0 \exp\left(-\frac{1}{N_0 V_0}\right) \tag{6.14}$$

$$\Delta_0 = \frac{\pi}{\gamma} T_c \approx 1,75 T_c \tag{6.15}$$

$$\frac{1}{N_0 V_0} = \int_0^{\varepsilon_0} \frac{d\xi}{\sqrt{\xi^2 + \Delta^2}} - 2 \int_0^{\varepsilon_0} \frac{f(E) d\xi}{\sqrt{\xi^2 + \Delta^2}}$$

$$\ln \frac{2\varepsilon_0}{\Delta_0} = \ln \frac{2\varepsilon_0}{\Delta} - 2 \int_0^{\varepsilon_0} \frac{f(E) d\xi}{\sqrt{\xi^2 + \Delta^2}}$$

$$\ln \frac{\Delta_0}{\Delta} = 2 \int_0^{\varepsilon_0} \frac{d\xi}{\left(\exp\left(\sqrt{\xi^2 + \Delta^2}/T\right) + 1\right) \sqrt{\xi^2 + \Delta^2}} \tag{6.16}$$

$\varepsilon \approx \infty, T \approx 0,$

$$\ln \frac{\Delta_0}{\Delta} \approx \frac{2}{\Delta_1} e^{-\Delta_0/T} \int_0^{\infty} e^{-\xi^2/(2\Delta T)} d\xi = \sqrt{2\pi \frac{T}{\Delta}} e^{-\Delta_0/T}$$

$$\Delta = \Delta_0 \left(1 - \sqrt{\frac{2\pi T}{\Delta}} e^{-\Delta_0/T}\right) \tag{6.17}$$

$$\ln \frac{\Delta_0}{\Delta} = \ln \frac{\pi T}{\gamma \Delta} + \frac{7\zeta(3)}{8\pi^2} \left(\frac{\Delta}{T}\right)^2 + \dots$$

$\Delta_0 = \pi T_c / \gamma,$

$$\ln \frac{T_c}{T} \approx \frac{T\zeta(3)}{8\pi^2} \left(\frac{\Delta}{T}\right)^2$$

$$\Delta(T) \approx \left(\frac{8\pi^2}{7\zeta(3)}\right)^{1/2} T_{\mathrm{c}} \left(\frac{T_{\mathrm{c}} - T}{T_{\mathrm{c}}}\right)^{1/2} \tag{6.18}$$

16.6.3 Advanced properties of basic UC SC

Temperature Dependence of Thermodynamic Quantities of UC SC for T → 0

$$C_{\mathrm{s}} = \sum_{\mathrm{k}\alpha} E_{\mathrm{k}} \frac{\partial f_{\mathrm{k}}}{\partial T} \tag{7.1}$$

$$C_{\mathrm{s}} = 2N_0 \int_{-\infty}^{+\infty} d\xi \sqrt{\xi^2 + \Delta^2} \frac{\partial}{\partial T} \left(\frac{1}{\exp\left(\sqrt{\xi^2 + \Delta^2}/T\right) + 1}\right) \tag{7.2}$$

$$S = -\sum_{ka} \{(1 - f_k) \ln (1 - f_k) + f_k \ln f_k\}$$

$T \to 0,$

$$C_s \approx \frac{2N_0 \Delta^2}{T^2} e^{-\Delta/T} \int_{-\infty}^{+\infty} d\xi e^{-\xi^2/(2\Delta T)} \approx N_0 \left(\frac{\Delta_0}{T}\right)^2 \sqrt{2\pi T \Delta_0} e^{-\Delta_0/T} \tag{7.3}$$

$$C_{\rm s} = 2N_0 \int\limits_{-\infty}^{+\infty} d\xi \int \frac{d\Omega}{4\pi} E_{\rm k} \frac{\partial}{\partial T} \frac{1}{c^{E_{\rm k}/T}+1} \tag{7.4}$$

$$\theta < \frac{\xi}{\Delta}, \quad \pi - \theta < \frac{\xi}{\Delta}.$$

$T \to 0$,

$$C_s = \frac{N_0}{T^2} \int\limits_{-\infty}^{+\infty} d\xi \int\limits_0^{\pi} \sin\theta d\theta \frac{E^2 e^{E/T}}{\left(e^{E/T}+1\right)^2} \approx$$

$$\approx \frac{N_0}{2T^2} \int\limits_{-\infty}^{+\infty} \frac{d\xi \xi^2}{\mathrm{ch}^2(\xi/2T)} \int\limits_0^{\xi/\Delta} \theta d\theta + O\left(\exp\left(-\frac{\Delta_0}{T}\right)\right) \approx$$

$$\approx \frac{N_0}{4T^2\Delta^2} \int\limits_{-\infty}^{+\infty} \frac{d\xi \xi^4}{\mathrm{ch}^2(\xi/2T)} = N_0 \frac{T^3}{\Delta_0^2} I \tag{7.5}$$

$$I = 8 \int\limits_{-\infty}^{+\infty} \frac{dz z^4}{\mathrm{ch}^2 z} = \frac{7\pi^4}{15}$$

$$g(\mathbf{k}) \propto \left(\hat{k}_x + i\hat{k}_y\right)^2 \tag{7.6}$$

$$\left.\frac{C_s}{C_n}\right|_{T\to 0} \sim \begin{cases} \left(\frac{T_c}{T}\right)^{5/2} e^{-\Delta_0/T}, & \text{щель в спектре не обращается в нуль,} \\ \left(\frac{T}{T_c}\right)^2, & \text{щель в спектре имеет нули первого порядка в изолированных точках,} \\ \frac{T}{T_c}, & \text{щель в спектре равна нулю на линиях или имеет нули второго порядка в изолированных точках.} \end{cases}$$

8 Effects of Electron Number Parity in Superconductors

16.6.4 9 Paramagnetic Susceptibility and Knight Shift

16.6.5 11 Superconducting States with Multicomponent Order Parameters

16.6.6 12 Ginzburg-Landau Equations and Upper Critical Field

16.6.7 13 Boundary Conditions and Surface Superconductivity

16.6.8 14 Meissner and Mixed States in Unconventional Superconductors

16.6.9 15 Magnetic Superconductors

16.6.10 18 Ginzburg-Landau Functional for UC SC

16.6.11 19 Upper Critical Field in a p-wave Superconductor

16.6.12 20 Boundary Conditions for the Order Parameter

16.6.13 21 Effect of Impurities on Unconventional Superconductivity

16.6.14 22 Electronic Thermal Conductivity of Unconventional Superconductors

16.7 Special effects

16.7.1 Thermoelectric effects

(??????)

The Seebeck effect in a superconductor and the possibility of measuring it.

“Superconducting thermocouple” and the magnetic flux in it.

The Nernst effect in the mixed state of a superconductor and the problem of entropy per vortex.

The Nernst fluctuation effect is above the transition point.

(???)

16.7.2 Heat Capacity from Fluctuation, Diamagnetism of SC II kind

Флуктуации вблизи температуры перехода (оценка ширины флуктуационной области, диамагнетизм, парапроводимость).

Переход Березинского-Костерлица-Таулеса в тонкой пленке.

(По Варламову Ларкину создам параграфы потом!)

2.2. Вклад флуктуаций в теплоемкость

2.2.1. Точное решение задачи в случае размерности $D = 0$
2.2.2. Произвольная размерность: случай $T \geqslant T_c$
2.2.3. Произвольная размерность: случай $T < T_c$

2.3. Флуктуационный диамагнетизм

2.3.1. Предварительные замечания

Что касается трехмерных образцов, то следует отметить, что выражение (1.10), будучи представленным посредством корреляционной длины $\xi(T)$, оказывается справедливым в области более широкой, чем обсуждаемая выше область слабых флуктуаций (ГЛ-область). Действительно, в ГЛ-области ($|\epsilon| \gtrsim Gi$) $\xi(\epsilon) \sim \epsilon^{-1/2}$ и такое представление тривиально. Ситуация изменяется в непосредственной близости точки перехода, где становится существенным взаимодействие флуктуаций. Здесь само присутствие куперовских пар начинает влиять на корреляционную длину. Согласно скэйлинговой гипотезе (которую мы подробно обсудим ниже) вблизи перехода единственным масштабом в системе остается корреляционная длина, по-прежнему степенным образом зависящая от температуры: $\xi(\epsilon) \sim \epsilon^{-\nu}$, однако взаимодействие флуктуаций изменяет критический индекс по сравнению с его ГЛ-величиной $\nu = 1/2$. Та же скэйлинговая гипотеза позволяет записать для диамагнитной восприимчивости общее соотношение:

$$\chi_{(3)} \sim -e^2 T \xi(T) \sim -\chi_P \epsilon^{-1/2} \begin{cases} 1, & \epsilon \gtrsim Gi \\ \left(\frac{\epsilon}{Gi}\right)^{1/2-\nu}, & \epsilon \lesssim Gi, \end{cases}$$

$$\chi_{(3c)} \left(T \gg T_c\right) \sim -e^2 T \xi(T) \sim -\chi_P$$

В двумерном случае выражение (1.10) применимо для оценки $\chi_{(2)}$, когда магнитное поле приложено перпендикулярно плоскости, позволяя флуктуационным куперовским парам вращаться в ней:

$$\chi_{(2c)}(T) \sim e^2 \frac{n}{m} < R^2 > \sim e^2 T \xi^2(T) \sim -\chi_P \frac{E_F}{T - T_c}.$$

$$\chi_{(\text{layer },\perp)}(\epsilon, H \to 0) \sim -e^2 T \frac{\xi_x(\epsilon)\xi_y(\epsilon)}{\max\{s, \xi_z(\epsilon)\}}$$

Из этой формулы очевидно существование кроссовера между $2D$ и $3D$ температурными режимами: по мере того, как температура приближается к T_c, зависимость диамагнитной восприимчивости от ϵ меняется с $1/\epsilon$ на $1/\sqrt{\epsilon}$. Это происходит тогда, когда приведенная температура достигает значения $\epsilon_{cr} = r\left(\xi_z\left(\epsilon_{cr}\right) \sim s\right)$. Параметр анизотропии:

$$r = \frac{4\xi_z^2(0)}{s^2} = \frac{J^2}{T} \begin{cases} \frac{\pi\tau}{4}, & T\tau \ll 1 \\ \frac{7\zeta(3)}{8\pi^2 T}, & T\tau \gg 1 \end{cases}$$

играет важную роль в теории слоистых сверхпроводников [5].

2.3.2. Флуктуационный диамагнетизм нульмерного образца

$$T_c(H) = T_c(0)\left(1 - \frac{4\pi^2\xi^2}{\Phi_0^2}\left\langle \mathbf{A}^2 \right\rangle\right)$$

По этой причине для описания сверхпроводящей гранулы в магнитном поле можно воспользоваться статистической суммой в той же форме (2.25), как и в его отсутствие, но с перенормированным параметром $a(H) = a + \frac{e^2}{m}\langle \mathbf{A}^2 \rangle$:

$$Z_{(0)}(H) = \pi \int d\,|\Psi_0|^2 \exp\left(-\frac{\left[a+\frac{e^2}{m}\left\langle \mathbf{A}^2\right\rangle\right]|\Psi_0|^2+\frac{b}{2V}|\Psi_0|^4}{T}\right) = \\ = \sqrt{\frac{\pi^3 VT}{2b}}\exp\left[\frac{a^2(H)V}{2bT}\right]\left\{1-\operatorname{erf}\left[a(H)\sqrt{\frac{V}{2bT}}\right]\right\}.$$

В области слабых флуктуаций $Gi_{(0)} \lesssim \epsilon$ для свободной энергии можно выписать асимптотическое выражение (2.27):

$$F_{(0)}(\epsilon, H) = -T\ln\frac{\pi}{\alpha\left(\epsilon + \frac{4\pi^2\xi^2}{\Phi_0^2}\langle \mathbf{A}^2\rangle\right)}$$

$$M_{(0)}(\epsilon, H) = -\frac{1}{V}\frac{\partial F_{(0)}(\epsilon, H)}{\partial H} = -\frac{6\pi T\xi^2}{5\Phi_0^2 d}\frac{H}{\left(\epsilon + \frac{\pi^2\xi^2}{10\Phi_0^2}H^2d^2\right)}$$

Легко видеть, что флуктуационная намагниченность отрицательна и линейно возрастает по абсолютной величине вплоть до некоторого поля кроссовера, при котором она достигает минимума. Это поле мы назовем температурно зависящим критическим полем гранулы $H_{c2(0)}(\epsilon) \sim \frac{\Phi_0}{d\xi(\epsilon)} \sim \sim \frac{\xi}{d}H_{c2}(0)\sqrt{\epsilon}$[7].

$$\chi_{(D)}(\epsilon) = -2\pi\frac{\xi T}{v_F}\chi_P\begin{cases}\frac{1}{\sqrt{\epsilon}}, & \text{проволока в параллельном}\\ \frac{2}{\sqrt{\epsilon}}, & \text{поле,}\\ \frac{d}{3\xi}\ln\frac{1}{\epsilon}, & \text{проволока в перпендикулярном}\end{cases}$$

2.3.3. Флуктуационный диамагнетизм в двумерном случае

$$F(\epsilon, H) = -\frac{SH}{\Phi_0}T\sum_{n,k_z}\ln\frac{\pi T}{\alpha T_c\epsilon + \omega_c\left(n+\frac{1}{2}\right)}.$$

Здесь S есть площадь сечения, перпендикулярного полю, а учет вырожденности уровней привел к появлению множителя HS/Φ_0, равного числу квантовых состояний, соответствующих определенной паре квантовых чисел n и k_z. Поскольку мы будем интересоваться лишь флуктуационным вкладом, сингулярным по степени близости системы к точке перехода, то, в интересующем нас случае тонкой пленки ($d \ll \xi_z(T)$), при суммировании по k_z в выражении (2.71) следует оставить лишь член с $k_z = 0$. Это приводит к появлению множителя $1/d$.

Выражение (2.51) удобно переписать, введя безразмерное магнитное поле:

$$h = \frac{\omega_c}{\alpha T_c} = \frac{eH}{2m\alpha T_c} = \frac{H}{\widetilde{H}_{c2}(0)}$$

после чего флуктуационная часть свободной энергии $2D$ сверхпроводника принимает вид:

$$F_{(2)}(\epsilon, H) = -\frac{TS}{2\pi\xi_{xy}^2}h\sum_{n=0}^{n_c-1}\ln\frac{\pi}{\alpha\left[\epsilon + 2h\left(n+\frac{1}{2}\right)\right]}$$

Мы ввели здесь удобное для нашего дальнейшего рассмотрения определение верхнего критического поля

$$\widetilde{H}_{c2}(0) = \frac{2m\alpha T_{\rm c}}{e} = \frac{\Phi_0}{2\pi\xi^2}$$

(??? дальше словами. Плюс указания на эти действия выше обязательно должны быть!!!)

2.4. Слоистый сверхпроводник в магнитном поле

2.4.1. Модель Лоуренса - Дониака

Обобщение функционала Гинзбурга - Ландау на случай слоистого сверхпроводника (функционал Лоуренса - Дониака, ЛД-функционал [50]) в перпендикулярном магнитном поле может быть записано в виде

$$\mathcal{F}_{LD}[\Psi] = \sum_l \int d^2r \left(a\left|\Psi_l\right|^2 + \frac{b}{2}\left|\Psi_l\right|^4 + \frac{1}{4m}\left|\left(\nabla_\parallel - 2ie\mathbf{A}_\parallel\right)\Psi_l\right|^2 + \mathcal{J}\left|\Psi_{l+1} - \Psi_l\right|^2 \right),$$

Ψ_l - параметр порядка в l-м сверхпроводящем слое, а феноменологический параметр $\mathcal{J}$ пропорционален энергии джозефсоновской связи между соседними слоями.

(дальше словами какие-то свойства напишу и указания на ходы. Вроде что-то похожее на типичные ходы дальше идет, но тут прямо специфика.)

2.4.2. Общая формула для флуктуационного вклада в свободную энергию в произвольном магнитном поле

(словами напишу, тут специфика)

2.4.3. Флуктуационная намагниченность и ее кроссоверы

2.4.4. Флуктуационная теплоемкость в магнитном поле

Дифференцирование общего выражения для флуктуационного вклада в свободную энергию слоистого сверхпроводника (2.74) по приведенной температуре позволяет найти наиболее сингулярную часть флуктуационной теплоемкости в магнитном поле:

$$C_{\rm LD}(\epsilon, h) = -\frac{1}{VT}\frac{\partial^2}{\partial^2\epsilon}F_{\rm LD}(\epsilon, h) = \frac{1}{4\pi s\xi_{xy}^2}\frac{1}{2h}\int\limits_0^{2\pi}\frac{d\theta}{2\pi}\psi^{(1)}\left(\frac{1}{2} + \frac{\widetilde{\epsilon}(\theta)}{2h}\right).$$

2.6. Скейлинг и ренормализационная группа

2.7. Влияние флуктуаций на сверхтекучую плот ность и критическую температуру
2.8. Флуктуации магнитного поля

16.7.3 Functional integral for Gor'kov and GL theories

(???)

Integral over Grassmann variables for SC

(!?!?)

A functional integral for a Fermi gas with attraction in an arbitrary channel. Effective action and functions of Gorkov.

Power decomposition of Δ: local terms.
The gradient term and the correlation length.

17 Very special theories and models

17.1 Very special SC junctions

(из "Applied Superconductivity: Josephson Effect and Superconducting Electronics" by Rudolf Gros)

17.1.1 Tight-biding models of SC junctions

(write here formulas from my master's thesis!)

17.1.2 Special Voltage States of JJ

(упрощенное это поставлю раньше! тут усложненные будут модели)

3.1 The Basic Equation of the Lumped Josephson Junction 90

3.1.1 The Normal Current: Junction Resistance 90 3.1.2 The Displacement Current: Junction Capacitance 92 3.1.3 Characteristic Times and Frequencies 93 3.1.4 The Fluctuation Current 94 3.1.5 The Basic Junction Equation 96

3.2 The Resistively and Capacitively Shunted Junction Model 97

3.2.1 Underdamped and Overdamped Josephson Junctions 100 3.3 Response to Driving Sources 102 3.3.1 Response to a dc Current Source 102 3.3.2 Response to a dc Voltage Source 107 3.3.3 Response to ac Driving Sources 107 3.3.4 Photon-Assisted Tunneling 112

3.4 Additional Topic: Effect of Thermal Fluctuations 115

3.4.1 Underdamped Junctions: Reduction of Ic by Premature Switching 117 3.4.2 Overdamped Junctions: The Ambegaokar-Halperin Theory 118

3.5 Secondary Quantum Macroscopic Effects 122

3.5.1 Quantum Consequences of the Small Junction Capacitance 122 3.5.2 Limiting Cases: The Phase and Charge Regime 125 3.5.3 Coulomb and Flux Blockade 128 3.5.4 Coherent Charge and Phase States 130 3.5.5 Quantum Fluctuations 132 3.5.6 Macroscopic Quantum Tunneling 133

3.6 Voltage State of Extended Josephson Junctions 139

3.6.1 Negligible Screening Effects 139 3.6.2 The Time Dependent Sine-Gordon Equation 140 3.6.3 Solutions of the Time Dependent Sine-Gordon Equation 141 3.6.4 Additional Topic: Resonance Phenomena

17.1.3 Fluctuation Effects in Weak Junctions

Тепловые флуктуации в джозефсоновском переходе, проскальзывание фазы и I(V,T).

Макроскопические квантовые эффекты: «туннелирование фазы» и переход в резистивное состояние.

Макроскопическая квантовая когерентность в СКВИДах.

17.1.4 SFS junctions

(много статей про это есть, нужно будет - выпишу все про это сюда)

SFS junctions Основные свойства

(нужно будет - начну с того, что из Шмидта выпишу, пока итак хватает занятий)

17.1.5 MTJJ methods and models

(maybe later I'll separate methods to the section above and here will be only their applications. currently it is fine)

MTJJ with QD

(copy of my masters)

MTJJ with general normal region

(copy of my masters)

Review of Multiterminal Topological Junctions

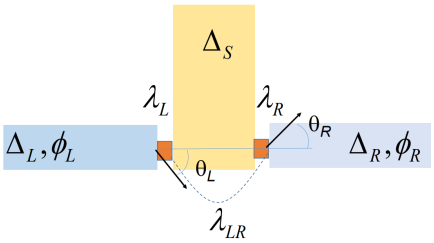


Figure 17.1: TS-S-TS junction setup. $\lambda_L, \lambda_r, \lambda_{LR}$ are the coupling strengths. Credit: [**?**].

$$H_t = \frac{1}{2}\Phi_L^\dagger W_{LR}\Phi_R + \sum_{j=L/R}\Psi^\dagger W_j \Phi_j + \text{h.c.},$$

$$\begin{aligned} W_{LR} &:= \lambda_{LR} e^{-i\sigma_z\phi/2}\sigma_z, \\ W_j &:= \lambda_j e^{i\sigma_z\phi_j/2}\mathrm{diag}(\alpha_j, -\beta_j^*) \\ \alpha_j &:= \cos(\theta_j/2) \\ \beta_j &:= \sin(\theta_j/2). \end{aligned}$$

$$\mathcal{G}^{-1}(\omega) = G^{-1}(\omega) - \Sigma(\omega), \tag{17.1}$$

$G := \mathrm{diag}(G_L, G_R)$

$$\Sigma_{LL/RR}(\omega) = -\frac{i\omega\lambda_{L/R}^2}{\sqrt{\omega^2+\Delta_S^2}}\,\sigma_0,$$

$$\Sigma_{LR}(\omega) = W_{LR} - \frac{\lambda_L\lambda_R}{\sqrt{\omega^2+\Delta_S^2}}\begin{pmatrix} i\omega\cos(\theta/2)e^{-i\phi/2} & \sin(\theta/2)\Delta_S e^{-i\tilde{\phi}/2} \\ -\sin(\theta/2)\Delta_S e^{i\tilde{\phi}/2} & i\omega\cos(\theta/2)e^{i\phi/2}\end{pmatrix},$$

$$I_j = -iT\ \mathrm{tr}\sum_\omega \sigma_z\left[\Sigma(\omega)\mathcal{G}(\omega)\right]_{jj}. \tag{17.2}$$

$I_{L/R}^{(\Delta_S\to\infty)}(\tilde{\phi}) = -\frac{\partial E_A}{\partial\tilde{\phi}}\tanh(E_A/2T)$
$E_A(\tilde{\phi}) := \sqrt{\tau(\theta)}\Delta_{TS}\cos(\tilde{\phi}/2)$

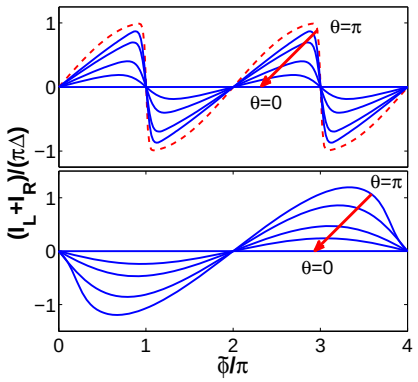


Figure 17.2: Current-phase relation of a TS-S-TS junction with fixed $\phi_L = \phi_R$ from [**?**]. The upper panel corresponds $\lambda_{LR} = 0$, the lower panel corresponds $\lambda_{LR} = 1$.

Review of Analysis of Multiterminal Josephson Junctions by Matute-Cañadas, et al.

$$H = \sum_\sigma \epsilon d_\sigma^\dagger d_\sigma + H_T + \sum_\nu H_\nu\,, \qquad H_T = \sum_{\nu,\sigma,k} t_\nu e^{-i\phi_\nu/2} d_\sigma^\dagger c_{\nu,k\sigma} + \text{h.c.}. \tag{17.3}$$

$$H^{\text{eff}} = \sum_\sigma \epsilon n_\sigma + U n_\uparrow n_\downarrow + \sum_{\nu=1}^{3}\left[\Gamma_\nu e^{-i\phi_\nu} d_\uparrow^\dagger d_\downarrow^\dagger + \text{h.c.}\right]. \tag{17.4}$$

$$H_{\text{even}}^{\text{eff}} \approx -(\epsilon+U/2)\tau_z + (\epsilon+U/2) + \sum_\nu \Gamma_\nu(\cos\phi_\nu\tau_x - \sin\phi_\nu\tau_y), \tag{17.5}$$

$$E_{0,1}(\{\phi_\nu\}) = -(\epsilon+U/2) \mp \sqrt{(\epsilon+U/2)^2 + \left|\sum_\nu \Gamma_\nu e^{-i\phi_\nu}\right|^2}. \tag{17.6}$$

$E_{0,1}(\phi_{12}) + \xi = \mp\sqrt{\xi^2+\Gamma^2}\sqrt{1 - T\sin^2(\phi_{12}/2)}$
$T := (\Gamma^2 - \delta\Gamma^2)/(\xi^2+\Gamma^2)$, where $\delta\Gamma := \Gamma_1 \pm \Gamma_2$.

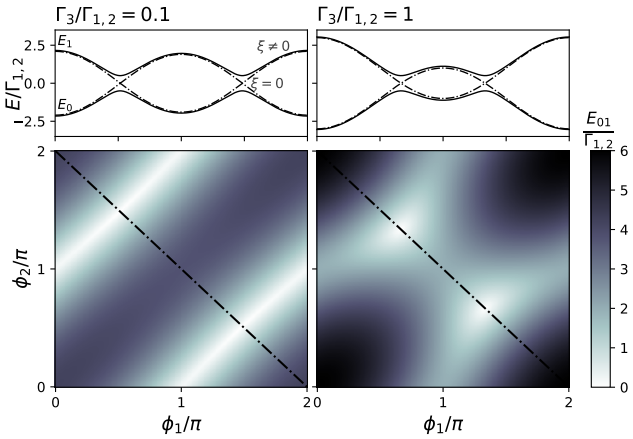


Figure 17.3: Top: transition energies $E_{0,1} := E_1 - E_0$ (up to a shift) of the Andreev states along the lines in the bottom diagrams, with solid (dash-dotted) lines; solid lines: $\epsilon + U/2 = 0.5\Gamma_{1,2}$; dot-dashed lines: $\epsilon = -U/2$. Bottom: E_{01} versus the phase differences $\phi_{1,2}$ for $\Gamma_1 = \Gamma_2$ and different Γ_3. Left: $\Gamma_3 \ll \Gamma_{1,2}$; right: $\Gamma_3 = \Gamma_1 = \Gamma_2$. Phase ϕ_3 is assumed equal to zero. Credit: [?].

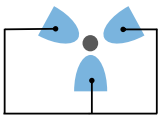
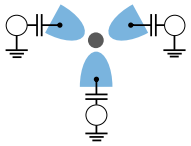
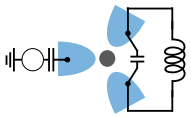
Configuration	Control parameters	Features
 Perfect phase bias	ϕ_{1e}, ϕ_{2e} ξ, Γ_ν	- Sensitivity of relaxation to phase drop distribution - Appearance of Weyl points - Connection with Bi-SQUID
 Charge islands	n_{g_ν} ξ, Γ_ν	- Mapping to a discrete lattice: platform for topology - Controllable disjointness
 Hybrid charge/flux	ϕ_e, n_{g_3} ξ, Γ_ν	- 0-π and bifluxon in the tunnel limit ⇕ - Simultaneous noise protection to relaxation and n_g, ϕ_e-dephasing

Table 1: Typical circuit configurations of possible three-terminal junctions. Here $\xi := \epsilon + U/2$ from the model in Eq. (17.4). Credit: [?].

17.1.6 Overview of other not so used methods for SC contacts

Andreeev's equation

$$|\varphi(\mathbf{r})\rangle = e^{i\mathbf{p}_F\cdot\mathbf{r}/\hbar}|\Psi_{\mathbf{p}}(\mathbf{r})\rangle$$

$$\left[\varepsilon\widehat{\tau}_3 - \widehat{\Delta}(\mathbf{p},\mathbf{r})\right]|\Psi_{\mathbf{p}}(\mathbf{r})\rangle + i\hbar\mathbf{v}_{\mathbf{p}}\cdot\left(\boldsymbol{\nabla} - i\frac{2e}{\hbar c}\mathbf{A}(\mathbf{r})\right)|\Psi_{\mathbf{p}}(\mathbf{r})\rangle = 0. \tag{17.7}$$

Here $\mathbf{p}_F$ is the Fermi momenta, $\widehat{\tau}_3$ is the third Pauli's matrix, $\mathbf{p} = p_F\hat{\mathbf{p}}$ and $\mathbf{v}_\mathbf{p} = v_F\hat{\mathbf{p}}$, $\mathbf{v}_\mathbf{p}$ is a Fermi momenta and velocity at different unit directions $\hat{\mathbf{p}}$, and $\widehat{\Delta}$ is a matrix with Δ parameters (it is different for different parity of the Cooper pairs). Finally, $|\Psi_\mathbf{p}(\mathbf{r})\rangle$ should ba understood as the Andreev spinor $|\Psi_\mathbf{p}(\mathbf{r})\rangle := \mathrm{col}\,(u_{\mathbf{p}\uparrow}(\mathbf{r})\ u_{\mathbf{p}\downarrow}(\mathbf{r})\ v_{\mathbf{p}\uparrow}(\mathbf{r})\ v_{\mathbf{p}\downarrow}(\mathbf{r}))$.

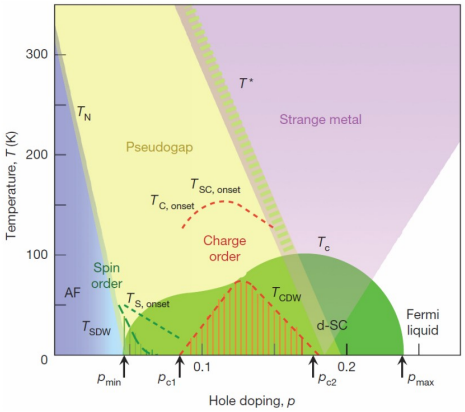
(see de Gennes book for example of application of it to the vortex. I don't know other applications of it.)

PPS's Green's functions method

(see my special note about it for now. it is a strange method, which is hard to use.)

17.2 Disorder in Superconductors in a Nutshell

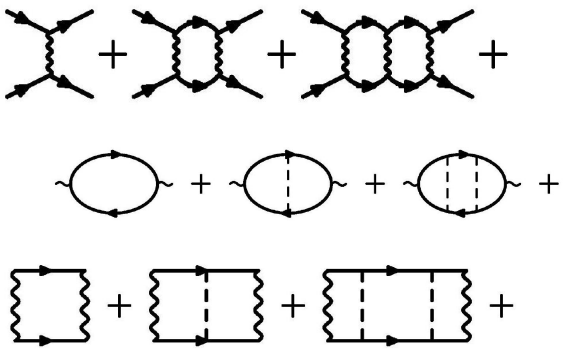
(нужно будет - прочитаю, сделаю потом подразделы)



Потенциальные примеси и их влияние на обычное s-спаривание.
Зависимость критических магнитных полей от беспорядка.
Спин-орбитальное примесное рассеяние и парамагнитный предел.
Нарушение T-инвариантности и распаривающий фактор.
Подавление сверхпроводимости магнитным полем. Бесщелевая сверхпроводимость.
Разрушение «необычных» сверхпроводящих фаз потенциальными примесями.

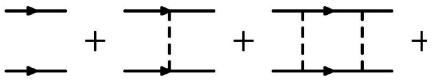
17.2.1 Disorder of superconductors: Basic Models

Теорема Андерсона.



$$\Gamma^C = -\frac{\lambda}{1+\lambda\Pi_c}$$

Π_c =



$$G\left(i\omega_n, \mathbf{p}\right) = \frac{1}{i\omega_n - \xi_p + \frac{1}{2\tau}\operatorname{sign}\omega_n}.$$

$$B_c\left(i\omega_n\right) = \int G\left(i\omega_n, \mathbf{p}\right) G\left(-i\omega_n, -\mathbf{p}\right) \frac{d^3p}{(2\pi)^3} = \int\limits_{-\infty}^{\infty} \frac{\nu_0 d\xi}{\left(\omega_n + \frac{1}{2\tau}\operatorname{sign}\omega_n\right)^2 + \xi^2} = \frac{2\pi\nu_0\tau}{1+2\tau\left|\omega_n\right|}$$

$$L\left(i\omega_n\right) = B_c\left(i\omega_n\right) + \frac{1}{2\pi\nu_0\tau}B_c^2\left(i\omega_n\right) + \ldots = \frac{B_c\left(i\omega_n\right)}{1 - B_c\left(i\omega_n\right)/\left(2\pi\nu_0\tau\right)} = \frac{\pi\nu_0}{\left|\omega_n\right|}$$

$$\langle n(\omega, \mathbf{q}) n(-\omega, -\mathbf{q})\rangle_{\mathbf{q}=0} = \pi\nu_0/(i\omega)$$

$$\Pi_c = -T\sum_{\omega_n} L\left(i\omega_n\right) = -2\pi\nu_0 T \sum_{\omega_n>0} \frac{1}{\left|\omega_n\right|} = -\nu_0 \ln\frac{2\gamma\omega_D}{\pi T}$$

$$T_c = \frac{2\gamma}{\pi}\omega_D e^{-1/\lambda\nu_0}$$

О методе матричных функций Грина и уравнении Намбу-Горькова

$$G_{\uparrow\uparrow}(r_1, r_2, \tau_1, \tau_2) = -\left\langle \mathrm{T}_\tau \psi_\uparrow(r_1, \tau_1)\psi_\uparrow^+(r_2, \tau_2)\right\rangle,$$
$$G_{\downarrow\downarrow}(r_1, r_2, \tau_1, \tau_2) = -\left\langle \mathrm{T}_\tau \psi_\downarrow(r_1, \tau_1)\psi_\downarrow^+(r_2, \tau_2)\right\rangle,$$

и, аналогично, $F_{\uparrow\downarrow}, F_{\downarrow\uparrow}$.

$$\widehat{G}_\omega\left(r_1, r_2\right) := \left[\begin{array}{cc} G_{\uparrow\uparrow} & F_{\uparrow\downarrow} \\ F_{\downarrow\uparrow} & G_{\downarrow\downarrow} \end{array}\right]$$

$$\left(i\omega - \tau_z\xi(\widehat{\mathbf{p}}) - \frac{1}{2}\left(\Delta\left(r_1\right)\tau_+ + \Delta^*\left(r_1\right)\tau_-\right)\right)\widehat{G}_\omega\left(\mathbf{r}_1, \mathbf{r}_2\right) = \widehat{\delta}\left(\mathbf{r}_1 - \mathbf{r}_2\right)$$

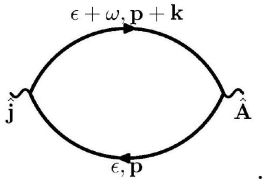
$$G_{\alpha\beta}(\varepsilon, \mathbf{p}) = G^0_{\alpha\beta}(\varepsilon, \mathbf{p}) + G^0_{\alpha\lambda}(\varepsilon, \mathbf{p})\Delta^*_{\lambda\mu}F_{\mu\beta}(\varepsilon, \mathbf{p})$$
$$F_{\alpha\beta}(\varepsilon, \mathbf{p}) = G^0_{\alpha\lambda}(-\varepsilon, \mathbf{p})\Delta_{\lambda\mu}G_{\mu\beta}(\varepsilon, \mathbf{p})$$

$$\widehat{\mathbf{j}}(\mathbf{r}) = c\frac{\delta}{\delta\mathbf{A}(\mathbf{r})}\widehat{G}^{-1}[\mathbf{A}(\mathbf{r})]$$

Лондоновская длина в сплаве

$$\langle\widehat{G}(i\omega p)\rangle = \left(\widehat{G}_0(i\omega\mathbf{p})^{-1} + \frac{i\omega - \Delta\tau_x}{2\tau\left(\omega^2 + \Delta^2\right)^{1/2}}\right)^{-1}$$

$\Delta^* = \Delta$.
$\widehat{G}_0^{-1}(i\omega\mathbf{p}) = i\omega - \tau_z\xi(\mathbf{p}) - \Delta\tau_x$.



.

$\mathrm{Tr}(\widehat{j}\widehat{G}\widehat{j}\widehat{G})\ Q(\mathbf{k})\ Q(\mathbf{k}=0)$.

65 a.



$$nu_0^2 \begin{pmatrix} 1 & 0 \\ 0 & 1 \end{pmatrix} = \frac{1}{2\pi\nu_0\tau}\widehat{1}$$

$$\widehat{\Sigma}\left(i\omega_n\right) = \frac{1}{2\pi\nu_0\tau}\int \widehat{G}\left(i\omega_n \mathbf{p}\right)\frac{d^3p}{(2\pi)^3} = -\frac{1}{2\pi\nu_0\tau}\int \frac{i\omega_n\widehat{1}+\xi_{\mathbf{p}}\widehat{\tau}_z-\Delta\widehat{\tau}_x}{\omega_n^2+\Delta^2+\xi_{\mathbf{p}}^2}\frac{d^3p}{(2\pi)^3} = -\frac{1}{2\tau}\frac{i\omega_n\widehat{1}+\Delta\widehat{\tau}_x}{\sqrt{\omega_n^2+\Delta^2}}$$

$$\widehat{G}^{-1} = \widehat{G}_0^{-1} - \widehat{\Sigma} = i\tilde{\omega}_n\widehat{1} - \xi\widehat{\tau}_z - \tilde{\Delta}\widehat{\tau}_x$$

$$\tilde{\omega}_n = \omega_n\left(1+\frac{1}{2\tau\sqrt{\omega_n^2+\Delta^2}}\right); \qquad \tilde{\Delta} = \Delta\left(1+\frac{1}{2\tau\sqrt{\omega_n^2+\Delta^2}}\right)$$

$$\tilde{\omega}_n/\tilde{\Delta} = \omega_n/\Delta$$

$\Delta_{\alpha\beta} = \lambda\int F_{\alpha\beta}(\varepsilon\mathbf{p})\frac{d\varepsilon d^3p}{(2\pi)^4}$

$$\Delta = \lambda T\sum_{\omega_n}\int_{-\infty}^{\infty}\frac{\nu_0 d\xi\tilde{\Delta}}{\tilde{\omega}_n^2+\tilde{\Delta}^2+\xi^2}$$

$$\Delta = \pi\lambda\nu_0 T\sum_{\omega_n}\frac{\tilde{\Delta}}{\sqrt{\tilde{\omega}_n^2+\tilde{\Delta}^2}} = \pi\lambda\nu_0 T\sum_{\omega_n}\frac{\Delta}{\sqrt{\omega_n^2+\Delta^2}}$$

65 .

$\omega_n \to \tilde{\omega}_n; \Delta \to \tilde{\Delta}$.

$$\frac{n-n_s}{n} = T\sum_{\omega_n}\int_{-\infty}^{\infty}\frac{\xi^2+\tilde{\Delta}-\tilde{\omega}_n^2}{\left(\xi^2+\tilde{\Delta}+\tilde{\omega}_n^2\right)^2}d\xi$$

$$\frac{n_s}{n} = \pi T\sum_{\omega_n}\frac{\tilde{\Delta}^2}{\left(\tilde{\omega}^2+\tilde{\Delta}^2\right)^{3/2}}$$

$$\frac{n_s}{n} = \pi T\sum_{\omega_n}\frac{\Delta^2}{\left(\omega_n^2+\Delta^2\right)^{3/2}\left(1+\frac{1}{2\tau\sqrt{\omega_n^2+\Delta^2}}\right)}.$$

$\tau\Delta_0 \gg 1$
$\tau\Delta_0 \ll 1$

$$\frac{n_s}{n} = 2\pi\tau T \sum_{\omega_n} \frac{\Delta^2}{\left(\omega_n^2 + \Delta^2\right)^2} = \pi\tau\Delta \,\mathrm{th}\, \frac{\Delta}{2T}.$$

$$\frac{n_s(T \to 0)}{n} = \pi\tau\Delta_0 \ll 1$$

$$\delta_\Lambda = \frac{1}{2\pi}\sqrt{mc^2/\left[e^2\Delta\tau \,\mathrm{th}(\Delta/2T)\right]}$$

Влияние магнитных примесей на сверхпроводимость.

$$H_{int} = \sum_{\mathbf{r}_a} J\psi^+\left(\mathbf{r}_a\right)\widehat{\sigma}^k\widehat{S}_a^k\psi\left(\mathbf{r}_a\right)$$

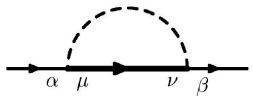
$n \approx T_c/(v_F\sigma)$

66.

$$\widehat{G} = -\begin{pmatrix} \langle \mathrm{T}_\tau\psi_\alpha^+(\mathbf{r}\tau)\psi_\beta(00)\rangle & \langle \mathrm{T}_\tau\psi_\alpha(\mathbf{r}\tau)\psi_\beta(00)\rangle \\ \left\langle \mathrm{T}_\tau\psi_\alpha^+(\mathbf{r}\tau)\psi_\beta^+(00)\right\rangle & \left\langle \mathrm{T}_\tau\psi_\alpha(\mathbf{r}\tau)\widehat{\psi}_\beta^+(00)\right\rangle \end{pmatrix}$$

$$\widehat{G}_0 = -\frac{1}{\omega_n^2 + \xi^2 + \Delta^2}\begin{pmatrix} \left(i\omega_n + \xi\right)\delta_{\alpha\beta} & -\Delta_{\alpha\beta} \\ -\Delta_{\alpha\beta}^+ & \left(i\omega_n - \xi\right)\delta_{\alpha\beta} \end{pmatrix}$$

$\Delta_{\alpha\beta} = i\Delta\sigma_{\alpha\beta}^y$.



$$\left\langle \sum_a J\delta\left(\mathbf{r} - \mathbf{r}_a\right)\sigma_{\alpha\beta}^i S_i^a \sum_b J\delta\left(\mathbf{r}' - \mathbf{r}_b\right)\sigma_{\mu\nu}^k S_k^b \right\rangle = n_{\mathrm{mag}} J^2\delta\left(\mathbf{r} - \mathbf{r}'\right)\left\langle S^i S^k\right\rangle \sigma_{\alpha\beta}^i\sigma_{\mu\nu}^k =$$
$$= \frac{S(S+1)}{3} n_{\mathrm{mag}} J^2\delta\left(\mathbf{r} - \mathbf{r}'\right)\sigma_{\alpha\beta}^i\sigma_{\mu\nu}^i$$

$\sigma_{\alpha\beta}^i\sigma_{\mu\nu}^i = 2\delta_{\alpha\nu}\delta_{\beta\mu} - \delta_{\alpha\beta}\delta_{\mu\nu}$,

$$\widehat{\Sigma}_{\alpha\beta}\left(i\omega_n\right) = -\frac{n_{\mathrm{mag}}}{3} J^2 S(S+1)\left(2\delta_{\alpha\beta}\delta_{\mu\nu} - \delta_{\alpha\mu}\delta_{\beta\nu}\right)\int_{-\infty}^{\infty}\widehat{G}_{\mu\nu}\left(i\omega_n\xi\right)\nu_0 d\xi$$

$$\widehat{\Sigma}_{\alpha\beta}\left(i\omega_n\right) = -\frac{1}{2\pi\tau_s}\frac{i\omega_n\widehat{1} - 2\delta_{\alpha\beta}\Delta_{\mu\nu}\delta_{\mu\nu}\widehat{\tau}_x + \Delta_{\alpha\beta}\widehat{\tau}_x}{\sqrt{\omega_n^2 + \Delta^2}}$$

$\tau_s = \frac{3}{\pi\nu_0 n_{\mathrm{mag}} J^2 S(S+1)}$
$\Delta_{\mu\nu}\delta_{\mu\nu} = 0$
$\widehat{G}^{-1} = \widehat{G}_0^{-1} - \widehat{\Sigma}$

$$\tilde{\omega}_n = \omega_n \left(1 + \frac{1}{2\tau_s \sqrt{\omega_n^2 + \Delta^2}}\right) \quad \tilde{\Delta} = \Delta \left(1 - \frac{1}{2\tau_s \sqrt{\omega_n^2 + \Delta^2}}\right)$$

$$\tilde{\omega}/\tilde{\Delta} \neq \omega/\Delta.$$

$$\widehat{\Sigma}_{\alpha\beta}\left(i\omega_n\right) = -\frac{1}{2\pi\tau_s} \frac{i\tilde{\omega}_n \widehat{1} - \tilde{\Delta}_{\alpha\beta}\widehat{\tau}_x}{\sqrt{\tilde{\omega}_n^2 + \tilde{\Delta}^2}}.$$

$$\tilde{\omega} = \omega + \frac{\tilde{\omega}}{2\tau_s \sqrt{\tilde{\omega}^2 + \tilde{\Delta}^2}}, \qquad \tilde{\Delta} = \Delta - \frac{\tilde{\Delta}}{2\tau_s \sqrt{\tilde{\omega}^2 + \tilde{\Delta}^2}}.$$

$$\Delta = \lambda T \sum_{\omega_n} \int_{-\infty}^{\infty} \nu_0 d\xi F\left(i\omega_n \xi\right) = \lambda T \sum_{\omega_n} \int_{-\infty}^{\infty} \frac{\tilde{\Delta}\nu_0 d\xi}{\tilde{\omega}_n^2 + \tilde{\Delta}^2 + \xi^2} = \pi\lambda\nu_0 T \sum_{\omega_n} \frac{\tilde{\Delta}}{\sqrt{\tilde{\omega}_n{}^2 + \tilde{\Delta}^2}}.$$

$$\tilde{\omega} = \omega + \frac{1}{2\tau_s} \operatorname{sign} \omega \quad \tilde{\Delta}\left(1 + \frac{1}{2\tau_s|\tilde{\omega}|}\right) = \Delta.$$

$$1 = 2\pi\lambda\nu_0 T_c^* \sum_{\omega_n > 0} \frac{\tilde{\Delta}}{\Delta\tilde{\omega}_n} = 2\pi\lambda\nu_0 T_c^* \sum_{\omega_n > 0} \frac{1}{\tilde{\omega}_n + 1/2\tau_s} = 2\pi\lambda\nu_0 T_c^* \sum_{\omega_n > 0} \frac{1}{\omega_n + 1/\tau_s}.$$

τ_s h/T_c^* T_c. $\tau_s \approx \hbar/T_c^*$. τ_s^* $T_c^* = 0$

$$\frac{1}{\lambda\nu_0} = \ln \frac{2\gamma\omega_D}{\pi T_c} = \int_0^{\omega_D} \frac{d\omega}{\omega + 1/\tau_s^*} = \ln\left(\omega_D \tau_s^*\right)$$

$$\tau_s^* = 2\gamma\hbar/\left(\pi T_c\right)$$

Верхнее критическое поле в грязном сверхпроводнике

(???)
Proof:

$$B_c = \iint \frac{d\Omega}{4\pi} \frac{\nu_0 d\xi}{\left(i\omega - \xi + \frac{i}{2\tau}\operatorname{sign}\omega\right)\left(-i\omega - \xi + \mathbf{sv} - \frac{i}{2\tau}\operatorname{sign}\omega\right)} = \int \frac{d\Omega}{4\pi} \frac{2\pi\nu_0\tau}{1 + 2|\omega|\tau + i\tau\mathbf{sv}} =$$
$$= \frac{2\pi\nu_0\tau}{1 + 2|\omega|\tau + \tau D\mathbf{s}^2}$$

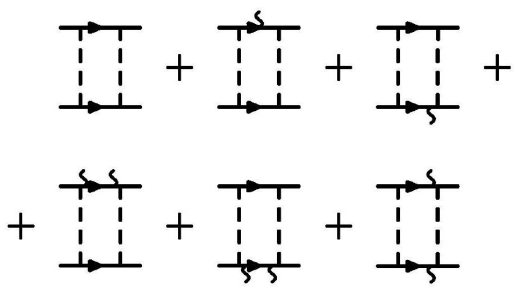
$$C_\omega(\mathbf{s}) = \frac{B_c}{1 - B_c/2\pi\nu_0\tau} = \frac{2\pi\nu_0}{2|\omega| + D\mathbf{s}^2}$$

$\mathbf{p} \to \mathbf{p} - e\mathbf{A}/c$

$$\widehat{C}_\omega = \frac{2\pi\nu_0}{2|\omega| + D\left(\mathbf{s} - \frac{2e}{c}\mathbf{A}\right)^2}.$$

$$\left[2|\omega| + D\left(-i\frac{\partial}{\partial\mathbf{r}} - \frac{2e}{c}\mathbf{A}\right)^2\right] C_\omega\left(\mathbf{r}\mathbf{r}'\right) = 2\pi\nu_0\delta\left(\mathbf{r} - \mathbf{r}'\right).$$

$$\left[2|\omega| + D\left(-i\frac{\partial}{\partial\mathbf{r}} - \frac{2e}{c}\mathbf{A}(\mathbf{r})\right)^2\right] C_\omega\left(\mathbf{r}\mathbf{r}'\right) = 2\pi\nu_0\delta\left(\mathbf{r} - \mathbf{r}'\right).$$



$$\Delta(\mathbf{r}) = \lambda \int\limits_{-\infty}^{\infty} F(\omega \mathbf{r}\mathbf{r}) \frac{d\omega}{2\pi}$$



$$F(\omega \mathbf{r}\mathbf{r}) = \int \Delta\left(\mathbf{r}'\right) C_\omega\left(\mathbf{r}\mathbf{r}'\right) d^3 r'$$

$$\Delta(\mathbf{r}) = \lambda \int\limits_{-\infty}^{\infty} \frac{d\omega}{2\pi} \int C_\omega\left(\mathbf{r}\mathbf{r}'\right) \Delta\left(\mathbf{r}'\right) d^3 r'$$

$$D\left(-i\frac{\partial}{\partial \mathbf{r}} - \frac{2e}{c}\mathbf{A}(\mathbf{r})\right)^2 \varphi_n(\mathbf{r}) = \mu_n \varphi_n(\mathbf{r})$$

$$\int \varphi_n(\mathbf{r}) \varphi_m^*(\mathbf{r}) d^3 r = \delta_{nm}$$

$$\Delta(\mathbf{r}) = \sum_n \Delta_n \varphi_n(\mathbf{r})$$

$$C_\omega\left(\mathbf{r}\mathbf{r}'\right) = 2\pi\nu_0 \sum_n \frac{\varphi_n(\mathbf{r}) \varphi_n^*\left(\mathbf{r}'\right)}{2|\omega| + \mu_n}$$

$$\Delta_n = \int\limits_{-\infty}^{\infty} \frac{2\pi\nu_0 \lambda \Delta_n}{2|\omega| + \mu_n} \frac{d\omega}{2\pi}.$$

$$\frac{1}{\nu_0 \lambda} = \int\limits_{-\infty}^{\infty} \frac{d\omega}{2|\omega| + \mu_n}$$

$\omega = \omega_D$.

$$\frac{1}{\nu_0 \lambda} = \ln \frac{2\omega_D}{\mu_n}.$$

$$E_n = \omega_H \left(n + \frac{1}{2}\right) + \frac{\hbar^2 k_z^2}{2m}; \quad \omega_H = \frac{qH}{mc}.$$

$$\mu_n = \frac{4DeH}{c}\left(n + \frac{1}{2}\right) + Dk_z^2.$$

$\mu_0 = 2DeH/c.$

$$\frac{1}{\nu_0\lambda} = \ln\frac{\omega_D c}{DeH_{c2}}.$$

$$H_{c2} = \frac{\pi}{2\gamma}\frac{T_c c}{De} = \frac{\pi}{\gamma}\frac{T_c}{\hbar D}\Phi_0$$

$\Phi_0 = \hbar c/2e$

$$\varphi_{nk_y}(xyz) = \frac{1}{\pi^{1/4}l_H^{1/2}}e^{ik_y y}e^{-(x-x_0)^2/2l_H^2}$$

$$l_H = \sqrt{\hbar c/(qH)} \quad x_0 = ck_y/(qH).$$

$$E_{\text{mag}} = H^2/8\pi$$

$$E_c \approx \nu_0\Delta^2 \approx \nu_0 T_c^2$$

$$H_c \approx T_c\sqrt{\nu_0}$$

$$\frac{H_c}{H_{c2}} \approx \sqrt{De\nu_0}c \approx \frac{v_F l\sqrt{mp_F/\hbar^3}}{c} \approx l\sqrt{\frac{e^2p_F^3}{mc^3\hbar^3}} \approx \frac{l}{\delta_\Lambda}$$

17.2.2 Superconductor-insulator Phase Transition

(a widely discussed topic)

Most Important Experimental Facts

(?? see some artivles about it, not important for now)

17.2.3 2D Superconductors

(there are a lot of experiments about it, I'll write later)

17.2.4 Materials with Localization and SC

(SC when there is a lot of disorder, the wf are localized. this is a research topic. how to combine BCS and localization?)

17.2.5 Superconductivity of a Graph

(see Feigelman's article)

Main Experimental Parameters

(remember what Khvaluk told me)

Main Experimental Facts for Materials

(see what Feigelman wrote)
And this is the only thing that we can describe by this whole theory.

Main Methods of the Theory

(main idea of Feigelman's theory)

17.3 Less currently applicable, but potentially useful theories

17.3.1 Kitaev's 1D chain

17.3.2 Majorana Fermions in a Superconductors

(много статей про это есть, выпишу что-то важное)

On Quantizing Majorana Fermions in a Superconductor C. Chamon, R. Jackiw, Y. Nishida, S.-Y. Pi, L. Santos

(выпишу основные потом формулы)

17.3.3 London's theory

(допишу потом, даже не знаю, где это нужно в настоящее время)

Уравнения Лондонов в двух словах

$$\mathbf{B} + \lambda_L^2 \text{ rot } \text{rot}\, \mathbf{B} = 0 \qquad \text{(ур. Лондонов)}$$

Суть их в том, что (?? мы описываем нелинейную электродинамику в сверхпроводнике??)
(!?!? абзац про связь их с ур Максвелла?? так и не додумал, потом додумаю!)
Получаются уравнения Лондонов так:

$$\text{rot}\, \mathbf{B} = \frac{4\pi}{c}\mathbf{j}_s, \qquad \mathbf{j}_s(\mathbf{r}) := n_s e \mathbf{v}(\mathbf{r})$$
$$\text{div}\, \mathbf{B} = 0.$$

$$\mathcal{F} = \int F_s dV + E_{kin} + E_{\text{mag}}\,,$$

$$E_{kin} = \frac{1}{2}\int n_s m v^2 dV = \frac{1}{2}\int n_s m \left(\frac{c}{4\pi n_s e}\,\text{rot}\,\mathbf{B}\right)^2 dV,$$

$$E_{\text{mag}} = \int \frac{\mathbf{B}^2}{8\pi} dV$$

В итоге:

$$\mathcal{F} = \int dV \left[\mathcal{F}_s + \frac{1}{8\pi}\left(\mathbf{B}^2 + \lambda_L^2 (\text{rot}\,\mathbf{B})^2\right)\right], \qquad \lambda_L := \left(\frac{mc^2}{4\pi n_s e^2}\right)^{1/2} \sim 10^{-5} \div 10^{-6}\text{cm}.$$

Варьируем (????), получаем уравнение Лондонов:

$$\mathbf{B} + \lambda_L^2 \text{ rot } \text{rot}\, \mathbf{B} = 0$$

(тут еще калибровку можно сделать, кстати.(????))

$$\text{rotrot}\, \mathbf{A} = -\frac{1}{\lambda_L^2}\mathbf{A},$$

О границе применимости уравнений Лондонов (????)

(напишу четко потом)

Вывод уравнений Лондонов и их свойств

(выпишу из Шмидта, все про них)

6. Глубина проникновения магнитного поля по Лондонам

Лондоновская глубина проникновения для некоторых сверхпроводников по Шмидту, со ссылкой на [Линтон Э. Сверхпроводимость. М.: Мир, 1971.]:

Элемент	Al	Cd	Hg	In	Nb	Pb	Sn	Tl
$\lambda(0), \text{Å}$	500	1300	$380 \div 450$ (анизотропия)	640	470	390	510	920

(?!!! проверю расчетами!)

Нелокальная электродинамика сверхпроводников по Шмидту

В общем виде нелокальная связь между j_s и $\mathbf{A}$ может быть записана в виде

$$\mathbf{j}_s(\mathbf{r}) = \int \widehat{Q}\left(\mathbf{r}-\mathbf{r}'\right)\mathbf{A}\left(\mathbf{r}'\right)d\mathbf{r}',$$

$\widehat{Q}$ - некоторый оператор, который, действуя на вектор $\mathbf{A}$, превращает его в вектор $\widehat{Q}\mathbf{A}$. Радиус действия оператора $\widehat{Q}(\mathbf{r}$ - $\mathbf{r}')$ берется равным ξ_0, т.е. $\widehat{Q}\left(\mathbf{r}-\mathbf{r}'\right)$ отличен от нуля только при $|\mathbf{r}-\mathbf{r}'| \lesssim \xi_0$. Так происходит усреднение действия вектора $\mathbf{A}$ на частицу (носитель сверхтока) больших размеров. Если этот размер устремить к нулю, то $\widehat{Q}$ превратится в δ-функцию, и мы вернемся к локальной электродинамике. Пиппард предложил $\widehat{Q}\mathbf{A}$ выбрать в виде

$$\widehat{Q}\left(\mathbf{r}-\mathbf{r}'\right)\mathbf{A}\left(\mathbf{r}'\right) = -\frac{3n_s e^2}{4\pi mc\xi_0}\frac{\left(\mathbf{r}-\mathbf{r}'\right)}{\left(\mathbf{r}-\mathbf{r}'\right)^4}\left(\mathbf{A}\left(\mathbf{r}'\right),\mathbf{r}-\mathbf{r}'\right)e^{-|\mathbf{r}-\mathbf{r}'|/\xi_0}$$

$$\lambda = \frac{1}{H_0}\int\limits_0^\infty H dx.$$

$H_0 = H_{\text{surface}}$

$$\mathbf{j}_s = -\frac{c}{4\pi\lambda^2}\frac{\lambda_{\mathrm{P}}}{\xi_0}\mathbf{A}.$$

$$= -\frac{c}{4\pi\lambda_{\mathrm{P}}^2}\mathbf{A},$$

$$\lambda_{\mathrm{P}} \simeq \left(\lambda^2\xi_0\right)^{1/3}.$$

Квантовое обобщение уравнения Лондонов. Квантование магнитного потока по Лондонам

$$\hbar\nabla\theta = 2m\mathbf{v}_s + \frac{2e}{c}\mathbf{A}$$

$$\mathbf{j}_s = n_s e\mathbf{v}_s$$

$$\mathbf{j}_s = \frac{1}{c\Lambda}\left(\frac{\Phi_0}{2\pi}\nabla\theta - \mathbf{A}\right)$$

$$\frac{\Phi_0}{2\pi}\oint_C \nabla\theta d\mathbf{l} = \oint_C \mathbf{A}d\mathbf{l}.$$

$$\oint_C \mathbf{A}d\mathrm{l} = \Phi,$$

$$\Phi = (\Phi_0/2\pi)\oint_C \nabla\theta d\mathbf{l}.$$

$$\Phi = n\Phi_0,$$

$$\Phi_0 = \frac{\pi\hbar c}{e} = \frac{hc}{2e}.$$

17.3.4 London equations, consequences

(все указания про них - тут. из Кириченко выпишу всё, когда дойду)

Пока считаю, что это почти бесполезная теория, окей, объясняет диамагнетизм, и не знаю, что больше из неё можно получить.

- The London equation

$$\mathbf{j} = -\frac{c}{4\pi\lambda_L^2}\mathbf{A} \quad \Leftrightarrow \quad \operatorname{curl}\mathbf{j} = -\frac{c}{4\pi\lambda_L^2}\mathbf{B}$$

leads to the Meissner effect through the penetration equation $\nabla^2 B = B/\lambda_L^2$, where $\lambda_L \approx (mc^2/4\pi ne^2)^{1/2}$ is the London penetration depth.

- In the London equation $\mathbf{A}$ or $\mathbf{B}$ should be a weighted average over the coherence length ξ. The intrinsic coherence length $\xi_0 = 2\hbar v_p/\pi E_g$.

17.3.5 On 1D superconductors

(есть статья Бычкова Горькова Дзялошинского, мб когда-то отвечу на этот вопрос. Говорят, что она может быть, но это спорно и при сильном кулоновском взаимодействии (???))

17.3.6 BCS-BEC Crossover

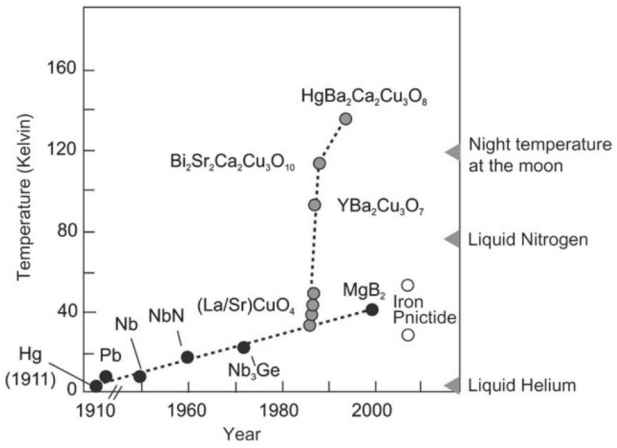
(??? what is it???)

17.4 High-T SC

(нужно будет - прочитаю, сделаю потом подразделы)

High-T SC: main methods

Overview of high-T sup cond



Compound	T_C(K)
$La_{2-x}Sr_xCuO_4$	38
$YBa_2Cu_3O_{7-x}$	92
$Bi_2Sr_2CaCu_2O_{8+x}$	110
$Tl_2Ba_2Ca_2Cu_3O_{10+x}$	125
$HgBa_2Ca_2Cu_3O_{8+x}$	133

(ниже пара тем курса “Введение в сверхпроводимость” от КАФЕДРы ФИЗИКИ НИЗКИХ ТЕМПЕРАТУР И сверхпроводимости МГУ)

№16, 2 часа.

Квазидвумерные и квазиодномерные системы.

Усиление электрон–фононного взаимодействия в системах с переменной валентностью.

Нефононные механизмы сверхпроводимости.

d-спаривание.

Высокотемпературная сверхпроводимость.

№17, 2 часа.

Высокотемпературные сверхпроводники на основе оксидов меди и их основные характеристики.

Аномалии нормального состояния купратов.

Температура сверхпроводящего перехода, длина когерентности и пространственная анизотропия.

Природа электронного спаривания и симметрия сверхпроводящего параметра порядка в ВТСП купратах.

№18, 2 часа.

Двухщелевая сверхпроводимость в MgB2 и твердых растворах на его основе.

Пниктиды железа – новый класс высокотемпературных сверхпроводников на основе слоистых соединений железа.

Сопоставление свойств ВТСП купратов, сверхпроводников на основе MgB2 и железосодержащих сверхпроводников

Main materials for high-T SC

18 Overview of special phenomena and applications

18.1 Other Phenomena In a Nutshell

18.1.1 Thermoelectric Effects in Superconductors

Эффект Зеебека в сверхпроводнике и возможность его измерения.

«Сверхпроводящая термопара» и магнитный поток в ней.

Эффект Нернста в смешанном состоянии сверхпроводника и проблема энтропии, приходящейся на один вихрь.

Флуктуационный эффект Нернста выше точки перехода.

18.1.2 Vortex Lattice Melting and Pinning in a Nutshell

Вихрь в потенциале точечных дефектов.

Скейлинговые соотношения.

Решетка вихрей: упругие модули.

Плавление решетки вихрей тепловыми флуктуациями.

Разрушение дальнего порядка решетки примесями и критический ток.

Крип магнитного потока и нелинейная проводимость в ВТСП.

18.1.3 Fluctuation Effects by Varlamov, Larkin in a Nutshell (????)

(по Варламову Ларкину, I'll write the most important concepts)

Fluctuations in Nanostructures and Special Superconducting Systems (????)

(по Варламову Ларкину. их часть 4. там огромное задротство)

18.1.4 Other Magnetic Phenomena

(пока как-то не актуально про них думать, но слышал про них)

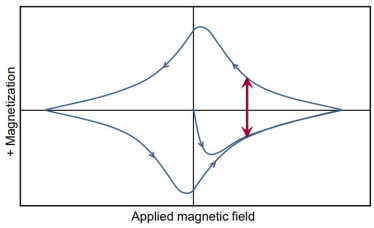
Magnetization curve of hard superconductors

(я не понял это, когда-то подумаю еще раз, все равно никакими формулами нас не обучали)

If flux lines are pinned in hard superconductors, their thermodynamic equilibrium positions can not settle, which results in irreversible magnetization curves with higher magnetization values.

Close relation between irreversible magnetization and critical current The 'Bean critical state model"' explains that under certain assumptions:

$$|M(B_a)| \sim \boldsymbol{j_c}(\boldsymbol{B_a})$$



18.1.5 On induced superconductivity of 2D materials (???)

(maybe I'll look later)

18.2 Superconductivity for quantum computation (???)

(тут очень многое можно указать потом)

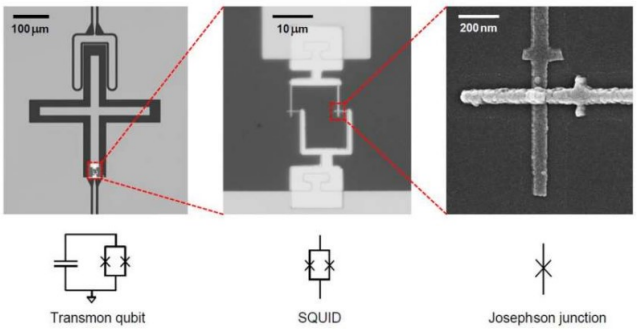
18.3 Applications of superconductivity

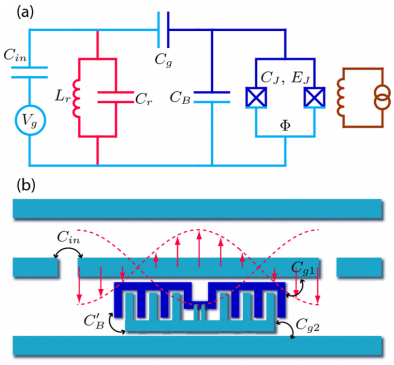
(из Applied Superconductivity: Josephson Effect and Superconducting Electronics by Prof. Dr. Rudolf Gross, пока не актуально в этом разбираться.)

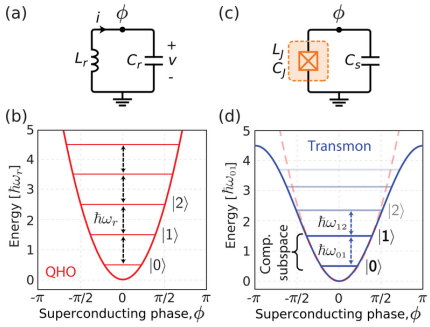
18.3.1 On superconductivity for qubits and quantum computers

(это же в кв теор инф)

Transmon qubits







LC circuit $E_{tot} = \frac{Q^2}{2C} + \frac{1}{2L}\Phi^2 = \frac{1}{2}C\dot{\Phi}^2 + \frac{1}{2}C\frac{1}{LC}\Phi^2 \quad \widehat{H} = \frac{Q^2}{2C} + \frac{1}{2L}\widehat{\Phi}^2$

$$E_n = \hbar\omega_0\left(n + \frac{1}{2}\right) \quad \omega_0 = \frac{1}{\sqrt{LC}}$$

Non-linear inductance $L_J = \frac{\hbar}{2eI_c\cos(\varphi)} = \pm L_c \frac{1}{\cos(\varphi)}$ Energy in JJ $E = E_J[1-\cos(\varphi)]$ $E_J \equiv \frac{\Phi_0}{2\pi} I_c$ $E_c = e^2/2C$ Transmon

$$\widehat{H} = \frac{\hat{Q}^2}{2C} + E_J[1-\cos(\hat{\varphi})]$$
$$\widehat{H} = 4E_c\hat{n}^2 + E_J[1-\cos(\hat{\varphi})] \qquad hf_{01} \approx \sqrt{8E_JE_c} - E_c$$
$$\widehat{H} = 4E_c\hat{n}^2 + E_J\frac{\widehat{\varphi}^2}{2} - E_J\frac{\widehat{\varphi}^4}{24} + \cdots \qquad hf_{12} \approx hf_{01} - E_c$$

Time dependence

$$|\Psi(t)\rangle = c_0(t)e^{-\frac{i\varepsilon_0 t}{\hbar}}|0\rangle + c_1(t)e^{-\frac{i\varepsilon_1 t}{\hbar}}|1\rangle$$
$$c_0(t) = e^{-i\Delta t/2}\left[\cos\frac{\Omega t}{2} + i\frac{\Delta}{\Omega}\sin\frac{\Omega t}{2}\right]$$
$$c_1(t) = i\frac{A}{\Omega\hbar}e^{i\Delta t/2}\sin\frac{\Omega t}{2} \qquad P_1(t) = |c_1(t)|^2 = \frac{A^2}{\hbar^2\Omega^2}\sin^2\left(\frac{\Omega}{2}t\right)$$

Rabi frequency $\Omega = \sqrt{\Delta^2 + A^2/\hbar^2}$ Detuning $\Delta = \omega_{01} - \omega$
Resonator $\omega_r = 2\pi\frac{v_p}{\lambda_n} = 2\pi\frac{1}{\sqrt{LC}}\frac{(n+1)}{2\ell}$ FWHM: $\kappa = \frac{\omega_r}{Q}$
Dispersive readout $\omega_r \pm \frac{g^2}{\Delta}$
(??? так пока и не разобрался, как это работает???)
Anharmonicity is required to isolate two levels
(тут абзац про эту идею)
We need an anharmonic energy spectrum
Non-linear circuit elements are required (diodes, transistors,) But typical non-linear elements are dissipating
Solution: Josephson junction The energy levels will be non-equidistant
A Josephson junction is a non-linear inductor
Inductance of a JJ:

$$V = L_J\frac{dI_S}{dt}$$
$$I_S = I_c\sin\varphi \Leftrightarrow \frac{dI_S}{dt} = I_c\cos\varphi\frac{d\varphi}{dt} = \frac{2eV}{\hbar}I_c\cos\varphi \quad L_J = \frac{\hbar}{2eI_C\cos\varphi}$$

voltage-phase relation: $\frac{d\varphi}{dt} = \frac{2\mathrm{eV}}{\hbar}$; $\cos\varphi = \pm\sqrt{1-\left(\frac{I_s}{I_c}\right)^2}$ the inductance of a JJ depends on the current (via the phase difference φ)
Total energy $\rightarrow$ Hamiltonian:

$$\widehat{H} = \frac{\widehat{Q}^2}{2C} + E_J[1-\cos\hat{\varphi}]$$
$$\widehat{H} = 4E_c\hat{n}^2 + E_J[1-\cos\hat{\varphi}]$$

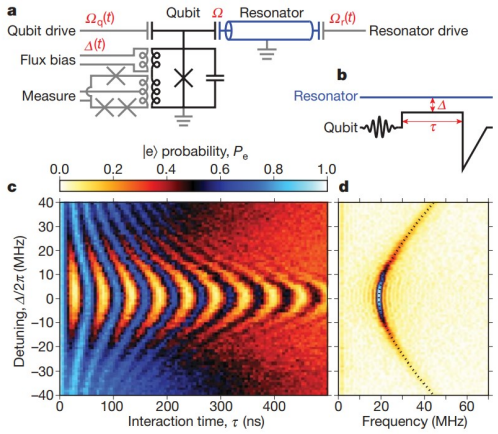
We consider $\varphi \ll 1$ and $E_J > E_C$ i.e. the transmon regime

$$\hat{H} = 4E_c\hat{n}^2 + E_J\left[1-\left(1-\frac{\hat{\varphi}^2}{2}+\frac{\hat{\varphi}^4}{24}\ldots\right)\right] \approx 4E_c\hat{n}^2 + E_J\frac{\hat{\varphi}^2}{2} - E_J\frac{\hat{\varphi}^4}{24}$$

Stored energy in JJ:

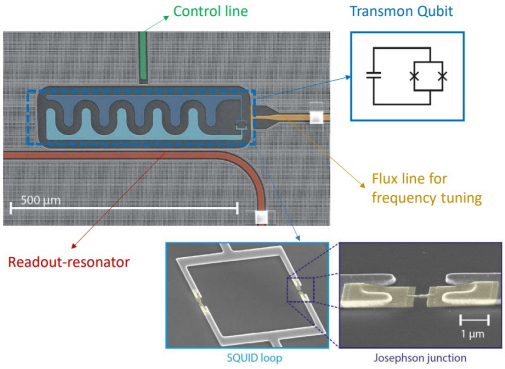
$$E = \int_0^t IV\,dt = \int_0^\varphi I_C\sin\varphi\frac{\hbar}{2e}d\varphi$$
$$E = \frac{\Phi_0}{2\pi}I_C[1-\cos(\varphi)] = E_J[1-\cos(\varphi)] \qquad E_J := \frac{\Phi_0}{2\pi}I_C = \text{ "Josephson energy"}$$

Two-level systems, basic quantum optics for quantum computing



Superconducting circuits as artificial atoms: frequency range

General circuit is as follows:



Qubit control

(допишу скоро уже, там минут 20 и сделаю это)

Qubit readout

When a qubit is coupled to a superconducting CPW resonator, dispersive readout allows to determine the qubit state: under the conditions:

- Strong coupling regime

$$\text{i.e. } g \gg \kappa, \frac{1}{T_1}, \frac{1}{T_2} \quad \left(\frac{1}{g} \sim 50 \text{ ns} \ll T_1,\ T_2 \right)$$

- Dispersive regime (detuned regime)

$$\text{i.e. } g \ll \omega_{\text{resonator}} - \omega_{\text{qubit}} \equiv \Delta$$

- Low photon numbers in cavity: $<< \Delta^2/4\ g^{2\sim100}$

18.3.2 Overview of typical applications of superconductivity

On applications in MRI (magnetic resonance imaging), where superconductors are used for Strong Magnetic Fields, Size and Design (???)

On applications in colliders where superconducting wires are used.

18.3.3 Digital Electronics

5.1 Superconductivity and Digital Electronics 216 5.1.1 Historical development 217 5.1.2 Advantages and Disadvantages of Josephson Switching Devices 219 5.2 Voltage State Josephson Logic 222 5.2.1 Operation Principle and Switching Times 222 5.2.2 Power Dissipation 225 5.2.3 Switching Dynamics, Global Clock and Punchthrough 226 5.2.4 Josephson Logic Gates 228 5.2.5 Memory Cells 234 5.2.6 Microprocessors 236 5.2.7 Problems of Josephson Logic Gates 237 5.3 RSFQ Logic 239 5.3.1 Basic Components of RSFQ Circuits 241 5.3.2 Information in RSFQ Circuits 246 5.3.3 Basic Logic Gates 247 5.3.4 Timing and Power Supply 249 5.3.5 Maximum Speed 249 5.3.6 Power Dissipation 250 5.3.7 Prospects of RSFQ 250 5.3.8 Fabrication Technology 253 5.3.9 RSFQ Roadmap 25 254 5.4 Analog-to-Digital Converters 255 5.4.1 Additional Topic: Foundations of ADCs 256 5.4.2 The Comparator 261 5.4.3 The Aperture Time 263 5.4.4 Different Types of ADCs 26

The Josephson Voltage Standard

6.1 Voltage Standards 270 6.1.1 Standard Cells and Electrical Standards 270 6.1.2 Quantum Standards for Electrical Units 271 6.2 The Josephson Voltage Standard 274 6.2.1 Underlying Physics 274 6.2.2 Development of the Josephson Voltage Standard 274 6.2.3 Junction and Circuit Parameters for Series Arrays 279 6.3 Programmable Josephson Voltage Standard 281 6.3.1 Pulse Driven Josephson Arrays 283

18.3.4 Superconducting Photon and Particle Detectors

7.1 Superconducting Microwave Detectors: Heterodyne Receivers 286
7.1.1 Noise Equivalent Power and Noise Temperature 286
7.1.2 Operation Principle of Mixers
7.1.5 Josephson Mixers 296
7.2 Superconducting Microwave Detectors: Direct Detectors 297
7.2.1 NEP of Direct Detectors 298
7.3 Thermal Detectors 300
7.3.1 Principle of Thermal Detection 300
7.3.2 Bolometers 302
7.3.3 Antenna-Coupled Microbolometers 307
7.4 Superconducting Particle and Single Photon Detectors 314
7.4.1 Thermal Photon and Particle Detectors: Microcalorimeters 314
7.4.2 Superconducting Tunnel Junction Photon and Particle Detectors 318
7.5 Other Detectors 328

18.3.5 Microwave Applications

8.1 High Frequency Properties of Superconductors 330
8.1.1 The Two-Fluid Model 330
8.1.2 The Surface Impedance 333
8.2 Superconducting Resonators and Filters 336
8.3 Superconducting Microwave Sources 3

18.3.6 Applications of SC junctions and SQUIDS

(просто раскрою плюсы приборов с ними, пока не особо про это думал)

The particular I-V dependence of a JJ and the possible hysteresis (∼memory) has a large number of applications in analog and digital electronics. (??? какие???)

Produce very fast switches (IC's), low power consumption

SQUID as a highly sensitive

sensors for the magnetic field

- Laboratory applications (magnetometry)
- Geophysical applications (earth magnetic field, rock magnetometry, . . .)
- Non-destructive tests and evaluations, structural characterization Scanning SQUID microscopy
- Medical applications

Scanning SQUID microscope

(хз, как это работает, потом допишу мб, пока знаю, что такой есть.)

Medical applications of SQUID magnetometers

(хз, продумаю потом)

Part VIII
Other Properties, Theories and Effects

19 Other Known Phenomena and Models

19.1 Unconventional Superconductivity by Mineev, V.P. Samokhin, K., part 1

19.1.1 1. Cooper Pairing in General

Сверхпроводимость - полное исчезновение электрического сопротивления постоянному току - наблодается во многих металлах при достаточно низких температурах. О сверхпроводимости можно говорить как о сверхтекучести, то есть полном исчезновении вязкости в жидкости, состоящей из электронов проводимости. Подобное явление имеет место и в ряде друтих квантовых жидкостен: сверхтекучих ^{4}He и ^{3}He, атомных ядрах и нейтронных звездах.

Теоретическое изучение сверхтекучих ферми-систем началось со времени создания в 1957 г. Дж. Бардиным, Л. Купером и Дж. Шриффером [1] геории сверхпроводимости (здесь и далее - теории БКШ). В основе этой теории лежит утверждение Л. Купера о нсустойчивости основного состояния электронного газа со сколь угодно слабым притяжением между частицами по отношению х образованию связанных состояний - пар электронов. Межэлектронное

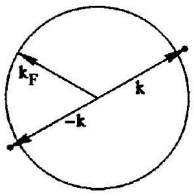


Рис. 1. Два электрона с противоположными импульсами над сферои Ферми притяжение, превосходящее кулоновское отталкивание, в большинстве сверхпроводников обязано своим происхождепием взаимодействию электронов с колебаниями кристаллической решетки (фононами), приводящему к образованиоо области избыточного положительного заряда, окружающщего данный электрон. Такое взаимодействие практически изотропно, поэтому куперовские пары образуются в состоянии с нулевым орбитальным момегтом (s-спаривание). Иначе дело обстоит в сверхтекучем ^{3}He, где куперовское спаривание возникает благодаря взаимодействию ядерных спинов атомов гетия-3 с флуктуациями намагниченности жидкости (парамагнонами). Парамагнонное взаимодействие существенно анизотропно и приводит к образованию куперовских пар с орбитальным моментом $L = 1$ (p-спаривание).

Несмотря на значительную разницу в природе притяжения между частицами, куперовское спаривание является общим механизмом, ответствеппыым за формирование сверхтекучего состояния в различных ферми-системах. Слепуя работе [2], рассмотрим квантово-мсханическую задачу о двух электронах в нормальном металле при нулево температуре. Будем считать, что пара электронов взаимодействует между собой посредством потенциала $V(\mathbf{r}_1 - \mathbf{r}_2)$, не зависящето от их спинов, а наличие остапьних электронов, заполняющих все состояния нисже уровня Ферми, проявляется только чсрез приншип Паули
(рис. 1). Для определения уровней эiергии и волновых функций $\psi(\mathbf{r}_1, \mathbf{r}_2)$ электроніо пары нсобходимо рсшшить уравеение Шредингера

$$-\frac{\hbar^2}{2m}\left(\boldsymbol{\nabla}_1^2+\boldsymbol{\nabla}_2^2\right)\dot{\psi}\left(\mathbf{r}_1,\mathbf{r}_2\right)+V\left(\mathbf{r}_1-\mathbf{r}_2\right)\psi\left(\mathbf{r}_1,\mathbf{r}_2\right)=\left(\Delta+\frac{\hbar^2k_F^2}{m}\right)\psi\left(\mathbf{r}_1,\mathbf{r}_2\right) \tag{1.1}$$

где Δ - эдергия электронной пары, отсчитанная от энергии двух свободныхх электронов, т. е. удвоенной энергии Ферми $h^2k_{\mathrm{F}}^2/m$.

Or координат электронов $\mathbf{r}_1$ и $\mathbf{r}_2$ можно перейти к координатам центра инерции $\mathbf{R}=\left(\mathbf{r}_1+\mathbf{r}_2\right)/2$ и относительного движения $\mathbf{r}=\mathbf{r}_1-\mathbf{r}_2$. Если счщтать, что центр инерции пары покоится, иными словами, что импульсы электронов противоположны ($\mathbf{k}$ и $-\mathbf{k}$), то зависимость ψ от $\mathbf{R}$ можно опустить, и уравнение Шредиигсра перепишется в виде

$$-\frac{\hbar^2}{m}\frac{\partial^2\psi(\mathrm{r})}{\partial\mathrm{r}^2}+V(\mathbf{r})\psi(\mathbf{r})=\left(\Delta+\frac{\hbar^2k_F^2}{m}\right)\psi(\mathbf{r}) \tag{1.2}$$

Персходя к импупьсному представлениго

$$g(\mathbf{k})=\int d^3re^{-i\mathbf{kr}}\psi(\mathbf{r}) \tag{1.3}$$

получаем:

$$\frac{\hbar^2}{m}h^2g(\mathbf{k})+\int\frac{d^3k'}{(2\pi)^3}V\left(\mathbf{k}-\mathbf{k}'\right)g\left(\mathbf{k}'\right)=\left(\Delta+\frac{\hbar^2k_F^2}{m}\right)g(\mathbf{k}) \tag{1.4}$$

Взаимодействие

$$V\left(\mathbf{k}-\mathbf{k}'\right)=\int d^3re^{-i(\mathbf{k}-\mathbf{k}')\mathbf{r}}V(\mathbf{r}) \tag{1.5}$$

зависящее от направлений импульсов

$$V\left(\mathbf{k}-\mathbf{k}'\right)=\sum_{l=0}^{\infty}V_l\left(k,k'\right)\sum_{m=-1}^{1}Y_{lm}(\hat{\mathbf{k}})Y_{lm}^*\left(\hat{\mathbf{k}}'\right) \tag{1.6}$$

будем считать притяжением в узком слое толщиной $\varepsilon_l\ll\varepsilon_{\mathrm{F}}=\hbar^2k_{\mathrm{F}}^2/(2\ \mathrm{m})$ над поверхностыо Ферми

$$V_l\left(k,k'\right)=\begin{cases}-V_l, & \text{при } \varepsilon_{\mathrm{F}}<\frac{\hbar^2k^2}{2m},\frac{\hbar^2k'^2}{2m}<\varepsilon_{\mathrm{F}}+\varepsilon_l\\ 0, & \text{вне интервала } \left(\varepsilon_{\mathrm{F}},\varepsilon_{\mathrm{F}}+\varepsilon_l\right)\end{cases} \tag{1.7}$$

Здесь $Y_{lm}(\hat{\mathbf{k}})$ - сферические функции с орбитадыным моментом l и его проекцией m на ось z, а $\hat{\mathbf{k}}=\mathbf{k}/k_{\mathrm{F}}$.

Осуществим в (1.4) обычный переход от интегрирования по волновому вектору к интегрированию по энергии $\xi=\hbar^2k^2/2m-\varepsilon_{\mathrm{E}}$ и направлениям $\mathbf{k}$

$$\int\frac{d^3k}{(2\pi)^3}\to N_0\int d\xi\int\frac{d\Omega}{4\pi} \tag{1.8}$$

где

$$N_0=\frac{mk_F}{2\pi^2\hbar^2} \tag{1.9}$$

• плотность состояний на поверхности Ферми на одну проекцию спина электрона. Имеем:

$$\left[\frac{\hbar^2}{m}\left(k^2-k_{\mathrm{F}}^2\right)-\Delta\right]_{\varepsilon_l} g(\mathbf{k})-$$
$$-N_0\int\limits_0^d d\xi'\int\frac{d\Omega'}{4\pi}\sum_{i=0}^{\infty}V_l\sum_{m=-1}^{1}Y_{im}(\hat{\mathbf{k}})Y_{lm}^*\left(\hat{\mathbf{k}}'\right)g\left(\mathbf{k}'\right)=0 \tag{1.10}$$

Нетрудно убедиться, что каждому значению орбитального момснта l соответствует определенное собственное состояние $\{g_l(\mathbf{k}),\Delta_l\}$ уравнения (1.10). Действительно, подставдяя разложение

$$g(\mathbf{k})=g_{l'}(\mathbf{k})=\sum_{m'=-l'}^{l'}a_{l'm'}(k)Y_{l'm'}(\hat{\mathbf{k}})$$

в (1.10) и попьзуясь ортонормированностью сферических функций

$$\int\frac{d\Omega'}{4\pi}Y_{lm}^*\left(\hat{k}'\right)Y_{l'm'}\left(\hat{k}'\right)=\delta_{ll}\delta_{mm'} \tag{1.11}$$

полупим:

$$\left[\frac{\hbar^2}{m}\left(k^2-k_{\Gamma}^2\right)-\Delta_l\right]g_l(\mathbf{k})-N_0V_l\int\limits_0^{\varepsilon_l}d\xi g_l(\mathbf{k})=0$$

Следоватетьно,

$$g_l(\mathbf{k})=\frac{N_0V_i\int\limits_0^{c_1}d\xi g_l(\mathbf{k})}{2\xi-\Delta_l} \tag{1.12}$$

Интегрируя по ξ левую и правуіо части этого уравнения, получим

$$1=N_0V_l\int\limits_0^{\varepsilon_l}\frac{d\xi}{2\xi-\Delta_l}=\frac{N_0V_l}{2}\ln\frac{\varepsilon_l-\frac{\Delta_l}{2}}{-\frac{\Delta_l}{2}}$$

Отсюда, полагая взаимодействие слабым $N_0V_1\ll 1$, находим

$$\Delta_l=-2\varepsilon_l\exp\left(-\frac{2}{N_0V_l}\right) \tag{1.13}$$

Итак, при сколб угодно слабом притяжении между двумя электронами возникает связаннос состояние, энергия которого зависит от орбитального момента.

Данное утверждение, доказаннюе для двух электронов, сохраняет свою силу и в многоэлектронной задаче (см. 6). Именно, сверхпроводящие состояния, соответствуошие куперовскому спариванипо с различными значениями орбитального момента, имеют различную критическую температуру. Сверхпроводящие состояния

$$g_l(\mathbf{k})=\sum_{m=-1}^{1}a_{lm}(k)Y_{lm}(\hat{\mathbf{k}}) \tag{1.14}$$

с данным l, отличагощиеся наборами коэффициентов $\{a_{3m}(k)\}$, имеют одинаковую критическуі температуру. Из всех таких состоянй при опредсленной температуре и определенном давлении реализуется наиболее эпергетически выгодіное.

Размер куперовской пары. Характерный интервал δk, на котором изменяюотя коэффициенты $a_{lm}(k)$, связан соотношешием неопрсделенности $\xi_0 \delta k \geq 1$ с характерным размером ξ_0 волновой функции в координатном пространстве - размером куперовской пары [1]. Неопределенность волнового вектора δk можно оценить через энсргиго связи пары:

$$\Delta \sim \delta\varepsilon \sim \frac{\hbar^2}{m} k_{\mathrm{F}} \delta k \sim \hbar v_{\mathrm{F}} \delta k$$

Следовательно,

$$\xi_0 \sim \frac{\hbar v_{\mathrm{F}}}{\Delta} \tag{1.15}$$

Неустойчивость нормального ферми-газа по отношению к куперовскому спариванио, очевидно, должпа проявляться при температуре ' $T_{\mathrm{c}} \sim \Delta$. Фермиевская скорость оценивается терез среднее расстояние между фермионами $n^{-1/3}$ (n - копцентрация) как $v_F \sim \hbar n^{1/3}/\mathrm{m}$. Для обычных сверхпроводников T_c порядка нескольких градусов, а масса электронов проводимости, грубо говоря, совпадает с массой электронов в вакууме, и $\xi_0 \approx 10^{-5}$ cm. В ^{3} Не критическая температура нххе на три порядка, но и масса атомов ^{3}Не в несколько тысяч раз больше массы электронов, поэтому $\xi_0 \approx 10^{-6}$с. В тяжелофермионних соединениях эффективная масса электронов в $10 - 100$ раз больше массы электронов в вакууме, а в высокотемпературных сверхпроводниках T_c достигает десятков и сотен градусов. Поэтому в этих соединениях $\xi_0 \approx 10^{-6} - 10^{-7}$ cm.

Во всех персчислснных случаях $\xi_0 \gg n^{-1/3}$, то есть изолированных куперовских пар нс существует, и задача о возникновении сверхпроводящего состояния является существенно многочастичной.

19.1.2 2. Spin Structure of Paired States

Во всех известіннх к пастоящему моменту сверхтекучих ферми-жидкостях куперовские пары состоят из частиц со спином $1/2$. Спиновое состояние пары может характеризоваться значением полного спина $S = 0$ (синглет) или $S = 1$ (триплет), либо же представлять суперпозицию этих двух состояний. Для сверхпроводяших систем, обладаюощих определенной пространственной четностью, последняя возможность искппочается. Удобно рассмотреть этот вопрос для сверхпроводящих состояний с определенным орбиташным моментом.

Орбитальная волновая функшия (1.14) является четной для четдых значений орбитального момента l и нечетной ддя нечетных l:

$$g_l(-\mathbf{k}) = (-1)^l g_i(\mathbf{k}) \tag{2.1}$$

В то же время, согласно принципу Паули, полная волновая функция пары, состояшая из произведений вида $g(\mathbf{k})\chi_{12}$, где χ_{12} - спиноовая волютовая фунаия частиц 1 и 2, должна менять знак при их перестановкс:

$$g(-\mathbf{k})\chi_{21} = -g(\mathbf{k})\chi_{12} \tag{2.2}$$

Из соотношений (2.1) и (2.2) следует, что спиновое состояние пары с четным (нечетным) орбитатьным моментом / должно быть антисимметричньмм (симметричным) по отношснио к перестановке частиц.

Спиновые состояния двух частиц со спином $1/2$ строятся из спиновых состояний

[11] Точнос шыражение $\xi_0 = \hbar v_F / (2\pi T_c)$ для размера куперовской пары будет получено в \$18.

$$\alpha_\lambda = \begin{pmatrix}1\\0\end{pmatrix} = |\uparrow\rangle \quad \text{и} \quad \beta_\lambda = \begin{pmatrix}0\\1\end{pmatrix} = |\downarrow\rangle$$

одной частицы, являющихся собственнціми для операторов квадрата спина s^2 и проекшии спина s_z на ось z:

$$s_z = \frac{h}{2}\begin{pmatrix}1 & 0\\ 0 & -1\end{pmatrix}, \quad s_z\alpha_\lambda = \frac{\hbar}{2}\alpha_\lambda, \quad s_z\beta_\lambda = -\frac{\hbar}{2}\beta_\lambda$$

Собственная функция спин-синглетного состояния пары, для которого $S = 0$, $S_z = 0$ (где $\mathbf{S} = \mathbf{s}_1 + \mathbf{s}_2$), антисимметричная по отношению к перестановке частиц, имеет вид

$$\alpha_{1\lambda}\beta_{2\mu} - \beta_{1\lambda}\alpha_{2\mu} = |\uparrow|\rangle - \left|\nu\vdots\right\rangle = \begin{pmatrix}0 & 1\\ -1 & 0\end{pmatrix} = \left\langle i\sigma_{\psi_{i\mu}}\right.$$

то есть выражается черсз матрицу Паули σ_y[1]. Полная волновая функиия пары с $S = 0$ выглядит при этом следующим образом:

$$\Psi^l_{\text{pair}} = g(\mathbf{k})i\sigma_y = \sum_{m=-l}^{1} a_{lm}Y_{lm}(\hat{\mathbf{k}})i\sigma_y \tag{2.3}$$

где l может принимать значения $0, 2, 4, \ldots$ Соответствующие парные состояния, как это принято в атомной физике, носят названия $s, d, g, \ldots$ состояний.

Комплексные коэффициенты a_{im}, входлшие в формулу (2.3), одинаковые для всех куперовских пар данного сверхпроводящего состояния, представляют собой параметр порядка сверхпроводника. В слабо неоднородиьх состояниях параметр порядка зависит or координат, то есть коэффициенты a_{lm} являются функциями r. Так, параметром порядка для сверхпроводника с s-спариванием спужит одна комплексная фупкдия

$$a_{00}(\mathbf{r}) = \psi(\mathbf{r}) = |\dot{\psi}|e^{i\varphi} \tag{2.4}$$

а, например, для сверхпроводника с d-спариванием ($l = 2$) таких функций пять.

Для спин-триплетного состояния пары ($S = 1$) волновые функции, соответствующие трем различным проекдиям спина пары иа ось квантования и симметричные по отiошенито к перестановке частиц, имеiот вид

$$S_z = \begin{cases} 1, & \alpha_{1\lambda}\alpha_{2\mu} = |\uparrow\uparrow\rangle = \begin{pmatrix}1 & 0\\ 0 & 0\end{pmatrix} \\ 0, & \alpha_{1\lambda}\beta_{2\mu} + \beta_{1\lambda}\alpha_{2\mu} = |\uparrow\downarrow\rangle + |\downarrow\uparrow\rangle = \begin{pmatrix}0 & 1\\ 1 & 0\end{pmatrix}, \\ -1, & \beta_{1\lambda}\beta_{2\mu} = |\downarrow\rangle = \begin{pmatrix}0 & 0\\ 0 & 1\end{pmatrix} \end{cases}$$

то есть являются симметричными матрицами. Полная волновая функция пары представляет собой линсйную комбинациюо этих состояний:

$$\Psi^l_{\text{pair}} = g_1(\mathbf{k})|\uparrow\uparrow\rangle + g_2(\mathbf{k})(|\uparrow\downarrow\rangle + |\downarrow\uparrow\rangle) + g_3(\mathbf{k})|\downarrow\rangle = \begin{pmatrix}g_1(\mathbf{k}) & g_2(\mathbf{k})\\ g_2(\mathbf{k}) & g_3(\mathbf{k})\end{pmatrix} \tag{2.5}$$

[11] Напомним опрелеление магриц Паули:

$$\sigma_x = \begin{pmatrix}0 & 1\\ 1 & 0\end{pmatrix}, \quad \sigma_y = \begin{pmatrix}0 & -i\\ i & 0\end{pmatrix}, \quad \sigma_z = \begin{pmatrix}1 & 0\\ 0 & -1\end{pmatrix}$$

Здесь

$$g_\alpha(\mathbf{k}) = \sum_{m=-1}^{1} a^\alpha_{lm} Y_{Im}(\hat{\mathbf{k}}) \tag{2.6}$$

• ампиитуды состояний с $S_z = 1, 0$ и -1, соответственно.

Квантовое число / в формуле (2.6) можст приниматъ значения $1, 3, \ldots$ Соответствующие состояния называют сверхпроводящими состояниями с $p, f, \ldots$ спариванием. Друтая форма записи выражения (2.5) связана с использованием базиса симметричных матриц $i\sigma\sigma_y = (i\sigma_x\sigma_y, i\sigma_y\sigma_y, i\sigma_z\sigma_y)$. Имеем:

$$\begin{aligned}\Psi'_{\text{pair}} &= i(\,\mathrm{d}(\mathbf{k})\sigma)\sigma_y = (d_x(\mathbf{k})\sigma_x + d_y(\mathbf{k})\sigma_y + d_x(\mathbf{k})\sigma_z)\, i\sigma_y = \\ &= \begin{pmatrix} -d_x(\mathbf{k}) + id_y(\mathbf{k}) & d_z(\mathbf{k}) \\ d_z(\mathbf{k}) & d_x(\mathbf{k}) + id_y(\mathbf{k}) \end{pmatrix}\end{aligned} \tag{2.7}$$

Компоненты всктора $\mathrm{d}(\mathbf{k})$, линейно выражающиеся через ампиитуды $g_\alpha(\mathbf{k})$:

$$g_1 = -d_x + id_y, \quad g_2 = d_2, \quad g_3 = d_x + id_y$$

могут быть разложены по сферическим гармоникам:

$$d_\alpha(\mathbf{k}) = \sum_{m=-1}^{1} b^\alpha_{lm} Y_{lm}(\hat{\mathbf{k}}) \tag{2.8}$$

Коэффициенты b^α_{lm} играют роль параметра порядка сверхпроводника с данным типом спаривания, то есть с данным значением квантового числа l. Так, в простейшем случае p-спаривания параметром порядка является набор девяти комплексных функиий $b^\alpha_{lm}(m = -1, 0, 1)$.

Упражнешие. Используя выражение (2.7) для спшиновой волновой функции триплетного состояния, доказать формулы для

а) среднего значения спина пары:

$$\mathbf{S} = i\hbar \int \frac{d\Omega}{4\pi} \mathrm{d}^*(\mathbf{k}) \times \mathrm{d}(\mathbf{k}) \tag{2.9}$$

б) срешлего значения орбитального момента пары:

$$\mathbf{L} = i\hbar \int \frac{d\Omega}{4\pi} \mathbf{d}^*(\mathbf{k}) \left[\mathbf{k} \times \frac{\partial}{\partial \mathbf{k}}\right] \mathbf{d}(\mathbf{k}) \tag{2.10}$$

19.1.3 3. Phases of Superfluid Helium-3

Сферические гармоники $Y_{\mathrm{lm}}(\hat{k})$ с $l = 1$

$$Y_{11}(\hat{\mathbf{k}}) \propto \left(\hat{k}_x + i\hat{k}_y\right)$$
$$Y_{1-1}(\hat{\mathbf{k}}) \propto \left(\hat{k}_x - i\hat{k}_y\right), \quad Y_{10}(\hat{\mathbf{k}}) \propto \hat{k}_x$$

линейно выражаются через компоненты вектора $\hat{\mathbf{k}}$, что порождает еще одну форму записи вектора d:

$$d_\alpha(\mathbf{k}) = A_{\alpha i}\hat{k}_i \tag{3.1}$$

Комплексная 3 × 3 матрица $A_{\alpha i}$ суть параметр порядка в сверхтекучих ферми-жидкостях с p-спариванием. Именно такой тип спаривания осуществляется в сверхтекучем ^{3} He [3-6], фазовая диаграмма которого изображена на рис. 2.

Вектор d в выражении (3.1) зависит от компонент вектора k в некоторой фиксированной системе координат. Пользуясь тем, что при трехмсрных по-

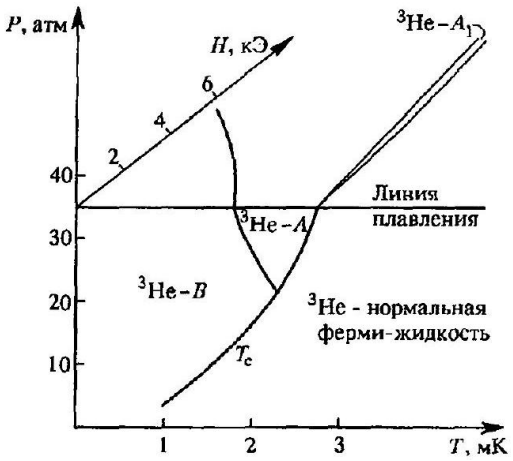


Рис. 2. Фазовая диаграмма жидкого гелия-3 в координатах: температура $-T$ (мК), давление P (атм), магнитное поле - H (кЭ)

воротах $\hat{R}^S$ и $\hat{R}^O$ в стиновом и орбитаном (координатном) пространствах, соответственно, компоненты векторов **d** и **k** линейно прсобразуются через самих себя, то есть

$$d_\alpha \to \tilde{d}_i = R^{\mathrm{S}}_{\alpha\beta} d_\beta$$
$$k_i \to \tilde{k}_i = R^{\mathrm{o}}_{ij} k_j$$

мы можем записать параметр порядка в произвольной сисгеме координат.

Перечислим возможные фазы сверхтекучей жидкости с p-спариванием, различалишиеся видом спшнового вектора d (или матрицы $A_{\alpha i}$).

B-фаза:

$$\mathrm{d}(\mathbf{k}) \propto \hat{\mathbf{k}} \tag{3.2}$$

то есть $A_{\alpha i} \propto \delta_{\alpha i}$ (в произвольной сисгеме координат $A_{\alpha i} \propto R_{\alpha i}$, где $\hat{R}$ матрица трехмерных вращений). Волновая функция пары (см. (2.7)) имеет в ХХд

$$\begin{aligned}\mathbf{\Psi}^B_{\mathrm{pair}} &\propto \begin{pmatrix} -\hat{k}_x + i\hat{k}_y & \hat{k}_z \\ \hat{k}_z & \hat{k}_x + i\hat{k}_y \end{pmatrix} = \\ &= \left(-\hat{k}_x + i\hat{k}_y\right)|\Pi\rangle + \hat{k}_z\left(\left|\prod \downarrow\right\rangle + |\,\lfloor\uparrow\rangle\right) + \left(\hat{k}_x + i\hat{k}_y\right)|\downarrow\downarrow\rangle\end{aligned} \tag{3.3}$$

Таким образом, B-фаза предсгавляет собой линеейную комбинацию трех равновероятных состояний $|S_z = +1, m = -1\rangle, |S_z = 0, m = 0\}$ и $|S_z = -1,\ m = +1\rangle$.

Имеюотся еше пве фазы, в которых реализуется часть состояний, из которых состоит B-фаза.

Планарная фаза:

$$\mathrm{d}(\mathbf{k}) \propto \left(\hat{k}_x, \hat{k}_y, 0\right) \tag{3.4}$$

Отсiода

$$\Psi_{\text{pair}}^{\text{pl}} \propto \left(-\hat{k}_x + i\hat{k}_y\right) |\Uparrow\rangle\Big\rangle + \left(\hat{k}_x + i\hat{k}_y\right) |U\rangle. \tag{3.5}$$

Планарная фаза является смесыо двух состояний: $|S_z = +1, m = -1\rangle$ и $|S_z = -1, m = +1\rangle$.

Полярпая фаза:

$$\mathbf{d}(\mathbf{k}) \propto \left(0, 0, \hat{k}_z\right) \tag{3.6}$$

Отсюода

$$\Psi_{\text{pair}}^{\text{pol}} \propto \hat{k}_z(|\uparrow\downarrow\rangle + |\downarrow\uparrow\rangle) \tag{3.7}$$

Полярная фаза состоит из пар с $S_z = 0$ и $m = 0$.

Имеются также фазы с ненулевыми орбитальным и спиновым моментами.

А-фаза:

$$\mathbf{d}(\mathbf{k}) \propto \left(\hat{k}_x + i\hat{k}_y, 0, 0\right) \tag{3.8}$$

то есть $A_{\alpha i}^{A} \propto V_\alpha \left(\Delta_i' + i\Delta_i''\right)$, где $\mathbf{V} = (1,0,0), \Delta' = (1,0,0), \Delta'' = (0,1,0)$. В произвольной систсме координат: V - единичныпи вектор в спиновом пространстве, а Δ' и Δ'' - единиqные взаимно перпендикулярные векторы в координатном пространстве. Парная волновая функция имеет вид

$$\Psi_{\text{pair}}^{A} \propto \left(\hat{k}_x + i\hat{k}_y\right) \begin{pmatrix} -1 & 0 \\ 0 & 1 \end{pmatrix} \propto \left(\hat{k}_x + i\hat{k}_y\right) \left(|\uparrow\rangle\rangle - |\downarrow\rangle\right\rangle \tag{3.9}$$

Таким образом, A-фаза представляет собой линейную комбинацино двух равновероятных состояний $|S_z = +1, m = 1\rangle$ и $|S_z = -1, m = 1\rangle$. Спиновый момент в этой фазе отсутствует. Орбитальный момент сосуда с A-фазой в основном состоянии должен быть порядка $N\hbar$, где N - число куперовских пар.

A_1 - фаза:

$$\mathbf{d}(\mathbf{k}) \propto \left(\hat{k}_x + i\hat{k}_y, i\left(\hat{k}_x + i\hat{k}_y\right), 0\right) \tag{3.10}$$

Отсюда $A_{\alpha i}^{A_1} \propto \left(V_\alpha' + iV_\alpha''\right)\left(\Delta_i' + i\Delta_i''\right)$, причем в произвольной системе координат $\mathbf{V}'$ и $\mathbf{V}''$ - единичные взаимно перпендикулярные спиновые векторы,
а Δ' и Δ'' опредепяюотся апалогично A-фазе. Парная волновая функиия имеет вид

$$\Psi_{\text{pair}}^{A_2} \propto \left(\hat{k}_x + i\hat{k}_y\right) \begin{pmatrix} 1 & 0 \\ 0 & 0 \end{pmatrix} = \left(\hat{k}_x + i\hat{k}_y\right) |\Pi\rangle \tag{3.11}$$

Следовательно, A_1-фаза состоит щз пар с $S_z = 1$ и $m = 1$. Эта фаза обладает как орбитальным, так и спиновым магнитным моментом.

$\beta - \phi aa$:

$$\mathrm{d}(\mathbf{k}) \propto \left(\hat{k}_x, i\hat{k}_x, 0\right) \tag{3.12}$$

Отсiода $A_{\alpha i}^{\beta} \propto \left(V_\alpha' + iV_\alpha''\right)\Delta_i$, и

$$\Psi_{\text{pair}}^{\beta} \propto \hat{k}_x \begin{pmatrix} 1 & 0 \\ 0 & 0 \end{pmatrix} = \left(\left(\hat{k}_x + i\hat{k}_y\right) + \left(\hat{k}_x - i\hat{k}_y\right)\right) |\Pi\rangle \tag{3.13}$$

то есть β-фаза состоит из пар с $S_z = 1, m = +1$ и $S_z = 1, m = -1$ и обладает ненулевым спиновым момснтом.

19.1.4 4. Superconducting States in Crystals

Из рассмотрсния в 2 следует, что свсрхпроводящие состояния, обладаэщие определениой пространственной четностыю, могут быть тибо спинсинглетными, либо спин-триплетными. Именно, парная волновая функция для пространственно-четных состояний

$$\Psi^{\mathrm{s}}_{\mathrm{pair}} \propto g(\mathbf{k}) i\sigma_y \tag{4.1}$$

$$g(\mathbf{k}) = g(-\mathbf{k}) \tag{4.2}$$

соответствует $S = 0$, а для пространственно-нечетных состоянид $S = 1$, то есть

$$\Psi^{\mathrm{t}}_{\mathrm{pair}} \propto (\mathbf{d}(\mathbf{k})\sigma) i\sigma_y \tag{4.3}$$

$$\mathbf{d}(\mathbf{k}) = -\mathrm{d}(-\mathbf{k}) \tag{4.4}$$

Симметрия системы в сверхпроводящем состоянии включает в себя пространственную инверсию, если парная волновая функция Ψ_{pair} под деюствием оператора инверсии I не менятся:

$$I\Psi_{\mathrm{pair}} = \Psi_{\mathrm{pair}} \tag{4.5}$$

что соответствует синглетному спариванию, или меняет знак:

$$I\Psi_{\mathrm{pair}} = -\Psi_{\mathrm{pair}} \tag{4.6}$$

при триплетном спаривании. Смешанные сверхпроводящие состояния вида

$$a\Psi^{\mathrm{s}} + b\Psi^{\mathrm{t}} \tag{4.7}$$

в этом случае запрещены.

Если же симметрия нормального состояния не включает пространственпууо инверсипо (кристалшi без цештра инверсии), или симметрия по отношению к инверсии нарушается при переходе в сверхпроводящее состояние (специальный вид спаривающего взаимодействия), то состояния типа (4.7) в
принципе могут реализовываться [7]. Мы будем предполагать наличие пространственной инверсии и работать со свсрхпроводящими состояниями вида (4.1) либо (4.3).

Как было показано в 1, в изотропном веществе темпсратуры перехода в сверхпроводящие состояния с разными зачениями орбитального момепта куперовских пар различны, то есть $T_{\mathrm{c}} = T_{\mathrm{c}}(l)$. Функции $g(\mathbf{k})$ и $\mathbf{d}(\mathbf{k})$ для синглетного и триплстного состояний, соотвстственно, имегт вид линейных комбинаций сферических функиий с даницм l:

$$g^l(\mathbf{k}) = \sum_{m=-l}^{l} a_{lm} Y_{lm}(\hat{k}), \qquad \text{при } l = 0, 2, 4, \ldots \tag{4.8}$$

$$\mathrm{d}^l(\mathbf{k}) = \sum_{m=-l}^{l} \mathrm{b}_{lm} Y_{lm}(\hat{\mathrm{k}}), \qquad \text{при } l = 1, 3, 5, \ldots \tag{4.9}$$

Как отмечалось в предыдущем параграфе, выбор системы координат, в которой записываются функции $Y_{lm}(\hat{k})$, роли не играет, поскольку при переходе от одного базиса

$(\hat{x}, \hat{y}, \hat{z})$ к другому $(\hat{x}', \hat{y}', \hat{z}')$, то есть при пространстзснных вращениях систсмы координат, функции $Y_{lm}\left(\hat{\mathbf{k}}'\right)$ линейно выражаются через сферические гармоники с тем же значением l:

$$Y_{lm}\left(\hat{\mathbf{k}}'\right) = \sum_{m'=-1}^{i} \Gamma_{mm'} Y_{lm'}(\hat{\mathbf{k}})$$

В общем стучас говорят, что набор функций $\{\psi_i(\mathbf{r})\}$ образует базис нсприводимого представления нскоторой трупшы пространственной симметрии G, если функции данного набора при любом преобразовании симметрии g из этой группы линейно выражаются только через самих себя [8]:

$$\psi_i(g\cdot) = \psi_i\left(\mathbf{r}'\right) = \sum_{j=1}^{d} c_{ij}\psi_j(\mathbf{r})$$

В изотропной системе, инвариантной относительно любшх пространственнвіх вращений, то есть преобразований из группы SO_3, неприводимые представления нумеруются значением орбитального момента l, а набор из $2l+1$ сферических гармоник с данным l образует базис представления. Типы куперовского спаривания при этом находятся во взаимнооднозначном соответствии с неприводимыми представлениями группы трехмерных вращений.

Принцип классификации сверхпроводпщих состояний согласно различным представлениям группы симметрии системы в нормальном состоянии полностью сохраняется и в присутствии кристаллической аиизотропии [9-14]. Именно, сверхпроводящие состояния с различными критическими температурами описываготся базисными функиими различных неприводимых представлении Γ группы G точечной симметрии кристалла [1], причем $T_c = T_c(\Gamma)$.

Разложения (4.8), (4.9) в этом случае принимают вид:

$$g(\mathbf{k}) = \sum_{i=1}^{d_\Gamma} \eta_i \psi_i^{\Gamma_s}(\hat{\mathbf{k}}) \tag{4.10}$$

$$\mathbf{d}(\mathbf{k}) = \sum_{i=1}^{d_\mathrm{r}} \eta_i \psi_i^{\Gamma_u}(\hat{\mathbf{k}}) \tag{4.11}$$

где $\psi_i^{\Gamma_\mathrm{s}}(\hat{\mathbf{k}})$ и $\psi_i^{\Gamma_\mathrm{u}}(\hat{\mathbf{k}})$ - базисные функции (g - четтые, au - нечетные по $\hat{\mathbf{k}}$) неприводимых представлений Γ размерности d_Γ группны G.

Для пренебрежимо малого спин-орбитального взаимодсйствия имеется вырождение состояний по отношенип к вращениям стиновьх векторов:

$$\eta_i^\alpha \to \tilde{\eta}_i^\alpha = R^S_{\alpha\beta}\eta_i^\beta.$$

В случае сильного спшн-орбиталного взаимодействия, которое имеет место в соединениях, содержащих элсменты с большими атомными номерами, удобно представить (4.11) в виде разложения

[11] Пространствешая группа симметрии кристалия вкточает комбинации операций точечной симметрии и трангляций. Постсдние мохно не принмать по внимание, так как никакой цопо:нительной пространствснноі модуляции при переходе в сверхпроводящсе состояине не возникаст.

$$\mathbf{d}^{\mathrm{I}}(\mathbf{k}) = \sum_{i=1}^{d_\Gamma} \eta_i \psi_i^{\Gamma_{\mathrm{u}}}(\hat{\mathbf{k}}) \tag{4.12}$$

по векторным базисным функциям

$$\begin{gathered}\psi_i^{\Gamma_u}(\hat{\mathbf{k}}) = \psi_i^x(\hat{\mathbf{k}})\hat{x} + \psi_i^y(\hat{\mathbf{k}})\hat{y} + \psi_i^z(\hat{\mathbf{k}})\hat{z} \\ \psi_i^{\Gamma_u}(-\hat{\mathbf{k}}) = -\psi_i^{\Gamma_u}(\hat{\mathbf{k}})\end{gathered} \tag{4.13}$$

неприводимого представления Г. Базис в спиновом пространстве задается единичными аксиалыпыми векторами $\hat{x}, \hat{y}, \hat{z}$, жестко связанными с кристаллическими осями. Здесь необходимо сделать слелующее замечание. Несмотря на то, что в кристаллах с сильным спин-орбитальным взаимодействием спиnі электрона становится «ллохим» квантовым числом, электронные состояния тем не менее остаются двукратно вырожденными (крамсрсовское вырождение - следствие симметрии по отношению к обращениоо времени), что позволяет характеризовать их «псевдоспином». В этом же смыслс следует понимать термин «спин-синглетное» или «спин-триплетное» сверхпроводящие состояния.

Совокупность комплексных коэффициентов η_i (или η_i) в разложениях (4.10), (4.11) или (4.12) прсдставляет собой параметр порядка в кристаллических сверхпроводниках. Таким образом, возможны как сверхпроводящие состояния с однокомпонентными параметрами порядка $\eta = |\eta|e^{i\varphi}$, так и с многокомпонентными параметрами порядка.

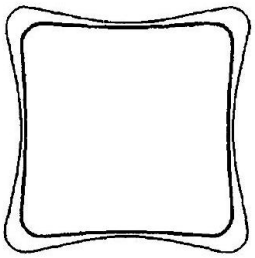
Помимо точечных преобразований, группа симметрии нормального состояния $\mathcal{G}$ включает операцию обращения времени R и калибровочные преобразования $U(1)$[2]:

$$\mathcal{G} = U(1) \times R \times G$$

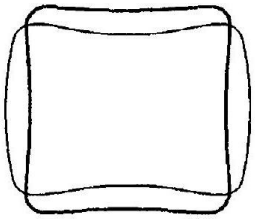
Переход в сверхгекулее или сверхпроводяшсе состояние означает появление фазовой когерентіости, то есть различия между состояниями с различными фазами φ параметра порядка $|\eta|e^{i\varphi}$, о чем говорят как о спонтанном нарушении калибровочной симметрии $U(1)$. При переходе в данное сверхтекучее состояние могут нарушаться также и другие симметрии из $\mathcal{G}$ (необыиная сверхмекучесть или сверхпроводимость). В результате сохраняется инвариантность лишгь по отношению к преобразованиям, образующим подгруппу H (сверхироводящий класс) группы $\mathcal{G}$. Таким образом, задача перечисления всех возможных сверхпроводящих (или сверхтекулих) фаз сводится к нахождению сверхпроводящих классов, соответствующих различным нарушенным симетриям нормалыной фазы [9].

Среди допустимьх по симметрии сверхпроводящих состояний следует выделять те, которые могут возникпуть непосредственно из нормальной фазы [3]. Согласно общей теории фазовых переходов Ландау, параметры порядка таких состояний должны преобразовываться по одному из неприводимых представлений точечной группы симметрии G нормальной фазы [9]. Обычное сверхпроводящее состояние обладает полной точечной симметрией кристалла, то есть относится к единичному представлению A_{1g} и описывается тривиальным сверхпроводящим классом $H = R \times G$. Точечная симметрия всех остальных сверхпроводящих состояний, относящихся к неслиничнцм представлениям

[12] В отсутствие спин-орбитального взаимодействия в группу $\mathcal{G}$ необходимо включать также преобразования свободных трехмериых вращений спинов, образуюиих группу SO_3^S.



a



6

Рис.3. Сечение ферми-поверхности (жирная линия) в базисной плоскости тетрагонаиного кристалла (группа симметрии D_{4h}. Тонкой линисй изображемы: а) аминитуда параметра порялка обычного сверхпроводящего состояния (прецставление Λ_{1g}), б) амплитуда парамстра порядка одного из нсобычиых снсрхироводяших состояний (представтение B_{1g}), поннжающего точечную симметрию кристаліа до D_{2h}

(или нечетному единичному представлению A_{1u}), нарушсна, и они пазываются нетривиальными или необычньми сверхпроводящими состоянияии (рис. 3).

В случае однокомпонентіого параметра порядка имеется взамнооднозначное соответствие между одномерными представлениями группы G и сверхпроводящими классами. Напротив, неодномерные представления порохдают несколько сверхпроводящих состояний, относящихся к различным сверхпроводяшшм классам и имеющих одинаковую критическуго температуру, но разную свободную энсргио (подробнее об этом см. 11). Это имеет место, нагример, для фаз с p-спариванисм, персисленнЬIX в 3.

Сверхпроводящие классы в гексагональном кристалле. В качестве примера, важного с точки зрения приложений к сверхпроводящему соединению с гяжельми фермионами LPt_3, обсудим сверхпроводящие состояния в кристалле с гексагонатьной симметрией, для которого $G = D_{6h} = D_6 \times I$, где I - преобразование инверсии. Здесь имеется 6 неприводимых представлений: 4 одномерных (A_1, A_2, B_1, B_2) и 2 пвумерных (E_1, E_2). Симметрия каждого сверхпроводящего состояния должна описываться подгруппой группы $\mathcal{G} = U(1) \times R \times D_{6h}$.

Группа $D_6 = \{C_n, U_n\}$ сосгоит из шести операций поворота C_n вокруг оси $\hat{z}$ на угол $\pi n/3$ $(n = 0, 1, \ldots, 5; C_0 = E$ - единичный элемент группы) и вращений U_n на угол π вокруг шести осей

$$- - \hat{x} \sin \frac{\pi n}{3} + \hat{y} \cos \frac{\pi n}{3}$$

Среди подгрупп группы $\mathcal{G}$ имеются четыре подгруппы H, которые соответствуот сверхпроводящим состояниям, описываемым функциями четырех одномерных представлений D_6. Это подтруппы $D_6 \times R, D_6\,(C_6) \times R$, $D_6\,(D_3) \times R$, и $D_6\,(D_3') \times R$.

[13] Сверхпроводящие классы, не относяицииеся к данной катсгория, соответствуот состояния, которые могут вознпкууть при дополиительных фазовых переходах внутри свсрхпроводяцей фазы.

Подгруппа, указанная в скобках, объединяет те элементы группы D_{6h}, которые не умножагтся на фазовый множитель из $U(1)$, то есть

$$D_6\left(C_6\right) = \left\{C_n, e^{i\pi}U_n\right\}$$
$$D_6\left(D_3\right) = \left\{C_{2k}, U_{2k}, e^{i\pi}C_{2k+1}, e^{i\pi}U_{2k+1}\right\}$$
$$D_6\left(D_3'\right) = \left\{C_{2k}, U_{2k+1}, e^{i\pi}C_{2k+1}, e^{i\pi}U_{2k}\right\}$$

гдс $k = 0, 1, 2$. Легко видеть, что подгруппа D_6 соответствует единичному представлснию A_1. Ровно половина элементов подгруппы $D_6\left(C_6\right)$ (или $D_6\left(D_3\right), D_5\left(D_3'\right)$) есть элементы группы D_6, друтая половина - комбинации операций точечной симметрии и калибровочного преобразования $c^{i\pi}$. Так, точечные преобразования U_n мсняют знак параметра порядка свсрхпроводящсго состояния с симметрией $D_6\left(C_6\right)$, которое, тем самым, соответствуст неединичному представлению A_2 групш D_6 (аналогично, $D_6\left(D_3\right)$ соответствует B_1, а $D_6\left(D_3'\right)$ соответствует B_2).

Высокотемпературиые сверхпроводиики. Еще одним примером необимной сверхпроводимости являются высокотемпературные сверхпроводники, к которым относятся металлооксидные материалы с T_c в пределах от 7 K до 100 K. Наиболее изученные представители этого класса - соединения $La_{2-x}Sr_xCuO_4$ и $YBa_2Cu_3O_{7-x}$, - обладают тетрагональной симметрией кристаллической решетки, то есть $G = D_{4h} = D_4 \times I$. В иттрий-бариевых соединениях имеются неболшие (порядка одного процента) орторомбические искажения кристалличсской рсшетки, влияние которых мы рассмотрим несколько ниже.

Группа D_4, вкпючаоошая операции поворотов C_n вокрут оси $\hat{z}$ на утол $\pi n/2$ и поворотов U_n на угол π вокруг осей

$$\hat{x}\cos\frac{\pi n}{2} + \hat{y}\sin\frac{\pi n}{2}$$

где $n = 0, 1, 2, 3$, имеет 5 неприводимых представлений: четыре одномерных (A_1, A_2, B_1, B_2) и одно двумерное (E).

Совокупность данных о низкотемпературном повепении тсрмолинамических характеристик [15, 16], а также измерения угловой зависимости амплитуды фотоэмиссии (ARPES) [17] и фазочувствительные SQUID-эксперименты [18-20] (см. 16) позволяют сделать вывод о том, что сверхпроводящцее состояние в этих соединсниях описывается однокомпонентным нетривиальным параметром порядка, отвечающим синглетному спариванито и преобразуіоциммся в соответствии с представлением B_{1g}, то есть

$$g(\mathbf{k}) \propto \hat{k}_x^2 - \hat{k}_y^2 \tag{4.14}$$

В устоявшейся терминологии такая импухьсная зависимость называется «dспариванием», что, однако, не совсем точно, поскольку в кристаллах нет классификации состояний по орбиталному момснту. В соответствуюощем сверхпроводящсм классе

$$\therefore \quad D_4\left(D_2\right) \times R = \left\{C_{2k}, U_{2k}, e^{i\pi}C_{2k+1}, e^{i\pi}U_{2k+1}\right\} \times R \quad (k = 0, 1)$$

фазовые множители $e^{i\pi} = -1$ компенсируют смену знака базиспой функшии при действии операцжй тотечной симметрии.

Орторомбичсскис кристаллы характеризуются группой симметрии $G = D_{2h}$, имеющей четыре одномерных неприводимьх представления. Простейшее из них - едипичное A_{1g}, соответствующсе обычной сверхпроводимости, описывается параметром порядка, инвариантным относительно вращений на угол π вокруг направлений $\hat{x}, \hat{y}, \hat{z}$. Для синглетного спаривания такими свойствами, в частности, обладает функция

$$g(\mathbf{k}) \propto a + b\left(\hat{k}_x^2 - \hat{k}_y^2\right)$$

представляющая собой смесь s и d-состояний - параметр порядка сверхпроводимости с так назьваемьм «s $+d$-спариванием». Интересно отметить, что это вполне обычное сверхпроводящее состояние в орторомбическом кристалле может оказаться довольно «близким» к необычному сверхпроводящему состоянию B_{1g} в тетрагональном кристалле. Так будет, когда неболыше орторомбические искажения в тетрагональном кристалле вызывают примешивание s-компонепты к исходной d - компоненте параметра порядка (4.14). Другое, часто фигурирующее в литературе «s $+id$-состояние», мы обсудим в следующем подразделе.

Мапнитные сверхпроводящие влассы. Приведенные выше примеры сверхпроводяших классов явно содержат операдию R, то есть соответствующие состояния инвариантны по отношению к обращению времени. Эго, в свою очередь, означает отсутствие спонтанного магнетизма куперовских пар. Однако действие операций точечной группы на параметр порядка может быть скомпенсировано умножснием не толкко на фазовый множитель из калибровочной группы $U(1)$, но и на операцито R, которая сводится к комплексному сопряжению: $g(\mathbf{k}) \to g^*(\mathbf{k})$ или $\mathbf{d}(\mathbf{k}) \to \mathbf{d}^*(\mathbf{k})$. Тем самым инвариантность по отношению к обращенио времени оказывается нарушенной, и симметрия таких сверхпроводящих состояний описывается магнитныии сверхпроводящими классами [9].

Легко видеть, что непосредственный переход из нормаьной фазы в сверхпроводяшую с однокомпонентвым параме тром порядка и нарушеннод симметрией по отношению к обращенио времени невозможен. В самом деле, вблизи
криттческой температуры сверхпроводящие классы находятся во взаимнооднозначном соответствии с представлениями точечной группы G, а операшия R переводит базисную функциі представления в комплексно-сопряженную и поэтому требует, чтобы размерность прсдставления d_Γ была не меньше двух.

Детальное обсуждение вопроса о магнетизме сверхпроводящих фаз с многокомпонентными параметрами порядка мы отложим до 15, а здесь приведем лишь один пример магнитного сверхпроводящего класса для тетрагонального кристалла. Нетрудно убедиться в том, что у группы $\mathcal{G} = U(1) \times R \times D_{4h}$ имеется подгруппа:

$$D_4\,(D_2) = \{C_{2k}, U_{2k}, RC_{2k+1}, RU_{2k+1}\} \quad (k = 0, 1)$$

содержащая операцию обращения времени лишь в комбинации с поворотами вокруг осей симметрии тетрагональной решетки. Указанной симметрией обладает, например, сверхпроводящая фаза синглетного спаривания с параметром порядка $g(\mathbf{k}) = \left(\Delta_s + i\Delta_d\left(\hat{k}_x^2 - \hat{k}_y^2\right)\right)e^{i\varphi}$, где Δ_s и Δ_d - произвольные когстанты. Такое состояние (тасто называемое $s + id$-спариванисм) может возникнуть в результате двух последоватешных фазовых переходов: сначала из нормальной фазы в сверхпроводящую с однокомпонентным параметром порядка $g_1(\mathbf{k}) = \Delta_s e^{i\varphi}$, соответствующим представлению $A_{1\ \mathrm{g}}$, а затем, при более низкой температуре - в другую сверхпроводяшую фазу, в которой к $g_1(\mathbf{k})$ примешивается параметр порядка $g_2(\mathbf{k}) = \Delta_d\left(\hat{k}_x^2 - \hat{k}_y^2\right)e^{i\varphi}$, соответствующий представлению $B_{1\ \mathrm{g}}$.

Нули в спектре элементарных возбуждений. Наличие нетривиальных элементов симметрии, вкпочающих калибровочное прсобразование, приводит к важному слелствию - существованито нулей параметра порядка. Обсудим это свойство для спин-синглетного параметра порядка $g(\mathbf{k})$ с симметрией $D_6\,(C_6) \times R$:

$$C_n g(\mathbf{k}) = g(\mathbf{k}) \tag{4.15}$$

$$e^{i\pi} U_n g(\mathbf{k}) = g(\mathbf{k}) \tag{4.16}$$

$$g(-\mathbf{k}) = g(\mathbf{k}) \tag{4.17}$$

В частности, значсний параметра порядка на плоскости (k_x, k_z), перпендикулярной оси $\hat{y}$, вокрут которой осуществляется поворот U_0, из (4.16) имеем:

$$U_0 g\left(k_x, k_z\right) = -g\left(k_x, k_z\right) \tag{4.18}$$

С друтой стороны, $U_0 k_x = -k_x, U_0 k_z = -k_z$, и

$$U_0 g\left(k_x, k_z\right) = g\left(-k_x, -k_z\right)$$

Используя свойство (4.17), получаем:

$$U_0 g\left(k_x, k_z\right) = g\left(k_x, k_z\right) \tag{4.19}$$

Равенства (4.18) и (4.19) могут быть выполнены ошіовременно лишь при условии

$$g\left(k_x, k_z\right) = 0 \tag{4.20}$$

Таким образом, параметр порядка обращается в нуль на плоскости (k_x, k_x), более того, он меняет знак при се пересечении. То же самое верно для всех плоскостей, перпендикулярных к осям поворотов U_n.

Т а.б ли и а 1. Базисные функции тетных ($S = 0$) и нстетных ($S = 1$, силыное спинорбутальное взаимодсйствие) представлений группы $D_{6\text{ п}}$

d	Γ	$\psi_i^\Gamma(\hat{\mathrm{k}}), \psi_i^\Gamma(\hat{\mathrm{k}})$	H
1	$A_{1\text{ g}}$	$ak_x^2 + b\left(k_x^2 + k_y^2\right) + c\left(k_x^6 - 15k_x^4k_y^2 + 15k_x^2k_y^4 - k_y^6\right)$	$D_6 \times R$
1	A_{1u}	$ak_z\hat{z} + b\left(k_x\hat{x} + k_y\hat{y}\right)$	$D_6\left(C_6\right) \times R$
1	A_{2g}	$\left(k_x^3 - 3k_xk_y^2\right)\left(k_y^3 - 3k_yk_x^2\right)$	
1	A_{2u}	$a\hat{z}k_x\left(k_x^3 - 3k_xk_y^2\right)\left(k_y^3 - 3k_yk_x^2\right) + b\left(\hat{x}k_y - \hat{y}k_x\right)$	$D_6\left(D_3\right) \times R$
1	B_{1g}	$k_x\left(k_x^3 - 3k_xk_y^2\right)$	
1	B_{1u}	$a\hat{z}\left(k_x^3 - 3k_xk_y^2\right) + bk_x\left[\hat{x}\left(k_x^2 - k_y^2\right) - 2\hat{y}k_xk_y\right]$	$D_6\left(D_3'\right) \times R$
1	B_{2g}	$k_z\left(k_y^3 - 3k_yk_x^2\right)$	
1	B_{2u}	$a\hat{z}\left(k_y^3 - 3k_yk_x^2\right) + bk_x\left[\hat{y}\left(k_x^2 - k_y^2\right) - 2\hat{x}k_xk_y\right]$	
2	$E_{1\text{ g}}$	k_zk_x, k_zk_y	
2	$E_{1\text{u}}$	$\hat{z}k_x, \hat{z}k_y$ или $k_z\hat{x}, k_z\hat{y}$	
2	E_{2g}	$k_x^2 - k_y^2, 2k_xk_y$	
2	E_{2u}	$k_x\hat{x} - k_y\hat{y}, k_x\hat{y} + k_y\hat{x}$ или $\hat{z}k_x\left(k_x^2 - k_y^2\right), 2\hat{z}k_xk_xk_y$	

Таблица 2. Базисныс функции нечетных ($S = 1$, слабос спиц-орбиталыюо взаимодействие) представлений группы D_{6h}

d	Γ	$\psi_i^\Gamma(\hat{\mathbf{k}})$	H
1	A_{1u}	$k_z\left(k_x^3 - 3k_xk_y^2\right)\left(k_y^3 - 3k_yk_x^2\right)$	$D_6 \times R \times SO_3^{\text{S}}$
1	$A_{2\text{u}}$	k_z	$D_6\left(C_6\right) \times R \times SO_3^{\text{s}}$
1	B_{1u}	$k_y^3 - 3k_yk_x^2$	$D_5\left(D_3\right) \times R \times SO_3^3$
1	B_{2u}	$k_x^3 - 3k_xk_y^2$	$D_6\left(D_3'\right) \times R \times SO_3^S$
2	E_{1u}	k_x, k_y	
2	E_{2u}	$k_z\left(k_x^2 - k_y^2\right), 2k_xk_yk_z$	

Щель в спектре элементарных возбуждений сверхпроводника пропорционална модуло параметра порядка [4]:

$$\Delta_{\mathbf{k}} \sim |g(\mathbf{k})| \quad \text{при } S=0, \quad \Delta_{\mathrm{k}} \sim |\mathbf{d}(\mathbf{k})| \quad \text{при } S=1$$

(см. ниже 5). Поэтому энергетический спектр квазичастиц в сверхпроводящем состоянии с симметрией $D_6\,(C_6) \times R$ является бесшелевым на линиях пересечения поверхности Ферми и плоскостей, перпендикулярных к осям поворотов U_n.

Для спин-триплетного параметра порядка $\mathbf{d}(\mathbf{k})$ с симметриеи $D_6\,(C_6) \times R$ имеем:

$$C_n\ \mathrm{d}(\mathbf{k}) = \mathrm{d}(\mathbf{k}) \tag{4.21}$$

$$e^{i\pi} U_n\ \mathrm{d}(\mathbf{k}) = \mathrm{d}(\mathbf{k}) \tag{4.22}$$

$$\mathrm{d}(-\mathbf{k}) = -\mathrm{d}(\mathbf{k}) \tag{4.23}$$

Таблица 3. Базисныс функции четных ($S=0$) и нечетных ($S=1$, силыое спинорбитальное взаимодействые) представлений группы $D_{4\text{ д}}$

d	Γ	$\psi_i^{\Gamma}(\hat{k}), \psi_1^{\Gamma}(\hat{k})$	H
1	$A_{1\text{ g}}$	$ak_z^2 + b\left(k_x^2 + k_y^2\right)$	$D_4 \times R$
1	A_{1u}	$a\hat{z}k_x + \hat{b}\left(\hat{x}k_x + \hat{y}k_y\right)$	
1	A_{2g}	$k_x k_y\left(k_x^2 - k_y^2\right)($	$D_4\,(C_4) \times R$
1	A_{2u}	$u\left(\hat{x}k_y + \hat{y}k_x\right)\left(k_x^2 - k_y^2\right) + b\left(\hat{x}k_y - \hat{y}k_x\right)$	
1	$B_{1\text{ g}}$	$k_x^2 - k_y^2$	$D_4\,(D_2) \times R$
1	B_{1u}	$a\left(\hat{x}k_x - \hat{y}k_y\right) + b\hat{z}k_x\left(k_x^2 - k_y^2\right)$	
1	B_{2g}	$k_x k_y$	$D_4\,(D_2') \times R$
1	B_{2u}	$u\left(\hat{x}k_y + \hat{y}k_x\right) + b\hat{z}k_x k_y k_z$	
2	E_g	$k_z k_x, k_z k_y$	
2	E_u	$\hat{z}k_x, \hat{z}k_y$	

Таблица 4. Базисные функции нечетных ($S=1$. слабое спин-орбитальнос взаимодействие) представлений трутпы D_{4h}

d	Γ	$\psi_i^{V_{\mathrm{s}}}(\hat{\mathrm{k}})$	H
1	A_{1u}	$k_x k_y k_x\left(k_x^2 - k_y^2\right)$	$D_4 \times R \times SO_3^{\mathrm{s}}$
1	A_{2u}	k_x	$D_4\,(C_4) \times R \times SO_3^{\mathrm{s}}$
1	B_{1u}	$k_x k_3 k_z$	$D_4\,(D_2) \times R \times SO_3^5$
1	B_{2u}	$k_z\left(k_x^2 - k_y^2\right)$	$D_4\,(D_2') \times R \times SO_3^5$
2	E_u	k_x, k_y	

Инвариантность параметра порядха по отношению к вращениям C_n означает, что для импульсов, направленных вдоль оси $\hat{z}$, отлична от нуля только z-компонента вектора $\mathrm{d}(\mathrm{k})$:

$$\mathbf{d}\,(k_z) = \hat{z}\psi^z\left(\hat{k}_z\right) \tag{4.24}$$

Из (4.22)

$$U_0 \mathbf{d}\,(k_z) = -\mathbf{d}\,(k_z) \tag{4.25}$$

но в то же время из (4.23) и (4.24) получаем:

[14] Данное утверждение справедливо аля уиитарных свгрхпроводящих состояний в отсутствие примесей (см. сноску 6 в 5 и 17).

$$U_0\mathbf{d}\left(k_z\right)=U_0\hat{z}\psi^z\left(\hat{k}_z\right)=-\hat{z}\psi^z\left(-\hat{k}_z\right)=\hat{z}\psi^z\left(\hat{k}_z\right)=\mathbf{d}\left(k_z\right) \tag{4.26}$$

Из сравнения соотношений (4.25) и (4.26) следует, что

$$\mathbf{d}\left(k_z\right)=0 \tag{4.27}$$

то есть параметр порядка равен нулоо на оси $\ddot{z}$, и поэтому спектр квазичастиц является бесщелевым на северном и южном полюсах ферми-поверхности.

Таким образом, имеется общая особенность сверхпроводяших состояний, симметрия которых включает комбинации точечных и калибровочных преобразований (или точечных преобразований и операции обращения времени). А именно, спектр элементарных возбуждений в таких сверхпроводниках является бесщелевым. Нули параметра порядка расположены на

таблица S. Базисные функции четных ($S=0$) и нечстных ($S=1$, сильное спин-орбиталынос взаимодействие) прелставлений группы $O_h(\varepsilon=\exp(2\pi i/3)$. $O(T)=(E,8C_3,3C_2,6\epsilon^{\imath\pi}U_2,6e^{t\pi}C_4))$

d	Γ	$\psi_i^\Gamma\varepsilon(\hat{k}),\psi_i^{\mathrm{Y}}(\hat{\mathrm{k}})$	H
1	A_{1s}	$k_x^2+k_y^2+k_z^2$	
1	A_{1u}	$\hat{x}k_x+\hat{y}k_y+zk_z$	$O\times R$
1	A_{2s}	$\left(k_x^2-k_y^2\right)\left(k_y^2-k_z^2\right)\left(k_z^2-k_x^2\right)$	$O(T)\times R$
1	A_{2u}	$\hat{x}k_x\left(k_z^2-k_y^2\right)+\hat{y}k_y\left(k_x^2-k_z^2\right)+\hat{z}k_z\left(k_y^2-k_x^2\right)$	
2	E_k	$k_x^2+\varepsilon k_y^2+\varepsilon^2k_z^2,k_x^2+\varepsilon^2k_y^2+\varepsilon k_z^2$	
2	E_u	$\hat{x}k_x+\varepsilon\hat{y}k_y+\varepsilon^2\hat{z}k_z,\hat{x}k_x+\varepsilon^2\hat{y}k_y+\varepsilon\hat{z}k_z$	
3	F_{1s}	$k_yk_z\left(k_y^2-k_z^2\right),k_zk_x\left(k_z^2-k_x^2\right),k_xk_y\left(k_x^2-k_y^2\right)$	
3	F_{1u}^2	$\hat{y}k_z-zk_y,\hat{k}k_x-\hat{z}k_z,\hat{x}k_y-\hat{y}k_x$	
3	F_{2s}	k_yk_z,k_zk_x,k_xk_y	
3	F_{3u}	$\hat{y}k_z+\hat{z}k_y,\hat{z}k_x+\hat{x}k_z,\hat{x}k_y+\hat{y}k_x$	

Таблица 6. Базисные функции нечстных ($S=1$, слабое спин-орбиталыюее взаимодежствие) прсдставлений группы O_h

d	Γ	$\psi_i^\Gamma\mathrm{s}(\hat{\mathrm{k}})$	II
1	A_{1u}	$k_xk_yk_z\left(k_x^2-k_y^2\right)\left(k_y^2-k_z^2\right)\left(k_z^2-k_x^2\right)$	$O\times R\times SO_3^s$
	A_{2u}	$k_xk_yk_z$	$O(T)\times R\times SO_3^s$
2	E_u	$k_xk_yk_x\left(k_x^2+\varepsilon k_y^2+\varepsilon^2k_z^2\right)$	
		$k_xk_yk_z\left(k_x^2+\varepsilon^2k_y^2+\varepsilon k_x^2\right)$	
3	F_{1u}	k_x,k_y,k_z	
3	F_{2u}	$k_x\left(k_y^2-k_z^2\right),k_y\left(k_z^2-k_x^2\right),k_z\left(k_x^2-k_y^2\right)$	

ферми-поверхности на линиях и в изолированных точках для $S=0$ и в точках лля $S=1$. Послешнее утверждсние всрно лишь для случая сильного спин-орбиталыного взаимодействия (коптрпример - параметр порядка для полярной фазы с p-спариванием).

Непременное наличие нулей в спеклре возбужпений есть прямое следствие определенной сдмметрии сверхпроводящего состомния. Поэтому нули этого типа назывзотся симметрийными нулями. Среди симметрийных нулей можно выделить осоБый подкласс топологических нулей. К последним относятся те симметрийные нули, которые не исчезают при непрерывных деформациях, нарушагоцих симметрию кристалла. Не утлубляясь особо в сей предмет, укажем без доказательства, что симметрийныс точки нулсй являются в то же время топологическими, линии - нст.

Симметрийный подход пставляет значительнуо свободу в выборе базисвых фуікдий неприводимых представлений. Конкретный выбор базисных функций данного предстазления Γ может быть сделап только п рамках какойибо микроскопической модели и опрсделяется тотностыо, с которой мы хотим описать параметр порядка даниого сверхпроволящего состояния. Наличие и положение симметрийных нудей в спектре элементарных возбуждений
определяется не видом базисних функций, а симметрией сверхпроводящего состояния. Опрслеленный же выбор базисных фупкший может искусственно породить дополнитслыые нефизические («случайныс») нули в спектрс элемснтарных возбуждений.

Примеры базисных функций для представлений грулпы D_{6h} собраны в табл. 1 и 2. Для илююстрации высказанных утверждений базиспые функции нсчетных представлепий в табл. 1 представлены в видс линейных комбинаций фупкций двух типов. При произвольных значениях коэффициснтов a и b базисные функции $\psi_i^{\Gamma'}(\hat{\mathbf{k}})$ обращаются в нуль только в изолированных точках на ферми-поверхности, лежаших па осях вращений, соответствующих комбитированшымм эдеменгам симметрии данного сверхпроводящего состояния (симметрийныс нули). С другой стороны, при $a = 0$ (или $b = 0$) в каждой из перечисленных сверхпроводящих фаз к симметрийшым пгудя добавлятотся случайные (в том числе и лежащие на линиях) нули параметра порядка.

Базисные функции прсдставлений лля кристаллов с тетрагональной (группа D_{4h}) и кубическон (группа O_h) симметрией приведены в табл. 3-6. Для одномерных представлений указаплы также соответствующие сверхпроводящис классы H. Классы сверхпроводящих состояний, описываемых неодномерными представлениями, будут введены в II, посвященном теории Ландау лля ашизотроптых сверхпроводников.

19.1.5 5. Energy of Elementary Excitations of a Superconductor

Задача о нахождении спектра элемснтарных возбуждений свсрхпроводника решается пугем диагонализации гамильтониаша системы ферми-частиц [1], в котором из всех видов взаимодействий оставлено только сушественное для сверхпроводимости парное притяжение частиц, имеющих противоположные импульсы (гамильтониан Бардина-Купера-Шриффера):

$$H = \sum_{\mathbf{k}} \xi_{\mathbf{k}} a^+_{\mathbf{k}\alpha} a_{\mathbf{k}\alpha} + \frac{1}{2} \sum_{\mathbf{k},\mathbf{k}'} V_{\alpha\beta,\lambda\mu}(\mathbf{k},\mathbf{k}')\, a^+_{-\mathbf{k}\alpha} a^+_{\mathbf{k}\beta} a_{\mathbf{k}'\lambda} a_{-\mathbf{k}'\mu} \tag{5.1}$$

Здесь и ниже по повторяющимся спиновым индексам подразумевается суммирование, $\xi_k = \hbar^2 k^2/(2m^*) - \varepsilon_F$ - эергия возбуждений в нормалыном металле, отсчитанная от энергии Ферми, m^* - эффективная масса. $V_{\alpha\beta,\lambda\mu}(\mathbf{k},\mathbf{k}')$ потенциал парного притяжения, обладаюощий симметрийными свойстзами:

$$V_{\alpha\beta,\lambda\mu}(\mathbf{k},\mathbf{k}') = -V_{\beta\alpha,\lambda\mu}(-\mathbf{k},\mathbf{k}') = -V_{\alpha\beta,\mu\lambda}(\mathbf{k},-\mathbf{k}') = V_{\mu\lambda,\beta\alpha}(\mathbf{k}',\mathbf{k}) \tag{5.2}$$

В отсутствие спин-орбиталшного взаимодействия потенциал факторизуется:

$$V_{\alpha\beta,\lambda\mu}(\mathbf{k},\mathbf{k}') = V(\mathbf{k},\mathbf{k}')\,\Gamma_{\alpha\beta,\lambda\mu} \tag{5.3}$$

[1] Для простоты мы будем рассматривать ферми-газ со сферической ферми-поверхиостью, ие иринимая во внимание влияние кристаллической решетки на энергегический спектр.

[2] Здссь и ниже мы испажьзусм шолновыс функции, нормированные на единичный объем, поэтому $\sum_{\mathbf{k}} \to \int \frac{d^3k}{(2\pi)^3} = N_0 \int d\xi \int \frac{d\Omega}{4\pi}$, где $N_0 = \frac{m^* k_{\mathrm{F}}}{2\pi^2\hbar^2}$ - пиютность состоянии на поверхности Ферми на одгу проекцию спина.

Функшию $V(\mathbf{k},\mathbf{k}')$ будсм счигать опличной от пуля, когда концы векторов $\mathbf{k}$ и $\mathbf{k}'$ лежат в узком слое вблизи ферми-поверхIости:

$$V(\mathbf{k},\mathbf{k}') = V_l(k,k') \sum_{m=-1}^{l} Y_{lm}(\hat{\mathbf{k}}) Y_{lm}^*\left(\hat{\mathbf{k}}'\right) \tag{5.4}$$

$$V_l(k,k') = \begin{cases} -V_l, & \text{при } \varepsilon_\mathrm{F} - \varepsilon_l \le k^2/(2m^*), k^2/(2m^*) \le \varepsilon_\mathrm{F} + \varepsilon_l \\ 0, & \text{вне указанного интервата.} \end{cases}$$

Здесь в разложении функции $V(\mathbf{k},\mathbf{k}')$ по сферическим гармоникам с разными l оставлено лишв взаимодействие V_7, приводящее k максимальной критической температуре (см. 1).

Что касается спиновой зависимости потенциала, то для четных l она записывается через антисимметричные по индексам $\alpha\beta(\lambda\mu)$ матрицы

$$\Gamma_{\alpha\beta,\lambda\mu} = \frac{1}{2} g_{\alpha\beta\beta} g^+_{\lambda\mu} \tag{5.5}$$

$g_{\alpha\beta} = (i\sigma_y)_{\alpha\beta}$, а для нечетных l - черсз симметричные:

$$\Gamma_{\alpha\beta,\lambda,\beta} = \frac{1}{2} \mathbf{g}_{\alpha\beta} \mathbf{b}^+_{\lambda\mu} \tag{5.6}$$

где $\mathrm{g}_{\alpha\beta} = (i\sigma\sigma_y)_{\alpha\beta}$, а g^+и g^+обозначают эрмитово-сопряжепные матрицы.

В кристаллах, где сущсстзешна инвариантность относительно преобразований точечной группы симметрии, парное взаимодействие имеет вид

$$V_{\alpha\beta,\lambda\mu}(\mathbf{k},\mathbf{k}') = V_\Gamma(k,k')\,\Gamma^2_{\alpha\beta,\lambda\mu} \sum_{i=1}^{d_\mathbf{r}} \psi_i^\Gamma(\hat{\mathbf{k}}) \psi_i^{\Gamma^\top}\left(\hat{\mathbf{k}}'\right) \tag{5.7}$$

Здесь оставлено лишь взаимодсйствие V_Γ, относящееся х неприводимому представлению Γ с базисными функциями $\psi_i^\Gamma(\hat{\mathbf{k}})$, которое приводит к спариваниго с максимальной критической тсмпературой. Функдии $\Gamma_{\alpha\beta,\lambda\mu}$ ддя четных и нечетных прсдставлсций задаготся формулами (5.5) и (5.6), соответственіно.

Вцражение (5.7) справедливо для синглетного спаривашия и триплетного спаривания со слабым спин-орбитальным взаимолсйствием. В случае $S = 1$ и сильного спин-орбитального взаимодействия (см. 4) парнос взаимодействие имеет вид

$$V_{\alpha\beta,\lambda\mu}(\mathbf{k},\mathbf{k}') = \frac{1}{2} V_\Gamma(k,k') \sum_{i=1}^{d_\Gamma} \left(\psi_i(\hat{\mathbf{k}}) \mathrm{g}_{\alpha\beta}\right) \left(\psi_i^*\left(\hat{\mathbf{k}}'\right) \mathrm{g}^+_{\lambda\mu}\right) \tag{5.8}$$

Неустойчивость электронного газа, описываемого гамильтонианом (5.1), по отношению к образованию куперовских пар можно учесть [1], записывая волновуо функииюо основного состояния в виде произведения

$$\Psi = \prod_\mathbf{k} \left(u_\mathbf{k} + v_\mathbf{k} a^+_{\mathbf{k}\uparrow} a^+_{-\mathbf{k}\downarrow}\right) |vac\rangle \tag{5.9}$$

Здесь $v_\mathbf{k}$ - амплитуда вероятности заполисния пары опночастичных состоянии ($\mathbf{k}\uparrow, -\mathbf{k}\downarrow$) (для простоты мы имеем в виду синглетное спаривание),
u_k - амплитуда вероятности обнаружить состояние ($\mathbf{k}\uparrow, -\mathbf{k}\downarrow$) незаполнеппым, а $\langle \mathrm{vac}\rangle$ - волновая функция вакуумного состояния, причем выполтяется условие

$$|u_\mathbf{k}|^2 + |u_\mathbf{k}|^2 = 1$$

В нормалыном металле

$$\begin{array}{ll} v_k = 1 : u_k = 0, & \text{при } |\mathrm{k}| < k_F, \\ u_k = 0, u_k = 1, & \text{при } |\mathrm{k}| > k_F, \end{array} \tag{5.10}$$

то есть все состояния иже ферми-уровня запотлсны, выше него - пусты.

В сверхпроводнике при лобом $\mathbf{k}$ имеется ненулевая вероятность обнаружить данное парное состояние пустым, и волновая функция основного состоs1дия (5.9) состоит из большого числа слагаемых, в каждом из которых с различной вероятностью заполнено $0, 2, \ldots, N, N \pm 2, \ldots$ парных одночастичных состояний. Иными словами, основное состояние сверхпроводника предстазляет собой суперпозициюо состояний с разлжчным пислом куперовских пар [3]. Стедствием этого фундаментального факта служит опличие от нуля так называемдх аномальных средних [21]:

$$F_{\mathbf{k},T\downarrow} = \langle \Psi \left| a_{\mathbf{k}\uparrow} a_{-\mathbf{k}\downarrow} \right| \Psi \rangle$$
$$F^{+}_{\mathbf{k},T\downarrow} = \left\langle \Psi \left| a^{+}_{-\mathbf{k}\uparrow} a^{+}_{\mathbf{k}\downarrow} \right| \Psi \right\rangle$$

Такие среднис можно опрсделить и при произволыной температуре [4]:

$$F_{\mathrm{k},\alpha\beta} = \langle a_{\mathbf{k}\alpha} a_{-\mathbf{k}\beta} \rangle$$
$$F^{+}_{\mathrm{k},\alpha\beta} = \left\langle a^{+}_{-k\alpha} a^{+}_{\mathrm{k}\beta} \right\rangle \tag{5.11}$$

Функция $F_{\mathrm{k},\alpha\beta}$, имегощая смысл вопіовой фуікции пары, антисимметрична относитетьно переставшовки частиг:

$$F_{\mathbf{k},\alpha\beta} \to P_{-\mathbf{k},\beta\alpha} = -F_{\mathbf{k},\alpha\beta\beta} \tag{5.12}$$

Для пространственно-четных функций F равенство (5.12) означает антисимметрию по спиновым индексам:

$$F^{\mathrm{g}}_{\mathbf{k}_1\alpha\beta} = -F^{\mathrm{g}}_{\mathbf{k},\beta\alpha}$$

то есть для спаривания в синглетном состояIIии имеем:

$$F^{\mathrm{g}}_{\mathbf{k},\alpha\beta} = F_{\mathbf{k}} g_{\alpha\beta}$$
$$F^{\mathrm{g}}_{\mathbf{k},\alpha\beta} = F^{*}_{\mathbf{k}} g^{+}_{\alpha\beta} \tag{5.13}$$

гле $F_{-\mathrm{k}} = F_{\mathrm{k}}$. Для пространственно-нечетных функший F равенство (5.12) справедливо линь в слугае симметрии по спиновым индексам:

$$F^{\mathrm{U}}_{\mathbf{k},\alpha\beta} = F^{\mathrm{u}}_{\mathbf{k},\beta\alpha}$$

[3] Гтавныд вклад в эту суперпозицию вносят состояния с тислом пар $N_{\mathrm{pairs}} \approx N_{\mathrm{particles}}/2$.

[4] Средиее в формулах (5.11) понимается как

$$\langle A \rangle = \frac{\sum\limits_{n} A_{nnc} - E_n/T}{\sum\limits_{n} e^{-E_n/T}}$$

то есть для спаривания в триплетном состоянии:

$$F^{\mathrm{u}}_{\mathbf{k},\alpha\beta} = \mathbf{F}_{\mathbf{k}}\mathbf{g}_{\alpha\beta}$$
$$F^{\mathrm{u}+}_{\mathbf{k},\alpha\beta} = \mathbf{F}^{*}_{\mathbf{k}}\mathbf{g}^{+}_{\alpha\beta} \tag{5.14}$$

где $\mathbf{F}_{-\mathbf{k}} = -\mathbf{F}_{\mathbf{k}}$.

Для диагонализации гамильтониана в приближении самосогласованного поля [21] предположим, что отклонения произведений пар операторов, входяших в (5.1), от их средних значений (5.11) малы. Воспользовавшись тождественными преобразовапиями:

$$a^{+}_{-\mathbf{k}\alpha}a^{+}_{\mathbf{k}\beta} = F^{+}_{\mathbf{k},\alpha\beta} + \left(a^{+}_{-\mathbf{k}\alpha}a^{+}_{\mathbf{k}\beta} - F^{+}_{\mathbf{k},\alpha\beta}\right) \tag{5.15}$$
$$a_{\mathbf{k}'\lambda}a_{-\mathbf{k}'\mu} = F_{\mathbf{k}',\lambda\mu} + \left(a_{\mathbf{k}'\lambda}a_{-\mathbf{k}'\mu} - F_{\mathbf{k}',\lambda\mu}\right)$$

перепишем гамильтониан (5.1) в линсйном приближении по указанным откдонетиям:

$$H = \sum_{\mathbf{k}} \xi_{\mathbf{k}} a^{+}_{\mathbf{k}\alpha}a_{\mathbf{k}\alpha} + \frac{1}{2}\sum_{\mathbf{k},\mathbf{k}'} V_{\alpha\beta,\lambda\mu}\left(\mathbf{k},\mathbf{k}'\right)\left(-F^{+}_{\mathbf{k},\alpha\beta}F_{\mathbf{k}',\lambda\mu} + \right.$$
$$\left. + F^{+}_{\mathbf{k},\alpha\beta}a_{\mathbf{k}'\lambda}a_{-\mathbf{k}'\mu} + F_{\mathbf{k}',\lambda\mu}a^{+}_{-\mathbf{k}\alpha}a^{+}_{\mathbf{k}\beta}\right) \tag{5.16}$$

Введем теперь функции

$$\Delta_{\mathbf{k},\alpha\beta} = -\sum_{\mathbf{k}'} V_{\beta\alpha,\lambda\mu}\left(\mathbf{k},\mathbf{k}'\right) F_{\mathbf{k}',\lambda,k}$$
$$\Delta^{+}_{\mathbf{k},\lambda,k} = -\sum_{\mathbf{k}'} V_{\alpha\beta,\mu\lambda}\left(\mathbf{k}',\mathbf{k}\right) F^{+}_{\mathbf{k}',\alpha\beta} \tag{5.17}$$

Из (5.2) и (5.12) получаем:

$$\Delta_{k,\alpha\beta} = -\Delta_{-k,\beta\alpha\alpha}.$$

Очевидго, что для четного по импудьсам потенциала взаимодействия функции $\Delta_{\mathbf{k},\alpha\beta}$ и $F_{\mathbf{k},\alpha\beta}$ также должны быть четньмми, что соответствует спариваник в синглетном состоянпи:

$$\Delta_{\mathbf{k},\alpha\beta} = \Delta g(\mathbf{k})\left(i\sigma_y\right)_{\alpha\beta} \tag{5.18}$$

Здесь

$$g(\mathbf{k}) = g'(\mathbf{k}) = \sum_{m=-1}^{l} a_{lm}(k)Y_{lm}(\mathbf{k})$$

а нормировка выбрана стедующим образом:

$$\int \frac{dS}{4\pi}\left|g'(\mathbf{k})\right|^2 = 1 \tag{5.19}$$

Заметим, что

$$\int \frac{d\Omega}{4\pi} g^{l}(\mathbf{k}) = 0$$

ддя всех значепий l, кроме s-спаривапия ($l = 0$).

В случае нечетного потешциала взаимодействия фупкции $\Delta_{\mathbf{k},\alpha\beta}$ и $F_{\mathbf{k},\alpha\beta}$ также нечетны и описывают триплетное спаривание:

$$\Delta_{\mathbf{k},\alpha\beta} = \Delta \mathrm{d}(\mathbf{k}) \left(i\sigma\sigma_y\right)_{\alpha,\beta k} \tag{5.20}$$

Здесь

$$\mathrm{d}(\mathbf{k}) = \mathrm{d}^l(\mathbf{k}) = \sum_{m=-1}^{1} \mathbf{b}_{lm}(k) Y_{lm}(\mathbf{k})$$

и

$$\int \frac{d\Omega}{4\pi} |\mathbf{d}(\mathbf{k})|^2 = 1 \tag{5.21}$$

Коэффициенты $a_{lm}(k)$ и $\mathrm{b}_{lm}(k)$ отличны от нуля лишв в узком слое толшиной $\delta k = \varepsilon_l / v_F$ вблизи поверхіости Ферми.

Испольэуя (5.17), для гамитониана (5.16) получаем [5]:

$$\begin{aligned} H = \frac{1}{2}\sum_{\mathbf{k}} \xi_{\mathbf{k}} \left(a^+_{\mathbf{k}\alpha} a_{\mathbf{k}\alpha} - a_{-\mathbf{k}\alpha} a^+_{-\mathbf{k}\alpha}\right) + \frac{1}{2}\sum_{\mathbf{k}\alpha} \xi_{\mathbf{k}} + \\ + \frac{1}{2}\sum_{\mathbf{k}} \left(\Delta_{\mathbf{k},\alpha\beta} a^+_{\mathbf{k}\alpha} a^+_{-\mathbf{k}\beta} + \Delta^+_{\mathbf{k},\alpha\beta} a_{-\mathbf{k}\alpha} a_{\mathbf{k}\beta} + \Delta_{\mathbf{k},\alpha\beta} F^+_{\mathbf{k},\beta\alpha}\right) \end{aligned} \tag{5.22}$$

Это выражение можно переписать в более компактном виде, определив векторные операторы [22]

$$\begin{aligned} A^+_{k,i} \equiv \left(a^+_{k\alpha}, a_{-k\alpha}\right) \equiv \left(a^+_{k\uparrow}, a^+_{k\downarrow}, a_{-k\uparrow}, a_{-k\downarrow}\right) \\ A_{k,i} \equiv \begin{pmatrix} a_{k\alpha} \\ a^+_{-k\alpha} \end{pmatrix} \equiv \begin{pmatrix} a_{k\uparrow} \\ a_{k\downarrow} \\ a^+_{-k\uparrow} \\ a^+_{-k\downarrow} \end{pmatrix} \end{aligned} \tag{5.23}$$

Имеем:

$$H = \frac{1}{2}\sum_{\mathbf{k}} A^+_{\mathbf{k},i} \varepsilon_{\mathbf{k},ij} A_{\mathbf{k},j} + \frac{1}{2}\sum_{\mathbf{k}} \Delta_{\mathbf{k},\alpha\beta} F^+_{\mathbf{k},\beta\alpha} + \frac{1}{2}\sum_{\mathbf{k}\alpha} \xi_{\mathbf{k}}$$

где мы ввели матрицу 4×4:

$$\varepsilon_{k,ij} = \begin{pmatrix} \xi_k \delta_{\alpha\beta} & \Delta_{k,\alpha\beta} \\ \Delta^+_{k,\alpha\beta} & -\xi_k \delta_{\alpha\beta} \end{pmatrix}$$

Гамильтониан (5.24) приводится к диагональному виду с помощью сохранятощего антикоммуташионные соотношения унитарного преобразования Боголобома [6], прсобразуэощего фермиевские операторы a_k в фермиевские опсраторы $b_{\mathbf{k}\alpha}$:

$$A_{k,i} = U_{ij} B_{k,j} \tag{5.25}$$

гдс

$$U_{ij} = \begin{pmatrix} u_{k,\alpha\beta} & v_{k,\alpha\beta} \\ v^*_{-k,\alpha\beta} & u^*_{-k,\alpha\beta} \end{pmatrix} \tag{5.26}$$

$$B_{k,i} = \begin{pmatrix} b_{k\beta} \\ b^+_{-k\beta} \end{pmatrix} \tag{5.27}$$

Элементы матрицы преобразования являются, в свою очередь, матрицами 2×2 в спиновом пространстве и определяются следующими формулами:

$$u_{k,\alpha\beta} = \frac{(E_k + \xi_k)\,\delta_{a\beta}}{\sqrt{(E_k + \xi_k)^2 + \Delta_k^2}} = u_k \delta_{\alpha\beta} \tag{5.28}$$

$$v_{k,\alpha\beta} = -\frac{\Delta_{k,\alpha\beta}}{\sqrt{(E_k + \xi_k)^2 + \Delta_k^2}}$$

где

$$E_{\mathbf{k}} = \sqrt{\xi_k^2 + \Delta_{\mathbf{k}}^2} \tag{5.29}$$

и введено обозначснис (см. (5.18) и (5.20))

$$\Delta^2_{\mathbf{k}} = \frac{1}{2}\,\mathrm{Sp}\,\Delta^+_{\mathbf{k}}\Delta_{\mathbf{k}} = \begin{cases} \Delta^2 |g(\mathbf{k})|^2, & \text{при } S = 0 \\ \Delta^2 \mathbf{d}(\mathbf{k})\mathbf{d}^*(\mathbf{k}), & \text{при } S = 1 \end{cases} \tag{5.30}$$

В результате получаем:

$$\sum_{\mathbf{k}} A^+_{\mathbf{k},i} \varepsilon_{\mathbf{k},ij} A_{\mathbf{k},j} = \sum_{\mathbf{k}} B^+_{\mathbf{k},i} E_{\mathbf{k},ij} B_{\mathbf{k},j}$$

где

$$E_{\mathrm{k},ij} = \begin{pmatrix} E_{\mathrm{k}}\delta_{\alpha\beta} & 0 \\ 0 & -E_{\mathrm{k}}\delta_{\alpha\beta} \end{pmatrix}$$

Перепишем послелисс выражение в терминах операторов рождения и уничтожения квазичастиц $b_{\mathbf{k}\alpha}$:

$$\frac{1}{2}\sum_{\mathbf{k}} B^+_{\mathbf{k},i}\hat{E}_{\mathbf{k},ij}B_{\mathbf{k},j} = \frac{1}{2}\sum_{\mathbf{k}} E_{\mathbf{k}} b^+_{\mathbf{k}\alpha} b_{\mathbf{k}\alpha} - \frac{1}{2}\sum_{\mathbf{k}} E_{\mathbf{k}} b_{-\mathbf{k}\alpha} b^+_{-\mathbf{k}\alpha} =$$
$$= \sum_{\mathbf{k}} E_{\mathbf{k}} b^+_{\mathbf{k}\alpha} b_{\mathbf{k}\alpha} - \frac{1}{2}\sum_{\mathbf{k}\alpha} E_{\mathbf{k}}$$

Таким образом, гамильтониаи свсрхпроводника окончательно приобретает следующий вид:

$$H = E_0 + \sum_{\mathbf{k}} E_{\mathbf{k}} b^+_{\mathbf{k}\alpha} b_{\mathbf{k}\alpha} \tag{5.31}$$

где

[1] Суммированис по спиновым индсхсам от функции ξ_k, не зависящсй от спинов, означаст $\sum_{k\alpha} \xi_k = 2\sum_k \xi_k$

[6] Все формулы, приводимые ииже, справедливы для произваыьного тита синглетного спаривания, а в случае триптетного спаривания - линъ птя тах называемых уннтарыых фаз. удовлстворяюицих условию: $(\Delta\Delta^+)_{\alpha\beta} \sim \delta_{\alpha\beta}$. Среди персчислснпых в §3 фаз с р-спариваиием к унитарым фазам относятся всс. кроме A_1 - и β-фазы. В неуинарном стучае диагонализация гамильтониана выглядит иесколько сложлее (см. [13], а также 17), и мы не будем здесь на этом останавливаться.

$$E_0 = \frac{1}{2}\sum_{\mathbf{k}} \Delta_{\mathbf{k},\alpha\beta} H^{+}_{\mathbf{k},3\alpha} + \frac{1}{2}\sum_{\mathbf{k}\alpha} (\xi_k - E_{\mathbf{k}}) \tag{5.32}$$

ссть эдергия основного состояния, а величины E_{k} представляют собой энергии элементарных возбуждсний сверхпроводника.

Для сверхпроводиика с синглетным спариваниси имесм:

$$E_{\mathbf{k}} = \sqrt{\xi_k^2 + \Delta^2 |g(\mathbf{k})|^2} \tag{5.33}$$

то есть в спектре элементарних возбуждений имеется щель. В полностью изотропном стучае (s-спаривание) $g(\mathbf{k}) = |\Delta| e^{i\varphi}$, и щел отлична от нуля на всей ферми-повсрхности. Как было показано в §4, s-спаривашию в кристалле соответствует сверхпроволящее состолние, преобразуоцееся согласно
единичному представлениюо точечной группы симметрии кристалла. В этом случае $g(k)$ может обращаться в нузь при некоторых значениях k (случайные нули). Для анизотропных типов спаривания с $l \neq 0$, таких, что сверхпроводящее состояние облапает комбинированной (например, поворотной и калибровочной) симметрией, обращение щели в нуль при некоторых $\mathbf{k}$ обязателшно (симметрийные нули).

Для сверхпроводника с триплетным спариванием:

$$E_{\mathrm{k}} = \sqrt{\xi_k^2 + \Delta^2 |\ \mathrm{d(k)}|^2} \tag{5.34}$$

В B-фазе $\mathbf{d} = \hat{\mathbf{k}}$ (см. (3.2) и (5.21)), и

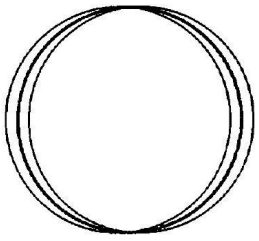
$$E_k^B = \sqrt{\xi_k^2 + |\Delta|^2} \tag{5.35}$$

то есть, как и в случае s-спаривания, на всей ферми-поверхности имеется щель, не зависящая от направления $\mathbf{k}$.

В A-фазе $\mathbf{d} = \sqrt{3/2}\left(\hat{k}_x + i\hat{k}_y, 0, 0\right)$ (см. (3.8) с учетом нормировочного міножителя), и

$$E^A_{\mathbf{k}} = \sqrt{\xi_k^2 + \frac{3}{2}\Delta^2\left(\hat{k}_x^2 + \hat{k}_y^2\right)} = \sqrt{\xi_k^2 + \frac{3}{2}\Delta^2 \sin^2\theta} \tag{5.36}$$

то есть щель в спектре обращается в нуль на северном и южном полюосах ($\theta = 0, \pi$) ферми-сферы (рис. 4). Наличие нулей в спектре A-фазы следует из



Ри с. 4. Щель в спектре A-фазы. Границы щели - товкие дишии, ферми-сфера - жирная линия комбинированной инвариантности состояния (3.8) относительно поворотов на утол α вокрут оси z и одновременного калибровочного преобразования домножения на $\epsilon^{-i\alpha}$ (более подробно см. 4).

Упражиеиие. Показать, что энергия основного состояния сверхпроводника (5.32) определяется следующими выражениями:

$$E_{0\ \mathrm{s}} = E_{0\mathrm{n}} - \frac{1}{2} N_0 \Delta^2 \tag{5.37}$$

для синглетного изотропного спаривания, и

$$E_{0\ \mathrm{s}} = E_{0\mathrm{n}} - \frac{1}{4} N_0\, \mathrm{Sp} \int \frac{d\Omega}{4\pi} \Delta_{\mathrm{k}}^{+} \Delta_{\mathrm{k}} \tag{5.38}$$

для произвольного типа спаривания, где $E_{0\mathrm{n}}$ есть энергия основного состояния нормального металла.

19.1.6 6. Gap in the Excitation Spectrum and Critical Temperature

Для определения температурной зависимости щели в спектре элементарных возбуждений обратимся к формуле (5.17):

$$\Delta_{\mathbf{k},\alpha\beta} = -\sum_{\mathbf{k}'} V_{\beta\alpha,\lambda\mu}\left(\mathbf{k},\mathbf{k}'\right) F_{\mathbf{k}',\lambda\mu} \tag{6.1}$$

Подставляя сода аномальное среднее (5.11) и применяя преобразование Боголобова (5.25), имеем:

$$F_{\mathbf{k},\lambda\mu} = \left\langle a_{\mathbf{k}\lambda} a_{-\mathbf{k}\mu} \right\rangle = \left\langle \left(u_{\mathbf{k},\lambda\gamma} b_{\mathbf{k}\gamma} + v_{\mathbf{k},\lambda\gamma} b_{-\mathbf{k}\gamma}^{+}\right) \left(u_{-\mathbf{k},\mu\delta} b_{-\mathbf{k}\delta} + v_{-\mathbf{k}}\mu\delta b_{\mathbf{k}\delta}^{+}\right) \right\rangle$$

Используя соотношения

$$u_{\mathbf{k},\alpha\beta} = u_{\mathbf{k}}\delta_{\alpha\beta}, \quad v_{\mathbf{k},\alpha\beta} = -v_{-\mathbf{k},\beta\alpha}$$
$$\left\langle b_{-\mathbf{k}\alpha} b_{\mathbf{k}\beta} \right\rangle = \left\langle b_{\mathbf{k}\alpha}^{+} b_{-\mathbf{k}\beta}^{+} \right\rangle = 0$$
$$\left\langle b_{\mathbf{k}\alpha}^{+} b_{\mathbf{k}\beta} \right\rangle = \delta_{\alpha\beta} - \left\langle b_{\mathbf{k}\beta} b_{\mathbf{k}\alpha}^{+} \right\rangle = f_{\mathbf{k}}\delta_{\alpha\beta}$$

где

$$f_{\mathrm{k}} = f\left(E_{\mathrm{k}}\right) = \frac{1}{\exp\left(E_{\mathrm{k}}/T\right) + 1} \tag{6.2}$$

есть фермиевская функция распределения возбуждений с энергией $E_{\mathbf{k}}$, определяемой формулой (5.29), получаем:

$$F_{\mathbf{k},\lambda\mu} = -u_{\mathbf{k}} v_{\mathbf{k},\lambda\mu}\left(1 - 2f_{\mathbf{k}}\right) = \frac{\Delta_{k,\lambda\mu}}{2E_{\mathbf{k}}}\left(1 - 2f_{\mathbf{k}}\right) \tag{6.3}$$

После подстановки в (6.1) окончательно приходим х следующему условию самосогласования:

$$\Delta_{\mathbf{k},\alpha\beta} = -\sum_{\mathbf{k}'} V_{\beta\alpha,\lambda\mu}\left(\mathbf{k},\mathbf{k}'\right) \frac{1 - 2f_{\mathbf{k}'}}{2E_{\mathbf{k}'}} \Delta_{\mathbf{k}',\lambda\mu} \tag{6.4}$$

называемому также «уравнением на щель. Вспоминая выражения (5.33) п (5.34), имеем:

$$g(\mathbf{k}) = -\sum_{\mathbf{k}'} \frac{V\left(\mathbf{k},\mathbf{k}'\right)\left(1 - 2f_{\mathbf{k}'}\right)}{2\sqrt{\xi_{k'}^2 + \Delta^2 \left|g\left(\mathbf{k}'\right)\right|^2}} g\left(\mathbf{k}'\right) \tag{6.5}$$

для синглетного спаривания и

$$\mathbf{d}(\mathbf{k}) = -\sum_{\mathbf{k}'} \frac{V\left(\mathbf{k},\mathbf{k}'\right)\left(1 - 2f_{\mathbf{k}'}\right)}{2\sqrt{\xi_{k'}^2 + \Delta^2 \left|\mathbf{d}\left(\mathbf{k}'\right)\right|^2}}\ \mathrm{d}\left(\mathbf{k}'\right) \tag{6.6}$$

для триплетного спаривания.

При $T \to T_c$ щель в спектре обращается в нуль, и уравнения (6.5) и (6.6) становятся линейными. Это означает, что любая комбинация сферических гармоник с данным l (в общем случае - функций данного неприволимого представления группы симметрии нормальной фазы), имеющая вид

$$g(\mathbf{k}) = \sum_{m=-1}^{l} a_{lm} Y_{lm}(\hat{\mathbf{k}}) \tag{6.7}$$

или

$$\mathrm{d}(\mathbf{k}) = \sum_{m=-l}^{1} \mathrm{b}_{lm} Y_{lm}(\hat{\mathbf{k}}) \tag{6.8}$$

является решением уравнений (6.5) и (6.6), соответственно. Мы вновь пришли к утвержденито, что все сзерхпроводящие состояния, относящисся к данному нсприводимому представлснию группы симметрии нормальной фазы, имеюо одинаковуоо критическуп тсмпературу. Опа определяется уравнением

$$1 = N_0 V_i \int_0^{\varepsilon_i} d\xi \frac{\mathrm{th}\,(|\xi|/2T_c)}{|\xi|} \tag{6.9}$$

которое получается при подстановке в уравиение на щель разложений (6.7) (или (6.8)). Интегрируя по частям правую часть (6.9) и заменяя на бесконсчность верхлий предел быстро сходящегося иптеграла, потучаем:

$$1 = N_0 V_l \left(\ln \frac{\varepsilon_l}{2T_\mathrm{c}} - \int_0^{\infty} dx \frac{\ln x}{\mathrm{ch}^2\, x} \right)$$

Следовательыio,

$$T_\mathrm{C} = \frac{2\gamma}{\pi} \varepsilon_l \,\mathrm{cxp} \left(-\frac{1}{N_0 V_l} \right) \tag{6.10}$$

Здссь $2\gamma/\pi \approx 1.14$, гдс

$$\ln \gamma = C \approx 0.577$$

носит пазвание постоянной Эннтера.

Подставляя в (6.5) и (6.6) разложения (5.4), (5.7) или (5.8) потенциала парного притяжения и используя ортогональность базисных функций неприводимого представления, получаем, что параметр порядка при всех $T < T_c$ имеет вид (6.7) или (6.8). Зависимость молуля параметра порядка и коэффициентов a_{lm} и $\mathbf{b}_{lm}$ от тсмпературы при этом определястся нслинейпыми уравнениями вида [1]:

$$a_{lm}(T) = N_0 V_i \int_0^{\varepsilon_1} d\xi \int \frac{d\Omega}{4\pi} \frac{\mathrm{lh}\left(\sqrt{\xi^2 + \Delta^2(T)|g(\mathbf{k})|^2}/2T \right)}{\sqrt{\xi^2 + \Delta^2\,(T')\,|g(\mathbf{k})|^2}} Y^*_{lm}(\hat{\mathbf{k}}) g(\mathbf{k}) \tag{6.11}$$

для синглстного спаризания, и

$$\mathbf{b}_{lm}(T) = N_0 V_l \int_0^{\varepsilon_1} d\xi \int \frac{d\Omega}{4\pi} \frac{\mathrm{th}\left(\sqrt{\xi^2 + \Delta^2(T)|\mathbf{d}(\mathbf{k})|^2}/2T \right)}{\sqrt{\xi^2 + \Delta^2(T)|\mathrm{d}(\mathbf{k})|^2}} Y^*_{im}(\hat{\mathbf{k}}) \mathrm{d}(\mathbf{k}) \tag{6.12}$$

для триплетного спаривания, дополтенными условиями нормировки (5.19) и (5.21).

В общсм случае необходимо решать аналогичные нелинейныс уравнения для коэффишлентов разложения параметра порядка по базисным функциям неприводимого представлсния группы симметрии кристалла. Ввиду ачитеднного произвола в выборе этих функций (см. 4), а также анизотропти ферми-поверхности, задача количественного описания температурного поведения параметра порядка, а, следовательно, термодиiтамических и кинетидеских свойств анизотропных сверхпроводников, является весьма неопределенiтой.

В некоторьх случаях величину щели в спсктре при $T = 0$ можто пайти аналитически. Так, для s-спаривания из (6.11) получаем:

$$\frac{1}{N_0 V_0} = \int_0^{\varepsilon_0} \frac{d\xi}{\sqrt{\xi^2 + \Delta_0^2}} \approx \ln \frac{2\varepsilon_0}{\Delta_0} \tag{6.13}$$

Следовательно,

$$\Delta_0 = \Delta(T = 0) = 2\varepsilon_0 \exp\left(-\frac{1}{N_0 V_0}\right) \tag{6.14}$$

и, сравнивая с (6.10), имеем:

$$\Delta_0 = \frac{\pi}{\gamma} T_c \approx 1,75 T_c \tag{6.15}$$

Температурнос повсдение шели в спектре для s-спаривапия опредепяется уравнением, следующим из (6.4):

$$\frac{1}{N_0 V_0} = \int_0^{\varepsilon_0} \frac{d\xi}{\sqrt{\xi^2 + \Delta^2}} - 2\int_0^{\varepsilon_0} \frac{f(E) d\xi}{\sqrt{\xi^2 + \Delta^2}}$$

Отсюда, воспользовавиись (6.13), получаем:

$$\ln \frac{2\varepsilon_0}{\Delta_0} = \ln \frac{2\varepsilon_0}{\Delta} - 2\int_0^{\varepsilon_0} \frac{f(E) d\xi}{\sqrt{\xi^2 + \Delta^2}}$$

ипи

$$\ln \frac{\Delta_0}{\Delta} = 2\int_0^{\varepsilon_0} \frac{d\xi}{\left(\exp\left(\sqrt{\xi^2 + \Delta^2}/T\right) + 1\right)\sqrt{\xi^2 + \Delta^2}} \tag{6.16}$$

Ввиду быстрой сходимости верхиий предел интегрирования в этом уравнении можно заменить на бесконечность.

При $T \to 0$ имеем $\Delta/T \to \infty$, и

[11] Если в разложенин потенинала парного притяжсния присутствучт сферические гармоники с другими значениями орбитального момента (в обшем случае - Базисные функции других леприводимых представлснии), соответствующие меньшим критическим температурам, то при $T < T_c$ сверхпроводящее состоянис будет представлять собой супсрпозицию гармоник с разными l. При этом допустимо, разумеетcs, зишь примешиваиие гармоник, не поиижающсе симметрии данного сверхпроводяццего состояния. В противном случае происходит фазовый переход из одной сверхпроводящей фазы в другую.

$$\ln \frac{\Delta_0}{\Delta} \approx \frac{2}{\Delta_1} e^{-\Delta_0/T} \int_0^\infty e^{-\xi^2/(2\Delta T)} d\xi = \sqrt{2\pi \frac{T}{\Delta}} e^{-\Delta_0/T}$$

$$\Delta = \Delta_0 \left(1 - \sqrt{\frac{2\pi T}{\Delta}} e^{-\Delta_0/T} \right) \tag{6.17}$$

Гри $T \to T_c$ иммеем $\Delta/T \to 0$, и

$$\ln \frac{\Delta_0}{\Delta} = \ln \frac{\pi T}{\gamma \Delta} + \frac{7\zeta(3)}{8\pi^2} \left(\frac{\Delta}{T} \right)^2 + \dots$$

Здесь $\zeta(3) = \sum_{n=1}^{\infty} n^{-3}$ - дзета-фуікция Рімана.

Поскольку $\Delta_0 = \pi T_c/\gamma$, го

$$\ln \frac{T_c}{T} \approx \frac{T\zeta(3)}{8\pi^2} \left(\frac{\Delta}{T} \right)^2$$

Отстода

$$\Delta(T) \approx \left(\frac{8\pi^2}{7\zeta(3)} \right)^{1/2} T_{\mathrm{c}} \left(\frac{T_{\mathrm{c}} - T}{T_{\mathrm{c}}} \right)^{1/2} \tag{6.18}$$

Ввиду условий нормировки (5.19) и (5.21) температурное поведение амплитуды энергетической щели в анизотропних сверхпроводниках при $T \to T_\varsigma$ такжс определяется формулой (6.18).

MC-6.1

Найти распрсделение электронов в сверхпроводнике по имгульсам: $n_{\mathrm{k},\alpha\theta} = \left\langle a^+_{\mathbf{k}\alpha} a_{\mathrm{k}\beta} \right\rangle$;

MC-6.2

Найти флуктуашио числа частиц при $J = 0 : \delta N = \frac{\sqrt{\langle N^2 \rangle - \langle N \rangle^2}}{\langle N \rangle}$, где $N = \sum_{\mathbf{k}} a^+_{\mathbf{k}\alpha} a_{\mathrm{k}\alpha}$.

19.1.7 7. Temperature Behavior of Thermodynamic Quantities as $T \to 0$

Наличие щели в спектре сверхпроводников с s-спариванием обуславтивает термоактивационное ($\sim \epsilon^{-\Delta_u/T}$) поведение всех термодинамических и кинетических величин при низких температурах.

Так, электронная теплоемкость сверхпроводника [1]

$$C_{\mathrm{s}} = \sum_{\mathrm{k}\alpha} E_{\mathrm{k}} \frac{\partial f_{\mathrm{k}}}{\partial T} \tag{7.1}$$

в случае s-спаривания равная

$$C_{\mathbf{s}} = 2N_0 \int_{-\infty}^{+\infty} d\xi \sqrt{\xi^2 + \Delta^2} \frac{\partial}{\partial T} \left(\frac{1}{\exp\left(\sqrt{\xi^2 + \Delta^2}/T \right) + 1} \right) \tag{7.2}$$

где

$$S = -\sum_{ka} \{(1 - f_k) \ln (1 - f_k) + f_k \ln f_k\}$$

в пределе $T \to 0$ принимает вид

$$C_s \approx \frac{2N_0\Delta^2}{T^2} e^{-\Delta/T} \int\limits_{-\infty}^{+\infty} d\xi e^{-\xi^2/(2\Delta T)} \approx N_0 \left(\frac{\Delta_0}{T}\right)^2 \sqrt{2\pi T\Delta_0} e^{-\Delta_0/T} \tag{7.3}$$

В необычных свсрхпроводниках с симметрийными нудями в спектре возбуждений естествешно ожидать степенное поведепие термодинамических всличин при низких температурах. Формула, обобщающая (7.2) на случай анизотропного спаривания, имеет вид

$$C_{\rm s} = 2N_0 \int\limits_{-\infty}^{+\infty} d\xi \int \frac{d\Omega}{4\pi} E_{\rm k} \frac{\partial}{\partial T} \frac{1}{c^{E_{\rm k}/T} + 1} \tag{7.4}$$

где спектр возбуждениii $E_{\rm k}$ определяется формулами (5.33) или (5.34).

Рассмотрим в качестве примера теплосмкость в A-фазе [3]. Спектр элементарных возбуждении имеет вид (5.36), то есть щель обращается в нуль на северном и южном полюсах ферми-сферы ($\theta = 0.\pi$), и главный вклал в теплоемкость дают окрестности этих точек [2]:

$$\theta < \frac{\xi}{\Delta}, \quad \pi - \theta < \frac{\xi}{\Delta}.$$

Отсюдда в пределе $T \to 0$ получаем:

$$C_s = \frac{N_0}{T^2} \int\limits_{-\infty}^{+\infty} d\xi \int\limits_0^{\pi} \sin\theta d\theta \frac{E^2 e^{E/T}}{\left(e^{E/T} + 1\right)^2} \approx \frac{N_0}{2T^2} \int\limits_{-\infty}^{+\infty} \frac{d\xi\xi^2}{\mathrm{ch}^2(\xi/2T)} \int\limits_0^{\xi/\Delta} \theta d\theta +$$

$$+ O\left(\exp\left(-\frac{\Delta_0}{T}\right)\right) \approx \frac{N_0}{4T^2\Delta^2} \int\limits_{-\infty}^{+\infty} \frac{d\xi\xi^4}{\mathrm{ch}^2(\xi/2T)} = N_0 \frac{T^3}{\Delta_0^2} I \tag{7.5}$$

где

$$I = 8 \int\limits_{-\infty}^{+\infty} \frac{dz z^4}{\mathrm{ch}^2\, z} = \frac{7\pi^4}{15}$$

Таким образом, элекгронная теплоемкость сверхпроводника, щель в спектре которого обращается в нуль в изолированиы точках на ферми-повсрхности, при $\bar{T} \to 0$ пропорциональна T^3. Аалогичное вычисление лия сверхпроводника с нулями щели на линиях на ферми-поверхности дает $C_{\rm s} \sim T^2$ при $T \to 0$.

[11] Iааломним, что формуду (7.1) ироще всего получить. диффсрепиируя комбинаторнос выражение для эитропин ферми-газа

$$C = T\frac{\partial S}{\partial T}$$

Возможны также сверхпроводящие состояния, в которых щель в спектре воэбуждений имеет изолированные точки нулей более высокого порядка. Например, для аксиальной фазы в случае d-спаривания:

$$g(\mathbf{k}) \propto \left(\hat{k}_x + i\hat{k}_y\right)^2 \tag{7.6}$$

имеюотя два нуля второго порядка на полюсах ферми-поверхности. Для этой фазы вычисления, подобные привсденным выше, дают $C_\mathrm{s} \sim T^2$.

Полученные рсзултаты можно сформулировать так:

$$\left.\frac{C_\mathrm{s}}{C_\mathrm{n}}\right|_{T\to 0} \sim \begin{cases} \left(\frac{T_c}{T}\right)^{5/2} e^{-\Delta_0/T}, & \text{щель в спектре не обращается в нуль,} \\ \left(\frac{T}{T_c}\right)^2, & \text{щель в спектре имеет нули первого порядка в изолированных точках,} \\ \frac{T}{T_c}, & \text{щель в спектре равна нулю на линиях или имеет цули второго порядка в изолированных точках.} \end{cases}$$

Здесь C_n - теплоемкость нормальной фазы.

Довольно просто установить степенное температурное поведение при $T \to 0$ и для друтих термодинамических величин, например, лондоновскоу глубины проникновения, сдвига Найта (парамагнитіоий воспрлимчивости), а такжс кинетических величиі, таких как коэффициент элсктронной теплопроводности или коэффнциент поглощения ультразвука.

Степенное поведснис перечисленных величих при зизких тсмпературах служит прямым указаншием на необычный характер свсрхпровопимости. Болес того, поскольку в случае сильного спин-орбитального взаимодействия для трдплетного спаривания симметрийные нули в спектре могут реализовываться лишь в изолированных точках на ферми-поверхіости (см. \$4), то различие показателей в степенных законах для линий и точек нулей даст принципиальнуюо возможносьь сделать выбор между спип-синглетной и спин-триплетной сверхпроводимостыоо.

На практике, применение этих простых результатов усложняется тсм, что паличис сколь угодно малого количестза примесей превращает линии нулей в полоски конечной ширины, что дает линейное поведенис теплосмкости в обдасти низких температур. Изолированные точки нулей под действием примесей также превращаготся в пятна конечного диаметра, окружающия исходные точки [23]. Эти процессы влияюот на низкотемпературное поведение всех величин, усложняя интсрпретацию эксперименттальных данных. Мы вернемся к этому вопросу в 2I, посвященном влиянио примсссй на свойства необычных сверхпроводников.

19.1.8 8. Parity Effects of the Number of Electrons in Superconductors

Согласно теории БКШ, основное состоянис сверхпроводника (5.9) представляет собой суперпозицию состояний с различньм числом куперовских пар. Энергия сверхпроводника при $T \to 0$ ниже энергии нормального металла на величину $\delta E_\mathrm{s} \sim N\Delta^2/\varepsilon_\mathrm{F}$ (см. упражнение к §), гдс N - полное число электронов. Возбужденные, то есть неспаренные, состояния в обычном сверхпроводнике отделены от основного состояния энергетической щелью $\triangle$. Поэтому при изменении числа электронов на единигу: $N \to N \pm 1$ велитиита δE_s должна измениться на $\pm\Delta$. Знак пиос иди минус здесь зависит от того, было исходное писло N тетіым или нечетньм. Поскопьку

[12] В этом параграфе для более компактной записи мы используем в A-фазе спектр вида $E_k^A = \sqrt{\xi^2 + \Delta^2 \sin^2\theta}$, отличающийся от (5.36) переопредслением модуля Δ.

величина Δ порядка нескольких гралусов (напомним, что $\Delta \sim T_c$), то измерение δE_s при изменении огромного числа N на единицу являстся, казалось бы, нереальной задачей. Тем ме менее это удалось сделать [24, 25] после создания так называемых транзисторов с кулоновской блокадой.

В этом параграфе мы опишем действие этого прибора, дающщего возможность непосредственно продемонстрировать существование куперовских пар, а таюже вычислим изменение термодинамического потендиала газа элементарных возбуждений сверхпроводника для различных сверхпроводящих состояний при изменении полного исла электронов на единицу [26-28].

Транзистор (электрометр) с кулоновской блокадо представляет собой прямоутольнуоо апоминиевую пленку (островок), занимающуо участок электрической цепи между двумя туннелынми контактами с емкостями C_1 и C_2. Размеры пленки в эксперименте, выполнен-

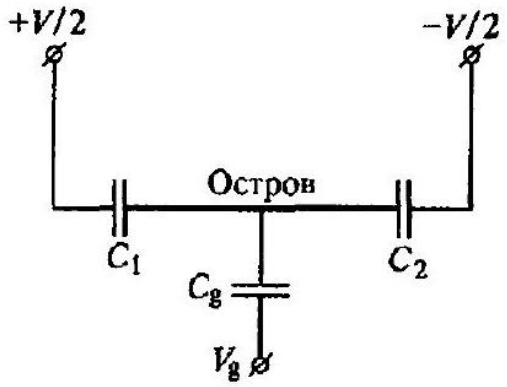
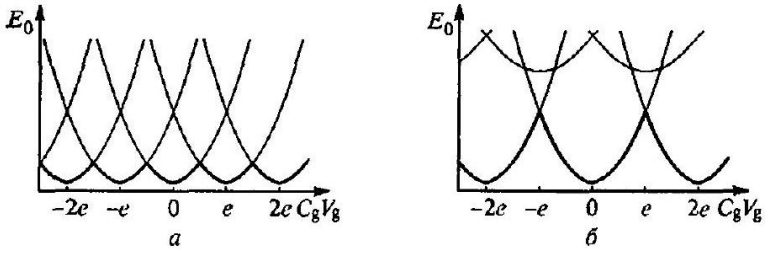


Рис. 5. Элехтрическая схема электрометра с кулоновско бловапой ном в Гарвардском университете [24], были таковы: толшина -200Å, ширина -600Å, длина $-2{\cdot}10^4$Å Островок связан емкостью C_g с затвором, позволянощим менять электростатический потенциал островка, прикладывая напряжение V_g (см. рис. 5).

При достаточно слабой связи островка с внештей цепью, когда сопротивленис каждого из контактов подчиняется условию $R > h/e^2$, квантовомеханические состояния островка характеризутотся определенным числом электронов [1]. Если полная емкость всех контактов $C = C_1 + C_2 + C_g$ достаточно мала, элементарна электростатическая энергия $E_c = e^2/2C$ превышает температуру, и можно пренебречь тепловыми флуктуациями. В этих условиях полная элекхростатическая энергия островка

$$U = \frac{Q^2}{2C} = \min_n \frac{(en + C_g V_g)^2}{2C} \tag{8.1}$$

является периодлческой функцией напряжения на затворе (рис. 6а), поэтому ток через островок при заданном напряжении во внешней цепи V будет также периодической функцией от $C_g V_g$ с псриодом e.



[11] Чтобы ие пирерывать сиязности изложения, вывод указанного неравенства отнесен в конце параграфа.

Ри с.6. Качественное поведение энергии островка как функции заряда $C_{\rm g}V_{\rm g}$ иа затворе: а) при $e^2/(2C) > T, \delta\Omega$; б) при $\delta\Omega > e^2/(2C) > 7$

Так обстоит лело, пока алюминиевый островок нахолится в нормальном состоянии. В свсрхпроводящем состоянии было обнаружено, что при тсмпературах ниже $0,3$ К (что соответствует $0.4T_{\rm c}$) пики тока, ссответствующие нечетному количеству электронов на островс, начинают подавляться, и зависимость $j\left(C_{\rm g}V_{\rm g}\right)$ становится $2e$-периодической. ЕстествеIiное объяснение этого явлешия состоит в том, что свободные энергии (более точно, термодинамические потенциалы Ω) островка в сверхпроводящем состоянии с четным и нечетным числами электронов $\Omega_{\rm odd} - \Omega_{\rm even}$ при $T \to 0$ отличаются на величину порядка щели Δ в спектре элемснтарных возбуждений. Поэтому при выполнении условия $\Delta > E_{\text{с па-}}$ па раболичсские участки, отвечающие нечетным значениям n в зависимости $U\left(C_{\rm g}V_{\rm g}\right)$, поднимутся на высоту $\Omega_{\rm odd} - \Omega_{\rm even}$ и станут ненаблюдаемыми (см. рис. 60). Соответственно, ток $j = j\left(C_{\rm g}V_{\rm g}\right)$ станет $2e$-периодической функцией $C_{\rm g}V_{\rm g}$.

Островок представляет собой два последоватслыо включенных лжозефсоновских контакта. Нас интересует зависимость тока через островок от энсргии островка. Проще всего она выглялит лля нулевой внешней разности потенциалов [2]:

$$j = \frac{2e}{\hbar}\sqrt{n_{\rm s1}n_{\rm s2}}\frac{K^2\sin\Phi}{E_0} \tag{8.2}$$

Здесь - джозефсоновская энергия (матричный элемепт перехода) каждого из контактов, которыс для простоты мы полагаем одинаковыми; $n_{\rm s1}$ и $n_{\rm s2}$ плотности сверхпроводящих электронов в подводящих проводах по обе стороны островка; Φ - «внелшняя» разность фаз (разность фаз между контактами, к которым подключен островок). E_0 - энергия островка, вклюотаюшая как э.ектростатическуюо часть (8.1), так и слагаемое, величина которого меняется на $\delta\Omega = \Omega_{\rm odd} - \Omega_{\rm even}$ при изменениях $C_{\rm g}V_{\rm g}$, сопровождающихся сменой четности числа электронов на островкс:

$$E_0 = U + \begin{cases} \delta\Omega, & \text{если } n \text{ нечетно,} \\ 0. & \text{если } n \text{ тетно.} \end{cases} \tag{8.3}$$

Для вычислсния $\delta\Omega$ заметим, что термодинамический потенциал сверхпровотника склапывается из энергии кондепсата куперовских пар и термодинамического потенциала газа элемсптарных возбуждений. Конденсат пар состоит из четного числа частиш, поэтому разность термодинамических потенциалов сверхпроводника с нечетным и четным числом эдектронов совпадает с разностью Ω-потенциалов ансамблей с нечетным и четньдм числом квазичастиц. Термодинамический потенциал для газа квазичастиц записывается как сумма потенциалов всех состоянии, нумеруемьх кванттовым пислом $i = (\mathbf{k}, \alpha)$, в каждом из котторых может быть $n_i = 0, 1$ квазичастиц с энергией E_i':

$$\Omega = -T\sum_i \ln\left(\sum_{n_i=0.1} e^{-BE_in_1}\right) \tag{8.4}$$

здесь $\beta = 1/T$. Эту формулу можио переписать иначе:

$$\Omega = -T\ln\prod_i\left(1+e^{-\beta E_1}\right) = -T\ln\left(1+\sum_i e^{-\beta E_1} + \frac{1}{2}\sum_i\sum_{j\neq i} e^{-\beta E_1-\beta E_j} + \right.$$

$$\left. +\frac{1}{6}\sum_i\sum_{j\neq i}\sum_{k\neq i,j} e^{-\beta E_1-\beta E_j-\beta E_k} + \ldots\right) = -T\ln\left(Z_{\rm odd} + Z_{\rm even}\right)$$

[12] Вывоп формулы пля тока приведен в конце параграфа.

где

$$Z_{\text{odd}} = \sum_i e^{-\beta E_i} + \frac{1}{6}\sum_i \sum_{j\neq i} \sum_{k\neq i,j} e^{-\beta E_1 - \beta E_j - \beta E_k} + \dots \tag{8.5}$$

$$Z_{\text{even}} = 1 + \frac{1}{2}\sum_i \sum_{j\neq i} e^{-\beta E_i - \beta E_1} + \dots \tag{8.6}$$

предстамлят собой больние статистическис суммы для ансамБлей систем с нечетным и четным числом квазинастиц. Соответствующие термолинамические потспциаы имсюот вид

$$\Omega_{\text{odd/even}} = -T \ln Z_{\text{oidd /even}} = -T \ln \frac{\prod_1 \left(1 + \epsilon^{-\beta E_i}\right) \mp \prod_i \left(1 - \mathrm{e}^{-3E_i}\right)}{2} =$$
$$= \Omega_{\text{BCs}} - T \ln \frac{1}{2}\left(1 \mp \prod_i \text{lh}\, \frac{\beta E_i}{2}\right)$$

Следовательно,

$$\delta\Omega = \Omega_{\text{odd}} - \Omega_{\text{even}} = -T \ln \frac{1 - f(T)}{1 + \rho(T)} \tag{8.8}$$

где

$$f(T) = \prod_{\text{k}\alpha} \text{th}\, \frac{\beta E_{\text{k}}}{2} \tag{8.9}$$

Рассмогрим теперь, как проявляются эффекты четности числа частиц в нормальном металле и различных сверхпроводниках. Для нормального металла

$$f(T) = \prod_{k\alpha} \text{th}\, \frac{\beta\,|\xi_k|}{2} = \exp\left(4N_0 V \int_0^\infty d\xi \ln \text{th}\, \frac{\xi}{2T}\right) = \exp\left(-2\pi^2 N_0 V T\right) \tag{8.10}$$

Здесь N_0 - плотность состояний на одну проскапию спина, а V - объем образиа. Эффекты тетности, таким образом, пренебрежимо маты:

$$\Omega_{\text{odd}} - \Omega_{\text{even}} \approx 2T' \exp\left(-2\pi^2 N_0 V T\right) \tag{8.11}$$

если температура велика по сравиениго с расстоянием между эиергетическими уровнями электронов в островке $\delta E = (N_0 V)^{-1}$ или точнее, если

$$T > T^* \approx \frac{\delta E}{2\pi^2} \tag{8.12}$$

Для микроостровков, испотьзованных в Гарвардских экспериментах, $\delta E \sim 2 \cdot 10^{-4}$ К.

В обычных сверхпроводниках щель в спектре элементарных возбуждений нигде не обращается в гуль, и

$$f_{\text{s}}(T) = \prod_{\mathbf{k}\alpha} \text{th}\, \frac{\beta E}{2} = \exp\left(4N_0 V \int_\Delta^\infty \frac{E dE}{\sqrt{E^2 - \Delta^2}} \ln \frac{1 - e^{-E/T}}{1 + e^{-E/T}}\right) \tag{8.13}$$

Последнее выражение при низких температурах $T < \Delta$ можно представить в виде

$$f_{\mathrm{s}}(T) = \left(\mathrm{th}\,\frac{\Delta}{2T}\right)^{N_{eff}} \tag{8.14}$$

где

$$N_{\mathrm{eff}} = 4N_0V\int\limits_{\Delta}^{\infty}\frac{EdE}{\sqrt{E^2-\Delta^2}}e^{-(E-\Delta)/T} \approx 2\sqrt{2\pi\Delta T}N_0V \tag{8.15}$$

что, в свого очередь, позволяет записать $\delta\Omega$ в виде

$$\delta\Omega \approx \Delta - T\ln N_{\mathrm{off}} \tag{8.16}$$

Эта формула имеет ясный физический смысл: свободная энсргия, связанная с появлением неспаренного электрона, ссть вежмчнна щели в спектре возбуждений минус температура, умноженная на логарифм эффективного числа состояний, в которых размешалотся тепловые возбуждения. В отличие от нормального металла, проявление эффектов четности (подавление нечетных пиков в токе через островок) начинается с температуры

$$T_{\mathrm{s}}^{**} \approx \frac{\Delta}{\ln N_{\mathrm{eff}}} \tag{8.17}$$

При этой температуре на островке будет порядка одной квазичастицы:

$$N_{\mathrm{qp}} \approx e^{-\delta\Omega/T} = N_{\mathrm{eff}}e^{-\Delta/T} \tag{8.18}$$

Для Гарвардских экспериментов $T_{\mathrm{s}}^{*} \approx 0,3$ K.

Обратимся теперь к сверхпроводникам, щель в спектре которых обращается в нуль в изолированных точках, как в A-фазе ^{3}He, ити па изолированных линиях на ферми-поверхности, как это имеет место в полярной фазе. Вычисления, аналогичные тем, что были проделаны для теплоемкости необычных сверхпроводников (см. 7), дают:

$$f_A(T) \approx \exp\left(-\frac{\pi^4}{18}N_0V\frac{T^3}{\Delta^2}\right) \tag{8.19}$$

$$f_{\mathrm{POl}}(T) \approx \exp\left(-CN_0V\frac{T^2}{\Delta}\right) \tag{8.20}$$

где C - постоянная порядка единицы. Следовательно, для сверхпроводников с нулями в изолированных точках имеем:

$$\Omega_{\mathrm{odd}} - \Omega_{\mathrm{even}} = \begin{cases} 2T\exp\left[-(T)T_A^{*}\right)^3], & \text{при } T > T_A^{*} \\ \delta E, & \text{при } T \ll T_A^{*} \end{cases} \tag{8.21}$$

Здесь

$$T_A^{*} = \left(\frac{18}{\pi^4}\Delta^2\delta E\right)^{1/3} \tag{8.22}$$

Мы видим, что значение $\delta\Omega$ в этом случае не достигает величины щели Δ. С понижением температуры $\delta\Omega$ возрастает, а затем начинает падать. В точке максимума $\delta\Omega\,(T_A^{*}) \approx T_A^{*}, T_A^{*}$ - температура, при которой число уровней в

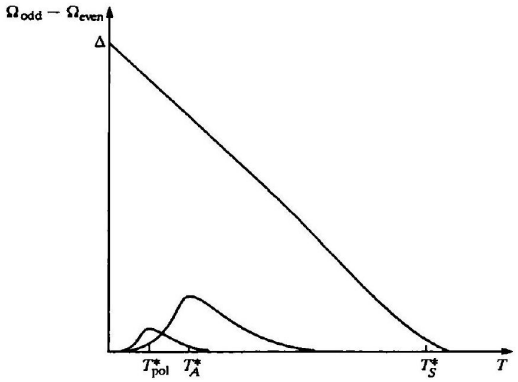


Рис.7. Качественная зависимость от температуры разности термодинамических потенциалов с нечетным и четным числом электронов для обычного сверхпроводника (верхняя линия) и для сверхпроводников, щель в спектре хоторых обращается в ноль в изолированных точках или на линиях

энергетическом интервале $E < T_A^*$ становится порядка единицы (сравните с (8.12)). При температурах $T < T_A^*$ пренебрсжение дискретностью спектра неоправдано, и в этой области $\Omega_{\text{odd}} - \Omega_{\text{even}} \approx \delta E$.

Для свсрхпроводников с нулями параметра порядка на линиях имеем:

$$\Omega_{\text{odd}} - \Omega_{\text{even}} = \begin{cases} 2T \exp\left[-\left(T/T_{\text{pol}}^*\right)^2\right], & \text{при } T > T_{\text{pol}}^* \\ \delta E, & \text{при } T \ll T_{\text{pol}}^* \end{cases} \tag{8.23}$$

где

$$T_{\text{pol}}^* = \left(\frac{\Delta \delta E}{C}\right)^{1/2} \tag{8.24}$$

Как и в предыдущем случае, имеет место немонотонное поведение $\delta\Omega(T)$. В точке максимума $\delta\Omega\left(T_{\text{pol}}^*\right) \approx T_{\text{pol}}^*$. В условиях эксперимента [24]: $T_A^* \approx 0,1 T_c$, $T_{\text{pol}}^* \approx 10^{-2} T_{\text{c}}$.

Качественное поведение $\delta\Omega$ в различных типах сверхпроводников изображено на рис. 7. Эффект четности числа электронов в микроостровках кз необычных сверхпроводников выражен заметно слабее. Он имеет место при существенно более низких температурах и существенно меньше, чем в микроостровках из обычных сверхпроводников.

Имеется и друтое ограничснис возможности наблюдения $2e$-периодичности тока через транзистор с кулоновской блокадой, изготовлешный из сверхпроводника с пулями в спсктре элсментарных возбуждений. Сверхпровопящее состояние в таком транзисторе скорее всего будст подавлено в поверхостном слос толщиной ξ_0. Плотность состояний в этом слое Будст близка к плотности состоянии нормального металла. Поэтому разность $\Omega_{\text{odd}} - \Omega_{\text{even}}$ может остаться экспоненциально малой.

Итак, удвоение периода тока через сверхпроволящий транзистор с кулоновской блокадой реализуемо, по-видимому, лиш в сверхпроводниках без нудей в спектре возбуждений.

В зактючение обсудим два вопроса, рассмотренис которых мы оставили в стороне, чтобы не прерывать связности изложения.

Условяе слабой связи островка с впешней цепью. Островок можно рассматривать как изолированный объект при условии отсутствия в контактах, связывающих островок с внешие й цепыо, делокализованных электронных состояниф, распространенных на весь объем контакта. Элекгронные состояния в контакте не должны испытьвать влияния границ, что количественно можно записать в виде неравенства $\delta E \gg \Delta E$ (условие лохализации). Здесь δE - расстояние между эпергетическими уровнями, $\triangle E$ - сдвит

уровней за счет влияния границы. В плоских контактах толшиной L и площадыо S, имеем $\delta E = 1/(SLN_0)$, где N_0 - плотность состояний, а $\triangle E \sim h/\tau \approx hD/L^2$, где τ - время диффузионного движсния электрона до границы ($L \ll \sqrt{S}$), D коэффициент диффузии, связанный с проводимостью контакта σ соотношением Эйниттейна

$$e^2 DN_0 = \sigma$$

Подставляя все перечисленные выражения в исходное неравснство, окогчательно получим условие локализации [29]:

$$R = \frac{L}{\sigma S} \gg \frac{h}{e^2} \approx 26\text{kO}$$

Ток чсрез два последовательыо включенных джжозефсоновских когтакта. Джозефсоновский ток в схеме, изображенной на рис. 8, легко пайти с помо-

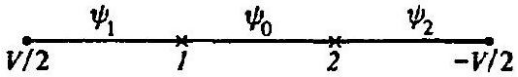


Рис. 8. Два постедовательно вклкчениві джозефсоиовсхих ковтакта щью этементарного обобщения фейнмановского подхода [30] к контакту Джозсфсона как к двухуровневой квантовомсханитеской системе. Вводя в двухуровневую систему с амплитудами состояний $\psi_1 = \sqrt{n_{\text{s1}}/2}e^{i\varphi_1}, \psi_2 = \sqrt{n_{\text{s2}}/2}e^{i\varphi_2}$ промежуточное састояние - острозок с волновой фунпцией ψ_0, запишем уравнения Шредингера:

$$i\hbar\frac{\partial\psi_1}{\partial t} = \frac{eV}{2}\psi_1 + K\psi_0$$
$$i\hbar\frac{\partial\psi_0}{\partial t} = K\psi_1 + K\psi_2 + E_0\psi_0$$
$$i\hbar\frac{\partial\psi_2}{\partial t} = K\psi_0 - \frac{eV}{2}\psi_2$$

Здесь V - внешняя разность потенциалов, K - джозефсоновская энергия (матричньий элемент перехода) каждого из контактов, E_0 - энергия островка. При нулевой внешней разности потеншиалов черсз контакты течет постоянный ток. В этих условиях волновая функция островка, такжс как и разность фаз 0 - φ_1 не зависят от времени. Требование сташионарности состояния ψ_0 приводит к условио

$$\dot{\psi}_0 = -\frac{K(\psi_1 + \psi_2)}{E_0}$$

с учетом которого система уравнений переписывается в виде:

$$i\hbar\frac{\partial\psi_1}{\partial t} = -\frac{K^{-2}}{E_0}(\psi_1 + \psi_2)$$
$$i\hbar\frac{\partial\psi_2}{\partial t} = -\frac{K^2}{E_0}(\psi_1 + \psi_2)$$

Подставляя в первое уравнеиие выражения для ψ_1 и ψ_2 и выделяя мнимуюо часть, получаем:

$$\hbar\frac{\partial\sqrt{n_{s1}}}{\partial t} = -\frac{K^2}{E_0}\sqrt{n_{\text{s2}}}\sin(\varphi_2 - \varphi_1)$$

Поскольку ток пропорционален $\dot{n}_{s1}$, то окончательное выражение для постоянного тока через два последовательно включенных джозефсоновских контакта при нулевой внешней разности потенниалов принимает вид

$$j = \frac{2e}{\hbar}\sqrt{n_{s1}n_{s2}}\frac{K^2\sin(\varphi_2-\varphi_1)}{E_0}.$$

19.1.9 9. Paramagnetic Susceptibility and Knight Shift

Измерение парамагнитной восприимчивости элсхтронного газа в сверхпроводнике является еще одним способом тестирования сверхпроводящего состояния. Хотя слабое магнитное поле, экранируемое незатухающими токами, не проникает в толиу сверхпроводника, тем не менее спиновый (паулиевский) парамагнетизм в сверхпроводниках (а тем более в нейтральной сверхтекучей ферми-жидкости ^{3}He) - наблюдаемое явление. В этом параграфе мы найдем температурную зависимость парамагнитной восприимчивости элекгронного газа в различных сверхпроводяших состояниях.

Для сверхпроводника с синглетным спариванием купсровсхие пары не дают вклада в спиновый парамагнетизм, и спиновый магнитныи момент электронного газа определяется томько вкладом элементарных возбуждений:

$$M = \mu_B \sum_{\mathbf{k}} \left[f\left(E_{\mathbf{k},-}\right) - f\left(E_{\mathbf{k},+}\right)\right] \tag{9.1}$$

Здесь $f(E)$ - фермиевская функиия распределения (6.2),

$$E_{\mathbf{k},\pm} = \sqrt{\xi^2 + \Delta^2|g(\mathbf{k})|^2} \pm \mu_B H \tag{9.2}$$

• энергии возбуждений с ориентацией спинов соответственно по и против направлсния поля H, μ_B - магнетон Бора (в случае ^{3}He - магниттый момент ядра). Из (9.1) имеем:

$$M = -2\mu_B^2 N_0 H \int \frac{d\Omega}{4\pi}\int d\xi \frac{\partial f\left(E_{\mathbf{k}}\right)}{\partial E} = 2\mu_B^2 N_0 H \int \frac{d\Omega}{4\pi} Y(\hat{\mathbf{k}}, T) \tag{9.3}$$

где

$$Y(\hat{\mathbf{k}}, T) = \frac{1}{4T}\int\limits_{-\infty}^{+\infty} \frac{d\xi}{\mathrm{ch}^2\left(E_k/2T\right)} \tag{9.4}$$

а $E_{\mathbf{k}} = \sqrt{\xi^2 + \Delta^2|g(\mathbf{k})|^2}$. Отсюда получаем выражение для магнитной восприимчивости:

$$\chi = \frac{\partial M}{\partial H} = \chi_n Y(T) \tag{9.5}$$

где $\chi_n = 2\mu_B^2 N_0$ - восприимчивость в нормальном состоянии [1], а функция

$$Y(T) = \int \frac{d\Omega}{4\pi} Y(\hat{\mathbf{k}}, T) = \begin{cases} 1, & \text{при } T = T_c \\ 0, & \text{при } T = 0 \end{cases} \tag{9.6}$$

называется функцией Иосида и описывает долю нормальных электронов в сверхпроводнике (рис. 9).

При $0 < T < T_c$ температурное поведение $Y(T)$ для разичшых сверхпроводящих состояний различно. В пределе $T \to 0$ вычисления, аналогичные проделанным в 7 для теплоемкости, дают:

$$Y(T) \sim \begin{cases} e^{-\Delta_0/T}, & g(\mathbf{k}) \neq 0, \\ \left(\frac{T}{T_c}\right)^2, & g(\mathbf{k}) \text{ обращается в нуль в изолирован-} \\ \frac{T}{T_c}, & g(\mathbf{k}) \text{ обращается в нуль на линиях.} \end{cases} \tag{9.7}$$

Парамагнитная восприимчивость сверхпроводника с синглетгым спариванием при $T \to 0$ обращается в нул, что обуславливает проигрыш в энергии $\chi_n H^2/2 = \mu_{\mathrm{B}}^2 N_0 H^2$ сверхпроводника, находящегося в магнитном поле, по сравнению с нормальным металлом. В то же время, при $T = 0$ сверхпроводящее состояние энергетически выгоднее нормального на $N_0\Delta_0^2/2$ (см. (5.37)). Сравнивая эти лве энергии, получаем, что в полях, больших, чем

$$H_{\mathrm{p}} = \frac{\Delta_0}{\sqrt{2}\mu_{\mathrm{B}}} \tag{9.8}$$

сверхпроводящее состояние заведомо невыгодно. В поле H_{p}, называемом парамагнитным пределом сверхпроводимости, происходит разрушение синглетного состояния куперовских пар. В обычных свсрхпроводниках $H_{\mathrm{p}} \approx 1$ Тесла. На практике сверхпроводимость разрушается в полях, прсвышаюоших верхнее критическое поле H_{c2} в сверхпроводнихах второго рода (см. ниже 12) или поле абсолютной неустойчивости сверхпроводящего состояния H_{c1} в сверхпроводниках первого рода, значительно меньших парамагнитного предела H_{p}. Кромс парамагнитного предела в сверхпроводниках с ненулевым орбитальным моментом куперовских пар, как при сишглетном $S = 0$, так и при триплетном $S = 1$ спаривании, имеется диамагнитный прсдел [2] $H_{\mathrm{D}} \approx \frac{m^*}{m} H_{\mathrm{p}}$. Поле H_{D} может как превосходить, так и быть меньше парамагнитного предела, в зависимости от отношения эффективной массы электрона к массе электропа в вакууме.

Температурная зависимость (9.5) пзмеряется следующим образом. Ядерные спины атомов вещества, из которого состоит сверхпроводнник, прецессируют в магнитном поле H с частотои

$$\omega = \gamma H \tag{9.9}$$

На этой частоте наблюдается ядерныи магнитный резонанс, то есть резонансное поглошение радиочастотного поля $\mathrm{H_{rf}}$, перпендикулярного постоянному полю $\mathbf{H}$[3]. Из-за конечной вероятности попадания электронов проводимости в точку нахождения ядра R_n, пропорционалшной $|\psi_e(\mathbf{R}_n)|^2$, имеется взаимодсйствие магнитных моментов ядер μ_{n} и магнитных моментов электронов проводимости μ_{e} (контактное взаимодействие):

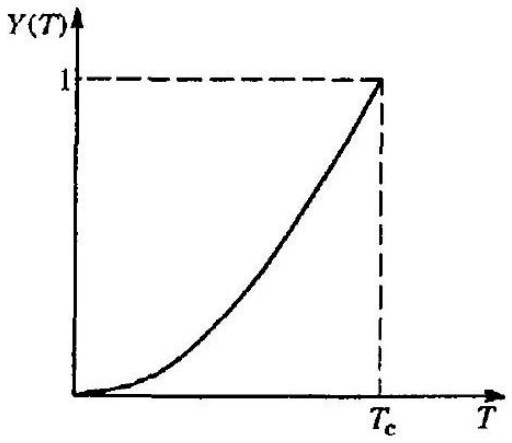
$$H_{\mathrm{int}} \sim \mu_{\mathrm{n}}\mu_{\mathrm{e}}\delta(\mathbf{r} - \mathbf{R}_{\mathfrak{n}}) \tag{9.10}$$

Среднее значение величины μ_{e} во внешнем поле дается выражением

$$\langle \mu_c \rangle = \frac{\chi \mathrm{H}}{n}$$

где χ есть парамагнитная восприимчи-

[11] Напомннм, что N_0 - плотность состояний на одну проекцию спина.



Ри с.9. Общцй вид функции Иосида вость, а n - плотность электронного газа.

Сдвиг уровней энергии ядерного спина вследствие взаиммодействия (9.10):

$$\delta E \sim \mu_{\mathrm{n}} \frac{\chi}{n} \left|\psi\left(\mathbf{R}_n\right)\right|^2 H$$

приводит к изменению резонансной частоты (9.9), то есть частоты переходов между уровнями в магнитном поле (сдвиг Найта) па величину:

$$\delta\omega \sim \frac{\mu_{\mathrm{n}}\chi}{n\hbar} \left|\psi\left(\mathbf{R}_{\mathrm{n}}\right)\right|^2 H \tag{9.11}$$

При переходе металла в сверхпроводящее состояние изменяется входящая в (9.11) парамагнитная восприимчивость χ, поэтому измерение отношения $\delta\omega_{\mathrm{s}}/\delta\omega_{\mathrm{n}} = \chi_{\mathrm{s}}/\chi_{\mathrm{n}}$ позволяет, согласно (9.5), определить плотность нормальных электронов. Из (9.6) следует, что слвиг Найта в сверхпроводнике с синглетным спариванием должен исчезать по мере уменьшения температуры.

Посмотрим теперь, как обстоит дело в сверхпроводликах с триплетным спариванием. Спиновое состояние куперовсхих пар во всем объеме сверхпроводника задается вектором d, зависящим от направления импульса на ферми-поверхности. Вероятность найти пару в состоянии с нулевой проекцией спина на ось квантования $\hat{z}$ пропорциональна $|d_z(\mathbf{k})|^2$ (см. (2.5) и (2.7)).

Очевидно, что если внешнее поле H (задающее ось квантования) направлено вдоль d)$\mathbf{k}$), то спин пар перпендикулярен $\mathbf{H}$ и не дает вклада в восприимчивость, которая, следовательно, определяется лиш вкладом возбужлений:

$$\chi_{\perp}(\mathbf{k}) = \chi_{\mathrm{n}} Y\left(\hat{\mathbf{k}}, T'\right) \tag{9.12}$$

где $Y(\hat{\mathbf{k}}, T)$ дастся формулой (9.4), а $E_{\mathbf{k}} = \sqrt{\xi^2 + \Delta^2 |\mathbf{d}(\mathbf{k})|^2}$.

Для направления поля (то есть оси $\hat{z}$) в плоскости, псрпендикулярной вектору d($\mathbf{k}$), будут отличны от нуля только x - и y-компонеиты всктора $\mathbf{d}(\mathbf{k})$, из которых составлены амплитуды вероятности $\pm d_x(\mathbf{k}) + i d_y(\mathbf{k})$ найти пары в состояниях с проскциями спина ± 1 на ось квантования. Очевидно, что для такого папранления поля вклад в восприимчивость дают как пары, так и возбуждения, и она совпадает с восприимчивостью ферми-жипкости в нормальном сосгоянии:

$$\chi_{\parallel} = \chi_{\mathrm{n}}. \tag{9.13}$$

[12] См. Н. А. Лjжьянчjж, В. Л. Миесв //Письма в ЖЭТФ, 44, 183 (1986).

[3] Для наблюдения этого эффекта поле в образце должно быть однородно, что имест место при условии матости размера образиа по сравценио с лоцщоновской глубиной проникиовения.

Для произвольной оринстации подл магнитный момент сверхтскучей жидкости определяется тснзором восприимчивости:

$$M_\alpha = \chi_{\alpha\beta} H_\beta,$$

который получается путсм комбинирования выраженнй (9.12) и (9.13):

$$\chi_{\alpha\beta} = \int \frac{d\Omega}{4\pi} \left\{ \chi_\perp(\mathbf{k}) \frac{d^*_\alpha(\mathbf{k}) d_\beta(\mathbf{k})}{\mathrm{d}^*(\mathbf{k})\mathrm{d}(\mathbf{k})} + \chi_\parallel(\mathbf{k}) \left[\delta_{\alpha\beta} - \frac{d^*_\alpha(\mathbf{k}) d_\beta(\mathrm{k})}{\mathbf{d}^*(\mathbf{k})\mathrm{d}(\mathbf{k})} \right] \right\} \tag{9.14}$$

В качестве примера приведем выражения для тензоров восприимчивости в A - и B-фазах гелия-3, которые потучаются из (9.14) после подстаповви соответствуоших параметров порядка [4] $\mathrm{d}^A(\mathbf{k})$ и $\mathrm{d}^B(\mathbf{k})$ (см. 3):

$$\chi^A_{\alpha,3} = \chi_\mathrm{n} \left[\delta_{\alpha\beta} + V_\alpha V_\beta \left(Y_A(T) - 1 \right) \right] \tag{9.15}$$

$$\chi^B_{\alpha\beta} = \chi_\mathrm{n} \delta_{\alpha\beta} \left(\frac{2}{3} + \frac{1}{3} Y_\mathrm{B}(T) \right) \tag{9.16}$$

Мы вилим, что в B-фазе восприимчивость изоропна, и при $T \to 0$ сдвиг Найга в сверхпроводнике со структурой B-фазы исчезает лиш частично. В А-фазе восприимчивость явлнется одиоосншм тензором. На практике, вдали от стенок сосуда с гелием-3, восприимчивость A-фазы всегда совпадает с χ_n, поскольку вектор V разворачивается перпендикулярно магнитному полю, чем достигается энергетически выгопное максимальнос значение восприимчивости. Вблизи стенок из-за спин-орбиталного взаимодействия вектор $\mathbf{V}$ псрпсндикулярен к поверхности, поэтому восприимчивость A-фазы зависит от направления.

Такой же эффект доджен иметь место и в сверхпроводниках с триплетным спариванием и силыпы спин-орбитальным взаимодействием, фиксирующим направление вектора d. Парамагнитные эффекты (в частности, сдзиг Найта) должны в этом случае сильно зависеть от направления внешнего магнитного поля [31-33]. Угловая зависимость восприимчивости лобой из триплетных фаз, переписленных в табл. 1-6, устанавливается после подстановки в (9.14) соответствуоших выражепий для параметров порядка $\mathrm{d}(\mathbf{k}) = \sum_i \eta_i \psi(\hat{k})$. Следует, однако, иметь в виду, что результат вычислений зависит от конкрстного вида базисных функций неприводимого представления. При этом температуріааа зависимость различиых компонент восприимчивости должна опредезяться с учетом зависимости $\eta_i(T)$, диктуемой уравнениями типа (6.12). Парамагнитная восприимчивость в сверхпроводниках с триплетным спариванием и слабым спин-орбитальньм заимодействием совпадает с паулиевской восприимчивостыо в нормальном состоянии.

MC-9.1

Доказать формулы (9.5) и (9.14) прямым выгчислепием спинового магнитного момента.
Указание. Найти прсобразование Боголобова, диагопализирующее гамиштопиан

$$H = H_\mathrm{BCS} - \mu_\mathrm{B} \sum_\mathbf{k} \mathrm{a}^+_{\mathbf{k}\alpha} \left(\sigma_{\alpha\beta} \mathrm{H} \right) a_{\mathbf{k}\beta}$$

[14] При вычислении восприимчивостей A - и B-фаз в реальном гелии-3 необходимо учитывать изменения внешнего поля за счет намагничивания самой жидкости (ферми-жыдкостные поправки) [3, 6]. Этот количественно довольно значительный эффект ие приволит, однако, к качественинм изменениям, и здесь мы сго учнтышать нс будем.

где H_{Bcs} - гамильтониан (5.1). Воспользовавшись этим преобразованием, найти линсйный по пото вктад в средное значешие операгора спинового магнитного момента

$$\mathbf{M} = \mu_B \sum_{\mathbf{k}} \left\langle a^+_{\mathbf{k}\alpha} \sigma_{\alpha\beta} a_{\mathbf{k}\beta} \right\rangle$$

MC-19.2

Найти поведенис функкший Иосида $Y_A(T)$ и $Y_B(T)$ для A - и B-фаз при $T \to 0$ и $T \to T_c$.

19.1.10 10. Landau Expansion of the Free Energy of Superconductors

Образование сверхпроводящего состояния из нормального происходит посредством фазового перехода второго рода. Согласно теории Ландау, изменение плотности свободной энергии при таком переходе может быть разложено в ряд по степеням параметра порядка. В случае однокомпонентной сверхпроводимости, когда параметром порядка является комплексная скалярная функция $\eta = |\eta| e^{i\varphi} = \Delta e^{i\varphi}$ (см. 4), это разложение имеет вид

$$F_{\text{cond}} = F_{\text{s}} - F_{\text{n}}^2 = \alpha |\eta|^2 + \frac{\beta}{2} |\eta|^4 = \alpha \Delta^2 + \frac{\beta}{2} \Delta^4 \tag{10.1}$$

где $\alpha(T) = \alpha_0 \left(T' - T_c\right) / T_{\text{c}}$ - меняет знак пря $T = T_c$; α_0, β - постоянные положителыные коэффициегты. Минимизация F_{s} по Δ дает следуоцие температурные зависимости щели (параметра порядка):

$$\Delta^2(T) = -\frac{\alpha_0}{\beta} \frac{T - T_c}{T_{\text{c}}} \tag{10.2}$$

и свободноны энергии:

$$F_{\text{cond}} = -\frac{\alpha_0^2}{2\beta} \left(\frac{T - T_c}{T_c} \right)^2 \tag{10.3}$$

вблизи критической температуры. Выражение (10.3) позволяет найти скачок теплоемкости при переходе в сверхпроводящее состояние:

$$(C_{\text{s}} - C_{\text{n}})|_{T=T_{\text{c}}} = -T_{\text{c}} \frac{\partial^2 F_{\text{cond}}}{\partial T^2} \bigg|_{T=T_{\text{c}}} = \frac{\alpha_0^2}{T_{\text{c}} \beta} \tag{10.4}$$

Формула (10.1) и ее обобщение на пространствепно-неоднородный случай ирают важнейшую роль в тсории свсрхпроводимости. Она может быть получена из микроскопической теории Бардина-Купера-Шриффера. Такой вывод для произвольного типа спаривапия и составляет предмет настоящего параграфа.

Свободная энергия сверхпроводника имеет вид

$$F_{\text{s}} = \langle H_{\text{BCS}} \rangle - TS \tag{10.5}$$

Здесь H_{BCS} - гамильтониал БКUU (5.31):

$$H_{\text{BCS}} = \sum_{\mathbf{k}} E_{\mathbf{k}} b^+_{\mathbf{k}\alpha} b_{\mathbf{k}\alpha} + \frac{1}{2} \sum_{\mathbf{k}} \Delta_{\mathbf{k},\alpha\beta} F^+_{\mathbf{k},\alpha\beta} + \frac{1}{2} \sum_{\mathbf{k}\alpha} (\xi_k - E_{\mathbf{k}}) \tag{10.6}$$

а S - энтропия электронного газа, определяемая формулой

$$S = -\sum_{\mathbf{k}\alpha} \left[f_{\mathbf{k}} \ln f_{\mathbf{k}} + (1 - f_{\mathbf{k}}) \ln (1 - f_{\mathbf{k}}) \right] \tag{10.7}$$

где $f_{\mathbf{k}}$ - фермиевская функция распределения (6.2).

Для опрсделенности мы будем рассматривать случай унитарных фаз с триплетным спариванием, когда параметр порядка и энергия элементарных возбуждений даются формулами

$$E_{\mathbf{k}} = \sqrt{\xi_k^2 + \Delta^2(T) \mathrm{d}(\mathbf{k}) \mathrm{d}^*(\mathbf{k})}$$
$$\Delta_{\mathbf{k},\alpha\beta} = \Delta(T) \mathrm{d}(\mathbf{k}) \mathbf{g}_{\alpha\beta}$$
$$F^+_{\mathbf{k},\alpha\beta} = \mathbf{F}^*_{\mathbf{k}} \mathbf{g}^+_{\alpha\beta}$$

(см. 5). Подставляя в (10.5) и выполняя статистическое усреднепие, имеем:

$$\langle H_{\mathrm{BCS}} \rangle = \sum_{\mathbf{k}\alpha} \left[E_{\mathbf{k}} f_{\mathbf{k}} + \frac{1}{2} \left(\Delta(T) \mathbf{d}(\mathbf{k}) \mathbf{F}^*_{\mathbf{k}} + \xi_k - E_{\mathrm{k}} \right) \right]$$

В то же время:

$$\begin{aligned} -TS &= T \sum_{\mathbf{k}\alpha} \ln (1 - f_{\mathbf{k}}) + T \sum_{\mathbf{k}\alpha} f_{\mathbf{k}} \ln \frac{f_{\mathbf{k}}}{1 - f_{\mathbf{k}}} = \\ &= T \sum_{\mathbf{k}\alpha} \ln (1 - f_{\mathbf{k}}) - \sum_{\mathbf{k}\alpha} E_{\mathbf{k}} f_{\mathbf{k}} \end{aligned} \tag{10.8}$$

После подстановки в (10.5) получаем:

$$F_{\mathbf{s}} = \sum_{\mathbf{k}} \left[\Delta(T) \mathrm{d}(\mathbf{k}) \mathbf{F}^*_{\mathbf{k}} + \xi_k + 2T \ln (1 - f_{\mathbf{k}}) - E_{\mathbf{k}} \right] \tag{11.9}$$

Первыдй член в этой формуле преобразуется с помошыо уравненияя (5.17):

$$\Delta \mathbf{d}^*(\mathbf{k}) = -\sum_{\mathbf{k}'} V_l (\mathbf{k}, \mathbf{k}') \mathbf{F}^*_{\mathbf{k}'}$$

Домножая здесь левупо и правую части на $\Delta d(k)$ и интегрируя по углам с помошъю условия нормировки и разложения (5.4) потешциала $V_l (\mathbf{k}, \mathbf{k}')$, имеем:

$$\frac{\Delta^2}{V_l} = \sum_{\mathbf{k}'} \Delta \mathrm{d} (\mathbf{k}') \mathbf{F}^*_{\mathbf{k}'}$$

Отсiода, в своIо очередь, учитывая выражение для критической температуры (6.10), получаем:

$$N_0 \Delta^2 \ln \frac{2\gamma\varepsilon_l}{\pi T_c} = \sum_{\mathbf{k}'} \Delta \mathrm{d} (\mathbf{k}') \mathbf{F}^*_{\mathbf{k}'}$$

Охонтательно:

$$F_{\mathrm{s}} = N_0 \Delta^2 \ln \frac{2\gamma\epsilon_l}{\pi T_k} + \sum_{\mathbf{k}} \left[\xi_k + 2T \ln (1 - f_{\mathbf{k}}) - E_{\mathbf{k}} \right] \tag{10.10}$$

Поскольку нас интересует только энергия конденсации, то есть отклонение энергии сверхпроводника от энергии нормального металла, то, принимая во внимание равснство

$$\frac{\partial}{\partial\Delta}\left[2T\ln\left(1-f_{\mathbf{k}}\right)-E_{\mathbf{k}}\right]=-2\ \mathrm{d}(\mathbf{k})\mathrm{F}_{\mathbf{k}}^{\nu}$$

можно переписать (10.10) в виде

$$F_{\mathrm{cond}}\ =N_0\Delta^2\ln\frac{2\gamma\epsilon_l}{\pi T_c}-2\sum_{\mathbf{k}}\int\limits_0^{\Delta}d\Delta\mathrm{d}(\mathbf{k})\mathbf{F}_{\mathbf{k}}^{*} \tag{10.11}$$

Интегрирование по волновым векторам выполняется в соответствии с правилом (1.8), при этом удобно сначала произвести интегрирование по энергии:

$$N_0\int\limits_{-\varepsilon_1}^{\varepsilon_1}\mathrm{F}_{\mathbf{k}}^{*}d\xi=N_0\Delta\mathrm{d}^{*}(\mathrm{k})\int\limits_{-\varepsilon_1}^{\varepsilon_1}d\xi\frac{1-2f_{\mathrm{k}}}{2E_{\mathrm{k}}}$$

Это выражсние при $\Delta\to 0$ приводится k виду (ср. с выводом формулы (6.18))
$N_0\Delta\mathrm{d}^{*}(\mathbf{k})\left[\ln\frac{2\varepsilon_0}{\Delta}-\ln\frac{\pi T}{\gamma\Delta}-\frac{7\zeta(3)}{8\pi^2}\ \mathrm{d}(\mathbf{k})\mathrm{d}^{*}(\mathbf{k})\left(\frac{\Delta}{T}\right)^2\right]=$

$$=N_0\Delta d^{*}(\mathbf{k})\left[\ln\frac{2\gamma\varepsilon_0}{\pi T}-\frac{7\zeta(3)}{8\pi^2}\ \mathrm{d}(\mathbf{k})\mathrm{d}^{*}(\mathbf{k})\left(\frac{\Delta}{T}\right)^2\right] \tag{10.12}$$

Подставляя (10.12) в (10.11) и выпоодіяя интегрирование по Δ, имеем:

$$F_{\mathrm{cond}}\ =N_0\Delta^2\ln\frac{T}{T_c}+\frac{7\zeta(3)}{16\pi^2}N_0\int\frac{d\Omega}{4\pi}\left(\mathbf{d}(\mathbf{k})\mathrm{d}^{*}(\mathbf{k})\right)^2\frac{\Delta^4}{T^2}$$

Учитывая близость T к T_c, получаем окончательно:

$$F_{\mathrm{cond}}\ =N_0\frac{T-T_c}{T_{\mathrm{c}}}\Delta^2+\frac{7\zeta(3)}{16\pi^2}N_0\int\frac{d\Omega}{4\pi}\left(\mathrm{d}(\mathbf{k})\mathrm{d}^{*}(\mathbf{k})\right)^2\frac{\Delta^4}{T_c^2} \tag{10.13}$$

Аналогичные рассуждения позволяют получить разложение Ландау и для случая синглетного спаривапия:

$$F_{\mathrm{cond}}\ =N_0\frac{T-T_c}{T_c}\Delta^2+\frac{7\zeta(3)}{16\pi^2}N_0\int\frac{d\Omega}{4\pi}\left(g(\mathbf{k})g^{*}(\mathbf{k})\right)^2\frac{\Delta^4}{T_c^2} \tag{10.14}$$

В частности, для обычного сверхпроводника с s-спариванием ($g(\mathbf{k})=e^{i\varphi}$)

$$F_{\mathrm{cond}}\ =N_0\frac{T-T_i}{T_{\mathrm{c}}}\Delta^2+\frac{7\zeta(3)}{16\pi^2}N_0\frac{\Delta^4}{T_{\mathrm{c}}^2} \tag{10.15}$$

Итак, ми полугіи разложения Лаппау шя сзерхпроводников с трипихетным [1] и сингле TILjм спариваниєм, следующие из тсории БКШ. Критическая тсмпература, входящая в (10.13) и (10.14), одинакова дхя всех сверхпроволящих состояний с данным l (относящихся k данному неприводимому представлению группи симметрии нормального состояния). В то же время, эпергии сверхпроводяших состояний с данным l, оличаюошихся паборами коэффициснтов в разложениях (4.8) или (4.9) параметра порядка по сферическим гармоникам (в сбщем случае - по функшиям базиса неприводимого представления (4.10) или (4.11)), будут различньми. В самом деле, равновесная энергия конденсации)10.3)

$$F_{\mathrm{cond}}\ =-\frac{\alpha_0^2}{2\beta}\left(\frac{T-T_c}{T_c}\right)^2\sim\left[\int\frac{d\Omega}{4\pi}\left(\mathrm{d}(\mathbf{k})\mathrm{d}^{*}(\mathbf{k})\right)^2\right]^{-1} \tag{10.16}$$

сушсственно зависит от вида сверхпроводящего состояния. Так, напрммер, для фаз с p-спариванием после подстаповки в (10.16) параметров порядка из 3 мы получаем, тто минимальной энергией среди фаз с p-спариванием будет обладать B-фаза ($\mathrm{d}(\mathbf{k}) = \hat{\mathbf{k}}$). В частности, се энергия оказывастся ниже эгергии A-фазы $\left(\mathrm{d}(\mathbf{k}) = \sqrt{3/2}\left(\hat{k}_x + i\hat{k}_y, 0, 0\right)\right)$ в $6/5$ раз [22].

Действительно, в жидком гелии-3 при низких давлениях фазовый переход из нормальной жидкости происходит в сверхтекучуп B-фазу. Однако, в области высоких давлений (рис. 2) сначала происхолит переход в A-фазу, которая загем сменяется на B-фазу посредством перехола первого рода. Эго означает, что при высоких давлепиях вблизи T_c именно A-фаза наиболес энергетически выгодна. Разренение противоречия с наиим результатом состоит в том, что формуда (10.13), на основании которой сделан вывод о мипимальности энсргии B-фазы, является на самом деле недостаточно общей. В процессе ее вывода использовалось, казалось бы, естественіное предположение о том, что спаривательнос взаимолействие не изменяется в сверхпроводящем состоянии, в частности, является одинаковым во всех сверхпроводящих фазах с данным l (приблискение слабой связи или приближение БКШ). На самом деле это не так, и $V(\mathbf{k}, \mathbf{k}')$ зависит от конкретного вида параметра порядка (сильная связь). Хотя этот факт не сказчвается на утверждении о том, что все фазы с данным l иметот одинаковую критическуюо температуру, вид члена четвертого порядка по Δ в разложении (10.13) прри этом меняется, что делает, вообще говоря, неверным вывод об энергетической вытодности B-фазы при побых температурах и давлениях. Учет влияния вида спаривания ша $V(\mathbf{k}, \mathbf{k}')$ может быть произведен тиш в рамках конкрстной микроскопитеской модели (см. [3, 6]) и мы не булем здесь этим запиматься, тем более что на практике нет возможности количественіо проверить справедливость той или иной модели сильной связи.

19.1.11 11. Superconducting States with Multicomponent Order Parameters

Из рассмотрения в §4 и 10 следует, что возможные сверхпроводящие или сверхтекучие фазы, параметр порядка которых прсобразуетея в соотве гствии с определснным (неодномерным) прсдставтением точечной группы симметрии G, имеют одинаковуто критическую температуру, но различную свободную энергию. Вычисления с помощыо той или иной микроскопичсской модели в принципе позволяют найпи коэффициенты в разложении Ландау и ответить на вопрос, в какос имснно состояние происходит фазовый переход, подобно тому, как это было сделапо в предыдущем параграфе в рамках теории БКШ. Одиако к выводу о том, тто минимальную свободную энергию могут иметь различные состояния, причем каждое - в своей области фазовой диаграммы (напримср, не только B-фаза, но и другие фазы p-спаривания на плоскости давлепие-температура), можно прийти не зависяцим от конкретной микроскопической мопели феноменологическим путем. При этом пля получения разложсния Ландау могут быть использованы лиш весьма общие симмстрийные соображения [34].

Разлжение свободной энергии Лацдау для фаз с p-спариваиием. Параметром порядка в сверхтекутей ферми-жилкости с p-спариванием являстся комплексная 3×3 матрица $A_{\alpha i}$ (см. 3), которая прсобразуется при спиновых вращениях как вектор по индексу α, а при вращениях в координатном пространстве - как вектор по индексу i. Свободиая

[11] Iапомним, что разложепие (10.13) страведтиво лишь дли так называемых уинитарных фаз (см. 5). Вывод разложения Ландау из теории БКI аля произвольныгх сверхпроводяипх фаз с триплетиым спаривапием проделан в 18.

энергия, будучи скалярнои величиной, не зависит от выбора систем координат, в которых заданы эти вектора. Иными словами, разложение должно быть иівариаітно относительно произвольных и независимдх (в отсутствие сппи-орбиталного взаимодействия) трехмерных вращений спинового и координатного пространств. Кроме этого, свободная энергия вещественна, то есть не должна меняться при комплексном сопряжении параметра порядка (симметрия по отношению к обращению времени), а также при домножении парамстра порядка на произвольный фазовый міожитель $e^{i\varphi}$ (калибровочная инвариантность).

Указанным свойствам инвариантности при преобразованиях параметра порядка вила

$$A_{\alpha i} \to \tilde{A}_{\alpha i} = R^{\mathrm{S}}_{\alpha\beta} R^{o}_{ij} e^{i\varphi} R A_{\beta j}$$

где $R^{S}_{\alpha\beta}$ и R^{O}_{ij} - матрицы трехмерных вращений в спиновом и координатном (орбитальном) пространствах, соответственно, а $RA_{\alpha i} = A^{*}_{\alpha i}$ - операция обращсния времени, удовлетворяет выраженис для плотности свободной энергии, содержащее всего пять инвариантных членов четвертого порялка:

$$\begin{aligned} F_{\mathrm{cond}} &= \alpha A_{\alpha i} A^{*}_{\alpha i} + \beta_1 \left|A_{\alpha i} A_{\alpha i}\right|^2 + \beta_2 \left(A^{*}_{\alpha i} A_{\alpha i}\right)^2 + \beta_3 A^{*}_{\alpha i} A_{\beta i} A^{*}_{\alpha j} A_{\beta j} + \\ &+ \beta_4 A^{*}_{\alpha i} A_{\beta i} A^{*}_{\beta j} A_{\alpha j} + \beta_5 A^{*}_{\alpha i} A_{\alpha j} A^{*}_{\beta i} A_{\beta j} \end{aligned} \tag{11.1}$$

Здесь матрицы A и A^{*} встречаются попарно, и во всех слагаемых произведена попарная свертка спиновых индексов со спиновыми, а орбитальных - с орбитальными.

Плотность свободной энергии (11.1) имеет несколько экстрсмумов, определяемых уравнениями $\delta F_{\mathrm{cond}} / \delta A_{\alpha i} = 0$. Какие из этих экстремумов есть минимумы, и какой из минимумов является абсолотным, зависит or соотношения между коэффициентами β_i, которые в свою очередь, зависят от температуры и давления [1]. A - и B-фазы входят в число минимумов F_{cond} Матрицы параметра порядка для них выглядят следующим образом (см. 3):

$$A^{A}_{\alpha i} = \sqrt{\frac{3}{2}} \Delta(T) V_\alpha \left(\Delta'_i + i\Delta''_i\right) \tag{11.2}$$

$$A^{B}_{\alpha i} = \Delta(T) R_{\alpha i} e^{i\varphi} \tag{11.3}$$

где $\mathbf{V}, \Delta', \Delta''$ - единичные векторы (причем $\Delta'\Delta'' = 0$), $R_{\alpha i}$ - матрица трехмерных вращений, а $\Delta(T)$ - модуль параметра порядка. Состояния A-фазы вырождены по ориентациям вектора V и пары векторов Δ' и Δ'', а состояния B-фазы вырождены по отнопению к трехмерным вращениям, задаваемым матрицей параметра порядка $R_{\alpha i}$, и к выбору фазы φ.

В отличие or (10.13), разложение (11.1) дает право на существование А-фазы. Действительо, подставляя (11.2) и (11.3) в (11.1), получаем:

$$\begin{aligned} F^{A}_{\mathrm{cond}} &= 3\alpha\Delta^2 + 9\Delta^4 \left(\beta_2 + \beta_3 + \beta_4\right) \\ F^{B}_{\mathrm{cond}} &= 3\alpha\Delta^2 + 9\Delta^4 \left(\beta_1 + \beta_2 + \frac{\beta_3 + \beta_4 + \beta_5}{3}\right) \end{aligned}$$

Отсюда видно, что A-фаза энергетически выгоднее B-фазы, если значение β_1 (или β_5) достаточно велико.

Многокомпоненттые сверхпроводяппие состояния в кристаллах. Пусть сверхпроводящее состояние соответствует одному из неодномерных представлений

группы точечной симметрии кристалла. В случае сильного спин-орбитального взаимодействия параметр порядка такого состояния имеет вид (см. 4)

$$\begin{array}{rl} g(\mathbf{k}) = \eta_1 \psi_1^{\mathrm{g}}(\hat{\mathbf{k}}) + \eta_2 \psi_2^{\mathrm{g}}(\hat{\mathbf{k}}) + \ldots & \text{при } S = 0 \\ \mathrm{d}(\mathbf{k}) = \eta_1 \psi_1^{\mathrm{u}}(\hat{\mathbf{k}}) + \eta_2 \psi_2^{\mathrm{u}}(\hat{\mathbf{k}}) + \ldots & \text{при } S = 1 \end{array} \tag{11.4}$$

Как для синглетного, так и для триплетного сверхпроводящего состояния плотность свободной эпергии вблизи температуры перехода записывается в виде разложения по степепям комплексных коэффициештов η_i, которое лотжно быть инвариантно относительно прсобразований гругппы симметрии нормапного состояния $\mathcal{G} = U(1) \times R \times G$. При выводе такого разложения необходимо принять во внимание, что транеформационные своиства базисных функкший $\psi_i^{\mathrm{g}}(\hat{\mathbf{k}})$ и $\psi_i^{\mathrm{u}}(\hat{\mathrm{k}})$ при преобразованиях симметрй можно отнести к коэффициентам η_i.

Напримср, для представлений $E_{1\,\mathrm{g}}$ и $E_{1\,\mathrm{и}}$ группы $D_{6\,\mathrm{h}}$ базисные функции пропорциональны компонентам вектора, лежацего в Базисиой плоскости (см. табл. 1), т.е.

$$\begin{array}{c} \left(\psi_1^{\mathrm{g}}(\hat{\mathbf{k}}), \psi_2^{\mathrm{g}}(\hat{\mathbf{k}})\right) \sim (k_z k_x, k_z k_y) \\ \left(\psi_1^{\mathrm{u}}(\hat{\mathbf{k}}), \psi_2^{\mathrm{u}}(\hat{\mathbf{k}})\right) \sim (\hat{z} k_x, \hat{z} k_y) \end{array} \tag{11.5}$$

Поэтому можно считать, что коэффициенты η_1, η_2 прсобразуются под действием эдементов группы $D_{6\,\mathrm{к}}$ как компонснты такого вектора [2]. Скалярные произведения $\boldsymbol{\eta}\boldsymbol{\eta}^*, \boldsymbol{\eta}\boldsymbol{\eta}, \boldsymbol{\eta}^*\boldsymbol{\eta}^*$ инвариантны относительно любых вращений из труппы D_6. Из них можно составить два вещественных инварианта четвертого порядка. Друтих инвариантов в случае гексагональной симметрии нс существует, следовательно, разложснис Ландау имест вид:

$$F = \alpha \boldsymbol{\eta} \eta^2 + \frac{\beta_1}{2} \left(\boldsymbol{\eta} \eta^2\right)^2 + \frac{\beta_2}{2} |\eta\eta|^2 \tag{11.6}$$

Минимуму свободной энергии (11.6) при $\beta_2 < 0$ соответствует параметр порядка

$$\begin{array}{c} \eta = \eta_0 (\cos\lambda, \sin\lambda) e^{i\varphi} \\ \eta_0^2 = -\dfrac{\alpha}{\beta_1 + \beta_2} \end{array} \tag{11.7}$$

где φ и λ - произволыне фазы. Снятие вырождения по отношению к λ происходит только при добавлешии к разложеник (11.6) инварианта шестого порядка:

$$\gamma \,\mathrm{Re}\left(\eta_1 + i\eta_2\right)^3 \left(\eta_1^* + i\eta_2^*\right)^3 \tag{11.8}$$

Если $\gamma < 0$, то минимум своболной энергии достигается при $\lambda = \lambda_n = \pi n/3$, $n = 0, 1, \ldots, 5$, если $\gamma > 0$, то - при $\lambda_n = \pi n/3 + \pi/6$. Все сверхпроводящие состояния, описываемые параметром порядка (11.7) с указанными значениями λ формально принадлежат одному сверхпроводящему классу $D_2\,(C_2) \times R$, однако направление оссй симметрии для разных λ_n различно. Так, например, при $\gamma < 0$ и $\lambda = 0$ сверхпроводящий класс выглядит следующим образом:

$$D_2\,(C_2) \times R = \left\{E, C_{2y}, e^{i\pi} C_{2x}, e^{i\pi} C_{2z}\right\} \times R$$

[11] Общая загача о нахождении всех экстремумов функционага (11.1) решена В. Березинским [35]. Те же результаты независимо получены в работе [36]

При $\beta_2 > 0$ минимум энергии (11.6) достигается при [3]

$$\eta = \eta_0(1, \pm i)e^{i\varphi} \qquad (11.9)$$
$$\eta_0^2 = -\frac{\alpha}{2\beta_1}$$

Этому решению соответствует сверхпроводяиий класс

$$D_6(E) = \left\{\exp\left(\frac{i\pi n}{3}\right) C_n, \exp\left(\frac{i\pi n}{3}\right) RU_n\right\}$$

гдс $n = 0, 1, \ldots, 5$. Аналогично А-фазе гелия-3, состояние (11.9) не илвариантно относитсдьно обращения врсмени, что означает напщчие спонтанного магнетизма купсровских пар. К этому вопросу мы еше вернемся в 15.

Для сверхпроводяших состояний, соответствутоших двумерным представлениям $E_{2\,\mathrm{g}}$ и $E_{2\mathrm{u}}$ группы D_{6h}, свободная энергия сохраняет вил (11.6). Ее минимумы определяготся формупами (11.7) и (11.9) и формалыно относятся к тем же сверхпроводяшим ктассам, вктючающим, оштако, другие элементы симметрии в соответствии с трансформационными свойствами базисных функций представления E_2.

В тетрагональном кристалле ($G = D_{4h}$) базисные функции единственного двумсрного представления E тоже пмеюот вид (11.5), то есть преобразуются как

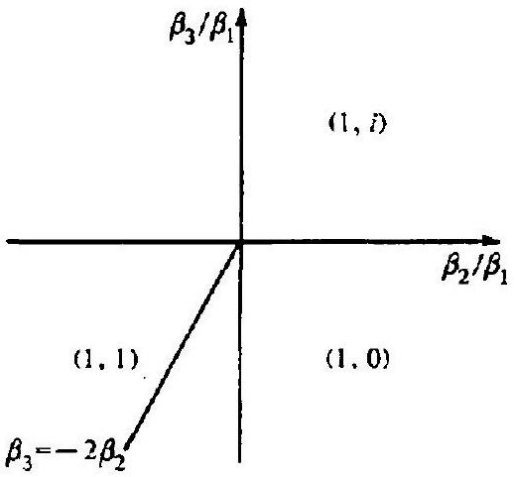


Рис. 10. бласти существования двухкомпонеппиых сверхроводяиих состоянии (1,0), (1,i) и (1,1) в тетрагонатыгом кристалле

компоненты вектора, лежащего в базисной плоскости. Однако, в этом случае симметрия допускает существование трех инвариантов четвергого порядка, и свободная энергия Лаидау принимает вид

$$F = a\eta\eta^* + \frac{\beta_1}{2}(\eta\eta'')^2 + \frac{\beta_2}{2}|\eta\eta|^2 + \frac{\beta_3}{2}\left(|\eta_1|^4 + |\eta_2|^4\right) \qquad (11.10)$$

В зависимости от отношения коэффициентов β_2 и β_3 (см. рис. 10) энергия достигает минимашных значенний на решениях трех типов:

[12] Действие операций хатибровочной группы сводится **x** умножению компонент парачетра порадка на обиций фазовый множитель: $(\eta_1, \eta_2) \to e^{1\varphi}(\eta_1, \eta_2)$, а обращение времени эквивалентно комплексному сопряжению: $(\eta_1, \eta_2) \to (\eta_1^*, \eta_2^*)$

[3] Пользуясь результатами предыдушего параграфа, нетрудно установить, что в теории БК (приближение слабой связи) выполняется соотношение $\beta_1 = 2\beta_2 > 0$.

$$\eta \sim (1.0)(\text{ илии } (0,1)). \quad (1.\pm 1), \quad (1,\pm i) \tag{11.11}$$

Веществепные фазы относятся х классам вида $D_2\,(C_2) \times R$, причсм, как и в гексагональном кристалле, направлсния осей симметрии для различных фаз различно. Комплексныс состояния принадлежат магнитному классу

$$D_4(E) = \left\{ \exp\left(\frac{i\pi n}{2}\right) C_n, \exp\left(\frac{i\pi n}{2}\right) RU_n \right\}$$

где $n = 0, 1, 2, 3$.

В кристаллах с кубической симметрией пля сверхтроводящих состояний, параметры порядка $\boldsymbol{\eta} = (\eta_1, \eta_2, \eta_3)$ которых преобразуются согласно одному из двух трехмсрных представлений труппы O_h (см. табл. 5, 6), плотность свободной энсргии записывается в виде, аналогичном (11.10):

$$F' = \alpha\eta\eta^{=} + \frac{\beta_1}{2}\left(\eta\eta^{-}\right)^2 + \frac{\beta_2}{2}|\eta\eta|^2 + \frac{\beta_3}{2}\left(|\eta_1|^4 + |\eta_2|^4 + |\eta_3|^4\right) \tag{11.12}$$

В случае же двухкомпонентного параметра порядка, сскответствуоощего двумсриому представлению, свободная эергия имеет вид

$$F = \alpha\eta\eta^* + \frac{\beta_1}{2}\left(\eta\eta^*\right)^2 + \frac{\beta_2}{2}|\eta\eta|^2 + \gamma\left(\eta_1^3\eta_2^{*3} + \eta_1^{*3}\eta_2^3\right) \tag{11.13}$$

где мы добавиш ипвариант шестого порядка, спиматощи вырожденис веществснігдх состояний.

Мы не будем здссь останавливаться на перечислении всех возможных минимумов (11.12) ии (11.13) и соответствующих им сверхпроволящих классов. Это может быть сделано (см. [9]) анатогично рассмотренному выие простому случаю тетрагонального кристалла.

Упражиение. Найти разложение Ландау свободиой энсргии изотропного сверхпроводника с d-спариванием.

19.1.12 12. Ginzburg–Landau Equations and the Upper Critical Field

В этом и нескольких следующих параграфах будет изложена теория Гинзбурга-Лапдау для анизотропных сверхпроводяиих состояний. Прелполагая, что читатель знаком с теорией Гинзбурга-Ландау для обычных сверхпроводников (см., например, [37]), мы сосредоточим вниманис на вопросах, специфическдх дия необычной свсрхпроводимости. Напем с постросния функционалов Гинзбурга-Лаплау и вычисления верхіих критических полей в необыгныхх сверхпроводиниках второго рода.

Однокомпопегтиые сверхпроводящие состояния в кристаллах. Функиионал Гинзбурга-Ландау, то есть разность энергий Гиббса [1] свсрхпроводника в неоднородном состоянии вблизи T_c и нормального металла, в стучае однокомпонентного параметра порядка $\eta(\mathbf{r}) = |\eta(\mathbf{r})|e^{i\varphi(\mathbf{r})}$ имеет вид

$$\mathcal{G} = \int d^3r G = \int d^3r \left(F - \frac{\mathbf{HB}}{4\pi}\right) \tag{12.1}$$

где плотность свободной энергии F отлитается от выражсния (10.1) тем, что здесь добавлсна градиегтная энергия и энергия магнитного поля:

$$F = \alpha_0 \left(\frac{T - T_c}{T_\varepsilon} \right) |\eta|^2 + \frac{3}{2}|\eta|^4 + K_{ij} \left(D_i \eta \right)^* \left(D_j \eta \right) + \frac{B^2}{8\pi} \tag{12.2}$$

Здесь

$$D_i = -i\nabla_i + \frac{2\pi}{\Phi_0} A_i \quad (i = x, y, z) \tag{12.3}$$

$\Phi_0 = \pi\hbar c/e$ - кваит магнитного потока [2], а $\mathbf{B} = \operatorname{rot} \mathbf{A}$ - всктор магнитной индукции.

Тепзор K_{ij}, называемый тензором эффективных масс, описывает анизотропию направлений в кристалле. Так, для одноосных кристалов с гексаго- нальной (илщ тетрагональной) симметрией:

$$K_{ij} = \left(\delta_{ij} - \hat{z}_i \hat{z}_j \right) K_1 + \hat{z}_i \hat{z}_j K_4 \tag{12.4}$$

В кристаллах с кубической симметрией $K_1 = K_4$, то есть $K_{ij} = K\delta_{ij}$. Вывод градиентных слагаемых в свободной энергии с помощью михроскопической теории проделан в параграфе 18.

Пространственные распределения параметра порядка η и векторпотенциала A должны обсспечивать минимальность функционала $\mathcal{G}$:

$$\frac{\delta \mathcal{G}}{\delta \eta^*} = 0, \quad \frac{\delta \mathcal{G}}{\delta \mathrm{A}} = 0 \tag{12.5}$$

Варьируя (12.1) по η^* и отбрасывая интеграл по поверхности сверхпроводника (мы обсудим поверхностные эффекты в следующем параграфе), приходим х уравнению Гинзбурга-Ландау:

$$\alpha_0 \left(\frac{T - T_c}{T_c} \right) \eta + \beta |\eta|^2 \eta + K_{ij} D_i D_j \eta = 0 \tag{12.6}$$

Сравнивая первый и последний члены в уравнении (12.6), мы вилим, что в теории имеется характерный пространственный масштаб - корреляционная длина $\xi(T)$, различная для различных кристаллографических направлений i:

$$\xi_i(T) \approx \hbar \left(\frac{K_{11}}{\alpha(T)} \right)^{1/2} \tag{12.7}$$

Буквенная оценка $\xi(T)$ для произвольного направлсния имеет вид

$$\xi(T) \sim \xi_0 \left(\frac{T_c - T}{T_c} \right)^{-1/2} \tag{12.8}$$

где $\xi_0 = \hbar v_{\mathrm{F}} / \left(2\pi T_{\mathrm{c}} \right)$ есть размер куперовской пары (см. 1).

Градиентная энергия сверхпроводника включаст, разумеется, и члены бодее высоких порядков по градиегтам, чем $K_{ij} \left(D_i \eta \right)^* \left(D_j \eta \right)$. Их игнорирование означает, что теория Гиізбурга-Ландау адекватно описывает достаточно медленные пространственные изменения параметра порядка с масшгтабом, превышающим ξ_0.

Верхнее критическое поле. Верхнее критическое поле $H_{c2}(T)$, при котором в сверхпроводниках второго рода происходит фазовый переход в сверхпроводящес состояние, соотвстствует наинизшему собственному значению дифференциаьного

[11] В задавном внешлем мжаннтном поте 11 иместо свободнои энергии $\mathcal{F}(T, B)$ улобно исполызрвать энергио Гиббса $\mathcal{G}(T, IT)$.

[2] Здесь и пиже е обозыачает абсолютнуо величину заряда электрона.

оператора в линеаризованном уравнении Гинзбурга-Ландау. Перед изучением анизотропии верхнего критического поля, специфической для некоторых кристаллических сверхпроводников с многокомпонентным параметром порядка, посмотрим сначала, как обстоит дело для однокомпонентной сверхпроводимости в одноосных кристаллах. В этом случае линеаризованное уравнение Гинзбурга-Лапдау имеет вил

$$\alpha_0 \left(\frac{T - T_c}{T_c} \right) \eta + K_1 \left(D_x^2 + D_y^2 \right) \eta + K_4 D_z^2 \eta = 0 \tag{12.9}$$

Выбирая магнитное поле лежащим в базисной плоскости:

$$\begin{aligned} \mathbf{H} &= H(\cos\varphi, \sin\varphi, 0) \\ \mathbf{A} &= Hz(\sin\varphi, -\cos\varphi, 0) \end{aligned} \tag{12.10}$$

из (12.9) получаем:

$$-K_4 \frac{d^2\eta}{dz^2} + K_1 \left(\frac{2\pi H}{\Phi_0} \right)^2 z^2 \eta + \alpha_0 \left(\frac{T - T_c}{T_\mathrm{c}} \right) \eta = 0 \tag{12.11}$$

Пользуясь тем, что данное уравнешиее формально совпадает с уравнением Шрсдингера для заряженной частицы в магнитном поле, собственные функции и собственные значения которого (уровни Ландау) хорошо известны, находим:

$$H_{c2}(T) = \frac{\Phi_0 \alpha_0}{2\pi\sqrt{K_1 K_4}} \frac{T_c - T}{T_c} \tag{12.12}$$

то есть ведичина верхнего критического поля, лежащего в базиспой плоскости гексагонального (тетрагонального) кристалла, не зависиг от направления.

Такая зависимость появляется лишь при выходе из базисной плоскости. Например, дхя поля, лежацего в плоскости (y, z):

$$\begin{aligned} \mathbf{H} &= H(0, \sin\theta, \cos\theta) \\ \mathbf{A} &= Hx(0, \cos\theta, -\sin\theta) \end{aligned} \tag{12.13}$$

решение уравнения (12.9) дает

$$H_{\mathrm{c}2}(T) = \frac{\Phi_0 \alpha_0}{2\pi\sqrt{K_1 \left(K_1 \cos^2\theta + K_4 \sin^2\theta \right)}} \frac{T_\mathrm{c} - T}{T_\mathrm{c}} \tag{12.14}$$

В кристаллах с кубической симметрией $K_1 = K_4$, и величина верхнего критического поля нс зависит от его ориснтации относительно осей кристаллической решетки.

Миогокомпонентиые сверхпроводящие состояния в кристаллах. Персйдем геперь к рассмотрегию двухкомпонентий сверхпроводимости с векторным параметром порядка $\eta = (\eta_x, \eta_y)$, соответствующим мибо представлению E_1 группы D_6, либо представлению группы E группы D_4 (см. 4). Функционалы Гиизбурга-Ландау записываются в виде разложения по степеням двух комплексных функций η_1 и η_2 и их градиентов, которос должно быть вещественным и инвариантндм относитежно всех преобразований точечной группы D_{6h} (или D_{4h}). Последнее требованис означает, что всякий член разложения имеет один и тот же вид во всех системах координат, связанных между собой преобразованиями из D_{6h} (или D_{4h}). Оставляя лишь квадратичные по параметру порядка слагаемые, существенные

для вычисления верхнего критического поля, запишем фупкционалы Гинзбурга-Ландау для векторного представления в гексагоналыном:

$$F_{\text{hex}} = \alpha_0 \left(\frac{T - T_c}{T_c} \right) \eta\eta^m + K_1 \left(D_i \eta_i \right)^* \left(D_i \eta_j \right) + K_2 \left(D_i \eta_i \right)^* \left(D_j \eta_j \right) + \\ + K_3 \left(D_i \eta_j \right)^* \left(D_j \eta_i \right) + K_4 \left(D_z \eta_i \right)^* \left(D_z \eta_i \right) + \frac{B^2}{8\pi} \tag{12.15}$$

и тетрагональном:

$$F_{\text{tetr}} = F_{\text{hex}} + K_5 \left[\left(D_x \eta_x \right)^* \left(D_x \eta_x \right) + \left(D_y \eta_y \right)^* \left(D_y \eta_y \right) \right] \tag{12.16}$$

кристаллах, $i = x, y$.

Плотность свободной энергии F_{hex} содержит только скалярнъе произведения двух лежащих в базисной плоскости векторов $\boldsymbol{\eta}$ и $\mathbf{D}$ ($\boldsymbol{\eta}\boldsymbol{\eta}^*, \mathrm{D}\boldsymbol{\eta}$ и т. д.),
и поэтому инвариантна относительно любих поворотов в базиспой плоскости. Члены, соответствуошие специфической гексагональной анизсгропии, появдяются только в болсе высоких порядках разложения по градиентам. Полная симметрия свободной энергии по отношению к врашениям на произвольный угол в базисной плоскости привопит к изотропии верхнего критического поля. В эгом можно убедиться нспосредственно, решая два уравнения. получающиеся варьированием (12.15) по η_j^*:

$$K_1 D_i^2 \eta_j + K_2 D_j D_i \eta_i + K_3 D_i D_j \eta_j + K_4 D_z^2 \eta_j + a_0 \left(\frac{T - T_c}{\tau_c} \right) \eta_j = 0 \tag{12.17}$$

в поле вида (12.10). Выбирая систему координат таким образом, чтобы ось $\ddot{x}$ была параллельна магнитному полю, из (12.17) полугаем систему двух независимых лифферснциальных уравнений:

$$\begin{cases} \cdots K_4 \frac{d^2 \eta_x}{dz^2} + K_1 \left(\frac{2\pi I l}{\Phi_0} \right)^2 z^2 \eta_x + \alpha_0 \left(\frac{T - T_c}{T_c} \right) \eta_x = 0 \\ -K_4 \frac{d^2 \eta_y}{dz^2} + \left(K_1 + K_2 + K_3 \right) \left(\frac{2\pi H}{\Phi_0} \right)^2 z^2 \eta_y + \alpha_0 \left(\frac{T - T_c}{T_c} \right) \eta_y = 0 \end{cases} \tag{12.18}$$

с собственыыми знаяениями, определяющиими дзс возможныс величины $H_{\text{c2}}(T)$:

$$H_{\text{c2}}^{(1)}(T) = \frac{\Phi_0 \alpha_0}{2\pi \sqrt{K_1 K_4}} \frac{T_{\text{c}} - T}{T_{\text{c}}} \tag{12.19}$$

$$H_{\text{c2}}^{(2)}(T) = \frac{\Phi_0 \alpha_{\text{G}}}{2\pi \sqrt{\left(K_1 + K_2 + K_3 \right) K_4}} \frac{T_{\text{c}} - T}{T_{\text{c}}} \tag{12.20}$$

Большая из них соответствует верхнему критическому полю, при котором происходит фазовый переход в сверхпроводящее состояние. Таким образом, всрхнее критичсское поле оказывастся изотропным в базисной плоскости гексагонального кристалла и в случае двухкомпонснтной свсрхпроводимости. Для состояния, преобразующегося согласпо представлению E_2, доказательство этого факта можно найти в рабоге [38].

Отмстим сще одно важнюе следствие из уравнений (12.18). Мы видим, что в магнитном поле фазовый переход из нормального состояния происходит в одну из двух сверхпроводяших фаз:

$$\boldsymbol{\eta}_x \propto (1, 0) f_0(z) \tag{12.21}$$

или

$$\eta_y \propto (0,1) f_0(z) \tag{12.22}$$

где $f_0(z)$ - фупкция осповіого состояния Ланлау лля заряженной частицы в мапнитіом поле. С друтой стороны, если переход в нулевом магнитном поле ляя векторного представления происходит в комплексную фазу (см. (11.9))

$$\eta \propto (1, \pm i) \tag{12.23}$$

то при уменышении магиитного поля (при $T < T_c$) трансформация состояния с параметром порядка (12.21) в в состояние (12.23) доджна обязательно сопровождаться переходом, связанным с зарождснисм фазы с параметром
порядка (12.22) (см. рис. 11). Аиалогитное явление должно наблюдаться, если в нулсвом полс переход происходит в вещественнуо фазу

$$\eta \propto (\cos \lambda_n, \sin \lambda_n) \tag{12.24}$$

где величины λ_n опрсдсляются кристаллической анизотропиcй (см. 11).

Свойство изотропии $II_{c2}(T)$ в базисной плоскости гексагонального кристалла, разумсстся, утрачивается при введешии л!обого внешпего воздействия, нарушающего гексагональную симметрию. Так например, слабое орторомбитеское возмущснис, характсризуемое вектором M, лежащим в базиспой птоскости, приводит к появлсиино в фупционале ГинзбургаЛандау слагаемого с орторомбитеской симметрией, имеющсго вил

$$\gamma(\mathbf{M}\boldsymbol{\eta})^*(\mathbf{M}\eta) \tag{12.25}$$

Учет такого вклада приводит как к расщептснию температуры псрсхода (компоненты η, параллельная и перпеідикулярная M, будут появляться при разных температурах), так и к заметной анизотропии верхнего критиче-

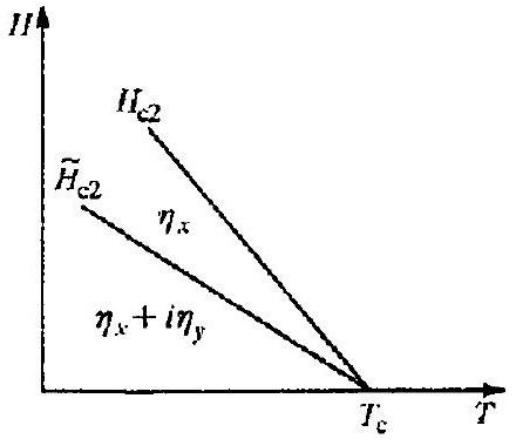


Рис. 11. Фазоsьіе переходы в маагиитгом полс для двухкомпонентіых сверхпроводяших состояин в гексагональном кристалле ского поля [39]. Последное свойство следует из того, что уравнения дпя компонент парамстра порядка перестают быть независимыми (кроме вылелснных направпений H$\|$M и H $\perp$ M).

Рассмотрим теперь кристалл с тетрагональной симметрией. Специфическим для него является дополшительныи млег в грапиенпой энсргии (12.16), обладаюшний симметрией четвсртого порядка относительно поворотов вокруг оси $\hat{z}$. Линеаризованшые уравнения Гинзбурга-Ландау в этом случае нмеюот вип

$$K_1 D_i^2 \eta_j + K_2 D_j D_i \eta_i + K_3 D_i D_j \eta_i + K_4 D_x^2 \eta_j + \\ + K_5 \left(\delta_{xj} D_x^2 \eta_x + \delta_{yj} D_y^2 \eta_y \right) + \alpha_0 \left(\frac{T - T_c}{T_c} \right) \eta_j = 0 \tag{12.26}$$

Положим для простоты $K_2 = K_3 = 0$, тогда уравнения для компонеіт парамета порядка расцспчяются, и, в случае поля вила (12.10), лсжащсго в базиспой плоскости, получаем следупощие значсния $H_{\text{с:2 для компонепт}}$ η_x и η_y, соответственно:

$$I_{c2}^{(1)}(T') = \frac{\Phi_0 \alpha_0}{2\pi \sqrt{K_4 \left(K_1 + K_s \sin^2 \rho \right)}} \frac{T_c - T}{T_c} \tag{12.27}$$

$$H_{c2}^{(2)}(T) = \frac{\Phi_0 \alpha_0}{2\pi \sqrt{K_1 \left(K_1 + K_5 \cos^2 \varphi \right)}} \frac{T_c - T}{T_c} \tag{12.28}$$

При каждом тгаправлении поля $H(\varphi)$ нужно выбрать из этих двух пачений больиес. Таким образом, в тетрагональном кристалле возникает анизотропия верхего критического поля, спешифическая для пвухкомпонснтной сверхпроводимости {40! (рис. 12).

Анизотропия верхнего критического поля той жс природы имеет место в кубитеских кристаллах в случае двух- или трехкомпонентных свсрхпроводя-

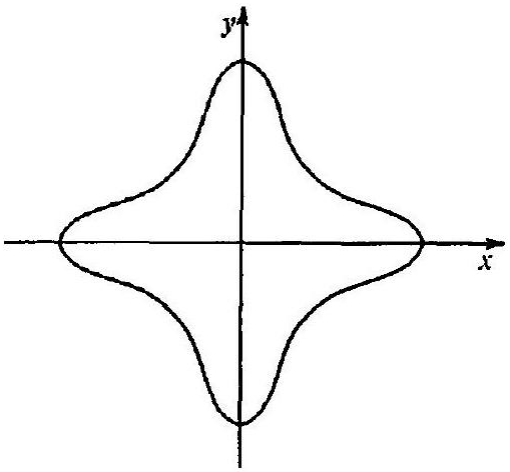


Рис. 12. Анизотрония верхігего критического поля в базисной плоскостн тетрагонального кристалла для двухкомпонентного сверхпроводяицего состояния щих состояний [38].

В общем случае, то есть при произволыной ориентацши внсшнего поля относительно осей кристаллической решетки, верхнее критическое поле для многокомпонентного параметра порядка в области применимости тсории Гицзбурга-Ландау может быпь найдено лишь путем численного апализа. Искточение составляет задача о вычислении $H_{c2}(T)$ для дзухкомпонентного параметра порядка в гексагональном (или тетрагональном) кристалле при $\mathbf{H}$, направленном вдоль оси шестого (или четвертого) порядка, допускающая аналитическое решение [41].

В этом случае постедний член в (12.16) не приводит к качественным отличиям, и мы будем решахь задачу при $K_5 = 0$. Поскольку магнитное поле направлено вдоль оси шестого порядка $\hat{z}$ (калибровка $\mathbf{A} = (0, Hx, 0)$), то можно считать, что параметр порядка от z нс зависит, и из (12.17) мы имеем следутощис уравнения:

$$\begin{cases} \left(K_{123}D_x^2 + K_1 D_y^2\right)\eta_x + \left(K_2 D_x D_y + K_3 D_y D_x\right)\eta_y + \alpha_0\left(\frac{T-T_c}{T_c}\right)\eta_x = 0 \\ \left(K_{123}D_y^2 + K_1 D_x^2\right)\eta_y + \left(K_3 D_x D_y + K_2 D_y D_x\right)\eta_x + \alpha_0\left(\frac{T-T_c}{T_c}\right)\eta_y = 0 \end{cases} \tag{12.29}$$

где $K_{123} = K_1 + K_2 + K_3$. Введем теперь новыс функции $\eta_\pm = \eta_x \pm i\eta_y$ и операторы $D_\pm = D_x \pm iD_y$, а также учтем, что $[D_x, D_y] = -2\pi iH/\Phi_0$. Тогда уравнения перписываются в виде

$$\begin{cases} \left(\alpha_0\left(\frac{T-T_c}{T_c}\right) + K_0\left(D_x^2 + D_y^2\right) - K_-\frac{2\pi H}{\Phi_0}\right)\eta_+ + K_+ D_+^2\eta_- = 0 \\ K_+ D_-^2\eta_+ + \left(\alpha_0\left(\frac{T-T_c}{T_c}\right) + K_0\left(D_x^2 + D_y^2\right) + K_-\frac{2\pi I}{\Phi_0}\right)\eta_- = 0 \end{cases} \tag{12.30}$$

где $K_0 = \left(K_{123} + K_1\right)/2, K_\pm = \left(K_2 \pm K_3\right)/2$.

Парамстр порялка ищем в виде

$$\eta_\pm = \exp(-ipy) f_\pm(x) \tag{12.31}$$

Тогда уравнения Гинзбурга-Лапдау имеют решения двух типов:

$$\begin{pmatrix} f_+(x) \\ f_-(x) \end{pmatrix} \sim \begin{pmatrix} F_{0.1}(x) \\ 0 \end{pmatrix}, \tag{12.32}$$

либо

$$\begin{pmatrix} f_+(x) \\ f_-(x) \end{pmatrix} \sim \begin{pmatrix} qF_{n+2}(x) \\ F_n(x) \end{pmatrix}, \tag{12.33}$$

где q - константа, а функция $F_n(x)$ связана с полиномами Эрмита $H_n(x)$ следующим соотношением:

$$F_n(x) = \exp\left[-\frac{\pi H}{\Phi_0}\left(x - p\frac{\Phi_0}{2\pi H}\right)^2\right] H_n\left[\sqrt{\frac{2\pi H}{\Phi_0}}\left(x - p\frac{\Phi_0}{2\pi H}\right)\right] \tag{12.34}$$

В том, что семейство (12.33) в самом деле является решением уравпений (12.30), легко убсдиться, используя тождества [42]:

$$D_-^2 F_n = -4n(n-1)\frac{2\pi H}{\Phi_0}F_{n-2}$$
$$D_+^2 F_n = -\frac{2\pi H}{\Phi_0}F_{n+2}$$
$$\left(D_x^2 + D_y^2\right)F_n = (2n+1)\frac{2\pi H}{\Phi_0}F_n$$

Подставляя (12.34) в (12.31), получаем выраженис для температур перехода, соответствуоших этому семейству решений:

$$\alpha_0\frac{T-T_c}{T_c} = \\ = \left[-(2n+3)K_0 + \sqrt{\left(2K_0 - K_-\right)^2 + 4(n+1)(n+2)K_+^2}\right]\frac{2\pi H}{\Phi_0} \tag{12.35}$$

Максимальная величина верхнего критического поля соответствует либо решению

$$\begin{pmatrix} f_+(x) \\ f_-(x) \end{pmatrix} \propto \begin{pmatrix} F_0(x) \\ 0 \end{pmatrix} \tag{12.36}$$

при котором

$$H_{c2}^{(1)}(T) = \frac{\Phi_0 \alpha_0}{2\pi \left(K_0 - K_-\right)} \frac{T_c - T}{T_c} \tag{12.37}$$

либо решенийо

$$\begin{pmatrix} f_+(x) \\ f_-(x) \end{pmatrix} \propto \begin{pmatrix} qF_2(x) \\ F_0(x) \end{pmatrix} \tag{12.38}$$

которому соответствует

$$H_{c2}^{(2)}\left(T'\right) = \frac{\Phi_0 \alpha_0}{2\pi \left(3K_0 - \sqrt{\left(2K_0 - K_-\right)^2 + 8K_+^2}\right)} \frac{T_c - T}{T_c} \tag{12.39}$$

Вид состояния, в которос происходит фазовый переход в магнитном поле, зависит от соотношения между коэффигиентами K_i. В частности, в теории БКШ $K_1 = K_2 = K_3$ (см. 18), и большее значение верхнего критического поля имеет состояние)12.38).

При уменьшении внешнего поля нихж $H_{c2}(T)$ сверхпроводящие зародышш, отвечающис различным значениям парамстра вырождения p, формируют периодическуо решетку вихрей Абрикосова, вид которой может существенно отличаться от обычной треугольной (подробнее об этом см. [43]).

Нарушение пространствешной четности и геликоидальные фазы. Всс рассмотренные многокомпонснтные сверхпроводящие состояния возникаюот из нормальной фазы, в группе симметрии которой имеется преобразование пространственной итверсии. В противном случае, во-первых, теряет смысл
разделение на четшые и нечетные сверхпроводящие состояния, ввиду возможности их перемешивания (см. 4), и, во-втирых, появтятся визможность постросния инвариантных слагаемвх в свободной эиергии, лигейных по прострацственным градиептам (инварианты Лифшица).

Например, ссли параметр порядка $\eta = (\eta_x, \eta_y)$ соответствует двумерному представтениio E_1 группы D_6, то кроме членов, входящих в разтожение (12.15), имеется итвариант вида

$$\gamma \left(\eta_1^* D_2 \eta_2 + \text{ k.c. }\right) \tag{12.40}$$

Учет подобных чтенов приводит к значительному изменению термодинамических и магнитных свойств системы, в частности, к возможности существования неоднородикх (геликоидалыьх) фаз в нулевом магнитном поле [7].

MC-12.1

Доказать, что функционал Гинзбурга-Ландау для двухкомпонентного параметра порялка, соответствующего представлению E_2 группы)$_6$ (базисныс функции см. в табл. 1,2), также можно записать в виде (12.15).)Указание. Составьте из компонент D и η комбинации, инвариантные относительно операций группы D_{6h} и найдите преобразование $\eta_i \to \chi_i$, такое, что для функиий $\chi_{1,2}$ градиептная энергия может быть приведена к виду (12.15).)

MC-19.2

Найти критическую температуру и состояния, в которые происходит фазовый переход в гсксагоналыном сверхпроводнике без центра инверсии с учетом слагаемого вида (12.40) в свободіо энергин.

19.1.13 13. Boundary Conditions and Surface Superconductivity

Вблизи поверхности заролыип сверхпроводящей фазы в сверхпроводниках второго рола возникают в магнитном поле, превышающем верхнее критическое поле. Дтя нахождешия поверхностного критичсского поля нсобходимо решить линеаризоваіное уравыение Гинзбурга-Ландау с учетом граничных условий для параметра поряпка. В этом параграфе будут получены граничные условия и изутеп вопрос о поверхостной сверхпрозолимости в кристаллах Возможность образования поверхностных зародыпей в необычных сверхпроводниках сущсственио зависит от ориептации поверхіости по опноченііо к кристаллическим осям. Обпаружение такой зависимости может служить способом илентификации сверхпроводяшпх фаз.

Граничные условия. Одиокомпонентная сверхпроводимоств. Уравнения Гинзбурга-Ландау были потучены в предыдущем параграфе из условия равенства нуло вариации свободной энсргии. Оставшаяся поверхностная часть:

$$\delta\mathcal{F}|_{S,\,\mathrm{grad}} = -i \oint dS n_i K_{ij} \left(D_j \eta\right) \delta\eta^m \tag{13.1}$$

где $\mathbf{n}$ - вектор нормали к поверхности, обращается в пуль при условии

$$n_i K_{ij} D_j \eta l_S = 0 \tag{13.2}$$

которое обеспечивает обращение в пуль нормацнои к поверхпости компоненты тока: $\mathbf{nj}|_{\mathrm{S}} = 0$. Полагая, что параметр порядка волизи поверхности в
нулевом магнитном поле может меняться лишіь вдоль направлешия нормали, получаем:

$$(\mathbf{n}\nabla)\eta|_{\mathrm{S}} = 0 \tag{13.3}$$

Отсюда следует, что на поверхности сверхпроводника в опсутствие магнитного поля параметр порядка имест ту же величиу, тто и в обьеме.

Одиако, даже для обьчных сверхпроводиков этот вывод, полученнъій в рамках теории Гинзбурга-Ландау, нуждается в проверке на основе микроскопитеской теории. Дело в том, что теория Гипзбурга-Лапдау применима лив на пространствепных масштабах, превышаюшпх длну когерентиости ξ_0 и поэтому не уитывает изменение условий возникновения сверхпроводимости непосредственно вблизи повсрхности. Микроскопическое рассмотрение (см. ниже 20) гоказывает, что вблизи границы, на расстояниях порядка атомпьх, волновые функции электронов существснно отличатотся от волновых фупкций в объсме. Это, в своюо очередь, приводит х появлению в свободной энсргии сверхпроводника дополнитслыьх слагаемьх, локатизованных на расстояииях порядка ξ_0 от границы. Даиный факт можно учесть феноменолюгичсски, ввопя в рассмотрепие поверхностную энсртко

$$\mathcal{F}_{\mathrm{S}} = \oint dS a(\mathbf{n}) |\eta|^2 \tag{13.4}$$

которая зависит от ориентации поверхности кристалла по отношению $\mathbf{k}$ осям кристалличсской решетки. Здесь $a(\mathbf{n}) \sim N_0 \xi_0 f(\mathbf{n})$, причем $f(\mathbf{n})$ есть безразмерная

скалярпая функция паправлений гормали, инвариантиая олносительно всех преобразований симмстрии точечной групты кристалла.

Граничныс условия для параметра порядка могут быть получены путем варьирования по η^* полной свободной энергии сверхпроводника

$$\mathcal{F} = \mathcal{F}_\mathrm{V} + \mathcal{F}_\mathrm{S} \tag{13.5}$$

состоящей из общчной обемной части (12.2) и поверхностнои эчергии (13.4). Условие исчезновения вариации на поверхности принимает вид

$$in_i K_{ij} D_j \eta|_\mathrm{S} = a(\mathbf{n})\eta\|_S \tag{13.6}$$

Таким образом, в залаче поямляется новый характерный масштаб - интерполяционная длина, которая зависит от направления нормат:

$$b_i(\mathbf{n}) \sim \frac{K_n}{u(\mathbf{n})} \tag{13.7}$$

Эффективное граничное условие дия параметра порядка вбтизи критической температуры может быть получено путем сравнения $b(\mathbf{n})$ с коррсляционной длиной $\xi(\mathbf{n})$(12.8).

Пусть направление нормали таково, что поверхностный инвариант $f(\mathrm{n})$ и, следовательыно, функция $a(\mathbf{n})$ равны нуло. Тогда из (13.6) мы получаем граничное условие (13.3). Итерполяционная дхина в этом случае обрацается в бесконечность.

Если же лля данного направлсния нормали $f(\mathbf{n}) \neq 0$, то интерполяиионная дпина $b(\mathbf{n})$ конегна и нс зависит от температуры. Следовательно, при $T \to T_c$ выполняется неравснство $b(\mathbf{n}) \ll \xi(\mathbf{n})$, которое, в свого очереш, означает,
что эффективное граничное условие для параметра порядка имеет следуюшбдй вид:

$$\eta l_\mathrm{s} = 0 \tag{13.8}$$

Вывод о том, что при $f(\mathbf{n}) \neq 0$ граничное условие (13.3) должно быть заменено на (13.8), может быть получен также с помошъю простых энергетических соображений. Проигрыш в энергии сверхпроводника вблизи поверхности определяется суммой градиентного (13.1) и поверхіостного (13.4) вкладов. Относителыіый величину этих слагаемых при $T \to T_c$ можно оценить, учитывая, что харахтериьм масшттабом простраплственного изменения параметра порядка является корреляционная длина $\xi(T) \sim \xi_0 (1 - T/T_c)^{-1/2}$, а его значение в объеме кристалла есть $|\eta_0| \propto (1 - T/T_\mathrm{c})^{1/2}$. Тогда из (13.1) имеем

$$\mathcal{F}_\mathrm{S,grad} \propto \left(1 - \frac{T}{T_\mathrm{c}}\right)^{3/2} \tag{13.9}$$

Если $f(\mathbf{n}) \neq 0$, и параметр порядка на позсрхности отличен от нуля, то из (13.4) иммеем

$$\mathcal{F}_\mathrm{S} \propto \left(1 - \frac{T}{T_\mathrm{c}}\right) \tag{13.10}$$

Сравнивая (13.9) и (13.10), мы видим, что вблизи критической температуры $\mathcal{F}_\mathrm{S}$ превосхолит $\mathcal{F}_\mathrm{S,grad}$. Этот существенный проигрыш в поверхностной энергии исчезает лишь при полном подавлении сверхпроводимости на поверхиости, тто приводит к граничному условию (13.8). Если $f(\mathbf{n}) = 0$, то проигрыпа в энергии (13.4) нет, и имеет место граничное условие (13.3).

Очевидно, что на границе сверхпроводника с нормальным металлом условия отражения и прохождения квазичастиц изменяют их волновые функции в поверхностном

слое, то есть $f(\mathbf{n}) \neq 0$ при любом направлении $\mathbf{n}$. Следовательно, в этом случае при $T \to T_c$ всегда имеют место граничныс условия (13.6). Для границы сверхпроводника с диэлектриком или вакуумом следует различать случаи зеркальiого и диффузного отражения квазичастиц от границы. Рассмотрим сначала зеркальное отражение.

В этом случае также $\int(\mathrm{n}) \neq 0$ пля всех ориентаций нормали по отношению к кристашографическим осям, кроме тех, для которых электронный спектр $\varepsilon(\mathbf{k})$ и функции $g(\mathbf{k})$ (или $\mathbf{d}(\mathbf{k})$), описывающие сверхпроводящие состояния и прсобразующиеся согласпо одному из одiомерных неприводимых представлегий группы симметрии кристалла, не меняготся при отражении в плоскости границы:

$$\varepsilon(\mathbf{k} - 2\mathbf{n}(\mathbf{kn})) = \varepsilon(\mathbf{k})$$
$$g(\mathbf{k} - 2\mathbf{n}(\mathbf{kn})) = g(\mathbf{k}), \quad \mathbf{d}(\mathbf{k} - 2\mathbf{n}(\mathbf{kn})) = \mathrm{d}(\mathbf{k}) \tag{13.11}$$

В самом деле, при выпоолнении этих условий траектории квазичастиш, отраженных от границы, представляюот собои зеркальное отражение в плоскости границы траекторий падаюощих на нее частиц, продолхенных в полупространство, занятое диэлектриком (подробнее об этом см. ниже 20). Поэтому задача становится эквиватентшой задаче о нахождснии параметра порядка в сверхпроводнике, заполняющем все пространство, и подавления сверхпроводимости на границе не происходит, то есть имеют место граничные условия (13.3).

Та 6 лица 7. Угловые зависимости парамстра порядка и поверхностной энергии для однокомпоненттых параметров порддка в тетрагональном кристаллс ($S = 0, G = D_{4h}$)

Γ	$g(\mathrm{k})$	$f(\mathrm{n})$
A_{1g}	$\left(k_x^4 + k_y^4\right)$	$an_x^2\left(n_x^2 + n_y^2\right) + bn_x^2 n_y^2\left(n_x^2 - n_y^2\right)^2$
A_{2g}	$k_x k_y\left(k_x^2 - k_y^2\right)$	$\left(n_x^2 + n_y^2\right)$
B_{1g}	$k_x^2 - k_y^2$	$an_z^2\left(n_x^2 + n_y^2\right) + bn_x^2 n_y^2$
B_{2g}	$k_x k_y$	$an_x^2\left(n_x^2 + n_y^2\right) + b\left(n_x^2 - n_y^2\right)^2$

Итак, нуля функции $f(\mathbf{n})$ для данного сверхпроводящего состояния должны соответствовать оринстациям плоскости границы, совпадающим с общими плоскостями симметрии ферми-поверхности и параметра порядка сверхпроводника. Для сферической ферми-поверхности и полностью изотропного сверхпроводяшего состояния (s-спаривание) $f(\mathbf{n})$ тождественно обрашается в нуль для всех ориентаций n. Поэтому общепринято, что в этом случае на транице сверхпроводник-диэлектрик выполнены грагничне условия (13.3).

Для обычной сверхпроводимости, соответствующей единичному представленик $A_{1\ \mathrm{g}}$ в анизотропном кристалле, симметрия параметра порядка совпадает с симметрией ферми-поверхности и включает в себя все преобразования точечной группы кристалла. Функции $f(\mathbf{n})$, обращающиеся в нуль для всех зеркально-симметричных направлений, в кристаллах с кубической, тетрагональнои и гексагональнод симметрией, соответственно, имеют вид

$$f_{A_{1\mathrm{g}}}^{\mathrm{cub}}(\mathbf{n}) = a\left[n_x^2 n_y^2\left(n_x^2 - n_y^2\right)^2 + n_x^2 n_z^2\left(n_x^2 - n_z^2\right)^2 + n_y^2 n_z^2\left(n_y^2 - n_z^2\right)^2\right] \tag{13.12}$$

$$f_{A_{1\mathrm{g}}}^{\mathrm{terr}}(\mathbf{n}) = an_z^2\left(n_x^2 + n_y^2\right)^2 + bn_x^2 n_y^2\left(n_x^2 - n_y^2\right)^2 \tag{13.13}$$

$$f_{A_{1\mathrm{g}}}^{\mathrm{hex}}(\mathbf{n}) = an_z^2\left(n_x^2 + n_y^2\right) + b\left(n_x^3 - 3n_x n_y^2\right)^2\left(n_y^3 - 3n_y n_x^2\right)^2 \tag{13.14}$$

Здесь a и b - числа, определяiошие меру анизотропити, то есть отличие формы ферми-поверхности и щели в спектре от сфсрической или цилиндрической.

Граничныс условия (13.3) имект место в узкой области направлений нормали с шириной $\sim \sqrt{\xi_0/\xi(T)}$[1], для которьх функции $f(\mathrm{n})$ обрашаются в нуль. Для всех остальных ориентаций поверхности сверхпроводникдиэлектрик граиичные условия имеют вид (13.6).

Если мы имеем дело с необычным сверхпроводяшим состоянием, параметр порядка которого преобразуется согласно неединичному представлению, то число ориентаций поверхности, для которых выполняется условие $f(\mathbf{n}) = 0$, может только уменьшиться по сравнению с обычным сверхпроводящим состоянием. В табл. 7 приведены соответствующие функции для однохомпонентных сверхпроводящих состояний с синглетным спариванием в тетрагоналыном кристалле, популярных в настоящее время в связи с исследованиями высокотемпературной сверхпроводимости.

Мы видим, что лля представления $A_{1\ \mathrm{g}}$ поверхностная энергия обрашаехся в нуль для восьми направлений $\mathbf{n}$ в базисной плоскости, а также при $\mathbf{n}\|\hat{z}$. Для представлеиий $B_{1\ \mathrm{g}}$ и $B_{2\ \mathrm{g}}$ из этих нулеи остается лишш по четыре нуля в Базисной плоскости и олин нуль при $\mathbf{n}\|\hat{z}$. Вертикальные плоскости зеркальной симметрии лтя представлений $A_{1\ \mathrm{g}}$ (ферми-поверхность) и $A_{2\ \mathrm{g}}$ (сверхпроводящее состоянис) не совпадаюот, поэтому если параметр порядка прсобразуется согласно $A_{2\ \mathrm{g}}$, то у функции $f_{A_{2g}}(\mathbf{n})$ остается лишь один нуль при $\mathbf{n}\|\hat{z}$, то есть вдоль направления, перпендикулярного обшей горизоптальной плоскости симметрии функцший $\varepsilon(\mathbf{k})$ и $g_{A_{28}}(\mathbf{k})$.

Для пространствешн-нечетных однокомпонентных сверхпроводяших состояний в тетрагональном кристалле ($S = 1$, сильное спин-орбитапьное взаимодействие, см. табл. 3) нет симметрииных причин, по которым функция $f(\mathbf{n})$ должа обратиться в нуль, и поэтому поверхностная энергия прсдставяят собой произвольную комбинацию всех скалярныхх инвариантов тетрагональной группы.

Мы не будем здесь находить функции $f(\mathbf{n})$ для нетривиальных сверхпроводящих состояний в гексагочапных и кубитеских кристаллах, предоставив это читателю (см. упражнение в конце параграфа).

Поверхностная сверхпроводимость. Найденные выие граничные условия (13.3) и (13.6) для параметра порядка позволяют вычислить критическое поле поверхностной сверхпроводимости в области применимости теории Гинзбурга-Ландау.

Рассмотрим тетрагональный сверхпроводних, занимающий полупространство $x > 0$ так, что тетрагональная ось лежит в плоскости границы, а нормашь к границе расположена в базисной плоскости кристалла. Выберем направление магнитного поля вдоль тетрагональной оси:

$$\mathbf{H} = H(0, 0, 1)$$
$$\mathbf{A} = (0, Hx, 0)$$

Подставляя в уравнение Гинзбурга-Ландау (12.9) параметр порядка в виде $\eta(x, y) = f(x)\exp(-ipy)$, получаем:

$$-K_1\frac{d^2f}{dx^2} + K_1\left(\frac{2\pi H}{\Phi_0}\right)^2\left(x - p\frac{\Phi_0}{2\pi H}\right)^2 f + \alpha_0\left(\frac{T - T_\mathrm{c}}{T_\mathrm{c}}\right)f = 0 \qquad (13.15)$$

Решение этого уравнения и величина поверхiостного критического поля определяются граничными условиями.

Для тех ориентаций поверхности, дтя которьх выпольется условие (13.8), ro ecTb

$$\eta(x = 0) = 0$$

[1] Эта оценка получается путем сравнеиня поверхностной градиегтьой энергии (13.1) и поверхностной экергии (13.4) вблизи наиравления, для которого $f(n)$ обраигается в нуль.

сверхпроводящий зародыш образуется вдати от поверхности ($p\xi(T) \gg 1$). Соответствующее решение уравнения (13.15) имеет вид

$$f(x) \propto \exp\left[-\frac{\pi H}{\Phi_0}\left(x - p\frac{\Phi_0}{2\pi H}\right)^2\right]$$

а поле, в котором зарождается сверхпроводящее состояние, совпадает с объемным верхним критичсским полем:

$$H_{c3}(T) = H_{c2}(T) = \frac{\Phi_0\alpha_0}{2\pi K_1}\frac{T_c - T}{T_c} \tag{13.17}$$

Если же поверхность ориентирована так, что выполняется граничное условие (13.3), то есть

$$\left.\frac{\partial\eta}{\partial x}\right|_{x=0} = 0 \tag{13.18}$$

то уравнение (13.15) имеет решение, локализованное вБлизи гранишы:

$$f(x) \propto F_\nu(x) \tag{13.19}$$

$$F_\nu(x) = \exp\left[-\frac{\pi H}{\Phi_0}\left(x - p\frac{\Phi_0}{2\pi H}\right)^2\right] H_\nu\left[\sqrt{\frac{2\pi H}{\Phi_0}}\left(x - p\frac{\Phi_0}{2\pi H}\right)\right]$$

где $H_\nu(x)$ - функция Эрмита (функция параболического цитиндра) с индексom

$$\nu(\lambda) = -\frac{1}{2} + \frac{\lambda}{2} \tag{13.20}$$

Здесь введена безразмерная величина

$$\lambda = \frac{\Phi_0\alpha_0}{2\pi K_1 H}\frac{T_c - T}{T_c}$$

Подстановка (13.19) в граничное условие (13.18) приводит к трансцендентному уравнениio

$$2\nu H_{\nu-1}(-r) = -rH_\nu(-r) \tag{13.21}$$

где

$$r = p\sqrt{\frac{\Phi_0}{2\pi H}}$$

которое позволяет найти зависимость $\lambda(r)$. При этом магнитно поле, в котором зарождается свсрхпроводящая фаза вблизи поверхности образца, соответствует минимальному значению функции $\lambda(r)$. Численнос решение уравнения (13.21) дает [78]: $\lambda_{\min} = 0,59, r = 0,77$, следовательоо,

$$H_{c3}(T) \approx 1,69H_{c2}(T) \tag{13.22}$$

Для обычного свсрхпровопящего состолния (прсдставленис $A_{1\ g}$) граничное условие (13.18) реатизуется, строго говоря, дхя поверхностей с ориентациями нормати $n = (\cos(\pi k/4), \sin(\pi k/4), 0)$, где $k = 0, 1, \ldots, 7$, или $\mathbf{n} = (0, 0, 1)$. Для поверхностей, нормапь к которым откгоняется от указанных значений на утлы, превышаащие

отношение $\sqrt{\xi_0/\xi(T)}$, граничиое условие (13.18) заменяется на условис (13.16), и поверхностной сверхпроводимости не возникает.

На практике анизотропия обычного сверхпроводящего состояния не очеиь выражена. Дело в том, что как рассеяние на примссях, так и усредняющее деистие диффузиого рассеяния на поверхиости, не подавляя сверхпроводимости, привопят к уменьшению функции $f_{A_{18}}(\mathbf{n})$, поэтому поверхностная сверхпроводимость наблюдается для произволыой ориеитации поверхности.

Не так обстоит дело для свсрхпроводяших состояний, преобразующихся согласно неединичным представлениям. Например, в тетрагоналышхх кристаллах для состояния, соотве тствугощего представлению B_{1g}, которос реализуется, по-видимому, в высокотемпературных свсрхпроводниках, поверхноствая сверхпроводимость в стучас зеркатьно отражающей позерхности имеет
место для следующих ориентаций нормали:

$$\mathbf{n} = \left(\cos\frac{\pi k}{2}, \sin\frac{\pi k}{2}, 0\right), \quad k = 0, 1, 2, 3$$

$$\mathbf{n} = (0, 0, 1)$$

Если поверхность отклоняется от указанных направлений на утлы, превышающие $\sqrt{\xi_0/\xi(T)}$, поверхностной сверхпроводимости нст. В отличие от состояния $A_{1\,\mathrm{g}}$, учет диффузности рассеяния на границе ие восстанавливает поверхностную сверхпроводимость для произвощной ориентации поверхности, а, напротив, вызывает усреднение параметра порядка по направлениям импульса и тем самым подавляет поверхностную сверхпроводимость.

Окончательный вывод таков: опсутствие поверхностной сверхпроводимости на диффузно-отражающих поверхостях может служить характерньм признаком необычных сверхпроводящих состоянии. По наличию же поверхностной сверхпроводимости лишв в узких угловьх окрестностях выделенных направлений $\mathbf{n}$ можно установить симметрию сверхпроводящего состояния.

Граничные условия для многокомлонентных параметров порядка. В этом случае выражение для поверхностной энергии находится точно так же, как это дедалось для получения градиентной энсргии в 12. Например, для сверхпроводящего состояния, преобразующегося согласно двумерному представлению E в тетрагональном кристалле, необходимо составить все возможные квадратичные по компонентам параметра порядка (η_x, η_y) и вектора нормали $\mathbf{n}$, комбинации, инвариантные относителыо всех преобразований группы симметрии нормального состояния $U(1) \times R \times D_{4h}$:

$$\mathcal{F}_{\mathrm{S}} = \oint dS \left[a_1(\mathbf{n})\boldsymbol{\eta}\boldsymbol{\eta}^* + a_2(\mathbf{n})|\eta_x n_x + \eta_y n_y|^2 + \right.$$
$$\left. + a_3(\mathbf{n})\left(|\eta_x n_x|^2 + |\eta_y n_y|^2\right)\right] \qquad (13.23)$$

Здесь $a_i(\mathbf{n}) \sim N_0\xi_0 f_i(\mathbf{n})$ $(i = 1, 2, 3)$ - функции, инвариатные относитежно всех преобразований из D_{4h}. За исключением ориегтаций границы, задаваемых кристаллографическими направлениями, обе компонснты параметра порядка, преобразующщеся как $(k_z k_x, k_z k_y)$, пе обладают определенной четностью при отражении в плоскости гранишы (ср. с (13.11)). Отсюда, так же, как и в однокомпонентном случас, следует обращенис в нуль обеих компонент параметра порядка па поверхности и отсутствие поверхностной сверхпроводимости. Ориентации границы, совпадающие с кристаллографическими направлениями, требуот специального исследования. Мы проделаем его для более простого объекта - двухкомпонентного сверхпровопящего состояния в

гексагональном кристалле, где выражение для поверхностной энергии имеет

вид (13.23) без последнего слагаемого, отсутствие которого означает инвариантность по отношениіо к вращениям на произвольный утол вокруг оси шестого порядка.

Поверхностное критическое поле для векторного лараметра порядка в гексагональном кристалле. Аналогично верхнсму критическому полю в объеме, поверхностное критическое поле для многокомпонентной сверхпроводимости может быть вычислено аналитически лиш в искпючительных случаях. В частности, это можно сделатъ для парамстра порядка, соответствующего
представлению E_1 в гексагональном кристалле, если поле иагравлено вдоль оси шестого порядка, а нормаь лежит в Базисной плоскости [44].

Поверхиостная энергия обладает симметрией шестого порядка относительно вращений вокрут гексагонашной оси. Поэтому, при совпадегии ориентации нормали к поверхности с одним из кристаллографических направлений, можно выбрать систему координат так, чтобы ьь $\dot{x}$ совпала с направлением нормали. Тогда перекрестные члены вида $\eta_1^*\eta_2$ исчезают, и поверхностная энергия принимает вид

$$\mathcal{F}_S = \oint dS \left(b_1 \left|\eta_1\right|^2 + b_2 \left|\eta_2\right|^2 \right) \tag{13.24}$$

Поскольку пара (η_1, η_2) преобразуется как $(k_z k_x, k_z k_y)$, то при отражении в плоскости yz компонснта η_1 меняет, а компонента η_2 сохраняет знак. Поэтому на зеркапно-отражающей границе векторный параметра порядка должен удовлетворять граничным условиям:

$$\eta_1\big|_{x=0} = 0, \quad \left.\frac{\partial \eta_2}{\partial x}\right|_{x=0} = 0 \tag{13.25}$$

Для вычисления поверхіостного критического поля сверхпроводника, заниматощего полупространство $x > 0$, в случае поля, направленного вдоль оси шестого порядка, необходимо решить уравнения Гинзбурга-Ландау (12.30)

$$\begin{cases} \left(\alpha_0 \left(\frac{T-T_c}{T_c}\right) + K_0 \left(D_x^2 + D_y^2\right) - K_- \frac{2\pi H}{\Phi_0}\right) \eta_+ + K_+ D_+^2 \eta_- = 0 \\ K_+ D_-^2 \eta_+ + \left(\alpha_0 \left(\frac{T-T_c}{T_c}\right) + K_0 \left(D_x^2 + D_y^2\right) + K_- \frac{2\pi H}{\Phi_0}\right) \eta_- = 0 \end{cases} \tag{13.26}$$

дополненние граничными условиями (13.25).

При нахождении верхнего критического поля в бесконечном объеме необходимо было наложить на параметр порядка условис убывания при $x \to -\infty$, вследствие чсго решение уравнений выражалось через полиномы Эрмита. Теперь же, при рассмотрении поверхностной задачи, мы не фиксируем поведение решения на $-\infty$ и, соответственно, отказьваемся от требования неотрицательности и целочисленности индекса полиномов Эрмита, которые, таким образом, становятся функциями Эрмита $H_\nu(x)$.

Итак, ищем решение уравнений (13.26) в виде

$$\begin{pmatrix} f_+(x) \\ f_-(x) \end{pmatrix} \sim \begin{pmatrix} qF_{\nu+2}(x) \\ F_\nu(x) \end{pmatrix}$$

где $F_\nu(x)$ даются формулой (13.19), а индекс ν должен удовлетворять уравнению

$$\alpha_0 \frac{T - T_c}{T_\mathrm{c}} = \left(-(2\nu+3)K_0 + + \sqrt{\left(2K_0 - K_-\right)^2 + 4(\nu+1)(\nu+2)K_+^2} \right) \frac{2\pi H}{\Phi_0} \tag{13.27}$$

При этом параметр q равен

$$q(\nu) = \frac{-(2K_0 - K_-) + \sqrt{(2K_0 - K_-)^2 + 4(\nu+1)(\nu+2)K_+^2}}{4(\nu+1)(\nu+2)K_+}$$

В отличие от однокомпонеитного случая (см. (13.20)), выражение (13.27) нс позволяет однозначно найти ν как функцию безразмерного параметра

$$\lambda = \frac{\Phi_0 \alpha_0}{2\pi/K_1 H} \frac{T_c - T}{T_c}$$

Будучи квадратпым по ν, это уравнение при заданном λ может иметь два корня:

$$\nu_{1,2}(\lambda) = -\frac{3}{2} + \frac{\lambda K_0 K_1 \pm \sqrt{D}}{2\left(K_0^2 - K_+^2\right)} \tag{13.28}$$

где

$$D = 4K_0^4 + K_+^4 - 5K_0^2 K_+^2 - K_-\left(K_0^2 - K_+^2\right)(4K_0 - K_-) + \lambda^2 K_+^2 K_1^2$$

Соответствующие значения $q_{1,2}$ есть

$$q_{1,2}(\lambda) = \frac{K + \left(K_0^2 - K_+^2\right)}{(2K_0 - K_-)\left(K_0^2 - K_+^2\right) + \lambda K_1 K_+^2 \pm \sqrt{D} K_0} \tag{13.29}$$

Ниже мы будем считать, что дискриминант положителен, а $\nu_{1,2}$ и $q_{1,2}$ вещественны [2].

Собственное значение уравнений (13.26) оказывается двукратно вырожденным, поэтому их общее решение записывается в виде

$$\begin{pmatrix} f_+(x) \\ f_-(x) \end{pmatrix} \propto \begin{pmatrix} q_1 F_{\nu_1+2}(x) \\ F_{\nu_1}(x) \end{pmatrix} + s \begin{pmatrix} q_2 F_{\nu_2+2}(x) \\ F_{\nu_2}(x) \end{pmatrix} \tag{13.30}$$

где s - свободный парамстр, который без потсри общности мы выбираем всщественным. Подстановка в граничные условия (13.25) даст нам систему двух трансцендситиьх уравнений для определения $\lambda(r, s)$ (ср. с (13.21)). Исклгочая из них s, получаем одшо уравнение на $\lambda(r)$:

$$\frac{A_1(\lambda, r)}{B_1(\lambda, r)} = \frac{A_2(\lambda, r)}{B_2(\lambda, r)} \tag{13.31}$$

где

$$\begin{gathered} A_i(\lambda, r) = rH_{\nu_1}(-r) + 2\nu_i H_{\nu_1 - 1}(-r) - \\ -rq_i H_{\nu_1+2}(-r) - 2q_i\left(\nu_i + 2\right) H_{\nu_1+1}(-r) \\ B_i(\lambda.r) = H_{\nu_1}(-r) + q_i H_{\nu_1+2}(-r) \end{gathered}$$

Здесь $\nu_{1,2}$ и $q_{1,2}$ являтотся функциями λ (см. (13.28) и (13.29)). Минимизация решения по r в принципе решает поставленную задату, то сеть позволяет найти температурную зависимость критического поля поверхностной сверхпроводимости $H_{c3}(T)$.

Важным свойством (13.31) является то, что это уравиение не содержит явно зависимости от H, и, следовательно, зависимость $H_{\text{сз}}(T)$, отвечающая $\lambda_{\min}$ - минимапьному по r решению - линейна, однако аналитически найти коэффициент не представляется возможным. Численный расчет для $K_1 = K_2 = K_3$ дает следующий результат: $\lambda_{\min} \approx 0,89, r \approx 0,55$, то есть

[12] Отказ от этого требовалия не вносит никаких принциниальных затрупнений, поскольку функции Эрмита попускают аитлитическос продолжение иа комплекстые значения инлскса. Заметим, что ссли $K_1 = K_2 = K_3$ (теория стабой связи, см. ннже 18), то $D > 0$.

$$H_{c3}(T) \approx 1,24 I_{c2}(T) \tag{13.32}$$

Здесь для всрхнего критичсского поля в объеме использовано выражение (12.39).

Отметим, что в предположении цилиндрической симметрии фермиповерхности поверхностнос критичсское поле одинаково для любых ориенташий поверхности, паралтелыных гексагональной оси. Полученный результат справедлив и для сверхпроводящих фаз с p-спариванием. В обшем случас, так же, как и для однокомпонентных сверхпроволящих состояний, поверхностная сверхпроводимость исчезает при отклонении пормали к поверхiости от кристаллографических направлений на весьма малые углы.

Упражнеиие. Персчислить поверхностныс инварианты $f(\mathbf{n})$ дя всех однокомпонентных сверхпроводящих состояний в гсксагональном и кубическом кристаллах.

19.1.14 14. Meissner and Mixed States in Unconventional Superconductors

Большая часть анизотропных сверхпроводников (высокотемпературные и органические сверхпроводники, сверхпроводящие соединения с тяжелыми фермионами) относится к ярко выраженным сверхпроводникам второго рода. Электродинамика таких сверхпроводников является лондоновской, то есть между плотностью тока и вектор-потенциалом имеется локальная связь во всем температурном интсрвалс вглоть до $T = 0$. В настоящем параграфе мы изучим ряд свойств необычных сверхпроводников, которые можно рассмотреть в рамках лондоновской элсктродинамики. Помимо обычных проявлений анизотропии здесь, как и в термодинамикс, имеются спешифические эффекты, связанные с наличием гулей в спектре элемегтарных возбужденик.

Эффект Мейсснера. Сравнсние уравиения

$$\frac{\delta \mathcal{G}}{\delta \mathbf{A}} = 0$$

(см. 12) с уравнением Максвелла

$$\mathrm{rot}\, B = \frac{4\pi j}{c} \tag{14.1}$$

позволяет найти выражение для плотности тока j. Так, для однокомпонситного сверхпроводящего состояния, гдс плотносгь свободной энергии имеет вид (12.2), плотность тока опрелелястся выражением

$$j_i = -2e\mathrm{Re}_{\,ij} \left[\eta^* \left(D_j \eta\right) + \eta \left(D_j \eta\right)^*\right] \tag{14.2}$$

Для двухкомпонентного сверхпроводящего состояния в гексагонашном кристалле (представление E_1) из (12.15) имесм:

$$j_i = -\frac{2e}{\hbar} \left\{ K_1 \eta_j^* D_i \eta_j + K_2 \eta_i^* D_j \eta_j + K_3 \eta_j^* D_j \eta_i + \text{ к.с. } \right\}, \quad i = x, y \tag{14.3}$$

$$j_z = -\frac{2e}{h} K_4 \left(\eta_i^* D_z \eta_i + \text{ к.с. } \right) \tag{14.4}$$

Подставляя в (14.2) параметр порядка $\eta(\mathbf{r}) = |\eta(\mathbf{r})| e^{i\varphi(\mathbf{r})} = \Delta(\mathbf{r}) e^{i\varphi(\mathbf{r})}$, получаем:

$$j_i = -e n_{ij}^{\mathbf{s}} w_j \tag{14.5}$$

где введены скорость конденсата купсровских пар (сверхгекучая скорость):

$$\mathbf{w} = \frac{\hbar}{2m}\left(\nabla\varphi + \frac{2e}{\hbar c}\mathbf{A}\right) \tag{14.6}$$

)m - масса электрона), и тензор плотности сверхпроводящих электронов (сверхтекучей плотности):

$$n_{ij}^{\mathrm{s}} = \frac{8m}{\hbar^2}\Delta^2 K_{ij} \tag{14.7}$$

Для двухкомпонентной сверхпроводимости с «вещественным» параметром порядка вида (11.7):

$$\boldsymbol{\eta} \sim (\cos\lambda_n, \sin\lambda_n)\, e^{i\varphi(r)}$$

характеризуемым общей фазой φ обеих компонент, плотность тока также можно записать в виде (14.5), причем тензор сверхтекучей плотности n_{ij}^{s} здесь выражастся через коэффиииенты K_1, K_2, K_3, K_4. В магнитных сверхпроводниках с комплексным параметром порядка (11.9) ситуация несколько сложнее, и мы рассмотрим ее в следующем параграфе.

Итак, в немагнитных сверхпроводниках с произвольным числом компонент параметра порядка связь тока с градиентом фазы и вектор-потенциалом в слабых полях имеет вид (14.5). Следует также подчеркнуть, что в немагнитных сверхпроводниках второго рода линейная связь (14.5) имеет место при любьхх температурах. Температурная зависимость тензора $n_{ij}^s(T)$ будет найдена ниже.

Плотность тока, также, как и плотность свободной энергии, инвариантна относителыо калибровочных преобразований:

$$\begin{aligned} \mathbf{A} &\to \mathbf{A} + \boldsymbol{\nabla}\chi \\ \varphi &\to \varphi - \frac{2e}{hc}\chi \end{aligned} \tag{14.8}$$

что позволяет записать (14.5) в виде

$$j_i = -\frac{e^2}{mc} n_{ij}^{\mathrm{s}} A_j \tag{14.9}$$

После подстановки (14.9) в (14.1) получаем уравнение для вектора B (уравнение Лондонов):

$$\frac{mc^2}{4\pi e^2}\,\mathrm{rot}\left((\leftrightarrow^s)^{-1}\,\mathrm{rot}\,\mathrm{B}\right) + \mathrm{B} = 0 \tag{14.10}$$

Для любьх сверхпроводяших состояний в одноосиLx кристаллах (гексагональном и тетрагональном), а также в случае многокомпонентных сверхпроводящих состояний в кубических кристаллах, тензор n_{ij}^{s} имеет одноосую анизотропию и его можно записать в виде

$$n_{ij}^s = n_0\delta_{ij} + n'\nu_i\nu_j \tag{14.11}$$

где ν - ось анизотропии. Подставляя (14.11) в уравиение (14.10), получаем:

$$\delta_0^2[\mathrm{rot}\,\mathrm{rot}\,\mathbf{B} + \lambda\,\mathrm{rot}(\nu(\nu\,\mathrm{rot}\,\mathbf{B}))] + \mathbf{B} = 0 \tag{14.12}$$

гДе

$$\delta_0 = \left(\frac{mc^2}{4\pi n_0 e^2} \right)^{1/2} \tag{14.13}$$

а $\lambda = -n'/(n_0 + n')$.

Пусть ось анизотропии $\nu = \hat{z}$ и внешшее поле $\mathbf{H} = (0, H_y, H_z)$ лежат в плоскости поверхности сверхпроводника, занимаюощего полупространство $x > 0$. Легко убедиться, что решение уравнения (14.12) имеет вид

$$B_y = H_y \exp\left(-\frac{x}{\delta_0 \sqrt{1+\lambda}} \right) \tag{14.14}$$

$$B_z = H_z \exp\left(-\frac{x}{\delta_0} \right) \tag{14.15}$$

то есть магнитнос поле затухает вглубь образца (эффект Мейсснера), при этом поворачиваясь, вследствие анизотропии, вокруг направления $\hat{x}$ [45]. Глубша проникновения поля $\delta(T)$, различная вдоль разнцх направлений, называется лондоновской глубиной проникновения и определяется тензором плотности сверхпроводящих элекгронов $n^{\mathrm{s}}_{ij}(T)$. Ее типичные значения при $T = 0$ порядка $10^{-5} - 10^{-6}$ cm.

Плотность сверхпроводдших электронов. Температурную зависимость тензора n^{s}_{ij} можно найти из следуюощих соображсний. Легко проверить, что формула (5.29) для энергии элементарнвх возбуждений сверххроводника при учете различия направлений $\mathbf{k}$ и $-\mathbf{k}$ прицимает вид

$$E_k = \frac{\xi_k - \xi_{-k}}{2} + \sqrt{\left(\frac{\xi_k + \xi_{-k}}{2} \right)^2 + \Delta_k^2} \tag{14.16}$$

В магиитном поле, достаточно медленно меняющемся в пространстве [1], импульсы эдементарных возбужденин приобретагот одинаковую добавку $m\mathbf{w}$ за счет ненупевои скорости движения сверхтекучей компоненты. С помощью (14.16) получаем:

$$E_{\mathbf{k}} \to E_{\mathbf{k}+m\mathbf{w}} \approx E_{\mathbf{k}} + m\mathbf{v}_F(\mathbf{k})\mathbf{w} \tag{14.17}$$

где $\mathbf{v}_{\mathrm{F}}(\mathbf{k}) = \partial\xi_{\mathrm{k}}/\partial\mathbf{k}$. Пдотность потока возбуждений есть

$$\mathbf{P} = \sum_{\mathbf{k}\alpha} \mathbf{v}_{\mathrm{F}}(\mathbf{k}) f\left(E_{\mathbf{k}} + m\mathbf{v}_{\mathbf{F}}(\mathbf{k})\mathbf{w} \right) \tag{14.18}$$

где $f(E)$ - фермиевская функция распределения. Введсм тензор плотности возбуждеий, как величину, определяющую отклик $\mathbf{P}$ на измснение скоросTY: $\mathbf{w}$:

$$\delta P_i = -n^{\mathrm{n}}_{ij} \delta w_j \tag{14.19}$$

Из (14.18) получаем:

$$n^{\mathrm{n}}_{ij} = -m \sum_{\mathbf{k}\alpha} v_{\mathrm{F},i}(\mathbf{k}) v_{\mathrm{F},j}(\mathbf{k}) \frac{\partial f\left(E_{\mathbf{k}} + m\mathbf{v}_F(\mathbf{k})\mathbf{w} \right)}{\partial E} \tag{14.20}$$

Разность тензоров n^{n}_{ij} в нормальном (то есть при $\Delta = 0$) и сверхпроводящем состояниях дает величину тензора плотности сверхпроводяших электроНОВ

[11] Более точно, в лононовском пределе, когда глубина проникновения превышает длину котерентности, что всегда имеет место в сверхпроводниках второго рода.

$$n_{ij}^{\mathbf{s}} = n_{ij}^{\mathrm{n}}(\Delta = 0) - n_{ij}^{\mathrm{n}} \tag{14.21}$$

Опуская эависимость n_{ij}^{n} от магнитного поля (мы вернемся к этому вопросу нише), получаем

$$n_{ij}^{\mathrm{s}}(T) = 2m \int \frac{dS_{\mathrm{F}}}{(2\pi\hbar)^3} \frac{v_{\mathrm{F},i}(\mathbf{k}) v_{\mathrm{F},3}(\mathbf{k})}{|\mathbf{v}_{\mathrm{F}}(\mathbf{k})|} [1 - Y(\hat{\mathbf{k}}, T)] \tag{14.22}$$

где $Y(\hat{\mathbf{k}}, T)$ - функция Иосида (9.4), а интегрирование происходит по ферми-повсрхности. Формула (14.22) определяет тензор $n_{i,}^{\mathrm{s}}$ для фермиповерхности произвольной формы и произволыгого типа спаривания. В области Гинзбурга-Ландау аналогичное выражение для обычной анизотропной сверхпроводимости впервые получепо в работе [46]. При $T = 0$

$$n_{ij}^{\mathbf{s}}(0) = 2m \int \frac{dS_{\mathbf{F}}}{(2\pi\hbar)^3} \frac{v_{\mathbb{F},i}(\mathbf{k}) v_{\mathbf{F},j}(\mathbf{k})}{|\mathbf{v}_{\mathbf{F}}(\mathbf{k})|} \tag{14.23}$$

При наличии нумей в спектре элементарных возбуждений изменение компонент тензора плотности сверхпроводящих электронов (или лондоновской глубины проникновения) с температурой при $T \to 0$ происходит по степенным законам, аналогично поведению теплоемкости, парамагнитной восприпмчивости и т.д. Так, для A-фазы, где $\Delta_{\mathrm{k}}^2 = \Delta^2 \sin^2\theta$, вычисления, подобные приведенным в 7, дают [47]:

$$[n_{zz}^{\mathrm{s}}(0) - n_{zz}^{\mathrm{s}}(T)]|_{T\to 0} \sim n \left(\frac{T}{T_c}\right)^2 \tag{14.24}$$

$$[n_{xx}^{\mathrm{s}}(0) - n_{xx}^{\mathrm{s}}(T)]|_{T\to 0} \sim n \left(\frac{T}{T_c}\right)^4 \tag{14.25}$$

где n - полная плотность частиц. Аналогично, для полярной фазы ($\Delta_{\mathbf{k}}^2 = \Delta^2 \cos^2\theta$) :

$$[n_{zz}^{\mathrm{s}}(0) - n_{zz}^{\mathrm{s}}(T)]|_{T\to 0} \sim n \left(\frac{T}{T_{\mathrm{c}}}\right)^{\mathbf{3}} \tag{14.26}$$

$$[n_{xx}^{\mathrm{s}}(0) - n_{xx}^{\mathbf{s}}(T)]|_{T\to 0} \sim n\frac{T}{T_c} \tag{14.27}$$

Нструдно установить закопы низкотемпературного поведения и для фаз с другим расположением нулей.

Вблизи критической температуры

$$n_{ij}^{\mathrm{s}}\left(T \to T_{\mathrm{c}}\right) = \frac{7\zeta(3)m}{2\pi^2} \left(\frac{\Delta(T)}{T_{\mathrm{c}}}\right)^2 \int \frac{dS_{\mathrm{F}}}{(2\pi\hbar)^3} \frac{v_{\mathrm{F},i}(\mathbf{k}) v_{\mathrm{F},j}(\mathbf{k})}{|\mathbf{v}_{\mathrm{F}}(\mathbf{k})|} |g(\mathbf{k})|^2 \tag{14.28}$$

Это выражение соответствует случаю синглетного спаривания, для триплетного спаривания надо произвести очевидную замену $|g(\mathbf{k})|^2 \to |\mathrm{d}(\mathbf{k})|^2$. Функция $\Delta(T)$ задана формулой (6.18). Для полностью изотроппого сверхпроводящего состояния из (14.23) и (14.28) получается известное соотношение [48]

$$n^{\mathrm{s}}\left(T \to T_{\mathrm{c}}\right) = 2n^{\mathrm{s}}(0) \left(1 - \frac{T}{T_{\mathrm{c}}}\right) \tag{14.29}$$

Обратим внимание на то, что согласно (14.7) матрица коэффициентов K_{ij}, определяощая пространственные масшштабы изменения параметра порядка (уравнение

(12.6)) и поля (уравпепие (14.10)) пе зависит от массы электрона m, но зависит (чсрез $\mathbf{v}_F(\mathbf{k})$) от той эффективной массы, которуо электрон приобретает в кристалле.

Заметим также, что мы здесь не принимали во внимание псрснормировку массы за счет ферми-жидкостного взаимодействия электрона с молекулярным полем, создаваемьмм током остальных электронов. Это можно сделать вклюочая в скорость w молекулярное поле:

$$w_i \to w_i - mF_{1,ij}P_j$$

и разрешая уравнения (14.18), (14.19) относителыо $\delta\mathbf{P}$. Здесь $F_{1,ij}$ - тензор плотности ферми-жидкостного взаимодействия в кристалле, являющийся обобщснисм всличины $F_1/\left(N_0k_F^2\right)$ в изотропной фсрми-жидкости. Учет ферми-жидкостных эффектов, вообще говоря, изменяет температурную зависимость n_{ij}^{s} даже в изсропном случас [49, 50]. Мы не будем в дальнейшем прииимать во віимание ферми-жидкостіые эффекты, предполагая, тто основная перенормировка массы электрона происходит за счет его взаимодействия с кристаллической решеткой.

Нелипейпый эффект Мейсснера [51]. Кроме степенного убывания лондоновской глубины проникновения $\delta(T)$ при $T \to 0$, наличие нулей в спектре возбуждений приводит к специфическому для каждой сверхпроводящей фазы и геометрии задачи увеличениио $\delta(0)$ с ростом магиитного поля. Для рассмотрения этого эффскта веріемся к формуле (14.20). При $T = 0$ входяшая в эту формулу производная фермисвской функции распредсления обращается в нулг для всех ненулевьхх знатений своего аргументта:

$$n_{ij}^{\mathrm{n}}(0) = m\sum_{\mathbf{k}a} v_{\mathrm{F},i}(\mathbf{k})v_{\mathrm{F},j}(\mathbf{k})\delta\left(E_{\mathbf{k}} + m\mathbf{v}_{\mathrm{F}}(\mathbf{k})\mathbf{w}\right) \tag{14.30}$$

Отсюда видно, что при $T = 0$ в сверхпроводниках с конечной величиной щели на всей ферми-поверхности тснзор нормальной плотности равсн нулю для скоростей $\mathbf{w}$, не превышающих критическуо скор $\propto$ ль Ландау $w_c \approx \Delta/mv_{\mathrm{F}}$.

Если щель обращается в нуль на некотором множестве точек на фермиповерхности, то конечная плотность возбуждений сохраняется и при $T = 0$. Для сверхпроводника со сферической ферми-поверхностью можяо переписать (14.30) следующим образом:

$$n_{ij}^{\mathrm{n}} = 3n\int\frac{d\Omega}{4\pi}\hat{k}_i\hat{k}_j\int\frac{dEE}{\sqrt{E^2-\triangle_{\mathrm{k}}^2}}\delta(E+\mathbf{kw}) = \\ = 3n\int\frac{d\Omega}{4\pi}\hat{k}_i\hat{k}_j\frac{|\mathbf{kw}|}{\sqrt{(\mathbf{kw})^2-\triangle_k^2}} \tag{14.31}$$

тде n - полная плотность электронов, а интегрирование шо утлам производится в пределах, задаваемьх условием $(\mathbf{kw})^2 > \Delta_{\mathbf{k}}^2$.

Пусть щель обращается в нулы на экваторе ферми-сферы, как это имеет место в полярной фазе ($\Delta_{\mathbf{k}}^2 = \Delta\cos^2\theta$), а сверхтекучая скорость $\mathbf{w} = [e/(mc)]\mathbf{A}$ направлена вдоль оси y (сверхпроводник занимает полупространство $z > 0$, внешнее поле направлено вдоль оси x, в выбранной калибровке фаза кон-
денсата постоянна). Тогда из (14.31) мы получаем, что при $T = 0$ имеется ненулевая плотность нормальной компоненты:

$$n_{yy}^{\mathrm{n}} \approx \frac{3nk_F\,|w_y|}{\Delta}\int\limits_0^{2\pi}\frac{d\varphi}{2\pi}\sin^2\varphi|\sin\varphi| = n\frac{4ek_F}{\pi mc\Delta}\,|A_y| \tag{14.32}$$

Следовательно,

$$n_{yy}^{\mathrm{s}} = n\left(1 - \frac{4ck_{\mathrm{F}}}{\pi mc\Delta}\,|A_y|\right) \tag{14.33}$$

Уравнение Максвелла (14.1), с учетом выражений для тока (14.9) и плотности сверхтекучей компоненты (14.33), принимает вид

$$\frac{\partial^2 A_y}{\partial z^2} = \frac{1}{\delta^2} A_y \tag{14.34}$$

где

$$\frac{1}{\delta^2} = \frac{mc^2}{4\pi nc^2}\left(1 - \frac{4ek_F}{\pi mc\Delta}\,|A_y|\right) \tag{14.35}$$

Таким образом, благодаря тому, что щель в спектре возбуждений обращается в нуль на экваторе ферми-сферы, в выражении для лондоповской глубины проникновения появляется неаналитичсское, линейно зависящее от модуля поля слагаемое [3]. Его удобно записать, выражая Δ через термодинамическое критическое поле H_c:

$$\frac{H_c^2}{8\pi} = \frac{N_0}{2}\Delta^2 \tag{14.36}$$

при котором работа по выталкиванию магнитного поля из сверхпроводника равняется выигрышу энергии (5.37) (или (5.38)) при переходе в сверхпроводящее состояние. Оценивая входящий в (14.35) вектор-потенциал как $|A_y| \sim H\delta_0$, гдс δ_0 дается формулой (14.13), получаем:

$$\delta(H) = \delta_0\left(1 + \frac{4}{\pi}\sqrt{\frac{3}{2}}\frac{H}{H_{\mathrm{c}}}\right) \tag{14.37}$$

Смешанное состояпие. Так же, как и в обычных сверхпроводниках второго рода, в полях, превышающих величину

$$H_{c1}(T) \sim \frac{\Phi_0}{4\pi\delta^2(T)} \ln\frac{\delta(T)}{\xi(T)} \tag{14.38}$$

мейсснеровское (цдеально диамагнитное) состояние в иеобычных сверхпроводниках перехоштт в смешанное состояние, в котором в толщу сверхпроводника начинают проникать абрикосовские вихри.

В отличие от изотропного случая, в анизотропных сверхпроводниках направление и расположение вихрей эависят от величины и направления внешиего поля по отношению к кристаллическим осям. Величина нижяего крити- ческого поля H_{c1} также зависит от направления внсшнего поля, а симметрия вихревых решеток может отличаться от правитьной треутольной. Теория смешанного состояния для необычных сверхпроводников в основном совпадает с соответствующей теорией для обычных анизотропных сверхпроводников, охватывающей большое разнообразие различных частных вопросов (распределения полей, утловые зависимости и пр.). Мы не будем останавливаться на этой части тсории (см. [45, 52-54]).

Среди явлений, специфических лля смешанного состояния в необычных сверхпроводниках, следует прежде всего указать на фазовые переходы, связанные с изменением симметрии многокомпонентных сверхпроводящих состояний [43]. Пример

[12] На появление при $T = 0$ плотности нормальной компоненты, неаналитически зависящсй от поля, в сверхтекучих фазах с нулями в щели в спектре возбуждений впервые указано в работе [58].

[3] В обычиых сверхпроводниках добавКа к элубине проникновения квадратична по помю.

такого перехода обсуждался в 12. Другой характеріой чертой многокомпонентіо сверхпроводимости является возможность существования свсрхпроводяших состояний со спонтанным магнетизмом [9]. Свойства таких сверхпроводников мы изучим в следующем параграфе. Наконец, еще один эффект, специфический для сверхпроводников с нетривиальным спариванием - это появление необычной зависимости теплоемкости от магнитного поля в смешанном состоянии [55]. Посмотрим сначала, как обстоит дело в обычных сверхпроводниках.

Как известно, параметр порядка сверхпроводника обращается в нуль на оси вихревой нити и восстанавливает свое равновесное постоянное значение на расстояниях $\rho \sim \xi(T)$ от оси вихря. Такая «яма» в потенциале $\Delta(\rho)$ приводит к образованито локализованных на ядре вихря связанных состояний квазичастиц. Наинизшгуо энергио связанных состояний можно оценить с помощью соотношения неопределенностей как

$$E_0 \approx \frac{\hbar^2}{2m\xi^2(T)} \approx \frac{\Delta^2}{\varepsilon_F} \tag{14.39}$$

Поскольку эта эпергия в $\Delta/\varepsilon_{\mathrm{F}}$ раз меньше наинизшей энергии возбуждений вдали от ядра вихря, то спектр возбуждений, локализованных в ядре, можно считать бесщелевым, практически совпадатошим со спектром возбуждений в нормальном металле. Таким образом, занимаемая ядрами вихрей часть объема сверхпроводника второго рода в смешанном состоянии обладает той же плотностью состояний [4], что и нормальный металл. Следовательно, дополнигельный вклад в плотность состояний пропорционален доле площади, занимаемой ядрами вихрей в плоскости, им перпендикудярной:

$$N_{\mathrm{loc}} \approx N_0 \frac{S_{\mathrm{cores}}}{S} = N_0 \pi \xi^2 n_v \tag{14.40}$$

Здесь N_0 - плотность состояний в нормальном металле, $n_\nu = B/\Phi_0$ - число вихрей на сдиницу площади, B - магнитная индукция (среднее значение микроскопического магнитного поля в образце).

В сильно выраженных сверхпроводниках второго рода, в которых выполняется условие $\delta(T)/\xi(T) \gg 1$, индукция B мало отличается от внешнего поля H практически во всем интервале полей $H_{\mathrm{c1}} < H < H_{\mathrm{c2}}$ (но не в непосредственной окрестности H_{c1}). Учитывая это обстоятельство, а также

[4] Длотность состояний определяется следуююиим образом:

$$N(E) = \sum_{\mathrm{k}\alpha} \delta\left(E - E_{\mathrm{k}}\right)$$

вспоминая, что переход в норманое состояние происходит в поле

$$H_{c2} \approx \frac{\Phi_0}{\pi \xi^2(T)} \tag{14.41}$$

когда расстояние между ядрами вихрсй становится порядка ξ, получаем:

$$N_{\mathrm{loc}} \approx N_0 \frac{II}{H_{c2}} \tag{14.42}$$

В результате, при низких тсмпературах ($T \ll T_c$), теплоемкость сверхпроводника в смешанном состоянии будет определяться в основном вкладом возбуждении, локализованных в ядрах вихрей:

$$C_{\mathrm{s}} \approx \frac{H}{H_{c2}} C_{\mathrm{n}} \tag{14.43}$$

гдс C_{n} - теплоемкость нормалыного металла, линейно зависящая от температуры.

В сверхпроводниках с нетривиальным спариванием результат (14.43), разумеется, сохраняет силу. Однако, если щель в спектре возбуждений обращается в нуль где-либо на ферми-повсрхности, то возможно появление дополнительmьх вкладов в теплоемкость, связанных с плотностьоо состояний в окрестности нулей. В пространстве между ядрами вихрсй текут незатухающие сверхтекучие токи $\mathbf{j} = -en_s\mathbf{w}$, что приводит к сдвигу энсргии элемештарных возбуждсний (14.17). В области полей $H_{c1} < H \ll H_{c2}$ расстояние между вихрями $a \sim n_V^{-1/2} \sim (\Phi_0/H)^{1/2}$ ограничено интервалом $\xi \ll a < \delta$, и распределение сзерхтекучей скорости

$$\mathrm{w} = -\frac{\mathrm{j}}{en_3} = -\frac{c}{4\pi en_3}\,\mathrm{rot\,B}$$

определяется вкладом ближайшего вихря:

$$\begin{aligned}\mathbf{B} &\approx \hat{z}\frac{\Phi_0}{2\pi\delta^2}\ln\frac{\delta}{\rho}\\ \mathbf{w} &= -\frac{\hbar}{2m}\frac{\hat{\varphi}}{\rho}\end{aligned} \tag{14.44}$$

Здесь ρ юбозначает расстояние до оси вихря, а $\hat{\varphi}$ - единичный вектор азимутального направления. Вновь, ограничиваясь для простоты случаем сферической ферми-поверхности, получаем вклад в плотность состояний за счет окрестностей нулей щели в спектре элементарных возбуждений:

$$N_{\mathrm{deloc}} = n_{\mathrm{v}}\int dS\sum_{\mathbf{k}\alpha}\delta\left(E_{\mathbf{k}} + \mathbf{kw}\right) \tag{14.45}$$

Интегрирование ведется здесь по площади элементарной ячейки решетки Абрикосова. Имеем (ср. с выводом формулы (14.31)):

$$\sum_{k\alpha}\delta\left(E_{\mathrm{k}} + \mathrm{kw}\right) = 2N_0\int\frac{d\Omega}{4\pi}\frac{|\mathrm{kw}|}{\sqrt{(\mathrm{kw})^2 - \Delta_{\mathrm{k}}^2}} \tag{14.46}$$

причем интегрирование происходит по области $(\mathrm{kw})^{\,2} > \Delta_{\mathbf{k}}^2$. Дальнейшие вычисления необходимо производить уже для конкретного вида сверхпроводящего состояния.

Рассмотрим в качестве примера полярнуто фазу с p-спариваниcм, гдс $\Delta_{\mathbf{k}}^2 = \Delta^2\cos^2\theta$. Главный вклад в плотность состояний возникает от окрестности экватора ферми-поверхілости. Выполняя в (14.46) интегрироваиие по углам, получаем:

$$N_0\frac{k_{\mathrm{F}}|\mathbf{w}|}{\pi\Delta}\int\limits_0^{2\pi}d\varphi|\cos\varphi| = N_0\frac{4k_{\mathrm{F}}|w|}{\pi\Delta}$$

Подставляя это выражение в (14.45), получаем (с учетом (14.44)):

$$N_{\mathrm{deloc}} \approx n_{\mathrm{v}}N_0\frac{1\hbar v_{\mathrm{F}}}{\Delta}a \sim N_0\sqrt{\frac{II}{H_{c2}}} \tag{14.47}$$

Полученный рсзультат показывает, что в смешанном состоянии при $H \ll H_{c2}$ главньй вклад в электронную плотность состояний свсрхпроводника, иметощего нули параметра порядка па линиях на ферми-поверхности, вносят не ядра вихрей, а пространство между ними, где текут сверхдроводящие токи:

$$\frac{N_{\rm deloc}}{N_{\rm loc}} \sim \sqrt{\frac{H_{\rm cc}}{H}} \gg 1 \tag{14.48}$$

Теплоемкость такого сверхпроводника в смешанном состоянии при достаточно низких температурах должна иметь вид [5]

$$\frac{C_{\rm s}}{C_{\rm n}} = b\sqrt{\frac{H}{H_{\rm c2}}} \tag{14.49}$$

где b - численный коэффициент. Подобная зависимость наблюдалась экспериментально в высокотсмпературных ($YBa_2Cu_3O_{7-6}$[16, 56]) и в тяжелофермионных (UPt_3 [57]) сверхпроводниках.

Упражнение. Показать, что для сверхпроводника с нулями щели в изолированнвх точках на ферми-поверхности имеет место следующее поведение теплоемкости в смешанном состоянии при низких температурах:

$$\frac{C_{\rm s}}{C_{\rm n}} = b\frac{H}{H_{\rm c2}} \ln \frac{H_{\rm c2}}{H} \tag{14.50}$$

19.1.15 15. Magnetic Superconductors

Сверхпроводящие состояния с многокомпонентным параметром порядка могут обладать спонтанным магнитным моментом. Так, орбитальный момент куперовской пары в состояниях, преобразующихся согласпо представлению E_1 группы D_6, с параметрами порядка:

$$g(\mathbf{k}) \propto \hat{k}_z \left(\hat{k}_x + i\hat{k}_y\right), \text{ при } S = 0 \tag{15.1}$$

$$\mathrm{d}(\mathbf{k}) \propto \hat{z} \left(\hat{k}_x + i\hat{k}_y\right), \text{ при } S = 1 \tag{15.2}$$

равеп. Имеются также состояния, обладаiшиие спонтанным спиновым моментом пары, например:

$$\mathbf{d}(\mathbf{k}) \propto \hat{k}_z(\hat{x} + i\hat{y}), \quad \text{при } S = 1 \tag{15.3}$$

С симметрийной точки зрения все такие состояния соответствуют магнитным сверхпроводящим классам (§§4, 11).

Магнитный момент $\mathcal{M}$ сверхпроводящего магнетика складывается из магнитнLx моментов всех куперовских пар и для образца объемом V, в болшшей части которого они ориентированы вдоль общего направления $\hat{\mu}$, дается выражснием

$$\mathcal{M} = \mathbf{MV}, \quad \mathbf{M} \sim \frac{\hbar\gamma n_8}{2}\hat{\boldsymbol{\mu}} \tag{15.4}$$

Здесь $n_{\rm s}$ есть плотность сверхпроводящих электронов, а $\gamma = e/(2mc)$ - гиромагнитное отношение. Легко проверить, что магнитный момент магнитного сверхпроводника с точностью до численного множителя совпадает с магнитным моментом обычного сверхпроводника такого же объема, в котором находится один абрикосовсгяй вихрь.

Магнитный момент (15.4) сверхпроводника создается незатухающими токами, текущими по его поверхности. В то же время магнитный момент единицы объема в толще сверхпроводника ничтожно мал. Дело в том, что спиновый момент пар

[15] См. также Н. Б. Копнин, Г. Е. Воловик //Письма в ЖЭТФ, 64, 641 (1996).

компенсируется моментом неспаренных частиц. С другой стороны, куперовские пары силнно перекрываются между собой, поскольку размер пары ξ_0 велик по сравнению с межатомным расстоянием. По этой причине локалные токи, создающие орбитальный момент, практически полностью компенсируюот друг друга в объеме сверхпроводника. Однако, на поверхности образца такая компенсация отсутствует, и поверхностные токи порождают магнитный момент [58, 59].

Локальный мапнстизм. Рассмотрим ситуацию количественно на примере двухкомпонентного векторного параметра порядка в гексагональном кристалле. Для вычисления плотности внутреннего спонтанного момента вблизи критической температуры мь должны явно выделить в функшионале свободной энергии Тинзбурга-Ландау (12.15) слагаемые, пропорциональные магнитному поло. Для этой цели перепишем градиентіые члены в (12.15) в следующсм виде:

$$\begin{aligned}\mathcal{F}_{\text{grad}} = \int d^3r \{ & K_1 \left(D_i\eta_j\right)^* \left(D_i\eta_j\right) + K_4 \left(D_z\eta_i\right)^* \left(D_z\eta_i\right) + \\ & \frac{K_2+K_3}{2}\left[\left(D_i\eta_i\right)^*\left(D_j\eta_j\right) + \left(D_i\eta_j\right)^*\left(D_j\eta_i\right)\right] + \\ & + \frac{K_2-K_3}{2}\left[\left(D_i\eta_i\right)^*\left(D_j\eta_j\right) - \left(D_i\eta_j\right)^*\left(D_j\eta_i\right)\right]\Big\} \end{aligned} \tag{15.5}$$

Интегрируя по частям последнее слагаемое в правой части и используя тождество

$$[D_i, D_j] \equiv D_iD_j - D_jD_i = -\frac{2\pi i}{\Phi_0} e_{ijk} (\text{rot}\,\mathbf{A})_k$$

находим, что вклад в плотность свободной энергии, пропорциональный магнитному полю, имеет вид

$$F_{MH} = -\frac{\pi i}{\Phi_0}\left(K_2 - K_3\right)\left(\eta^* \times \eta\right) \text{rot}\,\mathbf{A} \tag{15.6}$$

Отсюда получаем выражение дзя плотности внутреннего спонтапного момента:

$$\mathrm{M_i} = \frac{\pi i}{\Phi_0}\left(K_2 - K_3\right)\left(\eta^* \times \eta\right) \tag{15.7}$$

Как мы знаем (см. 11), минимуму свободной энсргии (11.6) при $\beta_2 > 0$ отвечает комплексная сверхпроводящая фаза $\eta = \eta_0(1, \pm i)e^{i\varphi}$. Согласно (15.7), эта фаза обладает ненулевым собственным магнитным моментом в однородном состоянии. Величина этого момента определяется значением разности $K_2 - K_3$ и оказывается ничтожно малой. Микроскопический ажализ (см. 18) показываст, что в теории БКІШ лия векторного параметра порядка $K_1 = K_2 = K_3$, и спонтанный магнетизм отсутствуст. Однако, при учете зависимости плотности состоянии вблизи ферми-повсрхности от энергии (электрон-дырочная асиммстрия), разность $K_2 - K_3$, а вместе с ней и плотность внутреннего момента, становится отличной от нуля:

$$K_2 - K_3 \sim N_0\xi_0^2\left(\frac{T_c}{\varepsilon_F}\right)^2 \ln\frac{\varepsilon_1}{T_c}$$

Можно убедиться в том, что плотность внутреннего магнитного момента сверхпроводника весьма мала и при нулевой температуре. Проще всего это сделать для состояния (15.3). В этом состоянии спарены только электроны со спинами «вверх» (см.

(2.7)). Испожзуя прсобразование Боголюбова ($5), нетрудно проверить, что распределение таких электронов по энергиям имеет вид

$$n_\uparrow(\xi) = \left\langle a^+_{\mathbf{k}\uparrow} a_{\mathbf{k}\uparrow} \right\rangle = \frac{1}{2}\left[1 - \frac{\xi}{E}(1 - 2f(E))\right] \tag{15.8}$$

где $f(E)$ - фсрмиевская функция распрсделения, $E = \sqrt{\xi^2 + \Delta^2_{\mathbf{k}}}$. При $T = 0$

$$n_\uparrow(\xi) = \frac{1}{2}\left(1 - \frac{\xi}{E}\right)$$

В то же время, электроны со спинами «вниз» не спарсны, и их распределение по энергиям

$$n_\downarrow(\xi) = \frac{1}{2}\left(1 - \frac{\xi}{|\xi|}\right)$$

есть фермиевская «ступенька». Спиновый магнитный момент единины объема такой жидкости дается выражением

$$\mathrm{M_i} = \hat{z}\mu_\mathrm{B} \int d\xi N(\xi)\left(n_\uparrow(\xi) - n_\downarrow(\xi)\right) \approx \hat{z}\mu_\mathrm{B} N_0' \Delta^2 \ln\frac{\varepsilon_1}{\Delta} \tag{15.9}$$

Здесь $N(\xi)$ - плотность электронных состояний, N_0' - производная плотности состояний на ферми-поверхности, а ε_1 - параметр обрезания логарифмически расходяшегося интеграла, соответствующий тому, что параметр порядка отличен от нуля в узком слое вблизи ферми-поверхности (см. 5). Таким образом, плотность спогттанного магнитного момента мала в меру малости $(T_c/\varepsilon_1)^2 \ln(\varepsilon_1/T_c)$ и отлична от нуля лишь при наличии асимметрии в раепределении частиц и дырок вблизи ферми-поверхности [3, 60].

Малая плотность внутреннего спинового момента возникает в результате компенсации спиновых моментов куперовских пар, состоящих иэ частиц со спинами вдоль поля и неспаренных частиц с противоположной ориентацией спина. Такой компенсации может и не быть. Для этого надо иметь либо гигантское спаривающее взаимодействие для одного из двух направлений спина, либо создать практически полностью поляризованную ферми жидкость с очень сильіо раздвинутыми ферми-поверхіостями для частиц со спинами «вверх» и «вниз». Для сверхпроводников обс эти возможности в настоящес время выглядят ие очень рсально. В нсйтральнй сверхтекучсй ферми-жидкости (^{3}He) создание силыно спин-поляризованной сверхтекуче ф фазы возможно.

Поверхностные токи и магнитіый момелт образца. Магнитные сверхпроводящие состояния в кристаллах, гдс существенны эффекты кристаллической анизотропии и сильного спин-орбитального взаимодействия, имегот пиить один вил пепрерывного вырождения - вырождение по фазе φ параметра порядка, обсспечивадощее возможность протекания бездиссипативных токов. Токи, іле связанные с градиегтами φ, могут протекать лишь в слоях толщиной порядка ξ вблизи границ образца или гранит магнитных доменов. Для их вычисления воспользуемся выражениsм (15.5) лля градиентной части свободной эергии, подставив в него параметр порядка с явно выделенньм фазовым множителем $\boldsymbol{\eta} \to \boldsymbol{\eta}(\mathbf{r})e^{i\varphi(\mathbf{r})}$. Опуская слагаемыс с K_4, с точностью до полных производных в попынтегральном выраженип ниеем:

$$\begin{aligned}\mathcal{F}_\mathrm{grad} = \int d^3r \Big\{ & K_1\left[v^2|\boldsymbol{\eta}|^2 + iv_i\left(\eta_k\nabla_i\eta_k^* - \eta_k^*\nabla_i\eta_k\right) + \left(\nabla_i\eta_j^*\right)\left(\nabla_i\eta_j\right)\right] + \\ & + \tfrac{K_2+K_3}{2}\left[2|\mathbf{v}\eta|^2 + i\mathbf{v}\,\mathrm{rot}\left(\boldsymbol{\eta}^*\times\eta\right) + \left|\nabla_i\eta_i\right|^2 + \left(\nabla_i\eta_j^*\right)\left(\nabla_j\eta_i\right)\right] - \\ & - \tfrac{K_2-K_3}{2}\tfrac{2\pi i}{\Phi_0}\left(\boldsymbol{\eta}^*\times\eta\right)\mathrm{rot}\,\mathbf{A}\Big\}\end{aligned} \tag{15.10}$$

Здесь

$$\mathbf{v} = \boldsymbol{\nabla}\varphi + \frac{2e}{\hbar c}\mathbf{A}$$

• калибровочно-инвариантньдй градиент фазы (ср. с (14.6)). Соответствующее выражение для плотности тока выгдядит следующим образом:

$$\begin{aligned}
\mathrm{j} &= --\frac{\delta \mathcal{F}_{\mathrm{grad}}}{\delta \mathrm{A}} = -\frac{2e}{\hbar}\frac{\delta \mathcal{F}_{\mathrm{grad}}}{\delta \mathbf{v}} = \\
&= -\frac{2e}{\hbar}\left\{K_1\left[2\mathbf{v}|\boldsymbol{\eta}|^2 + i\left(\eta_i\nabla\eta_i^* - \eta_i^*\nabla\eta_i\right)\right] + \frac{K_2+K_3}{2}\left[2\left(\boldsymbol{\eta}^*(\mathbf{v}\boldsymbol{\eta})+\right.\right.\right. \\
&\left.\left.\left. + (\mathbf{v}\boldsymbol{\eta}^*)\,\boldsymbol{\eta}\right) + i\,\mathrm{rot}\,(\boldsymbol{\eta}^*\times\boldsymbol{\eta})\right] + i\frac{K_2-K_3}{2}\,\mathrm{rot}\,(\boldsymbol{\eta}^*\times\boldsymbol{\eta})\right\} \qquad (15.11)
\end{aligned}$$

Неоднородности в распределении модуля или направления вектора $i\,(\eta^*\times\eta)$ на границе образца (на расстояниях порядка дтиыы когерентности $\xi(T)$) или на границах магнитных доменов порождают незатухаюощие поверхностныс токи, создающие полный магнитный момент:

$$\mathcal{M} = \frac{1}{2c}\int d^3r(r\times j) \qquad (15.12)$$

Величина $\mathcal{M}$ зависит, разумеется, от распределения компонент параметра порядка $\eta_i(\mathbf{r})$ вблизи границы образца.

Рассмотрим цилиндричсский образец радиуса R с осью $\hat{z}$ вдоль гексагональной кристалшческой оси. Для простоты будем считать, что параметр
порядка во всем объсме имеет вид $\eta = \eta_0(r)(1,i)$, где $\eta_0(r)$ в повсрхностном слое толипной ξ гладко спадает от объемного значения η_0 до нуля при $r = R$. В этом случае даже в отсутствие внешнего магнитного поля, то есть при $\mathbf{v} = 0$, выражение вд плотности тока приобретает вид

$$\mathrm{j} = c\,\mathrm{rot}\,\mathrm{M} = -\frac{4\epsilon}{\hbar}K_2\frac{\partial\eta_0^2(r)}{\partial r}\hat{\varphi}$$

где $\hat{\varphi}$ - единичный вектор азимуталного направления. Выполняя теперь интегрирование в (15.12), получаем оценку (15.4) для магнитного момента цилитдра обтема V:

$$\mathcal{M} = \frac{8e}{\hbar c}K2\eta_0^2 V\hat{z} \approx 2\hbar\gamma n_{\mathrm{s}}V\hat{z} \qquad (15.13)$$

Здесь использовано, что $K_2 \sim \hbar^2 n_{\mathrm{s}}/\left(m\eta_0^2\right)$ (см. (14.7)).

Заканчивая обсуждсние вопроса о спонтанном моменте магнитиных сверхпроводников, подчеркнсм, что в выражении для плотности тока (15.11) последнее слагаемое, соответствующее пдотности спонтанного впутреннего момента, и предпоследнее слагаемое, соответствующее поверхностному моменту, неотличимы по своей структуре. Поэтому формулы для плотности тока, полученные на основе микроскопической теории, приводили многих авторов к утверждению о существовании «большой» ($\sim \mu_{\mathrm{B}} n_{\mathrm{s}}$) плотности спонтанного внутреннего момента (см., например, [61]). Для правильной же интерпретации раздичных вкладов в ток необходимо производить микроскопическое вычисление градиентной энергин [62, 63].

Электродинамика магинтых сверхпроводников. При наличих внешнего поля $\mathbf{H}$, параллельного оси цилиндра, уравнение лондоновской электродинамики приобретает вид

$$\operatorname{rot} B = \frac{4\pi j}{c} = -\frac{A}{\delta^2} + 4\pi \operatorname{rot} M \tag{15.14}$$

где δ - лощдоновская глубина проникновсния. Поскольку вклад в ток, обусловленнюи слагаемым с rot M, сосредоточен в поверхностном слос толщиной $\xi \ll \delta \ll R$, то магнитное поле, как обыпно, затухает вглубь образца:

$$\mathbf{B}(r) = \mathbf{B}(R) \exp\left(-\frac{R-\tau}{\delta}\right) \tag{15.15}$$

Однако, за счет того, что по поверхности текут незатухающие токи, граничное условие для уравнении Лондонов приобрстает вид:

$$\mathbf{B}(R) = \mathbf{H} + 4\pi\mathbf{M} \tag{15.16}$$

Таким образом, даже в отсутствие внешнего поля на поверхности сверхпроводника имеется магнитное поле, индуцированное магнетизмом пар:

$$\mathbf{B}_0 = 4\pi\mathbf{M} = 4\pi\frac{c\hbar}{2mc} n_{\mathrm{s}} \hat{\boldsymbol{\mu}} = 4\pi\mu_{\mathrm{B}} n_{\mathrm{s}} \hat{\boldsymbol{\mu}} \tag{15.17}$$

которое подавлятся в толще сверхпроводника, причем величина $\mathbf{B}_0$ оказывается порядка нижнего критического поля:

$$H_{c1} = \frac{\Phi_0}{4\pi\delta^2} \ln\frac{\delta}{\xi} = 2\pi\mu_{\mathrm{B}} n_{\mathrm{s}} \ln\frac{\delta}{\xi} \tag{15.18}$$

Мы видим, что в магнитном сверхпроводнике достичь нижнего критического поля легче, прикладввая внешшее поле параллелыо $\hat{\mu}$, чем антипараллельно ему. Более того, если поверхностное поле (15.17) в каком-то сверхпроводнике окажется больше H_{c1}, то это будет означать отсутствие мсйсснеровского состояния. Вихревые нити будут проникать вглубь такого сверхпроводника при сколь утодно малом внешнем поле.

Вблизи поверхности однодоменного магнитного сверхпроводника конечных размеров должно возникать поле порядка H_{c1} , убывающее с расстоянием от поверхности по тому же закону, что и поле магнитного шиполя.

Мапистизм в сверхпроводниках с p-спариванием. Несколько иная ситуация, по сравнению с рассмотрснной выше, возникает в сверхпроводниках со слабым спин-орбитальным взаимодействием. В этом случае существенно не только вырождение по фазе, но и по пространственным ориенташиям параметра порядка. Так, например, в заряженной сверхтекучей ферми-жидкости со структурой A-фазы гелия-3 (см. §§3, 11), параметр порядка имеет вид

$$A_{\alpha i} \sim V_\alpha \left(\Delta_i' + i\Delta_i''\right) \tag{15.19}$$

где $\mathbf{V}, \Delta', \Delta''$ - сдиничные векторы, причем $\Delta' \perp \Delta''$, а $\Delta' \times \Delta'' = 1$ задает паправление орбиталыного момента куперовских пар. Неоднородная часть свободной энергии Гинзбурга-Ландау в сверхпроводниках с p-спариванием в магнитном поле записывается как

$$\begin{aligned}\mathcal{F}_{\mathrm{grad}} = \int d^3r \Big[& K_1 \left(D_i A_{\alpha j}\right)^* \left(D_i A_{\alpha j}\right) + K_2 \left(D_i A_{\alpha i}\right)^* \left(D_j A_{\alpha j}\right) + \\ & + K_3 \left(D_i A_{\alpha j}\right)^* \left(D_j A_{\alpha i}\right) + K_4 \frac{2e}{\hbar c} i e_{\alpha\beta\gamma} B_\alpha A^*_{\beta i} A_{\gamma i} + \frac{B^2}{8\pi}\Big]\end{aligned} \tag{15.20}$$

Состояния A-фазы вырождены по отношению к вращениям вектора V и репера $(\Delta', \Delta'', 1)$. Поэтому во всем объеме бездиссипативные токи определяются не только калибровочно-инвариантной скоростью $\mathbf{v}$, но и пространственным изменением (текстурой) векторов, задающих параметр порядка (ср. с (15.11)). Выводы, сделанные выпие о величине спонтанного магнетизма в таком сверхпроводнике, сохраняются, однако возможные типы вихрей и структура смешанного состояния оказываются существенно сложнее, нежели для многокомпонентных сверхпроводящих фаз в кристаллах, где ориентационное вырождение подавлсно сильной анизотропией и спин-орбитальным взаимоденствием.

Слагаемое в свободной энергии (15.20), содержащее K_4, описывает взаимодействие спонтанного спинового магнитного момента сверхпроводящей фазы с внешним полем. Для унитарных фаз (определение унитарной фазы см. в сноске 6 к 5), в частности, для A - и B-фаз, такое слагаемое отсутствует. Для неунитарных фаз спиновый момент отличен от нуля, что вызывает расщепление фазового перехода ^{3}He в сверхтекучее состояние на два. Сначала имеет место переход в A_1-фазу, а затем - в A-фазу (см. рис. 2) [64]. Расщепление перехода, однако, оказывается малым, поскольку коэффициент K_4 отличен от нуля лишв в меру малости электрон-дырочной асимметрии (см. §18).

Сверхпроводники с p-спариванием и со структурой A - или A_1-фазы в настоящий момент неизвестны. Отдельные вопросы теории таких сверхпроводящих состояний рассмотрены в работах [31, 65, 66].

19.1.16 16. Эффект Джозефсона

Обобщение феноменологитеской теории эффекта Джозефсона на случай контактов между двумя сверхтроводниками, облалающими различной симметрией, может быть построено в духе полхода, развитого в 13 при анализе поверхностных свойств. Проще всего рассмотреть это явление на примере плоского контакта между двумя сверхпроводниками, находящимися в различных сверхпроводящих состояниях с опнокомпонентными параметрами порядка

$$\eta_1 = |\eta_1|\, e^{i\varphi_1}, \quad \eta_2 = |\eta_2|\, e^{i\varphi_2} \tag{16.1}$$

Для одноосных (гексагональных и тетрагонапыых), а также кубических кристаллов свободная энергия системы дается выражением

$$\mathcal{F} = \mathcal{F}_1 + \mathcal{F}_2 + \mathcal{F}_\mathrm{J} \tag{16.2}$$

тде

$$\mathcal{F}_i = \int\limits_{\mathrm{rn},>0} d^3 r F_i \quad (i = 1, 2) \tag{16.3}$$

есть свободные энергии (12.2) сверхпроводников, занимающих левое и правое полупростраиства с плоской границей, проходящей через начало координат, $\mathbf{n_i}$ - векторы внсишей нормали к соответствующему полупространству ($\mathbf{n}_1 = -\mathbf{n}_2$), а $\mathcal{F}_3$ есть поверхностная (джозефсоновская) энергия, феноменологически описываюшая связь мсжду сверхпроводниками из-за возможности туннелирования куперовских пар:

$$\mathcal{F}_\mathbf{J} = A \oint dS g_1(\mathbf{n}_1)\, g_2(\mathbf{n}_2)\, (\eta_1^* \eta_2 + \eta_1 \eta_2^*) \tag{16.4}$$

Здесь интегрированис происходит по поверхности раздела. Вообще говоря, энергия джозефсоновского контакта представляется бесконечной суммой слагаемых вида (16.4):

$$\sum_{p,q} \oint dS g_1^p(\mathbf{n}_1)\, g_2^q(\mathbf{n}_2)\, (\eta_1^* \eta_2 + \eta_1 \eta_2^*)$$

где каждое произведсние $g_1^p(\mathbf{n}_1)\,\eta_1$ и $g_2^q(\mathbf{n}_2)\,\eta_2$ не должно меняться при всех преобразованиях группы точечной симметрии соответствующсго полупространства. Для дашнейшего, однако, достаточно рассмотреть лишв одно слагаемое в этой сумме.

Энергия $\mathcal{F}_\mathrm{J}$ инвариантна относительно всех преобразований группы симметрии как левого, так и правого кристаллов в нормальном состоянии. Для христаллов с сильным спин-орбиталыным взаимодеиствием всегда имеются -билинейные по η_1 и η_2 комбинации, обладающие ухазанной симметрией. Это означаст, что в принципе пет никаких ограничений на существование джозефсоновской связи между двумя сверхпроводниками с однокомпонентными параметрами порядка, в том числе - между сверхпроводниками с синглетным и триплетным спариванием. При этом, разумеется, возможны такие ориентации поверхности, при которых какая-то из функций $g_i(\mathbf{n}_i)$, а вместе с ней и $\mathcal{F}_\mathrm{J}$, обращаются в нуль. В этом случае нсобходимо принимать во внимание джозефсоновские энергии болес высоких порядков по η_i.

Симметрия $g(\mathbf{n})$ совпадает с симметрией соответствующего сверхпроводящего класса. Для синглетных состояний это означает, что $g(\mathbf{n}) = 0$ для направлении нормали, при которьх параметр порядка обрашается в нуль на ферми-поверхности (см. 4), то есть при $S = 0$ функции $g(\mathbf{n})$ можно считать совпадающими с базисньми функциями соответствуошего представления. Для случая триплетного спаривания функции $g(\mathbf{n})$ найдены в работе [67].

Точно таким же образом, составляя инвариантные комбинации из векторов $\mathbf{n}_i$ и компонент параметров порядка η_i в случае сильной спинорбиталыой связи, можно получить джозефсоновские эиергии $\mathcal{F}_\mathrm{J}$ для многокомпонентных сверхпроводящих состояний.

В отсутствие спин-орбитального взаимодействия, в сверхпроводнике с триплетным спариванием нельзя построить скалярггую линейную функцию из спинового всктора $\boldsymbol{\eta}$ параметра порядка и пространственного вектора нормали n, поэтому джозефсоновская связь вида (16.4) невозможна. Однако в этом случае можно рассмотреть связи (лжозефсоновские энергии) болес высоких порядков по η [68]. То жс самое справсдливо для тех ориентаций поверхности, дтя которых выражение (16.4) обращается в нуль по симметрийным соображениям.

Варьируя гралиентную часть (16.2) по A, находим выражения для плотности тока в правом и левом полупространствах:

$$\begin{aligned}
\mathrm{j}_1 &= -c\frac{\delta \mathcal{F}_{1,\mathrm{grad}}}{\delta \mathbf{A}} = -\frac{2\pi c}{\Phi_0} \operatorname{Re} \eta_1^* \left[K_{11}(D_x + D_y) + K_{12} D_z\right] \eta_1 \\
\mathrm{j}_2 &= -c\frac{\delta \mathcal{F}_{2,\mathrm{grad}}}{\delta \mathbf{A}} = -\frac{2\pi c}{\Phi_0} \operatorname{Re} \eta_2^* \left[K_{21}(D_x + D_y) + K_{22} D_z\right] \eta_2
\end{aligned} \tag{16.5}$$

Как и в 13, граничные условия для уравнений Гинзбурга-Ландау на поверхности коптакта получаготся варьированием полшой эпергии (16.2) по η_1^* и η_2^*:

$$\begin{aligned}
i\left[K_{11}(n_{1,x} D_x + n_{1,y} D_y) + K_{12} n_{1,z} D_z\right] \eta_1|_S &= -\,A g_1(\mathbf{n}_1)\, g_2(\mathbf{n}_2)\, \eta_2|_S \\
i\left[K_{21}(n_{2,x} D_x + n_{2,y} D_y) + K_{22} n_{2,z} D_z\right] \eta_2|_S &= -\,A g_1(\mathbf{n}_1)\, g_2(\mathbf{n}_2)\, \eta_1|_S
\end{aligned} \tag{16.6}$$

С помощьо (16.5) и (16.6) находим плотность тока через джозефсоновский контакт:

$$\mathbf{j} = (\mathbf{j}_1 + \mathbf{j}_2)\,\mathbf{n}_1|_S = \frac{4\pi c A}{\Phi_0} g_1(\mathbf{n}_1)\, g_2(\mathbf{n}_2)\, |\eta_1|\, |\eta_2| \sin(\varphi_2 - \varphi_1) \tag{16.7}$$

Согласно формуле (16.7), температурная зависимость максимаьного джозефсоновского тока определяется произведением модулей параметров порядка на границах контакта. Если правое и левое полупространства заняты сверхпроводниками с одинаковыми критическими температурами, и модуль параметра порядка принимает на границе объемное значение, то максимальный джозефсоновский ток пропорционален $T_c - T$. Ощнако, как мы знаем, в необычных сверхпроводниках величина параметра порядка на границе может быть сильно подавлена по сравнению с его объемным значением из-за проигрыиа в поверхностной энергии, что имеет место при условии $f(\mathbf{n}) \neq 0$, где функция $f(\mathbf{n})$ описываст зависимость поверхностной энсргии от ориеитации нормали (см. 13). В этом случае справедлива следующая оценка

$$\eta|_S \sim \frac{b(\mathrm{n})}{\xi(T)} \eta_0(T) \tag{16.8}$$

где $b(\mathrm{n})$ - интерполяционная длина, определяемая формулой (13.7), $\xi(T) \sim \xi_0 (1 - T/T_c)^{-1/2}$ - корреляционная ллина, $\eta_0(T) \propto (1 - T/T_c)^{1/2}$ - объемное значение модуля параметра порядка. Подставлия (16.8) в (16.7), мы видим, что максимальный джозефсоновский ток пропорционален $(T_c - T)^2$, если параметры порядка обоих сверхпроводников подавлены на границах контакта и пропорционалеи $(T_c - T)^{3/2}$, если подавление имеет место только на одной из границ.

Для обвтного сверхпроводящего состодния $g(\mathbf{n})$ преобразуется как базисная функция едиииичного прсдставления A_1, инвариантная относителыно всех преобразований точсчной группы кристалла. Традиииионно считастся, что $g_{A_1}(\mathbf{n})$ полностью изотропна, поэтому джозефсоновский ток не зависит от оринстации контакта по отношению к кристалтическим осям.

Напротив, для необычных свсрхпроводящих состояний $g(\mathbf{n})$ зависит от направления $\mathbf{n}$. Так, для любого из одномерных пеединичных представлений в тетрагональном кристале $g(n)$ мепяет зак при пересечении линии нудей. Например, $g_{B_1}(\mathbf{n}) \propto n_x^2 - n_y^2$ и меняет знак при изменении ориентации

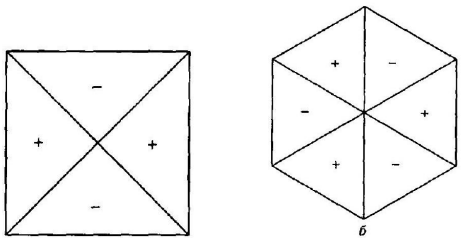


Рис. 13. Знакочередованис функции $g(\mathbf{n})$ для представлсний B_{1_g} па гравях: а) тетрагонатьного и б) гексагонального кристаллов

поверханости от одной боковой грани тетрагонального кристалла к другой (рис. 13а). То же самое происходит в гексагональном кристалде для сверхпроводящего состояния B_1 (рис. 130), поскольку $g_B \propto n_x^3 - 3n_x n_y^2$. Поэтому для контакта обычнного сверхпроводиика с различными боковыми гранями идеального тетрагопального или гексагонального кристала в свсрхпроводящем состоянии B_1 выражение для тока, используя формулу (16.7), можно записать в виде

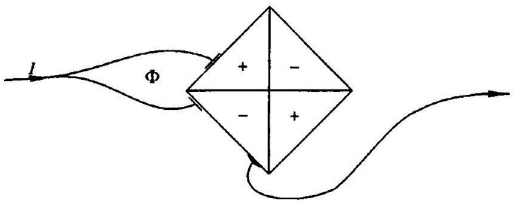
$$I = I_0 \sin(\varphi_1 - \varphi_2 + \pi n) \tag{16.9}$$

где n - номер боковой грани.

Этот результат позволил установить симметрию сверхпроводящего состояния иттриевьх высокотемпературных сверхпроводников. Наиболее надежными выглядят измерения [69, 70] тока через двухконтактный SQUID, в двух джозефсоновских контактах которого провода из обьтчного сверхпроводника (свинсц) подсоединены к двум боковым граням свсрхпроводящего тетрагонального кристалла $YBa_2Cu_3O_{7-x}$ (рис. 14). В предположении, что
контакты 1 и 2 одинаковы, полный ток через SQUID дается выражением

$$I = I_0 \left(\sin \Delta\varphi_1 + \sin \Delta\varphi_2\right) = 2I_0 \sin \frac{\Delta\varphi_1 + \Delta\varphi_2}{2} \cos \frac{\Delta\varphi_1 - \Delta\varphi_2}{2} \tag{16.10}$$

Здесь $\Delta\varphi_1$ и $\Delta\varphi_2$ - скачки фаз на контактах 1 и 2. Их разность, то есть полное измепение фазы параметра порядка при обходе по замкну-



Р и с. 14. Двухконтактны SQUID, подсоединенный к соседним граням тетрагонального кристалта с противоположными знаками параметра порядка

тому контуру SQUID'а, складывается из набега фазы в магнитном поле $(2e/\hbar c) \oint \mathbf{A} d\mathbf{r} = (2\pi\Phi/\Phi_0)$ и «внутрениего» набега фазы δ_{12} между контактамн 1 и 2:

$$\Delta\varphi_1 - \Delta\varphi_2 = \frac{2\pi\Phi}{\Phi_0} + \delta_{12} \tag{16.11}$$

Из формул (16.10) и (16.11) получаем выраженис для максималнного тока как функции внешнего поля:

$$I_{\max} = 2I_0 \cos\left(\frac{\pi\Phi}{\Phi_0} + \frac{\delta_{12}}{2}\right) \tag{16.12}$$

В случас обычной сверхпроводимости в $YBa_2Cu_3O_{7-x}\delta_{12} = 0$, так что в отсутствие внешнего поля ток $I_{\max}(\Phi = 0) = 2I_0$ принимает наибольшее значение. На опыте [69, 70] оказалось, что $I_{\max}(\Phi = 0) = 0$, то есть $\delta_{12} = \pi$, как должно быть в случае необычной синглетной сверхпроводимости, соотвстствующей представлению B_1.

Существование внутреннего набега фазы параметра порядка между боковыми гранями кристалта $YBa_2Cu_3O_{7-x}$ продемонстрировано также прямым измерением полуцелого кванта потока, захваченного сверхпроводящим кольцом, изготовленным из трех иттриевых сверхпроводящих монокристаллов с различной ориентацией [19].

Посколку простейшая функция неприводимого представления B_1 имеет вид

$$g(\mathbf{k}) \propto \hat{k}_x^2 - \hat{k}_y^2 \tag{16.13}$$

то в литературе принято говорить о сверхпроводимости в $YBa_2Cu_3O_{7-x}$ как о сверхпроводимости с d-спариванием (или $d_{x^2} - y^2$-спариванием). Иногда (см. ссылки в работе [18]) также обсуждается так называемое «s + id-спаривание»:

$$g(\mathbf{k}) = \Delta_s + i\Delta_d \left(k_x^2 - k_y^2\right) \tag{16.14}$$

для которого δ_{12} может отклоняться от π в меру отношения Δ_s/Δ_d. Как уже указывалось в 4, фаза вида (16.14) может образоваться непосредственно из

нормального состояния, только если фазовые переходы в сверхпроводящее состояние (нарушение калибровочной симметрии) и в ферромагнитное состояние (нарушение симметрии по отношению к обращению времени) происходят одновременно, для чего не видно особых причин. Поэтому возникновение состояния (16.14) из нормального должо идти через два последоватсльных фазовьдх перехода, что, насколько известио авторам, не наблюдается. Таким образом, интерпретация отклонений δ_{12} от π в терминах смеси s - и d-состояний представляется весьма условной.

19.2 Unconventional Superconductivity by Mineev, V.P. Samokhin, K., part 2

Во второй части книги мы строим теорию необычной сверхпроводимости, используя квантово-полевой подход. Формулировка теории в терминах функций Грина не только придает наглядность и компактиость процедурс вывода основныхх рсзультатов, но и позволяет решать значительно более шхрокчй крут задач, не поддающихся решению методами, изложениыми в первой части. Мы не ставим здесь своей целью систематическое введение в метол функций Грина в теории конденсированного состояния, в частности, в теории обычной свсрхпроволимости (см. [71]), предполагая знакомство читателя с основыыми идеями и понятиями этого метода.

19.2.1 17. Gor'kov Equations

Рассмотрим электрошшый газ с притяжением мсжлу частицами, описываемый следующим гамильтонианом:

$$H = H_0 + H_{\text{int}} = \sum_{\mathbf{k},\mathbf{k}'} (\mathbf{k}\alpha \,|H_0|\, \mathbf{k}'\beta)\, a^+_{\mathbf{k}\alpha} a_{\mathbf{k}'\beta} +$$
$$+\frac{1}{2}\sum_{\mathbf{k},\mathbf{k}',\mathbf{q}} V_{\alpha\beta,\lambda\mu}(\mathbf{k},\mathbf{k}')\, a^+_{-\mathbf{k}+\mathbf{q}/2,\alpha} a^+_{\mathbf{k}+\mathbf{q}/2,\beta} a_{\mathbf{k}'+\mathbf{q}/2,\lambda} a_{-\mathbf{k}'+\mathbf{q}/2,\mu} \tag{17.1}$$
$$H_0 = \frac{1}{2m}\left[-i\nabla + \frac{e}{c}\mathbf{A}(\mathbf{r})\right]^2 + U(\mathbf{r}) - \mu$$

Злссь мы использовали более общее выражение, нежели (5.1), включив в одночастичный гамильтониан H_0 возможную пространственнуто неоднородность системы, возникаюшупо за счет примсссй, поверхности, внешних полей и т. д. Спаривательнос взаимодействие V имеет вил (5.3), (5.7) или (5.8).

Функция Грина сверхпроводника при коиечных температурах (мацубаровская функция Грина) определяется следующим образом:

$$G_{\alpha\beta}(\mathbf{k},\tau_1;\mathbf{k}',\tau_2) = -\left\langle T_\tau a_{\mathbf{k}\alpha}(\tau_1)\, a^+_{\mathbf{k}'\beta}(\tau_2)\right\rangle \tag{17.2}$$

где утловые скобки означаюот гиббсовское усреднение с гамильтонианом (17.1) (см. сноску 4 в §5), $a_{\mathrm{k}\alpha}(\tau) = \exp(\tau H) a_{\mathrm{k}\alpha} \exp(-\tau II)$ - фермионные операторы в мацубаровском предсгавлении, а T'_τ - символ упорядочсния в мнимом времени τ. Через фуікиио Грина (17.2) непосредсгвенно выражаются физические характеристики системы.

Подобно тому, как это деластся в теории обычной сверхпроводимости, иведем еще две, так называемыс аномальные функции Грина:

$$F_{\alpha\beta}(\mathbf{k},\tau_1;\mathbf{k}',\tau_2) = \langle T_\tau a_{\mathbf{k}\alpha}(\tau_1)\, a_{-\mathbf{k}'\beta}(\tau_2)\rangle$$
$$F^+_{\alpha\beta}(\mathbf{k},\tau_1;\mathbf{k}',\tau_2) = \left\langle T_\tau a^+_{-\mathbf{k}\alpha}(\tau_1)\, a^+_{\mathbf{k}'\beta}(\tau_2)\right\rangle \tag{17.3}$$

Отличие от нуля аномальных средних следует из того, что в присутствии бозекондегсата купсровских пар рождснис илі унитгожепис пары электронов практичссски не меняет состояние системы (см. 5). В диаграммной технике нормальные и аномальныс функции Грина (17.2) и (17.3) изображаются липиями со стрелками (рис. 15).

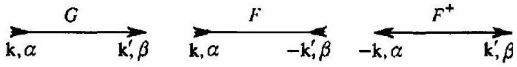


Рис. 15. Графичсскос изображение нормтьной и аномалыных функций Грина

При рассмотрснии статических задач фупкции Грина зависят лишь or разности мнимых времеIi $\tau_1 - \tau_2 = \tau$, и удобно перейти в импульспо-частотное представдение:

$$G_{\alpha\beta}\left(\mathbf{k},\mathbf{k}':\tau\right) = T\sum_n G_{\alpha\beta}\left(\mathbf{k},\mathbf{k}';\omega_n\right)e^{-i\omega_n\tau} \qquad \text{ит.д.}$$

где $\omega_n = (2n+1)\pi T$ - фермионная мацубаровская частота.

Функции G и F удовлетворяют систсме лиффсрснциалышьх уравнений, к выводу которой мы и переходим. Воспользуемся уравнениями движения для операторов $a_{\mathbf{k}\alpha}$:

$$\frac{\partial a_{\mathrm{ka}}}{\partial\tau} = [H, a_{\mathrm{k}\alpha}]$$

Дифференцируем фуікцпо G (17.2) по τ:

$$\frac{\partial G_{\alpha\beta}\left(\mathbf{k},\mathbf{k}';\tau\right)}{\partial\tau} = -\left\langle T_\tau\left[H(\tau), a_{\mathbf{k}\alpha}(\tau)\right]a^+_{\mathbf{k}'\beta}(0)\right\rangle - \delta(\tau)\delta\left(\mathbf{k}-\mathbf{k}'\right)\delta_{\alpha\beta}$$

Подставляя соода гамильтониау (17.1) и используя свойство (5.2), получаем:

$$\frac{\partial G_{\alpha\beta}\left(\mathbf{k},\mathbf{k}';\tau\right)}{\partial\tau} = -\sum_{\mathbf{k}_1}\left(\mathbf{k}\alpha\left|H_0\right|\mathbf{k}_1\gamma\right)G_{\gamma\beta}\left(\mathbf{k}_1,\mathbf{k}'\right) -$$
$$-\sum_{\mathbf{k}_1,\mathbf{q}} V_{\gamma_1\alpha,\gamma_2\gamma_3}\left(\mathbf{k},\mathbf{k}_1\right)\left\langle T_\tau a^+_{-\mathbf{k}+\mathbf{q},\gamma_1}(\tau)a_{\mathbf{k}_1+\mathbf{q}/2,\gamma_2}(\tau)a_{-\mathbf{k}}+\mathbf{q}/2,\gamma_3(\tau)a^+_{\mathbf{k}'\beta}(0)\right\rangle -$$
$$-\delta(\tau)\delta\left(\mathbf{k}-\mathbf{k}'\right)\delta_{\alpha\beta}.$$

Следующий шаг состоит в преобразовапии точного уравнения (17.4) с помощыо расцепления стоящей в правой части двухчаститной фупкции Грипа по следующему рецепту (приближепие средпего поля):

$$\left\langle T_\tau a^+_{-\mathbf{k}+\mathbf{q},\gamma_3}(\tau)a_{\mathbf{k}_1+\mathbf{q}/2,\gamma_2}(\tau)a_{-\mathbf{k}_1+\mathbf{q}/2,\gamma_3}(\tau)a^+_{\mathbf{k}'\beta}(0)\right\rangle \to$$
$$\to\left\langle I_\tau a^+_{-\mathbf{k}+\mathbf{q},\gamma_1}(\tau)a^+_{\mathbf{k}'\beta}(0)\right\rangle\left(T_\tau a_{\mathbf{k}_1+\mathbf{q}/2\cdot\gamma_2}(\tau)a_{-\mathbf{k}_1+\mathbf{q}/2,\gamma_3}(\tau)\right\rangle$$

Остальныс слагаемые в данном расцеплении дают линь алиитивную добавку к входящему в H_0 химическому потенциалу, и поэтому не учитываются.

Введем теперь функциго, являющуюся параметром порядка сверхпроводника:

$$\Delta_{\alpha\beta}(\mathbf{k},\mathbf{q}) = -\sum_{\mathbf{k}'} V_{\beta\alpha,\lambda\mu}\left(\mathbf{k};\mathbf{k}'\right)F_{\lambda\mu}\left(\mathbf{k}'+\frac{\mathbf{q}}{2},\tau;\mathbf{k}'-\frac{\mathbf{q}}{2},\tau\right) =$$
$$= -T\sum_n\sum_{\mathbf{k}'} V_{\beta\alpha,\lambda\mu}\left(\mathbf{k},\mathbf{k}'\right)F_{\lambda\mu}\left(\mathbf{k}'+\frac{\mathbf{q}}{2},\mathbf{k}'-\frac{\mathrm{q}}{2};\omega_n\right) \qquad (17.5)$$

а также

$$\Delta^+_{\lambda,}(\mathbf{k},\mathbf{q}) = -T\sum_n\sum_{\mathbf{k}'} V_{\alpha\beta,\mu\lambda}\left(\mathbf{k}';\mathbf{k}\right)F^+_{\alpha\beta}\left(\mathbf{k}'-\frac{\mathbf{q}}{2},\mathbf{k}'+\frac{\mathbf{q}}{2};\omega_n\right)$$

После этого уравнение для функции Грина G в импульсно-частотном прелставлении окончатеьо переписывается в виде

$$\sum_{\mathbf{k}_1} \left(\mathbf{k}\alpha \left| i\omega_n - H_0 \right| \mathbf{k}_1\gamma\right) G_{\gamma\beta}\left(\mathbf{k}_1, \mathbf{k}'; \omega_n\right) + \sum_{\mathbf{q}} \Delta_{\alpha\gamma}(\mathbf{k}, \mathbf{q}) F^{+}_{\gamma\beta}\left(\mathbf{k} - \mathbf{q}, \mathbf{k}'; \omega_n\right) = \\ = \delta\left(\mathbf{k} - \mathbf{k}'\right)\delta_{\alpha\beta} \tag{17.6}$$

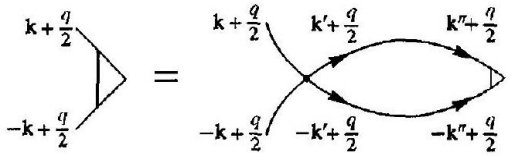
Рассуждая аналогичным образом, получаем уравнения для аномашных фукций Грина:

$$\sum_{\mathbf{k}_1} \left\langle -\mathbf{k}_1\gamma \left| i\omega_n + H_0 \right| - \mathbf{k}\alpha \right\rangle F^{+}_{\gamma\beta}\left(\mathbf{k}_1, \mathbf{k}'; \omega_n\right) + \\ + \sum_{\mathbf{q}} \Delta^{+}_{\alpha\gamma}(\mathbf{k}, \mathbf{q}) G_{\gamma\beta}\left(\mathbf{k} + \mathbf{q}, \mathbf{k}'; \omega_{r_n}\right) = \mathbf{0} \tag{17.7}$$

$$\sum_{\mathbf{k}_1} \left(\mathbf{k}\alpha \left| i\omega_n - H_0 \right| \mathbf{k}_1\gamma\right) F_{\gamma\beta}\left(\mathbf{k}_1, \mathbf{k}'; \omega_n\right) - \\ - \sum_{\mathbf{q}} \Delta_{\alpha\gamma}(\mathbf{k}, \mathbf{q}) G_{\beta\gamma}\left(-\mathbf{k}', -\mathbf{k} + \mathbf{q}; -\omega_n\right) = 0 \tag{17.8}$$

Уравнсния (17.6)-(17.8) (дифференциальныс в координатном представлении) называются уравиениями Горькова и составляют, вместе с условием согласования (17.5), основу тсоретичсского описания сверхпроводников.

В далынейшем нам часто придется использовать уравнение, определягощсе темпера-



туру сверхпроводящего персхода T_c для различных ситуаций (Iапример, в присутствие примесей или внешнего магнитного поля), получающееся из уравыений Горькова следутощим образом. Вблизи T_c параметр порядка мал и можно, используя (17.6) и (17.8), разложить аномальнуо фупкцию Грина F до первой степени по Δ, а затем подставить в условис согласования. При этом мы приходим к следующему уравнению:

$$\Delta_{\alpha\beta}(\mathbf{k}, \mathbf{q}) = -T_\mathrm{c} \sum_n \sum_{\mathbf{k}', \mathbf{k}'', \mathbf{q}'} V_{\beta\alpha,\lambda\mu}\left(\mathbf{k}, \mathbf{k}'\right) G^{(0)}_{\lambda\gamma}\left(\mathbf{k}' + \frac{\mathbf{q}}{2}, \mathbf{k}'' + \frac{\mathbf{q}'}{2}; \omega_n\right) \times \\ \times G^{(0)}_{\mu\delta}\left(-\mathbf{k}' + \frac{\mathbf{q}}{2}, -\mathbf{k}'' + \frac{\mathbf{q}'}{2}; -\omega_n\right) \Delta_{\gamma\delta}\left(\mathbf{k}'', \mathbf{q}'\right) \tag{17.9}$$

где $G^{(0)}$ есть функция Грина нормального металла с учетом всех внешних полей. Соответствутощее диаграммное выражение изображено на рис. 16. Критическая температура определяется как температура, при которой у линейного интегрального уравнения (17.9) появляется ненулевое решснис.

Для практичсских вычислсний важно знать функцдии Грина пространственно-однородной системы в опсутствие внешних возмущений. В этом случае уравнепия Горькова значительно упрощаются:

$$G_{\alpha\beta}\left(\mathbf{k}, \mathbf{k}'; \omega_n\right) = G_{\alpha\beta}\left(\mathbf{k}, \omega_n\right)\delta\left(\mathbf{k} - \mathbf{k}'\right) \quad \text{и т. д.} \tag{17.10}$$

Следоватешно, параметр порядка зависит лишь от направлсния импульсов $\hat{k}$ на повсрхности Ферми, но ие от прострапственных координат:

$$\Delta_{\alpha\beta}(\mathbf{k}, \mathbf{q}) = \Delta_{\alpha\beta}(\mathbf{k})\delta(\mathbf{q})$$

причем

$$\Delta_{\alpha\beta}(k) = -\Delta_{\beta\alpha}(-k)$$

Легко видеть, что ввсдснные в §5 аномальные средние пепосредственно выражатотся через функшии Грина однородной системы при совпадающих временніх аргумеIітах:

$$F_{\mathbf{k},\alpha\beta} = F_{\alpha\beta}(\mathbf{k},\tau;\mathbf{k},\tau) = T\sum_n F_{\alpha\beta}\left(\mathbf{k},\omega_n\right)$$
$$F^+_{\mathbf{k},\alpha\beta} = T\sum_n F^+_{\alpha\beta}\left(\mathbf{k},\omega_n\right)$$

Подставляя (17.10) в уравнения (17.6)-(17.8) и учитывая, что одночастичный гамилтониан певозмушенной системы диагопален по импупсам и спинам:

$$\langle \mathbf{k}\alpha \left|H_0\right| \mathbf{k}'\beta\rangle = \xi_{\mathbf{k}}\delta\left(\mathbf{k}-\mathbf{k}'\right)\delta_{\alpha\beta}$$

причем $\xi_{\mathbf{k}} = \xi_{-\mathbf{k}}$, получаем

$$\begin{aligned}
\left(i\omega_n - \xi_k\right) G_{\alpha\beta}\left(\mathbf{k},\omega_n\right) + \Delta_{\alpha\gamma}(\mathbf{k}) F^+_{\gamma\beta}\left(\mathbf{k},\omega_n\right) &= \delta_{\alpha\beta} \\
\left(i\omega_n + \xi_k\right) F^+_{\alpha\beta}\left(\mathbf{k},\omega_n\right) + \Delta^+_{\alpha\gamma}(\mathbf{k}) G_{\gamma\beta}\left(\mathbf{k},\omega_n\right) &= 0 \\
\left(i\omega_n - \xi_k\right) F_{\alpha\beta}\left(\mathbf{k},\omega_n\right) - \Delta_{\alpha\gamma}(\mathbf{k}) G_{\beta\gamma}\left(-\mathbf{k},-\omega_n\right) &= 0
\end{aligned} \tag{17.11}$$

Решение данной алгебраической системы уравнений выглядит следующим образом:

$$\begin{aligned}
G_{\alpha\beta}\left(\mathbf{k},\omega_n\right) &= -\left(i\omega_n + \xi_k\right)\left[\omega_n^2 + \xi_k^2 + \Delta(\mathbf{k})\Delta^+(\mathbf{k})\right]^{-1}_{\alpha\theta} \\
F_{\alpha\beta}\left(\mathbf{k},\omega_n\right) &= \Delta_{\alpha\gamma}(\mathbf{k})\left[\omega_n^2 + \xi_k^2 + \left(\Delta^+(\mathbf{k})\Delta(\mathbf{k})\right)\right]^{-1}_{\gamma\beta}
\end{aligned} \tag{17.12}$$

Для всех свсрхпроводящих фаз с синглетным спариванием, а также для унитарных фаз с триплетным спариванием, выполняется условие $\left(\Delta\Delta^+\right)_{\alpha\beta} \propto \delta_{\alpha\beta}$, и функции Грина принимагот вид

$$\begin{aligned}
G_{\alpha\beta}\left(\mathbf{k},\omega_n\right) &= -\frac{i\omega_n + \xi_k}{\omega_n^2 + \xi_k^2 + \Delta_k^2}\delta_{\alpha\beta} \\
F_{\alpha\beta}\left(\mathbf{k},\omega_n\right) &= \frac{\Delta_{\alpha\beta}(\mathbf{k})}{\omega_n^2 + \xi_k^2 + \Delta_k^2}
\end{aligned} \tag{17.13}$$

где

$$\Delta^2_{\mathbf{k}} = \frac{1}{2}\,\mathrm{Sp}\,\Delta^+(\mathbf{k})\Delta(\mathbf{k})$$

Отсюдда для функшии Грина нормального состояния (то есть при $\Delta = 0$) мы получаем

$$G^{(0)}_{\alpha\beta}\left(\mathbf{k},\omega_n\right) = \frac{\delta_{\alpha\beta}}{i\omega_n - \xi_k} \tag{17.14}$$

Для неунитарных фаз с триплетным спариванием

$$\left(\Delta\Delta^+\right)_{\alpha\beta} = \Delta^2\left(\mathrm{dd}^*\,\delta_{\alpha\beta} + \mathbf{m}\sigma_{\alpha\beta}\right)$$

здесь $\mathrm{m}(\mathbf{k}) = i\,\mathrm{d}(\mathbf{k}) \times \mathrm{d}^*(\mathbf{k}) \neq 0$, и выражения для функций Грина сверхпровопшика выглялят иесколько сложнее:

$$G_{\alpha\beta}\left(\mathbf{k},\omega_n\right)=-\left(i\omega_n+\xi_k\right)\frac{\left(\omega_n^2+\xi_k^2+\Delta^2|\ \mathrm{d}(\mathbf{k})|^2\right)\delta_{\alpha\beta}+\Delta^2\ \mathrm{m}(\mathbf{k})\sigma_{\alpha\beta}}{\left(\omega_n^2+E_{\mathrm{k},-}^2\right)\left(\omega_n^2+E_{k,-}^2\right)}$$

$$F_{\alpha\beta}\left(\mathbf{k},\omega_n\right)=\Delta\left(i\sigma\sigma_y\right)_{\alpha\beta}\frac{\left(\omega_n^2+\xi_k^2+\Delta^2|\ \mathrm{d}(\mathrm{k})|^2\right)\mathrm{d}(\mathbf{k})-i\Delta^2\ \mathrm{m}(\mathbf{k})\times\mathrm{d}(\mathbf{k})}{\left(\omega_n^2+E_{\mathbf{k},\mathrm{t}}^2\right)\left(\omega_n^2+E_{k,-}^2\right)} \tag{17.15}$$

где

$$E_{\mathbf{k},\pm}=\sqrt{\xi_k^2+\Delta^2\left(|\ \mathrm{d}(\mathbf{k})|^2\pm|\mathrm{m}(\mathbf{k})|\right)} \tag{17.16}$$

Уравненис, определяющщее температурное поведение параметра порядка, получается подстановкой выражения (17.13) для функции P в условис согласования (17.5):

$$\Delta_{\alpha\beta}(\mathbf{k})=-T\sum_n\sum_{k'}V_{\beta\alpha,\gamma\delta}\left(\mathbf{k},\mathbf{k}'\right)\frac{\Delta_{\gamma\delta}\left(\mathbf{k}'\right)}{\omega_n^2+\xi_{k'}^2+\Delta_{\mathbf{k}'}^2} \tag{17.17}$$

(аналогитным образом может быть получено и соответствующее уравненис в случае неунитарных фаз (см. [13]). Дчя вычисления суммы по частотам в (17.17) воспользусмся формулой

$$\sum_{n=-\infty}^{\infty}\frac{1}{(2n+1)^2\pi^2+x^2}=\frac{1}{2x}\ln\frac{x}{2} \tag{17.18}$$

Из (17.17) получаем:

$$\Delta_{\alpha\beta}(\mathrm{k})=-\sum_{\mathbf{k}'}V_{\beta\alpha,\gamma\delta}\left(\mathrm{k},\mathrm{k}'\right)\Delta_{\gamma\delta}\left(\mathrm{k}'\right)\frac{1}{2E_{\mathrm{k}'}}\ \mathrm{th}\left(\frac{E_{\mathrm{k}'}}{2T}\right) \tag{17.19}$$

откуда, учитывая, что $\mathrm{th}\ \left(E_{\mathbf{k}'}/2T\right)\ =\ 1-2f_{\mathbf{k}'}$, где $f_{\mathbf{k}'}$ - фермиевская функция распределения, возвращаемся к формулам (6.5) и (6.6). Уравпенис, определяющее критическуо температуру T_c, получается пугем подстановки $\Delta\ =\ 0$ (1. с. замены $E'_{\mathbf{k}'}\to|\varepsilon_{k'}|$) в (17.19).

Техника функций Грина для сверхпроводника может быть сформудирована в болсе компактном виде, формалыо напоминаоощсм диаграммную техику аля нормальной ферми-жидкости, если объединить G,F и F^+в
одну матричную функцию Грина $\hat{G}$, используя векторные операторы (5.23) в мацубаровском представлении. По опредслснию:

$$\hat{G}\left(\mathbf{k}_1,\mathbf{k}_2;\omega_n\right)=-\int_0^{1/T}d\tau e^{i\omega_n\tau}\left\langle T_\tau A_{\mathbf{k}_1}(\tau)A^+_{\mathbf{k}_2}(0)\right\rangle=$$

$$=\begin{pmatrix}G_{\alpha\beta}\left(\mathbf{k}_1,\mathbf{k}_2;\omega_n\right) & -F_{\alpha\beta}\left(\mathbf{k}_1,\mathbf{k}_2;\omega_n\right)\\ -F^+_{\alpha\beta}\left(\mathbf{k}_1,\mathbf{k}_2;\omega_n\right) & -G_{\beta\alpha}\left(-\mathbf{k}_2,-\mathbf{k}_1;-\omega_n\right)\end{pmatrix} \tag{17.20}$$

Матричные элементы $\hat{G}$ являотся, в свою очередь, матрицами 2×2 в спиновом пространстве. В пространственно-однородном случае имеем (см. (17.12)):

$$\hat{G}_0\left(\mathbf{k},\omega_n\right)=-\frac{1}{\omega_n^2+\xi_k^2+\Delta_k^2}\begin{pmatrix}\left(i\omega_n+\xi_k\right)\delta_{\alpha\beta} & \Delta_{\alpha\beta}(\mathbf{k})\\ \Delta^+_{\alpha\beta}(\mathbf{k}) & \left(i\omega_n-\xi_k\right)\delta_{\alpha\beta}\end{pmatrix}=$$

$$=-\frac{i\omega_n\hat{\tau}_0+\xi_k\hat{\tau}_3+\dot{\Delta}(\mathbf{k})}{\omega_n^2+\xi_k^2+\Delta_k^2} \tag{17.21}$$

где $\hat{\tau}_i$ - матрицы Паули в «пространстве» частица-дырка.

Спектральное представление и элергии возбуждепий. При решении конкретных задач необходимо уметь вычислять суммы по мацубаровским частотам. Для этого удобно использовать так называемое спектралыно разложение функций Грина, которое в матричных обозначениях имеет вид

$$\hat{G}\left(\mathbf{k}, \omega_n\right) = \int\limits_{-\infty}^{+\infty} \frac{dz}{2\pi} \frac{\hat{\rho}(\mathbf{k}, z)}{i\omega_n - z}$$

После этого суммы по фермионным частотам легко вычисляются с помощью тождества (ср. с (17.18))

$$T \sum_n \frac{1}{i\omega_n - z} = \frac{1}{2} \text{ th } \frac{z}{2T} \tag{17.22}$$

Вещественная спектралыая плотность $\hat{\rho}$ выражается черсз фурьс-образы запаздываощих и опережаіощих функций Грина [1] следующим образом:

$$\hat{\rho}(\mathbf{k}, \omega) = -2 \operatorname{Im} \hat{G}^R(\mathbf{k}, \omega) = i \left(\hat{G}^R(\mathbf{k}, \omega) - \hat{G}^A(\mathbf{k}, \omega) \right)$$

В свою очередь, запаздывающис (опережающие) функции Грина получаюотся из $\hat{G}\left(\mathbf{k}, \omega_n\right)$ путем аналитического прододжения па верхнюю (нижнюю) полуплоскость комплекстіхх ω:

$$\hat{G}^{R(\boldsymbol{A})}(\mathbf{k}, \omega) = \hat{G}\left(\mathbf{k}, \omega_n\right)\Big|_{i\omega_n \to \omega \pm i0} \tag{17.23}$$

Спектр элементарнцх возбуждений сверхпроводника определяется полюсами функции G^R. Выполняя аналитическое продолжение в (17.13), получаем уравнение, опрспсляющсе спектр:

$$\det \left\| E^2 - \xi_k^2 - \Delta(\mathbf{k}) \Delta^+(\mathbf{k}) \right\| = 0 \tag{17.24}$$

Подставляя сюда выражения (5.18) и (5.20), получаем, что энергии возбуждени даются формулами

$$E_{\mathbf{k}} = \sqrt{\xi_k^2 + \Delta^2 |g(\mathbf{k})|^2}$$

для синглетого спаривания и

$$E_{\mathbf{k}} = \sqrt{\xi_k^2 + \Delta^2 |\ \mathrm{d}(\mathbf{k})|^2}$$

для унитарных фаз с триплетньм спариванием, то есть возвращаемся к результатам (5.33) и (5.34).

Для неунитарных фаз спектр возбуждений расщепляется на две ветви аналогично тому, как это происходит в обычных магнитных материалах, поскольку неунитарные фазы обладают собственным магнитиым моментом:

$$E_{\mathrm{k},\pm} = \sqrt{\xi_k^2 + \Delta^2 \left(|\ \mathrm{d}(\mathbf{k})|^2 \pm |\mathrm{d}^*(\mathbf{k}) \times \mathrm{d}(\mathbf{k})| \right)} \tag{17.25}$$

Отсюда следует, что положение нулей спектра возбуждений для любых фаз триплетного спаривания определяется уравнением $\det \Delta(k) = 0$, то есть $\mathrm{d}^2(\mathbf{k}) = 0$.

[11] Наломним, тто функцни $\hat{G}^R \left(\hat{G}^A \right)$ отличаюгся от мацубаровской функции $\hat{G}$ (17.20) заменой τ-упорядоченного пронзведекия опсраторов на их запаздывающие (опережаюиие) антикоммутаторы.

Плотность состоянии. Плотность состояний квазичастиц по определению

$$N(E) = \sum_{\mathbf{k}\alpha} \delta\left(E - E_{\mathbf{k}}\right) \tag{17.26}$$

Эта величина следующим образом вьражается через функцию Грина:

$$N(E) = \frac{1}{2\pi} \sum_{\mathbf{k}\alpha} \rho(\mathbf{k}, E) = -\frac{1}{\pi} \operatorname{Im} \sum_{\mathbf{k}\alpha} G\left(\mathbf{k}, \omega_n\right) \Big|_{i\omega_n \to E + i0} \tag{17.27}$$

Из (17.26), с учетом вырaженiя (5.29) для спектра возбуждений, получаем:

$$\begin{aligned} N\left(E'\right) &= 2 \int \frac{d^3k}{(2\pi)^3} \delta\left(E - E_{\mathbf{k}}\right) = 2N_0 \int \frac{d\Omega}{4\pi} \int d\xi \delta\left(E - E_{\mathbf{k}}\right) = \\ &= 2N_0 \int \frac{d\Omega}{4\pi} \frac{dE'' E'}{\sqrt{E'^2 - \Delta_{\mathbf{k}}^2}} \delta\left(E' - E'\right) = 2N_0 \int \frac{d\Omega}{4\pi} \frac{E}{\sqrt{E^2 - \Delta_{\mathbf{k}}^2}} \end{aligned} \tag{17.28}$$

где N_0 есть плотность состояний на урозне Ферми в нормалыном металле на одну проекдию спина, а интсгрирование по утлам производится в пределах $\Delta_{\mathbf{k}}^2 < E^2$.

Для обычного изотропного свсрхпроводника с s-спариванием ($g(\mathbf{k}) = 1$) из (17.28) следует, что

$$N(E) = 2N_0 \begin{cases} 0, & \text{при } E < \Delta \\ \frac{E}{\sqrt{E^2 - \Delta^2}}, & \text{при } E > \Delta \end{cases} \tag{17.29}$$

то есть плотность квазичастичных состояний тождественно обращается в нуль при $E < \Delta$.

Посмотрим теперь, что изменится, если в спектре возбуждений имеются нули. В качестве примера рассмотрим сверхпроводник со структурой A-фазы,
параметр порядка в котором имеет вид (3.8), то есть щель обращастся в нуль на северном и юожном полюсах ферми-поверхности. Из (17.28) получаем:

$$N(E) = 2N_0 \int \frac{d\Omega}{4\pi} \frac{E}{\sqrt{E^2 - \Delta^2\left(\hat{k}_x^2 + \hat{k}_y^2\right)}} = N_0 \int \sin\theta d\theta \frac{E}{\sqrt{E^2 - \Delta^2 \sin^2\theta}}$$

причем $\sin\theta < E/\Delta$. При $E \to 0$ основной вклад в интеграл дают окрестности полюосов $\theta < E/\Delta$ и $\pi - \theta < E/\Delta$, следовательно,

$$N(E) \approx N_0 \int_0^{E/\Delta} 0 d\theta \frac{E}{\sqrt{E^2 - \Delta^2\theta^2}} \sim N_0 \left(\frac{E}{\Delta}\right)^2 \tag{17.30}$$

Таким образом, мы имеем ненулевуюо плотность состояний.

Можно убедиться в том, что если щепь в спектре обращается в нуль на целой линии (это имест место, например, для сверхпроводника со структурой полярной фазы), то

$$N(E) \sim N_0 \frac{E}{\Delta}. \tag{17.31}$$

Подобные степенные зависимости плотности состояний квазичастиц от энергии приводят к степенному (а не экспоненциальному) гемпературному поведению термодинамических и кинетических характеристик теобычных сверхпроводников.

19.2.2 18. Ginzburg–Landau Functional

Полученные в предыдущем параграфе уравнения для функций Грина сверхпроводника - уравнения Горькова - позволяют в принципе полностью описать свойства сверхпроводящего состояния. На практике, однако, существует широкий крут задач, в которых нет необходимости использовать эти достаточно сложные уравнения непосредственно. В частности, вблизи критической температуры, когда малы как сам сверхтроводящий параметр порядка ($\Delta \propto (T_c - T)^{1/2}$), так и его градиенты (то есть $\Delta(\mathrm{r})$ медленно меняяется на характсрном масштабе теории сверхпроводимости - размере куперовской пары ξ_0), удобно использовать уравения Гинзбурга-Лашдау (см. 12). Эти уравнения проще всего вывести с использованием техники функций Грина, вычисляя свободную энсргию сверхпроводника $\mathcal{F}_\mathrm{s}$ как функционал от параметра порядка, с последующей ее минимизацией по Δ.

Мы рассмотрим в качестве примера сверхпроводник с p-спариванием вблизи критической температуры в отсутствие примесей (см. [72]), для которого потенциал спаривательного взаимодействия, входящий в гамильтониан (17.1), выгдядит следугощим образом:

$$V(\mathbf{k}, \mathbf{k}') = -3V \frac{\mathbf{k}\mathbf{k}'}{k_\mathrm{F}^2} \tag{18.1}$$

где константа связи V отлична от нуля лишь в узком слое толщиной ε_1 вблизи ферми-сферы (см.)5.4)).

Свободная энергия определяется формупой $\mathcal{F} = -T \ln Z$, где $Z = \mathrm{Sp}\left(e^{-\beta H}\right)$ есть статистическая сумма1. Для гамитьтониапа H мы используем соответствующес приближению среднего поля выражение (5.22), переписав его в виде, содержащем только сверхпроводящий парамстр порядка Δ и фермионньге операторы рождения и уiичтожешия:

$$\begin{aligned} H = \sum_{\mathbf{k}} \xi_k a^+_{\mathbf{k}\alpha} a_{\mathbf{k}\alpha} + \frac{1}{2V} \sum_{\mathbf{k},\mathbf{q}} S_p \Delta^+(\mathbf{k},\mathbf{q}) \Delta(\mathbf{k},\mathbf{q}) + \\ + \frac{1}{2} \sum_{\mathbf{k},\mathbf{q}} \Big(\Delta_{\alpha\beta}(\mathbf{k},\mathbf{q}) a^+_{\mathbf{k}+\mathbf{q}/2,\alpha} a^+_{-\mathbf{k}+\mathbf{q}/2,\beta} + \\ + \Delta^+_{\alpha\beta}(\mathbf{k},\mathbf{q}) a_{-\mathbf{k}+\mathbf{q}/2,\alpha} a_{\mathbf{k}+\mathbf{q}/2,\beta} \Big) \end{aligned} \tag{18.2}$$

В отличие от (5.22), здесь учтена возможная пространственшая неоднородность парамстра порядка [2]

Рассматривая содержашие Δ слагаемыс в (18.2) как возмущение $\hat{H}_\mathrm{int}$ и переходя к мацубаровскому представлению, разложим разность свободных энергий свсрхпроводящсго и нормального состояний

$$-T \ln \left\langle \exp \left[-\int_0^{1/\tau} d\tau \hat{\Pi}_\mathrm{int}(\tau) \right] \right\rangle$$

вплоть до членов тетвертой степени по Δ. Имеем:

$$\mathcal{F}_\mathrm{cond} = \mathcal{F}_\mathrm{s} - \mathcal{F}_\mathrm{n} = \frac{1}{2V} \int d^3 r \int \frac{d\Omega}{4\pi} \mathrm{Sp}\, \Delta^+(\mathbf{k},\mathbf{r}) \Delta(\mathbf{k},\mathbf{r}) + \mathcal{F}_2 + \mathcal{F}_4 \tag{18.3}$$

Здесь

$$\Delta_{\lambda\mu}(\mathbf{k},\mathbf{r}) = \int \frac{d^3q}{(2\pi)^3}\Delta_{\lambda\mu}(\mathbf{k},\mathbf{q})e^{i\mathbf{qr}} = (i\sigma_\alpha\sigma_y)_{\lambda\mu} A_{\alpha i}(\mathbf{r})\hat{k}_i \tag{18.4}$$

• параметр порядка сверхпроводника с p-спариванием,

$$\mathcal{F}_2 = -\int d^3r_1 d^3r_2 A^*_{\alpha i}(\mathbf{r}_1)\, S_{ij,\alpha\beta}(\mathbf{r}_1,\mathbf{r}_2)\, A_{\beta j}(\mathbf{r}_2) \tag{18.5}$$

где ядро S выглядит следуоошим образом:

$$S_{ij,\alpha\beta}(\mathbf{r}_1,\mathbf{r}_2) = \lim_{\mathbf{r}'_{1,2}\to\mathbf{r}_{1,2}} \frac{T}{4k_\mathrm{F}^2}\sum_n \left(\frac{\partial}{\partial r_{1,i}} - \frac{\partial}{\partial r'_{1,i}}\right)\left(\frac{\partial}{\partial \mathbf{r}_{2,j}} - \frac{\partial}{\partial r'_{2,j}}\right)\times$$
$$\times (\sigma_y\sigma_\alpha)_{\lambda\mu} G^{(0)}_{\lambda\gamma}(\mathbf{r}_1,\mathbf{r}_2;\omega_n)(\sigma_\beta\sigma_y)_{\gamma\delta} G^{(0)}_{\mu\delta}(\mathbf{r}'_1,\mathbf{r}'_2;-\omega_n) \tag{18.6}$$

Входящие сюда фуункции $G^{(0)}$ прелставляюот собой функции Грина нормального металла с учетом взаимодействия как зарядов, так и спинов элсктронов с внешним магнитным полем. Наконец члеI четвертого порядка в разложении свободной энергии имеет вид

$$\mathcal{F}_4 = \frac{1}{4}T_\mathrm{c}\sum_n\sum_{\{\mathbf{q}_\mathrm{i}\}}\sum_{\mathbf{k}} \mathrm{Sp}\,\Delta^+(\mathbf{k},\mathbf{q}_1)\, G^{(0)}(\mathbf{k},\omega_n)\times$$
$$\times\,\Delta(\mathbf{k},\mathbf{q}_2)\, G^{(0)}(-\mathbf{k},-\omega_n)\,\Delta^+(\mathbf{k},\mathbf{q}_3)\, G^{(0)}(\mathbf{k},\omega_n)\times$$
$$\times\,\Delta(\mathbf{k},\mathbf{q}_4)\, G^{(0)}(-\mathbf{k},-\omega_n)\,\delta(\mathbf{q}_1+\mathbf{q}_3-\mathbf{q}_2-\mathbf{q}_4) \tag{18.7}$$

Все импупшсы $\mathbf{q}_i$ в функциях Грина положены равными пгулго, так как рассмотрение конечных импульсов пужно лишь при вычислении градиентных члснов чствертой степени по Δ, которыс нас нс интсрссуот.

Если пренебречь дсйствием поля на спины электронов (мы вернемся к этому вопросу позже), то

$$G^{(0)}_{\lambda\gamma}(\mathbf{r}_1,\mathbf{r}_2;w_n) = G^{(0)}(\mathbf{r}_1,\mathbf{r}_2;w_n)\,\delta_{\lambda\gamma}$$

Для квадратичного закона дисперсии при $H=0$ фурье-образ выражсния (17.14) есть

$$G^{(0)}(\mathbf{r},\omega_n) = -\frac{\pi N_0}{k_\mathrm{F} r}\exp\left(ik_\mathrm{F} r\sqrt{1+\frac{i\omega_n}{\varepsilon_\mathrm{F}}}\,\mathrm{sign}\,\omega_n\right)\approx$$
$$\approx -\frac{\pi N_0}{k_\mathrm{F} T}\exp\left(ik_\mathrm{F} r\,\mathrm{sign}\,\omega_n - \frac{|\omega_n|}{v_\mathrm{F}}r\right) \tag{18.8}$$

При $\Delta=0$, но $H\neq 0$, из (17.6) получаем следующее уравнение для функции Грина G:

[11] Более точио, таким образом определяется термодинамический нотенциал Ω, однако, согласно обшим принципам термодинамики, разность $\Omega_\mathrm{s}-\Omega_\mathrm{n}$ равна разности свободных энергий $\mathcal{F}_\mathrm{s}-\mathcal{F}_\mathrm{n}$.

[2] В общем случае второе слагаемое в правой части (18.2) имеет вид:

$$-\frac{1}{2}S_\mathbf{p}\sum \Delta^+(\mathbf{k},q)\hat{V}^{-1}(\mathbf{k},\mathbf{k}')\,\Delta(\mathbf{k}',q)$$

где $\dot{V}^{-1}$ удовлетворяет урависнию $\sum\limits_{\mathbf{k}''}\hat{V}^{-1}(\mathbf{k},\mathbf{k}'')\,\hat{V}(\mathbf{k}'',\mathbf{k}') = \delta(\mathbf{k}-\mathbf{k}')$. Используя ортогоналыость и полноту системы базиспих функций, приходим к выраженик (18.2).

$$\left[i\omega_n - \frac{h^2}{2m}\left(-i\frac{\partial}{\partial \mathbf{r}_1} + \frac{e}{\hbar c}\mathbf{A}\left(\mathbf{r}_1\right)\right)^2 + \epsilon_{\mathbf{F}}\right] G^{(0)}\left(\mathbf{r}_1, \mathbf{r}_2; \omega_n\right) = \delta\left(\mathbf{r}_1 - \mathbf{r}_2\right)$$

В последующих выкладках мы используем систему сдиниц, в которой $\hbar = 1$, при необходимости восстапавливая постоянную Планка в окогчателыных ответах.

Ищем решение этого уравнения в виде $G^{(0)}\left(\mathbf{r}_1, \mathbf{r}_2; \omega_n\right) =$

$$= G^{(0)}\left(\mathbf{r}_1 - \mathbf{r}_2, \omega_n\right) \exp\left[\frac{ie}{c}\int\limits_{\mathbf{r}_1}^{\mathbf{r}_2} \mathbf{A}(\mathbf{r}) d\mathbf{r} + i\psi\left(\mathbf{r}_1 - \mathbf{r}_2, \omega_n\right\}\right] \tag{18.9}$$

Интегрирование в показателе экспоненты идет по прямой линии, соединягощей точки $\mathbf{r}_1$ и $\mathbf{r}_2$. Для функции ψ получаем уравнение [73]:

$$k_F \hat{\mathbf{r}} \operatorname{sign} \omega_n \frac{\partial \psi\left(\mathbf{r}, \omega_n\right)}{\partial \mathbf{r}} + \frac{e^2}{4c^2}(\mathbf{H} \times \mathbf{r})^2 = 0$$

откуда видно, что в даже в полях порядка $H_{c\,2}(0) \sim \Phi_0 / \left(\pi \xi_0^2\right)$ добавка к фазе имест малость $\sim \left(k_{\mathbf{r}} \xi_0\right)^{-1}$ по сравнению с первым членом в показателе экспоненты в (18.9). Поэтому для функции Грина имеем:

$$\begin{aligned} G^{(0)}\left(\mathbf{r}_1, \mathbf{r}_2; \omega_n\right) &= G^{(0)}\left(\mathbf{r}_1 - \mathbf{r}_2; \omega_n\right) \exp\left(\frac{ie}{c}\int\limits_{\mathbf{r}_1}^{\mathbf{r}_2} \mathbf{A}(\mathbf{r}) d\mathbf{r}\right) \approx \\ &\approx G^{(0)}\left(\mathbf{r}_1 - \mathbf{r}_2; \omega_n\right) \exp\left(\frac{ie}{c}\mathbf{A}\left(\mathbf{r}_1\right)\left(\mathbf{r}_2 - \mathbf{r}_1\right)\right) \end{aligned} \tag{18.10}$$

Последнее равенство написано на том основании, что характерный масштаб изменения вектор-потенциала (лондоновская глубина проникновения) вблизи T_c значительно превышает расстояние, на котором спадают нулевые функции Грина (18.8).

Подставляя (18.8) и (18.10) в (18.6), убеждаемся, что главный вклад в ядро происходит от дифференцирования меняющихся на атомных масштабах множителей вида $\exp\left(ik_{\mathrm{F}} r \operatorname{sign} \omega_n\right)$, а поправки первого порядка малости по магнитному полю возникают при дифференцировании зависящих от поля фазовых множителей в (18.10). Имеем [31]:

$$\begin{aligned} &S_{ij,\alpha\beta}\left(\mathbf{r}_1, \mathbf{r}_2\right) = S_{ij}\left(\mathbf{r}_1, \mathbf{r}_2\right) \delta_{\alpha\beta} \\ &S_{ij}\left(\mathbf{r}_1, \mathbf{r}_2\right) = T\left(\frac{\pi N_0}{k_{\mathbf{F}} R}\right)^2 \sum_n \exp\left(-\frac{2\left|\omega_n\right|}{v_{\mathbf{F}}} R\right)\left(\hat{R}_i \hat{R}_j + \frac{ie}{2k_{\mathrm{F}}^2 c} e_{ijk} H_k\right) \times \\ &\times \exp\left(\frac{2ie}{c}\mathbf{A}\left(\mathbf{r}_1\right)\mathbf{R}\right) \end{aligned} \tag{18.11}$$

где $\mathbf{R} = \mathbf{r}_2 - \mathbf{r}_1$ и $\hat{\mathbf{R}} = \mathbf{R}/|\mathbf{R}|$.

Оценим второй член в квадратных скобках в правой части (18.11):

$$\frac{eH}{k_{\mathrm{F}}^2 c} \sim \frac{1}{\left(k_{\mathrm{F}} \xi_0\right)^2} \frac{H}{II_{c2}(0)}$$

В нулевом порядке по параметру квазиклассичности $\left(k_F \xi_0\right)^{-1}$ им можно пренсбречь, тогда

$$S_{ij}\left(\mathbf{r}_1,\mathbf{r}_2\right)=K_{ij}^{(0)}(\mathbf{R})\exp\left(\frac{2ie}{c}\mathbf{A}\left(\mathbf{r}_1\right)\mathbf{R}\right) \tag{18.12}$$

где

$$S_{ij}^{(0)}(\mathbf{R})=T\left(\frac{\pi N_0}{k_F R}\right)^2\sum_n\exp\left(-\frac{2\left|\omega_n\right|}{v_F}R\right)\hat{R}_i\hat{R}_j$$

Мы видим, что ядро $K^{(0)}$ эхспонснциально убывает на расстояниях между $\mathbf{r}_1$ и $\mathbf{r}_2$, превышающих

$$\xi_0=\frac{v_F}{2\pi T_c}$$

и тем самым в теории появляется характерный микроскопичсскй масштаб размер куперовской пары (или длина когерентности) ξ_0. С друтой стороны, параметр порядка сверхпроводника изменяется на масштабе порядка корреляционной длины $\xi(T)$, причем $\xi/\xi_0\sim(1-T/T_c)^{-1/2}\gg 1$ (см. 12). 100

Следовательно, вблизи T_c мы можем разложить в подынтегральном выражении в (18.5) как параметр порядка, так и фазовый множитель в ядре вплоть до второй степени по $\mathbf{r}_2-\mathbf{r}_1=\mathbf{R}$. Имеем:

$$\begin{aligned}\mathcal{F}_2=&-\int d^3r A_{\alpha i}^*(\mathbf{r})\int d^3R S_{ij}^{(0)}(\mathbf{R})\times\\&\times\left[1+\frac{2ie}{c}\mathbf{A}(\mathbf{r})\mathbf{R}+\frac{1}{2}\left(\frac{2ie}{c}\right)^2(\mathbf{A}(\mathbf{r})\mathbf{R})^2\right]\times\\&\times\left[A_{\alpha j}(\mathbf{r})+\frac{\partial A_{\alpha j}}{\partial\mathbf{r}}\mathbf{R}+\frac{1}{2}\frac{\partial^2 A_{\alpha j}}{\partial r_k\partial r_l}R_kR_l\right]\end{aligned}$$

Выделяя явно члсны пулевой степени по $\mathbf{R}$ и интегрируя члены второй степсни по тастям, получаем:

$$\mathcal{F}_2=\mathcal{F}_{\text{uniform}}+\mathcal{F}_{\text{grad}} \tag{18.13}$$

где

$$\mathcal{F}_{\text{uniform}}=-\int d^3r A_{\alpha i}^*(\mathbf{r})A_{\alpha j}(\mathbf{r})\int d^3R S_{ij}^{(0)}(\mathbf{R}) \tag{18.14}$$

$$\mathcal{F}_{\text{grad}}=\frac{1}{2}\int d^3r\left(D_kA_{\alpha i}\right)^*\left(D_lA_{\alpha j}\right)\int d^3R S_{ij}^{(0)}(\mathbf{R})R_kR_l \tag{18.15}$$

а $\mathbf{D}=-i(\partial/\partial\mathbf{r})+(2e/c)\mathbf{A}(\mathbf{r})$ - ковариантная производная.

Вычислим входящие в (18.14) и (18.15) интегралы по R. Для однородной части имеем:

$$\begin{aligned}\int d^3R S_{ij}^{(0)}(\mathbf{R})=&T\left(\frac{\pi N_0}{k_F}\right)^2\sum_n\int_0^\infty dR\exp\left(-\frac{2\left|\omega_n\right|}{v_F}R\right)\int d\Omega\hat{R}_i\hat{R}_j=\\=&\frac{2\pi}{3}\delta_{ij}v_F\left(\frac{\pi N_0}{k_F}\right)^2T\sum_n\frac{1}{|\omega_n|}=\frac{2\pi}{3}\delta_{ij}N_0T\sum_{n\geq 0}\frac{1}{\omega_n}\end{aligned} \tag{18.16}$$

Обрезая логарифмически расходящупося сумму на граничной частоте ε_1, получаем:

$$2\pi T\sum_{n\geq 0}\frac{1}{\omega_n}=\ln\frac{\varepsilon_1}{2\pi T}+\ln 4\gamma=\frac{1}{N_0V}+\ln\frac{T_c}{T}=\frac{1}{N_0V}-\frac{T-T_c}{T_c} \tag{18.17}$$

Здесь мы воспользовались формулой (6.10) и тождеством

$$\lim_{N\to\infty}\sum_{n\geq 0}^{N}\frac{1}{n+1/2}=\ln N+\ln 4\gamma$$

Подставдяя (18.16) и (18.17) в (18.14), получаем:

$$\mathcal{F}_{\text{uniform}}=\frac{1}{3}\left(-\frac{1}{V}+N_0\frac{T-T_c}{T_c}\right)\int d^3rA^*_{\alpha i}(\mathbf{r})A_{\alpha i}(\mathbf{r}) \tag{18.18}$$

Подставляя (18.18) в (18.3), убеждаемся, что однородные слагаемые, явно содержащие константу связи, сокращают друг друга.

Для градиентной части имеем:

$$\begin{aligned}\int d^3RS^{(0)}_{ij}(\mathbf{R})R_kR_l=T\left(\tfrac{\pi N_0}{k_F}\right)^2\sum_n\int_0^\infty dRR^2\exp\left(-\tfrac{2|\omega_n|}{v_{\text{F}}}R\right)\times\\ \times\int d\Omega\hat{R}_i\hat{R}_j\hat{R}_k\hat{R}_l=\tfrac{\pi}{15}\left(\delta_{ij}\delta_{kl}+\delta_{ik}\delta_{jl}+\delta_{il}\delta_{jk}\right)v_{\text{F}}^2N_0T_c\sum_{n\geq 0}\tfrac{1}{\omega_n^3}=\\ =\tfrac{7\zeta(3)}{120}\left(\delta_{ij}\delta_{kl}+\delta_{ik}\delta_{jl}+\delta_{il}\delta_{jk}\right)\tfrac{N_0v_{\text{F}}^2}{\pi^2T_c^2}\end{aligned} \tag{18.19}$$

Сравнивая полученный результат с феномснологическим выражением (15.20) для свободной энергии сверхпроводника с p-спариванием, получаем окончательно следующие значения констант [72]:

$$K_1=K_2=K_3=\frac{7\zeta(3)N_0v_F^2}{240\pi^2T_c^2}=\frac{7\zeta(3)}{60}N_0\xi_0^2 \tag{18.20}$$

Рассмотрим теперь член четвертого порядка в разложении свободной энергии. Подставляя в $\mathcal{F}_4$ выражения (18.4) и (17.13), а затем вычисляя интеграл по углам и след по спиновым индексам с использованием тождества

$$\text{Sp}\left(\boldsymbol{\sigma}\mathbf{d}_1\right)\left(\sigma\mathbf{d}_2\right)\left(\sigma\mathbf{d}_3\right)\left(\sigma\mathbf{d}_4\right)=2\left(\mathbf{d}_1\mathbf{d}_2\right)\left(\mathbf{d}_3\mathbf{d}_4\right)-2\left(\mathbf{d}_1\times\mathbf{d}_2\right)\left(\mathbf{d}_3\times\mathbf{d}_4\right)$$

получаем:

$$\begin{aligned}\mathcal{F}_4=&\frac{B}{4}\sum_{\mathbf{q}_1}\left(-A^*_{\alpha i}A_{\beta j}A^*_{\alpha i}A_{\beta j}+2A^*_{\alpha i}A_{\alpha i}A^*_{\beta j}A_{\beta j}-2A^*_{\alpha i}A_{\beta i}A^*_{\alpha j}A_{\beta j}+\right.\\ &\left.+2A^*_{\alpha i}A_{\beta i}A^*_{\beta j}A_{\alpha j}+2A^*_{\alpha i}A_{\alpha j}A^*_{\beta i}A_{\beta j}\right)\delta\left(\mathbf{q}_1+\mathbf{q}_3-\mathbf{q}_2-\mathbf{q}_4\right)\end{aligned} \tag{18.21}$$

где все слагаемые в фигурных скобках зависят от импульсов следующим образом: $A^*_{\alpha i}A_{\beta j}A^*_{\alpha i}A_{\beta j}=A^*_{\alpha i}\left(\mathrm{q}_1\right)A_{\beta j}\left(\mathrm{q}_2\right)A^*_{\alpha i}\left(\mathrm{q}_3\right)A_{\beta j}\left(\mathrm{q}_4\right)$ и т. п., а

$$B=\frac{2}{15}N_0T_c\sum_n\int d\xi\frac{1}{\left(\omega_n^2+\xi^2\right)^2}=\frac{7\zeta(3)}{60}\frac{N_0}{\pi^2T_{\text{c}}^2}$$

Возвращаясь в (18.21) в координатное представление и сравнивая результат с (11.1), получаем значения коистант [34, 74]:

$$-2\beta_1=\beta_2=-\beta_3=\beta_4=\beta_5=\frac{7\zeta(3)}{120}\frac{N_0}{\pi^2T_6^2} \tag{18.22}$$

Таким образом, плотность функционала (18.3) принимаст следующий окончательный вид:

$$F_{\text{cond}} = \frac{N_0}{3}\frac{T-T_c}{T_c}A_{\alpha i}A^*_{\alpha i} + \frac{7\zeta(3)}{120\pi^2}\frac{N_0}{T_c^2}\left[-\frac{1}{2}\left|A_{\alpha i}A_{\alpha i}\right|^2 + \left(A^*_{\alpha i}A_{\alpha i}\right)^2 - \right.$$
$$\left. - A^*_{\alpha i}A_{\beta i}A^*_{\alpha j}A_{\beta j} + A^*_{\alpha i}A_{\beta i}A^*_{\beta j}A_{\alpha j} + A^*_{\alpha i}A_{\alpha j}A^*_{\beta i}A_{\beta j}\right] +$$
$$+ \frac{7\zeta(3)}{60}N_0\xi_0^2\left[\left(D_iA_{\alpha j}\right)^*\left(D_iA_{\alpha j}\right) + \left(D_iA_{\alpha i}\right)^*\left(D_jA_{\alpha j}\right) + \left(D_iA_{\alpha j}\right)^*\left(D_jA_{\alpha i}\right)\right] \tag{18.23}$$

Найденные параметры функционала Гинзбурга-Ландау соответствуот приближению слабой связи (см. конец 10).

Поправки к квазиклассическому приближению. Орбитальпый магнетизм. Сравнивая (18.20) и (15.7), мы видим, что в рассматриваемом приближении внутренний спонтанный орбитальный магнитный момент в сверхпроволнике с p-спариванием отсутствует в силу равенства $K_2 = K_3$. Посмогрим, что произойдет, если учесть второе слагаемое в квадратной скобке в выражениил (18.11), антисимметричное по индексам i, j и представяющее собой, как уже отмсчалось, поправку второго порядка малости по парамстру квазиктассичности.

Опуская зависящий от поля фазовый множитель в (18.11), получаем следуошую поправку к плотности свободной энсргии:

$$\delta F_{MH} = i\frac{e}{2k_{\text{F}}^2c}\left(\frac{\pi N_0}{k_{\text{F}}}\right)^2 e_{ijk}A^*_{\alpha i}A_{\alpha j}H_k 2\pi T_{\text{c}}\sum_n\int_0^\infty dR\exp\left(-\frac{2\left|\omega_n\right|}{v_{\text{F}}}R\right) =$$
$$= i\frac{e}{4k_{\text{F}}^2c}N_0\ln\frac{\varepsilon_1}{2\pi T_c}e_{ijk}A^*_{\alpha i}A_{\alpha j}H_k$$

Отсюода, восстанавливая постояннуо Планка, полутаем выражение для плотности внутреннего орбитального магнитного момента [75]

$$M_i = -i\frac{ch}{4k_{\text{F}}^2c}N_0\ln\frac{\varepsilon_1}{2\pi T_c}e_{ijk}A^*_{\alpha j}A_{\alpha k}$$

Сравнивая с (15.7), приходим к выводу о том, что при учете поправок порядка $\left(k_F\xi_0\right)^{-2}$ k квазиклассическому приближению разность $K_2 - K_3$, а вместе с ней и плотность внутрсннего спонтанного орбитального момента, становятся отличнымми от пгуля.

Спиновый магнетизм. Рассмотрим теперь эффект взаимодействия спинов электроiов с магнитным полем. В пренебрежении орбитальными эффектами ядро (18.6) зависит только от разности координат. Параметр порядка тогда можно считать ие зависящим от $\mathbf{r}$, и из (18.5) имеем следуощее выражение для плотности свободной энергии:

$$F_{SH} = -\frac{1}{2}A^*_{\alpha i}S_{ij,\alpha\beta}A_{\beta j} \tag{18.24}$$

Входящий сюда коэффицисит K удобно вычислять в импульсном представлснии:

$$S_{ij,\alpha\beta} = T_c\sum_n\int\frac{d^3k}{(2\pi)^3}\hat{k}_i\hat{k}_j\left(\sigma_y\sigma_\alpha\right)_{\lambda\mu}\times$$
$$\times G^{(0)}_{\lambda\gamma}\left(\mathbf{k},\omega_n\right)\left(\sigma_\beta\sigma_y\right)_{\gamma\delta}G^{(0)}_{\mu\delta}\left(-\mathbf{k},-\omega_n\right) \tag{18.25}$$

Выбирая ось квантования (направление магнитного поля $\mathbf{H}$) вдоль оси $\hat{z}$, функции Грина можно записать в следуощем видс (ср. с (17.14) при $\mathbf{H} = 0$):

$$G^{(0)}_{\lambda\gamma}(\mathbf{k},\omega_n) = \frac{i\omega_n - \xi_k}{(i\omega_n - \xi_k)^2 - (\mu_{\rm B}H)^2}\delta_{\lambda\gamma} - \\ - \frac{\mu_{\rm B}H}{(i\omega_n - \xi_k)^2 - (\mu_{\rm B}H)^2}(\sigma_z)_{\lambda\gamma} \qquad (18.26)$$

где $\mu_{\rm B}$ есть магнетон Бора (или магнитный момегтт ядра в ^{3}). Подставляя (18.26) в (18.25) и вычисляя след по спиновым индскcам, получаем линейнупо
по полю поправху к коэффициенту :

$$\delta S_{ij,\alpha\beta} = -ie_{\alpha\beta z}\mu_B H T_c \sum_n \int \frac{d^3k}{(2\pi)^3}\hat{k}_i\hat{k}_j\left[\frac{1}{i\omega_n - \xi_k}\frac{1}{(i\omega_n + \xi_k)^2} + \text{ к.с. }\right] = \\ = -\frac{1}{3}i\delta_{ij}e_{\alpha\beta z}\mu_{\rm B}HT_{\rm c}\sum_n \int d\xi N(\xi)\left[\frac{1}{i\omega_n - \xi}\frac{1}{(i\omega_n + \xi)^2} + \text{ к.с. }\right]$$

где $N(\xi)$ есть плотность электронных состояний. Записывая ее в виде разложения $N(\xi) = N_0 + N_0'\xi$ вблизи энергии Ферми и выполняя интегрирование по ξ, получаем:

$$\delta S_{ij,\alpha\beta} = -\frac{\pi}{2}\delta_{ij}e_{\alpha\beta z}\mu_{\rm B}HN_0T_c\sum_n \frac{\operatorname{sign}\omega_n}{\omega_n^2} - \\ - i\frac{\pi}{2}\delta_{ij}e_{\alpha\beta z}\mu_{\rm B}HN_0'T_c\sum_n \frac{\operatorname{sign}\omega_n}{\omega_n} \qquad (18.27)$$

Первое слагаемое в правой части тождественно обращается в нуль, а расходяшаяся сумма во в'гором слагаемом обрезается на граничной частоте ε_1. Подставляя полученный результат в (18.24), приходим к ответу:

$$\delta F_{SH} = i\frac{\pi}{4}\mu_{\rm B}N_0'\ln\frac{\varepsilon_1}{2\pi T_c}e_{\alpha\beta\gamma}A^*_{\alpha i}A_{\beta i}H_\gamma \qquad (18.28)$$

Сравнивая это выражение с (15.20), видим, что зачение коэффициента K_4, а, следовательно, и плотность внутреннего слонтанного спинового магнитного момента малы в меру малости асимметрии в распределснии части и дырок вблизи поверхности Ферми.

Упражнение. Вычислить коэффициенты в разложении Гинзбурга-Ландау для изотропного сверхпроводника с d-спариванием в модели слабой связи.

19.2.3 19. Upper Critical Field in p-wave Superconductors

В области применимости теории Гинзбурга-Ландау верхнис крититеские поля для сверхпроволников с необычньм параметром порядка вычислялись в § 12. При понивкснии температуры корреляционная длина $\xi(T)$, задающая пространственный масштаб измснения параметра порямка, уменьшается и при $T \ll T_{\rm c}$ становится сравнимой с длиной когерентности ξ_0. В этих условиях градиентное разложенис свободной энергии становится неприменимым, и для вычисления $H_{c2}(T)$ необходимо использовать методы микроскопической теории. В настоящем параграфе мы проведем вычисления для анизотропного сверхпроводника с p-спариванием. В этом случае, также как в случас обычного изотропного сверхпроводиика можно получить аналитические выражепия для верхнего критического поля при $T = 0$. Для многих друтих необытчых сверхпроводящих состояний, даже с однокомпонепттиыми параметрами порядка, не

являтощихся собственными функциями уравпенния типа (19.5) (см. ниже), например, для тетрагоналыного сверхпроводника с $\Delta(\mathbf{r}) \sim \Delta\left(\hat{x}^2 - \hat{y}^2\right)$, верхнее критическое полс можно найти лишь приближенно.

Для вычисления верхнего критического поля $H_{c2}(T)$ в сверхпроводнике с p-спариванием воспользуемся уравнением (17.9). Переходя в координатное представление, с учетом выражения (18.4) для параметра порядка и разложения (18.1) притягивающего взаимодействия, получаем линейное интегральное уравнение [76]:

$$A_{\alpha i}(\mathbf{r}_1) = \int d^3 r_2 K_{ij}(\mathbf{r}_1, \mathbf{r}_2) A_{\alpha j}(\mathbf{r}_2) \tag{19.1}$$

где ядро имеет вид (ср. с (18.5))

$$K_{ij}(\mathbf{r}_1, \mathbf{r}_2) = \lim_{\mathbf{r}'_{1,2} - \mathbf{r}_{1,2}} \frac{3VT}{4k_F^2} \sum_n \left(\frac{\partial}{\partial r_{1,i}} - \frac{\partial}{\partial r'_{1,i}}\right)\left(\frac{\partial}{\partial r_{2,3}} - \frac{\partial}{\partial r'_{2,j}}\right) G(\mathbf{r}_1, \mathbf{r}_2; \omega_n) G(\mathbf{r}'_1, \mathbf{r}'_2; -\omega_n) \tag{19.2}$$

Повторяя дословно рассуждения, использованные в предыдудем параграфе при выводе формулы (18.12), получаем:

$$K_{ij}(\mathbf{r}_1, \mathbf{r}_2) = 3VT\hat{R}_i R_j \left(\frac{\pi N_0}{k_{\mathrm{F}} R}\right)^2 \sum_n \exp\left(-\frac{2|\omega_n|}{v_{\mathbf{F}}} R\right) \exp\left(\frac{2ie}{c} \int\limits_{\mathbf{r}_1}^{\mathbf{r}_2} \mathbf{A}(\mathbf{r}) d\mathbf{r}\right) \tag{19.3}$$

где $\hat{R} = (\mathbf{r}_2 - \mathbf{r}_1) / |\mathbf{r}_2 - \mathbf{r}_1|$.

Воспользовавшись тождеством

$$\exp\left(\frac{2ie}{c} \int\limits_{\mathbf{r}_1}^{\mathbf{r}_2} \mathbf{A}(\mathbf{r}) d\mathbf{r}\right) f(\mathbf{r}_2) = \exp\left(i(\mathbf{r}_2 - \mathbf{r}_1)\mathbf{D}(\mathbf{r}_1)\right) f(\mathbf{r}_1) \tag{19.4}$$

где $\mathbf{D}(\mathbf{r}) = -i(\partial/\partial\mathbf{r}) + (2e/c)\mathbf{A}(\mathbf{r})$ - оператор ковариантного лифференцирования, переписываем уравнение (19.1) в виде

$$A_{\alpha i}(\mathbf{r}) = 3VT\left(\frac{\pi N_0}{k_{\mathrm{F}}}\right)^2 \int d^3 R \frac{\hat{R}_{\mathrm{r}} \hat{R}_3}{R^2} \sum_n \exp\left(-\frac{2|\omega_n|}{\psi_{\mathrm{F}}} R\right) \exp(i\mathbf{R}\mathbf{D}(\mathbf{r})) A_{\alpha j}(\mathbf{r}) \tag{19.5}$$

Заметим, что (19.5) является дифференциалным уравнением бесконечно высокого порядка [77], причсм линсаризованные уравнения Гинзбурга-Ландау получаются, если мы разложим экспонснту в правой части до членов второго порядка по D.

Пусть внешнее полс H направлено вдоль оси z, тогда ищем решение уравнения (19.5) в виде

$$A_{\alpha i}(\mathbf{r}) = e^{ip_z z} A_{\alpha i}(\rho)$$

где $\rho = (x, y)$.

Естественно прсдположить, что максимальному значению верхнего критического поля отвечает $p_z = 0$. Переходя в интеграле в (19.5) к сферическим координатам с полярной осью вдоль z, дегко убедиться, что уравнения расцепляются, т.с. z-компонснты параметра порядка $A_{\alpha z}$ могут быть рассмотрены независимо от x, y-компонент.

Полярная фаза [76]. Начнем с вычисления $H_{c2}(T)$ для сверхпроводящего состояния вида

$$d_{\alpha x} = A_{\alpha z}\hat{k}_z$$

Поскольку уравнение (19.5) диагоналыо по спиновым индсксам, то всем компонентам вектора d соответствует одинаковое значение верхнего критического поля. Полагая $d_1 = d_2 = 0$, убеждаемся, что рассматриваемый случай соответствует полярнои фазе [1]. Итак, пусть $\mathcal{A}_{zz}(\rho) = \int(\rho)$. Метод решения аналогичен применяемому в соответствующей задаче для изотропного сверхпроводника с s-спариваниcм [77].

Введем повышающий и понижающий операторы:

$$D_{\pm} = \frac{D_x \pm iD_y}{\sqrt{2}} \tag{19.6}$$

удовлетворякщие коммутаиионному соотношению $[D_-, D_+] = 2\pi H/\Phi_0$, гдс Φ_0 - квант потока. Тогда уравнение (19.5) принимает вил

$$f(\rho) = 3VT\left(\frac{\pi N_0}{k_F}\right)^2 \sum_n \int_0^\infty dR \exp\left(-\frac{2\left|\omega_n\right|}{v_{\mathrm{F}}}R\right) \int_0^\pi \sin\theta\cos^2\theta d\theta \times$$
$$\times \int_0^{2\pi} d\varphi \exp\left(i\frac{R}{\sqrt{2}}\sin\theta\left(e^{-i\varphi}D_+ + e^{i\varphi}D_-\right)\right) f(\rho) \tag{19.7}$$

Воспользуемся теперь операторным тождеством:

$$e^{\Lambda+B} = e^A e^B e^{-(1/2)[A\cdot B]}$$

верным, если коммутатор операторов A и B есть c-число, и перепишем содержащую $D_\pm$ экспоненту в (19.7) в следующем виде:

$$\exp\left(i\frac{R}{\sqrt{2}}\sin\theta\left(e^{-i\varphi}D_+ + e^{i\varphi}D_-\right)\right) =$$
$$= \exp\left(-\frac{\pi H}{2\Phi_0}R^2\sin^2\theta\right)\exp\left(i\frac{R}{\sqrt{2}}\sin\theta e^{-i\varphi}D_+\right)\exp\left(i\frac{R}{\sqrt{2}}\sin\theta e^{i\varphi}D_-\right) \tag{19.8}$$

Если мы разложим правую часть в ряд по степеням $D_\pm$и подставим в (19.7), то после интегрирования по утлу φ в этом разложении останутся только члены вида $D_+^n D_-^n$, содержащие одитаковое число повышаюоших и понижающих операторов. Эго означает, что рсшгсниями уравiения (19.7) являются соБственные функции $|N\rangle$ оператора D_+D_-, являющегося оператором Гамильтона для гармонического осциллятора:

$$D_+D_-|N\rangle = N\frac{2\pi H}{\Phi_0}|N\rangle$$
$$D_+^n D_-^n|N\rangle = \frac{N!}{(N-n)!}\left(\frac{2\pi H}{\Phi_0}\right)^n|N\rangle$$

В калибровке Ландау $\mathbf{A} = (0, Hx, 0)$ эти собственiые функции выглядят следующим образом:

$f_{N,p}(\rho) \propto e^{ipy}\exp\left[-\frac{\pi H}{\Phi_0}\left(x - \frac{p\Phi_0}{2\pi H}\right)^2\right] \times$

[11] Это справедливо в пренебрсжении взаимодействием $\mu_{\mathrm{B}}H$ спинов электронов с магнитным полем. Если учесть такое взаимодействие, то переход происходит в β-фазу (см. 3) [31].

$$\times H_N\left[\sqrt{\frac{2\pi H}{\Phi_0}}\left(x-\frac{p\Phi_0}{2\pi H}\right)\right] \tag{19.9}$$

где $H_N(x)$ - полиномы Эрмита. С учетом сказанного получаем:

$$\begin{aligned}\int\limits_0^{2\pi} d\varphi \operatorname{cxp}\left(i\tfrac{R}{\sqrt{2}}\sin\theta e^{-i\varphi}D_+\right)\exp\left(i\tfrac{R}{\sqrt{2}}\sin\theta e^{i\varphi}D_-\right)|N\rangle = \\ = 2\pi\sum_{n=0}^{N}\tfrac{N!}{(n!)^2(N-n)!}\left(-\tfrac{\pi H}{\Phi_0}R^2\sin^2\theta\right)^n|N\rangle = \\ = 2\pi L_N\left(\tfrac{\pi H}{\Phi_0}R^2\sin^2\theta\right)|N\rangle\end{aligned} \tag{19.10}$$

где $L_N(x)$ - полиномы Лагерра. Уравнение на собственные значения (19.7) принимает вид

$$\begin{aligned}1 = 6\pi VT\left(\tfrac{\pi N_0}{k_{\mathrm{F}}}\right)^2\sum_n\int\limits_0^{\infty}dR\exp\left(-\tfrac{2|\omega_n|}{v_{\mathrm{F}}}R\right)\times \\ \times\int\limits_0^{\pi}\sin\theta\cos^2\theta d\theta\exp\left(-\tfrac{\pi H}{2\Phi_0}R^2\sin^2\theta\right)\times \\ \times L_N\left(\tfrac{\pi H}{\Phi_0}R^2\sin^2\theta\right)\end{aligned} \tag{19.11}$$

Можно показать, что максималыно значение верхдего критического поля получается пля рсшения, отвсчающцсго нулсвому ($N=0$) уровню гармонического осциллятора, при этом параметр порядка имест вид

$$\mathbf{d}\propto f_{0,p}(x,y)\tilde{k}_z \tag{19.12}$$

Для устранения логарифмической расходимости при суммировании по n в (19.11) вычтем из обеих частей выражения в нулевом поле. Тогла, учитывая (18.17), получаем окончательнос уравнение, опрсделяющсе зависимость $H_{\mathrm{c}2}(T)$ для полярной фазы:

$$\begin{aligned}\ln\frac{T_c}{T} = \sum_n\left[\frac{1}{|2n+1|}-\frac{6\pi T}{N_0}\left(\frac{\pi N_0}{k_F}\right)^2\int\limits_0^{\infty}dR\exp\left(-\frac{2\,|\omega_n|}{v_{\mathrm{F}}}R\right)\times\right. \\ \left.\times\int\limits_0^{\pi}\sin\theta\cos^2\theta d\theta\exp\left(-\frac{\pi H}{2\Phi_0}R^2\sin^2\theta\right)\right]\end{aligned} \tag{19.13}$$

При выводе (19.13) использовапю определение критической температуры T_{c} в нулевом поле:

$$\pi VN_0T_c\sum_n\frac{1}{|\omega_n|}=1$$

где сумма по частотам обрезана на граничной энергии ε_1 (см. предыдущий параграф).

А-фаза и фаза Парнберга-Клемма [76]. Рассмотрим теперь x - и y-компоненты параметра порядка. Обозначим $A_{\alpha i}(\rho)=f_i(\rho)$ и введем новые функции

$$f_{\pm}(\rho)=\frac{1}{\sqrt{2}}\left(f_x\pm if_y\right)$$

тогда уравнение (19.5) принимает вид

$$\begin{pmatrix} f_+ \\ f_- \end{pmatrix} = \frac{3VT}{2}\left(\frac{\pi N_0}{k_{\rm F}}\right)^2 \sum_n \int_0^\infty dR \exp\left(-\frac{2\left|\omega_n\right|}{v_{\rm F}}R\right) \times$$

$$\times \int_0^\pi \sin^3\theta d\theta \int_0^{2\pi} d\varphi \begin{pmatrix} 1 & e^{21\varphi} \\ e^{-21\varphi} & 1 \end{pmatrix} \exp\left(i\frac{R}{\sqrt{2}}\sin\theta\left(e^{-i\varphi}D_+ + e^{i\varphi}D_-\right)\right)\begin{pmatrix} f_+ \\ f_- \end{pmatrix} \qquad (19.14)$$

Если воспользоваться формулой (19.8), разложить зависящие от φ экспоненты в ряд Тейлора, а затем проинтегрироватъ по φ, то диагональные элементы матричного оператора в правой части содержат слагаемые вида $D_+^n D_-^{\rm n}$, наддиагональный элемент - слагаемые вида $D_+^{n+2}D_-^n$, а поддиагоналыный слагаемые вида $D_+^n D_-^{n+2}$. По этой причине ищем решснис уравнения (19.14) в следующем виде:

$$\begin{pmatrix} f_+ \\ f_- \end{pmatrix} = \begin{pmatrix} p_N|N+2\rangle \\ q_N|N\rangle \end{pmatrix}, \quad N \geq 0 \qquad (19.15)$$

где $|N\rangle$ определяется формулой (19.9).

Имеем:

$$\int_0^{2\pi} d\varphi \begin{pmatrix} 1 & e^{2i\varphi} \\ e^{-2i\varphi} & 1 \end{pmatrix} \exp\left(i\frac{R}{\sqrt{2}}\sin\theta e^{-i\varphi}D_+\right)\exp\left(i\frac{R}{\sqrt{2}}\sin\theta e^{i\varphi}D_-\right)\begin{pmatrix} p_N|N+2\rangle \\ q_N|N\rangle \end{pmatrix} =$$

$$= 2\pi \begin{pmatrix} p_N\sqrt{(N+1)(N+2)}\sum_{n=0}^N \frac{N!}{n!(n+2)!(N-n)!}\left(-\frac{\pi H}{\Phi_0}R^2\sin^2\theta\right)^{n+1}|N+2\rangle + \\ +q_N L_{N+2}\left(\frac{\pi H}{\Phi_0}R^2\sin^2\theta\right)|N+2\rangle \\ p_N L_N\left(\frac{\pi H}{\Phi_0}R^2\sin^2\theta\right)|N\rangle + \\ +q_N\sqrt{(N+1)(N+2)}\sum_{n=0}^N \frac{N!}{n!(n+2)!(N-n)!}\left(-\frac{\pi H}{\Phi_0}R^2\sin^2\theta\right)^{n+1}|N\rangle \end{pmatrix}$$

Мы получили линейную однородную систему уравпепий на коэффициенты p_N и q_N, условие разрсшимости которой имсст вид

$$(1-\alpha_N)(1-\alpha_{N+2}) - \beta_N^2 = 0 \qquad (19.16)$$

где

$$\alpha_N(H,T) = 3\pi VT\left(\frac{\pi N_0}{k_F}\right)^2 \sum_n \int_0^\infty dR \exp\left(-\frac{2\left|\omega_n\right|}{v_{\rm F}}R\right) \times$$

$$\times \int_0^\pi \sin^3\theta d\theta \exp\left(-\frac{\pi H}{2\Phi_0}R^2\sin^2\theta\right) L_N\left(\frac{\pi H}{\Phi_0}R^2\sin^2\theta\right)$$

$$\beta_N(H,T) = 3\pi VT\left(\frac{\pi N_0}{k_{\rm F}}\right)^2 \sum_n \int_0^\infty dR \exp\left(-\frac{2\left|\omega_n\right|}{v_{\rm F}}R\right) \times$$

$$\times \int_0^\pi \sin^3\theta d\theta \exp\left(-\frac{\pi H}{2\Phi_0}R^2\sin^2\theta\right)\sqrt{(N+1)(N+2)}\times$$

$$\times \sum_{m=0}^N \frac{N!}{m!(m+2)!(N-m)!}\left(-\frac{\pi H}{\Phi_0}R^2\sin^2\theta\right)^{m+1}$$

при этом $q_N = \left(\left(\alpha_N - 1\right)/\beta_N\right) p_N$.

Итак, мы получили уравненис, определяющее температурпую зависимость верхнего критического поля для решения вида (19.15). Можно показать, что максиматное значение $H_{c2}\left(T\right)$ достигается при $N = 0$. Соответствуоший параметр порядка:

$$\mathrm{d} \propto \left[f_{2,p}(x,y) \left(\hat{k}_x - i\hat{k}_y \right) + \frac{\alpha_0 - 1}{\beta_0} f_{0,p}(x,y) \left(\hat{k}_x + i\hat{k}_y \right) \right] \tag{19.17}$$

описывает так называемую фазу Шариберга-Клсмма. В отсутствие спиновыхх эффектов верхнее критичсскос поле одилаково для всех компонент вектора $\mathbf{d}$.

Осталось рассмотрсть состояние

$$\begin{pmatrix} f_+ \\ f_- \end{pmatrix} = \begin{pmatrix} |0\rangle \\ 0 \end{pmatrix} \tag{19.18}$$

которое также является решешием (19.14), но не принадлежит к семсйству (19.15)[2]. Подставляя (19.18) в (19.14), убсждаемсяя в том, что уравнение на верхнее критическое поле для параметра поряшка

$$\mathbf{d} \propto f_{0,p}(x,y) \left(\hat{k}_x - i\hat{k}_y \right) \tag{19.19}$$

соответствуощщего, как легко видеть, A-фазе [3], имест вид

$$1 - \alpha_0 = 0 \tag{19.20}$$

Мы приходим, таким образом, к следупошему выводу: в заряженной ферми-жидкости с p-спариванием переход из нормального в сверхпроводящее состояние в магнитном поле может произойтн в одлу из трех фаз: полярную фазу, A-фазу или фазу Шарнберга-Клемма. Для ответа на вопрос, какая именно из них имеет максимальнос критическос полс, нсобходимо решить урависния (19.13), (19.20) и (19.16). Хотя в общем случае эта задача может быть решена лишь путсм числснного анализа, оказывается возможным получить аналитические выражения для H_{c2} при $T \to T_c$ (см. §12, 18, а также упражнение в конце параграфа) и при нулевой температуре.

вычисление $H_{c2}\left(0\right)$ [76]. Начнем с исследования полярной фазы. Для сокращения обозначений удобно ввести следующие безразмерные переменные:

$$h = \frac{2H}{H_0}. \quad \rho = \frac{r\sqrt{h}}{\xi_0}, \quad t = \frac{T}{T_{\circ 0}}$$

гдс $H_0 = \Phi_0/\left(\pi\xi_0^2\right)$, а $T_{c:0}$ - критическая темпсратура при $II = 0$. Из (19.13) имеем

$$\ln t = \sum_n \left[\frac{3t}{2\sqrt{h}} \int_0^\infty d\rho \int_0^\pi \sin\theta \cos^2\theta d\theta \times \right.$$
$$\left. \times \exp\left(-\frac{t\rho|2n+1|}{\sqrt{h}} - \frac{\rho^2 \sin^2\theta}{4} \right) - \frac{1}{|2n+1|} \right] \tag{19.21}$$

Прсдслыный переход $t \to 0$ в этом уравнении выполнястся следующим образом. Перепииеем сумму по частотам в виде

[12] у (19.14) имеется также решение вида $\binom{f_+}{f_-} = \binom{|1\rangle}{0}$, однако можно похазать, что оно приводит х заведомо мсныиему значснию верхнего критического погя.

[3] В сверхпроводящей A-фазе орбитальый момент пар орисщтирован против паправлсния поля H.

$$\sum_n \{\ldots\} = 2 \lim_{y\to 1} \sum_{n=0}^{\infty} y^{2n+1} \{\ldots\}$$

Обозначая $x = \cos\theta$ и суммируя по n, получаем:

$$\ln t = \lim_{y\to 1} \left[\frac{3i}{\sqrt{h}} \int_0^1 x^2 dx \int_0^\infty d\rho \frac{2y \exp\left(-\frac{t\rho}{\sqrt{h}} - \frac{\rho^2\left(1-x^2\right)}{4} \right)}{1 - y^2 \exp\left(-\frac{2t\rho}{\sqrt{h}} \right)} - \ln \frac{1+y}{1-y} \right]$$

Разложим теперь экспопегты в подыитегральном выражении по стспеням t при $t \to 0$ и запишем правую часть в виде

$$\lim_{y\to 1} \left[3 \int_0^1 dx x^2 \cdot \int_0^\infty d\rho \frac{\exp\left(-\frac{\rho^2\left(1-x^2\right)}{4} \right)}{\rho + \frac{\sqrt{h}(1-y)}{t}} - \ln \frac{2}{1-y} \right] =$$

$$= \lim_{y\to 1} \left\{ 3 \int_0^1 dx x^2 \left[\ln \frac{t}{\sqrt{h}(1-y)} - \frac{1}{2} \left(\ln \frac{1-x^2}{4} + C \right) \right] - \ln \frac{2}{1-y} \right\} =$$

$$= \ln \frac{t}{2\sqrt{h}} - \frac{C}{2} - \frac{3}{2} \int_0^1 dx x^2 \ln \frac{1-x^2}{4} = \ln \frac{t}{2\sqrt{h}} - \frac{C}{2} + \frac{4}{3}$$

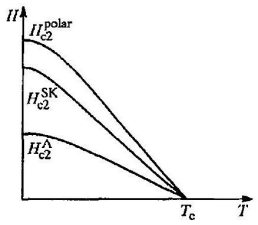
где $C = \ln \gamma$ - постоянная Эйлера. Отсюода окончательно получаем, что

$$h = \frac{e^{8/3}}{4\gamma}$$

Вычисления лтя A-фазы и фазы Шариберга-Клемма выполняются аналогитіто. Возвращаясь к размерным величипам, приведем сводку результатов:

$$H_2(T=0) = \frac{e^2}{4\gamma} \frac{\Phi_0}{2\pi\xi_0^2} \begin{cases} e^{2/3}, & \text{полярная фаза,} \\ e^{-1/3}, & \text{A-фаза,} \\ e^{\sqrt{3}-4/3}, & \text{фаза Шариберга-Клемма.} \end{cases} \tag{19.22}$$

Для удобства сравиения мв явно выдслили перед фигурной скобкой значение верхего критического поля при $T = 0$ для изотропного сверхпроводпика



Р ис. 17. Качественное новедение $H_2(T)$ в различных фазах с p-спариванием

с s-спариванием. Мы видим, что максималыое значенис верхнего критипеского поля получается для полярной фазы. Графики $H_{c2}(T)$ для фаз с р-спариванием изображены пта рис. 17.

MC-19.1

Доказать тождество (19.4).

MC-19.2

С помощыо уравнений (19.13), (19.16) и (19.20) зычислить значсние H_{c2} для сверхпроводника с p-спариванисм вблизи критической температуры.

19.2.4 20. Boundary Conditions for the Order Parameter

Из феноменодогического анализа в 13 следует, что ввиду внутренней анизотропии параметра порядка, граничные условия для уравнений ГинзбургаЛандау, определяющие повсрхиостные свойства сверхпроводника, также оказываются существенно анизотропными. Предмет настоящего параграфа составляет микроскопический вывод траничных условий для параметров порядка, соответствующих нетривиалыім типам спаривания. При этом мы ограничимся рассмотрснием сверхпроводников со слабцм спин-орбиталыным взаимодействием и сферической ферми-повсрхностыг.

Зеркалыю отражаюшая поверхность [79, 80]. В области применимости тсории Гиізбурга-Ландау задача сводится к решению линейного иітеграпного уравнения (17.9), в которое входят мацубаровские функции Грина нормального металла в полупространствс $x > 0$, обращающиеся в нуль на поверхности (то ссть при $x = 0$) и имеющис в отсутствис примесей и магнитного поля
следующий вид:

$$G^{(0)}\left(x_1, x_2; \mathrm{k}_{\parallel}, \omega_n\right) = \sum_q \frac{F_q\left(x_1, x_2\right)}{i\omega_n - \xi\left(q, \mathbf{k}_{\parallel}\right)} \tag{20.1}$$

где

$$F_q\left(x_1, x_2\right) = \theta\left(x_1\right)\theta\left(x_2\right)\sin qx_1 \sin qx_2$$

а

$$O(x) = \begin{cases} 1, & \text{при } x > 0 \\ 0, & \text{при } x < 0 \end{cases}$$

Мы использовали смешапное координатчо-импульсное представление, в котором функсии Грина диагональны по компонентам импульса вдоль поверхности.

Рассмотрим ситуашяio па примерс сверхпроводника с синглетным спариванисм, параметр порядка в котором соотвстствует одномерному нетривиальному представлению точечной группы симметрии кристалла (см. 4). Обобщение пга остальные случаи нс составляет труда. Входяший в (17.9) параметр порядка выглядит в смешанном координатно-импульсном представлении следулощим образом:

$$\Delta_{\alpha\beta}(\mathbf{k}, \mathbf{r}) = \left(i\sigma_y\right)_{\alpha\beta} \eta(\mathbf{r})\psi(\hat{\mathbf{k}})$$

Подставляя в (17.9) разложение (5.7) и возвращаясь в координатпое предсгавление по x, получаем линейное интегралыно уравнение для параметра порядка:

$$\eta\left(x_1\right) = \int_0^{\infty} dx_2 K\left(x_1, x_2\right)\eta\left(x_2\right) \tag{20.2}$$

ялро которого имеет вид

$$K\left(x_1,x_2\right)=-VT_c\sum_n\sum_{\mathbf{k}_1,\mathbf{k}_2,q_1,q_2}\exp\left(iq_1x_1-iq_2x_2\right)\times$$
$$\times\psi^*\left(\hat{\mathbf{k}}_1\right)\psi\left(\hat{\mathbf{k}}_2\right)\delta\left(\mathbf{k}_{1,\parallel}-\mathbf{k}_{2,\parallel}\right)G^{(0)}\left(k_{1,x}+\frac{q_1}{2},k_{2,x}+\frac{q_2}{2};\mathbf{k}_{\parallel},,w_n\right)\times$$
$$\times G^{(0)}\left(-k_{1,x}+\frac{q_1}{2},-k_{2,x}+\frac{q_2}{2};-\mathbf{k}_{\parallel},-\omega_n\right)\tag{20.3}$$

гдс $V>0$ есть констапта связи, а базисные фупкции ψ зависят от направлений векторов $\mathbf{k}_i=\left(k_{i,x},\mathbf{k}_{\parallel}\right)$.

Выполняя в (20.1) прсобразование Фурье и подставляя результат в (20.3), полугаем, после интегрирования спачала по модулям k_1, а затем по $q_{1,2}$, следующее выражение для ядра [1]:

$$K\left(x_1,x_2\right)=\frac{\pi VN_0T_c}{v_F}\sum_n\int\limits_0^1\frac{ds}{s}\left[\exp\left(-\frac{2\left|\omega_n\right|}{v_{\mathrm{F}}s}\left|x_1-x_2\right|\right)F^{(-)}(s)+\right.$$
$$\left.+\exp\left(-\frac{2\left|\omega_n\right|}{v_Fs}\left(x_1+x_2\right)\right)F^{(+)}(s)\right]\tag{20.4}$$

где $s=\cos\theta$, а

$$F^{(\pm)}(s)=\int\limits_0^{2\pi}\frac{d\varphi}{2\pi}f^{(\pm)}(s,\varphi)$$

Функшии направлений $f^{(\pm)}(\hat{\mathbf{k}})=f^{(\pm)}(s,\varphi)$ определяются следующим образом. Для фиксчрованных значении углов $0\leq\varphi<2\pi,0\leq\theta<\pi/2$ вводим два единичных вектора:

$$\hat{\mathbf{k}}_{\pm}=\left(\pm\cos\theta,\sin\theta\cos\varphi,\sin\theta\sin\varphi\right)=\left(\pm s,\sqrt{1-s^2}\cos\varphi,\sqrt{1-s^2}\sin\varphi\right)$$

связаиных отражением в плоскости границы. Тогда

$$f^{(\pm)}=\frac{1}{2}\left(\psi^*\left(\hat{\mathbf{k}}_+\right)\psi\left(\hat{\mathbf{k}}_{\mp}\right)+\psi^*\left(\hat{\mathbf{k}}_-\right)\psi\left(\hat{\mathbf{k}}_{\pm}\right)\right)$$

Таким образом, вид ядра $K\left(x_1,x_2\right)$ определяется трансформационными свойствами базисных функций представлешия при отражении в плоскости границы.

Для бесконечного однородного сверхпроводника ядро линейного интегрального уразнения, определяющее параметр порядка, имеет вид:

$$K^{(0)}\left(x_1-x_2\right)=\frac{\pi VN_0T_c}{v_F}\sum_n\int\limits_0^1\frac{ds}{s}\exp\left(-\frac{2\left|\omega_n\right|}{v_Fs}\left|x_1-x_2\right|\right)F^{(-)}(s)\tag{20.5}$$

причем из определения критической температуры:

$$\pi VN_0T_{\mathbf{c}}\sum_n\frac{1}{\left|\omega_n\right|}=1$$

[11] Ланное выражсние сцраведливо в квазиклассическом приближении. Это озпачает, что, поскольку характерный масыгтаб изменения ялра - длина когереттности о - значительно превосходит атомны масыштаб $k_{\bar{F}}^{-1}$, то можно прснебречь быстроосциллирующими вкладами в $K\left(x_1,x_2\right)$, пропордиональными $e^{\pm21k_{\mathrm{F}}x}$.

следует, что

$$\int\limits_{-\infty}^{+\infty} dx_1 K^{(0)}\left(x_1 - x_2\right) = 1 \tag{20.6}$$

По сравнению с бесконечным неограниченным сверхпроводником, учет поверхдости свелся к появлешиіо в правой части (20.4) второго слагаемого, убцваюощего на расстояниях порядка ξ_0 от поверхности и ответственного, как указывалось в §13, за подавление сверхпроводимости в приповерхностном слое.

Граничные условия для уравнений Гинзбурга-Ландау получаются из асимптотики решения интегрального уравнения (20.2) при $x \gg \xi_0$. Непосредственной подстановкой в (20.2) с учетом (20.5), убеждаемся, что искомым асимптотическим репиенисм является линейная функция $\eta(x) = \eta_0(1 + x/b)$ с вещественным b. Эффективное граничное условие тогда выглядит следующим образом:

$$\left.\frac{\partial\eta}{\partial x}\right|_{x=0} = \left.\frac{1}{b}\eta\right|_{x=0} \tag{20.7}$$

Параметр 6 совпадает с интерполяшионной длиной, введенной в 813.

Отметим два существенных симметрийных свойства граничных условий. Если базисная функция не менятся при отражении $x \to -x$, т.е. $\psi\left(\hat{\mathbf{k}}_-\right) = \psi\left(\hat{\mathbf{k}}_+\right)$, то $b = \infty$, т. е. $\partial\eta/\,\partial x|_{x=0} = 0$. Действителыно, в этом случае, распространяя параметр порядка четным образом на «нефизическую» область $x < 0 : \eta(-x) = \eta(x)$, попучим, что ядро (20.4) принимает вид однородного объемного ддра $K^{(0)}$, а уравнение (20.2) в попупространстве становится уравнением во всем пространстве:

$$\eta\left(x_1\right) = \int\limits_{-\infty}^{+\infty} dx_2 K^{(0)}\left(x_1 - x_2\right)\eta\left(x_2\right) \tag{20.8}$$

определяющим темпсратуру сверхпроводящего перехода для бесконечного одлородного кристалла. Четное рештение этого уравнения в силу (20.5) есть просто константа. Граничное условие, таким образом, имеет вид (13.18):

$$\left.\frac{\partial\eta}{\partial x}\right|_{x=0} = 0. \tag{20.9}$$

Покажем, что в другом предельном случа, когда базисная функция меняет ак при отражении, имеем $b = 0$. Параметр порядка теперь также можно продолжить в область $x < 0$, но уже нечетным образом: $\eta(-x) = -\eta(x)$. Тогда уравнение (20.2) вновь переходит в обхемное уравнение, нечетное решетие которого есть линейная функшия x, что дает граничное условие вида (13.16):

$$\left.\eta\right|_{x=0} = 0 \tag{20.10}$$

В общем случае, ссл: базисные функции не имегот опрсделенной четности при отражении в плоскости границы, то интегральнос уравнение, определячощее параметр порядка, не сводится к простому вилу и грашичные условия не совпалакт с (20.9) или (20.10). В этой ситуации можно пользоваться следующцвм приближенньім выражением для интерполяционной дтины b:

$$\frac{b}{\xi_0} = \frac{1}{7\zeta(3)} \frac{1}{\int\limits_0^1 dss^2 F^{(-)}(s)} \left\{ \frac{\pi^4}{24} \int\limits_0^1 dss^3 \left(F^{(-)}(s) + F^{(+)}(s) \right) + \right.$$
$$\left. + \frac{\left[7\zeta(3) \int\limits_0^1 dss^2 \left(P^{(-)}(s) + F^{(+)}(s) \right) \right]^2}{2\pi^2 \int\limits_0^1 dss \left(F^{(-)}(s) - F^{(+)}(s) \right)} \right\} \tag{20.11}$$

Чтобы не прерывать связности изложения, вывод этой формулы вынесен в конец параграфа.

Для сдиничного представления A_{1g}, соответствующего ббычному s волновому параметру порядка, базисная фупкиия $\psi(\hat{\mathbf{k}}) \sim \text{const}$ не изменяет знака при отражении в плоскости транишы, и мы имеем $b = \infty$, что означает существование изотропной в базисной плоскости поверхностной сверхпроводимости.

Совсем по-друтому обстоит дело в случас неединимних представлений. Рассмотрим ситуацию на примере параметра порядка, соответствующсго представлснипо B_{1g} группы $D_{6\,\%}$. В главних осях (X, Y, Z) (см. рис. 18) базисная функция имеет следующий вид:

$$\psi(\hat{\mathbf{k}}) \propto \hat{k}_Z \left(\hat{k}_X^3 - 3\hat{k}_X \hat{k}_Y^2 \right) \tag{20.12}$$

Если поверхдость кристалла совпадает с плоскостью XZ, т.с. $\varphi = \pi/2$, то отражснию в плоскости гранины соответствуст замена $Y \to -Y$. При таком преобразовании Базисная функиия не меняет знак, и мы потучаем $b = \infty$. Следовательно, поверхностнос критическое поле максимально и определяется формулой (13.22). Эгот же результат мы получим, если угол φ принимает значения $\pi/6, 5\pi/6$ и т. д., поскольку во всех элих случаях $\psi(\hat{\mathbf{k}})$ не менятся при отражении в плоскости границы.

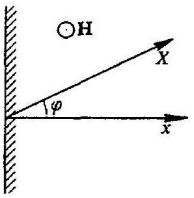


Рис. 18. Ориентация поверхности сверхпроводника (внутренняя нормаль - вдоль $\dot{x}$) относителыо осей кристаллической решетки. Поле H паратлельно оси шестого порядка, внутренняя нормаль направлена вдоль оси x.

Если же поверхность сверхпроводника совпадает с кристаллографической плоскостью YZ, т.е. $\varphi = 0$, то при замене $X \to -X$ базисная функция (20.15) меняет знак. Поэтому $b = 0$ и $f(0) = 0$. В этом случае (а также при $\varphi = \pi/3, 2\pi/3$ и т. д.) поверхностное критическое поле минимально и совпадает с верхним критическим полем в ойъеме (см. (13.17)).

Окончательный вывод:

$$\frac{H_{c3}(T)}{H_{c2}(T)} = \begin{cases} \approx 1,69, & \text{при } \varphi = \frac{(2n+1)\pi}{6} \\ 1, & \text{при } \varphi = \frac{n\pi}{3} \end{cases} \tag{20.13}$$

где $n = 0, 1, \ldots, 5$. Таким образом, граничные условия и поверхностное критическос поле демонстрируіт существенную анизотропию (в данном случае - шестого порядка) [2]. Следует отметить, что результат (20.13) вытекает из общих свойств четности или нечетности базисной функции представления B_1 при отражении в пооскости грапицы и поэтому не зависит от выбора $\psi(\hat{\mathbf{k}})$.

При промсжуточшьх значениях угла φ необходимо пользоваться граничными условиями общего вида (20.7), причсм для вычисления $b(\varphi)$ периодической функции с

периодом $\pi/3$, измсняющейся в пределах 0 до ∞, важе, разумеется, конкретный выбор базисной фупкции. Зависимость $H_{c3}(\varphi)$ должна при этом иметь достаточно резкие пики. Дело в том, что вблизи T_c существует характерный масштаб изменения параметра порядка корредяшопная длина $\xi \gg \xi_0$. Если $b(\varphi) < \xi$, что имеет месго почти всюоду, кроме узких окрсстностей шириной $\delta\varphi$ вблизи угла $\varphi = \pi/2$ и т. д., то эффективное граничное условие имеет вид (20.10) и $H_{c:3} = H_{\mathrm{c}\,2}$ в целом иттервале углов. С другой стороны, при $|\varphi - (2n+1)\pi/6| < \delta\varphi$ имеем $b(\varphi) > \xi$, т.е. эффективно $b = \infty$ и $H_{c3} \approx 1,69H_{c2}$. Ширина пика определяется конкретным видом функции $b(\varphi)$. Для базиспой функции (20.12) вычисление с помошюо (20.11) дает:

$$\frac{b(\varphi)}{\xi_0} \sim \frac{1}{\cos^2 3\varphi}, \qquad \text{при } \varphi \to \frac{(2n+1)\pi}{6}$$

откуда $\delta\varphi \sim \sqrt{\xi_0/\xi}$.

В указанной узкой переходной области утлов, где 6 нзменяется от 0 до ∞, следует ожидать, что сверхпроводящее состояние вблизи поверхіноти будет возникать в некотором поле между $H_{c2}(T)$ и $1,69H_{c2}(T)$, наклон которого становится функцией H. Следует заметить, что анизотропия интерполяционной длины, а следовательно и поверхностной энергии, выгчисленная с помощыо формулы (20.11), не описывается, вообще говоря, простейшими допустимыми по симметрии функциями $f(\mathbf{n})$ (см. (13.12)-(13.14)). Однако, положение нуле этих функций (то есть пиков интерполяшонной длины) обусловлено симметрийными требованиями.

Диффузно-отражагомая поверхность. Для получения граничных условий на диффузно-отражающей поверхности удобно использовать метод квазиклассических траекторий (см. [81, 82]). Исходным пунктом, как и при рассмотрении случая зеркалынй границы, является интегральное уравнение вида (17.9) для компонент параметра порядка.

Принимая во внимание слабую зависимость плотности состояний вблизи ферми-поверхости от энергии и сохраняя только медленно мсняющиеся на атомных масштгабах вклады, получаем слслуюющее выражение для ядра $K(\mathbf{r}_1, \mathbf{r}_2)$:

$$K(\mathbf{r}_1, \mathbf{r}_2) = \pi V N_0 T \sum_n \int_0^\infty dt \exp(-2|\omega|t) \left\langle \psi^*(\hat{\mathbf{n}}_1)\, \psi_j(\hat{\mathbf{n}}_2) \right\rangle_{\varepsilon\mathbf{F},\text{classical}} \tag{20.14}$$

где $\psi(\hat{\mathbf{n}})$ - базисные функции выбранного представлсния. Угловые скобки означают усреднение по всем траекториям классической частишы, движущейся с фермисвской скоростью v_F, которые соединяют точки $\mathbf{r}_1$ и $\mathbf{r}_2$ и удовлетворятот условию $\mathbf{r}(0) = \mathbf{r}_1$. При этом мы должіы рассматривать как траектории, стартующие в момешт врсмени $t = 0$ из r_1 и через время t закапчивающиеся в $\mathbf{r}_2$, так и обращенные во времени, то есть те, которые стартуют при $-t$ из $\mathbf{r}_2$ и заканчиваются в $\mathbf{r}_1$ при $t = 0$ (нихе мы выписываем явные выражения только дъя траекторий псрвого типа, поскольку обращенные во времени дающт лишв эрмитово-сопряженный вклад в ядро). Едипичные векторы $\hat{\mathbf{n}}_1 = \mathbf{n}(\mathbf{r}_1)$ и $\hat{\mathbf{n}}_2 = \mathbf{n}(\mathbf{r}_2)$ обозпачают направления $\mathbf{n}$ скорости частишы в соответствующих точках.

Для того, чтобы вывести формулу (20.14), начнем с микроскопического определения ядра K:

[12] Во избежание недоразумений подчеркнем, что под ацизотропие поверхостной сверхпроводимости здесь имеется в виду анизотропия ваклона ликии $H_{c3}(T)$ ири фиксированном направлении внецисго поля - вдоль главно оси - и разлитчнх направлениях нормали в поверхпости в базисной плоскосги.

$$K(\mathbf{r}_1,\mathbf{r}_2)=VTT_{\mathbf{r}'_{1,2}\to r_{1,2}}\sum_n\psi^*\left(\frac{\nabla_{r_1}-\nabla_{\mathbf{r}'_1}}{2ik_{\mathrm{F}}}\right)\psi\left(\frac{\nabla_{\mathbf{r}'_2}-\nabla_{\mathbf{r}_2}}{2ik_{\mathrm{F}}}\right)\times$$
$$\times G^{(0)}(\mathbf{r}_1,\mathbf{r}_2;\omega_n)\,G^{(0)}(\mathbf{r}'_1,\mathbf{r}'_2;-\omega_n) \tag{20.15}$$

(ср. с выражением (19.2) для случая p-спаривания). Здесь $G^{(0)}$ есть функции Грина нормального состояния, для которых мы используем следуощее представление:

$$G^{(0)}(\mathrm{r}_1,\mathbf{r}_2;\omega_n)=\sum_i\frac{\Psi_i^*(\mathrm{r}_1)\,\Psi_i(\mathrm{r}_2)}{i\omega_n-\varepsilon_i} \tag{20.16}$$

где Ψ_i - собственные функцин однотастичного гамильтониана H_0 (см. 17), а ε_i - соответствутощие собственные значения. Здесь и нижс мы опускаем спиновые индексы.

Подставляя (20.16) в (20.15), получаем:

$$K(\mathbf{r}_1,\mathbf{r}_2)=\frac{VT}{k_{\mathrm{F}}^2}\sum_n\sum_{ij}\frac{(i\,|\psi_i^*\ \mathrm{J}(\mathbf{r}_2)|\,j\rangle\,\langle j\,|\psi\mathrm{J}(\mathbf{r}_2)|\,i\rangle}{(i\omega_n-\varepsilon_i)(-i\omega_n-\varepsilon_j)} \tag{20.17}$$

где $\mathbf{J}(\mathbf{r})$ есть оператор тока:

$$J(r)=\frac{1}{2i}\lim_{r'\to r}\left(\frac{\partial}{\partial r}-\frac{\partial}{\partial r'}\right)$$

Следутошии шаг состоит в использовании того факта, что только медленно меняющщиеся части волновьх функций дают вклады в сверхпроводящее ядро, и поэтому можно применять квазиклассическос приближение. Можно показать [81, 82], что в данном приближении произведение двух матричных элементов в числителе (20.17) может быть переписано в виде

$$\langle i|\hat{A}|j\rangle\langle j|\hat{B}|i\rangle=\frac{1}{2\pi N_0}\int\limits_{-\infty}^{+\infty}dt\exp\left(-i\left(\varepsilon_i-\varepsilon_j\right)t\right)\left\langle\hat{A}(\mathbf{r}_1)\,\hat{B}(\mathbf{r}(t))\delta(\mathbf{r}_2-\mathbf{r}(t))\right\rangle_{\varepsilon_{\mathrm{P}},\ \mathrm{classical}} \tag{20.18}$$

гдс усреднение проводится по всем классическим траекториям $r(t)$, таким, что $\mathbf{r}(0)=\mathbf{r}_1$. Разделим теперь область интегрирования в (20.18) на две части: $(-\infty,0)$ и $(0,\infty)$, и произведем в первой из них замену $t\to -t$. Таким образом, мді получаем интеграл по положительным t от суммы двух вкладов - от «прямых и «обращенных во времени» траекторий, сосдиняіших тодки r_1 и $\mathbf{r}_2$ (t при этом имеет смысл времени пролета частицы по траектории). После суммирования по i и j приходим к формуле (20.14).

Рассмотрим оба типа рассеяния квазичастиц на поверхности: зеркапьнос и диффузное.

Кроме того, мы ограничимся спучаем чистьх свсрхпроводников, следовательно, квазиклассические траектории в объеме образда являются

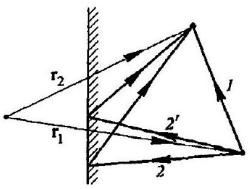


Рис. 19. Прямая (1) и отражсниыс (2 и 2') траектории из точки r_1 в точку $\mathbf{r}_2$ в случас диффузного отражения на границе прямыми линиями, а все вклады в ддро могут быть разделены на два класса: «прямые» и «отраженные» (см. рис. 19).

Первый вклад определяется тривиальной трасктсрией: $\mathbf{r}(t) = \mathbf{r}_1 + \mathbf{v}_\mathrm{F} t$. Ее подстановка в (20.17) дает следующее выражение:

$$K^{(0)}(x_1, x_2) = \frac{\pi V N_0 T}{v_F} \sum_n \int_0^1 \frac{ds}{s} \exp\left(-\frac{2|\omega_n|}{v_F s}|x_1 - x_2|\right) F^{(0)}(s) \tag{20.19}$$

где

$$F^{(0)}(s) = \int_0^{2\pi} \frac{d\varphi}{4\pi} \left(\psi^*(s,\varphi)\psi(s,\varphi) + \psi'^*(-s,\varphi)\psi(-s,\varphi)\right) \tag{20.20}$$

Как и выше, мы ввели обозначение: $s = \cos\theta$, где θ, φ ссть полярный и азимуталыный углы, соответственно (полярная ось направлена вдоль оси $\hat{x}$ - нормали к поверхности). Подразумевастся также, что все суммы по частотам обрезаны на граничной частоте ε_l.

Что касается второго вклапа в ядро, которыдй дают все возможные отраженные траектории, то его вил существснно зависит от характера отражения квазичастиц на поверхности. В случае зеркального отражения мы имеем дело лишь с одной траекторией:

$$\mathbf{r}(t) = \begin{cases} \mathbf{r}_1 + \mathbf{v}_F t, & t < t_0 = -\frac{x_1}{v_{F,x}} \\ \bar{\mathbf{v}}_F (t - t_0), & t > t_0 \end{cases}$$

где t_0 соответствует моменту соударения с поверхностью, а $\bar{\mathbf{v}}_\mathrm{F} = (-v_{F,x}, v_{F,y}\ v_{F,z})$. Подставляя это выражение для $\mathbf{r}(t)$ в (20.17) и выполняя интегрирования, окончательно прихолим к следутошему резуштату:

$$K^{(\mathrm{spec})}(x_1, x_2) = \frac{\pi V N_0 T}{v_F} \sum_n \int_0^1 \frac{ds}{s} \exp\left(-\frac{2|\omega_n|}{v_F s}(x_1 + x_2)\right) F^{(\mathrm{spec})}(s) \tag{20.21}$$

rae

$$F^{(\mathrm{spec})}(s) = \int_0^{2\pi} \frac{d\varphi}{4\pi} \left(\psi^*(-s,\varphi)\psi(s,\varphi) + +\psi^*(s,\varphi)\psi(-s,\varphi)\right) \tag{20.22}$$

Сумма выражений (20.19) и (20.21) совпадает, как и слеловало ожидатъ, с формулой (20.4), полученіой путем непосредственного интегрирования фулкий Грина.

В случае диффузного отражения, принимая во внимание вклады от всех возможных траекторий вида:

$$\mathbf{r}(t) = \begin{cases} \mathrm{r}_1 + \mathbf{v}_\mathrm{F}^{(1)} t, & t < t_0 = -\frac{x_1}{v_{\mathrm{F},x}^{(1)}} \\ v_\mathrm{F}^{(2)}(t - t_0), & t > t_0 \end{cases}$$

где $\mathbf{v}_\mathbf{F}^{(1)}$ и $\mathbf{v}_\mathbf{F}^{(2)}$ - скорости частицы на двух прямых отрезках данной траектории, и интегрируя по всем отраженным траекториям с весовым множителем $(1/\pi)\cos\theta$, получаем:

$$K^{(\mathrm{diff})}(x_1,x_2)=\frac{\pi V N_0 T_c}{v_F}\times$$
$$\times\sum_n^1\int_0^1 ds_1\int_0^1 ds_2\exp\left(-\frac{2|\omega_n|}{v_F}\left(\frac{x_1}{s_1}+\frac{x_2}{s_2}\right)\right)F^{(\mathrm{diff})}(s_1,s_2) \tag{20.23}$$

где

$$F^{(\mathrm{diff})}(s_1,s_2)=\int_0^{2\pi}\frac{d\varphi_1}{2\pi}\int_0^{2\pi}\frac{d\varphi_2}{2\pi}\left(\psi^*(-s_1,\varphi_1)\psi(s_2,\varphi_2)+\right.$$
$$\left.+\psi^*(s_1,\varphi_1)\psi(-s_2,\varphi_2)\right)$$

Окончательно получаем:

$$K(x_1,x_2)=K^{(0)}(x_1,x_2)+K^{(\mathrm{diff})}(x_1,x_2) \tag{20.24}$$

В общем случае анизотропного спаривания и произвольной ориентации поверхоости уравнение (20.2) с ядром (20.24) ие может быть решено точно [3], однако для вычисления b можно использовать вариационный метод. В результате интерполяционная ллина b всегда оказывается порядка длины когерентности ξ_0, то есть эффективное граничное условие в области Гинзбурга-Ландау имеет вид (20.10), и поверхноспная сверхпроводимость отсутствует для всех направлений нормали. В слуqае изотропного s-спаривания можно показать [83], что граничное условие имест вид (20.9) вне зависимости от характера отражения электронов.

Таким образом, поверхостная сверхпроволимость на диффузно отражающей границе оказывается весьма чувствительной к внутренней симметрии параметра порялка, поскольку случайный характер отражения электронов приводит к его изотропизации, а это может быть достигнуто лишв путем подавления сверхпроводимости вблизи поверхности.

Вывод формулы (20.11). Для вычисления коэффициента b в линейной асимптотике параметра порядка воспользуемся вариационным методом.

Перейдем в (20.4) к безразмерной переменной $X=x/\xi_0$. Тогда

$$K(X_1,X_2)=\frac{1}{2}VN_G\sum_n\int_0^1\frac{ds}{s}\left[F_i^{(-)}(s)\exp\left(-\frac{|2n+1|}{s}|X_1-X_2|\right)+\right.$$
$$\left.+F_i^{(+)}(s)\exp\left(-\frac{|2n+1|}{s}(X_1+X_2)\right)\right] \tag{20.25}$$

При $X\gg 1$, ишем решение в виде (индекс i оптскаем): $\eta(X)=C(X+q(X))$, причем $b/\xi_0=\lim_{X\to\infty}q(X)$. Уравнение для $q(X)$ имеет вид

$$q(X_1)=\frac{1}{2}E(X_1)+\int_0^\infty dX_2K(X_1,X_2)\,q(X_2) \tag{20.26}$$

$$E(X_1)=VN_0\sum_n\frac{1}{(2n+1)^2}\int_0^1 ds\,s\left[F^{(-)}(s)+F^{(+)}(s)\right]\exp\left(-\frac{|2n+1|}{s}X_1\right)$$

[13] Если параметр порядка преобразуется согласно неединичному прелставленню точечной группы

Для формулировки вариационного принципа заметим, что интегральное уравнение на параметр порядка получается вариашией функционала: $\delta\Phi/\delta q = 0$, гдс

$$\Phi[q] = \frac{\int\limits_0^\infty dX q(X)\left[q(X) - \int\limits_0^\infty dX'\Psi\left(X,X'\right)q\left(X'\right)\right]}{\left[\int\limits_0^\infty dX q(X)E(X)\right]^2} \tag{20.27}$$

При этом экстремалыне (минимальное) значение функционала есть

$$\Phi_{\min} = \frac{1}{2\int\limits_0^\infty dX E(X)q(X)}$$

Покажем теперь, что нужное нам пределное значение решения уравнения (20.25) при $X \to \infty$ выражается как раз через $\Phi_{\min}$. Пусть $q(X) = b/\xi_0 + Q(X)$, где $Q(X) \to 0$ при $X \to \infty$. Подставляя $q(X)$ в (20.25), получаем уравнение на $Q(X)$, затсм умножаем обе его части на X_1 и, интегрируя по X_1 от 0 до ∞, окончательно имеем:

$$\frac{b}{\xi_0} = \frac{1}{7\zeta(3)}\frac{1}{\int\limits_0^1 dss^2F^{(-)}(s)}\left\{\frac{\pi^4}{24}\int\limits_0^1 dss^3\left[F^{(-)}(s) + F^{(+)}(s)\right] + \frac{1}{VN_0\Phi_{\min}}\right\}$$

Величину $\Phi_{\min}$ можно вычислять, используя вариаднонны принцип. Выбирая в качестве пробной функции пулевого приближения произвольную константу и подставляя ее в (20.26), приходим к формуле (20.11).

19.2.5 21. Influence of Impurities on Unconventional Superconductivity

Хорошо известно, что немагнитные примеси нс влияют на термодинамические свойства обычных сверхпроводников. В частности, критическая температура не зависит от концентрации пемагнитных примесей. Эффскт подавления сверхпроводимости возникаст только за счет рассеяния на магнитных примесях, разрушающих когерентность спиновых состояний электронов в куперовских парах с $S = 0$. в необычных сверхпроводпиках к такому же эффекту приводит и рассеяние на обычных примесях, разрушаюощее когсрентность орбитальных состояний спаренных электронов.

Здесь мы рассмотрим два эффекта, связанных с примесями в необычных сверхпроводниках: во-первых, умсньшение критической температуры немагнитными примесями, во-вторцх, изменение плотности состояний квазичастиц и, соответственно, термодинамических и кинетических свойстi при $T \to 0$.

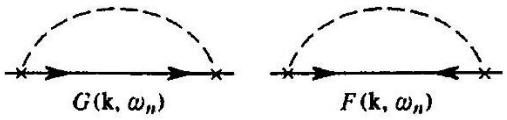
Уравнения Горькова и температура перехода. Функции Грина сверхпроводника при произвольной температуре $T \le T_c$ при наличии примессй определяются путем решения уравнений Горькова (17.6)-(17.8). При этом в одночастичный гамильтониан следует добавить слагаемое вида

$$II_{\text{imp}} = \sum_{\mathbf{k},\mathbf{k}'} u_{\alpha\beta}\left(\mathbf{k},\mathbf{k}'\right)a^+_{\mathbf{k}\alpha}a_{\mathbf{k}'\beta} \tag{21.1}$$

симметрии кристалла, то штя некоторьх выделенных направленнй нормалн вклад K (difi) (x_1, x_2) тохлественно обращается в пуль в результате интегрирования по утлам. Ананотичная ситуация ямеет место аля фаз p-спаривавия при любой ориентации поверхности [72]. Негралыое уравнение (20.2) в этом случае может быть решено методом Виnера-Хопфа.

где $u_{\alpha\beta}(\mathbf{k},\mathbf{k}')$ есть амплитуда рассеяния электрона в поле примесей, в общем случае зависящая от спина.

Поскольку мы интересуемся лишь характеристиками, усреднснными по реализациям случайного потенциала (по положениям примессй), то для нахождения функций Грина следуст воспользоваться уравнениями (17.11), включив в них примесные собственно-энергетические части (см. рис. 20), причем усреднение производится в точности так же, как и в теории обычных сверхпро-



б

Рис. 20. Примесные собственно-энергетические функция. Борновское приближение водящих сплавов [71]. Мы не принимаем во внимание интерференцию волн, рассеянных на разных примесях, предполагая выполнение условия слабого беспорядка $k_F l \gg 1$, где $l = v_F\tau$ - длина свободного пробега. Кроме того, мы пренебрегаем возможностью многократного рассеяния на одлой и той же примеси, что справедливо в слутае малости потенциала примесей по сравнению с характерной энергией электронов ε_F (борновское приближение) [1].

В указанных условиях диаграммы для усредненных собственноэнергетических частей содержат по два примесных креста, соединенных пунктирной линией (рис. 21). Если рассеяние на примесях изотропно и не зависит от спина, то пунктириой лиiии соответствует выражение

$$n_{\text{imp}}u^2 = \frac{1}{2\pi N_0\tau}$$

где n_{imp} - концентрация примессй, u - входящая в (21.1) амплитуда рассеяния, а τ есть время свободного пробега квазичастиц.

В анизотропном сверхпроводнике амплитуда рассеяния на примеси зависит от углов, и пунктиру отвечает выражсние $\hat{\tau}^{-1}(\mathbf{k},\mathbf{k}')$, обладающее точечной симметрией кристалла (см. 4). Мы можем представить его в виде разложения по мепривоДимым представлениям группы G:

$$\tau^{-1}_{\alpha\beta,\gamma\delta}(\mathbf{k},\mathbf{k}') = \sum_{\Gamma}\left(\frac{1}{\tau_{\Gamma,1}}\delta_{\alpha\beta}\delta_{\gamma\delta} + \frac{1}{\tau_{\Gamma,2}}\boldsymbol{\sigma}_{\alpha\beta}\sigma_{\gamma\delta}\right)\sum_{i=1}^{d_\Gamma}\psi_i^\Gamma(\hat{\mathbf{k}})\psi_i^{\Gamma*}\left(\hat{\mathbf{k}}'\right) \tag{21.2}$$

для случая слабого спин-орбитального взаимодействия, или

$$\tau^{-1}_{\alpha\beta,\gamma\delta}(\mathbf{k},\mathbf{k}') = \sum_{\Gamma}\frac{1}{\tau_\Gamma}\sum_{i=1}^{d\text{r}}\left(\psi_i^\Gamma(\hat{\mathbf{k}})\sigma\right)_{\alpha\beta}\left(\psi_i^{\Gamma*}\left(\hat{\mathbf{k}}'\right)\sigma\right)_{\gamma\delta}$$

для случая сильного спин-орбитального взаимодействия. Индекс Г обозначает неприводимыге представления размерности d_Γ группы G, а i нумерует базисные функции $\psi_i^\Gamma(\hat{k})$. Коэффициенты разложения τ^{-1} пропорциональны концентрагии примесей, причем слагаемые с τ_2 в выражении (21.2) соответствуют рассеянию с переворотом спина.

Для простоты ограничимся рассмотрением изотропного рассеяния на немагнитных примесях. Тогда усредиенная нормальная собственноэнергетическая часть (см. рис. 20а) имеет вид:

[11] Iекоторые следствия выхода за пределы борновского приближения будут рассмотрены нихе.

$$\Sigma_{1,\alpha\beta}(\omega_n) = \Sigma(\omega_n)\,\delta_{\alpha\beta} = \frac{1}{2\pi N_0 \tau}\int \frac{d^3k}{(2\pi)^3} G(\mathbf{k},\omega_n)\,\delta_{\alpha\beta} \tag{21.3}$$

Аномальная собственно-энергетическая часть, соответствующая диаграмме на рис. 206:

$$\Sigma_{2,\alpha\beta}(\omega_n) = \frac{1}{2\pi N_0 \tau}\int \frac{d^3k}{(2\pi)^3} F_{\alpha\beta}(\mathbf{k},\omega_n) \tag{21.4}$$

обращается в нуль в результате интегрирования по направлениям k в случас изотропного примесного рассеяния для любого сверхпроводящего состояния с параметром порядка, преобразующимся согласно неединичному представлениоо.

Уравнения Горькова теперь записываются как

$$\begin{gathered}
(i\omega_n - \xi_k - \Sigma(\omega_n))\,G(\mathbf{k},\omega_n)\,\delta_{\alpha\beta} + \Delta_{\alpha\gamma}(\mathbf{k}) F^{+}_{\gamma\beta}(\mathbf{k},\omega_n) = \delta_{\alpha\beta} \\
(i\omega_n + \xi_k - \Sigma(\omega_n))\,F^{+}_{\alpha\beta}(\mathbf{k},\omega_n) + \Delta^{+}_{\alpha\beta}(\mathbf{k}) G(\mathbf{k},\omega_n) = 0 \\
(i\omega_n - \xi_k - \Sigma(\omega_n))\,F_{\alpha\beta}(\mathbf{k},\omega_n) - \Delta_{\alpha\beta}(\mathbf{k}) G(-\mathbf{k},-\omega_n) = 0
\end{gathered} \tag{21.5}$$

Отсгода мы получаем следующие выражения для функций Грина сверхпроводника:

$$\begin{aligned}
G(\mathbf{k},\omega_n) &= -\frac{i\bar{\omega}_n + \xi_k}{\tilde{\omega}_n^2 + \xi_k^2 + \Delta_k^2} \\
F_{\alpha\beta}(\mathbf{k},\omega_n) &= \frac{\Delta_{\alpha\beta}(k)}{\tilde{\omega}_n^2 + \xi_k^2 + \Delta_k^2}
\end{aligned} \tag{21.6}$$

где

$$i\tilde{\omega}_n = i\omega_n - \Sigma(\omega_n) \tag{21.7}$$

Собственно-энергетическая часть должна быть вычислена самосогласованнымм образом. Подставляя выражение для функции G из (21.6) в (21.3) и выполняя интегрирование по энергии в предположснии электрон-дырочной симметрии, приходим к следуюощему уравненио:

$$\Sigma(\omega_n) = -\frac{i\bar{\omega}_n}{2\tau}\int \frac{d\Omega}{4\pi} \frac{1}{\sqrt{\tilde{\omega}_n^2 + \Delta_k^2}} \tag{21.8}$$

При $T < T_c$ решение уравнений (21.7), (21.8) определяется конкретным видом параметра порядка.

Вблизи критической температуры параметр порядка мал, и можно пренебречь зависимостью правой части уравнения (21.8) от Δ_k. Учитывая (21.7), получаем:

$$\tilde{\omega}_n = \omega_n + \frac{1}{2\tau}\operatorname{sign}\tilde{\omega}_n$$

Опсюда

$$\bar{\omega}_n = \omega_n + \frac{1}{2\tau}\operatorname{sign}\omega_n$$

и, следовательно, собственно-энергетическая часть при $\Delta_k \to 0$ имеет вид:

$$\Sigma(\omega_n) = -\frac{i}{2\tau}\operatorname{sign}\omega_n \tag{21.9}$$

то есть совпадает, как и допжно быть, с соответствуошпим выражением дя нормального металла.

Усредненная аномальная функция Грина выглядит тогда следующим образом:

$$F_{\alpha\beta}\left(\mathbf{k},\omega_n\right)=\frac{\Delta_{\alpha\beta}(\mathbf{k})}{\left[\omega_n+(1/2\tau)\operatorname{sign}\omega_{rn}\right]^2+\xi_k^2} \tag{21.10}$$

Подставляя (21.10) в условие самосогласования (17.5) и выполняя интегрирование по ξ, паходим:

$$\Delta_{\alpha\beta}(\mathbf{k})=\pi N_0 VT\sum_n\frac{\operatorname{sign}\omega_n}{\omega_n+(1/2\tau)\operatorname{sign}\omega_n}\int\frac{d\Omega'}{4\pi}V_{\beta\alpha,\gamma\delta}\left(\mathbf{k},\mathbf{k}'\right)\Delta_{\gamma\delta}\left(\mathbf{k}'\right)$$

После подстановки сюода разложсний потенниала парного притяжения V из §5, получаем:

$$\begin{aligned}1&=\pi N_0 VT\sum_n\frac{\operatorname{sign}\omega_n}{\omega_n+(1/2\tau)\operatorname{sign}\omega_n}=\\&=2\pi N_0 VT\sum_{n\geq 0}\frac{1}{\omega_n}+2\pi N_0 VT\sum_{n\geq 0}\left(\frac{1}{\omega_n+1/2T}-\frac{1}{\omega_n}\right)\end{aligned} \tag{21.11}$$

Логарифмически расходящаяся сумма в первом слагаемом обрезается на граничной частоте ε_1. Вспоминая определение критической температуры T_{c0} в чистом сверхпроводнике (см. (18.17)), и переписывая второе (сходящееся) слагаемое в (21.11) с учетом определения дигамма-функции $\psi(x)$, мы приходим к окончательному результату [84]:

$$\ln\frac{T_{\mathrm{c}0}}{T_{\mathrm{c}}}=\psi\left(\frac{1}{2}+\frac{1}{4\pi\tau T_{\mathrm{c}}}\right)-\psi\left(\frac{1}{2}\right) \tag{21.12}$$

Полученное уравнение определяет понижение критической температуры для произвольного сверхпроводящего состояния с нетривиальньм спариванием за счет изотропного рассеяния на немагнитных примесях относительно температуры перехода $T_{\mathrm{c}0}$ чистого сверхпроводника, характерной для представления Г, согласно которому преобразуется параметр порядка. Обратим вниманис на то, что (21.12) (с точностью до обозначений) совпадает с уравнением, описывающим подавление критической температуры парамагнитными примесями в обычном сверхпроводнике [85].

В случае малой концентрации примесей получаем:

$$T_{\mathrm{c}}=T_{c0}-\frac{\pi}{8\tau} \tag{21.13}$$

(мы воспользовались тем, что $\psi'(1/2)=\pi^2/2$).

Таким образом, немагнитные примеси в сверхпроводнике с нетривиальным спариванием подавляют сверхпроводимостъ. Качественно данный эффект можно объяснить следующим образом. Внесение примесей приводит
к изотропизации щели в спектре возбуждений. Однако, если куперовское спаривание происходит в состоянии с нарушенной пространственной симметрией, то единственной возможвостью сделать щель изотропной является тождественное обращение ее в нуль на всей поверхности Ферми, что и происходит при некоторон концснтрации примесей $\tau\Delta_0\sim 1$, гдс Δ_0 - мопуль щели при $T=0$ в отсутствие примесей.

Плотность состоний. Представлет интерес проследить, каким образом происходит подавление параметра порядка и что происходит с нулями щели при увеличении

концентрации примссей. Для ответа на эти вопросы найдем плотность состояний квазитастиц $N(E)$ (см. 17) при $E \to 0$. При этом мы не будем принимать во внимание уравнение самосогласования для параметра порядка в присутствие примесей, так как это пе влияет на поведение $N(E)$ при $E \to 0$, а лиш меняет величину модуля параметра порядка.

Выполним в (21.7) аналитическое прололжение и введем обозначение

$$t(E) = (i\tilde{\omega}_n)|_{i\omega_n \to E+i0} = E - \Sigma^R(E) \tag{21.14}$$

Тогда выражение (17.27) для плотности состояниді может бытть с учетом (21.3), записано следующим образом:

$$N(E) = -\,2N_0\tau\,\mathrm{Im}\,\Sigma\,(\omega_n)|_{i\omega_n+E+i0} = 2N_0\tau\,\mathrm{Im}\,t(E) \tag{21.15}$$

Таким образом, задача свелась к нахождению зависимости $\mathrm{Im}\,t(E)$. Для ее вытисления необходимо произвести в (21.8) аналитическое продолжение на ось вещественных частот. В результате получается зависящее от структуры сверхпроводящего параметра порядка $\Delta(\mathrm{k})$ уравнение самосогласования для функции $t(E)$:

$$t = E + \frac{i}{2\tau} g(t) \tag{21.16}$$

где

$$g(t) = \int \frac{d\Omega}{4\pi} \frac{t}{\sqrt{t^2 - \Delta_k^2}} \tag{21.17}$$

(знак корня при аналитическом продолжении выбирается таким образом, чтобы $\mathrm{Im}\,\Sigma^R < 0$).

В качестве примеров, илшострирупших поведение плотности состояний в необычных сверхпроводниках с примесями, найдем решения уравнения (21.16) для различных фаз с p-спариванием.

B-фаза. Анатогично случато обычной сверхпроводимости, для B-фазы мы имеем $\Delta_{\mathrm{k}}^2 = \Delta^2 = \mathrm{const}$, и (21.16) принимает вид

$$t = E + \frac{i}{2\tau} \frac{t}{\sqrt{t^2 - \Delta^2}}$$

Мнимая часть у решения $t(E)$ данного уравнения (а, следовательно, и ненулевая плотность состояний) появляется лишш при $E > E_c$, где величина порога соответствует максимальному значению функции $E(t) = t - t/2\tau\sqrt{\Delta^2 - t^2}$ (см. [85]):

$$E_c^2 = \Delta \left[1 - \left(\frac{1}{2\tau\Delta} \right)^{2/3} \right]^{3/2} \tag{21.18}$$

Мы видим, что при достаточно высокой концентрации немагнитных примесей такод, что $\tau < 1/2\Delta$, щель в спектре обращается в нул. При этом, однако, критическая темпсратура, определяемая уравнением (21.12), все еще больше нуля, что соответствует бесщелевой свсрхпроводимости, совсршенно аналогично тому, что имеет место в обычных сверхпроводниках с парамагнитными примесями (см. упражнение в конце параграфа).

A-фаза. Параметр порядка имеет вид $\Delta_{\mathrm{k}}^2 = \Delta^2 \sin^2\theta$ (мы выбрали такую же нормировку модуля Δ, как и в 7). Выполняя интегрирование по утлам в (21.17), получаем:

$$t = E + \frac{i}{4\tau\Delta} t \ln \frac{t+\Delta}{t-\Delta}$$

Это уравнение может быть решено при $E \to 0$:

$$t = \frac{E}{1 - \pi/(4\tau\Delta)} + \frac{iE^2}{2\tau\Delta^2[1 - \pi/(4\tau\Delta)]^3}$$

откуда следует, что

$$N(E) = N_0 \frac{1}{[1 - \pi/(4\tau\Delta)]^3} \left(\frac{E}{\Delta}\right)^2$$

С увеличением слепени загрязнения, то есть уменьшением времени пробега τ, коэффициент при E^2 растет и при $\tau\Delta = \pi/4$ обращается в бесконечность. Этим определяется критическая концентрация примесей, выше которой

$$N(E = 0) = 2N_0\tau\Delta \operatorname{tg}\left(\frac{\pi}{2} - 2\tau\Delta\right) \tag{21.19}$$

Физический смысл полученного результата становится ясным при сравнении с (17.30): нули в спектре квазичастиц для A-фазы остатотся изолированньми точками при малом количестве примесей и размываются в «пятна» нулей [23, 86] только выиге критической концснтрации.

Полярная фаза. Параметр порядха имеет вид $\Delta_k^2 = \Delta^2 \cos^2\theta$. Из (21.16) имеем:

$$t = E + \frac{i}{2\tau\Delta} t \arcsin\frac{\Delta}{t}$$

Легко убедиться в том, что это уравнение имеет при $E = 0$ следующее решение

$$t(E = 0) = \frac{i\Delta}{\operatorname{sh} 2\tau\Delta} \tag{21.20}$$

откуда

$$N(E = 0) = N_0 \frac{2\tau\Delta}{\operatorname{sh} 2\tau\Delta} \tag{21.21}$$

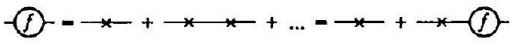
Это означает, что при сколь угодно слабом загрязнении линии нулей становятся цельми полосами [23, 86]. Такой эффект приведет к изменению термодинамических свойств сверхпроводника с подобной структурой щели при $T \to 0$, в частности, электронная теплоемкость станет пропорциональной температуре.

Упражнение. С помощью уравнения (21.12) вцчислить значение критической концентрации примесей, при которой T_c обращается в нуль, и найти область существования бесщелевой сверхпроводимости в B-фазе.

Выход за пределы борновского приближения. Приведенный выше анализ базировался на использовании борновского приблихения, то есть на пренебрежении возможностью многократного рассеяния электрона на одной и той же примеси. При учете такого рассеяния необходимая модификация теории сводится к замене собственно-энергетических частей, найденных в борновском приближении, на точпые. Для обычных сверхпроводников при этом сохраняегся основной вывод об отсутствии подавления сверхпроводимости немагнитными примесями. Для необычных сверхпроводников рассеяние на примесях подавляет свсрхпроводимость, а выход за пределы борновского приближения приводит к существенным изменениям в поведении функаий Грина, а, следовательно, и физических величин [87, 88].

Мы рассмотрим случа слабого беспоряшка, то есть достаточно малой концентации примесей, когда выполняется условие $k_F l \gg 1$, позволяющее не учитывать диаграммы с пересекающимися пунктирными линиями. Физически это означает пренебрежение интерференцией волн, рассеянных на разных примесях, и ответ для $\Sigma(\omega_n)$ получается

просто умножением вклада одной примеси $\Sigma_0(\omega_n)$ на их концентрацию: $\Sigma(\omega_n) = n_{\text{imp}}\,\Sigma_0(\omega_n)$. Величина $\Sigma_0(\omega_n)$ непосредственно связана с точной ампитудой рассеяния на нулевой утол на одной примеси, которая определяется суммой диаграмм



Ри с. 21. Диаграммное уравнение для точной амплитуды рассеяния на одной примеси

на рис. 21. Для изотропного точечного потенциала примесей аномальная собственно-энергетическая часть обрашается в нуль для любых сверхпроводящих состояний с параметрами порядка, соответствующими неединичным прсдставлениям группы симметрии кристалла. В этом случае амплитуда рассеяния характеризуется единственной скалярной функаией $f(\omega_n)$, причем

$$\Sigma(\omega_n) = n_{\text{imp}} f(\omega_n) \tag{21.22}$$

В общем же случае амплитуда рассеяния зависит от импульсов и является матрицей 4×4 (T-матрицей) в спиновом пространстве и «пространстве» частица-дырка (см. 17).

Суммирование диаграммного ряда на рис. 21 позволяет выразить $f(\omega_n)$ через затравочную амплитуду рассеяния $\boldsymbol{u}$. Удобнее, однако, записать точную амплитуду рассеяния в несколько ином виде, вводя фазовыи сдвиг δ_0 рассеянной s-волны в нормальном состоянии:

$$f(\omega_n) = \frac{k_{\text{n}}}{1 - k_{\text{n}} \sum\limits_{\mathbf{k}} G(\mathbf{k}, \omega_n)} \tag{21.23}$$

где $k_{\text{n}} = -\operatorname{tg}\delta_0/(\pi N_0)$, а $G(\mathbf{k}, \omega_n)$ есть усредненная функция Грина сверхгроводника [2]. Подставляя (21.23) в (21.22), включая вещественную (четную по ω_n) часть собственно-энергетической функции в перенормировку химического потенциала и выдсляя явно мнимую (нечетную по ω_n) часть, получаем:

$$\Sigma(\omega_n) = \frac{n_{\text{imp}} k_{\text{n}}^2 \sum\limits_{\mathbf{k}} G(\mathbf{k}, \omega_n)}{1 - k_n^2 \left(\sum\limits_{\mathbf{k}} G(\mathbf{k}, \omega_n) \right)^2} \tag{21.24}$$

Здесь мы использовали тот факт, что в случас элскгрон-дырочной симмстрии $\sum\limits_{\mathbf{k}} G(\mathbf{k}, -\omega_n) = -\sum\limits_{\mathbf{k}} G(\mathbf{k}, \omega_n)$ (см. (21.6)). Подставляя в (21.24) выражение для функции Грина (21.6), интегрируя по ξ и выполняя аналитическое продолжение с jчетом (21.14), получаем окончательно уравнение для функции $t(E)$, обобщающее (21.16) на случай неборновского рассеяния:

$$t = E + i\Gamma \frac{g(t)}{\cos^2\delta_0 + \sin^2\delta_0 g^2(t)} \tag{21.25}$$

где

$$\Gamma = \frac{n_{\text{imp}}}{\pi N_0} \sin^2\delta_0$$

а $g(t)$ определяется формулой (21.17). В прсделе слабого рассеяния, устремляя δ_0 К нулюо, имеем:

[12] Чтобы не прерывать связности излохения, вывод формулы (21.23) вынесен в конец параграфа.

$$\Gamma \to \frac{n_{\rm imp}}{\pi N_0}\delta_0^2 = \pi N_0 n_{\rm imp} u^2 = \frac{1}{2\tau_{\rm Born}}$$

и (21.25) переходит в (21.16).

Выражение (21.15) для плотности состояний квазичастиц справедливо лиш в борновском приближении. Для вычисления $N(E)$ в случае произвольных фазовых сдвигов вернемся к опрсделению (17.27):

$$N(E) = -\frac{1}{\pi}\,{\rm Im}\sum_{\mathbf{k}} G\left(\mathbf{k},\omega_n\right)\Big|_{i\omega_n\to E+i0} = -\frac{1}{\pi}\,{\rm Im}\sum_{\mathbf{k}} G^R(\mathbf{k},E) \tag{21.26}$$

Входящая сюда функция Грина получается путем аналитического продолжения в (21.5):

$$G^R(\mathbf{k},E) = \frac{t(E)+\xi_k}{t^2(E)-\Delta_{\mathbf{k}}^2-\xi_k^2} \tag{21.27}$$

Из (21.26), (21.27) и (21.17) окончательно получаем:

$$N(E) = N_0\,{\rm Re}\,g(t(E)) \tag{21.28}$$

В борновском приближении, как мы видели, изолированные точки нулей в сверхпроводнике со структурой, например, A-фазы, являтся устойчивыми по отношению к слабому загрязнению. Покажем теперь, что для достаточно сильного потенциала примессй это не так.

Рассмотрим противоположныи борновскому случай резонансного рассеяния, то есть больших фазовых сдвигов: $\delta_0 \to \pi/2$. Подставляя в (21.25) $\Delta_{\mathbf{k}}^2 = \Delta^2\sin^2\theta$, получаем для $t(E)$ уравнение:

$$t = E + 2i\Gamma\Delta\frac{1}{t}\left(\ln\frac{t+\Delta}{t-\Delta}\right)^{-1} \tag{21.29}$$

имеющее при $E=0$ и $\Gamma \ll \Delta$ следующее решение:

$$t(E) = i\sqrt{\frac{2\Gamma\Delta}{\pi}} \tag{21.30}$$

Подставляя его в (21.17), получаем:

$${\rm Re}\,g(t(E=0)) = \sqrt{\frac{\pi\Gamma}{2\Delta}}$$

Окончательно:

$$N(E=0) = N_0\sqrt{\frac{\pi\Gamma}{2\Delta}} \tag{21.31}$$

Мы видим, что плотность состояний при $E=0$ оказывается конечной, но, разумеется, обращается в нуль при уменьшении степени загрязнения, то есть при $\Gamma \to 0$. Это означает, что внесение сколь утодно малого количества резонансных примссей превращает изолированные нули щели в спектре сверхпроводника в пятна конечного размера [88].

MC-21.1

Найти понижение критической температуры сверхпроводника с p-спариванием вследствие резонансного рассеяния на примесях. Как изменится в этом случае уравнение (21.12)?

MC-21.2

Вычислить плотность состоянnй при $E = 0$ для полярной фазы при резонансном рассеянии на примесях [3].

Вывод формулы (21.23). Диаграммный ряд на рис. 21 сводится, как легко видеть, к следующему уравнению на амплитуду рассеяния:

$$f(\omega) = u + u \sum_{\mathbf{k}} G(\mathbf{k}, \omega) f(\omega) \tag{21.32}$$

Запишем входяшую сюда функцию Грина сверхпроводника как

$$G = G_{\text{off}}^{(0)} + G - G_{\text{off}}^{(0)} \tag{21.33}$$

где

$$G_{\text{off}}^{(0)} = \frac{1}{2}\left(G^{(0)R} + G^{(0)A}\right)$$

есть всщественная часть функции Грина для расссяния на одной примеси в нормалном состоянии. В соответствии с определением функции Грина уравнения Шредингера:

$$G^{(0)}(\omega) = \frac{1}{\omega - \varepsilon + i0} = P\frac{1}{\omega - \varepsilon} - i\pi\delta(\omega - \varepsilon) = G_{\text{off}}^{(0)} + G_{\text{on}}^{(0)}$$

гдс ε есть энергии свободных электронов, взаимодействующих с примесью, а P - символ главного значения интеграла. Индекс «off («оп») у вещественной (мнимой) части функции Грина означает, что промежуточные состояния пе находятся (находятся) на массовой поверхiости.

[3] См. Ю. С. Бараи, В. П. Минеев, А. А. Свидзииский //Письма в ЖЭТФ. 1997. 65. 606.

Подстановка (21.33) в (21.32) и перегруппировка слагаемьх даюот:

$$\begin{aligned} f(\omega) &= \left(u + u^2 \sum_{\mathbf{k}} G_{\text{off}}^{(0)}(\mathbf{k}, \omega) + \ldots\right)\left(1 + \sum_{\mathbf{k}} \left[G(\mathbf{k}, \omega) - G_{\text{off}}^{(0)}(\mathbf{k}, \omega)\right] f(\omega)\right) = \\ &= k_{\text{n}} + k_{\text{n}} \sum_{\mathbf{k}} \left[G(\mathbf{k}, \omega) - G_{\text{off}}^{(0)}(\mathbf{k}, *\omega)\right] f(\omega) \end{aligned} \tag{21.34}$$

Здесь мы ввели величину k_{n}, описываюшую рассеянис на примеси в нормальном металле и удовлетворяющую соотношенино:

$$k_{\text{n}} = u + u G_{off}^{(0)} k_{\text{n}}$$

В общем случае вместо одной скалярной функции k_{n} нсобходимо рассматривать матрицу 4×4 (-матрицу) [88].

Величина k_{n} параметризуется с помошьго фазового сдвига рассеянных волн следующим образом:

$$k_{\text{n}} = -\frac{\operatorname{tg} \delta_0}{\pi N_0} \tag{21.35}$$

Стоящая в правой части (21.34) сумма по димпулесам от $G_{\text{ofT}}^{(0)}(\mathbf{k}, \omega)$ равна нулю и мы приходим к формуле (21.23).

19.2.6 22. Electronic Thermal Conductivity of Unconventional Superconductors

Наличие симметрийпых нулей в спсктре элементарных возбуждений приводит, как мы убсдились выше, к существенному измешению термодинамичсских характсристик сверхпроводиика при низких температурах. В кинетике необычных сверхпроводников нули в спсктре также итраюот важнуо роль.

Наиболее просго неравновесные свойства сверхпроводников описываются с помощью кинетического уравнения Больцмана, которому удовлстворяет функция распределения возбуждсний. Разумеется, больцмановская кинетическая теория справедлива лишш для газа хорошо определешших элементарных возбуждений, энсргия которых велика по сравнснию с обратным врсменсм их жизни. Это условие заведомо нарушается в необычных сверхпроводниках с нулями в спектре элсмен'гарных возбуждений, обладающих конечной плотностью состояний при нулевой энергии. Поэтому описанис релаксационных процессов с помощью уравнения Больцмана справедливо только в области достаточно высоких температур, гдс средняя тепловая энергия возбуждений велика по сравнению с их затуханием γ. В чистьх сверхпроводниках данная область охватывает почти весь диапазон температур, кроме депосредстзенной охрестности нуля, поэтому здесь можно пользоваться уравнением Болцмана. Следует, однако, иметь в виду, что и в этой области вычислсние энергетической зависимости времени свободного пробега возбуждений, черсз которое выражактся кинстические коэффишиенты, требует привлечения микроскопической теории. При $T < \gamma$ кинетические коэффициенты можно выгчислить только теоретико-полевыми методами. Мы изложим здесь оба подхода к кинетике сверхпроводников на примере вычисления электронной теплопроводности.

Метод кинетического уравления. Напомним опрелеление коэффициента теплопроводности §. Поток тепла, переносимый неравновесными возбуждениями, определяется формулой

$$\mathbf{Q}(\mathbf{r}) = 2\int \frac{d^3k}{(2\pi)^3} E_{\mathbf{k}}(\mathbf{r})\mathbf{v}_{\mathbf{k}}(\mathbf{r})f_{\mathbf{k}}(\mathbf{r}) \tag{22.1}$$

где E - энергия, $\mathbf{v} = \partial E/\partial\mathbf{k}$ - скорость квазичастиц в свсрхпроводнике [1], а $f_k(\mathbf{r})$ - неравновесная фупкция распределения возбуждений, взаимодействующих с примесями. Коэффицисит теплопроводности x связывает поток тепла с градиентом температуры

$$Q = -x\nabla T \tag{22.2}$$

Функция $f_{\mathbf{k}}(\mathbf{r}, t)$ удовлетворяет хинетическому уравнению Больцмана, которое имеет следующий вид:

$$\frac{\partial f}{\partial t} + \frac{\partial E}{\partial \mathrm{k}}\nabla f - \nabla E\frac{\partial f}{\partial \mathrm{k}} = \left(\frac{\partial n}{\partial t}\right)_{\mathrm{imp}} \tag{22.3}$$

где в правой части стоит интеграл сголкновений возбуждений с примесями [2]. В сташионарном случас и для слабо неравновесных распределений это уравнение может быть упрощсно. Поскольку интеграл столкновений обрашается в нуль при подстановке локальио-равновесной функции распределения $f^{(0)}_{\mathbf{k}}(\mathbf{r}) = f\left(E_{\mathbf{k}}(\mathbf{r})/T(\mathbf{r})\right)$, где f - фермиевская функция (6.2), то в линейном по отклонению от равновесия приближении в левой части уравнения (22.3) мы можем заменить f на $f^{(0)}$. Имеем

$$\frac{\partial E}{\partial \mathbf{k}}\nabla f_{\mathrm{k}}^{(0)} - \nabla E\frac{\partial f_{\mathbf{k}}^{(0)}}{\partial \mathbf{k}} = \frac{\partial E}{\partial \mathbf{k}}\frac{\partial f_{\mathrm{k}}^{(0)}}{\partial E}T\left(\frac{1}{T}\nabla E - \frac{E}{T^2}\nabla T\right) -$$
$$- \nabla E\frac{\partial f_{\mathrm{k}}^{(0)}}{\partial E}\frac{\partial E}{\partial \mathbf{k}} = -\frac{E}{T}\frac{\partial f_{\mathbf{k}}^{(0)}}{\partial E}\frac{\partial E}{\partial \mathbf{k}}\nabla T \tag{22.4}$$

ОБратим внимание на то, что члены, содержащие градиенты щели Δ, в точности сократили друт друга.

Интеграл столкновений в случае слабого беспорядка получается умножением вклада одной примеси на их концентрацию:

$$\left(\frac{\partial f_{\mathbf{k}}}{\partial t}\right)_{\mathrm{imp}} = n_{\mathrm{imp}}\int\frac{d^3k'}{(2\pi)^3}w\left(\mathbf{k},\mathbf{k}'\right)\left(\delta f_{\mathbf{k}'} - \delta f_{\mathbf{k}}\right) \tag{22.5}$$

где $w\left(\mathbf{k},\mathbf{k}'\right)$ - вероятность упрутого рассеяния квазичастиц, а δf - отклоненис функчии распределения от равновесгой, входящее, согласно (22.1), в формулу для теплового погока:

$$\mathbf{Q} = 2\int\frac{d^{\hat{s}}k}{(2\pi)^3}E_{\mathbf{k}}\mathbf{v}_{\mathbf{k}}\delta f_{\mathbf{k}}(\mathbf{r}) \tag{22.6}$$

В борновском приближснии вероятность w вычисляется с помощью «золотого правила Фермиж:

$$w\left(\mathbf{k},\mathbf{k}'\right) = \frac{2\pi}{\hbar}\left|\left(\mathbf{k}'\left|H_{\mathrm{imp}}\right|\mathbf{k}\right\rangle\right|^2\delta\left(E_{\mathbf{k}} - E_{\mathbf{k}'}\right)$$

Применяя прсобразование Боголюбова (5.25) к гамильтониану (21.1), описывающему взаимодействис электронов с немагнитно примссью, получаем:

$$w\left(\mathbf{k},\mathbf{k}'\right) = \frac{2\pi}{h}u^2\mathcal{C}\left(\mathbf{k},\mathbf{k}'\right)\delta\left(E_{\mathbf{k}} - E_{\mathbf{k}'}\right) \tag{22.7}$$

где так называемый фактор когерентности дается выражением:

$$\mathcal{C}\left(\mathbf{k},\mathbf{k}'\right) = \begin{cases}\frac{1}{2}\left(1 + \frac{\xi_k\xi_{k'} - \mathrm{Re}\,\Delta^2 g(\mathbf{k})g(\mathbf{k}')}{E_{\mathbf{k}}E_{\mathbf{k}'}}\right), & \text{при } S=0\\ \frac{1}{2}\left(1 + \frac{\xi_k\xi_{k'} - \mathrm{Re}\,\Delta^2\mathbf{d}(\mathbf{k})\mathbf{d}(\mathbf{k}')}{E_{\mathbf{k}}E_{\mathbf{k}'}}\right), & \text{при } S=1\end{cases}$$

Мы видим, что в случае анизотропного спаривания вероятность w зависит от утлов даже для изотропной амплитуды рассеяния $u\left(\mathbf{k},\mathbf{k}'\right) = u = \mathrm{const}$.

Перепишем кинетическое уравнение (22.3) с учетом (22.4) и (22.5) в следующем виде:

$$\delta f_{\mathbf{k}} - \tau_{\mathbf{k}}\int\frac{d^3k'}{(2\pi)^3}\tau^{-1}\left(\mathbf{k},\mathbf{k}'\right)\delta f_{k'} = \tau_k E_k\mathbf{v}_{\mathbf{k}}\frac{\partial f_{\mathbf{k}}^{(0)}}{\partial E}\frac{\nabla T}{T} \tag{22.8}$$

где

[11] Пространственная зависчмость E и $\mathbf{v}$ возникает из-за зависимости энергетической щели $\triangle$ от температуры, которая, в свож очередь, является фупгсиней r. Предполагастся, что T медленно меняется на масшттабе корреляционно д длины.

[2] Вывод кннетических уравнении для сверхпррводника представляет собо доволыо слодную задачу, поскольку необходимо учитывать динамику самого параметра порядка. Уравнение (22.3) справедлкво в предлолохении, что возбухдения распространяются в заданном, не зависящем от времени, слабо неоднородном потенциале $\Delta(r)$, а $E_{\mathrm{k}}(\mathrm{r}) = \sqrt{\xi^2 + \Delta_{\mathrm{k}}^2(\mathrm{r})}$.

$$\tau^{-1}(\mathbf{k},\mathbf{k}') = n_{\rm imp}\, w(\mathbf{k},\mathbf{k}')$$
$$\tau_{\mathbf{k}}^{-1} = \int \frac{d^3k'}{(2\pi)^3}\tau^{-1}(\mathbf{k},\mathbf{k}') = \frac{2\pi}{\hbar} n_{\rm imp} u^2 \int \frac{d^3k'}{(2\pi)^3}\mathcal{C}(\mathbf{k},\mathbf{k}')\,\delta(E_{\mathbf{k}} - E_{\mathbf{k}'}) \tag{22.9}$$

причем τ_k имеег смысл времени свободного пробега квазичастиц. Поскольку как при замене частица-дырка (т. е. $\xi_k \to -\xi_k$), так и при пространственной инверсии τ^{-1} остается инвариантнвм, а правая часть (22.8) меняет знак, получаем, что $\delta f_{\rm k}$ долхна быть нечетной относительно ухазанных преобразовании. По этой причине второе слагаемое в левой части (22.8) обращдается в нуль, и

$$\delta f_{\rm k} = \tau_{\rm k} E_{\rm k} \mathbf{v}_{\rm k} \frac{\partial f_{\rm k}^{(0)}}{\partial E}\frac{\nabla T}{T}$$

Подставляя пайденное решение кинетического уравнения в (22.6) и вспоминая определение коэффициента теплопроводности (22.2), окоичательно имеем:

$$\varkappa_{ij} = -\frac{2}{T}\int \frac{d^3k}{(2\pi)^3}\frac{\partial f_{\mathbf{k}}^{(0)}}{\partial E} E_{\mathbf{k}}^2 v_{\mathbf{k},i} v_{\mathbf{k},j}\tau_{\mathbf{k}} \tag{22.10}$$

причем скорость квазичастиц определяется следующим образом

$$\mathbf{v}_{\mathbf{k}} = \frac{\partial E_{\rm k}}{\partial \mathbf{k}} = v_{\rm F}\hat{\mathbf{k}}\frac{\xi_k}{E_{\mathbf{k}}} + O\left(\frac{\Delta}{\varepsilon_{\rm F}}\right) \tag{22.11}$$

Из всех величинт, входящих в (22.10), неизвестным пока осталось лишш время свободного пробега квазичастиц $\tau_{\rm k}$. Для синглетного изотропного спаривания из (22.9) имеем:

$$\begin{aligned}\frac{1}{\tau_{\rm k}} &= \frac{2\pi}{\hbar} n_{\rm imp} u^2 \int \frac{d^3k'}{(2\pi)^3}\left(1 - \frac{\Delta^2}{E_{\rm k}E_{\rm k'}}\right)\delta(E_{\rm k} - E_{\mathbf{k}'}) = \\ &= \frac{1}{\tau_{\rm n}}\frac{1}{N_0}\frac{E_{\rm k}^2 - \Delta^2}{E_{\rm k}^2}\int \frac{d^3k'}{(2\pi)^3}\delta(E_{\rm k} - E_{\rm k'}) = \frac{1}{\tau_{\rm n}}\frac{N(E_{\rm k})}{N_0}\frac{\xi_{\rm k}^2}{E_{\rm k}^2}\end{aligned} \tag{22.12}$$

где

$$\tau_{\rm n}^{-1} = \frac{2\pi}{\hbar} n_{\rm imp}\, N_0 u^2 \tag{22.13}$$

есть время свободного пробега в нормальной фазе [3], а плотность состояний $N(E_{\mathbf{k}}) = \int d^3k'\delta(E_{\mathbf{k}} - E_{\mathbf{k}'})/(2\pi)^3$(cm.(17.26)).

Подставляя (22.11) и (22.12) в (22.10) и учитывая (17.28), находим выражение для коэффициегта теплопроводности [89, 90]:

$$x = \frac{2\tau_n N_0 v_{\rm F}^2}{3T^2}\int\limits_{-\infty}^{\infty} d\xi \frac{E_k^2 e^{E_k/T}}{\left(e^{E_k/T}+1\right)^2}\frac{N_0}{N(E_k)} = \frac{\tau_{\rm n} N_0 v_{\rm F}^2}{3T^2}\int\limits_{\Delta}^{\infty}\frac{dEE^2}{{\rm ch}^2[E/(2T)]} \tag{22.14}$$

При $T \ll \Delta$

$$x(T) = \frac{4}{3}v_F^2\tau_{\rm n}N_0 T\left(\frac{\Delta}{T}\right)^2 \exp\left(-\frac{\Delta}{T}\right)$$

что можно переписать также в виде:

$$\frac{\varkappa(T)}{\varkappa_n\left(T_c\right)}=\frac{T}{T_c}\left(\frac{\Delta}{T}\right)^2\exp\left(-\frac{\Delta}{T}\right)I^{-1} \tag{22.15}$$

где теплопроводность в нормальном состоянии есть

$$\varkappa_{\mathrm{n}}\left(T_{\mathrm{c}}\right)=\frac{1}{3}v_{\mathrm{F}}^2\tau_{\mathrm{n}}N_0T_{\mathrm{c}}I \tag{22.16}$$

а

$$I=\int\limits_0^{+\infty}\frac{dzz^2}{\mathrm{ch}^2(z/2)}=\frac{2\pi^2}{3}$$

В случае анизотропного спаривания параметр порядка преобразуется в соответствии с неединичным представлением группы симметрии, и интеграл от фактора когерентности по направлениям $\mathbf{k}'$ в (22.9) равен единице. Следовательно,

$$\frac{1}{\tau_{\mathrm{k}}}=\frac{2\pi}{\hbar}n_{\mathrm{imp}}u^2\int\frac{d^3k'}{(2\pi)^3}\delta\left(E_{\mathrm{k}}-E_{\mathrm{k}'}\right)=\frac{1}{\tau_{\mathrm{n}}}\frac{N\left(E_{\mathrm{k}}\right)}{N_0} \tag{22.17}$$

Подставляя это выражение в (22.10), получаем, с учетом (22.11):

$$\begin{aligned}x_{ij}&=\frac{2\tau_{\mathrm{n}}v_F^2}{T^2}\int\frac{d^3k}{(2\pi)^3}\frac{\xi_k^2E_{\mathrm{k}}/T}{\left(e^{E_k/T}+1\right)^2}\frac{N_0}{N\left(E_{\mathrm{k}}\right)}\hat{k}_i\hat{k}_j=\\&=\frac{\tau_{\mathrm{n}}N_0v_{\mathrm{F}}^2}{T^2}\int\limits_0^{\infty}\frac{EdE}{\mathrm{ch}^2(E/2T)}\frac{N_0}{N(E)}\int\frac{d\Omega}{4\pi}\hat{k}_i\hat{k}_j\sqrt{E^2-\Delta_{\mathbf{k}}^2}\end{aligned} \tag{22.18}$$

причем интегрирование по углам производится в пределах, задаваемых условием $\Delta_{\mathbf{k}}^2<E^2$.

Для сверхпроводника со структурой B-фазы коэффициент теплопроводности изотропен и экспоненциально мал при $T\to 0$ (см. (22.15)).

Для сверхпроводников с нулями щели на поверхности Фсрми температурное поведение теплопроводности, напротив, будет не экспоненцианым, а степенным, подобно многим другим физическим характеристикам (см. 7). Кроме того, следует ожидать, что ввиду анизотропии щели коэффициенты теплопроводности будут зависеть от направления. В качестве примера рассмотрим сверхпроводник со структурой A-фазы, параметр порядка в котором обращается в нул на полюсах ферми-сферы: $\Delta_k^2=\Delta^2\sin^2\theta$. Ввиду одноосной анизотропии спсктра возбуждений теплопроводность описывается двумя коэффициентами: $x_{\parallel}=x_{zz}$ и $x_{\perp}=x_{xx}=x_{yy}$. Из (22.18) получаем:

$$\begin{aligned}\varkappa_{\parallel}&=\frac{\tau_{\pi}N_0v_{\mathrm{F}}^2}{T^2}\int\limits_0^{\infty}\frac{dEE}{\mathrm{ch}^2(E/2T)}\frac{N_0}{N(E)}\int\frac{d\Omega}{4\pi}\sqrt{E^2-\Delta^2\sin^2\theta}\cos^2\theta\approx\\&\approx\frac{\tau_{\mathrm{n}}N_0v_{\mathrm{F}}^2}{T^2}\int\limits_0^{\infty}\frac{dEE}{\mathrm{ch}^2(E/2T)}\frac{N_0}{N(E)}\int\limits_0^{E/\Delta}\theta d\theta\sqrt{E^2-\Delta^2\theta^2}\sim\\&\sim\frac{\tau_{\mathrm{n}}N_0v_{\mathrm{F}}^2}{T^2}\int\limits_0^{\infty}\frac{dEE}{\mathrm{ch}^2(E/2T)}\frac{N_0}{N(E)}\frac{E^3}{\Delta^2}\end{aligned}$$

[13] С учетом выражения для скорости возбуждснии $v=\partial E/\partial k=v_k\xi_k/E_k$ и формулы (17.28) из (22.13) следует, что длина свободного пробега в сверхпроводящем состоянии с s-спариванием равна длине прробега в нормтьном состояии.

Вспоминая выражение (17.30) для плотности состояний в A-фазе, окончательно получаем:

$$\frac{x_{\parallel}(T)}{x_{\pi}(T_c)} \sim \frac{T}{T_c} \tag{22.19}$$

Аналогично выполняются выписления для поперечного коэффициента теплопроводности:

$x_{\perp} = \frac{\tau_{\mathrm{n}} N_0 v_{\mathrm{F}}^2}{T^2} \int\limits_0^{\infty} \frac{dEE}{\mathrm{ch}^2(E/2T)} \frac{N_0}{N(E)} \int \frac{d\Omega}{4\pi} \sqrt{E^2 - \Delta^2 \sin^2\theta} \sin^2\theta \sim$

$\sim \frac{\tau_{\mathrm{n}} N_0 v_{\mathrm{F}}^2 T^3}{\Delta}$.

Следовательно,

$$\frac{x_{\perp}(T)}{x_n(T_c)} \sim \left(\frac{T}{T_c}\right)^3 \tag{22.20}$$

Если щель в спектрс обращается в нуль на цельх линиях на фермиповерхности, как это имеет место, например, в сверхпроводнике со структурой
полярной фазы: $\Delta_{\mathrm{k}}^2 = \Delta^2 \cos^2\theta$, то выписления с помощыо формулы (22.18), аналогичные проведенным выиге, дают следуишие результаты:

$$\frac{x_{\parallel}(T)}{\varkappa_n(T_c)} \sim \left(\frac{T}{T_c}\right)^3; \quad \frac{\varkappa_1(T)}{x_n(T_c)} \sim \frac{T}{T_c}. \tag{22.21}$$

Из (22.19)-(22.21) видно, что в свсрхпроводниках с нулями щели как на полюсах, так и на экваторе фсрми-поверхности, максимальный коэффицисит теплопроводности линейно зависит от тсмпературы, т. е. $x(T)/T \to \mathrm{const}$ при $T \to 0$.

Резонанснос рассяяние на примесях [87, 91]. Выражение (22.10) для электронной теплопроводности, полученное из кинетического уравнения, справсдливо и при резонансном рассеянии на примесях. Отличие от случая борновского рассеяния состоит в существенно иной зависимости времени свободного пробега возбуждений от энергии $\tau(E)$, которуюо нуждо найти из решения уравнения самосогласования для собственно-энергетической части, выведенного в 21. В этом разделе мы получим $\tau(E)$ и определим область справедливости описания релаксационных явленини в нсобычных сверхпроводниках с помощью уравнения Больдмана.

При наличии рассеяния на примесях квазичастицы приобретаюот консчное время жизпи, которос определяется мнимой частыю запаздывающей собственно-энергетической функции:

$$\frac{1}{\tau(E)} = -2\,\mathrm{Im}\,\Sigma^R(E) = 2\,\mathrm{Im}\,t(E) \tag{22.22}$$

Здесь мы воспользовались определением (21.14). Величина $t(E)$ удовлетворяет уравненио (21.25).

В случае резонансного рассеяния ($\delta_0 \to \pi/2$) уравнение (21.25) принимает вид

$$t = E + i\Gamma \frac{1}{g(t)}$$

где

$$g(t) = \int \frac{d\Omega}{4\pi} \frac{t}{\sqrt{t^2 - \Delta_k^2}}$$

В нормальном состоянии $g(t) = 1$, и

$$t_{\rm n}(E) = E + i\Gamma$$

Сравнивая это выражение с (22.22), получаем, что величина I связана с временем жизни квазичастиц в нормальном металле с резонансными примесями следующим образом:

$$\frac{1}{\tau_n} = 2\Gamma \tag{22.23}$$

и уравнение на функцию $t(E)$ в сверхпроводящем состоянии может быть записано как

$$t = E + \frac{i}{2\tau_{\rm n}}\frac{1}{g(t)} \tag{22.24}$$

Из (22.22), (22.24) и (21.28) имеем

$$\frac{1}{r(E)} = \frac{1}{\tau_{\rm n}}\,{\rm Re}\,\frac{1}{g(t)} = \frac{1}{\tau_{\rm n}}\frac{N(E)}{N_0}\frac{1}{|g(t(E))|^2} \tag{22.25}$$

Таким образом, нахождение врсмени жизни квазичастиц трсбует, вообщс говоря, самосогласованного вычисления собственио-энергетической части с помошию уравнения (22.24). Опнако, в случае достаточно слабого беспорядка лля энергий, превышающих некоторое критическое значение (точный критерий зависит от конкретного вида сверхпроводящего состояния, см. ниже), залача может быть упрощена. В самом деле, если при $E \to 0$

$${\rm Im}\, t(E) \to \gamma = \ {\rm const}\ \neq 0 \tag{22.26}$$

то при $E < \gamma$, как следуст из (22.22), время жизни почти не зависит от энергии, и:

$$\frac{1}{\tau} = 2\gamma \tag{22.27}$$

Энергия квазичастиц становится малой по сравненино с их затуханием, и при $T < \gamma$ больцмановское описание кинетики неприменимо.

Если же $E > \gamma$, то при вычислении малой мнимой добавки к $t(E)$ можно ограничиться низшим порядком теории возмушений по потенциалу примесей. Это, в частности, означает, что в выражении (22.25) мы можем пренебречь оттичием $t(E)$ от E. Тогда

$$\left.\frac{1}{\tau(E)}\right|_{\delta_0 \to \pi/2} = \frac{1}{\tau_{\rm n}}\frac{N(E)}{N_0}\frac{1}{|g(E)|^2} \tag{22.28}$$

причем в правую часть здесь следует подставлять плотность состояний для чистого сверхпроводника.

При вычислении коэффициента теплопроводности в случае резонансного рассеяния на примесях с помощью кинетического уравнения необходимо использовать выражение (22.28). Проделаем эти вычисления для различных фаз с p-спариванием.

Для сверхпроводника со структурой A-фазы из (22.26) и (21.30) имеем

$$\gamma = \sqrt{\frac{2\Gamma\Delta}{\pi}} = \sqrt{\frac{\Delta}{\pi\tau_{\rm n}}} \tag{22.29}$$

Из (21.17) находим функциго $g(E)$ (при $\gamma < E \ll \Delta$):

$$g(E) = \int \frac{d\Omega}{4\pi}\frac{E}{\sqrt{E^2 - \Delta^2\sin^2\theta}} \approx -i\frac{\pi E}{2\Delta}$$

Подставляя это выражение в (22.28) и учитывая (17.30), получаем:

$$\tau(E) \sim \tau_{\mathrm{n}} \tag{22.30}$$

Для сверхпроводника со структурой полярной фазы решение уравиения (22.24) дает с тогарифмической точностью при $\Gamma \ll \Delta$:

$$\gamma = \sqrt{\frac{\Delta}{\tau_{\mathrm{n}}}} \left(\ln \tau_{\mathrm{n}} \Delta\right)^{-1/2} \tag{22.31}$$

Из (21.17) получаем (при $\gamma < E \ll \Delta$):

$$g(E) = \frac{E}{\Delta} \ln \frac{2\Delta}{E}$$

Из (22.28) тогда имеем

$$\tau(E) \sim \tau_{\mathrm{n}} \frac{E}{\Delta} \ln^2 \frac{E}{\Delta} \tag{22.32}$$

Как и следовало ожидать, в случае сильного рассеяния на резонансных примесях время жизни квазичастиц уменьшается по сравнению с борновским случаем. Подставляя (22.30) в (22.10), получаем, что в выражениях для коэффициента теплопроводности в A-фазс появляется дополнительная вторая сгепень тсмпсратуры:

$$\frac{x_{\parallel}(T)}{x_{\mathrm{n}}\left(T_c\right)} \sim \left(\frac{T}{T_c}\right)^3; \quad \frac{x_{\perp}(T)}{x_n\left(T_c\right)} \sim \left(\frac{T}{T_c}\right)^5 \tag{22.33}$$

Аналогичные вычисления с помощью (22.32) для полярной фазы дающот

$$\frac{x_{\parallel}(T)}{x_{\mathrm{n}}\left(T_c\right)} \sim \left(\frac{T}{T_c}\right)^5 \ln^2 \frac{T}{T_{\mathrm{c}}}; \quad \frac{\varkappa_{\perp}(T)}{\varkappa_{\mathrm{n}}\left(T_c\right)} \sim \left(\frac{T}{T_c}\right)^3 \ln^2 \frac{T}{T_{\mathrm{c}}} \tag{22.34}$$

Найденные температурыые зависимости (22.33) и (22.34) согласуются с результатами измерений теплопроводности на монокристаллах $\mathrm{UPt_3}$ [92-94], в соотвстствии с которыми $x(T)/T \propto T^2$ для всех направлений. Совокупность эксперименталынхх данных свидетельствует о том, что сверхпроводящий параметр порядка в $\mathrm{UPt_3}$ прсобразуется согласно представлснию E_{1g} (или E_{2u}) группы $D_{6\,\mathrm{h}}$ (см. 4). В этом случае продольный (вдоль оси шестого порядка) коэффициент теплопроводности опрсдслястся формулой (22.33), а поперечный - формулой (22.34).

Подчеркнем еще раз, что результаты, полученные с помощью кинетического уравнения, справедливы при не слишком низких температурах $\gamma \ll T < \Delta$. При $T < \gamma$ выччисление кинетических коэффипиентов может быть произведено лишь в рамках теории линейного отклика, к иэложениг которой мы и переходим.

Упражнение. Вывести формулу (22.7).

Метод функций Грина: теория линейного отклика. Другой способ вычисления теплопроводности, а также многих друтих термодинамических и кинетических характеристик свсрхпроводника, основан на использовании теории линейного отктика в терминах фупкший Грина [95]. Согласно этой теории, рсакция систсмы на малос возмущение ее параметров (в нашем случае - на градисит тсмпсратуры) описывается запаздывающими коррелятораии сопряженных потоков.

Коэффиииент теплопровошности в этом формапизме выччисляется следующим образом. Введем прежде всего мацубаровскую корреляционную функшпю потоков тепла:

$$K_{ij}\left(\mathbf{r}_1, \tau_1; \mathbf{r}_2, \tau_2\right) = \left\langle T_\tau Q_i\left(\mathbf{r}_1, \tau_1\right) Q_j\left(\mathbf{r}_2, \tau_2\right)\right\rangle \tag{22.35}$$

где Q_i - оператор потока тепла. В реальном времени имеем:

$$Q_i(\mathbf{r},t) = -\frac{1}{2m}\left(\frac{\partial\dot{\psi}_\alpha^+(\mathbf{r},t)}{\partial t}\frac{\partial\psi_\alpha(\mathbf{r},t)}{\partial r_i} + \frac{\partial\psi_\alpha^+(\mathbf{r},t)}{\partial r_i}\frac{\partial\psi_\alpha(\mathbf{r},t)}{\partial t}\right) \tag{22.36}$$

Справедливость такого определения вытекает из операторного уравнения непрерывности для плотности гамильтониана $h(\mathbf{r},t)$ $\left(H=\int d^3r\right.$, глс II - гамильтониан БКШ (17.1) в координатном представлении):

$$\frac{\partial h}{\partial t} + \operatorname{div}\mathbf{Q} = 0$$

Фурье-образ уравнения (22.36) имеет вил $K_{ij}(\mathbf{q},\omega_n)$, где $\omega_n = 2\pi nT$ - бозонная мацубаровская частота. Запаздыватощая коррсляционная функшия потоков тепліа $K_{ij}^R(\mathbf{q},\omega)$ находится путем аналитического продолжения мацубаровской функции на ось вещественных частот $i\omega_n \to \omega + i0$. Согласно теории линейного отклика, коэффишеент теплопроводности связан с $K_{ij}^R(\mathbf{q}=0,\omega)$ следуюшшим образом [95]:

$$\varkappa_{ij} = -\frac{1}{T}\lim_{\omega\to 0}\operatorname{Im}\frac{K_{ij}^R(\omega)-K_{ij}^R(0)}{\omega} = -\left.\frac{1}{T}\frac{d\operatorname{Im}K_{ij}^R(\omega)}{d\omega}\right|_{\omega=0} \tag{22.37}$$

Подставим (22.36) в (22.35) и используем для расцепления стоящего в правой части (22.35) τ-упорядоченного произведения четырех фермионньдх операторов (двухчастичной функции Грина) приближение среднего поля:

$$\begin{aligned}
&\left\langle T_\tau\psi_\alpha^+(\mathbf{r}_1',\tau_1)\,\psi_\alpha(\mathbf{r}_1,\bar{\tau_1})\,\psi_\beta^+(\mathbf{r}_2',\tau_2)\,\psi_\beta(\mathbf{r}_2,\tau_2)\right\rangle \to\\
&\to -G_{\alpha\beta}(\mathbf{r}_1,\tau_1;\mathbf{r}_2',\tau_2)\bar{G}_{\beta\alpha}(\mathbf{r}_2,\tau_2;\mathbf{r}_1',\tau_1) -\\
&- I_{\alpha\beta}(\mathbf{r}_1,\tau_1;\mathbf{r}_2,\tau_2)\bar{F}_{\alpha\beta}^+(\mathbf{r}_1',\tau_1;\mathbf{r}_2',\tau_2) =\\
&= -G_{\alpha\beta}(\mathbf{r}_1,\tau_1;\mathbf{r}_2',\tau_2)\bar{G}_{\beta\alpha}(\mathbf{r}_2,\tau_2;\mathbf{r}_1',\tau_1) +\\
&+ F_{\alpha\beta}(\mathbf{r}_1,\tau_1;\mathbf{r}_2,\tau_2)\bar{F}_{\beta\alpha}^+(\mathbf{r}_2',\tau_2;\mathbf{r}_1',\tau_1)
\end{aligned}$$

где чсрта свсрху обозначает усреднение по положениям примесей. Переходя в импульсно-частотнос представление, перепишем коррелятор (22.35) в следующем виле:

$$\begin{aligned}
K_{ij}(\omega_n) = T\sum_m\int\tfrac{d^3k}{(2\pi)^3}(2\varepsilon_m+\omega_n)^2\tfrac{k_ik_j}{4m^2}\Big(&G_{\alpha\beta}(\mathbf{k},\varepsilon_m+\bar{\omega_n})\,G_{\beta\alpha}(\mathbf{k},\varepsilon_m) -\\
&-F_{\alpha\beta}(\mathbf{k},\varepsilon_m+\bar{\omega_n})\,F_{\beta\alpha}^+(\mathbf{k},\varepsilon_m)\Big) + K_{ij}^{(\text{sing})}
\end{aligned}$$

где $\varepsilon_m = (2m+1)\pi T$. Последпее слагаемое в правой части объепиняет сингупярные вклады вида $\delta(\tau_1-\tau_2)$, происходящие от дифференширования по времени τ-упорядоченівх произведений. Учет таких вклапов позволяет сократить расходимости при суммировании по m в первом слагаемом.

Данную трудность удобнее обойти, используя спектральное разложение (17.22) для функиит Грина. При этом можно показать [96], что апалитически продолженное выражсние для коррелятора имеет вид:

$$\begin{aligned}
K_{ij}^R(\omega) = &\int\frac{d\omega_1}{2\pi}\frac{d\omega_2}{2\pi}\frac{(\omega_1+\omega_2)^2}{\omega_1-\omega_2-\omega-i0}\left(\operatorname{th}\frac{\omega_1+\omega}{2T}-\operatorname{th}\frac{\omega_2}{2T}\right)\times\\
&\times\int\frac{d^3k}{(2\pi)^3}\frac{k_ik_j}{4m^2}\left(\operatorname{Im}G_{\alpha\beta}(\mathbf{k},\omega_1+\bar{\omega})\operatorname{lm}G_{\beta\alpha}(\mathbf{k},\omega_2) -\right.\\
&\left.-\operatorname{Im}F_{\alpha\beta}(\mathbf{k},\omega_1+\bar{\omega})\operatorname{Im}F_{\beta\alpha}^+(\mathbf{k},\omega_2)\right)
\end{aligned}$$

Подставляя сгода вцражение (17.23) для спектральной плотности, можно убедиться, что интеграл по ξ от слагаемых вида $G^R G^R$ и т. д. обращается в нул. Для коэффициента теплопроводиости тогда получаем:

$$\varkappa_{ij} = \frac{1}{4m^2T^2}\int \frac{dE}{2\pi}\frac{E^2}{\mathrm{ch}^2(E/2T)}\int \frac{d^3k}{(2\pi)^3}k_i k_j \left(G^R_{\alpha\beta}(\mathbf{k},E)\bar{G}^A_{\beta\alpha}(\mathbf{k},E) - F^R_{\alpha\beta}(\mathbf{k},E)\bar{F}^{+A}_{\beta\alpha}(\mathbf{k},E)\right) \tag{22.38}$$

Интеграл по импульсам в правой части определяется суммой диаграмм, изображенных на рис. 22, причем сплошным линиям соответствуоот усредненные запаздываюощие и опережающие функции Трина.

Если, как и выше, ограничиться случаем изотропного рассеяния на точечных примесях, то пунктирные линии пе несут никакой зависимости от импульсов. Поэтому для пространственно-четных сверхпроводящих фаз все диаграммы, кроме первой, обращаются в нуль при интегрировании по направлениям k ввиду нечетности вериины k_i.

Дхя пространственно-нечетных фаз, в частности, для p-спаривания, диаграммы с поперечными примесными линиями (так называемые вершинные поправки), вообще говоря, в пуль не обращаются, что значительно усложняет задачу. Однако, здесь мы интересуемся лишш поведением максимального

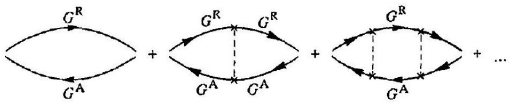


Рис. 22. Совокупность диаграмм, опредсляющих электронную теплопроводность сверхпроводииха при рассеянии электрона на примесях.

коэффицисита теплопроводности $\chi_{\max} = \chi_{ii}$, совпадающего с$\chi_{zz} = \chi_{\|}$для А-фазы, и с $x_{xx} = x_{yy} = x_\perp$ для полярной фазы. В этом случае непосредственное вычисление показывает, что вершинные поправки равны нулю [88] в результате интегрирования по азимутальному углу. Следователыво,

$$\varkappa_{ii} = \frac{1}{8\pi m^2T^2}\int\limits_0^\infty \frac{dEE^2}{\mathrm{ch}^2(E/2T)}L_{ii}(E) \tag{22.39}$$

гпе

$$L_{ii}(E) = \int \frac{d^3k}{(2\pi)^3}k_i^2\left(G^R_{\alpha\beta}(\bar{\mathbf{k}},E)G^A_{\beta\alpha}(\bar{\mathbf{k}},E) - F^R_{\alpha\beta}(\bar{\mathbf{k}},E)F^{+A}_{\beta\alpha}(\bar{\mathbf{k}},E)\right) \tag{22.40}$$

(суммирования по повторяющимся латинским индексам нет).

Усредненные запаздыватощие и опережаюощие функции Грина получаются путем аналитического продолжения в (21.6) и выглядят следующим образом:

$$G^R(\bar{\mathbf{k}},E) = \tfrac{t(E)+\xi_k}{t^2(E)-\Delta^2_{\mathbf{k}}-\xi^2_k},\quad F^R_{\alpha\beta}(\bar{\mathbf{k}},E) = \tfrac{\Delta_{\alpha\beta}(\mathbf{k})}{t^2(E)-\Delta^2_{\mathbf{k}}-\xi^2_k}$$
$$G^A(\mathbf{k},E) = G^{R*}(\mathbf{k},E),\quad F^A(\mathbf{k},E) = F^{R_*}(\mathbf{k},E)$$

причем $t(E)$ находится из уравпения самосогласования (21.16) (или (21.25)). После полстановки в (22.40) потучаем [88]:

$$L_{ii}(E) = 2N_0k_{\mathrm{F}}^2\int\frac{dS}{4\pi}\hat{k}_i^2\int d\xi\frac{|t|^2+\xi^2-\Delta_k^2}{(\xi^2-t^2+\Delta_k^2)(\xi^2-t^{*2}+\Delta_k^2)} =$$
$$= \frac{2\pi N_0k_F^2}{\mathrm{Re}\,i\,\mathrm{Im}\,t}\int\frac{d\Omega}{4\pi}\hat{k}_i^2\,\mathrm{Re}\,\frac{|t|^2+t^2-2\Delta_k^2}{\sqrt{t^2-\Delta_k^2}} \tag{22.41}$$

Подставляя (22.41) в (22.39), приходим к окогчательному ответу:

$$\varkappa_{ii} = \frac{N_0 v_F^2}{4T^2} \int\limits_0^\infty \frac{dE E^2}{\mathrm{ch}^2(E/2T)} \frac{1}{\mathrm{Re}\, t(E) \ln t\,(E^2)} \times$$
$$\times \int \frac{d\Omega}{4\pi} \hat{k}_i^2\, \mathrm{Re}\, \frac{|t(E)|^2 + t^2(E) - 2\Delta_k^2}{\sqrt{t^2(E) - \Delta_k^2}} \tag{22.42}$$

Дашшое выражение определяет максимальный коэффициент теплопроводности лля нечетных фаз и всс компоненты тснзора теплопроводности для четных фаз.

Поскольку основной вклад в интеграл (22.42) происходит от области энергий $E \sim T$, поэтому при не слишком низких температурах и для достаточно малой коншентрации примесей можно, как показано выше, пренебречь опличием $\mathrm{Re}\, t(E)$ от E. Тогда, вводя время жизни квазичастиц согласно (22.22), получаем

$$x_{ii} = \frac{N_0 v_F^2}{T^2} \int\limits_0^\infty \frac{dE E}{\mathrm{ch}^2(E/2T)} \tau(E) \int \frac{d\Omega}{4\pi} \hat{k}_i^2 \sqrt{E^2 - \Delta_{\mathbf{k}}^2} \tag{22.43}$$

Данное выражение справедливо как для борновского, так и для неборновского рассеяния на примесях. В случае борновского рассеяпия, используя (22.17), приходим к формуле (22.18), полученной путсм решения кинетического уравнения.

Уиверсалыность кишстических коэффициентов при очешь низких температурах [97]. Если $T < \gamma$ (то еств $\mathrm{Re}\, t(E) < \gamma$), то, подставляя $t(E) = \mathrm{Re}\, t + i\gamma$ в (22.41), полутаем:

$$I_{ii}(E \to 0) = \frac{4\pi N_0 k_\mathrm{F}^2}{\gamma\, \mathrm{Re}\, t} \int \frac{d\Omega}{4\pi} \ddot{k}_i^2\, \mathrm{Re}\, \frac{i\gamma\, \mathrm{Re}\, t - \Delta_\mathrm{k}^2}{\sqrt{2i\gamma\, \mathrm{Re}\, t - \gamma^2 - \Delta_\mathrm{k}^2}} =$$
$$= 4\pi N_0 k_\mathrm{F}^2 \int \frac{d\Omega}{4\pi} \hat{k}_i^2 \frac{\gamma^2}{(\gamma^2 + \Delta_\mathrm{k}^2)^{3/2}}$$

Отсюда

$$x_{ii} = 4 N_0 v_\mathrm{F}^2 T I \int \frac{d\Omega}{4\pi} \hat{k}_i^2 \frac{\gamma^2}{(\gamma^2 + \Delta_\mathrm{k}^2)^{3/2}} \tag{22.14}$$

где

$$I = \int\limits_0^{+\infty} \frac{dz z^2}{\mathrm{ch}^2 z} = \frac{\pi^2}{12}$$

Таким образом, для сверхпроводящих фаз с нетривиальным спариванием имеет место линейное по T поведение теплопроводности при очень низких температурах, а коэффициент этой линейной зависимости определяется конкретным видом параметра порядка.

Так, для полярной фазы ($\Delta_\mathrm{k}^2 = \Delta^2 \cos^2\theta$) из (22.44) имеем (при условии $\gamma \ll \Delta$) :

$$x_{\parallel\parallel} = 4 N_0 v_\mathrm{F}^2 T I \int\limits_0^\pi \sin\theta d\theta \int\limits_0^{2\pi} \frac{d\varphi}{4\pi} \cos^2\theta \frac{\gamma^2}{(\gamma^2 + \Delta^2 \cos^2\theta)^{3/2}} \approx$$
$$\approx 4 N_0 v_\mathrm{F}^2 T I \frac{\gamma^2}{\Delta^3} \ln \frac{2\Delta}{\gamma e} \tag{22.45}$$

$$x_\perp = 4 N_0 v_\mathrm{F}^2 T I \int\limits_0^\pi \sin\theta d\theta \int\limits_0^{2\pi} \frac{d\varphi}{4\pi} \sin^2\theta \cos^2\varphi \frac{\gamma^2}{(\gamma^2 + \Delta^2 \cos^2\theta)^{3/2}} \approx$$
$$\approx 2 N_0 v_\mathrm{F}^2 I \frac{T}{\Delta} \left(1 + O\left(\frac{\gamma}{\Delta}\right)\right) \tag{22.46}$$

Для фаз с изолированными нулями первого или второго порядка аналогичные вычисления дают:

$$x_{\parallel} = 4N_0 v_{\rm F}^2 TI\frac{\gamma}{\Delta^2}, \quad x_{\perp} = \pi N_0 v_{\rm F}^2 TI\frac{\gamma^2}{\Delta^3}, \quad \text{для } \Delta_{\mathbf{k}}^2 = \Delta^2 \sin^2\theta \tag{22.47}$$
$$x_{\parallel} = 2N_0 v_{\rm F}^2 I\frac{T}{\Delta}, \quad x_{\perp} = N_0 v_{\rm F}^2 TI\frac{\gamma}{\Delta^2}, \quad \text{для } \Delta_{\mathbf{k}}^2 = \Delta^2 \sin^4\theta$$

Мы приходим к заключению, что если тепловой поток направлен параллелыо плоскости, в которой параметр порядка обращается в нуль, или вдоль линии, соединяюощей точечныс нули второго порядка, то коэффициент теплопроводности не зависит от концентрации примесей. Подобная универсальность имеет место и для друтих кинетических коэффициентов [98].

19.3 Eliashberg Theory: a short review by F. Marsiglio

Eliashberg theory is a theory of superconductivity that describes the role of phonons in providing the attractive interaction between two electrons. Phonon dynamics are taken into account, thus giving rise to retardation effects that impact the electrons, in the form of a frequency-dependent electron self-energy. In the superconducting state, this means that the order parameter, generally considered to be a static quantity in the Bardeen-Cooper-Schrieffer (BCS) theory, also becomes frequency dependent. Here we review the finite temperature formulation of Eliashberg theory, both on the imaginary and real frequency axis, and briefly display some examples of the consequences of a dynamical, as opposed to static, interaction. Along the way we point out where further work is required, concerning the validity of some of the assumptions used.

19.3.1 Introduction

Superconductivity is a remarkable phenomenon, not least because it represents a manifestation of the quantum world on a macroscopic scale. It is spectacularly demonstrated with levitating train sets,[1] and indeed this property and many others of superconductors are slowly being utilized in everyday applications.[2] However, the established practice of incorporating superconductors into the real world should not be taken as an indication that "the last nail in the coffin [of superconductivity]"[3] has been achieved. On the contrary, in the intervening half-century since this quote was written, many new superconductors have been discovered, and we have reached a point where it is clear that a deep lack of understanding[4] of superconductivity currently exists. Reference [[5]] compiles a series of articles reviewing the various "families" or classes of superconductors, where one can readily see common and different characteristics. At the moment many of these classes require a class-specific mechanism for superconductivity, a clearly untenable situation, in my opinion. Further classes have been discovered or expanded upon since, such as nickelates,[7] and the hydrides under pressure,[6] for example.

Our "deep lack of understanding" should not be taken to indicate that theoretical contributions have not been forthcoming. In fact there have been remarkable contributions to key theoretical ideas in physics that stem from research in superconductivity, starting with London theory[8] and Ginzburg-Landau[**?**] theory, through to BCS theory.[10] When Gor'kov[11] recast the BCS theory of superconductivity in the language of Green functions, then the stage was set for Eliashberg[12, 13] to formulate the theory that bears his name. It is fitting that we honour the lasting impact of his work with this brief review, on the occasion of his 90th birthday, and the 60th anniversary of the publication of two papers that paved the path for considerable future quantitative work in superconductivity. Based on an index I am fond of

using for famous people, his name appears in titles of papers 248 times, and in abstracts and keywords 1439 times.[16]

Before proceeding further, we wish to make some remarks about the nature of this review. It will necessarily repeat material from previous reviews, which we catalogue as follows. Scalapino[17] and McMillan and Rowell[18] perhaps gave one of the first comprehensive reviews of both calculations and experiments that provide remarkable evidence for the validity of Eliashberg theory for various superconductors. These reviews were provided in the comprehensive monogram by Parks;[19] the reader should refer to this monogram and the references therein, as we cannot possibly properly reference all the primary literature sources before "Parks", as this would consume too many pages here. The author list in Parks is a who's who of experts in superconductivity, with two notable exceptions, John Bardeen and Gerasim (Sima) Eliashberg.

A subsequent very influential review was that of Allen and Mitrović,[20] where mostly superconducting T_c was discussed. These authors highlighted the expediency of doing many calculations on the imaginary frequency axis, a possibility first noted in Ref. [[21]] and utilized to great advantage in subsequent years.[22, 23, 24, 25]

A few years later Rainer wrote a "state-of-the-union" address[26] on first principles calculations of superconducting T_c in which a challenge was issued to both band structure and many-body theorists. For the former, the missing ingredient was a *complete* (italics are mine) calculation of the electron-phonon coupling. These were first calculated in the 1960's (e.g. Ref. [[27]]) but have experienced vast improvement over the past 50 years, through the adoption and improvement of Density Functional Theory methods, plus the increased computational ability achieved in the intervening decades. Excellent summaries of this progress is provided in Refs. [[28],[29],[30]], where two alternative procedures are described. The first follows the original route of determining the electron-phonon interaction and including this as input to the Eliashberg equations, while the second aims to treat both the electron-phonon-induced electron-electron interaction *and* the direct Coulomb interaction on an equal footing. The result is advertised to meet Rainer's challenge and calculate T_c and other superconducting properties without any experimental input. It is noteworthy that in the second formulation (see also Refs. [[31]] and [[32]]) the equations are BCS-like and do *not* depend on frequency, but only momentum. In the usual formulation, the calculation of μ^*, the effective direct electron-electron Coulomb interaction, is often simply assigned a (small) numerical value, and therefore is treated phenomenologically as a fitting parameter. The challenge to many-body theorists remains, as more superconductors have been discovered that seem to extend beyond the weak coupling regime, and likely require descriptions beyond BCS and Eliashberg theory.

In 1990 the review by Carbotte[33] provided a comprehensive update for a number of thermodynamic properties of various superconductors known at the time, including the high temperature cuprate materials. Partly for this reason his review is titled "*Properties of boson-exchange superconductors*," since there was a feeling at the time (and still is in parts of the community) that the Eliashberg framework might apply to these superconductors, but with exchange of a boson other than the phonon. Quite a few years later we wrote a review jointly,[34] focusing on "*electron-phonon superconductivity*." This review summarized known properties and extended results to dynamical properties such as the optical conductivity, building on earlier work in Ref. [[35]] and mini-reviews in Ref. [[36]]. More recently Ummarino has published a mini-review with some generalizations to multi-band and the iron pnictide superconductors.[37]

The other remark we should make is that while Eliashberg theory has been extremely successful, we will also point out the limitations that exist. Indeed, these were recognized right from the beginning, with both Eliashberg[12] and Migdal[38] emphasizing that limitations exist on the value of the dimensionless coupling parameter, λ, due to the expected phonon softening that would occur as λ increases. They claimed an upper limit of $\lambda \approx 1$, which then significantly restricts the domain of validity of the theory. Constraints on the parameters would be a constant

theme over the ensuing years. In 1968 McMillan[39] gave more quantitative arguments for a maximum T_c, based on the expected relationship between the coupling strength and the phonon frequency. This was reinforced by Cohen and Anderson[40] and has been discussed critically a number of times since.[41, 42] Alexandrov[43] has also raised objections, based on polaron collapse, a topic we will revisit later.

Some of the early history regarding the origins of the electron-phonon interaction was provided in Ref. [[34]] and will be omitted here. By the early to mid 1950's Fröhlich[44] and Bardeen and Pines[45] had established that the effective Hamiltonian for the electron-phonon interaction had a potential interaction of the form[46]

$$V^{\rm eff}_{\mathbf{k},\mathbf{k}'} = \frac{4\pi e^2}{(\mathbf{k}-\mathbf{k}')^2 + k^2_{\rm TF}}\left[1 + \frac{\hbar^2\omega^2(\mathbf{k}-\mathbf{k}')}{(\epsilon_{\mathbf{k}}-\epsilon_{\mathbf{k}'})^2 - \hbar^2\omega^2(\mathbf{k}-\mathbf{k}')}\right], \tag{19.1}$$

where $k_{\rm TF}$ is the Thomas–Fermi wave vector, and $\omega(\mathbf{q})$ is the dressed phonon frequency. This part of the Hamiltonian represents the pairing interaction between two electrons with wave vectors $\mathbf{k}$ and $\mathbf{k}'$ in the First Brillouin Zone (FBZ) and energies $\epsilon_{\mathbf{k}}$ and $\epsilon_{\mathbf{k}'}$. The interaction Hamiltonian written in this form is often said to have "the phonons integrated out." It was on the basis of this Hamiltonian that Bardeen, Cooper and Schrieffer (BCS)[10] formulated a model Hamiltonian with an attractive (negative in sign) interaction for electron energies near the Fermi energy, ϵ_F.

19.3.2 The Eliashberg Equations

Eliashberg,[12] following what Migdal[38] had calculated in the normal state, did not "integrate out the phonons," but instead adopted the Hamiltonian

$$\begin{aligned} H &= \sum_{\mathbf{k}\sigma}(\epsilon_{\mathbf{k}}-\mu)c^\dagger_{\mathbf{k}\sigma}c_{\mathbf{k}\sigma} + \sum_{\mathbf{q}}\hbar\omega_{\mathbf{q}}a^\dagger_{\mathbf{q}}a_{\mathbf{q}} \\ &\quad + \frac{1}{\sqrt{N}}\sum_{\substack{\mathbf{k}\mathbf{k}'\\ \sigma}} g(\mathbf{k},\mathbf{k}')\left(a_{\mathbf{k}-\mathbf{k}'} + a^\dagger_{-(\mathbf{k}-\mathbf{k}')}\right)c^\dagger_{\mathbf{k}'\sigma}c_{\mathbf{k}\sigma} \quad . \end{aligned} \tag{19.2}$$

where $c_{\mathbf{k}\sigma}$ ($c^\dagger_{\mathbf{k}\sigma}$) is the annihilation (creation) operator for an electron with spin σ and wave vector $\mathbf{k}$, and $a_{\mathbf{q}}$ ($a^\dagger_{\mathbf{q}}$) is the annihilation (creation) operator for a phonon with wave vector $\mathbf{q}$. The electron-phonon coupling function, $g(\mathbf{k},\mathbf{k}')$ is generally a function of both wave vectors (and not just their difference), and in principle is calculable with the Density Functional Theory Methods mentioned earlier. Very often models are adopted based on simple (e.g. tight-binding) considerations.

Eliashberg then applied the apparatus of field theory to formulate a pairing theory that accounts for the dynamics of the interaction, i.e. for retardation effects. A sketch of the derivation, taken from Rickayzen[47] (see also Ref. [[34]]), is provided in the Appendix. This is my favourite derivation, as it does not rely on a formalism (e.g. the Nambu formalism) whose validity requires an act of faith (or, you simply work through everything anyways, to ensure that the formalism "works").

Following Eliashberg[13] with more modern notation,[17, 20] the "normal" self energy $\Sigma(\mathbf{k}, i\omega_m)$ is separated out into even and odd (in Matsubara frequency) parts, so that two new functions, Z and χ are defined:

$$\begin{aligned} i\omega_m\left[1 - Z(\mathbf{k},i\omega_m)\right] &\equiv \frac{1}{2}\left[\Sigma(\mathbf{k},i\omega_m) - \Sigma(\mathbf{k},-i\omega_m)\right] \\ \chi(\mathbf{k},i\omega_m) &\equiv \frac{1}{2}\left[\Sigma(\mathbf{k},i\omega_m) + \Sigma(\mathbf{k},-i\omega_m)\right]. \end{aligned} \tag{19.3}$$

The equations that emerge are

$$Z(\mathbf{k}, i\omega_m) = 1 + \frac{1}{N\beta}\sum_{\mathbf{k}',m'} \frac{\lambda_{\mathbf{k}\mathbf{k}'}(i\omega_m - i\omega_{m'})}{g(\epsilon_F)} \frac{\left(\omega_{m'}/\omega_m\right) Z(\mathbf{k}', i\omega_{m'})}{\omega_{m'}^2 Z^2(\mathbf{k}', i\omega_{m'}) + \left(\epsilon_{\mathbf{k}'} - \mu + \chi(\mathbf{k}', i\omega_{m'})\right)^2 + \phi^2(\mathbf{k}', i\omega_{m'})} \tag{19.4}$$

$$\chi(\mathbf{k}, i\omega_m) = -\frac{1}{N\beta}\sum_{\mathbf{k}',m'} \frac{\lambda_{\mathbf{k}\mathbf{k}'}(i\omega_m - i\omega_{m'})}{g(\epsilon_F)} \frac{\epsilon_{\mathbf{k}'} - \mu + \chi(\mathbf{k}', i\omega_{m'})}{\omega_{m'}^2 Z^2(\mathbf{k}', i\omega_{m'}) + \left(\epsilon_{\mathbf{k}'} - \mu + \chi(\mathbf{k}', i\omega_{m'})\right)^2 + \phi^2(\mathbf{k}', i\omega_{m'})} \tag{19.5}$$

along with the equation for the order parameter:

$$\phi(\mathbf{k}, i\omega_m) = \frac{1}{N\beta}\sum_{\mathbf{k}',m'} \left[\frac{\lambda_{\mathbf{k}\mathbf{k}'}(i\omega_m - i\omega_{m'})}{g(\epsilon_F)} - V_{\mathbf{k},\mathbf{k}'}\right] \frac{\phi(\mathbf{k}', i\omega_{m'})}{\omega_{m'}^2 Z^2(\mathbf{k}', i\omega_{m'}) + \left(\epsilon_{\mathbf{k}'} - \mu + \chi(\mathbf{k}', i\omega_{m'})\right)^2 + \phi^2(\mathbf{k}', i\omega_{m'})}. \tag{19.6}$$

These are supplemented with the electron number equation, which determines the chemical potential, μ:

$$n_e = 1 - \frac{2}{N\beta}\sum_{\mathbf{k}',m'} \frac{\epsilon_{\mathbf{k}'} - \mu + \chi(\mathbf{k}', i\omega_{m'})}{\omega_{m'}^2 Z^2(\mathbf{k}', i\omega_{m'}) + \left(\epsilon_{\mathbf{k}'} - \mu + \chi(\mathbf{k}', i\omega_{m'})\right)^2 + \phi^2(\mathbf{k}', i\omega_{m'})}. \tag{19.7}$$

Written in this way both Z and χ are even functions of $i\omega_m$ (and, as we've assumed from the beginning, they are also even functions of $\mathbf{k}$). With electron-phonon pairing the anomalous self energy, which determines the anomalous pairing amplitude $\phi(\mathbf{k}, i\omega_m)$, is also an even function of Matsubara frequency. A generalization of this latter result, giving rise to so-called Berezinskii[**?**] "odd-frequency" pairing, is beyond the scope of this review. A survey of Berezinskii pairing is given in Ref. [[49]].

Other symbols in Eqs. (19.4-19.7) are as follows.The number of lattice sites is given by N, the parameter $\beta \equiv 1/(k_B T)$, where k_B is the Boltzmann constant and T is the temperature, μ is the chemical potential, and $g(\epsilon_F)$ is the electronic density of states at the Fermi level in the band. These equations are generally valid for multi-band systems, and then the labels $\mathbf{k}$ and $\mathbf{k}'$ are to be understood to include band indices. However, we shall proceed for simplicity with the assumption of a single band, with single particle energy $\epsilon_{\mathbf{k}}$. Because we are assuming finite temperature right from the start, the equations are written on the imaginary frequency axis, and are functions of the Fermion Matsubara frequencies, $i\omega_m \equiv \pi k_B T(2m-1)$, with m an integer. Similarly the Boson Matsubara frequencies are given by $i\nu_n \equiv 2\pi k_B T n$, where n is an integer. Finally, we have also included a direct Coulomb repulsion in the form of $V_{\mathbf{k},\mathbf{k}'}$, which in principle represents the full (albeit screened) Coulomb interaction between two electrons.

The key ingredient of Eliashberg theory (as opposed to BCS theory) is the presence of the electron-phonon propagator, contained in

$$\lambda_{\mathbf{k}\mathbf{k}'}(z) \equiv \int_0^\infty \frac{2\nu\alpha^2_{\mathbf{k}\mathbf{k}'}F(\nu)}{\nu^2 - z^2} d\nu \tag{19.8}$$

with $\alpha^2_{\mathbf{k}\mathbf{k}'}F(\nu)$ the spectral function of the phonon Green function. This function is sometimes written as $\alpha^2_{\mathbf{k}\mathbf{k}'}(\nu)F(\nu)$ to emphasize that the coupling part (α^2) can have significant frequency dependence. This spectral function is often called the Eliashberg function. Equation (19.8) has been used as a "bosonic glue" to generalize the application of the Eliashberg/BCS formalism to beyond that of phonon exchange. Very often the boson is a collective mode of the very degrees of freedom that are superconducting, i.e. the conduction electrons. Examples include spin fluctuations or plasmons, but this work is on more questionable footing.[50]

A significant anisotropy may exist, specifically through the nature of the coupling in the Eliashberg function. Since the important physical attribute of the Eliashberg formalism beyond BCS is retardation, and therefore in the frequency domain, we will nonetheless neglect anisotropy in what follows.[51] More nuanced arguments for the wave vector dependence of the electron-phonon coupling are provided in Ref. [[20]], connected to the energy scale hierarchy $\epsilon_F \gg \nu_{\rm phonon} \gg T_c$, where $\nu_{\rm phonon}$ is a typical phonon energy scale (note that we have adopted the standard practice of dropping $\hbar$ and k_B, and therefore we refer to temperatures and phonon frequencies as energies). Indeed very often the neglect of anisotropy was justified by the study of so-called "dirty" superconductors, where the presence of impurities served to self-average over anisotropies. We will also drop the wave vector dependence in the direct Coulomb repulsion, although this step is less justified. It means that the direct Coulomb repulsion is represented by a single parameter, which we will call U, since this is what we would obtain by reducing the long-range Coulomb repulsion with an on-site Hubbard interaction with strength given by U. This is one of the weak points of the Eliashberg description of superconductivity — an inadequate description of correlations due to Coulomb interactions. In what follows we will focus more attention on the retardation effects, since this is the part that Eliashberg theory is best designed to handle properly.

Once we drop the wave vector dependence in the coupling function, all quantities (Z, χ and ϕ) become independent of wave vector. The integration over the First Brillouin Zone can then be performed, although here a series of approximations are utilized. The result can lead to confusion, so we provide some detail here. First, once it is determined that the unknown functions in Eqs. (19.4-19.7) do not depend on wave vector, we can replace the sum over wave vectors in the first Brillouin zone with an integration over the electronic density of states,

$$\frac{1}{N}\sum_k \rightarrow \int_{\epsilon_{\rm min}}^{\epsilon_{\rm max}} d\epsilon \; g(\epsilon), \tag{19.9}$$

where $g(\epsilon)$ is the single electron density of states and $\epsilon_{\rm min}$ and $\epsilon_{\rm max}$ are the minimum and maximum energies of the electronic band. Since typically the energy scales are such that $T_c << \nu_{\rm phonon} << \epsilon_F$, the variation of the electronic density of states away from the Fermi level is of little importance, so the approximation $g(\epsilon) \approx g(\epsilon_F)$ is used. Exceptions to this case have been discussed previously, and one is referred to Ref. [[34]] for references. The remaining integration is now elementary and yields a combination of inverse tangent and logarithmic functions.[52]

However, the "standard" practice is to extend these integrations over energy to $\pm\infty$ (and similarly adopt particle-hole symmetry so $\epsilon_{\rm min} \equiv -\epsilon_{\rm max}$, along with $\mu = 0$, and now $\epsilon_{\rm max} \rightarrow \infty$) with the philosophy that the remainder of the integrand ensures that these additional contributions are negligible. This is in fact *not true* and the term proportional to $V_{\mathbf{k},\mathbf{k}'}$ in Eq. (19.6) (now replaced by U as described above) will result in a Matsubara sum that diverges if this procedure is carried out without thought. So in fact the bandwidth parameters are required in the integration for this term and the resulting inverse tangent function results in a soft cutoff at $\omega_m \approx \epsilon_{\rm max}$. This is most often replaced with a hard (step-function) cutoff. Because of the assumptions about particle-hole symmetry the function $\chi(\mathbf{k}, i\omega_m)$ in Eq. (19.5) is identically zero, and Eq. (19.7) becomes meaningless (so the occupation is no longer considered an input parameter).

The more highly simplified equations that result are

$$Z(i\omega_m) = 1 + \frac{\pi T_c}{\omega_m}\sum_{m'=-\infty}^{+\infty} \lambda(i\omega_m - i\omega_{m'}) \frac{\omega_{m'} Z(i\omega_{m'})}{\sqrt{\omega_{m'}^2 Z^2(i\omega_{m'}) + \phi^2(\omega_{m'})}} \tag{19.10}$$

$$\phi(i\omega_m) = \pi T_c \sum_{m'=-\infty}^{+\infty} \left[\lambda(i\omega_m - i\omega_{m'}) - u\ \theta)\frac{W}{2} - |\omega_{m'}|)\right] \frac{\phi(i\omega_{m'})}{\sqrt{\omega_{m'}^2 Z^2(i\omega_{m'}) + \phi^2(\omega_{m'})}}. \quad (19.11)$$

where W is the bandwidth (i.e. $\epsilon_{\max} = -\epsilon_{\min} \equiv W/2$ and the band has been centred around zero for convenience), and $\theta(x)$ is the usual step function, and $u \equiv Ug(\epsilon_F)$. Very often a different order parameter is favoured over $\phi(\omega_m)$, defined as $\Delta(\omega_m) \equiv \phi(\omega_m)/Z(\omega_m)$. Then Eqs. (19.10,19.11) are written as

$$Z(i\omega_m) = 1 + \frac{\pi T_c}{\omega_m} \sum_{m'=-\infty}^{+\infty} \lambda(i\omega_m - i\omega_{m'}) \frac{\omega_{m'}}{\sqrt{\omega_{m'}^2 + \Delta^2(\omega_{m'})}} \quad (19.12)$$

$$Z(i\omega_m)\Delta(i\omega_m) = \pi T_c \sum_{m'=-\infty}^{+\infty} \left[\lambda(i\omega_m - i\omega_{m'}) - u\ \theta)\frac{W}{2} - |\omega_{m'}|)\right] \frac{\Delta(i\omega_{m'})}{\sqrt{\omega_{m'}^2 + \Delta^2(\omega_{m'})}}. \quad (19.13)$$

These are the standard Eliashberg equations, written on the imaginary axis. These components of the self energy (refer back to Eq. (19.3)) are all real functions. One further 'simplification' is usually made before computations are performed. The Matsubara summation is in principle infinite; in practice the summation with the electron-phonon kernel converges with relatively few terms, corresponding to a frequency cutoff $\omega_c << W/2$. Yet in the term with the Coulomb interaction one is required to carry out a summation over many more terms, corresponding to a frequency cutoff of $W/2$. Inspection of Eqs (19.12,19.13) shows that over this range ($\omega_c < \omega_m < W/2$), the gap function is a constant, i.e. $\Delta(\omega_m) \approx \Delta_\infty$, and $Z(\omega_m) \approx 1$. Making use of this allows one to sum this part analytically, with the result that U changes to an effective $U^*(\omega_c)$, where

$$U^*(\omega_c) \equiv \frac{U}{1 + U\ln(\frac{W/2}{\omega_c})}, \quad (19.14)$$

and we have approximated digamma functions with their asymptotic logarithmic form, since it is assumed that both $W/2 \gg T_c$ and $\omega_c \gg T_c$. Now the equations are

$$Z(i\omega_m) = 1 + \frac{\pi T_c}{\omega_m} \sum_{m'=-\infty}^{+\infty} \lambda(i\omega_m - i\omega_{m'}) \frac{\omega_{m'}}{\sqrt{\omega_{m'}^2 + \Delta^2(\omega_{m'})}} \quad (19.15)$$

$$Z(i\omega_m)\Delta(i\omega_m) = \pi T_c \sum_{m'=-\infty}^{+\infty} [\lambda(i\omega_m - i\omega_{m'}) - u^*(\omega_c)\theta)\omega_c - |\omega_{m'}|)] \frac{\Delta(i\omega_{m'})}{\sqrt{\omega_{m'}^2 + \Delta^2(\omega_{m'})}}, \quad (19.16)$$

where $u^*(\omega_c) \equiv g(\epsilon_F)U^*(\omega_c)$. One should note that $U^*(\omega_c) < U$, physically corresponding to the fact that retardation effects allow two electrons to exchange a phonon with one another while not being at the same place at the same time. This means they do not feel the full direct Coulomb interaction with one another.

Thus far we have written the Eliashberg equations as functions of imaginary frequency. As we will see in the next subsection one can solve these equations as they are, to determine many thermodynamic quantities of interest, in particular T_c. However, later we will extend these equations to the upper half-plane, and in particular just above the real axis. This is required for the evaluation of dynamic quantities like the tunneling density of states and the optical conductivity.[17, 36, 34] In anticipation of these results we note here that we use functions $Z(z)$ and $\phi(z)$ [and therefore $\Delta(z)$] with the following properties[53] as a function of complex frequency z

$$Z(z^*) = Z^*(z); \qquad Z(-z) = Z(z), \quad (19.17)$$

$$\phi(z^*) = \phi^*(z); \qquad \phi(-z) = \phi(z), \quad (19.18)$$

$$\Delta(z^*) = \Delta^*(z); \qquad \Delta(-z) = \Delta(z). \quad (19.19)$$

19.3.3 Results on the imaginary axis: T_c

To compute actual results for T_c, along with the gap function $\Delta(\omega_m)$ and the renormalization function $Z(\omega_m)$, we need to specify $\alpha^2F(\nu)$ (now assumed to be isotropic) and $u^*(\omega_c)$. The latter quantity is very difficult to compute, and the former is more tractable through Density Functional Theory. Historically it has been "measured" through tunnelling measurements.[18] We use quotation marks around the word "measured" because in fact the current is measured while the spectral function is extracted through an inversion process that requires theoretical input through the Eliashberg equations themselves.[18] We will simply adopt a model spectral function given by

$$\alpha^2F(\nu) = \frac{\lambda_0\nu_0}{2\pi}\left[\frac{\epsilon}{(\nu-\nu_0)^2+\epsilon^2} - \frac{\epsilon}{\nu_c^2+\epsilon^2}\right]\theta(\nu_c - |\nu-\nu_0|), \tag{19.20}$$

that is, a Lorentzian line shape cut off in such a way that the function goes smoothly to zero in the positive frequency domain. This Lorentzian has a centroid given by ν_0 and a half-width given by ϵ. The cutoff frequency parameter ν_c makes the Lorentzian go to zero at frequency $\nu_0+\nu_c$ and frequency $\nu_0-\nu_c$. For concreteness we will use a variety of values of ν_0 with $\epsilon = 0$, or $\epsilon \approx \nu_0/10$. The first choice results in a δ-function spectrum with weight such that the mass enhancement parameter, λ, defined by

$$\lambda \equiv 2\int_0^\infty d\nu \frac{\alpha^2F(\nu)}{\nu} \tag{19.21}$$

is simply given by λ_0. As ϵ increases λ decreases from λ_0; however in what follows we will adjust λ_0 to keep λ constant.[54] Since the main focus of Eliashberg theory is the effect of retardation, we will often set $u^*(\omega_c) = 0$, but we will nonetheless note how this quantity affects the gap function and T_c.

Superconducting T_c is determined by linearizing the gap equations, Eqs. (19.15,19.16) so that they become

$$Z(i\omega_m) = 1 + \frac{\pi T_c}{\omega_m}\left\{\lambda + 2\sum_{n=1}^{m-1}\lambda(i\nu_n)\right\}. \tag{19.22}$$

$$Z(i\omega_m)\Delta(i\omega_m) = \pi T_c \sum_{m'=-\infty}^{+\infty}\left[\lambda(i\omega_m - i\omega_{m'}) - u^*(\omega_c)\theta)\omega_c - |\omega_{m'}|\right]\frac{\Delta(i\omega_{m'})}{|\omega_{m'}|}. \tag{19.23}$$

The latter of these two equations is an eigenvalue equation and can be solved as such. We use a power method that iterates the eigenvalue and eigenvector simultaneously by requiring that the gap function at the lowest Matsubara frequency,[55] $\Delta(i\omega_1)$, remain at unity. This procedure tends to converge very quickly for stronger coupling, but requires more care for weaker coupling.[56]

We begin with a standard plot of T_c vs λ in Fig. 1, for a simple δ-function spectral function with frequency as shown. There are scaling relations for T_c with typical phonon frequency, but we choose to show the results explicitly in real units to make the result clear. The possibility of determining an expression for T_c analytically has been discussed extensively in the literature[20] and will not be done here. The trends are clear; higher T_c comes from higher values of λ and from higher values of the characteristic phonon frequency, which in the present case is provided by ν_0. The width of the spectrum plays a minor role, and the Coulomb repulsion suppresses T_c, as indicated by the marked points. It is well known that Eliashberg theory predicts that T_c increases with both frequency and coupling strength as $T_c \approx \nu_0\sqrt{\lambda}$ in the asymptotic limit.[57, 24]

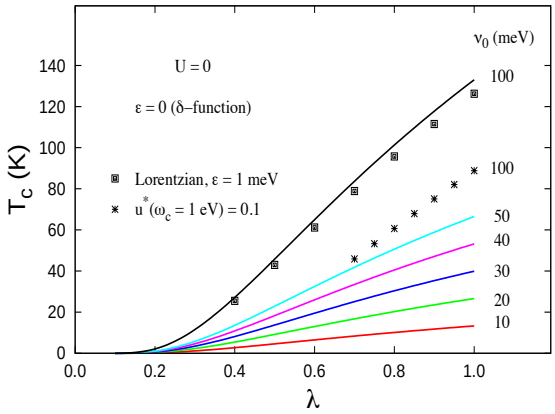


Figure 19.1: The superconducting critical temperature, T_c (K) vs. the dimensionless mass enhancement parameter, λ, for a variety of characteristic phonon frequencies, as indicated. The solid curves are for the Einstein spectrum with $U = 0$. The square points indicate how T_c changes (for $\nu_0 = 100$ meV only) when a Lorentzian is used instead with $\epsilon = 10$ meV and $\nu_c = 80$ meV, according to Eq. (19.20). For the same value of λ there is only a slight reduction in the value of T_c. The points marked with asterisks are again for the same broadened Lorentzian centred at $\nu_0 = 100$ meV, but now with $u^*(\omega_c = 1$ eV. Note that ν_c is used as a practical cutoff for the phonon spectrum whereas ω_c is used for the Matsubara cutoff for the direct Coulomb repulsion. See the discussion in the text for how plausible these parameters might or might not be.

19.3.4 Validity of the Theory

A perhaps more important question is the validity of the parameters used in the calculation. We have shown results up to a value of $\lambda = 1$. Are higher values allowed? In particular, is it possible for a material to have a sizeable value of electron-phonon coupling while maintaining a large phonon frequency? As discussed in the introduction, this question has been the subject of previous investigation,[40, 41, 42] although with only qualitative conclusions. The discovery of (very) high temperature superconductivity in the hydrides[58, 59] under intense pressure has spurred a reassessment of this type of analysis, since a part of the community believes that these superconductors are electron-phonon driven. The main evidence has been an observed isotope shift.[58] Moreover, the prediction of superconductivity in some of these compounds through density functional theory calculations[60] adds plausibility to this explanation. However, very high characteristic phonon frequencies (60 - 120 meV) and rather large electron-phonon coupling values ($\lambda \approx 2$ or more) are required. The latter is well outside the range considered reasonable, *especially* given that the characteristic phonon energy remains so high. Moreover, the superconductivity literature has unfortunately lapsed into simply accepting as "standard" or "conventional" a value for the Coulomb pseudopotential $u^* = 0.1$, and, *especially* given the high value of phonon frequency, the anticipated reduction of the Coulomb interaction through retardation will be much lower than previously thought, and the value of the direct Coulomb repulsion is undoubtedly higher when the phonon frequency is so high.

An additional direction of addressing this question comes from microscopic calculations involving Quantum Monte Carlo (QMC) and Exact Diagonalization (ED) techniques, utilizing specific microscopic models. These methods provide controlled approximations and are therefore suitable for benchmarking more approximate theories like Eliashberg theory. By far the most work in this direction has been done on the Holstein model.[61] The Holstein model retains only the short-range (on-site) interaction between local (Einstein) oscillators and the electron charge density. Because it is a very local model it is more amenable to the exact or controlled methods developed over the past 40 years, and therefore is a "favourite" for understanding the electron-phonon interaction, much like the Hubbard model[62] is heavily used for the study of electron-electron interactions. A short historical account of this activity is provided in the Appendix of Ref. [[34]].

Briefly, early Quantum Monte Carlo studies in one dimension[63] and two dimensions[64, 65] established that charge-density-wave (CDW) correlations dominate at half-filling and close to half-filling. The critical question is whether, sufficiently away from half-filling, where the susceptibility for superconductivity is stronger than that for CDW formation, do the "remnant" CDW correlations *enhance* or *suppress* suppress superconducting T_c? In Ref. [[66]] the present author, based on a comparison of QMC and Migdal-Eliashberg calculations on (very!) small lattices, argued that CDW fluctuations actually *suppress* superconducting T_c. In the so-called *renormalized* Migdal-Eliashberg calculations a phonon self-energy was included; in this manner CDW fluctuations impacted the phonon propagator, resulting in softer phonons and an enhanced coupling constant. Comparisons with the QMC results served to benchmark the Eliashberg-like calculations.

Figure 2, reproduced from Ref. [[66]], illustrates that the so-called *renormalized* calculations agree with the QMC results. These calculations (solid curves) include phonon self-energy effects which are essentially the CDW fluctuations.[65] In contrast, the *unrenormalized* calculations (dashed curves) are the standard Migdal-Eliashberg calculations that omit phonon self-energy effects. Figure 2(a) illustrates that the renormalized calculations are more accurate, and Fig. 2(b) shows that including CDW fluctuations *suppresses* the pairing susceptibility, $\chi^{\rm SP}$. We understand these results to indicate that in the vicinity of a CDW instability, while the effective coupling constant ($\lambda^{\rm eff}$ in Ref. [[65, 66]]) *increases*, superconducting T_c *actually decreases*.

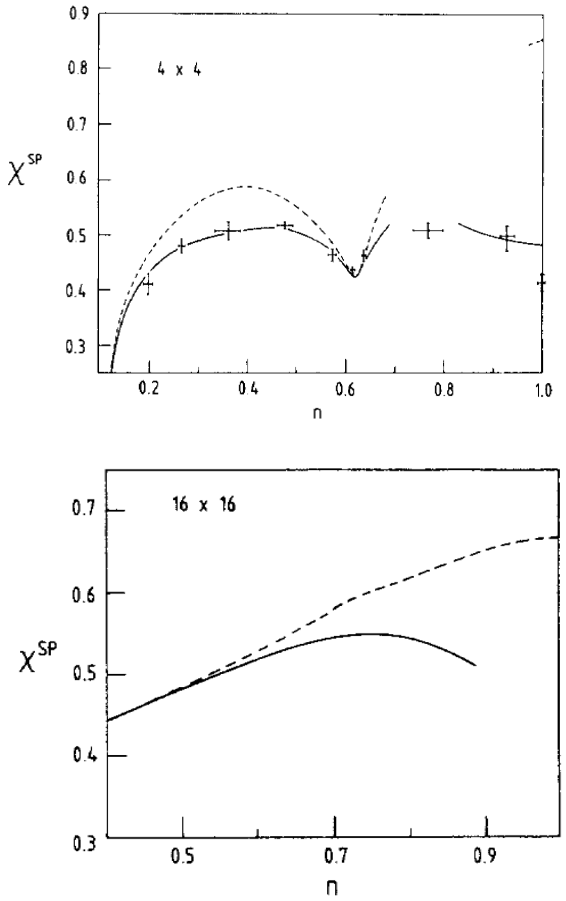


Figure 19.2: The singlet pairing susceptibility vs. electron density for the Holstein model on a 4×4 lattice. See Refs. [[65, 66]] for pertinent definitions. Here a bare dimensionless coupling strength $\lambda_0 = 2$ and phonon (Einstein) frequency $\omega_E = 1t$ are used, and the susceptibility is plotted for a temperature $T = t/6$, where t is the nearest neighbour hopping parameter. In the topmost figure, QMC results are indicated with error bars. The solid curves are the result for Migdal-Eliashberg theory with a renormalized phonon propagator and the dashed curves are the result for the unrenormalized calculations. The renormalized calculations agree very well with the QMC results (both done for a 4×4 lattice), indicating that this (combined Migdal-Eliashberg plus phonon self-energy in the bubble RPA approximation) result accurately captures the impact of CDW fluctuations on the pairing susceptibility. In the bottom figure the renormalized (solid curve) and unrenormalized (dashed curves) are plotted for a larger system. The renormalized calculations stop at an electron density close to $n \approx 0.9$ because a CDW instability occurs there. The unrenormalized calculations carry on to half-filling, because they are oblivious to the CDW instability (and fluctuations). This result indicates that CDW fluctuations at densities less than $n = 0.9$ suppress pairing, and presumably T_c, even though $\lambda^{\text{eff}} \to \infty$. Reproduced from Ref. [[66]].

More recently similar calculations have been performed[67] and other methodologies have been employed.[68] In the latter reference the role of retardation in reducing the direct Coulomb interaction was also addressed; while they found qualitative agreement with the standard arguments, quantitative agreement was lacking, especially for the expected large values of direct Coulomb repulsion. An older calculation with just two electrons,[69] based on Exact Diagonalization studies, also found qualitative support for a retardation-related reduction in the direct Coulomb repulsion. It is worth mentioning that finding this insensitivity to increased Coulomb repulsion, known as the "pseudopotential effect,"[70, 71] has been looked for in QMC studies, but these have mostly been unsuccessful. They may still be there; part of the problem is that QMC results become more difficult as the electronic and phonon energy scales differ from one another by a significant amount. Moreover, it may be that if larger lattices and more realistic phonon frequencies (i.e. significantly less than the electron hopping parameter, t) are used, the result illustrated in Fig. 29.2 could change qualitatively.

An additional concern has been raised about the electron-phonon coupling becoming too strong — that of polaron collapse.[43] Exact studies in the thermodynamic limit[72] have established that a single electron, interacting with Einstein oscillators through the Holstein model, acquires an additional mass which is modest for $\lambda \lessapprox 1$, but becomes quickly (though smoothly!) very, very large beyond this point. This is true independent of dimension,[73, 74] and is especially acute when $\nu_0 << W$,[75] where W is the electronic bandwidth. So we have the intriguing situation where the standard Migdal approximation (upon which Eliashberg theory is based) utilizes a Fermi sea of electrons strongly coupled to phonons, while close examination of *just one* of these constituent quasiparticles (polarons) shows that it acquires a tremendous effective mass. Thus, the properties of the single polaron, out of which a Fermi sea is constructed, appear to be incompatible with the properties of the electrons in that Fermi sea.

For example, in Migdal theory, the effective mass for electrons near the Fermi energy is $m^*/m_e \approx 1 + \lambda$, even for $\lambda \approx 2$ or more, whereas a single electron with this coupling would have an effective mass many orders of magnitude higher. It is important to note that in the quantum treatment polarons never "self-localize," essentially because of Bloch's Theorem. However, with such large effective mass ratios, any impurities (including surfaces), would readily act as localization sites.

There are perhaps a few scenarios to work one's way out of this dilemma. First, as we have already mentioned, perhaps the Holstein model itself is pathological. For this reason it is important to study other models. Unfortunately other models are more difficult to work with, but thus far the conclusions arrived at with the Holstein model seem to hold for these other models as well. For example, in Ref. [[76]] a variational approach was used with the Fröhlich Hamiltonian in the continuum with acoustic phonons, and in Refs. [[77, 78]] the Barisić-Labbé-Friedel/Su-Schrieffer-Heeger (BLF/SSH) model was examined with perturbation theory and the adiabatic approximation. In either case more definitive results as achieved with the Holstein model are still lacking, although all indications are that these models have strong polaronic tendencies as well.

A second scenario is that as one assembles a Fermi sea of polarons, they somehow become increasingly undressed, presumably due to some argument involving Pauli blocking. There are no calculations that we are aware of, however, that provide a demonstration of this.[79] Part of the reason may be psychological; the Migdal approximation is more often called the Migdal Theorem, and so one may be inclined to take it for granted that this is what will happen when we assemble a Fermi sea — the "theorem" will be fulfilled. However, in my opinion this is more a belief than an established argument, as the Migdal approximation does not foresee or account for polaron physics.

This discussion has been a long digression concerning the domain of applicability of Eliashberg theory, and clearly a lot more investigation is required on this question. For now we return

to the properties of the solutions to the Eliashberg equations.

19.3.5 Results on the imaginary axis: in the superconducting state

Returning to Eqs. (19.15,19.16), or their linearized counterparts, Eqs. (19.22,19.23), once T_c is determined then the gap function can be determined both at T_c and below T_c. The gap function is a generalized (frequency-dependent) order parameter. It will grow continuously from zero at T_c to its full value at zero temperature, but it depends on frequency. In Fig. 29.3(a) we show the gap function as a function of Matsubara frequency for a variety of temperatures, for $\lambda = 1$ and $\nu_0 = 10$ meV. Note that these functions are defined on a discrete set of points (the Fermion Matsubara frequencies) that become more closely spaced as the temperature is lowered. For temperatures close to T_c the gap function diminishes gradually to zero at all frequencies, while at the lowest temperature the gap function attains a maximum. In Fig. 29.3(b) we plot the normalized values, $\Delta(i\omega_m)/\Delta(i\omega_1)$ vs. Matsubara frequency, and it is clear that they differ from one another by very little. Returning to Fig. 29.3(a), the lowest frequency function value can be thought of as an order parameter. In Fig. 29.4 we show the lowest frequency gap function value, $\Delta(i\omega_1)$, now normalized to the value at $T = 0$ vs. reduced temperature, T/T_c. These are shown as blue squares, for about 9 temperatures. Also shown is the BCS weak coupling result, given as a red curve. One can see that the differences are small. We have also a plotted many more points (green asterisks) for a weaker coupling, $\lambda = 0.3$ (same phonon frequency), which fall exactly on the BCS curve. The main point is that deviations from the weak coupling BCS result are minor. For much stronger coupling than given here deviations are similarly very small, and experiment confirms this to be the case.[80]

Many measurable properties of the superconducting state can be calculated from the imaginary axis solutions to the gap function. The renormalization function, $Z(i\omega_m)$, is also required but this does not change by very much in the superconducting state. Examples of measurable properties include all thermodynamic quantities like the specific heat, and various critical fields. Systematic changes with coupling strength, as measured by λ, or alternatively the ratio of the critical temperature to a particular phonon frequency moment, $T_c/\omega_{\ln}$, have been reviewed elsewhere,[33, 34] and will not be repeated here.

19.3.6 Results on the real axis

For any dynamical property (tunneling current, optical response, dynamical penetration depth, etc.), the relevant Green function (and therefore self-energy) is required as a function of real frequency. More precisely, for the retarded Green function it is needed at $\omega + i\delta$, i.e. infinitesimally above the real axis. In the original literature[12, 13, 71, 81, 82] the spectral representation was introduced to replace Matsubara sums with real frequency integrals, and these equations were then solved, either analytically (with approximations) or numerically. This was a difficult task (especially with the computers available at that time), and eventually the procedure was adopted that first required a solution on the imaginary axis and then analytic continuation ($i\omega_m \to \omega + i\delta$) through some approximate process. For this type of analytic function, the method of Padé approximants was used,[83] although the degree of precision needed for the gap function on the imaginary axis was very stringent (10^{-12} for relative errors) in order to achieve accurate results on the real axis.

An appreciation for the information imbedded in imaginary axis solutions can be attained by considering the simple example of $g(i\omega_m) = \mathrm{sech}(\omega_m/\nu_0)$, a very smooth function without structure, and monotonically decreasing with frequency on the positive imaginary axis. The analytic continuation can be easily done analytically; it is $g(\omega + i\delta) = \sec[(\omega + i\delta)/\nu_0]$. This function, in contrast to its imaginary axis counterpart, is riddled with divergences and discon-

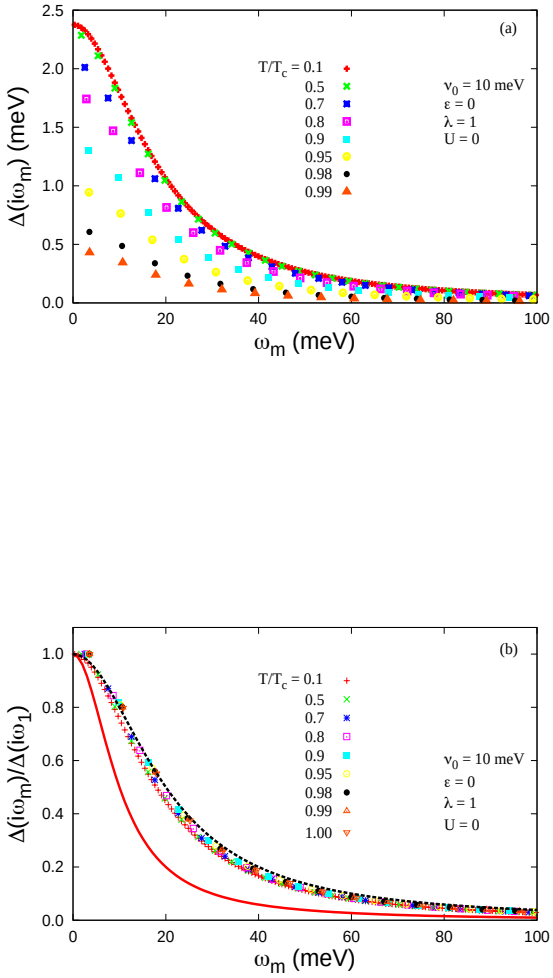


Figure 19.3: (a) The gap function $\Delta(i\omega_m)$ vs. Matsubara frequency, ω_m, for various temperatures. We have used a δ-function phonon spectrum ($\epsilon = 0$) with $\nu_0 = 10$ meV, electron-phonon coupling strength, $\lambda = 1$ and $U = 0$. For these parameters, $T_c = 13.3$ K. Clearly the gap function increases in amplitude with decreasing temperature, and below about $T/T_c = 0.5$ there is very little change in the amplitude and in the frequency dependence. With a broadened phonon spectrum there would be only minor changes. With a nonzero U, the gap function would have a negative asymptote as $\omega_m \to \infty$. In (b), to illustrate that there is very little change in the frequency dependence *at all temperatures* we show the normalized gap function, $\Delta(i\omega_m)/\Delta(i\omega_1)$ vs. ω_m. Now the results look very similar to one another, which makes convergence from one temperature to the next relatively easy. Also shown is the weak coupling expectation[56] at T_c, $\Delta(i\omega_m)/\Delta(i\omega_1) = \omega_E^2/(\omega_E^2 + \omega_m^2)$, indicated with a solid red curve. This result clearly does not resemble the data, since we the numerical results are for $\lambda = 1$. However, the slightly modified result, $\Delta(i\omega_m)/\Delta(i\omega_1) = \omega_E^2/(\omega_E^2 + \omega_m^2/(1+\lambda)^2)$, shown as a dashed black curve, is a fairly good fit.

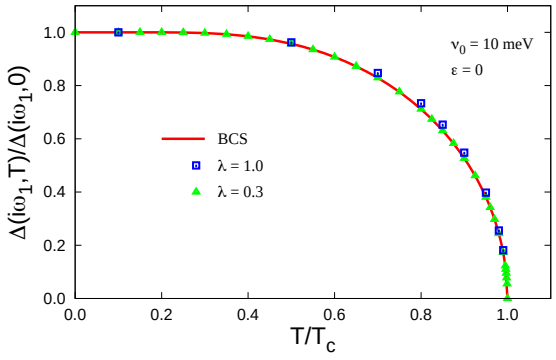


Figure 19.4: The gap function at the first Matsubara frequency (serving as an order parameter), normalized to the zero temperature gap function at the first Matsubara frequency, vs. reduced temperature T/T_c. The blue squares are the results at a few temperatures for calculations using a phonon δ-function spectrum with $\nu_0 = 10$ meV, $\lambda = 1$, and $U = 0$. Shown for comparison is the weak coupling BCS result (red curve). The deviations are very slight. Also shown for comparison are the Eliashberg results for the same phonon spectrum but with $\lambda = 0.3$ (green triangles). These results fall right on the BCS weak coupling result.

tinuities. And yet, in principle at least, this information is embedded in the (smooth) results on the imaginary axis. In practice, the information is contained in the 10^{th} significant digit and beyond.

An alternative, numerically exact procedure was developed in the late 1980's.[84] Here we simply write down the resulting expressions, the derivation of which is available in Ref. [[84]]. They are

$$\begin{aligned}\phi(\omega+i\delta) &= \pi T\sum_{m=-\infty}^{\infty}\left[\lambda(\omega-i\omega_m)-u^*(\omega_c)\theta(\omega_c-|\omega_m|)\right]\frac{\Delta(i\omega_m)}{\sqrt{\omega_m^2+\Delta^2(i\omega_m)}}\\ +i\pi\int_0^\infty d\nu\,\alpha^2F(\nu)\qquad &\left\{\left[N(\nu)+f(\nu-\omega)\right]\frac{\phi(\omega-\nu+i\delta)}{\sqrt{(\omega-\nu)^2Z^2(\omega-\nu+i\delta)-\phi^2(\omega-\nu+i\delta)}}\right.\\ &\left.+\left[N(\nu)+f(\nu+\omega)\right]\frac{\phi(\omega+\nu+i\delta)}{\sqrt{(\omega+\nu)^2Z^2(\omega+\nu+i\delta)-\phi^2(\omega+\nu+i\delta)}}\right\},\end{aligned} \tag{19.24}$$

and

$$Z(\omega+i\delta) = 1+\frac{i\pi T}{\omega}\sum_{m=-\infty}^{\infty}\lambda(\omega-i\omega_m) \tag{19.25}$$

$$\frac{\omega_m}{\sqrt{\omega_m^2+\Delta^2(i\omega_m)}} + \frac{i\pi}{\omega}\int_0^\infty d\nu\,\alpha^2F(\nu)\left\{\left[N(\nu)+f(\nu-\omega)\right]\frac{(\omega-\nu)Z(\omega-\nu+i\delta)}{\sqrt{(\omega-\nu)^2Z^2(\omega-\nu+i\delta)-\phi^2(\omega-\nu+i\delta)}}\right.$$
$$\left.+\left[N(\nu)+f(\nu+\omega)\right]\frac{(\omega+\nu)Z(\omega+\nu+i\delta)}{\sqrt{(\omega+\nu)^2Z^2(\omega+\nu+i\delta)-\phi^2(\omega+\nu+i\delta)}}\right\} \tag{19.26}$$

and of course $\Delta(\omega+i\delta)\equiv\phi(\omega+i\delta)/Z(\omega+i\delta)$. Here $f(\omega)\equiv 1/(\exp(\beta\omega)+1)$ and $N(\nu)\equiv 1/(\exp(\beta\nu)-1)$ are the Fermi and Bose functions respectively. Note that in cases where the square–root is complex, the branch with positive imaginary part is to be chosen. The reason for this can be traced back to Eq. (19.6) [or Eq. (19.4)] where the integration over $\epsilon_{\mathbf{k}'}$ (with the assumptions made there) requires that the pole (given the same square–root that appears here) be *above* the real axis.

It can easily be verified that substituting $\omega+i\delta\to i\omega_n$ instantly recovers the imaginary axis equations (all the Fermi and Bose factors cancel to give zero contributions beyond the initial terms that require Matsubara summations). Clearly the inverse is not true — replacing the Matsubara frequency $i\omega_m$ where it appears in Eqs. (19.15,19.16) produces the first lines in Eqs. (19.24,19.26) involving Matsubara sums, but leaves out the remaining two lines in each case. The strategy for solving these equations is straightforward; the imaginary axis equations [Eqs. (19.15,19.16)] are first solved self-consistently. These are then used in Eqs. (19.24,19.26) and these equations are iterated to convergence. The presence of the first lines in these equations provides a "driving term" that makes the iteration process quite rapid. For example, performing the entire operation (solution of imaginary axis and real axis equations) for a given temperature takes about a tenth of a second on a laptop.

Moreover, $T=0$ is a special case, as is clear from these equations. In fact, this was recognized a long time ago,[85] where they established the following low frequency behaviour at $T=0$,

$$\begin{aligned}\mathrm{Re}\Delta(\omega+i\delta) &= c,\\ \mathrm{Im}\Delta(\omega+i\delta) &= 0,\\ \mathrm{Re}Z(\omega+i\delta) &= d,\\ \mathrm{Im}Z(\omega+i\delta) &= 0.\end{aligned}\qquad T=0 \tag{19.27}$$

where c and d are constants. In contrast, the behaviour at any non-zero temperature is

$$\begin{aligned}\mathrm{Re}\Delta(\omega+i\delta) &\propto \omega^2,\\ \mathrm{Im}\Delta(\omega+i\delta) &\propto \omega,\\ \mathrm{Re}Z(\omega+i\delta) &= d(T),\\ \mathrm{Im}Z(\omega+i\delta) &\propto 1/\omega.\end{aligned}\qquad T>0 \tag{19.28}$$

For conventional parameter choices this distinction has very little consequence, as the differences are barely discernible. For example, the expression of the imaginary part of $Z(\omega+i\delta)$ in the normal state is given by

$$\mathrm{Im}Z(\omega+i\delta)=2\pi\lambda\frac{\nu_0}{\omega}[N(\nu_0)+f(\nu_0)] \tag{19.29}$$

for a δ-function spectrum [$\epsilon \to 0$ in Eq. (19.20)] with strength λ and central frequency ν_0. For $\nu_0 = 10$ meV and $\lambda = 1$ then Fig. 29.1 indicates $T_c \approx 10$ K, and at $T/T_c = 0.1$, the exponent in the Bose and Fermi functions makes this part $\approx 10^{-50}$. Thus, true to Eq. (19.28) the limiting behaviour is $\propto \nu_0/\omega$. However, to see this requires $\omega/\nu_0 < 10^{-45}$, making it unobservable, and indistinguishable from the $T = 0$ case.

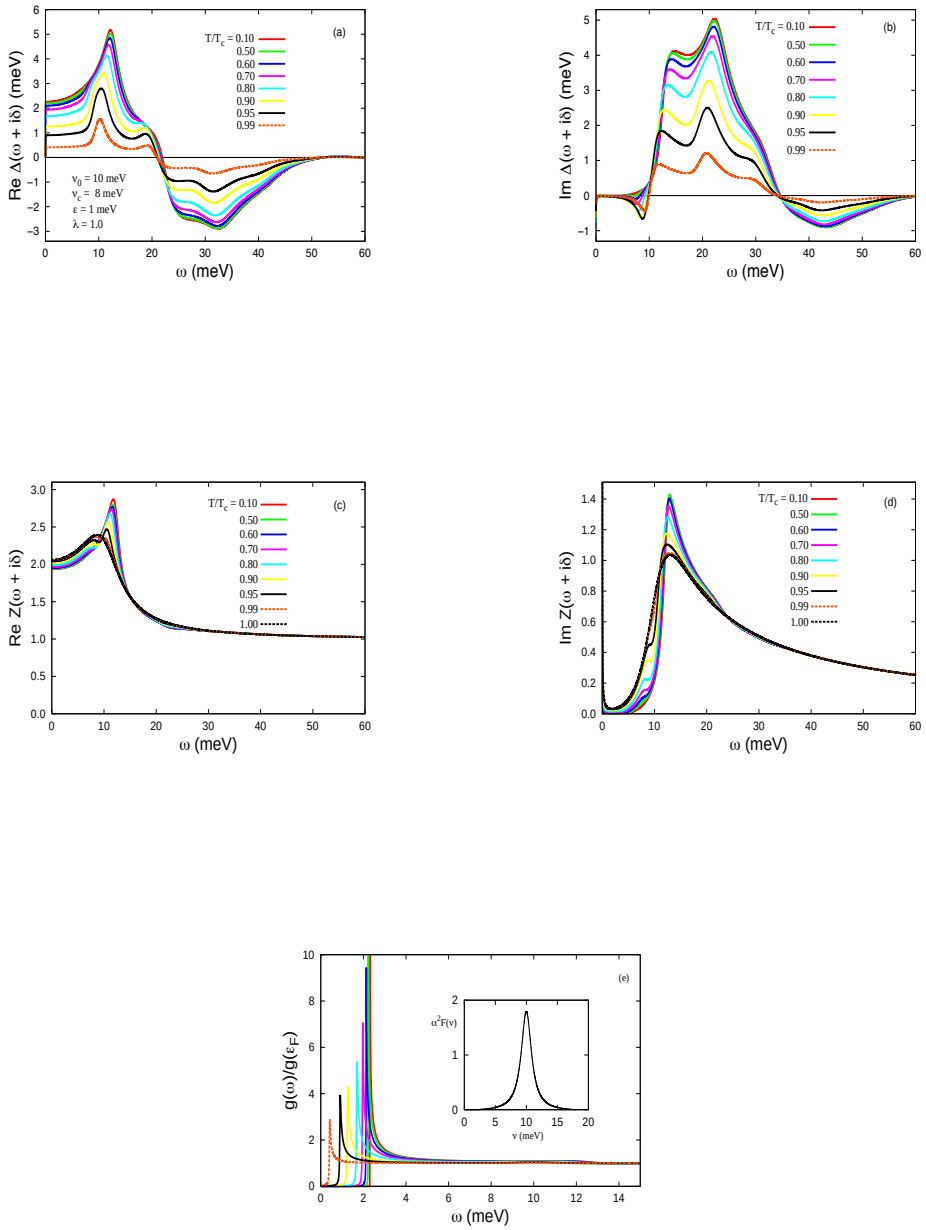


Figure 19.5: Frequency dependence of (a) Re $\Delta(\omega + i\delta)$, (b) Im $\Delta(\omega + i\delta)$, (c) Re $Z(\omega + i\delta)$, (d) Im $Z(\omega + i\delta)$, and (e) $g(\omega)/g(\epsilon_F)$, for various temperatures in the superconducting state. Features are discussed in the text. For the spectral function we have used Eq. (19.20) with $\lambda = 1$, $\nu_0 = 10$ meV, and $\epsilon = 1$ meV. It is displayed in the inset of (e) and was used for all these figures. The colour coding in (e) is the same as the others. We used $U = 0$.

While this expression is for the normal state, the corresponding one of the superconducting state is even more severe, due to the development of the superconducting order parameter, which gives rise to a gap in the spectrum. Again, given the first two lines in Eq. (19.28) there is technically *no gap*, but in practice for reasons like we have just indicated, the practical results more closely follow the behaviour indicated in Eq. (19.27). Where the finite temperature result becomes pronounced and noticeably different than the zero temperature behaviour is in the strong coupling limit,[86] but in this case the parameters are not realistic and undoubtedly beyond the domain of validity of the theory.

Returning to $T = 0$, for cases like the present where the phonon spectrum has a gap there is a special simplification. Basically, no iteration is required — the low frequency gap and renormalization functions come entirely from the first lines of Eqs. (19.24,19.26), and these can be constructed explicitly from the imaginary axis results. For a δ-function phonon spectrum, however, one has to be careful to convert the Matsubara summation to an actual integral, as a discontinuity will occur at the phonon frequency (at non-zero temperature this discontinuity is broadened into a gradual drop). Once the low frequency gap and renormalization functions are so constructed, higher frequency values require the Matsubara sum *and* real axis values of these functions at *lower frequencies only*. Eventually the entire functional forms are so constructed, without the need for iteration. As we will see, low temperature results converge quite rapidly to the zero temperature result, so this non-iterative method can be used as an alternative, for the lowest temperatures. Nonetheless, we will proceed with fully converged (iterative) finite temperature results, since these require such few iterations anyways.

To show real axis results, we utilize a phonon spectrum as in Eq. (19.20) with $\nu_0 = 10$ meV, $\nu_c = 8$ meV, and $\epsilon = 1$ eV, and $\lambda = 1$. Results with a δ-function spectrum tend to have a series of singularities, that are anyways artifacts of the singular spectrum, so we prefer to show results corresponding to this model spectrum. A series of such plots was also shown in Ref. [[34]] for the tunneling-derived Pb spectrum, with a much larger value of λ, and many more such results have been shown in the literature, often using this same method.[87] In Fig. 29.5 we show (a) the real part of the gap function, (b) the imaginary part of the gap function, (c) the real part of the renormalization function, (d) the imaginary part of the renormalization function, and (e) the tunneling density of states,

$$\frac{g(\omega)}{g(\epsilon_F)} = \mathrm{Re}\frac{\omega}{\sqrt{\omega^2 - \Delta^2(\omega + i\delta)}}, \tag{19.30}$$

which is measurable in single-particle tunneling experiments. The first observation, difficult to make with just these results, is that an image of the $\alpha^2F(\nu)$ spectrum is contained in both the real and imaginary parts of the gap function. Here it is the peak structure clearly evident in (a) centred around 10 meV *for the highest temperature shown.* As the temperature decreases this peak shifts to higher frequency, roughly by an amount equal to the value of the gap function at low frequency (about 2 meV in the present case). Experimentation with different spectral functions makes this observation more self-evident. See, for example, the distinctive spectrum for Pb in Fig. 4.35(a) of Ref. [[34]].

Both functions in (a) and (b) go to zero as the critical temperature is approached from below. As discussed earlier, they both go to zero at zero frequency at all temperatures shown, according to Eqs. (19.28), although one cannot see this on the scale shown. Even for the highest temperatures shown this behaviour can barely be seen, but becomes evident when one expands the low frequency scale. For the lowest temperatures shown even expanding the frequency scale by a few orders of magnitude is not enough to reveal the low-frequency behaviour indicated by Eqs. (19.28). For this reason one cannot use $\Delta(\omega + i\delta)$ as an order parameter at any frequency; either one has to revert to $\phi(\omega + i\delta)$ at zero frequency, or one can use the imaginary axis result for $\Delta(i\omega_m)$, as we did in Fig. 29.4. Also note that these functions approach zero at high

frequency. If a Coulomb repulsion is included then the real part of $\Delta(\omega + i\delta)$ approaches a negative constant at high frequency.

In contrast the real and imaginary parts of $Z(\omega + i\delta)$ plotted in (c) and (d) have changed very little in the superconducting state, and remain non-zero at the superconducting critical temperature, as indicated by the black curve. An image of $\alpha^2F(\nu)$ is present in this function as well, particularly in the imaginary part (see also Fig. 4.35 (c) and (d) in Ref. [[34]]). Finally, the tunneling density of states is shown in Fig. 29.5(e), and reveals a "gap" that opens from zero at $T = T_c$ rather quickly and then saturates to a low temperature value as indicated. In fact a plot of this "gap" vs. temperature would follow the result displayed in Fig. 29.4 very closely. However, as first pointed out by Karakozov et al.[85] there is no "gap" (hence the parentheses) and in fact this is evident in Fig. 29.5(e), where there is a noticeable rounding of the curves at frequencies below the sharp peak at almost all temperatures shown. The peak is a remnant of the square-root singularity known from BCS theory, which is evident from Eq. (19.30) if a constant gap function is used, $\Delta(\omega + i\delta) = \Delta_0$. In fact Eliashberg theory predicts smearing of this singularity simply due to the presence of imaginary components of all the functions involved in Eqs. (19.28) for all finite temperatures. It is also worth pointing out that the BCS limit of Eliashberg theory is *not* achieved by setting the gap function to a constant, $\Delta(\omega + i\delta) \to \Delta_0$, but in fact the gap function is a decaying function of frequency in this limit.[85] This frequency dependence and its implications for the weak coupling limit has been further explored in Refs. [[88, 56, 89]].

Finally, though not so evident in Fig. 29.5(e), there are "ripples" in the density of states beyond the "gap" region, caused by the coupling of electrons to phonons. The presence of these ripples in experiments (see, in particular, Refs. [[90, 91, 18]]) is perhaps the strongest evidence of the validity of Eliashberg theory. In fact the most intense scrutiny has been superconducting Pb, where the electron-phonon coupling is particularly strong, $\lambda \approx 1.5$, with a value well beyond the expected domain of validity. These experiments, coupled with an inversion technique that use the Eliashberg equations themselves, result in a consistent description of the superconducting state for Pb and other so-called "strong coupling" superconductors.

Many systematic deviations from BCS theory have been characterized, for example the gap ratio, $2\Delta_0/(k_BT_c)$,[92] the specific heat jump, and many other dimensionless ratios[93, 94] These have all been reviewed in Ref. [[33]], and show very systematic behaviour as a function of the strong coupling index, $T_c/\omega_{\ln}$. On the other hand, when systematics are examined with purely experimental parameters, the picture is not so clear.[95]

19.3.7 Summary and Outlook

I have provided just a sketch of what we consider the essence of Eliashberg theory — retardation effects, in the context of a single featureless band. The generalization of these types of calculations to more complicated scenarios is well documented in a number of places, and have not been reviewed here. These include order parameter anisotropy, multi-band superconductivity, Berezinskii "odd-frequency" pairing, sharply varying electronic density of state, impurity effects, and so on. These additional complications are increasingly taken into account to understand new classes of compounds that exhibit superconductivity, such as the hydrides, MgB_2, and the pnictides. In some cases, these additional effects have been invoked to explain higher critical temperatures as well, but for the most part they are motivated by matching theory to experiment.

In its bare form, Fig. 29.1 presents the possibilities for T_c provided by Eliashberg theory. The conscious decision was made to extend the domain of coupling strength to unity *only* and not beyond, because there are reasons to believe that going beyond this regime is not viable. At the same time, large values of the characteristic phonon frequency have been used, and this is

why the plot extends to beyond ≈ 50 K for the vertical axis, T_c. Are these values of frequency, together with large values of $\lambda \approx 1$ viable? Probably not, but given these sorts of parameter values, this is what Eliashberg in its standard form predicts.

I have also tried to touch on aspects of the theory where more critical scrutiny is possible, by comparing results to those obtained with microscopic models, such as the Holstein model. We believe there are significant difficulties that arise when these comparisons are made. One reaction is to dismiss such comparisons, as the Holstein model (or the Hubbard model, for that matter) may be regarded as "toy models," possibly fraught with pathologies. However, if the Holstein model is lacking in some way, it is important to know why, and what other aspect of the electron-phonon interaction (wave-vector dependence?) is essential to the success of Eliashberg theory. For example, if the super-high-T_c of the hydrides is confirmed to originate in the electron-phonon interaction, then clearly one or more missing gaps in our understanding of how this happens needs to be filled.

Moreover, as presented here, Eliashberg theory focusses on the superconducting instability, and does not consider other, possibly competing, or potentially enhancing, instabilities. This possibility has come up as more and more phase diagrams of families of materials exhibit a nearby antiferromagnetic or charge-density-wave instability, as a function of some tuning parameter (doping, pressure, etc.). It would be desirable to generalize Eliashberg theory to be more "self-regulating," and have the theory itself indicate when a competing instability is limiting superconducting T_c, for example.

The other aspect that goes hand in hand with the electron-phonon coupling is the direct Coulomb interaction. We cannot claim to understand superconductivity to the point of having predictive power until we understand the role of Coulomb correlations, and their detrimental (or perhaps favourable?) effects on pairing. A key advancement has to come in further understanding the role that competitive tendencies or instabilities play in superconductivity. Many of the modern-day methods (Dynamical Mean Field Theory, for example) seek to address the question of competing interactions. Studies with Quantum Monte Carlo methods, like the ones mentioned here, will also aid in furthering our understanding of interacting electrons, and similar studies with the now-accessible much larger lattice sizes would be welcome.

This work was supported in part by the Natural Sciences and Engineering Research Council of Canada (NSERC). I would like to thank the many students and postdoctoral fellows in my own group who have contributed to the work described here. I also want to thank in particular Jules Carbotte, who first taught me about Eliashberg theory, and Ewald Schachinger, who was instrumental in teaching me about programming the Eliashberg imaginary axis equations. I also want to thank Sasha Alexandrov, who over the years continued to question the validity of MIgdal-Eliashberg theory. In the same way, Jorge Hirsch, with whom I have worked a great deal on other matters, has been instrumental in discussions concerning the validity of the work reviewed here. I also want to thank him for critical comments concerning parts of this review. Finally, Jules sadly passed away earlier this year (April 5, 2019), and this review is dedicated to his memory. He was a wonderful man, and I feel extremely fortunate to have first entered the physics world under his guidance.

APPENDIX: Derivation of Eliashberg Theory

In this Appendix, we will first outline a derivation of Eliashberg theory, based on a weak coupling approach. Our primary source for this derivation is Ref. [[47]]. Migdal theory of the normal state follows by simply dropping the anomalous amplitudes in what follows.

If we know the many-body wave function of system, we can calculate the expectation value for any observable. However, usually this is something we do not know, and instead we calculate multi-electron Green functions, which are themselves related to observables. The Green

functions are necessarily almost always approximate, and those computed in Eliashberg theory are no exception. In fact, Eliashberg theory is essentially a mean-field theory, though because of the inherent frequency dependence in the self energy, it is in many ways a precursor to Dynamical Mean Field Theory.[96]

We begin with the definition of the one-electron Green function, defined in momentum space,[97] as a function of imaginary time, τ,

$$G(\mathbf{k}, \tau - \tau') \equiv - < T_\tau c_{\mathbf{k}\sigma}(\tau) c^\dagger_{\mathbf{k}\sigma}(\tau') >, \tag{19.31}$$

where $\mathbf{k}$ is the momentum and σ is the spin. The angular brackets denote a thermodynamic average. We can Fourier-expand this Green function in imaginary frequency:

$$\begin{aligned} G(\mathbf{k}, \tau) &= \frac{1}{\beta} \sum_{m=-\infty}^{\infty} e^{-i\omega_m \tau} G(\mathbf{k}, i\omega_m) \\ G(\mathbf{k}, i\omega_m) &= \int_0^\beta d\tau G(\mathbf{k}, \tau) e^{i\omega_m \tau}. \end{aligned} \tag{19.32}$$

The frequencies $i\omega_m$ are the Fermion Matsubara frequencies, given by $i\omega_m = i\pi T(2m-1)$, $m = 0, \pm 1, \pm 2, ...$, where T is the temperature. Because the c's are Fermion operators, the Matsubara frequencies are *odd* multiples of $i\pi$T. The imaginary time τ takes on values from 0 to $\beta \equiv 1/(k_B T)$.

A similar definition holds for the phonon Green function,

$$D(\mathbf{q}, \tau - \tau') \equiv - < T_\tau A_{\mathbf{q}}(\tau) A_{-\mathbf{q}}(\tau') >, \tag{19.33}$$

where

$$A_{\mathbf{q}}(\tau) \equiv a_{\mathbf{q}}(\tau) \quad + \quad a^\dagger_{-\mathbf{q}}(\tau). \tag{19.34}$$

The Fourier transform is similar to that given in (19.32) except that the Matsubara frequencies are $i\nu_n \equiv i\pi T 2n$, $n = 0, \pm 1, \pm 2, ...$ and occur at *even* multiples of $i\pi T$. These are the Boson Matsubara frequencies.

To derive the Eliashberg equations, we follow Ref. [[47]], and use the equation-of-motion method. The starting point is the time derivative of Eq. (19.31),

$$\frac{\partial}{\partial \tau} G(\mathbf{k}, \tau) = -\delta(\tau) \quad - \quad < T_\tau \big[H - \mu N, c_{\mathbf{k}\sigma}(\tau) \big] c^\dagger_{\mathbf{k}\sigma}(0) >, \tag{19.35}$$

where we have put $\tau' = 0$, without loss of generality. We use the Hamiltonian (19.2), and assume, for the Coulomb interaction, the simple Hubbard model, $H_{Coul} = U \sum_i n_{i\uparrow} n_{i\downarrow}$. Including the Coulomb repulsion, the result is repeated here,

$$\begin{aligned} H \quad = \quad & \sum_{\mathbf{k}\sigma} \epsilon_{\mathbf{k}} c^\dagger_{\mathbf{k}\sigma} c_{\mathbf{k}\sigma} \\ & + \sum_{\mathbf{q}} \hbar\omega_{\mathbf{q}} a^\dagger_{\mathbf{q}} a_{\mathbf{q}} \\ & + \frac{1}{\sqrt{N}} \sum_{\substack{\mathbf{k}\mathbf{k}' \\ \sigma}} g(\mathbf{k}, \mathbf{k}') \big(a_{\mathbf{k}-\mathbf{k}'} + a^\dagger_{-(\mathbf{k}-\mathbf{k}')} \big) c^\dagger_{\mathbf{k}'\sigma} c_{\mathbf{k}\sigma} \\ & + \frac{U}{N} \sum_{\mathbf{k},\mathbf{k}',\mathbf{q}} c^\dagger_{\mathbf{k}\uparrow} c^\dagger_{-\mathbf{k}+\mathbf{q}\downarrow} c_{-\mathbf{k}'+\mathbf{q}\downarrow} c_{\mathbf{k}'\uparrow}, \end{aligned} \tag{19.36}$$

where the various symbols have already been defined in the text. We consider only the Green function with $\sigma =\uparrow$; the commutator in Eq. (19.35) is straightforward and we obtain

$$\left(\frac{\partial}{\partial\tau}+\epsilon_{\mathbf{k}}\right)G_{\uparrow}(\mathbf{k},\tau) =$$
$$-\delta(\tau)-\frac{1}{\sqrt{N}}\sum_{\mathbf{k}'}g_{\mathbf{k}\mathbf{k}'} < T_\tau A_{\mathbf{k}-\mathbf{k}'}(\tau)c_{\mathbf{k}'\uparrow}(\tau)c^\dagger_{\mathbf{k}\uparrow}(0) >$$
$$+\frac{U}{N}\sum_{\mathbf{p}\mathbf{p}'} < T_\tau c^\dagger_{\mathbf{p}'-\mathbf{k}+\mathbf{p}\downarrow}(\tau)c_{\mathbf{p}'\downarrow}(\tau)c_{\mathbf{p}\uparrow}(\tau)c^\dagger_{\mathbf{k}\uparrow}(0) > . \tag{19.37}$$

Various higher order propagators now appear; to determine them another equation of motion can be written, which would, in turn, generate even higher order propagators, and this eventually leads to an infinite set of equations with hierarchical structure. This infinite series is normally truncated at some point by the process of decoupling, which is simply an approximation procedure. For example, in (19.37) the Coulomb term is normally decoupled at this point and becomes

$$< T_\tau c^\dagger_{\mathbf{p}'-\mathbf{k}+\mathbf{p}\downarrow}(\tau)c_{\mathbf{p}'\downarrow}(\tau)c_{\mathbf{p}\uparrow}(\tau)c^\dagger_{\mathbf{k}\uparrow}(0) >\rightarrow$$
$$< T_\tau c^\dagger_{\mathbf{p}'-\mathbf{k}+\mathbf{p}\downarrow}(\tau)c_{\mathbf{p}'\downarrow}(\tau) >< T_\tau c_{\mathbf{p}\uparrow}(\tau)c^\dagger_{\mathbf{k}\uparrow}(0) >\rightarrow$$
$$-\delta_{\mathbf{k}\mathbf{p}}G_{\downarrow}(\mathbf{p}',0)G_{\uparrow}(\mathbf{k},\tau). \tag{19.38}$$

The case of the electron–phonon term is more difficult; in this case we define a 'hybrid' electron/phonon Green function,

$$G_2(\mathbf{k},\mathbf{k}',\tau,\tau_1) \equiv< T_\tau A_{\mathbf{k}-\mathbf{k}'}(\tau)c_{\mathbf{k}'\uparrow}(\tau_1)c^\dagger_{\mathbf{k}\uparrow}(0) >, \tag{19.39}$$

and write out an equation of motion for it. We simply get

$$\frac{\partial}{\partial\tau}G_2(\mathbf{k},\mathbf{k}',\tau,\tau_1) = -\omega_{\mathbf{k}-\mathbf{k}'} < T_\tau P_{\mathbf{k}-\mathbf{k}'}(\tau)c_{\mathbf{k}'\uparrow}(\tau_1)c^\dagger_{\mathbf{k}\uparrow}(0) >, \tag{19.40}$$

where $P_{\mathbf{q}}(\tau) = a_{\mathbf{q}}(\tau) - a_{-\mathbf{q}}(\tau)$. Taking a second derivative yields

$$\left[\frac{\partial^2}{\partial\tau^2}-\omega_{\mathbf{k}-\mathbf{k}'}\right]G_2(\mathbf{k},\mathbf{k}',\tau,\tau_1) =$$
$$\sum_{\mathbf{k}''\sigma}2\omega_{\mathbf{k}-\mathbf{k}'}g_{\mathbf{k}-\mathbf{k}'} < T_\tau c^\dagger_{\mathbf{k}''-\mathbf{k}+\mathbf{k}'\sigma}(\tau)c_{\mathbf{k}''\sigma}(\tau)c_{\mathbf{k}'\uparrow}(\tau_1)c^\dagger_{\mathbf{k}\uparrow}(0) > . \tag{19.41}$$

At this point we *do not simply* decouple the last line of Eq. (19.41). We first need to take the phonon propagator into account, and the standard procedure is to use the "non-interacting" phonon propagator. The adjective "non-interacting" is in quotes because part of the philosophy of proceeding in this way was a desire to *not* compute corrections to the phonon propagator, because the information going into this part of the calculations (e.g. the phonon spectral function) was going to come from experiment. Coming from experiment means that nature "had already done the calculation," and we did not want to double count. Clearly, if the purpose of this calculation is to compare to Quantum Monte Carlo calculations where this is *not* the case, then something different should be done, and this is what motivated the *renormalized* Migdal-Eliashberg calculations of Refs. [[65, 66]].

For now, we proceed with the standard Eliashberg calculations. The equation of motion for the non-interacting phonon propagator is

$$\left)\frac{\partial^2}{\partial\tau^2}-\omega^2_{\mathbf{q}}\right)D(\mathbf{q},\tau-\tau') = 2\omega_{\mathbf{q}}\delta(\tau-\tau'). \tag{19.42}$$

(?? ниже формула испорчена версткой, см. оригинальную статью его!)
Inserting this expression into Eq. (19.41) then yields

$$G_2(\mathbf{k},\mathbf{k}',\tau,\tau) = \frac{1}{N}\sum_{\mathbf{k}''\sigma}\int_0^\beta d\tau' g_{\mathbf{k}'',\mathbf{k}''+\mathbf{k}-\mathbf{k}'} g_{\mathbf{k}\mathbf{k}'} D(\mathbf{k}-\mathbf{k}',\tau-\tau')$$
$$\times < T_\tau c^\dagger_{\mathbf{k}''\sigma}(\tau') c_{\mathbf{k}''+\mathbf{k}-\mathbf{k}'\sigma}(\tau') c^\dagger_{\mathbf{k}''-\mathbf{k}+\mathbf{k}'\sigma}(\tau') c_{\mathbf{k}''\sigma}(\tau') c_{\mathbf{k}'\uparrow}(\tau) c^\dagger_{\mathbf{k}\uparrow}(0) >, \tag{19.43}$$

where now τ_1 has been set equal to τ as is required in (19.37). It is important that this be done only *after* applying Eq. (19.42). The result can be substituted into Eq. (19.37), and then Fourier transformed (from imaginary time to imaginary frequency). Before doing this however, we recall that Gor'kov[11] realized the important role of the so-called Gor'kov anomalous amplitude, in the Wick decomposition [97] of the various two–particle Green functions encountered above. We therefore have to account for these in addition to the pairing of fermion operators used in Eq. (19.38).

The anomalous amplitudes are defined to be

$$F(\mathbf{k},\tau) \equiv - < T_\tau c_{\mathbf{k}\uparrow}(\tau) c_{-\mathbf{k}\downarrow}(0) > \tag{19.44}$$

and

$$\bar{F}(\mathbf{k},\tau) \equiv - < T_\tau c^\dagger_{-\mathbf{k}\downarrow}(\tau) c^\dagger_{\mathbf{k}\uparrow}(0) > . \tag{19.45}$$

Now we need to repeat the same steps as above with F and $\bar{F}$ as we did with G. Skipping the intermediate steps, the result is an equation analogous to Eq. (19.37)

$$\left(\frac{\partial}{\partial\tau} - \epsilon_{\mathbf{k}}\right)\bar{F}(\mathbf{k},\tau) =$$
$$-\frac{1}{\sqrt{N}}\sum_{\mathbf{k}'} g_{-\mathbf{k}',-\mathbf{k}} < T_\tau A_{\mathbf{k}-\mathbf{k}'}(\tau) c^\dagger_{-\mathbf{k}'\downarrow}(\tau) c^\dagger_{\mathbf{k}\uparrow}(0) >$$
$$+\frac{U}{N}\sum_{\mathbf{k}'',\mathbf{q}}(????) < T_\tau c^\dagger_{\mathbf{p}'-\mathbf{k}+\mathbf{p}\downarrow}(\tau) c_{\mathbf{p}'\downarrow}(\tau) c_{\mathbf{p}\uparrow}(\tau) c^\dagger_{\mathbf{k}\uparrow}(0) >, < T_\tau c^\dagger_{\mathbf{k}''\uparrow}(\tau) c^\dagger_{-\mathbf{k}''+\mathbf{q}\downarrow}(\tau) c_{\mathbf{k}+\mathbf{q}\uparrow}(\tau) c^\dagger_{\mathbf{k}\uparrow}(0) > \tag{19.46}$$

and similarly for the function F. This leads to the need for another 'hybrid' electron/phonon anomalous Green function,

$$\bar{F}_2(\mathbf{k},\mathbf{k}',\tau,\tau_1) \equiv < T_\tau A_{\mathbf{k}-\mathbf{k}'}(\tau) c^\dagger_{-\mathbf{k}'\downarrow}(\tau_1) c^\dagger_{\mathbf{k}\uparrow}(0) >, \tag{19.47}$$

and, following the same process as for the regular Green function, we find
(?? ниже формула испорчена версткой, см. оригинальную статью его!)

$$\bar{F}_2(\mathbf{k},\mathbf{k}',\tau,\tau) = \frac{1}{N}\sum_{\mathbf{k}''\sigma}\int_0^\beta d\tau' g_{\mathbf{k}'',\mathbf{k}''+\mathbf{k}-\mathbf{k}'} g_{\mathbf{k}\mathbf{k}'} D(\mathbf{k}-\mathbf{k}',\tau-\tau')$$
$$\times < T_\tau c^\dagger_{\mathbf{k}''\sigma}(\tau') c_{\mathbf{k}''+\mathbf{k}-\mathbf{k}'\sigma}(\tau') c^\dagger_{\mathbf{k}''-\mathbf{k}+\mathbf{k}'\sigma}(\tau') c_{\mathbf{k}''\sigma}(\tau') c^\dagger_{-\mathbf{k}'\downarrow}(\tau) c^\dagger_{\mathbf{k}\uparrow}(0) >, \tag{19.48}$$

where again τ_1 has been set equal to τ *after* applying Eq. (19.42).

The Fourier definitions of the anomalous Green function are the same as Eq. (19.32):

$$\bar{F}(\mathbf{k},\tau) = \frac{1}{\beta}\sum_{m=-\infty}^{\infty} e^{-i\omega_m\tau}\bar{F}(\mathbf{k},i\omega_m)$$
$$\bar{F}(\mathbf{k},i\omega_m) = \int_0^\beta d\tau \bar{F}(\mathbf{k},\tau) e^{i\omega_m\tau}, \tag{19.49}$$

and similarly for F. In frequency space one finds that two self energies naturally arise,

$$\Sigma(\mathbf{k}, i\omega_m) = -\frac{1}{N\beta}\sum_{\mathbf{k}',m'} g_{\mathbf{k}\mathbf{k}'}g_{\mathbf{k}'\mathbf{k}}D(\mathbf{k}-\mathbf{k}', i\omega_m - i\omega_{m'})G(\mathbf{k}', i\omega_{m'}), \tag{19.50}$$

$$\phi(\mathbf{k}, i\omega_m) = -\frac{1}{N\beta}\sum_{\mathbf{k}',m'} g_{\mathbf{k}'\mathbf{k}}g_{-\mathbf{k}'-\mathbf{k}}D(\mathbf{k}-\mathbf{k}', i\omega_m - i\omega_{m'})F(\mathbf{k}', i\omega_{m'}). \tag{19.51}$$

One can show that $g_{\mathbf{k}'\mathbf{k}} = g^*_{\mathbf{k}\mathbf{k}'}$; normally one expects a similar relation with negative wave vectors, and we assume it in what follows. These equations are then written self-consistently and lead to Eqs. (19.4-19.7) once Eq. (19.3) is used.

19.4 Open superconductive systems

(???? write what is known about it???)

19.4.1 Choice of the Dissipator and the Model

(write what are the options)

19.4.2 Models of Open Superconductors

(overview or results of models from articles, 5-10 paragraphs with them)

19.4.3 Experimental Results of Open Superconductors

(overview or results from articles, 5-10 paragraphs with them)

19.5 Some phenomena by Abrikosov, Gor'kov, Dzyaloshinsky

19.5.1 Superconductor in an Arbitrary Magnetic Field Near the T_c

(специфика)

Теория (???)

Особый случай представляют свойства сверхпроводника вблизи критической температуры. Величина щели при этом достаточно мала, вследствие чего все уравнения значительно упрощаются. Из результатов 36 (выражение (36.4)) легко усмотреть, что в данном случае возможно разложение уравнений по величине $1 - T/T_c \ll 1$. Кроме того, как мы уже отмечали в предыдущем параграфе, вблизи T_c глубина проникновения слабого магнитного поля $\delta \gg \xi_0$, т. е. все величины в поле, в том числе и само поле, меняются на расстояниях, гораздо больших параметра теории $\xi_0 \sim \tau/T_c$. Указанное обстоятельство позволит в этой области температур построить теорию (Горьков [66]), описывающую поведение сверхпроводников в произвольных магнитных полях (порядка величины критического поля).

С этой целью перепишем снова уравнения (37.6)

$$\left\{ i\omega + \frac{1}{2m}\left(\frac{\partial}{\partial r} - ieA(r)\right)^2 + \mu \right\} \mathfrak{G}_\omega(\boldsymbol{r}, \boldsymbol{r}') + \Delta(\boldsymbol{r})\mathfrak{F}^+_\omega(\boldsymbol{r}, \boldsymbol{r}') = \delta(\boldsymbol{r} - \boldsymbol{r}'),$$

$$\left\{-i\omega+\frac{1}{2m}\left(\frac{\partial}{\partial \boldsymbol{r}}+ieA(\boldsymbol{r})\right)^2+\mu\right\}\mathfrak{F}_\omega^+(\boldsymbol{r},\boldsymbol{r}')-\Delta^*(\boldsymbol{r})\mathfrak{G}_\omega(\boldsymbol{r},\boldsymbol{r}')=0$$

вместе с уравнением, определяющим величину щели:

$$\Delta^*(\boldsymbol{r})=|\lambda|T\sum_\omega \mathfrak{F}_\omega^+(\boldsymbol{r},\boldsymbol{r})$$

Поскольку $|\Delta|$ мало, разложим функцию $\mathfrak{J}_\omega^+(\boldsymbol{r},\boldsymbol{r}')$ по степеням $|\Delta|$ и, подставляя это разложение в (38.1), найдем уравнение для $\Delta^*(r)$. При этом полезно ввести компоненты Фурье функции Грина $\tilde{\mathfrak{G}}_\omega^{(0)}(\boldsymbol{r},\boldsymbol{r}')$ для электронов в нормальном металле (в данном поле $\boldsymbol{A}(\boldsymbol{r})$). Уравнение, которому удовлетворяет $\tilde{\mathfrak{G}}_\omega^{(0)}(r,r')$, можно записать двояким образом:

$$\left\{i\omega+\frac{1}{2m}\left(\frac{\partial}{\partial \boldsymbol{r}}-ieA(\boldsymbol{r})\right)^2+\mu\right\}\tilde{\mathfrak{G}}_\omega^{(0)}(\boldsymbol{r},\boldsymbol{r}')=\delta(\boldsymbol{r}-\boldsymbol{r}')$$

или

$$\left\{i\omega+\frac{1}{2m}\left(\frac{\partial}{\partial \boldsymbol{r}'}+ieA(\boldsymbol{r}')\right)^2+\mu\right\}\tilde{\mathfrak{G}}_\omega^{(0)}(\boldsymbol{r},\boldsymbol{r}')=\delta(\boldsymbol{r}-\boldsymbol{r}').$$

С помощью функции

$$\tilde{\mathfrak{G}}_\omega^{(0)}(\boldsymbol{r},\boldsymbol{r}'),$$

привлекая второе из этих уравнений, приведем систему уравнений для $\boldsymbol{G}_\omega$ к интегральной форме:

$$\mathfrak{F}_\omega(\boldsymbol{r},\boldsymbol{r}')=\tilde{\mathfrak{G}}_\omega^{(0)}(\boldsymbol{r},\boldsymbol{r}')-\int\tilde{\mathfrak{G}}_\omega^{(0)}(\boldsymbol{r},\boldsymbol{l})\Delta(\boldsymbol{l})\mathfrak{G}_\omega^+(\boldsymbol{l},\boldsymbol{r}')\,d\boldsymbol{l},$$

$\mathfrak{F}_\omega^+(r,r')=\int\tilde{\mathfrak{G}}_{-\omega}^{(0)}(l,r)\Delta^*(l)\left(\xi_\omega(l,r')\,dl\right.$.

Прежде чем переходить к дальнейшему, найдем, чему: равна функция $\tilde{\mathfrak{G}}_\omega^{(0)}(\boldsymbol{r},\boldsymbol{r}')$. В отсутствие магнитного поля $\left(\overset{(0)}{\omega}(\boldsymbol{r}-\boldsymbol{r}')\right.$ равна ($R=|\boldsymbol{r}-\boldsymbol{r}'|$)

$$\mathfrak{G}_\omega^{(0)}(R)=\begin{cases}-\frac{m}{2\pi R}e^{ip_0R-\frac{|\omega|}{v}R} & \text{при } \omega>0,\\ -\frac{m}{2\pi R}e^{-ip_0R-\frac{|\omega|}{v}R} & \text{при } \omega<0.\end{cases}$$

В этом можно убедиться или непосредственной подстановкой (38.4) в уравнение (38.2) в стсутствие поля, или воспользовавшись известным нам выражением для компоненты Фурье $\mathfrak{G}_\omega^{(0)}(p)=[i\omega-\xi]^{-1}$:

$$\mathfrak{G}_\omega^{(0)}(R)=\frac{1}{(2\pi)^3}\int\mathfrak{G}_\omega^{(0)}(\boldsymbol{p})dpe^{ipR}=\frac{m}{(2\pi)^2iR}\int\frac{e^{ip_0R+i\frac{\xi}{v}R}-e^{-ip_0R-i\frac{\xi}{v}R}}{i\omega-\xi}d\xi$$

(нас интересует, разумеется, вид функции $\mathfrak{G}_\omega^{(0)}(R)$ на расстояниях, больших по сравнению с атомными: $Rp_0\gg1$). Интегрируя по ξ, непосредственно получаем (38.4).

Функция $\mathfrak{G}_\omega^{(0)}(R)$ быстро осциллирует. Поскольку $p_0R\gg1$. это обстоятельство позволяет для определения функции $\tilde{\mathfrak{G}}_\omega^{(0)}(\boldsymbol{r},\boldsymbol{r}')$ в магнитном поле применить своего рода квазиклассическое приближение. В самом деле, будем искать $\tilde{\mathfrak{z}}_\omega^{(0)}(\boldsymbol{r},\boldsymbol{r}')$ в виде

$$\tilde{\mathfrak{G}}_\omega^{(0)}(\boldsymbol{r},\boldsymbol{r}')=e^{i\varphi(\boldsymbol{r},\boldsymbol{r}')}\mathfrak{G}_\omega^{(0)}(\boldsymbol{r}-\boldsymbol{r}'),$$

где $\varphi(\boldsymbol{r},\boldsymbol{r})=0$. Подставляя (38.5) в (38.2) и дифференцируя только главные члены, найдем уравнение для добавки $\varphi(\boldsymbol{r},\boldsymbol{r}')$ к действию

$$(\boldsymbol{n},\nabla_r\varphi(\boldsymbol{r},\boldsymbol{r}'))=e(\boldsymbol{n},A(\boldsymbol{r}));\left(n=\frac{R}{|R|}\right).$$

В этом уравнении мы отбросили квадратичные по $\boldsymbol{A}$ члены, поскольку радиус закручивания электронов $\frac{ep_0}{H}$ в интересующих нас полях очень велик по сравнению с глубиной проникновения: $p_0 \gg eA \sim eH\delta$(δ - порядок глубины проникновения). Вернемся теперь к уравнениям (38.3) и произведем в них разложение по степеням $|\Delta(r)|$. Как видно из (38.4) и (38.6), это разложение в $\mathfrak{F}_\omega^+(\boldsymbol{r},\boldsymbol{r}')$ достаточно произвести до членов третьего порядка по $|\Delta|$ включительно. Что касается функции Грина $\mathfrak{G}_\omega(\boldsymbol{r},\boldsymbol{r}')$, то ее достаточно знать с точностью до членов второго порядка по $|\Delta|$:

$$\mathfrak{G}_\omega(\boldsymbol{r},\boldsymbol{r}') = (\tilde{\mathfrak{G}}_\omega^{(0)}(\boldsymbol{r},\boldsymbol{r}') - \int \tilde{\mathfrak{G}}_\omega^{(0)}(\boldsymbol{r},\boldsymbol{l})\Delta(\boldsymbol{l})\tilde{\mathfrak{G}}_\omega^{(0)}(\boldsymbol{m},\boldsymbol{r}')\,\Delta^*(\boldsymbol{m})\tilde{\mathfrak{G}}_{-\omega}^{(0)}(\boldsymbol{m},\boldsymbol{l})d\boldsymbol{m}d\boldsymbol{l}. \qquad (38.7)$$

Подставляя это выражение во второе из уравнений (38.3), найдем разложение $\mathfrak{F}_\omega^+(\boldsymbol{r},\boldsymbol{r}')$, с помощью которого из (38.1) получаем следующее уравнение относительно $\Delta^*(\boldsymbol{r})$:

$$\Delta^*(\boldsymbol{r}) = |\lambda|T\sum_\omega \int \tilde{\mathfrak{G}}_\omega^{(0)}(\boldsymbol{l},\boldsymbol{r})\Delta^*(\boldsymbol{l})(\tilde{\mathfrak{G}}_{-\omega}^{(0)}(\boldsymbol{l},\boldsymbol{r})d\boldsymbol{l} =$$
$$- |\lambda|T\sum_\omega \iint \tilde{\mathfrak{G}}_\omega^{(0)}(l,m)\Delta(m)\tilde{\mathfrak{G}}_\omega^{(0)}(s,r)\Delta^*(s)\tilde{\mathfrak{G}}_{-\omega}^{(0)}(s,m)\Delta^*(\boldsymbol{l})\tilde{\mathfrak{G}}_{-\omega}^{(0)}(\boldsymbol{l},\boldsymbol{r})d\boldsymbol{l}dmds. \qquad (38.8)$$

Существенные расстояния в интегралах в этом уравнении порядка ξ_0, поскольку, как это видно из (38.4) и (38.5), функция $\tilde{\mathfrak{G}}_\omega^{(0)}(\boldsymbol{r},\boldsymbol{r}')$ экспоненциально убывает при $|\boldsymbol{r}-\boldsymbol{r}'| > \xi_0$. Между тем изменение щели $\Delta(\boldsymbol{r})$ и поля $\boldsymbol{A}(\boldsymbol{r})$ происходит на расстояниях порядка глубины проникновения, которая вблизи критической температуры много больше ξ_0. По тем же причинам фаза $\varphi(\boldsymbol{r},\boldsymbol{r}')$ в (38.5) может быть написана в виде

$$\varphi(r,\dot{r}') \simeq e\left(A(r), r-r'\right).$$

Вблизи $T_cA(\boldsymbol{r}) \sim H\delta \backsim \sqrt{1-\frac{T}{T_c}}$, поэтому фаза $\varphi(\boldsymbol{r},\boldsymbol{r}')$ мала и экспоненту можно разложить по φ.

Рассмотрим сначала первый член в правой части. Пусть

$$K(\boldsymbol{l},\boldsymbol{r}) = T\sum_\omega \tilde{\mathfrak{G}}_\omega^{(0)}(\boldsymbol{l},\boldsymbol{r})\tilde{\mathfrak{G}}_{-\omega}^{(0)}(\boldsymbol{l},\boldsymbol{r}) = K_0(\boldsymbol{l}-\boldsymbol{r})e^{2ie(\boldsymbol{A}(\boldsymbol{r}),\boldsymbol{l}-\boldsymbol{r})}.$$

Воспользовавшись представлением (38.4) для функции Грина в координатном пространстве и произведя суммирование по частотам, найдем для $K_0(R)$ следующее выражение:

$$K_0(R) = \frac{m^2T}{(2\pi R)^2}\frac{1}{\operatorname{sh}\frac{2\pi TR}{v}}.$$

Поскольку, как мы уже отмечали, все величины меняются мало на расстояниях порядка ξ_0, можно в интеграле

$$\int K_0(\boldsymbol{l}-\boldsymbol{r})e^{2ie(\boldsymbol{A}(\boldsymbol{r}),\boldsymbol{t}-\boldsymbol{r})}\Delta^*(\boldsymbol{l})d\boldsymbol{l}$$

разложить все величины в ряд по степеням $(\boldsymbol{l}-\boldsymbol{r})$ около точки $\boldsymbol{r}$. Ограничиваясь членами второго порядка по $(\boldsymbol{l}-\boldsymbol{r})$, получим:

$\Delta^*(\boldsymbol{r})\int K_0(R)d\boldsymbol{R} + \frac{1}{6}\left(\frac{\partial}{\partial\boldsymbol{r}} + 2ieA(\boldsymbol{r})\right)^2\Delta^*(\boldsymbol{r})\int K_0(R)R^2dR.$

Функция $K_0(R)$, согласно (38.9), при $R=0$ обращается

в бесконечность как $1/R^3$. Поэтому формально первый из этих двух интегралов расходится. Обрезание расходящегося выражения удобнее произвести в импульсном пространстве. В результате мы получаем знакомое выражение:

$$\int K_0(R)dR = \frac{mp_0}{2\pi^2}\int\limits_0^{\omega_D} \mathrm{th}\left(\frac{\xi}{2T}\right)\frac{d\xi}{\xi}.$$

Второй член при интегрировании вблизи $R = 0$ особенностей не содержит. Вычисляя этот интеграл непосредственно в координатном представлении, получим:

$$\int R^2 K_0(R)dR = \frac{7\zeta(3)v^2}{8(\pi T)^2}\cdot\frac{mp_0}{2\pi^2}.$$

В члене третьего порядка по $|\Delta|$ в уравнении (38.8) зависимостью $\Delta(\boldsymbol{r})$ от координат можно пренебречь. Этот член равен поэтому

$$\left(\frac{mp_0}{2\pi^2}\right)\Delta^*(\boldsymbol{r})|\Delta(\boldsymbol{r})|^2 T\sum_\omega \int d\xi \frac{1}{\left(\omega^2+\xi^2\right)^2} = \left(\frac{mp_0}{2\pi^2}\right)\frac{7\zeta(3)}{8(\pi T)^2}\Delta^*(\boldsymbol{r})|\Delta(\boldsymbol{r})|^2.$$

Собирая вместе полученные результаты, найдем, что вблизи критической температуры функция $\Delta^*(r)$ удовлетворяет следующему уравнению:

$$\left\{\frac{1}{4m}\left(\frac{\partial}{\partial \boldsymbol{r}}+2ieA(\boldsymbol{r})\right)^2+\frac{1}{\eta}\left[\frac{T_c-T}{T_c}-\frac{7\zeta(3)}{8\left(\pi T_c\right)^2}|\Delta(\boldsymbol{r})|^2\right]\right\}\Delta^*(\boldsymbol{r})=0$$

где

$$\eta = \frac{7\zeta(3)}{6\left(\pi T_c\right)^2}\varepsilon_F$$

В отсутствие поля Δ постоянно по пространству и уравнение (38.10) совпадает с первыми членами разложения (36.4).

Перейдем теперь к вычислению плотности тока $\boldsymbol{j}(\boldsymbol{r})$. Формула (37.5) предыдущего параграфа, конечно, верна и в данном случае. Пользуясь, однако, тем, что величина Δ мала по сравнению с T_c, мы будем и здесь производить раэложение по A и Δ до первых неисчезающих членов. Заметим, что член в плотности тока (37.5)

$$-\frac{2e^2A(\boldsymbol{r})}{m}\mathfrak{G}_{t'=t+0}(\boldsymbol{r},\boldsymbol{r}) \equiv -\frac{e^2}{m}\boldsymbol{A}(\boldsymbol{r})N.$$

Здесь N - плотность полного числа электронов, которая равна своему значению для нормального металла. Изменение N противоречило бы условию электронейтральности. (Решение (38.7) удовлетворяет этому требованию, т. е. если

$\Big(\mathfrak{G}_\omega(\boldsymbol{r},\boldsymbol{r}') = \Big(\tilde{\mathfrak{G}}_\omega^{(0)}(\boldsymbol{r},\boldsymbol{r}')+\delta\mathfrak{G}_\omega(\boldsymbol{r},\boldsymbol{r}')$,

то

$T\sum\limits_\omega \delta\mathfrak{G}_\omega(\boldsymbol{r},\boldsymbol{r}) \equiv 0\Big)$

Подставляя (38.7) в (37.5), найдем:

$$T\sum_\omega \frac{ie}{m}\left(\nabla_{\boldsymbol{r}'}-\nabla_{\boldsymbol{r}}\right)\tilde{\mathfrak{G}}_\omega^{(0)}(\boldsymbol{r},\boldsymbol{r}')\underset{\boldsymbol{r}'\to r}{} - \frac{e^2}{m}NA(\boldsymbol{r})\equiv 0,$$

поскольку в постоянном магнитном поле ток в нормальном металле равен нулю. Таким образом,

$$j(\boldsymbol{r}) = \frac{ie}{m}\left(\nabla_{\boldsymbol{r}'}-\nabla_{\boldsymbol{r}}\right)_{\boldsymbol{r}'\to\boldsymbol{r}} T\sum_\omega^{\top}\delta\left(S_\omega(\boldsymbol{r},\boldsymbol{r}')\right.$$

где

$$\delta\mathfrak{G}_\omega(r,r') = -\int \tilde{\mathfrak{G}}^{(0)}_\omega(\boldsymbol{r},l)\Delta(l)\tilde{\mathfrak{G}}^{(0)}_\omega(\boldsymbol{m},\boldsymbol{r}')\,\Delta^*(\boldsymbol{m})\tilde{\boldsymbol{G}}^{(0)}_{-\omega}(\boldsymbol{m},l)d\boldsymbol{m}d\boldsymbol{l}.$$

Подставляя сюда (38.5), разлагая все величины около точки r до членов лервого порядка и опуская члены, которые дают нуль при интегрировании по углам, получим:

$$\boldsymbol{j}(\boldsymbol{r}) = \left[\frac{ie}{m}\left(\Delta\frac{\partial\Delta^*}{\partial\boldsymbol{r}} - \Delta^*\frac{\partial\Delta}{\partial\boldsymbol{r}}\right) - \frac{4e^2|\Delta|^2}{m}A(\boldsymbol{r})\right]C,$$

где

$$C = \tfrac{T}{3}\sum_\omega \iint \left(\left[\left(\nabla_r\mathfrak{G}^{(0)}_\omega(\boldsymbol{r}-\boldsymbol{l})\right)\mathfrak{G}^{(0)}_\omega(\boldsymbol{m}-\boldsymbol{r}) - \mathfrak{G}^{(0)}_\omega(r-l)\left(\nabla_{\boldsymbol{r}}\mathfrak{G}^0_\omega(\boldsymbol{m}-\boldsymbol{r})\right)\right]\cdot\boldsymbol{m}\right)\mathfrak{G}^{(0)}_{-\omega}(\boldsymbol{m}-\boldsymbol{l})d\boldsymbol{m}d\boldsymbol{l}$$

Вычисление C удобно произвести в компонентах Фурье, заменяя обычным образом $r \to i\frac{d}{dp}$. Не останавливаясь на этом довольно простом вычислении, приведем окончательный результат:

$$C = \frac{7\zeta(3)N}{16\left(\pi T_c\right)^2}$$

Система уравнений (38.10) и (38.11) описывает свойства сверхпроводников в постоянном магнитном поле вблизи T_c. Введем волновую функцию $\psi(\boldsymbol{r})$, пропорциональную $\Delta(\boldsymbol{r})$:

$$\psi(r) = \sqrt{\frac{7\bar{\zeta}(3)N}{8\left(\pi T_c\right)^2}}\Delta(r).$$

Взяв комплексно сопряженное от уравнения (38.10) и подставляя всюду выражение (38.12), приведем эти уравнения к следующему виду:

$$\left\{\frac{1}{4m}\left(\frac{\partial}{\partial\boldsymbol{r}} - 2leA(\boldsymbol{r})\right)^2 + \frac{1}{\eta}\left[\frac{T_c-T}{T_c} - \frac{1}{N}|\psi|^2\right]\right\}\psi(\boldsymbol{r}) = 0$$

$$\boldsymbol{j}(\boldsymbol{r}) = -\frac{2ie}{4m}\left(\psi^*\frac{\partial\psi}{\partial\boldsymbol{r}} - \psi\frac{\partial\psi^*}{\partial\boldsymbol{r}}\right) - \frac{(2e)^2}{2m}A(\boldsymbol{r})|\psi|^2.$$

Теперь становится понятным смысл введения волновой функции $\psi(\boldsymbol{r})$: получающиеся уравнения имеют вид, похожий на квантовомеханические уравнения для частицы с массой $2m$ и зарядом 2e. Физически этот результат совершенно ясен, поскольку $\Delta(\boldsymbol{r})$ имеет смысл величины, пропорциональной волновой функции связанной пары, или, точнее, волновой функции относительно координат ее центра инерции. Интересно, что подобного вида уравнения были предложены в феноменологической теории Гинзбурга-Ландау [67], где, однако, фигурировал однократный элементарный заряд: Помимо этого существенного изменения, новая теория сверхпроводимости, подтверждая правильность теории Гинзбурга Ландау вблизи T_v, дает возможность вычислить фигурирующие в последней теории постоянные.

В заключение отметим еще раз тот факт, что при выводе мы использовали малость изменения всех величин на расстояниях порядка ξ_0. Поскольку, как легко видеть из (38.13) и (37.19), все величины меняются в общем случае на расстояниях порядка лондоновской глубины проникновения вблизи T_c, а для пиппардовских металлов эта глубина проникновения становится больше ξ_0 только в самой близости от T_c, то область применимости этих уравнений для металлов пиппардовского типа представляет собой очень незначительную окрестность температур вблизи критической температуры перехода. Для металлов лондоновского типа, или промежуточных, эти уравнения

справедливы в довольно широкой области температур вблизи T_c. С экспериментальной точки зрения это - весьма интересная область температур, и следует отметить, что уравнения (38.13) приводят к очень хорошему согласию теории с результатами измерений в этой области.

19.5.2 Theory Of Superconducting Alloys by AGD [see cond matter about it]

20 Fluctuation Phenomena in Superconductors by Larkin, Varlamov

20.1 Introduction

A major success of low temperature physics was achieved with the introduction by Landau of the notion of quasiparticles. According to his hypothesis, the properties of many body interacting systems at low temperatures are determined by the spectrum of some low energy, long living excitations (quasiparticles). Another milestone of many body theory is the Mean Field Approximation (MFA), which permitted achieving considerable progress in the theory of phase transitions. Phenomena which cannot be described by the quasiparticle method or by MFA are usually called fluctuations. The BCS theory of superconductivity is a bright example of the use of both the quasiparticle description and MFA. The success of the BCS theory for traditional superconductors was determined by the fact that fluctuations give small corrections with respect to the MFA results.

During the first half of the century after the discovery of superconductivity the problem of fluctuation smearing of the superconducting transition was not even considered. In bulk samples of traditional superconductors the critical temperature T_c sharply divides the superconducting and the normal phases. It is worth mentioning that such behavior of the physical characteristics of superconductors is in perfect agreement both with the Ginzburg-Landau (GL) phenomenological theory (1950) [1] and the BCS microscopic theory of superconductivity (1957)[2].

The characteristics of high temperature and organic superconductors, low dimensional and amorphous superconducting systems studied today, strongly differ from those of the traditional superconductors discussed in textbooks. The transitions turn out to be much more smeared out. The appearance of superconducting fluctuations above critical temperature leads to precursor effects of the superconducting phase occurring while the system is still in the normal phase, sometimes far from T_c. The conductivity, the heat capacity, the diamagnetic susceptibility, the sound attenuation, etc. may increase considerably in the vicinity of the transition temperature.

The first numerical estimation of the fluctuation contribution to the heat capacity of a superconductor in the vicinity of T_c was done by Ginzburg in 1960 [3]. In that paper he showed that superconducting fluctuations increase the heat capacity even above T_c. In this way fluctuations change the temperature dependence of the specific heat in the vicinity of critical temperature, where, in accordance with the phenomenological GL theory of second order phase transitions, a jump should take place. The range of temperatures where the fluctuation correction to the heat capacity of a bulk clean conventional superconductor is relevant was

estimated by Ginzburg [2] to be

$$Gi = \frac{\delta T}{T_c} \sim \left(\frac{T_c}{E_F}\right)^4 \sim 10^{-12} \div 10^{-14}, \tag{20.1}$$

where E_F is the Fermi energy. The correction occurs in a temperature range δT many orders of magnitude smaller than that accessible in real experiments.

In the 1950s and 60s the formulation of the microscopic theory of superconductivity, the theory of type-II superconductors and the search for high-T_c superconductivity attracted the attention of researchers to dirty systems, superconducting films and filaments. In 1968, in the papers of L. G. Aslamazov and A. I. Larkin [5], K.Maki [6] and a little later in the paper of R.S.Thompson [7] the fundaments of the microscopic theory of fluctuations in the normal phase of a superconductor in the vicinity of the critical temperature were formulated. This microscopic approach confirmed Ginzburg's evaluation [3] for the width of the fluctuation region in a bulk clean superconductor. Moreover, was found that the fluctuation effects increase drastically in thin dirty superconducting films and whiskers. In the cited papers was demonstrated that fluctuations affect not only the thermodynamical properties of superconductor but its dynamics too. Simultaneously the fluctuation smearing of the resistive transition in bismuth amorphous films was experimentally found by Glover [8], and it was perfectly fitted by the microscopic theory.

In the BCS theory [2] only the Cooper pairs forming a Bose-condensate are considered. Fluctuation theory deals with the Cooper pairs out of the condensate. In some phenomena these fluctuation Cooper pairs behave similarly to quasiparticles but with one important difference. While for the well defined quasiparticle the energy has to be much larger than its inverse life time, for the fluctuation Cooper pairs the "binding energy" E_0 turns out to be of the same order. The Cooper pair life time τ_{GL} is determined by its decay into two free electrons. Evidently at the transition temperature the Cooper pairs start to condense and $\tau_{GL} = \infty$. So it is natural to suppose from dimensional analysis that $\tau_{GL} \sim \hbar/k_B(T - T_c)$. The microscopic theory confirms this hypothesis and gives the exact coefficient:

$$\tau_{GL} = \frac{\pi\hbar}{8k_B(T - T_c)}. \tag{20.2}$$

Another important difference of the fluctuation Cooper pairs from quasiparticles lies in their large size $\xi(T)$. This size is determined by the distance on which the electrons forming the fluctuation Cooper pair move away during the pair life-time τ_{GL}. In the case of an impure superconductor the electron motion is diffusive with the diffusion coefficient $\mathcal{D} \sim v_F^2\tau$ (τ is the electron scattering time[3]), and $\xi_d(T) = \sqrt{\mathcal{D}\tau_{GL}} \sim v_F\sqrt{\tau\tau_{GL}}$. In the case of a clean superconductor, where $k_BT\tau \gg \hbar$, impurity scattering does not affect any more the electron correlations. In this case the time of electron ballistic motion turns out to be less than the electron-impurity scattering time τ and is determined by the uncertainty principle: $\tau_{bal} \sim \hbar/k_BT$. Then this time has to be used in this case for determination of the effective size instead of τ: $\xi_c(T) \sim v_F\sqrt{\hbar\tau_{GL}/k_BT}$. In both cases the coherence length grows with the approach to the critical temperature as $(T - T_c)^{-1/2}$, and we will write it down in the unique way ($\xi = \xi_{c,d}$):

[2]The expression for the width of the strong fluctuation region in terms of the Landau phenomenological theory of phase transitions was obtained by Levanyuk [4]. So in the modern theory of phase transitions the relative temperature width of fluctuation region is called the Ginzburg-Levanyuk parameter $Gi_{(D)}$, where D is the effective space dimensionality.

[3]Strictly speaking τ in the most part of future results should be understood as the electron transport scattering time τ_{tr}. Nevertheless, as it is well known, in the case of isotropic scattering these values coincide, so for sake of simplicity we will use hereafter the symbol τ.

$$\xi(T) = \frac{\xi}{\sqrt{\epsilon}}, \quad \epsilon = \frac{T - T_c}{T_c}.. \tag{20.3}$$

The microscopic theory in the case of an isotropic Fermi surface gives for ξ the precise expression:

$$\xi^2_{(D)} = -\frac{v_F^2\tau^2}{D}\left\{\psi(\frac{1}{2} + \frac{\hbar}{4\pi k_B T\tau}) - \psi(\frac{1}{2}) - \frac{\hbar}{4\pi k_B T\tau}\psi^{'}(\frac{1}{2})\right\}, \tag{20.4}$$

where $\psi(x)$ is the digamma function and $D = 3, 2, 1$ is the space dimensionality. In the clean (c) and dirty (d) limits:

$$\xi_c = 0.133\frac{\hbar v_F}{k_B T_c}\sqrt{\frac{3}{D}} = 0.74\xi_0\sqrt{\frac{3}{D}}, \tag{20.5}$$

$$\xi_d = 0.36\sqrt{\frac{\hbar v_F l}{k_B T_c}\frac{3}{D}} = 0.85\sqrt{\xi_0 l}\sqrt{\frac{3}{D}}. \tag{20.6}$$

Here $l = v_F\tau$ is the electron mean free path and $\xi_0 = \hbar v_F/\pi\Delta(0)$ is the conventional BCS definition of the coherence length of a clean superconductor at zero temperature. One can see that (20.5) and (20.6) coincide with the above estimations [4].

Finally it is necessary to recognize that fluctuation Cooper pairs can be really treated as classical objects, but these objects instead of Boltzmann particles appear as classical fields in the sense of Rayleigh-Jeans. This means that in the general Bose-Einstein distribution function only small energies $E(p)$ are involved and the exponent can be expanded:

$$n(p) = \frac{1}{\exp(\frac{E(p)}{k_B T}) - 1} = \frac{k_B T}{E(p)}. \tag{20.7}$$

This is why the more appropriate tool to study fluctuation phenomena is not the Boltzmann transport equation but the GL equation for classical fields. Nevertheless at the qualitative level the treatment of fluctuation Cooper pairs as particles with the density $n_{(D)} = \int n(p)\frac{d^D p}{(2\pi\hbar)^D}$ often turns out to be useful [5].

Below will be demonstrated both in the framework of the phenomenological Ginzburg-Landau theory and the microscopic BCS theory that in the vicinity of the transition

$$E(p) = \alpha k_B(T - T_c) + \frac{\mathbf{p}^2}{2m^*} = \frac{1}{2m^*}\left[\hbar^2/\xi^2(T) + \mathbf{p}^2\right]. \tag{20.8}$$

Far from transition temperature the dependence $n(p)$ turns out to be more sophisticated than (20.7), nevertheless one can always write it in the form

[4] Let us stress some small numerical difference between our Exp. (20.4) and the usual definition of the coherence length. We are dealing near the critical temperature, so the definition (20.4) is natural and permits us to avoid many numerical coefficients in further calculations. The cited coherence length $\xi_0 = \hbar v_F/\pi\Delta(0) = 0.18\hbar v_F/k_B T_c$, as is evident, was introduced for zero temperature and an isotropic $3D$ superconductor.

It is convenient to determine the coherence length also from the formula for the upper critical field: $H_{c2}(T) = A(T)\Phi_0/2\pi\xi^2(T)$. $A(T_c) = 1$, while its value at $T = 0$ depends on the impurities concentration. For the dirty case the appropriate value was found by K.Maki [9] $A_d(0) = 0.69$, for the clean case by L.Gor'kov [10] $A_c^{2D}(0) = 0.59$, $A_c^{3D}(0) = 0.72$.

[5] This particle density is defined in the (D)-dimensional space. This means that it determines the normal volume density of pairs in $3D$ case, the density per square unit in $2D$ case and the number of pairs per unit length in $1D$. The real three dimensional density n can be defined too: $n = d^{D-3}n_{(D)}$, where d is the thickness of the film or wire.

$$n(p) = \frac{m^* k_B T}{\hbar^2} \xi^2 (T) \, f \left(\frac{\xi(T) p}{\hbar} \right). \tag{20.9}$$

In classical field theory the notions of the particle distribution function $n(p)$ (proportional to $E^{-1}(p)$ in our case) and Cooper pair mass m^* are poorly determined. At the same time the characteristic value of the Copper pair center of mass momentum can be defined and it turns out to be of the order of $p_0 \sim \hbar/\xi(T)$. So for the combination $m^* E(p_0)$ one can write $m^* E(p_0) \sim p_0^2 \sim \hbar^2/\xi^2(T)$. In fact the particles density enters into many physical values in the combination n/m^*. As the consequence of the above observation it can be expressed in terms of the coherence length:

$$\frac{n_{(D)}}{m^*} = \frac{k_B T}{m^* E(p_0)} (\frac{p_0}{\hbar})^D \sim \frac{k_B T}{\hbar^2} \xi^{2-D}(T), \tag{20.10}$$

p_0^D here estimates the result of momentum integration.

For example we can evaluate the fluctuation Cooper pairs contribution to conductivity by using the Drude formula

$$\sigma = \frac{n e^2 \tau}{m^*} \Rightarrow \frac{k_B T}{\hbar^2} d^{D-3} \xi^{2-D}(T) (2e)^2 \tau_{GL}(\epsilon) \sim \epsilon^{D/2-2}. \tag{20.11}$$

Analogously a qualitative understanding of the increase in the diamagnetic susceptibility above the critical temperature may be obtained from the well-known Langevin expression for the atomic susceptibility[6]:

$$\chi = -\frac{e^2}{c^2} \frac{n}{m^*} \left\langle R^2 \right\rangle \Rightarrow -\frac{4e^2}{c^2} \frac{k_B T}{\hbar^2} d^{D-3} \xi^{4-D}(T) \sim -\epsilon^{D/2-2}. \tag{20.12}$$

Besides these examples of the direct influence of fluctuations on superconducting properties, indirect manifestations by means of quantum interference in the pairing process and of renormalization of the density of one-electron states in the normal phase of superconductor take place. These effects, being much more sophisticated, have a purely quantum nature, and in contrast to the direct Cooper pair contributions require microscopic consideration. This is why, in developing phenomenological methods through the first five Sections of this review, we will deal with the direct fluctuation pair contributions only. The sixth Section is devoted to the microscopic justification of the time dependent Ginzburg-Landau equation. The description of the microscopic theory of fluctuations, including indirect fluctuation effects, discussion of their manifestations in various physical properties of superconductors will be given in the Sections 7-8.

The first seven Sections are written in detail, so they can serve as a textbook. On the contrary, in the last (eighth) Section a wide panorama of fluctuation effects in different physical properties of superconductors is presented. Thus this Section has more of a handbook character, and the intermediate calculations often are omitted.

Finally we would like to mention that the number of articles devoted to superconducting fluctuations published in the last 33 years is of the order of ten thousands, so our bibliography list does not pretend nor at the completeness nor at the establishment of the rigorous priorities.

[6]This formula is valid for the dimensionalities $D = 2, 3$, when fluctuation Cooper pair has the possibility to "rotate" in the applied magnetic field and the average square of the rotation radius is $< R^2 > \sim \xi^2(T)$. "Size" effects, important for low dimensional samples, will be discussed later on.

20.2 Ginzburg-Landau formalism. Thermodynamics

20.2.1 Fluctuation contribution to heat capacity

GL functional.

The complete description of the thermodynamic properties of a system can be done through the exact calculation of the partition function[7]:

$$Z = \mathrm{Tr}\left\{\exp\left(-\frac{\widehat{\mathcal{H}}}{T}\right)\right\}. \tag{20.13}$$

As discussed in the Introduction, in the vicinity of the superconducting transition, side by side with the fermionic electron states, fluctuation Cooper pairs of a bosonic nature appear in the system. As already mentioned, they can be described by means of classical bosonic fields $\Psi(\mathbf{r})$ which can be treated as "Cooper pair wave functions". So the calculation of the trace in (20.13) can be separated into a summation over the "fast" electron degrees of freedom and a further functional integration carried out over all possible configurations of the "slow" Cooper pairs wave functions:

$$Z = \int D\Psi(\mathbf{r})\mathcal{Z}[\Psi(\mathbf{r})], \tag{20.14}$$

where

$$\mathcal{Z}[\Psi(\mathbf{r})] = \exp\left(-\frac{\mathcal{F}[\Psi(\mathbf{r})]}{T}\right) \tag{20.15}$$

is the system partition function in a fixed bosonic field $\Psi(\mathbf{r})$, already summed over the electronic degrees of freedom. Here it is assumed that the classical field dependent part of the Hamiltonian can be chosen in the spirit of the GL approach[8]:

$$F[\Psi(r)] = F_N + \int dV\left\{a|\Psi(\mathbf{r})|^2 + \frac{b}{2}|\Psi(\mathbf{r})|^4 + \frac{1}{4m}|\nabla\Psi(\mathbf{r})|^2\right\}.. \tag{20.16}$$

Let us discuss the coefficients of this functional. In accordance with the Landau hypothesis, the coefficient a goes to zero at the transition point and depends linearly on $T - T_c$. Then $a = \alpha T_c\epsilon$; all the coefficients α,b and m are supposed to be positive and temperature independent. Concerning the magnitude of the coefficients it is necessary to make the following comment. One of these coefficients can always be chosen arbitrary: this option is related to the arbitrariness of the Cooper pair wave function normalization. Nevertheless the product of two of them is fixed by dimensional analysis: $ma \sim \xi^{-2}(T)$. Another combination of the coefficients, independent of the wave function normalization and temperature, is α^2/b. One can see that it has the dimensionality of the density of states. Since these coefficients were obtained by a summation over the electronic degrees of freedom, the only reasonable candidate for this value is the one electron density of states ν. The microscopic theory gives the precise coefficients for the above relations:

$$4m\alpha T_c = \xi^{-2};\ \alpha^2/b = \frac{8\pi^2}{7\zeta(3)}\nu, \tag{20.17}$$

where $\zeta(x)$ is the Riemann zeta function, $\zeta(3) = 1.202$. One can notice that the arbitrariness in the normalization of the order parameter amplitude leads to the unambiguity in the choice

[7] Hereafter $\hbar = k_B = c = 1$.

[8] For simplicity the magnetic field is assumed to be zero.

of the Cooper mass introduced in (20.16) as $2m$. Indeed, this value enters in (20.17) in the product with α so one of these parameters has to be fixed. In the case of a clean D-dimensional superconductor it is natural to suppose that the Copper pair mass is equal to two free electron masses what results in

$$\alpha_{(D)} = \frac{2D\pi^2}{7\zeta(3)}\frac{T_c}{E_F}. \tag{20.18}$$

As the first step in the Landau theory of phase transitions Ψ is supposed to be independent of position. This assumption in the limit of sufficiently large volume V of the system permits a calculation of the functional integral in (20.14) by the method of steepest descent. Its saddle point determines the equilibrium value of the order parameter

$$|\widetilde{\Psi}|^2 = \begin{cases} -\alpha T_c \epsilon/b, & \epsilon < 0 \\ 0, & \epsilon > 0 \end{cases}. \tag{20.19}$$

Choosing α in accordance with (20.18) one finds that this value coincides with the superfluid density n_s of the microscopic theory [2].

The fluctuation part of the free energy related to the transition is determined by the minimum of the functional (20.16):

$$F = (\mathcal{F}[\Psi])_{\min} = \mathcal{F}[\widetilde{\Psi}] = \begin{cases} F_N - \frac{\alpha^2 T_c^2 \epsilon^2}{2b} V, & \epsilon < 0 \\ F_N, & \epsilon > 0 \end{cases}. \tag{20.20}$$

From the second derivative of (20.20) one can find an expression for the jump of the specific heat capacity at the phase transition point:

$$\begin{aligned} \Delta C &= C_S - C_N = \frac{T_c}{V}\left(\frac{\partial S_S}{\partial T}\right) - \frac{T_c}{V}\left(\frac{\partial S_N}{\partial T}\right) = \\ &= -\frac{1}{VT_c}\left(\frac{\partial^2 F}{\partial \epsilon^2}\right) = \frac{\alpha^2}{b}T_c = \frac{8\pi^2}{7\zeta(3)}\nu T_c. \end{aligned} \tag{20.21}$$

Let us mention that the jump of the heat capacity was obtained because of the system volume was taken to infinity first, and after this the reduced temperature ϵ was set equal to zero.

Zero dimensionality: the exact solution.

In a system of finite volume fluctuations smear out the jump in heat capacity. For a small superconducting sample with the characteristic size $d \ll \xi(T)$ the space independent mode $\Psi_0 = \Psi\sqrt{V}$ defines the main contribution to the free energy:

$$\begin{aligned} Z_{(0)} &= \int d^2\Psi_0 \mathcal{F}[\Psi_0] = \pi \int d|\Psi_0|^2 \exp\left(-\frac{(\, a|\Psi_0|^2 + \frac{b}{2V}|\Psi_0|^4)}{T}\right) = \\ &= \sqrt{\frac{\pi^3 VT}{2b}} \exp(x^2)(1 - \mathrm{erf}(x))|_{x=a\sqrt{\frac{V}{2bT}}}. \end{aligned} \tag{20.22}$$

By evaluating the second derivative of this exact result [11] one can find the temperature dependence of the superconducting granular heat capacity (see Fig. 20.1). It is evident that the smearing of the jump takes place in the region of temperatures in the vicinity of transition where $x \sim 1$, i.e.

Figure 20.1: Temperature dependence of the heat capacity of superconducting grains in the region of the critical temperature

$$\epsilon_{cr} = Gi_{(0)} = \frac{\sqrt{7\zeta(3)}}{2\pi} \frac{1}{\sqrt{\nu T_c V}} \approx 13,3 \left(\frac{T_{c0}}{E_F}\right) \sqrt{\frac{\xi_0^3}{V}},$$

where we have supposed that the granule is clean; T_{c0} and ξ_0 are the critical temperature and the zero temperature coherence length (see the footnote 3 in Introduction) of the appropriate bulk material. From this formula one can see that even for granule with the size $d \sim \xi_0$ the smearing of the transition still is very narrow.

Far above the critical region, where $Gi_{(0)} \ll \epsilon \ll 1$, one can use the asymptotic expression for the $\mathrm{erf}(x)$ function and find

$$F_{(0)} = -T \ln Z_{(0)} = -T \ln \frac{\pi}{\alpha\epsilon}. \tag{20.23}$$

Calculation of the second derivative gives an expression for the fluctuation part of the heat capacity in this region:

$$\delta C_{(0)} = 1/\epsilon^2. \tag{20.24}$$

The experimental study of the heat capacity of small Sn particles in the vicinity of transition was done in [12]

Arbitrary dimensionality: case $T \geq T_c$.

It is possible to estimate the fluctuation contribution to the heat capacity for a specimen of an arbitrary effective dimensionality on the basis of the following observation. The volume of the specimen may be divided into regions of size $\xi(T)$, which are weakly correlated with each other. Then the whole free energy can be estimated as the free energy of one such zero-dimensional specimen (20.23), multiplied by their number $N_{(D)} = V\xi^{-D}(T)$:

$$F_{(D)} = -TV\xi^{-D}(T) \ln \frac{\pi}{\alpha\epsilon}. \tag{20.25}$$

This formula gives the correct temperature dependence for the free energy for even dimensionalities. A more accurate treatment removes the $\ln \epsilon$ dependence from it in the case of the odd dimensions.

Let us begin with the calculation of the fluctuation contribution to the heat capacity in the normal phase of a superconductor. We restrict ourselves to the region of temperatures beyond the immediate vicinity of transition, where this correction is still small. In this region one can omit the fourth order term in $\Psi(\mathbf{r})$ with respect to the quadratic one and write down the GL functional, expanding the order parameter in a Fourier series:

$$F[\Psi_{\mathbf{k}}] = F_N + \sum_{\mathbf{k}} [a + \frac{\mathbf{k}^2}{4m}]|\Psi_{\mathbf{k}}|^2 = \alpha T_c \sum_{\mathbf{k}} \left(\epsilon + \xi^2 \mathbf{k}^2\right) |\Psi_{\mathbf{k}}|^2. \tag{20.26}$$

Here $\Psi_{\mathbf{k}} = \frac{1}{\sqrt{V}} \int \Psi(\mathbf{r}) e^{-i\mathbf{kr}} dV$ and the summation is carried out over the vectors of the reciprocal space. Now we see that the free energy functional appears as a sum of energies of the independent modes $\mathbf{k}$. The functional integral for the partition function (20.15) can be separated to a product of Gaussian type integrals over these modes:

$$Z = \prod_{\mathbf{k}} \int d^2\Psi_{\mathbf{k}} \exp\left\{-\alpha(\epsilon + \frac{\mathbf{k}^2}{4m\alpha T_c}\ )|\Psi_{\mathbf{k}}|^2\right\}. \tag{20.27}$$

Carrying out these integrals, one gets the fluctuation contribution to the free energy:

$$F(\epsilon > 0) = -T \ln Z = -T \sum_{\mathbf{k}} \ln \frac{\pi}{\alpha(\epsilon + \frac{\mathbf{k}^2}{4m\alpha T_c})}. \tag{20.28}$$

The appropriate correction to the specific heat capacity of a superconductor at temperatures above the critical temperature may thus be calculated. We are interested in the most singular term in ϵ^{-1}, so the differentiation over the temperature can be again replaced by that over ϵ :

$$\delta C_+ = -\frac{1}{VT_c}\left(\frac{\partial^2 F}{\partial \epsilon^2}\right) = \frac{1}{V} \sum_{\mathbf{k}} \frac{1}{(\epsilon + \frac{\mathbf{k}^2}{4m\alpha T_c})^2}. \tag{20.29}$$

The result of the summation over $\mathbf{k}$ strongly depends on the linear sizes of the sample, i.e. on its effective dimensionality. As it is clear from (20.29), the scale with which one has to compare these sizes is determined by the value $(4m\alpha T_c \epsilon)^{-\frac{1}{2}}$ which, as was already mentioned above, coincides with the effective size of Cooper pair $\xi(T)$. Thus, if all dimensions of the sample considerably exceed $\xi(T)$, one can integrate over $(2\pi)^{-3} L_x L_y L_z dk_x dk_y dk_z$ instead of summing over n_x, n_y, n_z. In the case of arbitrary dimensionality the fluctuation correction to the heat capacity turns out to be

$$\delta C_+ = \frac{V_D}{V} \int \frac{1}{(\epsilon + \frac{\mathbf{k}^2}{4m\alpha T_c})^2} \frac{d^D\mathbf{k}}{(2\pi)^D} = \vartheta_D \frac{V_D}{V} \frac{(4m\alpha T_c)^{\frac{D}{2}}}{\epsilon^{2-\frac{D}{2}}}, \tag{20.30}$$

where $V_D = V, S, L, 1$ for $D = 3, 2, 1, 0$. For the coefficients ϑ_D it is convenient to write an expression valid for an arbitrary dimensionality D, including fractional ones. For a space of fractional dimensionality we just mention that the momentum integration in spherical coordinates is carried out according to the rule: $\int d^D\mathbf{k}/\,(2\pi)^D = \mu_D \int k^{D-1} dk$, where

$$\mu_D = \frac{D}{2^D \pi^{D/2} \Gamma(D/2+1)} \tag{20.31}$$

and $\Gamma(x)$ is a gamma-function. The coefficient in (20.30) can be expressed in terms of the gamma-function too:

$$\vartheta_D = \frac{\Gamma(2 - D/2)}{2^D \pi^{D/2}} \tag{20.32}$$

yielding $\vartheta_1 = 1/4, \vartheta_2 = 1/4\pi$ and $\vartheta_3 = 1/8\pi$.

In the case of small particles with characteristic sizes $d \lesssim \xi(\epsilon)$ the appropriate fluctuation contribution to the free energy and the specific heat capacity coincides with the asymptotics of the exact results (20.23) and (20.24). From the formula given above it is easy to see that the role of fluctuations increases when the effective dimensionality of the sample or the electron mean free path decrease.

Arbitrary dimensionality: case $T < T_c$.

The general expressions (20.14) and (20.16) allow one to find the fluctuation contribution to heat capacity below T_c. For this purpose let us restrict ourselves to the region of temperatures not very close to T_c from below, where fluctuations are sufficiently weak. In this case the order parameter can be written as the sum of the equilibrium $\widetilde{\Psi}$ (see (20.19)) and fluctuation $\psi(\mathbf{r})$ parts:

$$\Psi(\mathbf{r}) = \widetilde{\Psi} + \psi(\mathbf{r}). \tag{20.33}$$

Keeping in (20.16) the terms up to the second order in $\psi(\mathbf{r})$ and up to the fourth order in $\widetilde{\Psi}$, one can find

$$\begin{aligned} \mathcal{Z}[\widetilde{\Psi}] \;=\; & \exp(-\frac{a\widetilde{\Psi}^2 + b/2\widetilde{\Psi}^4}{T}) \prod_{\mathbf{k}} \int d\mathrm{Re}\psi_{\mathbf{k}} d\mathrm{Im}\psi_{\mathbf{k}} \times \\ & \times \exp\left\{ -\frac{1}{T}[(3b\widetilde{\Psi}^2 + a + \frac{\mathbf{k}^2}{4m})\mathrm{Re}^2\psi_{\mathbf{k}} + (b\widetilde{\Psi}^2 + a + \frac{\mathbf{k}^2}{4m})\mathrm{Im}^2\psi_{\mathbf{k}}] \right\}. \end{aligned} \tag{20.34}$$

Carrying out the integral over the real and imaginary parts of the order parameter one can find an expression for the fluctuation part of the free energy:

$$F = -\frac{T}{2} \sum_{\mathbf{k}} \left\{ \ln \frac{\pi T_c}{3b\widetilde{\Psi}^2 + a + \frac{\mathbf{k}^2}{4m}} + \ln \frac{\pi T_c}{b\widetilde{\Psi}^2 + a + \frac{\mathbf{k}^2}{4m}} \right\}. \tag{20.35}$$

Let us discuss this result. It is valid both above and below T_c. The two terms in it correspond to the contributions of the modulus and phase fluctuations of the order parameter. Above T_c $\widetilde{\Psi} \equiv 0$ and these contributions are equal: phase and modulus fluctuations in the absence of $\widetilde{\Psi}$ represent just two equivalent degrees of freedom of the scalar complex order parameter. Below T_c, the symmetry of the system decreases (see (20.19)). The order parameter modulus fluctuations remain of the same diffusive type as above T_c, while the character of the phase fluctuations, in accordance with the Goldstone theorem, changes dramatically.

Substitution of (20.19) to (20.35) results in the disappearance of the temperature dependence of the phase fluctuation contribution and, calculating the second derivative, one sees that only the fluctuations of the order parameter modulus contribute to the heat capacity. As a result the heat capacity, calculated below T_c, turns out to be proportional to that found above:

$$\delta C_- = 2^{\frac{D}{2}-2} \delta C_+.$$

Hence, in the framework of the theory proposed we found that the heat capacity of the superconductor tends to infinity at the transition temperature. Strictly speaking, the restrictions of the above approach do not permit us to discuss seriously this divergence at the critical point itself. The calculations in principle are valid only in that region of temperatures where the fluctuation correction is small. We will discuss in the next Section the quantitative criteria for the applicability of this perturbation theory.

20.2.2 Ginzburg-Levanyuk criterion

The fluctuation corrections to the heat capacity obtained above allow us to answer quantitatively the question: where are the limits of applicability of the GL theory?

This theory is valid not too near to the transition temperature, where the fluctuation correction is still small in comparison with the heat capacity jump. Let us define as the Ginzburg-Levanyuk number $Gi_{(D)}$ [4, 3] the value of the reduced temperature at which the fluctuation correction (20.30) equals the value of ΔC (20.21)[9]:

$$Gi_{(D)} = \frac{1}{\alpha}\left[\frac{V_D}{V}\vartheta_D b(4m)^{\frac{D}{2}}T_c^{\frac{D}{2}-1}\right]^{\frac{2}{4-D}}. \tag{20.36}$$

Substituting into this formula the microscopic values of the GL theory parameters (20.17) one can find

$$Gi_{(D)} = \left[\frac{7\zeta(3)\vartheta_D}{8\pi^2}\left(\frac{V_D}{V}\right)\frac{1}{\nu_D T_c \xi^D}\right]^{\frac{2}{4-D}}. \tag{20.37}$$

Since $\nu_D T_c \sim \nu_D v_F/\xi_c \sim p_F^{D-1}\xi_c^{-1} \sim \mathfrak{a}^{1-D}\xi_c^{-1}$ one can convert this formula to the form

$$Gi_{(D)} \sim \left[\frac{7\zeta(3)\vartheta_D}{8\pi^2}\left(\frac{V_D}{V}\right)\frac{\xi_c \mathfrak{a}^{D-1}}{\xi^D}\right]^{\frac{2}{4-D}},$$

where $\mathfrak{a}$ is the interatomic distance. It is worth mentioning that in bulk conventional superconductors, due to the large value of the coherence length ($\xi_c \sim 10^{-6} \div 10^{-4} cm$), which drastically exceeds the interatomic distance ($\mathfrak{a} \sim 10^{-8} cm$), the fluctuation correction to the heat capacity is extremely small. However, the fluctuation effect increases for small effective sample dimensionality and small electron mean free path. For instance, the fluctuation heat capacity of a superconducting granular system is readily accessible for experimental study.

Using the microscopic expression for the coherence length (20.4), the Ginzburg-Levanyuk number (20.37) can be evaluated for different cases of clean (c) and dirty (d) superconductors of various dimensionalities and geometries (film, wire, whisker and granule are supposed to have $3D$ electronic spectrum):

$Gi_{(3)}$	$Gi_{(2)}$	$Gi_{(1)}$	$Gi_{(0)}$
$80\left(\frac{T_c}{E_F}\right)^4$, (c) $\frac{1.6}{(p_F l)^3}\left(\frac{T_c}{E_F}\right)$, (d)	$\left(\frac{T_c}{E_F}\right)$, (c) $\frac{0.27}{p_F l}$, (d) $\frac{1.3}{p_F^2 l d}$, (d) film	0.5, (c) $1.3\left(p_F^2 S\right)^{-2/3}\left(T_c\tau\right)^{-1/3}$, (d) wire $2.3\left(p_F^2 S\right)^{-2/3}$, (c) whisker	$\frac{\sqrt{7\zeta(3)}}{2\pi}\frac{1}{\sqrt{\nu T_c V}} \approx$ $13.3\frac{T_{c0}}{E_F}\sqrt{\frac{\xi_0^3}{V}}$

Table 1.

One can see that for the three dimensional clean case the result coincides with the original Ginzburg evaluation and demonstrates the negligibility of the superconducting fluctuation effects in clean bulk materials.

[9] One can see that some arbitrariness occurs in this definition. For instance the Gi number could be defined as the reduced temperature at which the AL correction to conductivity is equal to the normal value of conductivity (as it was done in [13, 14]). Such definition results in the change of the numerical factor in Gi number: $Gi_{(2,\sigma)} = 1.44 Gi_{(2,h.c.)}$.

20.2.3 Scaling and renormalization group

In the above study of the fluctuation contribution to heat capacity we have restricted ourselves to the temperature range out of the direct vicinity of the critical temperature: $|\epsilon| \gtrsim Gi_{(D)}$. As we have seen the fluctuations in this region turn out to be weak and neglecting their interaction was justified. In this Section we will discuss the fluctuations in the immediate vicinity of the critical temperature ($|\epsilon| \lesssim Gi_{(D)}$) where this interaction turns out to be of great importance.

We will start with the scaling hypothesis, i.e. with the belief that in the immediate vicinity of the transition the only relevant length scale is $\xi(T)$. The temperature dependencies of all other physical quantities can be expressed through $\xi(T)$. This means, for instance, that the formula for the fluctuation part of the free energy (20.25) with the logarithm omitted is still valid in the region of critical fluctuations[10]

$$F_{(D)} \sim -\xi^{-D}(\epsilon), \tag{20.38}$$

the coherence length is a power function of the reduced temperature: $\xi(\epsilon) \sim \epsilon^{-\nu}$. The corresponding formula for the fluctuation heat capacity can be rewritten as

$$\delta C \sim -\frac{\partial^2 F}{\partial \epsilon^2} \sim \epsilon^{D\nu-2}. \tag{20.39}$$

As was demonstrated in the Introduction, the GL functional approach, where the temperature dependence of $\xi(T)$ is determined only by the diffusion of the electrons forming Cooper pair, $\xi(\epsilon) \sim \epsilon^{-1/2}$ and $\delta C \sim \epsilon^{-1/2}$. These results are valid for the GL region ($|\epsilon| \gtrsim Gi$) only, where the interaction between fluctuations can be neglected. In the immediate vicinity of the transition (so-called critical region), where $|\epsilon| \lesssim Gi$, the interaction of fluctuations becomes essential. Here fluctuation Cooper pairs affect the coherence length themselves, changing the temperature dependencies of $\xi(\epsilon)$ and $\delta C(\epsilon)$. In order to find the heat capacity temperature dependence in the critical region one would have to calculate the functional integral with the fourth order term, accounting for the fluctuation interaction, as was done for $0D$ case. For the $3D$ case up to now it is only known how to calculate a Gaussian type functional integral. This was done above when, for the GL region, we omitted the fourth order term in the free energy functional (20.16).

The first evident step in order to include in consideration of the critical region would be to develop a perturbation series in b [11]. Any term in this series has the form of a Gaussian integral and can be represented by a diagram, where the solid lines correspond to the correlators $\left\langle \Psi(r)\Psi^*(r')\right\rangle$. The "interactions " b are represented by the points where four correlator lines intersect (see Fig. 20.2).

This series can be written as

$$C \sim \sum_{n=0} c_n \left(\frac{Gi_{(D)}}{\epsilon}\right)^{\frac{4-D}{2}n}.$$

For $\epsilon \gtrsim Gi$ it is enough to keep only the first two terms to reproduce the perturbational result obtained above. For $\epsilon \lesssim Gi$ all terms have to be summed. It turns out that the coefficients c_n can be calculated for the space dimensionality $D \to 4$ only. In this case the complex diagrams from Fig. 20.2 (like the diagram similar to an envelope) are small by the parameter $\varepsilon = 4 - D$ and in order to calculate c_n it is sufficient to sum the relatively simple "parquet" type diagrammatic series. Such a summation results in the substitution of the "bare" vertex b by some

[10] The logarithm in (20.25) is essential for the case $D = 2$. This case will be discussed later.

[11] Let us mention that this series is an asymptotic one, i.e. it does not converge even for small b. One can easily see this for small negative b, when the integral for the partition function evidently diverges. This is also confirmed by the exact $0D$ solution (20.22).

Figure 20.2: Examples of diagrams for the fluctuation contribution to b.

effective interaction $\widetilde{b}$ which diminishes and tends to zero when the temperature approaches the transition point. Such a method was originally worked out in quantum field theory [15, 16, 17]. For the problem of a phase transition such a summation was first accomplished in [18].

Instead of a direct summation of the diagrams it is more convenient and physically obvious to use the method of the renormalization group. In the case of quantum field theory this method was known long ago [19, 20]. For phase transition theory it was proposed in [18, 21] but the most simple and evident formulation was presented by Wilson [22]. The idea of the renormalization group method consists in separating the functional integration over "fast" ($\psi_{|k|>\Lambda}$) and "slow"($\psi_{|k|<\Lambda}$) fluctuation modes. If the cut off Λ is large enough the fast mode contribution is small and the integration over them is Gaussian. After the first integration over fast modes the functional obtained depends on the slow ones only. They can, in their turn, be divided on slow ($|k| < \Lambda_1$) and fast ($\Lambda_1 < |k| < \Lambda$), and the procedure can be repeated. Moving step by step ahead in this way one can calculate the complete partition function.

As an example of the first step of renormalization, the partition function calculation below T_c can be recalled. There we separated the order parameter into the space-independent part $\widetilde{\Psi}$ ("slow" mode) and the fluctuation part $\psi(r)$ ("fast" mode) which was believed to be small in magnitude. Being in the GL region it was enough to average over the fast variables just once, while in the critical region the renormalization procedure requires subsequent approximations.

The cornerstone of the method consists in the fact that in the critical region at any subsequent step the free energy functional has the same form. For D close to 4 this form coincides with the initial free energy GL functional but with the coefficients a_Λ and b_Λ depending on Λ. We will perform these calculations by the method of mathematical induction. Let us suppose that after the $(n-1)-$st step the free energy functional has the form:

$$\begin{aligned}\mathcal{F}[\widetilde{\Psi}_{\Lambda_{n-1}}] &= F_{N,\Lambda_{n-1}} + \int dV \left\{ a_{\Lambda_{n-1}} |\widetilde{\Psi}_{\Lambda_{n-1}}|^2 + \right. \\ &\left. + \frac{b_{\Lambda_{n-1}}}{2} |\widetilde{\Psi}_{\Lambda_{n-1}}|^4 + \frac{1}{4m} |\nabla \widetilde{\Psi}_{\Lambda_{n-1}}|^2 \right\}. \end{aligned} \tag{20.40}$$

Writing $\widetilde{\Psi}_{\Lambda_{n-1}}$ in the form $\widetilde{\Psi}_{\Lambda_{n-1}} = \widetilde{\Psi}_{\Lambda_n} + \psi_{\Lambda_n}$ and choosing Λ_n close enough to Λ_{n-1} it is possible to make ψ_{Λ_n} so small, that one can restrict the functional to the quadratic terms in ψ_{Λ_n} only and perform the Gaussian integration in complete analogy with (20.34). The important property of the spaces with dimensionalities close to 4 is the possibility to choose $\Lambda_n \ll \Lambda_{n-1}$ and still to have $\psi_{\Lambda_n} \ll \widetilde{\Psi}_{\Lambda_n}$. In this case $\widetilde{\Psi}_{\Lambda_n}$can be taken as coordinate independent, and one can use the result directly following from (20.34):

$$\mathcal{F}[\widetilde{\Psi}_{\Lambda_n}] = F_{N,\Lambda_{n-1}} + \int dV \left\{ a_{\Lambda_n}|\widetilde{\Psi}_{\Lambda_n}|^2 + \frac{b_{\Lambda_n}}{2}|\widetilde{\Psi}_{\Lambda_n}|^4 + \frac{1}{4m}|\nabla\widetilde{\Psi}_{\Lambda_n}|^2 \right\}$$
$$-\frac{T}{2}\sum_{\Lambda_n<|\mathbf{k}|<\mathbf{\Lambda}_{n-1}} \left\{ \ln\frac{\pi T_c}{(3b_{\Lambda_n}|\widetilde{\Psi}_{\Lambda_n}|^2 + a_{\Lambda_n} + \frac{\mathbf{k}^2}{4m})} + \right.$$
$$\left. \ln\frac{\pi T_c}{b_{\Lambda_n}|\widetilde{\Psi}_{\Lambda_n}|^2 + a_{\Lambda_n} + \frac{\mathbf{k}^2}{4m}} \right\}. \tag{20.41}$$

Expanding the last term in (20.41) in a series in $\widetilde{\Psi}_{\Lambda_n}$ one can get for $\mathcal{F}[\widetilde{\Psi}_{\Lambda_n}]$ the same expression (20.40) with the substitution of $\Lambda_{n-1} \to \Lambda_n$. From (20.41) follows that

$$F_{n,\Lambda_n} = F_{n,\Lambda_{n-1}} - T\sum_{\Lambda_n<|\mathbf{k}|<\mathbf{\Lambda}_{n-1}} \ln\frac{\pi T_c}{(a_{\Lambda_n} + \frac{\mathbf{k}^2}{4m})},$$
$$a_{\Lambda_n} = a_{\Lambda_{n-1}} + 2T\sum_{\Lambda_n<|\mathbf{k}|<\mathbf{\Lambda}_{n-1}} \frac{b_{\Lambda_n}}{(a_{\Lambda_n} + \frac{\mathbf{k}^2}{4m})} \tag{20.42}$$
$$b_{\Lambda_n} = b_{\Lambda_{n-1}} - 5T\sum_{\Lambda_n<|\mathbf{k}|<\mathbf{\Lambda}_{n-1}} \frac{b^2_{\Lambda_n}}{(a_{\Lambda_n} + \frac{\mathbf{k}^2}{4m})^2}.$$

Passing to a continuous variable $\Lambda_n \to \Lambda$ one can rewrite these recursion equations as the set of differential equations:

$$\frac{\partial F(\Lambda)}{\partial\Lambda} = -T\mu_D\Lambda^{D-1}\ln\frac{\pi T_c}{(a(\Lambda) + \frac{\Lambda^2}{4m})}, \tag{20.43}$$

$$\begin{cases} \frac{\partial a(\Lambda)}{\partial\Lambda} = -2T\mu_D\frac{b(\Lambda)\Lambda^{D-1}}{(a(\Lambda)+\frac{\Lambda^2}{4m})} \\ \frac{\partial b(\Lambda)}{\partial\Lambda} = 5T\mu_D\frac{b^2(\Lambda)\Lambda^{D-1}}{(a(\Lambda)+\frac{\Lambda^2}{4m})^2} \end{cases}. \tag{20.44}$$

These renormalization group equations are evidently valid for small enough Λ only, where the transition from discrete to continuous variables is justified. This means at least

$$\Lambda^2/4m \ll T_{c0}Gi_{(D)}. \tag{20.45}$$

in order to move away from the first approximation.

Let us recall that in the framework of the Landau theory of phase transitions the coefficient $a(T_{c0}) = 0$ at the transition point and this can be considered as the MFA definition of the critical temperature T_{c0}. The same statement for the function $a = a(\Lambda)$ in the framework of the renormalization group method can be written as the $a(T_{c0}, \Lambda \sim \xi^{-1}) = 0$. With the decrease of Λ the effect of critical fluctuations more and more is taken into account and the renormalized value of the critical temperature decreases, being defined by the equation: $a(T_c(\Lambda), \Lambda) = 0$. Finally, after the application of the complete renormalization procedure, one can define the real critical temperature T_c, shifted down with respect to T_{c0} due to the effect of fluctuations, from the equation:

$$a(T_c, \Lambda = 0) = 0. \tag{20.46}$$

It is easy to find this shift in the first approximation. Indeed, let us integrate the first equation of (20.44) over Λ in limits $[0, \xi^{-1}]$. The main contribution to the integral will be determined

by the region where $a(\Lambda) \ll \frac{\Lambda^2}{4m}$. Being far from the critical point one can assume that the coefficient $b = const$ and then

$$a(\xi^{-1}) = \alpha\delta T_c = \int\limits_{a(0)}^{a(\xi^{-1})} da = -8mT\mu_D b \int\limits_0^{1/\xi} \Lambda^{D-3} d\Lambda.$$

For the $3D$ case this gives the shift of the critical temperature δT_c due to fluctuations [12]

$$\frac{\delta T_c^{(3)}}{T_c} \sim -\frac{2mb}{\pi\alpha\xi} = -\frac{b}{2\pi T_c\alpha^2}\frac{1}{\xi^3} = -\frac{7\zeta(3)}{16\pi^3\nu T_c\xi^3} = -\frac{8}{\pi}\sqrt{Gi_{(3)}}. \tag{20.48}$$

Let us come back to study of properties of the system of equations (20.44). One can find its partial solution at $T = T_c$ in the form:

$$\begin{aligned} a(T_c,\Lambda) &= \frac{4-D}{4m[5+(4-D)]}\Lambda^2 \\ b(T_c,\Lambda) &= \frac{5}{16m^2T\mu_D}\frac{4-D}{[5+(4-D)]^2}\Lambda^{4-D}. \end{aligned} \tag{20.49}$$

These power solutions are correct in the domain of validity of the system (20.44) itself, i.e. for small enough Λ defined by the condition (20.45). Nevertheless, in a space of dimensionality close to 4 ($D = 4-\varepsilon, \varepsilon \ll 1$) it is possible to extend their validity up to the GL region and to observe their crossover to the GL results: $a(T_c) = 0$; $b(T_c) = b_0 = const$. Indeed, in this case, due to proportionality of $a(\Lambda)$ to $\varepsilon \to 0$, one can omit it in the denominators of the system (20.44) and to write down the solution for $b(\Lambda)$ in the form

$$b^{-1}(T_c,\Lambda) = b_0^{-1} + \frac{80m^2}{(4-D)}T\mu_D(\Lambda^{D-4} - \xi^{4-D}). \tag{20.50}$$

We have chosen the constant of integration as b_0^{-1} - $\frac{80m^2}{(4-D)}T\mu_D\xi^{4-D}$ in order to match the renormalization group and GL solutions at the value of $\Lambda = \Lambda_{\max} \sim \xi^{-1}$.

Now let us pass to study of the function $a(T,\Lambda)$ for the same interesting case of space dimensionality $D \to 4$ for temperatures slightly different (but still close enough) from T_c, where one can write

$$a(T,\Lambda) = a(T_c,\Lambda) + \alpha(T_c,\Lambda)T_c\epsilon.$$

The first term on the right hand side is determined by Eq.(20.49). In order to determine $\alpha(T_c,\Lambda)$ let us expand the first equation in (20.44) in terms of ϵ

$$\frac{\partial\alpha(T_c,\Lambda)}{\partial\Lambda} = 2T\mu_D\frac{b(T_c,\Lambda)\Lambda^{D-1}}{\left(a(T_c,\Lambda)+\frac{\Lambda^2}{4m}\right)^2}\alpha(T_c,\Lambda). \tag{20.51}$$

For

$$\Lambda^2/4m \gtrsim \alpha(T_c,\Lambda)T_c\epsilon \tag{20.52}$$

[12] In the same way we can analyze the shift of the critical temperature in $2D$ case too and obtain:

$$\frac{\delta T_c^{(2)}}{T_c} = -2Gi_{(2)}\ln\frac{1}{4Gi_{(2)}}. \tag{20.47}$$

As we will show below both $3D$ and $2D$ results for δT_c coinside with those obtained by the analysis of the effect of fluctuations on superconducting density in the perturbation approach.

we can again use the solution (20.50) for $b(T_c, \Lambda)$ and omit $a(T_c, \Lambda)$ in the denominator of (20.51). The constant of integration, appearing in the process of solution of (20.51), is chosen in accordance with the condition that for $\Lambda = \Lambda_{\max} \sim \xi^{-1}$ we match $\alpha(T_c, \Lambda) = \alpha(T_{c0}, \xi^{-1}) = \alpha_0$ with the GL theory:

$$\alpha(T_c, \Lambda) = \alpha_0 \left[1 + \frac{80 m^2 b_0}{(4-D)} T \mu_D (\Lambda^{D-4} - \xi^{4-D})\right]^{-2/5}. \tag{20.53}$$

The condition (20.52) can be written as $\Lambda \gtrsim \xi^{-1}(T)$, where $\xi(T)$ is the generalized coherence length, determined by the equation:

$$\xi^{-2}(T) = 4m\alpha\left(T_c, \xi^{-1}(T)\right) T_c \epsilon.$$

Such a definition is valid at any temperature. For example, far enough from the critical point, in the GL region, $\alpha\left(T_c, \xi^{-1}(T)\right) = \alpha_0$ and one reproduces the result (20.3). Vice versa, in the critical region the main contribution on the right hand side of the Eq. (20.53) results from the second term containing Λ^{D-4} so, putting $\xi^{-1}(T) = \Lambda$, one can rewrite the self-consistent equation for $\xi(T)$ and get

$$\xi(T) = (4m)^{(1-D)/2} \frac{4-D}{20 b_0 T \mu_D \sqrt{T_c \alpha_0}} \epsilon^{-\nu}, \tag{20.54}$$

where $2\nu = [1-(4-D)/5]^{-1}$. As was already mentioned, strictly speaking this result was carried out for $\varepsilon = 4 - D \ll 1$, so it is confident up to the first in ε expansion only: $\nu = 1/2 + \varepsilon/10$. Nevertheless extending it to $\varepsilon = 1$ $(D = 3)$ one can obtain $\nu_3 = 3/5$.

Let us pass to the calculation of the critical exponent of the heat capacity in the immediate vicinity of the transition. For this purpose one can calculate the second derivative of equation (20.43) with respect to ϵ:

$$\frac{\partial C(\Lambda)}{\partial \Lambda} = T^2 \mu_D \frac{\Lambda^{D-1} \alpha^2(\Lambda)}{(\alpha(\Lambda) T_c \epsilon + \frac{\Lambda^2}{4m})^2} \tag{20.55}$$

The heat capacity renormalized by fluctuations has the value $C(\Lambda = 0)$ which is the result of integration over all fluctuation degrees of freedom. Carrying out the integration of (20.55) over all $\Lambda \lesssim \xi^{-1}$ one can divide the domain of integration on the right hand side in two: $\Lambda \lesssim \xi^{-1}(T)$ and $\xi^{-1}(T) \lesssim \Lambda \lesssim \xi^{-1}$. In the calculation of the integral over the region $\xi > \Lambda \gtrsim \xi^{-1}(T)$ the inequality $\alpha(\Lambda) T_c \epsilon \ll \frac{\Lambda^2}{4m}$ holds, and the function $\alpha(\Lambda)$ can be omitted in the denominator. In the numerator of (20.55) one can use for $\alpha(\Lambda)$ the solution (20.53). In the region $\Lambda \lesssim \xi^{-1}(T)$ one has to use the partial solution (20.49) for $\alpha(\Lambda)$ and can find that the contribution of this domain has the same singularity as that from the region $\Lambda \gtrsim \xi^{-1}(T)$, but with a coefficient proportional to $(4-D)^2 = \varepsilon^2$, hence negligible in our approximation. The result is:

$$C(\Lambda = 0) = \alpha_0^2 [(4mT)^2 \mu_D]^{\frac{1}{5}} \left[\frac{4}{5} \frac{(4-D)}{b_0}\right]^{4/5} \frac{5}{4-D} \xi^{\frac{4-D}{5}}(T).$$

Substituting the expression for $\xi(T)$ one can finally find

$$C = 2^{12/5} \alpha_0^2 [5 \mu_D \frac{m^2 T^2}{b_0^4 (4-D)}]^{\frac{1}{5}} \epsilon^{-\alpha}, \tag{20.56}$$

confirming the validity of the scaling hypothesis and the relation (20.39). The critical exponent in (20.56) is

$$\alpha = \frac{(4-D)}{10[1-(4-D)/5]} \approx \varepsilon/10.$$

One can see that generally speaking the critical exponents ν and α appear in the form of series in powers of ε. More cumbersome calculations permit finding the next approximations for them in $\varepsilon = 4 - D$. Nevertheless it is worth mentioning that even the first approximation, giving $\nu_3 = 3/5$ and $\alpha_3 = 1/10$ for $\varepsilon = 1$, is already weakly affected by the following steps of the expansion in powers of ε [23].

One can notice that the exercise performed in this Section has more academic than practical character. Indeed, the results obtained turn out applicable to the analysis of the critical region of a $3D$ superconductor only if Gi is so small that the theoretical predictions are hardly experimentally observable. Nevertheless we demonstrated the RG method which helps to see the complete picture of the fluctuations manifestation in the vicinity of the critical temperature.

20.2.4 Fluctuation diamagnetism

Qualitative preliminaries.

In this Section we discuss the effect of fluctuations on the magnetization and the susceptibility of a superconductor above the transition temperature. Being the precursor effect for the Meissner diamagnetism, the fluctuation induced magnetic susceptibility has to be a small correction with respect to the diamagnetism of a superconductor but it can be comparable to or even exceed the value of the normal metal diamagnetic or paramagnetic susceptibility and can be easily measured experimentally. As was already mentioned in the Introduction the temperature dependence of the fluctuation induced diamagnetic susceptibility can be qualitatively analyzed on the basis of the Langevin formula, but some precautions in the case of low dimensional samples have to be made.

As regards the $3D$ case we would like just to mention here that Exp.(20.12), presented in terms of $\xi(T)$, has a wider region of applicability than the GL one. Namely, the scaling arguments are valid for diamagnetic susceptibility too and one can write the general relation

$$\chi_{(3)} \sim -e^2 T\xi(T) \sim -\chi_P \epsilon^{-1/2} \begin{cases} 1, & \epsilon \gtrsim Gi \\ \left(\frac{\epsilon}{Gi}\right)^{1/2-\nu}, & \epsilon \lesssim Gi \end{cases}, \tag{20.57}$$

which is valid in the region of critical fluctuations in the immediate vicinity of the transition temperature too. Here, in order to define the scale of fluctuation effects, we have introduced the Pauli paramagnetic susceptibility $\chi_P = e^2 v_F/4\pi^2$. Moreover, the Langevin formula permits us to extend the estimation of the fluctuation diamagnetic effect to the other side beyond the GL region: to high temperatures $T \gg T_c$. The coherence length far from the transition becomes a slow function of temperature. In a clean superconductor, far from T_c, $\xi(T) \sim v_F/T$, so one can write

$$\chi_{(3c)}(T \gg T_c) \sim -e^2 T\xi(T) \sim -\chi_P \tag{20.58}$$

and see that the fluctuation diamagnetism turns out to be of the order of the Pauli paramagnetism even far from the transition. More precise microscopic calculations of $\chi_{(3)}(T \gg T_c)$ lead to the appearance of $\ln^2(T/T_c)$ in the denominator of (20.58).

In the $2D$ case Exp.(20.12) is applicable for the estimation of $\chi_{(2)}$ in the case when the magnetic field is applied perpendicular to the plane, permitting $2D$ rotations of fluctuation Cooper pairs in it:

$$\chi_{(2c)}(T) \sim e^2 \frac{n}{m} < R^2 > \sim e^2 T\xi^2(T) \sim -\chi_P \frac{E_F}{T - T_c}. \tag{20.59}$$

This result is valid for a wide range of temperatures and can exceed the Pauli paramagnetism by factor $\frac{E_F}{T}$ even far from the critical point (we consider the clean case here).

For a thin film ($d \ll \xi(T)$) perpendicular to the magnetic field the fluctuation Cooper pairs behave like effective $2D$ rotators, and the formula (20.12) still can be used, though one has to take into account that the susceptibility in this case is calculated per unit square of the film. So for the realistic case (from the experimental point of view) of the dirty film, one has just use in (20.59) the expression (20.6) for the coherence length:

$$\chi_{(2d)} \sim \frac{e^2 T}{d}\xi^2(T) \sim -\chi_P \left(\frac{l}{d}\right)\frac{T_c}{T-T_c}. \tag{20.60}$$

Let us discuss now the important case of a layered superconductor (for example, a high temperature superconductor). It is usually supposed that the electrons move freely in conducting planes separated by a distance s. Their motion in the perpendicular direction has a tunneling character, with effective energy J. The related velocity and coherence length can be estimated as $v_z = \partial E(\mathbf{p})/\partial p_\perp \sim J/p_\perp \sim sJ$ and $\xi_{z,(c)} \sim sJ/T$ for clean case. In dirty case the anisotropy can be taken into account in the spirit of formula (20.6) yielding $\xi_{z,(d)} \sim \sqrt{D_\perp/T} \sim sJ\sqrt{\tau/T}$.

We start from the case of a weak magnetic field applied perpendicular to layers. The effective area of a rotating fluctuation pair is $\xi_x(\epsilon)\xi_y(\epsilon)$. The density of Cooper pairs in the conducting layers (20.10) has to be modified for the anisotropic case. Its isotropic $3D$ value is proportional to $1/\xi(\epsilon)$, that now has to be read as $\sim 1/\sqrt{\xi_x(\epsilon)\xi_y(\epsilon)}$. The anisotropy of the electron motion leads to a concentration of fluctuation Cooper pairs in the conducting layers and hence, to an effective increase of the Cooper pairs density of $\sqrt{\xi_x(\epsilon)\xi_y(\epsilon)}/\xi_z(\epsilon)$ times its isotropic value. This increase is saturated when $\xi_z(\epsilon)$ reaches the interlayer distance s, so finally the anisotropy factor appears in the form $\sqrt{\xi_x(\epsilon)\xi_y(\epsilon)}/\max\{s, \xi_z(\epsilon)\}$ and the square root in its numerator is removed in the Langevin formula (20.12), rewritten for this case

$$\chi_{(layer,\perp)}(\epsilon, H \to 0) \sim -e^2 T \frac{\xi_x(\epsilon)\xi_y(\epsilon)}{\max\{s, \xi_z(\epsilon)\}}. \tag{20.61}$$

The existence of a crossover between the $2D$ and $3D$ temperature regimes in this formula is evident: as the temperature tends to T_c the diamagnetic susceptibility temperature dependence changes from $1/\epsilon$ to $1/\sqrt{\epsilon}$. This happens when the reduced temperature reaches its crossover value $\epsilon_{cr} = r$ ($\xi_z(\epsilon_{cr}) \sim s$). The anisotropy parameter

$$r = \frac{4\xi_z^2(0)}{s^2} = \frac{J^2}{T}\begin{cases} \frac{\pi\tau}{4}, & T\tau \ll 1 \\ \frac{7\zeta(3)}{8\pi^2 T}, & T\tau \gg 1 \end{cases} \tag{20.62}$$

plays an important role in the theory of layered superconductors [13].

It is interesting to note that this intrinsic crossover, related to the spectrum anisotropy, has an opposite character to the geometric crossover which happens in thick enough films when $\xi(T)$ reaches d. In the latter case the characteristic $3D$ $1/\sqrt{\epsilon}$ - dependence taking place far enough from T_c (where $\xi(T) \ll d$), is changed to the $2D$ $1/\epsilon$ law (see (20.60)) in the immediate vicinity of transition (where $\xi(T) \gg d$) [24]. It is worth mentioning that in a strongly anisotropic layered superconductor the fluctuation-induced susceptibility may considerably exceed the normal metal dia- and paramagnetic effects even relatively far from T_c [25, 26].

Let us consider a magnetic field applied along the layers. First it is necessary to mention that the fluctuation diamagnetic effect disappears in the limit $J \sim \xi_z \to 0$. Indeed, for the formation of a circulating current it is necessary to tunnel twice, so

$$\chi_{(layer,\parallel)} \sim -e^2 T \frac{\xi_z^2}{\max\{s, \xi_z(T)\}} \sim -\chi_P\left(\frac{sJ}{v_F}\right)\frac{J/T}{\sqrt{\epsilon}\max\{\sqrt{\epsilon}, J/T\}}.$$

[13] We use here a definition of r following from microscopic theory (see Section 6).

In the general case of an anisotropic superconductor, choosing the z axis along the direction of magnetic field H, the following extrapolation of the results obtained may be written

$$\chi \sim -e^2 T \frac{\xi_x^2(\epsilon)\xi_y^2(\epsilon)}{\max\{\mathfrak{a}, \xi_x(\epsilon)\}\max\{\mathfrak{b}, \xi_y(\epsilon)\}\max\{\mathfrak{s}, \xi_z(\epsilon)\}}. \tag{20.63}$$

This general formula is useful for the analysis of the fluctuation diamagnetism of anisotropic superconductors or samples of some specific shape: granular, quasi-1D, quasi-2D, and 3D. It is also applicable to the case of a thin film ($d \ll \xi_z(\epsilon)$) placed perpendicular to the magnetic field: it is enough to replace $\xi_z(\epsilon)$ by d in (20.63). Nevertheless the formula (20.63) cannot be applied to the cases of thin films in parallel fields, wires and granules. In those cases the Langevin formula (20.12) can still be used with the replacement of $\langle R^2 \rangle \to d^2$:

$$\chi_{(D)} \sim -\chi_P \left(\frac{T}{v_F}\right) \xi^{2-D} d^{D-1} \sim \epsilon^{D/2-1}.$$

The magnetic field dependence of the fluctuation part of free energy in these cases is reduced only to account for the quadratic shift of the critical temperature versus magnetic field.

For 3D systems or in the case of a film in a perpendicular magnetic field the critical temperature depends on H linearly, while the magnetic field dependent part of the free energy for $H \ll H_{c2}^*(-\epsilon)$ (the line $H_{c2}^*(-\epsilon)$ is mirror-symmetric to the $H_{c2}(\epsilon)$ with respect to y-axis passing through $T = T_c$) is proportional to H^2. This is why the magnetic susceptibility is determined by Eq.(20.63) for weak enough magnetic fields $H \ll \Phi_0/[\xi_x(\epsilon)\xi_y(\epsilon)] = H_{c2}(\epsilon) \ll H_{c2}(0)$ only. In the vicinity of T_c these fields are small enough.

Zero-dimensional diamagnetic susceptibility.

For quantitative analysis of the fluctuation diamagnetism we start by writing down the GL functional for the free energy (see Exp.(20.16)) in the presence of the magnetic field

$$\begin{aligned} \mathcal{F}[\Psi(\mathbf{r})] &= F_n + \int dV \left\{ a|\Psi(\mathbf{r})|^2 + \frac{b}{2}|\Psi(\mathbf{r})|^4 + \frac{1}{4m}|\left(-i\nabla - 2e\mathbf{A}\right)\Psi(\mathbf{r})|^2 + \right. \\ &\left. + \frac{\mathbf{B}^2}{8\pi} - \frac{\mathbf{H}\cdot\mathbf{B}}{4\pi} \right\}. \end{aligned} \tag{20.64}$$

where $\mathbf{A}$ is vector potential. As long as fluctuation effects are comparatively small, the average magnetic field in the metal $\mathbf{B}$ may be assumed to be equal to the external field $\mathbf{H}$. Thus we omit the last two terms in (20.64) (see later on).

The fluctuation contribution to the diamagnetic susceptibility in the simplest case of a "zero-dimensional" superconductor (spherical superconducting granule of diameter $d \ll \xi(\epsilon)$) was considered by V.Shmidt [11]. In this case the order parameter does not depend on the space variables and the free energy can be calculated exactly for all temperatures including the critical region in the same way as was done for the case of the heat capacity in the absence of a magnetic field. Formally the effect of a magnetic field in this case is reduced to the renormalization of the coefficient a, or, in other words, to the suppression of the critical temperature. This is why one can use the same formula (20.22) for the partition function with the critical temperature T_c shifted by magnetic field as[14]:

$$T_c(H) = T_c(0)(1 - \frac{4\pi^2\xi^2}{\Phi_0^2} < \mathbf{A}^2 >). \tag{20.65}$$

[14]Let us stress the difference between the H^2 shift of the critical temperature for a zero-dimensional granule and the linear shift in the case of bulk material.

Here $\Phi_0 = \frac{\pi}{e}$ is the magnetic flux quantum and $< ..... >$ means the averaging over the sample volume.

Such a trivial dependence of the properties of $0D$ samples on magnetic field immediately allows one to understand its effect on the heat capacity of a granular sample. Indeed, with the growth of the field the temperature dependence of the heat capacity presented in Fig. 20.1 just moves in the direction of lower temperatures.

In the GL region $Gi_{(0)} \lesssim \epsilon$ one can write the asymptotic expression (20.23) for the free energy:

$$F_{(0)}(\epsilon, H) = -T \ln \frac{\pi}{\alpha(\epsilon + \frac{4\pi^2\xi^2}{\Phi_0^2} < \mathbf{A}^2 >)}.$$

In the case of a spherical particle the relation $< \mathbf{A}^2 >= \frac{1}{10} H^2 d^2$ can be used in full analogy with the calculation of the moment of inertia of a solid sphere. In this way an expression for the $0D$ fluctuation magnetization valid for all fields $H \ll H_{c2}(0)$ can be found:

$$M_{(0)}(\epsilon, H) = -\frac{\partial F_{(0)}(\epsilon, H)}{\partial H} = -T \frac{\frac{2\pi^2\xi^2}{5\Phi_0^2} d^2}{(\epsilon + \frac{\pi^2\xi^2}{5\Phi_0^2} H^2 d^2)} H. \tag{20.66}$$

One can see that the fluctuation magnetization turns out to be negative and linear up to some crossover field, which can be called the temperature dependent upper critical field of the granule $H_{c2(0)}(\epsilon) \sim \frac{\Phi_0}{d\xi(\epsilon)} = \frac{\xi}{d} H_{c2}(0)\sqrt{\epsilon}$ at which it reaches a minimum. At higher fields $H_{c2(0)}(\epsilon) \lesssim H \ll H_{c2}(0)$ the fluctuation magnetization of the $0D$ granule decreases as $1/H$. In the weak field region $H \ll H_{c2(0)}(\epsilon)$ the diamagnetic susceptibility is:

$$\chi_{(0)}(\epsilon, H) = -\frac{12\pi T \xi_0^2}{5\Phi_0^2 d} \frac{1}{\epsilon} \approx -2 \cdot 10^2 \chi_P \left(\frac{\xi}{d}\right) \frac{1}{\epsilon}$$

which coincides with our previous estimate in its temperature dependence but the numerical factor found is very large. Let us underline that the temperature dependence of the $0D$ fluctuation diamagnetic susceptibility turns out to be less singular than the $0D$ heat capacity correction: ϵ^{-1} instead of ϵ^{-2}.

The expression for the fluctuation part of free energy (20.28) is also applicable to the cases of a wire or a film placed in a parallel field: as was already mentioned above all its dependence on magnetic field is manifested by the shift of the critical temperature (20.65). In the case of the wire in a parallel field one has to choose the gauge of the vector-potential $\mathbf{A} = \frac{1}{2}\mathbf{H} \times \mathbf{r}$ yielding $\langle \mathbf{A}^2 \rangle_{(wire,\|)} = \frac{H^2 d^2}{32}$ (the calculation of this average is analogous to that of the moment of inertia of a solid sphere). For a wire in a perpendicular field, or a film in a parallel field, the gauge has to be chosen in the form $\mathbf{A} = (0, Hx, 0)$ (to avoid the appearance of currents perpendicular to surface). One can find $\langle \mathbf{A}^2 \rangle_{(wire,\perp)} = \frac{H^2 d^2}{16}$ for a wire and $\langle \mathbf{A}^2 \rangle_{(film,\|)} = \frac{H^2 d^2}{12}$ for a film.

Calculating the second derivative of Eq.(20.28) with the appropriate magnetic field dependencies of the critical temperature one can find the following expressions for the diamagnetic susceptibility:

$$\chi_{(D)}(\epsilon) = -2\pi \frac{\xi T}{v_F} \chi_P \begin{cases} \frac{1}{\sqrt{\epsilon}}, \text{ wire in parallel field} \\ \frac{2}{\sqrt{\epsilon}}, \text{ wire in perpendicular field} \\ \frac{d}{3\xi} \ln \frac{1}{\epsilon}, \text{ film in parallel field} \end{cases}. \tag{20.67}$$

GL treatment of fluctuation magnetization.

Let us analyze quantitatively, on the basis of the GL functional, the temperature and field dependencies of the fluctuation magnetization. We will carry on the discussion for a layered superconductor. As was already mentioned this system has a great practical importance because of its direct applicability to high temperature superconductors, where the fluctuation effects are very noticeable. Moreover, the general results obtained will allow us to analyze $3D$ and $2D$ situations as limiting cases. The effects of a magnetic field are more pronounced for perpendicular orientation, so let us consider first this case.

The generalization of the GL functional for a layered superconductor (Lawrence-Doniach (LD) functional [27]) in a perpendicular magnetic field can be written as

$$\begin{aligned}\mathcal{F}_{LD}\left[\Psi\right] &= \sum_{l}\int d^2r\left(a\left|\Psi_l\right|^2+\frac{b}{2}\left|\Psi_l\right|^4+\frac{1}{4m}\left|\left(\nabla_{\parallel}-2ie\mathbf{A}_{\parallel}\right)\left|\Psi_l\right|^2\right.\right.\\ &\left.\left.+\mathcal{J}\left|\Psi_{l+1}-\Psi_l\right|^2\right),\end{aligned} \tag{20.68}$$

where Ψ_l is the order parameter of the $l-$th superconducting layer and the phenomenological constant $\mathcal{J}$ is proportional to the Josephson coupling between adjacent planes. The gauge with $A_z=0$ is chosen in (20.68). In the immediate vicinity of T_c the LD functional is reduced to the GL one with the effective mass $M=(4\mathcal{J}s^2)^{-1}$ along c-direction, where s is the interlayer spacing. One can relate the value of $\mathcal{J}$ to the coherence length along the c-direction: $\mathcal{J}=2\alpha T_c\xi_z^2/s^2$. Since we are dealing with the GL region the fourth order term in (20.68) can be omitted.

As it is well known the Landau representation is the most appropriate for problems related with the motion of a charged particle in a uniform magnetic field. The fluctuation Cooper pair wave function $\phi_{nk_z}(\mathbf{r})$ can be written as the product of a plane wave propagating along the magnetic field direction and a Landau state wave function. Let us expand the order parameter $\Psi_l(\mathbf{r})$ on the basis of these eigenfunctions:

$$\Psi_l(\mathbf{r})=\sum_{\mathbf{n},k_z}\Psi_{n,k_z}\phi_{nk_z}(\mathbf{r})\exp(ik_zl), \tag{20.69}$$

where $\mathbf{n}$ is the quantum number related with the degenerate Landau state and k_z is the momentum component along the direction of the magnetic field. Substituting this expansion into (20.68) one can find the LD free energy as a functional of the Ψ_{n,k_z} coefficients:

$$\mathcal{F}_{LD}\left[\Psi_{n,k_z}\right]=\sum_{\mathbf{n},k_z}\left\{\alpha T_c\epsilon+\frac{H}{2m\Phi_0}\left(n+\frac{1}{2}\right)+\mathcal{J}\left(1-\cos(k_zs)\right)\right\}\left|\Psi_{n,k_z}\right|^2. \tag{20.70}$$

In complete analogy with the case of an isotropic spectrum the functional integral over the order parameter configurations Ψ_{n,k_z} in the partition function can be reduced to a product of ordinary Gaussian integrals, and the fluctuation part of the free energy in a magnetic field takes the form:

$$F(\epsilon,H)=-\frac{2\pi SH}{\Phi_0}T\sum_{n,k_z}\ln\frac{\pi T}{\alpha T_c\epsilon+\frac{H}{2m\Phi_0}\left(n+\frac{1}{2}\right)+J\left(1-\cos(k_zs)\right)}. \tag{20.71}$$

Here the summation over the degenerate states of each Landau level was performed (S is the sample cross-section) and results in appearance of the number of particle states $(2\pi HS/\Phi_0)$ with the definite quantum numbers n and k_z. The summation over n has to be performed through all occupied states, i.e. the upper limit of the sum is $N\sim 2m\Phi_0E_F/H$.

In the limit of weak fields one can carry out the summation over the Landau states by means of the Euler-Maclaurin's transformation

$$\sum_{n=0}^{N} f(n) = \int_{-1/2}^{N+1/2} f(n) - \frac{1}{24}\left[f^{'}(N+1/2) - f^{'}(-1/2)\right]$$

and obtain

$$F(\epsilon, H) = F(\epsilon, 0) + \frac{\pi S T H^2}{24 m \Phi_0^2} \int_{-\pi/s}^{\pi/s} \frac{\mathcal{N} s dk_z}{2\pi} \left\{ \frac{1}{\alpha T_c \epsilon + \mathcal{J}\left(1 - \cos(k_z s)\right)} \right\}. \tag{20.72}$$

Here $\mathcal{N}$ is the total number of layers. After the momentum integration one gets:

$$F(\epsilon, H) = F(\epsilon, 0) + \frac{\pi V H^2}{24 m \alpha s \Phi_0^2} \frac{1}{\sqrt{\epsilon(\epsilon + r)}}$$

with the anisotropy parameter defined as[15]

$$r = \frac{2\mathcal{J}}{\alpha T} = \frac{4\xi_z^2(0)}{s^2}. \tag{20.73}$$

The magnetic susceptibility in a weak field turns out [28, 29] to be

$$\chi_{(layer,\perp)} = -\frac{e^2 T}{3\pi s} \frac{\xi_{xy}^2}{\sqrt{\epsilon(\epsilon + r)}}. \tag{20.74}$$

These results confirm the qualitative estimation (20.61) additionally providing the exact value of the numerical coefficient and the temperature dependence in the crossover region. In the limit $r \gg \epsilon$ Exp.(20.74) transforms into the diamagnetic susceptibility of the $3D$ anisotropic superconductor [30].

For a film of thickness d the integral over k_z in Exp.(20.72) has to be replaced by a summation over the discrete k_z and when $\xi_z(T) \gg d$ only the term with $k_z = 0$ has to be taken into account:

$$\chi_{(film,\perp)} = -\frac{e^2 T}{3\pi d} \frac{\xi_{xy}^2}{\epsilon}. \tag{20.75}$$

Note that these formulas predict a nontrivial increase of diamagnetic susceptibility for clean metals [29]. The usual statement that fluctuations are most important in dirty superconductors with a short electronic mean free path does not hold in the particular case of susceptibility because here ξ turns out to be in the numerator of the fluctuation correction.

Now we will demonstrate that, besides the crossovers in its temperature dependence, the fluctuation induced magnetization is a nonlinear function of magnetic field too, and these nonlinearities, different for various dimensionalities, take place at relatively low fields. This, strong in comparison with the expected scale of $H_{c2}(0)$, manifestation of the nonlinear regime in fluctuation magnetization and hence, field dependent fluctuation susceptibility, was the subject of the intensive debates in early seventies [30, 31, 32, 33, 34, 35, 36, 37, 38, 39] (see also the

[15] Let us stress the difference between J and $\mathcal{J}$ in the two definitions (20.62) and (20.73) of the anisotropy parameter r. The first one was introduced as the electron tunneling matrix element, while the second one enters in the LD functional as the characteristic Josephson energy for the order parameter. Later on, in the framework of the microscopic theory, it will be demostrated that, in accordance with our qualitative definition, $r \sim J^2$, while $\mathcal{J}$ turns out to be proportional to J^2 too. In the dirty case it depends on the relaxation time of the electron scattering on impurities: $\mathcal{J} \sim \alpha J^2 \max\{\tau, 1/T\}$. Hence both definitions (20.62), appearing in the qualitative consideration, and (20.73), following from the LD model, are consistent.

old but excellent review of W.J. Skocpol and M. Tinkham [40]) and after the discovery of HTS [41, 42, 43, 44] (see also very recent detailed essay of T.Mishonov and E.Penev [45] with references there). We will mainly follow here the paper of Buzdin et al. [46], dealing with the fluctuation magnetization of a layered superconductor, which permits observing in a unique way all variety of the crossover phenomena in temperature and magnetic field.

Let us go back to the general expression (20.71) and evaluate it without taking the magnetic field to small. The difficulty in dealing with it consists in the divergence of the sum over Landau levels n. This divergence can be regularized (see [45, 47]), but let us observe that in order to calculate the magnetization we must know the magnetic field dependent part of the free energy only. So a very convenient method to bypass the divergence problem [48] is to calculate the difference $F(H) - F(0)$, turning the sum over Landau states in $F(\epsilon, 0)$ into an integral and then, in its turn, turning this integral into a sum of integrals over the unit length intervals $x \in [n - 1/2, n + 1/2]$. Then

$$F(\epsilon,0) = -\lim_{H\to 0}\frac{2\pi VH}{\Phi_0}T\int\limits_{-\pi/s}^{\pi/s}\frac{dk_z}{2\pi}\sum_{n=0}^{\infty}\int\limits_{-1/2}^{1/2}dx\times \\ \times\ln\frac{\pi T}{\alpha T_c\epsilon+\frac{H}{2m\Phi_0}\left(x+n+\frac{1}{2}\right)+\mathcal{J}\left(1-\cos(k_z s)\right)}.$$

and by introducing the dimensionless variable [16]

$$h=\frac{H}{H_{c2}(0)},\ H_{c2}(0)=2m\alpha T_c/e=\Phi_0/2\pi\xi_{xy}^2, \tag{20.76}$$

one can write

$$F(\epsilon,H)-F(\epsilon,0)= \tag{20.77}$$
$$=-\frac{TV}{2\pi s\xi_{xy}^2}h\int\limits_{-\pi}^{\pi}dz\sum_{n=0}\int\limits_{-1/2}^{1/2}dx\ln\frac{(2n+1+2x)h+r/2(1-\cos z)+\epsilon}{(2n+1)h+r/2(1-\cos z)+\epsilon}.$$

Performing the integrations over z and x in (20.77) and differentiating with respect to h we finally obtain a very convenient general expression for the fluctuation magnetization in a layered superconductor:

$$M(\epsilon,H)=\frac{T}{\Phi_0 s}\sum_{n=0}^{\infty}\left\{n\ln\frac{\varphi(R_n+1)}{\varphi(R_n)}+\right. \\ \left.\ln\frac{\varphi(R_n+1)}{\varphi(R_n+1/2)}-\frac{n+1/2}{\sqrt{(R_n+1/2)^2-\rho^2}}\right\} \tag{20.78}$$

with $\varphi(x)=x+\sqrt{x^2-\rho^2}$, $R_n=n+\epsilon/2h+\rho$ and $\rho=r/2h$. The sum in (20.78) converges as $1/n^2$ and it provides a volume magnetization expression that can be compared with experiment.

Let us comment on the different crossovers in the $M(\epsilon, H)$ field dependence analyzing the general formula (20.78). Let us fix the temperature $\epsilon \ll r$. In this case the c-axis coherence length exceeds the interlayer distance ($\xi_z \gg s$) and in the absence of a magnetic field the

[16] Let us remind that the exact definition of $H_{c2}(0)$ contains the numerical coefficient $A(0)$ (see footnote 3).

fluctuation Cooper pairs motion has a $3D$ character. Supposing the magnetic field to be not too high ($h \ll r$) we may perform an expansion in (20.78) in$1/\rho$ and obtain

$$M_{(3)}(\epsilon \ll r, h \ll r) = \frac{T\sqrt{2}h^{1/2}}{\Phi_0 \xi_z} \times \sum_n \left\{ (n+1)\left(n+1+\frac{\epsilon}{2h}\right)^{1/2} - n\left(n+\frac{\epsilon}{2h}\right)^{1/2} - \frac{3}{2}\frac{(n+1+\frac{2\epsilon}{3h})}{\sqrt{n+\frac{1}{2}+\frac{\epsilon}{2h}}} \right\}. \tag{20.79}$$

For weak fields ($h \ll \epsilon$) the magnetization grows linearly with magnetic field, justifying our preliminary qualitative results. Nevertheless, this linear growth is changed to the nonlinear $3D$ high field regime $M \sim \sqrt{H}$ already in the region of a relatively small fields $H_{c2}(\epsilon) \lesssim H$ ($\epsilon \lesssim h$). The further increase of magnetic field leads to the next crossover in the magnetization field dependence at $h \sim r$. However the Exp.(20.79) was obtained in the assumption $h \ll r$ as an expansion over $1/\rho$, and it does not work any more. Handling with the Hurvitz zeta-function the summation in (20.78) for $3D$ case can be carried out for an arbitrary field [34]:

$$M_{(3)}(\epsilon \ll r, h) = 3\frac{T}{\Phi_0 s}\left(\frac{2}{r}\right)^{1/2}\sqrt{h} \times \left[\zeta\left(-\frac{1}{2}, \frac{1}{2}+\frac{\epsilon}{2h}\right) - \zeta\left(\frac{1}{2}, \frac{1}{2}+\frac{\epsilon}{2h}\right)\frac{\epsilon}{6h}\right]. \tag{20.80}$$

One can see from this formula that for large fields the magnetization saturates at the value M_∞ [49]:

$$M(h \gg r) \to M_\infty = -\frac{\ln 2}{2}\frac{T}{\Phi_0 s} = -0.346\frac{T}{\Phi_0 s}, \tag{20.81}$$

that is a typical for $2D$ superconductors. Therefore at $h \sim r$ we have a $3D \to 2D$ crossover in $M(H)$ behavior in spite of the fact that all sizes of fluctuation Cooper pair exceed considerably the lattice parameters. The effective "bidimensionalization" of the fluctuations is related to the effect of a strong magnetic field which "freezes out" the rotations along its direction. Let us stress that this crossover occurs in the region of already strongly non-linear dependence of $M(H)$ and therefore for a rather strong magnetic field from the experimental point of view in HTS.

Fixing the temperature $\epsilon \gg r$ in the formula (20.78) one can find the general formula for $2D$ fluctuation regime [45]:

$$M_{(2)}(\epsilon \gg r, h) = \frac{T}{\Phi_0 s}\left\{\ln\Gamma\left(\frac{1}{2}+\frac{\epsilon}{2h}\right) - \frac{1}{2}\ln(2\pi) - \frac{\epsilon}{2h}\left[\psi\left(\frac{1}{2}+\frac{\epsilon}{2h}\right) - 1\right]\right\}, \tag{20.82}$$

where $\Gamma(x)$ is the Euler gamma-function and $\psi(x) = d\ln\Gamma(x)/dx$ is already cited in Introduction digamma-function. Using (20.82) one can directly pass from the linear regime in a weak magnetic field corresponding to (20.59) to the saturation of magnetization (20.81) in strong fields.

Near the line of the upper critical field ($h_{c2}(\epsilon) = -\epsilon$) the contribution of the term with $n = 0$ in the sum (20.78) becomes most important and for the magnetization the expression

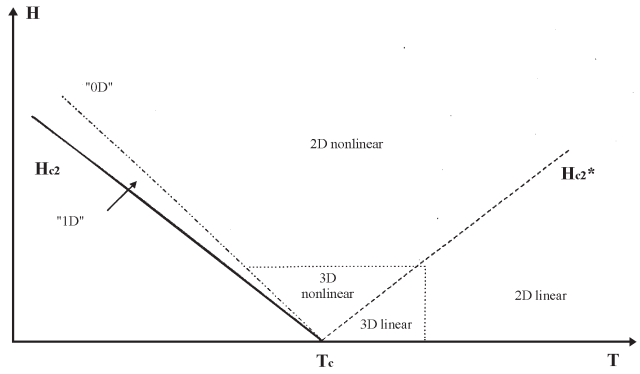


Figure 20.3: Schematic representation of the different regimes for fluctuation magnetization in the (H,T) diagram. The line $H^*_{c2}(T)$ is mirror-symmetric to the $H_{c2}(T)$ line with respect to a y-axis passing through $T = T_c$. This line defines the crossover between linear and non-linear behavior of the fluctuation magnetization above T_c.

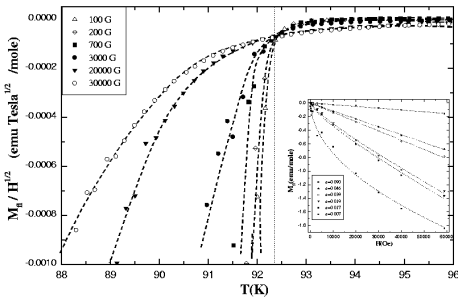


Figure 20.4: Fluctuation magnetization of a YBaCO123 normalized on $\sqrt{H}$ as the function of temperature in accordance with the described theory shows the crossing of the isofield curves at $T = T_c(0) = 92.3K$. The best fit obtained for anisotropy parameter r=0.09. In the inset the magnetization curves as the function of magnetic field are reported.

$$-M(h) \sim \frac{h}{\sqrt{(h-h_{c2})(h-h_{c2}+r)}}$$

can be obtained. It contains the already familiar for us "$0D$" regime ($r \ll h - h_{c2} \ll 1$), where the magnetization decreases as $-M(h) \sim \frac{1}{h-h_{c2}}$ (compare with (20.66)), while for $h - h_{c2} << r$ the regime becomes "$1D$" and the magnetization decreases slower, as $-M(h) \sim \frac{1}{\sqrt{h-h_{c2}}}$.

Such an analogy is observed in the next orders in Gi too. In the Ref. [50] the analogy was demonstrated for the example of the first eleven terms for the $2D$ case and nine for the $3D$ case. Summation of the series of high order fluctuation contributions to the heat capacity by the Pade-Borel method resulted in its temperature dependence similar to the $0D$ and $1D$ cases without magnetic field. Nevertheless a considerable difference has not be forgotten: in the $0D$ and $1D$ cases no phase transition takes place while in the $2D$ and $3D$ cases in a magnetic field a phase transition of first order to the Abrikosov vortex lattice state occurs.

In conclusion, the fluctuation magnetization of a layered superconductor in the vicinity of the transition temperature turns out to be a complicated function of temperature and magnetic field, and it evidently cannot be factorized on these variables. The fit of the experimental data is very sensitive to the anisotropy parameter r and allows determination of the latter with a rather high precision [51, 52]. In Fig. 20.4 the successful application of the described approach to fit the experimental data on $YBa_2Cu_3O_7$ is shown [53].

20.3 Ginzburg-Landau theory of fluctuations in transport phenomena

The appearance of fluctuating Cooper pairs above T_c leads to the opening of a "new channel" for charge transfer. In the Introduction the fluctuation Cooper pairs were treated as carriers with charge $2e$ while their lifetime τ_{GL} was chosen to play the role of the scattering time in the Drude formula. Such a qualitative consideration results in the Aslamazov-Larkin (AL) pair contribution to conductivity (20.11) (so-called paraconductivity[17]).

Below we will present the generalization of the phenomenological GL functional approach to transport phenomena. Dealing with the fluctuation order parameter, it is possible to describe correctly the paraconductivity type fluctuation contributions to the normal resistance and magnetoconductivity, Hall effect, thermoelectric power and thermal conductivity at the edge of transition. Unfortunately the indirect fluctuation contributions are beyond the possibilities of the description by Time-Dependent GL approach and they will be calculated in the framework of the microscopic theory (see Sections 6-8).

20.3.1 Time dependent GL equation

In previous Sections we have demonstrated how the GL functional formalism allows one to account for fluctuation corrections to thermodynamical quantities. Let us discuss the effect of fluctuations on the transport properties of a superconductor above the critical temperature.

In order to find the value of paraconductivity, some time-dependent generalization of the GL equations is required. Indeed, the conductivity characterizes the response of the system to the applied electric field. It can be defined as $\mathbf{E} = -\partial\mathbf{A}/\partial t$ but, in contrast to the previous Section, $\mathbf{A}$ has to be regarded as being time dependent. The general non-stationary BCS equations are very complicated, even in the limit of slow time and space variations of the field and the order parameter. For our purposes it will be sufficient, following [66, 67, 68, 69, 70, 71, 72], to write a model equation in the vicinity of T_c, which in general correctly reflects the qualitative aspects of the order parameter dynamics and in some cases is exact.

Let us keep in mind the GL functional formalism introduced above. If a deviation from equilibrium is assumed, then it is no more possible to derive the GL equations starting from the condition that the variational derivative of the free energy is zero. At the same time, in the absence of equilibrium Ψ begins to depend on time. For small deviations from the equilibrium it is natural to assume that in the process of order parameter relaxation its time derivative $\partial\Psi/\partial t$ is proportional to the variational derivative of the free energy $\delta\mathcal{F}/\delta\Psi^*$, which is equal to zero at the equilibrium. But this is not all: side by side with the normal relaxation of the order parameter the effect of thermodynamical fluctuations on it has to be taken into account. This can be done by the introduction the Langevin forces $\zeta(\mathbf{r}, t)$ in the right-hand side of equation describing the order parameter dynamics. Finally, gauge invariance requires that $\partial\Psi/\partial t$ should be included in the equation in the combination $\partial\Psi/\partial t + 2ie\varphi\Psi$, where φ is the scalar potential of the electric field. By concluding all these speculations one can write the model time-dependent GL equation (TDGL) in the form

$$-\gamma_{GL}\left(\frac{\partial}{\partial t} + 2ie\varphi\right)\Psi = \frac{\delta\mathcal{F}}{\delta\Psi^*} + \zeta(\mathbf{r}, t). \tag{20.83}$$

with the GL functional $\mathcal{F}$ determined by (20.16),(20.64),(20.68). The dimensionless coefficient γ_{GL} in the left-hand-side of the equation can be related to pair life-time τ_{GL} (20.2): $\gamma_{GL} =$

[17] This term may have different origins. First of all, evidently, paraconductivity is analogous to paramagnetism and means excess conductivity. Another possible origin is an incorrect onomatopoeic translation from the Russian "paroprovodimost' " that means pair conductivity

$\alpha T_c \epsilon \tau_{GL} = \pi\alpha/8$ by the substitution in (20.83) of the first term of (20.16) only[18].

Neglecting the fourth order term in the GL functional, equation (20.83) can be rewritten in operator form as

$$[\widehat{L}^{-1} - 2ie\gamma_{GL}\varphi(r,t)]\Psi(\mathbf{r},t) = \zeta(\mathbf{r},t) \tag{20.84}$$

with the TDGL operator $\widehat{L}$ and Hamiltonian $\widehat{\mathcal{H}}$ defined as

$$\widehat{L} = \left[\gamma_{GL}\frac{\partial}{\partial t} + \widehat{\mathcal{H}}\right]^{-1}, \widehat{\mathcal{H}} = \alpha T_c\left[\epsilon - \widehat{\xi}^2(\widehat{\nabla} - 2ie\mathbf{A})^2\right]. \tag{20.85}$$

We have introduced here the formal operator of the coherence length $\widehat{\xi}$ to have the possibility to deal with an arbitrary type of spectrum. For example, in the most interesting case for our applications to layered superconductors, the action of this operator is defined by the Exp.(20.68).

In the absence of an electric field one can write the formal solution of equation (20.84) as

$$\Psi^{(0)}(\mathbf{r},t) = \widehat{L}\zeta(\mathbf{r},t). \tag{20.86}$$

The Langevin forces introduced above must satisfy the fluctuation-dissipation theorem, which means that the correlator $< \Psi^{(0)*}_{\mathbf{p}}(t')\Psi^{(0)}_{\mathbf{p}}(t) >$ at coinciding moments of time has to be the same as $< |\Psi_{\mathbf{p}}|^2 >$, obtained by averaging over fluctuations in thermal equilibrium. This requirement is fulfilled if the Langevin forces $\zeta(\mathbf{r},t)$ and $\zeta^*(\mathbf{r},t)$ are correlated by the Gaussian white-noise law

$$< \zeta^*(\mathbf{r},t)\zeta(\mathbf{r}',t') >= 2T\mathrm{Re}\gamma_{GL}\delta(\mathbf{r}-\mathbf{r}')\delta(t-t'). \tag{20.87}$$

To show it let us restrict ourselves for sake of simplicity to the case of $A = 0$ and calculate the correlator

$$\begin{aligned} &< \Psi^*(\mathbf{r},t)\Psi(\mathbf{r}',t) >=< \zeta^*(\mathbf{r},t)\widehat{\widehat{L}^*}\widehat{L}\zeta(\mathbf{r}',t) >= \\ &= 2T\mathrm{Re}\gamma_{GL}\int\frac{d\mathbf{p}}{(2\pi)^D}e^{i\mathbf{p}(\mathbf{r}-\mathbf{r}')}\int_{-\infty}^{\infty}\frac{d\Omega}{2\pi}L^*(\mathbf{p},\Omega)L(\mathbf{p},\Omega). \end{aligned} \tag{20.88}$$

$L(\mathbf{p},\Omega)$ can be found by making the Fourier transform in (20.85):

$$L(\mathbf{p},\Omega) = (-i\gamma_{GL}\Omega + \varepsilon_{\mathbf{p}})^{-1}, \tag{20.89}$$

resulting in

$$\left\langle\Psi^*(\mathbf{r},t)\Psi(\mathbf{r}',t)\right\rangle_{\mathbf{p}} = 2T\mathrm{Re}\gamma_{GL}\int_{-\infty}^{\infty}\frac{d\Omega}{2\pi}\frac{1}{\gamma_{GL}^2\Omega^2 + \varepsilon_{\mathbf{p}}^2} = \left\langle|\Psi_{\mathbf{p}}|^2\right\rangle, \tag{20.90}$$

where

$$\varepsilon_{\mathbf{p}} = \alpha T_c(\epsilon + \widehat{\xi}^2\mathbf{p}^2). \tag{20.91}$$

is the Cooper pair energy spectrum.

[18]It will be shown below that taking into account the electron-hole asymmetry leads to the appearance of an imaginary part of γ_{GL} proportional to the derivative $\partial\ln(\rho v^2\tau)/\partial E|_{E_F} \sim \mathcal{O}(1/E_F)$. This is important for such phenomena as fluctuation Hall effect or fluctuation thermopower and, having in mind writing the most general formula, we will suppose $\gamma_{GL} = \pi\alpha/8 + i\mathrm{Im}\gamma_{GL}$, where necessary.

20.3.2 Paraconductivity

Let us try to clear up the reason why the simple Drude formula works so well for complex phenomenon like paraconductivity. For this purpose let us try to derive the Boltzmann master equation for the fluctuation Cooper pair distribution function

$$n_{\mathbf{p}}(t) = \int \langle \Psi(\mathbf{r},t)\Psi^*(\mathbf{r}',t)\rangle \exp(-i\mathbf{p}(\mathbf{r}-\mathbf{r}'))d(\mathbf{r}-\mathbf{r}'). \tag{20.92}$$

Let us recall that in the state of thermal equilibrium $n_{\mathbf{p}}^{(0)} =< |\Psi_{\mathbf{p}}|^2 >= T/\varepsilon_{\mathbf{p}}$.

In order to determine the electric field dependence of $n_{\mathbf{p}}$ let us write its time derivative using (20.83)

$$\begin{aligned}\frac{\partial n_{\mathbf{p}}(t)}{\partial t} &= \int d(\mathbf{r}-\mathbf{r}')e^{-i\mathbf{p}(\mathbf{r}-\mathbf{r}')}\left[< \frac{\partial\Psi(\mathbf{r},t)}{\partial t}\Psi^*(\mathbf{r}',t) > + < \Psi(\mathbf{r}',t)\frac{\partial\Psi^*(\mathbf{r},t)}{\partial t} >\right] = \\ &= \int d(\mathbf{r}-\mathbf{r}')e^{-i\mathbf{p}(\mathbf{r}-\mathbf{r}')}\left[2\frac{e}{i}[\varphi(\mathbf{r})-\varphi(\mathbf{r}')] < \Psi(\mathbf{r},t)\Psi^*(\mathbf{r}',t) > + \right. \\ &\left. +\frac{2}{\gamma_{GL}}\mathrm{Re}\left\langle \Psi(\mathbf{r},t)\frac{\delta\mathcal{F}}{\delta\Psi}(\mathbf{r}',t)\right\rangle + \frac{2}{\gamma_{GL}}\mathrm{Re}\left\langle\zeta(\mathbf{r},t)\Psi^*(\mathbf{r}',t)\right\rangle\right],\end{aligned} \tag{20.93}$$

where $\mathcal{F}$ is determined by (20.64). Expressing the scalar potential by the electric field E one can transform the first term of the last integral into $-2e\mathbf{E}\frac{\partial n_{\mathbf{p}}}{\partial\mathbf{p}}$. The term with the variational derivative can be evaluated by means of (20.26) and expressed in the form $-\frac{2}{\gamma_{GL}}\varepsilon_{\mathbf{p}}n_{\mathbf{p}}$. More cumbersome is the evaluation of the last term, containing the Langevin force. To the first approximation it is possible to use here the order parameter $\Psi^{(0)}(\mathbf{r},t)$ (see (20.86)) unperturbed by the electric field as the convolution $\widehat{L}\zeta(\mathbf{r},t)$. In this way, using (20.87) and (20.88) we calculate the last average in (20.93)

$$\begin{aligned}\frac{2}{\gamma_{GL}}\int d(\mathbf{r}-\mathbf{r}')e^{-i\mathbf{p}(\mathbf{r}-\mathbf{r}')}\mathrm{Re}\left\langle\zeta^*(\mathbf{r},t)\widehat{L}\zeta(\mathbf{r},t)\right\rangle &= \\ 4T\int\frac{d\mathbf{p}}{(2\pi)^D}e^{i\mathbf{p}(\mathbf{r}-\mathbf{r}')}\mathrm{Re}\int\limits_{-\infty}^{\infty}\frac{d\Omega}{2\pi}L(\mathbf{p},\Omega) &= \frac{2T}{\gamma_{GL}} = \frac{2}{\gamma_{GL}}\varepsilon_{\mathbf{p}}n_{\mathbf{p}}^{(0)}\end{aligned}$$

and obtain the transport equation

$$\frac{\partial n_{\mathbf{p}}}{\partial t} + 2e\mathbf{E}\frac{\partial n_{\mathbf{p}}}{\partial\mathbf{p}} = -\frac{2}{\gamma_{GL}}\varepsilon_{\mathbf{p}}\left(n_{\mathbf{p}}-n_{\mathbf{p}}^{(0)}\right) = -\frac{2}{\tau_{\mathbf{p}}}\left(n_{\mathbf{p}}-n_{\mathbf{p}}^{(0)}\right). \tag{20.94}$$

In the absence of a magnetic field $\varepsilon_{\mathbf{p}}$ was determined by (20.91) and the momentum dependent lifetime, corresponding to the Ginzburg-Landau one, can be introduced:

$$\tau_{\mathbf{p}} = \gamma_{GL}/\varepsilon_{\mathbf{p}} = \frac{\tau_{GL}(\epsilon)}{1+\xi^2(\epsilon)\mathbf{p}^2}.$$

Let us stress the appearance of the coefficient 2 on the right hand side of the equation (20.94). This means that the real Cooper pair lifetime, characterizing its density decay, is $\tau_{\mathbf{p}}/2$.

The effect of a weak electric field on the fluctuation Cooper pair distribution function in the linear approximation is determined by

$$n_{\mathbf{p}}^{(1)} = -\frac{e\mathbf{E}\gamma_{GL}}{\varepsilon_{\mathbf{p}}}\frac{\partial n_{\mathbf{p}}^{(0)}}{\partial\mathbf{p}} = \frac{eT\gamma_{GL}}{\varepsilon_{\mathbf{p}}^3}\mathbf{E}\cdot\frac{\partial\varepsilon_{\mathbf{p}}}{\partial\mathbf{p}}. \tag{20.95}$$

Substituting this formula into the expression for the electric current side by side with the Cooper pair velocity $\mathbf{v_p} = \partial\varepsilon_\mathbf{p}/\partial\mathbf{p}$ one can find

$$\mathbf{j}^\alpha = \sum_\mathbf{p} (2e\mathbf{v}^\alpha n_\mathbf{p}) = \sigma^{\alpha\beta} E^\beta,$$

where the paraconductivity tensor components are:

$$\sigma^{\alpha\beta}_{(D)} = \frac{\pi}{4} e^2 \alpha T \sum_\mathbf{p} \frac{\mathbf{v}^\alpha_\mathbf{p} \mathbf{v}^\beta_\mathbf{p}}{\varepsilon^3_\mathbf{p}}. \tag{20.96}$$

In the case of isotropic spectrum

$$\sigma^{\alpha\beta}_{(D)} = \frac{\pi}{4} e^2 \alpha T \sum_\mathbf{p} \frac{\mathbf{v}^\alpha_\mathbf{p} \mathbf{v}^\beta_\mathbf{p}}{\varepsilon^3_\mathbf{p}} = \begin{cases} \dfrac{e^2}{32\xi} \dfrac{1}{\sqrt{\epsilon}} & \text{3D case,} \\ \dfrac{e^2}{16d} \dfrac{1}{\epsilon} & \text{2D film, thickness } : d \ll \xi, \\ \dfrac{\pi e^2 \xi}{16 S} \dfrac{1}{\epsilon^{3/2}} & \text{1D wire, cross} - \text{section } : S \ll \xi^2. \end{cases} \tag{20.97}$$

One can compare this result with that carried out in the Introduction from qualitative consideration, based on the Drude formula. Those simple speculations reflect correctly the physics of the phenomenon but were carried out with the assumption of the momentum independence of the relaxation time $\tau_\mathbf{p}$, taken as $\tau_\mathbf{0} = \frac{\pi}{8(T-T_c)}$. As we have just seen, in reality $\tau_\mathbf{p}$ decreases rapidly with increase of the momentum, the excess "2" appeared in (20.94) because of the wave nature of fluctuation Cooper pairs; accounting for this circumstance results in the precise coefficients of (20.97), different from (20.11).

An especially simple form the paraconductivity results in the $2D$ case, where, calculated per unit square, it depends on the reduced temperature only:

$$\sigma_\square(T) = \frac{e^2}{16\hbar} \frac{T}{T - T_c}. \tag{20.98}$$

The coefficient in this formula turns out to be a universal constant and is given by the value $\hbar/e^2 = 4.1k\Omega$. For electronic spectra of other dimensionalities this universality is lost, and the paraconductivity comes to depend on the electron mean free path.

Let us compare $\sigma_\square(T)$ with the normal electron Drude part $\sigma_n = n_e e^2 \tau/m$ by writing the total conductivity

$$\sigma = \frac{e^2}{\hbar} \left(\frac{p_F l}{2\pi\hbar} + \frac{1}{16\epsilon} \right). \tag{20.99}$$

One sees that at $\epsilon_{cr} = 0.4/(p_F l) \sim Gi_{(2c)}$ the fluctuation correction reaches the value of the normal conductivity. Let us recall that the same order of magnitude for the $2D$ Ginzburg-Levanyuk number was obtained above from the heat capacity study. We will discuss the region of applicability of (20.99) below in Section 8.6.

It is worth mentioning that the results derived here for paraconductivity are valid with the assumption of weak fluctuations: for the temperature range $\epsilon \lesssim Gi_{(D)}$ they are not anymore applicable. Nevertheless, one can see that for not very dirty films, with $p_F^2 ld \gg 1$, a wide region of temperatures $Gi_{(2d)} \ll \epsilon \ll 1$ exists where the temperature dependence of conductivity is determined by fluctuations and in this region the localization effects are negligible.

The transport equation (20.94) was originally derived many years ago by L.G.Aslamazov and A.I.Larkin [73]. Recently T.Mishonov et al. [74] rederived Eq.(20.94) and solved it for $n_\mathbf{p}$ in the case of an arbitrary electric field.

20.3.3 General expression for paraconductivity

Unfortunately the applicability of the master equation derived is restricted to weak magnetic fields ($H \ll H_{c2}(\epsilon)$). For stronger fields $H_{c2}(\epsilon) \lesssim H \ll H_{c2}(0)$ the simple evaluation of averages in (20.93) turns out to be incorrect, the density matrix has to be introduced and the master equation loses its attractive simplicity. At the same time, as we already know, namely these fields, quantizing the fluctuation Cooper pair motion, present special interest. This is why in order to include in the scheme the magnetic field and frequency dependencies of the paraconductivity, we return to the analysis of the general TDGL equation (20.83) without the objective to reduce it to a Boltzmann type transport equation.

Let us solve it in the case when the applied electric field can be considered as a perturbation. The method will much resemble an exercise from a course of quantum mechanics. To carry out the necessary generality side by side with a formal simplicity of expressions we will introduce some kind of subscript $\{i\}$ which includes the complete set of quantum numbers and time. By a repeated subscript a summation over a discrete and integration over continuous variables (time in particular) will be supposed.

We will look for the response of the order parameter to a weak electric field applied in the form

$$\Psi_{k_z}(\mathbf{r},t) = \Psi^{(0)}_{\{i\}} + \Psi^{(1)}_{\{i\}}, \tag{20.100}$$

where $\Psi^{(0)}_{\{i\}}$ is determined by (20.86). Substituting this expression into (20.84) and restricting our consideration to linear terms in the electric field we can write

$$(\widehat{L}^{-1})_{\{ik\}}\Psi^{(1)}_{\{k\}} = 2ie\gamma_{GL}\varphi_{\{il\}}\Psi^{(0)}_{\{l\}}$$

with the solution in the form

$$\Psi^{(1)}_{\{i\}} = 2ie\gamma_{GL}\widehat{L}_{\{ik\}}\varphi_{\{kl\}}\widehat{L}_{\{lm\}}\zeta_{\{m\}}.$$

Let us substitute the order parameter (20.100) in the quantum mechanical expression for current

$$\mathbf{j} = 2e\mathrm{Re}\left[\Psi^{(0)*}_{\{i\}}\widehat{\mathbf{v}}_{\{ik\}}\Psi^{(1)}_{\{k\}} + \Psi^{(1)*}_{\{i\}}\widehat{\mathbf{v}}_{\{ik\}}\Psi^{(0)}_{\{k\}}\right], \tag{20.101}$$

where $\widehat{\mathbf{v}}_{\{ik\}}$ is the velocity operator which can be expressed by means of the commutator of $\mathbf{r}$ with Hamiltonian (20.85):

$$\widehat{\mathbf{v}}_{\{ik\}} = i\{\widehat{\mathcal{H}}, \mathbf{r}\}_{\{ik\}}. \tag{20.102}$$

The second term of (20.101) can be written by means of a transposed velocity operator (which is Hermitian) as the complex conjugated value of the first one:

$$\Psi^{(1)*}_{\{i\}}\widehat{\mathbf{v}}_{\{ik\}}\Psi^{(0)}_{\{k\}} = (\Psi^{(0)*}_{\{k\}}\widetilde{\widehat{\mathbf{v}}}_{\{ik\}}\Psi^{(1)}_{\{i\}})^*, \tag{20.103}$$

which results in

$$\begin{aligned}\mathbf{j} &= 2\mathrm{Re}\{\Psi^{(0)*}_{\{i\}}(2e\widehat{\mathbf{v}}_{\{ik\}})\Psi^{(1)}_{\{k\}}\} = \\ &= -8e^2\mathrm{Im}\{\gamma_{GL}\widehat{L}^*_{\{ki\}}\widehat{\mathbf{v}}_{\{il\}}\widehat{L}_{\{lm\}}\varphi_{\{mn\}}\widehat{L}_{\{np\}}\zeta^*_{\{k\}}\zeta_{\{p\}}\}.\end{aligned} \tag{20.104}$$

Let us average now (20.104) over the Langevin forces moving the operator $\widehat{L}^*_{\{ki\}}$ from the beginning to the end of the trace and using (20.87). One finds

$$\mathbf{j} = -16Te^2\mathrm{Re}(\gamma_{GL})\mathrm{Im}\{\gamma_{GL}\widehat{\mathbf{v}}_{\{il\}}\widehat{L}_{\{lm\}}\varphi_{\{mn\}}\widehat{L}_{\{np\}}\widehat{L}^*_{\{pi\}}\}. \tag{20.105}$$

Now we choose the representation where the $\widehat{L}_{\{lm\}}$ operator is diagonal (it is evidently given by the eigenfunctions of the Hamiltonian (20.85)):

$$L_{\{m\}}(\Omega) = \frac{1}{\varepsilon_{\{m\}} - i\Omega\gamma_{GL}}, \tag{20.106}$$

where $\varepsilon_{\{m\}}$ are the appropriate energy eigenvalues. Then we assume that the electric field is coordinate independent but is a monochromatic periodic function of time:

$$\varphi(r,t) = -E^{\beta}r^{\beta}\exp(-i\omega t). \tag{20.107}$$

In doing the Fourier transform in (20.105) one has to remember that the time dependence of the matrix elements $\varphi_{\{mn\}}$ results in a shift of the frequency variable of integration $\Omega \to \Omega - \omega$ in both L-operators placed after $\varphi_{\{mn\}}$ or, what is the same, to a shift of the argument of the previous $\widehat{L}_{\{lm\}}$ for ω :

$$\begin{aligned} \mathbf{j}^{\alpha}_{\omega} &= 16Te^2\mathrm{Re}(\gamma_{GL}) \times \\ &\times \int \frac{d\Omega}{2\pi}\mathrm{Re}\left\{\gamma_{GL}\widehat{\mathbf{v}}^{\alpha}_{\{il\}}\widehat{L}_{\{l\}}(\Omega+\omega)[-ir^{\beta}_{\{li\}}]\widehat{L}_{\{i\}}(\Omega)\widehat{L}^{*}_{\{i\}}(\Omega)\right\}\mathbf{E}^{\beta}, \end{aligned} \tag{20.108}$$

where $\mathrm{Re}\, f(\omega) \equiv [f(\omega) + f^{*}(-\omega)]/2$.

Let us express the matrix element $\mathbf{r}_{\{li\}}$ by means of $\widehat{\mathbf{v}}_{\{li\}}$ using the commutation relation (20.102). One can see that in the representation chosen

$$\widehat{\mathbf{r}}^{\beta}_{\{li\}} = i\frac{\widehat{\mathbf{v}}^{\beta}_{\{li\}}}{\varepsilon_{\{i\}} - \varepsilon_{\{l\}}} \tag{20.109}$$

and, carrying out the frequency integration in (20.108), finally write for the fluctuation conductivity tensor ($\mathbf{j}^{\alpha}_{\omega} = \sigma^{\alpha\beta}(\omega)\mathbf{E}^{\beta}$) :

$$\begin{aligned} \sigma^{\alpha\beta}(\epsilon,H,\omega) &= 8e^2T\mathrm{Re}(\gamma_{GL})\sum_{\{i,l\}=0}^{\infty} \\ &\mathrm{Re}\left[\gamma_{GL}\frac{\widehat{\mathbf{v}}^{\alpha}_{\{il\}}\widehat{\mathbf{v}}^{\beta}_{\{li\}}}{\varepsilon_{\{i\}}(\gamma_{GL}\varepsilon_{\{i\}} + \gamma^{*}_{GL}\varepsilon_{\{l\}} - i|\gamma_{GL}|^2\omega)(\varepsilon_{\{l\}} - \varepsilon_{\{i\}})}\right]. \end{aligned} \tag{20.110}$$

This is the most general expression which describes the d.c., galvanomagnetic and high frequency paraconductivity contribution. In the case when we are interested in diagonal effects only, where it is enough to accept γ_{GL} as real ($\gamma_{GL} = \mathrm{Re}\gamma_{GL} = \pi\alpha/8$) omitting its small imaginary part, the last expression can be simplified by means of symmetrization of the summation variables):

$$\sigma^{\alpha\alpha}(\epsilon,H,\omega) = \frac{\pi}{2}\alpha e^2T\sum_{\{i,l\}=0}^{\infty}\mathrm{Re}\left[\frac{\widehat{\mathbf{v}}^{\alpha}_{\{il\}}\widehat{\mathbf{v}}^{\alpha}_{\{li\}}}{\varepsilon_{\{i\}}\varepsilon_{\{l\}}(\varepsilon_{\{i\}} + \varepsilon_{\{l\}} - i\gamma_{GL}\omega)}\right]. \tag{20.111}$$

Let us demonstrate the calculation of the d.c. paraconductivity in the simplest case of a metal with an isotropic spectrum. In this case we choose a plane wave representation. By using $\varepsilon_{\mathbf{p}}$ defined by (20.91) one has

$$\widehat{\mathbf{v}}_{\{\mathbf{pp}'\}} = \mathbf{v}_{\mathbf{p}}\delta_{\mathbf{pp}'},\ \mathbf{v}_{\mathbf{p}} = \frac{\partial\varepsilon_{\mathbf{p}}}{\partial\mathbf{p}} = 2\alpha T_c\xi^2\mathbf{p}. \tag{20.112}$$

We do not need to keep the imaginary part of γ_{GL}, which is necessary to calculate particle-hole asymmetric effects only. Then the fluctuation conductivity calculated from (20.111) coincides exactly with (20.96).

20.3.4 Fluctuation conductivity of layered superconductor

Let us return to the discussion of our general formula (20.111) for the fluctuation conductivity tensor. A magnetic field directed along the c-axis still permits separation of variables even in the case of a layered superconductor. The Hamiltonian in this case can be written as in (20.70), (20.85):

$$\widehat{\mathcal{H}} = \alpha T_c \left(\epsilon - \xi_{xy}^2 (\nabla_{xy} - 2ie\mathbf{A}_{xy})^2 - \frac{r}{2}(1 - \cos(k_z s)) \right). \tag{20.113}$$

It it is convenient to work in the Landau representation, where the summation over $\{i\}$ is reduced to one over the ladder of the Landau levels $i = 0, 1, 2..$ (each is degenerate with a density $2eH$ per unit square) and integration over the c-axis momentum in the limits of the Brillouine zone. The eigenvalues of the Hamiltonian (20.113) can be written in the form

$$\varepsilon_n = \alpha T_c [\epsilon + \frac{r}{2}(1 - \cos(k_z s)) + h(2n+1)] = \varepsilon_{k_z} + \alpha T_c h(2n+1), \tag{20.114}$$

where $h = \frac{eH}{2m\alpha T_c}$ was already defined by Eq. (20.76). For the velocity operators one can write

$$\widehat{\mathbf{v}}^{x,y} = \frac{1}{2m}(-i\nabla - 2ie\mathbf{A})^{x,y};\ \widehat{\mathbf{v}}^z = -\frac{\alpha r s}{2} T_c \sin(k_z s). \tag{20.115}$$

In-plane conductivity.

Let us start from the calculation of the in-plane components. The calculation of the velocity operator matrix elements requires some special consideration. First of all let us stress that the required matrix elements have to be calculated for the eigenstates of a quantum oscillator whose motion is equivalent to the motion of a charged particle in a magnetic field. The commutation relation for the oscillator's velocity components is well known (see [75]):

$$[\widehat{\mathbf{v}}^x, \widehat{\mathbf{v}}^y] = i\frac{eH}{2m^2} = \frac{i\alpha T_c}{m} h. \tag{20.116}$$

In order to calculate the necessary matrix elements let us present the velocity operator components in the form of boson-type creation and annihilation operators $\widehat{a}^+, \widehat{a}$ with commutation relation $[\widehat{a}, \widehat{a}^+] = 1$:

$$\widehat{\mathbf{v}}^{x,y} = \sqrt{\frac{\alpha T_c h}{2m}} \begin{pmatrix} \widehat{a}^+ + \widehat{a} \\ i\widehat{a}^+ - i\widehat{a} \end{pmatrix}$$

One can check that the correct commutation relation (20.116) is fulfilled. Taking into account that

$$< l|\widehat{a}|n > = < n|\widehat{a}^+|l > = \sqrt{n}\delta_{n,l+1}$$

it is seen that the only non-zero matrix elements of the velocity operator are

$$< l|\widehat{\mathbf{v}}^{x,y}|n > = \sqrt{\frac{\alpha T_c h}{2m}} \begin{pmatrix} \sqrt{l}\delta_{l,n+1} + \sqrt{n}\delta_{n,l+1} \\ i\sqrt{l}\delta_{l,n+1} - i\sqrt{n}\delta_{n,l+1} \end{pmatrix}.$$

Using these relations the necessary product of matrix elements can be calculated:

$$< l|\widehat{\mathbf{v}}^x|n >< n|\widehat{\mathbf{v}}^x|l > = \frac{\alpha T_c h}{2m}(l\delta_{l,n+1} + n\delta_{n,l+1}).$$

Its substitution into (20.111) and accounting of the degeneracy of the Landau levels $2eH = 4m\alpha T_c h$ gives for the diagonal component of the in-plane conductivity tensor

$$\sigma^{xx}(\epsilon,H,\omega) = \frac{\pi\alpha^2T_c^2e^2}{4m}h\sum_{\{n\}=0}^{\infty}\sum_{\{l\}=0}\mathrm{Re}\,[\frac{(l\delta_{l,n+1}+n\delta_{n,l+1})}{\varepsilon_l\varepsilon_n(\varepsilon_l+\varepsilon_n-i\gamma_{GL}\omega)}] \tag{20.117}$$

$$= \pi e^2\left(\alpha T_c\right)^3h^2\int_{-\frac{\pi}{s}}^{\frac{\pi}{s}}\frac{dk_z}{2\pi}\sum_{n=0}^{\infty}\mathrm{Re}\,[\frac{n+1}{\varepsilon_{n+1}\varepsilon_n(\varepsilon_{n+1}+\varepsilon_n-i\gamma_{GL}\omega)}].$$

Expanding the denominator into simple fractions we reduce the problem to the calculation of the c-axis momentum integral, which can be carried out in the general case by use of the identity:

$$\int_0^{2\pi}\frac{dx}{2\pi}\frac{1}{\cos x-z}=-\frac{1}{\sqrt{z^2-1}} \tag{20.118}$$

valid for any complex parameter $z\neq 1$ with the proper choice of the square root branch. Using it we write the general expression for the in-plane component of the fluctuation conductivity tensor

$$\sigma^{xx}(\varepsilon,h,\omega) = \frac{e^2h}{16s}\sum_{n=0}^{\infty}(n+1)\left\{\frac{1}{h-i\widetilde{\omega}}\frac{1}{\sqrt{[\epsilon+h(2n+1)][r+\epsilon+h(2n+1)]}}+\right.$$
$$\frac{1}{h+i\widetilde{\omega}}\frac{1}{\sqrt{[\epsilon+h(2n+3)][r+\epsilon+h(2n+3)]}}- \tag{20.119}$$
$$\left.\frac{2h}{h^2+\widetilde{\omega}^2}\frac{1}{\sqrt{[\epsilon+h(2n+2)-i\widetilde{\omega}][r+\epsilon+h(2n+2)-i\widetilde{\omega}]}}\right\}.$$

where $\widetilde{\omega}=\frac{\pi\omega}{16T_c}$.

Out-of plane conductivity.

The situation with the out-of plane component of paraconductivity turns out to be even simpler because of the diagonal structure of the $\widehat{\mathbf{v}}^z_{\{in\}}=-\frac{\alpha rs}{2}T_c\sin(k_zs)\times\delta_{in}\times\delta(k_z-k_{z'})$. Taking into account that the Landau state degeneracy $2eH=h\xi_{xy}^{-2}$ we write

$$\sigma^{zz}(\epsilon,H,\omega) = \frac{1}{2}\pi\alpha e^2T\sum_{\{i,l\}=0}^{\infty}\mathrm{Re}\left[\frac{\widehat{\mathbf{v}}^{\alpha}_{\{il\}}\widehat{\mathbf{v}}^{\alpha}_{\{li\}}}{\varepsilon_{\{i\}}\varepsilon_{\{l\}}(\varepsilon_{\{i\}}+\varepsilon_{\{l\}}-i\alpha T_c\widetilde{\omega})}\right]=$$
$$= \frac{\pi e^2\left(\alpha T_c\right)^3}{16}\left(\frac{sr}{\xi_{xy}}\right)^2h\sum_{n=0}^{\infty}\int_{-\frac{\pi}{s}}^{\frac{\pi}{s}}\frac{dk_z}{2\pi}\mathrm{Re}\,[\frac{\sin^2(k_zs)}{\varepsilon_n^2(k_z)[\varepsilon_n(k_z)-i\alpha T_c\widetilde{\omega}]}].$$

The following transformations are similar to the calculation of the in-plane component: we expand the integrand into simple fractions and perform the k_z-integration by means of the identity (20.118). The final expression can be written as

$$\sigma^{zz}(\epsilon,H,\omega) = \frac{\pi e^2}{32s}\left(\frac{sr}{\xi_{xy}}\right)^2 h\sum_{n=0}^{\infty}\left(-\frac{\partial}{\partial\lambda}\right)\times \tag{20.120}$$
$$\mathrm{Re}\left(\frac{1}{\lambda+i\widetilde{\omega}}\right)\left\{\frac{1}{\sqrt{(\epsilon+h(2n+1)+\lambda)(\epsilon+h(2n+1)+\lambda+r)}}-\right.$$
$$\left.\frac{1}{\sqrt{(\epsilon+h(2n+1)-i\widetilde{\omega})(\epsilon+h(2n+1)-i\widetilde{\omega}+r)}}\right\}|_{\lambda=0}\,.$$

Analysis of the general expressions.

In principle the expressions derived above give an exact solution for the a.c.($\omega \ll T$) paraconductivity tensor of a layered superconductor in a perpendicular magnetic field $H \ll H_{c2}$ ($h \ll 1$) in the vicinity of the critical temperature ($\epsilon \ll 1$). The interplay of the parameters r, ϵ, ω h entering into (20.119)-(20.120), as we have seen in the example of fluctuation magnetization, yields a variety of crossover phenomena.

1. The simplest and most important results which can be derived are the components of the *d.c.* paraconductivity ($\omega = 0$) of layered superconductor in the absence of magnetic field. Keeping $\omega = 0$ and setting $h \to 0$ one can change the summations over Landau levels into integration and find

$$\sigma^{xx}(\varepsilon, h\to 0, \omega=0) = \frac{e^2}{16s}\frac{1}{\sqrt{[\epsilon(r+\epsilon)]}},$$
$$\sigma^{zz}(\epsilon, h\to 0, \omega=0) = \frac{e^2 s}{32\xi_{xy}^2}\left(\frac{\epsilon+r/2}{[\epsilon(\epsilon+r)]^{1/2}}-1\right).$$

2. The Aslamazov-Larkin contribution to the magnetoconductivity can be studied by putting $\omega = 0$ and keeping magnetic field as arbitrary. We will not go into details and just report the results (following [154] with some revision of the coefficient in $3D$ case)

	$h \ll \epsilon$	$\epsilon \ll h \ll r$ $(3D)$	$\max\{\epsilon, r\} \ll h$ $(2D)$
σ^{xx}	$\sigma^{xx}(\epsilon, h=0) - \frac{e^2}{2^8 s}\frac{[8\epsilon(\epsilon+r)+3r^2]}{[\epsilon(\epsilon+r)]^{5/2}}h^2$	$\frac{e^2}{4s}\frac{1}{\sqrt{2hr}}$	$\frac{e^2}{8s}\frac{1}{h}$
σ^{zz}	$\sigma^{zz}(\epsilon, h=0) - \frac{e^2 s}{2^8\xi_{xy}^2}\frac{r^2(\epsilon+r/2)}{[\epsilon(\epsilon+r)]^{5/2}}h^2$	$\frac{3.24e^2 s}{\xi_{xy}^2}\sqrt{\frac{r}{h}}$	$\frac{7\zeta(3)e^2 s}{2^9\xi_{xy}^2}\frac{r^2}{h^2}$

Table 2.

Here it is worth making an important comment. The proportionality of the fluctuation magnetoconductivity to h^2 is valid when using the parametrization $\epsilon = (T - T_{c0})/T_{c0}$ only. As it well known, a weak field shifts the critical temperature linearly, which often makes it attractive to analyze the experimental data by choosing as the reduced temperature parameter $\epsilon_h = (T - T_c(H))/T_c(H)$. In this parametrization one can get a term in the magnetoconductivity linear in h , which previously was cancelled out by the magnetic field renormalization of the critical temperature. So it is important to recognize that the effect of a weak magnetic field on the fluctuation conductivity cannot be reduced to a simple replacement of T_{c0} by $T_c(H)$ in the appropriate formula without the field. Vice versa, this effect is exactly compensated by the change in the functional dependence of the paraconductivity in magnetic field, and finally it contains the negative quadratic contribution only.

3. Letting the magnetic field go to zero and considering nonzero frequency of the electromagnetic field one can find general expressions for the components of the *a.c* paraconductivity

tensor. They are cumbersome enough and in the complete form can be found, for instance, in [76]. We recall here the simplified asymptotics for the Reσ in the $2D$ regime only:

$$\begin{aligned} \mathrm{Re}\sigma^{xx}_{(2D)}(r \ll \epsilon, \widetilde{\omega}) = \\ = \frac{e^2}{16s}\frac{1}{\epsilon}\left[\frac{2\epsilon}{\widetilde{\omega}}\arctan\frac{\widetilde{\omega}}{\epsilon} - \left(\frac{\epsilon}{\widetilde{\omega}}\right)^2 \ln\left[1+\left(\frac{\widetilde{\omega}}{\epsilon}\right)^2\right]\right] \end{aligned} \tag{20.121}$$

$$\mathrm{Re}\sigma^{zz}_{(2D)}(r \ll \epsilon, \widetilde{\omega}) = \frac{e^2}{2^8 s}\left(\frac{sr}{\xi_{xy}}\right)^2\left(\frac{1}{\widetilde{\omega}}\right)^2 \ln[1+\left(\frac{\widetilde{\omega}}{\epsilon}\right)^2]. \tag{20.122}$$

The general formulas (20.119)-(20.120) allow one to study the different crossovers in the *a.c.* conductivity of layered superconductor in the presence of magnetic field of various intensity. We leave this exercise for the reader having some practical interest in the problem.

20.3.5 Magnetic field angular dependence of paraconductivity

We have seen above that in the case of a geometry with a magnetic field directed along the c-axis many sophisticated fluctuation features of layered superconductors can be studied in the most general form. Nevertheless even the attempt to explore the d.c. conductivity in a longitudinal magnetic field (directed in ab plane) [77] or, moreover, with the field directed at some arbitrary angle θ with the c-axis leads to the appearance of the a vector potential component in the argument of $\cos(k_z s)$ and the problem requires a nontrivial calculation of the matrix elements over the Mathieu functions.

We already learned that at temperatures very near to the critical one ($\epsilon \ll r$) the $3D$ fluctuation regime takes place. Here the size of the Cooper pairs along the c-axis is so large that the peculiarities of the layered structure do not play any more role. This means that only small values of k_z are important in the k_z-integrations, where the $\cos(k_z s)$ in (20.70) can be expanded and the LD functional is reduced to its traditional GL form with an anisotropic effective mass tensor:

$$\begin{aligned} \mathcal{F}[\Psi] = \int d^3\mathbf{r}\left\{a|\Psi|^2 + \frac{B}{2}|\Psi|^4 + \sum_{\mu=1}^{3}\frac{1}{4m_\mu}\left|\left(\frac{1}{i}\frac{d}{dx_\mu} - 2eA_\mu\right)\Psi\right|^2 + \right. \\ \left. + \frac{B^2}{8\pi} - \frac{\mathbf{H}\cdot\mathbf{B}}{4\pi}\right\}. \end{aligned} \tag{20.123}$$

We will demonstrate below that in this case a scaling approach provides a direct access to the most general results by rescaling the anisotropic problem to the corresponding isotropic one on the initial level of the GL approach [78].

Let us suppose that the external field $\mathbf{H}$ is chosen to lie in the $y-z$ plane and makes angle θ with the z - axis. For sake of simplicity and because the oxide superconductors are within high accuracy uniaxial materials, we choose $m_x = m_y = m^*$, while $m_z^{-1} = 2\alpha s^2 r$ (compare with (20.68)). The effective anisotropy parameter $\gamma_a^2 = m^*/m_z = 2\alpha s^2 r m^* < 1$ is introduced. In (20.123) the anisotropy enters only in the gauge-invariant gradient term, so the simple rescaling of the coordinate axes: $x = \widetilde{x}, y = \widetilde{y}, z = \gamma_a\widetilde{z}$ together with the scaling of the vector potential: $\mathbf{A} = (\widetilde{A}_x, \widetilde{A}_y, \widetilde{A}_z/\gamma_a)$ will render this term isotropic. The magnetic field evidently is rescaled to $\mathbf{B} = (\widetilde{B}_x/\gamma_a, \widetilde{B}_y/\gamma_a, \widetilde{B}_z)$ and the last three terms in (20.123), describing the magnetic-field energy, are transformed to

$$\delta\mathcal{F}[\Psi] = \frac{\gamma_a}{8\pi}\int d^3\widetilde{\mathbf{r}}\left[\frac{1}{4m}\sum_{\mu=1}^{3}\left|\left(\frac{\hbar}{i}\frac{d}{d\widetilde{x}_\mu}-\frac{2e}{c}\widetilde{A}_\mu\right)\Psi\right|^2+(\frac{\widetilde{\mathbf{B}}_{xy}^2}{\gamma_a}+\widetilde{B}_z^2)- -2(\frac{\widetilde{\mathbf{B}}_{xy}\cdot\mathbf{H}_{xy}}{\gamma_a}+\widetilde{B}_z H_z)\right].$$

In short, we have removed the anisotropy from the gradient term but reintroduced it into the magnetic energy term. In general it is not possible to make both terms isotropic in the Gibbs energy simultaneously. However, depending on the physical question addressed, we can neglect fluctuations in the magnetic field, as was mostly done above.

Let us demonstrate how the method works for the example of the d.c. fluctuation conductivity tensor which was calculated above for a magnetic field directed along the c-axis. We restrict our consideration to the $3D$ region ($\epsilon \ll r$). One can write the scaling relations between the electric field and current components before and after the scaling transformation by means of a conductivity tensor and the anisotropy parameter:

$$\begin{aligned} j_{x,y} &= \widetilde{j}_{x,y} \qquad j_z \sim ev_z \sim \gamma_a\widetilde{j}_z \\ E_{x,y} &= \widetilde{E}_{x,y} \qquad E_z \sim \frac{\partial\varphi}{\partial z}\sim\frac{1}{\gamma_a}\widetilde{E}_z. \end{aligned} \tag{20.124}$$

Now let us rewrite the relations between the current and electric field vectors before and after the scale transformation

$$\begin{aligned} j_\alpha &= \sigma_{\alpha\beta}E_\beta \\ \widetilde{j}_\alpha &= \widetilde{\sigma}_{\alpha\beta}\widetilde{E}_\beta. \end{aligned}$$

Comparing them with (20.124) and introducing the operator of the direct scaling transformation $T_{\alpha\beta}$

$$T_{\alpha\beta} = \begin{pmatrix} 1 & 0 & 0 \\ 0 & 1 & 0 \\ 0 & 0 & \gamma_a \end{pmatrix},$$

one can write $j_\alpha = T_{\alpha\mu}\widetilde{j}_\mu,\ E_\alpha = (T^{-1})_{\alpha\mu}\widetilde{E}_\mu$ and express the conductivity tensor as

$$\sigma_{\alpha\beta} = T_{\alpha\mu}\widetilde{\sigma}_{\mu\rho}T_{\rho\beta}.$$

Now let us work in the already isotropic coordinate frame. We suppose that initially the magnetic field was directed along the c-axis and now we rotate it in the X-Z plane by the angle $\widetilde{\theta}$ with respect to the initial direction. The conductivity tensor will be transformed by the usual matrix law:

$$\widetilde{\sigma}_{\alpha\beta}(\widetilde{\theta}) = R^T_{\alpha\mu}\widetilde{\sigma}_{\mu\rho}(0)R_{\rho\beta} = R^T_{\alpha\mu}(T^{-1})_{\mu\varsigma}\sigma_{\varsigma\eta}(0)(T^{-1})_{\eta\delta}R_{\delta\beta}$$

and

$$\sigma_{\alpha\beta}(\widetilde{\theta}) = T_{\alpha\gamma}\widetilde{\sigma}_{\gamma\delta}(\widetilde{\theta})T_{\delta\beta} = T_{\alpha\gamma}R^T_{\gamma\mu}(T^{-1})_{\mu\varsigma}\sigma_{\varsigma\eta}(0)(T^{-1})_{\eta\delta}R_{\delta\kappa}T_{\kappa\beta},$$

where

$$R_{\alpha\beta} = \begin{pmatrix} \cos\widetilde{\theta} & 0 & -\sin\widetilde{\theta} \\ 0 & 1 & 0 \\ \sin\widetilde{\theta} & 0 & \cos\widetilde{\theta} \end{pmatrix}.$$

Finally the fluctuation conductivity tensor $\sigma_{\alpha\beta}(\theta)$ in the initial tetragonal system with the magnetic field directed at the angle θ with respect to the c-axis can be expressed by means of the effective transformation operator $M_{\alpha\beta}$:

$$\sigma_{\alpha\beta}(\theta) = M^{T}_{\alpha\varsigma}(\widetilde{\theta})\sigma_{\varsigma\eta}(0,\widetilde{H})M_{\eta\beta}(\widetilde{\theta}),$$

with

$$M_{\alpha\beta}(\widetilde{\theta}) = (T^{-1})_{\alpha\delta}R_{\delta\kappa}T_{\kappa\beta} = \begin{pmatrix} \cos\widetilde{\theta} & 0 & -\frac{1}{\gamma}\sin\widetilde{\theta} \\ 0 & 1 & 0 \\ \gamma_a\sin\widetilde{\theta} & 0 & \cos\widetilde{\theta} \end{pmatrix}.$$

The angle $\widetilde{\theta}$ can be expressed via the renormalized magnitude of the magnetic field $\widetilde{H} = \sqrt{H_c^2 + \gamma_a^2 H_x^2}$:

$$\cos\widetilde{\theta} = \frac{\widetilde{H}_z}{\widetilde{H}} = \frac{\cos\theta}{\sqrt{\cos^2\theta + \gamma_a^2\sin^2\theta}}; \sin\widetilde{\theta} = \frac{\gamma_a\sin\theta}{\sqrt{\cos^2\theta + \gamma_a^2\sin^2\theta}}.$$

In the case of the paraconductivity of a layered superconductor with the magnetic field applied at an arbitrary angle θ the answer can be written in the general form by means of the three diagonal components of conductivity $\sigma_{ii}(0,\widetilde{H})$ in the perpendicular field $\widetilde{H}$:

$$\sigma_{\alpha\beta}(\theta) = \frac{1}{\cos^2\theta + \gamma_a^2\sin^2\theta} \times$$
$$\times \begin{pmatrix} \sigma_{xx}\cos\theta + \\ +\gamma_a^4\sigma_{zz}\sin^2\theta & 0 & \sigma_{zz}^2\gamma_a\sin^2\theta\cos\theta - \\ & & -\sigma_{xx}\sin\theta \\ 0 & \sigma_{yy}(\cos^2\theta + \gamma_a^2\sin^2\theta) & 0 \\ \sigma_{zz}^2\gamma_a\sin\theta\cos\theta & 0 & \sigma_{zz}\cos^2\theta \end{pmatrix}$$

In the simplest case of a longitudinal field $\theta = 90^0$:

$$\sigma_{\alpha\beta}(90^0, H) = \begin{pmatrix} \gamma_a^2\sigma_{zz}(0,\gamma_a H) & 0 & -\gamma_a^{-2}\sigma_{zz}(0,\gamma_a H) \\ 0 & \sigma_{yy}(0,\gamma_a H) & 0 \\ 0 & 0 & 0 \end{pmatrix}. \tag{20.125}$$

20.4 Fluctuations near superconductor-insulator transition

20.4.1 Quantum phase transition

It is usually supposed that the temperature of the superconducting transition does not depend on the concentration of non-magnetic impurities (Anderson's theorem [79, 80]). Nevertheless when the degree of disorder is very high Anderson localization takes place, and it would be difficult to expect that under conditions of strong electron localization superconductivity can exist, even if there is inter-electron attraction. This means that at $T = 0$ the phase transition takes place with a change of the disorder strength or carrier concentration. Such a transition is called a quantum phase transition since at zero temperature the classical fluctuations are

absent. Indeed, one can see from (20.7) that in the limit $T \to 0$ the thermal fluctuation Cooper pairs vanish.

In the metallic phase of a disordered system the conductivity is mostly determined by the weakly decaying fermionic excitations, their dynamics yielding the familiar Drude formula (the method which accounts for the fermionic excitations will be referred to as the Fermi approach later on). Inside the critical region the charge transfer due to fluctuation Cooper pairs turns out to be more important. In some approximation, the pairs may be considered as Bose particles. Therefore the approach dealing with the fluctuation pairs will be called below the Bose approach.

Let us suppose that at temperature $T = 0$ the superconducting state occurs in a weakly disordered system. In principle two scenarios of the development of the situation are possible with an increase of the disorder strength: the system at some critical disorder strength can go from the superconducting state to the metallic state or to the insulating state. The first scenario is natural and takes place in the following cases: if the effective constant of the inter-electron interaction changes its sign with the growth of the disorder; if the effective concentration of magnetic impurities increases together with the disorder growth; if the pairing symmetry of superconducting state is nontrivial it can be destroyed even by the weak disorder level. We will study here the second scenario where the superconductor becomes an insulator with disorder increase. This means that at some disorder degree range, higher than the localization edge when the normal phase does not exist any more at finite temperatures, superconductivity can still survive. From the first glance this statement seems strange: what does superconductivity mean if the electrons are already localized? And if it really can take place beyond the metallic phase, at what value of disorder strength and in which way does the superconductivity finally disappears?

One has to have in mind that localization is a quantum phenomenon in its nature and with the approach to the localization edge the coherence length of localization ℓ grows. From the insulator side of the transition vicinity this means the existence of large scale regions where delocalized electrons exist. If the energy level spacing in such regions does not exceed the value of superconducting gap Cooper pairs still can be formed by the delocalized electrons of this region.

The problem can be reformulated in other, already familiar, way: how does the critical temperature of the superconducting transition decrease with the increase of the disorder strength? In the previous Sections we have already tried to solve it by discussing the critical temperature fluctuation shift. We have seen that the fluctuation shift of the critical temperature is proportional to $\sqrt{Gi_{(3)}}$ for a $3D$ superconductor and to $Gi_{(2)} \ln\{1/Gi_{(2)}\}$ for $2D$. This means that the critical temperature is not changed noticeably as long as the Ginzburg-Levanyuk number remains small. So one can expect the complete suppression of superconductivity when $Gi \sim 1$ only. For further consideration it is convenient to separate the $3D$ and $2D$ cases because the physical pictures of the superconductor-insulator transition for them are quite different.

20.4.2 3D superconductors

As one can see from Table 1 in the $3D$ case the Ginzburg-Levanyuk number remains small at $p_F l \sim 1$: $Gi_{(3d)} \approx \left(\frac{T_c}{E_F}\right) \ll 1$. Nevertheless, approaching the edge of localization, the width of the fluctuation region increases [81]. In the framework of the self-consistent theory of localization [82] such growth of the width of the fluctuation region was found in paper [83].

Instead of the cited self-consistent theory let us make some more general assumptions concerning the character of the metal-insulator (M-I) transition in the absence of superconductivity [13]. We suppose that in the case of very strong disorder and not very strong Coulomb interaction the M-I transition is of second order. The role of "temperature" for this transition is

played by the "disorder strength" which is characterized by the dimensionless value $g = \frac{p_F l.}{2\pi}$ With its decrease the conductivity of the metallic phase decreases and at some critical value g_c tends to zero as

$$\sigma = e^2 p_F (g - g_c)^{\varkappa}. \tag{20.126}$$

This is the critical point of the Anderson (M-I) transition. We assume that the thermodynamic density of states remains constant at the transition point.

The electron motion in metallic phase far enough from the M-I transition has a diffusion character and the conductivity can be related to the diffusion coefficient $\mathcal{D} = p_F l/3m$ by the Einstein relation: $\sigma = \nu e^2 \mathcal{D}$. One can say that diffusion like "excitations" with the spectrum $\omega(q) = iDq^2$ propagate in the system. At the point of the M-I transition normal diffusion terminates and conductivity, together with $\mathcal{D}$, turns zero. In accordance with scaling ideas, the diffusion coefficient can be assumed here to be a power function of q: $\mathcal{D}(q) \sim q^{z-2}$, with the dynamical critical exponent $z > 2$. The anomalous diffusion excitation spectrum in this case would take the form $\omega \sim q^z$.

In the insulating phase ($g < g_c$) some local, anomalous diffusion, confined to regions of the scale ℓ, is still possible. It cannot provide charge transfer through out all the system, so $\mathcal{D}(q = 0) = 0$, but for small distances ($q \gtrsim \ell^{-1}$) anomalous diffusion takes place. Analogously, in the metallic phase ($g > g_c$) the diffusion coefficient in the vicinity of the transition has an anomalous dependence on q for $q \gtrsim \ell^{-1}$ and weakly depends on it for $q \lesssim \ell^{-1}$. So one can conclude that the diffusion coefficient for $q \gtrsim \ell^{-1}$ from both sides of the transition has the same q-dependence as for all q in the transition point. It can be written in the form

$$\mathcal{D}(q) = \frac{g}{3m}\left[\frac{\varphi(q\ell)}{p_F \ell}\right]^{z-2}, \quad \varphi(x) = \begin{cases} x, \ x \gg 1 \\ 1, \ x \ll 1, g > g_c \\ 0, \ x \ll 1, g < g_c \end{cases}, \tag{20.127}$$

where the dimensionless localization length ℓ, characterizing the spatial scale near the transition, grows with the approach to the transition point like

$$\ell(g) = \frac{1}{p_F}(g - g_c)^{-\frac{\varkappa}{z-2}}. \tag{20.128}$$

The critical exponent in this formula is found from the Einstein relation in the vicinity of the M-I transition.

At finite temperatures, instead of the critical point g_c,a crossover from metallic to insulating behavior of $\sigma(g)$ takes place. The width of the crossover region is $\widetilde{g} - g_c$,where $\widetilde{g}$ is determined from the relation $\mathcal{D}\ell^{-2}(\widetilde{g}) \sim E_F[p_F \ell(\widetilde{g})]^{-z} \sim T$ (we have used the second asymptotic of (20.127)). In this region the diffusion coefficient is

$$\mathcal{D}(T) \sim T\ell^2 \sim \frac{T}{p_F^2}\left(\frac{E_F}{T}\right)^{\frac{2}{z}} \tag{20.129}$$

and it depends weakly on the $g - g_c$. Beyond this region the picture of the transition remains the same as at $T = 0$.

Let us consider now what happens to superconductivity in the vicinity of the localization transition. In the mean field approximation (BCS) the thermodynamic properties of a superconductor do not depend on the character of the diffusion of excitations. This should be contrasted with the fluctuation theory, where such a dependence clearly exists. We will show that the type of superconducting transition depends on the dynamical exponent z. If $z > 3$, the transition to superconductivity occurs on the metallic side of the localization transition (we will refer to such a transition as S-N transition). If $z < 3$, the transition to superconductivity occurs from the insulating state directly (S-I transition).

Let us study how the superconducting fluctuations affect the transition under discussion. In spirit of the GL approach fluctuation phenomena in the vicinity of the transition can be described in the framework of the GL functional (20.26). The coherence length in the metallic region, far enough from the Anderson transition, was reported in Introduction to be equal $\xi^2 = \xi_c l = 0.42\mathcal{D}/T$. In the vicinity of the M-I transition we still believe in the diffusive character of the electron motion resulting in the pair formation. The only difference from the previous consideration is the anomalous character of the quasiparticle diffusion. So in order to describe the superconducting fluctuations simultaneously near superconducting (in temperature) and Anderson (in g) transitions let us use the GL functional (20.26) with the k-dependent diffusion coefficient (20.127).

The value of Gi can be estimated from the expression for the fluctuation contribution to heat capacity (20.30) taken at $\epsilon \sim Gi$, where the fluctuation correction reaches the value of the heat capacity jump:

$$1 \sim \frac{T}{\nu}\int \frac{d^3q}{\left(TGi + \mathcal{D}(q)q^2\right)^2}, \tag{20.130}$$

with $T \simeq T_c$. Let us approach the M-I transition from the metallic side. If we are far enough from transition, Gi is small and the integral in (20.130) is determined by the region of small momenta $\mathcal{D}(q)q^2 \lesssim TGi$:

$$Gi \sim \frac{T}{\nu^2\mathcal{D}^3(q=0)}. \tag{20.131}$$

Two scenarios are possible: Gi becomes of the order of 1 in the metallic phase, or it remains small up to the crossover region, where finally reaches its saturation value. In the first case we can use the second asymptotic of (20.127) for $D(q)$ and find:

$$Gi \sim \frac{T_c}{E_F}(p_F\ell)^{3z-6}. \tag{20.132}$$

One can see that Gi becomes of the order of 1 at $p_F\ell_M \sim (E_F/T)^{\frac{1}{3z-6}}$. Comparing this value with $p_F\ell(\widetilde{g}) \sim (E_F/T)^{1/z}$ at the limit of the crossover region we see that for $z > 3$ the first scenario is realized. Concluding the first scenario discussion we see that the superconducting critical temperature goes to zero at $\ell = \ell_M$, still in the metallic phase, so at $T = 0$ a superconductor-normal phase (S-N) type quantum phase transition takes place.

The second scenario takes place for $z < 3$ when Gi remains small even at the edge of crossover region, reaching there the value

$$Gi \sim \left(\frac{T_c}{E_F}\right)^{\frac{2(3-z)}{z}} \ll 1. \tag{20.133}$$

In the crossover region the diffusion coefficient, and hence Gi, almost do not vary. This is why the temperature of superconducting transition remains almost frozen with further increase of disorder driving the system through the Anderson transition. The abrupt growth of Gi and decrease of T_c take place when the system finally goes from the crossover to the insulating region. In the insulator phase the diffusion coefficient $D(q \lesssim l^{-1}) = 0$ and from (20.130) one can find for Gi :

$$Gi \sim \sqrt{\frac{E_F}{T_c}}\frac{1}{(p_F\ell)^{3/2}} \tag{20.134}$$

Comparing this result with the Table 1 it is easy to see that it coincides with the Ginzburg-Levanyuk number for a zero-dimensional granule of size $\ell \ll \xi(T)$. Hence we see that in the

Figure 20.5: Phase diagram in the temperature – disorder plane for a three-dimensional superconductor.

second scenario the Ginzburg number reaches 1 and, respectively, $T_c \to 0$ at $p_F \ell_I \sim \left(\frac{E_F}{T_c}\right)^{1/3}$, which is far enough from the M-I transition point. This is why in this case one can speak about the realization at $T = 0$ of a superconductor-insulator (S-I) type quantum phase transition. The scale ℓ_I determines the size of the "conducting" domains in the insulating phase, where the level spacing reaches the order of the superconducting gap. It is evident that in the domain of scale $\ell \lesssim \ell_I$ superconductivity cannot be realized.

In the vicinity of a quantum phase transition one can expect the appearance of non monotonic dependencies of the resistance on temperature and magnetic field. Indeed, starting from the zero resistance superconducting phase and increasing temperature from $T = 0$, the system passes through the localization region, where the resistance is high, to high temperatures where some hopping charge transfer will decrease the resistance again. The analogous speculations are applicable to the magnetic field effect: first the magnetic field "kills" superconductivity and increases the resistance, then it destroys localization and decreases it.

The phase diagram in the (T, g) plane has the form sketched in Fig. 20.5. For $g_I = g_c - (T_c/E_F)^{3(z-2)/\varkappa}$, an S-I transition takes place at $T = 0$. Increasing the temperature from $T = 0$ in the region $0 \lesssim g \lesssim g_I$ we remain in the insulating phase with exponential dependence of resistance on temperature. For $g_I \lesssim g \lesssim \widetilde{g}_-$ at low temperatures $0 \le T < T_c(g)$ the system stays in the superconducting state which goes to the insulating phase at higher temperatures. In the vicinity of the Anderson transition ($\widetilde{g}_- \lesssim g \lesssim \widetilde{g}_+$) the superconducting state goes with growth of the temperature to some crossover metal-insulator state which is characterized by a power decrease of the resistivity with the increase of temperature. Finally at $g_c \lesssim g$ the superconducting phase becomes of the BCS type and at $T = T_c$ it goes to a metallic phase.

The phase diagram in the magnetic field – disorder plane is similar to that in the (T, g) plane

with the only difference that at $T = 0$ there is no crossover region, instead a phase transition takes place.

20.4.3 2D superconductors

Preliminaries.

As was demonstrated in Section 4, according to the conventional theory of paraconductivity, the sheet conductivity in the vicinity of the superconducting transition is given by a sum of the electron residual conductivity ge^2 (Fermi part) and the conductivity of the Cooper pair fluctuations (Bose part) (see (20.99)). This expression is valid in the Ginzburg Landau region when the second term is a small correction to the first one. The width of the critical region can be determined from the requirement of equality of both contributions in (20.99)[19]:

$$\epsilon_{cr} = \frac{1}{16g} = 1.3Gi_{(2d)}. \tag{20.135}$$

In accordance with general scaling ideas one can believe that inside the fluctuation region the conductivity should obey the form:

$$\sigma(T) = ge^2 f\left(\frac{\epsilon}{Gi_{(2d)}}\right). \tag{20.136}$$

Concerning the scaling function $f(x)$, we know its asymptotes in the mean field region ($x \gg 1$) and just above the BKT transition [56, 57]:

$$f(x) = \begin{cases} 1 + x^{-1}, & x \gg 1 \\ \exp\left[-b(x - x_{\rm BKT})^{-1/2})\right], & x \to x_{\rm BKT} = -4 \end{cases}. \tag{20.137}$$

The BKT transition temperature $T_c^{\rm BKT}$ is determined by

$$n_{s2}(T_c) = \frac{4mT_c}{\pi}. \tag{20.138}$$

and one can find its value by comparing the superfluid density n_s from (20.138) with that found in the BCS scheme:

$$T_c^{\rm BKT} = T_{c0}(1 - 4Gi). \tag{20.139}$$

Here we assumed that the Ginzburg parameter is small, so that the BKT transition temperature does not deviate much from the mean-field BCS transition temperature T_{c0}.

Boson mechanism of the T_c suppression.

The classical and quantum fluctuations reduce n_s and therefore, suppress $T_c^{\rm BKT}$. At some $g = g_c \sim 1$, the superfluid density n_s, and simultaneously $T_c^{\rm BKT}$, go to zero. In the vicinity of this critical concentration of impurities $T_c^{\rm BKT} \ll T_{c0}$. Thus a wide new window of intermediate temperatures $T_c^{\rm BKT} \ll T \ll T_{c0}$ opens up. In this window, according the dynamical quantum scaling conjecture [84], one finds

$$\sigma = e^2\varphi\left(\frac{T}{T_c^{BKT}}\right). \tag{20.140}$$

At $T - T_c^{\rm BKT} \ll T_c^{\rm BKT}$ the Berezinski-Kosterlitz-Thouless law (20.136)-(20.137) should hold, so $\varphi(x) = f(x)$ and is exponentially small. In the intermediate region $T_c^{\rm BKT} \ll T \ll T_c^{\rm BCS}$ the duality hypothesis gives $\varphi(x) = \pi/2$. Let us derive this relation.

[19] It is worth mentioning that this definition of the Ginzburg Levanyuk number ($\widetilde{Gi}_{(2d)} = \frac{\pi}{8p_F l}$) agrees with that defined from the heat capacity fluctuations ($Gi_{(2d)} = \frac{0.3}{p_F l}$).

We will start from the assumption that in the region $T_c^{\rm BKT} \ll T \ll T_{c0}$ the conductivity is a universal function of temperature which does not depend on the pair interaction type. Being in the framework of the classical approach, let us suppose that in a weak electric field pairs move with the velocity $\mathbf{v} = \mathbf{F}/\eta$, where $\mathbf{F} = 2e\mathbf{E}$ is the force acting on the pairs. The current density $\mathbf{j} = 2en\mathbf{v} = \sigma\mathbf{E}$, (here n is the pair density), so one can relate the conductivity with the effective viscosity η: $\sigma = 4e^2 n/\eta$.

Let us recall that we are dealing with a quantum fluid, so another, superconducting, view on the problem of its motion near the quantum phase transition exists. One can say that with the increase of Gi the role of quantum fluctuations grows too and fluctuation vortices carrying the magnetic flux quantum $\Phi_0 = \pi/e$ are generated. With electric current flow in the system the Lorentz (Magnus) force acts on a vortex: $F = j\Phi_0$. The electric field is equal to the rate of magnetic flux transfer, i.e. to the density of the vortex current: $\mathbf{E} = \Phi_0 n_v \mathbf{v}_v = \Phi_0 n_v \mathbf{F}/\eta_{\mathbf{v}}$, where n_v is the density and η_v is the viscosity of the vortex liquid. As a result $\mathbf{E} = \Phi_0^2 n_v \mathbf{j}/\eta_{\mathbf{v}} = \mathbf{j}/\sigma$. So one can conclude that for vortices the velocity is proportional to the voltage, and the force is proportional to the current. For Cooper pairs (bosons) the situation is exactly the opposite.

The duality hypothesis consists in the assumption that at the critical point the pair and the vortex liquid density flows are equal: $n_v \mathbf{v}_v = n\mathbf{v}$. Comparing these quantities, expressed in terms of the conductivity from the above relations, one can find a universal value for the conductivity at the critical point

$$\sigma = \frac{2e}{\Phi_0} = \frac{2e^2}{\pi}. \tag{20.141}$$

One can restrict oneself to a less strong duality hypothesis, supposing the product $n\eta = CT^\delta$ with a universal δ exponent both for the pair and the vortex liquids, while the constant C for them is different. In this case, based on duality, is possible to demonstrate that $\delta = 0$ and the conductivity is temperature independent up to T_{c0} but its value is not universal any more and can vary from one sample to another.

To conclude, let us emphasize that in the framework of the boson scenario of superconductivity suppression, the BCS critical temperature is changed insignificantly, while the "real" superconducting transition temperature $T_c^{\rm BKT} \to 0$.

Fermion mechanism of T_c suppression.

Apart from the above fluctuation (boson) mechanism of the suppression of the critical temperature in the $2D$ case, there exists another, fermionic mechanism. The suppressed electron diffusion results in a poor dynamical screening of the Coulomb repulsion which, in turn, leads to the renormalization of the inter-electron interaction in the Cooper channel. and hence to the dependence of the critical temperature on the value of the high-temperature sheet resistivity of the film. As long as the correction to the non-renormalized BCS transition temperature T_{c0} is still small, one finds [85, 86, 87]:

$$T_c = T_{c0}\left(1 - \frac{1}{12\pi^2 g}\ln^3\frac{1}{T_{c0}\tau}\right). \tag{20.142}$$

At small enough T_{c0} this mechanism of critical temperature suppression turns out to be the principal one. The suppression of T_c down to zero in this case may happen in principle even at $g \gg 1$. A renormalization group analysis gives [88] the corresponding critical value of conductance

$$g_c = \left(\frac{1}{2\pi}\ln\frac{1}{T_{c0}\tau}\right)^2. \tag{20.143}$$

Here we should recall that the typical experimental [89] values of g_c are in the region $g_c \sim 1-2$, and do not differ dramatically from the predictions of the boson duality assumption

$g_c = \frac{2}{\pi}$. If one attempts to explain the suppression of T_c within the fermion mechanism, one should assume that $\ln \frac{1}{T_{c0}\tau} > 5$. Then, according to Eq. (20.143), $g_c > 2/\pi$ and the boson mechanism is not important. On the contrary, if $\ln \frac{1}{T_{c0}\tau} < 4$, then Eq. (20.142) gives a small correction for T_c even for $g_c = 2/\pi$ and the fermion mechanism becomes unimportant. The smallness of the critical temperature T_c compared to the Fermi energy is the cornerstone of the BCS theory of superconductivity and it is apparently satisfied even in high-T_c materials. Nevertheless it is necessary to use the theoretically large logarithmic parameter with care, if one needs $\ln \frac{1}{T_{c0}\tau}$ to be as large as 4.

20.5 Microscopic derivation of the Time-Dependent Ginzburg-Landau equation

20.5.1 Preliminaries

We have seen above how the phenomenological approach based on the GL functional allows one to describe fluctuation Cooper pairs (Bose particles) near the superconducting transition and to account for their contribution to different thermodynamical and transport characteristics of the system. Now we pass to the discussion of the microscopic description of fluctuation phenomena in superconductors. The development of the microscopic approach is necessary for the following reasons:

1. This description permits microscopic determination of the values of the phenomenological parameters of the GL theory.

2. This method is more powerful than the phenomenological GL approach and permits treatment of fluctuation effects quantitatively even far from the transition point and for magnetic fields strong as H_{c2}, taking into account the contributions of dynamical and short wavelength fluctuations.

3. The electron energy relaxation times in metals are relatively large ($\tau_\varepsilon \gg \hbar/T$) which causes the electron low frequency dynamics to be sensitive to the nearness to the superconducting transition. This is why the temperature dependence of fluctuation corrections can be determined generally speaking not only by the Cooper pair motion but also by changes in the single-electron properties.

4. There are some fluctuation phenomena in which the direct Cooper pair contribution is considerably suppressed or even absent altogether. Among them we can mention the nuclear magnetic relaxation rate, tunnel conductivity, c-axis transport in strongly anisotropic layered metals, thermoelectric power and heat conductivity where the fluctuation pairing manifests itself by means of the indirect influence on the properties of the single-particle states of electron system.

Formally in the above consideration averaging over the superconducting order parameter has been accomplished by means of a functional integration over all its possible bosonic field configurations. In this description we have dealt with the fluctuation Cooper pair related effects only and the method of the functional integration turned out to be simple and effective for their description. In the following Sections we will develop the diagrammatic method of Matsubara temperature Green functions which is more adequate for the description of the properties of a Fermi system of interacting electrons.

20.5.2 The Cooper channel of electron-electron interaction

Let us start the microscopic description of fluctuation phenomena in a superconductor from the electron Hamiltonian. We will choose it in the simple BCS form[20]:

$$\mathcal{H} = \sum_{\mathbf{p},\sigma} E(\mathbf{p}) \widetilde{\psi}^{+}_{\mathbf{p},\sigma} \widetilde{\psi}_{\mathbf{p},\sigma} + g \sum_{\mathbf{p},\mathbf{p}',\mathbf{q},\sigma,\sigma'} \widetilde{\psi}^{+}_{\mathbf{p}+\mathbf{q},\sigma} \widetilde{\psi}^{+}_{-\mathbf{p},-\sigma} \widetilde{\psi}_{-\mathbf{p}',-\sigma'} \widetilde{\psi}_{\mathbf{p}'+\mathbf{q},\sigma'}. \tag{20.144}$$

The momentum conservation law side by side with singlet pairing are already taken into account in the interaction term. Here $E(\mathbf{p})$ is the quasiparticle spectrum of the normal metal; g is the negative constant of electron-electron attraction which is supposed to be momentum independent and different from zero in a narrow domain of momentum space in the vicinity of the Fermi surface where

$$p_F - \frac{\omega_D}{v_F} < |\mathbf{p}|, |\mathbf{p}'| < p_F + \frac{\omega_D}{v_F}.$$

$\widetilde{\psi}^{+}_{\mathbf{p},\sigma}$ and $\widetilde{\psi}_{\mathbf{p},\sigma}$ are the creation and annihilation field operators in the Heisenberg representation, so the first term is just the kinetic energy of the non-interacting Fermi gas. The interaction term is chosen in the traditional form characteristic for the electron-phonon mechanism of superconductivity[21].

For the description of the properties of an interacting electron system with the Hamiltonian (20.144) we will use the formalism of the Matsubara temperature diagrammatic technique. The state of a non-interacting quasiparticle is described by its Green function

$$G(\mathbf{p}, \varepsilon_n) = \frac{1}{i\varepsilon_n - \xi(\mathbf{p})}, \tag{20.145}$$

where $\varepsilon_n = (2n+1)\pi T$ is a fermion Matsubara frequency and $\xi(\mathbf{p}) = E(\mathbf{p}) - E_F$ is the quasiparticle energy measured from the Fermi level.

As it is well known the effective electron-electron attraction leads to a reconstruction of the ground state of the electron system which formally manifests itself by the appearance at the critical temperature of a pole in the two particle Green function

$$\mathcal{L}(p, p', q) = < T_\tau [\widetilde{\psi}_{p+q,\sigma} \widetilde{\psi}_{-p,-\sigma} \widetilde{\psi}^{+}_{p'+q,\sigma'} \widetilde{\psi}^{+}_{-p',-\sigma'}] >,$$

where T_τ is the time ordering operator and $4D$ vector notations are used [92]. As it well known the two particle Green function can be expressed in terms of the vertex part [92]. In the case under consideration it is the vertex part of the electron-electron interaction in the Cooper channel $L(\mathbf{q}, \Omega_k)$, which will be called below the fluctuation propagator**.** The Dyson equation for $L(\mathbf{q}, \Omega_k)$, accounting for the e-e attraction in the ladder approximation, is represented graphically in Fig.20.6. It can be written down analytically as

$$L^{-1}(\mathbf{q}, \Omega_k) = g^{-1} - \Pi(\mathbf{q}, \Omega_k), \tag{20.146}$$

where the polarization operator $\Pi(\mathbf{q}, \Omega_k)$ is defined as a loop of two single-particle Green functions:

[20] We suppose that reader is familiar with the BCS formulation of the theory of superconductivity (see for example, [92]).

[21] Fluctuations in the framework of more realistic Eliashberg [90] model of superconductivity were studied by B.Narozhny [91]. He demonstrated that the strong coupling does not change drastically the results of the weak coupling approximation. The critical exponents turn out to be exactly the same as in the framework of the GL theory, which provides an adequate description of paraconductivity in strong coupling superconductors. The robustness of the critical exponents and their dependence in GL region on the space dimensionallity only was stressed in [83] in relation to the discussion of the paraconductivity at the edge of the superconductor-insulator transition.

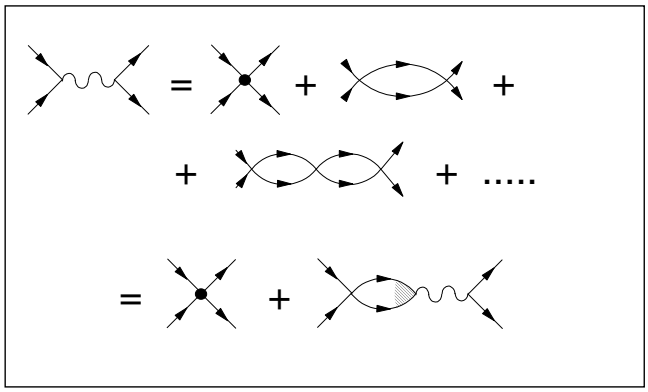


Figure 20.6: The Dyson equation for the fluctuation propagator (wavy line) in the ladder approximation. Solid lines represent one-electron Green functions, bold points correspond to the model electron-electron interaction.

$$\Pi(\mathbf{q},\Omega_k) = T\sum_{\varepsilon_n}\int \frac{d^3\mathbf{p}}{(2\pi)^3} G(\mathbf{p}+\mathbf{q},\varepsilon_{n+k})G(-\mathbf{p},\varepsilon_{-n}). \tag{20.147}$$

Let us emphasize, that the two quantities introduced above, $\mathcal{L}(p,p',q)$ and $L(q)$, are closely connected with each other. The former being integrated over momenta p and p' becomes an average of the product of two order parameters:

$$\int dpdp'\mathcal{L}(p,p',q) = \frac{1}{g^2}\left\langle \Delta_q\Delta_q^*\right\rangle, \tag{20.148}$$

where Δ_q is the superconducting gap proportional to the condensate wave function Ψ. Thus, this quantity represents the coefficient in the linear term in the GL equation. In terms of the polarization operator introduced above it can be written as

$$\int dpdp'\mathcal{L}(p,p',q) \propto \frac{\Pi}{1-g\Pi}.$$

Comparing this equation with Eq.(20.146) for the fluctuation propagator we see that the corresponding expressions are very similar. After analytical continuation to the real frequencies the fluctuation propagator $L(q,i\Omega)$ coincides with the quantity defined by Eq.(20.148) (up to a constant).

One can calculate the propagator (20.146) using the one-electron Green functions of the normal metal (20.145). For sake of convenience of future calculations let us define the correlator of two one-electron Green functions

$$\begin{aligned}\mathcal{P}(\mathbf{q},\varepsilon_1,\varepsilon_2) &= \int \frac{d^3\mathbf{p}}{(2\pi)^3} G(\mathbf{p}+\mathbf{q},\varepsilon_1)G(-\mathbf{p},\varepsilon_2) = \\ &= 2\pi\nu\Theta(-\varepsilon_1\varepsilon_2)\left\langle \frac{1}{|\varepsilon_1-\varepsilon_2| + i\Delta\xi(\mathbf{q},\mathbf{p})|_{\epsilon(\mathbf{p})=E_F}}\right\rangle_{F.S.},\end{aligned} \tag{20.149}$$

where $\Theta(-\varepsilon_1\varepsilon_2)$ is Heavyside step function, ν is the one-electron density of states, $<>_{F.S.}=\int\frac{d\Omega_{\mathbf{p}}}{4\pi}$ means the averaging over the Fermi surface,

$$\Delta\xi(\mathbf{q},\mathbf{p})|_{\epsilon(\mathbf{p})=E_F} = [\xi(\mathbf{q}+\mathbf{p})-\xi(-\mathbf{p})]|_{\epsilon(\mathbf{p})=E_F} \approx (\mathbf{v_p q})_{\xi(\mathbf{p})=0}.$$

The last approximation is valid not too far from the Fermi surface, i.e. when $(\mathbf{v_p q})_{\xi(\mathbf{p})=0} \ll E_F$.

It is impossible to carry out the angular averaging in (20.149) for a general anisotropic spectrum. Nevertheless in the following calculations of fluctuation effects in the vicinity of critical temperature only small momenta $\mathbf{v_p q} \ll T$ will be involved in the integrations, so we can restrict our consideration here to this region, where one can expand the integrand in powers of $\mathbf{v_p q}$. Indeed, the presence of $\Theta(-\varepsilon_1\varepsilon_2)$ leaves the difference of the two fermionic frequencies in (20.149) to be of the order of the temperature which permits this expansion. The first term in $\mathbf{v_p q}$ will evidently be averaged out, so with quadratic accuracy one can find:

$$\mathcal{P}(\mathbf{q},\varepsilon_1,\varepsilon_2) = 2\pi\nu\frac{\Theta(-\varepsilon_1\varepsilon_2)}{|\varepsilon_1-\varepsilon_2|}\left(1-2\frac{\langle(\mathbf{v_p q})^2\rangle_{F.S.}}{|\varepsilon_1-\varepsilon_2|^2}\right). \tag{20.150}$$

Now one can calculate the polarization operator

$$\begin{aligned}\Pi(\mathbf{q},\Omega_k) &= T\sum_{\varepsilon_n}\mathcal{P}(\mathbf{q},\varepsilon_{n+k},\varepsilon_{-n}) = \\ &= \nu\left[\sum_{n\geq 0}\frac{1}{n+1/2+\frac{|\Omega_k|}{4\pi T}} - 2\frac{\langle(\mathbf{v_p q})^2\rangle_{F.S.}}{(4\pi T)^2}\sum_{n=0}^{\infty}\frac{1}{\left(n+1/2+\frac{|\Omega_k|}{4\pi T}\right)^3}\right].\end{aligned} \tag{20.151}$$

The calculation of the sums in (20.151) can be carried out in terms of the logarithmic derivatives of the Γ-function $\psi^{(n)}(x)$. It worth mentioning that the first sum is well known in the BCS theory, one can recognize in it the so-called "Cooper logarithm"; its logarithmic divergence at the upper limit ($\psi(x\gg 1)\approx \ln x$) is cut off by the Debye energy ($N_{\max} = \frac{\omega_D}{2\pi T}$) and one gets:

$$\begin{aligned}\frac{1}{\nu}\Pi(\mathbf{q},\Omega_k) &= \psi\left(\frac{1}{2}+\frac{|\Omega_k|}{4\pi T}+\frac{\omega_D}{2\pi T}\right)-\psi\left(\frac{1}{2}+\frac{|\Omega_k|}{4\pi T}\right)- \\ &\quad -\frac{\langle(\mathbf{v_p q})^2\rangle_{F.S.}}{(4\pi T)^2}\psi''\left(\frac{1}{2}+\frac{|\Omega_k|}{4\pi T}\right).\end{aligned} \tag{20.152}$$

The critical temperature in the BCS theory is determined as the temperature T_c at which the pole of $L(0,0,T_c)$ occurs

$$L^{-1}(\mathbf{q}=0,\Omega_k=0,T_c) = g^{-1}-\Pi(0,0,T_c) = 0,$$

$$T_c = \frac{2\gamma_E}{\pi}\omega_D\exp\left(-\frac{1}{\nu g}\right), \tag{20.153}$$

where $\gamma_E = 1.78$ is the Euler constant. Introducing the reduced temperature $\epsilon = \ln(\frac{T}{T_c})$ one can write the propagator as

$$L^{-1}(\mathbf{q},\Omega_k) = -\nu\left[\epsilon+\psi(\frac{1}{2}+\frac{|\Omega_k|}{4\pi T})-\psi(\frac{1}{2})-\frac{\langle(\mathbf{v_p q})^2\rangle_{F.S.}}{(4\pi T)^2}\psi''\left(\frac{1}{2}+\frac{|\Omega_k|}{4\pi T}\right)\right]. \tag{20.154}$$

We found (20.154) for bosonic imaginary Matsubara frequencies $i\Omega_k = 2\pi i T k$. These frequencies are necessary for the calculation of fluctuation contributions to any thermodynamical characteristics of the system.

In the vicinity of the transition point one can restrict oneself in summations of the expressions with $L(\mathbf{q},\Omega_k)$ over Matsubara frequencies to the so-called static approximation, taking into account the term with $\Omega_k = 0$ only, which turns out to be the most singular term in $\epsilon \ll 1$. This approximation physically means that the product of Heisenberg field operators

$\widetilde{\psi}_{p,\sigma}\widetilde{\psi}_{-p,-\sigma}$ appears here like a classical field Ψ, which in the phenomenological approach describes the Cooper pair wave function and in the vicinity of critical temperature is proportional to the fluctuation order parameter. Having in mind namely this GL region of temperatures we restricted ourselves above by the assumption of small momenta $\mathbf{v_p q} \ll T$. In these conditions the static propagator reduces to

$$L(\mathbf{q},0) = -\frac{1}{\nu}\frac{1}{\epsilon + \xi^2\mathbf{q}^2}. \tag{20.155}$$

With an accuracy of a numerical factor and the total sign this correlator coincides with the expression for $\langle|\Psi_{\mathbf{q}}|^2\rangle$. By this expression we also have finally obtained the microscopic value of the coherence length ξ for a clean superconductor with an isotropic D-dimensional Fermi surface which was often mentioned previously (compare with (20.5))

$$\xi^2_{(D)} = \frac{7\zeta(3)\mathbf{v}_\mathbf{F}^2}{16D\pi^2T^2}.. \tag{20.156}$$

In order to describe the fluctuation contributions to transport phenomena one has to start from the analytical continuation of the propagator (20.154) from the discrete set of $\Omega_k \geq 0$ to the whole upper half-plane of imaginary frequencies. The analytical properties of $\psi^{(n)}(x)-$functions (which have poles at $x = 0, -1, -2...$) permit one to obtain the retarded propagator $L^R(\mathbf{q}, -i\Omega)$ by simple substitution $i\Omega_k \to \Omega$. For small $\Omega \ll T$ the $\psi-$functions can be expanded in $-i\Omega/4\pi T$ and the propagator acquires the simple pole form:

$$L^R(\mathbf{q},\Omega) = -\frac{1}{\nu}\frac{1}{-\frac{i\pi}{8T}\Omega + \epsilon + \xi^2\mathbf{q}^2} = \frac{8T}{\pi\nu}\frac{1}{i\Omega - \left(\tau_{GL}^{-1} + \frac{8T}{\pi}\xi^2\mathbf{q}^2\right)}. \tag{20.157}$$

This expression provides us with the microscopic value of the GL relaxation time $\tau_{GL} = \frac{\pi}{8(T-T_c)}$, widely used above in the phenomenological theory. Moreover, comparison of the microscopically derived (20.157) with the phenomenological expressions (20.85), (20.89) and (20.106) shows that $\alpha T_c = \nu$ and $\gamma_{GL} = \pi\nu/8T_c$.

In evaluating $L(\mathbf{q}, \Omega_k)$ we neglected the effect of fluctuations on the one-electron Green functions. This is correct when fluctuations are small, i.e. not too near to the transition temperature. The exact criterion of this approximation will be discussed in the following.

20.5.3 Superconductor with impurities

Account for impurities.

In order to study fluctuations in real systems like superconducting alloys or high temperature superconductors one has to perform an impurity average in the graphical equation for the fluctuation propagator (see Fig. 20.6). This procedure can be done in the framework of the Abrikosov-Gorkov approach [92], which we shortly recall below.

Let us start from the equation for the electron Green function in the potential of impurities $U(\mathbf{r})$:

$$\left(E - U(\mathbf{r}) - \widehat{H}\right) G_E(\mathbf{r},\mathbf{r}') = \delta(\mathbf{r}-\mathbf{r}') \tag{20.158}$$

If we solve this equation using the perturbation theory for the impurity potential and average the solution, then the average product of two Green functions, can be presented as series, each term of which is associated with a graph drawn according the rules of diagrammatic technique (see Fig. 20.7). In this technique solid lines correspond to bare Green functions and dashed lines to random potential correlators. We assume that the impurity system random potential

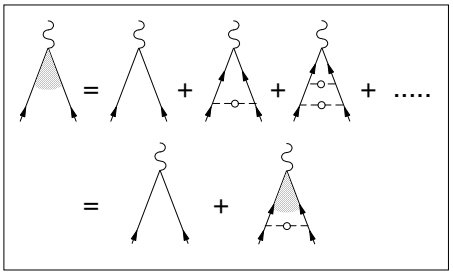


Figure 20.7: The equation for the vertex part $\lambda(q, \omega_1, \omega_2)$ in the ladder approximation. Solid lines correspond to bare one-electron Green functions and dashed lines to the impurity random potential correlators.

$U(r)$ is distributed according to the Gauss $\delta-$correlated law. Then all the correlators can be represented as the products of pair correlators

$$\langle U(r)\rangle = 0,\ \langle U(r)U(r')\rangle = \left\langle U^2\right\rangle \delta(r-r'), \tag{20.159}$$

where the angle brackets denote averaging over the impurity configuration. Equation 20.159 corresponds to the Born approximation for the electron interaction with short range impurities, and $\langle U^2\rangle = C_{imp}\left(\int V(\mathbf{r})d\mathbf{r}\right)^2$ where C_{imp} is the impurity concentration and $V(\mathbf{r})$ is the potential of the single impurity.

In conductors (far enough from the metal-insulator transition) the mean free path is much greater than the electron wavelength $l \gg \lambda = 2\pi/p_F$ (which in practice means the mean free path up to tens of interatomic distances). As is well known [92] for the electron spectra with dimensionality $D > 1$ the angular integration in momentum space reduces considerably the contribution of the diagrams with intersecting impurity lines what permits to omit them to the leading approximation in $(p_F l)^{-1}$. In this approximation the one-electron Green function keeps the same form as the bare one (20.145) with the only substitution

$$\varepsilon_n \Rightarrow \widetilde{\varepsilon}_n = \varepsilon_n + \frac{1}{2\tau} sign(\varepsilon_n), \tag{20.160}$$

where $1/\tau = 2\pi\nu\left\langle U^2\right\rangle$ is the frequency of elastic collisions.

Another effect of the coherent scattering on the same impurity by both electrons forming a Cooper pair is the renormalization of the vertex part $\lambda(\mathbf{q}, \varepsilon_1, \varepsilon_2)$ in the particle-particle channel. Let us demonstrate the details of its calculation. The renormalized vertex $\lambda(\mathbf{q}, \varepsilon_1, \varepsilon_2)$ is determined by a graphical equation of the ladder type (see Fig. 20.7). Here after the averaging over the impurity configurations the value $\langle U^2\rangle = \frac{1}{2\pi\nu\tau}$ is associated with the dashed line. In the momentum representation this, generally speaking, integral equation is reduced to the algebraic one

$$\lambda^{-1}(\mathbf{q}, \varepsilon_1, \varepsilon_2) = 1 - \frac{1}{2\pi\nu\tau}\mathcal{P}(\mathbf{q}, \widetilde{\varepsilon}_1, \widetilde{\varepsilon}_2), \tag{20.161}$$

where $\mathcal{P}(\mathbf{q}, \widetilde{\varepsilon}_1, \widetilde{\varepsilon}_2)$ was defined above by (20.149).

Now one has to perform a formal averaging of the general expression (20.149) over the Fermi surface ($\langle ...\rangle_{F.S.}$). Restricting consideration to small momenta

$$\Delta\xi(\mathbf{q}, \mathbf{p})|_{|\mathbf{p}|=p_F} \ll |\widetilde{\varepsilon}_1 - \widetilde{\varepsilon}_2|. \tag{20.162}$$

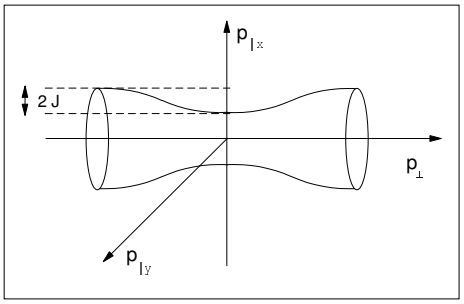


Figure 20.8: The Fermi surface in the form of a corrugated cylinder

the calculation of $\lambda(\mathbf{q},\omega_1,\omega_2)$ for the practically important case of an arbitrary spectrum can be done analogously to (20.150). Indeed, expanding the denominator of (20.149) one can find

$$\lambda(\mathbf{q},\omega_1,\omega_2)=\frac{|\widetilde{\varepsilon}_1-\widetilde{\varepsilon}_2|}{|\varepsilon_1-\varepsilon_2|+\frac{\langle(\Delta\xi(\mathbf{q},\mathbf{p})|_{|\mathbf{p}|=p_F})^2\rangle_{F.S.}}{\tau|\tilde{\omega}_1-\tilde{\omega}_2|^2}\Theta(-\varepsilon_1\varepsilon_2)}. \tag{20.163}$$

It is easy to see that assumed restriction on momenta is not too severe and is almost always satisfied in calculations of fluctuation effects at temperatures near T_c. In this region of temperatures the effective propagator momenta are determined by $|\mathbf{q}|_{eff}\sim[\xi^{GL}(T)]^{-1}=\xi^{-1}\sqrt{\epsilon}\ll\xi^{-1}$, while the Green function $\mathbf{q}$-dependence becomes important for much larger momenta $q\sim\min\{\xi^{-1},l^{-1}\}$, which is equivalent to the limit of the condition (20.162).

The average in (20.163) can be calculated for some particular types of spectra. For example in the cases of $2D$ and $3D$ isotropic spectra it is expressed in terms of the diffusion coefficient $\mathcal{D}_{(D)}$:

$$\langle(\Delta\xi(\mathbf{q},\mathbf{p})|_{|\vec{p}|=p_F})^2\rangle_{F.S.(D)}=\tau^{-1}\mathcal{D}_{(D)}q^2=\frac{v_F^2q^2}{D}. \tag{20.164}$$

Another important example is already familiar case of quasi-two-dimensional electron motion in a layered metal:

$$\xi(\mathbf{p})=E(\mathbf{p}_\parallel)+J\cos(p_zs)-E_F, \tag{20.165}$$

where $E(\mathbf{p}_\parallel)=\mathbf{p}_\parallel^2/(2m)$, $\mathbf{p}\equiv(\mathbf{p}_\parallel,p_z)$, $\mathbf{p}_\parallel\equiv(p_x,p_y)$, J is the effective nearest-neighbor interlayer hopping energy for quasiparticles. We note that J characterizes the width of the band in the c-axis direction taken in the strong-coupling approximation and can be identified with the effective energy of electron tunneling between planes (see (20.62) and footnote 14). The Fermi surface, defined by the condition $\xi(\mathbf{p})=0$, is a corrugated cylinder (see Fig. 20.8). In this case the average (20.164) is written in a more sophisticated form:

$$\langle(\Delta\xi(\mathbf{q},\mathbf{p})|_{|\vec{p}|=p_F})^2\rangle_{F.S.}=\frac{1}{2}(v_F^2\mathbf{q}^2+4J^2\sin^2(q_zs/2))=\tau^{-1}\widehat{\mathcal{D}}q^2, \tag{20.166}$$

where we have introduced the definition of the generalized diffusion operator $\widehat{\mathcal{D}}$ in order to deal with an arbitrary anisotropic spectrum.

Propagator.

In Section 4, in the process of the microscopic derivation of the TDGL equation, the fluctuation propagator was introduced. This object is of first importance for the microscopic fluctuation theory and it has to be generalized for the case of an impure metal with an anisotropic

electron spectrum. This is easy to do using the averaging procedure presented in the previous Section. Formally it is enough to use in equation (20.146) the polarization operator $\Pi(\mathbf{q},\Omega_k)$ averaged over impurity positions, which can be expressed in terms of $\mathcal{P}(\mathbf{q},\widetilde{\varepsilon}_{n+k},\widetilde{\varepsilon}_{-n})$ introduced above:

$$\begin{aligned}\Pi(\mathbf{q},\Omega_k) &= T\sum_{\omega_n}\lambda(q,\varepsilon_{n+k},\varepsilon_{-n})\mathcal{P}(\mathbf{q},\widetilde{\omega}_{n+k},\widetilde{\omega}_{-n}) = \\ &= T\sum_{\omega_n}\frac{1}{\left[\mathcal{P}(\mathbf{q},\widetilde{\varepsilon}_{n+k},\widetilde{\varepsilon}_{-n})\right]^{-1}-\frac{1}{2\pi\nu\tau}}.\end{aligned} \tag{20.167}$$

For relatively small $\mathbf{q}$ ($\Delta\xi(\mathbf{q},\mathbf{p})|_{|E(\mathbf{p})|=E_F} \ll |\widetilde{\varepsilon}_{n+k}-\widetilde{\varepsilon}_{-n}| \sim \max\{T,\tau^{-1}\}$) and $\Omega \ll T$ one can find an expression for the fluctuation propagator, which can be useful in studies of fluctuation effects near T_c ($\epsilon \ll 1$) for the dirty and intermediate but not very clean case ($T\tau \ll 1/\sqrt{\epsilon}$). Expanding (20.163) in powers of $\left(\Delta\xi(\mathbf{q},\mathbf{p})|_{|E(\mathbf{p})|=E_F}/|2\widetilde{\varepsilon}_n+\Omega_k|\right)^2$ it is possible write $L^R(q,\Omega)$ in a form almost completely coinciding with Exp.(20.157):

$$L^R(\mathbf{q},\Omega) = -\frac{1}{\nu}\frac{1}{\epsilon - i\frac{\pi\Omega}{8T}+\xi^2(T\tau)\mathbf{q}^2}. \tag{20.168}$$

Let us stress that the phenomenological coefficient γ_{GL} turns out to be equal to the same value $\frac{\pi\nu}{8T}$ as in clean case, and hence does not depend on the impurity concentration. The only difference in comparison with the clean case is in appearance of a dependence of the natural effective coherence length on the elastic relaxation time. In the isotropic D-dimensional case it can be written as

$$\begin{aligned}\xi^2_{(D)}(T\tau) &= (4m\alpha T)^{-1} = \eta_{(D)} = \\ &-\frac{\tau^2 v_F^2}{D}\left[\psi(\frac{1}{2}+\frac{1}{4\pi T\tau})-\psi(\frac{1}{2})-\frac{1}{4\pi T\tau}\psi'(\frac{1}{2})\right]\end{aligned} \tag{20.169}$$

(we introduced here the parameter $\eta_{(D)}$ frequently used in the microscopic theory)[22].

The generalization of (20.168) for the case of a layered electronic spectrum is evident:

$$L^R(q,\Omega) = -\frac{1}{\nu}\frac{1}{\epsilon - i\frac{\pi\Omega}{8T}+\eta_{(2)}\mathbf{q}_\parallel^2 + r\sin^2(q_z s/2)}. \tag{20.170}$$

One has to remember that the Exp. (20.168) was derived in the assumption of small momenta $\Delta\xi(\mathbf{q},\mathbf{p})|_{|E(\mathbf{p})|=E_F} \ll |\widetilde{\varepsilon}_{n+k}-\widetilde{\varepsilon}_{-n}| \sim \max\{T,\tau^{-1}\}$, so the range of its applicability is restricted to the GL region of temperatures $\epsilon = \ln(\frac{T}{T_c}) \ll 1$, where the integrands of diagrammatic expressions have singularities at small momenta of the Cooper pair center of mass.

Finally let us express the Ginzburg-Levanyuk parameter for the important $2D$ case in terms of the microscopic parameter $\eta_{(2)}$. In accordance with (20.37) and the definition (20.169):

$$Gi_{(2)}(T\tau) = \frac{7\zeta(3)}{16\pi^2}\frac{1}{mT_c\eta_{(2)}(T\tau)}. \tag{20.171}$$

One can see that this general definition in the limiting cases of a clean and dirty metal results in the same values $Gi_{(2c)}$ and $Gi_{(2d)}$ as was reported in Table 1.

[22]Let us recall that its square determines the product of the GL parameter α and the Cooper pair mass entering in the GL functional. In clean case we supposed the letter equal to two free electron masses and defined α in accordance with (20.18). As we just have seen in the case of the impure superconductor ξ depends on impurity concentration and this dependence, in principle, can be attributed both to α or m. For our further purposes it is convenient to leave α in the same form (20.18) as in the case of a clean superconductor. The Cooper pair mass in this case becomes dependent on the electron mean free pass what physically can be attributed to the diffusion motion of the electrons forming the pair.

20.5.4 Microscopic theory of fluctuation conductivity of layered superconductor

Qualitative discussion of different fluctuation contributions

In Section 4 the direct fluctuation effect on conductivity, related with the charge transfer by means of fluctuation Cooper pairs, was discussed in details. Nevertheless, below in this Section we return to its discussion and will demonstrate its calculation by means of the microscopic theory. This will be done in purpose to prepare the basis for studies of the Aslamazov-Larkin contribution in the variety of physical values like magnetoconductivity near the upper critical field, conductivity far from transition point, fluctuation conductivity in ultra-clean limit, Hall conductivity etc.

Microscopic approach permits also to calculate the cited above indirect fluctuation effects like so called DOS and MT contributions. We will start now from their qualitative discussion.

The important consequence of the presence of fluctuating Cooper pairs above T_c is the decrease of the one-electron density of states at the Fermi level. Indeed, if some electrons are involved in pairing they can not simultaneously participate in charge transfer and heat capacity as single-particle excitations. Nevertheless, the total number of the electronic states can not be changed by the Cooper interaction, and only a redistribution of the levels along the energy axis is possible [93, 94]. In this sense one can speak about the opening of a fluctuation pseudo-gap at the Fermi level. The decrease of the one-electron density of states at the Fermi level leads to a reduction of the normal state conductivity. This, indirect, fluctuation correction to the conductivity is called the *density of states (DOS)* contribution and it appears side by side with the *paraconductivity (or Aslamazov-Larkin contribution)*. It has the opposite (negative) sign and turns out to be much less singular in $(T-T_c)^{-1}$ in comparison with the AL contribution, so that in the vicinity of T_c it was usually omitted. However, in many cases [29, 95, 96, 97, 98, 99], when for some special reasons the main, most singular, corrections are suppressed, the DOS correction becomes of major importance. Such a situation takes place in many cases of actual interest (quasiparticle current in tunnel structures, c-axis transport in strongly anisotropic high temperature superconductors, NMR relaxation rate, thermoelectric power).

The correction to the normal state conductivity above the transition temperature related with the fluctuation DOS renormalization for the dirty superconductor can be evaluated qualitatively. Indeed, the fact that some electrons ($\Delta\mathcal{N}_e$ per unit volume) participate in fluctuation Cooper pairing means that the effective number of carriers taking part in one-electron charge transfer diminishes leading to a decrease of conductivity (we deal here with the longitudinal component):

$$\delta\sigma_{xx}^{DOS} = -\frac{\Delta\mathcal{N}_e e^2\tau}{m} = -\frac{2n_s e^2\tau}{m}, \tag{20.172}$$

where n_s is the superfluid density coinciding with the Cooper pairs concentration. The latter can be identified with the average value of the square of the order parameter modulus already calculated as the correlator

$$\langle\Psi^*(0)\Psi(\mathbf{r})\rangle\,(T>T_{c0}) = \sum_{\mathbf{k}}\left\langle|\Psi_k|^2\right\rangle\exp\left(i\mathbf{kr}\right) = \frac{1}{4\pi\alpha\xi^2}\mathbf{K}_0\left(\frac{r}{\xi(\epsilon)}\right), \tag{20.173}$$

with $r\sim\xi$. For the $2D$ case, which is of the most interest to us, one finds:

$$n_s = \frac{1}{4\pi\alpha\xi^2}\frac{1}{s}\mathbf{K}_0(\sqrt{\epsilon}) = \frac{7\zeta\left(3\right)}{\pi^4 v_F^2}\frac{E_F}{s\tau}\ln\ \frac{1}{\epsilon}, \tag{20.174}$$

where we have used the explicit expression (20.18) for α and ξ. As we will see the corresponding expression for the fluctuation DOS correction to conductivity (20.172) coincides with the accuracy of 2 with the microscopic expression (20.185) which will be carried out below.

The third, purely quantum, fluctuation contribution is generated by the coherent scattering of the electrons forming a Cooper pair on the same elastic impurities. This is the so called *anomalous Maki-Thompson (MT)* contribution [6, 7] which can be treated as the result of Andreev scattering of the electron by fluctuation Cooper pairs. This contribution often turns out to be important in conductivity and other transport phenomena. Its temperature singularity near T_c is similar to that of the paraconductivity, although being extremely sensitive to electron phase-breaking processes and to the type of orbital symmetry of pairing it can be suppressed. Let us evaluate it.

The physical origin of the Maki-Thompson correction consists in the fact that the Cooper interaction of electrons with the almost opposite momenta changes the mean free path (diffusion coefficient) of electrons. As we have already seen in the previous Section the amplitude of this interaction increases drastically when $T \to T_c$:

$$g_{eff} = \frac{g}{1 - g \ln \frac{\omega_D}{2\pi T}} = \frac{1}{\ln \frac{T}{T_c}} \approx \frac{T}{T - T_c} = \frac{1}{\epsilon}.$$

What is the reason of this growth? One can say that the electrons scatter one at another in resonant way with the virtual Cooper pairs formation. Or it is possible to imagine that the electrons undergo the Andreev scattering at fluctuation Cooper pairs binding in the Cooper pair themselves. The probability of such induced pair irradiation (let us remind that Cooper pairs are Bose particles) is proportional to their number in the final state, i.e. $n(p)$ (20.7). For small momenta $n(p) \sim 1/\epsilon$.

One can ask why such interaction does not manifest itself considerably far from the transition point? The matter of fact that so intensively interacts just small number of electrons with the total momentum $q \lesssim \xi^{-1}(T)$. In accordance with the Heisenberg principle the minimal distance between such electrons is of the order of $\sim \xi(T)$. From the other hand such electrons in purpose to interact have to approximate one another up to the distance of the Fermi length $\lambda_F \sim 1/p_F$. The probability of such event may be estimated in the spirit of the self-intersection trajectories contribution evaluation in the weak localization theory [100, 102].

In the process of diffusion motion the distance between two electrons increases with the time growth in accordance with the Einstein law: $R(t) \sim (Dt)^{1/2}$. Hence the scattering probability

$$W \sim \int\limits_{t_{\min}}^{t_{\max}} \frac{\lambda_F^{D-1}}{R^D(t)} v_F \, dt.$$

The lower limit of the integral can be estimated from the condition $R(t_{\min}) \sim \xi(T)$ (only such electrons interact in the resonant way). The upper limit is determined by the phase breaking time τ_φ since for larger time intervals the phase coherence, necessary for the pair formation, is broken. In result the relative correction to conductivity due to such processes is equal to the product of the scattering probability on the effective interaction constant: $\delta\sigma^{MT}/\sigma = W \; g_{eff}$. In the $2D$ case

$$\delta\sigma^{MT} \sim \frac{e^2}{8\epsilon} \ln \frac{D\tau_\varphi}{\xi^2(T)}.$$

This result will be confirmed below in the frameworks of the microscopic consideration.

Generalities

Let us pass to the microscopic calculation of the fluctuation conductivity of the layered superconductor. We begin by discussing the quasiparticle normal state energy spectrum. While models with several conducting layers per unit cell and with either intralayer or interlayer

pairing have been considered [103], it has been shown [104] that all of these models give rise to a Josephson pair potential that is periodic in k_z, the wave-vector component parallel to the c-axis, with period s, the c-axis repeat distance. While such models differ in their superconducting densities of states, they all give rise to qualitatively similar fluctuation propagators, which differ only in the precise definitions of the parameters and in the precise form of the Josephson coupling potential. Ignoring the rather unimportant differences between such models in the Gaussian fluctuation regime above $T_c(H)$, we therefore consider the simplest model of a layered superconductor, in which there is one layer per unit cell, with intralayer singlet s-wave pairing. These assumptions lead to the simple spectrum (20.165) and hence to a Fermi surface having the form of a corrugated cylinder (see Fig.20.8).

Some remarks regarding the normal-state quasiparticle momentum relaxation time are necessary. In the "old" layered superconductors the materials were generally assumed to be in the dirty limit (like $TaS_2(\text{pyridine})_{1/2}$). In the high-$T_c$ cuprates, however, both single crystals and epitaxial thin films are nominally in the "intermediate" regime, with $l/\xi_{xy} \approx 2-5$. In addition, the situation in the cuprates is complicated by the presence of phonons for $T \simeq T_c \simeq 100K$, the nearly localized magnetic moments on the Cu^{2+} sites, and by other unspecified inelastic processes. In this Section we assume simple elastic intralayer scattering and restrict our consideration to the local limit in the fluctuation Cooper pair motion. This means that we consider the case of not too clean superconductors, keeping the impurity concentration n_i and reduced temperature such that the resulting mean-free path satisfies the requirement $l < \xi_{xy}(T) = \frac{\xi_{xy}}{\sqrt{\varepsilon}}$ and the impurity vertex can be taken in the local form (20.163) with $\langle(\Delta\xi(\mathbf{q},\mathbf{p})|)^2\rangle_{F.S.}$ determined by (20.166). The phase-breaking time τ_φ is supposed to be much larger than τ.

The most general relation between the current density $\mathbf{j}(\mathbf{r},t)$ and vector-potential $\mathbf{A}(\mathbf{r}',t')$ is given through the so-called electromagnetic response operator $Q_{\alpha\beta}(\mathbf{r},\mathbf{r}',t,t')$ [92]:

$$\mathbf{j}(\mathbf{r},t) = \int Q_{\alpha\beta}(\mathbf{r},\mathbf{r}',t,t')\mathbf{A}(\mathbf{r}',t')\ \mathbf{dr}'\ dt,$$

Assuming space and time homogeneity, one can take the Fourier transform of this relation and compare it with the definition of the conductivity tensor $j_\alpha = \sigma_{\alpha\beta}E_\beta$. This permits us to express the conductivity tensor in terms of the retarded electromagnetic response operator

$$\sigma_{\alpha\beta}(\omega) = -\frac{1}{i\omega}[Q_{\alpha\beta}]^R(\omega). \tag{20.175}$$

The electromagnetic response operator $Q_{\alpha\beta}(\omega_\nu)$, defined on Matsubara frequencies $\omega_\nu = (2\nu+1)\pi T$, can be presented as the correlator of two exact one-electron Green functions [92] averaged over impurities and accounting for interactions, in our case the particle-particle interactions in the Cooper channel. The appropriate diagrams corresponding to the first order of perturbation theory in the fluctuation amplitude are shown in Fig. (20.9).

With each electromagnetic field component A_α we associate the external vertex $ev_\alpha(p) = e\frac{\partial\xi(p)}{\partial p_\alpha}$. For the longitudinal conductivity tensor elements (parallel to the layers, for which $\alpha = x, y$), the resulting vertex is simply ep_α/m. For the c-axis conductivity, the vertex is given by

$$ev_z(p) = e\frac{\partial\xi(p)}{\partial p_z} = -eJs\sin(p_z s). \tag{20.176}$$

Each solid line in the diagrams represents a one-electron Green function averaged over impurities (20.145), a wavy line represents a fluctuation propagator $L(\mathbf{q},\Omega_k)$ (20.168), three-leg vertices were defined by the Exp.(20.163). The four-leg impurity vertex**,** appearing in diagrams 3-4, 9-10 of the Fig. 20.9, is called the Cooperon in the weak localization theory (see, for example,[105]) It is easy to see that it differs from the above three-leg vertex only by the additional factor $(2\pi\nu\tau)^{-1}$. We do not renormalize the current vertices: it is well known (see [92])

Figure 20.9: Feynman diagrams for the leading-order contributions to the fluctuation conductivity. Wavy lines are fluctuation propagators, thin solid lines with arrows are impurity-averaged normal-state Green's functions, shaded semicircles are vertex corrections arising from impurities, dashed lines with central crosses are additional impurity renormalisations and shaded rectangles are impurity ladders. Diagram 1 represents the Aslamazov-Larkin term; diagrams 2–4 represent the Maki-Thompson type contributions; diagrams 5–10 arise from corrections to the normal state density of states.

that this renormalization only leads to the substitution of the scattering time τ by the transport one τ_{tr}. We integrate over the internal Cooper pair momentum $\mathbf{q}$ and electron momentum $\mathbf{p}$ and sum over the internal fermionic and bosonic Matsubara frequencies, with momentum and energy conservation at each internal vertex (fluctuation propagator endpoint) in the analytical expressions for the diagrams presented in Fig. (20.9).

After these necessary introductory remarks and definitions we pass to the microscopic calculation of the different fluctuation contributions.

Aslamazov-Larkin contribution

We first examine the AL paraconductivity (diagram 1 of Fig.(20.9)). Actually this contribution was already studied in the Section 4 in the framework of the TDGL equation but, in order to demonstrate how the method works, we will carry out here the appropriate calculations in the microscopic approach, as was originally done by Aslamazov and Larkin [5].

The AL contribution to the electromagnetic response operator tensor has the form:

$$\begin{aligned} Q^{AL}_{\alpha\beta}(\omega_\nu) &= 2e^2T\sum_{\Omega_k}\int\frac{d^3\mathbf{q}}{(2\pi)^3}B_\alpha(\mathbf{q},\Omega_k,\omega_\nu)L(\mathbf{q},\Omega_k)\times \\ &\times B_\beta(\mathbf{q},\Omega_k,\omega_\nu)L(\mathbf{q},\Omega_k+\omega_\nu), \end{aligned} \tag{20.177}$$

where the three Green function block is given by

$$\begin{aligned} B_\alpha(\mathbf{q},\Omega_k,\omega_\nu) &= T\sum_{\varepsilon_n}\lambda(\mathbf{q},\varepsilon_{n+\nu},\Omega_k-\varepsilon_n)\lambda(\mathbf{q},\varepsilon_n,\Omega_k-\varepsilon_n)\times \\ &\times\int\frac{d^3\mathbf{p}}{(2\pi)^3}v_\alpha(\mathbf{p})G(\mathbf{p},\varepsilon_{n+\nu})G(\mathbf{p},\varepsilon_n)G(\mathbf{q}-\mathbf{p},\Omega_k-\varepsilon_n). \end{aligned} \tag{20.178}$$

Expanding $G(\mathbf{q}-\mathbf{p},\Omega_k-\varepsilon_n)$ over $\mathbf{q}$ one find that the angular integration over the Fermi surface kills the first term and leaves nonzero the second term of the expansion only. Then the $\xi-$integration is performed by means of the Cauchy theorem. The further summation over the fermionic frequency is cumbersome, so we will show it for the example of the simplest case of a dirty superconductor with $T\tau\ll 1$. In this case the main sources of the ε_n-dependence in (20.178) are the λ-vertices and that originating from the Green functions can be neglected by the parameter $T\tau\ll 1$ (indeed, one can see that $\varepsilon_n\sim T$ are important in vertices, while in Green functions $\varepsilon_n\gtrsim\tau^{-1}$ only). The remaining summation in (20.178) is performed in the same way as was done in (20.168) and results in:

$$\begin{aligned} B_\alpha(\mathbf{q},\Omega_k,\omega_\nu) &= \nu\frac{\eta_{(2)}}{v_F^2}\left\langle v_\alpha q_\beta v_\beta\right\rangle_{FS}\times \\ &\times\frac{8T}{\pi\omega_\nu}\left[\psi(\frac{1}{2}+\frac{|\Omega_k|+\omega_\nu+\widehat{D}q^2}{4\pi T})-\psi(\frac{1}{2}+\frac{|\Omega_k|+\widehat{D}q^2}{4\pi T})+\right. \\ &\left.+\psi(\frac{1}{2}+\frac{|\Omega_{k+\nu}|+\omega_\nu+\widehat{D}q^2}{4\pi T})-\psi(\frac{1}{2}+\frac{||\Omega_{k+\nu}|+\widehat{D}q^2}{4\pi T})\right]. \end{aligned} \tag{20.179}$$

Now let us return to the general expression for $Q^{AL}_{\alpha\beta}(\omega_\nu)$ and transform the Ω_k - summation into a contour integral, using the identity [106]

$$T\sum_{\Omega_k}f(\Omega_k)=\frac{1}{4\pi i}\oint_C dz\coth\frac{z}{2T}f(-iz),$$

Figure 20.10: The contour of integration in the plane of complex frequencies.

where $z = i\Omega_k$ is a variable in the plane of complex frequency and the contour C encloses all bosonic Matsubara frequencies over which the summation is carried out. In our case the contour C can be chosen as a circle with radius tending to infinity (see Fig. 20.10):

$$Q^{AL}_{\alpha\beta}(\omega_\nu) = \frac{e^2}{2\pi i}\int \frac{d^3\mathbf{q}}{(2\pi)^3}\oint_C dz \coth\frac{z}{2T} B_\alpha(\mathbf{q}, -iz+\omega_\nu, -iz)\times \\ \times L(\mathbf{q}, -iz) B_\beta(\mathbf{q}, -iz+\omega_\nu, -iz) L(\mathbf{q}, -iz+\omega_\nu). \tag{20.180}$$

One can see that the integrand function in (20.180) has breaks of analyticity at the lines $\mathrm{Im}z = 0$ and $\mathrm{Im}z = -i\omega_\nu$. Indeed, the fluctuation propagator $L(\mathbf{q}, \Omega_k)$ and Green function blocks $B_\alpha(\mathbf{q}, \Omega_k, \omega_\nu)$ were defined on the bosonic Matsubara frequencies only, while now we have to use them as functions of the continuous variable z. As it is well known from the properties of Green functions in the complex plane z two analytical functions, related with $L(\mathbf{q}, \Omega_k)$, can be introduced. The first one, $L^R(\mathbf{q}, -iz)$ (retarded), is analytic in the upper half-plane ($\mathrm{Im}z > 0$), while the second one, $L^A(\mathbf{q}, -iz)$ (advanced), has no singularities in the lower half-plane ($\mathrm{Im}z < 0$). As we have seen above the same lines separate the domains of the analyticity of the Green function blocks, so the functions B^{RR}, B^{RA}, B^{AA} analytic in each domain can be introduced (with the appropriate choices of the $|\Omega_{k+\nu}|$ and $|\Omega_k|$ signs in the arguments of the $\psi-$ functions, see (20.179)). This means that by cutting the z-plane along the lines $\mathrm{Im}z = 0$ and $\mathrm{Im}z = -i\omega_\nu$ we can reduce the calculation of the contour integral in (20.180) to the sum of three integrals along the contours C_1, C_2, C_3 which enclose domains of well defined analyticity of the integrand function. The integral along the large circle evidently vanishes and the contour integral is reduced to four integrals along the cuts of the plane in Fig.20.10:

$$
\begin{aligned}
I(\mathbf{q},\omega_\nu) &= \oint_{C_1+C_2+C_3} dz \coth\frac{z}{2T} B_\alpha(\mathbf{q},-iz)L(\mathbf{q},-iz)B_\beta(\mathbf{q},-iz)L(\mathbf{q},-iz+\omega_\nu) = \\
&= \int_{-\infty}^{\infty} dz \coth\frac{z}{2T} L^R(\mathbf{q},-iz+\omega_\nu)\left[B_\alpha^{RR}B_\beta^{RR}L^R(\mathbf{q},-iz)-\right. \\
&\quad \left. -B_\alpha^{RA}B_\beta^{RA}L^A(\mathbf{q},-iz)\right] + \int_{-\infty-i\omega_\nu}^{\infty-i\omega_\nu} dz \coth\frac{z}{2T} L^A(\mathbf{q},-iz)\times \\
&\quad \left[B_\alpha^{RA}B_\beta^{RA}L^R(\mathbf{q},-iz+\omega_\nu) - B_\alpha^{AA}B_\beta^{AA}L^A(\mathbf{q},-iz+\omega_\nu)\right] ..
\end{aligned}
$$

Now one can shift the variable in the last integral to $z = z' - i\omega_\nu$, take into account that $i\omega_\nu$ is the period of $\coth\frac{z}{2T}$ and get an expression analytic in $i\omega_\nu \to \omega$.

In the vicinity of T_c, due to the pole structure of the fluctuation propagators in (20.177), the leading contribution to the electromagnetic response operator $Q_{\alpha\beta}^{AL(R)}$ arises from them rather than from the frequency dependence of the vertices B_α, so we can neglect the Ω_k- and ω_ν-dependencies of the Green functions blocks and use the expression for $B_\alpha(\mathbf{q},0,0)$ valid for small $\mathbf{q}_{ab}$ only:

$$
B_\alpha(\mathbf{q}) = -2\nu\frac{\eta_{(2)}}{v_F^2}\begin{cases} v_F^2 q_\alpha, & \alpha = x,y \\ sJ^2 \sin q_z s, & \alpha = z \end{cases} .
$$

Detailed calculations demonstrate that this result can be generalized to an arbitrary impurity concentration just by using the expression (20.169) for $\eta_{(2)}$. Finally:

$$
\begin{aligned}
Q_{\alpha\beta}^{AL(R)}(\omega) = \frac{2e^2}{\pi}\int\frac{d^3q}{(2\pi)^3}B_\alpha(\mathbf{q})B_\beta(\mathbf{q}) \quad & \int_{-\infty}^{\infty} dz \coth\left(\frac{z}{2T}\right)\left[L^R(\mathbf{q},-iz-i\omega)\right. \\
& \left. +L^A(\mathbf{q},-iz+i\omega)\right]\mathrm{Im}L^R(\mathbf{q},-iz).
\end{aligned}
$$

Being interested here in the d.c. conductivity one can expand the integrand function in ω. It is possible to show that the zeroth order term is cancelled by the same type contributions from all other diagrams (this cancellation confirms the absence of anomalous diamagnetism above the critical temperature). The remaining integral can be integrated by parts and then carried out taking into account that the contribution most singular in ϵ comes from the region $z \sim \epsilon \ll T$:

$$
\begin{aligned}
\sigma_{xx}^{AL} &= \frac{e^2}{2\pi T}\int\frac{d^3\mathbf{q}}{(2\pi)^3}B_{x,z}^2(\mathbf{q},0,0)\int_{-\infty}^{\infty}\frac{dz}{\sinh^2\frac{z}{2T}}\left[\mathrm{Im}L^R(\mathbf{q},-iz)\right]^2 = \\
&= \frac{\pi^2e^2\eta_{(2)}^2}{s}\int\frac{d^2\mathbf{q}}{(2\pi)^2}\frac{\mathbf{q}^2}{\left[(\eta_{(2)}\mathbf{q}^2+\epsilon)(\eta_{(2)}\mathbf{q}^2+\epsilon+r)\right]^{3/2}} \\
&= \frac{e^2}{16s}\frac{1}{[\epsilon(\epsilon+r)]^{1/2}} \to \frac{e^2}{16s}\begin{cases} 1/\sqrt{\epsilon r}, & \epsilon \ll r \\ 1/\epsilon, & \epsilon \gg r \end{cases} .
\end{aligned}
\tag{20.181}
$$

where the Lawrence-Doniach anisotropy parameter r [27] was already defined by (20.62).

In the same way one can evaluate the AL contribution to the transverse fluctuation conductivity [107, 95, 108]:

$$
\begin{aligned}
\sigma_{zz}^{AL} &= \frac{\pi e^2 s r^2}{32}\int\frac{d^2\mathbf{q}}{(2\pi)^2}\frac{1}{\left[(\eta_{(2)}\mathbf{q}^2+\epsilon)(\eta_{(2)}\mathbf{q}^2+\epsilon+r)\right]^{3/2}} = \\
&= \frac{e^2 s}{32\eta_{(2)}}\left(\frac{\epsilon+r/2}{[\epsilon(\epsilon+r)]^{1/2}}-1\right) \to \frac{e^2 s}{64\eta_{(2)}}\begin{cases} \sqrt{r/\epsilon}, & \text{for } \epsilon \ll r \\ (r/2\epsilon)^2, & \text{for } \epsilon \gg r \end{cases} .
\end{aligned}
\tag{20.182}
$$

Note, that contrary to the case of in-plane conductivity, the critical exponent for σ_{zz} above the Lawrence-Doniach crossover temperature T_{LD} (for which $\epsilon(T_{LD}) = r$) is 2 instead of 1, so the crossover occurs from the 0D to 3D regimes. This is related with the tunneling (so from the band structure point of view effectively zero dimensional) character of electron motion along the c-axis.

Contributions from fluctuations of the density of states

In original paper of Aslamazov and Larkin [5] the most singular AL contribution to conductivity, heat capacity and other properties of a superconductor above the critical temperature was considered. The diagrams of the type 5-6 were pictured and correctly evaluated as less singular in ϵ. Nevertheless the specific form of the AL contribution to the transverse conductivity of a layered superconductor, which may be considerably suppressed for small interlayer transparency, suggested to re-examine the contributions from diagrams 5-10 of Fig.20.9 which are indeed less divergent in ϵ, but turn out to be of lower order in the transmittance and of the opposite sign with respect to the AL one [95, 96]. These, so-called DOS, diagrams describe the changes in the normal Drude-type conductivity due to fluctuation renormalization of the normal quasiparticles density of states above the transition temperature (see Section 8.5). In the dirty limit, the calculation of contributions to the longitudinal fluctuation conductivity σ_{xx} from such diagrams was discussed in [109, 99]. Contrary to the case of the AL contribution, the in-plane and out-of-plane components of the DOS contribution differ only in the square of the ratio of effective Fermi velocities in the parallel and perpendicular directions. This allows us to calculate both components simultaneously. The contribution to the fluctuation conductivity due to diagram 5 is

$$\begin{aligned} Q^5_{\alpha\beta}(\omega_\nu) &= 2e^2T\sum_{\Omega_k}\int\frac{d^3\mathbf{q}}{(2\pi)^3}L(\mathbf{q},\Omega_k)T\sum_{\varepsilon_n}\lambda^2(\mathbf{q},\varepsilon_n,\Omega_k-\varepsilon_n)\times \\ &\int\frac{d^3\mathbf{p}}{(2\pi)^3}v_\alpha(\mathbf{p})v_\beta(\mathbf{p})G^2(\mathbf{p},\varepsilon_n)G(\mathbf{q}-\mathbf{p},\Omega_k-\varepsilon_n)G(\mathbf{p},\varepsilon_{n+\nu}), \end{aligned}$$

and diagram 6 gives an identical contribution. Evaluation of the integrations over the in-plane momenta $\mathbf{p}$ and the summation over the internal frequencies ε_n are straightforward. Treatment of the other internal frequencies Ω_k is less obvious, but in order to obtain the leading singular behavior in the vicinity of transition it suffices to set $\Omega_k = 0$ [99]. After integration over q_z, we have [95, 97]:

$$\begin{aligned} \sigma^{5+6}_{\alpha\beta} &= -\frac{\pi e^2}{2s}A_{\alpha\beta}\kappa_1\eta_{(2)}\int\limits_{|\mathbf{q}|\le\xi^{-1}}\frac{d^2\mathbf{q}}{(2\pi)^2}\frac{1}{\left[(\epsilon+\eta_{(2)}\mathbf{q}^2)(\epsilon+r+\eta_{(2)}\mathbf{q}^2)\right]^{1/2}} \\ &\approx -\frac{e^2\kappa_1}{8s}A_{\alpha\beta}\ln\left(\frac{2}{\epsilon^{1/2}+(\epsilon+r)^{1/2}}\right), \end{aligned} \tag{20.183}$$

where $A_{xx} = A_{yy} = 1, A_{zz} = (sJ/v_F)^2, A_{\alpha\neq\beta} = 0$ and

$$\kappa_1 = \frac{2(v_F\tau)^2}{\pi^2\eta_{(2)}}\left[\psi'\left(\frac{1}{2}+\frac{1}{4\pi T\tau}\right)-\frac{3}{4\pi T\tau}\psi''\left(\frac{1}{2}\right)\right].$$

In order to cut off the ultra-violet divergence in q we have introduced here a cut off parameter $q_{\max} = \xi^{-1} = \eta_{(2)}^{-1/2}$ in complete agreement with Section 3. Let us stress that in the framework of the phenomenological GL theory we attributed this cut off to the breakdown of the GL approach at momenta as large as $q \sim \xi^{-1}$. The microscopic approach developed here permits

to see how this cut off appears: the divergent shortwave-length contribution arising from GL-like fluctuation propagators is automatically restricted by the q-dependencies of the impurity vertices and Green functions, which appear at the scale $q \sim l^{-1}$.

In a similar manner, the equal contributions from diagrams 7 and 8 sum to

$$\begin{aligned}\sigma_{\alpha\beta}^{7+8} &= -\frac{\pi e^2}{2s} A_{\alpha\beta}\kappa_2\eta_{(2)} \int\limits_{|\mathbf{q}|\le q_{\max}} \frac{d^2\mathbf{q}}{(2\pi)^2} \frac{1}{\left[(\epsilon+\eta_{(2)}\mathbf{q}^2)(\epsilon+r+\eta_{(2)}\mathbf{q}^2)\right]^{1/2}} \\ &\approx -\frac{e^2\kappa_2}{8s} A_{\alpha\beta} \ln\left(\frac{2}{\epsilon^{1/2}+(\epsilon+r)^{1/2}}\right), \end{aligned} \tag{20.184}$$

$$\kappa_2 = \frac{(v_F\tau)^2}{2\pi^3 T\tau}\psi''\left(\frac{1}{2}\right).$$

Comparing (20.183) and (20.184), we see that in the clean limit, the main contributions from the DOS fluctuations arise from diagrams 5 and 6. In the dirty limit, diagrams 7 and 8 are also important, having -1/3 the value of diagrams 5 and 6, for both σ_{xx} and σ_{zz}. Diagrams 9 and 10 are not singular in $\epsilon << 1$ at all and can be neglected. The total DOS contribution to the in-plane and c-axis conductivity is therefore

$$\sigma_{\alpha\beta}^{DOS} = -\frac{e^2}{2s}\kappa(T\tau)A_{\alpha\beta}\ln\left(\frac{2}{\epsilon^{1/2}+(\epsilon+r)^{1/2}}\right), \tag{20.185}$$

where

$$\begin{aligned}\kappa(T\tau) &= \kappa_1+\kappa_2 = \frac{-\psi'\left(\frac{1}{2}+\frac{1}{4\pi\tau T}\right)+\frac{1}{2\pi\tau T}\psi''\left(\frac{1}{2}\right)}{\pi^2\left[\psi\left(\frac{1}{2}+\frac{1}{4\pi\tau T}\right)-\psi\left(\frac{1}{2}\right)-\frac{1}{4\pi\tau T}\psi'\left(\frac{1}{2}\right)\right]} \\ &\to \begin{cases} 56\zeta(3)/\pi^4 \approx 0.691, & T\tau \ll 1 \\ 8\pi^2\left(T\tau\right)^2/\left[7\zeta(3)\right] \approx 9.384\left(T\tau\right)^2, & 1 \ll T\tau \ll 1/\sqrt{\epsilon} \end{cases} \end{aligned} \tag{20.186}$$

is a function of τT only. As it will be shown below at the upper limit $T\tau \sim 1/\sqrt{\epsilon}$ the DOS contribution reaches the value of the other fluctuation contributions and in the limit of $T\tau \to \infty$ exactly eliminates the Maki-Thompson one.

Maki-Thompson contribution

We now consider another quantum correction to fluctuation conductivity which is called the Maki-Thompson (MT) contribution (diagram 2 of Fig. 20.9). It was firstly discussed by Maki [6] in a paper which appeared almost simultaneously with the paper of Aslamazov and Larkin [5]. Both these articles gave rise to the microscopic theory of fluctuations in superconductor. Maki found that, in spite of the seeming weaker singularity of diagram 2 with respect to the AL one (it contains one propagator only, while the AL one contains two of them) it can contribute to conductivity comparably or even stronger than AL one.

Since the moment of its discovery the MT contribution became the subject of intense controversy. In its original paper Maki found that in $3D$ case this fluctuation correction is four times larger than the AL one. In $2D$ case the result was striking**:** the MT contribution simply diverged. This paradox was, at least at the level of recipe, resolved by Thompson [7]: he proposed to cut off the infra-red divergence in the Cooper pair center of mass momentum integration by the introduction of the finite length l_s of inelastic scatterings of electrons on paramagnetic impurities. In the further papers of Patton [110], Keller and Korenman [111] it was cleared up that the presence of paramagnetic impurities or other external phase-breaking sources is not necessary: the fluctuation Cooper pairing of two electrons results in a change

of the quasiparticle phase itself and the corresponding phase-breaking time τ_φ appears as a natural cut off parameter of the MT divergence in the strictly 2D case. The minimal quasi-two-dimensionality of the electron spectrum, as we will show below, automatically results in a cut off of the MT divergence.

Although the MT contribution to the in-plane conductivity is expected to be important in the case of low pair-breaking, experiments on high-temperature superconductors have shown that the excess in-plane conductivity can usually be explained in terms of the fluctuation paraconductivity alone. Two possible explanations can be found for this fact. The first one is that the pair-breaking in these materials is not weak. The second is related with the $d-$wave symmetry of pairing which kills the anomalous Maki-Thompson process [112, 113]. We will consider below the case of s-pairing, where the Maki-Thompson process is well pronounced.

The appearance of the anomalously large MT contribution is nontrivial and worth being discussed. We consider the scattering lifetime τ and the pair-breaking lifetime τ_φ to be arbitrary, but satisfying $\tau_\varphi > \tau$. In accordance with diagram 2 of Fig.(20.9) the analytical expression for the MT contribution to the electromagnetic response tensor can be written as

$$Q_{\alpha\beta}^{MT}(\omega_\nu) = 2e^2T\sum_{\Omega_k}\int\frac{d^3\mathbf{q}}{(2\pi)^3}L(\mathbf{q},\Omega_k)I_{\alpha\beta}(\mathbf{q},\Omega_k,\omega_\nu), \tag{20.187}$$

where

$$I_{\alpha\beta}(\mathbf{q},\Omega_k,\omega_\nu) = T\sum_{\varepsilon_n}\lambda(\mathbf{q},\varepsilon_{n+\nu},\Omega_{k-n-\nu})\lambda(\mathbf{q},\varepsilon_n,\Omega_{k-n})\times \tag{20.188}$$

$$\times\int\frac{d^3\mathbf{p}}{(2\pi)^3}v_\alpha(\mathbf{p})v_\beta(\mathbf{q}-\mathbf{p})G(\mathbf{p},\varepsilon_{n+\nu})G(\mathbf{p},\varepsilon_n)G(\mathbf{q}-\mathbf{p},\Omega_{k-n-\nu})G(\mathbf{q}-\mathbf{p},\Omega_{k-n})\ .$$

In the vicinity of T_c, it is possible to restrict consideration to the static limit of the MT diagram, simply by setting $\Omega_k = 0$ in (20.187). Although dynamic effects can be important for the longitudinal fluctuation conductivity well above T_{LD}, the static approximation is correct very close to T_c, as shown in [98, 125]. The main $q-$dependence in (20.187) arises from the propagator and vertices λ. This is why we can assume $q = 0$ in Green functions and to calculate the electron momentum integral passing, as usual, to a $\xi(\mathbf{p})$ integration:

$$\begin{aligned} I_{\alpha\beta}(q,0,\omega_\nu) &= \pi\nu\left\langle v_\alpha(p)v_\beta(q-p)\right\rangle_{FS}\times \\ &\times T\sum_{\varepsilon_n}\frac{1}{\left(|2\varepsilon_{n+\nu}|+\widehat{D}q^2\right)}\frac{1}{\left(|2\varepsilon_n|+\widehat{D}q^2\right)}\frac{1}{|\widetilde{\varepsilon}_{n+\nu}|+|\widetilde{\varepsilon}_n|}\ . \end{aligned} \tag{20.189}$$

In evaluating the sum over the Matsubara frequencies ε_n in (20.189) it is useful to split it into the two parts. In the first ε_n belongs to the domains $]-\infty,-\omega_\nu[$ and $[0,\infty[$, which finally give two equal contributions. This gives rise to the *regular* part of the MT diagram. The second, *anomalous*, part of the MT diagram arises from the summation over ε_n in the domain $[-\omega_\nu,0[$. In this interval, the further analytic continuation over ω_ν leads to the appearance of an additional diffusive pole:

$$\begin{aligned} I_{\alpha\beta}(q,0,\omega_\nu) &= I_{\alpha\beta}^{(reg)}(q,\omega_\nu)+I_{\alpha\beta}^{(an)}(q,\omega_\nu) = \nu\left\langle v_\alpha(p)v_\beta(q-p)\right\rangle_{FS} \\ &\times\left[2\pi T\sum_{n=0}^{\infty}\frac{1}{\left(2\varepsilon_{n+\nu}+\widehat{D}q^2\right)}\frac{1}{\left(2\varepsilon_n+\widehat{D}q^2\right)}\frac{1}{2\varepsilon_n+\omega_\nu+\tau^{-1}}+\right. \\ &\left.+\frac{\pi T}{\omega_\nu+\tau^{-1}}\sum_{n=-\nu}^{-1}\frac{1}{\left(2\varepsilon_{n+\nu}+\widehat{D}q^2\right)}\frac{1}{\left(-2\varepsilon_n+\widehat{D}q^2\right)}\right]. \end{aligned}$$

The limits of summation in the first sum do not depend on ω_ν, so it is an analytic function of this argument and can be continued to the upper half-plane of the complex frequency by the simple substitution $\omega_\nu \to -i\omega$. Then, tending $\omega \to 0$, one can expand the sum over powers of ω and perform the summation in terms of digamma-function:

$$\begin{aligned} I_{\alpha\beta}^{(reg)}(q,\omega_\nu) &= \nu \left\langle v_\alpha(\mathbf{p}) v_\beta(\mathbf{q}-\mathbf{p}) \right\rangle_{FS} \times \\ &\left\{ const + \frac{i\omega}{2} \frac{\partial}{\partial\left(\widehat{D}q^2\right)} \left(\frac{\partial}{\partial\left(\widehat{D}q^2\right)} + \frac{\partial}{\partial\left(\tau^{-1}\right)} \right) \cdot \right. \\ &\left. \frac{1}{\tau^{-1} - \widehat{D}q^2} \left[\psi\left(\frac{1}{2} + \frac{\omega_\nu + \widehat{D}q^2}{4\pi T} \right) - \psi\left(\frac{1}{2} + \frac{\widehat{D}q^2}{4\pi T} \right) \right] \right\}. \end{aligned} \tag{20.190}$$

The values of characteristic momenta $q \ll l^{-1}$ are determined by the domain of convergibility of the final integral of the propagator $L(\mathbf{q},0)$ in (20.187) (analogously to (20.184) and one can neglect $\widehat{D}q^2$ with respect to τ^{-1}. In result

$$\begin{aligned} I_{\alpha\beta}^{(reg)R}(q,\omega \to 0) &= \nu \left\langle v_\alpha(\mathbf{p}) v_\beta(\mathbf{q}-\mathbf{p}) \right\rangle_{FS} \times \\ &\left\{ const + \frac{i\omega\tau^2}{4} \left[\psi'\left(\frac{1}{2} + \frac{1}{4\pi\tau T} \right) - \psi'\left(\frac{1}{2} \right) - \frac{\psi''\left(\frac{1}{2}\right)}{4\pi T\tau} \right] \right\}. \end{aligned} \tag{20.191}$$

The appearance of the constant in $Q_{\alpha\beta}(\omega_\nu)$ was already discussed in the case of the AL contribution and, as was mentioned there, it is cancelled with the similar contributions of the other diagrams [98] and we will not consider it any more.

Now let us pass to the calculation of $I_{\alpha\beta}^{(an)}(q,\omega_\nu)$. Expanding the summing function in simple fractions one can express the result of summation in terms of digamma-functions

$$\begin{aligned} I_{\alpha\beta}^{(an)}(q,\omega_\nu) &= \frac{1}{4} \frac{\nu \left\langle v_\alpha(\mathbf{p}) v_\beta(\mathbf{q}-\mathbf{p}) \right\rangle_{FS}}{\omega_\nu + \tau^{-1}} \frac{1}{\omega_\nu + \widehat{D}q^2} \times \\ &\left[\psi\left(\frac{1}{2} + \frac{2\omega_\nu + \widehat{D}q^2}{4\pi T} \right) - \psi\left(\frac{1}{2} + \frac{\widehat{D}q^2}{4\pi T} \right) \right]. \end{aligned} \tag{20.192}$$

Doing the analytical continuation $i\omega_\nu \to \omega \to 0$ and taking into account that in the further q-integration of $I_{\alpha\beta}^{(an)R}(q,\omega \to 0)$, due to the singular at small q propagator, the important range is $\widehat{D}q^2 \ll T$, one can find

$$I_{\alpha\beta}^{(an)R}(q,\omega \to 0) = -\frac{i\pi\omega\tau}{16T} \frac{\nu \left\langle v_\alpha(\mathbf{p}) v_\beta(\mathbf{q}-\mathbf{p}) \right\rangle_{FS}}{-i\omega + \widehat{D}q^2}. \tag{20.193}$$

Because of the considerable difference in the angular averaging of the different tensor components we discuss the MT contribution to the in-plane and out of plane conductivities separately.

Taking into account that $\left\langle v_x(\mathbf{p}) v_x(\mathbf{q}-\mathbf{p}) \right\rangle_{FS} = -v_F^2/2$ one can find that the calculation of the regular part of MT diagram to the in-plane conductivity is completely similar to the corresponding DOS contribution and here we list the final result [97] only:

$$\sigma_{xx}^{MT(reg)} = -\frac{e^2}{2s}\tilde{\kappa} \ln\left(\frac{2}{\epsilon^{1/2} + (\epsilon + r)^{1/2}} \right),$$

where

$$\begin{aligned}\tilde{\kappa}(T\tau) &= \frac{-\psi'\left(\frac{1}{2}+\frac{1}{4\pi\tau T}\right)+\psi'\left(\frac{1}{2}\right)+\frac{1}{4\pi T\tau}\psi''\left(\frac{1}{2}\right)}{\pi^2\left[\psi\left(\frac{1}{2}+\frac{1}{4\pi\tau T}\right)-\psi\left(\frac{1}{2}\right)-\frac{1}{4\pi\tau T}\psi'\left(\frac{1}{2}\right)\right]} \\ &\to \begin{cases} 28\zeta(3)/\pi^4 \approx 0.346, \text{ for } T\tau \ll 1 \\ \pi^2/\left[14\zeta(3)\right] \approx 0586, \text{ for } 1 \ll T\tau \ll 1/\sqrt{\epsilon} \end{cases}\end{aligned} \tag{20.194}$$

is a function only of τT. We note that this regular MT term is negative, as is the overall DOS contribution.

For the anomalous part of the in-plane MT contribution we have:

$$\begin{aligned}\sigma_{xx}^{MT(an)} &= 8e^2\eta_{(2)}T\int\frac{d^3q}{(2\pi)^3}\frac{1}{[1/\tau_\varphi+\hat{D}q^2][\epsilon+\eta_{(2)}\mathbf{q}^2+\frac{r}{2}(1-\cos q_z s)]} \\ &= \frac{e^2}{4s(\epsilon-\gamma_\varphi)}\ln\left(\frac{\epsilon^{1/2}+(\epsilon+r)^{1/2}}{\gamma_\varphi^{1/2}+(\gamma_\varphi+r)^{1/2}}\right),\end{aligned} \tag{20.195}$$

where, in accordance with [7], the infra-red divergence for the purely 2D case ($r=0$) is cut off at $Dq^2 \sim 1/\tau_\varphi$[23]. The dimensionless parameter

$$\gamma_\varphi = \frac{2\eta}{v_F^2\tau\tau_\varphi} \to \frac{\pi}{8T\tau_\varphi}\begin{cases} 1, & T\tau \ll 1 \\ 7\zeta(3)/\left(2\pi^3 T\tau\right), & 1 \ll T\tau \ll 1/\sqrt{\epsilon} \end{cases}$$

is introduced for simplicity. If $r \neq 0$ the MT contribution turns out to be finite even with $\tau_\varphi = \infty$. Comparison of the expressions (20.181) and (20.195) indicates that in the weak pair-breaking limit, the MT diagram makes an important contribution to the longitudinal fluctuation conductivity: it is four times larger than the AL contribution in the 3D regime, and even logarithmically exceeds it in the 2D regime above T_{LD}. For finite pair-breaking, however, the MT contribution is greatly reduced in magnitude.

We now consider the calculation of the MT contribution to the transverse conductivity. The explicit expressions for $v_z(p)$ and $v_z(q-p)$ (see Exp. (20.176)), result in $\langle v_x(p)v_x(q-p)\rangle_{FS} = \frac{1}{2}J^2s^2\cos q_z s$. We take the limit $J\tau << 1$ in evaluating the remaining integrals, which may then be performed exactly.

The regular part of the MT contribution to the transverse conductivity is

$$\begin{aligned}\sigma_{zz}^{MT(\text{reg})} &= -\frac{e^2s^2\pi r\tilde{\kappa}(T\tau)}{4}\int\frac{d^3q}{(2\pi)^3}\frac{\cos q_z s}{\epsilon+\eta_{(2)}\mathbf{q}^2+\frac{r}{2}(1-\cos q_z s)} \\ &= -\frac{e^2sr\tilde{\kappa}(T\tau)}{16\eta_{(2)}}\left(\frac{(\epsilon+r)^{1/2}-\epsilon^{1/2}}{r^{1/2}}\right)^2\end{aligned}$$

This term is smaller in magnitude than is the DOS one, and therefore makes a relatively small contribution to the overall fluctuation conductivity. In the 3D regime below T_{LD}, it is proportional to J^2, and in the 2D regime above T_{LD}, it is proportional to J^4.

[23] The detailed study of the phase-breaking time, its energy dependence and the effect on the MT contribution was done in [115]

For the anomalous part of the MT diagram one can find

$$\begin{aligned}\sigma_{zz}^{MT(\mathrm{an})} &= \frac{\pi e^2 J^2 s^2 \tau}{4}\int\frac{d^3q}{(2\pi)^3}\frac{\cos q_z s}{[1/\tau_\varphi+\hat{\mathbf{D}}q^2][\epsilon+\eta_{(2)}\mathbf{q}^2+\frac{r}{2}(1-\cos q_z s)]}\\ &= \frac{\pi e^2 s}{4(\epsilon-\gamma_\varphi)}\int\frac{d^2\mathbf{q}}{(2\pi)^2}\left[\frac{\gamma_\varphi+\eta_{(2)}\mathbf{q}^2+r/2}{\left[(\gamma_\varphi+\eta_{(2)}\mathbf{q}^2)(\gamma_\varphi+\eta_{(2)}\mathbf{q}^2+r)\right]^{1/2}}-\right.\\ &\left.-\frac{\epsilon+\eta_{(2)}\mathbf{q}^2+r/2}{\left[(\epsilon+\eta_{(2)}\mathbf{q}^2)(\epsilon+\eta_{(2)}\mathbf{q}^2+r)\right]^{1/2}}\right]\\ &= \frac{e^2 s}{16\eta_{(2)}}\left(\frac{\gamma_\varphi+r+\epsilon}{[\epsilon(\epsilon+r)]^{1/2}+[\gamma_\varphi(\gamma_\varphi+r)]^{1/2}}-1\right). \qquad (20.196)\end{aligned}$$

In examining the limiting cases of (20.196), it is useful to consider the cases of weak ($\gamma_\varphi << r$, $\Longleftrightarrow J^2\tau\tau_\varphi \gg 1/2$) and strong ($\gamma_\varphi \gg r$,$\Longleftrightarrow J^2\tau\tau_\varphi << 1/2$) pair-breaking separately[24]. For weak pair-breaking, we have

$$\sigma_{zz}^{MT(\mathrm{an})} \to \frac{e^2 s}{16\eta_{(2)}}\begin{cases}\sqrt{r/\gamma_\varphi}, & \epsilon \ll \gamma_\varphi \ll r\\ \sqrt{r/\epsilon}, & \gamma_\varphi \ll \epsilon \ll r\\ r/(2\epsilon), & \gamma_\varphi \ll r \ll \epsilon\end{cases}.$$

In this case, there is the usual 3D to 2D dimensional crossover in the anomalous MT contribution at T_{LD}. There is an additional crossover at T_φ(where $T_c < T_\varphi < T_{LD}$), characterized by $\epsilon(T_\varphi)=\gamma_\varphi$, below which the anomalous MT term saturates. Below T_{LD}, the MT contribution is proportional to J, but in the 2D regime above T_{LD}, it is proportional to J^2.

For strong pair-breaking

$$\sigma_{zz}^{MT(\mathrm{an})} \to \frac{e^2 s}{32\eta_{(2)}}\begin{cases}r/\gamma_\varphi, & \epsilon \ll r \ll \gamma_\varphi\\ r^2/(4\gamma_\varphi\epsilon), & r \ll \min\{\gamma_\varphi,\epsilon\}\end{cases}.$$

In this case, the 3D regime (below T_{LD}) is not singular, and the anomalous MT contribution is proportional to J^2, rather than J for weak pair-breaking. In the 2D regime, it is proportional to J^4 for strong pair-breaking, as opposed to J^2 for weak pair-breaking. In addition, the overall magnitude of the anomalous MT contribution with strong pair-breaking is greatly reduced from that for weak pair-breaking.

Let us now compare the regular and anomalous MT contributions. Since these contributions are opposite in sign, it is important to determine which will dominate. For the in-plane resistivity, the situation is straightforward: the anomalous part always dominates over the regular and the latter can be neglected. The case of $c-$axis resistivity requires more discussion. Since we expect $\tau_\varphi \geq \tau$, strong pair-breaking is likely in the dirty limit. When the pair-breaking is weak, the anomalous term is always of lower order in J than the regular term, so the regular term can be neglected. This is true for both the clean and dirty limits. The most important regime for the regular MT term is the dirty limit with strong pair-breaking. In this case, when $\tau_\varphi T \sim 1$, the regular and anomalous terms are comparable in magnitude. In short, it is usually a good approximation to neglect the regular term, except in the dirty limit with relatively strong pair-breaking and only for the out-of-plane conductivity.

Finally let us mention that the contributions from the two other diagrams of the MT type (diagrams 3 and 4 of Fig. 20.9) in the vicinity of critical temperature can be omitted: one can

[24] Physically the value $J^2\tau.$ characterizes the effective interlayer tunneling rate [97, 114]. When $1/\tau_\phi << J^2\tau << 1/\tau$, the quasiparticles scatter many times before tunneling to the neighboring layers, and the pairs live long enough for them to tunnel coherently. When $J^2\tau << 1/\tau_\phi$, the pairs decay before both paired quasiparticles tunnel.

Figure 20.11: The normalised excess conductivity for samples of YBCO-123 (triangles), BSSCO-2212(squares) and BSSCO-2223 (circles) plotted against $\epsilon = \ln T/T_c$ on a ln-ln plot as described in [124]. The dotted and solid lines are the AL theory in 3D and 2D respectively. The dashed line is the extended theory of [125]..

check that they have an additional square of the Cooper pair center of mass momentum q in the integrand of q-integration with respect to diagram 2 and hence turn out to be less singular in ϵ.

Discussion

Although the in-plane and out-of plane components of the fluctuation conductivity tensor of a layered superconductor contain the same fluctuation contributions, their temperature behavior may be qualitatively different. In fact, for σ_{xx}^{fl}, the negative contributions are considerably less than the positive ones in the entire experimentally accessible temperature range above the transition, and it is a positive monotonic function of the temperature. Moreover, for HTS compounds, where the pair-breaking is strong and the MT contribution is in the overdamped regime, it is almost always enough to take into account only the paraconductivity to fit experimental data. Some examples of the experimental findings for in-plane fluctuation conductivity of HTS materials on can see in [116, 117, 118, 119, 120, 121, 122, 123].

In Fig. 20.11 the fluctuation part of in-plane conductivity σ_{xx}^{fl} is plotted as a function of $\epsilon = \ln T/T_c$ on a double logarithmic scale for three HTS samples (the solid line represents the $2D$ AL behavior $(1/\epsilon)$, the dotted line represents the $3D$ one: $3.2/\sqrt{\epsilon})$ [124]. One can see that paraconductivity of the less anisotropic YBCO compound asymptotically tends to the 3D behavior $(1/\epsilon^{1/2})$ for $\epsilon < 0.1$, showing the LD crossover at $\epsilon \approx 0.07$; the curve for more anisotropic 2223 phase of BSCCO starts to bend for $\epsilon < 0.03$ while the most anisotropic 2212 phase of BSCCO shows a $2D$ behavior in the whole temperature range investigated. All three compounds show a universal $2D$ temperature behavior above the LD crossover up to the limits of the GL region. It is interesting that around $\epsilon \approx 0.24$ all the curves bend down and follow the same asymptotic $1/\epsilon^3$ behavior (dashed line). Finally at the value $\epsilon \approx 0.45$ all the curves fall down indicating the end of the observable fluctuation regime.

Reggiani et al. [125] extended the $2D$ AL theory to the high temperature region by taking into account the short wavelength fluctuations. The following universal formula for $2D$ para-

conductivity of a clean 2D superconductor as a function of the generalized reduced temperature $\epsilon = \ln T/T_c$ was obtained[25]:

$$\sigma_{xx}^{fl} = \frac{e^2}{16s} f(\epsilon)$$

with $f(\epsilon) = \epsilon^{-1}$, $\epsilon \ll 1$ and $f(\epsilon) = \epsilon^{-3}$, $\epsilon \gtrsim 1$.

In the case of the out-of-plane conductivity the situation is quite different. Both positive contributions (AL and anomalous MT) are suppressed by the interlayer transparency, leading to a competition between positive and negative terms. This can lead to a maximum in the c-axis fluctuation resistivity which occurs in the 2D regime (in the case discussed $J\tau << 1, r\kappa << 1$ and $\gamma_\varphi \kappa > 1$):

$$\epsilon_m/r \approx \frac{1}{(8r\kappa)^{1/2}} - \frac{1}{8\kappa}\left[\tilde{\kappa} - \frac{1}{2\gamma_\varphi}\right].$$

This nontrivial effect of fluctuations on the transverse resistance of a layered superconductor allows a successful fit to the data observed on optimally and overdoped HTS samples (see, for instance, Fig.20.12) where the growth of the resistance still can be treated as the correction.

The fluctuation mechanism of the growth of the transverse resistance can be easily understood in a qualitative manner. Indeed to modify the in-plane result (20.98) for the case of c-axis paraconductivity one has to take into account the hopping character of the electronic motion in this direction. If the probability of one-electron interlayer hopping is $\mathcal{P}_1$, then the probability of coherent hopping for two electrons during the fluctuation Cooper pair lifetime τ_{GL} is the conditional probability of these two events: $\mathcal{P}_2 = \mathcal{P}_1(\mathcal{P}_1\tau_{GL})$. The transverse paraconductivity may thus be estimated as $\sigma_\perp^{AL} \sim \mathcal{P}_2\sigma_\parallel^{AL} \sim \mathcal{P}_1^2\frac{1}{\epsilon^2}$, in complete accordance with (20.182). We see that the temperature singularity of $\sigma_\perp^{AL}$ turns out to be stronger than that in $\sigma_\parallel^{AL}$, however for a strongly anisotropic layered superconductor $\sigma_\perp^{AL}$ is considerably suppressed by the square of the small probability of inter-plane electron hopping which enters in the pre-factor. It is this suppression which leads to the necessity of taking into account the DOS contribution to the transverse conductivity. The latter is less singular in temperature but, in contrast to the paraconductivity, manifests itself in the first, not the second, order in the interlayer transparency $\sigma_\perp^{DOS} \sim -\mathcal{P}_1 \ln \frac{1}{\varepsilon}$. The DOS fluctuation correction to the one-electron transverse conductivity is negative and, being proportional to the first order of $\mathcal{P}_1$, can completely change the traditional picture of fluctuations just rounding the resistivity temperature dependence around transition. The shape of the temperature dependence of the transverse resistance mainly is determined by competition of the opposite sign contributions: the paraconductivity and MT term, which are strongly temperature dependent but are suppressed by the square of the barrier transparency and the DOS contribution which has a weaker temperature dependence but depends only linearly on the barrier transparency.

20.6 Manifestation of fluctuations in various properties

In this Section we will demonstrate the applications of the microscopic theory of fluctuations. The limited volume does not permit us to deliver here the systematic review of the modern theory and we restrict ourselves only by presentation of the several representative recent studies. The details one can find in the articles cited in subtitles.

It is necessary to underline that the comparison of the results of fluctuation theory with the experimental findings on HTS materials has to be considered sooner in qualitative than quantitative context. Indeed, as is clear now, the superconductivity in the most of HTS compounds has the nontrivial symmetry. Moreover, as was discussed in the previous Section, these

[25] In Section 7.2 we will demonstrate how such a dependence $\left(1/\ln^3(T/T_c)\right)$ appears by accounting for short wavelength fluctuations for the $2D$ fluctuation susceptibility.

Figure 20.12: Fit of the temperature dependence of the transverse resistance of an underdoped BSCCO c-axis oriented film with the results of the fluctuation theory [126]. The inset shows the details of the fit in the temperature range between T_c and 110K.

compounds are rather clean than dirty. Both these complications can be taken into account (see for example [112, 97]) but this was not done in the majority of the cited papers.

20.6.1 The effects of fluctuations on magnetoconductivity [97, 127, 154, 155]

The experimental investigations of the fluctuation magnetoconductivity are of special interest first because this physical value weakly depends on the normal state properties of superconductor and second due to its special sensitivity to temperature and magnetic field. The role of AL contribution for both the in-plane and out-of-plane magnetoconductivities was studied above in the framework of the phenomenological approach. The microscopic calculations of the other fluctuation corrections to the in-plane magnetoconductivity conductivity show that the MT contribution has the same positive sign and temperature singularity as the AL one. In the case of weak pair-breaking it can even considerably exceed the latter. The negative DOS contribution, like in the case of the zero-field conductivity, turns out to be considerably less singular and many authors (see e.g. Refs. [136, 137, 138, 139, 142, 140, 141, 143, 144, 145],[146, 147]) successfully explained the in-plane magnetoresistance data in HTS using the AL and MT contributions only [148, 149, 150, 151].

Turning to the out-of-plane magnetoconductivity of a layered superconductor one can find a quite different situation. Both the AL and MT contributions turn out to be here of the second order in the interlayer transparency and this circumstance makes the less singular DOS contribution, which remains however of first order in transparency, to be competitive with the main terms [127]. The large number of microscopic characteristics involved in this competition, like the Fermi velocity, interlayer transparency, phase-breaking and elastic relaxation times, gives rise to the possibility of occurrence of different scenarios for various compounds. The c-axis magnetoresistance of a set of HTS materials shows a very characteristic behavior above T_{c0}. In contrast to the ab-plane magnetoresistance which is positive at all temperatures, the magnetoresistance along the c-axis has been found in many HTS compounds (BSSCO [128, 130, 131, 132], LSSCO [133], YBCO [134] and TlBCCO [135]) to have a negative sign not too close to T_{c0} and turn positive at lower temperatures. We will show how this behavior find its explanation within the fluctuation theory [97].

We consider here the effect of a magnetic field parallel to the c-axis. In this case both quasiparticles and Cooper pairs move along Landau orbits within the layers. The c-axis dispersion remains unchanged from the zero-field form. In the chosen geometry one can generalize the zero-field results reported in the previous Section to finite field strengths simply by the

replacement of the two-dimensional integration over $\mathbf{q}$ by a summation over the Landau levels

$$\int \frac{d^2\mathbf{q}}{(2\pi)^2} \to \frac{H}{\Phi_0}\sum_n = \frac{h}{2\pi\eta_{(2)}}\sum_n$$

(let us remind that $\eta_{(2)} = \xi_{xy}^2$). So the general expressions for all fluctuation corrections to the c-axis conductivity in a magnetic field can be simply written in the form [97]:

$$\sigma_{zz}^{AL} = \frac{e^2 s r^2 h}{64\xi_{xy}^2}\sum_{n=0}^{\infty}\frac{1}{\{[\epsilon + h(2n+1)][r+\epsilon+h(2n+1)]\}^{3/2}} \tag{20.197}$$

$$\sigma_{zz}^{DOS} = -\frac{e^2 s r\kappa h}{8\xi_{xy}^2}\sum_{n=0}^{1/h}\frac{1}{\{[\epsilon + h(2n+1)][r+\epsilon+h(2n+1)]\}^{1/2}} \tag{20.198}$$

$$\sigma_{zz}^{MT(reg)} = -\frac{e^2 s\tilde{\kappa} h}{4\xi_{xy}^2}\sum_{n=0}^{\infty}\left(\frac{\epsilon + h(2n+1) + r/2}{\{[\epsilon + h(2n+1)][r+\epsilon+h(2n+1)]\}^{1/2}} - 1\right) \tag{20.199}$$

$$\sigma_{zz}^{MT(an)} = \frac{e^2 s h}{8\xi_{xy}^2(\varepsilon-\gamma_\varphi)}\sum_{n=0}^{\infty}\left(\frac{\gamma_\varphi + h(2n+1) + r/2}{\{[(\gamma_\varphi + h(2n+1)][\gamma_\varphi + h(2n+1)+r)]\}^{1/2}} - \right.$$
$$\left. - \frac{\epsilon + h(2n+1) + r/2}{\{[\epsilon + h(2n+1)][r+\epsilon+h(2n+1)]\}^{1/2}}\right). \tag{20.200}$$

For the in-plane component of the fluctuation conductivity tensor the only additional problem appears in the AL diagram, where the matrix elements of the harmonic oscillator type, originating from the $B_\parallel$ ($q_\parallel$) blocks, have to be calculated. How to do this was demonstrated in details in Section 4. The other contributions are essentially analogous to their c-axis counterparts:

$$\sigma_{xx}^{AL} = \frac{e^2}{4s}\sum_{n=0}^{\infty}(n+1)\left(\frac{1}{\{[\epsilon + h(2n+1)][r+\epsilon+h(2n+1)]\}^{1/2}} - \right.$$
$$\frac{2}{\{[\epsilon + h(2n+2)][r+\epsilon+h(2n+2)]\}^{1/2}} +$$
$$\left.\frac{1}{\{[\epsilon + h(2n+3)][r+\epsilon+h(2n+3)]\}^{1/2}}\right), \tag{20.201}$$

$$\sigma_{xx}^{DOS} + \sigma_{xx}^{MT(reg)} = -\frac{e^2 h(\kappa+\tilde{\kappa})}{2s}\sum_{n=0}^{1/h}\frac{1}{\{[\epsilon + h(2n+1)][r+\epsilon+h(2n+1)]\}^{1/2}}, \tag{20.202}$$

and

$$\sigma_{xx}^{MT(an)} = \frac{e^2 h}{4s(\epsilon-\gamma_\varphi)}\sum_{n=0}^{\infty}\left(\frac{1}{\{[(\gamma_\varphi + h(2n+1)][\gamma_\varphi + h(2n+1)+r)]\}^{1/2}} - \right.$$
$$\left.\frac{1}{\{[\epsilon + h(2n+1)][r+\epsilon+h(2n+1)]\}^{1/2}}\right). \tag{20.203}$$

These results can in principle be already used for numerical evaluations and fitting of the experimental data which was indeed successfully done in a series of papers [134, 152, 135].

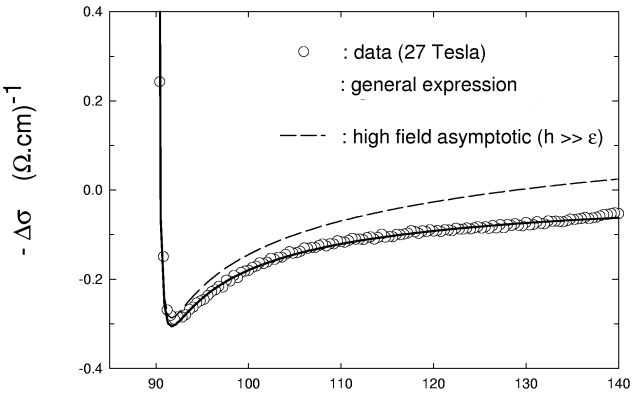


Figure 20.13: Magnetoconductivity versus temperature at 27 T for an underdoped Bi-2212 single crystal. The solid line represents the theoretical calculation. The symbols are the experimental magnetoconductivity $\Delta\sigma_{zz}(B \shortparallel c \shortparallel I)$[155]

The detailed comparison of the cited results with the experimental data [134, 153], especially in strong fields, raised the problem of regularization of the DOS contribution. If in the absence of the magnetic field its ultra-violet divergence was successfully cut off at $q \sim \xi^{-1}$, in the case under consideration the cut off parameter depends on the magnetic field and makes the fitting procedure ambiguous. The solution of this problem was proposed in [154], where the authors calculated the difference $\Delta\sigma_{zz}^{DOS} = \sigma_{zz}^{DOS}(h,\epsilon) - \sigma_{zz}^{DOS}(0,\epsilon)$ applying to formulas (20.198) and (20.202) the same trick which was already used in Section 2 for the regularization of the free energy in magnetic field (Eq. (20.77)). The corresponding asymptotics for all out-of-plane fluctuation contributions are presented in the following table:

	$h \ll \epsilon$	$\epsilon \ll h \ll r \quad (3D)$	$\max\{\epsilon, r\} \ll h \quad (2D)$
$\Delta\sigma_{zz}^{DOS}$	$\frac{e^2 s\kappa}{3\,2^5\xi_{xy}^2}\frac{r(\epsilon+r/2)}{[\epsilon(\epsilon+r)]^{3/2}}h^2$	$0.428\frac{e^2 s\kappa}{16\xi_{xy}^2}r\sqrt{\frac{h}{r}}$	$\frac{e^2 s\kappa}{8\xi_{xy}^2}r\ln\frac{\sqrt{h}}{\sqrt{\epsilon}+\sqrt{\epsilon+r}}$
$\Delta\sigma_{zz}^{MT(reg)}$	$\frac{e^2 s\tilde{\kappa}}{3\,2^6\xi_{xy}^2}\frac{r^2}{[\epsilon(\epsilon+r)]^{3/2}}h^2$	$0.428\frac{e^2 s\tilde{\kappa}}{8\xi_{xy}^2}r\sqrt{\frac{h}{r}}$	$-\sigma_{zz}^{MT(reg)}(0,\epsilon) - \frac{\pi^2 e^2 s\tilde{\kappa}}{2^8\xi_{xy}^2}\frac{r^2}{h}$
$-\Delta\sigma_{zz}^{AL}$	$\frac{e^2 s}{2^8\xi_{xy}^2}\frac{r^2(\epsilon+r/2)}{[\epsilon(\epsilon+r)]^{5/2}}h^2$	$\sigma_{zz}^{AL}(0,\epsilon) - \frac{3.24e^2 s}{\xi_{xy}^2}\sqrt{\frac{r}{h}}$	$\sigma_{zz}^{AL}(0,\epsilon) - \frac{7\zeta(3)e^2 s}{2^9\xi_{xy}^2}\frac{r^2}{h^2}$
$-\Delta\sigma_{zz}^{MT(an)}$ $\min\{\epsilon, r\} \ll \gamma_\varphi$	$\frac{e^2 s}{3\,2^7\xi_{xy}^2}\frac{r^2}{[\epsilon(\epsilon+r)]^2}h^2$	$\sigma_{zz}^{MT(an)}(0,\epsilon) - \frac{e^2 s}{32\xi_{xy}^2}\sqrt{\frac{r}{\gamma_\varphi}}$	$\sigma_{zz}^{MT(an)}(0,\epsilon) - \frac{3\pi^2 e^2 s}{2^8\xi_{xy}^2}\frac{\max\{r,\gamma_\varphi\}}{h}$
$-\Delta\sigma_{zz}^{MT(an)}$ $\gamma_\varphi \ll \min\{\epsilon, r\}$	$\frac{e^2 s}{3\,2^7\xi_{xy}^2}\frac{\sqrt{r}}{\epsilon\gamma_\varphi^{3/2}}h^2$	$\sigma_{zz}^{MT(an)}(0) - \frac{3.24e^2 s}{64\xi_{xy}^2}\sqrt{\frac{r}{h}}$	$\sigma_{zz}^{MT(an)}(0,\epsilon) - \frac{3\pi^2 e^2 s}{2^8\xi_{xy}^2}\frac{(r+\epsilon)}{h}$

Table 3

The procedure described gives an excellent fitting up to very high fields [155] which is shown in Fig. 20.13.

Let us start the analysis from the $2D$ case ($r \ll \epsilon$). One can see that here the positive DOS contribution to magnetoconductivity turns out to be dominant. It grows as H^2 up to $H_{c2}(\epsilon)$ and then crosses to a slow logarithmic asymptote. At $H \sim H_{c2}(0)$ the value of $\Delta\sigma_{zz}^{DOS}(h \sim 1, \epsilon) = -\sigma_{zz}^{DOS}(0,\epsilon)$ which means the total suppression of the fluctuation correction in such a strong field. The regular part of the Maki-Thompson contribution does not manifest itself in this case while the AL term can compete with the DOS one in the immediate vicinity of T_c, where the small anisotropy factor r can be compensated by the additional ϵ^3 in the denominator. The anomalous MT contribution can contribute in the case of small pairbreaking only, which is opposite to what is expected in HTS.

In the $3D$ case ($\epsilon \ll r$) the behavior of the magnetoconductivity is more complex. In weak and intermediate fields the main, negative, contribution to the magnetoconductivity occurs from

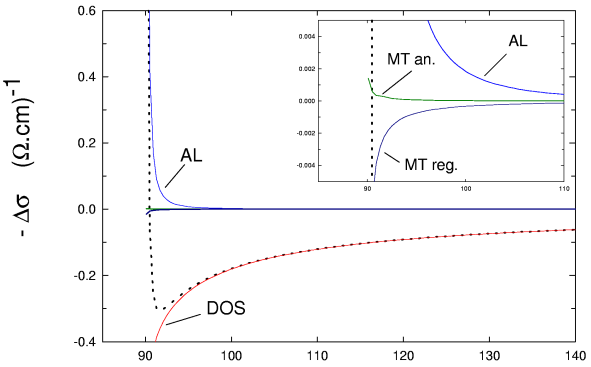


Figure 20.14: Decomposition of the calculation of total theoretical magnetoconductivity for an underdoped Bi-2212 single crystal at 27 T. The inset shows the regular and anomalous parts of the MT contribution which are too small to be presented in the same scale as the AL and DOS contributions [155].

the AL and MT terms. At $H \sim H_{c2}(\epsilon)(h \sim \epsilon)$ the paraconductivity is already considerably suppressed by the magnetic field and the h^2 - dependence of the magnetoconductivity changes through the $\sqrt{\frac{r}{h}}$ tendency to the high field asymptote $-\sigma_{zz}^{(fl)}(0,\epsilon)$. In this intermediate region of fields ($\epsilon \ll h \ll r$), side by side with the decrease ($\sim \sqrt{\frac{r}{h}}$) of the main AL and MT contributions, the growth of the still relatively small DOS term takes place. At the upper limit of this region ($h \sim r$) its positive contribution is of the same order as the AL one and at high fields ($r \ll h \ll 1$) the DOS contribution determines the slow logarithmic decay of the fluctuation correction to the conductivity which is completely suppressed only at $H \sim H_{c2}(0)$. The regular part of the Maki- Thompson contribution is not of special importance in the $3D$ case. It remains comparable with the DOS contribution in the dirty case at fields $h \lesssim r$, but decreases rapidly ($\sim \frac{r}{h}$) at strong fields ($h \gtrsim r$), in the only region where the robust $\Delta\sigma_c^{DOS}(h,\epsilon) \sim \ln\frac{h}{r}$ shows up surviving up to $h \sim 1$.

The temperature dependence of the different fluctuation contributions to the magnetoconductivity calculated for an underdoped Bi-2212 single crystal at the magnetic field 27 T is presented in Fig. 20.14.

The formulas for the in-plane magnetoconductivity are presented in the table:

	$h \ll \epsilon$	$\epsilon \ll h \ll r;\quad \max\{\epsilon, r\} \ll h$
$\Delta\sigma_{xx}^{AL}$	$-\frac{e^2}{2^8 s}\frac{[8\epsilon(\epsilon+r)+3r^2]}{[\epsilon(\epsilon+r)]^{5/2}}h^2$	$-\sigma_{xx}^{AL}(0,\epsilon)+\frac{e^2}{4s}\frac{1}{\sqrt{2hr}};\quad -\sigma_{xx}^{AL}(0,\epsilon)+\frac{e^2}{8s}\frac{1}{h}$
$\Delta\sigma_{xx}^{MT(an)}$ $(\min\{\epsilon, r\} \ll \gamma_\varphi)$	$-\frac{e^2}{3\,2^5 s}\frac{(\epsilon+r/2)}{[\epsilon(\epsilon+r)]^{3/2}}h^2$	$-\sigma_{xx}^{MT}(0,\epsilon)+\frac{e^2}{8s}\frac{1}{\gamma_\varphi}\ln\frac{\sqrt{\gamma_\varphi}}{\sqrt{2h}+\sqrt[4]{2h+r}}$
$\Delta\sigma_{xx}^{MT(an)}$ $(\gamma_\varphi \ll \min\{\epsilon, r\})$	$-\frac{e^2}{3\,2^5 s}\frac{1}{\epsilon\gamma^{3/2}r^{1/2}}h^2$	$-\sigma_{xx}^{MT}(0,\epsilon)+\frac{0.2e^2}{s}\frac{1}{\sqrt{hr}};\quad -\sigma_{xx}^{MT}(0,\epsilon)+\frac{3\pi^2e^2}{32s}\frac{1}{h}$
$\Delta(\sigma_{xx}^{DOS}+$ $\sigma_{xx}^{MT(reg)})$	$\frac{e^2(\kappa+\tilde{\kappa})}{3\,2^7 s}\frac{(\varepsilon+r/2)}{[\varepsilon(\varepsilon+r)]^{3/2}}h^2$	$0.428\frac{e^2(\kappa+\tilde{\kappa})}{2^6 s}\sqrt{\frac{h}{r}};\qquad \frac{e^2(\kappa+\tilde{\kappa})}{32s}\ln\frac{\sqrt{h}}{(\sqrt{\epsilon}+\sqrt{\epsilon+r})}$

Table 4

Analyzing it one can see that in almost all regions the negative AL and MT contributions govern the behavior of in-plane magnetoconductivity. Nevertheless, similar to the c-axis case, the high field behavior is again determined by the positive logarithmic $\Delta(\sigma_{xx}^{DOS}+\sigma_{xx}^{MT(reg)})$ contribution, which is the only one to survive in strong field. It is important to stress that the suppression of the DOS contribution by a magnetic field takes place very slowly. Such robustness with respect to the magnetic field is of the same physical origin as the slow logarithmic dependence of the DOS-type corrections on temperature.

Another important problem which appears in the fitting of the resistive transition shape in relatively strong fields with the fluctuation theory is the much larger broadening of the transition than predicted by the Abrikosov-Gorkov theory [156]. Kim and Gray [96] explained the broadening of the c-axis peak with increasing magnetic field in terms of Josephson coupling, describing a layered superconductor as a stack of Josephson junctions. In Refs. [157, 71] the self-consistent Hartree approach was proposed for the extension of fluctuation theory beyond the Gaussian approximation. It results in the considerable shift of $T_c(H)$ toward low temperatures with a corresponding broadening of the transition. The renormalized reduced temperature $\tilde{\varepsilon}_h$ is determined according to the self-consistent equation [71]:

$$\varepsilon_h = \tilde{\varepsilon}_h - \frac{1}{4}\, Gi_{(2)}\; h \sum_{n=0}^{1/h} \frac{1}{[(\tilde{\varepsilon}_h + hn)(\tilde{\varepsilon}_h + h(n+1) + r)]^{1/2}} \tag{20.204}$$

The authors of [158], following the procedure proposed by Dorsey and Ullah [71], modified the expressions (20.197)- (20.203) by account for (20.204). In result they succeeded to fit quantitatively both in-plane resistivity transition and the transverse resistivity peak for BSCCO films strongly broadened by applied magnetic field.

20.6.2 Fluctuations far from T_c or in strong magnetic fields

As was mentioned above the role of fluctuations is especially pronounced in the vicinity of the critical temperature. Nevertheless for some phenomena they can be still considerable far from the transition too. In these cases the GL theory is certainly unapplicable since the short-wave and dynamical fluctuation contributions have to be taken into account. It can be done in the microscopic approach which we will demonstrate in several examples.

Fluctuation magnetic susceptibility far from transition [29].

The given above qualitative estimations (20.57)-(20.63) for the fluctuation diamagnetic susceptibility, based on the Langevin formula, demonstrate that even at high temperatures $T \gg T_c$ it turns to be of the order of χ_P for clean $3D$ superconductors and exceeds noticeably this value for $2D$ systems. In order to develop the microscopic theory [159, 29, 161] let us start from the general expression for free energy in the one-loop approximation:

$$F = T \sum_{\Omega_k} \mathrm{Tr}\{\ln[1 - g\Pi(\Omega_k, \mathbf{r}, \mathbf{r}')]\}, \tag{20.205}$$

where g is the effective interaction constant related with the transition critical temperature by (20.153). This approximation corresponds to the ladder one (see (20.146)) for the fluctuation propagator. The polarization operator $\Pi(\Omega_k, \mathbf{r}, \mathbf{r}')$ is determined by expression (20.147) but in the case of an applied magnetic field the homogeneity of the system is lost and $\Pi(\Omega_k, \mathbf{r}, \mathbf{r}')$ depends not on the space variable difference $\mathbf{r} - \mathbf{r}'$ but on each separately. Expanding $\Pi(\Omega_k, \mathbf{r}, \mathbf{r}')$ one can express the magnetic susceptibility of a layered superconductor in a weak magnetic field perpendicular to the layers in terms of the derivatives $\Pi_x = \frac{\partial}{\partial q_x}\Pi(\mathbf{q})$ [29]:

$$\chi = -\frac{\partial^2 F}{\partial H^2} = -\frac{2}{3} e^2 T \sum_{\Omega_k} \int \frac{d^3\mathbf{q}}{(2\pi)^3} L^3 \Pi_x (\Pi_x \Pi_{yy} - \Pi_y \Pi_{xy}). \tag{20.206}$$

The final expressions for the fluctuation diamagnetic susceptibility in the clean and dirty cases for wide range of temperatures can be written as:

$$\chi_{fl}^{(3)}(T) = \frac{\chi_P}{3} \begin{cases} 0.05(\ln^{-2}(\omega_D/T_c)) - \ln^{-2}(T/T_c)), & \tau^{-1} \ll T \ll \omega_D \\ 2\sqrt{T\tau}\,\ln^{-1}(T/T_c), & T_c \ll T \ll \tau^{-1} \end{cases} \tag{20.207}$$

$$\chi_{fl}^{(2)}(T) = \frac{0.05}{p_F s}\chi_P \left(\frac{E_F}{T}\right) \frac{1}{\ln^3(T/T_c)} \tag{20.208}$$

Let us stress that these results are valid for the fluctuation diamagnetism of a normal metal with $g > 0$ too, if by T_c one uses the formal value $T_c \sim E_F \exp(\frac{1}{\nu g})$.

Fluctuation magnetoconductivity far from transition [162].

Let us discuss the conductivity of the $2D$ electron system with impurities in a magnetic field at low temperatures. Even in the absence of the field the effects of quantum interference of the non-interacting electrons in their scatterings on elastic impurities already results in the appearance of a nontrivial temperature dependence of the resistance. This result contradicts the statement of the classical theory of metals requiring the saturation of the resistance at its residual value at low temperatures. In a superconductor above the critical temperature this, so-called weak localization (WL), effect is amplified by the Andreev reflection of electrons on the fluctuation Cooper pair leading to appearance of the MT correction to the conductivity. The characteristic feature of both the MT and WL corrections is their extreme sensitivity to the dephasing time τ_φ and to weak magnetic fields.

Beyond the GL region ($T \gtrsim T_c$) the MT correction is determined by the same diagram 2 of Fig. 20.9 but now the dynamic ($\Omega_k \neq 0$) and short-wave-length ($q \sim \xi^{-1}$) fluctuation modes have to be taken into account. The corresponding calculations were performed in [98, 162] and the result can be written in the form:

$$\delta\sigma_{WL+MT} = \frac{e^2}{2\pi^2}\left[\alpha - \beta(T)\right] Y\left(\Omega_L \tau \epsilon\right), \tag{20.209}$$

where we introduced the effective Larmour frequency for the diffusion motion $\Omega_L = 4\mathcal{D}eH$ with the diffusion coefficient $\mathcal{D}$ [26] and the function

$$Y(x) = \ln x + \psi(\frac{1}{2} + \frac{1}{x}) = \begin{cases} \frac{x^2}{24}, & x \ll 1 \\ \ln x, & x \gg 1 \end{cases}. \tag{20.210}$$

The first term in this formula corresponds to the WL contribution ($\alpha = 1$ if the spin-orbit interaction of the electrons with the impurities is small while in the opposite limiting case $\alpha = -1/2$), the second describes the MT contribution to magnetoconductivity. The function $\beta[\ln(T/T_c)]$ was introduced in Ref.[162]. At $T \to T_c$ $\beta(x) = 1/x$ and (20.209) reduces to the already studied MT correction in the vicinity of critical temperature. For $T \gg T_c$ $\beta(x) = 1/x^2$ and the MT contribution gives a logarithmically small correction to the WL result. Its zero-field value, being proportional to $\ln^{-2}(T/T_c)$, decreases with the growth of the temperature faster than both the AL contribution (in the dirty case $\delta\sigma_{AL} \sim 1/\ln(T/T_c)$) and the especially slow DOS contribution ($\delta\sigma_{DOS} \sim \ln\ln(1/T_c\tau) - \ln\ln(T/T_c)$) (see Ref. [98, 99]).

It worth mentioning that for the region of temperatures $T \gg T_c$, analogous to Exp.(20.207)-(20.208), the result (20.209) can be applied both to superconducting and normal metals ($g > 0$), if in place of the critical temperature the formal value $T_c \sim E_F \exp(\frac{1}{\nu g})$ is undermined. The interplay of the localization and fluctuation corrections was extensively studied (see, for example, [163, 164, 165, 166, 167])

[26] Comparison of the expressions (20.76), (20.114) and (20.209) relates the Larmour frequency with the dimensionless field: $h = \Omega_L/2T_c$ introduced in section 2 and the diffusion coefficient with the phenomenological GL constants $\mathcal{D} = 1/m\alpha$.

Fluctuations in magnetic fields near $H_{c2}(0)$ [168].

As one can see from (20.201)- (20.203), in the vicinity of the upper critical field $H_{c2}(T)$ the fluctuation corrections diverge as ϵ_h^{-1} for the $2D$ case and as $\epsilon_h^{-1/2}$ for the $3D$ case [27] (it is enough to keep just the terms with $n = 0$ in these formulas). This behavior is preserved in strong magnetic fields too, but the coefficients undergo changes. A case of special interest is $T \ll T_c$ (which means $H \to H_{c2}(0)$) which represents an example of a quantum phase transition [168]. Microscopic analysis of the magnetoconductivity permits us to study the effect of fluctuations in magnetic fields of the order of $H_{c2}(0)$, where the GL functional approach is inapplicable.

We restrict our consideration to the case of a dirty metal ($T\tau \ll 1$). In this limit $|\tilde{\omega}_{n+\mu} - \tilde{\omega}_{-n}| \approx \tau^{-1}$ and the Green function correlator (20.149) can be written in the form

$$\mathcal{P}(\mathbf{q}, \varepsilon_1, \varepsilon_2) = 2\pi\nu\tau^2\theta(-\varepsilon_1\varepsilon_2)\left(\tau^{-1} - |\varepsilon_1 - \varepsilon_2| - \widehat{\mathcal{D}}q^2\right). \tag{20.211}$$

Expressing $\Pi(\mathbf{q}, \Omega_k)$ in terms of $\mathcal{P}(\mathbf{q}, \varepsilon_1, \varepsilon_2)$ by means of (20.167) and using the definition of the critical temperature one can find an explicit formula for the fluctuation propagator

$$\begin{aligned} L^{-1}(\mathbf{q}, \Omega_k) &= g^{-1} - \Pi(\mathbf{q}, \Omega_k) = \\ &= -\nu\left[\ln\frac{T}{T_c} + \psi\left(\frac{1}{2} + \frac{|\Omega_k| + \widehat{\mathcal{D}}\mathbf{q}^2}{4\pi T}\right) - \psi\left(\frac{1}{2}\right)\right]. \end{aligned} \tag{20.212}$$

The prominent characteristic of this expression is that it is valid even relatively far from the critical temperature (for temperatures $T \ll \min\{\tau^{-1}, \omega_D\}$) and for $|\mathbf{q}| \ll l^{-1}, |\Omega_k| \ll \omega_D$.

One can rewrite this expression in a magnetic field applied along the c-axis in the Landau representation by simply replacing $\left(\widehat{\mathcal{D}}\mathbf{q}^2\right)_{\|} \Rightarrow \Omega_L(n + 1/2)$ [159]:

$$\begin{aligned} L_n^{-1}(q_z, \Omega_k) &= -\nu\left[\ln\frac{T}{T_c} + \psi\left(\frac{1}{2} + \frac{|\Omega_k|}{4\pi T} + \right.\right. \\ &\left.\left. + \frac{\Omega_L(n + 1/2) + 4\tau J^2 \sin^2(q_z s/2)}{4\pi T}\right) - \psi\left(\frac{1}{2}\right)\right]. \end{aligned} \tag{20.213}$$

In the case of arbitrary temperatures and magnetic fields the expression for the AL contribution to the conductivity takes the form:

$$\begin{aligned} \sigma_{xx}^{AL}(\omega_\nu) &= \nu e^2 T \sum_{\Omega_k} \sum_{n,m=0}^{\infty} B_{n,m}(\Omega_k + \omega_\nu, \Omega_k) L_m(\Omega_k) \times \\ &\times B_{m,n}(\Omega_k, \Omega_k + \omega_\nu) L_n(\Omega_k + \omega_\nu) \end{aligned} \tag{20.214}$$

(we have restricted our consideration to the $2D$ case). The expression for $B_{n,m}(\Omega_k, \omega_\nu)$ can be rewritten as

$$\begin{aligned} B_{n,m}(\Omega_k + \omega_\nu, \Omega_k) &= -\frac{2\pi\nu}{\sqrt{eH}}\tau^2\mathcal{D}_{(2)} T \sum_{\varepsilon_i}\left[\sqrt{n+1}\delta_{m,n+1} + \sqrt{n}\delta_{m,n-1}\right] \times \\ &\lambda_n(\varepsilon_i + \omega_\nu, \Omega_k - \varepsilon_i)\lambda_m(\varepsilon_i, \Omega_k - \varepsilon_i) \end{aligned} \tag{20.215}$$

with

[27] ϵ_h is the renormalized by the magnetic field reduced temperature $\epsilon_h = \epsilon + h$

$$\lambda_m(\varepsilon_1,\varepsilon_2)=\frac{1}{\tau}\frac{\Theta\left(-\varepsilon_1\varepsilon_2\right)}{\left|\varepsilon_1-\varepsilon_2\right|+\Omega_L(m+1/2)}. \tag{20.216}$$

The critical field $H_{c2}(T)$ is determined by the equation $L_0^{-1}(q_z=0,\Omega_k=0)=0$. This is why in the vicinity of $H_{c2}(T)$ the singular contribution to (20.214) originates only from the terms with $L_0(0,\Omega_k)$. The frequency dependencies of the functions $B_{n,m}(\Omega_k+\omega_\nu,\Omega_k)$ and $L_1(\Omega_k)$ are weak although we cannot omit them to get nonvanishing answer. It is enough to restrict ourselves to the linear approximation in their frequency dependencies. If the temperature $T\ll T_{c0}$ the sum over frequencies in (20.215) can be approximated by an integral. Transforming the boson frequency Ω_k summation to a contour integration as was done above and making the analytic continuation in the external frequency ω_ν one can get an explicit expression for the d.c. paraconductivity. In the same spirit the contributions of all other diagrams from the Fig. 20.9 which contribute to fluctuation conductivity in the case under discussion are calculated side by side with the AL one. The final answer can be presented in the form:

$$\begin{aligned}\delta\sigma_{tot} \;=\; & \frac{2e^2}{3\pi^2}\left\{-\ln\frac{\pi T_{c0}}{2\gamma T}+\frac{3\gamma_E T}{T_{c0}}\left(\frac{H_{c2}(T)}{H-H_{c2}(T)}\right)+\right.\\ & +\psi\left[\frac{T_{c0}}{2\gamma_E T}\left(\frac{H-H_{c2}(T)}{H_{c2}(T)}\right)\right]+\\ & \left.+\,4\left(\frac{T_{c0}}{2\gamma_E T}\frac{H_{c2}(T)}{H-H_{c2}(T)}\psi'\left[\frac{T_{c0}}{2\gamma_E T}\left(\frac{H-H_{c2}(T)}{H_{c2}(T)}\right)\right]-1\right)\right\},\end{aligned} \tag{20.217}$$

where γ_E is the Euler constant. Let us consider some limiting cases. If the temperature is relatively high $T/T_{c0}\gg\left(H-H_{c2}(T)\right)/H_{c2}(T)$, we obtain the following formula for the fluctuation conductivity:

$$\delta\sigma=\frac{2\gamma_E e^2}{\pi^2}\frac{T}{T_{c0}}\left(\frac{H_{c2}(T)}{H-H_{c2}(T)}\right). \tag{20.218}$$

If $H<H_{c2}(0)$, we can introduce $T_c(H)$ and rewrite Eq.(20.218) in the usual way

$$\delta\sigma=\frac{3e^2}{2\gamma_E\pi^2}\frac{T_{c0}}{T-T_c(H)}. \tag{20.219}$$

If $H>H_{c2}(0)$, in the low-temperature limit $T/T_{c0}\ll\left(H-H_{c2}(T)\right)/H_{c2}(T)$ we have

$$\delta\sigma=-\frac{2e^2}{3\pi^2}\ln\frac{H_{c2}(T)}{H-H_{c2}(T)}. \tag{20.220}$$

One can see, that even at zero temperature a logarithmic singularity remains and the corresponding correction is negative. It results from all three fluctuation contributions, although the DOS one exceeds the others by numerical factor. Let us recall that in the case of the c-axis conductivity of a layered superconductor, or in granular superconductors above T_c, the DOS contribution exceeds the MT and AL ones parametrically [160].

20.6.3 The effect of fluctuations on the Hall conductivity[174]

Let us start with a discussion of the physical meaning of the Hall resistivity ρ_{xy}. In the case of only one type of carriers it depends on their concentration n and turns out to be independent of the electron diffusion coefficient: $\rho_{xy}=H/(en)$. The fluctuation processes of the MT and DOS types contribute to the diffusion coefficient, so their expected contribution to the Hall resistivity is zero. For the Hall conductivity in a weak field one can write

$$\sigma_{xy} = \rho_{xy}\sigma_{xx}^2 = \rho_{xy}\sigma_{xx}^{(n)2} + 2\rho_{xy}\sigma_{xx}^{(n)}\delta\sigma_{xx} = \sigma_{xy}^{(n)}\left(1 + 2\frac{\delta\sigma_{xx}}{\sigma_{xx}}\right) \tag{20.221}$$

so, evidently, the relative fluctuation correction to Hall conductivity is twice as large as the fluctuation correction to the diagonal component. This qualitative speculation is confirmed by the direct calculation of the MT type diagram [169].

The AL process corresponds to an independent charge transfer which cannot be reduced to a renormalization of the diffusion coefficient. It contributes weakly to the Hall effect, and this contribution is related to the Cooper pair particle-hole asymmetry. This effect was investigated in a set of papers: [169, 170, 171, 172, 71, 173, 174]. Let us recall that the proper general expression describing the paraconductivity contribution to the Hall conductivity in the general case of arbitrary magnetic fields and frequencies (in the TDGL theory limits) was already carried out above in the phenomenological approach (see Eq. (20.110)). The microscopic consideration of this value can be done in the spirit of the calculation of σ_{xx}^{AL} (see (20.180)) and after the analytical continuation results in

$$\begin{aligned}\sigma_{xy}^{AL} &= \left(\frac{2h\nu(0)}{\pi}\right)^2 \sum_{n=0}^{\infty}(n+1)\int\limits_{-\pi/s}^{\pi/s}\frac{dk_z}{2\pi}\int\limits_{-\infty}^{\infty}\coth\frac{z}{2T}dz \times \\ &\times\left[\mathrm{Im}L_n^R(z)\frac{\partial}{\partial z}\mathrm{Re}L_{n+1}^R(z) - \mathrm{Im}L_{n+1}^R(z)\frac{\partial}{\partial z}\mathrm{Re}L_n^R(z)\right].\end{aligned} \tag{20.222}$$

where dimensionless magnetic field h was introduced by (20.76). The phenomenological expression (20.110) can be obtained from this formula by carrying out the frequency integration in the same way as was done in the calculation of (20.180) (the essential region of integration is $z \ll T$).

One can see from (20.222) that if $\mathrm{Im}L_n^R(-z) = -\mathrm{Im}L_n^R(z)$ and $\mathrm{Re}L_n^R(-z) = \mathrm{Re}L_n^R(z)$ the Hall conductivity is equal to zero, or, in terms of the phenomenological parametrization, the reality of γ_{GL} results in a zero Hall effect. Physically it is possible to say that this zero is the direct consequence of electron-hole symmetry. However, from the formula (20.147) one can see that an energy dependence of the density of states or the electron interaction constant g immediately results in the appearance of an imaginary part of γ_{GL}. In the weak interaction approximation

$$\mathrm{Im}\gamma_{GL} = \frac{\nu(0)}{2}\left(\frac{\partial \ln T_c}{\partial E}\right)_{E=E_F}. \tag{20.223}$$

Usually this value is small in comparison with $\mathrm{Re}\gamma_{GL}$ by a ratio of the order of T_c/E_F. Taking into account the terms of the order of $\mathrm{Im}\gamma_{GL}$ in (20.222) and using the explicit form of the fluctuation propagator for layered superconductor (20.170) one can find

$$\begin{aligned}\sigma_{xy}^{AL} &= e^2T\frac{\mathrm{Im}\gamma_{GL}}{2\nu(0)}h \\ &\times\int\limits_{-\pi/s}^{\pi/s}\frac{dk_z}{2\pi}\frac{1}{\left[\epsilon + r\sin^2(k_zs/2))\right]^2}F\left(\frac{\epsilon + r\sin^2(k_zs/2))}{2h}\right),\end{aligned} \tag{20.224}$$

where

$$F(x) = 4x^2\left[\psi(x) + x\psi'(x) - 1 - \psi(\frac{1}{2} + x)\right].. \tag{20.225}$$

For $H \to 0$ the expression for the fluctuation Hall paraconductivity takes the form

$$\sigma_{xy}^{AL} = \frac{e^2 T}{6s}\left(\frac{\mathrm{Im}\gamma_{GL}}{\nu(0)}\right) h \frac{\epsilon + r/2}{\left[\epsilon\left(\epsilon + r\right)\right]^{3/2}} = \frac{e^3 \Phi_0 T}{6\pi s}\left(\frac{\mathrm{Im}\gamma_{GL}}{\nu(0)}\right) \frac{\epsilon + r/2}{\left[\epsilon\left(\epsilon + r\right)\right]^{3/2}} h. \tag{20.226}$$

One can see that in the $2D$ case the temperature dependence of the AL fluctuation correction to the Hall conductivity

$$\sigma_{xy}^{AL} \approx \frac{e^3 \Phi_0}{12\pi s}\left(\frac{T_c}{E_F}\right)\frac{h}{\epsilon^2}$$

turns out to be more singular than the MT one.

20.6.4 Fluctuations in the ultra-clean case [175]

When dealing with the superconductor electrodynamics in the fluctuation regime, it is necessary to remember that in the vicinity of the critical temperature the role of the effective size of a fluctuation Cooper pair is played by the GL coherence length $\xi_{GL}(T) = \xi_0/\sqrt{\epsilon}$. So, as was already mentioning above, the case of a pure enough superconductor with electron mean free path $\ell \gg \xi_0$ has to be formally subdivided into the clean ($\xi_0 \ll \ell \ll \xi_{GL}(T)$) and ultra-clean ($\xi_{GL}(T) \ll \ell$) limits. The nontrivial cancellation of the contributions, previously divergent in $T\tau$ (see, for example, (20.186)), will be shown in this Section. This results in a reduction of the total fluctuation correction in the ultra-clean case to the AL term only. We will base on [175] restricting our consideration to the case of a 2D electron system.

In terms of the parameter $T\tau$, used in the theory of disordered alloys, three different domains of the metal purity can be distinguished: $T\tau \ll 1$ (dirty case), $1 \ll T\tau \ll 1/\sqrt{\epsilon}$ (clean case) and $1/\sqrt{\epsilon} \ll T\tau$ (ultra-clean case of non-local electrodynamics). The latter case was rarely discussed in the literature [150, 176, 177] in spite of the fact that it becomes of primary importance for metals of very modest purity, let us say, with $T\tau \approx 10$. Really, in this case the condition $T\tau \geq 1/\sqrt{\epsilon}$, which in terms of the reduced temperature is read as $10^{-2} \leq \epsilon \ll 1$, practically covers all the experimentally accessible range of temperatures for the fluctuation conductivity measurements. As regards the usually considered local clean case ($1 \ll T\tau \ll 1/\sqrt{\epsilon}$) for the chosen value $T\tau \approx 10$, it would not have any range of applicability. Indeed, the equivalent condition for the allowed temperature interval is $\epsilon \ll (T\tau)^{-2}$, and it almost contradicts the $2D$ thermodynamical Ginzburg-Levanyuk criterion for the mean field approximation applicability ($Gi_{(2)} = \frac{T_c}{E_F} \ll \epsilon$). Moreover, as we will show below, for transport coefficients the higher order corrections become comparable with the mean field results much before they are important for thermodynamical quantities, namely at $\epsilon \sim \sqrt{Gi_{(2)}}$ [178, 179]. So in practice one can speak about the dirty and the non-local ultra-clean limits only.

As we saw above the 2D AL contribution turns out to be completely independent of the electron mean free path ℓ [5]. The anomalous Maki-Thompson contribution, being induced by the pairing on the Brownian diffusive trajectories [76], naturally depends on $T\tau$, but in an indirect way. It turns out to be $\tau-$independent up to $T\tau \sim 1/\sqrt{\epsilon}$, (see (20.195)) and diverges as $T\tau \ln(T\tau)$ for $T\tau \gg 1/\sqrt{\epsilon}$ [150, 176]. The analogous problem takes place in the case of the DOS contribution: its standard diagrammatic technique calculations lead to a negative correction (20.186) [95] evidently strongly divergent when $T\tau \to \infty$. In the derivation of all these results the local form of the fluctuation propagator and Cooperons were used. This is why the direct extension of their validity for $T\tau \gg 1/\sqrt{\epsilon} \to \infty$ is incorrect.

One can notice [175] that at the upper limit of the clean case, when $T\tau \sim 1/\sqrt{\epsilon}$, both the DOS and anomalous MT (20.195) contributions turn out to be of the same order of magnitude but of opposite signs. So one can suspect that in the case of a correct procedure of impurity

averaging in the ultra-clean case the large negative DOS contribution can be cancelled with the positive anomalous MT one. In the case of a $2D$ electron spectrum the Cooperon can be calculated exactly for the case of an arbitrary electron mean free path:

$$\lambda(\mathbf{q},\varepsilon_1,\varepsilon_2)=\left(1-\frac{\Theta(-\varepsilon_1\varepsilon_2)}{\tau\sqrt{(\widetilde{\varepsilon}_1-\widetilde{\varepsilon}_2)^2+v_F^2q^2}}\right)^{-1}. \tag{20.227}$$

One can see that this expression can be reduced to (20.163) in the case of $v_Fq\ll|\widetilde{\varepsilon}_1-\widetilde{\varepsilon}_2|$. Let us stress that this result was carried out without any expansion over the Cooper pair center of mass momentum $\mathbf{q}$ and is valid in the $2D$ case for an arbitrary ℓq.

The fluctuation propagator in the $2D$ case of an arbitrary mean free path can be written as [175]

$$\begin{aligned}-[\nu L(\mathbf{q},\Omega_k)]^{-1} &= \ln\frac{T}{T_c}+\sum_{n=0}^{\infty}\left\{\frac{1}{n+1/2}\right. \\ &\left.-\frac{1}{\sqrt{\left(n+\frac{1}{2}+\frac{\Omega_k}{4\pi T}+\frac{1}{4\pi T\tau}\right)^2+\frac{v_F^2\mathbf{q}^2}{16\pi^2T^2}}-\frac{1}{4\pi T\tau}}\right\}.\end{aligned} \tag{20.228}$$

Near T_c $\ln\frac{T}{T_c}\approx\epsilon$ and in the local limit, when only small momenta $\ell q\ll 1$ are involved in the final integrations, the Exp. (20.228) can be expanded in $v_Fq/\max\{T,\tau^{-1}\}$ and reduces to the appropriate local expression.

Let us demonstrate the specifics of the non-local calculations for the example of the Maki-Thompson contribution. We restrict our consideration to the vicinity of the critical temperature, where the static approximation is valid. Using the non-local expressions for the Cooperon and the propagator one can find after integration over electronic momentum:

$$\begin{aligned}Q^{(MT)}(\omega_\upsilon) &= -4\pi\nu v_F^2e^2T^2\sum_{\varepsilon_n}\int\frac{d^2\mathbf{q}}{(2\pi)^2}L(\mathbf{q},0)\times \\ &\times\left[\mathcal{M}\left(\widetilde{\epsilon}_n,\widetilde{\epsilon}_{n+\nu},\mathbf{q}\right)+\mathcal{M}\left(\widetilde{\epsilon}_{n+\nu},\widetilde{\epsilon}_n,\mathbf{q}\right)\right],\end{aligned} \tag{20.229}$$

where

$$\mathcal{M}(\alpha,\beta,\mathbf{q})=\frac{R_q(2\alpha)R_q(\alpha+\beta)-\Theta(\alpha\beta)R_q(2\alpha)R_q(2\beta)}{(\beta-\alpha)^2\left(R_q(2\alpha)-\frac{1}{\tau}\right)\left(R_q(2\beta)-\frac{1}{\tau}\right)R_q(\alpha+\beta)}$$

and $R_q(x)=\sqrt{x^2+v_F^2\mathbf{q}^2}$. The analogous consideration of the DOS diagrams 2 and 4 which are the leading ones in the clean case [95] results in similar expressions.

One can see that, after analytical continuation over the external frequency $\omega_\nu\to-i\omega$ and the consequent tending $\omega\to0$, each of the DOS or MT type diagrams is written in the form of a Laurent series of the type $C_{-2}(T\tau)^2+C_{-1}(T\tau)+C_0+C_1(T\tau)^{-1}+...$ and is divergent at $T\tau\to\infty$ in accordance with (20.186). Nevertheless the expansion in a Laurent series of the sum of these non-local diagrams leads to the exact cancellation of all divergent contributions. The leading order of the sum of the MT and DOS contributions in the limit of $T\tau\gg1$ turns out to be proportional to $(T\tau)^{-1}$ only and disappears in the ultra-clean limit. So the correct accounting for non-local scattering processes in the ultra-clean limit results in a total quantum correction negligible in comparison with the AL contribution. Nevertheless, its formal independence on impurities concentration (see (20.97)) was re-examined for ultra-clean case too in [174] and there it was demonstrated that this statement is valid in a rigorous sense only in the case of direct current and absence of a magnetic field. Let us recall that the normal Drude conductivity in the ultra-clean case takes the form

$$\sigma_{\pm}(\omega) = \sigma_{xx} \pm i\sigma_{xy} = \frac{e^2 n\tau/m}{1 - i(\omega \mp \omega_c)\tau}, \tag{20.230}$$

where ω_c is the cyclotron frequency. When $\tau \to \infty$ the real part of the conductivity vanishes. The analysis of the AL diagram in the ultra-clean case demonstrates that each of the Green functions blocks B acquires the same denominator. As a result the expression for the fluctuation conductivity contains the same Drude like pole but of second order

$$\sigma_{\pm}^{AL}(\omega) = \frac{\sigma_{xx}^{AL(l)} \pm i\sigma_{xy}^{AL(l)}}{(1 - i(\omega \mp \omega_c)\tau)^2} \tag{20.231}$$

($\sigma_{\alpha\beta}^{AL(l)}$ is the component of the paraconductivity tensor calculated above in the local limit (20.97-(20.226)). The origin of this pole can be recognized by means of the following speculation. The electric field does not interact directly with the fluctuation Cooper pairs, but it produces the effect by interaction with the quasiparticles forming these pairs only. The characteristic time of the change of a quasiparticle state is of the order of τ. Consequently the single-particle Drude type conductivity in an a.c. field has a first order pole, while in the AL paraconductivity it is of second order [174]. In spite of this difference one can see that the AL conductivity, like the Drude one, vanishes at $\omega \neq 0, \tau \to \infty$ because in the absence of impurities the interaction of the electrons does not produce any effective force acting on the superconducting fluctuations, while the d.c. paraconductivity conserves its usual $\tau-$independent form. It is impossible to distinguish the motion of the electron liquid from the condensate motion in current experiments without additional scattering.

The non-local form of the Cooperon and fluctuation propagator have to be taken into account not only for the ultra-clean case but in every problem where relatively large bosonic momenta are involved: the consideration of dynamical and short wavelength fluctuations beyond the vicinity of critical temperature, the effect of relatively strong magnetic fields on fluctuations etc. Recently such an approach was developed in a number of studies [176, 175, 180, 181].

20.6.5 The effect of fluctuations on the one-electron density of states and on tunneling measurements

Density of states [94].

The appearance of non-equilibrium Cooper pairing above T_c leads to a redistribution of the one-electron states around the Fermi level. A semi-phenomenological study of the fluctuation effects on the density of states (DOS) of a dirty superconducting material was first carried out while analyzing the tunneling experiments of granular Al in the fluctuation regime just above T_c [182]. The second metallic electrode was in the superconducting regime and its well developed gap gave a bias voltage around which a structure, associated with the superconducting fluctuations of Al, appeared. The measured DOS energy dependence has a dip at the Fermi level [28], reaches its normal value at some energy $E_0(T)$, show a maximum at an energy value equal to several times E_0, finally decreases towards its normal value at higher energies. The characteristic energy E_0 was found to be of the order of the inverse of the GL relaxation time τ_{GL} introduced above.

The presence of a depression at $E = 0$ and of a peak at $E \sim (1/\tau_{GL})$ in the DOS above T_c are precursor effects of the appearance of the superconducting gap in the quasiparticle spectrum at temperatures below T_c. The microscopic calculation of the fluctuation contribution to the one-electron DOS can be carried out within the diagrammatic technique [93, 94].

[28] Here we refer the energy E to the Fermi level, where we assume $E = 0$.

Figure 20.15: The one-electron Green function with the first order fluctuation correction.

Let us start from the discussion of a clean superconductor. As is well known the one-electron DOS is determined by the imaginary part of the retarded Green function integrated over momentum. This definition permits us to express the appropriate fluctuation correction in terms of the fluctuation propagator:

$$\delta\nu^{(c)}(E,\epsilon) = -\frac{1}{\pi}\mathrm{Im}\int\frac{d^D\mathbf{p}}{(2\pi)^D}\delta G^R(\mathbf{p},E) = -\frac{1}{\pi}\mathrm{Im}R^R(E) \tag{20.232}$$

where $R^R(E)$ is the retarded analytical continuation of the expression corresponding to the diagram of Fig. 20.15:

$$R(\varepsilon_n) = T\sum_{\Omega_k}\int\frac{d^D\mathbf{q}}{(2\pi)^D}L(\mathbf{q},\Omega_k)\int\frac{d^D\mathbf{p}}{(2\pi)^D}G^2(\mathbf{p},\varepsilon_n)G(\mathbf{q}-\mathbf{p},\Omega_k-\varepsilon_n). \tag{20.233}$$

The result of the integration of the last expression depends strongly of the electron spectrum dimensionality: for the two important cases of isotropic $3D$ and $2D$ electron spectra one finds [94]

$$\frac{\delta\nu^{(c)}_{(3)}(E,\epsilon)}{\nu_{(3)}(0)} = -\frac{(4\pi)^{3/2}}{7\zeta(3)}\sqrt{Gi_{(3,c)}}\mathrm{Re}\frac{\sqrt{T_c}}{\sqrt{\tau_{GL}^{-1}-2iE+\varkappa_3^2T_c}}\times \left\{\frac{1}{\tau_{GL}^{-1}-iE+\tau_{GL}^{-1/2}\left[\tau_{GL}^{-1}-2iE+\varkappa_3^2T_c\right]^{1/2}}\right\}, \tag{20.234}$$

$$\frac{\delta\nu^{(c)}_{(2)}(E,\epsilon)}{\nu_{(2)}(0)} = -\frac{(4\pi)^2}{7\zeta(3)}Gi_{(2,c)}\frac{T_c^2}{\left[E^2+\varkappa_2^2T_c\tau_{GL}^{-1}\right]}\times \left\{1-\frac{E}{\sqrt{E^2+\varkappa_2^2T_c\tau_{GL}^{-1}}}\ln\frac{E+\sqrt{E^2+\varkappa_2^2T_c\tau_{GL}^{-1}}}{\varkappa\sqrt{T_c\tau_{GL}}}\right\}, \tag{20.235}$$

where $\varkappa_D = \pi\sqrt{\pi D/7\zeta(3)}$.

In a dirty superconductor the calculations may be carried out in a similar way with the only difference that the impurity renormalization of the Cooper vertices has to be taken into account [93]. The value of the fluctuation dip at the Fermi level can be written in the form:

$$\frac{\delta\nu^{(d)}(0)}{\nu(0)} \sim -\begin{cases}\sqrt{Gi_{(3,d)}}\epsilon^{-3/2}, & D=3\\ Gi_{(2,d)}\epsilon^{-2}, & D=2\end{cases}. \tag{20.236}$$

At large energies $E \gg \tau_{GL}^{-1}$ the DOS recovers its normal value, according to the same laws (20.236) but with the substitution $\epsilon \to E/T_c$. It is interesting that the critical exponents of the fluctuation correction of the DOS change when moving from a dirty to a clean superconductor [94]: the analysis of (20.234)-(20.235) gives

Figure 20.16: The theoretical curve of the energy dependence for the normalised correction to the single-particle density of states vs energy for a clean two-dimensional superconductor above T_c.

$$\frac{\delta\nu^{(c)}(0)}{\nu(0)} \sim -\begin{cases} \sqrt{Gi_{(3,c)}}\epsilon^{-1/2}, & D=3 \\ Gi_{(2,c)}\epsilon^{-1}, & D=2 \end{cases} . \tag{20.237}$$

Another important respect in which the character of the DOS renormalization differs strongly for the clean and dirty cases is the energy scale at which this renormalization occurs. In the dirty case this energy turns out to be [93] $E_0^{(d)} \sim T - T_c \sim \tau_{GL}^{-1}$, while in the clean case $E_0^{(c)} \sim \sqrt{T_c(T-T_c)}$ [94]. To understand this important difference one has to study the character of the electron motion in both cases [94]. The relevant energy scale in the dirty case is the inverse of the time necessary for the electron to diffuse over a distance equal to the coherence length $\xi(T)$. This energy scale coincides with the inverse relaxation time: $t_\xi^{-1} = \mathcal{D}\xi^{-2}(T) \sim \tau_{GL}^{-1} \sim T - T_c$. In the clean case, the ballistic motion of the electrons gives rise to a different characteristic energy scale $t_\xi^{-1} \sim v_F\xi^{-1}(T) \sim (T_c\tau_{GL}^{-1})^{1/2} \sim \sqrt{T_c(T-T_c)}$.

One can check that the integration of (20.234)-(20.235) over all positive energies gives zero:

$$\int_0^\infty \delta\nu(E)dE = 0 \tag{20.238}$$

This "sum rule" is a consequence of a conservation law: the number of quasiparticles is determined by the number of cells in the crystal and cannot be changed by the interaction. So the only effect which can be produced by the inter-electron interaction is a redistribution of the energy levels near the Fermi energy. The sum rule (20.238) plays an important role in the understanding of the manifestation of the fluctuation DOS renormalization in the observable phenomena. As we will see in the next Section the singularity in the tunneling current (at zero voltage), due to the density of states renormalization, turns out to be much weaker than that in the DOS itself ($\ln\epsilon$ instead of ϵ^{-1} or ϵ^{-2}, see (20.236)-(20.237)). A similar smearing of the DOS singularity occurs in the opening of the pseudo-gap in the c-axis optical conductivity, in the NMR relaxation rate etc. These features are due to the fact that we must always form the convolution of the DOS with some slowly varying function: for example, a difference of Fermi functions in the case of the tunnel current. The sum rule then leads to an almost perfect cancellation of the main singularity at low energies. The main non-zero contribution then comes from the high energy region where the DOS correction has its 'tail'. Another important

consequence of the conservation law (20.238) is the considerable increase of the characteristic energy scale of the fluctuation pseudo-gap opening with respect to E_0: this is $eV_0 = \pi T$ for tunneling and $\omega \sim \tau^{-1}$ for the c-axis optical conductivity.

The effect of fluctuations on the tunnel current [179].

It is quite evident that the renormalization of the density of states near the Fermi level, even of only one of the electrodes, will lead to the appearance of anomalies in the voltage-current characteristics of a tunnel junction. The quasiparticle current flowing through it may be written as a convolution of the densities of states with the difference of the electron Fermi distributions in each electrode (L and R):

$$I_{qp} = \frac{1}{eR_n\nu_L(0)\nu_R(0)} \times \int_{-\infty}^{\infty} \left(\tanh\frac{E+eV}{2T} - \tanh\frac{E}{2T}\right)\nu_L(E)\nu_R(E+eV)dE, \tag{20.239}$$

where R_n is the Ohmic resistance per unit area and $\nu_L(0)$, $\nu_R(0)$ are the densities of states at the Fermi levels in each of electrodes in the absence of interaction. One can see that for low temperatures and voltages the expression in parenthesis is a sharp function of energy near the Fermi level. Nevertheless, depending on the properties of the DOS functions, the convolution (20.239) may exhibit different properties. If the energy scale of the DOS correction is much larger than T , the expression in parenthesis in (20.239) acts as a delta-function and the zero-bias anomaly in the tunnel conductivity strictly reproduces the anomaly of the density of states around the Fermi level:

$$\frac{\delta G(V)}{G_n(0)} = \frac{\delta\nu(eV)}{\nu(0)}, \tag{20.240}$$

where $G(V)$ is the differential tunnel conductance and $G_n(0)$ is the background value of the Ohmic conductance supposed to be bias independent, $\delta G(V) = G(V) - G_n(0)$. This situation, for instance, occurs in a junction with one amorphous electrode [183], where the dynamically screened Coulomb interaction is strongly retarded, which leads to a considerable suppression of the density of states in the vicinity of the Fermi level, within $\tau^{-1} \gg T$.

It is worth stressing that the proportionality between the tunneling current and the electron DOS of the electrodes is widely accepted as an axiom, but generally speaking this is not always so. As one can see from the previous subsection, the opposite situation occurs in the case of the DOS renormalization due to the electron-electron interaction in the Cooper channel: in this case the DOS correction varies strongly already in the scale of $E_0 \sim E_{\rm ker} \ll T$ and the convolution in (20.239) with the DOS (20.235) has to be carried out without the simplifying approximations assumed to obtain (20.240). We will show that the fluctuation induced pseudo-gap like structure in the tunnel conductance differs drastically from the anomaly of the density of states (20.235), both in its temperature singularity near T_c and in the energy range of its manifestation.

Let us first discuss the effect of the fluctuation suppression of the density of states on the properties of a tunnel junction between a normal metal and a superconductor above T_c. The effect under discussion turns out to be most pronounced in the case of thin superconducting films ($d \ll \xi(T)$) and layered superconductors like HTS cuprates. In order to derive the explicit expression for the fluctuation contribution to the differential conductance of a tunnel junction with one thin film electrode close to its T_c we differentiate (20.239) with respect to voltage, and

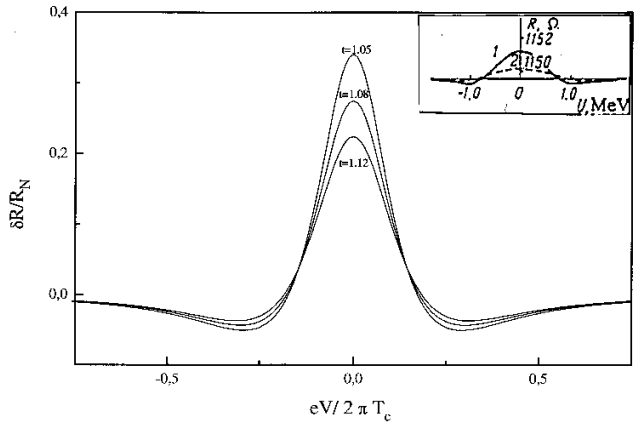


Figure 20.17: The theoretical prediction for the fluctuation-induced zero-bias anomaly in tunnel-junction resistance as a function of voltage for reduced temperatures $\epsilon = 0.05$ (top curve), $\epsilon = 0.08$ (middle curve) and $\epsilon = 0.12$ (bottom curve). The insert shows the experimentally observed differential resistance as a function of voltage in an Al-I-Sn junction just above the transition temperature

substitute the DOS correction given by (20.235). This results in (see [179]):

$$\frac{\delta G_{fl}(V,\epsilon)}{G_n(0)} = \frac{1}{2T}\int_{-\infty}^{\infty}\frac{dE}{\cosh^2\left(\frac{E+eV}{2T}\right)}\delta\nu^{(2)}(E,\epsilon) \sim \tag{20.241}$$

$$\sim Gi_{(2)}\ln\left(\frac{2}{\sqrt{\epsilon}+\sqrt{\epsilon+r}}\right)\mathrm{Re}\psi''\left(\frac{1}{2}-\frac{ieV}{2\pi T}\right).$$

It is important to emphasize several nontrivial features of the result obtained. First, the sharp decrease ($\epsilon^{-2(1)}$) of the density of electron states in the immediate vicinity of the Fermi level generated by fluctuations surprisingly results in a much more moderate growth of the tunnel resistance at zero voltage ($\ln 1/\epsilon$). Second, in spite of the manifestation of the DOS renormalization at the characteristic scales $E_0^{(d)} \sim T - T_c$ or $E_0^{(cl)} \sim \sqrt{T_c(T-T_c)}$, the energy scale of the anomaly developed in the $I-V$ characteristic is much larger: $eV = \pi T \gg E_0$ (see Fig. 20.17).

In the inset of Fig. 20.17 the result of measurements of the differential resistance of the tunnel junction $Al - I - Sn$ at temperatures slightly above the critical temperature of Sn electrode is presented. This experiment was done [184] with the purpose of checking the theory proposed [179]. The non-linear differential resistance was precisely measured at low voltages which permitted the observation of the fine structure of the zero-bias anomaly. The reader can compare the shape of the measured fluctuation part of the differential resistance (the inset in Fig. 20.17) with the theoretical prediction. It is worth mentioning that the experimentally measured positions of the minima are $eV \approx \pm 3T_c$, while the theoretical prediction following from (20.241) is $eV = \pm\pi T_c$. Recently similar results on an aluminium film with two regions of different superconducting transition temperatures were reported [185]. The observations of the pseudogap anomalies in tunneling experiments at temperatures above T_c obtained by a variety of experimental techniques were reported in [186, 187, 188, 189, 190]..

We will now consider the case of a symmetric junction between two superconducting electrodes at temperatures above T_c. In this case, evidently, the correction (20.241) has to be multiplied by a factor of "two" because of the possibility of fluctuation pairing in both electrodes. Furthermore, in view of the extraordinarily weak ($\sim \ln 1/\epsilon$) temperature dependence of the first order correction, different types of high order corrections may manifest themselves

on the energy scale $eV \sim T - T_c$ or $\sqrt{T_c(T-T_c)}$. Among them are the familiar AL and MT corrections which take place in the first order of Gi but in the second order of the barrier transparency. Another type of higher order correction appears in the first order of barrier transparency but in the second of fluctuation strength ($\sim Gi^2$) [179]. Such corrections are generated by the interaction of fluctuations through the barrier and they can be evaluated directly from (20.239) applied to a symmetric junction. The second order correction in Gi can be written as [179]:

$$\delta G_{fl}^{(2)}(0,\epsilon) \sim \int_{-\infty}^{\infty} \frac{dE}{\cosh^2\left(\frac{E}{2T}\right)} \left[\delta\nu^{(2)}(E,\epsilon)\right]^2 \sim \frac{Gi_{(2)}^2}{\epsilon^3} \tag{20.242}$$

This nonlinear fluctuation correction turns out to be small by Gi^2 but its strong singularity in temperature and opposite sign with respect to $\delta G_{fl}^{(1)}$ make it interesting. Apparently it leads to the appearance of a sharp maximum at zero voltage in $G(V)$ with a characteristic width $eV \sim T - T_c$ in the immediate vicinity of T_c (one can call this peak as the hyperfine structure). This result was confirmed in [191] but to our knowledge such corrections were never observed in tunneling experiments.

One can see that $\delta G_{fl}^{(1)}$ and $\delta G_{fl}^{(2)}$ become of the same order at $\epsilon_{cr}^* \sim \sqrt[3]{Gi}$, i.e. the critical region where nonlinear fluctuations effects become important in the problem under consideration starts much before the thermodynamical criterion $\epsilon_{cr} \sim Gi$. In the next Section we will discuss this early manifestation of nonlinear fluctuation effects in transport phenomena.

20.6.6 Nonlinear fluctuation effects [14]

As we have already seen in the temperature region $Gi \ll \epsilon \ll 1$ the thermodynamic fluctuations of the order parameter Ψ can be considered to be Gaussian. Nevertheless the example of the previous Section demonstrates that in transport phenomena nonlinear effects, related with the interaction of fluctuations (higher order corrections) can manifest themselves much earlier. It has been found in paper [178], that nonlinear fluctuation phenomena restrict the Gaussian region in the fluctuation conductivity of a superconducting film to a new temperature scale: $\sqrt{Gi_{(2d)}} \ll \epsilon \ll 1$ (see also [110, 111, 179, 115, 192]). In this Section we obtain expressions for the conductivity in the temperature region $Gi_{(2d)} < \epsilon < \sqrt{Gi_{(2d)}}$, where both the perturbation theory works well and the nonlinear fluctuation effects are important.

Let us start from the correlator (20.168) which can be expressed by means of the $Gi_{(2d)}$ number:

$$\langle \Psi_{\mathbf{k}}^* \Psi_{\mathbf{k}} \rangle = \frac{T}{\nu} \frac{1}{\epsilon + \frac{\pi\mathcal{D}}{8T}\mathbf{k}^2} = \frac{32\pi^3}{7\zeta(3)} Gi_{(2d)} \frac{T^2}{k^2 + \frac{8T\epsilon}{\pi\mathcal{D}}}. \tag{20.243}$$

The long-wave-length fluctuations with $k^2 < k_{\min}^2 = 8T\epsilon/\pi\mathcal{D}$ can be considered as a local condensate. They lead to the formation of the pseudogap

$$\Delta_{pg} = \left[\int_{k^2 \lesssim k_{\min}^2} \frac{d^2k}{(2\pi)^2} \langle \Psi_{\mathbf{k}}^* \Psi_{\mathbf{k}} \rangle\right]^{1/2} \simeq T\sqrt{Gi_{(2d)}}. \tag{20.244}$$

in the single-particle spectrum of excitations.

Not very close to the transition ($\epsilon > \sqrt{Gi_{(2d)}}$) only excitations with energies $E > \Delta_{pg}$ are important. The pseudogap does not play any role for them. Thus, in this region of temperatures it is sufficient to consider fluctuations in the linear approximation only (see [5, 6, 7]). However, in the temperature region $\epsilon < \sqrt{Gi_{(2d)}}$ the nonlinear fluctuation contribution of the excitations with energies $E < \Delta_{pg}$ becomes essential.

To take into account the spatial dependence of the order parameter we will use the results obtained in [193]. It was shown there that the spatial variations of Δ_{pg} act on single-particle excitations in the same way as magnetic impurities do (the analogy between the effect of fluctuations and magnetic impurities was observed in many papers, see for example, [194]). In this case, the total pairbreaking rate Γ can be written as a sum of the pairbreaking rate due to the magnetic impurities and the fluctuation term. Thus, the self-consistent equation for Γ can be written in the following form [193]:

$$\Gamma = \int \frac{d^2k}{(2\pi)^2} \frac{\langle \Psi_k^* \Psi_k \rangle}{E + \frac{1}{2}\mathcal{D}k^2 + \Gamma} + \frac{1}{\tau_s}. \tag{20.245}$$

In the region $E \lesssim \Gamma$, $\Gamma \gg T\epsilon$ we obtain from Eqs.(20.245), (20.243):

$$\Gamma \sim T \left(Gi_{(2d)} \right)^{1/2} \simeq \Delta_{pg}, \tag{20.246}$$

which coincides with the results obtained in [110, 101].

Let us note, that the pair-breaking rate Γ was found to be of the order of the pseudogap Δ_{pg}. Thus, a wide maximum appears in the density of states at $E \sim \Delta_{pg}$. As we already saw (20.195), in purely $2D$ case the Maki-Thompson correction to the conductivity saturates for $T\epsilon < \Gamma$ (where $\Gamma = 8T\gamma_\varphi/\pi$) and takes the form [14]:

$$\frac{\delta\sigma^{MT}}{\sigma_n} \sim \frac{T}{\Gamma} Gi_{(2d)} \ln \frac{\pi\Gamma}{8T\epsilon}. \tag{20.247}$$

As it can be seen from Eqs.(20.246) such a saturation takes place when $\epsilon < \sqrt{Gi_{(2d)}}$. Similar results have been obtained in [110, 111, 115], with slightly different numerical coefficients[29]. However, its exact value is not very important since in the region $T\epsilon < \Gamma$ the Maki-Thompson correction is less singular than the Aslamazov-Larkin one and can be neglected. The latter does not saturate when T tends to T_c but becomes more and more singular.

In the presence of the pseudogap if there is no equilibrium, the fluctuating Cooper pair lifetime increases with respect to the GL one: $\tau_{fl} = a\tau_{GL}$ $(a > 1)$. Recall, that analogous changes in the coefficient a in the TDGL equations appear below the transition temperature (see e.g. [66, 72, 195, 196, 197]). The growth of the coefficient a and, consequently, the increase of the fluctuation lifetime is because the quasiparticles require more time to attain thermal equilibrium (the corresponding time we denote as τ_e). A rough estimate gives $a \sim \Delta_{pg}\tau_e$. In the case of weak energy relaxation, τ_e has to be determined from the diffusion equation taking account of the pseudogap (see [196, 197, 198]). Note, that in this complicated case the coefficient a becomes a non-local operator. Rough estimates give the following value for the thermal equilibrium transition time $\tau_e \sim (\mathcal{D}k_{\min}^2)^{-1} \sim (T\epsilon)^{-1}$. Taking into account Eq.(20.244) we obtain from (20.11) for the paraconductivity contribution in the discussed limit of the weak energy relaxation [14]:

$$\frac{\delta\sigma}{\sigma_n} \sim \frac{Gi_{(2d)}^{3/2}}{\epsilon^2}. \tag{20.248}$$

Let us discuss now the role of the energy relaxation processes, characterized by a quasiparticle lifetime τ_ε. Nonelastic electron scattering off phonons and other possible collective excitations can decrease τ_ε significantly. These processes together with additional pairbreaking processes (due to magnetic impurities or a magnetic field) lead to a decrease of the nonlinear

[29] Note, that the numerical coefficient in Eq.(20.247) depends on the definition of $Gi_{(2d)}$ and how the summation of higher order diagrams is made.

effects. In view of these processes, one can write the following interpolation formula for the non-linear fluctuation conductivity [14]:

$$\frac{\delta\sigma}{\sigma_n} \sim \frac{Gi_{(2d)}^{3/2}}{\epsilon\left(\epsilon+\frac{1}{T\tau_\varepsilon}\right)\left(1+\frac{\Gamma}{T\sqrt{Gi_{(2d)}}}\right)}. \tag{20.249}$$

Note that Eqs.(20.248-20.249) are valid only if the parameters Γ and τ_ε are such that the correction to conductivity $\delta\sigma$ is larger than the usual Aslamazov-Larkin correction Eq.(20.97). If $\Gamma > T$, $T\tau_\varepsilon < \sqrt{Gi_{(2d)}}$ or if $T^2\tau_\varepsilon/\Gamma < Gi_{(2d)}$, than nonlinear effects are negligible and the usual result (20.97) is valid for all $\epsilon > Gi_{(2d)}$.

We see that the paraconductivity can exceed the value of the normal conductivity σ_n in the region $Gi_{(2d)} < \epsilon < Gi_{(2d)}^{3/4}$. Let us recall, that in this region corrections to all the thermodynamic coefficients are still small and the linear theory is well applicable.

20.6.7 The effect of fluctuation on the optical conductivity [199]

The optical conductivity of a layered superconductor can be expressed by the same analytically continued electromagnetic response operator $Q_{\alpha\beta}^{(R)}(\omega)$ (see Exp.(20.175)) but in contrast to the d.c. conductivity case, calculated without the assumption $\omega \to 0$. Let us recall that the paraconductivity tensor in an a.c. field was already studied in Section 4 in the framework of the TDGL equation [31] and the most interesting asymptotics for our discussion (20.121)-(20.122), valid for $\omega \ll T$ in the $2D$ regime, were calculated there. The microscopic calculation of the AL diagram [98] shows that in the vicinity of T_c and for $\omega \ll T$ the leading singular contribution to the response operator $Q_{\alpha\beta}^{AL\,(R)}$ arises from the fluctuation propagators rather than from the B_α blocks, which confirms the TDGL results. Nevertheless the DOS and MT corrections can be calculated only by the microscopic method, as was done in [98, 199]..

Let us note that the external frequency ω_ν enters in the expression for the DOS contribution to $Q_{\alpha\beta}(\omega)$ only by means of the Green's function $G(\mathbf{p},\omega_{n+\nu})$ and it is not involved in q integration. So, near T_c, even in the case of an arbitrary external frequency, we can restrict consideration to the static limit, taking into account only the propagator frequency $\Omega_k = 0$, and to get [199]:

$$\mathrm{Re}\sigma_{\alpha\beta}^{DOS}(\omega) = -\frac{e^2}{2\pi s}\hat{\kappa}\left(\omega,T,\tau\right)A_{\alpha\beta}\ln\left[\frac{2}{\sqrt{\epsilon+r}+\sqrt{\epsilon}}\right],$$

where the anisotropy tensor $A_{\alpha\beta}$ was introduced in (20.183). Let us stress that, in contrast to the AL frequency dependent contribution, this result has been found with only the assumption $\epsilon \ll 1$, so it is valid for any frequency, and impurity concentration. The function $\hat{\kappa}\left(\omega,T,\tau\right)$ was calculated in [199] exactly but we present here only its asymptotics for the clean and dirty cases:

$$\hat{\kappa}_d\left(\omega,T\ll\tau^{-1}\right) = \frac{8}{\pi}\begin{cases}\frac{7\zeta(3)}{2\pi^2}, & \omega\ll T\ll\tau^{-1}\\ \left(\frac{T}{\omega}\right)^2, & T\ll\omega\ll\tau^{-1}\\ -\frac{\pi T^2}{\omega^3\tau}, & T\ll\tau^{-1}\ll\omega\end{cases},$$

$$\hat{\kappa}_{cl}\left(\omega,T\gg\tau^{-1}\right) = \frac{\pi^3}{28\zeta(3)}\begin{cases}(T\tau)^2, & \omega\ll\tau^{-1}\ll T\\ \left(\frac{T}{\omega}\right)^2, & \tau^{-1}\ll\omega\ll T\\ -4\left(\frac{T}{\omega}\right)^3, & \tau^{-1}\ll T\ll\omega\end{cases}.$$

The general expression for the MT contribution is too cumbersome, so we restrict ourselves here to the important $2D$ overdamped regime ($r \ll \epsilon \leq \gamma_\varphi$):

$$\sigma_{zz}^{MT(an)(2D)}(\omega) = \frac{e^2 s}{2^7 \eta_{(2)}} \frac{r^2}{\gamma_\varphi \epsilon} \begin{cases} 1, & \tilde{\omega} \ll \tau_\varphi^{-1} \\ \left(\frac{8T_c\gamma_\varphi}{\pi\omega}\right)^2, & \tilde{\omega} \gg \tau_\varphi^{-1} \end{cases}$$

$$\sigma_{xx}^{MT(an)(2D)}(\omega) = \frac{e^2}{8s} \begin{cases} \frac{1}{\gamma_\varphi} \ln \frac{\gamma_\varphi}{\epsilon}, & \omega \ll \tau_\varphi^{-1} \\ \left(\frac{8T_c\gamma_\varphi}{\pi\omega}\right)^2, & \omega \gg \tau_\varphi^{-1} \end{cases} .$$

Let us discuss the results obtained. Because of the large number of parameters entering the expressions we restrict our consideration to the most interesting c-axis component of the fluctuation conductivity tensor in the $2D$ region (above the Lawrence-Doniach crossover temperature).

The AL contribution describes the fluctuation condensate response to the applied electromagnetic field. The current associated with it can be treated as the precursor phenomenon of the screening currents in the superconducting phase. As was demonstrated above the characteristic "binding energy " of fluctuation Cooper pair is of the order of $T - T_c$, so it is not surprising that the AL contribution decreases when the electromagnetic field frequency exceeds this value. Indeed $\omega^{AL} \sim T - T_c$ is the only relevant scale for σ^{AL}: its frequency dependence does not contain T, τ_φ and τ. The independence from the latter is due to the fact that elastic impurities do not present obstacles for the motion of Cooper pairs. The interaction of the electromagnetic wave with the fluctuation Cooper pairs resembles, in some way, the anomalous skin-effect where the reflection is determined by the interaction with the free electron system.

The anomalous MT contribution also is due to fluctuation Cooper pairs, but this time they are formed by electrons moving along self-intersecting trajectories. Being the contribution related with the Cooper pair electric charge transfer it does not depend on the elastic scattering time but it turns out to be extremely sensitive to the phase-breaking mechanisms. So two characteristic scales turn out to be relevant in its frequency dependence: $T - T_c$ and τ_φ^{-1}. In the case of HTS, where τ_φ^{-1} has been estimated as at least $0.1T_c$, for temperatures up to $5 \div 10K$ above T_c the MT contribution is overdamped, it is determined by the value of τ_φ and is almost temperature independent.

The DOS contribution to $\mathrm{Re}\sigma(\omega)$ is quite different from those above. In the wide range of frequencies $\omega \ll \tau^{-1}$ the lack of electron states at the Fermi level leads to the opposite sign effect in comparison with the AL and MT contributions: $\mathrm{Re}\sigma^{DOS}(\omega)$ turns out to be negative and this means an increase of the surface impedance, or, in other words, decrease of the reflectance. Nevertheless, the applied electromagnetic field affects the electron distribution and at very high frequencies $\omega \sim \tau^{-1}$ the DOS contribution changes its sign. It is interesting that the DOS contribution, as a one-electron effect, depends on the impurity scattering in a similar manner to the normal Drude conductivity. The decrease of $\mathrm{Re}\sigma^{DOS}(\omega)$ starts at frequencies $\omega \sim \min\{T, \tau^{-1}\}$ which for HTS are much higher than $T - T_c$ and τ_φ^{-1}.

The ω-dependence of $\mathrm{Re}\sigma_{zz}^{tot}$ with the most natural choice of parameters ($T_c r \ll T_c\epsilon \leq \tau_\varphi^{-1} \ll \min\{T, \tau^{-1}\}$) is presented in Fig. 20.18.

Let us discuss it referring to a strongly anisotropic layered superconductor. The positive AL and MT contributions to σ_{zz}^{tot} , being suppressed by the square of the interlayer transparency, are small in magnitude and they vary in the low frequency region $\omega \sim \min\{T - T_c, \tau_\varphi^{-1}\}$. The DOS contribution is proportional to the first order of transparency and remains in this region almost invariable. With a further increase of frequency $\min\{T - T_c, \tau_\varphi^{-1}\} \lesssim \omega$ the AL and MT contributions decay; $\mathrm{Re}\sigma_\perp$ remains negative up to $\omega \sim \min\{T, \tau^{-1}\}$, then it changes its sign at $\omega \sim \tau^{-1}$, reaches maximum and rapidly decreases. The following high frequency behavior is governed by the Drude law. So one can see that the characteristic pseudo-gap-like behavior in

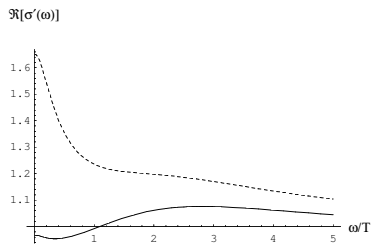


Figure 20.18: The theoretical dependence [199] of the real part of the conductivity, normalized by the Drude normal conductivity, on ω/T, Re $[\sigma'(\omega)]$ = Re $[\sigma(\omega)]/\sigma^{\rm n}$. The dashed line refers to the *ab*-plane component of the conductivity tensor whose Drude normal conductivity is $\sigma^{\rm n}_{\parallel} = N(0)e^2\tau v_F^2$. The solid line refers to the *c*-axis component whose Drude normal conductivity is $\sigma^{\rm n}_{\perp} = \sigma^{\rm n}_{\parallel} J^2 s^2/v_F^2$. In this plot we have put $T\tau = 0.3, E_F/T = 50, r = 0.01, \epsilon = 0.04, T\tau_\varphi = 4$.

the frequency dependence of the c-axis optical conductivity takes place: a transparency window appears in the range $\omega \in [T - T_c, \tau^{-1}]$.

In the case of the *ab*-plane optical conductivity the two first positive contributions are not suppressed by the interlayer transparency, and exceed considerably the negative DOS contribution in a wide range of frequencies. Any pseudo-gap like behavior is therefore unlikely in $\sigma^{tot}_{xx}(\omega)$: the reflectivity will be of the metallic kind.

20.6.8 Thermoelectric power above the superconducting transition [203, 201]

Thermoelectric effects are difficult both to calculate and to measure if compared with electrical transport properties. At the heart of the problem lies the fact that the thermoelectric coefficients in metals are the small resultant of two opposing currents which almost completely cancel. In calculating the thermoelectric power one finds that the electrons above the Fermi level carry a heat current that is nearly the negative of that carried by the electrons below E_F. In the model of a monovalent metal in which band structure and scattering probabilities are symmetric about E_F, this cancellation would be exact; in a real metal a small asymmetry survives. Because of their compensated nature, thermoelectric effects are very sensitive to the characteristics of the electronic spectrum, presence of impurities and peculiarities of scattering mechanisms. The inclusion of many-body effects, such as electron-phonon renormalization, multi-phonon scattering, drag effect, adds even more complexity to the problem of calculating the thermoelectric power. Among such effects, there is also the influence of thermodynamical fluctuations on the thermoelectric transport in a superconductor above the critical temperature. This problem has been attracting the attention of theoreticians for more than twenty years, since the paper of Maki [202] appeared, where the logarithmically divergent AL contribution was predicted for the two-dimensional case. So the AL term turns out to be less singular compared with the corresponding correction to conductivity.

In every case where the main AL and MT fluctuation corrections are suppressed for some reason, the contribution connected with fluctuation renormalization of the one-electron density of states (DOS) can become important. The analogous situation also occurs in the case of the thermoelectric coefficient [200, 201]. Although the DOS term has the same temperature dependence as the AL contribution [202, 203], it turns out to be the leading fluctuation contribution in both the clean and dirty cases, due to its specific dependence on the electron mean free path.

We introduce the thermoelectric coefficient ϑ in the framework of linear response theory as

$$\vartheta = \frac{1}{T}\lim_{\omega\to 0}\frac{\mathrm{Im}[Q^{(eh)R}(\omega)]}{\omega}$$

where $Q^{(eh)R}(\omega)$ is the Fourier representation of the retarded correlation function of electric J^e and heat J^h current operators in Heisenberg representation:

$$Q^{(eh)R}(X-X') = -\Theta(t-t')\langle\langle\left[J^h(X), J^e(X')\right]\rangle\rangle.$$

Here $X = (\mathbf{r}, t)$ and $\langle\langle\cdots\rangle\rangle$ represents both thermodynamical averaging and averaging over random impurity positions. The correlation function $Q^{(eh)R}$ in the diagrammatic technique is represented by a bubble with two exact electron Green's functions and two external field vertices, the first, $e\mathbf{v}$, associated with the electric current operator and the second, $\frac{i}{2}(\varepsilon_n+\varepsilon_{n+\nu})\mathbf{v}$, associated with the heat current operator (ε_n is fermionic Matsubara frequency) [172]. The first order fluctuation corrections to $Q^{(eh)}(\omega_\nu)$ are represented by the same diagrams as for conductivity (see Fig.20.9).

The first diagram describes the AL contribution to thermoelectric coefficient and was calculated in [202, 203] with the electron-hole asymmetry factor taken into account in the fluctuation propagator. Diagrams 2-4 represent the Maki-Thompson contribution, neither anomalous nor regular parts of these diagrams contribute to ϑ in any order of electron-hole asymmetry [172, 203]. The contribution from diagrams 5-10 describes the correction to ϑ due to fluctuation renormalization of the one-electron density of states. Evaluating it in the same way as (20.187) but with one heat current vertex one obtains a vanishing result if electron-hole asymmetry is not taken into account. The first possible source of this factor is contained in the fluctuation propagator; it was used in [203] for the AL diagram but for the DOS contribution this correction results in non-singular contributions to ϑ only and can be neglected. Another source of electron-hole asymmetry is connected with expansion of energy-dependent functions in powers of ξ/E_F near the Fermi level:

$$\nu(\xi)\mathbf{v}^2(\xi) = \nu(0)\mathbf{v}^2(0) + \xi\left[\frac{\partial(\nu(\xi)\mathbf{v}^2(\xi))}{\partial\xi}\right]_{\xi=0}. \tag{20.250}$$

Only the second term in Eq. (30.74) contributes to the thermoelectric coefficient. Performing the integration over ξ, summations over fermionic frequencies and analytical continuation of the result obtained we find that the contribution to the thermoelectric coefficient associated with the DOS renormalization takes the form

$$\vartheta_{2D}^{\mathrm{DOS}} = \frac{1}{4\pi^2}\frac{eT_c}{\nu(0)\mathbf{v}_F^2}\left[\frac{\partial(\nu\mathbf{v}^2)}{\partial\xi}\right]_{\xi=0}\kappa^*(T\tau)\ln[\frac{2}{\sqrt{\epsilon}+\sqrt{\epsilon+r}}], \tag{20.251}$$

where

$$\begin{aligned}\kappa^*(T\tau) &= -\frac{1+\frac{\pi}{8T\tau}}{T\tau\left[\psi\left(\frac{1}{2}+\frac{1}{4\pi T\tau}\right)-\psi\left(\frac{1}{2}\right)-\frac{1}{4\pi T\tau}\psi'\left(\frac{1}{2}\right)\right]} \\ &= \begin{cases}\frac{8\pi^2}{7\zeta(3)}T\tau \approx 9,4T\tau & T\tau\gg 1\\ (T\tau)^{-1} & T\tau\ll 1\end{cases}.\end{aligned} \tag{20.252}$$

Summing Eq. (20.251) with the AL contribution [203] one can find the total correction to the thermoelectric coefficient in the case of a 2D superconducting film of thickness d:

$$\frac{\vartheta^{DOS}+\vartheta^{AL}}{\vartheta_0} = -0.17\frac{1}{E_F\tau}\frac{1}{p_F d}\ln\left(\frac{T_c}{T-T_c}\right)\left[\kappa^*(T_c\tau)+5.3\ln\frac{\omega_D}{T_c}\right],$$

Assuming $\ln(\omega_D/T_c) \approx 2$ one finds that the DOS contribution dominates the AL one for any value of impurity concentration: κ^* has a minimum at $T\tau \approx 0.3$ and even at this point the DOS term is twice as large. In both limiting cases $T\tau \ll 1$ and $T\tau \gg 1$ this difference strongly increases.

In practice, although the Seebeck coefficient $S = -\vartheta/\sigma$ is probably the easiest to measure among the thermal transport coefficients, the comparison between experiment and theory is complicated by the fact that S cannot be calculated directly; it is rather a composite quantity of the electrical conductivity and thermoelectric coefficient. As both ϑ and σ have corrections due to superconducting fluctuations, the total correction to the Seebeck coefficient is given by

$$\Delta S = S_0 \left(\frac{\Delta\vartheta}{\vartheta_0} - \frac{\Delta\sigma}{\sigma_0} \right) \tag{20.253}$$

We see that the fluctuations result in a decrease of the absolute value of the overall Seebeck coefficient as the temperature approaches T_c.

The situation is complicated additionally in HTS materials, where the temperature behavior of the background value of the thermoelectric power remains unknown. This does not permit to extract precisely from the experimental data the fluctuation part $\Delta\vartheta$ to compare it with the theoretical prediction. Nevertheless the very sharp maximum in the Seebeck coefficient experimentally observed in a few papers [204, 205, 206] seems to be unrelated to the fluctuation effects. This conclusion is supported by recent analysis of the temperature dependence of the thermoelectric coefficient close to the transition in Refs. [207].

20.6.9 The effect of fluctuations on NMR characteristics [176]

Preliminaries.

In this Section we discuss the contribution of superconducting fluctuations to the spin susceptibility and the NMR relaxation rate. For both these effects the interplay of different fluctuation contributions is unusual with respect to the case of the conductivity. Like in the case of the optical conductivity, the fluctuation contributions to the spin susceptibility and the NMR relaxation rate can manifest themselves as the opening of a pseudogap already in the normal phase, a phenomenon which is characteristic to HTS compounds.

We begin with the dynamic spin susceptibility $\chi_{\pm}^{(R)}(\mathbf{k},\omega) = \chi_{\pm}(\mathbf{k}, i\omega_\nu \to \omega + i0^+)$ where

$$\chi_{\pm}(\mathbf{k},\omega_\nu) = \int_0^{1/T} d\tau e^{i\omega_\nu\tau} \langle\langle \hat{T}_\tau \left(\hat{S}_+(\mathbf{k},\tau)\hat{S}_-(-\mathbf{k},0) \right) \rangle\rangle. \tag{20.254}$$

Here $\hat{S}_\pm$ are the spin raising and lowering operators, $\hat{T}_\tau$ is the time ordering operator, and the brackets denote thermal and impurity averaging in the usual way. The uniform, static spin susceptibility is given by $\chi_s = \chi_{\pm}^{(R)}(\mathbf{k} \to 0, \omega = 0)$ while the dynamic NMR relaxation rate is given by

$$\frac{1}{T_1 T} = \lim_{\omega\to 0} \frac{A}{\omega} \int \frac{d^3\mathbf{k}}{(2\pi)^3} \mathrm{Im}\chi_{\pm}^{(R)}(\mathbf{k},\omega) \tag{20.255}$$

where A is a positive constant involving the gyromagnetic ratio.

For non-interacting electrons $\chi_{\pm}^0(\mathbf{k},\omega_\nu)$ is determined by the usual loop diagram. Simple calculations lead to the well known results for $T \ll E_F$: $\chi_s^0 = \nu$ (Pauli susceptibility) and $(1/T_1T)^0 = A\pi\nu^2$ (Korringa relaxation). We will present the fluctuation contributions in a dimensionless form by normalizing to the above results.

To leading order in Gi the fluctuation contributions to $\chi_\pm$ can be discussed with the help of the same diagrams drawn for the conductivity in Fig. 20.9. It is important to note that

the role of the external vertices (electron interaction with the external field) is now played by the $\hat{S}_{\pm}(\mathbf{k},\tau)$ operators. This means that the two fermion lines attached to the external vertex must have opposite spin labels (up and down). Consequently, the Aslamazov-Larkin diagram for $\chi_{\pm}$ does not exist since one cannot consistently assign a spin label to the central fermion for spin-singlet pairing. The next set of diagrams to consider is the Maki-Thompson contribution. While the MT diagrams for $\chi_{\pm}$ appear to be identical to those for the conductivity, there is an important difference in topology which arises from their spin structure. It is easy to see, by drawing the fluctuation propagator explicitly as a ladder of attractive interaction lines, that the MT diagram is a non-planar graph with a single fermion loop. In contrast the MT graph for the conductivity is planar and has two fermion loops. The number of loops, in accordance with the rules of diagrammatic technique [92], affects the sign of the contribution.

The diagrams 5 and 6 represent the effect of fluctuations on the single-particle self energy, leading to a decrease in the DOS. The DOS diagrams 7 and 8 include impurity vertex corrections (note that these have only a single impurity scattering line as additional impurity scattering in the form of a ladder has a vanishing effect). Finally 9 and 10 are the DOS diagrams with the Cooperon impurity corrections.

Spin Susceptibility[208, 176].

We note that, when the external frequency and momentum can be set to zero at the outset, as is the case for χ_s, there is no anomalous MT piece (which as we shall see below is the most singular contribution to $1/T_1$). The MT diagram 2 then yields a result which is identical to the sum of the DOS diagrams 5 and 6.

In the clean limit ($T_c\tau \gg 1$) the fluctuation contribution is given by $\chi_s^{\rm fl} = \chi_{s2} + \chi_{s5} + \chi_{s6}$; all other diagrams turn out to be negligible. In the dirty case ($T_c\tau \ll 1$), the DOS diagrams 5 and 6, together with the regular part of the MT diagram (2), yield the same result as in the clean limit (of the order $\mathcal{O}(T_c/E_F)$). One can see, that this contribution is negligible in comparison with the expected dominant one for the dirty case of the order $\mathcal{O}(1/E_F\tau)$. A thorough study of all diagrams shows that the important graphs in the dirty case are those with the Cooperon impurity corrections MT 3 and 4, and the DOS ones 9 and 10. This is the unique example known to us where the Cooperons, which play a central role in the weak localization theory, give the leading order result in the study of superconducting fluctuations. Diagrams 3 and 4 give one half of the final result given below; diagrams 9 and 10 provide the other half. The total fluctuation susceptibility is $\chi_s^{\rm fl} = \chi_{s3} + \chi_{s4} + \chi_{s9} + \chi_{s10}$. Interesting, that in both the clean and dirty cases $\chi_s^{\rm fl}/\chi_s{}^{(0)}$ can be expressed by the same formula if one expresses the coefficient in terms of the GL number $Gi_{(2)}$ (20.171):

$$\frac{\chi_s^{\rm fl}}{\chi_s{}^{(0)}} = -2Gi_{(2)} \ln\left(\frac{2}{\sqrt{\epsilon}+\sqrt{\epsilon+r}}\right). \tag{20.256}$$

It is tempting to explain the negative sign of the fluctuation contribution to the spin susceptibility in Eq. (20.256) as arising from a suppression of the DOS at the Fermi level. But one must keep in mind that only the contribution of diagrams 5 and 6 can strictly be interpreted in this manner; the MT graphs and the coherent impurity scattering described by the Cooperons do not permit such a simple interpretation.

Relaxation Rate[209, 210, 204, 176].

The calculation of the fluctuation contribution to $1/T_1$ requires rather more care than χ_s because of the subtleties of analytic continuation. Let us define the local susceptibility

$$K(\omega_\nu) = \int (d\mathbf{k}) \chi_{+-}(\mathbf{k},\omega_\nu).$$

In order to write down the fluctuation contribution to $1/T_1$ for the case of an arbitrary impurity concentration including the ultra-clean case let us start from the anomalous MT contribution and evaluate it using the standard contour integration techniques

$$\lim_{\omega\to 0}\frac{1}{\omega}\mathrm{Im}K^{(an)R}(\omega)=-\frac{\pi\nu^2}{8}\int(d\mathbf{q})L(\mathbf{q},0)\mathcal{K}(\mathbf{q}), \tag{20.257}$$

$$\mathcal{K}(\mathbf{q}) = 2\tau\int\limits_{-\infty}^{\infty}\frac{dz}{\cosh^2(z/4T\tau)}\frac{1}{\left(\sqrt{l^2q^2-(z-i)^2}-1\right)}\times \frac{1}{\left(\sqrt{l^2q^2-(z+i)^2}-1\right)}. \tag{20.258}$$

We have used the impurity vertices in the general form (20.227). The first simple limiting case for (20.258) is $lq\ll 1$, when the square roots in the denominator can be expanded and $\mathcal{K}(\mathbf{q})=2\pi/\mathbf{D}q^2$. As we already know from Section 8.4 this corresponds to the usual local approximation and covers the domain $T_c\tau\ll 1/\sqrt{\epsilon}$. Introducing the pair breaking rate γ_φ as an infrared cut off one can find:

$$\frac{\delta\left(1/T_1\right)^{MT(an)}}{\left(1/T_1\right)^0}=\frac{28\zeta(3)}{\pi^4}Gi_{(2,d)}\frac{1}{\epsilon-\gamma_\varphi}\ln(\epsilon/\gamma_\varphi). \tag{20.259}$$

The other limiting case is the "ultra-clean limit" when the characteristic q-values satisfy $lq\gg 1$. This is obtained when $T\tau\gg 1/\sqrt{\epsilon}\gg 1$. From (20.258) we then find $\mathcal{K}(\mathbf{q})=4\ln(lq)/vq$, which leads to

$$\frac{\delta(1/T_1)^{MT(an)}}{(1/T_1)^0}=\frac{\pi^3}{\sqrt{14\zeta(3)}}Gi_{(2,cl)}\frac{1}{\sqrt{\varepsilon}}\ln(T\tau\sqrt{\epsilon}). \tag{20.260}$$

We note that in all cases the anomalous MT contribution leads to an *enhancement* of the NMR relaxation rate over the normal state Korringa value. In particular, the superconducting fluctuations above T_c have the *opposite* sign to the effect for $T\ll T_c$ (where $1/T_1$ drops exponentially with T). One might argue that the enhancement of $1/T_1$ is a precursor to the coherence peak just below T_c. Although the physics of the Hebel-Slichter peak (pile-up of the DOS just above gap edge and coherence factors) appears to be quite different from that embodied in the MT process, we note that both effects are suppressed by strong inelastic scattering.

We now discuss the DOS and the regular MT contributions which are important when strong dephasing suppresses the anomalous MT contribution discussed above. The local susceptibility arising from diagrams 5 and 6 can be easily evaluated. The other remaining contribution is from the regular part of the MT diagram. It can be shown that this regular contribution is exactly one half of the total DOS contribution from diagrams 5 and 6. All other diagrams either vanish (as is the case for graphs 7 and 8) or contribute at higher order in $1/E_F\tau$ (this applies to the graphs with the Cooperon corrections). The final results can be presented in a unique way for the clean (but not ultra-clean) and dirty cases by means of the $Gi_{(2)}$ number:

$$\frac{\delta(1/T_1)^{DOS}}{(1/T_1)^0}=-12Gi_{(2)}\ln\left(\frac{2}{\sqrt{\epsilon}+\sqrt{\epsilon+r}}\right). \tag{20.261}$$

The negative DOS contribution to the NMR relaxation rate is evident from the Korringa formula and it sign seems very natural while the sign of the positive Maki-Thompson contribution can generate a questions about its physical origin. Let us consider a self-intersecting trajectory and the motion of the electron along it with fixed spin orientation (let us say "spin

up"). If, after passing a full turn, the electron interacts with the nucleus and changes its spin state and momentum to the opposite value it can pass again along the previous trajectory moving in the opposite direction. Interaction of the electron with itself on the previous stage of the motion is possible due to the retarded character of the Cooper interaction and such a pairing process, in contrast to the AL one, turns out to be an effective mechanism for relaxation near T_c. This purely quantum process opens a new mechanism of spin relaxation, and so contributes positively to the relaxation rate $1/T_1$.

In the case of the nuclear magnetic relaxation rate calculations, the electron interaction causing nuclear spin flip is considered. If one would try to imagine an AL process of this type he would be in trouble, because the electron-nuclei scattering with spin-flip evidently transforms the initial singlet state of the fluctuation Cooper pair in a triplet-one, which is forbidden in the scheme discussed. So the formally discovered absence of the AL contribution to the relaxation rate is evident enough.

It is worth mentioning that the cancellation of the MT and DOS contributions to conductivity found in Section 8.4 is crucial for the fluctuation contributions to the NMR relaxation rate. In fact, the MT and DOS contributions here have the same structure as in the conductivity while the AL contribution is absent. So the full fluctuation correction to the NMR relaxation rate in clean superconductor simply disappears.

Discussion.

The main results of this Section, valid for $\epsilon \ll 1$, can be summarized as follows:

(1) Fluctuations lead to a suppression of the spin susceptibility χ_s, due to the combined effect of the reduction of the single particle density of states arising from the self energy contributions, and of the regular part of the MT process.

(2) "Cooperon" impurity interference terms, involving impurity ladders in the particle-particle channel, are crucial for the χ_s suppression in the dirty limit.

(3) The processes which dominate the results in (1) and (2) above have usually been ignored in fluctuation calculations (conductivity, $1/T_1$, etc.). The spin susceptibility is unusual in that the AL and the anomalous MT terms, which usually dominate, are absent.

(4) For weak pair-breaking ($1/\tau_\varphi \ll T_c$), an enhancement of $1/T_1T$, coming from the positive anomalous MT term, takes place [210, 176].

(5) Strong dephasing suppresses the anomalous MT contribution, and $1/T_1$ is then dominated by the less singular DOS and the regular MT terms. Being negative, these contributions lead to a suppression of spectral weight and a decrease in $1/T_1$.

An intensive controversy took place in recent years in relation to the magnetic field dependence of the fluctuation contribution to $1/T_1$. The situation here resembles much the situation with the magnetoconductivity: a positive MT contribution is suppressed by the magnetic field while the magnetic field dependent part of the DOS contribution increases with the growth of the field. But in contrast to the magnetoconductivity, which can be measured extremely precisely, the NMR relaxation rate measurements are much more sophisticated. The result of this delicate competition, depending on many parameters $(r, \gamma_\varphi, \tau,)$, was found in HTS materials to be qualitatively different in experiments of various groups. The absence of a strong positive AL contribution, possible d-pairing, killing the MT contribution [210], small magnitude of the sum of MT and DOS effects even in the case of s-pairing, lack of the precise values of r, γ_φ, τ, leading to contradictive theoretical predictions[176, 113, 180, 212], the dispersion in the quality of samples and experimental methods were the reason of this discussion [113, 213, 214, 215, 44, 216].

20.7 Conclusions

Several comments should be made in conclusion. As was mentioned in the Introduction the first "fluctuation boom" took place at the end of 60's - beginning of 70's, just after the discovery of the fluctuation smearing of the superconducting transition and formulation of the microscopic theory of fluctuations. The discovery of HTS reanimated this interest and, in order to account for the specifics of these layered structures with high critical temperatures, low charge carrier concentration and other particularities, considerable progress in studies of fluctuation phenomena was achieved (see for instance the conference proceedings [217, 218] and the extensive review article [76]). As it is recognized now the optimally or overdoped phases of HTS compounds present an example of a "bad" Fermi liquid. The accounting for superconducting fluctuations is identical to including of the electron-electron interaction beyond the Fermi-liquid approximation. As a result a lot of anomalies of the normal state properties of such HTS compounds can be explained. The situation was found to be much more sophisticated in underdoped phases where the quasiparticle approach, which from we have started this Chapter, fails.

In the fluctuation theory discussed above, as in modern statistical physics in general, two methods have been used mainly: they are the diagrammatic technique and the method of functional (continual) integration over the order parameter. Each of them as we have seen, has its own advantages and disadvantages and in different parts of this review we used the former or the latter.

The years of the fluctuation boom coincided with the maximum development of the diagrammatic methods of many body theory in Condensed Matter Theory. This methods turns out to be extremely powerful: any physical problem, after its clear formulation and writing down the Hamiltonian, can be reduced to the summation of some classes of diagrams. The diagrammatic technique is especially comfortable for problems containing some small parameter. In the theory of superconducting fluctuations such a small parameter exists: as we have seen, it is the Ginzburg-Levanyuk number $Gi_{(D)}$ which is expressed as some powers of the ratio $\max\{T_c, \tau^{-1}\}/E_F$. This is why superconducting fluctuations led to the appearance of the small corrections to different physical values in a wide range of temperatures, and due to this smallness these corrections can be evaluated quantitatively. On the other hand their specific dependence on nearness to the critical temperature $T - T_c$ permits to separate them in experiment from other effects.

In those cases when fluctuations are small it is possible to restrict their summation to the ladder approximation only. The diagrammatic technique permits in a unique way to describe the quantum and classical fluctuations, the thermodynamical and transport effects

In the description of thermodynamic fluctuations the method of functional integration turned out to be simpler. The ladder approximation in the diagrammatic approach is equivalent to the Gaussian approximation in functional integration. The method of functional integration turns out to be more effective too in the case of strong fluctuations, for instance, in the immediate vicinity of the phase transition. The final equations of the renormalization group carried out by means of functional integrations turn out to be equivalent to the result of the summation of the parquet diagrams series. Nevertheless the former derivation is much more simple.

There is one another reason why we have tried to use both methods and even to carry out some results in both ways. In its explosive development of the last decades physics became an "oral science". In the process of such direct communication near a blackboard it is difficult to write and to read some cumbersome formulas. The language of diagrams is much more comprehensive: by drawing them the speaker demonstrates that this one is small and that one has to be taken into account for this and that reasons clear for the experienced listener. The success of the diagrammatic technique in some sense is similar to the success of geometry in

Ancient Greece, where the science was "oral" too.

This advantage of the diagrammatic technique transforms into its disadvantage when there is no direct communication between the speaker and listener. It is difficult to learn the diagrammatic technique by a textbook on your own, when no one helps you to find the necessary insight on a complex graph. May be because of similar reasons geometry disappeared in Middle Ages when direct communications between scientists was minimal while the "written" algebra had continued to develop. Operating with Osvald Spengler "prosymbols" we can say that the diagrammatic technique belongs more to the Ancient Greece culture style with its "finite body" prosymbol, while functional integration, side by side with the Vikings travels to unknown lands and Leibnitz analysis of infinitesimals, is an evident modern contribution to West-European culture with its "infinite space" prosymbol.

That is why, suspecting that the modern physics in the near future can fall down to a "New Middle Ages" period, we have carried out some results by means of functional integration instead of the diagrammatic technique.

21 Nonequilibrium SC

21.1 General Properties of Nonequilibrium Superconductors

21.1.1 General Understanding of Physics in Nonequilibrium SC

(here, I'll write many paragraphs about which one will work and which one will not. a very important section!)

Suppose the distribution of Bogoliubov particles $\langle n \rangle$ was changed because of an action on the superconductor of laser (or somehow else). Should the $\langle n \rangle$ change during the equilibration?

It will be only because of collision integral, which takes into account collisions with phonons, other excitations, impurities. If this integral is zero or absent in the model because of some restrictions, then there is no change of $\langle n \rangle$ and only the gap will be updated. So, we'll be still in the nonthermal state.

The gap adjusts "instantly" to the change of distribution of excitations

By "instantly" I mean that the update of the gap happens with the speed of Fermi velocity, because there are particles near Fermi surface which are responsible for it.

(???? why - I have no idea, really.)

But it is important to understand that there is no any delay. And there is no numerical discretization which would produce some equations where there are effects of not updated gap and Hamiltonian. All of this equations can be written only because of a not understanding of basics of nonequilibrium superconductivity.

Applicability of GGE ansatz

How exactly the density matrix comes back to the updated GGE manifold during the equilibration?

(write better question and answer)

GGE - это приближение, которое работает, потому что так проверено для пары других моделей, и скорее всего не будет проблем с этой моделью тоже. equilibration - просто обновление щели, потому что у нас обновилась функция распределения, а они всегда

связаны ур самосогласования, которое всегда используется. почему физически так - это я уже не знаю, но все используют это свойство, так что очень вряд ли оно не верное. если бы был не 1д случай и были бы фононы, то были бы еще интегралы столкновений, была бы термализация, но в нашем случае ничего особенного не происходит, просто пишем ур. самосоласования и сделана equilibration.

In a nutshell, all is ok with it.

(examples of proofs that GGE is good)

21.1.2 Choosing a Framework for Nonequilibrium SC

(some extra ideas about what to use and what not to use)

Formalism of Dissipative SC by Lindblad operators

(write here what we are using with Zala)

Formalism of Dissipative SC by non-hermitian Hamiltonians

(see Beenakker and his refs)

Dissipative BCS theory from "Collective Excitations and Nonequilibrium Phase Transition in Dissipative Fermionic Superfluids" by Yamamoto, Nakagawa, et al.

We consider ultracold fermionic atoms described by the three-dimensional attractive Hubbard model

$$H = \sum_{\boldsymbol{k}\sigma} \epsilon_{\boldsymbol{k}} c^\dagger_{\boldsymbol{k}\sigma} c_{\boldsymbol{k}\sigma} - U_{\rm R} \sum_i c^\dagger_{i\uparrow} c^\dagger_{i\downarrow} c_{i\downarrow} c_{i\uparrow}, \tag{21.1}$$

where $U_{\rm R} > 0$, $\epsilon_{\boldsymbol{k}}$ is the single-particle energy dispersion, and $c_{\boldsymbol{k}\sigma}$ ($c_{i\sigma}$) denotes the annihilation operator of a spin-σ fermion with momentum $\boldsymbol{k}$ (at site i). When the system is subject to inelastic collisions, scattered atoms are lost to a surrounding environment, resulting in dissipative dynamics as observed experimentally [**? ? ? ?**] (??? I am not sure, if this is true). Here, we study the time evolution of the density matrix ρ which is described by the Lindblad equation [**? ?**]

$$\frac{d\rho}{dt} = \mathcal{L}\rho = -i[H,\rho] - \frac{\gamma}{2}\sum_i (\{L_i^\dagger L_i, \rho\} - 2L_i \rho L_i^\dagger), \tag{21.2}$$

where $L_i = c_{i\downarrow} c_{i\uparrow}$ is a Lindblad operator that describes two-body loss with loss rate $\gamma > 0$. We note that the kinetic energy of lost atoms is large because of large internal energy of atoms before inelastic collisions. Under such situations, atoms after inelastic collisions are quickly lost into the surrounding environment and the Born-Markov approximation is justified [**? ? ?**].

Figure 21.1: [I'll add it later] (a) Schematic illustration of the amplitude and phase modes in a Mexican-hat free-energy potential as a function of the complex order parameter Δ, when either the interaction $U_{\rm R}$ or the dissipation γ is suddenly switched on. A sudden quench of the interaction $U_{\rm R}$ and that of the dissipation γ kick Δ in a direction parallel and perpendicular to the radial direction, respectively. Note that a finite change of γ excites both the phase and amplitude modes. (b) Two superfluids coupled via a Josephson junction, where one superfluid (system 2) is subject to two-body loss.

We first study how the standard BCS theory is generalized in open dissipative systems by formulating a time-dependent mean-field theory in terms of a closed-time-contour path integral [? ?]. We start with a generating functional defined as

$$Z = \mathrm{tr}\rho = \int \mathcal{D}[c_-, \bar{c}_-, c_+, \bar{c}_+] e^{iS} = 1, \tag{21.3}$$

with an action

$$\begin{aligned} S = \int_{-\infty}^{\infty} dt \Big[\sum_{\boldsymbol{k}\sigma} (\bar{c}_{\boldsymbol{k}\sigma+} i\partial_t c_{\boldsymbol{k}\sigma+} - \bar{c}_{\boldsymbol{k}\sigma-} i\partial_t c_{\boldsymbol{k}\sigma-}) - H_+ \\ + H_- + \frac{i\gamma}{2} \sum_i (\bar{L}_{i+} L_{i+} + \bar{L}_{i-} L_{i-} - 2L_{i+} \bar{L}_{i-}) \Big], \end{aligned} \tag{21.4}$$

where the subscripts + and - denote forward and backward paths, $H_\alpha = \sum_{\boldsymbol{k}\sigma} \epsilon_{\boldsymbol{k}} \bar{c}_{\boldsymbol{k}\sigma\alpha} c_{\boldsymbol{k}\sigma\alpha} - U_{\mathrm{R}} \sum_i \bar{c}_{i\uparrow\alpha} \bar{c}_{i\downarrow\alpha} c_{i\downarrow\alpha} c_{i\uparrow\alpha}$, $L_{i\alpha} = c_{i\downarrow\alpha} c_{i\uparrow\alpha}$, and $\bar{L}_{i\alpha} = \bar{c}_{i\uparrow\alpha} \bar{c}_{i\downarrow\alpha}$ $(\alpha = +, -)$. Note that the action has U(1) symmetry under $c_{i\sigma\alpha} \to e^{i\theta} c_{i\sigma\alpha}$ though the particle number is not conserved [? ?]. By introducing auxiliary fields via the Hubbard-Stratonovich transformation, we rewrite the action in a quadratic form of fermionic Grassmann fields as [? ?]

$$\begin{aligned} S = \int dt \Big\{ \sum_{\boldsymbol{k}} \Big[\bar{\psi}^t_{\boldsymbol{k}+} \begin{pmatrix} i\partial_t - \epsilon_{\boldsymbol{k}} & -\Delta \\ -\Delta^* & -i\partial_t + \epsilon_{\boldsymbol{k}} \end{pmatrix} \psi_{\boldsymbol{k}+} \\ - \bar{\psi}^t_{\boldsymbol{k}-} \begin{pmatrix} i\partial_t - \epsilon_{\boldsymbol{k}} & -\Delta \\ -\Delta^* & -i\partial_t + \epsilon_{\boldsymbol{k}} \end{pmatrix} \psi_{\boldsymbol{k}-} \Big] \Big\}, \end{aligned} \tag{21.5}$$

where $\bar{\psi}_{\boldsymbol{k}\alpha} = (\bar{c}_{\boldsymbol{k}\uparrow\alpha}, \ \ c_{-\boldsymbol{k}\downarrow\alpha})^t$ and $\psi_{\boldsymbol{k}\alpha} = (c_{\boldsymbol{k}\uparrow\alpha}, \ \ \bar{c}_{-\boldsymbol{k}\downarrow\alpha})^t$ $(\alpha = +, -)$. Here Δ is the superfluid order parameter which can be determined from the requirement that the action be extremal as [?]

$$\Delta = -\frac{U}{N_0} \sum_{\boldsymbol{k}} \mathrm{tr}(c_{-\boldsymbol{k}\downarrow} c_{\boldsymbol{k}\uparrow} \rho) \equiv -\frac{U}{N_0} \sum_{\boldsymbol{k}} \langle c_{-\boldsymbol{k}\downarrow} c_{\boldsymbol{k}\uparrow} \rangle, \tag{21.6}$$

where $U = U_R + i\gamma/2$ is an effective complex coupling constant including a contribution from the atom loss [?], and N_0 is the number of sites. Importantly, the order parameter includes the loss rate γ, which leads to dissipation-induced collective modes as discussed below. The action (21.5) describes the mean-field time-evolution equation of the density matrix as

$$\frac{d\rho}{dt} = -i[H_{\mathrm{eff}}, \rho], \tag{21.7}$$

$$H_{\mathrm{eff}} = \sum_{\boldsymbol{k}} \Psi^\dagger_{\boldsymbol{k}} \begin{pmatrix} \epsilon_{\boldsymbol{k}} & \Delta \\ \Delta^* & -\epsilon_{\boldsymbol{k}} \end{pmatrix} \Psi_{\boldsymbol{k}}, \tag{21.8}$$

where $\Psi_{\boldsymbol{k}} = (c_{\boldsymbol{k}\uparrow}, \ \ c^\dagger_{-\boldsymbol{k}\downarrow})^t$ is the Nambu spinor. In the Supplemental Material [?], we show that Eq. (21.7) can be derived from two different methods, i.e. the mean-field theory for the Lindblad equation and the time-dependent Bogoliubov-de Gennes analysis. While Eq. (21.7) appears to describe unitary evolution, it is consistent with the original Lindblad equation (21.2) as a consequence of the time-dependent BCS ansatz [?].

We use Anderson's pseudospin representation defined by $\boldsymbol{\sigma}_{\boldsymbol{k}} = \frac{1}{2} \Psi^\dagger_{\boldsymbol{k}} \cdot \boldsymbol{\tau} \cdot \Psi_{\boldsymbol{k}}$ and $H_{\mathrm{eff}} = 2 \sum_{\boldsymbol{k}} \boldsymbol{b}_{\boldsymbol{k}} \cdot \boldsymbol{\sigma}_{\boldsymbol{k}}$, where $\boldsymbol{\tau} = (\tau_x, \ \ \tau_y, \ \ \tau_z)$ is the vector of the Pauli matrices. The pseudospins satisfy the commutation relations $[\sigma^j_{\boldsymbol{k}}, \sigma^k_{\boldsymbol{k}}] = i\epsilon_{jkl} \sigma^l_{\boldsymbol{k}}$. For simplicity of notation, we omit the

bracket and regard $\boldsymbol{\sigma}_{\boldsymbol{k}}$ as the expectation value of the pseudospin operator. By using the commutation relation of the pseudospins, Eq. (21.7) is mapped to the Bloch equation:

$$\frac{d\boldsymbol{\sigma}_{\boldsymbol{k}}}{dt} = 2\boldsymbol{b}_{\boldsymbol{k}} \times \boldsymbol{\sigma}_{\boldsymbol{k}}, \tag{21.9}$$

$$\boldsymbol{b}_{\boldsymbol{k}} = (\mathrm{Re}\Delta, \quad -\mathrm{Im}\Delta, \quad \epsilon_{\boldsymbol{k}}). \tag{21.10}$$

Equation (21.9) shows that the superfluid dynamics is characterized by precession of a pseudospin in an effective magnetic field $\boldsymbol{b}_k$. Here, the order parameter is determined self-consistently from the pseudospin expectation value as

$$\Delta = |\Delta| e^{i\theta} = -\frac{U}{N_0} \sum_{\boldsymbol{k}} (\sigma^x_{\boldsymbol{k}} - i\sigma^y_{\boldsymbol{k}}). \tag{21.11}$$

It is noteworthy that the norm of the pseudospin is conserved by the Bloch equation (21.9). The time evolution of the particle number due to particle loss is obtained from Eq. (21.7) as

$$\frac{1}{N_0}\frac{dN}{dt} = -\frac{2\gamma|\Delta|^2}{|U|^2}, \tag{21.12}$$

which reflects the dynamics of the order parameter.

Other fundamental questions about construction of models of dissipative SC

In which range the dissipator acts?

(??? should it act in the also Debye's window or how??? or it does not matter? My code was breaking down because of something related to it)

Overview of other literature of dissipative SC

(see special note about it)

21.2 Typical Experiments with Nonequilibrium Superconductors

(write intro to many experimental articles)

21.3 7. Some Nonequilibrium Effects in Superconductors by Shmidt

The question of what happens to a superconductor when its equilibrium is disturbed and how it relaxes back to the equilibrium state has been a subject of intense discussions. Why is this? Why are nonequilibrium properties of superconductors so interesting and important? One would think that the answer lies in the fact that the superconductor comprises several groups of electrons: superconducting electrons, electron-like excitations, and holes. What was elucidated following the publication of the BCS theory was the equilibrium situation, in which all electron groups are in equilibrium not only with each other but also with the crystal lattice. If the equilibrium is disturbed, the behavior of the system becomes more complex. Then, through analyzing the processes of relaxation back to equilibrium, we can learn more about the very basics of the theory and gain insight into the nature of the phenomena. In addition, one should bear in mind that many successful cryoelectronic devices normally operate under conditions which are far from equilibrium. This attaches to studies of nonequilibrium phenomena a practical importance, too.

In this chapter we shall discuss a number of cases in which a nonequilibrium state of a superconductor plays a decisive role in determining its physical properties.

21.3.1 7.1 Quasiparticles: Electrons and Holes

Theory by Schmidt

Elementary excitations in superconductors (electrons and holes) already were the subject of our discussion in Chap. 6. Now we shall define them more accurately.

Consider first the normal metal. Its ground state (at $T = 0$, without elementary excitations) is such that all free electrons occupy all the states inside the Fermi surface while all states outside it are empty. Let us now add one extra electron to the metal. It will occupy one of the states, k_1 in momentum space ($k > k_{\mathrm{F}}$, where k_F is the radius of the Fermi sphere), and the total energy of the electron system will increase by $\hbar^2 \left(k^2 - {k_{\mathrm{F}}}^2\right)/2m$. The energy, as before, is measured from the Fermi energy $\hbar^2 {k_{\mathrm{F}}}^2/2m$. The increase in total energy will therefore be equal to the energy of the elementary excitation and the system's momentum will be k, the momentum of the

Consider once again the ground state of the normal metal, but this time after one electron has been removed from the state $k\,(k < k_F)$. This state can also be treated as an elementary excitation of the system, because its energy is greater than the ground-state energy of electrons remaining in the metal, by $\hbar^2 \left({k_F}^2 - k^2\right)/2m$. Indeed, we can restore the ground state by taking an electron from the Fermi surface and putting it in the vacant state k. The momentum of this elementary excitation is equal to the momentum of the entire electron system, that is, to $-k$. Such an excitation (quasiparticle) behaves in the same way as a positive charge and is called a hole. The elementary excitation energy spectrum for the normal metal is shown in Fig. 7.1 by dashed lines.

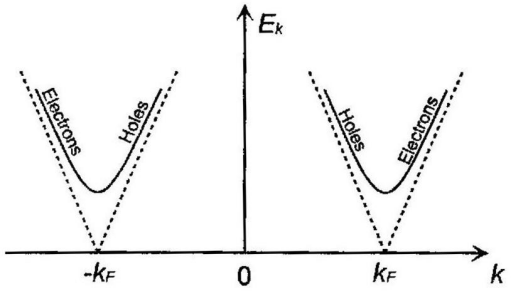


Fig. 7.1. Energy spectrum of the quasiparticles in the superconductor. Dashed lines show the spectrum for the normal metal

In the superconductor, things are somewhat more complicated. We already know (Chap. 6) that the ground state of the superconductor is described by a function ${v_k}^2$ representing the probability that the pair states $(k, -k)$ are occupied by electrons. The behavior of this function is illustrated in Fig. 6.5. Let us now add one extra electron to a superconductor. It will occupy one of the vacant k states in momentum space, while the state $-k$ will remain empty. But, unlike the normal metal, in the superconductor, the state k can be either inside or outside the Fermi surface. Because some of the k states with $k < k_F$ remain empty in the ground state, too! Thus, in the superconductor, the momentum of an electron-like quasiparticle can be not only greater than, but also less than, k_F.

Conversely, if we remove one electron from, say, the state $-k$ in the ground state of a superconductor, the complementary electron in the state k will become uncoupled and start behaving in the same manner as a hole with momentum k which, again, can be not only greater than, but also less than, k_{F}.

Therefore, in the superconductor, an elementary excitation corresponding to the state $\boldsymbol{k}$ being occupied and the state $-\boldsymbol{k}$ being empty behaves partly
relative probabilities of the two states. The probability of its behaving as a hole must be proportional to the probability of the state k being occupied by a superconducting electron, that is, to ${v_k}^2$. On the other hand, its behavior as an electron-like quasiparticle is governed by

the probability that one of the k states in the ground state is vacant, that is, by ${u_k}^2 = 1 - {v_k}^2$.

One may define a quasiparticle of electron type in the superconductor (an almost pure electron) as a quasiparticle with momentum k satisfying the conditions $|k - k_\mathrm{F}|/k_\mathrm{F} \gg \Delta/\varepsilon_\mathrm{F}$ and $k > k_\mathrm{F}$. And an almost pure hole is an excitation with momentum k such that it satisfies the inequalities $|k - k_\mathrm{F}|/k_\mathrm{F} \gg \Delta/\varepsilon_\mathrm{F}$ and $k < k_\mathrm{F}$.

The electron and hole branches of the quasiparticle spectrum for the superconductor are sketched in Fig. 7.1 by solid lines.

It only remains to add that, in real space, the propagation velocity of a quasiparticle is the group velocity well known to be

$$s_k = \frac{\mathrm{d}E_k}{\mathrm{d}p_k} = \frac{1}{\hbar}\frac{\mathrm{d}E_k}{\mathrm{d}k}$$

This means that at $k > 0$ (in the notation of Fig. 7.1) the holes move to the left and the electrons to the right.

21.3.2 7.2 Charge of a Quasiparticle in the Superconductor

Theory by Schmidt

We have just seen that a quasiparticle in the superconductor is an elementary excitation which can be treated to a certain extent as an electron and to a certain extent as a hole. As one moves along the curve of the elementary excitation spectrum, as in Fig. 7.1, the transition from the pure electron to the pure hole happens gradually. This simple observation suggests that one should assign a fractional electric charge to the quasiparticle. In the argumentation below we shall follow Pethick and Smith [67] who were apparently the first to propose this approach. We shall find very soon how convenient it is and how much easier it makes a qualitative analysis of nonequilibrium processes in superconductors. For the sake of simplicity, we agree to measure all charges in normalized units, taking the electron charge equal to unity.

Consider a superconductor at a finite temperature and assume that it contains both coupled (superconducting) electrons and elementary excitations. Suppose that the distribution of the elementary excitations in k space is defined by a distribution function f_k, that is, f_k gives the probability that the state k is occupied by an excited electron. Since the probability that this state was free of a superconducting electron before is ${u_k}^2$, the net probability to find an excited electron in the state k is given by $f_k {u_k}^2$. On the other hand, this state can be filled with one of the superconducting electrons. For this, two conditions must be satisfied simultaneously: first, that this state does not contain an excited electron (the probability of this is $1 - f_k$), and second - it contains a superconductive electron (the probability equals ${v_k}^2$).

Thus, the net probability to find a superconducting electron in the state k is $(1 - f_k)\,{v_k}^2$ and the total charge associated with this state is $f_k {u_k}^2 + (1 - f_k)\,{v_k}^2$. The total charge associated with all electrons in the superconductor is then

$$Q_\mathrm{tot} = \sum_k f_k u_k^2 + \sum_k (1 - f_k)\, v_k^2 \tag{7.1}$$

Suppose that, as a result of an external perturbation, the distributions of both the quasiparticles and the superconducting electrons have changed (the former by the value of δf_k and the latter by the value of $\delta {v_k}^2$). Such a change will result in a variation of the total charge of the electron system by

$$\delta Q_\mathrm{tot} = \sum_k \left(u_k^2 - v_k^2\right) \delta f_k + \sum_k (1 - 2f_k)\, \delta v_k^2. \tag{7.2}$$

Here the first term is obviously a variation of the total charge of the quasiparticles. More specifically, the probability of finding a quasiparticle in the state k has changed by the value of δf_k and been accompanied by a change of the charge associated with this state by $({u_k}^2 - {v_k}^2)\,\delta f_k$. It is obvious then that the quantity

$$q_k = u_k^2 - v_k^2 \tag{7.3}$$

can be treated as the charge of a quasiparticle with momentum k. According to (6.12),

$$v_k^2 = \frac{1}{2}\left(1 - \frac{\varepsilon_k}{E_k}\right) \tag{7.4}$$

Then

$$u_k^2 = \frac{1}{2}\left(1 + \frac{\varepsilon_k}{E_k}\right) \tag{7.5}$$

This leads to

$$q_k = \frac{\varepsilon_k}{E_k} = \frac{\varepsilon_k}{(\varepsilon_k^2 + \Delta^2)^{1/2}} \tag{7.6}$$

The dependence of q_k on k is shown in Fig. 7.2. It implies that the charge of a quasiparticle varies continuously from +1 (pure electron) to -1 (pure hole) and is completely determined by which particular state in k space the quasiparticle occupies. A rather odd result at first sight! But let us add one extra electron to the superconductor and place it in the state k.

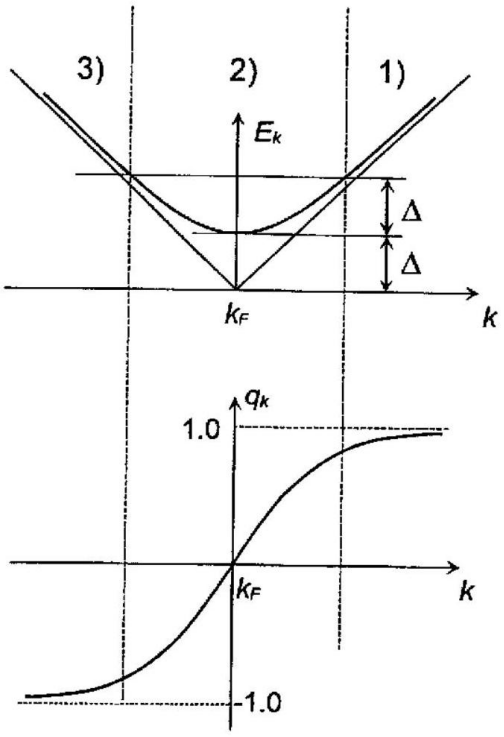


Fig. 7.2. Energy spectrum E_k of quasiparticles in the superconductor and their charge q_k. In region 1 , the quasiparticle charge q_k is close to +1 , in region 3 it is close to -1 , and in region 2 it may assume any value from +1 to -1

As a result, the superconductor as a whole has acquired a charge +1 (recall that it is this value that we agreed to regard as the electron charge), while the state $\boldsymbol{k}$ has got a charge q_k. But where is the difference $1 - q_k$? We know that the total charge must be conserved! The answer is that the charge $1 - q_k$ has been transferred to the superconducting electrons thereby increasing their charge. The whole process can be described as follows. An electron is added

to $-\boldsymbol{k}$ which belongs to the condensate [1] and the pair subsequently joins the condensale. But an electron in the state $\boldsymbol{k}$ is left without a partner, that is, a hole is formed.

We use the name 'condensate' for the entire sea of superconducting electrons, all of them described by a single wavefunction. It is, however, not entirely correct. Not all electron pairs, despite being Bose particles, can make a transition to the lowest energy level (i.e., to join the Bose condensate, in the strict meaning of the word). Owing to their interaction with each other, some of the Bose particles have energies above that of the condensate. Together with the condensate particles, they form the sea of superconducting electrons. There is no sense to see these excitations as a elementary excitations (?????).

Thus the condensate and the elementary excitations in the superconductor are closely interrelated and cannot be treated as independent in the relaxation process. Quasiparticle transitions between different $\boldsymbol{k}$ states are accompanied by changes of their charges q_k resulting in a change of the total charge of the condensate or, in other words, of the number of electrons in the condensate.

21.3.3 7.3 Relaxation Time for the Quasiparticle Charge

Theory by Schmidt

Let us try to estimate the time required for relaxation of the quasiparticle charge, that is, the time required for the charge of a system of quasiparticles to attain its equilibrium value, after the equilibrium has been disturbed by some external perturbation. At this stage, we assume that the total number of quasiparticles remains constant. With this assumption, one may consider an elementary act of charge relaxation as a transition of a quasiparticle from one k state in momentum space to another. Such a transition must be accompanied by either emission or absorption of phonons. If τ_E is the relaxation time, the inverse quantity, τ_E^{-1}, represents the frequency of inelastic collisions between electrons and phonons in a metal, which is independent of whether the metal is in the normal or superconducting state. The order of magnitude of this frequency is [68]

$$\tau_E^{-1} \sim \frac{k_\mathrm{B}T}{\hbar} - \left(\frac{T}{\Theta_\mathrm{D}}\right)^2$$

where k_B is the Boltzmann constant and Θ_D the Debye temperature. Suppose that the temperature of the superconductor is close to T_c. This means that $\Delta \ll k_\mathrm{B}T_\mathrm{c}$. Let us ask: Will every electron-phonon collision then contribute to the charge relaxation? Obviously, it will not. Indeed, if the states of an electron, before and after a collision, are both in region 1 (see Fig. 7.2), the transition leaves its charge practically unaltered. The same applies to region 3. But the electrons in region 2 are completely different. Their transitions, initiated by collisions with phonons, alter the quasiparticle charge by values of the order of unity. At a finite temperature T, the fraction of excitations in region 2 out of the total number of excitations is of the order $\Delta/k_\mathrm{B}T$ since, by definition, the excitation energies E_k in this region fall into the range $\Delta \le E_k \le 2\Delta$. The frequency of transitions resulting in a considerable change of the quasjparticle charge is therefore

$${\tau_Q}^{-1} \sim \frac{\Delta}{k_\mathrm{B}T}{\tau_E}^{-1}$$

At $T \approx T_\mathrm{c}$, rigorous calculations of the quasiparticle charge relaxation time [69] yield

$$\tau_Q = \frac{4}{\pi}\frac{k_\mathrm{B}T_\mathrm{c}}{\Delta}\tau_E \tag{7.7}$$

According to (7.7), the quasiparticle charge relaxation time diverges at $T \to T_c$. Typical values of τ_E are of the order 10^{-10} s. For example, for superconducting tin, $\tau_E = 3 \times 10^{-10}$ s; for lead $\tau_E = 10^{-11}$ s. The above values of τ_E correspond to the respective critical temperatures of the materials. The relaxation time τ_Q can be much longer. It depends entirely on how close one approaches the critical temperature.

21.3.4 7.5 Branch Imbalance of the Elementary Excitation Spectrum and Electric Field in the Superconductor

Theory by Schmidt

At equilibrium, the electron and hole branches of the elementary excitation spectrum are symmetrically populated with quasiparticles. For this reason, at equilibrium, the number of electron-like quasiparticles is exactly equal to the number of holes, and the total charge is zero. Furthermore, the distribution function for the quasiparticles is given by the Fermi distribution

$$f_k = \frac{1}{\exp\left(E_k/k_B T\right) + 1}$$

The equilibrium distribution can be disturbed as a result of an external perturbation. If, for example, a superconductor is exposed to electromagnetic radiation, the latter does not affect the symmetry of the distribution of electrons and holes over the branches of the spectrum. What happens is that the quasiparticles, having absorbed the electromagnetic energy, move up to higher energy levels, which may result in an alteration of the energy gap. Nonequilibrium processes of this type will be considered in Sect.7.8.

Another way to disturb the equilibrium in the neighborhood of the NS interface is to have a flow of electrons coming from the normal metal. Indeed, in this process, electrons with energies $E_k > \Delta(T)$ penetrate the interior of the superconductor and occupy some of the k states on the electron branch of the spectrum. This causes a population imbalance on the two branches. In this section we want to investigate the consequences of this branch imbalance and the characteristic distances for its relaxation.

It is obvious that the existence of the branch imbalance leads to the appearance of a finite quasiparticle charge Q at a given location in the superconductor:

$$Q = \sum_k q_k f_k$$

where f_k is some (in the general case, nonequilibrium) distribution function for the electrons in momentum space.

But the net charge of all electrons at every point of the superconductor must be identical and equal in absolute value to the local charge on the ions of the crystal lattice. This condition assures electroneutrality of the material. Thus, an increase (compared to equilibrium) of the quasiparticle charge at some location by an amount Q must be compensated by a decrease, by the same amount, of the charge of the condensate, thereby modifying the distribution function of the superconducting electrons, ${v_k}^2$. The dotted line in Fig. 7.4 indicates the initial distribution function ${v_k}^2$ corresponding to equilibrium, when $Q = 0$ and the chemical potential of the superconducting electrons, μ_s, coincides with the Fermi energy ε_F of the metal. [2] Since the area under the ${v_k}^2$ curve is proportional to the number of superconducting electrons, a decrease of the latter ought to shift the distribution boundary to the left. This will result in a decrease of the chemical potential μ_5 by the amount $\varepsilon_F - \mu_s$. The new distribution ${v_k}^2$ is shown in Fig. 7.4 by the solid line. Now we can easily count the number of states that have become

free of superconducting electrons: $2N(0)\,(\varepsilon_F - \mu_s)$, where $N(0)$ is the density of states at the Fermi level, and the factor 2 takes into account that there are

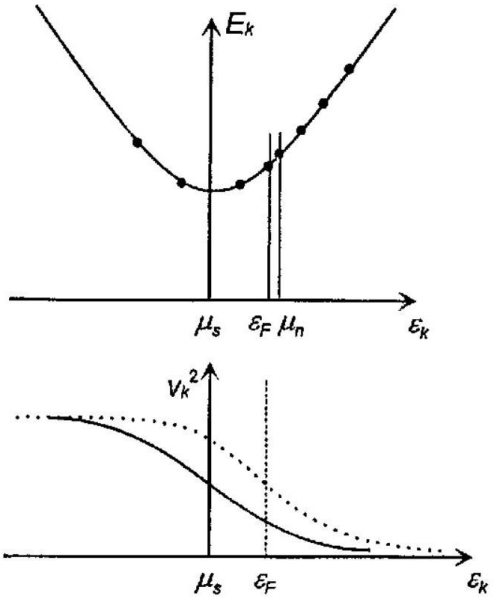


Fig. 7.4. Nonequilibrium distribution of superconducting electrons, ${v_k}^2$, and quasiparticle spectrum E_k for the superconductor in a nonequilibrium state. The dotted line shows the equilibrium distribution ${v_k}^2$ for $\mu_\mathrm{s} = \varepsilon_F$. In the latter case, the energy gap Δ retains its value while the chemical potential μ_n becomes greater than ε_F

two electrons with opposite spins at each energy level. It follows that the condensate has lost the charge

$$Q = 2N(0)\,(\varepsilon_\mathrm{F} - \mu_\mathrm{s})\,, \tag{7.8}$$

which has subsequently been added to the quasiparticles.

Let us analyze the consequences of this process. Since the nonequilibrium quasiparticle charge Q becomes a function of the coordinate x, it is obvious from (7.8) that, in real space, the nonequilibrium chemical potential of the superconducting electrons, μ_s, also becomes a function of x. But this is equivalent to the possibility of having an electric field $\boldsymbol{E}$ in the superconductor, such that it does not accelerate the condensate. Indeed, the most general form of the equation of motion for a superconducting electron reads

$$\frac{\mathrm{d}}{\mathrm{d}t}\,(m\boldsymbol{v}_\mathrm{s}) = -\frac{e}{c}\frac{\mathrm{d}\boldsymbol{A}}{\mathrm{d}t} - e\nabla\varphi - \nabla\mu_\mathrm{s}. \tag{7.9}$$

Here e is the electron charge, m the electron mass, v_s the superfluid velocity of the condensate, φ the electrostatic potential, and $\boldsymbol{A}$ the vector potential. Under stationary conditions, $\mathrm{d}\,(m\boldsymbol{v}_\mathrm{s})\,/\mathrm{d}t = \mathrm{d}\boldsymbol{A}/\mathrm{d}t = 0$, and the superconducting electrons do not accelerate. This implies that the electrochemical potential of the superconducting electrons, $\varphi_{\mathrm{ech}\,,s}$, must be constant in space:

however, it does not oppose the existence of the electric field. The latter is, from (7.10),

$$\boldsymbol{E} = -\nabla\varphi = \frac{1}{e}\nabla\mu_\mathrm{s}$$

Using (7.8) we have

[292] In the nonequilibrium case, the form of the electron distribution function for the condensate is the same as at equilibrium, i.e., ${v_k}^2 = (1 - \varepsilon_k/E_k)\,/2$, but with $\varepsilon_k = \hbar^2k^2/2m - \mu_s$ and $E_k = \left({\varepsilon_k}^2 + \Delta^2\right)^{1/2}$. That is, we assume that there is enough time for the condensate to adjust to a given nonequilibrium distribution of the quasiparticles. One can easily verify that the branch imbalance does not

$$E = -\frac{1}{2eN(0)}\nabla Q \tag{7.11}$$

The above analysis infers that a gradient of the quasiparticle charge in a superconductor under nonequilibrium conditions brings about an electric field. However, this field does not cause the condensate to accelerate, because it is compensated by a gradient of the chemical potential of superconducting electrons. We emphasize once again that superconducting electrons are only affected by the gradient of their electrochemical potential $\nabla\varphi_{\text{ech, s}}$ which, by (7.10), is zero.

For a given site in the superconductor, the presence of a stationary but nonequilibrium quasiparticle charge of density Q indicates that there exists a continuous flow of quasiparticles through this site. The quasiparticles bring with them a certain charge which is immediately transferred to the condensate through the relaxation process.

The entire process can be expressed by a simple relation

$$\operatorname{div} j_{\text{n}} = -eQ/\tau_Q \tag{7.12}$$

where $\boldsymbol{j}_{\text{n}}$ is the normal component of the total current. The relation (7.12) is only approximately valid when the gap is small ($\Delta \ll k_{\text{B}}T_{\text{c}}$), that is, when the temperature is close to T_c. One can find a more rigorous treatment of this process in [67]. In the same approximation, at $T \approx T_c$, the change in the chemical potential of the quasiparticles is small compared to that of the superconducting electrons, and can be neglected, i.e., $\varepsilon_{\text{F}} - \mu_{\text{s}} \gg \mu_{\text{n}} - \varepsilon_{\text{F}}$ (see Fig. 7.4). Indeed, at $T \approx T_{\text{c}}$, the number of superconducting electrons in the condensate is small, while that of normal electrons is substantial. Therefore, the removal of a few electrons from the condensate and their transfer to the sea of normal electrons will result in a considerable alteration of the properties of the condensate (a decrease in μ_s) while leaving the normal electrons almost unaffected.

In view of this, one may write Ohm's law for the excitations in the usual form

$$j_{\text{n}} = \sigma E$$

where σ is the normal conductivity at low temperatures: $\sigma^{-1} = \rho_{\text{res}}$, and ρ_{res} the residual resistivity. [3] Taking the divergence of both sides of this equation and substituting (7.11) and (7.12) yields

$$\nabla^2 Q = \frac{1}{{\lambda_Q}^2} Q \tag{7.13}$$

where

$${\lambda_Q}^2 = \frac{\sigma\tau_Q}{2e^2N(0)} \tag{7.14}$$

Taking into account that the conductivity of the normal metal can be written as [4]

$$\sigma = \frac{2}{3}e^2N(0)lv_{\text{F}}$$

where l is the electron mean free path and v_{F} is the electron velocity on the Fermi surface, we finally have

$$\lambda_Q = \left(\frac{lv_F\tau_Q}{3}\right)^{1/2} = (D\tau_Q)^{1/2} \tag{7.15}$$

where D is the electron diffusion coefficient, $D = lv_{\text{F}}/3$.

Consider now the simplest case. Suppose that the sample is a filament so thin that the problem

can be considered one-dimensional. Let us take the x axis along the filament and assume the material of the filament to be normal for $x < 0$ and superconducting for $x > 0$. Further, suppose that the filament carries a current in the positive x direction. Equation (7.13) then takes the form

$$\frac{\mathrm{d}^2 Q}{\mathrm{d}x^2} = \frac{1}{{\lambda_Q}^2} Q \tag{7.16}$$

It is obvious that far away from the interface (at $x \to \infty$) the charge is $Q \to 0$, because there the superconductor is at equilibrium and the quasiparticle charge is zero. The solution of (7.16) is then given by the function

$$Q \propto \mathrm{e}^{-x/\lambda_Q} \tag{7.17}$$

Accordingly, the charge gradient gives rise to an electric field in the interior of the superconductor which, by (7.11), will be

$$E = E_0 \mathrm{e}^{-x/\lambda_Q} \tag{7.18}$$

where E_0 is the electric field at the interface. If one ignores the Andreev reflection, which is indeed permitted at $T \approx T_\mathrm{c}$, the field E_0 at the interface will be equal to the electric field in the interior of the normal metal, i.e., at $x < 0$.

Thus the quantity λ_Q represents the depth to which the electric field penetrates into the superconductor. According to (7.18), the electric field is exponentially damped over a distance λ_Q from the interface. Let us estimate the electric field penetration depth. According to (7.14), $\lambda_Q \propto {\tau_Q}^{1/2}$ and, according to (7.7), τ_Q is proportional to Δ^{-1}. Taking into account that $\Delta \propto (1 - T/T_c)^{1/2}$, we have

$$\lambda_Q \propto \left(1 - \frac{T}{T_c}\right)^{-1/4} \tag{7.19}$$

that is, the depth λ_Q diverges at $T \to T_c$. Thus, at temperatures sufficiently close to the critical temperature, the electric field can penetrate the superconductor to large distances. Recalling that the characteristic value of τ_Q is of the order $10^{-9} - 10^{-10}$ s, we obtain for $v_\mathrm{F} \sim 10^8$ cm s^{-1} and, say, $l \sim 10^{-5}$ cm: $\lambda_Q \sim 10^{-4} - 10^{-3}$ cm. This means that the electric field penetration depth can surpass all other characteristic lengths of the superconductor. Not too close to T_c, it is possible to have $\lambda_Q \gg \xi(T)$.

Let us summarize. An electric current passing through the interface between a superconductor and a normal metal gives rise to an electric field in the superconductor. The field decays over the distance λ_Q from the interface, where λ_Q can be of a macroscopically large value. Within this region, the divergence of the normal current, $\nabla \boldsymbol{j}_\mathrm{n}$, is nonzero (see (7.12)). But for the total current $\boldsymbol{j} = \boldsymbol{j}_\mathrm{g} + \boldsymbol{j}_\mathrm{n}$ (where $\boldsymbol{j}_\mathrm{g}$ is the supercurrent density) under stationary conditions, the divergence is, naturally, zero. Therefore, we have

$$\nabla j_\mathrm{n} = -\nabla j_\mathrm{s}$$

It means that within the layer of a superconductor of thickness λ_Q near the interface with the normal metal, the normal current is converted into the supercurrent. This can also be interpreted in a different way. According to Fig. 7.4, the chemical potentials in this 'nonequilibrium' region are: $\mu_\mathrm{n} > \mu_\mathrm{g}$. Therefore, one may say that this region hosts a 'chemical reaction' in which a substance with chemical potential μ_n transforms into a substance with chemical potential μ_8.

All the processes analyzed in this section relate to the case where there is a current of electrons passing from a normal metal to a superconductor. However, it is easy to verify

that the entire pattern is symmetric with respect to current reversal. In that case, the particles moving from the normal metal towards the superconductor and entering the interface are holes, and the Andreev-reflected particles are electron-like. Furthermore, the branch imbalance of the elementary excitations in the superconductor, in the region $\sim \lambda_Q$ near the interface, is such that the population of the hole branch exceeds that of the electron branch.

21.3.5 7.6 Experimental Study of a Nonequilibrium State at a Normal Metal-Superconductor Interface

7.6.1 The Experiments of Yu and Mercereau

In this section we shall describe particularly elegant experiments due to Yu and Mercereau [71]. These experiments have clearly demonstrated that, in the presence of an electric current passing through an NS interface, the elec (????? missing text) differ from each other within a region of the superconductor adjacent to the normal metal.

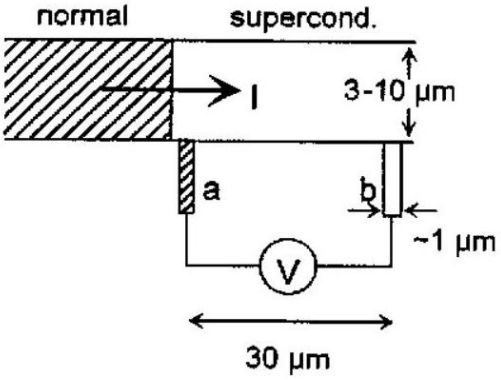


Fig. 7.5. Schematic diagram of the experiment by Yu and Mercereau [71]. Voltage leads a and b are connected to the voltmeter. If lead a is normal, the voltmeter registers the difference between electrochemical potentials of the quasiparticles and the condensate. If lead a is superconducting, the voltmeter reading is zero. Note that the readings do not depend on whether lead b is in the normal or superconducting state

The critical temperature of a thin film of tantalum of thickness of about 250Å is approximately 4.1 K . If a part of the film is made thinner (about 100Å) by anodization, the critical temperature of this part will fall to 3.5 K . Further, if the temperature of the film is kept between 3.5 K and 4.1 K , one part of the film will be normal and the other superconducting.

If we now apply a current to the film, the electrochemical potential of the superconducting electrons, $\varphi_{\text{ech},}$ s, will be constant in space, according to (7.10). Therefore, the superconducting voltage leads a and b (see Fig. 7.5)

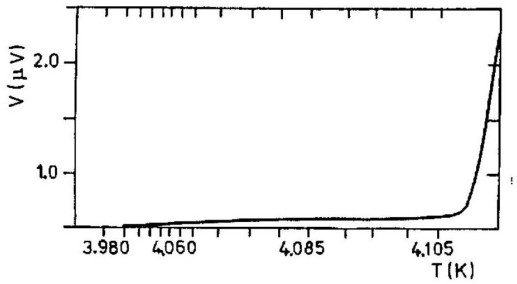


Fig. 7.6. Results of the Yu-Mercereau experiment [71]. The voltmeter registers the difference between the electrochemical potentials of the quasiparticles and the

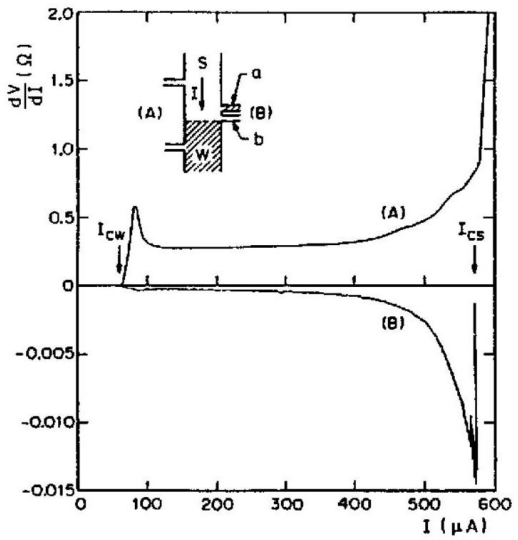


Fig. 7.7. Results of the Yu -Mercereau experiment [71]: differential resistance as a function of current through the film. Voltage A is opposite in sign to voltage B. Current flows in the direction from the superconducting to the normal (dashed area) lead

will convey to the voltmeter equal electrochemical potentials. That is, the voltmeter will register zero voltage. If, however, one of the voltage leads, a, immediately adjacent to the NS interface is made of a normal metal, it will convey to the left input contact of the voltmeter the electrochemical potential of the normal electrons, which in this region differs from $\varphi_{\text{ech.s}}$. This difference relaxes over the distance λ_Q from the interface. If the distance between the voltage leads a and b exceeds λ_Q, the lead b will send to the right contact of the voltmeter the electrochemical potential of the superconducting electrons (in equilibrium conditions, the latter is equal to the electrochemical potential of the quasiparticles). As a result, the voltmeter will measure the difference in electrochemical potential between the normal and superconducting electrons in the vicinity of the NS interface.

The result of the experiment with the lead a normal is shown in Fig. 7.6.

Another experiment by the same authors proved to be even more elegant. By placing the voltage contacts in the nonequilibrium region of a superconductor close to each other (as illustrated in Fig. 7.7) and in such a way that the superconducting lead b was very close to the interface and the normal lead a was some distance away from it, they were able to observe a reversal of the voltage sign for the same direction of current as before.

These experiments have provided ample verification of the ideas discussed in the foregoing sections.

Indeed, if the current in the film passes from S to N (see Fig. 7.7), a 'chemical reaction' takes place in the region of nonequilibrium near the interface: superconducting electrons convert into normal electrons. That is, the chemical potential μ_8 in this region is larger than μ_{n}. As a result, the reading of the voltmeter changes sign.

7.6.2 Excess Resistance of the Normal-Superconducting Interface

Another interesting manifestation of nonequilibrium processes in the vicinity of an NS interface, initiated by a current, is the excess electrical resistance of the interface. Physically, it is easy to understand.

Suppose that there is a current of electrons passing from a normal metal N to a superconductor S. Electrons from N with energies less than the gap $\Delta(T)$ in S will be Andreev-reflected and the current they were carrying will convert into a current of superconducting electrons. This process will take place within a distance $\xi(T)$ from the interface and its contribution to the resistivity will be zero.

But things will be different for the electrons in N of energies higher than the gap $\Delta(T)$.

Upon arriving in S , they move, in momentum space, to the electron branch of the elementary excitation spectrum of the superconductor. This, as was established in the previous section, results in an imbalance of the quasiparticle charge Q and gives rise to an electric field E which extends into the superconductor over a distance λ_Q from the interface. Furthermore, the presence of an electric field in the region λ_Q near the interface implies that this region contributes to the net voltage drop, that is, to the net resistance of the circuit. This additional resistance is called the excess resistance of an NS interface. If all electrons carrying the current were accelerated by the electric field, the excess resistance would simply be

$$R_{\text{exc}} = \rho\lambda_Q/S$$

where ρ is the normal-state resistivity of the superconductor and S its crosssectional area. One should bear in mind, however, that not all electrons are accelerated by the electric field E.

Indeed, as we already know, the electrons of the condensate are not accelerated by the field E, because the effect of the field on superconducting electrons is exactly compensated by the gradient of their chemical potential $\nabla\mu_5$. This property is a characteristic of all electrons passing from N into S with energies that are below the gap $\Delta(T)$ (they are Andreev-reflected), and also of the quasiparticles with energies above the gap: $E_k \geq \Delta(T)$. The number of quasiparticles which do not contribute to the excess resistance is determined by the following process. Consider an electron having a charge g_k which is injected from N into S . Upon entering S , the electron will have 'lost' a part of its charge $1 - q_k$ which has been transferred to the condensate. The transmission of this part of the charge through the NS interface occurs
excess resistance. The latter should then be written as

$$R_{\text{exc}} = \frac{Z(T)}{S}\ \frac{\rho\lambda_{\text{Q}}}{S},$$

where the coefficient $Z(T)$ accounts for the number of electrons which ar not Andreev-reflected at the interface.

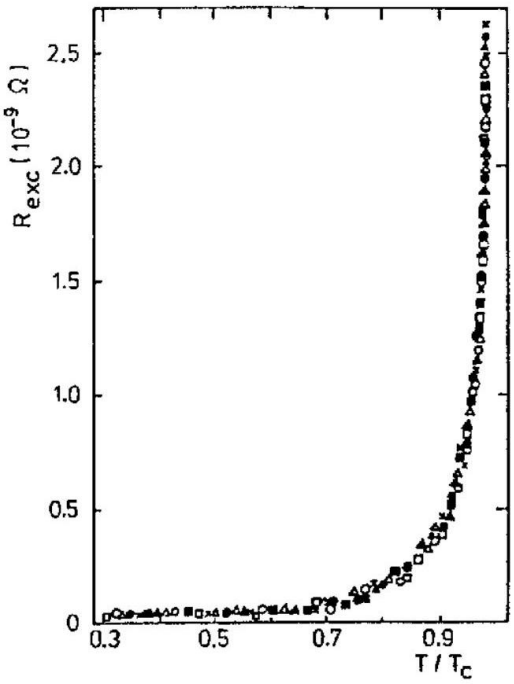


Fig. 7.8. Excess resistance of an NS interface as a function of temperature, me sured on Ta -Cu-Ta sandwiches [72]. The data were obtained from seven differen samples

It is obvious that as $T \to 0$ all electrons passing through the interfac are Andreev-reflected and $Z \to 0$. Conversely, as $T \to T_{\text{c}}$ we have $\Delta(T) \to$ so that the overwhelming majority of

electrons pass through the interfa without being Andreev-reflected and therefore contribute to the resistanc In this limit $Z \to 1$.

Therefore, in the entire temperature range: $R_{\text{cxc}}(T)$ is a monotonic fun tion of temperature:
5

$$R_{\text{exc}}\,(T \to 0) = 0, \quad R_{\text{exc}}\,(T \to T_{\text{c}}) = \rho\lambda_{\text{Q}}/S$$

In the latter case ($T \to T_{\text{c}}$), the temperature dependence of R_{exc} is governe by the temperature dependence of λ_Q (7.19):

$$\lambda_Q \propto \left(1 - \frac{T}{T_{\text{c}}}\right)^{-1/4}$$

This conclusion agrees well with experiment.
As an illustration, the results of experiments on seven different SNS sandwiches are shown in Fig. 7.8. The excess resistances of NS interfaces are plotted as functions of temperature.

21.3.6 7.7 Phase-Slip Centers

Theory by Schmidt

In the present chapter, we have so far considered stationary nonequilibrium processes. Now we are going to address nonstationary nonequilibrium processes.

It was demonstrated in Sect. 3.6, where we examined the critical current of a thin film, that a film driven to the normal state by critical pair-breaking current does not undergo a phase transition. It was established that what happens at $I = I_{\text{c}}$ is simply that the number of superconducting carriers becomes insufficient to sustain a given current I. This means that, at $I > I_c$, there appears a peculiar resistive state which we are going to examine now.

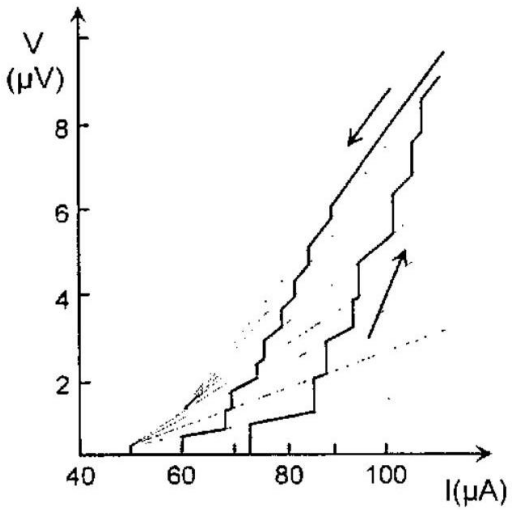


Fig. 7.9. Current-voltage characteristic of a single-crystalline Sn filament: the length of the flament is 0.8 mm and its cross-sectional area is 1.93 mm^2 [75]

Let us start with experimental results. The most suitable objects to study this kind of resistive state are quasi-one-dimensional objects, such as long thin superconducting filaments of diameter $d \leq \xi(T)$. The diameter of such a flament is so small that an Abrikosov vortex having a normal core fof radius
$\sim \xi(T)$) cannot fit into it. Therefore, the resistive state of the filament is not masked by effects typical of the resistive state of type-II superconductors. The current-voltage characteristic of a

[29]–The function $Z(T)$ is calculated in a number of theoretical papers. See, for e: 1 im-1 -11

thin single-crystalline whisker of tin is shown in Fig. 7.9. One can see that the voltage builds up in a stepwise fashion and each upward jump of the voltage is accompanied by an increase of the sample resistivity (the slope of the $I - V$ characteristic).

This behavior in the resistive state is explained by the model proposed by Skocpol, Beasley and Tinkham [76], the so-called phase slip center model,

Suppose that at a certain location (weak spot) in the filament the critical current is somewhat smaller than elsewhere. Then, as we increase the current through the filament, the current will first reach its critical value at the weak spot. A further increase of the current will result in a flow of normal electrons which will induce an electric field. The latter, in turn, will accelerate the normal electrons to the critical velocity. Electron pairs at the weak spot will be broken, the amplitude of the order parameter $|\psi|$ will go to zero and the current will be carried by the normal component alone. But formation of electron pairs remains favored. Therefore, the amplitude of the order parameter $|\psi|$ will become nonzero again and the current will again be carried partly by superconducting electrons, i.e., a supercurrent will appear. Then the entire process will repeat itself. On completion of each cycle, the phase difference of the superconducting electron wavefunctions to the left and to the right of the weak spot will vary by 2π; hence the name phase slip center. The size of the center is given, of course, by the size of the region where the oscillations of $|\psi|$ take place, which is $\sim 2\xi(T)$.

At the moment when $|\psi| = 0$, a phase slip center is in the normal state and the electric field penetrates the parts of the superconductor adjacent to it, to a depth $\sim \lambda_Q$ (see Sect. 7.5). Therefore, formation of one phase slip center is accompanied by the appearance of a finite resistance $\rho 2\lambda_Q/S$, where ρ is the normal-state resistivity of the material of the filament and S is its crosssectional area. The voltage drop across this resistance is produced solely by the normal component of the current: $I_{\rm n} = I - I_{\rm s}$. Let us find the average of this expression over time. I is a given constant current independent of time. The supercurrent $I_{\rm s}$ oscillates between $I_{\rm c}$ and 0 . Therefore, we assume $\bar{I}_{\rm s} = \beta I_{\rm c}$, where $\beta \sim 0.5$. Then, for the average voltage across one phase slip center we have

$$\bar{V} = \frac{2\lambda_Q \rho\,(1 - \beta I_{\rm c})}{S} \tag{7.20}$$

Despite its simplicity, this formula describes the experimental results very well.

A further increase of the current will give rise to a second phase slip center, then a third and so on. The arrival of every new center will cause the total voltage across the filament to increase in a jump, and the slope of the current-voltage characteristic will increase, too, owing to the increased number of resistive regions. One can trace this behavior in the Fig. 7.9.

21.3.7 7.8 Nonequilibrium Enhancement of Superconductivity

Theory by Schmidt

In this section we shall examine the case of a symmetric deviation from the equilibrium distribution function, such that the nonequilibrium distributions of the quasiparticles for the two branches of the elementary excitation spectrum are identical. Contrary to the other nonequilibrium processes which we have already analyzed, a deviation from equilibrium in this case brings about a change of the energy gap Δ.

A symmetric nonequilibrium distribution can be realized, for instance, by exposing a superconductor to electromagnetic radiation of frequency $\omega < 2\Delta/\hbar$. Then a quantum of electromagnetic energy incident on the superconductor will be insufficient to break a pair but will still be enough to move elementary excitations up to the higher energy levels of the excitation spectrum. Such a nonequilibrium distribution of quasiparticles ought to cause an increase of both the energy gap and the critical temperature.

Indeed, by making the lower energy levels of the elementary excitation spectrum vacant, we open the way for the electron pairs of the condensate to make transitions to these k states thereby increasing the number of terms in the sum of (6.34), which defines the energy gap. A number of experimental results support these ideas. For instance, an increase of the critical current of narrow superconducting constrictions was observed in [77], after the sample had been subjected to ultra-high-frequency radiation. Theoretical treatment of these effects can be found in works by Eliashberg [78].

21.3.8 7.9 Thermoelectric Effect in Superconductors

Theory by Schmidt

For a long time it was believed that there are no thermoelectric effects in superconductors. However, this is not true. To find out what really happens in superconductors, let us first consider the ordinary thermoelectric effect in a normal metal.

Suppose that the two ends of a bulk piece of a normal metal have different temperatures, T_1 and T_2, that is, there is a temperature gradient $\nabla T'$ across the metal. Free electrons in the metal are acted upon by a force pushing them in the direction from the 'hot' to the 'cold' end. A subsequent accumulation of opposite charges at the opposite ends of the superconductor produces an electric field in its interior which, in turn, exerts a force on the electrons in the reverse direction, i.e., from the cold to the hot end. Under stationary conditions, the two forces balance each other resulting in a constant voltage drop across the specimen, V, referred to as the thermo-electromotive force (thermo-emf):

$$V = \alpha\,(T_1 - T_2)$$

whare n:- the shoulitathnemanlontrie nower (thermnnower) of the metal.

In the superconductor, the process of heat transfer relates to entirely different electron phenomena. [6] Suppose, again, that two ends of a bulk piece of metal (this time of a superconductor) are at different temperatures, T_1 and T_2. Again, the temperature gradient ∇T will produce a force on normal excitations of the superconductor initiating a current of the normal excitations

$$j_{\mathrm{n}} = \sigma\alpha\nabla T \tag{7.21}$$

where σ is the normal-state conductivity of the superconductor. As an immediate response, a countercurrent of the superconducting component, $\boldsymbol{j}_{\mathrm{s}}$, will start, thereby compensating the normal current $\boldsymbol{j}_{\mathrm{n}}$. Indeed, according to (7.21), the current $\boldsymbol{j}_{\mathrm{n}}$ is a potential current, i.e., curl $\boldsymbol{j}_{\mathrm{n}} = 0$. This means that for the total current $\boldsymbol{j}$ defined as

$$\boldsymbol{j} = \boldsymbol{j}_{\mathrm{n}} + \boldsymbol{j}_{\mathrm{s}}$$

we have curl $\boldsymbol{j} = \operatorname{curl} \boldsymbol{j}_s$. The supercurrent $\boldsymbol{j}_g$ must, under stationary conditions, satisfy the London equation. Taking the curl of both sides of (2.17) we get

$$\operatorname{curl} A j_{\mathrm{s}} = -\frac{1}{c}\boldsymbol{H}$$

which means that in our case the equation

$$\operatorname{curl} A j = -\frac{1}{c}H \tag{7.22}$$

is valid. Using Maxwell's equations curl $\boldsymbol{H} = \frac{4\pi}{c}\boldsymbol{j}$ and div $\boldsymbol{H} = 0$, we then arrive at the well-known equation for the magnetic field:

$$\nabla^2 \boldsymbol{H} = \frac{1}{\lambda^2}\boldsymbol{H}$$

from which the Meissner-Ochsenfeld effect follows directly. This implies that, in the presence of heat flow, the total current in the interior of a bulk isotropic homogeneous superconductor must be zero, too:

$$\boldsymbol{j} = \boldsymbol{j}_{\mathrm{n}} + \boldsymbol{j}_{\mathrm{s}} = 0$$

that is, $j_{\mathrm{n}} = -j_{\mathrm{s}}$.
This means that, as they approach the edge of the superconductor, normal excitations driven by the temperature gradient convert into superconducting carriers, i.e., electron pairs, and move in the reverse direction, thereby forming the countercurrent $\boldsymbol{j}_{\mathbf{s}}$. A graphic illustration of this process is given by the equivalent circuit shown in Fig. 7.10.

Let us assume that the normal excitations are acted upon by an electromotive force (emf) E_T produced by the temperature gradient:

$$E_T = \alpha\,(T_1 - T_2)$$

The emf induces a current $I_{\mathrm{n}} = E_T/R_{\mathrm{n}}$ in the circuit, which flows back

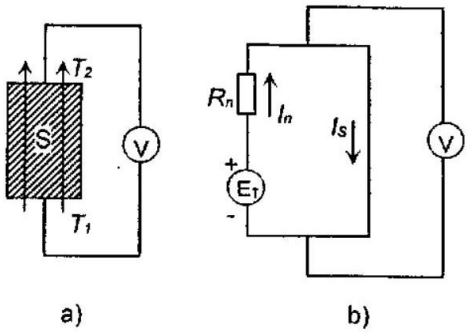


Fig. 7.10. (a) Superconductor carrying a heat flow, $T_1 > T_2$; (b) equivalent circuit for a superconductor subjected to a temperature gradient. R_{n} is the specimen resistance in the normal state, E_T is the thermo-emf acting upon the normal excitations
through the superconducting region as a supercurrent I_5. With this in mind, we can understand why the reading of the voltmeter incorporated in the circuit of Fig. 7.10 is zero: it is shunted by the supercurrent. That is why it was presumed for a long time that there are no thermoelectric effects in superconductors.

21.3.9 7.10 Superconducting 'Thermocouple' and the Magnetic Flux Induced by a Heat Flow

Theory by Schmidt

Now we shall see that thermoelectric effects can indeed be observed in superconductors. Consider two bulk specimens of two dissimilar superconductors, S_1 and S_2, which are brought into contact in such a way that together they form a closed ring, as in Fig. 7.11. We assume that the contact regions have different temperatures, T_1 and T_2.

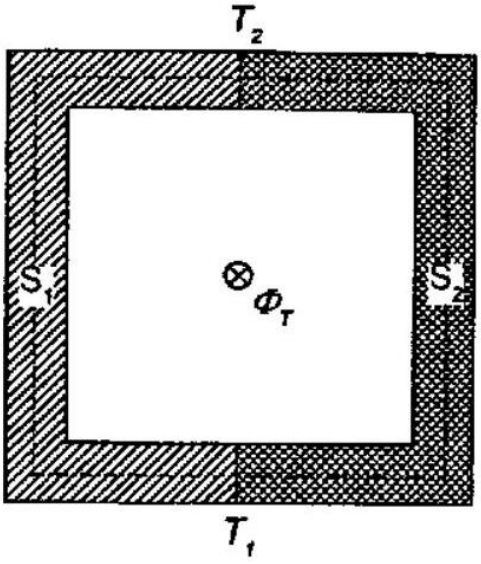


Fig. 7.11. Superconducting 'thermocouple'. The magnetic flux Φ_T through the ring is proportional to the temperature difference $(T_1 - T_2)$

The temperature gradient induces a current $\boldsymbol{j}_{\mathbf{n}} = \sigma\alpha\nabla T$ in each half of the ring, S_1 and S_2. The supercurrent, which starts in response in the interior of the superconductor, is $\boldsymbol{j}_{\mathrm{s}} = -\boldsymbol{j}_{\mathrm{n}}$ and, according to the second Ginzburg-

$$j_{\mathrm{s}} = \frac{\hbar n_8 e}{2m}\nabla\theta - \frac{e^2}{mc}n_{\mathrm{s}}A \tag{7.23}$$

where n_{s} is the superconducting electron density, e and m are the charge and mass of a free electron, respectively, θ is the phase of the superconducting wavefunction of the GL, theory, and A is the vector potential.

Taking into account (7.21), we have

$$\nabla\theta = \frac{2m}{\hbar n_\varepsilon e}(-\sigma\alpha\nabla T) + \frac{2e}{\hbar c}\boldsymbol{A} \tag{7.24}$$

As a next step, we integrate this equation over the dashed contour which passes through the interior of our bimetallic superconducting ring in such a way that its distance from the surfaces of the ring everywhere exceeds the penetration depth λ (see Fig. 7.11). Taking into account the requirement of the GL theory that the wavefunction must be single-valued leads to an equation which is already well-known to us:

$$\oint \nabla\theta \mathrm{d}l = 2\pi n, \quad n = 0, 1, 2, \ldots \tag{7.25}$$

Integrating the right-hand side of (7.24) and using (7.25) yields

$$2\pi n = -\frac{2m}{\hbar e}\int_{T_1}^{T_2}\left(\frac{\sigma_1\alpha_1}{n_{\mathrm{s}1}} - \frac{\sigma_2\alpha_2}{n_{\mathrm{s}2}}\right)\mathrm{d}T + \frac{2\pi\Phi}{\Phi_0}$$

This means that the total magnetic flux through the bimetallic ring can be expressed as

$$\Phi = \Phi_0 n + \Phi r \tag{7.26}$$

where

$$\Phi_T = \Phi_0\frac{m}{\pi e\hbar}\int_{T_1}^{T_2}\left(\frac{\sigma_1\alpha_1}{n_{\mathrm{s}1}} - \frac{\sigma_2\alpha_2}{n_{\mathrm{s}2}}\right)\mathrm{d}T \tag{7.27}$$

The indices 1 and 2 in the integrand refer to S_1 and S_2, respectively.
It follows from (7.26) and (7.27) that even in the case $n = 0$, that is, when the magnetic flux through the ring is zero, the difference in temperature between the contact regions S_1 and S_2 induces a magnetic flux Φ_T. This flux is generated by the supercurrent circulating along the inner surface of the binnetallic ring. If the quantities σ, α and n_s are assumed to be independent of temperature in the interval $T_1 < T < T_2$, (7.27) can be simplified to

$$\Phi_T = \Phi_0 \frac{m}{\pi e \hbar} \left(\frac{\sigma_1 \alpha_1}{n_{s1}} - \frac{\sigma_2 \alpha_2}{n_{82}} \right) \Delta T$$

where $\Delta T' = T_2 - T_1$.
Taking $\sigma \sim 10^7 (\Omega\ \mathrm{m})^{-1}, \alpha \sim 10^{-6} \mathrm{VK}^{-1}$, and $n_s \sim 10^{28} \mathrm{ml}^{-3}$ we obtain for $\Phi_T / \Delta T$ a value of the order $10^{-5} \Phi_0$ per Kelvin. Measuring such tiny

At temperatures close to T_c, the effect is enhanced, since the superconducting electron density there tends to zero. A magnetic flux Φ_T induced by a temperature gradient in a bimetallic ring was indeed observed in the experiments reported in [82, 83]. Its value, however, proved to be much larger that the theoretical estimate. The cause of this discrepancy is not clear yet.

21.3.10 7.11 Thermoelectric Effects in Josephson Junctions

One encounters very interesting and striking thermoelectric effects in Josephson junctions. They are most pronounced in superconductor-normal metalsuperconductor (SNS) junctions. As we are soon to find out, the reason for this lies in the fact that phase coherence in this type of Josephson junctions is established through a fairly thick normal layer ($\sim 10^{-3}$ cm). The typically very low resistance of the normal layer results in very small characteristic values of the voltage across the junction, V_c. In this section we shall first consider the behavior of an SNS junction when its S electrodes have different temperatures or, in other words, when there is a heat flow through the junction. After that, we shall discuss the thermoelectric effects arising when, in addition to carrying a heat flow, the junction is placed in a magnetic field.

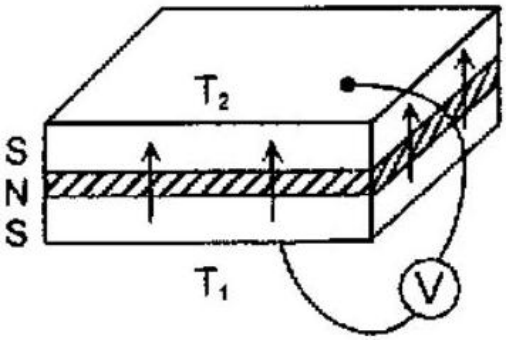
7.11.1 SNS Josephson Junction in a Temperature Gradient

Let us consider an SNS Josephson junction placed in a temperature gradient (Fig. 7.12 (a)). Again, the question to be asked is: what will be the reading of a voltmeter connected in parallel with such an autonomous junction? The answer is suggested by an equivalent circuit of such a junction (Fig. 7.12 (b)) which has been constructed by adding a source of thermo-emf $E_T = \alpha\,(T_1 - T_2)$ to the equivalent circuit of the Josephson junction shown in Fig. 4.5. Here α is the absolute thermopower of the material of the normal layer and T_1 and T_2 are the temperatures of the superconducting electrodes where they make contact with the normal layer. It is clear from Fig. 7.12 (b) that the thermoemf E_T included in the closed circuit produces a current which passes through the normal layer in the form of a normal current I_n; and through the true Josephson part of the junction in the form of a supercurrent $I_s = I_c \sin \varphi$. Here φ is the phase difference between the superconducting electron wavefunctions in the two S electrodes and I_c the critical current of the junction.

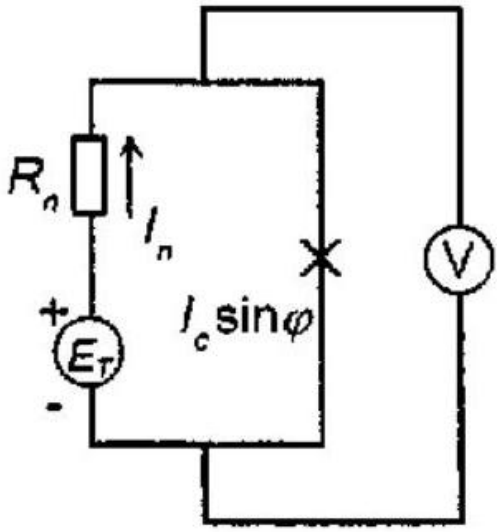
The voltage V_{AB} between the points A and B in Fig. 7.12 (b) must satisfy the equation

$$E_T - I_n R_n = V_{AB} \tag{7.28}$$

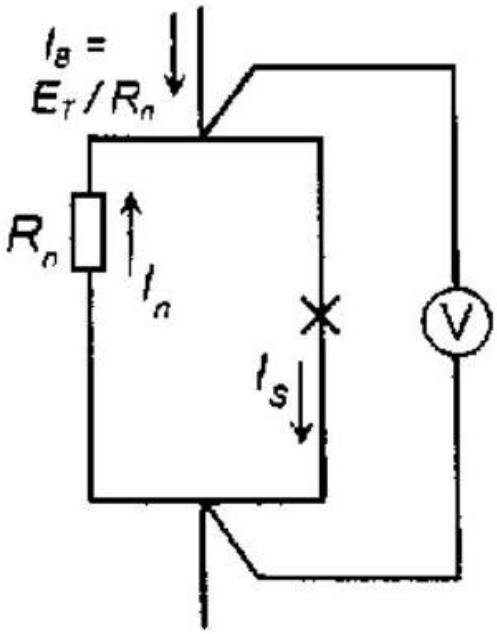
where R_n is the resistance of the normal layer. On the other hand, Kirchhoff's first law must hold for both the point A and the point B:



a)



b)



c)

Fig. 7.12. (a) SNS Josephson junction with heat flow. The temperature drop across the normal layer is $(T_1 - T_2)$; (b) equivalent circuit for such a junction: E_T is the thermo-emf due to the heat flow across the normal layer; (c) the circuit corresponding to (7.32)

Finally, the part of the circuit carrying the Josephson current ought to obey the Josephson relations:

$$I_{\mathrm{B}} = I_{\mathrm{C}} \sin \varphi \tag{7.30}$$

$$2eV_{\mathrm{AB}} = \hbar \frac{\mathrm{d}\varphi}{\mathrm{d}t} \tag{7.31}$$

Together, equations (7.28-31) give a complete definition of the problem. They can be easily reduced to

$$\frac{\hbar}{2eR_{\mathrm{n}}} \frac{\mathrm{d}\varphi}{\mathrm{d}t} + I_{\mathrm{c}} \sin \varphi = \frac{E_T}{R_{\mathrm{n}}}. \tag{7.32}$$

But the last equation is equivalent to the equation of the Josephson junction in the resistively shunted model (which is already known to us from Chap. 4). The current applied to the Josephson junction from an external source (in our case E_T/R_{rl}) is divided into two branches: a Josephson current $I_{\mathrm{c}} \sin \varphi$ and a current through the normal layer $(\hbar/2eR_{\mathbf{n}})\,\mathrm{d}\varphi/\mathrm{d}t$; see Fig. 7.12 (c). The behavior of such a system with identical temperatures of the S electrodes is well known (see Sect. 4.3). If the external current is less than I_{c}, it flows through the superconducting (Josephson) part of the junction only and the voltage between the points A and B is zero. Hence the reading of the voltmeter will be zero, too. If, however, the current exceeds I_c, an oscillating voltage of frequency $\omega = 2e\bar{V}_{\mathrm{AB}}/\hbar$ appears across the junction, where $\bar{V}_{\mathrm{AB}}$ is the dc component of the oscillating voltage registered by the voltmeter.

Now we are in a position to give a complete description of the behavior of a Josephon junction placed in a temperature gradient. As long as the temperature drop between the two surfaces of the normal layer, $\Delta T = T_1 - T_2$, is less than a certain critical value
the reading of the voltmeter connected to the superconducting electrodes remains zero. If, however, ΔT exceeds ΔT_c, an oscillating voltage appears across the junction, with frequency ω given by

$$\omega = \frac{2e}{\hbar} R_{\mathrm{n}} \left[\left(\frac{\alpha \triangle T}{R_{\mathrm{n}}^{-}} \right)^2 - I_{\mathrm{c}}^2 \right]^{1/2} \tag{7.34}$$

Here we have used (4.20). These thermoelectric effects were proposed by Aronov and Galperin in [84] based on theoretical considerations.

One can see from (7.33) that such effects become observable if the critical difference in temperature $\triangle T_{\mathrm{c}}$ is sufficiently small. This implies that the characteristic voltage across the junction $V_{\mathrm{c}} = I_{\mathrm{c}} R_{\mathrm{n}}$ must also be small. In practice, it is not difficult to fabricate an SNS junction with $V_{\mathrm{c}} \sim 10^{-13}$ V. With $\alpha \sim 10^{-8}\mathrm{VK}^{-1}$, this corresponds to $\Delta T_{\mathrm{c}} \sim 10^{-5}$ K. Such a temperature difference can be fairly easily attained in experiment. Experimental studies of the thermoelectric effects in SNS Josephson junctions [85] have provided ample verification of the above ideas.

7.11.2 Thermoelectric Effects in SNS Josephson Junctions in the Presence of a Magnetic Field

Suppose that, in addition to the heat flow, our SNS Josephson junction is placed in a magnetic field parallel to the plane of the junction (the xz plane). In this case it turns out that one can witness interesting and beautiful phenomena.

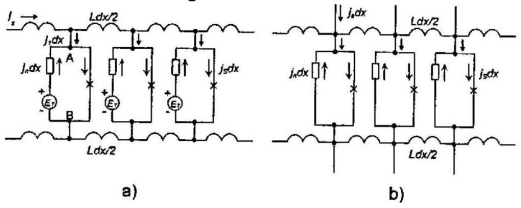


Fig. 7.13. (a) Equivalent circuit for a distributed SNS Josephson junction under a heat flow; (b) alternative representation of the same junction. The source of thermo-emf E_T is replaced by a uniform current j_e

Let us take into account the finite size of the junction, say, along the x axis. Let this size be w. The heat flow is directed along the y axis, perpendicular to the junction, and the magnetic field is in the z direction. The equivalent circuit for such a junction is shown in Fig. 7.13 (a). Here L is the total induc-
and I_x is the current in the direction of the x axis, per unit width. Now, in the same manner as we went from the equivalent circuit of Fig. 7.12 (b) to the circuit of Fig. 7.12 (c), we can go from the circuit of Fig. 7.13 (a) to the equivalent circuit of Fig. 7.13 (b). The latter is the equivalent circuit of an extended (distributed) Josephson junction of uniform temperature (that is, without heat flow) to which an external current of density $j_e = E_T/R_n$ is applied. Here R_n is the resistance per unit area of the normal layer. The behavior of such an object in an external magnetic field parallel to the y axis is well known (see Sect. 4.4). Therefore, one can foresee [86] that the critical temperature difference ΔT_c, corresponding to the appearance of a voltage across the junction, will be a nommonotonic function of the magnetic field. In the ideal case, the dependence to be observed should have the form (see (4.46))

$$\Delta T_c = \frac{j_c R_{n1}}{\alpha} \left| \frac{\sin(\pi\Phi/\Phi_0)}{\pi\Phi/\Phi_0} \right| \tag{7.35}$$

where $\Phi = B_0 w d$. Here B_0 is the magnetic induction of the external field, w is the dimension of the junction along the x axis and $d = d_0 + 2\lambda_L$, with d_0 being the thickness of the normal layer.

The above prediction was verified in the following experiment [87]. The SNS Josephson junction under study was a tantalum-copper-tantalum sandwich with the thickness of the normal layer about 10^{-3} cm, the resistance of the normal layer about $10^{-9}\Omega$, and a critical current of about 10^{-4} A. With these parameters, the characteristic voltage across the junction, V_c, was about 10^{-13} V. The voltage V_c was measured by a SQUID voltmeter. The temperature difference between the two surfaces of the normal layer, $\Delta T'$, was produced by a heater attached to one of the superconducting electrodes of the junction and was therefore proportional to the power supplied by the heater. The critical power of the heater, P_c, was proportional to the critical temperature difference $\triangle T_c$.

The measured critical power P_c as a function of an external magnetic field parallel to the plane of the junction is shown in Fig. 7.14 (the upper curve). The lower curve shows the dependence of the maximum zero-voltage current I_c through the junction on the external magnetic field, corresponding to a uniform temperature over the junction. The position of maximum I_c in Fig. 7.14 is shifted from $B_e = 0$ due to the effect of a background dc magnetic field. Nevertheless, when the scale of the plot was chosen in such a way that the two curves coincided at least at one point, they proved to coincide along their entire lengths. This provided convincing evidence of the validity of the above argumentation.

Let us summarize the main results of this section. Beginning from a certain critical value of the heat flow through an SNS Josephson junction, the latter starts to generate a voltage of thermoelectric nature. The critical value of the heat flow is a nonmonotonic function of the magnetic field. This phenomenom

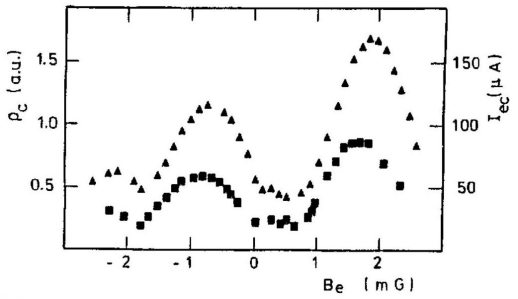


Fig. 7.14. Measurements of the magnetothermoelectric effect in an SNS Josephson junction [87]

It turned out that there also exists a thermal analog of the ac Josephson effect: a steady heat flow through an SNS Josephson junction gives rise to Josephson radiation, that is, to an oscillating voltage across the junction. This effect was observed experimentally [88] two years after the first edition of this book was published in Russian. Later on, several related thermoelectric effects, due to superconducting phase slippage, were observed in the new highT_c materials. The most recent review on this topic is that of Huebener [81].

Problems

Problem 7.1. Find the relaxation time for the quasiparticle charge in Sn if the temperature of the material is 0.01 K below the critical temperature T_c ($T_c = 3.8$ K).

Problem 7.2. Proceeding from the requirement of electroneutrality, we have found that there exists an electric field E in the vicinity of the interface between a superconductor and a normal metal, provided there is an electric current passing through the interface. According to (7.18), div $\boldsymbol{E} \neq 0$. But this suggests that there must exist a finite volume density of the electric charge ρ, in a region of size $\sim \lambda_Q$ near the interface. The charge density is defined by Poisson's equation div $\boldsymbol{E} = 4\pi\rho$. Does this contradict the initial assumption of electroneutrality?

21.3.11 Solutions

Chapter 1

1.1. The surface current density j_{surf} is defined by (1.6). The field H_0 should be set equal to the critical field at $T = 4.2$ K, according to (1.1). As a result we obtain $j_{\text{gurf}} = 422$ A cm^{-1}.
1.2. The difference in free energy is defined by (1.12). The value of H_{cm} at 4.2 K can be calculated using (1.1). Finally, using data from Table 1.1, we have $F_{\text{n}} - F_{\text{s0}} = 1.1 \times 10^4$ergcm^{-3}.
1.3. The latent heat given up by the specimen is $Q = T\,(S_{\text{n}} - S_0)$. Using (1.1) and (1.18), we obtain $Q = 2.30 \times 10^4$erg.

Note. Formula (1.18) expresses the difference in entropy through the quantity $(\partial H_{\text{cm}}/\partial T)_R$. Under the conditions of this particular problem, when the fixed quantity is the external field at infinity, the superconductor does not do any work on external bodies when its temperature changes. Indeed, the only kind of work on external bodies possible for such a superconductor is radiation of electromagnetic waves, which may occur as a result of a change in its internal state. But this is only possible if the integral of the Poynting vector $(c/4\pi)[\boldsymbol{E} \times \boldsymbol{H}]$ over the surface of the superconductor is nonzero. An electric field E can only appear as a result of variations in the magnetic induction B, but $B = 0$. This implies that a change in temperature of a superconductor placed in a magnetic field cannot be accompanied by electromagnetic radiation and $(\partial H_{\text{cm}}/\partial T)_n = (\partial H_{\text{cm}}/\partial T)_H$. That is, we can indeed use (1.18).
1.4. Searching for a minimum of the entropy difference (1.18), we find that the temperature in question is $T_c/\sqrt{3} = 4.16$ K.
1.5. 108 Oe .

1.6. $2.8 \times 10^4 \text{ergcm}^{-3}$.

Chapter 2

2.1. $H = 1.84 \times 10^{-2}\text{Oe}$.
2.2. $A = 75\text{Gcm}; \nabla\theta = 2.36 \times 10^9 \text{radcm}^{-1}$.
2.3. Since $d \ll \lambda$, the current distribution over the film is uniform. Therefore, integrating (2.32) over a closed circular contour of radius R yields

$$\Phi = \Phi_0 n - \frac{2\pi mcR}{n_s e^2} j_s \tag{S.1}$$

On the other hand, the magnetic field in the interior of the cylinder and the current at its surface are related to each other by

$$H = \frac{4\pi}{c} j_s d$$

so that the magnetic flux through the cylinder is $\Phi = (4\pi^2/c)\, j_s d R^2$. Using this to express j_s and substituting it into (S.1) finally yields

$$\Phi = \Phi_0 n \left(1 + \frac{2\lambda^2}{Rd}\right)^{-1}$$

Note. At $Rd \gg 2\lambda^2$, quantization of the magnetic flux through a thin-wolled cylinder ($d \ll \lambda$) is totally analogous to that through a bulk cylinder. In all other cases, the 'flux quantum' is less than Φ_0.
2.4. See Fig. S.1.

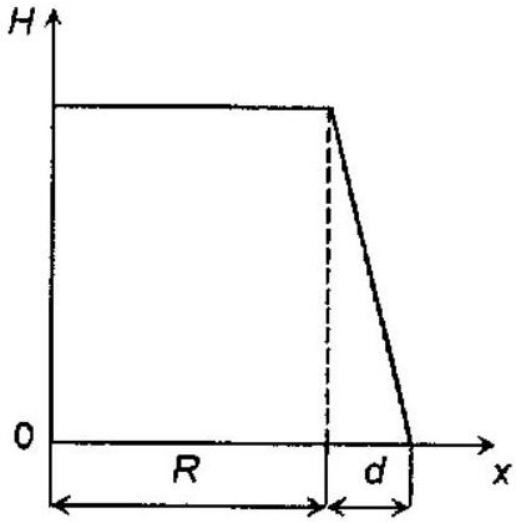


Fig. S.1. Distribution of the magnetic field trapped by a thin-walled superconducting cylinder

Chapter 3

3.1. If $\lambda(0) = 390\text{Å}$, we have $\lambda(4.2\text{ K}) = 415\text{Å}$. The magnetic field at a distance 300Å from the surface will then be $H = H_0 \text{e}^{-x/\lambda} = 145.6$ Oe and $w = H^2/8\pi = 844\text{ergcm}^{-3}$.
3.2. $\lambda(7.10\text{ K})/\lambda(4.2\text{ K}) = 4.49$; $\quad n_s(7.10\text{ K}) = 8.06 \times 10^{20}\text{ cm}^{-3}$.
3.3. Since $\lambda \ll \xi$, we can use (3.56). Finding H_{cm} from (3.38) and substituting it into (3.56), we obtain $\sigma_{\text{ns}} = 1.24 \times 10^{-2}\text{ergcm}^{-2}$.
3.4. Since $\lambda\,(T = 0.9T_c) = 870\text{Å}$ (see Problem 3.3) we have, according to (3.61), $H(x =$

0) = 8.55 Oe. Here we have assumed that the magnetic field is sufficiently small ($H_0 \ll H_{cm}\,(T = 0.9T_c) \approx 60$Oe) so that the order parameter ($\psi = 1$) remains unaffected.

The density of the diamagnetic moment is $M(x) = (1/4\pi)\,[H(x) - H_0]$. Taking, according to (3.61), $H(x) = H_0 \cosh(x/\lambda)/\sinh(x/\lambda)$ and integrating the diamagnetic moment over the thickness of the film, we find M_0:

$$M_0 = \frac{H_0 d}{4\pi}\left(\frac{2\lambda}{d}\tanh\frac{d}{2\lambda} - 1\right). \tag{S.2}$$

It follows that $M_0 = -7.74 \times 10^{-7}$Gcm.

3.5. It follows from (S.2) that the average density of the diamagnetic moment is $\bar{M} = (1/4\pi)H_0[(2\lambda/d)\tanh(d/2\lambda) - 1]$. The work done by the source of magnetic field equals

$$W\,(H_0) = -\int_0^{H_4} \bar{M}\ \mathrm{d}H_0$$

The transition to the normal state occurs when this work becomes equal to $F_\mathrm{n}\ F_{80} = H_{cm}^2/(8\pi)$. Therefore

$$H_{c|} = H_\mathrm{cm}\left(1 - \frac{2\lambda}{d}\tanh\frac{d}{2\lambda}\right)^{-1/2}.$$

Recalling that $\lambda \ll d$, we have $H_\mathrm{cl} = H_\mathrm{cm}(1 + \lambda/d) = 1.087 H_\mathrm{cm}$.

3.6. $H_{J_\mathrm{e}} = 12.5$ Oe; $H_{\mathrm{c}\|} = 1015$ Oe.

3.7. $j_\mathrm{c} = 2.30 \times 10^8$ A cm^{-2}.

3.8. The critical current density is defined by (3.67) and the critical velocity by (3.69). Using (2.7) and (3.37), we have

$$v_\mathrm{c} = \frac{\hbar\kappa}{3\sqrt{3}m\lambda} = 2.81 \times 10^3 \text{ cm s}^{-1}$$

3.9. According to (2.22), $j_\mathrm{M} = cH_\mathrm{cm}/4\pi\lambda$ and $j_\mathrm{M}/j_\mathrm{c} = 3\sqrt{3}/2\sqrt{2} = 1.837$. This means that, if the field at the surface is equal to H_cm, the density of the Meissner current exceeds the pair-breaking current by 1.84 times. This happens because (2.22) does not take into account the decrease of the superconducting electron density n_s caused by the magnetic field H_cm.

Chapter 4

4.1. Since the junctions are connected in parallel, the phase differences φ_1 and φ_2 across them are identical and the currents through the junctions are distributed in proportion to their critical currents: $I_1 = 0.417$ mA, $I_2 = 0.583$ mA.

4.2. $V_\mathrm{max}\ - V_\mathrm{tinin}\ = 2I_\mathrm{c}R$.

4.3. $\bar{V} = 1.33\mathrm{mV}; \nu = 641\mathrm{GHz}$.

4.4. We seek the phase difference across the junction in the form $\varphi = \varphi_0 + \varphi_1$, where φ_0 is the phase difference due to the dc current I_0. The voltage across the junction is $V = (\Phi_0/2\pi)\,\mathrm{d}\varphi/\mathrm{d}t = (\Phi_0/2\pi)\,\mathrm{d}\varphi_1/\mathrm{d}t$, where $\mathrm{d}\varphi_1/\mathrm{d}t = (\mathrm{d}I/\mathrm{d}t)\,(\mathrm{d}I/\mathrm{d}\varphi_1)^{-1}$. Substituting this expression into the expression for V, we obtain

$$V = \frac{\Phi_0}{I_\mathrm{c}\cos\varphi_0}\nu I_1 \sin(2\pi\nu t + \pi/2)$$

With the parameters given in the problem, the amplitude of the ac voltage will be 0.58 nV

.

Note. It follows from the above solution that there is a positive phase angle of $\pi/2$ between the voltage V and the current through the junction. This implies that the junction behaves as

an inductance $L = \Phi_0/(2\pi I_c \cos\varphi_0)$.
4.5. $H_{c1} = 0.290\text{Oe}; H(0) = 0.455\text{Oe}$.
4.6. The first maximum will appear at $H_1 = 1.85$ Oe and the second at $H_2 = 3.18$ Oe.
4.7. The dependence of Φ on Φ_e will not show hysteresis if the critical current of the junction is less than $\Phi_0/(2\pi L) = 0.165 \times 10^{-6}$ A.
4.8. The current in the ring is determined by the phase difference φ across the junction: $\varphi = 2\pi L I_R/\Phi_0$. The current through the junction is $I_J = I_c \sin\varphi$. The total current is $I = 1.34 \times 10^{-6}$ A.
4.9. $\varphi_{AB} = 1.60$ rad, see Fig.S.2.

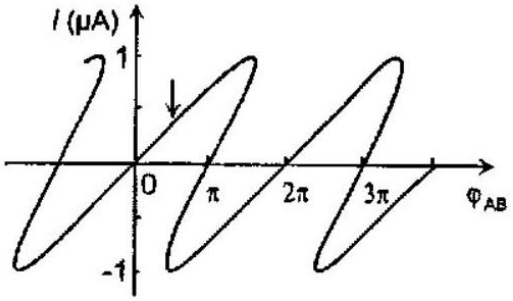


Fig. S.2. Answer to Problem 4.9. Current as a function of the phase difference between points A and B. The arrow marks the phase difference sought, $\varphi_{AB} = 1.60$rad

Chapter 5

5.1. The magnetic field generated by one of the vortices at a distance $r \ll \lambda$ from its center is, according to (5.6) and (5.7),

$$H = \frac{\Phi_0}{2\pi\lambda^2} \ln\frac{\lambda}{r}$$

The density of the current generated by the vortex at the same point is

$$j = \frac{c}{4\pi}\frac{\Phi_0}{2\pi\lambda^2 r}.$$

Finally, using (5.23), we find that the vortex will experience a repulsive force

$$f = \frac{\Phi_0^2}{4\pi^2\lambda^2}\frac{x}{x^2 + (d/2)^2}$$

directed away from the line ab, along the dashed line in Fig. 5.22.
5.2. $\lambda = \frac{1}{H_{cm}}\sqrt{\frac{\Phi_0 H_{c2}}{4\pi}} = 1.48 \times 10^{-5}$ cm.
5.3. $H_{c1} = 244\text{Oe}$.
5.4. Taking into account that $\xi \ll \lambda$ and using (5.6) and (3.38), we find that the field at a distance $r \sim \xi$ is

$$H(r) = \frac{\sqrt{2}H_{cm}}{\kappa} K_0\left(\frac{r}{\lambda}\right)$$

The current density will then be $j = (c/4\pi)\mathrm{d}H/\mathrm{d}r$. This gives

$$|j| = \frac{\sqrt{2}}{4\pi}\frac{cH_{cm}}{\lambda}$$

Note. It follows from the above that, by the order of magnitude, the current density at a distance ξ from the center of the vortex is equal to the pair-breaking current (compare with (3.67)).

5.5. Knowing H_{c2}, we find $\xi = 4.69 \times 10^{-7}$ cm and knowing κ, we find $\lambda = 4.50 \times 10^{-5}$ cm. Further, using (5.12), we find $\varepsilon = 6.12 \times 10^{-7}\text{ergcm}^{-1}$. The vortex core is normal, which implies that its energy density exceeds that of the surrounding medium by $H_{\text{cm}}^2/8\pi$. Therefore, the energy of the core equals $H_{\text{cm}}^2\xi^2/8$, if its radius is assumed equal to ξ. With the parameter values of our problem, the energy is $3.33 \times 10^{-8}\text{ergcm}^{-1}$, that is, many times less than the electromagnetic energy of the vortex, ε.
5.6. $M = -0.445\text{G}$.
5.7. It is evident from Fig. 5.23 that H_{c1} is given by the solution of the following equation: $H_{\text{c1}} = k\,(H_{c2} - H_{\text{c1}})$, where $k^{-1} = 1.16\,(2\kappa^2 - 1)$. Then $H_{\text{cl}} = 193\text{Oe}$. Further, an evaluation of H_{cm} can be obtained from the area enclosed by the magnetization curve, as follows from (5.35). This gives $H_{\text{cm}} = [k/(1+k)]^{1/2} H_{c2} = 879$ Oe. The exact value of H_{cm} can be found using (5.25): $H_{\text{cm}} = 942$ Oe.
5.8. $H_{\text{c3}} = 51900\text{Oe}$.
5.9. $H_{\text{c3}} = 68700\text{Oe}$.
5.10. $f = \frac{(\Phi_0/4\pi\lambda)^2}{l} = 6.03 \times 10^{-2}\text{dyncm}^{-2}$.
5.11. $f_x = -0.208\text{dyncm}^{-1}$; $f_y = -6.20 \times 10^{-2}\text{dyncm}^{-1}$.
5.12. $f = \frac{\Phi_0 H_0}{4\pi\lambda}\text{e}^{-l/\lambda} = 5.52 \times 10^{-2}\text{dyncm}^{-1}$.
5.13. $H_p = \frac{\Phi_0\kappa}{2\sqrt{2}\pi\lambda^2} = 1.40 \times 10^3\text{Oe}$.
5.14. Using (5.17) and (5.26), we find $\kappa = 31$. From (5.17) we find $\lambda = 2.1 \times 10^{-5}$ cm. Finally, approximating the magnetization curve $|M|$ by two triangles (see Fig. 5.23) and using (5.57), we have

$$I_c = \frac{2c\sqrt{\Phi_0}l}{\lambda\sqrt{B}}\frac{H_{c1}}{4\pi}\frac{H_{c2} - B}{H_{c2} - H_{c1}} \approx 13 \text{ A}$$

5.15. It follows from (5.67) and (5.68) that $\rho_{\text{f}} = \rho_{\text{u}} B/H_{\text{c2}}(0)$. Taking approximately $H_{\text{c2}}(T) = H_{\text{c2}}(0)\,(1 - T^2/{T_{\text{c}}}^2)$ and $B = H_0$, we find $\rho_{\text{f}} = 3 \times 10^{-6}\Omega$ cm.
5.16. $v_{\text{L}} = \frac{U}{iB} = 3.75 \times 10^{-5}$ m s^{-1}.

Chapter 6

6.1. $\rho/N(0) = 7.12; 1.34; 1.15$.
6.2. Using (6.37), we obtain $g = 0.245$.
6.3. The critical temperature will decrease by 0.01 K .
6.4. $T_{\text{c}} = \frac{2\Delta_0}{3.52k_{\text{B}}} = 3.49$ K.
6.5. $K_{\text{c}} = \frac{2\Delta_0}{\hbar v_{\text{F}}} = 2.61 \times 10^4$ cm^{-1}, $k_{\text{F}} = \frac{mv_{\text{F}}}{\hbar} = 5.6 \times 10^7$ cm^{-1}.

Chapter 7

7.1. Using the expression for the gap (at $T \approx T_{\text{c}}$): $\Delta(T) = 1.74\Delta(0)\,(1 - T/T_{\text{c}})^{1/2}$, we obtain for Sn : $\tau_Q \approx 2.4 \times 10^{-9}$ s.
7.2. Let us show that the volume charge density ρ, which will indeed appear in the transitional region of width $\sim \lambda_Q$ at the interface, will be many orders of magnitude less than the volume charge density of the quasiparticles, eQ. Poisson's equation can be written approximately as $E/\lambda_Q \sim 4\pi\rho$, or $\rho \sim E/4\pi\lambda_Q$. On the other hand, we have from (7.12):

$$Q \sim \frac{j_{\text{n}}T_Q}{e\lambda_Q} = \frac{\sigma\tau_Q E}{e\lambda_Q}$$

which leads to

$$\frac{\rho}{\varepsilon\bar{Q}} \sim \frac{1}{4\pi\tau_Q\sigma} = \left(\frac{8\pi\tau_Q e^2 N(0) l_{v_F}}{3}\right)^{-1}$$

With the values $\tau_Q \approx 10^{-10}$ s, $N(0) \approx 10^{33}\text{erg}^{-1}$ cm^{-1}, $l \approx 10^{-8}$ cm, and $v_\text{F} \approx 10^8$ cm s^{-1}; we obtain $\rho/eQ \sim 10^{-5}$.

References

1. A.C. Rose-Innes, E.H. Rhoderick: Introduction to Superconductivity (Pergamon Press, Oxford 1978)
2. E.A. Lynton: Superconductivity (Methuen, London 1962)
3. M. Tinkham: Introduction to Superconductivity (MacGraw-Hill, New York 1996)
4. P.G. de Gennes: Superconductivity of Metals and Alloys (Benjamin, New York 1966)
5. D.R. Tilley, J. Tilley: Superfluidity and Superconductivity (Hilger, Bristol 1986)
6. H. Kamerlingh Onnes: Leiden Comm. 122b, 124 (1911)
7. B.W. Roberts: J. Plyys. Chem. Ref. Data 5, 581 (1976)
8. B.S. Deaver, Jr., W.M. Fairbank: Phys. Rev. Lett. 7, 43 (1961)
9. R. Doll, M. Nbaner: Phys. Rev. Lett. 7, 51 (1961)
10. B.D. Josephson: Phys. Lett. 1, 251 (1962)
11. I.K. Yanson, V.M.Svistunov, I.M. Dmitrenko: Zh. Eksp. Teor. Fiz. 48, 976 (1965) [English transl.: Sov. Plyys. JETP 21, 650 (1965)]
12. W. Meissner, R. Ochsenfeld: Naturwiss. 21, 787 (1933)
13. L.D. Landau, E.M. Lifshitz: Electrodynamics of Continuous Media (Nauka, Moscow 1972) (English transl.: 2nd edn., Pergamon Press, Oxford 1968]
14. A.(i. Meshkovskii, A.I.Shalnikov: Zh. Eksp. Teor. Fiz. 17, 851 (1947)
15. A.G. Meshkovskii, A.I. Shalnikov: Zh. Eksp. Teor. Fiz. 19, 1 (1949)
16. A. Bodmer, U. Essmann, H. Trable: Phys. Status Solidi (a) 13, 471 (1972)
17. F. London, H. London: Proc. Roy. Soc. A149, 71 (1935)
18. A.B. Pippard: Proc. Roy. Soc. A216, 547 (1953)
19. V.L. Newhonse, J.W. Bremer, H.H. Edwards: Proc. IRE 48, 1395 (1960)
20. K.K. Likharev, B.T. Ulrich: Systems with Josephson Junctions. The Basics of the Theory (Moscow State Univ. Press, Moscow 1978)
21. T. van Duzer, C.W. Turner: Principles of Superconductive Devices and Circuits (Flsevier, New York 1981)
22. J.I. Gittlemann, B. Rosenblum: Proc. IEEE 52, 1138 (1964)
23. V.L. Ginzburg, L.D. Landau: Zh. Eksp. Teor. Fiz. 20, 1064 (1950)
24. L.D. Landa, E.M. Lifshitz: Statistical Physics, 3rd edn., part 1 (Nauka, Moscow 1976) [English transl.: Pergamon Press, Oxford 1980]

25. K.K. Likharev, L.A. Yakobson: Zh. Teor. Fiz. 45, 1503 (1975)

26. G. Deutscher, P.G. de Gennes: In Superconductivity, ed. by R.D. Parks, Vol. 2, p. 1005 (Marcel Dekker Inc., New York 1969)

27. Z.G. Ivanov, M.Yu. Kupriyanov, K.K. Likharev, O.V. Snigirev: J. de Physique C-6, 556 (1978)

28. J.J. Hauser, H.C. Theuerer: Phys. Lett. 14, 270 (1965)

29. N.V. Zavaritzkii: Doklady Akad. Nauk SSSR 78, 665 (1951)

30. S. Shapiro: Plys. Rev. Lett. 11, 80 (1963)

31 KK Jikloirew. Rov Mand. Phys. 51. 101 (1979)

21.4 Nonequlibrim Superconductors: Other Models, Features, Approaches

(there are many articles, so I'll write some ideas here. For them, see a special note, where they will be discussed in detail.)

22 Disorder SC

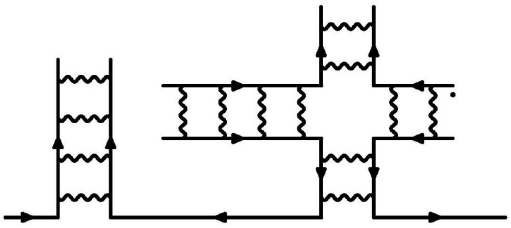
22.1 Usadel theory

(I'll study it later)

23 Other theoretical models

23.0.1 Strange, useless statements about typical theories of SC

Strange diagram from Levitov Shitov



(??? maybe ones I'll think to what does it correspond to?)

23.1 Possibility of superconductivity type phenomena in a one-dimensional system

(почитаю потом, интересная статья)

23.2 Very exotic models and properties of superconductors

23.3 Interesting Ideas, which are proven to be unphysical

23.3.1 On proposal by W. Heisenberg: Z. Naturforsch. 2a, 185 (1947)

(I'll maybe read this article later and describe this attempt)

23.3.2 On proposal by H. Welker: Z. Phys. 114, 525 (1939)

(I'll maybe read this article later and describe this attempt)

23.3.3 On proposal by M. Born, K. C. Cheng: Nature (London)

(I'll maybe read this article later and describe this attempt)

24 BCS-BEC Crossover: From High Temperature Superconductors to Ultracold Superfluids by Chen, Stajic, Tan, Levin

Abstract

We review the BCS to Bose Einstein condensation (BEC) crossover scenario which is based on the well known crossover generalization of the BCS ground state wavefunction Ψ_0. While this ground state has been summarized extensively in the literature, this Review is devoted to less widely discussed issues: understanding the effects of finite temperature, primarily below T_c, in a manner consistent with Ψ_0. Our emphasis is on the intersection of two important problems: high T_c superconductivity and superfluidity in ultracold fermionic atomic gases. We address the "pseudogap state" in the copper oxide superconductors from the vantage point of a BCS-BEC crossover scenario, although there is no consensus on the applicability of this scheme to high T_c. We argue that it also provides a useful basis for studying atomic gases near the unitary scattering regime; they are most likely in the counterpart pseudogap phase. That is, superconductivity takes place out of a non-Fermi liquid state where preformed, metastable fermion pairs are present at the onset of their Bose condensation. As a microscopic basis for this work, we summarize a variety of T-matrix approaches, and assess their theoretical consistency. A close connection with conventional superconducting fluctuation theories is emphasized and exploited.

24.1 Conclusions

In this Review we have summarized a large body of work on the subject of the BCS-BEC crossover scenario. In this context, we have explored the intersection of two very different fields: high T_c superconductivity and cold atom superfluidity. Theories of cuprate superconductivity can be crudely classified as focusing on "Mott physics" which reflects the anomalously small zero temperature superfluid density and "crossover physics", which reflects the anomalously short coherence length. Both schools are currently very interested in explaining the origin of the mysterious pseudogap phase. In this Review we have presented a case for its origin in crossover physics. The pseudogap in the normal state can be associated with meta-stable pairs of fermions; a (pseudogap) energy must be supplied to break these pairs apart into their separate components. The pseudogap also persists below T_c in the sense that there are non

condensed fermion pair excitations of the condensate. These concepts have a natural analogue in self consistent theories of superconducting fluctuations, but for the crossover problem the width of the "critical region" is extremely large. This reflects the much stronger-than-BCS attractive interaction.

It was not our intent to shortchange the role of Mott physics which will obviously be of importance in our ultimate understanding of the superconducting cuprates. There is, however, much in this regard which is still uncertain associated with establishing the simultaneous relevance and existence of spin-charge separation [3], stripes [91], and hidden order parameters [25]. What we do have in hand, though, is a very clear experimental picture of an extremely unusual superconductor in which superconductivity seems to evolve gradually from above T_c to below. We have in this Review tried to emphasize the common ground between high T_c superconductors and ultracold superfluids. These Mott issues may nevertheless, set the agenda for future cold atom studies of fermions in optical lattices [70].

The recent discovery of superfluidity in cold fermion gases opens the door to a new set of fascinating problems in condensed matter physics. Unlike the bosonic system, there is no ready-made counterpart of Gross-Pitaevskii theory. A new mean field theory which goes beyond BCS and encompasses BEC in some form or another will have to be developed in concert with experiment. *As of this writing, there are four experiments where the simple mean field theory discussed in this review is in reasonable agreement with the data.* These are the collective mode studies over the entire range of accessible magnetic fields [74, 66]. In addition in the unitary regime, RF spectroscopy-based pairing gap studies [89], as well as density profile [160] and thermodynamic studies [88] all appear to be compatible with this theory.

The material in this Review is viewed as the first of many steps in a long process. It was felt, however, that some continuity should be provided from another community which has addressed and helped to develop the BCS-BEC crossover, since the early 1990's when the early signs of the cuprate pseudogap were beginning to appear. As of this writing, it appears likely that the latest experiments on cold atoms probe a counterpart to this pseudogap regime. That is, on both sides, but near the resonance, fermions form in long lived metastable pair states at higher temperatures than those at which they Bose condense.

24.2 Introduction to Qualitative Crossover Picture

This review addresses an extended form of the BCS theory of superfluidity (or superconductivity) known as "BCS-Bose Einstein condensation (BEC) crossover theory". Here we contemplate a generalization of the standard mean field description of superfluids now modified so that one allows attractive interactions of arbitrary strength. In this way one describes how the system smoothly goes from being a superfluid system of the BCS type (where the attraction is arbitrarily weak) to a Bose Einstein condensate of diatomic molecules (where the attraction is arbitrarily strong). One, thereby, sees that BCS theory is intimately connected to BEC. Attractive interactions between fermions are needed to form "bosonic-like" molecules (called Cooper pairs) which then are driven statistically to Bose condense. BCS theory is a special case in which the condensation and pair formation temperatures coincide.

The importance of obtaining a generalization of BCS theory which addresses the crossover from BCS to BEC at general temperatures $T \leq T_c$ cannot be overestimated. BCS theory as originally postulated can be viewed as a paradigm among theories of condensed matter systems; it is complete, in many ways generic and model independent, and well verified experimentally. The observation that a BCS-like approach goes beyond strict BCS theory, suggests that there is a larger mean field theory to be addressed. Equally exciting is the possibility that this mean field theory can be discovered and simultaneously tested in a very controlled fashion using ultracold fermionic atoms. We presume here that it may also have applicability to other short

coherence length materials, such as the high temperature superconductors.

This Review is written in order to convey important new developments from one subfield of physics to another. Here it is hoped that we will communicate the recent excitement felt by the cold atom community to condensed matter physicists. Conversely we wish to communicate a comparable excitement in studies of high temperature superconductivity to atomic physicists. There has been a revolution in our understanding of ultracold fermions in traps in the last few years. The milestones in this research were the creation of a degenerate Fermi gas (1999), the formation of dimers of fermions (2003), Bose-Einstein condensation (BEC) of these dimers (late 2003) and finally superfluidity of fermionic pairs (2004).

In high temperature superconductors the BCS-BEC crossover picture has been investigated for many years now. It leads to a particular interpretation of a fascinating, but not well understood phase, known as the "pseudogap state". In the cold atom system, this crossover description is not just a scenario, but has been realized in the laboratory. This is because one has the ability (via Feshbach resonances) to apply magnetic fields in a controlled way to tune the strength of the attraction. We note, finally, that research in this field has not been limited exclusively to the two communities. One has seen the application of these crossover ideas to studies of excitons in solids [101], to nuclear physics [9, 65] and to particle physics [94, 92, 76] as well. There are not many problems in physics which have as great an overlap with different subfield communities as this "BCS-BEC crossover problem".

In this Review, we begin with an introduction to the qualitative picture of the BCS-BEC crossover scenario which is represented schematically in Fig. 24.1. We discuss this picture in the context of both high T_c superconductivity and ultracold atomic superfluidity, summarizing experiments in both. In Section II, we present a more quantitative study of this crossover primarily at and below the superfluid transition temperature T_c. Section III contains a detailed discussion of the superfluid density and gauge invariance issues, in large part to emphasize self consistency checks for different theoretical approaches to crossover. These alternative theories are summarized and compared in Section IV. Sections V and VI, respectively, present the physical implications of crossover physics, in one particular rendition, in the context of ultracold fermionic superfluids and high temperature superconductors. Our conclusions are presented in Section VII and a number of Appendices are included for clarity. A reader interested in only the broad overview may choose to omit Sections II-IV.

The convention and notation as well as a list of abbreviations used in this Review are listed in Appendix 24.11 at the end.

24.2.1 Fermionic Pseudogaps and Meta-stable Pairs: Two Sides of the Same Coin

A number of years ago Eagles [49] and Leggett [187] independently noted[30] that the BCS ground state wavefunction

$$\Psi_0 = \Pi_{\mathbf{k}}(u_{\mathbf{k}} + v_{\mathbf{k}} c^\dagger_{k,\uparrow} c^\dagger_{-k,\downarrow})|0\rangle \tag{24.1}$$

had a greater applicability than had been appreciated at the time of its original proposal by Bardeen, Cooper and Schrieffer (BCS). As the strength of the attractive pairing interaction U (< 0) between fermions is increased, this wavefunction is also capable of describing a continuous evolution from BCS like behavior to a form of Bose Einstein condensation. What is essential is that the chemical potential μ of the fermions be self consistently computed as U varies.

The variational parameters $v_{\mathbf{k}}$ and $u_{\mathbf{k}}$ which appear in Eq. 24.1 are usually represented by the two more directly accessible parameters $\Delta_{sc}(0)$ and μ, which characterize the fermionic system. Here $\Delta_{sc}(0)$ is the zero temperature superconducting order parameter. These fermionic

[30] Through private correspondence it appears that F. Dyson may have made similar observations even earlier.

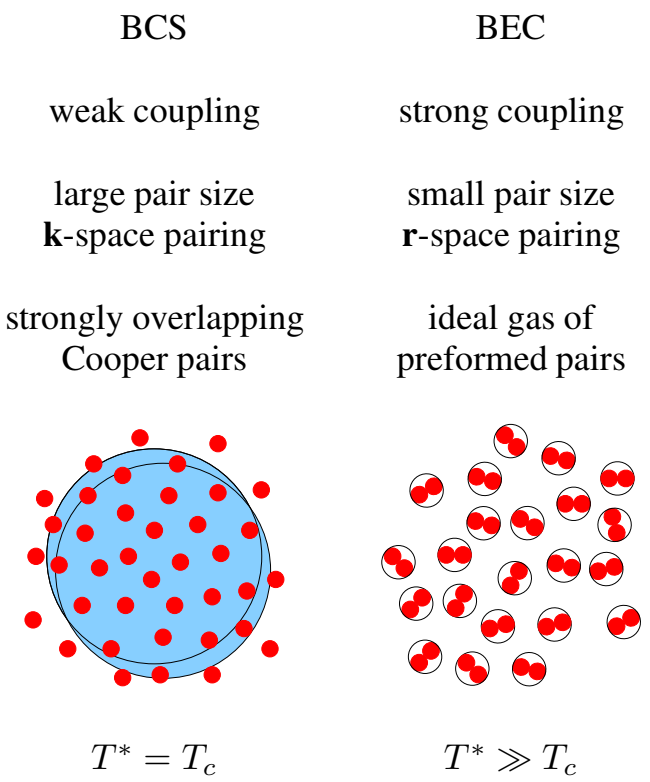


Figure 24.1: Contrast between BCS- and BEC-based superfluids. Here T^* represents the temperature at which pairs form, while T_c is that at which they condense.

parameters are uniquely determined in terms of U and the fermionic density n. The variationally determined self consistency conditions are given by two BCS-like equations which we refer to as the "gap" and "number" equations respectively.

$$\Delta_{sc}(0) = -U \sum_{\mathbf{k}} \Delta_{sc}(0) \frac{1}{2E_{\mathbf{k}}} \tag{24.2}$$

$$n = \sum_{\mathbf{k}} \left[1 - \frac{\epsilon_{\mathbf{k}} - \mu}{E_{\mathbf{k}}} \right] \tag{24.3}$$

where [31]

$$E_{\mathbf{k}} \equiv \sqrt{(\epsilon_{\mathbf{k}} - \mu)^2 + \Delta_{sc}^2(0)} \tag{24.4}$$

and $\epsilon_{\mathbf{k}} = k^2/2m$ is the fermion energy dispersion.[32] Within this ground state there have been extensive studies of collective modes [120, 144, 39], effects of two dimensionality [144], and, more recently, extensions to atomic gases [182, 136]. Noziéres and Schmitt-Rink were the first [128] to address nonzero T. We will outline some of their conclusions later in this Review. Randeria and co-workers reformulated the approach of Noziéres and Schmitt-Rink (NSR) and moreover, raised the interesting possibility that crossover physics might be relevant to high temperature superconductors [144]. Subsequently other workers have applied this picture to the high T_c cuprates [28, 121, 146] and ultracold fermions [123, 131] as well as formulated alternative schemes [61, 139] for addressing $T \neq 0$. Importantly, a number of experimentalists, most notably Uemura [178], have claimed evidence in support [149, 46, 81] of the BCS-BEC crossover picture for high T_c materials.

[31] In general, the order parameter Δ_{sc} and the excitation gap may have a $\mathbf{k}$-dependence, $\Delta_k = \Delta\varphi_{\mathbf{k}}$, except for a contact potential. To keep the mathematical expressions simpler, however, we neglect $\varphi_{\mathbf{k}}$ for the s-wave pairing under investigation of this Review. It can be easily reinserted back when needed in actual calculations. In particular, we use $\varphi_{\mathbf{k}} = \exp(-k^2/2k_c^2)$ with a large cutoff k_c in most of our numerical calculations.

[32] Throughout this Review, we set $\hbar = 1$ and $k_B = 1$.

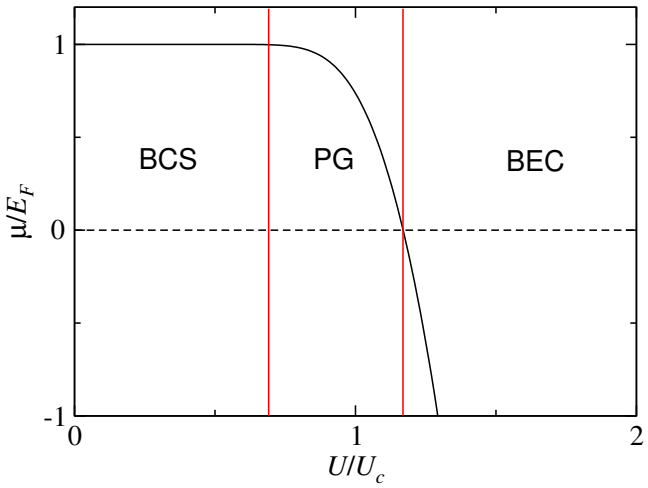


Figure 24.2: Typical behavior of the $T = 0$ chemical potential in the three regimes. As the pairing strength increases from 0, the chemical potential μ starts to decrease and then becomes negative. The character of the system changes from fermionic ($\mu > 0$) to bosonic ($\mu < 0$). The PG (pseudogap) case corresponds to non-Fermi liquid based superconductivity, and U_c corresponds to critical coupling for forming a two fermion bound state in vacuum, as in Eq. (24.17) below.

Compared to work on the ground state, considerably less has been written on crossover effects at nonzero temperature based on Eq. (24.1). Because our understanding has increased substantially since the pioneering work of NSR, and because they are the most interesting, this review is focussed on these finite T effects, at the level of a simple mean field theory. Mean field approaches are always approximate. We can ascribe the simplicity and precision of BCS theory to the fact that in conventional superconductors the coherence length ξ is extremely long. As a result, the kind of averaging procedure implicit in mean field theory becomes nearly exact. Once ξ becomes small, BCS is not expected to work at the same level of precision. Nevertheless even when they are not exact, mean field approaches are excellent ways of building up intuition. And further progress is not likely to be made without investigating first the simplest of mean field approaches, associated with Eq. (24.1).

The effects of BEC-BCS crossover are most directly reflected in the behavior of the fermionic chemical potential μ. We plot the behavior of μ in Fig. 24.2, which indicates the BCS and BEC regimes. In the weak coupling regime $\mu = E_F$ and ordinary BCS theory results. However at sufficiently strong coupling, μ begins to decrease, eventually crossing zero and then ultimately becoming negative in the BEC regime, with increasing $|U|$. We generally view $\mu = 0$ as a crossing point. For positive μ the system has a remnant Fermi surface, and we say that it is "fermionic". For negative μ, the Fermi surface is gone and the material is "bosonic".

The new and largely unexplored physics of this problem lies in the fact that once outside the BCS regime, but before BEC, superconductivity or superfluidity emerge out of a very exotic, non-Fermi liquid normal state. Indeed, it should be clear that Fermi liquid theory must break down somewhere in the intermediate regime, as one goes continuously from fermionic to bosonic statistics. This intermediate case has many names: "resonant superfluidity", the "unitary regime" or, as we prefer (because it is more descriptive of the many body physics) the "pseudogap (PG) regime". The PG regime plotted in Fig. 24.2 is drawn so that its boundary on the left coincides with the onset of an appreciable excitation gap at T_c, called $\Delta(T_c)$; its boundary on the right coincides with where $\mu = 0$. This non-Fermi liquid based superconductivity has been extensively studied[28, 30, 78, 114].

Fermi liquid theory is inappropriate here principally because there is a gap for creating fermionic excitations. The non-Fermi liquid like behavior is reflected in that of the fermionic

spectral function [114] which has a two-peak structure in the normal state, broadened somewhat, but rather similar to its counterpart in BCS theory. Importantly, the onset of superconductivity occurs in the presence of fermion pairs, which reflect this excitation gap. Unlike their counterparts in the BEC limit, these pairs are not infinitely long lived. Their presence is apparent even in the normal state where an energy must be applied to create fermionic excitations. This energy cost derives from the breaking of the metastable pairs. Thus we say that there is a "pseudogap" at and above T_c. But pseudogap effects are not restricted to this normal state. Pre-formed pairs have a natural counterpart in the superfluid phase, as noncondensed pairs.

It will be stressed throughout this Review that gaps in the fermionic spectrum and bosonic degrees of freedom are two sides of the same coin. A particularly important observation to make is that the starting point for crossover physics is based on the fermionic degrees of freedom. Bosonic degrees of freedom are deduced from these; they are not primary. A nonzero value of the excitation gap Δ is equivalent to the presence of metastable or stable fermion pairs. And it is only in this indirect fashion that we can probe the presence of these "bosons", within the framework of Eq. (24.1).

In many ways this crossover theory appears to represent a more generic form of superfluidity. Without doing any calculations we can anticipate some of the effects of finite temperature. Except for very weak coupling, *pairs form and condense at different temperatures*. The BCS limit might be viewed as the anomaly. Because the attractive interaction is presumed to be arbitrarily weak, in BCS the normal state is unaffected by U and superfluidity appears precipitously, that is without warning at T_c. More generally, in the presence of a moderately strong attractive interaction it pays energetically to take some advantage and to form pairs (say roughly at temperature T^*) within the normal state. Then, for statistical reasons these bosonic degrees of freedom ultimately are driven to condense at $T_c < T^*$, just as in BEC.

Just as there is a distinction between T_c and T^*, *there must be a distinction between the superconducting order parameter Δ_{sc} and the excitation gap Δ*. The presence of a normal state excitation gap or pseudogap for fermions is inextricably connected to this generalized BCS wavefunction. In Figure 24.3 we present a schematic plot of these two energy parameters. It may be seen that the order parameter vanishes at T_c, as in a second order phase transition, while the excitation gap turns on smoothly below T^*. It should also be stressed that there is only one gap energy scale in the ground state [187] of Eq. (24.1). Thus at zero temperature

$$\Delta_{sc}(0) = \Delta(0) \; . \tag{24.5}$$

In addition to the distinction between Δ and Δ_{sc}, another important way in which *bosonic degrees of freedom are revealed is indirectly through the temperature dependence of Δ. In the BEC regime where fermion pairs are pre-formed, Δ is essentially constant for all $T \leq T_c$ (as is μ)*. By contrast in the BCS regime it exhibits the well known temperature dependence of the superconducting order parameter. This is equivalent to the statement that bosonic degrees of freedom are only present in the condensate for this latter case. This behavior is illustrated in Fig. 24.4.

Again, without doing any calculations we can make one more inference about the nature of crossover physics at finite T. *The excitations of the system must smoothly evolve from fermionic in the BCS regime to bosonic in the BEC regime*. In the intermediate case, the excitations are a mix of fermions and meta-stable pairs. Figure 24.5 characterizes the excitations out of the condensate as well as in the normal phase. This schematic figure will play an important role in our thinking throughout this review. In the BCS and BEC regimes one is led to an excitation spectrum with a single component. For the PG case it is clear that the excitations now have two distinct (albeit, strongly interacting) components.

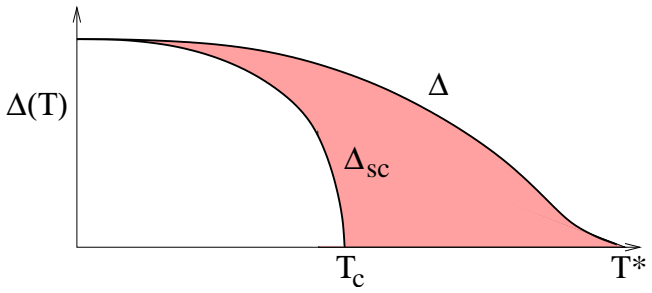


Figure 24.3: Contrasting behavior of the excitation gap $\Delta(T)$ and superfluid order parameter $\Delta_{sc}(T)$ versus temperature. The height of the shaded region roughly reflects the density of noncondensed pairs at each temperature.

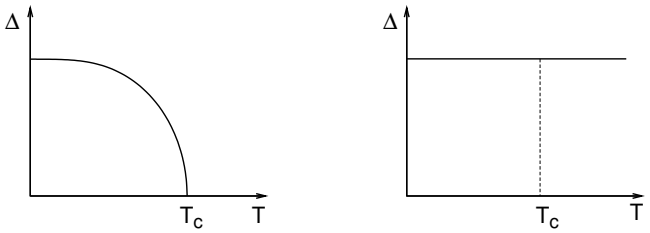


Figure 24.4: Comparison of typical temperature dependences of the excitation gaps in the BCS (left) and BEC (right) limits. For the former, the gap is small and vanishes at T_c; whereas for the latter, the gap is very large and essentially temperature independent.

24.2.2 Introduction to high T_c Superconductivity: Pseudogap Effects

This Review deals with the intersection of two fields and two important problems: high temperature superconductors and ultracold fermionic atoms in which, through Feshbach resonance effects, the attractive interaction may be arbitrarily tuned by a magnetic field. Our focus is on the broken symmetry phase and how it evolves from the well known ground state at $T = 0$ to $T = T_c$. We begin with a brief overview [174, 169] of pseudogap effects in the hole doped high temperature superconductors. A study of concrete data in these systems provides a rather natural way of building intuition about non-Fermi liquid based superfluidity, and this should, in turn, be useful for the cold atom community.

It has been argued by some [29, 121, 146, 140, 189] that a BCS-BEC crossover-induced pseudogap is the origin of the mysterious normal state gap observed in high temperature superconductors. Although, this is a highly contentious subject, a principal supporting rationale is that this above-T_c excitation gap seems to evolve smoothly into the fermionic gap within the

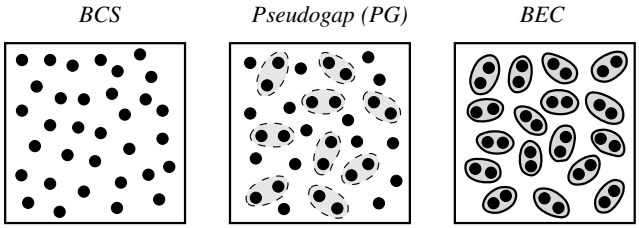


Figure 24.5: The character of the excitations in the BCS-BEC crossover both above and below T_c. The excitations are primarily fermionic Bogoliubov quasiparticles in the BCS limit and bosonic pairs (or "Feshbach bosons") in the BEC limit. In the PG case the "virtual molecules" consist primarily of "Cooper" pairs of fermionic atoms.

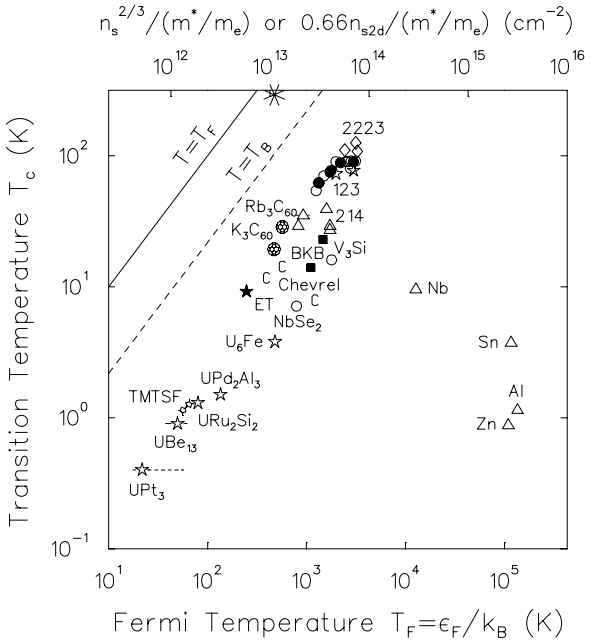


Figure 24.6: Uemura plot [178] of the superconducting transition temperature as a function of Fermi temperature (lower axis) and of the low T superfluid density (upper axis) for various superconductors. The plot indicates how "exotic" superconductors appear to be in a distinct category as compared with more conventional metal superconductors such as Nb, Sn, Al and Zn. Note the logarithmic scales.

superconducting state. This, in conjunction with a panoply of normal state anomalies which appear to represent precursor superconductivity effects, suggests that the pseudogap has more in common with the superconducting phase than with the insulating magnetic phase associated with the parent compound.

The arguments in favor of this (albeit, controversial) crossover viewpoint rest on the following observations: (i) the transition temperature is anomalously high and the coherence length ξ for superconductivity anomalously short, around 10Å as compared more typically with 1000Å. (ii) These systems are quasi-two dimensional so that one might expect pre-formed pairs or precursor superconductivity effects to be enhanced. (iii) The normal state gap has the same d-wave symmetry as the superconducting order parameter [42, 20], and (iv) to a good approximation its onset temperature, called T^*, satisfies [98, 129] $T^* \approx 2\Delta(0)/4.3$ which satisfies the BCS scaling relation. (v) There is widespread evidence for pseudogap effects both above [174, 169] and below [113, 163] T_c. Finally, it has also been argued that short coherence length superconductors may quite generally exhibit a distinctive form of superconductivity [178]. Figure 24.6 shows a plot of data collected by Uemura which seems to suggest that the traditional BCS superconductors stand apart from other more exotic (and frequently short ξ) forms of superconductivity. From this plot one can infer, that, except for high T_c, there is nothing special about the high T_c superconductors; they are not alone in this distinctive class which includes the organics and heavy fermion superconductors as well. Thus, to understand them, one might want to focus on this simplest aspect (short ξ) of high T_c superconductors, rather than invoke more exotic and less generic features.

In Fig. 24.7 we show a sketch of the phase diagram for the copper oxide superconductors. Here x represents the concentration of holes which can be controlled by adding Sr substitutionally, say, to $La_{1-x}Sr_xCuO_4$. At zero and small x the system is an antiferromagnetic (AFM) insulator. Precisely at half filling ($x = 0$) we understand this insulator to derive from Mott effects. These Mott effects may or may not be the source of the other exotic phases indicated

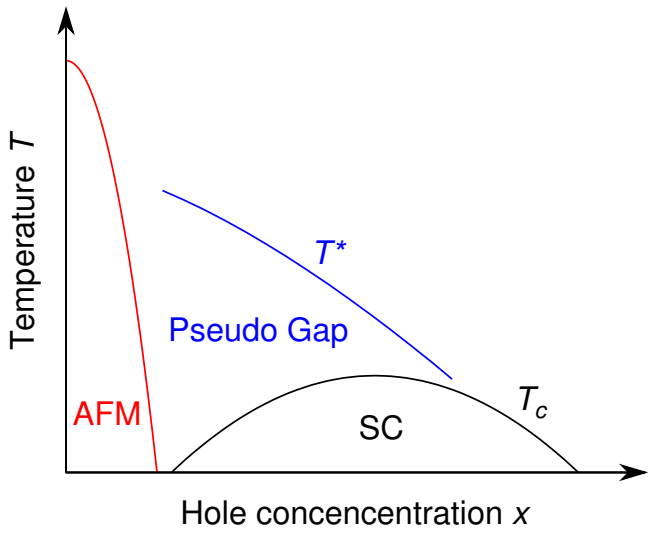


Figure 24.7: Typical phase diagram of hole-doped high T_c superconductors. There exists a pseudogap phase above T_c in the underdoped regime. Here SC denotes superconductor, and T^* is the temperature at which the pseudogap smoothly turns on.

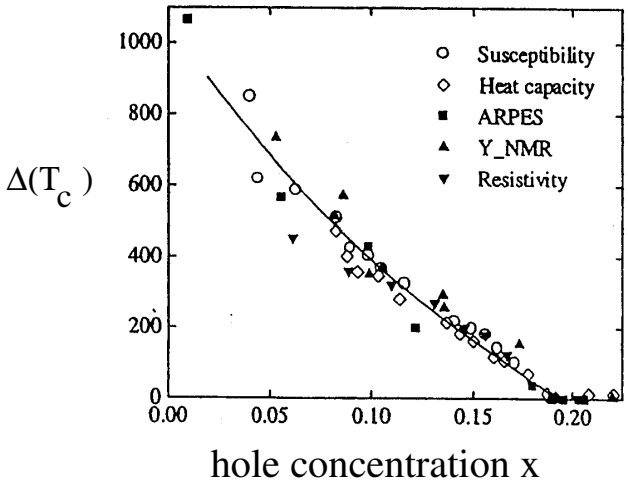


Figure 24.8: Pseudogap magnitude at T_c versus doping concentration in hole doped high T_c superconductors measured with different experimental techniques (from [169]). Units on vertical axis are temperature in degrees K.

in the diagram, as "SC" for superconductivity and the pseudogap phase. Once AFM order disappears the system remains insulating until a critical concentration (typically around a few percent Sr) when an insulator-superconductor transition is encountered. Here photoemission studies [42, 20] suggest that once this line is crossed, μ appears to be positive. For $x \leq 0.2$, the superconducting phase has a non-Fermi liquid (or pseudogapped) normal state [169]. We note an important aspect of this phase diagram at low x. As the pseudogap becomes stronger (T^* increases), superconductivity as reflected in the magnitude of T_c becomes weaker. One way to think about this competition is through the effects of the pseudogap on T_c. As this gap increases, the density of fermionic states at E_F decreases, so that there are fewer fermions around to participate in the superconductivity.

Importantly, there is a clear excitation gap present at the onset of superconductivity which is called $\Delta(T_c)$ and which vanishes at $x \approx 0.2$. The magnitude of the pseudogap at T_c is shown in Fig. 24.8, from [169]. Quite remarkably, as indicated in the figure, a host of different probes seem to converge on the size of this gap.

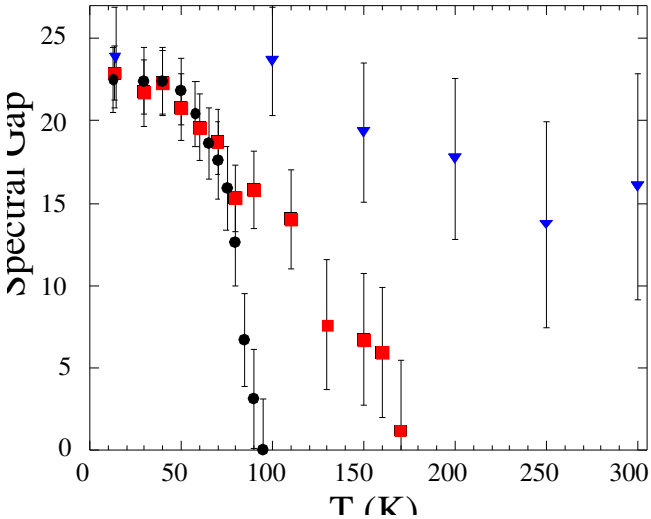


Figure 24.9: (Color) Temperature dependence of the excitation gap from ARPES measurements for optimally doped (filled black circles), underdoped (red squares) and highly underdoped (blue inverted triangles) single-crystal BSCCO samples (taken from [47]). There exists a pseudogap phase above T_c in the underdoped regime.

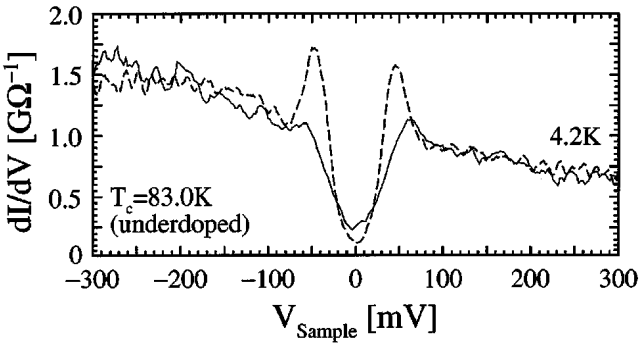


Figure 24.10: STM measurements of the dI/dV characteristics of an underdoped BSCCO sample inside (solid) and outside (dashed) a vortex core at low T from [149]. dI/dV is proportional to the density of states.

Figure 24.9 indicates the temperature dependence of the excitation gap for three different hole stoichiometries. These data were taken [47] from angle resolved photoemission spectroscopy (ARPES) measurement on single-crystal $Bi_2Sr_2CaCu_2O_{8+\delta}$ (BSCCO) samples. For one sample shown as circles, (corresponding roughly to "optimal" doping) the gap vanishes roughly at T_c as might be expected for a BCS superconductor. At the other extreme are the data indicated by inverted triangles in which an excitation gap appears to be present up to room temperature, with very little temperature dependence. This is what is referred to as a highly underdoped sample (small x), which from the phase diagram can be seen to have a rather low T_c. Moreover, T_c is not evident in these data on underdoped samples. This is a very remarkable feature which indicates that from the fermionic perspective there appears to be no profound sensitivity to the onset of superconductivity.

While the high T_c community has focussed on pseudogap effects above T_c, there is a good case to be made that these effects also persist below. Shown in Fig. 24.10 are STM data [149] taken below T_c within a vortex core (solid lines) and between vortices in the bulk (dashed lines). The quantity dI/dV may be viewed as a measure of the fermionic density of states at energy E given by the voltage V. This figure shows that there is a clear depletion of the density of states around the Fermi energy ($V = 0$) in the normal phase within the core. Indeed the size of

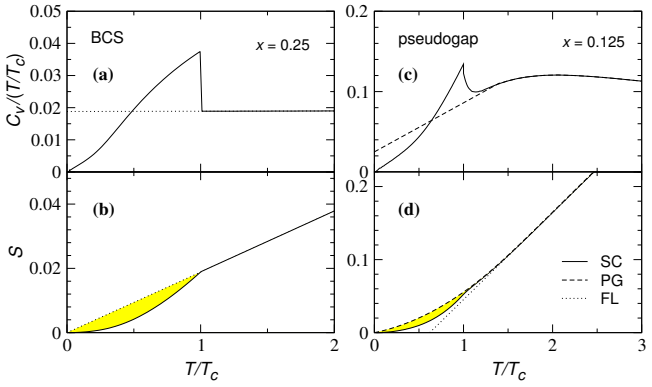


Figure 24.11: Behavior of entropy S and specific heat coefficient $\gamma \equiv C_v/T$ as a function of temperature for (a)-(b) BCS and (c)-(d) pseudogapped superconductors. Dotted and dashed lines are extrapolated normal states below T_c. The shaded areas were used to determine the condensation energy.

the inferred energy gap (or pseudogap) corresponds to the energy separation between the two maxima in dI/dV; this can be seen to be the same for both the normal and superconducting regions (solid and dashed curves). This figure emphasizes the fact that the existence of an energy gap has little or nothing to do with the existence of phase coherent superconductivity. It also suggests that pseudogap effects effectively persist below T_c; the normal phase underlying superconductivity for $T \leq T_c$ is not a Fermi liquid.

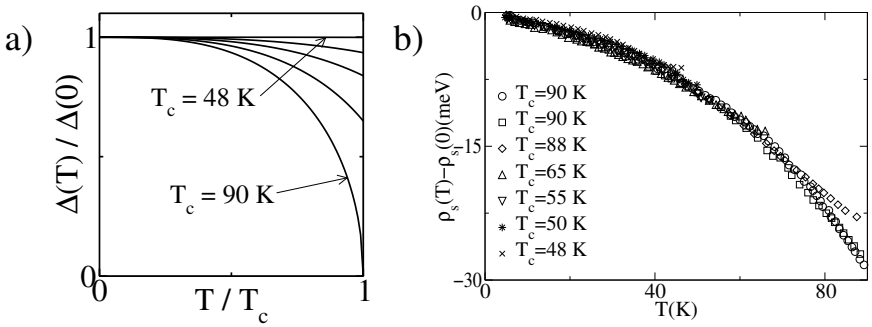


Figure 24.12: Temperature dependence of (a) the fermionic excitation gap Δ and (b) superfluid density ρ_s from experiment for various doping concentrations (from [163]). Figure (a) shows a schematic plot of Δ as seen in the ARPES and STM tunneling data. When $\Delta(T_c) \neq 0$, there is little correlation between $\Delta(T)$ and $\rho_s(T)$; this figure suggests that something other than fermionic quasiparticles (*e.g.*, bosonic excitations) may be responsible for the disappearance of superconductivity with increasing T. Figure (b) shows a quasi-universal behavior for the slope $d\rho_s/dT$ at different doping concentrations, despite the highly non-universal behavior for $\Delta(T)$.

Analysis of thermodynamical data [113, 169] has led to a similar inference. Figure 24.11 presents a schematic plot of the entropy S and specific heat for the case of a BCS superconductor, as contrasted with a pseudogapped superconductor. Actual data are presented in Fig. 24.38. Figure 24.11 makes it clear that in a BCS superconductor, the normal state which underlies the superconducting phase, *is* a Fermi liquid; the entropy at high temperatures extrapolates into a physically meaningful entropy below T_c. For the PG case, the Fermi liquid-extrapolated entropy becomes negative. In this way Loram and co-workers [113] deduced that the normal phase underlying the superconducting state is not a Fermi liquid. Rather, they claimed to obtain proper thermodynamics, it must be assumed that this state contains a persistent pseudogap. They argued for a distinction between the excitation gap Δ and the superconducting

order parameter, within the superconducting phase. To fit their data they presumed a modified fermionic dispersion

$$E_{\mathbf{k}} = \sqrt{(\epsilon_{\mathbf{k}} - \mu)^2 + \Delta^2(T)} \tag{24.6}$$

where

$$\Delta^2(T) = \Delta_{sc}^2(T) + \Delta_{pg}^2 \tag{24.7}$$

Here Δ_{pg} is taken on phenomenological grounds to be T-independent. The authors argue that the pseudogap contribution may arise from physics unrelated to the superconductivity. While others [25, 127] have similarly postulated that Δ_{pg} may in fact derive from another (hidden) order parameter or underlying band structure effect, in general the fermionic dispersion relation $E_{\mathbf{k}}$ will take on a different character from that assumed above, which is very specific to a superconducting origin for the pseudogap.

Finally, Fig. 24.12 makes the claim for a persistent pseudogap below T_c in an even more suggestive way. Figure 24.12(a) represents a schematic plot of excitation gap data such as are shown in Fig. 24.9. Here the focus is on temperatures below T_c. Most importantly, this figure indicates that the T dependence in Δ varies dramatically as the stoichiometry changes. Thus, in the extreme underdoped regime, where PG effects are most intense, there is very little T dependence in Δ below T_c. By contrast at high x, when PG effects are less important, the behavior of Δ follows that of BCS theory. What is most impressive however, is that these wide variations in $\Delta(T)$ are *not* reflected in the superfluid density $\rho_s(T)$, which is proportional to the inverse square of the London magnetic penetration depth and can be measured by, for example, muon spin relaxation (μSR) experiments. Necessarily, $\rho_s(T)$ vanishes at T_c. What is plotted [163] in Fig. 24.12(b) is $\rho_s(T) - \rho_s(0)$ versus T. That these data all seem to sit on a rather universal curve is a key point. The envelope curve in $\rho_s(T) - \rho_s(0)$ is associated with an "optimal" sample where $\Delta(T)$ essentially follows the BCS prediction. Figure 24.12 then indicates that, *despite the highly non-universal behavior for $\Delta(T)$, the superfluid density does not make large excursions from its BCS- predicted form.* This is difficult to understand if the fermionic degrees of freedom through $\Delta(T)$ are dominating at all x. Rather this figure suggests that something other than fermionic excitations is responsible for the disappearance of superconductivity, particularly in the regime where $\Delta(T)$ is relatively constant in T. At the very least pseudogap effects must persist below T_c.

Driving the superconductivity away is another important way to probe the pseudogap. This occurs naturally with temperatures in excess of T_c, but it also occurs when sufficient pair breaking is present through impurities [168, 192, 169] or applied magnetic fields [6]. An important effect of temperature needs to be stressed. With increasing $T > T_c$, the d-wave shape of the excitation gap is rapidly washed out [20, 42]; the nodes of the order parameter, in effect, begin to spread out, just above T_c. The inverse of this effect should also be emphasized: when approached from above, T_c *is marked by the abrupt onset of long lived quasiparticles.*

One frequently, and possibly universally, sees a superconductor-insulator (SI) transition when T_c is driven to zero in the presence of a pseudogap. This suggests a simple scenario: that *the pseudogap may survive when superconductivity is suppressed.* In this way the ground state is no longer a simple metal. This SI transition is seen upon Zn doping [168, 192, 169], as well as in the presence of applied magnetic fields [6]. Moreover, the intrinsic change in stoichiometry illustrated in the phase diagram of Fig. 24.7 also leads to an SI transition. One can thus deduce that the effects of pair-breaking on T_c and T^* are very different, with the former being far more sensitive than the latter.

It is clear that pseudogapped fermions are in evidence in a multiplicity of experiments. Are there indications of bosonic degrees of freedom in the normal state of high T_c superconductors? The answer is unequivocally yes: *meta-stable bosons are observable as superconducting fluctuations.* These bosons are intimately connected to the pseudogap; in effect they are the

other side of the same coin. These bosonic effects are enhanced in the presence of the quasi-two dimensional lattice structure of these materials. Very detailed analyses [103] of thermodynamic and transport properties of the highest T_c or "optimal" samples reveal clearly these pre-formed pairs. Moreover they are responsible [100] for divergences at T_c in the dc conductivity σ and in the transverse thermoelectric [179] response α_{xy}. These transport coefficients are defined more generally in terms of the electrical and heat currents by

$$\mathbf{J}^{\mathbf{elec}} = \sigma \mathbf{E} + \alpha(-\nabla T) \tag{24.8}$$

$$\mathbf{J}^{\mathbf{heat}} = \tilde{\alpha} \mathbf{E} + \kappa(-\nabla T) \tag{24.9}$$

Here σ is the conductivity tensor, κ the thermal conductivity tensor, and $\alpha, \tilde{\alpha}$ are thermoelectric tensors. Other coefficients, while not divergent, exhibit precursor effects, all of which are found to be in good agreement [103] with fluctuation theory. As pseudogap effects become more pronounced with underdoping much of the fluctuation behavior appears to set in at a higher temperature scale associated with T^*, but often some fraction thereof [188, 170].

Figures 24.13 and 24.14 make the important point that precursor effects in the transverse thermoelectric response (α_{xy}) and conductivity σ appear at higher temperatures ($\propto T^*$) as pseudogap effects become progressively more important; the dotted lines which have the strongest pseudogap continue to the highest temperatures on both Figures. Moreover, both transport coefficients evolve smoothly from a regime where they are presumed to be described by conventional fluctuations [103, 179] as shown by the solid lines in the figures into a regime where their behavior is associated with a pseudogap. A number of people have argued [188, 38] that normal state vortices are responsible for the so called anomalous transport behavior of the pseudogap regime. We will argue in this Review that these figures may alternatively be interpreted as suggesting that bosonic degrees of freedom, not vortices, are responsible for these anomalous transport effects.

24.2.3 Introduction to High T_c SC: Mott Physics and Possible Ordered States

Most workers in the field of high T_c superconductivity would agree that we have made enormous progress in characterizing these materials and in identifying key theoretical questions and constructs. Experimental progress, in large part, comes from transport studies [174, 169] in addition to three powerful spectroscopies: photoemission [20, 42], neutron [33, 53, 86, 1, 2, 125, 151, 175] and Josephson interferometry [187, 176, 116]. These data have provided us with important clues to address related theoretical challenges. Among the outstanding theoretical issues in the cuprates are (i) understanding the attractive "mechanism" that binds electrons into Cooper pairs, (ii) understanding the evolution of the normal phase from Fermi liquid (in the "overdoped" regime) to marginal Fermi liquid (at "optimal" doping) to the pseudogap state, which is presumed to occur as doping concentration x decreases, and (iii) understanding the nature of that superconducting phase which evolves from each of these three normal states.

The theoretical community has concentrated rather extensively on special regions and x-dependences in the phase diagram which are presumed to be controlled by "Mott physics". There are different viewpoints of precisely what constitutes Mott physics in the metallic phases, and, for example, whether or not this is necessarily associated with spin-charge separation. For the most part, one presumes here that the insulating phase of the parent compound introduces strong Coulomb correlations into the doped metallic states which may or may not also be associated with strong antiferromagnetic correlations. There is a recent, rather complete review [106] of Mott physics within the scenario of spin-charge separation, which clarifies the physics it entails.

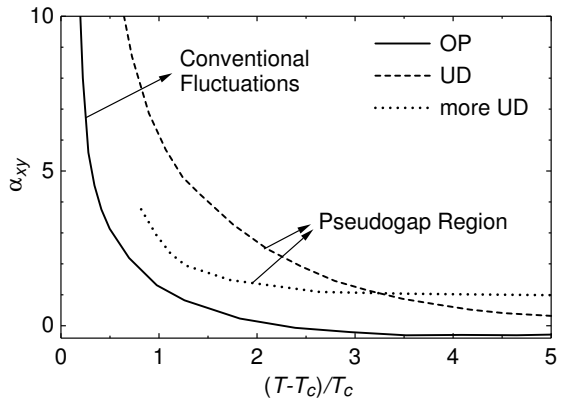


Figure 24.13: Transverse thermoelectric response (which relates to the Nernst coefficient) plotted here in fluctuation regime above T_c. Here OP and UD correspond to optimal and underdoping, respectively. Data were taken from [188].

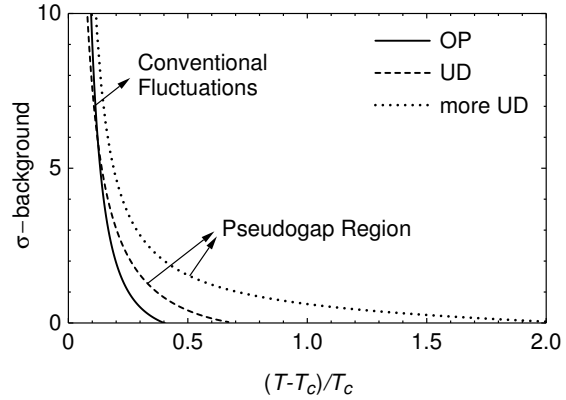


Figure 24.14: Conductivity in fluctuation regime for optimally (OP) and underdoped (UD) cuprate superconductors. Data from [186].

Concrete experimental signatures of Mott physics are the observations that the superfluid density $\rho_s(T = 0, x) \to 0$ as $x \to 0$, as if it were reflecting an order parameter for a metal insulator transition. More precisely it is deduced that $\rho_s(0, x) \propto x$, at low x. Unusual effects associated with this linear- in- x dependence also show up in other experiments, such as the weight of coherence features in photoemission data [20, 42], as well as in thermodynamical signatures [169].

While there is no single line of reasoning associated with these Mott constraints, the low value of the superfluid density has been argued [50] to be responsible for soft phase fluctuations of the order parameter, which may be an important contributor to the pseudogap. However, recent concerns about this "phase fluctuation scenario" for the origin of the pseudogap have been raised [105]. It is now presumed by a number of groups that phase fluctuations alone may not be adequate and an additional static or fluctuating order of one form or another needs to be incorporated. Related to a competing or co-existing order are conjectures [25] that the disappearance of pseudogap effects around $x \approx 0.2$ is an indication of a "quantum critical point" associated with a hidden order parameter which may be responsible for the pseudogap. Others have associated small [183] x or alternatively optimal [180] x with quantum critical points of a different origin. The nature of the other competing or fluctuating order has been conjectured to be RVB [5], "d-density wave" [25], stripes [24, 190] or possibly antiferromagnetic spin fluctuations [141, 36, 45]. The latter is another residue of the insulating phase.

What is known about the "pairing mechanism"? Some would argue that this is an ill-defined question, and that superconductivity has to be understood through condensation energy argu-

ments based for example on the data generated from the extrapolated normal state entropy [113, 169] discussed above in the context of Fig. 24.11. These condensation arguments are often built around the non-trivial assumption that there is a thermodynamically well behaved but meta-stable normal phase which coexists with the superconductivity. Others would argue that Coulomb effects are responsible for d-wave pairing, either directly [108, 111], or indirectly via magnetic fluctuations [153, 141]. Moreover, the extent to which the magnetism is presumed to persist into the metallic phase near optimal doping is controversial. Initially, NMR measurements were interpreted as suggesting [122] strong antiferromagnetic fluctuations, while neutron measurements, which are generally viewed as the more conclusive, do not provide compelling evidence [158] for their presence in the normal phase. Nevertheless, there are interesting neutron-measured magnetic signatures [191, 112, 85] below T_c associated with d-wave superconductivity. There are also analogous STM effects which are currently of interest [184].

24.2.4 Overview of the BCS-BEC Picture of High T_c SC in the Underdoped Regime

We summarize here the physical picture associated with the more controversial BCS-BEC crossover approach to high T_c superconductors, based on the standard ground state of Eq. (24.1). One presumes that the normal state (pseudo)gap arises from pre-formed pairs. This gap $\Delta(T)$ is thus present at the onset of superconductivity, and reflects the fact that Cooper pairs form before they Bose condense, as a result of sufficiently strong attraction. Below T_c, Δ evolves smoothly into the excitation gap of the superconducting phase.

This behavior reflects the fact that T_c corresponds to the condensation of the $q = 0$ pairs, while finite momentum pairs persist into the order phase as excitations of the condensate. As the temperature is progressively lowered below T_c, there are fewer and fewer such bosonic excitations. Their number vanishes precisely at $T = 0$, at which point the system reaches the ground state of Eq. (24.1). Here the superconducting order parameter and the excitation gap become precisely equal. This approach is based on a mean field scheme and is thus not equivalent to treating phase fluctuations of the order parameter. In general, below T_c, the superconducting order parameter Δ_{sc} and the pseudogap contributions add in quadrature in the dispersion of Eq. (24.6) as

$$\Delta^2(T) = \Delta_{sc}^2(T) + \Delta_{pg}^2(T) \tag{24.10}$$

where $\Delta_{pg} \to 0$ as $T \to 0$; this behavior should be contrasted with that in Eq. (24.7).

Transport and thermodynamics in the normal and superconducting phases are determined by two types of quasiparticles: fermionic excitations which exhibit a gap $\Delta(T)$, and noncondensed pairs or bosonic excitations. Contributions from the former are rather similar to their (low T) counterparts in BCS theory, except that they are present well above T_c as well, with substantially larger Δ than in strict BCS theory. In this way, experiments which probe the opening of an excitation gap (such as Pauli susceptibility in the spin channel, and resistivity in the charge channel) will exhibit precursor effects, that is, the gradual onset of superconductivity from around T^* to below T_c.

The contributions to transport and thermodynamics of the bosonic excitations are rather similar to those deduced from the time dependent Ginsburg-Landau theory of superconducting fluctuations, provided that one properly extends this theory, in a quantum fashion, away from the critical regime. It is these contributions which often exhibit divergences at T_c, but unlike conventional superconductors, bosonic contributions (pre-formed pairs) are present, up to high temperatures of the order of $T^*/2$, providing the boson density is sufficiently high. Again, these bosons do not represent fluctuations of the order parameter, but they obey a generically similar dynamical equation of motion, and, in the more general case which goes beyond Eq. (24.1),

they will be coupled to order parameter fluctuations. Here, in an oversimplified sense there is a form of spin-charge separation. The bosons are spin-less (singlet) with charge $2e$, while the fermions carry both spin and charge, but are non-Fermi-liquid like, as a consequence of their energy gap.

In the years following the discovery of high T_c superconductors, attention focused on the so-called marginal Fermi liquid behavior of the cuprates. This phase is associated with near-optimal doping. The most salient signature of this marginality is the dramatically linear in temperature dependence of the resistivity from just above T_c to very high temperatures, well above room temperature. Today, we know that pseudogap effects are present at optimal doping, so that the precise boundary between the marginal and pseudogap phases is not clear. As a consequence, addressing this normal state resistivity in the BCS-BEC crossover approach has not been done in detail, although it is unlikely to yield a strictly linear T dependence at a particular doping. Nevertheless, the bosonic contributions lead to a *decrease* in resistivity as temperature is lowered, while the opening of a d-wave gap associated with the fermionic terms leads to an *increase*, which tends to compensate. These are somewhat analogous to Aslamazov-Larkin and Maki-Thompson fluctuation contributions [103]. The bosons generally dominate in the vicinity of T_c, but at higher T, in the vicinity of T^*, the gapped fermions will be the more important.

The vanishing of T_c with sufficiently large T^* (extreme underdoping) occurs in an interesting way in this crossover theory. This effect is associated with the localization of the bosonic degrees of freedom. Pauli principle effects in conjunction with the extended size of d-wave pairs inhibit pair hopping, and thus destroy superconductivity. One can speculate that, just as in conventional Bose systems, once the bosons are localized, they will exhibit an alternative form of long range order. Indeed, "pair density wave" models have been invoked [26] to explain recent STM data [181, 56]. In contrast to the cold atom systems, for the d-wave case the BEC regime is never accessed. This superconductor-insulator transition takes place in the fermionic regime where $\mu \approx 0.8E_F$.

In the context of BCS-BEC crossover physics, it is not essential to establish the source of the attractive interaction. For the most part we skirt this issue in this Review by taking the pairing onset temperature $T^*(x)$ as a phenomenological input parameter. At the simplest level one may argue that as the system approaches the Mott insulating limit ($x \to 0$) fermions become less mobile; this serves to increase the effectiveness of the attractive interaction at low doping levels.

The variable x in the high T_c problem should be viewed then, as a counterpart to the magnetic field variable in the cold atom problem which tunes the system through a Feshbach resonance; both x and field strength modulate the size of the attraction. However, for the cuprates, in contrast to the cold atom systems, one never reaches the BEC limit of the crossover theory.

It is reasonable to presume based on the evidence to date, that pairing ultimately derives from Coulombic effects, not phonons, which are associated with $l = 0$ pairing. While the widely used Hubbard model ignores these effects, longer ranged screened Coulomb interactions have been found [111] to be attractive for electrons in a d-wave channel. In this context, it is useful to note that, similarly, in He^3 short range repulsion destroys s-wave pairing, but leads to attraction in a higher ($l = 1$) channel [4]. There is, however, no indication of pseudogap phenomena in He^3, so that an Eliashberg extended form of BCS theory appears to be adequate. Eliashberg theory is a very different form of "strong coupling" theory from crossover physics, which treats in detail the dynamics of the mediating boson. Interestingly, there is an upper bound to T_c in both schemes. For Eliashberg theory this arises from the induced effective mass corrections [110], whereas in the crossover problem this occurs because of the presence of a pseudogap at T_c.

Other analogies have also been invoked in comparing the cuprates with superfluid He^3, based on the propensity towards magnetism. In the case of the quantum liquid, however, there is a positive correlation between short range magnetic ordering [110] and superconductivity while the correlation appears negative for the cuprates (and some of their heavy fermion "cousins") where magnetism and superconductivity appear to compete.

Searching for the Definitive High T_c Theory

In no sense should one argue that the BCS-BEC crossover approach precludes consideration of Mott physics. Nor should it be viewed as superior. Indeed, many of the experiments we will address in this Review have alternatively been addressed within the Mott scenario. Presumably both components are important in any ultimate theory. We have chosen in this Review to focus on one component only, and it is hoped that a comparably detailed review of Mott physics will be forthcoming. In this way one could compare the strengths and weaknesses of both schemes. A summary [21] of some aspects of the Mott picture with emphasis on one dimensional stripe states should be referred to as a very useful starting point. Also available now is a new Review [106] of Mott physics, based on spin charge separation.

Besides those discussed in this Review, there is a litany of other experiments which are viewed as requiring explanation in order for a high T_c theory to be taken seriously. Among these are the important linear resistivity in the normal state (at optimal doping) and unusual temperature and x dependences in Hall data. While there has been little insight offered from the crossover scheme to explain the former, aspects of the latter have been successfully addressed within pre-formed pair scenarios [57]. Using fermiology based schemes the major features of photoemission[126] and of neutron scattering and NMR data were studied theoretically and rather early on [158, 191, 85], along with a focus on the now famous 41 meV feature [112]. These and other related approaches to the magnetic data, make use of a microscopically derived [157] random phase approximation scheme which incorporates the details of the Fermi surface shape and d-wave gap. Among remaining experiments in this litany is the origin of incoherent transport along the c-axis [150].

On the basis of the above cited literature which addressed magnetic and c-axis [33] data we are led to conclude that pseudogap effects and related crossover physics are not central to their understanding. The presence of a normal state gap will lead to some degree of precursor behavior above T_c, but d-wave nesting related effects such as reflected in neutron data [191, 85, 112] will be greatly weakened above T_c by the blurring out of the d-wave gap nodes [42, 20]. It should be said, however, that c-axis optical data do appear to reflect pseudogap effects [75] above T_c. (The ab-plane counterparts are discussed in Section 24.7.3). In summary, we are far from the definitive high T_c theory and the field has much to gain by establishing a collaboration with the cold atom community where BCS-BEC crossover as well as Mott physics [70] can be further elucidated and explored.

24.2.5 Many Body Hamiltonian and Two Body Scattering Theory: Mostly Cold Atoms

The existence of Feshbach resonances in a gas of ultracold fermionic atoms allows the interaction between atoms to be tuned arbitrarily, via application of a magnetic field. Figure 24.15 presents a characteristic plot of the two body interaction potentials which are responsible for this resonance. These interaction potentials represent an effective description of all Coulomb interactions between the electrons and nuclei. For definiteness, we consider the case of ^{6}Li

[33] Here the ab-plane refers to the crystal plane in parallel with the layers of the cuprate compounds, and the c-axis refers to the axis normal to the layers.

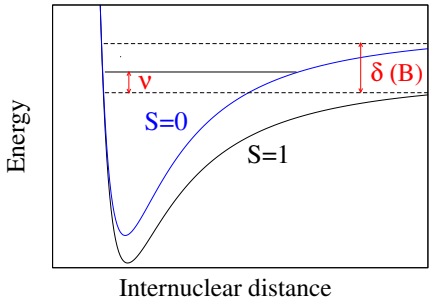


Figure 24.15: A schematic representation of the Feshbach resonance for ^{6}Li. The effective interaction between the scattering of atoms in the triplet state is greatly enhanced, when the energy level of the singlet bound state approaches the continuum of the $S = 1$ channel.

here. In the region of magnetic fields near the "wide" Feshbach resonance, $\approx 837G$, we may focus on the two lowest atomic levels characterized by $|F, m_F\rangle$, where the two quantum numbers correspond to the total spin and its z component. We specify the two states $|1\rangle \equiv |\frac{1}{2}, \frac{1}{2}\rangle$ and $|2\rangle \equiv |\frac{1}{2}, -\frac{1}{2}\rangle$. In place of these quantum numbers one can alternatively characterize the two states in terms of the projections of the electronic (m_s) and nuclear (m_i) spins along the magnetic field. In this way the states 1 and 2 have $m_s = -\frac{1}{2}$ and $m_i = 1$ and 0, respectively.

The curve in Fig. 24.15 labelled $S = 1$ represents the interaction between these two states. This corresponds to the so-called "open" channel and is associated with a triplet (electronic) spin state. A Feshbach resonance requires that there be an otherwise unspecified near-by state which we refer to as in the "closed" channel. The potential which gives rise to this singlet (electronic) spin state is shown by the $S = 0$ curve in Fig. 24.15. A Feshbach resonance arises when this bound state lies near the zero of energy corresponding to the continuum of scattering states in the triplet or open channel. The electronic Zeeman coupling to the triplet state makes is possible to shift the relative position of the two potentials by application of a magnetic field. This shift is indicated by δ in Fig. 24.15. In this way, the resonance is magnetically tunable and the scattering length of the system will vary continuously with field, diverging at that magnetic field which corresponds to the Feshbach resonance. We represent the deviation of this field from the resonance condition by the "detuning parameter" ν. When ν is large and positive, the singlet state is substantially raised relative to the triplet– and it plays relatively little role. By contrast when the magnitude of ν is large, but with negative sign, then the physics is dominated by the singlet or closed channel.

The most general form for the Hamiltonian contains two types of particles: fermions which represent the open channel and "molecular bosons" which represent the two fermion bound state of the closed channel. We will also refer to the latter as "Feshbach bosons". These, in turn, lead to two types of interaction effects: those associated with the direct attraction between fermions, parameterized by U, and those associated with "fermion-boson" interactions, whose strength is governed by g. The latter may be viewed as deriving from hyperfine interactions which couple the (total) nuclear and electronic spins. In the high T_c applications, one generally, but not always, ignores the bosonic degrees of freedom. Otherwise the Hamiltonians are the same, and can be written as

$$\begin{aligned} H \quad - \quad \mu N &= \sum_{\mathbf{k},\sigma} (\epsilon_{\mathbf{k}} - \mu) a^\dagger_{\mathbf{k},\sigma} a_{\mathbf{k},\sigma} + \sum_{\mathbf{q}} (\epsilon^{mb}_{\mathbf{q}} + \nu - 2\mu) b^\dagger_{\mathbf{q}} b_{\mathbf{q}} \\ &+ \sum_{\mathbf{q},\mathbf{k},\mathbf{k}'} U(\mathbf{k},\mathbf{k}') a^\dagger_{\mathbf{q}/2+\mathbf{k},\uparrow} a^\dagger_{\mathbf{q}/2-\mathbf{k},\downarrow} a_{\mathbf{q}/2-\mathbf{k}',\downarrow} a_{\mathbf{q}/2+\mathbf{k}',\uparrow} \\ &+ \sum_{\mathbf{q},\mathbf{k}} \left(g(\mathbf{k}) b^\dagger_{\mathbf{q}} a_{\mathbf{q}/2-\mathbf{k},\downarrow} a_{\mathbf{q}/2+\mathbf{k},\uparrow} + h.c. \right) \end{aligned} \tag{24.11}$$

Here the fermion and boson kinetic energies are given by $\epsilon_{\mathbf{k}} = k^2/(2m)$, and $\epsilon^{mb}_{\mathbf{q}} = q^2/(2M)$, and ν is an important parameter which represents the magnetic field "detuning". $M = 2m$ is the bare mass of the Feshbach bosons. For the cold atom problem $\sigma = \uparrow, \downarrow$ represents the two different hyperfine states ($|1\rangle$ and $|2\rangle$). One may ignore [173] the non-degeneracy of these two states, since there is no known way for state 2 to decay into state 1. In the two channel problem the ground state wavefunction is slightly modified and given by

$$\bar{\Psi}_0 = \Psi_0 \otimes \Psi_0^B \tag{24.12}$$

where the normalized molecular boson contribution Ψ_0^B is

$$\Psi_0^B = e^{-\lambda^2/2 + \lambda b_0^\dagger}|0\rangle \, . \tag{24.13}$$

as discussed originally by [95]. Here λ is a variational parameter. We present the resulting variational conditions for the ground state in Appendix 24.8.

Whether both forms of interactions are needed in either the high T_c or cold atom systems is still under debate. The bosons ($b^\dagger_{\mathbf{k}}$) of the cold atom problem [71, 173] will be referred to as Feshbach bosons. These represent a separate species, not to be confused with the fermion pair ($a^\dagger_{\mathbf{k}} a^\dagger_{-\mathbf{k}}$) operators. Thus we call this a "two channel" model. In this review we will discuss the behavior of crossover physics both with and without these Feshbach bosons (FB). Previous studies of high T_c superconductors have invoked a similar bosonic term [146, 120, 57] as well, although less is known about its microscopic origin. This fermion-boson coupling is not to be confused with the coupling between fermions and a "pairing-mechanism"-related boson ($[b + b^\dagger]a^\dagger a$) such as phonons. The coupling $b^\dagger aa$ and its conjugate represents a form of sink and source for creating fermion pairs, inducing superconductivity in some ways, as a by-product of Bose condensation. We will emphasize throughout that crossover theory proceeds in a similar fashion with and without Feshbach bosons.

It is useful at this stage to introduce the s-wave scattering length, a_s. This parameter is associated with the scattering amplitude in the low energy limit, for a two body scattering process. This scattering length can, in principle, be deduced from Figure 24.15. It follows that a_s is negative when there is no bound state, it tends to $-\infty$ at the onset of the bound state and to $+\infty$ just as the bound state stabilizes. It remains positive but decreases in value as the interaction becomes increasingly strong. The magnitude of a_s is arbitrarily small in both the extreme BEC and BCS limits, but with opposite sign (See Fig. 24.16). *The fundamental postulate of crossover theory is that even though the two-body scattering length changes abruptly at the unitary scattering condition ($|a_s| = \infty$), in the N-body problem the superconductivity varies smoothly through this point.* Throughout this Review, we presume an equivalence between the "pseudogap" and unitary scattering regimes.

An important goal is to understand how to incorporate all the constraints of the two body physics into the superfluid gap equation. As a by-product, one avoids implicit divergences which would also appear in the problem. To begin we ignore Feshbach effects. The way in which the two body interaction U enters to characterize the scattering (in vacuum) is different from the way in which it enters to characterize the N-body processes leading to superfluidity. In each case, however, one uses a T-matrix formulation to sum an appropriately selected but infinite series of terms in U. For the two-body problem in vacuum, we introduce the scattering length, a_s,

$$\frac{m}{4\pi a_s} \equiv \frac{1}{U_0} \, , \tag{24.14}$$

which is related to U via the Lippmann-Schwinger equation

$$\frac{m}{4\pi a_s} \equiv \frac{1}{U} + \sum_{\mathbf{k}} \frac{1}{2\epsilon_{\mathbf{k}}} \, . \tag{24.15}$$

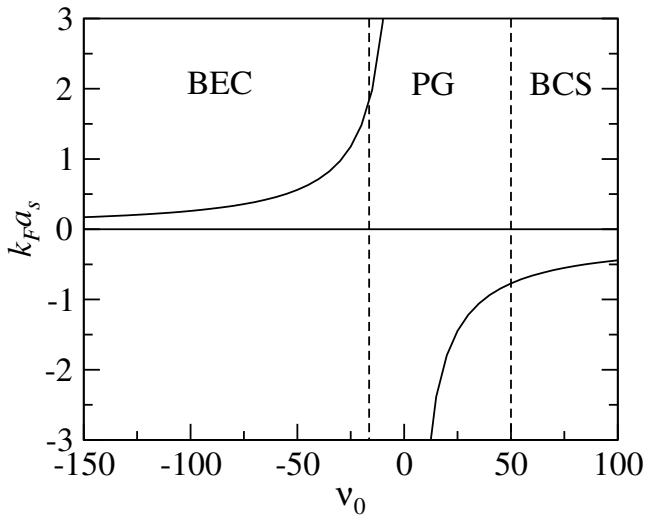


Figure 24.16: Characteristic behavior of the scattering length a_s in the three regimes. a_s diverges when $\nu_0 = 2\mu$. Here, and in subsequent figures ν_0 is always in units of E_F and we estimate 1 G $\approx 60 E_F$ for a typical $E_F = 2\,\mu$K, for either ^{6}Li or ^{40}K.

In this way one may solve for the unknown U in terms of a_s or U_0. The two-body T-matrix equation [Eq. (24.15)] can be rewritten as

$$U = \Gamma U_0, \qquad \Gamma = \left(1 + \frac{U_0}{U_c}\right)^{-1} , \tag{24.16}$$

where we define the quantity U_c as

$$U_c^{-1} = -\sum_{\mathbf{k}} \frac{1}{2\epsilon_{\mathbf{k}}} . \tag{24.17}$$

Here U_c is the critical value of the potential associated with the binding of a two particle state in vacuum. Specific evaluation of U_c requires that there be a cut-off imposed on the above summation, associated with the range of the potential.

Now let us turn to the Feshbach problem, where the superfluidity is constrained by a more extended set of parameters U, g, ν and also μ. Provided we redefine the appropriate "two body" scattering length, Equation (24.15) holds even in the presence of Feshbach effects [131, 123]. It has been shown that U in the above equations is replaced by U_{eff} and a_s by a_s^*

$$\frac{m}{4\pi a_s^*} \equiv \frac{1}{U_{eff}} + \sum_{\mathbf{k}} \frac{1}{2\epsilon_{\mathbf{k}}} . \tag{24.18}$$

Here it is important to stress that many body effects, via the fermionic chemical potential μ enter into a_s^*.

More precisely the effective interaction between two fermions is Q dependent. It arises from a second order process involving emission and absorption of a molecular boson. The net effect of the direct plus indirect interactions is given by

$$U_{eff}(Q) \equiv U + g^2 D_0(Q) , \tag{24.19}$$

where

$$D_0(Q) \equiv 1/[i\Omega_n - \epsilon_{\mathbf{q}}^{mb} - \nu + 2\mu] \tag{24.20}$$

is the non-interacting molecular boson propagator. What appears in the gap equation, however, is

$$U_{eff}(Q = 0) \equiv U_{eff} = U - \frac{g^2}{\nu - 2\mu} . \tag{24.21}$$

Experimentally, the two body scattering length a_s^* varies with magnetic field B. Near resonance, it can be parameterized [93] in terms of three parameters of the two body problem U_0, g_0 and the magnetic field which at resonance is given by B_0. One fits the scattering length to $a_{bg}(1-\frac{w}{B-B_0})$ so that the width w is related to g_0 and the background scattering length a_{bg} is related to U_0. Away from resonance, the crossover picture requires that the scattering length vanish asymptotically as

$$a_s^* \approx 0\,, \qquad \text{in extreme BEC limit,} \tag{24.22}$$

so that the system represents an ideal Bose gas. Here it should be noted that this BEC limit corresponds to $\nu \to \mu^+$. The counterpart of Eq. (24.22) also holds for the one channel problem. Note that the actual resonance of the many body problem will be somewhat shifted from the atomic-fitted resonance parameter B_0.

It is convenient to define the parameter ν_0 which is directly related to the difference in the applied magnetic field B and B_0

$$\nu_0 = (B - B_0)\Delta\mu^0, \tag{24.23}$$

where $\Delta\mu^0$ is the difference in the magnetic moment of the singlet and triplet paired states. *We will use the parameter ν_0 as a measure of magnetic field strength throughout this Review.* The counterpart of Eq. (24.14) is then

$$\frac{m}{4\pi a_s^*} \equiv \frac{1}{U_0 - \frac{g_0^2}{\nu_0 - 2\mu}} \equiv \frac{1}{U^*}\,, \tag{24.24}$$

where $U_0 = \frac{4\pi a_{bg}}{m}$ and $g_0^2 = U_0\Delta\mu^0 w$. For the purposes of this Review we will use the scattering length a_s^*, although for simplicity we often drop the asterisk and write it as a_s.

We can again invert the Lippmann-Schwinger or T-matrix scattering equation [93, 18] to arrive at the appropriate parameters g and ν which enter into the Hamiltonian and thus into the gap equation. Just as in Eq. (24.16), one finds a connection between measurable parameters (with subscript 0) and their counterparts in the Hamiltonian (without the subscript):

$$U = \Gamma U_0, \quad g = \Gamma g_0, \quad \nu - \nu_0 = -\Gamma\frac{g_0^2}{U_c}\,. \tag{24.25}$$

To connect the various energy scales, which appear in the problem, typically $1\text{G} \approx 60\text{E}_\text{F}$ for both ^{6}Li and ^{40}K. Here it is assumed that the Fermi energy is $E_F \approx 2\,\mu$K.

In Fig. 24.16 and using Eq. (24.18), we plot a prototypical scattering length $k_F a_s \equiv k_F a_s^*$ as a function of the magnetic field dependent parameter, ν_0. This figure indicates the BEC, BCS and PG regimes. Here, as earlier, the PG regime is bounded on the left by $\mu = 0$ and on the right by $\Delta(T_c) \approx 0$.

A key finding associated with this plot is that *the PG regime begins on the so-called "BEC side of resonance", independent of whether Feshbach effects are included or not.* That is, the fermionic chemical potential reaches zero while the scattering length is positive. This generic effect of the ground state self consistent equations arises from the Pauli principle. For an isolated system, two particle resonant scattering occurs at $U = U_c$, where U_c is defined in Eq. (24.17). In the many body context, because of Pauli principle repulsion between fermions, it requires an effectively stronger attraction to bind particles into molecules. Stated alternatively, the onset of the fermionic regime ($\mu > 0$) occurs for more strongly attractive interactions, than those required for two body resonant scattering. As a consequence of $\mu > 0$, *there is very little condensate weight in the Feshbach boson channel near the unitary limit, for values of the coupling parameter g_0, appropriate to currently studied (and rather wide) Feshbach resonances.*

Finally, it is useful to compare the two interaction terms which we have defined above, (U_{eff} and U^*), and to contrast their behavior in the BEC and unitary limits. The quantity U^* is

proportional to the scattering length; it reflects the two body physics and necessarily diverges at unitarity, where $U_{eff} = U_c$. By contrast, in the BEC regime, U^*, or a_s^* approaches zero, (under the usual presumption that the interaction is a contact interaction). This vanishing of U^* should be compared with the observation that the quantity U_{eff}, which reflects the many body physics, must diverge in this BEC limit.

Differences Between One and Two Channel Models: Physics of Feshbach bosons

The main effects associated with including the explicit Feshbach resonance are twofold. These Feshbach bosons provide a physical mechanism for tuning the scattering length to be arbitrarily large, and in the BEC limit, they lead to different physics from the one channel problem. As will be illustrated later via a comparison of Figures 24.23 and 24.25, in an artificial way one can capture most of the salient physics of the unitary regime via a one channel approach in which one drops all molecular boson related terms in the Hamiltonian, but takes the interaction U to be arbitrary. In this way there is very little difference between fermion-only and fermion-boson models. There is an important proviso, though, that one is not dealing with narrow resonances which behave rather differently near unitarity, as will be seen in Fig. 24.32. In addition, as in the one channel model a form of universality [68] is found in the ground state at the unitary limit, provided g is sufficiently large. This is discussed later in the context of Fig. 24.30.

We emphasize that, within the BEC regime there are three important effects associated with the Feshbach coupling g. As will become clear later, (i) in the extreme BEC limit when g is nonzero, there are no occupied fermionic states. The number constraint can be satisfied entirely in terms of Feshbach bosons. (ii) The absence of fermions will, moreover, greatly weaken the inter-boson interactions which are presumed to be mediated by the fermions. In addition, as one decreases $|U_{eff}|$ from very attractive to moderately attractive (i.e., increases a_s^* on the BEC side) the nature of the condensed pairs changes. Even in the absence of Feshbach bosons (FB), the size of the pairs increases. But in their presence the admixture of bosonic (i.e., molecular bosons) and fermionic (i.e., Cooper pair) components in the condensate is continuously varied from fully bosonic to fully fermionic. Finally (iii) the role of the condensate enters in two very different ways into the self consistent gap and number equations, depending on whether or not there are FB. The molecular boson condensate appears principally in the number equation, while the Cooper pair condensate appears principally in the gap equation. To make this point clearer we can refer ahead to Eq. (24.81) which contains the FB condensate contribution n_b^0. By contrast the Cooper condensate contribution Δ_{sc} enters into the total excitation gap Δ as in Eq. (24.10) and Δ is, in turn, constrained via Eq. (24.69). Points (i) and (iii), which may appear somewhat technical, have essential physical implications, among the most important of these is point (ii) above.

We stress, however, that *for the PG and BCS regimes the differences with and without FB are, however, considerably less pronounced.*

24.2.6 Cold Atom Experiments: Crossover in the Presence of Feshbach Resonances

There has been an exciting string of developments over the past few years in studies of ultracold fermionic atoms, in particular, ^{6}Li and ^{40}K, which have been trapped and cooled via magnetic and optical means. Typically these traps contain $\sim 10^5$ atoms at very low densities $\approx 10^{13}$ cm^{-3} when cooled to very low T. Here the Fermi temperature E_F in a trap can be estimated to be of the order of a micro-Kelvin. It was argued on the basis of BCS theory alone [73], and rather early on (1997), that the temperatures associated with the superfluid

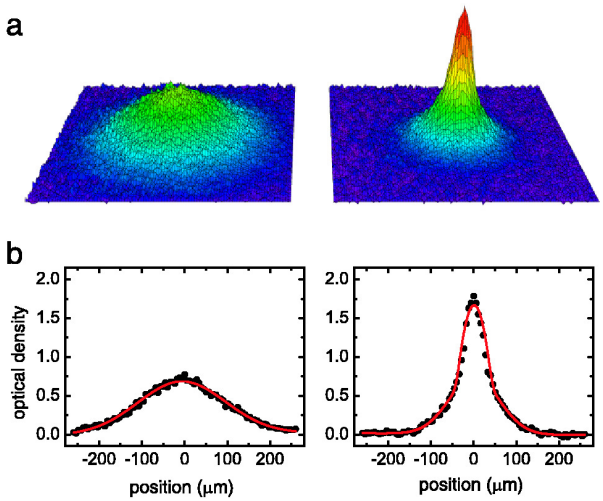


Figure 24.17: (Color) Spatial density profiles of a molecular cloud of trapped ^{40}K atoms in the BEC regime in the transverse directions after 20 ms of free expansion (from [59]), showing thermal molecular cloud above T_c (left) and a molecular condensate (right) below T_c. (a) shows the surface plots, and (b) shows the cross-sections through images (dots) with bimodal fits (lines).

phases may be attainable in these trapped gases. This set off a search for the "holy grail" of fermionic superfluidity. That a Fermi degenerate state could be reached at all is itself quite remarkable; this was was first reported [44] by Jin and deMarco in 1999. By late 2002 reports of unusual hydrodynamics in a degenerate Fermi gas indicated that strong interactions were present [130]. This strongly interacting Fermi gas (associated with the unitary scattering regime) has attracted widespread attention independent of the search for superfluidity, because it appears to be a prototype for analogous systems in nuclear physics [8, 65] and in quark-gluon plasmas [76, 94]. Moreover, there has been a fairly extensive body of analytic work on the ground state properties of this regime [64, 22], which goes beyond the simple mean field wave function ansatz.

As a consequence of attractive s-wave interactions between fermionic atoms in different hyperfine states, it was anticipated that dimers could also be made. Indeed, these molecules formed rather efficiently [148, 165, 40] as reported in mid-2003 either via three body recombination [79] or by sweeping the magnetic field across a Feshbach resonance. Moreover, they are extremely long lived [165]. From this work it was relatively straightforward to anticipate that a Bose condensate would also be achieved. Credit goes to theorists such as Holland [71] and to Timmermans [173] and their co-workers for recognizing that the superfluidity need not be only associated with condensation of long lived bosons, but in fact could also derive, as in BCS, from fermion pairs. In this way, it was argued that a suitable tuning of the attractive interaction via Feshbach resonance effects would lead to a realization of a BCS-BEC crossover.

By late 2003 to early 2004, four groups [59, 80, 193, 16] had observed the "condensation of weakly bound molecules" (that is, on the $a_s > 0$ side of resonance), and shortly thereafter a number had also reported evidence for superfluidity on the BCS side [147, 194, 87, 34]. The BEC side is the more straightforward since the presence of the superfluid is reflected in a bi-modal distribution in the density profile. This is shown in Fig. 24.17 from [59], and is conceptually similar to the behavior for condensed Bose atoms [41]. On the BEC side but near resonance, the estimated T_c is of the order of 500 nK, with condensate fractions varying from 20% or so, to nearly 100%. The condensate lifetimes are relatively long in the vicinity of resonance, and fall off rapidly as one goes deeper into the BEC. However, for $a_s < 0$ there is no clear expectation that the density profile will provide a signature of the superfluid phase.

These claims that superfluidity may have been achieved on the BCS side ($a_s < 0$) of resonance were viewed as particularly exciting. The atomic community, for the most part, felt the previous counterpart observations on the BEC side were expected and not significantly different from condensation in Bose atoms. The evidence for this new form of "fermionic superfluidity" rests on studies [147, 194] that perform fast sweeps from negative a_s to positive a_s across the resonance. The field sweeps allow, in principle, a pairwise projection of fermionic atoms (on the BCS side) onto molecules (on the BEC side). It is presumed that in this way one measures the momentum distribution of fermionic atom pairs. The existence of a condensate was thus inferred. Other experiments which sweep across the Feshbach resonance adiabatically, measure the size of the cloud after release [16] or within a trap [11]. Evidence for superfluidity on the BCS side, which does not rely on the sweep experiments, has also been deduced from collective excitations of a fermionic gas [87, 10]. Pairing gap measurements with radio frequency (RF) probes [34] have similarly been interpreted [89] as evidence for superfluidity, although it appears more likely that these experiments establish only the existence of fermionic pairs. Quite recently, evidence for a phase transition has been presented via thermodynamic measurements and accompanying theory [88]. The latter, like the theory [89] of RF experiments [34], is based on the formalism presented in this Review.

Precisely what goes on during the sweep is not entirely understood. It should be stressed again that where the scattering length changes sign is not particularly important to the N-body physics. *Thus starting on the "BCS side of resonance" and ending on the "BEC side of resonance" involves a very continuous sweep in which the physics is not qualitatively changed.* It has been speculated that for this sweep procedure to work a large percentage of the Cooper pair partners must be closer than the inter-atomic spacing. Others have alternatively viewed the sweep as having little to do with the large Cooper pairs of BCS superconductivity.

It is useful to establish the various pair sizes here. In the PG regime the normal state consists of a significant number of small (compared to BCS) pre-formed pairs. Below T_c, the condensate pair size is also small. Finally, there are excited pair states in the superfluid phase, with characteristic size ξ_{pg}. The Cooper pair size ξ as plotted in Fig. 24.18 was deduced from the condensate [144] at $T = 0$, but this can be shown to be rather similar to ξ_{pg}, corresponding to the size of excited pair states [28, 27] both above and below T_c. It seems plausible that during the sweep there is some rearrangement of excited states (both fermionic and bosonic) and condensate. In addition, all pairs (excited and condensate) contract in size. When, at the end of a sweep, they are sufficiently small, then they are more "visible". What appears to be essential, however, is that the sweep time scales are rapid enough so that the existence of a condensate at the initial starting point is a necessary and sufficient condition for observing a condensate at the end of a sweep.

24.2.7 T-Matrix-Based Approaches to BCS-BEC Crossover in the Absence of Feshbach Effects

In this subsection we introduce the concept of a T-matrix within the pairing channel. This is defined in Eq. (24.26) below and it represents an effectively screened interaction in which the appropriate polarizability (χ) is associated with the particle-particle rather than the particle-hole channel, as in the more conventional dielectric susceptibility. The T-matrix thus appears as an infinite series of two particle "ladder" diagrams.

Away from zero temperature, a variety of different many body approaches have been invoked to address the physics of BCS-BEC crossover. For the most part, these revolve around T-matrix schemes. Here one solves self consistently for the single fermion propagator (G) and the pair propagator (t). That one stops at this level without introducing higher order Green's functions (involving three, and four particles, etc) is believed to be adequate for addressing a leading

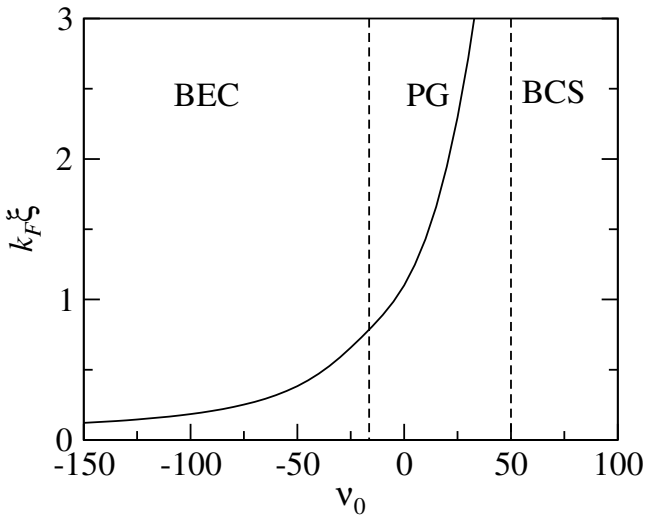


Figure 24.18: Characteristic behavior of Cooper pair size ξ in the condensate in the three regimes. The dotted vertical lines are not sharp transitions but indicate where $\mu = 0$ (left line) and where $\Delta(T_c) \approx 0$ (right line). The dimensionless $k_F\xi$ gives the ratio between pair size ξ and the mean inter-particle spacing $1/k_F$. Pairs shrink and become tightly bound in the deep BEC regime.

order mean field theory such as that represented by Eq. (24.1). One can see that pair-pair (boson-boson) interactions are only treated in a mean field averaging procedure; they arise exclusively from the fermions and are presumed to be sufficiently weak so as not to lead to any incomplete condensation in the ground state, as is compatible with Eq. (24.1).

One can view this approach as the first step beyond BCS in a hierarchy of mean field theories. In BCS, above T_c one includes only the bare fermion propagator G_0. Below T_c, pairs play a role but only through the condensate. At the next level one accounts for the interaction between particles and noncondensed pairs in both the normal and superconducting states. The pairs introduce a self energy Σ into the particles, which represents a correction to BCS theory. The pairs are treated at an effective mean field level. By truncating the equations of motion in this way, the effects of all higher order Green's functions are subsumed into t in an averaged way.

Below we demonstrate that at this T-matrix level there are a number of distinct schemes which can be implemented to address BCS-BEC crossover physics. These same alternatives have also entered into a discussion of pre-formed pairs as they appear in treatments of superconducting fluctuations. Above T_c, quite generally one writes for the T-matrix

$$t(Q) = \frac{U}{1 + U\chi(Q)} \tag{24.26}$$

and theories differ only on what is the nature of the pair susceptibility $\chi(Q)$, and the associated self energy of the fermions. Here and throughout we use Q to denote a four-vector and write $\sum_Q \equiv T\sum_{i\Omega_n}\sum_{\mathbf{q}}$, where Ω_n is a Matsubara frequency. Below T_c one can also consider a T-matrix approach to describe the particles and pairs in the condensate. For the most part we will defer extensions to the broken symmetry phase to Section 24.3.2.

Review of BCS Theory Using the T-matrix Approach

In order to assess alternative schemes, it is useful to review BCS theory within a T-matrix formalism. In BCS theory, pairs explicitly enter into the problem below T_c, but only through

the condensate. These condensed pairs are associated with a T-matrix given by

$$t_{sc}(Q) = -\Delta_{sc}^2 \delta(Q)/T \tag{24.27}$$

with fermionic self energy

$$\Sigma_{sc}(K) = \sum_Q t_{sc}(Q) G_0(Q-K) \tag{24.28}$$

so that $\Sigma_{sc}(K) = -\Delta_{sc}^2 G_0(-K)$. Here, and throughout, G_0 is the Green's function of the non-interacting system. The number of fermions in a BCS superconductor is given by

$$n = 2\sum_K G(K) \tag{24.29}$$

and

$$G(K) = [G_0^{-1}(K) - \Sigma_{sc}(K)]^{-1} \tag{24.30}$$

Doing the Matsubara summation in Eq. (24.29), one can then deduce the usual BCS expression for the number of particles, which determines the fermionic chemical potential

$$n = \sum_{\mathbf{k}} \left[1 - \frac{\epsilon_{\mathbf{k}} - \mu}{E_{\mathbf{k}}} + 2\frac{\epsilon_{\mathbf{k}} - \mu}{E_{\mathbf{k}}} f(E_{\mathbf{k}}) \right] \tag{24.31}$$

where

$$E_{\mathbf{k}} = \sqrt{(\epsilon_{\mathbf{k}} - \mu)^2 + \Delta_{sc}^2(T)} \tag{24.32}$$

We need, however, an additional equation to determine $\Delta_{sc}(T)$. The BCS gap equation can be written as

$$1 + U\chi_{BCS}(0) = 0, \quad T \leq T_c \tag{24.33}$$

where

$$\chi_{BCS}(Q) = \sum_K G(K) G_0(Q-K) \tag{24.34}$$

This suggests that one consider the uncondensed or normal state pair propagator to be of the form

$$t(Q) = \frac{U}{1 + U\chi_{BCS}(Q)} \tag{24.35}$$

then in the superconducting state we have a BEC like condition on the pair chemical potential μ_{pair} defined by

$$t^{-1}(Q=0) = \mu_{pair} \times const. \tag{24.36}$$

where the overall constant is unimportant for the present purposes. Thus we say that the pair chemical potential satisfies

$$\mu_{pair} = 0, \qquad T \leq T_c \, . \tag{24.37}$$

That μ_{pair} vanishes at *all* $T \leq T_c$ is a stronger condition than the usual Thouless condition for T_c. Moreover, it should be stressed that *BCS theory is associated with a particular asymmetric form for the pair susceptibility.* These uncondensed pairs play virtually no role in BCS superconductors but the structure of this theory points to a particular choice for a pair susceptibility. We can then write the self consistent condition on Δ_{sc} which follows from Eq. (24.33). Using Eqs. (24.27- 24.34), we find the expected form for the BCS gap equation. This represents a constraint on the order parameter Δ_{sc}:

$$\Delta_{sc}(T) = -U\sum_{\mathbf{k}} \Delta_{sc}(T) \frac{1 - 2f(E_{\mathbf{k}})}{2E_{\mathbf{k}}} \, . \tag{24.38}$$

The above discussion was presented in a somewhat different way in a paper by Kadanoff and Martin [82].

Three Choices for the T-matrix of the Normal State: Problems with the Noziéres Schmitt-Rink Approach

On general grounds we can say that there are three obvious choices for $\chi(Q)$ which appears in the general definition of the T-matrix in Eq. (24.26). Each of these has been studied rather extensively in the literature. All of these introduce corrections to BCS theory and all were motivated by attempts to extend the crossover ground state to finite T, or to understand widespread pseudogap effects in the high T_c superconductors. In analogy with Gaussian fluctuations, one can consider

$$\chi_0(Q) = \sum_K G_0(K)G_0(Q-K) \tag{24.39}$$

with self energy

$$\Sigma_0(K) = \sum_Q t(Q)G_0(Q-K) \tag{24.40}$$

which appears in G in the analogue of Eq. (24.30). The number equation is then deduced by using Eq. (24.29).

This scheme was adopted by Noziéres and Schmitt-Rink (NSR), although these authors [128, 144] approximated the number equation [155] by using a leading order series for G in Eq. (24.30) with

$$G = G_0 + \ G_0\Sigma_0 G_0 \ . \tag{24.41}$$

It is straightforward, however, to avoid this approximation in Dyson's equation, and a number of groups [78, 139] have extended NSR in this way.

Similarly one can consider

$$\bar{\chi}(Q) = \sum_K G(K)G(Q-K) \tag{24.42}$$

with self energy

$$\bar{\Sigma}(K) = \sum_Q t(Q)G(Q-K) \ . \tag{24.43}$$

This latter scheme (sometimes known as fluctuation-exchange or FLEX) has been also extensively discussed in the literature, by among others, Haussmann [63], Tchernyshyov [171], Micnas and colleagues [119] and Yamada and Yanatse [189].

Finally, we can contemplate the asymmetric form [28, 58] for the T-matrix, so that the coupled equations for $t(Q)$ and $G(K)$ are based on

$$\chi(Q) = \sum_K G(K)G_0(Q-K) \tag{24.44}$$

with self energy

$$\Sigma(K) = \sum_Q t(Q)G_0(Q-K) \tag{24.45}$$

Each of these three schemes determines the superfluid transition temperature via the Thouless condition. Thus $\mu_{pair} = 0$ leads to a slightly different expression for T_c, based on the differences in the choice of T-matrix which appears in Eq. (24.36).

A central problem with the NSR scheme ($\chi \approx G_0G_0$) is that it incorporates self energy effects only through the number equation. The absence of self energy effects in the gap equation is equivalent to the statement that pseudogap effects only indirectly affect T_c: the particles acquire a self energy from the pairs but these self energy effects are not fed back into the propagator for the pairs. On physical grounds one anticipates that the pseudogap must have a direct effect on T_c as a consequence of the associated reduction in the density of states. Other problems related

to the thermodynamics were pointed out [159] when NSR was applied to a two dimensional system. Finally, because only the number equation contains self energy effects, it is not clear if one can arrive at a proper vanishing of the superfluid density ρ_s at T_c within this approach. This requires a precise cancellation between the diamagnetic current contributions (which depend on the number equation) and the paramagnetic terms (which reflect the gap equation).

One might be inclined, then, to prefer [155] the FLEX ($\chi \approx GG$) scheme since it is ϕ-derivable, in the sense of Baym [12]. This means that it is possible to write down a closed form expression for the thermodynamical potential, from which one derives other physical quantities via functional derivatives of this potential. Theoretical consistency issues in this approach have been rather exhaustively discussed by Haussmann [63] above T_c. We are not aware of a fully self consistent calculation of ρ_s below T_c, at the same level of completeness as Haussmann's normal state analysis (or, for that matter, of the counterpart discussion to Section 24.4.1 and accompanying Appendix 24.9). However, in principle, it should be possible to arrive at a proper expression for the superfluid density, providing Ward identities are imposed. There is some ambiguity [14, 171, 119] about whether pseudogap effects are present in the FLEX approach; a consensus has not been reached at this time. Numerical work based on FLEX is more extensive [43, 14] than for the other two alternative schemes.

It will be made clear in what follows that, if one's goal is to extend the usual crossover ground state of Eq. (24.1) to finite temperatures, then one must choose the asymmetric form for the pair susceptibility. Here $\chi \approx GG_0$. This is different from the approach of Noziéres and Schmitt-Rink in which there is no evident consistency between their finite T treatment and the presumed ground state. Some have claimed [144] that an NSR-based approach, when extended below T_c, reproduces Eqs. (24.69) and (24.70). But elsewhere in the literature it has been shown that these ground state self consistency conditions are derived from a lower level theory [95]. They arise from a $T = 0$ limit of what is called the saddle point approximation, or mean field approach. When pairing fluctuations beyond the saddle point [128] are included, the number equation is changed. Then the ground state is no longer that of Eq. (24.1) [139]. In the cold atom literature, the distinction between the NSR-extrapolated ground state and the ground state of Eq. (24.1) has been pointed out in the context of atomic density profiles [137] within traps.

It should be evident from Eq. (24.34) and the surrounding discussion that the asymmetric form is uniquely associated with the BCS-like behavior implicit in Eq. (24.1). The other two T-matrix approaches lead to different ground states which should, however, be very interesting in their own right. These will need to be characterized in future.

Additional support for the asymmetric form, which will be advocated here, was provided by Kadanoff and Martin. In their famous paper they noted that several people had surmised that the form for $\chi(Q)$ involving GG would be more accurate. However, as claimed in [82], "This surmise is not correct." Aside from theoretical counter-arguments which they present, the more symmetric combination of Green's functions "can also be rejected experimentally since they give rise to a T^2 specific heat." Similar arguments in support of the asymmetric form were introduced [62] into the literature in the context of addressing specific heat jumps.

24.2.8 Superconducting Fluctuations: a type of Pre-formed Pairs

While there are no indications of bosonic degrees of freedom, (other than in the condensate), within strict BCS theory, it has been possible to access these bosons via probes of superconducting fluctuations. Quasi-one dimensional, or quasi-2D superconductors in the presence of significant disorder exhibit fluctuation effects [103] or precursor pairing as seen in "paraconductivity", fluctuation diamagnetism, as well as other unusual behavior, often consisting of divergent contributions to transport. One frequently computes [100] these bosonic contribu-

tions to transport by use of a time dependent Ginzburg-Landau (TDGL) equation of motion. This is rather similar to a Gross-Pitaevskii (GP) formalism except that the "bosons" here are highly damped by the fermions.

Alternatively T-matrix based approaches (involving all three choices of $\chi(Q)$) have been extensively used to discuss conventional superconducting fluctuations. The advantage of these latter schemes is that one can address both the anomalous bosonic and fermionic contributions to transport through the famous Aslamazov-Larkin and Maki-Thompson diagrams [103]. We defer a discussion of these issues until Appendix 24.9.

It is useful to demonstrate first how conventional superconducting fluctuations behave at the lowest level of self consistency, called the Hartree approximation. This scheme is closely associated[162] with a GG_0 T-matrix, as is discussed in more detail in Appendix 24.10. It is also closely associated with BCS theory, for one can show that, in the spirit of Eq. (24.1), at this Hartree level the excitation gap $\Delta(T_c)$ and T_c lie on a specific BCS curve (specified by n and U). What is different from strict BCS theory is that the onset of superconductivity takes place in the presence of a finite excitation gap (ie, pseudogap), just as shown in Fig. 24.3. This, then, reflects the fact that there are pre-formed pairs at T_c. By contrast with high T_c superconductors, however, in conventional fluctuation effects, the temperature T^* at which pairs start to form is always extremely close to their condensation temperature T_c. We thus say that there is a very narrow critical region.

In Hartree approximated Ginzburg Landau theory [62] the free energy functional is given by

$$F[\Psi] = a_0(T - T^*)|\Psi|^2 + b|\Psi|^4 \approx a_0(T - T^*)|\Psi|^2 + 2b\Delta^2|\Psi|^2 \tag{24.46}$$

Here Δ^2 plays the role of a pseudogap in the normal state. It is responsible for a lowering of T_c relative to the mean field value T^*. Collecting the quadratic terms in the above equation, it follows that

$$T_c = T^* - \frac{2b}{a_0}\Delta^2(T_c) \; . \tag{24.47}$$

Moreover, self consistency imposes a constraint on the magnitude of $\Delta(T_c)$ via

$$\Delta^2(T) = \int D\Psi e^{-\beta F[\Psi]}\Psi^2 \Big/ \int D\Psi e^{-\beta F[\Psi]} \; . \tag{24.48}$$

It should be noted that Eq. (24.47) is consistent with the statement that $\Delta(T_c)$ and T_c lie on the BCS curve, since for small separation between T_c and T^*, this curve is, below T_c, defined by

$$\Delta^2_{BCS}(T) \approx \frac{a_0}{2b}(T^* - T) \; . \tag{24.49}$$

The primary effect of fluctuations at the Hartree level is that pairing takes place in the presence of a finite excitation gap, reflecting the presence of very short lived, but pre-formed pairs. It should be clear that Δ is not to be confused with the superconducting order parameter Δ_{sc}, as should be evident from Fig. 24.3. We refer the reader to a more detailed discussion which is presented in Appendix 24.10.

Figure 24.19 illustrates how this pseudogap appears experimentally, via a plot of the normalized density of states [37] $\nu_1 \equiv N(E)$ in the normal state. This figure derives from tunneling measurements on Al-based films. Note the depression of $N(E_F)$ at low energies. This is among the first indications for a pseudogap reported in the literature.

Alternatively, fluctuations have also been discussed at the Gaussian (G_0G_0) level in which there is no need for self consistency, in contrast to the above picture. Here because the calculations are so much more tractable there have been very detailed applications [103] of essentially all transport and thermodynamic measurements. This Gaussian analysis led to unexpected

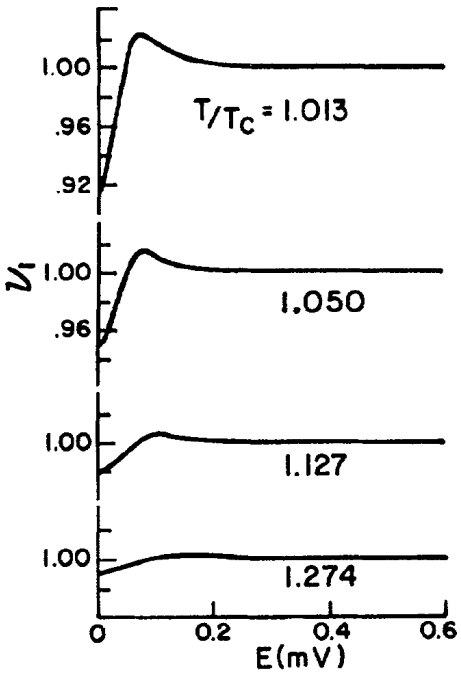


Figure 24.19: Pseudogap in the density of states above T_c in conventional superconductors, from [37]. $\nu_1 \equiv N(E)$ is the normalized density of states.

divergences in the para-conductivity from the so-called Maki-Thompson term which then provided a motivation to go beyond leading order theory. Patton [134, 133] showed how this divergence could be removed within a more self consistent GG_0 scheme, equivalent to self consistent Hartree theory. Others argued [154, 177] that Hartree-Fock (GG) was more appropriate, although in this weak coupling, narrow fluctuation regime, the differences between these latter two schemes are only associated with factors of 2. Nevertheless with this factor of 2, $\Delta(T_c)$ and T_c are no longer on the BCS curve. It should be noted that a consensus was never fully reached [62] by the community on this point.

Dynamics of Pre-formed Pairs Above T_c: Time Dependent Ginzburg-Landau Theory

We turn again to Fig. 24.5 which provides a useful starting point for addressing bosonic degrees of freedom and their implications for experiment. It is clear that transport in the unusual normal state, associated with the pseudogap (PG) phase (as well as thermodynamics) contains contributions from both fermionic and bosonic excitations. The bosons are not infinitely long lived; their lifetime is governed by their interactions with the fermions. In some instances [103], the bosonic contributions to transport become dominant or even singular at T_c. Under these circumstances one can ignore the fermionic contributions except insofar as they lead to a lifetime for the pairs.

To address the transport properties of these more well established pre-formed pairs, one appeals to a standard way of characterizing the dynamics of bosons – a phenomenological scheme known as time dependent Ginsburg- Landau (TDGL) theory. This theory has some microscopic foundations in diagrammatic T-matrix approaches in which one considers only the Aslamazov-Larkin terms (which are introduced in Appendix 24.9). At the Gaussian level both TDGL and the T-matrix approaches are tractable. At the Hartree level things rapidly become more complicated, and it is far easier to approach the problem [170] by adopting a strictly phenomenological TDGL.

The generic Hartree-TDGL equation of motion for classical charged bosons interacting with

electromagnetic fields $(\phi, \mathbf{A})$ is given by

$$\gamma\left(i\frac{\partial}{\partial t} - e^*\phi(\mathbf{x},t)\right)\psi(\mathbf{x},t) = \frac{\left(-i\nabla - e^*\mathbf{A}(\mathbf{x},t)\right)^2}{2M^*}\psi(\mathbf{x},t) - \mu_{pair}(T)\psi(\mathbf{x},t) + D(\mathbf{x},t), \quad (24.50)$$

Here $\psi(\mathbf{x},t)$ is a classical field variable representing the bosons which have vanishing chemical potential μ_{pair} at T_c. The function $D(\mathbf{x},t)$ introduces a noise variable into the equation of motion. Generally γ is complex.

We will explore the implications of this equation in our more quantitative discussion of Section 24.7.5.

24.3 Quantitative Details of Crossover

24.3.1 $T = 0$, BEC Limit without Feshbach Bosons

We begin by reviewing $T = 0$ crossover theory in the BEC limit. Our starting point is the ground state wavefunction Ψ_0 of Eq. (24.1), along with the self consistency conditions of Eq. (24.2). For positive chemical potential μ, the quantity $\Delta_{sc}(0)$ also corresponds to the energy gap for fermionic excitations. In the ground state the two energy scales $\Delta(0)$ and $\Delta_{sc}(0)$ are degenerate, just as they are (at all temperatures) in strict BCS theory.

It is convenient to rewrite these equations [34] in terms of the inter-fermion scattering length a_s

$$\frac{m}{4\pi a_s} = \sum_{\mathbf{k}}\left[\frac{1}{2\epsilon_{\mathbf{k}}} - \frac{1}{2E_{\mathbf{k}}}\right], \quad (24.51)$$

$$n = \sum_{\mathbf{k}}\left[1 - \frac{\epsilon_{\mathbf{k}} - \mu}{E_{\mathbf{k}}}\right], \quad T = 0\,. \quad (24.52)$$

In the fermionic regime ($\mu > 0$) these equations are essentially equivalent to those of BCS theory, although at weak coupling appropriate to strict BCS, little attention is paid to the number equation since $\mu = E_F$ is always satisfied. The more interesting regime corresponds to $\mu \leq 0$ where these equations take on a new interpretation. Deep inside the BEC regime it can be seen that

$$n = \Delta_{sc}^2(0)\frac{m^2}{4\pi\sqrt{2m|\mu|}}, \quad (24.53)$$

which, in conjunction with Eq. (24.51) (expanded in powers of $\Delta_{sc}^2(0)/\mu^2$):

$$\frac{m}{4\pi a_s} = (2m)^{3/2}\frac{\sqrt{|\mu|}}{8\pi}\left[1 + \frac{1}{16}\frac{\Delta_{sc}^2(0)}{\mu^2}\right], \quad (24.54)$$

yields

$$\mu = -\frac{1}{2ma_s^2} + \frac{a_s\pi n}{m}. \quad (24.55)$$

[34] To make the equations simpler, in much of what we present in this review we will consider a contact potential interaction. The momentum sums are assumed to run to infinity. More generally, one can include a cutoff function $\varphi_{\mathbf{k}}$ for the momentum integrals. The gap function thus becomes $\Delta_{\mathbf{k}} = \Delta\varphi_{\mathbf{k}}$. For the cuprate d-wave cuprate superconductors, $\varphi_{\mathbf{k}} = \cos k_x a - \cos k_y a$. For our numerical work on atomic gases we use a Gaussian cutoff $\varphi_{\mathbf{k}}^2 = e^{-k^2/k_0^2}$ with k_0 taken to be as large as is numerically feasible.

This last equation is equivalent [182, 136] to its counterpart in Gross-Pitaevskii theory. This theory describes true bosons, and is associated with the well known equation of state

$$n_{pairs} = \frac{m_B}{4\pi a_B}\mu_B \, . \tag{24.56}$$

To see the equivalence we associate the number of bosons $n_{pairs} = n/2$, the boson mass $m_B = 2m$ and the bosonic scattering length $a_B = 2a_s$. Here the bosonic chemical potential $\mu_B = 2\mu + \epsilon_0$ and we define $\epsilon_0 = 1/(2ma_s^2)$. This factor of 2 in a_B/a_s has received a fair amount of attention in the literature. Although it will be discussed later in the Review, it should be noted now that this particular numerical value is particular to the one channel description[161], and different from what is observed experimentally [138].

Despite these similarities with GP theory, the fundamental parameters are the fermionic $\Delta_{sc}(0)$ and chemical potential μ. It can be shown that in this deep BEC regime the number of pairs is directly proportional to the superconducting order parameter

$$n_{pairs} = \frac{n}{2} = Z_0 \Delta_{sc}^2(0) \tag{24.57}$$

where

$$Z_0 \approx \frac{m^2 a_s}{8\pi} \, . \tag{24.58}$$

One may note from Eq. (24.57) that the "gap equation" now corresponds to a number equation (for bosons). Similarly the number equation, or constraint on the fermionic chemical potential defines the excitation gap for fermions, once the chemical potential is negative. In this way the roles of the two constraints are inverted [144] relative to the BCS regime.

That a Gross-Pitaevskii approach captures the leading order physics at $T = 0$ can also be simply seen by rewriting the ground state wavefunction, as pointed out by Randeria [144]. Define $v_{\mathbf{k}}/u_{\mathbf{k}} \equiv \eta_{\mathbf{k}}$

$$\begin{aligned} \Psi_0 &= const \times \Pi_k (1 + \eta_{\mathbf{k}} c_k^\dagger c_{-k}^\dagger)|0\rangle \\ &= const \times \exp\left(\sum_k \eta_{\mathbf{k}} c_k^\dagger c_{-k}^\dagger\right)|0\rangle \, . \end{aligned} \tag{24.59}$$

Projecting onto a state with fixed particle number N yields

$$\Psi_0 = const \times \left(\sum_{\mathbf{k}} \eta_{\mathbf{k}} c_k^\dagger c_{-k}^\dagger\right)^{N/2} |0\rangle \, . \tag{24.60}$$

This is a GP wavefunction of composite bosons with the important proviso: that the characteristic size associated with the internal wavefunction $\eta_{\mathbf{k}}$ is smaller than the inter-particle spacing. It should be stressed that, except in the BEC asymptotic limit, (where the "bosons" are non-interacting) there are essential differences between Eq. (24.60) and the Gross-Pitaevskii wavefunction. Away from this extreme limit, pair-pair interactions (arising indirectly via the fermions and the Pauli principle), as well as the finite size of the pairs, will differentiate this system from that of true interacting bosons. This same issue arises more concretely in the context of the collective mode spectrum of ultracold gases, as discussed in Section 24.6.3.

24.3.2 Extending conventional Crossover Ground State to $T \neq 0$: BEC limit without Feshbach Bosons

How do we extend [28] this picture to finite T? In the BEC limit, as shown in Fig. 24.4, fermion pairs are well established or "pre-formed" within the entire range of superconducting

temperatures. The fundamental constraint associated with the BEC regime is that: *for all $T \leq T_c$, there should, thus, be no temperature dependence in fermionic energy scales. In this way Eqs. (24.51) and (24.52) must be imposed at all temperatures T.*

$$\frac{m}{4\pi a_s} = \sum_{\mathbf{k}} \left[\frac{1}{2\epsilon_{\mathbf{k}}} - \frac{1}{2E_{\mathbf{k}}} \right], \tag{24.61}$$

$$n = \sum_{\mathbf{k}} \left[1 - \frac{\epsilon_{\mathbf{k}} - \mu}{E_{\mathbf{k}}} \right], \quad T \leq T_c \,. \tag{24.62}$$

It follows that the number of pairs at $T = 0$ should be equal to the number of pairs at $T = T_c$. However, all pairs are condensed at $T = 0$. Clearly, the character of these pairs changes so that at T_c, all pairs are noncondensed. To implement these physical constraints (and to anticipate the results of a more microscopic theory) we write

$$n_{pairs} = \frac{n}{2} = Z_0 \Delta^2 \tag{24.63}$$

$$n_{pairs} = n_{pairs}^{condensed}(T) + n_{pairs}^{noncondensed}(T) \tag{24.64}$$

so that we may decompose the excitation gap into two contributions

$$\Delta^2 = \Delta_{sc}^2(T) + \Delta_{pg}^2(T) \tag{24.65}$$

where $\Delta_{sc}(T)$ corresponds to condensed and $\Delta_{pg}(T)$ to the noncondensed gap component. Each of these are proportional to the respective number of condensed and noncondensed pairs with proportionality constant Z_0. At T_c,

$$n_{pairs}^{noncondensed} = \frac{n}{2} = \sum_{\mathbf{q}} b(\Omega_q, T_c) \,, \tag{24.66}$$

where $b(x)$ is the usual Bose-Einstein function and Ω_q is the unknown dispersion of the noncondensed pairs. Thus

$$\Delta_{pg}^2(T_c) = Z_0^{-1} \sum b(\Omega_q, T_c) = \frac{n}{2} Z_0^{-1} \,. \tag{24.67}$$

We may deduce directly from Eq. (24.67) that $\Delta_{pg}^2 = -\sum_Q t(Q)$, if we presume that below T_c, the noncondensed pairs have propagator

$$t(Q) = \frac{Z_0^{-1}}{\Omega - \Omega_q} \,. \tag{24.68}$$

It is important to stress that the dispersion of the pairs Ω_q cannot be put in by hand. It is not known a priori. Rather, it has be to *derived* according to the constraints imposed by Eqs. (24.61) and (24.62). We can only arrive at an evaluation of Ω_q after establishing the nature of the appropriate T-matrix theory. In what follows we derive this dispersion using the two channel model. We state the one channel results here for completeness. In the absence of FB, $\Omega_q \equiv B_0 q^2$, where $B_0 \equiv 1/(2M_0^*)$. As a consequence of a "bosonic" self energy, which arises from fermion-boson (as distinguished from boson-boson) interactions, the bosonic dispersion is found to be quadratic. This quadratic dependence persists for the two channel case as well.

24.3.3 Extending Conventional Crossover Ground State to $T \neq 0$: T-matrix Scheme in the Presence of Feshbach Bosons

To arrive at the pair dispersion for the noncondensed pairs, Ω_q, we need to formulate a generalized T-matrix based scheme which is consistent with the ground state conditions, and

with the T dependence of strict BCS theory. It is useful from a pedagogical point to now include the effects of Feshbach bosons [164]. Our intuition concerning how true bosons condense is much better than our intuition concerning the condensation of fermion pairs, except in the very limited BCS regime. We may assume that Δ and μ evolve with temperature in such a way as to be compatible *with both the temperature dependences of BCS and with the above discussion for the BEC limit.* We thus take

$$\Delta(T) = -U_{eff} \sum_{\mathbf{k}} \Delta(T) \frac{1 - 2f(E_{\mathbf{k}})}{2E_{\mathbf{k}}}, \tag{24.69}$$

$$n = \sum_{\mathbf{k}} \left[1 - \frac{\epsilon_{\mathbf{k}} - \mu}{E_{\mathbf{k}}} + 2\frac{\epsilon_{\mathbf{k}} - \mu}{E_{\mathbf{k}}} f(E_{\mathbf{k}}) \right], \tag{24.70}$$

where $E_{\mathbf{k}} = \sqrt{(\epsilon_{\mathbf{k}} - \mu)^2 + \Delta^2(T)}$. Note that in the presence of Feshbach bosons, we use n to denote the density of fermionic atoms which is to be distinguished from the constituents of the Feshbach bosons. The total density of particles will be denoted by n^{tot}. *Equations (24.69) and (24.70) will play a central role in this review. They have been frequently invoked in the literature, albeit under the presumption that there is no distinction between $\Delta(T)$ and $\Delta_{sc}(T)$.*

Alternatively one can rewrite Eq. (24.69) as

$$\frac{m}{4\pi a_s^*} = \sum_{\mathbf{k}} \left[\frac{1}{2\epsilon_{\mathbf{k}}} - \frac{1 - 2f(E_{\mathbf{k}})}{2E_{\mathbf{k}}} \right]. \tag{24.71}$$

Clearly Eqs. (24.69) and (24.70) are consistent with Eqs. (24.61) and (24.62) since Fermi functions are effectively zero in the BEC limit. Our task is to find a T-matrix formalism which is compatible with Eqs. (24.69) and (24.70), and to do this we focus first on the *noncondensed* molecular bosons. Their propagator may be written as

$$D(Q) \equiv \frac{1}{i\Omega_n - \epsilon_q^{mb} - \nu + 2\mu - \Sigma_B(Q)}. \tag{24.72}$$

We presume that the self energy of these molecules can be written in the form

$$\Sigma_B(Q) \equiv -g^2 \chi(Q) / [1 + U\chi(Q)], \tag{24.73}$$

where $\chi(Q)$ is as yet unspecified. This RPA-like self energy arises from interactions between the molecular bosons and the fermion pairs, and this particular form is required for self-consistency.

noncondensed bosons in equilibrium with a condensate must necessarily have zero chemical potential.

$$\mu_{boson}(T) = 0, \qquad T \leq T_c. \tag{24.74}$$

This is equivalent to the Hugenholtz-Pines condition that

$$D^{-1}(0) = 0, \quad T \leq T_c. \tag{24.75}$$

Using Eqs. (24.73) and (24.75) it can be seen that

$$U_{eff}^{-1}(0) + \chi(0) = 0, \qquad T \leq T_c. \tag{24.76}$$

This equation can be made compatible with our fundamental constraint in Eq. (24.69) provided we take

$$\chi(Q) = \sum_K G(K) G_0(Q - K), \tag{24.77}$$

where $G(K)$

$$G(K) \equiv [G_0^{-1}(K) - \Sigma(K)]^{-1} \tag{24.78}$$

includes a self energy given by the BCS-form

$$\Sigma(K) = -G_0(-K)\Delta^2\,, \tag{24.79}$$

which now involves the quantity Δ to be distinguished from the order parameter Δ_{sc}. Note that with this form for $\Sigma(K)$, the number of fermions is indeed given by Eq. (24.70).

More generally, we may write the constraint on the total number of particles as follows. The number of noncondensed molecular bosons is given directly by

$$n_b(T) = -\sum_Q D(Q)\,. \tag{24.80}$$

For $T \leq T_c$, the number of fermions is given via Eq. (24.70). The *total* number (n^{tot}) of particles is then

$$n + 2n_b + 2n_b^0 = n^{tot}\,, \tag{24.81}$$

where $n_b^0 = \phi_m^2$ is the number of molecular bosons in the condensate, and ϕ_m is the order parameter for the molecular condensate.

Thus far, we have shown that the condition that noncondensed molecular bosons have zero chemical potential, can be made consistent with Eqs. (24.69) and (24.70) provided we constrain $\chi(Q)$ and $\Sigma(K)$ as above. We now want to examine the counterpart condition on the fermions and their condensate contribution. The analysis leading up to this point should make it clear *that we have both condensed and noncondensed fermion pairs, just as we have both condensed and noncondensed molecular bosons.* Moreover, these fermion pairs and Feshbach bosons are strongly admixed, except in the very extreme BCS and BEC limits. Because of noncondensed pairs, we will see that the excitation gap is distinct from the superconducting order parameter, although in the literature this distinction has not been widely recognized.

Just as the noncondensed molecular bosons have zero chemical potential below T_c we have the same constraint on the noncondensed fermion pairs which are in chemical equilibrium with the noncondensed bosons

$$\mu_{pair} = 0, \qquad T \leq T_c\,. \tag{24.82}$$

The T-matrix scheme in the presence of the Feshbach bosons is shown in Fig. 24.20. Quite generally, the T-matrix consists of two contributions: from the condensed (sc) and noncondensed or "pseudogap"-associated (pg) pairs,

$$t = t_{pg} + t_{sc}\,, \tag{24.83}$$

$$t_{pg}(Q) = \frac{U_{eff}(Q)}{1 + U_{eff}(Q)\chi(Q)}, \qquad Q \neq 0\,, \tag{24.84}$$

$$t_{sc}(Q) = -\frac{\tilde{\Delta}_{sc}^2}{T}\delta(Q)\,, \tag{24.85}$$

where we write $\tilde{\Delta}_{sc} = \Delta_{sc} - g\phi_m$, with $\Delta_{sc} = -U\sum_{\mathbf{k}}\langle a_{-\mathbf{k}\downarrow}a_{\mathbf{k}\uparrow}\rangle$ and $\phi_m = \langle b_{\mathbf{q}=0}\rangle$. Here, the order parameter is a linear combination of both paired fermions and condensed molecules. Similarly, we have two contributions for the fermion self energy

$$\Sigma(K) = \Sigma_{sc}(K) + \Sigma_{pg}(K) = \sum_Q t(Q)G_0(Q-K)\,, \tag{24.86}$$

where, as in BCS theory,

$$\Sigma_{sc}(K) = \sum_Q t_{sc}(Q)G_0(Q-K)\,. \tag{24.87}$$

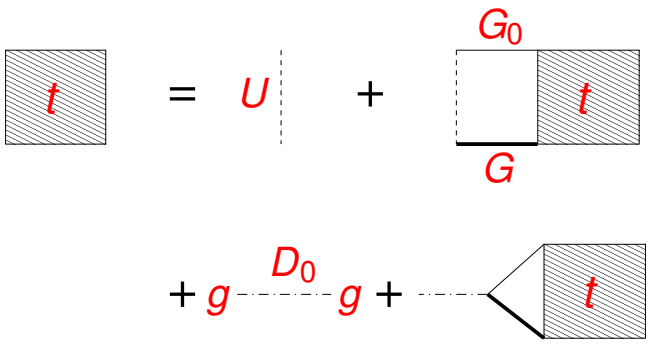


Figure 24.20: Diagrammatic scheme for present T-matrix theory. Here U is the open-channel interaction, g is the coupling between open and closed channels. G_0, G and D_0 are bare fermion, full fermion, and bare Feshbach boson Green's functions, respectively. U and $g_0^2 D_0$ yield an effective pairing interaction, U_{eff}.

Without loss of generality, we choose order parameters $\tilde{\Delta}_{sc}$ and ϕ_m to be real and positive with $g < 0$. Importantly, these two components are connected [93] by the relation $\phi_m = g\Delta_{sc}/[(\nu - 2\mu)U]$.

The vanishing of the pair chemical potential implies that

$$t_{pg}^{-1}(0) = U_{eff}^{-1}(0) + \chi(0) = 0, \qquad T \leq T_c \, . \tag{24.88}$$

This same equation was derived from consideration of the bosonic chemical potential. Most importantly, we argued above that this was consistent with Eq. (24.69) provided the fermion self energy assumes the BCS form. We now verify the assumption in Eq. (24.79). A vanishing chemical potential means that $t_{pg}(Q)$ is strongly peaked around $Q = 0$. Thus, we may approximate [114] Eq. (24.86) to yield

$$\Sigma(K) \approx -G_0(-K)\Delta^2 \, , \tag{24.89}$$

where

$$\Delta^2(T) \equiv \tilde{\Delta}_{sc}^2(T) + \Delta_{pg}^2(T) \, , \tag{24.90}$$

and we define the pseudogap Δ_{pg}

$$\Delta_{pg}^2 \equiv -\sum_{Q \neq 0} t_{pg}(Q). \tag{24.91}$$

This bears a close resemblance to Eq. (24.80), if we write the number of noncondensed fermion pairs and molecular bosons as

$$n_p(T) = Z\Delta_{pg}^2(T) \, . \tag{24.92}$$

Note that in the normal state (where μ_{pair} is nonzero) one cannot make the approximation of Eq. (24.89). Referring back to our discussion of Hartree-approximated TDGL, a strong analogy between Eq. (24.91) and (24.48) should be observed. There is a similar analogy between Eq. (24.69) and (24.49); more details are provided in Appendix 24.10. We thus have that Eqs. (24.51) and (24.89) with Eq. (24.78) are alternative ways of writing Eqs. (24.69) and (24.70). Along with Eq. (24.91) we now have a closed set of equations for addressing the ordered phase. Moreover the propagator for noncondensed pairs can now be quantified, using the self consistently determined pair susceptibility. At moderately strong coupling and at small four-vector Q, we may expand to obtain

$$t_{pg}(Q) = \frac{Z^{-1}}{\Omega - \Omega_q + \mu_{pair} + i\Gamma_Q}, \tag{24.93}$$

Consequently, one can rewrite Eq. (24.91) as

$$\Delta_{pg}^2(T) = Z^{-1} \sum b(\Omega_q, T) \,. \tag{24.94}$$

Here we introduce a simple notation for the small Q expansions:

$$\begin{aligned} \chi(Q) - \chi(0) &= Z_0(i\Omega_n - B_0 q^2), \\ U_{eff}^{-1}(Q) - U_{eff}^{-1}(0) &= Z_g(i\Omega_n - B_g q^2) \end{aligned}$$

with

$$\begin{aligned} Z_0 &= \frac{1}{2\Delta^2}\left[n - 2\sum_{\mathbf{k}} f(\epsilon_{\mathbf{k}} - \mu)\right], \\ Z_g &= \frac{g^2}{[(2\mu - \nu)U + g^2]^2} \,. \end{aligned}$$

We have that $Z = Z_0 + Z_g$, $Z_b = (Z_0 + Z_g)/Z_0$, and the q^2 coefficient $B \equiv 1/(2M^*)$ in $\Omega_q \equiv Bq^2$ is such that

$$B = \frac{B_0 Z_0 + \frac{1}{2M} Z_g}{Z} \,.$$

The strong hybridization between the molecular bosons and fermion pairs should be stressed. Indeed, there is just one branch Ω_q for bosonic-like excitations, so that at small Q

$$D(Q) = \frac{Z_b^{-1}}{\Omega - \Omega_q + \mu_{boson} + i\Gamma_Q}, \tag{24.95}$$

where below T_c, $\mu_{pair} = \mu_{boson} = 0$. Here Γ_Q contains all the imaginary part of the inverse T-matrix and it vanishes rapidly as $Q \to 0$. As the coupling is decreased from the BEC limit towards BCS, the character of the pairs changes from pre-dominantly molecular-boson like to (noncondensed) Cooper pairs, composed only of the fermionic atoms.

24.3.4 Nature of the Pair Dispersion: Size and Lifetime of noncondensed Pairs Below T_c

We may rewrite the pair susceptibility [28, 29] of Eq. (24.77) (after performing the Matsubara sum and analytically continuing to the real axis) in a relatively simple form as

$$\begin{aligned} \chi(Q) = \sum_{\mathbf{k}} \Big[& \frac{1 - f(E_{\mathbf{k}}) - f(\xi_{\mathbf{k}-\mathbf{q}})}{E_{\mathbf{k}} + \xi_{\mathbf{k}-\mathbf{q}} - \Omega - i0^+} u_{\mathbf{k}}^2 \\ & - \frac{f(E_{\mathbf{k}}) - f(\xi_{\mathbf{k}-\mathbf{q}})}{E_{\mathbf{k}} - \xi_{\mathbf{k}-\mathbf{q}} + \Omega + i0^+} v_{\mathbf{k}}^2 \Big] \,, \end{aligned} \tag{24.96}$$

where $u_{\mathbf{k}}^2$ and $v_{\mathbf{k}}^2$ are given by their usual BCS expressions in terms of Δ and $\xi_{\mathbf{k}} \equiv \epsilon_{\mathbf{k}} - \mu$. In the long wavelength, low frequency limit, the inverse of t_{pg} can be written as

$$a_1\Omega^2 + Z_0(\Omega - \frac{q^2}{2M^*} + \mu_{pair} + i\Gamma_Q). \tag{24.97}$$

We are interested in the moderate and strong coupling cases, where we can drop the $a_1\Omega^2$ term in Eq. (24.97), and hence we have Eq. (24.93) with

$$\Omega_{\mathbf{q}} \equiv \frac{q^2}{2M^*} = \frac{q^2 \xi_{pg}^2}{Z_0} \,. \tag{24.98}$$

This establishes a quadratic dispersion and defines the effective pair mass, M^*. Analytical expressions for this mass are possible via a small $\mathbf{q}$ expansion of χ, in Eq. (24.96). It is important to note that the pair mass reflects the effective *size* ξ_{pg} of noncondensed pairs. This serves to emphasize the fact that the q^2 dispersion derives from the compositeness of the "bosons", in the sense of their finite spatial extent. A description of the system away from the BEC limit must accommodate the fact that the pairs have an underlying fermionic character. This pair mass has a different origin from the mass renormalization associated with real interacting bosons. There one finds a mass shift which comes from a Hartree approximate treatment of their q-dependent interactions. Finally, we note that ξ_{pg} is comparable to the size ξ of pairs in the condensate. In the weak coupling BCS limit, a small Q expansion of χ_0 shows that, because the leading order term in Ω is purely imaginary, the Ω^2 contribution cannot be neglected. The T-matrix, then, does not have the propagating q^2 dispersion, discussed above.

It follows from Eq. (24.96) that the pair lifetime

$$\begin{aligned}\Gamma_Q &= \frac{\pi}{Z_0}\sum_{\mathbf{k}}\left[1-f(E_{\mathbf{k}})-f(\xi_{\mathbf{k}-\mathbf{q}})\right]u_{\mathbf{k}}^2\delta(E_{\mathbf{k}}+\xi_{\mathbf{k}-\mathbf{q}}-\Omega)\\ &\quad+\left[f(E_{\mathbf{k}})-f(\xi_{\mathbf{k}-\mathbf{q}})\right]v_{\mathbf{k}}^2\delta(E_{\mathbf{k}}-\xi_{\mathbf{k}-\mathbf{q}}+\Omega)\,. \end{aligned} \tag{24.99}$$

Here Γ_Q reflects the rate of decay of noncondensed bosons into a bare and dressed fermion. Note that the excitation gap in $E_{\mathbf{k}}$ significantly restricts the contribution from the δ functions. Thus, *the decay rate of pair excitations is greatly suppressed, due to the excitation gap (for fermions) in the superconducting phase*. Even in the normal phase pairs live longer than one might have anticipated from "Pauli blocking" arguments which are based on evaluating Γ_Q in a Fermi liquid state. However, the same equations are not strictly valid above T_c, because Eq. (24.89) no longer holds. To compute the pair lifetime in the normal state requires a more extensive calculation involving the full T-matrix self consistent equations and their numerical solution [78, 114, 115].

24.3.5 T_c Calculations: Analytics and Numerics

Calculations of T_c can be performed using Eqs. (24.69) and (24.70) along with Eq. (24.91). The T-matrix is written in the expanded form of Eq. (24.93), which is based on the pair dispersion as derived in the previous section. For the most part the calculations proceed numerically.

A typical curve is plotted in Fig. 24.21, where the three regimes BCS, BEC and PG are indicated. For positive, but decreasing the magnetic detuning ν_0, T_c follows the BCS curve until the "pseudogap" or $\Delta(T_c)$ becomes appreciable. After its maximum (near the unitary limit, at slightly negative ν_0), T_c decreases, (as does μ), to reach a minimum at $\mu \approx 0$. This decrease in T_c reflects the decreasing number of low energy fermions due to the opening of a pseudogap. Beyond this point, towards negative ν_0, the system is effectively bosonic, and the superconductivity is no longer hampered by pseudogap effects. In the presence of FB, the condensate consists of two contributions, although the weight of the fermion pair component rapidly disappears. Similarly T_c rises, although slowly, towards the ideal BEC asymptote, following the inverse effective boson mass. The corresponding curve based on the NSR approach [128] has only one extremum, but nevertheless the overall magnitudes are not so different [131, 123].

Analytic results are obtainable in the near-BEC limit only. The general expression for the effective mass $1/M_0^*$ in this limit is given by

$$\frac{1}{M_0^*} = \frac{1}{Z_0\Delta^2}\sum_{\mathbf{k}}\left[\frac{1}{m}v_{\mathbf{k}}^2 - \frac{4E_{\mathbf{k}}k^2}{3m^2\Delta^2}v_{\mathbf{k}}^4\right], \tag{24.100}$$

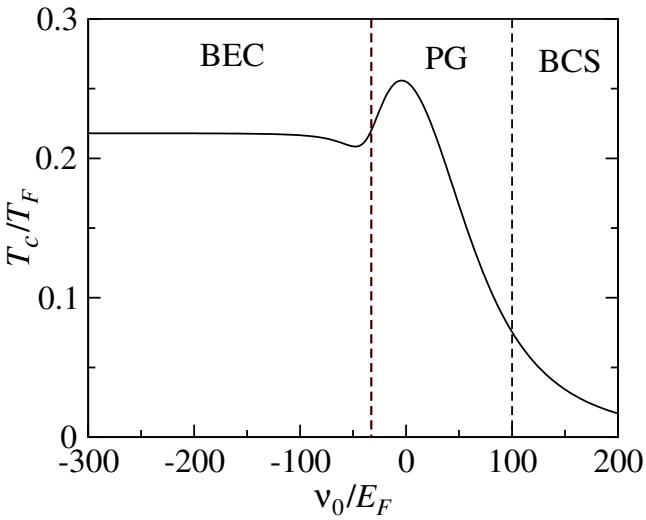


Figure 24.21: Typical behavior of T_c in the homogeneous case. For the purposes of illustration, this calculation includes Feshbach effects. T_c follows BCS for large magnetic detuning parameter ν_0 and approaches the BEC asymptote 0.218 for large negative ν_0. It reaches a maximum at unitarity, and has a minimum when the fermionic chemical potential μ changes sign.

where here FB effects have been dropped for simplicity. In what follows, we expand Eq. (24.100) in powers of na_s^3 and obtain after some algebra

$$M_0^* \approx 2m \left(1 + \frac{\pi a_s^3 n}{2}\right) . \tag{24.101}$$

We now invoke an important constraint, derived earlier in Eq. (24.66) which corresponds to the fact that at T_c all fermions are constituents of uncondensed pairs

$$\frac{n}{2} = \sum_{\mathbf{q}} b(\Omega_{\mathbf{q}}, T_c) . \tag{24.102}$$

From the above equation it follows that $(M^* T_c)^{3/2} \propto n = const.$ which, in conjunction with Eq. (24.101) implies

$$\frac{T_c - T_c^0}{T_c^0} = -\frac{\pi a_s^3 n}{2}. \tag{24.103}$$

Here T_c^0 is the transition temperature of the ideal Bose gas with $M_0 = 2m$. This downward shift of T_c follows the effective mass renormalization, much as expected in a Hartree treatment of GP theory at T_c. Here, however, in contrast to GP theory for a homogeneous system with a contact potential [41], there is a non-vanishing renormalization of the effective mass. This is a key point which underlines the importance in this approach of the fermionic degrees of freedom, even at very strong coupling.

24.4 Self Consistency Tests

All T-matrix approaches to the BCS-BEC crossover problem must be subject to self consistency tests. Among these, one should demonstrate that *normal state* self energy effects within a T-matrix scheme are not associated with superfluidity or superconductivity [96]. While this seems at first sight straightforward, all theories should be put to this test. Thus for a charged system, a meaningful result for the superfluid density ρ_s requires that there be an exact cancellation between diamagnetic and paramagnetic current contributions at T_c. In this way self

energy effects in the number equation and gap equation must be treated in a consistent fashion. In the following we address some of these self consistency issues in the context of the asymmetric ($\chi \approx GG_0$) BCS-BEC crossover scheme. Other crossover theories with different forms for the pair susceptibility should also be subjected to these tests. We begin with a summary of calculations [97, 162] of the Meissner effect, followed by a treatment of the collective mode spectrum. Our discussion in this section is presented for the one channel problem, in the absence of Feshbach effects.

24.4.1 Important check: behavior of ρ_s

The superfluid density may be expressed in terms of the local (static) electromagnetic response kernel $K(0)$

$$n_s = \frac{m}{e^2} K(0) = n - \frac{m}{3\,e^2} P_{\alpha\alpha}(0) \; , \tag{24.104}$$

with the current-current correlation function given by

$$\begin{aligned} P_{\alpha\beta}(Q) &= -2\,e^2 \sum_K \lambda_\alpha(K, K+Q)\, G(K+Q) \\ &\quad \times \Lambda^{EM}_\beta(K+Q, K)\, G(K) \; . \end{aligned} \tag{24.105}$$

Here the bare vertex $\lambda(K, K+Q) = \frac{1}{m}(\mathbf{k} + \mathbf{q}/2)$ and we consider $Q = (\mathbf{q}, 0)$, with $\mathbf{q} \to 0$. We write $\mathbf{\Lambda}^{EM} = \lambda + \delta\mathbf{\Lambda}_{pg} + \delta\mathbf{\Lambda}_{sc}$, where the pseudogap contribution $\delta\mathbf{\Lambda}_{pg}$ to the vertex correction will be shown in Appendix 24.9 to satisfy a Ward identity below T_c

$$\delta\mathbf{\Lambda}^{pg}(K, K) = \frac{\partial \Sigma_{pg}(K)}{\partial \mathbf{k}} \; . \tag{24.106}$$

By contrast for the superconducting contributions, one has

$$\delta\mathbf{\Lambda}^{sc}(K, K) = -\frac{\partial \Sigma_{sc}(K)}{\partial \mathbf{k}} \; . \tag{24.107}$$

This important difference in sign is responsible for the fact that the Meissner effect is associated with superconductivity, and not with a normal state self energy.

The particle density n, after partial integration can be rewritten as $n = -(2/3)\sum_K \mathbf{k} \cdot \partial_{\mathbf{k}} G(K)$. Then, as a result of Dyson's equation, one arrives at the following general expression which relates to the diamagnetic contribution

$$n = -\frac{2}{3} \sum_K G^2(K) \left[\frac{k^2}{m} + \mathbf{k} \cdot \frac{\partial \Sigma_{pg}(K)}{\partial \mathbf{k}} + \mathbf{k} \cdot \frac{\partial \Sigma_{sc}(K)}{\partial \mathbf{k}} \right] \; . \tag{24.108}$$

Now, inserting Eqs. (24.108) and (24.105) into Eq. (24.104) one can see that the pseudogap contribution to n_s drops out by virtue of Eq. (24.106); we find

$$n_s = \frac{2}{3} \sum_K G^2(K)\, \mathbf{k} \cdot \left(\delta\mathbf{\Lambda}_{sc} - \frac{\partial \Sigma_{sc}}{\partial \mathbf{k}} \right) \; . \tag{24.109}$$

We emphasize that the cancellation of this pseudogap contribution to the Meissner effect is the central physics of this analysis, and it depends on treating self energy effects in a Ward-identity-consistent fashion.

We also have that

$$\delta\mathbf{\Lambda}_{sc}(K+Q, K) = \Delta_{sc}^2 G_0(-K-Q) G_0(-K) \lambda(K+Q, K) \; . \tag{24.110}$$

Inserting Eqs. (24.87), (24.89), and (24.110) into Eq. (24.109), after calculating the Matsubara sum, one arrives at

$$n_s = \frac{4}{3}\sum_{\mathbf{k}} \frac{\Delta_{sc}^2}{E_{\mathbf{k}}^2}\epsilon_{\mathbf{k}} \left[\frac{1-2\,f(E_{\mathbf{k}})}{2\,E_{\mathbf{k}}} + f'(E_{\mathbf{k}})\right] . \tag{24.111}$$

This expression can be simply rewritten in terms of the BCS result for the superfluid density

$$\left(\frac{n_s}{m}\right) = \frac{\Delta_{sc}^2}{\Delta^2}\left(\frac{n_s}{m}\right)^{BCS} . \tag{24.112}$$

Here $(n_s/m)^{BCS}$ is just (n_s/m) with the overall prefactor Δ_{sc}^2 replaced with Δ^2.

Finally we can rewrite Eq. (24.112) using Eq. (24.90) as

$$\left(\frac{n_s}{m}\right) = \left[1 - \frac{\Delta_{pg}^2}{\Delta^2}\right]\left(\frac{n_s}{m}\right)^{BCS} . \tag{24.113}$$

In this form it is evident that (via Δ_{pg}^2) *pair excitations out of the condensate are responsible for a suppression of the superfluid density relative to that obtained from fermionic excitations only [163].*

24.4.2 Collective Modes and Gauge Invariance

The presence of pseudogap self energy effects greatly complicates the computation of collective modes [97]. This is particularly apparent at nonzero temperature. Once dressed Green's functions G enter into the calculational schemes, the collective mode polarizabilities and the electromagnetic (EM) response tensor must necessarily include vertex corrections dictated by the form of the self-energy Σ, which depends on the T-matrix which, in turn depends on the form of the pair susceptibility χ. These necessary vertex corrections are associated with gauge invariance in the same way, as was seen for ρ_s, and discussed in Appendix 24.9. Collective modes are important in their own right, particularly in neutral superfluids, where they can be directly detected as signatures of long range order. They also must be invoked to arrive at a gauge invariant formulation of electrodynamics. It is relatively straightforward to introduce these collective mode effects into the electromagnetic response in a completely general fashion that is required by gauge invariance. The difficulty is in the implementation.

In the presence of a weak externally applied EM field, with four-vector potential $A^\mu = (\phi, \mathbf{A})$, the four-current density $J^\mu = (\rho, \mathbf{J})$ is given by

$$J^\mu(Q) = K^{\mu\nu}(Q)A_\nu(Q) , \tag{24.114}$$

where $K^{\mu\nu}(Q)$ is the EM response kernel.

The incorporation of gauge invariance into a general microscopic theory may be implemented in several ways. Here we do so via a generalized matrix Kubo formula [99] in which the perturbation of the condensate is included as additional contributions $\Delta_1 + i\Delta_2$ to the applied external field. These contributions are self consistently obtained (by using the gap equation) and then eliminated from the final expression for $K^{\mu\nu}$. We now implement this procedure. Let $\eta_{1,2}$ denote the change in the expectation value of the pairing field $\hat{\eta}_{1,2}$ corresponding to $\Delta_{1,2}$. For the case of an s-wave pairing interaction $U < 0$, the self-consistency condition $\Delta_{1,2} = U\eta_{1,2}/2$ leads to the following equations:

$$J^\mu = K^{\mu\nu}A_\nu = K_0^{\mu\nu}A_\nu + R^{\mu 1}\Delta_1 + R^{\mu 2}\Delta_2 , \tag{24.115a}$$

$$\eta_1 = -\frac{2\Delta_1}{|U|} = R^{1\nu}A_\nu + Q_{11}\Delta_1 + Q_{12}\Delta_2 , \tag{24.115b}$$

$$\eta_2 = -\frac{2\Delta_2}{|U|} = R^{2\nu}A_\nu + Q_{21}\Delta_1 + Q_{22}\Delta_2 , \tag{24.115c}$$

where

$$K_0^{\mu\nu}(\omega,\mathbf{q}) = P^{\mu\nu}(\omega,\mathbf{q}) + \frac{ne^2}{m} g^{\mu\nu}(1-g^{\mu 0}) \tag{24.116}$$

is the usual Kubo expression for the electromagnetic response. We define the current-current correlation function $P^{\mu\nu}(\tau,\mathbf{q}) = -i\theta(\tau)\langle[j^\mu(\tau,\mathbf{q}), j^\nu(0,-\mathbf{q})]\rangle$. In the above equation, $g^{\mu\nu}$ is a (diagonal) metric tensor with elements $(1,-1,-1,-1)$. We define

$$R^{\mu i}(\tau,\mathbf{q}) = -i\theta(\tau)\langle[j^\mu(\tau,\mathbf{q}), \hat{\eta}_i(0,-\mathbf{q})]\rangle \tag{24.117}$$

with $\mu = 0,\ldots,3$, and $i,j = 1,2$; and

$$Q_{ij}(\tau,\mathbf{q}) = -i\theta(\tau)\langle[\hat{\eta}_i(\tau,\mathbf{q}), \hat{\eta}_j(0,-\mathbf{q})]\rangle \tag{24.118}$$

Finally, it is convenient to define

$$\tilde{Q}_{ii} = 2/U + Q_{ii}\ . \tag{24.119}$$

In order to demonstrate gauge invariance and reduce the number of component polarizabilities, we first rewrite $K^{\mu\nu}$ in a way which incorporates the effects of the amplitude contributions via a renormalization of the relevant generalized polarizabilities,

$$K'^{\mu\nu}_0 = K^{\mu\nu}_0 - \frac{R^{\mu 1}R^{1\nu}}{\tilde{Q}_{11}}\ , \tag{24.120}$$

It can be shown, after some analysis, that the gauge invariant form for the response tensor is given by

$$K^{\mu\nu} = K'^{\mu\nu}_0 - \frac{\left(K'^{\mu\nu'}_0 q_{\nu'}\right)\left(q_{\nu''}K'^{\nu''\nu}_0\right)}{q_{\mu'}K'^{\mu'\nu'}_0 q_{\nu'}}\ . \tag{24.121}$$

The above equation satisfies two important requirements: it is manifestly gauge invariant and, moreover, it has been reduced to a form that depends principally on the four-current-current correlation functions. (The word "principally" appears because in the absence of particle-hole symmetry, there are effects associated with the order parameter amplitude contributions that add to the complexity of the calculations).

The EM response kernel of a superconductor contains a pole structure that is related to the underlying Goldstone boson of the system. Unlike the phase mode component of the collective mode spectrum, this Anderson-Bogoliubov (AB) mode is independent of Coulomb effects. The dispersion of this amplitude renormalized AB mode is given by

$$q_\mu K'^{\mu\nu}_0 q_\nu = 0\ . \tag{24.122}$$

For an isotropic system $K'^{\alpha\beta}_0 = K'^{11}_0\delta_{\alpha\beta}$, and Eq. (24.122) can be rewritten as

$$\omega^2 K'^{00}_0 + \mathbf{q}^2 K'^{11}_0 - 2\omega q_\alpha K'^{0\alpha}_0 = 0\ , \tag{24.123}$$

with $\alpha = 1,2,3$, and in the last term on the left hand side of Eq. (24.123) a summation over repeated Greek indices is assumed.

It might seem surprising that from an analysis which incorporates a complicated matrix linearized response approach, the dispersion of the AB mode ultimately involves only the amplitude renormalized four-current correlation functions, namely the density-density, current-current and density-current correlation functions. The simplicity of this result is, nevertheless, a consequence of gauge invariance.

At zero temperature $K'^{0\alpha}_0$ vanishes, and the sound-like AB mode has the usual linear dispersion $\omega = \omega_{\mathbf{q}} = c|\mathbf{q}|$ with the "sound velocity" given by

$$c^2 = K'^{11}_0/K'^{00}_0\ . \tag{24.124}$$

We may, thus, interpret the AB mode as a special type of collective mode which is associated with $A_\nu = 0$. This mode corresponds to free oscillations of $\Delta_{1,2}$ with a dispersion $\omega = cq$ given by the solution to the equation

$$\det|Q_{ij}| = \tilde{Q}_{11}\tilde{Q}_{22} - Q_{12}Q_{21} = 0 \; . \tag{24.125}$$

The other collective modes of this system are derived by including the coupling to electromagnetic fields. Within self-consistent linear response theory the field $\delta\phi$ must be treated on an equal footing with $\Delta_{1,2}$ and formally can be incorporated into the linear response of the system by adding an extra term $K_0^{\mu 0}\delta\phi$ to the right hand side of Eqs. (24.115a), (24.115b), and (24.115c). Note that, quite generally, the effect of the "external field" $\delta\phi$ amounts to replacing the scalar potential $A^0 = \phi$ by $\bar{A}^0 = \bar{\phi} = \phi + \delta\phi$. In this way one arrives at the following set of three linear, homogeneous equations for the unknowns $\delta\phi$, Δ_1, and Δ_2

$$0 = R^{10}\delta\phi + \tilde{Q}_{11}\Delta_1 + Q_{12}\Delta_2 \; , \tag{24.126a}$$

$$0 = R^{20}\delta\phi + Q_{21}\Delta_1 + \tilde{Q}_{22}\Delta_2 \; , \tag{24.126b}$$

$$\delta\rho = \frac{\delta\phi}{V} = K_0^{00}\delta\phi + R^{01}\Delta_1 + R^{02}\Delta_2 \; , \tag{24.126c}$$

where V is an effective particle-hole interaction which may derive from the pairing channel or, in a charged superconductor, from the Coulomb interaction. The dispersion of the collective modes of the system is given by the condition that the above equations have a nontrivial solution

$$\begin{vmatrix} Q_{11} + 1/U & Q_{12} & R^{10} \\ Q_{21} & Q_{22} + 1/U & R^{20} \\ R^{01} & R^{02} & K_0^{00} - 1/V \end{vmatrix} = 0 \; . \tag{24.127}$$

In the BCS limit where there is particle-hole symmetry $Q_{12} = Q_{21} = R^{10} = R^{01} = 0$ and, the amplitude mode decouples from the phase and density modes; the latter two are, however, in general coupled.

The above formalism (or its equivalent RPA variations [39, 13]) has been applied to address collective modes in the crossover scenario. The most extensive studies have been at $T = 0$ based on the ground state of Eq. (24.1). There one finds a smooth change in the character of the Anderson-Bogoliubov (AB) mode. At weak coupling one obtains the usual BCS value $c = v_F/\sqrt{3}$. By contrast at strong coupling, the collective mode spectrum reflects [13] an effective boson-boson interaction deriving from the Pauli statistics of the constituent fermions. This is most clearly seen in jellium models [61, 97] where the AB sound velocity is equivalent to that predicted for a 3D interacting Bose gas $c = [4\pi n a_B/m_B^2]^{1/2}$. Here, as earlier, the inter-boson scattering length is twice that of the inter-fermionic counterpart, at strong coupling.[35]

The effects of finite temperature on the AB mode have been studied in [97], by making the approximation that the temperature dependence of the order parameter amplitude contribution is negligible. Then the calculation of this dispersion reduces to calculations of the electromagnetic response, as discussed, for example in ρ_s. See also Appendix 24.9. At finite T, the AB mode becomes damped and the real and imaginary parts of the sound velocity have to be calculated numerically. Here one finds, as expected, that the complex $c \to 0$ as $T \to T_c$. The results are plotted in Fig. 24.22 for both moderate and weak coupling. Because the real and imaginary parts are comparable there, the mode is highly damped near T_c.

[35] In the neutral case, for the full collective modes of Eq. (24.127), there are numerical differences (of order unity) in the prefactors of the mode frequency, so that the collective modes of the crossover theory are not strictly the same as in GP theory. In these calculations V in Eq. (24.127) should be associated with the pairing interaction, which enters in the context of fermionic density-density correlation effects within the particle-hole channel.

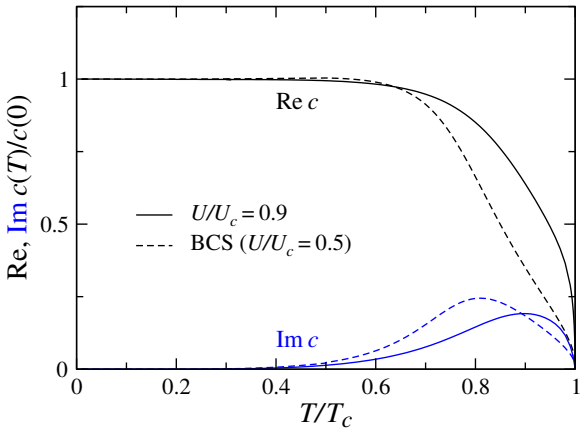


Figure 24.22: Temperature dependence of the real and imaginary parts of the AB collective mode velocity for moderate (solid lines) and weak (dashed lines) coupling. The velocity vanishes at T_c for both cases.

24.4.3 Investigating the Applicability of a Nambu Matrix Green's Function Formulation

Diagrammatic schemes appropriate to BCS superconductors are based on a Nambu matrix Green's function approach. The off-diagonal or anomalous Green's functions in this matrix are given by

$$F(K) \equiv \Delta_{sc} G(K) G_0(-K) \tag{24.128}$$

as well as its Hermitian conjugate. This Nambu formalism was designed to allow study of perturbations to the BCS state, due to, for example, external fields or impurities. For these perturbations the central assumption is that they act on both the "normal" (with BCS Green's function $G(K)$ from Eq. (24.30)) and anomalous channels in a symmetrical way.

Understanding as we now do that BCS theory is a very special case of superconductivity, this raises the caution that once one goes beyond BCS, some care should be taken to justify this Nambu approach. At the very least the distinction between the order parameter Δ_{sc} and the excitation gap Δ raises ambiguity about applying a diagrammatic theory based on Nambu-Gor'kov Green's functions.

More importantly, in treating the effects of the pseudogap self energy Σ_{pg} as we do here, it should be clear that this self energy does *not* play a symmetric role in the anomalous and normal channels. It is viewed here as an entirely normal state effect. However this theory accommodates the equivalent [97] of the Nambu-Gor'kov "F"- function in general response functions such as in the Maki-Thompson diagrams of Appendix 24.9 through the asymmetric combination GG_0 which always arises in pairs (for example, as the FF combinations of BCS theory). In this regard the GG_0 formalism appears to differ from all other T-matrix schemes which are designed to go below T_c, in that the Nambu scheme is not assumed at the start. Nevertheless, many features of this formalism seem to naturally arise in large part because of Eq. (24.128), which demonstrates an intimate connection between GG_0 and the conventional diagrams of BCS theory.

24.5 Other Theoretical Approaches to the Crossover Problem

24.5.1 $T \neq 0$ Theories

We have noted in Section 24.2.7 that there are three main theoretical approaches to the crossover problem based on T-matrix theories. Their differences are associated with differ-

ent forms for the pair susceptibility χ. The resulting calculations of T_c show similar variations. When two full Green's functions are present in χ (as in the FLEX approach), T_c varies monotonically [63] with increasing attractive coupling, approaching the ideal gas Bose-Einstein asymptote from below. When two bare Green's functions are present in χ, as in the work of Noziéres and Schmitt-Rink, and of Randeria and co-workers, then T_c overshoots [128, 144, 118] the BEC asymptote and ultimately approaches it from above. Finally when there is one bare and one dressed Green's function, T_c first overshoots and then decreases to a minimum around $\mu = 0$, eventually approaching the asymptote from below [115]. This last appears to be a combination of the other two approaches. Overall the magnitudes are relatively similar and the quantitative differences are small. There is, finally, another body of work [58] based on the GG_0 scheme which should be noted here. The approach by the Swiss group seeks to make contact with the phase fluctuation scenario for high T_c superconductors and addresses STM and ARPES data.

Bigger differences appear when these T-matrix theories are extended below T_c. Detailed studies are most extensive for the NSR approach. Below T_c one presumes that the T-matrix (or χ) contains only bare Green's functions, but these functions are now taken to correspond to their Nambu matrix form, with the order parameter Δ_{sc} appearing in the dispersion relation for excited fermions [144, 139]. A motivation for generalizing the below- T_c T-matrix in this way is that one wants to connect to the collective mode spectrum of the superconductor, so that the dispersion relation for pair excitations is $\Omega_q \approx cq$. In this way the system would be more directly analogous to a true Bose system.

Self energy effects are also incorporated below T_c but only in the number equation, either in the approximate manner of NSR [144, 61] or through use of the full Dyson resummation [139] of the diagonal Nambu-matrix component $G(\Sigma_0)$. For the latter scheme, Strinati's group has addressed pseudogap effects in some detail with emphasis on the experimentally observed fermionic spectral function. Some concern can be raised that the fermionic excitations in the gap equation do not incorporate this pseudogap, although these pairs are presumed to emerge out of a normal state which has a pseudogap. Indeed, this issue goes back to the original formulation of NSR, which includes self energy effects in the number equation, and not in the gap equation.

Tchernyshyov [171] presented one of the first discussions below T_c for the FLEX-based T-matrix scheme. He also addressed pseudogap effects and found a suppression of the fermion density of states at low energy which allows for long-lived pair excitations inside this gap. At low momenta and frequencies, their dispersion is that of a Bogoliubov-sound-like mode with a nonzero mass. Some of these ideas have been recently extended [48] to apply to the boson-fermion model.

The work of Micnas and collaborators [119] which is also based on the FLEX scheme predates the work of Tchernyshyov, although their initial focus was above T_c in two dimensional Hubbard models. Here the fermionic spectral functions were studied in detail, using a numerically generated solution of the T-matrix equations. A nice review of their large body of work on "real space pairing" in the cuprates was presented based on a variety of different model Hamiltonians [121].

An extensive body of work on the FLEX scheme has been contributed by Yamada and Yanatse [189] both above and below T_c. They point out important distinctions between their approach and that of NSR. The effects of the broken symmetry are treated in a generalized Nambu formalism, much as assumed by Pieri *et al.* ([139]) and by Griffin and Ohashi ([61]), but here the calculations involve self energy effects in both the number and gap equations. Their work has emphasized the effects of the pseudogap on magnetic properties, but they have discussed a wide variety of experiments in high T_c and other exotic superconductors.

The nature of the ground states which result from these two alternatives ($\chi \approx GG$ and

$\chi \approx G_0 G_0$) has yet to be clearly established. It should be noted that, despite the extensive body of work based on the NSR or $G_0 G_0$ scheme, no detailed picture has been presented in the literature of the nature of the ground state which results when their calculations at T_c are extrapolated [139] down to $T = 0$. In large part, the differences between other work in the literature and that summarized in Sections 24.3.3 are due to the whether (as in NSR-based papers) or not (as here) the superconducting order parameter Δ_{sc} alone characterizes the fermionic dispersion below T_c.

One might well ask the question: because the underlying Hamiltonian [Eq. (24.11)] is associated with inter-fermionic, not inter-bosonic interactions, will this be reflected in the near-BEC limit of the crossover problem? The precise BEC limit is, of course, a non-interacting, or ideal Bose gas, but away from this limit, fermionic degrees of freedom would seem to be relevant in ways that may not be accounted for by the analogue treatment of the weakly interacting Bose gas. The most extensive study (albeit, above T_c) of this issue is due to Pieri and Strinati [140]. Their work, importantly, points out the inadequacies of T-matrix schemes, particularly at strong coupling. While the ground state in their calculations is unknown, it is necessarily different from the conventional crossover state of Eq. (24.1). There is much intuition to be gained by studying this simplest of all ground states, as outlined in this Review, but it will clearly be of great value in future to consider states, in which, for example, there is less than full condensation.

Finally, we note that studies of non-s wave orbital pairing states in the context of the BCS-BEC crossover problem have rapidly proliferated in the literature. This is, in large part because of the observed d-wave pairing in the cuprates. Indeed, Leggett's initial work [187], addressed p-wave pairing in ^3He. Randeria and co-workers [144] also considered non-s wave pairing. Studies [7, 67] of this crossover for a d-wave lattice case are plentiful at $T = 0$. Even earlier work was done [29] on extensions of this ground state to include nonzero temperature. Moreover, a d-wave continuum model has also been considered [143]. It is expected that in the near future cold atom experiments will begin to address $l \neq 0$ pairing via appropriate choices of the Feshbach resonances [69].

24.5.2 Boson-Fermion Models for High T_c Superconductors

The notion that it might be appropriate to include bosonic degrees of freedom in high T_c superconductors goes back to T.D. Lee and R. Friedberg who introduced [54, 55] the "boson-fermion" model within three years of the discovery of cuprate superconductivity. The work of Lee and colleagues is based on the Hamiltonian of Eq. (24.11) without the direct fermion-fermion interaction U. To our knowledge this is the first study which argues for something akin to "real space pairing" in these materials. Interestingly, this work was motivated only by the observed short coherence length. Pseudogap effects, which make this case much stronger, had not yet been properly characterized. The analogies with He^4 and a more BEC-like picture of superconductivity were discussed, as well as the superfluid density, and energy gap structure, albeit for s-wave pairing.

Subsequent work on this model Hamiltonian in the context of the high T_c copper oxides was pursued by Ranninger and Micnas and their collaborators. Indeed, Ranninger and Robaszkiewicz [145] were the first to write down the boson-fermion model, although initially, in an entirely different context, the bosons were associated with phonons rather than electron pairs, and they were presumed to be localized. In this context they addressed mean field theoretic solutions below T_c as well as more recently [48] an approach based on renormalization group techniques. The physical picture which emerges leads to two gap structures below T_c, one associated with a pseudogap and another with the superconductivity. In this way it appears to be very different from approaches based on Eq. (24.1).

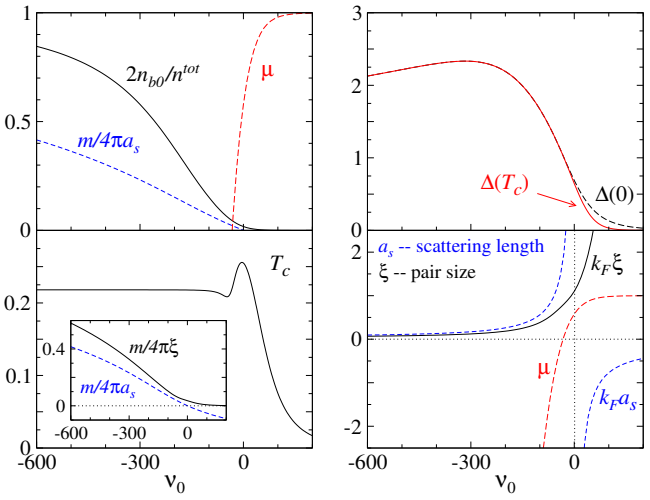


Figure 24.23: (Color) Characteristics of the ground state and T_c as a function of the magnetic detuning ν_0 in a homogeneous case. Shown are the chemical potential μ, fraction of molecular condensate $2n_{b0}/n^{tot}$, inverse scattering length $m/4\pi a_s$, gap $\Delta(0)$, inverse pair size $m/4\pi\xi$, dimensionless relative pair size $k_F\xi$ at $T = 0$ as well as T_c and $\Delta(T_c)$. The pair size is roughly the same as inter-particle spacing, $k_F\xi = 1$, at unitarity. As ν_0 decreases, the gap Δ increases and reaches a maximum, and then decreases slowly and approaches its BEC asymptote (not shown) from above. Here we take $g_0 = -40E_F/k_F^{3/2}$ and $U_0 = -3E_F/k_F^3$, and we use the convention for units $E_F = k_F = \hbar = k_B = 2m = 1$. A large exponential momentum cutoff, $k_c/k_F = 80$ is assumed in the calculations.

24.6 Physical Implications: Ultracold Atom Superfluidity

24.6.1 Homogeneous case

In this section we summarize the key characteristics of fermionic superfluidity in ultracold gases, in the homogeneous situation, without introducing the trap potential. Our results are based on numerical solution of the coupled Eqs. (24.69), (24.70) and (24.91). The upper left panel of Fig. 24.23 plots the fermionic chemical potential, the Feshbach boson condensate ratio and the inverse scattering length as a function of ν_0. Here we have chosen what we believe is the physically appropriate value for the Feshbach coupling $g_0 = -40E_F/k_F^3$ for ^{40}K, as determined from the experimentally measured scattering length data and resonance width.[36] This parameter is roughly an order of magnitude larger for ^{6}Li. Here ν_0, the gaps and μ are all in units of E_F, and the plots, unless indicated otherwise, are at zero temperature.

The upper right panel plots the excitation gap at T_c as well as the gap at $T = 0$. The lower left hand panel indicates T_c along with the inverse pair size ξ^{-1} in the condensate. Finally the lower right panel plots ξ itself, along with a_s.

One can glean from the figure that the Feshbach boson fraction decreases, becoming negligible when the chemical potential passes through zero. This latter point marks the onset of the PG regime, and in this regime the condensate consists almost entirely of fermionic pairs. The upper limit of the PG regime, that is, the boundary line with the BCS phase, is reached once the pseudogap, $\Delta(T_c)$ is essentially zero. This happens when μ is close to its saturation value at E_F. At this point the pair size rapidly increases.

[36] We note that the precise values of g_0 and U_0 are not critical for either ^{6}Li or ^{40}K as long as they give roughly the right (large) resonance width ΔB and background scatter length a_{bg}. In fact, these parameters usually change during experiment since the total particle number N (and hence E_F and k_F) decreases in the process of evaporative cooling. In order to compare with experiment, one needs to compare at the correct value of $k_F a_s$.

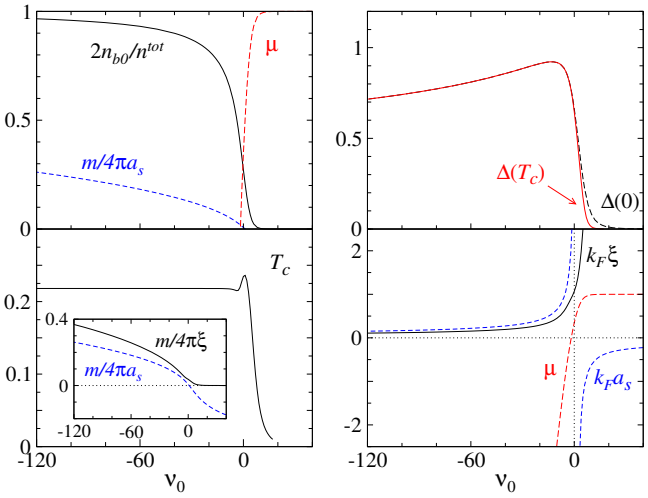


Figure 24.24: (Color) Characteristics of the ground state and T_c, as in Fig. 24.23 except for a smaller g_0. In comparison with Fig. 24.23, the Feshbach resonance becomes much narrower. Here $g_0 = -10E_F/k_F^{3/2}$ and $U_0 = -3E_F/k_F^3$.

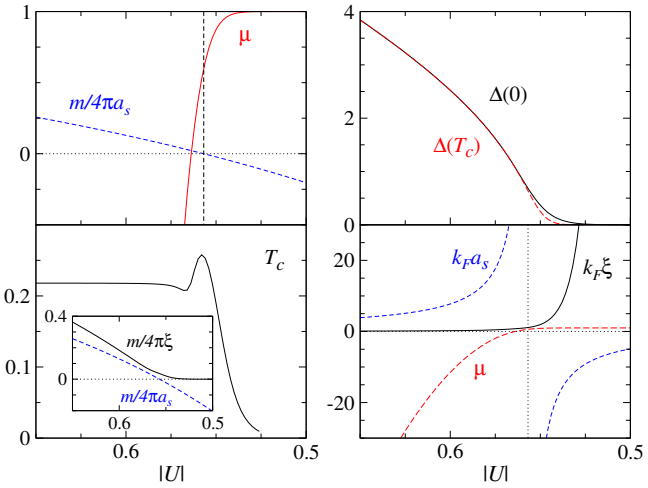


Figure 24.25: (Color) Characteristics of the ground state and T_c in the one-channel model, as in Fig. 24.23 but as a function of the attraction strength U. Here $g_0 = 0$. Different from the two-channel shown in Figs. 24.23-24.24 case, the gap Δ increases indefinitely with $|U|$. The units for U are E_F/k_F^3. Note that $|U|$ increases to the left.

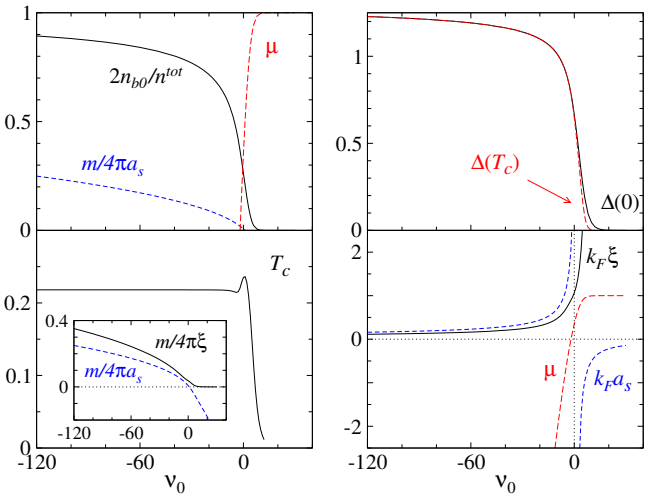


Figure 24.26: (Color) Characteristics of the ground state and T_c, as in Fig. 24.24, except now $U_0 = 0$. As a consequence of the vanishing of U_0, the gap Δ is monotonic and approaches its BEC asymptote from below as ν_0 decreases. Here $g_0 = -10E_F/K_F^{3/2}$.

These results can be compared with those derived from a smaller value of the Feshbach coupling constant $g_0 = -10E_F/k_F^{3/2}$ shown in Fig. 24.24. Now the resonance is effectively narrower. Other qualitative features remain the same as in the previous figure.

One can plot the analogous figures in the absence of Feshbach effects. Here the horizontal axis is the inter-fermionic interaction strength $|U|$, as is shown in Fig. 24.25. Three essential differences can be observed. Note, first the obvious absence of the Feshbach boson or molecular condensate n_{b0}. There is, of course, a condensate associated with pairs of fermions (Δ_{sc}) and these pairs will become bound into "fermionic molecules" for sufficiently strong attraction. Secondly, note that the excitation gap $\Delta(0)$ is monotonically increasing as $|U|$ increases towards the BEC limit. By contrast, from the upper right panels of Fig. 24.24 one can see that when Feshbach effects are present $\Delta(0) \approx \Delta(T_c)$ decreases towards zero in the extreme BEC limit. It can also be seen that the shape of the scattering length curve *vs* U is different from the plots in the previous two figures. Here a_s more rapidly increases in magnitude on either side of the unitary limit. Nevertheless it is important to stress that, *except for the nature of the Bose condensate in the BEC limit, the physics of the Feshbach resonance-induced superfluidity is not so qualitatively different from that associated with a direct inter-fermionic attraction.*

Figure 24.26 presents the analogous plots for the case when the direct attraction between fermions U vanishes. Here the coupling constant g_0 is the same as in Fig. 24.24, and pseudogap effects are present here just as in all other cases. The most notable difference in the physics is that the formation of the Cooper condensate is driven exclusively by coupling to the molecular bosons. A contrast between the two figures is in the behavior of $\Delta(T_c)$ and $\Delta(0)$. For the $U = 0$ case and in the BEC limit, $\Delta(0)$ approaches the asymptotic value $(|g|\sqrt{n_b^0})$ from below. When the system is the fermionic regime ($\mu > 0$), aside from quantitative details, there is very little to distinguish the effects of U from those of g, except when these parameters are taken to very extreme limits.

Finally, in Fig. 24.27 we plot T_c vs ν_0 in the presence of Feshbach effects with variable U_0, from weak to strong background coupling. The lower inset shows the behavior of the excitation gap at T_c. With very strong direct fermion attraction U, we see that T_c has a very different dependence on ν_0. In this limit there is a molecular BEC to PG crossover (which may be inaccessible in actual experiments, since U is not sufficiently high). Nevertheless, it is useful for completeness to illustrate the entire range of theoretical behavior.

Figures 24.28(a)-24.28(c) show the fermionic density of states for the BEC, PG and BCS

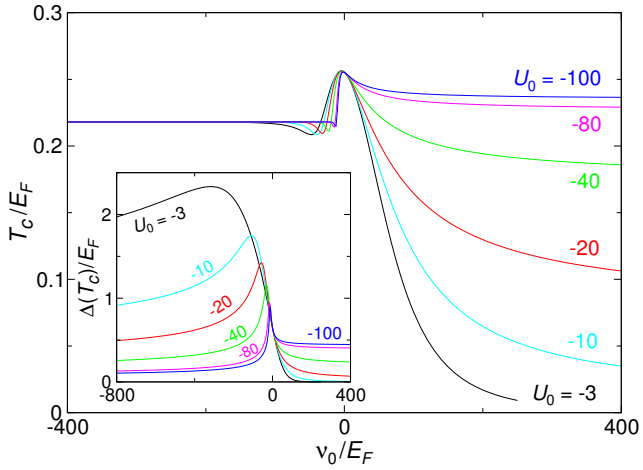


Figure 24.27: (Color) Behavior of T_c (main figure) and $\Delta(T_c)$ (inset) at fixed $g_0 = -40E_F/k_F^{3/2}$ with variable U_0. As $U_0 \to -\infty$, unitarity is approached from the BCS side at large positive ν_0. At the same time, $\Delta \propto |g|$ also decreases.

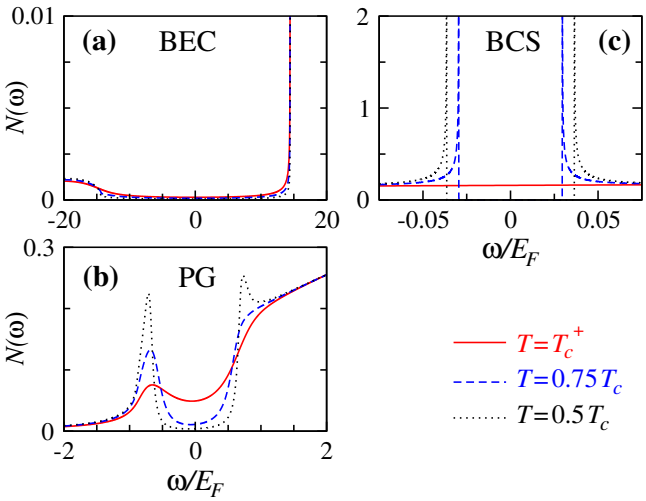


Figure 24.28: Typical density of states (DOS) $N(\omega)$ *vs* energy ω in the three regimes at indicated temperatures. There is no depletion of the DOS at T_c in the BCS case. By contrast, in the BEC case, there is a large gap in DOS at T_c, roughly determined by $|\mu|$. In the intermediate, i.e., pseudogap, regime, there is a strong depletion of the DOS already at T_c. Once T decreases below T_c, the DOS decreases rapidly, signalling the superfluid phase transition.

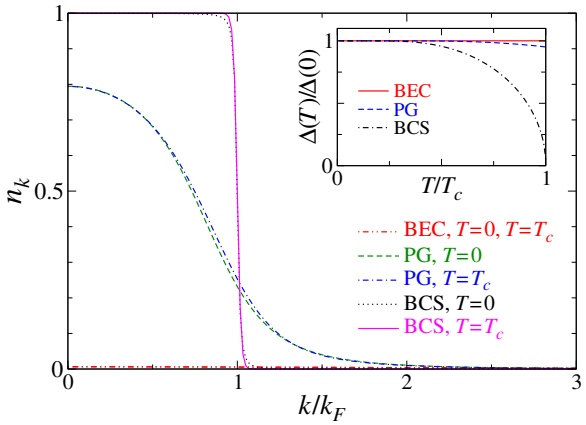


Figure 24.29: Typical behavior of the fermionic momentum distribution function n_k at $T = 0$ and T_c in the three regimes for a homogeneous system. The inset indicates the corresponding normalized gaps as a function of T/T_c. In all three regimes, n_k barely changes between $T = T_c$ and $T = 0$.

limits. These figures are important in establishing a precise visual picture of a "pseudogap". The temperatures shown are just above T_c, and for $T = 0.75T_c$ and $T = 0.5T_c$. The methodology for arriving at these plots will be discussed in the following section, in the context of high T_c superconductors. Only in the BCS case is there a clear signature of T_c in the density of states, but the gap is so small and T_c is so low, that this is unlikely to be experimentally detectable. Since the fermionic gap is well established in the BEC case, very little temperature dependence is seen as the system goes from the normal to the superfluid states. Only the PG case, where T_c is maximal, indicates the presence of superfluidity, not so much at T_c but once superfluid order is well established at $T = 0.5T_c$, through the presence of sharper coherence features, much as seen in the cuprates.

The inset of Fig. 24.29 plots the temperature dependence of $\Delta(T)$. It should be stressed that T_c is only apparent in $\Delta(T)$ in the BCS case. To underline this point, in the main body of Fig. 24.29 we plot the fermionic momentum distribution function n_k, which is the summand in the number equation, Eq. (24.70), at $T = 0$ and $T = T_c$. The fact that there is very little change from $T = 0$ to $T = T_c$ makes the important point that this momentum distribution function in a homogeneous system is not a good indicator of phase coherent pairing. For the PG case, this, in turn, derives from the fact that $\Delta(T)$ is nearly constant. For the BEC limit the excitation gap, which is dominated by μ, similarly, does not vary through T_c. In the BCS regime, $\Delta(T)$ is sufficiently small so as to be barely perceptible on the scale of the figure.

Unitary Limit and Universality

There has been considerable emphasis on the behavior of fermionic gases near the unitary limit where $a_s = \pm\infty$. Attention [68, 182] has concentrated on this limit in the absence of Feshbach bosons. We now want to explore the more general two-channel problem here. At unitarity we require that

$$\frac{4\pi a_s^*}{m} = U_0 + \frac{g_0^2}{2\mu - \nu_0} \tag{24.129}$$

diverges. This will be consistent, provided

$$\nu_0 = 2\mu\,. \tag{24.130}$$

It should be clear that the parameter U_0 is of no particular relevance in the unitary limit. This is to be contrasted with the one channel problem, where Feshbach bosons are absent and unitarity is achieved by tuning the direct inter-fermion interaction, U.

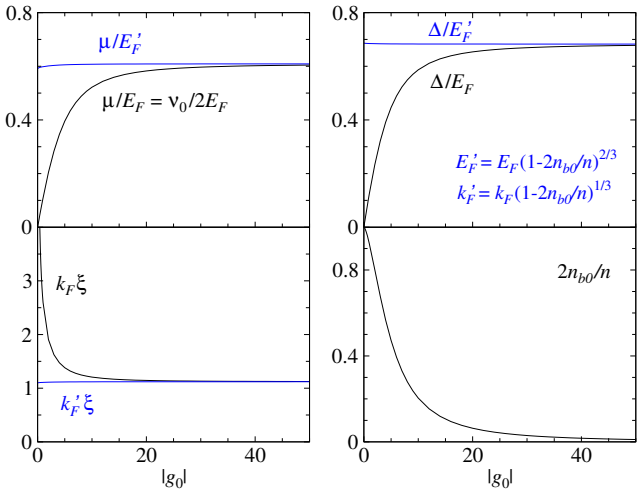


Figure 24.30: (Color) Characteristics of the unitary limit at $T = 0$ as a function of $|g_0|$ in the two-channel problem. Here n_{b0} is the density of condensed Feshbach bosons. $E'_F = k'^2_F/2m$ defines an effective Fermi energy of the fermionic component with a density $n = n^{tot} - 2n_{b0}$. After rescaling, μ/E'_F, Δ/E'_F, and $k'_F\xi$ are essentially a constant in g_0. This indicates that at unitarity, the system can be treated effectively as a two-fluid model at $T = 0$. The units for g_0 are $E_F/k_F^{3/2}$.

In the unitary limit, the $T = 0$ gap and number equations become

$$1 + U_c \sum_{\mathbf{k}} \frac{1}{2E_{\mathbf{k}}} = 0, \tag{24.131}$$

and

$$n^{tot} = 2n_b^0 + n = \frac{2\Delta_0^2}{g_0^2} + \sum_{\mathbf{k}} \left(1 - \frac{\epsilon_{\mathbf{k}} - \mu}{E_{\mathbf{k}}}\right), \tag{24.132}$$

where we have used the fact that at unitarity

$$n_b^0 = \frac{g^2\Delta_0^2}{[(2\mu - \nu)U + g^2]^2} = \frac{\Delta_0^2}{g_0^2}, \tag{24.133}$$

and we define $\Delta_0 \equiv \tilde{\Delta}_{sc}(T = 0)$. Here U_c is the critical coupling, given in Eq. (24.17). From these equations it follows that in this limit the values of μ and Δ_0 in the ground state are entirely determined by the Feshbach coupling g_0.

Figure 24.30 presents a plot of zero temperature properties showing their dependence on g_0. The two endpoints of the curves are of interest. For arbitrarily small but finite g_0 the unitary limit corresponds roughly to $\mu \approx 0$. Moreover, here the condensate consists exclusively of Feshbach bosons. At large g_0, (which appear to be appropriate to current experiments on ^{6}Li and ^{40}K), the behavior at unitarity is closer to that of the one channel problem [68]. Here one finds the so-called universal behavior with parameters $\mu/E_F = 0.59$, and $\Delta/E_F = 0.69$ associated with the simple crossover ground state and a contact potential interaction[37].

To what extent is the unitary limit of the two channel problem universal? It clearly is not in an absolute sense. However, there is a kind of universality implicit in these $T = 0$ calculations, as can be seen from Fig. 24.30 if we take into account the fact that there are a reduced number of fermions, as a result of the Bose condensate. We, thus, divide the two zero temperature energy scales by an effective Fermi energy defined by $E'_F = E_F(n/n^{tot})^{2/3}$ with $n = n^{tot} - 2n_b^0$. Figure 24.30 shows that as g_0 decreases, the effective or rescaled Fermi energy E'_F decreases while the

[37] In our plots we find small numerical corrections associated with our non-infinite cutoff.

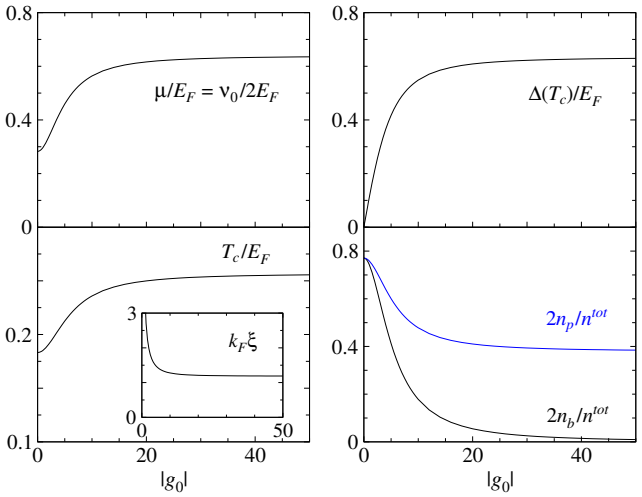


Figure 24.31: (Color) Characteristics of the unitary limit at $T = T_c$ as a function of $|g_0|$ in the two channel problem. In contrast to the previous figure for $T = 0$, there is no rescaling which would lead to universal behavior of μ, Δ or ξ with respect to g_0. More than 20% of the system is composed of fermionic quasiparticles when $|g_0| \to 0$. Here n_b and n_p denote the density of noncondensed Feshbach bosons and of the sum of FB and fermion pairs, respectively. The units for g_0 are $E_F/k_F^{3/2}$.

Bose condensate fraction increases. The rescaled quantities μ/E'_F and Δ/E'_F are universal, that is, they are essentially independent of g_0, as seen in the Figure. A similar scaling can be done for the Cooper pair size ξ. With a reduced effective Fermi momentum $k'_F = k_F(n/n^{tot})^{1/3}$, the dimensionless product $k'_F\xi$ is also independent of g_0. We can arrive at some understanding of this modified universality, by referring back to Sec. 24.6.1. In summary, the breakdown of universality seen in Fig. 24.30 is to be associated with a reduced number of fermions, which, in turn derives from the Bose condensate n_b^0. Once n_b^0 is negligible, the distinction between one and two channel models disappears.

Finite temperature properties, such as T_c and $\Delta(T_c)$ can also be calculated in the unitary limit, as a function of g_0. These are plotted in Fig. 24.31. Just as for the zero temperature energy scales, these parameters [along with $\mu(T_c)$] increase monotonically with g_0. However, at finite temperatures there are noncondensed Feshbach bosons as well as noncondensed fermion pairs, which interact strongly with each other. These noncondensed states are represented in the lower right inset. Plotted there is the fraction of noncondensed bosons $[n_b(T_c)]$ and sum of both noncondensed fermion pairs and noncondensed bosons $[n_p(T_c)]$ at T_c. These quantities correspond to the expressions shown in Eqs. (24.80) and (24.92), respectively.

These noncondensed particles are responsible for the fact that at T_c a simple rescaling will not yield the universality found at $T = 0$. Moreover, these noncondensed bosons and fermion pairs influence calculations of T_c, itself, via pseudogap effects which enter as $\Delta(T_c)$. These pseudogap effects, which are generally ignored in the literature, compete with superconductivity, so that T_c is bounded with its a maximum given by $\approx 0.25T_F$, just as seen in Fig. 24.25, for the one channel problem. Despite the fact that there is no universality, even in the rescaled sense, at T_c one can associate the large g_0 limits with the behavior of the one channel system which has been rather extensively studied in the unitary limit [68]. This large g_0 limit seems to be reasonably appropriate for the currently studied Feshbach resonances in ^{6}Li and ^{40}K. In this sense, these particular atomic resonances are well treated by a one channel problem, near the unitary limit.

In summary, comparison between Fig. 24.30 and Figure 24.31 reveals that (i) at $T = 0$, all Feshbach bosons and pairs are condensed and the two (fermionic and bosonic) condensates

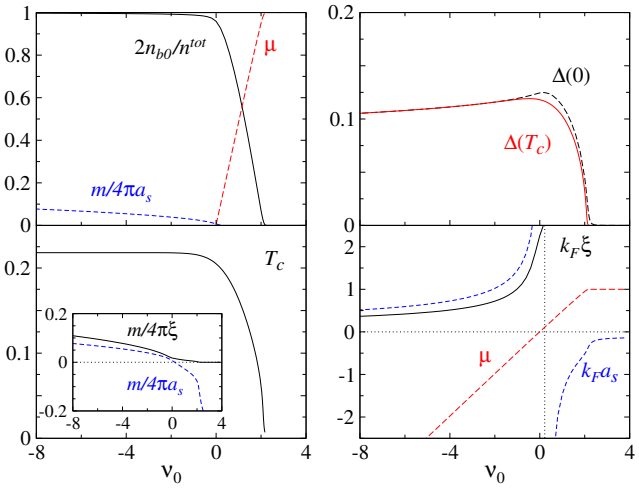


Figure 24.32: (Color) Characteristics of the small g_0 limit as a function of ν_0 in the two-channel model. Unless indicated otherwise the plots correspond to $T = 0$. The molecular condensate fraction is very high and there is no maximum at unitarity. The gap Δ is very small ($\propto g_0$). Here we take $g_0 = -1E_F/k_F^{3/2}$ and $U_0 = -3E_F/k_F^3$. Note the very different scales for the abscissa when comparing with Figs. 24.23 and 24.24.

are relatively independent of each other. (ii) By contrast, at $T = T_c$, fermionic quasiparticles, noncondensed fermion pairs and Feshbach bosons all coexist and interact strongly with each other. This destroys the simple scaling found at $T = 0$.

Weak Feshbach Resonance Regime: $|g_0| = 0^+$

The effects of very small yet finite g_0 lead to a nearly bi-modal description of crossover phenomena. Figure 24.32 presents the behavior for very narrow Feshbach resonances. It shows that there is a rather abrupt change as a function of magnetic field (via ν_0) from a regime in which the condensate is composed only of Feshbach bosons, to one in which it contains only fermion pairs. Depending on the size of g_0, this transition point (taken for concreteness to be where $2n_b^0/n^{tot} \approx 0.5$, for example) varies somewhat, but it seems to occur close to the unitary limit and, importantly, for negative scattering lengths *i.e.*, on the BCS side. This should be contrasted with the large g_0 case). This small g_0 regime of parameter space was explored by Ohashi and Griffin [131]. Indeed the behavior shown in the figure is similar to the physical picture which Falco and Stoof [51] presented.

This figure represents a natural evolution in the behavior already indicated by Figs. 24.23 and 24.24. Here, however, in contrast to these previous figures the behavior of T_c is essentially monotonic, and the weak maximum and minimum found earlier has disappeared. For this regime, the small pseudogap which can be seen in the upper right panel arises predominantly from the contribution of Feshbach bosons via Eqs. (24.84) and (24.91). At the same time it should be noted that the transition from mostly molecular bosons to mostly fermion pairs in the condensate is continuous. While it may look sharp particularly for a plot with a more extended range of ν_0 than shown here, this closeup view gives a more precise picture of a smooth crossover transition.

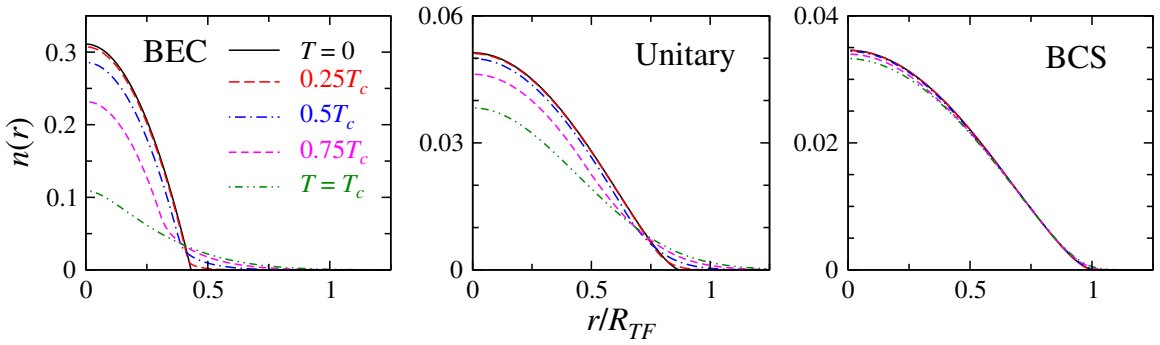


Figure 24.33: (Color) Representative spatial profiles of fermions in a harmonic trap potential at various temperatures from T_c to $T = 0$ in the three indicated regimes. As the system evolves from the BCS to the deep BEC regime, the fermion cloud shrinks, and a bimodal distribution of the density develops below T_c. Note the different scales for the vertical axes.

We end by noting that in this small g_0 regime, the system is far from the one channel limit obtained when g_0 is identically 0, as shown in Fig. 24.25. It should be clear from the above discussion that *Feshbach bosons play a more important role in the regime of unitary scattering the smaller is g_0, provided that it does not strictly vanish.*

24.6.2 Superfluidity in Traps

Most experiments on fermionic superfluids are done in the presence of a trap potential $V(r)$. For the most part, this is most readily included at the level of the local density approximation (LDA). In this section, we summarize the self consistent equations for spherical traps $V(r) = \frac{1}{2}m\omega^2 r^2$. T_c is defined as the highest temperature at which the self consistent equations are satisfied precisely at the center. At a temperature T lower than T_c the superfluid region extends to a finite radius R_{sc}. The particles outside this radius are in a normal state. Also important is the radius R_Δ beyond which the excitation gap is effectively zero, to a chosen level of numerical accuracy.

The self consistent equations (with simplified units $\hbar = 1$, fermion mass $m = \frac{1}{2}$, and Fermi energy $E_F = \hbar\omega(3N)^{\frac{1}{3}} = 1$, where ω is the trap frequency) are given in terms of the Feshbach coupling constant g and inter-fermion attractive interaction U by a gap equation

$$1 + \left[U + \frac{g^2}{2\mu - 2V(r) - \nu}\right] \sum_{\mathbf{k}} \frac{1 - 2f(E_{\mathbf{k}})}{2E_{\mathbf{k}}} = 0 \ . \tag{24.134}$$

which characterizes the excitation gap $\Delta(r)$ at positions r such that $\mu_{pair}(r) = 0$. Moreover, the pseudogap contribution to $\Delta^2(T) = \tilde{\Delta}^2_{sc}(T) + \Delta^2_{pg}(T)$ is given by

$$\Delta^2_{pg} = \frac{1}{Z} \sum_{\mathbf{q}} b(\Omega_q - \mu_{pair}) \ . \tag{24.135}$$

Here b represents the usual Bose function. The density of particles at radius r:

$$\begin{aligned} n(r) \ &= \ 2n_b^0 + \frac{2}{Z_b} \sum_{\mathbf{q}} b(\Omega_q - \mu_{boson}) \\ &\quad + 2 \sum_{\mathbf{k}} \left[v^2_{\mathbf{k}}(1 - f(E_{\mathbf{k}})) + u^2_{\mathbf{k}} f(E_{\mathbf{k}}) \right] \ . \end{aligned} \tag{24.136}$$

The important quantity $\mu_{pair} = \mu_{boson}$ is identically zero in the superfluid region $r < R_{sc}$, and must be solved for self consistently at larger radii. Here M is the bare boson mass equal to $2m$, and the various residues, Z and Z_b and pair dispersion Ω_q are described in Section 24.3.3.

The transition temperature T_c is numerically determined as follows: (i) A chemical potential is assigned to the center of the trap $\mu(0)$. The chemical potential at radius r will then be $\mu(r) = \mu(0) - V(r)$. (ii) The gap equation [Eq. (24.134)] and pseudogap equation [Eq. (24.135)] are solved at the center (setting $\Delta_{pg} = \Delta$) to find T_c and $\Delta(0, T_c)$ (iii) Next the radius R_Δ is determined. (It can be defined as the point where the gap has a sufficiently small value, such as $\Delta(0, T_c)/1000$). (iv) Following this, the pseudogap equation (Eq. (24.135)) is solved for $\Delta(r, T_c)$ up to the radius R_Δ. Then $n(r)$ is determined using Eq. (24.136). (v) Finally, $n(r)$ is integrated over all space ($\int d^3\mathbf{r} n(r)$) and compared with the given total number of fermions N. The procedure is repeated until the prescribed accuracy has been reached. To extend this algorithm below T_c a similar approach is used which now includes an additional step in which R_{sc} is computed.

Figure 24.33 shows a plot of the density profiles obtained from solving the self consistent equations. Here the Thomas-Fermi radius, called R_{TF}, is calculated for the non-interacting case. In the BCS regime there is virtually no temperature dependence in the density profile as expected from the small values for Δ. In the unitary and BEC regimes as the system approaches T_c, $n(r)$ can be reasonably well fit to a Gaussian. A bi-modality in the distribution is evident in the BEC regime, thus providing a clear signature of the superfluid phase. However, in the PG or unitary it is more difficult to establish superfluidity, since the profiles do not show a clear break at the position where the condensate first appears [160].

These observations differ somewhat from other theoretical predictions in the literature [68, 35]. The differences between the present theory and this other work can be associated with the inclusion of noncondensed pairs or pseudogap effects. These noncondensed pairs smooth out the otherwise abrupt transition between the condensate and the fermionic excitations. In contrast to earlier work [137] these studies, which are based on the standard crossover ground state [187], yield only monotonic density distributions. Future experiments will be needed to look for the secondary maxima predicted by Strinati and co-workers [135] in the BEC and unitary regimes.

Finally, Fig. 24.34 shows the behavior of T_c (inset) in a trap, together with the superfluid density (main figure). The latter is computed following the discussion in Sec. 24.4. From the inset one can read off that $T_c/E_F \approx 0.3$ at resonance, which is very close to [135], or slightly smaller than other estimates [132] in the literature.

The structure seen in the plot of T_c for the trapped gas reflects the minimum and maximum found for the homogeneous solution (Fig. 24.23); these are related, respectively, to where $\mu \approx 0$ and where unitary scattering occurs. The T_c curve follows generally the decrease in the density at the center of the trap from BEC to BCS. The temperature dependences of the (integrated over r) superfluid density reflect the nature of excitations of the condensate. The BEC limit has only bosonic, while the BCS has only fermionic excitations. The unitary case is somewhere in between. The fermionic contributions are apparent in the BCS regime, where N_s decreases almost linearly at low T. For an s-wave superfluid this reflects the contributions from low $\Delta(r) \leq T$ regions, near the edge of the trap. These are present to a lesser degree in the unitary case. The bosonic contribution to N_s and to thermodynamics (in both the BEC and unitary regimes) is governed by the important constraint that $\mu_{pair}(r)$ vanishes at positions r where there is a co-existent superfluid. A similar constraint is imposed at the level of Hartree-Fock-Bogoliubov theory for true bosons [156]. These gapless pair excitations are responsible for a $T^{3/2}$ temperature dependence in N_s. In this way the low T power law dependences are similar to their analogues in the homogeneous case of Section 24.7.4, much as found for true Bose gases [23] in a trap.

As for the BEC regime there is an interesting observation to make about the contribution to the density profile associated with the condensate. Experimentalists generally assume a Gaussian form throughout the trap for the noncondensed pairs. In this way they estimate the

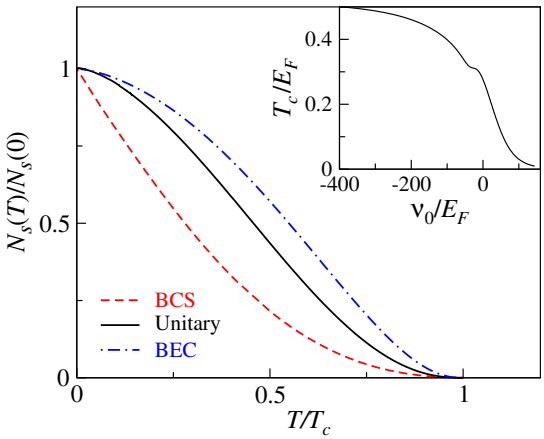


Figure 24.34: Behavior of superfluid density N_s as a function of T in the three different regimes. Note that the negative curvatures at low T for the unitary and BEC cases are different from the linear behavior in the BCS case. In the BEC limit, $N - N_s \propto T^{3/2}$. In the inset we show T_c as a function of magnetic detuning ν_0 in a trap. We have taken $U_0 = -0.9E_F/k_F^3$ and $g_0 = -35E_F/k_F^{3/2}$, based on experimental data for ^{40}K.

condensate fraction. Here we find [160] that this Gaussian form is not correct in the superfluid region of the trap, and that this Gaussian approximation will underestimate (by $\approx$ a factor of 1.5) the condensate fraction in the BEC regime.

24.6.3 Comparison Between Theory and Experiment: Cold Atoms

As time progresses it will be important to assess the assumed ground state wavefunction [187] and its two channel variant [123, 131, 161] in more detail. A first generation set of measurements and theories have indicated an initial level of success in addressing four experiments: RF pairing gap spectroscopy and collective mode measurements, as well as more recently, the particle density profiles [160] and thermodynamics [88] of Fermi gases in the unitary regime. The first of these experiments [34] seem to provide some support for the fact that the Bogoliubov excitations with dispersion, $E_{\mathbf{k}} \equiv \sqrt{(\epsilon_{\mathbf{k}} - \mu)^2 + \Delta^2(T)}$ have a "gap parameter" or pseudogap, $\Delta(T)$ which is in general different from the superconducting order parameter, as a consequence of noncondensed pairs at and above T_c. Törmä and colleagues [90] have used the formalism outlined in Section 24.3.2, to address RF spectroscopy. Subsequently [89] they have combined this analysis with an approximate LDA treatment of the trap to make contact with RF experiments [34]. Important to their work is the fact that the edges of a trap have a free atom character, where there is a vanishing $\Delta(r)$.

Additional support for the wavefunction comes from the collective mode behavior near $T = 0$. The mode frequencies can be connected to an equation of state [166]. Numerical studies [74, 66] of this equation for the standard crossover ground state demonstrate a good fit to the measured breathing mode frequencies [87, 10]. Importantly, in the near-BEC limit the frequencies decrease with increasing magnetic field; this is opposite to the behavior predicted for true bosons [166], and appears to reinforce the notion that for the magnetic fields studied thus far, the "BEC" regime should be associated with composite rather than real bosons.

At $T = 0$, calculations of the collective mode frequencies are based on an equation of state. Moreover, the zero temperature equation of state associated with the mean field ground state can be computed analytically in the near-BEC limit

$$\mu = -\frac{1}{2ma_s^2} + \frac{\pi a_s n}{m} - \frac{3(\pi n a_s^3)^2}{4ma_s^2} + O(n^3),$$

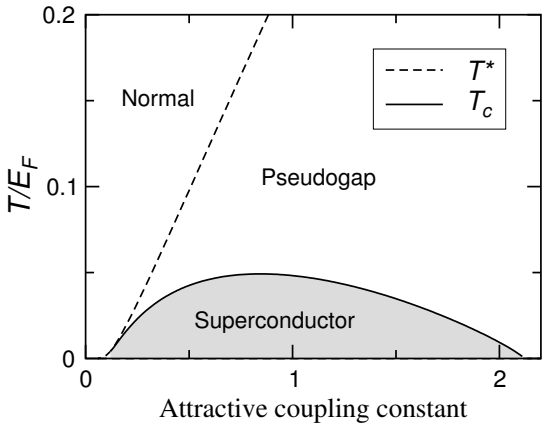


Figure 24.35: Phase diagram for a quasi-two-dimensional (2D) d-wave superconductor on a lattice. Here the horizontal axis corresponds to the strength of attractive interaction $-U/4t$, where t is the in-plane hopping matrix element.

where the first two terms on the right hand side were previously discussed following Eq. (24.55). Importantly, the third term is responsible for the observed agreement between theory and collective mode experiments, in the near-BEC regime.

A serious shortcoming of the wavefunction ansatz has been emphasized in the literature. This is associated with the ratio of the inter-boson to the fermionic scattering length near the unitary regime, but on the BEC side of the Feshbach resonance. Experimentally the numbers are considerably smaller [11, 194] (0.6) than the factor of 2 predicted for the one channel model discussed below Eq. (24.55). They are consistent, however, with more exact few body calculations [138]. These few body calculations apply to a regime of magnetic fields where $k_F a_s$ is smaller than about 0.3 -0.4. This seems to be close to the boundary for the "quasi-BEC" regime which can be accessed experimentally [11] in ^{6}Li.

It is interesting to repeat the $T = 0$ many body calculations now with the inclusion of FB, since these two channel effects begin to be important at $k_F a_s$ smaller than around 0.2 -0.25. Here, one sees [161], that the factor of 2 found in the one channel calculations is no longer applicable, and the values of the ratio (of bosonic to fermionic scattering lengths) are considerably smaller, and, thus, tending in the direction which is more in line with experiment. This reflects the decrease in the number of fermionic states which mediate the interaction between molecular bosons.

In this way the mean field theory presented here looks promising. Nevertheless, uncertainties remain. Current theoretical work [89] on the RF experiments is limited to the intermediate coupling phase, while experiments are also available for the near-BEC and near-BCS regimes, and should be addressed theoretically. In addition, the predictions of alternative approaches [137] which posit a different ground state will need to be compared with these RF data. The collective mode calculations [74, 66] which have been performed have not yet considered the effects of Feshbach bosons, which may change the behavior in the near-BEC regime.

It is, finally, quite possible that incomplete $T = 0$ condensation will become evident in future experiments. If so, an alternative wavefunction will have to be contemplated. Indeed, it has been argued [72] that the failure of the one channel model to match the calculations of Petrov and co-workers [138] is evidence that there are serious weaknesses. At an experimental level, new pairing gap spectroscopies appear to be emerging at a fairly rapid pace [60, 17] which will further test these and subsequent theories.

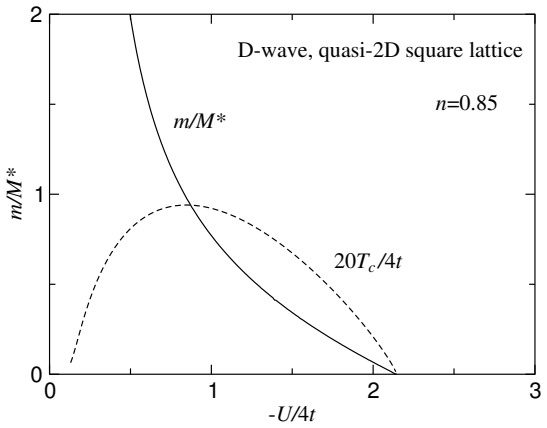


Figure 24.36: Inverse pair mass (solid line) and T_c (dashed line) as a function of coupling strength $-U/4t$ for a d-wave superconductor on a quasi-2D square lattice, where t is the in-plane hopping matrix element. T_c vanishes when the pair mass diverges, before the bosonic regime is reached. The electron density is taken to be $n = 0.85$ per unit cell, corresponding to optimal hole doping in the cuprate superconductors.

24.7 Physical Implications: High T_c Superconductivity

We begin with an important caveat that many of the experiments outlined in this section can alternatively be addressed from a Mott physics point of view [106]. Here we summarize the interpretation of these experiments within BCS-BEC crossover theory with the hope that this discussion will be of value to the cold atom community, and that ultimately, it will help to establish precisely how relevant is the BCS-BEC crossover scenario for understanding high temperature superconductivity.

24.7.1 Phase Diagram and Superconductor-Insulator Transition: Boson Localization Effects

The high T_c superconductors are different from the ultracold fermionic superfluids in one key respect; they are d-wave superconductors and their electronic dispersion is associated with a quasi-two dimensional tight binding lattice. In many ways this is not a profound difference from the perspective of BCS-BEC crossover. Figure 24.35 shows a plot of the two important temperatures T_c and T^* as a function of increasing attractive coupling. On the left is BCS and the right is PG. The BEC regime is not apparent. This is because T_c disappears before it can be accessed. At the point where T_c vanishes, $\mu/E_F \approx 0.8$.

A competition between increasing T^* and T_c is also apparent in Fig. 24.35. This is a consequence of pseudogap effects. There are fewer low energy fermions around to pair, as T^* increases. It is interesting to compare Fig. 24.35 with the experimental phase diagram plotted as a function of x in Fig. 24.7. If one inverts the horizontal axis (and ignores the AFM region, which is not addressed here) the two are very similar. To make an association between the coupling U and the variable x, it is reasonable to simply fit $T^*(x)$. We do not dwell on this last step here, since we wish to emphasize crossover effects which are not complicated by "Mott physics".

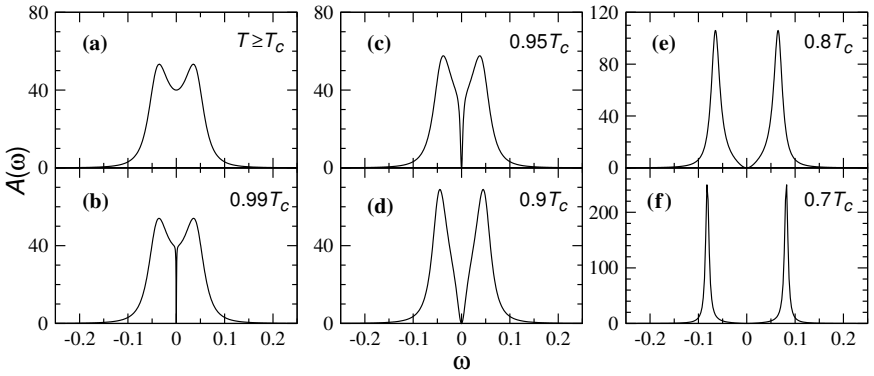


Figure 24.37: Evolution of spectral functions of a pseudogapped superconductor with temperature. As soon as T drops below T_c, the spectral peaks split up rapidly, signalling the onset of phase coherence.

Because of quasi-two dimensionality, the energy scales of the vertical axis in Fig. 24.35 are considerably smaller than their three dimensional analogues. Thus, pseudogap effects are intensified, just as conventional fluctuation effects are more apparent in low dimensional systems. This may be one of the reasons why the cuprates are among the first materials to clearly reveal pseudogap physics. Moreover, the present calculations show that in a strictly $2D$ material, T_c is driven to zero, by bosonic or fluctuation effects. This is a direct reflection of the fact that there is no Bose condensation in $2D$.

Figure 24.36 presents a plot [29] of boson localization effects associated with d-wave pairing. A divergence in the effective mass m/M^* occurs when the coupling strength, or equivalently T^* becomes sufficiently large. Once the bosons localize the system can no longer support superconductivity and T_c vanishes. It is generally believed that a system of bosons with short range repulsion is either a superfluid or a Mott insulator in its ground state [52]. Moreover, the insulating phase is presumed to contain some type of long range order. Interestingly, there are recent reports of ordered phases [56, 181] in the very underdoped cuprates. These appear on the insulating side and possibly penetrate across the superconductor-insulator boundary; they have been interpreted by some as Cooper pair density waves [26, 172, 117]. The observation of boson localization appears to be a natural consequence of BCS-BEC theory; it should be stressed that it is associated with the d-wave lattice case. Because d-wave pairs are more spatially extended (than their s-wave counterparts) they experience stronger Pauli repulsion [29] and this inhibits their hopping.

24.7.2 Superconducting Coherence Effects

The presence of pseudogap effects raises an interesting set of issues surrounding the signatures of the transition which the high T_c community has wrestled with, much as the cold atom community is doing today. For a charged superconductor there is no difficulty in measuring the superfluid density, through the electrodynamic response. Thus one knows with certainty where T_c is. Nevertheless, people have been concerned about precisely how the onset of phase coherence is reflected in thermodynamics, such as C_V or in the fermionic spectral function. One understands how phase coherence shows up in BCS theory, since the ordered state is always accompanied by the appearance of an excitation gap. When a gap is already well developed at T_c, how do these signatures emerge?

To address these coherence effects one has to introduce a distinction between the self energy [31] associated with noncondensed and condensed pairs. This distinction is blurred by the approximation of Eq. (24.89). Above, but near T_c, or at any temperature below we now use an

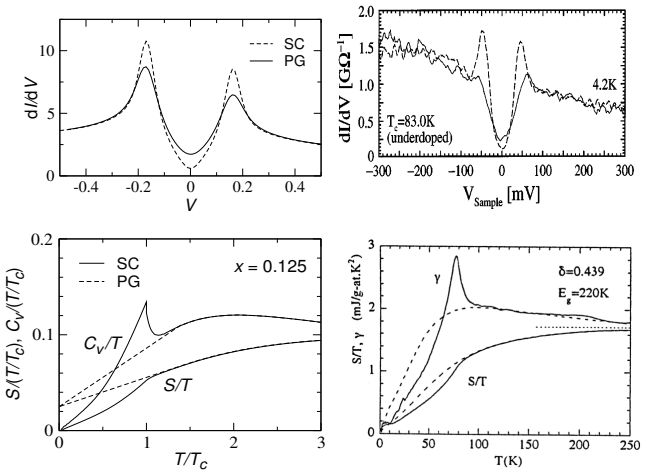


Figure 24.38: Superconducting state (SC) and extrapolated normal state (PG) contributions to SIN tunneling characteristics dI/dV (upper panels) and thermodynamics S/T and C_v/T (lower panels). We compare theoretical calculations (left) with experiments (right) on tunneling for BSCCO from [149] and on specific heat for $Y_{0.8}Ca_{0.2}Ba_2Cu_3O_{7-\delta}$ (YBCO) from [169]. The theoretical SIN curve is calculated for $T = T_c/2$, while the experimental curves are measured outside (dashed line) and inside (solid line) a vortex core. The *dashed and solid* curves in the upper left panel are for SC and PG state, respectively. In both lower panels, the *solid and dashed* curves indicate the SC and PG state, respectively.

improved approximation [114, 115]

$$\Sigma_{pg} \approx \frac{\Delta^2}{\omega + \xi_{\mathbf{k}} + i\gamma} \tag{24.137}$$

This is to be distinguished from Σ_{sc} where the condensed pairs are infinitely long-lived and there is no counterpart for γ. The value of this parameter, and even its T-dependence is not particularly important, as long as it is nonzero.

Figure 24.37 plots the fermionic spectral function at $\xi_{\mathbf{k}} = 0$, called $A(\omega)$, as the system passes from above to below T_c. One can see in this figure that just below T_c, $A(\omega)$ is zero at a point $\omega = 0$, and that as temperature further decreases the spectral function evolves smoothly into approximately two slightly broadened delta functions, which are just like their counterparts in BCS. In this way there is a clear signature associated with superconducting coherence. To compare with experimental data is somewhat complicated, since measurements of the spectral function [42, 20] in the cuprates also reveal other higher energy features ("dip, hump and kink"), not specifically associated with the effects of phase coherence. Nevertheless, this Figure, like its experimental counterpart, illustrates that sharp gap features can be seen in the spectral function, but only below T_c.

Analogous plots of superconducting coherence effects are presented in Fig. 24.38 in the context of more direct comparison with experiment. Shown are the results of specific heat and tunneling calculations and their experimental counterparts [169, 149]. The latter measures, effectively, the density of fermionic states. Here the label "PG" corresponds to an extrapolated normal state in which we set the superconducting order parameter Δ_{sc} to zero, but maintain the the total excitation gap Δ to be the same as in a phase coherent, superconducting state. Agreement between theory and experiment is satisfactory. We present this artificial normal state extrapolation in discussing thermodynamics in order to make contact with its experimental counterpart. However, it should be stressed that in zero magnetic field, there is no coexistent non-superconducting phase. BCS theory is a rather special case in which there are two possible phases below T_c, and one can, thereby, use this coexistence to make a reasonable estimate of

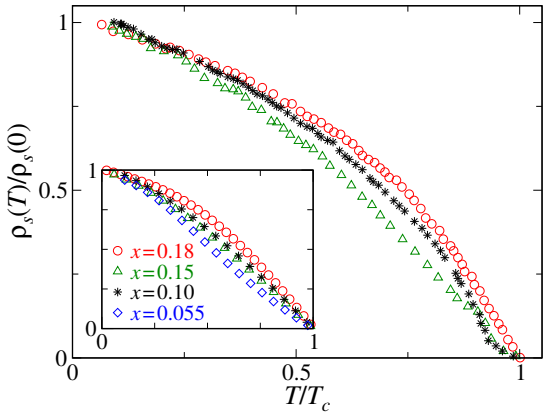


Figure 24.39: Comparison of normalized superfluid density $\rho_s/\rho_s(0)$ versus T/T_c for experiment (main figure) and theory (inset) in high T_c superconductors with variable doping concentration x. Both experiment and theory show a quasi-universal behavior with respect to doping.

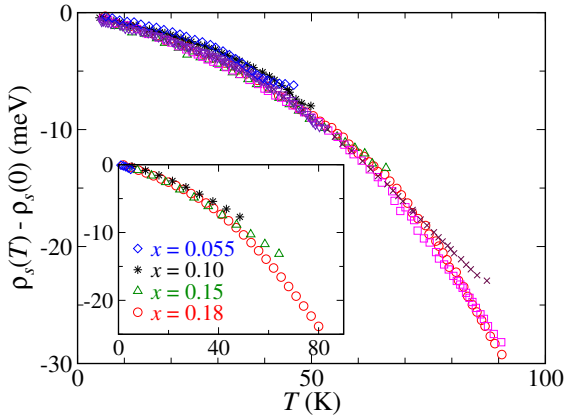


Figure 24.40: Offset plot of superfluid density ρ_s comparing experiment (main figure) with theory (inset). Both experiment and theory show the same quasi-universal slope $d\rho_s/dT$ for different hole concentrations x.

the condensation energy. When Bose condensation needs to be accommodated, there seems to be no alternative "normal" phase below T_c.

24.7.3 Electrodynamics and Thermal Conductivity

In some ways the subtleties of phase coherent pairing are even more perplexing in the context of electrodynamics. Figure 24.12 presents a paradox in which the excitation gap for fermions appears to have little to do with the behavior of the superfluid density. To address these data [163] one may use the formalism of Sec. 24.4.1. One has to introduce the variable x (which accounts for Mott physics) and this is done via a fit to $T^*(x)$ in the phase diagram. Here for Fig. 24.40 it is also necessary to fit $\rho_s(T=0,x)$ to experiment, although this is not important in Fig. 24.39. The figures show a reasonable correspondence [163] with experiment. The paradox raised by Fig. 24.12 is resolved by noting that there are bosonic excitations of the condensate, as in Eq. (24.113) and that these become more marked with underdoping, as pseudogap effects increase. In this way ρ_s does not exclusively reflect the fermionic gap, but rather vanishes "prematurely" before this gap is zero, as a result of pair excitations.

The optical conductivity $\sigma(\omega)$ is similarly modified [174, 77]. Indeed, there is an intimate relation between ρ_s and $\sigma(\omega)$ known as the f-sum rule. Optical conductivity studies in the literature, both theory and experiment, have concentrated on the low ω, T regime and the

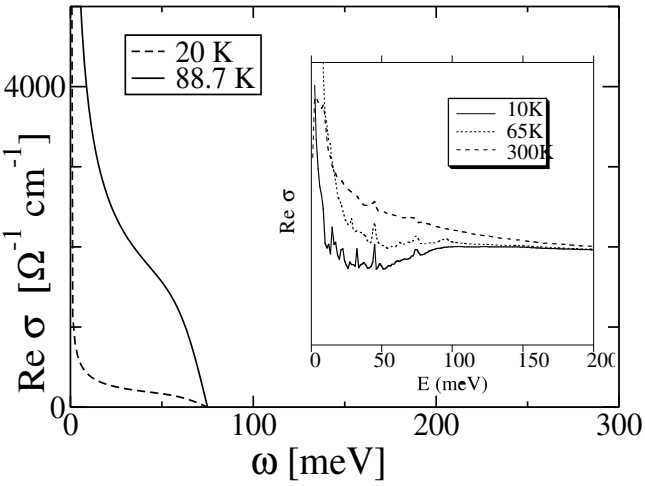


Figure 24.41: Real part of ac conductivity at low and high T below T_c. Here pseudogap effects, which insure that $\Delta(T) \approx$ *constant* below T_c, require that one go beyond BCS theory to explain the data shown in the inset [142]. In the theory, inelastic and other effects which presumably lead to the large constant background term observed in the data have been ignored.

interplay between impurity scattering and d wave superconductivity [15]. Also of interest are unusually high ω tails [124, 152] in the real part of $\sigma(\omega)$ which can be inferred from sum-rule arguments and experiment. Figure 24.12 raises a third set of questions which pertain to the more global behavior of σ. In the strong PG regime, where Δ has virtually no T dependence below T_c, the BCS-computed $\sigma(\omega)$ will be similarly T-independent. This is in contrast to what is observed experimentally where $\sigma(\omega)$ reflects the same T dependence as in $\rho_s(T)$, as dictated by the f-sum rule.

One may deduce a consequence of this sum rule, based on Eq. (24.113). If we associate the fermionic contributions with the first term in square brackets in this equation, and the bosonic contributions with the second. Note that the fermionic transport terms reflect the full Δ just as do the single particle properties. (This may be seen by combining the superconducting and Maki Thompson or PG diagrams in Appendix 24.9). We may infer a sum rule constraint on the bosonic contributions, which vanish as expected in the BCS regime where Δ_{pg} vanishes. We write

$$\frac{2}{\pi}\int_0^\infty d\Omega\, \sigma^{bosons}(\Omega,T) = \frac{\Delta_{pg}^2}{\Delta^2}\left(\frac{n_s}{m}\right)^{BCS}(T)\,. \tag{24.138}$$

The bosonic contributions can be determined most readily from a framework such as time dependent Ginzburg Landau theory, which represents rather well the contributions from the Aslamazov-Larkin diagrams, discussed in Appendix 24.9. The bosons make a maximum contribution at T_c.

The resulting optical conductivity [77] in the superconducting state is plotted in Fig. 24.41 below. The key feature to note is the decrease in width of the so-called Drude peak with decreasing temperature. In the present picture this pseudogap effect can be understood as coming from the contribution of bosonic excitations of the condensate, which are present at T_c, but which disappear at low T. This behavior is reasonably consistent with what is reported experimentally [174], where "the effect of the opening of a pseudogap is a narrowing of the coherent Drude peak at low frequency". The calculations leading to Fig. 24.41, indicate that by 20 K most of the conductivity is fermionic except for a high frequency tail associated with the bosons. This tail may be responsible in part for the anomalously high ω contributions to σ required to satisfy the sum rule [124, 152].

Although the normal state calculations have not been done in detail, once the temperature

is less than T^*, pseudogap effects associated with the fermionic contribution will also lead to a progressive narrowing in the Drude peak with decreasing T, down to T_c, due to the opening of an excitation gap. This mechanism (which is widely ascribed to [174] in the literature) reflects longer lived electronic states, associated with the opening of this gap. However, it cannot be applied to explain the progressive narrowing of the conductivity peaks, once $\Delta(T)$ becomes temperature independent, as is the case at low T. In this way, one can see that pseudogap effects show up in the optical conductivity of underdoped samples, both from the fermionic contributions (near and below T^*) and the bosonic contributions (below T_c) as a narrowing of the Drude peak.

The data shown in the inset of Fig. 24.41 reveal that the condensate is made from frequency contributions primarily up to ≈ 0.15 eV. These data pose a challenge for applying strict BCS theory to this problem, since one consequence of a temperature independent Δ in the underdoped phase is the absence of T dependence in the optical conductivity. This is the same challenge as posed by Fig. 24.12. Strikingly there is no explicit "gap feature" in the optical conductivity in the normal state. Such a gap feature, that is a near vanishing of σ for an extended range of frequencies, will occur in models where the pseudogap is unrelated to superconductivity; it is not seen experimentally, thus far

By contrast with the electrical conductivity, the thermal conductivity is dominated by the fermionic contributions at essentially all T. This is because the bosonic contribution to the heat current (as in standard TDGL theory [103]), is negligibly small, reflecting the low energy scales of the bosons. Thermal conductivity, experiments [167] in the high T_c superconductors provide some of the best evidence for the presence of fermionic d-wave quasiparticles below T_c. In contrast to the ac conductivity, here one sees a universal low T limit [104], and there is little to suggest that something other than conventional d-wave BCS physics is going on here. This cannot quite be the case however, since in the pseudogap regime, the temperature dependence of the fermionic excitation gap is highly anomalous, as shown in Fig. 24.3, compared to the BCS analogue.

24.7.4 Thermodynamics and Pair-breaking Effects

The existence of noncondensed pair states below T_c affects thermodynamics, in the same way that electrodynamics is affected, as discussed above. Moreover, one can predict [30] that the q^2 dispersion will lead to ideal Bose gas power laws in thermodynamical and transport properties. These will be present in addition to the usual power laws or (for s-wave) exponential temperature dependences associated with the fermionic quasiparticles. Note that the q^2 dependence reflects the spatial extent ξ_{pg}, of the composite pairs, and this size effect has no natural counterpart in true Bose systems. It should be stressed that numerical calculations show that these pair masses, as well as the residue Z are roughly T independent constants at low T. As a result, Eq. (24.94) implies that $\Delta_{pg}^2 = \Delta^2(T) - \Delta_{sc}^2(T) \propto T^{3/2}$.

The consequences of these observations can now be listed [30]. For a quasi-two dimensional system, C_v/T will appear roughly constant at the lowest temperatures, although it vanishes strictly at $T = 0$ as $T^{1/2}$. The superfluid density $\rho_s(T)$ will acquire a $T^{3/2}$ contribution in addition to the usual fermionic terms. By contrast, for spin singlet states, there is no explicit pair contribution to the Knight shift. In this way the low T Knight shift reflects only the fermions and exhibits a scaling with $T/\Delta(0)$ at low temperatures. Experimentally, in the cuprates, one usually sees a finite low T contribution to C_v/T. A Knight shift scaling is seen. Finally, also observed is a deviation from the predicted d-wave linear in T power law in ρ_s. The new power laws in C_v and ρ_s are conventionally attributed to impurity effects, where $\rho_s \propto T^2$, and $C_v/T \propto const.$ Experiments are not yet at a stage to clearly distinguish between these two alternative explanations.

Pair-breaking effects are viewed as providing important insight into the origin of the cuprate pseudogap. Indeed, the different pair-breaking sensitivities of T^* and T_c are usually proposed to support the notion that the pseudogap has nothing to do with superconductivity. To counter this inference, a detailed set of studies was conducted, (based on the BEC-BCS scenario), of pair-breaking in the presence of impurities [32, 84] and of magnetic fields [83]. These studies make it clear that the superconducting coherence temperature T_c is far more sensitive to pair-breaking than is the pseudogap onset temperature T^*. Indeed, the phase diagram of Fig. 24.35 which mirrors its experimental counterpart, shows the very different, even competing nature of T^* and T_c, despite the fact that both arise from the same pairing correlations.

24.7.5 Anomalous Normal State Transport: Nernst and Other Precursor Transport Contributions

Much attention is given to the anomalous behavior of the Nernst coefficient in the cuprates [188]. This coefficient is rather simply related to the transverse thermoelectric coefficient α_{xy} which is plotted in Fig. 24.13. In large part, the origin of the excitement in the literature stems from the fact that the Nernst coefficient behaves smoothly through the superconducting transition. Below T_c it is understood to be associated with superconducting vortices. Above T_c if the system were a Fermi liquid, there are arguments to prove that the Nernst coefficient should be essentially zero. Hence the observation of a non-negligible Nernst contribution has led to the picture of normal state vortices.

Another way to view these data is that there are bosonic degrees of freedom present in the normal state, as in the BCS-BEC crossover approach. To describe this dynamics we begin with the TDGL scheme outlined in Sec. 24.2.8. This formalism must be modified somewhat however. When "pre-formed" pairs are present at temperatures T^* high compared to T_c, the classical bosonic fields of conventional TDGL must be replaced by their quantum counterparts [170]. We investigate this fairly straightforward extension of TDGL in the next sub-section, and subsequently explore the resulting implications for transport.

Quantum Extension of TDGL

To make progress on the quantum analogue of TDGL we study a Hamiltonian describing bosons coupled to a particle reservoir of fermion pairs. The latter are addressed in a quantum mechanical fashion. Our treatment of the reservoir has strong similarities to the approach of Caldeira and Leggett [19]. These bosons are in the presence of an electromagnetic field, which interacts with the fermion pairs of the reservoir as well, since they have charge $e^* = 2e$. For simplicity we assume that the fermions are dispersionless. This Hamiltonian is given by

$$H = \sum_{\mathbf{lm}} \varepsilon_{\mathbf{lm}} \psi_{\mathbf{l}}^\dagger(t) \exp\bigl(-ie^* C_{\mathbf{lm}}(t)\bigr) \psi_{\mathbf{m}}(t) + \sum_{\mathbf{l}} e^* \phi \psi^\dagger \psi + \sum_{i\mathbf{l}} \Bigl\{ (a_i + e^*\phi) w_i^\dagger w_i + \eta_i \psi^\dagger w_i + \eta_i^* w_i^\dagger \psi \Bigr\} + \sum_{i\mathbf{l}} \Bigl\{ (b_i - e^*\phi) v_i^\dagger v_i + \zeta_i \psi^\dagger v_i^\dagger + \zeta_i^* v_i \psi \Bigr\}. \quad (24.139)$$

Here $\varepsilon_{\mathbf{lm}}$ is the hopping matrix element for the bosons. $C_{\mathbf{lm}}(t)$ is the usual phase factor associated with the vector potential. Annihilation operators for the reservoir, w_i and v_i (with infinitesimal coupling constants η_i and ζ_i), represent positive and negative frequencies respectively and need to be treated separately. The energies a_i and b_i of the reservoir are both positive.

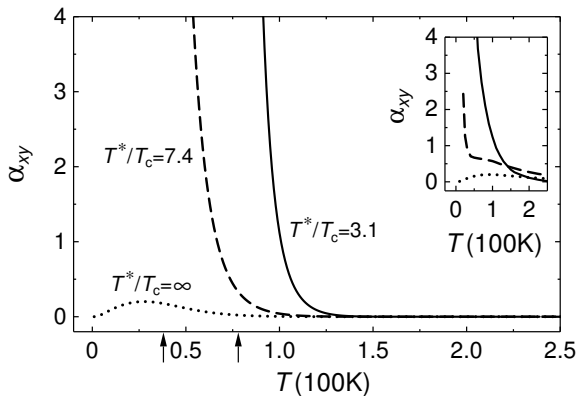


Figure 24.42: Calculated transverse thermoelectric response, which appears in the Nernst coefficient. Inset plots experimental [188] data. Both the theoretical and experimental values of α_{xy} are normalized by the value of α_{xy} for an optimally doped sample at $2T_c$, $0.0232(B/\mathrm{T})$ V/(KΩm).

The bosonic propagator $T(\mathbf{k},\omega)$ can be exactly computed from the equations of motion. Here $A(\mathbf{k},\omega) = \mathrm{Re}2iT(\mathbf{k},\omega)$ is the boson spectral function, and

$$T(\mathbf{k},\omega) \equiv \Big(\omega - \varepsilon(\mathbf{k}) - \Sigma_1(\omega) + \frac{i}{2}\Sigma_2(\omega)\Big)^{-1} \tag{24.140}$$

We have

$$\Sigma_2(\omega) \equiv 2\pi \sum_i |\eta_i|^2 \delta(\omega - a_i) - 2\pi \sum_i |\zeta_i|^2 \delta(\omega + b_i), \tag{24.141}$$

with $\Sigma_1(\omega)$ defined by a Kramers Kronig transform.

The reservoir parameters a_i, b_i, η_i and ζ_i which are of no particular interest, are all subsumed into the boson self energy $\Sigma_2(\omega)$. From this point forward we may ignore these quantities in favor of the boson self energy. We reiterate that this theory makes an important simplification, that the reservoir pairs have no dispersion. *For this case one can solve for the exact transport coefficients.*

For small, but constant magnetic and electric fields and thermal gradients we obtain the linearized response. For notational convenience, we define $v_{ab}(\mathbf{k}) \equiv \frac{\partial^2}{\partial k_a \partial k_b}\varepsilon(\mathbf{k})$. Then we can write a few of the in-plane transport coefficients which appear in Eqs. (24.8) and (24.9) as

$$\sigma = -\frac{e^{*2}}{2} \int \frac{\mathrm{d}^3k}{(2\pi)^3} \frac{\mathrm{d}\omega}{2\pi} v_x v_x A^2(\mathbf{k},\omega) \frac{\partial b(\omega)}{\partial \omega} \tag{24.142}$$

and

$$\alpha_{xy} = -\frac{e^{*2} B_z}{6T} \int \frac{\mathrm{d}^3k}{(2\pi)^3} \frac{\mathrm{d}\omega}{2\pi} v_x v_x v_{yy} \omega A^3(\mathbf{k},\omega) \frac{\partial b(\omega)}{\partial \omega}\,. \tag{24.143}$$

These equations naturally correspond to their TDGL counterparts (except for different phenomenological coefficients) when $T \approx T_c$.

Comparison with Transport Data

The formalism of the previous sub-section and in particular, Eqs. (24.142) and (24.143), can be used to address transport data within the framework of BCS-BEC crossover. The results for α_{xy}, which relates to the important Nernst effect, are plotted in Fig. 24.42 with a subset of the data plotted in the upper right inset. It can be seen that the agreement is reasonable. In this way a "pre-formed pair" picture is, at present, a viable alternative to "normal state vortices".

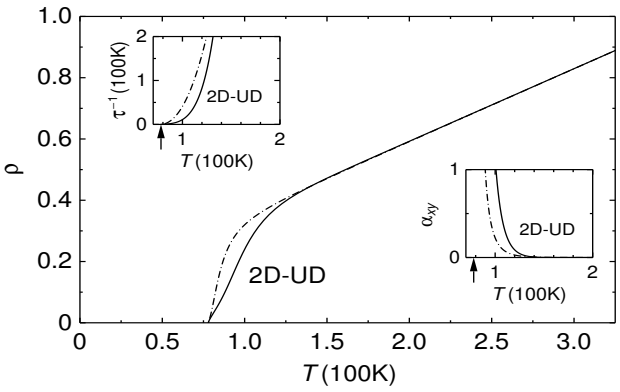


Figure 24.43: dc resistivity ρ (normalized by $\rho_Q \equiv s/e^2$) vs. T, for quasi-2D underdoped (UD) samples with two different forms for $\mu_{\rm pair}$. These are shown plotted in the left inset as $\tau^{-1} \equiv -\mu_{\rm pair}/{\rm Im}\gamma$. The right inset shows corresponding α_{xy}, and arrows indicate T_c.

Within the crossover scenario, just as in TDGL, there are strong constraints on other precursor transport effects: paraconductivity, diamagnetism and optical conductivity are all indirectly or directly connected to the Nernst coefficient, in the sense that they all derive from the same dynamical equation of motion for the bosons. Analogous inferences have been made [57], based on similar bosonic generalizations of TDGL.

The calculated behavior of a number of these other properties is summarized [170] in Figs. 24.43 and 24.44 below, which indicate both quasi-two dimensional and more three dimensional behavior. In the plots for the resistivity, ρ, a fairly generic [109] linear-in-T contribution [38] from the fermions has been added, as a background term. A central theme of concern in the literature is whether one can understand the behavior of ρ simultaneously with that of α_{xy}. Experiments [109, 186] indicate that there is a small feature corresponding to T^* at which ρ deviates from the background linear fermionic term, but that the deviation is not noticeably large except in the immediate vicinity of T_c. This is in contrast to the behavior of α_{xy} which shows a significant high temperature onset. A key observation from the theoretical calculations shown in the figures is that the onset temperatures for the Nernst coefficient and the resistivity are rather different with the former being considerably higher than the latter. Moreover all onsets appear to be significantly less than T^*. Qualitative agreement with experiment is not unreasonable. However, a more quantitative comparison with experiment has not been established, since it depends in detail on a phenomenological input: the temperature dependence of the pair chemical potential $\mu_{\rm pair}$.

Another important feature of these plots is the fact that there is virtually no diamagnetic precursor, as was also found to be the case in simple TDGL. To see this, note that the magnetization can be written [154, 170]

$$\frac{\mu_0 M}{B} = -\frac{4}{3}\frac{\alpha k_B T}{\hbar c}\frac{\xi_{ab}^2}{s\sqrt{1+(2\xi_c/s)^2}},$$

where α is the fine structure constant, c is the speed of light, s is the interlayer spacing, and ξ_{ab} (ξ_c) are coherence lengths in the direction parallel (perpendicular) to the planes. From this result we can estimate the order of magnitude of the diamagnetic susceptibility due to preformed pairs. For a typical high T_c superconductor, $T \sim 50$K, so that $\lambda \equiv \frac{hc}{k_B T} \sim 3\times 10^{-4}$m, and $\lambda/\alpha \sim 4\times 10^{-2}$m. Because the coherence lengths and the interlayer spacing are on the nanometer length scale, precursor effects in the diamagnetic susceptibility are of the order 10^{-6}, and thus extremely small, as is consistent with experiment [185].

[38] In reality, one should include an additional temperature dependence from pseudogapped fermions which presumably has a small upturn, relative to a linear curve, as T decreases.

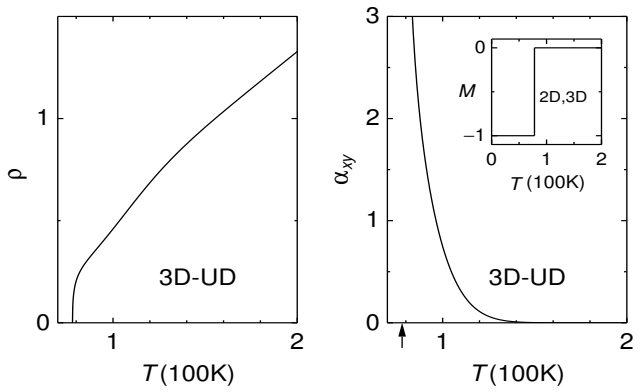


Figure 24.44: dc resistivity and α_{xy}, for an underdoped, more three-dimensional, system like YBCO. The arrow indicates T_c. The magnetization M is plotted as the inset, and is independent of dimensionality.

In order to make the BCS-BEC scenario more convincing it will be necessary to take these transport calculations below T_c. This is a project for future research and in this context it will ultimately be important to establish in this picture how superconducting state vortices are affected by the persistent pseudogap. Magnetic field induced magnetic order which has been associated with vortices [102] will, moreover, need to be addressed. The analogous interplay of vortices and pseudogap will also be of interest in the neutral superfluids.

24.8 Derivation of the $T = 0$ variational conditions

The ground state wavefunction is given by

$$\bar{\Psi}^0 = e^{-\lambda^2/2+\lambda b_0^\dagger}|0\rangle \otimes \Pi_{\mathbf{k}}(u_{\mathbf{k}} + v_{\mathbf{k}} a_{\mathbf{k}}^\dagger a_{-\mathbf{k}}^\dagger)|0\rangle \tag{24.144}$$

Thus one has three variational parameters $\lambda, u_{\mathbf{k}}, v_{\mathbf{k}}$ with normalization condition $u_{\mathbf{k}}^2 + v_{\mathbf{k}}^2 = 1$. We can define $\theta_{\mathbf{k}}$ such that $u_{\mathbf{k}} = \sin\theta_{\mathbf{k}}$ and $v_{\mathbf{k}} = \cos\theta_{\mathbf{k}}$, so that we have only two variational parameters, λ and $\theta_{\mathbf{k}}$.

We then have

$$\begin{aligned}\langle\bar{\Psi}^0|H-\mu N|\bar{\Psi}^0\rangle &= (\nu-2\mu)\lambda^2 + 2\sum_{\mathbf{k}}(\epsilon_{\mathbf{k}}-\mu)v_{\mathbf{k}}^2 \\ &+ 2U\sum_{\mathbf{k},\mathbf{k}'} u_{\mathbf{k}}v_{\mathbf{k}}u_{\mathbf{k}'}v_{\mathbf{k}'} + 2g\lambda\sum_{\mathbf{k}} u_{\mathbf{k}}v_{\mathbf{k}}\ ,\end{aligned}$$

where we have chosen $\varphi_{\mathbf{k}} = 1$ in Eq. (24.11) for simplicity.

Let us define

$$\Delta_{sc} = -2U\sum_{\mathbf{k}} u_{\mathbf{k}}v_{\mathbf{k}}. \tag{24.145}$$

The variational conditions are

$$\frac{\delta\langle H-\mu N\rangle}{\delta\lambda} = 0 \tag{24.146}$$

and

$$\frac{\delta\langle H-\mu N\rangle}{\delta\theta_{\mathbf{k}}} = 0 \tag{24.147}$$

These conditions yield two equations: a relationship between the two condensates

$$\frac{g\lambda}{\Delta_{sc}} = \frac{1}{U}\frac{g^2}{\nu-2\mu} \tag{24.148}$$

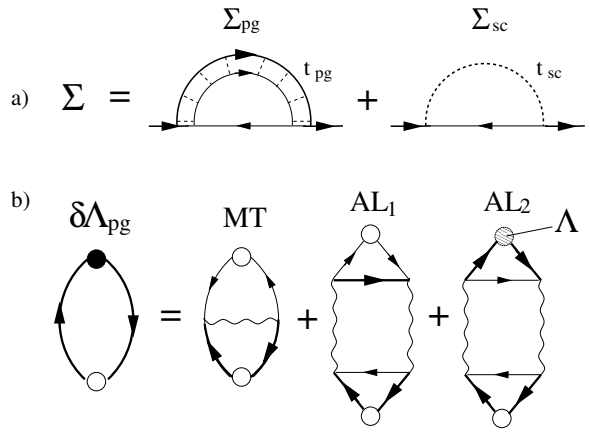


Figure 24.45: Self energy contributions (a) and response diagrams for the vertex correction corresponding to Σ_{pg} (b). Heavy lines are for dressed, while light lines are for bare Green's functions. Wavy lines indicate t_{pg}. See text for details.

and the $T = 0$ gap equation:

$$1 + (U + \frac{g^2}{2\mu - \nu}) \sum_{\mathbf{k}} \frac{1}{2E_{\mathbf{k}}} = 0 \; . \tag{24.149}$$

Similarly, we can write an equation for the total number of fermions

$$\begin{aligned} n^{tot} &= \langle \bar{\Psi}^0 | 2 \sum_{\mathbf{k}} b^\dagger_{\mathbf{k}} b_{\mathbf{k}} + 2 \sum_{\mathbf{k}} a^\dagger_{\mathbf{k}} a_{\mathbf{k}} | \bar{\Psi}^0 \rangle = 2\lambda^2 \\ &+ \sum_{\mathbf{k}} \left[1 - \frac{\epsilon_{\mathbf{k}} - \mu}{E_{\mathbf{k}}} \right] \end{aligned}$$

where

$$E_{\mathbf{k}} = \sqrt{(\epsilon_{\mathbf{k}} - \mu)^2 + \tilde{\Delta}^2_{sc}}, \tag{24.150}$$

with $\tilde{\Delta}_{sc} = \Delta_{sc} - g\lambda$. Thus we have obtained the three equations which characterize the system at $T = 0$. It should be clear that the variational parameter λ is the same as the condensate weight so that $\lambda = \phi_m \equiv \langle b_{\mathbf{q}=0} \rangle$.

24.9 Proof of Ward Identity Below T_c

We now want to establish that the generalized Ward identity in Eq. (24.106) is correct for the superconducting state as well. The vertex $\delta\mathbf{\Lambda}_{pg}$ may be decomposed into Maki-Thompson (MT) and two types of Aslamazov-Larkin (AL_1, AL_2) diagrams, whose contribution to the response is shown here in Fig. 24.45b. We write

$$\delta\mathbf{\Lambda}_{pg} \equiv \delta\mathbf{\Lambda}_{MT} + \delta\mathbf{\Lambda}^1_{AL} + \delta\mathbf{\Lambda}^2_{AL}(\mathbf{\Lambda}) \; . \tag{24.151}$$

Using conventional diagrammatic rules one can see that the MT term has the same sign reversal as the anomalous superconducting self energy diagram. This provides insight into Eq. (24.107). Here, however, the pairs in question are noncondensed and their internal dynamics (via t_{pg} as distinguished from t_{sc}) requires additional AL_1 and AL_2 terms as well, which will ultimately be responsible for the absence of a Meissner contribution from this normal state self energy effect.

Note that the AL_2 diagram is specific to our GG_0 scheme, in which the field couples to the full G appearing in the T-matrix through a vertex $\mathbf{\Lambda}$. It is important to distinguish the vertex $\mathbf{\Lambda}$ which appears in the AL_2 diagram from the full EM vertex Λ^{EM}.

In particular, we have

$$\mathbf{\Lambda} = \boldsymbol{\lambda} + \delta\mathbf{\Lambda}_{pg} - \delta\mathbf{\Lambda}_{sc}\,, \tag{24.152}$$

where the sign change of the superconducting term (relative to $\mathbf{\Lambda}^{EM}$) is a direct reflection of the sign in Eq. (24.107).

We now show that there is a precise cancellation between the MT and AL_1 pseudogap diagrams at $Q = 0$. This cancellation follows directly from the normal state Ward identity

$$Q \cdot \lambda(K, K+Q) = G_0^{-1}(K) - G_0^{-1}(K+Q)\,, \tag{24.153}$$

which implies

$$Q \cdot [\delta\Lambda^1_{AL}(K, K+Q) + \delta\Lambda_{MT}(K, K+Q)] = 0 \tag{24.154}$$

so that $\delta\mathbf{\Lambda}^1_{AL}(K,K) = -\delta\mathbf{\Lambda}_{MT}(K,K)$ is obtained exactly from the $Q \to 0$ limit.

Similarly, it can be shown that

$$Q \cdot \Lambda(K, K+Q) = G^{-1}(K) - G^{-1}(K+Q) \tag{24.155}$$

The above result can be used to infer a relation analogous to Eq. (24.154) for the AL_2 diagram, leading to

$$\delta\mathbf{\Lambda}_{pg}(K,K) = -\delta\mathbf{\Lambda}_{MT}(K,K)\,, \tag{24.156}$$

which expresses this pseudogap contribution to the vertex entirely in terms of the Maki-Thompson diagram shown in Fig. 24.45b. It is evident that $\delta\mathbf{\Lambda}_{MT}$ is simply the pseudogap counterpart of $\delta\mathbf{\Lambda}_{sc}$, satisfying

$$-\delta\mathbf{\Lambda}_{MT}(K,K) = \frac{\partial\Sigma_{pg}(K)}{\partial\mathbf{k}}\,. \tag{24.157}$$

Therefore, one observes that for $T \leq T_c$

$$\delta\mathbf{\Lambda}_{pg}(K,K) = \frac{\partial\Sigma_{pg}(K)}{\partial\mathbf{k}}\,, \tag{24.158}$$

which establishes that Eq. (24.106) applies to the superconducting phase as well. As expected, there is no direct Meissner contribution associated with the pseudogap self-energy.

24.10 Quantitative Relation between BCS-BEC crossover and Hartree-TDGL

In this appendix we make more precise the relation between Hartree-approximated TDGL theory and the T-matrix of our GG_0 theory. The Ginzburg-Landau (GL) free energy functional in momentum space is given by [62]

$$\begin{aligned} F[\Psi] &= N(0)\sum_{\mathbf{q}} |\Psi_{\mathbf{q}}|^2(\epsilon + \xi_1^2 q^2) \\ &\quad + \frac{b_0}{2}\sum_{\mathbf{q}_i} \Psi^*_{\mathbf{q}_1}\Psi^*_{\mathbf{q}_2}\Psi_{\mathbf{q}_3}\Psi_{\mathbf{q}_1+\mathbf{q}_2-\mathbf{q}_3}\,, \end{aligned} \tag{24.159}$$

where $\Psi_{\mathbf{q}}$ are the Fourier components of the order parameter $\Psi(\mathbf{r},t)$, $\epsilon = \frac{T-T^*}{T^*}$, ξ_1 is the GL coherence length, $b_0 = [1/T^2\pi^2]\frac{7}{8}\zeta(3)$, T^* is the critical temperature when feedback effects from the quartic term are neglected, and $N(0)$ is the density of states at the Fermi level in the normal state. The quantity $\langle|\Psi_{\mathbf{q}}|^2\rangle$ is determined self-consistently via

$$\langle|\Psi_{\mathbf{q}}|^2\rangle = \frac{\int D\Psi e^{-\beta F[\Psi]}|\Psi_{\mathbf{q}}|^2}{\int D\Psi e^{-\beta F[\Psi]}}\,, \tag{24.160}$$

where $F[\Psi]$ is evaluated in the Hartree approximation [163]. Our self consistency condition can be then written as

$$\langle|\Psi_{\mathbf{q}}|^2\rangle = \frac{T}{N(0}\left[\epsilon + b_0 \sum_{\mathbf{q}'}\langle|\Psi_{\mathbf{q}'0}|^2\rangle + \xi_1^2 q^2\right]^{-1} . \tag{24.161}$$

If we sum Eq. (24.161) over $\mathbf{q}$ and identify $\sum_{\mathbf{q}}\langle|\Psi_{\mathbf{q}0}|^2\rangle$ with Δ^2, we obtain a self-consistency equation for the energy "gap" (or pseudogap) Δ above T_c

$$\Delta^2 = \sum_{\mathbf{q}} \frac{T}{N(0)}\left[\epsilon + b_0\Delta^2 + \xi_1^2 q^2\right]^{-1} , \tag{24.162}$$

$$\Delta^2 = \sum_{\mathbf{q}} \frac{T}{N(0)} \frac{1}{-\bar{\mu}_{pair}(T) + \xi_1^2 q^2} , \tag{24.163}$$

where

$$\bar{\mu}_{pair}(T) = -\epsilon - b_0\Delta^2 . \tag{24.164}$$

Note that the critical temperature is renormalized downward with respect to T^* and satisfies

$$\bar{\mu}_{pair}(T_c) = 0 . \tag{24.165}$$

To compare with GL theory we expand our T-matrix equations to first order in the self energy correction. The T-matrix can be written in terms of the attractive coupling constant U as

$$t(Q) = \frac{U}{1 + U\chi_0(Q) + U\delta\chi(Q)} , \tag{24.166}$$

where

$$\chi_0(Q) = \sum_K G_0(Q-K)G_0(K) . \tag{24.167}$$

Defining

$$\Delta^2 = -\sum_Q t(Q) \tag{24.168}$$

we arrive at the same equation as was derived in Section 24.3.3

$$\Sigma(K) \approx -G_0(-K)\Delta^2 \tag{24.169}$$

where one can derive a self consistency condition on Δ^2 in terms of the quantity $\delta\chi(0)$ (which is first order in Σ), which satisfies

$$\delta\chi(0) = -b_0 N(0)\Delta^2, \tag{24.170}$$

implying that

$$\delta\chi(0) = -b_0 T\sum_{\mathbf{q}} \frac{1}{\epsilon + \xi_1^2 q^2 - \delta\chi(0)/N(0)} , \tag{24.171}$$

which coincides with the condition derived earlier in Eq. (24.162).

24.11 Convention and Notation

24.11.1 Notation

We follow standard notations as much as possible. They are summarized below.
E_F — Fermi energy
k_F — Fermi momentum
$\hbar$ — Planck constant
k_B — Boltzmann constant
c — Speed of light
e — Electron charge
T_c — Critical temperature for (superfluid/superconducting) phase transition
T^* — Pair formation or pseudogap onset temperature.
T — Temperature
μ, μ_{pair}, μ_B — Fermionic, pair and bosonic chemical potential, respectively.
Δ — Fermionic excitation gap
Δ_{sc} — Superconducting/superfluid order parameter
Δ_{pg} — Pseudogap
Four vector $K \equiv (i\omega_n, \mathbf{k})$, $\sum_K \equiv T\sum_n \sum_{\mathbf{k}}$, where $\omega_n = (2n+1)\pi T$ is the odd (fermionic) Matsubara frequency.
Four vector $Q \equiv (i\Omega_n, \mathbf{q})$, $\sum_Q \equiv T\sum_n \sum_{\mathbf{q}}$, where $\Omega_n = 2n\pi T$ is the even (bosonic) Matsubara frequency.
$f(x) = 1/(e^{x/k_BT}+1)$ — Fermi distribution function
$b(x) = 1/(e^{x/k_BT}-1)$ — Bose distribution function
$G(K)$, $G_0(K)$ — Full and bare Green's functions for fermions
$D(Q)$, $D_0(Q)$ — Full and bare Green's functions for Feshbach bosons.
$\Sigma(K)$, $\Sigma_B(Q)$ — Self energy of fermions and bosons, respectively.
$\chi(Q)$ — Pair susceptibility
$t(Q)$ — T-matrix
$\boldsymbol{\lambda}$, $\boldsymbol{\Lambda}$ — Bare and full vertex, respectively.
ν, ν_0 — Magnetic detuning parameter.
a_s, a_s^* — S-wave inter-fermion scattering length
U, U_0 — Renormalized and bare strength of the attractive interaction between fermions in the open-channel. $U_0 \propto a_s(\nu = +\infty)$.
U_c — Critical coupling strength at which the two-body scattering length diverges.
$A = (\phi, \mathbf{A})$ — Four vector potential
$J = (\rho, \mathbf{J})$ — Four current
$K^{\mu\nu}(Q)$ — Electromagnetic response kernel
$\epsilon_{\mathbf{k}} = k^2/2m$ — Bare fermion dispersion in free space
$\xi_{\mathbf{k}} = \epsilon_{\mathbf{k}} - \mu$ — Bare fermion dispersion measured from chemical potential.
$E_{\mathbf{k}}$ — Bogoliubov quasiparticle dispersion
$u^2_{\mathbf{k}} = \frac{1}{2}(1 + \xi_{\mathbf{k}}/E_{\mathbf{k}})$, $v^2_{\mathbf{k}} = \frac{1}{2}(1 - \xi_{\mathbf{k}}/E_{\mathbf{k}})$ — Coherence factor as given in BCS theory.
$n^{tot} = n + 2(n_b + n_{b0})$ — Total, fermion, finite momentum boson, condensed boson density, respectively.
$V(r) = \frac{1}{2}m\omega^2 r^2$ — Harmonic trap potential
We use alphabetic ordering when multiple authors appear together.
We always refer to the absolute value when we refer to the interaction parameters U, U_0, g, g_0 as increasing or decreasing.

24.11.2 Convention for units

Throughout this Review, we use the convention for units where it is not explicitly spelled out:

$\hbar = k_B = c = 1$.

$E_F = T_F = k_F = 2m = 1$.

In a harmonic trap, E_F, T_F and k_F are defined by the noninteracting Fermi gas with the same total particle number N. $E_F = \hbar\omega(3N)^{1/3}$. We further take the Thomas-Fermi radius $R_{TF} = 1$.

In this convention, the fermion density in a homogeneous gas in three dimensions is $n = 1/3\pi^2$, the harmonic trap frequency $\omega = 2$, and the total fermion number in a trap is $N = 1/24$.

In the two-channel model, the units are E_F/k_F^3 for U and U_0, and $E_F/k_F^{3/2}$ for g and g_0.

Our fermionic chemical potential μ is measured with respect to the bottom of the energy band, which leads to (i) $\mu = E_F$ in the non-interacting limit at $T = 0$, and (ii) μ changes sign when the system crosses the boundary between fermionic and bosonic regimes.

24.11.3 Abbreviations

BCS — Bardeen-Cooper-Schrieffer (theory)
BEC — Bose-Einstein condensation
GL — Ginzburg-Landau (theory)
TDGL — Time-dependent Ginzburg-Landau (theory)
RPA — Random phase approximation
LDA — Local density approximation
GP — Gross-Pitaevskii
TF — Thomas-Fermi (approximation)
NSR — Noziéres and Schmitt-Rink
FLEX — FLuctuation EXchange
AB — Anderson-Bogoliubov (mode)
PG — Pseudogap
SC — Superconductor
AFM — Antiferromagnet
FB — Feshbach boson
LSCO — $La_{1-x}Sr_xCuO_4$
BSCCO — $Bi_2Sr_2CaCu_2O_{8+\delta}$
YBCO — $YBa_2Cu_3O_{7-\delta}$
ARPES — Angle-resolved photoemission spectroscopy
STM — Scan tunneling microscopy
RF – Radio frequency (spectroscopy)
SIN — Superconductor-insulator-normal metal (tunneling junction)
SI — Superconductor-insulator (transition)
3D — Three dimensions

Part IX
High Temperature Superconductivity

25 High Temperature Superconductivity in the Cuprates: Materials, Phenomena and a Mechanism by Banerjee, Dasgupta, Mukerjee, Ramakrishnan, Sarkar

Abstract

Superconductivity in the cuprates, discovered in the late 1980's and occurring at unprecedentedly high temperatures (up to about 140K) in about thirty chemically distinct families, continues to be a major problem in physics. In this article, after a brief introduction of these square planar materials with weak interlayer coupling, we mention some of the salient electronic properties of hole doped cuprates such as the pseudogap phase and the Fermi arc . We then outline a phenomenological, Ginzburg Landau like theory developed by some of us for the emergent d-wave symmetry superconductivity in these materials, and confronted successfully with a large amount of experimental information. A more recent application of the approach to fluctuation diamagnetism and to the anomalously large Nernst effect is also discussed.

25.1 Introduction

Superconductivity was discovered more than a century ago, and seemed to be a very low temperature phenomenon confined to temperatures below about 20K. Therefore the discovery of high temperature superconductivity in a family of cuprates around 1987 or so took the Physics world by surprise, not only because the temperatures (T_c) for transition to superconductivity are high (by values prevalent till then in the field; the cuprate T_c's range from about 30K to about 140K), but also because these materials have unusual physical properties. Major unexpected experimental discoveries continue to be made, and there is no single broadly accepted theoretical framework in which the wide range of observed properties can be understood and calculated. In this article, we will outline some of the broad materials characteristics of these systems, some of their basic properties, and outline a novel phenomenological approach which is used to compute a wide range of experimental properties.

The article is organized as follows. Section 25.2 of this article is an introduction to the family of cuprate materials with a description of their structure and a *minimal* electronic model appropriate to the cuprates. A long section (Section 25.3) describes the phase diagram of the hole doped cuprates, which in addition to antiferromagnetically ordered insulating phase and a superconducting region, hosts 'pseudogap' and strange metal regions. The unusual electronic properties of these phases are also described. (This is what makes the section long). Section 25.4 introduces our phenomenological, superficially Ginzburg-Landau-like approach to the system. In Section 25.5, we outline further extensions of this phenomenological theory to describe transport properties (especially the unusual Nernst or thermo-magneto-electric effect) and electron spectra as measured in ARPES (Angle Resolved Photo Emission Spectroscopy). Section 25.6 mentions some of the major results obtained from the theory for a broad range of equilibrium and nonequilibrium phenomena, above and below T_c and for a range of doping x. The concluding section (Section 25.7) mentions some future directions.

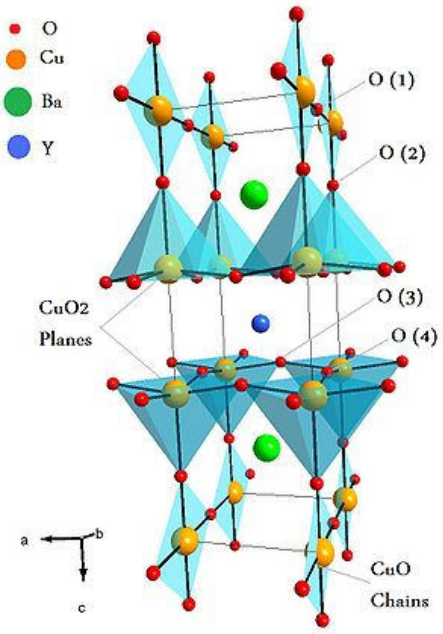


Figure 25.1: Orthorhombic unit cell of $YBa_2Cu_3O_{7-x}$ (YBCO or Y123) with $a = 3.82$ Å along [100] and $b = 3.89$ Å along [010]. The c axis dimension is around 12 Å.

25.2 Materials, structure and minimal electronic model

The cuprates , e.g. $La_{2-x}Sr_xCuO_4$, $YBa_2Cu_3O_{7-x}$, $Bi_2Sr_2Ca_{n-1}Cu_nO_{2n+4+x}$ (n=1,2,3) can be thought of as being made up of highly distorted corner sharing octahedra derivable from the ABO_3 perovskite family. The O^{2-} ions are at the corners of the octahedron, the Cu^{2+} ions at the centre, and the transition metal or rare-earth ions in the space between the octahedra. The Jahn-Teller distortion due the Cu^{2+} ions is very large; the plane of the octahedron is split in two, with a large splitting. (Fig.25.1 shows the structure of $YBa_2Cu_3O_{7-x}$). A good approximation for the electronic properties of these systems is to regard the materials as consisting of Cu-O planes; the Cu and O ions are arranged in squares in the plane, with O ions at the midpoint of the nearest Cu-Cu line. The low energy electronic degrees of freedom arise from the unfilled d shell electrons of the Cu^{2+} ions which are in the d^9 configuration. The Cu ions are at the vertices of a square whose length in most cuprates is about 3.9Å. Crudely, at the single site level, the occupation of the nine d electrons of the Cu^{2+} ion can be described as follows. The tenfold atomically degenerate d level is split into t_{2g} and e_g configurations, with the former lying lower in energy. Its six states are fully occupied by d electrons. That they do not take part in any low energy electron processes, and are strongly bonded with O^{2-} electrons, is clear from the fact that the relevant bond lengths, reflected in the Cu-Cu distances, are about the same in almost all cuprates. The twofold degenerate e_g level is strongly split in two by the Jahn-Teller distortion mentioned above; the lower one is fully occupied and the higher one is half occupied in the d^9 configuration.

For large local Coulomb repulsion or Mott Hubbard U (as is widely believed to be the case in cuprates from both theoretical and experimental evidence) the fluctuations in the number of local d electrons is strongly suppressed, and the material is an insulator for exactly one e_g electron per site (Mott insulator). If the cuprate is hole doped (for example, the trivalent La is partially substituted by the divalent Sr) both naively, and from a more sophisticated model which includes the oxygen p electrons, it is clear that the system can be thought of electronically as consisting (on the average) of $(1 - x)$ electrons per unit cell where a fraction x of the trivalent La ions is substituted by Sr ions. These electrons move on a square lattice,

and in a tight binding picture can be regarded as hopping from one site to another on a square planar lattice with hopping amplitudes t, t' etc.. There is an energy penalty of U for double occupation of a particular site by electrons. There is an amplitude λt ($\lambda << 1$) for electron hopping perpendicular to the plane. We will neglect this in what follows. Based on the above picture, a one-band Hubbard model on a square lattice is believed to be a reasonable microscopic description for most of the universal aspects of the cuprate phase diagram. The most widely used values for these parameters which define the electron dynamics of the model are, $t = 300$ meV, $t'/t = -1/4$ [1] and $U = 2 - 4$ eV [2]. The large value of U ($U \gg 4t$, the half bandwidth) implies that the material is a strongly correlated metal in which the electron of the Cu hops from site to site, avoiding other d electrons. In the large U limit the one-band model Hubbard model reduces to the well-known $t - J$ model,

$$\hat{\mathcal{H}}_{t-J} = -\sum_{<ij>,\sigma} \mathbb{P}_G \left(t_{ij} a^\dagger_{i\sigma} a_{j\sigma} + \text{h.c.} \right) \mathbb{P}_G + J \sum_{<ij>} (\hat{\mathbf{S}}_i . \hat{\mathbf{S}}_j - \frac{1}{4} \hat{n}_i \hat{n}_j), \tag{25.1}$$

which has been used extensively [3] in the context of cuprates. Here the $a^\dagger_{i\sigma}$ is the usual fermion creation operator on site i, $n_i = \sum_\sigma a^\dagger_{i\sigma} a_{i\sigma}$ and $\hat{\mathbf{S}}_i$ are the electron number and spin operators, respectively, and $\mathbb{P}_G = \prod_i (1 - \hat{n}_{i\uparrow} \hat{n}_{i\downarrow})$ is a projection operator excluding double occupancy of any site; J can be estimated to be around 0.13 eV [4].

25.3 Phase diagram and phenomena

An idealized 'phase diagram' of hole doped cuprates, in the hole density x and temperature T plane, is shown in Fig.25.2. Interestingly, it is nearly the same for the entire cuprate family. The parent compound is a Mott insulator which undergoes a Ne'el transition at T_N to an antiferromagnetic state. Upon doping, the T_N drops very rapidly and goes to zero beyond a small value of doping ($x \simeq 0.03$). The superconducting state sets in, preceded by a messy disordered low-temperature phase exhibiting spin glass like behavior till $x \simeq 0.05$. The superconducting transition temperature, $T_c(x)$, detected unambiguously by the onset of the zero resistance state, exhibits a well known parabolic (the 'superconducting dome') dependence with increasing x and reaches a maximum at $x \simeq 0.16$ and ultimately declines to zero for $x \gtrsim 0.25$. The x value corresponding to the maximum T_c is called the *optimal doping* (x_{opt}) and the regimes, $x < x_{\text{opt}}$ and $x > x_{\text{opt}}$, are denoted as *underdoped* and *overdoped* regions, respectively. The high temperature region corresponding to the *normal states* of the superconductor above the superconducting dome is rather *abnormal* ones among known states of matter found in Nature. This region can be broadly classified into three parts, the so-called *pseudogap* region for small x (underdoped), the *strange metal* phase for intermediate values of x and a more 'normal' (i.e. conventional) metal for large x, i.e. the overdoped region. The pseudogap state goes into the strange metal phase, above a temperature scale depicted as the pseudogap sclae T^* (see Fig.25.2), which seems more like a crossover (as opposed to a true phase transition) from variety of measurements. Below, we briefly discuss superconducting, strange metal phases and pseudogap phases and summarize some of their unusual features. We also include a separate detailed discussion of spectroscopic characteristics of these phases, as probed by angle-resolved photoemission (ARPES) and scanning tunneling (STS) spectroscopies.

25.3.1 Superconducting state

The superconducting state is less unconventional compared to the other parts of high-T_c phase diagram. The superconducting order parameter is a charge $2e$ complex field with d-wave symmetry as has been unambiguously demonstrated by phase sensitive measurements [6, 7]. In conventional superconductors the Cooper pair amplitude or the energy gap [8] that appears

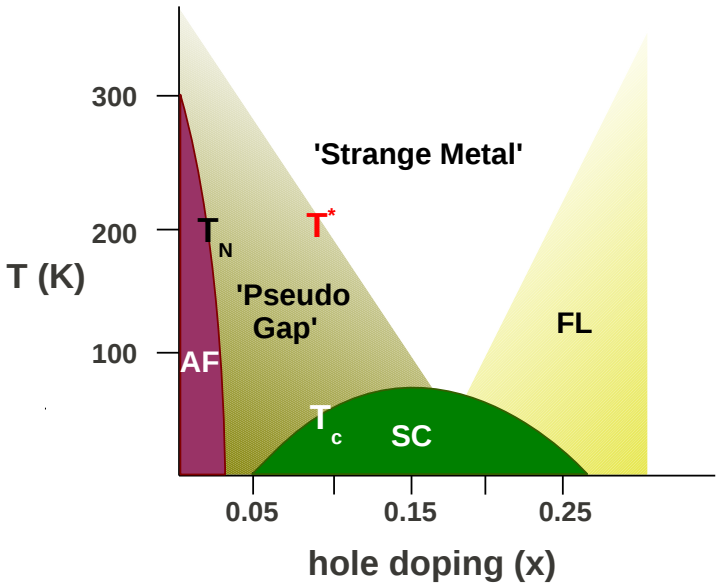


Figure 25.2: The famous phase diagram of hole doped cuprates, showing superconductive (SC), antiferromagnetic (AF), *pseudogap*, *strange metal* and more conventional Fermi liquid (FL) metal regions. Also indicated are the Ne'el temperature (T_N), superconducting transition temperature (T_c) and somewhat *ill defined* pseudogap temperature scale (T^*).

in the spectrum of electronic excitations with momentum $\mathbf{k}$ on the Fermi surface, namely $\Delta_{\mathbf{k}}$, is generally independent of $\mathbf{k}$, whereas in cuprates it is strongly $\mathbf{k}$ dependent and has nodes i.e. vanishes along certain $\mathbf{k}$ directions. An approximate two dimensional representation of d-wave symmetry superconducting gap, whose validity for cuprates has been established by ARPES [9, 10, 11] and phase-sensitive Josephson junction measurements (see later), is $\Delta_{\mathbf{k}} = (\Delta_0/2)(\cos k_x a - \cos k_y a)$ (see Fig.25.3, a is Cu-O-Cu bond length in the plane and Δ_0 is the maximum gap magnitude). This can arise in a lattice system through nearest neighbor pairing such that magnitude of pair amplitude (a complex number) along x and y bonds is same but the phases differ by π (see Fig.25.1). A gap function of this kind implies nodal Bogoliubov quasiparticles leading to substantial density of gapless excitations (see Fig.25.3) and these would dominate the behavior of various physical properties at low temperatures ($T \ll T_c$). Particularly, since the density of states (DOS) vanish linearly in energy, the nodal excitations give rise to, e.g., a non-activated T^2 term in electronic specific heat[12] and similar power law T dependences of various other quantities [13, 14], unlike that in a s-wave superconductor. An interesting effect [15] can be seem in the presence of a magnetic field H due to a shift of the quasiparticle spectrum by an amount $\propto H^{1/2}$; this has been verified experimentally [16].

The superconductivity in cuprates has several unusual characteristics. Here we list a few of them.

1. Short coherence length: The length scale associated with pairing, namely the coherence length (ξ_0), is very small in cuprate superconductors - around $15 - 20$ Å in the plane and, between planes 2 Å, even smaller than the interlayer spacing, implying that the superconductivity related phenomena in the cuprates can be thought of as effectively having Josephson coupled [8] planes.

2. Low superfluid density: Cuprates superconductors are characterized by very small

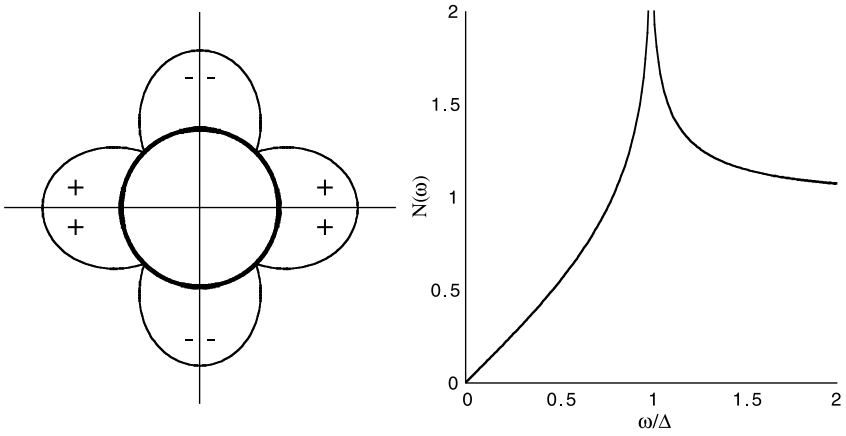


Figure 25.3: Variation of the d-wave gap on the Fermi surface is shown in the left figure, $k_x = \pm k_y$ is the nodal direction. The density of states (DOS) is plotted in the right figure. A DOS divergence appears at the maximum gap magnitude $\omega = \Delta$. (From Ref.[5])

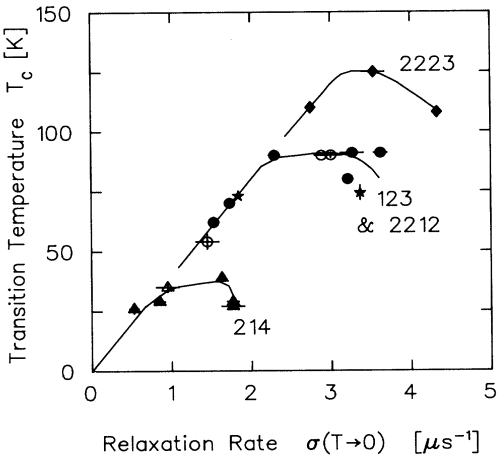


Figure 25.4: The superconducting transition temperature T_c as a function of low temperature muon spin-relaxation rate $\sigma(T \to 0) \propto 1/\lambda_{ab}^2(0) \propto \rho_s(0)$ for different cuprate compounds. At the low doping values data fall on the *universal* straight line indicating the Uemura correlation $\rho_s \propto T_c$. (See Ref.[17] for more details).

in-plane superfluid density or stiffness ρ_s. The low temperature superfluid density ρ_s for small doping goes as x, as also does T_c. This is the so-called Uemura scaling [17], $\rho_s \propto T_c$ for small x (see Fig.25.4). Such a scaling is unusual for conventional superconductors, typically having very large ρ_s and much smaller T_c [18]. Since the in-plane penetration depth $\lambda_{ab} \propto 1/\rho_s^{1/2}$, cuprates have very large penetration depth (~ 1500 Å), implying the extreme type-II limit [8] for these superconductors. Small superfluid density of phase stiffness indicates the importance of phase fluctuations, which are expected to be very strong, especially in the underdoped regime. This fact is corroborated by the observation of large Nernst effect[19] and enhanced fluctuation diamagnetism[20] by Ong and coworkers over an unusually large temperature range above T_c. A phase fluctuation related theory for this is described later here.

3. Gap to T_c ratio: Another important experimental observation about the superconducting state is that the zero temperature superconducting gap Δ_0 inferred, e.g., from STM [21] or ARPES [10, 11] increases, whereas T_c declines, as mentioned above, in the underdoped side with decreasing doping. Both the measured ratio $(2\Delta_0/k_B T_c)$ and the x dependence imply the violation of the BCS relation between Δ_0 and T_c i.e. $2\Delta_0/k_B T_c \simeq 4.3$ for d-wave[22]. However, of late, the large gap seen via spectroscopy has been attributed to other competing

order [23, 24] or as having non-pairing origin [25, 26, 27].

4. Emergence from pseudogap state: In the underdoped side, the precedence of *pseudogap phase* (see Fig.25.2) while approaching the superconducting state from high temperatures suggests that the transition is not a sudden gap appearance one, as in BCS. This is related with the pseudogap phenomena which we discuss below in more detail.

5. Anomalous high-field vortex states: The mixed state of cuprate superconductor at high field and low temperature is rather anomalous, showing mangetoconductivity (Shubnikov-deHaas (SdHvA)) and magnetization (deHaas-van Alphen (dHvA)) oscillations as a function of $(1/H)$, e.g. in clean $YBa_2Cu_4O_8$ and $HgBa_2CuO_{4+\delta}$ [28, 29, 30]. These quantum oscillations have been seen with an accompanying long-range charge-density wave (CDW) order even far below the irreversiblity field for superconducting to non-superconducting transition [31, 32, 33], presumably related to vortex lattice or vortex glass depinning [34].

25.3.2 Strange metal

The strange metal is one of the most enigmatic phases in the cuprate phase diagram (Fig.25.2). Transport measurements reveal that the resistivity is linear in temperature over a large range, the most fascinating example being the single layer Bi2201, where linearity persists down to $T_c \simeq 7$ K [35], starting from an amazingly high temperature (~ 700 K). This behaviour is in strong contrast to what one expects on the basis of Fermi liquid theory. We discuss a few of the strange properties of the strange metal phase below.

1. T-linear resistivity: In conventional low-temperature superconductors, the temperature dependence of resistivity ρ is well described by $\rho \approx \rho_0 + bT^5$, at low T ($> T_c$). This T dependence well below the phonon Debye temperature θ_D arises from the scattering of electrons by phonons. At higher temperatures ($T \gtrsim \theta_D$), a linear behavior is expected, and the interpolation between the two regimes is given by the Grüneisen-Bloch formula. The residual resistivity ρ_0 at $T = 0$ is caused by scattering by impurities. However, the behaviour of ρ observed in high-T_c superconductors is strikingly different. Resistivity in the CuO_2 planes for several different cuprate compounds near optimal doping exhibits an approximate linear behavior over a large temperature window [36, 37] as shown in Fig.25.5. The resistivity values are very large at high temperature, e.g., in comparison to that of copper at room temperature, which has a resistivity of 1.7 $\mu\Omega$cm. This seems to be one of the defining characteristics of strongly correlated metals i.e. typical resistivity values are quite large, often of the same order or even larger than the Ioffe-Regel limit and increase linearly with temperature without any saturation. Fig.25.5 demonstrates clear linear behaviour with very similar slopes for the various compounds, suggesting a possible common origin for in-plane transport.

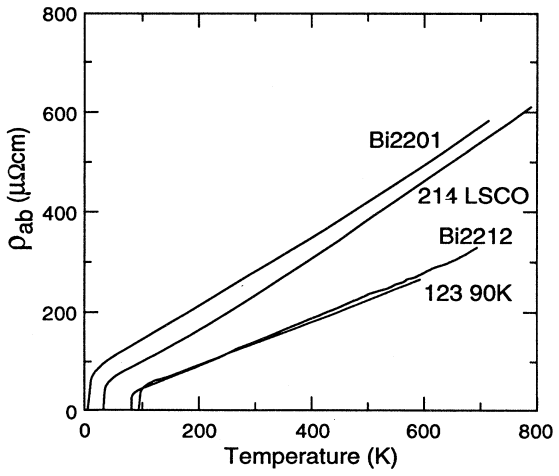


Figure 25.5: Temperature dependence of the in-plane resistivity ρ_{ab} for various optimally doped cuprates. (From Ref.[36]).

The linear T dependence [37] is something not fundamentally understood, and is generally associated with strong correlation in the system. As is well known, electron-electron interaction in Fermi liquid systems leads to a T^2 dependence of resistivity, unlike what is observed in optimally doped cuprates. With increasing doping, the temperature dependence is of the form $\rho_{ab} \propto T^{\alpha}$ with α increasing smoothly from 1 to 2 from optimum to overdoped [38]. This behaviour is also not understood, but presumably can be broadly described as due to the system changing from strongly correlated non-Fermi liquid to weakly interacting Fermi liquid.

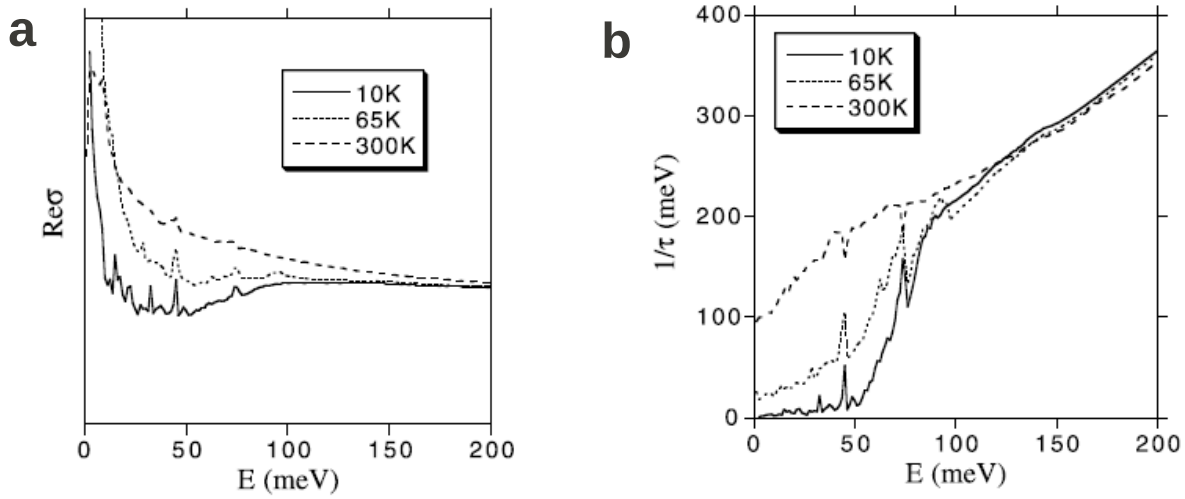


Figure 25.6: **a**, Real part of in-plane infrared optical conductivity of underdoped YBCO for the superconducting state (10 K), pseudogap phase (65 K), and normal state (300 K). A gap-like suppression develops at around 50 meV in the pseudogap regime. **b**, Variation of extracted optical scattering rate $1/\tau(\omega)$ with frequency for underdoped YBCO. (From Ref.[39]).

2. ω-linear scattering rate: Optical conductivity, which probes the current-current correlation function, gives further evidence of the unconventional nature of the strange metal phase. In plane, the normal state (both strange metal and pseudogap states) of cuprates is characterized by a broad, Drude-like response centered at frequency $\omega = 0$ (Fig.25.6 **a**) for optical conductivity $\sigma(\omega)$. The data are phenomenologically represented by a generalized Drude form [39]

$$\sigma(\omega) = \frac{1}{4\pi} \frac{\omega_{\rm pl}^2}{1/\tau(\omega) - i\omega[1+\lambda(\omega)]}, \tag{25.2}$$

where $\omega_{\rm pl}$ (the plasma frequency) is given by the sum rule $\int_0^\infty d\omega {\rm Re}\sigma(\omega) = (\omega_{\rm pl}^2/8)$ (here, $\sigma = {\rm Re}\sigma + i{\rm Im}\sigma$ and the integral has a high frequency cut off ~ 1 eV). In the above form, $1/\tau(\omega)$ and $1+\lambda(\omega)$ are the frequency dependent scattering rate and mass renormalization, respectively. The analysis of the experimental data using eq.(25.2) reveals that the scattering rate has the form $a + b\omega$ (see Fig.25.6 **b**), unlike a Fermi liquid where $1/\tau \sim \omega^2$. The ω-linear term is expected from a marginal Fermi liquid theory [40, 41].

25.3.3 Pseudogap phase

One of the most controversial aspects of the cuprate phase diagram is the nature of *pseudogap phase*. This is associated with a set of ill-understood apparent crossover phenomena [42, 43, 44, 45], which are widely observed in underdoped cuprates and, to some extent, in optimally and even slightly overdoped materials. As we summarize below, signatures of gap

are observed through different experimental probes, e.g., spin susceptibility, thermodynamic, transport and optical measurements, and in the quasiparticle excitations investigated through ARPES and scanning tunneling microscopy (STM),. As shown in Fig.25.2, these gap-like features ('pseudogap' as opposed to true gap) become prominent below a temperature scale T^* (the pseudogap temperature), which varies somewhat when detected using different probes. In the underdoped samples, T^* is way above the superconducting transition temperature T_c, which is traditionally detected through the onset of zero resistance state, indicating that superconducting long range order (LRO) is not present in the pseudogap state even though there are clear hallmarks of a gap of the kind resembling that of the d-wave symmetry superconducting state. Below, we touch upon some of the salient fetures of the pseudogap phase.

1. "Spin gap" in spin susceptibility: The first experimental indication [46] of a pseudogap phase came from NMR measurements in underdoped YBCO, which showed that the spin lattice relaxation rate (which depends on the number of conduction electron spin states at the Fermi energy) starts to decrease much above T_c. A similar decrease is seen in the related Knight shift [47] (Fig.25.7). NMR experiments probe the spin channel, unlike optical conductivity which probes the charge degrees of freedom. The decrease of Knight shift indicates decrease of spin susceptibility with temperature in the pseudogap state of cuprates, initially supporting the hypothesis of spin gap [46]. Subsequent experiments, however, have demonstrated that the pseudogap exists in both spin and charge channels, as evident from, e.g., ARPES or optical conductivity.

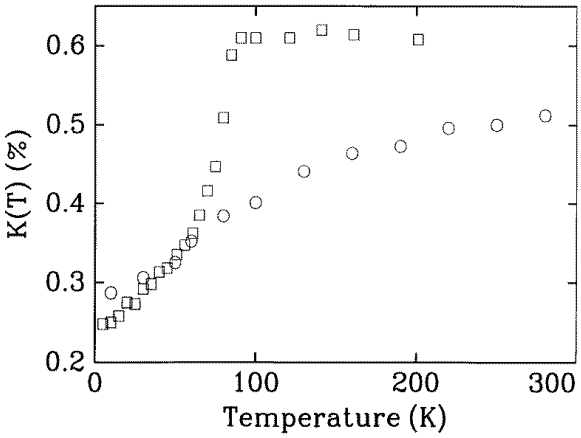


Figure 25.7: Knight shift in $YBa_2Cu_3O_{6.95}$ (squares) and underdoped $YBa_2Cu_3O_{6.64}$ (circles). The normal-state susceptibility is temperature independent above T_c in the optimally doped compound, but decreases with temperature in the underdoped compound even above T_c. (From Ref.[42]).

2. Suppression of specific heat: Another evidence of pseudogap comes from the electronic specific heat [45, 42]. The electronic specific heat provides thermodynamic evidence for a gap in the normal state of the cuprates [49]. The specific heat is generally found to be linear in temperature $C_v \approx \gamma T$ above the pseudogap temperature scale T^*. Below T^*, C_v/T begins to decrease with decreasing temperature (Fig.25.25), indicating presence of a normal state gap. For YBCO, above T_c, overdoped samples show (Fig.25.25 **a**) a temperature- and doping-independent γ. The underdoped samples have a depression of the specific heat coefficient in the normal state below T^* (Fig.25.25 **b**) [49] and the specific heat jump at T_c is diminished with decreasing doping. Evidence of pseudogap in specific heat measurements has also been found in other cuprates [50, 51].

3. Transport signatures of pseudogap: There is a significant deviation of in-plane or the ab-plane resistivity from the T linear temperature dependence of strange metal at higher temperature. A pseudogap temperature [37] is identified as the point below which temperature-dependence of in-plane resistivity deviates significantly from its high temperature behavior (see, e.g., Fig.25.9 **a**). A similar temperature scale can be inferred from the Hall resistance which,

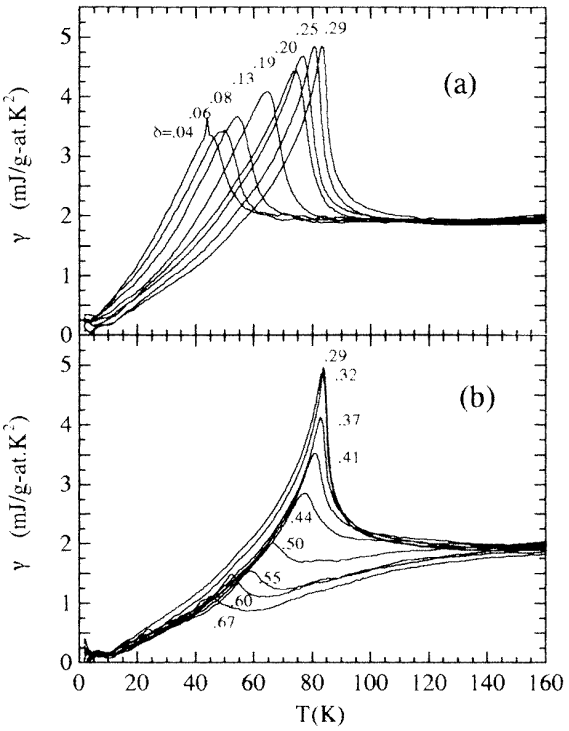


Figure 25.8: Specific heat coefficient γ for (a) overdoped and (b) underdoped $Y_{0.8}Ca_{0.2}Ba_2Cu_3O_{7-\delta}$. In the overdoped material a gap opening, signalled by a peak and the subsequent suppression of γ, occurs below T_c. In the underdoped materials a gap appears to form much above T_c, around 140K, in the normal state itself. (From Ref.[48]).

quite remarkably, is strongly temperature dependent [52]. The pseudogap also appears in the c-axis resistivity ρ_c [53, 54] as an insulator-like increase with decreasing temperature.

4. Optical gap: A signature of a gap is also observed in infrared measurements exhibiting a suppression in the ab-plane optical conductivity $\sigma'_{ab}(\omega)$ separating the low energy Drude peak from 'bump'-like feature at mid-infrared [55, 56] (see Fig.25.6 **a**). Interestingly, c-axis optical conductivity $\sigma_c(\omega)$ reveals more dramatic effect of a pseudogap; $\sigma_c(\omega)$ does not have a Drude peak at low energies and shows a significant gap below a characteristic frequency scale. The gap becomes more prominent as one approaches T_c.

5. Temperature and doping dependent Drude peak: The other interesting observation is that the width of the Drude peak in σ_{ab} decreases with temperature, but the area (spectral weight) under it is independent of temperature [57]. Intriguingly, the integrated area under the Drude peak is found to be linear in x [58, 59] indicating a connection to the doped holes [3] and this weight transforms to form the delta function superfluid peak in the superconducting state suggesting $\rho_s \propto x$. However, as we discuss below, ARPES shows a Fermi surface with an area corresponding to $1-x$ electrons [3].

6. Anomalous Nernst and fluctuation diamagnetism regime in the pseudogap phase: Experiments have found a very large diamagnetic and Nernst response in the pseudogap phase of the cuprates. A large diamagnetic signal naturally points towards fluctuating superconductivity as one of the possible origins. Also, the fact that the Nernst response is usually very small in typical nonmagnetic metals and a much stronger response is observed in the vortex-liquid regime of superconductors supports this point of view. Compared to conventional superconductors, the Nernst and diamagnetic response have been found to exist over an anomalously large region [61, 60] in the pseudogap phase, extending to temperatures far above the superconducting transition temperature T_c (see however ref. [62, 63, 64]). Another important piece of the debate is related to the fact that the putative boundary [61, 60] of the large Nernst and diamagnetic response regime, the so-called 'onset' temperature $T_{\rm onset}$, tracks $T_c(x)$ and so follows a dome-shaped curve as a function of doping x instead of tracking the pseudogap temperature scale $T^*(x)$, which monotonically decreases with x (see Fig.25.12) .

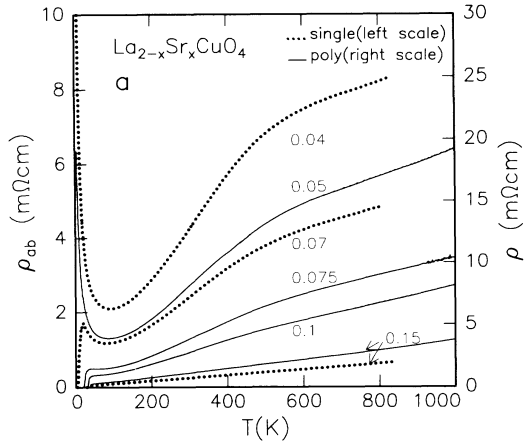


Figure 25.9: Temperature dependence of in-plane resistivity for underdoped LSCO ($0 \leq x \leq 0.15$). Around the pseudogap temperature scale, the resistivity starts deviating from nearly linear in T high-temperature behavior. (From Ref.[37]).

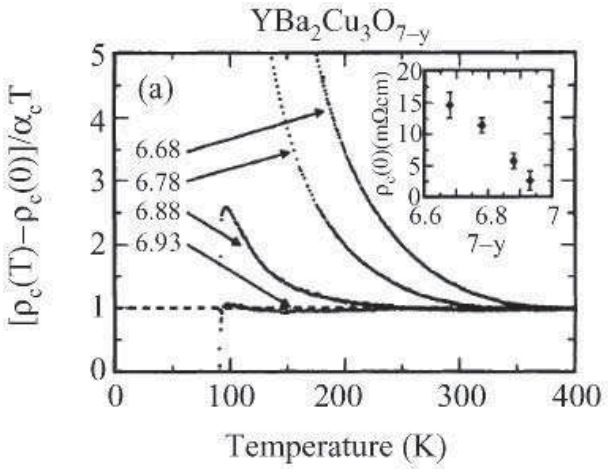


Figure 25.10: The temperature dependence of the c-axis resistivity in underdoped and optimally doped $YBa_2Cu_3O_{7-\delta}$ after the subtraction of the intercept of a approximately linear-T metallic part; α_c is the slope of the linear-T part. (From Ref.[53]).

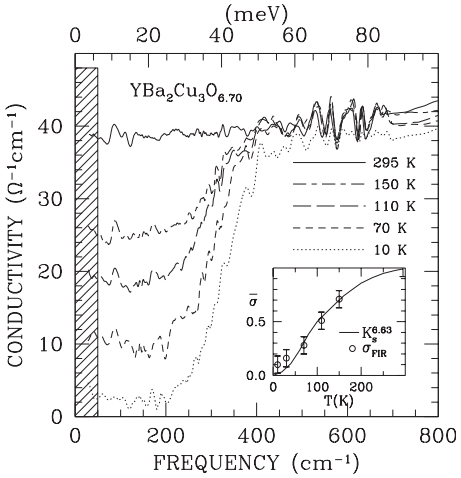


Figure 25.11: c-axis optical conductivity for underdoped YBCO demonstrating a pseudogap which fills in with temperature (From Ref.[39])

This has been argued as evidence against a pairing origin of the pseudogap, mainly due to the expectation that if the pseudogap arises from pairing then superconducting fluctuations and associated Nernst and diamagnetic responses should persist all the way up to pseudogap temperature [3].

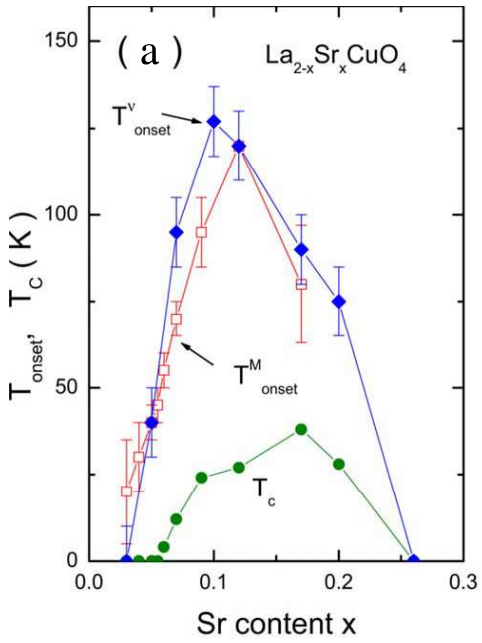


Figure 25.12: The phase diagram of LSCO showing the onset temperatures, $T^{\nu}_{\rm onset}$ and $T^{M}_{\rm onset}$, determined by enhanced Nernst and diamagnetic signal, respectively, as a function of doping. $T_c(x)$ is shown for comparison (From Ref.[60]).

25.3.4 Spectroscopic characteristics of superconducting, strange metal and pseudogap phases

Angle-resolved photoemission spectroscopy (ARPES) and scanning tunneling microscopy (STM) have emerged as two of the major tools for probing condensed matter systems mainly due to their success in directly accessing electronic excitations in cuprates. Here we discuss in somewhat more detail the major findings and phenomenologies that have emerged out of the ARPES and STM studies on cuprates.

1. ARPES: It is really the ARPES experiments [10, 11] that unambiguously demonstrated the pseudogap. Reviews by Damascelli *et al.* [10] and Campuzano *et al* [11] provide an in-depth discussion on this topic. Cuprates are ideal candidates for ARPES experiments owing to their approximate 2d nature that enables easy cleavage and possibility of experiments on atomically 2d surfaces that are representative of the bulk. One can also infer the in-plane electron momentum **k** with high precision. ARPES, a modern version of familiar photoelectric effect, measures the spectrum of electrons (photoemission intensity as a function of energy ω and momentum **k** of electron in the sample) ejected due to incident photons. In this way, ARPES probes the electronic spectral function or spectral density $A(\mathbf{k},\omega)$, that quantifies the probability of finding an electron with momentum **k** and energy ω (measured from the Fermi energy or the chemical potential). The energy corresponding to the position of a peak (if there is one, as in the case of a quasiparticle in a Fermi liquid) in $A(\mathbf{k},\omega)$ for a fixed **k** gives the information of energy of electronic excitations for that **k**, and their dispersion; the width of the peak is a measure of the life time of such excitations. ARPES can map out the Fermi surface from the **k**-space locus of the minimum energy excitation [10, 11] in the Brillouin zone. Peak in $A(\mathbf{k},\omega)$ for a particular **k** on the Fermi surface appearing at a nonzero energy indicates a gap in the electronic excitation. The gap can either be traced from the raw data of energy distribution curve (EDC, photoemission intensity as a function of energy for a fixed **k**) through the pulling back of the leading edge of the electronic spectrum from the Fermi energy (Figs.25.27 **a-c**) or

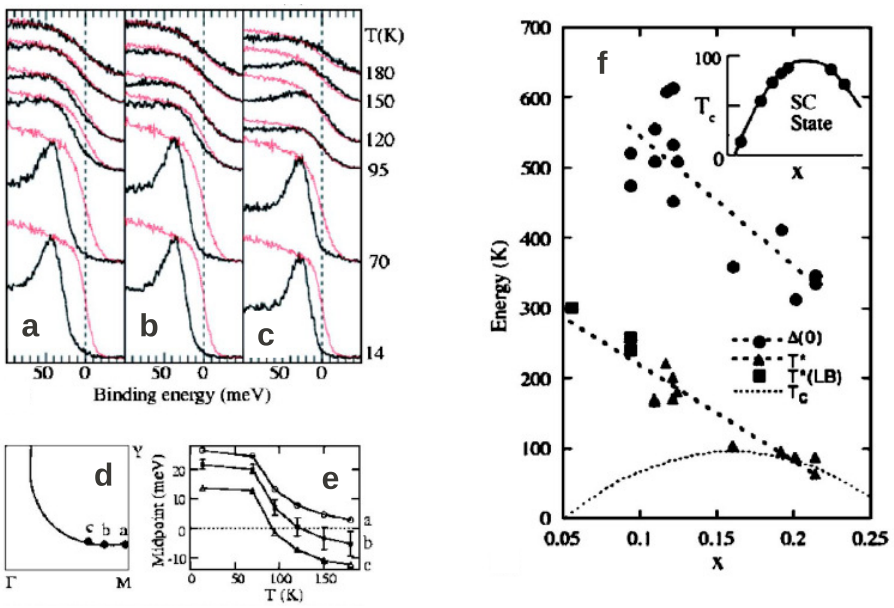


Figure 25.13: ARPES of underdoped cuprates. **a-c** Unsymmetrized energy distribution curves (EDC) for underdoped Bi2212 $T_c = 85$ K at different **k** points on the Fermi surface (panel **d**). The existence of a gap for $T > T_c$ is signaled by the pullback of the spectrum from the Fermi surface determined by the Pt reference (red lines). **e**, Temperature dependence of the gap determined from the leading-edge midpoints. (From Ref.[65]). **f**, The temperature T^* corresponding to the appearance of the pseudogap is plotted as a function of doping for Bi2212. Triangles are determined from data shown in **a**. Circles show the energy gap $\Delta(0)$ measured at the antinodal point at low temperatures in the superconducting state. (From Ref.[11]).

from the peak position of symmetrized EDC [10, 11] (Figs.25.14 **a-e**).

Angle-resolved photoemission spectroscopy shows that an energy gap is observed on the Fermi surface crossing along the direction $(\pi, 0)$ to (π, π) i.e. at the antinodal point, even above T_c for underdoped sample (Figs.25.27 **a-c**). Although, above T_c, a finite spectral weight can be detected at zero energy ($\omega = 0$), justifying the nomenclature 'pseudogap'. With increasing temperature the pseudogap *fills in* rather than closing in. Intriguingly, the spectral line width is large implying an incoherent spectra above T_c. The appearance of a coherent peak at the gap edge (Figs.25.27 **a-c**) indicates the appearance of superconductivity. The size of the pullback of the leading edge and the energy gap measured by the location of the coherence peak in the superconducting state are basically same. As shown in Fig.25.27 **f**, the estimated gap increases with decreasing doping in contrast to T_c which decreases.

As shown in Fig.25.14, below T_c, the energy gap is maximal near $(0, \pi)$ and vanishes along the line connecting $(0, 0)$ and (π, π) i.e. the nodal direction ($k_x = k_y$), giving rise to gapless nodal quasiparticles, confirming the d-wave nature of the superconductivity. Above T_c the gapless region expands to cover a finite region near the nodal point giving rise to the so-called 'Fermi arcs'[67, 68, 69] (see Fig.25.14 **f**). Strangely, spectral line shape is relatively sharp in the nodal direction even above T_c, unlike that along the antinodal direction.

The spectral weight of the antinodal coherence peak, that marks the onset of superconductivity, decreases with decreasing doping [11]. This behaviour is unlike that in any conventional superconductors [3]. A more recent and very detailed ARPES study [70] gives an overall perspective (Fig.25.15) of the cuprate phase diagram based on the existence of gap and/or sharp spectral peak in the ARPES spectra. For example, the strange metal phase is characterized as

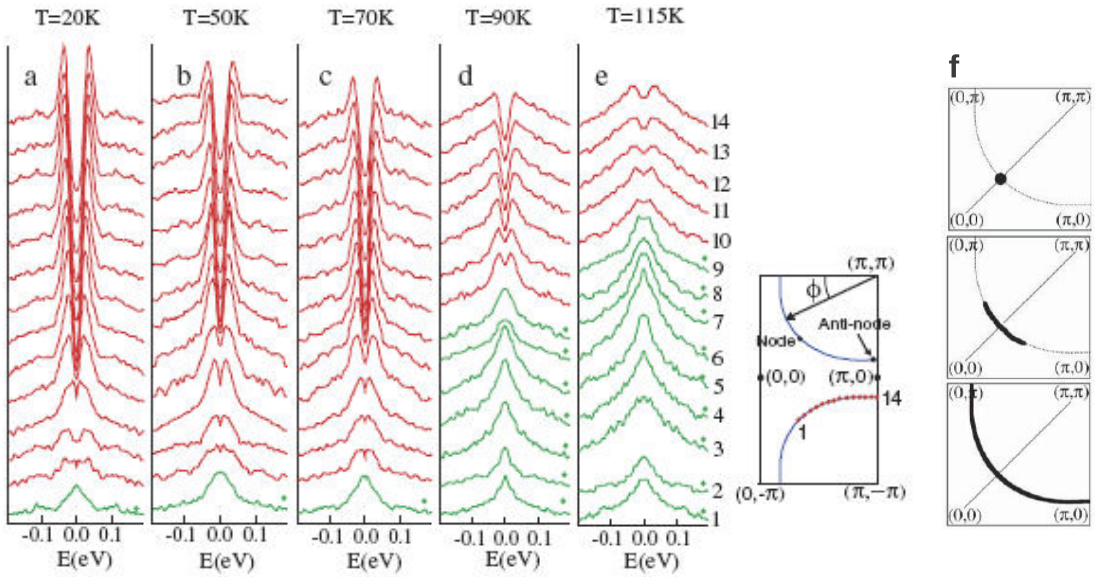


Figure 25.14: **a-e**, Evolution of the symmetrized energy distribution curves (EDCs) for underdoped Bi2212 $Tc = 80$ K with temperature. The different EDCs correspond to different **k** points from the node (lowest curve) to the antinode (uppermost curve). Gapless spectra having a peak at zero energy are shown in green. (From Ref.[66]). **f**, Schematic illustration of the development of Fermi arcs with temperature in the pseudogap phase. The d-wave node below T_c (top panel) becomes an extended gapless arc above T_c (middle panel) which expands in length with increasing T to form the full Fermi surface at T^* (bottom panel). (From Ref.[11]).

the one with neither gap nor sharp peak, whereas the pseudogap has a gapped spectrum but no sharp peak. Interestingly, there is a narrow region above the superconducting dome around optimal doping having both gap and sharp spectral peak, similar to the superconducting state below T_c.

2. Tunneling spectroscopy: In scanning tunneling spectroscopy (STS) or scanning tunneling microscopy (STM) one measures the tunneling current that flows between a sharp metallic tip and typically a conducting sample separated by thin insulating barrier, generally vacuum [8, 21]. STM allows one to probe the local density of states (LDOS) $\rho(\omega = eV, \mathbf{r})$ at position $\mathbf{r}$ directly from the differential tunneling conductance dI/dV obtained by measuring tunneling current $I(V, \mathbf{r})$ due to applied voltage difference V between the tip and the sample i.e. $dI(V, \mathbf{r})/dV \propto \rho(\omega = eV, \mathbf{r})$.

STM provides direct real-space information and hence is complementary to ARPES. By virtue of probing the local density of states with very high energy resolution, STM gives direct information [21] about the gap in the excitation spectrum as well as other spectroscopic features such as scattering rate etc. The Pseudogap was first detected in tunneling spectroscopy by Tao *et al.* [72]. A gap-like suppression of LDOS was found in the tunneling conductance of Bi2212 in the normal state. STM studies [71] on underdoped Bi2212 have again shown a disappearance of the coherence peaks at T_c and the existence of a V-shaped LDOS suppression in the normal state up to room temperature (see Fig.25.16). This feature can be identified with the signature of pseudogap.

The magnitude of the gap in the superconducting state, measured via the separation between the peaks, is effectively temperature independent, unlike that of a BCS gap which closes as the temperature is raised through T_c. The same phenomenology applies to the magnitude of the

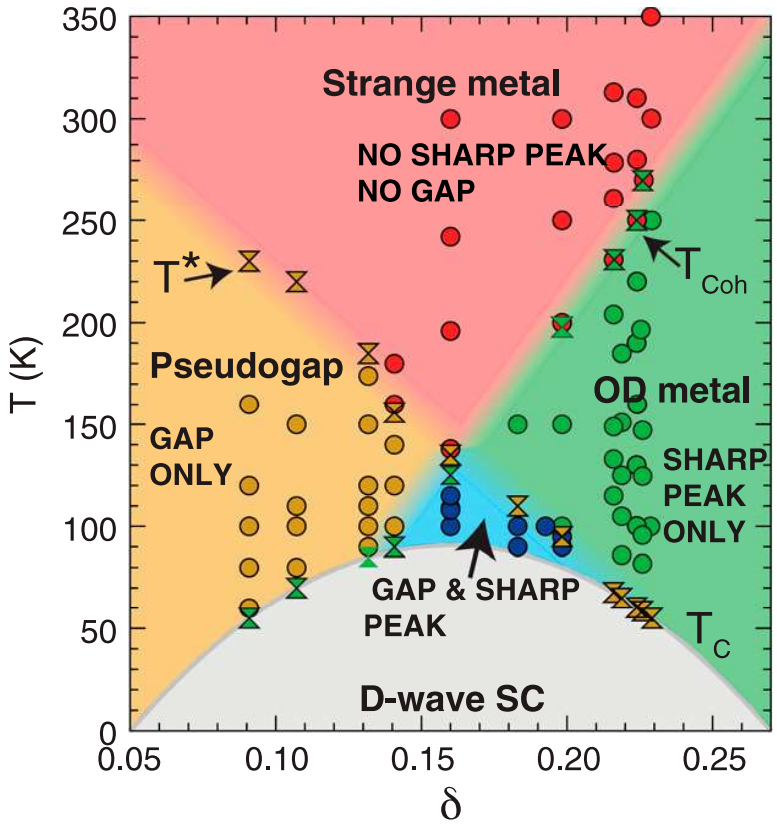


Figure 25.15: The cuprate phase diagram based on either the presence or absence of spectral gap and/or sharp peak. The latter indicates the existence of well-defined quasiparticle excitations, e.g., as in the more conventional metallic state in the overdoped region (From Ref.[70]).

pseudogap which, as in ARPES, fills in with temperature but retains its magnitude up to room temperature in underdoped samples. The magnitude of the gap however does decrease with increasing x (Fig.25.17). This is just the opposite to what is expected from BCS theory when the dome-shaped doping dependence of T_c is taken into account (Fig.25.27 **f**).

STM reveals several important relations between the superconducting gap below T_c and pseudogap above T_c and between T_c and T^* [73].Firstly, the superconducting gap and pseudogap has the same scaling with doping, i.e. increasing with decreasing doping. However the ratios of these two gaps are nearly the same over different compounds and doping in spite of the fact that their absolute magnitudes change substantially between different compounds and doping. Also the ratio $2\Delta_p/k_{\rm B}T_c \approx 4.3$ amazingly follows the BCS d-wave relation [22] with T^* replacing T_c (Fig.25.18). Here Δ_p denotes half of the separation between two superconducting peaks.

25.4 Phenomenological theory of superconducting and pseudogap states

A variety of approximate microscopic theories based on many different scenarios and ideas, from both strong and weak coupling perspectives, have been proposed to understand the cuprate phase diagram, and numerical techniques at various levels of sophistication have been tried to

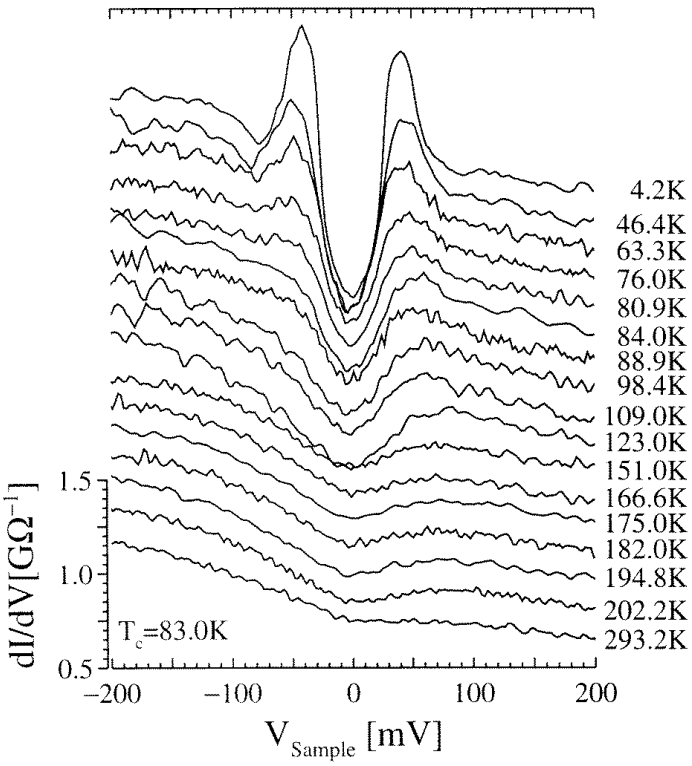


Figure 25.16: LDOS measured via differential tunneling conductance for an underdoped Bi2212 with $T_c = 83$ K and pseudogap temperature $T^* \simeq 300K$). A gap-like feature indicated by the suprresion of LDOS at low energies is seen even above T_c till T^* indicating a pseudogap. Two coherence peaks can be seen below T_c. (From Ref.[71]).

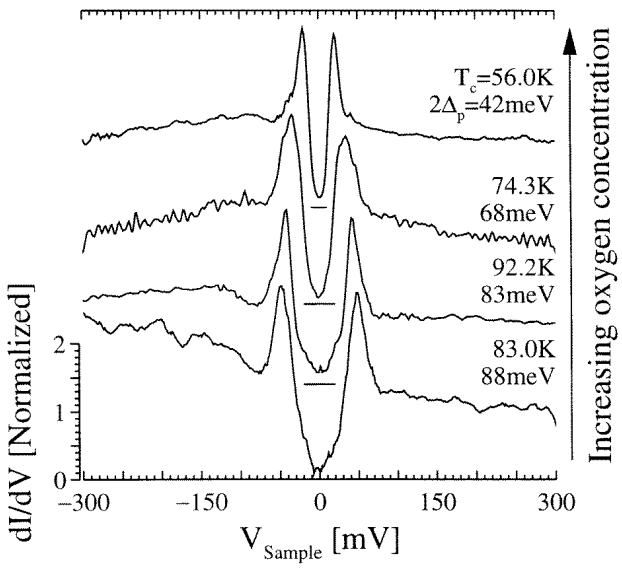


Figure 25.17: Doping dependence of LDOS measured through STS at low temperature. The separation between the peaks $2\Delta_p$ quantifies a superconducting gap that decreases with x. (From Ref.[71]).

address the issue of strong correlations in Hubbard and $t-J$ models. On the other hand, in conventional superconductors and, in general, for the study of phase transitions, phenomenological Ginzburg-Landau (GL) functionals [74] written down from very general symmetry grounds have provided useful descriptions for a variety of systems [75]. Specially, Ginzburg-Landau theory has been proven to be complementary to BCS theory for attacking a plethora of situations in superconductors, e.g., inhomogeneities, structures of isolated vortex and vortex lattice etc. [8].

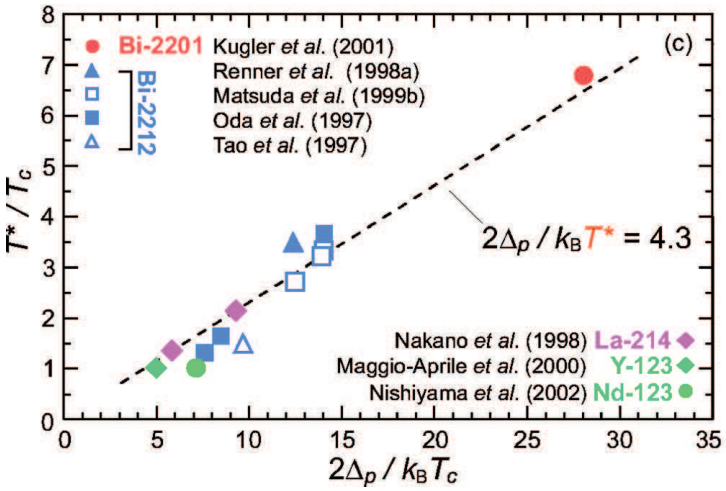


Figure 25.18: T^*/T_c as a function of $2\Delta_p/k_BT_c$ obtained for various cuprates from STS. Dashed line corresponds to the mean-field d-wave relation $2\Delta_p/k_BT^* = 4.3$, but with T_c replaced by pseudogap temperature scale T^*. (From Ref.[73], see Ref.[21] for references within the figure).

In the same spirit, some of us have proposed and developed a phenomenological approach [76] for the superconducting and pseudogap states of the cuprates.

In the phenomenological theory we attribute the pseudogap to short-range local spin-singlet pairing. This is in line with a large number of theories for cuprate superconductivity within the so-called "preformed pair scenarios" [5], especially those from the strong coupling point of view [3]. We discuss below a possible microscopic underpinning of our theory from a strong correlation picture. However, we emphasize that we do not tie ourselves down to any particular microscopic calculation. Our theory essentially has two main empirical inputs, namely

1. A pairing temperature scale $T^*(x)$, mimicking the pseudogap temperature scale (Fig.25.2), below which local pairing amplitude becomes substantial.

2. A 'bare' superfluid density $\rho_s \propto x$, that linearly increases with doping for small x, as implied by the Uemura correlation [17] discussed before.

As we discuss below, based on the above basic ingredients built into the proposed GL functional, we can encapsulate a large number of well known cuprate phenomenologies in the form of a low-energy effective lattice functional of complex spin-singlet pair amplitudes that resides on the Cu-Cu bonds of the CuO_2 planes of cuprates. We summarize our results for average pairing amplitude in the superconducting and pseudogap phases, superfluid density, specific heat, vortex properties , fluctuation diamagnetism as well as thermoelectric transport quantity like Nernst coefficient [76, 77, 78] obtained using the proposed functional and compare them successfully with experiments.

Motivated by the picture that emerges from our GL-like approach, we have also extended [79] it to obtain the electron spectral density that inevitably results from coupling between electrons and Cooper pair fluctuations. These results, and their implications for low energy electronic spectra measured through ARPES and STM, are also discussed.

25.4.1 Phenomenological GL-like functional

Based on our central assumption of the pairing origin of pseudogap, we propose that, as a minimal description, the free energy of a cuprate in the superconducting and pseudogap states can be expressed as a functional solely of the complex pair amplitude. We hypothesize a lattice free-energy functional similar in structure to the conventional GL functional [8], but defined

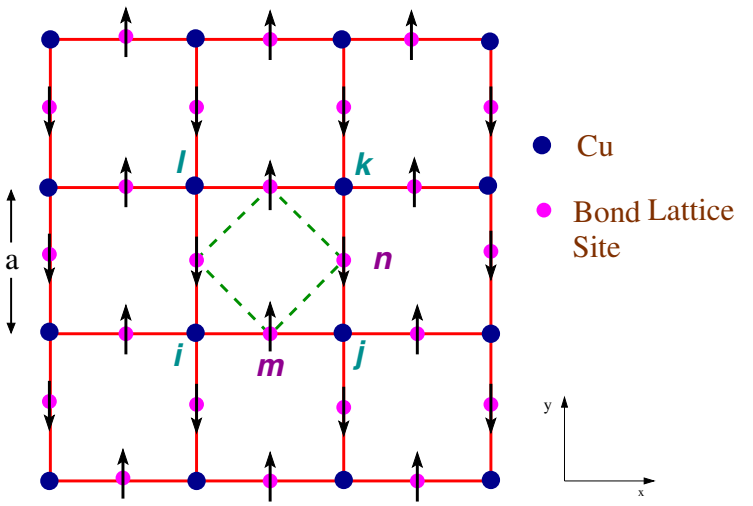


Figure 25.19: The square Cu lattice sites in the CuO_2 plane and construction of the bond-centre lattice out of the centers of the Cu-O-Cu bonds. The arrows indicate the direction of equivalent planar spins, with $\mathbf{S}_m = (\Delta_m \cos\phi_m, \Delta_m \sin\phi_m)$ representing the complex order parameter $\psi_{ij} \equiv \psi_m = \Delta_m \exp(i\phi_m)$ and antiferromagnetic ordering of spins translating into a long-range d-wave superconducting order.

on the CuO_2 square lattice. Fig.25.19 shows the square planar lattice schematically. The free energy is assumed to be a functional of the complex spin-singlet pair amplitude $\psi_{ij} \equiv \psi_m = \Delta_m \exp(i\phi_m)$, where i and j are nearest-neighbour sites of the square planar Cu lattice and m labels the bond-center lattice site located at the bond between the lattice site i and j (see Fig.25.19). The highly anisotropic cuprate superconductivity is modelled as a weakly coupled stack of CuO_2 planes and we ignore, as a first approximation, the interplane coupling. The free-energy functional for a single plane is assumed to have the lattice version of the conventional GL functional [8], i.e.

$$\mathcal{F}(\{\Delta_m, \phi_m\}) = \sum_m \left(A\Delta_m^2 + \frac{B}{2}\Delta_m^4 \right) + C \sum_{<mn>} \Delta_m \Delta_n \cos(\phi_m - \phi_n), \qquad (25.3)$$

We posit the above lattice functional to be more fundamental, in principle, than the conventional continuum GL functional due to underlying strongly correlated nature of the cuprate superconductors and owing to the fact that they have very short coherence length ($\sim 15-20$Å). A Gor'kov like [80] microscopic interpretation of ψ_{ij} is as an average spin-singlet nearest-neighbor Cooper pair amplitude, i.e., $\psi_{ij} \equiv \langle \hat{b}_{ij} \rangle / \sqrt{2} \equiv (1/2)\langle a_{i\downarrow} a_{j\uparrow} - a_{i\uparrow} a_{j\downarrow} \rangle$. The sites i and j are different because strong electron repulsion U disfavors on-site pairing, while the existence of large nearest-neighbor antiferromagnetic spin-spin interaction in the parent (undoped) cuprate is identically equivalent for spin-$\frac{1}{2}$ electrons to attraction between nearest-neighbor pairs, i.e. $J(\hat{\mathbf{S}}_i.\hat{\mathbf{S}}_j - \frac{1}{4}\hat{n}_i\hat{n}_j) = -J\hat{b}_{ij}^\dagger \hat{b}_{ij}$. This favours the formation of nearest-neighbour bond spin-singlet pairs.

The 'on-site' part of the above functional [eq.(25.3)] has been written down in a bare minimum form, as a sum of quadratic and quartic terms in Δ_m in the image of conventional GL theory, for simplicity. We remark that unlike in the original GL theory where the parameters A and B are proposed near T_c, we propose this simple form for all T and all x, as a qualitatively correct one. The parameters A and B depend, in general, on x and T. We assume that B is a positive constant independent of x and T and choose $A(x,T) \propto (T - T^*(x))$ to change sign along a straight line $T^*(x) = T_0(1 - x/x_c)$ running from $T = T_0$ at $x = 0$ to $T = 0$ at $x = x_c$. As a first approximation, this line can be identified with the pseudogap temperature $T^*(x)$ because the magnitude of the local pair ampliitude, $\langle \Delta_m \rangle$, can increase dramatically as the temperature crosses this line due to sign change of A.

The occurrence of superconductivity in the model is characterized by a nonzero stiffness for long-wavelength phase fluctuations and is determined by the phase coupling term C [eq.(25.3)]. The parameter C is taken to be proportional to x in conformity with the Uemura correlation

[17]. Also, $C > 0$ so that the zero-temperature superconducting state has d-wave symmetry [see Fig.25.19]. We discuss the choice of doping and temperature dependences of the parameters A, B and C in more detail in Appendix 25.8.

Effect of magnetic field: An applied magnetic field perpendicular to the CuO_2 planes giving rise to, e.g., the orbital magnetization and magnetothermoelectric effects [77, 78], is incorporated in our model through a bond flux $A_{mn} = (2\pi/\Phi_0)\int_m^n \mathbf{A}\cdot d\mathbf{r}$, which modifies $(\phi_m - \phi_n)$ to $(\phi_m - \phi_n - A_{mn})$ in eq.(25.3), as usual in a lattice GL functional. Here $\mathbf{A}$ is the vector potential. Assuming extreme type-II limit as appropriate for the cuprate superconductors, the magnetic field H is given by the condition $\sum_\square A_{mn} = \Phi$, where $\sum_\square$ is a sum over a plaquette of the lattice and $\Phi = Ha^2/\Phi_0$ is the magnetic flux per plaquette in units of the universal flux quantum.

Effect of quantum phase fluctuations: As we discuss below, the superconducting transition temperature T_c obtained in our model follows a dome-shaped curve as a function of x. However, on the extreme underdoped and overdoped regimes the superfluid density becomes small in our model [76]. In these regimes, one needs to take into account the effect of quantum phase fluctuations. These would renormalize T_c to zero at finite doping in the underdoped side and their importance is well-supported by experiments [81, 82] and theoretical analysis [83]. We can incorporate quantum phase fluctuation effects in our formalism [76] by supplementing the free-energy functional of eq.(25.3) with the following term

$$\mathcal{F}_Q(\{\hat{q}_m\}) \;=\; \frac{1}{2}\sum_{mn}\hat{q}_m V_{mn}\hat{q}_n \tag{25.4}$$

Here $\hat{q}_m$ is the Cooper pair number operator at site m, and ϕ_m in eq.(25.3) should be treated as a quantum mechanical operator $\hat{\phi}_m$, canonically conjugate to $\hat{q}_m$ so that $[\hat{q}_m, \hat{\phi}_n] = i\delta_{mn}$. We take the simplest possible form for V_{mn} i.e. $V_{mn} = V_0\delta_{mn}$, where V_0 is the strength of on-site Cooper pair interaction, an additional phenomenological parameter that can fixed such that $T_c(x)$ curve computed in the phenomenological theory matches the experimental one [76]. We do not include these quantum fluctuations explicitly for calculating thermodynamic quantities, e.g. specific heat, magnetization etc., associated with pairing fluctuations, since quantum phase fluctuations bring about qualitative changes only at the extreme end of the dome on the underdoped side. For other values of x, these fluctuations only renormalize the values of the parameters A, B and C of our functional (25.3). We assume that such renormalizations have already been taken into account while choosing these parameters in tune with experiments. Next we discuss some general aspects of our model and its possible microscopic origin.

General aspects of the phenomenological theory: As clearly evident from eq.(25.3), since $\Delta_m\Delta_n\cos(\phi_m - \phi_n) = -(|\psi_m - \psi_n|^2 - \Delta_m^2 - \Delta_n^2)$, the intersite term can be readily identified with the discretized version of usual spatial derivative term $|\nabla\psi|^2$. The model is thus of the form of a conventional GL model, albeit one that is defined on a lattice at the outset. As discussed above, defining the complex singlet pair amplitude to reside on the $Cu-Cu$ bonds (Fig.25.19) and choosing the phase coupling term C to be positive, we immediately get a d-wave superconducting order at low temperature. The negative sign of C corresponds to more conventional s-wave BCS like case. For quantitative comparison with experiments, the lattice should be thought of more appropriately as a phenomenological one that emerges upon coarse graining, albeit with a coarse graining length only three to five times larger than microscopic lattice spacing a [77]. Hence, our model, in practice, can be thought of as the discretized version of a continuum theory with the lattice spacing a as a suitable ultraviolet cutoff to describe long wavelength physics. In the presence of magnetic field H, the lattice constant is also equivalent to a field scale $H_0 = \Phi_0/(2\pi a^2)$, defined through the flux quantum $\Phi_0 = hc/2e$. In principle, the field scale H_0 can be obtained by fitting the field dependence of magnetization with that of experiment [77].

The free-energy functional in eq. (25.3) can also be viewed as the Hamiltonian of an XY model with fluctuations in the magnitude of 'planar spin' ψ_m, where the on-site term in eq.(25.3) simply controls the temperature and doping dependence of the magnitude. The form of the free-energy functional might seem superficially similar to the widely used model of granular superconductors [84]. However, we would like to re-emphasize that we do not assume any underlying granularity of our system, as mentioned above. Such phenomenological lattice models, in the extreme XY limit, have been employed in the past to study superconductivity in non-granular lattice systems, especially in the context of cuprates [85, 86, 83, 87].

Additionally, even though the form of our functional is mainly motivated by cuprate phenomenology, as we discuss below, a similar functional arises quite naturally in a strong correlation framework for a doped Mott insulator [88, 89, 90]. In general, in such a functional, the single-site term of eq.(25.3) will have more complicated form[89, 90], having many terms in a power series expansion of Δ_m, in addition to the quadratic and quartic ones that our functional does. But, as we discuss below, the superconducting dome is reproduced quite reasonably by truncating the functional to quartic order. In addition, several other experimentally observed thermodynamic properties of the cuprates over the entire pseudogap regime are also reproduced by this simplified form of the functional [76].

Microscopic underpinning: GL theories for cuprates have been proposed by a large number of authors, arising either out of a particular model for electronic behavior and often coupled with the assumption of a particular 'glue' for binding electrons into pairs [88, 89, 91], or out of lattice symmetry considerations [92, 93]. The functional in eq.(25.3) is consistent with square lattice symmetry and, in principle, does not assume any particular electronic approach, e.g. weak coupling or strong correlation. However, some of the properties of the coefficients are natural in a strong electron correlation framework. For example, mobile holes in such a system can cause a transition between a state in which there is a Cooper pair in the x directed ij bond (Fig.25.19) to one in which the Cooper pair is in an otherwise identical but y directed bond jk nearest to it (or vice versa), thus leading to a nonzero intersite phase coupling term in eq.(25.3). This is probably connected with the observed [94] empirical correlation between T_c and the diagonal or next-nearest-neighbor hopping amplitude t' of electrons in the Cu lattice.

A phenomenological approach such as ours does not point to a specific 'glue' which binds electrons on nearest-neighbor sites into spin singlet pairs. However, as mentioned before, in a strong correlation picture, a natural source is J. In general therefore, the nearest-neighbor interaction can be thought of as a mixture of antiferromagnetic spin exchange and pair attraction. As the Mott insulator is doped and the holes become mobile, it seems likely (from experiment) that the interaction is more conveniently described as latter than the former in a mean-field sense. A number of microscopic variational $T = 0$ calculations appropriate for competing spin density wave and d-wave superconducting ground states as a function of hole doping exist in the literature [95, 96, 97]; they generally suggest a magnetic ground state or a coexistence of magnetism and superconductivity for low hole doping and a superconducting ground state for higher doping. Here, we consider only the pair degrees of freedom and disregard the spin. So, if this description is appropriate, the limiting ($x \to 0$) pseudogap or bound pair energy scale T_0 is expected to be of order J from which the pair attraction originates in the strong correlation picture. Nevertheless, T_0 is a factor of two or three smaller than J. The decrease of the pseudogap energy scale with x is presumably due to holes because their presence implies at the very least a decrease in the number of nearest-neighbor electron pairs that can be formed. Some early results [98] suggest a mean-field 'effective' $J_{\rm eff} \simeq J - xt$ where t is the nearest-neighbor hopping. This may be relevant to the linear decrease of $T^*(x)$ with doping x.

25.4.2 Thermodynamic quantities obtained from the phenomenological theory

The main objective of our phenomenological approach is to investigate whether the free energy functional defined in eq.(25.3) provides a good description of experimental results over a wide range of x and T. To this end, we have calculated large number of thermodynamic quantities associated with pairing fluctuations [76, 77] and directly compared them with the experimental observations discussed in section 25.3. Here we list some of the quantities computed within the phenomenological theory. The details of the calculations and the results can be found in Refs.[76, 77, 78]. In section 25.6, we summarize our main results and briefly discuss how these compare with the cuprate phenomena discussed in section 25.3.

We have calculated the zero-temperature gap $\Delta_0(x)$ and superfluid density $\rho_s^0(x)$ as a function of doping by minimizing the free-energy functional (25.4) with respect to pairing amplitude Δ_m at $T = 0$ for the uniform d-wave state shown in Fig.25.19. Thermodynamic quantities, such as average local pairing amplitude $\langle\Delta_m\rangle$, specific heat C_v and orbital magnetization M etc., are calculated via canonical thermal averages, $\langle\dots\rangle = (1/Z)\int\prod_m d\phi_m d\Delta_m(\dots)e^{-\beta\mathcal{F}(\Delta_m,\phi_m)}$, where Z is the partition function. The calculations have been done via standard techniques like mean-field theory, Monte-Carlo (MC) simulation etc. We have also calculated properties, e.g. core-structure and core-energy $E_c(x)$, of topological defects, i.e. a superconducting vortex, via numerical optimization with appropriate boundary condition [76]. The vortex core-energy has important implications for the transport coefficients in the underdoped regime, as discussed in Ref.[77].

25.5 Extensions of the phenomenological theory to describe thermoelectric transport and low-energy electronic spectra

We have extended the phenomenological theory in several ways, e.g., to study the contributions of pairing fluctuations to thermoelectric transport, such as Nernst coefficient, and also to look into the effects of these fluctuations on low-energy electronic spectral density as directly probed via ARPES and STM. We discuss these extensions below.

25.5.1 Relaxation dynamics using the phenomenological theory

To study the influence of pairing fluctuations on transport properties we implement[78] "model A" dynamics [74] for a time-dependent complex pair amplitude $\psi_m(t) = \Delta_m(t)e^{i\phi_m(t)}$ given by the stochastic equation

$$\tau D_t\psi_m(,t) = -\frac{\partial\mathcal{F}(\{\psi_m,\psi_m^*\})}{\partial\psi_m^*(t)} + \eta_m(t). \tag{25.5}$$

Here $\mathcal{F}(\{\psi,\psi^*\})$ is a the free energy functional [eq.(25.3)], that incorporates the effect of electromagnetic field in the inter-site phase coupling term, as discussed earlier, via a vector potential $\mathbf{A}_{mn}(t)$, which can be time-dependent in general. We define a covariant time derivative $D_t = (\frac{\partial}{\partial t} + iV_m(t))$, where $V_m(t)$ is a scalar potential at site m. The time scale τ, which provides the characteristic temporal relaxation scale of the order parameter dynamics, can in general be complex. However it is required to be real in the presence of particle-hole symmetry, that translates to the requirement that the equation of motion for ψ_m^* be the same as for ψ_m under the simultaneous transformation of complex conjugation ($\psi_m \to \psi_m^*$) and magnetic field inversion ($H \to -H$). Evidence of particle-hole symmetry in the form of no appreciable Hall or Seebeck effect is seen in the experimentally accessible regime of the superconductors we study here, and

thus we take τ to be real in our calculations. The thermal fluctuations are introduced through $\eta_m(t)$ with the complex Gaussian white noise correlator $\langle \eta_n^*(t)\eta_m(t')\rangle = 2k_{\rm B}T\tau\delta_{mn}\delta(t-t')$.

The dynamical model Eq. 25.5 is the simplest one which yields an equilibrium state in the absence of driving potentials. For conventional superconductors, it can be derived microscopically within BCS theory above and close to the transition temperature T_c. However, it has been used phenomenologically to study transport previously in situations where the microscopic theory is not known, such as for the cuprates [99, 100, 87]. We employ the model in a similar spirit here.

Transport coefficients: To compute transport coefficients, we numerically integrate the dynamical equations (25.5), in the presence of either temperature gradient ∇T or electric field $\mathbf{E}$, applied via suitable choice of gauge potentials $A_{mn}(t)$ and $V_m(t)$. The transport current densities, obtained in our model after appropriate subtractions of magnetization currents [78], can be related to ∇T and $\mathbf{E}$ using standard linear response relations

$$\begin{pmatrix} \mathbf{J}^e_{\rm tr} \\ \mathbf{J}^Q_{\rm tr} \end{pmatrix} = \begin{pmatrix} \hat{\sigma} & \hat{\alpha} \\ \hat{\tilde{\alpha}} & \hat{\kappa} \end{pmatrix} \begin{pmatrix} \mathbf{E} \\ -\nabla T \end{pmatrix},$$

where $\hat{\sigma}$, $\hat{\alpha}$, $\hat{\tilde{\alpha}}$, $\hat{\kappa}$ are the electrical, thermoelectric, electro-thermal and thermal conductivity tensors, respectively. We have mainly studied the Nernst signal e_N, which is the electric field (E_y) response to a temperature gradient ($\nabla_x T$) in the direction transverse to the electric field in the presence of a magnetic field H along z-direction, i.e. $e_N \equiv E_y/\nabla_x T$ with open circuit boundary conditions. Under reasonable assumptions [78], the Nernst coefficient, $\nu = e_N/H$ can be connected to the thermoelectric coefficients via the simple relation $\nu = \alpha_{xy}/(H\sigma_{xx})$, that we use. We summarize our results of Nernst coefficient calculated over the whole doping-temperature range in section 25.6.

25.5.2 Pairing fluctuations and low-energy electronic spectra in cuprates

Decipherment of the physics of high-T_c cuprates should necessarily involve the understanding of electronic excitations and properties related to them in the various parts of cuprate phase diagram (Fig.25.2). Hence a phenomenological theory, such as ours, which aims to describe the pseudogap phase as one consisting of preformed pairs of *a specific type*, is required to include both electrons and Cooper pairs of the same electrons coexisting and *necessarily* coupled with each other. In our GL-like approach only the latter are explicit, while the former are *integrated out*. However, effects connected with the pair degrees of freedom are often explored via their coupling to electrons, e.g. via ARPES and STM, as discussed earlier. Here we develop a unified theory of electronic excitations in the superconducting and pseudogap phases, using a model of electrons coupled to spatially and temporally fluctuating nearest-neighbor bond singlet Cooper pairs. We discuss the theory, its basic principles and assumptions here, and a number of its consequences with respect to cuprate phenomena are summarized in section 25.6.

Basic notions and assumptions behind the approach: The main difficulty in a theory of the above kind is the description of electrons in a presumably strongly correlated system such as a cuprate, which is perhaps best described as a doped Mott insulator [3] with strong low-energy antiferromagnetic correlation between electrons as well as various other types long-and short-range ordering tendencies. This is the major problem for constructing a microscopic theory in the entire field of strongly correlated electrons and dealing with such problems in a controlled manner would probably continue to be an active field of research and one of the most challenging tasks in condensed matter physics for years to come .

However, irrespective of the microscopic origin, the interacting pair degrees of freedom probably still can be described by a phenomenological theory of the kind described here. To

pursue this path, one needs to commit to some kind of model for electron dynamics which therefore implies an approach to the coupling between single electronic and pair degrees of freedom. We develop what we believe is a minimal theory, appropriate for low-energy physics. We assume that for energies $|\omega| \lesssim \Delta$ (Δ is of the order of zero temperature superconducting gap), well defined electronic states, namely tight binding lattice states with a renormalized hopping/bandwidth exist and couple to low energy pair fluctuations. Superconducting ordering/phase stiffness and fluctuations are reflected in the pair-pair correlation function. This correlation function has a generic form, especially near T_c, which, for example, may be obtained from the GL-like functional [eq.(25.3)] or, as we show in Ref.[79], can be deduced from various experiments. The *inevitable* coupling between electrons and low lying fluctuations of pairs, made of the same electrons leads to a self energy with a significant structure for electron momentum $\mathbf{k}$ along the Fermi surface and low electronic excitation energy ω.

Physically, we have electrons (e.g. those with energy near the Fermi energy) moving in a medium of evanescent pairs which have finite range d-wave correlation for $T > T_c$ and have long range order of this kind for $T < T_c$ in addition to 'spin wave' like fluctuations. On approaching T_c from above, collective d-wave symmetry superconducting correlations develop among the pairs with a characteristic superconducting coherence length scale ξ which diverges at the second-order transition temperature T_c. These correlations have a generic form at large distances (>> the lattice spacing a). Our theory captures the effects of these correlations on low-energy unpaired electronic degrees of freedom in the superconducting and pseudogap phases.

Model: To motivate the microscopic coupling between the spin-singlet bond pair and electrons, we take the tJ model (25.1) as the basic starting point. However to circumvent the daunting task of treating the no double occupancy constraint discussed in section 25.2, we use the following simplified Hamiltonian, the so-called 'plain vanilla' [101] version of tJ model, i.e.

$$\hat{\mathcal{H}} \;=\; -\sum_{ij,\sigma} \tilde{t}_{ij} a^{\dagger}_{i\sigma} a_{j\sigma} - \tilde{J} \sum_{<ij>} \hat{b}^{\dagger}_{ij} \hat{b}_{ij}. \tag{25.6}$$

Here the effective hopping $\tilde{t}_{ij} = g_t t_{ij}$ and effective antiferromagnetic exchange $\tilde{J} = g_s J$, which acts as a pair attraction, are strongly affected by correlations via single-site Gutzwiller renormalization factors $g_t = 2x/(1+x)$ and $g_s = 4/(1+x^2)$ [101]. The bare hopping amplitude t_{ij} involves the nearest neighbor (t), next-nearest neighbor (t') and further neighbor (t'') hopping terms. In our calculations, we use the above mentioned homogeneous Gutzwiller approximation with standard values for t_{ij} ($t = 300$ meV, $t'/t = -1/4$ and $t'' = 0$, see e.g. [1]).

Very generally, assuming pairing fluctuations to be relevant at low energies, the bond-pair attraction term term eq.(25.6), can be written via Hubbard-Stratonovich transformation as a time and space dependent bond pair potential acting on electrons and characterized by a field $\psi_m(\tau)$ [τ is the imaginary time; $0 < \tau < \beta = 1/(k_B T)$]. The saddle point of the resulting action in the static limit gives rise to the conventional mean field approximation in which the second term in eq.(25.6) is written as

$$-\tilde{J}_{ij}(\langle \hat{b}^{\dagger}_{ij} \rangle \hat{b}_{ij} + \hat{b}^{\dagger}_{ij} \langle \hat{b}_{ij} \rangle - \langle \hat{b}^{\dagger}_{ij} \rangle \langle \hat{b}_{ij} \rangle) \tag{25.7}$$

and the average $\psi_m = \psi_{ij} \equiv \tilde{J}_{ij} \langle \hat{b}_{ij} \rangle$ is determined self-consistently (mean field theory).

The effective Hamiltonian we use is of the form of eq.(25.6) with the second term in it replaced by eq.(25.7). This describes two coupled fluids, namely a fermionic fluid and a bosonic fluid, represented respectively by the on-site electron field $a^{\dagger}_{i\sigma}$ and the bond Cooper pair field $\psi_{ij} = \psi_m$. The properties of ψ_m needed in our calculation are its mean value $\langle \psi_m \rangle$ (nonzero below T_c) and the fluctuation part of the correlation function $\langle \psi_m \psi^*_n \rangle$, whose *universal* form for large $|\mathbf{R}_m - \mathbf{R}_n|$ near T_c is what we use. These arise from an inter-site term of the form shown in eq.(25.3).

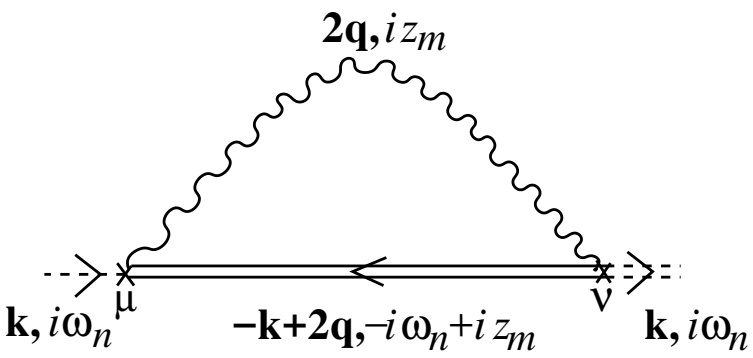


Figure 25.20: **The pair fluctuation exchange process for the self energy of electrons.** Feynman diagram of the process in which an electron $(\mathbf{k}, i\omega_n)$ virtually becomes another electron $(-\mathbf{k}+2\mathbf{q}, -i\omega_n + iz_m)$ and absorbs a Cooper pair $(2\mathbf{q}, iz_m)$ in the intermediate state. The curly line denotes the Cooper pair propagator $D_{\mu\nu}(2\mathbf{q}, iz_m)$ (here $z_m = 2m\pi/\beta$ is the bosonic Matsubara frequency, m being an integer).

For a translationally invariant system described by eq.(25.6), the electron Green's function satisfies the Dyson equation

$$G^{-1}(\mathbf{k}, i\omega_n) \;=\; (G_0)^{-1}(\mathbf{k}, i\omega_n) - \Sigma(\mathbf{k}, i\omega_n), \tag{25.8}$$

where $\Sigma(\mathbf{k}, i\omega_n)$ [$\omega_n = (2n+1)\pi/\beta$ is the fermionic Matsubara frequency with n as an integer] is the irreducible self energy, originating from the coupling between bond pairs and electrons with bare propagator $G_0(\mathbf{k}, i\omega_n) = (i\omega_n - \xi_{\mathbf{k}})^{-1}$, $\xi_{\mathbf{k}} = \epsilon_{\mathbf{k}} - \mu$ and $\epsilon_{\mathbf{k}}$ is the Fourier transform of the hopping $\tilde{t}_{ij} = \tilde{t}_{\mathbf{i-j}}$ (μ is the chemical potential). We use the well-known lowest-order bosonic fluctuation exchange approximation for $\Sigma(\mathbf{k}, i\omega_n)$ shown diagrammatically in Fig.25.20.

Close to T_c, the temporal decay of long-wavelength fluctuations is specially slow due to critical slowing down [74], so that they can be regarded as quasistatic. The self energy Σ can then be expressed as [76]

$$\Sigma(\mathbf{k}, i\omega_n) \;=\; -\frac{1}{N}\sum_{\mathbf{q},\mu,\nu} G_0(-\mathbf{k}+2\mathbf{q}, -i\omega_n) D_{\mu\nu}(2\mathbf{q}) f_\mu(\mathbf{k}, \mathbf{q}) f_\nu(\mathbf{k}, \mathbf{q}) \tag{25.9}$$

where N is the total number of Cu sites on a single CuO_2 plane and μ, ν refer to the direction of the bond i.e. x or y (see Fig.25.19). $D_{\mu\nu}(2\mathbf{q}) = \sum_{\mathbf{R}} D_{\mu\nu}(\mathbf{R}) \exp(-i2\mathbf{q}.\mathbf{R})$ is the static pair propagator of Cooper pair fluctuations with

$$D_{\mu\nu}(\mathbf{R}_{i\mu} - \mathbf{R}_{j\nu}) = \langle \psi_{i\mu} \psi^*_{j\nu} \rangle. \tag{25.10}$$

The quantity $f_\mu(\mathbf{k}, \mathbf{q}) = \cos[(k_\mu - q_\mu)a]$ is a form factor arising from the coupling between a tight-binding lattice electron and a nearest-neighbour bond pair. Because of the d-wave long-range order (LRO) described as 'Ne′el' order (Fig.25.19) of the 'planar spin' ψ_m in the bipartite bond-centre lattice, the standard sublattice transformation [i.e. $\psi_m \rightarrow \tilde{\psi}_m = \Delta_m \exp(i\tilde{\phi}_m)$ where $\tilde{\phi}_m = \phi_m$ for x-bonds and $\tilde{\phi}_m = \phi_m + \pi$ for y-bonds] implies

$$D_{xx}(\mathbf{R}) = D_{yy}(\mathbf{R}) = -D_{xy}(\mathbf{R}) = -D_{yx}(\mathbf{R}) \equiv D(\mathbf{R}), \tag{25.11}$$

where $D(\mathbf{R})$ can be written as

$$D(\mathbf{R}_m - \mathbf{R}_n) = \langle \tilde{\psi}_m \rangle \langle \tilde{\psi}^*_n \rangle + \widetilde{D}(\mathbf{R}_m - \mathbf{R}_n)\,. \tag{25.12}$$

Here $\widetilde{D}(\mathbf{R})$ is the fluctuation term. The LRO part $\langle \tilde{\psi}_m \rangle \equiv \Delta_d$ leads to a d-wave Gor'kov like gap with $\Delta_{\mathbf{k}} = (\Delta_d/2)(\cos k_x a - \cos k_y a)$; the corresponding electron self energy is $\Sigma(\mathbf{k}, i\omega_n) = \Delta^2_{\mathbf{k}}/(i\omega_n + \xi_{\mathbf{k}})$. In widely used phenomenological analyses [102] of ARPES data, this form is

used above T_c with lifetime effects, both diagonal and off-diagonal in particle number space added to Σ, i.e.

$$\Sigma(\mathbf{k},\omega) \;=\; -i\Gamma_1 + \frac{\Delta_{\mathbf{k}}^2}{\omega + \xi_{\mathbf{k}} + i\Gamma_0} \tag{25.13}$$

Here Γ_1 is single-particle scattering rate and Γ_0 is assumed to originate due to finite life-time of *preformed* d-wave pairs [102].

We propose here that as described above, the electrons move (above T_c) *not* in a pair field with d-wave LRO which decays in time at a rate put in by hand, but in a nearly static pair field with growing correlation length ξ. We assume, as appears quite natural for a system with characteristic length scale ξ that $\widetilde{D}(\mathbf{R}) \sim \exp(-R/\xi)$ for large R, while ξ diverges at T_c. This natural form for $\widetilde{D}(R)$ is found, for example, in the Berezinskii-Kosterlitz-Thouless (BKT) theory [74] for two dimensions and in a GL theory for all dimensions. For large correlation lengths, $\Sigma(\mathbf{k}, i\omega_n)$ obtained in our theory is nearly the same as that for preformed d-wave symmetry pairs. Below T_c, $\widetilde{D}(R)$ decays as a power law (i.e. $\widetilde{D}(R) \sim R^{-\eta}$ with $\eta > 0$) due to order parameter phase or 'spin wave'-like fluctuations [79]. We find here the consequences of these for the spectral function, i.e.

$$A(\mathbf{k},\omega) \;\equiv\; -\frac{2}{\pi}\mathrm{Im}\left[G(\mathbf{k}, i\omega_n \to \omega + i\delta)\right], \tag{25.14}$$

measured in ARPES. $G(\mathbf{k}, i\omega_n)$ is obtained from eq.(25.8) with the self energy calculated from eq.(25.9) using the aforementioned forms of the pair propagator $\widetilde{D}(\mathbf{R})$ (or $D(\mathbf{R})$) for temperatures above and below T_c.

In a regime where the fluctuations in the real pair magnitude Δ_m are short ranged,

$$D(\mathbf{R}) \simeq \langle \Delta(\mathbf{R})\Delta(\mathbf{0})\rangle \langle e^{i[\tilde{\phi}(\mathbf{R}) - \tilde{\phi}(\mathbf{0})]}\rangle \equiv \bar{\Delta}^2 \bar{D}(R) \tag{25.15}$$

for large R ($R >> a$) [as evident from eq.(25.12), $\widetilde{D}(R) \simeq \bar{\Delta}^2(\bar{D}(R) - |< e^{i\tilde{\phi}(\mathbf{0})} >|^2)$]. This decoupling between magnitude and long distance phase correlations is accurate for $x \lesssim x_{\rm opt}$, a manifestation of which is the separation between T^* and T_c. Our calculations based on eq.(25.15) are therefore reliable in this doping range. For strictly two-dimensional system mostly considered here, we use the general form [74] for the phase correlator,

$$\bar{D}(R) = (\tilde{\Lambda}R)^{-\eta} \exp\left(-R/\xi\right) \tag{25.16}$$

(with $\tilde{\Lambda} \sim a^{-1}$) in eq.(25.9). An analytical expression can be obtained for the self energy in this case [79], namely

$$\Sigma(\mathbf{k}, i\omega_n) \;\simeq\; \frac{-i\ \mathrm{sgn}(\omega_n)\Gamma(1-\eta)\bar{\Delta}_{\mathbf{k}}^2}{\left(\tilde{\Lambda} \mathrm{v}_{\mathbf{k}}\right)^{\eta} \left(v_{\mathbf{k}}/\xi - i\ \mathrm{sgn}(\omega_n)(i\omega_n + \xi_{\mathbf{k}})\right)^{1-\eta}} \tag{25.17}$$

In this equation, Γ is the well known gamma function and $\mathbf{v}_{\mathbf{k}} = \frac{1}{a}\frac{\partial \xi_{\mathbf{k}}}{\partial \mathbf{k}}$ (with $v_{\mathbf{k}} = |\mathbf{v}_{\mathbf{k}}|$) is the velocity (expressed in units of energy) obtainable from the energy dispersion $\xi_{\mathbf{k}}$. The above self energy does not affect the nodal quasiparticles owing to the $\mathbf{k}$ dependence of $\bar{\Delta}_{\mathbf{k}} = (\bar{\Delta}/2)(\cos k_x a - \cos k_y a)$. We have also obtained electronic self-energy for an anisotropic three-dimensional system with small interlayer coupling, as appropriate for the cuprates [79]. We have used inputs from our phenomenological theory as well as from experimental data to estimate various parameters, such as $\bar{\Delta}$, ξ, η, that enter into the self-energy [79]. We summarize the main results of our calculations for low-energy electronic spectral properties in the next section.

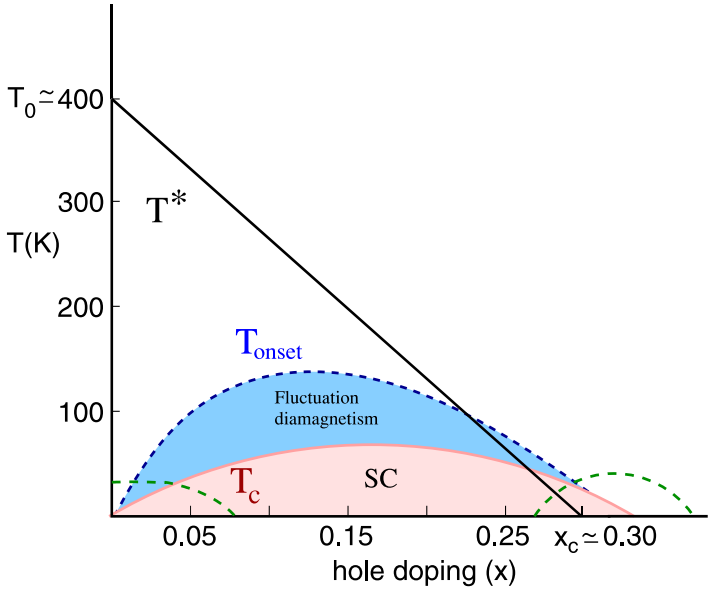


Figure 25.21: A schematic phase diagram for the model [eq. (25.3)] in the hole doping x and temperature T plane. The local pairing temperature scale $T^*(x)$, (solid black line) is an input to our phenomenological model [eq. (25.3)] and it mimics the experimental pseudogap temperature scale. The model reproduces a dome-shaped superconducting region (drawn in pink). The region of enhanced fluctuation diamagnetism and Nernst signal (shaded in blue) in the pseudogap phase and corresponding onset temperature $T_{\rm onset}$ are shown. Between T_c and T^*, electronic spectral functions shows an antinodal pseudogap. The pseudogap state is also characterized by Fermi arcs that emerges from d-wave node at T_c and persist all the way up to T^*. The two arcs shown by dotted lines denote regions where quantum fluctuation effects, as well as other low-energy degrees of freedom, such as electronic and spin plus their coupling with pair degrees of freedom, need to be explicitly included in the free energy functional.

25.6 Results from the phenomenological theory and comparison with experiments

Fig.25.21 shows overall phase diagram obtained from our phenomenological theory and its extensions to capture thermoelectric transport and low-energy electronic spectra. We summarize our main results below and indicate how they compare with the cuprate phenomenology discussed in Section 25.3.

1. Superconducting and pseudogap phases: The pseudogap and superconducting states are both described by a non-zero thermal average of local pairing amplitude, i.e. $\Delta(T) = \langle \Delta_m \rangle \neq 0$. The superconducting state has long-range phase coherence characterized by superfluid density $\rho_s(x,T)$ becoming non-zero below a transition temperature $T_c(x)$ (Fig.25.21), that reproduces the nearly parabolic superconducting dome of Fig.25.2. The results for the zero-temperature gap, T_c as a function of x and superfluid density as function of x and T are shown in Figs.25.22,25.23. We have also calculated the effect of quantum phase fluctuations on T_c in the underdoped regime; T_c is pushed to zero at nonzero x, leading to a $T_c(x)$ dome [76] in close agreement with experiment.

2. Pseudogap crossover: The onset of pesudogap state is characterized by rapid but smooth crossover of various quantities across $T^*(x)$ which is an input incorporated via change of sign of the coefficient A [eq.(25.3)] in our theory. For example, the local pairing amplitude $\Delta(T)$ rises rapidly with decreasing temperature across $T^*(x)$ and the pairing contribution to the specific heat has a broad 'hump' around the same temperature [76]. Both of these are consistent with experiments, namely spin gap seen in Knight shift (Section 25.3.3) and broad feature seen in specific heat measurements [103]. In our theory, a similar crossover also appears at a

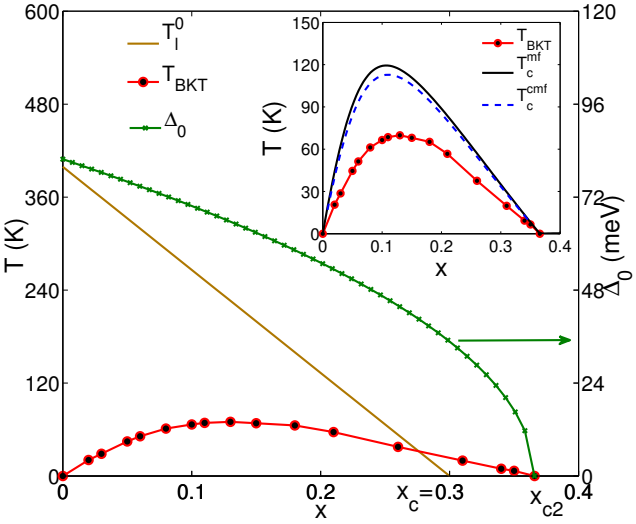


Figure 25.22: Doping dependence of different temperature scales ($T^* = T_l^0$ and $T_{\rm BKT}$, the Berezinskii-Kosterlitz-Thouless transition temperature, as appropriate for the purely 2d system considered here) and the zero temperature gap Δ_0 are shown in the main plot.

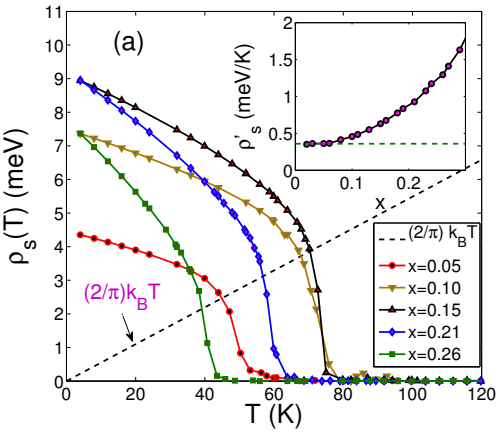


Figure 25.23: Finite temperature superfluid density calculated via MC simulation for different x values. The dashed line corresponds to the size of universal Nelson-Kosterlitz jump expected at a BKT transition. $T_{\rm BKT}(x)$ has been obtained from the intersection of this line with $\rho_s(x,T)$ vs. T curves.

temperature where the antinodal pseudogap in electronic spectral function is completely filled up or, in other words, the Fermi arc extends over the full Fermi surface [79]. All these various crossovers appears around temperature $T^*(x)$, however not all at exactly same temperature but over a somewhat broad range around $T^*(x)$ [76](see Fig.25.21), justifying the pseudogap temperature scale as a crossover rather than a sharp transition, as seen in the experiments 25.3.3. The results for pseudogap crossover seen in local pairing amplitude and specific heat are shown in Figs.25.24,25.25.

3. Large region of fluctuation diamagnetism and Nernst effect above T_c: We obtain a region of enhanced fluctuation diamagnetism in the pseudogap phase extending far above (around 1.5 times) the transition temperature T_c and show that the boundary of the region, namely the onset temperature $T_{onset}(x)$, follows a dome shaped curve tracking T_c as a function of doping (Fig.25.21). The results for Nernst regime computed from our theory is shown in Fig.25.26. Similar feature is also seen for magnetization [77].

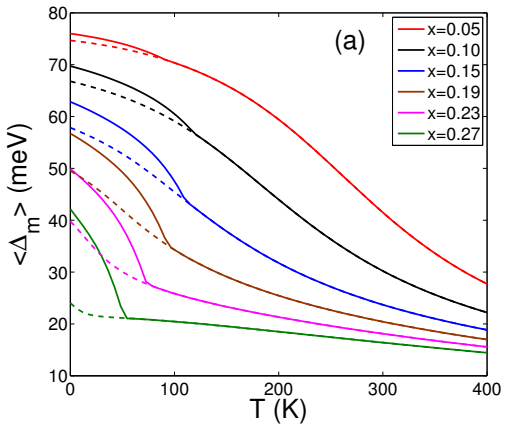


Figure 25.24: The figure shows a crossover $\langle \Delta_m \rangle$ from small to large values around $T^*(x)$ and an onset of the second gap feature at T_c.

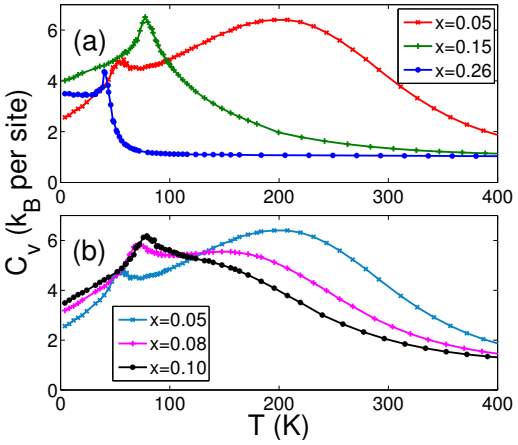


Figure 25.25: (a) Specific heat obtained from MC simulation of our model. Panel (b) shows the evolution of the broad maximum around T^* with doping in the underdoped region.

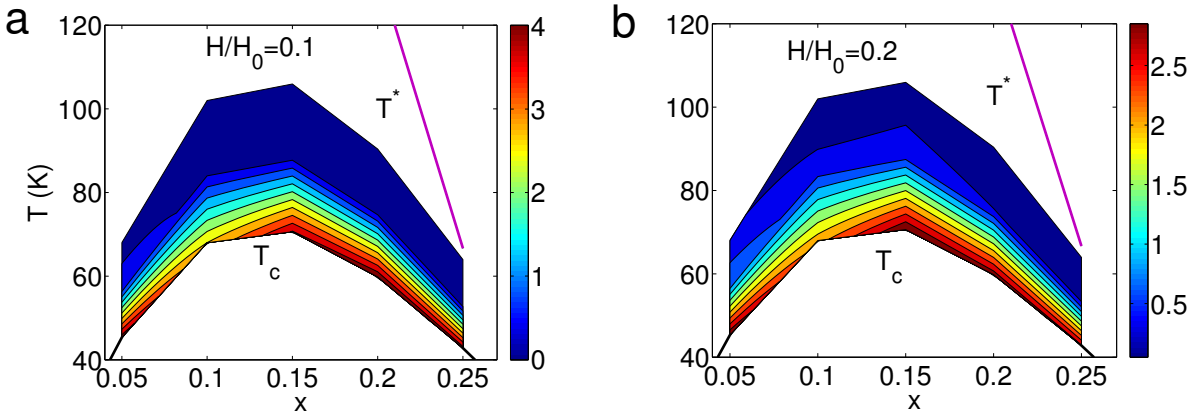


Figure 25.26: α_{xy} in the $x-T$ plane for two different values of the magnetic field (a) $H/H_0 = 0.1$ and (b) $H/H_0 = 0.2$. The lines of constant α_{xy} follow the superconducting dome. This indicates that the equilibrium superconducting fluctuations responsible for the suppression of the superfluid stiffness also determine the thermoelectric response.

Experimentally, both the Nernst effect [61] and diamagnetism [60] have been seen to track the superconducting dome. As mentioned earlier, the persistence of the Nernst and diamagnetism signal over a dome-shaped region above T_c, instead of the entire pseudogap state till $T^*(x)$, has been argued as evidence against the pairing origin of the pseudogap line. This is due to the expectation that if the pseudogap line is related to pairing then superconducting fluctuations should continue till T^*. However, on the basis of our results, we can argue that this expectation is not justified since pairing fluctuations identifiable as superconducting fluctuations, e.g. those detected through Nernst or diamagnetism, are mainly controlled by ρ_s or the T_c scale. The GL-like model we study has the pseudogap temperature $T^*(x)$ explicitly set as the local pairing scale by construction, but, even then, the diamagnetic signal tracks the superconducting T_c that is governed by the superfluid density rather than the pairing scale T^* on the underdoped side. The suggestion is that the long wavelength anomalies in Nernst effect and fluctuation diamagnetism require a large correlation length for superconducting phase fluctuations as happens near T_c.

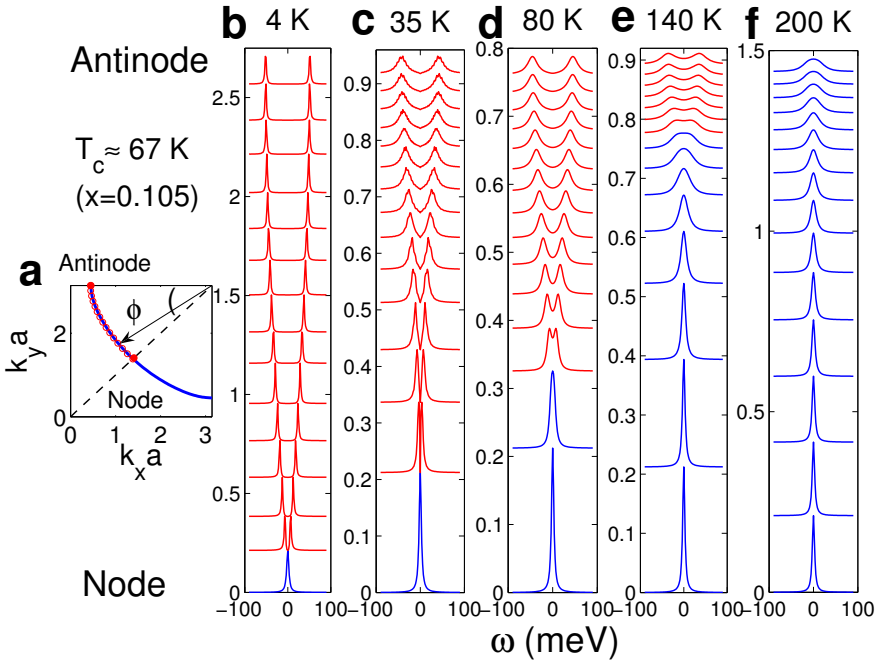


Figure 25.27: **The Fermi surface and the spectral density along it.** **a**, Fermi surface (FS) in the first quadrant of the Brillouin zone for $x \simeq 0.11$, a typical value. The angular position ϕ on the Fermi surface is shown. **b-f**, Single-particle spectral density $A(\mathbf{k}, \omega)$ at 15 equally spaced points (red circles) on the Fermi surface in **a** shown vertically shifted from node (bottom) to antinode (top), as a function of temperature at $x \simeq 0.11$. Blue and red lines correspond to Fermi arc and gapped portions of FS, respectively. (From Ref.[76])

4. Filling up of pseudogap and evolution of Fermi arc with doping and temperature: We show that, in remarkable agreement with ARPES experiments, non-zero local pairing amplitude above T_c manifests itself as pseudogap in the electronic spectral function on the *putative* Fermi surface that exists above the pseudogap temperature scale. Two spectral peaks appear away from the $\omega = 0$, however their is finite spectral weight at the zero energy. Above T_c, finite near-nodal gapless regions on the Fermi surface, or Fermi arcs, emerges from the d-wave node below T_c. The arcs expands with increasing temperatures and finally take over the whole Fermi surface at a temperature $T_{\rm an} \approx T^*(x)$, where the antinodal pseudogap gets completely filled up. The results are shown in Figs.25.27,25.28.

5. Deviation from d-wave gap structure below T_c due to phase fluctuations: 'Two gaps' from one gap:

Possibly the most widely explored property of a superconductor is the energy gap $\Delta_{\mathbf{k}}$ or $\Delta(\phi)$. The apparent deviation ('bending') of the gap below T_c, inferred from ARPES [105], from the d-wave form has been the subject of a great deal of current interest, leading to speculation

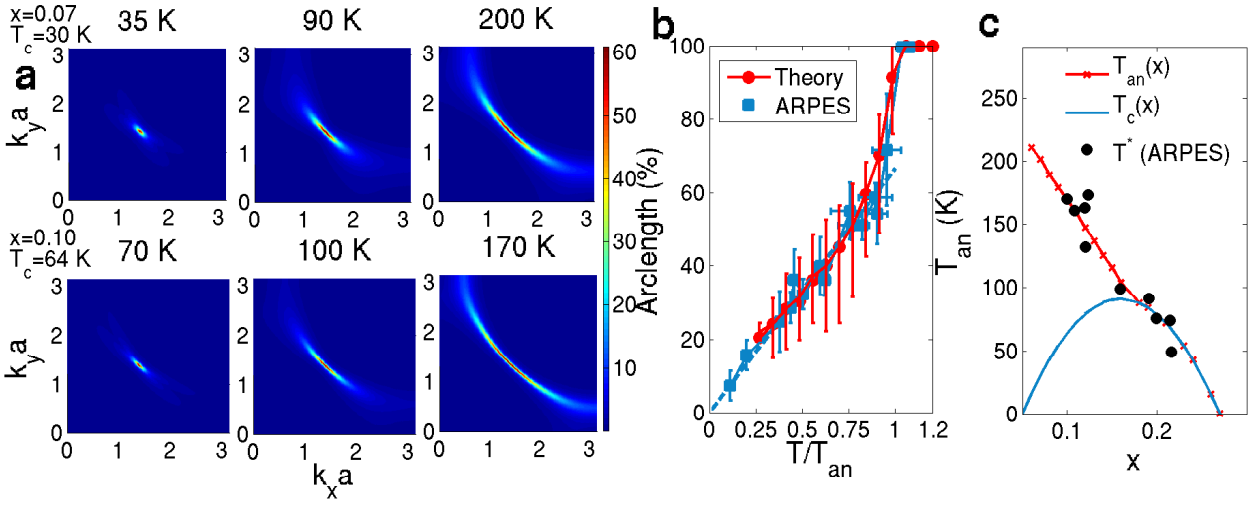


Figure 25.28: **Fermi arcs above T_c.** **a**, Colourmap of $A(\mathbf{k}, \omega = 0)$ over the first quadrant of the Brillouin zone for two values of x at different temperatures. The Fermi arc is easily picked out visually. The color bar indicates the value of $A(\mathbf{k}, \omega = 0)$. **b**, The arc length vs. $T/T_{\rm an}$ curve, averaged over the entire doping range ($x \lesssim x_{\rm opt}$). On the y-axis, 0% is the node and 100% is the antinode. The experimental data are from Ref.[104]. The vertical error bars in the theoretical points indicate the variation of the arc length at different x for a given $T/T_{\rm an}(x)$. **c**, The antinodal pseudogap filling temperature $T_{\rm an}$ as a function of x is compared with the data for the pseudogap temperature T^* from ARPES [66]. (From Ref.[79])

that there are two gaps in high-T_c superconductors [106]. We have obtained the gap $\Delta_{\mathbf{k}}$ from the peak position of the calculated spectral function $A(\mathbf{k}, \omega)$ for a fixed $\mathbf{k}$ as mentioned earlier and conclude from the results (see Fig.25.29**a**) that the 'bending' is due to the coupling of the electron to thermal phase fluctuations ('spin waves') below T_c. As expected from such an origin, it is large close to T_c, and small as $T \to 0$. These results confirm that there is only one gap, but that to 'uncover' it, effects of coupling to pair fluctuations ('spin waves') have to be factored in.

25.7 Conclusion and future directions

The cuprate superconductors are unusual materials both in their superconducting and non-superconducting states. After a description of some of their strangeness (Section 25.3), we have described a phenomenological theory that focuses on their superconductivity and on the properties connected with pairing fluctuations. We have also described a simple model which couples the fluctuations to electrons. Our aim has been to show that such an approach, in principle and in practice, successfully makes sense of the large amount of experimental information accumulated over decades on these materials, and that it does this both qualitatively and quantitatively. Given that such an approach is made in the background of our already strong and increasing knowledge of electrons in condensed matter, and given the repeated discovery of major novel experimental facts, some directions suggest themselves, in addition to several extensions, such as the inclusion of quantum phase fluctuations in the GL theory, already mentioned. One direction, within the ambit of phenomenological theory, is to enlarge it to include competing order. In the last several years, CDW (charge density wave) correlations have been clearly seen in these materials [107, 108, 62, 109]. Their dependence on doping, temperature and magnetic field [108, 62, 109, 31, 32, 33], whether the order is short or long range [108, 62, 109], whether they are bond CDW's or not [110], have all been documented extensively. Whether this is a competing order and whether there is ineluctable complexity in

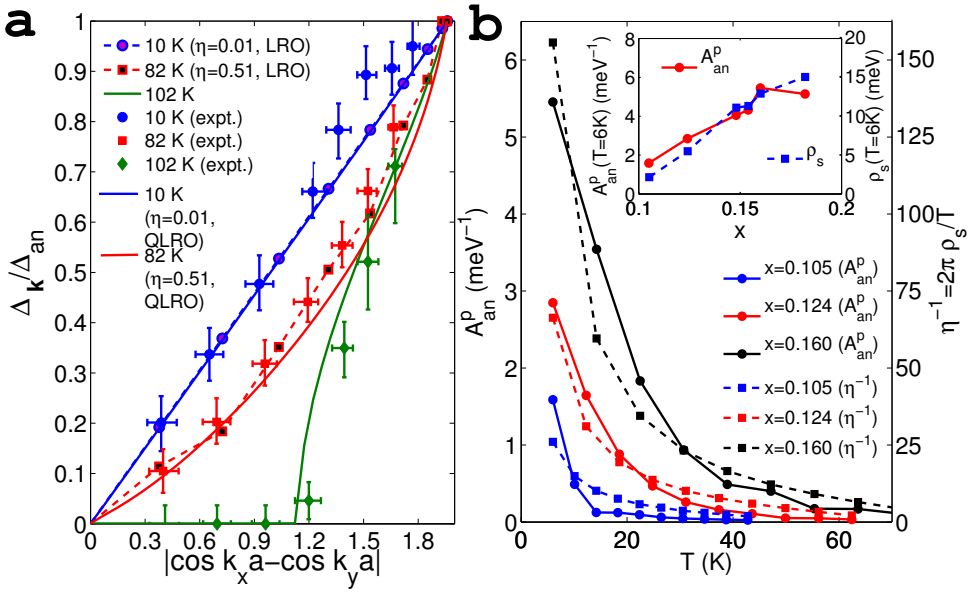


Figure 25.29: **Spectral properties below T_c. a**, Deviation of $\Delta_{\mathbf{k}}$ from the d-wave form, $|\cos k_x a - \cos k_y a|$, below T_c for $x = 0.16$ is compared with $\Delta_{\mathbf{k}}$ obtained in ARPES [105]. At low temperature ($T = 10$ K), $\Delta_{\mathbf{k}}$ follows the canonical d-wave form (a straight line), but bends away considerably from it close to T_c. For $T < T_c$, we have shown $\Delta_{\mathbf{k}}$ obtained for both the true LRO phase [i.e. $D(R \to \infty) = |\langle\psi_m\rangle|^2 \neq 0$] and the quasi-LRO or QLRO phase [i.e. $D(R) \sim R^{-\eta} \xrightarrow{R\to\infty} 0$]. **b**, The antinodal peak height $A^p_{\rm an}$ vs. T tracks $\rho_s(T)/T$ vs. T. **Inset** At low temperatures ($T = 6$ K) $A^p_{\rm an}(x)$ closely follows $\rho_s(x)$, especially in the underdoped side ($x \lesssim 0.16$).

these compounds, are important questions. There is again considerable experimental support for other non Cooper pair correlations such as electronic liquid crystal like effects [111, 107], SDW (spin density wave) like correlations [112].

The approach emphasizes the importance of phase fluctuations and is really a theory in which Cooper pair magnitude Δ_m and the phase ϕ_m are both relevant low-energy degrees of freedom whose significance varies with doping x and temperature T. For small x, the amplitude fluctuations are not important. This is like in interacting spin models where spin length fluctuations are not important, only there directional fluctuations which are like phase angle (ϕ_m) fluctuations are thermally excited. As x increases, amplitude Δ_m fluctuations have decreasing energies, till presumably for large x, one has the BCS like limit where both these are indistinguishable energetically. This raises several important questions. One is that there are and must be other phase angle fluctuations besides the d-wave like ones in which we constrain the nearest neighbor x, y-bond angles to be $(\pi/2)$ out of phase. These have been investigated recently [] and have important consequences. The other is whether there is indeed a BCS limit, given the short coherence length. Questions connected with time-reversal symmetry breaking [113, 114], anomalous Kerr effect [115] etc. are other basic directions. Can the effects be understood in the above framework?

An overarching issue is the need for a microscopic theory with *electrons* as basic ingredients. The analogue is the celebrated BCS theory which followed the original GL theory in seven or so years. Here, nearly a quarter of century after the discovery of cuprate superconductivity, and in the background of a large number of well developed many-body electronic approaches, a phenomenological theory has been proposed. The underlying question is the well known problem of a theoretical description of strongly correlated mobile electrons. Many phenomena of the strange metal phase itself, depend for their theoretical understanding on the development of such a theory, so that the development of a 'reliable' many-particle approach for strongly cor-

related electrons with inevitable pairing correlations is a pressing necessity for a comprehensive theory of electronic matter.inductable

25.8 Parameters of the phenomenological theory

As natural in a phenomenological theory, the parameters of the functional in eq.(25.3) are chosen to be consistent with experiment. The doping and temperature dependence of the coefficients are parametrized as $A(x,T) = (f/T_0)^2[T - T^*(x)]e^{T/T_0}$, $B = bf^4/T_0^3$ and $C(x) = xcf^2/T_0$; f, b, c are dimensionless and $T^*(x) = T_0(1 - x/x_c)$ with the single energy scale T_0 and doping concentration $x_c = 0.3$ controlling the pseudogap temperature scale. The phenomenological parameters f, b, c vary for different cuprates and T_0 is the bare pseudogap temperature extrapolated to zero doping. The exponential factor e^{T/T_0} appearing in A is not very crucial in the temperature range of our interest, i.e. below the pseudogap temperature. This factor suppresses average local gap magnitude $\langle \Delta_m \rangle$ at high temperatures ($T \gtrsim T^*(x)$) with respect to its otherwise temperature independent equipartition value $\sqrt{T/A(x,T)}$ which will result from the simplified form of the functional [Eq.(25.3)] being used over the entire range of temperature. Such a suppression is natural in a degenerate Fermi system; the relevant local electron pair susceptibility is rather small above the pair binding temperature and below the degeneracy temperature.

The forms of the parameters A, B and C specified above allow us to reproduce the superconducting dome. However, it is also important to mention that having chosen A, B and C to reproduce the superconducting dome, the doping and temperature dependences of other physical properties like the superfluid density, the magnitude of the local gap, specific heat, orbital magnetization and Nernst coefficient also agree very well with experiments [76, 77, 78].

While, underdoped phenomenology plays an important part in determining the form of our model, e.g. to determine the doping dependence of the parameter C as mentioned above, it also produces the standard GL theory for conventional superconductors on the overdoped side. The amplitude of pairing approaches zero at T_c, or in other words the actual or 'renormalized' pairing scale $\widetilde{T}^*(x) \approx T_c(x)$, on the overdoped side in our theory [76]. This is in conformity with the common expectation that the BCS theory or mean-field GL theory is more appropriate for overdoped cuprates.

For specific values of the parameters, e.g. for Bi2212, which has a $T_c^{\rm opt} \simeq 91$ K at $x = x_{\rm opt} \simeq 0.15$, we choose $f \simeq 1.33$, $b = 0.1$, $c \simeq 0.3$ with $T_0 \simeq 400$ K. This choice of parameters leads to an optimal BKT transition temperature $T_{\rm KT}^{\rm opt} \approx 75K$ for the 2D system that we study. In the cuprates, the small but finite inter-layer coupling between CuO_2 planes is expected to lead to a slightly higher T_c. The interlayer coupling can be easily incorporated in our model in the manner of Lawrence and Doniach[116]. Since this coupling is, in practice, quite small (e.g. the measured anisotropy ratio in Bi2212 is about 100), it makes very little difference quantitatively to most of our estimates.

Part X
Experiments and Other Applications

26 Devices with Superconductivity

(тут скорее всего еще много тем будет)

26.0.1 Levitation over superconductors

(????)

27 Experiments with Superconductors

27.1 Measurement methods

(тут про то, как вообще можно что-то мерить в сверхпроводимости)

27.1.1 Measurement of a resistance by microwave photons (???)

(Kittel wrote this, I'll look again later)

27.2 "Classical" Experiments with Superconductors

27.2.1 Meissner's Experiment

27.3 Some Modern Well-Known Experiments

(статей много, вот на некоторые и создам параграфы тут)

28 Other Phenomena and Applications

(пока они не актуальны, а подумать про них можно итак много)

28.0.1 Levitation over a superconductor

????
хз

28.0.2 Superconducting Train: Main Ideas

(??? just in a nutshell, how to create it?)

29 Atomic physics and quantum optics using SC circuits by You, Nori

Abstract

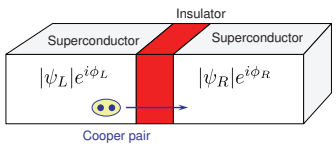
Superconducting circuits based on Josephson junctions exhibit macroscopic quantum coherence and can behave like artificial atoms. Recent technological advances have made it possible to implement atomic-physics and quantum-optics experiments on a chip using these artificial atoms. This review presents a brief overview of the progress achieved so far in this rapidly advancing field. We not only discuss phenomena analogous to those in atomic physics and quantum optics with natural atoms, but also highlight those not occurring in natural atoms. In addition, we summarize several prospective directions in this emerging interdisciplinary field.

Superconducting circuits with Josephson junctions can behave as artificial atoms. In these quantum circuits, the Josephson junctions act as nonlinear circuit elements (see Box 1). Such nonlinearity in a circuit ensures an unequal spacing between energy levels, so that the lowest levels can be individually addressed by using external fields (see, e.g., [5, 6, 7, 8, 9, 1, 2, 3, 4]). Experimentally, these circuits are fabricated on a micrometer scale and operated at mK temperatures. Because of the reduced dimensionality and thanks to the superconductivity, the environment-induced dissipation and noise are greatly suppressed, so the circuits can behave quantum mechanically.

Superconducting circuits based on Josephson junctions have recently become subjects of intense research because they can be used as qubits—controllable quantum two-level system—for quantum computing (see, e.g., [1, 2, 3, 4] for reviews). Even though the typical decoherence times of these circuits fall short of the requirements for quantum computation, their macroscopic quantum coherence is sufficient for them to exhibit striking quantum behaviors. These circuits can have a number of superconducting eigenstates with discrete eigenvalues lower than the energy levels of the quasi-particle excitations that involve breaking Cooper pairs. This property allows these circuits to behave like superconducting artificial atoms. Indeed, there is a deep analogy between natural atoms and the artificial atoms made from superconducting circuits (see Box 2). Both have discrete energy levels and can exhibit coherent quantum oscillations between these levels. Whereas natural atoms may be controlled using visible or microwave photons that excite electrons from one state to another, the artificial atoms in the circuits are driven by currents, voltages and microwave photons that excite the system from one macroscopic quantum state to another.

Differences between superconducting circuits and natural atoms include the different energy scales in the two systems, and how strongly each system couples to its environment; the coupling is weak for atoms and strong for circuits. In contrast to naturally occurring atoms, artificial atoms can be designed with specific characteristics and fabricated on a chip using standard lithographical technologies. With a view to applications, this degree of tunability is an important advantage over natural atoms. Thus, in a controllable manner, superconducting circuits can be used to test fundamental quantum mechanical principles at a macroscopic scale, as well as to demonstrate atomic physics and quantum optics on a chip. Moreover, artificial atoms can be designed to have exotic properties that do not occur in natural atoms.

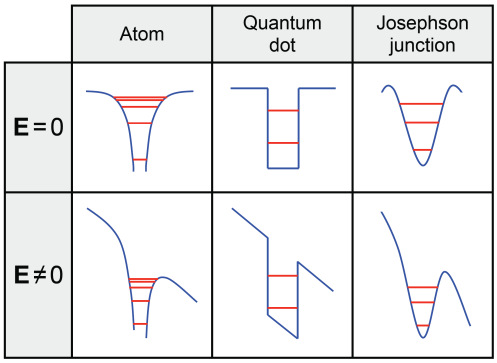
Box 1. The Josephson junction as a nonlinear inductor



A superconductor contains many paired electrons, called Cooper pairs, which condense into the same macroscopic quantum state described by the wavefunction $|\psi|e^{i\phi}$, with $|\psi|^2$ being the density of Cooper pairs. In the absence of applied currents or magnetic fields, the phase ϕ is the same for all Cooper pairs. A Josephson junction is composed of two bulk superconductors separated by a thin insulating layer through which Cooper pairs can tunnel (see the figure

above). The supercurrent through the junction is $I = I_c \sin\varphi$, where the critical current I_c is related to the Josephson coupling energy E_J of the junction by $I_c = (2e/\hbar)E_J$, and $\varphi = \phi_L - \phi_R$ is the phase difference of the two superconductors across the junction. The time variation of this phase difference is related to the potential difference V between the two superconductors: $\dot{\varphi} = \left(\frac{2\pi}{\Phi_0}\right) V$, where $\Phi_0 = h/2e$ is the magnetic-flux quantum. From the definition of the inductance $V = L_J \dot{I}$, it follows that $L_J = \frac{\Phi_0}{2\pi I_c \cos\varphi}$, indicating that the Josephson junction behaves like a nonlinear inductor.

Box 2. Artificial and natural atoms



Potential energy (in blue) and discrete energy levels (in red) for an atom, a quantum dot and a Josephson junction in the absence ($\mathbf{E} = 0$) and presence ($\mathbf{E} \neq 0$) of an externally applied electric field, respectively (see the figure above). Owing to their confinement, the electrons in the atom and the quantum dot have discrete energy levels. The Cooper pairs confined in the potential well of the Josephson coupling energy also have discrete energy levels and the junction can be regarded as a superconducting artificial atom.

In this review, we highlight the atomic-physics and quantum-optics phenomena found in superconducting circuits. The novel physics in these artificial atoms will be emphasized, including phenomena that do not occur in natural atoms. We also summarize several prospective directions in this emerging interdisciplinary field. Some of the examples in this brief overview relate to our work, because we are more familiar with them.

Superconducting circuits as artificial atoms

Two important energy scales determine the quantum mechanical behavior of a Josephson-junction circuit: The Josephson coupling energy E_J and the electrostatic Coulomb energy $E_c = (2e)^2/2C$ for a single Cooper pair, where e is the electronic charge, and C is either the capacitance C_J of a Josephson junction or the capacitance of a superconducting island called a Cooper-pair box (i.e., the sum of the gate capacitance C_g and the relevant junction capacitance), depending on the circuit. Figure 29.1 summarizes three kinds of superconducting circuits implemented in different regimes of E_J/E_c; Fig. 1(a) shows the voltage-driven box (also known as a Cooper-pair box) for a charge qubit [5], Fig. 1(b) the flux-driven three-junction loop for a flux qubit [6] and Fig. 1(c) the current-driven junction for a phase qubit [8, 9]. As a typical example, energy levels of the flux qubit are shown in Fig. 1(d). Moreover, hybrid superconducting qubits are possible. For instance, a Cooper-pair box can behave like a charge-flux qubit [7] when $E_J/E_c \sim 1$. As for the flux qubit, by reducing the ratio E_J/E_c, the charge noise can become dominant over the flux noise [10] and the circuit behaves more like a charge qubit. In this circuit, when $\alpha < 0.5$ (here α is the ratio of the Josephson coupling energy between the smaller and larger junctions in the loop), the double-well potential converts to a single-well potential and the circuit behaves like a phase qubit [10, 11]. One can shunt a large

capacitance to the small junction [10, 11] to suppress the charge noise in this circuit. Also, this large capacitance shunted to the Josephson junction can be used to reduce the charge noise in the Cooper-pair box [12], so as to implement the circuit in the phase regime. Below we highlight several aspects of the atomic-physics and quantum-optics phenomena found in superconducting circuits.

Cavity quantum electrodynamics. A quantized electromagnetic field can coherently exchange energy with a two-level system, usually in a tiny (micrometer-scale) cavity. This energy exchange process involves a fundamental phenomenon called Rabi oscillation; the two-level system and the field exchange a quantum of energy back and forth at a characteristic frequency known as the Rabi frequency. When the field is in resonance with the system, the Rabi frequency is proportional to the system-field coupling strength. The most elementary of such coherent processes involves the interaction of a two-level system with a single photon in the cavity. The exchange of energy between the system and the single photon is observable when the Rabi frequency is larger than the decay rates of the two-level system and the cavity. This photon-atom coupling has been achieved for a variety of atoms interacting with the light field in a cavity and forms the basis of cavity quantum electrodynamics (QED). Cavity QED with superconducting circuits was proposed [13, 14] and experimentally achieved [15, 16] in systems where superconducting qubits were employed as two-level artificial atoms. For the cavity, a single-mode LC resonator [15] and a multi-mode coplanar waveguide resonator [16] have been used. Significantly, the strong-coupling limit for a superconducting qubit in a cavity can be attained much more easily than for a natural atom in a cavity [4, 14] by suitably designing the system parameters. It allows, e.g., the observation of the Lamb shift for a superconducting qubit in the cavity [17]. Moreover, both the superconducting qubit and the cavity can be fabricated on the same chip. For a review on cavity QED with superconducting qubits, see, e.g., [4].

Because they can be designed with specific system parameters, superconducting quantum circuits are suited for achieving the so-called ultrastrong-coupling regime, where the qubit-photon coupling strength is comparable to the energy scales of the qubit and the photon [18]. Indeed, there have been a number of theoretical studies of this system, analyzing some of its rich static and dynamical properties (see, e.g., [19, 20, 21]). Also, the ultrastrong coupling between a superconducting flux qubit and a coplanar waveguide [22] or an LC resonator [23] has recently been demonstrated in experiments. One can expect to find new phenomena in this ultrastrong-coupling regime which are not present in the conventional weak- and moderately strong-coupling regimes. In addition, dressed states of a superconducting charge qubit and an intense microwave field were experimentally observed by embedding the circuit in an LC oscillator [22]. The tunability of these dressed states allows one to explore both resonant and dispersive coupling regimes.

Selecting quantum transitions. In natural atoms, the electronic state at each orbital level has a well-defined parity symmetry, either even or odd. Under the dipole approximation, the interaction Hamiltonian between the atom and the time-dependent electric field has an odd parity. Thus, to have a nonzero dipole transition matrix element, there should be a parity change between the initial and final states, in addition to the constraints on azimuthal and magnetic quantum numbers of the electronic states. This optical selection rule dictates that only three types of three-level systems, called Λ-, V-, and Ξ-type atoms [see Fig. 29.2(a)], exist for the natural atoms, where no dipole transition between electronic states with the same parity are allowed. However, selection rules can be different for superconducting artificial atoms. For instance, in the dipole approximation, the interaction Hamiltonian between a flux qubit circuit and a time-dependent magnetic field does not have a well-defined parity, except at the point with a static magnetic flux $f \equiv \Phi/\Phi_0 = \frac{1}{2}$, where Φ is the static magnetic flux applied to the

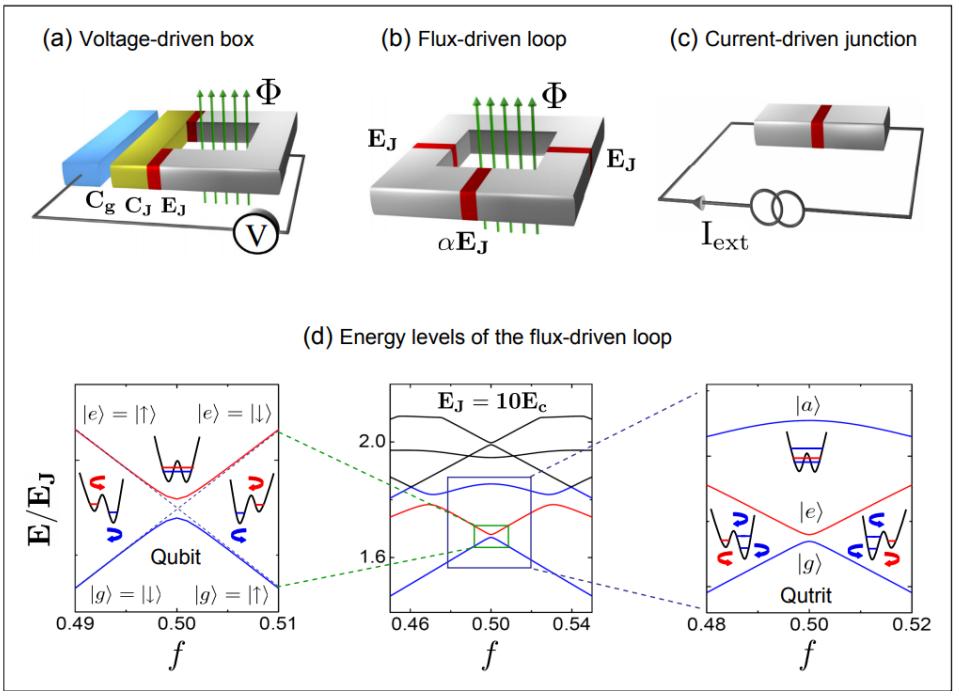


Figure 29.1: **Superconducting circuits as artificial atoms. (a)** A Cooper-pair box biased by a gate voltage V_g and implemented in the charge regime $E_J/E_c \ll 1$. The SQUID loop provides an effective Josephson coupling energy tuned by the threading magnetic flux Φ. See main text for nomenclature. **(b)** A superconducting loop interrupted by three Josephson junctions and implemented in the phase regime $E_J/E_c \gg 1$. The two identical Josephson junctions have coupling energy E_J and capacitance C, while both the Josephson coupling energy and the capacitance of the smaller junction are reduced by a factor α, where $0.5 < \alpha < 1$. The three-junction loop is biased by a flux Φ such that $f \equiv \Phi/\Phi_0 \sim \frac{1}{2}$. **(c)** A Josephson junction biased by a current $I_{\rm ext}$, which is also implemented in the phase regime and has a much larger ratio E_J/E_c. **(d)** Energy levels of the flux-driven three-junction loop (the curves in the middle panel). With the lowest two energy levels involved (the curves in the left panel, which are enlarged from the smaller rectangle in the middle panel), the flux-driven loop can behave like a coherent and controllable quantum two-level system (qubit), while the circuit can behave like a coherent and controllable three-level system (qutrit) when using the lowest three levels (the curves in the right panel, which are enlarged from the larger rectangle in the middle panel). Moreover, in the left, top and right insets of the left (right) panel, the two (three) energy levels are also displayed in the double potential well for $f < \frac{1}{2}$, $f = \frac{1}{2}$ and $f > \frac{1}{2}$, where the clockwise and anticlockwise arrows represent the circulating supercurrent states in the flux-driven three-junction loop. In **(a)-(c)**, the qubit employs the charge states on a single island, the persistent-current states in a double potential well, and the anharmonic-oscillator states in a single potential well, respectively. Also, a flux-driven superconducting loop with a different number of Josephson junctions, e.g., one [89] or four junctions [90], can be used for a flux qubit. Furthermore, a flux-driven single-junction loop can be used as a phase qubit when working with the energy levels in a tilted potential well [91], as in a current-driven junction.

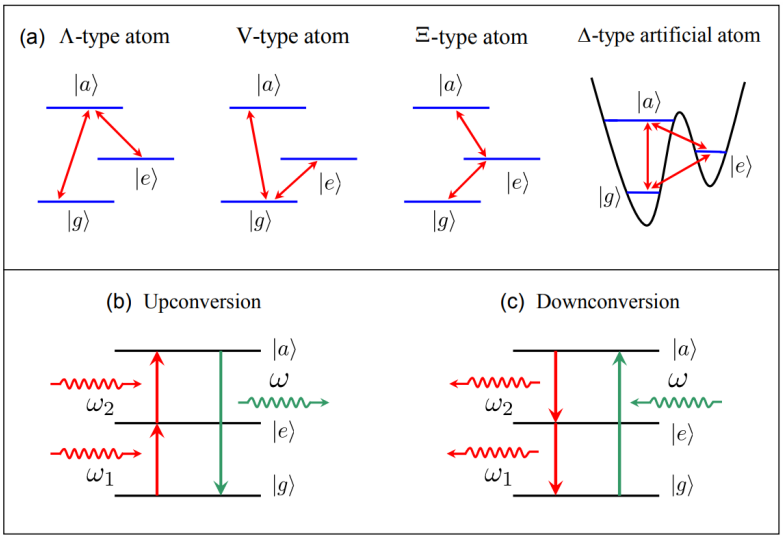


Figure 29.2: **Three-level atoms and frequency conversion.** **(a)** Energy levels of natural atoms of the Λ, V, and Ξ types, as well as a Δ-type artificial atom consisting of a flux-driven three-junction loop. The allowed dipole transitions between energy levels are indicated in red. In contrast to naturally occurring atoms, the three dipole transitions among the states $|g\rangle$, $|e\rangle$ and $|a\rangle$ are all allowed in the Δ-type three-level artificial atom. Here $|g\rangle$ and $|e\rangle$ denote the ground and first excited states, while $|a\rangle$ denotes either the second or another excited state. **(b)** Frequency upconversion in a Δ-type artificial atom. Here $\omega_1 = (E_e - E_g)/\hbar$, $\omega_2 = (E_a - E_e)/\hbar$, and $\omega = (E_a - E_g)/\hbar$, with E_i ($i = g, e$ or a) being the energy level of the state $|i\rangle$. When two microwave photons, one with frequency ω_1 and the other with ω_2, are successively absorbed by the artificial atom, it can emit a microwave photon with frequency $\omega = \omega_1 + \omega_2$ via the transition $|a\rangle \to |g\rangle$. **(c)** Frequency downconversion in the Δ-type artificial atom. When a microwave photon with frequency ω is absorbed by the artificial atom, the sequential transitions $|a\rangle \to |e\rangle$ and $|e\rangle \to |g\rangle$ can produce two microwave photons with frequencies ω_1 and ω_2, respectively. In particular, when $E_a - E_e = E_e - E_g$, the upconversion in **(b)** converts two photons with frequency $\frac{1}{2}\omega$ to one photon with frequeny ω, while the downconversion in **(c)** converts one photon with frequency ω to two photons with frequeny $\frac{1}{2}\omega$. Natural atoms cannot perform up- or down-conversion, unless aided by nonlinear effects. However, artificial atoms can.

loop and Φ_0 the magnetic-flux quantum. At this particular point, the interaction Hamiltonian has an odd parity. Owing to the parity symmetries of the artificial-atom states at $f = \frac{1}{2}$, the lowest three levels of the circuit behave like a Ξ-type or ladder-type artificial atom [25]. In this case, the dipole transition between $|g\rangle$ and $|a\rangle$ is forbidden, while the other two transitions (among states $|g\rangle$, $|e\rangle$ and $|a\rangle$) are allowed [see Fig. 2(a) for nomenclature]. However, when $f \neq \frac{1}{2}$, the parity symmetry is broken for the interaction Hamiltonian. Therefore, all three dipole transitions among $|g\rangle$, $|e\rangle$ and $|a\rangle$ are possible, allowing the atom to be Δ-type because of the triangle-shaped transitions among the three energy levels. Now (when $f \neq \frac{1}{2}$) the superconducting circuit behaves as a Δ-type cyclic artificial atom, where one- and two-photon processes can coexist [25].

This Δ-type artificial atom can be used for the upconversion and downconversion of the photon frequency [see Figs. 29.2(b) and 29.2(c)]. In these frequency conversions, all transitions involve only linear processes; this is in sharp contrast to the conventional frequency conversion in nonlinear optics, where a nonlinear medium is used and the nonlinear effect facilitates converting the frequency of the photons. Recently, the frequency upconversion of a microwave photon was experimentally demonstrated in a flux qubit [26]. This experiment explained the observed coexistence of one- and two-photon processes as due to the symmetry-breaking of the system Hamiltonian, when varying the applied magnetic flux away from $f = \frac{1}{2}$.

In the experiment reported in [27], two microwave fields were applied simultaneously to a superconducting circuit containing two coupled flux qubits. The interference between the processes that correspond to a selected excitation by the applied microwave fields can be controlled and used to activate or suppress a given transition. Thus, this method effectively creates artificial and controllable selection rules.

Electromagnetically induced transparency. Quantum interference can be introduced to control the propagation of light through an atomic medium consisting of three-level atoms or qutrits. We now consider a Λ-type three-level atom; to control the propagation of a probe light field in resonance with the dipole transition $|a\rangle \leftrightarrow |g\rangle$ (that is, at the probe frequency ω_p), one can drive the atom by a second (control) field that is in resonance with the transition $|a\rangle \leftrightarrow |e\rangle$ at the control frequency ω_c (see Fig. 29.3). Now the amplitude of the wavefunction for the state $|a\rangle$ is driven by two terms; one proportional to the probability amplitude of the ground state $|g\rangle$ and the other proportional to the probability amplitude of state $|e\rangle$. The combined effect of these two fields is to pump the atom into a coherent superposition of the states $|g\rangle$ and $|e\rangle$ known as a dark state. In such a case, the two driving terms can interfere and cancel each other, i.e., they have equal magnitudes but opposite signs. Under this destructive quantum interference, the occupation probability at state $|a\rangle$ is zero, leading to a vanishing light absorption even in the presence of light fields. This effect is called electromagnetically induced transparency (EIT) in quantum optics [28, 29] and also applies to V- and Ξ-type atoms. This important effect has a variety of applications. For instance, a medium with EIT can slow down and even stop or trap light.

We now consider EIT in a more quantitative manner. Let Ω_p (Ω_c) be the Rabi frequency that quantifies the coupling strength between the probe (control) light and the atom. Here we assume that a Λ-type atom can be prepared in the initial state $|\Psi(0)\rangle = (\Omega_c|g\rangle - \Omega_p|e\rangle)/\Omega$, where $\Omega = \sqrt{\Omega_p^2 + \Omega_c^2}$. When the EIT occurs, the atom will be trapped in this dark state, i.e., $|\Psi(t)\rangle = (\Omega_c|g\rangle - \Omega_p|e\rangle)/\Omega$, for a time which is dependent on the decoherence rate of the atom. Usually, it is not easy for an atom to be prepared in the initial state $|\Psi(0)\rangle$, when Ω_p is comparable to Ω_c. Instead, the atom can be naturally prepared in the ground state $|g\rangle$. If strong control and weak probe fields are chosen so that $\Omega_c \gg \Omega_p$, the dark state $|\Psi(t)\rangle$ is close to the initial state $|g\rangle$. In such a case, the combined action of the control and probe fields can easily drive the atom from the ground state into the dark state [29]. This is the reason why

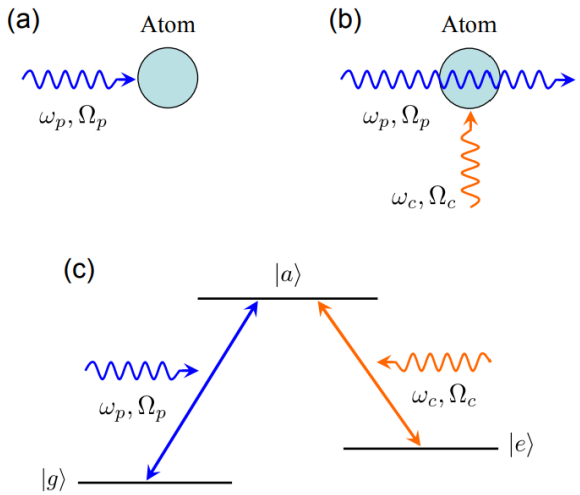


Figure 29.3: **Electromagnetically induced transparency. (a)** A probe light field is absorbed by natural or artificial atoms when the frequency of the light field is resonant with a particular separation between two atomic energy levels. **(b)** However, the probe light field can go through the natural or artificial atoms when a suitable control light field also drives the atoms. **(c)** Λ-type three-level atomic system for EIT. The frequency ω_p of the probe light field is resonant with the energy separation between states $|a\rangle$ and $|g\rangle$, and the frequency ω_c of the control light field is resonant with the energy separation between states $|a\rangle$ and $|e\rangle$. The Rabi frequency Ω_p (Ω_c) quantifies the coupling strength between the probe (control) light field and the atom.

a strong control field and a weak probe field are used to experimentally implement EIT in an atomic medium.

At $f = \frac{1}{2}$, the flux qubit circuit can behave like a Ξ-type artificial atom [25, 30]. The circuit can also behave approximately like a Λ-type artificial atom when $f \neq \frac{1}{2}$, if the dipole transition rate between $|g\rangle$ and $|e\rangle$ is much smaller than the rates for the other two transitions [30]. As discussed above, these selection rules are related to the parity symmetries of the artificial-atom states. In contrast to natural atoms, the tunability of a superconducting circuit can be used to prepare the artificial atom in an initial state that is close to the dark state $|\Psi\rangle$ with arbitrary Ω_c and Ω_p. Therefore, it is experimentally feasible to produce EIT in a single artificial atom for either strong or weak control and probe fields. This is an important advantage of superconducting circuits compared to natural atoms. EIT using superconducting circuits has been studied theoretically (e.g., [31, 32, 33]) and experimentally [34, 35]. In [35], this phenomenon was experimentally shown using a four-junction loop biased at $f = \frac{1}{2}$, where the circuit behaves as a Ξ-type artificial atom.

State population inversion and lasing. A laser is composed of an amplifying medium inside a resonant optical cavity. When the system is driven, a state population inversion (SPI) can be achieved for the atoms or molecules in the amplifying medium. Moreover, there is a positive feedback between the emitted light and the amplifying medium. Because of this positive feedback and the nature of the stimulated photon emission, the laser has a large net optical gain and the emitted photons have the same direction, phase and polarization. These advantages mean that the laser has a variety of applications in different fields. Recently, several studies have considered lasing using only a single artificial atom, both theoretically [30, 36, 37, 38] and experimentally [39, 40].

With suitable junction parameters, the flux qubit circuit can have the following dipole transition rates [30] when $f \neq \frac{1}{2}$: $\Gamma_{ga} > \Gamma_{ae} \gg \Gamma_{eg}$, where the rate Γ_{ij} is proportional to

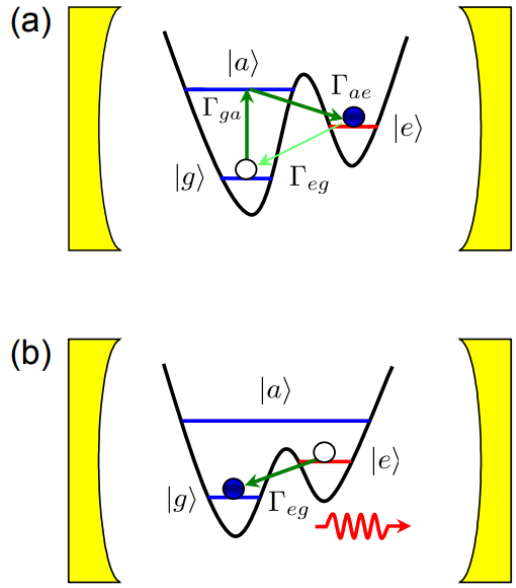


Figure 29.4: **Lasing. (a)** State population inversion (for lasing) between states $|e\rangle$ and $|g\rangle$ in a three-junction loop at $f > \frac{1}{2}$, where the artificial atom is quickly pumped from $|g\rangle$ to $|a\rangle$ by a strong microwave pulse (for example, by a quick Rabi oscillation) and then decays from $|a\rangle$ to $|e\rangle$ via photon emission. Here the dipole transition rate from $|e\rangle$ to $|g\rangle$ is small because of a higher inter-well barrier between them; the dipole transition rate from $|a\rangle$ to $|e\rangle$ is larger owing to a lower barrier; and the rate is even larger for the dipole transition $|g\rangle \to |a\rangle$ because no potential barrier is involved in the single well. **(b)** Photon emission of the artificial atom to build up a lasing field, where the inter-well barrier is lowered so as to have a strong transition rate between $|e\rangle$ and $|g\rangle$ and to tune the transition $|e\rangle \to |g\rangle$ into resonance with the cavity.

$|t_{ij}|^2$, with t_{ij} being the dipole transition matrix element between states $|i\rangle$ and $|j\rangle$. Because the transition $|a\rangle \to |e\rangle$ can be dominant over $|e\rangle \to |g\rangle$, an SPI between states $|e\rangle$ and $|g\rangle$ [Fig. 29.4(a)] can be quickly achieved by pumping the artificial atom (via the transition $|g\rangle \to |a\rangle$) using a strong microwave field. Here the artificial atom can be placed in, e.g., a coplanar waveguide resonator [16] by sharing a segment of the circuit loop with the transmission line. In the process of SPI, the weak-coupling regime is assured by having the flux qubit circuit off-resonant with respect to the cavity.

While the SPI is being established, the biasing flux can be adjusted to give a value of f near $\frac{1}{2}$, where the rate Γ_{eg} for the transition $|e\rangle \to |g\rangle$ becomes large and the cavity is resonant with this transition. However, the adiabatic condition is not easy to satisfy near this anticrossing point ($f = \frac{1}{2}$), where the Landau-Zener transition is strong, so the biasing flux cannot be changed very fast while approching this point. Fortunately, away from this anticrossing point, the Landau-Zener transition is weak, so it is easy to satisfy the adiabatic condition [30] and the flux can be changed very quickly. To take advantage of this property, the small Josephson junction in the flux-driven loop can be replaced by a tunable superconducting quantum interference device (SQUID). In this d.c. SQUID, the magnetic field applied to the loop causes the critical current to oscillate with period $2\Phi_0$. With the SPI established at a biasing flux away from $f = \frac{1}{2}$, one can quickly change the flux in the SQUID loop to lower the inter-well barrier, so as to both increase the transition rate Γ_{eg} and tune this transition $|e\rangle \to |g\rangle$ into resonance with the cavity mode [Fig. 29.4(b)]. This can yield a strong coupling between the circuit and the cavity.

To build up a lasing field, in addition to the above two conditions for quickly establishing SPI and then achieving a strong circuit-cavity coupling, the cavity used should have a high quality factor Q (Q-factor), i.e., a small leak or decay rate. This can be implemented using a

coplanar waveguide resonator [16].

Indeed, lasing was experimentally observed using a Cooper-pair box in an on-chip cavity [39]. In contrast to the proposal [30] using a flux-driven loop, this experiment [39] employs a different three-level system: the two lowest superconducting states $|g\rangle$ and $|e\rangle$ and a quasi-particle state $|a\rangle$. The gate voltage is tuned to $V_g > e/C_g$ (above the degeneracy point), so the state $|2\rangle$ with an extra Cooper pair in the box becomes the ground state $|g\rangle$ of the artificial atom, and the state $|0\rangle$ with zero extra Cooper pair in the box is the excited state $|e\rangle$. Also, the box is connected to a lead via a tunnel barrier. When driving the box with a voltage across the tunnel barrier, an SPI between $|e\rangle \equiv |0\rangle$ and $|g\rangle \equiv |2\rangle$ is achieved, following quasi-particle tunneling processes [36]. In [39], lasing was achieved continuously, with emitted light escaped from one end of the cavity.

Cooling. There are different methods for cooling atoms, including Dopper cooling, Sisyphus cooling, side-band cooling, subrecoil cooling, and evaporative cooling. Some of these techniques can be adapted to cool a solid-state artificial atom. For instance, the Sisypus cooling technique was used to cool a flux qubit (i.e., a flux-driven three-junction or four-junction loop) [40].

Another important advancement [42] is the cooling of a flux qubit implemented via the inverse process of SPI. In [42], the temperature of the superconducting qubit was lowered by up to two orders of magnitude when its surroundings reached a temperature as low as tens of mK. This cooling of the flux qubit is achieved when the biasing flux is shifted away from $f = \frac{1}{2}$, where the dipole transition rates for the lowest three levels of the flux qubit satisfy the relations $\Gamma_{ag} > \Gamma_{ea} \gg \Gamma_{ge}$. By optically pumping the qubit via the transition $|e\rangle \to |a\rangle$, the qubit is excited to the high-energy state $|a\rangle$ and then decays to the ground state by way of the transition $|a\rangle \to |g\rangle$ [see Fig. 29.5(a)], with a net energy, extracted from the qubit, emitted to the outside environment. This experiment also provides fine analogies between solid-state artificial atoms and natural atoms, as well as showing how these analogies can inspire new applications.

Although the superconducting qubit in [42] was greatly cooled ($k_B T \ll E_e - E_g$) in experiments, the noise sources surrounding the qubit were not. So the qubit will quickly return to the temperature of its environment. To overcome this difficulty, the superconducting qubit can be redesigned to increase its controllability by replacing the small Josephson junction in the flux-driven loop with a tunable SQUID [43]. The cooling process can now be described as follows [see Figs. 29.5(b)-29.5(d)]: First, as in the experiment [42], the qubit is initially cooled, following the inverse process of the SPI. Then, the tunable qubit is switched on for a period of time in order to resonantly interact with the noise source (e.g., local two-level fluctuators) surrounding the qubit. This process extracts energy from the noise source to heat the qubit. Repeating these two processes [43], both the qubit and its neighboring noise source can be simultaneously cooled. This will significantly enhance the quantum coherence of the qubit, because the cooled qubit is then thermally activated only very slowly to the first excited state.

Recent technical advances allow the fabrication of a nanomechanical resonator with both a high Q-factor and a sufficiently high frequency, close to the typical frequencies of superconducting circuits [44]. This has stimulated researchers to propose different ways to use superconducting circuits to achieve the ground-state cooling of coupled nanomechanical resonators [45, 46, 47, 37, 43, 48]. Moreover, the experimental cooling of such a resonator, by coupling it to a superconductor single-electron transistor [49] or to a microwave-frequency superconducting resonator [50], has also been reported. When a nanomechanical resonator is cooled to the ground state [51], it provides a good platform for exploring various quantum phenomena and for observing the quantum-to-classical transition in such a macroscopic object. This will give rise to the new subject of quantum acoustics.

Photon generation. Superconducting qubits have the advantage of manipulating quantum states in a controllable manner. If these stationary qubits are spatially separated, one

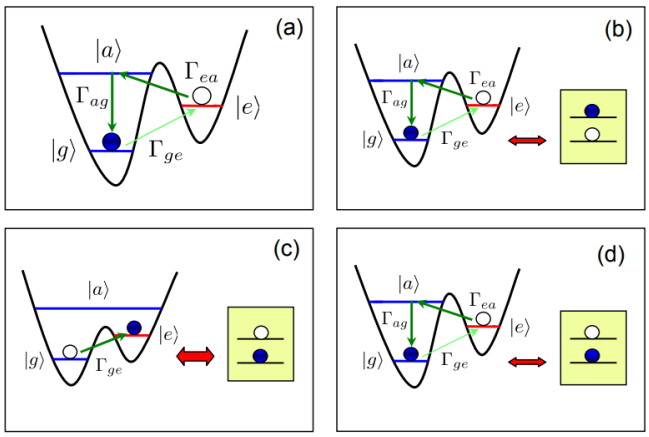


Figure 29.5: **Cooling a three-level artificial atom and a nearby two-level system. (a)** Cooling the three-junction loop to its ground state $|g\rangle$. While the artificial atom is thermally excited to $|e\rangle$, one can drive the atom to $|a\rangle$ by a microwave field. Because of a large transition rate for $|a\rangle \rightarrow |g\rangle$, the atom can decay quickly from the unstable state $|a\rangle$ to the ground state, emitting net energy, extracted from the atom, to the outside environment. The levels in the double potential well correspond to the lowest three energy levels of a three-junction loop biased at $f > \frac{1}{2}$. **(b)** While the noise source is thermally excited, the artificial atom is shifted off-resonance to the noise source by tuning the externally applied flux and also driven to the cooled state via the inverse process of the state population inversion in (a). The box to the right of the energy level diagram represents a two-level fluctuator acting as a noise source. **(c)** The inter-well barrier of the artificial atom is lowered by tuning the externally applied flux so as to have both a strong transition rate between $|g\rangle$ and $|e\rangle$ and the transition $|g\rangle \rightarrow |e\rangle$ in resonance with the two-level system, so as to extract energy from the two-level system. **(d)** Shifting the artificial atom off-resonance from the two-level system and cooling the atom again, with the net energy extracted from the two-level system emitted to the outside environment.

can use single photons generated in an extended cavity as a quantum bus, similar to a flying qubit, to implement quantum communication among them [see Fig. 29.6(a)]. Technologically, this requires the generation of single photons by manipulating a superconducting qubit and the transfer of information between the superconducting qubits and the photons. Using an on-chip cavity, it becomes feasible to achieve this quantum communication process on a chip.

Recent experiments show that a single-photon source can be achieved using a superconducting qubit coupled to an on-chip cavity [52, 53, 54, 55]. When the qubit is prepared in the excited state $|e\rangle$ by a control pulse, it can decay to the ground state $|g\rangle$ by emitting one (and only one) photon in the on-chip cavity; this decay is possible because of the interaction between the qubit and the cavity. If the cavity was originally in the vacuum state $|0\rangle$, it now changes to the single-photon state $|1\rangle$. When the qubit is prepared in an arbitrary superposition state $\alpha|g\rangle + \beta|e\rangle$, in an ideal manner, the coupling between the qubit and the cavity can map the qubit state into a superposition state of zero and one photon in the cavity: $\alpha|0\rangle + \beta|1\rangle$ [see Figs. 29.6(b)-29.6(d)]. Furthermore, the experiment in [52] shows how to transfer the information from a cavity to a stationary qubit [see Figs. 29.6(d)-29.6(f)]. These experiments demonstrate that both single-photon sources and quantum communication between superconducting qubits can be achieved on a chip. However, because of the relaxation and decoherence in both qubit and cavity, after each step for transferring the information between a stationary qubit and a cavity, the amplitudes α and β of the photon (qubit) state can be different from the amplitudes α and β of the previous qubit (photon) state. Improving relaxation rates and qubit decoherence times would allow higher-fidelity state transfers between qubits and cavities.

In addition to single-photon generation, one can also generate, as proposed in [56, 57], multi-photon Fock states $|n\rangle$ (i.e., the number states of photons) and arbitrary superposition states $\sum_n c_n|n\rangle$. Indeed, in a recent experiment [58], the controlled generation of pure Fock states with up to 15 photons was achieved using a superconducting phase qubit coupled to a microwave on-chip cavity. Moreover, thanks to the advantages of both on-chip cavity and tunable superconducting circuits, complex superpositions of states with different number of photons were also generated in a controlled and deterministic manner [55], which is a beautiful experimental realization of the protocol described in [56]. Recently, the N-photon entangled NOON states, $|N0\rangle + |0N\rangle$, have also been generated in two superconducting resonator [59]. These experiments further reveal the quantum behavior of the on-chip cavity and provide a useful on-demand multi-photon source for future quantum-technology applications.

Quantum state tomography. A crucial step in quantum information processing is the measurement of the output quantum states. However, a quantum state cannot be ascertained by a single quantum measurement. This is because quantum states may comprise many complementary features which cannot be measured simultaneously and precisely, owing to uncertainty relations. Nevertheless, all complementary aspects can in principle be observed by a series of measurements on a large enough number of identically prepared copies of the quantum system. Then, one could reconstruct an unknown quantum state from such a complete set of measurements of system observables. Such a process of reconstructing quantum states is called quantum state tomography. Using state tomography, the noisy channel of the quantum system can also be determined. This procedure of determining the dynamics of an open quantum system is known as quantum process tomography.

Tomographic measurements on the quantum states of superconducting charge qubits, either single or multiple qubits, were proposed in [60]. Recently, there were many experiments on the quantum state tomography of single superconducting phase qubits [61, 62] and of two coupled superconducting phase [63] and charge [64] qubits. Also, quantum process tomography was experimentally implemented on single [65] and two [66] phase qubits. Indeed, quantum state tomography is an essential tool in qubit-state measurements, and quantum process tomography

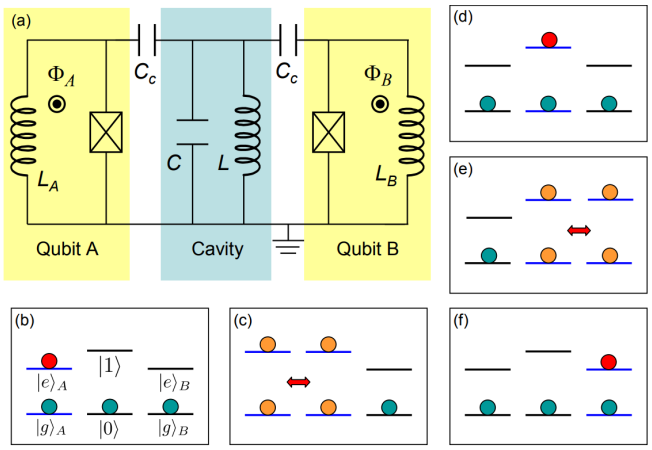


Figure 29.6: **Transferring quantum information between two stationary qubits via a cavity**. **(a)** Schematic diagram of two flux-driven phase qubits capacitively coupled by an on-chip cavity (an LC resonator). **(b)** Qubit A is prepared in a superposition state $\alpha|g\rangle_A + \beta|e\rangle_A$, while both qubit B and the resonator are prepared in their ground states. In this step, both qubits A and B are off-resonance with the cavity. **(c)** Qubit A is shifted into resonance with the resonator, for a time interval $t_1 = \pi/2g_A$, with $\hbar g_A$ being the interaction energy between qubit A and the resonator. This step maps the state of qubit A to the superposition state $\alpha|0\rangle + \beta|1\rangle$ of the resonator, where $|0\rangle$ and $|1\rangle$ are two Fock states of the resonator with zero and one photon, respectively. **(d)** Shift qubit A off-resonance with the resonator again, and store the quantum information in the resonator for a time duration t_2. **(e)** Shift qubit B in resonance with the resonator for a time interval $t_3 = \pi/2g_B$, where $\hbar g_B$ is the interaction energy between qubit B and the resonator. This step maps the state of the resonator to the superposition state $\alpha|g\rangle_B + \beta|e\rangle_B$ of qubit B. **(f)** Shift qubit B off-resonance with the resonator again, and store the quantum information in qubit B. Note that a high-fidelity state transfer between qubits A and B can be implemented if both the relaxation and decoherence of the state are negligibly small during the above processes.

can be used to probe the noise properties and temporal dynamics of qubit systems.

Future prospects

With technological advances, superconducting circuits can be used to test quantum mechanics on a macroscopic scale (see Box 3). Also, they can be used to demonstrate many novel phenomena in quantum science. A few examples are listed below.

Dynamical Casimir effect. When two mirrors are placed in empty space, their presence affects the vacuum fluctuations of the electromagnetic field. Because of the different densities of the vacuum modes inside and outside of the space between the two mirrors, a net force on the mirrors can be generated. This effect of quantum electrodynamics is known as the static Casimir effect.

If the mirrors move, there is also a mismatch between vacuum modes at different times. It has been predicted that this may result in the creation of real photons out of vacuum fluctuations. This dynamical Casimir effect also holds for a single mirror subject to a nonuniform acceleration in empty space. Although receiving considerable interest since its theoretical prediction, there is still no experimental verification of the dynamical Casimir effect. This is mainly due to the fact that the rate of photon production is non-negligible only when the mirror velocity approaches the speed of light, making the use of massive mirrors very challenging. A coplanar waveguide terminated by a SQUID was proposed [67] for experimentally observing the dynamical Casimir effect. Changing the magnetic flux threading the SQUID loop parametrically modulates the boundary condition of the waveguide and thereby its effective length. Because there is no massive mirror moving, the velocity of the effective boundary can approach the speed of light. Photon production from the vacuum can thus be made experimentally detectable.

Coherent population transfer. Elementary logic gates in quantum computing networks are usually implemented using precisely-designed resonant pulses. However, the various fluctuations and operational imperfections that exist in practice limit these designs. Also, the difficulty of switching interqubit couplings on and off strongly limits the precise design of the required pulses for two-qubit gates. To overcome these difficulties, Ref. [68] proposes an approach to coherently transfer the populations of qubit states by using Stark-chirped rapid adiabatic passages. As in the case of geometric phases, these population transfers are insensitive to the dynamical evolution times of the qubits, as long as they are adiabatic. The rapid adiabatic passages of populations could offer an attractive approach to implementing high-fidelity single- and two-qubit gates for quantum computing.

The key of these rapid adiabatic passages is how to produce time-dependent detunings by chirping the qubit levels. For most natural atomic or molecular systems, where each bound state possesses a definite parity, the required detuning chirps could be achieved by making use of the Stark effect via, eg., two-photon excitations of the qubit levels [69]. The breaking of parity symmetries in the bound states in superconducting circuits such as current-biased Josephson junctions provides an advantage [68], because the desirable detuning chirps can be produced by single-photon pulses. Recently, rapid adiabatic passage was achieved for the tranfer of a single photon in a superconducting circuit [70].

Tunable mirrors and interferometers. Superconducting circuits can be used for Landau-Zener-Stückelberg interferometry [71], but they can also be used for other types of interferometry—including Fano and Fabry-Perot interferometry [72, 73]—by coupling superconducting qubits to a coplanar waveguide. When injected into the waveguide, the photons interact with the qubits along the way, controlled by changing the applied electric

and/or magnetic fields on the qubits. These artificial atoms, working as tunable mirrors, can change the reflection and transmission coefficients of the photons confined in the waveguide.

Box 3. Testing quantum mechanics with macroscopic superconducting circuits

Bell inequality

The Bell inequality shows that the predictions of quantum mechanics can contradict those of local hidden variable theories (see, e.g., [92]) if one looks at correlations between spatially separated measurements. It can alternatively be stated that no physical theory of local hidden variables can reproduce all of the predictions of quantum mechanics. Tests of the Bell inequality have been proposed, using superconducting circuits such as charge [93] and phase qubits [94]. Recently, the violation of the Bell inequality has been experimentally verified [95] in phase qubits. Because the Bell inequality is violated by a quantum mechanical prediction, this experiment provides strong evidence that these macroscopic superconducting circuits indeed behave quantum mechanically. Recent experimental results [96, 97] on Greenberger-Horne-Zeilinger states do not require statistical arguments for a violation of the Bell inequality to be seen.

Leggett-Garg inequality

Leggett and Garg derived an inequality for a single degree of freedom undergoing coherent oscillations and being measured at successive times [98]. The Leggett-Garg inequality can be regarded as a temporal version of Bell's inequality, and it should be violated by a quantum two-level system. Very recently, this has been verified experimentally [99] using a voltage-driven box (i.e., the Cooper-pair box) acting as a quantum two-level system, showing that the time correlations present at the detector output violate the inequality.

Kochen-Specker theorem

This theorem elucidates the conflict between quantum mechanics and noncontextual hidden-variable theories [92]. Noncontextuality means that the measured value of an observable is independent of the choice of other co-measurable (commuting) observables that are measured previously or simultaneously. Quantum mechanics is contextual, because outcomes depend on the context of measurement. This theorem is an important complement to Bell's theorem; testing it can disprove noncontextual hidden-variable theories without referring to locality. To confirm such a counterintuitive phenomenon on a macroscopic scale, it was proposed [100] to use two charge qubits which are controllably coupled by a two-level data-bus built from a phase qubit. The analysis [100] showed that by performing joint nondestructive quantum measurements of two distinct qubits, the proposed superconducting circuits could demonstrate quantum contextuality at a macroscopic level.

For a system consisting of a superconducting qubit in an array of coupled cavities, the photon transmission exhibits a more general line shape [72], beyond the Breit-Wigner and Fano line shapes, because of the nonlinear photonic dispersion relation. At a particular matching condition between the photon wavelength and the lattice constant [72], the photonic dispersion relation can become linear and the photon transmission has the Breit-Wigner line shape, just as in an open transmission line [74]. Recently, this phenomenon was observed in a superconducting flux qubit coupled to an open transmission line [75]. When two superconducting qubits are placed in an array of coupled cavities, they can be used as tunable mirrors to form a Fabry-Perot interferometer [73]. Such a controllable on-chip interferometer is expected to have various applications in quantum optics.

Quantum nondemolition measurements. In a quantum measurement, a signal observable of a quantum system is measured by detecting the change in an observable of the detector that is coupled to the quantum system during the process of measurement. Generally, the

process of measurement will disturb the state of the quantum system owing to the interplay between the system and the detector. A quantum nondemolition (QND) measurement does not perturb the subsequent evolution of the quantum system; this can be achieved by using a particular type of system-detector coupling that preserves the eigenstates of the signal observable in the quantum system. In quantum optics, a QND measurement of the photon number can be implemented using the optical Kerr effect and a dispersive atom-field coupling (see, e.g., [29]).

The first successful QND measurement on a superconducting qubit was implemented using the dispersive atom-field coupling technique [16, 76]. Recent experiments [77, 78] show that QND measurements can also be implemented for a single superconducting qubit by using a nonlinear resonator as the detector. In [77], the detector was composed of a SQUID shunted with a capacitance, while in [78] the detector was a bifurcation amplifier, which is a r.f.-driven Josephson junction working near the dynamical bifurcation point [79]. Very recently, a fast QND measurement of a flux qubit was implemented in the weakly-projective regime by employing a hysteretic d.c. SQUID detector [80]. A quantum device can have multiple qubits, so QND measurements on quantum states of multiple qubits (e.g., entangled states) should be an appealing topic for future investigations.

Generating squeezed states. Squeezed states have been extensively studied in quantum optics, and are now being studied in condensed matter systems. Owing to their tunable nonlinearity and low losses in the microwave regime, Josephson-junction superconducting circuits are promising devices for producing squeezed states. In superconducting circuits, LC oscillators have been successfully used for quantum control and readout devices in conjunction with superconducting qubits. As parametric transducers (essentially, a radio-frequency auto-oscillator), superconducting resonant tank circuits have been used to measure the quantum state of flux qubits [81]. When squeezed states are generated in these resonant tank circuits acting as quantum-state detectors, the noise of the detectors can be decreased below the standard quantum limit. A recent theoretical study [82] shows that a superconducting parametric transducer can naturally implement this approach, as it can be used both to produce squeezed states and to use them in order to minimize quantum fluctuations. An immediate application of this method would be to suppress the effective noise temperature of the amplifier connected to the parametric transducer, at least to the nominal temperature of the cooling chamber.

Topological phases. A topologically-protected quantum state degeneracy cannot be lifted by any local perturbations [83]. It is therefore natural to consider using topological phases for applications requiring a high degree of quantum coherence. With superconducting circuits as building blocks, various artificial lattices can be constructed that possess interesting topological phases. For instance, it has been proposed that a triangular Josephson junction array may have a two-fold degenerate ground state, which could be used for constructing topologically-protected qubits [75]. Recently, an experiment [85] was implemented for a prototype device that consisted of twelve physical qubits made of nanoscale Josephson junctions. Owing to properly tuned quantum fluctuations, this system was protected against magnetic flux variations well beyond linear order. This suggests that topologically protected superconducting qubits are feasible. Also, superconducting circuits were proposed [86] as a way to construct the Kitaev honeycomb model, which requires that the spin (natural or artificial) at each node of a honeycomb lattice interacts with its three nearest neighbors through three different types of interactions [87]. Depending on the bond parameters, this anisotropic spin model supports both Abelian and non-Abelian anyons, which are particles obeying unusual statistics (they are neither bosons nor fermions). Its realization would provide exciting opportunities for experimentally demonstrating anyons.

Final remarks. The superconducting circuits that we have described above contain Josephson junctions that can act as nonlinear inductors. Using suitably designed superconducting circuits, it is therefore possible to fabricate field-controlled nonlinear resonators, which can be used to demonstrate the Kerr effect (either quadratic electro-optic or quadratic magneto-optic). If such circuits were used as a Kerr medium, one could carry out a variety of nonlinear optics experiments, e.g., coupling microwave photons, implementing quantum gates for photon qubits, and performing QND measurement. Superconducting circuits could have many other applications. For instance, it has been suggested that a coplanar waveguide with the center conductor replaced by an array of SQUIDs could be used to simulate Hawking radiation [88]. Indeed, superconducting circuits have the advantage of enabling the study of complex controllable quantum dynamics. This could lead to quantum simulations and on-chip studies of many-body physics. Numerous new phenomena and applications will continue to be discovered using superconducting circuits, and these will play an important part in future quantum technologies.

30 Spin-polarized supercurrents for spintronics: a review of current progress by Eschrig

Abstract

During the past 15 years a new field has emerged, which combines superconductivity and spintronics, with the goal to pave a way for new types of devices for applications combining the virtues of both by offering the possibility of long-range spin-polarized supercurrents. Such supercurrents constitute a fruitful basis for the study of fundamental physics as they combine macroscopic quantum coherence with microscopic exchange interactions, spin selectivity, and spin transport. This report follows recent developments in the controlled creation of long-range equal-spin triplet supercurrents in ferromagnets and its contribution to spintronics. The mutual proximity-induced modification of order in superconductor-ferromagnet hybrid structures introduces in a natural way such evasive phenomena as triplet superconductivity, odd-frequency pairing, Fulde-Ferrell-Larkin-Ovchinnikov pairing, long-range equal-spin supercurrents, π-Josephson junctions, as well as long-range magnetic proximity effects. All these effects were rather exotic before 2000, when improvements in nanofabrication and materials control allowed for a new quality of hybrid structures. Guided by pioneering theoretical studies, experimental progress evolved rapidly, and since 2010 triplet supercurrents are routinely produced and observed. We have entered a new stage of studying new phases of matter previously out of our reach, and of merging the hitherto disparate fields of superconductivity and spintronics to a new research direction: super-spintronics.

30.1 Introduction: historical background

30.1.1 Superconductivity interacting with magnetism

Quantum phenomena fascinate us and challenge our imagination for over 100 years since the theoretical foundations of quantum physics were laid. The two prime examples for macroscopic quantum phenomena are magnetism and superconductivity. Soon after the discovery of superconductivity in 1911 in Leiden by Kamerlingh-Onnes [1, 2] it became clear that a magnetic field acts in peculiar ways on superconductors. Silsbee unified in 1927 the observations of Kamerlingh-Onnes of a critical transport current density and a critical magnetic field [3], and in 1933, following a suggestion by von Laue, Meißner and Ochsenfeld performed experiments showing that the new state of matter is a true thermodynamic phase and that it expels magnetic

fields from its interior [4]. Following this pivotal discovery, Shubnikov pioneered in the 1930's the field of interplay between superconductivity and magnetic field, culminating in the discovery of what is now called the intermediate state, or the Shubnikov phase [5],[39] where magnetic flux partially penetrates the superconductor in a well defined region of the temperature-field phase diagram. After the notion of a macroscopic quantum wave function was introduced for the superconducting state by Ginzburg and Landau in 1950 [9], Abrikosov theoretically explained in the 1950's type II superconductivity, where a magnetic field penetrates the superconductor in a regular array of flux lines carrying quantized flux [7]. Abrikosov's vortex phase exists between the upper critical field H_{c2} and the lower critical field H_{c1} in type II superconductors.

Soon the microscopic theories of superconductivity by Bardeen, Cooper, and Schrieffer (BCS) in 1957 [8], by Bogoliubov in 1958 [9], and by Gor'kov in 1958-59 [10] brought all previous studies on a firm ground.

Ginzburg, in an attempt to formulate a theory for ferromagnetic superconductors (he considered the possibility of superconductivity in gadolinium), concentrated in 1956 on the electromagnetic (or so-called orbital) mechanism, where a suppression of superconductivity occurs via the interaction of the Cooper pairs with the vector potential of the magnetic field due to their charge [11]. In the orbital mechanism the magnetic field leads to an additional kinetic energy of the condensate, and when this energy exceeds the condensation energy, the superconducting state is destroyed. As shown in 1966 by Werthamer, Helfand, and Hohenberg, the orbital critical field for conventional isotropic, diffusive superconductors in the absence of spin-orbit and spin paramagnetic effects is $H_{\rm orb} \equiv H_{c2}|_{T=0} \approx 0.7 T_c [-dH_{c2}/dT]_{T=T_c}$ [12], where T_c is the superconducting transition temperature.

An alternative mechanism, the exchange mechanism, was suggested in 1958 by Matthias, Suhl, and Corenzwit [13] in order to explain the variation of T_c in lanthanum with rare earth impurities and the correlation between the appearance of ferromagnetism and superconductivity in ruthenides. They observed that it is not the dipole field of the effective moments of the rare earth elements that causes decrease of superconductivity in these systems, but the spin of the solute atoms; the T_c does not correlate with van Vleck's famous curve of $\mu_{\rm eff}$ [14], but rather with spin. In these cases an exchange interaction mediated by conduction electrons, responsible for ferromagnetism, occurs in a material that by itself is superconducting. The exchange interaction via conduction electrons tries to align spins in a ferromagnet, whereas the spins in a Cooper pair are opposite for the usual case of singlet superconductors. These antagonistic tendencies led to the so-called paramagnetic effect of pair breaking.

In 1959, Anderson and Suhl showed in a seminal paper [15] that in a system with coexisting superconductivity and ferromagnetism the magnetism is modified due to the suppression of the spin susceptibility at small wavevectors. As a consequence, magnetism becomes under certain conditions inhomogeneous with a new, finite, wavevector. This new state was termed the cryptoferromagnetic state. The wavelength of the magnetic inhomogeneity is much smaller than the superconducting coherence length (the typical extend of a Cooper pair) and much larger than the lattice spacing, thus keeping neighboring spins almost parallel, however reducing the exchange field averaged over a typical Cooper pair volume. In real (anisotropic) materials the corresponding magnetic structure is often a one-dimensional magnetic domain structure.

30.1.2 Pair breaking by paramagnetic impurities and external fields

If one introduces paramagnetic impurities into a singlet superconductor, there is the effect of pair breaking due to scattering from paramagnetic impurities, which reduces T_c with increasing

[39] Unfortunately, Shubnikov's work ended abruptly when he was arrested on the 6th of August and executed on the 10th of November 1937 during the Stalin-Yezhov terror on the basis of falsified charges of antirevolutionary activities; he was officially rehabilitated in 1957.

impurity concentration. Following previous works by Herring [16] and by Suhl and Matthias [17] for the limit of small concentrations, Abrikosov and Gor'kov developed in 1960 a theory covering the full range of concentrations up to the critical value, when superconductivity is destroyed; the T_c dependence vs. concentration is described in terms of a single "pair breaking parameter" ρ by the Abrikosov-Gor'kov formula [18]. In particular, these authors showed that the possibility of gapless superconductivity exists in metals with paramagnetic impurities (this peculiar state was further studied in 1964 by Skalski, Betbeder-Matibet, and Weiss [19], by Maki [20], and by de Gennes [21]). The Abrikosov-Gor'kov model, which employs the Born approximation, works well, e.g. for rare earth (except cerium) impurities. For transition metal impurities in superconductors Yu [22], Shiba [23], and Rusinov [24] discovered within the framework of a full t-matrix treatment of the problem that local states (now called the Yu-Shiba-Rusinov states) are present within the BCS energy gap due to multiple scattering between conduction electrons and paramagnetic impurities.

De Gennes and Tinkham noted in 1964 [25] that for a time-reversal invariant superconducting order parameter, pair breaking can be related to the asymptotic long-time behavior of the time-reversal correlation function, $\eta(t) = \lim_{t\to\infty}\langle\hat{\Theta}^\dagger(0)\hat{\Theta}(t)\rangle$, with the time reversal operator $\hat{\Theta}$. An exponential decay, $\eta(t) = \exp^{-2t/\tau_\Theta}$, with τ_Θ some correlation time, corresponds to pair breaking with pair breaking parameter $\rho = (2\pi T\tau_\Theta)^{-1}$. If, on the other hand, a nonzero limiting value $0 < \eta < 1$ appears, then this leads to an effective weakening of the pairing interaction.

When applying a magnetic field to a superconductor, apart from the orbital effect of the penetrating field, there is also an appreciable Zeeman coupling between the electronic spins and the magnetic field. It leads to a splitting between the electronic spin bands similarly as in a weak ferromagnet the exchange energy leads to a band splitting. This effect has been experimentally studied in the early 1970's by Meservey and Tedrow in a series of classical papers (see [26] for a review). If the magnetic field exceeds a certain value, superconductivity becomes energetically unfavorable due to this Zeeman coupling. This limiting field is the Pauli paramagnetic limiting field or the so-called Chandrasekhar-Clogston limiting field, and was predicted independently in 1962 by Chandrasekhar [27] and by Clogston [28]. It amounts to $H_p = \sqrt{2}\Delta(T = 0)/g\mu_B$, where Δ is the excitation gap in the superconductor at zero magnetic field, $g \approx 2$ the electron g-factor, and μ_B the Bohr magneton. The ratio $\alpha = \sqrt{2}\tilde{H}_{orb}/H_p$, where $\tilde{H}_{orb}$ is the upper critical field in the absence of the Pauli term, was discussed in 1966 by Maki, and is known as the Maki parameter [29].

30.1.3 Ferromagnetic superconductors

Coexisting singlet superconductivity and ferromagnetism is rare, and can be achieved either by finding suitable crystalline materials (classical examples are the rare-earth ternary compounds $ErRh_4B_4$ [30] and $HoMo_6S_8$ [31] in a narrow temperature region below the Curie temperature), or by introducing magnetic ions in a superconducting material that order ferromagnetically. In the latter case, at high impurity concentrations, the possibility to obtain coexistence between ferromagnetism and superconductivity was theoretically predicted in 1964 by Gor'kov and Rusinov [32]. Furthermore, for the case that ferromagnetism and superconductivity coexist or an external magnetic field is applied, Fulde and Maki [33] showed that the Abrikosov-Gor'kov formula holds with a modified pair breaking parameter. For an early review on magnetic superconductors see [34].

In addition to the above cases of conventional singlet superconductors, there has been discovered a large number of unconventional superconductors, which are distinguished from the conventional ones by the fact that they break additional symmetries, e.g. the lattice symmetry of the normal state, or the spin rotational symmetry. The latter is the case for superconductors exhibiting spin-triplet pairing (see figure 30.1). In particular ferromagnetic

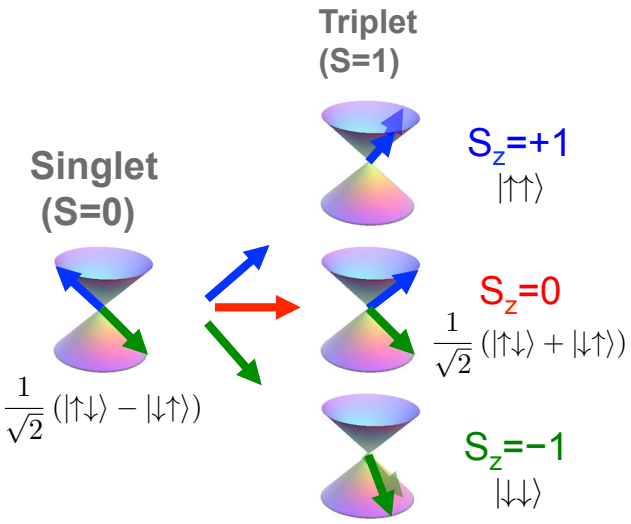


Figure 30.1: Two electrons, each of which has spin $s = \frac{1}{2}$, can combine their spin angular momenta $\mathbf{s}_1$ and $\mathbf{s}_2$ to build a pair with total spin $S = 0$ or a pair with total spin $S = 1$. In the first case, the pair is in a spin-singlet state (shown on the left). In the second case, the pair is in one of the three possible spin-triplet states: with spin projection $S_z = 0, \pm 1$ (shown on the right). The pairs with $S_z = \pm 1$ are called "equal-spin" pairs with respect to the spin quantization axis (here z-axis). The spin state $|S, S_z\rangle$ is fully characterized by the two quantum numbers S and S_z. We use a spin-vector representation to visualize pair angular momenta, where the expectation value of the cosine of the relative angle between the two spin vectors within a pair, $\langle S, S_z|\mathbf{s}_1 \cdot \mathbf{s}_2|S, S_z\rangle / \sqrt{\mathbf{s}_1^2 \mathbf{s}_2^2}$, is -1 for singlet states, and $\frac{1}{3}$ for triplet states. Thus, angular momenta can be visualized as antiparallel for singlet pairs, whereas for triplet pairs they enclose in average a relative angle of $\approx 70.53^o$ (even for "equal spin" pairs).

superconductors are under suspicion of such a pairing state, as equal-spin triplet pairing is not sensitive to the exchange mechanism in the way singlet pairing is. This refers to some heavy fermion compounds, like UGe_2 [35], URhGe [36], UCoGe [37], and UIr [38], in which superconductivity can coexist with ferromagnetism, and which have been studied in the past 15 years [39].

The main problem for coexistence between superconductivity and ferromagnetism is that a strong exchange effect destroys superconductivity unless the pairing is of the triplet kind. However, not many superconductors support triplet pairing. Furthermore, such systems are typically p-wave superconductors [40], which are very sensitive to pair breaking by normal impurities (conventional superconductors are insensitive to scattering from normal impurities, which is the content of a theorem by Abrikosov, Gor'kov, and Anderson [41, 42]). For this reason new avenues have been chosen to study such systems for s-wave and d-wave superconductors, which are much more common in nature. These avenues combine the phenomena of proximity induced superconductivity, Cooper pairs with finite center of mass momentum, and odd-frequency s-wave spin-triplet pairs.

30.1.4 Cooper pairs with finite center of mass momentum

When the paramagnetic limiting field is smaller than the orbital critical field, then the possibility of an inhomogeneous superconducting state with finite pair momentum arises near H_p. Such a state was theoretically predicted in 1964 independently by Fulde and Ferrell [43] and by Larkin and Ovchinnikov [44]. It is known in the western literature as FFLO state and

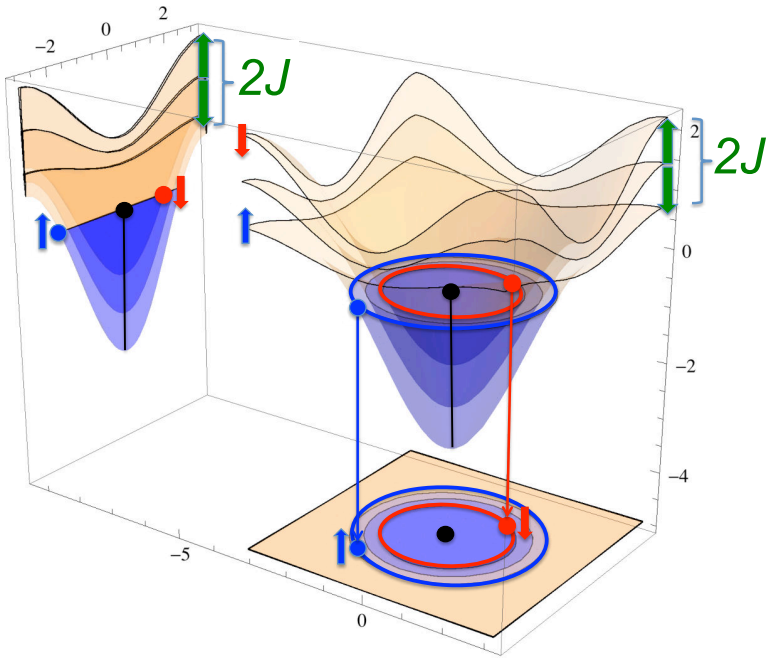


Figure 30.2: The FFLO effect: due to the exchange splitting of the energy bands (filled states are shaded blue in the picture) by $\pm J$ the Fermi surfaces split as well. A Cooper pair with opposite spins can be accommodated at the Fermi surface only on the cost of a finite center of mass momentum. Note that spin is quantized here in direction of the exchange field $\boldsymbol{J}$, entering the Hamiltonian as $\mathcal{H}_{\text{exch}} = -\boldsymbol{J} \cdot \boldsymbol{\sigma}$.

in the eastern as LOFF state.

Consider superconductivity in a weakly spin-polarized ferromagnetic material (or in an external magnetic field). Electronic spin bands are shifted in energy with respect to each other by an amount $2J$ (which in general can be anisotropic): $\varepsilon(\boldsymbol{p}) \to \varepsilon(\boldsymbol{p}) - \boldsymbol{J}(\boldsymbol{p}) \cdot \boldsymbol{\sigma}$. The exchange field can be related to an effective magnetic field via $\mu \boldsymbol{B}_{\text{eff}} = \boldsymbol{J}$ (for free electrons the magnetic moment is $\mu = \mu_{\text{e}} < 0$). We use the convention that spin is quantized in direction of the exchange field. The energy shift translates into a splitting of the Fermi surface for the two spin species (see Figure 30.2), which results e.g. for small J from the relation

$$\hbar \boldsymbol{v}_f \cdot \boldsymbol{Q} = \boldsymbol{v}_f \cdot (\boldsymbol{p}_{f\uparrow} - \boldsymbol{p}_{f\downarrow}) = 2J(\boldsymbol{p}_f) \tag{30.1}$$

obtained by linearizing the dispersion relation around the Fermi energy [here the Fermi velocity $\boldsymbol{v}_f$ is assumed to be approximately equal for the two spin bands due to the small splitting, and $\boldsymbol{p}_f = (\boldsymbol{p}_{f\uparrow} + \boldsymbol{p}_{f\downarrow})/2$]. Thus, the system only allows for opposite-spin Cooper pairs $\{\boldsymbol{p}_{f\uparrow}, -\boldsymbol{p}_{f\downarrow}\}$ and $\{\boldsymbol{p}_{f\downarrow}, -\boldsymbol{p}_{f\uparrow}\}$ built from electrons at the Fermi energy if they carry a finite center of mass momentum $\pm\hbar\boldsymbol{Q}/2 = \pm(\boldsymbol{p}_{f\uparrow} - \boldsymbol{p}_{f\downarrow})/2$ ($\hbar\boldsymbol{Q}$ is the momentum of the Cooper pair). This can lead to an order parameter characterized by a linear combination of terms with different Cooper pair momenta

$$\Delta_{\text{FFLO}}(\boldsymbol{R}) = \sum_{\nu} \Delta_\nu e^{i\boldsymbol{Q}_\nu \cdot \boldsymbol{R}}. \tag{30.2}$$

The preferred directions are chosen by the system (spontaneously or due to crystal anisotropy and boundary conditions). Fulde and Ferrell suggested an order parameter characterized by only one wavevector $\boldsymbol{Q}$, leading to a spatially homogeneous modulus and a spatially varying phase. If the order parameter is characterized by more than one wavevector $\boldsymbol{Q}_\nu$, then the FFLO state exhibits an inhomogeneous order showing a periodic structure. Larkin and Ovchinnikov proposed that the ground state may show a one-dimensional modulation (neglecting orbital

effects). However, more complex structures are possible in the general case of anisotropic metals. In general, the pair amplitudes develop an $|S = 1, S_z = 0\rangle$ spin-triplet component, and the inhomogeneous modulus of the order parameter is accompanied by an oscillation of the magnetization around its average, determined by the product of the singlet and triplet pair amplitudes.

Originally the state had been studied for a superconductor with ferromagnetically aligned impurities. However, it is known today that the FFLO state is very sensitive to disorder [45, 46], and thus most likely is found in clean materials in an external field. Gruenberg and Gunther studied in 1966 the influence of orbital effects in type II superconductors on the possibility to observe an FFLO state and found that although orbital effects are detrimental to the formation of the FFLO state, such a state can exist at finite temperatures in the mixed state of a pure superconductor provided the Maki parameter α exceeds 1.8 [47]. Interesting candidates are quasi-two-dimensional superconductors in a magnetic field applied nearly parallel to the conducting layers. The theory for such systems was developed by Bulaevskiĭ [48] in 1973, by Burkhardt and Rainer [49] and by Shimahara [50] in 1994, and by Buzdin and Brison [51] in 1996. For quasi-one-dimensional systems theories in terms of soliton lattice solutions were developed by Buzdin and Tugushev in 1983 [52], by Buzdin and Polonskii in 1987 [53], and by Dupuis in 1995 [54]. In compounds with large spin susceptibility and high H_{c2}, as in heavy fermion and intermediate-valence systems, a generalized FFLO state was discussed by Tachiki and co-workers, where the order parameter is spatially modulated, and planar nodes of the order parameter are periodically aligned perpendicular to the vortices [55].

The FFLO state only appears below a certain temperature T^*, which determines a tri-critical point (T^*, H^*) in the (T, H)-diagram at which the normal, BCS, and the FFLO phases meet. A generalized Ginzburg-Landau theory for the vicinity of this tri-critical point was derived by Buzdin and Kachkachi [56]. A self-consistent calculation of the field versus temperature phase diagram and order parameter structures for the FFLO states of quasi-two-dimensional d-wave superconductors is presented in Ref. [57]. Recently, a symmetry classification of the pairing amplitudes in FFLO states coexisting with vortices was suggested [58]. For reviews on this topic see Refs. [59, 60, 61, 62].

The FFLO state has not been unambiguously found in bulk materials to date, although there are currently candidates under debate, as the heavy fermion material $CeCoIn_5$ [63, 64, 65, 66], or some organic superconductors such as κ-(BEDT-TTF)$_2$Cu(NCS)$_2$ [67, 68, 69, 70]. However, a similar state can be realized in superconductor-ferromagnet hybrid structures, where superconducting pairs leak into a ferromagnet due to the superconducting proximity effect, as we discuss in detail further below (for earlier reviews see [71, 72, 73, 74, 75]).

30.1.5 Proximity effect

The pivotal role for realizing the FFLO state in such hybrid structures is played by the proximity effect between a superconducting and a normal conducting material. The theory for the proximity effect was developed largely by de Gennes [76, 77, 78, 79], and by Werthamer [80, 81] in the 1960's. It describes the effect of penetration of Cooper pairs in a normal metal where the two conduction electrons (or holes) of the pair stay correlated with each other over a distance that depends on the amount of disorder in the normal material and on temperature. In a clean material, the penetration depth is determined by the thermal coherence length $\xi_{N,c} = \hbar v_f / 2\pi k_B T$. It gives the distance, a quasiparticle with velocity v_f travels during time $\hbar/2\pi k_B T$, before thermal decoherence sets in. For ballistic motion and atomically smooth interfaces, the penetration depth depends on the angle of impact of the quasiparticles, i.e. the Fermi velocity should be replaced by the Fermi velocity component in the normal metal perpendicular to the interface, $v_{f,x}$. The notion of a coherence length determined by the Fermi

velocity and a characteristic superconducting energy scale was introduced by Pippard in 1953 [82].

In the presence of impurities, scattering decreases the penetration of Cooper pairs into the normal metal. If the mean free path is ℓ, and the motion is diffusive, then the quasiparticle travels in average between two scattering events a time $\tau = \ell/v_f$. For a random walk, the variance for the x-component is given by $\sigma_x^2 = \frac{1}{3}\frac{t}{\tau}\ell^2 = tv_f\ell/3$, where t is the elapsed time. Coherence is lost when the total path traversed during the random walk is equal to $\xi_{\rm N,c}$, i.e. $v_f t = \xi_{\rm N,c}$. If we define the diffusive coherence length by $\xi_{\rm N,d}^2 = \sigma_x^2$, we obtain $\xi_{\rm N,d}^2 = \xi_{\rm N,c}\ell/3$. Hence, the diffusive coherence length is given by $\xi_{\rm N,d} = \sqrt{\xi_{\rm N,c}\ell/3}$, or in other words, $\xi_{\rm N,d} = \sqrt{\hbar D/2\pi k_{\rm B}T}$ with the diffusion constant $D = v_f\ell/3$.[40]

The proximity amplitude is proportional to the pair potential in the superconductor, Δ, and the product of the transmission amplitudes through the interface of the two particles comprising a pair. Inversely, the loss of Cooper pairs in the superconductor leads to the so-called inverse proximity effect of a weakening of the superconducting pair potential near the interface in the superconductor.

30.1.6 Andreev reflection

A very closely related phenomenon is the so-called Andreev reflection, discovered by Andreev in 1964 [83] and by de Gennes and Saint-Jaimes in 1963/64 [84, 85] (see Ref. [86] for a review). It describes the correlations between particles and holes at the normal side of the interface due to penetration of pairs. In fact, Andreev reflection and proximity effect are two sides of one and the same coin.

Let us assume that a spin $\uparrow$ conduction electron in the normal metal with energy $\mu + \varepsilon$ near the chemical potential μ moves in positive x-direction towards a superconductor. The excitation energy ε is assumed to be within the energy gap Δ of the superconductor. The electron can be transmitted into the superconductor only together with another electron with spin $\downarrow$, energy $\mu-\varepsilon$, and momentum approximately opposite, to build a Cooper pair that enters the condensate at the pair chemical potential 2μ (after some momentum relaxation has taken place). For $\Delta \ll \mu$ it is possible to approximate the electronic dispersion $E(\boldsymbol{p}) \approx \mu + \boldsymbol{v}_f\cdot(\boldsymbol{p}-\hat{\boldsymbol{p}}_f)$, with the Fermi momentum $\hat{\boldsymbol{p}}_f$ and Fermi velocity $\boldsymbol{v}_f \equiv \boldsymbol{v}(\hat{\boldsymbol{p}}_f)$. Within this approximation, the group velocity of the incoming electron is equal to $\boldsymbol{v}_f$, and its excitation energy $\varepsilon = \boldsymbol{v}_f\cdot(\boldsymbol{p}-\hat{\boldsymbol{p}}_f)$.

Let us consider a Landau quasiparticle with momentum $\boldsymbol{p}_1 = \boldsymbol{p}_{f1} + \delta\boldsymbol{p}_1$, spin $\uparrow$, and excitation energy $\varepsilon_1 = \boldsymbol{v}_{f1}\cdot\delta\boldsymbol{p}_1$. We will consider pairing with another quasiparticle with momentum $\boldsymbol{p}_2 = -\boldsymbol{p}_{f1} + \delta\boldsymbol{p}_2$, spin $\downarrow$, and excitation energy $\varepsilon_2 = -\boldsymbol{v}_{f1}\cdot\delta\boldsymbol{p}_2$ (see Figure 30.3). We require that $\varepsilon_2 = -\varepsilon_1$. This leads to the relation $\boldsymbol{v}_{f1}\cdot(\delta\boldsymbol{p}_2 - \delta\boldsymbol{p}_1) = 0$, which allows us to choose $\boldsymbol{p}_{f1}$ such that $\delta\boldsymbol{p}_1 = \delta\boldsymbol{p}_2 = \delta\boldsymbol{p}$ holds[41]. The missing electron in the spin-$\downarrow$ band is equivalent to a hole excitation characterized by energy $-\varepsilon_2 = +\varepsilon_1$, momentum $-\boldsymbol{p}_2 = \boldsymbol{p}_{f1} - \delta\boldsymbol{p}$, group velocity $\boldsymbol{v}(\boldsymbol{p}_2) \approx -\boldsymbol{v}_{f1}$, and spin $\uparrow$ (a missing spin $\downarrow$). The process can be considered as a scattering of a particle with charge e, momentum $\boldsymbol{p}_f + \delta\boldsymbol{p}$, and velocity $\boldsymbol{v}_f$ into a hole with charge $-e$, momentum $\boldsymbol{p}_f - \delta\boldsymbol{p}$ and velocity $-\boldsymbol{v}_f$. The electron-hole pair gives rise to a current density of $e\boldsymbol{v}_f + (-e)(-\boldsymbol{v}_f) = 2e\boldsymbol{v}_f$, twice the current density of the incoming particle. The incoming electron (velocity $\boldsymbol{v}_{f1}$) is approximately "retro-reflected" (velocity $\approx -\boldsymbol{v}_{f1}$) as a hole [83]. This process is called Andreev reflection, contrasting the familiar specular reflection.

A possible small angle between the reflected hole and the incoming particle is due to variation of the Fermi velocity between the momenta $\boldsymbol{p}_f$ and $\boldsymbol{p}_f \pm \delta\boldsymbol{p}$, and is of order of ε/E_f, with Fermi

[40] In d dimensions the factor of 3 is replaced by a factor of d.

[41] Choose $\tilde{\boldsymbol{p}}_{f1} = \boldsymbol{p}_{f1} + (\delta\boldsymbol{p}_1 - \delta\boldsymbol{p}_2)/2$, then $\boldsymbol{p}_1 - \tilde{\boldsymbol{p}}_{f1} = \boldsymbol{p}_2 + \tilde{\boldsymbol{p}}_{f1} = \delta\boldsymbol{p} = (\delta\boldsymbol{p}_1 + \delta\boldsymbol{p}_2)/2$. This is again (in leading order) a Fermi surface point due to $\boldsymbol{v}_{f1}\cdot(\tilde{\boldsymbol{p}}_{f1} - \boldsymbol{p}_{f1}) = 0$, i.e. the shift is tangential to the Fermi surface.

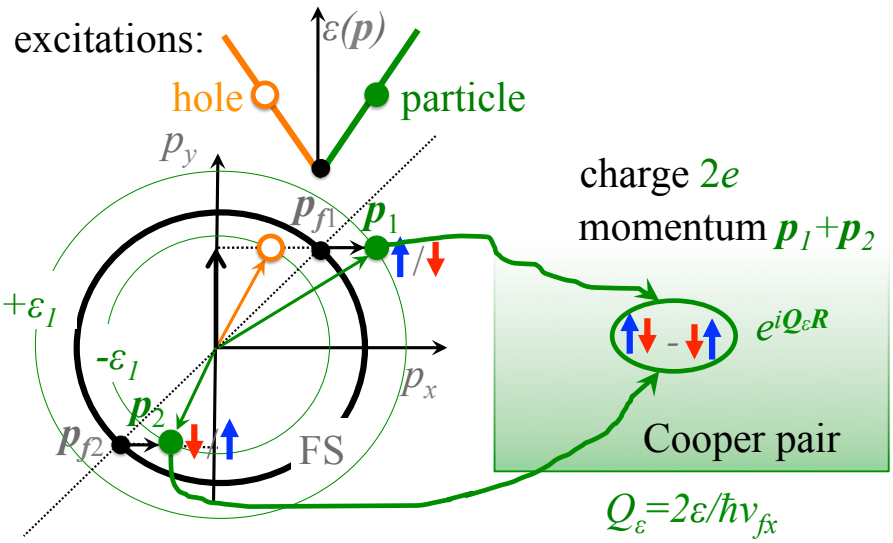


Figure 30.3: Andreev reflection: An electron at crystal momentum $\boldsymbol{p}_1$ pairs with another one at $\boldsymbol{p}_2$ under the conditions that their energies and p_y-component of momentum are opposite to each other. This leads to a finite p_x component and a resulting center of mass momentum $\hbar\boldsymbol{Q}_\varepsilon/2$ of the Cooper pair. A hole is reflected, which is drawn in this plot at the negative momentum and energy of the missing electron (in the excitation picture all excitation states inside the Fermi surface have reversed momentum and energy and are considered as hole excitation with positive excitation energy). The resulting Cooper pair transfers its momentum partially to the interface between the normal metal and the superconductor (for the case that there is a Fermi surface or Fermi velocity mismatch), and partially to the condensate in the superconductor when entering it. The amount transferred to the condensate results in a supercurrent consistent with current conservation in the scattering process.

energy E_f [87]. Retroreflection is perfect for perpendicular impact if no supercurrent flows along the surface. In the Andreev particle-hole conversion process, energy and spin are conserved, however charge is not, and momentum is only approximately conserved. The charge $2e$ and (partially) the momentum $\hbar\boldsymbol{Q} = 2\delta\boldsymbol{p}$ are transferred to the superconducting condensate: two electrons with opposite spin enter the superconductor to create a Cooper pair with non-zero pair momentum, which joins the condensate, leading to a (small) supercurrent for finite excitation energies. The momentum $\hbar\boldsymbol{Q}$ is thereby partially transferred to the interface (provided a Fermi surface or Fermi velocity mismatch exists), and partially to the condensate resulting into a supercurrent consistent with total charge conservation. In equilibrium, and in the absence of a macroscopic supercurrent, this current is exactly canceled by the inverse process when a Cooper pair enters the normal metal and converts a hole into an electron.

For an atomically clean interface, if there is a macroscopic supercurrent with Cooper pair momentum $\boldsymbol{p}_S$ parallel to the interface present in the superconductor, then momentum conservation requires that the created Cooper pair enters the condensate with the required Cooper pair momentum parallel to the interface, such that $2\delta\boldsymbol{p}_{||} = \boldsymbol{p}_S$. One obtains (we assume $v_{fx} > 0$) $2\delta p_x = (2\varepsilon - \boldsymbol{v}_f \cdot \boldsymbol{p}_S)/v_{fx}$. In particular, for $\boldsymbol{p}_S = 0$ only p_x can change in the Andreev scattering process. In this case, as $\delta\boldsymbol{p}_{||}$ must be zero, the Cooper pair momentum is given by $Q_\varepsilon = 2\varepsilon/v_{fx}$ (see Figure 30.3).

The Andreev reflection process is phase coherent, i.e. the phases of the incoming particle and the Andreev-reflected hole are correlated. For a superconducting order parameter $\Delta = |\Delta|e^{i\chi}$, the phase difference is $\varphi(\varepsilon) - \chi$, between an incoming electron and retroreflected hole, and is $\varphi(\varepsilon) + \chi$ between an incoming hole and retroreflected electron, where $\varphi(\varepsilon) = -\arccos(\varepsilon/|\Delta|)$ describes the phase delay due to the fact that during Andreev reflection the particle and hole amplitudes penetrate into the superconductor over a length scale $\xi_\varepsilon^{(\mathrm{S})} = \hbar v_f^{(\mathrm{S})}/\sqrt{|\Delta|^2 - \varepsilon^2}$.[42]

During their motion in the normal metal, the phase coherence is lost due to the slight difference in momentum of the electron and the hole, given by $2\delta p_x = 2\varepsilon/v_{fx}$. When averaged over all momentum directions, the pair correlation function decays away from the interface algebraically $\sim \xi_{\mathrm{c}}^{(\mathrm{N})}/x$ as function of x, where we define $\xi_{\mathrm{c}}^{(\mathrm{N})} = \hbar v_f/2\varepsilon$. For observables in equilibrium, the decay length can be obtained by replacing ε in the expression for the momentum δp_x by the lowest Matsubara energy [89] $i\pi k_{\mathrm{B}}T$. This leads to an exponential decay on the length scale $\hbar v_f/2\pi k_{\mathrm{B}}T$ along each ballistic trajectory, which is precisely the coherence length from the proximity effect.

For diffusive motion, non-magnetic scattering events conserve the time reversal symmetry, and thus scatter time-reversed states in a similar way. In particular a particle-hole pair with momenta both close to $\boldsymbol{p}_f$ will scatter in a particle hole pair with momenta both close to $\boldsymbol{p}'_f$ (as scattering amplitude for $\boldsymbol{p}_f \to \boldsymbol{p}'_f$ is the same as for $-\boldsymbol{p}'_f \to -\boldsymbol{p}_f$ due to time reversal symmetry). Thus, scattering events change the momentum of particle and hole by the same amount, however do not destroy their coherence. This means, the dephasing between the particle and hole takes place on a semiclassical trajectory as in the clean case, however the trajectory changes direction multiple times in a random way. The diffusive process away from the interface is characterized by a diffusion equation for the pair amplitude f, given by $\partial_t f = D\partial_x^2 f$. With $f \sim e^{i(k_x x - 2\varepsilon t/\hbar)}$ this implies $-2i\varepsilon = -\hbar D k_x^2$, resulting in a complex wave vector given for decay in positive x direction by $k_x = (i \pm 1)\sqrt{|\varepsilon|/\hbar D}$. This gives rise to an exponential decay on the length scale $\sqrt{\hbar D/|\varepsilon|}$, accompanied by an oscillation on the same length scale. For observables in equilibrium we can replace $\varepsilon \to i\pi k_{\mathrm{B}}T$, leading to $k_x^2 = -2\pi k_{\mathrm{B}}T/\hbar D$ and an exponential decay on the length scale $\xi_{\mathrm{d}}^{(\mathrm{N})} = \sqrt{\hbar D/2\pi k_{\mathrm{B}}T}$, again matching the length scale for the proximity

[42] For a supercurrent along the interface, $\chi(\boldsymbol{R}) = \chi(\boldsymbol{R}_0) + \frac{1}{\hbar}\boldsymbol{p}_{\mathrm{S}} \cdot (\boldsymbol{R} - \boldsymbol{R}_0)$, with $\boldsymbol{R}$ the spatial coordinate on the interface. The time the Cooper pair needs to enter the condensate is $\tau_\varepsilon^{(\mathrm{S})} = \xi_\varepsilon^{(\mathrm{S})}/v_f^{(\mathrm{S})}$, which also determines the time delay between the maximum of an incoming electron wave packet and the maximum of the retroreflected hole wave packet, $\tau_\varepsilon^{(\mathrm{S})} = \hbar\partial_\varepsilon\varphi(\varepsilon) = \hbar/\sqrt{|\Delta|^2 - \varepsilon^2}$ [88].

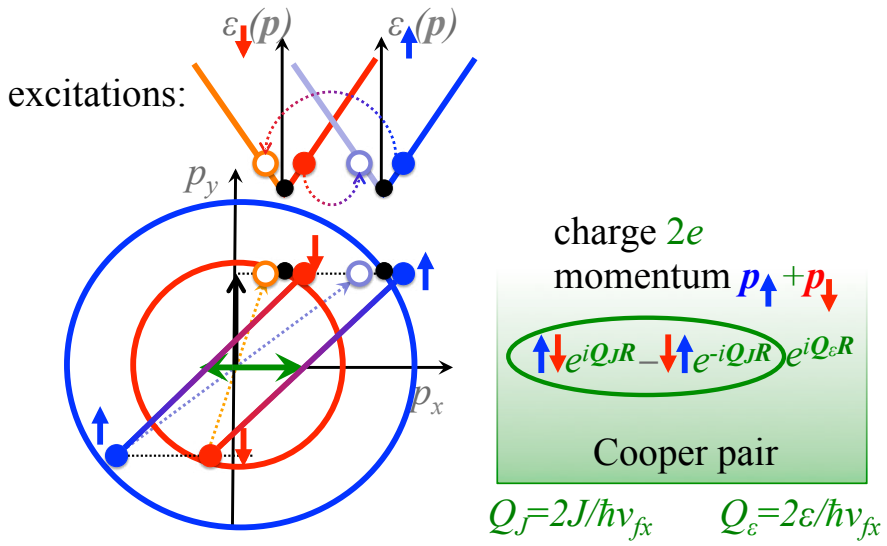


Figure 30.4: Andreev reflection in a ferromagnet: an electron with energy ε and spin $\uparrow$ pairs with an electron with energy $-\varepsilon$ and spin $\downarrow$, resulting into a total momentum of $\hbar(\boldsymbol{Q}_\varepsilon \pm \boldsymbol{Q}_J)$. For sufficiently small spin band splitting a Cooper pair of the form shown to the right results, which contains singlet and triplet components with amplitudes $\cos(Q_J x)$ and $i\sin(Q_J x)$, respectively. The Cooper pair enters the condensate in the superconductor, transferring its momentum partially to the interface and partially to the singlet condensate, ensuring current conservation. The triplet component decays on the superconducting coherence length scale into the superconductor.

effect in diffusive metals. The two phenomena, proximity effect and Andreev reflection are intertwined and cannot be discussed separately from each other. The above discussion assumes that the phase coherence is not weakened by additional effects. If phase coherence is weakened by inelastic processes, as for example magnetic scattering, this puts limitations on the proximity effect. In this case, one has to replace ε by $\bar{\varepsilon} = \varepsilon + i\alpha_s$ with the spin-flip scattering rate $\alpha_s = \hbar/\tau_s$, where τ_s is the corresponding life time. This means that in the ballistic limit exponential decay of pair correlations sets in on the length scale $\hbar v_f/2\alpha_s = v_f\tau_s/2$ (the factor 2 takes into account that both particles and holes are affected). The corresponding coherence lengths are obtained by replacing $\pi k_B T$ by $\pi k_B T + \alpha_s$.

A similar mechanism works for a weakly ferromagnetic normal metal, as for example a ferromagnetic alloy (see Figure 30.4) [90]. In this case, the electronic bands are spin-split due to the exchange interaction by an amount of $\pm J \ll E_f$. The Andreev reflection mechanism now requires that the x-component of the momentum of the incoming electron with spin $\uparrow$ is $p_{1x} = p_{fx} + (\varepsilon + J)/v_{fx}$, which pairs with an electron with momentum $p_{2x} = -p_{fx} + (\varepsilon + J)/v_{fx}$. This leads to a Cooper pair momentum of $2(\varepsilon + J)/v_{fx}$. On the contrary, if the incoming electron has spin $\downarrow$, it pairs with a spin $\uparrow$ electron, and the sign of J reverses in the above expressions, leading to a center of mass momentum of $2(\varepsilon - J)/v_{fx}$. Denoting $Q_J = 2J/\hbar v_{fx}$ and $Q_\varepsilon = 2\varepsilon/\hbar v_{fx}$, we see that instead of a singlet Cooper pair $(\uparrow\downarrow - \downarrow\uparrow)e^{iQ_\varepsilon x}$ as in the case of a non-magnetic normal metal, a Cooper pair of the form

$$(\uparrow\downarrow e^{iQ_J x} - \downarrow\uparrow e^{-iQ_J x})e^{iQ_\varepsilon x} \tag{30.3}$$

is created. This is exactly the FFLO type of pair, as it was considered in the original work. Only it is now induced as a proximity amplitude instead of a bulk phase. It can be decomposed into a spin singlet $(\uparrow\downarrow - \downarrow\uparrow) \equiv |S = 0, S_z = 0\rangle$ and a spin triplet $(\uparrow\downarrow + \downarrow\uparrow) \equiv |S = 1, S_z = 0\rangle$

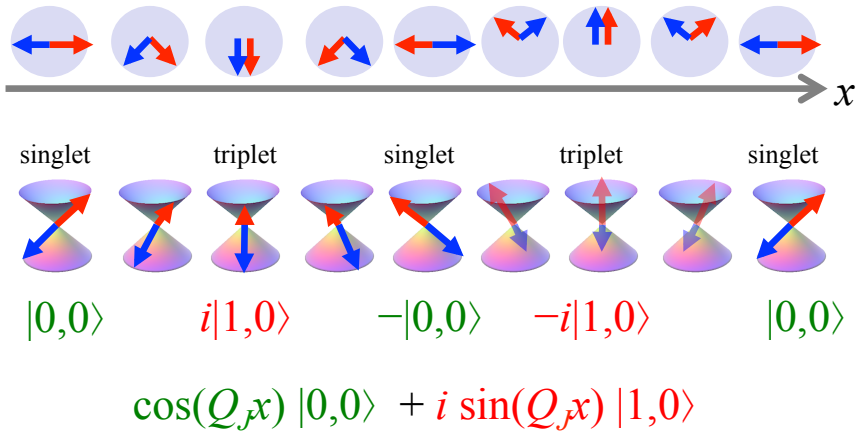


Figure 30.5: Singlet-triplet mixtures between $|S=0, S_z=0\rangle$ and $|S=1, S_z=0\rangle$ spin angular momentum states in an exchange field (or in an applied external magnetic field) in z-direction. Singlet and triplet spin states oscillate spatially out of phase relative to each other. Within the spin-vector representation the relative azimuthal angle between the two spin vectors within a pair varies as $\pi + 2Q_J x$, and its deviation from 0 (triplet) and π (singlet) is a measure for the degree of singlet-triplet mixing. The top row shows a top-view of the bottom row.

(where S is the total spin of the pair and S_z its projection on the z-axis), leading to (see figure 30.5)

$$[\cos(Q_J x)|0,0\rangle + i\sin(Q_J x)|1,0\rangle]\, e^{iQ_\varepsilon x}. \tag{30.4}$$

The proximity amplitudes in the ferromagnet are such mixtures. The triplet component also penetrates over a coherence length into the singlet superconductor, thus leading to singlet-triplet mixing in the superconductor close to the interface. The excess momentum during the Andreev reflection process is transferred partially to the interface and partially to the condensate (with the rate determined by the continuity equation for total charge conservation).

In the diffusive limit the wave vector is given by $Q_\pm = (i+1)\sqrt{(\varepsilon \pm J)/\hbar D}$ (where a small positive imaginary part of ε determines the root), i.e. the pair amplitudes oscillate and decay on the same length scale.

30.1.7 Josephson effect

If two superconducting materials are brought in contact via a sufficiently narrow non-superconducting region (or via a weak link), the macroscopic wave functions of the two superconductors may overlap. Under the condition that a phase difference exists between the superconductors, a supercurrent may flow between them directly through the non-superconducting region even under zero applied voltage. This effect was discovered by Josephson in 1962 [91, 92] and first observed by Anderson and Rowell in 1963 [93]. The Josephson effect is a hallmark of macroscopic quantum coherence, proving the macroscopic character of the pair wave function as originally predicted by Ginzburg and Landau [9]. Originally, the effect described the zero resistance tunneling of Cooper pairs between two superconductors through an insulating barrier, an SIS junction. The Josephson current from superconductor 2 to superconductor 1 (i.e.

electrons are flowing from 1 to 2), I, is given by the set of Josephson relations

$$I = F(\Delta\chi), \quad F(\Delta\chi + 2\pi) = F(\Delta\chi), \tag{30.5a}$$

$$\Delta\chi = \chi_2 - \chi_1 - \frac{q^*}{\hbar}\int_1^2 \boldsymbol{A}\cdot d\boldsymbol{r}, \tag{30.5b}$$

$$\frac{\partial\Delta\chi}{\partial t} = -\frac{q^*}{\hbar}(\Phi_2 - \Phi_1) \tag{30.5c}$$

where $q^* = 2e = -2|e|$, χ_1 and χ_2 are the phases of the superconducting condensate wave function on either side of the contact, $\boldsymbol{A}$ is the electromagnetic vector potential, and $q^*\Phi$ is the pair electrochemical potential ($\Phi_2 - \Phi_1 = V$ is the voltage across the junction). The function F describes the current-phase relation. The critical Josephson currents in positive and negative flow directions are defined via

$$I_{c+} = \max_{\Delta\chi} F(\Delta\chi), \qquad I_{c-} = -\min_{\Delta\chi} F(\Delta\chi). \tag{30.6}$$

For non-magnetic barriers in the *tunneling limit*, $I_{c+} = I_{c-} = I_c$ and $I = I_c\sin(\Delta\chi)$, where I_c is positive. The relations (30.5a)-(30.5c) are invariant against gauge transformations $\boldsymbol{A}' = \boldsymbol{A} + \nabla\zeta$, $\Phi' = \Phi - \partial_t\zeta$, $\chi' = \chi + \frac{q^*}{\hbar}\zeta$. The function $F(\Delta\chi)$ may not be single valued, for example for the case of a weak link multiple solutions can exist, and a hysteresis when sweeping $\Delta\chi$ may appear. If a flux Φ penetrates the junction, a characteristic Fraunhofer pattern appears when I_c is plotted vs. the flux. A multitude of interesting effects and devices based on the Josephson relations exist, and the reader is referred to review articles, e.g. [94, 95, 96, 97, 98].

Here we are mainly concerned with the dc Josephson effect for the case when the non-superconducting material is an extended region of normal metal or metallic ferromagnet. With the help of the proximity effect via Andreev reflections, the Josephson effect can also occur in such devices. The current passing through the normal region is carried by the Andreev states, which build bound states below the superconducting gaps within the normal conducting region. The number and distribution of the bound states depend on details such as interface transmission, mean free path, and length of the normal metal. In general, there is a characteristic energy, the Thouless energy [99], given by $\hbar v_f/L$ for the clean limit, and by $\hbar D/L^2$ for the diffusive limit. In normal metals coupled to conventional superconductors, there will be a low-energy gap in the spectrum of Andreev states, which for long junctions approximately scales with the Thouless energy and the transmission probabilities between the superconductors and the normal metal (possibly further reduced by inelastic scattering processes). This is the so-called minigap, found first by McMillan [100]. This minigap can be probed by scanning tunneling microscopy [101, 102]. When a supercurrent flows across the junction, or when an external magnetic field is applied, the minigap is reduced and eventually closes.

In the ballistic limit, each Andreev bound state with energy $E_{\text{b.s.}}$ disperses as function of phase difference $\Delta\chi$, and the current is given by $(q^*/\hbar)\partial E_{\text{b.s.}}/\partial\Delta\chi$. Apart from the current carried by the Andreev bound states, there is also a contribution from continuum states above the gap.

The current-phase relation $F(\Delta\chi)$ is in general strongly dependent on the details of the Josephson junction. Sinusoidal behavior is only observed under special circumstances, like for example in the tunneling limit. The critical Josephson current depends strongly on the length of the junction. For more details I refer the reader to the above mentioned review articles.

30.2 Symmetry classification of Cooper pairs in superconductors

30.2.1 Consequences of Pauli principle and Fermi statistics

Due to the Fermi statistics the pair correlation function, or the Gor'kov "anomalous Green function" [10], fulfills fundamental symmetries following from fermionic anti-commutation re-

lations of the field operators. For fermions, the definition of the anomalous Green function [92, 104] in Matsubara representation [89] is given by

$$\begin{aligned} -F^{\mathrm{M}}_{\alpha\beta}(\mathbf{r}_1,\mathbf{r}_2;\tau) &= \langle \mathbf{T}_\tau \left\{ \Psi_\alpha(\mathbf{r}_1,-i\tau)\Psi_\beta(\mathbf{r}_2,0)\right\}\rangle \\ &\equiv \theta(\tau)\langle \Psi_\alpha(\mathbf{r}_1,-i\tau)\Psi_\beta(\mathbf{r}_2,0)\rangle - \theta(-\tau)\langle \Psi_\beta(\mathbf{r}_2,0)\Psi_\alpha(\mathbf{r}_1,-i\tau)\rangle \end{aligned} \tag{30.7}$$

where the θ-function is defined as $\theta(\tau)=1$ for $\tau\geq 0$ and 0 for $\tau<0$, and where $|\tau|<|\hbar/k_{\mathrm{B}}T|$. The function F^{M} fulfills the fundamental identity

$$F^{\mathrm{M}}_{\alpha\beta}(\mathbf{r}_1,\mathbf{r}_2;\tau) \;=\; -F^{\mathrm{M}}_{\beta\alpha}(\mathbf{r}_2,\mathbf{r}_1;-\tau). \tag{30.8}$$

which expresses the fermionic nature of the constituents of a pair. Going over to relative and center of mass coordinates, $\mathbf{r}=\mathbf{r}_1-\mathbf{r}_2$, $\mathbf{R}=(\mathbf{r}_1+\mathbf{r}_2)/2$, the corresponding relation reads

$$F^{\mathrm{M}}_{\alpha\beta}(\mathbf{r},\tau;\mathbf{R}) \;=\; -F^{\mathrm{M}}_{\beta\alpha}(-\mathbf{r},-\tau;\mathbf{R}), \tag{30.9}$$

or after Fourier transformation in the relative coordinates $\mathbf{r}\to\mathbf{p}$, $\tau\to z$,

$$F^{\mathrm{M}}_{\alpha\beta}(\mathbf{p},z;\mathbf{R}) \;=\; -F^{\mathrm{M}}_{\beta\alpha}(-\mathbf{p},-z;\mathbf{R}). \tag{30.10}$$

Kubo-Martin-Schwinger (KMS) boundary conditions [105, 106] allow for anti-periodicity in τ with period $\hbar/k_{\mathrm{B}}T$: $F^{\mathrm{M}}_{\alpha\beta}(\mathbf{r},\tau-i\hbar/k_{\mathrm{B}}T;\mathbf{R})=-F^{\mathrm{M}}_{\alpha\beta}(\mathbf{r},\tau;\mathbf{R})$. This leads to discrete Matsubara energies $z=\varepsilon_n=(2n+1)\pi k_{\mathrm{B}}T$,

$$F^{\mathrm{M}}_{\alpha\beta}(\mathbf{p},\varepsilon_n;\mathbf{R}) \;=\; -F^{\mathrm{M}}_{\beta\alpha}(-\mathbf{p},-\varepsilon_n;\mathbf{R}). \tag{30.11}$$

We consider now spin-singlet (spin-antisymmetric) and spin-triplet (spin-symmetric) components:

$$F^{\mathrm{M}}_{s/t} = \frac{1}{2}\left(F^{\mathrm{M}}_{\alpha\beta} \mp F^{\mathrm{M}}_{\beta\alpha}\right) \tag{30.12}$$

(suppressing the spin indices hereafter), which fulfill

$$F^{\mathrm{M}}_{s}(\mathbf{p},\varepsilon_n;\mathbf{R}) \;=\; F^{\mathrm{M}}_{s}(-\mathbf{p},-\varepsilon_n;\mathbf{R}) \tag{30.13a}$$

$$F^{\mathrm{M}}_{t}(\mathbf{p},\varepsilon_n;\mathbf{R}) \;=\; -F^{\mathrm{M}}_{t}(-\mathbf{p},-\varepsilon_n;\mathbf{R}). \tag{30.13b}$$

Each of these we can classify according to parity. We define even-parity and odd-parity functions

$$F^{\mathrm{M}}_{\pm}(\varepsilon_n;\mathbf{R}) \;=\; \frac{1}{2}\left(F^{\mathrm{M}}(\mathbf{p},\varepsilon_n;\mathbf{R}) \pm F^{\mathrm{M}}(-\mathbf{p},\varepsilon_n;\mathbf{R})\right) \tag{30.14}$$

(we suppress the momentum argument hereafter) and find

$$F^{\mathrm{M}}_{s+}(\varepsilon_n;\mathbf{R}) \;=\; F^{\mathrm{M}}_{s+}(-\varepsilon_n;\mathbf{R}) \tag{30.15a}$$

$$F^{\mathrm{M}}_{s-}(\varepsilon_n;\mathbf{R}) \;=\; -F^{\mathrm{M}}_{s-}(-\varepsilon_n;\mathbf{R}) \tag{30.15b}$$

$$F^{\mathrm{M}}_{t+}(\varepsilon_n;\mathbf{R}) \;=\; -F^{\mathrm{M}}_{t+}(-\varepsilon_n;\mathbf{R}) \tag{30.15c}$$

$$F^{\mathrm{M}}_{t-}(\varepsilon_n;\mathbf{R}) \;=\; F^{\mathrm{M}}_{t-}(-\varepsilon_n;\mathbf{R}). \tag{30.15d}$$

Thus, $F^{\mathrm{M}}_{s+}(\varepsilon_n;\mathbf{R})$ and $F^{\mathrm{M}}_{t-}(\varepsilon_n;\mathbf{R})$ are even in Matsubara frequency, whereas $F^{\mathrm{M}}_{s-}(\varepsilon_n;\mathbf{R})$ and $F^{\mathrm{M}}_{t+}(\varepsilon_n;\mathbf{R})$ are odd.

After it was realized that in diffusive heterostructures with ferromagnets the type $F^{\mathrm{M}}_{t+}(\varepsilon_n;\mathbf{R})$ appears, which is according to the above a so-called odd-frequency pair amplitude (for a review see [73]), a systematic classification according to symmetry of pairing correlations was undertaken along the lines explained above. Pair amplitudes are classified into four types according

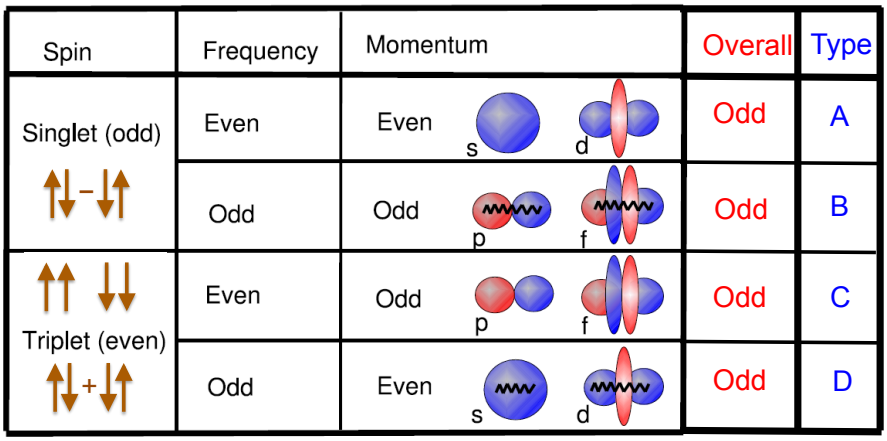


Figure 30.6: Symmetry classification of Cooper pairs in inhomogeneous systems. The wavy lines symbolize odd-frequency symmetry of the pair amplitude. After [107, 133].

to their behavior with respect to frequency, momentum (parity), and spin (see Fig. 30.6) [107]:

Type A:	spin singlet, even frequency, even parity
Type B:	spin singlet, odd frequency, odd parity
Type C:	spin triplet, even frequency, odd parity
Type D:	spin triplet, odd frequency, even parity.

An identical classification scheme was independently proposed in Refs. [108, 109]. The four symmetry states above exhaust all possibilities compatible with Fermi statistics and the Pauli exclusion principle.[43] The usual spin singlet, s-wave Bardeen-Cooper-Schrieffer (BCS) superconductor [8] is of type A, while the spin triplet, p-wave superfluid formed in ^{3}He [110, 111] is of type C. Type D was first considered by Berezinskiĭ [112] in connection with early research on superfluid ^{3}He. Finally, type B was introduced in connection with unconventional superconductors by Balatsky, Abrahams and others [116, 117, 118].

Suggestions for realization of Type B superconductivity include generalized one-dimensional $t-J$ and Hubbard models [119, 120], two-channel Kondo models and Kondo lattices [121, 122, 123, 124], and quantum critical points [125]. Realizations suggested for the Type D state include disordered two-dimensional electron fluids in semiconductors [113, 114, 115], triangular antiferromagnets [126], composite spin and orbital triplet superconductivity in two-channel Anderson lattices [127], Hund's coupled pairing in double orbital Hubbard models [128], strong-coupling triplet superconductivity in Holstein Hubbard models [129], and one-dimensional systems with strong charge fluctuations [130].

30.2.2 Odd-frequency pairing amplitudes

To date an odd-frequency superconductor has not been found in nature. However, in contrast to all cases discussed above, where the appearance of an order parameter due to spontaneous symmetry breaking (global phase symmetry in superconductors) was in the focus, in this review we are interested in the case of explicit symmetry breaking taking place locally in some spatial region, e.g. near interfaces, line defects, or inclusions. For this case an overwhelming

[43] If more discrete degrees of freedom than the ones considered here are relevant (e.g. orbital) then the classification must be extended accordingly.

number of experiments support the picture of the existence of proximity induced pairing states of type D. In its pure form (i.e. without additional components of different symmetry), it has been first predicted theoretically for a superconductor-ferromagnet proximity structure with a spiral inhomogeneous magnetization near the interface in Ref. [131]. Previous work had predicted the appearance of similar odd-frequency triplet anomalous functions in a model of coexistence of a superconducting phase and a helical ordering of localized spins, motivated by experiments on the superconductor $ErRh_4B_4$ [132].

In fact, the Pauli principle requires odd-frequency amplitudes to be present in any inhomogeneous superconducting state, not necessarily spin-polarized [107]. For example, the case of a normal metal coupled to a superconductor involves pair amplitudes of Type B. Thus, odd-frequency amplitudes appear in heterostructures naturally due to breaking of translational symmetry at interfaces (similarly as Rashba spin-orbit coupling appears at interfaces in semiconductor heterostructures). They have been present in all treatments of inhomogeneous superconductivity for a long time, however were not explicitly named as such. Similarly, pair amplitudes of Type D appear as soon as spin rotational symmetry is broken, e.g. by an external magnetic field via the Zeeman coupling. If both spin rotational symmetry and parity are broken, e.g. at an interface between a superconductor and a ferromagnet, all four types of pair amplitudes are generated at the interface [107, 133]. Similar conclusions have been reached in Refs. [108, 109]. The important issue in discussing odd-frequency amplitudes in Ref. [131] is not the presence of Type D correlations per se, but their only presence. Thus, in diffusive structures those s-wave odd-frequency triplet pair amplitudes have a definite symmetry, and thus are of special interest for fundamental research. In regions where all amplitudes are mixed, simply all symmetries are absent, and a symmetry classification is not very useful. However, once such regions are coupled to reservoirs in which symmetries are asymptotically (far away from the spatial regions where the symmetry breaking takes place) re-established, then it is useful to discuss processes at interfaces in the light of those asymptotic symmetries.

To date it remains a great challenge to find direct experimental verification of the odd-frequency symmetry. There have been a number of proposals for indirect experimental verification via tunneling density of states studies, by inducing odd-frequency triplet superconducting correlations in a normal metal [134, 135, 136].

The odd-frequency pairing aspect in superconductor ferromagnet heterostructures was reviewed in Ref. [73]. A recent review dealing with odd-frequency pairing states and their relation to topological edge states can be found in Ref. [137]. Newer developments in finding odd-frequency order parameters include odd-frequency pairing states in multi-band superconductors [138, 139], at the surface of topological insulators [140], in a controllable double-quantum dot system [141], and in two-particle Bose-Einstein condensates [142], as well as odd-frequency density wave states [143, 144].

Odd-frequency symmetry requires that the equal time pair correlator vanishes, i.e. electrons in a pair avoid each other in time. It has been argued that in such a case certain particle-hole symmetries based on a Green function approach are not appropriate and a Lagrangian formalism must be used [145, 146]. In particular, these arguments were brought forward for homogeneous odd-frequency states with an odd-frequency pair potential appearing due to spontaneous symmetry breaking. However, these arguments do not take into account that symmetries following from the full many body Hamiltonian of the system are fundamental. Should they be violated in a model Lagrangian approach, for which a corresponding model Hamiltonian cannot be found, then this simply means that the model Lagrangian is not appropriate for the problem in question [147]. It has also been pointed out that spatially homogeneous odd-frequency states might be thermodynamically unstable in reality [148].

30.3 Magnetically active interfaces

30.3.1 Scattering phase delays

Let us consider the basic quantum mechanical problem of a (quasi)-particle being reflected from an insulating region (which we assume at $x > 0$, potential V). Let us assume the particle has energy $0 < E < V$ with $E = (k^2 + k_{||}^2)/2m = V + (-\kappa^2 + k_{||}^2)/2m$, and thus $\kappa(E) = [2m(V-E) + k_{||}^2]^{1/2}$, $k(E) = [2mE - k_{||}^2]^{1/2}$. It is described by a wave function $\Psi(x, \mathbf{r}_{||}) = e^{i\mathbf{k}_{||}\mathbf{r}_{||}}(e^{ikx} + r\, e^{-ikx})$ at $x < 0$ and $\Psi(x, \mathbf{r}_{||}) = te^{i\mathbf{k}_{||}\mathbf{r}_{||}}e^{-\kappa x}$ at $x > 0$. The reflection amplitude for such a process is $r = (k - i\kappa)/(k + i\kappa) = e^{-2i\arctan(\kappa/k)}$, where k is the momentum component perpendicular to the interface and κ determines the exponential decay of the wave function in the insulating region. In the limit for large κ the phase of the reflected wave is flipped by π with respect to the incoming wave. For finite κ there is a *phase delay* with respect to this, given by $\varphi(E) = \pi - 2\arctan(\kappa/k)$. This phase delay results from the fact that the particle penetrates the insulator over a length scale $\hbar/\kappa$, and it corresponds to a *time delay* between the maximum of an incoming wave packet and the corresponding reflected wave packet [149] of $\tau_d = \hbar\partial_E\varphi(E) = 2m\hbar/(\kappa k)$ (accompanied by a Goos-Hänchen shift along the interface of $s = 2\hbar k_{||}/(\kappa k)$ [150]).

30.3.2 Spin-mixing angle and spin-dependent scattering phase shifts

We now assume that an exchange field $\boldsymbol{J}$ is present, leading to a contribution to the Hamiltonian given by $\mathcal{H}_{\text{exch}} = -\boldsymbol{J}\cdot\boldsymbol{\sigma}$. This can also be written as $\mathcal{H}_{\text{exch}} = -\mu\, \boldsymbol{B}_{\text{eff}}\cdot\boldsymbol{\sigma}$, with $\boldsymbol{B}_{\text{eff}} = \boldsymbol{J}/\mu$, and μ is the (effective) magnetic moment of the charge carriers (negative for free electrons). Let us now consider a ferromagnetic insulating region, so that the two spin directions σ have different reflection amplitudes $r_\sigma = (k - i\kappa_\sigma)/(k + i\kappa_\sigma) = e^{-2i\arctan(\kappa_\sigma/k)}$, with $\Psi_\sigma \sim e^{-\kappa_\sigma x}$ in the ferromagnetic insulating region (see Figure 30.7). As throughout this review, we take the spin quantization axis along the exchange field, i.e. $\kappa_\sigma(E) = [2m(V - E - \sigma J) + k_{||}^2]^{1/2}$, such that the majority Fermi surface is assigned spin projection $\sigma = 1$.[44] The scattering phase delays now are spin dependent, $\varphi_\sigma(E) = \pi - 2\arctan(\kappa_\sigma/k)$, and we can define a quantity $\vartheta = \varphi_\uparrow - \varphi_\downarrow$, which is called *spin-mixing angle* [151] or *spin dependent interface scattering phase shift* [152] in the literature (it is associated with a delay time $\tau_\vartheta = \hbar\partial_E\vartheta(E) = 2m\hbar/(\kappa_\uparrow k) - 2m\hbar/(\kappa_\downarrow k)$ between the two spin components). For our example we have $\kappa_\uparrow < \kappa_\downarrow$, and consequently $\vartheta > 0$, $\tau_\vartheta > 0$. Together with the spin-independent averaged phase $\varphi = (\varphi_\uparrow + \varphi_\downarrow)/2$, we write the reflection amplitude in a more general way as [151]

$$r(\varphi, \vartheta, \hat{\mathbf{n}}) = -e^{i\varphi}\cdot e^{i\frac{\vartheta}{2}\hat{\mathbf{n}}\cdot\boldsymbol{\sigma}} \tag{30.16}$$

with respect to a spin quantization axis $\hat{\mathbf{n}}$. The spin-mixing angle also describes the rotation angle of the spin components perpendicular to the axis $\hat{\mathbf{n}}$ under reflection. This can be interpreted as a precession that the spins undergo around the axis $\hat{\mathbf{n}}$ as a result of quantum mechanical penetration into the magnetic and insulating region.

If one considers the Cooper instability in the presence of an interface with a ferromagnetic insulator, it becomes clear that pairing near the interface will be affected by these spin-mixing angles. In particular, a spin-up electron with momentum pointing towards the interface will have a relative phase shift with respect to a spin-down electron with momentum pointing away from the interface if the Cooper pair volume overlaps with the interface region. As the Cooper pair's size is determined by the superconducting coherence length, Cooper pairs in a layer that extends a coherence length from the interface into the bulk will feel the spin-mixing phase

[44] For free electrons (negative magnetic moment) this quantization axis would point opposite to the effective magnetic field. For a quantization axis in field direction, spin up and down would simply switch their roles.

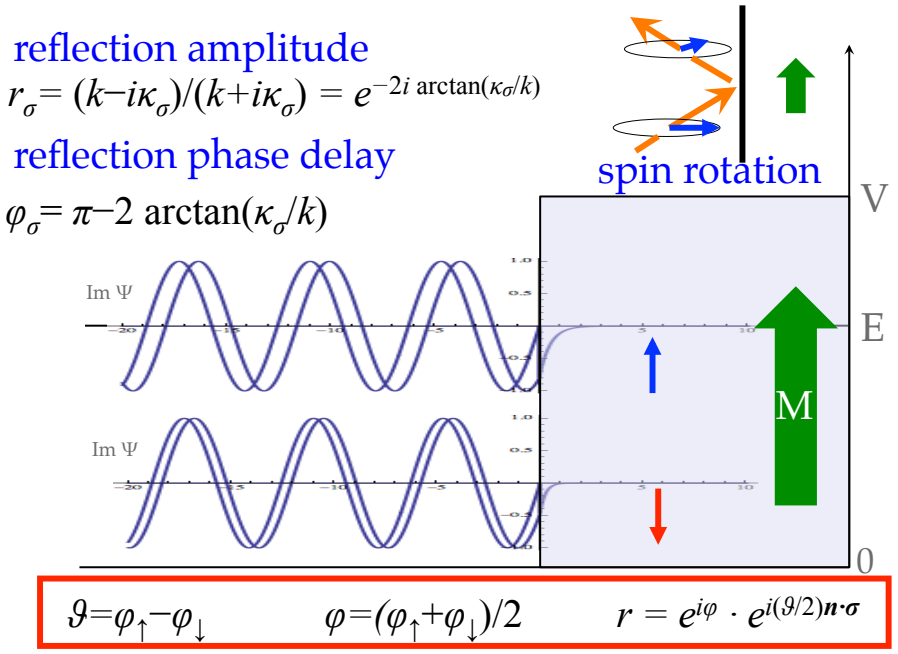


Figure 30.7: When a Bloch wave is reflected from a ferromagnetic insulator, a phase delay appears between the reflected waves and the incoming waves, which differs for both spin directions. As a result, the spin-down reflected wave is delayed with respect to the spin-up reflected wave. If the incoming wave is polarized perpendicular to the ferromagnet's magnetization, then the reflected wave has its spin rotated with respect to the spin of the incoming wave (see top part of the drawing).

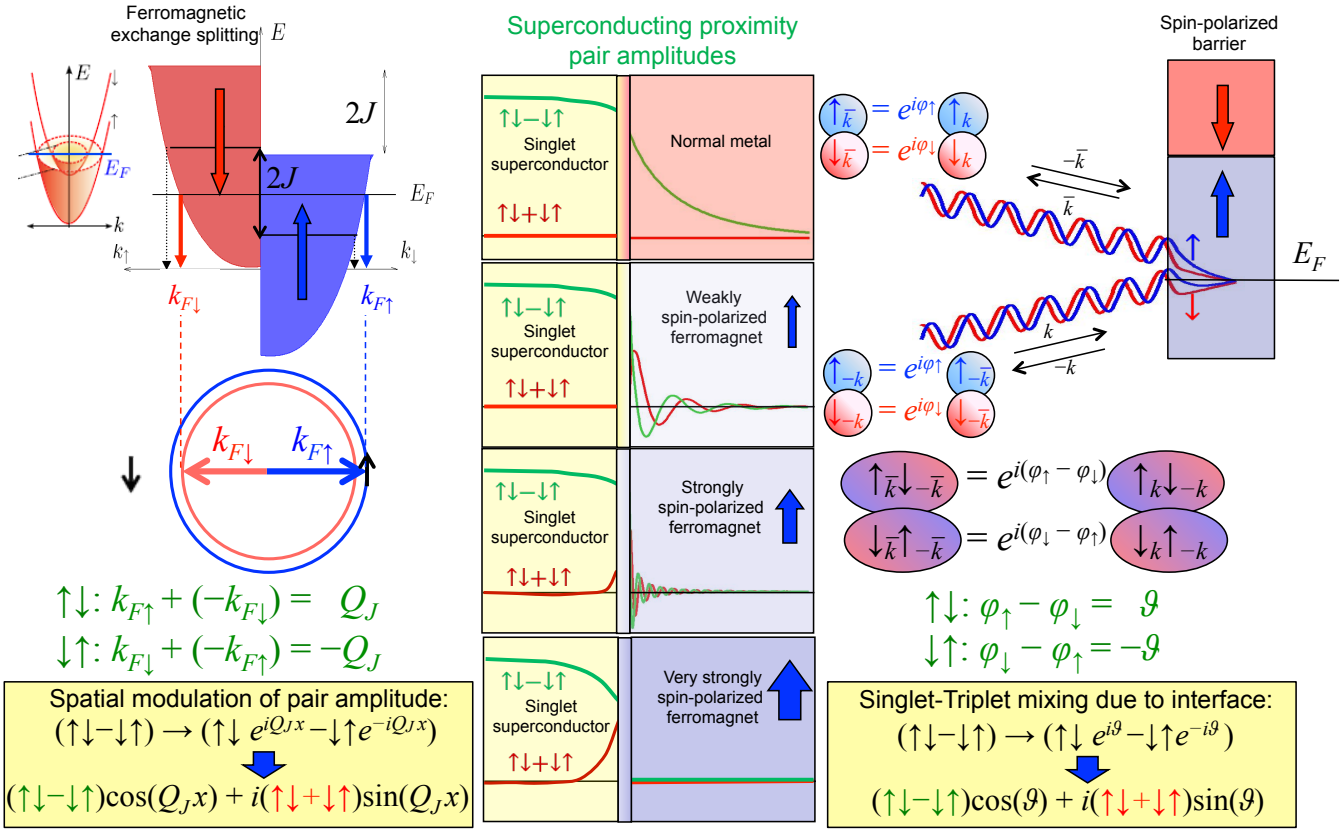


Figure 30.8: Creation mechanisms for triplet pair correlations by direct and inverse proximity effect. See text for explanation. Reproduced and modified with permission from [153]. Copyright (2011) American Institute of Physics.

shifts of the interface. This is shown in Figure 30.8 on the right. Near the interface, only a singlet-triplet mixed Cooper pair of the form

$$(\uparrow\downarrow e^{i\vartheta} - \downarrow\uparrow e^{-i\vartheta}) \equiv \cos(\vartheta)|0,0\rangle + i\sin(\vartheta)|1,0\rangle \tag{30.17}$$

can be present. According to this, we can consider the parameter ϑ also as the parameter that governs the *degree of singlet-triplet mixing* at a spin-active interface. As seen in Figure 30.8, there is a certain analogy between the creation of FFLO correlations in a ferromagnetic metal and the creation of singlet-triplet mixtures near a magnetically active interface in a superconductor. The role of the phase $Q_J x$ in the former is played by the spin-mixing angle ϑ in the latter. As demonstrated in the middle column of Figure 30.8, with increasing spin polarization of the ferromagnet in a superconductor-ferromagnet heterostructure, a shift from the creation of FFLO correlations in the ferromagnet to the creation of singlet-triplet mixtures in the superconductor takes place. This is because for very weak spin polarizations, the spin-mixing angle of the interface usually is of similarly small order and should be neglected in a consistent expansion in small parameters of the theory. For strong spin-polarization it is important and must be taken into account. The FFLO correlations in the ferromagnet show an inverse behavior: they are important for weak spin polarizations, however are restricted to atomically small distances from the interface for strongly spin polarized ferromagnets.

The presence of spin-mixing angles has many consequences. For example, it leads to Andreev bound states at the interface, as predicted theoretically [154, 155, 156, 157, 158, 159], and verified experimentally [160]. It also is responsible for giant thermoelectric effects in non-local setups [161, 162] and is the main ingredient for creating triplet supercurrents in strongly spin-polarized ferromagnets [155, 133]. It also crucially affects point contact spectra [163, 164, 158,

165, 166, 167, 168, 169]. Finally, it is the main cause of the inverse proximity effect and the magnetic proximity effect in strongly spin polarized hybrid structures [155, 133, 170, 171].

30.3.3 Scattering matrix and induced triplet correlations

The interface scattering matrix connects incoming Bloch waves with outgoing Bloch waves at an interface between two itinerant electron materials (metals, half metals, itinerant ferromagnets), or at a surface of such a material with an insulator. Relevant for transport are Bloch waves with energy close to the Fermi energy and momentum close to the Fermi momentum, in which case the Bloch waves are assumed to describe quasiparticle excitations. "Incoming" and "outgoing" refers to the projection of the quasiparticle's Fermi velocity on the surface normal. We distinguish between electron-like and hole-like quasiparticles. For electron-like quasiparticles the projection of the group velocity on the Fermi momentum is positive, for hole-like quasiparticles it is negative. This means that electron-like and hole-like quasiparticles associated with the same Fermi momentum have opposite group velocity projections on the surface normal and consequently have different scattering matrices. For atomically ordered interfaces the crystal momentum component parallel to the interface, $\boldsymbol{p}_{||}$, is conserved, and then the relation between hole (h) and electron (e) like scattering matrices is $S_{\rm h}^{\dagger}(\boldsymbol{p}_{||}) = S_{\rm e}^{*}(-\boldsymbol{p}_{||})$.

In relation to superconductivity, it is sufficient to consider the normal state scattering matrix for quasiparticles at Fermi momentum and Fermi energy. This results from a systematic classification of all terms during a perturbation expansion in the small phase space volume associated with quasiparticles, which leads to quasiclassical theory of superconductivity [188, 196]. In terms of the normal-state scattering matrix,

$$\hat{\mathbf{S}} = \begin{pmatrix} \hat{R}_1 & \hat{T}_1 \\ \hat{T}_2 & -\hat{R}_2 \end{pmatrix} \tag{30.18}$$

we can study the superconducting amplitudes induced by the presence of a singlet pair potential on either side of the interface. To simplify algebra and to gain some intuition we limit ourselves to the case of small pair amplitudes, in which case one can linearize the boundary conditions in the pair amplitudes. In our notation, $\hat{R}_1$ describes reflection into the superconductor, and $\hat{R}_2$ describes reflection into the ferromagnet. All reflection and transmission parameters in Eq. (30.18) are 2x2 spin matrices. We consider the ballistic case, for which the reflected and transmitted pair amplitudes $\hat{f}_{\rm out}^{\rm SC}$, $\hat{f}_{\rm out}^{\rm FM}$ are given in terms of the incoming singlet pair amplitude $\hat{f}_{\rm in}^{\rm SC} = f_0(i\sigma_y)$ by boundary conditions at the interface between the superconductor and the magnetic material, which in linear order read

$$\hat{f}_{\rm out}^{\rm SC} = f_0\, \hat{R}_1\, (i\hat{\sigma}_y)\, \hat{R}_1^{*} \tag{30.19}$$

$$\hat{f}_{\rm out}^{\rm FM} = f_0\, \hat{T}_2\, (i\hat{\sigma}_y)\, \hat{T}_1^{*}. \tag{30.20}$$

The simplest case is that of total reflection from an interface with a magnetic insulator. In this case we have (choosing the quantization axis appropriately, and with a scalar phase ψ)

$$\hat{R}_1 = e^{i\psi} \begin{pmatrix} e^{\frac{i}{2}\vartheta} & 0 \\ 0 & e^{-\frac{i}{2}\vartheta} \end{pmatrix}. \tag{30.21}$$

The reflected amplitudes for this case follow from Eq. (30.19) and are given by

$$\hat{f}_{\rm out}^{\rm SC} = [f_0 \cos(\vartheta) + i f_0 \sin(\vartheta)\hat{\sigma}_z]\, i\hat{\sigma}_y. \tag{30.22}$$

This justifies the expression obtained by the simple arguments leading to Eq. (30.17).

symmetry	even frequency	odd frequency
even parity	Type A, singlet$\|0,0\rangle$ $f_s^s = \frac{\pi\Omega_n\Delta\left(1-\sin^2\frac{\vartheta}{2}\right)}{\Omega_n^2-\|\Delta\|^2\sin^2\frac{\vartheta}{2}}$	Type D, triplet$\|1,0\rangle$ $f_{t_0}^s = \frac{i\pi\varepsilon_n\Delta\,\frac{1}{2}\sin\vartheta}{\Omega_n^2-\|\Delta\|^2\sin^2\frac{\vartheta}{2}}$
odd parity	Type C, triplet$\|1,0\rangle$ $f_{t_0}^a = \frac{-i\pi\Omega_n s_\mu\Delta\,\frac{1}{2}\sin\vartheta}{\Omega_n^2-\|\Delta\|^2\sin^2\frac{\vartheta}{2}}$	Type B, singlet$\|0,0\rangle$ $f_s^a = \frac{\pi\varepsilon_n s_\mu\Delta\sin^2\frac{\vartheta}{2}}{\Omega_n^2-\|\Delta\|^2\sin^2\frac{\vartheta}{2}}$

Table 2: Symmetry components of the interface amplitudes inside a ballistic superconductor in contact with a ferromagnetic insulator, assuming a constant singlet order parameter Δ. Here, $\Omega_n = \sqrt{|\Delta|^2+\varepsilon_n^2}$, $\vartheta \equiv \vartheta(\mu)$, and $s_\mu = \mathrm{sign}(\mu)$ (μ is the cosine of the impact angle). From Supplementary Material of Ref. [133].

Next, we consider the case of arbitrarily large pair amplitudes in a ballistic superconductor with spatially constant pair potential. This is justified for sufficiently small spin-mixing angles ϑ. Incoming and reflected directions are parameterized by the polar angle $\theta_{\hat{\boldsymbol{p}}_f}$, measured from the surface normal. The cosine of this angle is called μ. Defining even parity (symmetric) and odd parity (antisymmetric) functions with respect to the propagation direction, $f^a = [f(\mu)-f(-\mu)]/2$ and $f^s = [f(\mu)+f(-\mu)]/2$, we obtain all four possible symmetry components as summarized in Table 2. It can be seen that the corrections to the singlet amplitudes are $\sim \sin^2(\vartheta/2)$. Thus, to linear order in ϑ the pair potential stays unaffected. With increasing ϑ the singlet pair potential is reduced, leading to corrections to the expressions in Table 2.

For the case of an interface with a strongly spin-polarized ferromagnet, one has to consider Fermi surface geometry, due to the presence of different Fermi surfaces for the two spin projections in the ferromagnet. Various cases can occur, depending on the scattering channel (parameterized in the ballistic case by $\boldsymbol{p}_{||}$, see figure 30.9): for example for reflection from the interface on the superconducting side, there can occur total reflection from the ferromagnet, total reflection of only one spin component from the ferromagnet (so-called half-metallic channels), or partial reflection for both spin components. Depending on the geometry of the Fermi surface in the superconductor, one, two, or all three cases may occur.

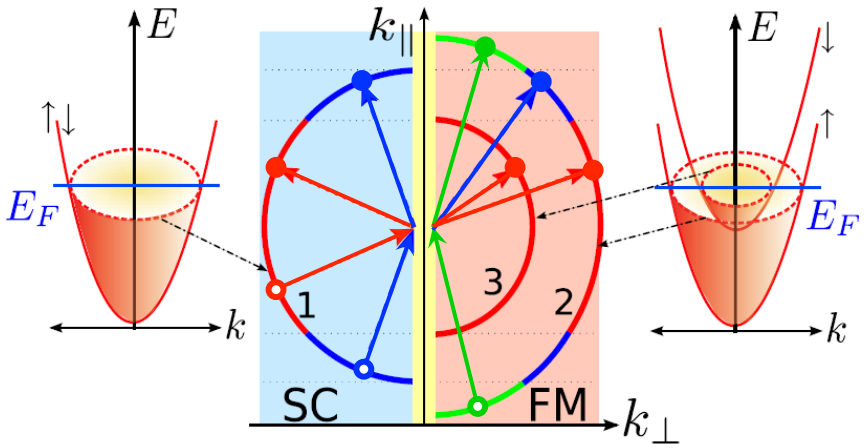


Figure 30.9: Fermi surface geometry for a superconductor (left)-ferromagnet (right) interface. Various types of scattering events include total reflection (green), involvement of only one (blue) or of both spin bands (red). After [172], Copyright (2009) by the American Physical Society.

For illustrative purposes we will consider a simple model of an interface potential of width d

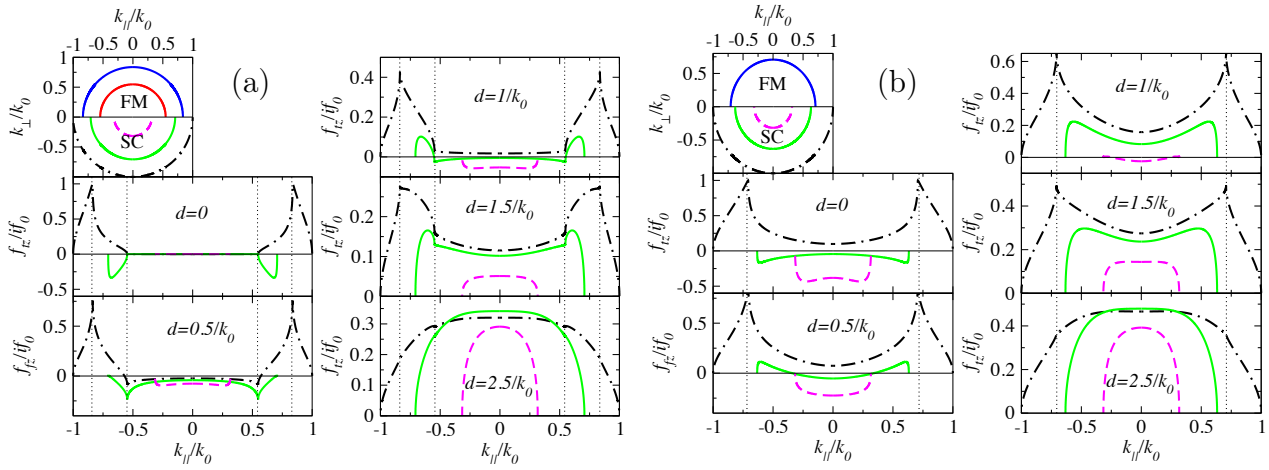


Figure 30.10: Induced triplet components at a superconductor-ferromagnet interface with an interface barrier of width d. Model free-electron dispersions are: $V_{\rm S}+\boldsymbol{k}^2/2m$ (superconductor), $V_{\rm I}-\sigma J+\boldsymbol{k}^2/2m$ (barrier), $V_{\rm FM}-\sigma J+\boldsymbol{k}^2/2m$ (ferromagnet). The singlet amplitude in the superconductor is f_0, the induced triplet component is f_{tz} (and f_{tz}/f_0 is purely imaginary). The Fermi wavevectors for the spin bands in the ferromagnet are fixed in (a) and (b). The various curves correspond to various Fermi wavevectors in the superconductor (as illustrated in the top left diagram in each panel). Wavevectors are normalized to $k_0=\sqrt{2mE_F}$. For (a) $V_{\rm I}=1.3$, $V_{\rm FM}=0.5$, $J=0.2$, $V_{\rm S}=0$ (black dashed-dotted), 0.5 (green full line), 0.9 (magenta dashed); for (b) $V_{\rm I}=1.4$, $V_{\rm FM}=0.8$, $J=0.3$, $V_{\rm S}=0$ (black dashed-dotted), 0.6 (green full line), 0.9 (magenta dashed); energies are in units of the Fermi energy E_F. (b) corresponds to a half-metallic ferromagnet, with only one spin projection itinerant (i.e. a Fermi surface exists only for $\sigma=1$).

between a superconductor and a ferromagnet, with corresponding (free) electronic dispersions $V_{\rm S}+\boldsymbol{k}^2/2m$ in the superconductor, $V_{\rm I}-\sigma J+\boldsymbol{k}^2/2m$ in the interface region, and $V_{\rm FM}-\sigma J+\boldsymbol{k}^2/2m$ in the ferromagnet. If the magnetization in the interface region is collinear with that in the ferromagnet, there will be no transmitted pair amplitudes, as for a strongly spin-polarized ferromagnet only $\uparrow\uparrow$ and $\downarrow\downarrow$ pairs are supported, which both are not generated in such a system. There is, however, an induced triplet component on the superconducting side, with spin projection zero on the spin quantization axis. It is shown in Figure 30.10, for the case of a strongly spin polarized ferromagnet in (a), and for the case of a half-metallic ferromagnet (with only spin projection $\sigma=1$ itinerant) in (b). When the barrier is absent, there is no induced triplet component for the regions connecting wave vectors that support Bloch waves for both spin projections. Only wave vectors for which maximally one spin projection in the ferromagnet supports Bloch waves contribute to the induced triplet amplitudes in the superconductor. This shows that for high-transmission contacts half-metallic ferromagnets are most effective for including triplet correlations in the superconductor. If a spin-polarized barrier is present, triplet amplitudes are created also in the barrier region, and their sign depends on the relative size of the Fermi surfaces in the superconductor and in the ferromagnet. In the tunneling limit, the creation of triplet correlations happens mainly in the barrier region, such that they become insensitive to the Fermi surface geometry.

In order to allow for proximity induced triplet amplitudes in the ferromagnet, one needs an inhomogeneous non-collinear magnetization in the interface region. We study a simple model where the interface barrier is magnetized in direction perpendicular to the magnetization in the ferromagnet. We again assume a spin quantization axis in direction of the exchange field in the ferromagnet, which we take as the z-axis, and a barrier exchange field pointing along the x-axis in spin space. In Figure 30.11 we show for two values of barrier thickness all triplet amplitudes

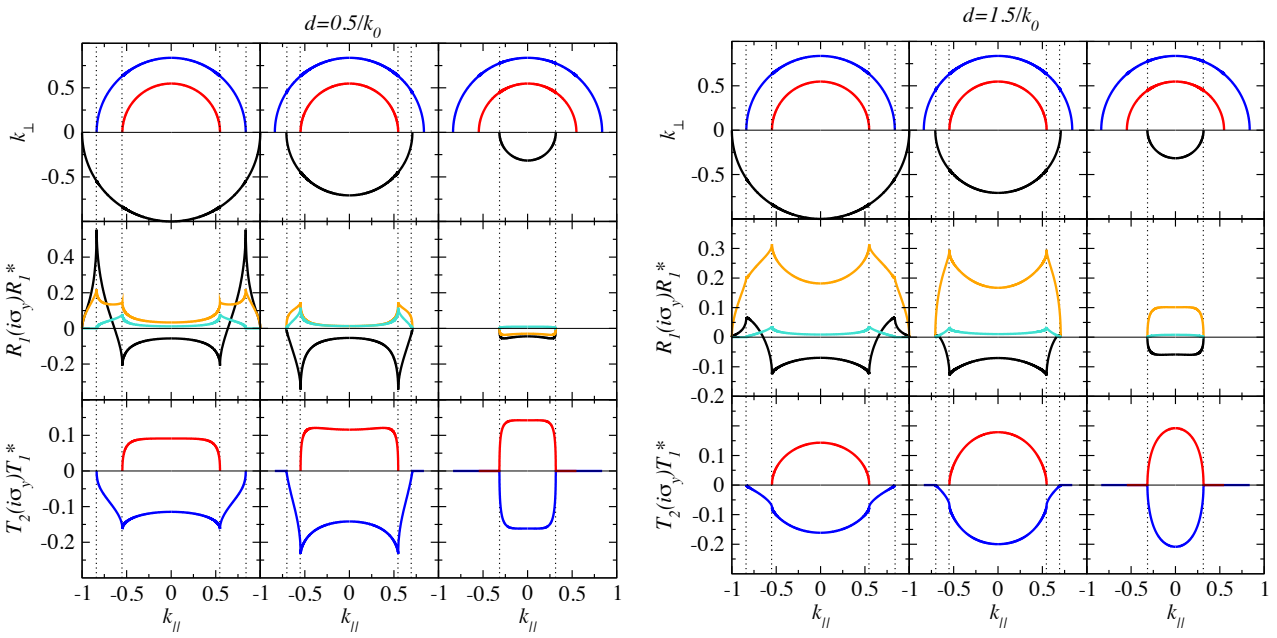


Figure 30.11: Induced triplet components at a superconductor-ferromagnet interface with an interface barrier of width d, spin polarized in x-direction, perpendicular to the ferromagnet's spin polarization in z-direction. Other parameters are as in Fig. 30.10 (a), with $V_{\rm S} = 0, 0.5E_F, 0.9E_F$ for each thickness d. The components shown are: in the superconductor $f^{\rm SC}_{tz}/(if_0) = f^{\rm SC}_{\frac{1}{2}(\uparrow\downarrow+\downarrow\uparrow)}/(if_0)$ (black); $f^{\rm SC}_{tx}/(if_0) = f^{\rm SC}_{\frac{1}{2}(-\uparrow\uparrow+\downarrow\downarrow)}/(if_0)$ (orange); $f^{\rm SC}_{ty}/f_0 = f^{\rm SC}_{\frac{1}{2i}(\uparrow\uparrow+\downarrow\downarrow)}/f_0$ (turquoise); in the ferromagnet $f^{\rm FM}_{\uparrow\uparrow}/(if_0)$ (blue); $f^{\rm FM}_{\downarrow\downarrow}/(if_0)$ (red).

generated in the superconductor and in the ferromagnet. For each value of barrier thickness we show three representative Fermi surface geometries. In the ferromagnet the spin bands support only triplet amplitudes of the form $f^{\rm FM}_{\uparrow\uparrow}$ and $f^{\rm FM}_{\downarrow\downarrow}$, whereas in the superconductor we show all three triplet amplitudes $f^{\rm SC}_{tz} = f^{\rm SC}_{\frac{1}{2}(\uparrow\downarrow+\downarrow\uparrow)}$, $f^{\rm SC}_{tx} = f^{\rm SC}_{\frac{1}{2}(-\uparrow\uparrow+\downarrow\downarrow)}$, and $f^{\rm SC}_{ty} = f^{\rm SC}_{\frac{1}{2i}(\uparrow\uparrow+\downarrow\downarrow)}$.

It is interesting to note that for intermediate barrier thicknesses, also a component $f^{\rm SC}_{ty}$ is generated, although the magnetization always lies in the $x-z$ plane. This is due to the fact that spins polarized in z-direction, precessing around the x-direction, develop a y-component (and similarly for spins polarized in x-direction and precessing around the z-direction). In a real gauge of the singlet pair potential, $f^{\rm SC}_{tz}$ and $f^{\rm SC}_{tx}$ are purely imaginary, and $f^{\rm SC}_{ty}$ is purely real. As a consequence, only the former two contribute to the magnetization in the superconductor.

Furthermore, depending on the barrier thickness, the vector of the triplet amplitudes in the superconductor changes direction rapidly as function of impact angle with respect to the surface normal. Only for tunneling barriers the direction of the triplet vector is dominated by the barrier exchange field.

The equal-spin triplet amplitudes generated in the ferromagnet have opposite sign for the two spin projections. This reflects the fact that a triplet component with zero spin projection along the exchange field in the barrier region (x-direction) decomposes into equal-spin pairs with respect to the z-direction with equal magnitude and opposite sign: $(\uparrow\downarrow + \downarrow\uparrow)_x = (-\uparrow\uparrow + \downarrow\downarrow)_z$. Whereas in the tunneling limit the largest contributions to triplet amplitudes arise from near-normal impact, for thin barriers the dominating contributions arise from wavevectors that have for at least one spin projection evanescent solutions in the ferromagnet.

For a general orientation of the interface barrier exchange field we parameterize its direction by polar and azimuthal angles, α and φ,[45] respectively, measured from the z-axis in spin space.

[45] In the following the scalar scattering phase φ will not appear anymore in this review, such that no confusion

	microscopic model	**quasiclassical**
wave function methods:	Bogoliubov-de Gennes equations	Andreev equations
Green function methods:	Gor'kov equations	Eilenberger-Larkin-Ovchinnikov equations

Table 3: Theories for inhomogeneous superconductivity can be classified into four types, as shown in this table.

The well-known transformation formulas for basis vectors quantized along the direction α, φ in terms of basis vectors quantized along the z-axis read

$$\uparrow_{\alpha,\varphi} = \cos\frac{\alpha}{2}e^{-i\frac{\varphi}{2}}\uparrow_z + \sin\frac{\alpha}{2}e^{i\frac{\varphi}{2}}\downarrow_z \tag{30.23a}$$

$$\downarrow_{\alpha,\varphi} = -\sin\frac{\alpha}{2}e^{-i\frac{\varphi}{2}}\uparrow_z + \cos\frac{\alpha}{2}e^{i\frac{\varphi}{2}}\downarrow_z \tag{30.23b}$$

and can be used to find the transformation for pair amplitudes, for example

$$(\uparrow\downarrow - \downarrow\uparrow)_{\alpha,\varphi} = (\uparrow\downarrow - \downarrow\uparrow)_z \tag{30.24a}$$

$$(\uparrow\downarrow + \downarrow\uparrow)_{\alpha,\varphi} = -\sin\alpha\left[e^{-i\varphi}(\uparrow\uparrow)_z - e^{i\varphi}(\downarrow\downarrow)_z\right] + \cos\alpha(\uparrow\downarrow + \downarrow\uparrow)_z. \tag{30.24b}$$

It can be seen from this that if a triplet component of the form (30.24b) is created in the barrier region, it gives rise to $f_{\uparrow\uparrow}^{\mathrm{FM}}$ and $f_{\downarrow\downarrow}^{\mathrm{FM}}$ correlations in the ferromagnet with relative phase of $\pi + 2\varphi$. This leads to a non-trivial current-phase relation in Josephson devices, in which two singlet superconductors are connected by the two spin bands of the ferromagnet, each with their own separate current-phase relation [172]. The azimuthal angle φ plays a crucial role in such devices [107, 133, 173].

For the case of a long-wavelength magnetic inhomogeneity one has to deal with the spatial variation of the pair amplitudes, which can be done within the framework of quantum transport equations, which we discuss in the next section. In general, the scattering matrix should be calculated from first principles or from microscopic models, taking into account disorder, band anisotropy, and micromagnetics.

30.4 Theoretical tools

Theoretical treatments of superconductor-ferromagnet heterostructures can be separated into two types: microscopic treatments and quasiclassical treatments. There are two main methods, which both can be applied to the two types of theories: wave-function methods and Green function methods. Green function methods are based on an asymptotic expansion of the fundamental many-body Hamiltonian, whereas wave function methods work preferably with an effective mean-field Hamiltonian. Green function methods allow in an easier way for the treatment of disorder, and for generalization to strong coupling with bosonic excitations and to non-equilibrium situations. The resulting four theoretical frameworks with their corresponding equations of motion are shown in table 3. The Bogoliubov-de Gennes equations [78, 9] lead in quasiclassical approximation to the Andreev equations for the envelopes of the waves [83]. Alternatively, one can start from the microscopic Nambu-Gor'kov matrix Green functions obeying the Gor'kov equations [10, 174]. These lead in quasiclassical approximation to the

with the azimuthal angle φ should arise.

Eilenberger-Larkin-Ovchinnikov equations [175, 176], where the concepts of BCS pairing theory of superconductors [8] were merged with the concepts of Boltzmann transport equations within Landau's Fermi-liquid theory [177]. An extension to non-equilibrium was developed by Eliashberg [178] and by Larkin and Ovchinnikov [179]. In quasiclassical approximation the Gor'kov equations result into envelope Green functions that vary on the superconducting coherence length scale and are free of irrelevant fine-scale structures on the Fermi wavelength scale. Dynamical phenomena are described in Green function methods within the Keldysh technique [180].

In this review we concentrate on two, which have been mostly used so far in the literature: microscopic wave function methods based on the Bogoliubov-de Gennes equations, and quasiclassical Green function methods, based on Eilenberger-Larkin-Ovchinnikov equations and their counterpart for diffusive systems, the Usadel equations. The two other frameworks, not covered in this review, are formulated in terms of Andreev equations and in terms of Gor'kov equations.

30.4.1 Bogoliubov-de Gennes equations

The Hartree-Fock-Bogoliubov (HFB) mean-field Hamiltonian

$$\mathcal{H}_{\rm HFB} = \int\int d^3\mathbf{r}d^3\mathbf{r}' \sum_{\sigma\sigma'\in\{\uparrow,\downarrow\}} \Big(H_{\mathbf{r}\sigma,\mathbf{r}'\sigma'}\, \psi^\dagger_{\mathbf{r}\sigma}\psi_{\mathbf{r}'\sigma'} + \frac{1}{2}\Delta_{\mathbf{r}\sigma,\mathbf{r}'\sigma'}\psi^\dagger_{\mathbf{r}\sigma}\psi^\dagger_{\mathbf{r}'\sigma'} + \frac{1}{2}\Delta^*_{\mathbf{r}\sigma,\mathbf{r}'\sigma'}\psi_{\mathbf{r}'\sigma'}\psi_{\mathbf{r}\sigma}\Big) \tag{30.25}$$

is the basis for the Bogoliubov-de Gennes theory. Hermiticity requires $H_{\mathbf{r}\sigma,\mathbf{r}'\sigma'} = H^*_{\mathbf{r}'\sigma',\mathbf{r}\sigma}$, and Fermi statistics leads to $\Delta_{\mathbf{r}\sigma,\mathbf{r}'\sigma'} = -\Delta_{\mathbf{r}'\sigma',\mathbf{r}\sigma}$. The Hamiltonian can be rewritten in a compact form using the 4×4 matrix

$$\hat{H}(\mathbf{r},\mathbf{r}') \equiv \begin{pmatrix} [H_{\mathbf{r}\sigma,\mathbf{r}'\sigma'}]_{2\times2} & [\Delta_{\mathbf{r}\sigma,\mathbf{r}'\sigma'}]_{2\times2} \\ -[\Delta^*_{\mathbf{r}\sigma,\mathbf{r}'\sigma'}]_{2\times2} & -[H^*_{\mathbf{r}\sigma,\mathbf{r}'\sigma'}]_{2\times2} \end{pmatrix} \tag{30.26}$$

where, for example,

$$[H_{\mathbf{r}\sigma,\mathbf{r}'\sigma'}]_{2\times2} = \begin{pmatrix} H_{\mathbf{r}\uparrow,\mathbf{r}'\uparrow} & H_{\mathbf{r}\uparrow,\mathbf{r}'\downarrow} \\ H_{\mathbf{r}\downarrow,\mathbf{r}'\uparrow} & H_{\mathbf{r}\downarrow,\mathbf{r}'\downarrow} \end{pmatrix}. \tag{30.27}$$

With the definitions $\hat{\Psi}^\dagger(\mathbf{r}) = (\psi^\dagger_{\mathbf{r}\uparrow}, \psi^\dagger_{\mathbf{r}\downarrow}, \psi_{\mathbf{r}\uparrow}, \psi_{\mathbf{r}\downarrow})$, $\hat{\Psi}(\mathbf{r}) = (\psi_{\mathbf{r}\uparrow}, \psi_{\mathbf{r}\downarrow}, \psi^\dagger_{\mathbf{r}\uparrow}, \psi^\dagger_{\mathbf{r}\downarrow})^{\rm T}$ (here T denotes a transpose) the Hartree-Fock-Bogoliubov Hamiltonian reads

$$\mathcal{H}_{\rm HFB} = \frac{1}{2}\int\int d^3\mathbf{r}d^3\mathbf{r}' \left(\hat{\Psi}^\dagger(\mathbf{r})\, \hat{H}(\mathbf{r},\mathbf{r}')\, \hat{\Psi}(\mathbf{r}')\right) + \text{const.} \tag{30.28}$$

This Hamiltonian is diagonalized by a Bogoliubov-Valatin transformation [181, 182]. To achieve this, we introduce the notation for the Bogoliubov amplitudes ($\alpha \in \{+,-\}$)

$$U_{n\alpha}(\mathbf{r}) \equiv \begin{pmatrix} u_{\mathbf{r}\uparrow,n\alpha} \\ u_{\mathbf{r}\downarrow,n\alpha} \\ v_{\mathbf{r}\uparrow,n\alpha} \\ v_{\mathbf{r}\downarrow,n\alpha} \end{pmatrix}, \quad \bar{U}_{n\alpha}(\mathbf{r}) \equiv \begin{pmatrix} v^*_{\mathbf{r}\uparrow,n\alpha} \\ v^*_{\mathbf{r}\downarrow,n\alpha} \\ u^*_{\mathbf{r}\uparrow,n\alpha} \\ u^*_{\mathbf{r}\downarrow,n\alpha} \end{pmatrix}. \tag{30.29}$$

Here, the index α may, e.g., refer to another spin basis, or to a helicity basis if strong spin-orbit interactions are present. The quantum numbers n, α fully characterize the eigenstates of the

set of Bogoliubov-de Gennes equations given by

$$\int d^3\mathbf{r}'\hat{H}(\mathbf{r},\mathbf{r}')U_{n\alpha}(\mathbf{r}') = E_{n\alpha}U_{n\alpha}(\mathbf{r}) \tag{30.30a}$$

$$\int d^3\mathbf{r}'\hat{H}(\mathbf{r},\mathbf{r}')\bar{U}_{n\alpha}(\mathbf{r}') = -E_{n\alpha}\bar{U}_{n\alpha}(\mathbf{r}). \tag{30.30b}$$

For each eigenvalue $E_{n\alpha} > 0$ there exists an eigenvalue $-E_{n\alpha}$, with corresponding eigenvectors obtained by the substitution $u_{\mathbf{r}\sigma,n\alpha} \to v^*_{\mathbf{r}\sigma,n\alpha}$, $v_{\mathbf{r}\sigma,n\alpha} \to u^*_{\mathbf{r}\sigma,n\alpha}$. One can divide the quantum numbers n in disjunct sets $\mathcal{Z}$, $\mathcal{P}$ and $\mathcal{N}$ (and relabel them if necessary) such that for $n \in \mathcal{Z}$ we have $E_{n\alpha} = 0$, for $n \in \mathcal{P}$ we have $E_{n\alpha} > 0$ and for $n \in \mathcal{N}$ we have $E_{n\alpha} < 0$. The eigenvectors can be chosen to build an orthonormal set, e.g. for n, n' within $\mathcal{P}$

$$\int d^3\mathbf{r}\sum_\sigma \left(u_{\mathbf{r}\sigma,n\alpha}u^*_{\mathbf{r}\sigma,n'\alpha'} + v_{\mathbf{r}\sigma,n\alpha}v^*_{\mathbf{r}\sigma,n'\alpha'}\right) = \delta_{nn'}\delta_{\alpha\alpha'}, \tag{30.31a}$$

$$\int d^3\mathbf{r}\sum_\sigma \left(u_{\mathbf{r}\sigma,n\alpha}v_{\mathbf{r}\sigma,n'\alpha'} + v_{\mathbf{r}\sigma,n\alpha}u_{\mathbf{r}\sigma,n'\alpha'}\right) = 0. \tag{30.31b}$$

We build for $n \in \mathcal{P}$ a 4×4 matrix $\hat{U}_n(\mathbf{r})$ from the four orthogonal eigenvectors $U_{n+}(\mathbf{r}), U_{n-}(\mathbf{r}), \bar{U}_{n+}(\mathbf{r}), \bar{U}_{n-}(\mathbf{r})$ (or a 4×2 matrix if only one value for α belongs to n). Similarly, for $n \in \mathcal{Z}$ we build a 4×2 matrix $U_{n+}(\mathbf{r}), U_{n-}(\mathbf{r})$ (or a 4×1 matrix if only one value for α belongs to n). Then the completeness relation

$$\sum_{n\in\bar{\mathcal{P}}} \hat{U}_n(\mathbf{r})\hat{U}^\dagger_n(\mathbf{r}') = \delta(\mathbf{r}-\mathbf{r}')\hat{1} \tag{30.32}$$

(with the 4×4 unit matrix $\hat{1}$, and with $\bar{\mathcal{P}} = \mathcal{Z} \cup \mathcal{P}$) holds, which reads explicitly

$$\sum_{n\in\bar{\mathcal{P}},\alpha} \left(u_{\mathbf{r}\sigma,n\alpha}u^*_{\mathbf{r}'\sigma',n\alpha} + s_n v^*_{\mathbf{r}\sigma,n\alpha}v_{\mathbf{r}'\sigma',n\alpha}\right) = \delta_{\sigma\sigma'}\delta(\mathbf{r}-\mathbf{r}') \tag{30.33a}$$

$$\sum_{n\in\bar{\mathcal{P}},\alpha} \left(u_{\mathbf{r}\sigma,n\alpha}v^*_{\mathbf{r}'\sigma',n\alpha} + s_n v^*_{\mathbf{r}\sigma,n\alpha}u_{\mathbf{r}'\sigma',n\alpha}\right) = 0 \tag{30.33b}$$

($s_n = 0$ for $n \in \mathcal{Z}$, $s_n = 1$ else). With this, the Hartree-Fock-Bogoliubov Hamiltonian is diagonalized by

$$\hat{\Psi}(\mathbf{r}) = \sum_{n\in\bar{\mathcal{P}}} \hat{U}_n(\mathbf{r})\hat{\gamma}_n, \quad \hat{\gamma}_n = \int d^3\mathbf{r}\; \hat{U}^\dagger_n(\mathbf{r})\hat{\Psi}(\mathbf{r}), \tag{30.34}$$

with, e.g., $\hat{\gamma}^\dagger_n = (\gamma^\dagger_{n+}, \gamma^\dagger_{n-}, \gamma_{n+}, \gamma_{n-})$, $\hat{\gamma}_n = (\gamma_{n+}, \gamma_{n-}, \gamma^\dagger_{n+}, \gamma^\dagger_{n-})^{\mathrm{T}}$ denoting Bogoliubov quasiparticle operators and $\hat{E}_n \equiv \mathrm{diag}(E_{n+}, E_{n-}, -E_{n+}, -E_{n-})$ corresponding energies, leading to

$$\hat{H}(\mathbf{r},\mathbf{r}') = \sum_{n\in\mathcal{P}} \hat{U}_n(\mathbf{r})\hat{E}_n\hat{U}^\dagger_n(\mathbf{r}') \tag{30.35}$$

$$\mathcal{H}_{\mathrm{HFB}} = \frac{1}{2}\sum_{n\in\mathcal{P}} \hat{\gamma}^\dagger_n\hat{E}_n\hat{\gamma}_n. \tag{30.36}$$

Explicitly, Eq. (30.34) reads

$$\psi_{\mathbf{r}\sigma} = \sum_{n\in\bar{\mathcal{P}},\alpha} \left(u_{\mathbf{r}\sigma,n\alpha}\gamma_{n\alpha} + s_n v^*_{\mathbf{r}\sigma,n\alpha}\gamma^\dagger_{n\alpha}\right) \tag{30.37a}$$

$$\gamma_{n\alpha} = \int d^3\mathbf{r}\sum_\sigma \left(u^*_{\mathbf{r}\sigma,n\alpha}\psi_{\mathbf{r}\sigma} + v^*_{\mathbf{r}\sigma,n\alpha}\psi^\dagger_{\mathbf{r}\sigma}\right). \tag{30.37b}$$

The Majorana property $\gamma_{n\alpha} = \gamma_{n\alpha}^\dagger$ holds if $v_{\mathbf{r}\sigma,n\alpha} = u_{\mathbf{r}\sigma,n\alpha}^*$; for $n \in \mathcal{Z}$ a solution of the Bogoliubov-de Gennes equations can always be chosen of this form provided this is compatible with the boundary conditions. The single-particle part $H^0_{\mathbf{r}\sigma,\mathbf{r}'\sigma'}$ of $H_{\mathbf{r}\sigma,\mathbf{r}'\sigma'}$ has typically the form

$$H^0_{\mathbf{r}\sigma,\mathbf{r}'\sigma'} = \delta(\mathbf{r}-\mathbf{r}')\left\{\varepsilon(\hat{\mathbf{P}}) - \mu + \mathbf{g}(\hat{\mathbf{P}})\cdot\boldsymbol{\sigma} - \mathbf{h}(\mathbf{r})\cdot\boldsymbol{\sigma}\right\}_{\sigma\sigma'} \tag{30.38}$$

with $\hat{\mathbf{P}} = -i\hbar\nabla_{\mathbf{r}} - e\mathbf{A}(\mathbf{r})$. Here, $\varepsilon(\hat{\mathbf{P}})$ is even in $\hat{\mathbf{P}}$ and $\mathbf{g}(\hat{\mathbf{P}})$ is odd in $\hat{\mathbf{P}}$. The last two terms in Eq. (30.38) describe spin-orbit coupling and Zeeman coupling, and μ is the electrochemical potential. The order parameter is given self-consistently by

$$\Delta_{\mathbf{r}\sigma,\mathbf{r}'\sigma'} = \int\int d^3\mathbf{r}_1 d^3\mathbf{r}_1' \sum_{\sigma_1\sigma_1'} V_{\sigma\sigma'\sigma_1\sigma_1'}(\mathbf{r},\mathbf{r}',\mathbf{r}_1,\mathbf{r}_1')\langle\psi_{\mathbf{r}_1'\sigma_1'}\psi_{\mathbf{r}_1\sigma_1}\rangle. \tag{30.39}$$

with

$$\langle\psi_{\mathbf{r}'\sigma'}\psi_{\mathbf{r}\sigma}\rangle = -\frac{1}{2}\sum_{n\in\mathcal{P},\alpha}\left\{u_{\mathbf{r}\sigma,n\alpha}v^*_{\mathbf{r}'\sigma',n\alpha} - v^*_{\mathbf{r}\sigma,n\alpha}u_{\mathbf{r}'\sigma',n\alpha}\right\}\tanh\frac{E_{n\alpha}}{2k_{\mathrm{B}}T}. \tag{30.40}$$

The spin-dependence of these equations simplifies when the pairing interaction can be split into singlet and triplet parts,

$$V_{\sigma\sigma'\sigma_1\sigma_1'} = \frac{1}{2}(i\sigma_2)_{\sigma\sigma'}V^s(i\sigma_2)^*_{\sigma_1\sigma_1'} + \frac{1}{2}(\boldsymbol{\sigma}i\sigma_y)_{\sigma\sigma'}\cdot\overleftrightarrow{V}^t\cdot(\boldsymbol{\sigma}i\sigma_y)^*_{\sigma_1\sigma_1'}, \tag{30.41}$$

and similarly for the order parameter,

$$\Delta_{\mathbf{r}\sigma,\mathbf{r}'\sigma'} = \Delta^s_{\mathbf{r},\mathbf{r}'}(i\sigma_2)_{\sigma\sigma'} + \boldsymbol{\Delta}^t_{\mathbf{r},\mathbf{r}'}\cdot(\boldsymbol{\sigma}i\sigma_y)_{\sigma\sigma'}. \tag{30.42}$$

The gap equation for spin singlet and triplet ferromagnetic superconductors has been scrutinized by Powell, Annett, and Györffy [183].

In order to study odd-frequency amplitudes one uses a Heisenberg representation

$$\psi_{\mathbf{r}\sigma}(t) = \sum_{n\in\bar{\mathcal{P}},\alpha}\left(u_{\mathbf{r}\sigma,n\alpha}e^{\frac{i}{\hbar}E_{n\alpha}t}\gamma_{n\alpha} + s_n v^*_{\mathbf{r}\sigma,n\alpha}e^{-\frac{i}{\hbar}E_{n\alpha}t}\gamma^\dagger_{n\alpha}\right) \tag{30.43}$$

and evaluates the pair correlation function [184]

$$F_{\mathbf{r}\sigma,\mathbf{r}'\sigma'}(t) = \langle\psi_{\mathbf{r}\sigma}(t)\psi_{\mathbf{r}'\sigma'}(0)\rangle \tag{30.44}$$

using $\langle\gamma^\dagger_{n\alpha}\gamma_{n\alpha}\rangle = f(E_{n\alpha})$, $\langle\gamma_{n\alpha}\gamma^\dagger_{n\alpha}\rangle = 1 - f(E_{n\alpha})$, with $f(E_{n\alpha}) = [1-\tanh(E_{n\alpha}/2k_{\mathrm{B}}T)]/2$ the fermionic distribution function. Concentrating on local correlation functions, one obtains [184, 185]

$$F_{\mp}(\mathbf{r},t) \equiv F_{\mathbf{r}\uparrow,\mathbf{r}\downarrow}(t) \mp F_{\mathbf{r}\downarrow,\mathbf{r}\uparrow}(t) = \sum_{n\in\mathcal{P},\alpha}\left(u_{\mathbf{r}\uparrow,n\alpha}v^*_{\mathbf{r}\downarrow,n\alpha} \mp u_{\mathbf{r}\downarrow,n\alpha}v^*_{\mathbf{r}\uparrow,n\alpha}\right)\zeta^{\mp}_{n\alpha}(t,T) \tag{30.45a}$$

$$F_{\sigma\sigma}(\mathbf{r},t) \equiv F_{\mathbf{r}\sigma,\mathbf{r}\sigma}(t) = \sum_{n\in\mathcal{P},\alpha}u_{\mathbf{r}\sigma,n\alpha}v^*_{\mathbf{r}\sigma,n\alpha}\zeta^{+}_{n\alpha}(t,T) \tag{30.45b}$$

for the singlet (F_-) and the three triplet ($F_+, F_{\uparrow\uparrow}, F_{\downarrow\downarrow}$) components, where

$$\zeta^-_{n\alpha}(t,T) \equiv \cos\left(\frac{E_{n\alpha}t}{\hbar}\right)\tanh\left(\frac{E_{n\alpha}}{2k_{\mathrm{B}}T}\right) - i\sin\left(\frac{E_{n\alpha}t}{\hbar}\right), \tag{30.46a}$$

$$\zeta^+_{n\alpha}(t,T) \equiv \cos\left(\frac{E_{n\alpha}t}{\hbar}\right) - 1 - i\sin\left(\frac{E_{n\alpha}t}{\hbar}\right)\tanh\left(\frac{E_{n\alpha}}{2k_{\mathrm{B}}T}\right). \tag{30.46b}$$

The triplet correlations show a time dependence according to $\zeta^{+}_{n\alpha}$ and consequently vanish identically for $t = 0$, whereas the singlet correlations, governed by $\zeta^{-}_{n\alpha}$, survive. This expresses the odd-frequency nature of the local triplet pair correlations in contrast to the even-frequency nature of the local singlet pair correlations. In particular, for $t \to -i\tau$ with $\hbar/k_{\rm B}T > \tau \geq 0$, and applying KMS boundary conditions $\zeta^{\mp}_{n\alpha}(-i\tau + i\hbar/k_{\rm B}T, T) = -\zeta^{\mp}_{n\alpha}(-i\tau, T)$, the relations $\zeta^{\mp}_{n\alpha}(i\tau, T) = \pm\zeta^{\mp}_{n\alpha}(-i\tau, T)$ follow.

Similarly, measurable quantities like magnetization, current density, and charge density can be expressed in terms of Bogoliubov quasiparticle operators using Eq. (30.37a) and evaluated using the solutions of the Bogoliubov-de Gennes equations.

30.4.2 Quasiclassical theory of superconductivity

The treatment of a superconductor in the presence of a Zeeman spin-splitting induced by an external magnetic field has been theoretically investigated in detail by Alexander, Orlando, Rainer, and Tedrow in 1985 [186] within quasiclassical theory of superconductivity. This theory, a generalization of previous studies for superfluid ^{3}He [187, 110, 188], includes Fermi liquid effects self-consistently, as well as impurity scattering (including ballistic and diffusive limits), internal exchange fields, and spin-orbit effects[46]. It is formulated in terms of generalized Landau parameters $A^{s,a}(\hat{\boldsymbol{p}}_f, \hat{\boldsymbol{p}}'_f)$ as well as singlet and triplet pairing interactions $V^{s,t}(\hat{\boldsymbol{p}}_f, \hat{\boldsymbol{p}}'_f)$, based on Leggett's treatment for clean systems [187, 110], and combines previous theories of Fulde [189] and Buchholtz and Zwicknagl [190]. First experimental tests of these theories were performed by Tedrow and Meservey [191]. Generalized Landau parameters lead for example to anisotropic renormalizations of the quasiparticle magnetic moment by coupling to electrons outside the phase space regions where quasiparticles live ("high-energy electrons").

For reviews of quasiclassical theory of superconductivity see Refs. [192, 193, 188, 194, 195, 196, 197, 198, 199, 200, 201]. Quasiclassical theory is an expansion in quantities like temperature or gap divided by Fermi energy, or Fermi wavelength divided by superconducting coherence length [188, 202, 203, 204, 205]. It predicts its own breakdown in low dimensions [206].

The central quantity in quasiclassical theory of superconductivity is the quasiclassical 4×4 matrix propagator or Green function $\hat{g}(\hat{\boldsymbol{p}}_f, \boldsymbol{R}; \varepsilon)$, which depends on the spatial coordinate $\boldsymbol{R}$, on energy ε, and on the momentum directions $\hat{\boldsymbol{p}}_f$ on the Fermi surface (out of equilibrium there is in addition a time dependence and the formalism can be extended to 8×8 Keldysh matrices [180]). The 2×2 Nambu-Gor'kov matrix structure of $\hat{g}$ reflects the particle-hole degree of freedom [10, 174]. Its matrix elements are 2×2 spin matrices (if the spin-splitting of the energy bands is not comparable to the energy band width, otherwise they are scalar). We will use a notation of unit matrices and Pauli matrices in spin space and particle hole space, where $(\sigma_0, \sigma_1, \sigma_2, \sigma_3)$ refers to spin and $(\hat{\tau}_0, \hat{\tau}_1, \hat{\tau}_2, \hat{\tau}_3)$ to particle-hole degrees of freedom. We expand the elements in Nambu-Gor'kov space into spin-scalars and spin-vectors,

$$\hat{g} = \begin{pmatrix} g\sigma_0 + \boldsymbol{g}\cdot\boldsymbol{\sigma} & (f\sigma_0 + \boldsymbol{f}\cdot\boldsymbol{\sigma})i\sigma_2 \\ i\sigma_2(\tilde{f}\sigma_0 - \tilde{\boldsymbol{f}}\cdot\boldsymbol{\sigma}) & \sigma_2(\tilde{g}\sigma_0 - \tilde{\boldsymbol{g}}\cdot\boldsymbol{\sigma})\sigma_2 \end{pmatrix}. \tag{30.47}$$

with e.g. $\boldsymbol{g} = (g_x, g_y, g_z)$ the vector part of $\hat{g}_{11}$, and g its scalar part. Of particular interest for this review are $\boldsymbol{f}$, $\tilde{\boldsymbol{f}}$, describing spin-triplet correlations, and $\boldsymbol{g}$, $\tilde{\boldsymbol{g}}$ describing the spin magnetization and the spin current that develop as a result of the generation of triplet correlations.

[46] The derivation in this work is more rigorous than in the later work by Demler *et al.* in 1997 [90].

30.4.3 Eilenberger equations

We discuss first the case when the spin splitting of the energy bands is small (comparable to the superconducting energy scales), so that it can be treated as a perturbation around the un-split Fermi surface. In this case one can integrate out the energy dependence of the Green's functions identically for the spins $\uparrow$ and $\downarrow$ [164] and assume spin-independent Fermi velocities $\boldsymbol{v}_f(\hat{\boldsymbol{p}}_f)$. The propagator $\hat{g}$ obeys the Eilenberger transport equation [175, 176]

$$\Big[\varepsilon\hat{\tau}_3 - \hat{h},\, \hat{g}\Big] + i\hbar\, \boldsymbol{v}_f \cdot \nabla_{\boldsymbol{R}}\, \hat{g} = \hat{0} \tag{30.48}$$

with the normalization condition [175]

$$\hat{g}^2 = -\pi^2 \hat{\tau}_0, \tag{30.49}$$

where $\boldsymbol{v}_f(\hat{\boldsymbol{p}}_f)$ is the Fermi velocity for the direction $\hat{\boldsymbol{p}}_f$ at the Fermi surface, and with

$$\hat{h} = \hat{v}_{\rm ext} + \hat{\sigma}_{\rm mf} + \hat{\sigma}_{\rm imp} \tag{30.50}$$

where $\hat{v}_{\rm ext}$ are external potentials, $\hat{\sigma}_{\rm mf}$ are Fermi liquid mean fields (both diagonal and off-diagonal), and $\hat{\sigma}_{\rm imp}$ is the impurity self energy. The matrix $\hat{h}(\hat{\boldsymbol{p}}_f, \boldsymbol{R}; \varepsilon)$ entering the Eilenberger equation (30.48) has a similar structure as $\hat{g}$,

$$\hat{h} = \begin{pmatrix} \nu\sigma_0 + \boldsymbol{\nu}\cdot\boldsymbol{\sigma} & (\Delta\sigma_0 + \boldsymbol{\Delta}\cdot\boldsymbol{\sigma})i\sigma_2 \\ i\sigma_2(\tilde{\Delta}\sigma_0 - \tilde{\boldsymbol{\Delta}}\cdot\boldsymbol{\sigma}) & \sigma_2(\tilde{\nu}\sigma_0 - \tilde{\boldsymbol{\nu}}\cdot\boldsymbol{\sigma})\sigma_2 \end{pmatrix} \tag{30.51}$$

The Nambu-Gor'kov matrix structure contains some redundancy, which results into symmetries between the particle and hole elements [188]. They are expressed by the tilde operation $\tilde{q}(\hat{\boldsymbol{p}}_f, \boldsymbol{R}; \varepsilon) = q(-\hat{\boldsymbol{p}}_f, \boldsymbol{R}; -\varepsilon^*)^*$ for $q \in \{g, f, \boldsymbol{g}, \boldsymbol{f}, \nu, \Delta, \boldsymbol{\nu}, \boldsymbol{\Delta}\}$. Matsubara propagators are obtained by $(\varepsilon \to i\varepsilon_n)$ (where $\varepsilon_n = \pi k_{\rm B} T(2n+1)$ is the Matsubara energy), retarded propagators by $(\varepsilon \to \varepsilon + i\delta)$, and advanced propagators by $(\varepsilon \to \varepsilon - i\delta)$. Further fundamental symmetry relations are: $g(\varepsilon^*) = g(\varepsilon)^*$, $\boldsymbol{g}(\varepsilon^*) = \boldsymbol{g}(\varepsilon)^*$, $f(\varepsilon^*) = \tilde{f}(\varepsilon)^*$, $\boldsymbol{f}(\varepsilon^*) = -\tilde{\boldsymbol{f}}(\varepsilon)^*$ (we omitted here for brevity the other arguments).

The self-consistency equations for the impurity self energy $\hat{\sigma}_{\rm imp}$ for impurity types i with impurity potential $\hat{v}_i$ and impurity concentration n_i is

$$\hat{\sigma}_{\rm imp}(\hat{\boldsymbol{p}}_f, \boldsymbol{R}; \varepsilon) = \sum_i n_i \hat{t}_i(\hat{\boldsymbol{p}}_f, \hat{\boldsymbol{p}}_f, \boldsymbol{R}; \varepsilon) \tag{30.52}$$

with the quasiclassical T-matrix equation

$$\begin{aligned} \hat{t}_i(\hat{\boldsymbol{p}}_f, \hat{\boldsymbol{p}}'_f, \boldsymbol{R}; \varepsilon) &= \hat{v}_i(\hat{\boldsymbol{p}}_f, \hat{\boldsymbol{p}}'_f) + \\ &+ \langle N_f(\hat{\boldsymbol{p}}''_f)\hat{v}_i(\hat{\boldsymbol{p}}_f, \hat{\boldsymbol{p}}''_f)\hat{g}(\hat{\boldsymbol{p}}''_f, \boldsymbol{R}; \varepsilon)\hat{t}_i(\hat{\boldsymbol{p}}''_f, \hat{\boldsymbol{p}}'_f, \boldsymbol{R}; \varepsilon)\rangle_{\hat{\boldsymbol{p}}''_f} \end{aligned} \tag{30.53}$$

$\langle \dots \rangle_{\hat{\boldsymbol{p}}_f} = \int d^2\hat{\boldsymbol{p}}_f/(2\pi\hbar)^2 \dots$ denotes a Fermi-surface integral, and $N_f(\hat{\boldsymbol{p}}_f) = (2\pi\hbar|\boldsymbol{v}_f|)^{-1}$ is for a fixed Fermi surface point the (one-dimensional) density of states in perpendicular direction to the Fermi surface, per spin projection, in the normal state.

The Fermi-liquid mean-field self energies $\hat{\sigma}_{\rm mf}$ are self-consistently determined from

$$\nu_{\rm mf}(\hat{\boldsymbol{p}}_f, \boldsymbol{R}) = k_{\rm B}T \sum_{\varepsilon_n} \big\langle N_f(\hat{\boldsymbol{p}}'_f) W^s(\hat{\boldsymbol{p}}_f, \hat{\boldsymbol{p}}'_f) g(\hat{\boldsymbol{p}}'_f, \boldsymbol{R}; \varepsilon_n)\big\rangle_{\hat{\boldsymbol{p}}'_f} \tag{30.54a}$$

$$\boldsymbol{\nu}_{\rm mf}(\hat{\boldsymbol{p}}_f, \boldsymbol{R}) = k_{\rm B}T \sum_{\varepsilon_n} \big\langle N_f(\hat{\boldsymbol{p}}'_f)\, \overleftrightarrow{W}^a\, (\hat{\boldsymbol{p}}_f, \hat{\boldsymbol{p}}'_f)\boldsymbol{g}(\hat{\boldsymbol{p}}'_f, \boldsymbol{R}; \varepsilon_n)\big\rangle_{\hat{\boldsymbol{p}}'_f} \tag{30.54b}$$

$$\Delta_{\rm mf}(\hat{\boldsymbol{p}}_f, \boldsymbol{R}) = k_{\rm B}T \sum_{\varepsilon_n} \big\langle N_f(\hat{\boldsymbol{p}}'_f) V^s(\hat{\boldsymbol{p}}_f, \hat{\boldsymbol{p}}'_f) f(\hat{\boldsymbol{p}}'_f, \boldsymbol{R}; \varepsilon_n)\big\rangle_{\hat{\boldsymbol{p}}'_f} \tag{30.54c}$$

$$\boldsymbol{\Delta}_{\rm mf}(\hat{\boldsymbol{p}}_f, \boldsymbol{R}) = k_{\rm B}T \sum_{\varepsilon_n} \big\langle N_f(\hat{\boldsymbol{p}}'_f)\, \overleftrightarrow{V}^t\, (\hat{\boldsymbol{p}}_f, \hat{\boldsymbol{p}}'_f)\boldsymbol{f}(\hat{\boldsymbol{p}}'_f, \boldsymbol{R}; \varepsilon_n)\big\rangle_{\hat{\boldsymbol{p}}'_f}. \tag{30.54d}$$

Fermi-liquid interactions are parameterized by dimensionless Fermi-liquid parameters $A^s(\hat{\boldsymbol{p}}_f,\hat{\boldsymbol{p}}'_f) = N_f W^s(\hat{\boldsymbol{p}}_f,\hat{\boldsymbol{p}}'_f)$ and $\overleftrightarrow{A}^a\ (\hat{\boldsymbol{p}}_f,\hat{\boldsymbol{p}}'_f) = N_f\ \overleftrightarrow{W}^a\ (\hat{\boldsymbol{p}}_f,\hat{\boldsymbol{p}}'_f)$, with $N_f = \langle N_f(\hat{\boldsymbol{p}}_f)\rangle_{\hat{\boldsymbol{p}}_f}$ the density of states per spin projection at the Fermi level, and the superconducting pair potentials by singlet and triplet pairing interactions V^s and $\overleftrightarrow{V}^t$ (where $\overleftrightarrow{W}^a$, $\overleftrightarrow{A}^a$, and $\overleftrightarrow{V}^t$ are in general tensors).

Finally, $\hat{v}_{\rm ext}$ contains the coupling to external fields, for example the electro-magnetic coupling to a magnetic vector potential $\boldsymbol{A}(\boldsymbol{R})$,

$$\hat{v}_{\rm orbital}(\hat{\boldsymbol{p}}_f,\boldsymbol{R}) = -e\boldsymbol{v}_f(\hat{\boldsymbol{p}}_f)\cdot\boldsymbol{A}(\boldsymbol{R})\hat{\tau}_3 \tag{30.55}$$

($e=-|e|$), and the Pauli-coupling to the quasiparticle spin

$$\hat{v}_{\rm spin}(\hat{\boldsymbol{p}}_f,\boldsymbol{R}) = -\boldsymbol{B}(\boldsymbol{R})\cdot\overleftrightarrow{\mu}_{\rm eff}\ (\hat{\boldsymbol{p}}_f)\cdot\hat{\boldsymbol{S}} \tag{30.56}$$

with the effective quasiparticle magnetic moment[47]

$$\overleftrightarrow{\mu}_{\rm eff}\ (\hat{\boldsymbol{p}}_f) = \big[\hat{1} - \overleftrightarrow{A}^a\ (\hat{\boldsymbol{p}}_f)\big]\mu_{\rm e} \tag{30.57}$$

where $\overleftrightarrow{A}^a\ (\hat{\boldsymbol{p}}_f) = N_f^{-1}\langle N_f(\hat{\boldsymbol{p}}'_f)\ \overleftrightarrow{A}^a\ (\hat{\boldsymbol{p}}_f,\hat{\boldsymbol{p}}'_f)\rangle_{\hat{\boldsymbol{p}}'_f}$, and the spin matrix in particle-hole space

$$\hat{\boldsymbol{S}} = \begin{pmatrix} \boldsymbol{\sigma} & 0 \\ 0 & -\sigma_2\boldsymbol{\sigma}\sigma_2 \end{pmatrix}. \tag{30.58}$$

$\mu_{\rm e}$ is the electron magnetic moment ($\mu_{\rm e} = -|\mu_{\rm e}|$).[48] The vector potential $\boldsymbol{A}$ and hence the magnetic field ($\boldsymbol{B} = \nabla\times\boldsymbol{A}$) are calculated from the current density as

$$\nabla\times\nabla\times\boldsymbol{A}(\boldsymbol{R}) = \mu_0\boldsymbol{j}(\boldsymbol{R}) \tag{30.59}$$

with the permeability of free space μ_0. The scalar electrochemical potential follows from local charge quasi-neutrality, and is zero in equilibrium. The charge current density is obtained from $\hat{g}(\hat{\boldsymbol{p}}_f,\boldsymbol{R};\varepsilon_n)$ via

$$\boldsymbol{j}(\boldsymbol{R}) = 2ek_{\rm B}T\sum_{\varepsilon_n}\big\langle N_f(\hat{\boldsymbol{p}}_f)\boldsymbol{v}_f(\hat{\boldsymbol{p}}_f)g(\hat{\boldsymbol{p}}_f,\boldsymbol{R};\varepsilon_n)\big\rangle_{\hat{\boldsymbol{p}}_f}, \tag{30.60}$$

the spin current density for spin projection along the axis $\boldsymbol{e}_\alpha$ via

$$\boldsymbol{J}_\alpha(\boldsymbol{R}) = 2ek_{\rm B}T\sum_{\varepsilon_n}\big\langle N_f(\hat{\boldsymbol{p}}_f)\boldsymbol{v}_f(\hat{\boldsymbol{p}}_f)[\boldsymbol{e}_\alpha\cdot\boldsymbol{g}(\hat{\boldsymbol{p}}_f,\boldsymbol{R};\varepsilon_n)]\big\rangle_{\hat{\boldsymbol{p}}_f} \tag{30.61}$$

and the spin magnetization via

$$\boldsymbol{M}(\boldsymbol{R}) = \overleftrightarrow{\chi}_{\rm n}\,\boldsymbol{B}(\boldsymbol{R}) + 2k_{\rm B}T\sum_{\varepsilon_n}\big\langle N_f(\hat{\boldsymbol{p}}_f)\ \overleftrightarrow{\mu}_{\rm eff}(\hat{\boldsymbol{p}}_f)\boldsymbol{g}(\hat{\boldsymbol{p}}_f,\boldsymbol{R};\varepsilon_n)\big\rangle_{\hat{\boldsymbol{p}}_f}, \tag{30.62}$$

where $\overleftrightarrow{\chi}_{\rm n} = 2N_f(\hat{1} - \overleftrightarrow{A}^a_0)\mu_{\rm e}^2$ is the normal state spin susceptibility, defined in terms of the parameter $\overleftrightarrow{A}^a_0 = N_f^{-1}\langle N_f(\hat{\boldsymbol{p}}_f)\overleftrightarrow{A}^a\ (\hat{\boldsymbol{p}}_f)\rangle_{\hat{\boldsymbol{p}}_f}$. The local density of states for a given spin direction $\boldsymbol{e}$ is calculated at real energies as

$$N_{\boldsymbol{e}}(\boldsymbol{R};\varepsilon) = -\frac{1}{\pi}{\rm Im}\langle N_f(\hat{\boldsymbol{p}}_f)[g(\hat{\boldsymbol{p}}_f,\boldsymbol{R};\varepsilon_+) + \boldsymbol{e}\cdot\boldsymbol{g}(\hat{\boldsymbol{p}}_f,\boldsymbol{R};\varepsilon_+)]\rangle_{\hat{\boldsymbol{p}}_f} \tag{30.63}$$

[47] $\hat{1}$ denotes a 3×3 unit tensor.

[48] $\mu_{\rm e} = -g\mu_{\rm B}/2$, with the Bohr magneton $\mu_{\rm B} = |e|\hbar/2m_e c$ and $g = 2.0$

with $\varepsilon_+ = \varepsilon + i\delta$ ($\delta > 0$ infinitesimal). The Eilenberger equation for $\hat{g}$, its normalization condition, the equations for the self energies $\hat{\sigma}$, and Maxwell's equation for $\boldsymbol{A}$, must be solved self consistently by iteration together with the appropriate boundary conditions imposed on the propagator and the vector potential [207, 208, 209, 210, 211]. Boundary conditions in quasiclassical theory are notoriously difficult to derive, as the quasiclassical propagators show in general jumps at interfaces (see figure 30.12), in contrast to microscopic propagators which are continuous.

A powerful way to implement boundary conditions and to solve Eilenberger equations is the Riccati method [212, 213, 214, 215]. Modern versions of boundary conditions for Eilenberger equations using these techniques are presented e.g. in Refs. [214, 154, 216, 215].

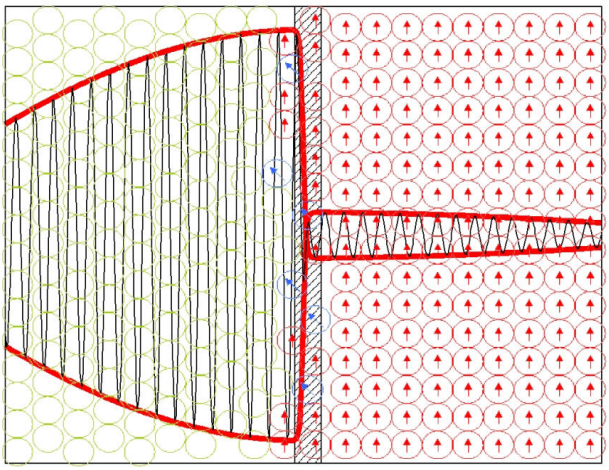


Figure 30.12: In quasiclassical approximation boundary conditions involve relations between the envelope functions of Bloch waves on the two sides of an interface. These envelope functions in general show a jump, even when the Bloch wave functions themselves are continuous.

Instead of applying an external field $\boldsymbol{B}(\boldsymbol{R})$, a superconductor can be spin-polarized via the inverse (or magnetic) proximity effect when in contact with a ferromagnetic material. This effect already appears when the ferromagnet is insulating. A theory for the spin polarization and the associated induced exchange field in the superconductor has been developed by Tokuyasu, Sauls, and Rainer in 1988 [151]. Although differing in details, the general mechanism presented there is essentially the same as for all subsequent studies of the inverse proximity effect in superconductor/ferromagnet heterostructures in the last decade: the appearance of a Cooper pair spin polarization, or of triplet pair correlations, in the superconductor creates a finite spin magnetization inside the superconducting region, extending roughly a coherence length away from the interface. This decay length is dictated by the decay of triplet pair correlations as the bulk of the singlet superconductor is approached.

30.4.4 Normalization condition and transport equation in spin-space

The interrelation between triplet amplitudes and induced magnetic moment can be understood within quasiclassical theory already by the normalization condition for the propagator. The normalization condition (30.49) encodes important information about the spin structure of the diagonal and off-diagonal propagators [217]. In equilibrium, physical solutions require the condition

$$\mathrm{Tr}\,(\hat{g}) = 0, \quad \text{i.e.} \quad \tilde{g}_0 = -g_0 \tag{30.64}$$

which also ensure local charge neutrality to leading order in the Fermi liquid expansion parameters. It is useful to introduce the notation $\boldsymbol{g}_\pm = (\boldsymbol{g} \pm \tilde{\boldsymbol{g}})/2$, $\boldsymbol{\nu}_\pm = (\boldsymbol{\nu} \pm \tilde{\boldsymbol{\nu}})/2$, $\nu_\pm = (\nu \pm \tilde{\nu})/2$. The external and internal fields are distributed according to: $\hat{v}_{\rm orbital}$ in ν_-; $\hat{v}_{\rm spin}$ in $\boldsymbol{\nu}_+$, which also contains the internal exchange field $\boldsymbol{J}$; spin-orbit band splitting in $\boldsymbol{\nu}_-$. In terms of measurable quantities, $\boldsymbol{g}_+$ determines the magnetization, $\boldsymbol{g}_-$ the spin current density, and g_0 the charge current density. One obtains from (30.49) and (30.64) for the spin components in (30.47) [217]

$$g_0^2 + \pi^2 = f\tilde{f} - \boldsymbol{f}\cdot\tilde{\boldsymbol{f}} - \boldsymbol{g}_+^2 - \boldsymbol{g}_-^2 \tag{30.65a}$$

$$2g_0\boldsymbol{g}_- = i\,\tilde{\boldsymbol{f}}\times\boldsymbol{f} \tag{30.65b}$$

$$2g_0\boldsymbol{g}_+ = \tilde{f}\boldsymbol{f} - f\tilde{\boldsymbol{f}} \tag{30.65c}$$

with $\boldsymbol{g}_\pm^2 = g_{x,\pm}^2 + g_{y,\pm}^2 + g_{z,\pm}^2 = \boldsymbol{g}_\pm\cdot\boldsymbol{g}_\pm$. It follows immediately that $\boldsymbol{g}_+\cdot\boldsymbol{g}_- = 0$, $f\boldsymbol{g}_- = i\boldsymbol{f}\times\boldsymbol{g}_+$ and $\boldsymbol{f}\cdot\boldsymbol{g}_- = \tilde{\boldsymbol{f}}\cdot\boldsymbol{g}_- = 0$. According to (30.65b), $\boldsymbol{g}_- = \boldsymbol{0}$ when $\boldsymbol{f} \parallel \tilde{\boldsymbol{f}}$. Moreover, from (30.65b)-(30.65c) it follows that $\boldsymbol{g}_+ = \boldsymbol{g}_- = \boldsymbol{0}$ when $\boldsymbol{f} = \tilde{\boldsymbol{f}} = \boldsymbol{0}$. The Eilenberger equations read

$$\frac{1}{2}\,i\hbar\,\boldsymbol{v}_f\cdot\nabla_{\boldsymbol{R}}\,f + (\varepsilon - \nu_-)\,f = \boldsymbol{\nu}_+\cdot\boldsymbol{f} - g\Delta - \boldsymbol{g}_+\cdot\boldsymbol{\Delta} \tag{30.66a}$$

$$\begin{aligned}\frac{1}{2}\,i\hbar\,(\boldsymbol{v}_f\cdot\nabla_{\boldsymbol{R}})\,\boldsymbol{f} + (\varepsilon - \nu_-)\,\boldsymbol{f} &- i\boldsymbol{\nu}_-\times\boldsymbol{f} = \\ &= \boldsymbol{\nu}_+ f - \boldsymbol{g}_+\Delta - g\boldsymbol{\Delta} - i\boldsymbol{g}_-\times\boldsymbol{\Delta},\end{aligned} \tag{30.66b}$$

which must be solved together with (30.65a), (30.65b) and (30.65c). These equations have to be complemented by self-consistency equations for the self-energies. Near $T_{\rm c}$ all off-diagonal quantities (f, $\boldsymbol{f}$, Δ, $\boldsymbol{\Delta}$) are small, and then from (30.65a)-(30.65c) follows that $\boldsymbol{g}_\pm$ can be neglected being second order in $\boldsymbol{f}$, $\tilde{\boldsymbol{f}}$, and g can be replaced by its normal state value [$-i\pi{\rm sign}(\varepsilon_n)$ in Matsubara representation]. If one introduces the matrices

$$\overleftrightarrow{V} = \begin{pmatrix} \nu_- & \nu_{+,x} & \nu_{+,y} & \nu_{+,z} \\ \nu_{+,x} & \nu_- & i\nu_{-,z} & -i\nu_{-,y} \\ \nu_{+,y} & -i\nu_{-,z} & \nu_- & i\nu_{-,x} \\ \nu_{+,z} & i\nu_{-,y} & -i\nu_{-,x} & \nu_- \end{pmatrix} \tag{30.67}$$

and

$$\overleftrightarrow{G} = \begin{pmatrix} g & g_{+,x} & g_{+,y} & g_{+,z} \\ g_{+,x} & g & ig_{-,z} & -ig_{-,y} \\ g_{+,y} & -ig_{-,z} & g & ig_{-,x} \\ g_{+,z} & ig_{-,y} & -ig_{-,x} & g \end{pmatrix} \tag{30.68}$$

as well as the vectors

$$\mathbf{F} = \begin{pmatrix} f \\ f_x \\ f_y \\ f_z \end{pmatrix}, \quad \mathbf{\Delta} = \begin{pmatrix} \Delta \\ \Delta_x \\ \Delta_y \\ \Delta_z \end{pmatrix}, \tag{30.69}$$

then the system (30.66a)-(30.66b) can be written compactly as

$$(i\hbar\,\boldsymbol{v}_f\cdot\nabla_{\boldsymbol{R}} + 2\varepsilon - 2\overleftrightarrow{V})\mathbf{F} = 2\overleftrightarrow{G}\,\mathbf{\Delta}. \tag{30.70}$$

The four eigenvalues of $2(\varepsilon - \overleftrightarrow{V})/\hbar v_f$ determine the wavevectors in the system, and can be calculated as

$$\left[2(\varepsilon - \nu_-) \pm \sqrt{\nu_x^2 + \nu_y^2 + \nu_z^2} \pm \sqrt{\tilde{\nu}_x^2 + \tilde{\nu}_y^2 + \tilde{\nu}_z^2}\right]/(\hbar v_f). \tag{30.71}$$

For a singlet superconductor in proximity contact with a ferromagnet with exchange field $\boldsymbol{J}$, assuming for the following discussion $\nu_- = 0$, $\boldsymbol{\nu}_- = \mathbf{0}$, $\boldsymbol{\nu}_+ = -\boldsymbol{J}$, $\boldsymbol{\Delta} = 0$, the Eilenberger equations simplify to

$$\left(\tfrac{1}{2}\, i\hbar\, \boldsymbol{v}_f \cdot \nabla_{\boldsymbol{R}} + \bar{\varepsilon}\right) f = -\boldsymbol{J}\cdot\boldsymbol{f} - g\Delta \tag{30.72a}$$

$$\left(\tfrac{1}{2}\, i\hbar\, \boldsymbol{v}_f \cdot \nabla_{\boldsymbol{R}} + \bar{\varepsilon}\right) \boldsymbol{f} = -\boldsymbol{J} f - \boldsymbol{g}_+ \Delta. \tag{30.72b}$$

where we have introduced $\bar{\varepsilon} = \varepsilon + i\alpha_\mathrm{s}$ for $\mathrm{Im}(\varepsilon) > 0$ and $\bar{\varepsilon} = \varepsilon - i\alpha_\mathrm{s}$ for $\mathrm{Im}(\varepsilon) < 0$ to account for possible spin-flip scattering with rate $\alpha_\mathrm{s} = \hbar/\tau_\mathrm{s}$, and τ_s is the spin-flip scattering time. The wavevectors are then given by

$$k_{1,2} = 2(\bar{\varepsilon} \pm |\boldsymbol{J}|)/\hbar v_f, \quad k_{3,4} = 2\bar{\varepsilon}/\hbar v_f. \tag{30.73}$$

In a superconductor-ferromagnet hybrid structure, the superconducting order parameter vanishes in the ferromagnetic regions, $\Delta_\mathrm{mf} = 0$. The proximity effect manifests itself in nonzero pair amplitudes $f, \boldsymbol{f} \neq 0$ in the ferromagnet. In the superconductor, the exchange field vanishes, $\boldsymbol{J} = \mathbf{0}$, expressing the non-coexistence of superconducting and ferromagnetic orders. 30.73 defines the propagation and decay of Cooper pairs into the ferromagnet. If one replaces ε by the first Matsubara energy $i\pi k_\mathrm{B}T$, then one obtains an exponential decay on the length scale $\xi_T = \hbar v_f/2(\pi k_\mathrm{B}T + \alpha_\mathrm{s})$. In addition, two of the components oscillate on the length scale $\xi_J = \hbar v_f/2|\boldsymbol{J}|$ (with wavelength $2\pi\xi_J$) along the direction $\boldsymbol{v}_f$. After averaging over all directions, this leads to an algebraic decay $\sim 1/x$ in x-direction away from the interface, before on a larger length scale ξ_T exponential decay sets in [107]. The components with wavevectors $k_{1,2}$, oscillating on the scale ξ_J, correspond to eigenvectors with $\boldsymbol{f} = \pm f\boldsymbol{J}/|\boldsymbol{J}|$ (i.e. $\boldsymbol{f}\times\boldsymbol{J} = \mathbf{0}$), and represent an equal weight superposition of the singlet amplitude ($S = 0, S_z = 0$) and the triplet amplitude with zero spin-projection to $\boldsymbol{J}$ ($S = 1, S_z = 0$). The (degenerate) components with wavevectors $k_{3,4}$, insensitive to $\boldsymbol{J}$, correspond to an eigenvector where $f = 0$, $\boldsymbol{f}\cdot\boldsymbol{J} = 0$, and represent equal-spin pairing amplitudes with respect to the quantization axis $\boldsymbol{J}$ ($S = 1, S_z = \pm 1$). For increasing exchange field, the pre-factor for the proximity amplitudes oscillating with wavelength ξ_J is of order $\Delta/|\boldsymbol{J}|$, and thus vanishes in the limit of large exchange splitting.

30.4.5 Usadel equations

In the dirty (diffusive) limit, the transport equation (30.48) can be greatly simplified. A strong scattering by impurities averages the quasiclassical propagator over momentum directions. The Green's function may be expanded in the small parameter τT_c (τ is the momentum relaxation time) following the standard procedure [218, 186]

$$\hat{g}(\hat{\boldsymbol{p}}_f, \boldsymbol{R}, \varepsilon_n) \approx \hat{g}^{(0)}(\boldsymbol{R}, \varepsilon_n) + \hat{g}^{(1)}(\hat{\boldsymbol{p}}_f, \boldsymbol{R}, \varepsilon_n) \tag{30.74}$$

where the magnitude of $\hat{g}^{(1)}$ is small compared to that of $\hat{g}^{(0)}$. The impurity self-energy is related to an (in general anisotropic) lifetime function $\tau(\hat{\boldsymbol{p}}_f', \hat{\boldsymbol{p}}_f)$ [186]. Substituting (30.74) into (30.48) and (30.49), multiplying with $N_f(\hat{\boldsymbol{p}}_f')v_{f,j}(\hat{\boldsymbol{p}}_f')\tau(\hat{\boldsymbol{p}}_f', \hat{\boldsymbol{p}}_f)$, averaging over momentum directions, and considering that $J\tau/\hbar \ll 1$, one obtains (with the help of the normalization condition) $\langle N_f(\hat{\boldsymbol{p}}_f)v_{f,j}(\hat{\boldsymbol{p}}_f)\hat{g}^{(1)}(\hat{\boldsymbol{p}}_f)\rangle_{\hat{\boldsymbol{p}}_f} = N_f \sum_k (D_{jk}/i\pi)\hat{g}^{(0)}\nabla_k\hat{g}^{(0)}$, where

$$D_{jk} = \frac{1}{N_f^2}\Big\langle\Big\langle N_f(\hat{\boldsymbol{p}}_f')v_{f,j}(\hat{\boldsymbol{p}}_f')\,\tau(\hat{\boldsymbol{p}}_f', \hat{\boldsymbol{p}}_f)\,N_f(\hat{\boldsymbol{p}}_f)v_{f,k}(\hat{\boldsymbol{p}}_f)\Big\rangle_{\hat{\boldsymbol{p}}_f}\Big\rangle_{\hat{\boldsymbol{p}}_f'} \tag{30.75}$$

is the diffusion constant tensor. The function $\hat{g}^{(0)}$ obeys the Usadel transport equation (hereafter we omit the superscript (0) and apply the Einstein summation convention)

$$\left[\varepsilon\hat{\tau}_3 - \hat{h}_0,\, \hat{g}\right] + \frac{\hbar D_{ij}}{\pi}\nabla_i\left(\hat{g}\nabla_j\hat{g}\right) = 0 \tag{30.76}$$

where $\hat{h}_0 = \langle N_f(\hat{\boldsymbol{p}}_f)[\hat{v}_{\rm ext}(\hat{\boldsymbol{p}}_f) + \hat{\sigma}_{\rm mf}(\hat{\boldsymbol{p}}_f)]\rangle_{\hat{\boldsymbol{p}}_f}/N_f$, together with the normalization condition

$$\hat{g}^2 = -\pi^2\hat{\tau}_0. \tag{30.77}$$

The diffusion constant is a material property. It is spin independent in agreement with the approximation of treating all exchange energy effects as perturbation. In the diffusive limit, the different components of g and f in the spin space are related through (30.65a), (30.65b) and (30.65c), since the Green's function $\hat{g}$ averaged over momentum fulfills the same normalization condition as before averaging. A vector potential enters in a gauge invariant manner by replacing the spatial derivative operators by (see e.g. [219])

$$\nabla_i\hat{X} \to \hat{\partial}_i\hat{X} \equiv \nabla_i\hat{X} - i\left[\frac{e}{\hbar}\hat{\tau}_3 A_i, \hat{X}\right]. \tag{30.78}$$

The charge current density is obtained from $\hat{g}(\boldsymbol{R};\varepsilon_n)$ via

$$j_k = \frac{2eN_f D_{kj}}{\pi} k_{\rm B}T \sum_{\varepsilon_n} {\rm Im}\left[f^*\,\overline{\partial}_j f - \boldsymbol{f}^*\,\overline{\partial}_j \boldsymbol{f}\right], \tag{30.79}$$

with $\overline{\partial}_j = \nabla_j - \frac{2ie}{\hbar}A_j$, and the spin-vector current density in spatial k-direction

$$\boldsymbol{J}_k = \frac{2eN_f D_{kj}}{\pi} k_{\rm B}T \sum_{\varepsilon_n} {\rm Re}\left[\boldsymbol{g}\times\nabla_j\boldsymbol{g} + \boldsymbol{f}^*\times\overline{\partial}_j\boldsymbol{f}\right]. \tag{30.80}$$

Note that from Eqs. (30.65b)-(30.65c) follows that $\boldsymbol{g} = \left[{\rm Im}(f^*\boldsymbol{f}) + i{\rm Re}(\boldsymbol{f})\times{\rm Im}(\boldsymbol{f})\right]/{\rm Im}(g_0)$ at Matsubara frequencies. As for the case of Eilenberger equations, an important part of the problem is the formulation of appropriate boundary conditions [220, 221]. In quasiclassical theory this is usually a highly non-trivial task, as boundary conditions are in general non-linear. A powerful way to implement boundary conditions and to solve Usadel equations is also here the Riccati method [72, 222, 223]. Modern versions of boundary conditions for Usadel equations are found in Ref. [152] for weak spin polarization, small spin-dependent scattering phase shifts, and small transmission. A general formulation appropriate for arbitrary transmission, spin polarization, and spin-dependent phase shifts has been derived in Ref. [224]. The tunneling limit of this boundary condition has been used in Ref. [161], and was independently introduced in Ref. [359].[49]

Near the critical temperature T_c, the pair amplitudes f and $\boldsymbol{f}$ are small and the Green's function g deviates only slightly from its value in the normal state, so that the Usadel equations can be linearized and take the simpler form [73, 226, 74]

$$\left(\tfrac{\hbar}{2i}\nabla_j D_{jk}\nabla_k + \bar{\varepsilon}\right) \quad f = \quad -\mathbf{J}\cdot\boldsymbol{f} + i\pi\Delta \tag{30.81}$$

$$\left(\tfrac{\hbar}{2i}\nabla_j D_{jk}\nabla_k + \bar{\varepsilon}\right) \quad \boldsymbol{f} = \quad -\mathbf{J}f, \tag{30.82}$$

where $\bar{\varepsilon}$ is defined as after Eq. (30.72b). The characteristic wavevectors for isotropic systems ($D_{ij} \to D\delta_{ij}$) are now given by (we chose the roots such that ${\rm Im}(k) > 0$)

$$k_{1,2} = (1+i)\sqrt{(\bar{\varepsilon} \pm |\boldsymbol{J}|)/\hbar D}, \quad k_{3,4} = (1+i)\sqrt{\bar{\varepsilon}/\hbar D}. \tag{30.83}$$

If we again substitute $\varepsilon \to i\pi k_{\rm B}T$, this leads to exponential decays for all four solutions. However, there are two long-range solutions with decay length

$$\xi_T = \left(\frac{\hbar D}{2(\pi k_{\rm B}T + \alpha_{\rm s})}\right)^{\frac{1}{2}}, \tag{30.84}$$

[49] A recently suggested alternative boundary condition [225] assumes the simplified case of coinciding spin-quantization axes for reflection and transmission matrix elements of each scattering channel within a channel-conserving approximation, and has a considerably narrower range of applicability.

and two short-range solutions showing damped spatial oscillations with decay length [239]

$$\xi_1 = \left(\frac{\hbar D}{\sqrt{(\pi k_\mathrm{B} T + \alpha_\mathrm{s})^2 + |\boldsymbol{J}|^2} + (\pi k_\mathrm{B} T + \alpha_\mathrm{s})} \right)^{\frac{1}{2}} \tag{30.85}$$

and inverse oscillation wavevector

$$\xi_2 = \left(\frac{\hbar D}{\sqrt{(\pi k_\mathrm{B} T + \alpha_\mathrm{s})^2 + |\boldsymbol{J}|^2} - (\pi k_\mathrm{B} T + \alpha_\mathrm{s})} \right)^{\frac{1}{2}} . \tag{30.86}$$

Note that $\xi_1 < \xi_2$ except when $T = 0$ and $\hbar/\tau_\mathrm{s} = 0$, thus the oscillations are strongly damped, so that one cannot expect to observe many oscillation periods. This is in contrast to the clean case, where the oscillation wavelength is entirely decoupled from the decay length, which can become very long for low temperatures. Thus, many oscillation periods are expected to be observable in experiment. For the diffusive case, on the other hand, both length scales are temperature dependent. This allows for oscillatory behavior as a function of temperature, an effect absent in the clean limit. For $|\boldsymbol{J}| \gg k_\mathrm{B} T, \alpha_\mathrm{s}$ both length scales merge and approach [227]

$$\xi_{1,2} = \sqrt{\frac{\hbar D}{|\boldsymbol{J}|}} \left(1 \mp \frac{\pi k_\mathrm{B} T + \alpha_\mathrm{s}}{2|\boldsymbol{J}|} \right) .$$

With increasing exchange splitting, the decay length shrinks to zero and the short-range proximity amplitudes are expected to be suppressed to unmeasurable size, unless one finds a mechanism to create new types of proximity amplitudes.

30.4.6 General features of the S/F proximity effect

It can be noticed from the transport equation (30.72b) or (30.82) that the triplet vector $\boldsymbol{f}$ obeys in the ferromagnet an inhomogeneous differential equation, implying that $\boldsymbol{f}$ is necessarily non-zero if the singlet component f penetrates in the ferromagnet. For spatially constant exchange field $\boldsymbol{J}$, the triplet vector aligns with $\boldsymbol{J}$. The singlet component and the triplet component with the zero spin-projection on $\boldsymbol{J}$ coexist always in the ferromagnet near the S/F interface. As they both involve electrons from both spin bands, both are characterized by short-range penetration lengths in the ferromagnet.

On the contrary, if the triplet vector $\boldsymbol{f}$ is non-collinear with $\boldsymbol{J}$, triplet components with nonzero spin-projection on $\boldsymbol{J}$ are produced. Since these correspond to equal-spin pairing, they are not limited locally by the paramagnetic interaction with the local exchange field and have long-range scales in the ferromagnet. A misalignment between the triplet vector $\boldsymbol{f}$ and the moment $\boldsymbol{J}$ occurs in presence of sudden changes in orientation of $\boldsymbol{J}$. The reason is that $\boldsymbol{f}$ obeys a differential equation and its variations in orientation have thus to be relatively smooth.

The counterpart for the production of triplet components ($\boldsymbol{f} \neq \boldsymbol{0}$) in the pair amplitudes is the presence of $\boldsymbol{g} \neq \boldsymbol{0}$ in the diagonal components of the Green function [217]. As a direct consequence, the density of states for the up and down spin projections differs [see 30.63]. This feature of the S/F proximity effect has been found numerically as early as in 1999 [228]. In the presence of long-range triplet components, the particle-hole diagonal Green function components contain also off-diagonal terms in the spin-space, a signature of a spin-flip scattering process.

As a result of the spin splitting in the density of states generated by the S/F proximity effect, a spin magnetization $\delta\boldsymbol{M}$ is also induced near the S/F interface. This magnetization

leakage has been investigated in Ref. [229] within a model considering a fixed exchange field. In the dirty limit the spin magnetization induced by the proximity effect is given by [186, 151]

$$\delta \boldsymbol{M}(\boldsymbol{R}) = 2N_f k_{\mathrm{B}} T \overleftrightarrow{\mu}_{\mathrm{eff}} \sum_n \mathrm{Re}\left[\boldsymbol{g}\left(\boldsymbol{R}, \varepsilon_n\right)\right], \tag{30.87}$$

with $\overleftrightarrow{\mu}_{\mathrm{eff}} = (\hat{1} - \overleftrightarrow{A}_0^a)\mu_{\mathrm{e}}$. Since the triplet vector $\boldsymbol{f}$ is also induced in the superconductor near the S/F interface via an inverse proximity effect, the vector $\boldsymbol{g}$ characterizing the magnetic correlations penetrates also in the superconductor according to the relation (30.65c), which for the diffusive limit reads $\mathrm{Im}(g_0)\mathrm{Re}(\boldsymbol{g}) = \mathrm{Im}(f^* \boldsymbol{f})$ (all functions of ε_n).

It is possible to convince oneself that the sum over Matsubara frequencies in the expression (30.87) is nonzero. Indeed, as noticed in Refs. [131, 230, 231], in the diffusive limit the triplet components are odd functions of the Matsubara frequencies ε_n, while the singlet amplitude f is an even function of ε_n. Note that in the diffusive limit

$$g_0(-\varepsilon_n) = -g_0(\varepsilon_n), \quad \boldsymbol{g}(-\varepsilon_n) = \tilde{\boldsymbol{g}}(\varepsilon_n). \tag{30.88}$$

For unitary pairing states, $\boldsymbol{f} \times \tilde{\boldsymbol{f}} = \boldsymbol{0}$, the relations (30.65b)-(30.65c) between the vectors $\boldsymbol{g}$ and $\boldsymbol{f}$ get simplified. In this case, it can be seen that if the gap Δ can be chosen real (and thus the singlet amplitude $f(\varepsilon_n)$ is real), then the triplet vector $\boldsymbol{f}(\varepsilon_n)$ is purely imaginary, i.e. $\tilde{\boldsymbol{f}} = \boldsymbol{f}^* = -\boldsymbol{f}$ (taking into account that $\tilde{g}_0 = -g_0$, i.e. g_0 is purely imaginary). As a result, one obtains the simpler relations

$$\boldsymbol{g} = \tilde{\boldsymbol{g}}, \qquad g_0 \boldsymbol{g} = f \boldsymbol{f}. \tag{30.89}$$

These simplifications arise also when $\boldsymbol{f} \parallel \boldsymbol{J}$ [229]. Combining the relations (30.89) and (30.88), it follows that the spin-vector part $\boldsymbol{g}$ is an even function of ε_n in the diffusive limit, which demonstrates that the induced spin magnetization $\delta \boldsymbol{M}$ is in general non-zero.

Near T_c, the singlet amplitude f and the triplet vector amplitude are small so that $\boldsymbol{g}$ and thus $\delta \boldsymbol{M}$ appear to be second order terms [see 30.65c]. Accordingly, the induced spin magnetization $\delta \boldsymbol{M}$ penetrating the superconductor, which is negligibly small near T_c, increases significantly by reaching temperatures well below T_c.

30.4.7 Strongly spin-polarized ferromagnets

In the case that the spin splitting of the spin bands in a ferromagnet is much larger than the superconducting gap in the adjacent superconductor, the above mentioned theories must be modified in various respects. First, Usadel approximation assumes that the inverse life time of quasiparticles due to impurity scattering averaged over the Fermi surface, $\hbar/\tau$, is much larger than all energy scales appearing in the Usadel equation, including the magnitude of the exchange field $|\boldsymbol{J}|$. If this is not the case, the spatial variation of superconducting correlations into the ferromagnet happens on length scales comparable to or shorter than the mean free path, and Usadel theory cannot be used within the ferromagnet on the same footing as the exchange field. One must resort to Eilenberger equations in this case. If the exchange splitting is, however, not much smaller than the Fermi energy scale, then even Eilenberger-Larkin-Ovchinnikov theory cannot accommodate the exchange field in the way described in the previous sections. A modified version of Eilenberger and Usadel equations can be used for the case that $|\boldsymbol{J}| \sim E_F$. In this case, there exist two well separated fully spin-polarized Fermi surfaces in the system, and the length scale associated with $\hbar/|\hat{\boldsymbol{p}}_{f\uparrow} - \hat{\boldsymbol{p}}_{f\downarrow}|$ is much shorter than the coherence length scale in the ferromagnet. Superconducting pairs of the type $\uparrow\uparrow$ and $\downarrow\downarrow$ are still long-ranged in such a system, however pairs of the type $\uparrow\downarrow$ and $\downarrow\uparrow$ are negligible within quasiclassical approximation. Both Fermi velocity and density of states at the Fermi level are spin-dependent. The same holds

for diffusion constant, and coherence length. The quasiclassical propagator is then spin-scalar for each quasiclassical trajectory in the ferromagnet,

$$\hat{g}_{\uparrow\uparrow} = \begin{pmatrix} g_{\uparrow\uparrow} & f_{\uparrow\uparrow} \\ \tilde{f}_{\uparrow\uparrow} & \tilde{g}_{\uparrow\uparrow} \end{pmatrix}, \quad \hat{g}_{\downarrow\downarrow} = \begin{pmatrix} g_{\downarrow\downarrow} & f_{\downarrow\downarrow} \\ \tilde{f}_{\downarrow\downarrow} & \tilde{g}_{\downarrow\downarrow} \end{pmatrix}, \tag{30.90}$$

and only has a particle-hole discrete degree of freedom. Similarly, all mean field self energies have the same structure (spin-scalar, only 2x2 particle-hole matrices), and the Fermi liquid interactions are replaced by spin-scalar interactions, which in the simplest case do not mix the spin bands: $A^s, \overset{\leftrightarrow}{A^a} \to A_{\uparrow\uparrow}, A_{\downarrow\downarrow}$, $V^s, \overset{\leftrightarrow}{V^t} \to V_{\uparrow\uparrow}, V_{\downarrow\downarrow}$ (in a more general case, the Fermi liquid interactions could be of the form $A_{\uparrow\uparrow,\uparrow\uparrow}$, $A_{\uparrow\uparrow,\downarrow\downarrow}$ etc). Eilenberger equation and Usadel equation have the same form as before for each separate spin band. The spin-resolved current densities are given in the ballistic case by

$$\boldsymbol{j}_{\uparrow} = ek_{\mathrm{B}}T \sum_{\varepsilon_n} \left\langle N_{f\uparrow} \boldsymbol{v}_{f\uparrow} g_{\uparrow\uparrow} \right\rangle_{\hat{\boldsymbol{p}}_{f\uparrow}}, \quad \boldsymbol{j}_{\downarrow} = ek_{\mathrm{B}}T \sum_{\varepsilon_n} \left\langle N_{f\downarrow} \boldsymbol{v}_{f\downarrow} g_{\downarrow\downarrow} \right\rangle_{\hat{\boldsymbol{p}}_{f\downarrow}}, \tag{30.91}$$

and the spin magnetization by

$$M_z \;=\; M_{\mathrm{n}}(B_z) + k_{\mathrm{B}}T \sum_{\varepsilon_n} \left(\left\langle N_{f\uparrow} \mu_{\mathrm{eff}\uparrow} g_{\uparrow\uparrow} \right\rangle_{\hat{\boldsymbol{p}}_{f\uparrow}} - \left\langle N_{f\downarrow} \mu_{\mathrm{eff}\downarrow} g_{\downarrow\downarrow} \right\rangle_{\hat{\boldsymbol{p}}_{f\downarrow}} \right). \tag{30.92}$$

The expressions in the diffusive limit are modified accordingly: e.g. for the spin-resolved current density one obtains

$$j_{k\uparrow} = -\frac{e}{\pi} k_{\mathrm{B}}T \sum_{\varepsilon_n} \mathrm{Im} \left[N_{f\uparrow} D_{kj\uparrow} f^*_{\uparrow\uparrow} \, \overline{\partial}_j f_{\uparrow\uparrow} \right], \tag{30.93}$$

and analogously for spin down.

30.5 Pair amplitude oscillations and π-Josephson junctions

30.5.1 $0-\pi$ transitions in Josephson junctions

Proximity-induced pairs in a superconductor-ferromagnet bilayer are subject to the FFLO effect, leading to spatially oscillating pair amplitudes in the ferromagnetic regions. These act back on the superconducting singlet pair potential in the superconducting region. How exactly this interaction between pair potential and FFLO amplitudes takes place depends on details of the interfaces and must be determined numerically, however for a sufficiently thin superconducting layer the oscillating nature of the FFLO amplitudes ultimately leads to oscillations in the modulus of the pair potential of the superconductor (and thus in the transition temperature) as function of the geometric dimensions of the hybrid structure. In addition, the oscillatory nature of the FFLO pairs in the ferromagnet affects the properties of superconductor-ferromagnet-superconductor Josephson devices, leading to the possibility of oscillations between junctions with a phase difference of zero and junctions with a phase difference of π in the ground state when a certain control parameter is changed.

The idea of Josephson junctions with a π phase difference in its ground state when a magnetic impurity is inserted in the junction was introduced by Bulaevskiĭ, Kuziĭ, and Sobyanin in 1977 [232]. Similar ideas had also been proposed by Kulik in 1965 [233]. In 1982 it was also shown in a classical paper by Buzdin, Bulaevskiĭ, and Panyukov that the pair amplitude oscillates in ferromagnets in contact with a superconductor [234]. Further early studies of this effect followed in Refs. [235, 236, 237]. One technological problem that became evident quickly was that weakly spin-polarized systems, like ferromagnetic Cu-Ni or Pd-Ni alloys, are better suited to observe $0-\pi$ oscillations, as otherwise the proximity amplitudes become

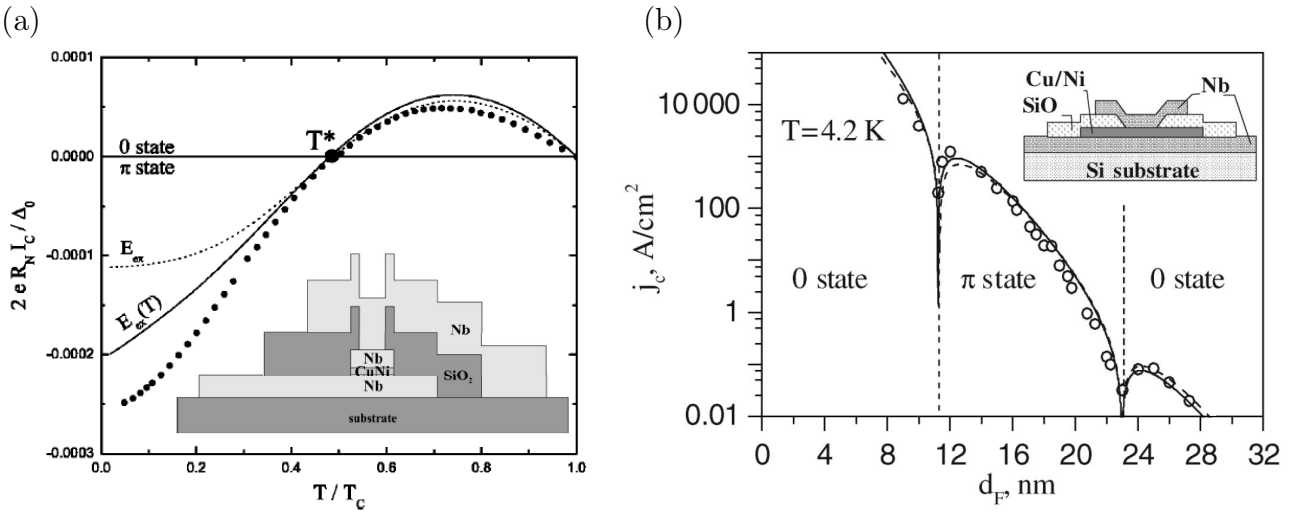


Figure 30.13: (a) Temperature dependence of the critical Josephson current in a $Nb/Cu_{52}Ni_{48}/Nb$ trilayer device, shown in the inset, for a ferromagnet layer thickness $d = 18$ nm. (The lines correspond to theoretical models with constant (dotted line) or temperature dependent (solid line) exchange energy.) From Sellier *et al.* [243]. Copyright (2003) by the American Physical Society. (b) The ferromagnet-layer thickness dependence of the critical current density for $Nb/Cu_{0.47}Ni_{0.53}/Nb$ junctions at temperature 4.2 K. Open circles represent experimental results; solid and dashed lines show model calculations. The inset shows a schematic cross section of the SFS junctions. From Oboznov *et al.* [227]. Copyright (2006) by the American Physical Society.

so short ranged that extremely thin layers are necessary. Typical ferromagnetic alloys that have been used are $Cu_{1-x}Ni_x$ (CuNi) and $Pd_{1-x}Ni_x$ (PdNi). The real break-through came in the beginning of the 2000's with the experimental verification of the switching between 0 and π-Josephson junctions based on the effect predicted theoretically before. Pioneering work was done by Ryazanov and co-workers who studied transitions between zero- and π-states as function of temperature [238, 239, 240, 227] and thickness of the ferromagnet layer [240, 227] in Nb/CuNi/Nb trilayers (see Figure 30.13). Closely following were experiments by Kontos and co-workers who studied the zero-π transition as function of barrier thickness in $Nb/Al/Al_2O_3/PdNi/Nb$ junctions [241], by Blum *et al.* [242], who use Nb/Cu/Ni/Cu/Nb junctions and vary both temperature and thickness of the Ni layer (thus employing a much stronger spin-polarized ferromagnet than the ferromagnetic alloys that were used by the other groups), and by Sellier *et al.* studying a temperature induced $0-\pi$ transition in Nb/CuNi/Nb (see Figure 30.13), as well as the appearance of half-integer Shapiro steps [243, 244].

The critical Josephson current density as function of layer thickness in the limit $k_B T, \alpha_s \ll |\boldsymbol{J}|$ is described in the clean limit by formula [74]

$$I_c(d_F) \sim \frac{\sin\left(\frac{2|\boldsymbol{J}|}{\hbar v_f}(d_F - d_0)\right)}{\frac{2|\boldsymbol{J}|}{\hbar v_f}(d_F - d_0)} \tag{30.94a}$$

where d_0 is a fit parameter which is usually assigned to a "dead layer",i.e. a layer of suppressed magnetism at the interface. In the diffusive limit the corresponding expression for long ($d_F \gg \xi_1$) junctions is

$$I_c(d_F) \sim e^{-d_F/\xi_1} \cos\left(\frac{d_F - d_0}{\xi_2}\right) \tag{30.94b}$$

with the length scales $\xi_{1,2}$ as in (30.85) and (30.86). A study by Pugach *et al.* [245] bridging the two limiting cases showed that the two length scales ξ_1 and ξ_2 may exhibit a non-monotonic

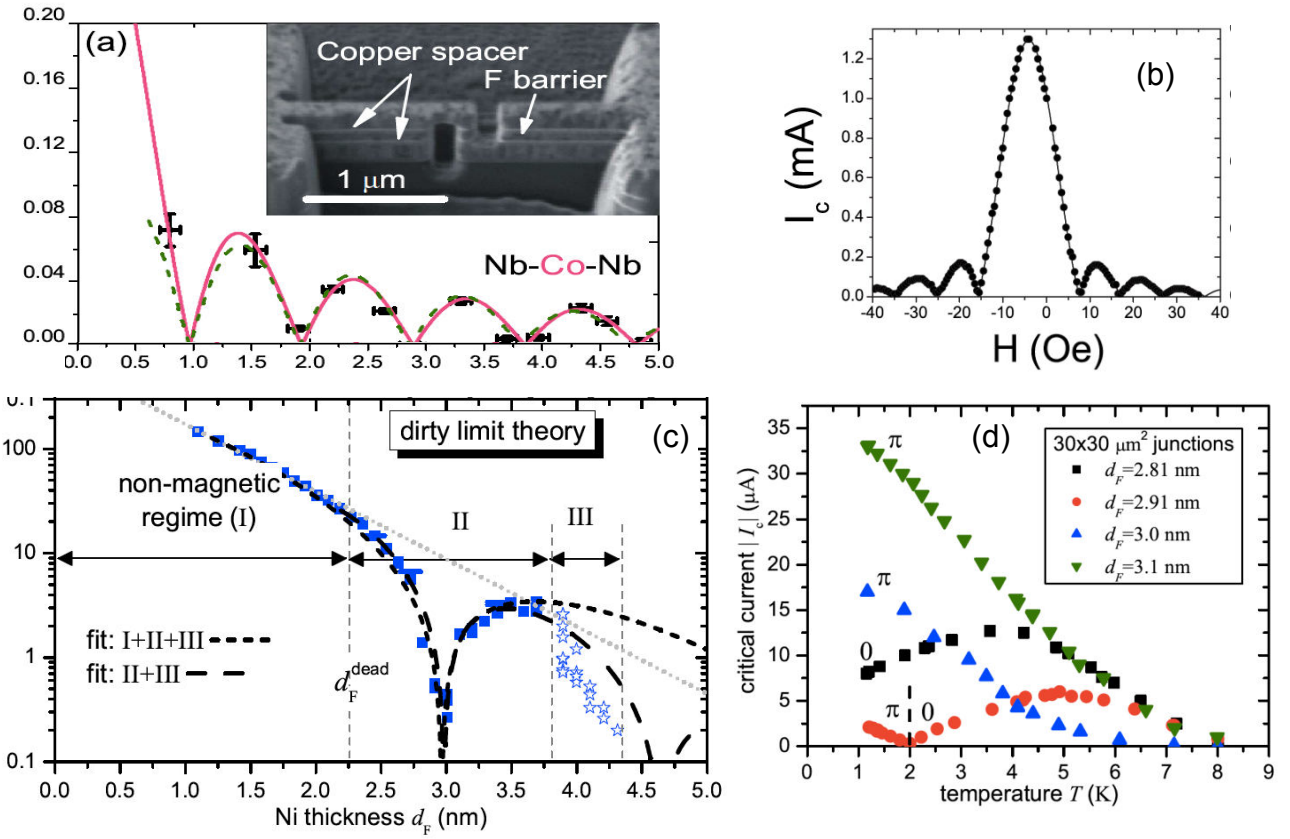


Figure 30.14: (a) Characteristic voltage of a Nb/Co/Nb Josephson junction as a function of Co thickness at 4.2K. The dashed line is a fit to theory. Inset: A focused ion beam micrograph of a typical Nb/Co/Nb Josephson junction. From Robinson *et al.* [247]. Copyright (2006) by the American Physical Society. (b) Critical current vs applied magnetic field obtained for Nb/Cu/Co/Ru/Co/Cu/Nb circular Josephson junctions with total Co layers thickness of 6.1 nm. From Khasawneh *et al.* [250]. Copyright (2009) by the American Physical Society. (c) $j_c(d_F)$ dependence for an SFS junction with F=Ni. Two fits appropriate for the dirty limit theory for data from regimes I+II+III and just II+III are shown as dashed lines. (d) $I_c(T)$ dependence for SFS Josephson junctions. A temperature induced 0 to π transition is observed (sample $d_F = 2.91$ nm). (c) and (d) from Bannykh *et al.* [249]. Copyright (2009) by the American Physical Society.

dependence on the properties of the ferromagnetic layer such as exchange field or electron mean-free path.

Further studies of strongly spin-polarized interlayers were performed, using various materials, among those Ni in Ref. [246], Co, Ni, and Py ($Ni_{80}Fe_{20}$) in Ref. [247], and Py ($Fe_{0.75}Co_{0.25}$) barriers in Ref. [248]. A detailed study, presented in Ref. [249], with Ni interlayers using the formulas (30.94a), (30.94b) above has been done recently, indicating that these structures are in the dirty limit. The thicknesses of the Ni layers ranged between 1 and 5 nm. In Figure 30.14 examples for $0-\pi$ oscillations in a Nb/Co/Nb structure are shown. In order to eliminate unwanted effects due to the variation of the electromagnetic vector potential across the junction due to the intrinsic magnetic flux in the junction, a special geometry was used where two Co layers were exchange coupled by a thin Ru layer in between to align antiferromagnetically. This cancels all the unwanted effects to a high degree, and a previously wildly fluctuating critical current vs. magnetic field curve turns into an excellent Fraunhofer pattern when the Ru interlayer present, as seen in Figure 30.14 (b) [250]. With this improvement high-quality $0-\pi$ transitions are observed both as function of temperature and of ferromagnet thickness. These

results complement the results shown in Figure 30.13, which are for ferromagnetic alloys. The main difference is a one order of magnitude smaller ferromagnet layer thickness necessary to observe the effect, which is an experimental challenge.

The effect of additional normal and/or insulating layers between the superconductor and the ferromagnet was studied theoretically in detail in Ref. [251]. It was found that even a thin additional normal conducting layer may shift the 0-π transitions to larger or smaller values of the thickness of the ferromagnet, depending on its conducting properties, and for certain parameter ranges a 0-π transition can even be achieved by changing only the normal layer thickness.

A promising setup are so-called double-proximity structures, in which two superconductors are connected by a weak link of a normal-metal/ferromagnet bilayer or a ferromagnet/normal-metal/ferromagnet trilayer forming a bridge between the superconducting banks. The proximity effect acts here twice: first to provide pair amplitudes from the superconducting banks into the bilayer or trilayer, and second at the interface between the normal metal and ferromagnet. Such structures have been proposed by Karminskaya and Kupriyanov [252], and experimental realization in terms of hybrid planar Al-(Cu/Fe)-Al submicron bridges is reported in Ref. [253]. The oscillation periods and damping lengths of the critical Josephson current can be much longer in such devices than in the conventional setup. Various geometries have been theoretically studied in subsequent work, including (SN)-(NF)-(SN), (SNF)-(NF)-(SNF), (SNF)-N-(SNF), and S-(NF)-S junctions, in order to optimize practical performance [254].

30.5.2 Phase sensitive measurements

The current-phase relation (CPR) as a function of temperature in a Nb/CuNi/Nb junction was measured by Frolov *et al.* (see Figure 30.15) [255]. Using an rf SQUID, the change of the current-phase relation from zero to π-junction behavior is clearly visible. This allows to observe the *sign* of the supercurrent. A π-junction is a Josephson junction with a negative critical current I_c, as its current-phase relation (CPR) is $I_J(\varphi) = |I_c| \sin(\varphi + \pi) = -|I_c| \sin(\varphi)$. As conventional measurement of the current-voltage characteristic of a Josephson junction is not sensitive to the sign of the supercurrent, it was necessary to include the Josephson junction in a multiply connected geometry. The sign was in Ref. [255] observed in an rf SQUID configuration [see Figure 30.15(a)] by shorting the electrodes of the junction with a superconducting loop. If that loop contains a π junction in zero external field it will exhibit a spontaneous circulating current, generating a flux of $\Phi_0/2$ which can be detected by a SQUID magnetometer or a Hall probe. In Figure 30.15 (b) the transition between a zero and a π state is unambiguously observed (although residual magnetic fields leading to shifts in the CPR curves did not allow to pin down if it was a 0-π or a π-0 transition).

Phase sensitive measurements of the ground state of ferromagnetic Josephson junctions using a single dc SQUID have been performed by Ryazanov and co-workers [256] for Nb/NbO_y/CuNi/Nb junctions, and by Guichard *et al.* [257] for Nb/NbO_y/PdNi/Nb junctions, showing that the sign change of the Josephson coupling is observed as a shift of half of a flux quantum $\Phi_0 = \frac{h}{2|e|}$ in the SQUID diffraction pattern (see Figure 30.15). A 0-0 and a π-π junction show identical critical current modulations with flux, whereas a 0-π junction exhibits a pattern shifted by $\Phi_0/2$ with respect to that for 0-0 and π-π junctions. In this experiment a single dc SQUID with two SFS junctions embedded. The ferromagnetic layer thickness d_{F1} and d_{F2} can then be chosen to correspond to zero or π coupling independently, leading to the possibility of a $0-0$, a π-π, a 0-π, or a π-0 SQUID. For a dc SQUID with negligible loop inductance and equal junction critical currents the modulation of

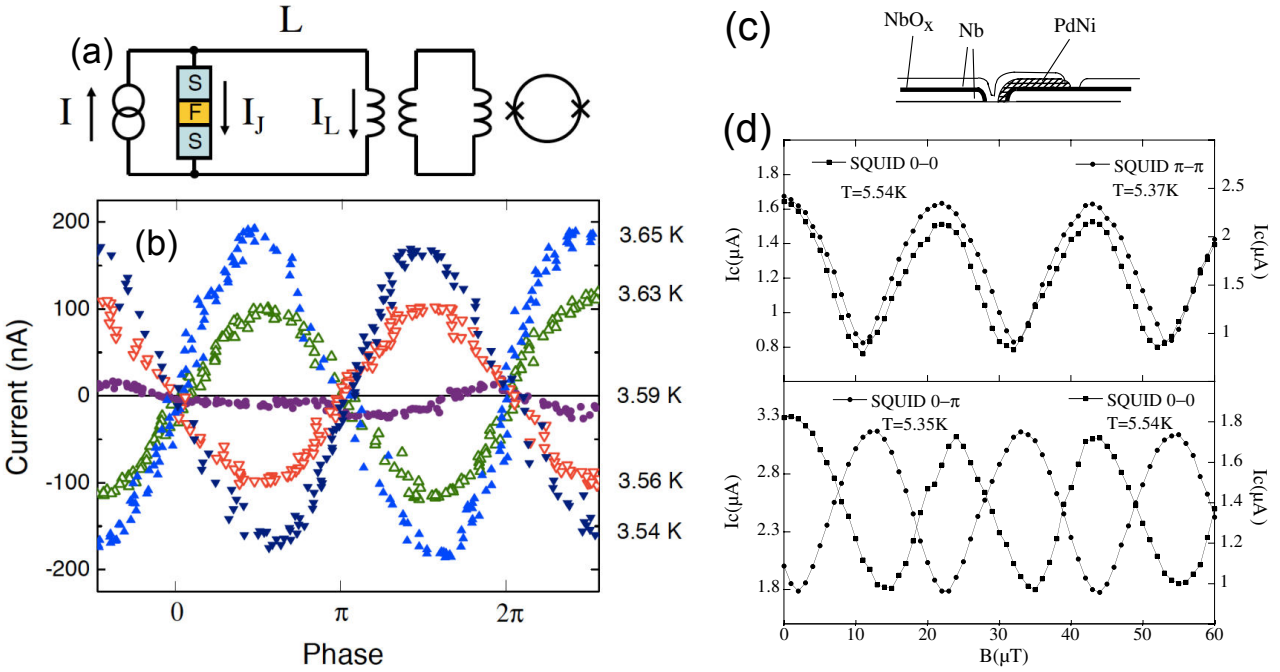


Figure 30.15: (a)Circuit for measuring the current-phase relations of a SFS junction. (b) Current-phase relation derived from rf SQUID modulation curves showing the transition to a π Josephson junction as the temperature is lowered. (a) and (b) from Frolov *et al.* [255]. Copyright (2004) by the American Physical Society. (c) A drawing of the cross section of a single SQUID junction. (d) Critical current modulations showing the expected no-shift between a $0-0$ SQUID and a π-π SQUID and a shift of $\Phi_0/2$ between a $0-\pi$ SQUID and a $0-0$ SQUID. As the T_c of the $0-0$, $0-\pi$, and π-π SQUIDs are different the $I_c(B)$ curves are observed at different temperatures in order to measure in the same range of critical currents for each couple. (c) and (d) from Guichard *et al.* [257]. Copyright (2003) by the American Physical Society.

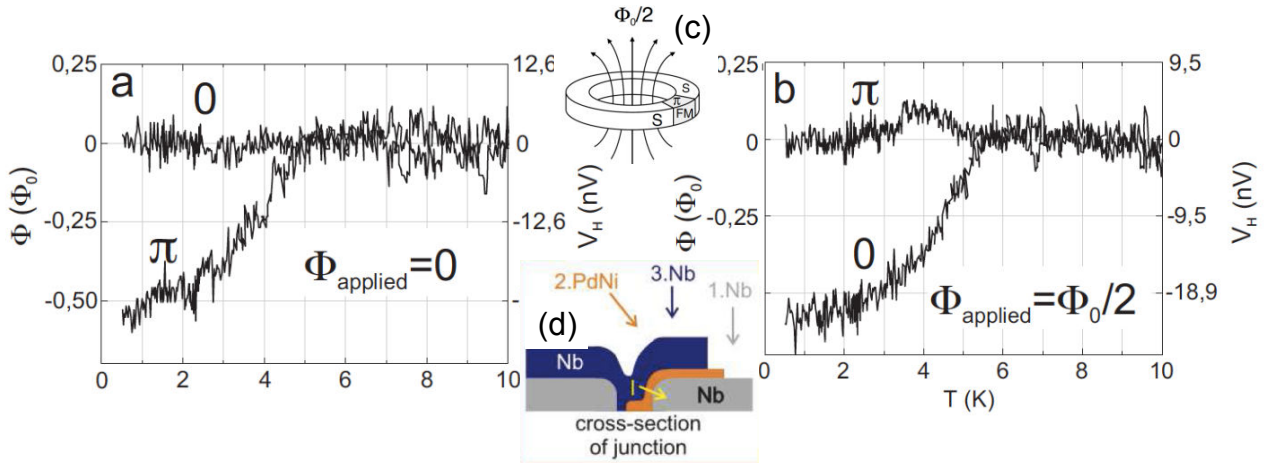


Figure 30.16: Temperature dependent magnetic flux produced by a π- and a 0-loop when cooling (a) in zero field and (b) in a magnetic field equal to half a flux quantum in the loop. Below $T \approx 5$ K the loop develops a spontaneous current when cooling down in zero field, while the magnetic flux through the 0−loop remains zero. When applying a field equal to half a flux quantum Φ_0 the roles of the π- and the 0-loops are interchanged. At low temperatures the spontaneous flux saturates at a value close to $\Phi_0/2$ in each case. (c) In zero external magnetic field, a spontaneous flux $\Phi = \Phi_0/2$ is required to maintain the condition of fluxoid quantization if a π-junction is inserted into a superconducting loop (d) Cross section of the planar Josephson junction. From Bauer *et al.* [258]. Copyright (2004) by the American Physical Society.

the critical current with applied flux is given by [96]

$$I_c(\Phi_{ext}) = 2I_0 \left| \cos\left(\pi \frac{\Phi_{ext}}{\Phi_0} + \frac{\delta_{12}}{2} \right) \right| \tag{30.95}$$

where δ_{12} is the sum of the internal phases (0 or π) in the two junctions of the SQUID. Thus, for a $0-0$ and a π-π SQUID the $I_c(\Phi_{ext})$ patterns are identical, whereas they are shifted by half a flux quantum if $\delta_{12} = \pi$, i.e. a $0-\pi$ or a π-0 SQUID. This shift is shown in Figure 30.15 (d).

The presence of spontaneous magnetic moments in superconducting (Nb) loops containing a ferromagnetic (PdNi) π junction was experimentally demonstrated by Bauer *et al.* (see Figure 30.16) [258]. The loops were prepared on top of a micro-Hall sensor. The authors observed asymmetric switching of the loop between different magnetization states when reversing the sweep direction of the magnetic field. The presence of a spontaneous current near zero applied field was studied as function of temperature, and the magnetic moment approached half a flux quantum at low temperatures.

An rf SQUID geometry where the macroscopic ground state of a ferromagnetic (PdNi) Josephson junction shorted by a 0 weak link was experimentally investigated by Della Rocca *et al.* and showed spontaneous half quantum vortices with random sign ($\pm\Phi_0/2$) [259]; it was found that $0-\pi$ junctions behave as classical spins.

30.5.3 φ-Josephson junctions

An interesting separate development concerns a geometry where a step in the thickness of the ferromagnet is present in a superconductor-ferromagnet bilayer, coupled to another superconductor via an insulating barrier. On one side of the step one has a 0 junction, on the other side a π junction. A half flux quantum (semifluxon) is trapped in such a structure at the step [260, 261, 262], and a supercurrent circulates in the structure, similarly as in a $0-\pi$

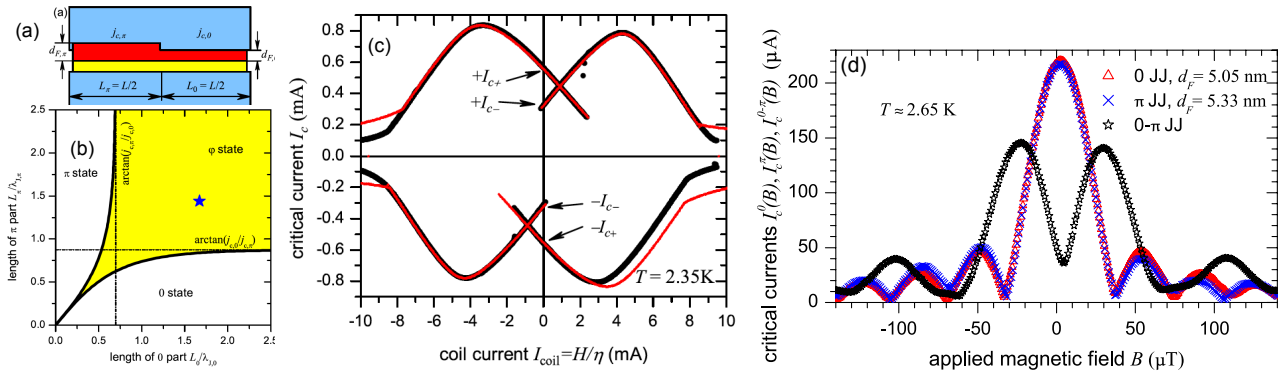


Figure 30.17: (a) Sketch (cross section) of the investigated SIFS 0-π Josephson junctions (Nb/Al-Al_2O_3/$Ni_{0.6}Cu_{0.4}$/Nb) with a step in the ferromagnet layer thickness. (b) Domains of existence of 0-, π- and φ-Josephson junctions. The star shows the position of the investigated Josephson junction in (c). (c) Experimentally measured $I_c(B)$ (black symbols) and theoretical predictions (red symbols). (a)-(c) from Sickinger *et al.* [268]. Copyright (2012) by the American Physical Society. (d) $I_c(B)$ of 0−junction (red triangles), π-junction (blue triangles), and 0-π junction (black spheres). From Weides *et al.* [264]. With kind permission from Springer Science and Business Media.

SQUID [263, 264, 265, 266]. Such structures were studied in detail by Weides, Kohlstedt, Koelle, Kleiner, Goldobin and co-workers. In particular, there exists in such structures the possibility of a φ-junction, which has neither 0 nor π phase difference as a ground state. A method to realize a φ Josephson junction by combining alternating 0 and π parts with intrinsically non-sinusoidal current-phase relation was suggested in Ref. [267]. The realization of an SIFS φ-junction has been experimentally achieved in 2012 (see Figure 30.17) [268]. Properties of zero-π junctions which act as a Josephson junction with an equilibrium phase difference $0 < \varphi < \pi$ are discussed in Ref. [269], where the current-phase relation is calculated numerically and in certain limiting cases analytically.

In Refs. [270, 271], a planar Josephson junction with a ferromagnetic weak link located on top of a thin normal metal film is considered. It is shown that this Josephson junction is a promising candidate for the realization of a φ-junction.

30.6 Long-range triplet supercurrents

30.6.1 Length scales for superconducting correlations in ferromagnets

As detailed in the sections 30.4.4 and 30.4.5, proximity induced superconducting correlations in ferromagnets with sufficiently strong exchange splitting $|\boldsymbol{J}|$ come in pairs of short-range and long-range amplitudes. The former ones are the singlet amplitude and the triplet pair amplitude with zero spin projection, $S_z = 0$, on the magnetization axis of the ferromagnet. These short-range amplitudes decay in ballistic structures algebraically with a reduced magnitude of order $\Delta/|\boldsymbol{J}|$, and in diffusive structures exponentially on the length scale $\xi_J = \sqrt{\hbar D/|\boldsymbol{J}|}$. The other two components, called long-range amplitudes, decay on the thermal coherence length scale ξ_T, given for ballistic structures by $\hbar v_f/(2\pi k_B T + 2\alpha_s)$ and for diffusive structures by $\sqrt{\hbar D/(2\pi k_B T + 2\alpha_s)}$. They are characterized by triplet amplitudes with a spin projection $S_z = \pm 1$ on the magnetization direction of the ferromagnet. Consequently, they are called equal-spin triplet pair correlations. Equal spin pairs do not suffer from having to populate spin-split pairs of Fermi surfaces. Both electrons of the pair are situated on the same spin

component of the Fermi surface. For this reason, they behave like in a normal metal, with the coherence length determined by the Fermi surface properties of one spin component only (which in general differ for $S_z = +1$ and $S_z = -1$). The quest for such long-range pair amplitudes has a long history, and is one of the success stories of interaction between experiment and theory.

30.6.2 Experimental "pre-history"

As in the 1990's the field of spintronics, i.e. functional nanometer-size devices based on spin-dependent transport phenomena, developed rapidly [272], a strong motivation to search for a long-range proximity effect in ferromagnets was established. Such long-range amplitudes would lead to long-range supercurrents in Josephson devices, and would ultimately lead to valuable applications. The ultimate goal is to obtain completely spin-polarized supercurrents, which would necessarily have to be triplet supercurrents.

It was for this reason that in the second half of the 1990's experimental efforts intensified to study proximity effects in strongly spin-polarized ferromagnets. Petrashov, Antonov, Maksimov, and Shaĭkhaĭdarov found in 1994 that the effect of superconducting islands, deposited on the surface of ferromagnetic Ni, can be still seen in the resistance of the Ni layer distances greater than 2 μm (exceeding by more than 30 times what the length $\hbar v_f/|\boldsymbol{J}|$ would suggest) away [273].

Lawrence and Giordano studied in 1996 the resistance as a function of temperature and magnetic field in structures containing a narrow ($\sim 2\mu$m) ferromagnetic strip connecting two superconducting films (In/Ni/In and Pb/Ni/Pb) [274]. They observed a magnetoresistance dip as function of magnetic field much too large to be accounted for by weak localization effects. In addition they found implausibly long phase coherence lengths, inconsistent with the usual superconducting proximity effect. In a later study of Sn/Ni/Sn structures, where the Ni was a narrow wire (~ 40 nm wide), they measured an unexpectedly long proximity length of about 50 nm (theory predicted 4 nm for these structures) when the Sn/Ni interfaces are clean, however with an oxide layer at the interfaces they observed an unexplained re-entrant behavior [275]. They also noted that their proximity length was of the order of the thermal length $\sqrt{\hbar D/k_{\rm B}T}$ which would appear in a normal metal.

Giroud and co-workers studied in 1998 Co/Al structures with a ferromagnetic Co wire in contact with superconducting Al [276]. They observed below the superconducting transition that the Co resistance exhibited a significant dependence on temperature and voltage, and the differential resistance showed that the decay length for the proximity effect was much larger than expected from the exchange field of Co.

Petrashov and co-workers found in 1999 a giant mutual proximity effect in Ni/Al structures with an proximity-induced conductance on the Ni side two orders of magnitude larger than predicted by theory [277]. Aumedato and Chandrasekhar, by performing multi-probe measurements on Ni/Al structures, re-evaluated these studies and came to the conclusion that superconducting correlations cannot extend into a ferromagnet over distances larger than the exchange length, and associated the large changes in resistance seen in the previous experiments with the superconductor/ferromagnet interface or the superconductor, which had been measured in series or in parallel with the ferromagnet [278]. The controversy lead to a vivid discussion about the existence of such long-range proximity components.

30.6.3 Theory of long-range proximity amplitudes

Spiral magnetic inhomogeneities and domain walls

The renewed interest created by the lack of understanding of long-range superconducting proximity effects in ferromagnets lead in the beginning of the 2000's to new theoretical develop-

ments. Pivotal was a series of papers by Bergeret, Volkov, Efetov, and coworkers, who studied the effect of a spiral Bloch-type inhomogeneity close to an S/F interface, where the magnetization vector rotates along the junction direction. They found that an equal-spin triplet pair amplitude shows a long-range penetration into the ferromagnet [131, 73, 222, 279, 280]. The authors also noted that this, as an isotropic ("s-wave") triplet pair component, must be a realization of odd-frequency pairing. As impurities suppress all anisotropic pairing components, this odd-frequency amplitude is the only superconducting pairing amplitude present in the ferromagnet. Shortly after that, Kadigrobov, Shekhter and Jonson found a similar effect [281]. A realization of these ideas motivated by experiment [282] was studied in Ref. [283], where the focus of study was a setup of a Ho/Co/Ho trilayer sandwiched between conventional s-wave superconducting leads. Holmium is a conical ferromagnet with an intrinsic spiral structure. In Ref. [284] a bilayer consisting of an ordinary singlet superconductor and a magnet with a spiral magnetic structure of the holmium or erbium type was investigated by solving self-consistently Bogoliubov-de Gennes equations. A re-entrance behavior as function of temperature is observed for certain parameter ranges.

Another type of magnetic structure discussed in the literature is a domain structure of the Néel type, in which the magnetization vector lies parallel to the interface and rotates along a direction parallel to the interface. A setup with a chiral ferromagnet, exhibiting a homogeneous cycloidal spiral, placed between two conventional superconductors was studied in Ref. [285]. Depending on the spiral wave length, 0-π transitions can be induced. In the case of a uniformly rotating spiral, however, it was shown that only short-range components exist [285]. In a more general case, with magnetic domains separated by Néel walls, long-range triplet components are present and arise at the domain walls, decaying inside the domains [286, 287].

Refs. [288, 289] investigate diffusive SF and SFS structures with a domain wall in the F layer, using a Riccati representation of the non-linear Usadel equations [72] and including spin-mixing parameters for interfaces. They study local density of states, induced magnetization, and spin-polarized Josephson currents. It is found that the spin polarization of the spin current in SFS structures is determined by the magnetization profile and that the spin current shows discontinuities at the zero-π transition points of the critical Josephson current. Similar as in Ref. [172], a non-zero spin-current even for zero superconducting phase difference is reported. In Ref. [290] the contribution of domain walls to the Josephson current through a ferromagnetic metal is examined for both ballistic and diffusive systems. It is found that in the clean limit domain walls enhance the Josephson current even for a collinear magnetic domain structure, whereas in the diffusive limit a non-collinear domain structure is necessary to enhance the effect. In Ref. [291] the influence of the location of a domain wall within a Josephson junction on the ground state properties of the junction was the topic of investigation. The authors considered both the diffusive and ballistic limits. They find that the location of the domain wall determines if the junction is in a zero-state or in a π-state and influences the transition temperature of the junction.

A different type of system with inhomogeneous magnetic structure was studied in Refs. [292, 293], where a ferromagnetic vortex in a mesoscopic ferromagnetic disc is brought in contact with a singlet superconductor. Proximity-induced long-range triplet components are generated by the ferromagnetic vortex under certain circumstances, leading to zero- or π-junction behavior depending on the contact geometry.

Multi-layer geometries

Instead of considering inhomogeneous magnetization profiles within a ferromagnetic layer as sources of long-range triplet correlations, one can also obtain the same effect in a multi-layer geometry with non-collinear arrangement of the magnetizations of the various layers. In Ref. [294] a diffusive SFIFS junction is investigated by self-consistently solving Usadel equations

with appropriate boundary conditions. It is found that for antiparallel ferromagnet magnetizations the critical current is enhanced by the exchange energy, and for parallel magnetization the junction exhibits a transition to a π-state. A switching behavior between zero- and π-state can be observed when going from the antiparallel to the parallel alignment. In Refs. [230, 231] a multilayered superconductor-ferromagnet structure with non-collinear alignment of the magnetizations of the ferromagnetic layers is considered, and the resulting long-range odd-frequency triplet condensate amplitude is calculated. It is found that this setup allows for a Josephson effect with possible zero- or π-junction behavior. It is also pointed out that the chirality of the magnetization profile matters for the direction of the Josephson current. In Ref. [295] a fully self-consistent calculation was performed for a ferromagnet-superconductor-ferromagnet trilayer setup with non-collinear magnetization, and the induced spin magnetization in the entire structure was determined. This work includes self-consistency of the order parameter in the superconducting layer at arbitrary temperatures, arbitrary interface transparency, and any relative orientation of the exchange fields in the two ferromagnets. The long-range Josephson effect through a ferromagnetic trilayer was the topic of Ref. [296], where conditions were derived under which the long-range triplet proximity effect dominates the short-range proximity effect. Both diffusive and clean limits were studied.

Halterman and Valls have investigated numerically ballistic S/F/S trilayer and S/F/S/F/S pentalayer Josephson junctions by self-consistently solving Bogoliubov-de Gennes equations, concentrating on the thermodynamic stability of zero- and π-junctions as function of material parameters and geometry [297, 298].

Zero-π transitions in Josephson junctions with a diffusive pentalayer-structure of the form F/S/F/S/F with misaligned magnetizations in the three ferromagnetic layers were explored in Ref. [299]. The transition temperatures for zero- and π-junctions as function of misalignment angle were determined numerically using an effective and fast procedure, which is described in detail in this publication. In Ref. [300] a diffusive S/F′/FF/F′/S structure is discussed, with two different ferromagnetic materials F and F′. The middle FF double layer is considered to be parallel or antiparallel magnetized, whereas the F′ layers were allowed to be non-collinear. This setup is in particular adapted to the experiments by Khaire *et al.* [301]. A similar study for clean or moderately diffusive materials was performed in Ref. [302].

An SF_1F_2S junction in the ballistic case (including moderate disorder in the ferromagnets) was considered in Refs. [303, 304], with misaligned ferromagnetic layers F_1 and F_2. It was found that the long-range spin-triplet correlations lead to a dominant second harmonic in the Josephson current-phase relation of asymmetric junctions [305], an effect also found for diffusive structures in Ref. [306]. In the latter reference this phenomenon is traced to the long-range coherent propagation of two triplet pairs of electrons, a process first pointed out and discussed in Ref. [172], and called there "crossed pair transmission".

Magnetic moment manipulation by triplet Josephson currents in Josephson junctions with multilayered ferromagnetic weak links is discussed in Ref. [307]. It is reported that by tuning the Josephson current, one may control a long-range induced magnetic moment, which appears due to non-collinear magnetization of the layers. Alternatively, applying a voltage one can in such a geometry generate an oscillatory magnetic moment. The spin-switching behavior as function of rotation of the magnetization in one ferromagnetic layer in diffusive SFSFS and SFSFFS Josephson junctions was investigated in Ref. [308].

The proximity effect in clean superconductor-ferromagnet structures caused by either the spatial or momentum dependence of the exchange field was discussed in Ref. [309]. It was shown that in symmetric junctions the long-ranged proximity effect is present for any non-collinear ferromagnetic moment orientation and a dominant second harmonic appears for any asymmetric junction. The Josephson coupling between two s-wave superconductors separated by a ferromagnetic trilayer with non-collinear magnetization was reconsidered in Ref. [310], where

in particular the dependence on strength of the exchange field and thickness of the interface layers was studied, and the competition between long-range and short-range components was investigated.

The appearance of a spin supercurrent in a diffusive SF_1F_2S Josephson junction was subject of study in Ref. [311]. It was found that a spin current with spin polarization normal to the magnetization vectors flows between the ferromagnetic domains. This spin current is even as function of superconducting phase difference, and odd as function of misalignment angle between F_1 and F_2.

A diffusive S-(FNF)-S double proximity structure, in which an FNF trilayer with mutually misaligned ferromagnetic magnetization vectors bridges two superconducting banks, was investigated in Ref. [312]. In this case long-range equal-spin triplet correlations are generated by the misalignment of the two ferromagnetic layers in the bridge.

Singlet-Triplet conversion at interfaces

The mechanisms discussed in the previous subsections employ a quasiclassical approximation, which is not valid for length scales as small as the Fermi wavelength. In fact, for the mechanism to work it is crucial that short-range components can enter the ferromagnet over a sufficiently long distance to feel the magnetic inhomogeneity, which was assumed to vary on the scale much larger than the Fermi wavelength. This poses the problem of what happens at interfaces between a superconductor and a ferromagnet with large exchange splitting, so that the length scale ξ_J becomes comparable to the Fermi wave length.

An appropriate mechanism for structures with strong exchange splittings was proposed, and first exemplary studied for the extreme case of a half-metallic ferromagnet (where one spin band is insulating and one spin band metallic), in [155, 164, 107, 215]. The mechanism is based on spin-dependent scattering phases under reflection and transmission, which in combination with a misalignment with respect to the ferromagnetic bulk magnetization of the interface magnetic moment in an atomically thin interface layer leads to the creation of long-range triplet pairs. It was shown subsequently, that this mechanism persists for the full range from ballistic to diffusive systems [133]. Note that such a mechanism invokes the magnetic inhomogeneity directly in an *interface barrier*, rather than in a metallic region. It thus differs from the mechanism suggested by Bergeret *et al.* Indeed, the two mechanisms are complementary, with the first one being important for ferromagnets where the exchange splitting is small compared to the Fermi energy, and the second one being important for the case of comparable exchange splitting and Fermi energy, both being much larger than all superconducting energy scales. The crossover between these two asymptotic cases cannot be described within either theory, as no useful expansion parameter is present in the crossover region.

The mechanism of long-range triplet pair creation at interfaces was generalized to Josephson structures involving strongly spin-polarized ferromagnets with two itinerant spin bands in Ref. [172].

Supercurrents in strongly spin-polarized itinerant ferromagnets and half metals

We discuss first the main predictions of a long-range Josephson effect in a structure involving a long half-metallic ferromagnetic region, as discussed in Refs. [155, 107, 133, 215, 224]. As shown in Fig. 30.18, which is for a fully self consistent calculation using a model barrier as in Fig. 30.10 (b), all possible symmetry components shown in Fig. 30.6 are indeed generated at the interface. This simply reflects the fact that both spin rotational symmetry and inversion symmetry are broken by the interface. The calculation assumes that the effective magnetic moment of the interfaces is perpendicular to the bulk magnetization of the half-metallic ferromagnet. As a consequence, according to Eq. (30.24b), long-range amplitudes are generated,

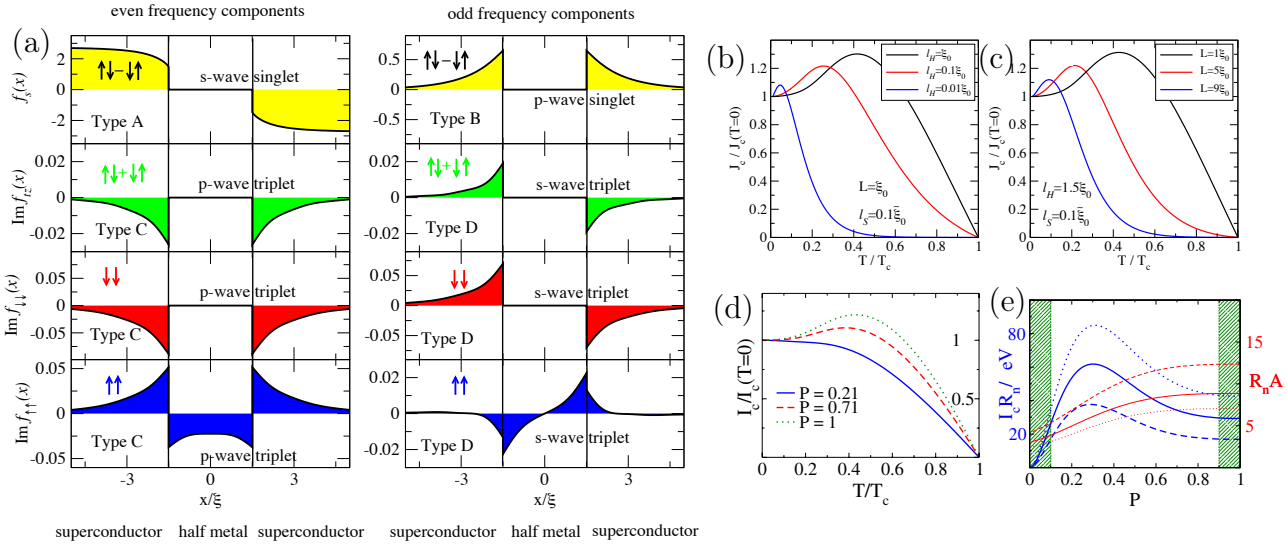


Figure 30.18: (a) All symmetry components in a ballistic S/F/S π-Josephson junction with a half-metallic ferromagnet (H) as F-layer (self-consistent calculation for model barrier as in Fig. 30.10 (b), with $V_S = 0.5$, $d = 0.5/k_0$); barrier spin-polarized in x-direction, half-metal spin-polarized in z-direction; temperature $T = 0.2T_c$; (b)-(e) Non-monotonic temperature dependence of critical Josephson current density in an S/F/S junction, normalized to its value at zero temperature; (b) for half-metallic ferromagnet, dependence on the mean free path ℓ_H in H for a fixed junction length $L = \xi_c = \hbar v_H/2\pi T_c$, where v_H is the Fermi velocity in H; (c) as in (b), but showing the dependence on junction length L for fixed $\ell_H = 1.5\xi_c$; (d) for a ferromagnet in the ballistic limit, with various spin polarizations $P = (p_{F\downarrow} - p_{F\uparrow})/(p_{F\downarrow} + p_{F\uparrow})$; $L = \hbar v_F/2\pi T_c$ with v_F the Fermi velocity in F. (e) I_cR_n product and normal-state resistance R_nA [in units of $(e^2N_Sv_S)^{-1}$, where N_S and v_S are density of states per spin at the Fermi level and the Fermi velocity in the superconductor, respectively] as function of P for $T = 0.5T_c$, and various strengths of interface transmission. In all plots the interface misalignment angle is $\alpha = \pi/2$. (b) and (c) after [133], (d) and (e) from [215]. Copyright (2009) by the American Physical Society.

linking the two singlet superconductors [see lower panels in Fig. 30.18 (a)]. Thus, we have an example of an *indirect* Josephson coupling [155], via a long-range triplet component which is generated in the first place from the singlet component by microscopic processes in the interface region. Note also, that the thermodynamically stable configuration for identical interfaces is a π-junction (for asymmetric junctions the appearence of a φ_0-junction is predicted [107, 133]), for which the system tries to minimize the odd-frequency triplet amplitudes of Type D in the structure. This is a general principle, as odd-frequency amplitudes *increase* the free energy density, instead of decreasing it as even-frequency singlet amplitudes do. Only if the p-wave components (and all higher orbital components) are suppressed by impurity scattering, can the odd-frequency triplet amplitude dominate.

A prominent feature in such a structure is a non-monotonous temperature dependence of the critical Josephson current density, with a pronounced maximum at a temperature which can be linked to the Thouless energy of the ferromagnetic layer (see Fig. 30.18 (c) and Ref. [133]). When the junction becomes effectively long compared with the diffusive-limit coherence length, $L \gg \xi_d = \sqrt{\xi_0 \ell_H/3}$, the current is dramatically suppressed and the peak is shifted to a lower temperature. This maximum moves also to low temperatures in diffusive structures, as is seen in Fig. 30.18 (b), which shows its dependence on the mean free path in the ferromagnet. If one replaces the half-metallic ferromagnet by a strongly spin-polarized ferromagnet with two itinerant spin bands, then the maximum remains only for sufficiently strong spin polarization, as seen in Fig. 30.18 (d). If one projects the Fermi surfaces on the contact plane, then only the "half-metallic" momentum directions contribute to the maximum, which are inside the Fermi sea for one spin projection and outside for the other [172]. Furthermore, there is an optimal spin polarization which maximizes the $I_c R_n$-product of the Josephson junction, which for the particular model interface studied in Ref. [172] is around $P \sim 0.3$. The green shadowed regions in Fig. 30.18 (d) for small and large spin polarizations are regions beyond the validity of the theory, as other processes which are neglected become relevant.

Following the early theoretical work on triplet supercurrents in half-metallic ferromagnets [155, 164], which treats a fully developed triplet proximity effect self-consistently, numerous groups confirmed the existence of triplet supercurrents under various conditions in half-metallic ferromagnets. In Ref. [133] the work of Refs. [155, 164, 107] was generalized to include impurity disorder bridging between the two limits of ballistic and diffusive transport. In this work, the full Eilenberger equations with impurity self energy in self-consistent Born approximation was solved. In Ref. [173] a fully developed triplet proximity effect, just like in Ref. [155] for the clean limit, was treated for the diffusive limit. Further studies in the diffusive limit were performed in Refs. [313, 314, 224]. The role of magnon creation in the half-metallic ferromagnet was studied in [315], with a resulting temperature dependence of the critical current reproducing the temperature dependence found in [155, 107]. The case when the superconductor is unconventional was studied in [316, 317, 318]. In Refs. [319, 215] the problem was advanced on the analytical level assuming a constant singlet order parameter in the superconductor. Self-consistent solution of Bogoliubov-de Gennes equations in the clean limit [320] found results in agreement with Ref. [155, 107], including a strong influence of the junction behavior by subgap Andreev bound states.

Most of these theoretical studies deal with either the diffusive limit within the Usadel approximation or the clean limit. The full range of impurity scattering from clean to diffusive limit for a superconductor-half metal proximity structure was first covered in the theory of Ref. [133]. A treatment in the quantum limit was given by Béri *et al.* [321].

In Ref. [172] a number of effects were pointed out that are absent in the half-metallic case, and which are due to the phase coherent transport of Cooper pairs in the two itinerant spin bands of a ferromagnet. These are illustrated in Fig. 30.19. As seen from Eq. (30.24b), equal-spin triplet correlations in the ferromagnet acquire an additional phase from the configuration

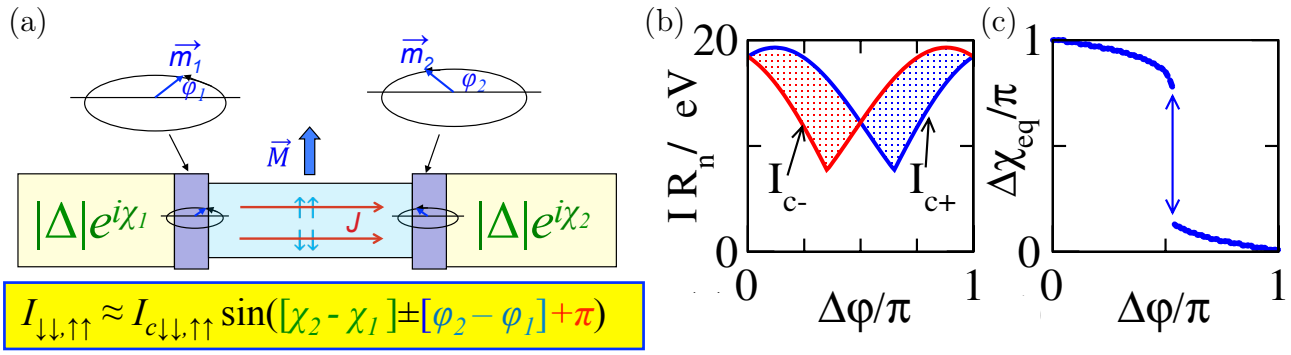


Figure 30.19: (a) S/F/S Josephson junction with a strongly spin-polarized ferromagnet with magnetization $\mathbf{M}$, having interface barriers with misaligned magnetic moments $\mathbf{m}_1$ and $\mathbf{m}_2$. Only equal-spin pair amplitudes are present in each of the spin bands of the ferromagnet. The azimuthal angles of $\mathbf{m}_1$ and $\mathbf{m}_2$ with respect to the magnetization axis $\mathbf{M}$ are denoted φ_1 and φ_2. (b) Critical current in positive (I_{c+})/negative (I_{c-}) bias direction vs $\Delta\varphi = \varphi_2 - \varphi_1$. (c) The zero current equilibrium phase difference $\Delta\chi_{\rm eq} = (\chi_2 - \chi_1)_{\rm eq}$ vs $\Delta\varphi$ varies from π to 0. Here, $T = 0.2T_c$, $P = 0.21$. The polar angle of $\mathbf{m}_1$ and $\mathbf{m}_2$ is $\alpha = \pi/2$. The length of the junction is $L = \hbar v_S/2\pi T_c$, with v_S the Fermi velocity of the superconductor. (b) and (c) from [172]. Copyright (2009) by the American Physical Society.

of the magnetic moments in the interface region, $\mathbf{m}_1$ and $\mathbf{m}_2$, with respect to the bulk magnetization $\mathbf{M}$. If the three magnetizations are *non-coplanar*, there is an important geometric phase involved, which is related to the projection of the interface magnetic moments of the two interfaces to the plane perpendicular to the bulk ferromagnetic magnetization[50]. The relative angle between these two projected magnetic moments defines the angle $\Delta\varphi = \varphi_2 - \varphi_1$, which is a gauge invariant quantity independent of the choice of the global spin quantization axis. This angle directly enters the current-phase relation for each spin band, and precisely with opposite sign for the two spin projections. Thus, the first-order processes (single Cooper pair tunneling) lead to contributions of the form

$$I_{\uparrow\uparrow} = -I_{c\uparrow\uparrow} \sin(\Delta\chi + \Delta\varphi) \tag{30.96a}$$

$$I_{\downarrow\downarrow} = -I_{c\downarrow\downarrow} \sin(\Delta\chi - \Delta\varphi) \tag{30.96b}$$

with $\Delta\chi = \chi_2 - \chi_1$ the difference of the superconducting phases of the singlet pair potential on either side of the Josephson junction. The equilibrium configuration for zero current amounts to[51]

$$\Delta\chi_{\rm eq} = \pi - \arctan\left(\frac{I_{c\uparrow\uparrow} - I_{c\downarrow\downarrow}}{I_{c\uparrow\uparrow} + I_{c\downarrow\downarrow}} \tan\Delta\varphi\right). \tag{30.97}$$

Thus, the system can act as a phase battery. For the half-metal case ($I_{c\downarrow\downarrow} = 0$) this has been noted using Eilenberger equations in Refs. [107, 133] and using Usadel equations in Ref. [224]. Going beyond the tunneling limit, we find a non-zero equilibrium phase difference between the superconducting leads, which shows a jump as function of $\Delta\varphi$, indicating a first order transition (two competing minima of the free energy located at different values of phase difference $\Delta\chi$), which is illustrated in Fig. 30.19 (c). Note that the current-phase relation fulfills the symmetry $I(-\Delta\chi, \Delta\varphi) = -I(\Delta\chi, -\Delta\varphi)$ following from the behavior of the current density under time reversal. The equilibrium configuration carries a non-zero spin current density

[50] In the coplanar but non-collinear case there still can be an important geometric phase of π introduced by the triple of magnetic vectors if $(\mathbf{m}_1 \times \mathbf{M}) \cdot (\mathbf{m_2} \times \mathbf{M}) < 0$.

[51] For zero phase difference a spontaneous current $I(\Delta\chi = 0) = -(I_{c\uparrow\uparrow} - I_{c\downarrow\downarrow}) \sin(\Delta\varphi)$ appears.

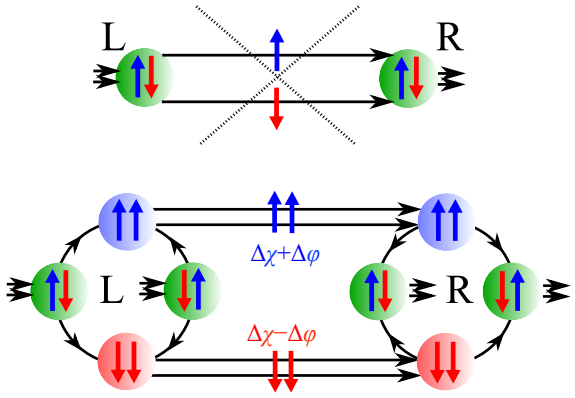


Figure 30.20: Schematic drawing of the crossed pair transmission process. Cooper pairs with opposite spin projection on the magnetization vector do not contribute to the spin supercurrent in strongly spin-polarized ferromagnets (top panel). However, due to magnetic inhomogeneity across the interfaces singlet-triplet conversion processes generate out of two singlet pairs two equal-spin triplet pairs with opposite spin polarization. These two equal-spin pairs are transmitted simultaneously in a crossed pair transmission process (bottom panel). Their phases correspond to $\Delta\chi \pm \Delta\varphi$. A geometric phase shift $2\Delta\varphi$ appears between the two types of Cooper pairs. Copyright (2009) by the American Physical Society [172].

$I_s = 2I_{\uparrow\uparrow}(\Delta\chi_{\rm eq}, \Delta\varphi) \neq 0$. The presence of a Josephson current at zero superconducting phase difference $\Delta\chi$ was confirmed in calculations using Bogoliubov-de Gennes equations in a tri-layer geometry [322]. A study of a superconductor/ferromagnetic-insulator/superconductor junction on the surface of a three-dimensional topological insulator revealed similar effects [323].

The first-order processes described by Eqs. (30.96a)-(30.96b) compete with a second order process, where two (or an even number of) pairs are transmitted simultaneously. In analogy to the so-called crossed Andreev reflection process, we call this process *crossed pair transmission* (see figure 30.20). For transmission of all pairs in equal direction, this process involves phases which are multiples of $(\Delta\chi+\Delta\varphi)+(\Delta\chi-\Delta\varphi) = 2\Delta\chi$, for which the dependence on $\Delta\varphi$ drops out. Consequently, the corresponding contribution to the Josephson current, $I_{\rm cp}$, is independent of $\Delta\varphi$ and π-periodic. More generally, a transmission process of m spin-$\uparrow\uparrow$ pairs and n spin-$\downarrow\downarrow$ pairs involves a phase $(m+n)\Delta\chi+(m-n)\Delta\varphi+(m+n)\pi$. Thus, the corresponding Josephson charge current can be written as

$$I = 2e\,\frac{1}{2}\sum_{mn}(m+n)(-1)^{n+m} I_{mn}\sin[(m+n)\Delta\chi+(m-n)\Delta\varphi] \qquad (30.98a)$$

whereas the spin current is

$$I_s = \hbar\,\frac{1}{2}\sum_{mn}(m-n)(-1)^{n+m} I_{mn}\sin[(m+n)\Delta\chi+(m-n)\Delta\varphi]. \qquad (30.98b)$$

As $I_{-m,-n} = I_{mn}$, the factor $\frac{1}{2}$ can be omitted if we restrict the summation to $m \geq 0$, and for $m = 0$ to positive n. Note that the spin-current is even present in the case $\Delta\chi = 0$, provided that $\Delta\varphi \neq 0$. An example of such a case was discussed in [172], where one of the superconductors was replaced by an insulator, and a pure spin supercurrent remains, giving rise to a *spin-Josephson effect*. In this case only terms with $m+n=0$ remain, with a pure spin supercurrents $I_s = \hbar\sum_m 2mI_{m,-m}\sin(2m\Delta\varphi)$. On the other hand, crossed pair transmission processes in equal direction have zero spin current and correspond to $m = n$, leading to a contribution to charge current of the form $2e\sum_m 2mI_{mm}\sin(2m\Delta\chi)$. For illustrative purposes

we consider the example of only first order terms and leading order crossed pair transmission terms, i.e. only terms associated with I_{01},I_{10}, I_{11}, and $I_{1,-1}$. Then

$$I/2e = -I_{10}\sin(\Delta\chi+\Delta\varphi) - I_{01}\sin(\Delta\chi-\Delta\varphi) + 2I_{11}\sin(2\Delta\chi) \quad (30.99a)$$

$$I_s/\hbar = -I_{10}\sin(\Delta\chi+\Delta\varphi) + I_{01}\sin(\Delta\chi-\Delta\varphi) + 2I_{1,-1}\sin(2\Delta\varphi). \quad (30.99b)$$

The last term in each of these equations corresponds to the crossed pair transmission process (in equal and opposite direction, correspondingly). The critical current density for positive and negative current bias differs for this case, similar as shown in Fig. 30.19 (b). Furthermore, for sufficiently large I_{11} multiple minima of the free energy as function of $\Delta\chi$ appear, leading to the characteristic jump at a certain value of $\Delta\varphi$ as illustrated in Fig. 30.19 (c). If $\Delta\varphi$ were continuously varied, a hysteresis would occur, typical for a first order phase transition. Finally, when one of the superconductors is replaced by an insulating material then $I = 0$ and the spin-Josephson current is $I_s = 2\hbar I_{1,-1}\sin(2\Delta\varphi)$ [172].

30.6.4 Recent experimental observations

Triplet supercurrents in half-metallic ferromagnets

Half-metallic ferromagnets are especially promising for applications, as they are fully spin polarized and thus give the largest spin filtering effect possible. The recent developments and applications for half-metallic ferromagnets have been reviewed e.g. in Refs. [324, 325, 326].

First indications for an coupling of superconductors through a half-metallic ferromagnet came from experiments by Peña *et al.* on ferromagnetic $La_{0.7}Ca_{0.3}MnO_3$, coupled with the high-temperature d-wave singlet superconductor $YBa_2Cu_3O_{7-\delta}$ in trilayers and superlattices [327, 328]. These authors found a long-range proximity effect over a length scale of 100 nm.

In 2006, Keizer *et al.* reported a triplet supercurrent in the half metal CrO_2 [329]. The authors used NbTiN as superconducting electrodes and CrO_2 grown on TiO_2. After it had proved difficult to reproduce the effect, it was in 2010 when finally Anwar *et al.* in the group of Aarts reported that they had found long-range supercurrents through CrO_2 grown on Al_2O_3 (sapphire) [330]. The current was observed over a distance of 700 nm between two superconducting amorphous $Mo_{70}Ge_{30}$ electrodes. The effect was interpreted in terms of odd-frequency pairing correlations (although really the experiment only indicates equal-spin pairing correlations and does not provide experimental insight about the orbital and frequency symmetry of the pairs). However, the group was not able to find the long-range supercurrent in CrO_2 grown on TiO_2, the material used by Keizer *et al.* They noted that their CrO_2 films showed a uniaxial anisotropy in contrast to the biaxial anisotropy present in the Keizer *et al.* samples [330, 331].

There had been criticism that based on previous point contact spectroscopy experiments, CrO_2 might not be fully spin-polarized. These data were summarized by Löwfander *et al.* in 2010, and it was shown that all point contact data on CrO_2 are indeed consistent with full spin polarization, if the theory is extended to take into account realistic interfaces [158].

Anwar *et al.* have in a subsequent study extended their work [332] and find that if a Ni/Cu sandwich between the CrO_2 film and the $Mo_{70}Ge_{30}$ electrodes is used, a long-range supercurrent is observed also for TiO_2 substrate over a distance of almost a micrometer. The critical current density is 100 times larger in these Ni/Cu/CrO_2 junctions on TiO_2 substrate than if sapphire is used as a substrate, and is comparable to that observed by Keizer *et al.* This proves that in addition to the substrate on which CrO_2 is grown, the interface characteristics between CrO_2 and the superconductor play a decisive role, and spin-mixing due to misaligned spins as predicted before by theory [155] is the crucial ingredient for explaining the singlet-triplet conversion in these structures.

Further evidence for triplet supercurrents came from a report by Sprungman *et al.*, who found a Josephson effect with ferromagnetic Cu_2MnAl Heusler barriers [333]. It was observed

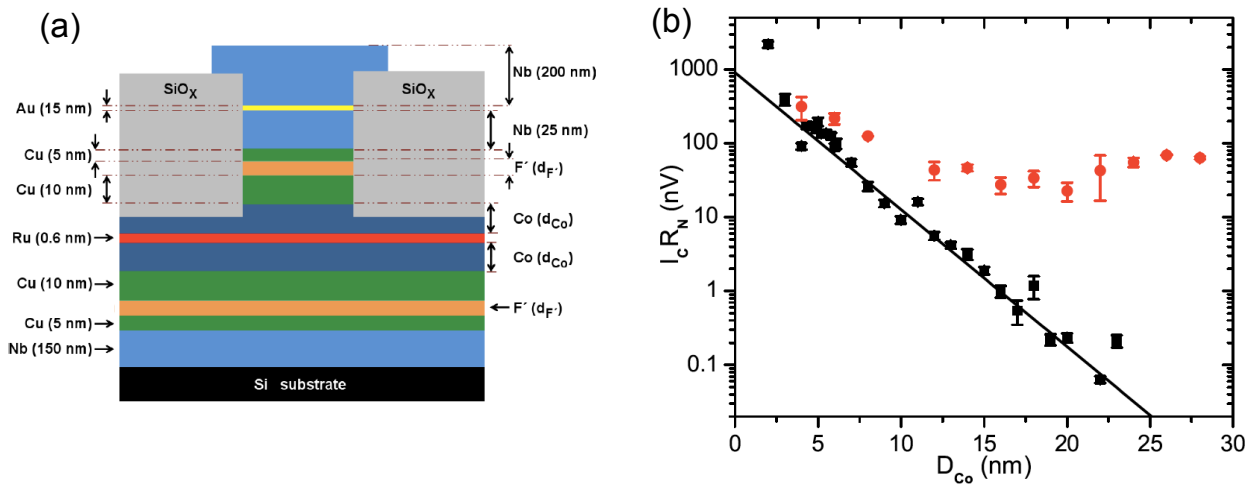


Figure 30.21: (a) Schematic diagram of the Josephson junctions used in the work of Khaire *et al.*, shown in cross-section. From Klose *et al.* [337]. Copyright (2012) by the American Physical Society. (b) Product of critical current times normal state resistance, I_cR_N, as a function of total Co thickness, $D_{Co} = 2d_{Co}$. Red circles represent junctions with F'=PdNi and d_{PdNi} =4 nm, whereas black squares represent junctions with no F' layer (taken from Ref. [250]). As D_{Co} increases above 12 nm, I_cR_N hardly drops in samples with PdNi, but drops very rapidly in samples without. (The solid line is a fit of the data without PdNi to a decaying exponential, from Ref. [250].) From Khaire *et al.* [301]. Copyright (2010) by the American Physical Society.

that the critical current density versus temperature shows a pronounced peak around 4.5 K (electrodes were Nb), decreasing towards lower and higher temperatures. Such a maximum was predicted in [155, 133, 215]. However, there is some intrinsic gradient of the degree of $L2_1$-type Heusler structure ordering inside the Heusler layers, with a low degree if order at the interfaces and higher degree of order in the interior [333]. For that reason, it is too early to decide about the origin of this maximum in $I_c(T)$ in these experiments.

Another half-metallic ferromagnet is $La_{0.7}Ca_{0.3}Mn_3O$, which has been studied in the context of $YBa_2Cu_3O_7/La_xCa_{1-x}MnO_3$ multilayers by Peña *et al.* in 2005. Kalcheim *et al.* [334] performed scanning tunneling spectroscopy experiments on $La_{0.7}Ca_{0.3}Mn_3O$ film epitaxially grown on superconducting $Pr_{1.85}Ce_{0.15}CuO_4$, and find long-range penetration of superconductivity into half-metallic $La_{0.7}Ca_{0.3}Mn_3O$. Visani *et al.* [335] find quasiparticle and electron interference effects in the conductance across a $La_{0.7}Ca_{0.3}Mn_3O/YBa_2Cu_3O_7$ interface that demonstrate long-range propagation of superconducting correlations across the half metal. The effect is interpreted in terms of equal-spin Andreev reflections (equal-spin Andreev reflection was introduced in Ref. [165] under the term "spin-flip Andreev reflection", or SAR). The peculiarities of Andreev reflection at a half-metal interface with a singlet superconductor are connected with the spin-active interfaces that unavoidably will be involved, and have been clarified in Appendix C of Ref. [215], and in Refs. [165, 158, 167, 168].

Multilayer converter

Experiments utilizing a multilayer geometry, in some sense manufacturing an inhomogeneous magnetization profile by using different materials for the various layers, led to a successful generation of triplet supercurrents in a thick Co layer by the group of Birge in 2010 [301]. In these experiments two layers of ferromagnetic alloys were used to generate triplet amplitudes, which then are passed as long-range supercurrent through a strongly spin-polarized ferromag-

net. The crucial role of the misalignment of the magnetizations was demonstrated. With this breakthrough a simple and reliable way was found to produce long-range triplet supercurrents. The geometry is shown in Figure 30.21 together with the results. It makes use of the previously acquired knowledge of the group that a Co/Ru/Co trilayer instead of a single Co layer will give much better control over the junction behavior [see Figure 30.14(b)] [250]. When the extra outer layers are present, a long-range effect persists, whereas if they are absent, there are only short-range supercurrents present [301, 336]. It was later shown experimentally that the triplet supercurrent is enhanced up to 20 times after the samples are subject to a large in-plane magnetizing field aligning the two Co layers perpendicular to the magnetizations of the two thin outer layers [337], exactly as predicted e.g. in [155, 107, 296]. In Ref. [338] a triplet supercurrent in S/F'/F/F'/S Josephson junctions was studied, where S was superconducting Nb, F' a thin Ni layer with in-plane magnetization, and F a Ni/$[Co/Ni]_n$ multilayer with out-of-plane magnetization. It was found that the supercurrent decays very slowly with F-layer thickness and is much larger when the F' layer are present than if not. This confirmed that the spin-triplet supercurrent is maximized by the orthogonality of the magnetizations in the F and F' layers.

Theoretical treatments of the geometry used by Khaire *et al.* have appeared in Refs. [300, 302, 283]. It was subsequently demonstrated experimentally that the critical current scales linearly with area in magnetized junctions, confirming the homogeneity of the superconducting phase difference across the junction area [339].

Long-range effects in ferromagnetic nanowires

There have been also reports for a long-range proximity effect in long ferromagnetic nanowires. An early overview over studies of ferromagnetic nanowires with superconducting electrodes was given by Petrashov *et al.* [340]. The controlled growth of nanowires has improved over the last decade, allowing to create crystalline nanowires of several hundreds nanometers length. Wang and coworkers used a single-crystalline ferromagnetic Co nanowire and reported zero resistance in wires up to 600 nm length [341]. A theory for a long-range singlet proximity effect in ferromagnetic nanowires was given by Konschelle *et al.* [342]. Takei *et al.* developed a theory of a ferromagnetic nanowire-superconductor proximity structure based on Rashba spin-orbit coupling in the barrier that induces p-wave superconductivity in the ferromagnet [343].

Almog *et al.* [344] report measurements of the dynamical conductance of a double In/Co/In device, where two Co wires are connected to superconducting In electrodes, running parallel less than a coherence length apart from each other. They find a spin polarization of the superconducting order parameters at the interfaces which depends on the relative spin polarization of the two wires. Colci *et al.* [345] study a similar structure with two superconducting electrodes being bridged by two parallel ferromagnetic wires forming an SFFS junction. They concentrate on the phenomenon of crossed Andreev reflection. At low temperatures and excitation energies below the superconducting gap, they find that the resistance corresponding to antiparallel alignment of the magnetization of the ferromagnetic wires is higher than that of parallel alignment. Spin-dependent interface scattering was found to be important in order to understand these findings [346].

Spiral magnetic order

A realization of the ideas by Bergeret, Volkov, and Efetov was reported in Ref. [347], by employing the conical ferromagnet holmium. A long-range proximity effect was observed. In this work, superconducting phase-periodic conductance oscillations in ferromagnetic Ho wires in contact with conventional superconductors were measured. The distance between the interfaces

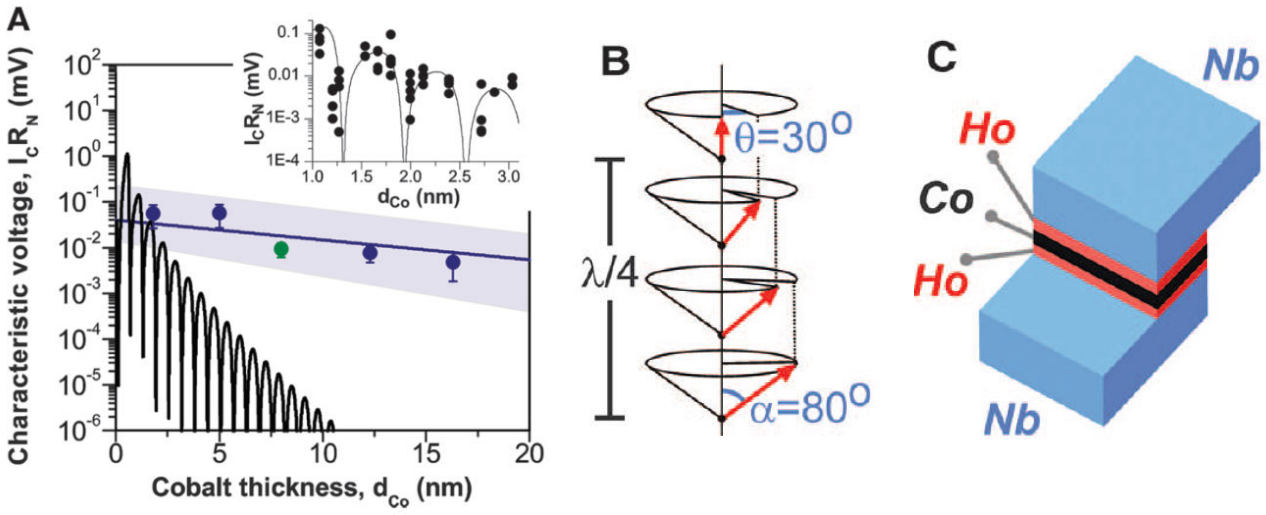


Figure 30.22: (A) Slow decay at 4.2 K in the characteristic voltage I_cR_N of Nb/Ho(4.5 nm)/Co(d_{Co})/Ho(4.5 nm)/Nb junctions (blue circles) and a Nb/Ho(10 nm)/Co(d_{Co})/Ho(10 nm)/Nb junction (green circle) versus Co barrier thickness (d_{Co}). Inset: Comparative data (black circles) from [348] showing the behavior of Nb/Rh/Co/Rh/Nb junctions. The oscillating curves in the inset and main panel are theoretical fits to the experimental data in the inset, as described in [348]. (B) The conical magnetic configuration of idealized Ho below its Curie temperature (20 K), showing an antiferromagnetic spiral rotating in-plane $\theta = 30^o$ per atomic plane and pitched $\alpha = 80^o$ out-of-plane. The moments (arrows) rotate about the surface of a cone with the spiral wavelength, λ, corresponding to a Ho thickness of 3.4 nm. (C) Device layout consisting of two superconducting Nb electrodes coupled via a Ho/Co/Ho trilayer. From Robinson *et al.* [282]. Reprinted with permission from AAAS.

was much larger than the singlet superconducting penetration depth.

A triplet supercurrent has been found by Robinson, Witt, and Blamire with a setup using a cobalt layer sandwiched between two holmium layers, constituting another breakthrough in 2010 [282]. The main results of this work are shown in Fig. 30.22. Without the Ho layers between the Nb and Co (or with the Ho replaced by Rh) the characteristic voltage I_cR_N shows fast oscillations and a short-range decay over six orders of magnitude on a scale of 10 nm. If additional Ho layers are inserted between Nb and Co, the characteristic voltage decays very slowly, by about an order of magnitude on a scale of 50 nm. The effect is spectacular especially for Co thicknesses above 10 nm. Theoretical treatments of this geometry have been given in Refs. [349, 350, 185].

Further reports concentrate on creating artificial non-collinear magnetic structures that can be brought in contact with superconductors. In Ref. [351] it is reported that a new structure using an exchange-spring magnet was fabricated that can be tuned from a collinear to a non-collinear state by a rotating external magnetic field in a controllable way. With this setup the authors found an increase of superconductivity in the structure (transition temperature and conductance) when going to a non-collinear state.

Robinson *et al.* studied Nb/Fe/Cr/Fe/Nb junctions where the thickness of the Cr layer determines the relative alignment of the Fe layers, and find a substantial enhancement of the critical Josephson current when a non-parallel configuration was realized [352].

Witt *et al.* find that in structures with a conical magnetic spacer layer of Ho the critical Josephson current decays exponentially with layer thickness, corresponding to a coherence length of 4.34 nm in Ho, and without showing any oscillatory behavior [353]. Comparing this with the mean free path of 0.28-0.87 nm, they conclude that their Ho structures are in the dirty

limit.

A realization of field-tunable in-plane Bloch domain walls in the rare-earth magnet gadolinium if grown between non-collinearly aligned ferromagnets was suggested in Ref. [354]. It was found that supercurrents flow through magnetic Ni/Gd/Ni nanopillars, the magnitude of which strongly depends on the domain wall state in Gd. The authors explain this result in terms of the inter-conversion of triplet and singlet pairs, the efficiency of which depends on the magnetic helicity of the structure.

For a recent review by Blamire and Robinson see [355].

30.7 Modern developments

In the following I selectively give examples for exciting modern developments of the field, without claiming to cover the entire spectrum of activities.

30.7.1 Spin-valve devices and spin-filter junctions

Although currently the research still concentrates on studying fundamental questions, applications can be imagined in various ways. The most obvious application would be the development of a spin-valve device. Re-entrant phenomena are predicted not only as function of thickness of the adjacent ferromagnetic layers, but also as function of other parameters, e.g. the degree of magnetic inhomogeneity, as in ferromagnets with spiral order. A high degree of experimental control has been achieved in producing large batches of samples with gradually varying thicknesses, allowing for a tailoring of the Fulde-Ferrell-Larkin-Ovchinnikov state [356]. A controllable Josephson spin-valve has been realised recently [357].

Superconducting spin-filter tunnel junctions have been studied recently experimentally [358] and theoretically [359]. In Ref. [358], GdN barriers are used as ferromagnetic insulator barriers, and it is shown that the field and temperature dependence of the critical Josephson current is strongly modified by the ferromagnetic insulator. It is found that the strong suppression of Cooper pair tunneling by the spin filtering of the barrier can be modified by magnetic inhomogeneity in the barrier. In theoretical work [359] it was also demonstrated that the differential conductance may exhibit peaks at different values of the voltage depending on the polarization of the spin filter, and the relative angle between the exchange fields and the magnetization of the barrier.

30.7.2 Flux Qubits and semifluxons

Superconducting electronics is undergoing a revival at present, with pressing need for cryogenic memory for flux quantum logic applications as well as new superconducting Qubit applications. Metal spintronics is already widely employed in computer hard disc technology, and superconducting spintronics may lead to energy efficient memory and logic for supercomputing applications. Superconducting digital single-flux-quantum circuits using superconductor-ferromagnet-superconductor sandwich technology to insert π-Josephson junctions into a circuit is promising due to its high operation speed and low energy consumption [360]. Such systems also solve the problem of high element densities on-chip for operating and holding magnetic flux quanta. A combination of magnetic Josephson junctions and conventional Josephson junctions can be used to form addressable memory cells, energy-efficient memory periphery circuits and programmable logic elements [361, 362].

Another interesting development is semifluxon physics in zero-π Josephson junctions. Fluxons are traveling, solitonic waves of magnetic flux in long Josephson junctions, created by external magnetic fields. In a zero-π-junction a Josephson vortex of fractional magnetic flux

is pinned at the zero-π-boundary. A memory cell based on a φ-Josephson junction has been suggested [363], where writing is done by applying a magnetic field and reading by applying a bias current. Storage at low temperatures is passive, without any bias or magnetic field applied.

A high-frequency cryogenic generator operating at about 200 GHz, and based on flipping a semifluxon in a Josephson junction has recently been demonstrated in Ref. [366]. A π junction is artificially created by current injection using a technique by Ustinov [364], giving rise to a semifluxon [365]. A conversion efficiency of $\sim 10\%$ of dc input power to ac output power was achieved, including the losses on the way from the generator to the on-chip detector. This type of Josephson oscillator is comparable with those based on flux-flow, with advantages like small size and insensitivity to injection current.

Realization of a 0-π junction in an atomic bosonic quantum gas has been proposed in Refs. [367, 368]. In Ref. [368] it is suggested that two-state atoms in a double-well trap are coupled and an all-optical 0-π Josephson junction is created by the phase of a complex-valued Rabi frequency, exhibiting modes similar to semifluxons. It is suggested that pairs of semifluxons can be created by starting from a flat-phase state in long, optical 0-π-0 Josephson junctions formed with internal electronic states of atomic Bose-Einstein condensates [369].

30.7.3 Non-equilibrium quasiparticle distribution

A particular exciting subject is the possibility to utilize non-equilibrium quasiparticle distribution in conjunction with quantum coherence in so-called Andreev interferometer geometries. These devices were introduced by Petrashov, Antonov, Delsing, and Claeson in 1994 [370]. A superconducting wire (e.g. aluminum) is attached at two points to a normal mesoscopic conductor (e.g silver or antimony) to form a loop. The conductance of the wire then oscillates as function of the magnetic flux through the loop. The oscillations are attributed to phase transfer from the superconducting condensate to normal electrons via Andreev reflections at the N-S interfaces. The so-called π-SQUID employs an idea of Volkov [371], where by applying a control voltage directly to a normal metal the electron distribution function in the normal metal is modified. This non-equilibrium distribution spreads to the superconductor and influences the transport in a nonlocal way. This allows for a direct control of the supercurrent through the device, including switching between zero-junction and π-junction behavior. Such a device was realized experimentally by Morpurgo, Baselmans, van Wees, and Klapwijk in 1998-99 [372, 373]. Corresponding effects are intricately connected with non-locality. Cadden-Zimansky, Wei, and Chandrasekhar [374] combined an Andreev interferometer arrangement with injection of non-equilibrium excitations into a normal wire, giving rise to a current that adds to the supercurrent in the Andreev interferometer and leads to a voltage at the contacts. Due to current conservation each current influences the other, and together they allow for tuning of the contact voltage by changing the flux through the Andreev interferometer that controls the supercurrent [375]. Coherent voltage oscillations as functions of external flux are the result.

The combination of non-equilibrium quasiparticle distribution with the Josephson effect seems particularly exciting, and is largely unexplored so far. Recent studies by Bobkova and Bobkov [376, 377] address the problem of spin-dependent non-equilibrium quasiparticle distribution. It is found that the interplay between the spin-dependent quasiparticle distribution and the triplet superconducting correlations induced by the proximity effect between the superconducting leads and ferromagnetic elements of the interlayer leads to the appearance of an additional contribution to the Josephson current. The interplay between short-range and long-range proximity effect is elucidated, and a long-range penetration of opposite-spin Cooper pairs under non-equilibrium conditions is proposed. An increase of the critical Josephson current by few orders of magnitude as a result of the non-equilibrium population in the ferromagnetic layer is suggested. Long-range spin and charge accumulation in mesoscopic superconductors

with Zeeman splitting was recently also studied by Silaev *et al.* [378].

A quantum interference transistor involving textured ferromagnets was suggested in Ref. [379]. It was shown that such a device acts as an ultra-sensitive magnetometer and allows for singlet-triplet switching by tuning a bias voltage. A combination of two spin injectors with an SFS Josephson junction was discussed in Refs. [380, 381].

30.7.4 Dynamical effects

Dynamical effects in superconductor-ferromagnet structures have moved in the focus of interest recently. In particular, it is clear that magnetization dynamics will be linked closely with Josephson dynamics, leading to potentially new effects. The geometric phases discussed in section 30.6.3, when time dependent, are expected to lead to spin accumulation effects via an imbalance between the equal-spin pair electrochemical potentials, very similar to the voltage linked to a dynamical superconducting phase in the ac Josephson effect [172].

The Josephson current in a diffusive superconductor-ferromagnet-superconductor junction with precessing bulk magnetization was calculated in Ref. [382]. It was found that when the junction is phase biased, a dc Josephson current without ac component can still flow under this non-equilibrium condition. Long-range triplet amplitudes are induced by the precessing magnetization.

In Refs. [383, 384] non-equilibrium effects in a Josephson junction with two s-wave singlet superconducting leads coupled via a precessing spin in a quantum dot was examined. An external magnetic field leads to a Larmor precession of the spin, rendering the magnetically active interface time-dependent. The authors analyze the non-equilibrium population of Andreev sidebands and dynamical spin currents. It is found that the supercurrent is enhanced and the critical Josephson current density shows a non-monotonous behavior as function of temperature, accompanied by a corresponding change in spin-transfer torques acting on the precessing spin.

Supercurrent-induced magnetization dynamics in superconductor-ferromagnet Josephson junctions was explored in Refs. [385, 386, 387, 388, 389, 390]. It is found that the spin supercurrent can induce magnetization switching that is controlled by the superconducting phase difference. The authors in Refs. [388, 389] confirm the finding of Ref. [172], that the effect of chiral spin symmetry breaking of the structure leads to additional geometric phases that allow for the stabilization of a φ-junction.

In Ref. [391] the dynamics of superconductor-ferromagnet-insulator-ferromagnet-superconductor (SFIFS) junctions with a thin ferromagnetic layers investigated. The coupled dynamics of the magnetization and the Josephson phase leads to Josephson plasma waves coupled to oscillations of the magnetization, affecting the form of the current-voltage characteristics in weak magnetic fields.

30.7.5 Spin-orbit coupling and topological materials

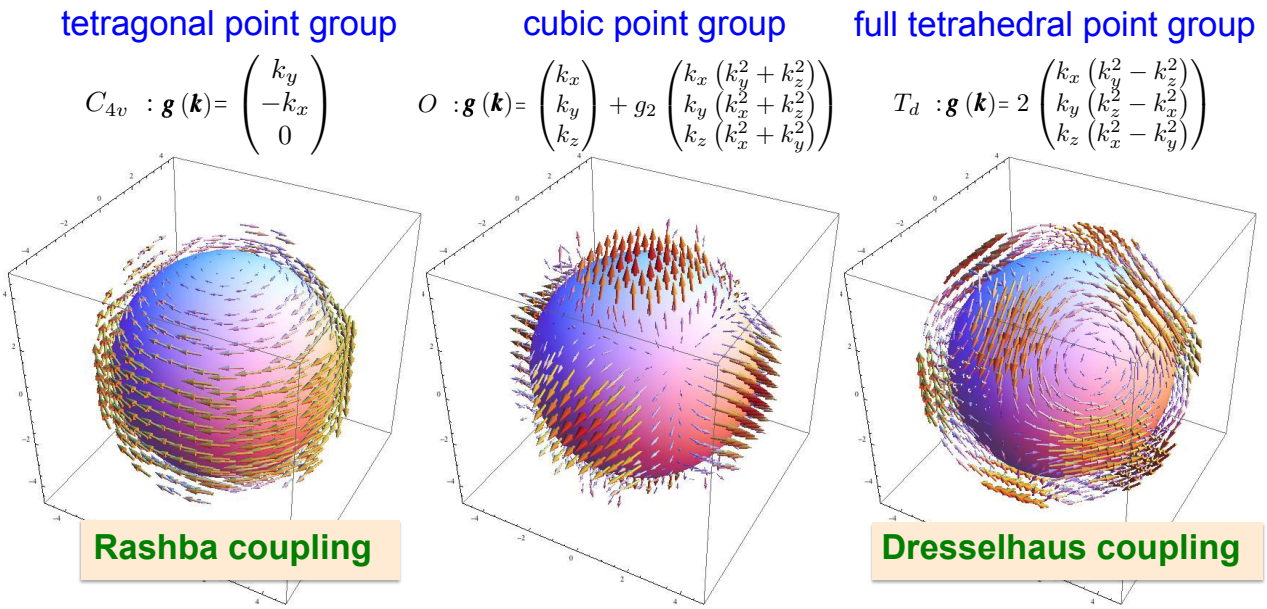


Figure 30.23: Various types of spin-orbit coupling in crystals, relevant for topological superconductivity. The crystal point group sets restrictions to the allowed spin-orbit vector fields. The lowest order expansion terms in crystal momentum are shown.

Spin-orbit effects play an important role whenever the inversion symmetry is broken, either in the bulk material (when it is lacking a center of inversion), or at interfaces and surfaces [392]. A prominent example for spin-orbit effects at surfaces is the Rashba-Bychkov spin-orbit coupling [393], and in the bulk an example is the Dresselhaus coupling due to bulk-inversion asymmetry [394].

Whereas in materials with a center of inversion all band-diagonal matrix elements of the spin-orbit coupling vanish, this is not the case in non-centrosymmetric materials. Spin-orbit coupling in non-centrosymmetric materials is strongly enhanced due to band-diagonal contributions, leading to a splitting of the Fermi surface into spin-orbit bands, sometimes also called 'helicity bands' (although a well defined helicity is only in special cases present). The kinetic part of the Hamiltonian in a one-band model has the form

$$\mathcal{H}_{\text{kin}} = \sum_{\mathbf{k}} \sum_{\sigma\sigma' \in \{\uparrow,\downarrow\}} \left[\varepsilon(\mathbf{k}) + \mathbf{g}(\mathbf{k}) \cdot \boldsymbol{\sigma}\right]_{\sigma\sigma'} a^\dagger_{\mathbf{k}\sigma} a_{\mathbf{k}\sigma'} \tag{30.100}$$

with the spin-orbit vector being odd in $\mathbf{k}$: $\mathbf{g}(-\mathbf{k}) = -\mathbf{g}(\mathbf{k})$. In figure 30.23 various spin-orbit vector fields compatible with the point group of the crystal are visualized on a hypothetical spherical Fermi surface. All three cases are relevant for materials: C_{4v} for $CePt_3Si$ [395], $CeRhSi_3$ [396] and $CeIrSi_3$ [397], T_d for Y_2C_3 [398], and O for $Li_2(Pd_{1-x}Pt_x)_3B$ [399]. The kinetic part of the Hamiltonian can be diagonalized, leading to the above-mentioned helicity bands. The spin-orbit interaction locks the orientation of the quasiparticle spin with respect to its momentum in each band.

One interesting aspect of a non-centrosymmetric ferromagnetic Josephson junction is the modification of the Josephson relation from an odd function in the superconducting phase difference to a current-phase relation where this symmetry is broken. For example, near the critical temperature the current-phase relation $I = I_c \sin(\Delta\chi)$ can be modified to

$$I = I_c \sin(\Delta\chi - \varphi_0), \tag{30.101}$$

where $\Delta\chi$ is the superconducting phase difference, and φ_0 is a phase shift proportional to the magnetic moment perpendicular to the gradient of the asymmetric spin-orbit potential [401]. The possibility of a φ_0-junction has been already taken into account by Josephson [91], and was later considered in Josephson junctions involving unconventional superconductors [400]. Examples in Josephson junctions with half-metals and strongly spin-polarized ferromagnets we discussed in Section 30.6.3. A similar effect has also been predicted for Josephson junctions with a spin-polarized quantum point contact in a two-dimensional electron gas with spin-orbit coupling in an external magnetic field [402]. The spin-dynamics with such a φ_0 Josephson junction has been discussed in Ref. [386]. The competition between a Zeeman interaction and a Rashba spin-orbit interaction has been in the center of attention since a while. In connection with one-dimensional quantum wires, an anomalous φ_0 shift was predicted in Refs. [403, 404]. In a model for a mesoscopic multilevel quantum dot the conditions for an anomalous Josephson current Eq. (30.101) were found to be a finite spin-orbit coupling, a suitably oriented Zeeman field, and the dot being a chiral conductor [405, 406]. In Refs. [322, 407] an anomalous Josephson current was predicted in junctions coupled with a two-dimensional electron gas exhibiting coexistence of spin-orbit coupling and Zeeman field.

A recent development concerns a gauge-covariant approach to establish the transport equations, treating the charge and spin degrees of freedom on equal footing. In this approach both the electromagnetic and spin interactions are described in terms of U(1) Maxwell and SU(2) Yang-Mills equations, respectively [408, 409]. The starting point is a quasiclassical expansion of the microscopic Gor'kov equations in a gauge-covariant manner [410, 411]. The idea is that one can re-write a Hamiltonian of the type

$$H_{\rm kin} = \frac{p_x^2 + p_y^2}{2m} - \mu + \mathbf{h}\cdot\boldsymbol{\sigma} + v_{\rm s.o.}(\hat{\mathbf{z}}\times\mathbf{p})\cdot\boldsymbol{\sigma} \tag{30.102}$$

as

$$H_{\rm kin} = \frac{(p_x - mv_{\rm s.o.}\sigma_y)^2}{2m} + \frac{(p_y + mv_{\rm s.o.}\sigma_x)^2}{2m} - \mu - \frac{mv_{\rm s.o.}^2}{2} + \mathbf{h}\cdot\boldsymbol{\sigma}, \tag{30.103}$$

which motivates to introduce $A_x = -mv_{\rm s.o.}\sigma_y/\hbar$ and $A_y = mv_{\rm s.o.}\sigma_x/\hbar$ as two non-abelian gauge potentials. In this approach, the covariant derivative

$$\mathfrak{D}G = \partial_{\mathbf{R}}G + i[\mathbf{A}, G] \tag{30.104}$$

with the gauge potential $\mathbf{A}$ is associated with the gauge field

$$\mathbf{F}_{\mu\nu} = \partial_\mu\mathbf{A}_\nu - \partial_\nu\mathbf{A}_\mu + i[\mathbf{A}_\mu, \mathbf{A}_\nu] \tag{30.105}$$

which is antisymmetric in its indices, and has only one component, $\mathbf{F}_{xy} = -2(mv_{\rm s.o.})^2\sigma_z/\hbar^2$. This leads in the transport equation to the modification

$$i\hbar\mathbf{v}_f\cdot\nabla_{\mathbf{R}}\hat{g} \to i\hbar\mathbf{v}_f\cdot\nabla_{\mathbf{R}}\hat{g} + imv_{\rm s.o.}^2\partial_\varphi\{\sigma_z, \hat{g}\} \tag{30.106}$$

with ∂_φ the derivative along the Fermi surface (which is assumed a circle for simplicity). Using this modified equation, the role of spin-orbit coupling as source of long-range triplet proximity effect in superconductor-ferromagnet structures has been explored in Ref. [411]. Furthermore, the connection to φ_0 Josephson junction behavior has been elucidated [412, 413]. It should be, however, cautened that the modification in Eq. (30.106) does not contain all terms of the same order as the additional term. A quasiclassical theory of disordered Rashba superconductors has also been proposed in Ref. [414].

One way to manipulate spin in spintronics devices is the so-called spin Hanle effect [415, 416, 417], which describes the coherent rotation of a spin in an external magnetic field. A recent theoretical study of this effect is given in Ref. [418]. It is demonstrated that superconductivity

can strongly influence the coherent spin rotation, depending on the type of spin relaxation mechanism being dominated either by spin-orbit coupling or spin-flip scattering at impurities.

Another manifestation of coherence in systems with spin-orbit coupling is the Aharonov-Casher effect [419], leading to a phase on the Josephson current through a semiconducting ring attached to superconducting leads [420]. This effect is the charge-spin dual effect to the Aharonov-Bohm effect [421], which describes the relative phase shift between two charged particle paths enclosing a magnetic flux. Both effects are manifestations of geometric phases acquired by the quantum mechanic wave function under adiabatic changes [422, 423]. The particle's spin acquires such a geometric phase in systems with spin-orbit interaction [424, 425, 426, 427, 428, 429, 430]. The Aharonov-Casher effect was, e.g., observed experimentally in ring structures of HgTe/HgCdTe quantum wells [431]. In superconducting Josephson rings, or closed Josephson junction arrays, such phases lead to oscillations of the Josephson current due to the Aharonov-Casher phase [432, 420, 433, 434]. The effect allows for control of the Josephson current through the control of the Aharonov-Casher phase by the gate voltage. Thus, this effect is a promising candidate for realizing new types of controllable devices in superconducting spintronics based on geometric phases.

Recently Mironov *et al.* [435] studied double path interference during Cooper pair transport through a single nanowire with two conductive channels. It is found that multi-period magnetic oscillations appear due to quantum mechanical interference between channels affected by spin-orbit coupling and Zeeman coupling. The model is relevant to recent observations of interference phenomena in Bi nanowires [436].

A Josephson junction containing a spacer with strong spin-orbit interaction was considered in Ref. [437]. A nonlinear dynamical coupling between magnetic moment and charge current was found, and magnetic torque and charge pumping was investigated in such a system. The intricate coupling between spin and charge currents in systems with strong spin-orbit coupling is previously known from non-centrosymmetric superconductors, where spin-polarized Andreev states play a prominent role [438].

This connects to the current hot topic of topological materials, in particular topological insulators and superconductors, both systems with strong spin-orbit coupling. As an example for the extremely rich plethora of effects involving topological materials we mention here the possibility to observe chiral Majorana modes in one-dimensional channels built at a superconductor/ferromagnetic-insulator/superconductor junction on top of a topological insulator [323], where a φ_0 junction is predicted. The effect is interpreted as tunneling process between two Majorana edge channels at the two interfaces between the superconductor and the ferromagnetic insulator. Majorana fermions have the property of being their own antiparticle, i.e. their field operators fulfill $\gamma_\alpha = \gamma_\alpha^\dagger$ [439, 440]. A non-trivial superconducting phase is also obtained in proximity junctions involving semiconductors with Rashba spin-orbit coupling and a time-reversal symmetry breaking Zeeman term in the Hamiltonian [441, 442].

The combined effect of spin-orbit interaction, magnetic field, and Coulomb charging for a multilevel quantum dot tunnel contacted by two superconductors was analyzed in Ref. [443]. Majorana bound states in a double dot variant of this system are predicted to leave a clear signature in the 2π-periodic current-phase relation. Majoranas in spin-orbit coupled ferromagnetic Josephson junctions were investigated in Ref. [444], were it was shown that two delocalized Majorana fermions with no excitation gap appear in a π-junction. Josephson currents through Majorana bound states in topological insulators have been studied in Refs. [445, 446, 447, 448, 449, 450, 451, 452, 453, 454]. Such Josephson junctions carry 4π-periodic bound states [445]. It has been shown that under certain conditions this periodicity manifests itself by an even-odd effect in Shapiro steps [447, 453]. In addition, a peak in the current noise spectrum at half the Josephson frequency has been predicted [454].

The diverse spectrum of effects and phenomena in hybrid systems between singlet super-

conductors and topological insulators (see e.g. Refs. [455, 456, 457, 458, 459, 137, 460, 461]) are promising examples of how the field can be brought forward, playing a prominent role in various modern developments at the forefront of international research.

Part XI
Appendix

A Introduction to Superconductivity

A.1 Other Motivation

Обсудим всю мотивацию, которая позволит нам познать предмет без проблем.

A.1.1 Other General Motivation

(I'll write it very not soon)

Польза в плане развития как профессионала

(потом раскрою)

Польза в плане саморазвития

(потом раскрою)

Результаты

A.1.2 Amazing Facts

(потом раскрою)

A.1.3 Motivation for Specific Topics in SC

(потом раскрою в параграфах)

A.2 Thinking as a Professional in Superconductivity

(потом раскрою)

A.2.1 Essence of Superconductivity

A.2.2 Ways to Earn Money Using Superconductivity

A.2.3 Everyday-Life Uses of Superconductivity

Укажем, как предмет используется в обычной жизни.

A.2.4 Overview of Most Relevant Applications

(???)

A.2.5 Ways to Guess All Main Ideas

незаменимая часть нормального понимания предмета.
(потом раскрою)

A.2.6 Thinking for Effective Learning

Осудим, какое мышление наиболее эффективное для усвоение предмета.

Способы изучения предмета

(потом раскрою)

Необходимые темы для

(потом раскрою)

Дополнительные темы для

(потом раскрою)

A.3 Acknowledgements

Currently, no one except me has worked on the sections of this note (with the exception of sections taken from books).

A.4 Literature

A.4.1 Main Literature

Основная обучающая

[1] В.В. Шмидт Введение в физику сверхпроводников
Большая книга, где многое разобрано, лучше книг для начала и общего обзора не знаю. Note that English version don't have many chapters that Russian have, so here I refer to the Russian version.

[2] Kittel C. Introduction to Solid State Physics, 8th 2005
Отличная книга, где есть раздел с основами сверхпроводимости, этих тем и достаточно для минимального знакомтсва.

Основная профессиональная

[3] Abrikosov Fundamentals of Theory of Metals
A big book that tells a lot about superconductors (and not only) that one would never read somewhere else.

[4] Mineev, V.P. Samokhin, K. Introduction to Unconventional Superconductivity
Очень крутая книга, где описывается много явлений и методов, о которых ну уж очень сложно подумать, пройдя обычный вводный курс сверхпроводимости.

Books With Many Solved Problems

Таких прямо отдельных задачников нет, но тут приведу книги, в которых много задач решено.
(потом напишу)

A.4.2 Additional Literature and Articles on Various Phenomena and Methods

Дополнительная обучающая

[5] Ya. V. Fominov, N. M. Shchelkachev The Josephson Effect: An educational and methodological guide

32 страницы про эффект Джозефсона, интересное изложение, описываются некоторые детали, которые мало кто обсуждает.

[6] Варламов Ларкин Теория флуктуаций в сверхпроводниках

Очень крутая книга, где много ответов и специфических явлений. Можно было бы брать ее основным учебником, но так не делают наверное, потому что слишком много информации появится. Но точно попробовать найти в ней ответ на какой-то вопрос - отличная идея.

[7] Li, Chuan Superconducting proximity effect in graphene and Bi nanowire based junctions

кандидатская просверхпроводящие контакты, очень хорошее изложение много чего, наверняка еще многое прочту из нее.

[8] Gross, R. and Marx, A. and Deppe, F. Applied Superconductivity: Josephson Effect and Superconducting Electronics

В открытом доступе только 60 страниц 2005го года, полистал, понял, что много там деталей, которую минимум неделю учить пришлось бы. Просто много теории, может, на самом деле приложения и раскрыты, не знаю.

[9] Lifshitz, E.M. and Pitaevskii, L.P. Statistical Physics: Theory of the Condensed State

Типичный учебник по код. средам, в котором многому можно научиться, в том числе некоторым важным, но не супер актуальным вопросам про сверхпроводимость.

Дополнительная по теоретической сверхпроводимости

Reinhold Kleiner and Werner Buckel. Superconductivity: A An Introduction, Third Edition.

Big book about basics of superconductivity with overview with many experiments. KU Leuven course was following it. Use Annas' archive to get it, as usual.

[10] Blatter, G. and Feigel'man, M. V. and Geshkenbein, V. B. and Larkin, A. I. and Vinokur, V. M. Vortices in high-temperature superconductors

По сути книга про вихри в high-temperature superconductors, там очень много всякого, минимум месяца 4 изучал ее бы, если бы нужно было.

[11] Suppression of the Josephson current through a narrow, mesoscopic, semiconductor channel by a single impurity Bagwell, Philip F.

Мне показалось, что тут хорошо написано про Андреевские уровни, так что добавил эту статью, потом поизучаю, не на пару дней тема.

[12] McMillan, W. L. Transition Temperature of Strong-Coupled Superconductors

Статья с умными формулами и таблицами экспериментальных данных. Обычной подготовки по Левитову Шитову достаточно для понимания её, в ней всего 2 страницы сложных формул. Если буду заниматься теорией и будет свободное время - изучу её.

Articles about superconductive junctions: theoretical methods

Barone A., Paterno G. Physics and aplication of the josephson effect
A big and very good book about Josephson junctions, maybe it is top 5 books one should read about them.

Blonder Tinkham Klapwijk Transition from metallic to tunneling regimes in SC microconstrictions: Excess current, charge imbalance, and supercurrent conversion
One of the most famous articles about superconducting weak leaks.

[13] Chamon, C. and Jackiw, R. and Nishida, Y. and Pi, S.-Y. and Santos, L. Quantizing Majorana fermions in a superconductor
Кирилл сказал, что там про Намбу базис и про Боголюбова де Жена хорошая теория, потом почитаю пару раз, не такая полезная статья, но тоже вроде как что-то там есть, чему можно поучиться.

C. W. J. Beenakker Universal limit of critical-current fluctuations in mesoscopic Josephson junctions
A very famous article with a very useful method.

Articles about superconductive junctions: experiments, applications

I.K. Yanson, V.M. Svistunov, I.M. Dmitrenko Experimental Observation of the Tunnel Effect for Cooper Pairs with the Emission of Photons 1964
First observation of Josephson radiation.

Статьи о других теоретических методах и особых моделях

[14] Likharev, K. K. Superconducting weak links
Очень известная статья на 60 страниц про сверхпроводимость и джозефсонику, когда-то поизучаю скорее всего.

[15] Yu. A. Bychkov and l. P. Gor'kov and I. E. Dzyaloshinskiĭ Possibility of superconductivity type phenomena in a one-dimensional system
Статья про 1Д сверхпроводимость, интересная, по идее учебник их как раз дает полностью к этому подготовку.

[16] Possibility of Synthesizing an Organic Superconductor Little, W. A.
Статья про 1Д сверхпроводимость, интересная и самая первая.

[17] Marsiglio, F. Eliashberg theory: A short review
Вроде хороший обзор этой теории, когда-то поизучаю, интересно, но не на пару дней.

Статьи про разные явления, специфические конструкции

[18] Doll, R. and Näbauer, M. Experimental Proof of Magnetic Flux Quantization in a Superconducting Ring
Кольцом можно доказать, что поток квантуется, на 2 страницы это написано, я так и не дошел разобраться в этом.

[19] Deaver B, Fairbank W. Experimental Evidence for Quantized Flux in Superconducting Cylinders

Самая известная и мб первая статья про квантование потока. Я так и не понял, потратив 15 минут, что там за странные графики есть? Потом когда-то еще почитаю, статья на 4 страницы.

[20] Andreev, A F Thermal conductivity of the intermediate state of superconductors

Оригинальная небольшая статья Андреева про его связные состояния, наверняка есть много хороших идей.

[21] Ryazanov, V. V. et al. Coupling of Two Superconductors through a Ferromagnet: Evidence for a π Junction

Известная статья про SFS контакт, там вообще много статей про это, может, когда-то изучу, пока нечего сказать про это.

[22] Magnetization of Hard Superconductors Bean, C. P.

Очень цитируемая статья, видел из нее график, доступа к ней не нашел. Видимо, там какие-то явления интересные происходят.

[23] Magnetization of multiple-quanta vortex lattices Moshchalkov, V. V. et. al.

Там график, что типа намагниченность возрастает в некоторых точках скачками, когда число его квантов равно числу вихрей. Видел на лекции, статью не читал, не актуально.

[24] Wiedenmann, J. 4π-periodic Josephson supercurrent in HgTe-based topological Josephson junctions

Статья про особый эффект Джозефсона со многим про шаги Шапиро. Много интересных графиков, но нет времени в ней пока разбираться, все равно нужно основы доучивать.

[25], Giaever, Ivar Energy Gap in Superconductors Measured by Electron Tunneling

Статья на страницу, за которую автор получил часть Нобелевской премии, потому что предложил по производной мерить щель. Я доучу наконец-то, как конкретно это делать?

[26], Hamilton, Clark A Josephson voltage standards

Статья с обзором применений эф. Джозефсона, про схемы с тысячами СКВИД-ами, джозефсоновские стандарты. Я совсем мало что знаю про это, нужно будет - отдельно читать нужно будет несколько дней. Во многих статьях видел картинки из нее, видимо, известная.

[27] Schulz, R. Chesca, B. et.al. Design and realization of an all d-wave dc π-superconducting quantum interference device

Небольшая статья, где есть график тока от потока для пи-СКВИДов, а также умные мысли про них.

[28] Jaklevic, R. C. and Lambe, J. and Mercereau, J. E. and Silver, A. H. Macroscopic Quantum Interference in Superconductors

Одна из первых статей про СКВИД-ы, есть несколько графиков интерференции. Киттель потом его у себя тоже привел. Вообще, типичная теория про них там, основные идеи в ней уже в учебниках.

References from de Gennes

Macroscopic description of 1st type superconductors:

F. London, Superfluids (New York: Wiley, 1950), Vol. I.

L. Landau and I. M. Lifschitz, Electrodynamics of Continuous Media (Pergamon, 1960), Chap. 6.

Relation between current and vector potential:

A. B. Pippard, Proc. Roy. Soc. (London), A216, 547 (1953).

Measurements of penetration depths:

A. L. Schawlow and G. Devlin, Phys. Rev., 113, 120 (1959).

A. B. Pippard, Proc, 7th Intern. Conf. Low Temp. Phys. (Toronto: Toronto Univ. Press, 1960), p. 320.

Intermediate state:

Optical Observation of Domains:

W. De Sorbo, Phys. Rev. Letters, 4, 406 (1960).

W. De Sorbo, Proc. 7th Intern. Conf. Low Temp. Phys. (Toronto: Toronto Univ. Press, 1960), p. 370.

Measurement of Wall Energy:

A. L. Schawlow, Phys. Rev., 101, 573 (1956).

Kinetics of the normal → superconducting phase transition:

T. E. Faber and A. B. Pippard, Progress in Low Temp. Physics, edited by C. G. Gorter (Amsterdam: North Holland, 1959), Vol. I, Chap. 9.

Литература по другим наукам, использующим сверхпроводимость

Литература о приложениях

[29] Clarke, J. and Braginski, A.I The SQUID Handbook: Fundamentals and Technology of SQUIDs and SQUID Systems

Библия сквидов, какие только возможно придумать детали про них обсуждены в их книге. Много ссылок и картинок.

[30] Fagaly, R. L. Superconducting quantum interference device instruments and applications

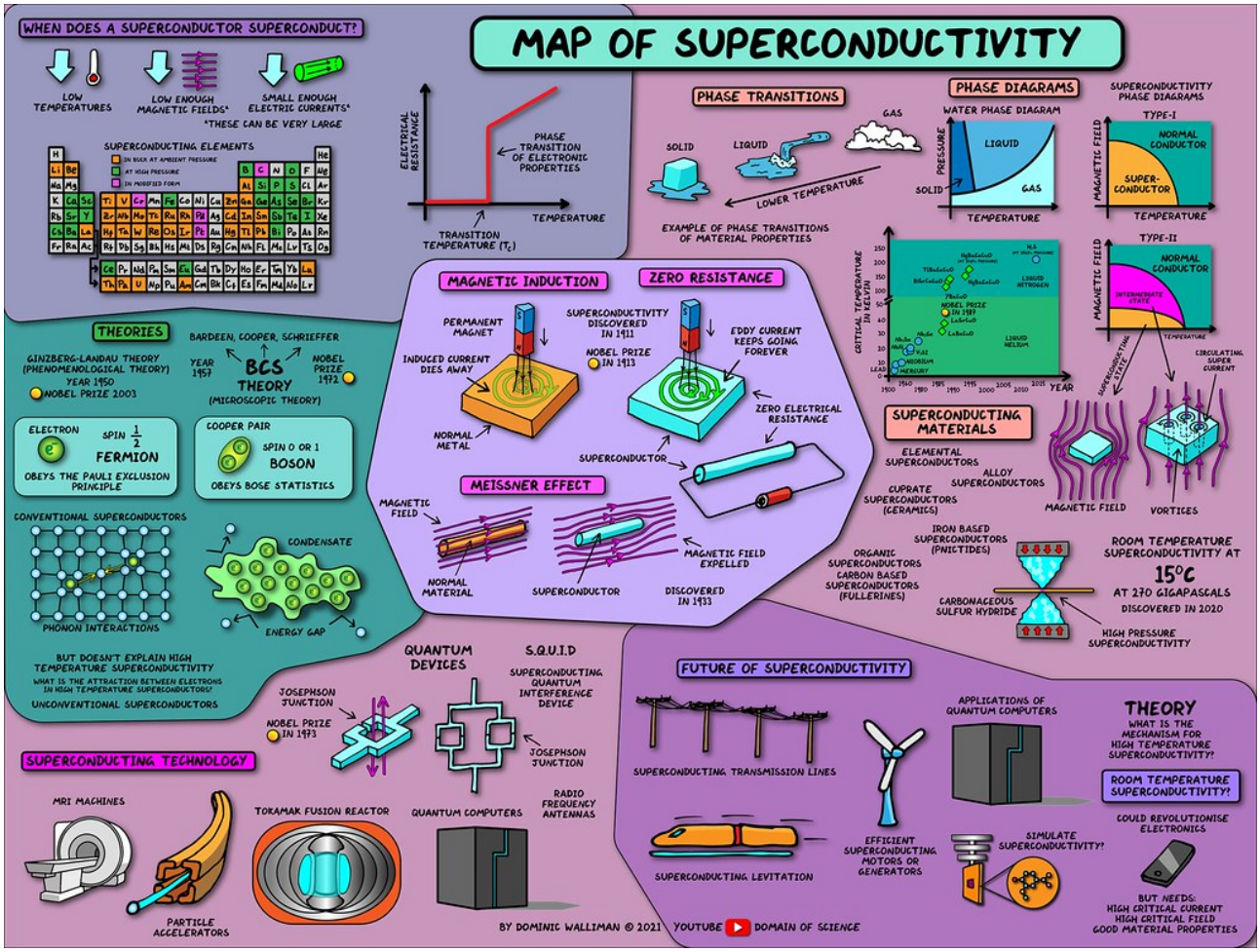
Обзор приложений СКВИД-ов с картинками. Нам на лекции в Левене из неё показывали пару картинок.

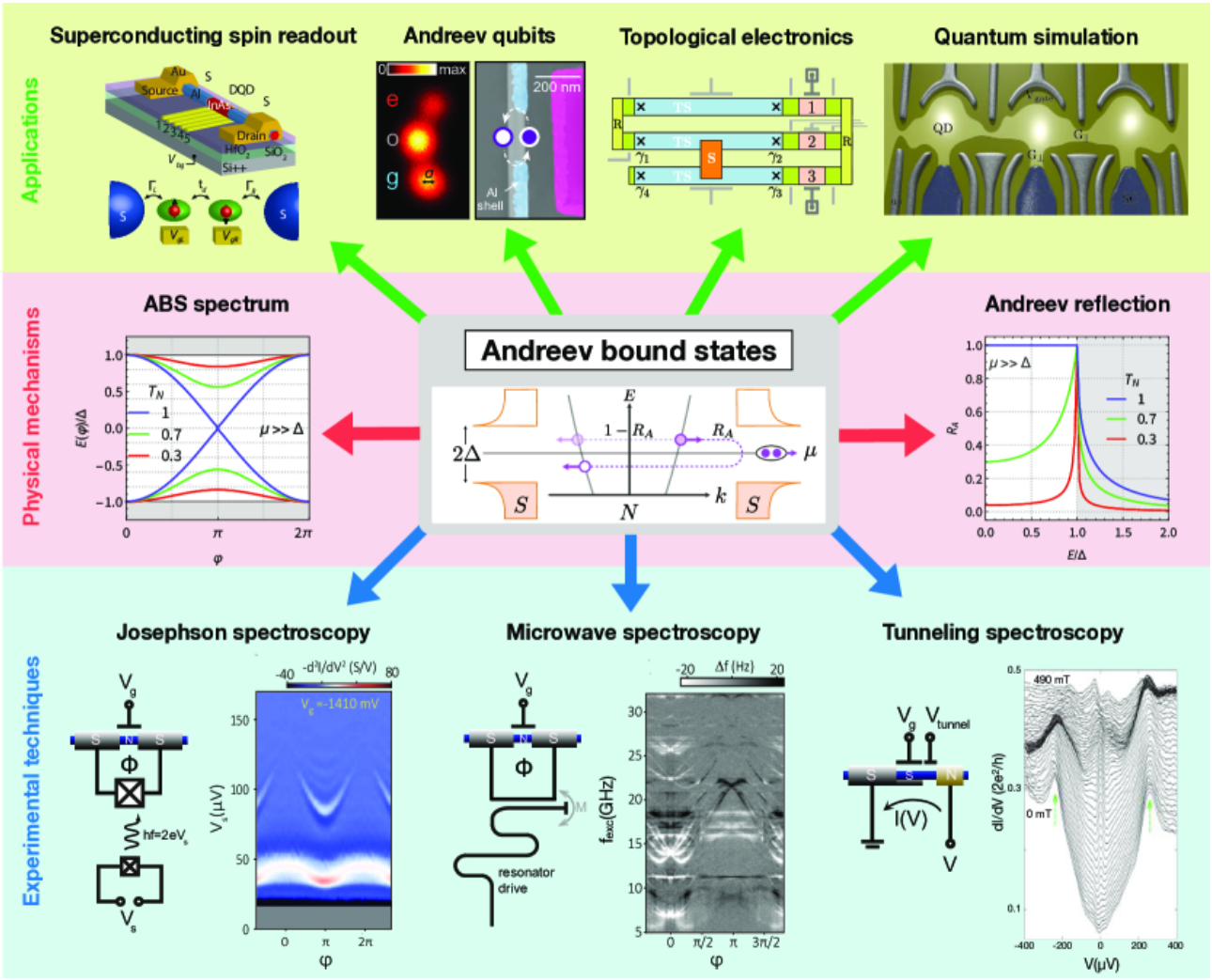
Литература в помощь по физике и математике

A.5 General overview of superconductivity

(потом раскрою)

A.5.1 Popular Introduction to Superconductivity





A.5.2 Overview of Rare Phenomena in Superconductivity

(по идее тут словами, что такие-то вещи могут быть и для них такие-то формулы и графики)

A.5.3 Overview of Theoretical Approaches

такие-то есть, такие полезные, такие - нет.

A.5.4 Overview of Further Developments

A.5.5 Connections with Other Sciences

Обсудим связи с разделами
(потом раскрою)

A.6 Description of the Note

Общее описание записи

Общие особенности записи

Особенности глав и разделов

Первая часть про предмет в двух словах

Вторая часть

Часть про приложения

какие вообще приложения я разбирал?

Обозначения и константы

A.7 History of Superconductivity in a Nutshell

Overview of the Development of the Theory of Superconductivity by Shmidt

The first theory which proved successful in describing the electrodynamics of superconductors was the London theory (1935). The theory was phenomenological, that is, it had introduced two equations, in addition to Maxwell's equations, governing the electromagnetic field in a superconductor. These equations provided a correct description of the two basic properties of superconductors: absolute diamagnetism and zero resistance to a dc current. The London theory did not attempt to resolve the microscopic mechanism of superconductivity on the level of electrons, that is, the question: "Why does a superconductor behave according to the London equations?" remained beyond its scope.

According to the London theory, electrons in a superconductor may be considered as a mixture of two groups: superconducting electrons and normal electrons. The number density of the superconducting electrons, n_s, decreases with increasing temperature and eventually becomes zero at $T = T_c$. At $T = 0$ it is the other way round, that is, n_s is equal to the total density of conduction electrons. These are the postulates of the so-called two-fluid model of a superconductor. A flow of superc ducti g ele trons meets no
in a superconductor because, if it did, it would cause the superconducting electrons to accelerate infinitely. Therefore, under stationary conditions, that is, without an electric field, the normal electrons are at rest. In contrast, in the presence of an ac electric field, both the normal and the superconducting components of the current are finite and the normal current obeys Ohm's law.

In the framework of this concept, a real superconductor can be modeled by an equivalent circuit consisting of a normal resistor and an ideal conductor connected in series. The ideal conductor in the circuit must have a finite inductance to mimic the inertia of the superconducting electrons.

The London equations provided a description for the behavior of the superconducting component of the electronic liquid in both dc and ac electromagnetic fields. They also helped to understand a number of aspects of the superconductors' behavior in general. However, by the end of the 1940s, it was clear that to one question at least the London theory gave a wrong answer. For an interface between adjacent normal and superconducting regions, the theory predicted a negative surface energy $\sigma_{ns} < 0$. This implied that a superconductor in an external magnetic field could decrease its total energy by turning into a mixture of alternating normal and superconducting regions. In order to make the total area of the interface within

the superconductor as large as possible, the size of the regions must be as small as possible. This was supposed to be the case even for a long cylinder in a longitudinal magnetic field, in contradiction to experimental evidence existing at that time. Experiment showed that such a separation of the normal and superconducting regions occurred only for specimens having a nonzero demagnetizing factor (the intermediate state, see Sect. 1.2.2). In addition, the layers were rather thick (~ 1 mm as in Fig. 1.7), which could only be the case if $\sigma_{\rm ns} > 0$, again in contradiction to the predictions of the London theory.

The above contradiction was reconciled by a theory proposed by V.L. Ginzburg and L.D. Landau (the so-called GL theory) which was also phenomenological but took account of quantum effects. Why it is so important to include quantum effects will become clear in a moment. Assume that there exists a wavefunction Ψ describing the superconducting electrons quantum-mechanically. Then the squared amplitude of this function (which is proportional to $n_{\rm s}$) must be zero in a normal region, increase smoothly through the normal-superconducting (NS) interface and finally reach a certain equilibrium value in a superconducting region. Therefore, a gradient of Ψ must appear at the interface. At the same time, as is well known from quantum mechanics, $|\nabla\Psi|^2$ is proportional to the density of the kinetic energy. Thus, by taking into account quantum effects, we also take into account an additional positive energy stored at the NS interface, which creates the opportunity to obtain $\sigma_{\rm ns} > 0$.

The GL theory will be discussed in detail in Chap. 3. Here we shall only outline its most important ideas which have determined the tremendous importance of the GL theory for the entire field of superconductivity.

The GL theory introduced quantum mechanics into the description of superconductors. It assigned to the entire number of superconducting electrons a wavefunction depending on a single spatial coordinate [recall that, generally speaking, a wavefunction of n electrons in a metal is a function of n coordinates, $\Psi(r_1, r_2, \ldots, r_n)$]. By doing so, the theory established the coherent behavior of all superconducting electrons. Indeed, in quantum mechanics, a single electron in the superconducting state is described by a function $\Psi(r)$. If we now have n_8 absolutely identical electrons (where n_8, the superconducting electron number density, is a macroscopically large number) and all these electrons behave coherently, it is clear that the same wavefunction of a single parameter is sufficient to describe all of them. This idea was a breakthrough that enabled the prediction of many beautiful quantum, and at the same time macroscopic, effects in superconductivity.

The GL theory was built on the basis of the theory of second-order phase transitions (the Landau theory) and, therefore, it is valid only in the vicinity of the critical temperature, that is, within the temperature range $T_{\rm c} - T \ll T_{\rm c}$. The scope of its validity will be discussed in more detail in Sect. 6.6.

Having applied the GL theory to superconducting alloys, A.A. Abrikosov developed a theory of the so-called type-II superconductors (1957). It turned out that superconductors do not necessarily have to have $\sigma_{\rm ns} > 0$. Those that do have $\sigma_{\rm rs} > 0$ are type-I superconductors. But the majority of superconducting alloys and chemical compounds show $\sigma_{\rm nB} < 0$; they are type-II superconductors. For type-II superconductors, there is no Meissner effect and the magnetic field does penetrate inside the material, but penetrates in a very unusual way, that is, in the form of quantized vortex lines (quantum effect on the macroscopic scale!). Superconductivity in these materials can survive up to very high magnetic fields.

Still, neither the London, nor the GL theory could answer the question: "What are those 'superconducting electrons' whose behavior they were intended to describe?" It was 46 years since the discovery of superconductivity but at the microscopic level a superconductor remained a mystery.

This question was finally resolved in 1957 by the work of J. Bardeen, L. Cooper and J. Schrieffer (the BCS theory). An important contribution was also made by N.N. Bogolyubov

(1958) who developed a mathematical method now widely used in studies of superconductivity.

The decisive step in understanding the microscopic mechanism of superconductivity is due to L. Cooper (1956). The essence of his work can be outlined as follows. Consider a normal metal in the ground state: in k space, all states for non-interacting electrons inside the Fermi sphere are occupied, while all those outside it are empty. Then an extra pair of electrons is brought
face (the arrows indicate the directions of electron spins). It turned out that if, for whatever reason, the two electrons become attracted to each other, they form a bound state regardless of how weak the attraction is. In real space, these electrons form a bound pair - a Cooper pair.

What the BCS theory has demonstrated is that taking into account the interaction between electrons and phonons can, under certain circumstances, lead to electron-electron attraction. As a result, a part of the electrons form Cooper pairs. The total spin of a Cooper pair is zero, which means that it represents a Bose particle (that is, obeys Bose-Einstein statistics). Such particles possess a remarkable property: if the temperature of a system falls below a certain temperature T_c, they can all gather at the lowest energy level (in the ground state). Furthermore, the larger the number of the particles that have accumulated there, the more difficult it is for one of them to leave this state. This process is called Bose condensation. All the particles in the condensate have the same wavefunction, depending on a single spatial coordinate. One can easily understand that the flow of such a condensate must be superfluid, that is, dissipation-free. Indeed, it is not easy at all for one of the particles to be scattered by, say, an impurity atom or by any other defect of the crystal lattice. In order to become scattered, the particle would first have to overcome the 'resistance' of the rest of the condensate.

Thus one can briefly describe the phenomenon of superconductivity as follows. At $T < T_c$, there exists a condensate of the Cooper pairs. This condensate is superfluid. It means that the dissipation-free electric current is carried by the Cooper pairs, i.e., the charge of an elementary current carrier is $2e$.

The microscopic theory of superconductivity was elaborated further by L.P. Gorkov (1958) who developed a method to solve the model BCS problem using Green's functions. He applied this method, in particular, to find microscopic interpretations for all phenomenological parameters of the GL theory as well as to define the theory's range of validity (see Sect.6.6). The works by Gorkov have completed the development of the Ginzburg-Landau-Abrikosov-Gorkov theory (the GLAG theory).

Then everything seemed to be settled until the critical temperature made a quantum leap. In 1987 J. Bednorz and K.A. Mller discovered the first high- T_c superconductor ($LaBaCuO_4, T_c \sim$ 40 K). Subsequently, materials have been found that raise T_c to temperatures of up to ~ 130 K ($HgBa_2Ca_2Cu_3O_8$). The classic BCS theory was unable to account for many of the properties of the high- T_c materials. The electron-phonon mechanism became questionable. New mechanisms - such as the so-called d-wave pairing - have been proposed. At present, the question of why the high- T_c superconductors have such high T_c values is still largely unanswered. Let us hope that the definitive answer need not be awaited for another 46 years.

A.8 Puzzles for Different Situations in Life

Обсудим в порядке интересности задачки и вопросы

A.8.1 Typical Puzzles

A.8.2 Everyday Puzzles

A.8.3 Fundamental Puzzles

A.8.4 Puzzles about Details

A.8.5 Puzzles for Mastering Typical Concepts

Допустим, видим человека, который в принципе хотел бы понять суть, опишем, какие в какой последовательности будем задавать, чтобы в типичном случае ему было бы интереснее въезжать. В частности это могут быть младшие студенты или редко школьники.

Головоломки для освоения школьного уровня

Головоломки для освоения уровня теормина

Головоломки для освоения других особенностей

B Mathematics and Physics for Reference

B.0.1 Quantum Mechanics for Superconductivity (??)

Особое понимание квантовой механики для сверхпроводимости

Волновая функция как очевидный ответ к природе сверхпроводимости (??????)

(??? почему выгодно пользоваться волновой функцией??? почему именно с ней решится задача??? напишу четко, пока что не понимаю, что такое макроскопическая волновая функция огромного количества электронов.)

B.0.2 Some Mathematics for Superconductivity (??)

(тут многое может быть)

Типичный интеграл БКШ

(?? строчка - откуда он???)

$$I(u) = \int\limits_0^\infty \frac{dx}{\sqrt{x^2+u^2}\left(e^{\sqrt{x^2+u^2}}+1\right)}.$$

Получим его асимптотики при низких температурах ($u \gg 1$) и при температурах вблизи точки перехода ($u \ll 1$). При $u \gg 1$ раскладываем по степеням u^{-1}:

$$I(u) \approx \int\limits_0^\infty \frac{dx}{u} e^{-u\left(1+\frac{x^2}{2u^2}\right)} = \left(\frac{\pi}{2u}\right)^{1/2} e^{-u}.$$

При малых $u \ll 1$ представим $I(u) \equiv I_1(u) + I_2(u)$, в

$$I_1(u) := \frac{1}{2}\int\limits_0^\infty \left(\frac{1}{\sqrt{x^2+u^2}} - \frac{1}{x}\ \mathrm{th}\ \frac{x}{2}\right) dx$$

первый член подынтегрального выражения интегрируется элементарно, а второй интегрируется по частям, в итоге

$$I_1(u) = \frac{1}{2}\ln\frac{u}{2} + \frac{1}{4}\int\limits_0^\infty \frac{\ln x dx}{\mathrm{ch}^2(x/2)}.$$

(?у Пухова тут видимо опечатка, перерешаю??) Стоящая в (16.4) константа равна $(1/2)$ $\ln(\pi/2\gamma)$, $\ln\gamma = C = 0,577$.

$$I_2(u) := \frac{1}{2}\int\limits_0^\infty \left(\frac{1}{x}\mathrm{th}\frac{x}{2} - \frac{1}{\sqrt{x^2+u^2}}\mathrm{th}\frac{\sqrt{x^2+u^2}}{2}\right) dx$$

$$I_2(0) = 0 \qquad\qquad I_2(u) \approx \frac{u^2}{2}\int\limits_0^\infty \frac{dx}{x}\left(\frac{1}{x}\ \mathrm{th}\ \frac{x}{2}\right)'.$$

Интеграл в (16.6) равен $7\zeta(3)/4\pi^2$. Таким образом, для обоих предельных случаев имеем

$$I(u) = \begin{cases} \left(\frac{\pi}{2u}\right)^{1/2} e^{-u} & \text{при } u \gg 1, \\ \ln\frac{\pi}{\gamma u} + \frac{7\zeta(3)}{8\pi^2}u^2 & \text{при } u \ll 1. \end{cases}$$

C References

References

[1] Shmidt, V.V.: *The Physics of Superconductors: Introduction to Fundamentals and Applications*. Springer, 1997, ISBN 9783540612438. https://books.google.be/books?id=8O8svNo_tWoC.

[2] Kittel, C.: *Introduction to Solid State Physics*. Wiley, 8th edition, 2004, ISBN 9780471415268. http://www.amazon.com/Introduction-Solid-Physics-Charles-Kittel/dp/047141526X/ref=dp_ob_title_bk.

[3] Abrikosov, A.A.: *Fundamentals of the Theory of Metals*. Dover Publications, 2017, ISBN 9780486819013. https://books.google.si/books?id=tTo2DwAAQBAJ.

[4] Mineev, V.P and Samokhin, K.: *Introduction to Unconventional Superconductivity*. Taylor & Francis, 1999, ISBN 9789056992095. https://books.google.be/books?id=2BXYWT8m068C.

[5] Фоминов, Я. В., Щелкачёв, Н. М. : *Эффект Джозефсона: Учебно-методическое пособие*. МФТИ, page 32, 2010. https://mipt.ru/education/chair/theoretical_physics/upload/b7f/Josephson-arpggxmxhr7.pdf.

[6] Larkin, A and Varlamov, A.: *Theory of Fluctuations in Superconductors*. International Series of Monographs on Physics. OUP Oxford, 2009, ISBN 9780199564835. https://books.google.be/books?id=ITyPPwAACAAJ.

[7] Li, Chuan: *Superconducting proximity effect in graphene and bi nanowire based junctions*. page 175, November 2014.

[8] Gross, R, Marx, A, Deppe, F.: *Applied Superconductivity: Josephson Effect and Superconducting Electronics*. De Gruyter Textbook Series. Walter De Gruyter Incorporated, 2016, ISBN 9783110417067. https://books.google.be/books?id=4SIzrgEACAAJ.

[9] Lifshitz, E.M, Pitaevskii, L.P.: *Statistical Physics: Theory of the Condensed State*. Number т. 9 in *Course of Theoretical Physics*. Elsevier Science, 2013, ISBN 9780080503509. https://books.google.be/books?id=lgiBDAAAQBAJ.

[10] Blatter, G, Feigel'man, M. V, Geshkenbein, V. B, Larkin, A. I, Vinokur, V. M.: *Vortices in high-temperature superconductors*. Rev. Mod. Phys., 66:1125–1388, Oct 1994. https://link.aps.org/doi/10.1103/RevModPhys.66.1125.

[11] Bagwell, Philip F.: *Suppression of the josephson current through a narrow, mesoscopic, semiconductor channel by a single impurity*. Phys. Rev. B, 46:12573–12586, Nov 1992. https://link.aps.org/doi/10.1103/PhysRevB.46.12573.

[12] McMillan, W. L.: *Transition temperature of strong-coupled superconductors*. Phys. Rev., 167:331–344, Mar 1968. https://link.aps.org/doi/10.1103/PhysRev.167.331.

[13] Chamon, C, Jackiw, R, Nishida, Y, Pi, S.-Y, Santos, L.: *Quantizing majorana fermions in a superconductor*. Phys. Rev. B, 81:224515, Jun 2010. https://link.aps.org/doi/10.1103/PhysRevB.81.224515.

[14] Likharev, K. K.: *Superconducting weak links.* Rev. Mod. Phys., 51:101–159, 1979.

[15] Bychkov, Yu. A., P. Gor'kov l., and Dzyaloshinskiĭ, I. E.: *Possibility of superconductivity type phenomena in a one-dimensional system*, pages 1–13. https://www.worldscientific.com/doi/abs/10.1142/9789814317344_0001.

[16] Little, W. A.: *Possibility of synthesizing an organic superconductor.* Phys. Rev., 134:A1416–A1424, Jun 1964. https://link.aps.org/doi/10.1103/PhysRev.134.A1416.

[17] Marsiglio, F.: *Eliashberg theory: A short review.* Annals of Physics, 417:168102, June 2020, ISSN 0003-4916. http://dx.doi.org/10.1016/j.aop.2020.168102.

[18] Doll, R, Näbauer, M.: *Experimental proof of magnetic flux quantization in a superconducting ring.* Phys. Rev. Lett., 7:51–52, Jul 1961. https://link.aps.org/doi/10.1103/PhysRevLett.7.51.

[19] Deaver, Bascom S and Fairbank, William M.: *Experimental evidence for quantized flux in superconducting cylinders.* Phys. Rev. Lett., 7:43–46, Jul 1961. https://link.aps.org/doi/10.1103/PhysRevLett.7.43.

[20] Andreev, A F: *Thermal conductivity of the intermediate state of superconductors.* Zh. Eksperim. i Teor. Fiz., Vol: 46, May 1964. https://www.osti.gov/biblio/4071988.

[21] Ryazanov, V. V, Oboznov, V. A, Rusanov, A. Yu, Veretennikov, A. V, Golubov, A. A, Aarts, J.: *Coupling of two superconductors through a ferromagnet: Evidence for a π junction.* Phys. Rev. Lett., 86:2427–2430, Mar 2001. https://link.aps.org/doi/10.1103/PhysRevLett.86.2427.

[22] Bean, C. P.: *Magnetization of hard superconductors.* Phys. Rev. Lett., 8:250–253, Mar 1962. https://link.aps.org/doi/10.1103/PhysRevLett.8.250.

[23] Moshchalkov, V. V, Baert, M, Metlushko, V. V, *et al.*: *Magnetization of multiple-quanta vortex lattices.* Phys. Rev. B, 54:7385–7393, Sep 1996. https://link.aps.org/doi/10.1103/PhysRevB.54.7385.

[24] Wiedenmann, J, Bocquillon, E, Deacon, R., *et al.*: *4π-periodic josephson supercurrent in hgte-based topological josephson junctions.* Nature Communications, 7(1), January 2016, ISSN 2041-1723. http://dx.doi.org/10.1038/ncomms10303.

[25] Giaever, Ivar: *Energy gap in superconductors measured by electron tunneling.* Phys. Rev. Lett., 5:147–148, Aug 1960. https://link.aps.org/doi/10.1103/PhysRevLett.5.147.

[26] Hamilton, Clark A: *Josephson voltage standards.* Review of scientific instruments, 71(10):3611–3623, 2000.

[27] Schulz, R, Chesca, B, Goetz, B, Schneider, C, Schmehl, *et al.*: *Design and realization of an all d-wave dc π-superconducting quantum interference device.* Applied Physics Letters, 76:912–914, February 2000.

[28] Jaklevic, R. C., Lambe, J., Mercereau, J. E., and Silver, A. H.: *Macroscopic quantum interference in superconductors.* Phys. Rev., 140:A1628–A1637, Nov 1965. https://link.aps.org/doi/10.1103/PhysRev.140.A1628.

[29] Clarke, J and Braginski, A.I.: *The SQUID Handbook: Fundamentals and Technology of SQUIDs and SQUID Systems*. Wiley, 2006, ISBN 9783527604586. https://books.google.bg/books?id=BsTTM-nU-JkC.

[30] Fagaly, R. L.: *Superconducting quantum interference device instruments and applications*. Review of Scientific Instruments, 77(10):101101, October 2006, ISSN 0034-6748. https://doi.org/10.1063/1.2354545.

[31] Kleiner, R, Buckel, W, Huebener, R.: *Superconductivity: An Introduction*. Wiley, 2016, ISBN 9783527411627. https://books.google.be/books?id=eaUvCgAAQBAJ.

[32] Gennes, P.G. de: *Superconductivity of Metals and Alloys*. Frontiers in physics. W.A. Benjamin, 1966. https://books.google.be/books?id=M8A8AAAAIAAJ.

[33] Bose, S. and García-García, A. M., Ugeda, M. M., Urbina, J. D., Michaelis, Christian H, Brihuega, Ivan and Kern, Klaus: *Observation of shell effects in superconducting nanoparticles of sn*. Nature Materials, 9(7):550–554, May 2010, ISSN 1476-4660. http://dx.doi.org/10.1038/nmat2768.

C.1 References from Very Useful Books

References from Jian-Xin Zhu Bogliubov-de Gennes Equations, Bogliubov-de Gennes Equations for Superconductors in the Continuum Model

1. J. Hubbard, Proc. R. Soc. (Lond.) A276, 238 (1963)
2. F. Gebhard, The Mott Metal-Insulator Transition: Models and Methods (Springer, Berlin, 1997)
3. E. Abrahams, P.W. Anderson, D.C. Licciardello, T.V. Ramakrishnan. Phys. Rev. Lett. 42, 673 (1979)
4. B.L. Altshuler, P.A. Lee, R.A. Webb (eds.), Mesoscopic Phenomena in Solids (Elsevier, Amsterdam, 1991)
5. E. Abrahams, 50 Years of Anderson Localization (World Scientific, Singapore, 2010)
6. A. Tsukada et al., Solid State Commun. 133, 427 (2005)
7. L.N. Cooper, Phys. Rev. 104, 1189 (1956)
8. J. Bardeen, L.N. Cooper, J.R. Schrieffer, Phys. Rev. 108, 1175 (1957)
9. P.G. de Gennes, Superconductivity of Metals and Alloys (W.A. Benjamin, New York, 1966)
10. M. Born, J.R. Oppenheimer, Ann. Phys. 84, 457 (1927)
11. R.M. Martin, Electronic Structure: Basic Theory and Practical Methods (Cambridge University Press, Cambridge, 2004)
12. W. Kohn, L.J. Sham, Phys. Rev. 137, A1441 (1965)
13. P. Hohenberg, W. Kohn, Phys. Rev. 136, B864 (1964)
14. J.P. Perdew, MRS Bull. 38, 743 (2013)

15. E. Fradkin, Field Theories of Condensed Matter Systems (Addison-Wesley, Redwood City, 1991)

16. A. Auerbach, Interacting Electrons and Quantum Magnetism (Springer, Berlin, 1994)

17. A.L. Fetter, J.D. Walecka, Quantum Theory of Many-Particle Systems (McGraw-Hill, New York, 1971)

18. G.D. Mahan, Many-Particle Physics, 3rd edn. (Kluwer Academic/Plenum, New York, 2000)

19. A. Hewson, The Kondo Problem to Heavy Fermions (Cambridge University Press, Cambridge, 1993)

20. A. Georges, G. Kotliar, W. Krauth, M. Rozenberg, Rev. Mod. Phys. 68, 13 (1996)

21. G. Kotliar, S. Savrasov, V. Oudovenko, O. Parcolet, C. Marianetti, Rev. Mod. Phys. 78, 865 (2006)

22. K. Held, Adv. Phys. 56, 829 (2007)

23. V. Anisimov, Y. Izyumov, Electronic Structure of Strongly Correlated Materials (Springer, Berlin, 2010)

24. A.R. Bishop, P.S. Lomdahl, J.R. Schrieffer, S.A. Trugman, Phys. Rev. Lett. 61, 2709 (1988)

25. N.N. Bogoliubov, Sov. Phys. -JETP 7, 41 (1958)

26. J.G. Valatin, Nuovo Cimento 7, 843 (1958)

27. C. Bruder, Phys. Rev. B 41, 4017 (1990)

28. R.D. Parks, Superconductivity (Dekker, New York, 1969)

29. P.A. Lee, N. Nagaosa, X.-G. Wen, Rev. Mod. Phys. 78, 17 (2006)

30. P.J. Hirschfeld, M.M. Korshunov, I.I. Mazin, Rep. Prog. Phys. 74, 124508 (2011)

31. J.D. Thompson, Z. Fisk, J. Phys. Soc. Jpn. 81, 011002 (2012)

32. J. L. Sarrao et al., Nature 420, 297 (2002)

33. N.J. Curro et al., Nature 434, 622 (2005)

34. E.I. Bount, Phys. Rev. B 32, 2935 (1985)

35. K. Ueda, T.M. Rice, Phys. Rev. B 31, 7114 (1985)

36. P.W. Anderson, W.F. Brinkman, in The Physics of Liquid and Solid Helium, ed. by K.H. Bennemann, J.B. Ketterson (Wiley, New York, 1978)

37. K. Ishida et al., Nature 396, 658 (1998)

38. C.M. Varma, in Moment Formation in Solids, ed. by W. J. L. Buyers (Plenum, New York, 1984)

39. H.R. Ott et al., Phys. Rev. Lett. 52, 1915 (1984)

40. P.W. Anderson, Phys. Rev. B 30, 1549 (1984)

41. D. Vollhardt, P. Wölfle, The Superfluid Phases of Helium 3 (Taylor and Francis, London, 1990)

42. R. Balian, N.R. Werthamer, Phys. Rev. 131, 1553 (1963)

43. P.W. Anderson, P. Morel, Phys. Rev. 123, 1911 (1961)

44. Y. Nambu, Phys. Rev. 117, 648 (1960)

45. J.R. Schrieffer, The Theory of Superconductivity (Benjamin, New York, 1964)

46. A.A. Abrikosov, L.P. Gorkov, I.E. Dzyaloshinski, Methods of Quantum Field Theory in Statistical Physics (Dover Publications, New York, 1963)

References from Jian-Xin Zhu Bogliubov-de Gennes Equations, BdG Equations in Tight-Binding Model

1. N.W. Ashcroft, N.D. Mermin, Solid State Physics (Saunders College, Philadelphia, 1976)

2. R. Micnas, J. Ranninger, S. Robaszkiewicz, Rev. Mod. Phys. 62, 113 (1990)

3. G. Kotliar, J. Liu, Phys. Rev. B 38, 5142(R) (1988)

4. T. Xiang, J.M. Wheatley, Phys. Rev. B 51, 11721 (1995)

5. Y. Wang, A.H. MacDonald, Phys. Rev. B 52, 3876 (1995)

6. M. Franz, C. Kallin, A.J. Berlinsky, Phys. Rev. B 54, R6897 (1996)

7. M. Franz, C. Kallin, A.J. Berlinsky, M.I. Salkola, Phys. Rev. B 56, 7882 (1997)

8. M. Takigawa, M. Ichioka, K. Machida, Phys. Rev. Lett. 83, 3057 (1999)

9. J.-X. Zhu, T.K. Lee, C.S. Ting, C.-R. Hu, Phys. Rev. B 61, 8667 (2000)

10. A. Ghosal, M. Randeria, N. Trivedi, Phys. Rev. B 65, 014501 (2001)

11. S. Takahashi, A. Shoyama, M. Tachiki, Physica C 185-189, 1677 (1991)

12. D.J. Scalapino, S.R. White, S.C. Zhang, Phys. Rev. Lett. 68, 2830 (1992)

13. D.J. Scalapino, S.R. White, S.C. Zhang, Phys. Rev. B 47, 7995 (1993)

References from Jian-Xin Zhu Bogliubov-de Gennes Equations, Local Electronic Structure Around a Single Impurity in Superconductors

1. A.V. Balatsky, I. Vekhter, J.-X. Zhu, Rev. Mod. Phys. 78, 373 (2006)

2. A.L. Fetter, Phys. Rev. A 140, 1921 (1965)

3. K. Machida, F. Shibata, Prog. Theor. Phys. 47, 1817 (1972)

4. H. Shiba, Prog. Theor. Phys. 50, 50 (1973)

5. K. Machida, Prog. Theor. Phys. 51, 1667 (1974)

6. L. Yu, Acta Phys. Sin. Ch.-Ed. 21, 75 (1965)

7. H. Shiba, Prog. Theor. Phys. 40, 435 (1968)

8. A.I. Rusinov, Zh. Eksp. Teor. Fiz. Pis'ma Red. 9, 146 (1968) [JETP Lett. 9, 85 (1969)]

9. A.I. Rusinov, Zh. Eksp. Teor. Fiz. 56, 2047 (1969) [Sov. Phys. JETP 29, 1101 (1969)]

10. V. Mourik et al., Science 336, 1003 (2012)

11. A. Das et al., Nat. Phys. 8, 887 (2012)

12. L. Rokhinson, X. Liu, J.K. Furdyna, Nat. Phys. 8, 795 (2012)

13. C.W. J. Beenakker, Annu. Rev. Condens. Matter Phys. 4, 113 (2013)

14. C. Nayak, S.H. Simon, A. Stern, M. Freeman, S. Das Sarma, Rev. Mod. Phys. 80, 1083 (2008)

15. N.B. Kopnin, M.M. Salomaa, Phys. Rev. B 44, 9667 (1991)

16. G. Volovik, JEPT Lett. 70, 609 (1999)

17. S.R. Elliott, M. Franz, Rev. Mod. Phys. 87, 137 (2015)

18. I. Martin, A.F. Morpurgo, Phys. Rev. B 85, 144505 (2012)

19. S. Nadj-Perge, I.K. Drozdov, B.A. Bernevig, A. Yazdani, Phys. Rev. B 88, 020407 (2013)

20. F. Pientka, L.I. Glazman, F. von Oppen, Phys. Rev. B 89, 180505(R) (2014)

21. I. Reis, D.J.J. Marchand, M. Franz, Phys. Rev. B 90, 085124 (2014)

22. A.Y. Kitaev, Phys. Usp. 44, 131 (2001)

23. B. Braunecker, P. Simon, Phys. Rev. Lett. 111, 147202 (2013)

24. J. Klinovaja, P. Stano, A. Yazdani, D. Loss, Phys. Rev. Lett. 111, 186805 (2013)

25. M.M. Vazifeh, M. Franz, Phys. Rev. Lett. 111, 206802 (2013)

26. D.J. Scalapino, Phys. Rep. 250, 329 (1995)

27. D.J. van Harlingen, Rev. Mod. Phys. 67, 515 (1995)

28. P.A. Lee, Phys. Rev. Lett. 71, 1887 (1993)

29. J.M. Byers, M.E. Flatté, D.J. Scalapino, Phys. Rev. Lett. 71, 3363 (1993)

30. C.H. Choi, Phys. Rev. B 50, 3491 (1994)

31. A.V. Balatsky, M.I. Salkola, A. Rosengren, Phys. Rev. B 51, 15547 (1995); A.V. Balatsky, M.I. Salkola, Phys. Rev. Lett. 76, 2386 (1996)

32. M.I. Salkola, A.V. Balatsky, D.J. Scalapino, Phys. Rev. Lett. 77, 1841 (1996); M.I. Salkola, A.V. Balatsky, J.R. Schrieffer, Phys. Rev. B 55, 12648 (1997)

33. M. Franz, C. Kallin, A.J. Berlinsky, Phys. Rev. B 54, R6897 (1996)

34. Y. Onishi et al., J. Phys. Soc. Jpn. 65, 675 (1996)

35. M.E. Flatté, J.M. Byers, Phys. Rev. Lett. 80, 4546 (1998)

36. A. Yazdani, C.M. Howald, C.P. Lutz, A. Kapitulnik, D.M. Eigler, Phys. Rev. Lett. 83, 176 (1999)

37. E.W. Hudson, S.H. Pan, A.K. Gupta, K.-W. Ng, J.C. Davis, Science 258, 88 (1999)

38. A. Shnirman, I. Adagideli, P.M. Goldbart, A. Yazdani, Phys. Rev. B 60, 7517 (1999)

39. H. Tanaka, K. Kuboki, M. Sigrist, Int. J. Mod. Phys. B 12, 2447 (1998)

40. H. Tsuchiura, Y. Tanaka, M. Ogata, S. Kashiwaya, J. Phys. Soc. Jpn. 68, 2510 (1999)

41. S.H. Pan, E.W. Hudson, K.M. Lang, H. Eisaki, S. Uchida, J.C. Davis, Nature (London) 403, 746 (2000)

42. G. Kotliar, J. Liu, Phys. Rev. B 38, 5142 (1988)

43. J.-X. Zhu, T.K. Lee, C.S. Ting, C.-R. Hu, Phys. Rev. B 61, 8667 (2000)

References from Jian-Xin Zhu Bogliubov-de Gennes Equations, Disorder Effects on Electronic and Transport Properties in Superconductors

1. P.W. Anderson, Phys. Rev. Lett. 3, 325 (1959)

2. J.-X. Zhu, W. Kim, C.S. Ting, Phys. Rev. B 57, 13410 (1998)

3. M. Ma, P.A. Lee, Phys. Rev. B 32, 5658 (1985)

4. P.J. Hirschfeld, N.D. Goldenfeld, Phys. Rev. B 48, 4219 (1993)

5. H. Kim, G. Preosti, P. Muzikar, Phys. Rev. B 49, 3544 (1994)

6. R.J. Radtke, et al., Phys. Rev. B 48, 653 (1993)

7. P. Arberg, J.P. Carbotte, Phys. Rev. B 50, 3250 (1994)

8. C.J. Pethick, D. Pines, Phys. Rev. Lett. 57, 118 (1986)

9. S. Schmitt-Rink, K. Miyaki, C.M. Varma, Phys. Rev. Lett. 57, 2575 (1986)

10. P. Hirschfeld, D. Vollhardt, P. Wölfle, Solid State Commun. 59, 111 (1986)

11. H. Monien, et al., Solid State Commun. 61, 581 (1987)

12. P. Hirschfeld, P. Wölfle, D. Einzel, Phys. Rev. B 37, 83 (1988)

13. A.V. Balatsky, M.I. Salkola, A. Rosengren, Phys. Rev. B 51, 15547 (1995)

14. M. Franz, C. Kallin, A.J. Berlinsky, M.I. Salkola, Phys. Rev. B 56, 7882 (1997)

15. P.J. Hirschfeld, J. Phys. Chem. Solids 56, 1605 (1995)

16. T. Das, J.-X. Zhu, M. J. Graf, Phys. Rev. B 84, 134510 (2011)

17. E. Abrahams, P.W. Anderson, D.C. Licciardello, T.V. Ramakrishnan, Phys. Rev. Lett. 42, 673 (1979)

18. E. Abrahams, 50 Years of Anderson Localization (World Scientific, Singapore, 2010)

19. A. MacKinnon, B. Kramer, Z. Phys. B 53, 1 (1983)

20. V.I. Oseledec, Trans. Mosc. Math. Soc. 19, 197 (1968)

21. R. Carmona, J. Lacroix, Spectral Theory of Random Schrödinger Equations (Birkhauser, Boston, 1990)

22. J.-X. Zhu, D.N. Sheng, C.S. Ting, Phys. Rev. Lett. 85, 4944 (2000)

23. T. Senthil, et al., Phys. Rev. Lett. 81, 4704 (1998)

24. C.W.J. Beenakker, Rev. Mod. Phys. 69, 731 (1997)

References from Jian-Xin Zhu Bogliubov-de Gennes Equations, Local Electronic Structure in Superconductors Under a Magnetic Field

1. J.M. Luttinger, Phys. Rev. 84, 814 (1951)

2. R.E. Peierls, Z. Phys. 80, 763 (1933)

3. C. Caroli, P.G. de Gennes, J. Matricon, Phys. Lett. 9, 307 (1964)

4. C. Caroli, J. Matricon, Phys. Kondens. Mater. 3, 380 (1965)

5. C. Caroli, Ann. Inst. Henri Poincaré A 4, 159 (1966)

6. J. Bardeen, R. Kümmel, A.E. Jacobs, L. Tewordt, Phys. Rev. 187, 556 (1969)

7. J.D. Shore, M. Huang, A.T. Dorsey, J.P. Sethna, Phys. Rev. Lett. 62, 3089 (1989)

8. F. Gygi, M. Schlüter, Phys. Rev. B 41, 822 (1990)

9. J.B. Ketterson, S.N. Song, Superconductivity (Cambridge University Press, Cambridge, 1999)

10. F. Gygi, M. Schlüter, Phys. Rev. B 43, 7609 (1990)

11. F. Gygi, M. Schlüter, Phys. Rev. B 43, 7609 (1991)

12. N. Hayashi, T. Isoshima, M. Ichioka, K. Machida, Phys. Rev. Lett. 80, 2921 (1998)

13. L. Kramer, W. Pesch, Z. Phys. 269, 59 (1974)

14. H.F. Hess, et al., Phys. Rev. Lett. 62, 814 (1989)

15. H.F. Hess, et al., Phys. Rev. Lett. 64, 2711 (1990)

16. H.F. Hess, in Scanning Tunneling Microscopy, ed. by J.A. Stroscio, W.J. Kaiser (Academic Press, San Diego, 1993), p. 427

17. J.-P. Xu, et al., Phys. Rev. Lett. 112, 217001 (2014)

18. J.-P. Xu, et al., Phys. Rev. Lett. 114, 017001 (2015)

19. T. Kawakami, X. Hu, Phys. Rev. Lett. 115, 177001 (2015)

20. C.K. Chiu, M.J. Gilbert, T.L. Hughes, Phys. Rev. B 84, 144507 (2011)

21. Z.-Z. Li, F.-C. Zhang, Q.-H. Wang, Sci. Rep. 4, 6363 (2014)

22. T. Mizushima, K. Machida, Phys. Rev. A 82, 023624 (2010)
23. A.A. Abrikosov, Sov. Phys. JETP 35, 1090 (1957)
24. Yu.A. Bychkov, E.I. Rashba, Sov. Phys. JETP 58, 1062 (1983)
25. V.N. Nicopoulos, P. Kumar, Phys. Rev. B 44, 12080 (1991)
26. S. Dukan, Z. Tešanović, Phys. Rev. B 49, 13017 (1994)
27. M.R. Norman, A.H. MacDonald, H. Akera, Phys. Rev. B 51, 5927 (1995)
28. P. Miller, Z. Tesanovic, J. Phys. Condens. Matter 7, 5579 (1995)
29. M.R. Norman, A.H. MacDonald, Phys. Rev. B 54, 4239 (1996)
30. G.M. Bruun, V.N. Nicopoulos, N.F. Johnson, Phys. Rev. B 56, 809 (1997)
31. J.E. Graebner, M. Robbins, Phys. Rev. Lett. 36, 422 (1976)
32. F. Mueller, et al., Phys. Rev. Lett. 68, 3928 (1992)
33. R. Corcoran, et al., Phys. Rev. Lett. 72, 701 (1994)
34. N. Harrison, et al., Phys. Rev. B 50, 4208 (1994)
35. M. Franz, Z. Tešanović, Phys. Rev. Lett. 80, 4763 (1998)
36. P.I. Soininen, C. Kallin, A.J. Berlinsky, Phys. Rev. B 50, 13883 (1994)
37. Y. Wang, A.H. MacDonald, Phys. Rev. B 52, R3876 (1995)
38. M. Takigawa, M. Ichioka, K. Machida, Phys. Rev. Lett. 83, 3057 (1999)
39. J.-X. Zhu, C.S. Ting, Phys. Rev. Lett. 87, 147002 (2001)
40. I. Maggio-Aprile, et al., Phys. Rev. Lett. 75, 2754 (1995)
41. S.H. Pan, et al., Phys. Rev. Lett. 85, 1536 (2000)
42. R.B. Laughlin, Phys. Rev. Lett. 80, 5188 (1998)
43. K. Yasui, T. Kita, Phys. Rev. Lett. 83, 4168 (1999)
44. D.P. Arovas, et al., Phys. Rev. Lett. 79, 2871 (1997)
45. J.H. Han, D.-H. Lee, Phys. Rev. Lett. 85, 1100 (2000)
46. J.-X. Zhu, I. Martin, A.R. Bishop, Phys. Rev. Lett. 89, 067003 (2002)
47. H.-D. Chen, O. Vafek, A. Yazdani, S.-C. Zhang, Phys. Rev. Lett. 93, 187002 (2004)
48. A.M. Clogston, Phys. Rev. Lett. 3, 266 (1962)
49. B.S. Chandrasekhar, Appl. Phys. Lett. 1, 7 (1962)
50. P. Fulde, R.A. Ferrell, Phys. Rev. 135, A550 (1964)
51. A.I. Larkin, Yu.N. Ovchinnikov, Sov. Phys. JETP 20, 762 (1965)

52. Y. Matsuda, H. Shimahara, J. Phys. Soc. Jpn. 76, 051005 (2007)

53. R. Casalbuoni, G. Nardulli, Rev. Mod. Phys. 76, 263 (2004)

54. A. Bianchi, R. Movshovich, C. Capan, P.G. Pagliuso, J.L. Sarrao, Phys. Rev. Lett. 91, 187004 (2003)

55. Q. Wang, H.-Y. Chen, C.-R. Hu, C.S. Ting, Phys. Rev. Lett. 96, 11706 (2006)

References from Jian-Xin Zhu Bogliubov-de Gennes Equations, Transport Across Normal-Metal/Superconductor Junctions

1. A.F. Andreev, Zh. Eksp. Teor. Fiz. 46, 1823 (1964) [Sov. Phys. JETP 19, 1228 (1964)]; 49, 655 (1965) [22, 455 (1966)]; 51, 1510 (1966) [24, 1019 (1967)]

2. G.E. Blonder, M. Tinkham, T.M. Klapwijk, Phys. Rev. B 25, 4515 (1982)

3. W.N. Mathews, Jr., Phys. Status Solidi B 90, 327 (1978)

4. P.F. Bagwell, Phys. Rev. B 49, 6841 (1994)

5. C.W.J. Beenakker, H. van Houten, in Nanostructures and Mesoscopic Systems, ed. by W.P. Kirk, M.A. Reed (Academic Press, New York, 1992)

6. R. Landauer, Philos. Mag. 21, 863 (1970)

7. M. Büttiker, Phys. Rev. Lett. 57, 1761 (1986)

8. C.W.J. Beenakker, Phys. Rev. Lett. 67, 3836 (1991); 68, 1442(E) (1992)

9. C.W.J. Beenakker, Phys. Rev. B 46, 12841 (1992)

10. C.J. Lambert, J. Phys.: Condens. Matter 3, 6579 (1991)

11. B.J. van Wees, P. de Vries, P. Magn'ee, T.M. Klapwijk, Phys. Rev. Lett. 69, 510 (1992)

12. Y. Takane, H. Ebisawa, J. Phys. Soc. Jpn. 61, 1685 (1992); 61, 2858 (1992); 61, 3466 (1992); 62, 1844 (1993)

13. A. Kastalsky, A.W. Kleinsasser, L.H. Greene, R. Bhat, F.P. Milliken, J.P. Harbison, Phys. Rev. Lett. 67, 3026 (1991)

14. C. Nguyen, H. Kroemer, E.L. Hu, Phys. Rev. Lett. 69, 2847 (1992)

15. S.J.M. Bakker, E. van der Drift, T.M. Klapwijk, H.M. Jaeger, S. Radelaar, Phys. Rev. B 49, 13275 (1994)

16. I.K. Marmorkos, C.W.J. Beenakker, R.A. Jalabert, Phys. Rev. B 48, 2811 (1993)

17. C.W.J. Beenakker, Rev. Mod. Phys. 69, 731 (1997)

18. J. Geerk, X.X. Li, G. Linker, Z. Phys. B 73, 329 (1988)

19. J. Lesueur, L.H. Greene, W.L. Feldmann, A. Imam, Physica C 191, 325 (1992)

20. M. Covington, R. Scheuerer, K. Bloom, L.H. Greene, Appl. Phys. Lett. 68, 1717 (1996)

21. M. Covington, M. Aprili, E. Paraoanu, L.H. Greene, F. Xu, J. Zhu, C.A. Mirkin, Phys. Rev. Lett. 79, 277 (1997)

22. C.R. Hu, Phys. Rev. Lett. 72, 1526 (1994)

23. Y. Tanaka, S. Kashiwaya, Phys. Rev. Lett. 74, 3451 (1995).

24. S. Kashiwaya, Y. Tanaka, M. Koyanagi, H. Takashima, K. Kajimura, Phys. Rev. B 51, 1350 (1995); J. Phys. Chem. Solids 56, 1721 (1995)

25. S. Kashiwaya, Y. Tanaka, M. Koyanagi, K. Kajimura, Phys. Rev. B 53, 2667 (1996)

26. J. Kurkijärvi, D. Rainer, in Modern Problems in Condensed Matter Sciences, ed. by W.P. Halperin, L.P. Pitaerskii (Elsevier, Amsterdam, 1989)

27. P. Koorevaar, Y. Suzuki, R. Coehoorn, J. Aarts, Phys. Rev. B 49, 441 (1994).

28. G. Verbanck, C.D. Potter, R. Schad, P. Belien, V.V. Moschalkov, Y. Bruynseraede, Physica C 235-240, 3295 (1994)

29. C. Struck, C. Sürgers, U. Paschen, H.V. Löhneysen, Phys. Rev. B 49, 4053 (1994)

30. J.S. Jiang, D. Davidović, D.H. Reich, C.L. Chuen, Phys. Rev. Lett. 74, 314 (1995)

31. Z. Radović, L. Dobrosavljević-Grujíc, A.I. Buzdin, J.R. Clem, Phys. Rev. B 38, 2388 (1988)

32. Z. Radović, M. Ledvij, L. Dobrosavljević-Grujíc, A.I. Buzdin, J.R. Clem, Phys. Rev. B 44, 759 (1991)

33. A.I. Buzdin, M.Y. Kupriyanov, Pis'ma Zh. Eksp. Teor. Fiz. 52, 1089 (1990) [JETP Lett. 52, 487 (1990)]; 53, 308 (1991) [53, 321 (1991)]

34. A.I. Buzdin, M. Yu. Kupriyanov, B. Vujícíc, Physica C 185, 2025 (1991)

35. A.I. Buzdin, L.N. Bulaevski, S.V. Panyukov, Pis'ma Zh. Éksp. Teor. Fiz. 35, 147 (1982) [JETP Lett. 35, 178 (1982)]

36. A.I. Buzdin, B. Bujicic, M.Y. Kupriyanov, Zh. Éksp. Teor. Fiz. 101, 231 (1992) [Sov. Phys. JETP 74, 124 (1992)]

37. E.A. Demler, G.B. Arnold, M.R. Beasley, Phys. Rev. B 55, 15174 (1997)

38. M.O. Visscher, G.E.W. Bauer, Phys. Rev. B 54, 2798 (1996)

39. O. Sipr, B.L. Grorffy, J. Phys.: Condens. Matter 7, 5239 (1995)

40. C.A.R. Sá de Melo, Phys. Rev. Lett. 79, 1933 (1997)

41. R. Meservey, P.M. Tedrow, Phys. Rep. 238, 173 (1994)

42. M.J.M. de Jong, C.W.J. Beenakker, Phys. Rev. Lett. 74, 1657 (1995)

43. M. Leadbeater, C.J. Lambert, K.E. Nagaev, R. Raimondi, A.F. Volkov, Phys. Rev. B 59, 12264 (1999)

44. S.K. Upadhyay, A. Palanisami, R.N. Louie, R.A. Buhrman, Phys. Rev. Lett. 81, 3247 (1998)

45. V.A. Vas'ko, K.R. Nikolaev, V.A. Larkin, P.A. Kraus, A.M. Goldman, Appl. Phys. Lett. 73, 844 (1998)

46. J.-X. Zhu, B. Friedman, C.S. Ting, Phys. Rev. B 59, 9558 (1999)

47. I. Zutic, O.T. Valls, Phys. Rev. B 60, 6320 (1999)

48. M.Z. Hasan, C.L. Kane, Rev. Mod. Phys. 82, 3045 (2010)

49. X.-L. Qi, S.-C. Zhang, Rev. Mod. Phys. 83, 1057 (2011)

50. Y.S. Hor, A.J. Williams, J.G. Checkelsky, P. Roushan, J. Seo, Q. Xu, H.W. Zandbergen, A. Yazdani, N.P. Ong, R.J. Cava, Phys. Rev. Lett. 104, 057001 (2010)

51. L. Fu, C.L. Kane, Phys. Rev. Lett. 100, 096407 (2008)

52. L. Fu, C.L. Kane, Phys. Rev. Lett. 102, 216403 (2009)

53. X.-L. Qi, T.L. Hughes, S.-C. Zhang, Phys. Rev. B 82, 184516 (2010)

54. A.R. Akhmerov, J. Nilsson, C.W.J. Beenakker, Phys. Rev. Lett. 102, 216404 (2009).

55. Y. Tanaka, T. Yokoyama, N. Nagaosa, Phys. Rev. Lett. 103, 107002 (2009)

56. K.T. Law, P.A. Lee, T.K. Ng, Phys. Rev. Lett. 103, 237001 (2009)

57. J. Linder, Y. Tanaka, T. Yokoyama, A. Sudbø, N. Nagaosa, Phys. Rev. Lett. 104, 067001 (2010)

58. P.A. Ioselevich, M.V. Feigel'man, Phys. Rev. Lett. 106, 077003 (2011)

59. J. Ren, J.-X. Zhu, Phys. Rev. B 87, 165121 (2013)

References from Jian-Xin Zhu Bogliubov-de Gennes Equations, Topological and Quantum Size Effects in Superconductors at Reduced Length Scale

1. Y. Aharonov, D. Bohm, Phys. Rev. 115, 485 (1959)

2. R. Landauer, M. Büttiker, Phys. Rev. B 54, 2049 (1985)

3. V. Chandrasekhar, et al., Phys. Rev. Lett. 67, 3578 (1991)

4. R. Doll, M. Näbauer, Phys. Rev. Lett. 7, 51 (1961)

5. B.S. Deaver, W.M. Fairbank, Phys. Rev. lett. 7, 43 (1961)

6. N. Byers, C.N. Yang, Phys. Rev. Lett. 7, 46 (1961)

7. W. Brenig, Phys. Rev. Lett. 7, 337 (1961)

8. C.E. Gough, et al., Nature (London) 326, 855 (1987)

9. J.-X. Zhu, Z.D. Wang, Phys. Rev. B 50, 7207 (1994)

10. J.-X. Zhu, H.T. Quan, Phys. Rev. B 81, 054521 (2010)

11. F. Loder, et al., Nat. Phys. 4, 112 (2008)

12. D. Ralph, et al., Phys. Rev. Lett. 74, 3241 (1995)

References from Jian-Xin Zhu Bogliubov-de Gennes Equations, Atomic physics and quantum optics using superconducting circuits by You, Nori

References

[1] Makhlin, Y., Schön, G. & Shnirman, A. Quantum-state engineering with Josephson-junction devices. *Rev. Mod. Phys.* **73**, 357-400 (2001).

[2] You, J.Q. & Nori, F. Superconducting circuits and quantum information. *Phys. Today* **58**(11), 42-47 (2005).

[3] Clarke, J. & Wilhelm, F.K. Superconducting quantum bits. *Nature* **453**, 1031-1042 (2008).
A review of superconducting circuits as qubits.

[4] Schoelkopf, R.J. & Girvin, S.M. Wiring up quantum systems. *Nature* **451**, 664-669 (2008).

[5] Nakamura, Y., Pashkin, Yu.A. & Tsai, J.S. Coherent control of macroscopic quantum states in a single-Cooper-pair box. *Nature* **398**, 786-788 (1999).

[6] van der Wal, C.H. *et al.* Quantum superposition of macroscopic persistent-current states. *Science* **290**, 773-777 (2000).

[7] Vion, D. *et al.* Manipulating the quantum state of an electrical circuit. *Science* **296**, 886-889 (2002).

[8] Yu, Y., Han, S.Y., Chu, X., Chu, S.I. & Wang, Z. Coherent temporal oscillations of macroscopic quantum states in a Josephson junction. *Science* **296**, 889-892 (2002).

[9] Martinis, J.M., Nam, S., Aumentado, J. & Urbina, C. Rabi oscillations in a large Josephson-junction qubit. *Phys. Rev. Lett.* **89**, 117901 (2002).

[10] You, J.Q., Hu, X., Ashhab, S. & Nori, F. Low-decoherence flux qubit. *Phys. Rev. B* **75**, 140515 (2007).

[11] Steffen, M. *et al.* High-coherence hybrid superconducting qubit. *Phys. Rev. Lett.* **105**, 100502 (2010).
Report of a low-decoherence flux qubit experiment.

[12] Koch, J. *et al.* Charge-insensitive qubit design derived from the Cooper pair box. *Phys. Rev. A* **76**, 042319 (2007).

[13] You, J.Q. & Nori, F. Quantum information processing with superconducting qubits in a microwave field. *Phys. Rev. B* **68**, 064509 (2003).

[14] Blais, A., Huang, R.-S., Wallraff, A., Girvin, S.M. & Schoelkopf, R.J. Cavity quantum electrodynamics for superconducting electrical circuits: An architecture for quantum computation. *Phys. Rev. A* **69**, 062320 (2004).

[15] Chiorescu, I. *et al.* Coherent dynamics of a flux qubit coupled to a harmonic oscillator. *Nature* **431**, 159-162 (2004).
Report of the strong-coupling regime between a superconducting flux qubit and a resonator composed of an inductance and a capacitance.

[16] Wallraff, A. *et al.* Strong coupling of a single photon to a superconducting qubit using circuit quantum electrodynamics. *Nature* **431**, 162-167 (2004).
Report of the strong-coupling regime between a superconducting charge qubit and a coplanar waveguide resonator composed of a transmission line.

[17] Fragner, A. *et al.* Resolving vacuum fluctuations in an electrical circuit by measuring the Lamb shift. *Science* **28**, 1357-1360 (2008).

[18] Devoret, M.H., Girvin, S. & Schoelkopf, R. Circuit-QED: How strong can the coupling between a Josephson junction atom and a transmission line resonator be? *Ann. Phys. (Leipzig)* **16**, 767-779 (2007).

[19] Zueco, D., Reuther, G.M., Kohler, S. & Hänggi, P. Qubit-oscillator dynamics in the dispersive regime: Analytical theory beyond the rotating-wave approximation. *Phys. Rev. A* **80**, 033846 (2009).

[20] Ashhab, S. & Nori, F. Qubit-oscillator systems in the ultrastrong-coupling regime and their potential for preparing nonclassical states. *Phys. Rev. A* **81**, 042311 (2010).

[21] Nataf P. & Ciuti, C. Vacuum degeneracy of a circuit QED system in the ultrastrong coupling regime. *Phys. Rev. Lett.* **104**, 023601 (2010).

[22] Niemczyk, T. *et al.* Circuit quantum electrodynamics in the ultrastrong-coupling regime. *Nature Phys.* **6**, 772-776 (2010).

[23] Forn-Diaz, P. *et al.* Observation of the Bloch-Siegert shift in a qubit-oscillator system in the ultrastrong coupling regime. *Phys. Rev. Lett.* **105**, 237001 (2010).

[24] Wilson, C.M. *et al.* Coherence times of dressed states of a superconducting qubit under extreme driving. *Phys. Rev. Lett.* **98**, 257003 (2007).
Report of dressed states of a superconducting charge qubit and an intense microwave field.

[25] Liu, Y.X., You, J.Q., Wei, L.F., Sun, C.P. & Nori, F. Optical selection rules and phase-dependent adiabatic state control in a superconducting quantum circuit. *Phys. Rev. Lett.* **95**, 087001 (2005).
Analysis of parity symmetry and selection rules in flux qubit circuits.

[26] Deppe, F. *et al.* Two-photon probe of the Jaynes-Cummings model and controlled symmetry breaking in circuit QED. *Nature Phys.* **4**, 686-691 (2008).

[27] de Groot, P.C. *et al.* Selective darkening of degenerate transitions demonstrated with two superconducting quantum bits, *Nature Phys.* **6**, 763-766 (2010)

[28] Harris, S.E. Electromagnetically induced transparency. *Phys. Today* **50**(7), 36-42 (1997).

[29] Scully M.O. & Zubairy, M.S. *Quantum Optics* (Cambridge University Press, 1997).

[30] You, J.Q., Liu, Y.X., Sun, C.P. & Nori, F. Persistent single-photon production by tunable on-chip micromaser with a superconducting quantum circuit. *Phys. Rev. B* **75**, 104516 (2007).

[31] Murali, K.V.R.M., Dutton, Z., Oliver, W.D., Crankshaw, D.S. & Orlando, T.P. Probing decoherence with electromagnetically induced transparency in superconductive quantum circuits. *Phys. Rev. Lett.* **93**, 087003 (2004).

[32] Dutton, Z., Murali, K.V.R.M., Oliver, W.D. & Orlando, T.P. Electromagnetically induced transparency in superconducting quantum circuits: Effects of decoherence, tunneling, and multilevel crosstalk. *Phys. Rev. B* **73**, 104516 (2006).

[33] Ian, H., Liu, Y.X. & Nori, F. Tunable electromagnetically induced transparency and absorption with dressed superconducting qubits. *Phys. Rev. A* **81**, 063823 (2010).

[34] Sillanpää, M.A. *et al.* Autler-Townes effect in a superconducting three-level system. *Phys. Rev. Lett.* **103**, 193601 (2009).

[35] Abdumalikov, Jr., A.A. *et al.* Electromagnetically induced transparency on a single artificial atom. *Phys. Rev. Lett.* **104**, 193601 (2010).

[36] Rodrigues, D.A., Imbers, J. & Armour, A.D. Quantum dynamics of a resonator driven by a superconducting single-electron transistor: A solid-state analogue of the micromaser. *Phys. Rev. Lett.* **98**, 67204 (2007).

[37] Hauss, J., Fedorov, A., Hutter, C., Shnirman, A. & Schön, G. Single-qubit lasing and cooling at the Rabi frequency. *Phys. Rev. Lett.* **100**, 037003 (2008).

[38] Ashhab, S., Johansson, J.R., Zagoskin, A.M. & Nori, F. Single-artificial-atom lasing using a voltage-biased superconducting charge qubit. *New J. Phys.* **11**, 023030 (2009).

[39] Astafiev, O. *et al.* Single artificial-atom lasing. *Nature* **449**, 588-590 (2007).

[40] Grajcar, M. *et al.* Sisyphus cooling and amplification by a superconducting qubit. *Nature Phys.* **4**, 612-616 (2008).

[41] Meystre, P. *Atom Optics* (Springer, New York, 2001).

[42] Valenzuela, S.O. *et al.* Microwave-induced cooling of a superconducting qubit. *Science* **314**, 1589-1592 (2006).
Report of cooling for a flux qubit using an inverse process of state population inversion.

[43] You, J.Q., Liu, Y.X. & Nori, N. Simultaneous cooling of an artificial atom and its neighboring quantum system. *Phys. Rev. Lett.* **100**, 047001 (2008).

[44] Huang, X.M.H., Zorman, C.A., Mehregany, M. & Roukes, M.L. Nanodevice motion at microwave frequencies. *Nature* **421**, 496 (2003).

[45] Martin, I., Shnirman, A., Tian, L. & Zoller, P. Ground-state cooling of mechanical resonators. *Phys. Rev. B* **69**, 125339 (2004).

[46] Zhang, P., Wang, Y.D. & Sun, C.P. Cooling mechanism for a nonmechanical resonator by periodic coupling to a Cooper pair box. *Phys. Rev. Lett.* **95**, 097204 (2005).

[47] Marquardt, F., Chen, J.P., Clerk, A.A. & Girvin, S.M. Quantum theory of cavity-assisted sideband cooling of mechanical motion. *Phys. Rev. Lett.* **99**, 093902 (2007).

[48] Grajcar, M., Ashhab, S., Johansson, J.R. & Nori, F. Lower limit on the achievable temperature in resonator-based sideband cooling. *Phys. Rev. B* **78**, 035406 (2008).

[49] Naik, A. *et al.* Cooling a nanomechanical resonator with quantum back-action. *Nature* **443**, 193-196 (2006).

[50] Rocheleau, T. *et al.* Preparation and detection of a mechanical resonator near the ground state of motion. *Nature* **463**, 72-75 (2010).

[51] O'Connell, A.D. *et al.* Quantum ground state and single-phonon control of a mechanical resonator. *Nature* **464**, 697-703 (2010).

[52] Sillanpää, M.A., Park, J.I. & Simmonds, R.W. Coherent quantum state storage and transfer between two phase qubits via a resonant cavity. *Nature* **449**, 438-442 (2007).
Report of quantum-information transfer between two superconducting qubits using single photons generated in a cavity as a quantum bus.

[53] Houck, A.A. *et al.* Generating single microwave photons in a circuit. *Nature* **449**, 328-331 (2007).

[54] Hofheinz, M. *et al.* Generation of Fock states in a superconducting quantum circuit. *Nature* **454**, 310-314 (2008).

[55] Hofheinz, M. *et al.* Synthesizing arbitrary quantum states in a superconducting resonator. *Nature* **459**, 546-549 (2009).
Report of the controllable and deterministic generation of complex superposition of states with different number of photons by using superconducting circuits.

[56] Law, C.K. & Eberly, J.H. Arbitrary control of a quantum electromagnetic field. *Phys. Rev. Lett.* **76**, 1055-1058 (1996).

[57] Liu, Y.X., Wei, L.F. & Nori, F. Generation of nonclassical photon states using a superconducting qubit in a microcavity. *Europhys. Lett.* **67**, 941-947 (2004).

[58] Wang, H. *et al.* Measurement of the decay of Fock states in a superconducting quantum circuit. *Phys. Rev. Lett.* **101**, 240401 (2008).

[59] Wang, H. *et al.* Deterministic entanglement of photons in two superconducting microwave resonators. *Phys. Rev. Lett.* **106**, 060401 (2011).

[60] Liu, Y.X., Wei, L.F., & Nori, F. Tomographic measurements on superconducting qubit states. *Phys. Rev. B* **72**, 014547 (2005).

[61] Steffen, M. *et al.* State tomography of capacitively shunted phase qubits with high fidelity. *Phys. Rev. Lett.* **97**, 050502 (2006).

[62] Katz, N. *et al.* Coherent state evolution in a superconducting qubit from partial-collapse measurement. *Science* **312**, 1498-1500 (2006).

[63] Steffen, M. *et al.* Measurement of the entanglement of two superconducting qubits via state tomography. *Science* **313**, 1423-1425 (2006).

[64] Filipp, S. *et al.* Two-qubit state tomography using a joint dispersive readout. *Phys. Rev. Lett.* **102**, 200402 (2009).

[65] Neeley, M. *et al.* Process tomography of quantum memory in a Josephson-phase qubit coupled to a two-level state. *Nature Phys.* **4**, 523-526 (2008).

[66] Bialczak, R.C. *et al.* Quantum process tomography of a universal entangling gate implemented with Josephson phase qubits. *Nature Phys.* **6**, 409-413 (2010).

[67] Johansson, J.R., Johansson, G., Wilson, C.M. & Nori, F. Dynamical Casimir effect in a superconducting coplanar waveguide. *Phys. Rev. Lett.* **103**, 147003 (2009).

[68] Wei, L.F., Johansson, J.R., Cen, L.X., Ashhab, S. & Nori, F. Controllable coherent population transfers in superconducting qubits for quantum computing. *Phys. Rev. Lett.* **100**, 113601 (2008).

[69] Rangelov, A.A. *et al.* Stark-shift-chirped rapid-adiabatic-passage technique among three states. *Phys. Rev. A* **72**, 053403 (2005).

[70] Johnson, B.R. *et al.* Quantum non-demolition detection of single microwave photons in a circuit. *Nature Phys.* **6**, 663-667 (2010).

[71] Shevchenko, S.N., Ashhab, S. & Nori, F. Landau-Zener-Strückelberg interferometry. *Phys. Rep.* **492**, 1-30 (2010).

[72] Zhou, L., Gong, Z.R., Liu, Y.X., Sun, C.P. & Nori, F. Controllable scattering of a single photon inside a one-dimensional resonator waveguide. *Phys. Rev. Lett.* **101**, 100501 (2008).

[73] Zhou, L., Dong, H., Liu, Y.X., Sun, C.P. & Nori, F. Quantum supercavity with atomic mirrors. *Phys. Rev. A* **78**, 063827 (2008).

[74] Shen J.T. & Fan, S. Coherent single photon transport in a one-dimensional waveguide coupled with superconducting quantum bits. *Phys. Rev. Let.* **95**, 213001 (2005).

[75] Astafiev, O. *et al.* Resonance fluorescence of a single artificial atom. *Science*, **327**, 840-843 (2010).

[76] Wallraff, A. *et al.* Approaching unit visibility for control of a superconducting qubit with dispersive readout. *Phys. Rev. Lett.* **95**, 060501 (2005).

[77] Lupascu, A. *et al.* Quantum non-demolition measurement of a superconducting two-level system. *Nature Phys.* **3**, 119-125 (2007).

[78] Boulant, N. *et al.* Quantum nondemolition readout using a Josephson bifurcation amplifier. *Phys. Rev. B* **76**, 014525 (2007).

[79] Siddiqi, I. *et al.* RF-driven Josephson bifurcation amplifier for quantum measurement. *Phys. Rev. Lett.* **93**, 207002 (2004).

[80] Picot, T., Schouten, R., Harmans, C.J.P.M. & Mooij, J.E. Quantum nondemolition measurement of a superconducting qubit in the weakly projective regime. *Phys. Rev. Lett.* **105**, 040506 (2010).

[81] Il'ichev, E. *et al.* Continuous monitoring of Rabi oscillations in a Josephson flux qubit. *Phys. Rev. Lett.* **91**, 097906 (2003).

[82] Zagoskin, A.M., Il'ichev, E., McCutcheon, M.W., Young, J.F. & Nori, F. Controlled generation of squeezed states of microwave radiation in a superconducting resonant circuit. *Phys. Rev. Lett.* **101**, 253602 (2008).

[83] Nayak, C., Simon, S.H., Stern, A., Freedman, M. & Das Sarma, S. Non-Abelian anyons and topological quantum computation. *Rev. Mod. Phys.* **80**, 1083 (2008),

[84] Ioffe, L.B. *et al.* Topologically protected quantum bits using Josephson junction arrays. *Nature* **415**, 503-506 (2002).

[85] Gladchenko, S. *et al.* Superconducting nanocircuits for topologically protected qubits. *Nature Phys.* **5**, 48-53 (2009).

[86] You, J.Q., Shi, X.F., Hu, X. & Nori, F. Quantum emulation of a spin system with topologically protected ground states using superconducting quantum circuits. *Phys. Rev. B* **81**, 014505 (2010).

[87] Kitaev, A. Anyons in an exactly solved model and beyond. *Ann. Phys. (N.Y.)* **321**, 2-111 (2006).

[88] Nation, P.D., Blencowe, M.P., Rimberg, A.J. & Buks, E. Analogue Hawking radiation in a dc-SQUID array transmission line. *Phys. Rev. Lett.* **103**, 087004 (2009).

[89] Friedman, J.R., Patel, V., Chen, W., Tolpygo, S.K. & Lukens, J.E. Quantum superposition of distinct macroscopic states. *Nature* **406**, 43-46 (2000).

[90] Bertet, P. *et al.* Dephasing of a superconducting qubit induced by photon noise. *Phys. Rev. Lett.* **95**, 257002 (2005).

[91] Simmonds, R.W. *et al.* Decoherence in Josephson phase qubits from junction resonators. *Phys. Rev. Lett.* **93**, 077003 (2004).

[92] Genovese, M. Research on hidden variable theories: A review of recent progresses. *Phys. Rep.* **413**, 319-396 (2005).

[93] Wei, L.F., Liu, Y.X. & Nori, F. Testing Bell's inequality in a constantly coupled Josephson circuit by effective single-qubit operations. *Phys. Rev. B* **72**, 104516 (2005).

[94] Kofman A.G. & Korotkov, A.N. Analysis of Bell inequality violation in superconducting phase qubits. *Phys. Rev. A* **77**, 104502 (2008).

[95] Ansmann, M. *et al.* Violation of Bell's inequality in Josephson phase qubits. *Nature* **461**, 504-506 (2009).

[96] Neeley, M. *et al.* Generation of three-qubit entangled states using superconducting phase qubits. *Nature* **467**, 570-573 (2010).

[97] DiCarlo, L. *et al.* Preparation and measurement of three-qubit entanglement in a superconducting circuit. *Nature* **467**, 574-578 (2010).

[98] Leggett, A.J. & Garg, A. Quantum mechanics versus macroscopic realism: Is the flux there when nobody looks? *Phys. Rev. Lett.* **54**, 857-860 (1985).

[99] Palacios-Laloy, A. *et al.* Experimental violation of a Bell's inequality in time with weak measurement. *Nature Phys.* **6**, 442-447 (2010).

[100] Wei, L.F., Maruyama, K., Wang, X.B., You, J.Q. & Nori, F. Testing quantum contextuality with macroscopic superconducting circuits. *Phys. Rev. B* **81**, 174513 (2010).

C.2 References from Theoretical Articles and Books about Specific Models

Refs from Gorkov's article about derivation of GL from BCS

[1] V. L. Ginzburg and L. D. Landau, J. Exptl. Theoret. Phys. (U.S.S.R.) 20, 1064 (1950).
[2] L. P. Gor'kov, J. Exptl. Theoret. Phys. (U.S.S.R.) 34, 735 (1958), Soviet Phys. JETP 7, 505 (1958).
[3] T. Matsubara, Progr. Theoret. Phys. 14, 352 (1954).
[4] Abrikosov, Gor'kov, and Dzyaloshinskiĭ, J. Exptl. Theoret. Phys. (U.S.S.R.) 36, 900 (1959), Soviet Phys. JETP 9, 636 (1959).
[5] Bardeen, Cooper, and Schrieffer, Phys. Rev. 108, 1175 (1957).
[6] N. N. Bogolyubov, J. Exptl. Theoret. Phys. (U.S.S.R.) 34, 58 (1958), Soviet Phys. JETP 7, 41 (1958).
[7] V. L. Ginzburg, J. Exptl. Theoret. Phys. (U.S.S.R.) 36, 1930 (1959), Soviet Phys. JETP this issue, p 1372.
[8] V. L. Ginzburg, J. Exptl. Theoret. Phys. (U.S.S.R.) 30, 593 (1956), Soviet Phys. JETP 3, 621 (1956).
[9] Yu. V. Sharvin, J. Exptl. Theoret. Phys: (U.S.S.R.) 33, 1341 (1957), Soviet Phys. JETP 6, 1031 (1958).
[10] T. E. Faber, Proc. Roy. Soc. (London) A248, 460 (1958).
Translated by D. ter Haar 380

References from Eliashberg Theory: a short review by F. Marsiglio

References

[1] See, for example, Superconducting Quantum Levitation on a 3π Möbius Strip.

[2] See, for example, Applications with Superconductivity.

[3] R.D. Parks, in the Preface of *Superconductivity*, edited by R.D. Parks (Marcel Dekker, Inc., New York, 1969) page v.

[4] This phrase was first used by an anonymous referee in appraising a colleague's understanding of the subject matter of his grant proposal (in 1990). I have plagiarized it ever since.

[5] See the various articles in the Special Issue of Physica C, 'Superconducting Materials: Conventional, Unconventional and Undetermined', edited by J.E. Hirsch, M.B. Maple, and F. Marsiglio, Physica C 514, 1-444 (2015).

[6] See, for example, P. P. Kong, V. S. Minkov, M. A. Kuzovnikov, S. P. Besedin, A. P. Drozdov, S. Mozaffari, L. Balicas, F.F. Balakirev, V. B. Prakapenka, E. Greenberg, D. A. Knyazev, M. I. Eremets, '*Superconductivity up to 243 K in yttrium hydrides under high pressure*,' in https://arxiv.org/abs/1909..

[7] Danfeng Li, Kyuho Lee, Bai Yang Wang, Motoki Osada, Samuel Crossley, Hye Ryoung Lee, Yi Cui, Yasuyuki Hikita and Harold Y. Hwang, '*Superconductivity in an infinite-layer nickelate*', Nature 572, 624 (2019).

[8] As summarized in F. London, In: *Superfluids Volume I: Macroscopic Theory of Superconductivity* (John Wiley and Sons, New York, 1950).

[9] V. L. Ginzburg and L. D. Landau, Zh. Eksperim. i. Teor. Fiz. 20, 1064 (1950).

[10] J. Bardeen, L.N. Cooper and J.R. Schrieffer, *Microscopic Theory of Superconductivity*, Phys. Rev. **106**, 162 (1957); *Theory of Superconductivity* Phys. Rev. **108**, 1175 (1957).

[11] L.P. Gor'kov, *On the energy spectrum of superconductors,* Zh. Eksperim. i Teor. Fiz. **34** 735 (1958); [Sov. Phys. JETP **7** 505 (1958)]. Zh. Eksperim. i Teor. Fiz. **34** 735 (1958); [Sov. Phys. JETP **7** 505 (1958)].

[12] G.M. Eliashberg, *Interactions between Electrons and Lattice Vibrations in a Superconductor,* Zh. Eksperim. i Teor. Fiz. **38** 966 (1960); Soviet Phys. JETP **11** 696-702 (1960).

[13] G.M. Eliashberg, *Temperature Green's Function for Electrons in a Superconductor,* Zh. Eksperim. i Teor. Fiz. **38** 1437-1441 (1960); Soviet Phys. JETP **12** 1000-1002 (1961). Nambu independently formulated the same theory.[15]

[14] Based on Web of Science, Oct. 1, 2019. These numbers are a little high, as a (very) few of these pertain to a mathematician with the same name.

[15] Yoichiro Nambu, *Quasi-Particles and Gauge Invariance in the Theory of Superconductivity* Phys. Rev. **117** 648-663 (1960).

[16] Based on Web of Science, Oct. 1, 2019. These numbers are a little high, as a (very) few of these pertain to a mathematician with the same name.

[17] D.J. Scalapino, *The Electron-Phonon Interaction and Strong-coupling Superconductivity,* In: *Superconductivity*, edited by R.D. Parks (Marcel Dekker, Inc., New York, 1969)p. 449.

[18] W.L. McMillan and J.M. Rowell, *Tunneling and Strong-coupling Superconductivity*, In: *Superconductivity*, edited by R.D. Parks (Marcel Dekker, Inc., New York, 1969)p. 561.

[19] *Superconductivity in Two Volumes*, edited by R.D. Parks (Marcel Dekker, Inc., New York, 1969) p. 1-1412.

[20] P.B. Allen and B. Mitrović, *Theory of Superconducting T_c*, in *Solid State Physics*, edited by H. Ehrenreich, F. Seitz, and D. Turnbull (Academic, New York, 1982) Vol. 37, p.1.

[21] C.S. Owen and D.J. Scalapino, *S-state instabilities for retarded interactions*, Physica **55** 691 (1971).

[22] G. Bergmann and D. Rainer, *The sensitivity of the transition temperature to changes in $\alpha^2F(\omega)$*, Z. Physik **263** 59 (1973).

[23] D. Rainer and G. Bergmann, *Temperature dependence of H_{c2} and κ_1 in strong coupling superconductors*, J. Low Temp. Phys. **14** 501 (1974).

[24] P.B. Allen and R.C. Dynes, *Transition temperature of strong-coupled superconductors reanalyzed*, Phys. Rev. B**12** 905 (1975).
See also R.C. Dynes, *McMillan's equation and the T_c of superconductors*, Solid State Commun. **10**, 615 (1972).

[25] J.M. Daams and J.P. Carbotte, *Thermodynamics of strong coupling superconductors including the effect of anisotropy*, J. Low Temp. Phys. **43** 263 (1981).

[26] D. Rainer, *Principles of Ab Initio Calculations of Superconducting Transition Temperatures,* Progress in Low Temperature Physics Volume 10, edited by D.F. Brewer (North-Holland, 1986), Pages 371-424.

[27] J.P. Carbotte and R.C. Dynes, *Superconductivity in Simple Metals*, Phys. Rev. **172**, 476-484 (1968).

[28] Lilia Boeri, *Understanding Novel Superconductors with Ab Initio Calculations,* In: Andreoni W., Yip S. (eds) Handbook of Materials Modeling. Springer, Cham. pp. 1-41.

[29] Antonio Sanna, *Introduction to Superconducting Density Functional Theory* E. Pavarini, E. Koch, R. Scalettar, and R. Martin (eds.) The Physics of Correlated Insulators, Metals, and Superconductors Modeling and Simulation Vol. 7 Forschungszentrum Julich, 2017, ISBN 978-3-95806-224-5

[30] F. Giustino, *Electron-phonon interactions from first principles*, Rev. Mod. Phys. 89, 015003 (2017).

[31] M. Lüders, M. A. L. Marques, N. N. Lathiotakis, A. Floris, G. Profeta, L. Fast, A. Continenza, S. Massidda, and E. K. U. Gross, *Ab initio theory of superconductivity. I. Density functional formalism and approximate functionals,* Phys. Rev. B 72, 024545 (2005).

[32] M. A. L. Marques, M. Lüders, N. N. Lathiotakis, G. Profeta, A. Floris, L. Fast, A. Continenza, E. K. U. Gross, and S. Massidda, *Ab initio theory of superconductivity. II. Application to elemental metals*, Phys. Rev. B 72, 024546 (2005).

[33] J.P. Carbotte, *Properties of boson-exchange superconductors*, Rev. Mod. Phys. **62**, 1027-1157 (1990).

[34] F. Marsiglio and J.P. Carbotte, 'Electron-Phonon Superconductivity', Review Chapter in *Superconductivity, Conventional and Unconventional Superconductors*, edited by K.H. Bennemann and J.B. Ketterson (Springer-Verlag, Berlin, 2008), pp. 73-162. Note that an earlier version of this review was published by the same editors in 2003, but the author order was erroneously inverted, and one of the author affiliations was incorrect in that version.

[35] W. Lee, D. Rainer and W. Zimmermann, *Holstein effect in the far-infrared conductivity of high Tc superconductors*, Physica C **159**, 535-544 (1989).

[36] F. Marsiglio and J.P. Carbotte, *Aspects of Optical Properties in Conventional and Oxide Superconductors*, Aust. J. Phys. **50**, 975 (1997);
Quasiparticle Lifetimes and the Conductivity Scattering Rate Aust, J. Phys. **50**, 1011 (1997).

[37] Giovanni A.C. Ummarino, *Eliashberg Theory*, In Emergent Phenomena in Correlated Matter Modeling and Simulation Vol. 3 Forschungszentrum Julich, 2013, ISBN 978-3-89336-884-6, edited by E. Pavarini, E. Koch, and U. Schollwock.

[38] A.B. Migdal, *Interaction between electrons and lattice vibrations in a normal metal*, Zh. Eksp. Teor. Fiz. **34**, 1438 (1958) [Sov. Phys. JETP **7**, 996 (1958)].

[39] W.L. McMillan, *Transition Temperature of Strong-Coupled Superconductors*, Phys. Rev. 167, 331 (1968).

[40] M. Cohen and P.W. Anderson, in *Superconductivity in d– and f–Band Metals*, edited by D.H. Douglass (AIP, New York, 1972)p. 17.

[41] Jonathan E. Moussa and Marvin L. Cohen, *Two bounds on the maximum phonon-mediated superconducting transition temperature,* Phys. Rev. B 74, 094520 (2006).

[42] I. Esterlis, S. A. Kivelson and D. J. Scalapino, *A bound on the superconducting transition temperature,* npj Quantum Materials (2018) 3:59, p1-4.

[43] A.S. Alexandrov, *Breakdown of the Migdal-Eliashberg theory in the strong-coupling adiabatic regime,* Europhys. Lett., 56, 92 (2001). See also A.S. Alexandrov, *Superconducting Polarons and Bipolarons*, in Polarons in Advanced Materials, edited by A.S. Alexandrov, Springer, 2007, p. 257.

[44] H. Fröhlich, *Electrons in Lattice Fields,* Advances in Physics **3**, 325 (1954)

[45] J. Bardeen and D. Pines, *Electron-Phonon Interaction in Metals*, Phys. Rev. **99** 1140 (1955).

[46] N.W. Ashcroft and N.D. Mermin, In: *Solid State Physics* (Saunders College Publishing, New York 1976) p. 518.

[47] G. Rickayzen, In: *Theory of Superconductivity* (John Wiley and Sons, New York, 1965).

[48] V. L. Berezinskii, *New model in the anistotropic phase of superfluid He-3,* Pisma Zh. Eksp. Teor. Fiz. 20, 628 (1974).

[49] J. Linder and A.V. Balatsky, Reviews of Modern Physics, accepted, Sept. 2019.

[50] Having said this, in the spirit of phenomenological exploration even the present author has used this formalism to explore other types of "bosonic glue." See, for example, S. Verga, A. Knigavko and F. Marsiglio, *Inversion of angle-resolved photoemission measurements in high-Tc cuprates* Phys. Rev. B**67**, 054503 (2003).

[51] This is not without irony, as one of the most celebrated electron-phonon-driven superconductors is MgB_2, with a $T_c \approx 39$ K. Ab initio calculations have explained this by finding *considerable* anisotropy in the coupling function. See Hyoung Joon Choi, David Roundy, Hong Sun, Marvin L. Cohen and Steven G. Louie, *The origin of the anomalous superconducting properties of MgB_2*, Nature **418**, 758-760 (2002).
Not everyone agrees with this interpretation. See, for example, J.E. Hirsch and F. Marsiglio, *Electron-phonon or hole superconductivity in MgB_2*, Phys. Rev. B **64**, 144523 (2001).

[52] F. Marsiglio, *Eliashberg Theory of the Critical Temperature and Isotope Effect. Dependence on Bandwidth, Band-Filling, and Direct Coulomb Repulsion,* J. Low Temp. Phys. **87** 659-682 (1992).

[53] Vinay Ambegaokar and Ludwig Tewordt, *Theory of the Electronic Thermal Conductivity of Superconductors with Strong Electron-Phonon Coupling*, Phys. Rev. **134**, A805 (1964).

[54] We could have elected to keep the area, $\int_0^\infty d\nu \alpha^2 F(\nu)$ constant as well, for example.

[55] There are undoubtedly references that describe this procedure in more detail, but I learned it primarily from a mentor at the time, Ewald Schachinger, who was a frequent visitor at McMaster University during the course of my PhD.

[56] F. Marsiglio, *Eliashberg theory in the weak-coupling limit*, Phys. Rev. B**98**, 024523 (2018).

[57] D. Rainer first obtained the asymptotic result noted in the text in 1973 (private communication).

[58] A. P. Drozdov, M. I. Eremets, I. A. Troyan, V. Ksenofontov, S. I. Shylin, *Conventional superconductivity at 203 kelvin at high pressures in the sulfur hydride system,* Nature **525**, 73 (2015)

[59] Maddury Somayazulu, Muhtar Ahart, Ajay K. Mishra, Zachary M. Geballe, Maria Baldini, Yue Meng, Viktor V. Struzhkin, and Russell J. Hemley, *Evidence for Superconductivity above 260 K in Lanthanum Superhydride at Megabar Pressures*, Phys. Rev. Lett. **122**, 027001 (2019).

[60] D. Duan, Y. Liu, F. Tian, D. Li, X. Huang, Z. Zhao, H. Yu, B. Liu, W. Tian, and T. Cui, *Pressure-induced metallization of dense* $(H_2S)_2H_2$ *with high-*T_c *superconductivity*, Sci. Rep. 4, 6968 (2014).

[61] T. Holstein, *Studies of Polaron Motion Part I. The Molecular-Crystal Model*, Ann. Phys. **8**, 325-342 (1959).
T. Holstein, *Studies of Polaron Motion Part II. The "Small" Polaron*, Ann. Phys. **8**, 343-389 (1959).

[62] J. Hubbard, *Electron Correlations in Narrow Energy Bands*, Proc. Roy. Soc. London, Ser. A, **276**, 238 (1963); see also **277**, 237 (1964); **281**, 401 (1964).

[63] J.E. Hirsch and E. Fradkin, *Effect of Quantum Fluctuations on the Peierls Instability: A Monte Carlo Study*, Phys. Rev. Lett. **49** 402 (1982).
J.E. Hirsch and E. Fradkin, *Phase diagram of one-dimensional electron-phonon systems. II. The molecular-crystal model*, Phys. Rev. B **27** 4302 (1983).

[64] R.T. Scalettar, N.E. Bickers and D.J. Scalapino, *Competition of pairing and Peierls-charge-density-wave correlations in a two-dimensional electron-phonon model,* Phys. Rev. B **40** 197 (1989).
R.M. Noack, D.J. Scalapino and R.T. Scalettar, *Charge-density-wave and pairing susceptibilities in a two-dimensional electron-phonon model*, Phys. Rev. Lett. **66** 778 (1991).
R.M. Noack and D.J. Scalapino, *Green's function self-energies in the two-dimensional Holstein model*, Phys. Rev. B **47** 305 (1993).

[65] F. Marsiglio, *Pairing and charge-density-wave correlations in the Holstein model at half-filling*, Phys. Rev. B **42** 2416 (1990);
see also F. Marsiglio, *Monte Carlo Evaluations of Migdal-Eliashberg Theory in two dimensions*, Physica C **162-164**, 1453 (1989).

[66] F. Marsiglio, *Phonon Self-energy Effects in Migdal-Eliashberg Theory*, In: *Electron–Phonon Interaction in Oxide Superconductors*, edited by R. Baquero (World Scientific, Singapore, 1991) p.167. See also Figure 1 in Z. Li and F. Marsiglio, *The Polaron-Like Nature of an Electron Coupled to Phonons*, J Supercond Nov Magn 25:1313 - 1317 (2012).

[67] I. Esterlis, B. Nosarzewski, E.W. Huang, B. Moritz T.P. Devereaux, D.J. Scalapino, and S.A. Kivelson, *Breakdown of the Migdal-Eliashberg theory: A determinant quantum Monte Carlo study*, Phys. Rev. **B97**, 140501(R) (2018).

[68] J. Bauer, J.E. Han and O. Gunnarsson, *Quantitative reliability study of the Migdal-Eliashberg theory for strong electron-phonon coupling in superconductors*, Phys. Rev. **B84**, 184531 (2011).
J. Bauer, J.E. Han and O. Gunnarsson, *The theory of electron-phonon superconductivity: does retardation really lead to a small Coulomb pseudopotential?*, J. Phys.: Condens. Matter **24**, 492202 (2012).
J. Bauer, J.E. Han and O. Gunnarsson, *Retardation effects and the Coulomb pseudopotential in the theory of superconductivity*, Phys. Rev. **B87**, 054507 (2013).

[69] F. Marsiglio, *Pairing in the Holstein model in the dilute limit*, Physica C **244**, 21 (1995).

[70] See the English translation of N.N. Bogoliubov, N.V. Tolmachev, and D.V. Shirkov in: *A New Method in the Theory of Superconductivity*, (Consultants Bureau, Inc., New York, 1959), p. 278-355, particularly Section 5.

[71] P. Morel and P.W. Anderson, *Calculation of the Superconducting State Parameters with Retarded Electron-Phonon Interaction*, Phys. Rev. **125** 1263 (1962).

[72] J. Bonča, S. A. Trugman, and I. Batistić, *Holstein polaron* Phys. Rev. B 60, 1633 (1999).

[73] Li-Chung Ku, S. A. Trugman, and J. Bonča, *Dimensionality effects on the Holstein polaron*, Phys. Rev. B 65, 174306 (2002).

[74] Z. Li and F. Marsiglio, *The Polaron-Like Nature of an Electron Coupled to Phonons*, J Supercond Nov Magn 25: 1313, (2012).

[75] Zhou Li, D. Baillie, C. Blois, and F. Marsiglio, *Ground-state properties of the Holstein model near the adiabatic limit*, Phys. Rev. **B81**, 115114 (2010).

[76] F. M. Peeters and J. T. Devreese, *Acoustical polaron in three dimensions: The ground-state energy and the self-trapping transition*, Phys. Rev. B 32, 3515 (1985).
W.B. da Costa and F.M. Peeters, *The polaron - bipolaron transition for acoustical three-dimensional polarons*, Journal of Physics: Condensed Matter, 8, 2173 (1996).
G. A. Farias, W. B. da Costa, and F. M. Peeters, *Acoustical polarons and bipolarons in two dimensions*, Phys. Rev. B 54, 12835 (1996).

[77] Zhou Li, Carl J. Chandler, and F. Marsiglio, *Perturbation theory of the mass enhancement for a polaron coupled to acoustic phonons*, Phys. Rev. B 83, 045104 (2011).

[78] Carl J. Chandler and F. Marsiglio, *BLF-SSH polarons coupled to acoustic phonons in the adiabatic limit*, Phys. Rev. B 90, 245149 (2014).

[79] There is, however, a calculation that describes the "undressing" of polarons as the number of carriers is increased when those carriers are holes, but this occurs due to an inherent electron-hole asymmetry in the model that is not present in the Holstein model. See J.E. Hirsch, *Polaronic superconductivity in the absence of electron-hole symmetry,* Phys. Rev. B**47**, 5351 (1993), and J.E. Hirsch, *Electron-hole asymmetric polarons*, in *"Polarons and Bipolarons in High-T_c Superconductors and Related Materials"*, ed. by E.K.H. Salje, A.S. Alexandrov and W.Y. Liang, Cambdrige University Press, Cambridge (1995), p. 234-257.

[80] R. F. Gasparovic, B. N. Taylor and R. E. Eck, *Temperature dependence of the superconducting energy gap of Pb*, Solid State Communications **4**, 59-63 (1966).

[81] J. R. Schrieffer, D. J. Scalapino, and J. W. Wilkins, *Effective Tunneling Density of States in Superconductors*, Phys. Rev. Lett. 10, 336 (1963).

[82] D. J. Scalapino, J. R. Schrieffer, and J. W. Wilkins, *Strong-Coupling Superconductivity. I* Phys. Rev. 148, 263 (1966).

[83] H.J. Vidberg and J. Serene, *Solving the Eliashberg equations by means of N-point Padé approximants*, J. Low Temp. Phys. 29, 179 (1977).

[84] F. Marsiglio, M. Schossmann, and J. P. Carbotte, *Iterative analytic continuation of the electron self-energy to the real axis,* Phys. Rev. B 37, 4965 (1988).

[85] A.E. Karakozov, E.G. Maksimov and S.A. Mashkov, *Effect of the frequency dependence of the electron-phonon interaction spectral function on the thermodynamic properties of superconductors*, [ZhETF 68, 1937 (1975)] Sov. Phys. JETP **41** 971 (1976).

[86] F. Marsiglio and J.P. Carbotte, *Gap function and density of states in the strong-coupling limit for an electron-boson system*, Phys. Rev. B**43** 5355 (1991).

[87] An $\alpha^2F(\nu)$ spectrum with $\lambda = 1.7$ and a large peak near 200 meV was used in J. P. Carbotte, E. J. Nicol, and T. Timusk, *Spectroscopic signatures of phonons in high pressure superconducting hydrides*, Phys. Rev. B 100, 094505 (2019).

[88] Yuxuan Wang and Andrey Chubukov, *Quantum-critical pairing in electron-doped cuprates*, Phys. Rev. B**88**, 024516 (2013). See particularly Appendix A.

[89] S. Mirabi and F. Marsiglio, unpublished (2019).

[90] J.M. Rowell, P.W. Anderson, and D.E. Thomas, *Image of the Phonon Spectrum in the Tunneling Characteristic Between Superconductors*, Phys. Rev. Lett. **10** 334 (1963).

[91] W.L. McMillan and J.M. Rowell, *Lead Phonon Spectrum Calculated from Superconducting Density of States*, Phys. Rev. Lett. **14** 108 (1965).

[92] B. Mitrović, H.G. Zarate, and J.P. Carbotte, *The ratio* $\frac{2\Delta_0}{k_BT_c}$ *within Eliashberg theory*, Phys. Rev. B **29** 184 (1984).

[93] F. Marsiglio and J.P. Carbotte, *Strong-coupling corrections to Bardeen-Cooper-Schrieffer ratios* , Phys. Rev. B **33** 6141 (1986).

[94] F. Marsiglio, *Eliashberg Theory and the High* T_c *Oxides,* PhD thesis, McMaster University (1988).

[95] For example, contrast Figures 4 and 6 in G.W. Webb, F. Marsiglio and J.E. Hirsch, 'Superconductivity in the elements, alloys and simple compounds', Physica C 514, 17-27 (2015).

[96] A. Georges, G. Kotliar, W. Krauth and M. Rozenberg, *Dynamical mean-field theory of strongly correlated fermion systems and the limit of infinite dimensions*, Reviews of Modern Physics. 68, 13 (1996).

[97] G.D. Mahan., In:*Many–Particle Physics, Third Edition* (Plenum Press, New York, 2000).

From BCS-BEC Crossover: From High Temperature Superconductors to Ultracold Superfluids

References

[1] Aeppli, G., T. E. Mason, S. M. Hayden, H. A. Mook, and J. Kulda, 1997, Science **278**(5342), 1432.

[2] Aeppli, G., T. E. Mason, H. A. Mook, A. Schroeder, and S. M. Hayden, 1997, Physica C **282-287**, 231.

[3] Anderson, P. W., 1997, *The Theory of Superconductivity in the High-T_c Cuprate Superconductors* (Princeton University Press, Princeton).

[4] Anderson, P. W., and W. F. Brinkman, 1973, Phys. Rev. Lett. **30**(1), 1108.

[5] Anderson, P. W., P. A. Lee, M. Randeria, T. M. Rice, N. Trivedi, and F. C. Zhang, (2004), J. Phys. - Condens. Matter. **16**, R755.

[6] Ando, Y., G. S. Boebinger, P. A, T. Kimura, and K. Kishio, 1995, Phys. Rev. Lett. **75**(25), 4662.

[7] Andrenacci, N., A. Perali, P. Pieri, and G. C. Strinati, 1999, Phys. Rev. B **60**, 12410.

[8] Baker, J. G. A., 1999, Phys. Rev. C **60**, 054311.

[9] Baldo, M., U. Lombardo, and P. Schuck, 1995, Phys. Rev. C **52**, 975.

[10] Bartenstein, M., A. Altmeyer, S. Riedl, S. Jochim, C. Chin, J. Denschlag, and R. Grimm, 2004, Phys. Rev. Lett. **92**, 203201.

[11] Bartenstein, M., A. Altmeyer, S. Riedl, S. Jochim, C. Chin, D. Hecke, and G. R, 2004, Phys. Rev. Lett. **92**, 120401.

[12] Baym, G., 1962, Phys. Rev. **127**(4), 1391.

[13] Belkhir, L., and M. Randeria, 1992, Phys. Rev. B **45**(1), 5087.

[14] Benard, P., L. Chen, and A. M. S. Tremblay, 1993, Phys. Rev. B **47**(22), 15217.

[15] Berlinsky, A., D. Bonn, R. Harris, and C. Kallin, 2000, Phys. Rev. B **61**(13), 9088.

[16] Bourdel, T., L. Khaykovich, J. Cubizolles, J. Zhang, F. Chevy, M. Teichmann, L. Tarruell, S. J. Kokkelmans, and C. Salomon, 2004, Phys. Rev. Lett. **93**, 050401.

[17] Bruun, G. M., and G. Baym, 2004, Phys. Rev. Lett. **93**, 150403.

[18] Bruun, G. M., and C. J. Pethick, (2004), Phys. Rev. Lett. **92**, 140404.

[19] Caldeira, A., and A. Leggett, 1983, Physica **121A**(4), 587.

[20] Campuzano, J. C., M. R. Norman, and M. Randeria, 2004, *Physics of Superconductors* (Springer-Verlag, Springer, Berlin), volume II, chapter Photoemission in the High Tc Superconductors, pp. 167–273.

[21] Carlson, E. W., V. J. Emery, S. A. Kivelson, and D. Orgad, 2002, Concepts in high temperature superconductivity, preprint; cond-mat/0206217.

[22] Carlson, E. W., S. A. Kivelson, V. J. Emery, and E. Manousakis, 1999, Phys. Rev. Lett. **83**(3), 612.

[23] Carr, L. D., G. V. Shlyapnikov, and Y. Castin, 2004, Phys. Rev. Lett. **92**(15), 150404.

[24] Castellani, C., C. DiCastro, and M. Grilli, 1995, Phys. Rev. Lett. **75**(25), 4650.

[25] Chakravarty, S., R. B. Laughlin, D. K. Morr, and C. Nayak, 2001, Phys. Rev. B **63**(10), 094503.

[26] Chen, H.-D., O. Vafek, A. Yazdani, and S. C. Zhang, 2004, Phys. Rev. Lett. **93**, 187002.

[27] Chen, Q. J., 2000, *Generalization of BCS theory to short coherence length superconductors: A BCS-Bose-Einstein crossover scenario*, Ph.D. thesis, University of Chicago, (unpublished).

[28] Chen, Q. J., I. Kosztin, B. Jankó, and K. Levin, 1998, Phys. Rev. Lett. **81**(21), 4708.

[29] Chen, Q. J., I. Kosztin, B. Jankó, and K. Levin, 1999, Phys. Rev. B **59**(10), 7083.

[30] Chen, Q. J., I. Kosztin, and K. Levin, 2000, Phys. Rev. Lett. **85**(14), 2801.

[31] Chen, Q. J., K. Levin, and I. Kosztin, 2001, Phys. Rev. B **63**, 184519.

[32] Chen, Q. J., and J. R. Schrieffer, 2002, Phys. Rev. B **66**, 014512.

[33] Cheong, S. W., G. Aeppli, T. E. Mason, H. A. Mook, S. M. Hayden, P. C. Canfield, Z. Fisk, K. N. Clausen, and J. L. Martinez, 1991, Phys. Rev. Lett. **67**, 1791.

[34] Chin, C., M. Bartenstein, A. Altmeyer, S. Riedl, S. Jochim, J. Hecker-Denschlag, and R. Grimm, 2004, Science **305**, 1128.

[35] Chiofalo, M. L., S. J. J. M. F. Kokkelmans, J. N. Milstein, and M. J. Holland, 2002, Phys. Rev. Lett. **88**, 090402.

[36] Chubukov, A. V., D. Pines, and B. P. Stojkovic, 1996, J. Phys. Cond. Matt. **8**, 10017.

[37] Cohen, R. W., B. Abeles, and C. R. Fuselier, 1969, Phys. Rev. Lett. **23**, 377.

[38] Corson, J., R. Mallozzi, J. Orenstein, J. N. Eckstein, and I. Bozovic, 1999, Nature **398**, 221.

[39] Cote, R., and A. Griffin, 1993, Phys. Rev. B **48**(14), 10404.

[40] Cubizolles, J., T. Bourdel, S. Kokkelmans, G. Shlyapnikov, and C. Salomon, 2003, Phys. Rev. Lett. **91**(24), 240401.

[41] Dalfovo, F., S. Giorgini, L. P. Pitaevskii, and S. Stringari, 1999, Rev. Mod. Phys. **71**, 463.

[42] Damascelli, R., Z. Hussain, and Z.-X. Shen, 2003, Rev. Mod. Phys. **75**(2), 473.

[43] Deisz, J. J., D. W. Hess, and J. W. Serene, 1998, Phys. Rev. Lett. **80**(2), 373.

[44] DeMarco, B., and D. S. Jin, 1999, Science **285**, 1703.

[45] Demler, E., and S.-C. Zhang, 1995, Phys. Rev. Lett. **75**(22), 4126.

[46] Deutscher, G., 1999, Nature **397**(20), 410.

[47] Ding, H., T. Yokoya, J. C. Campuzano, T. Takahashi, M. Randeria, M. R. Norman, T. Mochiku, K. Hadowaki, and J. Giapintzakis, 1996, Nature **382**(6586), 51.

[48] Domanski, T., and J. Ranninger, 2003, Phys. Rev. Lett. **91**(25), 255301.

[49] Eagles, D. M., 1969, Phys. Rev. **186**(2), 456.

[50] Emery, V. J., and S. A. Kivelson, 1995, Nature **374**(6521), 434.

[51] Falco, G. M., and H. T. C. Stoof, 2004, Phys. Rev. Lett. **92**, 130401.

[52] Fisher, M., P. B. Weichman, G. Grinstein, and D. S. Fisher, 1989, Phys. Rev. B **40**, 546.

[53] Fong, H. F., B. Keimer, P. W. Anderson, D. Reznik, F. Dogan, and I. A. Aksay, 1995, Phys. Rev. Lett. **75**(2), 316.

[54] Friedberg, R., and T. D. Lee, 1989, Phys. Lett. A **138**(8), 423.

[55] Friedberg, T., and T. D. Lee, 1989, Phys. Rev. B **40**(10), 6745.

[56] Fu, H. C., J. C. Davis, and D.-H. Lee, 2004, On the charge ordering observed by recent STM experiments, preprint, cond-mat/0403001.

[57] Geshkenbein, V., L. Ioffe, and A. Larkin, 1997, Phys. Rev. B **55**(5), 3173.

[58] Giovannini, B., and C. Berthod, 2001, Phys. Rev. B **63**(2), 144516.

[59] Greiner, M., C. A. Regal, and D. S. Jin, 2003, Nature **426**, 537.

[60] Greiner, M., C. A. Regal, and D. S. Jin, 2005, Phys. Rev. Lett. **94**, 070403.

[61] Griffin, A., and Y. Ohashi, 2003, Phys. Rev. A **67**, 063612.

[62] Hassing, R. F., and J. W. Wilkins, 1973, Phys. Rev. B **7**, 1890.

[63] Haussmann, R., 1993, Z. Phys. B **91**(3), 291.

[64] Heiselberg, H., 2001, Phys. Rev. A **63**, 043606.

[65] Heiselberg, H., 2004, J. Phys. B **37**, 141.

[66] Heiselberg, H., 2004, Phys. Rev. Lett. **93**, 040402.

[67] den Hertog, B., 1999, Phys. Rev. B **60**, 559.

[68] Ho, T.-L., 2004, Phys. Rev. Lett. **92**(9), 090402.

[69] Ho, T.-L., and N. Zahariev, 2004, High temperature universal properties of atomic gases near feshbach resonance with non-zero orbital angular momentum, preprint cond-mat/0408469.

[70] Hofstetter, W., J. I. Cirac, P. Zoller, E. Demler, and M. D. Lukin, 2002, Phys. Rev. Lett. **89**(22), 220407.

[71] Holland, M., S. J. J. M. F. Kokkelmans, M. L. Chiofalo, and R. Walser, 2001, Phys. Rev. Lett. **87**, 120406.

[72] Holland, M. J., C. Menotti, and L. Viverit, 2004, The role of boson-fermion correlations in the resonance theory of superfluids, preprint, cond-mat/0404234.

[73] Houbiers, M., R. Ferwerda, H. T. C. Stoof, W. McAlexander, C. A. Sackett, and R. G. Hulet, 1997, Phys. Rev. A **56**, 4864.

[74] Hu, H., A. Minguzzi, X.-J. Liu, and M. P. Tosi, 2004, Phys. Rev. Lett. **93**, 190403.

[75] Ioffe, L. B., and A. J. Millis, 1999, Science **285**, 1241.

[76] Itakura, K., 2003, Nucl. Phys A **715**, 859.

[77] Iyengar, A., J. Stajic, Y.-J. Kao, and K. Levin, 2003, Phys. Rev. Lett. **90**, 187003.

[78] Jankó, B., J. Maly, and K. Levin, 1997, Phys. Rev. B **56**(18), R11407.

[79] Jochim, S., M. Bartenstein, A. Altmeyer, G. Hendl, C. Chin, J. H. Denschlag, and R. Grimm, 2003, Phys. Rev. Lett. **91**(24), 240402.

[80] Jochim, S., M. Bartenstein, A. Altmeyer, G. Hendl, S. Riedl, C. Chin, J. H. Denschlag, and R. Grimm, 2003, Science **302**, 2101.

[81] Junod, A., A. Erb, and C. Renner, 1999, Physica C **317-318**(20), 333.

[82] Kadanoff, L. P., and P. C. Martin, 1961, Phys. Rev. **124**(3), 670.

[83] Kao, Y.-J., A. Iyengar, Q. J. Chen, and K. Levin, 2001, Phys. Rev. B **64**(14), 140505.

[84] Kao, Y.-J., A. Iyengar, J. Stajic, and K. Levin, 2002, Phys. Rev. B **68**, 214519.

[85] Kao, Y.-J., Q. M. Si, and K. Levin, 2000, Phys. Rev. B **61**(18), R118980.

[86] Kastner, M. A., R. J. Birgeneau, G. Shirane, and Y. Endoh, 1998, Rev. Mod. Phys. **70**, 897.

[87] Kinast, J., S. L. Hemmer, M. E. Gehm, A. Turlapov, and J. E. Thomas, 2004, Phys. Rev. Lett. **92**, 150402.

[88] Kinast, J., A. Turlapov, J. E. Thomas, Q. J. Chen, J. Stajic, and K. Levin, 2005, Science **307**, 1296, published online 27 January 2005; doi:10.1126/science.1109220.

[89] Kinnunen, J., M. Rodriguez, and P. Törmä, 2004, Science **305**, 1131.

[90] Kinnunen, J., M. Rodriguez, and P. Törmä, 2004, Phys. Rev. Lett. **92**(23), 230403.

[91] Kivelson, S. A., I. P. Bindloss, E. Fradkin, V. Oganesyan, J. M. Tranquada, A. Kapitulnik, and H. C, 2003, Rev. Mod. Phys. **75**(4), 1201.

[92] Klinkhamer, F. R., and G. E. Volovik, 2004, Emergent cpt violation from the splitting of fermi points, preprint hep-th/0403037.

[93] Kokkelmans, S. J. J. M. F., *et al.*, 2002, Phys. Rev. A **65**, 053617.

[94] Kolb, P. F., and U. Heinz, 2003, Hydrodynamic description of ultrarelativistic heavy ion collisions, preprint nucl-th/0305084.

[95] Kostyrko, T., and J. Ranninger, 1996, Phys. Rev. B **54**, 13105.

[96] Kosztin, I., Q. J. Chen, B. Jankó, and K. Levin, 1998, Phys. Rev. B **58**(10), R5936.

[97] Kosztin, I., Q. J. Chen, Y.-J. Kao, and K. Levin, 2000, Phys. Rev. B **61**(17), 11662.

[98] Kugler, M., O. Fischer, C. Renner, S. Ono, and Y. Ando, 2001, Phys. Rev. Lett. **86**(21), 4911.

[99] Kulik, I. O., O. Entin-Wohlman, and R. Orbach, 1981, J. Low Temp. Phys. **43**(20), 591.

[100] Kwon, H.-J., and A. Dorsey, 1999, Phys. Rev. B **59**(9), 6438.

[101] Lai, C. W., Z. J, A. C. Gossard, and D. S. Chemla, 2004, Science **303**(5273), 503.

[102] Lake, B., H. M. Ronnow, N. B. Christensen, G. Aeppli, K. Lefmann, D. F. McMorrow, P. Vorderwisch, P. Smeibidl, N. Mangkorntong, T. Sasagawa, M. Nohara, H. Takagi, *et al.*, 2002, Nature **415**, 299.

[103] Larkin, A., and A. Varlamov, 2001, Fluctuation phenomena in superconductors., cond-mat/0109177.

[104] Lee, P. A., 1993, Phys. Rev. Lett. **71**, 1887.

[105] Lee, P. A., 2004, Physica C **408-10**, 5.

[106] Lee, P. A., N. Nagaosa, and X.-G. Wen, 2004, Doping a mott insulator: Physics of high temperature superconductivity, preprint, cond-mat/0410445.

[187] Leggett, A. J., 1980, in *Modern Trends in the Theory of Condensed Matter* (Springer-Verlag, Berlin), pp. 13–27.

[108] Leggett, A. J., 1999, Phys. Rev. Lett. **83**(2), 392.

[109] Leridon, B., A. Defossez, J. Dumont, and J. Lesueur, 2001, Phys. Rev. Lett. **87**(19), 197007.

[110] Levin, K., and O. T. Valls, 1983, Physics Reports **98**(1), 1.

[111] Liu, D. Z., and K. Levin, 1997, Physica C **275**, 81.

[112] Liu, D. Z., Y. Zha, and K. Levin, 1995, Phys. Rev. Lett. **75**(22), 4130.

[113] Loram, J. W., K. Mirza, J. Cooper, W. Liang, and J. Wade, 1994, J. Superconductivity **7**(1), 243.

[114] Maly, J., B. Jankó, and K. Levin, 1999, Physica C **321**, 113.

[115] Maly, J., B. Jankó, and K. Levin, 1999, Phys. Rev. B **59**(2), 1354.

[116] Mathai, A., Y. Gim, R. C. Black, A. Amar, and F. C. Wellstood, 1995, Phys. Rev. Lett. **74**(22), 4523.

[117] Melikyan, A., and Z. Tešanović, 2004, A model of phase fluctuations in a lattice d-wave superconductor: application to the Cooper pair charge-density-wave in underdoped cuprates, preprint cond-mat/0408344.

[118] Sá de Melo, C. A. R., M. Randeria, and J. R. Engelbrecht, 1993, Phys. Rev. Lett. **71**(19), 3202.

[119] Micnas, R., M. H. Pedersen, S. Schafroth, T. Schneider, J. Rodriguez-Nunez, and H. Beck, 1995, Phys. Rev. B **52**(22), 16223.

[120] Micnas, R., J. Ranninger, and S. Robaszkiewicz, 1990, Rev. Mod. Phys. **62**(1), 113.

[121] Micnas, R., and S. Robaszkiewicz, 1998, Cond. Matt. Phys. **1**, 89.

[122] Millis, A. J., H. Monien, and D. Pines, 1990, Phys. Rev. B **42**(1), 167.

[123] Milstein, J. N., S. J. J. M. F. Kokkelmans, and M. J. Holland, 2002, Phys. Rev. A **66**, 043604.

[124] Molegraaf, H. J., C. Presura, D. van der Marel, P. H. Kes, and M. Li, 2002, Science **295**, 2239.

[125] Mook, H. A., P. Dai, S. M. Hayden, G. Aeppli, T. G. Perring, and F. Dogan, 1998, Nature **395**(6702), 580.

[126] Norman, M. R., and C. Pepin, 2003, Rep. Prog. Phys. **66**, 1547.

[127] Nozieres, P., and F. Pistolesi, 1999, Eur. Phys. J. B **10**, 649.

[128] Nozières, P., and S. Schmitt-Rink, 1985, J. Low Temp. Phys. **59**, 195.

[129] Oda, M., K. Hoya, R. Kubota, C. Manabe, N. Momono, T. Nakano, and M. Ido, 1997, Physica C **281**(1), 135.

[130] O'Hara, K. M., S. L. Hemmer, M. E. Gehm, S. R. Granade, and J. E. Thomas, 2002, Science **298**(1), 2179.

[131] Ohashi, Y., and A. Griffin, 2002, Phys. Rev. Lett. **89**(13), 130402.

[132] Ohashi, Y., and A. Griffin, 2003, Phys. Rev. A **67**, 033603.

[133] Patton, B. R., 1971, *The Effect of Fluctuations in Superconducting Alloys Above the Transition Temperature*, Ph.D. thesis, Cornell University, (unpublished).

[134] Patton, B. R., 1971, Phys. Rev. Lett. **27**(19), 1273.

[135] Perali, A., P. Pieri, L. Pisani, and G. C. Strinati, 2004, Phys. Rev. Lett. **92**(22), 220404.

[136] Perali, A., P. Pieri, and G. C. Strinati, 2003, Phys. Rev. A **68**(3), 031601R.

[137] Perali, A., P. Pieri, and G. C. Strinati, 2004, Phys. Rev. Lett. **93**(10), 100404.

[138] Petrov, D. S., C. Salomon, and G. V. Shlyapnikov, 2004, Phys. Rev. Lett. **93**, 090404.

[139] Pieri, P., L. Pisani, and G. C. Strinati, 2004, Phys. Rev. Lett. **92**, 110401.

[140] Pieri, P., and G. C. Strinati, 2000, Phys. Rev. B **61**(22), 15370.

[141] Pines, D., 1997, Physica C **282-287**, 273.

[142] Puchkov, A. V., B. D. N, and T. T, 1996, Jour. of Phys. Cond. Matter **8**(48), 10049.

[143] Quintanilla, J., B. L. Gyorffy, J. F. Arnett, and J. P. Wallington, 2002, Phys. Rev. B **66**, 214526.

[144] Randeria, M., 1995, in *Bose Einstein Condensation*, edited by A. Griffin, D. Snoke, and S. Stringari (Cambridge Univ. Press, Cambridge), pp. 355–92.

[145] Ranninger, J., and S. Robaszkiewicz, 1985, Physica B **135**(2), 468.

[146] Ranninger, J., and J. M. Robin, 1996, Phys. Rev. B **53**(18), R11961.

[147] Regal, C. A., M. Greiner, and D. S. Jin, 2004, Phys. Rev. Lett. **92**(1), 040403.

[148] Regal, C. A., C. Ticknor, J. L. Bohn, and D. S. Jin, 2003, Nature **424**(1), 47.

[149] Renner, C., B. Revaz, K. Kadowaki, I. Maggio-Aprile, and O. Fischer, 1998, Phys. Rev. Lett. **80**(16), 3606.

[150] Rojo, A., and K. Levin, 1993, Phys. Rev. B **48**(22), 16861.

[151] Rossat-Mignod, J., L. P. Regnault, C. Vettier, P. Bourges, P. Burlet, J. Bossy, J. Y. Henry, and G. Lapertot, 1991, Physica C **185**, 86.

[152] Santander-Syro, A. F., R. P. S. M. Lobo, N. Bontemps, Z. Konstantinovic, A. A. Li, and H. Raffy, 2003, Europhys. Lett. **62**(4), 568.

[153] Scalapino, D. J., J. E. Loh, and H. J. E, 1986, Phys. Rev. B **34**(2), 8190.

[154] Schmid, A., 1969, Phys. Rev. **180**(2), 527.

[155] Serene, J. W., 1989, Phys. Rev. B **40**(16), 10873.

[156] Shi, H., and A. Griffin, 1998, Phys. Rep. **304**, 1.

[157] Si, Q. M., J. P. Lu, and K. Levin, 1992, Phys. Rev. B. **45**, 4930.

[158] Si, Q. M., Y. Y. Zha, K. Levin, and J. P. Lu, 1993, Phys. Rev. B **47**(14), 9055.

[159] Sofo, J. O., and C. A. Balseiro, 1992, Phys. Rev. B **45**(14), 8197.

[160] Stajic, J., Q. J. Chen, and K. Levin, 2005, Phys. Rev. Lett. **94**, 060401.

[161] Stajic, J., Q. J. Chen, and K. Levin, 2005, Phys. Rev. A **71**, 033601.

[162] Stajic, J., A. Iyengar, Q. J. Chen, and K. Levin, 2003, Phys. Rev. B **68**, 174517.

[163] Stajic, J., A. Iyengar, K. Levin, B. R. Boyce, and T. R. Lemberger, 2003, Phys. Rev. B **68**(9), 024520.

[164] Stajic, J., J. N. Milstein, Q. J. Chen, M. L. Chiofalo, M. J. Holland, and K. Levin, 2004, Phys. Rev. A **69**, 063610.

[165] Strecker, K. E., G. B. Partridge, and R. Hulet, 2003, Phys. Rev. Lett. **91**(8), 080406.

[166] Stringari, S., 2004, Europhys. Lett. **65**, 749.

[167] Sutherland, M., D. G. Hawthorn, R. W. Hill, F. Ronning, S. Wakimoto, H. Zhang, C. Proust, E. Boaknin, C. Lupien, and L. Taillefer, 2003, Phys. Rev. B **67**(17), 174520.

[168] Tallon, J. L., C. Bernhard, G. V. M. Williams, and J. W. Loram, 1997, Phys. Rev. Lett. **79**, 5294.

[169] Tallon, J. L., and J. W. Loram, 2001, Physica C **349**, 53.

[170] Tan, S., and K. Levin, 2004, Phys. Rev. B **69**(1), 064510(1).

[171] Tchernyshyov, O., 1997, Phys. Rev. B **56**(6), 3372.

[172] Tešanović, Z., 2004, Phys. Rev. Lett. **93**, 217004.

[173] Timmermans, E., K. Furuya, P. W. Milonni, and A. K. Kerman, 2001, Phys. Lett. A **285**, 228.

[174] Timusk, T., and B. Statt, 1999, Rep. Prog. Phys. **62**(20), 61.

[175] Tranquada, J. M., P. M. Gehring, G. Shirane, S. Shamoto, and M. Sato, 1992, Phys. Rev. B **46**(9), 5561.

[176] Tsuei, C. C., J. R. Kirtley, C. C. Chi, L. S. Yu-Jahnes, A. Gupta, T. Shaw, J. Z. Sun, and M. B. Ketchen, 1994, Phys. Rev. Lett. **73**(4), 593.

[177] Tucker, J. R., and B. I. Halperin, 1971, Phys. Rev. B **3**(1), 3768.

[178] Uemura, Y. J., 1997, Physica C **282-287**, 194.

[179] Ussishkin, I., S. Sondhi, and D. Huse, 2002, Phys. Rev. Lett. **89**(28), 287001.

[180] Varma, C., 1999, Phys. Rev. Lett. **83**(17), 3538.

[181] Vershinin, M., S. Misra, S. Ono, Y. Abe, A. Yoichi, and A. Yazdani, 2004, Science **303**, 1995.

[182] Viverit, L., S. Giorgini, L. P. Pitaevskii, and S. Stringari, 2004, Phys. Rev. A **69**(1), 013607.

[183] Vojta, M., Y. Zhang, and S. Sachdev, 2000, Phys. Rev. Lett. **85**(23), 4940.

[184] Wang, Q.-H., and D.-H. Lee, 2003, Phys. Rev. B **67**(2), 020511.

[185] Wang, Y., Z. A. Xu, T. Kakeshita, S. Uchida, and N. P. Ong, 2001, Phys. Rev. B **64**(22), 224519.

[186] Watanabe, T., T. Fujii, and A. Matsuda, 1997, Phys. Rev. Lett. **79**(11), 2113.

[187] Wollman, D. A., D. J. Van, Harlingen, J. Giapintzakis, and D. M. Ginsberg, 1995, Phys. Rev. Lett. **74**(5), 797.

[188] Xu, Z., N. Ong, Y. Want, T. Kakeshita, and S. Uchida, 2000, Nature **406**(5), 486.

[189] Yanase, Y., J. Takanobu, T. Nomura, H. Ikeda, T. Hotta, and K. Yamada, 2003, Phys. Rep. **387**(1-4), 1.

[190] Zachar, O., S. A. Kivelson, and V. J. Emery, 1997, J. Supercond. **10**(4), 373.

[191] Zha, Y., K. Levin, and Q. M. Si, 1993, Phys. Rev. B **47**(14), 9124.

[192] Zhao, Y., H. Liu, G. Yang, and S. Dou, 1993, J. Phys. condens. Matter **5**(20), 3623.

[193] Zwierlein, C. A., M. W. andStan, C. H. Schunck, S. M. F. Raupach, S. Gupta, Z. Hadzibabic, and W. Ketterle, 2003, Phys. Rev. Lett. **91**, 250401.

[194] Zwierlein, M. W., C. A. Stan, C. H. Schunck, S. M. F. Raupach, A. J. Kerman, and W. Ketterle, 2004, Phys. Rev. Lett. **92**, 120403.

From High Temperature Superconductivity in the Cuprates: Materials, Phenomena and a Mechanism

References

[1] A. Paramekanti, M. Randeria, and N. Trivedi, Phys. Rev. B **70**, 054504 (2004).

[2] A. Fujimori, E. Takayama-Muromachi, Y. Uchida, and B. Okai, Phys. Rev. B **35**, 8814 (1987).

[3] P. A. Lee, N. Nagaosa, and X. G. Wen, Rev. Mod. Phys. **78**, 17 (2006).

[4] P. Bourges, H. Casalta, A. S. Ivanov, and D. Petitgrand, Phys. Rev. Lett. **79**, 4906 (1997).

[5] M. R. Norman and C. Pépin, Rep. Prog. Phys **66**, 1547 (2003).

[6] D. A. Wollman, D. J. van Harlingen, W. C. Lee, D. M. Ginsberg, and A. J. Leggett, Phys. Rev. Lett. **71**, 2134 (1993).

[7] C. C. Tsuei *et al.*, Phys. Rev. Lett. **73**, 593 (1994).

[8] M. Tinkham, *Introduction to Superconductivity* (McGraw-Hill, New York, 1996).

[9] Z.-X. Shen *et al.*, Phys. Rev. Lett. **70**, 1553 (1993).

[10] A. Damascelli, Z. Hussain, and Z.-X. Shen, Rev. Mod. Phys. **75**, 473 (2003).

[11] J. C. Campuzano, M. R. Norman, and M. Randeria, *in The Physics of Superconductors*, edited by K. H. Bennemann and J. B. Ketterson (Springer, Berlin, 2003).

[12] N. Momono et al., Physica C **233**, 395 (1994).

[13] J. A. Martindale, S. E. Barrett, K. E. O'Hara, C. P. Slichter, W. C. Lee, and D. M. Ginsberg, Phys. Rev. B **47**, 9155 (1993).

[14] W. N. Hardy, D. A. Bonn, D. C. Morgan, R. Liang, and K. Zhang, Phys. Rev. Lett. **70**, 3999 (1993).

[15] G. Volovik, JETP Lett. **58**, 469 (1993).

[16] K. A. Moller, D. J. Baar, J. S. Urbach, R. Liang, W. N. Hardy, and A. Kapitulnik, Phys. Rev. Lett. **73**, 2744 (1994).

[17] Y. J. Uemura *et al.*, Phys. Rev. Lett. **62**, 2317 (1989).

[18] V. J. Emery and S. A. Kivelson, Nature **374**, 434 (1995).

[19] Y. Wang, L. Li, and N. P. Ong, Phys. Rev. B **73**, 024510 (2006).

[20] L. Li *et al.*, Phys. Rev. B **81**, 054510 (2010).

[21] O. Fischer et al., Rev. Mod. Phys. **79**, 353 (2007).

[22] H. Won and K. Maki, Phys. Rev. B **49**, 1397 (1994).

[23] L. Taillefer, J. Phys.: Condens. Matter **21**, 164212 (2009).

[24] Patrick A. Lee, "Amperean pairing and the pseudogap phase of cuprate superconductors," Phys. Rev. X **4**, 031017 (2014).

[25] B. Kyung *et al.*, Phys. Rev. B **73**, 165114 (2006).

[26] M. Ferrero *et al.*, Phys. Rev. B **80**, 064501 (2009).

[27] W. Wu, M. Ferrero, A. Georges, and E. Kozik, Phys. Rev. B **96**, 041105(R) (2017).

[28] N. Doiron-Leyraud et al., Nature **447**, 565 (2007).

[29] S. E. Sebastian *et al.*, Nature **454**, 200–203 (2008).

[30] N. Barisic et al., Nature Physics **454**, 9 (2013).

[31] T. Wu et al., Nature **477**, 191 (2011).

[32] D. LeBoeuf et al., Nature Physics **9**, 79 (2013).

[33] S. Gerber et al., Science **350**, 949 (2015).

[34] F. Yu *et al.*, Proc. Nat. Acd. Sci **113**, 12667 (2016).

[35] S. Martin, A. T. Fiory, R. M. Fleming, L. F. Schneemeyer, and J. V. Waszczak, Phys. Rev. B **41**, 846 (1990).

[36] B. Batlogg nd H. Takagi, L. Kao, and J. Kwo, *in Electronic Properties of High-T_c Superconducting State*, edited by Kuzmany *et al.* (Springer-Verlag, Berlin, 1992).

[37] H. Takagi *et al.*, Phys. Rev. Lett. **69**, 2975 (1992).

[38] N. E. Hussey *et al.*, arXiv:0912.2001 **0**, 0 (0).

[39] A. V. Puchkov, D. N. Basov, and T. Timusk, J. Phys.: Condens. Matter **8**, 10049 (1996).

[40] E. Abrahams and C. M. Varma, Proc. Natl. Acad. Sci. **97**, 5714 (2000).

[41] C. M. Varma, P. B. Littlewood, S. Schmitt-Rink, E. Abrahams, and A. E. Ruckenstein, Phys. Rev. Lett. **63**, 1996 (1989).

[42] T. Timusk and B. Statt, Rep. Prog. Phys. **62**, 61 (1999).

[43] S. Hüfner *et al.*, Rep. Prog. Phys. **71**, 062501 (2008).

[44] M. R. Norman, D. Pines, and C. Kallin, Adv. Phys. **54**, 715 (2005).

[45] J. L. Tallon and J. W. Loram, Physica C **349**, 53 (2001).

[46] W. W. Warren Jr *et al.*, Phys. Rev. Lett. **62**, 1193 (1989).

[47] H. Alloul, T. Ohno, and P. Mendels, Phys. Rev. Lett. **63**, 1700 (1989).

[48] J. W. Loram, K. A. Mirza, J. R. Cooper, and J. L. Tallon, Physica C **282-287**, 1405 (1997).

[49] J. W. Loram, K. A. Mirza, J. R. Cooper, W. Y. Liang, and J. M. Wade, J. Supercond. **7**, 243 (1994).

[50] J. W. Loram, K. A. Mirza, J. R. Cooper, and W. Y. Liang, Phys. Rev. Lett. **71**, 1740 (1993).

[51] J. W. Loram, K. A. Mirza, J. R. Cooper, and J. L. Tallon, J. Phys. Chem. Solids **59**, 2091 (1998).

[52] H. Y. Hwang *et al.*, Phys. Rev. Lett. **72**, 2636 (1994).

[53] K. Takenaka, K. Mizuhashi, H. Takagi, and S. Uchida, Phys. Rev. B **50**, 6534 (1994).

[54] A. N. Lavrov, Y. Ando, and S. Ono, Euro. Phys. Lett. **57**, 267 (2002).

[55] S. L. Cooper *et al.*, Phys. Rev. B **40**, 11358 (1989).

[56] L. D. Rotter *et al.*, Phys. Rev. Lett. **67**, 2741 (1991).

[57] A. F. Santander-Syro *et al.*, Phys. Rev. Lett. **88**, 097005 (2002).

[58] J. Orenstein *et al.*, Phys. Rev. B **42**, 6342 (1990).

[59] S. Uchida *et al.*, Phys. Rev. B **43**, 7942 (1991).

[60] L. Li *et al.*, Phys. Rev. B **81**, 054510 (2010).

[61] Y. Wang, L. Li, and N. P. Ong, Phys. Rev. B **73**, 024510 (2006).

[62] J. Chang *et al.*, Nat. Phys. **8**, 751 (2012).

[63] G. Yu *et al.*, arXiv:1210.6942 [cond-mat.supr-con] 10.1103/RevModPhys.55.331.

[64] Kokanovic et al., Phys. Rev. B **88**, 060505(R) (2013).

[65] M. R. Norman *et al.*, Nature **392**, 157 (1998).

[66] A. Kanigel *et al.*, Phys. Rev. Lett. **99**, 157001 (2007).

[67] H. Ding *et al.*, Nature **382**, 51 (1996).

[68] A. C. Loeser *et al.*, Science **273**, 325 (1996).

[69] D. S. Marshall *et al.*, Phys. Rev. Lett. **76**, 4841 (1996).

[70] U. Chatterjee *et al.*, Proc. Nat. Soc. Sci. **108**, 9346 (2011).

[71] C. Renner, B. Revaz, J.-Y. Genoud, K. Kadowaki, and O. Fischer, Phys. Rev. Lett. **80**, 149 (1998).

[72] H. J. Tao *et al.*, Physica C **282–287**, 1507 (1997).

[73] M. Kugler, C. Renner, S. Ono, Y. Ando, and O. Fischer, Phys. Rev. Lett. **86**, 4911 (2001).

[74] P. M. Chaikin and T. C. Lubensky, *Principles of condensed matter physics* (Cambridge University Press, Cambridge, 1998).

[75] I. S. Aranson and L. Kramer., Rev. Mod. Phys. **74**, 99 (2002).

[76] S. Banerjee, T. V. Ramakrishnan, and C. Dasgupta, Phys. Rev. B **83**, 024510 (2011).

[77] K. Sarkar, S. Banerje, S. Mukerjee, and T. V. Ramakrishnan, Ann.Phys **365**, 7 (2016).

[78] K. Sarkar, S. Banerje, S. Mukerjee, and T. V. Ramakrishnan, New J. Phys. **19**, 073009 (2017).

[79] S. Banerjee, T. V. Ramakrishnan, and C. Dasgupta, Phys. Rev. B **84**, 144525 (2011).

[80] L. P. Gorkov, Sov. Phys. JETP **36**, 1364 (1959).

[81] D. M. Broun *et al.*, Phys. Rev. Lett. **99**, 237003 (2007).

[82] T. R. Lemberger I. Hetel and M. Randeria, Nat. Phys. **3**, 700 (2007).

[83] M. Franz and A.P. Iyengar, Phys. Rev. Lett. **96**, 047007 (2006).

[84] D. Stroud C. Ebner, Phys. Rev. B **23**, 6164 (1981).

[85] E.W. Carlson, S.A. Kivelson, V.J. Emery, and E. Manousakis, Phys. Rev. B **83**, 612 (1999).

[86] A. Paramekanti, M. Randeria, T.V. Ramakrishnan, and S.S. Mandal, Phys. Rev. B **62**, 6786 (2000).

[87] D. Podolsky, S. Raghu, and A. Vishwanath, Phys. Rev. Lett. **99**, 117004 (2007).

[88] G. Baskaran and P. W. Anderson, Phys. Rev. B **37**, 580 (1988).

[89] M. Drzazga et al., Z. Phys. B: Condens. Matter **74**, 67 (1989).

[90] M. Drzazga et al., Phys. Lett. A **143**, 267 (1990).

[91] L. Tewordt, S. Wermbter, and Th. Wölkhausen, Phys. Rev. B **40**, 6878 (1989).

[92] D. L. Feder and C. Kallin, Phys. Rev. B **55**, 559 (1997).

[93] A. J. Berlinsky *et al.*, Phys. Rev. Lett. **75**, 2200 (1995).

[94] E. Pavarini *et al.*, Phys. Rev. Lett. **87**, 047003 (2001).

[95] M. Ogata and H. Fukuyama, Rep. Prog. Phys. **71**, 036501 (2008).

[96] T. Giamarchi and C. Lhuiller, Phys. Rev. B **43**, 12943 (1991).

[97] A. Himeda and M. Ogata, Phys. Rev. B **60**, R9935 (1999).

[98] P. W. Anderson, J. Phys. Chem. Sol. **63**, 2145 (2002).

[99] I. Ussishkin, S. L. Sondhi, and D. A. Huse., Phys. Rev. Lett. **89**, 287001 (2002).

[100] S. Mukerjee and D. A. Huse, Phys. Rev. B **70**, 014506 (2004).

[101] P. W. Anderson *et al.*, J. Phys. Condens. Matter **16**, R755 (2004).

[102] H. Ding M. R. Norman, M. Randeria and J. C. Campuzano, Phys. Rev. B **57**, R11093 (1998).

[103] T. Matsuzaki *et al.*, J. Phys. Soc. Jpn. **73**, 2232 (2004).

[104] A. Kanigel *et al.*, Nature Phys. **2**, 447 (2006).

[105] W. S. Lee *et al.*, Nature **450**, 81 (2007).

[106] A. J. Millis, Science **314**, 1888 (2006).

[107] E. Fradkin, S. A. Kivelson, and J. M. Tranquada, Rev. Mod. Phys. **87**, 457 (2015).

[108] G. Ghiringhelli *et al.*, Science **337**, 821 (2012).

[109] A.J. Achkar *et al.*, Phys. Rev. Lett. **109**, 167001 (2012).

[110] M. H. Hamidian *et al.*, Nature Physics **12**, 150 (2016).

[111] S. A. Kivelson, E. Fradkin, and V. J. Emery, Nature **393**, 550 (1998).

[112] S. A. Kivelson *et al.*, Rev. Mod. Phys. **75**, 1201 (2003).

[113] C. M. Varma, Phys. Rev. B **73**, 155113 (2006).

[114] B. Fauque *et al.*, Phys. Rev. Lett. **96**, 197001 (2006).

[115] J. Xia *et al.*, Phys. Rev. Lett. **100**, 127002 (2008).

[116] W. E. Lawrence and S. Doniach, *Proc. 12th Int. Conf. Low Temp. Phys.*, edited by E. Kanada (Keigaku Publ. Co., Kyoto, 1970).

From Spin-polarized supercurrents for spintronics: a review of current progress by Eschrig

References

[1] D. van Delft and P. Kes, Physics Today **63**, 38-43 (2010), *The discovery of superconductivity*

[2] H. Kamerlingh-Onnes, Commun. Phys. Lab. Univ. Leiden **122b** (May 1911), reprinted in Proc. K. Ned. Akad. Wet. **14**, 113-114 (1911), *Further experiments with liquid helium. D. On the change of electric resistance of pure metals at very low temperatures, etc. V. The disappearance of the resistance of mercury.* http://www.dwc.knaw.nl/DL/publications/PU00013111.pdf

[3] F. B. Silsbee, Scientific Papers of the Bureau of Standards **22**, 293-314 (S556) (1927), *Current distribution in supraconductors*, http://dx.doi.org/10.6028/nbsscipaper.242

[4] W. Meissner and R. Ochsenfeld, Naturwissenschaften **21** (44): 787-788 (1933), *Ein neuer Effekt bei Eintritt der Supraleitfähigkeit (A new effect at the onset of superconductivity)* doi:10.1007/BF01504252

[5] J. N. Rjabinin and L. W. Schubnikow, Nature, **135**, 581-582 (1935), *Magnetic Properties and Critical Currents of Supra-conducting Alloys*; L. V. Shubnikov, V. I. Khotkevich, Yu. D. Shepelev, Yu. N. Ryabinin, Zh. Eksp. Teor. Fiz. **7**, 221-237 (1937), *Магнитные свойства сверхпроводящих металлов и сплавов*, Engl. transl.: Ukrainian Journal of Physics **53** 42-52 (2008), *Magnetic properties of superconducting metals and alloys*

[6] V. L. Ginzburg and L. D. Landau, Zh. Eksp. Teor. Fiz. **20**, 1064-1082 (1950), *К теории сверхпроводимости*, Engl. transl.: Collected Papers of L. D. Landau, edited by D. ter Haar, ISBN: 978-0-08-010586-4, Pergamon Press, Oxford, UK, 546-568 (1965), *On the theory of superconductivity*

[7] A. A. Abrikosov, Doklady Akademii Nauk SSSR **86(3)**, 489-492 (1952). *Влияние размеров на критическое поле сверхпроводников второй группы* (*Influence of size on the critical field of superconductors of the second group*); Zh. Eksp. Teor. Fiz. **32**, 1442-1452 (1957), *О магнитных свойствах сверхпроводников второй группы*, Engl. transl.: Sov. Phys. JETP **5**, 1174-1182 (1957), *On the magnetic properties of superconductors of the second group*; Rev. Mod. Phys. **76** 975-979 (2004), *Nobel Lecture: Type-II superconductors and the vortex lattice*

[8] J. Bardeen, L. N. Cooper, and J. R. Schrieffer, Phys. Rev. **108**, 1175-1204 (1957), *Theory of superconductivity*

[9] N. N. Bogoliubov, Zh. Eksp. Teor. Fiz. **34**, 58-65 (1958), *О новом методе в теории сверхпроводимости*: *I*, Engl. transl.: Sov. Phys. JETP **7**, 41-46 (1958), *Concerning a new method in the theory of superconductivity: I*

[10] L.P. Gor'kov, Zh. Eksp. Teor. Fiz. **34**, 735-739 (1958), *Об энергетическом спектре сверхпроводников*, Engl. transl.: Sov. Phys. JETP **7**, 505-508 (1958), *On the energy spectrum of superconductors*; Zh. Eksp. Teor. Fiz. **36**, 1918-1923 (1959), *Микроскопический вывод уравнений Гинзбурга-Ландау в теории сверхпроводимости*, Engl. transl.: Soviet Phys. JETP **9**, 1364-1367 (1959), *Microscopic derivation of the Ginzburg-Landau equations in the theory of superconductivity*

[11] V. L. Ginzburg, Zh. Eksp. Teor. Fiz. **31**, 202-210 (1956), *О ферромагнитных сверхпроводниках*, Engl. transl.: Sov. Phys. JETP **4**, 153-161 (1957), *Ferromagnetic superconductors*

[12] N. R. Werthamer, E. Helfand, and P. C. Hohenberg, Phys. Rev. **147**, 295-302 (1966), *Temperature and Purity Dependence of the Superconducting Critical Field, H_{c2}. III. Electron Spin and Spin-Orbit Effects*

[13] B. T. Matthias, H. Suhl, and C. Corenzwit, Phys. Rev. Lett. **1**, 92-94 (1958) [Erratum: Phys. Rev. Lett. **1**, 152 (1958)], *Spin exchange in superconductors*

[14] T. H. Van Vleck, *Magnetic and Electric Susceptibilities*, (Oxford University Press, Oxford, 1932), pp. 243-244.

[15] P. W. Anderson and H. Suhl, Phys. Rev. **116**, 898-900 (1959), *Spin Alignment in the Superconducting State*

[16] C. Herring, Physica **24**, Suppl. 1, S184 (1958), *Spin exchange in superconductors*

[17] H. Suhl and B. T. Matthias, Phys. Rev. **114**, 977-988 (1959), *Impurity Scattering in Superconductors*

[18] A. A. Abrikosov and L. P. Gor'kov, Zh. Eksp. Teor. Fiz. **39**, 1781-1796 (1960), *К теории сверхпроводящих сплавов с парамагнитными примесями*, Engl. transl.: Sov. Phys. JETP **12**, 1243-1253 (1961), *Contribution to the theory of superconducting alloys with paramagnetic impurities*

[19] S. Skalski, O. Betbeder-Matibet, and P. R. Weiss, Phys. Rev. **136**, A1500-A1518 (1964), *Properties of Superconducting Alloys Containing Paramagnetic Impurities*

[20] K. Maki, Physics (Long Island City, N.Y.) **1**, 21-30 (1964), *The magnetic properties of superconducting alloys, I*

[21] P. G de Gennes, Phys. Kondens. Mater. **3**, 79-90 (1964), *Behavior of dirty superconductors in high magnetic fields*

[22] Yu Luh, Acta Physica Sinica **21**, 75-91 (1965), *Bound state in superconductors with paramagnetic impurities*, http://wulixb.iphy.ac.cn/EN/Y1965/V21/I1/075

[23] H. Shiba, Prog. Theor. Phys. **40**, 435-451 (1968), *Classical Spins in Superconductors*

[24] A. I. Rusinov, Pis'ma Zh. Eksp. Teor. Fiz. **9**, 146-149 (1969), *Сверхпроводимость вблизи парамагнитной примеси*, Engl. transl.: JETP Lett. **9**, 85-87 (1969), *Superconductivity near a paramagnetic impurity*; Zh. Eksp. Teor. Fiz. **56**, 2047-2056 (1969), Engl. transl.: Sov. Phys. JETP **29**, 1101-1106 (1969), *On the theory of gapless superconductivity in alloys containing paramagnetic impurities*

[25] P. G. de Gennes and M. Tinkham, Physics (Long Island City, N.Y.) **1**, 107-126 (1964), *Magnetic behavior of very small superconducting particles*

[26] R. Meservey and P. M. Tedrow, Phys. Rep. **238**, 173-243 (1994), *Spin-polarized electron tunneling*

[27] B. S. Chandrasekhar, Appl. Phys. Letters **1**, 7-8 (1962), *A note on the maximum critical field of high-field superconductors*

[28] A. M. Clogston, Phys. Rev. Letters **9**, 266-267 (1962), *Upper Limit for the Critical Field in Hard Superconductors*

[29] K. Maki, Phys. Rev. **148**, 362-369 (1966), *Effect of Pauli Paramagnetism on Magnetic Properties of High-Field Superconductors*

[30] W. A. Fertig, D. C. Johnston, L. E. DeLong, R. W. McCallum, M. B. Maple, and B. T. Matthias, Phys. Rev. Lett. **38**, 987-990 (1977), *Destruction of Superconductivity at the Onset of Long-Range Magnetic Order in the Compound* $ErRh_4B_4$

[31] M. Ishikawa and Ø. Fischer, Solid State Commun. **24**, 747-751 (1977), *Magnetic ordering in the superconducting state of rare earth molybdenum sulphides,* $(RE)_{1.2}Mo_6S_8$ *(RE = Tb, Dy and Er)*

[32] L. P. Gor'kov and A. I. Rusinov, Zh. Eksp. Teor. Fiz. **46**, 1363-1378 (1964), *Ферромагнетизм в сверхпроводящих сплавах*, Engl. transl.: Sov. Phys. JETP **19**, 922-931 (1964), *Ferromagnetism in superconducting alloys*

[33] P. Fulde and K. Maki, Phys. Rev. **141** 275-280 (1966) [Erratum: Phys. Rev. 147, 414 (1966)], *Theory of Superconductors Containing Magnetic Impurities*

[34] A. I. Buzdin, L. N. Bulaevskiĭ, M. L. Kulić, and S. V. Panyukov, Usp. Fiz. Nauk **144**, 597-641 (1984), *Магнитные сверхпроводники*, Engl. transl.: Sov. Phys. Usp. **27** 927-953 (1984), *Magnetic superconductors*

[35] S. S. Saxena, P. Agarwal, K. Ahilan, F. M. Grosche, R. K. W. Haselwimmer, M. J. Steiner, E. Pugh, I. R. Walker, S. R. Julian, P. Monthoux, G. G. Lonzarich, A. Huxley, I. Sheikin, D. Braithwaite, and J. Flouquet, Nature (London) **406**, 587-592 (2000), *Superconductivity on the border of itinerant-electron ferromagnetism in* UGe_2

[36] D. Aoki, A. Huxley, E. Ressouche, D. Braithwaite, J. Flouquet, J.-P. Brison, E. Lhotel, and C. Paulsen, Nature **413**, 613-616 (2001), *Coexistence of superconductivity and ferromagnetism in URhRe*

[37] N. T. Huy, A. Gasparini, D. E. de Nijs, Y. Huang, J. C. P. Klaasse, T. Gortenmulder, A. de Visser, A. Hamann, T. Görlach, and H. v. Löhneysen, Phys. Rev. Lett. **99**, 067006-(1-4) (2007), *Superconductivity on the Border of Weak Itinerant Ferromagnetism in UCoGe*

[38] T. Akazawa, H. Hidaka, T. Fujiwara, T. C. Kobayashi, E. Yamamoto, Y. Haga, R. Settai, and Y. Ōnuki, J. Phys. Condens. Matter **16**, L29-L32 (2004), *Pressure-induced superconductivity in ferromagnetic UIr without inversion symmetry*

[39] D. Aoki, F. Hardy, A. Miyake, V. Taufour, T. D. Matsuda, and J. Flouquet, Comptes Rendus Physique **12**, 573-583 (2011), *Properties of ferromagnetic superconductors*

[40] R. Balian and N. R. Werthamer, Phys. Rev. **131**, 1553-1564 (1963), *Superconductivity with Pairs in a Relative p-Wave*

[41] A. A. Abrikosov and L. P. Gor'kov, Zh. Eksp. Teor. Fiz. **35**, 1558-1571 (1958), *К теории сверхпроводящих сплавов. I. Электродинамика сплавов при абсолютном нуле*, Engl. transl.: Sov. Phys. JETP **8**, 1090-1098 (1959), *On the theory of superconducting alloys, I. The electrodynamics of alloys at absolute zero*; Zh. Eksp. Teor. Fiz. **36**, 319-320 (1959), *Сверхпроводящие сплавы при температурах выше абсолютного нуля*, Engl. transl.: Sov. Phys. JETP **9**, 220-221 (1959), *Superconducting alloys at finite temperatures*

[42] P. W. Anderson, J. Phys. Chem. Solids **11**, 26-30 (1959), *Theory of dirty superconductors*

[43] P. Fulde and R. A. Ferrell, Phys. Rev. **135**, A550-A563 (1964). *Superconductivity in a Strong Spin-Exchange Field*

[44] A. I. Larkin and Yu. N. Ovchinnikov, Zh. Eksp. Teor. Fiz. **47**, 1136-1146 (1964), *Неоднородное состояние сверхпроводников*, Engl. transl.: Soviet Physics JETP **20**, 762-769 (1965), *Nonuniform state of superconductors*

[45] L. G. Aslamazov, Zh. Eksp. Teor. Fiz. **55**, 1477-1482 (1969), *Влияние примесей на существование неоднородного состояния в ферромагнитном сверхпроводнике*, Engl. transl.: Sov. Phys. JETP **28**, 773-775 (1969), *Influence of Impurities on the Existence of an Inhomogeneous State in a Ferromagnetic Superconductor*

[46] S. Takada, Prog. Theor. Phys. **43** 27-38 (1970), *Superconductivity in a Molecular Field. II: Stability of Fulde-Ferrel Phase*

[47] L. W. Gruenberg and L. Gunther, Phys. Rev. Lett. **16**, 996-998 (1966), *Fulde-Ferrell Effect in Type-II Superconductors*

[48] L. N. Bulaevskiĭ, Zh. Eksp. Teor. Fiz. **64**, 2241-2247 (1973), *Магнитные свойства слоистых сверхпроводников со слабым взаимодействием между слоями*, Engl. transl.: Sov. Phys. JETP **37**, 1133-1136 (1973), *Magnetic properties of layered superconductors with weak interaction between the layers*

[49] H. Burkhardt and D. Rainer, Ann. Phys. (Leipzig) **3** 181-194 (1994), *Fulde-Ferrell-Larkin-Ovchinnikov state in layered superconductors*

[50] H. Shimahara, Phys. Rev. B **50**, 12760-12765 (1994), *Fulde-Ferrell state in quasi-two-dimensional superconductors*

[51] A. I. Buzdin and J. P. Brison, Europhysics Letters **35**, 707-712 (1996), *Non-uniform state in 2D superconductors*

[52] A. I. Buzdin and V. V. Tugushev, Zh. Eksp. Teor. Fiz. **85**, 735-745 (1983), *Фазовая диаграмма при электронных и сверхпроводящих переходах в состояние солитонной решетки*, Engl. transl.: Sov. Phys. JETP **58**, 430-433 (1983), *Phase diagrams of electronic and superconducting transitions to soliton lattice states*

[53] A. I. Buzdin and S. V. Polonskiĭ, Zh. Eksp. Teor. Fiz. **93**, 747-761 (1987), *Неоднородное состояние в квазиодномерных сверхпроводниках*, Engl. transl.: Sov. Phys. JETP **66**, 422-429 (1987), *Nonuniform state in quasi-1D superconductors*

[54] N. Dupuis, Phys. Rev. B **51**, 9074-9083 (1995), *Larkin-Ovchinnikov-Fulde-Ferrell state in quasi-one-dimensional superconductors*

[55] M. Tachiki, S. Takahashi, P. Gegenwart, M. Weiden, M. Lang, C. Geibel, F. Steglich, R. Modler, C. Paulsen, and Y. Ōnuki, Z. Phys. B **100**, 369-380 (1996), *Generalized Fulde-Ferrell-Larkin-Ovchinnikov state in heavy-fermion and intermediate-valence systems*

[56] A.I. Buzdin and H. Kachkachi, Physics Letters A **225**, 341-348 (1997), *Generalized Ginzburg-Landau theory for nonuniform FFLO superconductors*

[57] A. B. Vorontsov, J. A. Sauls, and M. J. Graf, Phys. Rev. B **72**, 184501-(1-9) (2005), *Phase diagram and spectroscopy of Fulde-Ferrell-Larkin-Ovchinnikov states of two-dimensional d-wave superconductors*

[58] T. Yokoyama, M. Ichioka, and Y. Tanaka, J. Phys. Soc. Jpn. **79** 034702-(1-10) (2010), *Theory of Pairing Symmetry in Fulde-Ferrell-Larkin-Ovchinnikov Vortex State and Vortex Lattice*

[59] R. Casalbuoni and G. Nardulli, Rev. Mod. Phys. **76**, 263-320 (2004), *Inhomogeneous superconductivity in condensed matter and QCD*

[60] Y. Matsuda and H. Shimahara, J. Phys. Soc. Jpn. **76** 051005-(1-16) (2007), *Fulde-Ferrell-Larkin-Ovchinnikov State in Heavy Fermion Superconductors*

[61] G. Zwicknagl and J. Wosnitza, Int. J. Mod. Phys. B **24**, 3915-3949 (2010), *Breaking translational invariance by population imbalance: the Fulde-Ferrell-Larkin-Ovchinnikov states*

[62] R. Beyer and J. Wosnitza, Low Temperature Physics **39**, 225-231 (2013), *Emerging evidence for FFLO states in layered organic superconductors*

[63] H. A. Radovan, N. A. Fortune, T. P. Murphy, S. T. Hannahs, E. C. Palm, S. W. Tozer, and D. Hall, Nature **425**, 51-55 (2003), *Magnetic enhancement of superconductivity from electron spin domains*

[64] A. Bianchi, R. Movshovich, C. Capan, P. G. Pagliuso, and J. L. Sarrao, Phys. Rev. Lett. **91**, 187004-(1-4) (2003), *Possible Fulde-Ferrell-Larkin-Ovchinnikov Superconducting State in $CeCoIn_5$*

[65] M. Kenzelmann, Th. Strässle, C. Niedermayer, M. Sigrist, B. Padmanabhan, M. Zolliker, A. D. Bianchi, R. Movshovich, E. D. Bauer, J. L. Sarrao, and J. D. Thompson, Science **321**, 1652-1654 (2008), *Coupled Superconducting and Magnetic Order in $CeCoIn_5$*

[66] G. Koutroulakis, M. D. Stewart Jr., V. F. Mitrović, M. Horvatić, C. Berthier, G. Lapertot, and J. Flouquet, Phys. Rev. Lett. **104**, 087001-(1-4) (2010), *Field Evolution of Coexisting Superconducting and Magnetic Orders in $CeCoIn_5$*

[67] J. Singleton, J. A. Symington, M.-S. Nam, A. Ardavan, M. Kurmoo, and P. Day, J. Phys.: Condens. Matter **12**, L641-L648 (2000), *Observation of the Fulde-Ferrell-Larkin-Ovchinnikov state in the quasi-two-dimensional organic superconductor κ-(BEDT-TTF)$_2$Cu(NCS)$_2$ (BEDT-TTF = bis(ethylene-dithio)tetrathiafulvalene)*

[68] R. Lortz, Y. Wang, A. Demuer, P. H. M. Böttger, B. Bergk, G. Zwicknagl, Y. Nakazawa, and J. Wosnitza, Phys. Rev. Lett. **99**, 187002-(1-4) (2007), *Calorimetric Evidence for a Fulde-Ferrell-Larkin-Ovchinnikov Superconducting State in the Layered Organic Superconductor κ-(BEDT-TTF)$_2$Cu(NCS)$_2$*

[69] B. Bergk, A. Demuer, I. Sheikin, Y. Wang, J. Wosnitza, Y. Nakazawa, and R. Lortz, Phys. Rev. B **83**, 064506-(1-7) (2011), *Magnetic torque evidence for the Fulde-Ferrell-Larkin-Ovchinnikov state in the layered organic superconductor κ-(BEDT-TTF)$_2$Cu(NCS)$_2$*

[70] H. Mayaffre, S. Krämer, M. Horvatić, C. Berthier, K. Miyagawa, K. Kanoda, and V. F. Mitrović, Nature Physics **10**, 928-932 (2014), *Evidence of Andreev bound states as a hallmark of the FFLO phase in κ−(BEDT−TTF)$_2$Cu(NCS)$_2$*

[71] Yu. A. Izyumov, Yu. N. Proshin, and M. G. Khusainov, Usp. Fiz. Nauk **172**, 113-154 (2002), *Конкуренция сверхпроводимости и магнетизма в гетероструктурах ферромагнетик/сверхпроводник*, Engl. transl.: Phys. Usp. **45** 109-148 (2002), *Competition between superconductivity and magnetism in ferromagnet/superconductor heterostructures*

[72] M. Eschrig, J. Kopu, A. Konstandin, J. C. Cuevas, M. Fogelström, and G. Schön, Advances in Solid State Physics-Pergamon Press THEN Vieweg- **44**, 533-546 (2004), *Singlet-triplet mixing in superconductor-ferromagnet hybrid devices*

[73] F.S. Bergeret, A.F. Volkov, and K.B. Efetov, Rev. Mod. Phys. **77**, 1321-1373 (2005), *Odd triplet superconductivity and related phenomena in superconductor-ferromagnet structures*

[74] A. I. Buzdin, Pev. Mod. Phys. **77**, 935-976 (2005), *Proximity effects in superconductor-ferromagnet heterostructures*

[75] I. F. Lyuksyutov and V. L. Pokrovsky, Adv. Phys. **54**, 67-136 (2007), *Ferromagnet-superconductor hybrids*

[76] P.G. de Gennes and E. Guyon, Phys. Lett., **3** 168-169 (1963), *Superconductivity in "normal" metals*

[77] P. G. de Gennes, Rev. Mod. Phys. **36**, 225-237 (1964), *Boundary Effects in Superconductors*

[78] P. G. de Gennes, *Superconductivity of Metals an Alloys*, W. A. Benjamin Inc., New York (1966), Addison-Wesley, Reading, MA, (1989)

[79] G. Deutscher and P. G. de Gennes, *Proximity Effects*, in: R.D. Parks (Ed.), Superconductivity, Marcel Dekker, NY, pp. 1005-1034 (1969).

[80] N.R. Werthamer, Phys. Rev. **132** 2440-2445 (1963), *Theory of the superconducting transition temperature and energy gap function of superposed metal films*

[81] J. J. Hauser, H. C. Theuerer, and N. R. Werthamer, Phys. Rev. **136** A637-A641 (1964), *Superconductivity in Cu and Pt by means of superimposed films with lead*

[82] A. B. Pippard, Proc. R. Soc. London, Ser. A **216**, 547-568 (1953), *An Experimental and Theoretical Study of the Relation between Magnetic Field and Current in a Superconductor*

[83] A. F. Andreev, Zh. Eksp. Teor. Fiz. **46**, 1823-1828 (1964), *Теплопроводность промежуточного состояния сверхпроводников*, Engl. transl.: Sov. Phys. JETP **19**, 1228-1231 (1964), *Thermal conductivity of the intermediate state of superconductors*

[84] P. G. de Gennes and D. Saint-James, Phys. Lett. **4**, 151-152 (1963), *Elementary excitations in the vicinity of a normal metal-superconducting metal contact*

[85] D. Saint-James, J. Phys. (Paris) **25**, 899-905 (1964), *Excitations élémentaires au voisinage de la surface de séparation d'un métal normal et d'un métal supraconducteur (Elementary excitations in the vicinity of the surface separating a normal metal and a superconducting metal)*, https://hal.archives-ouvertes.fr/jpa-00205891

[86] G. Deutscher, Rev. Mod. Phys. **77**, 109-135 (2005), *Andreev-Saint-James reflections: A probe of cuprate superconductors*

[87] M. Stone, Phys. Rev. B **54**, 13222-13229 (1996), *Spectral flow, Magnus force, and mutual friction via the geometric optics limit of Andreev reflection*

[88] A. Jacobs and R. Kümmel, Phys. Rev. B **64**, 104515-(1-7) (2001), *Dynamics of conversion of supercurrents into normal currents and vica versa*

[89] T. Matsubara, Progress of Theoretical Physics **14**, 351-378 (1955), *A New Approach to Quantum-Statistical Mechanics*

[90] E. A. Demler, G. B. Arnold, and M. R. Beasley, Phys. Rev. B **55**, 15174-15182 (1997), *Superconducting proximity effects in magnetic metals*

[91] B. D. Josephson, Physics Letters **1**, 251-253 (1962), *Possible new effects in superconductive tunnelling*

[92] B. D. Josephson, Rev. Mod. Phys. **36**, 216-220 (1964), *Coupled Superconductors*

[93] P. W. Anderson and J. M. Rowell, Phys. Rev. Lett. **10**, 230-232 (1963), *Probable Observation of the Josephson Superconducting Tunneling Effect*

[94] I. O. Kulik and I. K. Yanson, *Эффект Джозефсона в сверхпроводящих туннельных структурах* (Москва: Наука. Гл. ред. физ.-мат. лит., 1970), Engl. transl.: *The Josephson effect in superconductive tunneling structures* (Jerusalem: Israel Program for Scientific Translations, 1972)

[95] K. K. Likharev and B. T. Ulrich, *Системы с джозефсоновскими контактами: основы теории (Systems with Josephson Junctions. The Basics of the Theory)* (Moscow State Univ. Press, Moscow, 1978); K. K. Likharev, Rev. Mod. Phys. **51**, 101-159 (1979), *Superconducting weak links*; K. K. Likharev, *Dynamics of Josephson Junctions and Circuits*, (New York: Gordon and Breach, 1986), ISBN 978-2881240423

[96] A. Barone and G. Paterno, *Physics and Applications of the Josephson Effect* (Wiley, New York, 1982) ISBN 978-0471014690

[97] A. A. Golubov, M. Yu. Kypriyanov, and E. Il'ichev, Rev. Mod. Phys. **76**, 411-469 (2004), *The current-phase relation in Josephson junctions*

[98] A. Posazhennikova, *Efecto Josephson en superconductores*, in *Superconductividad y correlaciones electrónicas*, edited by J. J. Rodríguez Núñez and C. I. Ventura, Inver-E-Group

Venezuela C.A., Maracaibo (2013), pp. 256-279, ISSN 9-6842-2054-5, ISBN 978-980-12-7409-4; in English: arXiv:0908.1761 (2009), *Josephson effect in Superconductors and Superfluids*

[99] J. T. Edwards and D. J. Thouless, J. Phys. C: Solid State Phys. **5**, 807-820 (1972), *Numerical studies of localization in disordered systems*

[100] W.L. McMillan, Phys. Rev. **175**, 537-542 (1968), *Tunneling Model of the Superconducting Proximity Effect*

[101] S. Guéron, H. Pothier, N. O. Birge, D. Esteve, and M.H. Devoret, Phys. Rev. Lett. **77**, 3025-3028 (1996), *Superconducting Proximity Effect Probed on a Mesoscopic Length Scale*

[102] B. Pannetier and H. Courtois, J. Low Temp. Phys. **118**, 599-615 (2000), *Andreev Reflection and Proximity effect*

[103] A. A. Abrikosov, L. P. Gor'kov, and I. E. Dzyaloshinskiĭ, *Методы квантовой теории поля в статистической физике* (Физматгиз, Москва, 1962), Engl. transl., incl. additional material: *Methods of Quantum Field Theory in Statistical Physics* (Dover, New York, 1975).

[104] E. M. Lifshits, and L. P. Pitaevskiĭ, *Статистическая физика. Часть 2. Теория конденсированного состояния* (Теоретическая физика, Том IX, Москва: Наука, 1951), Engl. transl.: *Statistical Physics Part 2: Theory of the Condensed State* (Course of Theoretical Physics Vol. 9) Butterworth-Heinemann (1980).

[105] R. Kubo, J. Phys. Soc. Jpn. **12**, 570-586 (1957), *Statistical-Mechanical Theory of Irreversible Processes. I. General Theory and Simple Applications to Magnetic and Conduction Problems*

[106] P. C. Martin and J. Schwinger, Phys. Rev. **115**, 1342-1373 (1959), *Theory of Many-Particle Systems. I*

[107] M. Eschrig, T. Löfwander, T. Champel, J. C. Cuevas, J. Kopu, and G. Schön, J. Low Temp. Phys. **147**, 457-476 (2007), *Symmetries of Pairing Correlations in Superconductor-Ferromagnet Nanostructures*

[108] Y. Tanaka and A. A. Golubov, Phys. Rev. Lett. **98**, 037003-(1-4) (2007), *Theory of the Proximity Effect in Junctions with Unconventional Superconductors*

[109] Y. Tanaka, Y. Tanuma, and A. A. Golubov, Phys. Rev. B **76**, 054522-(1-13) (2007), *Odd-frequency pairing in normal-metal/superconductor junctions*

[110] A. J. Leggett, Rev. Mod. Phys. **47**, 331-414 (1975), *A theoretical description of the new phases of liquid 3He*

[111] D. Vollhardt and P. Wölfle, New York: Taylor and Francis (1990), *The Superfluid Phases of 3He*

[112] V. L. Berezinskiĭ, Pis'ma Zh. Eksp. Teor. Fiz. **20**, 628-631 (1974), *Новая модель анизотропной фазы сверхтекучего He^3*, Engl. transl.: JETP Lett. **20**, 287-289 (1974), *New model of the anisotropic phase of superfluid He^3*

[113] T. R. Kirkpatrick and D. Belitz, Phys. Rev. Lett. **66**, 1533-1536 (1991), *Disorder-Induced Triplet Superconductivity*

[114] D. Belitz and T. R. Kirkpatrick, Phys. Rev. B **46**, 8393-8408 (1992), *Even-parity spin-triplet superconductivity in disordered electronic systems*

[115] D. Belitz and T. R. Kirkpatrick, Phys. Rev. B **60**, 3485-3498 (1999), *Properties of spin-triplet, even-parity superconductors*

[116] A. Balatsky and E. Abrahams, Phys. Rev. B **45**, 13125-13128 (1992), *New class of singlet superconductors which break the time reversal and parity*

[117] E. Abrahams, A. Balatsky, D. J. Scalapino, and J. R. Schrieffer, Phys. Rev. B **52**, 1271-1278 (1995), *Properties of odd-gap superconductors*

[118] H. P. Dahal, E. Abrahams, D. Mozyrsky, Y. Tanaka, and A. V. Balatsky, New J. Phys. **11**, 065005-(1-15) (2009), *Wave function for odd-frequency superconductors*

[119] A. V. Balatsky and J. Bonča, Phys. Rev. B **48**, 7445-7449 (1993), *Even- and odd-frequency pairing correlations in the one-dimensional t-J-h model: A comparative study*

[120] K. Shigeta, S. Onari, K. Yada, and Y. Tanaka, Phys. Rev. B **79**, 174507-(1-6) (2009), *Theory of odd-frequency pairings on a quasi-one-dimensional lattice in the Hubbard model*

[121] V. J. Emery and S. Kivelson, Phys. Rev. B **46**, 10812-10817 (1992), *Mapping of the two-channel Kondo problem to a resonant-level model*

[122] V. J. Emery and S. A. Kivelson, Phys. Rev. Lett. **71**, 3701-3704 (1993), *Solution of an orbital Kondo array*

[123] P. Coleman, E. Miranda, and A. Tsvelik, Phys. Rev. Lett. **70**, 2960-2963 (1993), *Possible realization of odd-frequency pairing in heavy fermion compounds*

[124] M. Jarrell, H. Pang, and D. L. Cox, Phys. Rev. Lett. **78**, 1996-1999 (1997), *Phase Diagram of the Two-Channel Kondo Lattice*

[125] Y. Fuseya, H. Kohno, and K. Miyake, J. Phys. Soc. Jpn. **72**, 2914-2923 (2003), *Realization of Odd-Frequency p-Wave Spin-Singlet Superconductivity Coexisting with Antiferromagnetic Order near Quantum Critical Point*

[126] M. Vojta and E. Dagotto, Phys. Rev. B **59**, R713-R716 (1999), *Indications of unconventional superconductivity in doped and undoped triangular antiferromagnets*

[127] F. B. Anders, Phys. Rev. B **66**, 020504-(1-4)(R) (2002), *Composite spin and orbital triplet superconductivity formed out of a non-Fermi-liquid phase*

[128] S. Sakai, R. Arita, and H. Aoki, Phys. Rev. B **70**, 172504-(1-4) (2004), *Numerical algorithm for the double-orbital Hubbard model: Hund-coupled pairing symmetry in the doped case*

[129] H. Kusunose, Y. Fuseya, and K. Miyake, J. Phys. Soc. Jpn. **80**, 044711-(1-6) (2011), *Possible Odd-Frequency Superconductivity in Strong-Coupling Electron-Phonon Systems*

[130] K. Shigeta, Y. Tanaka, K. Kuroki, S. Onari, and H. Aizawa, Phys. Rev. B **83**, 140509-(1-4)(R) (2011), *Competition of pairing symmetries and a mechanism for Berezinskiĭ pairing in quasi-one-dimensional systems*

[131] F. S. Bergeret, A. F. Volkov, and K. B. Efetov, Phys. Rev. Lett. **86**, 4096-4099 (2001), *Long-Range Proximity Effects in Superconductor-Ferromagnet Structures*

[132] L. N. Bulaevskiĭ, A. I. Rusinov, and M. Kulić, J. Low Temp. Phys. **39**, 255-272 (1980), *Helical Ordering of Spins in a Superconductor*

[133] M. Eschrig and T. Löfwander, Nature Physics **4**, 138-143 (2008); arXiv:cond-mat/0612533 (2006), *Triplet supercurrents in clean and disordered half-metallic ferromagnets*

[134] J. Linder, T. Yokoyama, A. Sudbø, and M. Eschrig, Phys. Rev. Lett. **102**, 107008-(1-4) (2009), *Pairing Symmetry Conversion by Spin-Active Interfaces in Magnetic Normal-Metal-Superconductor Junctions*

[135] J. Linder, A. Sudbø, T. Yokoyama, R. Grein, and M. Eschrig, Phys. Rev. B **81**, 214504-(1-13) (2010), *Signature of odd-frequency pairing correlations induced by a magnetic interface*

[136] A. Cottet, Phys. Rev. Lett. **107**, 177001-(1-5) (2011), *Inducing Odd-Frequency Triplet Superconducting Correlations in a Normal Metal*

[137] Y. Tanaka, M. Sato, and N. Nagaosa, J. Phys. Soc. Jpn. **81**, 011013-(1-34) (2012), *Symmetry and Topology in Superconductors -Odd-Frequency Pairing and Edge States-*

[138] A. M. Black-Schaffer and A. V. Balatsky, Phys. Rev. B **88**, 104514-(1-5) (2013), *Odd-frequency superconducting pairing in multiband superconductors*

[139] A. Aperis, P. Maldonado, and P. M. Oppeneer, Phys. Rev. B **92**, 054516-(1-8) (2015), *Ab initio theory of magnetic-field-induced odd-frequency two-band superconductivity in* MgB_2

[140] A. M. Black-Schaffer and A. V. Balatsky, Phys. Rev. B **86**, 144506-(1-5) (2012), *Odd-frequency superconducting pairing in topological insulators*; Phys. Rev. B **87**, 220506-(1-5) (2013), *Proximity-induced unconventional superconductivity in topological insulators*

[141] B. Sothmann, S. Weiss, M. Governale, and J. König, Phys. Rev. B **90**, 220501(R)-(1-5) (2014), *Unconventional superconductivity in double quantum dots*

[142] A. V. Balatsky, arXiv:1409.4875 (2014), *Odd-frequency Two Particle Bose-Einstein Condensate*

[143] E. Pivovarov and Ch. Nayak, Phys. Rev. B **64**, 035107-(1-6) (2001), *Odd-frequency density waves: Non-Fermi-liquid metals with an order parameter*

[144] Y. Kedem and A. V. Balatsky, arXiv:1501.07049 (2015), *Odd Frequency Density Waves*

[145] D. Solenov, I. Martin, and D. Mozyrsky, Phys. Rev. B **79**, 132502-(1-4) (2009), *Thermodynamical stability of odd-frequency superconducting state*

[146] H. Kusunose, Y. Fuseya, and K. Miyake, J. Phys. Soc. Jpn. **80**, 054702-(1-7) (2011), *On the Puzzle of Odd-Frequency Superconductivity*

[147] Ya. V. Fominov, Y. Tanaka, Y. Asano, and M. Eschrig, Phys. Rev. B **91**, 144514-(1-14) (2015), *Odd-frequency superconducting states with different types of Meissner response: problem of coexistence*

[148] R. Heid, Z. Phys. B **99**, 15-18 (1995), *On the thermodynamic stability of odd-frequency supercondutors*

[149] L. Eisenbud, Ph.D. thesis, Princeton University (1948), *The Formal Properties of Nuclear Collisions*; E. P. Wigner, Phys. Rev. **98**, 145-147 (1954), *Lower Limit for the Energy Derivative of the Scattering Phase Shift*; F. T. Smith, Phys. Rev. **118**, 349-356 (1960) [Erratum: Phys. Rev. **119**, 2098 (1960)], *Lifetime Matrix in Collision Theory*; C. A. A. de Carvalho and H. M. Nussenzveig, Physics Reports **364** 83-174 (2002), *Time delay*

[150] F. Goos and H. Hänchen, Ann. Phys. **436**, 333-346 (1947), *Ein neuer und fundamentaler Versuch zur Totalreflexion (A New and Fundamental Experiment on Total Reflection)*; H. Hora, Optic **17**, 409-415 (1960), *On the Side Shift at Total Reflection of Matter Waves*; M. Froissart, M. L. Goldberger, and K. M. Watson, Phys. Rev. **131**, 2820-2826 (1963), *Spatial Separation of Events in S-Matrix Theory*

[151] T. Tokuyasu, J. A. Sauls, and D. Rainer, Phys. Rev. B **38**, 8823-8833 (1988), *Proximity effect of a ferromagnetic insulator in contact with a superconductor*

[152] A. Cottet, D. Huertas-Hernando, W. Belzig, and Yu. V. Nazarov, Phys. Rev. B **80**, 184511-(1-17) (2009) [Erratum: Phys. Rev. B **83**, 139901 (2011)], *Spin-dependent boundary conditions for isotropic superconducting Green's functions*

[153] M. Eschrig, Physics Today **64**, 43-49 (2011), *Spin-polarized supercurrents for spintronics*

[154] M. Fogelström, Phys. Rev. B **62**, 11812-11819 (2000), *Josephson currents through spin-active interfaces*

[155] M. Eschrig, J. Kopu, J. C. Cuevas, and Gerd Schön, Phys. Rev. Lett. 90, 137003-(1-4) (2003), *Theory of Half-Metal/Superconductor Heterostructures*

[156] M. Krawiec, B. L. Györffy, and J. F. Annett, Phys. Rev. B **70**, 134519-(1-5) (2004), *Current-carrying Andreev bound states in a superconductor-ferromagnet proximity system*

[157] J. F. Annett, M. Krawiec, and B. L. Györffy, Physica C: Superconductivity **437-438**, 7-10 (2006), *Origin of spontaneous currents in a superconductor-ferromagnetic proximity system*

[158] T. Löfwander, R. Grein, and M. Eschrig, Phys. Rev. Lett. **105**, 207001-(1-4) (2010), *Is CrO_2 Fully Spin Polarized? Analysis of Andreev Spectra and Excess Current*

[159] G. Metalidis, M. Eschrig, R. Grein, and G. Schön, Phys. Rev. B **82**, 180503-(1-4)(R) (2010), *Nonlocal conductance via overlapping Andreev bound states in ferromagnet-superconductor heterostructures*

[160] F. Hübler, M. J. Wolf, T. Scherer, D. Wang, D. Beckmann, and H. v. Löhneysen, Phys. Rev. Lett. **109**, 087004-(1-5) (2012), *Observation of Andreev Bound States at Spin-active Interfaces*

[161] P. Machon, M. Eschrig, and W. Belzig, Phys. Rev. Lett. **110**, 047002-(1-5) (2013), *Nonlocal Thermoelectric Effects and Nonlocal Onsager relations in a Three-Terminal Proximity-Coupled Superconductor-Ferromagnet Device*

[162] P. Machon, M. Eschrig, and W. Belzig, New Journal of Physics **16**, 073002-(1-19) (2014), *Giant thermoelectric effects in a proximity-coupled superconductor-ferromagnet device*

[163] F. Pérez-Willard, J. C. Cuevas, C. Sürgers, P. Pfundstein, J. Kopu, M. Eschrig, and H. v. Löhneysen, Phys. Rev. B **69**, 140502-(1-4) (2004), *Determining the current polarization in Al/Co nanostructured point contacts*

[164] J. Kopu, M. Eschrig, J. C. Cuevas, and M. Fogelström, Phys. Rev. B **69**, 094501-(1-9) (2004), *Transfer-matrix description of heterostructures involving superconductors and ferromagnets*

[165] R. Grein, T. Löfwander, G. Metalidis, and M. Eschrig Phys. Rev. B **81**, 094508-(1-17) (2010), *Theory of superconductor-ferromagnet point-contact spectra: The case of strong spin polarization*

[166] S. Piano, R. Grein, C. J. Mellor, K. Výborný, R. Campion, M. Wang, M. Eschrig, and B. L. Gallagher, Phys. Rev. B **83**, 081305-(1-4)(R) (2011), *Spin polarization of (Ga,Mn)As measured by Andreev spectroscopy: The role of spin-active scattering*

[167] J. N. Kupferschmidt and P. W. Brouwer, Phys. Rev. B **83**, 014512-(1-14) (2011), *Andreev reflection at half-metal/superconductor interfaces with nonuniform magnetization*

[168] F. B. Wilken and P. W. Brouwer, Phys. Rev. B **85**, 134531-(1-10) (2012), *Impurity-assisted Andreev reflection at a spin-active half metal-superconductor interface*

[169] K. A. Yates, M. S. Anwar, J. Aarts, O. Conde, M. Eschrig, T. Löfwander, and L. F. Cohen, Europhysics Letters **103**, 67005-(1-5) (2013), *Andreev spectroscopy of CrO_2 thin films on TiO_2 and Al_2O_3*

[170] R. Grein, T. Löfwander, and M. Eschrig, Phys. Rev. B **88**, 054502-(1-11) (2013), *Inverse proximity effect and influence of disorder on triplet supercurrents in strongly spin-polarized ferromagnets*

[171] M. G. Flokstra, N. Satchell, J. Kim, G. Burnell, P. J. Curran, S. J. Bending, J. F. K. Cooper, C. J. Kinane, S. Langridge, A. Isidori, N. Pugach, M. Eschrig, H. Luetkens, A. Suter, T. Prokscha, and S.L. Lee, Nature Physics **12**, 57-61 (2016), *Remotely induced magnetism in a normal metal using a superconducting spin-valve*

[172] R. Grein, M. Eschrig, G. Metalidis, and G. Schön, Phys. Rev. Lett. **102** 227005-(1-4) (2009), *Spin-Dependent Cooper Pair Phase and Pure Spin Supercurrents in Strongly Polarized Ferromagnets*

[173] V. Braude and Yu. V. Nazarov, Phys. Rev. Lett. **98**, 077003-(1-4) (2007), *Fully developed triplet proximity effect*

[174] Y. Nambu, Phys. Rev. **117**, 648-663 (1960), *Quasi-Particles and Gauge Invariance in the Theory of Superconductivity*

[175] G. Eilenberger, Z. Phys. **214**, 195-213 (1968), *Transformation of Gor'kov's equation for type II superconductors into transport-like equations*

[176] A. I. Larkin and Yu. N. Ovchinnikov, Zh. Eksp. Teor. Fiz. **55**, 2262-2272 (1968), *О квазиклассическом методе в теории сверхпроводимости*, Engl. transl.: Sov. Phys.—JETP **28**, 1200-1205 (1969), *Quasiclassical Method in the Theory of Superconductivity*

[177] L. D. Landau, Zh. Eksp. Teor. Fiz. **30**, 1058-1064 (1956), *Теория ферми-жидкости*, Engl. transl.: Sov. Phys. JETP **3**, 920-925 (1957), *Theory of Fermi-liquids*; L. D. Landau, Zh. Eksp. Teor. Fiz. **32**, 59-66 (1957), *Колебания ферми-жидкости*, Engl. transl.: Sov. Phys. JETP **5**, 101-108 (1957), *Oscillations in a Fermi-liquid*; L. D. Landau, Zh. Eksp. Teor. Fiz. **35**, 97-103 (1958), *К теории ферми-жидкости*, Engl. transl.: Sov. Phys. JETP **8**, 70-74 (1959), *On the theory of the Fermi-liquid*

[178] G. M. Eliashberg, Zh. Eksp. Teor. Fiz. **61**, 1254-1272 (1971), *Неупругие столкновения электронов и неравновесные стационарные состояния в сверхпроводниках*, Engl. transl.: Sov. Phys. JETP **34**, 668-676 (1972), *Inelastic Electron Collisions and Nonequilibrium Stationary States in Superconductors*

[179] A. I. Larkin and Yu. N. Ovchinnikov, Zh. Eksp. Teor. Fiz. **68**, 1915-1927 (1975), *Нелинейная проводимость сверхпроводников в смешанном состоянии*, Engl. transl.: Sov. Phys. JETP **41**, 960-965 (1976), *Nonlinear conductivity of superconductors in the mixed state*; A. I. Larkin and Yu. N. Ovchinnikov, Zh. Eksp. Teor. Fiz. **73**, 299-312 (1977), *Нелинейные эффекты при движении вихрей в сверхпроводниках*, Engl. transl.: Sov. Phys. JETP **46**, 155-162 (1977), *Nonlinear effects during the motion of vortices in superconductors*

[180] L. V. Keldysh, Zh. Eksp. Teor. Fiz. **47**, 1515-1527 (1964), *Диаграммная техника для неравновесных процессов*, Engl. transl.: Sov. Phys. JETP **20**, 1018-1026 (1965), *Diagram Technique for Nonequilibrium Processes*

[181] N. N. Bogoliubov, Nuovo Cimento **7**, 794-805 (1958), *On a new method in the theory of superconductivity*

[182] J. G. Valatin, Nuovo Cimento **7** , 843-857 (1958), *Comments on the theory of superconductivity*

[183] B. J. Powell, J. F. Annett, and B. L. Györffy, J. Phys. A: Math. Gen. **36** 9289-9302 (2003), *The gap equations for spin singlet and triplet ferromagnetic superconductors*

[184] K. Halterman, P. H. Barsić, and O. T. Valls, Phys. Rev. Lett. **99**, 127002-(1-4) (2007), *Odd Triplet Pairing in Clean Superconductor/Ferromagnet Heterostructures*; K. Halterman, O. T. Valls, and P. H. Barsić, Phys. Rev. B **77**, 174511-(1-14) (2008), *Induced triplet pairing in clean s-wave superconductor/ferromagnet layered structures*

[185] D. Fritsch and J. F. Annett, New Journal of Physics **16**, 055005-(1-16) (2014), *Proximity effect in superconductor/conical magnet/ ferromagnet heterostructures*

[186] J. A. X. Alexander, T. P. Orlando, D. Rainer, and P. M. Tedrow, Phys. Rev. B **31**, 5811-5825 (1985), *Theory of Fermi-liquid effects in high-field tunneling*

[187] A. J. Leggett, Phys. Rev. **140**, A1869-A1888 (1965), *Theory of a Superfluid Fermi Liquid. I. General Formalism and Static Properties*, A. J. Leggett, Annals of Physics **46**, 76-113 (1968), *Inequalities, instabilities, and renormalization in metals and other fermi liquids*

[188] J. W. Serene and D. Rainer, Phys. Rep. **101**, 221-311 (1983), *The quasiclassical approach to superfluid ^3He*

[189] P. Fulde, Adv. Phys. **22**, 667-719 (1973), *High field superconductivity in thin films*

[190] L. J. Buchholtz and G. Zwicknagl, Phys. Rev. B **23**, 5788-5796 (1981), *Identification of p-wave superconductors*

[191] P. M. Tedrow and R. Meservey, Phys. Rev. Lett. **43**, 384-387 (1979), *Experimental Test of the Theory of High-Field Superconductivity*

[192] A. Schmid and G. Schön, J. Low Temp. Phys. **20**, 207-227 (1975), *Linearized Kinetic Equations and Relaxation Processes in Superconductors near T_c*

[193] A. Schmid, *Kinetic Equations for Dirty Superconductors* in *Nonequilibrium Superconductivity, Phonons and Kapitza Boundaries*, Proceedings of NATO Advanced Study Institute, edited by K. E. Gray (Plenum Press, New York, 1981), Chapter 14.

[194] A. I. Larkin and Yu. N. Ovchinnikov, *Vortex Motion in Superconductors* in *Nonequilibrium Superconductivity*, edited by D. N. Langenberg and A. I. Larkin (Elsevier Science Publishers, 1986), pp. 493-542

[195] J. Rammer and H. Smith, Rev. Mod. Phys. **58**, 323-359 (1986), *Quantum field-theoretical methods in transport theory of metals*

[196] J. A. Sauls, *Fermi-Liquid Theory for Unconventional Superconductors* in "Strongly Correlated Electronic Materials - The Los Alamos Symposium 1993", K. Bedell, Z. Wang, D. Meltzer, A. Balatsky, and E. Abrahams, eds., Addison-Wesley Publishing Co., New York (1994), pp. 106-132. ISBN 0-2-1-40930-5.

[197] P. Muzikar, D. Rainer and J. A. Sauls, *Fermi Liquid Theory of Non-S-Wave Superconductors*, NATO ASI series Vol. **438** on "The Vortex State", N. Bontemps, Y. Bruynseraede, G. Deutscher, and A. Kapitulnik, eds., Kluwer Academic Press, Dordrecht, The Netherlands (1994), pp. 245-264. ISBN 978-94-010-4422-6.

[198] Mineev V P and Samokhin K, *Introduction to Unconventional Superconductivity*, Gordon and Breach, (1999).

[199] W. Belzig, F. K. Wilhelm, C. Bruder, G. Schön, and A. D. Zaikin, Superlattices Microstruct. **25** 1251-1288 (1999), *Quasiclassical Green's function approach to mesoscopic superconductivity*

[200] M. Eschrig, J. A. Sauls, H. Burkhardt, and D. Rainer, *Fermi liquid superconductivity: concepts, equations, applications* , in *High-T_c Superconductors and Related Materials, Fundamental Properties, and Some Future Electronic Applications*, Proceedings of the NATO Advanced Study Institute, Vol **86**, edited by S.-L. Drechsler and T. Mishonov, Kluwer Academic, Norwell, MA (2001), pp. 413-446. ISBN 978-0-7923-6872-4.

[201] N. Kopnin, *Theory of Nonequilibrium Superconductivity* Oxford University Press (2009).

[202] D. Rainer, *Principles of AB Initio Calculations of Superconducting Transition Temperatures* in Progress in Low Temperature Physics X, Chapter 4: pp. 371-424, edited by D. F. Brewer (Elsevier Science Publishers, Amsterdam, 1986).

[203] D. Rainer and J. A. Sauls, *Strong Coupling Theory of Superconductivity*, in Superconductivity: From Basic Physics to New Developments, edited by P. N. Butcher and L. Yu (World Scientific, Singapore, 1995), pp. 45-78. ISBN 981-02-2456-7.

[204] M. Eschrig, D. Rainer, and J. A. Sauls, Phys. Rev. B **59**, 12095-12113 (1999), *Effects of strong magnetic fields on pairing fluctuations in high-temperature superconductors*, see Appendix C.

[205] M. Eschrig, C. Initoakis, and Y. Tanaka, *Properties of Interfaces and Surfaces in Noncentrosymmetric Superconductors*, in: "Non-Centrosymmetric Superconductors: Introduction and Overview", edited by E. Bauer and M. Sigrist, Lecture Notes in Physics, Vol. **847**, Berlin and Heidelberg: Springer-Verlag (2012), pp. 313-357. ISBN 978-3-642-24623-4.

[206] M. Eschrig, J. Heym, and D. Rainer, J. Low Temp. Phys. **95**, 323-327 (1994), *Corrections to Fermi-liquid theory of correlated metals*

[207] A. V. Zaitsev, Zh. Eksp. Teor. Fiz. **86**, 1742-1758 (1984), *Квазиклассические уравнения теории сверхпроводимости для контактирующих металлов и свойства микроконтактов с сужением*, Engl. transl.: Sov. Phys. JETP **59**, 1015-1024 (1984), *Quasiclassical equations of the theory of superconductivity for contiguous metals and the properties of constricted microcontacts*

[208] A. L. Shelankov, J. Low. Temp. Phys. **60**, 29-44 (1985), *On the derivation of quasiclassical equations for superconductors*

[209] W. Zhang, J. Kurkijärvi, and E. V. Thuneberg, Phys. Rev. B **36**, 1987-1995 (1987), *Order parameter of superfluid ^{3}He-B near surfaces*

[210] A. Millis, D. Rainer, and J. A. Sauls, Phys. Rev. B **38**, 4504-4515 (1988), *Quasiclassical theory of superconductivity near magnetically active interfaces*

[211] S.-K. Yip, J. Low Temp. Phys. **109**, 547-576 (1997), *Josephson Current Between d-Wave Superconductors Through an Interface with Finite Transmission*

[212] N. Schopohl and K. Maki, Phys. Rev. B **52**, 490-493 (1995), *Quasiparticle spectrum around a vortex line in a d-wave superconductor*

[213] M. Eschrig, J. A. Sauls, and D. Rainer, Phys. Rev. B **60**, 10447-10454 (1999), *Electromagnetic response of a vortex in layered superconductors*

[214] M. Eschrig, Phys. Rev. B **61**, 9061-9076 (2000), *Distribution functions in nonequilibrium theory of superconductivity and Andreev spectroscopy in unconventional superconductors*

[215] M. Eschrig, Phys. Rev. B **80**, 134511-(1-22) (2009), *Scattering problem in non-equilibrium quasiclassical theory of metals and superconductors: general boundary conditions and applications*

[216] E. Zhao, T. Löfwander, and J. A. Sauls, Phys. Rev. B **70**, 134510-(1-12) (2004), *Nonequilibrium superconductivity near spin-active interfaces*

[217] T. Champel and M. Eschrig, Phys. Rev. B **72**, 054523-(1-11) (2005), *Effect of an inhomogeneous exchange field on the proximity effect in disordered superconductor-ferromagnet hybrid structures*

[218] K. D. Usadel, Phys. Rev. Lett. **25**, 507-509 (1970), *Generalized Diffusion Equation for Superconducting Alloys*

[219] K. Tanaka and M. Eschrig, Supercond. Sci. Technol. **22** 014001-(1-11) (2009), *Abrikosov flux-lines in two-band superconductors with mixed dimensionality*

[220] M. Yu. Kupriyanov and V. F. Lukichev, Zh. Eksp. Teor. Fiz. **94**, 139-149 (1988), *Влияние прозрачности границна критический ток грязных SS'S структур*, Engl. transl.: Sov. Phys. JETP **67**, 1163-1168 (1988), *Influence of boundary transparency on the critical current of "dirty" SS'S structures*

[221] Yu. V. Nazarov, Superlatt. and Microstruc. **25**, 1221-1231 (1999), *Novel circuit theory of Andreev reflection*

[222] A. Konstandin, J. Kopu, and M. Eschrig, Phys. Rev. B **72**, 140501-(1-4)(R) (2005), *Superconducting proximity effect through a magnetic domain wall*

[223] J. C. Cuevas, J. Hammer, J. Kopu, J. K. Viljas, and M. Eschrig, Phys. Rev. B **73**, 184505-(1-6) (2006), *Proximity effect and multiple Andreev reflections in diffusive superconductor-normal-metal-superconductor junctions*

[224] M. Eschrig, A. Cottet, W. Belzig, and J. Linder, New Journal of Physics **17**, 083037-(1-21) (2015), *General Boundary Conditions for Quasiclassical Theory of Superconductivity in the Diffusive Limit: Application to Strongly Spin-polarized Systems*

[225] P. Machon and W. Belzig, arXiv:1502.05567v1 (2015), *Fully spin-dependent boundary condition for isotropic quasiclassical Green's functions*

[226] T. Champel and M. Eschrig, Phys. Rev. B **71**, 220506-(1-4)(R) (2005), *Switching superconductivity in superconductor/ferromagnet bilayers by multiple-domain structures*

[227] V. A. Oboznov, V. V. Bol'ginov, A. K. Feofanov, V. V. Ryazanov, and A. I. Buzdin, Phys. Rev. Lett **96**, 197003-(1-4) (2006), *Thickness Dependence of the Josephson Ground States of Superconductor-Ferromagnet-Superconductor Junctions*

[228] R. Fazio and C. Lucheroni, Europhys. Lett. **45**, 707-713 (1999), *Local density of states in superconductor-ferromagnetic hybrid systems*

[229] F. S. Bergeret, A. F. Volkov, and K. B. Efetov, Europhysics Letters **66**, 111-117 (2004), *Spin screening of magnetic moments in superconductors*; Phys. Rev. B **69**, 174504-(1-5) (2004), *Induced ferromagnetism due to superconductivity in superconductor-ferromagnet structures*

[230] A. F. Volkov, F. S. Bergeret, and K. B. Efetov, Phys. Rev. Lett. **90**, 117006-(1-4) (2003), *Odd Triplet Superconductivity in Superconductor-Ferromagnet Multilayered Structures*

[231] F. S. Bergeret, A. F. Volkov, and K. B. Efetov, Phys. Rev. B **68** 064513-(1-11) (2003), *Manifestation of triplet superconductivity in superconductor-ferromagnet structures*

[232] L. N. Bulaevskiĭ, V. V. Kuziĭ, and A. A. Sobyanin, Pis'ma Zh. Eksp. Teor. Fiz. **25**, 314-318 (1977), *Сверхпроводящая система со слабой связью с током в основном состоянии*, Engl. transl.: JETP Lett. **25**, 290-294 (1977), *Superconducting system with weak coupling to the current in the ground state*

[233] I. O. Kulik, Zh. Eksp. Teor. Fiz. **49**, 1211-1214 (1965), Engl. transl.: Sov. Phys. JETP **22**, 841-843 (1966), *Magnitude of the critical Josephson tunnel current*

[234] A. I. Buzdin, L. N. Bulaevskiĭ, and S. V. Panyukov, Pis'ma Zh. Eksp. Teor. Fiz. **35**, 147-152 (1982), *Осцилляции критического тока в зависимости от обменного поля и толщины ферромагнитного металла (F) в джозефсоновском контакте S-F-S*, Engl. transl.: JETP Lett. **35**, 178-180 (1982), *Critical-current oscillations as a function of the exchange field and thickness of the ferromagnetic metal (F) in an S-F-S Josephson junction*

[235] A. V. Andreev, A. I. Buzdin, and R. M. Osgood, Phys. Rev. B **43**, 10124-10131 (1991), *π phase in magnetic-layered superconductors*

[236] A. I. Buzdin and M. Yu. Kupriyanov, Pis'ma Zh. Eksp. Teor. Phys. **53**, 308-312 (1991), *Джозефсоновский контакт с ферромагнитной прослойкой*, Engl. trans.: JETP Lett. **53**, 321-326 (1991), *Josephson junction with a ferromagnetic layer*; A. I. Buzdin, B. Vujičić, and M. Yu. Kupriyanov, Zh. Eksp. Teor. Fiz. **101**, 231-240 (1992), *Структуры ферромагнетик-сверхпроводник*, Engl. transl.: Sov. Phys. JETP **74**, 124-128 (1992), *Superconductor-ferromagnet structures*

[237] N. M. Chtchelkatchev, W. Belzig, Yu. V. Nazarov, and C. Bruder, Pis'ma Zh. Eksp. Teor. Fiz. **74** 357-361 (2001), Reprinted in JETP Letters **74** 323-327 (2001), $\pi - 0$ *Transition in Superconductor-Ferromagnet-Superconductor Junctions*

[238] A. V. Veretennikov, V. V. Ryazanov, V. A. Oboznov, A. Y. Rusanov, V. A. Larkin, and J. Aarts, Physica B: Condensed Matter **284-288**, 495-496 (2000), *Supercurrents through the superconductor-ferromagnet-superconductor (SFS) junctions*

[239] V. V. Ryazanov, V. A. Oboznov, A. Yu. Rusanov, A. V. Veretennikov, A. A. Golubov, and J. Aarts, Phys. Rev. Lett **86**, 2427-2430 (2001), *Coupling of Two Superconductors through a Ferromagnet: Evidence for a π Junction*

[240] V. V. Ryazanov, V. A. Oboznov, A. S. Prokofiev, V. V. Bolginov, and A. K. Feofanov, J. Low Temp. Phys. **136**, 385-400 (2004), *Superconductor-Ferromagnet-Superconductor π-junctions*

[241] T. Kontos, M. Aprili, J. Lesueur, G. Genêt, B. Stephanidis, and R. Boursier, Phys. Rev. Lett **89**, 137007-(1-4) (2002), *Josephson Junction through a Thin Ferromagnetic Layer: Negative Coupling*

[242] Y. Blum, A. Tsukernik, M. Karpovski, and A. Palevski, Phys. Rev. Lett. **89**, 187004-(1-4) (2002), *Oscillations of the Superconducting Critical Current in Nb-Cu-Ni-Cu-Nb Junctions*

[243] H. Sellier, C. Baraduc, F. Lefloch, and R. Calemczuk, Phys. Rev. B **68**, 054531 (2003), *Temperature-induced crossover between 0 and π states in S/F/S junctions*

[244] H. Sellier, C. Baraduc, F. Lefloch, and R. Calemczuk, Phys. Rev. Lett. **92**, 257005-(1-11) (2004), *Half-Integer Shapiro Steps at the $0 - \pi$ Crossover of a Ferromagnetic Josephson Junction*

[245] N. G. Pugach, M. Yu. Kupriyanov, E. Goldobin, R. Kleiner, and D. Koelle, Phys. Rev. B **84**, 144513-(1-13) (2011), *Superconductor-insulator-ferromagnet-superconductor Josephson junction: From the dirty to the clean limit*

[246] V. Shelukhin, A. Tsukernik, M. Karpovski, Y. Blum, K. B. Efetov, A. F. Volkov, T. Champel, M. Eschrig, T. Löfwander, G. Schön, and A. Palevski, Phys. Rev. B **73**, 174506-(1-5) (2006), *Observation of periodic π-phase shifts in ferromagnet-superconductor multilayers*

[247] J. W. A. Robinson, S. Piano, G. Burnell, C. Bell, and M. G. Blamire, Phys. Rev. Lett. **97**, 177003-(1-4) (2006), *Critical Current Oscillations in Strong Ferromagnetic Pi-Junctions*

[248] D. Sprungmann, K. Westerholt, H. Zabel, M. Weides, and H. Kohlstedt, Journal of Physics D: Applied Physics **42**, 075005-(1-5) (2009), *Josephson tunnel junctions with ferromagnetic $Fe_{0.75}Co_{0.25}$ barriers*

[249] A. A. Bannykh, J. Pfeiffer, V. S. Stolyarov, I. E. Batov, V. V. Ryazanov, and M. Weides, Phys. Rev. B **79**, 054501-(1-7) (2009), *Josephson tunnel junctions with a strong ferromagnetic interlayer*

[250] M.A. Khasawneh, W.P. Pratt, and N. O. Birge, Phys. Rev. B **80**, 020506-(1-4)(R) (2009), *Josephson Junctions with a synthetic antiferromagnetic interlayer*

[251] D. M. Heim, N. G. Pugach, M. Yu. Kupriyanov, E. Goldobin, D. Koelle, R. Kleiner, N. Ruppelt, M. Weides, and H. Kohlstedt, New Journal of Physics **17**, 113022-(1-15) (2015), *The effect of normal and insulating layers on 0-π transitions in Josephson junctions with a ferromagnetic barrier*

[252] T. Yu. Karminskaya and M. Yu. Kupriyanov, Pis'ma Zh. Eksp, Teor. Fiz. **85**, 343-348 (2007), *Эффективное уменьшение обменной энергии в S-(FN)-S джозефсоновских структурах*, Engl. transl.: JETP Lett. **85**, 286-281 (2007), *Effective Decrease in the Exchange Energy in S−(FN)−S Josephson Structures*; Pis'ma Zh. Eksp, Teor. Fiz. **86**, 65-70 (2007), *Переход из 0 в π-состояние в S-(FNF)-S джозефсоновских структурах*, Engl. transl.: JETP Lett. **86**, 61-66 (2007), *Transition from the 0 State to the π State in S−FNF−S Josephson Structures*

[253] T. E. Golikova, F. Hübler, D. Beckmann, I. E. Batov, T. Yu. Karminskaya, M. Yu. Kupriyanov, A. A. Golubov, and V. V. Ryazanov, Phys. Rev. B **86**, 064416-(1-5) (2012), *Double proximity effect in hybrid planar Superconductor-(Normal metal/Ferromagnet)-Superconductor structures*

[254] T. Yu. Karminskaya, A. A. Golubov, M. Yu. Kupriyanov, and A. S. Sidorenko, Phys. Rev. B **79**, 214509-(1-13) (2009), *Josephson effect in superconductor/ferromagnet-normal/superconductor structures*; Phys. Rev. B **81**, 214518-(1-13) (2010), *Josephson effect in superconductor/ferromagnet structures with a complex weak-link region*

[255] S. M. Frolov, D. J. Van Harlingen, V. A. Oboznov, V. V. Bolginov, and V. V. Ryazanov, Phys. Rev. B **70**, 144505-(1-5) (2004), *Measurement of the current-phase relation of superconductor/ferromagnet/superconductor π Josephson junctions*

[256] V. V. Ryazanov, V. A. Oboznov, A. V. Veretennikov, and A. Yu. Rusanov, Phys. Rev. B **65**, 020501-(1-4)(R) (2001), *Intrinsically frustrated superconducting array of superconductor-ferromagnet-superconductor π junctions*

[257] W. Guichard, M. Aprili, O. Bourgeois, T. Kontos, J. Lesueur, and P. Gandit, Phys. Rev. Lett. **90**, 167001-(1-4) (2003), *Phase Sensitive Experiments in Ferromagnetic-Based Josephson Junctions*

[258] A. Bauer, J. Bentner, M. Aprili, M. L. Della Rocca, M. Reinwald, W. Wegscheider, and C. Strunk, Phys. Rev. Lett. **92**, 217001-(1-4) (2004), *Spontaneous Supercurrent Induced by Ferromagnetic π Junctions*

[259] M. L. Della Rocca, M. Aprili, T. Kontos, A. Gomez, and P. Spathis, Phys. Rev. Lett. **94**, 197003-(1-4) (2005), *Ferromagnetic* $0 - \pi$ *Junctions as Classical Spins*

[260] J. H. Xu, J. H. Miller, and C. S. Ting, Phys. Rev. B **51** , 11958-11961 (1995), *π-vortex state in a long 0−π Josephson junction*

[261] E. Goldobin, D. Koelle, and R. Kleiner, Phys. Rev. B **66**, 100508-(1-4)(R) (2002), *Semi-fluxons in long Josephson 0−π-junctions*

[262] H. Hilgenkamp, Ariando, H.-J. H. Smilde, D. H. A. Blank, G. Rijnders, H. Rogalla, J. R. Kirtley, and C. C. Tsuei, Nature (London) **422**, 50-53 (2003), *Ordering and manipulation of the magnetic moments in large-scale superconducting π-loop arrays*

[263] M. Weides, M. Kemmler, E. Goldobin, D. Koelle, R. Kleiner, H. Kohlstedt, and A. Buzdin, Applied Physics Letters **89**, 122511-(1-3) (2006), *High quality ferromagnetic 0 and π-Josephson tunnel junctions*

[264] M. Weides, H. Kohlstedt, R. Waser, M. Kemmler, J. Pfeiffer, D. Koelle, R. Kleiner, and E. Goldobin, Applied Physics A **89**, 613-617 (2007), *Ferromagnetic 0-π Josephson junctions*

[265] J. Pfeiffer, M. Kemmler, D. Koelle, R. Kleiner, E. Goldobin, M. Weides, A. K. Feofanov, J. Lisenfeld, and A. V. Ustinov, Phys. Rev. B **77**, 214506-(1-8) (2008), *Static and dynamic properties of 0, π, and 0–π ferromagnetic Josephson tunnel junctions*

[266] M. Kemmler, M. Weides, M. Weiler, M. Opel, S. T. B. Goennenwein, A. S. Vasenko, A. A. Golubov, H. Kohlstedt, D. Koelle, R. Kleiner, and E. Goldobin, Phys. Rev. B **81**, 054522-(1-8) (2010), *Magnetic interference patterns in 0–π superconductor/insulator/-ferromagnet/superconductor Josephson junctions: Effects of asymmetry between 0 and π regions*

[267] N. G. Pugach, E. Goldobin, R. Kleiner, and D. Koelle, Phys. Rev. B **81**, 104513-(1-7) (2010), *Method for reliable realization of a ϕ Josephson junction*

[268] H. Sickinger, A. Lipman, M. Weides, R. G. Mints, H. Kohlstedt, D. Koelle, R. Kleiner, and E. Goldobin, Phys. Rev. Lett. **109**, 107002-(1-5) (2012), *Experimental Evidence of a ϕ Josephson Junction*

[269] A. Lipman, R. G. Mints, R. Kleiner, D. Koelle, and E. Goldobin, Phys. Rev. B **90**, 184502-(1-9) (2014), *Josephson junctions with tunable current-phase relation*

[270] S. V. Bakurskiy, N. V. Klenov, T. Yu. Karminskaya, M. Yu. Kupriyanov, and A. A. Golubov, Superconductor Science and Technology **26**, 015005-(1-15) (2013), *Josephson ϕ-junctions based on structures with complex normal/ferromagnet bilayer*

[271] M. Heim, N. G. Pugach, M. Yu. Kupriyanov, E. Goldobin, D. Koelle, and R. Kleiner, Journal of Physics: Condensed Matter **25**, 215701-(1-7) (2013) [Erratum: Journal of Physics: Condensed Matter **25**, 239601 (2013)], *Ferromagnetic planar Josephson junction with transparent interfaces: a ϕ junction proposal*

[272] I. Žutic and S. Das Sarma, Phys. Rev. B **60**, R16322-R16325 (1999), *Spin-polarized transport and Andreev reflection in semiconductor/superconductor hybrid structures*

[273] V. T. Petrashov, V. N. Antonov, S. V. Maksimov, and R. Sh. Shaĭkhaĭdarov, Pis'ma Zh. Eksp. Teor. Fiz. **59**, 523-526 (1994), *Проводимость мезоскопических структур с ферромагнитными и сверхпроводящими областями*, Engl. transl.: JETP Lett. **59**, 551-555 (1994), *Conductivity of mesoscopic structures with ferromagnetic and superconducting regions*

[274] M.D. Lawrence and N. Giordano, J. Phys. Cond. Matt. **8**, L563-L568, (1996), *Weak-localization-like effects in superconductor-ferromagnet-superconductor structures*

[275] M.D. Lawrence and N. Giordano, J. Phys. Cond. Matt. **11**, 1089-1094 (1999), *Proximity effects in superconductor-ferromagnet junctions*

[276] M. Giroud, H. Courtois, K. Hasselbach, D. Mailly, and B. Pannetier, Phys. Rev. B **58**, R11872-R11875 (1998), *Superconducting proximity effect in a mesoscopic ferromagnetic wire*

[277] V. T. Petrashov, I. A. Sosnin, I. Cox, A. Parsons, and C. Troadec, Phys. Rev. Lett. **83**, 3281-3284 (1999), *Giant mutual proximity effects in ferromagnetic/superconducting nanostructures*

[278] J. Aumentado and V. Chandrasekhar, Phys. Rev. B **64**, 054505-(1-4) (2001), *Mesoscopic ferromagnet-superconductor junctions and the proximity effect*

[279] A. F. Volkov, A. Anishchanka, and K. B. Efetov, Phys. Rev. B **73**, 104412-(1-11) (2006), *Odd triplet superconductivity in a superconductor/ferromagnet system with a spiral magnetic structure*

[280] A. F. Volkov and K. B. Efetov, Phys. Rev. B **78**, 024519-(1-11) (2008), *Odd triplet superconductivity in a superconductor/ferromagnet structure with a narrow domain wall*

[281] A. Kadigrobov, R. I. Shekhter, and M. Jonson, Europhys. Lett. **54**, 394-400 (2001), *Quantum spin fluctuations as a source of long-range proximity effects in diffusive ferromagnet-superconductor structures*

[282] J. W. A. Robinson, J. D. S. Witt, and M. G. Blamire, Science **329**, 59-61 (2010), *Controlled Injection of Spin-Triplet Supercurrents into a Strong Ferromagnet*

[283] M. Alidoust and J. Linder, Phys. Rev. B **82**, 224504-(1-8) (2010), *Spin-triplet supercurrent through inhomogeneous ferromagnetic trilayers*

[284] C.-T. Wu, O. T. Valls, and K. Halterman, Phys. Rev. Lett. **108**, 117005-(1-5) (2012), *Reentrant Superconducting Phase in Conical-Ferromagnet-Superconductor Nanostructures*; Phys. Rev. B **86**, 184517-(1-15) (2012), *Proximity effects in conical-ferromagnet/superconductor bilayers*

[285] T. Champel, T. Löfwander, and M. Eschrig, Phys. Rev. Lett. **100**, 077003-(1-4) (2008), $0-\pi$ *Transitions in a Superconductor/Chiral Ferromagnet/Superconductor Junction Induced by a Homogeneous Cycloidal Spiral*

[286] A. F. Volkov, Ya. V. Fominov, and K. B. Efetov, Phys. Rev. B **72**, 184504-(1-9) (2005), *Long-range odd triplet superconductivity in superconductor-ferromagnet structures with Néel walls*

[287] Ya. V. Fominov, A. F. Volkov, and K. B. Efetov, Phys. Rev. B **75**, 104509-(1-12) (2007), *Josephson effect due to the long-range odd-frequency triplet superconductivity in SFS junctions with Néel domain walls*

[288] J. Linder, T. Yokoyama, and A. Sudbø, Phys. Rev. B **79**, 054523-(1-15) (2009), *Theory of superconducting and magnetic proximity effect in S/F structures with inhomogeneous magnetization textures and spin-active interfaces*

[289] M. Alidoust, J. Linder, G. Rashedi, T. Yokoyama, and A. Sudbø, Phys. Rev. B **81**, 014512-(1-9) (2010), *Spin-polarized Josephson current in superconductor/ferromagnet/superconductor junctions with inhomogeneous magnetization*

[290] A. I. Buzdin, A. S. Mel'nikov, and N. G. Pugach, Phys. Rev. B **83**, 144515-(1-8) (2011), *Domain walls and long-range triplet correlations in SFS Josephson junctions*

[291] J. Linder and K. Halterman, Phys. Rev. B **90**, 104502-(1-9) (2014), *Superconducting spintronics with magnetic domain walls*

[292] M. S. Kalenkov, A. D. Zaikin, and V. T. Petrashov, Phys. Rev. Lett. **107**, 087003-(1-5) (2011), *Triplet Superconductivity in a Ferromagnetic Vortex*

[293] M. A. Silaev, Phys. Rev. B **79**, 184505-(1-10) (2012), *Possibility of a long-range proximity effect in a ferromagnetic nanoparticle*

[294] A. A. Golubov, M. Yu. Kupriyanov, and Ya. V. Fominov, Pis'ma Zh. Eksp. Teor. Fiz. **75** 223-227 (2002), Reprinted in JETP Lett. **75**, 190-194 (2002), *Critical current in SFIFS junctions*

[295] T. Löfwander, T. Champel, J. Durst, and M. Eschrig, Phys. Rev. Lett. 95, 187003-(1-4) (2005), *Interplay of Magnetic and Superconducting Proximity Effects in Ferromagnet-Superconductor-Ferromagnet Trilayers*

[296] M. Houzet and A. I. Buzdin, Phys. Rev. B **76**, 060504-(1-4)(R) (2007), *Long range triplet Josephson effect through a ferromagnetic trilayer*

[297] K. Halterman and O. T. Valls, Phys. Rev. B **69**, 014517-(1-11) (2004), *Layered ferromagnet-superconductor structures: The π state and proximity effects*; Phys. Rev. B **70**, 104516-(1-14) (2004), *Stability of π-junction configurations in ferromagnet-superconductor heterostructures*

[298] P. H. Barsić, O. T. Valls, and K. Halterman, Phys. Rev. B **73**, 144514-(1-5) (2006), *First-order phase transitions in ferromagnet/superconductor layered structures*; Phys. Rev. B **75**, 104502-(1-12) (2007), *Thermodynamics and phase diagrams of layered superconductor/ferromagnet nanostructures*

[299] T. Löfwander, T. Champel, and M. Eschrig, Phys. Rev. B **75**, 014512-(1-18) (2007), *Phase diagrams of ferromagnet-superconductor multilayers with misaligned exchange fields*

[300] A. F. Volkov and K. B. Efetov, Phys. Rev. B **81**, 144522-(1-13) (2010), *Odd spin-triplet superconductivity in a multilayered superconductor-ferromagnet Josephson junction*

[301] T. S. Khaire, M. A. Khasawneh, W. P. Pratt Jr., and N. O. Birge, Phys. Rev. Lett. **104**, 137002-(1-4) (2010), *Observation of Spin-Triplet Superconductivity in Co-Based Josephson Junctions*

[302] L. Trifunovic and Z. Radović, Phys. Rev. B **82**, 020505-(1-4) (2010), *Long-range spin-triplet proximity effect in Josephson junctions with multilayered ferromagnets*

[303] L. Trifunovic, Z. Popović, and Z. Radović, Phys. Rev. B **84**, 064511-(1-7) (2011), *Josephson effect and spin-triplet pairing correlations in SF_1F_2S junctions*

[304] M. Knežević, L. Trifunovic, and Z. Radović, Phys. Rev. B **85**, 094517-(1-7) (2012), *Signature of the long range triplet proximity effect in the density of states*

[305] L. Trifunovic, Phys. Rev. Lett. **107**, 047001-(1-4) (2011), *Long-Range Superharmonic Josephson Current*

[306] C. Richard, M. Houzet, and J. S. Mayer, Phys. Rev. Lett. **110**, 217004-(1-5) (2013), *Superharmonic Long-Range Triplet Current in a Diffusive Josephson Junction*

[307] N. G. Pugach and A. I. Buzdin, Applied Physics Letters **101**, 242602-(1-4) (2012), *Magnetic moment manipulation by triplet Josephson current*

[308] M. Alidoust and K. Halterman, Phys. Rev. B **89**, 195111-(1-11) (2014), *Spin-controlled coexistence of 0 and π states in SFSFS Josephson junctions*

[309] A. S. Mel'nikov, A. V. Samokhvalov, S. M. Kuznetsova, and A. I. Buzdin, Phys. Rev. Lett. **109**, 237006-(1-5) (2012), *Interference Phenomena and Long-Range Proximity Effect in Clean Superconductor-Ferromagnet Systems*

[310] H. Meng, X. Wu, and Z. Zheng, Europhysics Letters **104**, 37003-(1-6) (2013), *Long-range triplet Josephson current modulated by the interface magnetization texture*

[311] Z. Shomali, M. Zareyan, and W. Belzig New Journal of Physics **13**, 083033-(1-14) (2011), *Spin supercurrent in Josephson contacts with noncollinear ferromagnets*

[312] T. Yu. Karminskaya, M. Yu. Kupriyanov, and A. A. Golubov, Pis'ma Zh. Eksp, Teor. Fiz. **87**, 657-663 (2007), *Критический ток S-(FNF)-S джозефсоновских структур с неколлинеарными векторами намагниченности ферромагнитных пленок*, Engl. transl.: JETP Lett. **87**, 570-576 (2007), *Critical Current in S−FNF−S Josephson Structures with the Noncollinear Magnetization Vectors of Ferromagnetic Films*

[313] Y. Asano, Y. Tanaka, and A. A. Golubov, Phys. Rev. Lett. **98**, 107002-(1-4) (2007), *Josephson Effect due to Odd-Frequency Pairs in Diffusive Half Metals*

[314] Y. Asano, Y. Sawa, Y. Tanaka, and A. A. Golubov, Phys. Rev. B **76**, 224525-(1-11) (2007), *Odd-frequency pairs and Josephson current through a strong ferromagnet*

[315] S. Takahashi, S. Hikino, M. Mori, J. Martinek, and S. Maekawa, Phys. Rev. Lett. **99**, 057003-(1-4) (2007), *Supercurrent Pumping in Josephson Junctions with a Half-Metallic Ferromagnet*

[316] T. Yokoyama, Y. Tanaka, and A. A. Golubov, Phys. Rev. B **75**, 094514-(1-10) (2007), *Theory of the Josephson effect in unconventional superconducting junctions with diffusive barriers*

[317] J. Linder, M. Cuoco, and A. Sudbø, Phys. Rev. B **81**, 174526-(1-12) (2010), *Spin-active interfaces and unconventional pairing in half-metal/superconductor junctions*

[318] H. Enoksen, J. Linder, and S. Sudbø, Phys. Rev. B **85**, 014512-(1-7) (2012), *Spin-flip scattering and critical currents in ballistic half-metallic d-wave Josephson junctions*

[319] A.V. Galaktionov, M.S. Kalenkov, and A.D. Zaikin, Phys. Rev. B **77**, 094520-(1-11) (2008), *Josephson current and Andreev states in superconductor-half metal-superconductor heterostructures*

[320] K. Halterman and O. T. Valls, Phys. Rev. B **80**, 104502-(1-13) (2009), *Emergence of triplet correlations in superconductor/half-metallic nanojunctions with spin-active interfaces*

[321] B. Béri, J. N. Kupferschmidt, C. W. J. Beenakker, and P. W. Brouwer, Phys. Rev. B **79**, 024517-(1-11) (2009), *Quantum limit of the triplet proximity effect in half-metal-superconductor junctions*

[322] J.-F. Liu and K. S. Chan, Phys. Rev. B **82**, 184533-(1-6) (2010), *Anomalous Josephson current through a ferromagnetic trilayer junction*

[323] Y. Tanaka, T. Yokoyama, and N. Nagaosa, Phys. Rev. Lett. **103**, 107002-(1-4) (2009), *Manipulation of the Majorana Fermion, Andreev Reflection, and Josephson Current on Topological Insulators*

[324] W.E. Pickett and J.S. Moodera, Physics Today **54**, No. 5, 39-44 (2001), *Half Metallic Magnets*

[325] C. Felser, G. H. Fecher, and B. Balke, Angewandte Chemie International Edition **46**, 668-699 (2007), *Spintronics: A Challenge for Materials Science and Solid-State Chemistry*

[326] M. I. Katsnelson, V. Yu. Irkhin, L. Chioncel, A. I. Lichtenstein, and R. A. de Groot, Rev. Mod. Phys. **80**, 315-378 (2008), *Half-metallic ferromagnets: From band structure to many-body effects*

[327] Z. Sefrioui, D. Arias, V. Peña, J. E. Villegas, M. Varela, P. Prieto, C. León, J. L. Martinez, and J. Santamaria, Phys. Rev. B **67**, 214511-(1-5) (2003), *Ferromagnetic/superconducting proximity effect in $La_{0.7}Ca_{0.3}MnO_3/YBa_2Cu_3O_{7-\delta}$ superlattice*

[328] V. Peña, Z. Sefrioui, D. Arias, C. Leon, J. Santamaria, M. Varela, S. J. Pennycook, and J. L. Martinez, Phys. Rev. B **69**, 224502-(1-4) (2004), *Coupling of superconductors through a half-metallic ferromagnet: Evidence for a long-range proximity effect*

[329] R. S. Keizer, S. T. B. Goennenwein, T. M. Klapwijk, G. Miao, G. Xiao, and A. Gupta, Nature (London) **439**, 825-827 (2006), *A spin triplet supercurrent through the half-metallic ferromagnet CrO_2*

[330] M. S. Anwar, F. Czeschka, M. Hesselberth, M. Porcu, and J. Aarts, Phys. Rev. B **82**, 100501-(1-4)(R) (2010), *Long-range supercurrents through half-metallic ferromagnetic CrO_2*

[331] M. S. Anwar and J. Aarts, Superconductor Science and Technology **24**, 024016-(1-9) (2011), *Inducing supercurrents in thin films of ferromagnetic CrO_2*

[332] M. S. Anwar, M. Veldhorst, A. Brinkman, and J. Aarts, Applied Physics Letters **100**, 052602-(1-3) (2012), *Long range supercurrents in ferromagnetic CrO_2 using a multilayer contact structure*

[333] D. Sprungmann, K. Westerhold, H. Zabel, M. Weides, and H. Kohlstedt, Phys. Rev. B **82**, 060505-(1-4)(R) (2010), *Evidence for triplet superconductivity in Josephson junctions with barriers of the ferromagnetic Heusler alloy Cu_2MnAl*

[334] Y. Kalcheim, O. Millo, M. Egilmez, J. W. A. Robinson, and M. G. Blamire, Phys. Rev. B **85**, 104504-(1-5) (2012), *Evidence for anisotropic triplet superconductor order parameter in half-metallic ferromagnetic $La_{0.7}Ca_{0.3}Mn_3O$ proximity coupled to superconducting $Pr_{1.85}Ce_{0.15}CuO_4$*

[335] C. Visani, Z. Sefrioui, J. Tornos, C. Leon, J. Briatico, M. Bibes, A. Barthélémy, J. Santamaría, and J. E. Villegas, Nature Physics **8**, 539-543 (2012), *Equal-spin Andreev reflection and long-range coherent transport in high-temperature superconductor/half-metallic ferromagnet junctions*

[336] M. A. Khasawneh, T. S Khaire, C. Klose, W. P. Pratt Jr, and N. O. Birge, Superconductor Science and Technology **24**, 024005-(1-7) (2011), *Spin-triplet supercurrent in Co-based Josephson junctions*

[337] C. Klose, T. S. Khaire, Yixing Wang, W. P. Pratt, Jr., Norman O. Birge, B. J. McMorran, T. P. Ginley, J. A. Borchers, B. J. Kirby, B. B. Maranville, and J. Unguris, Phys. Rev. Lett. **108**, 127002-(1-5) (2012), *Optimization of Spin-Triplet Supercurrent in Ferromagnetic Josephson Junctions*

[338] E. C. Gingrich, P. Quarterman, Yixing Wang, R. Loloee, W. P. Pratt, Jr., and N. O. Birge, Phys. Rev. B **86**, 224506-(1-4) (2012), *Spin-triplet supercurrent in Co/Ni multilayer Josephson junctions with perpendicular anisotropy*

[339] Yixing Wang, W. P. Pratt, Jr., and N. O. Birge, Phys. Rev. B **85**, 214522-(1-7) (2012), *Area-dependence of spin-triplet supercurrent in ferromagnetic Josephson junctions*

[340] V. T. Petrashov, I. A. Sosnin, I. Cox, A. Parsons, and C. Troadec, J. Low Temp. Phys. **118**, 689-698 (2000), *Ferromagnetic nanowires with superconducting electrodes*

[341] J. Wang, M. Singh, M. Tian, N. Kumar, B. Liu, Ch. Shi, J. K. Jain, N. Samarth, T. E. Mallouk, and M. H. W. Chan, Nat. Phys. **6**, 389-394 (2010), *Interplay between superconductivity and ferromagnetism in crystalline nanowires*

[342] F. Konschelle, J. Cayssol, and A. Buzdin, Phys. Rev. B **82**, 180509-(1-4) (2010), *Long-range singlet proximity effect in ferromagnetic nanowires*

[343] S. Takei and V. Galitski, Phys. Rev. B **86**, 054521-(1-14) (2012), *Microscopic theory for a ferromagnetic nanowire/superconductor heterostructure: Transport, fluctuations, and topological superconductivity*

[344] B. Almog, S. Hacohen-Gourgy, A. Tsukernik, and G. Deutscher, Phys. Rev. B **84**, 054514-(1-7) (2011), *Triplet order parameter component at Co/CoO/In contacts*

[345] M. Colci, Kuei Sun, N. Shah, S. Vishveshwara, and D. J. Van Harlingen, Phys. Rev. B **85**, 180512-(1-5) (2012), *Anomalous polarization-dependent transport in nanoscale double-barrier superconductor/ferromagnet/superconductor junctions*

[346] Kuei Sun, N. Shah, and S. Vishveshwara, Phys. Rev. B **87**, 054509 (1-11) (2013), *Transport in multiterminal superconductor/ferromagnet junctions having spin-dependent interfaces*

[347] I. Sosnin, H. Cho, V. T. Petrashov, and A. F. Volkov, Phys. Rev. Lett., **96**, 157002-(1-4) (2006), *Superconducting phase coherent electron transport in proximity conical ferromagnets*

[348] W. A. Robinson, Z. H. Barber, and M. G. Blamire, Appl. Phys. Lett. **95**, 192509-(1-3) (2009), *Strong ferromagnetic Josephson devices with optimized magnetism*

[349] G. B. Halász, J. W. A. Robinson, J. F. Annett, and M. G. Blamire, Phys. Rev. B **79**, 224505-(1-9) (2009), *Critical current of a Josephson junction containing a conical magnet*

[350] G. B. Halász, M. G. Blamire, and J. W. A. Robinson, Phys. Rev. B **84**, 024517-(1-5) (2011), *Magnetic-coupling-dependent spin-triplet supercurrents in helimagnet/ferromagnet Josephson junctions*

[351] J.Y. Gu, J. Kusnadi, and Ch.-Y. You, Phys. Rev. B **81**, 214435-(1-6) (2010) [Erratum: Phys. Rev. B **82**, 099905(E) (2010)], *Proximity effect in a superconductor/exchange-spring-magnet hybrid system*

[352] J. W. A. Robinson, G. B. Halász, A. I. Buzdin, and M. G. Blamire, Phys. Rev. Lett. **104**, 207001-(1-4) (2010), *Enhanced Supercurrents in Josephson Junctions Containing Nonparallel Ferromagnetic Domains*

[353] J. D. S. Witt, J. W. A. Robinson, and M. G. Blamire, Phys. Rev. B **85**, 184526-(1-6) (2012), *Josephson junctions incorporating a conical magnetic holmium interlayer*

[354] J. W. A. Robinson, F. Chiodi, M. Egilmez, Gábor B. Halász, and M. G. Blamire, Scientific Reports **2**, 699-(1-6) (2012), *Supercurrent enhancement in Bloch domain walls*

[355] M. G. Blamire and J. W. A. Robinson, J. Phys. Condens. Matter **26** 453201-(1-13) (2014), *The interface between superconductivity and magnetism: understanding and device prospects*

[356] M. Eschrig, Annalen der Physik **524**, A65-A67 (2012), *Tailoring the Fulde-Ferrell-Larkin-Ovchinnikov state*

[357] A. Iovan, T. Golod, and V. M. Krasnov, Phys. Rev B **90**, 134514-(1-9) (2014), *Controllable generation of a spin-triplet supercurrent in a Josephson spin valve*

[358] K. Senapati, M. G. Blamire, and Z. H. Barber, Nature Materials **10**, 849-852 (2011), *Spin-filter Josephson junctions*

[359] F. S. Bergeret, A. Verso, and A. F. Volkov, Phys. Rev. B **86**, 060506-(1-5) (2012), *Spin-polarized Josephson and quasiparticle currents in superconducting spin-filter tunnel junctions*

[360] A. K. Feofanov, V. A. Oboznov, V. V. Bol'ginov, J. Lisenfeld, S. Poletto, V. V. Ryazanov, A. N. Rossolenko, M. Khabipov, D. Balashov, A. B. Zorin, P. N. Dmitriev, V. P. Koshelets, and A. V. Ustinov, Nature Physics **6**, 593-597 (2010), *Implementation of superconductor/-ferromagnet/ superconductor π-shifters in superconducting digital and quantum circuits*

[361] V. V. Ryazanov, V. V. Bol'ginov, D. S. Sobanin, I. V. Vernik, S. K. Tolpygo, A. M. Kadin, and O. A. Mukhanov, Physics Procedia **36**, 35-41 (2012), *Magnetic Josephson Junction Technology for Digital and Memory Applications*

[362] I. V. Vernik, V. V. Bol'ginov, S. V. Bakurskiy, A. A. Golubov, M. Yu. Kupriyanov, V. V. Ryazanov, and O. A. Mukhanov, IEEE Transactions on Applied Superconductivity **23**, 1701208-(1-8) (2013), *Magnetic josephson junctions with superconducting interlayer for cryogenic memory*

[363] E. Goldobin, H. Sickinger, M. Weides, N. Ruppelt, H. Kohlstedt, R. Kleiner, and D. Koelle, Applied Physics Letters **102**, 242602-(1-4) (2013), *Memory cell based on a ϕ Josephson junction*

[364] A. V. Ustinov, Appl. Phys. Lett. **80**, 3153-3155 (2002), *Fluxon insertion into annular Josephson junctions*

[365] E. Goldobin, A. Sterck, T. Gaber, D. Koelle, and R. Kleiner, Phys. Rev. Lett. **92**, 057005-(1-4) (2004), *Dynamics of Semifluxons in Nb Long Josephson 0$-\pi$ Junctions*

[366] M. Paramonov, M. Yu. Fominsky, V. P. Koshelets, B. Neumeier, D. Koelle, R. Kleiner, and E. Goldobin, Appl. Phys. Lett. **104**, 062603-(1-4) (2014), *Radiation power and linewidth of a semifluxon-based Josephson oscillator*

[367] M. L. Kulić, Phys. Rev. A **76**, 053625-(1-4) (2007), *π-superconducting quantum interference device from ultracold fermionic atomic gases*

[368] R. Walser, E. Goldobin, O. Crasser, D. Koelle, R. Kleiner, and W. P. Schleich, New Journal of Physics **10**, 045020-(1-16) (2008), *Semifluxons in superconductivity and cold atomic gases*

[369] M. Grupp, W. P. Schleich, E. Goldobin, D. Koelle, R. Kleiner, and R. Walser, Physical Review A **87**, 021602-(1-5) (2013), *Emergence of atomic semifluxons in optical Josephson junctions*

[370] V. T. Petrashov, V. N. Antonov, P. Delsing, and T. Claeson, Zh. Eksp. Teor. Fiz. **60**, 589-594 (1994), Reprinted in JETP Lett. **60**, 606-611 (1994), *Phase controlled mesoscopic ring interferometer*; Phys. Rev. Lett. **74**, 5268-5271 (1995), *Phase Controlled Conductance of Mesoscopic Structures with Superconducting "Mirrors"*

[371] A. F. Volkov, Phys. Rev. Lett. **74**, 4730-4733 (1995), *New Phenomena in Josephson SINIS Junctions*

[372] A. F. Morpurgo, T. M. Klapwijk, and B. J. van Wees, Appl. Phys. Lett. **72**, 966-968 (1998), *Hot electron tunable supercurrent*

[373] J. J. A. Baselmans, A. F. Morpurgo, B. J. van Wees, and T. M. Klapwijk, Nature **397**, 43-45 (1999), *Reversing the direction of the supercurrent in a controllable Josephson junction*

[374] P. Cadden-Zimansky, J. Wei, and V. Chandrasekhar, Nature Physics **5**, 393-397 (2009), *Cooper-pair-mediated coherence between two normal metals*

[375] M. Eschrig, Nature Physics **5**, 384-385 (2009), *Superconductor-metal heterostructures: Coherent conductors at a distance*

[376] A. M. Bobkov and I. V. Bobkova, Phys. Rev. B **84**, 054533-(1-18) (2011), *Influence of spin-dependent quasiparticle distribution on the Josephson current through a ferromagnetic weak link*

[377] I. V. Bobkova and A. M. Bobkov Phys. Rev. Lett. **108**, 197002-(1-5) (2012), *Long-Range Proximity Effect for Opposite-Spin Pairs in Superconductor-Ferromagnet Heterostructures Under Nonequilibrium Quasiparticle Distribution*

[378] M. Silaev, P. Virtanen, F. S. Bergeret, and T. T. Heikkilä, Phys. Rev. Lett. **114**, 167002-(1-5) (2015), *Long-Range Spin Accumulation from Heat Injection in Mesoscopic Superconductors with Zeeman Splitting*

[379] M. Alidoust, K. Halterman, and J. Linder, Phys. Rev. B **88**, 075435-(1-5) (2013), *Singlet-triplet superconducting quantum magnetometer*

[380] A. G. Mal'shukov and A. Braatas, Phys. Rev. B **86**, 094517-(1-5) (2012), *Triplet supercurrent in ferromagnetic Josephson junctions by spin injection*

[381] Hao Meng, Xiuqiang Wu, and Feng Mei, Physics Letters A **378**, 2263-2269 (2014), *Long-range triplet Josephson current driven by the bias voltage*

[382] M. Houzet, Phys. Rev. Lett. 101, 057009-(1-4) (2008), *Ferromagnetic Josephson junction with precessing magnetization*

[383] C. Holmqvist, S. Teber, and M. Fogelström, Phys. Rev. B **83**, 104521-(1-18) (2011), *Nonequilibrium effects in a Josephson junction coupled to a precessing spin*

[384] C. Holmqvist, W. Belzig, and M. Fogelström, Phys. Rev. B **86**, 054519-(1-8) (2012), *Spin-precession-assisted supercurrent in a superconducting quantum point contact coupled to a single-molecule magnet*

[385] V. Braude and Ya. M. Blanter, Phys. Rev. Lett. **100**, 207001-(1-4) (2008), *Triplet Josephson effect with magnetic feedback in a superconductor-ferromagnet heterostructure*

[386] F. Konschelle and A. Buzdin, Phys. Rev. Lett. **102**, 017001-(1-4) (2009), *Magnetic Moment Manipulation by a Josephson Current*

[387] Liufei Cai and E. M. Chudnovsky, Phys. Rev. B **82**, 104429-(1-7) (2010), *Interaction of a nanomagnet with a weak superconducting link*

[388] J. Linder and T. Yokoyama, Phys. Rev. B **83**, 012501-(1-4) (2011), *Supercurrent-induced magnetization dynamics in a Josephson junction with two misaligned ferromagnetic layers*

[389] I. Kulagina and J. Linder, Phys. Rev. B **90**, 054504-(1-14) (2014), *Spin supercurrent, magnetization dynamics, and ϕ-state in spin-textured Josephson junctions*

[390] J. Linder and J. W. A. Robinson, Nature Physics **11**, 307-315 (2015), *Superconducting spintronics*

[391] S. Mai, E. Kandelaki, A. F. Volkov, and K. B. Efetov, Phys. Rev. B **84**, 144519-(1-12) (2011), *Interaction of Josephson and magnetic oscillations in Josephson tunnel junctions with a ferromagnetic layer*

[392] K. V. Samokhin, Ann. Phys. (N.Y.) **324**, 2385-2407 (2009), *Spin-orbit coupling and semiclassical electron dynamics in noncentrosymmetric metals*

[393] E. I. Rashba, Fizika Tverd. Tela **2** (6), 1224-1238 (1960), *Свойства полупроводников с петлей экстремумов. I. Циклотронный и комбинированный резонанс в магнитном поле, перпендикулярном плоскости петли*, Engl. transl.: Sov. Phys. Solid State **2**, 1109-1122 (1960), *Properties of semiconductors with an extremum loop .1. Cyclotron and combinational resonance in a magnetic field perpendicular to the plane of the loop*; Yu. L. Bychkov and E. I. Rashba, J. Phys. C **17**, 6039-6045 (1984), *Oscillatory effects and the magnetic susceptibility of carriers in inversion layers*

[394] G. Dresselhaus, Phys. Rev. **100**, 580-586 (1955), *Spin-Orbit Coupling Effects in Zinc Blende Structures*

[395] E. Bauer, G. Hilscher, H. Michor, Ch. Paul, E. W. Scheidt, A. Gribanov, Yu. Seropegin, H. Noël, M. Sigrist, and P. Rogl, Phys. Rev. Lett. **92**, 027003-(1-4) (2004), *Heavy Fermion Superconductivity and Magnetic Order in Noncentrosymmetric $CePt_3Si$*

[396] N. Kimura, K. Ito, K. Saitoh, Y. Umeda, H. Aoki, and T. Terashima, Phys. Rev. Lett. **95**, 247004-(1-4) (2005), *Pressure-Induced Superconductivity in Noncentrosymmetric Heavy-Fermion $CeRhSi_3$*

[397] I. Sugitani, Y. Okuda, H. Shishido, T. Yamada, A. Thamizhave l, E. Yamamoto, T. D. Matsuda, Y. Haga, T. Takeuchi, R. Settai, and Y. Ōnuki, J. Phys. Soc. Jpn. **75**, 043703-(1-4) (2006), *Pressure-Induced Heavy-Fermion Superconductivity in Antiferromagnet $CeIrSi_3$ without Inversion Symmetry*

[398] G. Amano, S. Akutagawa, T. Muranaka, Y. Zenitani, and J. Akimitsu, J. Phys. Soc. Jpn. **73**, 530-532 (2004), *Superconductivity at 18 K in Yttrium Sesquicarbide System, Y_2C_3*

[399] K. Togano, P. Badica, Y. Nakamori, S. Orimo, H. Takeya, and K. Hirata, Phys. Rev. Lett. **93**, 247004-(1-4) (2004), *Superconductivity in the Metal Rich Li-Pd-B Ternary Boride*; P. Badica, T. Kondo, and K. Togano, J. Phys. Soc. Jpn. **74**, 1014-1019 (2005), *Superconductivity in a New Pseudo-Binary $Li_2B(Pd_{1-x}Pt_x)_3$ ($x = 0 - 1$) Boride System*

[400] V. B. Geshkenbein and A. I. Larkin, Pis'ma Zh. Eksp. Teor. Fiz. **43**, 306-309 (1986), *Эффект Джозефсона в сверхпроводниках с тяжелыми фермионами*, Engl. transl.: JETP Lett. **43**, 395-399 (1986), *The Josephson effect in superconductors with heavy fermions*

[401] A. Buzdin, Phys. Rev. Lett. **101**, 107005-(1-4) (2008), *Direct Coupling Between Magnetism and Superconducting Current in the Josephson ϕ_0 Junction*

[402] A. A. Reynoso, Gonzalo Usaj, C. A. Balseiro, D. Feinberg, and M. Avignon, Phys. Rev. Lett. **101**, 107001-(1-4) (2008), *Anomalous Josephson Current in Junctions with Spin Polarizing Quantum Point Contacts*

[403] I. V. Krive, L. Y. Gorelik, R. I. Shekhter, and M. Jonson, Fiz. Nizk. Temp. **30**, 535-543 (2004), Reprinted in Low Temp. Phys. **30**, 398-404 (2004), *Chiral symmetry breaking and the Josephson current in a ballistic superconductor-quantum wire-superconductor junction*; I. V. Krive, A. M. Kadigrobov, R. I. Shekhter, and M. Jonson, Phys. Rev. B **71**, 214516-(1-13) (2005), *Influence of the Rashba effect on the Josephson current through a superconductor/Luttinger liquid/superconductor tunnel junction*

[404] T. Yokoyama, M. Eto, and Yu. V. Nazarov, J. Phys. Soc. Jpn. **82**, 054703-(1-9) (2013), *Josephson Current through Semiconductor Nanowire with Spin-Orbit Interaction in Magnetic Field*; Phys. Rev. B **89**, 195407-(1-14) (2014), *Anomalous Josephson effect induced by spin-orbit interaction and Zeeman effect in semiconductor nanowires*; T. Yokoyama and Yu. V. Nazarov, Europhysics Letters **108**, 47009-(1-5) (2014), *Magnetic anisotropy of critical current in nanowire Josephson junction with spin-orbit interaction*

[405] A. Zazunov, R. Egger, T. Jonckheere, and T. Martin, Phys. Rev. Lett. **103**, 147004-(1-4) (2009), *Anomalous Josephson Current through a Spin-Orbit Coupled Quantum Dot*

[406] A. A. Reynoso, Gonzalo Usaj, C. A. Balseiro, D. Feinberg, and M. Avignon, Phys. Rev. B **86**, 214519-(1-18) (2012), *Spin-orbit-induced chirality of Andreev states in Josephson junctions*

[407] A. G. Mal'shukov, S. Sadjina, and A. Brataas, Phys. Rev. B **81**, 060502-(1-4) (2010), *Inverse spin Hall effect in superconductor/normal-metal/superconductor Josephson junctions*

[408] J. Fröhlich and U. M. Studer, Commun. Math. Phys. **148**, 553-600 (1992), *U(1)×SU(2)-gauge invariance of non-relativistic quantum mechanics, and generalized Hall effects*; Rev. Mod. Phys. **65**, 733-802 (1993), *Gauge invariance and current algebra in nonrelativistic many-body theory*

[409] B. Berche and E. Medina, Eur. J. Phys. **34** 161-180 (2013), *Classical Yang-Mills theory in condensed matter physics*

[410] F. Konschelle, Eur. Phys. J. B **87** 119-(1-19) (2014), *Transport equations for superconductors in the presence of spin interaction*

[411] F. S. Bergeret and I. V. Tokatly, Phys. Rev. Lett. **110**, 117003-(1-6) (2013), *Singlet-Triplet Conversion and the Long-Range Proximity Effect in Superconductor-Ferromagnet Structures with Generic Spin Dependent Fields*; Phys. Rev. B **89**, 134517-(1-6) (2014), *Spin-orbit coupling as a source of long-range triplet proximity effect in superconductor-ferromagnet hybrid structures*

[412] F. Konschelle, arXiv:1408.4533 (2014), *Magneto-electric coupling in a two-dimensional ballistic Josephson junction with in-plane magnetic texture*; F. Konschelle, I. V. Tokatly, and F. S. Bergeret, Phys. Rev. B **92**, 125443 (2015), *Theory of the spin-galvanic effect and the anomalous phase-shift φ_0 in superconductors and Josephson junctions with intrinsic spin-orbit coupling*

[413] F. S. Bergeret and I. V. Tokatly, Europhys. Lett. **110**, 57005-(1-6) (2015), *Theory of diffusive φ_0 Josephson junctions in the presence of spin-orbit coupling*

[414] M. Houzet and J. S. Meyer, Phys. Rev. B **92**, 014509-(1-5) (2015), *Quasiclassical theory of disordered Rashba superconductors*

[415] W. Hanle, Naturwissenschaften **11**, 690-691 (1923), *Über den Zeemaneffekt bei der Resonanzfluoreszenz (On the Zeeman effect in resonance flourescence)*

[416] I. Žutić, J. Fabian, and S. Das Sarma, Rev. Mod. Phys. **76**, 323-410 (2004), *Spintronics: Fundamentals and applications*

[417] D. D. Awschalom and M. E. Flatté, Nature Physics **3**, 153-159 (2007), *Challenges for semiconductor spintronics*

[418] M. Silaev, P. Virtanen, T. T. Heikkilä, and F. S. Bergeret, Phys. Rev. B **91**, 024506-(1-7) (2015), *Spin Hanle effect in mesoscopic superconductors*

[419] Y. Aharonov and A. Casher, Phys. Rev. Lett. **53**, 319-321 (1984), *Topological Quantum Effects for Neutral Particles*

[420] Xin Liu, M. F. Borunda, Xiong-Jun Liu, and J. Sinova, Phys. Rev. B **80**, 174524-(1-12) (2009), *Control of Josephson current by Aharonov-Casher phase in a Rashba ring*

[421] Y. Aharonov and D. Bohm, Phys. Rev. **115** 485-491 (1959), *Significance of Electromagnetic Potentials in the Quantum Theory*

[422] M. V. Berry, Proc. R. Soc. A **392**, 45-57 (1984), *Quantal Phase Factors Accompanying Adiabatic Changes*

[423] Y. Aharonov and J. Anandan, Phys. Rev. Lett. **58**, 1593-1596 (1987), *Phase change during a cyclic quantum evolution*

[424] Y. Meir, Y. Gefen, and O. Entin-Wohlman, Phys. Rev. Lett. **63**, 798-800 (1989), *Universal effects of spin-orbit scattering in mesoscopic systems*

[425] H. Mathur and A. D. Stone, Phys. Rev. Lett. **68**, 2964-2967 (1992), *Quantum transport and the electronic Aharonov-Casher effect*

[426] A. G. Aronov and Y. B. Lyanda-Geller, Phys. Rev. Lett. **70**, 343-346 (1993), *Spin-orbit Berry phase in conducting rings*

[427] Tie-Zheng Qian and Zhao-Bin Su, Phys. Rev. Lett. **72**, 2311-2315 (1994), *Spin-orbit interaction and Aharonov-Anandan phase in mesoscopic rings*

[428] J. Nitta, F. E. Meijer, and H. Takayanagi, Appl. Phys. Lett. **75**, 695-697 (1999), *Spin-interference device*

[429] D. Loss, H. Schoeller, and P. M. Goldbart, Phys. Rev. B **59**, 13328-13337 (1999), *Observing the Berry phase in diffusive conductors: Necessary conditions for adiabaticity*; H.-A. Engel and D. Loss, Phys. Rev. B **62**, 10238-10254 (2000), *Conductance fluctuations in diffusive rings: Berry phase effects and criteria for adiabaticity*

[430] D. Frustaglia and K. Richter, Phys. Rev. B **69**, 235310-(1-7) (2004), *Spin interference effects in ring conductors subject to Rashba coupling*

[431] M. König, A. Tschetschetkin, E. M. Hankiewicz, Jairo Sinova, V. Hock, V. Daumer, M. Schäfer, C. R. Becker, H. Buhmann, and L. W. Molenkamp, Phys. Rev. Lett. **96**, 076804-(1-4) (2006), *Direct Observation of the Aharonov-Casher Phase*

[432] K. A. Matveev, A. I. Larkin, and L. I. Glazman, Phys. Rev. Lett. **89**, 096802-(1-4) (2002), *Persistent Current in Superconducting Nanorings*

[433] I. M. Pop, B. Doucot, L. Ioffe, I. Protopopov, F. Lecocq, I. Matei, O. Buisson, and W. Guichard, Phys. Rev. B **85**, 094503-(1-9) (2012), *Experimental demonstration of Aharonov-Casher interference in a Josephson junction circuit*

[434] M. T. Bell, W. Zhang, L. B. Ioffe, and M. E. Gershenson, arXiv:1504.05602 (2015), *Spectroscopic Evidence of the Aharonov-Casher effect in a Cooper Pair Box*

[435] S. V. Mironov, A. S. Mel'nikov, and A. I. Buzdin, Phys. Rev. Lett. **114**, 227001-(1-5) (2015), *Double path interference and magnetic oscillations in Cooper pair transport through a single nanowire*

[436] Chuan Li, A. Kasumov, A. Murani, Shamashis Sengupta, F. Fortuna, K. Napolskii, D. Koshkodaev, G. Tsirlina, Y. Kasumov, I. Khodos, R. Deblock, M. Ferrier, S. Guéron, and H. Bouchiat, Phys. Rev. B **90**, 245427-(1-5) (2014), *Magnetic field resistant quantum interferences in bismuth nanowires based Josephson junctions*

[437] S. Hoffman, Ya. M. Blanter, and Ya. Tserkovnyak, Phys. Rev. B **86**, 054427-(1-7) (2012), *Nonlinear dynamics in a magnetic Josephson junction*

[438] A. B. Vorontsov, I. Vekhter, and M. Eschrig Phys. Rev. Lett. **101**, 127003-(1-4) (2008), *Surface bound states and spin currents in noncentrosymmetric superconductors*; M. Sato and S. Fujimoto, Phys. Rev. B **79**, 094504-(1-16) (2009), *Topological phases of noncentrosymmetric superconductors: Edge states, Majorana fermions, and non-Abelian statistics*

[439] E. Majorana, Nuovo Cimento **14**, 171-184 (1937), *Teoria simmetrica dell'elettrone e del positrone*; English translation: Soryushiron Kenkyu **63**, 149-162 (1981), *A symmetric theory of electrons and positrons*, http://ci.nii.ac.jp/naid/110006469429/en

[440] F. Wilczek, Nature Physics **5**, 614-618 (2009), *Majorana returns*

[441] M. Sato, Y. Takahashi, and S. Fujimoto, Phys. Rev. Lett. **103**, 020401-(1-4) (2009), *Non-Abelian topological order in s-wave superfluids of ultracold fermionic atoms*; Phys. Rev. B **82**, 134521-(1-28) (2010), *Non-Abelian Topological Orders and Majorana Fermions in Spin-Singlet Superconductors*

[442] J. D. Sau, R. M. Lutchyn, S. Tewari, and S. Das Sarma, Phys. Rev. B **82**, 094522-(1-7) (2010), *Robustness of majorana fermions in proximity-induced superconductors*; R. M. Lutchyn, J. D. Sau, and S. Das Sarma, Phys. Rev. Lett. **105**, 077001-(1-4) (2010), *Majorana fermions and a topological phase transition in semiconductor-superconductor heterostructures*

[443] A. Brunetti, A. Zazunov, A. Kundu, and R. Egger, Phys. Rev. B **88**, 144515-(1-13) (2013), *Anomalous Josephson current, incipient time-reversal symmetry breaking, and Majorana bound states in interacting multilevel dots*

[444] A. M. Black-Schaffer and J. Linder, Phys. Rev. B **84**, 180509-(1-4)(R) (2011), *Majorana fermions in spin-orbit coupled ferromagnetic Josephson junctions*

[445] A. Yu. Kitaev, Uspekhi fiz. nauk **171** (Phys. Usp. **44**) (suppl.) 131-136 (2001), *Unpaired Majorana fermions in quantum wires*

[446] K. T. Law, and P. A. Lee, Phys. Rev. B **84**, 081304-(1-4)(R) (2011), *Robustness of Majorana fermion induced fractional Josephson effect*

[447] L. Jiang, D. Pekker, J. Alicea, G. Refael, Y. Oreg, and F. von Oppen, Phys. Rev. Lett. **107**, 236401-(1-5) (2011), *Unconventional Josephson signatures of Majorana bound states*

[448] P. A. Ioselevich and M. V. Feigel'man, Phys. Rev. Lett. **106**, 077003-(1-4) (2011), *Anomalous Josephson current via Majorana bound states in topological insulators*

[449] B. van Heck, F. Hassler, A. R. Akhmerov, and C. W. J. Beenakker, Phys. Rev. B **84**, 180502-(1-4)(R) (2011), *Coulomb stability of the 4π-periodic Josephson effect of Majorana fermions*

[450] P. San-Jose, E. Prada, and R. Aguado, Phys. Rev. Lett. **108**, 257001-(1-5) (2012), *AC Josephson effect in finite-length nanowire junctions with Majorana modes*

[451] D. I. Pikulin and Yu. V. Nazarov, Phys. Rev. B **86**, 140504-(1-5)(R) (2012), *Phenomenology and dynamics of Majorana Josephson junction*

[452] A. Zazunov and R. Egger, Phys. Rev. B **85**, 104514-(1-5) (2012), *Supercurrent blockade in Josephson junctions with a Majorana wire*

[453] F. Dominguez, F. Hassler, and G. Platero, Phys. Rev. B **86**, 140503-(1-5)(R) (2012), *On the dynamical detection of Majorana fermions in current-biased nanowires*

[454] D. M. Badiane, M. Houzet, and J. S. Meyer, Phys. Rev. Lett. **107**, 177002-(1-5) (2011), *Non-equilibrium Josephson effect through helical edge states*; M. Houzet, J. S. Meyer, D. M. Badiane, and L. I. Glazman, Phys. Rev. Lett. **111**, 046401-(1-5) (2013), *Dynamics of Majorana States in a Topological Josephson Junction*

[455] L. Fu and C. L. Kane, Phys. Rev. Lett. **100**, 096407-(1-4) (2008), *Superconducting Proximity Effect and Majorana Fermions at the Surface of a Topological Insulator*

[456] X.-L. Qi, T. L. Hughes, S. Raghu, and S.-C. Zhang, Phys. Rev. Lett. **102**, 187001-(1-4) (2009), *Time-Reversal-Invariant Topological Superconductors and Superfluids in Two and Three Dimensions*

[457] S. B. Chung, H.-J. Zhang, X.-L. Qi, and S.-C. Zhang, Phys. Rev. B **84**, 060510-(1-4) (2011), *Topological superconductivity and Majorana fermions in half-metal/superconductor heterostructure*

[458] J. Alicea, Rep. Prog. Phys. **75** 076501-(1-36) (2012), *New directions in the pursuit of Majorana fermions in solid state systems*

[459] R. Grein, J. Michelsen, and M. Eschrig, Journal of Physics: Conference Series **391**, 012149-(1-7) (2012), *A Numerical Study of the Superconducting Proximity Effect in Topological Surface States*

[460] C. W. J. Beenakker, Annu. Rev. Condens. Matter Phys. **4**, 113-136 (2013), *Search for Majorana Fermions in Superconductors*

[461] J.-P. Xu, C. Liu, M.-X. Wang, J. Ge, Z.-L. Liu, X. Yang, Y. Chen, Y. Liu, Z.-A. Xu, C.-L. Gao, D. Qian, F.-C. Zhang, and J.-F. Jia, Phys. Rev. Lett. **112**, 217001-(1-5) (2014), *Artificial Topological Superconductor by the Proximity Effect*

From Fluctuation Phenomena in Superconductors by Larkin, Varlamov

References

[1] V.L.Ginzburg, L.D.Landau, *Zh. Exp. & Teor. Fiz.* **20**, 1064 (1950).

[2] J.Bardeen, L.N.Cooper, J.R.Schrieffer, *Phys.Rev.* **106**, 162; **108**, 1175; (1957).

[3] V.L.Ginzburg, *Soviet Solid State* **2**, 61 (1960).

[4] A.P.Levanyuk, *Zh. Exp. & Teor. Fiz.* **36**, 810 (1959).

[5] L.G.Aslamazov, A.I.Larkin, *Soviet Solid State* **10**, 875 (1968); *Phys. Letters* **26A**, 238 (1968).

[6] K.Maki, *Progr. Theor. Phys.* (Kyoto) **39**, 897 (1968); **40**, 193 (1968).

[7] R.S.Thompson, *Phys. Rev.* **B1**, 327 (1970).

[8] R.E.Glover, *Phys. Rev. Lett.* **A25**, 542 (1967); *J. Low Temp. Phys.* **6**, (1970).

[9] K.Maki, in *Superconductivity,* edited by R.D.Parks (Dekker, New York), (1969).

[10] L.P.Gorkov, *Zh. Exp. & Teor. Fiz.* **37**, 1407 (1959).

[11] V.V.Schmidt, in *Proceedings of the 10th International Conference on Low Temperature Physics*, (VINITI, Moscow), **C2**, 205 (1967).

[12] Tsuboi Taketumi, Suzuki Takao, *Journ. of Phys. Soc. of Japan* **42**, (1977).

[13] A.I.Larkin, *Ann.Phys.*(Leipzig) **8**, 785 (1999).

[14] A.I. Larkin, Yu. N. Ovchinnikov. *Zh. Exp. & Teor. Fiz.* **119**, 595 (2001); *cond-mat/*0010014 (2000).

[15] L.D.Landau, A.A.Abrikosov, I.M.Khalatnikov, *DAN USSR.* **95**, 437, ibid.773, ibid 1177, (1954).

[16] I.T.Dyatlov, V.V. Sudakov, K.A.Ter-Martirosyan, *Zh. Exp. & Teor. Fiz.* **32**, 767 (1957).

[17] V.V.Sudakov, *DAN USSR.* **111**, 338 (1956).

[18] A.I.Larkin, D.E.Khmelnitski, *Zh. Exp. & Teor. Fiz.* **56**, 2087 (1969).

[19] M.Gel Man, F.E.Low, *Phys.Rev.* **95**, 1300 (1954).

[20] E.S.Stueckelberg, A.Peterman, *Helv. Phys. Acta* **24**, 153 (1951).

[21] C. Di Castro, G.Jona-Lasinio, *Physics Lett.* **A29**, 322 (1969).

[22] K.G.Wilson, *Phys.Rev.* **B4**, 3174, ibid. 3184(1971).

[23] A.S.Patashinski, V.L.Pokrovski, *The Fluctuation Theory of Phase Transitions,* Nauka, Moscow (1982).

[24] A.A.Varlamov, L.Yu, *Phys.Rev.* **44**, 7078 (1991).

[25] T.Tsuzuki, *Journ. Low Temp. Phys.* **9**, 525 (1972).

[26] D.E.Prober, M.R.Beasley, R.E.Schwall, *Phys. Rev.* **B15**, 5245 (1977).

[27] W.E.Lawrence and S.Doniach, *Proceedings of the Twelfth International Conference on Low Temperature Physics*, edited by E.Kanda, Academic Press of Japan, Kyoto, p.361 (1971).

[28] K.Yamaji, *Phys. Lett.* **A38**, 43 (1972).

[29] L.G.Aslamazov and A.I.Larkin, *Zh. Exp. & Teor. Fiz.* **67**, 647 (1973).

[30] A.Schmid, *Phys. Rev.* **180**, 527 (1969).

[31] H.Schmidt, *Z. Phys.* **B216**, 336 (1968).

[32] R.E.Prange, *Phys. Rev.* **B1**, 2349 (1970).

[33] B.R.Patton, V.Ambegaokar, J.W.Wilkins, *Solid St.Commun.* **7**, 1287, (1969).

[34] J.Kurkijarvi, V.Ambegaokar and G.Eilenberger, *Phys. Rev.* **B5**, 868 (1972).

[35] J.P. Gollub, M.R.Beasley, R.S.Newbower, M.Tinkham, *Phys. Rev.Lett.* **22**, 1288 (1969).

[36] J.P. Gollub, M.R.Beasley, M.Tinkham, *Phys. Rev.Lett.* **25**, 1646 (1970).

[37] J.P. Gollub, M.R.Beasley, R.Callarotti, M.Tinkham, *Phys. Rev.* **B7**, 3039 (1973).

[38] P.A.Lee, S.R.Shenoy, *Phys. Rev.Lett.* **28**, 1025 (1972).

[39] S.P.Farrant, C.E.Gough, *Phys. Rev.Lett.* **34**, 943 (1975).

[40] W.J.Skocpol and M.Tinkham, *Rep.Prog. Phys.* **38**, 1094 (1975).

[41] R.S.Thompson, V.Z.Kresin, *Mod. Phys. Lett.* **B2**, 1159 (1988).

[42] K.F.Quader, E.Abrahams, *Phys. Rev.* **B38**, 11977 (1988).

[43] W.C.Lee, R.A.Klemm, D.C.Johnson, *Phys. Rev.Lett.* **63**, 1012 (1989).

[44] P.Carretta, A.Lascialfari, A.Rigamonti, A.Rosso, A.Varlamov, *Phys. Rev.* **B61**, 12420 (2000).

[45] T.M.Mishonov, E.S.Penev, Thermodynamics of Gaussian Fluctuations and paraconductivity in layered superconductors. *International Journal of Modern Physics* **14,** 3831 (2000) (cond-mat N 0004023).

[46] A.Buzdin, V.Dorin in *"Fluctuation Phenomena in High Temperature Superconductors"*, ed. by M.Ausloos and A.A.Varlamov, NATO-ASI Series, Kluwer, Dordrecht (1997).

[47] T.Mishonov, in *"Physics and material Science of High Temperature Superconductors "* , NATO ASI E 181, Edited by R.Kossovski et al., (Kluwer, Dordrecht, 1990).

[48] A.Koshelev, *Phys. Rev.* **B50**, 506 (1994).

[49] R.A.Klemm, M.R.Beasley, A.Luther, *Phys. Rev.* **B8**, 5072 (1973).

[50] S.Hikami, A.Fujita, A.I. Larkin, *Phys. Rev.* **B44**, 10400 (1991).

[51] C.Baraduc, A.Buzdin, J-Y. Henry, J.P.Brison and L.Puech, *Physica* **C248**, 138 (1995).

[52] A.Junod, J-Y.Genoud, G.Triscone, *Physica* **C294**, 115 (1998).

[53] A.Lascialfari, A.Rigamonti, P.Tedesco, to be published (2001).

[54] A.I.Buzdin, B.Vuyichich, *Mod. Physics Letters* **B4,** 485 (1990).

[55] L.Glazman, A.Koshelev, *Soviet JETP* **70**, 774 (1990); A.Koshelev, private communication, (1999).

[56] V.S.Berezinskii, *Zh. Exp. & Teor. Fiz. Letters* **34**, 610 (1971).

[57] J.M.Kosterlitz and P.J.Thouless, *J. Phys.* **C6**, 1181 (1973).

[58] D.R.Nelson, J.M.Kosterlitz, *Phys. Rev.Lett.* **39**, 1201 (1977).

[59] P.C.Hohenberg, *Phys. Rev.* **158**, 383 (1967).

[60] P.Minnhagen, *Rev. Mod. Phys.* **59**, 1001 (1987).

[61] P.Minnhagen in *"Fluctuation Phenomena in High Temperature Superconductors"*, ed. by M.Ausloos and A.A.Varlamov, NATO-ASI Series, Kluwer (1997).

[62] V.Vaks, A.Larkin, *Soviet JETP* **22**, 678 (1966).

[63] W.A.Little, *Phys. Rev.* **166**, 398 (1967).

[64] J.S.Langer, V.Ambegaokar, *Phys. Rev.* **164**, 498 (1967).

[65] B.I.Halperin, T.C.Lubenski, Shang-keng Ma, *Phys. Rev.Lett.* **32**, 292 (1974).

[66] A. Schmid. *Phys. Konden. Mater.* **5**, 302 (1966).

[67] C.Caroli, K. Maki, *Phys. Rev.* **159**, 306,316 (1967).

[68] E. Abrahams, T. Tsuneto, *Phys. Rev.* **152**, 416 (1966).

[69] J.W.F.Woo, E. Abrahams, *Phys. Rev.* **169**, 407 (1968).

[70] C. Di Castro, W.Young, *Il Nuovo Cimento* **B62**, 273 (1969).

[71] S.Ullah, A.T.Dorsey, *Phys. Rev.* **B44**, 262 (1991).

[72] L.P. Gor'kov, G.M. Eliashberg. *Zh. Exp. & Teor. Fiz.* **54**, 612 (1968).

[73] L.G.Aslamazov, A.I.Larkin, Proceedings of the "1st European conference on condesed matter" European Phys.Soc, Geneva, Switzerland (1971).

[74] T.Mishonov, A.Pozheninnikova, J.Indekeu, to be published (2001).

[75] L.D.Landau, E.M.Lifshitz, *Course of Theoretical Physics, vol.3, "Quantum Mechanics "*, Pergamon Press, Oxford, (1978).

[76] A.A.Varlamov, G.Balestrino, D.Livanov, E.Milani, *Advances in Physics* **48,** 655 (1999).

[77] K.B.Efetov, *Zh. Exp. & Teor. Fiz.* **76**, 1781 (1979).

[78] G.Blatter, V.B.Geshkenbein, A.I.Larkin, *Phys. Rev. Lett.* **68**, 875 (1992).

[79] P.W.Anderson, *J. Phys. Chem. Sol.* **11**, 26 (1959).

[80] A.A.Abrikosov, L.P.Gorkov, *Soviet JETP* **8,** 1090; **9,** 220 (1959).

[81] A.Kapitulnik and G.Kotliar, *Phys. Rev. Lett.* **54**, 474 (1985).

[82] P.Wollhardt and D. Wolfle, " *Anderson localization ",* edited by Y. Nagaoka and H.Fukuyama, Springer Verlag, Berlin, (1982).

[83] L.N.Bulaevski, A.A.Varlamov, M.V.Sadovski, *Soviet Solid State Physics* **28**, 997 (1986).

[84] M.P.A.Fisher, *Phys. Rev. Lett.* **65**, 923 (1990).

[85] Yu.N.Ovchinnikov, *Soviet JETP* **36**, 366 (1973).

[86] S.Maekawa and H.Fukuyama, *Journ. of Phys. Soc. of Japan* **51**,1380 (1982); H.Takagi and Y.Kuroda, *Solid State Commun.* **41**, 643 (1982).

[87] A.A.Varlamov, V.V.Dorin, *Sov. JETP* **64**, 1159 (1986).

[88] A.M.Finkelstein, *Soviet JETP Letters* **45**, 37 (1987).

[89] A.Goldman and N.Markovic, *Physics Today*, November 1998 and refs.inside.

[90] G.M.Eliashberg, *Soviet JETP* **11**, 696 (1960).

[91] B.N.Narozhny, *Soviet JETP* **77**, 301 (1993); *Phys. Rev.* **B49**, 6375 (1994).

[92] A.A.Abrikosov, L.P.Gorkov, I.E.Dzyaloshinski, *"Methods of the quantum field theory in statistical physics "*, Dover Publications, New York (1963).

[93] E.Abrahams, M.Redi, and C.Woo, *Phys. Rev.* **B1**, 218 (1970).

[94] C.Di Castro, C.Castellani, R.Raimondi, A.Varlamov, *Phys. Rev.* **B49**, 10211 (1990).

[95] L.B.Ioffe, A.I.Larkin, A.A.Varlamov, L.Yu, *Phys. Rev.* **B47**, 8936 (1993); *Physica* **C 235-240**, 1963 (1994).

[96] K.E.Gray, D.H.Kim, *Phys. Rev. Lett.* **70**, 1693 (1993).

[97] V.V.Dorin, R.A.Klemm, A.A.Varlamov, A.I.Buzdin, D.V.Livanov, *Phys. Rev.* **B48**, 12951 (1993).

[98] L.G.Aslamazov, A.A.Varlamov, *Journ. of Low Temp. Phys.* **38**, 223 (1980).

[99] B.L.Altshuler, M.Yu.Reizer and A.A.Varlamov, *Soviet JETP* **57**, 1329 (1983).

[100] A.I.Larkin, D.E.Khmelnitski, *Soviet Phys. Uspekhi,* **136,** 536 (1982).

[101] W.Breing, M.C.Chang, E.Abrahams, P.Wolfle, *Phys.Rev.* **B 31**, 7001 (1985).

[102] A.A.Abrikosov, *Fundamentals of the Theory of Metals*, North-Holland, Elsevier, Groningen (1988).

[103] R.A.Klemm and S. H.Liu, *Phys. Rev.* **B49**, 6375 (1994).

[104] S. H.Liu and R.A.Klemm *Phys. Rev.* **B48**, 4080; ibid 10650 (1993).

[105] B.L.Altshuler and A.G.Aronov, *Electron-Electron Interaction in Disordered Conductors* in Efros, A.L. and Pollak, M. (eds.), Elseiver Scientific Publishing (1985).

[106] G.M.Eliashberg, *Zh. Exp. & Teor. Fiz.* **41**, 1241 (1961).

[107] R.A.Klemm, *J. Low Temp. Phys.* **16**, 381 (1974).

[108] C.Baraduc, V.Pagnon, A.Buzdin, J.Henry, C.Ayache, *Phys. Lett.* **A166,** 267 (1992).

[109] S.Ami, K.Maki, *Phys. Rev.* **B18**, 4714 (1978).

[110] B.R.Patton, *Phys. Rev. Lett.* **27,** 1273 (1971).

[111] J.Keller, V Korenman, *Phys. Rev. Lett.* **27,** 1270 (1971); *Phys. Rev.* **B5,** 4367 (1972).

[112] S.Yip, *Phys. Rev.* **B41**, 2612 (1990).

[113] P.Carretta, A.Rigamonti, A.A.Varlamov, D.V.Livanov, *Phys. Rev.* **B54**, R9682 (1996).

[114] A.Varlamov, *Europhysics Letters* **28**, 347 (1994).

[115] M. Reizer, *Phys. Rev.* **B45**, 12949 (1992).

[116] M.Ausloos, Ch.Laurent, *Phys. Rev.* **B37**, 611 (1988).

[117] P.P.Frietas, C.C.Tsuei, T.S.Plaskett, *Phys. Rev.* **B36**, 833 (1987).

[118] M.Hikita, M.Suzuki, *Phys. Rev.* **B41**, 834 (1990).

[119] M.Akinaga, D.Abukay, L.Rinderer, *Mod. Phys. Lett.* **2**, 891 (1988).

[120] A.Poddar, P.Mandal, A.N.Das, B.Ghosh, P.Choudhury, *Physica* **C159** , 231 (1989).

[121] D.H.Kim, A.M.Goldman, J.H.Kang, K.E.Gray, R.T.Kampwirth, *Phys. Rev.* **B39**, 12275 (1989).

[122] G.Balestrino, A.Nigro, R.Vaglio, *Phys. Rev.* **B39**, 12264 (1989).

[123] G.Kumm, K.Winzer, *Physica* **B165-166** , 1361 (1990).

[124] M.R.Cimberle, C.Ferdeghini, D.Marrè, M.Putti, S.Siri, F.Federici, A.Varlamov, *Phys. Rev.* **B55**, R14745 (1997).

[125] L.Reggiani, R.Vaglio, A.Varlamov, *Phys. Rev.* **B44**, 9541 (1991).

[126] G.Balestrino, E.Milani, A.Varlamov, *Physica* **C210** , 386 (1993).

[127] G.Balestrino, E.Milani, and A.A.Varlamov, *JETP Letters* **61**, 833 (1995).

[128] Y.F.Yan, P.Matl, J.M.Harris and N.P.Ong, *Phys. Rev.* **B52**, R751 (1995) ; N.P.Ong, Y.F.Yan, and J.M.Harris, *Procedings of CCAST Symposium on High Tc Superconductivity and the C60 Family*, Beijing, (1994).

[129] W.Lang, *Physica* **C282-287,** (1997).

[130] K.Nakao, K.Takamaku, K.Hashimoto, N.Koshizuka and S.Tanaka, *Physica* **B201**, 262 (1994).

[131] K.Hashimoto, K.Nakao, H.Kado and N.Koshizuka, *Phys. Rev.* **B53**, 892 (1996).

[132] G.Heine, W.Lang, X.L.Wang and X.Z.Wang, *J. Low Temp. Phys.* **105,** 945 (1996).

[133] T. Kimura, S. Miyasaka, H. Takagi, K. Tamasaku, H. Eisaki, S. Uchida, M. Hiroi, M. Sera, K. Kobayashi, *Phys. Rev.* **B53**, 8733 (1996).

[134] J.Axnas, W.Holm, Yu.Eltsev, and O.Rapp, *Phys Rev. Lett.* **77**, 2280 (1996).

[135] A. Wahl, D. Thopart, G. Villard, A. Maignan, V. Hardy, J.C. Soret, L.Ammor, A.Ruyter, *Phys. Rev.* **B59**, 7216 (1999).

[136] M.Suzuki and M. Hikita, *Phys. Rev.* **B39**, 4756 (1989); *Phys. Rev.* **B44**, 249 (1991).

[137] A.Matsuda, T.Ishii, K.Kinishita, T.Yamada, *Physica* **C162-164**, 371 (1989); A.Matsuda, T.Hirai, S.Komiyama, *Solid State Commun.* **68**, 103 (1988).

[138] J.Sugawara, H.Iwasaki, N.Kobayashi, H.Yamane and T.Hirai, *Phys. Rev.* **B46**, 14818 (1992).

[139] W.Holm, M.Andersson, O.Rapp, M.A.Kulikov and I.N.Makarenko, *Phys. Rev.* **B48**, 4227 (1993).

[140] W.Lang, G.Heine, W.Kula and R.Sobolewski, *Phys. Rev.* **B51**, 9180 (1995).

[141] W.Holm, O.Rapp, C.N.L.Johnson and U.Helmersson, *Phys. Rev.* **B52**, 3748 (1995).

[142] Yu.I.Latyshev, O.Laborde and P.Monceau, *Europhysics Letters* **29**, 495 (1995).

[143] W. Lang, *Z. Phys.* **B97**, 583 (1995).

[144] T.Watanabe, A.Matsuda, *Physica* **C263**, 313 (1996).

[145] W.Lang, *Physica* **C245**, 69 (1995).

[146] W. Volz, F.S. Razavi,G. Quiron, H.-U. Habermeier, A.L. Solovjov, *Phys. Rev.* **B55** 6631 (1997).

[147] C.Sekirnjak, W.Lang, S.Proyer, P.Schwab, *Physica* **C243**, 60 (1995).

[148] S.Hikami, A.I.Larkin, *Mod. Phys. Lett.* **B2**, 693 (1988).

[149] A.G.Aronov, S.Hikami and A.I.Larkin, *Phys. Rev. Lett.* **62**, 965 (1989).

[150] J.B.Bieri and K.Maki, *Phys. Rev.* **B42**, 4854 (1990).

[151] J.B.Bieri, K.Maki, and R.S.Thompson, *Phys. Rev.* **B44**, 4709 (1991).

[152] A.S.Nygmatulin, A.Varlamov, D.Livanov, G.Balestrino and E.Milani, *Phys. Rev* **B53** (1996).

[153] A. Wahl, D. Thopart, G. Villard, A. Maignan, Ch.Simon, J.C.Soret, L.Ammor, A.Ruyter, *Phys. Rev.* **B60**, 12495 (1999).

[154] A.Buzdin, A.Varlamov, *Phys. Rev.* **B58**, 14195 (1998).

[155] D.Thopart, A. Wahl, Ch.Simon, J.C.Soret, L.Ammor, A.Ruyter, A.Buzdin, A.A.Varlamov, S. de Brion, *Phys. Rev.* **B62**, 9721 (2000).

[156] A.A.Abrikosov, L.P.Gorkov, *Soviet JETP* **11**, 1781 (1960).

[157] R.Ikeda, T.Ohmi, and T.Tsuneto, *Journ. of Phys. Soc. of Japan Letters* **58**, 1377 (1989); ibid. **60**, 1051 (1991).

[158] D.Livanov, E.Milani, G.Balestrino and C.Aruta, *Phys. Rev.* **B55** R8701 (1997).

[159] K.Maki, *Phys. Rev. Lett.* **30**, 648 (1973).

[160] I.S.Beloborodov, K.B.Efetov, A.I.Larkin, *Phys. Rev.* **B61**, 9145 (2000).

[161] L.N.Bulaevski, *Zh. Exp. & Teor. Fiz.* **66,** 2212(1974).

[162] A.I.Larkin, *Zh. Exp. & Teor. Fiz. Letters* **31**, 219 (1980).

[163] E.Abrahams, *J. Stat. Phys.* **38**, 89 (1985); J.M.B. Lopes dos Santos, E.Abrahams, *Phys. Rev.* **B31**, 172 (1985).

[164] M.E.Gershenzon, V.N.Gubankov, Yu.E.Zhuravlev, *Solid State Commun.* **45**, 87 (1983).

[165] R.Rosenbaum, *Phys. Rev.* **B32**, 2190 (1985).

[166] N.Mori, *Jpn. J. Appl. Phys. Suppl.* **26**, 1339 (1987).

[167] B.I.Belevtsev, Yu.F.Komnik, A.V.Fomin, *J. Phys.* **B58**, 111 (1985); *Fiz. Nizk. Temp. (USSR)* **10,** 850 (1984).

[168] V.M.Galitski, A.I.Larkin, *Phys. Rev.* **B63**, 1745X (2001).

[169] H.Fukuyama, H.Ebisawa, and T.Tuzuki, *Prog. Theor. Phys.* **46**,1028 (1971).

[170] E.Abrahams, R.E.Prange, and M.E.Stephen, *Physica* **55,** 230 (1971).

[171] T.Inoue, S.Miwa, K.Okamoto, M.Awano, *Journ. of Phys. Soc. of Japan* **46**, 418 (1979).

[172] A.A.Varlamov and D.V.Livanov, *Soviet JETP* **71**, 325 (1990).

[173] A.G.Aronov and A.B. Rapoport, *Mod. Phys. Lett.* **B6**,1093 (1992).

[174] A.G.Aronov, S.Hikami and A.I.Larkin, *Phys. Rev.* **B51**, 3880 (1995).

[175] D.V.Livanov, G.Savona, A.A.Varlamov, *Phys. Rev.* **B62,** 8675 (2000).

[176] M.Randeria and A.A.Varlamov, *Phys. Rev.* **B50**, 10401 (1994).

[177] I.Aleiner, L.Glazman, A.Rudin, *Phys. Rev.* **B55**, 322 (1997).

[178] A.I.Larkin, Yu.A.Ovchinnikov, *J. Low Temp. Phys.* **10**, 407 (1973).

[179] A.A.Varlamov and V.V.Dorin, *Soviet JETP* **57**, 1089 (1983).

[180] M.Eschrig, D.Rainer, J.Souls, *Phys.Rev.* **B59**, 12095 (1999).

[181] J.Axnaes, *J. Low Temp. Phys.* **117**, 259 (1999).

[182] R.W.Cohen, B.Abels, *Phys. Rev.* **168**, 444 (1968).

[183] B.L.Altshuler and A.G.Aronov, *Soviet JETP* **50**, 968 (1979).

[184] M.Belogolovski, O. Chernyak and A.Khachaturov, *Fiz. Nizk. Temp. (USSR)* **12**, 630 (1986).

[185] M.Park, M.S.Isaacson, J.M.Parpia, *Phys. Rev. Lett.* **75**, 3740 (1995).

[186] H.J.Tao, Farun Lu, E.L.Wolf, *Physica C* **282-287,** 563 (1997).

[187] T.Watanabe et al., *Phys. Rev. Lett.* **79,** 2113 (1997); A.Matsuda, S.Sugita, T.Watanabe, *Phys. Rev.* **B60,** 1377 (1999); T.Watanabe, T.Fujii, A.Matsuda, *Phys. Rev. Lett.* **84,** 5848 (2000).

[188] M.Suzuki, S.Karimoto, K.Namekawa, *Journ. of Phys. Soc. of Japan* **67,** v.3 (1998).

[189] Ch.Renner, B.Revaz, J-Y. Genoud, K.Kadowaki and O.Fischer, *Phys. Rev. Lett.* **80,** 149 (1998).

[190] A.M.Cucolo, M.Cuoco, A.A.Varlamov, *Phys. Rev. Lett.* **59,** R11675 (1999).

[191] M. Yu. Reizer, *Phys. Rev.* **B48**, 13703 (1993).

[192] K.Maki, R.S.Thompson, *Physica* **C162-164,** 1441 (1989).

[193] A.I. Larkin, Yu.N. Ovchinnikov. *Zh. Exp. & Teor. Fiz.* **61**, 2147 (1971).

[194] A.A.Varlamov, V.V.Dorin and I.E.Smolyarenko, *Soviet JETP* **67**, 2536 (1988).

[195] A. Schmid, G. Schon. *J. Low Temp. Phys.* **20**, 207 (1975).

[196] A.I. Larkin, Yu. N. Ovchinnikov. *Zh. Exp. & Teor. Fiz.* **68**, 1916 (1975).

[197] A.I. Larkin, Yu.N. Ovchinnikov. In *"Nonequilibrium superconductivity"*. Edited by D.N. Langenberg and A.I. Larkin. Elsevier Science Publishers B.V. 1986.

[198] A.I. Larkin, Yu.N. Ovchinnikov. *Zh. Exp. & Teor. Fiz.* **73**, 299 (1977).

[199] F.Federici, A.A.Varlamov, *JETP Letters* **64**, 497 (1996); *Phys. Rev.* **B57**, 6071 (1997).

[200] A.Varlamov, D.Livanov, L.Reggiani, *Physics Letters* **A165**, 369 (1992).

[201] A.Varlamov, D.Livanov, F.Federici, *JETP Letters* **65**, 182 (1997).

[202] K.Maki, *J. Low Temp. Phys.* **14**, 419 (1974).

[203] M.Yu.Reizer and A.V.Sergeev, *Phys. Rev.* **B50**, 9344 (1994).

[204] M.A.Howson et al., *Phys. Rev.* **B41**, 300 (1990).

[205] N.V.Zavaritski, A.V.Samoilov, A.A.Yurgens, *JETP Letters* **55**, 127 (1992).

[206] S.Keshri, P.K.Barhai, *Chech. J. Phys.*, **47**, 249 (1997).

[207] J.Mosqueira, J.A.Viera, F.Vidal, *Physica* **C229,** 301 (1994); J.Mosqueira, J.A.Viera, J.Masa, O.Cabeza, F.Vidal, *Physica* **C253,** 1 (1995);

[208] T.Maniv, S.Alexander, *J. Phys.* **C10**, 2419 (1977).

[209] T.Maniv, S.Alexander, *Solid State Commun.* **18**, 1197 (1976).

[210] K.Kuboki, H.Fukuyama, *Journ. of Phys. Soc. of Japan* **58,** 376 (1989).

[211] J.Heym, *J. Low Temp. Phys.* **89**, 859 (1992).

[212] P.Mosconi, A.Rigamonti, A.Varlamov, *Applied Magnetic Resonance* **19,** 345 (2000).

[213] V. Mitrovic et al., *Phys. Rev. Lett.* **82**, 2784 (1999).

[214] H.Zimmermann, M.Mali, M.Bankey, D.Brinkmann, *Physica* **C185 - 189**, 1145 (1991); D. Brinkmann, *Appl. Magn. Resonance* **8**, 67 (1995).

[215] K.Gorny et al., *Phys. Rev. Lett.* **82**, 177 (1999).

[216] G.Zheng et al., *Phys. Rev.* **B60**, R9947 (1999); G.Zheng et al., *Phys. Rev. Lett.* **85**, 405 (2000).

[217] M.Ausloos and A.A.Varlamov, Editors of *"Fluctuation Phenomena in High Temperature Superconductors"*, ed. by NATO-ASI Series, Kluwer, Dordrecht (1997).

[218] J.Bok, G.Deutcher, D.Pavuna, S.A.Wolf, Editors of *"Gap Symmetry and Fluctuations in High Temperature Superconductors"* (Plenum, London) (1998).